The Crystal Structure of Quinolinium 2-Dicyanomethylene-1,1,3,3-tetracyanopropanediide, $[2(C_9NH_8)^+ \cdot (C_{10}N_6)^{2-}]$

Seiki SAKANOUE[1], Noritake YASUOKA, Nobutami KASAI[2], and Masao KAKUDO*

Department of Applied Chemistry, Faculty of Engineering, Osaka University, Yamadakami, Suita, Osaka

* *Institute for Protein Research, Osaka University, Joancho, Kita-ku, Osaka*

(Received April 2, 1970)

$[2(C_9NH^8)^+ \cdot (C_{10}N_6)^{2-}]$ crystallizes in the form of the space group of *Pbcn*, with four formula units in the unit cell, and the following unit-cell dimensions: $a=13.18$, $b=15.40$, and $c=11.56$ Å. The structure was determined by obtaining phases directly from the structure-factor magnitudes by means of the symbolic addition procedure. For 1580 non-zero reflections, the final R is 0.147. The crystal structure shows that the packing unit is an "ion-pair" consisting of one di-valent anion and two mono-valent cations. The anion is sandwiched by two cations with weak charge-transfer interaction between them; the closest atomic contact is 2.99 Å. These units stack infinitely, forming a column, along the a axis. Between these stacking columns, there exists a hydrogen bond (N–H···N, 2.84 Å) along the b axis. The $(C_{10}N_6)^{2-}$ anion has a C_2-2 symmetry; cyano-substituents are tilted out of the plane formed by four central carbon atoms, and the anion takes a propeller shape. The one arm is rotated 13° from the completely planar conformation, while the other two are rotated 24°. On the other hand, the $(C_9NH_8)^+$ cation seems not to be planar.

In the electronic spectra of some complexes, charge-transfer bands between organic cation and organic anion have been observed.[3] No studies have yet been reported, however, to explain the charge-transfer bands between organic cations and anions on the basis of the crystal structure.

The electronic spectra and the electrical and other physical properties of the salts of the 2-dicyanomethylene-1,1,3,3-tetracyanopropane anion and *N*-heteroaromatic cations have been studied by Sakanoue *et al.*[4] Among these substances is the quinolinium 2-dicyanomethylene-1,1,3,3-tetracyanopropanediide. The absorption maximum of this salt at 410 nm has been assumed, on the basis of the behavior of this band in solutions, to be due to the charge-transfer interaction between the anion and the cation. This band is also observed in the solid absorption spectrum in 415 nm; the polarized absorption spectrum of single crystals was measured.[4] In order to establish the relationship between the orientation of the ions in the crystal and the polarization behavior of the band, a single-crystal structure analysis of the salts was undertaken by means of X-rays; the preliminary results have already been reported.[5] Interest in the structure of the anion in this crystal also prompted the present study in relation to the structure of the anion in the calcium salt.[6]

Experimental

Yellow crystals were obtained from a saturated aqueous solution by slow evaporation at room temperature. A small, regular-shaped crystal (about $0.20\times0.22\times0.24$ mm) was selected.

Oscillation and Weissenberg X-ray photographs were taken, using nickel-filtered Cu$K\alpha$ radiation ($\lambda=1.5418$ Å), around the a and c axes. The unit-cell dimensions were determined from the Weissenberg photographs, on which powder diffraction patterns of tungsten ($a=3.16535$ Å) were superposed for calibration.

The crystals are orthorhombic, with the unit cell dimensions of $a=13.18$, $b=15.40$, and $c=11.56$ Å. The systematic absence of reflections, $0kl$ with $k\neq2n$, $h0l$ with $l\neq2n$, and $hk0$ with $h+k\neq2n$, uniquely determined the space group to be *Pbcn*. The density, measured at 14°C by flotation in a benzene-carbon tetrachloride mixture, was 1.318 g·cm^{-3}, whereas the calculated value, assuming four formula units, $[2(C_9NH_8)^+ \cdot (C_{10}N_6)^{2-}]$, per unit cell, was 1.314 g·cm^{-3}.

Using nickel-filtered Cu$K\alpha$ radiation, the intensity data were collected, by the multiple-film equi-inclination technique, for the layers from $0kl$ through $8kl$ and from $hk0$ through $hk8$.

The intensities were estimated visually, and were corrected for the Lorentz and polarization effects, but the absorption correction was ignored ($\mu=6.6$ cm^{-1} for Cu$K\alpha$). In all, 2003 independent (1580 non-zero) reflections were obtained.

Structure Determination

There were considerable difficulties in interpreting the sharpened and unsharpened Patterson maps computed from the three-dimensional data. The structure was established by obtaining phases directly from the structure-factor magnitudes by means of the symbolic addition procedure.[7]

The corrected intensity data were placed on an absolute scale, and both the structure-factor magnitude, $|F|$, and the normalized structure-factor magnitude, $|E|$, were computed (Table 1). Five reflections, with large $|E|$ magnitudes and also involving a large number of interactions in the $\sum_2$ relationship, were selected as a starting set. Positive signs were assigned to three linearly-independent reflections in order to specify the

1) Present address: Research Laboratories, Ashigara, Fuji Photo Film Co., Ltd., Minami-Ashigara, Kanagawa.

2) To whom any correspondence should be addressed.

3) M. Feldman and S. Winstein, *Tetrahedron Lett.*, **19**, 853 (1962); E. L. Golf and R. B. LaCount, *J. Amer. Chem. Soc.*, **85**, 1354 (1963).

4) S. Sakanoue, T. Tamamura, S. Kusabayashi, H. Mikawa, N. Kasai, M. Kakudo, and H. Kuroda, This Bulletin, **42**, 2407 (1969).

5) S. Sakanoue, N. Yasuoka, N. Kasai, M. Kakudo, S. Kusabayashi, and H. Mikawa, *ibid.*, **42**, 2408 (1969).

6) D. A. Bekoe, P. K. Gantzel, and N. K. Trueblood, *Acta Crystallogr.*, **22**, 657 (1967).

7) J. Karle and I. L. Karle, *ibid.*, **21**, 849 (1966).

TABLE 1. DISTRIBUTION OF NORMALIZED STRUCTURE FACTORS AND STATISTICAL AVERAGES

	Distribution of $\|E\|$		
	Theoretical (Centro-symmetric) (%)	Experimental (%)	Number of reflections
$\|E\| \geqq 3.0$	0.3	0.35	7
$\|E\| \geqq 2.0$	5.0	4.9	98
$\|E\| \geqq 1.8$		7.9	160
$\|E\| \geqq 1.6$		12.2	247
$\|E\| \geqq 1.5$		14.3	289
$\|E\| \geqq 1.0$	32.0	33.4	675
$<\|E\|>$	0.798	0.955	
$<\|E\|^2>$	1.000	0.709	
$<\|E\|^2-1>$	0.968	0.961	

TABLE 2. STARTING SET OF APPLICATION OF $\sum_2$ FORMULA

h	k	l	$\|E\|$	Phase
2	13	4	3.52	+
3	0	2	3.02	+
3	3	1	2.84	+
6	2	3	3.27	A
4	12	3	3.10	B

origin of the unit cell, and letter phases, A and B, were assigned to the remaining two reflections in order to facilitate the symbolic addition procedure (Table 2).

As a first step, the signs of 11 reflections out of 98, ($|E| \geqq 2$), were determined by hand calculations. The determination was then carried out on a HITAC 5020E computer. After six cycles, the signs of 161 reflections were determined out of 247 reflections with $|E| \geqq 1.6$ (Table 3). From the interaction list, the signs of the two letter phases were assigned as: $A=-$ and $B=+$. The E-map based on these signs permitted the approximate location of atoms, although a number of ghost peaks were present (Fig. 1). The signs of 21 reflections out of 161 were found to be falsely determined at the end of the structure determination.

Successive Fourier syntheses led to be identification of all the non-hydrogen atoms. At this stage, the calculation of structure factors with a single temperature factor, B, of 3.0 Å^2 for all the non-hydrogen atoms gave a discrepancy factor, R, of 0.34. The positional and thermal parameters of each atom were then refined by the block-diagonal least-squares procedure. In the refinement, the weight was taken as unity for all the reflections, and the hydrogen atoms were not included. Five cycles of refinement improved the R factor to 0.196. Anisotropic thermal parameters were introduced at this stage. After 3 cycles the R value converged to 0.147 for the observed non-zero reflections (the hydrogen atoms were not included in the refinement). The final atomic coordinates, along with their estimated standard deviations, are listed in Table 4. The thermal parameters are shown in Table 5, while the observed and calculated structure factors are given in Table 6. A composite drawing of the final electron density distributions viewed down along the

TABLE 3. PROCESS OF THE SYMBOLIC ADDITION PROCEDURE

Run number	Number of reflections	$\|E\|$	Number of phases determined
0			5 (starting set)
1	98	$\geqq 2.0$	11 (hand calculation)
2	160	$\geqq 1.8$	33 (cycle-1)
			77 (cycle-2)
			100 (cycle-3)
3	247	$\geqq 1.6$	142 (cycle-1)
			158 (cycle-2)
			161 (cycle-3)

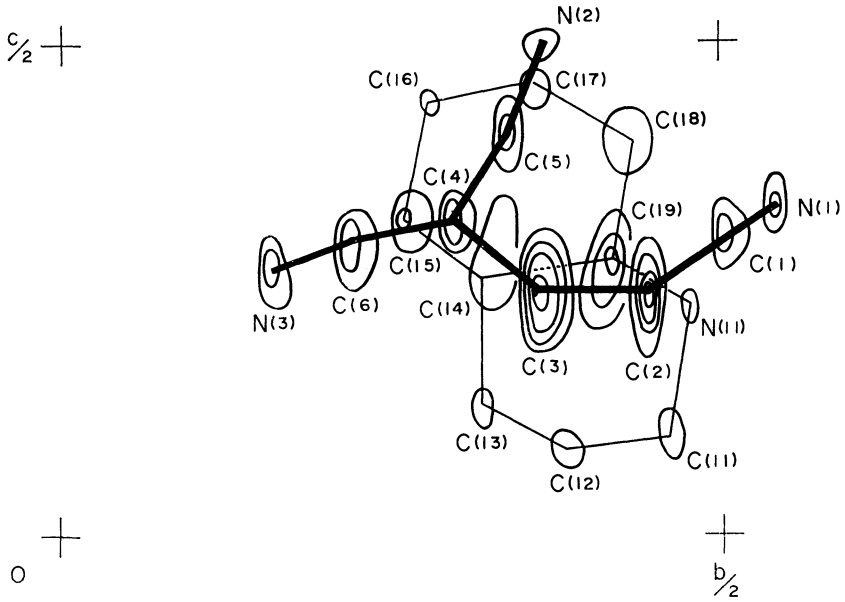

Fig. 1. The E-map computed by the use of 161 reflections (see text). Only the asymmetric unit is shown.

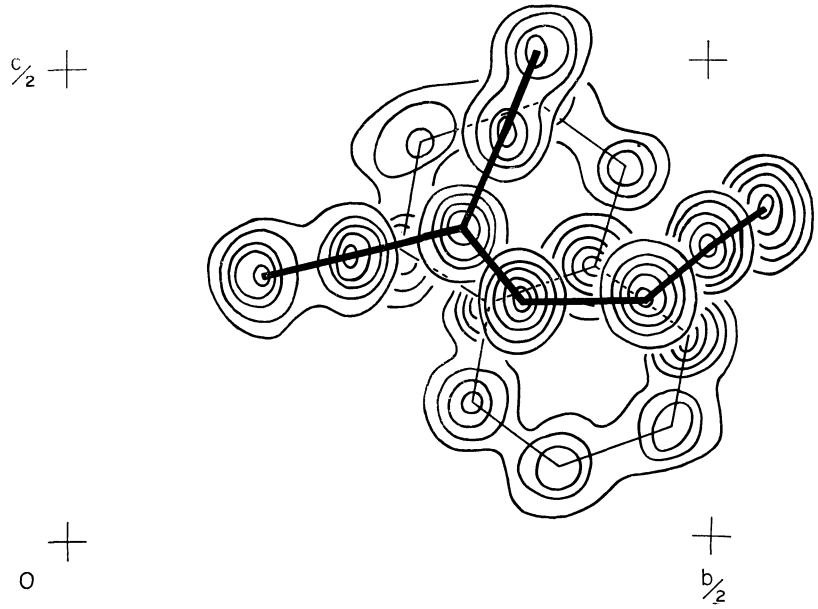

Fig. 2. The composite drawing of the final electron density viewed along the *a* axis. Contours at 1, 3, 5,···e.A^{-3}. Only the asymmetric unit is shown.

Table 4. The final atomic coordinates along with their estimated standard deviations within parentheses each multiplied by 10^4

Atom	*X*	*Y*	*Z*
N(1)	0.3600 (6)	0.5424 (4)	0.3445 (7)
N(2)	0.3516 (8)	0.3667 (5)	0.5104 (7)
N(3)	0.3741 (6)	0.1554 (4)	0.2773 (6)
C(1)	0.4223 (5)	0.4994 (4)	0.3032 (7)
C(2)	0.5	0.4494 (6)	0.25
C(3)	0.5	0.3571 (6)	0.25
C(4)	0.4324 (5)	0.3098 (4)	0.3241 (6)
C(5)	0.3879 (7)	0.3433 (5)	0.4267 (7)
C(6)	0.4015 (5)	0.2237 (5)	0.2963 (5)
N(11)	0.1772 (6)	0.4828 (6)	0.2130 (6)
C(11)	0.2265 (7)	0.4693 (6)	0.1145 (8)
C(12)	0.2454 (8)	0.3843 (7)	0.0754 (8)
C(13)	0.2133 (7)	0.3165 (5)	0.1409 (7)
C(14)	0.1607 (6)	0.3301 (4)	0.2461 (7)
C(15)	0.1252 (8)	0.2608 (6)	0.3184 (10)
C(16)	0.0776 (8)	0.2789 (8)	0.4201 (9)
C(17)	0.0606 (9)	0.3655 (8)	0.4569 (9)
C(18)	0.0920 (8)	0.4339 (7)	0.3878 (8)
C(19)	0.1430 (6)	0.4152 (5)	0.2824 (6)

Table 5. Thermal parameters along with their estimated standard deviations within parentheses each multiplied by 10^4

Atom	β_{11}	β_{22}	β_{33}	β_{12}	β_{13}	β_{23}
N(1)	65(5)	21(3)	89(7)	23(6)	8(11)	3(7)
N(2)	125(8)	23(3)	60(6)	28(8)	95(13)	17(7)
N(3)	64(5)	20(3)	97(8)	−20(6)	25(11)	−10(7)
C(1)	46(5)	11(2)	45(6)	−7(6)	−7(9)	19(6)
C(2)	37(6)	7(3)	40(8)	0	5(12)	0
C(3)	33(6)	10(3)	28(7)	0	−1(11)	0
C(4)	42(4)	14(3)	24(5)	−3(6)	8(8)	7(6)
C(5)	72(6)	12(3)	57(7)	7(7)	11(12)	23(7)
C(6)	39(4)	18(3)	50(6)	−1(6)	4(9)	8(7)
N(11)	62(5)	16(3)	50(5)	−6(5)	−24(9)	14(6)
C(11)	64(7)	42(4)	51(7)	−18(9)	−27(12)	38(9)
C(12)	63(6)	52(5)	48(7)	5(10)	2(13)	1(10)
C(13)	64(6)	26(3)	49(7)	10(8)	−16(11)	−10(8)
C(14)	43(5)	16(3)	36(5)	−4(6)	7(9)	13(7)
C(15)	63(6)	25(4)	115(11)	−15(8)	32(14)	57(11)
C(16)	65(7)	73(7)	76(9)	−13(12)	14(14)	96(14)
C(17)	70(8)	83(7)	50(8)	28(13)	27(14)	48(13)
C(18)	71(7)	58(5)	39(7)	59(11)	2(12)	−24(10)
C(19)	41(5)	21(3)	33(6)	8(6)	−2(9)	−10(6)

The expression used is:

$$\exp\{-(\beta_{11}h^2+\beta_{22}k^2+\beta_{33}l^2+\beta_{12}hk+\beta_{13}hl+\beta_{23}kl)\}$$

a axis is shown in Fig. 2.

Calculations of the symbolic addition procedure were done with the SSGM program revised by one of the present authors (N.Y.). Almost all the calculations in this study were done on a HITAC 5020E computer at the University of Tokyo. The atomic scattering factors used in the calculations were taken from those given by Hanson and his co-workers.[8]

Description and Discussion of the Structure

Structure of the Anion and Cation. The skeleton of the ions, together with interatomic distances and angles, is illustrated in Fig. 3. The estimated standard deviations of the bond lengths and angles are about 0.015 Å and 1°, respectively.

The $(C_{10}N_6)^{2-}$ anion in this crystal has a C_2-2 symmetry instead of the C_3-3 (or approximately D_3-32) in hexahydrated calcium salt.[6] The four central carbon atoms are exactly coplanar (Table 7(a)). The three cyano-substituents, $-C(CN)_2$, are, however, tilted out of this plane; the anion takes a propeller shape. The one arm which lies on the 2-fold axis is rotated 13° from the completely planar conformation, while the

8) H. P. Hanson, F. Herman, J. D. Lea, and S. Skillman, *Acta Crystallogr.*, **17**, 1040 (1964).

TABLE 6. THE OBSERVED AND CALCULATED STRUCTURE FACTORS

K	FO	FC	K	FO	FC	K	FO	FC	K	FO	FC	K	FO	FC	K	FO	FC	K	FO	FC	K	FO	FC	K	FO	FC
H=L= 0	0		5	26	-22	H=L= 5	1		4	0	4	7	55	46	8	54	-52	16	0	15	9	24	-20	10	34	-23	15	35	32
2	33	-22	7	44	43	1	108	-97	5	0	3	8	7	0	9	30	-30	H=L=	3	3	10	9	12	11	63	-48	H=L=	9	4
4	37	-11	9	23	-22	2	56	51	6	0	-1	9	0	1	10	21	15	1	121	-109	11	0	0	12	50	-48	0	94	-84
6	286	273	11	21	25	3	96	78	7	0	10	10	40	31	11	31	-28	2	25	-17	12	0	2	13	105	95	1	84	83
8	71	51	13	17	18	4	16	11	8	43	47	11	67	61	12	49	54	3	75	-68	13	0	-4	14	13	-17	2	13	-12
10	111	-109	H=L=	12	0	5	118	106	9	0	-9	12	81	78	13	10	-15	4	19	-11	14	38	38	15	56	-73	3	0	5
12	41	38	0	60	54	6	106	-88	H=L=	13	1	13	0	10	14	30	-26	5	18	7	H=L=	10	3	16	0	1	4	42	36
14	13	18	2	32	31	7	112	-107	1	0	-14	14	21	-24	15	16	-17	6	126	109	1	42	-35	17	22	-28	5	39	39
16	8	-10	4	20	16	8	0	3	2	0	11	15	36	34	H=L=	11	2	7	42	-29	2	19	15	H=L=	3	4	6	43	48
18	14	9	6	0	12	9	7	2	3	0	-14	16	31	-29	0	23	-19	8	32	-20	3	9	8	0	98	-92	7	0	3
H=L= 1	0		8	8	12	10	26	24	4	0	-10	17	0	7	1	25	-24	9	8	-11	4	22	-19	1	148	133	8	0	-6
1	56	-14	10	27	28	11	49	-47	5	0	9	18	8	18	2	9	-1	10	73	-71	5	31	-30	2	30	12	9	38	-37
3	147	152	H=L=	13	0	12	0	-4	6	0	-20	H=L=	5	7	3	19	23	11	29	30	6	39	39	3	44	26	10	36	34
5	39	21	1	13	11	13	65	-61	7	0	-2	0	106	-91	4	29	-20	12	74	75	7	0	5	4	189	-182	11	0	12
7	175	155	3	24	20	14	0	3	8	16	-16	1	25	15	5	36	29	13	42	-39	8	0	-18	5	50	40	12	0	11
9	80	-64	5	26	29	15	42	-42	9	0	5	2	79	-69	6	16	-21	14	0	-5	9	0	-3	6	37	-39	13	24	-26
11	11	7	7	24	23	16	9	0	10	16	17	3	143	126	7	0	-4	15	19	-25	10	30	-34	7	11	5	14	18	22
13	83	-82	9	12	15	H=L=	6	1	H=L=	14	1	4	24	20	8	23	25	16	0	7	11	20	-18	8	11	7	H=L=	10	4
15	73	77	H=L=	14	0	1	31	19	1	0	-4	5	97	76	9	15	19	17	0	-10	12	0	-5	9	81	-74	0	35	-27
17	0	3	0	62	57	2	23	18	2	27	31	6	60	40	10	43	-41	18	36	36	13	10	-3	10	53	-52	1	79	76
19	31	36	2	0	10	3	18	5	3	0	-2	7	36	20	11	0	-9	H=L=	4	3	14	34	36	11	0	14	2	19	14
H=L= 2	0		4	11	-2	4	6	-4	4	0	-18	8	16	10	12	0	-1	1	124	105	H=L=	11	3	12	42	-37	3	24	-19
0	74	-42	6	10	9	5	136	-134	5	0	0	9	44	39	13	18	-20	2	26	-8	1	17	-18	13	43	44	4	26	32
2	170	-147	8	20	-25	6	12	-4	6	0	11	10	79	72	H=L=	12	2	3	25	-5	2	14	-20	14	0	-7	5	55	55
4	19	23	H=L=	15	0	7	61	-56	7	0	5	11	102	100	0	30	-27	4	105	97	3	10	4	15	43	-44	6	0	-9
6	72	-61	1	39	35	8	24	17	8	22	-25	12	19	17	1	29	-28	5	62	-56	4	28	31	16	33	-39	7	26	23
8	0	-8	3	0	8	9	40	31	9	13	-15	13	51	-41	2	30	-25	6	19	-10	5	44	-39	17	7	-9	8	22	16
10	21	-26	5	34	34	10	8	11	10	11	-13	14	48	49	3	16	-14	7	46	-40	6	20	-21	H=L=	4	4	9	25	28
12	0	-4	H=L=	16	0	11	26	-27	H=L=	15	1	15	31	32	4	21	-19	8	62	-49	7	40	38	0	154	-131	10	0	-11
14	83	84	0	13	13	12	31	-26	1	0	6	16	41	38	5	33	-34	9	8	-7	8	9	11	1	54	-51	11	27	25
16	23	20	2	0	0	13	27	-27	2	0	-2	17	18	23	6	47	-44	10	0	8	9	29	29	2	72	59	12	38	-43
18	24	19	4	10	-13	14	50	56	3	0	17	18	8	-2	7	20	20	11	0	7	10	29	30	3	64	63	13	32	31
H=L= 3	0		H=L=	0	1	15	29	36	4	0	-9	H=L=	6	2	8	8	3	12	103	115	11	16	24	4	74	75	H=L=	11	4
1	238	242	2	347	432	16	8	9	5	26	-27	0	185	-169	9	0	6	13	46	-48	12	10	-17	5	7	1	0	26	25
3	96	-41	4	23	-14	H=L=	7	1	6	0	7	1	69	59	10	0	-5	14	0	-12	13	24	27	6	95	-81	1	26	27
5	197	177	6	119	114	1	25	-16	7	37	40	2	78	-62	11	0	10	15	0	-12	H=L=	12	3	7	8	13	2	26	30
7	48	-29	8	29	28	2	27	-26	H=L=	0	2	3	40	-30	12	0	-6	16	0	-3	1	0	-2	8	48	-42	3	0	-6
9	95	-22	10	74	-61	3	41	25	0	392	-474	4	80	65	13	0	26	17	0	-1	2	22	-27	9	27	-24	4	0	-13
11	105	100	12	100	99	4	12	-5	2	79	-64	5	88	69	14	9	-9	18	37	44	3	9	11	10	55	-49	5	34	-36
13	64	60	14	31	28	5	75	-71	4	323	-314	6	26	-14	H=L=	13	2	H=L=	5	3	4	33	31	11	54	-45	6	34	33
15	39	-36	16	27	28	6	39	35	6	148	-114	7	44	-30	0	13	-15	1	50	50	5	26	29	12	43	-46	7	16	-15
17	10	15	18	70	66	7	24	21	8	118	83	8	42	32	1	31	-32	2	82	75	6	0	-2	13	9	0	8	21	-20
19	19	-15	H=L=	1	1	8	0	11	10	26	-16	9	98	94	2	0	-9	3	49	-47	7	18	-23	14	0	5	9	30	-36
H=L= 4	0		2	44	-47	9	53	46	12	122	-125	10	56	51	3	0	-3	4	21	-9	8	60	-69	15	47	-51	10	29	28
0	403	-473	3	101	-100	10	24	-29	14	9	8	11	98	93	4	0	0	5	56	53	9	21	18	16	0	9	11	7	-14
2	138	119	4	102	99	11	33	-14	16	16	13	12	19	-18	5	28	-27	6	27	24	10	13	20	17	18	-17	12	0	11
4	49	-39	5	193	-202	12	23	-13	18	12	-22	13	9	-2	6	0	1	7	26	-19	H=L=	13	3	H=L=	5	4	13	0	17
6	11	-6	6	113	112	13	19	-36	H=L=	1	2	14	39	34	7	0	-16	8	83	78	1	16	-16	0	44	34	14	0	-6
8	10	-20	7	53	44	14	19	23	0	103	116	15	0	3	8	15	-8	9	20	-15	2	0	7	1	60	57	H=L=	12	4
10	89	90	8	41	34	15	8	12	1	24	-17	16	35	33	9	0	-13	10	23	22	3	0	-7	2	62	-53	0	44	42
12	90	-88	9	13	0	H=L=	8	1	2	103	-95	17	6	16	10	0	0	11	33	24	4	16	13	3	108	-93	1	0	10
14	47	-44	10	25	18	1	21	14	3	161	-152	H=L=	7	2	11	19	21	12	10	13	5	0	-14	4	41	-34	2	0	3
16	41	47	11	19	-10	2	35	-31	4	66	54	0	107	-93	H=L=	14	2	13	14	-1	6	8	-12	5	27	24	3	43	-42
18	25	-22	12	77	84	3	0	0	5	40	-27	1	126	118	0	33	-33	14	42	-38	7	0	-6	6	106	-92	4	13	10
H=L= 5	0		13	65	-63	4	75	67	6	99	-93	2	31	26	1	0	5	15	22	24	8	25	29	7	32	23	5	40	41
1	83	-76	14	0	-4	5	0	-2	7	40	26	3	109	-107	2	0	-16	16	9	10	9	18	-23	8	18	-8	6	41	39
3	113	-106	15	12	14	6	58	-53	8	37	-24	4	70	-65	3	0	7	17	7	7	10	6	-9	9	55	-46	7	0	1
5	165	-141	16	26	-27	7	50	47	9	19	-10	5	24	16	4	0	18	H=L=	6	3	H=L=	14	3	10	76	-77	8	12	-8
7	159	-147	17	16	-21	8	52	-45	10	77	-77	6	0	-2	5	0	1	1	156	129	1	0	3	11	34	-31	9	0	3
9	82	75	H=L=	2	1	9	0	4	11	17	-5	7	56	52	6	0	-5	2	251	-243	2	29	-31	12	0	-3	10	0	-8
11	137	-144	1	45	-53	10	0	2	12	37	29	8	9	6	7	25	25	3	56	52	3	0	-16	13	13	-18	11	0	-16
13	69	65	2	17	-15	11	8	7	13	75	70	9	28	25	8	15	17	4	10	-16	4	0	-12	14	9	2	12	0	-2
15	10	-12	3	10	5	12	44	-42	14	51	45	10	41	35	H=L=	15	2	5	64	52	5	24	22	15	0	-8	13	9	0
17	0	-12	4	9	3	13	24	26	15	70	-67	11	76	64	0	13	9	6	41	-47	6	7	9	16	31	-33	H=L=	13	4
H=L= 6	0		5	251	250	14	0	-3	16	15	-21	12	33	-34	1	23	-22	7	57	49	7	0	-10	17	21	-20	0	23	18
0	137	-110	6	26	-24	15	0	-2	17	20	-20	13	44	44	2	14	19	8	26	-34	8	0	1	H=L=	6	4	1	0	21
2	118	107	7	60	-50	H=L=	9	1	18	24	20	14	26	-28	3	12	12	9	23	21	9	8	7	0	247	229	2	0	17
4	83	-61	8	9	-10	1	55	49	H=L=	2	2	15	11	8	4	12	7	10	34	-32	H=L=	15	3	1	79	-69	3	0	7
6	96	48	9	60	-40	2	39	38	0	50	-49	16	12	14	5	25	-30	11	26	24	1	0	-15	2	42	25	4	0	10
8	96	-22	10	28	-21	3	37	33	1	112	109	17	7	9	6	6	-13	12	35	28	2	0	1	3	128	118	5	0	0
10	79	-80	11	0	-5	4	27	24	2	39	-17	H=L=	8	2	H=L=	0	3	13	9	18	3	0	-4	4	49	-47	6	0	4
12	0	11	12	66	-67	5	52	-39	3	116	114	0	53	-45	2	191	194	14	37	-34	4	0	9	5	73	-65	7	0	14
14	37	-31	13	15	-6	6	26	23	4	44	26	1	21	-16	4	150	-142	15	37	-36	5	28	29	6	38	37	8	16	-15
16	22	-27	14	56	-55	7	22	17	5	167	152	2	62	53	6	38	-25	16	0	5	6	0	-10	7	15	-11	9	0	1
18	28	-31	15	24	-24	8	12	-2	6	31	23	3	37	30	8	28	-20	17	29	33	7	21	-24	8	37	-27	10	0	-5
H=L= 7	0		16	16	3	9	51	47	7	146	131	4	55	46	10	44	43	H=L=	7	3	H=L=	0	4	9	9	-14	11	0	-25
1	100	91	17	14	-13	10	0	1	8	40	-24	5	22	-19	12	80	-69	1	127	101	0	121	117	10	48	-40	H=L=	14	4
3	7	-4	18	29	-30	11	29	-32	9	95	-77	6	81	65	14	10	12	2	7	-2	2	46	-44	11	31	-29	0	0	6
5	37	-33	H=L=	3	1	12	0	1	10	22	15	7	69	-60	16	22	-23	3	16	-11	4	210	-191	12	19	24	1	0	-1
7	23	-17	1	192	216	13	0	-5	11	70	65	8	13	11	18	31	-34	4	40	-34	6	114	103	13	57	-62	2	0	10
9	21	-21	2	337	-367	14	9	-14	12	46	45	9	19	11	H=L=	1	3	5	45	41	8	132	126	14	9	-1	3	0	-7
11	138	-149	3	144	152	15	47	51	13	80	-73	10	80	83	1	174	-189	6	0	8	10	31	-30	15	8	16	4	35	-29
13	67	-67	4	76	64	H=L=	10	1	14	36	-24	11	51	-56	2	185	-186	7	0	-7	12	45	47	H=L=	7	4	H=L=	15	4
15	0	-1	5	178	173	1	40	-37	15	0	6	12	0	6	3	31	-22	8	13	-13	14	71	77	0	127	128	0	18	-12
17	19	-17	6	30	11	2	14	-12	16	26	-26	13	9	8	4	43	32	9	51	-48	16	17	-13	1	99	-83	1	0	-1
H=L= 8	0		7	136	129	3	16	-17	17	7	-5	14	8	-14	5	60	-45	10	10	-11	H=L=	1	4	2	0	9	2	23	-25
0	121	86	8	13	-15	4	39	35	18	6	-5	15	0	-8	6	62	-46	11	10	11	0	165	-169	3	27	-25	3	0	-10
2	7	-3	9	31	32	5	25	23	H=L=	3	2	16	35	32	7	0	-1	12	17	-18	1	12	6	4	51	39	4	0	-8
4	104	-90	10	26	-24	6	17	13	0	606	738	H=L=	9	2	8	162	-155	13	44	49	2	11	3	5	61	-55	5	0	13
6	88	-75	11	29	26	7	0	-1	1	367	-368	0	47	-35	9	52	-40	14	0	-2	3	65	55	6	9	-5	6	17	-16
8	0	8	12	0	-5	8	64	62	2	40	-34	1	37	-31	10	86	-82	15	8	11	4	0	8	7	35	31	H=L=	0	5
10	127	-136	13	60	57	9	0	-8	3	227	233	2	15	17	11	0	-10	H=L=	8	3	5	54	-51	8	65	68	2	193	191
12	13	-16	14	0	3	10	0	8	4	115	79	3	56	-50	12	13	-13	1	91	-81	6	124	100	9	37	45	4	110	101
14	8	-8	15	22	-23	11	0	1	5	66	-55	4	0	6	13	85	93	2	0	12	7	28	-18	10	9	13	6	64	-39
16	49	-52	16	0	-4	12	0	-12	6	60	51	5	20	19	14	10	2	3	0	-1	8	38	-34	11	59	-63	8	83	75
H=L= 9	0		17	33	33	13	0	1	7	145	-128	6	9	6	15	9	7	4	39	-33	9	37	24	12	0	-11	10	35	31
1	21	9	H=L=	4	1	14	27	-31	8	26	-21	7	13	-16	16	12	-9	5	9	-9	10	0	3	13	13	-16	12	41	-36
3	8	-1	1	151	144	H=L=	11	1	9	44	32	8	21	-19	17	12	7	6	13	-5	11	57	-55	14	0	0	14	0	22
5	60	-49	2	117	107	1	54	47	10	8	-9	9	30	33	18	0	2	7	13	-19	12	9	15	15	40	45	16	0	-6
7	56	58	3	71	67	2	17	14	11	15	7	10	37	-35	H=L=	2	3	8	57	52	13	0	-3	H=L=	8	4	18	33	-42
9	44	-39	4	16	-12	3	15	13	12	13	9	11	9	-7	1	17	13	9	10	-4	14	0	4	0	29	22	H=L=	1	5
11	35	6	5	5	-15	4	26	-26	13	73	-73	12	0	3	2	66	-49	10	10	2	15	45	49	1	0	-2	1	12	-13
13	14	23	6	41	29	5	45	39	14	0	-5	13	0	15	3	160	-153	11	24	-21	16	0	-12	2	61	-51	2	64	-67
H=L= 10	0		7	17	-12	6	0	12	15	16	4	14	31	-29	4	68	-58	12	23	29	17	18	13	3	15	11	3	65	47
0	27	-20	8	118	110	7	0	-14	16	10	5	15	6	-3	5	134	-117	13	0	5	H=L=	2	4	4	51	-45	4	50	-39
2	30	-25	9	47	42	8	0	-14	17	15	7	16	16	-21	6	31	22	14	32	36	0	106	104	5	0	-8	5	75	67
4	63	64	10	85	76	9	0	7	18	7	11	H=L=	10	2	7	104	92	H=L=	9	3	1	145	-132	6	9	-15	6	81	78
6	9	-2	11	20	16	10	0	-3	H=L=	4	2	0	18	-26	8	33	-37	1	51	-52	2	40	47	7	22	-18	7	45	44
8	0	-2	12	36	-35	11	0	-5	0	245	203	1	20	18	9	64	-71	2	18	-18	3	172	-150	8	0	-9	8	49	38
10	24	-21	13	0	-15	12	0	6	1	151	-132	2	13	6	10	25	-19	3	48	-40	4	12	1	9	9	7	9	78	73
12	0	-7	14	47	-49	13	17	-20	2	45	-27	3	9	-9	11	61	56	4	13	-13	5	144	-111	10	0	-14	10	0	-4
14	82	90	15	10	6	H=L=	12	1	3	11	-7	4	0	2	12	0	-15	5	35	-25	6	29	32	11	60	62	11	39	-52
H=L= 11	0		16	19	-16	1	0	-5	4	96	83	5	16	-17	13	42	33	6	0	-4	7	57	-41	12	9	8	12	31	-29
1	26	25	17	8	20	2	52	51	5	42	-28	6	0	3	14	50	52	7	49	-55	8	8	-5	13	0	3	13	37	-28
3	92	-32	18	38	-41	3	0	2	6	34	-23	7	21	-21	15	23	24	8	48	-49	9	39	-31	14	21	21	14	48	51

TABLE 6 (continued)

K	FO	FC	K	FO	FC	K	FO	FC	K	FO	FC	K	FO	FC	K	FO	FC	K	FO	FC	K	FO	FC	K	FO	FC
15	0	8	10	26	-29	9	0	2	11	22	-17	15	24	31	8	0	5	3	51	-45	2	24	26	12	39	38	8	15	-37
16	0	-1	11	16	-21	10	62	60	12	0	-1	16	0	-4	9	0	8	4	45	-35	3	24	20	H=L=	3	10	9	0	-15
H=L=	2	5	12	0	7	11	55	54	13	20	-21	17	36	-50	10	0	-5	5	26	25	4	75	65	0	39	-29	10	20	28
1	115	-121	13	8	-17	12	24	18	14	0	-6	H=L=	3	7	11	17	-23	6	68	64	5	24	17	1	15	7	H=L=	7	11
2	66	62	14	34	-35	13	0	-3	15	29	-26	1	22	-19	12	24	21	7	0	1	6	43	-40	2	55	57	1	0	-14
3	20	19	15	6	10	14	30	-29	H=L=	9	6	2	39	32	H=L=	11	7	8	29	23	7	29	-24	3	80	75	2	0	-3
4	93	-29	H=L=	9	5	15	37	37	0	15	-7	3	47	-41	1	0	17	9	0	3	8	14	6	4	0	9	3	0	1
5	32	20	1	117	113	16	8	12	1	66	-53	4	49	49	2	0	17	10	0	2	9	93	-92	5	14	-2	4	0	-6
6	19	10	2	57	-45	17	18	23	2	23	23	5	34	27	3	0	-13	11	18	17	10	43	49	6	20	-16	5	0	10
7	53	-46	3	19	15	H=L=	3	6	3	75	72	6	46	-34	4	0	-9	12	0	0	11	29	-34	7	14	-21	6	0	-3
8	38	42	4	45	-45	0	102	111	4	10	-15	7	35	-36	5	0	1	13	0	-16	12	32	-30	8	0	-12	7	27	29
9	39	-33	5	39	-38	1	149	-142	5	52	-51	8	0	0	6	0	-18	14	24	26	13	10	7	9	30	34	H=L=	0	12
10	0	13	6	9	-10	2	87	-88	6	47	-40	9	0	-1	7	0	-20	H=L=	7	8	14	9	-12	10	17	-15	0	0	5
11	47	-43	7	72	69	3	7	10	7	21	-15	10	10	10	8	20	21	0	64	64	H=L=	3	9	11	0	0	2	64	-62
12	33	-31	8	51	46	4	11	-2	8	23	-17	11	20	24	H=L=	12	7	1	59	63	1	65	60	12	14	10	4	58	-49
13	43	48	9	0	15	5	48	32	9	27	25	12	10	3	1	38	36	2	0	-3	2	31	31	13	8	0	6	27	20
14	0	-10	10	30	-35	6	51	34	10	26	-24	13	10	5	2	27	-27	3	30	23	3	28	15	H=L=	4	10	8	19	-29
15	15	-24	11	27	-26	7	61	-55	11	0	-3	14	10	8	H=L=	13	7	4	23	13	4	111	-121	0	57	-61	10	33	-36
16	9	8	12	18	18	8	9	8	12	31	32	H=L=	4	7	1	16	21	5	23	20	5	45	-42	1	40	-48	H=L=	1	12
H=L=	3	5	13	7	7	9	62	56	13	7	-14	1	38	30	2	24	-28	6	35	32	6	28	-26	2	15	16	0	0	12
1	27	-25	14	24	-23	10	41	32	H=L=	10	6	2	7	6	H=L=	0	8	7	0	8	7	57	54	3	0	6	1	60	58
2	116	103	H=L=	10	5	11	52	46	0	10	-12	3	0	8	0	21	-17	8	16	11	8	0	-12	4	0	4	2	0	-20
3	67	64	1	64	56	12	36	32	1	77	-77	4	0	2	2	69	64	9	0	2	9	14	10	5	45	-46	3	31	-32
4	0	1	2	24	-29	13	0	4	2	0	-14	5	28	-29	4	79	-70	10	0	-5	10	0	2	6	14	18	4	26	19
5	39	-21	3	9	-3	14	50	53	3	34	-28	6	0	-2	6	10	17	11	0	7	11	12	-26	7	0	-19	5	0	-9
6	51	49	4	0	-9	15	12	-2	4	0	-1	7	25	-21	8	79	-68	12	20	18	12	11	-10	8	14	-22	6	0	8
7	44	-34	5	48	48	16	7	-11	5	45	-42	8	17	-15	10	82	-75	H=L=	8	8	13	10	-17	9	0	12	7	0	-1
8	12	17	6	9	-10	H=L=	4	6	6	0	0	9	23	-22	12	16	-16	0	51	39	H=L=	4	9	H=L=	5	10	8	0	0
9	9	-10	7	17	18	0	76	-72	7	10	-20	10	27	-24	14	19	-23	1	11	9	1	14	23	0	0	-3	H=L=	2	12
10	34	28	8	0	6	1	42	35	8	0	4	11	34	-29	H=L=	1	8	2	31	28	2	35	39	1	0	-18	0	17	14
11	13	-13	9	0	2	2	74	-63	9	13	-2	12	11	4	0	16	-13	3	26	29	3	0	19	2	21	17	1	0	-10
12	64	-60	10	0	7	3	32	26	10	36	35	13	11	-14	1	24	-21	4	16	18	4	14	3	3	47	-50	2	0	6
13	0	4	11	0	15	4	32	-20	11	28	-29	14	10	2	2	79	80	5	39	-31	5	14	16	4	15	-20	3	16	8
14	37	36	12	23	-22	5	0	3	12	26	29	H=L=	5	7	3	32	-19	6	40	42	6	0	9	5	0	-7	4	36	32
15	8	14	13	22	28	6	76	59	13	10	-13	1	11	-16	4	53	51	7	0	7	7	46	49	6	14	-5	5	16	12
16	27	-27	H=L=	11	5	7	32	-27	H=L=	11	6	2	0	0	5	57	-45	8	0	-15	8	46	41	7	49	-47	6	0	13
17	0	14	1	0	3	8	65	-65	0	0	6	3	0	-11	6	10	24	9	15	-12	9	20	14	8	45	54	7	14	-4
18	21	-24	2	47	47	9	36	-36	1	40	-33	4	87	-80	7	10	-15	10	0	11	10	13	-4	9	12	-9	8	23	-23
H=L=	4	5	3	28	27	10	32	25	2	28	-27	5	45	-32	8	28	22	11	0	5	11	0	10	10	26	-22	9	0	9
1	113	-90	4	13	-12	11	55	52	3	0	6	6	9	4	9	47	37	12	26	-23	12	0	-15	11	0	-2	10	0	-2
2	0	10	5	22	-15	12	87	91	4	18	0	7	10	-6	10	0	0	H=L=	9	8	13	10	16	12	12	-14	11	18	30
3	48	46	6	16	-12	13	16	2	5	20	17	8	60	48	11	91	-95	0	0	9	H=L=	5	9	13	6	7	H=L=	3	12
4	0	-7	7	21	-27	14	9	10	6	10	2	9	29	25	12	51	-48	1	0	-3	1	29	25	H=L=	6	10	0	23	8
5	85	-79	8	0	7	15	0	20	7	0	-9	10	33	33	13	0	-1	2	0	-2	2	62	47	0	62	-63	1	16	-24
6	88	-82	9	0	-2	16	32	-32	6	0	0	11	10	10	14	44	-37	3	48	-15	3	46	37	1	48	50	2	0	20
7	0	2	10	0	-3	17	0	13	9	24	24	12	0	-1	H=L=	2	8	4	0	40	4	25	14	2	0	-5	3	23	-36
8	41	-32	11	0	-11	H=L=	5	6	10	25	-18	13	30	36	0	72	-64	5	11	13	5	14	-5	3	0	-7	4	66	51
9	74	74	12	0	-6	0	88	75	11	32	31	14	13	9	1	31	23	6	22	-9	6	0	14	4	33	-36	5	15	0
10	47	48	13	24	-25	1	63	-54	H=L=	12	6	H=L=	6	7	2	47	44	7	0	-20	7	0	7	5	13	-2	6	14	-14
11	0	11	H=L=	12	5	2	65	54	0	44	-47	1	69	-69	3	32	-31	8	0	-2	8	0	-1	6	13	-7	7	0	-1
12	56	-52	1	0	-10	3	8	-3	1	38	41	2	56	-54	4	40	-38	9	0	4	9	45	39	7	0	21	8	0	0
13	0	12	2	45	43	4	64	59	2	10	8	3	26	29	5	0	-12	10	0	-5	10	0	-4	8	0	17	9	11	-26
14	28	-29	3	23	-23	5	29	-19	3	0	12	4	58	60	6	80	-76	11	0	6	11	0	0	9	22	-21	10	13	11
15	17	12	4	25	-27	9	105	105	4	0	0	5	34	36	7	105	-109	12	22	-20	12	0	7	H=L=	0	11	H=L=	4	12
H=L=	5	5	5	44	-44	7	36	33	5	21	-19	6	20	17	8	23	18	H=L=	10	8	13	35	-36	2	71	-59	0	16	21
1	42	25	6	0	3	8	27	23	6	13	13	7	76	-77	9	31	-39	0	11	7	14	27	-34	4	123	130	1	0	12
2	25	-24	7	0	6	9	0	12	7	9	11	8	49	-41	10	31	-33	1	30	27	H=L=	6	9	6	45	37	2	16	19
3	0	-1	8	16	19	10	15	23	8	8	7	9	25	-14	11	0	-5	2	23	20	1	13	22	8	20	5	3	16	-16
4	32	27	H=L=	13	5	11	0	-2	9	23	-21	10	25	25	12	25	-22	3	22	20	2	50	42	10	12	2	4	15	-8
5	16	-10	1	27	-28	12	42	-43	H=L=	13	6	11	9	21	H=L=	3	8	4	0	-14	3	40	-43	12	37	45	5	51	51
6	42	-44	2	15	21	13	20	24	0	33	-39	12	31	-11	0	102	-92	5	0	5	4	23	-30	H=L=	1	11	6	48	-36
7	0	10	3	15	16	14	9	-6	1	18	23	13	0	8	1	47	37	6	0	-15	5	0	-14	1	0	-13	7	13	17
8	93	-87	4	0	3	15	43	-42	2	18	-19	14	14	26	2	22	-20	7	17	26	6	0	-7	2	0	-24	H=L=	5	12
9	30	-30	5	20	20	16	7	25	3	20	-19	H=L=	7	7	3	37	-36	8	0	-14	7	9	4	3	62	-63	0	39	44
10	9	-7	6	25	32	17	16	-2	4	32	11	1	71	-64	4	0	-9	9	0	-3	H=L=	7	9	4	58	54	1	0	15
11	48	38	7	0	1	H=L=	6	6	5	8	27	2	13	10	5	17	24	10	0	-1	1	28	24	5	0	8	2	0	2
12	52	-59	8	11	-15	0	0	-5	H=L=	14	6	3	9	-6	6	21	27	11	20	18	2	0	-1	6	28	-26	3	26	38
13	9	-20	9	13	18	1	41	20	0	13	14	4	0	-9	7	19	16	H=L=	11	8	3	0	1	7	13	0	4	0	-26
14	0	3	H=L=	14	5	2	12	12	1	15	12	5	52	-48	8	52	-42	0	42	-39	4	34	32	8	34	-30	5	0	11
15	36	-31	1	7	-14	3	4	1	2	13	1	6	17	-12	9	82	-76	1	0	7	5	0	3	H=L=	2	11	6	0	-4
16	0	11	2	0	2	4	31	-22	3	7	-5	7	25	-26	10	16	17	2	0	13	6	0	6	1	0	-11	7	22	26
17	28	28	3	0	14	5	19	-13	4	10	-1	8	49	-47	11	0	8	3	0	-5	7	0	7	2	15	-7	H=L=	6	12
H=L=	6	5	4	27	27	6	62	-64	5	6	-8	9	25	-19	12	15	-24	4	20	18	8	0	1	3	49	-46	0	42	35
1	17	2	5	18	-14	7	10	-11	6	16	20	10	0	9	13	0	6	5	24	19	9	12	-10	4	0	-7	H=L=	0	13
2	59	49	H=L=	0	6	8	51	45	H=L=	0	7	11	0	0	14	37	-37	6	30	-31	10	11	-11	5	21	21	2	26	7
3	30	22	0	109	-93	9	32	32	2	107	-83	12	15	-21	15	0	-20	7	12	-6	11	10	2	6	30	-43	4	29	-38
4	32	18	2	32	-9	10	21	-19	4	100	-101	13	0	19	16	27	31	H=L=	12	8	12	25	30	7	0	3	6	29	26
5	39	-36	4	41	109	11	10	-4	6	44	-51	14	15	-15	H=L=	4	8	0	0	6	H=L=	0	10	8	31	-29	H=L=	2	13
6	90	82	6	37	-14	12	45	-46	8	50	-58	H=L=	8	7	0	64	54	1	0	-9	0	39	31	9	26	22	1	15	-17
7	0	18	8	19	15	13	36	30	10	10	-7	1	32	-23	1	13	7	2	0	-5	2	42	42	10	27	-26	2	15	28
8	57	55	10	67	61	14	0	4	12	50	38	2	69	-64	2	27	-19	3	0	-4	4	77	78	11	10	-3	3	0	-18
9	37	29	12	51	-54	15	0	-4	14	13	-15	3	35	-22	3	9	16	4	22	-23	6	65	-52	H=L=	3	11	4	20	-6
10	37	-38	14	22	-23	16	21	-24	16	30	25	4	0	-3	4	76	74	H=L=	13	8	8	67	66	1	15	-22	5	36	40
11	0	10	16	70	70	H=L=	7	6	H=L=	1	7	5	0	13	5	47	44	0	0	8	10	29	40	2	0	-10	H=L=	3	13
12	0	11	18	4	-44	0	79	-69	1	7	5	6	10	-8	6	15	11	1	0	-10	12	22	22	3	15	16	1	20	30
13	37	-39	H=L=	1	6	1	0	3	2	8	-17	7	49	54	7	23	-25	2	0	12	14	30	35	4	21	20	2	14	1
14	0	1	0	119	123	2	4	7	3	54	-51	8	32	-33	8	0	0	3	20	-12	H=L=	1	10	5	15	16	3	0	-4
H=L=	7	5	1	96	89	3	0	-5	4	7	6	9	0	-9	9	20	18	4	0	-11	0	41	-42	6	14	-17	4	30	30
1	45	42	2	101	-92	4	65	-66	5	39	34	10	0	-10	10	23	-17	5	28	-28	1	0	-17	7	0	-24	5	22	-32
2	37	-32	3	27	-25	5	29	-31	6	70	62	11	31	25	11	0	-11	H=L=	0	9	2	0	11	8	13	9	6	16	10
3	15	8	4	7	-8	6	40	-41	7	30	29	12	0	-10	12	0	8	2	23	-4	3	31	-24	9	12	8	7	10	12
4	41	51	5	68	56	7	28	29	8	9	-9	13	27	28	H=L=	5	8	4	37	-38	4	65	-62	10	11	1	8	9	25
5	9	5	6	0	17	8	37	-33	9	92	-91	H=L=	9	7	0	45	42	6	28	14	5	27	21	H=L=	5	11	H=L=	4	13
6	0	0	7	0	-16	9	34	-31	10	74	-77	1	45	-38	1	55	55	8	20	21	6	73	-69	1	15	-2	1	0	12
7	0	11	8	23	-19	10	0	-4	11	0	4	2	0	-11	2	36	-25	10	33	-32	7	59	59	2	0	19	2	0	13
8	0	13	9	10	7	11	0	7	12	14	11	3	10	20	3	21	20	H=L=	1	9	8	0	0	3	0	17	3	27	-36
9	49	47	10	0	3	12	13	-19	13	30	28	4	48	50	4	101	-105	1	43	-40	9	0	13	4	0	1	4	37	38
10	26	26	11	53	44	13	0	-6	H=L=	2	7	5	31	27	5	19	-22	2	0	-9	10	0	0	5	32	-39	5	12	-11
11	0	2	12	43	39	14	0	-9	1	0	11	6	96	93	6	28	-16	3	18	0	11	49	51	6	37	-34	H=L=	5	13
12	64	67	13	28	-23	15	18	-23	2	35	35	7	20	-16	7	92	85	4	61	-60	H=L=	2	10	7	13	-8	1	27	26
13	42	-31	14	17	8	H=L=	8	6	3	0	-3	8	9	-7	8	0	0	5	42	50	0	21	-16	8	33	40	2	29	27
14	0	-3	15	13	22	0	66	-65	4	38	-39	9	9	16	9	31	-32	5	37	44	1	67	-60	9	32	-31	3	12	8
H=L=	8	5	H=L=	2	6	1	14	-19	5	21	15	10	0	-7	10	0	-4	7	32	-29	2	39	-35	10	31	33	4	0	2
1	90	26	0	5	-1	2	0	-9	6	0	11	11	24	22	11	0	1	8	42	45	3	67	58	11	25	-31	5	41	9
2	24	28	1	11	-14	3	31	-18	7	89	90	H=L=	10	7	12	0	3	9	13	12	4	42	29	H=L=	6	11			
3	30	-29	2	22	16	4	59	59	8	25	21	1	10	16	13	16	13	10	18	25	5	47	41	1	0	-7			
4	35	33	3	169	152	5	63	62	9	78	69	2	0	-18	14	0	9	11	0	-5	6	0	1	2	0	-8			
5	77	64	4	0	0	6	52	-50	10	10	-5	3	0	-7	15	37	40	12	0	16	7	20	-6	3	0	11			
6	91	24	5	74	59	7	10	-9	11	14	-9	4	14	-2	H=L=	6	8	13	0	-6	8	24	-19	4	0	-16			
7	44	-41	6	0	11	8	10	17	12	50	54	5	26	-27	0	133	135	14	31	31	9	33	39	5	0	11			
8	0	5	7	56	47	9	0	18	13	14	11	6	19	-7	1	61	-55	H=L=	2	9	10	32	40	6	0	9			
9	49	-49	8	0	9	10	0	-3	14	0	-4	7	0	-3	2	49	-54	1	28	-28	11	0	-5	7	0	5			

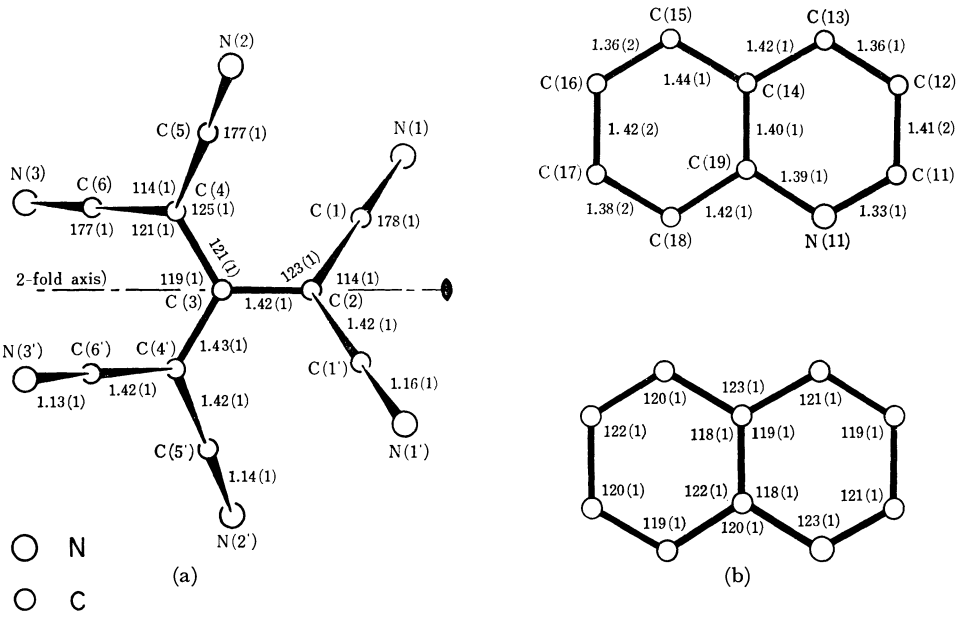

(c) Non-bonded distances in the anion (Å)

N(1)–N(1′)	4.29(2)	C(1)–C(1′)	2.39(2)
N(1)–N(2)	3.32(1)	C(1)–C(5)	2.83(1)
N(2)–N(3)	4.24(1)	C(5)–C(6)	2.39(1)
N(3)–N(3′)	3.38(2)	C(6)–C(6′)	2.81(2)
		C(2)–C(4)	2.48(1)
		C(4)–C(4′)	2.47(2)

Fig. 3. Interatomic distances and angles in the anion and the cation, together with the e.s.d.'s in parentheses.

TABLE 7.

(a) Equations of the least-squares planes through atoms in the ion pair

Least-squares plane[a]	Atom	Deviation (Å)	Least-squares plane[a]	Atom	Deviation (Å)
$(C_{10}N_6)^{2-}$ ion:				C(6)	−0.008
1) $-0.6934X-0.0000Y-0.7205Z+6.6499=0$	C(2)	0.000		N(3)	0.008
	C(3)	−0.000		C(3)	0.007
	C(4)	0.000	$(C_9NH_8)^{+}$ ion:		
	C(4′)	0.000	4) $-0.8794X-0.0007Y-0.4762Z+3.2136=0$	N(11)	−0.016
2) $-0.5109X-0.0000Y-0.8596Z+5.4854=0$	N(1)	0.003		C(11)	−0.045
	C(1)	−0.006		C(12)	−0.048
	C(2)	0.000		C(13)	−0.036
	C(3)	0.000		C(14)	−0.006
	C(1′)	0.006		C(15)	0.008
	N(1′)	−0.004		C(16)	−0.001
3) $-0.7732X+0.3597Y-0.5224Z+4.6323=0$	N(2)	0.001		C(17)	−0.001
	C(5)	0.006		C(18)	0.009
	C(4)	−0.014		C(19)	−0.002

(b) Dihedral angles

between the planes 1) and 2):	13.2°	between the planes 1) and 3):	24.2°

a) X, Y, and Z are the coordinates corresponding to the crystal axes a, b, and c, respectively.

rest are 24° (Table 7(b)). In the calcium salt[6] all the tilt angles are reported to be 24°. Each bond distance and bond angle show an accordance, within the limits of error, with the corresponding distance of the same anion in the calcium salt,[6] except for the C(2)–C(1)–N bond angle, where the difference slightly exceeds three times the estimated standard deviation. The non-bonded N···N distances show a shortening due to the above-mentioned tilt of the cyano-substituents: the N(1)···N(2) distance is 3.32(2), and the N(3)···N(3′) distance, 3.38(2) Å, while 3.48 and 3.48 Å are the corresponding distances in the calcium salt.

Table 8. Interatomic distances within the ion-pair (less than 3.8 Å), along with their e.s.d.'s in parentheses

N(1)–N(11)	2.99(1) Å
C(6)–C(13)	3.38(1)
N(1)–C(11)	3.38(1)
C(1)–N(11)	3.40(1)
C(1)–C(11)	3.41(1)
N(1)–C(19)	3.54(1)
C(4)–C(13)	3.58(1)
C(6)–C(14)	3.62(1)
N(3)–C(13)	3.62(1)
C(5)–C(14)	3.66(1)
N(3)–C(15)	3.69(1)
C(6)–C(15)	3.69(1)
C(4)–C(14)	3.71(1)
C(5)–C(19)	3.80(1)

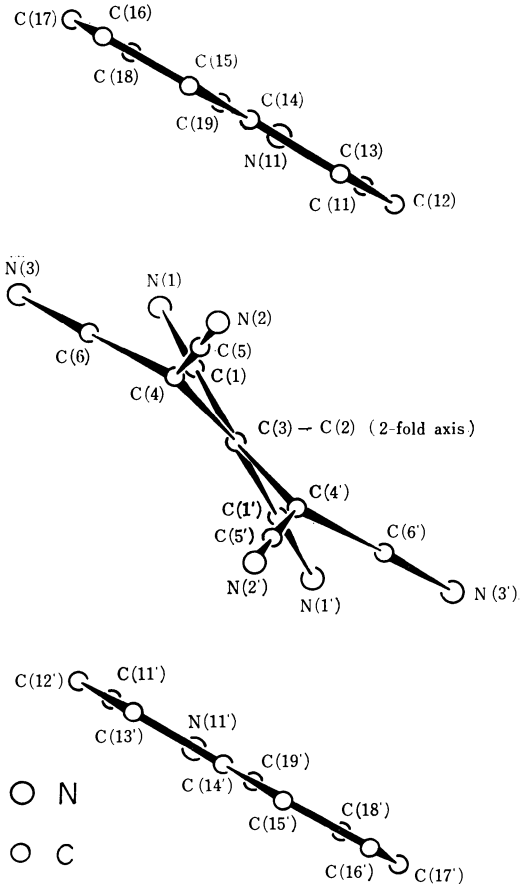

Table 9. Interatomic distances between the ion-pairs (less than 3.8 Å) along with their e.s.d.'s in parentheses

C(19)–C(18)^{i}	3.68(1) Å
C(14)–C(17)^{i}	3.78(2)
C(15)–C(15)^{i}	3.66(2)
C(14)–C(16)^{i}	3.76(2)
N(1)–N(3)^{ii}	3.63(1)
N(1)–C(15)^{ii}	3.38(1)
C(19)–N(3)^{ii}	3.71(1)
N(11)–N(3)^{ii}	2.84(1) (hydrogen bond)
C(11)–N(3)^{ii}	3.68(1)
N(1)–C(11)^{iii}	3.59(1)
N(1)–C(12)^{iii}	3.27(1)
N(2)–C(11)^{iii}	3.25(1)
C(18)–C(11)^{iii}	3.50(2)
C(16)–C(4)^{iv}	3.78(1)
C(16)–C(5)^{iv}	3.59(2)
C(17)–C(6)^{iv}	3.80(2)
C(13)–C(5)^{v}	3.74(1)

Key for superscripts:

i	$-x$,	y,	$1/2-z$
ii	$1/2-x$,	$1/2+y$,	z
iii	x,	$1-y$,	$1/2+z$
iv	$-1/2+x$,	$1/2-y$,	$1-z$
v	$1/2-x$,	$1/2-y$,	$-1/2+z$

From these facts, it may be concluded that the steric repulsions between cyano-groups in adjacent arms are considerably increased by the reduction of the tilt angle of the arm which lies on the 2-fold axis from 24° to 13°, while the π-overlap is increased a little, and that these effects may be due to weak interaction between the anion and the cation.

The quinolinium cation, $(C_9NH_8)^+$, was expected to be planar, but an intersting tendency is observed for the C(11), C(12), and C(13) atoms to deviate slightly toward the anion from the least-squares plane (Table 7(a)). Of these deviated atoms, C(11) makes close contact with N(1) and C(1), which belong to the arm of the anion having the smallest tilt angle. C(13) is also located close to C(6), C(4), and N(3) of a different arm of the anion (Table 8).

Crystal Structure. The crystal structure viewed down the *a* and *b* axes is shown in Fig. 4. The packing unit of the crystal is an ion pair consisting of one di-valent anion and two mono-valent cations, and the anion lies on a crystallographic 2-fold axis between two cations forming a sandwich structure. The tilt angle of the plane of the cation to the *a* axis is about 60°. The N(1)–N(11) distance is 2.99(1) Å (Fig. 5), which is the closest atomic contact between ions in this unit. These sandwiched units stack infinitely, forming a column, along the *a* axis (Fig. 4(b)). The polarized absorption spectra of a single crystal of this

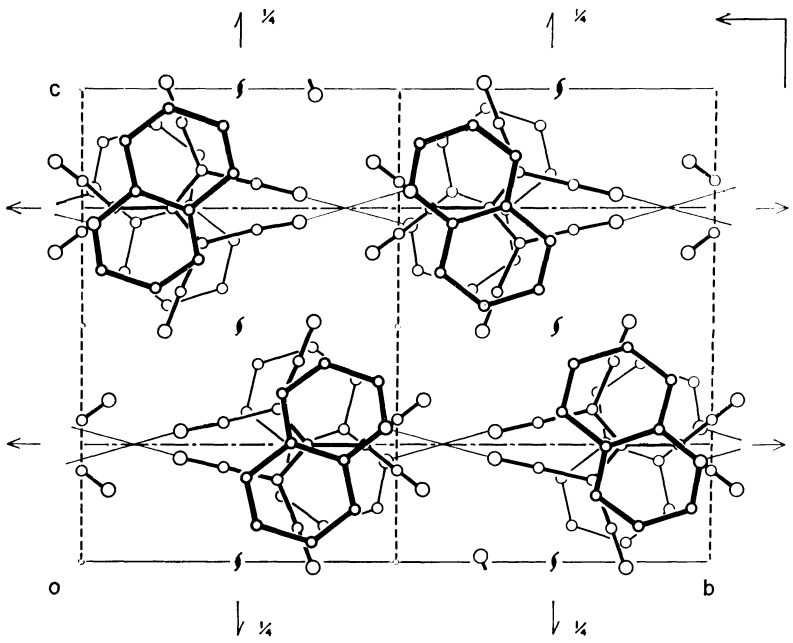

Fig. 4(a). Crystal stustructure viewed down along the *a* axis. Hydrogen bondings are shown by thin solid lines.

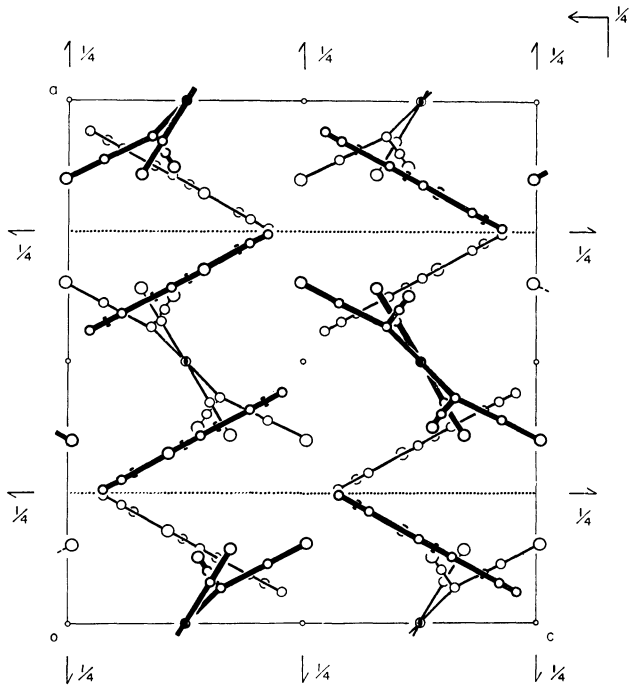

Fig. 4(b). Crystal structure viewed down along the *b* axis.

complex was measured.[4] The optical density of the charge-transfer band at 415 nm is much higher in the *a*-polarization spectrum than in the *c*-polarization spectrum. This result can be explained well in terms of the crystal structure (see Fig. 4(b)) as being due to the charge-transfer phenomenon between ions within the ion pair.

In the contacts between these stacks, the hydrogen bond exists along the *b* axis between the N(3) atom of one unit and the N(11) of the other unit, and the distance is 2.84(1) Å. Some close inter-ionic atomic contacts, including the hydrogen bond, are shown in Table 9.

The authors wish to express their deep thanks to Professor Hiroshi Mikawa for his kindness of supplying crystals and for his helpful discussions.

Polarized Absorption Spectra of Single Crystals of Ion Radical Salts. II. K(TCNQ) and $Cs_2(TCNQ)_3$

Shoji HIROMA, Haruo KURODA, and Hideo AKAMATU

Department of Chemistry, Faculty of Science, The University of Tokyo, Hongo, Tokyo

(Received June 2, 1970)

Polarized absorption spectra in the 10—40 kK region were observed on single crystals of the ion radical salts of tetracyano-*p*-quinodimethane (TCNQ), potassium·(TCNQ) and cesium$_2$·(TCNQ)$_3$. The crystal spectra are shown to be markedly different from the solution spectra of the monomer and dimer of TCNQ ion. It is shown that the 7.8 kK band of K(TCNQ) and the 11.1 kK band of $Cs_2(TCNQ)_3$ are charge-transfer bands associated with the transfer of an electron from a $TCNQ^-$ ion to the neighboring $TCNQ^-$ ion. The first-order and second-order effects were calculated on the local-excitation bands in order to explain the general feature of the observed spectra.

In a previous paper,[1] we reported the polarized absorption spectra of ionic solids composed of the radical anion of 7,7,8,8-tetracyano-*p*-quinodimethane (TCNQ) and the radical cation of a π-electron donor such as *N,N,N',N'*-tetramethyl-*p*-phenylenediamine (TMPD). We showed that the crystal spectra are composed of the local-excitation (LE) bands associated with the transition of each component ion, and the charge-transfer (CT) band associated with the transfer of an electron from an anion to the adjacent cation. In these crystals, the cation and anion are stacked face-to-face on each other to form a molecular column developed along one of the crystal axes, and there is a relatively strong charge-transfer interaction between them. There is another kind of TCNQ salt, composed of the TCNQ radical anion and a closed-shell cation, in which the closely packed molecular column is formed by the stacking of the TCNQ anion, not by the alternate stacking of the anion and cation. In this case, the charge-transfer interaction is expected to occur primarily between the neighboring TCNQ anions, which should have bearing on the electrical and magnetical properties of the TCNQ salts.

Recently, the absorption spectra of the crystalline powder obtained by use of the diffuse reflection method have been reported by Iida[2] on several TCNQ salts of this kind. He described some characteristic features distinguishing the spectra of the TCNQ salts of high electrical conductivity from those of the TCNQ salts of low conductivity, and pointed out that the latter resembles in several respects the absorption spectrum of the TCNQ ion dimer. However, care should be taken in comparing the crystal spectra with the spectrum of the ion dimer, since, in the crystal, the interaction by the TCNQ ions other than the nearest-neighbor ones might influence the absorption spectrum.

In the present study, we have observed the polarized absorption spectra of single crystals of two TCNQ salts, K(TCNQ) and $Cs_2(TCNQ)_3$, and carried out some theoretical considerations on the exciton states in these salts.

Experimental

We measured the polarized absorption spectra of the 9—40 kK region at room temperature by using single crystals of microscopic size with an apparatus modified from a commercial microspectrophotometer, Olympus MSP-A-IV. The details of the appratus have been described elsewhere.[3]

The TCNQ salts were prepared according to the procedures reported by Melby *et al.*[4] We recrystallized the powders of the salts to obtain very small single crystals suitable for the measurement of spectrum. The recrystallized powder occacionally contains a small amount of the crystal of free TCNQ, but is easily distinguishable from salt crystals by the crystal habits and optical properties.

We observed also the absorption spectrum of crystalline powder by means of the liquid-paraffin-mull method. The spectra thus obtained were used only for the purpose of examining the location of an absorption maximum in the low energy part outside the applicable region of our microspectrophotometer.

Experimental Results

(1) Spectrum of K(TCNQ). A preliminary analysis of crystal structure has been done by Anderson

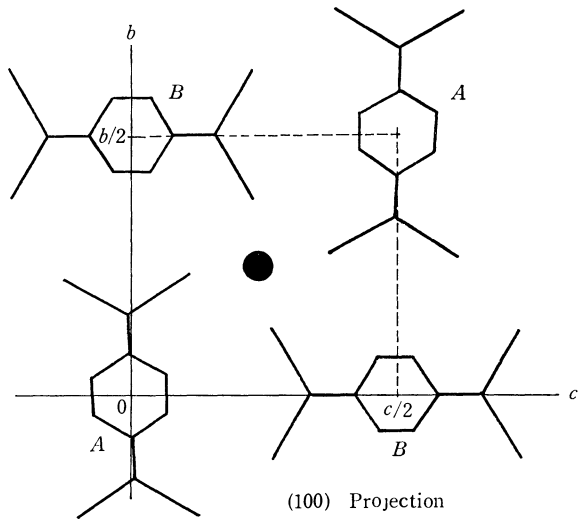

Fig. 1. Model of the crystal structure of K(TCNQ), after Anderson *et al*: ● indicates K^+ ion. $TCNQ^-$ are stacked along the *a*-axis. Two different groups of $TCNQ^-$ sites are indicated as *A* and *B*.

1) H. Kuroda, S. Hiroma, and H. Akamatu, This Bulletin, **41**, 2855 (1968).

2) Y. Iida, *ibid.*, **42**, 71, 673 (1969).

3) H. Kuroda, T. Kunii, S. Hiroma, and H. Akamatu, *J. Mol. Spectrosc.*, **22**, 60 (1967).

4) L. R. Melby, R. J. Harder, W. R. Hertler, W. Mahler, R. E. Benson, and W. E. Mochel, *J. Amer. Chem. Soc.*, **84**, 3374 (1962).

and Fritchie,[5] who reported that the K(TCNQ) crystal is monoclinic of $P2_1/n$ space group, with the lattice constants; $a=7.10$ Å, $b=18.80$ Å, $c=17.88$ Å and $\beta=94°54'$. The unit cell contains eight formula units. Of the eight TCNQ ions, four are mutually transferable by the symmetry operation of $P2_1/n$ space group, and the other four are mutually transferable among themselves. We shall call the former TCNQ sites *A*-site, and the latter *B*-site (see Fig. 1).

We observed the *a*- and *b*-axis polarized spectra from the direction normal to the developed face (001). The spectra are shown in Fig. 2, and the wave number of peak and the polarization ratio are given in Table 1.

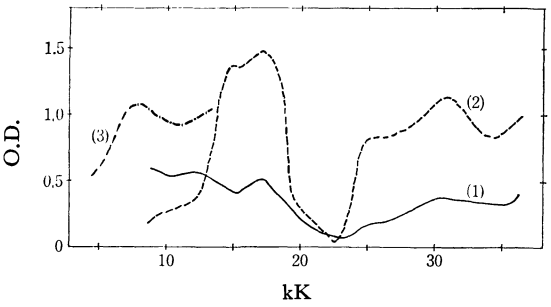

Fig. 2. Crystal absorption spectra of K(TCNQ): (1) *a*-spectrum, (2) *b*-spectrum, (3) spectrum of powder sample.

TABLE 1. WAVE NUMBERS OF THE ABSORPTION PEAKS AND POLARIZATION RATIOS OF CRYSTAL SPECTRA OF K(TCNQ)
(wave numbers in kK)

Band in crystal		I_a/I_b
$\tilde{\nu}_a$	$\tilde{\nu}_b$	
7.8		>2.5
12.5	15.0	0.43
17.3	17.3	0.36
25.0	25.0	0.17
30.8	30.8	0.33

For the sake of comparison, the absorption spectrum of the acetonitrile solution of K(TCNQ) and the spectrum of the dimer of TCNQ anion formed in aqueous solution are shown in Fig. 3. It should be noted that the crystal spectra differ markedly from the spectra of both the monomer and the dimer. The former are extended into a lower-energy region well outside the absorption limit of the latter, while the absorption bands of the crystal in the visible and ultraviolet region are located at appreciably higher energy in comparison with the monomer and dimer. A marked difference is also found in the band shape.

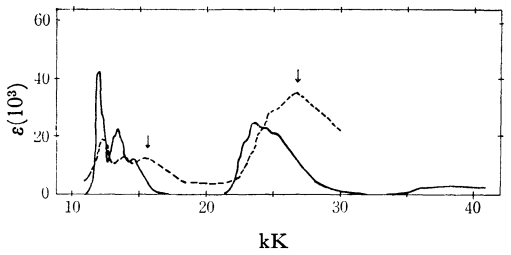

Fig. 3. Solution absorption spectrum of K(TCNQ): ——monomer in acetonitrile, ---- dimer in water (The absorption peaks of the dimer band are indicated by arrows.).

From the spectrum of the powder, we found that the absorption maximum of the low-energy band is located at about 7.8 kK. The polarization ratio, I_a/I_b, is 2.5 at 10 kK, and increases with the decrease of wave number. Thus we can consider that the 7.8 kK band is strongly polarized in the *a*-axis direction, along which $TCNQ^-$ ions are stacked face-to-face on each other. The polarization indicates that the 7.8 kK band is an absorption band associated with the charge-transfer (CT) between $TCNQ^-$ ions. Polarization is quite different in the case of the absorption bands found in the 15—40 kK region. It seems most reasonable to assign them to ones mainly associated with the transition of $TCNQ^-$ ion, which we will call the local-excitation (LE) bands. The bands in the 15—20 kK region appear to be due to the lowest transition of $TCNQ^-$ ion, and those in the 25—35 kK region to the second one.

However, for making a definite interpretation of the observed results, we need to make a theoretical consideration as regards the energy of the CT band, and the crystal shift and factor group splitting of each LE band. This will be discussed in the later part of this paper.

(2) Spectrum of $Cs_2(TCNQ)_3$. In this salt, formally, two electrons are shared among three molecules of TCNQ. The crystal structure has been determined by Fritchie and Arther.[6] According to them, the crystal is monoclinic belonging to $P2_1/c$ space group, with the lattice constants; $a=7.34$ Å, $b=10.40$ Å, $c=21.98$ Å, and $\beta=97.18°$. Two formula units are contained in a unit cell. The projection of the crystal structure from the direction normal to the (001) plane is schematically shown in Fig. 4. It has been concluded from the observed bond lengths that the TCNQ site at the center of symmetry is occupied by a neutral molecule, and is sandwiched by two TCNQ ions

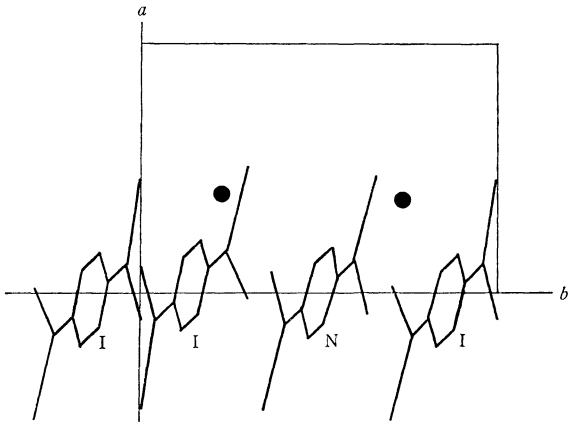

Fig. 4. Stacking of TCNQ ions and molecules in the $Cs_2(TCNQ)_3$ Crystal. (I: ion, N: neutral, ●: Cs)

5) G. R. Anderson and C. J. Fritchie, Jr., 2nd National Meeting of the Society of Applied Spectroscopy, San Diego (1963), Paper 111.

6) C. J. Fritchie, Jr., and P. Arther, Jr., *Acta Crystallogr.*, **21**, 139 (1966).

mutually transferable by the inversion operation.[6]

We observed the *a*-axis and *b*-axis spectra on the (001) plane. The observed spectra are shown in Fig. 5, and the wave numbers and polarization ratios of absorption bands are listed in Table 2.

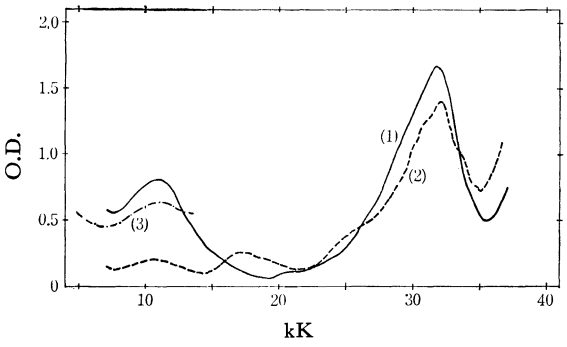

Fig. 5. Crystal absorption spectra of $Cs_2(TCNQ)_3$: (1) *b*-spectrum, (2) *a*-spectrum, (3) spectrum of powder sample.

Table 2. Wave numbers of the absorption peaks and polarization ratios of crystal spectra of $Cs_2(TCNQ)_3$ (wave numbers in kK)

$\tilde{\nu}_a$	$\tilde{\nu}_b$	I_a/I_b
11.1	11.1	0.25
17.3	~21.5	~2.1
25.0	—	*a*-axis polarized
32.3	31.9	0.84

The 11 kK band is strongly polarized in the *a*-axis direction, and other bands exhibit a different polarization. This suggests that the 11 kK band is the CT band whereas others are the LE bands associated either with the transitions of $TCNQ^-$ ion or with those of TCNQ° molecule. However, the relative intensities of the LE bands are markedly different from the ones expected from the oscillator strengths of transitions of the free component according to the oriented-gas model (Table 4). It should be noted also that the crystal spectra exhibit no strong absorption band at the wavelength corresponding to the second absorption band of $TCNQ^-$ ion and the first band of TCNQ° molecule, both of which are at about 25 kK in the solution spectra. Instead, we found one strong absorption band at about 32 kK in the *a*-axis spectrum as well as in the *b*-axis spectrum.

The large difference between the crystal spectra and the spectra of the components makes it hard to give any simple interpretation of the observed spectra. Thus it is particularly interesting in this case to estimate the crystal shift, factor group splitting, and crystal induced mixing.

The absorption spectrum of the crystalline powder shows that there is no absorption maximum from 5 kK to 10 kK, but the absorption increases with the decrease of wave number in the region below 7 kK, suggesting the presence of another low-energy absorption band. This seems to be associated with the charge transfer between an ion and a molecule of TCNQ.

Discussions

(1) Transitions of the Molecule and Anion of TCNQ. Before discussing the exciton states of salt crystals, we will first consider the transitions of TCNQ molecule and its anion. Although their π-electron states have been theoretically studied by Lowitz[7] by means of the semiempirical self-consistent-field molecular orbital (SCF-MO) method, his results are not satisfactory for the analysis of crystal spectra. Recently, the SCF-MO calculation has been carried out in our laboratory on the molecule and anion of TCNQ using the variable-β,γ modification[8] of Pariser-Parr-Pople method carefully choosing semiempirical parameters.[9] Two different procedures were used: [Method I], all β terms are included and are estimated by using Katagiri-Sandorfy's formula[10] for β; [Method II], only the nearest-neighbor β terms are included, which are estimated by using Nishimoto-Forster's formula.[8] In both cases, the configuration interaction (CI) calculation was carried out by taking into account the lower forty singly-excited configurations. The Longuet-Higgins and Pople method[11] was applied in the case of the anion.

The singlet-singlet transitions of TCNQ predicted by this calculation are shown in Fig. 6, together with the observed results. We find that the theoretical predictions are in satisfactory agreement with the observations. Thus the first and second transitions of TCNQ are assigned to $^1B_{1u}\leftarrow{}^1A_{1g}$ (*long-axis* polarized) and $^1B_{2u}\leftarrow{}^1A_{1g}$ (*short-axis* polarized), respectively. In the case of the anion, the agreement with the observation is found to be better in Method I than in Method II, as seen in Fig. 7.

We can safely assign the first absorption band of the anion observed at 12.0 kK to $^2B_{3u}\leftarrow{}^2B_{2g}$ (*long-axis* polarized) predicted at 9.8 kK by Method I and at 11.2 kK by Method II. According to the calculation, the second absorption band should be considered to be the superposition of two transitions, $^2A_u\leftarrow{}^2B_{2g}$ (*short-axis* polarized) and $^2B_{3u}\leftarrow{}^2B_{2g}$ (*long-axis* polarized). The band shape suggests that this absorption band is composed of a weak component (23.5 kK) and a strong component (25.4 kK). We will assign the former to $^2A_u\leftarrow{}^2B_{2g'}$ and the latter to $^2B_{3u}\leftarrow{}^2B_{2g}$. The next absorption band is probably due to $^2A_u\leftarrow{}^2B_{2g}$ although there is a large discrepancy between the predicted and observed energies. In the later part, we will denote the 12.0, 23.5, 25.4, and 35.7 kK transitions respectively as R, S, U, and S'.

(2) Charge Transfer between TCNQ Anions. In the TCNQ salts studied here, the overlap of the π-orbitals between $TCNQ^-$ ions stacked on each other is large enough to give a fairly strong CT band. The energy

7) D. A. Lowitz, *J. Chem. Phys.*, **46**, 4698 (1967).
8) K. Nishimoto and L. S. Forster, *Theoret. Chim. Acta*, **3**, 407 (1965); **4**, 155 (1966).
9) The details of this calculation will be reported separately.
10) S. Katagiri and C. Sandorfy, *Theoret. Chim. Acta*, **4**, 203 (1966).
11) H. C. Longuet-Higgins and J. A. Pople, *Proc. Phys. Soc.* (London), **A68**, 591 (1955).

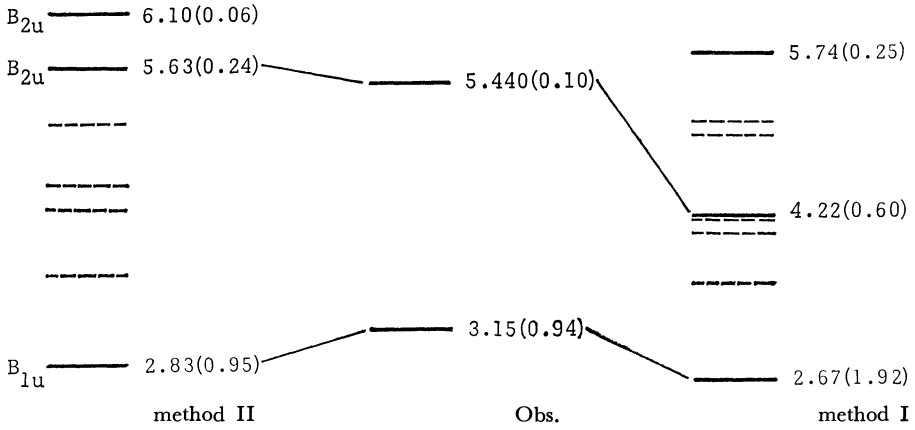

Fig. 6. Singlet excited levels of TCNQ molecule: (—— allowed, ---- forbidden). Excitation energies are given in eV. Oscillator strengths are shown in parentheses.

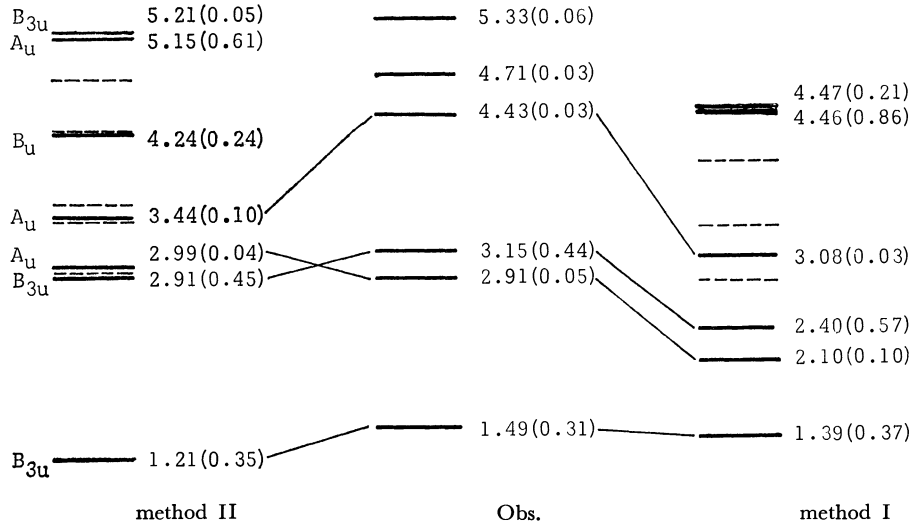

Fig. 7. Excited levels of TCNQ ions. (—— allowed, ---- forbidden). Symmetry of the ground state is B_{2g}. Excitation energies are given in eV. Oscillator strengths are shown in parentheses.

for transferring one electron from a $TCNQ^-$ ion to the neighboring $TCNQ^-$ ion to form a pair consisting of TCNQ° and $TCNQ^{2-}$ can be given by

$$\Delta E_{CT} = I - A - C \qquad (1)$$

where I and A are respectively the ionization potential and electron affinity of the $TCNQ^-$ ion, and C the Coulomb energy term. As can be easily seen, the difference, $I-A$, must be equal to the energy of the repulsion between the two electrons in the highest occupied orbital of the $TCNQ^{2-}$, which can be estimated from the molecular orbital by using the semiempirical values of the one-center and two-center repulsion integrals.[12] We obtained 3.9 eV for $I-A$. By considering the energy cycle of the charge-transfer process, we can show that the term C is approximately equal to the repulsion between the two $TCNQ^-$ ions in question. We estimated it by using the charge distribution obtained from the calculated molecular orbitals of $TCNQ^-$, and obtained the value of 3.0 eV for $Cs_2(TCNQ)_3$. It is almost the same also for K(TCNQ). Thus ΔE_{CT} is predicted to be 0.9 eV. We can therefore, expect the CT band to appear at about 7.2 kK. This is in agreement with the observed location of the CT band of K(TCNQ). In the case of $Cs_2(TCNQ)_3$, a CT band is found at 11 kK, which is considerably large as compared with the predicted values. It should be noted, however, that the actual location of the CT band will naturally be affected by the interactions with other CT states as well as by those with LE states.

In the crystal of $Cs_2(TCNQ)_3$, there can be another type of CT band, namely that associated with the transfer of an electron from $TCNQ^-$ to the adjacent TCNQ°. In this case, the value of $(I-A)$ in Eq. (1) becomes zero, and the term C must be very small. Therefore, this CT band should appear at a lower wave number, possibly in the infrared region. We will attribute the absorption below 5 kK to this CT band. A similar low-energy CT band can be expected to appear generally in the case of TCNQ salts which contain a neutral TCNQ molecule.

(3) Local Excitation Bands. Since the LE bands of the crystal spectra are markedly different from the

12) We have taken here the values of one-center repulsion integral, $\gamma_{\mu\mu}$, as 11.13, 10.09 and 11.52 respectively for carbon in the aromatic ring and carbon and nitrogen in C≡N group. The two-center repulsion integral $\gamma_{\mu\nu}$ was estimated by using the Nishimoto-Mataga method, *viz.*,

$$\gamma_{\mu\nu} = \frac{14.3897}{a_{\mu\nu} + R_{\mu\nu}}, \quad a_{\mu\nu} = 2\frac{14.3897}{\gamma_{\mu\mu} + \gamma_{\nu\nu}}$$

spectra of the free components, we will estimate the crystal shift and splitting of the LE bands by the calculation method within the usual approximation of the exciton theory of molecular crystal.[13,14] We will describe the zero-th order wavefunction of an exciton state, associated with the fth excited state of $TCNQ^-$ ion by the following equation neglecting the part associated with other components.

$$\Phi_r^f = \frac{1}{\sqrt{Nh}} \sum_{m=1}^{N} \sum_{\alpha=1}^{h} B_\alpha^r \psi_{m\alpha}^f \tag{2}$$

herewith

$$\psi_{m\alpha}^f = \phi_{m\alpha}^f \prod_{n\beta \neq m\alpha}{}' \phi_{n\beta}^\circ$$

where $\phi_{m\alpha}^f$ and $\phi_{m\alpha}^\circ$ are the wavefunctions of the fth excited state and the ground state of the $TCNQ^-$ ion at the αth site of the mth unit cell, respectively and B_α^r is the numerical factor characteristic of the rth representation of the symmetry group of the crystal.

In the first order approximation, the exciton level relative to the ground state is given as

$$\Delta E_r^f = \varepsilon^f + D^f + \sum_{n\beta \neq m\alpha} B_\alpha^r B_\beta^r I_{m\alpha,n\beta}^f \tag{3}$$

where ε^f is the transition energy of the free ion (or molecule), and D^f, $I_{m\alpha,n\beta}^f$ are defined as follows:

$$D^f = \sum_{n\beta \neq m\alpha} \{\langle \phi_{m\alpha}^f \phi_{n\beta}^\circ | V | \phi_{m\alpha}^f \phi_{n\beta}^\circ \rangle - \langle \phi_{m\alpha}^\circ \phi_{n\beta}^\circ | V | \phi_{m\alpha}^\circ \phi_{n\beta}^\circ \rangle\} \tag{4}$$

$$I_{m\alpha,n\beta}^f = \langle \phi_{m\alpha}^f \phi_{n\beta}^\circ | V | \phi_{m\alpha}^\circ \phi_{n\beta}^f \rangle \tag{5}$$

V being the perturbing potential due to the intermolecular interaction. The off-diagonal matrix element of the second-order calculation is given as

$$H_r^{fg} = \Delta^{fg} + \sum_{n\beta \neq m\alpha} B_\alpha^r B_\beta^r \Gamma_{m\alpha,n\beta}^{fg} \tag{6}$$

where

$$\Delta^{fg} = \sum_{n\beta} \langle \phi_{m\alpha}^f \phi_{n\beta}^\circ | V | \phi_{m\alpha}^g \phi_{n\beta}^\circ \rangle \tag{7}$$

$$\Gamma_{m\alpha,n\beta}^{fg} = \frac{1}{2} \left\{ \langle \phi_{m\alpha}^f \phi_{n\beta}^\circ | V | \phi_{m\alpha}^\circ \phi_{n\beta}^g \rangle + \langle \phi_{m\alpha}^g \phi_{n\beta}^\circ | V | \phi_{m\alpha}^\circ \phi_{n\beta}^f \rangle \right\} \tag{8}$$

Although the equations described above are the same as ones usually given in the exciton theory of molecular crystal, we have to take into account several aspects characteristic of the TCNQ salts in carrying out the numerical calculation. First, we should note that it is the electrostatic interaction between ions that gives the largest contribution to D^f, and, second, we are not allowed to use the dipole-dipole approximation for evaluating $I_{m\alpha,n\beta}^f$ and $\Gamma_{m\alpha,n\beta}^{fg}$ when two TCNQ ions or molecules are in direct contact with each other.

We estimated D^f by the following formula taking the point charge approximation.

$$D^f = \sum_\mu \sum_q \sum_\nu (\rho_{p\mu}^f \rho_{q\nu}^\circ - \rho_{p\mu}^\circ \rho_{q\nu}^\circ)(e^2/R_{p\mu,q\nu}) \tag{9}$$

where $\rho_{p\mu}^f$ and $\rho_{p\mu}^\circ$ are the charge density at the μth atom of the pth ion in the fth excited state and the ground state, respectively, and the summation over q is to include also the cations. We used the charge density of an atom in the $TCNQ^-$ ion estimated from the molecular orbitals. In the evaluation of $I_{m\alpha,n\beta}^f$ we used the following equation when the distance between the $m\alpha$ and $n\beta$ sites was within 10 Å, but used the dipole-dipole approximation when the distance was larger than 10 Å.

$$I_{p,q}^f = a_{i,j}^2 \sum_\mu \sum_\nu c_{i\mu} c_{j\mu} c_{i\nu} c_{j\nu} (e^2/R_{p\mu,q\nu}) \tag{10}$$

we have assumed here that the fth excited state is associated with the excitation of an electron from the ith molecular orbital to the jth molecular orbital; $a_{i,j}$ is the numerial factor equal to 1 or $\sqrt{2}$ depending on the type of orbitals concerned, and $c_{i\mu}$ is the coefficient in the ith molecular orbital. Similarly, when the gth excited state is associated with the excitation from the kth orbital to the lth orbital, $\Gamma_{m\alpha,n\beta}^{fg}$ was evaluated by the following equation for a distance up to 10 Å, and by the dipole-dipole approximation for a larger distance.

$$\Gamma_{p,q}^{fg} = a_{ij} a_{kl} \sum_\mu \sum_\nu c_{i\mu} c_{j\mu} c_{k\nu} c_{l\nu} (e^2/R_{p\mu,q\nu}) \tag{11}$$

The Δ^{fg} term is negligible unless $i=k$ or $j=l$. If $i=k$, it can be estimated by

$$\Delta^{fg} = b_{ij,k} \sum_\mu \sum_q \sum_\nu \rho_{p\mu}^{ij} \rho_{q\nu}^\circ (e^2/R_{p\mu,q\nu}) \tag{12}$$

where $b_{ij,k}$ is a numerical factor characteristic of the types of orbitals with respect to the fth and gth excitation, $\rho_{p\mu}^{ij}$ is a quantity defined as $\rho_{p\mu}^{ij} = c_{i\mu} c_{j\mu}$, and the summation over q is to include the cations.

(a) K(TCNQ): When we label the $TCNQ^-$ ions at A-sites as 1, 1′, 2, and 2′ so that 1 and 1′, or 2 and 2′ are in direct contact with each other, and the $TCNQ^-$ ions at B-sites as 3, 3′, 4, and 4′ in a similar way, the zero-th order wavefunctions are described as follows:

$$\Phi_A^\pm = \frac{1}{\sqrt{4N}} \sum_{m=1}^{N} \{(\psi_{m1} - \psi_{m1'}) \pm (\psi_{m2} - \psi_{m2'})\} \tag{13}$$

$$\Phi_B^\pm = \frac{1}{\sqrt{4N}} \sum_{m=1}^{N} \{(\psi_{m3} - \psi_{m3'}) \pm (\psi_{m4} - \psi_{m4'})\} \tag{14}$$

Φ_A^+ and Φ_B^+ belong to A_u representation, and Φ_A^- and Φ_B^- belong to B_u representation of C_{2h} symmetry group. Since the exact atomic coordinates were not reported by Anderson and Fritchie,[5] we carried out numerical calculation using the approximate coordinates we estimated from the data given in their report.

The exciton levels predicted by the second-order calculations are summarized in Table 3. Each transition of $TCNQ^-$ ion gives four exciton levels, two A_u and two B_u states. Each of them is associated mainly with either one of the wavefunctions given by Eqs. (13) and (14). We will denote the levels associated with

13) A. S. Davydov, "Theory of Molecular Excitons," McGraw-Hill, New York (1962).

14) D. P. Craig and S. H. Walmsley, "Physics and Chemistry of the Organic Solid State," Vol. 1, ed. by M. M. Labes, D. Fox, and A. Weissberger, Wiley, New York (1963), p. 585.

15) The same formula can be used for the exciton state associated with the TCNQ molecule in $Cs_2(TCNQ)_3$, if we replace $\phi_{m\alpha}^f$, $\phi_{m\alpha}^\circ$ with the corresponding wavefunction of the molecule.

Φ_A^+, Φ_A^-, Φ_B^+, and Φ_B^- as $A_u(A)$, $B_u(A)$, $A_u(B)$, and $B_u(B)$, respectively. It should be noted that the energies are almost equal between the $A_u(A)$ and $B_u(B)$ states and between the $B_u(A)$ and $A_u(B)$ states. This means that there will be little difference between the *b*-axis and *a*-axis spectra as regards the locations of LE bands. This is in agreement with the observation except for the difference between the $A_u(A)$ and $B_u(B)$ components of the R-band. The observed shifts of the transitions of $TCNQ^-$ ion are also well predicted by the present calculation.

TABLE 3. EXCITON LEVELS OF K(TCNQ) CRYSTAL PREDICTED BY THE SECOND ORDER CALCULATION[a)]
(in kK)

Band	Solution (obs.)	$A_u(\Psi_A)$	$A_u(\Psi_B)$	$B_u(\Psi_A)$	$B_u(\Psi_B)$
R	12.0	14.98	15.59	15.61	15.00
S	23.5	23.88	24.22	24.23	23.87
U	25.4	28.16	29.70	29.70	28.28
S′	35.7	36.01	35.84	35.84	36.04

a) A_u: *b*-axis polarized component.
B_u: *a*-axis polarized component.

A considerable discrepancy is found between prediction and observation in the case of the R-band. In the *b*-axis spectrum, we find peaks at 15.0 and 17.3 kK, which should correspond to the $A_u(A)$ and $B_u(B)$ components of the R-band predicted respectively at 15.0 and 15.6 kK. The 17.3 kK peak can be found also in the *a*-axis spectrum, but a peak does not appear at 15.0 kK. Instead, it is found at 12.5 kK. The wave number difference between this peak and the 17.3 kK one is very much larger than the predicted splitting between the $B_u(B)$ and $B_u(A)$ components of the R-band, the latter value being only 0.6 kK. However, it is difficult to find the origin of this peak other than the $B_u(B)$ component of the R-band. We can not attribute it to the second CT band, because the energy difference between the half-filled molecular orbital and the next filled orbital exceeds 2 eV, so that the second CT band is expected to appear at about 24 kK. Therefore, we will tentatively assign the 12.5 kK band to the $B_u(B)$ component of R-band. This discrepancy between prediction and observation could be associated with the interaction between the CT and LE exciton states.

(b) $Cs_2(TCNQ)_3$: As already mentioned, the unit cell contains four sites of $TCNQ^-$ ion and two sites of TCNQ° molecule. We will label the former sites 1, 1′, 2, and 2′, and the latter 3 and 4, so that the ions at sites 1 and 1′ are mutually transferable by inversion with respect to site 3. The zero-th order wave functions of the optically allowed states are then described as follows. For the exciton states associated with $TCNQ^-$ ion, we have

$$\Phi_{\mathrm{I}}^{\pm} = \frac{1}{\sqrt{4N}} \sum_{m=1}^{N} \{(\psi_{m1} - \psi_{m1'}) \pm (\psi_{m2} - \psi_{m2'})\} \qquad (15)$$

and, for those associated with TCNQ° molecule,

$$\Phi_{\mathrm{II}}^{\pm} = \frac{1}{\sqrt{2N}} \sum_{m=1}^{N} (\psi_{m3} \pm \psi_{m4}) \qquad (16)$$

We carried out the first-order and second-order calculations taking into account the lower four transitions of $TCNQ^-$ ion, *i. e.* R, S, U, and S′ transitions, and the lowest transition of TCNQ° molecule. We will denote the last one as the *N* transition. The results of the calculations are illustrated in Fig. 8, where the absorption bands predicted for the *a*-axis and *b*-axis spectra are shown as vertical lines with a length proportional to the predicted oscillator strength.

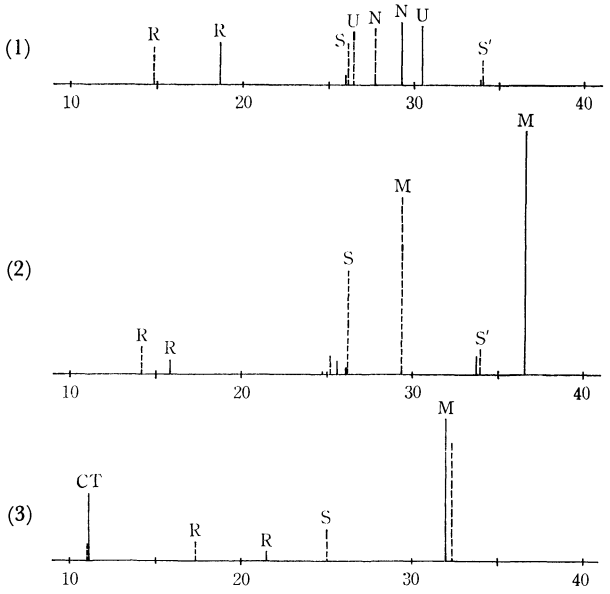

Fig. 8. Results of calculation on the first order and second order effects on the LE bands in $Cs_2(TCNQ)_3$ crystal. (1) Results of the first order calculation, (2) Results of the calculation including the second order effect, (3) Observed spectra. (energy unit in kK)

As shown in Fig. 8, the A_u and B_u components of each intramolecular transition are split appreciably by the first-order effect. The predicted spectra significantly change when the second-order effect is taken into account. Namely, the U- and N-transitions are mixed to give new absorption bands, which are denoted M and M′ in Fig. 8, and the oscillator strength of the R-band is markedly reduced. In Table 4, the oscillator strength of the absorption bands predicted by the second-order calculation are compared with the oriented-gas values. It can be seen that the oscillator strength of the M-band is larger than the sum of the oriented-gas values of the U- and N-bands, the former being about 1.3 times the latter in the *a*-axis spectrum and almost twice in the *b*-axis spectrum. This is mainly caused by the intensity stealing from the R-band.

The observed *a*-axis spectrum seems to be well explained by the present calculation. We will assign the absorption maxima found at 17.3, 25.0, and 32.3 kK to B_u components of R-, S-, and M-bands, respectively. According to the present calculation, the *b*-axis spectrum should exhibit one strong absorption band at 36.5 kK. This is not the case in the observed spectrum. Instead, we find a strong band at 31.9 kK. Within the approximation made in the present study, it seems difficult to find any good explanation for this discrepancy. We observed a very weak shoulder at about 20 kK, which can be assigned to the B_u component of the R-band.

TABLE 4. RESULTS OF CALCULATION ON THE ABSORPTION BANDS OF $Cs_2(TCNQ)_3$ CRYSTAL

Band	Solution spectrum		Crystal spectra								
			Oriented gas value			Calculation (including second order effect)					
	ΔE (kK)	$f^{a)}$	f_a	f_b	f_a/f_b	Band	ΔE_a (kK)	ΔE_b (kK)	f_a	f_b	f_a/f_b
R	12.0	0.63	0.243	0.253	0.96	R	14.23	15.91	0.162	0.076	2.13
S	23.5	0.10	0.250	0.049	5.17	S	26.22	25.65	0.621	0.083	7.48
U	25.4	0.88	0.389	0.354	0.96	M[b)]	25.22	26.26	0.110	0.032	3.44
N	25.4	0.94	0.317	0.368	0.86	M'[b)]	29.32	36.54	0.944	1.441	0.66
S'	35.7	0.06	0.150	0.029	5.17	S'	33.90	33.74	0.146	0.119	1.23

a) Oscillator strengths for $Cs_2(TCNQ)_3$, namely, the value of a band associated with $TCNQ^-$ is taken as twice of the corresponding value of $TCNQ^-$.
b) See text.

Summary and Conclusion

In the present study, we have observed the polarized absorption spectra of single crystals of K(TCNQ) and $Cs_2(TCNQ)_3$, and have shown that the 7.8 kK band of K(TCNQ) and the 11 kK band of $Cs_2(TCNQ)_3$ are the CT bands associated with the transfer of an electron from a $TCNQ^-$ ion to the neighboring $TCNQ^-$ ion. It is also shown that the LE bands observed in the crystal spectra are appreciably shifted from the locations of the corresponding absorption bands in the solution spectra. We have theoretically estimated the first-order and second-order effects on the LE bands of these crystals. In this calculation, we have adopted the method given for the ordinary molecular crystal, composed of neutral molecules, but have taken into account a few aspects associated with the ionic character of these crystals. Although discrepancies between prediction and observation are found in several respects, the general feature of the observed spectra seems to be explainable by the present calculation. From the various conclusions obtained by this study, we wish to point out, first, that the long-range interactions of Coulombic nature provide a large contribution to the crystal shift, and, second, that there is a marked mixing between the transitions of $TCNQ^-$ ion and those of $TCNQ^\circ$ molecule in the case of $Cs_2(TCNQ)_3$. These aspects should always be taken into account when we consider the interpretation of the crystal spectra of TCNQ salts. We have omitted exchange interaction between molecules, mixing between the CT and LE exciton states. This mixing could have a significant effect on the crystal spectra of TCNQ salts. A more sophisticated calculation might be needed to establish a quantitative interpretation of the crystal spectra of TCNQ salts.

Sound Velocity in Aqueous Solutions of Lead Nitrate and Ammonium Iodide

Otohiko NOMOTO*,** and Harumi ENDO*

* *Department of Applied Physics, Defence Academy, Yokosuka*

** *Kobayashi Institute of Physical Research, Kokubunji, Tokyo*

(Received June 3, 1970)

The sound velocity in aqueous solutions of NH_4I and $Pb(NO_3)_2$ is investigated in relation to the temperature and the concentration. In both solutions the $V(T)$ curves show maxima V_p at the peak temperature T_p, the T_p shifting to a lower temperature with an increase in the concentration. While the shift of T_p is sensibly linear with the concentration for $Pb(NO_3)_2$, the curve for NH_4I is almost constant up to 25 wt%, though it decreases linearly above this concentration. This corresponds to the rather abrupt change in the degree of dissociation obtained from the conductivity data. The constancy of T_p below 25 wt% is tentatively explained on the basis of Danford and Levy's X-ray diffraction study which concluded that NH_3 is included in cavities of the water framework and that the framework molecules are partially replaced by NH_3.

Generally speaking, the sound velocity (V) in a solution is dependent on both the temperature (T) and the concentration (C); *i. e.*, $V=V(T,C)$. No systematic study of the sound velocity in aqueous electrolyte solutions has, however, been made over a wide range of concentration and temperature, except for the studies of Tamm *et al.*[1] and Marks.[2,3] They found that the $V(T)$-curve at a constant concentration in electrolyte solutions exhibits its peak velocity (V_p) at a definite temperature — the peak temperature (T_p) — for each concentration, such as in the $V(T)$ curve of pure water. The $V(T)$ curve shifts upwards with an increase in the concentration, while there is a shift of T_p towards a lower temperature at the same time. This shift of T_p is linearly dependent on the concentration (molarity).

Reviews[4-7] of the water structure have appeared elsewhere. A water model closely related to a slightly-expanded ice-I lattice is proposed by Samoilov[8,9] and supported by Danford and Levy[10] on the basis of their X-ray diffraction studies. In this structure, each network molecule is tetrahedrally surrounded by an average of *ca.* 4.4 first neighbors.[11] The structure of this network is very bulky, with space within the framework of molecules in the tetrahedral coordination sufficiently large to accommodate additional water-molecules, and while these spaces—cavities— are not occupied in solid ice-I, about half the cavities in water are occupied by interstitial molecules which interact with the network by less directional, but by no means negligible, forces (Danford and Levy[10]).

As Debye[12] pointed out, the electrostatic field of the ions exerts an electrostrictive effect on the surrounding water molecules; this electrostatic pressure has the same effect as the application of an external pressure and diminishes the volume as well as the compressibility of water molecules. In general, the addition of an electrolyte to water results in a lowering of the peak temperature because of the destruction of the cluster by the solvation of the ions. In many electrolytes, the sound velocity increases as compared with that of pure water. However, there are electrolytes which exhibit a decrease in the sound velocity with an increase in the concentration, such as LiI, NaI, KI, NH_4I, $AgNO_3$[13]; CsCl, CsBr[14]; $Pb(NO_3)_2$[15]; $ZnBr_2$, ZnI_2[16]; UO_2Cl_2, $UO_2(NO_3)_2$, SnI_2, $(CH_3COO)_2Pb$[17]; $CdBr_2$[18]; CdI_2[19]; $TlNO_3$[20]; and RbBr, RbI.[21]

The purpose of the present study is to clarify the molecular mechanism of sound propagation in aqueous electrolyte solutions in connection with the accepted molecular structure of water and aqueous solutions, and to clarify the dissolved state and the properties of ions in aqueous solutions. We studied ammonium iodide and lead nitrate solutions, both electrolytes showing a decrease in the sound velocity with an increase in the concentration.

Experimental

Apparatus. The sound velocity is measured with a crystal-controlled ultrasonic interferometer equipped with a 5 MHz X-cut quartz transducer. The accuracy of this method depends on the number of standing waves counted. We counted one hundred standing waves. The interferometer cell is immersed in an oil bath controlled within ± 0.1°C at moderate temperatures and within ± 0.4°C at higher tem-

1) K. Tamm and H. G. Haddenhorst, *Acustica*, **4**, 653 (1954).
2) G. W. Marks, *J. Acoust. Soc. Amer.*, **31**, 936 (1959).
3) G. W. Marks, *ibid.*, **32**, 327 (1960).
4) L. Hall, *Phys. Rev.*, **73**, 775 (1948).
5) A. Eucken, *Angew. Physik. Chem.*, **53**, 102 (1949).
6) L. Pauling, "Nature of Chemical Bond," Cornell University Press, Ithaca, N. Y. (1960), p. 464.
7) G. Nemethy and H. A. Scheraga, *J. Chem. Phys.*, **36**, 3382, 3401 (1962).
8) O. Samoilov, *Zh. Fiz. Khim.*, **20**, 1411 (1946).
9) O. Samoilov, "Ion no Suiwa," (Translation from Russian by W. Uehira) Chigin Shokan, Tokyo, (1967), p. 21, 125.
10) M. D. Danford and H. A. Levy, *J. Amer. Chem. Soc.*, **84**, 3965 (1962).
11) J. Morgan and B. E. Warren, *J. Chem. Phys.*, **6**, 666 (1938).
12) P. Debye, Festschrift H. Zangger; II. Teil Verlag Rasher & Co., Zürich, (1935), p. 877.
13) D. S. Allam and W. H. Lee, *J. Chem. Soc., Suppl.*, 6049 (1964).
14) P. F. Cholpan, *Soviet Physics-Acoustics*, **12**, 72 (1966).
15) R. Barthel, *J. Acoust. Soc. Amer.*, **26**, 227 (1953).
16) S. V. Subrahmanyam, *Z. Phys. Chem.*, **219**, 5 (1962).
17) W. P. Mason, "Physical Acoustics" Part II-A, Academic Press, New York, London (1965), p. 355.
18) S. V. Subrahmanyam, *Trans. Faraday Soc.*, **56**, 971 (1960).
19) S. V. Subrahmanyam, *Nature*, **185**, 371 (1960).
20) B. Lunden, *Z. Physik. Chem.*, **192**, 345 (1943).
21) S. V. Subrahmanyam, *Z. Angew. Physik*, **15**, 352 (1963).

peratures. The dominant cause of error in sound velocity measurement is temperature fluctuations. The temperature coefficient of the sound velocity in usual aqueous solutions being *ca.* −2——3 m/sec/deg at room temperature, the estimated overall error in this study amounts to ±0.2 m/sec at moderate temperatures and ±1.5 m/sec at higher temperatures. Temperature measurement is made with a thermistor. The sound velocity is measured in terms of its dependence on the temperature for various electrolyte concentrations.

Materials. Lead nitrate and ammonium iodide, special reagent grade, are both recrystallized from water. Salts are prepared by maintaining the crystals at 95°C for two weeks under a reduced pressure of *ca.* 1 mmHg. After purification, ammonium iodide completely turned into colorless salt.

Results and Discussions

The $V(T)$-curves at various concentrations for lead nitrate and ammonium iodide aqueous solutions over the temperature range of 20—100°C are shown in Figs. 1 and 2 respectively. Measurements of the concentration dependence of the sound velocity $V(C)$ under a constant temperature in $Pb(NO_3)_2$ and NH_4I aqueous solutions has been reported, but there have, to our knowledge, been no measurements of the temperature dependence of the sound velocity. It is observed that the height of $V(T)$-curves of an aqueous solution of $Pb(NO_3)_2$ or NH_4I is lower than that of water and that the curves are displaced towards a lower temperature with an increase in the concentration in such a way as to maintain the parabolic shape of the $V(T)$-curve of water.

All kinds of somewhat dilute aqueous solutions,

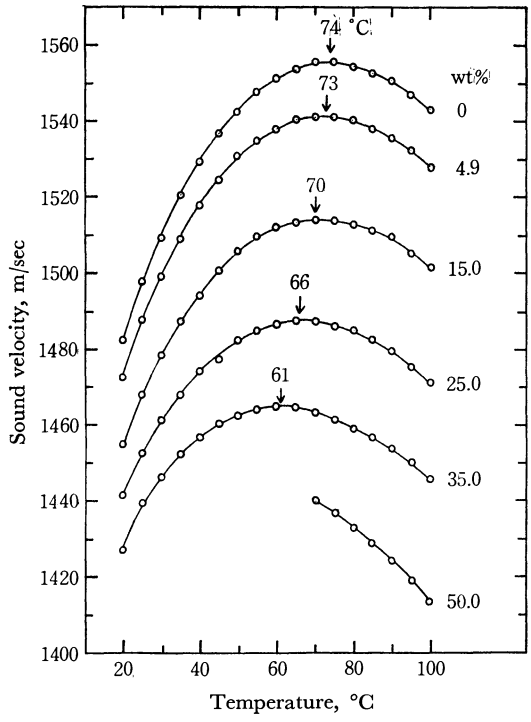

Fig. 1. Sound velocity of lead nitrate aqueous solutions. Arrows show the peak temperature.

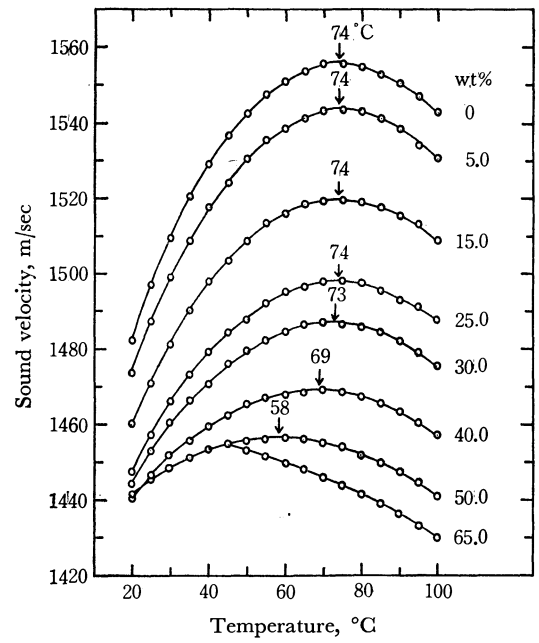

Fig. 2. Sound velocity of ammonium iodide aqueous solutions. Arrows show the peak temperature.

regardless of whether they are ionic[22,23] or non-ionic[24,25] substances, have parabolic curves like that of water. When a solute is added to water, the statistical equilibrium among different species is displaced and there is a partial destruction of the clusters; the decrease in the cluster by the solutes causes the peak temperature to become lower as compared with that of pure water.

The origin of an anomalous temperature dependence of the sound velocity in water and aqueous solutions can be sought in the structure of water. The cluster-part of water decreases with an increase in the temperature, resulting in a decrease in the structural compressibility. The increase in the molecular distance with the temperature-rise is accompanied by an increase in the ordinary compressibility due to the compression of the free space between non-associated water molecules. These opposite effects lead to a minimum of the compressibility at an intermediate temperature, or to the maximum of the sound velocity at a slightly different temperature.

The plot of the peak temperature against the concentration—$T_p(C)$—gives information on the water structure and the dissolved state, and also on the properties of ions in aqueous solutions. The relation between the peak temperature and the concentration has been extensively studied for various sulfates and hydroxides (*cf.* Marks[2,3]). In these solutions, the sound velocity rises with an increase in the concentration. On the other hand, the peak temperature (T_p) decreases with

22) W. Schaaffs, Landolt-Börnstein, Zahlenwerte und Funktionen aus Naturwissenshaften und Technik Gruppe II, Band 5, "Molekularakustik," Springer-Verlag, Berlin, Heidelberg, New York (1967), pp. 109—126.

23) J. Saneyoshi, K. Kikuchi, and O. Nomoto, "Tyoonpa Gizitu Binran," Nikkan Kogyo Sinbunsya, Tokyo (1966), pp. 1253—1258.

24) O. Nomoto and H. Endo, This Bulletin, **43**, 2718 (1970).

25) Nippon Kagaku Kai, "Jituken Kagaku Kouza," 5, Maruzen, Tokyo (1958), pp. 433—448.

an increase in molarity (m) along a straight line:

$$T_p = (T_p)_0 - km, \quad \text{where } (T_p)_0 = 74°C$$

with a common negative slope (k) for Li_2SO_4, Na_2SO_4, and K_2SO_4. Here $(T_p)_0$ is the peak temperature for water. Also, the $V(T)$-curves are nearly common for these three salts. The $T_p(m)$-curves for the other salts are straight lines, with a different slope for each salt. Marks concluded that the above-mentioned three salts affect the compressibility and the density of water in such a way that the maximum sound-velocity-changes (ΔV_p) with the concentration become nearly the same. This is evidence that the ionic charge is the determining property rather than the ionic size in electrolyte solutions. We have studied the shift of T_p with the concentration in organic aqueous solutions, and, by ascribing the T_p to the destruction of the water structure, we have found that, regardless of the kind of organic substance, there exists a simple linear relation between T_p and the geometical surface area of the solute.[24]

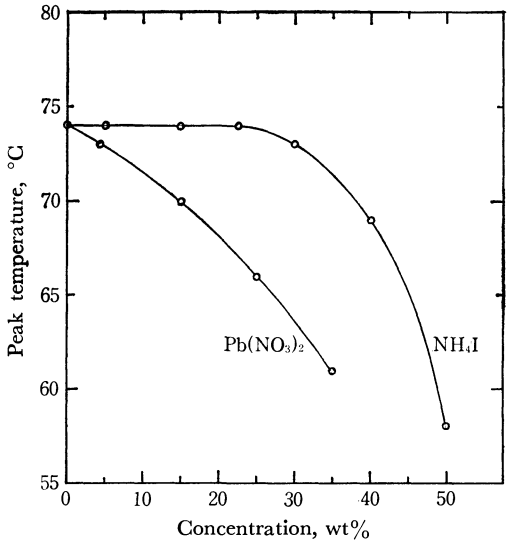

Fig. 3. Peak temperature in dependence of concentrations for lead nitrate and ammonium iodide aqueous solutions.

Figure 3 shows the $T_p(C)$-curves, with the weight-% as the abscissa. As may be seen, the peak temperature of the $Pb(NO_3)_2$ solution decreases linearly with the concentration. On the other hand, the behavior in the NH_4I-solution is very different from that in solutions of the other salts, such as sulfates, hydroxides, and $Pb(NO_3)_2$. The peak temperature in the NH_4I-solution does not change with the concentration up to *ca.* 25 wt%, with the T_p-value of water maintained at 74°C. Above this concentration, the T_p decreases as in other electrolyte-solutions.

The origin of the anomalous concentration dependence of the peak temperature in an NH_4I aqueous solution is to be explained on the basis of a slightly-expanded ice-1-model[8] of the water structure and the peculiarity of the dissolved state of NH_4^+ and I^- ions in an aqueous solution.

There are a number of parameters pertaining to the properties and dissolved state of ions in aqueous solutions, the hydration number being one such parameter. We have many experimental methods[25] for determining the hydration number of ions in aqueous solutions, such as mobility, entropy of mixing, and diffusion. Also, the hydration number has been acoustically determined from the sound velocity by many authors. It must be particularly emphasized, as regards the acoustically-determined hydration number, that the observed quantity is the overall bulk compression of the solution, and that no distinction between the effects to be ascribed to the nearest neighbors of the ions and the far distant molecular species as clusters of water, *etc.*, can be made. The so-called "hydration number," as determined by the acoustical method, is based on a model assuming incompressible hydrated water molecules and non-affected surrounding water. The physical interpretation of the acoustic hydration number is, however, rather the net destruction of the water structure. The hydration numbers for the ions, as obtained by various experimental methods, are remarkably different[26,27] from one another. The values obtained from the sound-velocity data are usually higher than those obtained by the other methods. Nevertheless, the acoustically-determined hydration number is a significant parameter for the study of the properties and the dissolved state of ions in aqueous solutions. Table 1

Tabel 1. The hydration number for various ions

Ion	Author	The other
NH_4^+	NH_4I 3.0	2.0[13]
I^-		0.2,[13] 0.1[27]
Pb^{2+}	$Pb(NO_3)_2$, 10.8	
NO_3^-		2.0,[13] 1.1[27]

shows the hydration numbers for $(NH_4^+ + I^-)$ and $(Pb^{2+} + 2NO_3^-)$ as obtained by acoustical means. Usual ions have acoustical hydration numbers between 5—16.[26] As may be seen in Table 1, NH_4I (NH_4^+ plus I^-) has exceptionally small hydration numbers. Therefore, it may be concluded that NH_4^+ and I^- ions do not destroy the water structure so much. Now we see from Fig. 3 that the peak temperature is not shifted, and that the water structure in the NH_4I-solution is not destroyed, for concentrations up to *ca.* 25 wt%. We reached the conclusion that the NH_4^+ and I^- ions can fill in the cavity positions in an expanded ice-1 structure of water without any serious destruction of the molecular arrangements. The NH_4^+ ion can replace the network-point of water molecules, too. Since the ions packed in the cavities serve only to expand the lattice, without destroying the water structure, the shift of T_p is expected to be small.

We have reported that, in the case of aqueous organic solutions, the shift of T_p is nearly proportional to the total surface area of the solutes. The shift of T_p is discernible for NH_4I solutions in the concentration range higher than *ca.* 30 wt%. This is presumably to be ascribed to the increase in neutral NH_4I molecules in this concentration range, as is also evidenced by

26) R. Robinson and R. Stokes, "Electrolyte Solutions," Butterworths, London (1959) p. 62.
27) 15th-Tyoonpa Kenkyukai Siryo, T. Yasunaga, Denki Tusin Gatukai (1964).

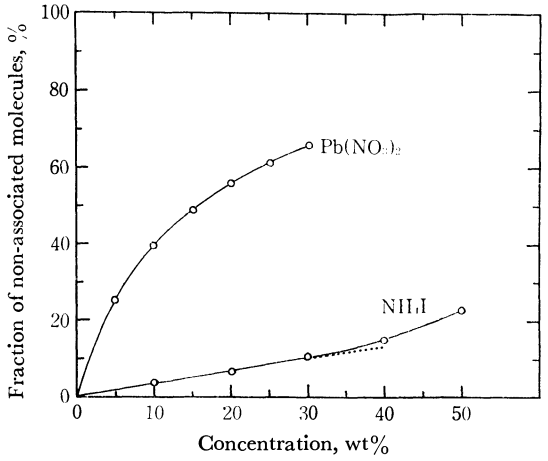

Fig. 4. Fraction of non-associated molecules in dependence of concentrations for lead nitrate and ammonium iodide aqueous solutions.

the change in the conductivity.[28] The fraction of non-dissociated solutes, as obtained from the conductivity data, is also indicated in Fig. 4. The curve shows a rather abrupt turn at 30 wt%. Both the turn of the T_p-curve and that of the degree of dissociation in the NH_4I aqueous solution at nearly the same concentration may correspond to the transformation of the properties and the dissolved state of ions in aqueous solutions.

The model used here is strongly supported by the results of investigations of water,[10,29] an aqueous ammonia[30] solution, and aqueous ammonium halide[31] solutions by the X-ray diffraction method (*cf.* also aqueous tetra-*n*-butylammonium fluoride[32]). That is, it is concluded by the X-ray method that the ammonia and ammonium ions can replace the water molecule in the network of the expanded ice-I structure and also fill up the cavities in this bulky structure. It has been stated that, in pure water,[10] the ratio of the framework to the free water molecules is 4 : 1, and that half the cavities in framework are filled by free water molecules. In the case of the water-ammonia[29] system of 28 mol%, it has been stated that 76% of the available cavities are occupied by ammonia molecules. Although the X-ray analysis may not be able to distinguish between the free single-water molecules and the single-water molecules filling in the cavities of the frameworks of the clusters, the X-ray results[30] do not contradict the present result.

We can see from Fig. 3 that T_p decreases in a $Pb(NO_3)_2$-solution sensibly and linearly with an increase in the concentration. Also, the non-dissociated fraction of $Pb(NO_3)_2$ molecules, as obtained from the conductivity[33] data, increases more rapidly than NH_4I with the concentration (*cf.* Fig. 4). The large hydration number of $Pb(NO_3)_2$ may be the reason why the ions do not fill in the cavities in water frameworks, but destroy the framework from the beginning.

28) J. Bartels *et al.*, Landolt-Börnstein, Zahlenwerte und Funktionen aus Physik. Chemie. Astronomie. Geophysik und Technik. II Band, 7 Teil "Electrische Eigenschaften" Springer-Verlag, Berlin, Göttingen, Heidelberg, (1960), p. 39.

29) A. Narten, M. Danford, and H. Levy, *Discuss. Faraday Soc.*, **43**, 97 (1967).

30) A. Narten and S. Lindenbaum, *J. Chem. Phys.*, **51**, 1108 (1969).

31) A. Narten, *J. Amer. Chem. Soc.*, **74**, 765 (1970).

32) A. Narten, *J. Chem. Phys.*, **49**, 1692 (1968).

33) Landolt-Börnstein II Band, 7 Teil "Elektrische Eigenschaften," Springer-Verlag, Berlin, Göttingen, Heidelberg (1960), p. 119.

Structure of Polynucleotide Complex with Non-Complementary Nucleosides.[1] II. Poly I, U + Poly C

Hideo AKUTSU and Masamichi TSUBOI

Faculty of Pharmaceutical Sciences, The University of Tokyo, Hongo, Bunkyo-ku, Tokyo

(Received July 18, 1970)

Three copolymers of riboinosinic acid and ribouridylic acid (poly I,U) with uridylic acid contents, 20, 32, and 44% were prepared. The ultraviolet absorption measurements were carried out with aqueous solutions of mixtures of poly I,U and polytribocytidylic acid (poly C) of various mole ratios. It has been shown that a double-helical structure is formed with an I···C type inter-base binding and with the U residue looping out of the helix. The structure was found to break on heating the solution. The process of break down was followed by means of ultraviolet absorption measurements.

Polyriboinosinic acid (poly I) and polyribocytidylic acid (poly C) are known to form a double-helical complex poly I·poly C in aqueous solution.[2,3] The structure involves specific hydrogen bonds (I···C) between inosine and cytidine residues. It can be schematically expressed as in Fig. 1(a). Here, inosine (I) and cytidine (C) are complementary nucleosides. The question now arises: what is the effect of introducting uridine (U) residue (which is complementary to neither I nor C) into this system. In a previous paper[4] we examined the effect of introducing the U residue into the poly C moiety. In this paper we describe the effect of its introduction into the poly I moiety.

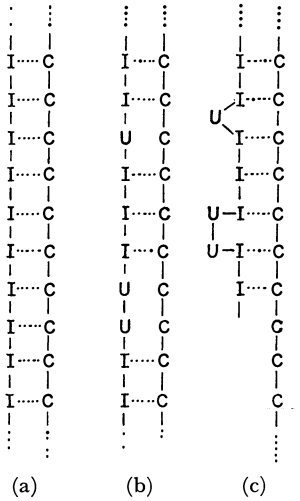

Fig. 1. Schematic drawings of (a) the double-helical structure of poly I·poly C complex, (b) a double-helical structure with the U residues inside, and (c) a double-helical structure with the U residues rotating out.

Preparation of Polynucleotide Samples

The polynucleotide samples were prepared by use of polynucleotide phosphorylase obtained from *Azotobacter vinelandii*. Compositions of the reaction mixtures and incubation times are given in Tables 1 and 2. The incubation temperature was 30°C. After the completion of enzymatic reaction, the product was precipitated with ethanol and then purified by phenol extraction.

Table 1. An example of reaction mixtures in enzymatic preparation of polynucleotides

Inosine-5′-diphosphate	(27 mg/m*l*)	0.8 m*l*
Uridine-5′-diphosphate	(26 mg/m*l*)	0.8
Tris buffer	(0.5M, pH 8.1)	1.5
EDTA[a]	(1 mM in β-mercaptoethanol)	0.05
$MgCl_2$	(50 mM)	0.6
Enzyme		0.7[b]
H_2O		0.55
	Total	5.0

a) Ethylenediamine tetraacetic acid
b) This amount contains 12 units of enzyme. 1 unit=amount of enzyme which can liberate 1μmol of orthophosphate in the enzymatic reaction (15 min)

Table 2. Enzymatic preparation of homopolymers of cytidylic acid and copolymers of inosinic and uridylic acids

Polymer	Substrate[a]		Amount of enzyme	Incubation time	Product				
					Yield				Sedimentation coeff.
	IDP mg	UDP mg	unit	min	mg	%	I %	U %	S_{20}
Poly I,U (1)	32.4	10.4	12	90	10.6	33	80	20	15.7
Poly I,U (2)	48.6	26.0	24	90	19.5	35	68	32	12.5
Poly I,U (3)	21.6	20.8	12	90	7.2	23	56	44	13.8
Poly C	CDP 40 mg		10	90	12.4	31			8.6

a) IDP: inosine-5′-diphosphate, UDP: uridine-5′-diphosphate, CDP: cytidine-5′-diphosphate

1) Paper I in this series, H. Akutsu and M. Tsuboi, This Bulletin, **43**, 3391 (1970).
2) D. R. Davies and A. Rich, *J. Amer. Chem. Soc.*, **80**, 1003 (1958).
3) D. R. Davies, *Nature*, **186**, 1030 (1960).
4) M. Tsuboi, K. Matsuo, and M. Nakanishi, *Biopolymers*, **6**, 123 (1968).

Base Composition and Degree of Polymerization of the Products

The base composition of each poly I,U sample was determined by its hydrolysis with 1 N HCl, paper chromatographic separation of the resulting hypoxanthine and uridylic acid and ultraviolet absorption measurements. The composition thus determined is given in Table 2.

The degrees of polymerization of the polymers were not determined, but they are considered to be sufficiently high from the sedimentation constants given in the last column of Table 2. The constants were determined in a solvent with 0.1 M NaCl and 0.01 M Na-cacodylate, pH 7.0.

Experimental

Ultraviolet absorption measurements were carried out with an Ito spectrophotometer Model QU-3. The temperature of the samples was controlled as previously descrived.[5] The polynucleotide concentration (in M) was determined by measuring phosphorus content.[6] The moles of polynucleotide means here moles of phosphorus (or the moles of nucleotide residue).

Mixing Curves

Solutions of poly I,U and poly C of various mole ratios were prepared, and their ultraviolet absorbances at a few points in the 240—250 mμ region were recorded. The results are shown in Fig. 2. From the absorbance *versus* mole-ratio profile, we can judge whether the two polymers in question form a complex or have no interaction. When a complex is formed, its stoichiometric ratio is determined from the observed profile of the mixing curve.

As may be seen in Fig. 2, each poly I,U, shows evidence of interaction with poly C. At room temperature, each of the mixing curves consists of two straight lines which intersect at a proper mole ratio. This should correspond to the stoichiometric mole ratio in which the two polynucleotides form a complex. The stoichiometric mole ratio, poly I,U/poly C, should be 50/50, if the complex has a structure, in which the non-complementary U residues are incorporated in the double-helix as shown schematically in Fig. 1(b). On the other hand, if the U residues rotate out of the helix and thus no C residue fails to form an I···C base-pair (see Fig. 1(c)), then the intersect (or the maximum hypochromicity) should take place at poly I,U/poly C=100/x. Here, x=mol% of I in the copolymer of I and U. The stoichiometric mole ratios expected for structures (b) and (c) in Fig. 1 are indicated by arrows in Fig. 2.

We see that each mixing curve shows its minimum at the mole ratio expected for structure (c) but not for structure (b) in Fig. 1.

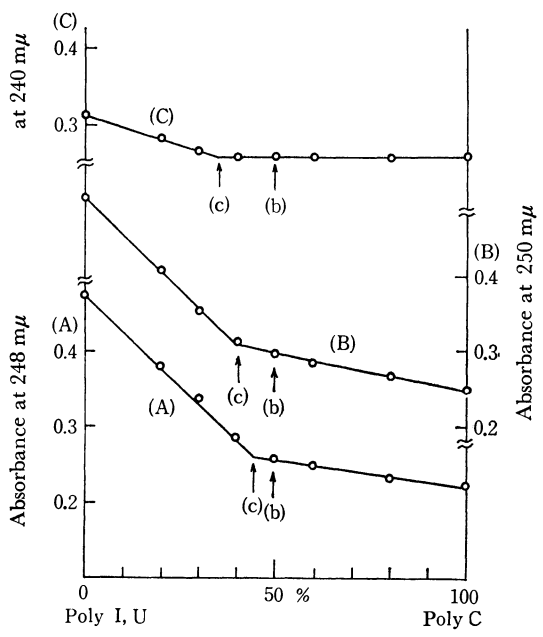

Fig. 2. Mixing curves of poly I,U and poly C.
Abscissa: mol% of poly C (determined by measuring phosphorus contents), ordinate: absorbance at 248, 250, or 240 mμ. Total nucleotide concentration in the solution was kept at 4.8×10^{-5} M. Solvent: 0.1 M NaCl+0.001 M $MgCl_2$+0.01 M Na-cacodylate buffer, pH 7.0. Temperature: 25°C.
(A) Poly I,U(1) and poly C, (B) poly I,U(2) and poly C, (C) poly I,U(3) and poly C.

Heating Curves

Absorbance-temperature profile of each of the poly

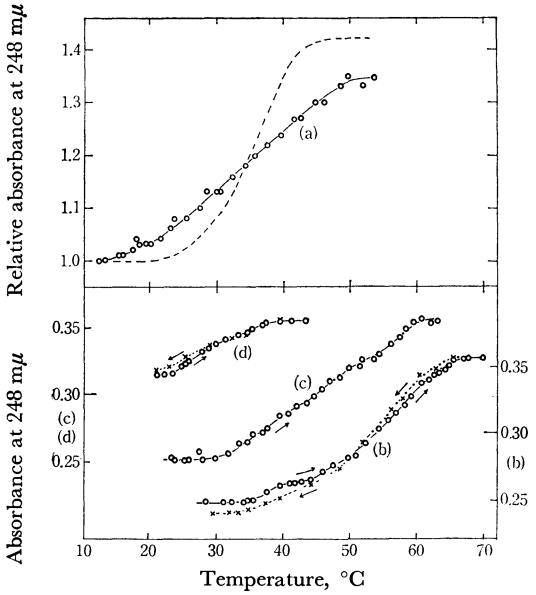

Fig. 3. Variation of the absorbance at 248 mμ with temperature of mixture solutions of poly I,U and poly C.
The mole ratio in each mixture solutions was that for the maximum hypochromicity (see Fig. 2). (a) Poly I,U(2) 2.9×10^{-5} M and poly C 1.9×10^{-5} M. Solvent: 0.1 M NaCl+0.01 M Na-cacodylate buffer, pH 7.0. (b) Poly I,U(1) 2.6×10^{-5} M and poly C 2.1×10^{-5} M. Solvent: 0.1 M NaCl+0.001 M $MgCl_2$ +0.01 M Na-cacodylate buffer, pH 7.0. (c) Poly I,U(2) 2.9×10^{-5} M and poly C 1.9×10^{-5} M. Solvent: the same as that for (b). (d) Poly I,U(3) 3.1×10^{-5} M and Poly C 1.7×10^{-5} M. Solvent: the same as that for (b). The dotted curve in the upper portion of this figure is the absorbance (at 248 mμ)-temperature profile of poly C,U (with 33% U) and poly I observed in the same solvent as that for (a).

5) K. Matsuo and M. Tsuboi, This Bulletin, **39**, 347 (1966).
6) B. N. Ames and D. T. Dubin, *J. Biol. Chem.*, **235**, 769 (1960).

I,U-poly C mixtures at the mole ratio with maximum hypochromicity are shown in Fig. 3. In general, such observed profiles do not always represent the melting profiles of the secondary structures of the complex molecules. As Fresco and Alberts[7] indicated, the absorbance of not only the complex but also the non-interacted constituent may depend upon the temperature. In the present case, however, the absorbance of poly I,U and of poly C would not depend too much on the temperature. Therefore, the observed profiles given in Fig. 3 would not greatly differ from the "true melting profile" of the complex molecule.

As may be seen in Fig. 3, the increase in absorbance takes place over a wide range of temperature for every complex even in a solvent with Mg^{2+}. This is in contrast with the case of the complex of poly C,U and poly I,[4] where a sharp rise in absorbance takes place. The midpoint (T_m) of the transition, however, is almost the same for poly C,U·poly I complex and poly I,U·poly C complex when the U contents in these two complexes are almost equal (32—33% in each copolymer). The T_m becomes lower as the U content in the copolymer increases. As in the case of the poly C,U·poly I complex, the cooling curve of each of these complexes was found to be almost equal to the heating curve.

We wish to express our thanks to Professor Sanae Mii for kindness in providing the wet cells of *Azotobacter vinelandii* and to Dr. Kimiko Matsuo for her valuable advice. This work was supported by a grant from the Ministry of Education of Japan and a grant from the United States Public Health Service (GM10024-06).

7) J. R. Fresco and B. M. Alberts, *Proc. Nat. Acad. Sci. U. S.*, **46**, 311 (1960).

BULLETIN OF THE CHEMICAL SOCIETY OF JAPAN, VOL. 44, 22—27 (1971)

Electronic Structure of Lone Pairs. III.[1] H_2S_2, H_2O_2, N_2H_4, and Diimides

Hiroko YAMABE, Hiroshi KATO,[2] and Teijiro YONEZAWA

Department of Hydrocarbon Chemistry, Faculty of Engineering, Kyoto University, Sakyo-ku, Kyoto

(Received June 25, 1970)

The electronic structure, the electronic transition, and the interaction of lone pairs of H_2S_2, H_2O_2, and N_2H_4 for several dihedral angles are studied by the semi-empirical ASMO SCF method, and their dependencies on the dihedral angle is discussed. Also, the interaction of the lone pairs of diimides, N_2H_2, N_2F_2, and $(CH_3)_2N_2$, the relative stability of the *cis* forms and of their *trans* form, and the electronic transition energies of these molecules are calculated. The stable forms of N_2H_2 and $(CH_3)_2N_2$ are calculated to be of the *trans* form, but that of N_2H_2 is the *cis* form. An energy component analysis of these compounds has been made. The main factor in the lack of stability of the *cis* form of N_2H_2 is shown to be the core-core repulsion term, V_{nn}. On the other hand, in H_2S_2 and N_2H_4 not only the V_{nn} term but also the electrostatic interaction term, $\sum_{i,j}^{occ}(2J_{ij}-K_{ji})$, contributes to their instability.

In a previous paper,[3] the electronic structure and the interaction of lone pairs of $(CH_3)_2S_2$ and cyclic disulfides were studied theoretically and their dependence on the dihedral angle, ϕ, was discussed.

Hydrogen peroxide, H_2O_2,[4,5] and hydrazine, N_2H_4,[5,6] are known to have dihedral angles of approximately 111° and 90° respectively from the investigation by means of X-ray analysis, by a study of the IR spectra, and so on. Recently, the dihedral angle of H_2S_2 was revealed to be 90°36′ by a microwave study.[7,8] In these molecules, the oxygen and the nitrogen atoms having lone pairs are bonded by a single bond, as in the case of disulfides. The problem of the rotational barriers of these compounds has been studied quantum-mechanically by many authors.[6,8-10] In the present paper, focusing our attention upon the electronic structure of the lone pair, calculations similar to the previous ones for several disulfides[3] are carried out for H_2S_2, H_2O_2, and N_2H_4. The dependence of the total energy and the interaction of the lone pairs on the dihedral angle is discussed, and an energy-component analysis of these molecules is reported.

In this paper we will also discuss the interaction of the lone pair of diimides, RN=NR, in which the nitrogen atoms are bonded by a double bond. The mutual

1) Presented at the Annual Meeting of the Chemical Society of Japan, April, 1968.

2) Present address: Department of General Education, Nagoya University, Chikusa-ku, Nagoya.

3) T. Yonezawa, H. Yamabe, and H. Kato, "Electronic Structure of Lone Pairs. II. Disulfides and Acyl Thiol" (to be published in this Bulletin).

4) L. Pauling, *Proc. Nat. Acad. Sci., U.S.*, **35**, 495 (1949); W. G. Penny, G. B. B. M. Sutherland, *J. Chem. Phys.*, **2**, 492 (1934); E. N. Lassettre and L. B. Dean, Jr., *ibid.*, **17**, 317 (1949).

5) L. Pedersen and K. Morokuma, *ibid.*, **46**, 3941 (1967).

6) A. Yamaguchi, I. Ichishima, T. Shimanouchi, and S. Mizushima, *ibid.*, **31**, 843 (1959).

7) G. Winnewisser, M. Winnewisser, and W. Gordy, *ibid.*, **49**, 3465 (1968).

8) M. S. Schwartz, *ibid.*, **51**, 4182 (1969).

9) W. H. Fink and L. C. Allen, *ibid.*, **46**, 2276 (1967).

10) W. E. Plke and R. M. Pitzer, *ibid.*, **46**, 3948 (1967).

stability of their *cis* and *trans* forms[11] and the electronic transition energy are calculated. Moreover, the substituent effect of an electronegative atom, such as the F atom, or of a CH_3 group to the lone pairs of the sp^2 type of nitrogen atom is investigated. As Robin *et al.* pointed out in their paper, a few works[12-14] on the electronic states of azoalkanes have been performed. They studied the electronic structure by a non-empirical SCF CI method, using Gaussian-type orbital basis functions. Here, the electronic states of *cis* and *trans* diimides, N_2H_2, $(CH_3)_2N_2$, and N_2F_2 are calculated by the semi-empirical ASMO SCF method.[15]

Calculations

In the calculation by the semi-empirical ASMO SCF method,[15] the approximation and parameters used in the case of the disulfides are adopted. The coordinate axes, bond lengths, and bond angles of H_2S_2, H_2O_2, and N_2H_4 are given in Fig. 1, together with their dihedral angles, ϕ's, while those of the diimides are given in Fig. 2. The conformation of N_2H_4 in the dihedral angle, $\phi=0°$, is assumed to be as follows: The atoms, H_4 and H_6, are placed downward to the x-y plane, as in Fig. 1. The $\angle$NNH angle is put as 112°. In the conformation of the 90° dihedral angle, the group containing the N_2 atom is rotated by 90° around the N–N bond.

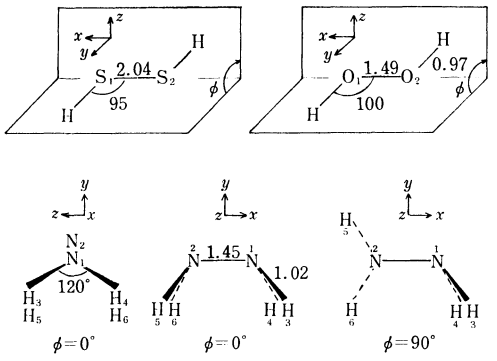

Fig. 1. Bond lengths (in Å) and bond angles (in degree), the dihedral angle ϕ of H_2S_2 and H_2O_2, the employed conformations of N_2H_4 for $\phi=0°$ and $\phi=90°$, and the coordinate axes are shown.

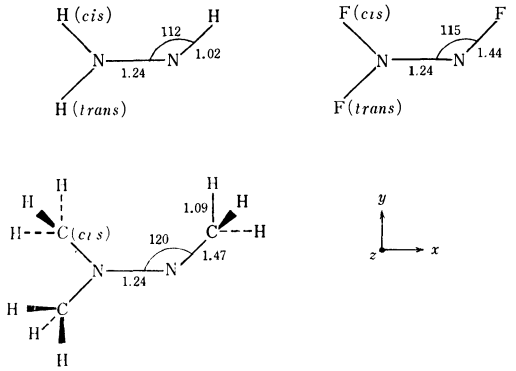

Fig. 2. Bond lengths (in Å), bond angles (in degree), and coordinate axes.

Results and Discussion

The angular dependencies of the atomic density and the atomic orbital (AO) densities of H_2S_2, H_2O_2, and N_2H_4 are given in Tables 1—3. The lone-pair levels and the lowest vacant level (LV) of H_2S_2 and H_2O_2 of various dihedral angles are given in Figs. 3 and 4 respectively.

Table 1. Electron densities of H_2S_2 and atomic bond order P_{s,p_i} of the sulfur for various configurations

	$\phi°$	0	45	90	180
Atomic density	S_1	6.171	6.172	6.177	6.184
	H_3	0.829	0.829	0.823	0.816
Atomic orbital density	S_1 s	1.623	1.625	1.627	1.630
	x	1.142	1.142	1.140	1.136
	y	1.406	1.406	1.411	1.417
	z	2.000	2.000	1.999	2.000
	S_2 s	1.623	1.625	1.627	1.630
	x	1.142	1.139	1.140	1.136
	y	1.406	1.710	1.999	1.417
	z	2.000	1.709	1.411	2.000
P_{s,p_i}	S_1 s-x	0.300	0.300	0.300	0.298
	s-y	−0.337	−0.338	−0.338	−0.339
	s-z	0.000	0.005	0.005	0.000
	S_2 s-x	−0.300	−0.299	−0.300	−0.298
	s-y	−0.337	−0.235	0.005	0.339
	s-z	0.000	−0.242	−0.338	0.000

Table 2. Electron densities of H_2O_2 and atomic bond order P_{s,p_i} of the oxygen atom for various configulations

	$\phi°$	0	45	90	180
Atomic density	O_1	6.323	6.329	6.337	6.349
	H_3	0.677	0.674	0.663	0.651
Atomic orbital density	O_1 s	1.808	1.807	1.807	1.806
	x	1.008	1.013	1.011	1.012
	y	1.507	1.509	1.519	1.531
	z	2.000	2.000	2.000	2.000
	O_2 s	1.808	1.807	1.807	1.806
	x	1.008	1.005	1.011	1.012
	y	1.507	1.767	2.000	1.531
	z	2.000	1.761	1.519	2.000
P_{s,p_i}	O_1 s-x	0.114	0.114	0.116	0.116
	s-y	−0.285	−0.285	−0.282	−0.278
	s-z	0.000	0.000	0.000	0.000
	O_2 s-x	−0.114	−0.114	−0.116	−0.116
	s-y	−0.285	−0.199	0.000	0.278
	s-z	0.000	−0.200	−0.282	0.000

11) M. R. Robin, R. R. Hart, and N. A. Kuebler, *J. Amer. Chem. Soc.*, **89**, 1564 (1967).
12) J. M. Lehn and B. Munsch, *Theor. Chim. Acta (Berl.)*, **12**, 91 (1968).
13) J. Alster and L. A. Burnelle, *J. Amer. Chem. Soc.*, **89**, 1261 (1967).
14) M. S. Gordon and H. Fischer, *ibid.*, **90**, 2471 (1968).
15) H. Konishi, H. Kato, and T. Yonezawa, Symposium on the electronic structure of molecules, Hokkaido, October, 1967; This Bulletin, **42**, 933 (1969).

TABLE 3. ELECTRON DENSITIES AND ATOMIC BOND ORDER P_{s,p_i} OF THE NITROGEN ATOM OF N_2H_4

$\phi°$		0	90	
Atom		N_1	N_1	N_2
Atomic density		5.509	5.516	5.516
Atomic orbital density	s	1.408	1.408	1.408
	x	0.979	0.983	0.983
	y	1.820	1.822	1.303
	z	1.301	1.303	1.821
P_{s,p_i}	s–x	0.076	0.079	−0.079
	s–y	0.292	0.290	0.004
	s–z	0.000	0.004	0.290

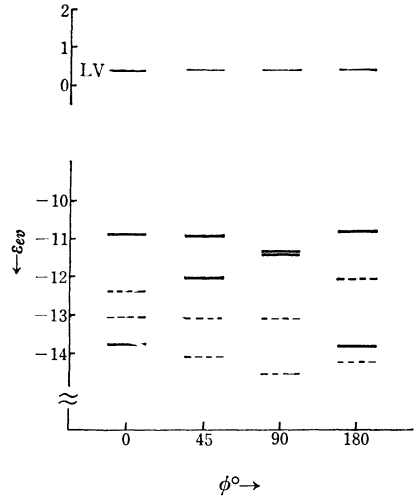

Fig. 3. Lone-pair levels and the lowest vacant level of H_2S_2 *vs.* dihedral angle ϕ. The heavy lines and the dashed lines designate the levels of the p-type lone pair and the sp^2-type lone pair, respectively.

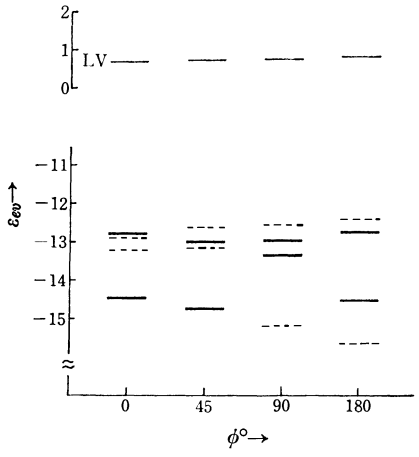

Fig. 4. Lone-pair levels and the lowest vacant level of H_2O_2 *vs.* dihedral angle ϕ. The heavy lines and the dashed lines designate the levels of the p-type lone pair and the sp^2-type lone pair, respectively.

1) H_2S_2: As is shown in Table 1, when the dihedral angle of H_2S_2 is equal to 0°, the p-type lone-pair AO becomes the p_z orbital of the S_1 atom (S_1z). The direction of the lone-pair orbital rotates, keeping its electron density approximately 2.00, following the change in the ϕ angle. When the dihedral angle increases, the atom density of the sulfur atom increases and that of the hydrogen atom decreases. That is, the electron flows from the s orbital of the hydrogen atom to the p_y orbital of the sulfur atom. This tendency has been pointed out for $(CH_3)_2S_2$ by the present authors[3] and for H_2O_2 by Morokuma *et al.* in their ab initio calculation[5] and also by Pitzer *et al.*[10] H_2S_2 also has sp^2-type lone pairs due to the hybridization of $3s$ and $3p$ electrons. These sp^2-type lone pairs rotate according to the change in the dihedral angle, ϕ. That is, the atomic density and the AO density of the sulfur atom of H_2S_2 and their angular dependence resemble those in the case of $(CH_3)_2S_2$. The lowest n–σ^* transition energies are given in Table 4. These

TABLE 4. DIFFERENCE OF TOTAL ENERGIES (eV)[a] AND TRANSITION ENERGIES[b] (eV)

	$\phi°$	0	45	90	180
H_2S_2	Difference of the total energy	0.17	0.14	0.00	−0.04
	Transition energy	4.23	4.30	4.82	4.22
H_2O_2	Difference of the total energy	0.27	0.22	0.00	−0.16
	Transition energy	2.99	4.65	5.73	5.93
N_2H_4	Difference of the total energy	0.16	—	0.00	—
	Transition energy	4.21	—	4.94[c]	—

a) Difference of total energies referred to that in 90°.
b) Lowest $n\rightarrow\sigma^*$ transition.
c) Observed value is about 5.39 eV (S. Imanishi, *Nature*, **127**, 782 (1931)).

transition energies are approximately equal to those of $(CH_3)_2S_2$. Therefore, it is noted that the main factor showing the angular dependency of the atomic density, the AO density, and the transition energy is not a group bonded to a sulfur atom, such as CH_3 and H, but a part of the S–S bond. The total energy decreases monotonically from a maximum at 0° to a minimum at 180°. The experimentally-obtained minimum (about 90.5°) can not be obtained.[16]

2) H_2O_2: The angular dependencies of the atomic density and the AO density of H_2O_2 (Table 2) are analogous to those of H_2S_2 and $(CH_3)_2S_2$.[3] That is the two p-type lone pairs are parallel at 0° and become orthogonal at 90°. The sp^2-type lone pairs are also seen. However, the AO density of the s orbital of the oxygen atom is larger than that of the sulfur atom (Table 2). The order of the lone-pair levels shown in Fig. 4 is different from that in the case of H_2S_2 of Fig. 3. The energy level of the sp^2-type lone pair becomes more unstable than the p type except for $\phi=0°$, which may correspond to the larger s character and the smaller sp^2-type hybridization of the oxygen atom (see Tables 1 and 2). The splitting

16) This may be due to the inappropriate approximation of the calculation for such a small molecule with lone pairs. Recently, by using the basic set of Gaussian orbitals and the ab initio SCF MO method, Schwartz obtained an energy minimum of H_2S_2 for a dihedral angle in the range 90°—100° in fair agreement with the experimental value (about 90.5°) (Ref. 8).

between the p-type lone-pair levels is large when $\phi=0°$ and small when $\phi=90°$. That is, the interaction of the lone pairs aligned parallel is larger than those aligned in a rectangular manner. The total energies referred to that at 90° are shown in Table 4 for the various dihedral angles. The total energy decreases monotonically from a maximum at 0° to a minimum at 180°. The experimentally-obtained minimum (approximately 111°) can not be obtained, such as in the case of H_2S_2.[17] The lowest n–σ^* transition energy in 90° is calculated to be 5.73 eV. Urey *et al.*[18] and Fergusson *et al.*[18] reported that H_2O_2 is decomposed by light in the UV region, thus, the transition energy was not observed experimentally.

3) N_2H_4: The total energy at the dihedral angle of 90° is lower than that at 0°, which is compatible with the observation that the dihedral angle of the stable form is approximately 90°. In Table 3, when $\phi=0°$, the atomic bond order is zero, and it is noted that the lone pair of the nitrogen atom lies on the x–y plane and has a large electron density in the y direction. When $\phi=90°$, the lone pairs of the nitrogen atoms are perpendicular to each other. The splitting between the lone-pair levels at 0° (2.23 eV) is larger than that at 90° (0.22 eV).

Table 5. Some calculated results of N_2H_2

		cis		*trans*	
		N	H	N	H
Atomic density		5.254	0.746	5.277	0.723
Atomic orbital density	s	1.578	0.746	1.583	0.723
	x	1.092	—	1.104	—
	y	1.583	—	1.590	—
	z	1.000	—	1.000	—
Atomic bond order	s–x	0.243	—	0.254	—
	s–y	−0.305	—	−0.304	—
P_{s,p_i}	s–z	0.000	—	0.000	—
Total energy (eV)		−413.02		−413.31	
Δn[a] (eV)		2.33		5.20	

a) Splitting of lone-pair levels.

Table 6. Some calculated results of N_2F_2

		cis		*trans*	
		N	F	N	F
Atomic density		4.865	7.135	4.877	7.123
Atomic orbital density	s	1.775	1.962	1.768	1.962
	x	1.040	1.874	1.122	1.835
	y	1.033	1.315	0.971	1.342
	z	1.017	1.983	1.015	1.985
Atomic bond order	s–x	0.280	—	0.323	—
	s–y	−0.240	—	−0.244	—
P_{s,p_i}	s–z	0.000	—	0.000	—
Total energy (eV)		−1361.46		−1360.64	
Δn[a] (eV)		0.83		3.12	

a) Splitting of lone-pair levels.

Table 7. Some calculated results of $N_2(CH_3)_2$

		cis		*trans*	
		N	C	N	C
Atomic density		5.197	4.066	5.231	4.013
Atomic orbital density	s	1.641	1.005	1.628	0.995
	x	1.044	1.041	1.066	1.032
	y	1.487	0.903	1.515	0.868
	z	1.026	1.116	1.023	1.118
Atomic bond order	s–x	0.225	—	0.239	—
	s–y	−0.308	—	−0.303	—
P_{s,p_i}	s–z	0.000	—	−0.001	—
Total energy (eV)		−740.23		−743.91	
Δn[a] (eV)		1.75		3.25	

a) Splitting of one-pair levels

Diimides. The electron density, the difference in the relative total energy, and the splitting of the lone-pair levels are listed in Tables 5—7 for the various diimides. Herzberg mentioned[19] that N_2H_2 should take a *trans* form in the ground state, and in our approximate calculation the *trans* form is calculated to be more stable.[20] For N_2F_2 and $(CH_3)_2N_2$, the stable forms are calculated to be the *cis* form and the *trans* form respectively. From the one-center bond orders of s–x, s–y, and s–z, the lone-pair orbital of the nitrogen atom may be approximately identified as a sp^2-type hybrid orbital for all the diimides studied here, and the lone pair of the N_1 atom lies on the molecular plane.

The splitting of the lone-pair levels is larger in the *trans* form than in the *cis* form for the three diimides, as is also pointed out by Robin *et al.*[11] This may be due to the fact that the overlap of the lone pairs is larger in the *trans* form than in the *cis* form. This tendency was also true in H_2S_2 and H_2O_2. (See the dotted line in Figs. 3 and 4. $\phi=0°$ and $\phi=180°$ correspond to the *cis* and *trans* forms respectively.) It is noted that, by the substitution of the fluorine atom, the lone-pair electron density of the nitrogen atom (mainly p_y AO) is greatly diminished and the splitting of the lone pair becomes small compared to N_2H_2. The atom density of the nitrogen atom of the *trans* diimide is larger in each case studied than that of the *cis* diimides, while that of the hydrogen atom of *trans* N_2H_2 is smaller than that of the *cis* form. Similar relations are shown for the atom density of the fluorine atom of N_2F_2 and that of the CH_3 group of $(CH_3)_2N_2$, which is the sum of the atom densities of the carbon atom and three hydrogen atoms.[21]

17) Pedersen and Morokuma have reported, in their ab initio calculation of H_2O_2 using a basic set of 26 Gaussian orbitals, that the energy decreases monotonically from a maximum at 0° to a minimum at 180° (Ref. 5).

18) H. C. Urey, L. H. Dawsey, and F. O. Rice, *J. Amer. Chem. Soc.*, **51**, 1371 (1929); W. C. Fergusson, L. Slotin, and D. W. G. Style, *Trans. Faraday Soc.*, **32**, 956 (1936).

19) G. Herzberg, *Kagaku to Kogyo*, **21**, 474 (1968).

20) Lehn *et al.*, by their ab initio SCF LCAO MO calculations, that *trans* N_2H_2 is more stable than *cis* N_2H_2 by 10.5 kcal/mol (Ref. 12). On the other hand, Gordon *et al.*, in their ab initio calculations, fond that *cis* N_2H_2 and *cis* N_2F_2 are more stable than the corresponding *trans* diimides (Ref. 14).

21) The atom densities of the CH_3 group of $(CH_3)_2N_2$ are 6.759 for the *trans* form and 6.803 for the *cis* form.

Some of the obtained transition energies are listed in Table 8, together with the values calculated and observed by Robin *et al.*[11] Among the calculated values of *trans* N_2F_2 and *trans* $(CH_3)_2N_2$, the lowest singlet-singlet transition is n–σ^* (^1B_g), and the next one is n–σ^* (^1B_u). This sequence is the same as that observed, but the values of these transitions are much smaller than the observed energies. Compared to the values calculated by Robin *et al.*,[11] our transition energies are small. The inclusion of the configuration interaction seems to be necessary. According to Herzberg,[19] the ground state of N_2H_2 is the triplet state. Our obtained transition energy of the $^3B_g(n$–$\sigma^*)$ of the *trans* N_2H_2 is remarkably low.

TABLE 8. TRANSITION ENERGIES (ΔE IN eV) AND TRANSITION MOMENTS (Q)

a) N_2H_2

	ΔE calcd	Q calcd	ΔE calcd[9]	Q calcd[9]
cis				
n_1–π^* $^1B_1$	1.52	0.17	3.36	0.20
n_2–π^* $^1A_2$	3.61	0.00	7.41	0.00
n_1–σ^* $^1A_1$	5.46	0.00	8.40,9.94	0.07,0.22
n_1–σ^{**} $^1B_2$	6.21	0.30	6.97,8.90	0.25,0.19
π–π^* $^1B_2$	6.64	0.88	—	—
n_1–π^* $^3B_1$	0.59	0.00	2.07	0.00
n_2–π^* $^3A_2$	2.64	0.00	—	—
n_1–σ^* $^3A_1$	4.46	0.00	—	—
n_1–σ^{**} $^3B_2$	5.65	0.00	—	—
π–π^* $^3B_2$	3.06	0.00	6.45	0.00
trans				
n_1–π^* ^1B_g	0.98	0.00	3.92	0.00
n_1–σ^* ^1B_u	5.02	0.09	7.80,8.53,9.68	0.23,0.19,0.16
n_2–π^* ^1A_u	6.36	0.24	10.94	0.26
n_1–σ^{**} ^1A_g	6.45	0.00	7.12,9.14	0.00,0.00
π–π^* ^1B_u	6.64	0.88	—	—
n_1–π^* ^3B_g	0.01		3.01	0.00
n_1–σ^* ^3B_u	4.01	0.00	—	—
n_2–π^* ^3A_u	5.17	0.00	—	—
n_1–σ^{**} ^3A_g	6.01	0.00	—	—
π–π^* ^3B_u	3.06	0.00	6.53	0.00

b) N_2F_2

	ΔE calcd	Q calcd	ΔE obsd[9]
cis			
n_2–π^* $^1A_2$	3.21	0.00	
n_1–π^* $^1B_1$	3.27	0.16	
n_2–σ^* $^1A_1$	3.79	0.10	
σ–σ^* $^1B_2$	5.24	0.04	
π–π^* $^1B_2$	5.99	0.84	
n_2–π^* $^3A_2$	2.44	0.00	
n_1–π^* $^3B_1$	2.74	0.00	
n_2–σ^* $^3A_1$	3.42	0.00	
σ–σ^* $^3B_2$	4.76	0.00	
π–π^* $^3B_2$	3.31	0.00	
trans			
n_1–π^* ^1B_g	1.99	0.00	>6.19
n_1–σ^* ^1B_u	3.15	0.82	8.06
n_1–σ^{**} ^1A_g	5.12	0.00	
n_2–π^* ^1A_u	5.83	0.13	
n_1–π^* ^3B_g	1.23	0.00	
n_1–π^* ^3B_u	1.31	0.00	
n_1–σ^{**} ^3A_g	3.85	0.00	
n_2–π^* ^3A_u	5.39	0.00	

c) $N_2(CH_3)_2$

	ΔE calcd	Q calcd	ΔE obsd[9]	ε max.[9]
cis				
n_1–π^* $^1B_1$	1.96	0.15		
n_2–π^* $^1A_2$	3.45	0.02		
n_1–σ^* $^1A_1$	5.56	0.29		
π–π^* $^1B_2$	5.82	0.93		
n_1–π^* $^3B_1$	1.15			
n_2–π^* $^3A_2$	2.71			
π–π^* $^3B_2$	3.09			
n_1–σ^* $^3A_1$	4.39			
trans				
n_1–π^* ^1B_g	1.21	0.03	3.65	5
π–π^* ^1B_u	5.73	0.94		
n_1–σ^* ^1B_u	4.52	0.23	6.7	
n_2–π^* ^1A_u	5.61	0.15		
n_1–σ^{**} ^1A_g	5.69	0.01		
n_1–π^* ^3B_g	0.37			
π–π^* ^3B_u	3.09			
n_2–π ^3A_u	4.96			
n_1–σ^{**} ^3A_g	5.03			

Energy Component Analysis. The total energies of $(CH_3)_2S_2$, H_2S_2, N_2H_4, and N_2H_2 have been analyzed to their various contributions; the results are given in Table 9, where W, V_{nn}, and E_e denote the total energy, the core-core repulsion energy, and the total electronic energy respectively. The orbital energy and the core integral of the ith MO are designated by ε_i and H_i. The Coulombic and exchange integrals between the ith and the jth MO's are indicated by J_{ij} and K_{ij} respectively. The W and E_e quantities are written as follows:

$$W = E_e + V_{nn} \tag{1}$$

$$E_e = 2\sum_i^{occ} \varepsilon_i - \sum_{ij}^{occ} (2J_{ij} - K_{ij}) \equiv \varepsilon - G \tag{2}$$

or

$$E_e = 2\sum_i^{occ} H_i^{core} + \sum_{ij}^{occ} (2J_{ij} - K_{ij}) \equiv H + G \tag{3}$$

where ε, H, and G imply $2\sum_i^{occ}\varepsilon_i$, $2\sum_i^{occ}H_i^{core}$, and $\sum_{ij}^{occ}(2J_{ij} - K_{ij})$ respectively. $\Delta H(E-H)$ in Table 9 denotes the electronic energy calculated by the extended Hückel method. We will first discuss the case of H_2S_2. As the dihedral angle, ϕ, decreases from 90° to 0°, the molecule becomes less stable. The unstabilization energy of H_2S_2 is given by the difference in the total energy, ΔW between 0° and 90°; it is 0.17 eV. Note that the difference in the core-core repulsion energy, ΔV_{nn}, is 1.26 eV, while that of the total electronic energy, ΔE_e, is −1.09 eV. Hence, the difference in the electronic interaction energy, ΔG, is 0.66 eV, which corresponds the fact that the two lone pairs become parallel at 0°. That is, the ΔW of H_2S_2 being decomposed to ΔV_{nn}, ΔH, and ΔG according to Eqs. (1) and (2), the tendencies of ΔV_{nn} and ΔG are parallel with that of ΔW.

Table 9. Energy component analysis (in eV)

	$(CH_3)_2S_2$			H_2S_2			N_2H_4		N_2H_2	
$\phi°$	0	45	90	0	45	90	0	90	0	180
ΔW	+ 1.98	+ 0.64	0	+0.17	+0.14	0	+0.16	0	+0.30	0
ΔV_{nn}	+47.46	+28.83	0	+1.26	+0.78	0	+0.84	0	+1.71	0
ΔE_e	−45.48	−28.19	0	−1.09	−0.64	0	−0.69	0	−1.41	0
ΔH	−88.87	−55.18	0	−1.75	−0.18	0	−0.82	0	−1.32	0
ΔG	+43.39	+26.99	0	+0.66	+0.54	0	+0.13	0	−0.09	0
$\Delta\varepsilon$	− 2.09	− 1.21	0	−0.43	−0.14	0	−0.56	0	−1.50	0
$\Delta H(E-H)$	+ 0.47	—	0	−0.03	−0.05	0	—	—	—	—

Table 10. Difference of $(2J_{ij}-K_{ij})$ between 0° and 90° of N_2H_4

	1	2	3	4	5	6(n)	7(n)
1	−0.01	+0.02	−0.26	+0.10	−0.15	+0.18	+0.05
2		+0.03	−0.05	+0.04	−0.14	+0.32	+0.04
3			−0.64	−0.02	−1.40	+0.66	−0.06
4				+0.36	+0.15	+0.17	−0.26
5					−0.46	+0.17	+0.43
6(n)						+0.43	+0.20
7(n)							+0.04

(n): (n) denotes a lone-pair MO.

It is also noted that the instability of H_2S_2 towards 0° is contributed to by an increase in ΔV_{nn} and ΔG.[22]

It is noted that the core-core repulsion energy does not cancel the electronic energy. The sum of the orbital energy does not exhibit the same trend as the total energy with regard to the variation in the dihedral angle[24] (see $\Delta\varepsilon$ and ΔW in Table 9). That is, in this case, the stabilization of the molecule at 90° can not be interpreted by the extended Hückel calculation, as is shown in Table 9.

Next, as for N_2H_2, *trans* N_2H_2 is more stable than *cis* N_2H_2. The unstabilization energy, ΔW, is 0.30 eV. In contrast to the other three compounds in Table 9, the difference in the electronic interaction energy, ΔG, is negative. That is, the electronic interaction in the *cis* form is smaller than that in the *trans* form.

In order to known whether the lone-pair levels have a definite relation to the value of $G=\sum_i^{occ}(2J_{ij}-K_{ij})$, each $(2J_{ij}-K_{ij})$ value of N_2H_4 and N_2H_2 is studied. In Table 10, the differences in these values of N_2H_4 between 0° and 90° are listed; they are also compared with the corresponding levels and a standard is made of the value of 90°.[25] That is, $\Delta(2J_{ij}-K_{ij})=(2J_{ij}-K_{ij})$ (at 0°) $-(2J_{ij}-K_{ij})$ (at 90°). The value of the $(2J_{ij}-K_{ij})$ is presented by the element of the ith raw and the jth column, namely, the (ij) element of Table 10. The order of the numbering is that of the level sequences obtained when $\phi=0$. Comparatively large repulsive values are seen in the elements with reference to the lone-pair levels, but they are not definitely large.

As has been noted in the previous section, the interaction of the lone pairs in N_2H_2 is larger at 180° (*trans* form) than at 0° (*cis* form), but the total energy at 180° is slightly lower than that at 0°. This relation between the interaction of the lone pair and the total energy is different from the previously-obtained relation that the stable conformation of such molecules as $(CH_3)_2S_2$, H_2S_2, H_2O_2, and N_2H_4 is the one where the interaction of the lone pairs is smaller. A similar relation appears in Table 9. That is, the electronic interaction, G, of N_2H_2 is large in the unstable conformation, while those of the other three compounds are small in the stable conformation.

Table 11. Difference of $(2J_{ij}-K_{ij})$ between 0° and 90° of N_2H_2

	1	2	3	4	5(n)	6(n)
1	−0.06	+0.11	−0.01	−0.07	−0.10	−0.20
2		+0.17	+0.18	+0.16	+0.70	+0.07
3			+0.23	−0.10	−0.03	−0.83
4				0.00	+0.24	−0.32
5(n)					−0.12	+0.26
6(n)						−0.41

(n): (n) denotes a lone-pair MO.

Comparing Tables 10 and 11, we can also see the following relations with regard to the different contributions of the electronic interaction term $(2J_{ij}-K_{ij})$ to the energies of N_2H_2 and N_2H_4. The 5th and 6th raws and columns of Table 11 are referred to the lone-pair levels of N_2H_2. Among the elements concerned with the lone-pair levels of N_2H_2,[25] negative values are more often seen than in the case of N_2H_4 in Table 10. In fact, the sum of the elements concerning the lone-pair MO's in Tables 10 and 11 is 2.37 eV (repulsive) for N_2H_4 and −0.74 eV for N_2H_2. From these discussions, it may be concluded that one of the main factors in the instability of N_2H_4 at $\phi=0°$ is the lone-pair interaction or the electrostatic interaction in the lone-pair MO's.

One of the authors (H.Y.) wishes especially to thank Mr. H. Nakatsuji for reading the manuscript and for his helpful discussions.

The calculations were carried out on the HITAC 5020 computer at the Computation Center of the University of Tokyo.

22) A parallelism between ΔV_{nn} and ΔW was also seen in the calculation of *cis*- and *trans*- butadienes and glyoxals (Ref. 23).

23) H. Kato, H. Konishi, H. Yamabe and T. Yonezawa, This Bulletin, **40**, 2761 (1967).

24) Fink and Allen also pointed out, in their SCF calculation of H_2O_2, the unparallel behavior of the sum of the orbital energies and the total energy. They said that this may be due to the highly localized ionic character associated with two sets of lone pairs in H_2O_2 (Ref. 9).

25) For N_2H_2, the difference between 0° and 180° is calculated as follows: $\Delta(2J_{ij}-K_{ij})=(2J_{ij}-K_{ij})$(at 0°) $-(2J_{ij}-K_{ij})$(at 180°).

The Crystal and Molecular Structure of *N*-Salicylidene-α-aminoisobutyratoaquocopper(II)

Hiroto FUJIMAKI,[1] Isao OONISHI, Fumio MUTO, Akitsugu NAKAHARA,* and Yoshimichi KOMIYAMA[2]

Department of Applied Chemistry, Faculty of Engineering, Yamanashi University, Kofu

* *Institute of Chemistry, College of General Education, Osaka University, Machikaneyama, Toyonaka*

(Received June 29, 1970)

The crystal structure of *N*-salicylidene-α-aminoisobutyratoaquocopper(II), [Cu{$OOCC(CH_3)_2N{=}CHC_6H_4O$}-($H_2O$)], has been determined from the three-dimensional X-ray diffraction data. The crystals are monoclinic. The cell dimensions are: $a=12.30$, $b=8.45$, $c=23.84$ Å, and $\beta=91.0°$. The space group is $P2_1/c$, with eight formula units in a unit cell. The structure has been refined by the least-squares method, with anisotropic temperature factors, to an *R*-value of 0.10. The molecular structures of the complex are essentially the same as those of *N*-salicylideneglycinatoaquocopper(II) hemihydrate and tetrahydrate. The environments of the copper(II) ions are square pyramidal, with one long and four short coordination bonds. The average distances of the two copper environments are: Cu–O, 1.912 and 1.945; Cu–N, 1.961; Cu–O(H_2O), 1.989, and Cu–O′ (the bond to the carboxyl oxygen of the adjacent molecule), 2.344 Å. The average bond distances of N=C in the salicylaldimine residue and of N–C in the α-aminoisobutyrate group are 1.271 and 1.504 Å respectively. Neighboring molecules related by a center of symmetry are linked together alternately by hydrogen bonds and coordination bonds (Cu–O′), an infinite chain being formed along the *b*-axis. However, there are no interactions other than van der Waals forces along the *a*- and *c*-axes.

An extensive study has recently been made of the copper(II) complexes with tridentate Schiff bases derived from salicylaldehyde and various amino acids by Nakahara and his co-workers.[3]

Kakudo and his co-workers have determined the structure of *N*-salicylideneglycinatoaquocopper(II) hemihydrate[4] (SGCH) and tetrahydrate (SGCT).[5] Concerning the transamination reaction, Kakudo *et al.* concluded, from their consideration of the bond distances around the nitrogen atom, that the N–C single bond of the salicylaldimine moiety and the N=C double bond of the glycine moiety are electron-rich.

It seemed that it would be of interest to investigate whether bulky groups such as the *t*-methyl group affect the bonds around the nitrogen atom of the Schiff-base linkage. Another point of interest is the coordination configuration about the copper atoms. In SGCH and SGCT, the coordination configurations about the copper atoms are both square pyramidal; however, in SGCH the fifth ligand atom is a 'free' carboxyl oxygen of the adjacent complex, while in SGCT it is a water oxygen atom.

In order to obtain more information about these aspects, we attempted to determine the crystal structure for *N*-salicylidene-α-aminoisobutyratoaquocopper(II), [Cu{$OOCC(CH_3)_2N{=}CHC_6H_4O$}($H_2O$)].

Experimental

N-Salicylidene-α-aminoisobutyratoaquocopper(II) was prepared and purified according to the procedure described in a previous paper.[3] The final pure product appears as green plates. The unit-cell dimensions were determined from the higher-order reflections of Weissenberg photographs (Cu$K\alpha$, $\lambda=1.5412$ Å). The systematic absences were: $h0l$ for l odd and $0k0$ for k odd. Hence, the space group was unequivocally determined. The crystal data are listed in Table 1. Sets of

Table 1. Crystal data

[Cu{$OOCC(CH_3)_2N{=}CHC_6H_4O$}($H_2O$)]
Monoclinic
$a=12.30\pm0.01$ Å
$b=8.45\pm0.01$ Å
$c=23.84\pm0.02$ Å
$\beta=91.0\pm0.5°$
$Dx=1.54$ g·cm^{-3}
$Dm=1.54$ g·cm^{-3}
$Z=8$
Space group $C_{2h}^5-P2_1/c$
Linear absorption coefficient for Cu$K\alpha$, $\mu=43.9$ cm^{-1}

multiple-film equi-inclination Weissenberg photographs were taken about the *b*-axis (0 to 6th layers), the *a*-axis, and the *c*-axis (0th layer). Cu$K\alpha$ radiation was employed throughout. The crystal used was a rod with dimensions of $0.1\times0.3\times1.0$ mm. The intensities were estimated visually with a standard film strip and were converted to $|F_o(hkl)|$ by applying the usual Lorentz, polarization, and spot-shape corrections. No correction was made for absorption and extinction. The range of relative intensities was from 1 to 7200. 2750 independent reflections fell within this range, whereas 1389 others were too weak to be observed.

Structure Analysis

The presence of eight formula units in a unit cell of the space group $P2_1/c$ requires that the complex molecules occupy two sets of general positions. Three-dimensional Patterson syntheses were performed. From these Patterson maps, the positions of the Cu atoms

1) Present address: Tokyo Laboratory, Kureha Chemistry Industry Co., Ltd., Hyakunin-cho, Shinjuku, Tokyo.

2) Deceased Aug. 1, 1968.

3) Y. Nakao, K. Sakurai, and A. Nakahara, This Bulletin **40**, 1536 (1967).

4) T. Ueki, T. Ashida, Y. Sasada, and M. Kakudo, *Acta Crystallogr.* **22**, 870 (1967).

5) T. Ueki, T. Ashida, Y. Sasada, and M. Kakudo, *ibid.*, **B25**, 328 (1969).

TABLE 2. ATOMIC PARAMETERS AND THEIR E.S.D.'S[a] ($\times 10^4$)

The expression of the temperature factor is given by
$\exp[-(h^2B_{11}+k^2B_{22}+l^2B_{33}+hkB_{12}+hlB_{13}+klB_{23})]$.

Molecule I

Atom	x/a	y/b	z/c	B_{11}	B_{22}	B_{33}	B_{12}	B_{13}	B_{23}
Cu(1)	1679(1)	240(3)	601(1)	42	210	15	35	− 7	14
O(1)	2090(7)	1857(14)	1125(4)	34	197	18	50	−10	−20
O(2)	1273(7)	−1473(14)	91(4)	37	202	14	21	−12	−34
O(3)	1969(8)	−3388(13)	− 443(4)	57	137	21	73	−22	−55
W(1)	122(6)	742(13)	742(4)	22	178	16	35	8	− 1
N(1)	3099(7)	− 829(13)	629(4)	24	83	11	55	− 6	− 8
C(1)	2053(10)	−2363(20)	− 76(5)	24	175	13	−11	6	−10
C(2)	3177(9)	−2199(20)	224(5)	17	181	9	5	− 6	−16
C(3)	4018(12)	−1801(22)	− 224(6)	54	213	16	−41	16	− 8
C(4)	3437(14)	−3758(22)	552(6)	103	117	13	88	− 4	12
C(5)	3901(9)	− 436(20)	935(5)	30	169	10	11	− 7	− 2
C(6)	3901(9)	943(18)	1310(5)	24	153	7	−21	− 6	− 8
C(7)	4880(12)	1177(25)	1628(6)	50	283	12	−19	− 6	5
C(8)	4983(14)	2444(26)	2001(7)	84	285	23	10	−15	−33
C(9)	4122(15)	3525(24)	2063(7)	102	193	20	− 9	−27	−53
C(10)	3147(13)	3258(22)	1777(6)	84	189	14	−36	−15	−31
C(11)	3017(11)	2017(20)	1386(6)	43	144	13	− 9	− 1	−11

Molecule II

Atom	x/a	y/b	z/c	B_{11}	B_{22}	B_{33}	B_{12}	B_{13}	B_{23}
Cu(2)	− 669(1)	4724(3)	963(1)	46	202	11	40	4	1
O(4)	− 430(7)	3046(14)	1488(4)	57	209	7	71	10	4
O(5)	− 935(7)	6452(14)	442(4)	47	208	12	108	8	4
O(6)	−2143(8)	8324(15)	223(4)	72	233	13	135	7	38
W(2)	788(6)	4307(13)	652(4)	27	195	10	48	13	− 2
N(2)	−1775(7)	5768(14)	1412(4)	30	99	8	38	8	− 3
C(12)	−1762(10)	7336(19)	547(6)	39	122	14	6	2	15
C(13)	−2267(11)	7189(21)	1131(6)	40	179	12	32	13	11
C(14)	−3512(12)	6859(25)	1060(7)	38	275	25	84	− 6	62
C(15)	−1973(16)	8713(25)	1466(7)	140	188	18	2	4	−48
C(16)	−2080(9)	5330(21)	1898(5)	35	183	10	31	7	− 6
C(17)	−1658(10)	3947(20)	2195(5)	30	184	6	11	9	2
C(18)	−2032(13)	3711(24)	2740(6)	76	230	13	−40	4	8
C(19)	−1656(14)	2453(26)	3077(7)	86	274	17	−19	23	27
C(20)	− 925(13)	1366(22)	2867(6)	79	187	14	15	8	− 9
C(21)	− 511(12)	1605(23)	2317(6)	68	228	10	12	−19	20
C(22)	− 850(10)	2878(19)	1986(5)	36	141	9	12	− 3	− 3

[a] e.s.d.'s in parentheses

were easily deduced, but those of lighter atoms could not be fixed. The structure factors, $h0l$, were calculated with the parameters of the Cu atoms. The discrepancy factor, R, was 0.50. The parameters of the eight lighter atoms coordinated to the Cu atoms were deduced from the two-dimensional electron density diagrams, $\rho(x,z)$ and $\rho(y,z)$, the signs of which were calculated from the parameter values of the copper atoms. After two cycles of calculations of the structure factors and the electron densities, $\rho(x,z)$ and $\rho(y,z)$, the parameters of all the atoms were fixed. At this stage, the discrepancy factors, R_{h0l} and R_{0kl}, dropped 0.20 and 0.25 respectively.

The structure thus obtained was refined by a block-diagonal, least-squares method with a HBLS-4 program written by T. Ashida. After three cycles of the refinements, the R-value was 0.14. Six more cycles of the refinements were carried out on the introduction of anisotropic temperature factors. The following weighting scheme was employed:

$$w = 0.2, \quad \text{if } F_0 \leqq F_{min}\ (=15.0);$$
$$w = 1.0, \quad \text{if } F_{min} < F_0 \leqq F_{max}\ (=200.0);$$

and

$$w = F_{max}/F_0, \text{ if } F_0 > F_{max}$$

The final discrepancy factor, $R=\sum||F_o|-|F_c||/\sum|F_o|$, was 0.10 for all the observed reflections. The atomic scattering factors were taken from the International Tables for X-ray Crystallography.[6] The final atomic parameters and their estimated standard deviations are summarized in Table 2. The agreement between the

6) International Tables for X-Ray Crystallography, Vol. III, Kynoch Press, Birmingham (1962), p. 202.

observed and calculated structure amplitudes is reasonable.[7]

Description of the Structure and Discussion

The intramolecular bond distances and angles are listed, with their estimated standard deviations, in Tables 3 and 4, and are shown in Figs. 1 and 2. These distances and angles were calculated by using the DAPH program written by T. Ashida.

The *N*-salicylidene-α-aminoisobutyrate groups is coordinated to the copper atom as a tridentate ligand; it is linked to the metal atom through the two oxygen atoms—carboxylic and phenolic—, and the one nitrogen atom of the Schiff-base linkage.

The coordination configurations about the copper atoms in the molecules I and II are both square pyramidal (Figs. 3 and 4). This type of 5-coordinated configuration has been already found in various copper(II) complexes, for instance, di-μ-hydroxobis[dimethylaminecopper(II)]sulfate monohydrate,[8] sodium glycylglycylglycinocuprate monohydrate,[9] and other copper(II) glycine-peptide complexes, pyruvidene-β-alaninatoaquocopper(II) dihydrate,[10] *N*-salicylidene-

Table 3. Bond distances and their estimated standard deviations[a]

Molecule I		Molecule II	
Cu(1)–O(1)	1.914(10) Å	Cu(2)–O(4)	1.910(10) Å
O(2)	1.948(19)	O(5)	1.941(10)
W(1)	1.996(9)	W(2)	1.982(9)
O(6″)	2.385(11)	O(3′)	2.302(10)
N(1)	1.966(10)	N(2)	1.956(10)
C(1)–O(2)	1.288(17)	C(12)–O(5)	1.289(17)
O(3)	1.235(17)	O(6)	1.226(18)
C(2)	1.551(19)	C(13)	1.539(21)
C(2)–C(3)	1.537(21)	C(13)–C(14)	1.562(23)
C(4)	1.562(21)	C(15)	1.556(24)
N(1)	1.511(16)	N(2)	1.497(18)
C(5)–N(1)	1.262(17)	C(16)–N(2)	1.279(17)
C(6)	1.469(18)	C(17)	1.457(19)
C(7)–C(6)	1.426(21)	C(18)–C(17)	1.399(22)
C(8)	1.395(25)	C(19)	1.406(25)
C(9)–C(8)	1.409(26)	C(20)–C(19)	1.385(25)
C(10)	1.387(25)	C(21)	1.429(23)
C(11)–C(10)	1.410(22)	C(22)–C(21)	1.393(21)
C(6)	1.429(19)	C(17)	1.439(19)
O(1)	1.297(18)	O(4)	1.312(17)

O(3′) and O(6″) are related to O(3) and O(6) through the operations $(-x, -y, -z)$ and $(-x, 1-y, -z)$ respectively.

a) e.s.d.'s × 10^3 in parentheses

Table 4. Bond angles and their estimated standard deviations[a]

Molecule I	
N(1)–Cu(1)–O(1)	94.7(4)°
N(1)–Cu(1)–O(2)	84.2(4)
W(1)–Cu(1)–O(1)	88.9(4)
W(1)–Cu(1)–O(2)	91.5(4)
O(6″)–Cu(1)–O(1)	96.3(4)
O(6″)–Cu(1)–O(2)	85.8(4)
O(6″)–Cu(1)–N(1)	92.1(4)
O(6″)–Cu(1)–W(1)	105.9(4)
Cu(1)–O(2)–C(1)	116.2(9)
O(2)–C(1)–O(3)	125.1(13)
O(3)–C(1)–C(2)	116.9(12)
O(2)–C(1)–C(2)	117.9(12)
C(1)–C(2)–C(3)	107.7(11)
C(1)–C(2)–C(4)	109.2(11)
C(3)–C(2)–C(4)	113.4(12)
C(3)–C(2)–N(1)	109.0(11)
C(4)–C(2)–N(1)	110.0(11)
C(1)–C(2)–N(1)	107.3(10)
C(2)–N(1)–Cu(1)	113.3(8)
C(5)–N(1)–Cu(1)	125.7(9)
N(1)–C(5)–C(6)	123.6(12)
C(5)–C(6)–C(11)	126.1(12)
C(7)–C(6)–C(11)	118.8(12)
C(6)–C(7)–C(8)	120.7(15)
C(7)–C(8)–C(9)	120.3(17)
C(8)–C(9)–C(10)	119.2(17)
C(9)–C(10)–C(11)	122.2(15)
C(10)–C(11)–C(6)	118.6(13)
C(6)–C(11)–O(1)	122.5(13)
C(11)–O(1)–Cu(1)	127.4(9)
Molecule II	
N(2)–Cu(2)–O(3)	94.4(4)°
N(2)–Cu(2)–O(5)	84.2(4)
W(2)–Cu(2)–O(4)	89.1(4)
W(2)–Cu(2)–O(5)	92.2(4)
O(3′)–Cu(2)–O(4)	94.9(4)
O(3′)–Cu(2)–O(5)	85.2(4)
O(3′)–Cu(2)–N(2)	91.8(4)
O(3′)–Cu(2)–W(2)	109.6(4)
Cu(2)–O(5)–C(12)	115.9(9)
O(5)–C(12)–O(6)	124.5(13)
O(6)–C(12)–C(13)	118.0(13)
O(5)–C(12)–C(13)	117.5(12)
C(12)–C(13)–C(14)	109.1(12)
C(12)–C(13)–C(15)	107.6(13)
C(14)–C(13)–C(15)	115.0(13)
C(14)–C(13)–N(2)	107.0(12)
C(15)–C(13)–N(2)	110.2(12)
C(12)–C(13)–N(2)	107.6(11)
C(13)–N(2)–Cu(2)	113.4(8)
C(16)–N(2)–Cu(2)	125.6(9)
N(2)–C(16)–C(17)	124.4(12)
C(16)–C(17)–C(22)	125.3(12)
C(18)–C(17)–C(22)	118.1(13)
C(17)–C(18)–C(19)	121.9(15)
C(18)–C(19)–C(20)	120.3(16)
C(19)–C(20)–C(21)	118.8(15)
C(20)–C(21)–C(22)	121.3(14)
C(21)–C(22)–C(17)	119.4(13)
C(17)–C(22)–O(4)	122.0(12)
C(22)–O(4)–Cu(2)	128.0(9)

a) e.s.d.'s × 10 in parentheses

7) A complete list of the observed and calculated structure factors has been submitted to, and is kept as Document No. 7101 at the office of the Bulletin of the Chemical Society of Japan, 1-5 Kanda-Surugadai, Chiyoda-ku, Tokyo. A copy may be secured by citing the Document number and by remitting, in advance, ¥200 for photoprints. Pay by check or money order payble to: The Chemical Society of Japan.

8) Y. Iitaka, K. Simizu, and T. Kwan, *Acta Crystallogr.* **20**, 803 (1966).

9) H. C. Freeman, J. C. Schoone, and J. G. Sime, *ibid.*, **18**, 381 (1965).

10) T. Ueki, T. Ashida, Y. Sasada, and M. Kakudo, *ibid.*, **B24**, 1361 (1968).

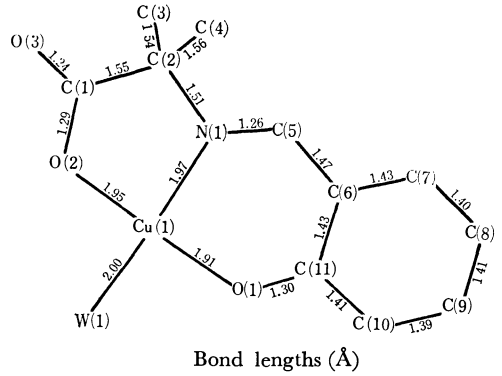

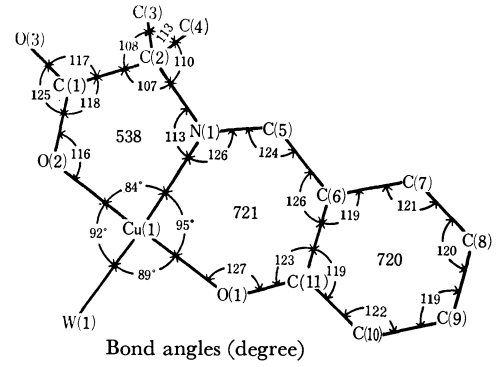

Fig. 1. Bond lengths and angles in the molecule I.

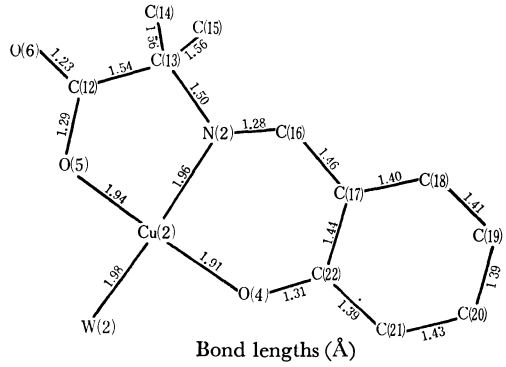

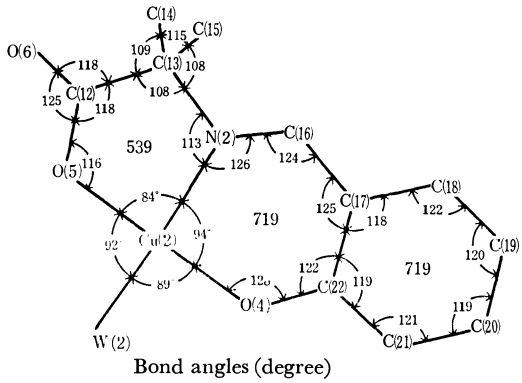

Fig. 2. Bond lengths and angles in the molecule II.

glycinatoaquocopper(II) hemihydrate,[4] and tetrahydrate,[5] and copper(II) yunainate trihydrate.[11]

The fifth coordination bond in one molecule is formed by the 'free' carboxyl oxygen atom of the adjacent, crystallographically-independent molecule, as

11) A. Furusaki and Y. Tomiie, This Bulletin, **43**, 736 (1970).

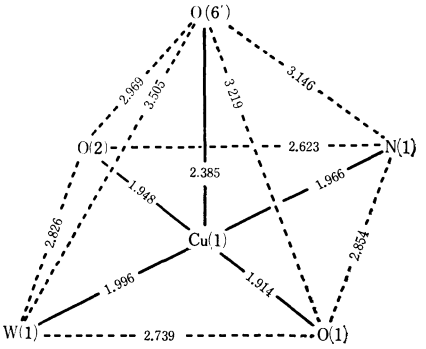

Fig. 3. Five ligand atoms disposed around the copper atom in the molecule I; bond distances are given in Å.

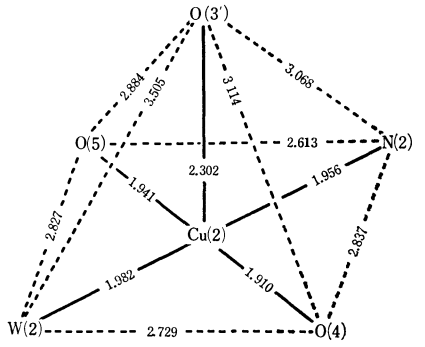

Fig. 4. Five ligand atoms disposed around the copper atom in the molecule II; bond distances are give in Å.

in the case of SGCH, while in SGCT and pyruvidene-β-alaninatoaquocopper(II) dihydrate it is formed by a water oxygen atom.

The Cu–O distances are 1.914 and 1.948 Å in the molecule I, and 1.910 and 1.941 Å in the molecule II, all shorter than those found in SGCH and SGCT. Cu–O distance is 1.966 Å in the molecule I and 1.956 Å in the molecule II, both values being longer than those found in SGCH and SGCT. The Cu–W (W represents the water oxygen atom) distance is 1.966 Å in the molecule I and 1.982 Å in the molecule II. These values are longer than that of 1.965 Å in SGCT, but shorter than that of 2.016 Å in SGCH. The fifth coordinating atoms, O(6'') and O(3'), lie at the apex of the square pyramid at distances of 2.385 and 2.302 Å respectively from the copper atoms in the molecules I and II.

The Cu–O' bond (O' means the apical oxygen atom mentioned above) makes an angle of 80.5° in the molecule I, and one of 79.1° in the molecule II, with the plane of the square base. In the present work, no significant displacement of the Cu atom toward the apical oxygen atom was observed such as is found in the cases of SGCH and SGCT. The angles of N(1)–Cu(1)–O(1) and N(1)–Cu(1)–O(2) in the molecule I are 94.7 and 84.2° respectively. The corresponding angles of N(2)–Cu(2)–O(4) and N(2)–Cu(2)–O(5) in the molecule II are 94.4 and 84.2°. These values are in good agreement with those observed in SGCH and SGCT. The other bond lengths and angles generally agree well with those found in SGCH and SGCT, except for the bond distances around the nitrogen

Table 5. Least-squares planes in the molecule I

Coefficients of least-squares plane equation, $AX+BY+CZ+D=0$

	A	B	C	$D(\times 10^4)$
P(1) (all the atoms except methyl groups)	2311	6371	−7354	6444
P(2) (square coordination atoms)	1399	6085	−7812	9074
P(3) (Cu-α-aminoisobutyrato)	2761	6099	−7428	4449
P(4) (benzene ring)	3528	5719	−7406	2006
P(5) (Cu-salicylaldimine)	3468	5761	−7402	2186

X(Å)$=ax+cz\cos\beta$ $Y=by$ $Z=cz\sin\beta$

Normal distances from the planes ($\times 10^3$ Å)

	P(1)	P(2)	P(3)	P(4)	P(5)
Cu(1)	192	(198)	69		−17
O(1)	255	120	(107)	(2)	12
O(2)	53	199	− 44		
O(3)	161		(157)		
W(1)	−229	− 75	(−453)		−(687)
N(1)	− 28	−159	− 49		19
C(1)	90		60		
C(2)	− 32		− 9		(105)
C(5)	−130		(−122)	(18)	6
C(6)	− 49			17	11
C(7)	−205			−11	−24
C(8)	−150			−17	−25
C(9)	78			22	23
C(10)	160			−22	−14
C(11)	144			17	22

( ) not included in the least-squares calculations

Table 6. Least-squares planes in the molecule II

Coefficients of least-squares plane equation, $AX+BY+CZ+D=0$

	A	B	C	$D(\times 10^4)$
P(1) (all the atoms except methyl groups)	−6167	−6323	−4689	32335
P(2) (square coordination atoms)	−5442	−6122	−5737	34892
P(3) (Cu-α-aminoisobutyrato)	−6765	−5918	−4383	28296
P(4) (benzene ring)	−7338	−5682	−3725	22987
P(5) (Cu-salicylaldimine)	−7228	−5637	−3997	24728

X(Å)$=ax+cz\cos\beta$ $Y=by$ $Z=cz\sin\beta$

Normal distances from the planes ($\times 10^3$ Å)

	P(1)	P(2)	P(3)	P(4)	P(5)
Cu(2)	165	(198)	44		−72
O(4)	308	201	(152)	(−51)	32
O(5)	12	183	− 69		
O(6)	168		(223)		
W(2)	−378	−143	(−643)		(−881)
N(2)	− 44	−205	− 13		1
C(12)	52		70		
C(13)	−123		− 29		(212)
C(16)	−109		(− 34)	(−10)	33
C(17)	− 15			18	42
C(18)	−200			2	−16
C(19)	−181			−23	63
C(20)	74			20	1
C(21)	233			3	25
C(22)	171			−19	25

( ) not included in the least-squares calculations

atoms.

Kakudo and his co-workers[5] concluded, from their consideration of the bond distances, that the N–C single bond and the N=C double bond in SGCT are electron-rich.

In the present work, the N–C single bonds have normal values, and the N=C double bonds are rather shorter than the normal double bond distance (1.29—1.30 Å), while in SGCT and SGCH the N–C bonds are rather shorter than the normal values (1.47—1.49 Å) and the N=C bonds are normal. Thus, such bulky groups as *t*-methyl will certainly affect the bonds around the nitrogen atom of the Schiff-base linkage.

The molecules may be described in terms of a set

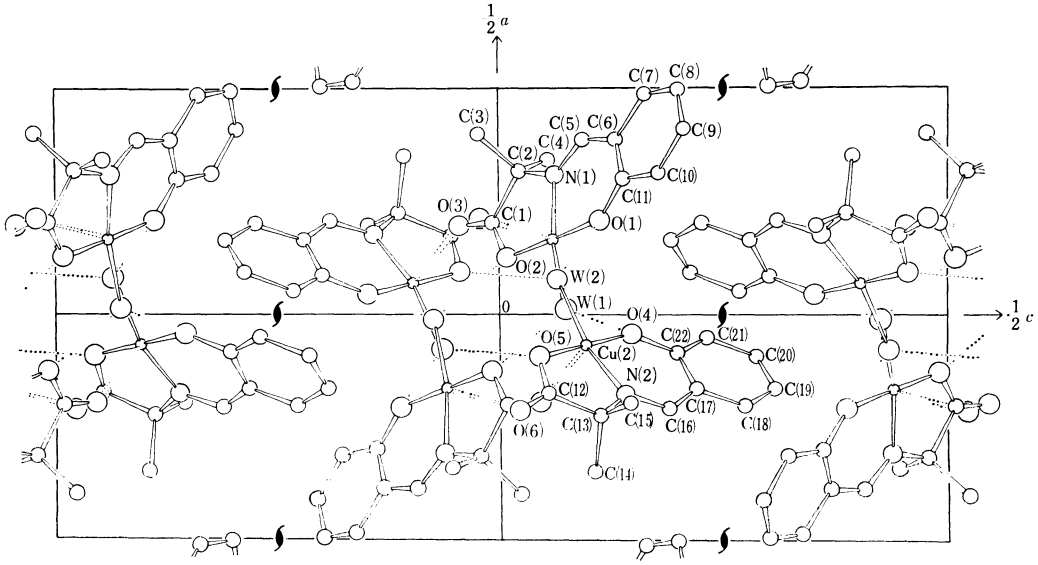

Fig. 5. Projection of the unit cell contents on the (010) plane.

of various plane groups. Tables 5 (molecule I) and 6 (molecule II) list the equations for various least-square planes and the deviations of the atoms therefrom. The largest deviation of any atom from the plane P(1), determined in any of the atoms of the molecule I (except for the two methyl groups) is 0.26 Å for the O(1) atom, whereas it is −0.38 Å for the W(2) atom in the molecule II. Thus, the planarity of the molecule I is slightly better than that of the molecule II, in which several atoms deviate by more than 0.3 Å from the plane. The plane through the α-aminoisobutyrate residue, P(3), and the one containing the salicylaldimine residue, P(5), make dihedral angles of 4.5° in the molecule I and 3.8° in the molecule II; these angles are considerably smaller than the corresponding values of 9.5° in SGCH and 16.5° in SGCT.

The structure projected upon a plane normal to the *b*-axis is shown in Fig. 5. The important intermolecular contacts are listed in Table 7.

The molecules are alternately linked together by the fifth coordination bonds described above to form zigzag chains along the *b*-axis. Two of these zigzag chains are related by the centres of symmetry and are bound laterally by the hydrogen bonds, indicated by dotted lines in Fig. 5. However, there is no interaction other than the van der Waals forces along the *a*- and *c*-axes.

Table 7. Intermolecular contacts not exceeding 3.6 Å

O(1)–O(4) (1)	3.385(14) Å	O(3)–C(12)(1)	3.355(17) Å
O(16) (2′)	3.219(15)	O(4)–W(1) (1)	2.731(13)
W(2) (1)	2.839(13)	C(20) (3)	3.596(19)
O(2)–O(5)(1″)	3.352(14)	O(5)–W(2) (2′)	2.697(13)
O(6) (2′)	2.969(14)	O(6)–W(1) (2′)	3.505(14)
W(1) (2)	2.674(13)	W(2) (2′)	3.492(14)
O(3)–O(4) (2)	3.114(14)	N(1) (2′)	3.146(15)
O(5) (2)	2.884(14)	C(1) (2′)	3.433(18)
W(1) (2)	3.472(14)	W(1)–W(2) (1)	3.130(13)
W(2) (1″)	3.586(14)	C(1) (2)	3.377(17)
W(2) (2)	3.505(14)	C(15)(1″)	3.566(21)
N(2) (2)	3.068(14)	W(2)–C(12)(1″)	3.415(17)

1) x, y, z 1′) $x, 1+y, z$ 1″) $x, -1+y, z$
2) $-x, -y, -z$ 2′) $-x, 1-y, -z$
3) $-x, \frac{1}{2}+y, \frac{1}{2}-z$
e.s.d.'s × 10^3 in parentheses

The numerical calculations were carried out on the FACOM231 computer at this University and the HITAC5020E computer at the Computer Center, the University of Tokyo.

Part of the cost of this investigation has been defrayed by a Scientific Research Grant of the Ministry of Education, for which the authors' thanks are due.

BULLETIN OF THE CHEMICAL SOCIETY OF JAPAN, VOL. 44, 33—37 (1971)

Infrared Absorption Spectra of Silica Gel - $H_2{}^{16}O$, $D_2{}^{16}O$, and $H_2{}^{18}O$ Systems

Masao HINO and Toshio SATO

Government Industrial Development Laboratory, Hokkaido, Higashi-Tsukisamu, Sapporo

(Received July 4, 1970)

Infrared absorption spectra of the systems of silica gel - $H_2{}^{16}O$, $D_2{}^{16}O$, $H_2{}^{18}O$, and some organic vapors were measured in order to assign the bands sensitive to adsorption at 870 and around 950 cm^{-1}. Deuteration of silica gel caused the absorption decrease at 870 cm^{-1} and the appearance of a band at 620 cm^{-1}. The band around 950 cm^{-1} appearing by adsorption not only of water but also of organic vapors showed no shift on deuteration, but shifted toward low frequency side by 25 cm^{-1} on the substitution of ^{16}O of surface silanol groups with ^{18}O. From these facts the bands at 870, 620 and 950 cm^{-1} were assigned to Si–OH bending, Si–OD bending and Si–O stretching vibrations of surface silanol groups, respectively. The oxygen atom of silanol groups of silica gel was found to exchange with that of adsorbed water molecules even at room temperature for a sample treated at temperature below 300°C. On the other hand, higher reaction temperature of *ca.* 200°C was necessary for a sample calcined at 800°C. Mechanism of the oxygen atom exchange reaction was discussed.

A number of investigations have been carried out to elucidate the structure and properties of silica gel surface by use of infrared spectroscopy.[1-3] They were concentrated on measurement of the OH stretching band between 4000 and 2500 cm^{-1}. However, there are very few investigations in other spectrum regions.

Beutelspacher[4] first pointed out that a wet silica gel had a 950 cm^{-1} band, which vanished by heat treatment at 1000°C. Soda[5] also found a 950 cm^{-1} absorption band sensitive to desiccation for a finely ground quartz powder sample. He assumed that it was due to the bending vibration of Si–OH groups on the surface of the particles. On the other hand, Benesi and Jones[6]

1) M. L. Hair, "Infrared Spectroscopy in Surface Chemistry," Marcel Dekker, Inc., New York (1967), p. 79.
2) M. R. Basila, "Applied Spectroscopy Reviews," Vol. 1, Marcel Dekker, Inc., New York (1968), p. 296.
3) A. V. Kiselev and V. I. Lygin, *Russian Chem. Rev.*, **31**, 175 (1962).
4) H. Beutelspacher, VI Congres International de la Science du sol, Vol. B 329 (1956).
5) R. Soda, This Bulletin, **34**, 1491 (1961).
6) H. A. Benesi and A. C. Jones, *J. Phys. Chem.*, **63**, 179 (1959).

assigned this bending vibration to the band at 870 cm^{-1}, from the fact that it disappeared on deuteration.

The purpose of the present work is to establish the assignment of these two bands more directly by measuring the isotopic shift in wider frequency region when H and ^{16}O atoms of silica gel are substituted with D and ^{18}O atoms, respectively, and also by measuring the adsorption effects of various vapors on the surface. The reactivity of the silica gel surface was also studied through the exchange reaction of water with surface silanol groups.

Experimental

Materials. Silica gel for chromatography (Kanto Chemical Co., Inc.) made from sodium silicate and sulfuric acid was ground in an agate mortar and then suspended in deionized water to get a very fine powder sample. The surface area of this material was 450 m^2/g, independent of the heat treatment at temperature lower than 600°C. $D_2{}^{16}O$ (Showa Denko Co., Ltd.) of 99.75 atom % in purity and $H_2{}^{18}O$ (Yeda R. & D., Co. Ltd.) of 97.9 atom % were used. Methanol, diethyl ether, acetone, and carbon disulfide, all of guaranteed reagent grade, were dried, distilled and degassed before the adsorption experiment. Pure hydrogen sulfide (Takachiho Chemical Industrial Co.) was used without further purification

Apparatus and Procedure. A JASCO Model 402-G double beam infrared spectrometer was used for recording the spectra in the wave number region between 4000 and 430 cm^{-1}. An all metal *in situ* cell used for measurement at room temperature is shown in Fig. 1. Another infrared cell with liquid nitrogen cooling system was also constructed by modifying the cell in Fig. 1 for measuring the adsorption of organic vapors and hydrogen sulfide at lower temperature down to −130°C.

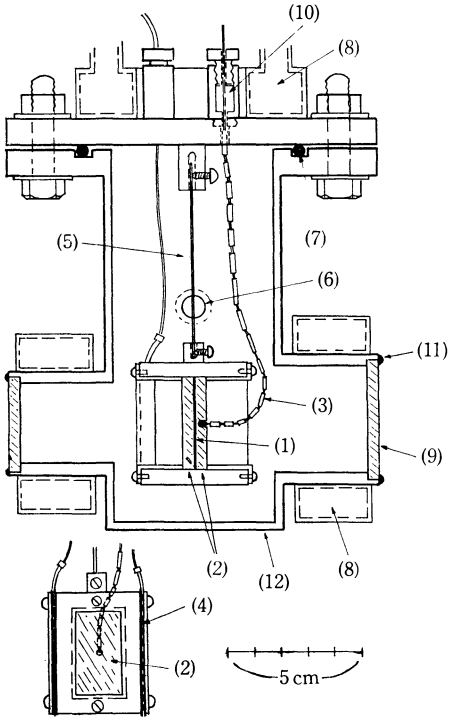

Fig. 1. All metal *in situ* cell.
1, adsorbent sample; 2, KBr plate; 3, thermocouple; 4, nichrome wire heater; 5, nichrome wire hanger; 6, evacuation outlet; 7, *O*-ring seal; 8, water jacket; 9, KBr window; 10, silicone rubber packing; 11, elastic epoxide resin seal; 12, chromium plated steel

A sandwich method was used for sample preparation; 6 to 20 mg of silical gel powder dispersed in a few drops of methanol was spread on the transparent KBr plate of 34 mm × 12 mm × 4 mm. After the methanol was evaporated, the silica powder on the plate was made even with a spatula and sandwiched by facing another KBr plate on the sample. As far as infrared spectrometer was used as a monitor, the silica gel was found not to react with methanol during the course of preparation. A vacuum reference cell was set in the light path of the reference side to eliminate the background effect of the spectra. To prepare a sufficiently deuterated silica gel sample, the sample was exposed to $D_2{}^{16}O$ vapor at 10 mmHg for 30 min and then evacuated, both at room temperature. The procedure was repeated six times.[6,7]

Results

1. Silica Gel - $H_2{}^{16}O$ System. Measurement of the spectra was carried out on the silica gel sample after evacuation at various temperatures and also on successive exposure to water vapor at room temperature. As shown in Fig. 2, evacuation at room temperature gave marked decrease of the OH stretching band at 3400 cm^{-1} and the HOH bending band at 1630 cm^{-1}, which were attributed to the hydrogen-bonded hydroxyl groups and physically adsorbed water molecules, respectively. A simultaneous decrease of the absorption at 950 cm^{-1} was observed, while the absorption at 870 cm^{-1} increased in intensity and a sharp OH stretching band at 3748 cm^{-1} due to the "free" silanol groups appeared. Evacuation at elevated temperatures, as represented by Curves 4 and 6 in Fig. 2, produced a similar but stronger effect in the spectral changes, although the band at 870 cm^{-1} exceptionally decreased in intensity. Admission of water vapor on these evacuated surfaces produced the reverse effect on the spectral changes (Curves 3, 5, and 7). However, these five absorptions were completely restored only when the sample was evacuated at room temperature (Curve 3). A small band shift from 950 to 960 cm^{-1} was observed, when the sample was evacuated at 200 and 300°C and then rehydrated at room temperature.

Organic vapors and hydrogen sulfide, which have no absorption around 960 cm^{-1}, were then admitted at low temperatures onto the silica gel samples evacuated at 200°C. In each case, as seen in Table 1, bands were found to come out around 960 cm^{-1} and in the wave number region from 3680 to 3300 cm^{-1}, the peak positions depending on the kind and the amount of adsorbate.

2. Silica Gel - $D_2{}^{16}O$ System. Appearance of a strong ^{16}OD stretching band at 2480 cm^{-1} together with the disappearance of the bands of ^{16}OH at 3400 and 1630 cm^{-1} after deuteration confirmed that the deuteration of the present silica gel sample was completed.[6,7] It should be emphasized that this treatment induced no spectral change at the 950 cm^{-1} band and

7) V. Ya. Davydov, A. V. Kiselev, and L. T. Zhuravlev, *Trans. Faraday Soc.*, **60**, 2254 (1964).

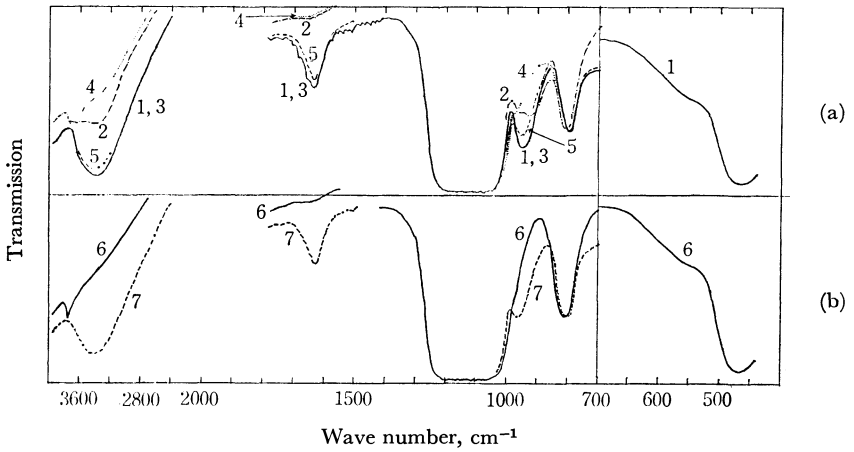

Fig. 2. Spectra of silica gel - $H_2{}^{16}O$ system.
a) 1——, before evacuation; 2-•-•-•, evacuated at room temperature for 26 hr; 3——, 5------, exposed to $H_2{}^{16}O$ at 12 mmHg; 4·····, evacuated at 200°C for 5 hr
b) 6——, evacuated at 300°C for 5 hr; 7------, exposed to $H_2{}^{16}O$ at 12 mmHg
Experiments were carried out in the order from 1 to 7. The spectra of lower wave number than 1400 cm^{-1} were recorded after the background was adjusted to a constant level at 1400 cm^{-1}.

Table 1. Peak position of the bands produced by adsorption of organic vapors

Adsorbate	OH stretching band of the surface silanol groups (cm^{-1})	The band around 960 cm^{-1} (cm^{-1})
CS_2	3680	970
H_2S	3460	914
$(C_2H_5)_2O$	3300	937
$(CH_3)_2CO$	3300	945
CH_3OH	a)	955

a) Not distinguishable from the OH stretching band of CH_3OH.

also much decrease of the absorption at 870 cm^{-1}. On evacuation of the sample at elevated temperatures, the band intensity at 950 cm^{-1} decreased and a new band grew up at 620 cm^{-1} (Curve 3 in Fig. 3). Introduction of $D_2{}^{16}O$ vapor to this evacuated sample gave a reverse spectral change, although the band at 950 cm^{-1} finally settled down to 960 cm^{-1} as in the case of silica gel - $H_2{}^{16}O$ system. The original spectra illustrated in Fig. 2 were restored by treating the deuterated sample with light water vapor.

3. Silica Gel - $H_2{}^{18}O$ System. A preliminary experiment showed that the introduction of $H_2{}^{18}O$ to a silica gel sample evacuated at 300°C for several hours gave small but definite isotopic shifts at the 3750 and 950 cm^{-1} bands, but not at any other bands. Evacuation and introduction of $H_2{}^{18}O$ were then repeated in the order from Curve 1 to Curve 12 in Fig. 4 in order to observe more precise spectral changes with time. As illustrated by Curve 3 of Fig. 4 (b), the band at

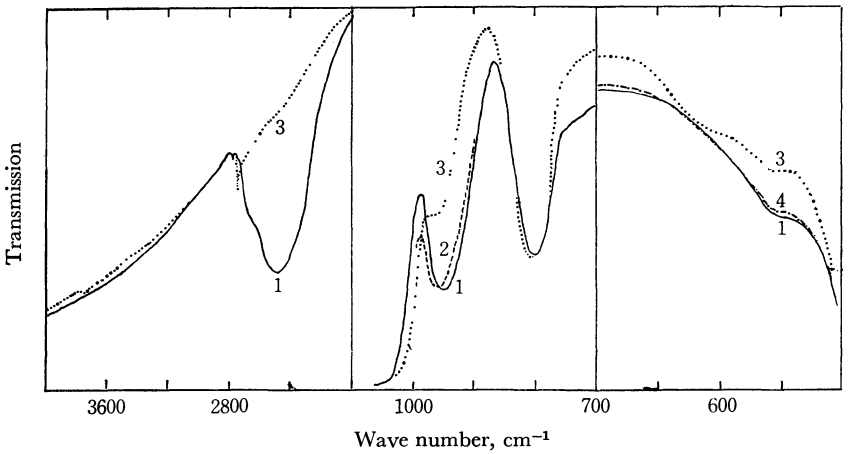

Fig. 3. Evacuation effect of a deuterated silica gel sample.
1——, on exposure to $D_2{}^{16}O$ at 5 mmHg; 2------, on exposure to D_2O^{16} at 9 mmHg after being evacuated at 200°C for 5 hr; 3·····, after being evacuated at 300°C for 5 hr; 4-•-•-•, on exposure to $D_2{}^{16}O$ at 12 mmHg after the 300°C evacuation

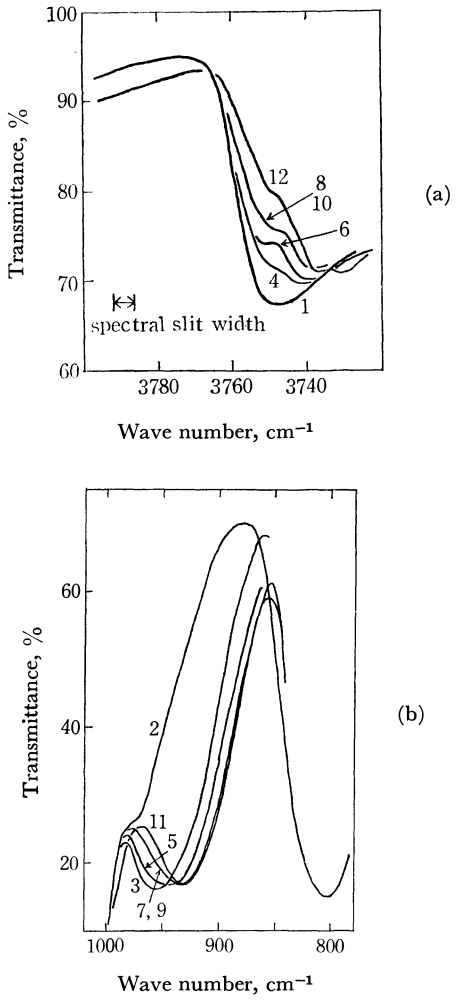

Fig. 4. Spectra of silica gel - $H_2{}^{18}O$ system.
1, evacuated; 2, evacuated at 200°C; 3, exposed to $H_2{}^{18}O$ vapor for 6 min; 4, evacuated; 5, exposed to $H_2{}^{18}O$ vapor for 25 min; 6, evacuated; 7, exposed to $H_2{}^{18}O$ vapor for 40 min; 8, evacuated; 9, exposed to $H_2{}^{18}O$ vapor for 100 min; 10, eavcuated; 11, exposed to $H_2{}^{18}O$ vapor at 100°C for 1 hr and cooled to room temperature in the vapor atmosphere; 12, evacuated.
Evacuation was conducted at room temperature for 5 hr and $H_2{}^{18}O$ vapor of 10 mmHg was introduced also at room temperature unless otherwise described.

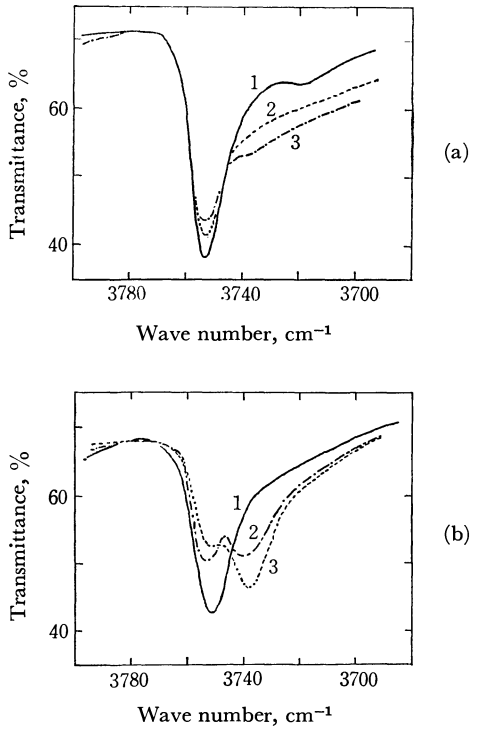

Fig. 5. Spectral changes in free OH stretching band of silica gel calcined at 800°C on exposure to $H_2{}^{18}O$ vapor at room temperature (a) and at higher temperatures (b).
a) before exposure (1), exposed to $H_2{}^{18}O$ vapor for 25 min (1), 2 hr more (2), 15 hr more (3), and 15 hr more (3). Each spectrum was recorded after evacuation at room temperature.
b) before exposure (evacuated at room temperature) (1), exposed to $H_2{}^{18}O$ vapor at 200°C for 20 hr and evacuated at room temperature (2), exposed at 260°C for 8 hr and evacuated at the same temperature (3).

960 cm^{-1} was produced immediately after the introduction of $H_2{}^{18}O$ at room temperature. This band, however, shifted to the lower wave number side with time and reached almost a steady value of 935 cm^{-1} after about 70 min. Successive treatment with $H_2{}^{18}O$ at 100°C gave more shifts, as seen in Curve 11. In a quite similar way, a new band around 3740 cm^{-1} grew up in accordance with the decrease of the OH stretching band at 3748 cm^{-1} with time and reached a steady state after 70 min (Curves 8 and 10, Fig. 4(a)). Treatment with $H_2{}^{18}O$ at 100°C gave a more distinct spectral change, as seen in Curve 12.

The exchange reaction with $H_2{}^{18}O$ was also conducted on a silica gel sample preliminarily calcined at 800°C for 30 hr, which gave very sharp free OH absorption on account of almost complete lack of background due to the broad hydrogen-bonded OH absorption around 3600 cm^{-1}. After the sample was evacuated at room temperature, it was exposed in $H_2{}^{18}O$ vapor at room temperature. As seen in Fig. 5(a), the free ^{16}OH absorption at 3751 cm^{-1} decreased very slowly in intensity and reached a steady state after 17 hr. A very small ^{18}OH absorption at 3737 cm^{-1} was observed. The result confirmed that the oxygen of the surface silanol groups was only partially exchanged by oxygen of $H_2{}^{18}O$ in adsorbed state at room temperature. Figure 5(b) shows the result on the same sample exposed in $H_2{}^{18}O$ vapor at 200 and 260°C and then evacuated. It turned out that the higher the temperature treatment with $H_2{}^{18}O$ the more promoted the oxygen exchange reaction.

Discussion

1. Assignment of the Bands at 960 and 870 cm^{-1}. The band at 870 cm^{-1} can definitely be attributed to the bending vibration of free Si–O–H groups on the surface, because the band increased in intensity on evacuation, at least at room temperature, and shifted to the position of 620 cm^{-1} on deuteration, its frequency being almost consistent with that calculated under the assumption that the band at 870 cm^{-1} was associated with Si–O–H bending vibration and that this can be

TABLE 2. SUMMARY OF THE INFRARED ABSORPTION BANDS OF SILICA GEL - WATER SYSTEM

Silica gel-$H_2{}^{16}O$ system (cm^{-1})	Silica gel-$D_2{}^{16}O$ system (cm^{-1})		Silica gel-$H_2{}^{18}O$ system (cm^{-1})		Assignment
Obsd	Obsd	Calcd	Obsd	Calcd	
* a) 3748	2755	2728	3740	3735	OH (or OD) stretching of free silanol groups
* b) 3751	—	—	3737	3737	
* 3400	2500	2474	**3400	3389	OH (or OD) stretching of water and hydrogen bonded silanol groups
* —	2780	—	—	—	OD asymmetric stretching of D_2O vapor
1870	1870	—	1870	—	Skeletal Si–O combination[c]
1640	1640	—	1640	—	Skeletal Si–O overtone[c]
* 1630	—	—	1630	—	HOH deformation of water
—	1440	—	—	—	HOD deformation[c]
1050 ~1200	1050 ~1200	—	1050 ~1200	—	Skeletal Si–O stretching[c,d]
* 950 ~960	950 ~960	—	935	916 ~925	Si–O stretching of silanol groups
* 870	620	633	870	—	Si–OH (or Si–OD) bending
805	805	—	805	—	Skeletal Si–O stretching[c,d]
560	560	—	560	—	Unknown, some skeletal vibration ?
470	470	—	470	—	Skeletal Si–O[d]

a) For silica gel without heat-treatment. b) For silica gel calcined at 800°C. c) Ref. 6. d) Ref. 5.
* Adsorption sensitive bands. **The band was so broad that an accurate determination of the small isotope shift was impossible.

treated by a simple harmonic oscillator model (Table 2).

The band at 960 cm^{-1} is conclusively assigned to the Si–O stretching vibration in surface silanol groups because of the following evidences. 1) No hydrogen isotopic effect was observed for this band. 2) The free OH stretching band and this band shifted quite simultaneously during the course of oxygen exchange reaction. 3) The observed values of the oxygen isotopic shift for these two bands were in harmony with those calculated according to a simple harmonic oscillator model, as illustrated in Table 2.

It should be pointed out, however, that no shift of the band at 960 cm^{-1} was observed immediately after the introduction of $H_2{}^{18}O$ on a silica gel sample. In other words, the band at 960 cm^{-1} was produced by rapid adsorption of $H_2{}^{18}O$ on the surface as in the case of $H_2{}^{16}O$ - silica gel system and then shifted gradually with the progress of the exchange reaction. The band is thus expected to be induced indirectly by the hydrogen bond formation of Si–OH with adsorbed water. This explanation was supported by the fact that the band around 960 cm^{-1} was produced by the introduction of various organic vapors which formed more or less hydrogen bonding with silanol groups. Such a stretching vibration sensitive to hydrogen bonding is not so strange; it is known that Si–O stretching vibration in silanol compounds[8] as well as C–O stretching vibration in alcohols[9] have a big dilution effect in nonpolar solvents.

We can safely rule out the possibility that the two bands at 960 and 870 cm^{-1} are associated with the overtone and combination of Si–O skeletal vibration, judging from their position and sensitivity to adsorption.

2. Reactivity of Silica Gel Surface. Mills and Hindin[10] have concluded indirectly from mass spectrometric analysis that the oxygen exchange reaction between surface silanol groups of silica gel and water takes place at a temperature above 100°C. The present work confirmed directly that the reaction proceeded considerably, but not completely, at room temperature on a silica gel treated at a low temperature below 300°C. Such a silica gel is readily dehydrated and rehydrated. The result can be explained as a consequence of the repetition of these two reactions according to the following scheme hitherto accepted[1]

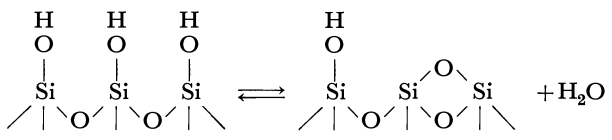

viz., the production of strained siloxan type species and some free OH groups from the clusters of OH groups adjacent to each other and the reverse reaction. Incomplete exchange of oxygen in the present case would be due to the presence of some genuinely free silanol groups, predominant for the silica gel treated at such a high temperature as 800°C.

8) K. Licht and H. Kriegsmann, *Z. Anorg. Allgem. Chem.*, **323**, 190, 239 (1963).

9) G. C. Pimentel and A. L. Mcclellan, "The Hydrogen Bond," W. H. Freeman & Company, San Francisco & London (1960), p. 140.

10) G. A. Mills and S. G. Hindin, *J. Amer. Chem. Soc.*, **72**, 5549 (1950).

Studies on the Electronic Spectra of the Semiquinones of Anthracene and Its Related Heterocycles. II

Hiroshi MASUHARA,[1] Michio OKUDA, and Masao KOIZUMI
Department of Chemistry, Faculty of Science, Tohoku University, Katahira, Sendai
(Received July 9, 1970)

The electronic structures of semiquinones of anthracene and its related heterocycles were calculated, using the open shell SCF procedure combined with configuration interaction calculations. A general classification and some peculiarities of the observed absorption spectra of these semiquinones can be readily explained by the present theoretical results. The effects of resonance integral and configuration interactions were examined in detail. The results obtained by considering the effect of hyperconjugation were added.

Semiquinones have been considered as reaction intermediates in photochemical reactions of aromatic compounds such as acridine dyes, xanthene dyes and triphenylmethane dyes. The photochemical behaviors and absorption spectra of anthracene semiquinone and its heterocycles have previously been reported.[2]

The absorption spectra of these semiquinones are classified into three groups; 1) the first band at 250 nm (4.9 eV in transition energy), 2) the second band at 350 nm (3.5 eV), and 3) the third band in the visible region (2.3—2.8 eV). However, some semiquinones have special features, *i. e.*, 1) anthracene semiquinone has no visible absorption, 2) acridine-*N* semiquinone has no first band, and 3) acridine-*C* semiquinone has a prominent peak at 281 nm.

Theoretical consideration of the electronic structures of their excited states is necessary for the assignment of each band. However, the electronic structures have not been reported because of the complexity of the treatment required for an open shell system.

Pople and Longuet-Higgins have proposed the method of semi-empirical SCF MO calculation with zero differential overlap approximation for open shell system and have calculated the transition energies of the benzyl radical.[3] The calculated energies are higher than the observed ones. Configuration interaction would be more important for the calculation of transition energies of open shell systems than for those of closed shell systems, as shown for the anion radicals of substituted benzenes.[4]

In this paper transition energies and oscillator strengths of the π-π^* transitions of anthracene semiquinone and its heterocycles will be reported and the assignment of absorption bands of the semiquinones will be decided by comparing those values with observed values.[2] The calculations were carried out with appropriate values of reasonance integrals β's. They were chosen by examining the effect of resonance integrals on the transition energies of anthracene anion radical, xanthene semiquinone, anion and cation radicals of six membered *N*-heterocycles. The effect of hyperconjugation of CH_2 group in the aromatic ring will be also examined for anthracene semiquinone and acridine-*N* semiquinone.

Method of Calculation

The method of calculation can be divided into two parts: 1) determination of LCAO-MO's by means of the semi-empirical open shell SCF method proposed by Pople and Longuet-Higgins,[3] and 2) generation of the spectroscopic states by configuration interaction.

The molecular orbitals obtained are the eigenfunctions of the Schrödinger equation

$$F\varphi_i = E_i\varphi_i \tag{1}$$

where F is the SCF Hamiltonian operator, E_i is the energy of ith molecular orbital. This equation can be derived by neglecting electronic repulsion integrals between the half occupied molecular orbital φ_m and other orbitals φ_i: (mi mm). The elements of the energy matrix (F) are given by the formulae

$$F_{pp} = -I_p + 0.5\times P_{pp}\times(pp\ pp) + \sum_{q\neq p}(P_{qq}-Z_q)\times(pp\ qq)$$
$$F_{pq} = \beta_{pq} - 0.5\times P_{pq}\times(pp\ qq) \tag{2}$$

where I_p and Z_p represent the ionization potential and the number of π electrons released from pth atom, respectively. The values of ionization potential and electron affinity of the π electron in the appropriate valence state are taken from the table of Pilcher and Skinner.[5]

Z_p is 1 for –C=, –N= and =O; is also 2 for –O– and –N–. Electronic Coulombic repulsion integrals between two atomic orbitals (pp qq) and resonance integrals β_{CX} were calculated using the Pariser-Parr approximation.[6]

The ground state and four types of excited states of the semiquinones are constructed as follows:

$$^2\Psi_G = |\varphi_1\bar{\varphi}_1\cdots\varphi_{m-1}\bar{\varphi}_{m-1}\varphi_m| \qquad G$$
$$^2\Psi_A = |\varphi_1\bar{\varphi}_1\cdots\varphi_i\bar{\varphi}_m\varphi_{m-1}\bar{\varphi}_{m-1}\varphi_m| \qquad A(i\text{–}m)$$
$$^2\Psi_B = |\varphi_1\bar{\varphi}_1\cdots\varphi_{m-1}\bar{\varphi}_{m-1}\varphi_k| \qquad B(m\text{–}k)$$
$$^2\Psi_{CA} = (|\varphi_1\bar{\varphi}_1\cdots\varphi_i\bar{\varphi}_k\cdots\varphi_{m-1}\bar{\varphi}_{m-1}\varphi_m| + |\varphi_1\bar{\varphi}_1\cdots\varphi_k\bar{\varphi}_i\cdots\varphi_m|)/\sqrt{2} \qquad CA(i\text{–}k)$$
$$^2\Psi_{CB} = (2|\varphi_1\bar{\varphi}_1\cdots\varphi_i\varphi_k\cdots\varphi_m| - |\varphi_1\bar{\varphi}_1\cdots\varphi_i\bar{\varphi}_k\cdots\varphi_m| - |\varphi_1\bar{\varphi}_1\cdots\varphi_k\bar{\varphi}_i\cdots\varphi_m|)/\sqrt{6} \qquad CB(i\text{–}k) \tag{3}$$

1) Present address: Department of Chemistry, Faculty of Engineering Science, Osaka University, Toyonaka, Osaka.

2) H. Masuhara, M. Okuda, and M. Koizumi, This Bulletin, **41**, 2319 (1968) (Series I).

3) H. C. Longuet-Higgins and J. A. Pople, *Proc. Roy. Soc., Ser. A*, **68**, 591 (1955).

4) A. Ishitani and S. Nagakura, *Theor. Chim. Acta*, **4**, 236 (1966).

5) G. Pilcher and H. A. Skinner, *J. Inorg. Nucl. Chem.*, **24**, 937 (1962).

6) R. Pariser and R. G. Parr, *J. Chem. Phys.*, **21**, 466 (1953).

where simple notations in the right column represent configurations in the left column, and i and k denote occupied and vacant orbitals, respectively.

Formulas of the transition energies and transition dipole moments are given in Ref. 3.

In the second step, configuration interaction calculations were carried out for 12 or 13 configurations of A and B types of singly excited states, and for 44 or 45 configurations of A, B, CA and CB types of singly excited states. The oscillator strength of each transition was evaluted by the equation

$$f = 1.085 \times 10^{-5} \times E \times M^2 \qquad (4)$$

where E represents the transition energy in cm^{-1} and M a transition dipole in Å.

Most calculations were carried out on the electronic computer HITAC 5020 in the electronic computer center of the University of Tokyo. The solution of CI determinant and other supplemental calculations were performed on the electronic computer NEAC 2230 in Tohoku University.

Parameterization: Effect of Resonance Integral

Calculated values of transition energies do not agree with observed ones in an open shell system as well as in a closed shell system. This discrepancy may be adjusted to some extent by the choice of the best experimental value of resonance integral, and by consideration of many configurations in the configuration interaction. The effects of both resonance integral and configuration interaction were examined carefully for some of the semiquinones and hydrocarbon anion radicals.

The Effect of Resonance Integral β_{CC}. The transition energies of the anthracene anion radical were calculated using the ordinary value of resonance integrals and by consideration of 13 excited configurations. The C–C bond distance and bond angles were taken as 1.39 Å and 120°, respectively. The value of β_{CC} used is −2.39 eV which corresponds to that of the neutral molecule. Using this value we obtained better agreement with the observed values. The results are shown in Table 1. Consequently, the value of β_{CC} for the neutral molecule was used in the following calculations.

Table 1. Transition energies of anthracene anion radical

E_{cal} (eV)	f_{cal}	E_{obs}[7] (eV)	f_{obs}[7]
1.830	— out of plane		
2.027	— x	1.686	0.95 x
2.538	— y	1.327	— y
3.382	— out of plane		
3.863	— y	3.161	— y
4.660	— x	3.781	1.50 x
4.834	— out of plane		
5.430	— out of plane		

7) R. S. Hoijtink, N. H. Velthorst, and P. J. Zandstra, *Mol. Phys.*, **3**, 534 (1961).

The Effect of β_{CX}. The transition energies of xanthene semiquinone were calculated using different β_{CO}'s (Fig. 1). Lower energy levels decrease and higher energy levels increase with the increase in the absolute value of resonance integral β_{CO}. The magnitude of the shift is about 0.2 eV for lower levels, which is within the accuracy of approximation in the calculations.

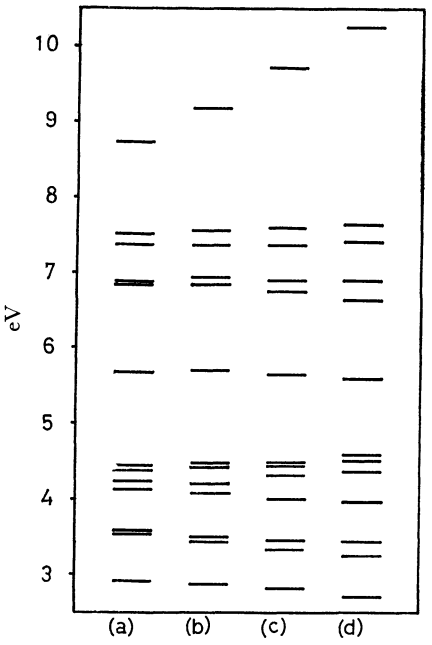

Fig. 1. The transition energies of xanthene semiquinone.
(a) $\beta_{CO} = -1.667$ eV (b) $\beta_{CO} = -1.945$ eV
(c) $\beta_{CO} = -2.223$ eV (d) $\beta_{CO} = -2.501$ eV

Small and more fundamental radicals such as anion and cation radicals of six-memberd *N*-heterocycles, allyl derivatives and pentadienyl derivatives were also used for examination of the effect of β_{CN} (Fig. 2). Although in the case of xanthene semiquinone the larger absolute value of β_{CO} gives the lower transition energies in ultraviolet region, the results for these radicals show the reverse effect. Thus, it is difficult to explain theoretically the shift of transition energy with the change of resonance integral. Consequently, the values of β_{CX} used in the calculations for semiquinones are also those for the neutral molecules.

Effect of Configuration Interaction

The results for the naphthalene anion radical with a different number of excited configurations in CI calculations are given in Table 2. This radical was chosen as a model for the examination of the effect of CI because it is intermediate in complexity between the benzyl radical and anthracene semiquinone. Our calculation of CI included 9 configurations of states A and B, and explained the observed absorption spectra rather well. The calculation including 29 configurations of states A, B, CA, and CB by Ishitani and Nagakura was more successful for explaining the transition energies.[4]

The contribution of states CA and CB becomes more

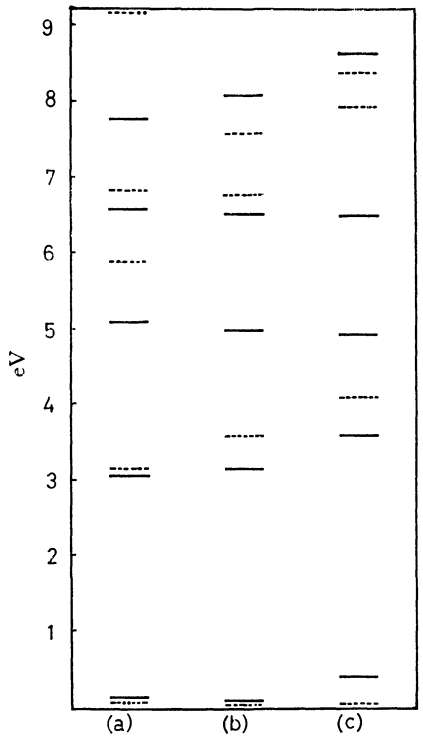

Fig. 2-A. The transition energies of anion radicals of pyridine and *s*-triazine.
——pyridine ·····*s*-triazine
(a) $\beta_{CN}=-2.576$ eV (b) $\beta_{CN}=-3.00$ eV
(c) $\beta_{CN}=-3.50$ eV

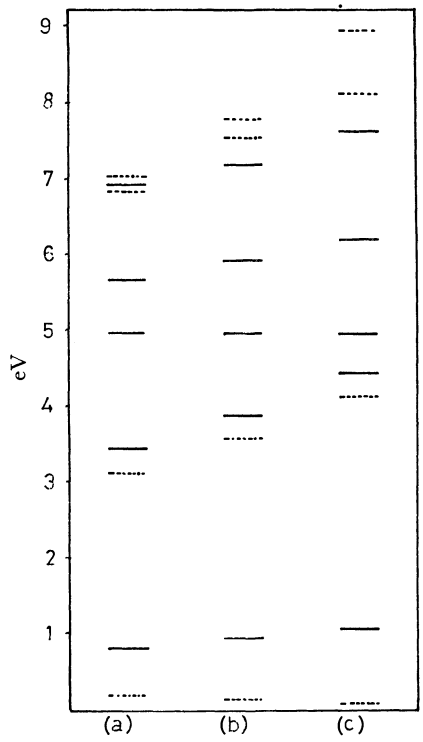

Fig. 2-B. The transition energies of cation radicals of pyridine and *s*-triazine.
——pyridine ------*s*-triazine
(a) $\beta_{CN}=-2.576$ eV (b) $\beta_{CN}=-3.00$ eV
(c) $\beta_{CN}=-3.50$ eV

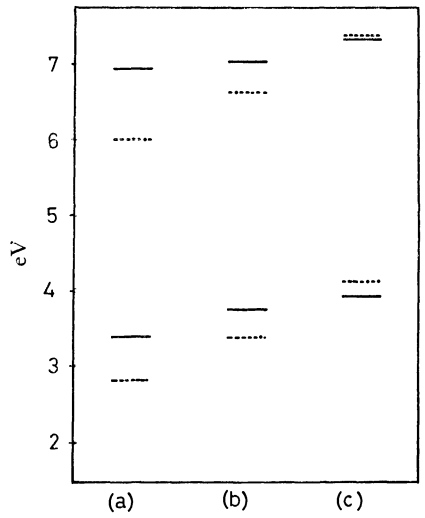

Fig. 2-C. The transition energies of allyl derivatives.
——N=C–C ------C=N–C
(a) $\beta_{CN}=-2.576$ eV (b) $\beta_{CN}=-3.00$ eV
(c) $\beta_{CN}=-3.50$ eV.

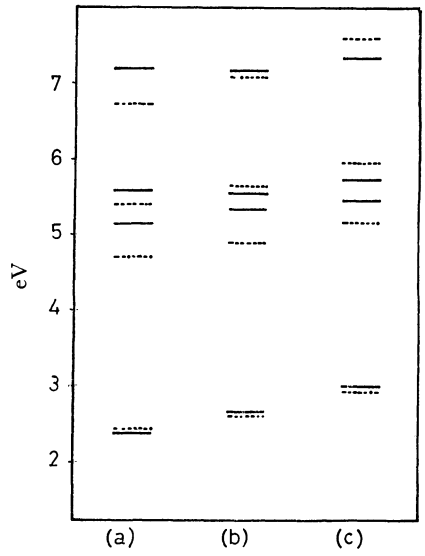

Fig. 2-D. The transition energies of pentadienyl derivatives.
——N=C–C=C–C ------C=N–C=C–C
(a) $\beta_{CN}=-2.576$ eV (b) $\beta_{CN}=-3.00$ eV
(c) $\beta_{CN}=-3.50$ eV

TABLE 2. RESULTS FOR THE NAPHTHALENE ANION RADICAL WITH DIFFERENT NUMBER OF EXCITED CONFIGURATIONS IN CI CALCULATIONS

a) E_{cal} (eV)	f_{cal}	b) E_{cal} (eV)	f_{cal}[4]	E_{obs}[7] (eV)	f_{obs}[7]
2.088	0.157	1.969	0.413	1.636	0.29(*x*)
2.989	0.015	2.657	0.057	hidded	
4.294	0.570	3.708	0.486	3.657	0.40(*y*)
		4.286	0.014	3.831	0.37(*x*)
5.051	0.734	5.032	0.876	4.228	
		6.374	2.516	5.443	

a) 9 configurations were taken into CI calculation.
b) 29 configurations were taken into CI calculation.

important for anthracene semiquinone and its heterocycles. Calculation of 12 or 13 configurations of states A and B could not explain the observed results. Generation of the spectroscopic states by including a number of configurations is indispensable for the calculations.

Results and Discussion

Transition energies and oscillator strengths of anthracence semiquinone and its heterocycles have been calculated with the same resonance integral as neutral molecules and also using the 44 or 45 configurations of singly excited states A, B, CA, and CB. The results are given in Table 3. The number of π electron in the semiquinones are 13 for anthracene and acridine-*N* semiquinones, and 15 for acridine-*C*, xanthene, and phenazine semiquinones. Molecular structures of these semiquinones assumed from a consideration of the experimental results are shown in Fig. 3 together with

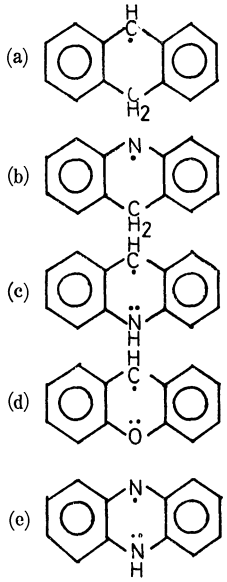

Fig. 3. Molecular structures.
(a) Anthracene semiquinone, 13π. (b) Acridine-*N* semiquinone, 13π. (c) Acridine-C semiquinone, 15π. (d) Xanthene semiquinone, 15π. (e) Phenazine semiquinone, 15π.
C–C, 1.39 Å. C–X, 1.36 Å.
Angles C–X–C, 117.5°. All otherangles, 120°.

the values of bond distances and bond angles. All the molecules are assumed to be planar. Calculated π–π^* transitions of these semiquinones can be divided into three groups. The first consists of strong transition (f=1.0) of about 6 eV transition energy, the second of moderate transitions (f=0.5—1.0) of about 4 eV and third of weak transitions of less than 3 eV. The calculated transitions correspond very well to the three groups of observed absorption bands. Discrepancies between theoretical and experimental results become smaller for lower transition energies. The magnitude of difference is about 1 eV for the 250 nm band (transition energy 4.9 eV), about 0.6 eV for the 350 nm band (3.5 eV) and 0.5 eV for the visible band (2.5 eV). The strong absorption band at 250 nm may be assigned to the π–π^* transition to the excited state, to which the CA configuration contributes predominantly. The other two bands may be assigned to the transition to the excited state which is a mixture of configurations A and B. By elimination of configurations which contribute to a small extent, each excited state can be expressed as follows.

$$\Psi(350\text{ nm}) = a\Psi_A - b\Psi_B$$
$$\Psi(\text{visible}) = b\Psi_A - a\Psi_B$$

The energy level of a half-occupied molecular orbital in an alternant hydrocarbon radical is located exactly in the center of the highest fully occupied orbital and the lowest vacant orbital, and then energies of configurations A and B are equal. When a carbon atom in this radical is replaced by a nitrogen atom, the half-occupied orbital is stabilized and its energy falls below its original level. The coefficient a for an alternant hydrocarbon radical is equal to $-b$, as proposed by Pople and Longuet-Higgins,[3] and thus f(visible) should be zero. This consideration explains well the experimental fact that anthracene semiquinone has no visible band. The line of argument is correct in the calculation which considers many configurations in CI calculations. The calculated oscillator strength of the visible band for anthracene semiquinone is 0.0000.

For heterocyclic radical, a is not equal to b, and f(visible) does not disappear. This is the reason why acridine-*N* semiquinone radical has a weak band in the visible region. It is possible to assign this weak band to a lone pair of N atom–π^* transition, but we have no evidence to show this.

The 350 nm and visible bands of acridine-*C*, phenazine and xanthene semiqunones are similarly interpreted, noting the difference of the number of molecular orbitals.

A special band at 281 nm of Acridine-*C* semiquinone can be assigned to the transition, whose excited state consists of CB(7—9) configuration predominantly and both CA(7—9) and A(6—8) configurations in a few percent. Although the transition to CB configurations is forbidden, this 281 nm transition has a moderate oscillator strength due to the contribution of CA(7—9) and A(6—8) configurations which have larger transition moments. A similar phenomenon can be expected in phenazine semiquinone, though this spectrum has not yet been observed.

The oscillator strength of the band at 250 nm for acridine-*N* semiquinone is 0.19 and much smaller than for other semiquinones. Thus, the other type of acridine semiquinone which has no band at 250 nm can be identified as acridine-*N* semiquinone.

The observed spectra of semiquinones are well explained by the present theoretical studies.

The Effect of Hyperconjugation

In the above section 13π type semiquinone structures were assumed for anthracene and acridine-*N* semiquinone, excluding the methylene group from the π-electron conjugated systems. The opposite extreme case is the one where electrons in the methylene group flow out to the π-electron conjugated systems. In this case it is appropriate to take the concept of hyper-

TABLE 3. THEORETICAL AND EXPERIMENTAL RESULTS

(a) Acridine-*C* semiquinone

	E_{cal} (eV)	f_{cal}	Direction	E_{obs} (eV)	Relative intensities
I	2.274	0.015	x	2.38	0.02
	2.769	0.071	x	2.52	0.08
	2.858	0.008	y		
	3.387	0.004	y		
II	3.840	0.103	y		
	3.917	0.093	x		
	4.048	0.282	x	3.42	0.16
III	4.852	0.089	x	4.45	0.24
	4.871	0.024	y	4.54	0.18
	5.238	0.003	y		
IV	5.707	0.127	x		
	5.771	0.000	y		
	5.794	2.139	x	4.95	1.00
	5.888	0.006	x		
	6.196	0.003	y		

(b) Xanthene semiquinone

	E_{cal} (eV)	f_{cal}	Direction	E_{obs} (eV)	R. I.
I	2.894	0.015	x	2.13	0.02
	3.050	0.004	y		
	3.171	0.016	x		
	3.234	0.000	y		
II	3.911	0.065	x		
	3.935	0.061	x		
	4.137	0.808	x	3.61	0.67
III	4.789	0.022	x		
	4.869	0.020	y		
	5.203	0.029	y		
IV	6.017	0.372	x	4.95	1.00
	6.100	0.225	y		
	6.301	0.064	y		

(c) Phenazine semiquinone

	E_{cal} (eV)	f_{cal}	Direction	E_{obs} (eV)	R. I.
I	2.669	0.000	x		
	2.758	0.021	y	2.06	0.05
	2.961	0.002	x		
II	3.619	0.005	y		
	3.724	0.045	x		
	3.870	0.068	y		
	3.947	0.515	x	3.35	0.36
III	4.844	0.016	y		
	5.032	0.220	x		
	5.230	0.002	y		
IV	5.739	0.661	x	5.27	1.00
	5.797	0.753	x	5.46	
	6.058	0.000	y		
	6.115	0.262	x	(ethylphenazil[8])	

8) K. H. Hausser and J. N. Murrell, *J. Chem. Phys.*, **27**, 500 (1957).

(d) Anthracene semiquinone

	13π model			15π model[a]			E_{obs} (eV)	R. I.
	E_{cal} (eV)	f_{cal}		E_{cal} (eV)	f_{cal}			
I	2.723	0.00002	x	2.916	0.000	x		
	3.251	0.000	y	3.131	0.004	y		
	3.274	0.000	x	3.650	0.001	x		
II	3.643	0.000	y	4.221	0.006	y		
	3.869	0.016	x	3.870	0.241	x		
	3.930	0.087	y	3.973	0.349	y	3.26	0.01
	4.129	0.985	x	4.220	0.721	x	3.54	0.72
III	4.753	0.000	x					
	4.824	0.000	y					
	5.244	0.023	y					
IV	5.640	0.000	y					
	5.691	0.000	x					
	6.207	0.922	x				4.95	1.00
	6.251	0.004	x					
	6.337	0.019	y					

a) Including the effect of hyperconjugation.

(e) Acridine-*N* semiquinone

	13π model			15π model[b]			E_{obs} (eV)	R. I.
	E_{cal} (eV)	f_{cal}		E_{cal} (eV)	f_{cal}			
I	2.538	0.126	x	2.654	0.136	x	2.19	0.17
	3.127	0.008	y	2.926	0.061	y		
	3.135	0.003	x	3.371	0.010	x		
II	3.731	0.005	y	4.127	0.081	y		
	4.068	0.026	x	4.124	0.244	x		
	4.126	0.086	y	4.366	0.292	y		
	4.286	0.870	x	4.504	0.629	x	3.52	1.00
III	4.776	0.021	x					
	4.940	0.009	y					
	5.471	0.010	y					
IV	5.770	0.001	y					
	5.782	0.001	x					
	6.161	0.190	x					
	6.225	0.070	y					

b) Including the effect of hyperconjugation.

NOTES.

1) The notations I, II, III, and IV in the tables, represent the groups of theoretical transition energies and differ from those appearing in the text.
2) In each group the observed bands are tentatively assigned to the theoretical bands whose f_{cal}'s are large.
3) R. I. denotes the relative intensity of observed band, the highest energy band being taken as a standard. It is easily estimated without precise molecular extinction coefficients.
4) As no data on phenazine semiquinone have been obtained for precise comparison, those on ethylphenazil are compared with theoretical results.
5) The transition with direction x is polarized along the long axis direction.

conjugation of methylene group into consideration. Here the 15π electron model was adopted for these semiquinones and the semi-empirical parameters used are the same as those reported by Morita.[9] This model treats the methylene group as a methylene cation. The real state of semiquinone molecule should be somewhere between these two models, which define the limits of delocalization of methylene electrons.

First the calculated orbital energies are compared with those of 13π electron models. The effect of hyperconjugation on transition energies appears on the orbitals, which have nothing to do with the observed electronic transitions. The difference of the orbital energies of the half-occupied orbitals in the 13π and 15π models is small (about 0.1 eV).

9) T. Morita, This Bulletin, **33**, 1486 (1960).

Calculated transition evergies and oscillator strengths are given in Table 3. The configurations included are 15 (cofigurations A and B) and the assignment of the 250 nm peak is omitted. The calculated intensity of the absorption polarized along the short axis direction is stronger in the 15π model. In the configurations of types A and B, calculated results are in better agreement with experimental ones in the 15π model than in the 13π model for both semiquinones. From the consideration of wave functions, it is concluded that the charge density of unpaired electron is lowered and more delocalized than that predicted by the 13π model. Although the larger conjugated systems, *i. e.* 15π model, have lower absorptions in general, it may be said that the unpaired electron and the electrons of methylene group are delocalized to some degree in anthracene and acridine-*N* semiquinones.

BULLETIN OF THE CHEMICAL SOCIETY OF JAPAN, VOL. 44, 43—48 (1971)

Modified INDO Calculations of the Electronic Structure of Organic Molecules. I. Electronic Excitation Energies of Some Carbonyl Compounds and Conjugated Dienes

Kizashi YAMAGUCHI and Takayuki FUENO

Department of Chemistry, Faculty of Engineering Science, Osaka University, Toyonaka, Osaka

(Received July 15, 1970)

The semi-empirical valence-shell SCF MO theory (the INDO method) by Pople *et al.* has been modified for the purpose of calculating the electronic excitation energies of organic compounds. All the necessary one-center parameters have been evaluated from the valence-state ionization data of Hinze and Jaffé, combined with the Slater-Condon atomic parameters. The INDO method thus modified has been applied to carbonyl compounds and conjugated dienes. The calculated excitation energies have been found to be satisfactory in many respects.

The all-valence-electrons SCF MO theory with intermediate neglect of differential overlaps (the INDO method) proposed by Pople *et al.*[1] is currently of gaining recognition as a promising route to theoretical estimation of dipole moments and unpaired spin distributions of various molecular species. Baird and Dewar[2] have modified the INDO method in order to calculate heats of formation and molecular geometry with "chemical" accuracy. This marked success of the theory in predicting the ground-state properties of molecules now urges chemists to explore the applicability of this theory to the calculations of electronic excitation energies of organic compounds.

Along the above line, Giessner-Prettre and Pullmann[3] have already examined the INDO method in its original form and found that the calculated transition energies are generally too great compared with the observed, despite extensive configuration interaction treatments. Thus, in order to be capable of reproducing the energies in fair agreement with observation, one is now required to take due consideration of electronic correlations, which have apparently been left out of account in the original INDO approximation.

One of the best approaches to the above problem will be a procedure involving semi-empirical evaluations of the two-electron repulsion integrals from the atomic spectroscopic data. The strategy is essentially the one that has already received wide acceptance in connection with the π-electron SCF MO theory of the Parier-Parr-Pople type.[4] Recently, Bene and Jaffé[5]

1) a) J. A. Pople, D. L. Beveridge, and P. A. Dobosh, *J. Chem. Phys.*, **47**, 2026 (1967). b) *Idem.*, *J. Amer. Chem. Soc.*, **90**, 4201 (1968). c) J. A. Pople and M. S. Gordon, *ibid.*, **89**, 4253 (1967). d) M. S. Gordon and J. A. Pople, *J. Chem. Phys.*, **49**, 4643 (1968). e) J. A. Pople, J. W. McIver, Jr., and N. S. Ostlund, *ibid.*, **49**, 2965 (1968). f) G. E. Maciel, J. W. McIver, Jr., N. S. Ostlund, and J. A. Pople, *J. Amer. Chem. Soc.*, **92**, 1 (1970). g) *Idem.*, *ibid.*, **92**, 11(1970).

2) a) N. C. Baird and M. J. S. Dewar, *J. Chem. Phys.*, **50**, 1262 (1969). b) *Idem.*, *J. Amer. Chem. Soc.*, **91**, 352 (1969). c) M. J. S. Dewar and S. D. Worley, *J. Chem. Phys.*, **50**, 654 (1969). d) N. Boden, M. J. S. Dewar, and S. D. Worley, *J. Amer. Chem. Soc.*, **92**, 19 (1970). e) M. J. S. Dewar and E. Haselbach, *ibid.*, **92**, 590 (1970).

3) C. Giessner-Prettre and A. Pullman, *Theoret. Chim. Acta* (Berl.), **13**, 265 (1969).

4) a) R. Pariser and R. G. Parr, *J. Chem. Phys.*, **21**, 466 (1953). b) J. A. Pople, *Trans. Faraday Soc.*, **149**, 1375 (1953).

have coupled this empiricism with Pople's simplest version of the all-valence-electrons SCF MO theory (the CNDO method)[6] Kato *et al.*[7] have also availed the empiricism in evaluating various integral parameters to be used in their own valence-shell theory analogous to the INDO method. In both these treatments, the transition energies obtained for various organic compounds are in satisfactory agreement with observation.

In this paper, a modification of the INDO method will be presented in order to calculate the excitation properties of conjugated compounds. All the necessary one-center parameters have been evaluated from the data for the valence-state ionization potentials and electron affinities compiled by Hinze and Jaffé,[8] in combination with the Slater-Condon atomic parameters.[1a] The procedure adopted for this parametrization is much the same as that in the MINDO method presented by Baird and Dewar.[2a] Our specific aim of the present treatment is to assess the applicability of the modified INDO theory to the calculations of electronic excitation energies of conjugated compounds, especially those of geometrical isomers. The results appear to be encouraging in most cases here investigated.

Method of Calculations

Since the INDO formulation has been described in detail by Pople *et al.*,[1a] there is no need to duplicate it here. Suffice it here to note that the Hamiltonian matrix elements for closed shell systems are given as follows:

$$F_{\mu\mu} = U_{\mu\mu} + \sum_{\lambda}^{A} [P_{\lambda\lambda}(\mu\mu|\lambda\lambda) - \frac{1}{2}P_{\lambda\lambda}(\mu\lambda|\mu\lambda)] + \sum_{B\neq A} (P_{BB} - Z_B)\gamma_{AB} \qquad (\mu \text{ on atom A}) \quad (1)$$

$$F_{\mu\nu} = \frac{3}{2}P_{\mu\nu}(\mu\nu|\mu\nu) - \frac{1}{2}P_{\mu\nu}(\mu\mu|\nu\nu) \qquad (\mu\ \nu, \text{ both on atom A}) \quad (2)$$

$$F_{\mu\nu} = \beta_{\mu\nu} - \frac{1}{2}P_{\mu\nu}\gamma_{AB} \qquad (\mu \text{ on atom A and } \nu \text{ on atom B}) \quad (3)$$

where P_{BB} and $P_{\mu\mu}$ are the atomic and orbital charge densities, respectively; $P_{\mu\nu}$ is the orbital bond order; Z_B is the core charge on atom B; γ_{AB} is the two-center electron repulsion integrals; $(\mu\mu|\lambda\lambda)$ and $(\mu\lambda|\mu\lambda)$ are one-center Coulomb and exchange integrals, respectively; $U_{\mu\mu}$ is the one-center core-electron attraction integral; and $\beta_{\mu\nu}$ is the core resonance integral.

In calculating the transition energies and moments, we have adopted the conventional virtual orbital approximations. The energies required to promote an electron from orbital i to virtual orbital j are given by the following expressions for singlet and triplet states, respectively:[5a]

$$\Delta^1 E = \varepsilon_j - \varepsilon_i - J_{ij} + 2K_{ij} \quad (4)$$

$$\Delta^3 E = \varepsilon_j - \varepsilon_i - J_{ij} \quad (5)$$

where ε_j and ε_i are the energies of the jth and ith molecular orbitals, and where J_{ij} and K_{ij} are the molecular Coulomb and exchange integrals. The dipole moment length for the i–j singlet-singlet transition is given by

$$M_{i-j} = 2\sum_{A}^{N}\sum_{\mu}^{A}\sum_{\nu}^{A} C_{i\mu}C_{j\mu}(\mu|\boldsymbol{r}_A|\nu) \quad (6)$$

where $\boldsymbol{r}_A$ is the coordinate vector operator of atom A.

Refinements of the transition energies by the configuration interaction treatments were not performed in the present calculations. For the geometries of the treated compounds, latest data from Ref. 9 were adopted. The solutions of the Hartree-Fock equations were required to be self-consistent to within 0.001 of all the resulting eigenvalues.

The above procedure was programmed in FORTRAN, and computations were carried out on the FACOM 230-60 Computer at the Kyoto University Computation Center.

Evaluation of Integral Parameters

One-center Parameters. The one-center integrals appropriate to the present calculations are (i) the core-electron attraction integrals, U_{ss} and U_{pp}, (ii) the Coulomb integrals, $(ss|ss)$, $(ss|xx)$, $(xx|xx)$ and $(xx|yy)$, and (iii) the exchange integrals of the types $(sx|sx)$ and $(xy|xy)$. In the framework of INDO approximations, all these energies are related with the Slater-Condon atomic parameters G^1 and F^2.[1a] The principle that we adopt for the evaluation of these one-center integrals is exactly the same as that of Pople *et al.*,[1a] except that we now follow a different semi-empirical procedure in estimating the average one-center electron repulsion integral, F^0.

For a second-row atom X with n valence electrons, the empirical electron repulsion energies may be estimated from[10]

$$g_{ss} = [E(X^-, s^2p^{n-1}) - E(X, sp^{n-1})] - [E(X, sp^{n-1}) - E(X^+, p^{n-1})] \quad (7)$$

$$g_{sp} = [E(X^-, s^m p^{n-m+1}) - E(X, s^{m-1}p^{n-m+1})] - [E(X, s^m p^{n-m}) - E(X^+, s^{m-1}p^{n-m})] \quad (8)$$

$$g_{pp} = [E(X^-, s^m p^{n-m+1}) - E(X, s^m p^{n-m})] - [E(X, s^m p^{n-m}) - E(X^+, s^m p^{n-m-1})] \quad (9)$$

where m may be 0, 1, or 2 wherever appropriate. The various g values can be evaluated from the valence-state ionization data of Hinze and Jaffé.[8] In the case

5) a) J. D. Bene and H. H. Jaffé, *J. Chem. Phys.*, **48**, 1807 (1968). b) *Idem., ibid.*, **48**, 4050 (1968). c) *Idem. ibid.*, **49**, 1221 (1968). d) *Idem., idem.*, **50**, 1126 (1969).

6) J. A. Pople, D. P. Santry, and G. A. Segal, *J. Chem. Phys.*, **43**, s129 (1965).

7) a) H. Kato, H, Konishi, and T. Yonezawa, This Bulletin, **40**, 1017 (1967). b) H. Kato, H. Konishi, H. Yamabe, and T. Yonezawa, *ibid.*, **40**, 2761 (1967).

8) a) J. Hinze and H. H. Jaffé, *J. Amer. Chem., Soc.*, **84**, 540 (1962). b) *Idem., J. Phys. Chem.*, **67**, 1501 (1963).

9) A. D. Mitchell, ed., "Table of Interatomic Distances and Configuration in Molecules and Ions," The Chemical Society, London (1958).

10) J. M. Sichel and M. A. Whitehead, *Theoret. Chim. Acta* (Berl.), **7**, 32 (1967).

of a valence-state carbon atom, for example, the g values are 12.10, 11.72, and 11.31 eV.

At the level of the INDO approximation, the empirical repulsion energies may be related with the Slater-Condon parameters by[11]

$$F^0(s,s) = g_{ss} \tag{10}$$

$$F^0(s,p) = g_{sp} + \frac{1}{6}G^1 \tag{11}$$

and

$$F^0(p,p) = g_{pp} + \frac{2}{25}F^2 \tag{12}$$

The parameter, F^0, for each atom with the ground state configuration, s^2p^{n-2}, may then be determined by averaging the values, $F^0(s,s)$, $F^0(s,p)$ and $F^0(p,p)$ over the electron pairs involved. Namely,

$$F^0 = \frac{1}{N}[F^0(s,s) + 2(n-2)F^0(s,p) + \frac{(n-2)(n-3)}{2}F^0(p,p)] \tag{13}$$

with

$$N = 1 + (n+1)(n-2)/2 \tag{14}$$

Using the F^0 values obtained as above and the G^1 and F^2 values given in Pople's INDO paper, the various two-electron parameters can be evaluated.

$$(ss\,|\,ss) = (ss\,|\,xx) = F^0 \tag{15}$$

$$(xx\,|\,xx) = F^0 + \frac{4}{25}F^2 \tag{16}$$

$$(xx\,|\,yy) = F^0 - \frac{2}{25}F^2 \tag{17}$$

$$(sx\,|\,sx) = \frac{1}{3}G^1 \tag{18}$$

$$(xy\,|\,xy) = \frac{3}{25}F^2 \tag{19}$$

The core-electron attraction integrals for atoms from boron to fluorine are[12a]

$$U_{ss} = -\frac{1}{2}(I_s+A_s) - \left(Z_A-\frac{1}{2}\right)F^0 + \frac{1}{6}\left(Z_A-\frac{3}{2}\right)G^1 \tag{20}$$

$$U_{pp} = -\frac{1}{2}(I_p+A_p) - \left(Z_A-\frac{1}{2}\right)F^0 + \frac{1}{3}G^1 + \frac{2}{25}\left(Z_A-\frac{5}{2}\right)F^2 \tag{21}$$

where I and A are the relevant valence-state ionization potential and electron affinity, respectively.

Table 1. Atomic parameters[a]

	H	C	N	O	F
U_{ss}	−13.595	−52.320	−72.078	−104.841	−131.248
U_{pp}		−44.648	−63.946	− 93.819	−116.272
F^0	12.845	11.715	12.860	15.897	17.233
G^1		7.285	9.416	11.817	14.486
F^2		4.727	5.961	7.250	8.594
I_s	13.595	19.603	23.777	33.234	39.922
I_p		12.309	16.598	20.013	20.452

a) Values given in units of eV.

11) Equations (7)—(9) in the present work, coupled with Eq. (3.16) of Ref. 1a, generate Eqs. (10)—(12). $F^0(p,p')$, where p and p' are different p orbitals centered on the same atom, were assumed to be equal to $F^0(p,p)$.

The one-center parameters evaluated as above for C, N, O, F atoms are listed in Table 1.

For an H atom, the parameters were $U_{ss}=-13.595$ eV and $F^0=12.845$ eV.

Two-center Parameters. The two-center repulsion integrals, γ_{AB}, between atoms A and B, which are R_{AB} apart, were evaluated by the Ohno approximation[12]

$$\gamma_{AB} = 14.397[R_{AB}^2+(\rho_A+\rho_B)^2]^{-1/2} \tag{22}$$

where

$$\rho_A = 7.199/F_A^0; \quad \rho_B = 7.199/F_B^0 \tag{23}$$

The core resonance integrals, $\beta_{\mu\nu}$, between atoms A and B were evaluated by the Wolfsberg-Helmholtz expression[13]

$$\beta_{\mu\nu} = \frac{1}{2}k^\omega S_{\mu\nu}(I_\mu^A+I_\nu^B) \tag{24}$$

where I_μ^A was taken as the valence-state ionization potential of μ AO of atom A. The parameters, k^ω, were so chosen as to reproduce the observed spectroscopic data, namely σ–π^* and π–π^* transition energies. For these purposes, discrimination between k^σ for σ orbitals and k^π for π orbitals was necessary, as was noted by Bene and Jaffé[5a] in their CNDO treatments of electronic spectra. The final values adopted were $k^\sigma=1.1$ and $k^\pi=0.9$.

Results and Discussion

The Values of k^σ *and* k^π. Bene and Jaffé[5] have shown in their CNDO treatments that, in order to obtain consistent spectroscopic data, the core resonance integrals $\beta_{\mu\nu}$ are necessary to be distinguished between σ and π orbitals. In order to examine whether or not

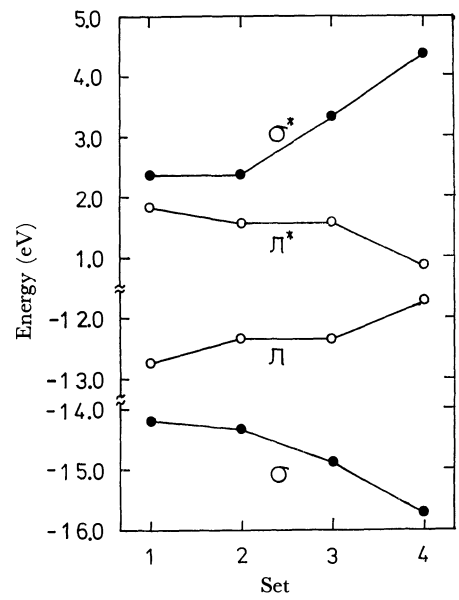

Fig. 1. Variations of the orbital energies of ethylene with the change in the resonance integral parameters used.
Set 1: $k^\sigma=1.0$ and $k^\pi=1.0$
Set 2: $k^\sigma=1.0$ and $k^\pi=0.9$
Set 3: $k^\sigma=1.1$ and $k^\pi=0.9$
Set 4: $k^\sigma=1.2$ and $k^\pi=0.7$

12) K. Ohno, *Theoret. Chim. Acta*, **2**, 219 (1964).
13) M. Wolfsberg and L. Helmholtz, *J. Chem. Phys.*, **20**, 837 (1952).

this discrimination will likewise be inevitable in the present INDO treatments, we have calculated Δ^1E of the ethylene molecule for various sets of k^σ and k^π values.

Shown in Fig. 1 are the highest occupied and lowest vacant orbital energies, both σ and π, calculated with different choices of k^σ and k^π.

Figure 1 clearly shows that both the σ–σ^* and π–π^* orbital energy separations tend to increase with the increasing k^σ and k^π values. Further, both the calculated π and π^* orbital heights are almost independent of k^σ. Likewise, the σ and σ^* orbital heights are relatively insensitive to the change in k^π. It is therefore obvious that both the σ–π^* and π–σ^* energy separations are dependent on both k^σ and k^π.

On the other hand, neither molecular Coulomb nor exchange integrals, J and K, shows material change with the variation of the core resonance integral parameters, as may be seen in Fig. 2. This facilitates adequate choice of k^σ and k^π values that may reproduce the observed transition energies.

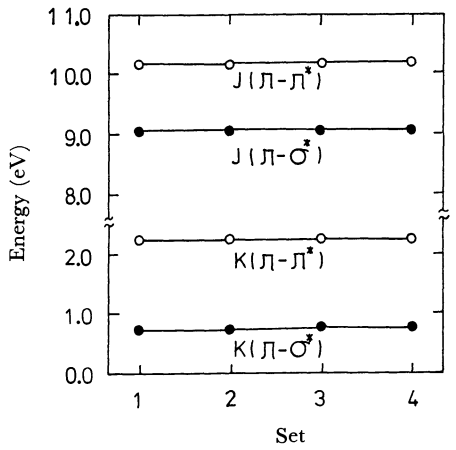

Fig. 2. Variations of the molecular repulsion integrals of ethylene with the change in the resonance integral parameters used.
The parameter sets are the same as those given in Fig. 1.

Similar analyses have been made for a few other compounds. It has been found that the parameter set $k^\sigma=1.1$ and $k^\pi=0.9$ are the most suitable to give consistent spectroscopic data in majority of cases here investigated. In the case of ethylene, the lower transition energies calculated with this parameter set were 8.27, 8.18, and 3.73 eV for the π–π^* ($^1B_{2u}$), σ–π^* ($^1A_{2u}$) and π–π^* ($^3B_{2u}$) transitions, respectively. Although these calculated values are somewhat deviated from the corresponding experimental data, 7.6, 6.4, and 4.8 eV,[3] these deviations are tolerable in view of the neglect of configuration interaction that may be important in such a highly symmetrical molecule.

Carbonyl Compounds. Formaldehyde, formic acid and formamide have been selected for test. The results obtained for lower transitions are summarized in Table 2, together with experimental data.

For each of the three compounds investigated, the calculated values of Δ^1E for both the n–π^* and π–π^* transitions have shown good agreement with the observed. Although the observed data for the triplet

TABLE 2. TRANSITION ENERGIES, ΔE, AND TRANSITION MOMENT LENGTHS, M, OF CARBONYL COMPOUNDS

Type	Symmertry[a]	Calcd		Obsd[b]	
		ΔE, eV	M, Å	ΔE, eV	f[c]
		Formaldehyde			
n–π^*	$^1A_2$	3.58	—	4.21	10^{-4}
σ–π^*	$^1B_2$	6.89	0.74	7.07	0.04
π–σ^*	$^1B_1$	7.75	0.65	8.18	
π–π^*	$^1A_1$	9.46	0.77	9.05	~0.1
n–π^*	$^3A_2$	3.14	0	3.12	
π–π^*	$^3A_1$	4.71	0		
		Formic acid			
n–π^*	S	4.68	0.22	5.5—5.8	
σ–π^*	S	6.87	0.27		
π–σ^*	S	7.60	0.32	7.4	
π–σ^*	S	7.64	0.70		
π–π^*	S	8.47	0.78	8.3	
n–π^*	T	4.34	0		
π–π^*	T	5.23	0		
		Formamide			
n–π^*	S	4.69	0.27	5.65	0.002
σ–π^*	S	7.24	0.56	6.80	0.06
π–σ^*	S	7.56	1.02	7.2—7.3, 7.8	0.240
π–π^*	S	7.80	0.76	8.6	~0.1
n–π^*	T	4.34	0		
π–π^*	T	5.26	0		

a) The symbols S and T denote that the excited states are singlet and triplet, respectively.
b) Observed values cited from Ref. 3.
c) Oscillator strength.

state excitation energies are limited, a good agreement is seen in formaldehyde. Therefore, the present parametrization seems to be satisfactory.

According to the present results, the second singlet-singlet transition band of the carbonyl spectra appearing at 7 to 8 eV is ascribed to a π–σ^* transition. As the assignment of this band is not entirely clear as yet,[3] no decisive assessment of the theory is permissive.

Butadiene and Glyoxal. Calculations have next been extended to butadiene and glyoxal. The electronic excitations of these compounds have already been the subject of the all-valence-electrons treatments by Kato *et al.*[7b] It will be of particular interest to compare the results between their treatments and the present.

The results of calculations for lower energy regions are summarized in Table 3, together with the experimental data. Agreements of the calculated results with the observed data are generally good, except for the energies for the singlet π–π^* transitions of the *s-trans* conformations of both butadiene and glyoxal, in which our calculated values are a little too great. For the n–π^* transitions of glyoxal, our results are more plausible than those of Kato *et al.*[7b]

In both treatments, the energies predicted for the n–π^* and π–π^* transitions of the *s-cis* conformers are lower than those of their *s-trans* counterparts. For the π–π^* transitions, the tendency agrees with observation.[14] Also in the n–π^* transition of glyoxal, there is

14) N. L. Allinger and M. A. Miller, *J. Amer. Chem. Soc.*, **86**, 2811 (1964).

TABLE 3. TRANSITION ENERGIES, ΔE, AND TRANSITION MOMENT LENGTHS, M, OF SOME CONJUGATED COMPOUNDS

Conformation	Type	Symmetry[a]	Calcd[b] ΔE, eV	Calcd[b] M, Å	Obsd ΔE, eV	Obsd f
			Butadiene			
s-trans	π–σ^*	^1A_u	6.52	0.24		
	π–π^*	^1B_u	6.61(6.38)	1.38(1.37)	5.7,[c] 6.0[d]	0.53[c]
	σ–π^*	^1A_u	6.83	0.47		
	π–π^*	^3B_u	3.65(4.18)	0 (0)	3.2[e]	
	π–σ^*	^3A_u	5.75	0		
s-cis	π–π^*	$^1B_1$	6.11(6.03)	0.93(0.95)		
	π–σ^*	$^1B_2$	6.51	0.42		
	σ–π^*	$^1B_2$	6.73	0.34		
	π–π^*	$^3B_1$	3.49(4.11)	0 (0)		
	π–σ^*	$^3B_2$	5.77	0		
			Glyoxal			
s-trans	n–π^*	^1A_u	2.79(3.22)	0.37(0.062)	2.72,[f] 3.23[g]	
	n–π^*	^1B_g	4.97(5.81)	— (0)	4.50,[f] 4.33[g]	
	n–π^*	^1B_g	6.10(7.20)	— (0)		
	n–σ^*	^1B_u	7.53	1.05		
	π–π^*	^1B_u	8.37(7.27)	1.09(1.167)	7.2—7.6[f]	
	n–π^*	^3A_u	2.44(2.68)	0 (0)	2.42[f]	
	n–π^*	^3B_g	4.61(5.22)	0 (0)		
	π–π^*	^3B_u	4.82(4.59)	0 (0)		
s-cis	n–π^*	$^1B_1$	2.78(3.18)	0.34(0.065)	2.66[g]	
	n–π^*	$^1A_2$	4.58(5.68)	— (0.034)	4.43[g]	
	n–π^*	$^1A_2$	6.03(7.08)	— (0.006)		
	n–σ^*	$^1B_1$	7.47	0.98		
	π–π^*	$^1B_2$	7.77(6.94)	0.66(0.805)		
	n–π^*	$^3B_1$	2.43(2.60)	0 (0)		
	n–π^*	$^3A_2$	4.20(5.07)	0		
	π–π^*	$^3B_2$	4.50(4.50)	0		
			trans-Crotonaldehyde			
s-trans	n–π^*	S	4.31	0.30	5.87[h]	
	π–π^*	S	6.91	1.38		
	n–π^*	T	4.07	0		
	π–π^*	T	4.08	0		
s-cis	n–π^*	S	4.29	0.28		
	π–π^*	S	6.57	1.08		
	n–π^*	T	4.06	0		
	π–π^*	T	4.07	0		

a) The symbols S and T denote that the excited states are singlet and triplet, respectively.
b) The values given in parentheses are those calculated by Kato *et al.* [7b]
c) Taken from Ref. 3.
d) Taken from Ref. 16b.
e) D. F. Evans, *J. Chem. Soc.*, **1960**, 1735.
f) J. W. Sidman, *J. Chem. Phys.*, **27**, 429 (1957).
g) Taken from Ref. 15.
h) H. H. Jaffé and M. Orchin, "Theory and Applications of Ultraviolet Spectroscopy," John Wiley & Sons, Inc., New York (1962), p. 213.

an indication of agreement between theory and experiment, if the Δ^1E values (2.66 and 4.43 eV) of a cyclic *cis*-α-diketone[15] may be assumed to closely approximate those of the *s-cis* conformation of glyoxal.

The trend that the π–π^* excitation energies calculated for *s-trans* conformation of a conjugated compound are greater than those for its *s-cis* conformer has long been noticed.[16–18] The trend now appears to be generally true with excitations including those of the n–π^* and σ–π^* types. This generalization seems not to be

15) N. J. Leonard and P. M. Mader, *J. Amer. Chem. Soc.*, **72**, 5388 (1950).

16) a) R. G. Parr and R. S. Mulliken, *J. Chem. Phys.*, **18**, 1338 (1950). b) R. Pariser and R. G. Parr, *ibid.*, **21**, 767 (1953).
17) M. Klessinger and W. Lüttke, *Z. Electrochem.*, **65**, 707 (1961).
18) A. Julg and J. C. Donadini, *Compt. rend.*, **252**, 1798 (1961).

affected by the level of sophistication at which the approximations used have been laid. The π–π^* and n–π^* transition energies calculated for *trans*-crotonaldehyde (I) have been included in Table 3, as an example that may serve to reinforce the above generalization.

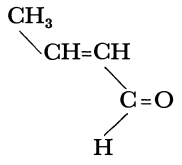

I (*s-trans*)

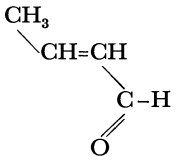

I (*s-cis*)

1,4-Disubstituted Butadienes. Butadiene derivatives that are substituted at the terminal carbon(s) have well-defined geometrical isomers, which can be separated from one another.

We here apply the present method of calculations to geometrical isomers of 1,4-difluorobutadiene (II) and sorbonitrile (III), to investigate the effect of geometrical isomerism on electronic spectra.

The reason for the choice of the F, CH_3, and CN groups as substituents is that they introduce no knotty problem of conformational multiformity with respect to the bond through which the substituents are linked with the sp^2 carbon. The butadiene framework will be assumed to be in the *s-trans* form, and various isomers will all be treated as having coplanar structure.

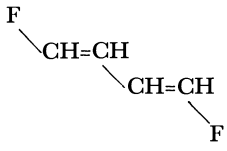

II (*trans,trans*)

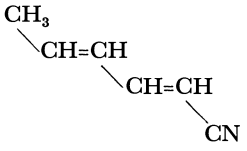

III (*trans,trans*)

The results of calculations for low energy transitions are summarized in Table 4, together with experimental data wherever available. The energies and moment lengths for the π–π^* transitions have also been calculated by the Pariser-Parr-Pople π-electron approximation (the PPP method).[4]

The singlet π–π^* transition energies and moment lengths calculated by the Modified INDO and the PPP methods are numerically almost equal. However, these energies are uniformly a little too great as compared with the observed values. Experimentally, the bathochromic (red) shifts are recognizable for the singlet π–π^* transitions on going from the *trans,trans* to *cis,cis* isomers. The theoretical results obtained by the PPP method agree with observation,[19] while those by the Modified INDO method partly fail to reproduce the tendency.

As for the triplet π–π^* transitions, there is no experimental data available. It will only be noted here that the values of Δ^3E calculated by the present method are all greater than those obtained from the PPP calculations.

Finally, according to the results of the present treatments, the singlet π–σ^* excited state of II is lower-lying than the singlet π–π^* excited state. Also, the moment lengths of the transitions leading to the former excited state is sufficiently great to warrant observation in usual cases. Since such transitions were not recorded together with the π–π^* transitions, the calculated values of ΔE are perhaps too small.

TABLE 4. TRANSITION ENERGIES, ΔE, AND TRANSITION MOMENT LENGTHS, M, OF BUTADIENE DERIVATIVES

Configuration	Type	Spin-state[a]	Calcd ΔE, eV	Calcd M, Å	Calcd (PPP)[b] ΔE, eV	Calcd (PPP)[b] M, Å	Obsd ΔE, eV
1,4-Difluorobutadiene-1,3							
cis,cis	π–σ^*	*S*	5.74	0.03			
	π–π^*	*S*	6.28	1.39	6.206	1.42	5.69[c]
	π–π^*	*T*	3.52	0	2.965	0	
trans,cis	π–σ^*	*S*	5.27	0.45			
	π–π^*	*S*	6.26	1.39	6.214	1.49	5.82[c]
	π–π^*	*T*	3.55	0	2.977	0	
trans,trans	π–σ^*	*S*	4.82	0.38			
	π–π^*	*S*	6.29	1.41	6.223	1.50	5.85[c]
	π–π^*	*T*	3.56	0	2.986	0	
Sorbonitrile							
cis,cis	π–π^*	*S*	5.65	1.49	5.137	1.83	5.17[b]
	π–π^*	*T*	3.51	0	2.880	0	
trans,trans	π–π^*	*S*	5.74	1.62	5.200	1.93	5.28[b]
	π–π^*	*T*	3.57	0	2.951	0	

a) The symbols *S* and *T* denote that the excited states are singlet and triplet, respectively.
b) Taken from Ref. 20.
c) Taken from Ref. 21.

Conclusions

The INDO method of Pople *et al.* is useful for the calculations of the quantities concerning the electronic transitions of unsaturated compounds, provided the two-electron repulsion integrals are evaluated from the atomic spectroscopic data. In particular, discrimination between the singlet and triplet states resulting from the n–π^* transition of carbonyl compound comes up with satisfactory accuracy. Success attained in the interpretations of the excited-state properties of molecules allows us to anticipate versatile usefulness of Dewar's MINDO method in various chemical problems.

19) In our separate piece of work, we have measured the lowest singlet π–π^* excitation energies of a great number of 1-substituted and 1,4-disubstituted butadienes and found that the *trans* and *trans,trans* isomers have greater excitation energies and oscillator strengths than do the corresponding *cis* and *cis,cis* isomers, with no exception whatsoever. The PPP calculations have been found to give results that are in accord with all these experimental data. Details will be presented elsewhere.[20]

20) T. Fueno and K. Yamaguchi, to be published.

21) H. G. Viehe, *Chem. Ber.*, **97**, 598 (1964).

The Infrared Spectra of Metallooctaethylporphyrins[1]

Hisanobu OGOSHI,* Naruhito MASAI,* Zen-ichi YOSHIDA,*
James TAKEMOTO,** and Kazuo NAKAMOTO**

* *Department of Synthetic Chemistry, Faculty of Engineering, Kyoto University, Yoshida, Kyoto*

** *Todd Wehr Chemistry Building, Marquette University, Milwaukee, Wisconsin* 53233

(Received July 16, 1970)

The infrared spectra of the Mg(II), Co(II), Cu(II), Zn(II), Pd(II), Ni(II), and Ge(IV)Cl_2 complexes of octaethylporphyrins have been studied over the range 4000—100 cm^{-1}. Metal sensitive bands have been observed at about 980, 920, 340, 230, and 130 cm^{-1}.

The metalloporphyrins constitute a large number of biologically important compounds. The wide range of biological activity is due in part to the nature of the interaction of the central metal atom with the porphyrine nucleus. Infrared spectroscopy provides one means by which the nature of metal-ligand interactions can be studied. Previous investigators have reported the infrared spectra of a number of naturally occurring porphyrins and chlorophylls.[2,3] We report here the results of an infrared investigation of the metal complexes of the symmetrical porphyrin, octaethylporphyrin (OEP).

Experimental

The preparation of the OEP complexes of Mg(II), Ni(II), Zn(II), Pd(II), Co(II), and Cu(II) have already been reported in the literature.[4,5] However, no micro analyses have been given for the Ni(II) and Pd(II) complexes.

Ni(II)-OEP. The Ni(II) complex was prepared by the treatment of OEP[6] with nickel acetate in glacial acetic acid.[7] Chromatography on alumina (neutral, activity II—III, Brockman) gave dark red crystals. Found: C, 73.78; H, 7,74; N, 8.91%. Calcd for $C_{36}H_{44}N_4Ni$: C, 73.10; H, 7.50; N, 9.47%.

Pd(II)-OED. The Pd(II) complex was prepared from 101 mg of OEP and 103 mg of $PdCl_2$ using the method of Theorell.[8] The NMR gave $\tau=8.08$ (24H, triplet, $-CH_2\underline{CH_3}$, $J=8.0$), $\tau=5.82$ (16H, quartet, $-\underline{CH_2}CH_3$, $J=7.2$) $\tau=-0.20$ (4H, singlet, $-CH=$).

Found: C, 66.29; H, 6.87; N, 8.32%. Calcd for $C_{36}H_{44}N_4Pd$: C, 67.65; H, 6.94; N, 8.77%.

Ge(IV)-OEP Dichloride. This complex was prepared from OEP and $GeCl_4$ in quinoline.[9] Purification was accomplished by chromatography of alumina using 3 : 1 benzene-chloroform mixture.

Found: C, 63.81; H, 6.56; N, 8.08%. Calcd for $C_{36}H_{44}N_4GeCl_2$: C, 63.94; H, 6.56; N, 8.28%.

Spectral Measurement. The infrared spectra were recorded on a Beckman IR 12 (4000—400 cm^{-1}, KBr pellet) and a Hitachi-Perkin-Elmer FIS-3 (400—100 cm^{-1}, Nujol mull). The UV spectra and NMR spectra were obtained by using a Hitachi EPS-3T spectrophotometer and a Jeolco JNM SH-60 spectrometer, respectively.

Results and Discussion

The observed frequencies of free OEP and its metal complexes are given in Table 1. All the OEP complexes show three weak absorptions above 3000 cm^{-1} which can be assigned to the C–H methine streching vibrations.[10,11] The three strong bands at about 2960, 2940 and 2870 cm^{-1} can be assigned to the C–H stretching vibrations of the ethyl group. Since the strong band at 2960 was very weak in the octamethylporphyrin complexes,[12] it can be attributed to the CH_2 stretching vibration. Free OEP also shows a medium band at 3320 cm^{-1} which is assigned to the N–H strecthing mode. This band disappears in the porphyrin complexes.[2,10]

As has been reported for etioporphyrin II[2,11] three medium to weak bands were observed at about 1670, 1600 and 1560 cm^{-1} and are assigned to the C=C and C=N stretching modes. The four bands at 1470, 1450, 1380, and 1370 cm^{-1} are probably due to the CH_2 asymmetric deformation and the CH_3 asymmetric and symmetric deformation vibrations. In general, the spectra of metal complexes are simpler than those of the free ligand in the region from 1500 to 1000 cm^{-1}. This is probably due to the fact that the symmetry of a metal complex is higher than that of the free ligand. For example, a weak band at 1412 cm^{-1} of OEP disappears on coordination to a metal. The two strong absorptions at 1268 and 1147 cm^{-1} are assigned tentatively to in-plane ring vibrations.[2,13] The latter is much stronger in the metal complex than in the free ligand. The two medium peaks at *ca.* 1150 and 1110 cm^{-1} are probably due to the ring deformation and CH in-plane bending mode of the pyrrole hydrogen, respectively. The bands at 1065 and 1057 cm^{-1} seem to be associated with the in-plane deformation of the porphyrin ring. The strong

1) This work was partly supported by an ACS-PRF unrestricted research grant (3318-C3,5).

2) L. J. Boucher and J. J. Katz, *J. Amer. Chem. Soc.*, **89**, 1340 (1967).

3) L. J. Boucher, H. H. Stain, and J. J. Katz, *ibid.*, **88** 1341 (1966).

4) J. H. Fuhrhop and D. Mauzerall, *ibid.*, **91**, 4174 (1969).

5) E. Samuels, R. Shuttleworth, and T. S. Stevens, *J. Chem. Soc., C*, **1968**, 145.

6) H. H. Inhoffen, J. H. Fuhrhop, H. Voigt, and H. Brockmann, Jr., *Ann. Chem.*, **695**, 133 (1966).

7) J. E. Falk, "Porphyrins and Metalloporphyrins," Elsevier, New York (1964), p. 137.

8) H. Theorell, *Enzymologia*, **4**, 192 (1932).

9) A. R. Kane, R. G. Yaleman, and M. E. Kennedy, *Inorg. Chem.*, **7**, 2588 (1968).

10) S. F Mason, *J. Chem. Soc.*, **1958**, 976.

11) W. S. Caughy, J. O. Alben, W. Y. Fujimoto, and L. J. York, *J. Org. Chem.*, **31**, 2631 (1966).

12) unpublished results.

13) J. E. Erdman, V. G. Ramsey, N. W. Kalenda, and W. E. Hanson, *J. Amer. Chem. Soc.*, **78** 5844 (1956).

Table 1. Observed frequencies of metal OEP complexes (cm^{-1})

Mg	Zn	Cu	Co	Ni	Pd	$GeCl_2$	OEP	Assignment
							3320	ν (N–H)
3132vw	3157vw	3195vw	3215vw	3185w	3185vw	3192w		
3175vw	3095vw	3123vw			3120vw	3150vw		ν $(C–H)_m$
3038vw	3045vw	3055w	3060w	3075w	3055w	3060w		
						3040w		
2965s	2962s	2965s	2955s	2965s	2965s	2965s	2970s	
2932s	2930s	2935s	2920s	2935s	2932s	2932s	2938s	ν $(C–H)_e$
2868s	2872s	2875s	2855s	2872s	2870s	2977s	2875s	
1708m		1720w	1715w					
1670m	1676w	1675w	1677m	1670w	1682m	1680m	1685w	
1604w		1602w	1615w	1618w	1608w	1621w	1675m	ν (C=C)
1580w	1580vw	1550w	1565w	1570w	1550m	1597w	1607m	ν (C=N)
	1532vw					1570w		
1467s	1467s	1478w	1465s	1467s	1469s	1501m	1503w	
		1465s				1480m	1469s	
1453s	1454s	1452s	1451s	1453s	1448s	1467s	1450s	δ (CH_2)
						1451s	1412w	δ (CH_3)
1390w	1378m	1381m	1381m	1385m	1382m	1386w	1397w	
1372m	1370m	1370m	1370m	1372m	1371m	1375m	1370m	
1317w	1317w	1317w	1316w	1318w	1318m	1320m	1317m	
	1303vw	1308vw	1306w	1309vw	1306w			
1268m	1268s	1271s	1271s	1272s	1273s	1272m	1277w	
							1260w	ring def.
1217m	1220m	1223m	1228m	1229m	1229m	1223m	1232w	
							1218m	
							1187m	
1148s	1147s	1148s	1147m	1147m	1152s	1152s	1147m	ring def.
							1140m	
1109m	1110m	1113m	1112m	1113m	1113m	1113m	1113s	δ $(C–H)_p$
1063sh	1064m	1066m	1064m	1064m	1064sh	1070s		
1057s	1057s	1058s	1057s	1054m	1055s	1057s	1057s	ring def.
1014s	1016s	1018s	1019s	1018s	1019s	1022s	1014s	ρ_t (C_2H_5)
							1003m	
977m	980m	985m	990m	992m	993m	990s	975w	ring. edf.
955s	953s	954s	955s	954s	958s	962	950s	ρ_r (C_2H_5)
911m	912m	919m	921w	923w	923w	920m		
	847w	846w	847sh	845sh		869w	892m	ν $(C–C)_e$
834s	836s	837s	837s	837s	839s	843m		π $(C–H)_m$
827s	827m	830s	830s	830s	835sh	809m	820m	ν $(C–C)_e$
746s	748m	750m	753m	754m	745s	787m	745s	π (ring)
						751m		
731m	730sh	730m	733m	732m	734m	730m		
	728m	717w	715w	713w	720m	707m	720m	π (ring)
703m	700m	697m	697m	700m	700w		698m	
						676m	675m	
						630m	667sh	
						613m	615w	
						607m	572	
	530w	535w				525w	512w	
	515w	520w					490w	
495vw	475vw	475vw	477vw	475wv	487w	480m	475w	
	400	443					447w	
347sh						375w		
336s	334s	336s	351s	355s	348s	348s	328m	ν (M–N)+ligand
	310w	313w			320w		320—310	
						306s	(w,br)	ν (Ge–Cl)
214s	203m	234m	264m	287w	275vw	245w		ν (M–N)
129s,b	121s	152w	157w			131w	159w	

$(C–H)_m$, methine hydrogen; $(C–H)_e$, ethyl hydrogen; $(C–H)_p$, pyrrole hydrogen; ν, stretching; δ; in-plane bending; π, out-of-plane bending; ρ_t, twisting; ρ_r, rocking

Table 2. Metal sensitive bands and electronic spectra

Metal	Frequency (cm^{-1})					λ_{max} (mμ) (log ε_{max})[c]		
						α	β	Soret
Mg	977[a]	911[a]	336[b]	214[b]	129[b]	582 (4.01),	544 (4.11),	410 (5.45)
Zn	980	912	334	203	121	570 (4.18),	533 (4.05),	402 (5.32)
Cu	985	919	336	234	152	562 (4.40),	526 (4.11),	399 (5.88)
Co	990	921	351	264	157	554 (4.29),	521 (3.99),	392 (5.14)
Ni	992	923	355	287	—	554 (4.39),	519 (3.99),	394 (5.24)
Pd	993	923	348	275	—	547 (4.48),	511 (4.00),	394 (5.19)

a) KBr pellet, b) Nujol mull, c) in $CHCl_3$

band at 1016 cm^{-1} is probably due to the CH_2 twisting vibration of the ethyl group which is slightly sensitive to the metal ion. In fact, it is absent in the spectra of Cu(II)-porphin[10] The increase in absorption intensity of 1016 cm^{-1} may be attributed to the coupling with the in-plane ring deformation vibration at 980 cm^{-1}.

Metal sensitive bands are usually observed near 1000 cm^{-1} in various types of metalloporphyrins.[2,14] OEP complexes show three bands at about 980, 955, and 912 cm^{-1}; the 980 and 912 bands are dependent on the nature of the metal (see Table 2). This metal ion dependence is not as large as that observed for proto- and hematoporphyrin dimethyl esters[2] and is of a comparable magnitude to that observed for tetraphenylporphyrin complexes.[14] The 955 and 912 cm^{-1} bands do not appear in the spectra of Cu(II)-porphyrin.[10] These two bands may therefore be assigned to the rocking vibrations of the ethyl groups. The 980 and 912 cm^{-1} bands shift to higher frequencies in the order Pd≈Ni>Co>Cu>Zn>Mg which is the same order as observed for the hypsochromic shift of the α, β, and soret bands in the electronic spectra (Table 2). Free OEP also shows bands in this region at 975, 950, and 892 cm^{-1}. The 980 cm^{-1} band may be due to a ring deformation vibration involving the motion of a metal atom. The metal dependence of the 912 cm^{-1} band may indicate that this ethyl rocking mode couples strongly with the in-plane deformation vibration of the porphyrin ring.

The strong bands at about 835 cm^{-1} are assigned to the CH out-of-plane deformation vibration of the methine group.[15] The bands at about 848 and 830 cm^{-1} are possibly assigned to the C–C streching of the ethyl group. Several strong bands are observed at about 750, 730, and 700 cm^{-1}. A similar set of bands has been observed for Cu-porphyrin.[10] Consequently, these bands may be assigned to the out-of-plane deformation of the porphyrin ring. The weak bands which occur in the 650—400 cm^{-1} range are difficult to assign empirically.

Far-Infrared Spectra. The metal nitrogen streching vibrations in metalloporphyrins are expected to appear in the far-infrared region. Free OEP shows weak bands at 328 and 320—310 cm^{-1}. The former band shifts to higher frequencies and becomes stronger by complex formation. It may be due to a ligand vibration coupled slightly with a metal-nitrogen stretching mode. The Ni, Co, and Pd complexes exhibit the highest frequencies at 355, 351, and 348 cm^{-1}, respectively, (Table 2), indicating that the metal-nitrogen bond is stronger in the Ni, Co, and Pd than in the Mg and Zn complexes.

In the 300—200 cm^{-1} region, medium to weak bands have been observed for metal complexes but not for free OEP ligand. The frequency of this band is most sensitive to the nature of the metal and increases in the order Zn<Mg<Cu<Co<Pd<Ni. This band may due to a relatively pure metal-nitrogen streching vibraration. However, the exact nature of this vibration cannot be determined without normal coordinate analysis. It is interesting to note that the frequency order of these metal-sensitive bands in a series of metal ions studied is similar to that found for the electronic transitions in the UV region (Table 2). The stronger coordination in metalloporphyrins causes the shift of the α, β, and soret bands to the shorter wave length.[16] This would be attributed to the stabilization in the ground state through π-conjugative interaction between $2p\pi$-orbitals of the ligand and *d*-orbitals of the metal ion.[16,17]

Finally, OEP–$GeCl_2$ exhibits the Ge–Cl stretching mode at 360 cm^{-1}. This frequency is similar to that reported for the $GeCl_6^{2-}$ ion (293 cm^{-1}).[18]

14) D. W. Thomas and A. E. Martell, *J. Amer. Chem. Soc.*, **81**, 5111 (1959).
15) R. Bonnett, A. D. Gale, and G. F. Stephenson, *J. Chem. Soc., C*, **1967**, 1168.
16) M. Gouterman, *J. Chem. Phys.*, **30**, 1139 (1956).
17) M. Zerner and M. Gouterman, *Theoret. Chim. Acta*, **4**, 44 (1966).
18) D. M. Adams, J. Chatt, J. M. Davison, and J. Gerratt, *J. Chem. Soc.*, **1963**, 2198.

Solvent Effects on the Spin-Lattice Relaxation Times and Chemical Shifts of *N*-Methylacetamide and *N,N*-Dimethylacetamide

Kazuo SATO and Atsuo NISHIOKA

Department of Polymer Engineering, Tokyo Institute of Technology, Meguro-ku, Tokyo

(Received July 20, 1970)

The spin-lattice relaxation time T_1 and chemical shift of *N*-methylacetamide (NMA) and *N,N*-dimethylacetamide (DMA) were measured in D_2O and CCl_4 solutions. In D_2O solution, it has been found that the weak interamide hydrogen bonding of NMA does not affect the spin-lattice relaxation entirely, and the molecular motion of NMA and DMA is almost identical. However, quite different results were obtained for CCl_4 solution. The molecular association of NMA in CCl_4 solution is strong enough to exhibit appreciable effects on spin-lattice relaxation. The life time of the associated molecules has been estimated to be longer than 10^{-10}—10^{-11} sec. The association of DMA at high concentration region in CCl_4 could be verified from the concentration dependence of the spin-lattice relaxation rate as well as chemical shift.

The contribution of the peptide bond character and the interamide hydrogen bonding to the conformational stability of the synthetic polypeptides and proteins in solutions have long been studied.[1] Quantitative information about model compounds which contain peptide bonds is expected to provide basic insight into the complexity of macromolecules.

So far, the interamide interaction, the double bond character and the hindered internal rotation of various amide compounds in solutions have been studied quantitatively, mainly by using IR, high resolution NMR and thermodynamic technique. IR studies of *N*-methylacetamide in various solvents by Klotz, Fransen, and Fornham[2,3] led us to conclude that in aqueous solution the interamide hydrogen bonding has no intrinsic strength, but is moderately strong in apolar solvent. Recently, Rabinovitz and Pines[4,5] and Neuman *et al.*[6] have studied the proton chemical shift of *N,N*-dimethylformamide, *N,N*-dimethylacetamide in CCl_4 and from the observed concentration dependence of chemical shift they argued the dimerization of amides. Equilibrium properties have been studied extensively, and quantitative features have been obtained and discussed. However, non-equilibrium properties such as microscopic molecular motion or relaxation process have not been studied in detail.

In this study, the proton spin-lattice relaxation time and chemical shift were measured on *N*-methylacetamide (NMA) and *N,N*-dimethylacetamide (DMA) in D_2O (aqueous environment) and CCl_4 (apolar environment). As is well known, the proton spin-lattice relaxation in diamagnetic liquid is mainly due to the dipole-dipole interactions between the nuclear magnetic moments both in the same molecule and in the neighboring molecules.

For most molecular liquids, the observed spin-lattice relaxation time T_1 can be expressed as[7,8]

$$(1/T_1) = (1/T_1)_{\text{rot.}} + (1/T_1)_{\text{transl.}} \quad (1)$$

$$(1/T_1)_{\text{rot.}} = \frac{3}{2}\hbar^2\gamma^4\sum_j \langle r_{ij}^{-6}\rangle \cdot \tau_c \quad (2)$$

$$(1/T_1)_{\text{transl.}} = 3\pi^2\hbar^2\gamma\eta N/kT \quad (3)$$

where $(1/T_1)_{\text{rot.}}$ represents the intramolecular contribution depending on the rotational motion of the molecule, and $(1/T_1)_{\text{transl.}}$ represents the intermolecular contribution which depends on the relative translational motions of the molecules. r_{ij} is the distance between ith and jth nucleus; τ_c is the rotational correlation time for molecule (including the effect of internal rotation in certain circumstances): η and N are solution viscosity and spin density, respectively, and all other notations have their usual meanings.

We measured T_1's and the chemical shifts at various solute concentrations, and obtained the intramolecular spin-lattice relaxation time $(T_1)_{\text{rot.}}$ by the dilution procedure.[9,10] We estimated τ_c values taking molecular geometry into consideration. Based on the results obtained on τ_c values, the concentration dependence of T_1 and the chemical shifts we would like to discuss the molecular motion, intramolecular interaction and the peptide bond character in aqueous and apolar environments.

Information on molecular motion or the relaxation process should help us understand the properties of these molecules in detail in relation to the information from equilibrium measurements.

Experimental

Materials. NMA and DMA were reagent grade samples from Tokyo Kasei Co., Ltd. and used without further purification, because their NMR spectra did not show any observable impurity signals. Heavy water and carbon tetrachloride were provided by E. Merck AG, Darmstadt and

1) For example S. Mizushima, "Structure of Molecules and Internal Rotation," Academic Press, New York (1954), Chap V 1, p. 117.

2) I. M. Klotz and J. S. Fransen, *J. Amer. Chem. Soc.*, **84**, 3461 (1962).

3) I. M. Klotz and S. B. Farnham, *Biochemistry*, **7**, 3879 (1968).

4) M. Rabinovitz and A. Pines, *J. Chem. Soc., B*, **1968**, 1110.

5) M. Rabinovitz and A. Pines, *J. Amer. Chem. Soc.*, **91**, 1585 (1969).

6) R. C. Neuman, Jr., W. R. Woolfenden, and V. Jonas. *J. Phys. Chem.*, **73**, 3177 (1969).

7) N. Bloembergen, E. M. Purcell, and R. V. Pound, *Phys. Rev.*, **73**, 679 (1948).

8) A. Abragam, "The Principle of Nuclear Magnetism," Oxford (1961).

9) G. Bonera and Rigamonti, *J. Chem. Phys.*, **42**, 171 (1965).

10) J. W. Emsley, J. Feeny, and L. H. Sutcliffe, "Progress in Nuclear Magnetic Resonance Spectroscopy," Vol. 3, Pergamon Press, London (1967), Chap. 5.

Tokyo Kasei Co., Ltd., respectively. The atmospheric oxygen dissolved in the sample was removed carefully by several freeze-pump-thaw cycles in NMR tube (ϕ=0.5 cm), and the sample tube then was sealed off in a vacuum (10^{-5}—10^{-6} mmHg). After sealing, the sample tube was immediately subjected to experiment.

NMR Measurements. A JNM-C-60H spectrometer of Japan Electron Optics Lab. operated at 60 MHz was used. Measurements of T_1 were carried out at 25±1°C in almost all cases by the adiabatic rapid passage and saturation recovery methods.

Experimental errors were smaller than ±3% for T_1 values longer than about 3 sec. For T_1 smaller than 3 sec, errors were smaller than ±5%. The signal of *N*-methyl protons of NMA splits into doublet due to the indirect spin-spin coupling with N–H proton. However, because of the small coupling constant ($J\simeq$4.8 Hz), only one recovery curve with a broad line width was observed.

trans- and *cis*-*N*-Methyl groups with respect to the carbonyl group of DMA undergo different shielding effects due to the double bond character of the central C–N bond. Thus, *N*-methyl proton resonance reveals a doublet ($\Delta\nu \simeq$ 9—10 Hz).

Two distinct recovery curves were then obtained, but almost all T_1 values calculated from these were equal within experimental errors. Thus we adopted the average value as T_1 for both *N*-methyl protons. The chemical shift was measured at 25±1°C by the usual side-band-technique using Tetramethylsilane (TMS) as an internal reference.

Results and Discussion

The concentration dependence of the relaxation rate $1/T_1$ for methyl protons of NMA and DMA in D_2O and CCl_4 solutions is shown in Figs. 1 and 2, respectively. T_1's of *C*-methyl and *N*-methyl protons in D_2O solutions of NMA or DMA and CCl_4 solution of NMA are equal within experimental errors, but not in CCl_4 solution of DMA. From the observed linear relation between $1/T_1$ and concentration, it is possible to estimate $(1/T_1)_{rot.}$ of the solute molecule for each solution, except for DMA in CCl_4 solution. However, at the concentration range above and below about 3 mol/*l*, linearity, appears again, and an estimation of $(1/T_1)_{rot.}$ or τ_c values is possible by extrapolating to infinite dilution. The results of $(T_1)_{rot.}$ thus obtained and τ_c

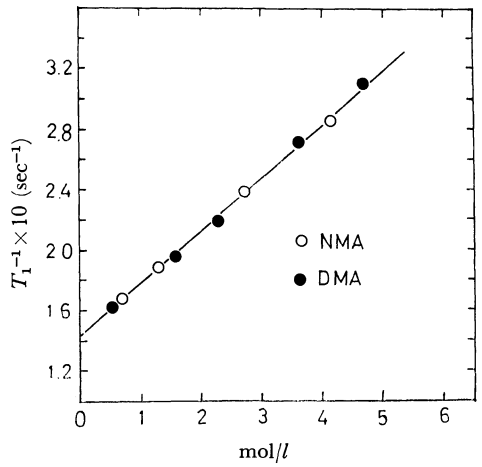

Fig. 1. Relaxation rate *vs.* solute concentration for MNA and DMA in D_2O solutions at 25°C.
T_1's of *C*- and *N*-methyl protons are equal within the experimental errors, so expressed by the same experimental points.

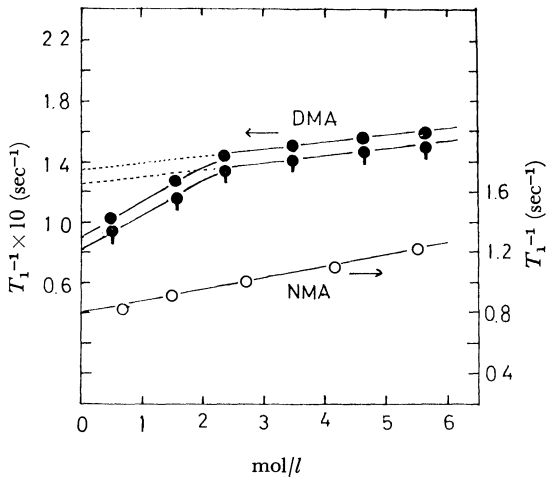

Fig 2. Relaxation rate *vs.* solute concentration for NMA and DMA in CCl_4 solutions at 25°C.
T_1's of *C*- and *N*-methyl protons of NMA are equal and expressed by the same experimental points (open circles). ●—T_1's of *C*-methyl protons of DMA. ◐—T_1's of *N*-methyl protons of DMA.

TABLE 1. T_1 AND τ_c VALUES OF NMA AND DMA IN D_2O, CCl_4 SOLUTION AT 25°C

Solvent	Solute					
	NMA			DMA		
	Observed protons	$(T_1)_{rot.}$	$\tau_c\times10^{12}$	Observed protons	$(T_1)_{rot.}$	$\tau_c\times10^{12}$
D_2O	$-\overset{O}{\overset{\|\|}{C}}-CH_3$	6.90 sec	2.58 sec	$-\overset{O}{\overset{\|\|}{C}}-CH_3$	6.90 sec	2.5_4 sec
	$-\overset{\|}{N}-CH_3$	6.90	2.50	$-\overset{\|}{N}(CH_3)_2$	6.90	2.4_8
CCl_4	$-\overset{O}{\overset{\|\|}{C}}-CH_3$	1.25	14.4	$-\overset{O}{\overset{\|\|}{C}}-CH_3$	11.1 7.40	τ_{c1}: 1.5_9 τ_{c2}: 2.4_0
	$-\overset{\|}{N}-CH_3$	1.2_5	$14._0$	$-\overset{\|}{N}(CH_3)_2$	12.2 7.8_0	τ_{c1}: 1.4_1 τ_{c2}: 2.2_0

τ_{c1} and τ_{c2} represent the correlation times estimated by extrapolating to infinite dilution from the low and high concentration regions, respectively.

estimated by using Eq. (2) are shown in Table 1. It was found that the relaxation process of NMA molecule in D_2O solution is very similar to that of DMA. Corresponding results and $\tau_c = 1.6 \times 10^{-12}$ sec were also obtained at 45°C. However, in CCl_4 solution a quite different relaxation tendency resulting from aqueous solution was observed for both NMA and DMA molecules.

In order to calculate the interprotonic distance, we adopted the molecular geometry of NMA proposed by Pauling.[11] We have assumed that the geometry of DMA is the same as that of NMA except for the substituted *N*-methyl proton. Moreover, internal rotation of methyl groups is assumed to be almost free. We adopted 1.78 Å for the interprotonic distance in methyl group.

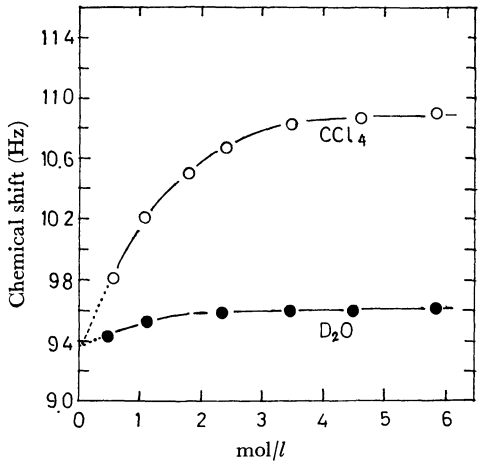

Fig. 3. Concentration dependence of the chemical shift between the two *N*-methyl resonance signals of DMA in CCl_4 (open circles) and D_2O (solid circles) solutions at 25°C.

The concentration dependence of the chemical shift of *N*-methyl protons of DMA both in D_2O and CCl_4 solutions at 25°C is shown in Fig. 3. The behavior in CCl_4 solution agrees qualitatively with the results of Neuman *et al.*[6] The concentration dependence of the chemical shift seems to be similar in its linearity to the concentration dependence of $1/T_1$. The concentration dependence of N–H proton chemical shift of NMA in CCl_4 solution is shown in Fig. 4 with the additional results[12] in $CDCl_3$ solution. It is easily seen that in CCl_4 solution the chemical shift of N–H proton appears at a lower field than that in $CDCl_3$ solution, and depends on the concentration slightly. Considering that the behavior of N–H proton chemical shift of NMA is mainly due to the interamide hydrogen bond and the proton participating in the hydrogen bonding resonates at a lower field, it is suggested that in CCl_4 solution this molecule could form relatively strong intermolecular hydrogen bonding at about 0.5 mol/*l*. This is in accordance with the conclusion of Klotz and Fransen[2] by IR method. They concluded that almost all the molecules (NMA) associate through the hydrogen bonding at 0.5 mol/*l* in CCl_4 solution. Therefore it may be considered that the extrapolated $(T_1)_{rot.}$ of NMA in CCl_4 solution represents the rotational correlation time of the molecule which is restricted in the associated form but not disturbed by the intermolecular dipole-dipole interactions.

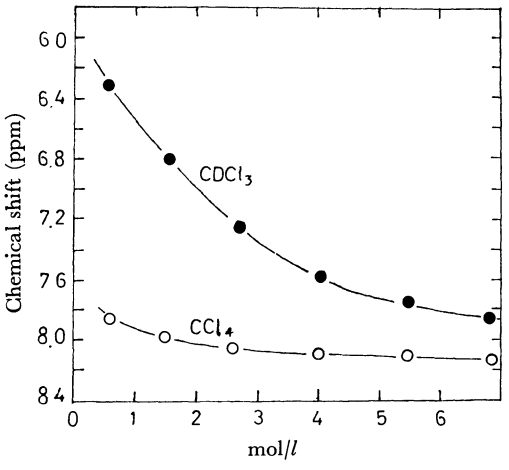

Fig. 4. Concentration dependence of the chemical shift (measured from internal TMS) of N–H protons of NMA in CCl_4 (open circlds) and $CDCl_3$ (solid circles) solutions at 25°C.

Since τ_c values as well as the concentration dependence of T_1 for NMA and DMA in aqueous solution are nearly equal and the chemical shift between the two *N*-methyl groups is almost independent of the solute concentration, the intermolecular interactions between solute molecules do not seem to be appreciable as discussed later. This leads us to the consideration that the estimated τ_c values may be related to the isolated molecule free from solute-solute interactions. Klotz and Fransen[2] also concluded that in aqueous solution the degree of association of NMA molecule is smaller than 10% even at moderately high concentration of about 5 mol/*l*. Their conclusion is in accordance with our present NMR results.

It is clear from Fig. 3 that the chemical shift, $\Delta\nu$, between the *N*-methyl protons of DMA in aqueous solution tends to coincide with that in CCl_4 solution at infinite dilution. This suggests that DMA molecules in dilute CCl_4 solution do not interact with each other as strongly as to affect the spin-lattice relaxation process. Neuman *et al.*,[6] and Rabinovitz and Pines[4,5] concluded from the observed dependence of the chemical shift of *N*-methyl doublet that DMA and *N*,*N*-dimethylformamide molecules dimerize at moderate concentration in CCl_4 solution. We also assume the behavior of $1/T_1$ at the moderate concentration region to be due to the dimerization of solute molecules. Thus it is considered that τ_c extrapolated from high concentration region may be associated with the DMA molecule weakly influenced by the molecular dimerization and not disturbed by the intermolecular dipole-dipole interactions.

Let us discuss the solvent effects in both aqueous and apolar solutions as follows.

Aqueous Solution. For both NMA and DMA molecules τ_c values of *C*-methyl and *N*-methyl groups are nearly equal. The fact that τ_c values of different methyl groups in the same molecule are equal means

11) L. Pauling, "The Nature of the Chemical Bond," Cornell University Press, Ithaca (1960), Chap, 8, p. 281.

12) K. Sato and A. Nishioka, unpublished data.

that the molecular rotational motion may be isotropic with respect to both methyl groups, provided that the internal rotation of methyl groups are almost in the same degree. τ_c values of NMA and DMA are about 2.5×10^{-12} sec, and the concentration dependence of T_1 or the contribution from intermolecular relaxation factors is equal. It can be concluded that the molecular rotational and translational motions are almost the same for NMA and DMA molecule in aqueous solution.

Recently, Anderson and Fryer[13,14] discussed the effect of the molecular association on the molecular rotational motion or the spin-lattice relaxation process, and concluded that if the lifetime of the associated molecules moving as a unit is longer than the rates of chemical exchange between the associated molecules, the effect of association is pronounced, whereas the effect is small if the lifetime of the molecular association is shorter. Thus it may be concluded that in aqueous solution the interamide hydrogen bonding is very weak, and if the molecular association is formed through the hydrogen bonding its lifetime is shorter than 10^{-11}—10^{-12} sec.

Thus the peptide bond character and the interamide interaction are not appreciable in aqueous solution, and do not affect entirely the microscopic molecular motion. From the concentration dependence of the chemical shift of *N*-dimethyl doublet of DMA solution, we conclude that the double bond character of the central C–N bond through the solute-solute interactions is not stabilized by the increase of solute concentration. This means implicitly that in contrast to CCl_4 solution the intermolecular interaction or the molecular association does not exist between DMA molecules in aqueous solution over the range of concentration studied.

Apolar Solution. The rotational correlation times of *C*-methyl and *N*-methyl groups of NMA are equal; $\tau_c=1.4\times10^{-11}$ sec. The concentration dependence of $1/T_1$ is also in the same order of magnitude. It is reasonable to consider that the molecular rotational and translational motions are isotropic as in the case of aqueous solution. τ_c of NMA seems to be about five to ten times longer than the values observed in ordinary low molecular weight compounds.[10] This provides another verification that τ_c estimated in the present study is related to the rotational correlation time of NMA molecule restricted in the associated form of chain. We might conclude that the interamide association through the hydrogen bonding is strong enough to affect the spin-lattice relaxation, and that the life time of the association is longer than 10^{-10}—10^{-11} sec. Considering the fact that the interamide association is strong, and the molecular rotational motion is isotropic with respect to both methyl groups, we conclude that the rotational motion is predominant around the associated chain.

(See below, the *trans* configuration of NMA has been verified and well known.[1])

According to Neuman and Rabinovitz, we may

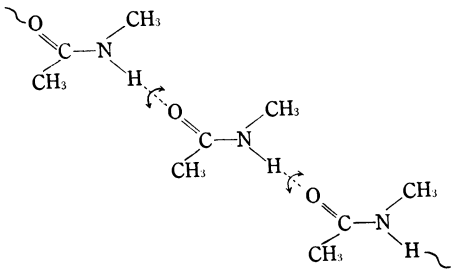

ascribe the peculiar concentration dependence of the chemical shift and T_1 to molecular dimerization. Another feature in CCl_4 solution differing from that in aqueous solution may be the fact that T_1 values of *C*-methyl and *N*-methyl protons are not equal over the experimental range of concentrations. This probably means that the molecular motion of DMA in CCl_4 is anisotropic with respect to both methyl groups. But the mechanism of this anisotropy is not clear. We might discuss from the effect of dimerization the reason for the concentration depedence of the relaxation rate in the dilute concentration region differing from that in the moderate concentration region. We consider that in dilute solutions the free DMA molecules are dominant and the fraction of the dimerized molecule increases linearly with increasing concentration (above about 3 mol/l). However, almost all DMA molecules dimerize and produce apparently different relaxation contributions from those at dilute solution region. τ_c values (denoted by τ_{c1}) obtained by extrapolating into infinite dilution from lower concentration region is plausible for most low molecular weight compounds. The value may correspond to the rotational correlation time of the isolated DMA molecule. τ_c (denoted by τ_{c2}) estimated from moderately concentration region is smaller than twice τ_{c1} of the isolated DMA.

The BPP theory[7] predicts $\tau_c=4\pi\eta a^3/3kT$ for the rigid molecule, where η and a represent solution viscosity and the radius of spherical molecule, respectively. If the dimerized molecule with a long lifetime is rigid enough to affect the spin-lattice relaxation process considerably, τ_{c2} must be roughly eight times greater than τ_{c1} according to BPP. Therefore we conclude that although the effect of association on spin-lattice relaxation is appreciable, it is not so significant, and that life time of association may be at most 10^{-11}—10^{-12} sec. It seems that both characters of monomer and dimer influence the relaxation process. This is also verified from the fact that T_1 values of *C*-methyl protons differ from those of *N*-methyl protons to the same degree as in dilute concentration region in moderately high concentrations where the fraction of associated molecule is expected to be larger.

τ_c of the isolated DMA is shorter in CCl_4 than in aqueous solution. The reasons might be as follows.

(1) The solution viscosity of aqueous solution at 25°C is larger than that of CCl_4 solution by factor about 1.5.[12] (2) The effect of solvation[10] of water molecules around the DMA molecules is expected to reduce molecular mobilities.

13) J. E. Anderson and P. A. Fryer, *J. Chem. Phys.* **50**, 3784 (1969).

14) J. E. Anderson, *ibid.*, **51**, 3578 (1969).

The Crystal and Molecular Structures of a 3 : 2 Adduct of Acetylene and Isonitrile Derivatives

Yoshio SUZUKI and Yōichi IITAKA

Faculty of Pharmaceutical Sciences, The University of Tokyo, Hongo, Tokyo

(Received July 24, 1970)

In order to determine the structure of the 3 : 2 adduct (acetylene : isonitrile) obtained by cycloaddition reaction of dimethyl acetylenedicarboxylate with 2,6-dimethylphenylisonitrile and to elucidate the route of the reaction, a heavy atom derivative of this adduct was prepared and subjected to X-ray diffraction analysis. The crystal grown from acetone solution has the composition $C_{36}H_{34}N_2O_{12}Br_2 \cdot CH_3COCH_3$ and belongs to monoclinic system with the lattice constants: $a=34.13\pm0.04$, $b=14.66\pm0.02$, $c=8.10\pm0.01$ Å, $\beta=90.5\pm0.2°$. The space group is $P2_1/n$ containing four formula units in the cell. The structure was solved by the heavy atom method and refined by the block-matrix least-squares method for 1482 observed reflections allowing the anisotropic thermal motions for each atom. It has been shown that the chemical structure of the adduct is 1-(4-bromo-2,6-dimethylphenyl)-2-(4-bromo-2,6-dimethylphenyl)imino-1,2-dihydro-3,4,5,5,6,7-hexacarbomethoxy-5*H*-1-pyrindine.

It has been shown that isonitrile reacts as nucleophile, but substituted acetylene, especially when it has electron withdrawing groups, reacts as electrophile giving rise to cyclic products. Takizawa, Obata, Suzuki, and Yanagida[1] synthesized cyclopententriimine and biskетenimine which correspond respectively to the 1 : 3 and 1 : 2 adducts of acetylene and isonitrile and elucidated the structures of these adducts as well as the reaction mechanism. However, this cycloaddition reaction is very complicated and gives many complex compounds in addition to 1 : 3 and 1 : 2 adducts. We have chosen one of the 3 : 2 adducts obtained in the reaction of dimethyl acetylenedicarboxylate and 2,6-dimethylphenylisonitrile for structure determination. However, the structure is so complicated that it proved to be difficult to solve it merely on the basis of spectral data and chemical reactions.

It was therefore decided to carry out X-ray diffraction analysis by applying the heavy atom method. In order to introduce a heavy atom into the adduct, 4-bromo-2,6-dimethylphenylisonitrile was reacted with dimethyl acethylenedicarboxylate and the 3 : 2 adduct containing heavy atoms was prepared.

Experimental

The crystals of the 3 : 2 adduct, $C_{36}H_{34}N_2O_{12}Br_2 \cdot CH_3COCH_3$, recrystallized from acetone solution are monoclinic deep violet prisms. The amount of the solvent of crystallization was calculated from elemental analysis and NMR spectrum. The lattice constants were determined from the $0kl$ and $h0l$ precession photographs taken with Cu$K\alpha$ radiation. Intensity data were collected from the *c*-axis multiple-film equi-inclination Weissenberg photographs of zero to six layers and the *b*-axis zero layer precession photographs of various exposures. All were taken with Cu$K\alpha$ radiation. The intensities were measured with the aid of a Narumi microdensitometer. From systematic absence, the space group was found to be $P2_1/n$. The unit cell contains four molecules of acetone. After Lorentz and polarization corrections were made, the structure factors of various layers of the *c*-axis were put on the same relative scale by use of $h0l$ structure factors obtained from the precession photographs. Since the cross-section of the crystal used for the *c*-axis Weissenberg photographs was about 0.08×0.10 mm and the μR value was calculated to be less than 0.2 for Cu$K\alpha$ radiation, no absorption correction was applied for the intensity data. All together 1482 independent reflections were observed out of 3085 possible reflections within the sphere of radius corresponding to $2\theta=90°$ in reciprocal space.

Crystal data

$C_{36}H_{34}N_2O_{12}Br_2 \cdot CH_3COCH_3$, MW 904.5, mp 254—255°C
Monoclinic
$a=34.13\pm0.04$, $b=14.66\pm0.02$, $c=8.10\pm0.01$ Å,
$\beta=90.5\pm0.2°$
Volume of the unit cell=4052.8 Å^3
Density (calculated)=1.483 g·cm^{-3}
Linear absorption coefficient for Cu$K\alpha$ radiation=33.2 cm^{-1}
Absent reflections: $h0l$ when $h+l$ is odd, $0k0$ when k is odd
Space group: $P2_1/n$
$Z=4$

Structure Determination

The ordinary heavy atom method was applied to phase determination. From the Harker and other vectors in the Patterson map, the positional parameters of the two independent bromine atoms were easily determined. Three-dimensional electron density map was then calculated on the basis of bromine contributions. Several cycles of Fourier and difference Fourier syntheses revealed the fifty-two atoms composing the whole molecule. Three cycles of least-squares refinement were made, in which individual isotropic temperature factors were assigned coding all atoms as carbon except for two bromine atoms. At this stage, twelve oxygen and two nitrogen atoms were distinguished by comparing their temperature factors. Using these positional parameters, difference Fourier synthesis was computed and the atomic parameters of the solvation molecule were determined. The *R* value at this stage was 0.17.

Refinement of the structural parameters for 1482 observed structure factors was carried out by the method of block-matrix least-squares using the program HBLS.[2] Six cycles of calculation with isotropic temperature factors and three cycles with anisotropic temperature factors for all atoms reduced the *R* value to

1) T. Takizawa, N. Obata, Y. Suzuki, and T. Yanagida, *Tetrahedron Lett.*, **1969**, 3407.

2) Y. Okaya and T. Ashida, *HBLSIV, The Universal Crystallographic Computing System (I)*, p. 65. Japanese Crystallographic Association (1967).

TABLE 1. THE FINAL ATOMIC PARAMETERS AND THEIR STANDARD DEVIATIONS

The thermal parameters are of the form

$$T = \exp\{-(\beta_{11}h^2+\beta_{22}k^2+\beta_{33}l^2+2\beta_{12}hk+2\beta_{13}hl+2\beta_{23}kl)\}.$$

ATOM	X	Y	Z	B11	B22	B33	B12	B13	B23
BR(18)	0.2795	0.6016	0.3091	0.0015	0.0048	0.0127	-0.0007	0.0015	-0.0000
	(1)	(2)	(3)	(0)	(2)	(5)	(1)	(1)	(3)
BR(28)	0.5477	0.3526	0.8813	0.0013	0.0082	0.0129	-0.0004	-0.0021	-0.0007
	(1)	(3)	(4)	(0)	(2)	(5)	(1)	(1)	(3)
O(30)	0.4678	0.0926	0.4712	0.0012	0.0060	0.0091	0.0006	-0.0006	-0.0026
	(5)	(12)	(18)	(2)	(12)	(31)	(4)	(6)	(16)
O(31)	0.4927	0.1774	0.2721	0.0008	0.0061	0.0091	-0.0003	-0.0002	-0.0022
	(5)	(12)	(17)	(2)	(13)	(29)	(4)	(6)	(15)
O(34)	0.4086	-0.0763	0.2239	0.0011	0.0032	0.0064	0.0003	0.0008	-0.0009
	(4)	(10)	(16)	(2)	(11)	(27)	(4)	(6)	(13)
O(35)	0.4635	-0.0066	0.1458	0.0008	0.0045	0.0058	-0.0001	0.0007	-0.0016
	(4)	(11)	(16)	(2)	(11)	(30)	(4)	(6)	(13)
O(38)	0.4061	-0.0101	-0.1474	0.0007	0.0081	0.0052	0.0002	0.0004	-0.0003
	(4)	(12)	(17)	(2)	(13)	(28)	(4)	(6)	(15)
O(39)	0.3512	0.0087	-0.2941	0.0010	0.0070	0.0057	0.0001	-0.0006	-0.0000
	(5)	(12)	(17)	(2)	(13)	(29)	(4)	(6)	(15)
O(42)	0.3150	-0.0417	0.2044	0.0011	0.0051	0.0076	-0.0005	0.0007	0.0005
	(5)	(11)	(17)	(2)	(12)	(29)	(4)	(6)	(15)
O(43)	0.3414	-0.1228	0.0063	0.0013	0.0028	0.0086	-0.0001	0.0004	-0.0010
	(5)	(10)	(17)	(2)	(11)	(28)	(4)	(6)	(14)
O(46)	0.2724	-0.0153	-0.1523	0.0008	0.0052	0.0088	0.0000	-0.0000	-0.0004
	(5)	(11)	(17)	(2)	(12)	(31)	(4)	(6)	(14)
O(47)	0.2620	0.1278	-0.2346	0.0013	0.0057	0.0017	-0.0001	-0.0014	-0.0002
	(5)	(11)	(16)	(2)	(13)	(25)	(4)	(6)	(14)
O(50)	0.3079	0.3212	-0.1443	0.0010	0.0054	0.0086	-0.0004	0.0003	0.0011
	(5)	(11)	(17)	(2)	(12)	(30)	(4)	(6)	(15)
O(51)	0.2622	0.2701	0.0390	0.0009	0.0040	0.0034	-0.0000	0.0007	0.0005
	(4)	(10)	(15)	(2)	(11)	(26)	(4)	(5)	(13)
N(1)	0.3705	0.2514	0.2000	0.0009	0.0021	0.0034	-0.0006	0.0004	-0.0012
	(5)	(13)	(18)	(2)	(12)	(31)	(4)	(6)	(15)
N(19)	0.4158	0.3115	0.3820	0.0006	0.0043	0.0030	-0.0003	0.0006	-0.0010
	(5)	(13)	(19)	(2)	(13)	(31)	(4)	(6)	(16)
C(2)	0.4054	0.2411	0.2984	0.0005	0.0038	0.0029	0.0002	0.0001	0.0006
	(7)	(16)	(23)	(3)	(16)	(40)	(5)	(8)	(20)
C(3)	0.4248	0.1553	0.2732	0.0004	0.0037	0.0023	-0.0002	0.0005	0.0024
	(6)	(16)	(23)	(2)	(15)	(36)	(5)	(7)	(19)
C(4)	0.4076	0.0827	0.1832	0.0008	0.0037	0.0000	-0.0005	0.0016	0.0025
	(6)	(16)	(23)	(3)	(17)	(39)	(6)	(8)	(19)
C(5)	0.3476	0.0385	-0.0093	0.0008	0.0036	0.0021	0.0001	0.0002	0.0002
	(7)	(16)	(24)	(3)	(16)	(39)	(5)	(8)	(19)
C(6)	0.3149	0.0990	-0.0591	0.0008	0.0043	0.0018	-0.0003	-0.0004	0.0018
	(7)	(17)	(23)	(3)	(16)	(39)	(6)	(8)	(21)
C(7)	0.3194	0.1858	0.0052	0.0008	0.0033	0.0027	-0.0001	0.0009	0.0003
	(7)	(16)	(23)	(3)	(16)	(40)	(5)	(8)	(19)
C(8)	0.3720	0.1012	0.1025	0.0004	0.0032	0.0000	0.0007	0.0000	-0.0025
	(6)	(15)	(20)	(2)	(14)	(33)	(5)	(6)	(17)
C(9)	0.3548	0.1810	0.1082	0.0005	0.0024	0.0000	-0.0002	0.0013	0.0004
	(6)	(14)	(22)	(2)	(15)	(35)	(5)	(7)	(17)
C(10)	0.3488	0.3374	0.2226	0.0006	0.0042	0.0010	-0.0006	-0.0009	0.0006
	(6)	(17)	(22)	(3)	(16)	(38)	(6)	(7)	(19)
C(11)	0.3594	0.4151	0.1322	0.0009	0.0023	0.0026	0.0006	0.0003	-0.0020
	(7)	(15)	(24)	(3)	(16)	(39)	(5)	(8)	(18)
C(12)	0.3380	0.4943	0.1573	0.0006	0.0065	0.0121	0.0014	-0.0003	-0.0009
	(7)	(18)	(28)	(3)	(19)	(50)	(7)	(9)	(25)
C(13)	0.3080	0.4899	0.2629	0.0008	0.0048	0.0116	0.0011	0.0007	-0.0031
	(7)	(18)	(28)	(3)	(19)	(51)	(6)	(10)	(24)
C(14)	0.2963	0.4155	0.3691	0.0009	0.0019	0.0052	-0.0002	-0.0010	-0.0014
	(7)	(15)	(24)	(3)	(15)	(41)	(5)	(8)	(19)
C(15)	0.3173	0.3332	0.3406	0.0007	0.0046	0.0000	-0.0004	0.0008	-0.0016
	(6)	(16)	(22)	(3)	(16)	(37)	(6)	(7)	(19)
C(16)	0.3077	0.2500	0.4367	0.0018	0.0043	0.0005	-0.0010	0.0024	0.0022
	(8)	(18)	(25)	(4)	(17)	(42)	(7)	(10)	(21)
C(17)	0.3913	0.4123	0.0056	0.0011	0.0052	0.0000	-0.0002	0.0013	-0.0025
	(7)	(18)	(24)	(3)	(18)	(39)	(6)	(8)	(20)
C(20)	0.4481	0.3140	0.4929	0.0013	0.0016	0.0032	-0.0002	-0.0007	-0.0022
	(7)	(15)	(23)	(3)	(15)	(41)	(6)	(9)	(19)
C(21)	0.4798	0.3625	0.4524	0.0010	0.0040	0.0068	-0.0006	-0.0001	-0.0028
	(7)	(17)	(26)	(3)	(18)	(43)	(6)	(9)	(21)
C(22)	0.5111	0.3738	0.5650	0.0006	0.0062	0.0105	0.0003	-0.0005	0.0001
	(7)	(18)	(27)	(3)	(21)	(47)	(6)	(8)	(24)
C(23)	0.5069	0.3374	0.7261	0.0009	0.0028	0.0169	0.0004	0.0002	0.0007
	(7)	(17)	(29)	(3)	(18)	(51)	(6)	(10)	(24)
C(24)	0.4740	0.2898	0.7758	0.0005	0.0091	0.0095	0.0003	0.0001	0.0002
	(7)	(20)	(28)	(3)	(22)	(48)	(6)	(9)	(25)
C(25)	0.4430	0.2793	0.6572	0.0010	0.0033	0.0041	0.0002	0.0009	0.0008
	(7)	(16)	(24)	(3)	(17)	(43)	(6)	(8)	(19)
C(26)	0.4048	0.2242	0.7054	0.0013	0.0037	0.0079	-0.0003	-0.0001	0.0030
	(8)	(17)	(27)	(4)	(18)	(48)	(6)	(10)	(22)
C(27)	0.4041	0.4039	0.2755	0.0008	0.0052	0.0053	-0.0006	-0.0001	0.0013
	(7)	(18)	(25)	(3)	(18)	(43)	(6)	(8)	(23)
C(29)	0.4041	0.1395	0.3505	0.0011	0.0029	0.0105	0.0001	-0.0001	-0.0010
	(7)	(17)	(27)	(3)	(17)	(47)	(6)	(9)	(22)
C(32)	0.5318	0.1558	0.3366	0.0006	0.0113	0.0179	0.0006	0.0008	-0.0022
	(8)	(23)	(32)	(3)	(26)	(58)	(8)	(10)	(31)
C(33)	0.4265	-0.0069	0.1860	0.0006	0.0062	0.0069	-0.0005	-0.0005	-0.0027
	(7)	(18)	(27)	(3)	(19)	(44)	(6)	(9)	(23)
C(36)	0.4833	-0.0943	0.1562	0.0013	0.0056	0.0169	0.0016	0.0017	0.0018
	(8)	(20)	(31)	(4)	(20)	(56)	(8)	(11)	(28)
C(37)	0.3730	0.0066	-0.1621	0.0003	0.0048	0.0008	-0.0001	0.0005	0.0007
	(6)	(17)	(24)	(3)	(18)	(39)	(6)	(7)	(21)
C(40)	0.3732	-0.0271	-0.4487	0.0010	0.0105	0.0000	-0.0004	0.0011	-0.0032
	(8)	(20)	(25)	(3)	(24)	(42)	(7)	(9)	(25)
C(41)	0.3535	-0.0457	0.0779	0.0010	0.0034	0.0007	-0.0004	0.0007	0.0006
	(7)	(16)	(24)	(3)	(16)	(39)	(6)	(8)	(20)
C(44)	0.3504	-0.2085	0.0845	0.0019	0.0023	0.0233	-0.0005	0.0008	0.0052
	(9)	(18)	(34)	(5)	(18)	(63)	(7)	(13)	(26)
C(45)	0.2811	0.0637	-0.1512	0.0012	0.0033	0.0041	0.0000	0.0011	0.0029
	(7)	(17)	(25)	(3)	(17)	(44)	(6)	(9)	(20)
C(48)	0.2249	0.0974	-0.3160	0.0010	0.0074	0.0147	-0.0000	-0.0019	0.0015
	(8)	(20)	(31)	(3)	(21)	(53)	(8)	(10)	(29)
C(49)	0.2940	0.2664	-0.0499	0.0010	0.0041	0.0019	-0.0003	-0.0004	-0.0029
	(7)	(17)	(24)	(3)	(17)	(41)	(6)	(8)	(20)
C(52)	0.2363	0.3484	-0.0104	0.0010	0.0057	0.0210	0.0007	-0.0004	0.0041
	(8)	(20)	(33)	(4)	(20)	(61)	(7)	(11)	(29)
O(56)	0.3808	0.6260	-0.1995	0.0038	0.0114	0.0401	0.0002	0.0022	-0.0042
	(9)	(20)	(34)	(5)	(25)	(67)	(9)	(15)	(32)
C(53)	0.3860	0.5197	-0.4167	0.0027	0.0054	0.0228	-0.0010	0.0003	-0.0014
	(11)	(22)	(39)	(6)	(24)	(71)	(9)	(16)	(32)
C(54)	0.3819	0.6102	-0.3474	0.0017	0.0127	0.0252	-0.0008	-0.0001	-0.0020
	(10)	(26)	(39)	(5)	(32)	(75)	(11)	(15)	(40)
C(55)	0.3750	0.6922	-0.4561	0.0019	0.0107	0.0632	-0.0003	-0.0002	0.0148
	(12)	(28)	(55)	(6)	(35)	(127)	(11)	(22)	(54)

TABLE 2. OBSERVED AND CALCULATED STRUCTURE FACTORS

H	K	L	|F(OBS)|	F(CAL)
4	0	0	53.23	49.13
6	0	0	43.38	38.20
8	0	0	31.52	16.68
12	0	0	116.16	-113.61
16	0	0	104.31	-95.97
20	0	0	25.01	-11.05
22	0	0	110.19	112.99
1	1	0	45.24	-49.70
2	1	0	117.59	124.15
3	1	0	36.11	44.62
4	1	0	31.92	-34.12
5	1	0	98.85	99.31
6	1	0	33.68	-24.05
7	1	0	97.88	-87.30
8	1	0	34.76	-20.48
9	1	0	95.53	83.04
10	1	0	83.67	-79.42
11	1	0	84.56	-88.03
12	1	0	110.09	99.16
13	1	0	58.74	-58.17
15	1	0	58.88	61.15
16	1	0	113.89	115.80
17	1	0	56.53	53.11
18	1	0	49.45	47.26
19	1	0	99.61	102.06
20	1	0	73.41	-71.05
22	1	0	47.43	48.88
24	1	0	42.24	-44.73
0	2	0	53.61	60.87
1	2	0	121.19	-128.29
2	2	0	103.41	-98.74
4	2	0	83.94	-82.11
5	2	0	174.36	-193.04
7	2	0	53.99	50.48
8	2	0	60.66	52.80
9	2	0	82.19	-82.96
11	2	0	56.74	-61.47
13	2	0	148.19	154.21
14	2	0	35.22	28.30
16	2	0	93.61	-87.35
17	2	0	102.98	104.32
19	2	0	52.18	-51.55
20	2	0	49.18	-48.76
21	2	0	63.20	62.16
23	2	0	48.26	-39.08
25	2	0	43.78	-36.06
1	3	0	262.87	-253.80
2	3	0	160.70	-156.33
4	3	0	23.63	18.45
6	3	0	150.06	-130.23
7	3	0	85.13	95.76
8	3	0	130.94	134.42
10	3	0	68.60	-66.55
11	3	0	127.83	129.70
12	3	0	57.39	56.09
13	3	0	46.18	45.52
14	3	0	42.27	-41.53
16	3	0	59.28	53.69
19	3	0	46.62	-39.61
21	3	0	49.75	-42.31
23	3	0	47.78	-54.30
24	3	0	58.42	-56.70
0	4	0	173.61	-169.20
1	4	0	68.98	-70.21
2	4	0	75.06	-70.87
3	4	0	127.69	135.66
4	4	0	212.82	-205.36
5	4	0	51.96	-47.46
8	4	0	35.52	-23.99
10	4	0	28.90	32.98
12	4	0	75.84	81.52
13	4	0	42.48	33.41
15	4	0	51.34	-47.41
17	4	0	37.30	32.46
18	4	0	77.97	-73.17
1	5	0	43.05	-41.28
2	5	0	72.92	67.87
3	5	0	73.38	65.39
4	5	0	77.11	69.31
5	5	0	63.12	-52.07
6	5	0	66.12	56.64
7	5	0	32.98	29.56
9	5	0	130.69	-129.97
10	5	0	91.13	88.63
11	5	0	87.13	92.61
12	5	0	51.67	-52.41
13	5	0	78.65	-72.49
14	5	0	70.09	-65.13
16	5	0	42.02	-38.40
18	5	0	69.11	-70.72
23	5	0	40.89	-45.56
25	5	0	44.27	43.73
26	5	0	48.29	43.04
27	5	0	52.77	-49.66
0	6	0	41.81	43.43
1	6	0	147.11	152.66
2	6	0	134.88	141.14
5	6	0	158.05	153.12
6	6	0	81.94	78.69
7	6	0	55.88	44.71
8	6	0	81.70	-72.34
10	6	0	101.90	-111.10
11	6	0	33.87	31.93
12	6	0	34.08	29.06
13	6	0	53.42	-50.64
14	6	0	48.83	-37.98
15	6	0	54.45	-49.91
16	6	0	63.87	61.59
17	6	0	46.05	-37.95
20	6	0	58.01	54.44
21	6	0	48.70	-50.36
1	7	0	43.92	38.64
3	7	0	36.06	33.17
4	7	0	83.16	-73.80
6	7	0	47.10	45.95
7	7	0	29.28	28.16
9	7	0	71.81	-68.23
11	7	0	77.51	73.78
12	7	0	69.90	-66.96
13	7	0	58.31	-64.95
14	7	0	60.96	55.21
19	7	0	63.42	59.40
20	7	0	44.97	46.49
0	8	0	112.03	106.63
1	8	0	64.87	66.85
3	8	0	98.98	-111.58
6	8	0	21.66	-32.38
7	8	0	52.37	-50.95
8	8	0	35.16	35.82
9	8	0	49.45	-51.05
10	8	0	34.00	-37.87
11	8	0	51.10	43.34
12	8	0	58.15	-58.79
16	8	0	54.21	-29.73
19	8	0	40.81	37.95
21	8	0	66.71	-69.95
2	9	0	59.17	-49.09
4	9	0	55.12	-54.30
5	9	0	58.36	63.41
7	9	0	51.34	-47.56
8	9	0	55.66	-63.37
9	9	0	81.13	77.09
13	9	0	47.94	45.05
14	9	0	47.97	48.41
0	10	0	60.28	60.01
2	10	0	60.93	-58.32
10	10	0	45.21	42.94
16	10	0	44.78	-45.31
20	10	0	44.10	-46.86
3	11	0	68.33	-70.40
4	11	0	60.39	63.60
8	11	0	51.32	47.68
0	12	0	70.46	66.42
3	12	0	71.19	63.34
-21	0	1	88.75	-87.03
-17	0	1	52.61	-48.11
-15	0	1	128.75	129.05
-11	0	1	18.15	35.61
-9	0	1	107.52	106.01
-7	0	1	192.24	174.07
-5	0	1	92.42	99.55
-3	0	1	214.58	270.37
-1	0	1	94.47	102.33
1	0	1	184.17	-252.53
3	0	1	75.76	78.62
5	0	1	121.32	-121.93
7	0	1	243.69	-212.64
9	0	1	208.29	179.93
19	0	1	42.43	-40.40
21	0	1	42.65	-40.35
23	0	1	45.54	-47.28
25	0	1	70.98	-71.59
-16	1	1	48.43	-49.38
-15	1	1	73.60	69.99
-14	1	1	84.35	82.18
-12	1	1	82.97	-74.18
-11	1	1	106.76	104.85
-10	1	1	210.56	203.19
-9	1	1	57.47	48.87
-8	1	1	37.46	-33.94
-7	1	1	21.69	-9.67
-6	1	1	181.41	158.75
-5	1	1	236.24	-234.48
-4	1	1	164.88	-168.23
-3	1	1	222.52	-215.55
4	1	1	112.87	112.50
5	1	1	16.99	-21.15
6	1	1	80.75	-77.06
7	1	1	322.13	308.78
8	1	1	27.47	39.71
12	1	1	197.21	189.78
17	1	1	96.28	-96.38
18	1	1	48.97	49.68
19	1	1	83.86	-87.27
20	1	1	57.28	-58.21
24	1	1	59.23	-53.45
25	1	1	53.15	50.65
-24	2	1	48.40	-47.48
-22	2	1	75.27	-66.58
-20	2	1	49.83	47.88
-18	2	1	76.30	-65.56
-16	2	1	84.99	79.71
-14	2	1	26.31	30.37
-12	2	1	157.86	132.04
-10	2	1	74.00	67.91
-9	2	1	57.66	-51.80
-8	2	1	31.19	27.99
-7	2	1	128.32	115.18
-6	2	1	41.38	-36.51
-5	2	1	126.45	112.69
-4	2	1	250.18	-246.51
-3	2	1	34.33	-38.35
-2	2	1	109.49	-117.31
-1	2	1	85.48	-79.34
0	2	1	68.36	-85.62
1	2	1	64.25	-59.18
2	2	1	94.34	-81.61
3	2	1	24.04	30.86
4	2	1	81.46	-77.08
5	2	1	27.58	-19.31
6	2	1	126.94	113.60
7	2	1	90.91	-94.59
8	2	1	104.76	94.74
9	2	1	78.38	80.55
11	2	1	80.35	-79.90
12	2	1	76.05	72.45
13	2	1	64.33	-62.71
14	2	1	137.34	-133.21
15	2	1	34.06	31.79
18	2	1	78.16	-76.77
20	2	1	42.83	-55.55
-22	3	1	45.56	36.07
-20	3	1	40.05	47.50
-16	3	1	43.05	33.64
-15	3	1	44.00	41.86
-14	3	1	50.45	-47.20
-13	3	1	94.42	-94.64
-12	3	1	53.48	-46.00
-11	3	1	65.55	61.20
-10	3	1	34.11	-39.65
-9	3	1	123.70	-111.36
-8	3	1	52.37	-54.58
-6	3	1	252.47	-227.78
-5	3	1	155.08	-146.69
-3	3	1	69.65	64.90
-2	3	1	70.63	69.23
-1	3	1	31.90	19.53
0	3	1	69.73	64.92
1	3	1	63.25	-38.59
2	3	1	19.09	21.54
3	3	1	41.00	39.50
4	3	1	191.49	161.22
5	3	1	28.36	-24.81
6	3	1	35.54	36.17
7	3	1	193.03	183.91
8	3	1	22.28	-16.51
10	3	1	60.47	-57.19
11	3	1	36.73	37.70
12	3	1	91.29	-87.57
13	3	1	33.38	-38.41
14	3	1	65.31	-72.42
16	3	1	89.32	-82.92
17	3	1	25.01	-26.72
18	3	1	25.90	-21.95
19	3	1	49.42	-43.58
23	3	1	81.92	-72.58
24	3	1	44.02	37.47
-20	4	1	28.47	33.47
-18	4	1	29.33	-42.22
-17	4	1	93.80	95.22
-15	4	1	51.45	-51.10
-12	4	1	30.98	-28.81
-11	4	1	36.06	-34.69
-9	4	1	134.34	-127.05
-6	4	1	166.29	158.86
-5	4	1	224.79	-203.66
-4	4	1	157.08	134.86
-3	4	1	98.58	-74.21
-2	4	1	190.52	177.17
-1	4	1	67.63	-73.61
0	4	1	152.51	139.95
1	4	1	98.85	89.12
2	4	1	71.06	59.92
3	4	1	27.06	27.37
4	4	1	40.89	-38.28
6	4	1	22.09	19.23
7	4	1	53.88	54.96
8	4	1	75.30	-81.54
9	4	1	56.80	-55.43
11	4	1	41.92	37.82
13	4	1	143.36	-127.10
15	4	1	140.12	120.57
16	4	1	108.14	101.78
17	4	1	49.29	-49.85
19	4	1	55.37	59.48
20	4	1	45.10	51.00
21	4	1	41.54	45.49
23	4	1	42.70	59.04
-14	5	1	42.21	-45.24
-13	5	1	77.59	-78.87
-12	5	1	40.46	31.89
-11	5	1	75.60	-72.64
-10	5	1	122.02	-113.88
-9	5	1	79.70	77.76
-6	5	1	230.00	-189.44
-5	5	1	55.58	53.79
-3	5	1	117.22	100.90
-2	5	1	114.33	115.34
1	5	1	26.31	-30.62
2	5	1	62.39	60.12
3	5	1	44.40	-47.84
4	5	1	122.83	-111.15
5	5	1	51.72	-49.71
6	5	1	137.71	136.23
7	5	1	61.96	-58.46
8	5	1	35.65	-36.59
9	5	1	48.56	-48.18
10	5	1	28.82	27.23
11	5	1	57.53	-53.66
12	5	1	50.21	-46.49
14	5	1	52.69	-54.78
15	5	1	37.08	38.10
17	5	1	62.50	66.63
19	5	1	53.75	45.21
20	5	1	40.70	38.59
21	5	1	37.11	36.40
-17	6	1	40.19	31.05
-16	6	1	81.70	-82.01
-15	6	1	47.51	-49.44
-13	6	1	40.54	33.62
-9	6	1	52.56	53.57
-8	6	1	73.46	-70.88
-7	6	1	183.44	172.87
-3	6	1	33.30	34.04
-1	6	1	115.08	-104.91
0	6	1	86.64	85.60
1	6	1	63.12	59.05
3	6	1	90.91	-83.00
5	6	1	73.89	-73.84
6	6	1	46.59	-36.32
7	6	1	74.84	-65.26
8	6	1	73.22	-67.44
9	6	1	61.23	56.38
11	6	1	105.36	99.07
12	6	1	66.71	-61.66
14	6	1	47.86	36.97
15	6	1	80.21	79.99
21	6	1	54.21	-45.02
-18	7	1	37.33	-45.90
-13	7	1	98.53	95.23
-12	7	1	35.89	35.71
-11	7	1	26.20	-30.67
-10	7	1	25.68	30.52
-9	7	1	82.40	83.97
-8	7	1	119.97	111.74
-7	7	1	34.44	-40.34
-2	7	1	59.60	51.40
-1	7	1	29.11	-31.10
0	7	1	36.35	-35.38
2	7	1	84.27	-80.62
5	7	1	120.43	104.17
7	7	1	96.58	-96.19
9	7	1	44.40	33.85
10	7	1	64.01	62.40
11	7	1	38.03	-34.12
13	7	1	54.75	53.05
15	7	1	40.46	-38.99
19	7	1	41.78	38.60
22	7	1	60.53	-60.98
-11	8	1	79.89	74.82
-10	8	1	40.94	-39.72
-7	8	1	75.22	75.16
-6	8	1	45.21	-47.52
-5	8	1	81.29	76.88
-3	8	1	42.56	-40.63
-2	8	1	137.50	-144.18
2	8	1	69.82	-61.59
6	8	1	42.13	42.09
7	8	1	39.24	-38.07
9	8	1	27.20	19.48
10	8	1	64.23	59.50
12	8	1	51.15	-47.29
13	8	1	52.10	43.36
16	8	1	64.50	-55.55
-9	9	1	55.34	51.22
-8	9	1	79.46	-75.85
-7	9	1	52.56	-57.19
-4	9	1	62.17	-58.07
-3	9	1	47.89	-49.26
-2	9	1	34.84	36.30
-1	9	1	40.73	-45.15
0	9	1	41.62	38.70
4	9	1	93.91	87.84
6	9	1	28.25	-24.80
8	9	1	53.96	53.25
9	9	1	56.91	52.67
10	9	1	29.57	-17.97
-7	10	1	50.13	-57.06
-3	10	1	48.94	-49.64
3	10	1	78.81	79.60
11	10	1	59.31	-71.31
12	10	1	32.03	29.81
14	10	1	32.68	-29.64
15	10	1	65.17	-55.21
-26	0	2	33.03	-40.72
-22	0	2	73.49	-79.01
-20	0	2	56.99	53.99
-18	0	2	42.78	38.20
-16	0	2	141.74	143.72
-14	0	2	8.91	-6.35
-12	0	2	52.67	47.62
-10	0	2	67.14	-63.08
-8	0	2	303.52	-320.29
-6	0	2	213.17	220.58
-4	0	2	245.88	-258.28
-2	0	2	124.89	-110.10
0	0	2	176.42	-202.86
2	0	2	91.56	105.43
4	0	2	127.87	146.22
6	0	2	46.05	-35.33
8	0	2	235.62	240.58
10	0	2	151.62	-149.37
12	0	2	96.69	-99.90
14	0	2	216.82	-202.66
16	0	2	34.06	-39.40
18	0	2	58.55	-51.21
22	0	2	25.65	-23.81
26	0	2	48.29	47.82
32	0	2	38.46	-38.84
-28	1	2	22.07	-26.15
-27	1	2	21.77	-31.84
-26	1	2	41.08	45.44
-20	1	2	28.49	27.71
-18	1	2	30.44	-28.18
-17	1	2	38.84	32.04
-16	1	2	47.75	45.84
-15	1	2	81.11	86.90
-14	1	2	73.65	-77.79
-12	1	2	31.22	-29.34
-11	1	2	137.66	121.10
-10	1	2	37.35	-37.89
-9	1	2	36.81	-41.22
-8	1	2	93.69	-87.35
-6	1	2	42.73	-43.85
-5	1	2	167.13	-151.15
-4	1	2	130.75	113.52
-3	1	2	26.36	26.26
-2	1	2	135.82	131.79
-1	1	2	96.34	87.06
0	1	2	138.74	149.60
1	1	2	32.38	-28.06
2	1	2	74.14	90.23
3	1	2	160.59	176.77
5	1	2	109.63	-104.81
6	1	2	143.82	133.41
7	1	2	44.56	-41.95
8	1	2	210.56	-219.08
9	1	2	46.35	49.10
10	1	2	24.44	26.27
11	1	2	12.42	15.29
12	1	2	39.62	-42.01
13	1	2	35.70	-35.27
14	1	2	132.28	-136.76
15	1	2	79.11	-76.05
17	1	2	48.10	-53.43
18	1	2	21.31	-28.29
19	1	2	48.51	-46.33
20	1	2	46.16	43.97
21	1	2	51.61	46.08
24	1	2	40.92	42.78
25	1	2	35.70	31.05
-27	2	2	34.57	-44.56
-26	2	2	21.50	-13.09
-25	2	2	24.90	27.80
-24	2	2	46.89	52.12
-21	2	2	64.55	69.52
-19	2	2	47.05	-51.32
-17	2	2	66.93	71.16
-16	2	2	49.24	-46.21
-13	2	2	60.80	-58.31
-12	2	2	86.64	-88.55
-11	2	2	32.60	26.84
-10	2	2	75.49	78.30
-9	2	2	132.37	-129.72
-8	2	2	18.77	11.69
-7	2	2	132.61	117.05
-6	2	2	58.47	57.97
-5	2	2	215.42	-191.09
-4	2	2	65.93	-53.17
-3	2	2	137.28	128.18
-2	2	2	134.12	108.88
-1	2	2	95.82	-73.24
0	2	2	84.10	-85.62
1	2	2	151.06	164.99
2	2	2	137.74	151.07
3	2	2	52.85	-44.54
4	2	2	78.54	-69.46
5	2	2	21.66	-18.16
7	2	2	147.09	-149.48
8	2	2	117.76	118.46
9	2	2	110.60	-105.98
10	2	2	83.32	-74.09
11	2	2	23.04	-25.05
12	2	2	95.37	85.84
13	2	2	142.76	-153.97
15	2	2	77.65	82.11
16	2	2	51.53	51.98
17	2	2	38.73	-44.46
19	2	2	100.39	93.89
21	2	2	69.41	72.69
25	2	2	42.78	42.42
-28	3	2	22.25	-19.97
-27	3	2	39.38	38.15
-26	3	2	46.53	52.03
-24	3	2	33.60	-31.72
-19	3	2	35.25	-40.88
-17	3	2	44.40	-42.29
-16	3	2	55.83	54.08
-15	3	2	121.89	-114.17
-14	3	2	95.64	-89.63
-13	3	2	49.69	-43.50
-12	3	2	34.68	-30.60
-11	3	2	63.78	-66.44
-10	3	2	141.47	-132.27
-9	3	2	70.79	67.37
-8	3	2	40.84	29.13
-7	3	2	110.76	106.45
-6	3	2	26.74	23.92
-5	3	2	146.68	129.70
-2	3	2	20.28	14.39
-1	3	2	79.03	-71.29
1	3	2	82.10	83.15
2	3	2	183.57	199.33
3	3	2	176.28	-203.41
4	3	2	41.19	39.31
5	3	2	76.62	-80.14
6	3	2	48.13	48.81
7	3	2	103.93	-107.38
8	3	2	110.08	-101.70
9	3	2	71.22	-73.09
11	3	2	51.13	48.48
13	3	2	79.59	81.08
14	3	2	53.26	-57.56
15	3	2	100.69	89.03
16	3	2	36.68	35.71
17	3	2	26.87	31.94
18	3	2	23.58	-31.24
19	3	2	33.52	40.14
20	3	2	32.49	31.56
22	3	2	52.99	-52.88
24	3	2	48.59	48.95
25	3	2	38.81	-44.19
26	3	2	31.52	-39.39
-26	4	2	26.87	35.80
-25	4	2	32.76	40.10
-22	4	2	34.52	35.83
-20	4	2	55.66	-57.58
-19	4	2	24.33	-20.89
-17	4	2	47.08	49.15
-16	4	2	39.13	-37.56
-13	4	2	53.07	60.46
-11	4	2	29.11	28.92
-8	4	2	58.07	57.44
-7	4	2	80.97	77.59
-6	4	2	96.26	-99.01
-4	4	2	197.51	190.93
-3	4	2	98.12	102.36
-2	4	2	113.97	-104.35
-1	4	2	101.52	-101.73
0	4	2	26.85	22.66
1	4	2	61.96	-63.16
2	4	2	78.73	-83.81
4	4	2	20.23	-14.45
5	4	2	99.23	-101.81
6	4	2	35.22	-33.17
7	4	2	28.90	35.17
9	4	2	42.51	36.90
10	4	2	55.02	45.09
11	4	2	44.54	50.28
13	4	2	39.11	-37.62
14	4	2	114.41	110.04
17	4	2	44.24	-43.68
18	4	2	81.32	82.54
21	4	2	42.97	-44.76
22	4	2	23.20	-23.18
23	4	2	29.44	-36.17
26	4	2	36.79	-38.22
27	4	2	29.82	-30.68
-25	5	2	39.84	-38.39
-24	5	2	26.47	30.14
-22	5	2	72.33	-73.10
-19	5	2	56.07	-59.13
-17	5	2	40.13	42.28
-15	5	2	57.64	-62.52
-13	5	2	70.38	74.89
-12	5	2	73.84	73.25
-11	5	2	131.18	-135.06
-10	5	2	113.89	115.14
-9	5	2	60.63	60.90
-8	5	2	53.34	51.56
-7	5	2	48.02	49.03
-3	5	2	37.38	33.38
-2	5	2	116.95	-111.86
0	5	2	84.89	-86.77
1	5	2	108.28	107.45
2	5	2	74.14	-78.55
3	5	2	84.24	-88.38
4	5	2	89.77	-88.16
5	5	2	92.07	91.34
6	5	2	102.25	101.38
7	5	2	144.79	-142.80
8	5	2	36.35	41.78
9	5	2	58.98	62.16
10	5	2	77.43	77.97
11	5	2	42.92	-45.04
12	5	2	15.91	18.73
14	5	2	80.57	83.46
15	5	2	45.97	43.77
17	5	2	39.03	-37.27
19	5	2	77.43	83.81
20	5	2	44.97	-51.37
23	5	2	42.02	46.43
24	5	2	39.92	-43.12
-25	6	2	31.41	-43.21
-22	6	2	48.67	52.16
-20	6	2	54.34	-55.04
-18	6	2	88.26	98.72
-17	6	2	61.55	-65.35
-14	6	2	27.01	33.45
-13	6	2	38.89	28.18
-12	6	2	32.57	32.17
-11	6	2	16.53	16.82
-10	6	2	27.04	-27.51
-9	6	2	95.82	89.97
-7	6	2	21.98	-25.36
-6	6	2	197.67	-208.86
-3	6	2	57.47	-65.77
-2	6	2	38.92	-40.93
-1	6	2	64.85	63.72
1	6	2	111.00	-102.27
6	6	2	46.99	45.84
8	6	2	57.20	54.31
9	6	2	83.27	92.29
10	6	2	53.02	51.71
11	6	2	24.04	24.66
12	6	2	82.59	-87.35
13	6	2	55.10	55.94
16	6	2	76.51	-81.05
18	6	2	30.52	-32.76
19	6	2	22.98	-32.36
26	6	2	47.45	-49.89
-17	7	2	52.37	52.83
-14	7	2	18.88	23.64
-12	7	2	52.45	-54.75
-11	7	2	41.21	-41.17
-10	7	2	76.81	75.60
-8	7	2	74.68	-74.01
-6	7	2	23.04	25.35
-4	7	2	38.32	-39.59
-1	7	2	38.62	-40.36
0	7	2	100.90	105.33
1	7	2	70.82	68.51
2	7	2	66.06	-58.82
3	7	2	87.26	83.91
4	7	2	52.37	51.92
5	7	2	82.29	88.38
6	7	2	77.41	-74.89
7	7	2	21.58	19.60
8	7	2	39.46	51.41
10	7	2	65.95	-64.57
11	7	2	47.05	-46.10
15	7	2	19.34	-25.99
17	7	2	48.51	-61.34
19	7	2	35.00	-40.51
20	7	2	40.38	-43.61
22	7	2	50.42	51.79
27	7	2	49.86	49.47
-17	8	2	29.65	-36.28
-12	8	2	36.57	39.01
-11	8	2	67.84	-67.75
-10	8	2	33.90	36.70
-9	8	2	29.63	-34.16
-8	8	2	31.38	-29.11
-7	8	2	96.36	-98.59
-5	8	2	38.35	41.04
-3	8	2	59.98	-60.73
-2	8	2	24.87	23.31
-1	8	2	115.59	121.66
0	8	2	36.68	-34.44
1	8	2	24.23	-25.26
2	8	2	29.74	27.06
3	8	2	47.59	52.38
4	8	2	60.71	62.82
5	8	2	43.29	42.75
6	8	2	48.18	53.05
7	8	2	30.52	-35.85
8	8	2	23.69	33.20
9	8	2	18.42	21.64
11	8	2	78.59	-71.98
13	8	2	42.16	37.97
14	8	2	34.06	-33.51
15	8	2	28.76	-33.88
17	8	2	82.46	82.89
21	8	2	44.75	42.90
-17	9	2	29.95	-32.58
-16	9	2	35.95	-43.04
-15	9	2	21.23	25.62
-13	9	2	33.36	-39.76
-12	9	2	79.08	-76.55
-11	9	2	43.24	41.76
-10	9	2	36.70	-35.64
-8	9	2	35.33	-34.54
-7	9	2	40.38	41.89
-2	9	2	62.04	67.35
0	9	2	52.64	54.83
1	9	2	32.19	-27.31
5	9	2	76.46	-84.75
9	9	2	19.69	-23.87
10	9	2	65.82	-70.93
13	9	2	49.91	51.52
15	9	2	32.95	-32.27
-14	10	2	42.48	-38.77
-8	10	2	42.38	-44.51
-6	10	2	72.80	73.77
-4	10	2	47.67	-49.25
-3	10	2	29.76	26.52
-2	10	2	61.98	59.79
-1	10	2	41.89	-48.35
0	10	2	30.84	-34.24
1	10	2	32.19	29.58
2	10	2	20.01	23.44
4	10	2	46.83	-45.79
6	10	2	47.37	-48.96
10	10	2	31.22	-26.01
12	10	2	39.54	40.89
16	10	2	62.63	66.68
-12	11	2	40.81	49.63
-8	11	2	46.48	51.67
-7	11	2	48.70	50.95
-5	12	2	35.03	-38.13
-1	11	2	36.68	39.59
0	12	2	36.89	-43.13
0	11	2	45.89	-47.35
1	11	2	34.14	-37.29
2	11	2	25.98	26.12
4	11	2	40.43	-43.16
5	11	2	104.58	-108.90
-21	0	3	50.72	57.88

TABLE 2 (cont.)

			15	
-17	0	3	34.98	-38.93
-15	0	3	44.40	-43.24
-13	0	3	80.30	-78.62
-11	0	3	119.62	-113.05
-9	0	3	83.40	83.37
-7	0	3	148.90	139.41
-5	0	3	7.62	-12.48
-3	0	3	125.18	136.08
-1	0	3	90.15	94.79
1	0	3	89.64	105.58
3	0	3	10.83	18.27
5	0	3	122.83	-137.22
7	0	3	77.73	-79.09
9	0	3	191.97	-196.51
11	0	3	13.04	-11.55
13	0	3	64.63	-69.95
15	0	3	59.58	68.98
17	0	3	72.71	73.16
21	0	3	54.66	48.36
-20	1	3	45.59	51.35
-19	1	3	75.27	-73.97
-16	1	3	41.11	42.53
-15	1	3	101.87	-101.66
-14	1	3	38.84	-42.38
-13	1	3	86.70	82.95
-12	1	3	66.52	70.15
-11	1	3	46.48	-45.11
-10	1	3	201.99	-175.56
-9	1	3	48.72	43.24
-8	1	3	57.37	-57.24
-7	1	3	18.80	-17.50
-6	1	3	167.10	150.93
-5	1	3	67.49	55.67
-4	1	3	21.53	19.50
-3	1	3	22.36	26.41
-2	1	3	90.96	95.49
-1	1	3	34.06	-38.28
0	1	3	110.09	-129.42
1	1	3	48.18	-47.09
2	1	3	33.33	47.90
3	1	3	100.44	-115.50
4	1	3	150.11	-161.43
5	1	3	80.48	-78.66
6	1	3	104.25	103.79
7	1	3	21.34	-18.38
8	1	3	28.47	-30.91
9	1	3	138.85	130.03
10	1	3	78.11	-79.87
11	1	3	27.49	30.54
15	1	3	32.95	38.42
16	1	3	31.57	32.51
19	1	3	40.43	-42.71
20	1	3	96.61	93.78
21	1	3	40.03	-33.14
22	1	3	32.95	-30.27
23	1	3	54.80	-53.70
-20	2	3	65.31	-66.67
-16	2	3	54.85	-56.92
-12	2	3	73.81	72.25
-11	2	3	41.35	41.17
-10	2	3	50.02	49.02
-9	2	3	74.14	68.07
-8	2	3	83.97	84.52
-7	2	3	45.21	-47.56
-6	2	3	29.92	-21.41
-5	2	3	82.89	-77.72
-4	2	3	137.07	115.21
-2	2	3	52.48	-53.91
-1	2	3	12.99	17.56
0	2	3	50.99	-48.77
1	2	3	132.96	140.95
2	2	3	76.65	-78.54
3	2	3	24.82	22.09
4	2	3	105.36	-94.27
5	2	3	20.45	23.50
6	2	3	37.49	43.60
7	2	3	69.38	-66.51
8	2	3	56.26	-58.26
10	2	3	127.34	125.92
11	2	3	60.39	59.11
12	2	3	58.66	52.70
13	2	3	39.49	41.70
14	2	3	111.76	110.58
15	2	3	81.70	-73.25
16	2	3	27.44	31.50
18	2	3	42.32	38.70
19	2	3	49.94	-43.95
20	2	3	46.51	-46.63
21	2	3	25.60	-21.86
22	2	3	42.40	-40.99
23	2	3	49.72	49.07
26	2	3	43.21	-44.35
-19	3	3	35.43	-32.97
-18	3	3	23.71	27.71
-17	3	3	51.32	53.96
-15	3	3	60.20	-68.17
-14	3	3	77.30	83.23
-13	3	3	47.94	42.35
-12	3	3	41.08	40.86
-11	3	3	34.46	-27.98
-9	3	3	75.87	74.58
-7	3	3	31.73	32.28
-6	3	3	54.50	-59.75
-5	3	3	67.66	-61.36
-4	3	3	120.27	-116.52
-2	3	3	137.12	-132.03
-1	3	3	69.11	-63.75
0	3	3	163.91	-149.79
1	3	3	59.58	69.10
2	3	3	89.50	-88.97
3	3	3	120.67	-123.17
4	3	3	92.75	99.04
5	3	3	27.33	29.00
6	3	3	91.91	84.43
7	3	3	75.35	-73.01
8	3	3	123.59	119.48
9	3	3	62.09	58.41
11	3	3	33.76	-36.66
12	3	3	86.64	78.58
15	3	3	72.25	72.90
16	3	3	46.89	-46.64
17	3	3	57.55	-56.76
21	3	3	40.35	-38.96
-24	4	3	40.76	-35.79
-23	4	3	42.83	38.02
-21	4	3	60.98	-67.35
-18	4	3	24.47	32.26
-15	4	3	47.94	56.20
-13	4	3	42.43	45.01
-11	4	3	31.83	-38.18
-10	4	3	76.87	-75.97
-8	4	3	33.27	-33.07
-7	4	3	40.46	-37.57
-3	4	3	163.64	-151.33
-2	4	3	96.61	-88.83
1	4	3	26.01	23.74
2	4	3	30.49	-32.64
5	4	3	84.89	85.62
8	4	3	49.07	-44.08
9	4	3	116.13	110.45
10	4	3	58.93	-53.37
11	4	3	38.54	36.70
12	4	3	129.53	-121.99
15	4	3	75.33	-73.29
16	4	3	44.67	-40.63
19	4	3	45.99	-47.35
21	4	3	67.39	-71.16
27	4	3	55.77	50.56
-21	5	3	69.28	72.43

[illegible]	[illegible]	[illegible]	76.59	74.76
-16	5	3	64.68	-61.99
-15	5	3	41.30	51.35
-14	5	3	65.33	66.13
-12	5	3	60.66	-62.85
-10	5	3	115.92	111.02
-9	5	3	54.48	-53.85
-8	5	3	31.87	-35.36
-7	5	3	49.37	-49.79
-6	5	3	39.70	40.41
-5	5	3	44.83	-43.47
-4	5	3	76.76	71.59
-2	5	3	82.32	-78.12
-1	5	3	96.47	98.96
0	5	3	58.72	66.13
1	5	3	41.40	45.36
3	5	3	53.25	56.55
5	5	3	28.82	29.36
8	5	3	44.46	44.59
13	5	3	71.30	-66.14
15	5	3	51.72	-50.35
-11	6	3	84.70	-85.34
-9	6	3	37.87	45.00
-8	6	3	46.18	-47.34
-7	6	3	84.51	-79.25
-5	6	3	70.49	70.67
-1	6	3	56.37	57.49
0	6	3	43.51	46.26
1	6	3	19.34	26.22
2	6	3	98.39	98.53
3	6	3	54.75	-59.70
4	6	3	42.97	49.35
5	6	3	20.09	-25.07
7	6	3	14.11	-116.75
8	6	3	95.15	90.02
10	6	3	92.39	-94.32
11	6	3	65.09	-62.04
13	6	3	23.66	25.47
14	6	3	51.40	-49.66
17	6	3	80.78	79.46
19	6	3	50.56	55.73
-20	7	3	37.78	39.14
-18	7	3	29.95	31.25
-17	7	3	38.97	-35.40
-16	7	3	46.51	-52.47
-15	7	3	47.10	50.08
-13	7	3	37.84	-40.61
-12	7	3	41.70	-31.20
-11	7	3	29.41	34.82
-7	7	3	30.14	33.40
-6	7	3	35.03	40.58
-5	7	3	41.54	-43.44
-4	7	3	70.25	69.09
-2	7	3	33.81	37.60
-1	7	3	71.95	81.42
0	7	3	74.97	76.90
1	7	3	88.18	-85.25
5	7	3	26.87	-32.42
6	7	3	39.13	-30.76
7	7	3	29.38	36.15
8	7	3	49.07	-58.58
10	7	3	38.92	-38.70
11	7	3	41.08	37.09
14	7	3	31.30	31.08
18	7	3	38.81	35.65
19	7	3	38.41	-39.74
21	7	3	40.38	41.65
-24	8	3	42.89	54.62
-22	8	3	35.52	-43.19
-10	8	3	59.61	62.22
-7	8	3	33.41	34.73
-6	8	3	35.54	40.99
-4	8	3	23.55	-28.56
-3	8	3	43.81	38.08
0	8	3	66.12	-65.32
2	8	3	41.08	45.41
3	8	3	23.44	29.73
5	8	3	56.31	-54.69
8	8	3	53.88	50.04
9	8	3	36.11	-44.44
12	8	3	64.28	61.44
-13	9	3	33.79	-36.12
-12	9	3	57.88	61.62
-5	9	3	81.48	82.08
-4	9	3	55.56	-61.14
0	9	3	72.71	-70.69
1	9	3	80.19	-84.05
2	9	3	30.82	30.47
4	9	3	31.09	-37.11
5	9	3	39.59	-36.66
6	9	3	75.95	74.51
10	9	3	41.46	24.27
-5	10	3	71.68	-76.80
-3	10	3	45.78	46.60
-16	11	3	40.92	55.10
0	11	3	60.28	-61.43
-6	12	3	76.70	-75.65
-4	12	3	44.83	36.37
-24	0	4	75.03	-73.22
-20	0	4	36.84	-40.07
-16	0	4	69.82	70.90
-12	0	4	202.64	199.90
-10	0	4	74.11	-71.34
-8	0	4	209.02	204.68
-6	0	4	13.37	-19.60
-4	0	4	92.48	92.11
-2	0	4	75.46	-77.87
2	0	4	42.86	-43.88
4	0	4	53.21	-60.28
6	0	4	85.48	82.48
8	0	4	15.75	-14.72
10	0	4	164.72	167.89
12	0	4	64.68	57.87
14	0	4	54.58	55.14
16	0	4	66.74	-63.30
22	0	4	100.01	-90.50
-18	1	4	56.61	42.57
-15	1	4	51.72	-45.03
-14	1	4	44.91	47.95
-12	1	4	69.33	-63.69
-11	1	4	43.29	-40.34
-10	1	4	32.30	-31.56
-9	1	4	155.97	119.98
-8	1	4	73.49	-71.72
-7	1	4	31.98	-15.95
-6	1	4	80.89	-79.78
-5	1	4	66.57	-63.45
-4	1	4	109.98	-97.34
-3	1	4	69.19	55.34
-2	1	4	70.63	-78.07
-1	1	4	97.18	-110.04
0	1	4	56.88	72.88
1	1	4	35.19	40.12
2	1	4	14.75	-22.51
4	1	4	73.08	79.85
5	1	4	52.80	54.84
6	1	4	79.05	72.63
7	1	4	47.32	43.51
8	1	4	47.91	39.45
9	1	4	51.13	42.96
10	1	4	34.71	32.90
11	1	4	56.50	54.52
12	1	4	77.98	-66.61
15	1	4	27.33	19.89
16	1	4	98.04	-96.37
17	1	4	33.95	-31.09
19	1	4	42.66	-38.22
21	1	4	62.31	-63.65
-25	2	4	46.97	-42.12
-24	2	4	45.48	-40.55

7	7	4	43.67	47.61
8	7	4	70.92	69.13
10	7	4	47.10	-46.25
11	7	4	43.46	39.38
13	7	4	32.87	-30.14
14	7	4	34.49	-33.97
17	7	4	44.10	-45.85
19	7	4	40.08	-41.21
20	7	4	47.24	45.85
-12	8	4	39.00	37.70
-11	8	4	60.93	58.13
-9	8	4	75.27	-67.18
-8	8	4	62.28	61.00
-5	8	4	59.44	-59.36
-4	8	4	32.14	-27.28
-3	8	4	37.46	31.29
-2	8	4	68.92	-66.26
2	8	4	80.46	-72.63
3	8	4	73.76	69.27
7	8	4	85.02	86.63
8	8	4	40.03	-39.86
13	8	4	74.65	-76.43
14	8	4	42.97	38.04
15	8	4	45.27	-37.74
18	8	4	41.46	-38.16
-20	9	4	44.46	40.28
-19	9	4	48.37	-49.79
-17	9	4	43.67	41.43
-15	9	4	41.35	-44.07
-8	9	4	27.76	30.17
-4	9	4	48.45	-41.75
-3	9	4	47.51	43.66
1	9	4	69.01	61.75
2	9	4	64.82	63.01
5	9	4	45.62	41.38
6	9	4	48.29	49.02
7	9	4	42.78	-43.23
12	9	4	46.32	-39.57
13	9	4	36.60	-35.76
15	9	4	38.16	38.98
-10	10	4	71.92	-62.24
-7	10	4	52.23	-50.83
-4	10	4	86.72	76.55
2	10	4	41.05	39.64
8	10	4	77.03	-71.22
-23	0	5	65.22	62.83
-19	0	5	78.67	68.32
-17	0	5	42.48	34.87
-13	0	5	69.17	67.34
-11	0	5	117.76	-99.27
-7	0	5	73.44	-82.10
-5	0	5	70.68	64.40
-3	0	5	44.54	38.93
-1	0	5	63.71	61.06
1	0	5	54.42	66.11
3	0	5	68.36	68.16
5	0	5	86.56	81.47
11	0	5	129.77	-119.48
13	0	5	82.70	-72.94
15	0	5	60.34	-53.03
17	0	5	33.98	-25.10
23	0	5	48.64	38.96
-22	1	5	69.82	70.51
-18	1	5	67.74	57.42
-6	1	5	51.50	-43.54
-5	1	5	80.19	80.01
-4	1	5	81.35	60.90
-2	1	5	58.96	-62.42
-1	1	5	74.25	86.40
0	1	5	67.14	75.37
1	1	5	15.99	-21.94
3	1	5	57.66	60.95
4	1	5	53.29	56.56
5	1	5	59.39	-44.69
7	1	5	53.80	-46.48
8	1	5	95.10	-82.50
9	1	5	44.64	-44.82
11	1	5	52.31	-41.90
12	1	5	64.87	-56.13
15	1	5	45.27	38.12
17	1	5	77.08	68.91
-12	2	5	82.05	-69.01
-8	2	5	66.71	-58.58
-6	2	5	52.96	42.46
-5	2	5	62.36	40.69
-4	2	5	36.70	29.33
-3	2	5	37.65	-19.82
-2	2	5	74.79	70.33
-1	2	5	41.13	-39.13
0	2	5	58.99	61.53
1	2	5	30.33	-31.82
2	2	5	93.37	-90.98
3	2	5	27.74	-27.32
5	2	5	32.36	22.71
6	2	5	107.20	-98.29
7	2	5	55.07	51.01
8	2	5	42.43	-33.50
9	2	5	43.78	40.15
10	2	5	108.28	-94.13
11	2	5	51.80	-46.74
18	2	5	76.16	67.91
22	2	5	49.86	37.70
28	2	5	58.47	-52.13
-22	3	5	46.97	-43.55
-21	3	5	46.40	-42.94
-18	3	5	80.13	-65.40
-17	3	5	114.97	-109.94
-15	3	5	52.37	38.31
-12	3	5	64.52	51.90
-8	3	5	75.65	70.86
-7	3	5	30.57	-31.90
-5	3	5	101.50	82.02
-1	3	5	34.46	34.76
0	3	5	39.35	-33.69
3	3	5	78.59	74.16
4	3	5	93.96	-86.38
5	3	5	50.88	-48.77
6	3	5	42.89	-36.64
10	3	5	84.18	74.66
12	3	5	70.14	62.18
14	3	5	88.99	81.67
17	3	5	48.67	49.68
-15	4	5	64.14	-60.81
-12	4	5	84.89	69.45
-11	4	5	74.03	64.02
-10	4	5	80.08	69.07
-9	4	5	57.23	-48.18
-8	4	5	41.73	-44.85
-7	4	5	46.56	40.45
-4	4	5	78.24	-63.14
-3	4	5	56.28	-52.75
1	4	5	115.43	-105.45
4	4	5	52.42	47.73
5	4	5	95.12	-91.29
6	4	5	35.03	-29.75
7	4	5	63.60	61.34
8	4	5	58.28	51.82
10	4	5	41.59	39.74
11	4	5	110.27	102.06
12	4	5	31.98	38.32
13	4	5	48.75	53.90
23	4	5	62.40	-78.64
-18	5	5	58.04	-48.79
-16	5	5	107.55	91.54
-14	5	5	86.75	-82.67
-12	5	5	63.25	-55.27
-9	5	5	38.11	35.20
-6	5	5	66.60	51.44
-5	5	5	60.88	-46.85
-4	5	5	28.25	-26.18

-23	2	4	31.01	30.76
-21	2	4	48.53	-50.34
-19	2	4	40.67	37.54
-17	2	4	59.69	55.41
-15	2	4	38.35	31.62
-14	2	4	39.97	37.34
-13	2	4	99.50	90.41
-11	2	4	103.36	-91.51
-10	2	4	90.96	-79.52
-7	2	4	104.20	-95.52
-6	2	4	31.49	25.15
-3	2	4	121.86	-100.35
-1	2	4	43.10	41.95
0	2	4	40.16	-35.50
1	2	4	45.10	51.26
3	2	4	71.81	78.52
4	2	4	49.37	-52.78
5	2	4	93.04	89.80
8	2	4	113.68	-118.31
9	2	4	144.44	127.98
10	2	4	37.51	38.69
11	2	4	113.68	-104.18
12	2	4	33.87	-27.87
14	2	4	46.53	-37.05
15	2	4	73.44	-68.67
17	2	4	96.36	-85.21
20	2	4	54.64	48.02
23	2	4	55.45	50.35
27	2	4	54.34	49.98
-20	3	4	44.21	-47.49
-18	3	4	51.69	51.04
-16	3	4	67.55	-63.87
-15	3	4	33.71	-26.50
-14	3	4	30.98	32.88
-13	3	4	52.69	-43.41
-12	3	4	30.30	-22.31
-11	3	4	34.89	45.36
-9	3	4	37.24	-30.53
-8	3	4	27.71	-17.07
-7	3	4	152.81	-131.42
-6	3	4	81.13	-72.00
-5	3	4	42.11	34.43
-2	3	4	65.36	-58.64
-1	3	4	118.70	110.95
0	3	4	53.07	56.70
1	3	4	54.53	53.63
2	3	4	84.13	-82.84
3	3	4	64.52	64.34
4	3	4	116.67	113.53
7	3	4	86.80	-87.82
8	3	4	60.07	53.14
9	3	4	22.31	-25.66
11	3	4	61.44	-54.90
13	3	4	25.95	-29.86
16	3	4	110.09	-97.20
17	3	4	91.88	78.89
18	3	4	31.52	28.68
21	3	4	94.77	89.37
22	3	4	34.60	37.42
23	3	4	37.43	40.14
-20	4	4	54.29	51.48
-19	4	4	45.81	-44.08
-18	4	4	40.67	-39.55
-16	4	4	36.08	37.66
-13	4	4	37.43	-36.65
-12	4	4	139.17	-135.05
-11	4	4	49.75	-49.02
-9	4	4	147.19	138.35
-8	4	4	89.86	-85.57
-6	4	4	99.23	87.47
-5	4	4	83.13	73.21
-4	4	4	62.77	-59.35
-3	4	4	45.37	-40.05
-2	4	4	77.49	72.58
-1	4	4	42.08	-38.43
1	4	4	30.98	-27.54
3	4	4	51.99	-47.88
4	4	4	49.75	51.86
6	4	4	48.99	-46.64
7	4	4	118.86	-103.72
8	4	4	27.79	-22.20
9	4	4	50.07	-41.48
10	4	4	62.44	-57.56
13	4	4	77.65	69.73
17	4	4	69.19	71.01
22	4	4	64.06	52.71
-19	5	4	40.05	41.06
-17	5	4	89.50	-88.09
-15	5	4	40.78	34.65
-14	5	4	47.45	-39.53
-13	5	4	36.46	-36.05
-9	5	4	41.16	-38.83
-8	5	4	25.93	22.25
-7	5	4	45.81	-32.87
-6	5	4	87.80	82.58
-5	5	4	41.67	43.04
-4	5	4	46.26	41.43
-3	5	4	45.64	-46.59
-1	5	4	100.69	99.87
0	5	4	14.69	26.21
1	5	4	67.52	-65.10
2	5	4	28.41	-23.41
3	5	4	46.21	45.01
4	5	4	104.06	-101.07
5	5	4	29.63	-31.91
6	5	4	56.18	-50.90
8	5	4	21.31	-24.89
11	5	4	81.65	-76.39
12	5	4	34.22	30.97
14	5	4	61.36	61.69
15	5	4	78.92	-74.31
16	5	4	62.28	53.29
17	5	4	33.76	25.84
19	5	4	35.16	-34.12
21	5	4	49.69	45.56
-14	6	4	118.75	112.02
-13	6	4	31.09	-26.32
-12	6	4	56.12	-52.75
-11	6	4	45.51	32.95
-10	6	4	66.98	60.93
-9	6	4	23.36	-30.21
-7	6	4	79.59	70.21
-6	6	4	87.48	81.87
-5	6	4	30.87	-30.76
-4	6	4	37.35	-30.41
-3	6	4	89.88	81.33
-2	6	4	68.41	-67.96
0	6	4	65.17	-63.39
1	6	4	38.41	-36.17
3	6	4	30.28	-28.93
5	6	4	34.65	-25.93
8	6	4	60.53	56.18
9	6	4	45.81	-45.77
11	6	4	72.62	62.19
12	6	4	99.07	97.36
15	6	4	59.47	53.58
16	6	4	47.75	42.14
17	6	4	45.37	46.36
20	6	4	53.99	-43.95
-12	7	4	90.61	85.48
-11	7	4	55.42	51.22
-10	7	4	25.41	-29.22
-9	7	4	51.91	39.92
-4	7	4	51.02	-43.62
-2	7	4	51.96	51.83
0	7	4	74.38	-72.01
1	7	4	47.53	-42.97
2	7	4	84.56	-78.72
4	7	4	41.54	-42.45
5	7	4	29.20	-32.83

-3	5	5	27.90	-26.82
-2	5	5	46.26	34.95
-1	5	5	55.72	-38.60
0	5	5	84.35	-72.46
1	5	5	27.55	-17.58
2	5	5	42.05	36.42
3	5	5	28.03	27.28
5	5	5	78.03	73.37
7	5	5	52.02	44.51
9	5	5	31.38	32.01
15	5	5	39.24	-42.31
16	5	5	74.81	65.06
19	5	5	79.05	-69.48
-15	6	5	59.39	50.81
-12	6	5	78.40	68.09
-9	6	5	74.38	-65.54
-6	6	5	66.57	-44.65
-5	6	5	52.42	-46.59
-2	6	5	51.96	-42.38
-1	6	5	52.67	49.57
3	6	5	63.12	58.61
4	6	5	43.97	-43.95
5	6	5	33.00	17.36
6	6	5	42.81	41.48
-5	7	5	58.47	-45.59
-3	7	5	45.89	39.01
0	7	5	16.50	24.76
1	7	5	33.08	40.20
2	7	5	33.19	33.05
3	7	5	69.17	-58.92
10	7	5	35.89	-44.72
12	7	5	43.56	-48.46
13	7	5	70.68	-51.19
14	7	5	53.29	-48.64
15	7	5	38.05	34.87
-10	8	5	72.76	-64.85
-8	8	5	63.58	53.45
-7	8	5	70.03	-64.20
-4	8	5	60.82	48.04
8	8	5	77.22	-68.58
17	8	5	57.64	-46.38
9	9	5	74.70	-67.81
14	9	5	38.86	40.37
15	9	5	38.81	40.10
-16	0	6	74.49	-68.86
-12	0	6	81.73	-64.86
-10	0	6	94.37	74.57
-6	0	6	103.55	80.94
-4	0	6	38.95	39.80
2	0	6	47.83	-52.76
4	0	6	41.78	-46.70
6	0	6	161.67	-150.50
8	0	6	85.24	-70.23
10	0	6	90.45	-73.28
14	0	6	41.75	35.78
18	0	6	46.26	40.50
24	0	6	77.49	-55.51
-10	1	6	71.25	61.26
-5	1	6	41.05	36.81
-4	1	6	51.96	-50.98
-3	1	6	33.19	-26.63
-1	1	6	34.95	37.84
0	1	6	39.65	-50.70
1	1	6	88.56	-97.64
3	1	6	56.91	-56.76
5	1	6	26.41	-27.80
6	1	6	45.05	38.33
8	1	6	60.61	45.94
12	1	6	73.22	64.19
17	1	6	92.12	67.46
18	1	6	62.25	-51.75
-17	2	6	67.52	-58.93
-16	2	6	66.03	-58.64
-15	2	6	64.39	55.26
-14	2	6	48.10	39.61
-13	2	6	40.86	-29.78
-12	2	6	57.23	-19.11
-11	2	6	74.14	63.15
-7	2	6	44.91	45.52
-5	2	6	32.57	-33.61
-1	2	6	96.47	-78.47
0	2	6	60.98	49.55
1	2	6	88.29	-87.08
3	2	6	44.75	49.81
4	2	6	27.71	25.05
5	2	6	41.38	-36.25
7	2	6	90.13	84.18
11	2	6	58.66	41.49
-9	3	6	82.29	-61.32
-6	3	6	73.89	53.62
-5	3	6	97.77	-67.65
-4	3	6	96.18	-75.07
1	3	6	55.88	-49.47
3	3	6	56.61	48.63
5	3	6	110.49	83.28
7	3	6	118.73	87.42
8	3	6	46.10	49.24
12	3	6	87.13	74.54
13	3	6	42.73	-41.73
14	3	6	43.83	-28.46
15	3	6	69.46	-66.09
16	3	6	61.42	47.83
17	3	6	98.80	-72.48
18	3	6	87.13	-69.18
-12	4	6	96.66	68.16
-10	4	6	111.54	-94.01
-6	4	6	65.74	-51.31
-1	4	6	71.11	57.75
2	4	6	124.67	101.60
5	4	6	56.18	-44.21
-14	5	6	71.44	-50.59
-9	5	6	83.37	-64.73
-8	5	6	72.95	-49.79
-7	5	6	71.63	61.10
-6	5	6	56.55	46.45
-3	5	6	88.40	62.92
-1	5	6	49.42	-39.81
0	5	6	66.14	61.55
2	5	6	68.36	59.06
8	5	6	74.73	-66.10
9	5	6	60.23	-44.77
12	5	6	77.92	-67.19
-14	6	6	47.32	-51.75
-11	6	6	69.38	-61.66
-1	6	6	50.72	35.88
4	6	6	80.13	-72.55
5	6	6	52.26	45.58
-6	7	6	79.94	-59.10
-4	7	6	85.05	68.14
-2	7	6	75.70	-66.35
0	7	6	54.31	25.64
-9	8	6	67.66	55.24
-6	8	6	68.47	52.55
-1	8	6	73.71	-55.70

0.077. In the final calculation, the following weight system was adopted.

$$\sqrt{w} = 76/F_o \quad \text{when } F_o > 76,$$
$$\sqrt{w} = 1.0 \quad \text{when } 76 \geq F_o \geq 7,$$
$$\sqrt{w} = 0 \quad \text{when } 7 \geq F_o.$$

The final atomic parameters and their standard deviations are given in Table 1 and the observed and calculated structure factors in Table 2.

Discussion of the Structure

The present X-ray structure determination has shown the chemical structure of the 3 : 2 adduct to be 1-(4-bromo-2,6-dimethylphenyl)-2-(4-bromo-2,6-dimethylphenyl)imino-1,2-dihydro-3,4,5,5,6,7-hexacarbomethoxy-5*H*-1-pyrindine (I). The chemical structure and conformation of the molecule are shown in Fig. 1. From the result of X-ray analysis, the mechanism of the reaction was clarified which enabled us to suppose the chemical structures of other reaction products. Details of the study have been published in a separate paper.[3]

The bond lengths and angles are shown in Figs. 2 and 3 along with their standard deviations. The average C–C, C–C(methyl) and C–Br bond lengths found in the substituted phenyl groups are 1.41 Å, 1.54 Å and 1.91 Å, respectively, which agree well with the standard values. The average bond lengths found in the ester groups are 1.50 Å for C(ring)–C, 1.20 Å for C=O, 1.31 Å for C–O and 1.49 Å for O–C(methyl) which are also in good agreement with those of normal carbomethoxy groups. The C–C bond lengths found in the pyrindine ring vary from 1.32 Å to 1.46 Å except for C(8)–C(5) and C(6)–C(5) bonds which correspond undoubtedly to single bonds. There are few examples of X-ray analysis of a compound containing the pyrindine ring. The only one we found is 1-methyl-6-[5-(1-methyl-1*H*-1-pyrindinyl)]-1-azoniaindan iodide (II)[4] which was found to consist of 1-methyl-1*H*-1-pyrindine and 1-methyl-1-azoniaindan iodide groups. The bond lengths in the former group

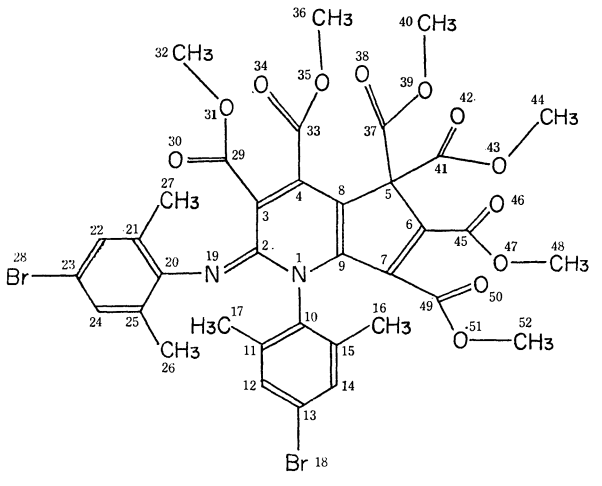

I

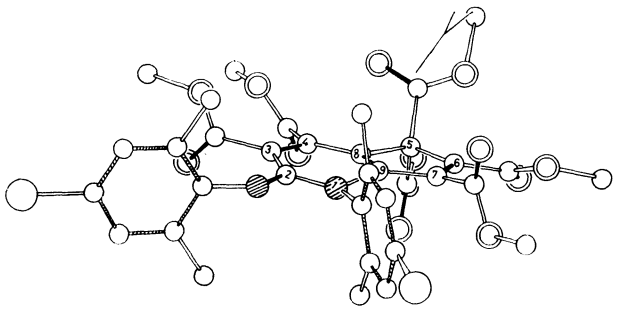

Fig. 1. Chemical structure (I) and conformation of the adduct.

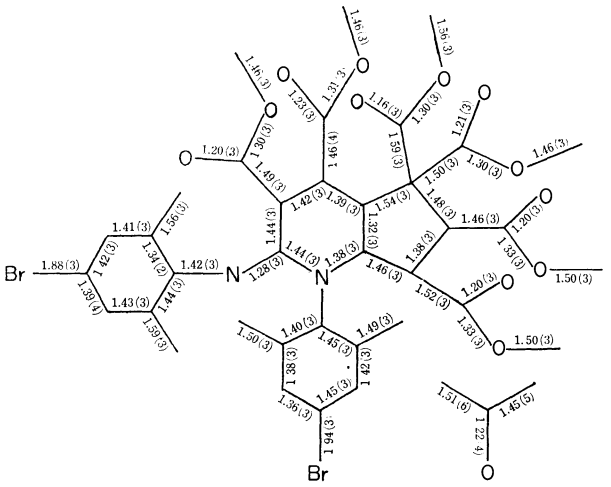

Fig. 2. Bond lengths and their estimated standard deviations. The e.s.d.'s are given in parentheses denoting the least significant digits in the bond lengths.

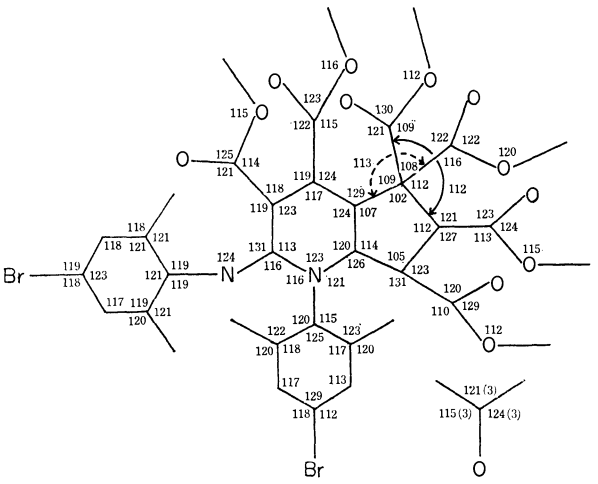

Fig. 3. Bond angles and their estimated standard deviations. The e.s.d.'s are 2° except those in acetone.

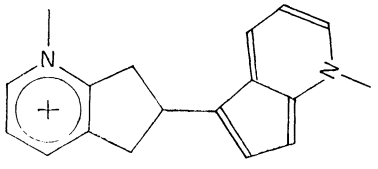

II

3) Y. Suzuki, N. Obata, and T. Takizawa, *Tetrahedron Lett.*, **1970**, 2667.

4) H. L. Ammon and L. H. Jensen, *J. Amer. Chem. Soc.*, **88** 681 (1966).

TABLE 3. LEAST-SQUARES PLANES AND DEVIATIONS OF THE ATOMS

The planes are of the form $AX+BY+CZ=D$, where X, Y, Z, and D are in Å unit relative to the axes a^*, b, and c.

Best plane through pyridine ring			
$-0.517X-0.311Y+0.798Z=-6.470$			
N(1)	−0.001 Å	C(6)	0.012 Å
C(2)	0.058	C(7)	−0.047
C(3)	−0.060	C(8)	0.015
C(4)	−0.005	C(9)	0.007
C(5)	0.023		
Distances from the above plane			
C(10)	0.141 Å	C(37)	−1.273 Å
N(19)	0.093	C(41)	1.223
C(29)	−0.191	C(45)	0.180
C(33)	0.084	C(49)	−0.330
Best planes through phenyl groups			
$0.637X+0.272Y+0.722Z=10.158$		$-0.419X+0.855Y+0.306Z=-1.261$	
C(10)	−0.006 Å	C(20)	−0.029 Å
C(11)	0.003	C(21)	0.023
C(12)	0.020	C(22)	−0.007
C(13)	−0.039	C(23)	−0.003
C(14)	−0.032	C(24)	−0.002
C(15)	−0.011	C(25)	0.017
Distances from the above planes			
C(16)	0.012 Å	C(26)	−0.003 Å
C(17)	−0.062	C(27)	0.040
Br(18)	0.064	Br(28)	−0.015
C(52)	−3.745	C(32)	−3.603

Best planes through ester groups	Distances from the planes		
$-0.107X+0.815Y+0.569Z=1.495$			
C(3)	−0.004 Å		
C(29)	0.013	C(32)	−0.115 Å
O(30)	−0.005		
O(31)	−0.004		
$0.256X+0.139Y+0.957Z=5.030$			
C(4)	0.000 Å		
C(33)	−0.001	C(36)	0.069 Å
O(34)	0.000		
O(35)	0.000		
$0.247X+0.954Y-0.168Z=3.496$			
C(5)	0.005 Å		
C(37)	−0.019	C(40)	−0.098 Å
O(38)	0.008		
O(39)	0.006		
$0.857X-0.049Y+0.514Z=10.045$			
C(5)	−0.003 Å		
C(41)	0.010	C(44)	0.064 Å
O(42)	−0.004		
O(43)	−0.003		
$-0.585X+0.153Y+0.796Z=-6.521$			
C(6)	−0.002 Å		
C(45)	0.007	C(48)	0.155 Å
O(46)	−0.003		
O(47)	−0.002		
$-0.443X+0.532Y+0.721Z=6.232$			
C(7)	0.013 Å		
C(49)	−0.049	C(52)	−0.048 Å
O(50)	0.020		
O(51)	0.016		

show a characteristic of aromatic systems, and most C–C bond lengths (average value of the seven peripheral bonds is 1.394 Å and the length of the transannular bond is 1.482 Å) are in good overall agreement with those found in azulenes. The bond lengths and angles in the latter group indicate that the five-membered ring can be best described as cyclopentenyl while the six-membered ring can be described as positively charged pyridinum, since the bond lengths involved in the six-membered ring agree with similar parameters in heterocyclic molecules having the character of sp^2 hybridization and electron delocalization. The structure of the pyrindine group in the present compound differs from that of the above two cases in that it has many substituents such as six carbomethoxy, a phenyl and a phenylimino group. Furthermore, the C(2)–N(19) bond length (1.28 Å) is significantly shorter than any other C–N lengths in the present molecule while the bond lengths of C(8)–C(5) and C(6)–C(5) (1.54 Å and 1.48 Å, respectively) are much longer than other C–C lengths involved in the ring. It is therefore reasonable to assume that the six-membered ring has an aromatic nature and the resonance structure is extended to N(19) on one side and to C(6) through C(7) on the other side of the ring. The mean C–C bond length in the six-membered ring (1.39 Å) is almost equal to that in 2-pyridone[5] (1.39 Å) and in pyridine[6] (1.395 Å) while the C–N bond lengths (1.38 Å and 1.44 Å) are longer than those in 2-pyridone (1.34 Å and 1.40 Å) and in pyridine (1.340 Å). The nitrogen atom, N(1), is undoubtedly in a state of sp^2 hybridization as evidenced by the nearly planar configuration of the substituent atoms (C(2), C(9) and C(10), see Table 3).

Least-squares planes through various groups of atoms and the deviations of atoms from each plane are shown in Table 3. Each of the pyrindine ring and the two substituted phenyl groups is almost planar within experimental error. These substituted phenyl groups are twisted with respect to the plane of the pyrindine ring at angles of 77° and 82°, respectively. Each C(ring)–COO– group is planar and the terminal methyl carbon deviates slightly from the plane. The six carbomethoxy groups are also twisted with respect to the plane of the pyrindine ring in various degrees ranging from 28° to 79°.

In the NMR spectrum of the present compound, two signals at 6.7 τ (s. 3H) and 6.9 τ (s. 3H) which are assigned to the methyl protons of C(32) and C(52), appear at a higher field than would be expected for

5) B. R. Penfold, *Acta Crystallogr.*, **6**, 591 (1953).
6) B. Bak, L. Hansen, and J. R. Rastrup-Andersen, *J. Chem. Phys.*, **22**, 2013 (1954).

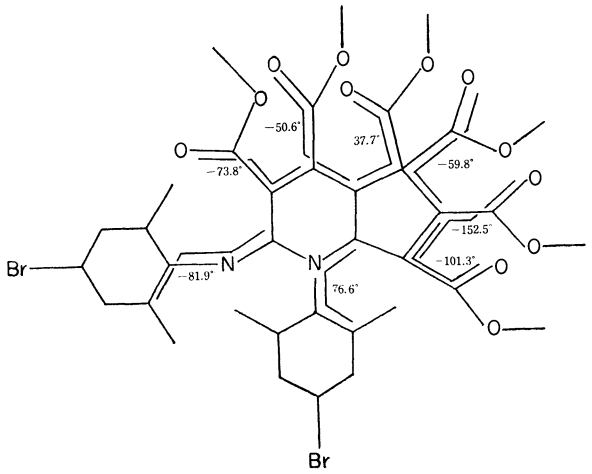

Fig. 4. Internal rotation angles about the bonds joining the pyrindine ring and the substituted groups.
Internal rotation angle A–B–C–D shown in Fig. 4 by bold line, is defined as the angle between the projections of A–B and C–D, when the projection is taken along the B–C bond. The positive angle is taken in the same sense as that of the turning direction of a right handed screw advancing along the B–C bond.

this kind of proton. The reason for this may be the effect of ring current of the proximate phenyl groups which are situated with their planes facing the methyl groups (see Fig. 1).

The crystal structure projected along the *b*-axis is shown in Fig. 5. Intermolecular short distances less than 3.6 Å are indicated in the Figure by dotted lines and are listed in Table 4. The molecules are denoted by Roman numerals and the subscript in parentheses indicates translations along the three edges of the unit cell. It is seen that the molecules lie along ($\bar{4}01$) plane and stack on top of the other mainly by the van der Waals force between the substituents of the phenyl group and carbomethoxy groups. The present molecule has so many bulky substituent groups of the pyrindine ring that there remains a wide space between the stacked molecules. The molecule of acetone is enclosed in the space as a solvent of crystallization and interacts with the surrounding adduct molecules by van der Waals force, the shortest distance being 3.55 Å found between O(56) I(000) and Br(28) III(000). Within ($\bar{4}01$) plane, the molecules are bound together through

TABLE 4. INTERMOLECULAR DISTANCES LESS THAN 3.6 Å

From molecule I	To atom	Of molecule	Translation	Distance
Br(18)	O(51)	II	010	3.11 Å
	C(45)	II	010	3.52
Br(28)	O(56)	III	000	3.55
O(30)	O(30)	III	$0\bar{1}0$	3.52
	C(36)	III	$0\bar{1}0$	3.44
O(35)	O(35)	III	$0\bar{1}\bar{1}$	3.46
	C(36)	III	$0\bar{1}\bar{1}$	3.40
O(38)	C(32)	III	$0\bar{1}\bar{1}$	3.39
O(42)	C(52)	II	000	3.45
O(46)	C(14)	II	000	3.45
	C(52)	II	$00\bar{1}$	3.40
O(47)	C(16)	I	$00\bar{1}$	3.58
O(50)	C(16)	I	$00\bar{1}$	3.55
C(17)	O(56)	I	000	3.56
C(22)	C(27)	III	000	3.51
C(24)	C(36)	III	$0\bar{1}0$	3.26
C(37)	C(26)	I	$00\bar{1}$	3.54
C(40)	O(34)	I	$00\bar{1}$	3.01
	O(42)	I	$00\bar{1}$	3.43
	C(4)	I	$00\bar{1}$	3.60
	C(33)	I	$00\bar{1}$	3.50

Molecule I at (x, y, z)
Molecule II at ($\frac{1}{2}-x$, $-\frac{1}{2}+y$, $\frac{1}{2}-z$)
Molecule III at ($1-x, 1-y$, $1-z$)
x, y and z are the fractional coordinates of atoms given in Table 1.

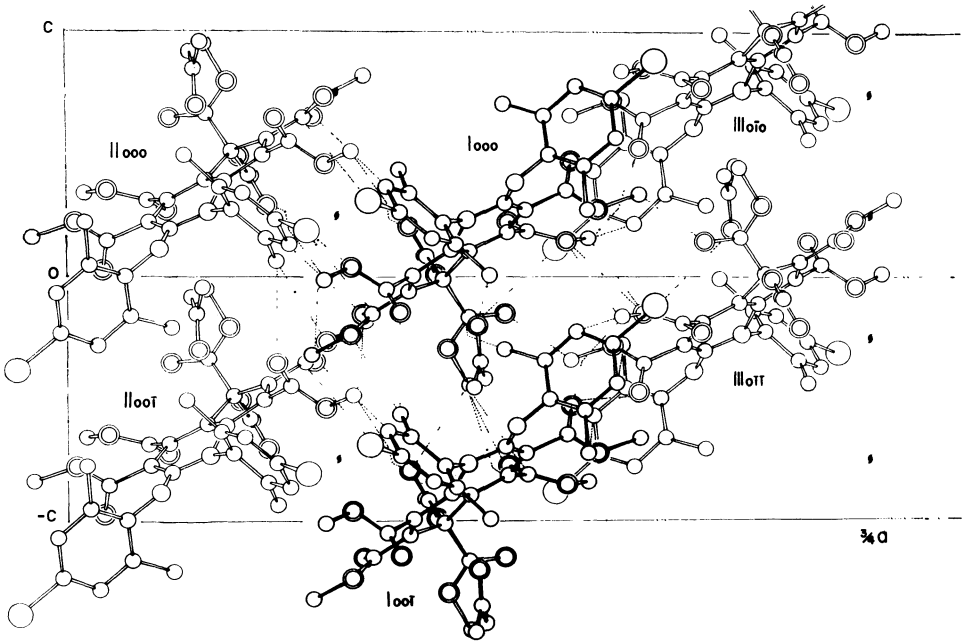

Fig. 5. Projection of the crystal structure along the *b* axis. Intermolecular short distances oi less than 3.6 Å are shown by dotted lines.

van der Waals interactions among the phenylimino groups and methyl groups. Remarkably short intermolecular distances to be noted are 3.01 Å found between C(40) I(000) and O(34) I(00$\bar{1}$) and 3.11 Å between Br(18) I(000) and O(51) II(010). Bolton[7] has already noted that very short distances are often found between a carbonyl oxygen atom and a carbon atom. In the present structure, the four atoms mentioned above belong to the ester carbon, carbonyl oxygen, *p*-substituent bromine of phenyl and ether oxygen atoms, respectively, indicating that they should be highly polarizable.

7) W. Bolton, *Nature*, **201**, 987 (1964).

The authors wish to express their sincere thanks to Professor Takeo Takizawa for valuable discussions.

BULLETIN OF THE CHEMICAL SOCIETY OF JAPAN, VOL. 44, 63—69 (1971)

Studies on Cobaloxime Compounds. I. Synthesis of Various Cobaloximes and Investigation on Their Infrared and Far-Infrared Spectra

Noboru YAMAZAKI and Yorikatsu HOHOKABE

Department of Polymer Science, Faculty of Engineering, Tokyo Institute of Technology, Ookayama, Meguro-ku, Tokyo

(Received July 31, 1970)

Cobaloximes with the general formula: $[CoX(DH)_2B]$ or $[RCo(DH)_2B]$ (X: Cl, CN. R: Alkyl groups such as methyl, ethyl, *n*-propyl, *i*-propyl, *n*-butyl, benzyl, or hydroxypropyl. DH: Dimethylglyoximato monoanion. B: Bases such as water, nicotinamide, *p*-toluidine, pyridine, γ-picoline, imidazole, or 4-vinylpyridine), and polymeric cobaloximes with the general formula: $[Co(OH)(DH)_2(Copoly\text{–}AM\text{-}VPy)]$ (Copoly–AM-VPy: a low molecular weight copolymer of acrylamide and 4-vinylpyridine), were synthesized and their infrared and far-infrared spectra were examined. The frequency shifts by changing the axial ligands were discussed.

The resemblance of cobaloxime compounds, including alkylcobaloximes, to cobalamin compounds in their chemical behavior has been clarified to a great extent by Schrauzer and Kohnle.[1,2] Compounds other than alkylcobaloximes, *e. g.*, the reduced states of cobaloximes, have been reported to serve as catalysts in some reduction reactions.[3,4]

In this paper we wish to report the synthesis of various cobaloximes including polymeric cobaloximes by improved methods and an investigation on their infrared spectra.

Results and Discussion

Synthesis of Cobaloximes. Some chlorocobaloximes were prepared by the general method similar to Tschugaeff's synthesis of $CoX(DH)_2B$:[5]

$$CoCl_2\cdot(6H_2O) + 2DH_2 + 2B + 1/4\,O_2 \rightarrow CoCl(DH)_2B + B\cdot HCl + 1/2\,H_2O\ (+6H_2O).$$

In these reactions, one equivalent amount of base is consumed to neutralize HCl produced in the reactions. Thus, instead of such organic bases, we could employ one equivalent of NaOH as follows:

$$CoCl_2\cdot(6H_2O) + 2DH_2 + B + NaOH + 1/4\,O_2 \rightarrow CoCl(DH)_2B + NaCl + 3/2\,H_2O\ (+6H_2O).$$

The results are summarized in Table 1. The product is essentially the same as those obtained by the former method. The latter method is preferable when the organic base is too invaluable to be used in such a side reaction, or when it is desirable for all basic residues such as polymeric ligands to form cobaloximes:

$$n\,CoCl_2\cdot(6H_2O) + 2n\,DH_2 + \text{(B)}_n + n\,NaOH + n/4\cdot O_2 \longrightarrow CoCl(DH)_2\text{(B)}_n + n\,NaCl + 3n/2\cdot H_2O\ (+6H_2O).$$

When two equivalent NaOH are used in the reaction in the absence of the organic base, hydroxoaquocobaloxime is produced:

$$CoCl_2\cdot(6H_2O) + 2DH_2 + 2NaOH + 1/4\,O_2 \rightarrow Co(OH)(DH)_2(H_2O) + 2NaCl + 1/2\,H_2O\ (+6H_2O).$$

As an extension of this idea, all pyridine residues in a low molecular weight copolymer of acrylamide-(AM) and 4-vinylpyridine(VPy) were completely complexed with cobaloxime, which was confirmed by Co analysis. The molecular weights and AM/VPy molar ratios of polymeric ligands are shown in Table 2.

Cyanocobaloximes were prepared by the general method:

$$Co(CH_3COO)_2\cdot(4H_2O) + 2DH_2 + NaCN + 2B + 1/4O_2 \rightarrow Co(CN)(DH)_2B + B\cdot HOOCCH_3 + CH_3COONa + 1/2H_2O\ (+4H_2O).$$

1) G. N. Schrauzer and J. Kohnle, *Chem. Ber.*, **97**, 3056 (1964).
2) G. N. Schrauzer, *Accounts Chem. Res.*, **1**, 97 (1968); and the references cited therein.
3) T. Mizuta and T. Kwan, *Nippon Kagaku Zasshi*, **88**, 471 (1967).
4) E. N. Sal'nikova and M. L. Khidekel, *Izv. Akad. Nauk. SSSR, Ser. Khim.*, 223 (1967); *Chem. Abstr.*, **66**, 104996*h* (1967).
5) L. Tschugaeff, *Ber*, **39**, 2694 (1906); *ibid.*, **40**, 3498 (1907).

TABLE 1. SYNTHESIS OF CHLOROCOBALOXIMES

Composition	Yield (%)	Formula (M. W.)	Found (Calcd) (%) C	H	N	Cl	Color
$CoCl(DH)_2(H_2O)$	34	$C_8H_{16}N_4O_5CoCl$ (342.63)	28.00 (28.04)	4.65 (4.71)	16.25 (16.35)	11.56 (10.35)	pale brown
$CoCl(DH)_2(nico)$[a]	58	$C_{14}H_{20}N_6O_5CoCl$ (446.74)	38.00 (37.64)	4.91 (4.51)	17.82 (18.81)	8.99 (7.94)	ocher
$CoCl(DH)_2(tolu)$[a]	95	$C_{15}H_{23}N_5O_4CoCl$ (431.77)	41.80 (41.73)	5.43 (5.37)	16.01 (16.22)	7.67 (8.21)	light brown
$CoCl(DH)_2(py)$[a]	63	$C_{13}H_{19}N_5O_4CoCl$ (403.71)	38.22 (38.68)	4.57 (4.74)	16.93 (17.35)	8.86 (8.78)	ocher
$CoCl(DH)_2(pico)$[a]	86	$C_{14}H_{21}N_5O_4CoCl$ (417.74)	40.20 (40.25)	5.28 (5.07)	16.56 (16.77)	8.21 (8.50)	light brown
$[CoCl(DH)_2(VPy)]\cdot H_2O$[a]	87	$C_{15}H_{23}N_5O_5CoCl$ (447.75)	40.60 (40.23)	5.16 (5.18)	15.86 (15.65)	8.18 (7.92)	ocher
$CoCl(DH)_2(imd)$[a]	68	$C_{11}H_{18}N_6O_4CoCl$ (392.69)	33.16 (33.65)	4.67 (4.62)	21.52 (21.40)	10.89 (9.03)	ocher

a) nico: nicotinamide, tolu: *p*-toluidine, py: pyridine, pico: *γ*-picoline, VPy: 4-vinylpyridine, imd: imidazole

TABLE 2. POLYMERIC COBALOXIMES [Co(OH)-(DH)$_2$(Copoly-AM-VPy)]

No.	Copoly-AM-VPy (Ligand) $\bar{M}_n \times 10^{-2}$ [a]	AM/VPy ratio[b]	Co(OH)(DH)$_2$ (Copoly-AM-VPy) $\bar{M}_n \times 10^{-2}$ [c]	Numbers of cobaloxime-unit/a polymer chain[d]
HC025	30	11.9	40	3.2
HC029	24	12.8	31	2.4
HC027	14	13.7	18	1.3
HC030	8.3	17.5	10	0.62

a) Determined by cryoscopic method.
b) Calculated by using the absorbance at 257 mμ due to the pyridine residue.
c), d) Estimated by using $\bar{M}_n$ and AM/VPy ratio of polymeric ligand.

In these reactions, one equivalent base is again consumed to neutralize acetic acid formed in the reaction. We found that without neutralizing acetic acid the cobaloximes are formed with one equivalent base to Co-$(CH_3COO)_2$:

$$Co(CH_3COO)_2\cdot(4H_2O) + 2DH_2 + NaCN + B + 1/4O_2 \rightarrow Co(CN)(DH)_2B + CH_3COOH + CH_3COONa + 1/2H_2O\ (+ 4H_2O).$$

The results of syntheses obtained by one of the two procedures are summarized in Table 3.

Various alkylcobaloximes were synthesized by the general methods according to Schrauzer and Windgassen,[6] from $CoCl_2\cdot 6H_2O$, DH_2, NaOH, and alkyl halide with or without $NaBH_4$ in an anaerobic condition. Some hydroxypropylcobaloximes, *i. e.*, *β*-hydroxy-isopropyl-, *β*-hydroxy-*n*-propyl-, and *β*,*γ*-dihydroxy-*n*-propyl-(pyridine)cobaloximes, were also synthesized with 2-bromo-1-propanol, 1-bromo-2-propanol, or glycerol α-monochlorohydrin, respectively, as the alkylating agents which are schematically described as:

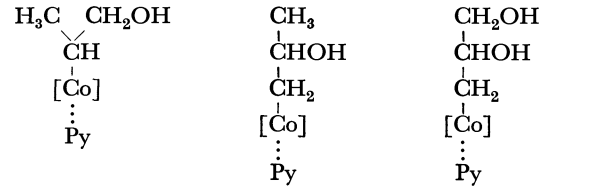

These cobaloximes might be considered as model compounds for possible intermediates in an enzymatic reaction, *i. e.*, in propanediol dehydratase system.

Base Substitution Reaction of Alkylaquocobaloximes. The water molecule coordinating to Co atom in alkylaquocobaloximes is readily displaced by another organic base:

TABLE 3. SYNTHESIS OF CYANOCOBALOXIMES

Composition	Yield (%)	Formula (M. W.)	Found (Calcd) (%) C	H	N	Color
$Co(CN)(DH)_2(H_2O)$	70	$C_9H_{16}N_5O_5Co$ (333.20)	31.39 (32.44)	4.23 (4.84)	20.48 (21.02)	brown
$Co(CN)(DH)_2(py)$[a]	26	$C_{14}H_{19}N_6O_4Co$ (394.28)	42.74 (42.65)	4.77 (4.86)	21.29 (21.32)	ocher
$Co(CN)(DH)_2(tolu)$[a]	94	$C_{16}H_{23}N_6O_4Co$ (422.33)	45.31 (45.50)	5.60 (5.49)	20.17 (19.90)	ocher
$Co(CN)(DH)_2(pico)$[a]	56	$C_{15}H_{21}N_6O_4Co$ (408.30)	42.91 (44.13)	5.15 (5.18)	20.48 (20.58)	yellow

a) py: pyridine, tolu: *p*-toluidine, pico: *γ*-picoline

6) G. N. Schrauzer and R. J. Windgassen, *J. Amer. Chem. Soc.*, **88**, 3738 (1966).

Table 4. Synthesis of alkylcobaloximes

$RCo(DH)_2B$ R	B[a]	Formula (M. W.)	Found (Calcd) (%) C	H	N	Color
CH_3	H_2O	$C_9H_{19}N_4O_5Co$ (322.21)	33.89 (33.55)	5.87 (5.94)	17.43 (17.39)	reddish orange
CH_3	nico	$C_{15}H_{23}N_6O_5Co$ (426.32)	42.01 (42.26)	5.46 (5.44)	19.73 (19.71)	orange
CH_3	tolu[b]	$C_{16}H_{28}N_5O_5Co$ (429.37)	44.73 (44.76)	6.52 (6.57)	16.34 (16.31)	orange
CH_3	py	$C_{14}H_{22}N_5O_4Co$ (383.30)	43.63 (43.87)	5.74 (5.79)	18.51 (18.27)	orange
CH_3	pico	$C_{15}H_{24}N_5O_4Co$ (397.32)	45.52 (45.35)	6.11 (6.09)	17.52 (17.63)	yellow
CH_3	imd	$C_{12}H_{21}N_6O_4Co$ (372.27)	38.70 (38.72)	5.67 (5.69)	22.72 (22.57)	yellow
CH_3CH_2	H_2O	$C_{10}H_{21}N_4O_5Co$ (336.24)	35.82 (35.72)	6.28 (6.30)	16.29 (16.66)	orange
CH_3CH_2	py	$C_{15}H_{24}N_5O_4Co$ (397.32)	44.95 (45.35)	6.17 (6.09)	17.50 (17.63)	orange
$CH_3CH_2CH_2$	H_2O	$C_{11}H_{23}N_4O_5Co$ (350.26)	37.19 (37.72)	6.48 (6.62)	16.26 (16.00)	reddish orange
$CH_3CH_2CH_2$	py	$C_{16}H_{26}N_5O_4Co$ (411.35)	47.06 (46.72)	6.42 (6.37)	17.06 (17.03)	orange yelllow
$CH_3CH_2CH_2$	pico	$C_{17}H_{28}N_5O_4Co$ (425.38)	48.21 (48.00)	6.37 (6.64)	16.56 (16.46)	yellow
$CH_3CH_2CH_2$	imd	$C_{14}H_{25}N_6O_4Co$ (400.33)	42.65 (42.00)	6.68 (6.29)	20.52 (20.99)	yellow
$CH_3CH_2CH_2CH_2$	H_2O	$C_{12}H_{25}N_4O_5Co$ (364.29)	39.58 (39.57)	7.08 (6.92)	15.61 (15.38)	reddish orange
$CH_3CH_2CH_2CH_2$	py	$C_{17}H_{28}N_5O_4Co$ (425.38)	48.53 (48.00)	6.61 (6.64)	15.99 (16.46)	orange yellow
$CH_3CH_2CH_2CH_2$	pico	$C_{18}H_{30}N_5O_4Co$ (439.40)	48.83 (49.20)	6.98 (6.88)	16.03 (15.94)	yellow
$CH_3CH(CH_3)$	H_2O	$C_{11}H_{23}N_4O_5Co$ (350.26)	37.43 (37.72)	6.66 (6.62)	16.37 (16.00)	reddish brown
$CH_3CH(CH_3)$	py	$C_{16}H_{26}N_5O_4Co$ (411.35)	46.82 (46.72)	6.50 (6.37)	17.24 (17.03)	orange
$C_6H_5CH_2$	py	$C_{20}H_{26}N_5O_4Co$ (459.39)	51.56 (52.29)	5.55 (5.71)	15.37 (15.25)	orange
$CH_3CH(OH)CH_2$	py	$C_{16}H_{26}N_5O_5Co$ (427.35)	44.36 (44.97)	6.22 (6.13)	17.24 (16.39)	yellow
$HOCH_2CH(CH_3)$	py	$C_{16}H_{26}N_5O_5Co$ (427.35)	44.46 (44.97)	6.18 (6.13)	15.85 (16.39)	dark ocher
$HOCH_2CH(OH)CH_2$	py	$C_{16}H_{26}N_5O_6Co$ (443.35)	43.11 (43.35)	5.87 (5.91)	15.34 (15.80)	orange yellow

a) nico: nicotinamide, tolu: *p*-toluidine, py: pyridine, pico: *γ*-picoline, imd: imidazole
b) This complex has a water of crystallization: $[CH_3Co(DH)_2(tolu)]\cdot H_2O$.

$$RCo(DH)_2(H_2O) + B \rightarrow RCo(DH)_2B + H_2O.$$

Thus, the addition of equimolar amount of imidazole to methylaquocobaloxime in methanol causes immediate color change in the solution from reddish orange to yellow. This indicates the immediate formation of methyl(imidazole)cobaloxime, which was actually isolated in quantitative yield. The alkylcobaloximes synthesized are summarized in Table 4.

Investigation on the Infrared and Far-Infrared Spectra. All the cobaloximes were identified by elemental analysis and infrared spectra. Characteristic absorption bands of chlorocobaloximes, methylcobaloximes, and (pyridine)cobaloximes are tabulated in Tables 5, 6, and 7, respectively.

The Band between 1700 and 1900 cm^{-1}: All the spectra of the complexes investigated contain a weak broad band between 1700 and 1900 cm^{-1}. It has been proved that this absorption is attributable to intramolecular hydrogen bridges[7] which are schematically shown below.

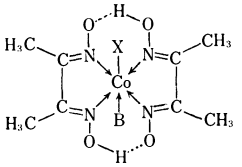

This conclusion has been supported by NMR spectra.[8] The hydrogen bonded OH frequencies indicated in

7) A. Nakahara, J. Fujita, and R. Tsuchida, This Bulletin, **29**, 296 (1956).
8) R. D. Gillard and G. Wilkinson, *J. Chem. Soc.*, **1963**, 6041.

TABLE 5. CHARACTERISTIC IR ABSORPTION BANDS OF CHLOROCOBALOXIMES (cm^{-1})

$CoCl(DH)_2B$: B	$\nu_{O-H\cdots O}$	$\nu_{C=N}$	ν_{N-O}	ν_{N-O}	$\nu_{Co-N(DH)}$
H_2O	1790	1570	1232	1080	508
p-Toludine	1760—50	1570—64	1229 or 1245	1092	513
Nicotinamide	—[a]	1570,[b] 1565—60, or 1550	1236	1090	513
Pyridine	1740	1563—53	1242	1091	512
Imidazole	1730—20	1561—51	1236	1087	511
γ-Picoline	1710	1562—53	1240	1092	513
4-Vinylpyridine	1700	1549—8	1241	1091	515

a) This band is obscure owing to the overlapping with strong $\nu_{C=O}$ band of nicotinamide at 1691 cm^{-1}.
b) It is not known which band is attributable to $\nu_{C=N}$. Others are characteristic bands of amide group.

TABLE 6. CHARACTERISTIC IR ABSORPTION BANDS OF CO-METHYL COBALOXIMES (cm^{-1})

$CH_3Co(DH)_2B$: B	$\nu_{O-H\cdots O}$	$\nu_{C=N}$	ν_{N-O}	ν_{N-O}	$\nu_{Co-N(DH)}$
H_2O	1780	1570	1230	1083	512
Nicotinamide	—[a]	1563	1233	1087	515
p-Toluidine	1770	1564	1234	1088	518
Pyridine	1760—50	1561	1239	1090	516
Imidazole	1760	1562—52	1234	1087	516
γ-Picoline	1760	1562	1238	1090	517

a) This band is obscure owing to the overlapping with strong $\nu_{C=O}$ band of nicotinamide at 1692 cm^{-1}.

TABLE 7. CHARACTERISTIC IR ABSORPTION BANDS OF (PYRIDINE)COBALOXIMES (cm^{-1})

$CoX(DH)_2$(pyridine): X	$\nu_{O-H\cdots O}$	$\nu_{C=N}$	ν_{N-O}	ν_{N-O}	$\nu_{Co-N(DH)}$
n-C_3H_7	1760	1563	1232	1088	515
$HOCH_2CH(OH)CH_2$	1760	1561	1233	1089	514
$CH_3CH(OH)CH_2$	1760	1562—55	1233	1088	515
C_2H_5	1760—50	1562—53	1235	1088	516
i-C_3H_7	1750—40	1561—52	1236	1081	515
CH_3	1760—50	1562	1239	1090	516
$C_6H_5CH_2$	1755	1560	1239	1090	516
n-C_4H_9	1750	1561—55	1232	1086	516
$HOCH_2(CH_3)CH$	1750—40	1563	1234	1089	515
Cl	1740	1563—53	1242	1092	512
CN	1730—20	1562—53	1244	1093	514

Tables 5, 6, and 7 are approximate values, nevertheless they showed the consecutive order of the strength of hydrogen bridges. These frequencies in chloro- or methyl-cobaloximes are shifted to lower wave numbers when the fifth ligand changes in the order H_2O> *p*-toluidine>pyridine>imidazole>*γ*-picoline. This is considered to be in the approximate order of the weakness of the electron donating power, whereas those in (pyridine)cobaloximes are shifted to lower wave numbers when the sixth ligand changes in the order alkyls>Cl>CN which is in the opposite direction from the donating power of the bases, *viz.*, the fifth ligands. This will be discussed later together with the shifts of other frequencies.

The Band at around 1560 cm^{-1}: The band at around 1560 cm^{-1} is attributed to C=N stretching frequency of dimethylglyoximato ligands.[7,9] The band is not affected by the change of the sixth ligand, *e. g.*, CN, Cl, alkyls. It is shifted to lower wave number when the fifth ligand changes in the order H_2O> *p*-toluidine>nicotinamide>pyridine>*γ*-picoline>imidazole>4-vinylpyridine, *i. e.*, with the increase of the interaction of the base with Co atom. Burger *et al.* reported on the basis of the frequency shift of the C=N vibration that the lower the C=N vibration frequency, the stronger the metal→N=C donor *π*-bond.[10] Our results suggest that the increase in electron density on the cobalt causes the increase of back donation from Co to nitrogen atoms of DH ligands, resulting in the increase in conjugation of the five membered chelate rings.

The Bands at around 1240 cm^{-1} and 1090 cm^{-1}: From the experiments by Blinc and Hadži,[9] we could assign the peaks of the spectra at around 1240 cm^{-1} and 1090 cm^{-1} to the N–O stretching vibrations. These two bands are shifted to lower wave numbers when the fifth ligand changes in the order 4-vinylpyridine> pyridine>*γ*-picoline>imidazole>*p*-toluidine>nicotinamide>H_2O, which is in the approximate order of the strength of electron donating power, as well as when the sixth ligand changes in the order CN>Cl> alkyls. Since the increase in the electron density in N–O bond is considered to cause the high frequency shift of the vibration, the high frequency shift caused by the change of the fifth ligand is explained by the electron donating power of the fifth ligands, *viz.*, the axial bases, while that caused by the change of the sixth ligand is unexpectedly in the opposite direction, which appears at first sight to be inconsistent with the effect of the fifth ligand, since cyanide is known as an electron withdrawing group stronger than others and hence it would cause the decrease in the electron density of N–O bond through the interaction with Co atom.

The Band at around 510 cm^{-1}: The band at around 510 cm^{-1} which is attributable to Co–N stretching frequency between Co and nitrogen atoms of dimethylglyoximato ligands is not affected by the change

9) R. Blinc and D. Hadži, *J. Chem. Soc.*, **1958**, 4536.
10) K. Burger, I. Ruff, and F. Ruff, *J. Inorg. Nucl. Chem.*, **27**, 179 (1965).

of the sixth ligand, *i. e.*, CN, Cl, alkyls similarly to the C=N vibration mentioned above, whereas it is shifted to higher wave number when the fifth ligand changes in the order H_2O<nicotinamide<pyridine, imidazole<*p*-toluidine, *γ*-picoline, which is not in an exact but approximate order of the strength of the interaction of the base with Co atom.

Other Bands Occurring in the Infrared Region: All the complexes show the weak broad bands between 2300 and 2400 cm^{-1}, which may be attributed to another hydrogen-bonded O–H frequency of bisdimethylglyoximato moiety according to Hadži.[9,11] The bands at around 1445 cm^{-1} and around 1375 cm^{-1} are due to asymmetric and symmetric deformation vibrations respectively, of methyl groups in dimethylglyoximes. The bands at around 980 cm^{-1} and 880 cm^{-1} may be attributed to deformation vibrations of OH in bisdimethylglyoximato moiety, and the band at around 740 cm^{-1} to C=N–O deformation vibration.

The characteristic absorption bands due to the axial ligands are also observed; pyridine derivatives show the weak bands at 3000—3150 cm^{-1} due to C–H stretching vibrations of pyridine ring, the band at 1600—1610 cm^{-1} to C=C and/or C=N stretching of pyridine ring, and the band at 750—780 cm^{-1} to C–H deformation of pyridine ring. The C–H stretchings of alkyl group linked to Co atom occurring at 2850—2960 cm^{-1} become distinct in intensity in the order CH_3<C_2H_5<C_3H_7<C_4H_9 as expected. In isopropyl(pyridine)cobaloxime, the characteristic absorption bands due to isopropyl group are clearly observed at 1375 and 1366 cm^{-1} which are symmetric deformation bands of CH_3 in isopropyl group, and 1187 and 1161 cm^{-1} which are skeleton vibrations of C–C–C in isopropyl group. In cyanocobaloximes, C≡N stretching vibration occurs at 2130—2200 cm^{-1}. Aquocobaloximes also show the characteristic bands due to H_2O molecule coordinating to Co atom; the ν_{O-H} at 2940—3110 cm^{-1}. δ_{O-H} at 830—838 cm^{-1}, and ν_{Co-O} at 357—378 cm^{-1}.

Other Bands Occurring in the Far-Infrared Region: The band at around 370 cm^{-1} in aquocobaloximes may be attributed to Co–O stretching vibration between Co atom and the coordinating water molecule. A few bands between 420—500 cm^{-1} other than that at around 510 cm^{-1} listed in Tables 5—7 may be attributable to Co–N stretching vibrations. All the alkylcobaloximes show an absorption band at around 325 cm^{-1}, which may be attributed to the Co–C stretching vibration, while methylcobalamin was reported to show the Co–C stretching band at 348 cm^{-1}.[12]

Polymeric Cobaloximes: Polymeric cobaloximes, *i. e.*, Co(OH)$(DH)_2$(Copoly–AM-VPy) showed characteristic absorption bands due to cobaloxime, other than due to the polymeric ligands; *e. g.*, ν_{N-O} at 1230 cm^{-1} and 1090 cm^{-1}, δ_{O-H} at 981 cm^{-1}, and ν_{Co-N} at 510—530 cm^{-1}.

Discussion on the Frequency Shift with Axial Ligands: The characteristic absorption bands mostly due to dimethylglyoximato ligands in these cobaloximes do not shift largely by the change of axial ligands. This suggests that the strength of the Co–N bonds in the equatorial position is not much affected by the change of the axial ligands because the Co–N(equatorial) bonds are very strong due to metal→N=C *π*-bond.

However, the definite relationship between the frequency shifts and the consecutive order of axial ligands was observed as mentioned above. In short, as the donating power of the base increases, $\nu_{O-H\cdots O}$ at around 1750 cm^{-1} and $\nu_{C=N}$ at around 1560 cm^{-1} shift to a lower wave number region, while ν_{N-O} at around 1240 cm^{-1} and 1090 cm^{-1}, and ν_{Co-N} at around 510 cm^{-1} to higher one. These results can be interpreted as follows. The coordination of more electron-donating base to Co atom causes the increase in electron density in Co atom. This facilitates the back donation from Co to the nitrogen atoms of dimethylglyoximato ligands, resulting in the increase in electron densities in C=N, and N–O bonds. The increase in electron density in N–O bonds causes the stronger hydrogen bridges of O–H···O and the higher frequency shifts of N–O stretching vibrations. The facilitated back donation from cobalt to nitrogen atoms of dimethylglyoxime means the increased metal-donor *π*-bond in the equatorial moiety of cobaloximes, which causes the stronger interaction of Co with equatorial N atoms, resulting in higher frequency shift of ν_{Co-N} vibration, and causes more conjugation in five membered chelate rings including Co atom, resulting in lower frequency shift of $\nu_{C=N}$ vibration.

On the contrary, the effects caused by the change of the sixth ligand, *e. g.*, CN, Cl, alkyls, were observed to be inverse. As the donating power of the sixth ligand decreases, $\nu_{O-H\cdots O}$ shifts to lower wave number, while ν_{N-O} to higher. This opposite tendency in the *cis*-effect of two axial ligands might be interpreted as follows: Since the bonding orbitals of both the fifth and sixth ligands are considered to interact most strongly with the d_{z^2} orbital of the central metal than the second probable one, *i. e.*, $d_{x^2-y^2}$ and than other *d* orbitals, the effect of one of the axial ligands is considered to be larger on another axial ligand (*trans*-effect) than on the equatorial ligands (*cis*-effect). More electron-withdrawing ligand in the sixth position causes stronger interaction between the central metal and the fifth ligand in the *trans* position, which could be caused by decrease in the cobalt-base bond length. Donation of electron from the base to Co atom is thus facilitated, which results in stronger back donation from Co to the equatorial nitrogen atoms and hence in increase

11) In principle the appearance of two OH bands could be admitted and explained by the splitting of the vibrational levels due to proton tunnelling. The structure of cobaloxime, $CoX(DH)_2B$, may be schematically described in a resonance as follows:

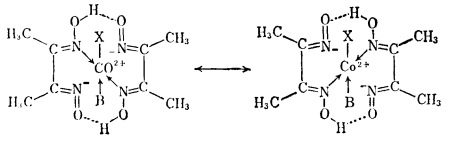

The hydrogen atoms in the hydrogen bridges may not occupy a central position between the oxygen atoms, which would result in the appearance of two OH bands in 1700—1900 cm^{-1} and in 2300—2400 cm^{-1}.[9]

12) H. P. C. Hogenkamp, J. E. Rush, and C. A. Swenson, *J. Biol. Chem.*, **240**, 3641 (1965).

in electron density in the equatorial bisdimethylglyoximato moiety. More electron-donating ligand in the sixth position causes weaker interaction between Co and the fifth ligand, which results in an increase in the Co-base bond length, and hence in the decrease in electron density in the equatorial moiety.

Similar effects of the axial ligands which were observed in the electronic spectra are considered to be consistent with the results, *viz.*, the stronger the interaction between Co and the axial base, the higher the *d-d* transition energy, whereas the stronger the donating power of another axial ligand, the lower the *d-d* transition energy.

Experimental

Synthesis of Cobaloximes. Chlorocobaloximes: a) Chloro(nicotinamide)cobaloxime: A typical method for the synthesis of chloro(nicotinamide)cobaloxime is as follows. To a hot solution of 2.55 g (0.022 mol) of dimethylglyoxime (abbreviated as DH_2 hereinafter) in 80 m*l* of ethanol, was added 2.38 g (0.010 mol) of $CoCl_2 \cdot 6H_2O$ in 10 m*l* of ethanol with stirring. After a while, 2.68 g (0.022 mol) of nicotinamide in 20 m*l* of ethanol was added to the mixture, followed by stirring with aeration for a few hours at room temperature, resulting in precipitation of the product. The precipitated ocher powders were collected, washed with water, ethanol, and finally with ether, and dried *in vacuo*. The yield was 1.56 g (35%).

Another method in which NaOH is used instead of organic base to neutralize HCl produced is as follows. To a hot solution of 2.55 g (0.022 mol) of DH_2 in 80 m*l* of ethanol, was added 2.38 g (0.010 mol) of $CoCl_2 \cdot 6H_2O$ in 10 m*l* of ethanol with stirring. After a while, 1.34 g (0.011 mol) of nicotinamide in 10 m*l* of ethanol and 0.40 g (0.010 mol) of NaOH in 10 m*l* of H_2O were successively added. The mixture was worked up as above. The yield was 2.60 g (58%).

Other chlorocobaloximes with organic bases were prepared using organic bases instead of nicotinamide.

b) Chloroaquocobaloxime: To a hot solution of 12.8 g (0.11 mol) of DH_2 in 300 m*l* of methanol, 11.9 g (0.050 mol) of $CoCl_2 \cdot 6H_2O$ in 50 m*l* of H_2O was added with stirring at room temperature. Fifty milliliters of a saturated aqueous solution of KCl was added to the mixture which was stood overnight, resulting in crystallization of the product in pale brown fine needles. The yield was 5.8 g (34%).

Cyanocobaloximes: A typical method for the preparation of cyano(pyridine)cobaloxime is as follows. To a hot solution of 6.40 g (0.055 mol) of DH_2 in 200 m*l* of methanol, 6.23 g (0.025 mol) of $Co(CH_3COO)_2 \cdot 4H_2O$ was added with stirring. After a while, 1.23 g (0.025 mol) of NaCN in 20 m*l* of H_2O, and 4.15 g (0.053 mol) of pyridine were added successively at room temperature, followed by stirring with aeration for a few hours, resulting in precipitation of the product. The yellow powders were collected, washed with water, methanol, and finally with ether and dried *in vacuo*. The yield was 1.80 g (18%).

Another method in which one equivalent base is enough to produce this complex instead of two is as follows: To a hot solution of 6.40 g (0.055 mol) of DH_2 in 150 m*l* of methanol, 6.23 g (0.025 mol) of $Co(CH_3COO)_2 \cdot 4H_2O$ was added with stirring. After a while, 2.08 g (0.026 mol) of pyridine and 1.23 g (0.025 mol) of NaCN in 20 m*l* of H_2O were added successively at room temperature, followed by stirring with aeration for a few hours, resulting in precipitation of the product. The product was worked up as above to give 2.55 g (26%) of yellow powders.

Other cyanocobaloximes with organic bases were prepared using organic bases, instead of pyridine.

Cyanoaquocobaloxime was prepared as above without adding any organic base but with additional 50 m*l* of H_2O.

Polymeric Cobaloximes——$Co(OH)(DH)_2$(Copoly-AM-VPy): Preparation of polymeric cobaloximes shown in Table 1 was reported.[13] A typical procedure is as follows: A hot solution of DH_2 in methanol was mixed with an aqueous solution of $CoCl_2 \cdot 6H_2O$ (DH_2: Co molar ratio 2) for an hour. An aqueous solution of the polymeric ligand (Copoly-AM-VPy) was then added to the reaction mixture (Co : VPy-residue ratio *ca.* 4), after the pH of the mixture was adjusted to 8.0—8.3. The reaction was complete within 3—4 hr. After concentration, the reaction mixture was applied to the Sephadex column (Sephadex LH-20 or G-25). From the first fraction, polymeric cobaloxime was recovered, followed by a by-product, *i. e.*, hydroxoaquocobaloxime. Alternatively the product was purified by repeated reprecipitation in water-acetone. The by-product was identified as $Co(OH)(DH)_2(H_2O)$ by elemental analysis and its infrared spectrum:

Found: C, 27.87; H, 5.25; N, 16.53%. Calcd for $C_8H_{17}N_4O_6Co$: C, 29.64; H, 5.29; N, 17.28%.

Hydroxoaquocobaloxime was also prepared as follows: To a hot solution of 12.8 g (0.11 mol) of DH_2 in 200 m*l* of methanol, was added 11.9 g (0.050 mol) of $CoCl_2 \cdot 6H_2O$ with stirring. After a while, 4.4 g (0.11 mol) of NaOH in 70 m*l* of H_2O was added to the mixture, followed by stirring with aeration for a few hours. The solution was evaporated to dryness and the residual product was applied to the Sephadex G-25 column to give dark brown hydroxoaquocobaloxime. The yield was 6.3 g (39%).

Found: C, 29.16; H, 3.95; N, 17.31%. Calcd for $C_8H_{17}N_4O_6Co$: C, 29.64; H, 5.29; N, 17.28%.

Alkylcobaloximes: Alkylcobaloximes were prepared according to two methods by Schrauzer and Windgassen;[6] by the reaction of alkyl halide with Co(I) species reduced by $NaBH_4$, and by that with Co(I) species formed by disproportionation of Co(II) species to Co(I) and Co(III) in alkaline media without any reducing agent. A typical method for the preparation of methylaquocobaloxime is as follows. To a stirred suspension of 29.0 g (0.250 mol) of DH_2 in 300 m*l* of methanol, 29.7 g (0.125 mol) of $CoCl_2 \cdot 6H_2O$ was added under nitrogen atmosphere. Methyl iodide, 25.4 g (0.180 mol), and 15.0 g (0.375 mol) of NaOH in 50 m*l* of H_2O were then successively added at $-20°C$, followed by stirring for an hour in a closed system. After evaporation of methanol under a reduced pressure, the remaining aqueous solution was stood overnight, resulting in the precipitation of dark red crystals. The yield was 15.8 g (80%).

When alkylaquocobaloxime was too soluble to isolate, pyridine or another organic base was added to the reaction mixture and alkyl(pyridine)cobaloxime or alkyl(B)cobaloxime was extracted with ether or methylene chloride. The yields obtained by the method with $NaBH_4$ were generally lower than those by alternative method, whereas alkyl iodides were more effective than bromides or chlorides in the preparation of alkylcobaloximes.

Base Substitution Reaction of Alkylaquocobaloxime. The coordinating water in alkylaquocobaloxime is readily displaced by another organic base only by the addition of an equivalent amount of base to the alkylaquocobaloxime. A typical displacement reaction is as follows. Methylaquocobaloxime, 0.967 g (3.00 mmol), was dissolved in 50 m*l* of methanol followed by addition of 0.204 g (3.00 mmol) of

13) N. Yamazaki and Y. Hohokabe, *Chem. Commun.*, **1968**, 829.

imidazole, resulting in immediate color change in the solution from reddish orange to yellow. By concentrating the solution, 1.05 g (94%) of yellow crystals of methyl(imidazole)-cobaloxime was obtained quantitatively.

Alkylcobaloximes prepared in this work are summarized in Table 4. The yields are not given in order to avoid complexity originating from the various preparatory methods.

Measurements. The infrared spectra were taken in KBr pellets with a JASCO, Model IR-G infrared spectrophotometer, and the far-infrared spectra with a JASCO, Model IR-F, far-infrared spectrophotometer.

BULLETIN OF THE CHEMICAL SOCIETY OF JAPAN, VOL. 44, 69—71 (1971)

Studies of Organic Peroxides. XI. The Reaction of Benzoyl Peroxide with Secondary Amines in Binary Mixed Solvents

Shigeo HASEGAWA, Setsuo KASHINO, and Yoshinobu MUKAHI

Department of Chemistry, Faculty of Science, Okayama University, Tsushima, Okayama

(Received July 31, 1970)

The rate constants of the reaction of benzoyl peroxide with some typical secondary amines, namely, diphenylamine, *N*-methylaniline, and piperidine, were measured in benzene-nitrobenzene binary mixed solvents. The reaction rates of diphenylamine and *N*-methylaniline are little influenced by the compositions of the solvents, while the reaction of piperidine proceeds more rapidly in nitrobenzene than in benzene. The isokinetic relationship holds for the reaction of piperidine in the binary mixed solvents. The isokinetic temperature is calculated to be 265°K. The analysis of the behavior of these reactions in the mixed solvents leads to the conclusion that, in the cases of diphenylamine and *N*-methylaniline, there are no specific interactions between the activated complexes and solvent molecules, whereas in the case of piperidine the activated complex is weakly solvated with the polar nitrobenzene. The reaction of benzoyl peroxide with *N*-methylaniline and *N*-*n*-butylaniline was also studied in benzene. These amines have a higher reactivity than would be expected from their basicity. This higher reactivity is probably due to the resonance stabilization of the activated complex besides the formation of a less-ionic activated complex.

In a previous work,[1] the reaction of benzoyl peroxide with some typical secondary amines was studied in benzene. It was ascertained that the reaction involves a nucleophilic attack by the amines on the peroxide, and it was noted that diphenylamine has rather a higher reactivity in spite of its lower basicity. This higher reactivity of diphenylamine was explained by the formation of a less-ionic activated complex. The explanation, however, was not conclusive.

In the present investigation, in order to obtain more clear-cut information on the activated complex, the reaction of benzoyl peroxide with *N*-methylaniline and *N*-*n*-butylaniline was studied in benzene, further, the rate constants of the reaction of benzoyl peroxide with diphenylamine, *N*-methylaniline, and piperidine were measured in benzene - nitrobenzene binary mixed solvents.

Experimental

The benzoyl peroxide, diphenylamine, piperidine, and benzene were the same as those described in the previous paper.[1] *N*-Methylaniline and *N*-*n*-butylaniline were commercially-available GR-grade reagents. The nitrobenzene was dried with anhydrous sodium sulfate and fractionated at reduced pressure.

The reaction rates were followed by means of the thermal-analysis method at temperatures between 20 and 35°C. The apparatus and procedure were also the same as those described in the previous paper.[1]

Results and Discussion

The reactions of benzoyl peroxide with amines were of the first order with respect to each reactant for all amines examined. It was reported previously[1] that diphenylamine and piperidine reacted with the peroxide in amine-peroxide ratios of 1.3 : 1 and 0.6 : 1 respectively. In the reaction of *N*-methylaniline and *N*-*n*-butylaniline, however, the stoichiometry was found to be 1 : 1.

The values of the second-order rate constants, k, for the reactions of *N*-methylaniline and *N*-*n*-butylaniline in benzene are shown in Table 1, together with those for the other amines studied previously;[1] the values of the enthalpy and entropy of activation are listed in Table 2.

TABLE 1. RATE CONSTANT $k \times 10^3$ (l mol^{-1} sec^{-1}) FOR BENZOYL PEROXIDE-SECONDARY AMINE REACTIONS IN BENZENE

	15°C	20°C	23°C	25°C	30°C	35°C
N-Methylaniline		14.5		20.2	26.9	33.6
N-*n*-Butylaniline		15.0		21.5	27.0	34.8
Diethylamine[a]	1.61	2.43		3.70	5.33	
Piperidine[a]	26.9	35.7		46.1	60.2	
Diphenylamine[a]	7.34		13.8		23.1	

a) Data from Ref. 1.

1) S. Kashino, Y. Mugino, and S. Hasegawa, This Bulletin, **40**, 2004 (1967).

TABLE 2. ENTHALPY AND ENTROPY OF ACTIVATION FOR THE REACTION OF BENZOYL PEROXIDE WITH SECONDARY AMINES IN BENZENE AT 25°C, kcal mol^{-1} or cal deg^{-1} mol^{-1}

	$\Delta H^{\neq}$	$\Delta S^{\neq}$
N-Methylaniline	7.9	−40.0
N-*n*-butylaniline	7.5	−41.4
Diethylamine[a)]	13.3	−25.1
Piperidine[a)]	8.6	−35.8
Diphenylamine[a)]	12.7	−24.2

a) Data from Ref. 1. $\Delta S^{\neq}$ is calculated from the rate constant at 30°C.

As may be seen in Tables 1 and 2, the alkylanilines have a slightly higher reactivity than diphenylamine. This can be explained by a mechanism which involves a nucleophilic attack by the amines on the peroxide,[1,2] because an inductive effect of the alkyl group would cause the increase in the electron density on the nitrogen atom of the amines, thus reducing the activation enthalpy and increasing the rate of the reaction.

The reactivities of both *N*-methylaniline and *N*-*n*-butylaniline are almost comparable to that of highly-basic piperidine, and are obviously higher than that of diethylamine. It can be said that the alkylanilines as well as diphenylamine have a rather higher reactivity than would be expected from the basicity. This suggests that the aromatic amines, that is, the alkylanilines and diphenylamine, form activated complexes somewhat different from those of the aliphatic amines.

TABLE 3. RATE CONSTANTS FOR BENZOYL PEROXIDE-SECONDARY AMINE REACTIONS IN BENZENE-NITROBENZENE MIXED SOLVENTS

Molar fraction of nitrobenzene x	Rate constant $k \times 10^3$ (l mol^{-1} sec^{-1})					
	Diphenylamine		*N*-Methylaniline	Piperidine		
	25°C	30°C	25°C	20°C	25°C	30°C
0.000	17.6	29.6	20.2	35.7	46.1	60.2
0.224	19.7	28.2	21.8	46.5	65.7	76.1
0.306	20.8	28.5	21.2	48.8	67.9	88.8
0.500	17.3	26.7	23.4	58.2	79.1	104.5
0.635	—	—	22.0	58.6	83.6	111.9
0.673	17.6	28.5	—	—	—	—
0.725	16.7	27.5	22.0	70.5	82.1	116.4
1.000	16.0	27.5	22.4	64.9	97.8	129.9

In order to clarify this difference, the solvent effect was examined. The experimental results are listed in Table 3 and are plotted in Fig. 1. It may be seen that, in the cases of *N*-methylaniline and diphenylamine, the compositions of the solvents have little influence on the rates of reactions, while in piperidine the rates obviously increase with the increase in the molar fraction of nitrobenzene.

These results are in line with the solvent effects

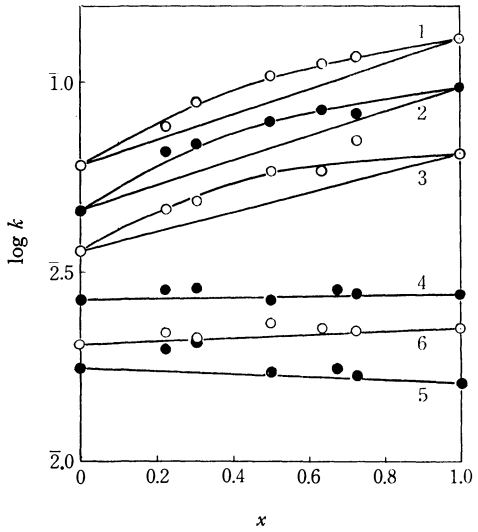

Fig. 1. Plot of log k *vs.* mole fraction of nitrobenzene, x, for the reaction of benzoyl peroxide with secondary amines in benzene-nitrobenzene mixed solvents.
1: piperidine, 30°C, 2: piperidine, 25°C, 3: piperidine, 20°C, 4: diphenylamine, 30°C, 5: diphenylamine, 25°C, 6: *N*-methylaniline, 25°C

observed by Chaltykyan *et al.*[3,4] They have shown that basic aliphatic amines react more rapidly in acetone than in ethyl ether, while diphenylamine has almost the same reactivity in these solvents.

For the reaction of piperidine in the binary mixed solvents, the values of the enthalpy and the entropy

TABLE 4. ENTHALPY AND ENTROPY OF ACTIVATION FOR THE REACTION OF PIPERIDINE WITH BENZOYL PEROXIDE IN BENZENE-NITROBENZENE MIXED SOLVENTS AT 25°C, kcal mol^{-1} or cal deg^{-1} mol^{-1}

Molar fraction of nitrobenzene	$\Delta H^{\neq}$	$\Delta S^{\neq}$
0.000	8.6	−35.7
0.224	8.7	−34.8
0.306	9.8	−31.0
0.500	10.0	−30.0
0.635	9.9	−30.3
0.725	10.8	−27.1
1.000	11.7	−23.9

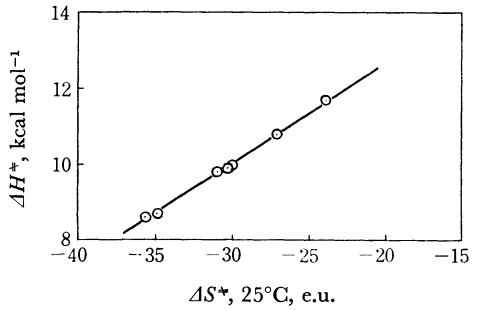

Fig. 2. Plot of $\Delta H^{\neq}$ *vs.* $\Delta S^{\neq}$ for the reaction of piperidine with benzoyl peroxide in benzene-nitrobenzene mixed solvents.

2) D. B. Denney and D. Z. Denney, *J. Amer. Chem. Soc.*, **82**, 1389 (1960).

3) O. A. Chaltykyan, E. N. Atanasyan, A. A. Sarksyan, and D. S. Gaibakyan, *Zhur. Fiz. Khim.*, **32**, 2601 (1958).

4) O. A. Chaltykyan, E. N. Atanasyan, N. M. Beileryan, and G. A. Marmaryan, *ibid.*, **33**, 36 (1959).

of activation are listed in Table 4. It may be noted that, in this reaction series, a higher enthalpy of activation does mean a higher rate; this is in contrast to the majority of reactions. The enthalpy of activation, $\Delta H^{\ddagger}$, is plotted against the entropy of activation, $\Delta S^{\ddagger}$, in Fig. 2. It may be seen that the isokinetic relationship holds for this reaction. The isokinetic temperature is calculated to be 265°K, below the experimental temperature. Pearson[5] has pointed out that the reactions in which ionic products are formed from neutral molecules frequently have an isokinetic temperature lower than the experimental temperature. Thus, it may be said that the reaction of piperidine with benzoyl peroxide has the same character as many ionic reactions.

Recently, Kondo and Tokura[6] have shown that, in the reactions in which the activated complexes have polar structures and are solvated in such polar solvents as nitrobenzene, the plot of log k *vs.* the composition of the mixed solvent deviates upward. Further, they have derived[7] theoretical expressions for the rate constants in binary mixed solvents on the basis of the theory of the non-electrolyte solution. An application of this theory was made in analyzing the reaction behavior of benzoyl peroxide with secondary amines.

According to Kondo and Tokura,[7] for the system in which all the solutes yield regular solutions the theoretical expression for the rate constant in a binary mixed solvent, k_{mix}, is given by:

$$\ln k_{mix} = x_1 \ln k_1 + x_4 \ln k_4 - \alpha_{14} x_1 x_4 \qquad (1)$$

where k_i and x_i stand for the rate constant in a pure solvent, i, and the mole fraction of the i solvent, respectively, and where α_{14} is a parameter expressing the deviation from the ideal-solution behavior of the solvent system.[8]

For the system in which there are specific interactions between the activated complex and the polar solvent, the expression for the rate constant can be given by:

$$\ln k_{mix} = x_1 \ln k_1 + x_4 \ln k_4 - \{x_1 \ln (K+1) - \ln(x_1 K+1) + x_1 x_4 \alpha_{14}\} \qquad (2)$$

where K is an equilibrium constant, defined in terms of the molar fraction, for the formation of a solvated activated complex from the unsolvated activated complex and the polar solvent.

The values of α_{14} for the benzene - nitrobenzene system have been estimated from the equilibrium vapour pressure data to be 0.10.[7] The values for K is so determined that the value calculated for k from Eq. (2) is equal to the experimental results at $x_1=x_4=0.5$.

The value of K for the reaction of piperidine was calculated to be 2.0. This means that, in pure nitrobenzene, the molar ratio of the solvated activated complex and the unsolvated one is 2 : 1.

The solid lines in Fig. 1 are calculated by means of Eqs. (1) and (2). It may be seen that, in the cases of *N*-methylaniline and diphenylamine, the relations between log k and the molar fraction of nitrobenzene are almost linear and agree with the lines calculated by Eq. (1), and that in piperidine the relation agrees well with the upward curved lines calculated by Eq. (2). Therefore, it can be concluded that, in the cases of diphenylamine and *N*-methylaniline, there are no specific interactions between the activated complex and the solvent molecules, whereas in the case of piperidine the activated complex is solvated with the polar nitrobenzene.

The results presented above show that the aromatic amines form a less-ionic intermediate, whereas aliphatic amines form a more-ionic intermediate, in the course of the reaction with benzoyl peroxide; this is in accordance with the previous proposition.[1]

However, even in the case of piperidine the solvent effect is much smaller than in typical ionic reactions, such as the Menschtkin reaction.[7] Kondo and Tokura[9] have also derived a theoretical expression for the activation energies in binary mixed solvents. In the reaction of piperidine with benzoyl peroxide, the solvent effect is too small to make it possible to discuss the changes in the activation energies in relation to the expression. That is, even in the case of highly basic piperidine the ionic character of the activated complex is rather small. Therefore, it is difficult to ascribe the higher reactivity of the aromatic amines only to the formation of the less-ionic activated complex. It is more reasonable to take other factors into consideration.

With regard to this higher reactivity of aromatic amines, another plausible reason is the resonance stabilization of the activated complex. Horner and Steppan[10] have proved that, by the reaction of *N*-ethylaniline with benzoyl peroxide at 20°C, *O*-benzoyl-*N*-ethyl-*N*-phenylhydroxyamine, *N*-benzoyl-*o*-hydroxy-*N*-ethylaniline, and *p*-benzoyloxy ethylaniline are formed; that the latter two products are not formed by the rearrangement of the former, but are formed directly by the reaction with benzoyl peroxide. Further, Denney and Denney[2] have shown that the reaction of diphenylamine with benzoyl peroxide labeled with oxygen-18 in the carbonyl positions forms, as the main product, *N*-(*o*-hydroxyphenyl)-*N*-phenylbenzamide, which contains 55% of oxygen-18 in the carbonyl oxygen and 45% of oxygen-18 in the phenol oxygen, and that, in the case of dibenzylamine, no such equilibration of oxygen-18 occurs. These facts may be evidence of the resonance of the activated complexes from aromatic amines.

5) R. G. Pearson, *J. Chem. Phys.*, **20**, 1478 (1952).
6) Y. Kondo and N. Tokura, This Bulletin, **37**, 1148 (1964).
7) Y. Kondo and N. Tokura, *ibid.*, **40**, 1433 (1967).
8) G. N. Lewis and M. Randall, "Thermodynamics," McGraw-Hill, New York (1923); 2nd Ed. (revised by K. S. Pitzer and L. Brewer, 1961), p. 287.
9) Y. Kondo and N. Tokura, This Bulletin, **40**, 1438 (1967).
10) L. Horner and H. Steppan, *Ann.*, **606**, 47 (1957).

Structure and Intramolecular Motions in Triethylenediamine as Studied by Gas Electron Diffraction

Akimichi YOKOZEKI and Kozo KUCHITSU

Department of Chemistry, Faculty of Science, The University of Tokyo, Hongo, Tokyo

(Received August 13, 1970)

The structure and intramolecular motions in triethylenediamine have been investigated by gas electron diffraction with a parallel study of bicyclo[2.2.2]octane in our previous paper. The structural parameters determined by a least-squares analysis on molecular intensities, with estimated limits of error, are as follows: r_g(C–N) = 1.472 ± 0.007 Å, r_g(C–C) = 1.562 ± 0.009 Å, ∠C–C–N = 110.2 ± 0.4°, ∠C–N–C = 108.7 ± 0.4°, r_g(C–H) = $1.11_0 \pm 0.01_2$ Å and ∠H–C–H = $111._5 \pm 5._6$°. The gas-phase structure is in good correspondence with that in the crystal phase determined by Weiss *et al.* by X-ray diffraction. The potential function with regard to the twisting motion around the C_3 symmetry axis is shown to have a broad minimum around the D_{3h} conformation, being quite analogous to that for bicyclo[2.2.2]octane; in terms of the torsional angle ϕ about the C–C axis, it probably has a small hump of the order of 100 cal/mol at $\phi = 0°$ and a double minimum around $\phi = 10°$. The above study was made with a new nozzle assembly, by which the sample can be heated to about 200°C. The detail of the design and operation is described.

According to our previous study of gas-phase electron diffraction,[1] bicyclo[2.2.2]octane (hereafter abbreviated as BO) has such a characteristic intramolecular motion with a large amplitude of twisting about the C_3 axis that the molecular symmetry should rightly be called "quasi-D_{3h}". Since triethylenediamine (TEDA), or 1,4-diazabicyclo[2.2.2]octane (Fig. 1), has an analogous

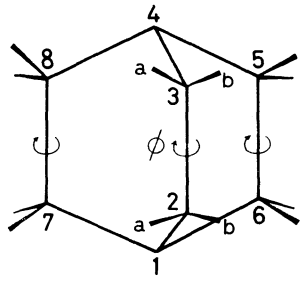

Fig. 1. Triethylenediamine, $(C_2H_4)_3N_2$; ϕ denotes a torsional angle defined by the dihedral angle between the planes N_1–C_2–C_3 and C_2–C_3–N_1.

skeleton, a similar problem of molecular dynamics is expected for TEDA. In fact, the intramolecular and overall motions in the crystal phase have been investigated by various experimental methods;[2-8] a particular attention has been paid to the solid-state properties of TEDA, since it belongs to the so-called "plastic crystals."[9,10]

In spite of such studies, however, the potential function for the twisting motion has not been explored in detail; nor has any conclusion regarding the equilibrium symmetry (D_{3h} or D_3) been reached. Therefore, an electron-diffraction study of gas-phase TEDA was initiated to parallel that of BO. In contrast to the case of BO, where closely-spaced C–C bond distances (C_1–C_2 and C_2–C_3) were hardly separable, the corresponding analysis for TEDA to separate N_1–C_2 and C_2–C_3 distances poses no serious problem.

In order to get a sufficient vapor pressure, a nozzle assembly, which can be heated to about 200°C, has been constructed. A detail of the design and operation is described in the Appendix.

Experimental

Anhydrous TEDA (classified as extra pure) was purchased from the Tokyo Chemical Industry Co. Ltd. The sample was loaded in a sample holder (Fig. 3a) in a dry atmosphere. Diffraction photographs were taken on Fuji Process Hard plates with the camera length of 113 mm at the temperature of 120°C (in the sample holder and on the nozzle tip) for 2 min with an apparatus equipped with an r^3-sector.[11] The accelerating voltage, about 40 kV, was stabilized within 0.1% during the experiment, and the beam current was 0.40 μA. The scale factor of the diffraction pattern was calibrated to

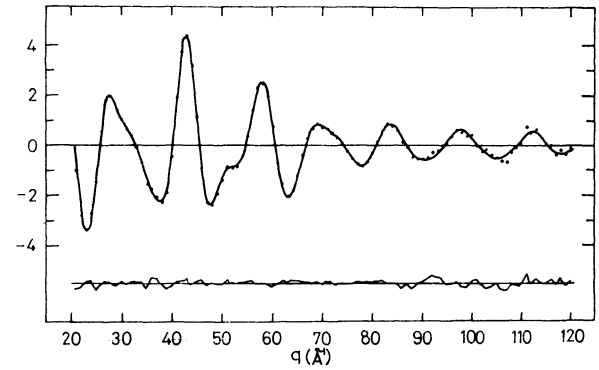

Fig. 2. Experimental (dots) and calculated (upper solid curve) molecular intensity functions for triethylenediamine; the lower curve represents $[qM(q)_{exp} - qM(q)_{calc}]$.

1) A. Yokozeki and K. Kuchitsu, This Bulletin, **43**, 2017 (1970).
2) P. Brüesch and Hs. H. Günthard, *Spectrochim. Acta*, **22**, 877 (1966).
3) M. P. Marzocchi, G. Sbrana, and G. Zerbi, *J. Amer. Chem. Soc.*, **87**, 1429 (1964).
4) G. S. Weiss, A. S. Parkes, E. R. Nixon, and R. E. Hughes, *J. Chem. Phys.*, **41**, 3759 (1964).
5) T. Wada, E. Kishida, Y. Tomiie, H. Suga, S. Seki, and I. Nitta, This Bulletin, **33**, 1317 (1960).
6) L. N. Becka, *J. Chem. Phys.*, **38**, 1685 (1963).
7) G. W. Smith, *ibid.*, **48**, 4325 (1965).
8) A. Zussman and S. Alexander, *ibid.*, **48**, 3534 (1968).
9) A. Farkas, G. A. Mills, W. E. Ermer, and J. B. Maerker, *Ind. Eng. Chem.*, **51**, 1299 (1959), *J. Chem. Eng. Data*, **4**, 334 (1959).
10) J. C. Trowbridge and E. F. Westrum, Jr., *J. Phys. Chem.*, **67**, 2381 (1963).

within 0.07% with reference to the r_a(C–O) bond length of carbon dioxide, 1.1646 Å,[11] and to the r_a(N–N) distance of the nitrogen gas, 1.1007 Å.[12] Other experimental and interpretational procedures are similar to those described in Ref. 1. A typical observed molecular intensity[13] and the difference between the observed and theoretical best-fit curves are shown in Fig. 2.

Analysis

The analytical procedures closely followed those empolyed in the study of BO. The mean amplitudes and nonlinear shrinkage corrections[14] on all the internuclear distances were calculated for a D_{3h} structure with sets of the Urey-Bradley force constants transferred from those for cyclohexane[15] and amides.[16] The vibrational frequencies calculated by the use of the force constants given in Table 1 are in fair agreement with the observed values reported in the literature,[2-4] as shown in Table 2. The mean amplitudes and vibrational corrections are insensitive to the moderate changes in the force constants, except for the torsional force constant Y.[1] Systematic variations in Y, 0.11 (estimated upper limit[1]), 0.08, 0.05 and 0.025 md·Å, yielded the lowest vibrational frequencies of 137, 118, 94 and 67 cm^{-1}, respectively. All the other frequencies were independent of Y; this indicates that the normal mode of twisting is separable almost completely from the other modes. The mean amplitudes and vibrational corrections calculated for 120°C are listed in Tables 3 and 4.

Least-Squares Analysis. On the assumption that the H–C–H plane is perpendicular to the N–C–C plane and bisects the N–C–C angle and *vice versa*, the molecular intensity (q=21 to 120) was first analyzed by a standard least-squares method[17] with the sets of constant mean amplitudes and shrinkage corrections, given in Tables 3 and 4, and with the following six variable parameters: the N–C and C–C bond distances, the N–C–C angle, the C–H distance, the H–C–H angle, and the equilib-

Table 1. Urey-Bradley force constants for triethylenediamine[a] (in md/Å).

K(C–N)	5.5	H(H–C–H)	0.42
K(C–C)	2.3	F(C···N)	0.70
K(C–H)	4.3	F(C···C)	0.30
H(C–C–N)	0.30	F(N···H)	0.52
H(C–N–C)	0.35	F(C···H)	0.41
H(C–C–H)	0.225	F(H···H)	0.07
H(N–C–H)	0.28	Y[b]	(0.11)

a) Estimated from the force constants for cyclohexane,[15] acctamide and thioamides[16]
b) See text; in md·Å units.

Table 3. Calculated mean amplitudes for triethylenediamine[a]

C_2-N_1	442	N_1-N_4	657	C_7-H_{2b}	1004
C_2-C_3	519	C-H	781	N_1-H_7	1014
C_3-N_1	602	C_2-H_{3a}	1069		
Set[b]	I	II	III	IV	V
C_2-C_7	695	695	699	704	709
C_3-C_7	728	877	922	1014	1222
C_7-H_{2a}	1562	1591	1623	1675	1774
C_7-H_{3a}	1514	2004	2165	2475	3142
C_7-H_{3b}	1043	1050	1053	1059	1069
N_1-H_8	1176	1276	1317	1399	1588

a) Calculated by using the force constants given in Table 1; in 10^{-4} units. The hydrogen-hydrogen amplitudes are omitted.
b) Sets I through V correspond to the torsional force constants Y (see text), assumed to be ∞, 0.11, 0.08, 0.05 and 0.025 md·Å respectively. Values listed in the upper section do not depend on the choice of Y.

Table 2. Vibrational frequencies of triethylenediamine

	Calcd[a]	Obsd[b]		Calcd	Obsd		Calcd	Obsd		Calcd	Obsd
A_1'	2970	2866	A_1''	3001	2920	E'	3017	2950	E''	3003	2930
	1465	1447		1222	1243		2971	2866		2985	2882
	1309	1335		966	1019		1490	1452		1516	—
	1121	965		137[c]	—		1442	1316		1446	1447
	957	800					1267	1295		1338	—
	571	600	A_2''	2984	2882		1203	1061		1210	—
				1457	1460		995	891		1008	—
A_2'	3014	—		1415	1350		781	825		601	580
	1224	—		1031	987		386	—		288	335
	750	—		890	765						

a) Calculated by the use of the force constants listed in Table 1; in cm^{-1} units.
b) Observed values[2] in CS_2 and CCl_4 solutions or solid state. Essentially similar values are given in Refs. 3 and 4 for some of the frequencies.
c) The value calculated in Ref. 3, 60 cm^{-1}, seems to be in error. See Ref. 1.

11) Y. Murata, K. Kuchitsu, and M. Kimura, *Japan. J. Appl. Phys.*, **9**, 591 (1970).
12) K. Kuchitsu, This Bulletin, **40**, 498 (1967).
13) Numerical experimental data of the levelled total intensity have been filed with the Chemical Society of Japan. A copy may be secured by citing the document number (Document No. 8002) and by remitting, in advance, ¥300 for photoprints. Payment may be made by check or money order payable to the Society.
14) Y. Morino, S. J. Cyvin, K. Kuchitsu, and T. Iijima, *J. Chem. Phys.*, **36**, 1109 (1962); K. Kuchitsu and S. Konaka, *ibid.*, **45**, 4342 (1966).
15) H. Takahashi and T. Shimanouchi, *J. Mol. Spectry.*, **13**, 43 (1964).
16) I. Suzuki, This Bulletin, **35**, 1279, 1449, 1456 (1962).
17) Y. Morino, K. Kuchitsu, and Y. Murata, *Acta Crystallogr.*, **18**, 549 (1965).

Table 4. Calculated corrections for nonlinear shrinkage effects for triethylenediamine[a)]

Set[b)]	I	II	III	IV	V
C_2-C_3	11	54	69	102	187
C_2-C_7	−4	17	24	40	80
C_3-C_7	−4	−11	−13	−18	−30
C_2-N_1	15	26	30	39	62
C_3-N_1	−1	5	8	13	26
N_1-N_4	−9	−9	−9	−9	−9
C-H	119	167	188	232	344
C_2-H_{3a}	48	134	168	239	423
C_7-H_{2a}	−27	16	29	60	143
C_7-H_{3a}	−18	−61	−78	−114	−208
C_7-H_{2b}	30	83	105	149	265
C_7-H_{3b}	28	43	50	63	97
N_1-H_7	55	104	125	167	276
N_1-H_8	16	38	46	63	108

a) Corrections r_a-r_a (Ref. 14) calculated by using the force constants given in Table 1; in 10^{-4} Å units. Corrections for the H-H pairs are omitted.
b) Sets I through V correspond to those in Table 3.

rium torsional angle ϕ_e defined in Fig. 1. The dependence of the ϕ_e parameters on Y was similar to that observed in the analysis of BO: By the use of Y=0.11, 0.08, and 0.05 md·Å, the cycles converged to nonzero sets (D_3) of ϕ_e, 9.8±1.1°, 8.5±0.9°, and 5.4±3.0° respectively, while ϕ_e tended to 0° (D_{3h}) for Y= 0.025 md·Å.

The situation that the alternative [twisted (D_3) or untwisted (D_{3h})] structures were derived from the analysis is in accordance with that encountered in the crystal-structure study of Weiss *et al.*,[4] where the D_{3h} and D_3 (with a twist angle of about 10° corresponding to $\phi_e\sim16°$) structures, both reasonable answers of their three-dimensional X-ray analysis, made them suggest a double-minimum potential for the twisting motion. A similar trend observed in BO has been explained by a potential with a broad trough and shallow double minima.[1] Therefore, TEDA is also expected to have a large-amplitude motion around the D_{3h} position, as is discussed below.

The rest of the independent parameters were unaffected by the choice of Y. The parameters obtained from the analysis are listed Table 5 with their limits of error (estimated as 2.5 times random errors plus systematic errors).[17-19] The corresponding error matrix is given in Table 6. In contrast to the case of BO,

Table 5. Structural parameters for triethylenediamine[a)]

N_1-C_2	1.472±0.007	∠N_1-C_2-C_3	110.2±0.4°
C_2-C_3	1.562±0.009	∠C_2-N_1-C_7	108.7±0.4°
C-H	1.11_0±0.01_2	∠H-C-H	$111._5$±$5._6$°
k[b)]	0.97 ±0.04		

a) Distances (r_g) in Å and r_α angles with estimated limits of error (See text).
b) Index of resolution (dimensionless).

Table 6. Error matrix[a)]

	C-N	C-C	C-H	∠N_1-C_2-C_3	∠H-C-H	ϕ_e	k
C-N	8	−6	−6	2	−17	10	−18
C-C		25	11	15	20	40	46
C-H			40	6	69	11	38
∠N_1-C_2-C_3				20	33	−44	−13
∠H-C-H					316	−53	63
ϕ_e						197	91
k							146

a) Error matrix for fixed mean amplitudes. Units ($\times10^{-4}$) for the distances are Å those for the angles are rad, and the index of resolution k is dimensionless. Elements of the matrix are given by $\sigma_{ij}=\mathrm{sgn}[(B^{-1})_{ij}]\cdot[|(B^{-1})_{ij}|\cdot V^*PV/(n-m)]^{1/2}$, where the notations follow Ref. 20. The diagonal element σ_{ii} represents the standard error for the parameter i.

the analysis evidenced that none of the distance and angle parameters had strong correlation with the mean amplitudes. Therefore, it was further possible to treat a number of mean amplitudes as variable parameters in the least-squares calculations, from which the amplitudes listed in Table 7 were obtained, with no significant influence on the distance and angle parameters and their uncertainties given in Table 5.

Table 7. Mean amplitudes for triethylenediamine (in Å units)

	Obsd[a)]	Calcd[b)]
C-C	0.051_8±0.004	0.0519
C-N	0.046_8±0.002	0.0442
C-H	0.076_4±0.002	0.0781
C_2-C_7	0.063_6±0.005	0.0695
C_3-C_7	0.083_4±0.009	0.0877
C_3-N_1	0.059_3±0.005	0.0601
N_1-H_7	0.110_5±0.007	0.1014

a) Errors represent random standard deviations obtained by a least-squares analysis (see text).
b) Calculated by Set II of Table 3.

Determination of the Potential Function. The potential function for the twisting motion around the C_3 symmetry axis, as characterized by a single torsional coordinate ϕ illustrated in Fig. 1, was assumed to have a quadratic-quartic type, $V(\phi)=k_2\phi^2+k_4\phi^4$. The molecular intensity function was averaged classically by the Boltzmann weight in regard to ϕ. The coefficients of $V(\phi)$ were determined by a least-squares method, by which the experimental molecular intensity was allowed to fit to the theoretical expression[1] by the use of the mean amplitudes of set I given in Table 3. The most probable set was found to be $k_2=-5.5\pm4.2$ kcal/mol rad^2 and $k_4=86.2\pm50.2$ kcal/mol rad^4. The parameters specifying the potential shape are compared in Table 8 with those for BO.

The radial distribution curve corresponding to the best-fit potential is in good agreement with the experimental curve, as shown in Fig. 3, where a theoretical curve corresponding to a D_{3h} structure with small amplitudes of twisting and frame vibrations is also

18) K. Kuchitsu, T. Fukuyama, and Y. Morino, *J. Mol. Structure*, **1**, 463 (1968).
19) K. Kuchitsu, This Bulletin, **32**, 748 (1959).
20) K. Hedberg and M. Iwasaki, *Acta Crystallogr.*, **17**, 529 (1964).

Table 8. Comparison of potential parameters[a)]

	k_2	k_4	$V(0)$[b)]	ϕ_e[c)]	ϕ_t[d)]	$\langle\phi^2\rangle^{1/2}$[e)]
TEDA[f)]	−5.5±4.2	86.2±50.2	87±100	10	19.5	11.0±1.5
BO[g)]	−4.0±3.3	54.2±34.5	75±100	11	21.5	12.0±1.5
units	kcal/mol	kcal/mol	cal/mol	deg.	deg.	deg.

a) The twisting potential function, $V(\phi)=k_2\phi^2+k_4\phi^4$ (ϕ in rad); errors for k_2 and k_4 represent standard deviations.
b) Potential hump at $\phi=0°$.
c) Potential minimum.
d) Classical turning point at 20°C (see Ref. 1).
e) Root-mean-square amplitude of twisting with limits of error estimated by a consideration of the correlation between the k_2 and k_4 parameters.[21)]
f) Triethylenediamine, determined in the present study (see text).
g) Bicyclo[2.2.2]octane (Ref. 1).

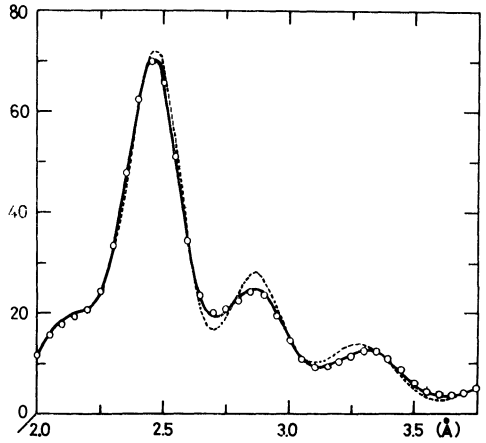

Fig. 3. Radial distribution curves for a region sensitive to the twisting motion.
Solid and broken lines represent synthetic curves calculated for the quadratic-quartic potential function $V(\phi)$ determined in the text and for a quadratic function, $V(\phi)=c\phi^2$ with $c=17$ kcal/mol rad^2, corresponding to the force constant for torsion, $Y=0.08$ md·Å,[1)] respectively; cirlces represent experimental values and their estimated uncertainties.

displayed. The distinct peak at about 2.8 Å is mainly composed of the nonbonded C_2–C_8 and C_3–C_7 pairs; a single sharp peak corresponding to a "rigid" D_{3h} conformation, where those pairs are equidistant, gets flattened as the system exerts a large-amplitude twisting motion. Thus, the contour of this peak offers a sensitive measure for the feature of the twisting potential.

Discussion

Structure. The C–N bond distance, 1.472±0.007 Å, is significantly longer than that of trimethylamine (1.451±0.003 Å)[22)] but is nearly equal to those of dimethylamine (1.466±0.005 Å),[23)] methylamine (1.467±0.002 Å),[24)] and ethylenediamine (1.468±0.005 Å).[25)] The rest of the parameters are almost identical with those for BO, as is contrasted in Table 9. The C_2–C_3 bond length, which has been determined with a much higher accuracy than that of BO, is significantly (about 0.02 Å) longer than that of cyclohexane.[26)] A similar lengthening has recently been observed in the C–C distance of ethylenediamine.[25)] The C–C–N bond angle is found to be equal to that in ethylenediamine, both slightly larger than the tetrahedral angle. The bridgehead angle (∠C–N–C) is about 2° smaller than that in trimethylamine.[22)]

A good correspondence has been observed between the gas-phase and crystal structures of TEDA, as compared in Table 9. A similar correspondence reported in Ref. 1 between the free BO and a crystal-phase BO derivative[27)] suggests that the intramolecular geometrical parameters for such globular molecules are little influenced by intermolecular interactions, which should exist in the solid state.

Potential Function. From the potential function determined in Table 8, one sees that TEDA has a "quasi-D_{3h}" structure analogous to that of BO (Fig. 4). Both molecules have potentials with double minima at $\phi\sim10°$ and small humps at $\phi=0°$. In this connection,

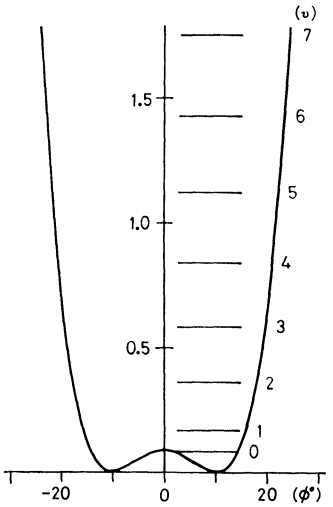

Fig. 4. The twisting potential function determined in terms of a torsional coordinate ϕ, $V(\phi)=-5.5\,\phi^2+86.2\,\phi^4$ (kcal/mol); horizontal lines, calculated energy levels for this potential function (see text).

21) Y. Morino and T. Nakagawa, *J. Mol. Spectry.*, **26**, 496 (1968).
22) J. E. Wollrab and V. W. Laurie, *J. Chem. Phys.*, **51**, 1580 (1969).
23) J. E. Wollrab and V.W. Laurie, *ibid.*, **48**, 5058 (1968). See also B. Beagley and T. G. Hewitt, *Trans. Faraday Soc.*, **64**, 2561 (1968).
24) H. K. Higginbotham and L. S. Bartell, *J. Chem. Phys.*, **42**, 1131 (1965).
25) A. Yokozeki and K. Kuchitsu, This Bulletin, **43**, 2664 (1970).
26) H. Kambara, K. Kuchitsu, and Y. Morino, *ibid.*, to be published.
27) O. Ermer and J. D. Dunitz, *Helv. Chim. Acta*, **52**, 1861 (1969).

Table 9. Comparison of the structures of triethylenediamine and related compounds

Molecule	TEDA		BO	EDA
Method	ED[a]	XD[b]	ED[c]	ED[d]
N-C[e]	1.472	1.46±0.013 (1.46)	1.538±0.015	1.468±0.005
C-C	1.562	1.57±0.014 (1.54)	1.552±0.029	1.556±0.010
∠N-C-C[e]	110.2°	110.0±1.0° (109.5°)	109.7±0.7°	110.2±0.8°
∠C-N-C[e]	108.7°	108.9±0.8° (108.2°)	108.9±0.6°	—
C-H	1.110	—	1.107±0.009	—
∠H-C-H	111.5°	—	110.1±5.6°	—

TEDA; triethylenediamine, BO; bicyclo[2.2.2]octane, EDA, ethylenediamine, ED; electron diffraction, XD; X-ray diffraction. (Units; in Å for distances.)

a) Present study (See Table 5), r_g distances and r_a angles.
b) Crystal structure in Ref. 4. Values in parentheses represent the average structure of an acentric (D_3) conformation with the twist angle of about 10°
c) Ref. 1, r_g distances and r_a angles.
d) Ref. 25, r_g distances and r_a angle.
e) For BO, the letter N should be replaced by C.

a similar potential for the 1-fluoro derivative of BO has recently been observed by Hirota from a microwave study.[28]

The origin of the hump at D_{3h} may be explained by a semi-empirical calculation of strain energy, if plausible models can be estimated for nonbonded N–N and N–H interactions. One of the primitive approaches to this problem is to assume that the N–N and N–H interactions are equal to those for the C–C and C–H pairs, respectively. Such a calculation of the strain energy, analogous to that for BO, yielded a potential hump of about 130 cal/mol with double minima at $\phi \sim 13.5°$, in reasonable agreement with the observed potential.

On the basis of the potential determined above, the energy levels for the twisting mode were estimated by the procedure described in Ref. 1. With an effective reduced mass of 26.8 amu calculated on the assumption of a semi-rigid framework, the levels given in Table 10 were obtained.

Table 10. Estimated energy levels of the twisting motion for triethylenediamine[a] (cm^{-1}).

v	E_v	v	E_v	v	E_v
0	28.8	3	205.6	6	500.2
1	59.9	4	295.1	7	613.7
2	128.0	5	393.7	8	733.3

a) Semiquantitative estimates based on the experimental potential function, $V = -5.5\phi^2 + 86.2\phi^4$ (kcal/mol, ϕ; in rad), determined in the present study.

Appendix

Construction of a High-Temperature Nozzle Assembly. A nozzle assembly which can be heated to about 200°C was constructed for structure studies of compounds with vapor pressures less than several Torr at room temperature. The assembly, illustrated in Fig. 1a, may be classified into three parts: a) the nozzle body equipped with a heating pipe 4 and a cooling pipe 5 with water ducts 12, and a mechanism

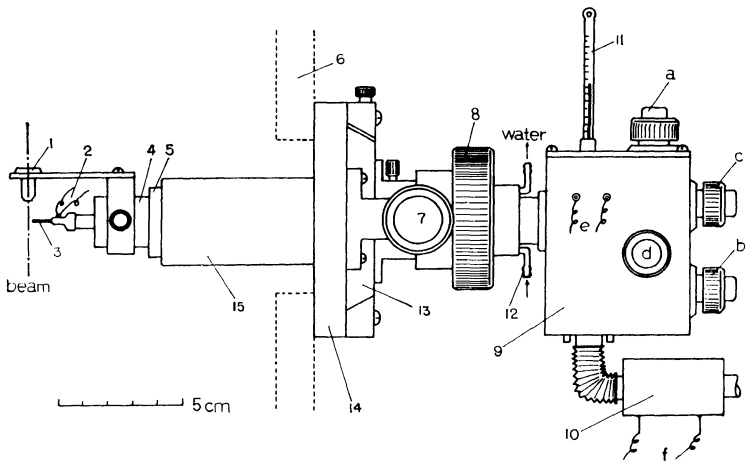

Fig. 1a. Nozzle assembly settled on a side-wall 6 of the diffraction chamber. The system is made vacuum-tight with metal *O*-ring contacts at 5—15, 13—14 (sliding) and 6—14 (fixed).

28) E. Hirota, Private communication (1970).

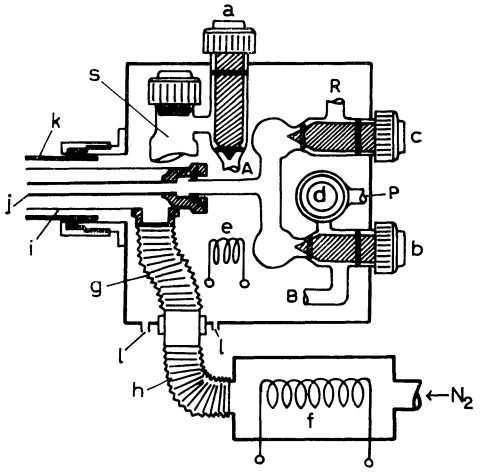

Fig. 2a. Inside section of the box 9 and the heater 10.
The walls are covered with asbestos. *a–d*: valves, *e*, *f*: electric heaters, *g–i*: paths of hot nitrogen gas, *j*: sample inlet, *k*: pipe corresponding to 4 in Fig. 1a, *l*: outlet of the nitrogen gas, *s*: sample holder with a connection *A*, *B* shown in Fig. 3a, *R*: reference gas inlet, *P*: outlet to a vacuum pump.

for adjustment 7, 8; b) an electric heater 10 supplying hot nitrogen gas as a thermal medium; c) values *a*—*d* (Fig. 2a) and a sample holder (Fig. 3a) installed in a box 9.

The sample is heated to a required temperature in the sample holder. Valves *a* and *b* are then opened, and the sample vapor is allowed to flow through a horizontal stainless-steel pipe (3 mm inside diameter) in the heating pipe 4 and emit through a capillary 3 (0.2 mm i. d.) into the diffraction chamber, where it crosses the vertical electron beam at a preset distance (0.4—0.6 mm) from the nozzle tip and condenses on a trap cooled with liquid nitrogen.[11]

Parts *b* and *c* are shown in Fig. 2a. The nitrogen gas heated by *f* (50Ω) flows through bellows *g* and *h* into a pipe *i*, heating the sample path *j*, and returns into the box, where the gas is again heated by *e* (125Ω) and ejected from the box (*l*) after heating the sample holder and the valves. At a normal flow rate of about 500 *l*·atm/min, and with A. C.

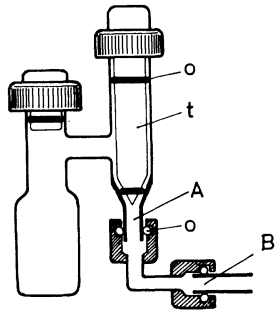

Fig. 3a. Cross section of the sample holder.
A, *B*: see corresponding parts in Fig. 2a, *o*: heat-resistant *O*-rings, *t*: teflon stopper.

voltages of 55 V applied on *f* and 25 V on *e*, the temperatures on the nozzle tip and inside the box reach 100°C. No disturbance on the electron beam caused by the heater currents is observed. The temperatures are measured with a copper-constantan thermocouple and a mercury thermometer, as shown in Fig. 1a. Thermal equilibrium is reached in several minutes, and a constant temperature (within ± 1°C) can be maintained during the experiment (of the order of 10 min). The values (*a*—*d*) made of glass and teflon with heat-resistant O-rings are set up in the box: *a* and *b* for the sample, *c* for a reference gas, and *d* for an exhaust valve. The sample holder with valve *a* can be removed from the other parts in the box (at positions *A* and *B* in Fig. 3a) in order that the sample may be loaded or unloaded outside the box.

The nozzle assembly can be moved in two directions perpendicular to the electron beam so as to make the beam pass through the aperture 1[11] by means of ball-bearing systems 7, 8 and sliding systems 13—15 with O-rings shown in Fig. 1a. The changes in the camera length by this adjustment and by thermal strain are found to be within 0.01 mm. The camera length is first estimated by a cathetometer and is later determined by the analysis of a diffraction pattern for a standard sample (CO_2 or N_2), which can be introduced into the diffraction chamber by the use of valve *c* in place of the sample to be studied at an identical experimental condition. In this way, the scale factor can be calibrated to within 0.07%.

Calorimetric Study of the Glassy State. VI. Phase Changes in Crystalline and Glassy-Crystalline 2,3-Dimethylbutane

Keiichiro ADACHI, Hiroshi SUGA, and Syûzô SEKI
Department of Chemistry, Faculty of Science, Osaka University, Toyonaka, Osaka, Japan
(Received August 14, 1970)

2,3-Dimethylbutane has two crystalline phases, high temperature form (crystal-I) and low temperature form (crystal-II). On account of the supercooling effect of crystal-I, its *glassy crystalline* state (non-equilibrium frozen-in state) is established below T_g (76 K) by rapid cooling. The heat capacities for various phases were determined from 13 to 300 K from principal interest in the thermodynamic properties of the glassy crystal. The transition temperature from crystal-II to crystal-I and melting point were determined to be 136.02 K and 145.05 K, respectively. The heats of transition and of fusion were determined to be 6427 J mol^{-1} and 788 J mol^{-1}, respectively. From these data, the residual entropy and T_2 temperature were determined to be 7.4 JK^{-1} mol^{-1} and 65 K, respectively. We also calculated the ratio of T_g to T_2 for several glassy crystals known hitherto, which amounts to 1.15—1.20. The stabilization effect was studied by the measurement of the change of the configurational enthalpy in the glassy crystalline state. Also, we discovered a new meta-stable intermediate phase (crystal-III) in the course of irreversible transition from the supercooled crystal-I to crystal-II. The thermal properties of this phase were also studied and its residual entropy was determined to be 2.7 JK^{-1} mol^{-1}.

Although the glass transition phenomenon is generally considered to be characteristic of the supercooled liquid state, it is known that the supercooled crystalline state of some materials also shows a similar behavior.[1-3] We studied the heat capacities of cyclohexanol and concluded that the anomalous jump of the heat capacity curve of the supercooled high-temperature form is attributed to the glass transition phenomenon. We have proposed a new term "*Glassy Crystal*" for the frozen-in state of the supercooled crystalline phase which has glass transition point. We would like to present the results of heat capacity measurements on the glassy crystalline state of 2,3-dimethylbutane as well as on various other stable phases and also on a metastable phase of this material. The thermal study of this substance has already been carried out by Douslin and Huffman.[4] They revealed that it has two crystalline phases, a high-temperature form (crystal-I) and a low-temperature form (crystal-II). The easy supercooling effect of the high-temperature form with rapid cooling has been confirmed in the study of nuclear magnetic resonance by Segall and Aston.[5] The thermal data of the supercooled crystal-I, however, were not given by Douslin and Huffman. In this article we report on the residual entropy of the glassy crystal as well as the T_2 temperature which was defined by Gibbs and Adam.[6] The relaxation phenomenon of the enthalpy was observed below glass transition temperature by annealing. An attempt has been also made to clarify the temperature dependence of the relaxation time. Furthermore, in the course of the irreversible transition from the supercooled crystal-I to crystal-II, we have discovered a metastable intermediate phase (crystal-III). Based on the heat capacity data of the crystal-III, the heat of transition from crystal-III to the supercooled crystal-I and the residual entropy of crystal-III have also been estimated.

Experimental

Material. The material was a mixture of two parts which had different purity. About 60 cc of 2,3-dimethylbutane (Tokyo Kagaku Seiki Co., Ltd. standard material 99.0%) was washed with concentrated sulfuric acid (including a small amount of potassium chromate) for ten hours at room temperatures to remove olefins involved. After this treatment the specimen was separated from the sulfuric acid solution by vacuum distillation and finally fractionally distilled. About 30 cc of the middle fraction of the distillate was obtained ——(A). On the other hand, 40 cc of the specimen which was claimed to have near 99.9% purity (Tokyo Kagaku Seiki Co., Ltd.) was purified by vacuum distillation at −70°C and about 20 cc of the middle fraction was obtained ——(B). The fractions (A) and (B) were mixed and the mixture was further distilled in a vacuum at −70°C. The purified specimen was introduced into the sample container for heat capacity measurements by vacuum distillation. The sample which had the same purity as that for heat capacity measurements was used for differential thermal analysis. The purity determined from equilibrium temperatures during fusion process was found to be 99.87% as will be described below.

Apparatus. The heat capacity was measured by a Nernst type adiabatic calorimeter with a platinum resistance thermometer. The details of the apparatus were reported previously.[7,8] The weight of the specimen employed in the measurement was 19.844 g (about 30 cc) after the correction for buoyancy due to air. A small amount of helium gas (0.2—0.5 cc at room temperature and 1 atm) was added as a heat exchange medium. After the sample and helium gas were introduced into the container, the filling tube (copper capillary) was pinched off and shielded with a soft solder. The apparatus for the differential thermal analysis has also been reported.[9]

1) K. Adachi, H. Suga, and S. Seki, This Bulletin, **41**, 1073 (1968).
2) H. M. Huffman, S. S. Todd, and G. D. Oliver, *J. Amer. Chem. Soc.*, **71**, 584 (1949).
3) J. G. Aston, H. Segall, and N. Fuscheillo, *J. Chem. Phys.*, **24**, 1061 (1956).
4) D. R. Douslin and H. M. Huffman, *J. Amer. Chem. Soc.*, **68**, 1704 (1946).
5) H. Segall and J. G. Aston, *J. Chem. Phys.*, **23**, 528 (1955).
6) J. H. Gibbs and G. Adam, *ibid.*, **43**, 139 (1965).
7) T. Matsuo, H. Suga, and S. Seki, Reported at The 3rd Japanese Calorimetry Conference 1967.
8) H. Suga and S. Seki, This Bulletin, **38**, 1000 (1965).
9) H. Suga, H. Chihara, and S. Seki, *Nippon Kagaku Zasshi*, **82**, 24 (1961).

Experimental Results

Differential Thermal Analysis (DTA). For the preliminary study of thermal behaviors of this material, differential thermal analyses have been carried out. The results are shown in Fig. 1. Run-1 is for a cooling

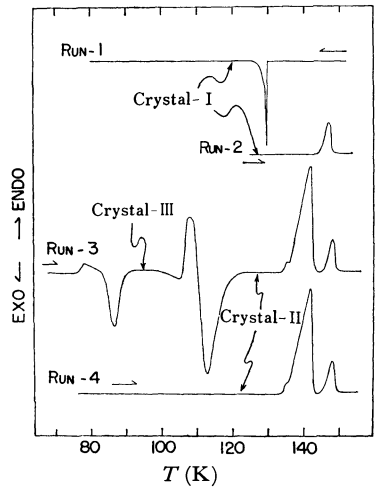

Fig. 1. DTA curves of 2,3-dimethylbutane.

curve with a rate about -1.4 K min^{-1}. The liquid state is supercooled to about 128 K where a sharp exothermic peak due to an abrupt crystallization has been observed. No remarkable thermal anomalies have been observed on further cooling. On account of noise effects and of a slow cooling rate between 80 K and 60 K, a reliable DTA curve has not been obtained. When the temperature was raised rapidly as soon as the sharp exothermic peak was observed at about 128 K in Run-1, only a peak due to the fusion effect was observed at about 145 K. This is shown by the curve for Run-2. From these DTA curves, it was confirmed that the high-temperature form (crystal-I) is easily supercooled. Run-3 is of a heating curve after slow cooling down to 65 K with a similar condition for Run-1. The heating rate of Run-3 is of about 1 K min^{-1}. It is seen that the supercooled crystal-I exhibits an anomaly resembling glass transition at about 78 K. The anomaly has been attributed to the glass transition phenomenon. An exothermic change was successively observed at about 89 K where the supercooled crystal-I was irreversibly transformed into another crystalline phase. We designate this crystalline phase as crystal-III, although we have not confirmed by X-ray analysis whether it is a pure single phase or a mixture of several modifications. After the formation of crystal-III, a gradual heat evolution was observed between 95 K and 105 K. It is considered that a part of crystal-III was transformed into a low temperature form (crystal-II) irreversibly in this temperature region. At about 107 K, the phase transition from crystal-III to an unknown crystalline phase was observed. This unknown phase is, however, unstable and irreversibly transformed to another crystalline phase. The resulting crystalline phase is evidently a stable modification below 136 K as shown by Run-4. Here Run-4 is for the heating curve determined after Run-3 has been stopped at about 125 K and cooled to a lower temperature. We designate this stable phase as crystal-II. Crystal-II was then transformed to crystal-I at 136 K, followed by the fusion of crystal-I at about 145 K. In this case we have always observed a small anomaly at about 135 K just before the II-I transition point in Fig. 1, and the anomaly is rather exaggerated. Occurrence of this anomalous hump[10] was influenced by previous

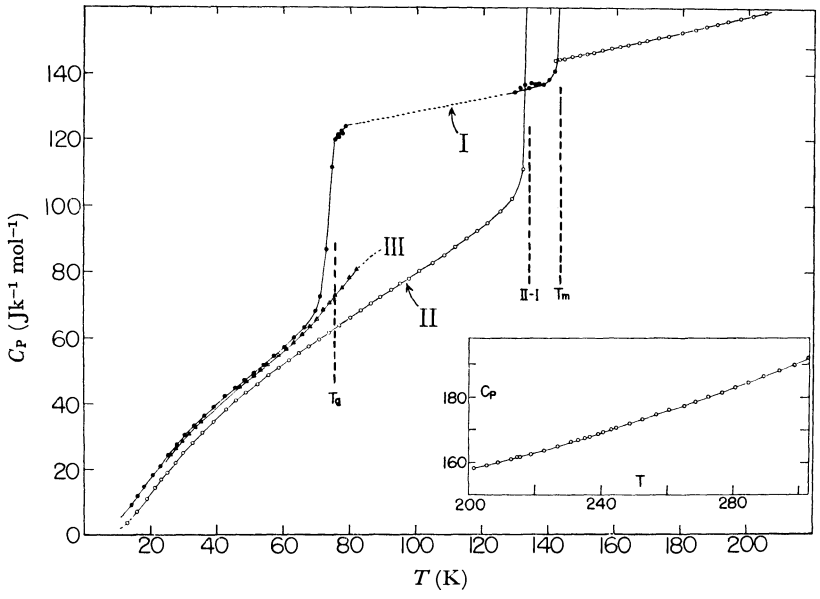

Fig. 2. The heat capacity curves of 2,3-dimethylbutane.
● the crystal-I, the supercooled crystal-I and the glassy crystal
○ the crystal-II (below 136 K) and the liquid (above 136 K)
△ the crystal-III

10) After the experiment was over, more clear and doubly separated peaks were observed by use of a new type DTA apparatus constructed in our laboratory. The details will be reported elsewhere.

TABLE 1. MOLAR HEAT CAPACITIES OF 2,3-DIMETHYLBUTANE

Mol wt=86.179 0°C=273.15K

T_{av}. K	$\Delta H/\Delta T$ $JK^{-1}mol^{-1}$	ΔT K	T_{av}. K	$\Delta H/\Delta T$ $JK^{-1}mol^{-1}$	ΔT K
Series 1					
(Glassy crystal and Supercooled crystal-I)					
14.481	9.420	1.62	16.259	11.817	1.92
18.444	14.826	2.45	20.972	18.374	2.61
23.381	21.623	2.20	25.681	24.567	2.40
27.949	27.368	2.13	30.596	30.443	3.16
33.584	33.678	2.82	36.281	36.423	2.58
39.313	39.268	3.48	42.662	42.234	3.21
45.764	44.861	3.00	48.673	47.289	2.82
51.429	49.595	2.69	54.404	51.975	3.26
57.589	54.706	3.10	60.635	57.447	2.96
63.570	60.269	2.83	66.638	63.509	3.16
69.823	68.428	2.98	72.813	78.974	2.69
75.198	98.343	1.98	76.849	117.104	1.74
78.547	125.021	1.65			
Series 2					
(Glassy crystal and Supercooled crystal-I)					
71.507	72.651	1.81	73.397	86.856	1.98
74.905	111.857	1.04	75.918	120.114	0.99
76.900	121.025	0.98	77.876	122.50	0.97
Series 3					
(Supercooled crystal-I)					
76.755	121.151	0.85	77.472	122.940	0.56
Series 4					
(Crystal-III)					
50.368	47.832	2.10	55.354	51.823	2.55
60.269	55.727	2.37	64.882	60.156	2.28
69.190	64.925	2.07	73.218	69.611	1.96
77.248	74.961	2.29	81.691	81.723	2.14
83.871	84.698	2.08			
Series 5					
(Crystal-III)					
26.399	24.485	1.11	27.988	26.300	2.05
29.946	28.532	1.87	31.886	30.708	2.01
33.824	32.827	1.87	35.634	34.725	1.75
47.239	45.191	1.75	51.319	48.561	2.08
55.342	51.792	1.95	59.124	54.745	1.84
63.566	58.697	2.30	67.997	64.017	2.14
72.153	69.016	2.01	76.075	73.267	1.91
80.018	79.013	2.25	82.254	82.122	2.18
Series 6					
(Crystal-II)					
13.033	3.865	3.24	16.061	6.966	2.82
18.989	10.566	3.04	21.662	14.062	2.30
23.607	16.616	1.58	25.445	18.982	2.09
27.769	21.962	2.56	30.170	24.854	2.25
32.944	28.033	3.30	36.056	31.398	2.92
39.372	34.699	3.71	42.911	37.975	3.37
46.151	40.775	3.12	49.170	43.324	2.92
52.366	45.890	3.47	55.742	48.500	3.28
58.948	50.932	3.13	62.009	53.295	2.99
64.940	55.471	2.88	67.936	57.568	3.12
70.996	59.696	3.01	73.958	61.707	2.92
77.067	63.926	3.30	80.324	66.310	3.21
83.483	68.534	3.10	86.546	70.744	3.02
89.534	72.707	2.95	92.458	74.562	2.89
95.323	76.420	2.74	98.134	78.253	2.78
101.344	80.333	3.64	104.939	82.752	3.55
108.451	85.240	3.47	111.888	87.751	3.40
115.248	90.157	3.33	118.542	92.571	3.26
121.402	95.416	3.54	125.444	98.430	3.46
128.855	102.503	3.36	132.188	111.636	3.30
134.814	216.86	1.95			
Series 7					
(Crystal-I)					
138.319	137.20	1.61	139.847	138.68	1.45
141.283	142.27	1.42			
Series 8					
(Supercooled crystal-I and Crystal-I)					
133.939	136.11	0.98	134.919	137.02	0.98
136.071	137.35	1.32	137.394	137.54	1.32
Series 9					
(Supercooled crystal-I)					
129.809	134.38	1.28	131.353	136.11	1.80
133.147	137.05	1.79	134.935	137.28	1.79
Series 10					
(Supercooled liquid and Liquid)					
141.900	144.02	0.86	142.908	144.40	1.15
144.630	144.77	2.29	146.915	145.31	2.28
149.192	145.73	2.27			
Series 11					
(Liquid)					
153.254	146.73	2.59	155.836	147.31	2.58
158.409	147.82	2.57	160.974	148.53	2.56
163.531	149.05	2.55	166.078	149.64	2.54
169.373	150.37	4.05	172.656	151.01	2.52
175.926	151.82	4.02	179.932	152.80	3.99
183.915	153.74	3.97			
Series 12					
(Liquid)					
187.462	154.61	3.95	190.662	155.39	2.45
193.843	156.21	3.91	197.730	157.14	3.89
201.617	158.20	3.87	205.474	159.15	3.85
208.595	159.98	2.39			
Series 13					
(Liquid)					
212.836	161.12	2.60	214.304	161.86	0.34
215.509	161.86	2.07	218.606	162.69	4.12
222.719	163.73	4.10	226.806	165.08	4.07
230.910	166.34	4.14	234.989	167.57	4.02
238.997	168.76	3.99	242.977	170.09	3.97
Series 14					
(Liquid)					
233.074	166.96	2.57	236.407	167.96	4.10
240.497	169.31	4.08	244.560	170.74	4.04
248.592	171.96	4.02	252.599	173.36	3.99
256.583	174.66	3.98	260.543	176.07	3.94
264.510	177.42	3.99	268.452	178.85	3.89
272.332	180.20	3.87	276.656	181.65	4.78
280.527	183.07	2.96	284.372	184.52	4.73
289.071	186.33	4.67	298.723	188.10	4.63
298.340	189.75	4.60	302.921	191.52	4.56

thermal history and may be attributed to the effect of impurities.

Measurement of Heat Capacity. The results of the heat capacities are listed in Table 1 and heat capacity curves are shown in Fig. 2, where direct results of the measured heat capacities are given by $\Delta H/\Delta T$, that is, an increment of the molar enthalpy divided by the corresponding temperature increment. Series-1 shows the heat capacities of the glassy crystalline state of crystal-I which has been established by supercooling the specimen with an average cooling rate of -2 K min^{-1} from 150 K to 75 K. In series-1 and series-2, the average heating rates were about 10 K/hr and 4 K/hr, respectively, in the glass transition region. The glass transition temperature was determined to be about 75 K from series-1 and 76 K from series-2. As is well known, it is considered that the discrepancy resulted from the difference in heating rates.[11,12] Series-2 also shows the heat capacity of the glassy crystalline state of crystal-I after supercooling with a cooling rate about -2 K min^{-1}. In the glass transition region, the measurements were disturbed by heat evolution due to the relaxation of enthalpy. This phenomenon was observed from 55 K and gradually increased up to 72 K. This heat evolution due to relaxation effect was removed by treating it as if it had arisen from heat inflow due to an incompleteness of adiabatic conditions. In other words, these relaxation effects were subtracted by the correction of a temperature drift in the computation of the heat capacities.[13] If we treat the heat due to the relaxation effect in this way, the calculated values of the heat capacities correspond to those of constant configuration; *i. e.* those measured with an infinitely rapid heating rate. The data of supercooled crystal-I which were obtained successively after the annealing experiments (described later) are shown in series-3. The aim of the measurements of this series was to see whether the irreversible transition from the glassy crystal to another phase had occurred or not during the course of annealing. Series-4 and series-5 give the selected values for crystal-III. The condition for establishing this phase is determined on the basis of the DTA measurements. Series-6 shows the heat capacities for crystal-II. The heat capacities of crystal-I and supercooled crystal-I are given in series-7,8 and 9. The heat capacities of supercooled crystal-I were measured after the specimen was slowly cooled (about -1 K min^{-1}) to about 133 K. However, below 133 K, the irreversible transition from supercooled crystal-I to the low temperature phase occurred gradually before the adiabatic condition for measurement was established. On account of this instability, the heat capacities of supercooled crystal-I between 80 K and 130 K could not be measured. The heat capacities of the liquid state are given in series-10—14. Heat capacities measured in this investigation have been compared with the data of Douslin and Huffman.[4] The deviation is found to be about $\pm 0.5\%$ below 20 K, whereas the data agree quite well within 0.1% between 25 K and 100 K for crystal-II. However, near transition temperature (136 K), our results are larger than those of Douslin and Huffman. The deviation between 110 K and 120 K is from 0.3% to 1% and between 120 K and 130 K about 2%. The deviation near the transition point might be due to impurity. In the region from 136 K to 220 K, the data of Douslin and Huffman is about 0.2% smaller and in the region from 220 K to 300 K, about 0.5% smaller.

Table 2. Equilibrium temperatures during fusion process

Fraction melted F (%)	$1/F$	Temperature (K)
46.8	2.137	144.488
58.7	1.704	144.578
71.2	1.404	144.646
84.1	1.189	144.702
97.1	1.030	144.752

Melting point of pure 2,3-Dimethylbutane 145.04± 0.01K
Mol % of impurity 0.13%

Table 3. Molar heat of fusion

	ΔH/J mol^{-1}
1st experiment	794.3
2nd experiment	793.1
mean	793.7±1.0

Table 4. Molar heat of transition

	ΔH/KJ mol^{-1}
1st experiment	6.423
2nd experiment	6.428
3rd experiment	6.430
mean	6.425±0.01

Molar Heats of Transition and Fusion. Equilibrium temperatures during fusion process and the molar heats of fusion and transition are given in Tables 2, 3, and 4, respectively. As shown in Table 2, the impurities in the specimen are determined to be 0.13% from the fractional melting data assuming no formation of solid solution. Compared with the data of Douslin and Huffman[4] both the melting point and the transition point of this study are somewhat lower. The values of the heat of fusion and the heat of transition are also smaller than those of Douslin and Huffman. A part of the disagreement may be attributed to the effect of the impurity. Another origin of the discrepancy may be attributed to the ambiguity in the estimation of the normal heat capacity curve. For the determination of the standard entropy, however, an error due to this ambiguity is small enough because the error of the entropy change at the transition point is corrected by heat capacity due to pre-transition. The increment of the molar entropy from 120 K (below transition point) to 150 K (above melting point) is compared with the value calculated from the data of Douslin and Huffman. The difference of these values is only 0.4 J K^{-1} mol^{-1}. Therefore the molar entropy may not be affected severely by the impurity of about 0.1% involved in the present specimen.

11) B. Wunderlich, *J. Polymer Sci.*, **C 6**, 137 (1963).
12) J. A. McMillan, *J. Chem. Phys.*, **42**, 3497 (1965).
13) For temperature drift, see Ref. 8.

Estimation of the Heat Capacity of Supercooled Crystal-I between 80 K and 130 K. The heat capacity of supercooled crystal-I between 80 K and 130 K is estimated to be

$$C_p = 0.18571T + 111.143\,\mathrm{JK^{-1}\,mol^{-1}} \quad (1)$$

which corresponds to the straight line obtained by connecting the values of the heat capacities at 80 and 130 K as shown in Fig. 2 (dotted line). Based on this interpolation equation, the molar enthalpy of supercooled crystal-I was calculated. Here, we have taken the value of the enthalpy of crystal-II at 0 K as 0 for the standard point of the enthalpy of this material. This value is compared with the directly determined value of the molar enthalpy of supercooled crystal-I at 77.72 K. Direct determination of the molar enthalpy of crystal-I was made as follows. If the temperature of glassy-crystal-I be raised up a little above T_g, say 77.7 K, a spontaneous exothermic transition takes place to another metastable phase which is finally transformed into the most stable crystal-II. If an adiabatic condition of the calorimeter cell is maintained during the irreversible changes, the molar enthalpy of supercooled crystal-I at 77.7 K can be determined by measuring the temperature at which the irreversible transitions terminate, since the enthalpy of crystal-II at this temperature is already known. In the actual measurement, an excess electric energy was supplied to terminate the phase change more rapidly. Assuming a complete adiabaticity, the calculation was made as follows.

$$H_{\mathrm{I}}(77.720) = H_{\mathrm{II}}(125.984) + \int_{77.720}^{125.984} C_p(\text{empty cell})\,dT - \sum(\text{supplied electric energy}) \quad (2)$$

Here, $H_{\mathrm{I}}(77.720)$ and $H_{\mathrm{II}}(125.984)$ are the enthalpies of supercooled crystal-I at 77.720 K and of crystal-II at 125.984 K, at which the irreversible transition ends completely under a specified condition for energy supply. Thus the enthalpy of supercooled crystal-I at 77.720 K was determined to be 6084.8 $\mathrm{Jmol^{-1}}$. Calculation from the integration of Eq. (1) gives, on the other hand, 6211.1 $\mathrm{Jmol^{-1}}$. For this discrepancy, the following three possibilities are considered; 1) True heat capacity curve of supercooled crystal-I is located above the estimated one. 2) The actual glassy crystal contains some amounts of the crystal-II phase due to insufficient cooling rate in the preparation of glassy crystal. 3) Experimental error due to the incompleteness of adiabatic conditions. In the calculation of various thermodynamic functions, the mean value 6150 ± 70 $\mathrm{Jmol^{-1}}$ has been employed.

The Residual Entropy of the Glassy Crystalline State. By comparison of the gaseous entropy determined from thermal data with that computed from spectroscopic data, it was concluded by Scott *et al.* that the crystal-II has no residual entropy at 0 K.[14] Based on this result the residual entropy of the glassy-crystalline state at 0 K has been determined by a well defined method. Contributions below 13 K have been determined from extrapolated heat capacities assuming the Debye theory. The Debye temperatures were taken to be 129.44 K and 101.35 K for crystal-II and the glassy crystal-I, respectively, by assuming 6 degrees of freedom. The increment of the entropy of the supercooled crystal-I between 80 and 136 K was calculated by using Eq. (1) with a slight correction (0.6 $\mathrm{JK^{-1}\,mol^{-1}}$) due to the uncertainty of this equation as described above. The calculation is shown in Table 5 and the residual entropy of the glassy crystal is determined to be 7.4 ± 1.3 J $\mathrm{K^{-1}\,mol^{-1}}$.

TABLE 5. THE THIRD LAW ENTROPY OF CRYSTAL-I AT 136.02 K *via* II-I TRANSITION AND *via* GLASSY CRYSTALLINE STATE

Temperature (K)	Contribution	ΔS ($\mathrm{JK^{-1}\,mol^{-1}}$)
via II-I transition		
0— 12.5	Debye extrapolation	1.16
12.5—136.02	$\int C_p(\mathrm{II})\,d\ln T$	98.22
136.02	Transition (6427/136.02)	47.25
		146.63
via glassy crystalline state		
0— 13.5	Debye extrapolation	2.92
13.5— 80.0	$\int C_p$ (Glassy cryst.) $d\ln T$	66.35
80.0—136.02	$\int C_p$ (I) $d\ln T+0.6$[a]	70.0
		139.27

a) Equation(1) is used for C_p(I) and 0.6 $\mathrm{JK^{-1}\,mol^{-1}}$ is added after integration for correction.

Crystal-III. On account of intricate irreversible transitions, the heat capacity of crystal-III between 80 K and 107 K and the heat of transition which occurs at 107 K from crystal-III to other unknown phase could not be measured. The molar enthalpy of the crystal-III at about 80 K has been measured by the same procedure as that employed in the determination of the enthalpy of supercooled crystal-I. The procedure gives 4990 ± 40 J $\mathrm{mol^{-1}}$ at 78.39 K. Using this value, we have attempted to estimate the heat of transition at 107 K. We assumed that the unknown crystalline phase into which crystal-III is transformed at 107 K is supercooled crystal-I. The heat capacity of crystal-III between 80 K and 107 K is estimated by the extrapolation equation which is represented by

$$C_p = 0.782T + 16.3\,\mathrm{JK^{-1}\,mol^{-1}} \quad (3)$$

From these assumptions, the heat of transition from crystal-III to supercooled crystal-I has been calculated to be 2370 J $\mathrm{mol^{-1}}$.

The residual entropy of crystal-III which amounted to 2.7 $\mathrm{JK^{-1}\,mol^{-1}}$ was calculated from the heat of transition determined above and the estimated heat capacity equations 1 and 3. The calculation is given

TABLE 6. THE THIRD LAW ENTROPY OF CRYSTAL-I AT 136.02K *via* III-I TRANSITION

Temperature (K)	Contribution	ΔS ($\mathrm{JK^{-1}\,mol^{-1}}$)
0— 24.5	Debye extrapolation	10.81
24.5— 82.0	$\int C_p$ (III) $d\ln T$	54.72
82.0—107	$\int C_p$ (III) $d\ln T$	23.8
107	Transition (2373/107)	22.2
107 —136.02	$\int C_p$ (I) $d\ln T$	32.4
		143.9

14) D. W. Scott, J. P. McCullough, K. D. Williamson, and G. Waddington, *J. Amer. Chem. Soc.*, **73**, 1707 (1951).

in Table 6 where contributions to the entropy below about 25 K has been estimated by using the Debye function with the value of 107.6 K for θ_D and by assuming 6 degrees of freedom. There appears an anomalous swelling in the heat capacity curve around 70 K. At this temperature range, a fairly long time was required to attain thermal equilibrium (about 25 min). Above 75 K, gradual heat liberation due to the irreversible transition to crystal-II was observed.

Thermodynamic Functions. Thermodynamic functions for the three crystalline phases and for the liquid phase are all listed in Table 7. The molar enthalpies and the molar entropies of respective phases are plotted in Figs. 3 and 4.

Relaxation of Enthalpy below the Glass-Transition Point. It is well known that the configurational degrees of freedom of the glass-forming materials are virtually frozen below T_g on account of the long relaxation time. However, if the temperature is regulated to be constant below glass transition point, the configurational

Table 7. Thermodynamic functions of 2,3-dimethylbutane (unit: $JK^{-1}mol^{-1}$)

T(K)	$C_p°$	$S°$	$(H°-H_0°)/T$	$-(G°-H_0°)/T$
		(Crystal-II)		
5	(0.224)	(0.0747)	(0.0569)	(0.0187)
10	(1.787)	(0.5976)	(0.4481)	(0.1495)
20	11.89	4.457	3.303	1.154
30	24.65	11.73	8.327	3.404
40	35.31	20.34	13.79	6.549
50	44.03	29.18	18.79	10.39
60	51.73	37.89	23.81	14.08
70	59.02	46.43	28.33	18.10
80	66.07	54.77	32.60	22.17
90	73.02	62.96	36.71	26.25
100	79.44	70.99	40.66	30.33
110	86.30	78.88	44.49	34.39
120	94.01	86.70	48.29	38.41
130	103.18	94.58	52.15	42.43
136.02		Transition		
		(Crystal-I)		
140	137.72	151.08	103.29	47.49
145.04		Fusion		
		(Liquid)		
150	145.92	166.81	110.69	56.12
160	148.16	176.30	112.97	63.33
170	150.43	185.35	115.11	70.24
180	152.81	194.01	117.11	76.90
190	155.22	202.34	119.06	83.28
200	157.73	210.37	120.94	89.43
210	160.23	218.12	122.76	95.36
220	163.03	225.64	124.52	101.12
230	165.98	232.95	126.26	106.69
240	169.09	240.08	127.98	112.10
250	172.39	247.05	129.69	117.36
260	175.83	253.88	131.40	122.48
270	179.32	260.58	133.11	127.47
280	182.91	267.16	134.82	132.34
290	186.61	273.65	136.54	137.11
300	190.40	280.03	138.27	141.76

T(K)	$C_p°$	$S°-S_0°$ (g)	$(H°-H_0°$ (g))$/T$	$-(G°-H_0°$ (g))$/T$
		(Glassy crystal and Supercooled crystal-I)		
5	(0.4669)	(0.1557)	(0.1167)	(7.6)
10	(3.637)	(1.234)	(0.9238)	(7.7)
20	17.01	7.71	5.54	9.6
30	29.75	17.10	11.56	12.9
40	39.91	27.10	17.42	17.1
50	48.40	36.93	22.78	21.5
60	56.84	46.49	27.71	26.2
70	68.88	56.03	32.63	30.8
80	126.00	69.27	41.32	35.4
90	(127.9)	(84.3)	(50.9)	(40.8)
100	(129.7)	(98.0)	(58.8)	(46.6)
110	(131.6)	(110.5)	(65.5)	(52.4)
120	(133.4)	(122.2)	(71.1)	(58.5)
130	(135.3)	(133.3)	(76.1)	(64.3)

T(K)	$C_p°$	$S°-S_0°$ (III)	$(H°-H_0°$ (III))$/T$	$-(G°-H°$ (III))$/T°$
		(Crystal-III)		
5	(0.3906)	(0.1302)	(0.0977)	(2.7)
10	(3.073)	(1.037)	(0.7768)	(3.0)
20	(16.27)	(6.90)	(5.00)	(4.6)
30	28.60	15.94	10.91	7.7
40	39.00	25.64	16.68	11.6
50	47.48	35.28	22.01	16.0
60	55.53	44.66	26.93	20.5
70	65.87	53.95	31.71	25.0
80	78.85	63.55	37.74	28.6

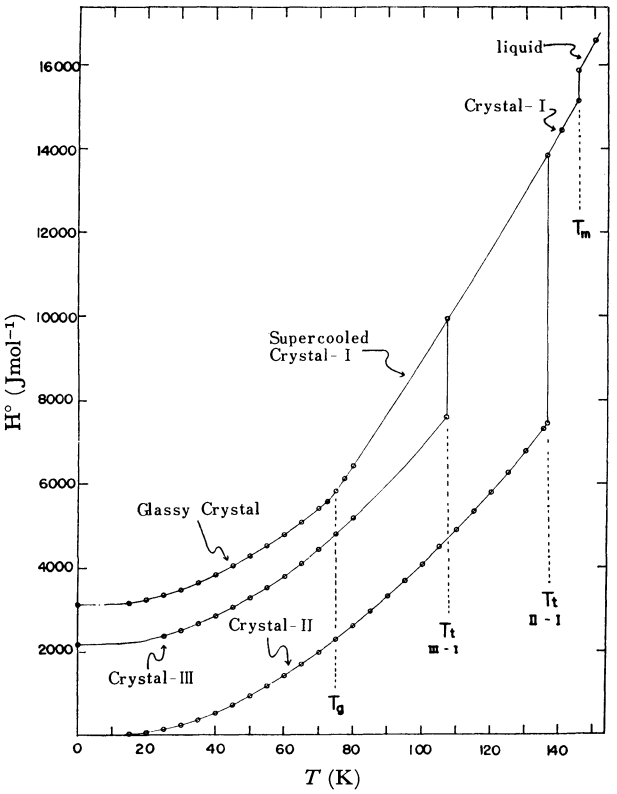

Fig. 3. The enthalpy curves.

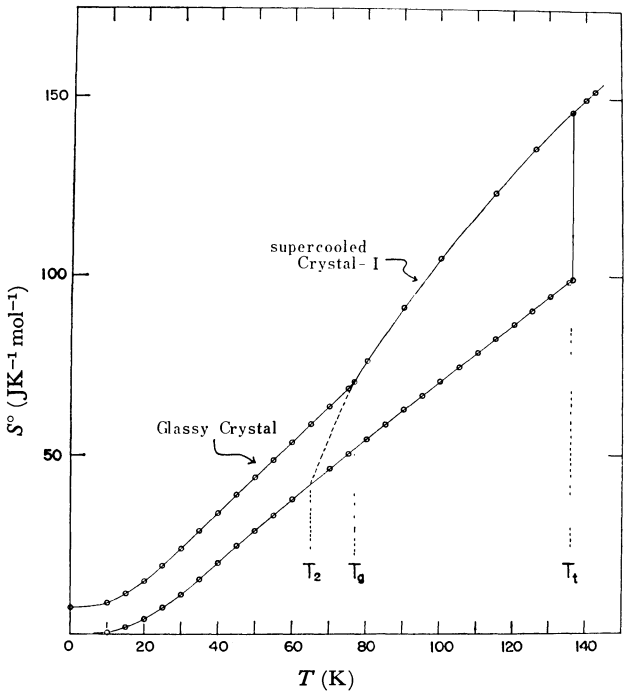

Fig. 4. The entropy curves.

enthalpy returns gradually to the equilibrium value from that of non-equilibrium frozen state.[15] We have revealed previously[1] that a similar behavior to ordinary glass is observed in the glassy crystalline state of cyclohexanol. The relaxation process for the glassy crystal of 2,3-dimethylbutane was investigated in the same way below T_g by annealing. The experiments were carried out as follows. Crystal-I was supercooled with the cooling rate of about -2 K min^{-1}. Cooling was stopped at a definite temperature below T_g and the temperature was regulated to maintain constant value for at least 20 hr. These studies were carried out at 60.7, 65.1, 69.7 and 72.0 K and the temperatures were regulated in the range of ± 0.3 K. After annealing for 20 hr, the temperature of the specimen was raised by supplying electric energy under adiabatic conditions to a temperature where an internal equilibrium was established, say 76 K. From the supplied energy, the difference in the enthalpies between the annealed glassy crystal at the initial temperature T_i and the supercooled crystal-I at T_f (about 76 K) was determined. Of course a part of the supplied electric energy is used to change the enthalpy of some degrees of freedom which is not frozen at the T_g. Thus, the enthalpy change due to this kind of degree of freedom (increment of the energy of vibrations or so) was subtracted from the total change of enthalpy in order to see directly the change of the configurational enthalpy. The heat capacity due to the vibrations (C_p(vib)) was estimated by the following equation between 60 and 80 K.

$$C_p(\text{vib}) = 0.9200\text{T} + 1.72 \text{ JK}^{-1}\text{ mol}^{-1} \quad (4)$$

The change of the configurational ΔH_c is given by

$$\Delta H_c = \Delta H - \int_{T_i}^{T_f} C_p(\text{vib})\text{d}T \text{ Jmol}^{-1} \quad (5)$$

15) R. O. Davies and G. O. Jones, Advances in Phys., **2**, 370 (1953).

where T_i and T_f were defined above and ΔH is the electric energy supplied per mol. The calculated values of ΔH_c are modified so that the final temperature T_f is 76.40 K by using the measured heat capacities near T_g. We take T_f=76.40 K as the reference point for ΔH_c=0. The results are shown in Fig. 5 and Table 8. During the course of annealing, the rates of the

TABLE 8. RELAXATION OF THE CONFIGURATIONAL ENTHALPY OF THE GLASSY CRYSTAL

	T_i(K)	T_f(K)	ΔH	ΔH(vib)	ΔH_c
1	69.669	76.425	671.7	465.6	206.0
2	65.138	76.346	913.7	748.7	165.0
3	60.692	76.327	1146.8	1012.3	134.4
4	72.028	76.328	493.4	300.9	192.6

The unit of ΔH is Jmol^{-1}. ΔH represents the supplied energy to raise the temperature from T_i where the specimen was annealed to T_f. ΔH(vib) indicates $\int_{T_i}^{T_f} C_p(\text{vib})\text{d}T$. C_p(vib) is given by Eq. (3). ΔH_c represents the difference of the configurational enthalpy, *i.e.* $\Delta H - \Delta H$ (vib).

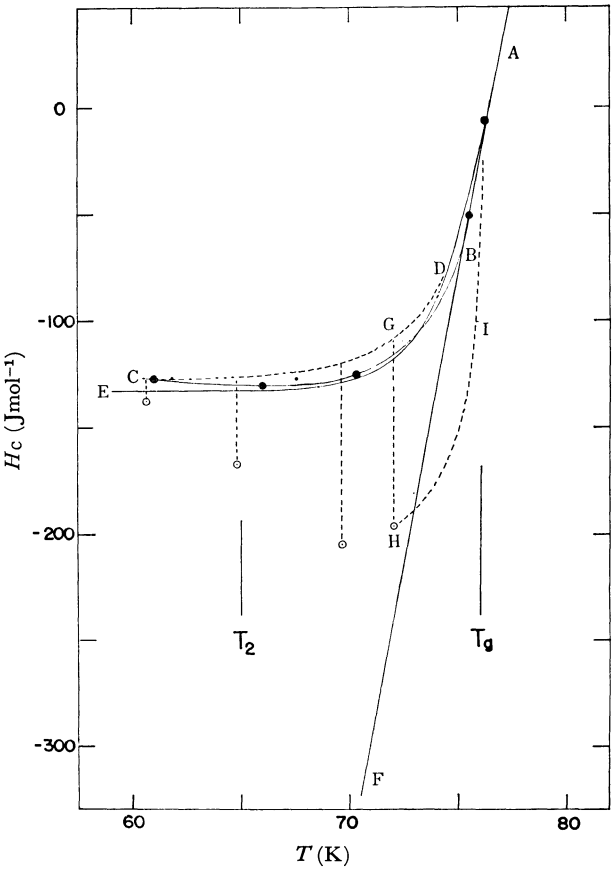

Fig. 5. The relaxation effect of the configurational enthalpy.
A-B-F Equilibrium curve calculated from Eq. (1).
A-B-C Change of the configurational enthalpy of the glassy crystal when it was heated with the rate of 4 K/hr after cooled down to about 50 K with the rate of -2 K/min.
A-D-G-C Estimated value of the enthalpy after cooling with the rate of -2 K/min.
G-H The point G shows the value of H_c just after the crystal-I was chilled to 72 K. After the annealing period of 20 hr the enthalpy changes to the point H.
H-I-A Estimated change of the configurational enthalpy when the specimen is heated from H with the rate of about 10 K/hr.

Table 9. The rate of change of configurational enthalpy

Annealed at 72.0K		69.7K		65.2K		60.7K	
Time	$-\dot{H}_c$	Time	$-\dot{H}_c$	Time	$-\dot{H}_c$	Time	$-\dot{H}_c$
0.53	54.4	1.33	27.9	1.33	9.99	0.83	3.25
0.66	48.0	3.09	14.2	4.58	3.20	2.17	2.35
2.58	14.5	4.33	10.4	5.50	4.32	5.00	1.74
5.42	7.50	5.58	8.22	18.75	1.94	6.25	1.58
8.42	4.07	7.00	6.86	19.50	2.16	11.17	1.22
10.66	3.43	9.09	5.09			14.25	1.04
20.00	1.29	15.09	3.88			17.25	1.35
		17.83	2.87			19.92	0.81
		19.83	2.22				

(time unit: hr; $-\dot{H}_c$: $10^{-2}J$ mol^{-1}min^{-1})

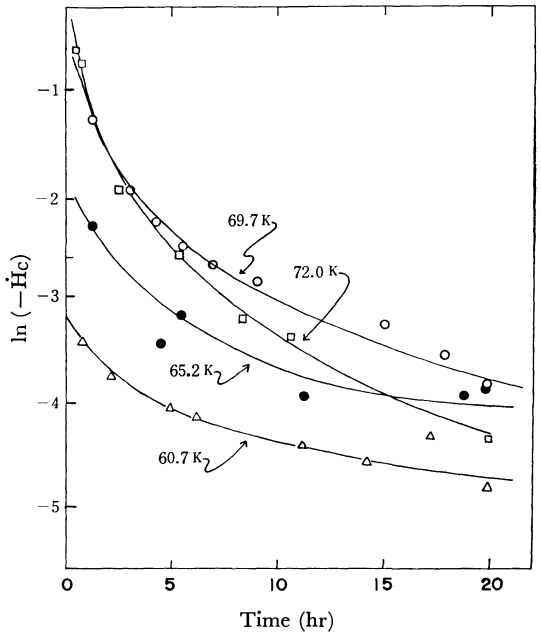

Fig. 6. Curves of the rate of the enthalpy change at various temperatures below T_g.

heat evolution due to the reversion of the enthalpy to the equilibrium state were determined from the rate of spontaneous temperature rise under the temporarily adjusted adiabatic conditions. The rates of the enthalpy change at various temperatures were calculated from these measurements and are shown in Fig. 6. and Table 9.

Discussion

Residual Entropy and Frozen-in State. Crystal-I of this material belongs to the so-called "plastic crystal" named by Timmermans.[16] It is known that in the plastic crystalline phase, the constituent molecules change their orientations rather rapidly at their lattice points. The self-diffusion phenomenon is also observed in many plastic crystals just below their melting points.[17,18] The second moment of NMR absorption line for crystal-I was reported to be 0.7 gauss^2 at about 140 K.[19] This may be explained also as a result of the rapid motion of molecules in the plastic crystal phase. It was also reported that the broadening of the line width of NMR spectrum was observed in the supercooled crystal-I at about 85 K, about 10 K higher than T_g (=76 K).[5] This behavior resembles that of ordinary glasses.[20] On the other hand, we have observed the relaxation effect of the configurational enthalpy below T_g where the relaxation time turns out to be 20 hr or more. These facts indicate that the probability of reorientation of molecules becomes smaller at lower temperatures due to the existence of hindering potential. At a temperature around 10 K higher than T_g, the frequency of the reorientation is estimated to be of the order of 10^3 times per second from the NMR data. Below T_g, on the other hand, the relaxation time becomes longer than the experimental time scale for heat capacity measurement, resulting in an establishment of non-equilibrium state. Therefore, it is expected that the main origin of the residual entropy can be attributed to the randomness of the orientation of molecules. If one calculates from the residual entropy the average number of configurational states permitted for a molecule in the glassy crystalline state by using the relation $S_0=R\ln W$, W amounts to 2.4 ± 0.3. Here, S_0, R and W are the residual entropy, the gas constant and the number of states, respectively. Unfortunately, the crystal structure of crystal–I is unknown and quantitative treatment for the orientational degree of freedom is impossible at the present stage. We should like to discuss, however, its contribution to the residual entropy briefly. If we assume the face-centered or body-centered lattice[21] for crystal-I and the center of gravity of the molecule located at the lattice point, it is plausible that the orientation of the molecular axis is directed to one of the three axis of the cubic cell with respect to their elongated sphere shape of a molecule. Here, the molecular axis is taken as the line parallel to the C–C bond connecting two $(CH_3)_2CH$-groups. There remains further the degree of freedom of the rotation of a whole molecule around this axis. The possible number of orientations permitted for this degree of freedom may be 4, at least even the conformation of the molecule being fixed. Thus, it may be concluded that at the limit of the most random state, the molecule will have about 12 kinds of orientations (3×4). In other word, the configurational entropy due to the orientational degree of freedom may be $R\ln 12$ (21 JK^{-1} mol^{-1}) at high temperature. Comparing this value with the residual entropy ($R\ln 2.4$), it may be said that the ordering of orientation should take place with the decrease of temperature. Furthermore, we may take into consideration the contribution of

16) J. Timmermans, *J. Phys. Chem. Solids*, **18**, 1 (1961).

17) H. Suga, M. Sugisaki, and S. Seki, *Mol. Cryst.*, **1**, 377 (1966).

18) C. P. Smyth, *J. Phys. Chem. Solids*, **18**, 40 (1961).

19) R. G. Eades, G. P. Jones, J. P. Llewellyn, and K. W. Terry, *Proc. Phys. Soc.*, **91**, 124 (1967).

20) for example, K. Luszczynski, J. A. E. Kail, and J. G. Powles, *ibid.*, **75**, 243 (1960).

21) W. J. Dunning, *J. Phys. Chem. Solids*, **18**, 21 (1967).

the molecular conformations to residual entropy. It is possible for the molecule of 2,3-dimethylbutane to have two different conformations by internal rotation,[22] *i.e.* one *trans*-form and two identical *gauche*-forms. The energy difference between them in the liquid state has been reported from the studies of the infrared and Raman spectra and from the absorption of sound wave. Szasz and Sheppard[23] proposed two possibilities for the energy difference between two conformations in the liquid state, *i.e.* either less than 100 cal/mol or very high value from the temperature dependence of the Raman spectra, based on the fact that no measureable intensity changes were observed in the spectra investigated at various temperatures. Brown and Sheppard studied further the IR and Raman spectra of the crystalline state and concluded the existence of only the *trans*-form.[24] They reported, however, that crystallization took place by raising the temperature of the "*glassy state.*"[25] They also reported that the spectrum in the "*glassy state*" closely resembled that in the liquid state. Accordingly, supercooled crystal-I is considered to be composed of a mixture of the *trans*-form and the *gauche*-form with the ratio of about one to two. On the other hand, Chen and Petrauskas determined the energy difference between two conformations to be 4.0 KJ mol^{-1} from their study of the absorption of the hypersonic sound wave in the liquid state.[26] The energy difference in the gaseous state was estimated to be 6.7 KJ mol^{-1} by Pitzer.[27] Scott *et al.* concluded, however, that it was very small (less than 100 cal mol^{-1}) from studies of the heat capacity and the entropy in the gaseous state.[14] We have reinvestigated the infrared spectrum of the glassy crystal at 40 ± 30 K and found that the spectrum was nearly the same as that of the liquid.[28] The study has been carried out in the region of 1050—800 cm^{-1}. If we assume that the mixing ratio of the isomers is frozen at the glass transition point and that the energy difference is 100 cal mol^{-1}, the contribution of this degree of freedom to the residual entropy amounts to 8.6 JK^{-1} mol^{-1}. Here, the *gauche* form is taken as the higher energy species. This value exceeds the actual value of the residual entropy. Thus, we understand from spectroscopic experiments that most of the residual entropy can be attributed to the randomness in the conformation of molecules. That the residual entropy can be explained only by the freezing of conformational degree of freedom was already observed in the case of the glassy crystalline state of cyclohexanol.[1] This seemingly strange result can be explained if we assume that the conformational degree of freedom is strongly coupled with the orientational degree. It should be noted that if the conformation be independent of the neighboring molecules, its contribution to heat capacity should be Schottky-type and may be much smaller than the actual jump of the heat capacity at T_g which is caused by the release from frozen-in state.

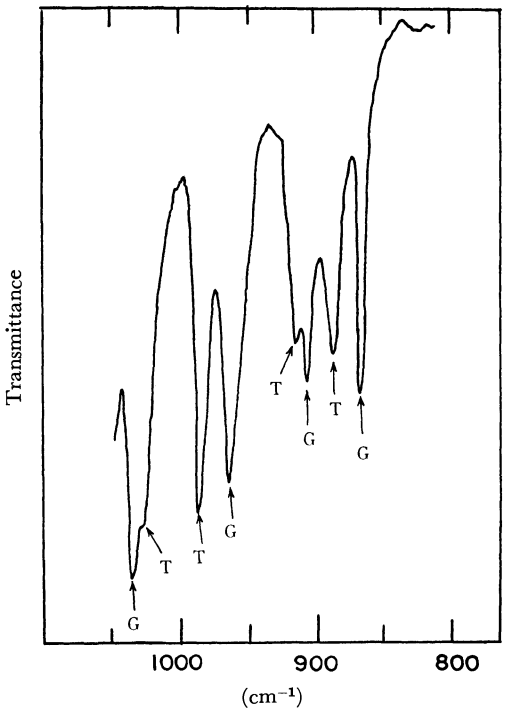

Fig. 7. Infrared spectra in the glassy crystalline state of 2,3-dimethylbutane.
T; the absorption band due to the *trans*-form.
G; the absorption band due to the *gauche*-form.

T_2 *Temperature.* In order to explain Kauzmann's paradox,[29] Gibbs and Adam have proposed an equation for the temperature dependence of the relaxation time in terms of the configurational entropy of the supercooled liquid.[6] The theory predicts that the relaxation time of viscoelastic properties becomes infinite at a temperature (T_2) where the configurational entropy disappears. T_2 temperature is determined from the equation described below by assuming that the equilibrium heat capacity is given by the extrapolation of the heat capacity curve above T_g.

$$S_0^\circ = \int_{T_2}^{T_g} [C_p(\mathrm{eq}) - C_p(\mathrm{gl})] \mathrm{d} \ln T, \qquad (6)$$

where S_0°, C_p(eq) and C_p(gl) are the residual entropy, the heat capacity of the supercooled crystal-I and that of the glassy crystal, respectively. Here, Eq. (1) extrapolated to lower temperature is used for C_p(eq). T_2 Temperature determined in this way amounts to 65.0 ± 0.7 K. It is known empirically that for ordinary amorphous glass, the ratio of T_g to T_2 is about 1.3.

22) R. I. Podlovchenko, L. M. Sverdlov, and M. M. Sushchinskii, *Optics. Spectr.*, **6**, 96 (1959).
23) G. J. Szasz and N. Sheppard, *J. Chem. Phys.*, **17**, 93 (1949).
24) J. K. Brown and N. Sheppard, *ibid.*, **19**, 976 (1951).
25) They decribed it as a "*glassy state*". It is, however, incorrect, because they did not find any glass transition point. This "*glassy state*" may be the supercooled crystal-I and the crystal (in their notation) is presumably crystal-II.
26) J. H. Chen and A. A. Petrauskas, *ibid.*, **30**, 304 (1959).
27) K. S. Pitzer, *Chem. Rev.*, **27**, 39 (1940).
28) The results are shown in Fig. 7. Almost the same spectra were observed in liquid state. Podlovchenko *et al.* concluded from calculation of the normal modes of vibration that these bands are attributed to those of *trans*-isomer and *gauche*-isomer as shown in Fig. 7. Since the specimen sealed in a polyethylene container was used, transmittance was rather bad. Accordingly, the intensity of each band is not very reliable.
29) W. Kauzmann, *Chem. Rev.*, **43**, 219 (1948).

Table 10. Values of ΔC_p, S_0, and T_g/T_2 for glassy crystals

	T_g(K)	ΔC_p	S_0	T_g/T_2
2,3-Dimethylbutane	76	51	7.4	1.17
Cyclohexanol[a)]	150	24	4.7	1.18
cis-1,2-Dimethylcyclohexane[b)]	94	54	8.6	1.15
Molecular compound[c] of 2,3-Dimethylbutane and 2,2-Dimethylbutane	69	56	10.0	1.19

The unit of ΔC_p and S_0; JK^{-1} mol^{-1}
a) From Ref. 1.
b) Calculated from Ref. 2.
c) Calculated from Ref. 3

For the glassy crystals including some other examples known hitherto the ratio T_g/T_2 amounts to about 1.15—1.20 as shown in Table 10. Angell discussed the value of T_g/T_2 for ordinary glass[30)] and considered the glass having the value of $T_g/T_2=1$ to be an ideal glass. The small value of T_g/T_2 for glassy crystal may be explained from the fact that glassy crystal has higher positional order than ordinary glass. It is interesting to compare the glassy crystal of 2,3-dimethylbutane with the glassy state of 2-methylbutane (isopentane), the study of which was reported previously.[31)] The values of T_g/T_2, ΔC_p and $S_0°$ of 2-methylbutane amount to 1.30, 52 JK^{-1} mol^{-1} and 14.1 JK^{-1} mol^{-1}, respectively. Although their structures differ slightly the difference between their residual entropies, 6.7 JK^{-1} mol^{-1}, seems to be attributable to the entropy of positional disorder of the glassy state of isopentane. The glassy crystal is considered to be positionally ideal glass from Angell's viewpoint.

Relaxation of Enthalpy. If one assumes an exponential decay for the change of configurational enthalpy in the period of annealing below T_g, it may be represented by the equation

$$\Delta H_c(t) = \Delta H_c(0) \exp(-t/\tau). \quad (7)$$

Here, ΔH_c is the difference between configurational enthalpy of frozen state and that of equilibrium state and τ the time constant. Differentiation of Eq. (7) with time gives

$$\log(-\dot{H}_c) = -t/\tau + \text{constant}, \quad (8)$$

where $\dot{H}_c$ represents dH_c/dt. The experimental result shown in Fig. 6, however, do not fit such a type of linear equation. From this figure, we recognize immediately that the rate of the enthalpy relaxation is more rapid at the initial stage than the corresponding exponential decay with a nearly equal time constant. This may be explained in two different ways. If one assumes the existence of different relaxation processes with different relaxation times, the results shown in Fig. 6 can be explained. For example, if there exist two relaxation processes, the equation will be given by

$$\Delta H_c(t) = \Delta H_1 \exp(-t/\tau_1) + \Delta H_2 \exp(-t/\tau_2). \quad (9)$$

Co-existence of two relaxation processes has been demonstrated experimentally by Macedo and Napolitano[32),33)] for boro-silicate glass. Another explanation is given by considering that the time constant is not only a function of temperature but also of the thermodynamic variables of the glassy state. Gibbs and Adam considered that the mechanical relaxation time in the supercooled liquid depends on the configurational entropy as well as on the temperature.[6)] We have examined the applicability of their theory to the relaxation of the configurational enthalpy. The $\dot{H}_c(t)$ at time t is given by

$$-\dot{H}_c(t) = \bar{W}(T)H_c(t). \quad (10)$$

Here, $\bar{W}(T)$ is the transition probability of the region in which molecules (or segments) change their configuration co-operatively. $\bar{W}(T)$ is given by

$$\bar{W}(T) = \bar{A} \exp(C/TS_c). \quad (11)$$

Here, $\bar{A}$ and C are constants and S_c the configurational entropy. From Eq. (10) and (11), we obtain

$$\log(-\dot{H}_c/\Delta H_c) = -C/(2.30TS_c) \quad (12)$$

From the data of annealing at 69.7 K and 72.0 K, the values of $\log(-\dot{H}_c/\Delta H_c)$ are plotted against $1/S_c$ in Fig. 8. The values of S_c at various time values are determined by the equation

$$S_c(t) = S_c(0) - \int_0^t (\dot{H}_c/T)dt + \Delta S_{irr}. \quad (13)$$

Here, $S_c(0)$ is equal to the residual entropy and ΔS_{irr} is, the irreversible entropy production.[15)] The latter is however, too small (less than 1% of the integral term) and can be neglected. As is seen in Fig. 8, the

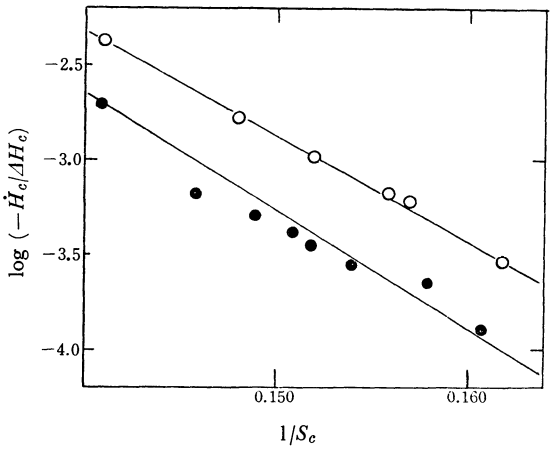

Fig. 8. The plot of ln $(-\dot{H}_c/\Delta H_c)$ *vs.* $1/S_c$.
○ calculated from the data of annealing experiment at 72.0 K
● calculated from the data at 69.7 K

agreement between theory and experiment is roughly established. From the slopes, the value of the constant C in Eq. (12) is determined to be about 9.9 KJ mol^{-1} for 69.7 K and 9.1 KJ mol^{-1} for 72.0 K. In the Gibbs-Adam theory, constant C is related to the number of

30) C. A. Angell, *J. Amer. Ceram. Soc.*, **51**, 117 (1968).
31) M. Sugisaki, K. Adachi, H. Suga, and S. Seki, This Bulletin, **41**, 593 (1968).
32) P. B. Macedo and A. Napolitano, *J. Res. Natl. Bur. Std.* (U. S. A.), **71A**, 231 (1967).
33) A. Napolitano and P. B. Macedo, *ibid.*, **72A**, 425 (1968).

molecules or segments Z^* in a minimum cooperative region by the equation

$$C = \Delta\mu S_c Z^*/R, \quad (14)$$

where $\Delta\mu$ is the activation free energy per mole and R the gas constant. We have assumed for a moment that the value of $\Delta\mu$ is equal to the difference between the Gibbs free energies of crystal-I just below melting point and of the glassy crystal at 70 K. It turns out to be 1.5 KJ mol^{-1}. This assessment on $\Delta\mu$ is rather small judging from the fact that the apparent activation energy for the rotational diffusion of molecule in the plastic crystals is known to be about 8 KJ mol^{-1}.[34] Therefore, we take 1.5—8 KJ mol^{-1} for the value of $\Delta\mu$ and determined the value of S_cZ^* to be 10—55 JK^{-1} mol^{-1} by putting 9.9 KJ mol^{-1} for the value of C. Taking the residual entropy (=7.4 JK^{-1} mol^{-1}) for S_c, Z^* is calculated to be 1—7. It may be noted that the relaxation effect was still observed below T_2 temperature as shown in Fig. 5. This fact does not contradict the Gibbs-Adam theory because the glassy crystalline state prepared in this way has a finite value of S_c.

The Heat Capacity Below T_g. As shown in Fig. 2, the heat capacity of the glassy crystal is anomalously large at low temperature compared with that of crystal-II. The frequency spectrum of lattice vibration for the glassy crystalline state seems to be of interest. The data of C_v (the heat capacity at constant volume) is necessary, but as the expansion coefficient and compressibility of this material are unknown at low temperature, it is impossible to know the C_p-C_v. Based upon the theory of Hovi[35] and Pautano, we have tried to find out the difference in the spectra of the glassy crystal and crystal-II from the difference of their heat capacity. Here, it is assumed that the C_p-C_v of each state are equal and all the vibrations are harmonic. According to the notation by Hovi and Pautano, the equations are given by

$$A \cdot X_1 = C_1 \text{ and} \quad (15)$$

$$A \cdot X_2 = C_2, \quad (16)$$

where X_1 and C_1 are the column vectors representing the magnitude of the histogram of the spectrum and that representing the heat capacities for the glassy crystal, respectively, and X_2 and C_2 are those for cystal-II. The difference between Eqs. (15) and (16) is given by

$$A \cdot \Delta X = \Delta C,$$

where ΔX is X_1-X_2 and ΔC is C_1-C_2. In the region from 0 to 30 cm^{-1}, the frequency spectrum is assumed to follow the Debye model. The cut-off frequency is then taken as 130 cm^{-1} judging from the Debye temperature 130 K (=90 cm^{-1}) for crystal-II. The region from 30 to 130 cm^{-1} is devided into five sections with equal width of 20 cm^{-1}. The values of the specific heat

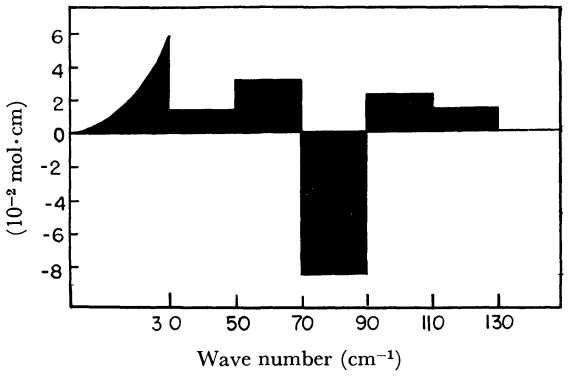

Fig. 9. The difference in the frequency spectrum of the lattice vibration between the glassy crystal and the crystal-II.

at 14, 17, 20, 25, 30 and 40 K are employed for ΔC in Eq. (14). The result is shown in Fig. 9. The positive value of the spectrum below 30 cm^{-1} can be explained by the lower density of the glassy crystal compared with that of crystal-II. Unfortunately, the data of the density of this material at low temperature is not available at present. It is known, however, that the large increase of the molar volume is associated with the transition from the low-temperature phase to the plastic phase, so the lower density of the glassy crystal may be the case. The large negative spectrum at 80 cm^{-1} suggests that a sharp peak (the vibrational mode —) exists in the spectrum of crystal-II whereas the spectrum is smoothed out in the glassy crystalline state. Dean[36] has shown this feature of the smoothing out effect of the spectrum of the perfect crystal by introducing a glass-like disorder.

The Entropy of Transition. Guthrie and McCullough discussed the transition entropy ΔS_t from the low temperature form to the plastic phase for various materials by considering molecular symmetry and symmetry of the crystal lattice of the plastic phases.[37] They interpreted ΔS_t from the viewpoint of the randomness of orientation and of the conformation of molecules. However, we can expect the contribution of entropy of the lattice vibration to be not negligible because the large change of the frequency spectrum is expected on account of softness of the plastic phase. It is considered that ΔS_t is the sum of ΔS_{or}, ΔS_c and ΔS_{vib}, where ΔS_{or} is the difference of entropy due to orientational change, ΔS_c that due to conformational change of the molecule and ΔS_{vib} that due to the change in lattice vibration. We calculated ΔS_{vib} for the 2,3-dimethylbutane from the difference in the spectrum of vibration which is given in Fig. 9. It amounts to 12.8 JK^{-1} mol^{-1} assuming the spectrum of the glassy crystalline state is retained even at transition temperature. ΔS_{or} and ΔS_c have been estimated to be 21 ($\simeq R\ln 12$) and 9 ($\simeq R\ln 3$) J K^{-1} mol^{-1}, respectively at the most random state (see page 85). Their sum becomes 43 JK^{-1} mol^{-1} which is comparable with the experimental value of ΔS_t (=47.25 JK^{-1} mol^{-1}).

34) A. Bondi, "Physical Properties of Molecular Crystals, Liquids and Glasses," J. Wiley and Sons, Inc., New York (1968), p. 106—121.
35) V. Hovi and Y. Pautano, *Ann. Acad. Sci. Fenn.* **Ser. A, 6**, 1, (1960).
36) P. Dean, *Proc. Phys. Soc.*, **84**, 727 (1960).
37) G. B. Guthrie and J. P. McCullough, *J. Phys. Chem. Solids*, **18**, 53 (1961).
38) J. R. Green and C. E. Sheie, *ibid.*, **28**, 383 (1967).

The agreement will be improved if we take account of the variation of the frequency spectra (Fig. 9) at a higher temperature. The data[38] of the elastic constant measured with high frequency ultrasonic wave for the plastic phase of the cyclohexanol will be helpful for this consideration. The Debye temperature calculated is 60 K around 265 K whereas the Debye temperature in the glassy crystalline state (at 50 K) has been determined to be about 90 K from thermal data.[1] If the effect is taken into account, the value of ΔS_{vib} becomes larger and a better agreement is obtained between experimental and calculated ΔS_t. We would like to point out that the contribution of ΔS_{vib} is not negligible for the explanation of the content of ΔS_t.

Crystal-III. It has been revealed that the residual entropy of crystal-III is determined to be 2.7 JK^{-1} mol^{-1} and that there exists an anomalous hump in the heat capacity curve around 70 K. From these facts, there is the possibility that the state of crystal-III below 70 K is also glassy crystalline. This can not be confirmed, however, as the relaxation phenomenon has not yet been observed.

BULLETIN OF THE CHEMICAL SOCIETY OF JAPAN, VOL. 44, 89—93 (1971)

Normal Coordinate Treatment and Force Constants of Alkanonitriles

Tsunetake FUJIYAMA

Department of Chemistry, Faculty of Science, The University of Tokyo, Hongo, Bunkyo-ku, Tokyo

(Received August 24, 1970)

Force constants of the Urey-Bradley type are calculated for a series of alkanonitriles. The calculation covers the mononitriles: CH_3CN, CH_3CH_2CN, $(CH_3)_2CHCN$, $(CH_3)_3CCN$, and the dinitriles: $NCCH_2CN$, $NCCHDCN$, $NCCD_2CN$, *trans*-$NCCH_2CH_2CN$, *gauche*-$NCCH_2CH_2CN$. The results show that the force constants can be transferred from molecule to molecule as a group. It is also shown that a group of force constants is characteristic of a corresponding chemical structure or a substituent.

One of the most important problems in the field of vibration spectroscopy is to find a reliable set of force constants which may explain the frequencies of many molecules with similar chemical structures. For the purpose of finding transferrable force constants of alkyl cyanides, a series of stadies have been made.

There exist some difficulties in the normal coordinate treatment of rather complicated molecules which are composed of many different atoms or substituents. The most important problem, from the viewpoint of force field, is that the number of force constants which should be considered in calculations often exceeds that of information obtained from vibration spectra. Consequently, the force constants obtained from the calculation are somewhat ambiguous and sometimes cause an erroneous conclusion when they are transferred to other molecules.

In the case of molecules consisting of a few atoms or of many but similar atoms or chemical bonds, the problem is easily settled or does not exist at all, because the number of force constants which should be determined is small, while many pieces of information can be obtained not only from the vibrational frequencies themselves but also from the other experimental results. One solution for this problem may be obtained by carrying out the normal coordinate treatment of many molecules having similar chemical structures. However, there still remain doubts as to whether the method can also be applied to the case in which two or more chemical structures are combined in one molecule.

In the present report the result of the normal coordinate treatment of some basic alkanonitriles will be discussed.

Calculation of Force Constants and Results

The infrared spectra and their frequency assignment necessary for the present work will be found in the references,[1-3] and are not discussed here. The method of calculation exactly follows that of the reference[4]

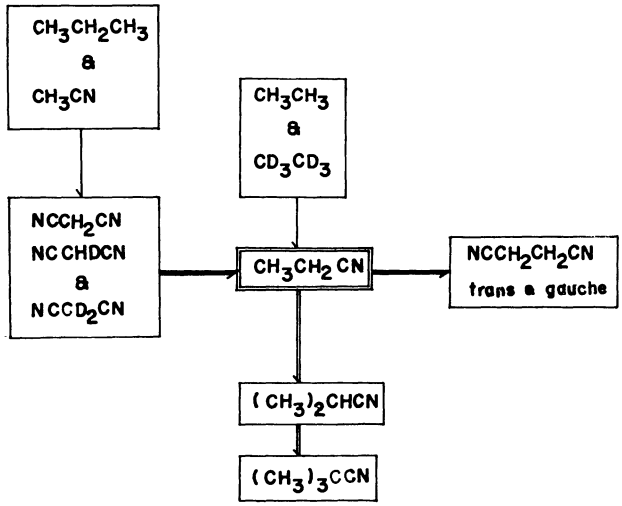

Fig. 1. The Diagram of the Determination of Force Constants of Alkylnitriles.

1) T. Fujiyama, the MA-thesis submitted to the University of Tokyo (1963).

2) T. Fujiyama and T. Shimanouchi, *Spectrochim. Acta*, **20**, 829 (1964).

3) T. Fujiyama, K. Tokumaru, and T. Shimanouchi, *ibid.*, **20**, 415 (1964).

4) T. Shimanouchi, *J. Chem. Phys.*, **17**, 245, 734, 848 (1949).

and is not repeated here.[5]

The process for the determination of the force constants is illustrated in Fig. 1. Prior to the explanation of the process, it is convenient to classify the force constants of alkanonitriles into three groups: a hydrocarbon group, an α-carbon group, and a cyanide group. The significance of these groups is illustrated in Fig. 2.

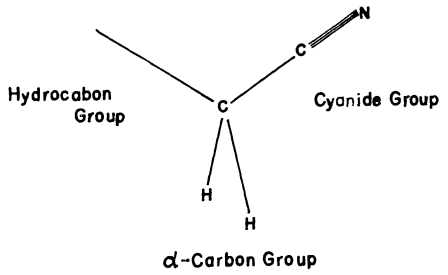

Fig. 2. Classification of Force Constants.

The α-carbon group is composed of the force constants associated with the α-carbon to any extent and the other two groups are composed of those associated with the β-carbon or with the cyanide radical. The force constants of acetonitrile obtained by Nakagawa[9] and those of normal hydrocarbons obtained by Takahashi[10] are a good starting set for the present calculation.

First, malononitrile and its deuterated compounds are treated using the force constants obtained from acetonitrile and propane. In this process, it was found necessary to make essential changes in the values of some force constants. The molecules studied next was ethylcyanide. The force constants determined for malononitrile were directly transferred to those associated with α-carbon and cyanide groups, while those for a methyl part were transferred from ethane. These two processes were designed for finding the force constants of alkanonitriles associated with the cyanide group and the α-carbon group. A little refinement of the force constants was necessary in the process from malononitrile to ethyl cyanide in order to obtain a good agreement between the observed and the calculated frequencies. However, the force constants of the hydrocarbon group and of the cyanide group remain unchanged.

Then the study was extended to larger molecules by two routes. One route was for succinonitrile in order to confirm the reliability of the force constants for the α-carbon and the cyanide groups. The results obtained were satisfactory both for the *trans* and the *gauche* conformations of succinonitrile. The other route was designed for finding the force constants associated with the secondary and the tertiary α-carbons. In this case also, the force constants were transferred from ethylcyanide. It must be emphasized here that in the treatment of the last three molecules, $NCCH_2CH_2CN$, $(CH_3)_2CHCN$, and $(CH_3)_3CCN$, the force constants of the hydrocarbon and the cyanide groups were not changed essentially.

The final set of force constants thus obtained are summarized in Table 1 and in Table 2. The calculated frequencies are compared with the observed frequencies in Figs. 3(a) and 3(b).

Interpretation

In the previous section, the difficulty of the normal coordinate treatment of rather complicated molecules has been emphasized. The alkyl cyanides are just such molecules which are composed of many chemically different atoms, H, C, and N. As easily be understood from many chemical phenomena, the chemical properties of the atoms associated with the α-carbon atoms are much different from those of the β-carbon atom. The effect of the substituent, the –CN radical, extends not only to the α-carbon but also to the atoms attached to the α-carbon atom.

One of the main object of this calculation is to see whether we can obtain a set of force constants which may be transferred as a group from one molecule to another. If the force constants of the hydrocarbon

Table 1. Force constants for the cyanide and the hydrocarbon groups

Molecule	Cyanide		Hydrocarbon				
	K(C≡N)	F(CCN) H(CCN)	K(C–H)	K(C–C)	F(HCH) H(HCH)	F(CCC) H(CCC)	$\kappa(CH_3)$
$NCCH_2CN$	18.159	0.501 0.141	—	—	— —	— —	—
$NCCH_2CH_2CN$	18.30	0.50 0.14	—	2.50	— —	— —	—
CH_3CH_2CN	18.47	0.50 0.15	4.48	2.00	0.07 0.44	— —	0.01
$(CH_3)_2CHCN$	18.47	0.55 0.15		2.00	0.07 0.44	0.33_5 0.27_5	0.01
$(CH_3)_3CCN$	18.47	0.50 0.15	4.48	2.00	0.07 0.44	0.33_5 0.27_5	0.01

The κ's are expressed in the unit of md · A. All the other parameters are in md/A.

5) After the completion of this work, a few papers were reported in which a few of the alkylnitriles of the present topics are discussed.[6-8] It is important to notice that their spectral assignments are often inconsistent with ours.[1]

6) J. J. Lucier, E. C. Tuazon, and F. F. Bentley, *Spectrochim. Acta*, **24**, 771 (1968).

7) P. Klaboe, *ibid.*, **26**, 87 (1970).

8) R. Yamadera and S. Krimm, *ibid.*, **24**, 1677 (1968).

9) I. Nakagawa and T. Shimanouchi, *ibid.*, **18**, 513 (1962).

10) H. Takahashi, *Nippon Kagaku Zasshi*, **82**, 1304 (1961).

TABLE 2. FORCE CONSTANTS FOR THE α-CARBON GROUP

Molecule	K(C–H)	K(C–CN)	F(HCH) H(HCH)	F(CCH)^{CH_3} H(CCH)	F(CCH)^{CN} H(CCH)	F(CCC) H(CCC)	F(CCH) H(CCH)	$\kappa(C_\alpha)$
$NCCH_2CN$	4.200	3.202	0.101 0.342	— —	0.507 0.210	0.300 0.430	— —	0.05
$NCCH_2CH_2CN$	4.20	3.10	0.10 0.34	0.54 0.16	0.51 0.21	0.32 0.36	— —	0.025
CH_3CH_2CN	4.34	2.60	0.10 0.36	0.54 0.19	0.51 0.21	0.34 0.38	0.48 0.14	0.05
$(CH_3)_2CHCN$	4.20	2.60	— —	0.54 0.19	0.51 0.21	0.44 9.35	0.48 0.14	0.11
$(CH_3)_3CCN$	—	2.60	— —	— —	— —	0.34 0.38	0.48 0.14	0.11

The κ's are expressed in the unit of md·A. All the other parameters are in md/A.

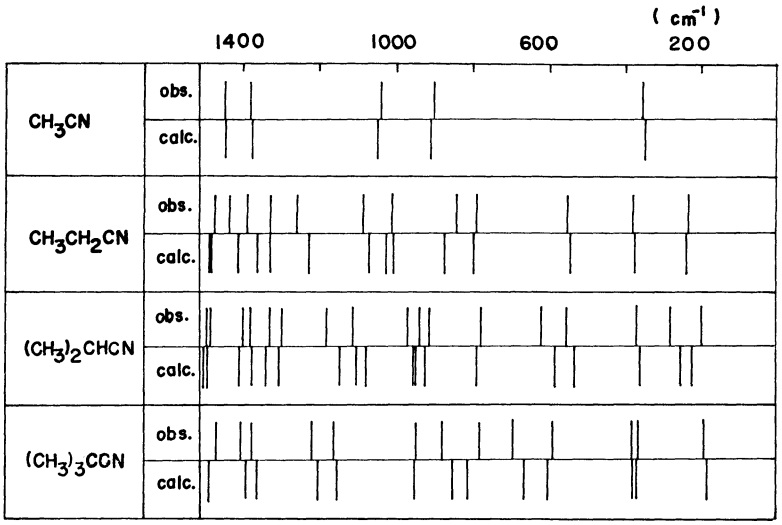

Fig. 3(a). Vibrational Frequencies for Alkanomononitriles.

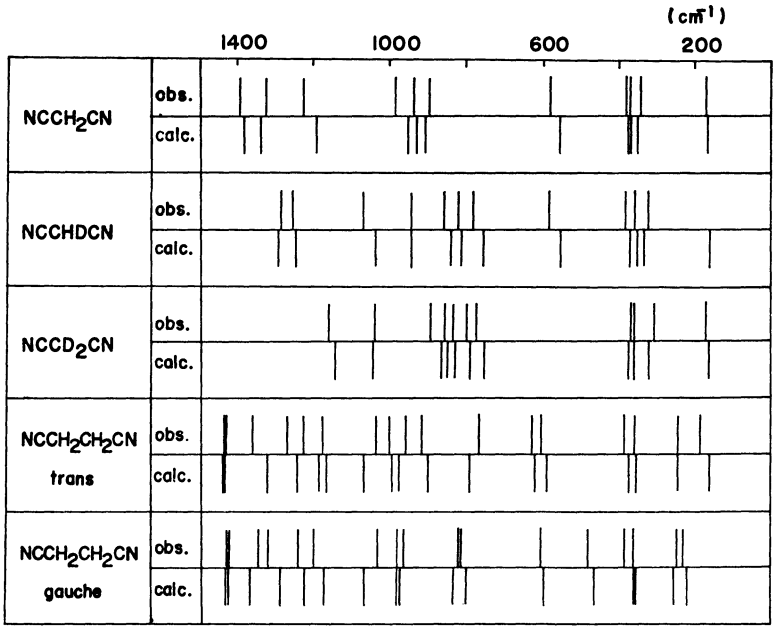

Fig. 3(b). Vibrational Frequencies for Alkanodinitriles.

group and the cyanide group are to be transferred unchanged from one molecule to the other, then the force constants which should be refined through the series of calculations are limited to those of the α-carbon group.

The Cyanide Group (see Table 1). The C≡N stretching vibration has little effect upon the other frequencies because it is an almost completely localized vibration. Consequently, the stretching force constants, K(C≡N), can be determined with good accuracy. The K(C≡N) changes its magnitude from the dinitriles to the mononitriles as is shown in Table 1. The tendency is interesting if the K(C≡N)'s are compared with the values of K(C–CN) of Table 2. The magnitude of K(C–CN) decreases from the dinitriles to the mononitriles, while that of K(C≡N) increases its magnitude. This implies that there exist some interactions between the C–CN and the C≡N bonds. As will be found elsewhere, this is also confirmed by the change of the bond length of the C–CN.

The force constants of the linear part, C–C≡N, are transferred quite successfully from one molecule to another in this series of calculations.

The Hydrocarbon Groups (see Table 1). The force constants belonging to this group have the same values as those of normal hydrocarbons. The K(C–H) of isobutylonitrile is not given in Table 1 because the high frequency separation has been made in the normal coordinate treatment of this molecule.

It may seem rather curious that the K(C–C) of succinonitrile has the value of 2.50 md/A, while the other K(C–C)'s have the values of 2.00 md/A. However the superposed effect from two adjacent α-carbon atoms on the C–C bond of succinonitrile certainly explains the relatively large value of the obtained force constant. The C–C bond of succinonitrile is sandwiched between two α-carbons, so that the effect of the substituents is supposed to be very large. Therefore, it should rather be classified into the cyanide group. Actually, some specific characters of the C–C bond have been reported and a hyperconjugation between the C–C and the C–N bonds has been proposed. Consequently, the anomalous value of this force constant does not spoil the transferability of this group force constants.

The α-Carbon Group (see Table 2). The stretching force constants, K(C–C)'s, are a little smaller than those of hydrocarbon group. This may suggest that the effect of the substituent extends to the nature of the bond between the α-carbon and the hydrogen atoms. A similar conclusion can be obtained from the values of F(H··H) and H(H·C·H). As the correlation between these two force constants is large, we cannot compare the magnitudes of these force constants separately. As a pair, however, an apparent decrease in the magnitude can be recognized for the F(H··H) and the H(H·C·H) values when they are compared with those of normal hydrocarbons.[11] The result is related with the fact that the CH_2 scissoring vibrations occur relatively lower frequencies for the alkanonitriles than for normal hydrocarbons.[12]

The molecular tension around the α-carbon atom does not satisfy the transferability in this group. In the case of a methyl group, the values of 0.01 md·A are commonly used for all the methyl parts of the molecules. According to the discussion of our laboratory, the reliable values are hardly be found as for the molecular tension of the skeletal part. For the purpose of finding reliable and transferable parameters, the result is not desirable (see the last column of Table 2).

In the 7th column of Table 2 the repulsive and the bending force constants, F(C··H) and H(CCH), are given. At first, they were expected to behave just like those for hydrocarbon molecules and were readily transferred from ethane. However, it was found through the calculation of ethylcyanide that their values must be reduced considerably in magnitude so as to obtain the reasonable frequencies for the C–C stretching, the C–CN stretching, and the methyl rocking vibrations. The force constants thus settled must be quite different from those for the simple hydrocarbon group. Nevertheless, they exhibit good transferability as the components of the α-carbon group (see Table 2). This result suggests that the effect of the substituent extends to the α-carbon or to the bond between α- and β-carbon atoms.

Discussion

Reliability of the Force Constants Obtained. The force constants obtained for each group may be quite reliable, because they show good transferability among the eight molecules treated in the present work. Moreover, the force constants of the hydrocarbon group are consistent with those of normal hydrocarbons. The cyanide group force constants are rather consistent with the results for acetonitrile. The agreement of the calculated frequencies with the observed frequencies given in Figs. 3(a) and 3(b) is very satisfactory. This gives ultimate supports for the reliability of the force constants obtained in this calculation.

Determination of the Force Field of a Complicated Molecule. The conclusions we have drawn from the present analysis of the force constants are itemized as follows:

1) Transferability of force constants is satisfied as a group.

2) Let there be two sets of force constants, one for a group A and another for a group B which is chemically different from A. If both sets of force constants are well determined, there is a reasonable hope of calculating the normal vibrations of such a molecule as A-B satisfactorily.

3) Moreover, the force constants of such molecules as A-C-B can be obtained rather definitely. We may well transfer the sets of force constants associated with the groups A and B, while the refinement should be made only for the set which is associated with C.

4) In this process, the number of force constants to be determined is rather small despite the com-

11) After this work was finished, quite different values were reported for the force constants of normal hydrocarbons. However, the magnitude of the F-matrix element does not change at all.

12) It was found later that the CH_2 scissoring vibration decreases its frequency in accordance with the magnitude of the electronegativity of the substituents.

plexities of the molecules.

5) If the force constants obtained from A and B are accurate, then the accuracy of the force constants obtained from the A-C-B will be confirmed. Thus, we can obtain the force constants associated with the C part with little ambiguity and the force constants thus obtained will be able to become good measures for considering the specific character of the C part.

The present work is completed under the guidance of Professor Takehiko Shimanouchi of the University of Tokyo. The author is grateful for his useful discussions.

BULLETIN OF THE CHEMICAL SOCIETY OF JAPAN, VOL. 44, 93—96 (1971)

Dissociation Constants of the Oxalato-Titanium(III) Complex as Determined from Spectrophotometric Measurements

Kuan PAN, Chin Chan LAI, and Teh-Shoon HUANG
Chemistry Research Center, National Taiwan University, Teipei, Taiwan, China

(Received August 25, 1970)

The dissociation constant of $Ti(C_2O_4)_2^-$ ions in hydrochloric acid media was evaluated from the data obtained by spectrophotometric measurements at 25°C. The average value of pK for the reaction, $Ti(C_2O_4)_2^- = Ti(III) + 2C_2O_4^{2-}$, at an infinite dilution was estimated as 9.0, while that for the $Ti(C_2O_4)_2^- = Ti^{3+} + 2C_2O_4^{2-}$ reaction was evaluated as 8.7_4.

The preparation of the oxalato-titanium(III) complex, $MTi(C_2O_4)_2 \cdot 2H_2O$ (M=K, Rb, NH_4), has been reported by Stahler.[1] The composition of the oxalato-titanium(III) ion in an aqueous solution was spectrophotometrically determined as $Ti(C_2O_4)_2^-$ by Pecsok,[2] while Subbanna, Rao, and Bhattacharya[3] asserted the molar ratio to be 1 : 1, corresponding to the formula, $H(TiOC_2O_4)$ from their spectrophotometric and conductometric measurements, however, they did not give an detailed data or the observed pH range. Afterwards, Jørgensen[4] suggested that the complexes $M^{I}Ti(C_2O_4)_2 \cdot 2H_2O$ contain a tetrahedral, $Ti(C_2O_4)_2^-$ anion, while Eve and Fowles[5] proposed the polymetric structure for $M^{I}Ti(C_2O_4)_2 \cdot 10H_2O$ on the basis of the diffuse reflectance spectra.

The present investigation was undertaken in order to redetermine the composition and to evaluate the dissociation constants of the oxalato-titanium(III) complex in a hydrochloric acid solution on the basis of spectrophotometric measurements at 25°C.

Experimental

Titanium(III) chloride was prepared by heating titanium sponge (99.9% purity, Alfa Inorganics, Inc., U. S. A.) with a 3N hydrochloric acid solution. Additional hydrochloric acid was added as the reaction progressed to prevent the hydrochloric acid concentration from falling below the point where hydrolysis could occur. The solution was then cooled and maintained under an atmosphere of nitrogen to prevent the formation of any appreciable quantity of Ti(IV). The Ti(III) content was determined by addition to an excess of ceric sulfate in a sulfuric acid solution, followed by potentiometric back-titration with a standard solution of ferrous sulfate. The chloride ion content was determined by potentiometric titration with silver nitrate. Hydrochloric acid, sodium chloride, and sodium hydroxide were used to adjust the H_3O^+ ion concentration and the ionic strength of the solution.

The oxalato-titanium(III) complex was prepared by the rapid addition of Ti(III) chloride to an aqueous solution of oxalic acid, according to Eve and Fowles,[5] and dried in a vacuum.

A Bausch & Lomb recording spectrophotometer, model 505, equipped with a constant temperature holder controlled to ±0.2°C was used.

For the spectrophotometric determination of the oxalato-titanium(III) complex, calibration curves for a series of solutions in an excess of oxalate at various H_3O^+ ion concentrations and ionic strengths were prepared. All the solutions were prepared from deaerated water and were kept in an atmosphere of nitrogen. All the reactants and their mixtures were kept in a thermostat whose temperature was controlled within ±0.2°C.

Since no time effect on the absorbance of the mixture of Ti(III) and oxalate ions in hydrochloric acid was observed in this pH range, and since the mixture of Ti(III) and oxalate as well as $KTi(C_2O_4)_2 \cdot 2H_2O$ in oxalic acid has the same absorption band at 440 mμ, a mixture containing a known content of Ti(III) in a HCl solution and a desired amount of a slight excess of oxalate was for the spectrophotometric measurements. The absorbance at 440 mμ was taken for the calculation of the dissociation constants.

Results and Discussion

Extinction Coefficients of Ti(III) Ions in Hydrochloric Acid Media. The titanium(III) ion has been known to form chloro-complexes such as $[TiCl(H_2O)_5]^{2+}$ and

1) A. Stahler, *Ber.*, **37**, 4405 (1904).
2) R. L. Pecsok, *J. Amer. Chem. Soc.*, **73**, 1304 (1951).
3) V. V. Subbanna, G. S. Rao, and Bhattacharya, *J. Sci. Ind. Res.*, **18B**, 127 (1959).
4) C. K. Jørgensen, "Inorganic Complexes," Academic Press, New York (1963).
5) D. J. Eve and G. W. A. Fowles, *J. Chem. Soc.*, **1966**, 1183.

$[TiCl_2(H_2O)_4]^+$ [6] even if the formation of the hydrolysis products, *e. g.* $[Ti(OH)(H_2O)_5]^{2+}$ and $[Ti(OH)_2(H_2O)_4]^+$, is neglegible in strong acid media. As a first degree of approximation, however, we may assume only the coexistence of $[Ti(H_2O)_6]^{3+}$ and $[TiCl(H_2O)_5]^{2+}$ (abbreviated as Ti^{3+} and $TiCl^{2+}$) in chloride media at pH 1—2.5 after the independence of the H_3O^+ ion concentration of the absorbance of the Ti(III) ions has been confirmed. Since no detailed data on the extinction coefficients of these ions is available, a series of spectrophotometric measurements were conducted for the determination of the extinction coefficients (ε_1) of Ti(III) ions in a mixture of 0.2—0.6N HCl and KCl solutions at 25°C.

Table 1. The extinction coefficients of Ti (III) in HCl and KCl at 25°C (ε_1 in $l\ mol^{-1}\ cm^{-1}$)

$[Cl^-]/\lambda$ mμ	0.2	0.3	0.4	0.5	0.6	Average
400	1.1	1.3	1.4	1.5	1.5	1.4
420	2.5	2.5	2.4	2.7	2.7	2.6
440	3.7	3.9	4.1	4.3	4.2	4.1
460	5.2	5.4	5.5	5.8	5.7	5.5
500	5.9	6.0	6.1	6.2	6.2	6.1
520	5.5	5.6	6.8	6.7	6.7	6.7
550	4.7	4.8	4.8	4.7	4.8	4.8

Since the extinction coefficient of Ti(III), ε_1, in the presence of a large excess of Cl^- ions was found to be practically independent of the H_3O^+ and Cl^- ion concentrations in the H_3O^+ ion concentration range mentioned above, we took the average value of 4.1 $l\ mol^{-1}\ cm^{-1}$ for ε_1 at 440 mμ.

Extinction Coefficients of Oxalato-Titanium(III) Complexes. Since, even in the acid media of pH 1.5—2.5, the mole ratio of the oxalato-titanium(III) complex was found to be 1 : 2 by the continuous variation plot (Fig. 1), the formation of the $Ti(C_2O_4)_2^-$ ion in the presence of HCl at pH 1.5 to 2.5 was assumed. The extinction coefficient of the complex was determined by plotting the absorbance against the total concentration of Ti(III) in a large excess of oxalate ions over this pH range at a constant ionic strength. The extinction coefficient of the oxalato-titanium(III) complex, ε_2, was found to be practically independent of the H_3O^+ and Cl^- ion concentrations, or of the ionic strength over the pH range of 1.5—2.5. We therefore, also took the average value of 320 $l\ mol^{-1}\ cm^{-1}$ for ε_2 in the calculation of this investigation.

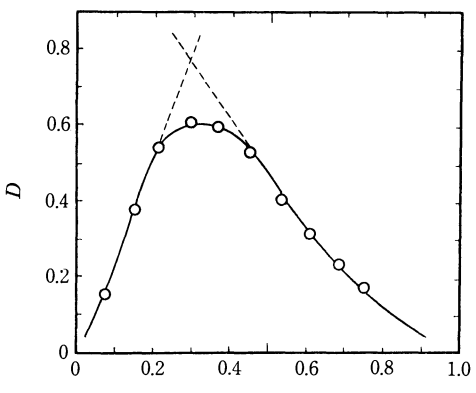

Fig. 1. Continuous variation plot for the Ti(III)-oxalate system. $[Ti(III)]+[H_2C_2O_4]=0.062M$ $[Cl^-]=0.254M$, pH 1.5

Dissociation Constants of the Oxalato-Titanium(III) Complex. When the $Ti(C_2O_4)_2^-$ ion is in equilibrium with Ti(III) and $HC_2O_4^-$ ions in a 10^{-3}—10^{-1}N hydrochloric acid solution, the stoichiometric equilibrium constants for the dissociation of $Ti(C_2O_4)_2^-$ and $HC_2O_4^-$ ions (denoted as TiX_2^- and HX^-),

$$TiX_2^- + 2H_3O^+ = Ti(III) + 2HX^- + 2H_2O \quad (I)$$

and $HX^- + H_2O = H_3O^+ + X^{2-}$

at a constant ionic strength are given by

$$K_1 = \frac{[Ti(III)][HX^-]^2}{[TiX_2^-][H^+]^2} \quad (1)$$

and

$$k_2 = \frac{[H^+][X^{2-}]}{[HX^-]} \quad (2)$$

where k_2 is the secondary ionization constant of the $HC_2O_4^-$ ion.

From Eq. (1) and Eq. (2), the apparent dissociation constant of $Ti(C_2O_4)_2^-$;

$$TiX_2^- = Ti(III) + 2X^{2-} \quad (II)$$

is given by

$$K_2 = K_1k_2^2 = \frac{[Ti(III)][X^{2-}]^2}{[TiX_2^-]} \quad (3)$$

where Ti(III) represents a mixture of Ti(III) ions other than the oxalate complexes.

The molar concentration of the unchelated oxalate ions is represented by

$$[X]_0 - 2[TiX_2^-] = [H_2X] + [HX^-] + [X^{2-}] \quad (4)$$

and that of the free $C_2O_4^{2-}$ ion concentration is given by

$$[X^{2-}] = \frac{[X]_0 - 2[TiX_2^-]}{1 + \frac{[H^+]}{k_2} + \frac{[H^+]^2}{k_1k_2}} \quad (5)$$

where $[X]_0$ is the total concentration of oxalate ions and $[TiX_2^-]$ is the concentration of oxalato-titanium-(III) ion as estimated from the spectrophotometric data.

When the absorption of the solution at 440 mμ is assumed to be associated with the equilibrium between the Ti(III) and TiX_2^- ions, the absorbance of the solution, D, can be expressed by;

$$D = \varepsilon_1(a-x) + \varepsilon_2 x \quad (6)$$

where a is the total molarity of the Ti(III) ions, x is that of the complexes, and ε_1 and ε_2 are the extinction coefficients of the unchelated and chelated ions respectively in a mixture of HCl and NaCl solutions.

From Eq. (6), therefore, the molar concentrations of TiX_2^- and Ti(III) ions can be given by;

$$x = [TiX_2^-] = \frac{D - D_0}{\varepsilon_2 - \varepsilon_1} \quad (7)$$

and;

$$a - x = [Ti(III)] = \frac{D_c - D}{\varepsilon_2 - \varepsilon_1} \quad (8)$$

where $D_0=\varepsilon_1 a$ for $x=0$ in the absence of oxalate ions and $D_c=\varepsilon_2 a$ for $x=a$ in a large excess of oxalate ions.

6) H. Hartmann and H. L. Schläfer, *Z. Phys. Chem.*, **197**, 116 (1951).

Thus, by substituting the ratio of Eq. (8) to Eq. (7) into Eq. (3), the apparent dissociation constant of the complex can be given by;

$$K_2 = \frac{(D_c - D)[X^{2-}]^2}{D - D_0} \tag{9}$$

The substitution of Eq. (5) into Eq. (9) gives;

$$K_2 = \frac{(D_c - D)\{[X]_0 - 2[TiX_2^-]\}^2}{(D - D_0)\left(1 + \frac{[H^+]}{k_2} + \frac{[H^+]^2}{k_1 k_2}\right)^2} \tag{10}$$

where k_1 and k_2 are the step-by-step ionization constants of oxalic acid, given by $k_1 = 5.38 \times 10^{-2}$ [7] and $k_2 = 5.18 \times 10^{-5}$ [8] at 25°C.

Taking the average values of the extinction coefficients, $\varepsilon_1 = 4.1$ and $\varepsilon_2 = 320\ l\ mol^{-1}\ cm^{-1}$ for the unchelated Ti(III) ions and the chelate ion, $Ti(C_2O_4)_2^-$, the values of D_0 and D_c at a specified total titanium(III) ion concentration, a, were evaluated. The substitution of the values of $[TiX_2^-]$ calculated by means of Eq. (7), and that of $[C_2O_4^{2-}]$ calculated by means of Eq. (5), into Eq. (10), the apparent dissociation constant of $Ti(C_2O_4)_2^-$ ion was evaluated. The results are summarized in Table 2.

Table 2. Spectrophotometric data for the Ti (III)-oxalate system at 25°C ($[KHC_2O_4] = 0.02$M)

I	$10^3\,a$	D	$[Cl^-]_0$	10^2 $[H^+]$	10^5 $[C_2O_4^{=}]$	$10^9\,K_2$	pK_2
0.1	0.656	0.1331	0.0844	1.244	6.480	2.457	8.61
	1.312	0.2798	0.0848	1.089	7.235	2.640	8.58
	4.868	0.9872	0.0939	0.933	6.537	2.520	8.59
	2.624	0.6308	0.0857	0.778	9.345	2.917	8.54
0.2	1.312	0.2604	0.1848	1.089	7.273	3.139	8.50
	4.868	0.9355	0.1939	0.933	6.691	3.042	8.52
	2.624	0.6021	0.1857	0.778	9.460	3.556	8.45
	3.280	0.8041	0.1861	0.622	11.192	3.824	8.42
0.3	0.679	0.1113	0.2850	1.656	6.251	3.826	8.42
	1.540	0.2596	0.2795	1.177	6.619	4.032	8.40
	3.079	0.5901	0.2751	0.954	7.501	3.856	8.41
	1.510	0.3468	0.2842	0.765	10.509	4.421	8.36
0.4	1.540	0.2496	0.3864	1.177	6.642	4.412	8.36
	1.588	0.2933	0.3823	1.147	6.770	4.579	8.34
	2.566	0.4498	0.3781	1.028	7.252	4.674	8.33
	0.927	0.1403	0.3853	0.656	13.390	4.989	8.30

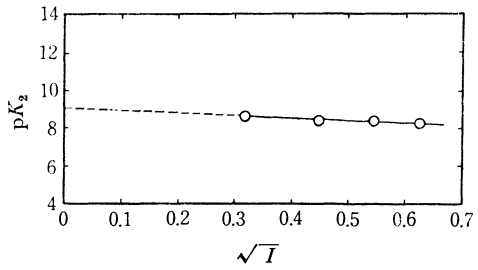

Fig. 2. Plot of pK_2 *vs.* $\sqrt{I}$ at 25°C.

7) W. J. Harned and L. D. Fallon, *J. Amer. Chem. Soc.*, **61**, 3111 (1939).

8) L. S. Darken, *ibid.*, **63**, 1007 (1941).

Table 3. Dependence of average pK_2 values *vs.* ionic strength

I (M)	0.1	0.2	0.3	0.4
$[Cl^-]_0$ (average) (M)	0.0872	0.1876	0.2809	0.3830
pK_2 (average)	8.58	8.47	8.40	8.33

By plotting the average values of pK_2 at each ionic strength against $\sqrt{I}$, as is shown in Fig. 2, and by extrapolating to zero ionic strength, the limiting value of $pK^\circ = 9.0$ at 25°C was obtained. Since the value of K_2 varies slightly with the H_3O^+ and Cl^- ion concentrations, as is shown in Table 2, however, we must also take into consideration the hydrolysis and the formation of chloro-complexes of Ti^{3+} ions;

$$Ti^{3+} + 3H_2O \overset{K_3}{\rightleftarrows} TiO^+ + 2H_3O^+ \tag{III}$$

$$Ti^{3+} + Cl^- \overset{K_4}{\rightleftarrows} TiCl^{2+} \tag{IV}$$

and;

$$TiO^+ + Cl^- \overset{K_5}{\rightleftarrows} TiOCl \tag{V}$$

and represent the stoichiometric equilibrium constants as;

$$K_3 = \frac{[TiO^+][H^+]^2}{[Ti^{3+}]} \tag{11}$$

$$K_4 = \frac{[TiCl^{2+}]}{[Ti^{3+}][Cl^-]} \tag{12}$$

and;

$$K_5 = \frac{[TiOCl]}{[TiO^+][Cl^-]} \tag{13}$$

respectively, at a constant ionic strength. Thus, the total concentration of Ti(III) ions other than the oxalato chelate may be given by;

$$[Ti(III)] = [Ti^{3+}]\left\{(1 + K_4[Cl^-]) + K_3(1 + K_5[Cl^-])\frac{1}{[H^+]^2}\right\} \tag{14}$$

and the apparent dissociation constant for the reaction (II) may be given by;

$$K_2 = \frac{[Ti^{3+}][X^{2-}]^2}{[TiX_2^-]}\left\{(1 + K_4[Cl^-]) + K_3(1 + K_5[Cl^-])\frac{1}{[H^+]^2}\right\} \tag{15}$$

by substituting Eq. (14) into Eq. (3). Therefore, when the true dissociation constant of $Ti(C_2O_4)_2^-$;

$$TiX_2^- = Ti^{3+} + 2X^{2-} \tag{VI}$$

is represented by;

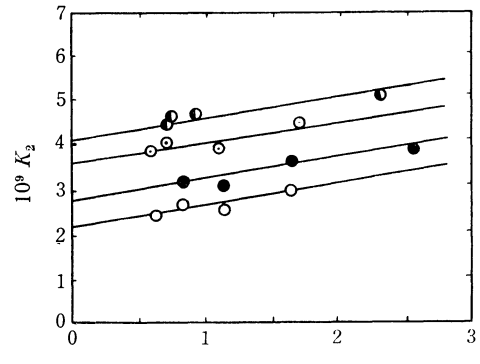

Fig. 3. Plots of K_2 *vs.* $1/[H^+]^2$ at various Cl^- ion concn.
$[Cl^-]_0$(average): ○ 0.085M, ● 0.184M, ⊙ 0.278M, ◑ 0.385M.

$$K_6 = \frac{[Ti^{3+}][X^{2-}]^2}{[TiX_2^-]} \quad (16)$$

the observed value of K_2 is related to that of K_6 by;

$$K_2 = K_6\left\{(1+K_4[Cl^-]) + K_3(1+K_5[Cl^-])\frac{1}{[H^+]^2}\right\} \quad (17)$$

By plotting the K_2 values against $1/[H^+]^2$ at a constant ionic strength and Cl^- ion concentration, as is shown in Fig. 3, a series of straight lines was obtained. The slope (S_1) corresponds to the value of $K_6K_3(1+K_5[Cl^-])$, and the intercept (A), to that of $K_6(1+K_4[Cl^-])$.

Since the slopes of these lines are practically independent of the Cl^- ion concentration, we may estimate that the value of K_4 is smaller than 0.1, and

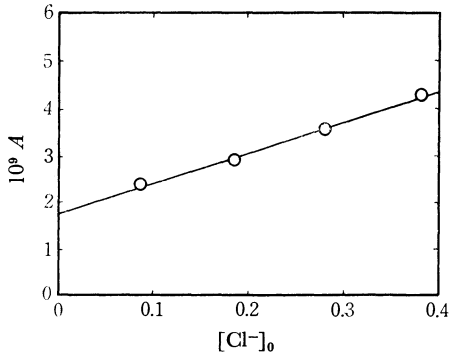

Fig. 4. Dependence of intercept (A) upon total Cl^- ion concn.

that the product, K_6K_3, corresponds to the slope of $S_1=5\times10^{-4}$. On the other hand, by plotting the value of the intercept, (A), obtained from Fig. 3, against the Cl^- ion concentration, a straight line was obtained (Fig. 4). From the intercept, $B=1.8\times10^{-9}$, and the slope, $S_2=6.4\times10^{-9}$, the values of K_6, K_4, and K_3 were evaluated to be 1.8×10^{-9}, 3.6, and 3×10^{-5} respectively. The formation constant of the $TiCl^{2+}$ ion, $K_4=3.6$, obtained in this experiment is in fair agreement with that of 2.18 estimated by Duke and Quinney[9] in their kinetic study of the reduction of the perchlorate ion by Ti(III).

Though there was some inevitable under-estimation of the H_3O^+ ion concentration, which caused some deviation in the evaluation of the K_2 values, the fact that the value of K_2 thus calculated decreases with an increase in the H_3O^+ ion concentration and increases with an increase in the Cl^- ion concentration seems to support the reaction mechanism proposed.

This work was carried out as a part of the research projects of Chemistry Research Center, National Taiwan University, CRC-5802 which was supported by the National Council on Science Development.

9) P. R. Duke and J. D. Quinney, *J. Amer. Chem. Soc.*, **76**, 3800 (1954).

BULLETIN OF THE CHEMICAL SOCIETY OF JAPAN, VOL. 44, 96—99 (1971)

Average Values of Bond Angles

KOZO KUCHITSU

Department of Chemistry, Faculty of Science, The University of Tokyo, Hongo, Tokyo

(Received August 29, 1970)

A number of definitions with clear physical significance regarding the "average bond angles" (nonlinear case) are presented. Simple expressions of the average angles in terms of the linear and quadratic mean values of the displacements in the internuclear distances are given. The differences in the various average angles for H_2O, D_2O, CH_4, CD_4 and SO_2 are estimated by means of a normal-coordinate analysis. The differences are shown to be small fractions of one degree. The root-mean-square angles for linear molecules (HCN, DCN, CO_2 and CS_2) are also calculated.

In a previous paper,[1] the merits and demerits of the two "average structures" (r_g and r_z) have been discussed. The r_g distance, which represents a thermal-average value of an instantaneous internuclear distance, is readily accessible from an experiment of gas electron diffraction.[2] A scheme has been devised relating the r_g distance to the r_e and r_z distances[3] defined as the distances between the "equilibrium" and "zero-point average" positions of the nuclei, respectively, with reference to a molecule-fixed coordinate system.[4] This scheme provides a theoretical basis of a comparative study of the molecular structures determined from electron-diffraction and spectroscopic data.[1,5,6] The purpose of the present paper is to extend the theory to the specification of bond angles: A similar scheme of conversion among the "average bond angles" based on various definitions is presented, and the orders of magnitude of their mutual differences are estimated.

Definitions of Bond Angles

Bond angles can simply be defined in terms of the r_e and r_z representations, since they are based on

1) K. Kuchitsu, *J. Chem. Phys.*, **49**, 4456 (1968).
2) L. S. Bartell, *ibid.*, **23**, 1219 (1955); K. Kuchitsu, This Bulletin, **40**, 498 (1967).
3) T. Oka, *J. Phys. Soc. Jap.*, **15**, 2274 (1960).
4) Y. Morino, K. Kuchitsu, and T. Oka, *J. Chem. Phys.*, **36**, 1108 (1962).
5) K. Kuchitsu and S. Konaka, *ibid.*, **45**, 4342 (1966).
6) K. Kuchitsu, T. Fukuyama, and Y. Morino, *J. Mol. Structure*, **1**, 463 (1968).

"nuclear positions." For a set of X—Y and Y—Z bonds in a molecule, the cosine rule can be applied to the bonded and nonbonded (r_e and r_z) distances, r_1(X—Y), r_2(Y—Z) and r_3(X—Z), to make equilibrium and zero-point average bond angles, ϕ_e and ϕ_z respectively,

$$\phi = \cos^{-1}[(r_1^2+r_2^2-r_3^2)/2r_1r_2] \quad (1)$$

An effective bond angle, ϕ_s, corresponding to the r_s coordinates[7] is often used in microwave spectroscopy. However, since no definite physical significance can be attached to the r_s coordinates, one needs to be content with a qualitative estimate[8] that ϕ_s should be very close to ϕ_e.

On the other hand, some consideration is needed in gas electron diffraction to define physically significant bond angles,[9] since only thermal-average internuclear distances, instead of angles or nuclear positions, are measured by this technique.[10] The r_g distance for a nonbonded pair does not correspond exactly to any geometrical arrangement consistent with the corresponding r_g distances for bonded pairs. As is known in terms of the linear and nonlinear shrinkage effect,[11,12] an "effective" bond angle (provisionally named ϕ_G) calculated from the bonded and nonbonded r_g distances by Eq. (1) is, in general, different from the ϕ_e or ϕ_z angles.[13,14] It should also be different from the "thermal-average value of an instantaneous bond angle" (here denoted as ϕ_g) defined in parallel with r_g

$$\phi_g = \langle\cos^{-1}[(r_1^2+r_2^2-r_3^2)/2r_1r_2]\rangle_T \quad (2)$$

where T represents the Boltzmann statistical average for temperature T over all the vibrational states of the molecule.[15] The differences between ϕ_g and ϕ_e for simple hydrides (water,[16,17] ammonia[17-20] and methane[21]), often denoted as $\langle\Delta\alpha\rangle$, have been investigated in detail in relation to the anharmonicity in the angle-bending vibrations and to the hydrogen-deuterium isotope effect.[22]

It may also be useful for some purpose to consider ϕ_c defined by

$$\phi_c \equiv \cos^{-1}\langle\cos\phi\rangle = \cos^{-1}\langle(r_1^2+r_2^2-r_3^2)/2r_1r_2\rangle \quad (3)$$

The angles ϕ_α and ϕ_α^0 corresponding to the r_α and r_α^0 structures,[4] which may be derived from electron-diffraction experiments, have been used in some previous studies;[1,6,23] ϕ_α is supposed to be essentially the angle composed of the thermal-average nuclear positions, so that ϕ_α^0, the angle extrapolated to 0°K, should be essentially equivalent to ϕ_z. For PF_3,[24] the ϕ_α^0 angle was estimated to be nearly equal to the ϕ_α within the experimental uncertainty of 0.2°.

Analytical Expressions

Nonlinear Case. For a nonlinear arrangement ($\phi_e<\pi$), Eq. (1) may be expanded in terms of the instantaneous displacements in the internuclear distances around ϕ_e,

$$\Delta r_i \equiv r_i - (r_e)_i \qquad (i=1, 2, 3) \quad (4)$$

$$\phi = \phi_e + \sum_{i=1}^{3} a_i\Delta r_i + \sum_{\substack{i=1\\ i\leq j}}^{3}\sum_{j=1}^{3} b_{ij}\Delta r_i\Delta r_j + \cdots \quad (5)$$

The coefficients a and b are functions of ϕ_e and $\sigma_i \equiv (r_e)_i^{-1}$,

$$\begin{aligned} a_k &= \sigma_k\cot\phi_e - \sigma_l\,\mathrm{cosec}\,\phi_e \\ a_3 &= (\sigma_1\sigma_2/\sigma_3)\,\mathrm{cosec}\,\phi_e \\ b_{kk} &= \frac{1}{2}\sigma_1\sigma_2\,\mathrm{cosec}\,\phi_e - \left(\sigma_k^2+\frac{1}{2}a_k^2\right)\cot\phi_e \\ b_{12} &= (\sigma_1^2+\sigma_2^2)\,\mathrm{cosec}\,\phi_e - (\sigma_1\sigma_2+a_1a_2)\cot\phi_e \\ b_{k3} &= (\sigma_1\sigma_2/\sigma_3)a_l\,\mathrm{cosec}^2\,\phi_e \\ b_{33} &= \frac{1}{2}(\sigma_1\sigma_2\,\mathrm{cosec}\,\phi_e - a_3^2\cot\phi_e) \end{aligned} \quad (6)$$

where $k=1$, 2 and $l=2$, 1 are to be taken in the same order. According to a simple order-estimation, higher-order terms of Eq. (5) do not contribute significantly to the following discussions.

By taking the thermal average of ϕ in Eq. (5), one gets a simple analytical expression of ϕ_g,

$$\phi_g = \phi_e + \sum_i a_i\langle\Delta r_i\rangle + \sum_{i\leq j}\sum b_{ij}\langle\Delta r_i\Delta r_j\rangle + \cdots \quad (7)$$

Since $(r_g)_i$ is defined as $\langle r_i\rangle$, ϕ_G defined above is given by

$$\phi_G = \cos^{-1}[(\langle r_1\rangle^2 + \langle r_2\rangle^2 - \langle r_3\rangle^2)/2\langle r_1\rangle\langle r_2\rangle] \quad (8)$$

so that it may be related to ϕ_g as

$$\phi_G = \phi_g - \sum_{i\leq j}\sum b_{ij}(\langle\Delta r_i\Delta r_j\rangle - \langle\Delta r_i\rangle\langle\Delta r_j\rangle) + \cdots \quad (9)$$

In a similar way, it follows from Eq. (3) that

$$\phi_c = \phi_g + \frac{1}{2}\cot\phi_e\sum_{i=1}^{3}\sum_{j=1}^{3}a_ia_j(\langle\Delta r_i\Delta r_j\rangle - \langle\Delta r_i\rangle\langle\Delta r_j\rangle) + \cdots \quad (10)$$

If ϕ is expanded around the zero-point average nuclear positions, instead of the equilibrium positions as is shown in Eq. (4), ϕ_g can be related to ϕ_z as

7) C. C. Costain, *J. Chem. Phys.*, **29**, 864 (1958); *Trans. Amer. Crystallogr. Soc.*, **2**, 157 (1966).
8) K. Kuchitsu, T. Fukuyama, and Y. Morino, *J. Mol. Structure*, **4**, 41 (1969).
9) K. Kuchitsu, This Bulletin, **32**, 748 (1959).
10) In most of the past electron-diffraction studies, an effective bond angle derived from Eq. (1) with bonded and nonbonded r_a distances[2] are reported without specification.
11) Y. Morino, J. Nakamura, and P. W. Moore, *J. Chem. Phys.*, **36**, 1050 (1962).
12) Y. Morino, S. J. Cyvin, K. Kuchitsu, and T. Iijima, *ibid.*, **36**, 1109 (1962).
13) L. S. Bartell and D. A. Kohl, *ibid.*, **39**, 3097 (1963).
14) Bartell and Kohl,[13] in their analysis of hydrocarbon structures, introduced a "mean" structure with a set of the r_G parameters, which consist of r_g bond distances and ϕ_G angles. They further estimated the shrinkages in the nonbonded r_G distances dependent on the torsional motions of the hydrocarbon chain as functions of the mean-square librational amplitudes.
15) For simplicity, the subscript T will be left out from the subsequent expressions.
16) K. Kuchitsu and L. S. Bartell, *J. Chem. Phys.*, **36**, 2460 (1962).
17) L. S. Bartell, *ibid.*, **38**, 1827 (1963).
18) E. A. Halevi, *Trans. Faraday Soc.*, **54**, 1441 (1958).
19) Y. Morino, K. Kuchitsu, and S. Yamamoto, *Spectrochim. Acta*, **24A**, 335 (1968).
20) K. Kuchitsu, J. P. Guillory, and L. S. Bartell, *J. Chem. Phys.*, **49**, 2488 (1968).
21) K. Kuchitsu and L. S. Bartell, *ibid.*, **36**, 2470 (1962).
22) M. Wolfsberg, *Ann. Rev. Phys. Chem.*, **20**, 449 (1969).
23) K. Kuchitsu, *J. Chem. Phys.*, **44**, 906 (1966).
24) Y. Morino, K. Kuchitsu, and T. Moritani, *Inorg. Chem.*, **8**, 867 (1969).

Table 1. Average values of displacements[a)]

	$\langle\Delta r_1\rangle$	$\langle\Delta r_3\rangle$	$\langle\Delta z_1\rangle_0$	$\langle\Delta z_3\rangle_0$	$\langle\Delta r_1^2\rangle$	$\langle\Delta r_3^2\rangle$	$\langle\Delta r_1\Delta r_2\rangle$	$\langle\Delta r_1\Delta r_3\rangle$	Ref.[b)]
H_2O	1713	2350	1431	2255	465	1282	10	334	16, 28
D_2O	1271	1649	1061	1587	337	913	3	231	
CH_4	2159	2810	1405	2294	618	1556	17	452	21
CD_4	1594	2048	1029	1681	446	1093	2	312	
SO_2	477	762	408	757	124	302	−10	80	29
HCN[c)]	1688	618	−431	25	570	601	−14	508	30
DCN[c)]	1250	395	−122	232	407	448	−21	357	
CO_2	503	471	235	471	121	156	−39	79	31
CS_2	448	196	98	196	151	170	−63	84	32

	$\langle\Delta r_2\rangle$	$\langle\Delta z_2\rangle_0$	$\langle\Delta r_2^2\rangle$	$\langle\Delta r_2\Delta r_3\rangle$	Ref.
HCN[c)]	538	456	117	96	30
DCN[c)]	515	354	117	89	

a) See text for notations: in 10^{-5} Å for the linear averages and 10^{-5} Å^2 for the quadratic averages.
b) References from which the potential constants were taken. See also Ref. 27.
c) The numbers 1 and 2 represent the C–H and C≡N bonds, respectively. They are equivalent for the other molecules.

$$\phi_g = \phi_z + \sum_i a_i\langle r_i-(r_z)_i\rangle + \sum_{i\le j}\sum b_{ij}\langle[r_i-(r_z)_i][r_j-(r_z)_j]\rangle + \cdots \quad (11)$$

which may be rewritten as

$$\phi_g = \phi_z + \sum_i a_i[(r_g)_i-(r_z)_i] + \sum_{i\le j}\sum b_{ij}(\langle\Delta r_i\Delta r_j\rangle_T + \langle\Delta z_i\rangle_0\langle\Delta z_j\rangle_0 - \langle\Delta r_i\rangle_T\langle\Delta z_j\rangle_0 - \langle\Delta r_j\rangle_T\langle\Delta z_i\rangle_0) + \cdots \quad (12)$$

by noting that $\phi_e\simeq\phi_z$ and that[4] $r_z\simeq r_e+\langle\Delta z\rangle_0$, where Δz is the projection of Δr onto the z axis taken in the direction of the equilibrium nuclear positions of the pair, and the average 0 is taken for the ground vibrational state.

Linear Case. For a linear arrangement, where ϕ_e tends to π, Eq. (5) is no longer valid. Although it is not impossible to define ϕ_g in a similar way to Eq. (2) providing that $\phi\le\pi$, the arccosine function in Eq. (2) can not readily be expanded in terms of the displacements around $\phi=\pi$, so that the problem deviates from that of the ordinary normal-coordinate analysis. It is much simpler, instead, to take the mean-square angle, $\langle(\pi-\phi)^2\rangle$, as a measure of the average bending displacement. It can be shown that

$$\langle(\pi-\phi)^2\rangle = \sum_i c_i\langle\Delta r_i\rangle + \sum_{i\le j}\sum d_{ij}\langle\Delta r_i\Delta r_j\rangle + \cdots \quad (13)$$

where

$$c_k = 2(\sigma_1+\sigma_2) = -c_3,\quad d_{kk} = -\sigma_k(2\sigma_k+\sigma_l),$$
$$d_{12} = -2(\sigma_1^2+\sigma_1\sigma_2+\sigma_2^2),\quad d_{k3} = 2\sigma_k(\sigma_1+\sigma_2),\quad (14)$$
$$d_{33} = -\sigma_1\sigma_2$$

The first sum may be rewritten as

$$\sum_i c_i\langle\Delta r_i\rangle = 2(\sigma_1+\sigma_2)\delta_g \quad (15)$$

where δ_g is the "linear shrinkage" defined by[11]

$$\delta_g = (r_g)_1 + (r_g)_2 - (r_g)_3 \quad (16)$$

One may also define ϕ_c given in Eq. (10) and another effective average angle ϕ_ρ,

$$\phi_\rho = \pi - [\langle\Delta\rho_1^2\rangle^{1/2}/(r_e)_1 + \langle\Delta\rho_2^2\rangle^{1/2}/(r_e)_2] \quad (17)$$

where $\Delta\rho_i$ represents a displacement perpendicular to the equilibrium molecular axis.

Application

The average displacements in the above equations can be calculated by means of a normal-coordinate analysis[16-21,25-27] provided the quadratic and higher-order potential constants for the molecule are known. Thus the present problem is, in principle, straightforward.

Table 1 lists the average displacements for a number of simple hydrides (with their full deuterides) and nonhydrides calculated by the use of the experimental anharmonic potential constants given in the literature.[28-35] It should be noted that the cross mean values of bonded and nonbonded displacements, $\langle\Delta r_1\Delta r_3\rangle$ and $\langle\Delta r_2\Delta r_3\rangle$, are comparable in the order of magnitude with the corresponding mean-square displacements, $\langle\Delta r_1^2\rangle$, $\langle\Delta r_2^2\rangle$ and $\langle\Delta r_3^2\rangle$.

The differences among the various angles calculated for nonlinear molecules are given in Table 2, together with their experimental ϕ_e.[28,36] The differences between the ϕ_g and ϕ_e for H_2O (D_2O) and CH_4 (CD_4) are essentially equal to their equivalents, $\langle\Delta\alpha\rangle$, re-

25) A. Reitan, *Acta Chem. Scand.*, **12**, 785 (1958); Thesis (Trondheim, Norway) (1958).
26) Y. Morino and T. Iijima, This Bulletin, **35**, 1661 (1962).
27) K. Kuchitsu, *ibid.*, **40**, 505 (1967).
28) W. S. Benedict, N. Gailar, and E. K. Plyler, *J. Chem. Phys.*, **24**, 1139 (1956).
29) Y. Morino, Y. Kikuchi, S. Saito, and E. Hirota, *J. Mol. Spectrosc.*, **13**, 95 (1964).
30) T. Nakagawa and Y. Morino, This Bulletin, **42**, 2212 (1969).
31) C. P. Courtoy, *Can. J. Phys.*, **35**, 608 (1957).
32) B. P. Stoicheff, *ibid.*, **36**, 218 (1958).
33) K. Kuchitsu and Y. Morino, This Bulletin, **38**, 805, 814 (1965).
34) S. J. Cyvin, "Molecular Vibrations and Mean Square Amplitudes," Universitetsforlaget, Oslo, and Elsevier, Amsterdam (1968), pp. 202, 311.
35) A part of the entries have already been published by the present author (Table 1 of Ref. 27). See Refs. 16, 21, 25, 26, and 34 for earlier calculations of the mean displacements. The mean-square amplitudes and shrinkages for HCN and DCN are in essential agreement with those calculated by Cyvin[34] by a harmonic approximation.
36) S. Saito, *J. Mol. Spectrosc.*, **30**, 1 (1969).

Table 2. Differences in average angles (Nonlinear Case) (in degrees)

	ϕ_e	$\phi_g-\phi_e$	$\phi_g-\phi_G$	$\phi_g-\phi_c$	$\phi_g-\phi_z$	$\phi_z-\phi_e$ [c]
H_2O	104.523[a]	0.022	0.367	0.176	0.025	−0.07[d]
D_2O	104.474[a]	−0.069	0.280	0.131	0.017	−0.12[d]
CH_4	109.471	−0.286	0.360	0.218	−0.295	0
CD_4	109.471	−0.228	0.286	0.164	−0.241	0
SO_2	119.33_0[b]	0.043	0.091	0.061	0.034	0.02_2[b]

a) Ref. 28.
b) Ref. 29 and 36.
c) Experimental estimates.
d) Refs. 19 and 23.

ported in previous studies.[16,21] In addition, the differences between the $\phi_g-\phi_e$ and $\phi_g-\phi_z$ calculated here are consistent with the corresponding experimental estimates of $\phi_z-\phi_e$ derived from the rotational constants by way of a slightly different procedure.[3,37] As is expected from the previous estimates of nonlinear shrinkages,[12,38] the differences among the various angles are as small as a few tenths of a degree, which are comparable with or smaller than ordinary experimental uncertainties. Nevertheless, it may not always be permissible to simply ignore the differences without discretion. The differences may be significantly larger when the molecule has a low-frequency, large-amplitude bending vibrations. This remark applies particularly to the dihedral angles of torsion[13] and the angles associated with ring-puckering motions, to which the above-mentioned definitions of the average angles can be extended.

Table 3. Average angles (Linear Case) (in degrees)

	$\langle(\pi-\phi)^2\rangle^{1/2}$	$\pi-\phi_c$ [a]	$\pi-\phi_\rho$ [b]
HCN	13.643	13.675	13.894
DCN	12.624	12.650	12.785
CO_2	7.747	7.753	7.786
CS_2	7.673	7.679	7.700

a) Equation (3) is applied on condition that $\phi \leq \pi$.
b) Equation (17).

The root-mean-square angles for linear molecules are listed in Table 3. The differences among them seem to be smaller than the uncertainties in their estimates.

37) D. R. Herschbach and V. W. Laurie, *J. Chem. Phys.*, **37**, 1668 (1962).
38) Ref. 34, p. 319ff.

BULLETIN OF THE CHEMICAL SOCIETY OF JAPAN, VOL. 44, 99—103 (1971)

A Remark on the Dipole Moment of Cyclohexane-1,4-dione in Relation to Its Flexible Molecular Conformation

Ariyuki AIHARA and Chikazu KITAZAWA

Department of Materials Science, Denki-Tsushin University, Chofu, Tokyo

(Received September 3, 1970)

A critical remark on the interpretation of the polarity of cyclohexane-1,4-dione molecule has been made taking into consideration a possible contribution of atomic polarization estimated from the electric permittivity of the compound in the solid state. The value 9.6 cc has been assigned as the minimum for atomic polarization which gives dipole moments, 1.16D (28.6°C), 1.20D (42.9°C), and 1.22D (60.8°C) obtained in benzene solutions. A theoretical calculation of the dipole moment has been made also with an assumed potential barrier of the form, $V(\theta)=V_0\cdot[(\pi-\theta)-2\beta]/2\alpha$, in relation to a flexing intramolecular movement of the molecule, where θ is the angle between two carbonyl groups substituted at the opposite sites of the molecule, V_0 is the potential for a boat form A (with two carbonyl groups at the bow and the stern), and α, β are constants to be determined by applying boundary conditions: $V(\theta)=0$ for $\theta=180°-137°$, and $V(91°)=V_0$. By taking 2.46D as the bond moment of carbonyl group, the best fit has been realized between the theoretical and experimental dipole moments when V_0 is assumed to be close to 6000 cal/mol, *i. e.*, twice as large as the hindering potential for the internal rotation of ethane molecule. Mention has also been made of the mechanism of dielectric absorption by this molecule in benzene solution with particular reference to the flexing motion suggested above.

X-ray crystal analyses of cyclohexane-1,4-dione by Mossel and Romers[1] and by Groth and Hassel[2] have revealed very clearly that the molecule exists as a twisted-boat conformation in the crystal. This is of particular interest in view of the peculiar dielectric behavior of the substance which has long been a subject of controversy. Fairly large values of dipole moment, 1.3—1.6 Debye,[3-9] have been obtained by a number

1) A. Mossel and C. Romers, *Acta Crystallogr.*, **17**, 1217 (1964).
2) P. Groth and O. Hassel, *Acta Chem. Scand.*, **18**, 923 (1964).
3) O. Hassel and E. Naeshagen, *Tids. Kjemi Bergvesen*, **10**, 81 (1930).
4) a) C. G. Le Fèvre and R. J. W. Le Fèvre, *J. Chem. Soc.*, **1935**, 1696; b) *ibid.*, **1956**, 3549.
5) S. Mizushima, "Structure of Molecules and Internal Rotation," Academic Press, New York (1950), p. 176.
6) Takehiko Chiba and Yonezo Morino, private Communication.
7) M. Rogers and J. M. Canon, *J. Phys. Chem.*, **65**, 1417 (1961).

of investigators both in solution and in gaseous state, in spite of the presumed nonpolar conformation of the molecule (chair form), while microwave measurement with benzene solutions[10] suggests a smaller dipole moment of ~0.4 Debye, dielectric loss of the solution being far less than the value which might be expected for a normal polar molecule with dipole moment of 1.3—1.6 Debye. An attempt to solve this problem by measuring the Kerr constant has proved to be unsatisfactory.[11,12]

The flexible conformation of cyclohexane-1,4-dione molecule, as revealed by X-ray analyses,[1,2] might explain the apparent dipole moment of the molecule when it is compared with the calculated values of the moment, assuming that the polarity of the molecule is due to a libration of the two polar moieties of the molecule in some range of angles,[8] or to a fixed polar form in which two carbonyl groups substituted at the opposite sites of the molecule make an angle of 155° between each other.[1]

However, we must not forget that most experimental values in literature have been deduced either neglecting the contribution of atomic polarization or assigning to it a small fraction of electronic polarization (5 to 10 percent); an appreciable contribution from atomic polarization should be considered with a flexible molecule such as cyclohexane-1,4-dione. In this respect, the conclusions of some authors[1,8] seem to be misleading.

Recently Cumper *et al.*[13] reported on the microwave measurement of the dipole moment as well as the relaxation time of cyclohexane-1,4-dione molecule in solutions. They refer to very small values of relaxation time ($\tau=0.57-0.71\times10^{-12}$ sec in benzene solutions) compared with observed dipole moment values, $\mu=1.28-1.32$ D, thereby suggesting some internal flexing motion concerning the dielectric absorption by the molecule. Attention should be paid to the fact that they neglect a possible large contribution of atomic polarization throughout their procedure to calculate μ and τ, and that their quotation of the present author's previous work[10] on the microwave absorption of this compound is somewhat erroneous.

It is appropriate, therefore, to make a critical remark on the interpretation of the polarity of the cyclohexane-1,4-dione molecule with particular reference to our recent work[14] on the estimation of atomic polarization by measuring the electric permittivity of this substance in the solid state.

Experimental

Material. Cyclohexane-1,4-dione was synthesized according to the procedure reported by Vincent *et al.*[15] and recrystallized from ethanol followed by vacuum sublimation, then purified through zone-refining: mp=78.5°C.

Apparatus. Measurement of electric permittivity of the compound in the solid state was performed with the use of a twin-T bridge,[16] (1—150 MHz), the sample being set as a compressed disc of 20 mm diameter and 2.42 mm in thickness. Measurement of the dipole moment in benzene solutions was made using a heterodyne, double-beat electric permittivity measuring equipment constructed in our laboratory (1 MHz), with a sample condenser of Sayce-Briscoe type. Details of these methods were reported before.[14]

Results

Electric Permittivity in the Solid State. Results of the measurement of electric permittivity of cyclohexane-1,4-dione in the solid state are shown in Fig. 1 as a function of temperature. Typical values of ε at 3 MHz are: $\varepsilon=3.10$ (35.0°C), 3.13 (45.0°C), 3.57 (55.0°C), 3.57 (65.0°C), 4.01 (72.0°C).

No appreciable dispersion was observed in the frequency and temperature ranges covered. We see that electric permittivity shows a distinct variation at the transition points 48°C and 69°C,[17] suggesting the onset of some molecular motion above the temperatures so as to give rise to the increase of electric permittivity, despite the increase of molar volume by 2.7% on the

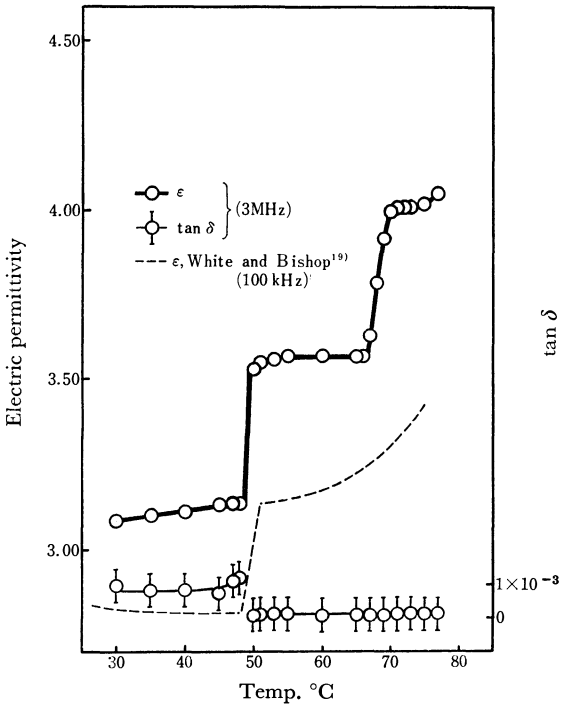

Fig. 1. Electric permittivity of cyclohexane-1,4-dione in the solid state (3 MHz).

8) a) N. L. Allinger, *J. Amer. Chem. Soc.*, **81**, 5727 (1959); b) N. L. Allinger and L. A. Freiberg, *ibid.*, **83**, 5028 (1961); c) N. L. Allinger, H. M. Blatter, L. A. Freiberg, and F. M. Karkowski, *ibid.*, **88**, 2999 (1966).

9) A. Aihara, K. Chitoku, and K. Higasi, unpublished data.

10) A. Aihara, K. Chitoku, and K. Higasi, This Bulletin, **35**, 2057 (1962).

11) C. G. Le Fèvre and R. J. W. Le Fèvre, *Rev. Pure and Appl. Chem.*, **5**, 261 (1955).

12) C. Y. Chen and R. J. W. Le Fèvre, *Australian J. Chem.*, **16**, 917 (1963).

13) a) C. W. N. Cumper, A. Melnikoff, and R. F. Rossiter, *Trans. Faraday Soc.*, **65**, 2892 (1969); b) C. W. N. Cumper and R. F. Rossiter, *ibid.*, **65**, 2900 (1969).

14) C. Kitazawa and A. Aihara, *Nippon Kagaku Zasshi*, **90**, 365 (1969).

15) J. R. Vincent, A. F. Thompson, Jr., and L. I. Smith, *J. Org. Chem.*, **3**, 603 (1939).

16) Fujisoku dielectrometer type 3.

17) A. Aihara, T. Chiba, and M. Kawano, *Nippon Kagaku Zasshi*, **86**, 708 (1965).

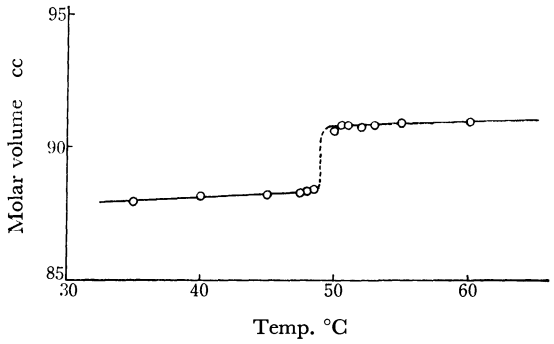

Fig. 2. Variation of the molar volume of cycloane-1,4-dione with temperature.

phase transition at 48°C (Fig. 2).

On the other hand there is a slight decrease in loss tangent (from tan $\delta = 1 \times 10^{-3}$ to ~ 0) at 48°C when the solid undergoes a transition from the low-temperature phase to the high-temperature one. This is in remarkable contrast with the abrupt increase in electric permittivity at this temperature.

The above fact is of importance in considering the mechanism of the phase transition of this compound,[14] although rather large experimental errors ($\pm 0.5 \times 10^{-4}$ in tan δ) prevent us from making any precise argument. It should be added here that Smyth[18] ascribed this transition to "half rotation" of the molecule referring to the experimental results by White and Bishop.[19] The variation of electric permittivity at 69°C is also remarkable, but no detectable changes were observed in tan δ.

Estimation of the Magnitude of Atomic Polarization. By assuming that the molecules of cyclohexane-1,4-dione are almost rigid at the crystalline lattice at temperatures below 48°C,[1,17] the molar distortion polarization may be calculated from the Clausius-Mossotti equation. With electric permittivity $\varepsilon = 3.13$ and molar volume = 88.22 cc (density = 1.271) both at 45°C, distortion polarization P_D has been found to be 36.6 cc. Subtracting electronic polarization $P_E = 27.01$ cc[20] from P_D, 9.6 cc can be assigned as the probable minimum value for the contribution of atomic polarization P_A. This value has been taken into consideration in calculating the dipole moment as measured in benzene solutions.

Dipole Moment in Benzene Solution. Electric permittivity and density as well as refractive index of cyclohexane-1,4-dione in benzene solutions were measured in the concentration range $2.67 \times 10^{-3} - 2.49 \times 10^{-2}$ (weight fraction) and at temperatures 28.6–60.8°C. The values of dipole moment were then calculated from the equations and methods of Halverstadt and Kumler[21] and of Guggenheim and Smith.[22] In Table 1, the values calculated both with and without due consideration of atomic polarization (9.6 cc) are shown. It should be noted that the μ values calculated neglecting P_A (Halverstadt-Kumlers' method) are in good agreement with those calculated by the Guggenheim-Smith equation. These values both correspond to the values in literatures.[3-9]

Table 1. Dipole moment of cyclohexane-1,4-dione in benzene solution (Debye)*

Temp. °C	μ_{H-K} ($P_A = 9.6$ cc)	μ_{H-K} ($P_A = 0$ cc)	μ_{G-S}
28.6	1.16	1.35	1.33
35.6	1.17	1.36	1.35
42.9	1.20	1.39	1.36
51.1	1.21	1.40	1.39
60.8	1.22	1.42	1.40

* Experimental errors in μ's are estimated to be ± 0.20 D. μ_{H-K} and μ_{G-S} refer to the dipole moment according to Halverstadt-Kumlers' and Guggenheim-Smiths' methods, respectively.

Discussion

The values of dipole moment, obtained with due consideration of atomic polarization, $P_A = 9.6$ cc, should be regarded as the maximum value of the experimental dipole moment, since we might expect a still greater contribution of atomic polarization for the molecule, in solution or in vapor phase, because of its large flexibility. For example, 14.9 cc can be obtained as P_A value if we use $\varepsilon = 3.57$ and molar volume = 90.94 cc both at 55°C, for the phase above 48°C, where the freedom of motion of the molecule is thought to be much larger as revealed by IR and NMR measurements.[17]

The flexing motion of the molecule could produce a very large increment of electric polarization making the distinction between atomic and orientation polarization ambiguous. Therefore, let us take the dipole moment values calculated with $P_A = 9.6$ cc as the most probable experimental values at the moment, and compare them with those calculated theoretically.

Calculation of the Theoretical Dipole Moment and the Geometry of the Molecule. The data of molecular dimensions of cyclohexane-1,4-dione, obtained by Mossel and Romers,[1] differ somewhat from the values usually adopted as normal bond lengths and valency angles: C(sp^3)–C(sp^2) 1.515 Å, C(sp^3)–C(sp^3) 1.536 Å, C=O 1.210 Å, $\angle$C(sp^3)C(sp^2)C(sp^3) 116.2°, $\angle$C(sp^2)C(sp^3)-C(sp^3) 112.2°.

Therefore it is necessary to estimate anew, with the above data, the angle between the two carbonyl groups substituted at the opposite sites of the molecule for the two conformations, boats A and B (Fig. 3).

A simple geometrical consideration leads to the following values of the angles between the two carbonyl groups for the two boat conformations: $\theta = 91.2°$ (boat A), $\theta = 136.9°$ (boat B). A comparison is made in Table 2 with the values adopted by Le Fèvre[4] and also by Allinger *et al.*[8c]

18) C. P. Smyth, "Dielectric Behavior and Structure," McGraw-Hill, New York (1955), p. 143.

19) A. H. White and W. S. Bishop, *J. Amer. Chem. Soc.*, **62**, 8 (1940).

20) The value was calculated as the sum of the bond electronic polarizations proposed by Le Fèrve and Steel [*Chem. Ind.* (London), **1961**, 670].

21) I. F. Halverstadt and W. D. Kumler, *J. Amer. Chem. Soc.*, **64**, 2988 (1942).

22) J. W. Smith, *Trans. Faraday Soc.*, **46**, 394 (1950).

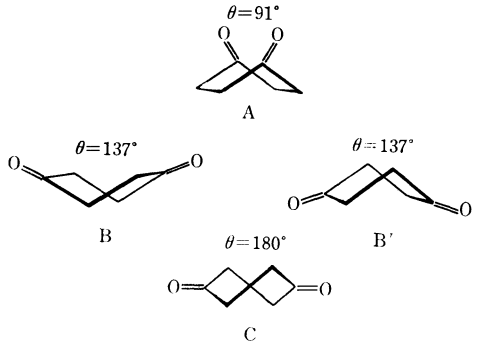

Fig. 3. Boat conformations of cyclohexane-1,4-dione molecule.

TABLE 2. THE ANGLE θ BETWEEN THE TWO CARBONYL GROUPS OF CYCLOHEXANE-1,4-DIONE MOLECULE CALCULATED FOR BOAT FORMS A AND B

	This work	Le Fèvre[4]	Allinger[8c]
Boat A	91.2°	86°	76°
Boat B	136.9°	130°	127°

The angle value observed with the actual molecular conformation in the crystalline state is 154.8°,[1] which means that the molecule is more flattened than boat B. Thus, if this conformation is taken as corresponding to the minimum internal energy even as a free molecule, the dipole moment of the molecule could be calculated with the use of an appropriate value of the C=O bond moment: $\mu=2\,\mu_{C=O}\times\cos(155°/2)$.

It should be noted, however, that the angle of 155° might not necessarily correspond definitely to the minimum of the potential energy of a free molecule, but could vary within an appreciable range of angles under the influence of external forces, as can be seen from the work by Groth and Hassel,[23] who report the value of 175° as the angle between the two carbonyl groups of cyclohexane-1,4-dione forming a molecular complex with $HgCl_2$, and 157° for the complex with C_2I_2.

An inspection of Dreiding model of this molecule reveals that the relative configuration of the two adjacent methylene groups (mutually gauche) does not change under the deformation of the molecule when the deformation is restricted within the two extreme conformations, boats B and B', including an intermediate boat C (nonpolar form). The methylene groups do not make any rotation relative to each other so far as the angle between the two carbonyl groups remains within the range 137°—180°. Furthermore, the relative configuration of a carbonyl group to the two adjacent methylene groups varies in such a way as to compensate each other the increase of the potential energy due to deformation. Allinger *et al.*[8c] also discussed the problem.

Thus, admittedly the Dreiding model should not be taken to represent the real molecular structure, we might safely assume that the polar moiety of the molecule "librates" almost freely in a shallow potential well so far as the angle θ does not decrease beyond 137°. If angle θ decreases further, the potential energy of the molecule will increase due presumably to the interaction between the two adjacent methylene groups known in the cases of ethane and its derivatives.[24]

According to the above reasoning, the dipole moment of the molecule can be expressed as follows:

$$\mu^2=\int_{\theta_1}^{\theta_2}\mu_\theta^2\exp(-V(\theta)/RT)\mathrm{d}\theta\Big/\int_{\theta_1}^{\theta_2}\exp(-V(\theta)/RT)\mathrm{d}\theta, \quad (1)$$

where μ_θ is the resultant moment of the molecule corresponding to the angle θ between the two dipole components $\mu_{C=O}$, the moment of the single carbonyl group, and is given by $\mu^2_\theta=2\,\mu^2_{C=O}\,(1+\cos\theta)$; $V(\theta)$ is the intramolecular potential as a function of θ, R is the gas constant, T is the absolute temperature and θ_1, θ_2 should be taken as the values for boat C (180°) and boat A (91°),[25] respectively.

It is necessary to make a proper choice of the value for the bond moment $\mu_{C=O}$ and also of the potential $V(\theta)$ as a function of θ. Allinger *et al.*[8c] took 3.0 D for $\mu_{C=O}$ and calculated μ values as 1.64 D (291°K) and 1.79 D (490°K), through a graphical integration of Eq. (1) from $\theta_1=76°$ to $\theta_2=180°$, with the assumption that the potential barrier for the boat A conformation is given either by 10.26 kcal/mol (291°K) or 12.00 kcal/mol (490°K). Their μ values are obviously too large compared with the values in literature, and do not give a reasonable explanation of the polarity of this molecule.

The authors have chosen a value 2.46 D for the C=O bond moment. The difference between experimental dipole moment of cyclohexanone, $\mu=2.87$ D, obtained by the measurement of Stark effect on the microwave absorption of the substance,[26] and the moment of methylene group, 0.46 D (the moment of $-CH_3$ is assumed to be 0.40 D), is 2.41 D, while we get $\mu_{C=O}=2.50$ D if we subtract $\mu_{-CH_3}=0.40$ D from the experimental dipole moment of acetone, $\mu=2.90$ D.[27] The average of these two values, 2.46 D, may be regarded as free from any contribution of atomic polarization and, therefore, must be more reasonable as the bond dipole moment of C=O for cyclohexane-1,4-dione molecule.

On the other hand, the following assumption has been made concerning the potential function of this molecule. The potential energy is zero for the range of θ values, 137° to 180°, but varies as $V(\theta)=V_0[(\pi-\theta)-2\beta]/2\alpha$ between 91° and 137°, where V_0 is the potential barrier for the conformation A ($\theta=91°$), α and β are constants. Converting the variable θ to $\varphi=(\pi-\theta)/2$, the potential becomes $V(\varphi)=V_0(\varphi-\beta)/\alpha$, (Fig. 4). α and β can be determined by applying the boundary conditions, $V(\varphi)=0$ for $\varphi=21.5°$ and $V(\varphi)=V_0$ for $\varphi=44.5°$.

Then, rewriting Eq. (1) as

23) P. Groth and O. Hassel, *Tetrahedron Lett.*, **1964**, 65.

24) S. Mizushima, *loc. cit.*, Chapters 1—3.

25) In the case of boat A, the two adjacent methylene groups become mutually "eclipsed," corresponding to the maximum of the intramolecular potential.

26) Y. Ohnishi and K. Kozima, This Bulletin, **41**, 1323 (1968).

27) J. W. Swalen and C. C. Costain, *J. Chem. Phys.*, **31**, 1562 (1959).

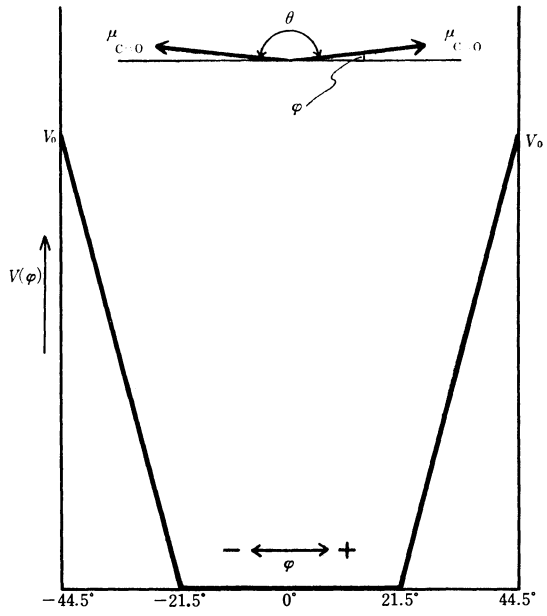

Fig. 4. Assumed potential curve for the flexing motion of cyclohexane-1,4-dione molecule.

$$\mu^2 = 2\mu^2_{C=O}\{1 + \langle\cos\theta\rangle\}, \quad (2)$$

the statistical average of $\cos\theta$, $\langle\cos\theta\rangle$, can be calculated in the following way:

$$\langle\cos\theta\rangle = \int_{0°}^{44.5°} -\cos 2\varphi \exp\{-V(\varphi)/RT\}d\varphi \Big/ \int_{0°}^{44.5°} \exp\{-V(\varphi)/RT\}d\varphi$$
$$= -\left[\int_{0°}^{21.5°} \cos 2\varphi d\varphi + \int_{21.5°}^{44.5°} \cos 2\varphi \exp\{-V_0(\varphi-\beta)/\alpha RT\}d\varphi\right] \Big/ \left[\int_{0°}^{21.5°} d\varphi + \int_{21.5°}^{44.5°} \exp\{-V_0(\varphi-\beta)/\alpha RT\}d\varphi\right] \quad (3)$$

Integration has been performed analytically for three temperatures (28.6°C, 42.9°C, 60.8°C) with the assumption that the potential barrier V_0 can be taken as 6000 cal/mol: the potential for the boat A conformer may approximately be chosen to be twice as large as the hindering potential barrier for the internal rotation of ethane molecule, 3000 cal/mol.[24] The results of calculation are shown in Table 3, together with the results obtained by using the potential barrier of $V_0=$ 5000 cal/mol and $V_0=10000$ cal/mol, the latter being of the same order of magnitude as those adopted by Allinger *et al.*[8c]

Table 3. Theoretical dipole moment of cyclohexane-1,4-dione as compared with experimental values (Debye)

Temp. °C	μ_{calc} $V_0=5000$ cal/mol	$V_0=6000$ cal/mol	$V_0=10000$ cal/mol	μ_{obs}
28.6	1.19	1.17	1.11	1.16±0.02
42.9	1.20	1.18	1.11	1.20±0.02
60.8	1.21	1.19	1.12	1.22±0.02

In spite of a simplified form of the potential function here adopted, the calculated values of dipole moment with $V_0=5000$—6000 cal/mol are in very good agreement with the experimental values with the consideration of atomic polarization. It is, therefore, most probable that the molecule of cyclohexane-1,4-dione behaves, in a solution, as a flexing twisted-boat conformation with the potential for the intramolecular movement of the form as shown in Fig. 4.

With the potential of this form, the molecule will be able to relax quite easily, under the action of high frequency electric field, without being subjected to appreciable hindrance in changing the direction of the molecular dipole. The flexing motion of this molecule could reverse the sense of polarity of the molecule instantaneously without performing rotation of the molecule as a whole, if the angle φ changes from positive to negative values (Figs. 3 and 4). This must be the reason why solutions of cyclohexane-1,4-dione give unexpectedly small dielectric loss[10] as well as small τ values,[13] but rather large increment of electric permittivity.[10]

On the Growth Rate of Selenium Spherulite

Shuichi HAMADA

Department of Chemistry, Faculty of Science, Science University of Tokyo, Kagurazaka, Shinjuku-ku, Tokyo

(Received March 13, 1970)

The radial growth rates of the selenium spherulites were measured by the microscopic method at temperatures ranging from 128.4°C to 192.3°C. The radial growth rate increased with an increase in the crystallization temperature up to about 180°C, reached a maximum value of 87.0 μ/min, and then decreased abruptly, judging from the observation of organic polymers at crystallization temperatures near their melting points. The process of the spherulite growth of selnium near the melting point could not be interpreted by only two elementary processes, that of the segmental jump and that of the formation of a two-dimensional nucleus of a critical size. The variation in the radial growth rates of selenium with the temperature was explained by considering the bond-breaking process as an elementary process. The estimated surface free energy at the liquid-crystal interface was 25.1 erg/cm^2; this value was a reasonable one.

When amorphous selenium is crystallized under atmospheric pressure, it grows in a spherulite form,[1] just like such organic polymers as polyethylene adipate, polyethylene succinate, and nylon 6. In general, the rate-determining step of the spherulite growth well below the melting point is considered to be the process of the segmental jump at the liquid-crystal interface, whereas the process of the spherulite growth near the melting point is governed mainly by the effort needed to overcome the surface free energy of the two-dimensional nucleus formed on the liquid-crystal interface.[2,3]

Because the temperature coefficient of the growth rate of the selenium spherulite is much larger than that expected from the process of the segmental jump well below the melting point, the process of the Se-Se bond breaking was suggested as one of the elementary processes associated with the spherulite growth.[4] In the present work, this concept will be discussed on the basis of the behavior of the selenium spherulite growth near the melting point.

Experimental

Materials. The selenium was obtained from the Yokozawa Chemical Company; its purity was guaranteed to be better than 99.999%. The selenium was melted at 230°C for 1 hr in an electric furnace and was then quenched on a microscopic cover-glass in order to prepare the sample. The samples were stored in a cooled desiccator.

Procedure. An Olympus reflecting microscope, Model STS, was used to measure the radial growth rates of selenium spherulites. The sample was at first melted at 230°C for 1 hr in a heating block mounted on the microscope, was cooled rapidly to 130°C in order to develop the nuclei, and was then heated again quickly to the specified temperatures. The selenium spherulites were grown isothermally at temperatures ranging from 128.4°C to 192.3°C. The radii of the spherulites formed on the surfaces of the selenium samples were estimated by measuring microscopic photographs. The temperatures of the heating block were calibrated by using materials of known melting points.

An X-ray diffractometer, Model JDX-5P, from the Japan Electron Optics Laboratory was used to obtain the X-ray powder diffraction patterns of the selenium crystallized in the temperature range from 99.5°C to 174.4°C.

Results

The radii of the spherulites varied linearly with the heating times, and the slopes of all the radius-time curves were nearly equal at a specified temperature, regardless of the developing periods of the nuclei, as was observed in a previous work.[4] Figure 1 shows the linear variations of the radius-time curve of the selenium spherulites at temperatures ranging from 128.4°C to 192.3°C. The slopes of the linear relationships increased as the crystallization temperatures increased up to about 180°C, whereas they decreased above 180°C. The radial growth rate, G, of the selenium spherulite was estimated from the slope of the radius-time relationship,

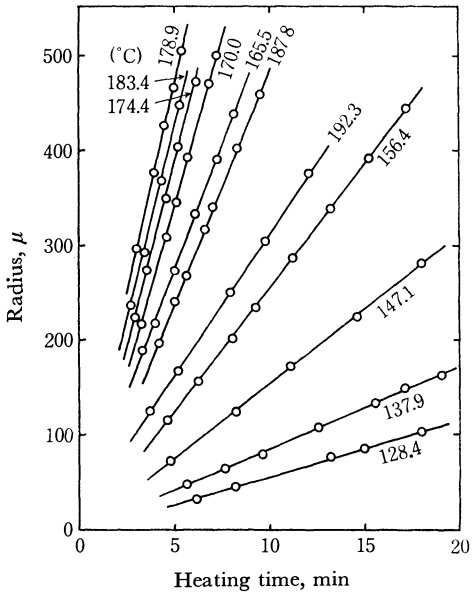

Fig. 1. Radial variation of selenium spherulite with heating time.
(The figure is illustrated by voluntary shifts of the heating times.)

1) P. T. Kozyrev, *Soviet Physics-Technical Physics*, **28**, 470 (1958).
2) M. Takayanagi, M. Nakao, and S. Machida, *Kogyo Kagaku Zasshi*, **59**, 549 (1956).
3) B. B. Burnet and W. F. McDevit, *J. Appl. Phys.*, **28**, 1101 (1957).
4) S. Hamada, T. Sato, and T. Shirai, This Bulletin, **40**, 864 (1967).

Table 1. Radial growth rates of selenium spherulites

Temp., °C	G, μ/min	Temp., °C	G, μ/min
128.4	6.0	174.4	77.9
137.9	8.7	178.9	87.0
147.1	15.8	183.4	81.0
156.4	26.2	187.8	50.3
165.5	52.0	192.3	29.7
170.0	72.6		

shown in Fig. 1. The values of G at the specified temperatures are given in Table 1.

The dependence of G on the crystallization temperature is shown in Fig. 2. The radial growth rate

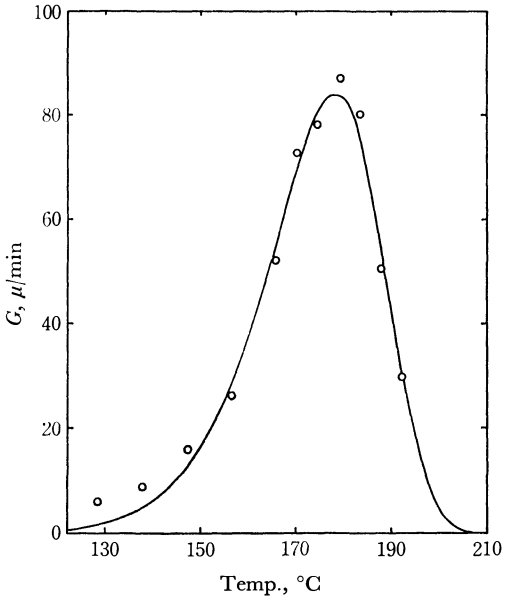

Fig. 2. Plot of radial growth rate of selenium spherulite against crystallization temperature.
○: observed —: calculated

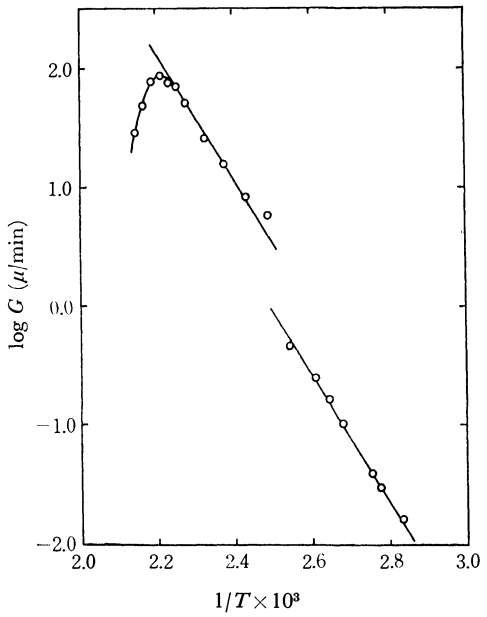

Fig. 3. Arrhenius plot of log G.
(The results below 120°C are reproduced from Ref. 4.)

increased with an increase in the crystallization temperature up to about 180°C, reached a maximum value, and then decreased abruptly. Figure 3 shows the dependence of log G on $1/T$. The relationship of log$G$ to $1/T$ at temperatures ranging from 128.4°C to 165.5°C is regarded as linear, and the slope in the temperature range is nearly equal to that at temperatures ranging from 70°C to 120°C.[4] The linear relationship varied discontinuously at about 125°C, though the slopes in the temperature ranges both above and below 125°C did not change. The results on the spherulite growth rate below 120°C presented in the previous work[4] were obtained from a crystallization without preheating, as has been described in the "Procedure" section of this paper. The discontinuity in the growth rate at approximately 125°C was also observed from the crystallization without preheating in the temperature range above 125°C, but slightly lower values were obtained than those with preheating. Such discontinuous changes in the radial growth rates, G, have often been observed in the growth of organic chain-polymer spherulites.[2]

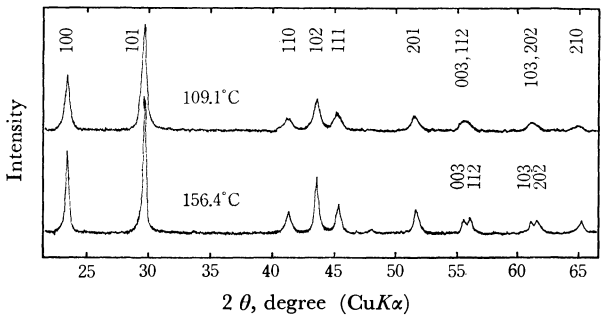

Fig. 4. X-Ray powder diffractograms of selenium crystallized at 109.1°C and 156.4°C.

Figure 4 shows X-ray powder diffraction intensity diagrams of the selenium crystallized at 109.1°C and 156.4°C, as examples for the samples obtained below and above 125°C respectively. A slight shift in the diffraction peaks was observed at crystallization temperatures between 118.9°C and 128.4°C. The values of the unit cell axes, a and c, were estimated by using the diffraction peaks of (003), (112), (103), and (202). The ratios of the axes, c/a, at the specified temperatures are given in Table 2.

The ratios of the axes, c/a, of the crystallized selenium changed discontinuously from 1.118 to 1.131 at temperatures between 118.9°C and 128.4°C, but the details of the change are obscure.

Discussion

Hoffman and Weeks[5] expressed the radial growth rate of spherulite, G, as follows:

$$G = G_0 \exp(-\Delta G^*/kT) \exp(-\Delta G_c/kT) \quad (1)$$

where G_0 is the specific rate; ΔG^*, the free energy of activation for the segmental jump process at the supercooled liquid-crystal interface, and ΔG_c, the free energy

5) J. D. Hoffman and J. J. Weeks, *J. Chem. Phys.*, **37**, 1723 (1962).

TABLE 2. RATIOS OF AXES IN HEXAGONAL SELENIUM

Cryst. temp., °C	99.5	109.1	118.9	128.4	137.9	147.1	156.4	165.5	174.5
c/a	1.118	1.118	1.118	1.131	1.133	1.134	1.134	1.133	1.134

of the formation of a two-dimensional nucleus of a critical size. The ΔG_c is expressed by the following equation:

$$\Delta G_c = 4\sigma_s\sigma_e h T_m/\Delta h_f \Delta T \quad (2)$$

where σ_s and σ_e are the lateral and end surface free energies of the two-dimensional, bundlelike nucleus respectively; h, the thickness of the nucleus; T_m, the melting point of the crystallized polymer; Δh_f, the heat of fusion at T_m, and ΔT, the difference in the melting point and the crystallization temperature, $T_m - T$. Therefore, the radial growth rate of spherulite may be expressed as follows:

$$\ln G = \ln G_0 - \Delta G^*/kT - CT_m/(\Delta T)T \quad (3)$$

where $C = 4\sigma_s\sigma_e h/k\Delta h_f$

Hoffman and Weeks[5] expressed the free energy of activation for the segmental jump process, ΔG^*, as follows, in conjunction with the WLF equation:

$$\Delta G^* = 2.303C_1^g C_2^g RT/(C_2^g + T - T_g) \quad (4)$$

In the crystallization of an organic-chain polymer, the radial growth rate of the spherulite near the melting point was considered to be governed by the third term on the right side of Eq. (3), and the variation in $(\ln G + \Delta G^*/kT)$ with $T_m/(\Delta T)T$ fit well into Eq. (3).

The application of Eq. (3) to selenium spherulite growth was examined. Harrison[6] reported the viscosities of the liquid selenium to be as follows:

TABLE 3. VISCOSITIES[6] AND DENSITIES[7] OF LIQUID SELENIUM

Temp. °K	η, poise	ρ, g/cm³	Temp. °K	η, poise	ρ, g/cm³
533	5.63	3.923	603	1.08	3.810
556	3.03	3.885	615	0.838	3.791
573	2.01	3.858	623	0.723	3.718
591	1.35	3.830			

The values in Table 3 were extremely adaptable to the WLF equation, though the temperatures in Table 3 were much higher than the glass transition temperature of amorphous selenium (305°K). The parameters, C_1^g and C_2^g, in the WLF equation were estimated to be 12.88 and 131.2 respectively from the shift factors calculated by means of the values in Table 3. These values for selenium were different from those for the usual polymers (17.44 and 51.6 respectively); it is probable that this difference arises from the fact that the temperatures used in the experiment were much higher than the T_g of amorphous selenium.

The apparent activation energy for the viscous flow of the liquid selenium was estimated to be 17.8 kcal/mol from the Arrhenius plot of the viscosities of the liquid selenium at temperatures ranging from 220°C to 240°C.[8] On the other hand, the calculated value of the activation energy for the viscous flow of liquid selenium at 230°C was found to be 17.3 kcal/mol by using the estimated parameters, C_1^g and C_2^g, and the following equation derived from the WLF equation:[5]

$$E_a = 2.303C_1^g C_2^g RT^2/(C_2^g + T - T_g)^2 - RT + \alpha RT^2 \quad (5)$$

where α is the expansion coefficient of liquid selenium, 4.8×10^{-4} °C^{-1}. Since the two values of the activation energy for the viscous flow nearly agreed with each other, the estimated values of the parameters, C_1^g and C_2^g, were considered to be reasonable.

The free energies of activation, ΔG^*, for the segmental jump process of amorphous selenium were estimated to be 17.10 and 13.35 kcal/mol at 401.6 and 465.5°K respectively, for example, by using Eq. (4). If the selenium spherulite growth obeys Eq. (3), the plots of $(\ln G + \Delta G^*/kT)$ should be linear with $T_m/(\Delta T)T$. Figure 5 shows the relationship between $(\ln G + \Delta G^*/RT)$ and $T_m/(\Delta T)T$. No linear relationship can be observed, as is shown in Fig. 5. It becomes clear that the process of the selenium spherulite growth can not be interpreted by only two terms, the segmental jump at the liquid-crystal interface and the free energy of the formation of a two-dimensional nucleus of a critical size.

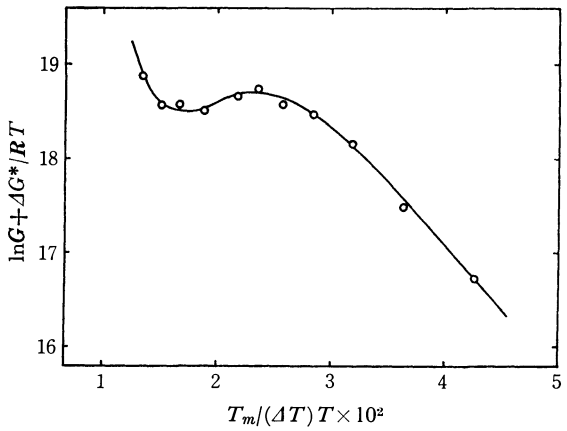

Fig. 5. Plot of $\ln G + \Delta G^*/RT$ against $T_m/(\Delta T)T$.

Turnbull and Cohen[9] pointed out that the crystallization of selenium was performed by the reconstruction of the irregularly-distributed chain molecules created by the breaking of the Se–Se bonds. The concept of the reconstruction in the selenium crystallization is due to a large barrier to internal rotation about Se–Se bonds,[10] which barrier is caused by the repulsion

6) D. E. Harrison, *J. Chem. Phys.*, **41**, 844 (1964).
7) "Gmelin's Handbuch der anorganischen Chemie," 8th ed., Selen, Teil A, Verlag Chemie, G. m. b. h., Weinheim (1953).
8) T. Shirai, S. Hamada, and K. Kobayashi, *Nippon Kagaku Zasshi*, **84**, 968 (1963).
9) D. Turnbull and M. H. Cohen, *J. Chem. Phys.*, **29**, 1049 (1958).
10) J. A. Semlyen, *Trans. Faraday Soc.*, **63**, 743 (1967).

between lone-pair electrons around selenium chains. Mamedov[11] reached the same conclusion on the basis of X-ray diffraction studies of the bulk crystallization in the selenium. Also, Hillig[12] doubted whether the treatment of Turnbull and Fisher[13] for the homogeneous nucleation on selenium, work based on the molecules across the phase boundary and work which needed to overcome the surface energy of a nucleus of a critical size, was applicable without modification.

Considering the breaking process of Se–Se bonds, that is, $Se_n \rightleftharpoons Se_{n-t} + Se_t$, the elementary processes of selenium crystallization at the liquid-crystal interface may be expressed as follows:

$$\underset{\text{(amorph. Se)}}{\text{State A}} \xrightarrow[k_1]{\text{seg. jump}} \text{State B} \underset{k_3}{\overset{k_2}{\rightleftharpoons}} \text{State C} \rightleftharpoons \underset{\text{(cryst. Se)}}{\text{State D}}$$

(bond breaking; build up)

where k_1, k_2, and k_3 are the rate constants. Since the activity of amorphous selenium, a_0, at the crystal-liquid interface is regarded as constant, the rate from the A state to the C state can be expressed as $k_1Ka_0/(1+K)$, where K is k_2/k_3, from the treatment of the reaction kinetics. If the bond-breaking process of an amorphous selenium chain is nearly equal to the opening process of the ring selenium molecule, the values[14] of K can be calculated to be of orders from 10^{-9} to 10^{-7} at the temperatures ranging from 128.4°C to 192.3°C; therefore, the rate from the state A to the state C can be expressed as k_1Ka_0.

Accordingly, the overall radial growth rate of selenium spherulite can be expressed as follows:

$$\ln G = \ln G_0 - \Delta G^*/kT - \Delta G_s^*/kT - CT_m/(\Delta T)T \quad (6)$$

where ΔG^* and C are the same as in Eq. (3), and ΔG_s^*, the free energy for the bond-breaking process of chain molecules. The ΔG_s^* is considered to be nearly equal to the ΔG for the process of opening ring molecules, Se_8. Eisenberg and Tobolsky[14] estimated the values of ΔH and ΔS for the ring-opening process to be 25 kcal/mol and 23.0 e. u. respectively. Assessing the ΔH_s^* and ΔS_s^* to be 25 kcal/mol and 23.0 e. u. respectively, the plots of the terms of $(\ln G + \Delta G^*/RT + \Delta G_s^*/RT)$ against $T_m/(\Delta T)T$ given in Fig. 6 are obtained. From the linear relationship in Fig. 6, it is clear that the selenium spherulite growth is governed by the breaking process of Se–Se bonds as well as by the processes of the segmental jump and the formation of a two-dimensional nucleus of a critical size.

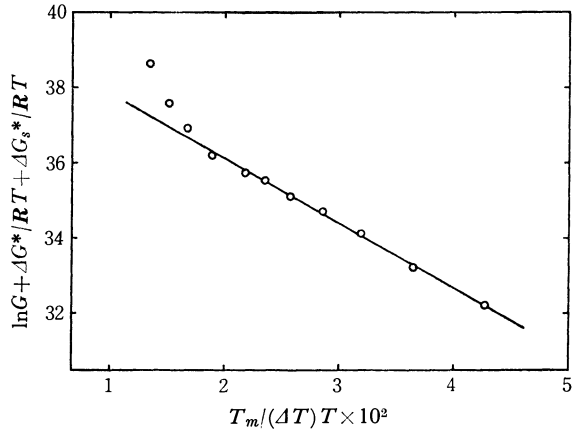

Fig. 6. Plot of $\ln G + \Delta G^*/RT + \Delta G_s^*/RT$ against $T_m/(\Delta T)T$.

The constant, C, was estimated to be 173.3 from the slope in Fig. 6. The radial growth rate of the selenium spherulite at temperatures ranging from 128.4°C to 192.3°C can be expressed by the following empirical formula:

$$\ln G = 39.60 - \Delta G^*/RT - (2500 - 23.0T)/RT - 173.3T_m/(\Delta T)T \quad (7)$$

The calculated values of G are plotted by the solid line in Fig. 2. The thickness of the two-dimensional nucleus at the liquid-crystal interface was calculated to be 3.78 Å on the basis of the crystal dimensions of hexagonal selenium, assuming the two-dimensional nucleus to be a monolayer of the selenium chain. The geometric average of $\sigma_s\sigma_e$, σ^*, was estimated to be 25.1 erg/cm^2 from the estimated value of the term of $4\sigma_s\sigma_e h/k\Delta h_f$ and from the values of h and Δh_f.[15]

Zadumkin[16] calculated the free energies of the melt-crystal interface for selenium and 36 metals to be 8—15% of the surface tension, σ, of their liquids at the melting points, except for Ge, Si, and Sb. The interfacial free energy of selenium at the liquid-crystal interface was calculated to be 15.9 erg/cm^2, assuming its value to be 15% of the surface tension of liquid selenium at the melting point, 217°C, 106 erg/cm^2.[17] Though the empirical value of the geometric average, σ^*, is slightly larger than the calculated value, it is considered to be reasonable.

11) K. P. Mamedov, *Akad. Nauk Azerb. SSR, Inst. Fiz.*, **1965**, 30.
12) W. B. Hillig, *J. Phys. Chem.*, **60**, 56 (1956).
13) D. Turnbull and J. C. Fisher, *J. Chem. Phys.*, **17**, 71 (1949).
14) A. Eisenberg and A. V. Tobolsky, *J. Polym. Sci.*, **46**, 19 (1960).
15) 3.98×10^9 erg/cm^3; "Handbook of Chemistry," ed. by N. A. Lange, McGraw-Hill, New York (1961), p. 107.
16) S. N. Zadumkin, *Akad. Nauk Ukr., SSR*, **1**, 21 (1961).
17) K. V. Astakhov, N. A. Penin, and E. Dobkina, *Zh. Fiz. Khim.*, **20**, 403 (1946).

Purity Determination of Organic Compounds by Time-temperature Freezing or Melting Curves with a Simplified Apparatus[1)]

Hisae ENOKIDO,[2)] Takako SHINODA, and Yo-ichiro MASHIKO
Government Chemical Industrial Research Institute, Tokyo, Shibuya-ku, Tokyo
(Received April 30, 1970)

A simplified apparatus has been constructed for determining the purity of organic compounds by time-temperature freezing or melting curves. The sample cell is small and the amount of the sample needed in only 0.2 m*l* or 2 m*l*. The thermometers used are a Shimadzu platinum resistance thermometer calibrated by the measurement of fixed points and a chromel *p*-constantan thermocouple calibrated against a standard platinum thermometer with a precision better than $\pm 0.03°$. Purities of several hydrocarbons were determined by measuring their freezing and melting curves.

The apparatus and procedure for determining the purity of compounds from time-temperature freezing and melting curves were developed by Taylor and Rossini, and Glasgow *et al.*,[3)] and are widely used. However, the temperature observed by the time-temperature technique is not real equilibrium temperature and differs from that observed with the use of a precision adiabatic calorimeter, especially in a simplified apparatus. Though purity determination by using the adiabatic calorimeter is more accurate, the apparatus and technique are complicated and the time required for measurement usually exceeds several hours.

This paper describes an apparatus and technique to simplify the method and save time in purity determination by means of time-temperature freezing and melting curves. The method was applied to the purity determination of several hydrocarbons. The results show that the well-known method of analyzing data should be improved to give highly accurate results.

Experimental

Apparatus. A small apparatus was constructed to obtain time-temperature freezing and melting curves. The general assembly is illustrated in Fig. 1. The sample cell and container are made of hard and pyrex glass, respectively. The details of the sample cells are shown in Fig. 2. The cells were closed in a vacuum system so that the sample could be analyzed in the absence of air and water vapor. A platinum thermometer or a thermocouple was inserted into the re-entrant well and the cells were then set in a hole of a copper cylindrical block, with wall of 0.2 mm thickness and heater wound around it. The cells were hung inside the container by means of three constantan wires. The container was evacuated, and the cooling and heating rates were controlled by adjusting the amount of helium gas inside the container. The whole assembly was mounted in a constant temperature cooling or heating bath. The temperature at the beginning of measurement was so selected that it differed from the freezing or melting point of a sample by approximately 10—50°C.

The sample temperature was measured with the platinum thermometer or the thermocouple. As the sample cell was small, a standard platinum thermometer could not be fitted. Instead, a small platinum-in-stainless steel resistance thermometer, 3.5 mm in diameter and 3 cm long, (Shimadzu Co.) was employed. It has four platinum leads, and was certified by the measurement of fixed points. The resistance value was about 100 ohms at room temperature. The thermocouple, a chromel *p*-constantan type, was calibrated by comparison with a Leeds & Northrup platinum thermometer certified by the National Bureau of Standards as well as against the melting point of benzoic acid and the freezing point of tin.

Each comparison was made under practically adiabatic conditions: the emf of the thermocouple and the resistance of the standard thermometer were measured at the same time. Some 40 comparisons were made in the temperature range of 15 to 500°K. Two formulas which each fit the data in the temperature regions above and below 0°C, are based on the expansion of emf in terms of absolute temperature T as follows:

$$\text{emf}\,(\mu\text{V}) = \sum_{n=0}^{m} A_n (T)^n \qquad (1)$$

where the upper limit of m is 4 and 9 for above and below 0°C, respectively. Coefficients determined are listed in Table 1. The deviations of the observed values from the calculated

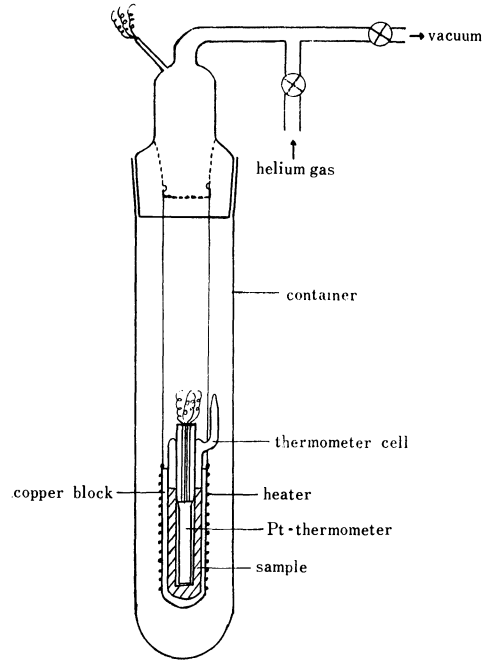

Fig. 1. Simplified apparatus for purity determination.

1) Presented at the Local Meeting of the Chemical Society of Japan, Niigata, July, 1969.

2) Present address: Tokyo Kasei Kogyo Co., Ltd., 6-Chome, Toshima, Kita-ku, Tokyo, Japan.

3) W. J. Taylor and F. D. Rossini, *J. Res. NBS*, **32**, 197 (1944); A. R. Glasgow, Jr., A. J. Streiff, and F. D. Rossini, *ibid.*, **35**, 355 (1945).

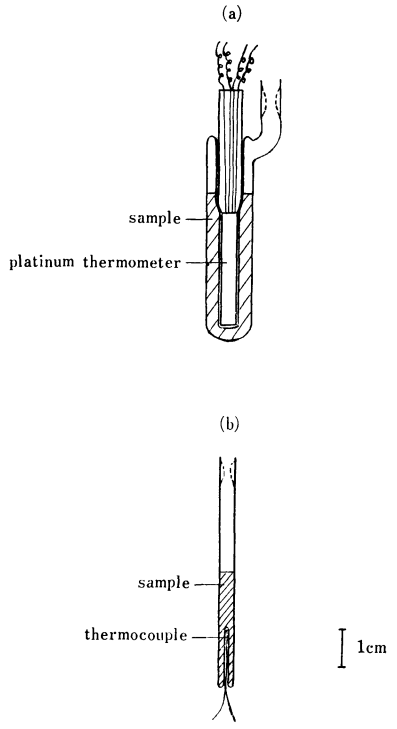

Fig. 2. Cross-sectional diagram of sample cells: (a) platinum thermometer cell (b) thermocouple cell.

TABLE 1. COEFFICIENTS DETERMINED BY FITTING EQ. (1) TO THE CALIBRATION DATA OF CHROMEL *p*-CONSTANTAN THERMOCOUPLE

	0°C$<T<$240°C	15°K$<T<$273°K
T	Celsius degree	Kelvin degree
A_0	−1.46271	9979.5
A_1	59.3394	−0.729544
A_2	0.0514691	−0.234398
A_3	-4.30948×10^{-5}	0.00180392
A_4	-7.06495×10^{-8}	-3.64454×10^{-5}
A_5	0.0	4.97434×10^{-7}
A_6	0.0	-3.85761×10^{-9}
A_7	0.0	1.68203×10^{-11}
A_8	0.0	-3.85227×10^{-14}
A_9	0.0	3.60646×10^{-17}

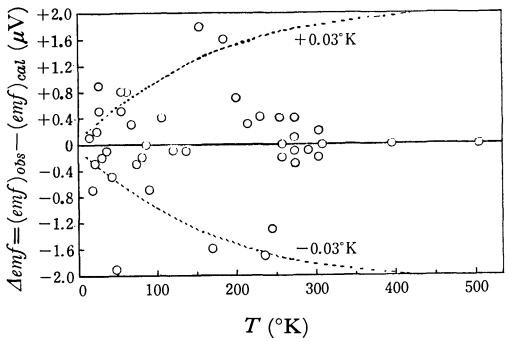

Fig. 3. Deviation of observed emf of a chromel *p*-constantan thermocouple from the calculated one by using Eq. (1).

ones by using Eq. (1) were within ±0.03° as shown in Fig. 3.

The resistance of the thermometer is recorded on a Shimadzu Precision Temperature Recorder CT3. An ice-water bath was used as a reference for the thermocouple, and the difference in emf between the cell thermocouple and a Yokogawa DC Potentiometer P-7B was amplified with an Ohkura DC Microvolt Meter AM-101, and then recorded on a Yamatake-Honneywell Recorder Electronic 19 as a function of time. All measurements were carried out automatically, except for the manual control of freezing or melting rates. The time required for the measurement of a sample was about fifteen minutes.

Material. The thermometer and thermocouple cells were filled at the same time with extra pure grade reagents *n*-octane, *n*-undecane, *n*-tridecane and *n*-docosane obtained from Tokyo Kasei Kogyo Co., Ltd. After removing the trace of air from the sample by pumping out at liquid nitrogen temperature, the cells were sealed in a vacuum system.

The amount of sample used was about 2 m*l* for the thermometer cell and 0.2 m*l* for the thermocouple cell.

Results and Discussion

Principle of Purity Determination from the Freezing or Melting Point. For impurities that are completely soluble in the liquid phase but insoluble in the solid phase, the thermodynamic relation between the amount of impurities and the equilibrium temperature in the case of an ideal or sufficiently dilute solution, is

$$-\ln(1-N)/r = (T^*_{f0}-T)\Delta H_m/R(T^*_{f0})^2 \qquad (2)$$

where N is mole fraction of the impurities, T^*_{f0} the melting point of pure compound, T the given temperature at equilibrium, r the fraction melted or crystallized, ΔH_m the heat of fusion at T^*_{f0} of pure compound and R the gas constant. However, the temperature T given by the time-temperature curve is not always at equilibrium, and the corresponding equation should be derived from irreversible thermodynamics as follows:[4]

$$-\ln(1-N)/r = (\Delta H_m/R)(1/T-1/T^*_{f0}) + (\Delta C_p/R)[\ln(T^*_{f0}/T) + 1 - (T^*_{f0}/T)] + A(T,r)/RT. \qquad (3)$$

Here ΔC_p denotes the difference of heat capacity of pure compound in liquid and solid states, and $A(T,r)$ the affinity. However, A usually has some finite value, and to estimate the value of A as a function of temperature or time is difficult, especially with a simplified apparatus and technique. If $A=0$, the temperature and fraction melted or crystallized are applicable for determining the purity of the sample by means of Eq. (2).

As a matter of principle it may be assumed that in the time-temperature curves of freezing or melting, the temperature of sample when $r=1/2$ is most nearly at equilibrium, and so Eq. (2) is applicable for determining the purity.

Purity Determination of Hydrocarbons. The time-temperature curves of freezing or melting for several hydrocarbons were obtained by using both the platinum thermometer and the thermocouple cells. As was described in the previous section, determination of

4) I. Prigogin and R. Defay, "Chemical Thermodynamics," Longmans Green and Ltd. (1954), p. 373; Y. Mashiko, T. Shinoda, and H. Enokido, to be published.

purity was made by measuring the temperature most nearly at equilibrium. The results were compared with those obtained by using the method of Rossini *et al.*[3]

As an example, time-temperature melting and freezing curves for *n*-undecane and *n*-docosane obtained by using the thermocouple cell are shown in Fig. 4.

i) Purity of n-*Undecane Obtained by the Melting Curve.* Temperature x, shown in Fig. 4(a), which is a point of inflexion of a quasi-equilibrium portion of the melting curve, seems to be the melting point of the sample. Also the temperature when $r=1/2$ seems to be given by the intersection y of the extension of the melting curve, where a major portion of the sample is melted, with the backward extension from the point x of the heating curve of liquid. The amounts of impurities in the sample of *n*-undecane estimated from the temperatures of point x and y corresponding to $r=1$ and 1/2, respectively, and the value of the melting point reported by Finke *et al.*[5] are in good agreement with each other within —0.03 mol%, and give the average value 99.2_3 mol%.

On the other hand, the melting points of the same sample and of zero impurity of *n*-undecane were calculated from the melting curve by Rossini's method. A GHI-line in Fig. 4(a) represents a quasi-equilibrium portion of melting curve which was explained by Rossini *et al.* The obtained values are 247.21_2°K and 248.30_0°K, respectively, and give a purity of 98.3_6 mol%. If the literature value 247.592°K is used as the melting point for zero impurity, the significantly different value of 95.3_7 mol% is obtained. Thus it can be seen that it is not appropriate to analyze the time-temperature melting curve obtained with a simplified apparatus in terms of Rossini's method, since it is difficult to observe the melting curve under equilibrium condition in a simplified apparatus as compared with Rossini's larger apparatus.

ii) Purity of n-*Docosane Obtained by the Freezing Curve.* If supercooling is successfully observed with a small peak, a major portion of the freezing curve may be assumed to be nearly at equilibrium. Therefore, analysis of the freezing curve was made for *n*-docosane by Rossini's method, as shown in Fig. 4(b). The result, 99.1_9 mol%, is in better agreement with ours (99.2_9 and 99.2_2 mol%) obtained by means of the melting curve than that determined by applying Rossini's method.

The results of the purity determination of hydrocarbons are given in Table 2 together with those obtained with a Yanagimoto Gas Chromatograph GCG-5DH.

It can be seen from Table 2 that of the four procedures for determining the purity from freezing and melting curves of the same sample, treatment of the melting curve, where the obtained temperature is not considered to be at equilibrium, gives results which are in good agreement with those obtained from the freezing curve when the sample was successfully supercooled. Application of Rossini's method to the melting curve was unsuccessful. This is probably due to the fact that it is easier to establish an equilibrium in the freezing process than in the melting one. However, if supercooling is carried out to the extent that a quasi-equilibrium portion of the freezing curve is not given, it is difficult to determine the purity with high accuracy. This will be seen in the purity determination of *n*-octane by the freezing curves using a thermocouple cell (97.4_0 mol%) and *n*-undecane using a platinum thermometer cell (97.4_7 mol%) with a high freezing rate. It was observed from many measurements that our treatment of the melting curve also could not give highly accurate results when the heating rate was greater than 0.5°C/min. Point y in Fig. 4(a) did not always give the temperature where $r=1/2$. It can be said that the melting curve may be obtained at an arbitrary heating rate as long as it is smaller than 0.5°C/min. However, results obtained without considering the equilibrium are less accurate than those obtained from a well-performed freezing curve.

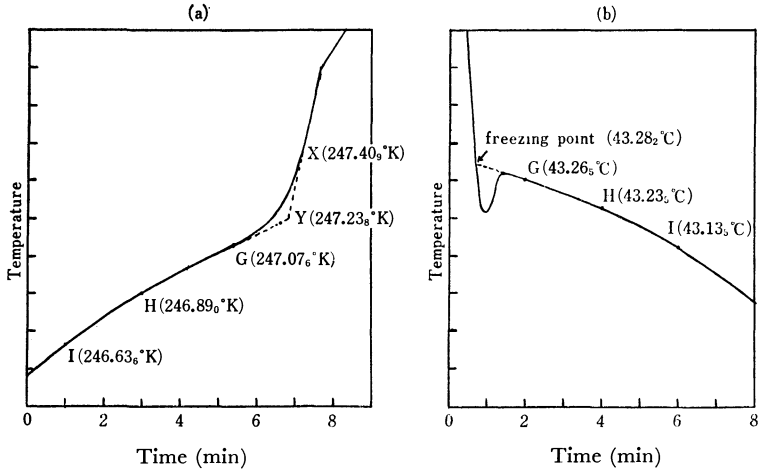

Fig. 4. Time-temperature melting and freezing curves for determining the purity: (a) melting curve of *n*-undecane (b) freezing curve of *n*-docosane.

5) H. L. Finke, M. E. Gross, Guy Waddington, and H. M. Huffman, *J. Amer. Chem. Soc.*, **76**, 333 (1954).

TABLE 2. PURITY DETERMINATION OF HYDROCARBONS

		n-Octane (n-C_8H_{18})			*n*-Undecane (n-$C_{11}H_{24}$)		
		Purity (Rossini's method mol %)	Purity (improved method mol %)	Rate (°C/min)	Purity (Rossini's method mol %)	Purity (improved method mol %)	Rate (°C/min)
Melting curve	Pt-therm. cell	(99.1_7)	99.4_2	0.45	(96.7_5)	99.2_5	0.20
	T. C. cell	(98.8_8)	99.4_3	0.19	(98.3_6)	99.2_3	0.17
Freezing curve	Pt-therm. cell	99.4_3	—	0.38	(97.4_7)	—	0.97
	T. C. cell	(97.4_0)	—	0.51	99.6_4	—	0.58
Gas chromatography			99.4			99.5	

		n-Tridecane (n-$C_{13}H_{28}$)			*n*-Docosane (n-$C_{22}H_{46}$)		
		Purity (Rossini's method mol %)	Purity (improved method mol %)	Rate (°C/min)	Purity (Rossini's method mol %)	Purity (improved method mol %)	Rate (°C/min)
Melting curve	Pt-therm. cell	(97.1_5)	96.5_7	0.46	—	99.2_9	0.29
	T. C. cell	(96.2_4)	96.1_9 97.9_1	0.23	(97.9_7)	99.2_2	0.40
Freezing curve	Pt-therm. cell	—	96.6_8	2.46	99.7_0	—	0.57
	T. C. cell	—	—	—	99.1_9	—	0.54
Gas chromatography			99.6			99.5	

The difference in the purity of *n*-tridecane obtained by thermodynamic methods and gas chromatography is probably due to some impurities which could not be observed by gas chromatography (Table 2).

Finally, from the results of the present experiments the following remarks are given for determining the purity of a compound from time-temperature freezing or melting curve with a simplified apparatus.

i) The sample cell should be closed in a vacuum system in order to carry out analysis in the absence of air and water vapor.

ii) The thermometer should be calibrated against a precision temperature scale, since the determination of melting point for zero impurity is less accurate than that obtained with the use of time-temperature curves. Thus, if we can find a value obtained with the use of a precision adiabatic calorimeter, it would be better to use it.

iii) The temperature of the equilibrium portion of the freezing or melting curve is not always at equilibrium. According to the accuracy required for purity determination, the observed curve should be analyzed on the basis of the theory of irreversible thermodynamics instead of by the well known method.

The authors wish to thank Mr. Tatsuhiko Ojima of Tokyo Kasei Kogyo Co., Ltd. for his measurement of gas chromatography.

The Reactions of Dihalogenoalkanes with Dimethyltin Bis-(*N,N*-dimethyldithiocarbamate) and Related Compounds

Toshio TANAKA, Koji TANAKA, and Tokio YOSHIMITSU

Department of Applied Chemistry, Faculty of Engineering, Osaka University, Yamada-kami, Suita

(Received May 7, 1970)

Dimethyltin-bis(*N,N*-dimethyldithiocarbamate), $(CH_3)_2Sn[S_2CN(CH_3)_2]_2$, reacts with dihalogenoalkanes to give 1,3-dithiacycloalkyl-2-dimethylimminium dimethyltin halides, $[(CH_3)_2SnX_{n+2}]^{n-}[(CH_2)_m\langle S \rangle C{=}N(CH_3)_2]^+_n$ ($n=1$ or 2; $m=2$, 3, or 4; X=Cl, Br, or I). On the other hand, the reactions between dimethyltin bis(*N*-methyl-*N*-phenyldithiocarbamate), $(CH_3)_2Sn[S_2CN(CH_3)(C_6H_5)]_2$, and dihalogenoalkanes yield preferentially alkylene bis-(*N*-methyl-*N*-phenyldithiocarbamate). The difference in reactivity between the two types of complexes is discussed. The infrared and NMR spectra indicate that the positive charge on the dithiacycloalkylimminium ions is more delocalized in the higher homologues. The configurations of dimethyltin trihalide and tetrahalide anions in the solid state and in solution are also presented on the basis of the infrared spectra; the results suggest that, in solution, dimethyltin trihalide anions are more likely to be formed than are dimethyltin tetrahalides.

We have previously reported that some *N,N*-dimethyldithiocarbamate complexes of tin(IV), $R_2Sn[S_2CN(CH_3)_2]_2$ (R=CH_3 and C_2H_5) and $(CH_3)_2SnCl[S_2CN(CH_3)_2]$, react with 1,2-dihalogenoethanes to give, preferentially, 1,3-dithiacyclopentyl-2-dimethylimminium compounds, (I) or (II):[1]

$$[R_2SnX_4]^{2-}\left[\begin{array}{l}CH_2{-}S\\ |\\ CH_2{-}S\end{array}\rangle C{=}N\langle\begin{array}{l}CH_3\\ CH_3\end{array}\right]^+_2 \quad (I)$$

(a): R=CH_3, X=Cl
(b): R=C_2H_5, X=Cl
(c): R=C_2H_5, X=Br

$$[(CH_3)_2SnBr_3]^-\left[\begin{array}{l}CH_2{-}S\\ |\\ CH_2{-}S\end{array}\rangle C{=}N\langle\begin{array}{l}CH_3\\ CH_3\end{array}\right]^+ \quad (II)$$

This reaction is different in selectivity from the previously-reported one between sodium *N,N*-dimethyldithiocarbamate and 1,2-dihalogenoethanes in some organic solvents, where ethylene bis(*N,N*-dimethyldithiocarbamate) was obtained as well as 1,3-dithiacyclopentyl-2-dimethylimminium salts.[2]

The purpose of the present study is to extend this type of reaction of a variety of dihalogenoalkanes with dimethyltin-bis(*N,N*-dimethyldithiocarbamate), $(CH_3)_2Sn[S_2CN(CH_3)_2]_2$, and -bis(*N*-methyl-*N*-phenyldithiocarbamate), $(CH_3)_2Sn[S_2CN(CH_3)(C_6H_5)]_2$ (abbreviated as $(CH_3)_2Sn(dmdtc)_2$ and $(CH_3)_2Sn(mpdtc)_2$ respectively). The former complex reacts with dihalogenoalkanes to form 1,3-dithiacycloalkyl-2-dimethylimminium dimethyltin halides. On the other hand, the reaction of $(CH_3)_2Sn(mpdtc)_2$ with dihalogenoalkanes gives, preferentially, alkylene bis(*N*-methyl-*N*-phenyldithiocarbamates); in the case of 1,2-dichloroethane, 1,3-dithiacyclopentyl-2-methylphenylimminium salt is also produced.

The infrared and PMR spectra of the compounds obtained are discussed from the viewpoint of the delocalization of the positive charge on the dithiacycloalkylimminium cations and of stereochemistry of the dimethyltin halide anions.

Results and Discussion

The reaction of $Cl(CH_2)_nCl$ ($n=3$, 4) with $(CH_3)_2Sn(dmdtc)_2$ without a solvent at elevated temperatures yielded 1,3-dithiacycloalkyl-2-dimethylimminium dimethyltin trichlorides, (III) and (IV), while $BrCH_2CHBrCH_3$, $Br(CH_2)_3Br$ and $I(CH_2)_3I$ reacted with $(CH_3)_2Sn(dmdtc)_2$ to give the uni-bivalent compounds, (V), (VI), and (VII), respectively.

$$[(CH_3)_2SnCl_3]^-\left[(CH_2)_3\langle S \rangle C{=}N\langle\begin{array}{l}CH_3\\ CH_3\end{array}\right]^+ \quad (III)$$

$$[(CH_3)_2SnCl_3]^-\left[(CH_2)_4\langle S \rangle C{=}N\langle\begin{array}{l}CH_3\\ CH_3\end{array}\right]^+ \quad (IV)$$

$$[(CH_3)_2SnBr_4]^{2-}\left[\begin{array}{l}CH_2{-}S\\ |\\ CH{-}S\\ |\\ CH_3\end{array}\rangle C{=}N\langle\begin{array}{l}CH_3\\ CH_3\end{array}\right]^+_2 \quad (V)$$

$$[(CH_3)_2SnBr_4]^{2-}\left[(CH_2)_3\langle S \rangle C{=}N\langle\begin{array}{l}CH_3\\ CH_3\end{array}\right]^+_2 \quad (VI)$$

$$[(CH_3)_2SnI_4]^{2-}\left[(CH_2)_3\langle S \rangle C{=}N\langle\begin{array}{l}CH_3\\ CH_3\end{array}\right]^+_2 \quad (VII)$$

The main products in these reactions were 1,3-dithiacycloalkyl-2-dimethylimminium salts, although the yields of III and IV were not very good. Another product expected to be formed, alkylene bis(*N,N*-dimethyldithiocarbamates), was not obtained under the present experimental conditions. Recently, the formation of ethylene bis(*N,N*-dimethyldithiocarbamate) (E) from 1,2-dichloroethane (A) and sodium *N,N*-dimethyldithiocarbamate (B) has been interpreted by the following reaction scheme, involving the intermediate of the isolated anchimetric cation (D), and in which the cyclization of the mono-substituted intermediate (C) occurs very rapidly ($k_c \gg k_a$):[2]

1) T. Tanaka and T. Abe, *Inorg. Nucl. Chem. Lett.*, **4**, 569 (1968).

2) T. Nakai, Y. Ueno, and M. Okawara, *Tetrahedron Lett.*, **1967**, 3831; This Bulletin, **43**, 165 (1970).

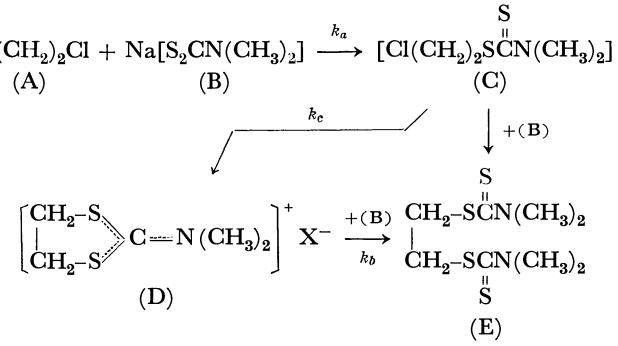

On the basis of this scheme, it may be explained that the reaction of $(CH_3)_2Sn(dmdtc)_2$ with dihalogenoalkanes mainly yielded I—VII, but not the di-substituted products; the I—VII obtained by the cyclization of the mono-substituted products are almost insoluble in dihalogenoalkanes; therefore, it is unlikely that any further reaction of those products with $(CH_3)_2Sn(dmdtc)_2$ will occur. This idea is supported by the results of the reaction of $(CH_3)_2Sn(mpdtc)_2$ with dihalogenoalkanes, as will be described below.

The $(CH_3)_2Sn(mpdtc)_2$ complex reacted with $Cl(CH_2)_2Cl$ to give ethylene bis(*N*-methyl-*N*-phenyldithiocarbamate) (VIIIa) as precipitates. From the filtrate we isolated 1,3-dithiacycloalkyl-2-methylphenylimminium salt (IXa). However, the reactions of $Cl(CH_2)_nCl$ (n=3, 4) with $(CH_3)_2Sn(mpdtc)_2$ yielded only alkylene bis(*N*-methyl-*N*-phenyldithiocarbamates) (VIIIb) and (VIIIc), not the corresponding imminium salts, (IXb) and (IXc).

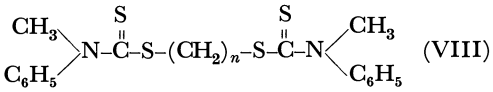

(a) n=2, (b) n=3, (c) n=4

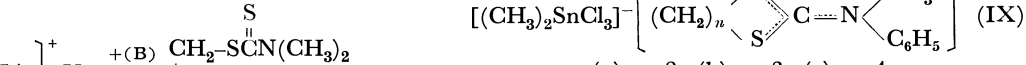

(a) n=2, (b) n=3, (c) n=4

In contrast to the dimethylimminium salts (I)—(VII), the methylphenylimminium salt (IXa) is appreciably soluble in dihalogenoalkanes, which act as solvents as well as reactants. IXb and IXc will be more soluble in dihalogenoalkanes than IXa, for they have more dithiacycloalkyl rings. In addition, the reaction rate, k_b, in the scheme described above is much faster than k_a in non-polar aprotic solvents.[2] It can reasonably be assumed from these facts that the further reaction of IX with $(CH_3)_2Sn(mpdtc)_2$ will occur to form the di-substituted product (VIII). The infrared spectrum of $(CH_3)_2Sn(mpdtc)_2$ shows the ν(Sn–S) band at 330 cm^{-1}, considerably lower than that of $(CH_3)_2Sn(dmdtc)_2$ (365 cm^{-1}). This lowering in frequency may be related to the bond weakening of the Sn–S bond, which will also enhance the reactivity of the former complex.

The capacity to form both $(CH_3)_2SnX_3^-$ and $(CH_3)_2SnX_4^{2-}$ ions has been known in fluoride,[3] chloride, and bromide,[4] where the counter cations are Cs^+, $N(CH_3)_4^+$, and $N(C_2H_5)_4^+$, but the iodo-complex has never been isolated. The compound VII is the first iodo-complex anion; this is suggests that some bulky

Table 1. Relevant infrared frequencies (cm^{-1})[a] of 1,3-dithiacycloalkyl-2-dimethylimminium dimethyltin halides and the related compounds[b]

	Compound	ν(C=N)	ν_{as}(Sn–C)	ν_s(Sn–C)	ν(Sn–X)
(Ia)	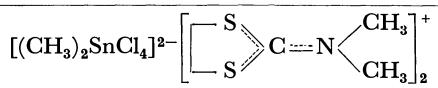	1590 s	560 s	515 vw	220 m
(II)	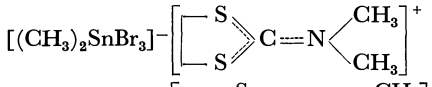	1587 s	559 s	511 s	215 s
(III)	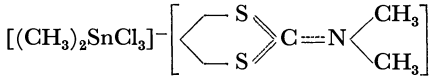	1541 s	571 m (565 m)	516 m (516 m)	312 s 241 s (325 s) (240 s)
(IV)	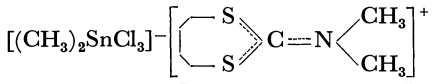	1461 s	565 m (566 m)	515 m (519 m)	325 s 240 s (326 s) (240 s)
(V)	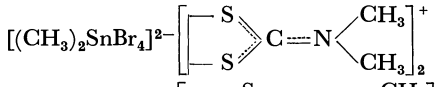	1590 s	568 m (562 m)	— (510 m)	210 s
(VI)	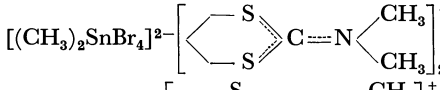	1538 s	562 m (561 m)	505 m (511 m)	215 s
(VII)	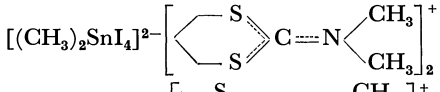	1530 s	560 s	518 vw	<200
(IXa)	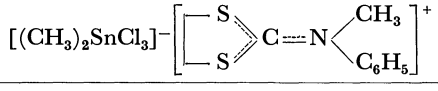	1524 s	578 m (566 m)	506 m (516 m)	256 s, br (326 s) (240 s)

a) Nujol mull and dichloromethane solution; the latter in parentheses.
b) The abbreviations used in this table are as follows: s, strong; m, medium; w, weak; vw, very weak; br, broad.

3) C. J. Wilkins and H. M. Haendler, *J. Chem. Soc.*, **1965**, 3174.

4) J. P. Clark and C. J. Wilkins, *J. Chem. Soc., A*, **1966**, 871.

TABLE 2. PROTON CHEMICAL SHIFTS (ppm) AND SPIN-SPIN COUPLING CONSTANTS BETWEEN THE ^{119}Sn AND THE METHYL PROTONS (Hz) OF 1,3-DITHIACYCLOALKYL-2-DIMETHYLIMMINIUM DIMETHYLTIN HALIDES AND THE RELATED COMPOUNDS[a]

Compound	τ(Sn–CH_3)	τ(C–CH_2–C)	τ(S–CH_2)	τ(N–CH_3)	τ(C_6H_6)	J(^{119}Sn–CH_3)	Solvent
(Ia)[b]	8.91 s	—	5.95 s	6.44 s	—	116	DMSO-d_6
(II)[b]	8.70 s	—	5.92 s	6.44 s	—	114	DMSO-d_6
(III)	8.73 s	7.70 t	6.56 t	6.37 s	—	90	CH_2Cl_2
(IV)	8.72 s	7.73 m	6.40 m	6.77 s	—	90	CH_2Cl_2
(V)[c]	8.27 s	—	[d]	6.25 [d]	—	86	$CHCl_3$
(VI)	8.34 s	7.58 m	6.51 t	6.33 s	—	86	CH_2Cl_2
(VII)	8.36 s	7.57 t	6.52 t	6.33 s	—	81	$CHCl_2CHCl_2$
(VIIIa)	—	—	6.45 s	6.20 s	2.30 m	—	DMSO-d_6
(VIIIb)	—	8.12 t	6.85 t	6.34 s	2.77 m	—	CH_2Cl_2
(VIIIc)	—	8.39 m	6.85 m	6.28 s	2.70 m	—	CH_2Cl_2
(IXa)	8.75 s	—	5.90 m	6.26 s	2.48 s	90	CH_2Cl_2

a) The abbreviations used in this table are as follows: s, singlet; d, doublet; t, triplet; m, multiplet; br, broad.
b) These compounds are too insoluble in less donor solvents to measure J(^{119}Sn–CH_3) values, but soluble in very polar solvents, such as dimethyl sulfoxide(DMSO). The values of these compounds in DMSO-d_6 are quite similar to those of $(CH_3)_2SnCl_2$ or $(CH_3)_2SnBr_2$ in the same solvent; W. Kitching, *Tetrahedron Lett.*, **1966**, 3689; T. Tanaka, *Inorg. Chim. Acta*, **1**, 217 (1967).
c) τ(C–CH_3), 8.26 d.
d) A complicated multiplet. This is also the case of the S–CH chemical shifts.

counter cations make it possible to form dimethyltin iodide anions.

Delocalization of the Positive Charge in the 1,3-Dithiacycloalkyl-2-imminium Cations. The relevant infrared frequencies are listed in Table 1. The compounds, Ia, II, and V all exhibit the ν(C=N) band at relatively high frequencies, suggesting an appreciable double-bond character of the C=N bond and, therefore, a high rotational barrier about it. This idea is supported, although qualitatively, by the PMR spectrum of the compound V (Fig. 1), in which the N–CH_3 proton signals are split due to their slightly different magnetic environments. The coalescene temperature is about 125°C in 1,1,2,2-tetrachloroethane, higher than those of most related compounds, such as *S*-methyl-*N*,*N*-dimethyldithiocarbamate, $CH_3SC(S)$-$N(CH_3)_2$ (2.5°C in hexane)[5] and *N*,*N*-dimethylacetamide, $CH_3C(O)$-$N(CH_3)_2$ (87°C as neat liquid),[6] although somewhat lower than that of *N*,*N*-dimethylformamide, HC(O)-$N(CH_3)_2$ (148°C as neat liquid).[6] As is shown in Table 1, the ν(C=N) band shifts to a lower frequency with an increase in the member of the 1,3-dithiacycloalkyl rings. This suggests that the higher homologues receive more contributions from the structure G, resulting in an increase in the electron density on the nitrogen atom. Consistently with this, the N–CH_3 proton signal in chloroalkanes is observed at a higher magnetic field with an increase in the size of the dithiacycloalkyl rings, as is shown in Table 2.[7] The participation of the lone-pair electrons of the sulfur atom in π-bonding is sterically more favorable in the higher homologues, resulting in the delocalization of the positive charge.

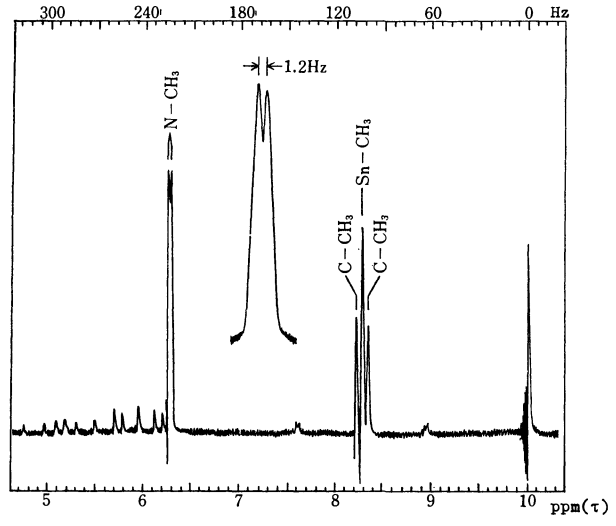

Fig. 1. PMR spectrum of $[(CH_3)_2SnBr_4]^{2-}$.

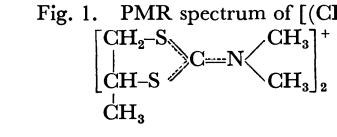

in chloroform, 6 wt %.

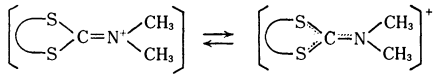

(F) (G)

With the compound IXa, the ν(C=N) band sppears at a somewhat lower frequency than those of the other compounds with five-membered dithiacycloalkyl rings, Ia, II, and V. This may be interpreted by assuming a conjugation between the C=N bond and the phenyl group.

Stereochemistry of the Dimethyltin Halide Anions. As is listed in Table 1, the 1 : 1 electrolytes, II, III, and IV, in the solid state exhibit two infrared bands due to ν(Sn–C), and the symmetric stretching bands are as strong as the asymmetric ones, indicating that the

5) C. E. Holloway and M. H. Gitlitz, *Can. J. Chem.*, **45**, 2659 (1967).
6) M. T. Rogers and J. C. Woodbrey, *J. Phys. Chem.*, **66**, 540 (1962).
7) This is not true fot Ia and II, whose τ(N–CH_3) values are those of a strong donor solvent; DMSO-d_6.

C–Sn–C moiety is not linear. The probable configuration of the $(CH_3)_2SnX_3^-$ anions is a trigonal bipyramid (H), with two methyl groups located in equatorial positions; this is analogous to the structure of the dimethyltin trichloride anion in $[(CH_3)_2SnCl\cdot terpyridyl]^+[(CH_3)_2SnCl_3]^-$, as determined by X-ray analysis.[8]

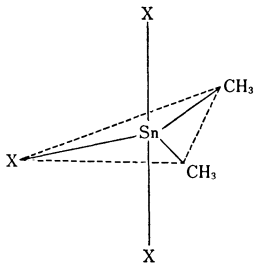

(H): X=Cl, Br

The spectra of III and IV in dichloromethane closely resemble those of their solid states, except for the region obscured by the solvent. It seems, therefore, that there is essentially no difference between the geometry in the solid state and that in solution for the two compounds. These compounds show a characteristic $J(^{119}Sn–CH_3)$ value of 90 Hz. Extrapolation from the function relating $J(^{119}Sn–CH_3)$ to the apparent *s*-character of the tin atomic orbital in the Sn–C bond[9] indicates a 41% *s*-character, which is much larger than that (33%) expected from the trigonal bipyramid (H). Such a large *s*-character of the tin atomic orbital in the Sn–C bond may possibly be explained by assuming the rehybridization of the tin atomic orbitals due to the electronegativity difference between the methyl group and the chlorine atom.[10] This idea is consistent with the present experimental results that $J(^{119}Sn–CH_3)$ value decreases with a decrease in the electronegativity of the X atom of $(CH_3)_2SnX_3^-$ anions, the bromide and iodide of which result from the dissociation of V, VI or VII in halogenoalkanes, as will be described below.

Of the uni-bivalent electrolytes, Ia, V and VII in the solid state exhibit an intense band due to ν_{as}(Sn–C), while their ν_s(Sn–C) bands are imperceptible. It seems, therefore, that the configuration J with an almost linear C–Sn–C moiety is most plausible for the dimethyltin tetrahalide anions.

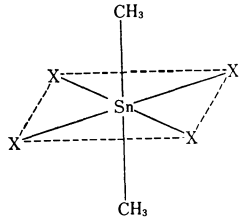

(J): X=Cl, Br or I

8) F. W. B. Einstein and B. R. Penfold, *Chem. Commun.*, **1966**, 780.

9) J. R. Holmes and H. D. Kaesz, *J. Amer. Chem. Soc.*, **83**, 3903 (1961).

10) H. A. Bent, *Can. J. Chem.*, **38**, 1235 (1960); *Chem. Rev.*, **61**, 275 (1961); *J. Inorg. Nucl. Chem.*, **19**, 43 (1961).

The spectrum of V in dichloromethane, however, shows the ν_{as}(Sn–C) band shifting to a lower frequency and the ν_s(Sn–C) band occurring distinctly, whereas there is no appreciable change is the spectrum in the other mid-infrared regions (Fig. 2).

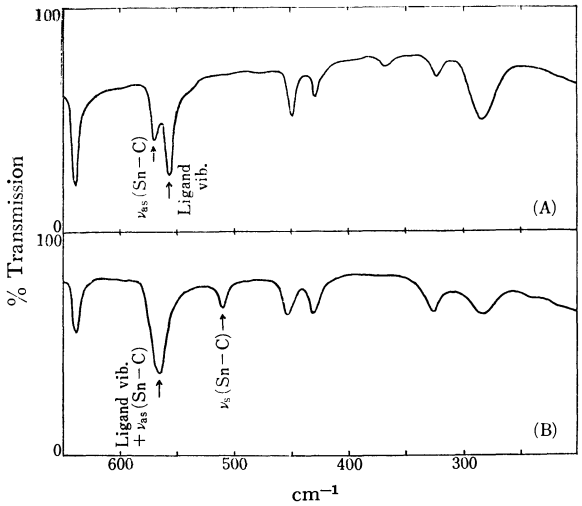

Fig. 2. Infrared spectra of $[(CH_3)_2SnBr_4]^{2-}$·

$$\left[\begin{array}{l} CH_2\text{–}S \\ | \\ CH\text{–}S \\ | \\ CH_3 \end{array}\!\!>\!C\!=\!N\!<\!\begin{array}{l} CH_3 \\ CH_3 \end{array}\right]_2^+$$

in Nujol (A) and in dichloromethane, 3 wt% (B).

These findings confirm that the $(CH_3)_2SnBr_4^{2-}$ dissociates partly into $(CH_3)_2SnBr_3^-$ and Br^-, and/or $(CH_3)_2SnBr_2$ and $2Br^-$. In view of the $J(^{119}Sn–CH_3)$ value of this compound in chloroform (Table 2), the predominant species may be the $(CH_3)_2SnBr_3^-$ rather than $(CH_3)_2SnBr_2$. The $(CH_3)_2SnI_4^{2-}$ anion of VII is assumed to dissociate similarly into $(CH_3)_2SnI_3^-$, $(CH_3)_2SnI_2$, and I^- in tetrachloroethane, judging from the $J(^{119}Sn–CH_3)$ value (Table 2).

Elemental analysis confirms that the reaction product between $(CH_3)_2Sn(dmdtc)_2$ and $Br(CH_2)_3Br$ has the composition VI, but it has no sharp melting point, even when the recrystallization is repeated. The infrared spectrum of this product in the solid state resembles closely that in solution; particularly, the intensity ratio of the two ν(Sn–C) bands dose not change from the solid state to that in solution. These observations and the $J(^{119}Sn–CH_3)$ value in dichloromethane (Table 2) suggest that VI is a 1 : 1 mixture of X and XI.

$$Br^-\left[(CH_2)_3\!<\!\begin{array}{l} S \\ S \end{array}\!>\!C\!=\!N\!<\!\begin{array}{l} CH_3 \\ CH_3 \end{array}\right]^+ \quad (X)$$

$$[(CH_3)_2SnBr_3]^-\left[(CH_2)_3\!<\!\begin{array}{l} S \\ S \end{array}\!>\!C\!=\!N\!<\!\begin{array}{l} CH_3 \\ CH_3 \end{array}\right]^+ \quad (XI)$$

There is a remarkable difference in the infrared spectra of IXa between in the solid state and in solution. The spectrum in dichloromethane shows two each of the ν(Sn–C) and ν(Sn–Cl) bands, which are close in frequency to those of III and IV. In the solid state, however, it gives only one broad band due to ν(Sn–Cl), at a very low frequency, and two ν(Sn–C) bands. as is shown in Fig. 3. This indicates that the

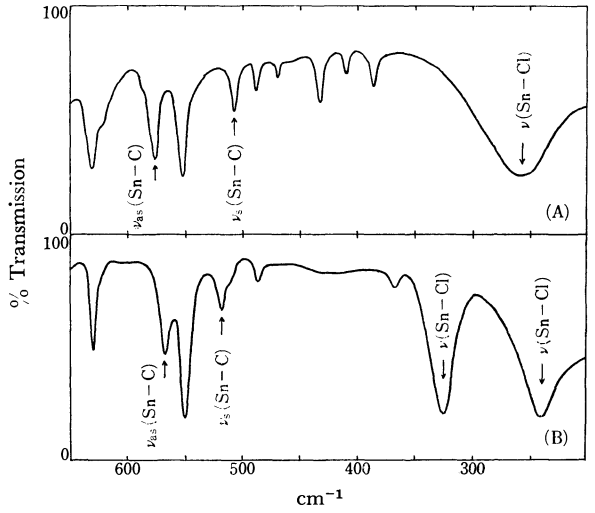

Fig. 3. Infrared spectra of $\left[(CH_3)_2 SnCl_3\right]^-\cdot\left[(CH_2)_2 \begin{matrix} S \\ S \end{matrix} \!\!>\!C\!=\!N\!<\!\begin{matrix} CH_3 \\ C_6H_5 \end{matrix}\right]^+$ in Nujol (A) and in dichloromethane, 3 wt% (B).

structure of the $(CH_3)_2SnCl_3^-$ ion of IXa in the solid state differs from that in solution, and that it is probably a distorted penta-coordinate.

It may be concluded, from above considerations, that the $(CH_3)_2SnX_4^{2-}$ ions are likely to dissociate into $(CH_3)_2SnX_3^-$ and X^-, and/or partly into $(CH_3)_2SnX_2$ and $2X^-$, even in less polar solvents, such as dichloromethane, and that, therefore, in solution the formation of dimethyltin trihalide anions is more likely than that of the tetrahalides. The electronic spectra of the present 1,3-dithiacycloalkyl-2-dimethylimminium compounds are now under investigation by the authors.

Experimental

Materials. The $(CH_3)_2Sn(dmdtc)_2$ was prepared as has previously been described.[11] The $(CH_3)_2Sn(mpdtc)_2$ was similarly synthesized by the reaction of $(CH_3)_2SnCl_2$ with sodium *N*-methyl-*N*-phenyldithiocarbamate in ethanol; mp 200°C (decomp.).

Found: C, 41.71; H, 4.41; N, 5.34%. Calcd for $C_{18}H_{22}N_2S_4Sn$: C, 42.07; H, 4.32; N, 5.46%.

NMR in dichloromethane: τ(Sn-CH_3), 8.55(singlet); τ(N-CH_3), 6.37(singlet); $\tau(C_6H_5)$, 2.72(multiplet) ppm; $J(^{119}Sn-CH_3)$, 84 Hz. The dihalogenoalkanes used in this experiment are commercially available, except for $I(CH_2)_3I$, which was obtained by the reaction of $Br(CH_2)_3Br$ with NaI in acetone.[12]

General Procedure of the Reactions. The dithiocarbamate complexes of tin(IV) were allowed to react with an excess of dihalogenoalkanes at elevated temperature, without any solvent and under dry nitrogen.

1,3-Dithiacyclohexyl-2-dimethylimminium-dimethyltin Trichloride (III). A solution of $(CH_3)_2Sn(dmdtc)_2$ (3.2 g) in 1,3-dichloropropane (20 m*l*) was refluxed for 3 hr. After the evaporation of an excess of 1,3-dichloropropane under reduced pressure, the resulting solid was repeatedly washed with carbon tetrachloride, and then recrystallized from acetonitrile to give colorless needles (1.0 g, 30% yield); mp 169°C.

Found: C, 23.75; H, 4.61; N, 3.58%. Calcd for $C_8H_{18}NS_2Cl_3Sn$: C, 23.03; H, 4.35; N, 3.36%.

1,3-Dithiacycloheptyl-2-dimethylimminium-dimethyltin Trichloride (IV). A solution of $(CH_3)_2Sn(dmdtc)_2$ (5.0 g) in 1,4-dichlorobutane (20 m*l*) was kept at a temperature of about 120°C for 3 hr. A procedure similar to that used in the case of III and recrystallization from a dichloromethane-petroleum ether mixture yielded colorless needles (1.0 g, 10% yield); mp 56—59°C.

Found: C, 24.87; H, 5.07%. Calcd for $C_9H_{20}NS_2Cl_3Sn$: C, 25.06; H, 4.67%.

Bis(1,3-dithia-4-methylcyclopentyl-2-dimethylimminium)-dimethyltin Tetrabromide (V). A solution of $(CH_3)_2Sn(dmdtc)_2$ (5.0 g) in 1,2-dibromopropane (20 m*l*) was heated to 120°C for 20 min to liberate a white precipitate. After the solution had then been cooled to room temperature, the precipitate V was filtered off and recrystallized from acetonitrile (6.8 g, 70% yield); mp 125—128°C.

Found: C, 20.93; H, 3.86; N, 3.48%. Calcd for $C_{14}H_{30}N_2S_4Br_4Sn$: C, 21.21; H, 3.81; N, 3.53%.

1,3-Dithiacyclohexyl-2-dimethylimminium-bromide (X) and -dimethyltin Tribromide (XI). A solution of $(CH_3)_2Sn(dmdtc)_2$ (5.0 g) in 1,3-dibromopropane (20 m*l*) was treated in a manner similar to that used in the case of V to give a white precipitate of a 1 : 1 mixture of X and XI. Recrystallization from acetonitrile yielded the same mixture (8.3 g, 80% yield).

Found: C, 20.62; H, 3.95; N, 3.42%. Calcd for $C_{14}H_{30}N_2S_4Br_4Sn$: C, 21.21; H, 3.81; N, 3.53%.

Bis(1,3-dithiacyclohexyl-2-dimethylimminium)-dimethyltin Tetraiodide (VII). A mixture of $(CH_3)_2Sn(dmdtc)_2$ (2.0 g) and 1,3-diiodopropane (3 m*l*) was heated at 130°C for 2 hr. After subsequent cooling to room temperature, an excess of 1,3-diiodopropane was filtered out; the solid product thus obtained was recrystallized from a dichloromethane-petroleum ether mixture to give colorless needles VII (4.6 g, 90% yield); mp 143—146°C.

Found: C, 16.76; H, 3.20; N, 2.67%. Calcd for $C_{14}H_{30}N_2S_4I_4Sn$: C, 17.14; H, 3.08; N, 2.85%.

Reaction of $(CH_3)_2Sn(dmdtc)_2$ with $Cl(CH_2)_2Cl$. A solution of $(CH_3)_2Sn(dmdtc)_2$ (5.3 g) in 1,2-dichloroethane was refluxed for 1 hr to give a white precipitate. After the mixture had then been cooled to room temperature, the precipitate VIIIa was filtered off, washed with diethyl ether, and dried *in vacuo* (1.2 g, 53% yield); mp 230°C (decomp.).

Found: C, 55.16; H, 5.34; N, 6.99%. Calcd for $C_{18}H_{20}N_2S_4$: C, 55.07; H, 5.13; N, 7.14%. The filtrate was evacuated under reduced pressure, and a light yellow viscous liquid thus obtained was shaken repeatedly with diethyl ether; the resulting insoluble materials in ether were collected by filtration and washed with carbon tetrachloride, giving a white powder IXa (1.9 g, 39% yield); mp 84—87°C.

Found: C, 30.87; H, 3.79; N, 2.89%. Calcd for $C_{12}H_{18}NS_2Cl_3Sn$: C, 30.97; H, 3.90; N, 3.01%.

Propylene Bis(N-methyl-N-phenyldithiocarbamate) (VIIIb). A solution of $(CH_3)_2Sn(mpdtc)_2$ (5.0 g) in 1,3-dichloropropane (20 m*l*) was heated on a bath at 120°C for 2 hr. After it had then been cooled to room temperature, the solution was evaporated to about a half volume under reduced pressure; the white precipitates which appeared were collected by filtration, and subsequent recrystallization from a dichloromethane - diethyl ether mixture gave colorless needles VIIIb (1.2 g, 37% yield); mp 169°C.

Found: C, 55.97; H, 5.33; N, 6.88%. Calcd for $C_{19}H_{22}N_2S_4$: C, 56.12; H, 5.45; N, 6.89%.

Butylene Bis(N-methyl-N-phenyldithiocarbamate) (VIIIc). This compound was obtained from $(CH_3)_2Sn(mpdtc)_2$ (5.1 g) and 1,4-dichlorobutane (20 m*l*) in a manner similar to that

11) M. Honda, M. Komura, Y. Kawasaki, T. Tanaka, and R. Okawara, *J. Inorg. Nucl. Chem.*, **30**, 3231 (1968).

12) H. Finkelstein, *Ber.*, **43**, 1528 (1910).

used in the case of VIIIb, and it was recrystallized from the same solvent (1.3 g, 38% yield); mp 135—137°C.

Found: C, 57.12; H, 5.80; N, 6.80%. Calcd for $C_{20}H_{24}N_2S_4$: C, 57.10; H, 5.75; N, 6.66%.

All the compounds isolated were identified by means of their NMR spectra, as are listed in Table 2.

Infrared and NMR Spectra. The infrared spectra were recorded on Hitachi EPI-2G (5000—400 cm^{-1}) and EPI-L (700—200 cm^{-1}) spectrophotometers. The NMR spectra were measured on a Japan Electron JNM-3H-60 spectrometer, operating at 60 MHz and at room temperature, and using tetramethylsilane as the internal standard.

BULLETIN OF THE CHEMICAL SOCIETY OF JAPAN, VOL. 44, 117—120(1971)

Extraction and Spectrophotometric Determination of Copper(II) with 2-Thenoyltrifluoroacetone

Hideo AKAIWA, Hiroshi KAWAMOTO, and Masanobu ABE

Department of Chemistry, Faculty of Technology, Gunma University, Kiryu, Gunma

(Received July 29, 1970)

A highly sensitive method for the spectrophotometric determination of copper(II) with 2-thenoyltrifluoroacetone (TTA) is described. Copper(II) is extracted with TTA in cyclohexane at pH 5.5 and the residual TTA in the organic phase is removed by washing with sodium hydroxide solution containing pyridine. Pyridine is added to the washing solution so that it forms an adduct and prevents the copper-TTA chelate from decomposing during the alkali treatment process. The absorbance of the organic phase is measured at 340 mμ. Beer's law is followed over the concentration range of 0.1 to 1.0 μg of Cu per m*l*, the sensitivity being 0.0023 μg Cu/cm^2 at 340 mμ. The present method was applied to the analysis of natural water.

So-called synergistic extraction of metal chelate has been utilized for various analytical purposes such as separation of metal ions,[1,2] extractive spectrophotometric[3-7] and fluorometric[8] determination of metals. In most cases, enhancement of the extractability could be explained by the formation of an adduct. In the work described below, the adduct formation in the synergistic extraction is shown to be useful for an improvement in the spectrophotometric sensitivity.

Two methods of the spectrophotometric determination of copper(II) with 2-thenoyltrifluoroacetone (TTA) have already been proposed.[9,10] However, the sensitivities of these methods are low compared with that of the well known dithizone method.[11] Although the dithizone method is very popular mainly due to its high sensitivity, it is not always free from interferences caused by coexisting ions and had a defect that the reproducibility of the method depends largely upon the experimental conditions.

Therefore, by the aid of the formation of pyridine adduct, the previous TTA extraction spectrophotometry for copper[10] has been revised into a method for the highly sensitive determination of the element.

Since the low sensitivity of the above mentioned TTA methods is caused by the presence of the residual TTA in the organic phase which interferes with absorption measurement around 340 mμ (an optimum wavelength for the extracted copper-TTA chelate), the residual reagent should be removed by washing the organic phase with an alkali solution. The above purpose can be attained only when pyridine is present in the washing solution, otherwise not only the residual reagent but the copper-TTA chelate is decomposed.

Experimental

Apparatus and Reagents. Absorption measurements were carried out with a Shimadzu Spectronic 20 type photoelectric photometer and 1.17-cm glass cells. The pH value of the aqueous phase was measured after extraction with a Hitachi-Horiba F-5 type pH-meter and a glass electrode. TTA (Wako Pure Chemical Inc.) and cyclohexane (Nippon Rikagakuyakuhin Co.) were used without further purification. Pyridine and all other materials used in this work were of guaranteed grade.

A 0.001M TTA solution was prepared by dissolving a weighed amount of the reagent in cyclohexane. Standard copper solution (100 mg/*l*) was prepared by dissolving copper sulfate pentahydrate in deionized water.

General Procedure. Transfer 50 m*l* of the sample solution containing 1-10 μg of copper to a separatory funnel and adjust the pH of the solution to about 5.5. Then extract with 10 m*l* of 0.001M TTA-cyclohexane solution by shaking for 3 minutes. Allow the phases to separate and remove the aqueous phase. Add 10 m*l* of aqueous solution of sodium

1) T. Sekine and D. Dyrssen, *Anal. Chim. Acta*, **37**, 217 (1967).
2) H. Akaiwa and H. Kawamoto, *ibid.*, **48**, 438 (1969).
3) T. Taketatsu and C. V. Banks, *Anal. Chem.*, **38**, 1524 (1966).
4) H. Akaiwa and H. Kawamoto, *Anal. Chim. Acta*, **40**, 407 (1968).
5) T. Shigematsu and T. Honjo, *Bunseki Kagaku*, **18**, 68 (1969).
6) K. S. Math, K. S. Bhatki, and H. Freiser, *Talanta*, **16**, 412 (1959).
7) H. Akaiwa, H. Kawamoto, and M. Hara, *Anal. Chim. Acta*, **43**, 297 (1968).
8) T. Shigematsu, M. Matsui, and R. Wake, *ibid.*, **46**, 101 (1969).
9) S. M. Khopkar and A. K. De, *Z. Anal. Chem.*, **171**, 241 (1959).
10) H. Akaiwa, *Bunseki Kagaku*, **12**, 457 (1963).
11) E. B. Sandell, "Colorimetric Determination of Traces of Metals," 3rd ed., Interscience Publishers, Inc., New York (1959), p. 437.

hydroxide (0.005M) containing 1% (v/v) of pyridine and shake the mixture for 3 minutes. Separate the phases and measure the absorbance of the organic phase at 340 mμ against the reagent blank.

Results and Discussion

Absorption Spectrum. The absorption spectrum of copper-TTA-pyridine complex in cyclohexane obtained by the above procedure is shown in Fig. 1. The spectrum of the extracted complex has a maximum absorbance at around 340 mμ, and the intensity is stable for at least 24 hrs. The absorbance of the reagent blank is considerably lowered by washing the organic phase with alkali solution.

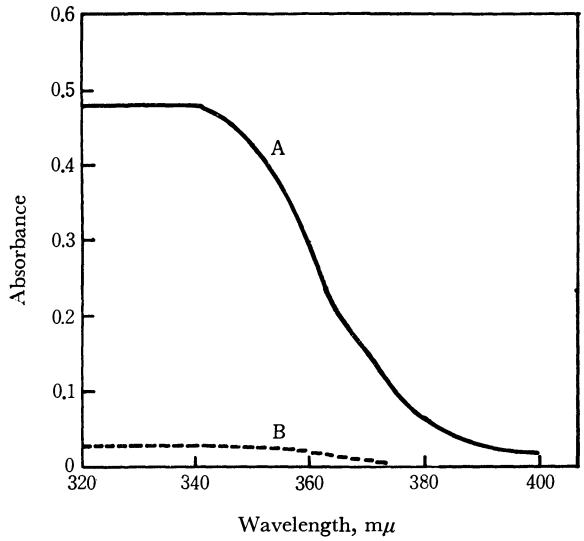

Fig. 1. Absorption spectra of copper-TTA-pyridine chelate (A) and the reagent blank (B).

Effect of pH. The extraction of copper into benzene proceeds according to the reaction: $Cu^{2+} + 2HTTA_{,org.} = Cu(TTA)_{2,org.} + 2H^+$, for which the extraction constant was reported to be 4.8×10^{-2}.[12] The above reaction indicates that the extractability of copper is affected by the TTA concentration and the pH.

Copper can be extracted quantitatively at pH 4.0 by using 0.01 M TTA in benzene.[10] However, since the residual TTA in the organic phase interferes with the absorption measurement, the TTA concentration for the extraction of copper was required to be as low as possible. Considering the above situation, the 0.001M TTA solution was adopted. The extraction curve obtained at the TTA concentration of 0.001M is shown in Fig. 2. As can be seen in the extraction curve, an increase in pH leads to an increase in the extractability of copper, and above 5.2 the absorbance becomes constant. Accordingly, a pH value of 5.5 was adopted.

Removal of Residual TTA. TTA has a strong absorption at around 340 mμ, and interferes with the absorption measurement of the extracted complex in the cyclohexane phase. In order to increase the spectrophotometric sensitivity, the residual TTA which does not combine with copper should be removed from the organic phase.

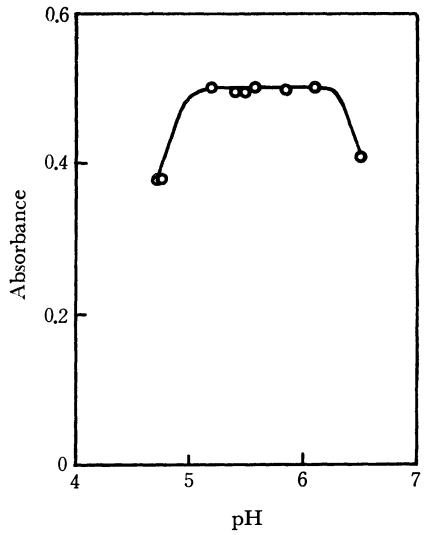

Fig. 2. Effect of pH on the absorbance of the organic phase.

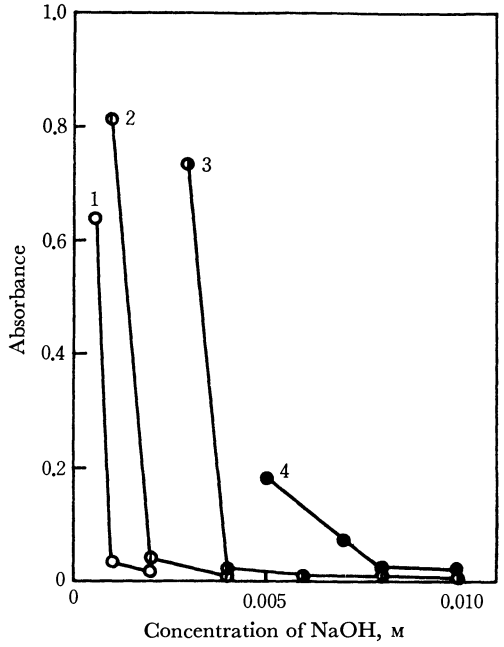

Fig. 3. Removal of the residual TTA.
TTA concentration - 1: 5×10^{-4}M, 2: 1×10^{-3}M, 3: 2×10^{-3}M, 4: 5×10^{-3}M.

By shaking TTA-cyclohexane solution with sodium hydroxide solution, the absorbance of the cyclohexane phase at 340 mμ decreases with increasing alkali concentration (Fig. 3). This decrease in the absorbance indicates the removal of the TTA from the cyclohexane solution, and shaking for 3 min with 0.005M sodium hydroxide solution is sufficient for the present purpose.

Effect of Pyridine. The copper-TTA chelate was decomposed by the alkali treatment of the cyclohexane phase in the absence of pyridine and copper was stripped into the alkali solution. However, the stripping of copper could be avoided by adding pyridine. As is shown in Fig. 4, the absorbance of the cyclohexane

12) R. A. Bolomey and L. Wish, *J. Amer. Chem. Soc.*, **72**, 4483 (1950).

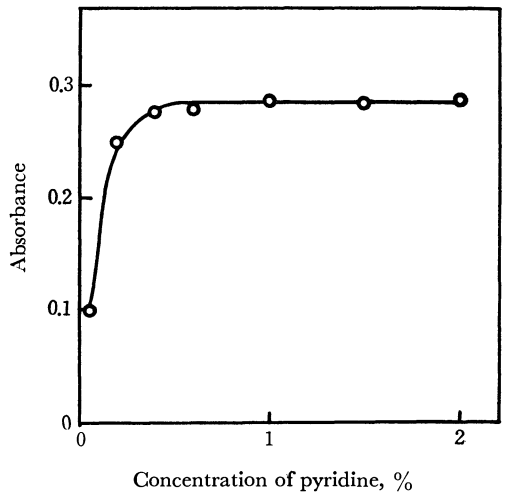

Fig. 4. Effect of pyridine concentration on the absorbance of the organic phase.

phase containing copper-TTA chelate increases along with an increase in the pyridine concentration in the alkali solution, and finally reaches a constant value in the pyridine concentration range above 0.5%. This indicates that the copper-TTA chelate in cyclohexane phase is stabilized by the presence of pyridine and the chelate was prevented from decomposition.

Pyridine Adduct. Visible spectra of benzene solutions of the copper-TTA chelate with various amounts of pyridine were measured and are shown in Fig. 5. The systematic variation in the spectra and

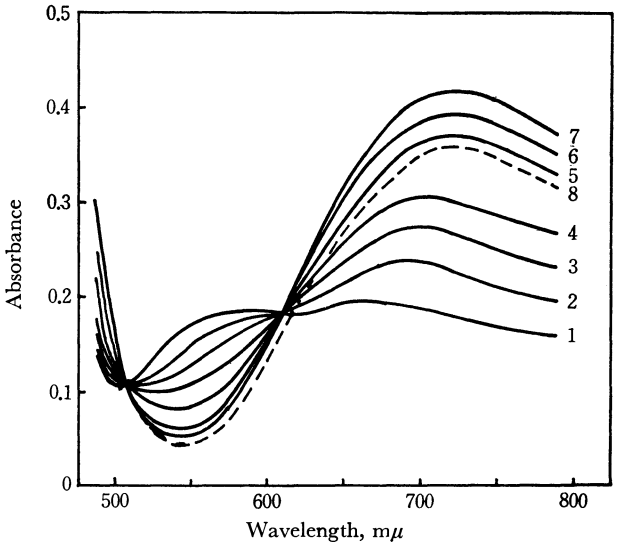

Fig. 5. Effect of pyridine concentration on the spectra of 5×10^{-3}M Cu $(TTA)_2$ in benzene.
Pyridine concentration - 1: 0, 2: 1×10^{-3}M, 3: 2×10^{-3}M, 4: 3×10^{-3}M, 5: 5×10^{-3}M, 6: 1×10^{-2}M, 7: 5×10^{-2}M, 8: 2.5×10^{-1}M.

the presence of two isosbestic points furnish the evidence for the formation of the pyridine adduct (1:1). The formation constant for the adduct was estimated to be $10^{3.45\pm0.25}$ by the method proposed by Ke and Li.[13]

13) C. H. Ke and N. C. Li, *J. Inorg. Nucl. Chem.*, **31**, 1383 (1969).

At high pyridine concentration (0.25M), the isosbestic points disappear probably because of the formation of the adduct (1:2), $Cu(TTA)_2$ $(pyridine)_2$.

In order to obtain further confirmation of the formation of pyridine adduct, the copper-TTA chelate $Cu(TTA)_2$ was prepared by adding the TTA-ethanol solution to the aqueous solution of copper and recrystallizing the resulting chelate from ethanol. The green crystalline solid was obtained by heating the copper-TTA chelate together with pyridine. Elemental analysis of the solid was given in Table 1. As is

Table 1. Elemental analysis of the adduct

	Cu(%)	C(%)	H(%)
Calculated*	9.56	46.7	2.71
Found	9.59	46.8	2.77

* Values for $Cu(TTA)_2(pyridine)_2$

seen in Table 1, the analytical results showed good agreement with the calculated value for $Cu(TTA)_2$-$(pyridine)_2$. These results indicate that the pyridine adduct is formed when the organic phase is treated with alkali solution containing pyridine and the formation of the adduct may prevent the copper-TTA chelate from decomposition.

Synergistic effect in the extraction of copper with TTA has been explained by the formation of an adduct.[14,15] Although the effect enhances the extractability of copper, the synergistic extraction is not suitable for the present case because co-extraction of divalent metal ions occurs. Therefore, the formation of the pyridine adduct should be performed at the stage after the completion of the extraction of the copper-TTA chelate.

Calibration Curve. Calibration curve obtained by the above mentioned procedure is linear for 0—1 ppm of copper in the organic phase and passes through the origin. The reproducibility of absorption mesurements is better than 1%. The sensitivity represented by Sandell's definition is 0.0023 $\mu g/cm^2$ at 340 mμ, which is nearly equal to that of the most sensitive dithizone method.[11] The sensitivity of the previous TTA method (0.7 $\mu g/cm^2$ at 430 mμ)[10] is remarkably improved. The present method is highly sensitive compared with the neocuproine method (0.008 $\mu g/cm^2$ at 457 mμ),[11] the diethyldithiocarbamate method (0.0046 $\mu g/cm^2$ at 436 mμ)[11] and the thiothenoyltrifluoroacetone method (0.01 $\mu g/cm^2$ at 490 mμ).[16]

Diverse Ions. The effect of diverse ions on the determination of copper was investigated by adding the known amount of test ion to a standard copper solution and by comparing the final absorbance with the standard. One milligram each of Ag(I), Ca(II), Cr(III), Mg(II), Mn(II), Pb(II), Sr(II), Tl(I), Zn(II), and 10 μg of Co(II) and Ni(II) gave no interference in the present method. Two hundred micrograms

14) H. Irving and D. N. Edgington, *ibid.*, **27**, 1359 (1965).
15) R. J. Casey, J. J. M. Fardy, and W. R. Walker, *ibid.*, **29** 1139 (1967).
16) Y. M. Shinde and S. M. Khopkar, *Anal. Chem.*, **41**, 342 (1969).

each of Al(III), Ce(III), Fe(III), Th(IV) interfered with the determination because of the formation of precipitate. However, these elements could be masked and kept in solution by adding 100 mg of fluoride ion.

Among anions, 100 mg each of fluoride and phosphate ions gave no interference, but the same amount of thiosulfate, thiocyanide, cyanide, tartrate and citrate ions interfered with the determination and could not be used for masking purpose.

Determination of Copper in Natural Waters. For determination of copper in natural water samples, 50 m*l* of the sample solution was taken and the general procedure was modified by adding 100 mg of fluoride ion (as NaF) before adjusting the pH. The analytical results are shown in Table 2. Recovery test and reproducibility indicate that the present procedure is applicable to these samples.

Table 2. Analytical results of natural water samples

Sample no.[a)]	Cu present[b)] (μg/m*l*)	Cu added (μg/m*l*)	Cu found[c)] (μg/m*l*)
1	0.102 ±0.009	0.100	0.201±0.004
2	0.0516±0.0039	0.100	0.154±0.015
3	0.0528±0.0022	0.100	0.154±0.002
4	0.0246±0.0041	0.100	0.135±0.045
5	0.0596±0.0035	0.250	0.335±0.017

a) Samples taken from the Watarase river.
b) Average value of 5 determinations and 95% confidence limit.
c) Average value of 3 determinations and 95% confidence limit.

This work was supported in part by Scientific Research Grant of the Ministry of Education.

BULLETIN OF THE CHEMICAL SOCIETY OF JAPAN, VOL. 44, 120—124 (1971)

Kinetics and Mechanism of Aquation and Anation of Some Amino Acid Pentamminecobalt(III) Complexes in Acid Aqueous Solutions

Tasuku MURAKAMI,[1a] Kazuko OGINO, Hiromi KOBAYASHI,[1a]
Hiroshi YAMAZAKI[1b], and Kazuo SAITO
Chemistry Department, Faculty of Science, Tohoku University, Sendai

(Received August 15, 1970)

Kinetics of aquation has been studied with pentamminecobalt(III) complexes containing aliphatic amino acids (γ-aminobutyric acid, ε-aminocaproic acid, α-amino-isobutyric acid, ornithine, and proline), aromatic acids (benzoate, anthranilic, and *p*-aminobenzoic acid), and α-substituted acetates (monochloroacetate and glycolate). Anation rate constants were obtained for glycine, β-alanine, and ε-aminocaproic acid, and equilibrium constants between $[CoH_2O(NH_3)_5]^{3+}$ and $[Co(NH_3)_5amH]^{3+}$ (amH=amino acid), K_{eq} were calculated. The free energy plot log k_{aq} *vs.* log K_{eq} gave a straight line with a gradient 0.6. This value has been discussed in terms of two possible mechanisms. The dependence of acid catalysed aquation rate constant, $k_H{}^+$ on pK_a of carboxylate group of the amino acid is written as log $k_H{}^+$=pK_a+const., while that for α-substituted acetates log $k_H{}^+$=0.5 pK_a+const. Such a difference in the slope is interpreted as due to the electrostatic influence of $-NH_3^+$ group of coordinated amino acid.

In our previous paper we reported on the kinetics of aquation of pentammine-amino acid cobalt(III) complexes, in which glycine, β-alanine, sarcosine, and betaine are combined with the cobalt(III) ion as unidentate through carboxylate oxygen.[2] The aquation had different characteristics from those of other carboxylate complexes.[3] We have now extended the study to some other pentammine cobalt(III) complexes containing various kinds of amino acid and α-substituted acetates, and the effect of positive charge of the ammonium group of coordinated amino acid upon aquation rate as well as the free energy relationship[4] has been discussed.

Aquation of amino acid pentamminecobalt(III) cations in an acid solution proceeds as follows:

$$[Co(NH_3)_5amH]^{3+} + H_2O \xrightarrow{k} [CoH_2O(NH_3)_5]^{3+} + amH \quad (1)$$

where amH denotes the amino acid. The pseudo first order rate constant k was obtained according to the method given in Experimental. When the values k are plotted against the concentration of perchloric acid, straight lines are obtained as exemplified in Fig. 1, the kinetics being expressed by

$$k = k_{H_2O} + k_{H^+}[H^+] \quad (2)$$

The intercept and the gradient correspond to k_{H_2O} and k_{H^+} respectively. The values are listed in Table 1.

Relationship between pK_a and k_{H^+}. The acid catalysed aquation of carboxylato and amino acid complexes is regarded to take place through the following two steps:

1) a) Present address; The Chemical Research Institute of Non-aqueous Solutions, Tohoku University, Sendai; b) Present Address; Research Institute, Japan Water Treatment Services Co., Hisamoto, Kawasaki.

2) K. Ogino, T. Murakami, and K. Saito, This Bulletin, **41**, 1615 (1968).

3) F. Basolo, J. G. Bergmann, and R. G. Pearson, *J. Phys. Chem.*, **56**, 22 (1952).

4) C. H. Langford, *Inorg. Chem.*, **4**, 265 (1965).

TABLE 1. RATE CONSTANT OF ACID-CATALYSED AND UNCATALYSED PATH OF THE AQUATION OF AMINO ACID AND α-SUBSTITUTED ACETATO PENTAMMINECOBALT(III) COMPLEXES (55°C)

Amino acid (other acid anion)	λ mμ	μ	k_{H_2O} 10^{-6}sec^{-1}	k_{H^+} 10^{-6}M^{-1}sec^{-1}	pK_a (25°C)
γ-Aminobutyric acid	285	0.1	0.2	32	4.03
		1.0	3.0	76	
ε-Aminocaproic acid	290	0.1	0.2	66	4.43
		1.0	4.0	140	
Proline	275	1.0	0.28	1.5	1.95
α-Amino-iso-butyric acid	280	1.0	0.18	1.3	2.36
Ornithine	275	0.1	0.5	≦1	1.94
		1.0	0.16	1.1	
Anthranilic acid	502	1.0	0.05	3.0	2.05
p-Aminobenzoic acid	502	1.0	1.4	15	2.38
Benzoate	315	1.0	1.0	28	4.20
Monochloroacetate	284	0.1	0.37	19	2.86
(65°C)			1.8	32	
(75°C)			6.2	130	
Glycolate	299	0.1	0.58	45	3.83
(65°C)			1.6	150	
(75°C)			8.0	440	

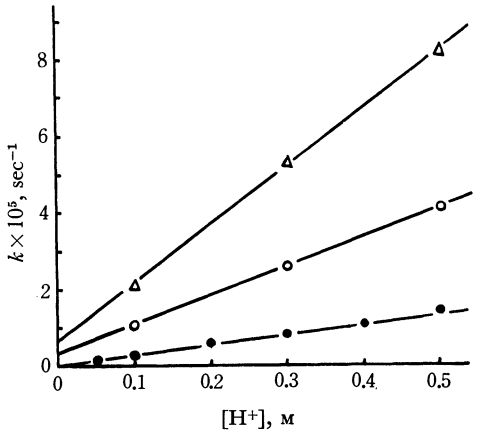

Fig. 1. Relationship between k_{obs} of aquation reactions and the hydrogen ion concentration. (55°C, μ=1.0)
—●— [Co $(NH_3)_5$ β-alaH]$^{3+}$ [2] —○— [Co $(NH_3)_5$ γ-ambutH]$^{3+}$ —△— [Co$(NH_3)_5$ ε-amcapH]$^{3+}$

$$[(NH_3)_5Co\text{-}O\text{-}\overset{\overset{O}{\|}}{C}\text{-}R]^{(n+2)+} + H^+ \overset{K}{\rightleftharpoons} [(NH_3)_5Co\text{-}O\text{-}\overset{\overset{OH}{|}}{C}\text{-}R]^{(3+n)+} \quad (3)$$

$$[(NH_3)_5Co\text{-}O\text{-}\overset{\overset{OH}{|}}{C}\text{-}R]^{(n+3)+} + H_2O \xrightarrow{k'} [(NH_3)_5CoH_2O]^{3+} + RCOOH^{n+} \quad (4)$$

and $$k_{H^+} = k'K. \quad (5)$$

In the previous paper we compared the k_{H^+} values of pentamminecobalt(III) complexes of glycine, sarcosine, and betaine and ascribed the small k_{H^+} value to the difficulty with which the protonated species are formed according to Eq. (3). Such a difficulty was considered to come from electrostatic effect due to ammonium group $-NH_xR_{3-x}^+$ rather than the hydrogen bonding between ammonium and carboxylate groups coordinated to cobalt(III).[2]

In Fig. 2, the log k_{H^+} values are plotted against

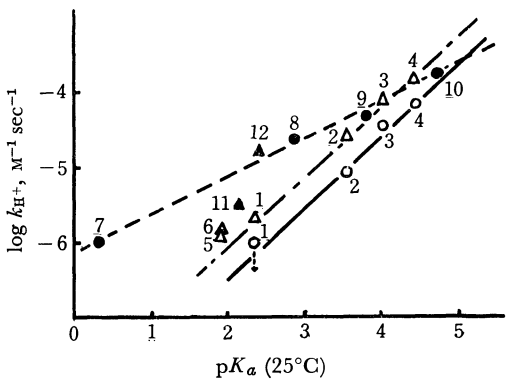

Fig. 2. Relationship between k_{H^+} of aquation reactions and pK_a of the ligands.
—○— (μ=0.1) and —△— (μ=1.0) [Co$(NH_3)_5$amH]$^{3+}$ 1. glycine,* 2. β-alanine,* 3. γ-aminobutyric acid, 4. ε-aminocaproic acid, 5. ornithine, 6. proline.
---●--- (μ=0.1)[Co$(NH_3)_5$(RCOO)]$^{2+}$ 7. trifluoroacetate,** 8. monochloroacetate, 9. glycolate, 10. acetate.**
—▲— (μ=1.0) [Co$(NH_3)_5$ aromatic amH]$^{3+}$ 11. anthranilic acid, 12. p-aminobenzoic acid.
* from Ref. 2. ** Ref. 3, values extrapolated to 55°C on the basis of $\Delta H^{\neq}$ values.

pK_a values of the acids. The diagram consists of two straight lines at a given ionic strength. Complexes of amino acids give one line with a gradient almost unity, and those of other α-substituted acetate anions, one with a gradient *ca.* 0.5. Aromatic amino acid complexes and benzoato complex fall on neither line. Complexes of glycolate and chloroacetate give plots on the line (broken line) together with acetato- and trifluoroacetato-complexes. The influence of substituting hydroxyl group and halogen atom seems to be appropriately reflected in pK_a values, and the kind of substituting group or atom give no particular influence upon k_{H^+} values.

Whenever the pK_a values are the same, the amino acid complexes give smaller k_{H^+} values than the substituted acetato complexes. The solid line in Fig. 2

indicates that the deviation from the broken line decreases with increase in carbon chain length between the $-NH_3^+$ and $-COO^-$ group of the amino acid, and is very small when the ammonium group is on the ε-carbon atom. It is noticeable that the complex of ornithine, which has two $-NH_3^+$ groups on α- and δ-carbon atom gives the plot on the same line as those of other amino acid complexes. The smaller k_{H^+} values of amino acid complexes must be due to the smaller tendency of forming protonated intermediate given by Eq. (3). Such a trend is brought about by the presence of $-NH_3^+$ group near the coordinated carboxylate. As the carbon chain length between $-NH_3^+$ and $-COO^-$ increases, the probability of such an approach would decrease because the freedom of rotation around the C–C axes increases. Our previous consideration that the electrostatic effect of $-NH_3^+$ group is reflected in the equilibrium constant K of Eq. (5), which is responsible in determining the k_{H^+} values, seems thus adequately reinforced.

There is a significant difference between k_{H^+} values of anthranilic and *p*-aminobenzoic acid complexes. The former gives a plot near the straight line for ω-amino acid complexes. Its $-NH_3^+$ group seems to be capable of giving a similar effect to that in ω-amino acids, because it is situated near the coordinated carboxylate. On the other hand, such an influence seems very unlikely for *p*-aminobenzoic acid complex.

The k_{H_2O} Values. Monacelli, Basolo, and Pearson reported that an antiparallel relationship is seen between the k_{H_2O} of carboxylatopentamminecobalt(III) complexes and the pK_a of the carboxylic acids.[3] Their results are well understood whenever the aquation takes place *via* S_N1(lim) mechanism, *i. e.* the ease with which the carboxylato-cobalt bond breaks depends fully on the bond strength predicted by the pK_a of the given acid. As shown in Fig. 3B, the k_{H_2O} values of ω-amino acid pentamminecobalt(III) ions do not seem to show significant difference from one another at an ionic strength 0.1. Neither do the α-substituted acetato complexes. At an ionic strength 1.0 (Fig. 3A), the k_{H_2O} seems to increase with rise of pK_a. Since the k_{H_2O} values are obtained by extrapolation, they can involve bigger experimental errors and may not be suitable for detailed discussion. However, the anthranilic acid- and the *p*-aminobenzoic acid complex give remarkably different values from each other, and a steric factor could be involved.

Relationship with the Equilibrium Quotient. The anation reaction of aquopentamminecobalt(III) complexes with amino acids (amH) is written as

$$[CoH_2O(NH_3)_5]^{3+} + amH \rightleftharpoons [Co(NH_3)_5amH]^{3+} + H_2O \quad (6)$$

and the rate constant k_{obs} is expressed by the following equation (see Experimental).

$$k_{obs} = k_{aq} + k_{an}[amH] \quad (7)$$

The k_{an} is obtained from the gradient of linear plot of k_{obs} *vs.* [amH], which stands for the concentration of amino acid zwitter ion (see Fig. 4). The equilibrium quotient K_{eq} is expressed by

$$K_{eq} = k_{aq}/k_{an} \quad (8)$$

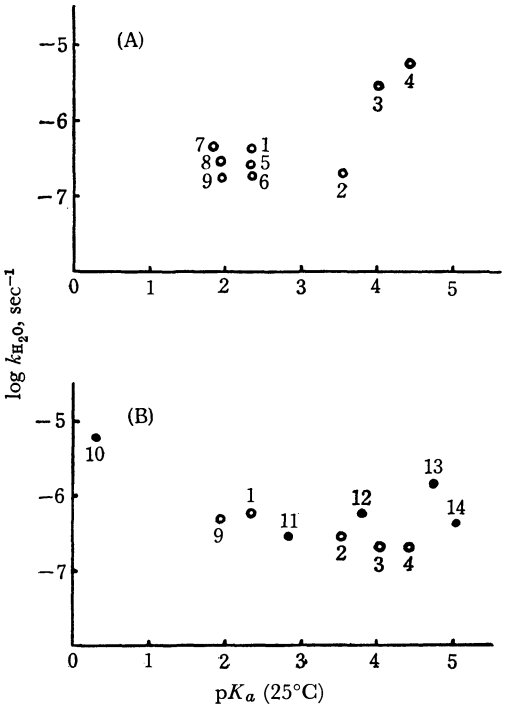

Fig. 3. Relationship between k_{H_2O} of aquation reactions and pK_a of the ligands. (55°C, (A), μ=1.0; (B), μ=0.1)
○ $[Co(NH_3)_5 amH]^{3+}$: 1. glycine,* 2. β-alanine,* 3. γ-aminobutyric acid, 4. ε-aminocaproic acid, 5. sarcosine,* 6. α-amino-iso-butyric acid, 7. betaine,* 8. proline, 9. ornithine.
● $[Co(NH_3)_5(RCOO)]^{2+}$: 10. trifluoroacetate,** 11. monochloroacetate, 12. glycolate, 13. acetate,** 14. trimethylacetate.** * from Ref. 2. ** Ref. 3, values extrapolated to 55°C.

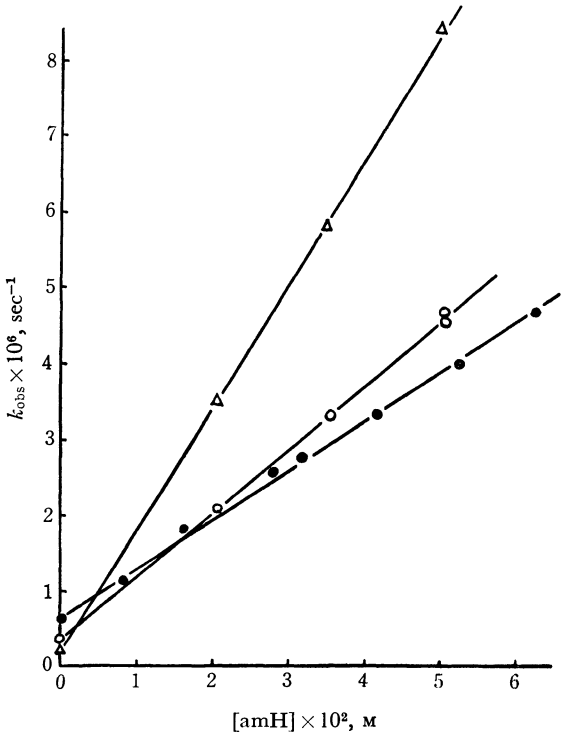

Fig. 4. Relationship between the k_{obs} of anation reactions and the concentration of amino acid zwitter ion. (55°C, μ=0.1)
—●— $[Co(NH_3)_5$ glyH$]^{3+}$ —○— $[Co(NH_3)_5$ β-alaH$]^{3+}$
—△— $[Co(NH_3)_5$ ε-aminocapH$]^{3+}$

In Table 2 are given k_{an} and K_{eq} values of some ω-amino acid pentamminecobalt(III) complexes.

Langford[4] and Haim[5] examined the linear free energy relationship[6] between the equilibrium quotient and the rate constant for aquation reactions of various acidopentamminecobalt(III) complexes and obtained a gradient unity on their log-log plot,

$$\Delta \ln k_{aq} = \alpha \Delta \ln K_{eq} \qquad (9)$$

Langford claimed that this value suggests a similarity between the transition state and the product, and that the role of the acido anion ligand in the transition state is very similar to that in the product, *i. e.* the solvated anion.

Table 2. Rate constants of anation and equilibrium quotients of aquation-anation reactions of some $[Co(NH_3)_5amH]^{3+}$ complex ions

Ligand	k_{an} $10^{-5}M^{-1}sec^{-1}$	k_{aq} $10^{-6}sec^{-1}$	K_{eq} $10^{-3}M$
Glycine	7±0.5[a]	0.57[b]	8.1[c]
(65°C)	25±1	1.8[b]	7.2
(75°C)	92±3	7.6[b]	8.3
β-Alanine	8.5	0.3[b]	3.5
ε-Aminocaproic acid	16	0.2	1.3

(55°C unless otherwise stated, μ=0.1)
a) The ΔH^* is 29 kcal/mol. b) from Ref. 2. c) $\Delta H^\circ \fallingdotseq 0$

A similar plot of our results for ω-amino acid pentamminecobalt(III) complexes is shown in Fig. 5. Although the number of plots is only three, an apparent α value 0.6 is obtained. The difference between this value and that for acidopentamminecobalt(III) complexes[4,5] seems significant, although the experimental conditions are not the same (data compiled by Haim[5] are at 25°C, ionic strength variable; ours at 55°C, ionic strength 0.1). It appears as if the transition state in the aquation of $[Co(NH_3)_5amH]^{3+}$ is between the initial and the final state of the reaction. We are thus inclined to consider that some mechanism such as solvent-assisted dissociation mechanism[7] is involved in the k_{H_2O} path. This mechanism was also suggested by Lincoln and Stranks[8] for the aquation of $[Co(NH_3)_5H_3PO_4]^{3+}$ in perchloric acid of medium strength. They found a good correlation between the aquation rate and the activity of water.

Haim[5] discussed the relation between k_{aq} and K_{eq} and gave the equation

$$\log k_{aq} = \log k_x Q_0 - \log K_{eq} \qquad (10)$$

where Q_o is the ion pair or outer sphere complex formation constant between $[CoH_2O(NH_3)_5]^{3+}$ and the incoming ligand, and k_x the inner sphere-outer sphere interchange velocity of the ion pair. He claimed that Q_o is principally dependent on the charge of the complex and the incoming ligand, and applied this correlation

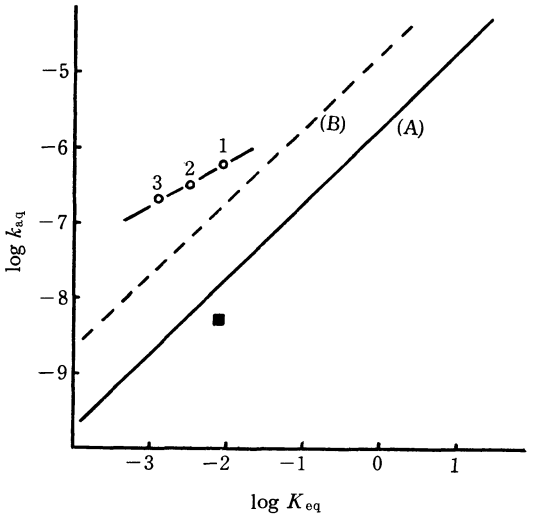

Fig. 5. Linear free energy relationship between the equilibrium quotient K_{eq} and the rate constant for aquation, k_{aq}.
—○— $[Co(NH_3)_5amH]^{3+}$ (55°C, μ=0.1): 1. glycine, 2. β-alanine, 3. ε-aminocaproic acid.
■ for $[Co(NH_3)_5glyH]^{3+}$ extrapolated to 25°C on the basis of ΔH^* and ΔH° value in Table 2.
—— (A) $[Co(NH_3)_5X]^{2+}$ (X, univalent anions, 25°C[5])
------ (B) $[Co(NH_3)_5Y]^{+}$ (Y, bivalent anions, 25°C[5])

to acidopentamminecobalt(III) complexes containing uni- and bivalent anions.

In the case of our amino acid complexes, Q_o is the outer sphere complex formation constant between $[CoH_2O(NH_3)_5]^{3+}$ and the amino acid zwitter ion. Although the net charge of an amino acid is zero, the zwitter ion has a separated minus charge on the carboxylate part, and can undergo ion-pair formation with multivalent complex cation.[9] However, the Q_o values for varying amino acids could be different, because the electrostatic effect of $-NH_3^+$ can differ according to the carbon chain length between $-NH_3^+$ and $-COO^-$ group. If Q_o increased with increase in this carbon chain length, the gradient of our diagram could deviate from unity, even if the inner sphere-outer sphere interchange velocity of the ion pair k_x were the same as those of uni- and bivalent incoming ligand. Hence the smaller α value (0.6) of our diagram does not necessarily indicate the participation of solvent assisted dissociation. These two possible interpretations cannot be distinguished at the present stage.

The ΔH^* value for anation reaction to give $[Co(NH_3)_5glyH]^{3+}$ was obtained to be 29 kcal/mol (Table 2). It is near that for the water exchange of $[CoH_2O(NH_3)_5]^{3+}$ ions,[10] which should involve cobalt-oxygen bond rupture. We can relevantly presume that our reactions also involve cobalt-oxygen bond rupture and formation. The same presumption was made in our previous paper[2] on the basis of comparison among ΔH^* values of $[Co(NH_3)_5glyH]^{3+}$,[2] $[Co(NH_3)_5(CH_3-$

5) A. Haim, *Inorg. Chem.*, **9**, 426 (1970).
6) J. E. Leffler and E. Grunwald, "Rates and Equilibrium of Organic Reactions," J. Wiley of Sons, New York (1963), p. 156.
7) R. G. Pearson and R. D. Lanier, *J. Amer. Chem. Soc.*, **85**, 765 (1964).
8) S. F. Lincoln and D. R. Stranks, *Austr. J. Chem.*, **21**, 67 (1968).
9) When the plot of $[Co(NH_3)_5glyH]^{3+}$ (glyH=glycine zwitter ion) in Fig. 5 is shifted from 55°C to 25°C on the basis of ΔH^*[2] and ΔH° value (Table 2), the plot given by full square is obtained. Since the net charge of glycine zwitter ion is zero, the Q_o value should be smaller than those for univalent anionic ligands.
10) H. R. Hunt and H. Taube, *J. Amer. Chem. Soc.*, **80**, 2642 (1958).

COO)]$^{2+}$,[11] and $[Co(NH_3)_5(HCO_3)]^{2+}$.[12,13] If a tracer study with ^{18}O were substantiated with our complexes, unambiguous conclusion could be obtained. Unfortunately, the oxygen exchange rate of free amino acid in water and the water exchange rate of $[CoH_2O(NH_3)_5]^{3+}$ are much greater than the aquation rate of $[Co(NH_3)_5amH]^{3+}$ ions in neutral and acid solutions and such a tracer study would not be very useful.

Experimental

Materials. Cobalt(III) pentammine complexes containing aliphatic amino acids were synthesized as perchlorate from $[CoH_2O(NH_3)_5](ClO_4)_3$ and the amino acids by the method of Fujita *et al.*[14] and identified by the analysis of carbon, hydrogen, and nitrogen, and visible and ultraviolet absorption spectra. Complexes containing aminobenzoic acids[15,16] and α-substituted carboxylates[2,17] were prepared by the methods given in literature. All other chemicals were of guaranteed grade and used without further purification.

Kinetic Runs. Aquation rate was measured spectrophotometrically at the given wavelengths (Table 1) as described previously.[2] Aromatic amino acids have marked absorptions in the ultraviolet region in the free state, and the reaction was followed at the *d–d* transition region.

The rate of anation given by Eq. (6) is expressed by the ordinary second order rate formula

$$dx/dt = k_{an}(a-x)(b-x) - k_{aq}x \qquad (11)$$

where x is the concentration of $[Co(NH_3)_5amH]^{3+}$ ion at time t, and a and b are the initial concentrations of $[CoH_2O(NH_3)_5]^{3+}$ and the amino acid in zwitter ion form, respectively. The last is known from the formal concentration and the acid dissociation constant under the given condition. Whenever b overwhelms a, Eq. (11) is integrated to give

$$\ln[(x_\infty - x)/x_\infty] = -(k_{aq}+bk_{an})t \qquad (12)$$

where the suffix ∞ denotes the equilibrated state. When the anation is measured by a spectrophotometric method, Eq. (12) is replaced by

$$\ln[(A_\infty - A_t)/(A_\infty - A_0)] = -(k_{aq}+bk_{an})t \qquad (13)$$

where A_0, A_t, and A_∞ are the extinctions of the reaction mixture at the initial state, time t and the final state, respectively. By plotting $\log(A_\infty - A_t)$ *vs.* t, the apparent rate constant k_{obs} given by Eq. (7) is obtained. The A_∞ value was not experimentally determined because the reaction was very slow. A tentative A_∞ was calculated on the basis of an assumed K_{eq},

$$K_{eq} = k_{aq}/k_{an} = (a-x_\infty)(b-x_\infty)/x_\infty \qquad (14)$$

and k_{obs} and k_{an} were obtained by means of Eqs. (13) and (7). The K_{eq} and A_∞ values were recalculated from this k_{an}. Such a stepwise approximation was repeated until a set of self-consistent k_{an} and K_{eq} was obtained.

Anation reactions were studied in weakly acid solutions (pH∼pK_a), where k_{H^+} path of aquation is negligible compared to k_{H_2O} path and k_{aq} can be approximated to be equal to k_{H_2O}. The rate was followed at the same wavelength at which the aquation was studied.

11) F. Monacelli, F. Basolo, and R. G. Pearson, *J. Inorg. Nucl. Chem.*, **24**, 1241 (1962).
12) T. P. Dasgupta and G. M. Harris, *J. Amer. Chem. Soc.*, **90**, 6360 (1968).
13) D. V. Francis and R. B. Jordan, *ibid.*, **89**, 5591 (1967).
14) J. Fujita, T. Yasui, and Y. Shimura, This Bulletin, **38**, 654 (1965).
15) E. S, Gould, *J. Amer. Chem. Soc.*, **87**, 4730 (1965).
16) E. S. Gould and H. Taube, *ibid.*, **86**, 1318 (1964).
17) R. D. Butler and H. Taube, *ibid.*, **87**, 5597 (1965).

The Reactions of Aroyl Peroxides with Grignard Reagents. II. Relative Reactivities of Substituted Benzoyl Peroxides.[1]

Masao Ōkubo,* Kazuhiro Maruyama,** and Jirō Ōsugi**

* *Government Industrial Research Institute, Nagoya, Kita-ku, Nagoya*

** *Department of Chemistry, Faculty of Science, Kyoto University, Sakyo-ku, Kyoto*

(Received October 20, 1969)

Benzoyl peroxide was found to react with Grignard reagents (RMgBr) in tetrahydrofuran at 0°C to form PhCOOR and PhCOOMgBr. The latter which was isolated as a complex containing two molecules of the solvent, can be coordinated by benzoyl peroxide to form an orange-colored complex. Similar complexes were found to be formed in the cases of some substituted benzoyl peroxides. The initial stage of the reaction was studied with the technique of competitive reaction. The results can be explained by assuming the coordination of the carbonyl oxygen atom of benzoyl peroxide to the Grignard magnesium atom. The effect of the substituent of the peroxide on the reaction was discussed.

The reactions of the carbanionic reagents with the peroxidic linkage are interesting, but scarcely any have been investigated so far.[2] We found that, when benzoyl peroxide was added to the tetrahydrofuran (THF) solution of phenylmagnesium bromide (PhMgBr), a pink color and the ESR signal were observed simultaneously.[3] This aroused our interest, and we investigated the reaction of aroyl peroxides with Grignard reagents. A stable complex containing benzoyl peroxide has been reported.[4] The initial stage of the reaction was investigated using the technique of competitive reaction, and the results are reported in this paper.

Results and Discussions

When benzoyl peroxide (BPO, 0.00184 mol in 50 m*l* THF) was mixed with nearly equimolar PhMgBr (0.612M, 3 m*l*) in THF (20 m*l*) under nitrogen stream at 0°C, about two thirds of BPO decomposed suddenly and the reaction mixture turned orange after being left to stand for about 2 hr. The products were benzoic acid (85—93%), phenyl benzoate(55—60%), small amounts of phenol, benzophenone and triphenylcarbinol. The orange color did not fade by contact with air, and it was confirmed to be not due to molecular bromine. Considering the products obtained in the preliminary experiment, we can construct the following reaction scheme (1) and (2)(R=Ph), though the reaction (2) is not yet confirmed.[5]

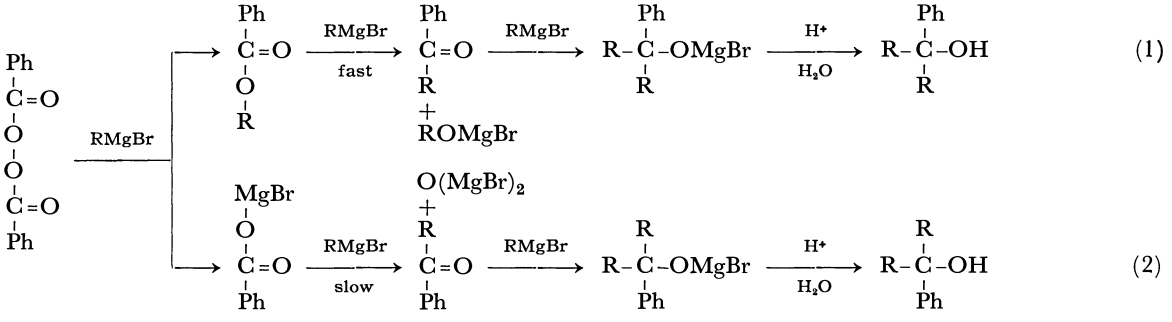

These formulas suggest that at least five moles of Grignard reagent is necessary to decompose one mole of benzoyl peroxide completely to form carbinol. When benzoyl peroxide in THF was added to the stirred solution of ten times moles of PhMgBr (solvent THF) under nitrogen stream, a pink color appeared after a few minutes. The color deepened gradually and did not fade after being left to stand overnight. Thus, the pink color and ESR signal can be attributed to the product resulting from interaction of PhMgBr with benzophenone which is produced during the course of the reaction.[6]

On the Complex Containing Peroxide. In the preceding paper,[4] it was reported that two complexes were isolated from the reaction between BPO and PhMgBr, white (Complex I) and orange (Complex II). The formulas previously proposed are written in an over-simplified form.[7] We should examine whether complexes similar to Complex II are formed in the reaction between analogous peroxides and other Grignard reagents.

When methyl- or ethylmagnesium bromide in THF was added to the solution of equimolar BPO, the mixture turned to a similar orange and Complex II was obtained. Substituted benzoyl peroxides such as

1) This work was carried out in the Department of Chemistry, Faculty of Science, Kyoto University.

2) N. C. Yang and S.-O. Lawesson, *J. Amer. Chem. Soc.*, **81**, 4230 (1959).

3) K. Maruyama and M. Ōkubo, unpublished work.

4) M. Ōkubo, K. Maruyama, and J. Ōsugi, This Bulletin, **42**, 1162 (1969).

5) Reaction (2) was confirmed later to proceed but much more slowly than reaction (1). See Experimental.

6) More details on this phenomenon will be published elsewhere. See K. Maruyama, This Bulletin, **37**, 897 (1964).

7) Their more precise structures will be discussed in the following paper.

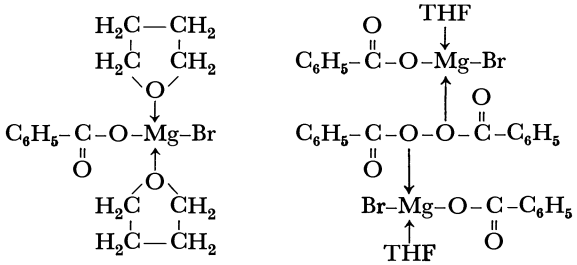

(Complex I) (Complex II)

p-methyl-, *p,p'*-dimethyl-, *p*-methoxy-, *p,p'*-dimethoxy-, *p*-fluoro-, and *p,p'*-difluorobenzoyl peroxides revealed a similar behavior when they were treated with equimolar PhMgBr. Of these, symmetrically substituted peroxides easily formed orange crystals when the reaction mixtures were left to stand for about 2 hrs at room temperature. However, with the unsymmetrically substituted peroxides, crystallization was difficult even though the solutions colored similarly. Furthermore, when *t*-butyl perbenzoate[2] in THF was added dropwise to the equimolar PhMgBr solution, it turned orange during the course of the reaction and faded by the time the addition was completed. This is also an indication of the transient formation of a similar complex to Complex II.

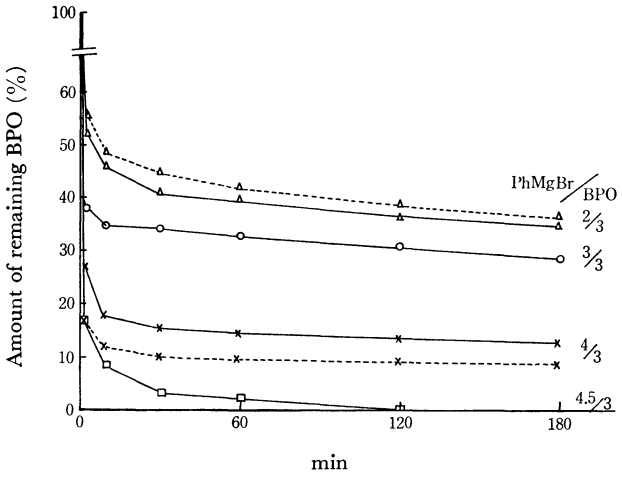

Fig. 1. Effect of molar ratio.
Temperature, 0°C Concentration, 0.007 mol/*l* (PhMgBr/BPO=3/3)

Effect of the Molar Ratio. Complex I was obtained when the molar ratio of PhMgBr : BPO was 1.5 : 1.0, while Complex II was obtained when it was 1 : 1.[4] Thus it is clear that the molar ratio of the two reactants has a remarkable effect on the course of reaction. Effect of the molar ratio on the consumption of BPO in the reaction system is shown in Fig. 1. The solid lines in Fig. 1 show the results obtained from the experiments when the amount of PhMgBr is fixed to 0.007 mol/*l* and that of BPO is varied, while the dotted lines show the results for the fixed amount of BPO and the varied amounts of PhMgBr. The difference between the solid and dotted lines for the same molar ratio shows the effect of concentration of the Grignard reagent. It should be noted that all the curves have creases between the initial and the second stages of the reaction. If the molar ratio is 3 : 3, the crease appears at the point where 35—37% of BPO remained, and hereafter the decomposition of BPO is markedly slowed down. The slow decomposition of BPO in the second stage may be attributed to the fact that benzoyl peroxide is stabilized through its complex formation with the reaction products, namely Complex I. If the molar ratio is 2 : 3, the crease rises up to 52—57% of remaining BPO, and the curve then goes down gradually to 33% of remaining BPO. If the molar ratio is 4 : 3, the crease falls down to 17—25% of remaining BPO. If 1.5 times molar Grignard reagent to the peroxide is used, BPO is completely decomposed after 2 hr. Though it is not shown in Fig. 1, when the two reactants were mixed at −15°C, the crease of the curve for the molar ratio of 2 : 3 rose up to about 66% of remaining BPO, and that for 4 : 3 to about 30%. If the molar ratio is 2 : 3, the reaction mixture turns orange very soon after mixing. Two conclusions can be derived from these facts; (i) Complex II is formed most effectively if the molar ratio is 2 : 3 and this ratio agrees with the composition of Complex II, (ii) twice moles of the Grignard reagent seems to be necessary for the rapid decomposition of one mole of Complex II.

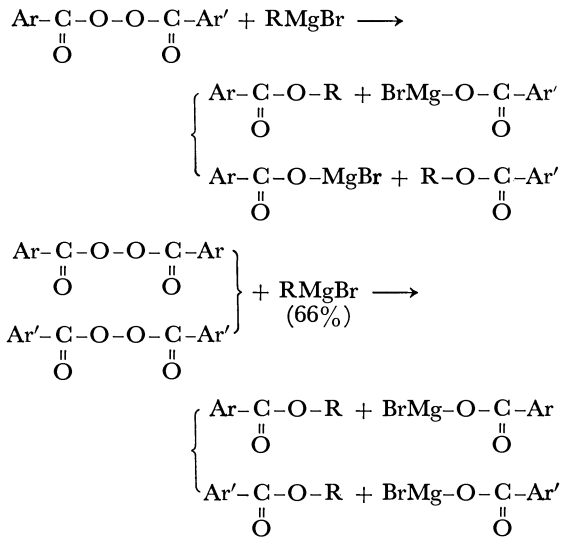

Table 1. Competitive reactions of substituted BPO with MeMgBr

Exp. No.	Peroxide	RMgBr	Ester	Molar ratio of esters
1.	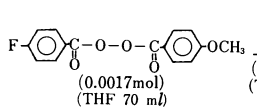 (0.0017mol) (THF 70 ml)	MeMgBr (0.0017mol) (THF 20 ml)	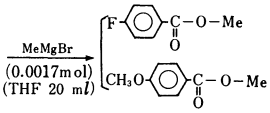	1.00 0.82
2.	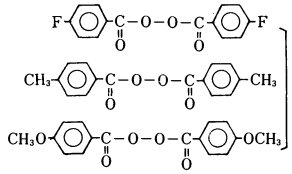	MeMgBr (66%)	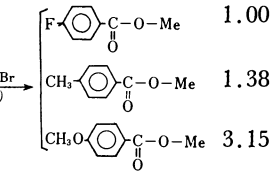	1.00 1.38 3.15

Table 2. Competitive reactions of substituted BPO with PhMgBr

Exp. No.	Peroxide	RMgBr	Ester	Molar ratio of esters
3.	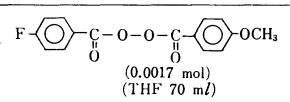 (0.0017 mol) (THF 70 ml)	PhMgBr (66%)	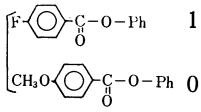	1.00 0.52
4.	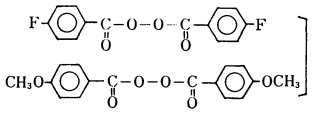	PhMgBr (0.0017 mol) (THF 20 ml)	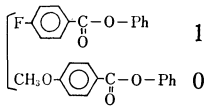	1.00 0.93

Table 3. Competitive reactions of acyl benzoyl peroxide with PhMgBr

Exp. No.	Peroxide	RMgBr	Ester	Molar ratio of esters
5.	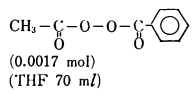 (0.0017 mol) (THF 70 ml)	PhMgBr (0.0017mol) (THF 20 ml)	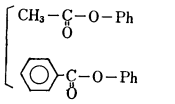	3.28 1.00
6.	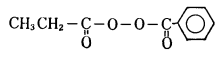	PhMgBr	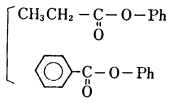	3.55 1.00
7.	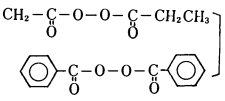	PhMgBr (66%)	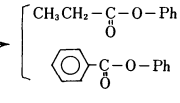	1.60 1.00

Table 4. Other competitive reactions

Exp. No.	Peroxide	RMgBr	Ester	Molar ratio of esters
8.	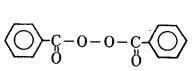	PhMgBr MeMgBr	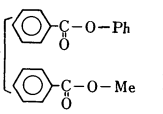	1.00 1.32
9.	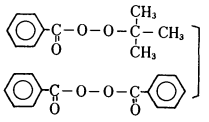	PhMgBr (66%)	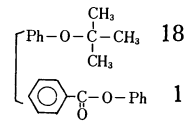	18.1 1.00

Effect of the Structure of Peroxide. The technique of competitive reaction was applied to investigate the first stage of the reaction. The experiments were conducted at −15°C. Although just equivalent moles of two reactants were used for the reaction between unsymmetrical acyl peroxide and the Grignard reagent, 66% equivalent moles of the Grignard reagent to the total moles of peroxides were mixed for the comparison of the reactivities of the two symmetrical peroxides.[8] Relative amounts of esters produced were used as a measure of the reactivity. The results are summarized in Tables 1, 2, 3 and 4.

Since RMgBr in THF is coordinated by solvent molecules, the initial stage of the reaction should be the replacement of THF molecules by peroxide molecules. The results of experiments Nos. 2, 4, and 7 may be used as a measure of the relative facility of the coordination of each peroxide. 2 and 7 show that the electron-donating substituent accelerates the reaction. If the results of 4 and 2 are compared, the difference between the yields of two esters is negligibly small in the case of PhMgBr. This seems to be explained on the basis of the following : —first, the phenyl group which is bulkier than the methyl group would make it difficult for PhMgBr-species to be coordinated by peroxide molecules, and would reduce the difference of the yields of phenyl esters. Second, the donation of π-electrons of the phenyl group would also bring about the same effect. Salinger and Mosher[9] found that the infrared absorption band of C_{Ph}-Mg bond appeared at 370—380 cm^{-1} and that of C_{Me}-Mg bond at 500—535 cm^{-1}, respectively. This means that the C_{Ph}-Mg bond is stronger than the C_{Me}-Mg bond. However, it is conceivable that the phenyl group might donate its π-electrons to the vacant *p*- and *d*-orbitals of magnesium atom, and then reduce the positive charge on the magnesium atom. Thus, the facility of the coordination of peroxide molecules to magnesium atom may be more strongly affected in the case of MeMgBr (No. 2) than in the case of PhMgBr (No. 4). The result of No. 8 supports the results.[10] Following the coordination of the peroxide molecule to the Mg-atom, the displacement of carbanionic alkyl or aryl group of Grignard reagent takes place so to form the esters of carboxylic acids. The difference between the values of 0.82(No. 1) and 0.52(No. 3) may also be ascribed to the smaller polarizability of C_{Ph}-Mg bond or to the bulkiness of the phenyl group, both of which may cause a higher selectivity to diaplacement of the carbanionic phenyl group from Mg-atom of Grignard reagent to one of the oxygen atoms in the peroxide molecule. The carbonyl and peroxidic oxygen atoms of peroxide molecules could not be distinguished in the discussions.

8) As the initial stage of reaction is very fast, even the less reactive peroxide was readily decomposed almost completely when the 100% equivalent moles of the Grignard reagent to the total moles of peroxides were used. When 2/3 mol of PhMgBr were used, unreacted BPO (1/3 mol) was converted into Complex II completely by the interaction with PhCOOMgBr (Complex I) produced.

9) R. M. Salinger and H. S. Mosher, *J. Amer. Chem. Soc.*, **86**, 1782 (1964).

10) The p_π-p_π and p_π-d_π delocalizations which have been proposed to explain the lower reactivities of vinyl-substituted boranes and silanes may be the same as the π-donation discussed here. cf. J. J. Eisch, "The Chemistry of Organometallic Compounds," Macmillan Co., New York (1967), Chap. IV.

The results of the intramolecular competitive reactions, Nos. 1, 3, 5, and 6 are considered to provide information on the facility of displacement of alkyl or aryl groups. At this stage, the possibility of the so-called four-center-type reaction as shown in formula

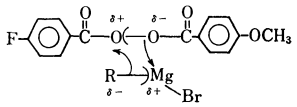

(3)

(3) may be small, since the actual Grignard reagent must have considerable bulkiness due to the coordination of solvent molecules. Thus, the six-membered ring structure for the transition state is more probable. If the carbonyl oxygen coordinates to Mg-atom, the mechanism is expressed as shown in formula (4). Another possible mechanism in which the peroxidic oxygen atom coordinates to Mg-atom is shown in formula (5). Both mechanisms lead to the same products. However, it may be difficult for the latter to occur

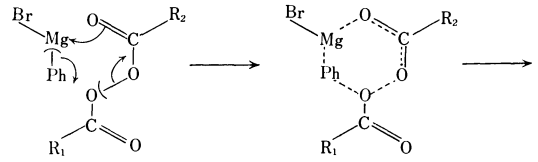

(4)

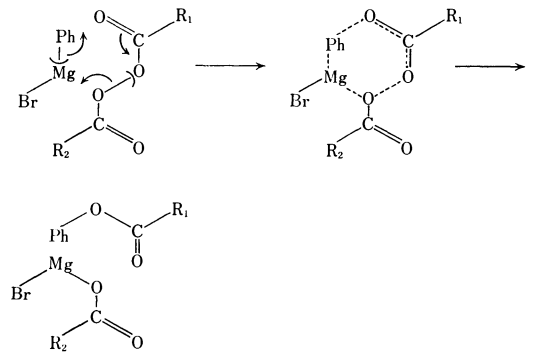

(5)

when the result of experiment No. 9 is taken into account. The fact that *t*-butyl perbenzoate is known to react with equimolar PhMgBr to produce exclusively *t*-butyl phenyl ether,[2] is explained solely by assuming the transition state in which the magnesium atom of the Grignard reagent is coordinated by the carbonyl oxygen atom as shown in formula (6). The predominant formation of *t*-butyl phenyl ether over phenyl benzoate in No. 9 is thus interpreted on the same assumption. The fact that di-*t*-butyl peroxide cannot react with PhMgBr under the same conditions,[2,11] means that peroxidic oxygen atoms are difficult to coordinate to the magnesium atom. Thus, the transition state can best be expressed by formula (4).

11) See experimental section. Baeyer and Villiger (*Ber.*, **33**, 3387 (1900)) observed that diethyl peroxide could not be decomposed by even sodium metal.

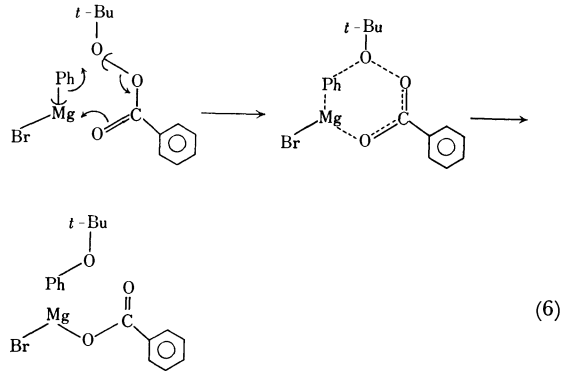

(6)

From this consideration, the more favorable structure for the transition state of No. 5 and No. 6 is expressed by formula (4) in which R_1 is CH_3 or CH_3CH_2 and R_2 is C_6H_5. Similarly, the results of No. 1 and No. 3 are expressed by formula (4) in which R_1 is *p*-FC_6H_4 and R_2 is *p*-$CH_3OC_6H_4$. These results cannot be interpreted if one assumes that the carbonyl group bearing the inductively more electron-donating substituent coordinates predominantly to Mg-atom. On the contrary, as shown in the above discussions, the "electromerically" more electron donating substituent favors the adjacent carbonyl group to coordinate to Mg-atom. Thus, the reaction of aroyl peroxides with the Grignard reagents can be illustrated by considering the electromeric polarizabilities caused by coordination of both the reagents.

Experimental

Grignard Reagents. THF solutions of phenyl-, ethyl- and methylmagnesium bromides were prepared in the usual manner using an excess of magnesium metal. They(about 0.5M, 300 ml) were stored in a tightly stoppered bottle and left standing overnight. A portion of clear solution was pipetted out, and its concentration was determined by alkaline titration.[12] Br^- and Mg^{2+} were also titrated by $AgNO_3$ and oxine-chelate[13] methods, respectively. Three values agreed with each other.

Peroxides. Commercial BPO was examined for its peroxide-content by iodometry, and purified, if necessary, by dissolving in chloroform and reprecipitated by methanol. *p,p'*-Difluoro-, *p,p'*-dimethyl- and *p,p'*-dimethoxy derivatives were prepared by treatment of the corresponding acid chlorides with sodium peroxide.[14] *p*-Fluoro-*p'*-methoxy derivative was prepared from sodium *p*-methoxyperbenzoate and *p*-fluorobenzoyl chloride.[15] *p*-Fluoro-, *p*-methyl- and *p*-methoxybenzoyl peroxides were prepared in the same manner from sodium perbenzoate and the corresponding acid chlorides. However, the differences in yields of the corresponding methyl esters on the reactions with MeMgBr were very small and the peroxide were not used.

Acetyl benzoyl peroxide and propionyl benzoyl peroxide were prepared by aerating the mixtures of acetic and/or

12) H. Gilman, P. D. Wilkinson, W. P. Fishel, and C. H. Meyers, *J. Amer. Chem. Soc.*, **45**, 150 (1923).

13) I. M. Kolthoff and E. B. Sandell, "Textbook of Quantitative Inorganic Analysis," Macmillan Co., N. Y. (1955), pp. 362, 607.

14) C. G. Swain, W. H. Stockmayer, and J. T. Clarke, *J. Amer. Chem. Soc.*, **72**, 5426 (1950).

15) J. E. Leffler and C. C. Petropoulos, *ibid.*, **79**, 3068 (1967).

propionic anhydride and benzaldehyde.[16] Dipropionyl peroxide was prepared by treating propionic anhydride with sodium peroxide.[17] *t*-Butyl perbenzoate was obtained by treating *t*-butyl hydroperoxide with benzoyl chloride and sodium hydroxide.[18] Di-*t*-butyl peroxide was prepared by adding *t*-butyl hydroperoxide to a cooled mixture of *t*-butyl alcohol and sulfuric acid.[19]

Reactions of Aroyl Peroxides with Grignard Reagents. From reaction schemes (1) and (2), we see that the primary products of the reaction are PhCOOMgBr and PhCOOPh (from BPO and PhMgBr). Phenyl benzoate reacts easily with the remaining Grignard reagent to produce benzophenone, which again reacts to produce triphenylcarbinol. It is necessary, therefore, to avoid these reactions as far as possible. Thus, the reaction flask as shown in Fig. 2 was used throughout

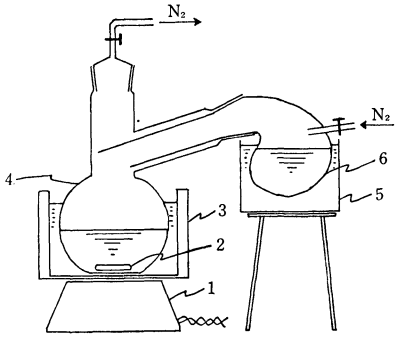

Fig. 2. Reaction flask for rapid mixing.
1. magnetic stirrer
2. stirring rod
3. ice bath
4. reaction flask (peroxide solution)
5. ice bath
6. reservoir (Grignard solution)

this work. After air in the flask was replaced with nitrogen and the equimolar peroxide and Grignard reagent were cooled to the desired temperature, the resevior was turned upside-down with vigorous stirring of the peroxide solution. After mixing, the one m*l* portions of the mixture were pipetted out at definite time intervals and quickly introduced into a CO_2-purged flask containing acetic acid and potassium iodide. The mixture was titrated with a standard thiosulfate solution according to Wibaut.[20] For comparison, di-*t*-butyl peroxide was added to PhMgBr and the mixture was left standing for 2 hr,* but the peroxide was recovered and no product other than benzene was detected.

The Competitive Reaction. Mixing of perodixe solution with Grignard reagents was conducted by using the devide in Fig. 2. After stirring for 30 min, the reaction mixture was concentrated and decomposed with ammonium chloride. Neutral products were extracted with ether, dried with anhydrous magnesium sulfate, and concentrated to an appropriate volume. For gas-chromatographic analysis, a suitable substance was added as an internal standard. The mixture of known amounts of authentic samples was analyzed under the same gas-chromatographic condition for the calculation of the calibration factor.

In experiments Nos. 2, 4, 7, and 9, in which 66% equivalent amounts of Grignard reagent were used, a considerable amount of peroxides were not decomposed. Since they might interfere with gas-chromatographic analysis, they had to be removed. For this purpose two methods were used. The first was to decompose the peroxide by treating with hydroquinone and palladium-black according to Wieland.[21] Peroxide can easily decomposed to benzoic acid (and its derivatives), and they were removed by alkaline extraction. However, there was some difficulty, since benzoquinone, which is formed from hydroquinone through hydrogen-fransfer, gave a large quantity of precipitates from a concentrated sample solution for gas-chromatographic analysis. The other method was as follows: peroxide which remains as Complex II (or its derivatives) can be almost quantitatively precipitated from the concentrated reaction mixture by addition of a sufficient amount of dry ethyl ether.[4] The precipitate was collected on a glass-filter and washed throughly with dry ether. The filtrate was concentrated for gas-chromatographic analysis.

Reaction of Complex I with PhMgBr. Five milliliters of *ca.* 0.5M PhMgBr was pipetted into a N_2-purged flask and diluted with 20 m*l* of THF. The solution was vigorously stirred and carbon dioxide was introduced. After the absorption of carbon dioxide was completed, 10 m*l* of PhMgBr (0.5M) was added and stirred gently. After a few hours the solution turned wine-red. The color faded after being left standing overnight. The solution was concentrated and decomposed with ammonium chloride. The products were benzoic acid (0.38 g), and the mixture of benzophenone and triphenylcarbinol (1.1 g). The latter was confirmed with TLC.

16) Yu. A. Ol'dekop, A. N. Sevchenko, I. P. Zyat'kov, and A. I. El'nitzkii, *Zh. Obshch. Khim.*, **31**, 2904 (1961).
17) A. Rennubaum and M. Szwarc, *J. Chem. Phys.*, **23**, 909 (1955).
18) N. A. Milas and D. M. Surgenor, *J. Amer. Chem. Soc.*, **68** 642 (1946).
19) N. A. Milas and D. M. Surgenor, *ibid.*, **68**, 205 (1946).
20) J. P. Wibaut, H. B. van Leeuwen, and B. van der Wal, *Rec. trav. chim.*, **73**, 1033 (1954).
21) H. Wieland, *Ber.*, **54**, 2369 (1921).

The Thermal Isomerization of Pinane and Its Products

Juntaro TANAKA, Takao KATAGIRI, and Kiyomi OZAWA[1]

Department of Synthetic Chemistry, Faculty of Engineering, Shizuoka University, Hamamatsu-shi

(Received March 6, 1970)

The stereochemistry of the reduced products of the iridenes was studied, and the main product produced by the thermal isomerization from pinane was confirmed to be 1-*trans*-2-dimethyl-*trans*-3-isopropenylcyclopentane, unlike as in the literatures. Moreover, the ozonolyses of the iridenes were reexamined in detail, and the following results were obtained: 1) When the ozonides were decomposed with Na_2CO_3-H_2O_2, the substituent on C-3 was epimerized. 2) On the other hand, when the ozonides were treated with Zn-CH_3COOH, no such epimerization occurred. Consequently, it was found that the former method when used for the confirmation of iridenes, did not give good results for assignments of these compounds.

l-cis-Pinane was isomerized at a high temperature to 3,7-dimethyl-1,6-octadiene (III)(=dihydromyrcene) and 1,2-dimethyl-3-isopropenylcyclopentanes (IVa—d) (=iridenes). The latter were the secondary products isomerized from the former. Those structures had been reported to be IVa and IVd.[2-5] Crowley,[6] however, reported that one of them was not IVa, but IVb, on the basis of his studies of the photochemical reactions of alloocimene. Furthermore, Ohloff[7] got plinols in which methyl on C-2 and isopropenyl on C-3 were *cis* configuration from ring-closure reactions of linalool.

In this paper, it will be reported on how, on the isomerization of pinane, the stereochemistry of iridenes was studied and IVb was obtained as the main product. Moreover, the determination of the structures through ozonolyses was reexamined, and the effect of epimerization on the process was reported.

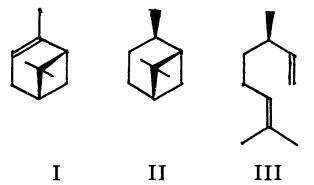

I II III

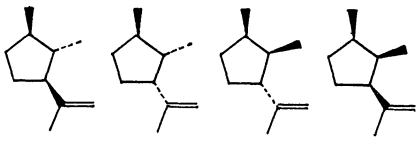

IVa IVb IVc IVd

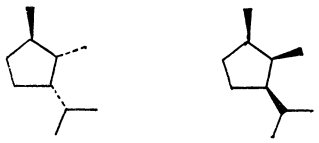

Vb Vd

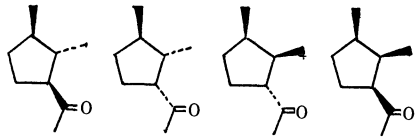

VIa VIb VIc VId

Experimental

Measurements. The measurements were carried out after glc fractionations. The PMR spectra were recorded on a Hitachi-Perkin Elmer Model R-20, using tetramethylsilane as the internal standard and CCl_4 as the solvent at an ordinary temperature. A Perkin Elmer Model 337 infrared spectrometer was used for the measurements of the infrared absorption spectra in the 4000—400 cm^{-1} region.

Preparation of l-cis-Pinane(II). Into a 300-m*l* autoclave equipped with a magnetic stirrer, 100 m*l* of *l*-α-pinene(I) (bp 52—53°C/20 mmHg, n_D^{20} 1.4675, d^{25} 0.8537, $[\alpha]_D^{20}$ −39.1°), 10 g of Raney nickel W-6 and ethanol (40 m*l*) were added, and then hydrogen was introduced from a pressure bomb (150 kg/cm^2). Reduction was carried out at room temperature.[8] After the reaction, pinane (bp 60.5—62.0°C/20 mmHg, n_D^{20} 1.4630, $d^{12.5}$ 0.8592, $[\alpha]_D^{24.6}$ −14.63. PMR; 8.85(s), 9.00(s), 9.01(d, J=6.5 Hz)) was obtained. These physical data corresponded to those for *l-cis*-pinane.[9]

Thermal Isomerization of II. II was isomerized in a silica tube (20 mm $\phi \times 300$ mm) at a feed rate of 21 m*l*/hr in the range of 400—500°C with preheating (210°C). The isomerization products were carefully distilled, and two fractions, A (bp 160.5—161.0°C, n_D^{20} 1.4480) and B (bp 169.0—170.0°C, n_D^{20} 1.4550), were collected. The fraction A contained 84% of the peak 6, and the fraction B contained 83% of peak 8.

Ozonolyses of the Isomerized Products. A 2.0 g portion of each fraction (A and B) was dissolved in dichloromethane and saturated with ozone at −80°C, and then the solutions were warmed to −20°C. To each solution, the following two methods were applied: *Method 1*: Acetic acid (50 m*l*) and zinc powder (8 g) were then stirred into the solutions. After one hour, carbonyl compounds were obtained (A′ and B′). *Method 2*: Into the solutions, 5 m*l* of 10% aqueous Na_2CO_3 and 5 m*l* of 30% H_2O_2 were stirred. After three hours, these solutions were neutralized with 1N HCl and extracted with ether.

Isomerization of the Carbonyl Compounds with Basic Reagents.

1) Present address: The Research Institute of Nissan Chemical Industries, Ltd., Toshima, Kita-ku, Tokyo.

2) V. N. Ipatieff, W. D. Huntsman, and H. Pines, *J. Amer. Chem. Soc.*, **75**, 6222 (1953).

3) H. Pines, N. E. Hoffman, and V. N. Ipatieff, *ibid.*, **76**, 4412 (1954).

4) W. D. Huntsman and T. H. Curry, *ibid.*, **80**, 2252 (1958).

5) W. D. Huntsman, V. C. Solomon, and D. Eros, *ibid.*, **80**, 5455 (1958).

6) K. J. Crowley, *Tetrahedron Lett.*, **1965**, 2863.

7) H. Strickler, G. Ohloff, and E. sz. Kovats, *Helv. Chim. Acta*, **50**, 759 (1967).

8) A low-temperature reduction was desirable in obtaining a stereospecific product.

9) a) A. Lipp, *Ber.*, **56**, 2089 (1923). b) W. Cocker, P. V. R. Shanon, and P. A. Staniland, *J. Chem. Soc., C*, **1966**, 41. c) H. C. Brown and G. Zweifel, *J. Amer. Chem. Soc.*, **86**, 393 (1964).

Table 1. Thermal isomerization of *l-cis*-pinane[a)]

No.	Temp. (°C)	Yield (g)	Product Ratio by the Peak Area on the Glc[b)]								
			1	2	3	4	5	6[c)]	7	8[d)]	9
1	400	3.0	—	0.9	2.7	—	15.3	5.6	73.1	2.4	—
2	425	3.0	—	3.1	3.8	—	29.0	3.3	57.3	3.3	—
3	455	2.9	—	1.2	5.2	—	44.2	21.3	18.6	5.0	4.1
4	480	2.8	—	4.8	5.7	—	31.9	38.4	2.7	13.7	2.3
5	500	2.8	0.5	2.3	2.8	3.7	25.5	42.8	2.3	14.8	5.3

a) 10 minutes feeding at the rate of 21 m*l*/hr. (*ca.* 3 g)
b) PEG 6000/celite, 120°C, H_2: 40 m*l*/min.
c) Peak 6: bp 160.5—161.0°C (lit.[3)] for IVa; 161.1—161.4°C), n_D^{20} 1.4480 (lit.[3)] for IVa; 1.4475), PMR 9.33 (3H, d, J=6.5 Hz), 8.99 (3H, d, J=4.8 Hz), 8.35 (3H, s), 8.70—7.20 (7H, m), 5.42 (1H, m), 5.30 (1H, m), IR 3080, 885 cm^{-1}.
d) Peak 8: bp 169.0—170.0°C (lit.[3)] for IVd; 169—170°C), n_D^{20} 1.4550(lit.[3)] for IVd; 1.4545—1.4560), PMR 9.50(3H, d, J=7.0 Hz), 9.08(3H, d, J=6.0 Hz), 8.31(3H, s), 8.70—7.30(7H, m), 5.42(1H, m), 5.28(1H, m), IR 3080, 885 cm^{-1}.

1) A mixture of A′ and B′ (1.5 g) was added to 30 m*l* of 10% aqueous Na_2CO_3 and refluxed for four hours with vigorous stirring. After the reaction, 1.0 g of an oily product was obtained.

2) A′ and B′ (0.5 g) were each dissolved in 20 m*l* of 1N alcoholic potash, and the mixtures was refluxed for four hours. Then, a 60 m*l* portion of water was added to each solution and they were neutralized with 1N HCl. The isomerized products were obtained by means of the usual treatment.

Results and Discussion

The results of the thermal isomerizations of II are listed in Table 1. The peaks 1,5, and 7 were identified as isoprene, III, and II respectively by reference to authentic samples. According to the literatures,[2,3)] the peaks 6 and 8 seem to be iridenes, IVa and IVd respectively; this assignment is based on the physical constants listed in Table 1. When, however, the fraction A was reduced by the same way as II was, the PMR spectrum of the main product was identical with that of iridane Vb.[10)] Therefore, the peak 6 may be identified as IVb, since, under our experimental conditions, the structure should be retained.

The formation of the iridenes has been considered to proceed through the polycenter-concerted mechanisms, and several 1,6-heptadienes have been cyclized intramolecularly at a high temperature to *cis*-products.[5,11,12)] However, the iridenes obtained from III have been reported to be *trans* IVa mainly.[2-5)] Therefore, Tabushi[12)] considered that the primary product, IVd, was converted thermally to IVa, and Huntsman[5)] presumed that the methyl group at the 3-position of III contributed to form IVa.

On the other hand, Ohloff and his coworkers[7)] obtained *cis*-plinols as the main products on the cyclization of linalool, and they presumed a reaction mechanism.

Since the cyclization of III seems to be the same as in the case of linalool, the following intermediate structures are presumed (Fig. 1). In the [III^c] series, C-7 methyl and terminal methylene are *cis*, while in the [III^t] series they are *trans*. The IV's must be produced from the respective [III's]. Among these, the [III^c_c] and [III^t_d] structures are unstable because of the ecliptic arrangement of methyl on C-3 and terminal vinyl. (With regard to the latter, the interaction of methyls on C-3 and C-7 must also be con-

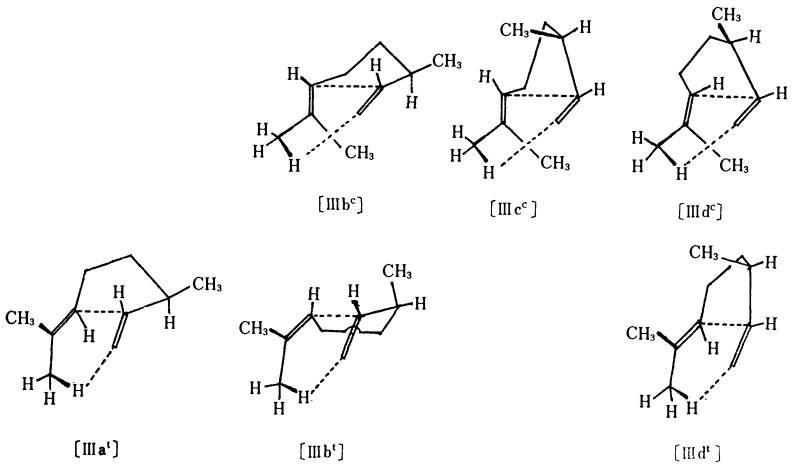

Fig. 1. The Presumptive Intermediates in the Cyclization of III.

10) K. Sisido, S. Kurozumi, K. Utimoto, and T. Isida, *J. Org. Chem.*, **31**, 2795 (1966).
11) H. M. R. Hoffman, *Angew. Chem.*, **81**, 597 (1969).
12) I. Tabushi and K. Fujita, *Yuki Gosei Kagaku Kyokai Shi*, **25**, 10 (1967).

sidered). Hence, from the standpoint of stability and from that of the number of intermediates, the ease of the formation of iridenes seems to be the following sequence:

$$IVb > IVd > IVa > IVc.$$

TABLE 2. THE RESULTS OF OZONOLYSES OF IRIDENES

Reactant[a]	Method[b]	Product (%)[c]				
		VIa	VIb	VIc	VId	others
A	1	17.3	63.1	7.1	12.5	
B	1	—	4.4	—	95.6	
A+B	2	31.4	30.5	16.3	21.8	
A	2	47.8	45.8	4.8	1.0	
Iridene fraction from thermally isomerized product of II	1	15.1	48.0	6.6	24.7	5.6

a) Fraction A containing 84% of IVb, and B did 83% of IVd.
b) Methods were described in the experimental part.
c) Analyses were carried out by glc (PEG 6000/celite, 126°C, H_2: 41 ml/min).

This agrees with the experimental results.

Moreover, the results of the ozonolyses (Table 2) show that VIb and VId were produced from IVb and IVd respectively; therefore, in the former, the methyl groups on C-1 and C-2 are *trans*, and in the latter, *cis*. On the other hand, VIb and VId were isomerized partly into VIa and VIc respectively by the action of alkalis (Table 3), so it seems that, concerning the methyl on C-2 and the acetyl on C-3, VIa and VIc have more stable configurations than do VIb and VId. Therefore, these two groups may be considered to be *trans* in VIa and VIc, and *cis* in VIb and VId. That is, in the ozonolyses in which the ozonides are decomposed with Zn–CH_3COOH, the configurations do not change, but with alkalis epimerizations occur.

TABLE 3. ISOMERIZATION WITH BASIC REAGENTS[a]

Reactant[b]	Reagent	Product (%)[c]			
		VIa	IVb	VIc	VId
A′	1 N-alc. potash	63.6	2.5	25.2	8.7
B′	1 N-alc. potash	1.0	—	54.4	44.6
A′+B′ (1:1)	10% aq. Na_2CO_3	22.2	38.3	14.9	24.6

a) Reaction conditions; refluxing for four hours.
b) A′ was obtained from fraction A by means of method 1, and B′ was from B.
c) The analyses were same as Table 2.

Furthermore, the Cotton effects of VIa and VId were positive, and those of VIb and VIc were negative. According to Djerassi,[13] the Cotton effects of pregnan-3β-ol-20-one were negative in the case of the α configuration at C-17 acetyl and positive in the case of the β. Since, on the steroid, the steric effects of A, B, and C rings make contributions, the data may be not strictly suitable for our experiments. However, when we use these data in connections with those obtained in our studies, it can be deduced that the configuration of C-3 acetyl is α in VIb and VIc, and β in VIa and VId.

From these results, the decomposition of ozonides with Zn–CH_3COOH may be concluded to give the sterically-corresponding ketones. On the other hand, when the decomposition of ozonides is carried out with Na_2CO_3–H_2O_2, VIa and VIb are obtained from IVb, and VIc and VId from IVd. When the former workers[2,3] studied the structures of iridenes through ozonolyses, they used Na_2CO_3–H_2O_2 as the decomposing reagent of ozonides, they thus deduced that IVa, which is an epimer of IVb, was the main product from the thermal isomerization of II.

13) C. Djerassi, *Bull. Soc. Chim. Fr.*, **1957**, 741; C. Djerassi, O. Halpern, V. Schindler, and Ch. Jamm, *Helv. Chim. Acta*, **41**, 250 (1958); C. Djerassi, I. Fornaguera, and O. Mancera, *J. Amer. Chem. Soc.*, **81**, 2383 (1959).

Side-chain Nitrooxylation of Polyalkylbenzenes through Ionic Process[1]

Kiyomi NAKAMURA

Department of Chemistry, Faculty of Science, Kyoto University, Sakyo-ku, Kyoto

(Received March 17, 1970)

The reaction of polyalkylated aromatic compounds with fuming nitric acid has been investigated with respect to the effects of substituents and added electrolytes on the ease and extent of the concurrent side-chain nitrooxylation and nuclear nitration. Relative reactivity of substituted pentamethylbenzenes $C_6(CH_3)_5X$ for side-chain substitution decreases from 1 to 2×10^{-2} to 4×10^{-4} to 3×10^{-6} with the change of substituent groups from methyl to hydrogen to bromine to nitro in accordance with the ionic character of the reaction. Added electrolytes have profound influence on the reaction rates, but the ratio of products from side-chain nitrooxylation and nuclear nitration remains almost unchanged, indicating that both processes share a common intermediate. The relative amount of side-chain substitution depends closely on the positional relationship of alkyl groups in the nucleus, and preferential formation of *p*-alkylbenzyl nitrates is always observed. It is concluded from the results, that the side-chain nitrooxylation products are formed by way of the polar intermediate common with the ring nitration products. Some plausible reaction sequences are briefly discussed.

Electrophilic reaction of highly alkylated aromatic compounds often gives products which are rather unexpected from the reaction of less substituted compounds. The acylation,[2] halogenation,[3] hydroxylation,[4] and nitration[5] of these systems have been studied by several workers to determine the pattern of electrophilic substitution. In a previous paper,[6] we showed that the actions of fuming nitric acid upon pentamethylbenzene and pentaethylbenzene give as the major product 2,3,4,5-tetramethylbenzyl nitrate and α-methyl-2,3,4,5-tetraethylbenzyl nitrate, respectively, and that these unusual nitrations are characterized by their high positional selectivity and peculiar orientation. In the present work, the effects of substituents, added electrolytes and structural features of the substrate upon the rate and extent of the concurrent side-chain nitrooxylation (SNO) and ring nitration (RNA) have been investigated with the aim of providing information on how the displacement of a side-chain proton by ONO_2 group occurs in preference to that of a ring proton by NO_2 group under typical ionic conditions. From the results the possible reaction sequences leading to the formation of side-chain substituted products are briefly discussed.

Experimental

Materials. Hexamethylbenzene,[7] hexaethylbenzene,[8] pentamethylbenzene[7] and its bromo[9] and nitro derivatives,[10] two ethyltetramethylbenzenes,[11] three tetramethylbenzenes[7,12] and thier mononitro derivatives,[13] bromodurene,[14] bromonitrodurene, ethylmesitylene,[15] 5-*t*-butylhemimellitene[16] and its mononitro derivative,[17] mesitylene,[18] pseudocumene,[19] and ethylxylenes[15] were prepared as described in literature. 5-Ethylhemimellitene was obtained by the Clemmensen reduction of 3,4,5-trimethylacetophenone.[20] Nitromethane was distilled after drying over anhydrous sodium sulfate. Nitric acid ($d=1.50$) of guaranteed grade was used without purification.

Kinetic Measurement and Product Analysis. All kinetic measurements were made on a Shimadzu QV-50 spectrophotometer. A volumetric flask containing a nitromethane solution of the reaction mixture was immersed in a constant-temperature bath at 25.0°C. Ten milliliters of aliquots was withdrawn periodically and quenched by pouring into aqueous sodium bicarbonate. The organic part was separated by extraction with ether. The aqueous part was analysed for nitrite ion by Shinn's method[21] and nitrate ion was determined spectrometrically[22] to obtain the amount of nitric acid consumed. The residue from the ether extract was diluted with nitromethane to a suitable concentration and the amount of ring nitration was determined by calculation from the optical densities of nitro compounds at appropriate wavelengths. Adherance to Beer's law was excellent. Since nitromethane used as a solvent had deep absorption below 350 mμ, a comparatively weak band ($\varepsilon=2\times10^2-4\times10^2$) at around 380 mμ was used for the determination of nitro compounds. The wavelengths λ_{max} used were

1) The Reaction of Polysubstituted Aromatics. XXI. Part XX: This Bulletin, **44**, 277 (1971).
2) H. Hopff and A. K. Wick, *Helv. Chim. Acta*, **43**, 1473 (1960); B. I. Mokrousov, A. N. Detsina, and V. A. Koptyug, *Zhur. Org. Khim.*, **4**, 1639 (1968).
3) L. J. Andrews and R. M. Keefer, *J. Amer. Chem. Soc.*, **86**, 4158 (1964); E. Baciocchi, A. Ciana. G. Illuminati, and C. Pasini, *ibid.*, **87**, 3953 (1965); R. M. Keefer, and L. J. Andrews, *J. Org. Chem.*, **31**, 541 (1966).
4) H. Hart and R. M. Lange, *J. Org. Chem.*, **31**, 3776 (1966); H. Hart and R. K. Murray, Jr., *ibid.*, **32**, 2448 (1967).
5) A. Huender, *Rec. Trav. Chim. Pays-Bas*, **34**, 1 (1915); I. J. Rinkes, *ibid.*, **57**, 1405 (1938); **58**, 538 (1939); **63**, 89 (1944); L. I. Smith and C. O. Guss, *J. Amer. Chem. Soc.*, **62**, 2635 (1940).
6) H. Suzuki and K. Nakamura, This Bulletin, **43**, 473 (1970).
7) L. I. Smith, "Organic Syntheses," Coll. Vol. II, 32 (1943).
8) E. Wertyporoch and T. Firla, *Ann. Chem.*, **500**, 293 (1933).
9) A. Kovczynski, *Ber.*, **35**, 868 (1902).
10) R. Willstatter and H. Kubli, *ibid.*, **42**, 4162 (1909).
11) M. S. Newman, J. R. Leblanc, H. A. Karnes, and G. Axelrad, *J. Amer. Chem. Soc.*, **86**, 868 (1964).
12) L. I. Smith and O. W. Cass, *ibid.*, **54**, 1609 (1932).
13) G. Illuminati, *ibid.*, **74**, 4951 (1952); G. Illuminati and G. Marino, *ibid.*, **75**, 4594 (1953).
14) O. Jacobsen, *Ber.*, **20**, 2837 (1887).
15) S. F. Birch, R. A. Dean, F. A. Fidler, and R. A. Lowry, *J. Amer. Chem. Soc.*, **71**, 1362 (1949).
16) M. J. Schlatter, *ibid.*, **76**, 4952 (1954).
17) R. C. Fuson, J. J. Denton, and J. W. Kneisley, *ibid.*, **63**, 2652 (1941).
18) R. Adams and R. W. Hufferd, "Organic Syntheses," Coll. Vol. I., p. 341 (1956).
19) R. W. Maxwell and R. Adams, *J. Amer. Chem. Soc.*, **52**, 2962 (1930); L. I. Smith and A. P. Lund, *ibid.*, **52**, 4147 (1930).
20) D. E. Pearson and J. D. Bruton, *J. Org. Chem.*, **19**, 961 (1954).
21) M. B. Shinn, *Ind. Eng. Chem., Anal. Ed.*, **13**, 33 (1941).
22) A. M. Hartley and R. I. Asai, *Anal. Chem.*, **35**, 1214 (1963).

nitropentamethylbenzene (380), nitrodurene (377), nitroisodurene (379), nitroprehnitene (381), nitromesitylene (379), bromonitrodurene (378), and 4-nitro-5-*t*-butylhemimellitene (378), respectively. Both nitrooxylated products and hydrocarbons exhibited no interference in this region. Nitromethane solutions were concentrated after optical density measurements, and the side-chain nitrooxylated compounds were hydrolyzed by refluxing with a mixture of sodium acetate (2 g), acetic acid (7 m*l*) and water (17 m*l*) for several hours. The organic part was removed by ether extraction and the aqueous part was analyzed for the nitrite ion derived from nitrooxylated products. Results of a typical run are summarized in Table 1. Since the amounts of nitrous acid[23] and benzyl nitrate are comparable at the initial stages of the reaction, the former can be used as a measure of side-chain nitrooxylation. Time t_{10} and t_1, which denote the time required for each of the substrates examined to attain 10% and 1% completion in SNO under identical conditions, were determined graphically. All runs were conducted at least twice and the values obtained were corrected by blank experiments.

Nitrations of polyalkylbenzenes for product analyses were carried out as described previously.[6] The structures of major nitration products were determined.

Mesitylene gave nitromesitylene. Pseudocumene[24] 4-ethyl-*o*-xylene, 4-ethyl-*m*-xylene, and 2-ethyl-*p*-xylene all underwent side-chain substitution at 4-alkyl group. Isodurene and its structure analogs were mainly nitrooxylated at 5-alkyl group: the major nitrooxylation product from 5-ethylhemimellitene was identified as α,3,4,5-tetramethyl-2-nitrobenzyl nitrate. No attempt was made to separate components of the product mixture from isodurene and ethylmesitylene because only small amounts of benzyl nitrates were formed. Prehnitene gave nitro compounds along with a small amount of side-chain substituted product, the structure of which has not yet been established. Durene gave a considerable amount of 2,4,5-trimethylbenzyl nitrate. 5-*t*-Butylhemimellitene yielded mono and dinitro derivatives as sole products.

Results and Discussion

Substituent Effects for Side-chain Nitrooxylation. In previous papers[25] of this series, the mode in which a substituent group determines the orientation of side-chain nitrooxylation (SNO) was briefly described. Strongly electron-withdrawing substituents such as nitro, carboxyl and carbomethoxy groups brought about almost exclusive ortho substitution to give 6-substituted tetramethylbenzyl nitrate, while halogen atoms were found to lead to comparable amounts of 5- and 6-halotetramethylbenzyl nitrates. Pentamethylphenol and its methyl ether gave mainly cyclohexadienones, with a concomitant formation of 3-substituted tetramethylbenzyl nitrate in a small amount.

In order to get further insight into the mechanism of SNO, the substituent effect on the reactivity has been examined for a series of pentamethylbenzene derivatives. The overall process of SNO may be expressed in the stoichiometric equation

$$C_6X_5CH_3 + 2HNO_3 = C_6X_5CH_2ONO_2 + HNO_2 + H_2O \quad (1)$$

Preliminary experiments carried out for dilute nitromethane solutions of hexamethylbenzene and fuming nitric acid at 10°C and 25°C have shown that the rate of SNO can be followed successfully by measuring the increase in the amount of nitrous acid (Table 1).

Table 1. Nitration of hexamethylbenzene in nitromethane at 10°C

$[C_6(CH_3)_6] = 2\times10^{-2}$ mol l^{-1}; $[HNO_3] = 10\times10^{-2}$ mol l^{-1}

Time (sec)	$[HNO_2$[23]$]$ (mol l^{-1})	[benzyl nitrate] (mol l^{-1})	[HNO_3 consumed] (mol l^{-1})
135	0.27×10^{-2}	0.24×10^{-2}	0.60×10^{-2}
210	0.41	0.46	1.06
230	0.47	0.45	1.12
300	0.67	0.63	1.46
324	0.74	0.62	1.66

With the lapse of time, the amount of nitrous acid gradually outweighs that of benzyl nitrate, indicating that nitrous acid can be no longer used as the measure of SNO. This would probably be due to the secondary reactions involving the oxidation or the condensation of the initially formed benzyl nitrate.[26] SNO of polyalkylbenzenes is quite sensitive to the reaction conditions, and the benzyl nitrates produced are usually highly reactive so that they can act as a benzylating agent in the presence of acid catalyst, or undergo further transformation with excess of nitric acid. Thus direct kinetic treatment of the nitration of polyalkylated aromatics for the purpose of determining their relative rates is very difficult. To avoid these complexities, relative rates of hydrocarbons were determined by comparing the time t_{10}, which denotes the time required for each of the substrates examined for 10% completion in SNO under identical conditions. Such a method has been successfully used by several groups of workers in some electrophilic aromatic substitutions.[27] Ob-

Table 2. Substituent effect on the rate of side-chain nitrooxylation of $C_6(CH_3)_5X$ in nitromethane at 25°C

$[C_6(CH_3)_5X] = 2\times10^{-2}$ mol l^{-1}; $[HNO_3] = 10\times10^{-2}$ mol l^{-1}

	X	Relative basicity (*p*-xylene=1)	t_{10}[a] (sec)
Hexamethylbenzene	CH_3	44500	15
Pentamethylbenzene	H	4350	660
Bromopentamethylbenzene	Br		4×10^4
Nitropentamethylbenzene	NO_2		5×10^6
Hexaethylbenzene		13500	800

a) t_{10} denotes the time required for 10% completion in SNO for each of the substrates examined.

23) The term "nitrous acid" used hereafter refers to all the products in the reaction mixture, which after dilution with water could be estimated as nitrous acid by ordinary procedures.

24) M. Dolinsky, J. H. Jones, C. D. Ritchie, R. L. Yates, and M. A. Hall, *J. Ass. Offic. Agri. Chem.*, **42**, 709 (1959).

25) H. Suzuki, This Bulletin, **43**, 481 (1970); K. Nakamura and H. Suzuki, *ibid.*, 227 (1971).

26) H. Suzuki, *ibid.*, **43**, 879 (1970).

27) H. C. Brown and L. M. Stock, *J. Amer. Chem. Soc.*, **79**, 1421 (1957); P. W. Robertson, P. B. D. de la Mare, and W. T. G. Johnston, *J. Chem. Soc.*, **1943**, 276; G. Illuminati and G. Marino, *J. Amer. Chem. Soc.*, **78**, 4975 (1956); E. Berliner and F. Berliner, *ibid.*, **71**, 1195 (1949).

Table 3. Comparison of substituent effects on the relative rates of side-chain nitrooxylation, ring nitration and dilute nitric acid oxidation

	X	Side-chain nitrooxylation of $C_6(CH_3)_5X$[a]	Ring nitration of C_6H_5X[b]	Oxidation by HNO_3 of $X\cdot C_6H_4CH_2OR$[c]
I	CH_3	1	1	1
II	H	2×10^{-2}	10^{-1}—10^{-2}	1—10^{-1}
III	Br	4×10^{-4}	10^{-3}	10^{-1}—10^{-2} [d]
IV	NO_2	3×10^{-6}	10^{-5}—10^{-8}	10^{-2}

a) II/I, III/I, and IV/I are reactivities of II, III, and IV relative to I calculated from the ratios of the reciprocals of t_{10} for each of them.
b) Ref. 29—31)
c) Ref. 28)
d) This value is the reactivity of chloro-substituted compound relative to methyl-substituted.

served t_{10} and reactivity relative to hexamethylbenzene are collected in Table 2. Comparisons are made with the substituent effects on the ring nitration of C_6H_5X, and on the oxidation of benzyl alcohols and their methyl ethers by dilute nitric acid (Table 3).

As is apparent from Table 2, the reactivity for SNO follows the order $C_6(CH_3)_6>C_6(CH_3)_5H>C_6(CH_3)_5Br>C_6(CH_3)_5NO_2$ and electron-withdrawing bromo and nitro groups remarkably retard the reaction. Similar orders are followed in ordinary nuclear nitrations, and in the oxidation of benzyl alcohols and their methyl ethers by dilute nitric acid to the corresponding benzaldehydes (Table 3). However, the magnitude of difference in relative rate for SNO differs remarkably from that of the latter process in which the hydrogen abstraction by radical is rate-determining.[28] Relative reactivities for SNO are $II/I=2\times10^{-2}$, $III/I=4\times10^{-4}$ and $IV/I=3\times10^{-6}$, and the overall reactivity range is covered by a factor of as large as 10^5. Marked dependence in the relative rates of SNO on the electronic effect of the substituent groups parallels that found in the nitration of C_6H_5X, $II/I=10^{-1}$—10^{-2},[29] $III/I=10^{-3}$,[30] and $IV/I=10^{-5}$—10^{-8},[31] where the attack of an electrophile to the nucleus to form benzenonium ion is rate-determining. In contrast, the relative rates of the hydrogen atom abstraction from side-chain vary very little with the change of substituents; $II/I=1$—10^{-1}, $III/I=10^{-1}$—10^{-2} and $IV/I=10^{-2}$.[28] A similar response of SNO and RNA to the change of substituents suggests that the processes of SNO and RNA are mechanistically alike and argues against any participation of free-radical pathway in the reaction. SNO proceeds with fuming nitric acid at low temperatures, while the nitric acid oxidation of alkylbenzenes can be effected with dilute aqueous nitric acid only at elevated temperatures. Additional support for the ionic process is put forward by the observation that SNO takes place with primary alkyl groups such as methyl and ethyl, but not with isopropyl or *t*-butyl group.[6] Excellent positional selectivity of SNO leads to the reaction products of simple composition and high purity,[6,25] which are opposed to the free-radical mechanism in which reactive benzyl nitrates would have been oxidized to a complicated mixture of benzaldehydes, benzoic acids and others.

Effects of Added Electrolytes on the Ease and Extent of Side-chain Nitrooxylation. Table 4 shows the effects of added electrolytes on SNO and RNA of pentamethylbenzene, which were carried out with nitric acid ($d=1.50$) in nitromethane at 5°C. The time required for 10% completion in the overall reaction—the sum of SNO and RNA — is indicated by t'_{10}. The relative percentage of the products from SNO and RNA at t'_{10} is also included. As is apparent from the Table, the ratios of both reaction products are almost independent of the concentration of nitric acid or the presence of the added electrolytes such as nitrite, nitrate or hydrogen sulfate. This might indicate that the reaction leading to RNA and SNO shares a common intermediate, presumably benzenonium ion (A) as described in the equation below:

Table 4. Effects of added electrolytes on the ease and extent of side-chain nitrooxylation of pentamethylbenzene with nitric acid in nitromethane at 5°C

$C_6(CH_3)_5H$ (mol l^{-1})	HNO_3 (mol l^{-1})	Added electrolytes (mol l^{-1})	t'_{10}[a] (min)	SNO (%)	RNA (%)	t_{10}[b] (min)
0.1	0.5	None	9.5	86	14	10.5
0.1	0.5	None	9	88	12	10
0.1	0.5	Et_4NHSO_4: 0.022	9	86	14	10
0.1	0.5	Et_4NNO_3: 0.022	15.5	90	10	16.5
0.1	0.5	$NaNO_2$: 0.0043	4	84	16	4.5
0.1	0.1	None	80	85	15	96
0.2	0.5	None	9.5	90	10	10
0.05	0.5	None	6.5	86	14	8
0.1	0.5	H_2SO_4: 0.01	7	76	24	8

a) The time required for 10% completion in the overall reaction—the sum of SNO and RNA—is indicated by t'_{10}.
b) The time required for 10% completion in SNO is indicated by t_{10}.

28) Y. Ogata, Y. Sawaki, F. Matsunaga, and H. Tezuka, *Tetrahedron*, **22**, 2655 (1966); Y. Ogata and Y. Sawaki, *J. Amer. Chem. Soc.*, **88**, 5832 (1966).
29) L. M. Stock, *J. Org. Chem.*, **26**, 4120 (1961).
30) J. D. Roberts, J. K. Sanford, F. L. J. Sixma, H. Cerfontain, and R. Zagt, *J. Amer. Chem. Soc.*, **76**, 4525 (1954).
31) P. B. D. de la Mare and J. H. Ridd, "Aromatic Substitution, Nitration and Halogenation," Butterworth Scientific Publications, London (1959), p. 83.

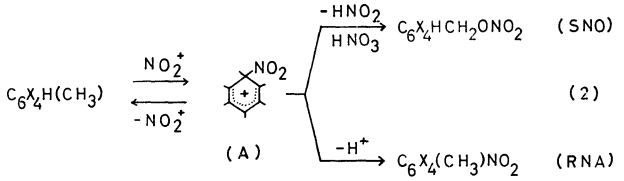

The reaction rates are subject to the influence of the added electrolytes. The reaction is accelerated by the addition of a small amount of sulfuric acid, the role of which is no doubt to form the nitric acidium ion $H_2NO_3^+$, the precursor of the reactive nitronium ion NO_2^+, HSO_4^- acting as a base. A negative effect has been shown by nitrate ion, which retards the reaction by decreasing the concentration of nitric acidium ion according to the equation

$$HNO_3 + HNO_3 \rightleftharpoons H_2NO_3^+ + NO_3^- \qquad (3)$$

Addition of a small amount of nitrite ion into the system brings about a remarkable enhancement of the reaction rate, but the relative ratio of SNO and RNA remains unchanged. Nitrooxylation of hexamethylbenzene and pentamethylbenzene according to Eq. (1) inevitably produces a large amount of nitrous acid with progress of the reaction, and the nitrous acid thus formed restricts the supply of the nitronium ion by lowering the concentration of the nitric acidium ion in the system following the equation[32]

$$H_2NO_3^+ + NO_2^- = N_2O_4 + H_2O \qquad (4)$$

Since the reaction of pentamethylbenzene is apparently autocatalysed, the nitrosonium ion may play some role in the substitution as has been suggested by Shofield and coworkers in the nitration of some activated aromatic systems.[33,34] The reaction rate of SNO is also more enhanced in nitromethane than in acetic acid. This trend has already been well substantiated for ordinary nuclear nitration.[32] Thus it is concluded that the effective species for SNO is the nitronium ion or its precursors ($H_2NO_3^+$ and N_2O_5) depending on the reagent and conditions employed, and the electrophilic attack of these ionic species on the aromatic substrate constitutes the initial stage of the reaction; the proton transfer from the nucleus leads to RNA and the proton removal from the side-chain results in SNO, as in Eq. (2).

Relative Reactivities of Polyalkylbenzenes towards Side-chain Nitrooxylation. Comparison of relative reactivities towards SNO has been made with 18 alkylbenzenes listed in Table 5. With durene and pentaalkylbenzenes, SNO predominates over RNA, but with the decreasing number of alkyl substituents, the situation is gradually reversed so that t_{10} should be replaced by t_1 to provide a sound basis of comparison for the diminished tendency of substrate towards side-chain substitution. In Table 5, a similar comparison of overall reactivities of seven polyalkylated aromatic systems has been made on the basis of t'_{10}, relative basicity and the percentage ratios of SNO and RNA at t'_{10}.

Tetralin and diphenylmethane, which have reactive hydrogen atoms and are readily oxidized by dilute nitric acid, remain mostly unchanged in support of the ionic process for SNO. The basicity of hydrocarbon decreases in the order: isodurene>mesitylene>prehnitene>durene>pseudocumene, whereas a partial reversal of the order was observed in the relative rates of these hydrocarbons for SNO: xylenes<mesitylene<pseudocumene<prehnitene<isodurene<durene. This is rather surprising since it means that mesitylene, which is highly reactive in ordinary electrophilic reactions, reacts more slowly for SNO than durene or pseudocumene, which are much less basic than the former and not so highly reactive in the ordinary sense. The reactivity for SNO is, therefore, closely related to the positional relationship of the substituents in the alkylated aromatic systems. The significance of this aspect of the reaction will be discussed in due course.

The percentage ratio of SNO tends to decrease in the following order: pentamethylbenzene>durene>isodurene>prehnitene>5-*t*-butylhemimellitene>mesitylene. From the results in Table 5 it appears that the more a hydrocarbon possesses a pair of alkyl groups located at ortho and/or para position, the more readily it undergoes SNO. This is clearly understood from the reactions of hexamethylbenzene, pentamethylbenzene, durene, pseudocumene and *p*-xylene. On the other hand, mesitylene and *m*-xylene which have no comparable alkyl group yield only RNA products. It follows, therefore, that a fine balance exists between SNO and RNA, and that the positional features of the substrate are likely to be an important factor for deciding the way the reaction will take place, SNO or RNA.

High positional selectivity for SNO is very likely connected with the slow step of the proton removal from the alkyl side-chain of the benzenonium ion intermediate. Although the nitration of benzene proceeds without any primary isotope effect,[35] sterically hindered compounds usually exhibit some effect since the slow proton transfer now becomes rate-determining.[36] The diminished facility of proton transfer from the nucleus necessarily increases the chance of hyperconjugative release of a proton from the alkyl side-chain. Thus, SNO and RNA are able to compete effectively in a crowded system such as durene, penta-alkylbenzenes and hexamethylbenzene. Taking the nitration of durene as an example, the process can be outlined as follows:

32) E. D. Hughes, C. K. Ingold, and R. I. Reed, *J. Chem. Soc.*, **1950**, 2400.

33) R. G. Coombes, R. B. Moodie, and K. Schofield, *ibid.*, *B*, **1968**, 800; J. G. Hoggett, R. B. Moodie, and K. Schofield, *ibid.*, *B*, **1969**, 1.

34) C. A. Bunton, E. D. Hughes, C. K. Ingold, D. I. H. Jacobs, M. H. Jones, G. J. Minkoff, and R. I. Reed, *J. Chem. Soc.*, **1950**, 2628.

35) H. Zollinger, "Advances in Physical Organic Chemistry," in V. Gold Ed., Academic Press, London, (1964), p. 163; H. Cerfontain, H. J. Hofman, and A. Telder, *Rec. Trav. Chim Pays-Bas*, **83**, 493 (1964).

36) H. Cerfontain and A. Telder, *ibid.*, **86**, 371 (1967); P. C. Myhre, M. Beug, and L. L. James, *J. Amer. Chem. Soc.*, **90**, 2105 (1968).

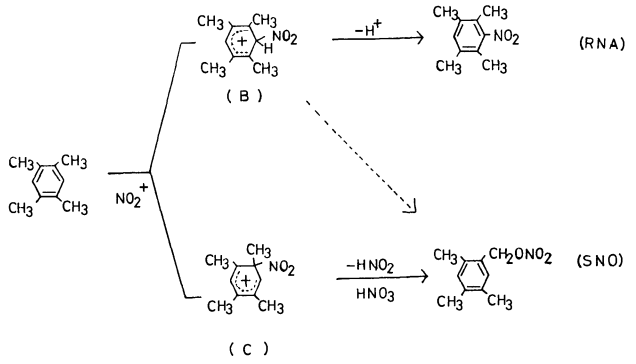

The attack of the nitronium ion upon durene will give two benzenonium intermediates (B) and (C), the latter outweighing the former in amount not only for statistical reasons, but also for more effective stabilization by one methyl group in an ortho position and one in para position than two methyl groups in ortho as (B). Steric factor also favors the formation of (C), in which the position of attack is flanked by one methyl group, over (B) where both sides are flanked. Ordinary proton removal from (B) will lead to RNA, and unusual proton removal from alkyl side-chain will result in the formation of SNO product. The predominance of the latter process in the reaction of durene may be rationalized by the greater contribution of the intermediate (C) over (B), and by the slower removal of the ring proton from (B). Further, the formation of nitrooxylated compound only as a minor product in the nitration of pentamethylphenol may be accounted for by easier proton transfer from the hydroxy group, leading to conversion into cyclohexadienone derivatives.

The methyl groups preferentially nitrooxylated and the most probable positions to be attacked initially by the nitronium ion are illustrated below for some polyalkylated aromatic systems.

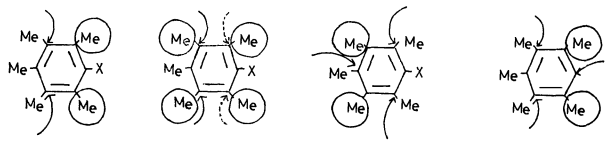

X=NO_2, COOH, $COOCH_3$ X=Cl, Br X=OH, OCH_3, NHAc

A circle indicates the methyl group preferentially nitrooxylated, and an arrow shows the preferred position for electrophilic attack by nitronium ion. Solid line —— the most preferred; dotted line ------ the next preferred.

As can be seen from the figures, the presence of methyl groups in positions ortho and/or para one another seems critical for the facile formation of benzyl nitrates. This might indicate that the hyperconjugative electron release from the methyl group will play some role for side-chain nitrooxylation. In fact, most benzyl nitrates obtained in high yields from the nitration products possess *p*-methyl group, and those having an electron-withdrawing substituent in para position are rarely formed.

On the basis of this study and related previous works,[6,25] we can tentatively construct some plausible sequences for side-chain substitution under heterolytic conditions. The cyclic process involving the migration of nitro group from nucleus to side-chain has been suggested for SNO of pentaalkylbenzenes.[6] This proceeds through a sort of allylic migration of nitro group from the attacking site to α-carbon of the alkyl group, from which the preferential proton removal took place. The benzyl nitrite thus formed will be transformed with nitric acid into the benzyl nitrate and nitrous acid.

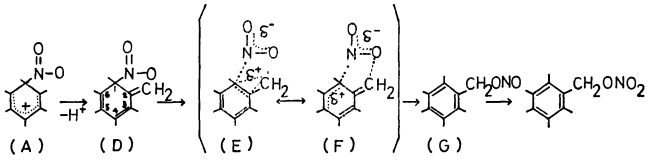

(5)

Many findings obtained from SNO are consistent with this mechanism, which has a formal resemblance to those proposed for some Claisen-type rearrangements[37] such as allyl amine oxides, nitramine and alkylpyridine *N*-oxide rearrangement. Transformation from the benzenonium intermediate (A) to the benzyl nitrite (G) can take place in two different ways; a direct conversion, and the intervention of an intermediate methylene cyclohexadiene, (D) and (H). The former process

TABLE 5. REACTIVITIES OF POLYALKYLBENZENES TOWARDS THE SIDE-CHAIN NITROOXYLATION IN NITROMETHANE AT 5°C

[Polyalkylbenzenes]=0.1 mol l^{-1}; [HNO_3]=0.5 mol l^{-1}

Polyalkylbenzenes	Basicity	t_{10}[a] (min)	t'_{10}[b] (min)	SNO (%)	RNA (%)
Pentamethylbenzene	4350	10.5	9.5	86	14
Ethyldurene		11			
Ethylprehnitene		15			
Pentaethylbenzene		15			
Durene	60	18	13.5	70	30
Tetralin		*ca.* 20 hr			
		t_1[c]			
Prehnitene	85	105	230	25	75
Isodurene	2800	45	200	43	57
5-*t*-Butylhemimellitene		600	690	12	88
Bromodurene		150[d]	450	38	62
Mesitylene	1400	very large			100
Ethylmesitylene		120			
5-Ethylhemimellitene		50			
Pseudocumene	18	570			
4-Ethyl-*o*-xylene		540			
4-Ethyl-*m*-xylene		660			
2-Ethyl-*p*-xylene		680			
Diphenylmethane		*ca.* 50 hr			

a) The time required for 10% completion in SNO is expressed by t_{10}.
b) The time required for 10% completion in the overall reaction the sum of SNO and RNA is indicated by t'_{10}.
c) The time required for 1% completion in SNO is indicated by t_1.
d) at 22.5°C

37) B. S. Thyagarajan, "Mechanisms of Molecular Migrations," Vol. II, Interscience Publishers, London, (1969); H. J. Shine, "Aromatic Rearrangements," Elsevier Publishing Company, London, (1967).

involves a simultaneous proton abstraction and nitro group migration in (A). Each pathway requires a transition state in which the scission of the C–N bond occurs in such a way that the departing nitrogen atom is accommodated with the unshared electron pair, leaving C-1 atom to be electron-deficient. This sort of π-σ electron interaction could occur through the overlap between C-1 carbon atom and the α or C-5 carbon atom.[38] The transition state for such a process may be depicted as (E) or (F). The C-5 methyl group at a position meta to C-1 and para to C-2 methylene can partly supplement this deficiency through the hyperconjugative electron release, thus facilitating the nucleophilic migration of the nitro group to the side-chain. Electron-withdrawing group at C-5, on the other hand, increases the electron deficiency at the carbon atom to which the nitro group is attached, making the departure of nitro group as a nucleophile more difficult. This is probably why the benzyl nitrate with the methyl group at para position is preferentially formed over the other isomeric products.

Two other possibilities are also conceivable, although they lack formal analogies in literature as far as the author is aware. One is a process in which a proton is removed hyperconjugatively from the side-chain to form a sort of methylene cyclohexadiene intermediate (D) and (H). Attachment of the nitrate anion to the terminal methylene carbon, departure of the nitro group as an anion, and rearomatization of the system, if occurring continuously, will lead to the formation of the benzyl nitrate.

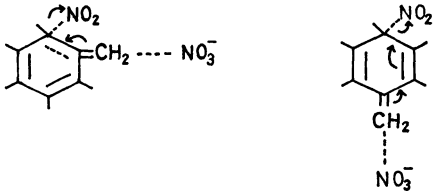

This intermolecular process is apparently difficult for justifying the fact that nitration carried out in dilute acetic acid solution affords a considerable amount of benzyl nitrate along with benzyl acetate at a very early stage of the reaction, and that the ratio of SNO and RNA is nearly independent of the concentration of nitric acid as well as added electrolytes. A speculative alternative may involve the ion-pair intramolecular path proposed for rearrangements of nitramine,[39] and 2- and 4-picoline oxides.[38,40] Formation of ion-pair requires a tight (solvent caged) association of these species, and their combination is required before separation to accommodate this intramolecular process, although the intramolecular nucleophilic cyclization leading to the formation of phthalide, or anthranil analog could not be observed during the nitration of pentamethylbenzoic acid, or pentamethylnitrobenzene.

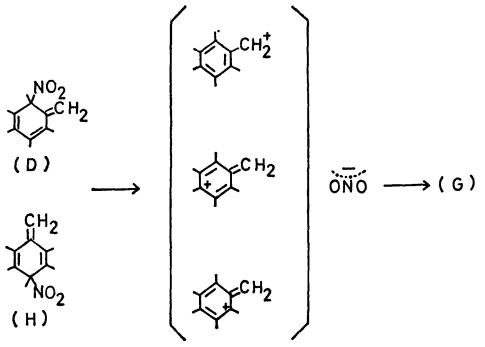

In view of a preferred attack on the 2-alkyl group in the reaction of 2,4-lutidine *N*-oxide[41] or 2,4-dimethylquinoline *N*-oxide with acetic anhydride, rearrangement to the neighboring ortho position could occur more readily than that to the remote para position. The former would probably proceed intramolecularly, while the latter possibly intermolecularly.[42]

Another possibility is a process similar to the Quinobenzylic rearrangement, where the attacking species migrates intramolecularly to the geminal methyl group to form the benzylic compound.

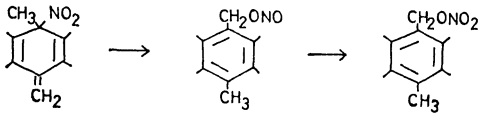

The principal disadvantage of this mechanism is that the nitropentamethylbenzene and pentamethylbenzoic acid undergo almost exclusive ortho nitrooxylation, because the most favored position for the attack of the nitronium ion in these compounds is not the ortho, but the meta position to the strongly electron-withdrawing nitro or carboxyl groups. Quinobenzylic rearrangement itself has recently been reported to proceed through a radical mechanism.[43]

The author wishes to thank Dr. H. Suzuki, Professor K. Maruyama and Professor J. Osugi for their discussions.

38) T. Koenig, *J. Amer. Chem. Soc.*, **88**, 4045 (1966).
39) W. N. White and J. T. Golden, *Chem. Ind.* (London) **1962**, 138.
40) T. Cohen and G. L. Deets, *J. Amer. Chem. Soc.*, **89**, 3939 (1967); T. Cohen and J. H. Fager, *ibid.*, **87**, 5701 (1965); R. Bodalski and A. R. Katritzky, *Tetrahedron Lett.*, **1968**, 257.
41) S. Furukawa, *Chem. Pharm. Bull* (Tokyo), **3**, 413 (1955).
42) S. Oae and S. Kozuka, *Tetrahedron*, **20**, 2694 (1964).
43) V.D. Pokhodenko and N.N. Kalibabchuk, *Zh. Org. Khim.*, **2**, 1397 (1966); N.N. Kalibabchuk, *ibid.*, **4**, 329 (1968).

A Modification of Red Blood Cells by Isocyanates[1)]

Masao KITAJIMA, Wataru SEKIGUCHI,[2)] and Asaji KONDO

Research Laboratories, Tokyo, Fuji Photo Film Co., Ltd., Asaka, Saitama

(Received April 23, 1970)

Modified red cells that have a reinforced membrane and hemoglobin which is difficult to denature are prepared by treating red cells with some isocyanates. These modified cells have the same shape as normal red cells, but they are not lysed by osmotic pressure or by the actions of any reagents except for some ionic surface-active agents. No agglutination was observed when they were mixed with the blood of foreign animals or with blood of different blood groups. The hemoglobin within the cell gave a reversible oxygenation curve and had a high oxygen affinity. Toluene-2,4-diisocyanate was found to be the most suitable reagent among the many isocyanates examined. A suspension reaction method which consists of the addition of an isocyanate emulsion to a red-cell suspension at 5°C is developed for the modification process.

The present authors have studied the preparation of artificial red blood cells by using microencapsulation techniques. A hemoglobin solution was microencapsulated with synthetic polymers, such as polystyrene, a silicone derivative, poly-γ-benzyl-L-glutamate, and dextrane stearate, into sphere particles five to ten microns in diameter.[3-5)] The hemoglobin contained in these microcapsules was found to be preserved in a normal state, and it gave an oxygenation curve identical with that of normal hemoglobin. The oxygen permeability of the hemoglobin-containing silicone microcapsules was comparable with that of natural red cells. They are free from problems of agglutination and hemolysis, and can be preserved over a long period. It is expected that the hemoglobins obtained from many mammalias can be used as artificial red cells when subjected to microencapsulation. The present authors are now studying the metabolism of the polymers used as capsulating materials and the rheology of the suspension containing such rigid particles.

This paper will describe a method of preparations and the properties of the modified red cells that have a reinforced membrane and normal hemoglobin. It is known that the shape of red cells can be fixed by treating them with some protein precipitants, such as aldehydes,[6,7)] tannic acid, or hydrogen peroxide.[8)] However, these reagents are soluble in water, so that they can penetrate into the cell to denature hemoglobin. These fixed cells have been used for studies of the morphology or the surface properties of red cells. In this modification reaction, water-immiscible isocyanates are used in the suspension reaction method that consists of the addition of an isocyanate emulsion to a red cell suspension. The modified red cells thus obtained show some specific behavior concerning hemolysis and agglutination. They are considered to be suitable as samples for a biological, physiological, or rheological study of erythrocytes. The present authors are now studying their use in the medical field as a kind of artificial red cell in a way similar to the hemoglobin-containing microcapsules.[9,10)] This modification technique can be employed generally in studying the nature of cell membranes other than that of the erythrocytes.

Experimental

Materials. Toluene-2,4-diisocyanate (TDI), from the Tokyo Kasei Co., was purified by distillation (146°C/38 mmHg). Phenyl and ethyl isocyanate, phenyl and ethyl isothiocyanate, hexamethylene diisocyanate (Tokyo Kasei Co.) and diphenylmethane diisocyanate (Hodogaya Chemicals) were obtained commercially.

Polyoxyethylene hydrogenated caster oil ether (Nikko Chemicals), Tween 20, sodium dodecylbenzenesulfonate (Kao-Atlas Co.), saponin, lecithin from eggs (Merck Co.), and cetyl, dodecyl and ethyl-pyridinium salt (Tokyo Kasei Co.) were obtained commercially. The other surface-active agents were synthesized and purified in our laboratories.

Reagent-grade chemicals were used in all the experiments.

Modification of Red Cells by TDI. The suspension reaction method developed by the authors was used to modify red cells suitably. Mammalian red cells were collected by centrifugation and washed three times with isotonic saline solution. In 200 m*l* of pH 7.2 phosphate-buffered isotonic saline, we suspended 10 g of the washed red-cell slurry at 5°C. The TDI emulsion was prepared by emulsifying 0.15 m*l* of the reagent in 30 m*l* of the saline, by means of an ultrasonic emulsifier, into microdroplets of about one micron in diameter. This TDI emulsion was quickly stirred into the red-cell suspension at 5°C. The modified cells were recovered after 5 min by centrifugal separation at 1500 rpm for 10 min and then washed with the saline twice.

The same method was employed in the cases of the other isocyanates, with varying amounts of the reagents and with varying reaction times.

Measurements of Properties. Hemolysis. Surface-active agents were dissolved in water to make a 1% solution, and the hydrogen-ion concentration was adjusted to neutral by adding dilute hydrochloric acid or a sodium hydroxide solution. In a test tube we placed 5 m*l* of this solution and then added several drops of the modified red cells. The suspension was

1) A part of this study was prestented at the 22nd Annual Meeting of the Chemical Society of Japan, Osaka, 1969, by M. Kitajima and A. Kondo.

2) Department of Surgery, Faculty of Medicine, the University of Tokyo, Hongo, Bunkyo-ku, Tokyo.

3) T. Toyoda, *Nihon Gekagaku Zasshi*, **67**, 36 (1966).

4) A. Kondo and S. Miyano, Japan. 529014 (1968).

5) M. Kitajima, S. Miyano, and A. Kondo, *Kogyo Kagaku Zasshi*, **72**, 493 (1969).

6) M. Moskowitz and S. Carb, *Nature*, **180**, 1049 (1957).

7) D. H. Heard and G. V. F. Seaman, *Biochem. Biophys. Acta*, **53**, 366 (1961).

8) H. Funaki, *Jap. J. Physiol.*, **7**, 153 (1957).

9) W. Sekiguchi, M. Kitajima, and A. Kondo, *Nihon Yuketsu Gakkai Zasshi*, **16**, 149 (1969).

10) W. Sekiguchi, M. Kitajima, and A. Kondo, Abstracts, the 12th Congress of the International Society of Blood Transfusion, Moscow, Aug. 1969, p. 512.

stirred for 5 min, and then observed under a microscope in order to see whether the cells were lysed, swelled, or unchanged.

Spectral Measurements. The visible absorption spectra for suspensions of the modified cells were taken with a Hitachi EPS-3T spectrophotometer, according to the opal glass method. A small amount of sodium hydrosulfite was added to deoxygenate hemoglobin. The infrared spectra were taken with a Hitachi Perkin-Elmer 125 spectrophotometer.

Oxygenation Curve. The modified cells were suspended in a solution phosphate-buffered at pH 6.5, and then put in a modified Wyman-type tonometer. The air inside the tonometer was replaced by nitrogen purified with Fieser's solution and saturated potassium chloride solutions. After the hemoglobin had been completely deoxygenated, a measured amount of air was introduced into the tonometer with a syringe. It was shaken for 20 min to equilibrate the hemoglobin with the gas, and then the sample was submitted to absorption spectrum measurements. The percentage of oxygenation, Y, of the hemoglobin was calculated from the spectra according to the following equation:

$$Y=\{[(E_a-E_b)-(D_a-D_b)]/[(O_a-O_b)-(D_a-D_b)]\}\times 100$$

where the terms O, D, and E represent the absorbance at the completely oxygenated state, the completely deoxygenated state, and the state between the two, respectively. The suffixes a and b represent the wavelength at which the absorption was measured: a, 578: b, 562.5 nm.

Results and Discussion

Modification Reaction. Various isocyanates were examined for use in modifying red cells, but most of them were found to be unsuitable. Monoisocyanates such as phenyl and ethyl isocyanate did not reinforce the membrane. The same was true with phenyl and ethyl isothiocyanate. Diisocyanates such as hexamethylene and diphenylmethane diisocyanate reinforced the membrane under some conditions, but they required too long a time to complete the modification, as their reactivity was not high enough,[11] and the hemoglobin within the cell was denatured. It was effective to add some catalysts, such as ferric chloride or sodium phenate, to accelerate the reaction, but they were undesirable because of their deleterious action on hemoglobin.

TDI was found to be the most suitable reagent. It gave modified cells that had a sufficiently reinforced membrane and hemoglobin which was hardly denatured at all. The reactivity of TDI is very high, so that the modification reaction is completed in a few minutes. The excess TDI is exhausted by reactions with water molecules and becomes inert solid particles in this suspension reaction. When the isocyanate is used as an organic solution, the shape of the cells changes into a sphere and a denaturation of the hemoglobin takes place. Actions based on the low surface tension of the solvent or on the extraction of lipids from the membrane must be the reason. Thus, both the high reactivity and the reaction method serve to prevent the reagent from penetrating into the cell to denature hemoglobin.

The amount of TDI to be used was determined by examining the degree of the reinforcement and that of the denaturation of hemoglobin. The optimum amount of TDI to modify 10 g of the red cell slurry properly was found to be 0.15 m*l*. When the amount was insufficient, the cells became more sensitive to hemolytic action than intact cells. A large excess of TDI caused serious denaturation. The use of small amount of surface-active agents served to keep the isocyanate emulsion stable. Polyoxyethylene hydrogenated caster oil ether, which is known to be inert to blood, was added to the suspension in an amount of 0.05%.

Shape. The shape of the modified cells was biconcave discoide, as is shown in Fig. 1. It cannot be distinguished from that of normal cells. These cells were neither ruptured nor deformed when suspended in a hypotonic or hypertonic salt solution.

It was assumed that the cells were fixed hard as rigid particles by the modification. However, viscometric measurements over a shear rate of 2 to 100 sec^{-1} showed that the flow behavior of the modified cell suspension was non-Newtonian, although to a lesser extent than with the intact red-cell suspension.[12] The result for the red cells hardened by formaldehyde was found to be Newtonian. These facts suggest that the membrane of the modified red cells has some flexibility.

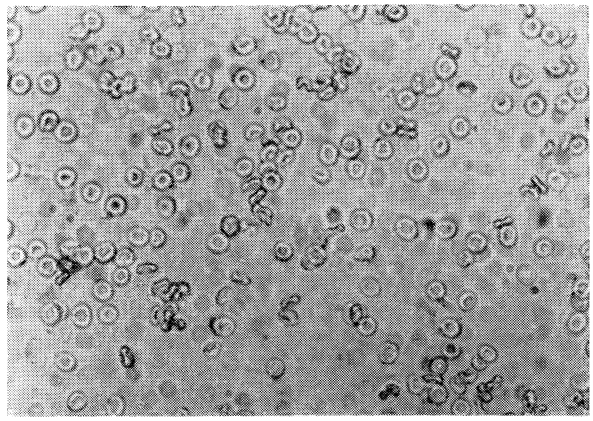

Fig. 1. Micro photograph of the modified human red cells suspended in distilled water.

Hemolysis. The modified cells showed some specific characteristics concerning hemolysis. They were not lysed by the action of osmotic pressure. They were recovered by centrifugation after being suspended in distilled water without releasing free hemoglobin into the medium. Neither lysis nor swelling was observed when they were suspended in a 50% aqueous solution of ethyl alcohol, acetone, or glycerine. No change in shape was observed in 2N sulfuric acid, but they swelled very much in 0.1N sodium hydroxide. Nonionic surface-active agents, such as Tween 20, polyoxyethylene hydrogenated caster oil ether, and saponin, were found not to affect the lysis of the modified cells. The same result was obtained with lecithin from eggs.

On the contrary, some of the ionic surface-active agents caused a lysis or swelling of the cells. The

11) W. Cooper, R. W. Pearson, and S. Drake, *Ind. Chemist*, **36**, 121 (1960).

12) M. Kaibara and E. Fukada, Institute of Physical and Chemical Research, Saitama, personal communication, 1969.

Table 1. Effect of ionic surface-active agents on the hemolysis of the red cells modified by TDI[a]

Anion	Result[b]	Cation	Result[b]
$C_{12}H_{25}SO_4Na$	H	$C_{12}H_{25}NH_2HCl$	H
$C_{12}H_{25}PhSO_3Na$[c]	H	$C_{12}H_{25}PyCl$[c]	H
$C_{11}H_{23}COONa$[d]	S	$C_{16}H_{33}PyCl$[c]	H
$C_{12}H_{25}PO_4Na_2$	U	$C_{12}H_{25}N(CH_3)_3Cl$	S
$C_{16}H_{33}O(CH_2)_3SO_3Na$	U	C_2H_5PyBr[c]	U
C_4H_9COONa	U	$C_{17}H_{35}(CONHC_2H_4)_2NH_2$[d]	U

a) Concentration of the detergents: 1%
b) H: hemolysed, S: swelled, U: unchanged.
c) Ph: phenylene, Py: pyridinium
d) A concentration below 1% was used because of the low solubility.

results are shown in Table 1.

There were clear differences among the hemolysed, the swelled, and the unchanged state. A hemolytically-active agent like dodecylpyridinium chloride caused lysis instantaneously, and a clear hemoglobin solution was obtained. Sodium laurate caused a swelling into a sphere and the hemoglobin within the cell was released into the medium, but a turbidity remained in the solution. No change in shape nor any release of hemoglobin was observed in the case of ethylpyridinium bromide. The hydrogen-ion concentration of the solution affected the hemolytic behavior sensitively. The modified cells were apt to lyse easily in a medium with a high pH value.

Although further investigations are required to establish the mechanism of the hemolysis of the modified cells, some tendencies can be seen in the table. There is some relationship between the structure of the ionic groups and the hemolytic effect. The orders are considered to be as follows: $-SO_4Na$ and $-SO_3Na > -COONa > -PO_4Na_2$ for the anionic series and $-NH_2HCl$ and $-PyCl > -N(CH_3)_3Cl$ for the cationic series. Hydrophobic groups are also considered to greatly affect the hemolytic action. Surface-active agents that have too short or too long alkyl chains cannot cause lysis. An alkyl chain that has ten to fifteen carbons is considered to be most effective.

These facts are in fair agreement with the results obtained for intact red cells. It has been reported that the order of the hemolytic activity of ionic surface-active agents according to the polar groups is as follows:[13]

$$-SO_4Na > -SO_3Na > -NH_2HCl > -COONa > -N(CH_3)_3I$$

Kondo and Tomizawa studied the hemolysis by cationic surface-active agents and proposed a mechanism.[14] They stated that lysis was caused by the adsorption of the detergent molecules onto the cell surface in terms of ionic attraction at first step, followed by the solubilization of lipids in the membrane in terms of hydrophobic interaction. They considered that the bulkiness of the hydrophobic group of reagents was an important factor in effective adsorption.

13) B. A. Pethica and J. H. Schulman, *Biochem. J.*, **53**, 177 (1953).
14) T. Kondo and M. Tomizawa, *J. Pharm. Sci.*, **58**, 255, 1378 (1969).

It is possible to consider that the mechanism of the hemolysis of the modified cells is the same as that for intact cells. This means that the isocyanate molecules do not affect the sites where the ionic surface-active agents attack to lyse. On the other hand, the sites where nonionic agents attack are assumed to be reinforced by the modification reaction.

Agglutination. The modified cells were found to be mixed with the blood of foreign animals or with that of different blood groups. Neither agglutination nor lysis was observed in the mixture. Figure 2 shows microphotographs of the modified human red cells of the A, B, O, and AB blood groups, suspended in plasma of the A blood group. Not much difference can be seen among them. It was also observed that the modified bovine red cells were mixed with the whole blood of a rabbit, homogeneously. No lysis nor agglutination was caused.

These facts suggest that red cells are inhibited or lose the power to agglutinate by the modification reaction. It has been reported that red cells lose their agglutinability towards appropriate antisera when they are treated with a formaldehyde solution.[5] It is expected that some information on the mechanism of the agglutination or other surface activities of red cells can be gotten by studying the properties of the modified cells further.

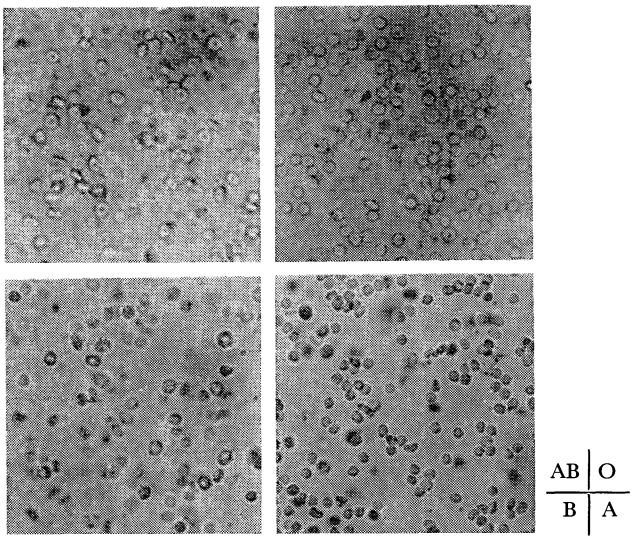

Fig. 2. Micro photographs of the modified red cells of the A, B, O, and AB blood group, suspended in plasma of the A blood group.

Properties of Hemoglobin. Figure 3 shows the visible absorption spectra of the red cells modified by TDI. The spectra for both the oxygenated state and the deoxygenated state are identical with that for normal blood, except that the peak intensity at 430 nm of the deoxygenated is slightly low. Figure 4 shows the oxygenation curves of the modified cells and intact cells. It is known that the hemoglobin within the modified cell retains the property to combine and to release molecular oxygen reversible in relation to the partial pressure of oxygen. It may be seen in the figure that hemoglobin within the modified cell has a higher oxygen affinity than normal hemoglobin, and that the

slope of the curve over the 10 to 90% oxygenated region is less steep. The n value, as calculated by using Hill's equation,[15] is 1.7. This is an intermediate value between 2.8 for normal hemoglobin and 1.0 for myoglobin. These changes in the oxygenation curve are considered to correspond to the decrease in the cooperation of hemoglobins or in the heme-heme interaction.

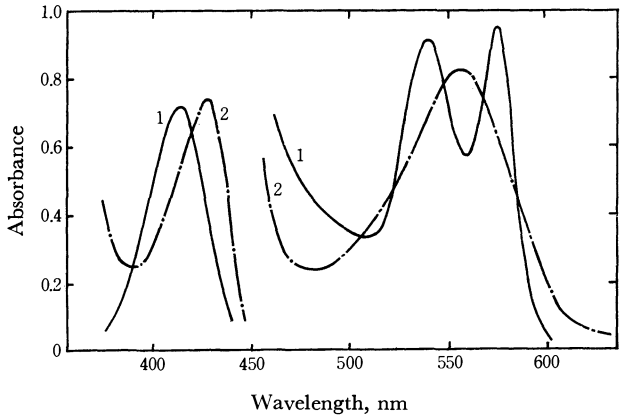

Fig. 3. Absorption spectra of the modified red cells.
(1) oxygenated; (2) deoxygenated with sodium hydrosulfite.
(The normal red cells give almost same absorption spectra as this figure.)

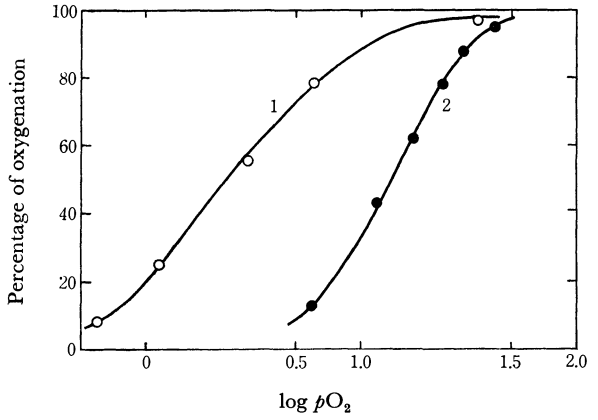

Fig. 4. Oxygenation curves of hemoglobin at pH 6.5. (1) the modified cells; (2) intact cells.

It is known that the absence of organic phosphates, such as D-2,3-diphosphoglycerate, or adenosine triphosphate, makes the oxygen affinity of hemoglobin higher.[16] It is considered that hemoglobins are not affected by the modification reaction, but some steric change or dissociation of the molecules may take place. On the other hand, it is also possible that the permeability of the cell membrane increases and that the organic phosphates within the cell come out, resulting in the high oxygen affinity. Further studies are necessary to ascertain the reasons and to find a way to protect hemoglobin from this change.

Reaction Sites. The facts described hitherto give us an idea of the modification reaction, that TDI reacts rapidly and selectively with specific components of the cell membrane to reinforce it, while the hemoglobin within the cell is kept unreacted. Figures 5 and 6 show the IR spectra of stroma and hemoglobin. The spectral samples of the modified cells were prepared through a process of lysis with sodium dodecylbenzenesulfonate, centrifugal separation of the stroma from the hemoglobin solution, and drying. Some differences can be seen between the spectrum of stroma separated from the modified cells and that for the intact cells. A sharp absorption band at 2250 cm^{-1} due to the stretching vibration of the isocyanate group, and additional bands at 805 and at 865 cm^{-1} corresponding to the out-of-plane deformation vibration of hydrogen on the 1,2,4-tri-substituted aromatic ring, appear in the spectrum for the modified stroma. On the other hand, the spectrum of the hemoglobin recovered from the modified cells is almost identical with that for the intact cells. This indicates that the hemoglobin is kept unreacted.

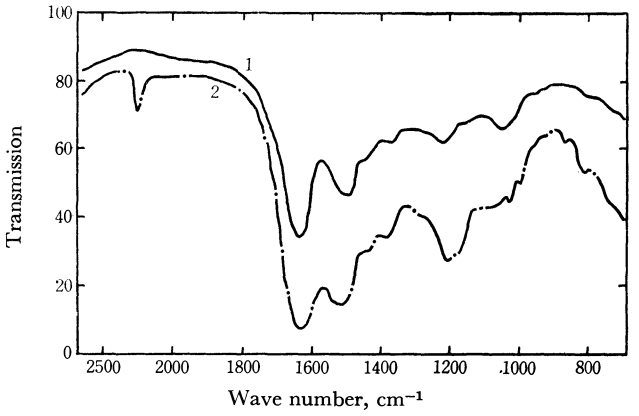

Fig. 5. IR spectra of stroma separated from (1) intact cells and (2) the modified cells.

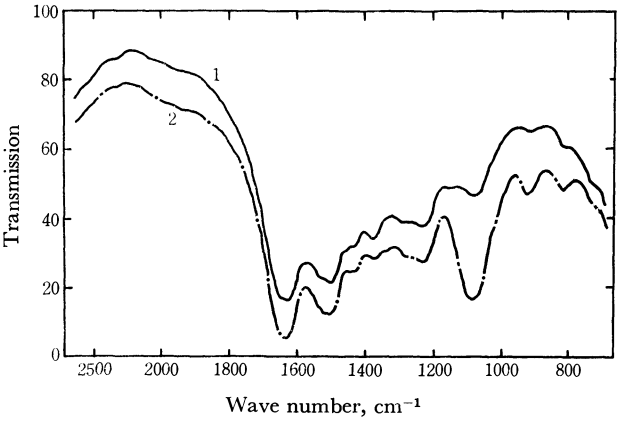

Fig. 6. IR spectra of hemoglobin separated from (1) intact cells and (2) the modified cells.

It is known that isocyanates react with compounds containing active hydrogen to give addition products. The order of reactivity on the bases of functional groups has been reported to be as follows:[17]

15) $Y=Kp^n/(1+Kp^n)$ where Y represents the oxygenated rate at partial pressure of oxygen being p mmHg, and K is the dissociation constant of oxygenated hemoglobin.

16) R. Benesch and R. E. Benesch, *Nature*, **221**, 618 (1969).

17) J. M. Buist and H. Dudgeon Ed., "Advances in Polyurethane Technology," J. Wiley and Sons Inc., New York (1968), p. 8.

Aliphatic NH_2>aromatic NH_2>primary OH>water>secondary OH>tertiary OH>phenolic OH>COOH and RNHCONHR'>RCONHR'>RNHCOOR'

As the modification reaction proceeds in an aqueous suspension, the reaction sites must have more isocyanate-reactive groups than water such as amino and primary hydroxy group. Other functional groups, carboxy, carbamoyl, imino, mercapto, formyl, *etc.*, may be kept unreacted. Diisocyanates are known as a kind of bridging reagents for enzymes and proteins.[18] It has been reported that the lysine residue was attacked exclusively in the treatment of pancreatic ribonuclease with hexamethylene diisocyanates.[19]

It has also been reported that comparatively large amounts of lysine and arginine residues are in the red-cell membrane as components of the protein.[20] Other components which have reactive groups are the cephalin and plasmalogens in the lipid layer and the serine residue in the protein. The isocyanate molecules must react with these components and reinforce the cell membrane through inter- or intra-molecular cross-linkings. It is reasonable to consider that ionic interaction between the polarized isocyanate group and polar group on the cell surface, or hydrophobic interaction between the hydrophobic group of the reagent and lipids in the membrane, gives some additional selectivity to the reaction.

One of the reactants must be the blood-group factor itself or one that is closely related to the agglutination phenomena. The isocyanate molecules may combine directly with it or mask the active site sterically, so that agglutination is inhibited. It is left for further studies now in progress to ascertain the exact mechanism of the modification reaction.

The authors wish to thank Professor S. Kimoto of the University of Tokyo, and Dr. S. Fujisawa and Dr. S. Ooba of Fuji Photo Film Co., Ltd., for their encouragements.

18) S. Petersen, *Angew. Chem.*, **59**, 266 (1947).
19) H. Ozawa, *J. Biochem.*, **62**, 419 (1967).
20) H. Behrendt, "Chemistry of Erythrocytes," C. C. Thomas, Springfield, I 11 (1957), p. 6.

BULLETIN OF THE CHEMICAL SOCIETY OF JAPAN, VOL. 44, 143—148 (1971)

Studies of Peptide Antibiotics. XXIII. Syntheses of Linear Decapeptide Analogs with Gramicidin S Sequence

Satoru MAKISUMI, Michinori WAKI, and Nobuo IZUMIYA

Laboratory of Biochemistry, Faculty of Science, Kyushu University, Hakozaki, Fukuoka

(Received June 13, 1970)

Six linear decapeptides having the same sequence of amino acids of gramicidin S, wherein the *N*-terminal amino acid is acylated with formyl or acetyl group, the *C*-terminal amino acid is in a form of its amide or ethanolamide and the *N*,*C*-terminal ones are free, were synthesized to obtain a more reliable picture of the cyclic structure to the antibacterial activity of gramicidin S. All these linear decapeptide analogs were found to be active to some extent against several microorganisms.

As a part of the program to synthesize linear analogs of gramicidin S, the syntheses of decapeptide analogs (II)[1] were undertaken. These compounds differ from gramicidin S in two ways: (a) they are non-cyclic and (b) both their terminal residues are blocked with an acyl and an amide group found in nature. Antibacterial assays of these analogs may clarify the influence of the cyclic structure of gramicidin S to its antibacterial activity.

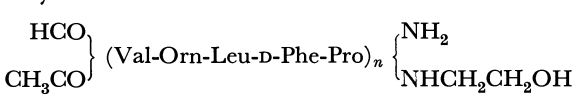

I (n=1), II (n=2)

H-(Val-Orn-Leu-D-Phe-Pro)$_2$-OH

III

It has been reported[2] that pentapeptide analogs (I) of this type were found to possess no antibacterial activity, although Erlanger and Goode[3] reported that *N*,*C*-terminal free linear decapeptide (III) having the gramicidin S sequence was found to possess weaker activity than gramicidin S itself. In order to obtain a more reliable picture of the cyclic structure to the antibacterial activity of gramicidin S, the activities of various synthetic linear peptides were compared with that of natural peptide. The present paper describes the syntheses and antibacterial properties of several acyl decapeptide amide analogs and the *N*,*C*-terminal free decapeptide which is used as a reference compound.

The steps involved in the syntheses of the acyl decapeptide amide analogs are shown in Fig. 1.[4] The reaction schemes are similar to those of the pentapeptide analogs[2] in general. For removal of the BOC

1) Amino acid symbols except D-Phe denote L configuration.

2) S. Makisumi, M. Waki, and N. Izumiya, *Mem. Fac. Sci., Kyushu Univ., Ser. C.* in press.

3) B. F. Erlanger and L. Goode, *Nature*, **174**, 840 (1954).

4) Abbreviations used: BOC, *t*-butyloxycarbonyl; Z, benzyloxycarbonyl; DCC, *N*,*N*'-dicyclohexylcarbodiimide; HOSu, *N*-hydroxysuccinimide; CM, carboxymethyl.

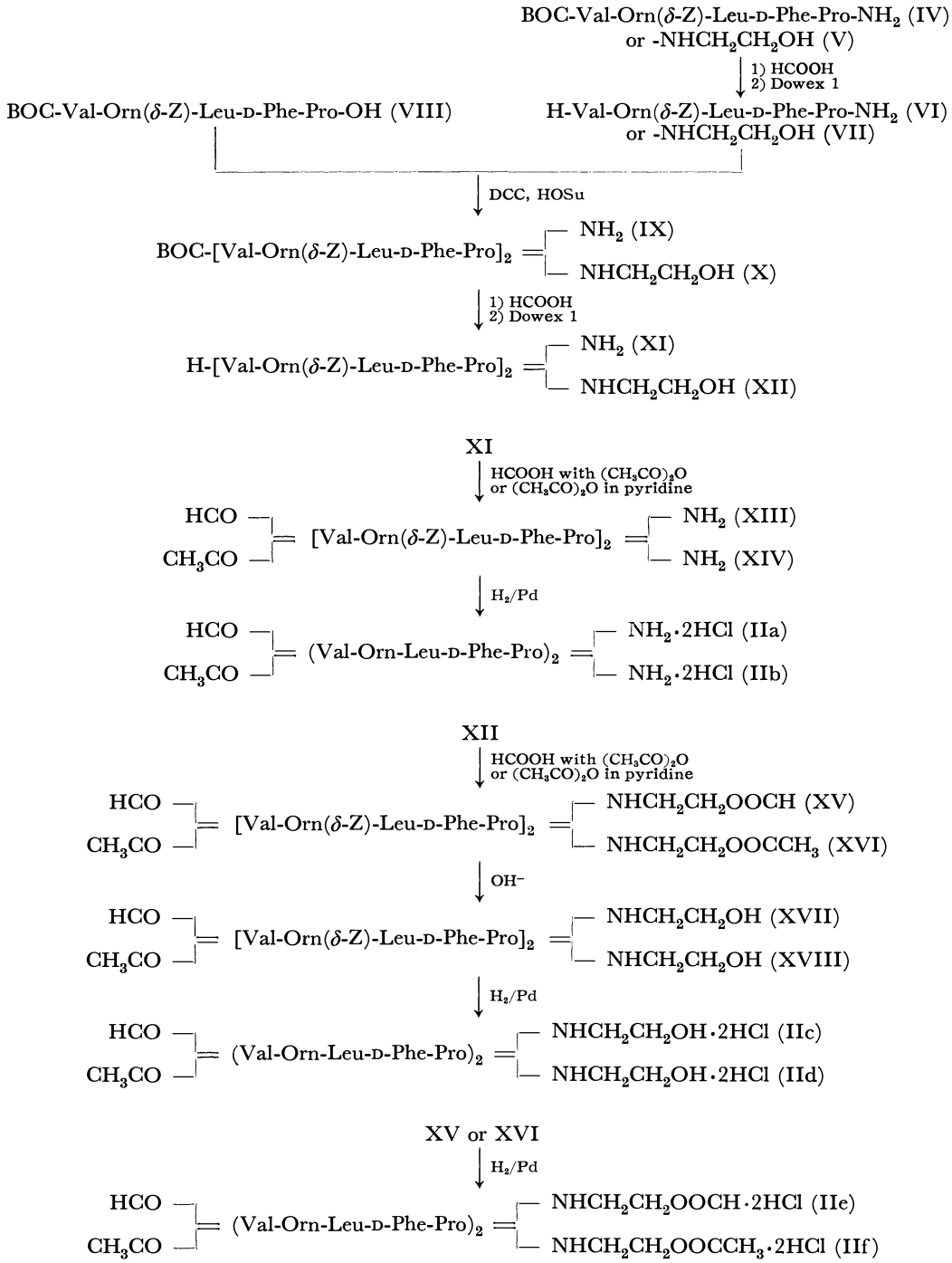

Fig. 1. Synthetic schemes of the acyl decapeptide amides.

group, 98% formic acid was used as reported by Halpern and Nitecki.[5] This method is good enough to prevent the partial deblocking of the Z groups in a peptide. Removal of the BOC group from BOC-pentapeptide amides (IV and V) by treatment with 98% formic acid and subsequent neutralization with Dowex 1 in methanol yielded free base of the pentapeptide amides (VI and VIII), respectively. Further purification of the products with column chromatography on CM-cellulose used in a previous work[2] was not needed in these cases, since the Z group remained intact.

Condensation of BOC-pentapeptide acid (VIII)[6] with VI or VII by the DCC-HOSu procedure[7] gave BOC-decapeptide amide derivative (IX or X) in a good yield. Purification of the crude product was performed by filtration over a column of Dowex 50 (H^+ form) and a Dowex 1 (OH^- form) in methanol. The method, reported by Sarges and Witkop,[8] was

5) B. Halpern and D. E. Nitecki, *Tetrahedron Lett.*, **1967**, 3031.

6) M. Ohno, T. Kato, S. Makisumi, and N. Izumiya, This Bulletin, **39**, 1738 (1966).

7) F. Weygand, D. Hoffmann, and E. Wünsch, *Z. Naturforsch.*, **21b**, 426 (1966); J. E. Zimmerman and G. W. Anderson, *J. Amer. Chem. Soc.*, **89**, 7151 (1967).

8) R. Sarges and B. Witkop, *J. Amer. Chem. Soc.*, **87**, 2020 (1965).

very useful for removing the contaminated amine and acid components in the fully protected peptide product obtained by coupling of the two components. Removal of the BOC group from IX or X by treatment with formic acid yielded a crystalline product of *N*-terminal free decapeptide amide derivative (XI or XII).

Acylation of the decapeptide amide (XI) with formic acid - acetic anhydride[9] or with acetic anhydride in pyridine[10] afforded formyl or acetyl decapeptide amide derivative (XIII or XIV). Removal of the Z groups from XIII or XIV by catalytic hydrogenation in the presence of hydrogen chloride in methanol provided formyl or acetyl decapeptide amide as dihydrochloride (IIa or IIb). On the other hand, acylation of decapeptide ethanolamide (XII) by the methods described above gave *N,O*-diacyl decapeptide derivative (XV or XVI) which was then converted to *N*-monoacyl derivative (XVII or XVIII) by saponification with alkali. Hydrogenolyses of XVII, XVIII, XV, and XVI in the presence of hydrogen chloride afforded *N*-acyl decapeptide ethanolamide analogs (IIc and IId) and *N,O*-diacyl decapeptide ethanolamide analogs (IIe and IIf) as hydrochloride, respectively. The final products IIa, IIb, IIc, IId, IIe, and IIf were shown to be practically homogeneous by thin-layer chromatography and paper electrophoresis. However, the formyl analogs (IIa, IIc, and IIe) were found to be contaminated with a minute amount of the deformylated peptides by paper electrophoresis as shown in Fig. 3. Attempts to remove these impurities have so far not been successful. It seems likely that the formyl group in these peptides is appreciably labile.

Erlanger *et al.* synthesized the *N,C*-terminal free decapeptide (III) by treatment of Z-[Val-Orn(δ-Tos)-Leu-D-Phe-Pro]$_2$-OH with sodium in liquid ammonia.[11] In this study, compound III was prepared *via* a different route shown in Fig. 2. Condensation of VIII with the formate (XIX) of neutral pentapeptide in the presence of two equivalents of triethylamine by the DCC-HOSu procedure gave BOC-decapeptide acid derivative (XX). Removal of BOC group from XX by an exposure to formic acid and subsequent crystallization in the presence of hydrogen chloride yielded *N,C*-terminal free decapeptide derivative as monohydrochloride (XXI). Catalytic hydrogenation of XXI gave III which was crystallized as trihydrochloride.

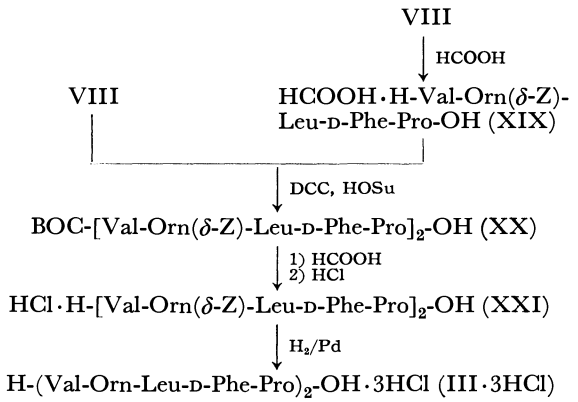

Fig. 2. Synthetic scheme of the *N,C*-terminal free decapeptide analog.

Comparison of the antibacterial activity of gramicidin S with that of the synthetic peptides showed that all of the linear decapeptide analogs have antibacterial activity against several microorganisms, though the activity is not so high compared with natural peptide (Table 1). It is of interest to note that the *N,C*-terminal free decapeptide (III) showed the same high activity as formyl-decapeptide amide (IIa) on Gram positive microorganisms, *S. aureus* and *B. subtilis*. The results we obtained have led us to conclude that even though the cyclic structure of gramicidin S is not essential for antibacterial activity, the specific activity of this compound is related to its unique cyclic structure.

Experimental

Melting points are uncorrected. The purity of the peptide intermediates after each synthetic step was ascertained by thin layer chromatography on silica gel plate. R_f^A refers to the solvent system chloroform-benzene-methanol (6 : 3 : 1, *v/v*) and R_f^B to the system chloroform-methanol (5 : 1, *v/v*). Homogeneity of the final product was confirmed by thin layer chromatography and by electrophoresis on paper. The solvent systems used are abbreviated as follows: C, ethyl acetate-pyridine-acetic acid-water (60 : 20 : 6 : 11, *v/v*); D, *n*-butanol-acetic acid-water (4 : 1 : 4, *v/v*); E, *sec*-buthanol-formic acid-

Table 1. Inhibitory activity of linear decapeptide analogs on microorganisms

Minimum inhibitory concentration, μg/ml

	Staphylococcus aureus FDA 209P	*Bacillus subtilis* ATCC 6633	*Escherichia coli* IAM 1253	*Proteus vulgalis* IAM 1052	*Shigella sonnei* 191—66	*Candida albicans* IAM 4888
GS·2HCl	1.56	0.79	25	>100	25	12.5
IIa	25	3.13	100	>100	100	50
IIb	50	6.25	100	>100	100	50
IIc	25	6.25	100	>100	>100	50
IId	50	12.5	100	>100	>100	100
IIe	50	6.25	100	>100	>100	50
IIf	25	12.5	100	>100	>100	100
III·3HCl	25	3.13	25	>100	50	50

9) J. C. Sheehan and D. D. H. Yang, *ibid.*, **80**, 1154 (1958).
10) H. Neumann, Y. Levin, A. Berger, and E. Katchalski, *Biochem. J.*, **73**, 33 (1959).
11) B. F. Erlanger, H. Sachs, and E. Brand, *J. Amer. Chem. Soc.*, **76**, 1806 (1954).

water (4 : 1 : 1, *v/v*). Gramicidin S was taken as the referene compound for the linear analogs and R_f^{GS} refers to the ratio of the distance which substances traveled to that which gramicidin S traveled from the origin on the same chromatogram. Paper electrophoresis was carried out on Toyo Roshi No. 50 with formic acid-acetic acid-methanol-water (1 : 3 : 6 : 10, *v/v*) buffer of pH 1.8. Electrophoretic mobilities are recorded as R^{His}, the ratio of the distance the compounds moved to that which a standard histidine spot moved on the same electrophoreogram. Compounds possessing free amino group were detected by spraying with ninhydrin and those with blocked amino groups by deblocking with 47% hydrobromic acid followed by staining with ninhydrin. Prior to microanalysis, desiccated samples were opened in air to a constant weight. Air dried samples were also subjected to measurement of specific rotation and $[\alpha]_D$ refers to 1% solution in methanol at 23°C unless otherwise noted.

The following compounds were prepared as described previously.[2] BOC-Val-Orn(δ-Z)-Leu-D-Phe-Pro-NH_2 (IV), BOC-Val-Orn(δ-Z)-Leu-D-Phe-Pro-$NHCH_2CH_2OH$ (V) and BOC-Val-Orn(δ-Z)-Leu-D-Phe-Pro-OH (VIII).

H-Val-Orn(δ-Z)-Leu-D-Phe-Pro-NH_2 (VI). BOC-pentapeptide amide (IV, 823 mg, 1 mmol) was dissolved in 25 m*l* of 98% formic acid and the solution kept at room temperature for 3 hr. The reagent was then removed *in vacuo* (bath temperature <30°C)and the residue was triturated with ether. The crude solid (formate) was dissolved in 10 m*l* of methanol and the solution was filtered over a column (1.2×8 cm) of Dowex 1 (OH^- form preserved in methanol). The effluent and washings were combined and the solution was evaporated *in vacuo*. The resulting residue was crystallized by addition of ether. The product was collected by filtration, yield 671 mg (93%), mp 118—122°C, $[\alpha]_D$ −68.1°, R_f^A 0.27, R_f^B 0.62.

Found: C, 62.12; H, 7.84; N, 13.02%. Calcd for $C_{38}H_{55}N_7O_7 \cdot H_2O$: C, 61.69; H, 7.77; N, 13.25%.

H-Val-Orn(δ-Z)-Leu-D-Phe-Pro-$NHCH_2CH_2OH$ (VII). Treatment of 866 mg (1 mmol) of V with 25 m*l* of 98% formic acid followed by crystallization and filtration over a column of Dowex 1 as described above gave 728 mg (95%) of peptide ethanolamide, mp 102—104°C, $[\alpha]_D$ −66.5°, R_f^A 0.29, R_f^B 0.63.

Found: C, 61.61; H, 7.99; N, 12.28%. Calcd for $C_{40}H_{59}N_7O_8 \cdot H_2O$: C, 61.28; H, 7.84; N, 12.51%.

BOC-[Val-Orn(δ-Z)-Leu-D-Phe-Pro]$_2$-NH_2 (IX). A suspension of 412 mg (0.5 mmol) of BOC-pentapeptide acid (VIII), 361 mg (0.5 mmol) of pentapeptide amide (VI) and 58 mg (0.5 mmol) of HOSu in a mixture of dioxane (5 m*l*) and dimethylformamide (4 m*l*) was cooled in an ice-salt bath. DCC (103 mg, 0.5 mmol) was added to the chilled solution and the mixture was stirred under cooling; meanwhile the suspension dissolved to form a clear solution. After it had been allowed to stand overnight at room temperature, the reaction mixture was stirred again with a few drops of water for 1 hr at 0°C. Crystals of dicyclohexylurea were removed by filtration and washed with cold dioxane. The filtrate and washings were evaporated to a small volume and the residual syrup was solidified by the addition of ice water. The solid obtained was collected by filtration, washed successively with water, 4% sodium bicarbonate, 10% citric acid and water, and dried. The product was dissolved in ethyl acetate and a small amount of insoluble dicyclohexylurea was removed. The filtrate was evaporated and the residue was crystallized by the addition of ether. Further purification was carried out as follow. The crystals were dissolved in 10 m*l* of methanol and the solution was filtered on a series of columns (1.2×8 cm, each) of Dowex 50 (H^+ form) and Dowex 1 (OH^- form) which were equilibrated with methanol. The effluent and the washings were evaporated and the residue was crystallized by the addition of ether and petroleum ether. The product was recrystallized from ethyl acetate-ether, yield 629 mg (82%), mp 203—205°C, $[\alpha]_D$ −123°, R_f^A 0.40.

Found: C, 63.19; H, 7.56; N, 11.64%. Calcd for $C_{81}H_{115}N_{13}O_{16} \cdot H_2O$: C, 62.97; H, 7.63; N, 11.79%.

BOC-[Val-Orn(δ-Z)-Leu-D-Phe-Pro]$_2$-$NHCH_2CH_2OH$ (X). By the DCC-HOSu method as described above, 823 mg (1 mmol) of VIII was allowed to couple with 766 mg (1 mmol) of pentapeptide ethanolamide (VII) in the presence of equimolar amount of DCC and HOSu. The product was purified as above to give 1399 mg (89%) of BOC-decapeptide ethanolamide, mp 127—130°C, $[\alpha]_D$ −110°, R_f^A 0.45.

Found: C, 62.45; H, 7.69; N, 11.28%. Calcd for $C_{83}H_{119}N_{13}O_{17} \cdot H_2O$: C, 62.74; H, 7.68; N, 11.46%.

H-[Val-Orn(δ-Z)-Leu-D-Phe-Pro]$_2$-NH_2 (XI). Treatment of 534 mg (0.35 mmol) of BOC-decapeptide amide (IX) with 10 m*l* of 98% formic acid followed by evaporation, crystallization and filtration on a column of Dowex 1 as described for the preparation of pentapeptide amide (VI) gave 481 mg (96%) of XI, mp 199—200°C, $[\alpha]_D$ −136°, R_f^A 0.30, R_f^B 0.66.

Found: C, 62.91; H, 7.56; N, 12.43%. Calcd for $C_{76}H_{107}N_{13}O_{14} \cdot 1.5H_2O$: C, 62.79; H, 7.63; N, 12.53%.

H-[Val-Orn(δ-Z)-Leu-D-Phe-Pro]$_2$-$NHCH_2CH_2OH$ (XII). Removal of the BOC group from 1304 mg (0.83 mmol) of BOC-decapeptide ethanolamide (X) by treatment with 98% formic acid followed by neutralization with Dowex 1 afforded 1185 mg (97%) of *N*-terminal free decapeptide ethanolamide, mp 114—116°C, $[\alpha]_D$ −123°, R_f^A 0.34, R_f^B 0.68.

Found: C, 62.52; H, 7.80; N, 11.93%. Calcd for $C_{78}H_{111}N_{13}O_{15} \cdot 1.5H_2O$: C, 62.55; H, 7.67; N, 12.16%.

HCO-[Val-Orn(δ-Z)-Leu-D-Phe-Pro]$_2$-NH_2 (XIII). To a solution of 200 mg (0.14 mmol) of decapeptide amide (XI) dissolved in 5 m*l* of 99.8% formic acid at 0°C was added 1.5 m*l* of acetic anhydride over a period of 15 min under stirring, and the mixture was kept at 0°C for 30 min at room temperature overnight. The solvent was removed *in vacuo* and the residue was triturated with ice water. The solid obtained was collected by filtration and dried. It was recrystallized from ethyl acetate-petroleum ether, yield 193 mg (95%), mp 215—216°C, $[\alpha]_D$ −145°, R_f^A 0.33.

Found: C, 62.03; H, 7.56; N, 12.05%. Calcd for $C_{77}H_{107}N_{13}O_{15} \cdot 2H_2O$: C, 62.04; H, 7.51; N, 12.21%.

CH_3CO-[Val-Orn(δ-Z)-Leu-D-Phe-Pro]$_2$-NH_2 (XIV). To a solution of 200 mg of XI in 5 m*l* of anhydrous pyridine, cooled in an ice-salt bath, 1.5 m*l* of acetic anhydride was added dropwise during a period of 10 min under stirring, and the mixture was kept in an ice-salt bath for 30 min at room temperature overnight. After the solvent had been evaporated, the oily product was solidified by the addition of ice water. The solid obtained was collected by filtration and dried. It was recrystallized from ethyl acetate-petroleum ether, yield 202 mg (98%), mp 230—232°C, $[\alpha]_D$ −133°, R_f^A 0.37.

Found: C, 62.48; H, 7.57; N, 12.00%. Calcd for $C_{78}H_{109}N_{13}O_{15} \cdot 2H_2O$: C, 62.26; H, 7.57; N, 12.10%.

HCO-(Val-Orn-Leu-D-Phe-Pro)$_2$-$NH_2 \cdot 2HCl$ (IIa). A solution of 102 mg (0.07 mmol) of formyl decapeptide amide (XIII) in 6 m*l* of methanol containing 0.7 m*l* of N/10 hydrochloric acid was hydrogenated in the presence of palladium black. After 3 hr, 0.7 m*l* of the hydrochloric acid was added and hydrogenation was continued. Completion of hydrogenolysis was confirmed by thin-layer chromatography. Palladium black was filtered off and the solution was evaporated *in vacuo*. When the residue was triturated with ether peptide was obtained as a crystalline hydrochloride. Recrystallization from methanol-ether gave 83 mg (94%), mp 247—

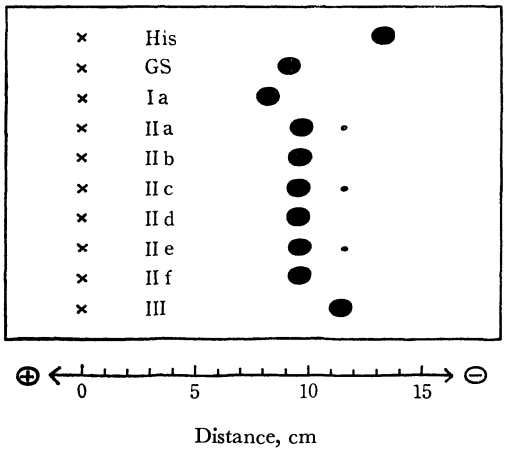

Fig. 3. Paper electrophoretic patterns of gramicidin S and its linear penta- and decapeptide analogs.
Buffer: formic acid-acetic acid-methanol-water (1 : 3 : 6 : 10, *v/v*) of pH 1.8. Duration: 600 V, 2 hr.

248°C, $[\alpha]_D$ −155°; R_f^{GS} 0.88(C), 0.90(D), 0.69(E); R^{His} 0.73.

Found: C, 53.42; H, 8.01; N, 13.32%. Calcd for $C_{61}H_{95}N_{13}O_{11}\cdot 2HCl\cdot 6H_2O$: C, 53.58; H, 8.03; N, 13.32%.

The product was contaminated with a minute amount of the deformylated derivative which was deduced from its higher electrophoretic mobility (R^{His} 0.87) (Fig. 3). Attempts to remove it have so far not been successful.

CH_3CO-(Val-Orn-Leu-D-Phe-Pro)$_2$-$NH_2\cdot 2HCl$ (IIb). When 103 mg (0.07 mmol) of XIV was hydrogenated as described above, after recrystallization from methanol - ether, 86 mg (97%) of the acetyl decapeptide amide dihydrochloride was obtained, mp 245—246°C, $[\alpha]_D$ −134°; R_f^{GS} 0.90(C), 0.80(D), 0.67(E); R^{His} 0.74.

Found: C, 53.59; H, 7.99; N, 13.16%. Calcd for $C_{62}H_{97}N_{13}O_{11}\cdot 2HCl\cdot 6H_2O$: C, 53.90; H, 8.10; N, 13.18%.

HCO-[Val-Orn(δ-Z)-Leu-D-Phe-Pro]$_2$-$NHCH_2CH_2OOCH$ (XV). Formylation of 441 mg (0.3 mmol) of the decapeptide ethanolamide (XII) was carried out in 10 m*l* of 99.8% formic acid with 3 m*l* of acetic anhydride in a similar manner to that employed for the preparation of XIII. Recrystallization from ethyl acetate-petroleum ether gave 441 mg (96%) of the diformyl decapeptide ethanolamide, mp 153—155°C, $[\alpha]_D$ −136°, R_f^A 0.38, R_f^B 0.60.

Found: C, 62.12; H, 7.44; N, 11.46%. Clacd for $C_{80}H_{111}N_{13}O_{17}\cdot H_2O$: C, 62.20; H, 7.37; N, 11.79%.

CH_3CO-[Val-Orn(δ-Z)-Leu-D-Phe-Pro]$_2$-$NHCH_2CH_2OOCCH_3$ (XVI). Acetylation of 441 mg of XII was carried out in 10 m*l* of pyridine with 3 m*l* of acetic anhydride in a similar manner to that employed for the preparation of XIV. Recrystallization from ethyl acetate-petroleum ether gave 444 mg (95%) of the diacetyl decapeptide ethanolamide, mp 179—181°C, $[\alpha]_D$ −123°, R_f^A 0.43. R_f^B 0.61.

Found: C, 62.54; H, 7.50; N, 11.45%. Calcd for $C_{82}H_{115}N_{13}O_{17}\cdot H_2O$: C, 62.62; H, 7.50; N, 11.58%.

HCO-[Val-Orn(δ-Z)-Leu-D-Phe-Pro]$_2$-$NHCH_2CH_2OH$ (XVII). A solution of 242 mg (0.16 mmol) of the diformyl derivative (XV) in 15 m*l* of methanol was saponified with 0.8 m*l* of N sodium hydroxide for 2 hr at room temperature. The reaction mixture was filtered over a column (1.8×8 cm) of Dowex 50 (H^+ form, equilibrated with methanol) and the effluent and washings were evaporated. The residue was dissolved in a mixture of methanol and ethyl acetate, and the solvent was removed. After this treatment had been repeated twice, the residue was crystallized by the addition of ether to yield 213 mg (89%), mp 148—150°C, $[\alpha]_D$ −132°, R_f^A 0.37.

Found: C, 62.47; H, 7.57; N, 11.74%. Calcd for $C_{79}H_{111}N_{13}O_{16}\cdot H_2O$: C, 62.56; H, 7.51; N, 12.00%.

CH_3CO-[Val-Orn(δ-Z)-Leu-D-Phe-Pro]$_2$-$NHCH_2CH_2OH$ (XVIII). Saponification of 233 mg (0.15 mmol) of XVI in 15 m*l* of methanol with 0.75 m*l* of N alkali as described above gave 219 mg (96%) of the monoacetyl derivative, mp 230—233°C, $[\alpha]_D$ −121°, R_f^A 0.40.

Found: C, 62.73; H, 7.57; N, 11.74%. Calcd for $C_{80}H_{113}N_{13}O_{16}\cdot H_2O$: C, 62.77; H, 7.57; N, 11.89%.

HCO-(Val-Orn-Leu-D-Phe-Pro)$_2$-$NHCH_2CH_2OH\cdot 2HCl$ (IIc). Hydrogenolysis of 105 mg (0.07 mmol) of XVII in 5 m*l* of methanol with 1.4 m*l* of N/10 hydrochloric acid as has been described for the preparation of IIa gave, after recrystallization from methanol - ether, 87 mg (96%) of the dihydrochloride of monoformyl decapeptide ethanolamide, mp 239—241°C, $[\alpha]_D$ −142°; R_f^{GS} 0.83(C), 0.82(D), 0.66(E); R^{His} 0.73.

Found: C, 53.99; H, 7.88; N, 13.02%. Calcd for $C_{63}H_{99}N_{13}O_{12}\cdot 2HCl\cdot 5H_2O$: C, 54.30; H, 8.03; N, 13.07%. This material was contaminated with a minute amount of the deformylated derivative (R^{His} 0.88).

CH_3CO-(Val-Orn-Leu-D-Phe-Pro)$_2$-$NHCH_2CH_2OH\cdot 2HCl$ (IId). By hydrogenolysis of 106 mg (0.07 mmol) of XVIII in methanol in the presence of hydrogen chloride, after recrystallization from methanol - ether, 88 mg (96%) of the dihydrochloride of monoacetyl decapeptide ethanolamide was obtained, mp 226—227°C, $[\alpha]_D$ −124°; R_f^{GS} 0.93(C), 0.76 (D), 0.58(E); R^{His} 0.72.

Found: C, 54.68; H, 8.09; N, 12.99%. Calcd for $C_{64}H_{101}N_{13}O_{12}\cdot 2HCl\cdot 5H_2O$: C, 54.61; H, 8.09; N, 12.94%.

HCO-(Val-Orn-Leu-D-Phe-Pro)$_2$-$NHCH_2CH_2OOCH\cdot 2HCl$ (IIe). Hydrogenolysis of 93 mg (0.06 mmol) of the diformyl derivative (XV) in 7 m*l* of methanol in the presence of hydrogen chloride for 5 hr gave, after recrystallization from methanolether, 76 mg (95%) of the diformyl decapeptide ethanolamide dihydrochloride, mp 234—236°C, $[\alpha]_D$ −138°; R_f^{GS} 0.91(C), 0.76(D), 0.65(E); R^{His} 0.71.

Found: C, 53.62; H, 7.83; N, 12.91%. Calcd for $C_{64}H_{99}N_{13}O_{13}\cdot 2HCl\cdot 6H_2O$: C, 53.39; H, 7.91; N, 12.65%.

The product was contaminated with a minute amount of the deformylated derivative (R^{His} 0.87).

CH_3CO-(Val-Orn-Leu-D-Phe-Pro)$_2$-$NHCH_2CH_2OOCCH_3\cdot 2HCl$ (IIf). By hydrogenolysis of 93 mg (0.06 mmol) of the diacetyl derivative (XVI) in 7 m*l* of methanol in the presence of hydrogen chloride 77 mg (94%) of the dihydrochloride of diacetyl decapeptide ethanolamide was obtained, mp 220—222°C, $[\alpha]_D$−119°; R_f^{GS} 0.84(C), 0.84(D), 0.71(E); R^{His} 0.73.

Found: C, 54.27; H, 7.83; N, 12.53%. Calcd for $C_{66}H_{103}N_{13}O_{13}\cdot 2HCl\cdot 6H_2O$: C, 54.01; H, 8.04; N, 12.41%.

H-Val-Orn(δ-Z)-Leu-D-Phe-Pro-OH·HCOOH (XIX). BOC-pentapeptide acid (VIII; 101 mg, 0.123 mmol) was dissolved in 2 m*l* of 98% formic acid and the solution was kept at room temperature for 2 hr. The solvent was removed *in vacuo* and the residue was solidified by the addition of ethyl acetate and ether. The product was collected by filtration and washed with ether. The very hygroscopic material was dried in a vacuum; yield 96 mg (99%), R_f^A 0.66, R_f^B 0.34. The formate was used for the next reaction without further purification, since the free pentapeptide had not been crystallized.[6]

BOC-[Val-Orn(δ-Z)-Leu-D-Phe-Pro]$_2$-OH (XX). To a solution of 101 mg of VIII and 14 mg (0.123 mmol) of HOSu in 2 m*l* of dioxane, 25 mg (0.123 mmol) of DCC was added at 5°C and the reaction mixture was stirred for 2 hr. To this solution was added a solution of pentapeptide formate (XIX; 96 mg, 0.122 mmol) in dioxane (3 m*l*) and dimethylformamide (2m*l*) containing 0.034 m*l* (0.244 mmol) of triethylamine, and the mixture was left to stand overnight in

a refrigerator. Crystals of dicyclohexylurea were removed by filtration and washed with dioxane. The filtrate and washings were concentrated to a small volume and the urea deposited further was filtred off. The filtrate was evaporated and the resulting syrup was solidified by the addition of water. The solid was collected by filtration, washed successively with water, 10% citric acid and water, and dried. The dried material was dissolved in 10 m*l* of methanol and filtered over a column (1.2×4 cm) of Dowex 50 (H^+ form) and the filtrate was evaporated. The residue crystallized upon the addition of ether. Recrystallization from methanol-ether gave 160 mg (95%) of the pure peptide, mp 173—175°C, $[\alpha]_D^{25}$ −109°, R_f^A 0.08, R_f^B 0.55.

Found: C, 61.56; H, 7.53; N, 10.86%. Calcd for $C_{81}H_{114}N_{12}O_{17}\cdot 3H_2O$: C, 61.50; H, 7.65; N, 10.63%.

*H-[Val-Orn(δ-Z)-Leu-*D*-Phe-Pro]$_2$-OH·HCl (XXI).* Compound XX (76 mg, 0.05 mmol) was dissolved in 3 m*l* of 98% formic acid and kept at room temperature for 90 min. The solvent was removed and the residue was dissolved in methanol containing 0.55 m*l* of N/10 hydrochloric acid. The solution was evaporated and the residue was dried over sodium hydroxide in a vaccum. The material obtained was then dissolved in a minute volume of methanol and precipitated by the addition of 10 m*l* of petroleum ether. Recrystallization from methanol-petroleum ether gave 69 mg (95%), mp 155—157°C, $[\alpha]_D^{30}$ −132°, R_f^A 0.10, R_f^B 0.57.

Found: C, 59.66; H, 7.30; N, 10.96%. Calcd for $C_{76}H_{106}N_{12}O_{15}\cdot HCl\cdot 4H_2O$: C, 59.42; H, 7.54; N, 10.94%.

*H-(Val-Orn-Leu-*D*-Phe-Pro)$_2$-OH·3HCl (III·3HCl).* By hydrogenolysis of 59 mg (0.04 mmol) of XXI in methanol containing an excess of hydrogen chloride in a similar manner to that employed for the preparation of IIa 49 mg (96%) of the trihydrochloride of the peptide was obtained, mp 233—234°C; $[\alpha]_D$ −135°; R_f^{GS} 0.77(C), 0.72(D), 0.70(E); R^{His} 0.86. Reported values, mp 233°C, $[\alpha]_D^{28}$ −89° (0.5N HCl).[11]

Found: C, 51.83; H, 7.90; N, 12.07%. Calcd for $C_{60}H_{94}N_{12}O_{11}\cdot 3HCl\cdot 6.5H_2O$: C, 52.00; H, 8.00; N, 12.13%.

Microbiological Assay.[12] The minimum amount of compounds needed for the complete inhibition of growth was determined by a dilution method with 10^3—10^4 organisms per milliliter using a Sabouraud bouillon as an incubation medium (Heart Infusion Broth for pre-incubation). The antibacterial activities of the decapeptide analogs are listed in Table 1.

12) We are indebted to Meiji Seika Co., Ltd. for the microbiological assays.

BULLETIN OF THE CHEMICAL SOCIETY OF JAPAN, VOL. 44, 148—152 (1971)

Studies on *s*-Triazines. VII. A New Method of Preparing 2-Methyl-4,6-bis(trichloromethyl)-*s*-triazine[1,2]

Ko WAKABAYASHI, Masaru TSUNODA, and Yasushi SUZUKI

Market Development Research Laboratory, Mitsubishi Chemical Industries Ltd., Kamoshida-cho, Midori-ku, Yokohama-shi, Kanagawa

(Received June 16, 1970)

During the liquid-phase chlorination of CH_3CN, a trimerization reaction occurred to yield four *s*-triazine derivatives, 2-methyl-4,6-bis(trichloromethyl)-*s*-triazine (I), 2-chloromethyl-4,6-bis(trichloromethyl)-*s*-triazine (II), 2-dichloromethyl-4,6-bis(trichloromethyl)-*s*-triazine (III), and 2,4,6-tris(trichloromethyl)-*s*-triazine (IV). The structure of each *s*-triazine derivative has been assigned on the basis of the results of elemental analysis and the spectral (particularly Mass and NMR) data after each derivative had been separated in a pure form using the gas-liquid chromatographic (GLC) method. The product composition was seen to depend upon the rate of the chrorination of CH_3CN and the presence of a catalyst. The *s*-triazine I was shown to be the precursor of the *s*-triazines II and III; the pathways for the formation of the *s*-triazine IV were also investigated. Then, the selective co-trimerization of CH_3CN with its chlorinated compounds was investigated; this yielded the *s*-triazine I, a useful intermediate of pesticides and resines. The reaction was found to provide a new method of preparing *s*-triazine I.

The *s*-triazine I is a valuable intermediate in the preparation of other substituted *s*-triazine derivatives, for example, the monoamino-[2,3] or diamino-*s*-triazines,[4,5] which are both extremely useful pesticides.[6-12] More-

1) Taken in part from the dissertation presented by K. Wakabayashi to the University of Tokyo, January 1969.

2) Previous paper of this series, K. Wakabayashi, M. Tsunoda and Y. Suzuki, *Yuki Gosei Kagaku Kyokai Shi*, **29**, in press (1971).

3) K. Wakabayashi, M. Tsunoda, and Y. Suzuki, *ibid.*, **27**, 868 (1969).

4) K. Wakabayashi, M. Tsunoda, and Y. Suzuki, *ibid.*, **28**, 252 (1970).

5) K. Wakabayashi, M. Tsunoda, and Y. Suzuki, *ibid.*, **28**, 333 (1970).

6) E. Knüsli, K. Rüfenacht, and H. Gysin, Ger. 1107448 (1961); U. S. 3086855 (1963).

7) H. Gysin and E. Knüsli, "Advance in Pest Control Research," Vol. III, ed. by R. L. Metcalf, Interscience, New York (1960), p. 289.

8) O. Weiberg, Ger. 1117131 (1961); Brit. 948175 (1964).

9) M. Okuzu, K. Wakabayashi, and T. Okada, Japan. 25170 (1967).

10) M. Okuzu, K. Wakabayashi, and T. Okada, *Japanese Appl.* 30187 (1965).

11) M. Okuzu, R. Hayashi, K. Wakabayashi, and Y. Suzuki, *ibid.*, 52006 (1967).

12) K. Matsui, H. Kasugai, K. Wakabayashi, and S. Motojima, *ibid.*, 74210 (1967).

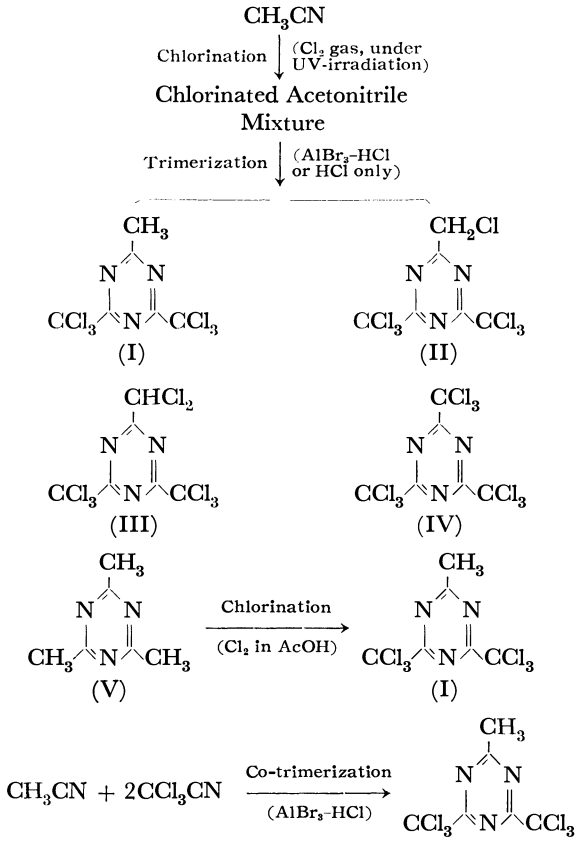

over, the *s*-triazine I itself shows remarkable nitrification inhibitory activity[13] in soil.

It is known that the *s*-triazine I can be prepared by the chlorination[14] of 2,4,6-trimethyl-*s*-triazine (V) or by the co-trimerization[15] of CCl_3CN and CH_3CN.

Schaefer and Ross[14] reported an 89% yield of the *s*-triazine I when chlorine was added to a solution of the *s*-triazine V in acetic acid. The same reaction has been repeated in our laboratory, but their very high yield was not always achieved and a complex mixture of all the possible *s*-triazines (I, II, III, IV, V, and other less chlorinated (Cl_{1-5}) 2,4,6-trimethyl-*s*-triazines) resulted.

In our earlier paper in this series,[15] we have reported that the co-trimerization of CCl_3CN with CH_3CN gave *s*-triazine I selectively in high yields. Therefore, we have investigated the preparation of CCl_3CN, the starting monomer, by the chlorination of CH_3CN, wherein the formation of a large amount of *s*-triazine derivatives as a by-product was observed. Gas-liquid chromatographic (GLC) and mass spectroscopic (Mass) analyses proved that the mixture contained *s*-triazines I, II, III, and IV.

Therefore we have investigated the preparation of the *s*-triazine I in a high yield and with a high selectivity by the co-trimerization of CH_3CN with its chlorinated mixture, without isolating them. It has now been found that the chlorinated mixture of CH_3CN can be co-trimerized with CH_3CN so as to selectively afford the *s*-triazine I. We wish here to report this first technical method for the preparation of the *s*-triazine I.

Results and Discussion

CH_3CN was chlorinated by chlorine in the presence of HCl under UV irradiation in order to prepare CCl_3CN. Table 1 shows some typical results of the chlorination experiments. CCl_3CN was the sole obtainable chlorinated nitrile; CH_2ClCN or $CHCl_2CN$ was detected to only a negligible extent in GLC. In addition, a large amount of a white solid was also obtained as a by-product. The GLC analysis of the solid revealed four peaks (A, B(minor), C(minor) and D); the relative R_t values were A=0.38, B=0.71, C=0.82, D=1.00 (based on D=1.00). The A and D relative R_t values were the same as those of the *s*-triazines I and IV respectively.[15] B, separated by GLC, was found to be the *s*-triazine II by Mass- (*m/e* 361(M^+, molecular peak), 326(M^+-Cl), 325(M^+-HCl) *etc.*); NMR-(τ 5.08 ppm(singlet, CH_2Cl)) and IR-data (1552, 1522, 1346 cm^{-1} (*s*-triazine ring)). C was found

Table 1. Chlorination of acetonitrile (Experimental A)

Chlorination time (hr)	Sp. gravity of chlorinated CH_3CN (D_4^{45})	Analysis of distillate: Total non-trimerized nitriles (mol)	Analysis of distillate: Yield of CCl_3CN (%)	Analysis of distillate: Selectivity of nitriles (%) CH_3CN	Analysis of distillate: Selectivity of nitriles (%) CCl_3CN	Analysis of residue: Total trimerized nitriles (mol)	Analysis of residue: Selectivity of *s*-triazines (%) I	II	III	IV
3	0.9010	100	8.7	91.3	8.7	0				
8	1.0004	100	18.2	81.8	18.2	0				
10	1.0512	100	24.4	76.5	24.4	0				
12	1.1004	100	30.6	69.4	30.6	0				
15	1.1502	99.4	36.8	63.0	37.0	0.6	100.0			
18	1.2010	97.9	43.6	55.5	44.5	2.0	100.0			
21	1.2504	82.6	40.3	51.2	48.8	17.3	94.8	3.4	1.8	
24	1.3006	68.5	38.8	43.4	56.6	31.5	85.7	5.7	6.7	1.9
29	1.3500	53.5	37.2	30.5	69.5	46.4	72.9	7.7	8.4	11.0
33	1.4020	42.7	36.8	13.8	86.2	57.3	62.8	8.5	9.9	18.8
38	1.4492	38.8	36.2	6.7	93.3	61.1	58.8	7.8	10.4	23.0

13) K. Wakabaysahi and M. Okuzu, *Nippon Dojo-Hiryogaku Zasshi*, **40**, 504 (1969).
14) F. C. Schaefer and J. H. Ross, *J. Org. Chem.*, **29**, 1527 (1964).
15) K. Wakabayashi, M. Tsunoda, and Y. Suzuki, This Bulletin, **42**, 2924 (1969).

TABLE 2. TRIMERIZATION OF CHLORINATED ACETONITRILE MIXTURE (Experimental B)

Chlorination time (hr)	Sp. gravity of chlorinated CH_3CN (D_4^{45})	$AlBr_3$-HCl catalyzed trimerization (Exp. B-1)					HCl catalylized trimerization (Exp. B-2)				
		Total yield of *s*-triazines (%)	Selectivity of *s*-triazines (%)				Total yield of *s*-triazines (%)	Selectivity of *s*-triazines (%)			
			I	II	III	IV		I	II	III	IV
12	1.1004	44.6	100.0				44.3	100.0			
15	1.1502	54.4	100.0				53.8	100.0			
18	1.2010	65.8	100.0				66.0	100.0			
21	1.2504	76.3	98.8	0.7	0.5		75.1	98.8	0.8	0.4	
24	1.3006	87.2	94.6	2.1	2.4	0.9	85.4	95.1	1.9	2.3	0.7
29	1.3500	92.3	81.4	3.8	4.1	10.7	90.5	86.6	4.0	4.1	5.3
33	1.4020	92.5	53.6	4.7	5.8	35.9	72.4	71.4	6.6	7.6	14.4
38	1.4492	94.0	43.5	4.7	6.4	45.4	64.3	63.5	7.3	8.8	20.4

to be the *s*-triazine III by Mass- (*m/e* 395 (M^+, molecular peak), 360(M^+—Cl), 359(M^+—HCl) *etc.*); NMR- (τ 3.12 ppm(singlet, $CHCl_2$)) and IR-data (1550, 1518, 1346 cm^{-1} (*s*-triazine ring)).

The following two pathways are possible for the formation of the *s*-triazine I:

1) by the chlorination of the *s*-triazine V or 2,4-dimethyl-6-trichloromethyl-*s*-triazine (VI), or

2) by the co-trimerization of 2 moles of CCl_3CN with 1 mole of CH_3CN.

The latter is more likely, since the *s*-triazines V[16] and VI were not detected during the chlorination of CH_3CN nor during the co-trimerization of CCl_3CN with CH_3CN,[15] whereas the *s*-triazine I was the sole product when the molar ratio,[17] CCl_3CN/CH_3CN, was less than two in the co-trimerization.[14]

The *s*-triazines II and III may be produced by the chlorination of the *s*-triazine I,[18] because CH_2ClCN and $CHCl_2CN$ were not detected in the chlorination mixture of CH_3CN and because neither CH_2ClCN nor $CHCl_2CN$ could co-trimerize with CCl_3CN.[19]

The trimerization of CCl_3CN does not proceed smoothly in the absence of a Friedel-Crafts catalyst-hydrogen halide complex under ordinary pressure.[15,20] The treatment of the chlorinated mixture of CH_3CN with $AlBr_3$-HCl or with HCl resulted in an increased formation of the *s*-triazine IV (*cf.* Table 2). Apparently a large part of the *s*-triazine IV could be formed by the chlorination of the *s*-triazine I,[18] while a small part of it could arise from the trimerization of CCl_3CN.

On the basis of this experimental result that a large amount of *s*-triazine derivatives was obtained during the chlorination of CH_3CN, we have tested to obtain the *s*-triazine I in a high yield and high selectivity by treating a chlorinated mixture of CH_3CN with a catalyst without isolating CCl_3CN. For this purpose several experiments were carried out under various reaction conditions (see Table 2).

When chlorine was introduced into CH_3CN for less than 15 hr, and when this chlorinated mixture was then treated with a catalyst, the total yield of the *s*-triazine I was lower, as is shown in Table 2, although the selectivity of the *s*-triazine I was higher. On the other hand, when chlorine was introduced into CH_3CN for more than 21 hr and it was then co-trimerized, the total yield was higher, although the selectivity was lower. The total yield of *s*-triazines in Exp. B-1 was higher when the chlorinated mixture was treated with the $AlBr_3$-HCl catalyst after a long chlorination time, since the CCl_3CN produced successively could be converted into the *s*-triazine I and IV smoothly by the aid of this catalyst. The total yield of *s*-triazines in Exp. B-2 was rather lower than that in Exp. B-1. This may have been because CCl_3CN could not be converted into the *s*-triazine I smoothly, because there was little CH_3CN over a long chlorination time, and also because it was hard to convert it into the *s*-triazine IV by means of the HCl catalyst alone.

The best way to obtain the *s*-triazine I is to co-trimerize both nitriles, CCl_3CN and CH_3CN, when the specific gravity of the chlorinated mixture of CH_3CN reaches *ca.* 1.2 — molar ratio, CCl_3CN/CH_3CN, 40/60. The detailed experimental conditions or techniques will be described in the experimental part. The results show that the *s*-triazine I can be prepared in high yields by a less costly and convenient method.

Experimental

All the boiling points and melting points are uncorrected. The gas-liquid chromatography was performed with a Shimadzu GC-2B apparatus fitted with a thermal conductivity detector, with 70 ml/min of helium, and using a ϕ 4 mm×2 m column containing 20% DOP on Shimalite C at 100°C (GLC-1), or with such an apparatus fitted with a flame ionization detector, with 40 ml/min of nitrogen and using a ϕ 4 mm× 2 m column containing 5% SE-30 on Gaschrom P at 170°C (GLC-2). The IR* spectra were obtained with a JASCO model IR-G spectrometer. The NMR spectra were determined

16) *s*-Triazine V are obtainable from CH_3CN under high pressure using alkaline catalyst.[15]

17) *s*-Triazine IV, beside *s*-triazine I, could be also obtained when the molar ratio is more than two and the co-trimerization is carried out in the presence of Friedel-Crafts catalyst.[14]

18) To ascertain this chlorination pathway, *s*-triazine I was chlorinated under UV-irradiation and we obtained *s*-triazines II, III and IV besides the unreacted *s*-triazine I. (See Exp.-E).

19) See Exp.-D.

20) T. R. Norton, *J. Amer. Chem. Soc.*, **72**, 3527 (1950).

* Abbreviation: vs, very strong; s, strong; m, medium; w, weak; vw, very weak; sh, shoulder.

at 60 Mc/Mc with a Varian A-60 spectrometer, using TMS the internal standard. The mass spectra were obtained on as a Hitachi RMU-6C spectrometer, using a direct inlet, an ion-accelerating voltage of 1800 V, an electron accelerating voltage of 80 eV, a total emission current of 80 μA, a temperature of the ionization chamber of 200°C, a sample temperature of 100°C, and a vacuum of 1×10^{-6} mmHg.

Materials. The CH_3CN was supplied by Kasei Mizushima, Ltd. The CCl_3CN was prepared by the chlorination of CH_3CN.[21] Authentic 2-methyl-4,6-bis(trichloromethyl)-*s*-triazine (I) and 2,4,6-tris(trichloromethyl)-*s*-triazine (IV) were prepared by the (co-)trimerization of CCl_3CN according to the previously-presented procedures of the present authors.[15] 2-Chloromethyl-4,6-bis(trichloromethyl)-*s*-triazine (II) and 2-dichloromethyl-4,6-bis(trichloromethyl)-*s*-triazine (III) were separated in a pure form with GLC-2 from the trimerized product of the chlorinated mixture of CCl_3CN.

A) Chlorination of CH_3CN. A 10-*l*, five-necked flask was equipped with an efficient mechanical stirrer, a thermometer, a gas-inlet tube reaching nearly to the bottom of the flask, an efficient reflux condenser protected at the top with a calcium chloride tube, and an immersion-type mercury lamp (10—15 W, 2537 Å, Taika Kogyo Co.). The gas-inlet tube was connected to a container of chlorine through a flow meter and a 500 m*l* bottle containing about 200 m*l* of concentrated H_2SO_4. The outlet tube at the back of the calcium chloride tube was connected with a gas-absorption trap in which the evolved HCl was absorbed by running water. It was best to set the apparatus up under a good hood.

In the flask 4.1 kg (100 mol) of CH_3CN were placed and saturated with 1.5 kg of dry HCl at 35—40°C. Then, a current of chlorine (22 kg, 310 mol) was introduced into the reaction mixture under UV irradiation, the temperature of which was maitained at 45—50°C. The rate of the flow of the chlorine (*ca.* 9.9 g per minute) had to be regulated, care being taken that the liquid remain as colorless as possible. This chlorination required about 38 hr; at intervals samples of the chlorinating mixture were taken out. By distillation, the samples were divided into two parts, the distillate (bp 56—88°C) and the residue, each of which was separated by GLC and analysed by spectroscopic methods.

Analysis of the Distillate. Two components were separated in GLC-1; their relative R_t values, 1.00 and 0.70 (based on R_t of CH_3CN, 1.00), were in fair agreement with those of authentic CH_3CN and CCl_3CN.

The component of $R_t=1.00$ (CH_3CN): Bp 81—83°C, n_D^{25} 1.34430, D_4^{15} 0.7875 (lit,[22] bp 81.6°C/760 mmHg, n_D^{30} 1.33934, D_4^{15} 0.78745). NMR ($CDCl_3$): τ 8.04 ppm (singlet, CH_3).

The Component of $R_t=0.70$ (CCl_3CN): Bp 84—86°C, n_D^{25} 1.43851, n_4^{15} 1.4418.

IR (liq. film, 0.05 mm): 2250 cm^{-1} (m, νC≡N), 1580(vw), 1374(vw), 1028(s), 971(m), 919(sh), 868(sh), 790(vs, νC–Cl), 648(w), 490(m).

NMR ($CDCl_3$): no signal.

Analysis of the Residue. Four components (A, B, C, D) were separated in GLC-2; their relative R_t values were A=0.38, B=0.71, C=0.82, D=1.00 (based on R_t of D, 1.00).

The Component A: The relative R_t value was same as authentic *s*-triazine I. Mp 96—97°C (lit,[15] mp 96—97°C).

Elemental analysis; Found: C, 21.95; H, 1.13; N, 12.70; Cl, 64.57%. Calcd for $C_6H_3N_3Cl_6$: C, 21.84; H, 0.92; N, 12.74; Cl, 64.49%.

IR (KBr): 2920 cm^{-1} (vw), 1570(s), 1551(vs), 1525(vs), 1490(sh), 1435(sh), 1406(s), 1350(m), 1341(s), 1048(m), 1011(sh), 1002(m), 992(m), 978(m), 852(m), 840(s), 828(vs), 818(sh), 790(vs), 771(vs), 746(sh), 722(sh), 696(vs), 600(m), 580(s), 500(m).

NMR ($CDCl_3$): τ 7.02 ppm (singlet, $C\underline{H}_3$).

Mass (relative intensity): *m/e* 335(0.8), 334(0.3), 333(2.8), 332(0.8), 331(6.2), 330(1.5), 329(7.7), 328(0.7), 327(4.0, M^+-peak), 300(3.8), 299(1.8), 298(20.5), 297(6.2), 296(64.2), 295(10.4), 294(100.0), 293(7.0), 292(61.8, M^+-Cl), 262(1.2), 261(6.5), 260(2.6), 259(15.0), 258(2.7), 257(12.1, M^+-Cl_2), 255(1.2), 253(1.8), 251(1.1), 220(1.5), 218(3.1), 216(2.4), 185(0.7), 183(1.5), 181(1.6), 173(0.7), 171(2.1), 169(2.1), 149(1.1), 147(0.6), 145(1.5), 143(1.7), 138(1.2), 137(0.8), 136(6.4), 135(0.9), 134(10.5), 133(0.3), 131.5(0.5), 131(1.5), 130.5(4.0), 130(1.1), 129.5(11.8), 129(1.5), 128.5(12.0), 123(0.8), 122(2.1), 121(5.3), 120(5.3), 119(16.5), 118(1.2), 117(17.3), 114(0.5), 113(0.6), 112(7.4), 111(2.1), 110(46.0), 109(2.8), 108(71.5, CCl_2CN), 102(1.2), 101(0.4), 100(3.0), 99(2.0), 98(1.8), 96(1.2), 94(2.0), 87(1.8), 86(2.0), 85(4.8), 84(10.8), 83(0.5), 82(15.1), 76(1.2), 75(3.8), 74(0.4), 73(12.0), 68(1.2), 67(14.7), 66(0.9), 64(0.8), 62(1.2), 61(0.7), 59(0.5), 57(1.0), 55(1.0), 53(1.0), 52(1.3), 51(1.2), 50(0.7), 49(5.2), 48(0.6), 47(15.8), 46(0.8), 45(1.2), 44(0.7), 43(1.1), 41(4.8), 40(4.8), 39(2.1), 38(3.2), 37(0.7), 36(10.2), 35(2.0), 31(0.7), 29(1.0), 28(1.6), 27(3.7), 26(2.5), 15(4.8).

The Component B: This compound was identified as *s*-triazine II on the basis of elemental analysis and spectroscopic data. Mp 62—64°C (from *n*-hexane), bp 175—180°C/2.0 mmHg (lit,[14] mp 63—64°C, bp 120—125°C/0.1 mmHg).

Elemental analysis; Found: C, 19.87; H, 0.55; N, 11.42; Cl, 68.29%. Calcd for $C_6H_2N_3Cl_7$: C, 19.78; H, 0.55; N, 11.54; Cl, 68.13%.

IR (KBr): 2961 cm^{-1} (vw), 1552(vs), 1522(vs), 1406(m), 1346(s), 1018(m), 990(w), 942(w), 850(m), 836(vs), 818(sh), 790(m), 768(vs), 746(sh), 730(sh), 696(vs), 578(w).

NMR ($CDCl_3$): τ 5.08 ppm (singlet, CH_2Cl).

Mass (relative intensity): *m/e* 369(0.6), 368(0.2), 367(1.9), 366(0.3), 365(3.8), 364(0.4), 363(3.9), 362(0.4), 361(1.7, M^+-peak), 360(0.2), 336(1.0), 335(0.5), 334(8.3), 333(1.0), 332(34.3), 331(4.5), 330(79.8), 329(11.0), 328(100.0), 327(12.6), 326(52.4, M^+-Cl), 325(6.5), 299(2.0), 298(0.6), 297(10.2), 296(3.0), 295(29.8), 294(9.5), 293(47.2), 292(15.0), 291(30.1, M^+-Cl_2), 290(9.0), 261(0.8), 260(2.0), 259(1.2), 258(3.7), 257(2.3), 256(2.9, M^+-Cl_3), 255(1.7), 220(0.7), 219(0.4), 218(1.4), 217(0.3), 216(1.1), 185(0.8), 184(0.9), 183(1.8), 182(0.8), 181(1.8), 173(0.6), 171(1.4), 169(1.4), 147(1.7), 146(1.5), 145(4.3), 144(6.7), 143(4.6), 138(1.2), 137(1.0), 136(5.1), 135(2.2), 134(8.4), 133(0.8), 130(1.5), 129.5(0.7), 129(1.0), 128.5(1.3), 128(2.1), 127.5(1.0), 127(1.0), 124(0.9), 123(0.7), 122(1.7), 121(4.5), 120(2.0), 119(13.8), 118(0.8), 117(14.1), 113(1.6), 112(5.0), 111(3.0), 110(31.8), 109(3.8), 108(48.2), 103(2.2), 102(1.1), 101(5.6), 100(1.9), 96(1.0), 95(0.9), 94(1.7), 88(0.7), 87(1.2), 86(1.3), 85(4.8), 84(6.8), 83(6.7), 82(10.9), 81(0.6), 79(0.7), 78(0.8), 77(1.2), 76(3.0), 75(4.3), 74(9.3), 73(7.2), 71(0.8), 69(0.7), 67(0.8), 66(2.4), 65(0.7), 64(1.0), 63(0.7), 62(1.0), 61(2.4), 60(1.1), 59(0.9), 57(0.5), 56(0.7), 55(1.0), 54(0.5), 53(0.8), 52(1.7), 51(4.2), 50(1.8), 49(8.3), 48(2.6), 47(10.3), 45(1.1), 44(3.2), 43(1.7), 42(0.6), 41(1.7), 40(2.9), 39(1.9), 38(2.9), 37(1.3), 36(8.8), 35(4.1), 31(0.8), 29(1.0), 28(1.8), 27(1.1), 26(1.1).

The Component C: This compound was identified as *s*-triazine III on the basis of elemental analysis and spectroscopic data. Mp 41—42°C (from *n*-hexane), bp 170—173°C/0.5 mmHg.

Elemental analysis; Found: C, 17.98; H, 0.32; N, 10.56;

21) K. Dachlauer, German 694479 (1942); *D. R. P. Org. Chem.*, **6**, 1384.

22) "The Merck Index," eighth edition, ed. by P. G. Stecher, Merck & Co., Inc., New Jersey, U. S. A. (1968), p. 8.

Cl, 71.30%. Calcd for $C_6HN_3Cl_8$: C, 18.07; H, 0.25; N, 10.54; Cl, 71.13%.

IR (KBr): 2970 cm^{-1}(vw), 1550(vs), 1518(s), 1410(w), 1346 (s), 1018(m), 930(w), 846(sh), 833(s), 818(sh), 790(m), 761(vs), 746(sh), 730(sh), 695(vs).

NMR ($CDCl_3$): τ 3.12 ppm (singlet, $CHCl_2$).

Mass (relative intensity): *m/e* 405(0.4), 404(0.5), 403(1.0), 402(0.9), 401(2.0), 400(2.0), 399(3.4), 398(3.0), 397(2.7), 396(2.5), 395(1.2, M^+-peak), 394(1.1), 370(6.2), 369(4.9), 368(17.9), 367(8.7), 366(54.9), 365(13.1), 364(96.4), 363(14.6), 362(100.0), 361(9.0), 360(45.9, M^+-Cl), 333(4.7), 332(4.4), 331(20.3), 330(9.0), 329(42.1), 328(20.6), 327(52.2), 326(24.9), 325(27.4, M^+-Cl_2), 324(12.8), 296(1.6), 295(1.4), 294(4.7), 293(4.0), 292(7.3), 291(6.0), 290(4.6), 289(3.7), 255(0.8), 253(1.2), 251(0.7), 222(0.3), 221(0.5), 220(1.0), 219(1.0), 218(2.1), 217(0.8), 216(1.6), 186(0.9), 185(0.7), 184(3.6), 183 (1.8), 182(3.8), 181(1.9), 173(0.5), 172(0.6), 171(1.3), 170(0.8), 169(1.3), 166(0.7), 165(2.7), 164(6.3), 163(7.8), 162(4.2), 160 (0.4), 159(1.3), 158(0.4), 157(1.3), 149(0.8), 148(1.3), 147 (3.2), 146(5.2), 145(4.4), 144(0.8), 143(1.3), 139(0.5), 138 (0.9), 137(2.3), 136(5.5), 135(3.9), 134(8.4), 133(0.4), 132 (1.6), 131(1.0), 130(1.5), 129(0.9), 128(1.8), 127(1.2), 123(1.0), 122(2.2), 121(7.1), 120(2.8), 119(21.1), 118(0.7), 117(21.5), 113(0.6), 112(5.6), 111(3.1), 110(37.7), 109(4.1), 108(54.6, CCl_2CN), 105(0.7), 104(0.3), 103(0.5), 102(1.7), 101(0.9), 100(5.4), 99(1.0), 98(0.8), 97(1.1), 96(1.4), 95(1.7), 94(2.1), 92(2.4), 91(0.5), 89(0.8), 88(1.2), 87(4.7), 86(4.3), 85(11.2), 84(9.6), 83(17.9), 82(14.4), 78(0.5), 77(1.7), 76(6.7), 75(2.8), 74(20.4), 73(9.0), 72(0.5), 71(0.5), 70(0.4), 69(0.5), 68(0.5), 67(0.5), 66(0.5), 65(0.7), 64(0.5), 63(0.5), 62(1.8), 61(0.9), 60(2.1), 59(1.0), 57(0.8), 55(1.0), 53(1.1), 52(1.1), 51(3.2), 50(2.0), 49(4.8), 48(5.5), 47(15.3), 45(0.5), 44(3.6), 43(1.1), 42(0.8), 41(0.4), 40(0.8), 39(1.8), 38(5.5), 37(1.1), 36(17.2), 35(3.3), 31(0.9), 29(1.3), 28(1.7), 27(1.3).

The Component D: Its relative R_t value was same as authentic *s*-triazine IV. Mp 94—95°C (from ethanol) (lit,[15] mp 93°C), bp 175—177°C/10 mmHg (lit,[23] bp 176—178°C/12 mmHg).

Elemental analysis; Found: C, 16.72; N, 9.65; Cl, 73.53%. Calcd for $C_6N_3Cl_9$: C, 16.64; N, 9.70; Cl, 73.66%.

IR (KBr): 1540 cm^{-1}(vs), 1508(sh), 1341(s), 1017(m), 846 (sh), 832(s), 818(sh), 756(vs), 744(sh), 726(sh), 692(vs).

NMR ($CDCl_3$): no signal.

Mass (relative intensity): *m/e* 439(0.9), 437(2.7), 435(5.6), 433(7.4), 431(5.8), 429(2.0, M^+-peak), 406(0.9), 405(0.5), 404(6.9), 403(2.4), 402(25.8), 401(4.7), 400(64.0), 399(8.8), 398(100.0), 397(8.0), 396(89.2), 395(3.2), 394(35.4, M^+-Cl), 369(0.8), 368(0.6), 367(3.9), 366(2.4), 365(12.0), 364(4.7), 363(21.8), 362(4.0), 361(23.0), 360(1.6), 359(10.2, M^+-Cl_2), 331(0.2), 330(2.7), 329(0.4), 328(0.4), 327(0.6), 326(8.0), 325(0.4), 324(4.2, M^+-Cl_3), 255(1.7), 253(2.6), 251(1.6), 220(0.6), 219(0.1), 218(1.2), 216(0.9), 185(1.3), 184(0.5), 183.5(1.6), 183(3.8), 182.5(4.4), 182(1.3), 181.5(8.4), 181 (4.0), 180.5(9.0), 180(0.8), 179.5(4.1), 167(0.4), 166(1.5), 165(5.4), 164(12.3), 163(16.4), 162(8.0), 147(0.2), 145(0.7), 143(0.7), 136(9.8), 135(0.8), 134(13.2), 133(1.3), 132(0.5), 131(3.9), 130(0.4), 129(4.0), 123(1.0), 122(2.4), 121(10.6), 120(4.8), 119(32.8), 118(0.8), 117(34.2), 112(7.0), 111(2.4), 110(42.5), 109(1.0), 108(69.2), 96(1.6), 95(0.1), 94(2.4), 88 (2.5), 87(2.8), 86(2.8), 85(9.0), 84(15.9), 83(0.8), 82(26.1), 76(1.7), 75(3.8), 74(0.3), 73(12.0), 71(0.5), 70(0.7), 69(1.2), 62(0.8), 61(1.5), 59(2.0), 57(1.7), 56(0.9), 55(2.1), 50(0.6), 49(8.7), 48(0.4), 47(28.4), 44(2.5), 43(3.2), 42(0.7), 41(1.6), 38(5.9), 37(1.9), 36(18.2), 35(6.0), 29(0.6), 28(0.8), 27(0.7).

B) Trimerization of Chlorinated Mixture. Each sample in Experimental-A) was also trimerized in the presence of $AlBr_3$-HCl (Exp. B-1) or HCl only (Exp. B-2). Dry HCl gas (*ca.* 100 g) was introduced into a mixture of the sampling solution (100 m*l*) and $AlBr_3$ (2 g) or the sampling solution (100 m*l*) only at −20—0°C with stirring. The reaction mixture was kept at room temperature for 12 hr to complete trimerization. After HCl gas was removed under reduced pressure by water pump, each residue was analized by GLC-2 (see Table 2).

C) Preparation of the s-Triazine I. In the manner similar to Exp.-A, 4.1 kg of CH_3CN was chlorinated by the use of 10.6 kg of chlorine. Thus, a chlorinated CH_3CN mixture (*ca.* 10 kg; D_4^{45} 1.1945, CCl_3CN/CH_3CN=43.3/56.7 by GLC-1) was obtained. Then 30 g of $AlBr_3$ was added to this mixture with stirring. The resultant mixture was saturated with anhydrous HCl (1 kg) at −20—0°C for 2 hr, and kept at room temperature for 12 hr to complete co-trimerization. The obtained solid was melted by heating at 100—110°C and poured into a large quantity of water to wash out HCl and catalyst. After being cooled to room temperature, the resolidified product was collected, dried in air and then analyzed by GLC-2. Yield 7.0 kg (63.6%). Mp 93—96°C (if a purer product is desired, it may be recrystallized from ethanol. mp 96—97°C).

Analysis of the Crude Product, Mp 93—96°C, by GLC-2. *Ca.* 100% purity of the *s*-triazine I, and trace of *s*-triazines II and III was indicated.

Elemental Analysis of the Recrystallized Product, Mp 96—97°C. Found: C, 21.96; H, 1.04; N, 12.62; Cl, 64.35%. Calcd for $C_6H_3N_3Cl_6$: C, 21.84; H, 0.92; N, 12.74; Cl, 64.49%.

D) Attempted Co-trimerization of CH_2ClCN or $CHCl_2CN$ with CCl_3CN. The mixture of CCl_3CN (2 mol), CH_2ClCN or $CHCl_2CN$ (1 mol), and $AlBr_3$ (5 g) was saturated with anhydrous HCl at −20—−10°C by cooling with a dry ice-methanol bath for 2 hr under stirring. The reaction mixture was then kept for 48 hr at room temperature. After a severe strong heating treatment[15] such as was used in the preparation of 2-alkyl-4,6-bis(trichloromethyl)-*s*-triazines, the *s*-triazine IV became the only trimerized product, while CH_2ClCN or $CHCl_2CN$ was recovered in every case.

E) Chlorination of the s-Triazine I. Chlorine (25 g, 3.5 mol) was passed into a solution of 330 g (1 mol) of the *s*-triazine I in 1000 m*l* of CH_3CN (or CH_3COOH) at 45—50°C under illumination from the same UV lamp as was used in Exp.-A for a 7 hr period. Then the reaction mixture was evaporated at ordinary pressure as completely as possible, leaving a semisolid residue of 354 g (or 375 g in the case of CH_3COOH solution). This residue, containing a small amount of the solvent, was then analyzed by GLC-2, Mass, and NMR.

NMR ($CDCl_3$): three singlets at τ 7.02 (CH_3), 5.08 (CH_2Cl), and 3.12 ppm ($CHCl_3$).

The Composition of the Product Mixture from the Chlorination of the s-Triazine I: GLC and Mass data showed the selectivity of the *s*-triazines to be as follows; I, 56.5; II, 8.7, III, 10.8, and IV, 24.0 mol%. (In the case of the CH_3COOH solution; I, 32.2; II, 14.1; III, 17.2, and IV, 36.5 mol%).

The authors are indebted to the Mitsubishi Chemical Industries Ltd. for their generous support of this publication. They also wish to express their thanks to Mr. Y. Takigawa, Mr. Y. Ihashi and Mr. T. Sato for obtaining and interpreting the spectra which were of great assistance in this work. Valuable technical assistance was also provided by Mr. M. Tsuda and Mr. M. Nakazawa.

23) H. Herlinger, *Angew. Chem.*, **76**, 437 (1964).

Studies of Seven-Membered Heterocyclic Compounds Containing Nitrogen. X. Syntheses of 5,6,8,9-Tetrahydro-7*H*-pyrimido[4,5-*d*]azepines

Hiroshi YAMAMOTO, Masaru NAKATA,[1] Shiro MOROSAWA, and Akira YOKOO

Department of Chemistry, Faculty of Science, Okayama University, Tsushima, Okayama

(Received June 17, 1970)

5,6,8,9-Tetrahydro-7*H*-pyrimido[4,5-*d*]azepine and some of its derivatives were synthesized. 6-Acetyl-3-hydroxy-4,5,7,8-tetrahydro-6*H*-pyrazolo[3,4-*d*]azepine was also synthesized.

The previously-known compounds which have pyrimido-azepine ring systems are 2,3,4,6,7,8,9,10-octahydropyrimido[1,2-*a*]azepine (I)[2] and 5,6,7,8-tetrahydro-9*H*-pyrimido[4,5-*b*]azepines (II).[3] As an extensive investigation of *N*-substituted 5-ethoxycarbonyl-1-azacycloheptan-4-one, which has been prepared from the corresponding *N*-substituted piperid-4-ones by ring expansion with ethyl diazoacetate,[4] and especially in order to obtain azepine compounds by the dehydrogenation of the corresponding hydroazepines, the syntheses of the tetrahydroazepines fused with the pyrimidine ring were undertaken.

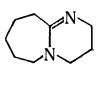

I

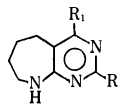

II

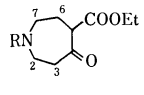

III

a: R=CH_2Ph
b. R=Ac

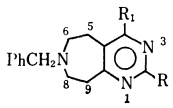

IV

a: R=SH, R_1=OH
b: R=Me, R_1=OH
c: R=NH_2, R_1=OH
d: R=NHCN, R_1=OH
e: R=NHAc, R_1=OH
f: R=H, R_1=OH
g: R=H, R_1=Cl
h: R=H, R_1=OMe
i: R=H, R_1=NH_2
j: R=H, R_1=$NHNH_2$
k: R=H, R_1=H
l: R=Me, R_1=Cl
m: R=Me, R_1=$NHNH_2$
n: R=Me, R_1=H

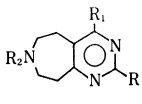

V

a: R=H, R_1=H, R_2=H
b: R=SH, R_1=OH, R_2=Ac
c: R=Me, R_1=OH, R_2=Ac
d: R=H, R_1=OH, R_2=Ac
e: R=H, R_1=OH, R_2=H
f: R=H, R_1=SH, R_2=CSMe

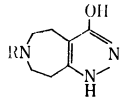

a: R=Ac
b: R=CH_2Ph

Upon the treatment of the *N*-benzyl-5-ethoxycarbonyl-1-azacycloheptan-4-one (IIIa) with thiourea, acetamidine, guanidine, and cyanoguanidine in the usual way, 2-mercapto-, 2-methyl-, 2-amino-, and 2-cyanamino-7-benzyl-4-hydroxy-5,6,8,9-tetrahydro-7*H*-pyrimido[4,5-*d*]azepines (IVa, b, c and d) were obtained. The structures of these compounds were derived by a study of the analytical and the spectral data. They all showed broad bands at 3100—2800 (medium) and 1665—1645 (strong) cm^{-1}, assignable to the amido group, indicating that the pyrimidine ring existed as a 3,4-dihydro-4-oxo form in solid states. The amino-pyrimido-azepine (IVc), when heated with acetic anhydride, readily gave a 2-acetamido derivative (IVe). The reduction of the mercapto compound (IVa) over Raney nickel yielded the hydroxypyrimido-azepine (IVf), and the IR spectrum indicated the presence of the 3,4-dihydro-4-oxo-pyrimidine structure (ν_{max} 2800 and 1660 cm^{-1}). The hydroxyl group of IVf could be replaced by a chlorine atom with phosphoryl chloride in the presence of diethylaniline, giving the chloro-pyrimido-azepine (IVg). The structure of this compound was confirmed by the IR (no absorption due to an amido group) and the NMR spectra. The assignment of the NMR signals is shown in the Table 1. On taking into account the chemical shift (τ 7.35) of the methylene protons at the 2 and 7 positions (*i. e.*, adjacent to the *N*-benzyl group) of 1-benzyl-1,4-diazacycloheptan-5-one,[5] the multiplet at τ 7.25—7.55 was assigned to the four protons at the 6 and 8 positions; thus, the multiplet at τ 6.80—7.10 was considered to be due to the methylene groups at the 5 and 9 positions.

Various nucleophilic substitution reactions took place on the IVg compound under conditions similar to those on 4,5-dialkyl-6-chloropyrimidines. Upon treatment with sodium methoxide in boiling methanol, ethanolic ammonia at 130°C, and hydrazine hydrate in boiling ethanol, 4-methoxy-, 4-amino-, and 4-hydrazino-pyrimido-azepine (IVh, i, and j respectively) were obtained. IVj gave 7-benzyl-5,6,8,9-tetrahydro-7*H*-pyrimido[4,5-*d*]azepine (IVk) on oxidation with silver oxide in methanol. The NMR spectrum of IVk was in conformity with the structure shown in Table 1. The assignment of the singlets at τ 1.20 and 1.74 to the protons at the 2 and 4 positions respectively was made on the grounds of the H(4) signal (τ 1.87) of the 2-methylpyrimido-azepine (IVn). A slight up-field shift of the signal of H(5) compared with that of IVg is

1) Present address: Nihon Kayaku Co., 1-6 Marunouchi, Chiyoda-ku, Tokyo.

2) a) H. Oediger and Fr. Moller, *Angew. Chem., Int. Ed. Engl.*, **6**, 76 (1967). b) Farbenfabriken Bayer A.-G., Fr. 1491791; *Chem. Abstr.*, **69**, 67412 (1968).

3) a) V. G. Granik and R. G. Glushkov, *Khim. -Farm. Zh.*, **1**, 21 (1967). b) K. Morita, S. Kobayashi, H. Shimadzu, and M. Ochiai, *Tetrahedron Lett.*, **1970**, 861.

4) T. Moriya, T. Oki, S. Yamaguchi, S. Morosawa, and A. Yokoo, This Bulletin, **41**, 230 (1968).

5) M. Sakakida, A. S. Kumanireng, H. Kawamoto, and A. Yokoo, to be published in This Bulletin.

TABLE 1. ASSIGNMENT OF NMR SIGNALS[a)]

Compound	τ Values[b)] for					
	H (2)	H (4)	H_2 (5)[c)]	H_2 (6, 8)[c)]	H_2 (9)[c)]	Substituent
IVg	1.41 s	—	6.80—7.10 m	7.25—7.55 m	6.80—7.10 m	2.75 s (C_6H_5) 6.42 s ($PhCH_2$)
IVk	1.20 s	1.74 s	7.10—7.60 m	7.10—7.60 m	6.80—7.10 m	2.73 s (C_6H_5) 6.39 s ($PhCH_2$)
IVn	—	1.87 s	7.10—7.60 m	7.10—7.60 m	6.80—7.10 m	2.75 s (C_6H_5) 6.40 s ($PhCH_2$) 7.46 s (CH_3)
Ve	1.98 s	—	6.55—7.30 m	6.55—7.30 m	6.55—7.30 m	—

a) Measured by a Hitachi High Resolution NMR Spectrometer, R-20A.
b) In CCl_4 with TMS as an internal standard, except for compound Ve (in D_2O). Suffixes: s, singlet; m, multiplet.
c) Too complicated to determine the accurate chemical shifts.

probably attributable to the removal of the influence of the chlorine atom at the 4 position. The catalytic debenzylation of IVk over 10% palladium on carbon yielded 5,6,8,9-tetrahydro-7*H*-pyrimido[4,5-*d*]azepine (Va) as a colorless oil.

The action of phosphoryl chloride on IVb similarly gave the chloropyrimido-azepine (IVl), but the product appeared to decompose appreciably on distillation. Therefore, the crude product, without purification, was treated with hydrazine hydrate, giving the hydrazinopyrimido-azepine (IVm) in a 67% yield (overall from IVb). IVm was converted into 7-benzyl-2-methyl-5,6,8,9-tetrahydro-7*H*-pyrimido[4,5-*d*]azepine (IVn) by oxidation with silver oxide. The structure was confirmed by the NMR spectrum, the assignment of which is given in Table 1. The catalytic debenzylation of IVn was attempted as in IVk, but the product expected to be similar to Va was not obtained. This is probably due to some decomposition of the starting material during the reaction.

1-Acetyl-1-azacycloheptan-4-one (IIIb) was prepared, by the ring expansion of 1-acetylpiperid-4-one with ethyl diazoacetate, in a relatively good yield (55—65%) compared with that of the same reaction[4)] of 1-benzyl- or 1-ethoxycarbonylpiperid-4-one. The IR spectrum of IIIb showed three strong bands, at 1735, 1715, and 1660 cm^{-1}, assignable to the ethoxycarbonyl, the ring carbonyl, and the acetyl groups respectively. Upon treatment with thiourea and acetamidine, IIIb afforded 2-mercapto- and 2-methyl-7-acetyl-4-hydroxy-5,6,8,9-tetrahydro-7*H*-pyrimido[4,5-*d*]azepine (Vb and c) respectively. The presence of a secondary amido absorption in the IR spectra showed that these compounds exist as the 4-oxo form. Vb was reduced to give the 7-acetyl-4-hydroxypyrimido-azepine (Vd). On refluxing with 6N hydrochloric acid, Vd yielded the hydrochloride of hydroxypyrimido-azepine (Ve) as colorless prisms. The NMR spectrum of the hygroscopic free base in heavy water showed a singlet (1H) at τ 1.98 due to the aromatic ring proton and a complicated multiplet (8H) at 6.55—7.30 due to the tetrahydroazepine ring protons. An attempt to replace the hydroxyl group of Vd with a chlorine atom under conditions similar to those used for the *N*-benzyl compounds (IVb and f) gave only a black, intractable tar. It was found, however, that phosphorus pentasulfide affected both the hydroxyl and acetyl groups of Vd, giving the 4-mercapto-7-thioacetylpyrimido-azepine (Vf). The IR spectrum showed no amido absorption.

6-Acetyl-3-hydroxy-4,5,7,8-tetrahydro-6*H*-pyrazolo-[3,4-*d*]azepine (VIa) was derived from IIIb and hydrazine hydrate as in the case of the benzyl derivative (VIb).[4)]

Experimental

The microanalyses were carried out by Miss H. Ohtani in this department, using a Yanagimoto C.H.N. Corder, MT-1. The solid materials for the analysis were dried over phosphorus pentoxide for 1—2 hr at 80°C/20 mmHg unless otherwise specified. Each of the analytical samples gave a single spot on a paper chromatogram (Toyo Roshi, No. 51) which was developed with 3% aqueous ammonium chloride or 5N acetic acid/1-butanol (29 : 71 v/v) and which was examined under ultraviolet light at 365 and 254 mμ alternately. The IR spectra were taken with a Nihon-Bunko IR-S spectrophotometer; the relatively intense absorption bands of each compound are shown by suffixes (s, strong; br, broad).

*4-Hydroxy-2-mercapto-5, 6, 8, 9-tetrahydro-7*H*-pyrimido[4, 5-d]-azepine (IVa).* Fifteen grams of IIIa hydrochloride[4)] were shaken with 100 m*l* of 10% aqueous potassium carbonate, and the mixture was extracted with ether. After the ether solution had been dried over anhydrous potassium carbonate and the solvent had been completely removed *in vacuo*, the residual oil was dissolved in 50 m*l* of absolute ethanol; a cold solution of 1.75 g (1.5 equiv) of sodium in 150 m*l* of absolute ethanol was then added. Four grams (1.25 equiv) of thiourea were then added, and the whole was refluxed for 7 hr with stirring. The solvent was evaporated *in vacuo*, and the viscous residue was stirred at 0°C with 50 m*l* of water until it became a powder (*ca.* 6 hr). It was collected, dried in a vacuum desiccator with calcium chloride, and boiled with 200 m*l* of methanol. After having been cooled, the precipitate was collected by filtration to give 6.65 g of IVa as an almost colorless powder; mp 232—236°C. On the concentration of the filtrate to *ca.* 30 m*l*, 0.4 g more of the material was obtained (total yield, 51%). Recrystallization from 50% aqueous ethanol gave almost colorless leaflets; mp 236—238°C. The material is moderately soluble in ethanol, and soluble with difficulty in cold water, 10% aqueous sodium carbonate, and N sodium hydroxide, and it gives a hydrochloride as a colorless powder in N hydrochloric acid.

Found: C, 62.83; H, 6.14; N, 14.43%. Calcd for $C_{15}H_{17}N_3OS$: C, 62.69; H, 5.96; N, 14.62%. ν_{max}^{KBr} 3060 br, 2920 br,

1645 sbr, 1590 sbr, 1560 s, 1230 s, 1215, 1118, 950, 910 br, 735 s, and 695 s cm^{-1}.

*7-Benzyl-4-hydroxy-2-methyl-5,6,8,9-tetrahydro-7*H*-pyrimido[4,5-d]azepine (IVb).* To a solution of 1.2 g (5 equiv) of sodium in 50 m*l* of absolute ethanol were added 3.1 g of IIIa hydrochloride and 1.4 g (1.5 equiv) of acetamidine hydrochloride; the mixture was then heated under reflux for 4 hr. The precipitate was removed by filtration, and the filtrate was evaporated to dryness *in vacuo*. Ten milliliters of water were added to the residue, and the resulting solution was washed with ether; then the aqueous layer was brought to pH 5 by the addition of acetic acid. The precipitate which appeared was collected by filtration, washed with a small amount of cold water, and recrystallized from ethanol, thus giving 1.8 g (67%) of IVb as colorless needles; mp 206—208°C. One more recrystallization from ethanol gave an analytical specimen; mp 211—212°C. The material is easily soluble in acetone, and moderately so in chloroform.

Found: C, 71.03; H, 7.08; N, 15.50%. Calcd for $C_{16}H_{19}N_3O$: C, 71.35; H, 7.11; N, 15.60%. ν_{max}^{KBr} 2800 br, 1656 sbr, 1610 s, 1570, 1435, 1352, 1343, 1308, 1222, 1159, 981, 959 s, 809, 751 s, 736, and 700 cm^{-1}.

*2-Amino-7-benzyl-4-hydroxy-5,6,8,9-tetrahydro-7*H*-pyrimido[4,5-d]azepine (IVc).* A mixture of 5.0 g of IIIa hydrochloride, 5.0 g (3.3 equiv) of guanidine hydrochloride, and 1.2 g (3.3 equiv) of sodium in 100 m*l* of absolute methanol was treated such as in the preparation of IVb. After recrystallization from methanol, 2.7 g (63%) of IVc were obtained as a colorless crystalline powder; mp 252—254°C. The material is soluble in water only with difficulty.

Found: C, 62.94; H, 7.34; N, 18.31%. Calcd for $C_{15}H_{18}N_4O\cdot CH_3OH$: C, 63.55; H, 7.33; N, 18.53%. The methanol of crystallization was not removed on drying even at 110°C. ν_{max}^{KBr} 3360 br, 3050 br, 2890 br, 1650 sbr, 1600 sbr, 1497, 1380, 1369, 1309, 1230, 1190, 1029 br, 948, 793, 779, 750 s, and 693 cm^{-1}.

*7-Benzyl-2-cyanamino-4-hydroxy-5,6,8,9-tetrahydro-7*H*-pyrimido-[4,5-d]azepine (IVd).* From 3.1 g of IIIa hydrochloride, 0.84 g (1.0 equiv) of cyanoguanidine, and 2.0 g (3.7 equiv) of sodium methoxide dissolved in 50 m*l* of absolute methanol, IVd was obtained according to the same precedures as those used for IVb. Two recrystallizations from methanol gave 0.7 g (24%) of IVd as a colorless crystalline powder; mp 254—256°C. The analytical specimen was dried at 25°C/20 mmHg.

Found: C, 65.61; H, 6.02; N, 23.78%. Calcd for $C_{16}H_{17}N_5O$: C, 65.07; H, 5.80; N, 23.71%. ν_{max}^{KBr} 2950 sbr, 2800 sbr, 2205 s, 1675 sbr, 1640 sbr, 1545, 1497, 1450, 1440, 1380, 1370, 1308, 1268, 1179, 1117, 948, 782, 770, 748, 733 s and 694 cm^{-1}.

*2-Acetamido-7-benzyl-4-hydroxy-5,6,8,9-tetrahydro-7*H*-pyrimido-[4,5-d]azepine (IVe).* A suspension of 0.5 g of IVc in 2 m*l* of acetic anhydride was heated on a steam bath for 10 min. The precipitate was then collected and recrystallized from methanol, giving 0.4 g (68%) of IVe as colorless prisms; mp 238°C. The analytical sample was dried at 20°C/20 mmHg.

Found: C, 65.37; H, 6.45; N, 17.94%. Calcd for $C_{17}H_{20}N_4O_2$: C, 65.01; H, 6.12; N, 17.77%. ν_{max}^{KBr} 3120 br, 1645 sbr, 1600 s, 1545 sbr, 1391, 1336, 1309, 1240, 1217, 1166 br, 1122, 941, 850, 792, 765, 737, and 692 cm^{-1}.

*7-Benzyl-4-hydroxy-5,6,8,9-tetrahydro-7*H*-pyrimido[4,5-d]azepine (IVf).* To a solution of 6.8 g of IVa in 120 m*l* of 28% aqueous ammonia and 600 m*l* of water were added *ca.* 18 g of freshly-prepared, wet Raney nickel W-2; the mixture was then refluxed for 2 hr. The catalyst was separated while hot and extracted with boiling water. The extract and the filtrate were combined and evaporated *in vacuo*. The recrystallization of the residue from methanol gave 4.8 g of IVf as colorless needles; mp 169—170°C. The concentration of the filtrate afforded a further solid, which was recrystallized from the same solvent to give 0.3 g of the product; mp 167—169°C (total yield, 85%).

Found: C, 70.12; H, 6.38; N, 16.37%. Calcd for $C_{15}H_{17}N_3O$: C, 70.56; H, 6.71; N, 16.46%. ν_{max}^{KBr} 2800 sbr, 1600 sbr, 1605 s, 1432, 1358 s, 1317, 1240, 1205, 1161, 1128, 979, 967 s, 925, 871, 739 s, and 706 cm^{-1}.

*7-Benzyl-4-chloro-5,6,8,9-tetrahydro-7*H*-pyrimido[4,5-d]azepine (IVg).* To a solution of 2.5 g of IVf previously dried for 1 hr at 80°C/20 mmHg in 30 m*l* of boiling phosphoryl chloride was added 1.0 m*l* (0.6 equiv) of diethylaniline during 1—2 min; the mixture was then refluxed for 2 hr. After the solvent had been removed *in vacuo*, 10 m*l* of cold water was added to the residue, and the mixture was stirred at 5°C until it became a solution (30 min). Enough solid sodium carbonate (*ca.* 1.8 g) was slowly stirred into the above ice-cooled solution, and then 30 m*l* of chloroform were added. After having been stirred for 15 min at 5°C, the aqueous layer was separated and extracted with chloroform (3×10 m*l*). The combined organic layer was dried over anhydrous potassium carbonate and evaporated *in vacuo*, and the residue was briefly boiled with 10 m*l* of benzene. After cooling, the precipitate was collected, washed with a small amount of benzene, and recrystallized from 10 parts of methanol, giving 1.7 g of IVg hydrochloride as colorless needles; mp 217—218°C. On concentration, the methanolic filtrate yielded an additional solid, which was recrystallized from the same solvent to give 0.6 g of the product; mp 218—219°C (total yield, 76%). The material is soluble only with difficulty in benzene, and slightly soluble in chloroform, methanol, and ethanol. Two more recrystallizations from methanol and drying at 100°C/20 mmHg gave an analytical specimen; mp 220°C.

Found: C, 58.35; H, 5.64; N, 13.99%. Calcd for $C_{15}H_{16}ClN_2\cdot HCl$: C, 58.07; H, 5.53; N, 13.55%. ν_{max}^{Nujol} 2520 sbr, 1560, 1537 s, 1430 s, 1415, 1383 s, 1320, 1290, 1205, 1080, 953, 917 s, 820 s, 780, 753 s and 705 cm^{-1}.

A mixture of 10 m*l* of 10% aqueous sodium carbonate and 1.75 g of the above crude hydrochloride was stirred for 15 min at 5°C. The mixture was then stirred with 30 m*l* of benzene for 10 min at the same temperature. The aqueous layer was extracted with benzene (3×15 m*l*), and the combined benzene layer, after being clarified by filtration, was evaporated *in vacuo* below 40°C (bath temp.), giving 1.48 g (96%) of the free base (IVg) as an almost colorless crystalline powder; mp 66—67.5°C. The material is easily soluble in ethanol, chloroform, and benzene, and slightly soluble in water. It sublimes at 100°C (bath temp.)/0.2 mmHg with a slight decomposition. The analytical specimen, twice recrystallized from light petroleum (30—70°C) and dried at 25°C/20 mmHg, consisted of colorless prisms; mp 67—68°C.

Found: C, 65.83; H, 5.60; N, 15.41%. Calcd for $C_{15}H_{16}ClN_3$: C, 65.80; H, 5.89; N, 15.35%. ν_{max}^{Nujol} 1555 s, 1540 s, 1498, 1450, 1381 s, 1370 s, 1355 s, 1342, 1335 s, 1310, 1292, 1160, 1121 s, 1000, 970, 950, 830, 819, 799, 741 s, and 705 cm^{-1}.

*7-Benzyl-4-methoxy-5,6,8,9-tetrahydro-7*H*-pyrimido[4,5-d]azepine (IVh).* A solution of 0.15 g of IVg in 5 m*l* of absolute methanol and another solution of 0.02 g (1.3 equiv) of sodium in 5 m*l* of the methanol were mixed and boiled for 1 hr. The solvent was evaporated *in vacuo*, and the residue was extracted with boiling benzene (3×5 m*l*). The evaporation of the solvent below 50°C under reduced pressure left 0.12 g (80%) of the crude product as a colorless liquid which did not solidify at −20°C. ν_{max}^{neat} 2980, 2910, 2860, 2765, 1575 sbr, 1555 s, 1460 sbr, 1380 s, 1350, 1338, 1305, 1190, 1168, 1155, 1138, 1080 s, 1039, 946, 860, 801, 781, 740 s, 700 s, 677, and

660 cm^{-1}.

The *picrate*: yellow leaflets (from methanol), mp 207—208°C (reddened). Drying at 20°C/20 mmHg gave an analytical sample.

Found: C, 46.25; H, 3.38; N, 17.62%. Calcd for $C_{16}H_{19}N_3O \cdot 2C_6H_3N_3O_7$: C, 46.22; H, 3.46; N, 17.33%. ν_{max}^{Nujol} 2550 br, 1625 sbr, 1605 sbr, 1560 sbr, 1540 sbr, 1515, 1480 sbr, 1455 sbr, 1430, 1388 s, 1361 s, 1330 sbr, 1295, 1265 sbr, 1143, 1111, 1080, 1041, 940, 910, 891, 789, 768, 746, and 710 s cm^{-1}.

4-Amino-7-benzyl-5,6,8,9-tetrahydro-7H-pyrimido[4,5-d]azepine (IVi). A solution of 0.10 g of IVg in 5 m*l* of ethanolic ammonia saturated at 0°C was heated in a sealed tube at 110°C for 2 hr, and then at 130°C for 8 hr. After the evaporation of the solvent *in vacuo*, the residue was stirred with 1 m*l* of 10% aqueous sodium carbonate. The precipitate was collected and recrystallized from benzene, giving 0.07 g (75%) of IVi as colorless fine prisms. One more recrystallization from the same solvent gave the analytical specimen as colorless leaflets; mp 200.5°C. The material is soluble in chloroform and ethanol, but soluble only with difficulty in water.

Found: C, 70.60; H, 6.87; N, 21.85%. Calcd for $C_{15}H_{18}N_4$: C, 70.83; H, 7.13; N, 22.03%. ν_{max}^{Nujol} 3355, 3170, 1663 s, 1583 s, 1550, 1420, 1380, 1343, 1316, 1262, 1168, 1151, 1130, 978, 951, 874, 801, 780, 740 s, and 700 cm^{-1}. No amination took place when IVg was heated under reflux with concentrated aqueous ammonia.

7-Benzyl-4-hydrazino-5,6,8,9-tetrahydro-7H-pyrimido[4,5-d]azepine (IVj). A mixture of 1.20 g of IVg, 5 m*l* of 80% hydrazine hydrate, and 40 m*l* of ethanol was refluxed for 2 hr. The solvent was then evaporated *in vacuo*, and 5 m*l* of water were added to the residue. After the mixture had been stirred for 5 min at 20°C, the precipitate was collected on a filter and washed with 1 m*l* of cold water, giving 1.12 g (95%) of IVj as a colorless powder; mp 162—165°C. Two recrystallizations from methanol gave an analytically-pure material as colorless plates, mp 165.5—166.5°C; this material is moderately soluble in methanol and ethanol, and slightly soluble in water and benzene.

Found: C, 67.09; H, 7.11; N, 26.11%. Calcd for $C_{15}H_{19}N_5$: C, 66.89; H, 7.11; N, 26.00%. ν_{max}^{Nujol} 3295 s, 3165, 1660, 1595 sbr, 1498 s, 1420 s, 1362, 1350 s, 1340 s, 1323, 1262, 1210, 1168, 990, 985, 961 s, 871, 810, 791, 751, 736 and 706 cm^{-1}. The reaction at 40°C recovered the starting material.

7-Benzyl-5,6,8,9-tetrahydro-7H-pyrimido[4,5-d]azepine (IVk). A suspension of 0.45 g of IVj and 3.5 g of freshly-prepared silver oxide in 30 m*l* of absolute ethanol was refluxed for 2 hr with stirring. The hot mixture was filtered, and the filtrate was treated with carbon. The solvent was evaporated *in vacuo*, and the residue was sublimed at 130°C (bath temp.)/0.1 mmHg, giving 0.33 (83%) of IVk as colorless prisms. Recrystallization from light petroleum (30—70°C) and drying at 25°C/20 mmHg gave an analytical specimen as colorless plates; mp 66.5—67.5°C. The material is soluble in most organic solvents, but soluble only with difficulty in water.

Found: C, 75.85; H, 7.14; N, 17.96%. Calcd for $C_{15}H_{17}N_3$: C, 75.28; H, 7.16; N, 17.56%. ν_{max}^{Nujol} 1580, 1555, 1410, 1398, 1375, 1359 s, 1312, 1128, 990, 951, 790, 746 s, and 706 cm^{-1}.

The *picrate* was obtained when IVk was added to an ethanolic solution of picric acid (2.1 equiv). It was recrystallized from ethanol and dried at 107°C/20 mmHg to give an analytical sample as yellow prisms; mp 170—171°C.

Found: C, 53.16; H, 4.10; N, 18.25%. Calcd for $C_{15}H_{17}N_3 \cdot C_6H_3N_3O_7$: C, 53.84; H, 4.30; N, 17.94%. ν_{max}^{Nujol} 2700 br, 2570 br, 1620 sbr, 1610 sbr, 1580, 1550 sbr, 1485, 1435, 1403, 1368 s, 1335 sbr, 1310 sbr, 1270 sbr, 1163, 1080, 907 s, 798, 776, 755, and 712 cm^{-1}.

5,6,8,9-Tetrahydro-7H-pyrimido[4,5-d]azepine (Va). A mixture of 0.20 g of IVk, 1 m*l* of acetic acid, and 20 m*l* of ethanol was shaken with hydrogen in the presence of 0.10 g of 10% palladium charcoal until the absorption of hydrogen ceased. The solid was then removed by filtration and washed with hot ethanol. The filtrate and the washings were combined and evaporated *in vacuo*. The residual liquid was suspended in 6 m*l* of 10% aqueous potassium carbonate and extracted with chloroform (3×7 m*l*). The dried extract was freed from the solvent at 60°C (bath temp.)/20 mmHg, giving 0.10 (80%) of Va as a colorless liquid. No crystallization occurred even at −20°C.

The oil was characterized by the *picrate*; yellow needles (from ethanol); mp 224°C (decomp.),.

Found: C, 44.56; H, 3.66; N, 22.00%. Calcd for $C_8H_{11}N_3 \cdot C_6H_3N_3O_7$: C, 44.45; H, 3.73; N, 22.22%. ν_{max}^{Nujol} 2580 br, 2450, 1635 s, 1608 sbr, 1545 sbr, 1480 br, 1450 sbr, 1397 s, 1365 sbr, 1310 sbr, 1270 sbr, 1162 s, 1152, 1079 s, 1026, 928, 912, 839, 780, 743, 721 s, and 710 s cm^{-1}.

7-Benzyl-4-chloro-2-methyl-5,6,8,9-tetrahydro-7H-pyrimido[4,5-d]azepine (IVl). This was prepared as in the case of IVg; the crude product (77%) was obtained as a pale yellow liquid. When purified by distillation, it gave pure IVl in a 30% yield as a colorless liquid, bp 170°C/0.7 mmHg, which crystallized in part.

Found: C, 67.81; H, 6.48; N, 15.05%. Calcd for $C_{16}H_{18}ClN_3$: C, 66.77; H, 6.30; N, 14.60%. ν_{max}^{neat} 2890 s, 2795, 2522, 2480, 1605, 1560 sbr, 1520 sbr, 1492, 1450 s, 1415 sbr, 1400 s, 1361, 1346, 1312 br, 1277 s, 1162, 1128, 1072, 1026, 942 s, 920, 908, 890, 829, 822, 790, 775, 750, 740, 721, and 698 s cm^{-1}.

7-Benzyl-4-hydrazino-2-methyl-5,6,8,9-tetrahydro-7H-pyrimido-[4,5-d]azepine (IVm). The procedure was similar to that used for IVj, except that benzene was used as the recrystallization solvent. The crude chloropyrimido-azepine (IVl) gave IVm as a colorless crystalline powder, mp 124—125°C, in an 87% yield. The material is easily soluble in methanol, ethanol, ethyl acetate, and chloroform, moderately soluble in benzene, and soluble only with difficulty in water. Drying at 60°C/20 mmHg gave an analytical sample.

Found: C, 68.60; H, 7.89; N, 25.42%. Calcd for $C_{16}H_{21}N_5$: C, 67.81; H, 7.47; N, 24.72%. ν_{max}^{Nujol} 3280 sbr, 3230 sbr, 3190 s, 1668, 1575 sbr, 1490 s, 1440 s, 1409 s, 1380, 1348, 1304, 1212, 1169, 1020, 970, 949 s, 797, 775, 760, 730, 700 s, and 660 cm^{-1}.

7-Benzyl-2-methyl-5,6,8,9-tetrahydro-7H-pyrimido[4,5-d]azepine (IVn). This was prepared in a 63% yield from IVm by much the same procedure as that used in preparing IVk. It was a colorless, viscous liquid, bp 155—156°C/0.20 mmHg, which did not crystallize on storage at −20°C.

The material gradually become a yellow viscous liquid in the air, while under ultraviolet light at 254 mμ, it was quickly destroyed and gave a substance which exhibited a blue fluorescence.

Found: C, 75.82; H, 7.79; N, 16.21%. Calcd for $C_{16}H_{19}N_3$: C, 75.85; H, 7.56; N, 16.59%. ν_{max}^{neat} 2980, 2880, 2855, 1579 s, 1563 sbr, 1495, 1450 sbr, 1445 sbr, 1402, 1372, 1345, 1272, 1163, 1120 br, 1031, 993, 968, 950 sbr, 782, 750 s, 725 and 701 cm^{-1}.

The *picrate*, yellow leaflets (from ethanol); mp 192.5—194°C (melted with darkening).

Found: C, 47.24; H, 3.87; N, 17.29%. Calcd for $C_{16}H_{19}N_3 \cdot 2C_6H_3N_3O_7$: C, 47.26; H, 3.54; N, 17.72%. ν_{max}^{Nujol} 2580 br, 1620 sbr, 1605 sbr, 1562 s, 1550 sbr, 1520, 1490, 1460 br, 1427, 1362 s, 1315 sbr, 1263 sbr, 1160, 1080, 900, 789, 760, 748, and 711 cm^{-1}.

The *hydrochloride* was obtained as a colorless crystalline

powder, mp 240—242°C (from methanol), when dry hydrogen chloride was passed through a solution of IVn in dry ether.

Found: C, 58.75; H, 6.50; N, 12.78%. Calcd for $C_{16}H_{19}N_3 \cdot 2HCl$: C, 58.90; H, 6.49; N, 12.88%. ν_{max}^{KBr} 2960, 2440 sbr, 2080, 1975 br, 1620, 1609 s, 1465, 1452 s, 1410, 1388, 1374, 1311, 1270, 1212, 1148, 1065 br, 1048, 1022, 971, 960, 932, 898 s, 790, 780, 753 s, 729, 710, and 698 cm^{-1}.

1-Acetylpiperid-4-one. A mixture of 20.0 g of piperid-4-one hydrochloride,[6] 30.0 g (2.0 equiv) of acetic anhydride and 220 m*l* of pyridine was heated under reflux for 2 hr. After cooling, 250 m*l* of water were added and the mixture was heated on a steam bath for 30 min and then concentrated to *ca.* 50 m*l* below 60°C (bath temp.) under reduced pressure. To this were added 20 m*l* of 10% aqueous sodium hydrogen carbonate and enough solid sodium hydrogen carbonate (*ca*, 6 g) to pH 7, after which the contents were thoroughly extracted with chloroform (6×50 m*l*). The combined extract was washed once with saturated aqueous sodium chloride and dried over anhydrous potassium carbonate. After the solvent had been removed, the residue was distilled to give 16.2 g (78%) of the acetylpiperidone as a colorless liquid; bp 122—125°C/0.20 mmHg. ν_{max}^{neat} 3450 br, 2960, 2890, 1735 sbr, 1715 sbr, 1660 s, 1640—1620 sbr, 1450—1420 sbr, 1362, 1349, 1310, 1260, 1230 sbr, 1140, 1032, 978, and 758 cm^{-1}

The liquid was identified by the 2,4-*dinitrophenylhydrazone* (yellow fine needles, 80% yield); mp 209—210°C.

Found: C, 48.72; H, 4.96; N, 21.35%. Calcd for $C_{13}H_{15}N_5O_5$: C, 48.59; H, 4.71; N, 21.80%.

1-Acetyl-5-ethoxycarbonyl-1-azacycloheptan-4-one (IIIb). The procedures of Moriya *et al.*[4] were followed. The treatment of 7.06 g of the above acetylpiperidone with 7.81 g (1.1 equiv) of freshly-distilled boron trifluoride and 17.1 g (3.0 equiv) of ethyl diazoacetate gave 7.35 g (65%) of IIIb as a pale yellow, voscous oil; bp 154°C/0.28 mmHg.

Found: C, 57.84; H, 7.78; N, 5.98%. Calcd for $C_{11}H_{17}NO_4$: C, 58.13; H, 7.54; N, 6.16%. ν_{max}^{neat} 2950 br, 1750 sbr 1710 sbr, 1645 sbr, 1480, 1455 br, 1425 br, 1370, 1315, 1295, 1230 br, 1195 sbr, 1100, 1025, 989 and 896 cm^{-1}.

7-Acetyl-4-hydroxy-2-mercapto-5,6,8,9-tetrahydro-7H-pyrimido[4,5-d]azepine (Vb). The procedure was essentially the same as that used for the benzyl compound IVa, but a slight modification was employed. To a cold solution of 0.40 g (1.5 equiv) of sodium in 70 m*l* of absolute ethanol was added a solution of 9.08 g of IIIb in 30 m*l* of absolute ethanol, and then 3.80 g (1.25 equiv) of finely-powdered thiourea. The mixture was shaken at room temperature until the thiourea had been almost completely dissolved (5 min), and then it was refluxed for 9 hr with stirring. The solvent was removed *in vacuo*, and the residue was dissolved in 20 m*l* of cold water and filtered. The filtrate was brought to pH 4 with 6N hydrochloric acid under cooling and kept at 5°C for two days to give 6.8 g of a precipitate. The concentration of the filtrate to *ca.* 10 m*l* yielded 1.8 g of the same material. Recrystallization from 50% aqueous ethanol gave 6.6 g (69%) of Vb as an almost colorless crystalline powder; mp 286—287°C. One more recrystallization from the same solvent raised the melting point to 288—289°C, and subsequent drying at 100°C/20 mmHg gave an analytical sample.

Found: C, 49.42; H, 5.41; N, 17.07%. Calcd for $C_{10}H_{13}N_3O_2S$: C, 50.18; H, 5.47; N, 17.54%. ν_{max}^{Nujol} 3120 br, 1660 sbr, 1610 sbr, 1550 sbr, 1425 sbr, 1340, 1276, 1212 s, 1198 s, 1121, 926 br, and 762 cm^{-1}.

7-Acetyl-4-hydroxy-2-methyl-5,6,8,9-tetrahydro-7H-pyrimido[4,5-d]azepine (Vc). A mixture of 2.27 g of IIIb, 0.70 g (1.2 equiv) of acetamidine hydrochloride, and 0.60 g (2.6 equiv) of sodium was similarly refluxed in 40 m*l* of absolute ethanol. After being changed to pH 4 with hydrochloric acid, the reaction mixture was well extracted with chloroform (5×10 m*l*). The combined and dried (over anhydrous potassium carbonate) extract was evaporated *in vacuo*, and the residue was recrystallized from ethanol to give 0.80 g (36%) of Vc as a colorless crystalline powder; mp 250—252°C. Two more recrystallizations from the same solvent afforded colorless needles, mp 254—255°C, an aliquot of which was then dried at 160°C/15 mmHg to give an analytical sample.

Found: C, 60.31; H, 7.07; N, 19.06%. Calcd for $C_{11}H_{15}N_3O_2$: C, 59.71; H, 6.83; N, 18.99%. The material dried below 120°C/20 mmHg still possessed the ethanol of crystallization. ν_{max}^{Nujol} 3070 br, 2760, 1660 sbr, 1590 sbr, 1455 sbr, 1425 s, 1380, 1337, 1294, 1282, 1251, 1219, 1201, 1144, 1045, 1037, 1030, 990, 943 s, 900, 795, and 734 cm^{-1}.

7-Acetyl-4-hydroxy-5,6,8,9-tetrahydro-7H-pyrimido[4,5-d]azepine (Vd). This was prepared according to the procedure described for IVf. The treatment of 2.0 g of Vb with 6.0 g of wet Raney nickel W-2, followed by the recrystallization of the crude product from ethanol, gave 1.5 g (87%) of Vd as colorless leaflets; mp 212—213°C. The material is easily soluble in water.

Found: C, 57.94; H, 6.17; N, 20.17%. Calcd for $C_{10}H_{13}N_3O_2$: C, 57.96; H, 6.32; N, 20.28%. ν_{max}^{Nujol} 3050 br, 2700, 1660 sbr, 1630, 1595 sbr, 1551, 1465 sbr, 1380 s, 1275, 1250, 1223, 1192, 1033, 997, 952, 937 s, 919, 864, 812, 785, and 665 br cm^{-1}.

4-Hydroxy-5,6,8,9-tetrahydro-7H-pyrimido[4,5-d]azepine (Ve). A solution of 0.20 g of Vd in 4 m*l* of 6N hydrochloric acid was refluxed for 4 hr. The solvent was removed under reduced pressure below 60°C (bath temp.), and the residue was boiled with 5 m*l* of ethanol. The precipitate was recrystallized from a mixture of N HCl–EtOH (1:30) to give 0.20 g (97%) of fine, colorless needles; mp 272—275°C (gradual decomp.). Likewise, one more recrystallization gave an analytical specimen; mp 272—274°C (foaming). The hydrochloride contained the water of crystallization, which was lost on drying above 110°C. Drying at 140°C/20 mmHg gave an analytical sample. It is very soluble in water and 10% aqueous sodium hydrogen carbonate.

Found: C, 46.71; H, 5.89; N, 20.52%. Calcd for $C_8H_{11}N_3O \cdot HCl$: C, 47.64; H, 6.00; N, 20.84%. ν_{max}^{Nujol} 3100—2400 br, 1650 sbr, 1630 sbr, 1605 s, 1595 s, 1552, 1450 sbr, 1428, 1403, 1373, 1308, 1250, 1230, 1180, 1129, 1101, 989, 976, 943 s, 890, 861, 831, and 795 cm^{-1}.

The *picrate*; yellow prisms (from 80% aqueous ethanol); mp 117—119°C. The analytical sample was dried at 60°C/20 mmHg.

Found: C, 36.09; H, 3.02; N, 18.98%. Calcd for $C_8H_{11}N_3O \cdot 2C_6H_3N_3O_7 \cdot HCl$: C, 36.40; H, 2.75; N, 19.10%. ν_{max}^{Nujol} 3470, 3230, 3070, 1685 s, 1675, 1630 s, 1615 s, 1565 sbr, 1540, 1465 sbr, 1383, 1373 s, 1355 s, 1335 s, 1303, 1284 s, 1172, 1098, 920, 863, 792, 750, and 720 br cm^{-1}.

A solution of 0.10 g of the hydrochloride in 10 m*l* of water was passed through a column of the Amberlite CC-413 and eluted with water. The eluate (*ca.* 80 m*l*) was evaporated *in vacuo*, giving the free base Ve as an almost colorless powder; this powder gradually melted at about 220°C. The material was very hygroscopic and became a pale yellow viscous tarry oil on being set aside in the air; thus, it was not analyzed. However, the NMR spectrum is shown in Table 1. It is very soluble in water, and slightly so in ethanol, but insoluble in chloroform.

4-Mercapto-7-thioacetyl-5,6,8,9-tetrahydro-7H-pyrimido[4,5-d]azepine (Vf). A mixture of 0.10 g of Vd and 2 m*l* of pyridine was heated at 110°C. After the resultant solution

6) A. Yokoo and S. Morosawa, This Bulletin, **29**, 631 (1956).

had been cooled to 90°C, 0.20 g (2.0 equiv) of powdered phosphoryl pentasulfide was added over a 1-min period and the mixture was heated under reflux for 30 min. The reaction mixture was treated with 2 m*l* of water and evaporated *in vacuo* at 60°C. The residue was stirred with 1 m*l* of water under cooling, and the precipitate was collected and recrystallized twice from ethanol to give 0.075 g (71%) of Vf as a yellow crystalline powder; mp 247—248°C (blackened). The drying of an aliquot of the powder at 140°C/20 mmHg afforded the analytical sample.

Found: C, 49.96; H, 5.32; N, 17.38%. Calcd for $C_{10}H_{13}N_3S_2$: C, 50.18; H, 5.47; N, 17.56%.

BULLETIN OF THE CHEMICAL SOCIETY OF JAPAN, VOL. 44, 158—161 (1971)

Studies of Peptide Antibiotics. XXIV. Synthesis of 4,4'-D-Alanine-gramicidin S

Sannamu LEE, Reiko OHKAWA[1], and Nobuo IZUMIYA[2]

Laboratory of Biochemistry, Faculty of Science, Kyushu University, Hakozaki, Fukuoka

(Received June 22, 1970)

In order to investigate the contribution to antibacterial activity of the D-phenylalanine residues at 4- and 4'-position in gramicidin S, 4,4'-D-alanine-gramicidin S (XX) and 4-D-alanine-semigramicidin S (XXI) were prepared and tested for antibacterial properties. XX exhibited recognizable activity though weaker than that of gramicidin S, whereas XXI showed no activity on any of the microorganisms tested.

We reported that 4,4'-glycine-gramicidin S possessed weak antibacterial activity toward several microorganisms.[3] On the other hand, 4,4'-D-valine- and 4,4'-D-leucine-gramicidin S were as active as natural gramicidin S (GS) (Fig. 1);[4] the results indicated that the aromatic side chains of D-phenylalanine residues of 4- and 4'-position can be replaced by the bulky aliphatic side chains without influencing the activity. From these findings, it seemed of interest to investigate the antibacterial properties of an analog of GS with D-amino acid residues at 4- and 4'-position which are larger than glycine and smaller than valine or leucine.

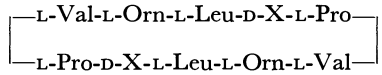

Fig. 1. Structure of GS (X=Phe) and 4,4'-D-Ala-GS (X=Ala).

This paper will describe the synthesis and antibacterial properties of 4,4'-D-alanine-GS besides those of a cyclic pentapeptide, 4-D-alanine-semigramicidin S.

The desired 4,4'-D-Ala-GS (XX) was obtained as a crystalline dihydrochloride by hydrogenolysis of a benzyloxycarbonyl-substituted cyclic decapeptide (XVII) wherein δ-amino functions of ornithine residues were protected with benzyloxycarbonyl groups. The protected cyclic decapeptide (XVII) was prepared from a corresponding decapeptide *p*-nitrophenyl ester trifluoroacetate (XVI) by treatment with pyridine. The trifluoroacetate (XVI) was obtained from *p*-methoxybenzyloxycarbonyl-decapeptide nitrophenyl ester (XV) which was derived from an acyl-decapeptide acid (XIV) and di-*p*-nitrophenyl sulfite.

Synthesis of the protected cyclic decapeptide (XVII) was attempted by possible dimerization reaction of a linear pentapeptide active ester (XVIII). Thus, treatment of the active ester with pyridine afforded a mixture of the protected monomer (XIX) and dimer (XVII) which was prepared as described before; the ratio in weight of XIX and XVII in the mixture was found to be 23 : 77. Separation of the two components was achieved by a Sephadex LH-20 column with methanol, the monomer (XIX) being obtained as a pure material. Hydrogenolysis of XIX in the presence of hydrogen chloride yielded a crystalline monohydrochloride of cyclic pentapeptide (XXI).

The antibacterial activities of the cyclic penta- and decapeptides (XXI and XX) toward several microorganisms were examined. Both compounds exhibited no activity toward Gram negative microorganisms (*e. g.*, *E. coli*). It was also found that 4-D-alanine-semiGS (XXI) possessed no activity toward Gram positive microorganisms (*St. aureus* and *B. subtilis*), whereas 4,4'-D-alanine-GS (XX) possessed recognizable activity though its degree was weaker than that of GS (Table 1). The results indicate that D-alanines can replace D-phenylalanines without drastic drop in activity. The optical rotatory dispersion (ORD) curves of the cyclic decapeptide (XX) and GS were measured with ethanol as a solvent.[5] Both decapeptide afforded a similar shape to a trough at approximately 232 mμ (Fig. 2). Since 4,4'-D-alanine-GS contains no aromatic amino acid residues, the only chromophores in the molecule are amide carbonyls and the shape of the ORD curve will reflect the spatial arrangement of chromophores in the molecule. The results suggest that 4,4'-D-alanine-

1) Present address: Division of Entomology, University of California, Berkeley, Calif., U.S.A.

2) To whom reprint requests should be addressed.

3) R. Nagata, M. Waki, M. Kondo, T. Kato, S. Makisumi, and N. Izumiya, This Bulletin, **40**, 963 (1967).

4) H. Aoyagi, T. Kato, M. Waki, O. Abe, R. Okawa, S. Makisumi, and N. Izumiya, *ibid.*, **42**, 782 (1969).

5) Several papers have given ORD curves on GS and its analogs: *e. g.*, D. Balasubramanian, *J. Amer. Chem. Soc.*, **89**, 5445 (1967); T. Kato, M. Waki, S. Matsuura, and N. Izumiya, *J. Biochem.* (Tokyo), **68**, 751 (1970).

GS possesses a conformation similar to GS. Further studies of the ORD measurements on other GS analogs are in progress.

Table 1. Inhibitory activity of the compounds on microorganisms

Minimum inhibitory concentration, μg/ml

	Staphylococcus aureus	*Bacillus substilis*
GS	6.25	3.13
4,4'-D-Ala-GS	50	25
4-D-Ala-semiGS	>100	>100

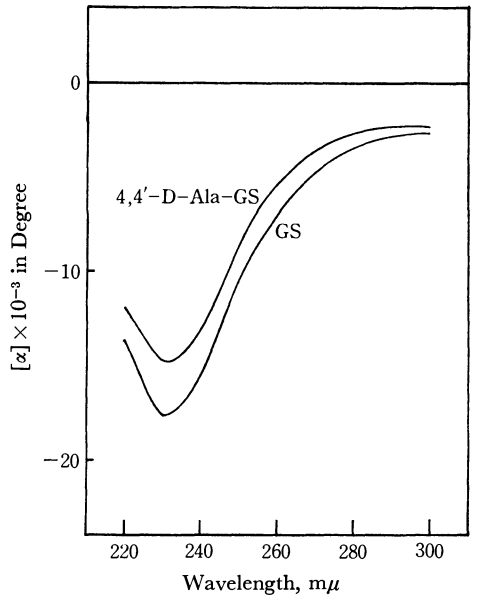

Fig. 2. ORD curves of GS and 4,4'-D-Ala-GS.

Experimental

All melting points are uncorrected. Thin layer chromatography was performed on Merck silica gel G with the following solvent systems: R_f^1, *n*-butanol - acetic acid - pyridine - water 4 : 1 : 1 : 2 v/v; R_f^2, chloroform-methanol 5 : 1 v/v. Paper chromatography was performed with the following solvent system: R_f^3, the same solvent used for R_f^1.

Z-D-Ala-Pro-OEt (I).[6] To a chilled solution of Z-D-Ala-OH (2.32 g, 10 mmol)[7] and TEA (1.4 ml, 10 mmol) in tetrahydrofuran (20 ml), isobutyl chloroformate (1.31 ml, 10 mmol) was added. After 10 min, a mixture of H-Pro-OEt·TsOH[8] (3.15 g, 10 mmol), TEA (1.4 ml, 10 mmol) and chloroform (20 ml) was added to the solution. The reaction mixture was allowed to stand overnight and then evaporated to dryness *in vacuo*. After the residual oil was dissolved in ethyl acetate, the solution was washed successively with water, 2% hydrochloric acid, 4% sodium bicarbonate and water, dried over sodium sulfate, and then evaporated. The product was obtained as oil; yield, 2.51 g (72%); R_f^1 0.98.

H-D-Ala-Pro-OEt·HCl (II). A solution of I (2.51, g 7.2 mmol) dissolved in 0.3N methanolic hydrogen chloride (28 ml) was hydrogenated in the presence of palladium black. The filtrate from the catalyst was evaporated to dryness; yield of oil, 1.80 g (100%); R_f^1 0.80.

Z-Leu-D-Ala-OEt (III). To a solution of Z-Leu-OH·DCHA[9] (6.69 g, 15 mmol) and H-D-Ala-OEt·HCl (1.96 g, 15 mmol)[10] in chloroform (100 ml) was added DCC (3.09 g, 15 mmol) at 0°C. The mixture was stirred for 3 hr at 0°C, and then kept overnight at room temperature. The mixture was evaporated and ethyl acetate was added to the residue. After dicyclohexylurea was filtered off, the filtrate was washed successively with water, 2% hydrochloric acid, 4% sodium bicarbonate, and water, and dried over sodium sulfate. The filtrate was evaporated and the residue was crystallized by addition of ether and petroleum ether. It was recrystallized from ethyl acetate-petroleum ether; yield, 4.45 g (83%); mp 93—94°C; $[\alpha]_D^{20}$ +3.3° (*c* 1, methanol); R_f^1 0.99.

Found: C, 62.49; H, 7.79; N, 7.73%. Calcd for $C_{19}H_{28}O_5N_2$: C, 62.62; H, 7.74; N, 7.73%.

Z-Leu-D-Ala-NHNH$_2$ (IV). A solution of III (4.02 g, 11 mmol) and hydrazine hydrate (5 ml) in DMF (20 ml) was allowed to stand at room temperature for one day. The solution was evaporated, and then water (300 ml) was added to the residue. The resulting crystals were collected by filtration; yield, 3.66 g (95%); mp 171—174°C; $[\alpha]_D^{20}$ −13.8° (*c* 1, DMF); R_f^1 0.87.

Found: C, 58.41; H, 7.58; N, 15.89%. Calcd for $C_{17}H_{26}O_4N_4$: C, 58.27; H, 7.48; N, 15.99%.

Z-Leu-D-Ala-Pro-OEt (V). (*a*) Z-Leu-OH·DCHA (3.2 g, 7.2 mmol) and II (1.8 g, 7.2 mmol) were condensed with DCC (1.48 g, 7.2 mmol) as described for the preparation of III; yield of oil, 2.6 g (77%); R_f^2 0.83.

(*b*) To a solution at −5°C of IV (3.5 g 10 mmol) in DMF (20 ml) containing 2.8N hydrogen chloride in dioxane (7.5 ml), isoamyl nitrite (1.4 ml, 10 mmol) was added.[11] After 10 min, TEA (2.8 ml, 20 mmol) was added. To the solution was added a mixture of H-Pro-OEt·TsOH (3.15g 10 mmol) and TEA (1.4 ml) in DMF (20 ml). The mixture was stirred for 3 days at 0°C and evaporated. The residue was dissolved in ethyl acetate, and the solution was washed successively with 2% hydrochloric acid, 4% sodium bicarbonate and water, dried over sodium sulfate, and then evaporated; yield of oil, 2.6 g (56%); R_f^2 0.83.

Z-Leu-D-Ala-Pro-OH (VI). To a solution of V (2.57 g, 5.6 mmol) in methanol (20 ml), N sodium hydroxide (9 ml) was added. The solution was allowed to stand for 3 hr at room temperature. After the addition of water (20 ml), the solution was evaporated to remove methanol. After the solution was extracted with ethyl acetate, the aqueous layer was acidified with 2N hydrochloric acid. The mixture was extracted with ethyl acetate and the organic layer was dried over sodium sulfate. The filtrate was evaporated to dryness; yield of a semi solid, 2.15 g (89%); R_f^2 0.56.

H-Leu-D-Ala-Pro-OH (VII). A solution of VI (2.15 g, 5 mmol) in a mixture of acetic acid (15 ml), methanol (12 ml) and water (2 ml) was hydrogenated. The filtrate was evaporated to dryness; yield of a semi solid, 1.39 g (93%); R_f^1 0.70.

H-Leu-D-Ala-Pro-OEt·HCl (VIII). This was obtained from V (1.84 g, 4 mmol) as described for the preparation

6) Abbreviations; Z, benzyloxycarbonyl; Z(OMe), *p*-methoxybenzyloxycarbonyl; DCC, dicyclohexylcarbodiimide; TEA, triethylamine: DMF, dimethylformamide; DCHA, dicyclohexylamine; CMC, carboxymethyl cellulose. Amino acid symbol denotes L configration unless otherwise noted.

7) C. S. Smith and A. E. Brown, *J. Amer. Chem. Soc.*, **63**, 2605 (1941).

8) T. Kato, S. Makisumi, M. Ohno, and N. Izumiya, *Nippon Kagaku Zasshi*, **83**, 1151 (1962).

9) E. Klieger, E. Schröder, and H. Gibian, *Liebigs Ann. Chem.*, **640**, 157 (1961).

10) D. A. Rowlands and G. T. Young, *J. Chem. Soc.*, **1950**, 3159.

11) J. Honzl and J. Rudinger, *Collect. Czech. Chem. Commun.*, **26**, 2333 (1961); E. Wünsch and A. Zwick, *Chem. Ber.*, **99**, 101 (1966).

of II; yield of oil, 1.46 g (100%); R_f^1 0.87.

Z-(OMe)-Val-Orn(δ-Z)-Leu-D-Ala-Pro-OH (IX). The azide[12] derived from Z(OMe)-Val-Orn(δ-Z)-$NHNH_2$ (XXII) (2.49 g, 4.4 mmol) was added to a solution of VII (1.19 g, 4 mmol) and TEA (1.12 ml, 8 mmol) in DMF (50 ml). The mixture was stirred for 2 days at 0°C and evaporated. The residue was triturated with 0.5M citric acid, and the precipitate was collected by filtration. It was recrystallized from methanol - ether; yield, 2.26 g (68%); mp 137—139°C; $[\alpha]_D^{20}$ −35.5° (*c* 1, methanol).

Found: C, 58.13; H, 7.24; N, 9.77%. Calcd for $C_{41}H_{58}O_{11}N_6 \cdot H_2O$: C, 58.14; H, 7.61; N, 9.92%.

Z-(OMe)-Val-Orn(δ-Z)-Leu-D-Ala-Pro-OEt (X). The azide[12] derived from XXII (2.49 g, 4.4 mmol) was condensed with VIII (1.50 g, 4.1 mmol) as described for the preparation of V. The precipitate which formed upon addition of water was collected, washed successively with 4% sodium bicarbonate, 0.5M citric acid and water; yield, 3.96 g (85%); mp 163—165°C; $[\alpha]_D^{20}$ −20.7° (*c* 1, DMF); R_f^1 0.98.

Found: C, 61.18; H, 7.45; N, 10.26%. Calcd for $C_{43}H_{62}O_{11}N_6$: C, 61.55; H, 7.45; N, 10.02%.

Z(OMe)-Val-Orn(δ-Z)-Leu-D-Ala-Pro-$NHNH_2$ (XI). A solution of X (4.12 g, 5 mmol) and hydrazine hydrate (2 ml) in DMF (20 ml) was allowed to stand for 5 days at 30°C. After evaporation, the hydrazide which precipitated upon addition of water (400 ml) was collected and recrystallized from dioxane - ether; yield, 1.98g (48%); mp 158—160°C; $[\alpha]_D^{20}$ −20.1° (*c* 1, DMF); R_f^1 0.65.

Found: C, 60.01; H, 7.40; N, 13.69%. Calcd for $C_{41}H_{60}O_{10}N_8$: C, 59.69; H, 7.33; N, 13.59%.

H-Val-Orn(δ-Z)-Leu-D-Ala-Pro-OH·HCl (XII). To a mixture of IX (2.05 g, 2.5 mmol) and anisole (0.3 ml), 2.7N hydrogen chloride in dioxane (20 ml) was added at room temperature. After 2 hr, the solution was evaporated, and the residue was triturated with ether; yield, 1.75 g (97%); mp 147—149°C (decomp.); $[\alpha]_D^{20}$ −36.3° (*c* 1, DMF); R_f^1 0.73.

Found: C, 53.39; H, 7.66; N, 11.52%. Calcd for $C_{32}H_{51}O_8N_6Cl \cdot 2H_2O$: C, 53.43; H, 7.56; N, 11.69%.

Z(OMe)-Val-Orn(δ-Z)-Leu-D-Ala-Pro-Val-Orn(δ-Z)-Leu-D-Ala-Pro-OH (XIV). The azide (XIII) was prepared from XI (2.06 g, 2.5 mmol), N hydrochloric acid (6 ml) and sodium nitrite (0.175 g, 2.5 mmol) in acetic acid (20 ml) as described for the preparation of the azide[12] from XXII. XIII was condensed with XII (1.73 g, 2.4 mmol) as described for the preparation of IX. The product was recrystallized from methanol - ether-petroleum ether; yield, 3.19 g (88%); mp 185—187°C; $[\alpha]_D^{20}$ −59.9° (*c* 1, methanol); R_f^1 0.92, R_f^2 0.66.

Found: C, 59.36; H, 7.26; N, 10.73%. Calcd for $C_{73}H_{106}O_{18}N_{12} \cdot 2H_2O$: C, 59.41; H, 7.51; N, 11.30%.

cyclo-*(Val-Orn(δ-Z)-Leu-D-Ala-Pro-)$_2$ (XVII).* *(a) From XIV.* To a solution of XIV (729 mg, 0.5 mmol) in pyridine (10 ml), di-*p*-nitrophenyl sulfite (1.61 g, 5 mmol) was added. After 8 hr at room temperature, the mixture was evaporated. The residual solid was collected by filtration with the aid of a mixture of ether-petroleum ether (1 : 1, v/v); yield of acyldecapeptide *p*-nitrophenyl ester (XV), 752 mg. To XV (745 mg) thus obtained, anisole (0.5 ml) and trifluoroacetic acid (5 ml) were added at 0°C. After 40 min, the solution was evaporated and the residual powder was collected by filtration with the aid of ether. Decapeptide *p*-nitrophenyl ester trifluoroacetate (XVI) (520 mg) thus obtained was dissolved in DMF (10 ml) and acetic acid (0.1 ml). The solution was added dropwise into pyridine (20 ml) at 50—60°C for 4 hr and stirring was continued for additional 2 hr. After the solvent was removed, the residue was dissolved in a mixture of methanol (40 ml) and water (10 ml). The solution was passed through the columns of Dowex 1 and 50. The effluent was evaporated, and the product was collected by filtration with the aid of water. It was recrystallized from methanol - ether; yield, 151 mg (23% from XIV); mp 234—236°C (decomp.); $[\alpha]_D^{20}$ −199° (*c* 1, methanol); R_f^1 0.95.

Found: C, 56.68; H, 7.61; N, 12.55%; mol wt 1240.[13] Calcd for $C_{64}H_{96}O_{14}N_{12} \cdot 3H_2O$: C, 58.60; H, 7.65; N, 12.81%; wt 1311.

(b) From IX. Acylpentapeptide acid (IX) (405 mg, 0.5 mmol) was converted to pentapeptide *p*-nitrophenyl ester trifluoroacetate (XVIII) (372 mg) as described for the preparation of XV and XVI. XVIII thus obtained was added to pyridine (150 ml) at 60°C as described above. After evaporation, the residue was treated with columns of Dowex 1 and 50, the effluent was evaporated, and the product was collected by filtration with the aid of water; yield of the crude product (XXIII), 110 mg. The solution of XXIII (100 mg) in methanol (5 ml) was applied to a column (2 × 110 cm) with Sephadex LH-20, and the development continued with methanol; a 2 ml fraction was collected in each test tube. The peak of XVII appeared from the test tube number 61 to 70 and the peak of XIX from 80 to 90. The fractions 61—70 were evaporated, and the product was collected by filtration with the aid of water (yield, 64 mg). It was recrystallized from methanol - ether; yield, 52 mg; mp 240—242°C; $[\alpha]_D^{20}$ −192° (*c* 1, methanol); R_f^1 0.95.

cyclo-*(Val-Orn(δ-Z)-Leu-D-Ala-Pro-) (XIX).* The fractions 80—90 were evaporated to afford an oily residue which was crystallized after several days. It was collected by the aid of a mixture of methanol and ether; yield, 19 mg; mp 130—133°C; $[\alpha]_D^{20}$ −64.6° (*c* 0.5, methanol); R_f^1 0.93.

Found: C, 59.49; H, 7.65; N, 13.01%; mol wt 596.[13] Calcd for $C_{32}H_{48}O_7N_6 \cdot H_2O$: C, 59.22; H, 7.74; N, 12.99%; mol wt 647.

cyclo-*(Val-Orn-Leu-D-Ala-Pro-)$_2$·2HCl (4,4′-D-Ala-GS·2HCl) (XX·2HCl).* A solution of XVII (50 mg, 0.038 mmol) in 0.01N methanolic hydrogen chloride (8.4 ml) was hydrogenated and the filtrate was evaporated. The product was recrystallized from methanol - ether - petroleum ether; yield, 31 mg (73%); mp 190—191°C (decomp.); $[\alpha]_D^{20}$ −189° (*c* 1, methanol); R_f^1 0.89.

Found: C, 51.58; H, 7.87; N, 14.05%. Calcd for $C_{48}H_{86}$-

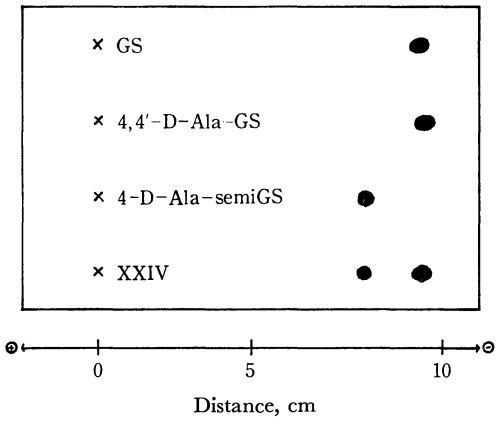

Fig. 3. Paper electrophoresis of the compounds.
XXIV, hydrogenated material after cyclization of pentapeptide active ester trifluoroacetate.

12) O. Abe and N. Izumiya, This Bulletin, **43**, 1202 (1970).

13) Molecular weight was determined on a Hitachi Osmometer type 115, using methanol as a solvent.

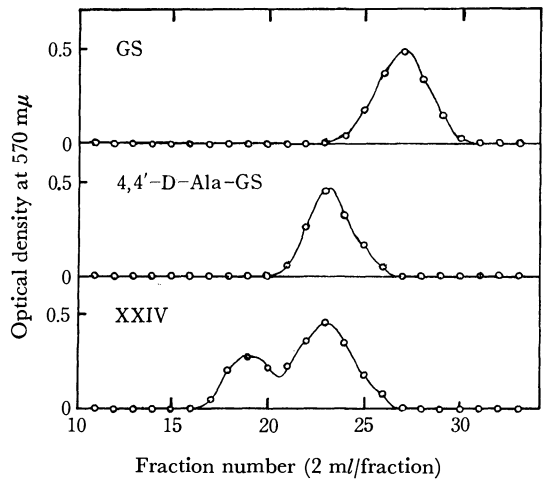

Fig. 4. CMC column chromatography of the compounds. XXIV, see Fig. 3.

$O_{10}N_{12}Cl_2 \cdot 3H_2O$: C, 51.64; H, 8.31; N, 14.33%.

cyclo-*(Val-Orn-Leu-*D*-Ala-Pro-)·HCl (4-*D*-Ala-semiGS·HCl)* *(XXI·HCl)*. XIX (15 mg, 0.02 mmol) was treated as described above; yield of a semi solid, 9.8 mg (98%); R_f^1 0.86.

Electrophoresis and CMC Chromatography. The experiments were carried out as described before.[4] A part of the crude product (XXIII) obtained after cyclization reaction of the pentapeptide active ester (XVIII), was hydrogenated and the product was designated as XXIV. As shown in Fig. 3, 4,4′-Ala-GS and 4-D-Ala-semiGS were clearly separated in the electrophoresis, whereas two compounds could be only partly separated with a column (0.9×50 cm) of CMC.

Microbiological Assays[14] *and ORD Measurements.*[15] The minimum amount of the compounds necessary for the complete inhibition of growth was determined by a dilution method using a bouillon agar medium and the results are shown in Table 1. ORD measurements were performed with JASCO Spectropolarimeter model ORD-CD/UV-5 over a wavelength range of 220 to 300 mμ in ethanol on the compound, and ORD curves are shown in Fig. 2.

14) We are indebted to Meiji Seika Co., Ltd. for the microbiological assays.

15) We are indebted to Mr. S. Matsuura and Dr. M. Waki in this laboratory for ORD measurements.

BULLETIN OF THE CHEMICAL SOCIETY OF JAPAN, VOL. 44, 161—166 (1971)

The Reactions of α-Substituted Carbonyl-stabilized Sulfonium Ylides with Succinic Anhydride

Teruaki MUKAIYAMA, Katsuaki HAGIO, Hisashi TAKEI, and Kazuhiko SAIGO

Laboratory of Organic Chemistry, Tokyo Institute of Technology, Ookayama, Meguro-ku, Tokyo

(Received June 25, 1970)

It was found that various kinds of α-substituted carbonyl-stabilized sulfonium ylides were conveniently prepared from the corresponding sulfonium salts by treating with 50% aqueous sodium hydroxide. The reactions of sulfonium ylides with succinic anhydride afforded furofuran derivative by one step procedure in yields ranging these from 5 to 14%. The structures of furofuran derivatives were confirmed by IR spectrum, NMR sepctrum, degradation, and its behavior toward alkali and acid.

It has been recently reported that 3-hydroxyfuran derivatives were obtained in good yields by the reactions of α-unsubstituted carbonyl-stabilized sulfonium ylides with ketene dimer.[1)]

In the present experiment, the reactions of carbonyl-stabilized ylides (I) with succinic anhydride were tried with the expectation that the six-membered lactone derivatives (III) would be formed by way of an intramolecular nucleophilic attack of carboxylate anion to α-carbon of the sulfonium compound (II). In the reactions of α-unsubstituted carbonyl-stabilized sulfonium ylides with succinic anhydride, it was found that the stable adducts (IV) were obtained in good yields instead of the expected six-membered lactone derivatives. These results indicate that the sulfonium ylide (II) is converted to the more stable tautomer (IV) by an intramolecular proton transfer from α-carbon to carboxylate anion.

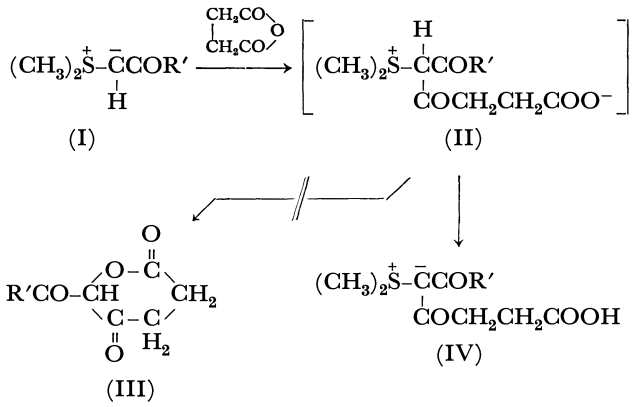

It was established that, unexpectedly, furofuran derivatives were obtained instead of six-membered lactone derivatives or stable adducts by the reactions of α-substituted carbonyl-stabilized sulfonium ylides with succinic anhydride.

Concerning to the preparation of α-substituted carbonyl-stabilized sulfonium ylides, there are few papers, except the cyclic ylide, dimethylsulfonium 2,6-diacetyl-

1) H. Takei, M. Higo, K. Saito, and T. Mukaiyama, This Bulletin **41**, 1738 (1968).

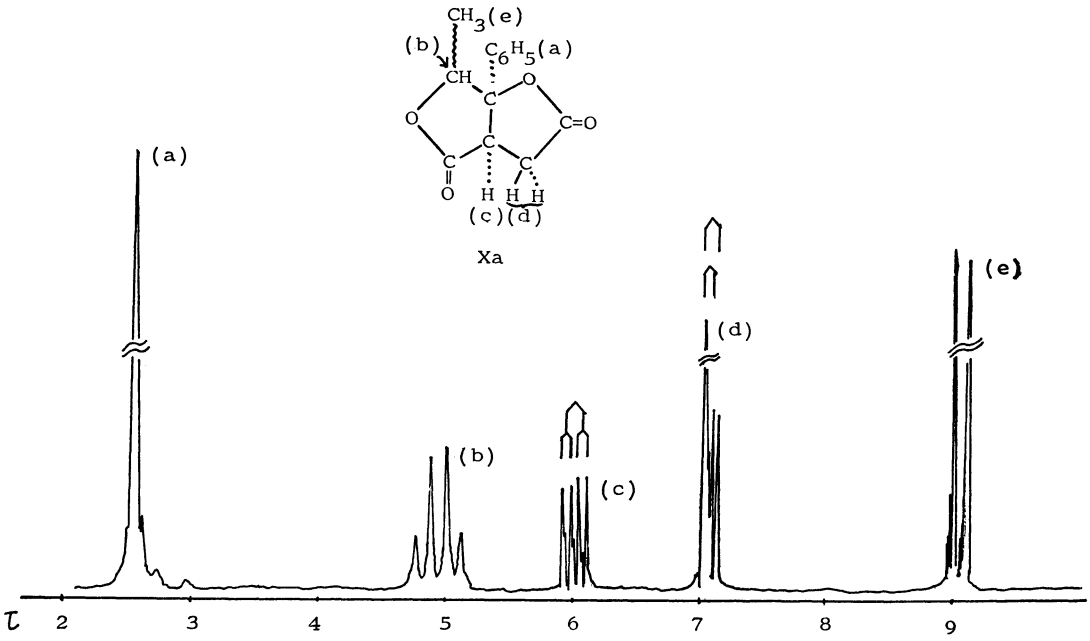

Fig. 1. NMR spectrum of Xa.

2,6-dimethyl-4-oxo-1,3-dioxan-5-ylide.[2] According to this procedure, the preparation of α-substituted sulfonium ylides were tried. When α-bromopropiophenone and dimethyl sulfide were mixed in acetone and allowed to stand for a week at room temperature, the crystalline sulfonium salt (IXa) was obtained in 76% yield. On the other hand, in the case of 3-bromo-2-oxobutane, the reaction took place very slowly and, even after ten days, the sulfonium salt (IXb) was produced only in 40% yield as syrup. When an equimolar amount of silver tetrafluoroborate was added to the resulting reaction mixture of 3-bromo-2-oxobutane and dimethyl sulfide in acetone, the sulfonium salt (IXb′) was obtained in almost quantitative yield within 16 hr. In a similar way, the sulfonium salts, IXc and IXd, were obtained in excellent yields from the corresponding bromides, VIIIc and VIIId. The desired sulfonium ylides (Va—d) were conveniently prepared from the corresponding sulfonium salts in chloroform by the action of 50% aqueous. sodium hydroxide according to the method of Payne.[3] The IR spectra of ylides (Va—d) show bands at 1500, 1505, 1555, and 1560 cm^{-1} attributable to carbonyl groups of sulfonium ylides respectively.

Next, the reaction of the sulfonium ylide with succinic anhydride was tried. When a mixture of the ylide (Va) and succinic anhydride in tetrahydrofuran (THF) was refluxed for 5 hr, evolution of dimethyl sulfide was observed by its characteristic odor and tarry residue remained after the solvent was evaporated. The crystals (Xa), mp 148—149°C, $C_{13}H_{12}O_4$, were isolated from the tarry residue by silica gel column chromatography. The IR spectrum of this compound shows bands at 1795 and 1775 cm^{-1} assigned to a five-membered lactone, and its NMR spectrum shows a singlet at 2.53 τ (5H), a quartet at 4.97 τ (1H), a double doublet at 6.09 τ (1H), a double doublet at 7.05 τ and 7.08 τ (2H) and a doublet at 8.95 τ (3H) (Fig. 1). This compound was stable toward hydrolysis in refluxing concentrated hydrochloric acid-ethanol (1 : 1). On the other hand, this affords acetaldehyde and ketoalcohol (XII) by reducing with lithium aluminum hydride in THF, followed by oxidation with sodium metaperiodate in aqueous ethanol. Acetaldehyde was identified by deriving to its 2,4-dinitrophenylhydrazone. The oily ketoalcohol (XII) reacted with *p*-nitrobenzoyl chloride to give the syrupy ketoester (XIII), which was confirmed by elemental analysis, IR spectrum showing bands at 1730 and 1682 cm^{-1}, and its NMR spectrum having a multiplet at 1.27—2.70 τ (13H), a doublet at 5.28 τ (2H), a triplet at 5.38 τ (2H), a multiplet at 5.72 τ (1H) and a multiplet at about 7.6 τ (2H). From these results, it seems reasonable to conclude that Xa is a furofuran derivative. In this case, Xa is a single product, but the configuration of a methyl group at C_6 in Xa can not be elucidated. Perhaps, a methyl group at C_6 exists in *trans* relation to a phenyl group at C_{6a}

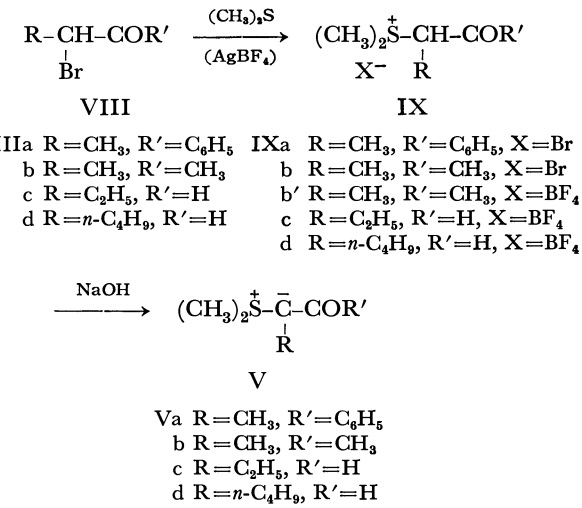

2) G. B. Payne, *J. Org. Chem.*, **33**, 3517 (1968).
3) G. B. Payne, *ibid.*, **32**, 3351 (1967).

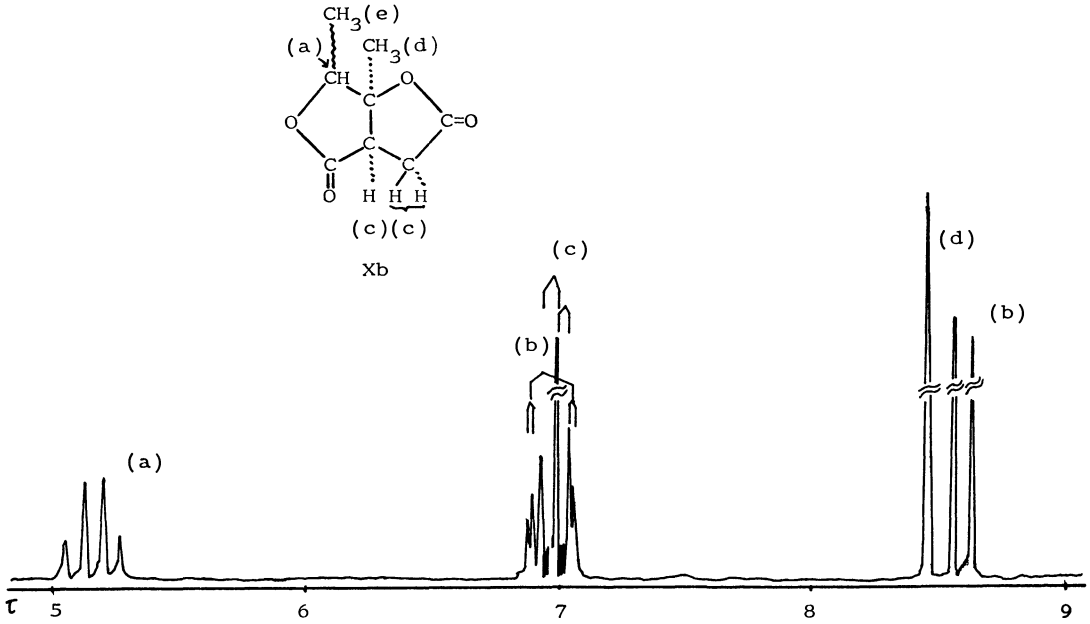

Fig. 2. NMR spectrum of Xb.

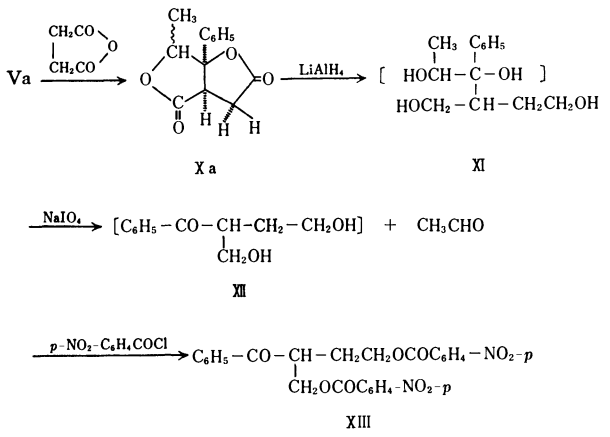

because of the steric hindrance.

Similarly, the ylide (Vb) reacted with succinic anhydride in THF-dimethylformamide (DMF) (1 : 1) to give the crystals (Xb), $C_8H_{10}O_4$, mp 144—146°C. The IR spectrum of Xb shows a band at 1770 cm^{-1} along with shoulder absorption at 1790 cm^{-1} and its NMR spectrum was similar to that of Xa as shown in Fig. 2. The compound (Xb) was stable toward acid hydrolysis, but a viscous oily carboxylic acid was obtained by hydrolysis of Xb with aqueous sodium hydroxide. This carboxylic acid is transformed to the original compound (Xb) by the treatment with acid. Based on these results, the structure of Xb was confirmed to be a furofuran derivative.

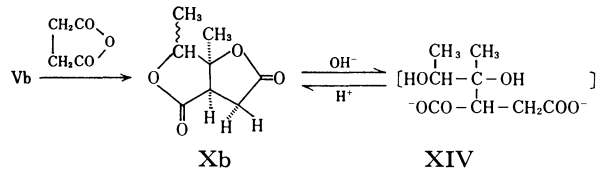

In the cases of the ylides, Vc and Vd, the reactions with succinic anhydride in THF-DMF (1 : 1) gave the furofuran derivatives, Xc, mp 107—108°C, $C_8H_{10}O_4$, and Xd, mp 86—87°C, $C_{10}H_{14}O_4$, in 10% and 5% yields respectively. The IR and NMR spectra of Xc and Xd were similar to those of Xb as shown in Figs. 3 and 4. The coupling constant between H_d and H_e (J_{de}=0 H_z) indicates that these protons have a *trans* relationship.

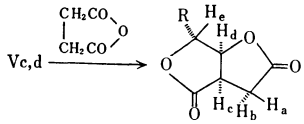

Xc R=C_2H_5 d R=*n*-C_4H_9

The reaction of Va and itaconic anhydride was tried in order to apply this reaction to the synthesis of the furofuran derivative[4] having an exocyclic double bond. However, the reaction under various conditions, such as with ice cooling or with dry-ice cooling, resulted in resinification of the reaction mixture. Consequently, the furofuran derivative (XVI) could not be isolated.

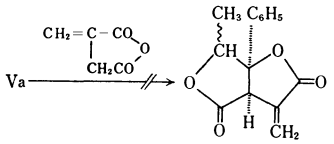

XVI

On the other hand, 2-methylsuccinic anhydride reacted with the ylide (Va) in THF-DMF (1 : 1) to give the furofuran derivative (XVII), mp 103—104°C, $C_{14}H_{14}O_4$, in only 10% yield. The IR spectrum of

4) These types of the skeletal structures exist in natural products, as Canadensolide (XV) which is one of metabolites produced by the fungi P. C.

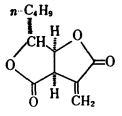

XV

N. J. McCorkindale, J. L. C. Wright, P. W. Brain, S. M. Clarke, and S. A. Hutihinson, *Tetrahedron Lett.*, **1968**, 727.

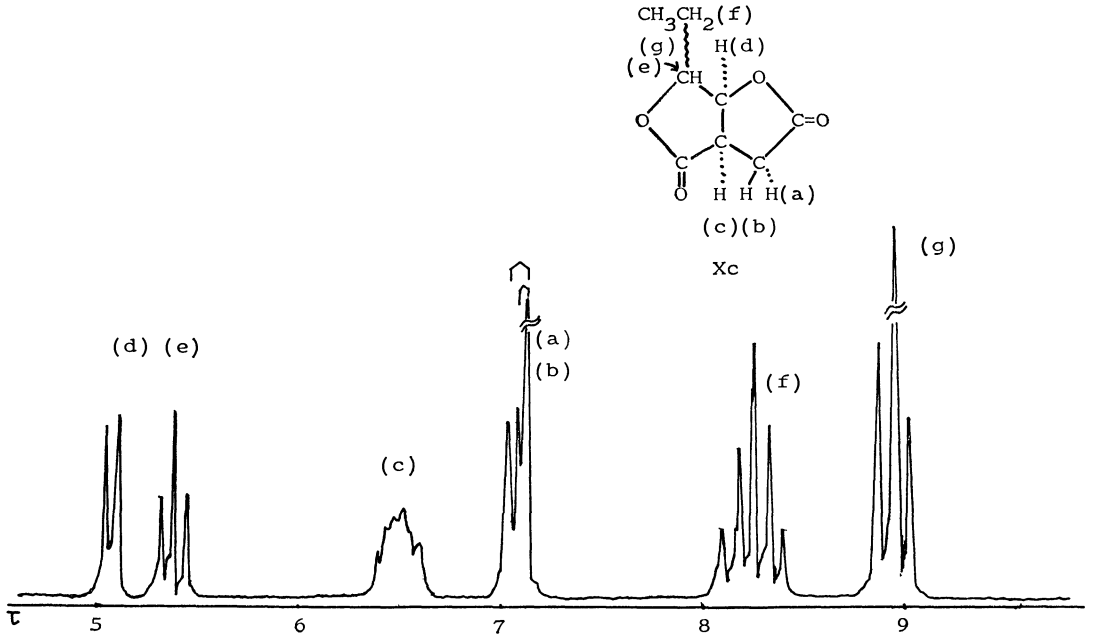

Fig. 3. NMR spectrum of Xc.

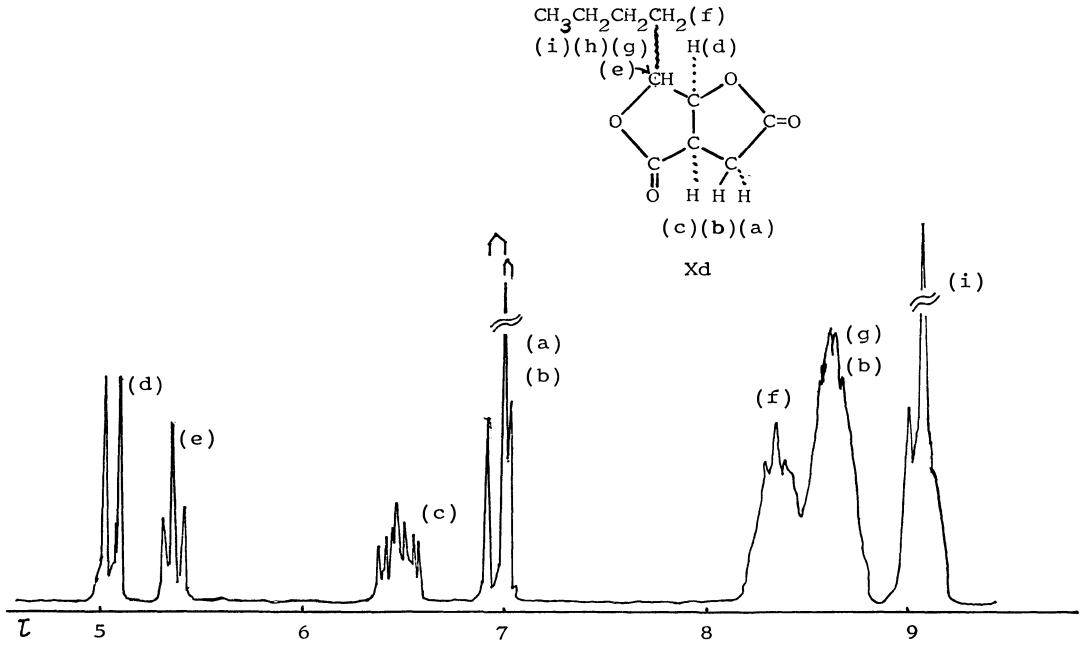

Fig. 4. NMR spectrum of Xd.

XVII shows a band at 1770 cm^{-1} along with shoulder absorption at 1790 cm^{-1} assigned to a five-membered lactone. The NMR spectrum of XVII shows a singlet at 2.55 τ (5H, C_6H_5), a quartet at 5.08 τ (1H, Hc), a doublet at 6.14 τ (1H, Hb), a quintet at 7.02 τ (1H, Ha), a doublet at 8.53 τ (3H, C_2–CH_3), and a doublet at 8.97 τ (3H, C_6–CH_3) (Fig. 5). From the coupling constant between Ha and Hb, it is concluded that Ha and Hb have a *cis* relationship.

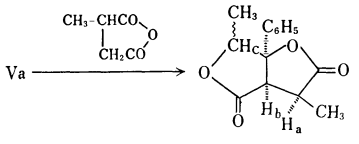

XVII

Experimental

All melting points are uncorrected.

Sulfonium Salts. The sulfonium salts were prepared by the following two methods, (A) and (B).

Method (A): A solution of α-bromopropiophenone (21.3 g, 0.1 mol) and dimethyl sulfide (6.8 g, 0.11 mol) in acetone (50 ml) was allowed to stand for a week. Filtration gave the sulfonium salt (IXa), 19.2 g (73%), mp 135—137°C (dec.). Recrystallization from ethanol gave colorless microcrystals, mp 138—139°C (dec.).

Method (B): A mixture of 3-bromo-2-oxobutane (11.7 g, 0.08 mol), dimethyl sulfide (9.3 g, 0.15 mol) and silver tetrafluoroborate (15.5 g, 0.08 mol) in acetone (50 ml) was stirred for 16 hr at room temperature. Silver bromide was filtered off and washed with ethanol. The combined filtrate was

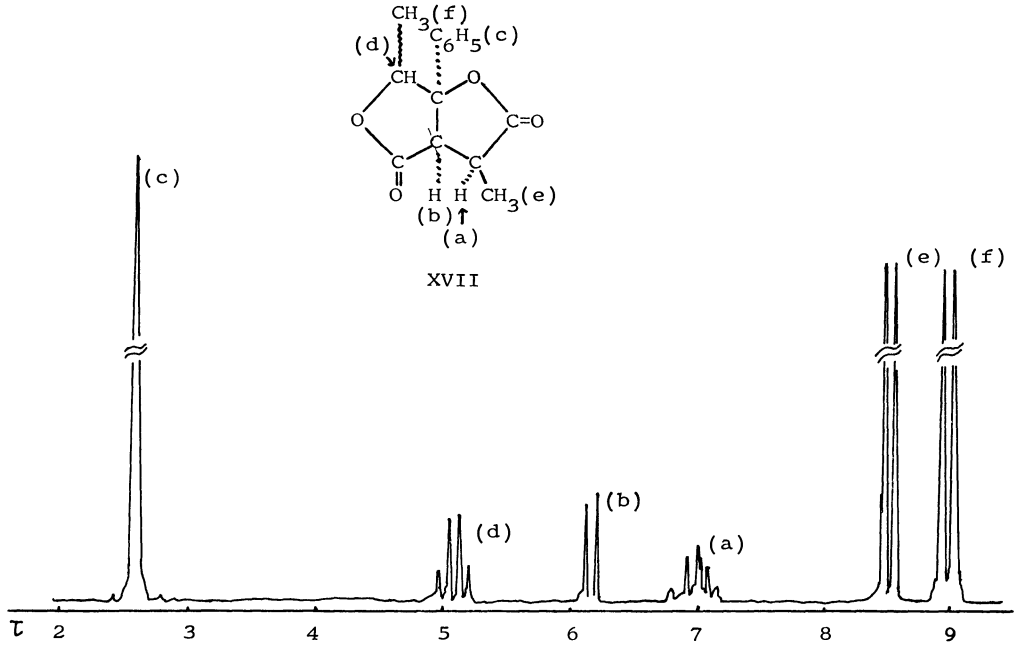

Fig. 5. NMR spectrum of XVII.

evaporated under reduced pressure to give an oily residue. After washing the residue with ether, evaporation of the ether under reduced pressure gave the sulfonium tetrafluoroborate (IXb′) as dark hygroscopic syrup with constant weight of 17.09 g (quantitative yield).

Similarly, various sulfonium salts were obtained by the reactions of α-bromoaldehydes with dimethyl sulfide. The results are listed in Table 1.

Table 1. Preparation of sulfonium salt

Sulfonium salt	IXa	IXb	IXb′	IXc	IXd
Time	1 week	10 days	16 hr	15 hr	2 weeks
Yield (%)	73	40	quant.	quant.	quant.
Mp (°C)	135—137	(syrup)	(syrup)	(syrup)	(syrup)
Method	A	A[a)]	B	B	B

a) After removal of supernatant liquid by decantation, the residue was washed with ether and dried under reduced pressure.

Sulfonium Ylides. The sulfonium ylides were prepared according to the method of Payne.[3] The results are listed in Table 2.

Table 2. Preparation of sulfonium ylide

Ylide	Va	Vb	Vb′	Vc	Vd
Yield (%)	96	59	68	38	50
Mp (°C)	110 (dec.) (sint. 60)	—	—	—	—
IR ($\nu_{C=O}$) cm^{-1}	1500	1505 a)	1505 b)	1555	1560

a) From the sulfonium salt (IXb)
b) From the sulfonium salt (IXb′)

The ylide was washed with ether, dried under reduced pressure, and used for the reaction with succinic anhydride without further purification.

6-Methyl-6a-phenyl-perhydrofuro[3,4-b]furan-2,4-dione (Xa). To a mixture of the ylide (Va) (10.8 g, 0.055 mol) and THF (50 m*l*) was added a solution of succinic anhydride (4.15 g, 0.41 mol) in THF (50 m*l*) with stirring at room temperature, and the reaction mixture was stirred for additional two hours. After refluxing for five hours (evolution of dimethyl sulfide was observed by its characteristic odor), removal of the solvent gave a tarry residue. The solution of the tarry residue in

Table 3. Reaction of sulfonium ylide with succinic anhydride or 2-methylsuccinic anhydride

Furofuran		Xa		Xb		Xc		Xd		XII	
Ylide		Va		Vb		Vc		Vd		Va	
Anhydride		succinic anhydride		succinic anhydride		succinic anhydride		succinic anhydride		2-methylsuccinic anhydride	
Solvent		THF		THF-DMF (1 : 1)		THF-DMF (1 : 1)		THF-DMF (1 : 1)		THF-DMF (1 : 1)	
Temp. and time		2 hr at r.t. and refl. for 5 hr		2 hr at r.t. and refl. for 2 hr		2 hr at r.t. and refl. for 2 hr		2 hr at r.t. and refl. for 2 hr		1 hr at r.t. and refl. for 3 hr	
Yield (%)		44		29		10		5		10	
Mp (°C)		148—149		144—146		107—108		86—87		103—104	
Solvent of recrystallization		ethanol		ethanol		carbon tetrachloride		carbon tetrachloride		cyclohexane	
		C	H	C	H	C	H	C	H	C	H
Anal.	Found	67.34	5.46	56.52	5.75	56.77	5.64	60.59	7.20	67.98	5.73
	Calcd	67.23	5.21	56.46	5.92	56.46	5.92	60.55	7.12	68.28	5.73

ethyl acetate was washed with aqueous sodium hydrogen carbonate followed by water, and dried over sodium sulfate. After removal of the solvent, the residue was chromatographed on silica gel, and elution with methylene chloride gave a yellow oil, which was crystallized from ether, and filtration gave colorless crystals, mp 146—148°C. Recrystallization from ethanol gave Xa, 4.22 g (44%), as colorless needles.

Similarly, various furofurans were obtained by the reaction of ylides with succinic anhydride or 2-methylsuccinic anhydride. The results are listed in Table 3.

Degradation of Xa. To a solution of lithium aluminum hydride (0.74 g) in dry THF (20 m*l*) was added a solution of Xa (1.70 g) in dry THF (10 m*l*). After refluxing for two hours, excess lithium aluminum hydride was decomposed by addition of small amount of water and the mixture was filtered. Evaporation of the solvent gave alcohol (XI), 1.45 g (81%), as syrup. A solution of XI (1.45 g) and sodium metaperiodate (1.33 g) in aqueous ethanol (1 : 1) (30 m*l*) was stirred in bubbling nitrogen atmosphere at room temperature for five hours. Evolved acetaldehyde was led into a solution of 2,4-dinitrophenylhydrazine in ethanol to give 2,4-dinitrophenylhydrazone, 1.04 g (75%), which was recrystallized from ethanol, mp 144—145°C. This hydrazone was identical with an authentic sample by comparing IR spectrum. The reaction mixture was extracted with ether. Evaporation of ether gave ketoalcohol (XII), 1.20 g (quantitative yield), as colorless oil, $\nu_{C=O}$ 1680 cm^{-1}. To a solution of XII (0.75 g) in pyridine (10 m*l*) was added *p*-nitrobenzoyl chloride (1.50 g) with stirring and heated at 70°C for fifteen minutes. After evaporation of pyridine, the reaction mixture was poured into water and extracted with methylene chloride which was washed with dilute hydrochloric acid and water. After evaporation of the solvent, the residue was chromatographed on silica gel, and elution with methylene chloride gave ketoester (XIII), 1.05 g (61%), as viscous syrup: $\nu_{C=O}$ 1730 and 1682 cm^{-1}; NMR (in $CDCl_3$): 1.27—2.70 τ (13H, multiplet), 5.28 τ (2H, doublet), 5.38 τ (2H, triplet), 5.72 τ (1H, multiplet), and 7.60 τ (2H, multiplet).

Found: C, 60.70; H, 3.86; N, 5.50% Calcd for $C_{25}H_{20}O_9N_2$: C, 60.97; H, 4.09; N, 5.69%.

Hydrolysis of Xb and Cyclization of XIV. A suspension of Xb (0.54 g) in 10% sodium hydroxide (40 m*l*) was heated at 70°C for two hours to give a clear solution, which was then cooled, washed with ether, acidified with hydrochloric acid, and immediately extracted with ethyl acetate. Removal of the ethyl acetate gave an oily carboxylic acid (XIV), 0.52 g, ν_{OH} 3430 cm^{-1} (broad) and $\nu_{C=O}$ 1705 cm^{-1}. A solution of 200 mg of the carboxylic acid (XIV) and one drop of conc. hydrochloric acid in ethyl acetate was refluxed for five hours. After removal of the ethyl acetate, the oily residue was crystallized from ether to give Xb; 120 mg, mp 142—144°C, which was identified by IR spectrum.

BULLETIN OF THE CHEMICAL SOCIETY OF JAPAN, VOL. 44, 166—172 (1971)

Hydrogenation and Hydrogenolysis. XIII.[1] The Hydrogenation of Ethyl 4-Methyl-1-cyclohexenyl Ether over Platinum Metal Catalysts

Shigeo NISHIMURA, Mamoru KATAGIRI, Tetsuo WATANABE, and Masayoshi URAMOTO
Department of Industrial Chemistry, Tokyo University of Agriculture and Technology, Koganei-shi, Tokyo

(Received June 29, 1970)

The hydrogenation and hydrogenolysis of ethyl 4-methyl-1-cyclohexenyl ether (I) have been investigated with six unsupported platinum metals as catalysts at 25°C under atmospheric pressure of hydrogen. The hydrogenation of I in ethanol was accompanied by the formation of 4-methylcyclohexanone diethyl acetal (II), the extent of which depended on the nature of the catalyst metals. The ratio of the acetal formation to hydrogenation increased with respect to the catalyst metals in the sequence Os$<$Ru$<$Ir$\ll$Rh$<$Pd$<$Pt. The amount of the hydrogenolysis to give methylcyclohexane increased in the order Pd$\cong$Ru$\ll$Os$<$Rh$<$Ir$\ll$Pt at an initial stage of the hydrogenation in ethanol. This order in hydrogenolysis was explained in terms of the action of the ionized hydrogen on the catalyst surface and the olefin isomerization activity of the catalyst metals. The stereochemistry of the hydrogenation of I was also studied and the results were interpreted on the basis of the proposed mechanism. I was also hydrogenated in *t*-butyl alcohol and isopropyl ether as solvents and, except in a few cases, the proportion of hydrogenolysis decreased with solvent in the order ethanol$>$*t*-butyl alcohol$>$isopropyl ether. The stereoselectivity in ether formation did not differ much among the solvents except over palladium.

Detailed studies on the catalytic hydrogenation of an enol ether seem rather few in the literature.[2-4] Howard and Brown, Jr.,[3] hydrogenated various acetals with supported platinum metal catalysts in the presence of hydrochloric acid and interpreted from the results that acetals hydrogenate *via* the corresponding enol ethers under the acidic conditions. Acke and Anteunis[4] hydrogenated some acetals and corresponding enol ethers, in relation to the study of the hydrogenation of cycloalkanones in acidic methanol, with Adams platinum as catalyst. They showed that in the presence of hydrochloric acid the products obtained on hydrogenation of acetals and enol ethers were almost the same and suggested that formation of these compounds would be responsible for the production of ethers and

1) Part XII: Y. Takagi, S. Ishii, and S. Nishimura, This Bulletin, **43**, 917 (1970).
2) P. N. Rylander, "Catalytic Hydrogenation over Platinum Metals," Academic Press Inc., New York (1967), p. 444.
3) W. L. Howard and J. H. Brown, Jr., *J. Org. Chem.*, **26**, 1026 (1961).
4) M. Acke and M. Anteunis, *Bull. Soc. Chim. Belges*, **74**, 41 (1965).

cycloalkanes on hydrogenation of the ketones in acidic methanol. It is also known from some examples in the literature that formation of alkanes on hydrogenation of enol ethers occurs over platinum, while this does not seem to occur with palladium.[2,4,5] However, no comparative study of the hydrogenation and hydrogenolysis of an enol ether over the six platinum metals seems to have ever been described and, especially, the nature of the rarer platinum metals in this reaction appears little known.

In this study, the catalytic hydrogenation and hydrogenolysis of ethyl 4-methyl-1-cyclohexenyl ether (I) over six unsupported platinum metals have been investigated in ethanol, *t*-butyl alcohol and isopropyl ether as solvents at 25°C and the atmospheric pressure of hydrogen. The properties of the six platinum metals have been compared mainly with respect to their activities for acetal formation in ethanol, their tendencies towards hydrogenolysis as well as their stereoselectivities in the formation of saturated ether. 4-Methylcyclohexanone diethyl acetal (II) has also been subjected to hydrogenation for comparison. We have been interested in the hydrogenation of I, because it is an important intermediate in the catalytic hydrogenation of ethyl *p*-tolyl ether, the results of which will be described in a forthcoming paper.[6]

Experimental

Materials. 4-Methylcyclohexanone Diethyl Acetal (II) was prepared by passing dry hydrogen chloride into a mixture of 4-methylcyclohexanone and ethyl orthoformate in absolute ethanol. Bp 96°C/21 mmHg; n_D^{20} 1.4347 (lit,[7] Bp 76—78°C/15 mmHg; n_D^{20} 1.4350).

Mthyl 4-Methyl-1-cyclohexenyl Ether (I) was prepared by heating II with 0.1% anhydrous *p*-toluenesulfonic acid and distilling off ethanol under the pressure of about 100 mmHg.[7] The residue was then distilled fractionally under reduced pressure. Bp 76—76.8°C/26 mmHg; n_D^{20} 1.4590 (lit,[7] Bp 58—60°C/15 mmHg; n_D^{20} 1.4537). The purity of this preparation was almost 100% as analyzed by gas chromatography. For hydrogenation, the enol ether of 97.3% purity, containing 2.3 mol% of II and 0.4 mol% of 4-methylcyclohexanone, was used throughout the experiments.

Solvents. S.S.G. ethanol of the Wako Pure Chemical Industries was further dehydrated by refluxing with sodium metal and diethyl phthalate.[8] *t*-Butyl alcohol and Isopropyl ether were dehydrated with sodium metal and then carefully distilled.

Catalysts. Unsupported ruthenium, rhodium and palladium catalysts were prepared by reducing the corresponding metal hydroxides in water with hydrogen under atmospheric pressure (at room temperature for rhodium and palladium and at 40—50°C for ruthenium). Unsupported iridium catalyst was prepared by reducing iridium hydroxide in water for 40 min at 90°C under the hydrogen pressure of 80 kg/cm². Unsupported osmium catalyst was obtained by reducing osmium tetroxide in water for 40 min at 90°C under the hydrogen pressure of 60 kg/cm². Unsupported platinum catalyst was prepared by the following procedure: Adams platinum oxide was reduced in water for 10 min at room temperature and atmospheric pressure. The upper layer of water was removed by decantation and a new portion of distilled water was added, and then the reduction was continued further for 5 min. By this procedure satisfactory removal of alkaline substances was effectuated for Adams platinum oxide. The catalyst metals thus prepared were all well washed with distilled water and then dried in vacuum over silica gel.

Hydrogenation. The substrate (0.2 m*l*) was hydrogenated with 10—40 mg of the catalyst metal in 10 m*l* of the solvent at 25°C and the atmospheric pressure of hydrogen in a glass bottle shaken at about 300—350 strokes per minute.

Analysis of Reaction Mixture. The reaction mixture was taken into a microsyringe through a silicone gum stopper during the course of hydrogenation and subjected to gas-chromatographic analysis as soon as possible. A column of 10% PEG 20M on Chromosorb W (column dimensions: 0.3 cm × 3.75 m; column temperature: programmed at 2°C/min for 36—100°C and 4°C/min for 100—160°C) was used except for the product in isopropyl ether, which was analyzed using a column consisting of PEG 6000 (2.25 m) and Apiezon L (1.5 m). The peaks of the *cis* and *trans* isomers of ethyl 4-methylcyclohexyl ether were assigned according to those of corresponding methyl ether, the *cis* isomer of which was reported by Hückel and Kurz to be of smaller retention time.[9] Correctness of this assignment was confirmed by ethylating a *cis*-rich 4-methylcyclohexanol with sodium amide and ethyl iodide in benzene and subjecting the resulting *cis*-rich ether to gas chromatography.

Results

Hydrogenation in Ethanol as the Solvent. Hydrogenation of I in ethanol is accompanied by the formation of the acetal II, the extent of which largely depends on the nature of the catalyst metal used. The rate of hydrogenation of the acetal is in most cases much lower than that of I and the product from the acetal often differs from that obtained from I. Accordingly, the composition of the reaction mixture at initial stages of hydrogenation is not always similar to that of subsequent hydrogenation. Table 1 shows only the composition of the reaction mixture at a final stage of hydrogenation. The varying composition of the reaction mixture during the course of hydrogenation is shown in Figs. 1—6. The results of the hydrogenation of the acetal II is given in Table 2.

1) Hydrogenation over Ruthenium Catalyst (Fig. 1): The acetal formation was slow over this metal, the maximum amount of it being 20.3 mol% at 79.4% hydrogenation. Accordingly, the greater part of I was hydrogenated without the accompanying formation of the acetal. Hydrogenolysis occurred only to the extent of 2.8 mol% and the selectivity for formation of ethyl 4-methylcyclohexyl ether (IV) was very high (95 mol%), until the acetal began to hydrogenate at about 70% hydrogenation. The rate of hydrogenation after this became very small and the main product of hydrogenation was 4-methylcyclohexanol (V), which

5) H. H. Inhoffen, G. Stoeck, G. Kölling, and U. Stoeck, *Ann. Chem.*, **568**, 52 (1950).

6) Presented at the 25th Symposium on Catalysis, Fukuoka, October, 1969. See also *Shokubai*, **11**, 149P (1969).

7) U. Schmidt and P. Grafen, *Ann. Chem.*, **656**, 97 (1962). The boiling point for II and the refractive index for I reported by these authors appear too low.

8) L. F. Fieser, "Experiments in Organic Chemistry," 3rd Ed., Heath and Company (1955), p. 285.

9) W. Hückel and J. Kurz, *Ann. Chem.*, **645**, 194 (1961).

TABLE 1. HYDROGENATION OF ETHYL 4-METHYL-1-CYCLOHEXENYL ETHER (I) CATALYZED BY PLATINUM METALS

Catalyst mg	Solvent	Reac. time (hr)	Hydrogenation[a] (%)	Composition of reac. mixture,[b] mol%						*Cis/trans*		Proportion of hydrogenolysis[c] (mol%)
				I	II	III	IV	V	VI	IV	V	
Ru, 25	EtOH	18.7	94.9	0.0	5.1	0.0	76.0	16.4	2.7	1.45	2.04	2.80
Rh, 25	EtOH	3.7	98.6	0.0	1.4	0.0	59.5	30.8	8.3	4.09	3.10	8.45
Pd, 25	EtOH	18.3	96.3	0.0	3.7	0.0	96.0	0.0	0.3	10.0	—	0.30
Os, 25	EtOH	3.8	88.9	2.2	8.9	0.0	67.4	0.8	20.8	2.11	1.03	23.3
Ir, 25	EtOH	15.3	88.3	0.0	11.7	0.0	75.3	2.2	10.9	2.87	1.02	12.3
Pt, 25	EtOH	2.9	100.0	0.0	0.0	0.0	46.3	14.6	39.1	2.56	1.01	39.1
Ru, 10	*t*-BuOH	1.9	97.3	0.0	2.7	0.0	96.2	0.74	0.45	1.85	0.90	0.46
Rh, 10	*t*-BuOH	2.2	99.6	0.13	0.17	0.11	96.3	2.3	1.1	3.13	1.19	1.1
Pd, 10	*t*-BuOH	1.9	92.5	0.0	0.61	6.8	91.8	0.0	0.73	4.54	—	0.79
Os, 15	*t*-BuOH	2.3	97.8	0.37	1.9	0.0	87.3	1.3	9.1	1.85	1.02	9.3
Ir, 10	*t*-BuOH	0.8	97.7	0.15	2.2	0.0	91.8	0.96	5.0	2.50	0.78	5.1
Pt, 10	*t*-BuOH	1.2	100.0	0.0	0.0	0.0	40.1	1.46	58.4	2.55	4.65	58.4
Ru, 10	*i*-Pr_2O	0.2	97.8	0.0	2.2	0.0	96.8	0.92	0.14	1.66	1.13	0.13
Rh, 10	*i*-Pr_2O	0.7	100.0	0.0	0.0	0.0	94.6	5.1	0.34	3.56	2.65	0.34
Pd, 10	*i*-Pr_2O	2.6	79.6	0.43	5.2	14.8	79.6	0.0	0.06	5.27	—	0.08
Os, 15	*i*-Pr_2O	2.9	97.8	0.0	1.9	0.3	94.8	1.42	1.7	1.84	1.04	1.7
Ir, 10	*i*-Pr_2O	2.1	98.2	0.0	1.8	0.0	92.9	0.88	4.4	2.40	1.04	4.45
Pt, 10	*i*-Pr_2O	1.6	91.6	1.1	4.1	3.2	63.9	0.0	27.8	2.83	—	30.3

a) "Hydrogenation" in this Table (and also in Table 2 and Figs. 1—6) is given by $\frac{100 \times \text{mol (IV+V+VI)}}{\text{mol } \sum(\text{I—VI})}$.

b) I: Ethyl 4-methyl-1-cyclohexenyl ether; II: 4-Methylcyclohexanone diethyl acetal; III: 4-Methylcyclohexanone; IV: Ethyl 4-methylcyclohexyl ether; V: 4-Methylcyclohexanol; VI: Methylcyclohexane.

c) Proportion of hydrogenolysis is given by $\frac{100 \times \text{mol (VI)}}{\text{mol (IV+V+VI)}}$.

probably resulted from hydrogenation of 4-methylcyclohexanone (III) formed by the hydrolysis of I or II. This type of hydrolysis was difficult to be avoided although hydrogenation was performed in carefully dehydrated ethanol under dry hydrogen. The alcohol formation was not observed during a much faster hydrogenation of I at earlier stages. The hydrogenation of II under the same conditions was also very slow and the predominant product was the alcohol IV, as expected from the results of the hydrogenation of I.

2) Hydrogenation over Rhodium Catalyst (Fig. 2): The acetal formation occurred to considerable extent during the hydrogenation of I with rhodium. The maximum amount of it formed was 44 mol% at 51% hydrogena-

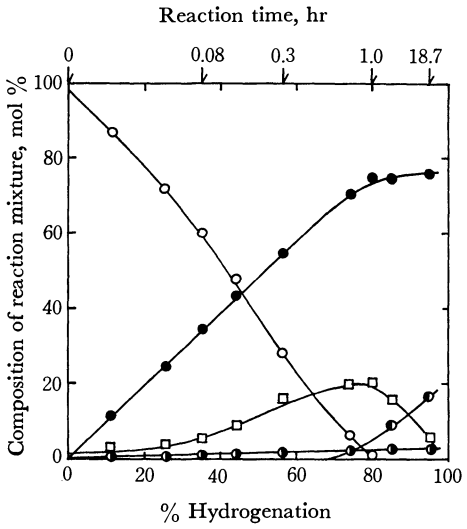

Fig. 1. The products in the hydrogenation of ethyl 4-methyl-1-cyclohexenyl ether (○) over ruthenium catalyst in ethanol at 25°C and 1 atm.
□ : 4-Methylcyclohexanone diethyl acetal
● : Ethyl 4-methylcyclohexyl ether
◐ : 4-Methylcyclohexanol
◑ : Methylcyclohexane

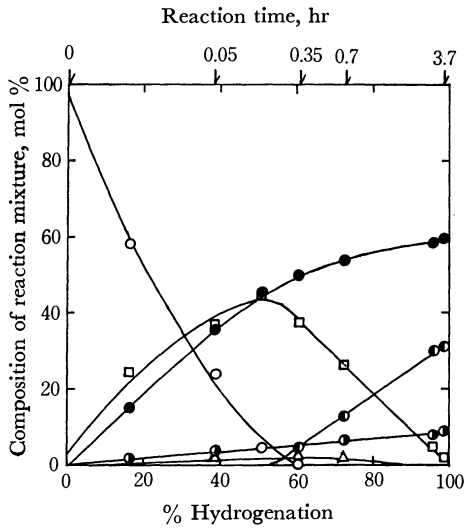

Fig. 2. The products formed in the hydrogenation of ethyl 4-methyl-1-cyclohexenyl ether over rhodium catalyst in ethanol at 25°C and 1 atm.
△: 4-Methylcyclohexanone. For other indications see Fig. 1.

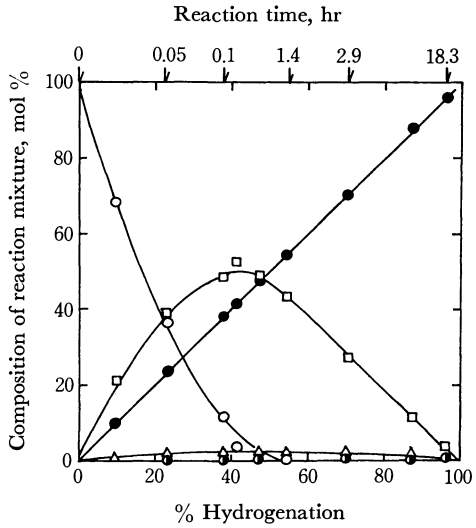

Fig. 3. The products formed in the hydrogenation of ethyl 4-methyl-1-cyclohexenyl ether over palladium catalyst in ethanol at 25°C and 1 atm. For indications see Figs. 1 and 2.

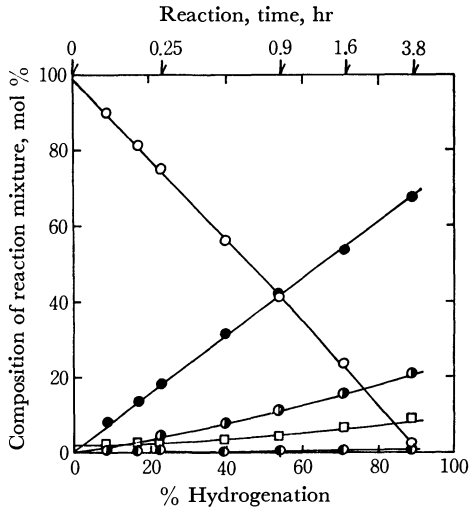

Fig. 4. The products formed in the hydrogenation of ethyl 4-methyl-1-cycohexenyl ether over osmium catalyst in ethanol at 25°C and 1 atm. For indications see Fig. 1.

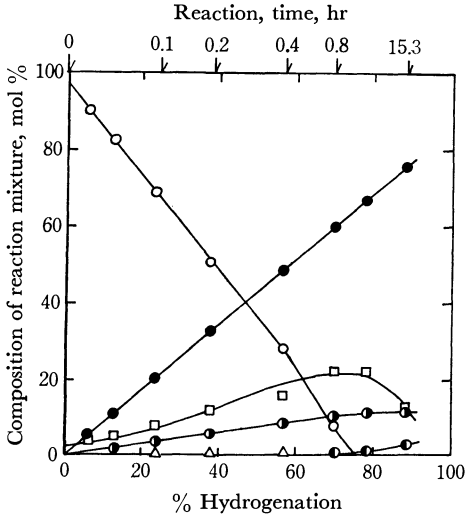

Fig. 5. The products formed in the hydrogenation of ethyl 4-methyl-1-cyclohexenyl ether over iridium catalyst in ethanol at 25°C and 1 atm. For indications see Figs. 1 and 2.

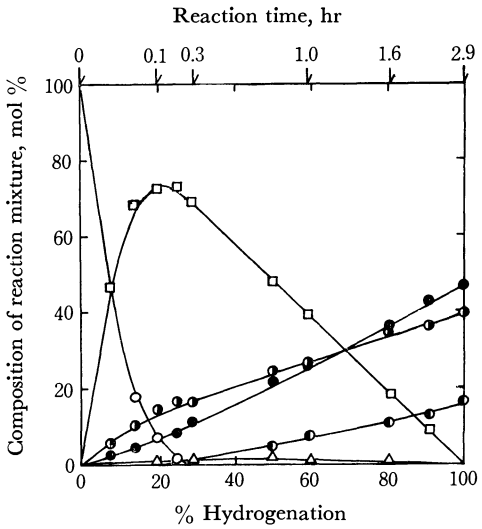

Fig. 6. The products formed in the hydrogenation of ethyl 4-methyl-1-cyclohexenyl ether over platinum catalyst in ethanol at 25°C and 1 atm. For indications see Figs. 1 and 2.

Table 2. Hydrogenation of 4-methylcyclohexanone diethyl acetal (II) with platinum metal catalysts[a)]

Catalyst mg	Reac. time (hr)	Hydrogenation[b)] (%)	Composition of hydrogenation product, mol%			*cis/trans*	
			IV	V	VI	IV	V
Ru, 40	3.8	17.0	6.5	93.5	0.0	6.2	1.5
Rh, 40	3.4	99.8	10.1	88.3	1.7	4.7	2.5
Pd, 30	6.1	88.6	99.0	0.7	0.3	8.9	2.4
Os, 40	3.5	43.0	73.4	25.3	1.3	3.0	1.0
Ir, 40	4.3	6.2	100.0	0.0	0.0	8.1	—
Pt, 15	13.7	17.7	29.5	10.6	60.0	3.3	1.0

a) Acetal II (0.2 m*l*) was hydrogenated in 10 m*l* ethanol at 25°C under an atmospheric pressure of hydrogen.
b) See the footnote (a) in Table 1.

tion. Similarly as with ruthenium catalyst, hydrogenation became slow after about 50% hydrogenation at which the acetal formed began to be hydrogenated and formation of the alcohol increased suddenly. As shown in Table 2, the main product of the hydrogenation of II was also the alcohol IV. Hydrogenolysis occurred to a much greater extent than over ruthenium catalyst and it decreased during the hydrogenation from 10 mol% at the initial stage to 8.5 mol% at a final stage. Hydrogenolysis occurred to a much lesser extent in hydrogenation of II as seen in Table 2. The *cis/trans* ratio of ether IV formed from I was 4.1 which was rather great as compared with those by other platinum metals except palladium.

3) Hydrogenation over Palladium Catalyst (Fig. 3): Hydrogenation of I with palladium catalyst was accompanied by a rapid formation of II which amounted to 53 mol% at 41% hydrogenation. In contrast to the results with ruthenium and rhodium, the product of the hydrogenation of I did not differ much from that formed from the acetal II (see Table 2). Noteworthy features of the palladium-catalyzed hydrogenation are that hydrogenolysis occurred only to a slight extent (0.3 mol%) and the selectivity for the formation

of ether IV was almost quantitative (99.7 mol%). The alcohol was not formed, although the ketone III was found in the reaction mixture in an amount of 2.3 mol% at the maximum in 41% hydrogenation. This is probably due to the fact that with palladium the ketone is hydrogenated to yield the ether IV as the predominant product as reported previously.[10] Another characteristic feature of the hydrogenation with palladium is a high stereospecificity in ether formation. The *cis*/*trans* ratio of the ether IV formed in ethanol was about 10 which was much greater than those obtained by other platinum metals.

4) Hydrogenation over Osmium Catalyst (Fig. 4).: Over this metal the acetal formation occurred to the least extent of the six metals investigated (8.9 mol% at 88.9% hydrogenation). The acetal formed appears not to be hydrogenated to any appreciable extent during hydrogenation as indicated by a linear increase of it with hydrogenation. Formation of the alcohol was also at a low level (0.86 mol%). Since the ketone III is readily hydrogenated to the alcohol V under these conditions, it seems that hydrolysis of I or II to give III did not occur or did only to a slight extent over osmium. Hydrogenolysis, however, occurred to considerable extent and the proportion of it increased from 8.2 mol% at an initial stage to 23 mol% at 88.9% hydrogenation.

5) Hydrogenation over Iridium Catalyst (Fig. 5): The acetal formation was not rapid, but somewhat faster than over osmium and ruthenium (24 mol% at 75.1% hydrogenation). Hydrogenolysis was 14.8% at the initial stage and decreased to about 12% towards the end of hydrogenation. The decrease in the proportion of hydrogenolysis may be due to the participation of the hydrogenation of II formed, since II was hydrogenolyzed to much lesser extent as seen in Table 2. A small amount of the alcohol V was produced after the hydrogenation of II began.

6) Hydrogenation over Platinum Catalyst (Fig. 6): The acetal was formed most rapidly over platinum. It amounted to 73 mol% at 24.8% hydrogenation. It is also noteworthy that hydrogenolysis occurred most extensively of the six platinum metals studied (71.6% at an initial stage and 39.1% at the end of hydrogenation). About 15 mol% of the alcohol V was formed along with 46 mol% of the ether. The ratio of the alcohol to the ether was almost the same with that obtained in hydrogenation of II (see Table 2). Thus the most part of the hydrogenation of I in ethanol is the same with that of II, but at the initial stage of hydrogenation a definitely more extensive hydrogenolysis was observed.

Hydrogenation in t-Butyl Alcohol and Isopropyl Ether as Solvents. The hydrogenation of I was performed in these solvents in order to see the behavior of I under the lack of formation of the acetal and also the effect of the solvent polarity. The results are given in Table 1. The acetal formation was observed only slightly except when hydrogenolysis occurred extensively. Hydrolysis to yield the ketone V occurred over rhodium, palladium and platinum catalysts. Except in a few cases the proportion of hydrogenolysis decreased with the solvents in the order ethanol>*t*-butyl alcohol> isopropyl ether. The *cis*/*trans* ratio of ether IV formed did not differ much among the three solvents except in hydrogenation over palladium where a definite decrease in the ratio was observed from in ethanol to in *t*-butyl alcohol and isopropyl ether.

Discussion

As illustrated in Figs. 1—6, hydrogenation of the enol ether I in ethanol is accompanied by the formation of the acetal II which results from the addition of ethanol to I. The ratio of the acetal formation to hydrogenation is indicated by the initial slope of the curves which show the amounts of the acetal varying with the extent of hydrogenation. The values of this ratio for the six platinum metals are in the following sequence: osmium (0.06)<ruthenium (0.11)<iridium (0.26)≪ rhodium (1.28)<palladium (1.87)<platinum (5.76). Thus, the six metals can be classified into two groups. Osmium, ruthenium and iridium belong to the group which catalyzes the acetal formation only weakly, while rhodium, palladium and platinum to the other group which catalyzes it efficiently. The addition of ethanol to I is an acid-catalyzed reaction. The action of the platinum metals to catalyze this addition is probably due to the presence of the adsorbed hydrogen which is ionized on the catalyst surface. It was previously shown that acetal is formed rapidly in the hydrogenation of cycloalkanones over some platinum metals in methyl or ethyl alcohol and also that the acetal formation is greatly depressed in the absence of hydrogen.[10]

With respect to hydrogenolysis, platinum was definitely more active than any other platinum metals. On the other hand, palladium and ruthenium showed only poor tendency towards hydrogenolysis. At an initial stage of hydrogenation of I in ethanol, the proportion of hydrogenolysis was in the following sequence for the six platinum metals: palladium≅ruthenium≪osmium<rhodium<iridium≪platinum (see Table 3). It is to be noted that palladium showed the lowest activity for hydrogenolysis although the same metal is known to be highly active for the hydrogenolysis of benzyl- and allyl-type ethers.[11]

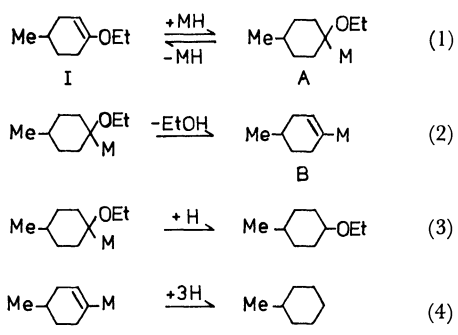

Scheme 1.

(M indicates catalyst metal)

10) S. Nishimura, T. Itaya, and M. Shiota, *Chem. Commun.*, **1967**, 422.

11) See for instance Ref. 2, p. 433.

The mechanism of the hydrogenation and hydrogenolysis of an enol ether appears not enough known. Probably, the half-hydrogenated state of I is the one which results from the addition of a hydrogen (or proton) to the C-2 carbon of I (A in Scheme 1), as assumed by Acke and Anteunis.[4] If the affinity of the carbon (or carbonium ion) and the catalyst metal is not strong in the resulting half-hydrogenated state, step (1) in Scheme 1 will readily be reversed and in this case the removal of ethanol from the half-hydrogenated state will not occur so easily. On the other hand, such affinity between the intermediate A and the catalyst metal is sufficiently strong, the reversal of step (1) would be inhibited and, rather, elimination of ethanol to give the adsorbed intermediate B would be favored [step (2)]. If we assume that the affinity mentioned above is expressed in terms of the olefin isomerization activity of the metal,[12] it is expected that hydrogenolysis will occur more easily over such metals which are less active in olefin isomerization. Since elimination of ethanol by step (2) would be promoted by acid and, accordingly, by the ionized hydrogen on the catalyst surface, hydrogenolysis will occur more extensively over such metals which can catalyze the acetal formation effectively on hydrogenation of I in ethanol. The activities of the six platinum metals in the acetal formation (r_1) and those in olefin isomerization (r_2) are summarized in

Table 3. Acetal formation and olefin isomerization activities of platinum metal catalysts and their tendency towards hydrogenolysis in hydrogenation of enol ether I

Catalyst	Ratio of acetal formation to hydrogenation[a] (r_1)	Ratio of olefin isomerization to hydrogenation[b] (r_2)	$\frac{r_1}{r_2}$	Proportion of hydrogenolysis in hydrogenation of I (mol%)[a]
Ru	0.11	0.12	0.92	1.9
Rh	1.28	0.125	10.2	10.0
Pd	1.87	2.05	0.91	1.1
Os	0.06	0.0093	6.45	8.2
Ir	0.26	0.025	10.4	14.8
Pt	5.76	0.025	230	71.6

a) These values were obtained at the initial stage of the hydrogenation of I in ethanol.
b) The ratio r_2 was obtained in the hydrogenation of 1-octene in isopropyl alcohol at 25°C under atmospheric presence of hydrogen and is given by the ratio of isomerized 2-octene to octane at about 20% conversion of 1-octene.

Table 3. The value of r_2 was obtained in the hydrogenation of 1-octene in isopropyl alcohol at 25°C under an atmospheric pressure of hydrogen, using the unsupported metals prepared by the same methods as used for the catalysts in this study.[13] Thus we can expect that the extent of hydrogenolysis observed in the hydrogenation of an enol ether would increase with increasing value of r_1/r_2 which is also given in Table 3. For the six platinum metals the value of r_1/r_2 is in the following sequence: Pd≅Ru≪Os<Rh<Ir≪Pt. It is seen that this sequence is in excellent accord with that obtained in the proportion of the hydrogenolysis which occurred at the initial stage of the hydrogenation of I in ethanol (see Table 3). Thus, the very low activity of palladium catalyst towards hydrogenolysis may be due to its weak affinity for the carbon atom as expressed by its unusually high olefin isomerization activity. The low activity of ruthenium in the hydrogenolysis may be explained by the poor action of the ionized hydrogen on that metal. The extremely high activity of platinum towards the hydrogenolysis will result from its properties as expressed by both of the high activity in the acetal formation and the low activity in the olefin isomerization.

The results of the stereochemistry of hydrogenation of I seem consistent with the mechanism described in Scheme 1. The hydrogenation of I over palladium catalyst is noteworthy in that *cis*-ether IV is formed with a high stereospecificity. If the rate-determining step over this metal is assumed to be formation of the saturated ether [step (3)], just as postulated in the hydrogenation of cycloolefins,[14] the preceding steps, including the adsorption of I to the catalyst, would be easily reversed as supposed by its weak affinity toward unsaturation. Under these circumstances, possible half-hydrogenated states A_c, A_t and A_t' (see Fig. 7) will be equilibrated on the catalyst surface. Since

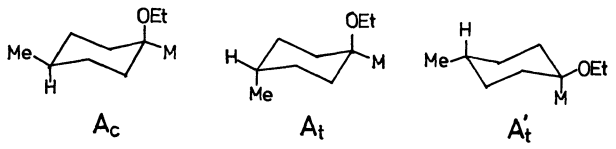

Fig. 7. Conformations of half-hydrogenated state A (M indicates catalyst metal).

the most stable one of them will be A_c, this will predominate at equilibrium and *cis*-ether will be formed in excess *via* A_c, if the rate constants for hydrogenation of them do not differ much among them. In this connection, it is of interest to note that hydrogenation of 1,4-dimethyl-1-cyclohexene, which has a methyl group instead of the ethoxyl group in I, gives the *trans* isomer as major product in the hydrogenation with palladium catalyst.[15] This result may be explained by the assumption made be Siegel and Smith that decreasing stabilities of various possible half-hydrogenated states are in the order primary>secondary>tertiary with respect to the carbon adsorbed on the catalyst surface.[14] On hydrogenation of I, the electromeric effect of the ethoxyl group will direct the first addition of hydrogen (or proton) to the C-2 carbon and this leads to the preferential formation of the half-hydrogenated state A. This assumption is strongly supported by the fact that hydrogenation of 3-

12) G. C. Bond and P. B. Wells, *Advan. Catal.*, **15**, 91 (1964).
13) Unpublished data by S. Nishimura and H. Nagamatsu.
14) S. Siegel and G. V. Smith, *J. Amer. Chem. Soc.*, **82**, 6087 (1960).
15) J.-F. Sauvage, R. H. Baker, and A. S. Hussey, *ibid.*, **83**, 3874 (1961).

methylcyclohexanone diethyl acetal (VII) in ethanol with palladium catalyst gave rise to *trans*-ether predominantly.[16] The acetal VII is probably hydrogenated *via* the corresponding enol ethers and over palladium the enol ethers are also expected to give the *trans*-ether in excess, as supposed from the comparison of the results obtained with palladium catalyst on their 4-methyl analogues (see Tables 1 and 2).

The stereoselectivity was much lower over the other platinum metals, although always *cis*-ether was formed in greater amount than *trans*-ether. It appears that the nature of the solvents does not have much influence on the stereochemistry of hydrogenation except with palladium. Over the metals other than palladium, the step which determines the stereochemistry of ether formation may be either adsorption of enol ether I or formation of the half-hydrogenated state, as postulated in the platinum-catalyzed hydrogenation of cycloolefins.[17]

16) unpublished results.
17) S. Siegel and G. V. Smith, *J. Amer. Chem. Soc.*, **82**, 6082 (1960).

It has been considered that acetals are hydrogenated *via* the corresponding enol ether in the presence of acid.[3,4] Although this reaction pathway will probably be true also in the absence of acid, hydrogenation of acetal II was in most cases much slower than that of enol ether I. This is also seen by the fact that I is hydrogenated at much greater rates in *t*-butyl alcohol and isopropyl ether than in ethanol (see Table 1). Since at an equilibrium in ethanol II is in a much greater amount than I, slow hydrogenation of II may be due to a slow formation of I by elimination of ethanol from I on the catalyst surface. It is also suggested that II is adsorbed to the catalyst much more weakly than I, since hydrogenation of II appears not to occur until almost all of I has disappeared as seen in Figs. 1—6. Slow hydrogenation of II also leads to the product considerably different from that obtained by hydrogenation of I and yields the saturated ether of a greater *cis*/*trans* ratio than formed from I, with the exception of the hydrogenation over palladium where almost the same product was formed on hydrogenation of I and II.

BULLETIN OF THE CHEMICAL SOCIETY OF JAPAN, VOL. 44, 172—177 (1971)

Cyclic Acetylenes. XI. The Syntheses of *p,p'*-Bridged Cyclic Tolans by the Fritsch-Buttenberg-Wiechell Rearrangement[1]

Takashi ANDO and Masazumi NAKAGAWA

Department of Chemistry, Faculty of Science, Osaka University, Toyonaka, Osaka

(Received July 13, 1970)

In order to ascertain the effect of ring strain on the electronic spectra of cyclic acetylenes, a series of *p,p'*-bridged cyclic tolans (V_n, $n=11$, 12, 13, 14, and 18) has been synthesized. It was found that the increasing ring strain exerted an appreciable hypochromic effect and also caused a slight bathochromic shift of the absorption band. The bathochromic shift observed in the *p,p'*-bridged cyclic tolans (V_n) forms a contrast with the hypsochromic shift observed in the strained *o,o'*-bridged cyclic diphenyldiacetylene (VI, $n=3$).

The formation of diarylacetylene from 1,1-diaryl-2-haloethylene by dehydrohalogenation, accompanied by rearrangement, has been well-known as the Fritsch-Buttenberg-Wiechell rearrangement.[2] The treatment of 1,1-diaryl-2,2-dihaloethylene with an organometallic compound also results in the formation of diarylacetylene.[3,4]

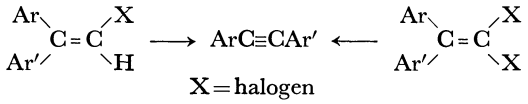

X=halogen

If a diarylhalo- or a diaryldihaloethylene in which the aryl groups are linked by a bridging chain (R) is subjected to the above-mentioned rearrangement, we can expect the formation of a cyclic diarylacetylene with a bridging chain between the aryl groups (I). As the distance between the *p*- and *p'*-positions of the two aryl groups in the ethylene is shorter than that of in the cyclic acetylene, the rearrangement

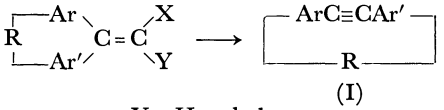

(I)

X=H or halogen
Y=halogen

reaction seems to offer a method of synthesizing highly-strained cyclic acetylene. Also, the rearrangement reaction in which the aryl group migrates with a bridging chain seems to be of interest in itself. An analogous

1) This paper is dedicated to Professor Munio Kotake in commemoration of his seventy-fifth birthday by one of his former students (M. N.).

2) P. Fritsch, *Ann.*, **279**, 319 (1894); W. Buttenberg, *ibid.*, **279**, 324 (1894); H. Wiechell, *ibid.*, **279**, 337 (1894).

3) D. Y. Curtin and E. W. Flym, *J. Amer. Chem. Soc.*, **81**, 4714 (1959).

4) B. Kirby, W. G. Kofron, and C. R. Hauser, *J. Org. Chem.*, **28**, 2176 (1963).

5) G. Wittig, W. Joos, and P. Rathfelder, *Ann.*, **610**, 180 (1957); G. Wittig and J. G. Grolig, *Chem. Ber.*, **94**, 2148 (1961).

type of rearrangement has been studied by Wittig[5] in the case of the benzidine rearrangement of *N,N'*-polymethylene hydrazobenzenes.

The present paper will deal with the syntheses of polymethylene ether derivatives of *p,p'*-dihydroxytolan according to the Fritsch-Buttenberg-Wiechell rearrangement reaction.

Syntheses. 1,1-Dichloro-2,2-bis(*p*-hydroxyphenyl)-ethylene,[6] which had been derived from 1,1,1-trichloro-

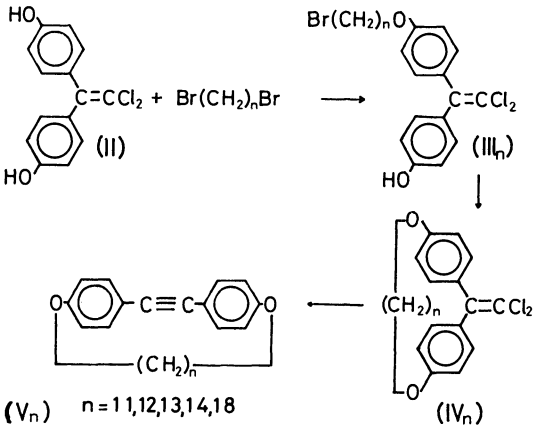

2,2-bis(*p*-hydroxyphenyl)ethane,[7] was treated with a large excess of polymethylene dibromide in the presence of potassium hydroxide to yield the monoether III.[8] The intramolecular alkylation of the monoether III to yield the cyclic ether derivative IV was achieved by the Lüttringhaus method[8] under highly diluted conditions. The monomeric nature of IV was confirmed by a molecular weight determination according to the Rast method. The reaction conditions, the yields, and the melting points of IV are summarized in Table 1. The decreasing yields of the cyclic ethers IV with the diminishing length of the bridging chain clearly indicate the increasing difficulty of the intramolecular alkylation with the shorter chain.

Generally, the rearrangement reaction was carried out in an ether solution by treating IV_n with a 10% excess of *n*-butyllithium at a temperature of −17—−18°C for 1 hr. In the case of IV_{14}, a 100% excess of *n*-butyllithium was employed. Also, in the case of IV_{18}, the dichloroethylene was treated with a 100% excess of *n*-butyllithium at 2°C for 1 hr, and then at 18°C for 1 hr. The yields and the melting points of the cyclic tolans (V_n) are tabulated in Table 2, along with those of the reference substance, 4,4'-di-*n*-butoxytolan.

In the case of IV_{10}, the cyclic tolan (V_{10}) could not be obtained. The amorphous yellow solid which was isolated from the reaction product seemed to be a complex mixture and could not be identified. The colorless crystals of V_{11} and V_{12} were found to be rather unstable. On exposure to a diffused light in the laboratory, the formation of a violet-colored layer on the surface of the crystals of V_{11} and V_{12} was observed. On the other hand, the cyclic tolans of the higher ring member, V_{13-18}, and the open-chain analogue were found to be stable compounds. The tendency toward sublimation observed in V_{12}, V_{13} and V_{14} seems to reflect the rigid structures of these molecules with a tightly-drawn polymethylene bridge.

Table 1. The intramolecular alkylation of III_n

n	III (mmol)	Reaction time (hr)	IV mp (°C)	IV Yield (%)
10	8.0	65	134.2—135.6	39
11	20.6	69	127.5—128.5	46
12	9.2	29	128.0—129.2	49
13	12.0	37	78.0— 78.8	60
14	9.0	40	89.5— 91.5[a]	60
			83.1— 84.0	
18	7.9	30	90.0— 91.0	94
		n-Bu	76.0— 77.0	

a) Dimorphism.

Table 2. The yields and the melting points of V_n

n	Yield (%)	Mp (°C)	Recovered IV_n(%)
10	0	—	29
11	23	166.0—167.0	46
12	47	151.0—152.0	49
13	75	158.5—159.5[a]	20
		160.0—161.2	
14	90	167.3—168.3	0
18	75	118.4—119.0	0
n-Bu	52	130.5—131.5	43

a) Dimorphism.

It is difficult to reach a definite conclusion from the results of the rearrangement reactions, as the reactions were carried out under different conditions. However, as it has been proved that the presence of a large excess of *n*-butyllithium had no influence on the rearrangement reaction,[3] it seems to be evident that the diminishing length of the bridging chain retards the rearrangement or enhances some side reactions, resulting in a decrease in the yields of the cyclic acetylenes. However, it should be noted that a much higher yield than that of the open-chain analogue was obtained in the case of $n=14$[9] Either the fixation of the phenyl groups in IV_{14} in a favorable position for the rearrangement, resulting from the presence of the bridging chain in an adequate length, or the increased intramolecular nature of the reaction brought about by the linking of the migrating moiety, seemed to be the cause of the high yield of V_{14}.

Electronic Spectra. The electronic spectral data of 1,1-dichloro-2,2-bis(*p*-hydroxyphenyl)ethylene polymethylene ethers (IV_n) are summarized in Table 3, together with those of the open-chain reference. Slight

6) H. Hubacher, *J. Org. Chem.*, **24**, 1949 (1959).
7) H. P. Kaufmann and J. Schierholt, *Pharm. Zentralhalle*, **96**, 443 (1957); *Chem. Abstr.*, **52**, 13686 (1958).
8) A. Lüttringhaus, *Ann.*, **528**, 211 (1937); A. Lüttringhaus and K. Ziegler, *ibid.*, **528**, 155(1937); K. Ziegler, A. Lüttringhaus, and K. Wohlgemuth, *ibid.*, **528**, 162 (1937).
9) An analogous result was obtained in the case of the synthesis of *o,p'*-bridged cyclic tolans by the same rearrangement. See the following paper.

Table 3. The elctronic spectral data of IV_n in *n*-hexane

IV_n	λ_{max} in mμ (ε)	
$n=10$	255.5(18,300)	277*(15,100)
11	254 (17,700)	276*(14,700)
12	255 (19,100)	275*(16,900)
13	254 (19,800)	275*(16,700)
14	254 (20,500)	275*(16,900)
18	254 (20,300)	275*(15,800)
n-Bu	254 (21,300)	275 (15,900)

The asterisks indicate the inflexions.

bathochromic and hypochromic effects were observed with a decrease in the ring size. A similar, but a more appreciable, spectral trend has been found in the case of [1,*n*]paracyclophanes and has been explained in terms of a transannular electronic coupling of the two phenyl groups and a modification of the benzenoid resonance due to the bending of the two benzene nuclei.[10] However, in the case of IV_n, the cross-conjugation of the phenyl groups with the dichloromethylene group and the interaction of the phenyl groups with the lone-pair electrons in the oxygen atoms in the ether linkages may be altered by the change in the ring size. Because of these situations, it seems to be difficult to deduce a definite correlation between the spectral behavior and the ring size of IV_n.

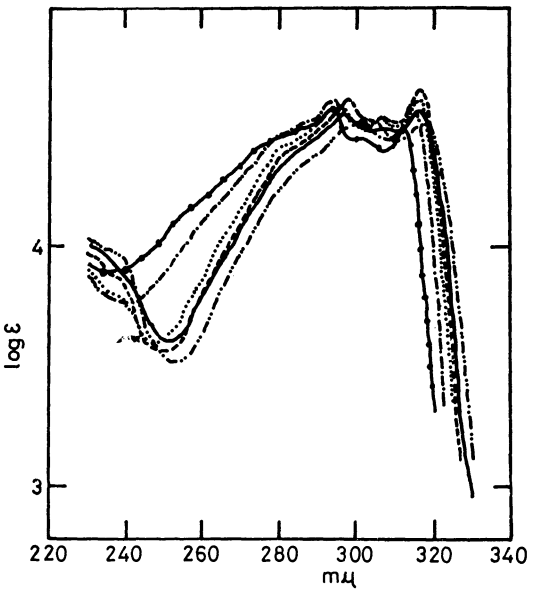

Fig. 1. The electronic spectra of V_n and *p,p'*-dibutoxytolan
$n=11$ -·-·-·- 14 ·····
12 ——— 18 -·-·-·
13 --------- *n*-Bu -•-•-•-

Figure 1 and Table 4 record the absorption curves and the data of the cyclic tolans (V_n) along with those of *p,p'*-dibutoxy-diphenylacetylene as a reference compound.

It will be seen that the ring formation causes an increase in the absorption intensity. The maximum intensity was observed in V_{13}. However, the absorption intensity decreased with a decrease in the number of *n*, accompanied by a slight bathochromic shift of λ_{max}. The increase in the absorption intensity can be rationalized by the increased coplanarity of the phenyl groups caused by the ring formation. On the other hand, the regular red shift of the λ_{max} with the diminishing ring size and the decrease in the extinction coefficient going from V_{13} to V_{11} seems to be attributable to the effect of strain on the electronic spectra. The bathochromic shift observed in V_n makes a sharp contrast with the hypsochromic shift observed in a strained diphenyldiacetylene derivative (VI, $n=3$).[11]

Table 4. The electronic spectal data of V_n in *n*-hexane

V_n	λ_{max} in mμ (ε)					
$n=11$	300	(33,700)			318	(33,400)
12	298	(37,000)	308	(31,400)	317	(36,900)
13	297.5	(42,300)	307	(34,800)	317	(44,300)
14	297	(42,300)	306.5	(35,300)	316	(42,600)
18	295.5	(41,700)	305	(33,500)	315	(35,500)
n-Bu	294	(37,700)	303	(29,200)	313	(31,900)

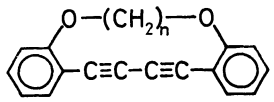

(VI)

Infrared Spectra. The 1580-cm^{-1} absorption band due to the skeletal in-plane vibration of an aromatic ring conjugated with the lone-pair electrons in a substituent, which could be observed in the spectrum of V_{18} at 1569 cm^{-1}, was found to be extremely weak in other members of V_n. This fact seems to indicate that the polymethylene bridge ($n=11$—14) would cause a fixation of the conformation of the oxygen atom at a position unfavorable for the conjugation with the aromatic ring. A regular shift of the absorption band due to the skeletal in-plane vibration of a benzene nucleus (*ca.* 1600 cm^{-1}) toward a lower wavenumber with a decrease in the ring size was observed; *i. e.*, the band appearing at 1609 cm^{-1} in the spectrum of V_{18} moved to 1596 cm^{-1} in that of V_{11}. Also, the fact that the spectra of V_{11} and V_{12} exhibit sharper absorption peaks than those of the other higher homologues seems to indicate the limited mode of vibration resulting from the fixed conformation and rigid structure of V_{11} and V_{12}. The characteristic peaks in the IR spectra of V_n are tabulated in Table 5, together

Table 5. The IR spectra of V_n (cm^{-1})

V_n	$\nu_{C=C}$ (arom.)		δ_{C-H} (arom.)	
11	1596	1561(w)	832(s)	
12	1600(s)	—		843(s)
13	1605(s)	—	830(s)	
14	1605(s)	—		836(s)
18	1609(s)	1569(m)	831(s)	836(s)
n-Bu	1611(s)	1571(m)	830(s)	848(s)

10) D. J. Cram and M. F. Antar, *J. Amer. Chem. Soc.*, **80**, 3103 (1958).

11) F. Toda and M. Nakagawa, This Bulletin, **34**, 862 (1961).

with that of the open-chain analogue, *p,p'*-dibutoxytolan.

Nuclear Magnetic Resonance Spectra. The most characteristic feature of the NMR spectra of V_n is the presence of strong and rather sharp peaks centered around 9 τ, as is illustrated in Fig. 2. The most well-

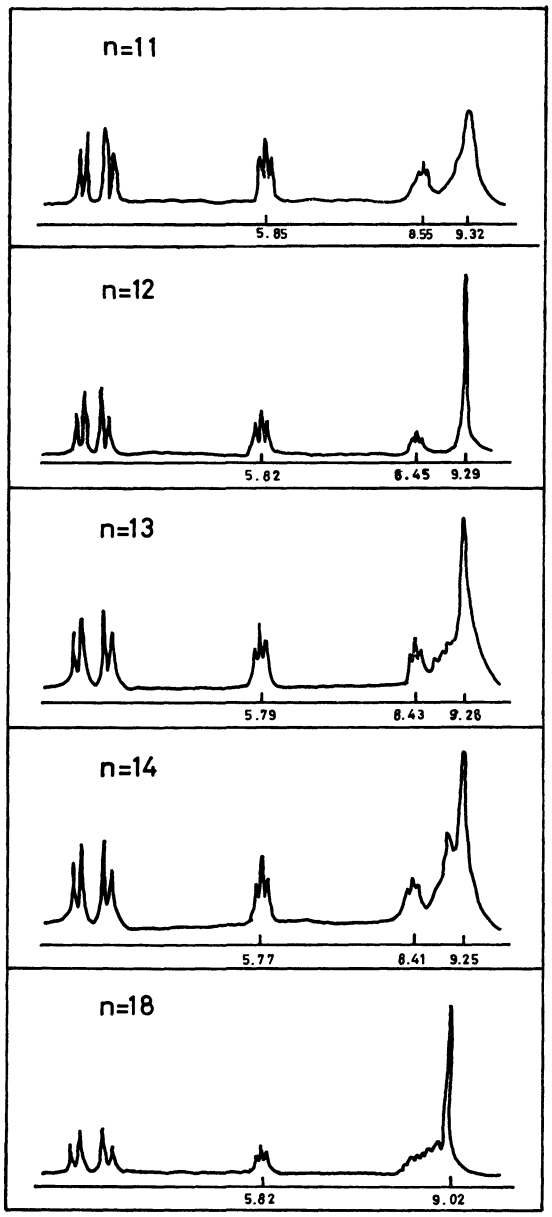

Fig. 2. The NMR spectra of V_n.

defined spectrum was obtained in V_{12}, and the triplet at 5.82 τ changed to a sharp singlet on the irradiation of the peak at 8.45 τ. On the basis of this finding, the triplet centered at 5.82 τ and 8.45 τ can be assigned to the protons of the α- and β-methylene groups of the oxygen atom respectively.[12] Therefore, the peak at 9.29 τ should be attributed to the protons of the other methylene groups. The aromatic nuclei and the triple bond should exert shielding[13] and deshielding effects[14] on the protons situated just on these structural units. However, the observed spectra indicate that an almost uniform magnetic environment is attained in the vicinity of the *p,p'*-disubstituted tolan system. This fact seems to be difficult to understand at first sight; however, the change in the electronic state caused by the conjugation of the phenyl nuclei with the triple bond may be responsible for the formation of the uniform magnetic environment.[15] The low-field shift of the peaks as compared with those of 4,4'-polymethylene biphenyls[16] seems to reflect the effect of acetylenic linkage.

Experimental

All the melting points are uncorrected. The infrared spectra were measured with a Hitachi EPI-2 Spectrophotometer by the KBr-disk method, the electronic spectra, with a Hitachi EPS-2 Spectrophotometer, and the NMR spectra, with a Varian A 60 Spectrometer.

*1,1-Dichloro-2,2-bis(*p*-hydroxyphenyl)ethylene (II).* 1,1,1-Trichloro-2,2-bis(*p*-hydroxyphenyl)ethane[7] was treated potassium hydroxide in methanol according to the reported method,[6] yielding II in a yield of 66.8%.

1,10-Dibromodecane. A commercial product was used.

1,11-Dibromoundecane. 10-Undecenol was prepared by the lithium aluminum hydride reduction of ethyl 10-undecenoate.[17] The acetate of 10-undecenol in benzene was treated with hydrogen bromide in the presence of benzoyl peroxide under the irradiation of UV light, thus affording 11-bromoundecanol acetate in a yield of 85%.[18] The hydrolysis of the bromo-acetate by means of potassium hydroxide in methanol resulted in the formation of a mixture of 11-bromoundecanol and 1,11-undecanediol (*ca.* 1 : 1), accompanied by a small amount of 11-undecenol. After the removal of the olefin under reduced pressure, hydrogen bromide was passed through the molten mixture of the alcohols at 130°C.[19] 1, 11-Dibromoundecane was obtained as a colorless liquid (bp 145—148°C/3 mmHg) in a yield of 81%.

1,12-Dibromododecane. Ethyl undecenoate[17] was converted to ethyl 11-bromoundecanoate according to the known method.[18] A mixture of the bromoester (350 g, 1.19 mol), powdered potassium cyanide (220 g, 3.38 mol), potassium iodide (5 g), cupric sulfate monohydrate (1 g), ethanol (1300 m*l*), and water (400 m*l*) was then refluxed for 8 hr. The crude ethyl 11-cyanoundecanoate obtained by working up the reaction mixture by an ordinary method was refluxed for 2 hr in a mixture of acetic acid (250 m*l*) and concentrated sulfuric acid (250 m*l*). The cooled reaction mixture was poured into ice water (3 *l*), yielding crude 1,12-dodecanedioic acid (251 g). The diethyl ester (241.4 g, 0.84 mol) which had been prepared from the crude dioic acid according to the usual

12) The double-resonance measurement was performed on a nuclear magnetic resonance spectrometer, C-60 of the Japan Electron-Optics Laboratory Co., Ltd. The authors wish to thank Professor Toshio Miwa, Department of Chemistry, Faculty of Science, Osaka City University, for the measurement and for his helpful advice.

13) C. E. Johnson and F. A. Bovey, *J. Chem. Phys.*, **29**, 1012 (1958); J. S. Waugh and R. W. Fassenden, *J. Amer. Chem. Soc.*, **79**, 846 (1957).

14) H. M. McConnell, *J. Chem. Phys.*, **27**, 226 (1957).

15) The same type of NMR spectra was obtained in the case of the polymethylene ether derivatives of 4,4'-dihydroxydiphenyldiacetylene. These results will be published in the near future.

16) M. Nakazaki and K. Yamamoto, *Chem. Ind.* (London), **1965**, 486.

17) G. H. Jeffery and A. I. Vogel, *J. Chem. Soc.*, **1948**, 658.

18) *Cf.* R. Huisgen, H. Walz, and I. Glogger, *Chem. Ber.*, **90**, 1437 (1957).

19) *Cf.* W. L. McEwen, "Organic Syntheses," Coll. Vol. III, p. 227 (1955).

method[20] was reduced by means of lithium alminum hydride to yield 1,12-dodecanediol[21] (159.9 g, 93.8%). The method used in the preparation of 1,11-dibromoundecane was used for the conversion of the diol (203.3 g, 1 mol) to 1,12-dibromododecane (248.6 g, 75.8%).

1,13-Dibromotridecane. 1,13-Tridecanedioic acid was prepared by the reaction of ethyl 11-bromoundecanoate (390.3 g, 1.33 mol) and diethyl sodiomalonate according to the reported method.[22] The crude diacid thus obtained was converted to the diethyl ester[20]; bp 159.0—163.0°C/2.7 mmHg, 295.8 g (74% based on the bromoundecanoate). The lithium alminum hydride reduction of the diethyl ester afforded 1,13-tridecanediol.[21] 1,13-Dibromotridecane, bp 162—164°C/3 mmHg, was obtained from the diol according to the above-stated method[19] in a yield of 59.8% (based on diethyl tridecanoate).

1,14-Dibromotetradecane. 1,12-Dibromododecane (164 g, 0.5 mol) was converted to crude 1,14-tetradecanedioic acid (126 g) *via* 1,12-dicyanododecane according to the method in the literature.[23] The diethyl ester derived from the dioic acid[20] was reduced to 1,14-tetradecanediol by means of lithium aluminum hydride.[21] 1,14-Dibromotetradecane was obtained from the diol in a yield of 57% (based on the diethyl ester) by treating it with hydrogen bromide at 130°C.[19]

1,18-Dibromooctadecane. Dimethyl octadecanedioate was prepared by the electrolysis of methyl hydrogen sebacate.[24] The lithium alminum hydride reduction of the dimethyl ester according to the above-described procedure[21] afforded 1,18-octadecanediol in a yield of 89%. The reaction of hydrogen bromide[19] with the diol at 120—135°C yielded 1,18-dibromooctadecane, bp 175—180°C/0.005 mmHg; mp 54—58°C, in a yield of 61%.

Preparation of ω-Bromoalkyl Ether of 1,1-Dichloro-2,2-bis(p-hydroxyphenyl)ethylene (III_{10-13}). The synthesis of ω-bromodecyl ether (III_{10}) will be described as a representative example. To a stirred and refluxing mixture of the bisphenol (II, 12.2 g, 0.0436 mol), anhydrous ethanol (100 m*l*), and 1,10-dibromodecane (91.5 g, 0.279 mol), we added 16.2 m*l* (0.0218 mol) of a 1.34N solution of potassium hydroxide in ethanol over a period of 15 min. The reaction mixture showed pH 5 after having been refluxed for a further 15 min. The cooled reaction mixture was then poured into water (300 m*l*) and extracted with ether. The extract was washed successively with water and a sodium hydrogen carbonate solution, and dried. After the solvent had been removed under reduced pressure, the excess of the dibromodecane was recovered by vaccum distillation under a nitrogen atmosphere (bp 131—137°C/3.7 mmHg, 80.6 g). The residue in benzene was chromatographed on alumina (300 g). The first fraction, on evaporation, gave a small amount of the dibromodecane. A minor amount of the substance obtained from the second fraction seemed to be 1,1-dichloro-2,2-bis(*p*-10-bromodecanoxyphenyl)ethylene; however, further investigation of this substance was not carried out. The crude mono-ether (III_{10}) which was obtained from the third fraction as a yellow waxy solid was rechromatographed on alumina to afford colorless III_{10} in a yield of 41.2% (based on the potassium hydroxide). This was used for the following reaction. The bisphenol (II) was recovered from the final fraction.

The other mono-ethers (III_{11}, III_{12} and III_{13}) were obtained according to the procedure described above. The yields may be summarized as follows: III_{11}: 22%; III_{12}: 33.3%; III_{13}: 34.7%.

Preparation of the Higher ω-Bromoalkyl Ether of the Dichloroethylene (III_{14} and III_{18}). Considering the high boiling and high melting points of 1,14-dibromotetradecane and 1,18-dibromooctadecane, the procedure of the recovery of the dibromoalkanes was slightly modified. After the reaction mixture had been mixed with water, the precipitated solid was repeatedly extracted with petroleum ether. The evaporation of the solvent then gave the crude dibromoalkanes. A material insoluble in petroleum ether was taken up in ether, and the aqueous layer was extracted with ether. The combined ethereal extracts were washed successively with water and a sodium hydrogen carbonate solution, and were then dried and evaporated under reduced pressure. The residue was combined with the distillation residue of the above-mentioned crude dibromoalkane and chromatographed on alumina to afford III_{14} (42%) and III_{18} (52%).

Synthesis of the Cyclic Ethers (IV_n). As all the intramolecular alkylations of III_n were carried out under almost the same conditions, the procedure employed for the preparation of IV_{10} will be described as a typical example. A solution of the mono-ether (III_{10}, 4.00 g, 0.008 mol) in isoamyl alcohol (250 m*l*) was added slowly to a vigorously-stirred and refluxing mixture of anhydrous potassium carbonate (3.3 g, 0.024 mol) and isomyl alcohol (300 m*l*) over a period of 65 hr, employing a high-dilution apparatus. After further refluxing for 2.5 hr, the cooled reaction mixture was filtered to remove any inorganic material. The yellowish-brown residue obtained by evaporating the solvent under reduced pressure was then redissolved in ether and washed thoroughly with a 10% aqueous solution of sodium hydroxide and water successively. The filtered ether solution was dried. The subsequent evaporation of the solvent resulted in a yellowish-brown liquid which crystallized on standing. The crude material was chromatographed on alumina, thus affording IV_{10} as light yellow crystals (1.3 g, 39.1%). The crystals were purified by rechromatography on alumina and by recrystallization from *n*-hexane to yield pure, colorless IV_{10}.

The reaction conditions of the intramolecular alkylation and the melting points and yields of IV_n are summarized in Table 1. Also, the electronic spectral data are recorded in

Table 6. The solvents of recrystallization, the analytical data, and the molecular weights of IV_n and the reference substance

IV_n	Solvent		Analytical data (%) C	H	Cl	Mol wt
$n=10$	*n*-hexane	Found	68.58	6.63	17.04	431
		Calcd	68.73	6.73	16.91	419
11	ethyl acetate	Found	69.04	6.83	16.22	418
		Calcd	69.28	6.98	16.36	433
12	ethyl acetate-methanol	Found	69.66	7.18	15.55	499
		Calcd	69.79	7.21	15.85	447
13	ethyl acetate-methanol	Found	70.12	7.39	15.27	442
		Calcd	70.27	7.34	15.37	461
14	ethyl acetate-methanol	Found	70.79	7.62	15.05	515
		Calcd	70.73	7.63	14.91	476
18	petroleum benzine	Found	72.46	8.47	13.15	480
		Calcd	72.30	8.34	13.34	531
n-Bu	ethanol	Found	67.08	6.61	17.90	
		Calcd	67.18	6.66	18.03	

20) *Cf.* V. M. Microvic, "Organic Syntheses," Coll. Vol. II, p. 264 (1943).
21) *Cf.* W. H. Huber, *J. Amer. Chem. Soc.*, **73**, 2730 (1951).
22) F. Kraft and R. Selidis, *Ber.*, **33**, 3571 (1900); J. Walker and J. S. Lumsden, *J. Chem. Soc.*, **79**, 1191 (1901).
23) R. G. Jones, *J. Amer. Chem. Soc.*, **69**, 2350 (1947).
24) S. Swann, Jr., and W. E. Garrison, Jr., "Organic Syntheses," **41**, 33 (1961).

Table 3. The solvents of recrystallization, the analytical data, and the molecular-weights are recorded in Table 6, together with those of the reference substance.

The Rearrangement Reaction of IV_n. The reactions were carried out under an atmosphere of nitrogen. The procedure used for the synthesis of the cyclic tolan (V_{12}) will be described as a representative instance. A solution of the cyclic ethylene (IV_{12}, 507.9 mg, 1.12 mmol) in anhydrous ether (30 m*l*) was chilled in an ice-salt bath to keep at −17—−18°C. To the stirred solution we then added a solution of *n*-butyllithium (0.0561 mol/*l*, 22 m*l*, 1.23 mmol) over a period of 7 min. After stirring for a further hour at this tempearture, methanol (2 m*l*) and then water were added to the mixture. The organic layer was separated and dried. The colorless crystals (447 mg) obtained by evaporating the solvent were chromatographed on alumina (40 g). The fractions eluted with carbon tetrachloride gave the recovered ethylene (IV_{12}, 200 mg, 48.4%). The cyclic tolan (V_{12}, 200 mg, 46.8%) was obtained as colorless crystals from the fractions eluted with benzene. In the case of the reaction was performed at a temperature of −35°C, the cyclic tolan (V_{12}) was obtained in a yield of 46.4%, together with the recovered ethylene (53.4%)

The reaction conditions used for the preparation of the other cyclic tolans have already been described. The melting points, the yields, and the recovery of the ethylenes are tabulated in Table 7, together with those of the open-chain analogue. The cyclic tolans (V_n) were recrystallized from *n*-hexane.

Table 7. The analytical and the molecular-weight data of V_n and the reference substance

V_n		Analytical data (%) C	H	Mol wt
$n=11$	Found	82.64	8.31	432
	Calcd	82.83	8.34	363
12	Found	82.70	8.44	352
	Calcd	82.94	8.57	377
13	Found	82.79	8.82	398
	Calcd	83.03	8.77	391
14	Found	82.80	8.90	448
	Calcd	83.21	8.97	405
18	Found	83.40	9.60	496
	Calcd	83.43	9.63	460
n-Bu[a)]	Found	81.97	8.02	
	Calcd	81.95	8.13	

a) Recrystallized from ethyl acetate.

Attempted Synthesis of the Cyclic Tolan V_{10}. The cyclic ethylene (IV_{10}, 436 mg, 1.04 mmol) was treated with a 10% excess of *n*-butyllithium under the above-described reaction conditions. The reaction mixture turned greenish-yellow and then deep green. The deep green color faded to yellow on the addition of methanol (2 m*l*). The reaction mixture was then worked up, resulting in a greenish-yellow, resinous material. The sole substance which could be identified was the recovered ethylene (IV_{10}, 126 mg, 28.9%).

BULLETIN OF THE CHEMICAL SOCIETY OF JAPAN, VOL. 44, 177—184 (1971)

Cyclic Acetylenes. XII. The Syntheses of *o,p'*-Bridged Cyclic Tolans by the Fritsch-Buttenberg-Wiechell Rearrangement[1]

Mutsuo KATAOKA, Takashi ANDO, and Masazumi NAKAGAWA
Department of Chemistry, Faculty of Science, Osaka University, Toyonaka, Osaka

(Received July 13, 1970)

The polymethylene ether derivatives of *o,p'*-dihydroxydiphenylacetylene (VII_n, $n=7,8,9,10,11$ and 12) have been synthesized by the Fritsch-Buttenberg-Wiechell rearrangement. The electronic, infrared, and NMR spectra of VII_n were examined. It was observed that the increasing ring strain had a hypochromic effect, with a hypsochromic shift of the long-wavelength band in the electronic spectra of VI_n making a contrast with the bathochromic shift in the strained *p,p'*-bridged cyclic tolans.

The successful preparation of *p,p'*-bridged cyclic tolans by the Fritsch-Buttenberg-Wiechell rearrangement[2] prompted the present authors to the syntheses of *o,p'*-bridged cyclic tolans according to the same reaction. Just as in the case of the *p,p'*-series, the distance between the *o*- and the *p'*-positions of the two phenyl groups in the tolans is longer than that of in the 1,1-diarylethylenes; therefore, the rearrangement reaction may provide a route for the synthesis of strained *o,p'*-bridged cyclic tolans. The two benzene nuclei in the *p,p'*-series with a suitably-long bridging chain are forced to take a coplanar conformation. On the other hand, in the case of *o,p'*-bridged tolans, the spanning of the *o*- and *p'*-positions with a short bridging chain should result in a twisting of the two benzene rings. Therefore, the comparison of the electronic and the NMR spectroscopic behavior of the *o,p'*-bridged tolans with those of the *p,p'*-series seemed to be of interest.

Synthesis. As is illustrated in Scheme 1, *o,p'*-dihydroxybenzophenone (I), which had been prepared by the intramolecular rearrangement of phenyl salicylate by stannic chloride,[3] was converted in a high yield to the *p'*-*ω*-bromopolymethylene ether derivative (II) by reaction with a large excess of polymethylene dibromide in the presence of equimolar potassium hydroxide.[4] Small amount of a diether derivative and the unreacted benzophenone (I) were also isolated. However, no *o*-alkylated compound could be obtained. This indicates the low reactivity of the *o*-hydroxyl group

1) This paper is dedicated to Professor Munio Kotake in commemoration of his seventy-fifth birthday by one of his former students (M. N.).

2) Preceding paper.

3) W. Stadel, *Ann. Chem.*, **283**, 179 (1894).

4) *Cf.* A. Lüttringhaus and K. Ziegler, *ibid.*, **528**, 155 (1937); A. Lüttringhaus, *ibid.*, **528**, 211 (1937).

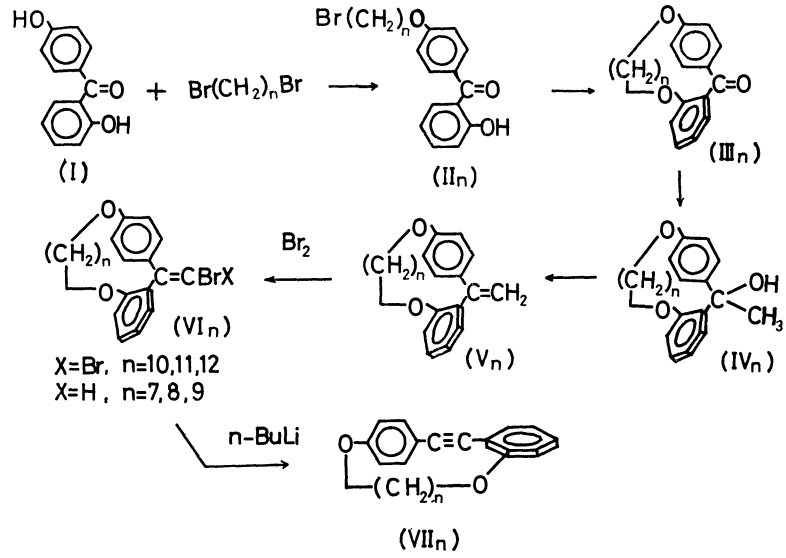

Scheme 1.

TABLE 1. THE REACTION CONDITIONS AND THE YIELDS OF III_n

	II_n			III_n	
n	Amount (mmol)	Solvent (ml)	Reaction time (hr)	Yield (%)	Mp (°C)
12	22	600	35	45	94—96
11	26	600	66	85	99.0—99.7
10	24	600	30	50	not crystallized
9	35	600	77	65	163.7—164.8
8	42	1300	78	34	125.3—126.3
7	24	1000	66	13	102.3—103.6
6[a)]	12	1300	69	31	144.5—145.5

a) III_6 has been prepared according to a modified procedure.

hydrogen-bonded with the carbonyl oxygen. The intramolecular alkylation of II_n to yield the cyclic benzophenone derivative (III_n) was carried out in isoamyl alcohol in the presence of 3 equivalents of potassium carbonate under high-dilution conditions.[4)] The reaction conditions and the yields of the intramolecular cyclization are summarized in Table 1, together with the melting points of the cyclic benzophenones (III_n). The low yields of III_{12} and III_{10} seemed to be due to the insufficient reaction period. On the other hand, the poor yields of III_8 and III_7 clearly indicate that the lengths of the bridging chains are unfavorable for the intramolecular alkylation. This suggests that the preparation of III_6 according to the above-mentioned procedure might not be feasible.

Consequently, the alternative procedure shown in Scheme 2 has been developed. The reaction of chloromethyl methyl ether with the monosodium salt of the dihydroxybenzophenone (I) in toluene afforded *o*-hydroxy-*p'*-methoxymethoxybenzophenone (VIII). The ω-bromohexyl ether (X) which was obtained by the reaction of hexamethylene dibromide with VIII according to the above-stated method, followed by an acid hydrolysis of the protective group, was subjected to intramolecular cyclization under high-dilution conditions to give the cyclic ether (III_6) in a reasonable yield.

The cyclic benzophenones (III_n and III_6) were converted to the corresponding methyl carbinols (IV_n and IV_6) by means of a large excess of methylmagnesium iodide. The 1,1-diarylethylenes (V_n and V_6) which were obtained by the acid dehydration of the carbinols were treated with bromine in carbon tetrachloride.[5)] In the cases of $n=12$ and 11, the dibromides (VI_{12} and VI_{11}) were obtained in good yields. The bromina-

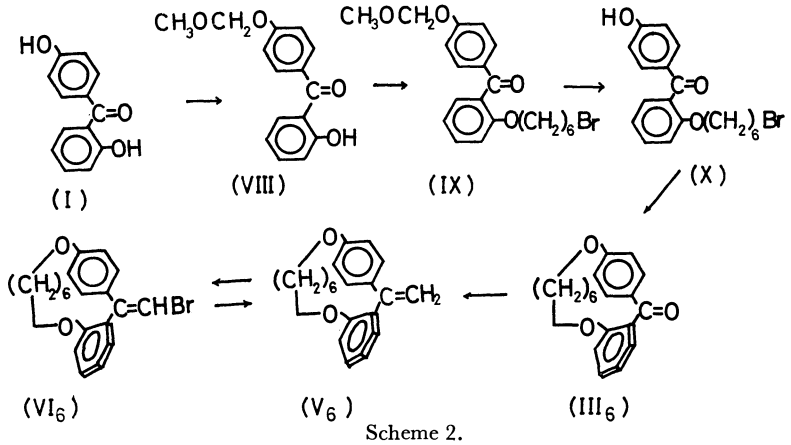

Scheme 2.

5) P. Pfeiffer and R. Wizinger, *Ann. Chem.*, **461**, 132 (1928).

tion of the decamethylene ether derivative (V_{10}) afforded the dibromide (VI_{10}, X=Br) contaminated with the monobromide (VI_{10}, X=H). The treatment of V_8 with 2 mole of bromine gave no crystalline product, and a prolonged reaction with an excess of bromine resulted in the formation of a product bearing a bromine atom in a phenyl group. Therefore, equimolar bromine was used to give a *cis-trans* mixture of the monobromide (VI_{9-6}) in the case of the lower homologue (V_{9-6}). The rearrangement reaction of VI_{12-6} was performed in ether employing 2 equivalents of *n*-butyllithium and at a temperature of −11——18°C. The yields and the melting points of the cyclic tolans (VII_n) are recorded in Table 2, together with those of an open-chain analogue, *o,p'*-dimethoxytolan.

Table 2. The yields and the melting points of the cyclic tolans (VII_n) and *o,p'*-dimethoxytolan

n	Yield (%)	Mp (°C)
7	22	121.7—122.7
8	42	137.0—137.6
9	56	127.6—128.0
10	73	143.8—144.4
11	75	101.4—102.0
12	63	120.0—120.6
CH_3O	17	68.0— 69.5

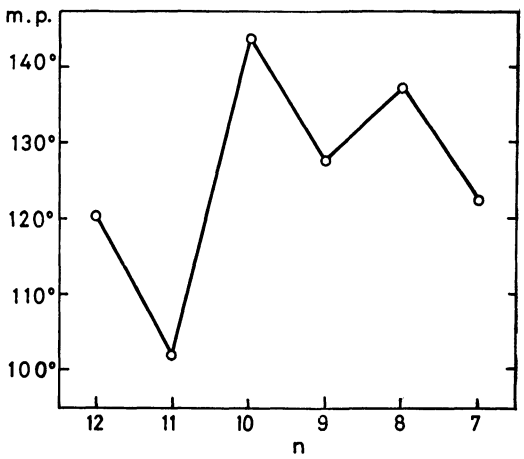

Fig. 1. The oscillation of the melting points of VII_n.

As is shown in Fig. 1, the cyclic tolans (VII_n) bearing an even number of methylene groups in the bridging chain exhibit higher melting points than the next higher or lower homologues having an odd number of methylene groups. This fact seems to indicate that the molecular geometry of VII_n is dependent not only on the length of the bridging chain, but also on whether the number of the methylene groups is odd or even.

In the case of VI_6, no cyclic tolan could be obtained, and the oily reaction product partly crystallized after standing overnight. The crystals were proved to be

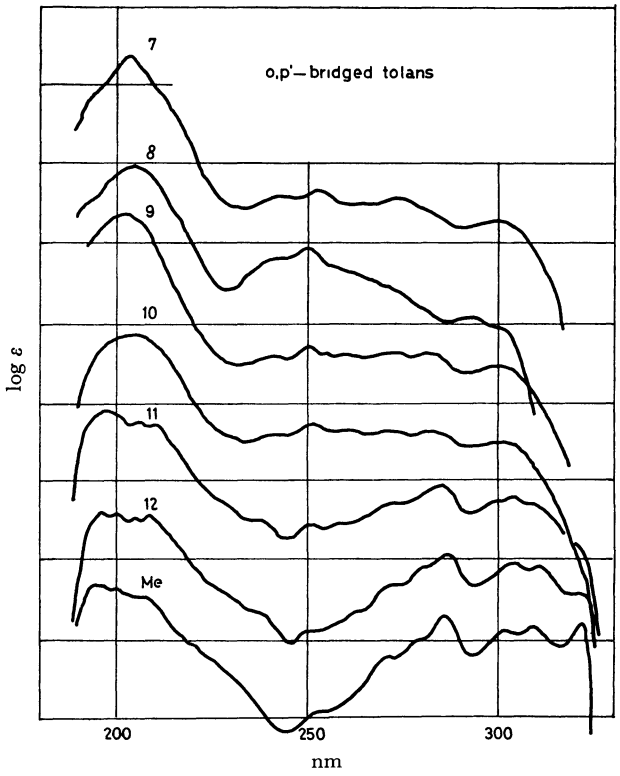

Fig. 2. The absorption curve of VII_n and *o,p'*-dimethoxytolan. The curves, with the exception of the dimethoxytolan at the bottom, have been displaced upward on the ordinate axis by 1/3 log ε unit increments from the curve immediately below, and the each horizontal lines correspond to log ε=4. (in *n*-hexane).

Table 3. The electronic spectral data of VII_n in *n*-hexane

n	λ_{max} in nm and $\varepsilon \times 10^{-4}$ in parentheses												
12	197 (3.89)	201.5 (3.73)	206.5 (3.63)	210.5 (3.64)	238 (1.39)	252.5 (1.19)		272.5 (1.81)	289.5 (2.37)		305 (2.08)	311.5 (2.06)	324 (1.54)
11	195 (4.27)	201.5 (4.05)	206 (3.89)	210 (3.79)	239 (1.46)	252 (1.47)		275 (1.82)	285.5 (2.09)		304 (1.89)		
10			206 (4.46)		241 (1.63)	251.5 (1.83)	260 (1.67)	272.5 (1.66)	283 (1.64)		302 (1.51)		
9		202 (6.74)	208 (6.93)		241.5 (1.57)	252 (1.74)	262 (1.60)	274 (1.63)	283.5 (1.59)		302 (1.41)		
8			207 (5.44)		244* (1.99)	252 (2.15)				292 (1.09)	301 (1.02)		
7		204.5 (6.05)			243 (1.58)	253 (1.64)	263 (1.45)	274 (1.51)		298 (1.20)	302* (1.22)		
CH_3O	196 (3.62)							271 (1.78)	286.5 (2.56)		302.5 (2.26)	310.5 (2.30)	321.5 (2.33)

The asterisks indicate the shoulders.

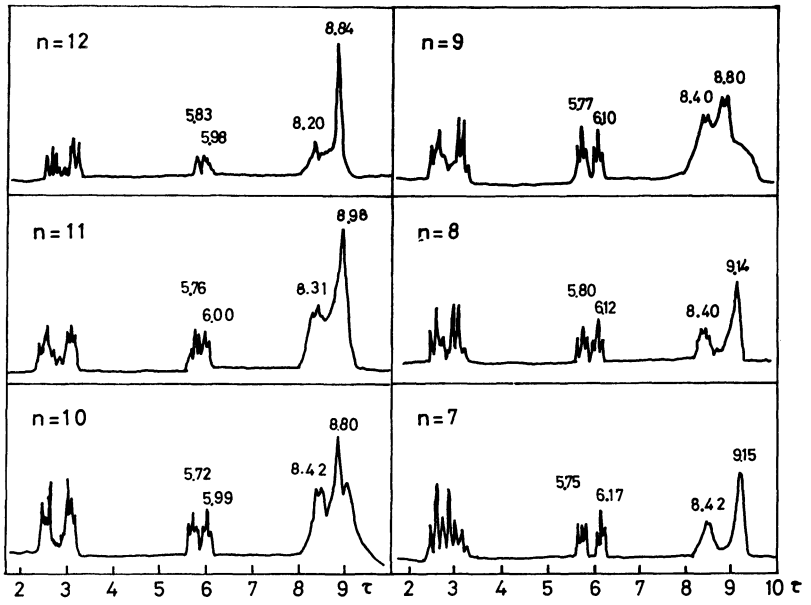

Fig. 3. The NMR spectra of VII_n.

the ethylene (V_6) on the basis of a mixed-melting-point determination and the thin-layer chromatographic, UV, IR, and NMR spectroscopic evidences. The structure of the oily product was not further studied. It is noteworthy that the yields of the cyclic tolans having a bridging chain of sufficient length are much higher than that of the open-chain analogue. As was pointed out previously,[1] the same trend has been observed in the case of the *p,p'*-series.

Electronic Spectra. The electronic spectral data of the cyclic tolans (VII_{12-7}), along with that of *o,p'*-dimethoxytolan as a reference, are recorded in Fig. 2 and Table 3. The reference substance exhibits a distinct, fine vibrational structure in the long-wavelength region. The gradual disappearanace of the fine structure according to the diminishing ring size is characteristic feature of the spectra of the cyclic tolans (VII_{12-7}).

Slight hypsochromic shifts of the absorption maxima at around 286 and 303 nm, accompanied by an appreciable hypochromic effect, were observed as the ring size decreased. On the other hand, the diminishing ring size exerted bathochromic and hyperchromic effects on the absorption peaks *ca.* 240 nm. The maximum ε-value of this peak was attained in the case of VI_{18}. The intensities of the peaks at *ca.* 250 nm gradually increased with the decrease in the number of *n*, and the maximum value was observed also in the case of VII_{18}.

The inspection of a molecular model of VII_7 indicates that the interplanar angle of the two benzene rings is almost rectangular. It is well-known that a twisted biphenyl derivative bearing bulky groups at the ortho positions exhibits an electronic spectrum resembling that of the ortho-substituted benzene moiety. However, no similarity was observed between the spectrum of VII_7 and that of *p*-methoxyphenylacetylene. This seems to indicate the presence of some conjugation of the two phenyl rings across the acetylenic linkage.

As the electronic spectra of the *o,p'*-bridged tolans (VII_n) suffer from the effects of both ring strain and the non-coplanarity of the two benzene nuclei, it is difficult to deduce the effect of strain from the above-mentioned spectral behavior. However, it seems to be pertinent to conclude that the increasing strain has hypsochromic and hypochromic effects on the long-wavelength band in the spectra of VII_n. The same tendency has been observed in the case of *o,o'*-bridged diphenyldiacetylenes.[6]

Nuclear Magnetic Resonance Spectra. The NMR spectra of the cyclic tolans (VII_n) are recorded in Fig. 3. The multiplets at around 2—3 τ can be assigned to the aromatic protons. Intense peaks, consisting of two poorly-resolved portions were observed at 8.0—9.7 τ in the spectra of VII_{12-9}. In the cases of VII_8 and VII_7, the peaks split into two peaks *ca.* 8.4 τ and *ca.* 9.15 τ. The higher-field peak can be assigned to the protons of methylene chain, except the α- and β-methylenes to the oxygen atoms. The peaks at 8.40 τ and 8.42 τ in VII_8 and VII_7 and the lower-field peaks in the poorly-resolved signals in VII_{12-9} were assigned to the protons of β-methylene to the oxygen atoms, considering the results of the assignment in *p,p'*-bridged tolans.[2] The two triplets observed around 6 τ were assigned to the methylene protons adjacent to the ortho- and para-oxygen atoms. The change in the chain length should alter the conformation of the tolan system as well as the relative configuration of $-O-CH_2-$ with respect to the planes of the benzene rings, resulting in a change in the shielding or deshielding effects of the benzene or the acetylene, and also in a change of the electron density on the oxygen atoms. This complicated situation makes it difficult to discriminate between the α-methylene attached to the para-oxygen and that linked with the ortho-oxygen. The above-mentioned assignments are summarized in Table 4, along with that of *o,p'*-dimethoxytolan.

6) F. Toda and M. Nakagawa, This Bulletin, **34**, 862 (1961).

The rather sharp peak at 8.84 τ in the poorly-resolved broad signal of VII_{12} seems to reflect the conformational mobility of the long bridging chain. The broadening of the corresponding signals in VII_{11-9} with the decrease in the number of n is attributable to some restriction of the conformational mobility of the bridging chain of a medium length. Consequently, the splitting of the two portions of the signals which was observed in the spectra of VII_8 and VII_7 seems to indicate a rigid structure in the cyclic tolans bearing short bridging chains.

Table 4. The assignment of the NMR spectra of VII_n (60 MHz in CCl_4, τ-value)

VII_n	Aromatic	α-Methylene		β-Methylene	Other methylene
12	2—3	5.98(2H)	5.83(2H)	8.20	8.84(20H)
11	2—3	6.00(2H)	5.76(2H)	8.31	8.98(18H)
10	2—3	5.99(2H)	5.72(2H)	8.42	8.80(16H)
9	2—3	6.10(2H)	5.77(2H)	8.40	8.80(14H)
8	2—3	6.12(2H)	5.80(2H)	8.40(4H)	9.14(8H)
7	2—3	6.17(2H)	5.75(2H)	8.42(4H)	9.15(6H)
CH_3O	2—3	6.06(3H)	5.77(3H)		

Infrared Spectra. It was observed that the cyclic tolans bearing a bridging chain with an odd number of methylene groups exhibit sharper IR spectra than those of the even-number homologues. This fact seems to have some correlation with the above-mentioned oscillation of the melting points (Fig. 1). The characteristic peaks in the IR spectra of VII_n are summarized in Table 5, along with the spectrum of *o,p'*-dimethoxytolan.

Table 5. The IR spectra of VII_n (KBr-disk)

VII_n	$\nu_{C\equiv C}$	$\nu_{C=C}$ (arom.)	δ_{CH} (arom.)	
12	2215 (w)	1605 (s) 1571 (w)	825 (s)	744 (s) cm^{-1}
11	2210 (w)	1604 (s) 1569 (m)	839 (s)	745 (s)
10	2220 (w)	1607 (s) 1570 (m)	829 (s)	750 (s)
9	2210 (w)	1603 (s) 1570 (w)	835 (s)	748 (s)
8	2210 (w)	1604 (s) 1573 (m)	836 (s)	749 (s)
7	2200 (w)	1602 (s) 1570 (w)	841 (s)	748 (s)
CH_3O	2220 (w)	1609 (s) 1574 (m)	830 (s)	749 (s)

Experimental

All the melting points are uncorrected. The electronic spectra were measured on a Hitachi EPS-2 Spectrophotometer; the infrared spectra, with a Hitachi EPI-2 Spectrophotometer, and the NMR spectra, with a Varian A 60 Spectrometer. The molecular weights were determined by the Rast method.

1,12-Dibromododecane and 1,11-Dibromoundecane. The polymethylene dibromides were prepared according to the method described in the preceding paper.[2]

1,10-Dibromodecane. A commercial product was used.

1,9-Dibromononane. Dimethyl 1,9-nonanedioate which had been prepared from azelaic acid[7] was reduced by means of lithium aluminum hydride; this yielded 1,9-nonanediol. The treatment of the diol (62.8 g, 0.39 mol) with hydrogen bromide (30% excess) at 130°C[8] afforded 1,9-dibromononane; bp 120—126°C/4 mmHg, 86.1 g (72%).

1,8-Dibromooctane. The Hunsdiecker reaction of silver sebacate[9] gave the dibromide in a yield of 40%.

1,7-Dibromoheptane. Silver 1,9-nonanedioate (200 g, 0.5 mol) in dry carbon tetrachloride was treated with bromine (56 m*l*, 1.1 mol) to yield the dibromide (61 g, 47%).[10]

1,6-Dibromohexane. To a stirred solution of lithium aluminum hydride (45 g, 1.2 mol) in dry ether (1 *l*), there was added a solution of dimethyl adipate (159 g, 0.92 mol) in ether (700 m*l*) at such a rate that the ether refluxed gently (100 min were required). After refluxing for 3 more hr, ethyl acetate (50 m*l*) was added to the cooled reaction mixture, and then 20% sulfuric acid (1.5 *l*) was added under ice-cooling. After the removal of the ether by distillation, the water was evaporated under reduced pressure. The crystalline solid obtained was dried *in vacuo* at 100°C for 8 hr. Ethanol (400 m*l*) was mixed the solid, and the mixture was refluxed for 4 hr. The ethanol was then separated by decantation. This procedure was repeated 6 times. The combined ethanol extracts were evaporated under reduced pressure. The residue was redissolved in anhydrous ethanol, and the insoluble material was removed by filtration. After the removal of the solvent from the filtrate *in vacuo*, the residue was distilled *in vacuo* to afford 1,6-hexanediol (bp 115—124°C/4—7 mmHg, mp 40—42°C, 68 g, 63%). The diol (79 g, 0.67 mol) was converted to 1,6-dibromohexane (bp 128—133°C/23—25 mmHg, 106 g, 65%) according to a previously described method.[8]

Preparation of o-*Hydroxy*-p'-*ω-bromoalkyloxybenzophenones* (II_n). As all the syntheses of *p'*-*ω*-bromopolymethylene ethers (II_n) were carried out under almost the same reaction conditions, the procedure used in the preparation of *p'*-10-bromodecyl ether (II_{10}) will be described as a representative example. To a stirred and refluxing solution of 1,10-dibromodecane (105 g, 0.35 mol) and *o,p'*-dihydroxybenzophenone (10 g, 47 mmol) in anhydrous ethanol (150 m*l*), there was added a solution of potassium hydroxide in ethanol (1.08N, 43.3 m*l*, 47 mmol) over a period of 1 hr. The reaction mixture immediately turned red, and then there was a deposition of fine crystals of potassium bromide. After the addition had been completed, refluxing was continued for a further 40 min. During this period, the reaction mixture turned yellowish brown and the pH-value of the mixture showed 5.5. The residue obtained by evaporating the solvent under reduced pressure was mixed with water (300 m*l*) and extracted with ether. The extract was then worked up according to the usual manner, and the excess of the dibromide was recovered by distillation (bp 138—141°C/5 mmHg). The yellow oily residue (15.2 g) in benzene was chromatographed on alumina (40 g). The fractions eluted with benzene afforded II_{10} (10.2 g, 68%) as a yellow liquid. Small amounts of the diether derivative and unreacted benzophenone (I) were obtained. These compounds could be easily discriminated by the difference in $\nu_{C=O}$ and ν_{O-H} as is shown in Table 6. The monoethers (II_n) were obtained as yellow liquid, except in the case of $n=12$, which gave yellow crystals in a yield of 46%. The yields of the other members were found to be

7) *Cf.* L. J. Durham, D. J. McLeod, and J. Cason, "Organic Syntheses," Coll. Vol. IV, p. 635 (1963).
8) *Cf.* W. L. McEwen, *ibid.*, Coll. Vol. III. p. 227 (1955).
9) F. L. M. Pattison, *J. Org. Chem.*, **21**, 745 (1956).
10) *Cf.* C. V. Wilson, "Organic Reactions," Vol. 9, ed. by R. Adams, John Wiley and Sons, New York, N. Y. (1957), p. 332.

TABLE 6. THE $\nu_{C=O}$ AND ν_{O-H} OF THE ETHERS AND I (cm^{-1})

	o,p'-Diether	*p'*-Ether (II_n)	*o*-Ether[a] (II_6)	I
$\nu_{C=O}$	1660	1630	1650	1630
ν_{O-H}	—	2900	3200	3250

a) This compound was prepared by a modified method. See below.

as follows: II_{11}: quantitative; II_{10}: 68%; II_9: 74%; II_8: 57% and II_6: 63%. The monoethers (II_n) thus obtained were subjected to the subsequent reaction without further purification.

Syntheses of the Cyclic Ethers (III_n). As the reaction conditions of the intramolecular cyclization of II_n and the yields of III_n have been shown in Table 1, the method of the synthesis of III_8 will be described as an example. The ω-bromoether (II_8, 17.1 g, 42 mmol) in isoamyl alcohol (310 m*l*) was added slowly to a vigorously-stirred and refluxing mixture of potassium carbonate (17.5 g, 0.13 mol) and isoamyl alcohol (960 m*l*) over a period of 74 hr, employing a high-dilution apparatus.[4] After the addition had been completed, the the reaction mixture was refluxed for a further 4 hr under stirring. The inorganic material was then removed by filtration. The resinous material obtained by evaporating the solvent under reduced pressure was dissolved in benzene and chromatographed on alumina (300 g). The fractions eluted with benzene - ether (1 : 1) gave III_8 (4.66 g, 34%) as colorless crystals. This substance was recrystallized twice from *n*-hexane - methanol to yield pure III_8 as colorless plates: mp 125.3—126.3°C. The analytical data, the molecular weights, and the solvents of the recrystallization of III_n are recorded in Table 7. The crude crystals of III_{12} and the liquid III_{10} were used for the following reaction without further purification.

TABLE 7. THE ANALYTICAL DATA, THE MOLECULAR WEIGHT, AND THE SOLVENTS OF RECRYSTALLIZATION OF III_n

III_n		Analytical data (%) C	H	Mol wt	Solvent
11	Found	78.93	8.26	358	H
	Calcd	78.65	8.25	366	
9	Found	77.84	7.69		H-B
	Calcd	78.07	7.74		
8	Found	77.63	7.50	318	H-B
	Calcd	77.75	7.46	324	
7	Found	77.76	7.18	314	H
	Calcd	77.39	7.14	310	
6[a]	Found	76.96	6.73	302	H-B
	Calcd	77.00	6.80	296	

a) This was prepared by a modified method. See below.
H=*n*-hexane; B=benzene

o-*Hydroxy*-p'-*methoxymethoxybenzophenone (VIII).* A solution of sodium ethoxide in ethanol, prepared from sodium (1.76 g, 73 mg atom) and ethanol (50 m*l*), was added to a solution of the dihydroxybenzophenone (I, 15.5 g, 73 mmol) in ethanol (150 m*l*). The mixture turned red, and the precipitation of a yellow solid was observed. The solvent was then removed under reduced pressure, and toluene (200 m*l*) was added to the residue. The toluene was subsequently evaporated again under reduced pressure. The procedure was repeated to remove the traces of ethanol and water. The sodium salt obtained as a yellow powder was mixed with toluene (200 m*l*), and then chloromethyl methyl ether (5.85 g, 73 mmol) was added dropwise under stirring. After having been stirred overnight, the reaction mixture was washed successively with a 10% sodium hydrogen carbonate solution, water, and a saturated sodium chloride solution, and then dried. The oily material (17.2 g) obtained by evaporating the solvent was chromatographed on alumina (190 g). The fractions eluted with benzene - ether (1:1), ether, and ether containing 3% of methanol, gave VIII (12.0 g 64%) as a liquid, IR (neat): ν_{O-H} 2900; $\nu_{C=O}$ 1630 cm^{-1}.

o-ω-*Bromo*-n-*hexyloxy*-p'-*methoxymethoxybenzophenone (IX).* Thirty-one m*l* of 1.03N solution of potassium hydroxide in ethanol was added, over a period of 1 hr, to a stirred and refluxing solution of VIII (7.99 g, 31 mmol) and 1,6-dibromohexane (105 g, 0.43 mol) in anhydrous ethanol (150 m*l*). After refluxing for further 1.5 hr, the solvent was removed under reduced pressure. Benzene was added to the residue, and it was washed with a 10% sodium hydroxide solution. The benzene solution was worked up in the usual manner, and the dibromohexane was removed by vaccum distillation; this yielded IX as a yellow liquid (5.63 g, 42%). IR (neat): ν_{O-H} absent; $\nu_{C=O}$ 1660 cm^{-1}. The aqueous layer was neutralized by dilute hydrochloric acid and extracted with benzene. The structure of *o*-ω-bromohexyloxy-*p'*-hydroxybenzophenone (X) was assigned to the oily substance obtained from the benzene layer on the basis of its IR spectrum (ν_{O-H} 3200; $\nu_{C=O}$ 1650 cm^{-1}). The prolonged reaction (7.5 hr) of VIII (11.5 g, 43 mmol) with the dibromohexane (73 g, 0.30 mol) in the presence of 64.5 mmol of potassium hydroxide resulted in the formation of *o,p'*-bis-ω-bromohexyloxybenzophenone (10.2 g, 47%) and *o*-ω-bromohexyloxy-*p'*-hydroxybenzophenone (X, 9.40 g, 58%). The cleavage of the acetal linkage in an alkaline medium seemed to be noteworthy.

o-ω-*Bromo*-n-*hexyloxy*-p'-*hydroxybenzophenone (X).* A mixture of IX (4.51 g, 12 mmol), acetic acid (25 m*l*), water (25 m*l*), and concentrated sulfuric acid (0.2 g) was refluxed for 15 min under stirring. The reaction mixture was then worked up according to the usual manner to afford crude X (4.80 g, 95%, IR (neat): ν_{O-H} 3200; $\nu_{C=O}$ 1650 cm^{-1}). This was subjected to the subsequent reaction without any further purification.

o,p'-*Dihydroxybenzophenone Hexamethylene Ether (III_6).* The intramolecular alkylation under high-dilution conditions described in the preparation of III_n was successfully adapted in this case. The product (4.50 g) obtained from X (4.51 g, 12 mmol) was chromatographed on alumina (135 g). The fractions eluted with benzene - ether (9 : 1～2 : 1) afforded, upon work-up, 1.08 g (31%) of III_6 as colorless crystals. This substance was recrystallized from *n*-hexane - benzene to give pure III_6 (for analytical data, see Table 7).

o,p'-*Dimethoxybenzophenone.* To a stirred and refluxing mixture of the dihydroxybenzophenone (I, 3.0 g, 14 mmol), methyl iodide (5 m*l*, 80 mmol), and anhydrous ethanol (25 m*l*), we added 28 m*l* of a 1N solution of potassium hydroxide in ethanol over a period of 70 min; refluxing was then continued for 1 hr. The presence of the hydroxyl group was revealed by the IR spectrum of the crude product. Therefore, the crude product was treated in the same way, and dimethoxybenzophenone (3.02 g, 89%) was afforded as a liquid.

o,p'-*Di*-n-*butoxybenzophenone.* According to the procedure described above, the reaction of the dihydroxybenzophenone with *n*-butyl bromide gave the dibutoxybenzophenone as a liquid in a yield of 74%.

Syntheses of the Methyl Carbinols (IV_n). The preparation of the methyl carbinol (IV_8) will be described as a re-

presentative example. To a stirred and ice-cooled solution of methylmagnesium iodide, prepared from magnesium (0.5g 0.021 g atom), methyl iodide (21 m*l*, 32 mmol) and ether (20 m*l*), we added, drop by drop a solution of III_8 (1.18 g, 5.6 mmol) in anhydrous benzene (30 m*l*). The mixture was refluxed for 2 hr; then a 10% aqueous solution of ammonium chloride was added to the ice-cooled reaction mixture. The benzene layer was then worked up to yield colorless crystals (1.80 g, 95%). This substance was recrystallized 4 times from *n*-hexane to yield pure IV_8; mp 84.0—86.0°C, colorless needles. The yields of the methyl carbinols were found to be as follows: IV_6: quantitative, IV_7*: 99%, IV_8: 95%, IV_9*: 85%, IV_{10}: quantitative, IV_{11}*: 87%, IV_{12}*: 90%, dimethoxy derivative: 94%, dibutoxy derivative*: 86%. The carbinols denoted by asterisks were obtained as liquids and could not be crystallized. The melting points, the analytical data, and the solvents of recrystallization are summarized in Table 8.

Table 8. The melting points, the analytical data, and the solvents of recrystallization of IV_n and the reference substance

IV_n	Mp (°C)		Analytical data (%) C	H	Solvent
10	76.3—77.0	Found	78.44	8.83	H
		Cacld	78.22	8.75	
8	84.0—86.0	Found	77.83	8.43	H
		Calcd	77.61	8.29	
6	143.0—143.9	Found	76.82	7.73	B-H
		Calcd	76.89	7.74	
CH_3O	99—103[a]				

a) Slightly impure material. H=*n*-hexane; B=benzene.

1-(o-Hydroxyphenyl)-1-(p'-hydroxyphenyl)ethylene Polymethylene Ethers (V_n). The Dehydration of the Methyl Carbinols (IV_n). The preparation of V_8 will be described as an example. A mixture of IV_8 (1.82 g, 54 mmol) and 8N sulfuric acid (60 m*l*) was refluxed for 1 hr under stirring, and then it was extracted with benzene. The extract afforded, upon work-up, 1.58 g (91%) of colorless crystals. This substance was recrystallized 3 times from *n*-hexane - methanol to give pure V_8, mp 80.0—81.0°C as colorless plates.

According to the same procedure, all the carbinols (IV_n) gave the ethylenes (V_n) in yields over 90%. The pure ethylenes (V_6, V_8 and V_{11}) were obtained by recrystallizing the crude materials from *n*-hexane - methanol (1 : 1). The melting points, the analytical data of V_n, and the reference substance are given in Table 9.

Table 9. The melting points and the analytical data of V_n and the reference compounds

V_n	Mp (°C)		Analytical data (%) C	H
6	126.0—126.7	Found	81.71	7.51
		Calcd	81.60	7.53
7	113—115[a]			
8	80.0—81.0	Found	81.73	8.13
		Calcd	81.95	8.13
9	crystalline solid[a]			
10	liquid[a]			
11	99.0—100.5	Found	82.38	8.86
		Calcd	82.37	8.85
CH_3O	75—77[a]			
n-BuO	liquid[a]			

a) The ethylenes denoted by asterisks were used for the subsequent reaction without further purification.

1-(o-Hydroxyphenyl)-1-(p'-hydroxyphenyl)-2,2-dibromoethylenes (VI_n, n=10, 11, 12, X=Br). The preparation of VI_{12} will be described as a representative instance. To a solution of V_{12} (2.36 g, 6.2 mmol) in carbon tetrachloride (30 m*l*), there was added a solution of bromine in the same solvent (0.63 mol/*l*, 19.8 m*l*, 13 mmol). The mixture was stirred for 1 hr under reflux, resulting in the disappearance of the color of the bromine. The same amount of the bromine solution was added to the reaction mixture, and the new mixture refluxed for 2 more hr. The residue obtained by evaporating the solvent under reduced pressure was mixed with benzene (50 m*l*). The benzene solution was washed successively with a 10% sodium hydroxide solution and water, and then dried. The evaporation of the solvent gave 2.96 g of an oily material. This was chromatographed on alumina (40 g) to afford yellowish crystals; 2.49 g (75%). The crystals were recrystallized 3 times from ethyl acetate - methanol to yield pure VI_{12} as colorless leaflets; mp 99.7—101.5°C.

The melting points, the analytical data, and the molecular weights of V_{10-12} and the reference substances are shown in Table 10, together with the solvents used for the recrystallization.

Table 10. The melting points, the analytical data, and the molecular weights of VI_{10-12} and the reference compounds

VI_n	Mp (°C)		Analytical data (%) C	H	Cl	Mol wt	Solvent
12	99.7—	Found	58.08	5.98	29.61	518	E-M
	101.5	Calcd	58.22	6.01	29.80	504	
11	103.6—	Found	58.07	5.87	29.52		H
	104.6	Calcd	57.48	5.79	30.60		
10	92.4—	Found	57.04	5.79	31.20	345	H
	94.6	Calcd	56.71	5.55	31.44	348	
CH_3O	93.5—	Found	48.47	3.56	40.83		E-M
	94.6	Calcd	28.27	3.54	40.15		
n-BuO	72.7—	Found	54.75	5.43	33.63		E-M
	73.4	Calcd	54.79	5.43	33.14		

E=ethyl acetate; M=methanol; H=*n*-hexane.

cis- and trans-1-(o-Hydroxyphenyl)-1-(p'-hydroxyphenyl)-2-bromoethylene Polymethylene Ethers (VI_n, n=9, 8, 7, 6, X=H). The procedure used for the preparation of VI_9 will be described as an example. A solution of V_9 (862 mg, 2.6 mmol) in carbon tetrachloride (40 m*l*) was mixed with a solution of bromine in the same solvent (0.249 mol/*l*, 10.3 m*l*, 26 mmol). After refluxing for 1 hr, the solvent was distilled out under reduced pressure. The residue in *n*-hexane - benzene was passed through a short column of alumina. The oily material obtained by evaporating the solvent *in vacuo* crystallized on standing overnight in a refrigerator. The crude crystals were chromatographed twice on alumina (30 g) to yield 600 mg (56%) of VI_9. An analytical specimen (colorless plates, mp 88—101°C) was obtained by recrystallizing the crystals 4 times from *n*-hexane.

Found: C, 66.99; H, 6.62; Br, 18.94%. Mol wt: 286. Calcd for $C_{23}H_{27}O_2Br$: C, 66.50; H, 6.55; Br, 19.24%. Mol wt: 415.

As the bromoethylenes (VI_8, VI_7, and VI_6) were obtained

as oily materials and could not be crystallized, the bromoethylenes purified by chromatography on alumina were subjected to the following reaction.

Formation of the Cyclic Tolans (VIII$_n$, n=12, 11, 10, 9, 8 and 7). The procedure of the rearrangement to form the cyclic tolan is exemplified by the case of $n=12$. To a solution of VI$_{12}$ (680 mg, 1.3 mmol) in anhydrous ether (30 m*l*) which had been cooled in an ice-salt-bath, there was added, drop by drop a solution of *n*-butyllithium in ether (0.15 mol/*l*, 17 m*l*, 2.6 mmol) under stirring. A rise of temperature from −16°C to −11°C was observed on the addition of the reagent. Stirring was continued for one more hr at a temperature of −16——17°C. The reaction mixture was then washed with water, and the aqueous layer was extracted with benzene. The extract was combined with the organic layer and was worked up in the usual manner to yield colorless crystals (460 mg, 96%). The crude crystals were recrystallized twice from *n*-hexane to afford 300 mg (63%) of pure VII$_{12}$, mp 120.0—120.6°C as colorless cubes.

In the cases of $n=8$ and 7, the crude crystals were subjected to chromatography on alumina 3 times, and the oily by-product could be removed by elution with petroleum benzine - benzene (1 : 1). The pure VII$_8$ and VII$_7$ were obtained from the fractions eluted with ether. Also, the reference substance, *o,p'*-dimethoxytolan, was obtained as liquid; crystallization was achieved after repeating the chromatography on alumina.

The analytical data, the molecular weights, and the solvents of the recrystallization of VII$_n$ are summarized in Table 11 (for the yields and the melting points of VII$_n$, see Table 2).

Attempted Synthesis of VII$_6$. The treatment of VI$_6$ (323 mg, 0.87 mmol) with *n*-butyllithium according to the above-mentioned procedure afforded a yellow, oily product (291 mg) which partly crystallized on standing overnight. The product gave a negative Beilstein test. Thin-layer chromatography of the reaction product 3 gave spots, R_f 6.1 (brown), R_f 5.5 (red), R_f 4.9 (purple), and R_f 1.5 (blue) (adsorbent: alumina; solvent: benzine - benzene (4 : 1); detection reagent: conc. sulfuric acid). It was found that the constituents which gave the spots at R_f 5.5 and 4.9 were the main products. The product which gave the spot at R_f 4.9 could be isolated as crystals by chromatography on alumina. This substance was proved to be identical with the cyclic ethylene (V$_6$) on the basis of the IR and NMR spectroscopic evidence and a mixed-melting-point determinaion. Another product (R_f 5.5), obtained as an oil, has not yet been chracterised.

TABLE 11. THE ANALYTICAL DATA, THE MOLECULAR WEIGHTS, AND THE SOLVENTS OF RECRYSTALLIZATION OF VII$_n$ AND THE REFERENCE COMPOUND

VII$_n$		Analytical data (%) C	H	Mol wt	Solvent
12	Found	83.09	8.59	368	H
	Calcd	82.93	8.57	378	
11	Found	82.52	8.26	352	H
	Calcd	82.83	8.34	362	
10	Found	82.82	8.09	345	B-H
	Calcd	82.72	8.10	348	
9	Found	82.44	7.82	325	H
	Calcd	82.59	7.84	334	
8	Found	82.55	7.60	334	H
	Calcd	82.46	7.55	320	
7	Found	82.12	7.28	288	H
	Calcd	82.32	7.24	306	
CH_3O	Found	80.58	5.92		H
	Calcd	80.64	5.92		

H=*n*-hexane; B=benzene

Studies on Heteroaromaticity. XLIV.[1] Reactivities of Benzoyl Cyanide *N*-Oxide and Some Derivatives Therefrom

Tadashi SASAKI, Toshiyuki YOSHIOKA, and Yasuyuki SUZUKI

Institute of Applied Organic Chemistry, Faculty of Engineering, Nagoya University, Chikusa-ku, Nagoya

(Received July 13, 1970)

ω-Chloroisonitrosoacetophenone was treated with ethylenic and acetylenic dipolarophiles to afford 3-benzoylisoxazolinines and -isoxazoles, respectively. With *m*-nitrobenzaldoxime or *m*-nitrobenzonitrile, it yielded 3-benzoyl-5-(*m*-nitrophenyl)-1,2,4-oxadiazole. The phenylhydrazones of the 3-benzoylisoxazole and -oxodiazole thus produced were converted to the corresponding 1,2,3-triazoles thermally or by the treatment with a base. The photo-induced rearrangement of 3-benzoyl-5-phenylisoxazole afforded 2-benzoyl-5-phenyloxazole. Treatment of *ω*-chloroisonitrosoacetophenone with aziridine afforded a new type of aziridine oximes, which was converted to 2-benzoyloxazoline.

It is surprising that there have been no reports on the preparation and reactions of benzoyl cyanide *N*-oxide (I) in contrast to abundant reports on benzonitrile oxide, though *ω*-chloroisonitrosoacetophenone (II, phenylglyoxylyl chloride oxime) is a readily available compound[2] and is regarded as its precursor. Holleman[3] postulated the intermediary formation of I in the preparation of 1,5-dibenzoylfuroxan from acetophenone. Because of the presence of a carbonyl conjugated with the nitrile oxide group, I is thought to be stabilized by the resonance, but presumably reactive enough to undergo the 1,3-dipolar cycloaddition reactions. In this paper, the results in the 1,3-dipolar cycloaddition reactions are discussed in comparison with those in similar reactions of benzonitrile oxide. The thermal and basic rearrangement of the phenylhydrazones of 3-benzoylisoxazole and -oxadiazole thus produce and the photo-induced rearrangement of 3-benzoylisoxazole are discussed. The ring-enlargement of the aziridine adduct of I is also described.

Results and Discussion

1,3-Dipolar Cycloadditivity. In order to examine 1,3-dipolar cycloaddition reactivity, II was treated in ether with triethylamine in the presence of a dipolarophile (styrene, for example) according to the general procedure for preparing the nitrile oxides.[4] The oily product was characterized as 3-benzoyl-5-phenylisoxazoline (III) after conversion to its crystalline picrate on the basis of analytical and spectral evidences. A further evidence was provided by its conversion to crystalline 3-benzoylisoxazole (XVIII) with *N*-bromosuccinimide (NBS). A similar treatment of II with acrylonitrile afforded 3-benzoyl-5-cyanoisoxazoline (IV); IV showed no nitril absorption in the IR spectrum, which supports 5-cyano structure.[5] An attempt to convert it to isoxazole with NBS was unsuccessful. Acidic hydrolysis of IV with sulfuric acid gave benzoic acid, while 3-(5-nitro-2-furyl)-5-cyanoisoxazole (V) was convertible to the corresponding amide under similar conditions. Treatment of II with two equivalent amounts of 1-morpholino-2-cyanoethylene in ether at room temperature afforded 3-benzoyl-4-cyanoisoxazole (VI) similar to the 1,3-dipolar cycloaddition of aromatic hydroxamoyl chlorides to the enamine after spontaneous elimination of a morpholine molecule from the initial 1 : 1 adduct.[6] VI was hydrolyzed to amide under acidic conditions. Treatment of II with *o*-aminophenol and methyl anthranilate afforded linear adducts, *N*-phenylglyoxylyl-*o*-aminophenol oxime (VII) and methyl *N*-phenylglyoxylylanthranilate oxime (VIII), respectively, but with *o*-phenylenediamine, a cyclized product, 3-benzoyl-1,4-dihydro-1,2,4-benzotriazine (IX), instead of the expected benzoxazole[7] or quinazoline[8] and benzimidazole[7] in the similar reactions of aromatic hydroxamoyl chlorides. VIII was cyclized, however, to 3-hydroxy-4-oxo-2-benzoyl-3,4-dihydroquinazoline (X) on treatment with hydrochloric acid. With 1-cyano-2-diethylaminoacetylene,[10] II afforded 3-benzoyl-4-cyano-5-diethylaminoisoxazole (XI) as in the case of aromatic hydroxamoyl chlorides,[9] but with ammonium thiocyanate in methanol, II unexpectedly[10] yielded *N*-benzoylthiourethane (XII). Since the products III and IV could be obtained by the thermal 1,3-dipolar cycloaddition reactions of II in almost quantitative yields, the thermal reactions were performed using several dipolarophiles; the results are summarized in Table 1.

As seen from this table, ethylenic and acetylenic dipolarophiles reacted with II to give the corresponding isoxazolidines, III, IV, and XIII—XV, and isoxazoles, XVI—XX, respectively; the yield of the latter was lower because of the thermal instability.[11] It should be mentioned that the yield of the former was almost quantitative.

In order to compare the reactivity of II with that

1) Part XLIII of this series: T. Sasaki, K. Kanematsu, Y. Yukimoto, and S. Ochiai, *J. Org. Chem.*, in press.

2) "Org. Synth.," Col. Vol. **3**, 191 (1955).

3) A. F. Holleman, *Ber.*, **20B**, 3359 (1887); **21B**, 2835 (1888).

4) For instance, see R. Huisgen and W. Mack, *Tetrahedron Lett.*, **1961**, 583.

5) The quenching effect of nitrile absorption intensity is greater when the oxygen-containing group is attached to the same carbon atom as the nitrile, see L. J. Bellamy, "The Infra-red Spectra of Complex Molecules," Methuen & Co., Ltd., New York (1969), p. 266.

6) T. Sasaki and T. Yoshioka, This Bulletin, **41**, 2212 (1968).

7) T. Sasaki and T. Yoshioka, *ibid.*, **42**, 3335 (1969).

8) T. Sasaki and T. Yoshioka, *ibid.*, **41**, 2206 (1968).

9) T. Sasaki and A. Kojima, *J. Chem. Soc., C*, **1970**, 476.

10) C. Musante, *Gazz. Chim. Ital.*, **68**, 331 (1938); T. Sasaki and T. Yoshioka, *Yukigosei Kagaku Kyokai-shi*, **27**, 877 (1969).

11) T. Sasaki and T. Yoshika, This Bulletin, **40**, 2604 (1967).

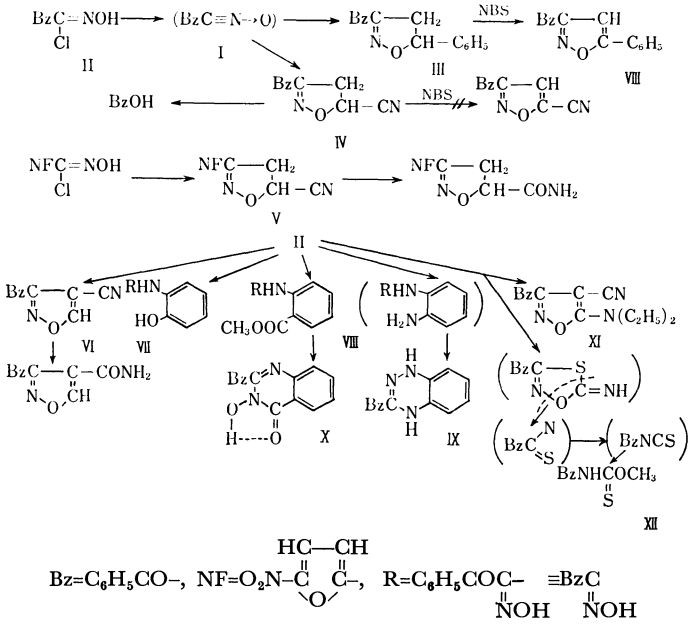

Bz=C_6H_5CO–, NF=O_2N–C_4H_2O–, R=$C_6H_5COC(=NOH)$–, ≡BzC(=NOH)

TABLE 1. THERMAL 1,3-DIPOLAR CYCLOADDITION OF II

Dipolarophiles	Products	Mp °C	Reflux time hr	Yield %	Analysis Found (Calcd) C%	H%	N%	IR (KBr) CO cm^{-1}	NMR ($CDCl_3$) τ (coupling const) C-5	C-4	UV λ_{max}^{EtOH} mμ (ε)
Ethylenic											
Styrene	III	oil[b]	16	q[a]	61.94	3.85	16.08	1655	4.50	6.70	262 (35900)
					(61.25	3.97	16.24)		(10.5 Hz)		233 (21900)
Acrylonitrile	IV	73—74	20	q[a]	65.96	4.15	13.90	1640	4.54	6.19	
					(65.99	4.03	13.99)		(10.5 Hz)		
Acenaphthylene	XIII	132	30	q[a]	80.45	4.15	4.68	1640	3.38	4.27	
					(80.25	4.38	4.68)		(9 Hz)		
Indene	XIV	91—92	6	85	78.00	5.06	5.48	1640	3.79	5.49	
					(77.55	4.98	5.32)		(12 Hz)		
Acrylic acid	XV	106	22	80	59.85	4.05	6.46	1640	4.79	6.35	6.63 (CH_2)
					(60.27	4.14	6.39)		(9.8 Hz)		
Acetylenic											
Phenylacetylene	XVIII	91	8	q[a]	77.26	4.35	5.91	1650	—	2.92	
					(77.09	4.45	5.62)				
Diphenylacetylene	XVI	148	17	5	81.32	4.50	4.45	1660	—	—	
					(81.21	4.65	4.31)				
Propargyl alcohol	XVII	oil[c]	7	30	55.70	3.45	19.15	1650	—	—	
					(55.59	3.57	19.07)				
Propargyl bromide	XIX	60	15	80	49.40	3.07	5.25	1650	—	—	
					(49.65	3.03	5.27)				
1-Ethynyl cyclohexanol	XX	oil[c]	12	40	71.05	6.45	5.20	1650	—	3.30	
					(70.83	6.32	5.16)				

a) quantitative yields b) analyzed as picrate
c) Analyzed as dinitrophenylhydrazones, mp 156°C for XVII and mp 250°C for XX.

of hydroxamoyl chlorides, II was treated with benzamidine to afford 55% yield of 2,4,6-triphenyl-1,3,5-triazine, a trimer of benzamidine. This indicates no reactivity of II with benzamidine, with which hydroxamoyl chlorides are known to afford oxadiazoles.[7] With *m*-nitrobenzonitrile II afforded 15% yield of 3-benzoyl-5-(*m*-nitrophenyl)-1,2,4-oxadiazole (XXI), while the same compound was prepared from II and *m*-nitrobenzaldoxime in 50% yield. With *m*-nitrobenzaldehyde, II underwent no cycloaddition, while benzonitrile oxide affords the corresponding dioxazole.[4,8] Even taking into consideration these different reactivities from benzhydroxamoyl chloride, II might be concluded to be a good starting material for the preparation of 3-benzoylisoxazolines and -isoxazoles.

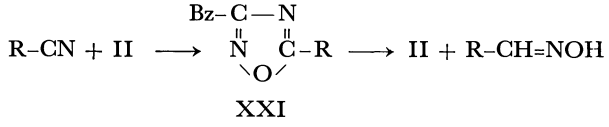

XXI

Rearrangement of 3-Benzoylisoxazole and 3-Benzoyloxadiazole. *a) Thermal and Basic Treatments*: Boulton *et al.*[12] have reported on the interesting thermal rearrangement reactions of one heterocycle to another as exemplified by those of 3-acetylisoxazole to 1,2,3-triazole *via* the phenylhydrazone and to 1,2,3-oxadiazole *via* the oxime. According to the modified procedure by Kano and Yamazaki,[13] *p*-nitrophenylhydrazone of XVIII was melted with copper powder to afford a quantitative yield of 2-(*p*-nitrophenyl)-4-phenyl-5-phenacyl-1,2,3-triazole (XXII), which was also obtained quantitatively by such a basic treatment as ammonia.[13] Similarly, 2,4-diphenyl-5-phenacyl-1,2,3-triazole (XXIII) was obtained from the phenylhydrazone of XVIII in 50% yield by thermal treatment. Thermal and basic treatments of the *p*-nitrophenylhydrazone of 3-benzoyl-1,2,4-oxadiazole (XXI) afforded 1,2,3-triazole (XXIV) in 60 and 90% yields, respectively. A similar rearrangement of *p*-nitrophenylhydrazone of VI failed, presumably because of the presence of a 4-substituent; thermal treatment afforded tarry polymer and the basic treatment resulted in recovery of the starting material. Attempts to obtain the oxime and the semicarbazone of XVIII were unsuccessful in contrast to the results given by Spiro and Ajello.[14]

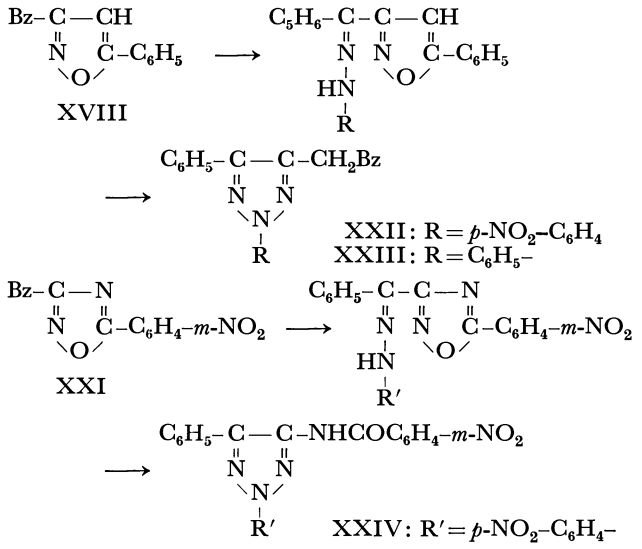

b) Photochemical Treatment: One feature in the photo-induced rearrangement of five-membered heterocycles is that two vicinal heteroatoms can interchange their positions to 1,3-system when irradiated with ultraviolet light. This example involves the photo-induced rearrangement of 3,5-diphenylisoxazole to 2,5-diphenyloxazole[15] and that of benzisoxazole to benzoxazole,[16] but not that of 3-acylisoxazoles. Thus, XVIII (UV λ_{max}^{EtOH} mμ (ε): 262 (35900) and 233 (21900)) was irradiated at room temperature under nitrogen stream. Chromatography of the reaction mixture afforded 2-benzoyl-5-phenyloxazole (XXV), *N*-benzoylbenzoylacetamide, dibenzoylacetonitrile, benzoic acid and/or benzamide. The product distributions under different conditions are summarized in Table 2.

The thermal and basic rearrangement reactions of XVIII and XXI might be explained by the radical and ionic mechanisms proposed by Kano and Yamazaki,[13] and Ullman and Singh.[15] For photoinduced rearrangement of XVIII, a similar explanation for that from 3,5-diphenylisoxazole to 2,5-diphenyloxazole[15] can be applied by postulating the intermediacy of 2,3-dibenzoylaziridine (A) and/or *N*-benzoylbenzoylketenimine (B) after its benzoyl migration (⌒). The exclusive formation of benzoic acid in the reaction of XVIII in ethanol might be originated from hydrolytic photocleavage by contaminated water in the solvent.

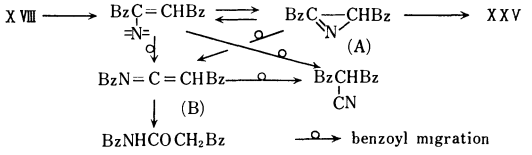

Ring-enlargement. II was treated with two equivalent amounts of aziridine in ether at room temperature to afford oily *N*-phenylglyoxylylaziridine oxime (XXVI), which was converted to crystalline *O*-*p*-nitrobenzoate (XXVII). Since XXVI is regarded as a new type of aziridine oximes,[17] ring-enlargement was carried out. Thus, XXVI was refluxed in acetone with a catalytic amount of sodium iodide to give an oily amine, which was characterized as 2-benzoyloxazoline (XXVIII) after conversion to the crystalline picrate.

Table 2. Photochemistry of 3-benzoyl-5-phenylisoxazole (XVIII)
(Yields % based on the converted XVIII)

Solvent	Mercury lamp	Reaction time hr	Recovered XVIII	Product distributions				
				XXV	*N*-Benzoyl-benzoyl-acetamide	Dibenzoyl-acetonitrile	Benzoic acid	Benzamide
Benzene	60-W low pressure	42	10	23	28	3	2	—
Ether	60-W low pressure	18	29	30	—	8	6	—
Ethanol	60-W low pressure	24	0	—	—	—	56	28
Benzene	100-W high pressure[a]	30	70	10	—	—	17	7

a) Using a liquid filter No 5. A. Schonberg, "Preparative Organic Photochemistry," Springer-Verlag New York Inc. 1968, p. 491.

12) A. J. Boulton, A. R. Katritzky, and A. M. Hamid, *J. Chem. Soc., C*, **1967**, 2005.
13) H. Kano and E. Yamazaki, *Tetrahedron*, **20**, 159, 461 (1964).
14) V. Spiro and E. Ajello, *Ann. Chim.* (Rome), **58**, 128 (1968).
15) E. F. Ullman and B. Singh, *J. Amer. Chem. Soc.*, **88**, 1844 (1966); **89**, 6911 (1967). D. W. Kurz and H. Shechter, *Chem. Commun.*, **1966**, 689.
16) M. Ogata, H. Matsuno, and H. Kano, Abstract of the Symposium on the Chemistry of Heterocyclic Compounds, p. 157 (Osaka, Oct., 1968).
17) T. Sasaki and T. Yoshioka, This Bulletin, **42**, 556 (1969).

The yield of the conversion to XXVIII was improved up to 60% by treating with concd. hydrochloric acid in acetone at room temperature.[17]

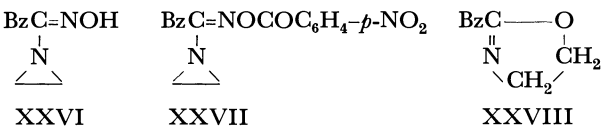

XXVI XXVII XXVIII

Experimental

All melting points were determined on a Yanagimoto electric micromelting point apparatus and are uncorrected. The ultraviolet (UV) and infrared spectra (IR) were recorded on a Jeolco Model ORD/UV-5 and a Jasco Model IR-S spectrometer. The NMR spectra were determined on a Varian A-60 and a Jeolco Minimar, with tetramethylsilane as an internal standard and the peak positions are expressed by τ-values. Column chromatography was carried out on a silica-gel (Mallinckrodt, 100 mesh) using benzene as an eluent.

3-Benzoyl-5-phenylisoxazoline (III). *a) Nitrile Oxide Method*: To a stirred solution of 1.84 g (0.01 mol) of ω-chloroisonitrosoacetophenone (II)[2] and 1.04 g (0.01 mol) of styrene in 50 m*l* of ether was added a solution of 1.2 g (0.012 mol) of triethylamine in 10 m*l* of ether under cooling with ice-water. The reaction mixture was stirred at room temperature overnight. The resulting precipitates (triethylamine hydrochloride) were removed and the filtrate was concentrated. The residual oil was converted to the crystalline picrate, mp 219—220°C, and analyzed (Table I). The yield was 30%.

b) Thermal Treatment: A solution of the same amounts of the two components as above in 50 m*l* of toluene was refluxed for 16 hr. The solvent was removed and the residual oil was purified as above to give a quantitative yield of III (Table 1).

Its Conversion to 3-Benzoyl-5-phenylisoxazole (XVIII). A solution of 1.0 g of III and 0.75 g of *N*-bromosuccinimide (NBS) in 20 m*l* of carbon tetrachloride was refluxed in the presence of a trace of azobisisobutyronitrile (AIBN) for 3 hr. The reaction mixture turned from red to pale yellow. The mixture was filtered and the filtrate was concentrated. The residue was treated with a solution of 0.25 g of potassium hydroxide in 10 m*l* of methanol to afford 0.5 g (50%) of XVIII, mp 91°C, which was identical with a specimen pre pared from II and phenylacetylene (Table 1). Phenylhydrazone, mp 106—107°C.

Found: C, 77.93; H, 5.60; N, 12.54%. Calcd for $C_{22}H_{27}ON_3$: C, 77.85; H, 5.05; N, 12.38%.

p-Nitrophenylhydrazone, mp 191—192°C. UV λ_{max}^{EtOH} mμ (ε): 396 (31700), 278 (16300) and 250 (22100).

Found: C, 68.95; H, 4.35; N, 14.45%. Calcd for $C_{22}H_{16}O_3N_4$: C, 68.74; H, 4.20; N, 14.58%.

3-Benzoyl-5-cyanoisoxazoline (IV). IV was obtained from II and acrylonitrile by the nitrile oxide method in 30% yield, but by the thermal procedure quantitatively. (Table 1).

3-(5-Nitro-2-furyl)-5-cyanoisoxazoline (V) and Its Conversion to Amide. *Thermal treatment*: A solution of 0.95 g (5 mmol) of 5-nitro-2-furylhydroxamoyl chloride[11] and 1.0 g (20 mmol) of acrylonitrile in 40 m*l* of toluene was refluxed for 15 hr. The chromatography afforded 0.74 g (70%) of V, mp 109°C, by recrystallization from ethanol. IR (KBr): no nitrile absorption at around 2200—2400 cm^{-1}.

Found: C, 46.53; H, 2.57; N, 20.41%. Calcd for $C_8H_5O_4N_3$: C, 46.38; H, 2.43; N, 20.29%.

The same compound was obtained in 65% yield by the nitrile oxide method.

Conversion of V to the amide was carried out as follows: a solution of 0.3 g of V in 4 m*l* of concd. sulfuric acid was stirred at room temperature for 2 days. The reaction mixture was poured onto ice-water and the resulting yellow crystals were collected and recrystallized from ethanol - THF to afford the amide in 75% yield, mp 225°C, which was identical with a specimen[11] by IR comparison.

3-Benzoyl-4-cyanoisoxazole (VI). A solution of 1.84 g (0.01 mol) of II and 2.8 g (0.02 mol) of 1-morpholino-2-cyanoethylene[18] in 50 m*l* of ether was stirred at room temperature for one week. The resulting precipitates were filtered and the solvent was removed from the filtrate. The residual solid was recrystallized from *n*-hexane to give 60% yield of VI, mp 73—74°C. IR (KBr) cm^{-1}: 2250 (ν_{CN}), and 1660 (ν_{CO}). NMR ($CDCl_3$) τ: 0.09 (s, 1H, C_5-H).

Found: C, 67.04; H, 3.25; N, 14.07%. Calcd for $C_{11}H_6O_2N_2$: C, 66.66; H, 3.05; N, 14.14%.

Its Conversion to Amide. Similar as in the case of V, VI was treated with concd. sulfuric acid to afford the amide, mp 174—175°C, in 70% yield. IR (KBr) cm^{-1}: 3400, 3350 (ν_{NH}) and 1670 (ν_{CO}).

Found: C, 60.89; H, 3.80; N, 13.05%. Calcd for $C_{11}H_8O_3N_2$: C, 61.11; H, 3.73; N, 12.96%.

N-Phenylglyoxylyl-o-aminophenol Oxime (VII). Treatment of II with two equivalent amounts of *o*-aminophenol in ether at room temperature for 1 day afforded 70% yield of VII, mp 162—163°C, by recrystallization from a 10 : 1 mixture of benzene and ethanol. IR (KBr) cm^{-1}: 1660 (ν_{CO}).

Found: C, 66.17; H, 4.91; N, 10.57%. Calcd for $C_{14}H_{12}O_3N_2$: C, 65.62; H, 4.72; N, 10.93%.

Methyl N-Phenylglyoxylylanthranilate Oxime (VIII). Similarly, a solution of 0.92 g (5 mmol) of II and 1.51 g (10 mmol) of methyl anthranilate in 70 m*l* of ether was left standing at room temperature for two months. Chromatography of the filtrate afforded 0.5 g (30%) of VIII, mp 162—164°C, by recrystallization from ethanol. IR (KBr) cm^{-1}: 3340 (ν_{NH}) and 1675 (ν_{CO}).

Found: C, 64.35; H, 4.75; N, 9.38%. Calcd for $C_{16}H_{14}O_4N_2$: C, 64.42; H, 4.73; N, 9.39%.

3-Benzoyl-1,4-dihydro-1,2,4-benzotriazine (IX). A similar treatment of II with *o*-phenylenediamine for 3 days afforded 75% yield of IX, mp 223—225°C, by recrystallization from a 3 : 1 mixture of benzene and ethanol. IR (KBr) cm^{-1}: 3200 (ν_{NH}) and 1640 (ν_{CO}).

Found: 71.03; H, 4.83; N, 17.57%. Calcd for $C_{14}H_{11}ON_3$: C, 70.87; H, 4.67; N, 17.71%.

Conversion of VIII to 3-Hydroxy-4-oxo-2-benzoyl-3,4-dihydroquinazoline (X). A solution of 0.2 g of VIII in 1 m*l* of concd. hydrochloric acid was warmed at 60—70°C in a sealed tube for 20 min. After cooling, the resulting crystals were collected and recrystallized from benzene - petroleum ether to afford 0.1 g (50%) of X, mp 76—78°C. IR (KBr) cm^{-1}: 3450, 2250 (broad, bound ν_{OH}[19]), 1670 and 1650 (ν_{CO}[8]).

Found: C, 67.75; H, 3.82; N, 10.60%. Calcd for $C_{15}H_{10}O_3N_2$: C, 67.66; H, 3.79; N, 10.52%.

3-Benzoyl-4-cyano-5-diethylaminoisoxazole (XI). Treatment of 1.84 g (0.01 mol) of II and 2.2 g (0.02 mol) of diethylaminocyanoacetylene[9] in 50 m*l* of ether at room temperature for one week afforded 40% yield of XI, mp 133—134°C, on chromatography. IR (KBr) cm^{-1}: 2240 (ν_{CN}) and 1650 (ν_{CO}).

18) T. Sasaki, T. Yoshioka, and K. Shoji, *J. Chem. Soc., C*, **1969**, 1086.

19) A. Dorner and K. Fisher, *Chem. Ber.*, **99**, 72 (1966).

Found: C, 66.90; H, 5.66; N, 15.62%. Calcd for $C_{15}H_{15}O_2N_3$: C, 66.90; H, 5.61; N, 15.61%.

N-Benzoylthiourethane (XII). A solution of 0.45 g (2.5 mmol) of II in 10 m*l* of methanol was added to a stirred solution of 0.35 g (5 mmol) of ammonium thiocyanate in 10 m*l* of methanol at room temperature. Chromatography afforded 0.3 g (70%) of XII, mp 98—99°C from benzene - petroleum ether, which was identical with a specimen prepared from benzoyl isothiocyanate and methanol.[20]

Reaction of II with Benzamidine. To a stirred mixture of a solution of 1.0 g of II in 30 m*l* of ether and a solution of 0.9 g of benzamidine hydrochloride in 20 m*l* of water was added a 5% aqueous potassium carbonate (1.6 g) under ice-cooling. Stirring was continued for 12 hr. Ether layer was separated, from which 0.6 g (55%) of 2,4,6-triphenyl-1,3,5-triazine, mp 240°C (lit,[21] 239°C) was isolated.

Found: C, 81.39; H, 5.03; N, 13.66%. Calcd for $C_{21}H_{15}N_3$: C, 81.53; H, 4.89; N, 13.58%.

3-Benzoyl-5-(m-nitrophenyl)-1,2,4-oxadiazole (XXI). This was prepared by refluxing in toluene for 20 hr of II with *m*-nitrobenzaldoxime and *m*-nitrobenzonitrile in 50 and 15% yields, respectively. Mp 174—175°C. IR (KBr) cm^{-1}: 1675 (ν_{CO}).

Found: C, 61.00; H, 3.21; N, 13.98%. Calcd for $C_{15}H_9O_4N_3$: C, 61.02; H, 3.07; N, 14.23%.

The *p*-nitrophenylhydrazone: mp 294—295°C.

Found: C, 58.65; H, 3.35; N, 19.47%. Calcd for $C_{21}H_{14}O_5N_6$: C, 58.60; H, 3.28; N, 19.53%.

Thermal Rearrangement of The Hydrazones of XVIII. General procedure: the hydrazone was melted with 1/3 of its weight of copper powder in a vacuum at a temperature slightly higher than the melting point for 10 min. The residue was extracted with hot ethanol to give the corresponding triazole.

Thus, 2,4-diphenyl-5-phenacyl-1,2,3-triazole (XXIII) was obtained in 50% yield as an oil from the phenylhydrazone of XVI. IR (KBr) cm^{-1}: 1685 (ν_{CO}). NMR ($CDCl_3$) τ: 5.42 (s, 2H, $-CH_2-$). Its 2,4-dinitrophenylhydrazone, mp 210—211°C.

Found: C, 64.87; H, 4.22; N, 18.52%. Calcd for $C_{28}H_{21}O_4N_7$: C, 64.79; H, 4.08; N, 18.89%.

A similar treatment of the *p*-nitrophenylhydrazone of XVIII afforded a quantitative yield of 2-(*p*-nitrophenyl)-4-phenyl-5-phenacyl-1,2,3-triazole (XXII), mp 137—138°C. UV λ_{max}^{EtOH} mμ (ε): 332 (22300), 242 (14800), and 230 (14200). IR (KBr) cm^{-1}: 1680 (νC_{CO}). NMR ($CDCl_3$) τ: 5.38 (s, 2H, $-CH_2-$).

Found: C, 68.75; H, 4.33; N, 14.44%. Calcd for $C_{22}H_{16}O_3N_4$: C, 68.74; H, 4.20; N, 14.58%.

Basic Rearrangement. The *p*-nitrophenylhydrazone of XVIII was dissolved in a minimum amount of acetone containing one drop of concd. ammonium hydroxide. The solution was refluxed for 5 hr; during that time the solution was kept alkaline by occasional addition of concd. ammonium hydroxide to the solution. By this procedure a quantitative yield of XXII was obtained.

Thermal and Basic Treatment of The p-Nitrophenylhydrazone of XXI. Similar thermal and basic treatments afforded XXIV, mp 280—281°C. IR (KBr) cm^{-1}: 3180 (ν_{NH}) and 1670 (ν_{CO}).

Found: 58.95; H, 3.54; N, 19.25%. Calcd for $C_{21}H_{14}O_5N_6$: C, 58.60; H, 3.28; N, 19.53%.

Photochemistry of XVIII. General procedure: A 0.01 mol/*l* solution of XVIII in a given solvent was irradiated at room temperature under nitrogen stream for a given reaction time. The resulting precipitates were filtered and recrystallized from ethanol - benzene to afford XXV, mp 134—136°C. IR (KBr) cm^{-1}: 1650 (ν_{CO}).

Found: C, 76.77; H, 4.45; N, 5.17%. Calcd for $C_{16}H_{11}O_2N$: C, 77.09; H, 4.45; N, 5.62%.

The solvent was removed from the filtrate and the residue was chromatographed. The first fraction gave unreacted starting material. Then, dibenzoylacetonitrile, mp 160°C,[22] XXV and benzoic acid were successively isolated.

Dibenzoylacetonitrile. IR (KBr) cm^{-1}: 3400 (broad, ν_{OH})[23] and 2220 (ν_{CN}).

Found: C, 77.32; H, 4.47; N, 5.85%. Calcd for $C_{16}H_{11}O_2N$: C, 77.09; H, 4.45; N, 5.62%.

When XVIII was irradiated with a 60-W low pressure mercury lamp in benzene, the main product was *N*-benzoylbenzoylacetamide, mp 170°C.[24] IR (KBr) cm^{-1}: 3250 (ν_{NH}), 1705 and 1680 (ν_{CO}). NMR (DMSO-d_6) τ: −0.82 (NH) and 5.42 ($-CH_2-$).

Found: C, 71.55; H, 4.86; N, 5.53%. Calcd for $C_{16}H_{13}O_3N$: C, 71.90; H, 4.90; N, 5.24%.

The results are summarized in Table 2.

N-Phenylglyoxylylaziridine Oxime (XXVI) and Its O-p-Nitrobenzoate (XXVII). To a stirred solution of 0.92 g (0.005 mol) of II in 50 m*l* of ether was added dropwise a solution of 1 m*l* of aziridine in 50 m*l* of ether under ice-cooling. The mixture was stirred for 30 min at this temperature and then for 24 hr at room temperature. After removal of the precipitates, the filtrate was concentrated to give 80% yield of XXVI as an oil. IR (neat) cm^{-1}: 3325 (ν_{OH}). NMR ($CDCl_3$) τ: 7.64 (s, 1H, OH) and 7.74 (s, 4H, $-CH_2-CH_2-$).[25]

To a stirred solution of 0.5 g (0.0025 mol) of XXVI and 0.5 g (0.05 mol) of triethylamine in 40 m*l* of dry benzene was added a solution of 0.5 g (0.0025 mol) of *p*-nitrobenzoyl chloride in 20 m*l* of dry benzene under ice-cooling. The reaction mixture was left standing overnight. After the solution was saturated with dry hydrogen chloride gas, the precipitates were filtered and the filtrate was concentrated. The residue was chromatographed to afford 0.41 g (50%) of XXVII, mp 147—149°C, by recrystallization from benzene - petroleum ether. IR (KBr) cm^{-1}: 1750 and 1665 (ν_{CO}). NMR ($CDCl_3$) τ: 7.42 (s, 4H, $-CH_2-CH_2-$).[25]

Found: C, 59.93; H, 3.94; N, 12.40%. Calcd for $C_{17}H_{13}O_5N_3$: C, 60.17; H, 3.86; N, 12.39%.

2-Benzoyloxazoline (XXVIII). A solution of 0.7 g of XXVI in 30 m*l* of acetone was refluxed in the presence of 0.2 g of sodium iodide for 30 min. The filtered solution was concentrated and chromatographed to give an oil (XXVIII). IR (neat) cm^{-1}: 1640 (ν_{CO}) and 1610 ($\nu_{C=N}$). Its picrate, mp 179—180°C; the yield was 0.3 g (25%). NMR (DMSO-d_6) τ: 4.8—5.6 (m, 4H, $-CH_2-CH_2-$)[26] and 1.8—2.5 (m, 5H, phenyl protons).

Found: C, 47.10; H, 3.24; N, 14.43%. Calcd for $C_{16}H_{14}O_9N_4$: C, 47.29; H, 3.47; N, 13.79%.

20) P. Miquel, *Ann. Chim.*, [v], **11**, 346 (1877).

21) B. W. Frizmmon, C. Hewlett, and R. A. Shaw, *J. Chem. Soc.*, **1965**, 47779.

22) Mp 156.5°C: E. v. Mayer, *J. prakt. Chem.*, [2], **42**, 267 (1890).

23) This indicates the presence of the tautomerism:

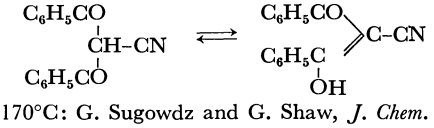

24) Mp 170°C: G. Sugowdz and G. Shaw, *J. Chem. Soc.*, **1954**, 665.

25) Equivalent two methylene protons of the aziridine ring are characteristics in these compounds. See H. Kessler, *Angew. Chem.*, **82**, 237 (1970).

26) Non-equivalent two methylene protons are a good proof of the aziridine ring rupture.

Reactions of Sulfonium and Pyridinium Salts with Alkyl Nitrite

Teruaki MUKAIYAMA, Kazuhiko SAIGO, and Hisashi TAKEI

Laboratory of Organic Chemistry, Tokyo Institute of Technology, Ookayama, Meguro-ku, Tokyo

(Received July 18, 1970)

It was found that α-bromo-α-hydroxyimino compounds were obtained in good yields by the reactions of sulfonium bromides, such as dimethylphenacylsulfonium bromide, acetonyldimethylsulfonium bromide and ethoxycarbonylmethyldimethylsulfonium bromide, with isopropyl nitrite. On the other hand, (α-hydroxyiminophenacyl and -acetonyl)pyridinium bromides were obtained in quantitative yields by the reactions of pyridinium bromides, such as phenacylpyridinium bromide and acetonylpyridinium bromide, with isopropyl nitrite. Further, the reactions of α-bromo-α-hydroxyimino compound or (α-hydroxyiminophenacyl)pyridinium bromide, which were obtained by the above mentioned reactions, with several nucleophiles were studied.

It is well known that dimethylphenacylsulfonium salt affords the corresponding stable ylide by treatment with alkali. The result indicates that hydrogen atom attached to α-carbon of the sulfonium salt becomes acidic by the influence of both positively charged sulfur atom and carbonyl group.

In the present experiment, the reactions of sulfonium salts with alkyl nitrite were tried in order to prepare hydroxyimino derivatives of the sulfonium compounds and to examine their reactions. When a mixture of phenacylsulfonium bromide (Ia) and isopropyl nitrite (II) in dichloromethane was stirred at room temperature, evolution of dimethyl sulfide was observed. After removal of the solvent, α-bromo-α-hydroxyiminoacetophenone (IVa) (93%) was unexpectedly obtained. It was identified by mixed melting point with authentic sample.[1] This result shows that the reaction proceeds by eliminating dimethyl sulfide from the initially formed α-hydroxyiminosulfonium salt by an intramolecular nucleophilic displacement with bromide ion. Similarly, α-bromo-α-hydroxyiminoacetone (IVb) and ethyl α-bromo-α-hydroxyiminoacetate (IVc) were obtained in quantitative yields from the reactions of the corresponding sulfonium salts, acetonyldimethylsulfonium bromide (Ib) and ethoxycarbonylmethyldimethylsulfonium bromide (Ic), with isopropyl nitrite. According to this method, α-bromo-α-hydroxyimino compounds can be prepared in higher yields than the previous methods.[1-3] Whereas, the reaction of benzyldimethylsulfonium bromide with isopropyl nitrite could not be observed and the starting materials were recovered quantitatively.

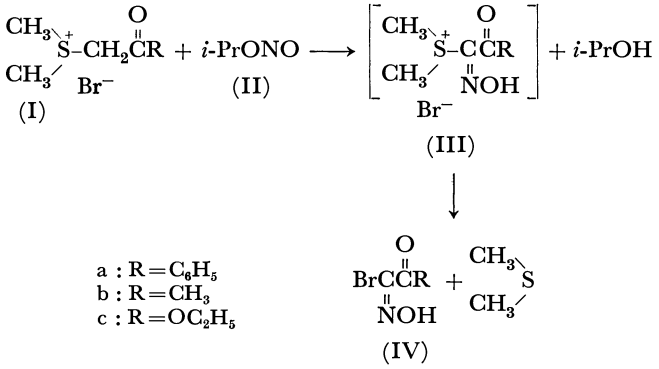

(I) (II) (III) (IV)

Then, the same reactions by the use of sulfonium tetrafluoroborates were tried with the expectation that the nucleophilic displacement by tetrafluoroborate anion at α-carbon of the sulfonium salts would be obstructed because of its lower nucleophilicity. But, α-hydroxyiminosulfonium tetrafluoroborates could not be obtained by the reactions of the sulfonium tetrafluoroborates, such as dimethylphenacylsulfonium tetrafluoroborate, ethoxycarbonylmethyldimethylsulfonium tetrafluoroborate and benzyldimethylsulfonium tetrafluoroborate, with isopropyl nitrite and the starting materials were recovered quantitatively.

Next, the several reactions[4] of α-bromo-α-hydroxyiminoacetophenone (IVa), produced by the above mentioned reaction, with some nucleophiles were investigated. When pyridine was added to a solution of α-bromo-α-hydroxyiminoacetophenone (IVa) in ether at room temperature, (α-hydroxyiminophenacyl)pyridinium bromide (V) precipitated readily in a quantitative yield. Similarly, when a solution of sodium thiophenolate in ethanol was added to a solution of α-bromo-α-hydroxyiminoacetophenone (IVa) in ethanol at 0°C, the yellow crystals, α-hydroxyimino-α-phenylthioacetophenone (VI), was obtained in an almost quantitative yield after removal of the solvent under reduced pressure.

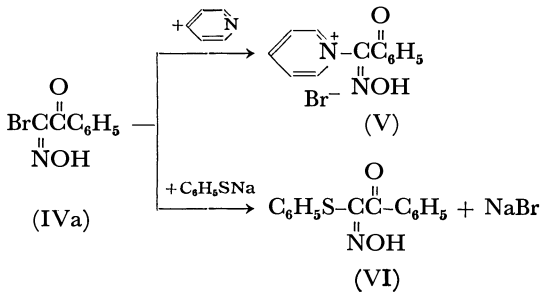

(IVa) (V) (VI)

On the other hand, it was found that dibenzoylfuroxane (VIII) was obtained in 48% yield by treating α-bromo-α-hydroxyiminoacetophenone (IVa) with an equimolar amount of triethylamine in ether. This result indicates that benzoyl cyanide *N*-oxide (VII) is formed as an intermediate by the elimination of hydrogen bromide from α-bromo-α-hydroxyiminoaceto-

1) G. C. Singhal and M. M. Bokadia, *J. Indian. Chem. Soc.*, **35**, 893 (1958).
2) G. C. Singhal and M. M. Bokadia, *ibid.*, **35**, 898 (1958).
3) M. Z. Jowitschitsch, *Ber.*, **39**, 785 (1906).
4) There has been recently reported by Dornow that α-anilino-α-hydroxyiminoacetophenone was obtained in good yield by the reaction of α-bromo-α-hydroxyiminoacetophenone with aniline. A. Dornow and W. Sassenberg, *Ann. Chem.*, **594**, 185 (1955).

phenone when it is treated with base. Similarly, by the reaction of α-bromo-α-hydroxyiminoacetophenone (IVa) with sodium salt of dibenzoylmethane, dibenzoylfuroxane (VIII) and dibenzoylmethane (IX) were obtained in 62% and 90% yields. In this reaction, sodium salt of dibenzoylmethane behaved as a base to accept hydrogen bromide from α-bromo-α-hydroxyiminoacetophenone instead of a nucleophilic reagent.

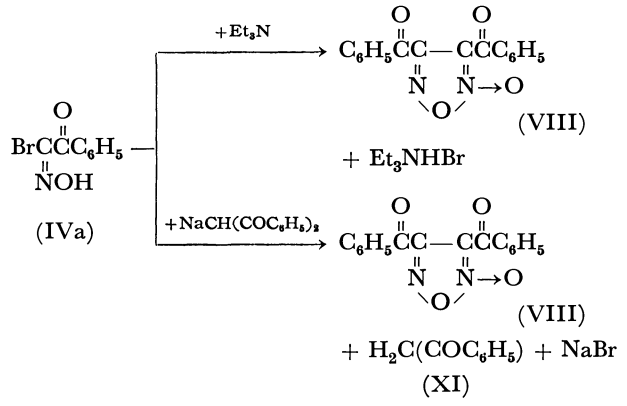

Next, the reactions of pyridinium bromides with isopropyl nitrite were tried with the expectation that the nucleophilic displacement by bromide ion at α-carbon of pyridinium salt would not occur because of the lower activity of α-carbon of the pyridinium salts than that of the sulfonium salts described before. When a mixture of phenacylpyridinium bromide (Xa) and isopropyl nitrite (II) in ethanol was allowed to stand at room temperature, the crystalline, (α-hydroxyiminophenacyl)pyridinium bromide (XIa) was obtained in a quantitative yield. Similarly (α-hydroxyiminoacetonyl)pyridinium bromide (XIb) was quantitatively obtained by the reaction of acetonylpyridinium bromide (Xb) with isopropyl nitrite (II). They were identified by the IR spectra and the elemental analyses. Whereas, ethoxycarbonylhydroxyiminomethylpyridinium bromide could not be isolated by the reaction of ethoxycarbonylmethylpyridinium bromide with isopropyl nitrite and the starting materials were recovered quantitatively.

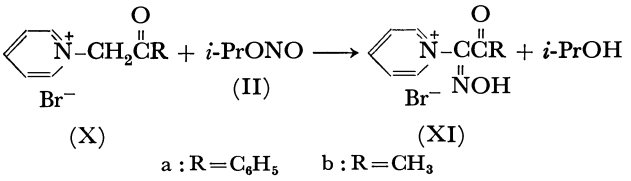

Then, the reactions of (α-hydroxyiminophenacyl)-pyridinium bromide, produced by the above mentioned reaction, with nucleophilic reagents were investigated. When a mixture of (α-hydroxyiminophenacyl)pyridinium bromide (XIa) and sodium thiophenolate in ethanol was allowed to stand at room temperature, α-hydroxyimino-α-phenylthioacetophenone (VI) was obtained in 71% yield. This was identical with that prepared by the reaction of α-bromo-α-hydroxyiminoacetophenone and sodium thiophenolate. Similarly, α-anilino-α-hydroxyiminoacetophenone (XII) was produced in 65% yield by the reaction of (α-hydroxyiminophenacyl)-pyridinium bromide (XIa) with two equimolar amounts of aniline in ethanol at room temperature. These reactions indicate that pyridine can be easily eliminated from the pyridinium salt by the nucleophilic displacement of the nucleophiles, such as aniline and sodium thiophenolate.

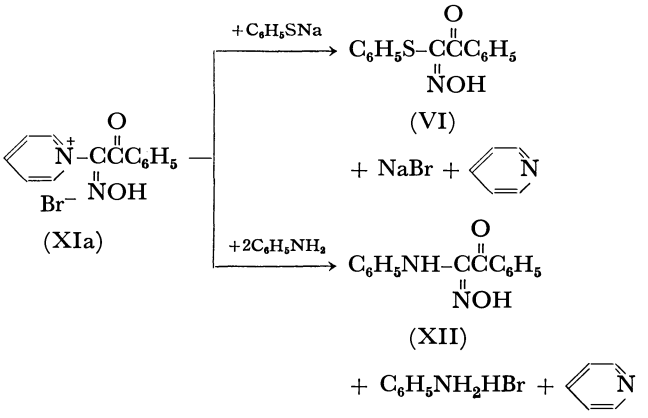

Experimental

Reaction of Dimethylphenacylsulfonium Bromide with Isopropyl Nitrite. A mixture of dimethylphenacylsulfonium bromide (1.31 g, 0.005 mol) and excess isopropyl nitrite (0.89 g, 0.01 mol) was stirred in dichloromethane (100 m*l*) for 12 hr at room temperature. The evolution of dimethyl sulfide was observed by its characteristic odor accompanied with disappearance of the crystals of the sulfonium salt. Evaporation of the solvent under reduced pressure gave white crystals, α-bromo-α-hydroxyiminoacetophenone (mp 138—139°C), 1.07 g (93%), recrystallized from cyclohexane. Similarly, various α-bromo-α-hydroxyimino compounds were obtained by the reactions of sulfonium bromides with isopropyl nitrite. The results are listed in Table 1. The α-bromo-α-hydroxyimino compounds were identified by their IR spectra and elemental analyses.

Table 1. The reaction of sulfonium bromides with isopropyl nitrite

Sulfonium bromide	Reaction time	Solvent	Yield	Mp, °C
$CH_3S^+(CH_3)CH_2COC_6H_5\ Br^-$	12 hr	CH_2Cl_2	93%	138—139
$CH_3S^+(CH_3)CH_2COCH_3\ Br^-$	1 day	CH_2Cl_2	quant.	119—120
$CH_3S^+(CH_3)CH_2COC_2H_5\ Br^-$	1 day	CH_2Cl_2	quant.	92—93

Reaction of α-Bromo-α-hydroxyiminoacetophenone with Pyridine. Into a solution of α-bromo-α-hydroxyiminoacetophenone (0.43 g, 0.0019 mol) in ether (50 m*l*), a solution of pyridine (0.15 g, 0.0019 mol) in ether (10 m*l*) was added drop by drop with stirring. After stirring for 30 min at room temperature, white precipitate deposited. The precipitate was collected by filtration and recrystallized from ethanol to give (α-hydroxyiminophenacyl)pyridinium bromide (mp 143.5°C (dec.)) in a quantitative yield.

Found: C, 51.07; H, 3.36; N, 9.31%. Calcd for $C_{13}H_{11}BrN_2O_2$: C, 50.83; H, 3.61; N, 9.12%.

Reaction of α-Bromo-α-hydroxyiminoacetophenone with Sodium Thiophenolate. A solution of sodium thiophenolate (0.66 g, 0.005 mol) in ethanol (50 m*l*) was added dropwise to a solution of α-bromo-α-hydroxyiminoacetophenone (1.14 g, 0.005 mol) in ethanol (50 m*l*) with stirring. After stirring for 12 hr at room temperature, solvent was evaporated. The residue was washed with water (100 m*l*) and extracted with ether (100 m*l*). Then, the solvent was evaporated under reduced pressure to give yellow crystals. Recrystallization from cyclohexane gave α-hydroxyimino-α-phenylthioacetophenone (mp 110—111°C) in an almost quantitative yield.

Found: C, 65.49; H, 4.56; N, 5.35; S, 12.20%. Calcd for $C_{14}H_{11}NO_2S$: C, 65.36; H, 4.31; N, 5.45; S, 12.44%.

Reaction of α-Bromo-α-hydroxyiminoacetophenone with Triethylamine. Into a solution of α-bromo-α-hydroxyiminoacetophenone (1.12 g, 0.005 mol) in ether (50 m*l*), an equimolar amount of triethylamine was added with stirring. The reaction mixture was stirred for 1 day at room temperature. After removal of the solvent, the residue was chromatographed on silica gel and elution with benzene gave dibenzoylfuroxane (mp 86—87°C, 48%).

Found: C, 65.51; H, 3.25; N, 9.27%. Calcd for $C_{16}H_{10}N_2O_4$: C, 65.30; H, 3.43; N, 9.52%.

Reaction of Phenacylpyridinium Bromide with Isopropyl Nitrite. A mixture of phenacylpyridinium bromide (2.78 g, 0.01 mol) and excess amount of isopropyl nitrite (1.78 g, 0.02 mol) in ethanol (50 m*l*) was stirred for 1 day at room temperature. After removal of the solvent, white crystals were obtained. Recrystallization from ethanol gave (α-hydroxyiminophenacyl)pyridinium bromide (mp 143.5°C (dec.)) in a quantitative yield. By a similar procedure, (α-hydroxyiminoacetonyl)-pyridinium bromide (mp 73.5—74.0°C) was obtained quantitatively.

Found: C, 39.48; H, 3.59; N, 11.36%. Calcd for $C_8H_9BrN_2O_2$: C, 39.20; H, 3.70; N, 11.43%.

Reaction of (α-Hydroxyiminophenacyl)pyridinium Bromide with Sodium Thiophenolate. To a suspension of (α-hydroxyiminophenacyl)pyridinium bromide (3.07 g, 0.01 mol) in ethanol (50 m*l*), a solution of sodium thiophenolate (1.32 g, 0.01 mol) in ethanol (20 m*l*) was added with stirring. After stirring for 12 hr, crystals of (α-hydroxyiminophenacyl)pyridinium bromide disappeared. The residue was chromatographed on silica gel after removal of the solvent under reduced pressure, and elution with dichloromethane gave yellow crystals, α-hydroxyimino-α-phenylthioacetophenone (mp 110—111°C), 1.82 g (71%).

Reaction of (α-Hydroxyiminophenacyl)pyridinium Bromide with Aniline. A mixture of (α-hydroxyiminophenacyl)pyridinium bromide (3.07 g, 0.01 mol) and two equimolar amounts of aniline (1.86 g, 0.02 mol) in ethanol (100 m*l*) was stirred for 5 days at room temperature. After removal of the solvent, the residue was washed with water (50 m*l*) and extracted with ether (50 m*l*). Then, the solvent was evaporated and crystalline solid of α-anilino-α-hydroxyiminoacetophenone (mp 145.0—146.5°C) was obtained in 65% yield after removal of the solvent under reduced pressure.

BULLETIN OF THE CHEMICAL SOCIETY OF JAPAN, VOL. 44, 192—196 (1971)

The Preparation of 4′,6′-Di- and 2′,4′,6′-Tri-*O*-acetates of Theophylline Nucleosides of 3′-Deoxy-3′-nitro-β-D-galacto-, gluco- and mannopyranose[1]

Toshio NAKAGAWA and Tetsuyoshi TAKAMOTO

Department of Chemistry, Tokyo Institute of Technology, O-okayama, Meguro-ku, Tokyo

(Received July 18, 1970)

7-(3′-Deoxy-3′-nitro-β-D-glucopyranosyl)theophylline (**1**) was treated with acetic anhydride in the presence of boron trifluoride, perchloric or phosphoric acid as a catalyst to afford the corresponding 2′,4′,6′-tri-*O*-acetate (**4**) in 87, 60 and 48% yields, respectively. With *galacto*-isomer (**2**), tri-*O*-acetate (**6**) was obtained in a high yield by the use of phosphoric acid or a large excess of perchloric acid as a catalyst, while 4′,6′-di-*O*-acetate (**5**) was selectively prepared in 82% yield when a trace of perchloric acid was used. The similar preparation of 4′,6′-di- and 2′,4′,6′-tri-*O*-acetates (**7** and **8**) of *manno*-isomer (**3**) was also carried out in the presence of boron trifluoride and phosphoric acid, respectively. The positions of the acetyl groups in the diacetates **5** and **7** were unequivocally deduced from NMR data.

On the acetylation of methyl 3-deoxy-3-nitro-hexopyranosides and their 4,6-*O*-benzylidene derivatives with acetic anhydride, Baer *et al*[2] pointed out the favorableness of boron trifluoride as a catalyst and mentioned the inadvisableness of acids such as sulfuric or perchloric acid, because these acids possess an inherent danger of acetolysis in the glycoside and benzylidene acetal structures. For the preparation of model compounds for our studies on aminations of nitro sugars,[3–5] we have examined the acid-catalysed acetylation of theophylline nucleosides of 3′-deoxy-3′-nitro-β-D-hexopyranoses (**1**—**3**) with boron trifluoride, perchloric or phosphoric acid and showed their merits, especially as a catalyst for a selective partial acetylation, and some limitations, as follows.

1) This paper was presented at the 23rd Annual Meeting of the Chemical Society of Japan, Tokyo, April, 1970.

2) H.H. Baer, F. Kienzle, and F. Rajabalee, *Can. J. Chem.*, **46**, 80 (1968).

3) T. Nakagawa, T. Sakakibara, and S. Kumazawa, *Tetrahedron Lett.*, **1970**, 1645.

4) T. Nakagawa, T. Sakakibara, and F. W. Lichtenthaler, This Bulletin, **43**, 3681 (1970).

5) T. Nakagawa, Y. Sato, T. Takamoto, F.W. Lichtenthaler, and N. Majer, *ibid.*, **43**, 3866 (1970).

Results and Discussion

Preparation of Acetates. When 7-(3′-deoxy-3′-nitro-β-D-glucopyranosyl)theophylline (**1**) was treated with acetic anhydride in the presence of boron trifluoride, the corresponding 2′,4′,6′-tri-*O*-acetate (**4**) was easily prepared in 87% yield, a favorable result over those in the case of perchloric or phosphoric acid (yields of **4**: 60 and 48%, respectively) as Baer *et al.* pointed out.[2]

The similar treatment of *galacto*-isomer **2** with boron trifluoride did not afford a single product but a mixture of two or more components including di- and tri-*O*-acetates of **2**. All attempts to isolate these components by a fractional recrystallisation were unsuccessful. When **2** was treated with acetic anhydride in the presence of a trace of perchloric acid, unexpected 4′,6′-di-*O*-acetate **5** was selectively prepared in 82% yield. If a large excess (*ca.* a molar amount) of this catalyst was used, only 2′,4′,6′-tri-*O*-acetate **6** precipitated in 89% yield. The triacetate **6** was also prepared in 60% yield by Fatiadi's method[6] using anhydrous phosphoric acid as a catalyst.

Similarly, the phosphoric acid-catalysed acetylation of *manno*-isomer **3** gave amorphous 2′,4′,6′-tri-*O*-acetate **8** in 45% yield, whereas 4′,6′-di-*O*-acetate **7** was exclusively obtained in 24% yield with boron trifluoride. Repeated trials of the perchloric acid-catalysed acetylation of **3** always produced a mixture of acetates containing both **7** and **8** at least on the basis of NMR spectra.

The 4′,6′-*O*-benzylidene derivatives of **1**—**3** were prepared in the usual manner and then treated with acetic anhydride in the presence of boron trifluoride to yield the corresponding 2′-*O*-acetyl-4′,6′-benzylidene derivatives (**12**—**14**), which were submitted for NMR studies described below.

NMR Studies. Recently, Lichtenthaler *et al.*[7,8] summarized the relationship between chemical shifts of the methyl resonances of *O*- and *N*-acetyl groups and their conformations in a series of pyranose- and cyclitolpolyacetates: In deuteriochloroform ($CDCl_3$), axial *O*-acetyl groups of polyacetates of sugars and aminosugars appear generally in a region of τ 7.80—7.87, equatorial *N*-acetyl groups in a relatively higher field, τ 8.03—8.10 and equatorial *O*-acetyl (including 6-*O*-acetyl group of aldopyranose derivatives) and axial *N*-acetyl groups in a middle region, τ 7.87—8.02.[8] By changing the solvent to dimethylsulfoxide-d_6 (DMSO-d_6) a diamagnetical shift of the signals of *O*-acetyl groups is in general permissible (0.05 ppm), but that of *N*-acetyl groups appreciable (ordinarily 0.15 ppm).[8] In the case of fully acetylated hexopyranosyl nucleosides, the anisotropy of the bases causes a diamagnetical shift of the 2′-acetyl singnals, *i.e.* generally in pyrimidines 0.1 ppm; in purines 0.3 ppm.[8]

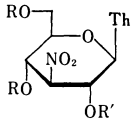

1 R=R′=H
4 R=R′=Ac
9 RR=PhCH<; R′=H
12 RR=PhCH<; R′=Ac

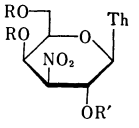

2 R=R′=H
5 R=Ac; R′=H
6 R=R′=Ac
10 RR=PhCH<; R′=H
13 RR=PhCH<; R′=Ac

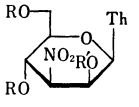

3 R=R′=H
7 R=Ac; R′=H
8 R=R′=Ac
11 RR=PhCH<; R′=H
14 RR=PhCH<; R′=Ac

Th=

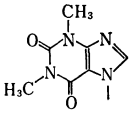

The lowest one of the three acetyl signals of *galacto*-isomer **6** (τ 7.82 in $CDCl_3$ and τ 7.86 in DMSO-d_6) is assigned to the axial 4′-*O*-acetyl group, the middle signal (τ 7.95 in $CDCl_3$ and τ 8.02 in DMSO-d_6) to the 6′-*O*-acetyl group, and the highest one (τ 8.11 in $CDCl_3$ and τ 8.18 in DMSO-d_6) to the equatorial 2′-*O*-acetyl group. These assignments are also confirmed by the facts that the 2′-*O*-acetyl signal of **13** appears at τ 8.11 in $CDCl_3$ and τ 8.20 in DMSO-d_6. The *galacto*-diacetate **5** has two acetyl signals at τ 7.82 and 7.94 in $CDCl_3$, and at τ 7.86 and 8.01 in DMSO-d_6, which are easily assigned to the 4′- and 6′-*O*-acetyl

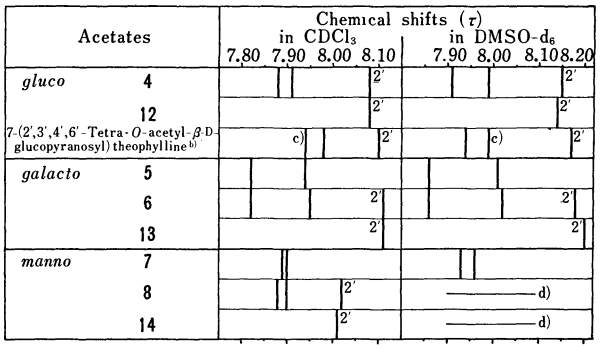

Fig. 1. Acetyl resonances of the acetates of 3′-deoxy-3′-nitro-β-D-hexopyranosyl theophylline at 100 MHz[a]
a) TMS as an internal standard.
b) Values cited in Ref. 9 (at 60 MHz).
c) 6H-Intensity.
d) Decomposition and/or acetyl migration occurred in DMSO in a considerable extent and complex spectra were observed.

6) A. J. Fatiadi, *Carbohyd. Res.*, **6**, 237 (1968).
7) F. W. Lichtenthaler and P. Emig, *Tetrahedron Lett.*, **1967**, 577; *Carbohyd. Res.*, **7**, 121 (1968).
8) F. W. Lichtenthaler, G. Bambach, and P. Emig, *Chem. Ber.*, **102**, 994 (1969).
9) F. W. Lichtenthaler and T. Nakagawa, *ibid.*, **100**, 1833 (1967).

TABLE 1. COMPARISON OF CHEMICAL SHIFTS OF THE RING PROTONS OF DIACETATES **5** AND **7** WITH THOSE OF TRIACETATES **6** AND **8**[a)]

Acetates	τ-Values in $CDCl_3$				τ-Values in DMSO-d_6			
	$H^{1'}$	$H^{2'}$	$H^{3'}$	$H^{4'}$	$H^{1'}$	$H^{2'}$	$H^{3'}$	$H^{4'}$
galacto **5**	3.94	(5.0—5.1)		3.98	4.06	4.99	4.53	4.28
6	3.71	3.77	4.84	3.95	(3.7—3.9)		4.08	4.14
Δτ	0.23	1.2—1.3	0.2—0.3	0.03	0.2—0.4	1.1—1.3	0.45	0.14
manno **7**	3.79	(5.0—5.1)		*ca.* 4.1	3.67	5.36	4.30	3.70
8	3.58	3.84	4.48	4.13	[b)]			
Δτ	0.21	1.2—1.3	0.2—0.3	0.0				

a) Assignments of the spectra are based on a first-oder analysis.
b) See footnote d) in Fig. 1.

groups, respectively, and shows no diamagnetically shifted signal corresponding to the 2'-*O*-acetyl group (*cf.* Fig. 1). Therefore, the structure of **5** is unequivocally deduced to be 4',6'-di-*O*-acetate.

On the other hand, the diamagnetically shifted axial 2'-*O*-acetyl signal of the *manno*-isomers appears at τ *ca.* 8.0 in $CDCl_3$ (*i. e.* compound **14**; τ 8.01: **8**; τ 8.02). From this reason, the two acetyl signals of *manno*-diacetate **7** (τ 7.89 and 7.90 in $CDCl_3$; τ 7.93 and 7.96 in DMSO-d_6) are assigned to the equatorial 4'- and 6'-*O*-acetyl groups and, therefore, the axial hydroxyl group on *C*-2' is free, which indicates the structure of **7** also to be 4',6'-di-*O*-acetate.

These structural elucidations of diacetates **5** and **7** are further confirmed by considerations on the spectra of their ring protons on *C*-2':

a) Their signals, resonated in DMSO-d_6 at τ 4.99 and 5.36 in **5** and **7**, respectively, appear as diffused bands as a result of the coupling with the 2'-hydroxylic proton in the presence of a trace of water in the solvent[10] (*cf.* Figs. 2 and 3);

b) On acetylation (**5**→**6**; **7**→**8**) the chemical shift of the proton on *C*-2' moves paramagnetically in a

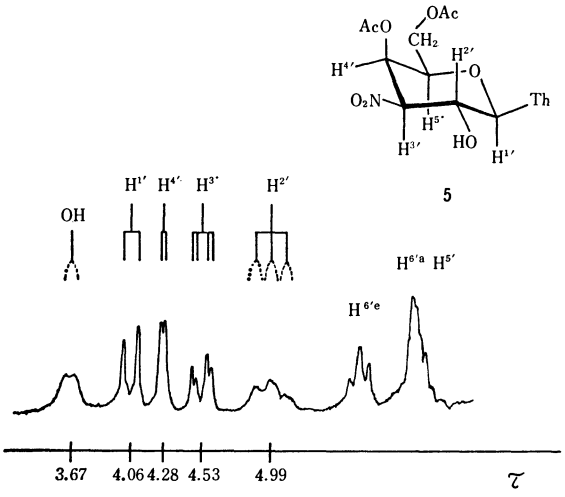

Fig. 2. NMR spectra of ring protons of *galacto*-diacetate **5** (100MHz; in DMSO-d_6).
$J_{1'2'}$: 9 Hz $J_{2'3'}$: 10 $J_{3'4'}$: 2.5 $J_{4'5'}$: ~0

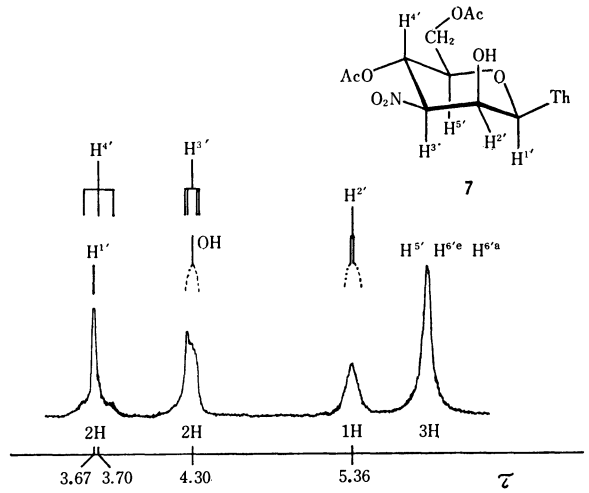

Fig. 3. NMR spectra of ring protons of *manno*-diacetate **7** (100 MHz; in DMSO-d_6).
$J_{1'2'}$: 1 (?) Hz $J_{2'3'}$: 2 (?) $J_{3'4'}=J_{4'5'}$: 10

considerable extent, 1.1—1.3 ppm,[11] and this effect diminishes remarkably with the degree of the distance from the 2'-carbon atom along the C–C bond, *i. e.* 0.2—0.45 ppm for $H^{1'}$ and $H^{3'}$; 0.0—0.14 ppm for $H^{4'}$ (Table 1), all of which indicate clearly the 2'-hydroxyl group in **5** and **7** to be free.

Experimental

General. All melting points were determined in a capillary and uncorrected. Optical rotations were measured with a CARL ZEISS photoelectric polarimeter. NMR spectra were recorded at 100 MHz with a JEOL spectrometer (Type JNM-4H-100), using tetramethyl silane as an internal standard.

7-(2',4',6'-Tri-O-acetyl-3'-deoxy-3'-nitro-β-D-glucopyranosyl)-theophylline (4). *a) Catalysed by Boron Trifluoride*: To a stirred suspension of **1**[9] (3.0 g, 8.1 mmol) in acetic anhydride (7 ml) was added boron trifluoride etherate (*ca.* 0.3 ml) dropwise. After standing overnight at room temperature the mixture was poured into ice water (200 ml) with sitrring. The acetate separated in gel-like form while the excess anhydride decomposed, was collected by filtration, suspended again in

10) L. M. Jackman, "Applications of Nuclear Magnetic Resonance Spectroscopy in Organic Chemistry," Pergamon Press, London (1959), p. 26—28.

11) Acylation of secondary alcohols causes the chemical shift of the α-proton to move paramagnetically by 1.0—1.15 τ and this effect is the same for axial and equatorial protons in steroid molecules [Ref. 10, p. 55; J. N. Shoolery and M. T. Rogers, *J. Amer. Chem. Soc.*, **80**, 5121 (1958)].

water (50 m*l*) with vigorous stirring and then filtered. After thorough washing with water and drying *in vacuo* at 40—50°C, the resulting colorless powder (3.5 g, 87%) was analytically pure. All attempts to crystallize were unsuccessful. $[\alpha]_D^{20}$ −7.4° (*c* 1.0, $CHCl_3$). IR (KBr): 1750 cm^{-1} ($\nu_{C=O}$ of Ac). NMR ($CDCl_3$): 3.73 (1H-*d*, $J_{1'2'}=9$ Hz, H$^{1'}$); 4.93 τ (1H-*t*, $J_{2'3'}=J_{3'4'}=10$ Hz, H$^{3'}$).

Found: C, 45.72; H, 4.72; N, 14.26%. Calcd for $C_{19}H_{23}O_{11}N_5$: C, 45.85; H, 4.66; N, 14.08%.

b) Catalysed by Perchloric Acid: To a well stirred suspension of **1**[9] (1.0 g, 2.7 mmol) in acetic anhydride (4 m*l*) were added two drops of 70% perchloric acid. The mixture was stirred for additional 12 hr at room temperature and then worked up as described above to yield 0.80 g (60%) of colorless powder, which was identified with the product obtained above.

c) Catalysed by Phosphoric Acid: To a mixture of Fatiadi's catalyst[6] (1 m*l*) and acetic anhydride (4 m*l*) was added **1**[9] (0.50 g, 1.35 mmol) and warmed with stirring at 50°C for 1 hr. The mixture was then worked up as described under *a*): Yield 0.32 g (48%).

*7-(2′,4′,6′-Tri-O-acetyl-3′-deoxy-3′-nitro-β-D-galactopyranosyl)-theophylline (**6**).* *a) In the Presence of a Large Excess of Perchloric Acid*: To a well stirred suspension of **2**[9] (2.0 g, 5.4 mmol) in acetic anhydride (8 m*l*) was added 70% perchloric acid (4.6 m*l*, 5.4 mmol) dropwise. The mixture became immediately a clear solution and then the acetate precipitated in crystalline form, which was filtered after stirring for 1 hr and washed well with ether. Additional crystals were deposited by further addition of 70% perchloric acid (3.0 m*l*) into the filtrate, filtered and washed with ether. The combined crystals were suspended in cold water (30 m*l*) with vigorous stirring for 1 hr, filtered, washed with water and then dried *in vacuo* at 50°C: 2.4 g (89%) of analytically almost pure, colorless needles, mp 191—193°C (decomp.).

Found: C, 45.95; H, 5.13; N, 14.02%. Calcd for $C_{19}H_{23}O_{11}N_5$: C, 45.85; H, 4.66; N, 14.08%.

Recrystallization from ethanol gave needles with lowered mp: 188—189°C (decomp.); $[\alpha]_D^{20}$ −1.8° (*c* 1.1, $CHCl_3$). (IR) (KBr): 1760 cm^{-1} ($\nu_{C=O}$ of Ac). NMR ($CDCl_3$): 3.71 (1H-*d*, $J_{1'2'}=9$ Hz, H$^{1'}$); 4.84 τ (1H-*q*, $J_{2'3'}=10$, $J_{3'4'}=3$ Hz, H$^{3'}$). Found: C, 45.75; H, 4.50; N, 14.17%.

b) Catalysed by Phosphoric Acid: To a mixture of Fatiadi's catalyst[6] (5 m*l*) and acetic anhydride (20 m*l*) was added **2**[9] (2.5 g, 6.7 mmol) and warmed with stirring at 50°C for 1.5 hr. The reaction mixture was poured into ice water with stirring and the resulting precipitates were filtered. Recrystallisation from ethanol gave 2.0 g (60%) of colorless needles, which were identified with the product obtained above.

*7-(2′,4′,6′-Tri-O-acetyl-3′-deoxy-3′-nitro-β-D-mannopyranosyl)-theophylline (**8**).* To a mixture of Fatiadi's catalyst[6] (2 m*l*) and acetic anhydride (8 m*l*) was added **3**[9] (1.0 g, 2.7 mmol) and stirred at room temperature for 1 hr. The reaction mixture was poured into ice water (100 m*l*) and stirred vigorously for 0.5 hr. The water layer was removed by decantation and the remnant was stirred with new cold water again. This operation was repeated three times more to afford colorless powder, which was collected by filtration and dried *in vacuo* at room temperature over phosphorous pentoxide: Yield 0.60 g (45%). The product obtained was analyticallly pure, but all attempts to crystallize were unsuccessful. $[\alpha]_D^{20}$ +108.6°C (*c* 1.0, $CHCl_3$). IR (KBr): 1750 cm^{-1} ($\nu_{C=O}$ of Ac). NMR ($CDCl_3$): 3.58 (1H-*d*, $J_{1'2'}=1.5$ Hz, H$^{1'}$); 4.84 τ (1H-*q*, $J_{2'3'}=3.5$, $J_{3'4'}=10.5$ Hz, H$^{3'}$).

Found: C, 45.56; H, 4.44; N, 14.38%. Calcd for $C_{19}H_{23}O_{11}N_5$: C, 45.85; H, 4.66; N, 14.08%.

*7-(4′,6′-Di-O-acetyl-3′-deoxy-3′-nitro-β-D-galactopyranosyl)theophylline (**5**).* To a suspension of **2**[9] (1.0 g, 2.7 mmol) in acetic anhydride (7 m*l*) was added a drop of perchloric acid and stirred at room temperature for 10 hr. To the reaction mixture was added 30 m*l* of ice water with vigorous stirring and the resulting precipitates were separated, washed well with water and dried *in vacuo* at 50°C to afford analytically pure, colorless needles (1.01 g, 82%) of mp 170—171°C (decomp.). Even after recrystallisation from ethanol/petroleum ether, the melting point did not change. $[\alpha]_D^{20}$ −19.2° (*c* 0.57, dioxane). IR (KBr): 3400 (ν_{OH}); 1750 and 1730 cm^{-1} ($\nu_{C=O}$ of Ac).

Found: C, 44.84; H, 4.68; N, 15.12%. Calcd for $C_{17}H_{21}O_{10}N_5$: C, 44.84; H, 4.65; N, 15.38%.

*7-(4′,6′-Di-O-acetyl-3′-deoxy-3′-nitro-β-D-mannopyranosyl)theophylline (**7**).* To a well stirred suspension of **3**[9] (0.50 g, 1.35 mmol) in acetic anhydride (10 m*l*) was added a few drops of boron trifluoride etherate and stirred for 3.5 hr at room temperature. To the reaction mixture was added ice water (30 m*l*) and vigorously stirred for 30 min. After extraction with methylene chloride (20 m*l*×4), washing with water and drying over sodium sulfate, the organic solvent was evaporated *in vacuo* at 40°C to dryness. The remained sirup was dissolved in chloroform (2 m*l*) and then allowed to stand overnight. The acetate deposited was collected by filtration and recrystallized from methanol: 0.15 g (24%) of colorless needles; mp 203—204°C (decomp.); $[\alpha]_D^{20}$ +73.4° (*c* 1.0, dioxane). IR (KBr): 3400 (ν_{OH}), 1741 cm^{-1} ($\nu_{C=O}$ of Ac).

Found: C, 44.93; H, 4.29; N, 15.48%. Calcd for $C_{17}H_{21}O_{10}N_5$: C, 44.84; H, 4.65; N, 15.38%.

*7-(4′,6′-O-Benzylidene-3′-deoxy-3′-nitro-β-D-glucopyranosyl)theophylline (**9**).* A mixture of **1**[9] (2.5 g, 6.7 mmol) and zinc chloride (2.5 g) in freshly distilled benzaldehyde (30 m*l*) was stirred for 2 days and then poured into ice water with stirring. The precipitates were collected by filtration washed well with water and petroleum ether, and then recrystallized from ethyl acetate to afford 1.95 g (63%) of colorless crystals; mp 255°C (decomp.); $[\alpha]_D^{20}$ −64.4° (*c* 1.23, dioxane). NMR (DMSO-d_6): 2.61 (5H-nallow *m*, phenyl); 3.52 (1H-*d*, J=6 Hz, OH); 4.07 (1H-*d*, $J_{1'2'}=8$ Hz, H$^{1'}$); 4.24 (1H-*s*, PhCH〈); 4.71 (1H-*t*, $J_{2'3'}=J_{3'4'}=10$ Hz, H$^{3'}$); 4.95 τ (1H-*m*, H$^{2'}$).

Found: C, 52.57; H, 4.53; N, 15.44%. Calcd for $C_{20}H_{21}O_8N_5$: C, 52.28; H, 4.61; N, 15.25%.

*7-(4′,6′-O-Benzylidene-3′-deoxy-3′-nitro-β-D-galactopyranosyl)-theophylline (**10**).* **2**[9] (1.0 g, 2.7 mmol) was treated with freshly distilled benzaldehyde (15 m*l*) in the presence of zinc chloride (1 g) in the same manner described above and then recrystallized from ethanol/petroleum ether to yield 0.78 g (63%) of **10**; mp 224—226°C (decomp.); $[\alpha]_D^{20}$ −86.0° (*c* 1.04, dioxane). NMR (DMSO-d_6): 2.61 (5H-*m*, phenyl); 3.78 (1H-*d*, J=6 Hz, OH); 4.04 (1H-*d*, $J_{1'2'}=9$ Hz, H$^{1'}$); 4.32 (1H-*s*, PhCH〈); 4.61 (1H-*q*, $J_{2'3'}=10$, $J_{3'4'}=3.5$ Hz, H$^{3'}$); 4.90 τ (1H-*m*, H$^{2'}$).

Found: C, 52.42; H, 4.35; N, 15.36%. Calcd for $C_{20}H_{21}O_8N_5$: C, 52.28; H, 4.61; N, 15.25%.

*7-(4′,6′-O-Benzylidene-3′-deoxy-3′-nitro-β-D-mannopyranosyl)-theophylline (**11**).* **3**[9] (2.0 g, 5.4 mmol) was treated with freshly distilled benzaldehyde (30 m*l*) in the presence of zinc chloride (2.5 g) in the same manner for preparing of **9** and recrystallized from methanol: 2.0 g (81%) of colorless crystals; mp 264—266°C (decomp.); $[\alpha]_D^{20}$ +94.8° (*c* 0.65, dioxane). NMR (DMSO-d_6): 2.61 (5H-*s*, phenyl); 3.62 (1H-nallow *d*, $J_{1'2'}=1.5$ Hz, H$^{1'}$); 3.66 (1H-*d*, J= 7 Hz, OH); 4.16 (1H-*s*, PhCH〈); 4.39 τ (1H-*q*, $J_{2'3'}=3.5$, $J_{3'4'}=10$ Hz, H$^{3'}$).

Found: C, 52.14; H, 4.39; N, 15.28%. Calcd for $C_{20}H_{21}O_8N_5$: C, 52.28; H, 4.61; N, 15.25%.

*7-(2′-O-Acetyl-4′,6′-O-benzylidene-3′-deoxy-3′-nitro-β-D-glucopyranosyl)theophylline (**12**).* To a suspension of **9** (1.0 g, 2.2 mmol) in acetic anhydride (5 m*l*) was added a few drops

of boron trifluoride etherate and stirred for 1 hr at room temperature. The reaction mixture was poured into ice water with vigorous stirring and the resulting precipitates were collected by filtration, washed well with water and recrystallized from ethyl acetate/petroleum ether to yield fine, colorless needles (0.91 g, 81%); mp 209—211°C (decomp.); $[\alpha]_D^{20}$ (decomp.); −59.1° (*c* 0.6, $CHCl_3$). IR (KBr): 1750 cm^{-1} ($\nu_{c=o}$ of Ac). NMR ($CDCl_3$): 2.61 (5H-nallow *m*, phenyl); 4.37 (1H-*s*, PhCH〈); 4.96 τ (1H-*t*, $J_{2'3'}=J_{3'4'}=10$ Hz, $H^{3'}$).

Found: C, 51.91; H, 4.48; N, 13.78%. Calcd for $C_{22}H_{23}O_9N_5 \cdot 1/2H_2O$: C, 51.78; H, 4.73; N, 13.73%.

*7-(2'-O-Acetyl-4',6'-O-benzylidene-3'-deoxy-3'-nitro-β-D-galactopyranosyl)theophylline (**13**).* **10** (0.46 g, 1.0 mmol) was acetylated in the similar manner described above and then recrystallized from ethyl acetate/ethanol to afford colorless crystals (0.31 g, 60%); mp 202—204°C (decomp.); $[\alpha]_D^{20}$ −22.6° (*c* 0.40, $CHCl_3$). IR (KBr): 1750 cm^{-1} ($\nu_{c=o}$ of Ac). NMR ($CDCl_3$): 2.58 (5H-nallow *m*, phenyl); 4.39 τ (1H-*s*, PhCH〈).

Found: C, 52.43; H, 4.39; N, 14.05%. Calcd for $C_{22}H_{23}O_9N_5$: C, 52.69; H, 4.62; N, 13.97%.

*7-(2'-O-Acetyl-4',6'-O-benzylidene-3'-deoxy-3'-nitro-β-D-mannopyranosyl)theophylline (**14**).* **11** (1.0 g, 2.2 mmol) was acetylated in the similar manner for preparing of **12** and recrystallized from ethyl acetate to give colorless prisms (0.75 g, 68%); mp 238°C (decomp.); $[\alpha]_D^{20}$ +108° (*c* 0.32, $CHCl_3$). IR (KBr): 1765 cm^{-1} ($\nu_{c=o}$ of Ac). NMR ($CDCl_3$): 2.60 (5H-nallow *m*, phenyl); 3.52 (1H-*d*, $J_{1'2'}=1.5$ Hz, $H^{1'}$); 4.26 (1H-*s*, PhCH〈); 4.87 τ (1H-*q*, $J_{2'3'}=3.5$, $J_{3'4'}=10.5$ Hz, $H^{3'}$).

Found: C, 52.66; H, 4.41; N, 14.21%. Calcd for $C_{22}H_{23}O_9N_5$: C, 52.69; H, 4.62; N, 13.97%.

The authors wish to thank associate Professor Y. Ishido for his interest and Mr. K. Fukukawa for his measurements of NMR spectra.

BULLETIN OF THE CHEMICAL SOCIETY OF JAPAN, VOL. 44, 196—199 (1971)

Phosphorylation of Alcohols and Phosphates by Oxidation-Reduction Condensation

Teruaki MUKAIYAMA and Mitsunori HASHIMOTO

Laboratory of Organic Chemistry, Tokyo Institute of Technology, Ookayama, Meguro-ku, Tokyo

(Received July 20, 1970)

Phosphorylation of alcohols and phosphates forming mixed esters of phosphoric acid and pyrophosphate by the oxidation-reduction condensation with triphenylphosphine and 2,2′-dipyridyl disulfide has been investigated. *n*-Butyl *p*-nitrophenyl phosphate was obtained in 80% yield when *p*-nitrophenyl dihydrogen phosphate was treated with one equiv. each of triphenylphosphine and 2,2′-dipyridyl disulfide in the presence of three equiv. of anhydrous *n*-butyl alcohol at room temperature. It was found that P^1,P^2-bis(*p*-nitrophenyl)pyrophosphate was obtained in 91% yield when *p*-nitrophenyl dihydrogen phosphate was treated with 1.5 equiv. each of triphenylphosphine and 2,2′-dipyridyl disulfide.

Recently, it was reported that peptides are synthesized in high yields with optical purity by use of triphenylphosphine and 2,2′-dipyridyl disulfied as the coupling reagents.[1] Dehydration from free carboxylic components and free amino components proceeds by eliminating one oxygen atom (reduction) and two hydrogen atoms (oxidation) with triphenylphosphine and 2,2′-dipyridyl disulfide, respectively, to afford peptides, triphenylphosphine oxide and 2 mol of 2-mercaptopyridine.

In the present study the phosphorylation of alcohols and phosphate was investigated. It was considered that the reaction of triphenylphosphine, 2,2′-dipyridyl disulfied and phosphates would yield a reactive intermediate, phosphoryloxyphosphonium salt, which in turn would further react with alcohols of phosphate to give mixed esters of phosphates and pyrophosphate, respectively, according to the following equation.

Selective phosphrylation can be effected successfully by this method without isolating the intermediate, since it reacts exclusively with nucleophilic reagents

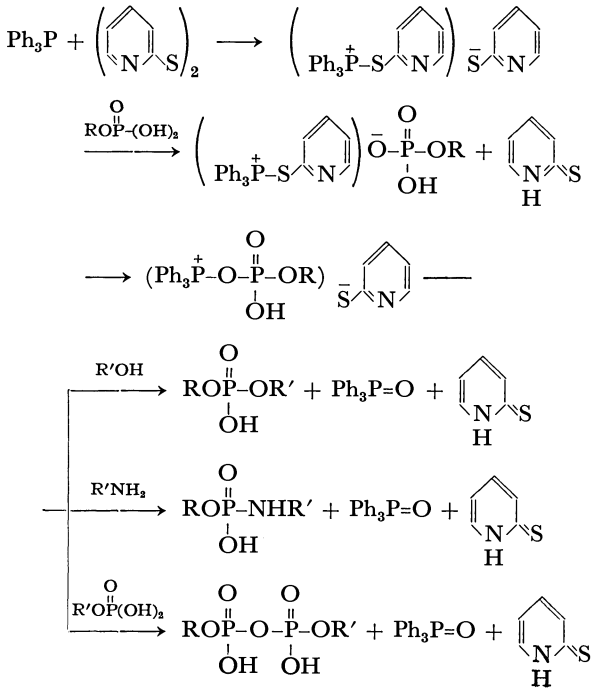

1) T. Mukaiyama, R. Matsueda, and M. Suzuki, *Tetrahedron Lett.*, **1970**, 1901.

such as alcohols, amines and phosphates under mild conditions.

When *p*-nitrophenyl dihydrogen phosphate was treated with triphenylphosphine and 2,2′-dipyridyl disulfide in excess anhydrous *n*-butyl alcohol at room temperature, an instantaneous reaction took place and *n*-butyl *p*-nitrophenyl phosphate was obtained in high yield along with a small amount of symmetrical P^1,P^2-bis(*p*-nitrophenyl) pyrophosphate.

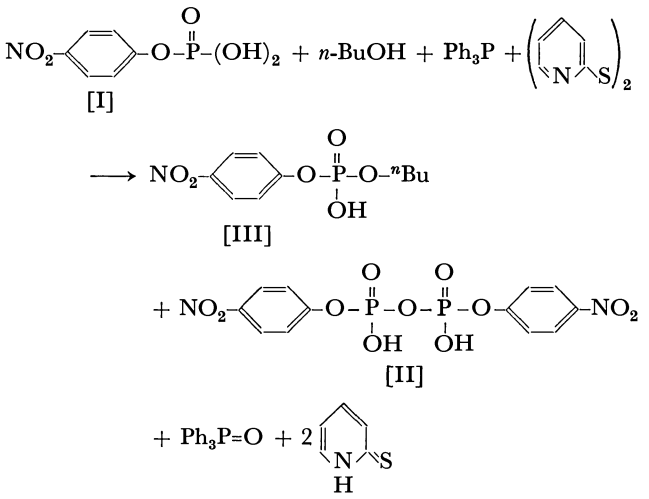

When I was treated with one equiv. each of triphenylphosphine and 2,2′-dipyridyl disulfide in the presence of ten equiv. of *n*-butyl alcohol, III was obtained in 80% yield. The results are nearly the same as those obtained when dicyclohexylcarbodiimide is used as a coupling reagent (see Table 1).

Table 1. Phosphorylation of *n*-butyl alcohol (10 equiv.) by means of triphenylphosphine (1 equiv.) and 2,2′-dipyridyl disulfide (1 equiv.)

Solvent (reaction at r.t.)	I(%)	II(%)	III(%)
THF	15	5	80
THF–  (2 : 1)	5	10	80
	5	15	80
Cf. DCC method			
THF	9	12	80

The effects of the solvent and base were examined in order to find a suitable condition for the preparation of III without accompanying the undesirable formation of II.

It was found that III was obtained in 50—70% yield together with 10—40% yield of II when phosphorylation was carried out in the presence of three equiv. of *n*-butyl alcohol (see Table 2). Of various solvents examined, it was found that the yield of II increased when pyridine is used as the solvent. However, when a catalytic amount of acetic anhydride was added to the pyridine solution, the formation of II decreased and III was obtained in fairly good yield.[2,3]

Table 2. Solvent effects in phosphorylation of *n*-butyl alcohol (3 equiv.) by means of triphenylphosphine (1 equiv.) and 2,2′-dipyridyl disulfide (1 equiv.)

Solvent	I(%)	II(%)	III(%)
THF	19	9	70
THF– 	5	30	65
	5	40	55
CH_3CN	24	25	49
DMF	40	25	35
	14	26	58
CH_2Cl_2	15	16	65
$CHCl_3$	18	20	62
	29	13	46
THF–(+ Ac_2O) (catalytic amounts)	17	2	80

Concerning the effect of bases, it was made clear that the reaction was accelerated in the presence of bases, but there was no remarkable difference on the products ratio of II to III (see Table 3).

Table 3. Effect of bases in phosphorylation of *n*-butyl alcohol (3 equiv.) by means of triphenylphosphine (1 equiv.) and 2,2′-dipyridyl disulfide (1 equiv.)

Base (Solvent THF)	I(%)	II(%)	III(%)
Et_3N (1 equiv.)	—	30	62
Bu_3N (1 equiv.)	—	25	65
$(HOCH_2CH_2)_3N$ (1 eqiuv.)	13	20	67
Me_2N–  (1 equiv.)	—	20	73
 (1 equiv.)	—	30	60
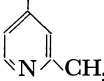 (1 equiv.)	—	25	65
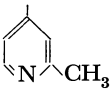 (1 equiv.)	—	30	57
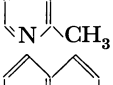 (1 eqiuv.)	—	30	60
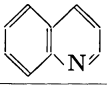 (1 equiv.)	10	20	70

When I was treated with just one eqiv. of *n*-butyl alcohol and 1.5 equiv. each of triphenylphosphine and 2,2′-dipyridyl disulfide, the result was almost

2) M. W. Moon and H. G. Khorana, *J. Amer. Chem. Soc.*, **88**, 1798 (1966).

3) H. G. Khorana and J. P. Vizasalyi, *ibid.*, **81**, 4660 (1959).

TABLE 4. PHOSPHORYLATION OF *n*-BUTYL ALCOHOL (1 equiv.) BY MEANS OF 1.5 equiv. EACH OF TRIPHENYLPHOSPHINE AND 2,2′-DIPYRIDYL DISULFIDE

Solvent	I(%)	II(%)	III(%)
THF	12	10	70
	17	30	52
DMF	24	25	45

TABLE 5. PHOSPHORYLATION OF *n*-BUTYL ALCOHOL (3 equiv.) BY MEANS OF TRIPHENYLPHOSPHINE AND 5,5′-DINITRO-2,2′-DIPYRIDYL DISULFIDE

Condition (Solvent)	I(%)	II(%)	III(%)
THF	25	3	72
THF - (Py-Ac_2O) - (catalytic amounts)	19	—	70
THF - Et_3N (1 mol)	—	15	80
THF - 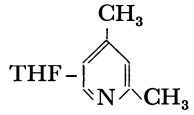 (1 mol)	10	5	71
	—	—	88
DMF	45	—	50

One equiv. each of reagents, triphenylphosphine and 2,2′-dipyridyl disulfide, were used.

the same as those obtained when 3 equiv. of *n*-butyl alcohol were used as shown in the above experiments. Thus, it can be said that the use of a small excess of the coupling reagents, triphenylphosphine and 2,2′-dipyridyl disulfied, is effective for this type of phosphorylation (see Table 4).

Phosphorylation of *n*-butyl alcohol was attempted with the use of 5,5′-dinitro-2,2′-dipyridyl disulfide in place of 2,2′-dipyridyl disulfide in oder to know the effect of the substituents of the disulfide component. It is worth mentioning that the undesirable by-pro-

TABLE 6. PHOSPHORYLATION OF ALCOHOL AND AMINES BY MEANS OF TRIPHENYLPHOSPHINE AND 2,2′-DIPYRIDYL DISULFIDE

Condition (Alcohol or amine) (Solvent THF)	I(%)	II(%)	III(%)
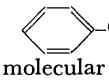 (3 molecular equivalents used)	—	—	90
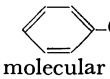 (3 molecular equivalents used)	10	—	80
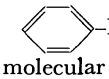 (3 molecular equivalents used)	—	—	90
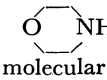 (3 molecular equivalents used)	15	—	75

One equiv. each of reagents, triphenylphosphine and 2,2′-dipyridyl disulfide, were used.

TABLE 7. P^1,P^2-BIS(p-NITROPHENYL) PYROPHOSPHATE SYNTHESIS

Conditions (Solvent, reagent)		I(%)	II(%)
THF	reagent Ph_3P- 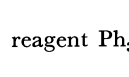 0.5 mol	55	45
THF, 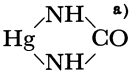 (0.5 mol)	reagent Ph_3P- 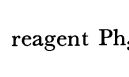 0.5 mol	55	45
	reagent Ph_3P- 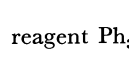 0.5 mol	19	81
 , 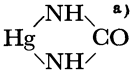 (0.5 mol)	reagent Ph_3P- 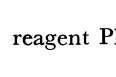 0.5 mol	20	80
CH_3CN	reagent Ph_3P- 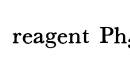 0.5 mol	40	60
DMF	reagent Ph_3P- 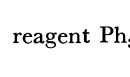 0.5 mol	38	62
THF	reagent Ph_3P- 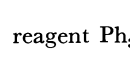 0.75 mol	10	85
	reagent Ph_3P- 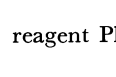 0.75 mol	9	91
THF	Ph_3P- 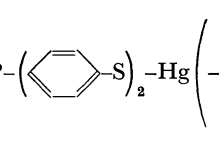 0.75 mol	7	93

a) mercaptan scavenger

duct, pyrophosphate II, was scarcely formed when 5,5′-dinitro-2,2′-dipyridyl disulfide was used as the disulfide component as shown in Table 5.

In a similar way, various disubstituted phosphates and phosphoramidates were prepared from I and benzyl alcohol or amines by using triphenylphosphine and 2,2′-dipyridyl disulfide as the coupling reagents. The results are summarized in Table 6.

Finally, the preparation of symmetrical pyrophosphate II was attempted. When a solution of one eqiuv. of I was treated with 1.5 equiv. each of triphenylphosphine and 2,2′-dipyridyl disulfide at room temperature, the reaction started instantly and symmetrical P^1,P^2-bis(*p*-nitrophenyl) pyrophosphate II was obtained in 91% yield. (see Table 7).

In conclusion, phosphorylation of alcohols and phosphates by oxidation-reduction condensation with triphenylphosphine and 2.2′-dipyridyl disulfide affords the corresponding mixed esters of phosphoric acid and pyrophosphate, respectively, in good yields under mild condition.

Differing from the case of the phosphorylation with the use of dicyclohexylcarbodiimide, the oxidation-reduction condensation proceeds rapidly even in the presence of strong bases such as triethylamine and tributylamine[4] to afford the phosphorylated products in good yields.

Experimental

Reagents. *p*-Nitrophenyl dihydrogen phosphate was prepared by hydrolysis of *p*-nitrophenyl phosphorodichloridate. *p*-Nitrophenyl phosphorodichloridate was prepared by an improved procedure, of which an example is given below. A mixture of 1 mol of *p*-nitrophenol, 3 mol of phosphorus oxychloride and 0.2 mol of potassium chloride was heated at 110°C for 28 hr. After removal of hydrogen chloride and excess phosphorus oxychloride, 179 g (70%) of *p*-nitrophenyl phosphorodichloridate bp 135°C/0.6 mmHg, was obtained. 2,2′-Dipyridyl disulfide[5,6] and 5,5′-dinitro-2,2′-dipyridyl disulfide[7,8] were prepared by procedures given in literature. Triphenylphosphine was obtained from a commercial source and purified by recrystallization.

General Methods. *Reaction of* n-*Butyl Alcohol and* p-*Nitrophenyl Dihydrogen Phosphate with Triphenylphosphine and 2,2′-Dipyridyl Diculfide*: To a solution of anhydrous *n*-butyl alcohol (111 mg, 1.5 mmol), *p*-nitrophenyl dihydrogen phosphate (110 mg, 0.5 mmol) and *2,2′*-dipyridyl disulfide (110 mg, 0.5 mmol) in anhydrous tetrahydrofuran 5 m*l*, triphenylphosphine (131 mg, 0.5 mmol) was added at room temperature with vigorous stirring. After stirring for 2 hr, the amount of III formed was determined by UV absorption after separation with paper chromatography. Yield 70%.

P^1,P^2-*Bis(*p-*nitrophenyl) Pyrophosphate*: To a solution of *p*-nitrophenyl dihydrogen phosphate (220 mg, 1 mmol) and 2, 2′-dipyridyl disulfide (165 mg, 0.75 mmol) in anhydrous pyridine 5 m*l*, triphenylphosphine (197 mg, 0.75 mmol) was added with vigorous stirring at room temperature. After 2 hr, the amount of II formed was determined by the method mentioned above. Yield 91%.

Paper chromatography was carried out by the desending technique on Toyo Roshi No. 50 paper using isopropyl alcohol-concentrated ammonium hydroxyde-water (7 : 1 : 2 (v/v)). In this solvent, *p*-nitrophenyl dihydrogen phosphate has R_F 0.3, ($\lambda_{max}^{H_2O}$ 310 mμ, $\varepsilon=0.96\times10^4$), P^1,P^2-bis(*p*-nitrophenyl) pyrophosphate R_F 0.65, ($\lambda_{max}^{H_2O}$ 288 mμ, $\varepsilon=1.95\times10^4$), *n*-butyl *p*-nitrphenyl phosphate R_F 0.80, ($\lambda_{max}^{H_2O}$ 290 mμ, $\varepsilon=10^4$), benzyl *p*-nitrphenyl phosphate R_F 0.80, ($\lambda_{max}^{H_2O}$ 290 mμ, $\varepsilon=1.05\times10^4$), *p*-nitrophenyl phosphoroanilidate R_F 0.82, ($\lambda_{max}^{H_2O}$ 291 mμ, $\varepsilon=10^4$), *p*-nitrophenyl phosphorobenzylamidate R_F 0.79, ($\lambda_{max}^{H_2O}$ 289 mμ, $\varepsilon=1.05\times10^4$) and *p*-nitrophenyl phosphoromorpholidate R_F 0.83, ($\lambda_{max}^{H_2O}$ 289 mμ, $\varepsilon=10^4$).

The authors wish to express their hearty thanks to Dr. Tsujiaki Hata, Dr. Rei Matsueda and Dr. Masaaki Ueki for their kind advice given during the course of this experiment.

4) M. Smith, J. G. Moffatt, and H. G. Khorana, *J. Amer. Chem. Soc.*, **80**, 6204 (1958).

5) R. A. Jones and A. R. Katritzky, *J. Chem. Soc.*, **1958**, 3610.

6) H. Kubota and T. Akita, *Yakugaku Zasshi* **81**, 511 (1961).

7) W. T. Caldusell and E. C. Kornfeld, *J. Amer. Chem. Soc.*, **64**, 1695 (1942).

8) C. Rath and L. L. Ware, *J. Chem. Soc.*, **1958**, 1853.

Macro Rings. III[1,2]. The Synthesis of [2.1.1.1]Paracyclophane

Toshio KAWATO,[3] Takahiko INAZU, and Tamotsu YOSHINO

Department of Chemistry, Faculty of Science, Kyushu University, Hakozaki, Fukuoka

(Received July 20, 1970)

Two new macrocyclic compounds, I and II, which incorporate, respectively, four or eight benzene rings and intervening methylene bridges attached to their *para* positions, were synthesized. The UV, IR, and NMR spectra of these paracyclophanes were compared with a corresponding open-chain compound, III.

Some paracyclophanes have been shown to have interesting characteristics compared with an open-chain analog because of the interaction of the π-electrons of adjacent benzene rings. An interesting characteristic of forming charge-transfer complexes and clathrate compounds may be expected, especially in a cyclophane in which the planes of benzene rings assume such a perpendicular configuration with each other as to form a square prism. The synthesis of [2.1.1.1]paracyclophane I was thus undertaken.

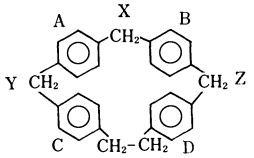

[2.1.1.1]Paracyclophane I

Formula 1

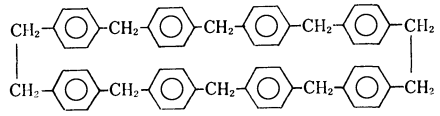

[2.1.1.1.2.1.1.1]Paracyclophane II

Formula 2

As is shown by a Dreiding molecular model of the paracyclophane I, four benzene rings are situated in planes so as to form a slightly deformed square prism whose respective parallel planes are slightly inclined to each other, and four pairs of adjacent benzene rings are connected by an ethylene and three separate methylene bridges, involving a slight strain in the valence angle of each methylene carbon and a slight warp in the planes of the benzene rings. The molecular model also shows that the [2.1.1.1]paracyclophane molecule should exist in the form of two nonsuperposable mirror-image conformers due to the pair of skew conformations of the 1,2-diphenylethane moiety in the macro ring.

A pair of such enantiomeric conformers appear to be interconverted so rapidly at an ordinary temperature by a flip that, because of the equalization of the shielding effects, the signals of the ethylene protons merge into one sharp peak, as will described later, in the NMR spectra. Judging from an inspection of the model of the cyclophane, I, the rocking motion of the benzene ring may be possible, but complete rotation about the para axis is considered to be extremely difficult. In the paracyclophane, II, the situation is quite different. The molecule may be free from strain and the macro ring may be so sufficiently flexible that the benzene rings in it may rotate about the para axis. This difference seems to be associated with the difference between the NMR spectra.

The synthetic routes are shown in Schemes 1 and 2. Diphenylmethane and ethyl *p*-chloroformylbenzoate IV were treated with anhydrous aluminum chloride to give a diketo diester, V. The carbonyl groups of V were then reduced by the Huang-Minlon modification of the Wolff-Kishner reduction to give a dicarboxylic acid, VIII, which was then esterified to give a diester, IX. The diester, IX, was also obtained by the Friedel-Crafts acylation of ethyl *p*-benzylbenzoate and phosgene and by subsequent Wolff-Kishner reduction and esterification. The diester, IX, was reduced with lithium aluminum hydride to a diol, X, which was then treated with phosphorus pentachloride or thionyl chloride to obtain a dichloro compound, XI. The *para*-substituted structures of Compounds V, VIII, IX, X and XI were

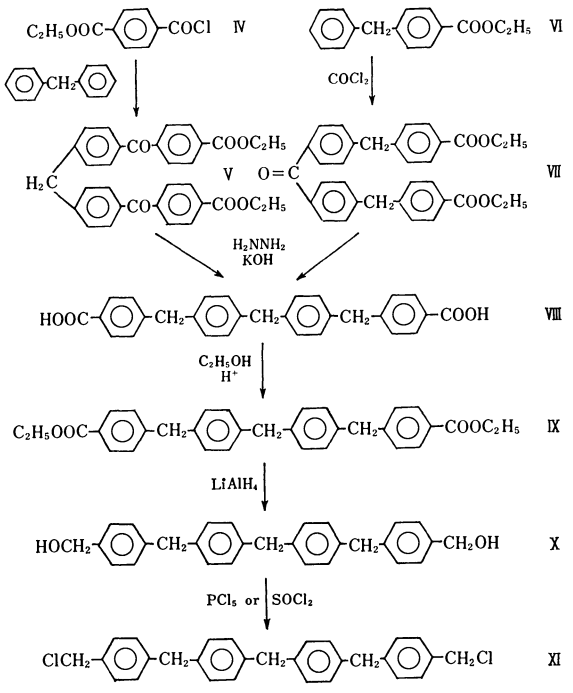

Scheme 1

1) Part II of this series: T. Inazu and T. Yoshino, This Bulletin, **41**, 652 (1968).

2) Presented at the 23rd Annual Meeting of the Chemical Society of Japan, Tokyo, April, 1970.

3) Present Address: Laboratory of Chemistry, College of General Education, Kyushu University, Ropponmatsu, Fukuoka.

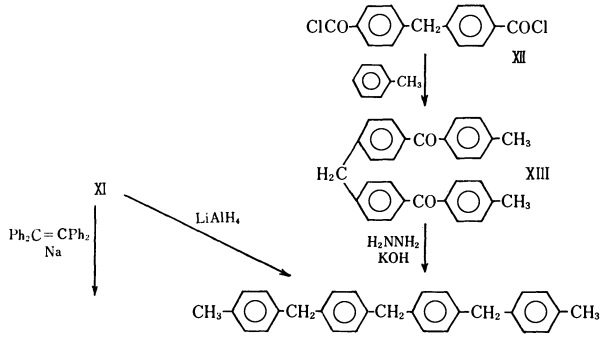

Paracyclophane I and II Open chain analog III

Scheme 2

shown by their characteristic infrared spectra over the 1650—2000 cm^{-1} range.

The [2.1.1.1]paracyclophane I and the dimeric [2.1.1.1.2.1.1.1]paracyclophane II were prepared by the cyclization of the dichloro compound, XIV, with a sodium adduct of tetraphenylethylene[4] in anhydrous tetrahydrofuran under nitrogen, using the high-dilution technique. The separation of the cyclophanes, I and II, was carried out by fractional crystallization.

An open-chain analog, III, was prepared by the reduction of the dichloro compound, XI, with lithium aluminum hydride or by the Wolff-Kishner reduction of a diketone, which had been produced by the Friedel-Crafts reaction of diphenylmethane-4,4′-dicarbonyl dichloride with toluene.

Between the IR spectra of the cyclophane, I or II, and that of the open-chain analog, III, small and yet characteristic differences were observed. Whereas weak absorption bands were observed in the spectra of the I and II cyclophanes at 1610 and 1575 cm^{-1} (double-bond region), they were not observed for the open-chain analog, III. From this fact, it was assumed that these bands are due to the vibrational transition which is

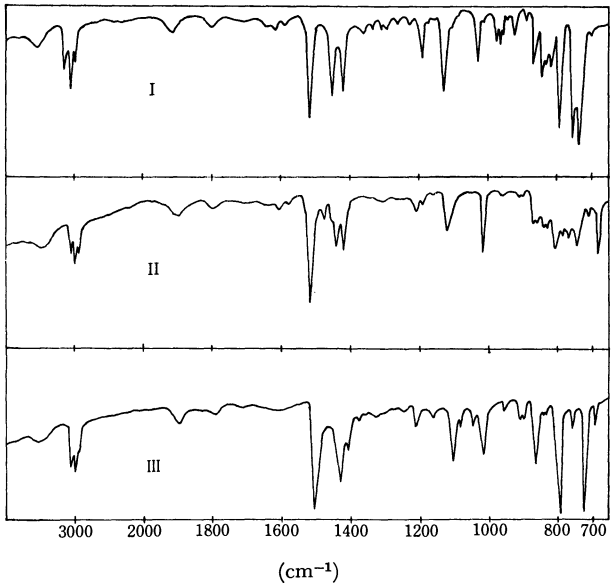

Fig. 1. The IR spectra of compound I, II, and III in KBr disk.

4) E. Müller and G. Röscheisen, *Chem. Ber.*, **90**, 543 (1957).

allowed for benzene rings in the macro ring compounds and forbidden for benzene rings in the open-chain analog. A weak absorption band assigned to the symmetric bending of the methyl group was observed at 1380 cm^{-1} for the open-chain analog, III; this band was necessarily absent in the IR spectra of the cyclic compounds. The intensity of the band at 1415 cm^{-1} due to the bending of the methylene groups increased upon ring closure. A similar tendency was observed in the region of the C–H in-plane bending of the benzene rings. In the 800—900 cm^{-1} region of the ring C–H out-of-plane bending vibration, more complicated spectra were observed for the I and II cyclophanes than for the open-chain compound, III. This complication in the spectra by ring closure may be attributable to the appearance of deformation vibrations not allowed for the open-chain compound.

The NMR spectra of the paracyclophanes, I and II, were different from that of the open-chain analog, III, in several respects. In the region of the alkyl protons, the open-chain compound, III, showed a peak due to methyl protons at τ 7.74 and one due to methylene protons at τ 6.16, in an equal area ratio.

On the other hand, the cyclophanes I and II showed no peak due to methyl protons, but, instead, showed a peak indicating the existence of an ethylene bridge resulting from cyclization. The peak of the ethylene protons was at τ 7.21 for the compound I and at τ 7.22 for the compound II. The fact that the peak due to ethylene protons is a singlet means that all the ethylene protons are equivalent. This fact may be readily understandable provided that the pair of conformers due to the two skew conformations of the 1,2-diphenylethane moiety of the macro ring is rapidly interconverted by flip rotation about the C–C axis of the ethylene group, as has been described before.

The singlets at τ 6.25 and 6.33 for the compound I and the singlet at τ 6.13 for Compound II are assigned to methylene protons. In Compound I, on the basis of the area ratio of 1 : 2, the peak at τ 6.25 is assigned to the protons of methylene remote from the ethylene bridge (indicated by X in formula 1), and the peak at τ 6.33, to those of methylenes near the ethylene bridge (indicated by Y and Z). Such a difference in the chemical shift between the methylene protons may be explained by their being shielded unequally by the ring current of the neighboring benzene rings.

The open-chain compound, III, showed a sharp singlet peak of benzene protons at τ 2.97, whereas the cyclophane I and II showed two different peaks. In the cyclophane I, the ring protons exhibit two well-separated peaks, at τ 3.45 and τ 3.10, equal in area. Such a difference in the chemical shift between aryl protons seems to be caused by the same reason as that in the case of methylene protons. From a molecular-model consideration of the cyclophane I, the lower-field peak was assigned to the protons of benzene rings remote from the ethylene bridge (indicated by A and B), and the higher-field peak, to those of benzene rings near the ethylene bridge (indicated by C and D).

In case of the cyclophane II, no such upfield shift of the aryl protons was observed. This fact may be

explained from an inspection of the molecular model, which shows that the molecule of the cyclophane II may be free from strain and that the macro ring may be so flexible that the benzene rings in it may rotate around the para axis.

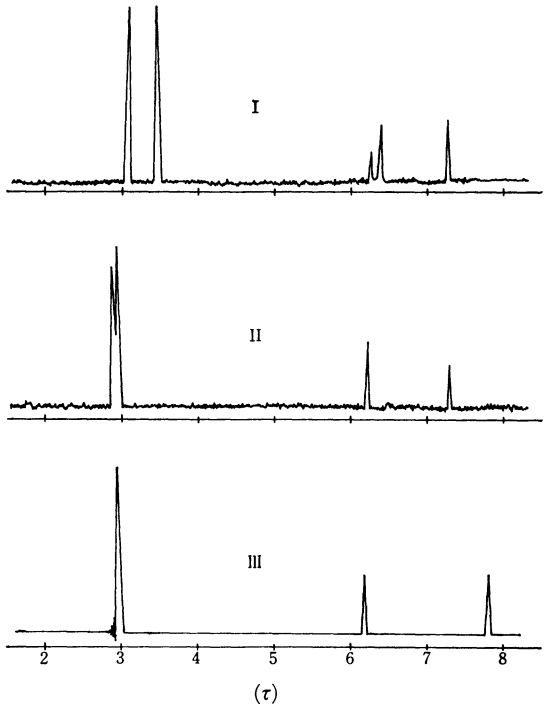

Fig. 2. The NMR spectra of compound I, II, and III in $CDCl_3$.

The UV spectra of the cyclophanes I and II were compared with that of the open-chain compound, III. A loss of the fine structure around 270 mμ in the cyclophane I is noticeable when its spectrum is compared with the spectrum of the open-chain compound, III. This fact is attributable to transannular electronic interactions of the benzene rings. In case of the compound I, compared with the compound III, the major peaks are observed to shift to longer wavelengths and to be weakened in intensity. Furthermore, the fine structure of the peaks becomes less apparent. The new absorption at 242 mμ for I indicates strong transannular electronic interactions of the benzene ring.

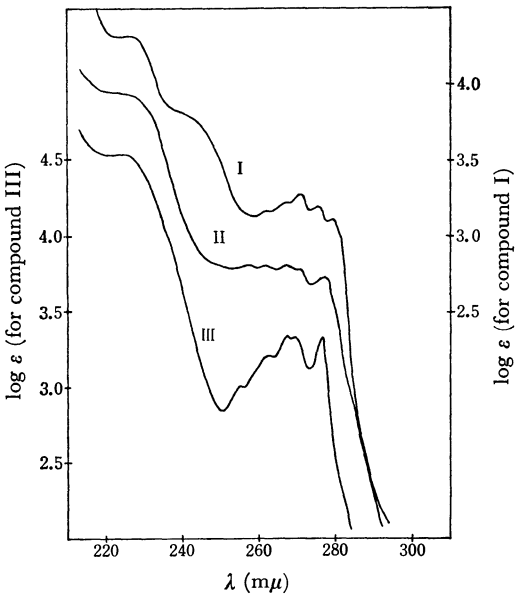

Fig. 3. The UV spectra of compound I, II, and III in ethanol.
I: λ_{max} 269.5 mμ, log ε=3.25
II: λ_{max} 266.5 mμ, log ε=3.30
III: λ_{max} 267.0 mμ, log ε=3.32
The graduation in the ordinate axis for compound II is displaced upward by 0.5 log ε unit increments from that for compound III.

The cyclic structures of the cyclophanes I and II were confirmed by the results of the elementary analysis and by molecular-weight determination, and by the absence of an end methyl group indicated by the IR and NMR spectra, as well as by a comparison of their IR, NMR and UV spectra with that of the open-chain analog, III.

The possibility of the formation of inclusion compounds is now under investigation.

Experimental

All the melting points are uncorrected. The IR spectra were determined in potassium bromide disks or films by means of a Hitachi EPI-S2 spectrophotometer, while the UV spectra were measured in ethanol by means of a Hitachi EPI-3T spectrophotometer. The NMR spectra were recorded at 60 MHz in $CDCl_3$ solution by means of a Varian Associates A-60 photometer. The chemical shifts are quoted as τ values relative to tetramethylsilane. The molecular weights were determined by means of a Hitachi Perkin-Elmer 115 molecular-weight-determination apparatus, using benzene as the solvent.

*4,4'-Bis(*p*-ethoxycarbonylbenzoyl)diphenylmethane, V.* Into an ice-cooled mixture of 70 g of ethyl *p*-chloroformylbenzoate, IV,[5] and 200 g of powdered anhydrous aluminum chloride in 600 m*l* of carbon disulfide, we stirred, drop by drop, a solution of 27 g of diphenylmethane in 200 m*l* of carbon disulfide at 0°C. The reaction mixture was then refluxed for 5 hr. The removal of carbon disulfide by distillation and the addition of crushed ice and hydrochloric acid yielded a pale yellow powder, which was then crystallized from ethanol to give 60 g (72% yield) of colorless needles; mp 130—130.5°C.

Found: C, 76.20; H, 5.47%. Calcd for $C_{33}H_{28}O_6$: C, 76.14; H, 5.42%.

*4,4'-Bis(*p*-ethoxycarbonylbenzyl)benzophenone, VII.* A mixture of 50 g of ethyl *p*-benzylbenzoate, VI, and 80 g of powdered anhydrous aluminum chloride in 500 m*l* of cabon disulfide was cooled to −15°C, and then 10 g of phosgene were slowly stirred into the mixture at a temperature below −10°C. The temperature was then allowed to rise slowly to room temperature. After a similar treatment of the reaction mixture, 44 g of the keto diester, VII, were obtained as a pale yellow powder, this powder was used without further purification for the preparation of the dicarboxylic acid, VIII.

*4,4'-Bis(*p*-carboxybenzyl)diphenylmethane, VIII.* A mixture of 50 g of the diketo diester, V, 200 g of potassium hydroxide, and 200 m*l* of 85% hydrazine hydrate in 500m*l* of ethylene glycol was refluxed for 1 hr. The water and excess hydrazine were removed by a take-off condenser until the temperature rose to 195—200°C, after which reflux was continued for 6 hr. The cooled solution was diluted with

5) J. B. Cohen and H. S. de Pennington, *J. Chem. Soc.*, **113**, 63 (1918).

water and acidified with concentrated hydrochloric acid. Almost a theoretical amount (42 g) of a white crystalline powder was thus obtained.

The same acid was also obtained by a similar reduction of Compound VII with potassium hydroxide and hydrazine hydrate in ethylene glycol.

*4,4'-Bis(*p*-ethoxycarbonylbenzyl)diphenylmethane, IX.* A mixture of 42 g of the dicarboxylic acid, VIII, 100 g of benzene, and 50 m*l* of concentrated sulfuric acid in 500 m*l* of ethanol was refluxed for 20 hr, the resultant water was removed as a volatile azeotrope composed of benzene, ethanol, and water. After working-up in the usual way, an almost theoretical amount (47 g) of the product was obtained; it was then purified by recrystallization from ethanol to colorless needles with a mp of 120—121.5°C.

Found: C, 80.51; H, 6.61%. Calcd for $C_{33}H_{32}O_4$: C, 80.46; H, 6.55%.

*4,4'-Bis(*p*-hydroxymethylbenzyl)diphenylmethane, X.* A solution of 40 g of the diester, IX, in 400 m*l* of anhydrous tetrahydrofuran was stirred, drop by drop, into a suspension of 5 g of lithium aluminum hydride in 400 m*l* of tetrahydrofuran at room temperature. After being refluxed for 1 hr, the mixture was cooled and treated with water and then with hydrochloric acid. The tetrahydrofuran was removed by distillation, and the resultant precipitate was collected and recrystallized from tetrahydrofuran to give an almost theoretical amount (33 g) of colorless needles; mp 180.5—181°C.

Found: C, 85.25; H, 7.08%. Calcd for $C_{29}H_{28}O_2$: C, 85.26; H, 6.91%.

*4,4'-Bis(*p*-chloromethylbenzyl)diphenylmethane, XI.* A mixture of 30 g of the diol, X, and 35 g of phosphorus pentachloride in 500 m*l* of chloroform was refluxed for 3 hr. After the removal of the solvent and phosphoryl chloride by distillation under reduced pressure, the residue was recrystallized from tetrahydrofuran to give 27 g (83% yield) of colorless needles; mp 164—164.5°C.

Found: C, 78.44; H, 5.98. Calcd for $C_{29}H_{26}Cl_2$: C, 78.20; H, 5.88%.

A mixture of 5 g of the diol, X, and 50 m*l* of thionyl chloride also gave the dichloro compound, XI, in an almost theoretical yield.

*4,4'-Bis(*p*-methylbenzyl)diphenylmethane, III.* To a stirred suspension of 0.03 g of lithium alminum hydride in 30 m*l* of anhydrous tetrahydrofuran, we slowly added a solution of 0.2 g of the dichloro compound, XI, in 20 m*l* of tetrahydrofuran at room temperature. After the usual treatment, 0.17 g (the theoretical amount) of the product was recrystallized from ethanol to give colorless crystals; mp 118—119°C.

Found: C, 92.36; H, 7.65%. Calcd for $C_{29}H_{28}$: C, 92.50; H, 7.50%.

This open-chain model compound was also prepared as follows. By the Friedel-Crafts reaction of 3 g of diphenylmethane-4,4'-dicarbonyl chloride, XII, 2 g of toluene, and 3.5 g of powdered anhydrous aluminum chloride in 70 m*l* of carbon disulfide, 3.1 g (73% yield) of the diketone, XIII, was obtained as pale yellow crystals with a mp of 140°C.

Found: C, 85.95; H, 6.14%. Calcd for $C_{29}H_{24}O_2$: C, 86.11; H, 5.98%.

A mixture of 0.75 g of the above-mentioned diketone, XIII, 3 m*l* of 85% hydrazine hydrate, and 5 g of potassium hydroxide in 50 m*l* of ethylene glycol was refluxed to give 0.7 g (the theoretical amount) of a colorless crystalline product, whose identity was confirmed by a mixed-melting-point determination (118°C) with the sample described above and by a comparison of their IR spectra.

[2.1.1.1]Paracyclophane I and [2.1.1.1.2.1.1.1]Paracyclophane, II. Into a dark-violet solution of 4 g of sodium and 1.5 g of tetraphenylethylene in 400 m*l* of anhydrous tetrahydrofuran, a solution of 5 g of the dichloro compound, XI, in 800 m*l* of anhydrous tetrahydrofuran was stirred, drop by drop, through a modified Hershberg dropping funnel[6] at room temperature under nitrogen over a period of 50 hr. After the careful addition of ethanol, and then water, the removal of the solvent from the mixture gave a white powder; when this powder was washed with water and fractionally crystallized from benzene-ethanol mixture, Compounds I and II were obtained in yields 200 mg and 120 mg respectively.

Compound I was crystallized from ethanol to give colorless crystals; mp 219—220°C.

Found: C, 92.95; H, 7.11%; mol wt, 390. Calcd for $C_{29}H_{26}$: C, 93.00; H, 7.00%; mol wt, 374.5. Compound II was recrystallized from benzene to give colorless needles.

Found: C, 92.87; H, 7.26%; mol wt, 742. Calcd for $C_{58}H_{52}$: C, 93.00; H, 7.00%; mol wt, 749.0.

6) R. E. Benson and B. C. Mukusick, "Organic Syntheses," Coll. Vol. IV, p. 747 (1963).

Stereochemical Studies of Monoterpene Compounds. X.[1] Intramolecular Interaction of Oxirane and Cyclopropane Rings with a Hydroxyl Group[2]

Satoru WATANABE, Takayuki SUGA,[3] Tsuyoshi SHISHIBORI, and Tamon MATSUURA
Department of Chemistry, Faculty of Science, Hiroshima University, Hiroshima
(Received July 20, 1970)

The intramolecular interaction of oxirane and cyclopropane rings with a hydroxyl group in the alicyclic α,β-epoxy-, β,γ-epoxy-, and cyclopropyl alcohols was investigated by means of the infrared spectroscopy. *cis*-α,β-Epoxyalcohols (II, IV and V) showed a free hydroxyl band, an interacted hydroxyl band with a C–O bond of the oxirane ring, and/or a band due to a O–H···O hydrogen bond, whereas *trans*-epoxyalcohols (I and III) showed only a free hydroxyl band. The interaction between the hydroxyl group and a C–C bond of the oxirane ring was likely to be absent. β,γ-Epoxyalcohols revealed a hydroxyl band interacting with lone-pair electrons of the oxirane oxygen, in addition to a free hydroxyl band. The O–H··· cyclopropane interaction was found with 2-(1-methylcyclopropyl)-5-methylcyclohexanols (VII and VIII). The correlation of the infrared spectra with the conformation of the interacting groups is also discussed.

A hydroxyl group interacts with the π-electrons of a double bond and a carbonyl group.[4-6] Cyclopropane and oxirane rings are known to show properties like those of the π-electron system. It seemed, therefore, that it would be interesting to investigate the intramolecular interaction between the hydroxyl group and the oxirane and cyclopropane rings. For acyclic epoxyalcohols, the interaction between the hydroxyl group and the oxirane ring can be created by using electrons of the C–O bond, and it is favored when the hydroxyl group approaches not from the top, but from the plane of the ring.[7] However, the correlation of the infrared spectrum with the geometry of the interacting groups has not yet been clarified for cyclic compounds, in which the approach of the hydroxyl group can be regulated both in site and in direction. This paper will report on the intramolecular interaction of the hydroxyl group with the oxirane and cyclopropane rings in cyclic monoterpene alcohols, such as *trans*- and *cis*-1,2-epoxy-*p*-menth-8-en-6-ols (I and II), *trans*- and *cis*-4,8-epoxy-*p*-menthan-3-ols (III, IV, and V), 8,9-epoxy-*p*-menthan-3-ol (VI), and 2-(1-methylcyclopropyl)-5-methylcyclohexanols (VII and VIII).

Results and Discussion

The structure and the infrared (IR) spectral data of α,β- and β,γ-epoxyalcohols are collected in Chart I.

We will first deal with the interaction between the hydroxyl group and the oxirane ring of the α,β-epoxyalcohols. The hydroxyl stretching absorption of *trans*-1,2-epoxy-*p*-menth-8-en-6-ol (I) showed only one peak, at 3635 cm^{-1}, which corresponds to the free, secondary hydroxyl group. The *trans*-epoxyalcohol I, therefore, takes a conformation in which the hydroxyl group is unable to interact with the oxirane ring, as is shown in Chart I. Now, the IR spectrum of *cis*-epoxy-*p*-menth-8-en-6-ol (II), an isomer of I in respect of the hydroxyl group, showed three bands, at 3629, 3594, and 3572 cm^{-1} (Fig. 1). The highest-frequency band is similar in position to the free hydroxyl absorption band of the isomer I. The remaining peaks are, thus, due to the intramolecularly-interacting hydroxyl group. The nuclear magnetic resonance (NMR) spectrum of the C-6 proton revealed the hydroxyl group to take an axial orientation, as is shown in Chart I. The molecular models suggest, then, that the interaction between an axial hydroxyl group and an oxirane ring would be possible in three cases, shown as A, B, and D in Chart

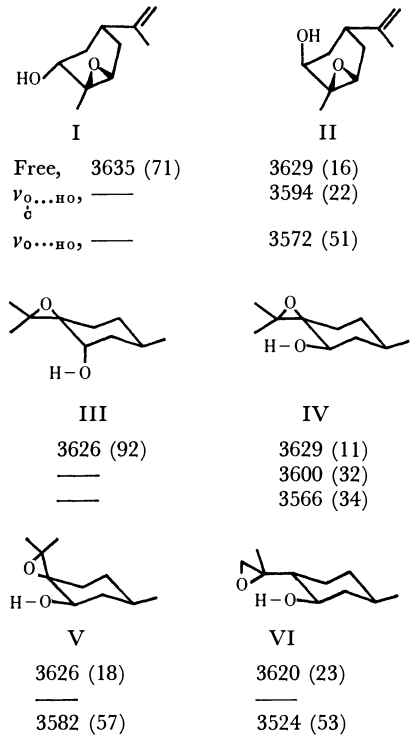

Chart I. Free and bonded peak positions of α, β- and β, γ-epoxyalcohols (I—VI), cm^{-1} (ε).

1) Paper IX of this series: T. Hirata and T. Suga, *J. Org. Chem.*, **36**, No. 3 (1971), in press.
2) Presented at the 22nd Annual Meeting of the Chemical Society of Japan, Tokyo, April, 1968.
3) To whom all inquiries regarding to this paper should be addressed.
4) M. Ōki, H. Iwamura, T. Onoda, and M. Iwamura, *Tetrahedron*, **24**, 1905 (1968).
5) M. Ōki, H. Iwamura, J. Aihara, and H. Iida, This Bulletin, **41**, 176 (1968).
6) T. Shishibori, *ibid.*, **41**, 1170 (1968).
7) M. Ōki and T. Murayama, *ibid.*, **40**, 1997 (1967).

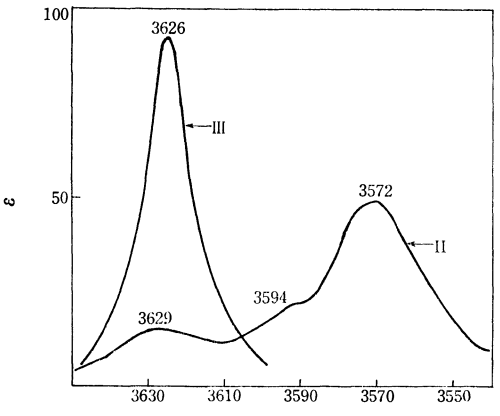

Fig. 1. IR spectra of epoxyalcohols (II and III) in a carbon tetrachloride solution.

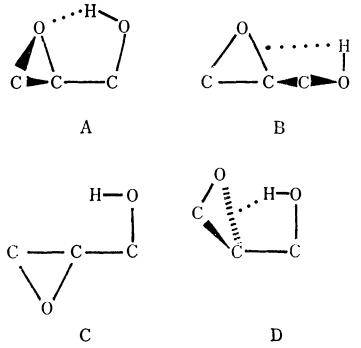

Chart II. Possible interactions between a hydroxyl group and an oxiran ring.

II. By comparison with the spectra of 2,3-epoxypropanols,[7] the peak at 3572 cm^{-1} ($\Delta\nu$=57 cm^{-1}) can be assigned to the interaction between the lone-pair electrons of an oxygen atom and the hydroxyl group which can approach the top of the oxirane ring surface; *cf.* A in Chart II. The other peak, at 3594 cm^{-1}, seems to be due to the hydroxyl group which interacts with electrons of the C–O bond in a plane of the oxirane ring; *cf.* B in Chart II.

The hydroxyl stretching absorption of *trans*-4,8-epoxy-*p*-menthan-3-ol (III), an exocyclic epoxide, showed only one peak, at 3626 cm^{-1} (Fig. 1); this peak is assignable to an absorption due to only the free secondary hydroxyl group. However, the hydroxyl group of III may interact with the C_4–C_8 bond in a plane of the oxirane ring, as in the case of C in Chart II; if any such interaction is present, however, it seems to be too little to detect by usual infrared measurements. *cis*-4,8-Epoxy-*p*-menthan-3-ol (IV), an isomer of III concerning the hydroxyl group, exhibited hereon three bands, at 3629, 3600, and 3566 cm^{-1}, which are similar in position to those of II. Thus, these were assigned to an absorption resulting from a free hydroxyl group and an interacted one, such as B and A (Chart II), respectively. On the other hand, epoxyalcohol V, an isomer of IV with respect to a methyl group, showed two bands, at 3626 and 3582 cm^{-1}, due to the free hydroxyl group and the intramolecular OH···O hydrogen-bonded hydroxyl group, shown in A, respectively. Although the hydroxyl group of V may approach the C–O bond from the top of the three-membered rings, as is shown in D, no such interaction was observed. This result indicates the impossibility of the interaction D for the epoxyalcohol V; this is in agreement with the literature.[7] The NMR spectrum of the C-3 proton of V showed double doublets (J_{vic}=10 and 6.5 Hz) at 3.88 ppm, which indicates the proton to be in a perfectly axial orientation. On the other hand, IV revealed the scarecely separated peak, suggesting some twisted conformations favorable for an approach of the hydroxyl group in a plane of the oxirane ring.

The IR spectrum of 8,9-epoxy-*p*-menthan-3-ol (VI) had two hydroxyl-stretching absorptions, at 3620 and 3524 cm^{-1}. The former was assigned to a free hydroxyl group, though the frequency of the band seems to be slightly low in comparison with a normal free secondary hydroxyl band; also, the hydroxyl proton may approach geometrically the C–O bond in a plane of the oxirane ring. On the other hand, the latter is shifted greatly from the free hydroxyl band. The extent of the shift is similar to that of *trans*- and *cis*-*p*-menthane-3,8-diols,[6] in which the hydroxyl group bonds intramolecularly with lone-pair electrons of the other hydroxyl oxygen atom. Thus, the band may be attributed to an intramolecular hydrogen bond between the hydroxyl group and the lone-pair electrons of an oxygen atom of the oxirane ring.

We now wish to deal with the interaction between the hydroxyl group and the cyclopropane ring of β,γ-cyclopropyl alcohols. The infrared spectral data are shown in Chart III. The spectrum of (−)-2-(1-methyl-

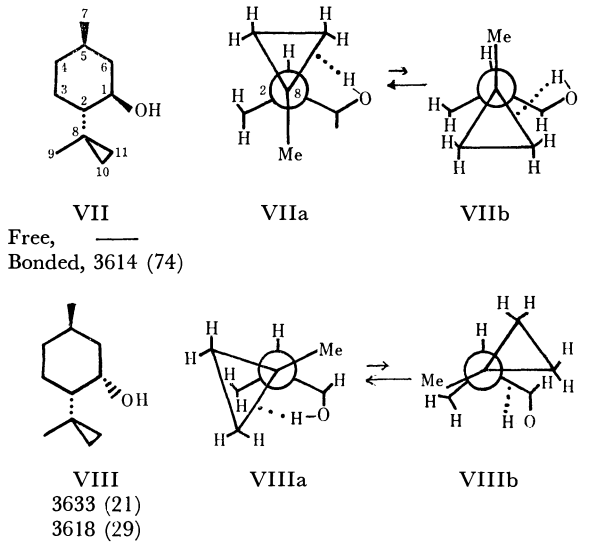

Chart III. Free and bonded peak possitiosn of cyclopropylalconhols (VII and VIII), cm^{-1} (ε).

cyclopropyl)-5-methylcyclohexanol (VII) has only one peak, at 3614 cm^{-1} (also Fig. 2). This shifted band was assigned on the basis of an internal O–H···cyclopropane interaction, since the free hydroxyl band of *l*-menthol[8] appears at 3628 cm^{-1}. Two conformers, VIIa and VIIb, can be considered for the preferred conformation of VII, because the preferred site for

8) Y. R. Naves and J. Lecomte, *Bull. Soc. Chim. Fr.*, **1955**, 792.

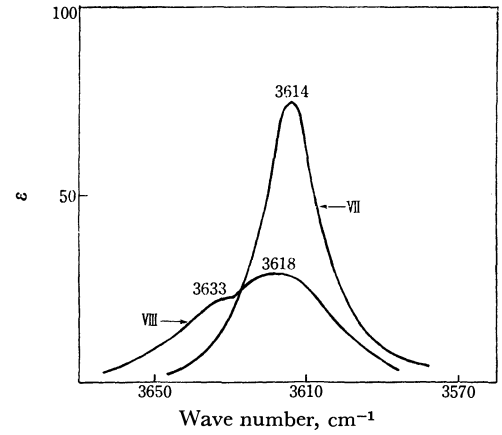

Fig. 2. IR spectra of cyclopropyl alcohols (VII and VIII) in a carbon tetrachloride solution.

the O–H···cyclopropane interaction is the "edge" of a plane of the ring.[9,10] Of those two, the *gauche* conformer VIIa is energetically more favorable than the *eclipsed* one, VIIb. On the other hand, (+)-2-(1-methylcyclopropyl)-5-methylcyclohexanol (VIII), an isomer of VII in respect of the hydroxyl group, had two peaks, at 3633 (weak) and 3618 cm^{-1} (*cf.* Fig. 2), attributable to the free hydroxyl group and the O–H··· cyclopropane interaction respectively. An interaction would be possible in both VIIIa and VIIIb. The interacted species may, then, be thought more populous in VII than in VIII, judging from the infrared spectra shown in Fig. 2. This may be interpreted as follows: a steric repulsion would be at a minimum in the *gauche* conformer VIIa, which is further stabilized by an internal O–H···cyclopropane interaction. On the other hand, the conformers, VIIIa and VIIIb, are favorable for the intraction, but are destabilized by the repulsion of the *eclipsed* groups. Therefore, both free and bonded hydroxyl absorptions appear in VIII.

Experimental

The IR spectra in the hydroxyl-stretching region were measured with a Perkin-Elmer Model 621 Infrared Spectrometer. A salt absorption cell (20 mm long) was used; the concentration of the carbon tetrachloride solution was 0.005 mol/*l*, at which concentration the association of the solute is negligible. The measurements were made at 25°C. The NMR spectra were recorded with a Hitachi Perkin-Elmer R-20 high-resolution spectrometer at 60 MHz, using tetramethylsilane as the internal standard. Gas-chromatographic analyses were made at 95—150°C, using a Hitachi Perkin-Elmer F6-D gas chromatograph with a flame ionization-type detector and a 3 mm × 1 m column packed with 3%-polyethylene glycol on Celite. Compounds I and II were separated preparatively using a Shimadzu (Kyoto) GC-2B gas chromatograph with a thermal conductor-type detector and a 4 mm × 3 m column packed with 10%-diethylene glycol succinate on Diasolid L (80—100 mesh). Helium was used as the carrier gas.

trans- *and* cis-*1,2-Epoxy*-p-*menth-8-en-6-ols (I and II).* (−)-Carvone (78.0°C/4 mmHg; n_D^{25} 1.4944; d_4^{25} 0.9539; $[\alpha]_D^{25}$ −61.14° (neat)) was epoxydized with 6 N sodium hydroxide and 30% hydrogen peroxide in methanol to (+)-α,β-epoxycarvone (107—109°C/8 mmHg; n_D^{25} 1.4788; d_4^{25} 1.0282; $[\alpha]_D^{25}$ +79.44° (neat), lit:[9] $[\alpha]_D^{25}$ +87.60° (neat)), according to the published procedure.[11] A mixture of $NaBH_4$ (2.0 g) and 700 m*l* of 80% dioxane in water was added to a solution of (+)-α,β-epoxycarvone (10 g) in 200 m*l* of 80% dioxane in water. After the entire reaction mixture has been left to stand at room temperature for three days, it was worked up in the usual manner to give 8.0 g of a mixture of I and II. The fractionation of the mixture was carried out by gas chromatography, as has been described above (peak area, I: 65%, II: 35%). The first peak was II: n_D^{25} 1.4831; NMR (CCl_4), $-\underset{|}{C}-CH_3$, 1.38 ppm (singlet, 3H), $>C\underline{H}-OH$ 3.70 (triplet, J=1.5 Hz, 1H), −OH 3.80 (broad singlet, 1H), $CH_2=\underset{|}{C}-C\underline{H}_3$ 1.72 (triplet, J=1.1 Hz, 3H), $=C\underline{H}_2$ 4.69 (multiplet, 2H); ν_{max}^{liq} 889 cm^{-1} (=CH_2), 3413 (OH). The second peak was I: n_D^{25} 1.4878; mp 31.0—31.5°C; NMR (CCl_4), −OH 3.14 ppm (broad singlet, 1H), $>C\underline{H}-OH$ 3.75 (double doublets, J_{vic}=11.0 and 6.0 Hz, 1H), $-\underset{|}{C}-CH_3$ 1.32 (singlet, 3H), $CH_2=\underset{|}{C}-C\underline{H}_3$ 1.69 (triplet, J=1.1 Hz, 3H), $=C\underline{H}_2$ 4.68 (multiplet, 2H); ν_{max}^{liq} 888 cm^{-1} (=CH_2), 3448 (OH).

4,8-Epoxy-p-*menthan-3-ol (III, IV, and V).* Two isomers, A (mp 55°C) and B (mp 59°C), of pulegone oxide were prepared[12] by the epoxidation of pulegone in the same manner as used for carvone. The reduction of the isomer A by the procedure described above afforded a mixture (2.0 g) of III and IV, which was then fractionated into two eluates by column chromatography on silica gel with a mixture of petroleum ether and ethyl ether (1 : 1). The initial eluate (1.0 g) was IV: mp 24.5—25.0°C; bp 80.0—81.0°C/2 mmHg; n_D^{25} 1.4770; d_4^{25} 1.115; $[\alpha]_D^{25}$ −3.97° (neat); NMR ($CDCl_3$), $>CH-C\underline{H}_3$ 1.05 ppm (doublet, J=6.0 Hz, 3H), −OH 1.61 (singlet, 1H), $>C\underline{H}-OH$ 3.64 (broad singlet, 1H), $>C(CH_3)_2$ 1.31 and 1.38 (each singlet, 6H); ν_{max}^{liq} 3441 cm^{-1} (OH). The second eluate was III: mp 54.0—55.0°C; $[\alpha]_D^{25}$ +52.8° (*c* 6.66, $CHCl_3$); NMR ($CDCl_3$), $>CH-C\underline{H}_3$ 0.91 ppm (doublet, J=6.0 Hz, 3H), −OH 1.61 (singlet, 1H), $>C\underline{H}-OH$ 3.64 (broad singlet, 1H), $>C(CH_3)_2$ 1.31 and 1.38 (each singlet, 6H); ν_{max}^{liq} 3394 cm^{-1} (OH). The isomer B (3.0 g) was reduced as above to afford V (2.0 g): bp 83.5—84.0°C/0.5 mmHg; n_D^{25} 1.4672; d_4^{25} 1.0007; $[\alpha]_D^{25}$ +3.30° (neat); NMR ($CDCl_3$), $>CH-C\underline{H}_3$ 1.04 ppm (doublet, J=6.0 Hz, 3H), $>C(CH_3)_2$ 1.33 and 1.56 (each singlet, 6H), $>C\underline{H}-OH$ 3.88 (double doublets, J_{vic}=10.0 and 6.0 Hz, 1H), −OH 2.38 (singlet, 1H); ν_{max}^{liq} 3438 cm^{-1} (OH).

(−)-8,9-Epoxy-p-*menthan-3-ol (VI).* (−)-Isopulegol (15.4 g, 93.0°C/10 mmHg, n_D^{25} 1.4676, d_4^{25} 0.9052, $[\alpha]_D^{25}$ −22.27° (neat)) was added to a solution of monoperphthalic acid (22.0 g) in ether (127 m*l*) below 0°C. The mixture was allowed to stand overnight at room temperature; subsequently, an usual working-up of the mixture afforded a crude product (15.3 g). The purification of the product by column chromatography and subsequent recrystallization afforded VI: mp 53.5—54.0°C; $[\alpha]_D^{25}$ −15.6° (*c* 3.33, $CHCl_3$), lit:[13] α_D = −14.5°; NMR ($CDCl_3$), $>CH-C\underline{H}_3$ 0.91 ppm (doublet, J=6.0 Hz, 3H), $>C\underline{H}-OH$ 3.25 (broad singlet, 1H), $-O-CH_2-$ 2.59 and 2.85 (each doublet, J=4.0 Hz, 2H), $-O-\underset{|}{C}-CH_3$

9) L. Joris, P. von R. Schleyer, and R. Gleiter, *J. Amer. Chem. Soc.*, **90**, 327 (1968).
10) M. Ōki, H. Iwamura, T. Murayama, and I. Oka, This Bulletin, **42**, 1986 (1969).
11) E. Klein and G. Ohloff, *Tetrahedron*, **19**, 1091 (1963).
12) W. Reusch and P. Mattison, *ibid.*, **24**, 4933 (1968).
13) K. H. Schulte and G. Ohloff, *Helv. Chim. Acta*, **50**, 153 (1967).

1.35 (singlet, 3H); ν_{max}^{KBr} 3523 cm^{-1} (OH).

(−)-2-(1-Methylcyclopropyl)-5-methylcyclohexanol (VII).[14] Methylene iodide (57.5 g) was added to a well-stirred suspension of anhydrous ether (125 m*l*), zinc-copper couple[15] (18.0 g), and iodine (0.1 g). To this gently-refluxing mixture, we then added a solution of (−)-isopulegol (15.4 g) in anhydrous ether (20 m*l*) over a period of 20 minutes. The mixture was stirred under reflux for an additional hour, and then it was worked up in the usual manner to yield VII (10.2 g): bp 105.0°C/15 mmHg; n_D^{25} 1.4696; d_4^{25} 0.9236; $[\alpha]_D^{25}$ −33.07° (neat); the 3,5-dinitrobenzoate derivative, mp 130.0—130.5°C; NMR ($CDCl_3$) >CH–C$\underline{H}_3$ 0.95 ppm (doublet, J=6.0 Hz, 3H), –C(–)–CH_3 0.99 (singlet, 3H), –OH 2.25 (singlet, 1H), >C$\underline{H}$–OH 3.55 (triple doublets, J_{vic}=11 and 4 Hz, 1H), $-CH_2-CH_2-$ (cyclopropane ring) 0.08—0.81 (4H); ν_{max}^{liq} 3589 cm^{-1} (OH);

(+)-2-(1-methylcyclopropyl)-5-methylcyclohexanol (VIII). The oxidation of VII with a chromium trioxide-pyridine complex afforded a ketone, which was then reduced by the Meerwein-Ponndorf-Verley method. The purification of the reaction mixture by column chromatography on silica gel with a mixture of 30% *n*-hexane in ethyl acetate gave VIII: bp 80.0—85.0°C/7 mmHg; n_D^{25} 1.4720; d_4^{25} 0.9294; $[\alpha]_D^{25}$ +28.72° (neat); mp 7.5—8.5°C; the 3,5-dinitrobenzoate derivative, mp 150.0—150.5°C; NMR ($CDCl_3$), >CH–C$\underline{H}_3$ 0.88 ppm (doublet, J=6.0 Hz, 3H), >C$\underline{H}$–OH 4.12 (multiplet, 1H), $-CH_2CH_2-$ (cyclopropane ring) 0.08—0.50 (4H), –OH 1.68 (singlet, 1H), –C(–)–CH_3 1.11 (singlet, 3H); ν_{max}^{liq} 3449 cm^{-1} (OH).

The authors wish to thank Dr. Motoichi Indō of the Takasago Perfumery Co. for his gifts of carvone, pulegone, and isopulegol.

14) W. G. Dauben and G. H. Berezin, *J. Amer. Chem. Soc.*, **85**, 468 (1963).

15) R. S. Shank and H. Shechter, *J. Org. Chem.*, **24**, 1825 (1959).

BULLETIN OF THE CHEMICAL SOCIETY OF JAPAN, VOL. 44, 207—210 (1971)

Ferrocene Polymers Obtained by the Polycondensation of Ferrocene with Dicarboxylic Acid Chlorides

Teruzo ASAHARA, Manabu SENŌ, Keiryo MITSUHASHI[1], and Yohsuke ICHIKAWA
The Institute of Industrial Science, The University of Tokyo, Roppongi, Minato-ku, Tokyo

(Received July 24, 1970)

The polycondensation reactions of ferrocene with terephthaloyl and adipoyl chloride were investigated in the presence of $AlCl_3$, $ZnCl_2$, or $FeCl_3$ as the catalyst and in dichloromethane, *n*-hexane, carbon tetrachloride, or dioxane as the solvent. With terephthaloyl chloride, the highest polymer yield was obtained when $AlCl_3$ in *n*-hexane was used, and the product was mainly of a polyketone structure. The polycondensation with adipoyl chloride afforded the most satisfactory result when ferrocene was treated in liquid adipoyl chloride with neither catalyst nor solvent, and a product with the expected structure was obtained. The average molecular weights of the products are in the range of 3000—7000. Polymers obtained by polycondensation with terephthaloyl and succinyl chloride are paramagnetic and show the temperature dependence characteristic of semi-conductivity.

Ferrocene possesses a high reactivity toward electrophilic substitution, especially toward the Friedel-Crafts acylation, and the acylation of monoacylated ferrocene affords 1,1′-disubstituted ferrocene as the main product. Therefore, it may be expected that a polyketone containing ferrocene nucleus will be produced through the polycondensation of ferrocene with a dicarboxylic acid chloride.

Recently, Neuse and Koda reported their findings on the polycondensation of ferrocene with terephthaloyl chloride.[2] They obtained the expected product, together with various by-products formed through the cleavage of the ferrocene nucleus and oxidation-reduction processes.

In the present investigation, the formation of polyketone was examined, under several sets of reaction conditions with various catalysts and solvents, by using adipoyl chloride or terephthaloyl chloride as the bifunctional acylating agent. The electric and magnetic properties of the products obtained were also measured. The results will be presented in this paper.

Experimental

Materials. Ferrocene was prepared according to the method reported by Hata *et al.*[3] and was purified by sublimation *in vacuo*; mp 172—173°C.

Terephthaloyl chloride and adipoyl chloride were prepared by the reaction of the corresponding acids with thionyl chloride in the presence of a small amount of pyridine; the former was purified by recrystallization from dry *n*-hexane, mp 81—82°C, and the latter by distillation at a reduced pressure, bp 120—123°C/12 mmHg.

Aluminum chloride, zinc chloride, and ferric chloride were dried and stored in a desiccator.

The solvents were purified by the usual methods.

Polycondensation Reactions. Ferrocene, dicarboxylic acid chloride, and a Lewis acid catalyst were mixed in a molar ratio of 1 : 1 : 2 (or >2) in a solvent and were heated at the prescribed temperature with stirring under a stream of

1) Present Address: Faculty of Engineering, Seikei University, Kichijoji, Musashino-shi, Tokyo.

2) E. W. Neuse and K. Koda, *J. Macromol. Chem.*, **1**, 595 (1966).

3) K. Hata, I. Motoyama, and H. Watanabe, This Bulletin, **38**, 853 (1965).

Table 1. Solution polycondensation of ferrocene with terephthaloyl chloride
[Ferrocene 0.02 mol, Terephthaloyl Chloride 0.02 mol]

Exp. No.	Solvent	Catalyst	(mol)	Temp. (°C)	Time (hr)	Yield of polymer[a] (%) Sol. in $CHCl_3$	Insol. in $CHCl_3$
1	dichloromethane	$AlCl_3$	0.04	35	3	3	52
5	carbon disulfide	$AlCl_3$	0.04	47	3	1.5	2
6	carbon disulfide	$AlCl_3$	0.04	47	6	2	3
7	carbon disulfide	$ZnCl_2$	0.04	47	6	<1	<1
8	carbon disulfide	$ZnCl_2$	0.04	47	20	1.5	1
9	*n*-hexane	$AlCl_3$	0.054	69	20	27	19
10	*n*-hexane	$AlCl_3$	0.054	69	30	33	25
11	*n*-hexane	$ZnCl_2$	0.073	69	10	<1	<1
12	*n*-hexane	$FeCl_3$	0.04	69	30	2	3.5
15	dimethylacetamide	$AlCl_3$	>0.04	5	100	0	0
31	cyclohexane	$AlCl_3$	0.06	83	7.5	15	5

a) The yield of product was calculated according to Eq. (1).

nitrogen gas. After a definite period, the reaction mixture was poured onto ice-water; the solid product was then collected by filtration and washed successively with water, dilute hydrochloric acid, a dilute sodium hydroxide solution, water, and hot methanol. After being dried, this product was fractionated into a soluble part and an insoluble part in chloroform. The soluble part was subsequently represipitated from methanol or *n*-hexane.

Analytical Procedures. The structure was analysed by means of a study of its IR spectrum (KBr disc). The molecular weight was measured with a vapor-pressure osmometer.

The electric conductivity and the magnetic susceptibility were measured using powdered samples packed under 1.5 kg/cm^{-1}.

Results and Discussion

Solution Polycondensation with Terephthaloyl Chloride. The results of polycondensation using various solvents and catalysts are summarized in Table 1. Each product is a reddish or dark brown powder. The products soluble in chloroform, obtained from polycondensation using $AlCl_3$ and *n*-hexane, were analysed to be as is shown in Table 2. The IR spectra of the soluble and insoluble products are shown in Fig. 1.

From these results, the main reaction to afford a soluble product may be assumed to be as follows:

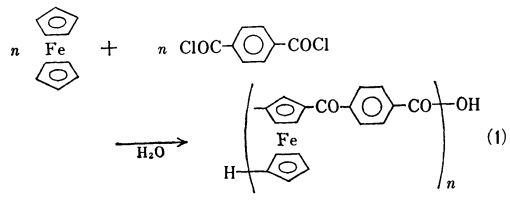

I

However, the results of the elemental analysis show a higher H content than the value calculated for I, and the IR spectrum shows a strong absorption at 2900 cm^{-1} which is assignable to a methylene group. These results suggest the occurrence of side reactions involving the cleavage of ferrocene nucleus and the reduction of carbonyl group to afford the compounds with structures II and III. This is in accord with the results obtained by Neuse and Koda.[1] They used sulfolane as the solvent.

Table 2. Analyses of polycondensation products of ferrocene with terephthaloyl chloride, soluble in $CHCl_3$

Exp. No.	Average mol wt	Degree of polymerisation[a]	Calcd for I (%) C	H	Found (%) C	H
9	3300	10	68.00	3.87	70.19	4.83
10	3600	11	86.03	3.86	68.57	5.13

a) calcd from mol wt by assuming structure I.

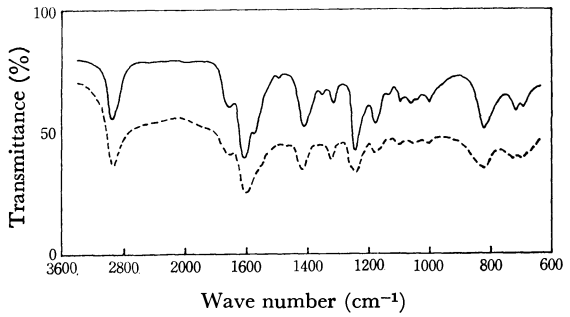

Fig. 1. IR spectra of polycondensation products of ferrocene with terephthaloyl chloride (Exp. No. 10).
—— : Sol. in $CHCl_3$, ------ : Insol. in $CHCl_3$

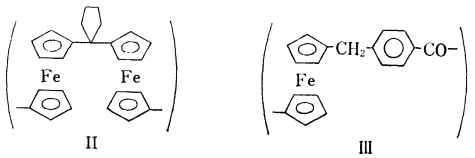

Such a dipolar aprotic solvent was considered to be favorable for this reaction, but no noticeable difference was observed in the present results, which were obtained using *n*-hexane, a nonpolar solvent.

When dichloromethane was used as a solvent, the product was mostly insoluble in chloroform. This solvent acts as a Friedel-Crafts alkylating agent to lead to cross-linking products. A similar reaction has been reported on ferrocene and dichloroethane.[4] Therefore,

4) A. N. Nesmeyanov and N. S. Kochetkova, *Dokl. Akad. Nauk SSSR*, **109**, 543 (1956); *ibid.*, **126**, 307 (1959).

an attempt to obtain a soluble methylene-bridged ferrocene polymer was made; such a polymer was indeed obtained, in 35% yield, from the reaction of ferrocene with dichloromethane catalysed by $AlCl_3$; mp 210—220°C; average molecular weight, 1600.

(Methylene group links at 1,1'-, 1,2-, or 1,3-position.)

Melt Polycondensation with Terephthaloyl Chloride. The polycondensation of ferrocene in liquid terephthaloyl chloride was carried out at 85°C without any solvent; the results are shown in Table 3. When $AlCl_3$ was used as a catalyst, a violent reaction occurred to give a decomposition product with a large carbon content. In the case of $ZnCl_2$ catalyst, a rather moderate reaction proceeded, with a low yield of polymers.

TABLE 3. MELT POLYCONDENSATION OF FERROCENCE WITH TEREPHTHALOYL CHLORIDE

[Ferrocene 0.01 mol, Terephthaloyl Chloride 0.01 mol, Temp. 85°C, Time 2 hr]

Exp. No.	Catalyst	(mol)	Yield of polymer (%) Sol. in $CHCl_3$	Insol.
20	none	—	0	0
21	$AlCl_3$	0.01	—	—
22	$ZnCl_2$	0.015	3	4

Polycondensation with Adipoyl Chloride. Ferrocene reacted with adipoyl chloride in a certain solvent or without any solvent in the manner shown in Eq. (1). The rseults are shown in Table 4.

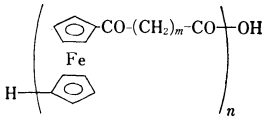

IVa: $m=4$ IVb: $m=2$

The products, the structures of which were assumed to be IVa, are pale or dark brown solids. The highest yield was obtained in the reaction at 80—100°C without any catalyst or solvent, whereas no polymeric product was obtained from the reaction with terephthaloyl chloride under similar conditions. This is likely to be the result of the difference in the solubility of ferrocene in liquid dicarboxylic acid chloride and the homogeneity of the reaction mixture.

The product (Exp. No. 43), purified by recrystallization from chloroform - *n*-hexane, was analysed as follows:

Average molecular weight, 7000 (Degree of polymerization assuming structure IVa, 24).

Found: C, 62.56; H, 5.48%. Calcd for IVa: C, 64.72; H, 5.46%.

The IR spectrum of this product shows absorptions at 2900 (CH_2), 1660 (C=O), 3050, 1440, 810 (ferrocene nucleus), 1100, and 1000 cm^{-1} (the unsubstituted cyclopentadienyl ring of terminal ferrocene) (Fig. 2). These results are in good accord with structure IVa.

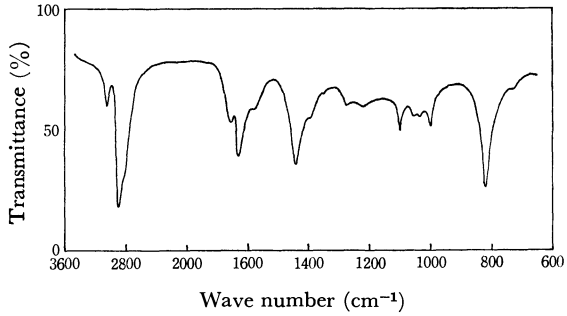

Fig. 2. IR spectrum of polycondensation product of ferrocene with adipoly chloride (Exp. No. 43).

TABLE 5. ELECTRIC CONDUCTIVITY AND MAGNETIC SUSCEPTIBILITY OF FERROCENE POLYMERS

Exp. No.	Compound	Yield of polymer (%)	σ (at room temp.) $ohm^{-1}\cdot cm^{-1}$	χ_g cgs units.	ΔE[a] eV
1	I	52	9×10^{-9}	7.3×10^{-6}	0.12
3	IV_b	75	7×10^{-9}	3.2×10^{-6}	0.52

a) ΔE was calculated from Fig. 3 by the following equation: $\rho=\rho_0 \exp(\Delta E/2kT)$ *i.e.* $\log\rho = (\Delta E/4.6k)(1/T) + \text{const.}$ where k is Boltzmann constant.

TABLE 4. POLYCONDENSATION OF FERROCENE WITH ADIPOYL CHLORIDE

[Ferrocene 0.02 mol, Adipoyl Chloride 0.02 mol]

Exp. No.	Solvent	Catalyst	(mol)	Temp. (°C)	Time (hr)	Yield of plolymer (%) Sol. in $CHCl_3$	Insol.
31	carbon tetrachloride	$AlCl_3$	0.04	30	15	12	5
32	carbon tetrachloride	$AlCl_3$ + pyridine	0.04 + 0.02	30	15	15	7
33	diethyl ether	$ZnCl_2$	0.04	0	140	0	0
34	dioxane	$ZnCl_2$	0.04	20	30	—[a]	0
40	none	$ZnCl_2$	0.02	r.t.	80	0[b]	0[b]
41	none	none	—	r.t.	45	—[a]	0
42	none	none	—	160	—[c]	—[c]	—[c]
42	none	none	—	80—100	4	55	0

a) dissolved in hot methanol.
b) As ferrocene was oxidized to ferricinium ion, condensation reaction didn't proceed to polymeric product.
c) A violet reaction proceeded to decomposition product with a large carbon content.

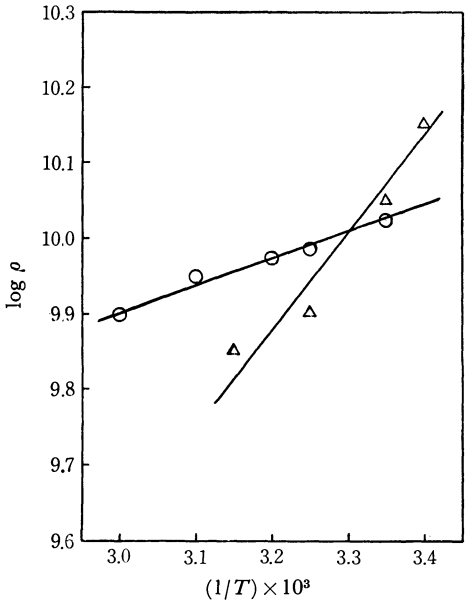

Fig. 3. The temperature dependences of specific resistance of ferrocene polymers.
○ : I, △ : IVb; T : °K

Electric and Magnetic Properties of Ferrocene Polymers. The electric conductivity and magnetic susceptibility of the products from the polycondensation reactions of ferrocene with terephthaloyl and succinyl chloride in dichloromethane are shown in Table 5. The temperature dependences of specific resistance, ρ, are shown in Fig. 3. This is characteristic of semi-conductive substances, and the order of specific conductivity agrees with the expected one. The magnetic susceptibility of ferrocene has been reported to be $\chi_a = -99.0 \times 10^{-6}$ cgs units,[5] while Karimov and Shchegolev stated that the magnetic properties of ferrocene polymers varied from paramagnetic to diamagnetic according to the method of preparation and purification.[6] Since the present specimens could not be completely purified because of insolubility, it was not possible to examine the relation of the magnetic properties to the chemical structures. In this respect, more detailed examinations are now in progress.

The authors wish to express their thanks to Professor Hiroo Inokuchi of The Institute for Solid State Physics for his kind suggestions regarding the measurement of the electric and magnetic properties.

5) L. N. Mulay and M. E. Fox, *J. Chem. Phys.*, **38**, 760 (1963).
6) Yu. S. Karimov and I. F. Shchegolev, *Dokl. Akad. Nauk SSSR*, **146**, 1370 (1962).

BULLETIN OF THE CHEMICAL SOCIETY OF JAPAN, VOL. 44, 210—214 (1971)

Studies of Peptide Antibiotics. XXV. Synthesis of an Immediate Precursor of Gramicidin S[1]

Satoru MAKISUMI, Shuji MATSUURA, Michinori WAKI, and Nobuo IZUMIYA
Laboratory of Biochemistry, Faculty of Science, Kyushu University, Hakozaki, Fukuoka

(Received July 29, 1970)

A linear decapeptide, HCO-D-Phe-Pro-Val-Orn-Leu-D-Phe-Pro-Val-Orn-Leu-$NHCH_2CH_2OH$, which has been identified as an immediate precursor of gramicidin S was synthesized in order to define the physical and biological properties of this peptide. The synthetic product possessed practically no antibacterial activity against any of the microorganisms tested, though the optical rotatory dispersion feature of this peptide was quite similar to that of gramicidin S. Stability of the terminal blocking groups of this peptide to the action of hydrogen chloride in methanol was also discussed.

For clarifying the influence of the cyclic structure of gramicidin S (GS) (I) on its antibacterial activity, several linear decapeptide analogs (II) having an amino acid sequence of the gramicidin S in which the α-amino group is acylated with formyl or acetyl and *C*-terminal amino acid in the form of its amide or ethanolamide have been synthesized in this laboratory.[2] Recently, Pollard *et al.*[3] observed the formation of another linear decapeptide (III), with formate linked to the *N*-terminal amino acid and ethanolamine to the *C*-terminus of the chain, in the cell-free biosynthesis systems as a possible intermediate of GS. However, they did not describe any of the physical and biological properties of this immediate precursor of GS. It can easily be seen that the natural analog (III) and the synthetic analogs (II) are very similar structurally, differing only in the sequence of amino acids. In connection with our original program it appeared of interest to synthesize the naturally occuring linear decapeptide and test its biological activity. This paper describes the details of the synthesis and properties of the product.

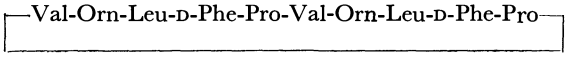

GS (I)

1) Part of this work has been briefly communicated: S. Makisumi and N. Izumiya, *Tetrahedron Letters*, **1970**, 227.

2) S. Makisumi, M. Waki, and N. Izumiya, This Bulletin, **44**, 143 (1971).

3) L. W. Pollard, N. V. Bhagovan, and J. B. Hall, *Biochemistry*, **7**, 1153 (1968).

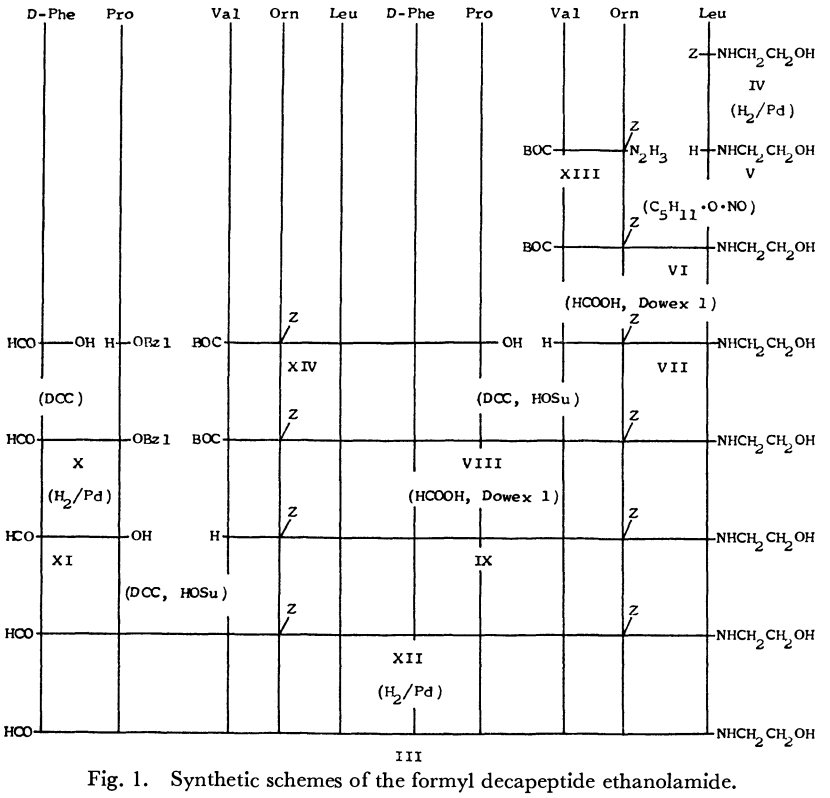

Fig. 1. Synthetic schemes of the formyl decapeptide ethanolamide.

$$\left.\begin{matrix}\text{HCO-}\\ \text{CH}_3\text{CO-}\end{matrix}\right\}\text{Val-Orn-Leu-D-Phe-Pro-}$$

$$\text{Val-Orn-Leu-D-Phe-Pro}\left\{\begin{matrix}\text{-NH}_2\\ \text{-NHCH}_2\text{CH}_2\text{OH}\end{matrix}\right.$$

Linear decapeptide analogs (II)

HCO-D-Phe-Pro-Val-Orn-Leu-D-Phe-Pro-
Val-Orn-Leu-$NHCH_2CH_2OH$

Immediate precursor of GS (III)

The steps involved in the synthesis of the formyl decapeptide ethanolamide are shown in Fig. 1.[4] Z-leucine ethanolamide (IV) was prepared by the reaction of Z-leucine with ethanolamine by means of the mixed anhydride method.[5] Compound (IV) was hydrogenolyzed to remove the Z-group and the product was isolated as the crystalline hydrochloride (V·HCl). BOC-tripeptide ethanolamide (VI) was synthesized from BOC-dipeptide hydrazide and V with the use of isoamylnitrite. Syntheses of BOC-dipeptide hydrazide (XIII) and BOC-pentapeptide acid (XIV) have already been described.[6]

Removal of the BOC-group from VI by treatment with 98% formic acid[7] and subsequent neutralization with Dowex 1 in methanol afforded free base of the tripeptide ethanolamide (VII). Condensation of BOC-pentapeptide acid with VII by the DCC–HOSu procedure[8] gave BOC-octapeptide ethanolamide (VIII) in a good yield. The BOC-group was removed from VIII by the method described above giving the free base of

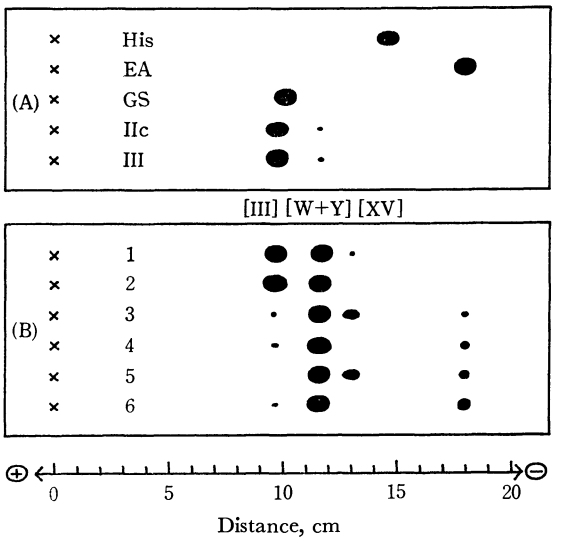

Fig. 2. Paper electrophoresis of the compounds. A: Synthetic peptide and reference compounds. EA, ethanolamine. B: Methanolysis products of the synthetic peptide; the odd numbers indicate the hydrolysates obtained before and the even after treatment with ammonia. 1,2: 0.8N HCl/MeOH, 50 min at room temperature; 3,4: 0.8N HCl/MeOH, 3 hr at room temperature; 5,6: 0.9N HCl/MeOH, 3 hr reflux.

4) Abbreviations used: Z, benzyloxycarbonyl; BOC, *t*-butyloxycarbonyl; OBzl, benzyl ester; DCC, dicyclohexylcarbodiimide; HOSu, *N*-hydroxysuccinimide. Amino acid symbol denotes L configuration otherwise noted.

5) J. R. Vaughan, Jr. and R. L. Osato, *J. Amer. Chem. Soc.*, **74**, 676 (1952).

6) M. Ohno and N. Izumiya, *ibid.*, **88**, 376 (1966); M. Ohno, T. Kato, S. Makisumi, and N. Izumiya, This Bulletin, **39**, 1738 (1966).

7) B. Halpern and D. E. Nitecki, *Tetrahedron Lett.*, **1967**, 3031.

8) F. Weyand, D. Hoffmann, and E. Wünsch, *Z. Naturforsch.*, **21b**, 426 (1966); J. E. Zimmerman and G. W. Anderson, *J. Amer. Chem. Soc.*, **89**, 7151 (1967).

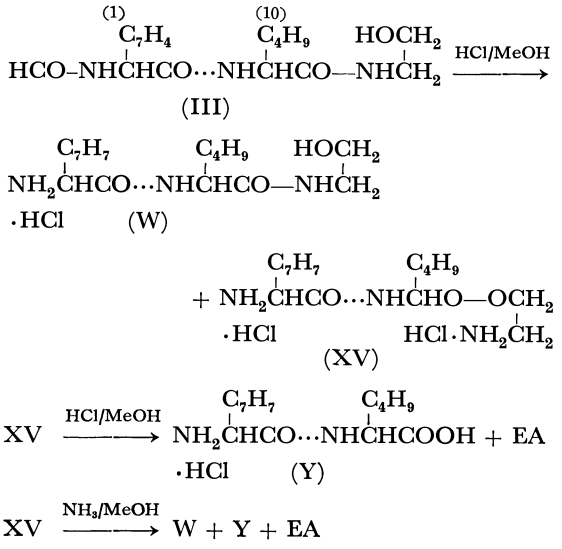

Fig. 3. Supposed reaction sequences of III by hydrogen chloride and subsequent treatment with ammonia.
EA, ethanolamine.

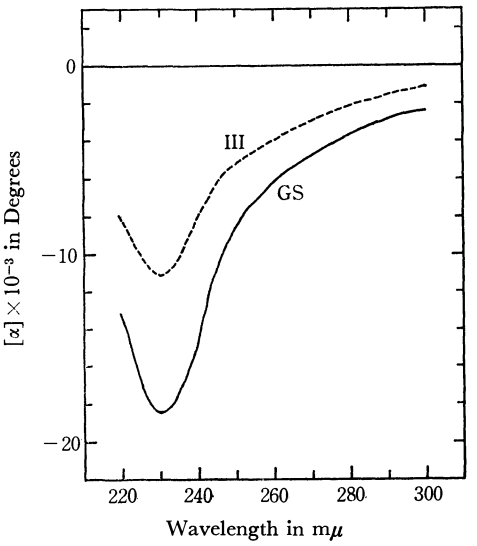

Fig. 4. Optical rotatory dispersion curves of GS (—) and linear decapeptide ethanolamide (···) in ethanol.

TABLE 1. INHIBITORY ACTIVITY OF SYNTHETIC DECAPEPTIDE AND RELATED COMPOUNDS ON MICROORGANISMS
Minimum inhibitory concentration, μg/ml

	Staphylococcus aureus FDA 209P	*Bacillus subtilis* ATCC 6633	*Escherichia coli* IMA 1253	*Proteus vulgaris* IAM 1025	*Shigella sonnei* 191—66	*Candida albicans* IAM 4888
GS·2HCl	1.56	0.75	25	>100	25	25
IIc·2HCl	25	6.25	100	>100	>100	50
III·2HCl	100	50	>100	>100	>100	>100

Octapeptide ethanolamide (IX).

Formyl dipeptide benzyl ester (X) was synthesized from formyl-D-phenylalanine and proline benzyl ester with the use of DCC.[9] Dipeptide (X) was obtained as an oil and could not be crystallized. X was hydrogenolyzed to remove the benzyl ester group and the product was isolated as crystalline dicyclohexylammonium salt. Pure formyl dipeptide (XI) obtained from the salt by treatment with Dowex 50 in methanol was coupled with IX by the DCC-HOSu procedure. This gave the protected decapeptide ethanoalmide (XII) in a good yield. Hydrogenolysis of XII in the presence of two equivalent amounts of hydrogen chloride in methanol provided the desired formyl decapeptide ethanolamide (III) as dihydrochloride.

The final product (III·2HCl) was found to be practically pure by means of elemental analysis and amino acid analysis. However, it was found to be contaminated with a minute amount of deformylated peptide by paper electrophoresis as shown in Fig. 2. It seems probable that the *N*-terminal formyl group of the peptide (III) is easily decomposed. This is comparable to the finding obtained for the formyl analogs of compound II.[2] On the contrary, Pollard *et al.*[3] reported that the formyl group in the natural peptide could not be removed from the peptide by treatment with 1.5N hydrogen chloride in methanol for 1 hr at room temperature. However, it was found that the formyl group in the synthetic peptide was relatively labile and removed easily under acidic conditions. It can be seen from Fig. 2 that the *C*-terminal ethanolamide group is apt to be rearranged by N→O acyl migration[10] with hydrogen chloride in methanol affording a deformylated decapeptide 2-aminoethyl ester (XV) to some extent. Peptide XV was easily converted to the parent peptide (W or Y) by treatment with ammonia. A supposed reaction sequence is summarized in Fig. 3.

Optical rotatory dispersion measurement at the region of 220—300 mμ revealed that the linear decapeptide exhibited apparent negative Cotton effect (see Fig. 4). This suggests that the conformational feature of the linear peptide is similar to that of GS, though the solution-state conformation of the latter compound has so far not been characterized completely.[11] In view of this experimental fact, it was expected that the linear peptide would have antibacterial activity. However, it was found that peptide (III) possessed practically no activity for any of microorganisms tested, whereas another formyl decapeptide ethanolamide (IIc) showed appreciable activity toward several strains of the Gram-positive microorganisms (Table 1). The result indicates that some linear decapeptide derivatives such as IIc possess substantial antibacterial activity though weaker than GS. Therefore, an amino acid sequence of a linear derivative affords important influence on the activity.

Experimental

Melting points are uncorrected. In thin-layer chromatography on a silica gel plate, the solvent systems used are abbreviated as follows: A, chloroform - benzene - methanol (6 : 3 : 1, *v/v*); B, chloroform - methanol (5 : 1, *v/v*); C, *s*-butanol - formic acid - water (4 : 1 : 1, *v/v*); D, ethyl acetate - pyridine - acetic acid - water (60 : 20 : 6 : 11, *v/v*); E, *n*-butanol - acetic acid - water (4 : 1 : 4, *v/v*) and F, *n*-butanol - acetic acid -

9) J. C. Sheehan and D.-D.H. Yang, *J. Amer. Chem. Soc.*, **80**, 1154 (1958).
10) A. P. Phillips and R. Baltzly, *ibid.*, **69**, 200 (1947).
11) D. Balasubramanian, *ibid.*, **89**, 5445 (1967).

pyridine - water (4 : 1 : 1 : 2, *v/v*). Paper electrophoresis was carried out on Toyo Roshi No. 50 with formic acid - acetic acid - methanol - water (1 : 3 : 6 : 10, *v/v*) buffer of pH 1.8 at 600 V/30 cm for 2 hr. Prior to analysis, desiccated samples were left in air to a constant weight. $[\alpha]_D$ of air dried samples refers to 1% solution in methanol at 23°C.

Z-Leu-NHCH$_2$CH$_2$OH (IV). To a mixed anhydride prepared at −20°C from 2.65 g (10 mmol) of Z-Leu-OH, 1.32 m*l* (10 mmol) of isobutyl chloroformate and 1.4 m*l* (10 mmol) of triethyamine in 40 m*l* of tetrahydrofuran, a chilled solution of 0.61 g (10 mmol) of ethanolamine dissolved in 5 m*l* of tetrahydrofuran was added. The mixture was then allowed to stand in a refrigerator overnight. The solvent was removed *in vacuo* and the residue was dissolved in 50 m*l* of ethyl acetate. The solution was washed successively with 3% sodium bicarbonate, 10% citric acid and water, dried over sodium sulfate, and then evaporated. The residual syrup was solidified by the addition of petroleum ether. The product was recrystallized from ethyl acetate - ether; yield 2.20 g (71%); mp 125—126°C; $(\alpha)_D$ −17.9°; R_f 0.32 (A).

Found: C, 62.23; H, 7.86; N, 8.99%. Calcd for $C_{16}H_{24}N_2O_4$: C, 62.32; H, 7.84; N, 9.08%.

H-Leu-NHCH$_2$CH$_2$OH·HCl (V·HCl). A solution of 1.23 g (4 mmol) of IV dissolved in 45 m*l* of methanol containing 4.2 m*l* of N hydrochloric acid was subjected to hydrogenolysis in the presence of palladium black. After 3 hr, the filtrate from the catalyst was evaporated to dryness and left in a desiccator over sodium hydroxide. The residue was crystallized from methanol-ethyl acetate-ether; yield 0.78 g (93%); mp 153—154°C; $[\alpha]_D$ +22.7°; R_f 0.09 (A), 0.43 (C).

Found: C, 45.42; H, 9.04; N, 13.11%. Calcd for $C_8H_{18}N_2O_2$·HCl: C,45.60; H, 9.09; N, 13.30%.

BOC-Val-Orn (δ-Z)-Leu-NHCH$_2$CH$_2$OH (VI). To a chilled solution of 959 mg (2 mmol) of BOC-Val-Orn(δ-Z)-N_2H_3 (XIII)[6] in 10 m*l* of dimethylformamide were added successively with stirring 1.45 m*l* (4 mmol) of 2.76N hydrogen chloride in dioxane and 0.272 m*l* (2 mmol) of isoamylnitrite at −5°C. After 10 min, 0.56 m*l* (4 mmol) of triethylamine and a solution of 421 mg (2 mmol) of V·HCl in 6 m*l* of dimethylformamide containing 0.28 m*l* (2 mmol) of triethylamine were added successively to the solution, and the mixture was stirred for 3 days at 0°C. After removal of the solvent, the residue was triturated with a mixture of ethyl acetate (5 m*l*) and water (50 m*l*). The product solidified was collected by filtation, washed successively with 4% sodium bicarbonate, 10% citric acid and water, and dried. It was recrystallized from methanol - ethyl acetate - ether; yield 949 mg (76%); mp 197—198°C; $[\alpha]_D$ −35.2°, R_f 0.41 (A), 0.95 (C).

Found: C, 60.09; H, 8.27; N, 11.12%. Calcd for $C_{31}H_{51}N_5O_8$: C, 59.88; H, 8.27; N, 11.26%.

H-Val-Orn(δ-Z)-Leu-NHCH$_2$CH$_2$OH (VII). BOC-tripeptide ethanolamide (VI, 622 mg, 1 mmol) was dissolved in 20 m*l* of 98% formic acid and the solution was kept at room temperature for 3 hr. The reagent was removed and the residue was triturated with ether. The crude solid (formate) was dissolved in 10 m*l* of methanol and the solution was filtered over a column (1.2×8 cm) of Dowex 1 (OH^- form, equilibrated with methanol). The effluents and the washings were evaporated. The resulting residue was crystallized by the addition of ether. The product was collected by filtration; yield 491 mg (94%); mp 180—182°C; $[\alpha]_D$ −19.8°; R_f 0.20 (A), 0.51 (B).

Found: C, 59.39; H, 8.24; N, 13.21%. Calcd for $C_{26}H_{43}N_5O_6$: C, 59.86; H, 8,31. N, 13.43%.

BOC-Val-Orn(δ-Z)-Leu-D-Phe-Pro-Val-Orn(δ-Z)-Leu-NHCH$_2$CH$_2$OH (VIII). A suspension of 412 mg (0.5 mmol) of BOC-pentapeptide acid (XIV),[6] 261 mg (0.5 mmol) of VII and 58 mg (0.5 mmol) of HOSu in a mixture of dioxane (5 m*l*) and dimethylformamide (5 m*l*) was cooled in an ice-salt bath. DCC (103 mg, 0.5 mmol) was added to the solution and the mixture was stirred under cooling; meanwhile the suspension dissolved to form a clear solution. After it had been allowed to stand overnight at room temperature, the reaction mixture was stirred again with one drop of acetic acid for 3 hr at 0°C. Crystals of dicyclohexylurea were removed by filtration and washed with cold dioxane. The filtrate and the washings were evaporated to a minute volume and the residual syrup was solidified by the addition of ice water. The solid obtained was collected by filtration, washed successively with water, 4% sodium bicarbonate, 10% citric acid and water, and dried. The product was dissolved in ethyl acetate and an isoluble material was removed. The filtrate was evaporated and the residue was crystallized by the addition of ether. The crystals obtained were dissolved in 10 m*l* of methanol and the solution was filtered over a series of columns (1.2×8 cm, each) of Dowex 50 (H^+ form) and Dowex 1 (OH^- form) which were equilibrated with methanol. The effluent and the washings were evaporated and the residue was crystallized by the addition of petroleum ether; yield 622 mg (94%); mp 156—158°C; $[\alpha]_D$ −91.0°; R_f 0.42 (A), 0.82 (B).

Found: C, 61.18; H, 7.79; N, 11.36%. Calcd for $C_{69}H_{103}N_{11}O_{15}\cdot 2H_2O$: C, 60.82; H, 7.91; N, 11.31%.

H-Val-Orn(δ-Z)-Leu-D-Phe-Pro-Val-Orn(δ-Z)-Leu-NHCH$_2$CH$_2$OH (IX). Treatment of 398 mg (0.3 mmol) of VIII with 6 m*l* of 98% formic acid followed by crystallization and filtration over a column of Dowex 1 as described above gave 335 mg (91%) of the octapeptide ethanolamide, mp 113—117°C; $[\alpha]_D$ −107°; R_f 0.22 (A), 0.56 (B).

Found: C, 60.99; H, 7.90; N, 11.84%. Calcd for $C_{64}H_{95}N_{11}O_{13}\cdot 2H_2O$: C, 60.88; H, 7.90; N, 12.20%.

HCO-D-Phe-Pro-OBzl (X). A solution of 0.97 g (5 mmol) of HCO-D-Phe-OH and 1.2 g (5 mmol) of H-Pro-OBzl·HCl in a mixture of 15 m*l* of chloroform and 15 m*l* of tetrahydrofuran containing 0.70 m*l* (5 mmol) of triethylamine was cooled in an ice-bath. With vigorous stirring 1.03 g (5 mmol) of DCC was introduced. After it had been allowed to stand overnight at 0°C, the mixture was evaporated, and ethyl acetate was added to the residue. After the insoluble dicyclohexylurea was filtered off, the filtrate was washed with 4% sodium bicarbonate, 10% citric acid and water, and dried over sodium sulfate. The filtrate was evaporated; yield of oil, 1.66 g (87%); R_f 0.44 (A).

HCO-D-Phe-Pro-OH·DCHA (XI·DCHA). A solution of 1.14 g (3 mmol) of X in 15 m*l* of methanol containing 3 drops of acetic acid was subjected to hydrogenolysis in the presence of palladium black. The filtrate was evaporated to dryness and the residue was dissolved in 10 m*l* of ethyl acetate. To the solution 0.6 m*l* (3 mmol) of dicyclohexylamine was added, and the mixture was allowed to stand in a refrigerator for 3 hr. The DCHA salt precipitated was collected, washed with ethyl acetate and ether, and dried; yield 1.02 g (72%); mp 177—178°C; $[\alpha]_D$ −51.1°.

Found: C, 66.19; H, 8.80; N, 8.58%. Calcd for $C_{27}H_{41}N_3O_4\cdot H_2O$: C, 66.23; H, 8.85; N, 8.58%.

HCO-D-Phe-Pro-Val-Orn(δ-Z)-Leu-D-Phe-Pro-Val-Orn(δ-Z)-Leu-NHCH$_2$CH$_2$OH (XII). The DCHA salt (94 mg, 0.2 mmol) of XI was dissolved in 5 m*l* of methanol and the solution was filtered through a column (1.2×4 cm) of Dowex 50 (H^+ form) in methanol. The effluent and the washings were evaporated. The formyl dipeptide acid (XI) thus obtained was reacted with 245 mg (0.2 mmol) of IX by the procedure using equimolar amount of DCC and HOSu as

has been described for the preparation of VIII. The product was purified by filtration over a series of columns of Dowex 50 and Dowex 1; yield 257 mg (86%); mp 132—135°C; $[\alpha]_D$ −81.0°; R_f 0.39 (A).

Found: C, 62.00; H, 7.50; N, 11.97%. Calcd for $C_{79}H_{111}N_{13}O_{16}\cdot 2H_2O$: C, 61.82; H, 7.55; N, 11.86%.

The molecular weight of a dried sample of XII was determined with a Hitachi Type 115 apparatus using methanol as a solvent. Found: 1477. Calcd: 1499.

HCO-D-Phe-Pro-Val-Orn-Leu-D-Phe-Pro-Val-Orn-Leu-NHCH$_2$-CH$_2$OH·2HCl (III·2HCl). A solution of 150 mg (0.1 mmol) of XII in 8 m*l* of methanol containing 0.4 m*l* of 0.25N methanolic hydrogen chloride was hydrogenolyzed over palladium black catalyst. After 3 hr, another portion of 0.4 m*l* of the hydrogen chloride was added and hydrogenolysis was continued. The progress of the reaction was checked by thin-layer chromatography. After additional 3 hr the filtrate was evaporated. When the residue was triturated with ether the peptide was obtained as a crystalline hydrochloride. Recrystallization from methanol - ether gave 107 mg (82%); mp 204—205°C; $[\alpha]_D$ −113°.

Found: C, 55.11; H, 8.06; N, 13.23; H_2O, 5.1%. Calcd for $C_{63}H_{99}N_{13}O_{12}\cdot 2HCl\cdot 4H_2O$: C, 55.01; H, 7.99; N, 13.24; H_2O, 5.2%.

The product was practically pure. However it was found to be contaminated with a minute amount of a ninhydrin positive compound which was deduced as a deformylated derivative (W) of III on the basis of electrophoretic mobility as shown in Fig. 2. The R_f values of III·2HCl and GS in several solvent systems are summarized in Table 2. Amino acid analysis of the hydrolysate of this peptide gave the molar ratios of the components as follows: Phe 2.2, Pro 1.9, Val 2.2, Orn 1.8, Leu 2.3 and ethanolamine 1.0.

TABLE 2. R_f VALUES OF SYNTHETIC LINEAR DECAPEPTIDE AND GS IN THIN LAYER CHROMATOGRAPHY

Solvent	III·2HCl	GS·2HCl
C	0.48	0.56
D[a)]	0.47	0.60
E	0.33	0.56
F	0.66	0.66

a) Pollard *et al.*[3] reported that the naturally occurring linear decapeptide (III) migrated in this solvent system with an R_f value of 0.82, whereas GS had an R_f of 0.45.

Methanolysis of III. A few mg of III·2HCl was dissolved in about 10 m*l* of 0.8N hydrogen chloride in methanol and the solution was allowed to stand at room temperature. After various periods of time two aliquots of the reaction mixture were withdrown and evaporated to dryness *in vacuo*. One of them was dissolved in methanol and the solution was subjected to paper electrophoresis. The other was dissolved in ammonia in methanol and evaporated immediately after mixing prior to electrophoretic analysis. Another few mg of III·HCl was dissolved in about 10 m*l* of 0.9N hydrochloric acid and the mixture allowed to reflux for 3 hr. The reaction products obtained before and after treatment with ammonia were subjected to electrophoresis on paper. A typical electrophoreogram is shown in Fig. 2 (B). Two unidentified peptides spots were detected. Peptide spot migrated a little more rapidly than peptide III was not characterized completely but deduced to be a mixture of a deformylated decapeptide (Y) and its ethanolamide (W) (Fig. 3). The second peptide (XV) in small amounts was not also characterized but was deduced as a 2-aminoethyl ester (Fig. 3) of Y. Occurrence of the spot corresponding to ethanolamine suggests the formation of deformylated decapeptide (Y) after the hydrolysis of 2-aminoethyl ester bond of XV. However, Y could not be distinguishable from W on this electrophoreogram because of their similar electric character under the conditions applied as for *N*, *C*-terminal free decapeptide and deformylated decapeptide ethanolamide.[2] XV peptide was not found in the reaction mixture after ammonia treatment, suggesting the loss of one basic group resulting from the reverse rearrangement of XV to W or the hydrolysis of XV to Y under alkaline condition. From the results it seems likely that the *N*-terminal formyl group is labile to be cleaved and that the *C*-terminal ethanolamide is apt to be rearranged by $N\rightarrow O$ acyl migration by mild methanolysis in presence of hydrogen chloride.

Optical Rotatory Dispersion. ORD measurements were performed with a JASCO Model ORD/UV-5 spectropolarimeter. Cell of path length 1.0 cm was used and the runs were made at ambient temperature. In Fig. 4 are reported the ORD curves (range 220—300 mμ) of the synthetic peptide and GS in ethanol solution (7.8 mg/50 m*l*).

Microbiological Assays.[12] Minimum amounts of the compounds for the complete inhibition of growth were determined by a dilution method with 10^3—10^4 organisms per milliliter using a Sabouraud bouillon as an incubation medium.

12) We are indebted to Meiji Seika Co., Ltd. for the microbiological assays.

Organic Photochemical Reactions. XIV. The Photocycloaddition of Acetone to Cyclooctene and 1,3-Cyclooctadiene[1]

Kensuke SHIMA, Yoshiki SAKAI, and Hiroshi SAKURAI
The Institute of Scientific and Industrial Research, Osaka University, Suita, Osaka

(Received August 1, 1970)

The photocycloaddition of acetone to cyclooctene (COE) or 1,3-cyclooctadiene (COD) yields isomeric *cis*- and *trans*-oxetanes in good yields. Kinetic studies of these reactions reveal that the photoaddition of acetone to COE proceeds *via* the attack of the triplet acetone on the ground state COE, while the addition to COD probably occurs by the attack of the excited singlet acetone on the ground state COD.

The photoaddition of carbonyl compounds to olefins to yield oxetanes (the Paterno-Büchi Reaction) has been the subject of much recent study. However, only a few papers on the photoreactions of ketones with eight-membered cyclic olefins or dienes have been published. The photocycloadditions of benzophenone, several *p*-quinones, and thiobenzophenone to cyclooctene and/or cyclooctadienes to yield oxetanes or thietanes have been reported.[2-4] We found that the photoaddition of acetone to cyclooctene (COE) or 1,3-cyclooctadiene (COD) afforded oxetanes in fairly good yields, while it is well-known that the photoreactions of acetone with cyclopentene or cyclohexene give mainly the products derived from hydrogen abstraction from these olefins by the acetone triplet, while oxetanes are minor products.[5] We also wish to report on the stereochemistry of oxetanes and on the kinetics of oxetane formation.

Results and Discussion

Photoaddition (Syntheses of Oxetanes). Acetone, when irradiated in the n–π^* region of the carbonyl group, readily adds to COE to give roughly equimolar mixtures of *cis*- and *trans*-oxetanes (**1** and **2**) in fairly good yields. Similarly, the irradiation of acetone and COD gives mainly *cis*- and *trans*-oxetanes (**3** and **4**, *ca.* 4 : 1).

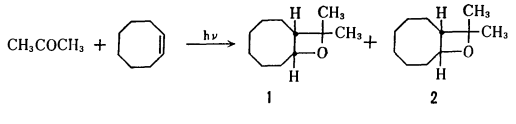

1 **2**

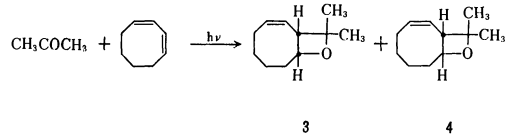

3 **4**

The products, **1**—**3**, were isolated by preparative VPC on a 3-m PEG-6000 column at 160°C. The structural identification of **1**—**4** is based on spectral analysis. The NMR spectra of **1**—**3** exhibit a low-field double triplet or septet at 5.45—5.65 τ. These absorptions are assigned to the ring hydrogen α to oxygen.[6] It is also well known that the coupling constant between H_a and H_b in *cis*-oxetanes are larger than that in *trans*-oxetanes.[7] The NMR data are shown in Table 1. These results support the stereochemical assignments for **1**, **2**, and **3**. **4** could not be separated by preparative VPC. Since the catalytic hydrogenation of **3** using an Adams catalyst gives **1**, and mixtures of **3** and **4** give those of **1** and **2**, **4** surely has a *trans*-configuration. The NMR data for **3** are similar to that of the thietane, **5**.[4,8] **1** and **2** give the same cracking patterns in the mass spectra.

TABLE 1. SUMMARY OF NMR DATA FOR OXETANES

	Chemical shift (τ)	Multiplicity	Proton assignment	Coupling constant (Hz)
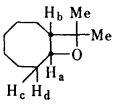	5.65	dt	H_a	$J_{ab}=J_{ac}=10$
	7.4—9.5	m	13H (Ring protons)	$J_{ad}=3.4$
	8.72	s	6H (Methyl)	
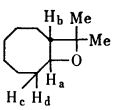	5.45	sept	H_a	$J_{ab}=6$
	7.4—9.4	m	13H (Ring protons)	$J_{ac}=10$
	8.63	s	3H (Methyl)	$J_{ad}=3.5$
	8.81	s	3H (Methyl)	
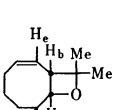	5.56	dt	H_a	$J_{ad}=J_{ac}=9$
	6.76	dd	H_b	$J_{ad}=3$
	4.48	m	2H (Vinyl)	$J_{be}=4$
	7.3—9.1	m	8H (Methylene)	
	8.61	s	6H (Methyl)	

Abbreviations used are as follows: m=multiplet; s=singlet; dt=doublet of triplets; dd=doublet of doublets; sept=septet.

The products from the photoreaction of acetone and

1) Presented at the 23rd Annual Meeting of the Chemical Society of Japan, Tokyo, April, 1970. Part XIII, Y. Nagao, K. Shima, and H. Sakurai, *Tetrahedron Lett.*, **1970**, 2221.

2) G. W. Griffin, unpublished results; D. R. Arnold, *Advan. Photochem.*, **6**, 373 (1968).

3) a) D. Bryce-Smith and A. Gilvert, *Proc. Chem. Soc.*, **1964**, 87. b) D. Bryce-Smith, A. Gilvert, and M. G. Johnson, *J. Chem. Soc., C*, **1967**, 383. c) D. Bryce-Smith, A. Gilvert, and M. G. Johnson, *Tetrahedron Lett.*, **1968**, 2863.

4) a) K. Yamada, M. Yoshioka, and N. Sugiyama, *J. Org. Chem.*, **32**, 3676 (1968). b) A. Ohno, Y. Ohnishi, and G. Tsuchihashi, *Tetrahedron Lett.*, **1969**, 283.

5) a) P. de Mayo, J. B. Stothers, and W. Templeton, *Can. J. Chem.*, **39**, 488 (1961). b) J. B. Bradshaw, *J. Org. Chem.*, **31**, 237 (1966). c) H.-D. Scharf and F. Korte, *Tetrahedron Lett.*, **1963**, 821; *Chem. Ber.*, **97**, 2425 (1964).

6) D. R. Arnold, R. L. Hinman, and A. H. Glick, *Tetrahedron Lett.*, **1964**, 1425.

7) a) N. J. Turro and P. A. Wriede, *J. Org. Chem.*, **34**, 3562 (1969). b) M. Karplus, *J. Amer. Chem. Soc.*, **85**, 2870 (1963).

8) Stereochemistry of **5** has not been mentioned in Ref. 4, but **5** is considered to have *cis*-configuration. The authors with to thank Dr. K. Yamada, Chiba University, for obtaining the NMR chart of the thietane **5**.

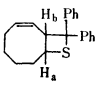 **5** $J_{ab}=10$ Hz

cyclopentene or cyclohexene are mainly unsaturated alcohols and dimers of olefins.[5] The photoreaction of acetone and COE, on the other hand, yields mainly oxetanes (**1** and **2**). These differences may be partly explained by the fact that the cycloocten-2-yl radical is less resonance-stabilized than the cyclohexen-2-yl or cyclopenten-2-yl radical, since it is well known that the two double bonds in COD are not coplanar.[4a] Consequently, in COE the addition of the acetone triplet to the double bond is more likely than the hydrogen abstraction.

Kinetic Studies. Degassed benzene solutions containing acetone (0.1—0.2 M) and varying amounts of COE or COD were irradiated using a 350-W high-pressure mercury lamp through quartz glass and a 10-mm filter solution of chromium potassium sulfate, which served to eliminate the absorption of the benzene used as a solvent. The quantum yields were determined by the simultaneous irradiation of actinometer solutions.[9] The quantum yield for oxetane formation in benzene was independent of the percentage of reaction up to 10%.

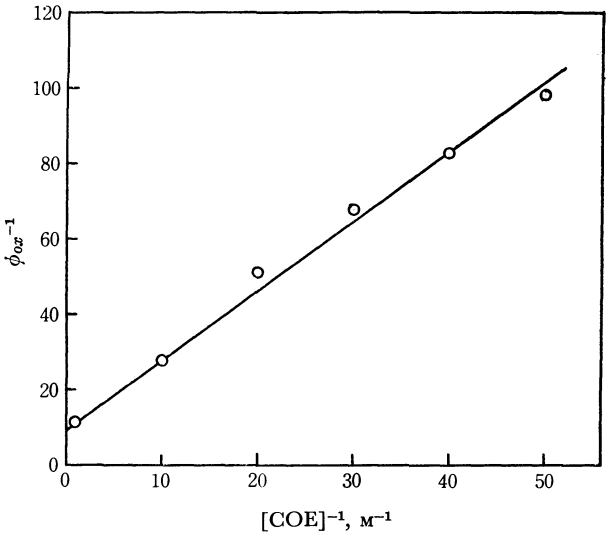

Fig. 1. Dependence of the reciprocal of the quantum yield for oxetane formation on the reciprocal of COE concentration.
Acetone (0.2 M) in benzene, Slope=1.83 M, Intercept=9.5.

Kinetics for the Acetone-COE System. Figure 1 shows the effect of the COE concentration on the quantum yields for oxetane formation.[11] Recently, Turro and Wriede have shown from kinetic analysis and quantum yield studies,[12] that the photocycloaddition of acetone to *trans*- or *cis*-1-methoxy-1-butene involves both the acetone singlet and the acetone triplet. In our experiment, however, the Stern-Volmer plot is linear, indicating that there are no significant contributions from either state of acetone under these reaction conditions. Since it is known that the acetone singlet is not measurably affected by low concentrations of piperylene, while the acetone triplet is quenched by piperylene at a rate close to that for diffusion-controlled quenching,[12] we examined the effect of piperylene on oxetane formation. The results are shown in Fig. 2. It is apparent that oxetane formation proceeds *via* the acetone triplet on the basis of the Stern-Volmer plots.

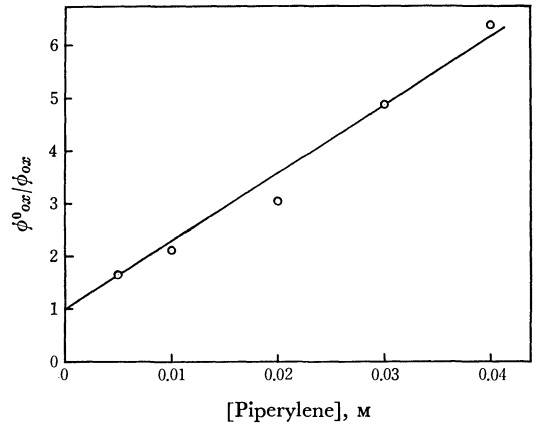

Fig. 2. Stern-Volmer plot of the quenching of oxetane formation by piperylene.
Acetone (0.2 M), COE (0.1 M) in benzene, Slope=132 M.

These observations are consistent with the following mechanism (Scheme 1):

$$A_0 \xrightarrow{h\nu} A_1 \quad (1)$$

$$A_1 \xrightarrow{k_f} A_0 + h\nu_f \quad (2)^{13}$$

$$A_1 \xrightarrow{k_{isc}} A_3 \quad (3)$$

$$A_3 \xrightarrow{k_t} A_0 \quad (4)$$

$$A_3 + O1 \xrightarrow{k^3_c} [A_3\text{-}O1] \quad (5)^{15}$$

$$[A_3\text{-}O1] \xrightarrow{k^3_{ox}} \text{Oxetane} \quad (6)$$

$$[A_3\text{-}O1] \xrightarrow{k^3_d} A_0 + O1 \quad (7)$$

$$A_3 + Q \xrightarrow{k_q} A_0 + Q_3 \quad (8)$$

Scheme 1

In this scheme, O1 represents COE, $[A_3\text{-}O1]$, a triplet 1,4-biradical intermediate, and Q, a triplet quen-

9) Acetone–2-methyl-2-butene system was employed as an actinometer. The limiting quantum yield for this system (0.50) was determined using ferrioxalate actinometry.[10]

10) H. Sakurai, K. Shima, and S. Toki, *Nippon Kagaku Zasshi*, **89**, 537 (1968).

11) In this paper, the quantum yields for oxetane formation are the sum of the quantum yields for oxetane **1** and **2** or oxetane **3** and **4**. We also have found that the ratio of **1** to **2** varies with the irradiation time, the concentration of cyclooctene, the amount of piperylene added, and the solvent used. These interesting problems are now under investigation and will be presented in near future.

12) N. J. Turro and P. W. Wriede, *J. Amer. Chem. Soc.*, **92**, 20 (1970).

13) Borkman and Kearns have shown that in the absence of singlet quenchers, all acetone singlets either intersystem cross or fluoresce and $k_{isc} \gg k_f$.[14] Therefore, unimolecular nonradiative decay process of the acetone singlet is negligible.

14) R. F. Borkman and D. R. Kearns, *J. Chem. Phys.*, **44**, 945 (1966); *J. Amer. Chem. Soc.*, **88**, 3467 (1966).

15) In other words, this is the quenching process of the acetone triplet by cyclooctene. We previously proposed the intermediacy of such 1,4-biradical intermediate in the photoaddition of benzophenone to furan.[16]

16) S. Toki and H. Sakurai, This Bulletin, **40**, 2885 (1967).

cher (piperylene). Since it has been established that the quenching of the acetone singlet by COE can very probably be excluded, kinetic analysis of Scheme 1 using the steady state approximation leads to the following expression:

$$\frac{1}{\phi_{ox}} = \left(1+\frac{k_f}{k_{isc}}\right)\left(1+\frac{k^3_d}{k^3_{ox}}\right)\left(1+\frac{k_t}{k^3_c[\mathrm{Ol}]}\right) \quad (9)$$

In the presence of a triplet quencher,

$$\frac{\phi^0_{ox}}{\phi_{ox}} = 1 + \frac{k_q[\mathrm{Q}]}{k_t + k^3_c[\mathrm{Ol}]} = 1 + k_q[\mathrm{Q}]\tau_t \quad (10)$$

where ϕ_{ox} is the quantum yield for oxetane formation and where ϕ^0_{ox} is the quantum yield for oxetane formation in the absence of an added quencher.

From the slope and intercept in Fig. 1 and $k_{isc} \gg k_f$,[14] we obtain the limiting quantum yield, $\phi_{ox}=0.11$, $k^3_d/k^3_{ox}=8.5$, $k^3_c/k_t=5.19$ M^{-1}. We can now calculate the value of the rate constants, k_t and k^3_c, from Fig. 2, since k_q, the rate constant for the quenching of A_3 by piperylene in benzene, is known to be equal to the diffusion-control quenching constant, which we shall estimate to be 5×10^9 M^{-1} sec^{-1}.[17] Thus, $k_t=2.5\times10^7$ sec^{-1} and $k^3_c=1.3\times10^8$ M^{-1} sec^{-1}. These values are in reasonable agreement with the values obtained from the photoaddition of the acetone triplet to 1-methoxy-1-butene by Turro *et al.*[12,18]

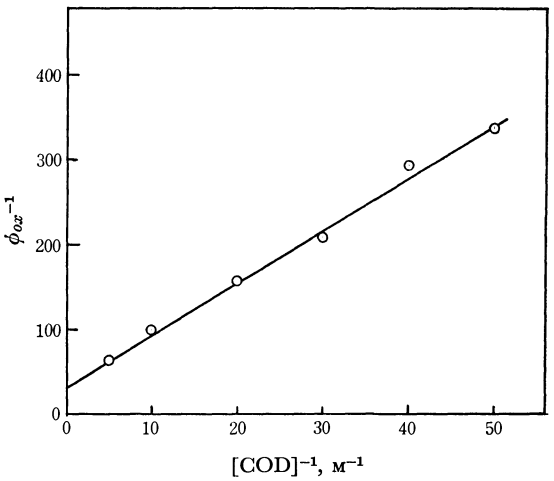

Fig. 3. Dependence of the reciprocal of the quantum yield for oxetane formation on the reciprocal of COD concentration. Acetone (0.2 M) in benzene, Slope=6.0 M, Intercept=32.

Kinetics for the Acetone-COD System. The quantum yields for oxetane formation at various COD concentrations are plotted as reciprocals in Fig. 3. In this acetone-COD system, the Stern-Volmer plot is also linear. Recently, we proposed that the photoaddition of propionaldehyde to conjugated dienes, such as 1,3-cyclohexadiene, 2,3-dimethyl-1,3-butadiene, isoprene, and piperylene, occurs from an excited singlet state of propionaldehyde.[19] The photoreaction of acetophenone with COD did not afford oxetanes at all, but gave the dimers of COD as the main products. These dimers are obtained from the attack of the triplet COD produced by acetophenone sensitization on the ground-state COD. These aromatic ketones have singlet state lifetimes of the order of 10^{-10} sec, too short for efficient bimolecular reactions to occur.[20] The oxetane formation from acetone and COD was little affected by the addition of 1,3-cyclohexadiene, which is very efficient triplet quencher.[21] These observations support the concept that oxetanes are produced from the interactions between an excited singlet state of acetone and ground state COD.

Scheme 2 accomodates our observations of the acetone-COD reaction:

$$A_0 \xrightarrow{h\nu} A_1 \quad (1)$$

$$A_1 \xrightarrow{k_f} A_0 + h\nu_f \quad (2)$$

$$A_1 \xrightarrow{k_{isc}} A_3 \quad (3)$$

$$A_1 + D \xrightarrow{k^1_c} [A_1\text{-}D] \quad (11)^{22}$$

$$[A_1\text{-}D] \xrightarrow{k^1_{ox}} \text{Oxetane} \quad (12)$$

$$[A_1\text{-}D] \xrightarrow{k^1_d} A_0 + D \quad (13)$$

Scheme 2

D is COD, and $[A_1\text{-}D]$, a singlet complex. A Stern-Volmer analysis of the oxetane formation from acetone and COD as a function of the COD concentration, assuming Scheme 2, results in Eq. (14).

$$\frac{1}{\phi_{ox}} = \left(1+\frac{k^1_d}{k^1_{ox}}\right)\left(1+\frac{k_f+k_{isc}}{k^1_c[\mathrm{D}]}\right) \quad (14)$$

From the slope and intercept in Fig. 3, we obtain the limiting quantum yield, $\phi_{ox}=0.031$, $k^1_d/k^1_{ox}=31$, and $k^1_c/(k_f+k_{isc})=5.3$ M^{-1}. $(k_f+k_{isc})^{-1}$ is equal to τ_s, the measured acetone singlet lifetime in the absence of the singlet quencher,[14] while τ_s has been reported to be *ca.* 2 nsec.[23,25] Using this value of τ_s, the calculated

Table 2. Limiting quantum yields and rate constants for oxetane formation

Carbonyl compounds	Diene	ϕ_{ox}	k^1_d/k^1_{ox}	$k^1_c/(k_f+k_{isc})$ M^{-1}
Acetone	COD	0.031	31	5.3
Propionaldehyde	COD	0.2	4	2.2
Propionaldehyde	CHD	0.086	10.6	7.3

17) P. J. Wagner and I. Kochevar, *J. Amer. Chem. Soc.*, **90**, 2232 (1968).

18) They report the value of $\sim1.7\times10^8$ and $\sim7\times10^7$ M^{-1} for rate constants for quenching of the acetone triplet by 1-methoxy-1-butene, and $\sim10^7$ sec^{-1} for k_t.

19) T. Kubota, K. Shima, S. Toki, and H. Sakurai, *Chem. Commun.*, **1969**, 1462.

20) D. R. Kearns and W. A. Case, *J. Amer. Chem. Soc.*, **88**, 5087 (1966).

21) L. M. Stephenson and G. S. Hammond, *Pure Appl. Chem.*, **16**, 125 (1968).

22) This is the quenching process of the acetone singlet by COD. The nature of the singlet complex is uncertain yet. We have considered that the inefficiency in this photocycloaddition is attributed to the formation of the intermediate complex, which combines to give oxetanes or dissociates to ground-state acetone and COD. This concept has been suggested by Turro *et al.*[23] and Singer *et al.*[24]

23) J. C. Dalton, P. A. Wriede, and N. J. Turro, *J. Amer. Chem. Soc.*, **92**, 1318 (1970).

24) L. A. Singer, G. A. Davis, and V. P. Muralidharan, *ibid.*, **91**, 897 (1969).

25) F. Wilkinson and J. T. Dubois, *J. Chem. Phys.*, **39**, 377 (1963).

rate constant for the formation of the singlet complex (k^1_c) is 2.7×10^9 M^{-1} sec^{-1}. This rate constant is within an order of magnitude of the diffusion-controlled rate constant in benzene, and it is in good agreement with that of the quenching of the singlet acetone by 1,2-dicyanoethylene.[23,26]

Table 2 summarizes the results of oxetane formation from the acetone singlet, as well as the preliminary results obtained from the singlet addition of propionaldehyde to 1,3-cyclohexadiene (CHD) and COD.

Since the rate constants for intersystem crossing or fluorescence in propionaldehyde are still unknown, a detailed comparison of the results is impossible, but the large limiting quantum yield in the case of propionaldehyde is probably due to the more efficient oxetane formation from a singlet complex.[27]

Experimental

General. The nuclear magnetic resonance spectra were taken on a Hitachi Perkin-Elmer R-20 High Resolution NMR Spectrometer, using tetramethylsilane as the internal standard. The gas-chromatographic analyses were run on a Shimadzu Gas Chromatograph, GC-3AF. The acetone (Wako Pure Chem. Co.) was purified by the ordinary method.[28] The COE and COD were purified by fractional distillation using a spinning-band column, and were redistilled prior to use. The benzene was purified by three successive crystallizations, with a rejection of about one-fourth of the benzene at each freezing, and by distillation with a spinning-band column.

Photoaddition of Acetone to Cyclooctene. Pyrex, doughnut-type vessels containing acetone (29 g) and COE (55 g) were placed outside a quartz immersion well and irradiated for 50 hr with a 350-W high-pressure mercury lamp at room temperature. The unreacted materials were then distilled off, and the portion boiling at 70—85°C/4 mmHg (10.8 g) was collected. Residues, 16.6 g. The adducts were isolated by preparative VPC on a 3-m PEG-6000 column (10 mm i. d.) at 160°C. Bp 73—74°C/4 mmHg; n_D^{27} 1.4644.

Found: C, 78.55; H, 11.91%; mol wt, 171. Calcd for $C_{11}H_{20}O$: C, 78.51; H, 11.98%; mol wt, 168.

Adduct **1** had a retention time of 11.2 min at 160° and was collected as a colorless oil by preparative VPC: IR spectra 970 and 945 cm^{-1}: NMR ($CDCl_3$) τ 5.65 (H_a, dt, $J_{ab}=J_{ac}=10$ Hz; $J_{ad}=3.4$ Hz), 8.72 ($2CH_3$, 6H, s), 7.4—9.5 (13H, m); $m/e=168$ (parent), 110 ($M-CH_3COCH_3$).

Adduct **2**: retention time, 12.5 min. (160°C); IR spectra 960 cm^{-1}; m/e, 168 (parent), 110 ($M-CH_3COCH_3$); NMR ($CDCl_3$), τ 5.45 (H_a, sept, $J_{ab}=6$ Hz; $J_{ac}=10$ Hz); $J_{ad}=3.5$ Hz), 8.63 and 8.81 (CH_3, s), 7.4—9.4 (13H, m).

Photoaddition of Acetone to 1,3-Cyclooctadiene. A mixture of acetone (34 g) and COD (53 g) was irradiated through Pyrex for 50 hr. After the removal of the unreacted materials, the fraction boiling at 100—110°C/18 mmHg was collected; yield, 19.0 g. Residue, 9.5 g. The 1 : 1 adducts were isolated by preparative VPC; bp 102—103°C/17 mmHg, n_D^{25} 1.4769.

Found: C, 79.63; H, 10.96%; mol wt, 169. Calcd for $C_{11}H_{18}O$: C, 79.46; H, 10.92%; mol wt, 166.

Quantum Yields. Benzene solutions (4 m*l*) containing 0.1—0.2 M acetone and 0.02—1.0 M COE or COD were degassed and sealed in 10-mm o. d. quartz tubes which had been attached to Pyrex tubes *via* graded seals. The sample tubes were then irradiated on a merry-go-round apparatus at room temperature, using a 350-W high-pressure mercury lamp and a filter solution with a path length of about 1 cm containing 150 g chromium potassium sulfate made up to 1 *l* with distilled water. This filter system completely eliminated the absorption of the benzene used as the solvent. Photolyses were carried out to 10% or less conversion (irradiation time, less than 6 hr); the conversion was linear to the irradiation time in these regions. Actinometers (acetone-2-methyl-2-butene system) were photolyzed simultaneously, and the quantum yields were computed relative to the actinometers. The solutions were analyzed on a Shimadzu Gas Chromatograph, GC-3AF, with a 3-m column packed with PEG-6000 (25%) on Shimalite at 160°C, using acetophenone (in the case of COE) or propiophenone(COD) as the internal standard.

Quenching Studies. The samples were prepared, degassed, and analyzed in the same way as in the quantum-yield determination, except that varying amounts of quenchers were added to the solution.

26) Turro *et al.* report the following values. $k^1_c/(k_f+k_{isc})=5.1$ M^{-1}, $k^1_c=2.5-5.0\times10^9$ M^{-1} sec^{-1}.

27) Quantum yields for oxetane formation from the propionaldehyde triplet and olefins are also as about 10 times as larger than those from the acetone triplet and olefins.[10] We have proposed that these differences are due to the more efficient oxetane formation from a triplet 1,4-biradical intermediate in the case of propionaldehyde.[10]

28) A. Bramley, *J. Chem. Soc.*, **59**, 10 (1916).

The Nitrosation of β-Keto Sulfoxides[1]

Yoshio Otsuji, Yasuhiro Tsujii, Akihiko Yoshida, and Eiji Imoto

Department of Applied Chemistry, College of Engineering, University of Osaka Prefecture, Sakai-shi, Osaka

(Received August 3, 1970)

β-Keto sulfoxides were prepared by the reaction of the esters with the methylsulfinyl carbanion. The nitrosation of the β-keto sulfoxides, $RCOCH_2SOCH_3$ ($R=C_6H_5$, $C_6H_5CH_2CH_2$, n-C_3H_7), with sodium nitrite and hydrochloric acid gave the corresponding α-chloro-α-isonitroso ketones, RCOC(=NOH)Cl, in high yields. However, the nitrosation of α-substituted β-keto sulfoxide, $RCOCH(R')SOCH_3$, in a similar manner afforded the α-isonitroso ketones, RCOC(=NOH)R′. The mechanisms of these reactions were studied.

Aliphatic and aromatic carboxylic esters have been converted to β-keto sulfoxides by the reaction of the esters with the methylsulfinyl carbanion.[2,3] The active methylene group lying between the keto and sulfoxide groups is very reactive toward electrophilic reagents and is readily brominated or alkylated to give the corresponding substituted β-keto sulfoxides.[4,5] In a previous communication[6] we reported that ω-(methylsulfinyl)-acetophenone (IIa), which can be prepared from ethyl benzoate (Ia), afforded ω-chloro-ω-isonitrosoacetophenone (IIIa) in a high yield upon treatment with sodium nitrite and hydrochloric acid.

In this paper we will describe the results of a detailed study of this reaction and of an extension of it to other compounds; it provides a useful general method for the preparation of α-keto-α-chloro-isonitroso compounds.

Results and Discussion

Preparation of β-Keto Sulfoxides. Four carboxylic esters (Ia—Id) were treated in dimethyl sulfoxide (DMSO) with 2 equiv. of the methylsulfinyl carbanion, prepared by the reaction of DMSO with sodium hydride.[2] This treatment afforded the corresponding β-keto sulfoxides (IIa—IId) in high yields.

$$\underset{\text{I}}{RCO_2C_2H_5} + {}^{-}CH_2SOCH_3 \longrightarrow \underset{\text{II}}{RCOCH_2SOCH_3}$$

a, $R=C_6H_5$; b, $R=C_6H_5CH_2CH_2$;
c, $R=n$-C_3H_7; d, $R=n$-C_6H_{13}

Ethyl phenylacetate could not be converted to the β-keto sulfoxide by this method, but it produced phenylacetic acid in an almost quantitative yield after the treatment of the reaction mixture with dilute hydrochloric acid. These results indicate that, in the case of ethyl phenylacetate, the proton transfer from the α-carbon of the ester to the methylsulfinyl carbanion predominates over the carbonyl addition of the anion because of the high acidity of the ester relative to the carbanion.

The treatment of the sulfoxide IIa with sodium hydride in tetrahydrofuran, followed by the addition of methyl iodide to the solution, gave a mixture of diastereoisomers of ω-methyl-ω-(methylsulfinyl)-acetophenone (IIe).[5] Upon the cooling of this mixture, one of the diastereoisomers crystallized; it was used for the successive reaction.

$$\underset{\text{IIa}}{C_6H_5COCH_2SOCH_3} + CH_3I \xrightarrow{NaH} \underset{\text{IIe}}{C_6H_5COCH(CH_3)SOCH_3}$$

Nitrosation of β-Keto Sulfoxides. When an aqueous solution of the sulfoxides (IIa, IIb, and IIc) containing an equiv. of sodium nitrite was acidified with hydrochloric acid and the mixture was then stirred for 1—3 hr at room temperature, α-chloro-α-isonitroso ketones (III) were obtained in the yields indicated in Table 1. No appreciable change in the yield of III was observed by the use of 2 equiv. of sodium nitrite. The application of this reaction to the sulfoxide IId produced a brown oil which could not be purified. It was also shown that the isonitroso compounds, III, can be obtained without the isolation of the sulfoxides, II, by starting with the carboxylic esters. For example, Ia afforded IIIa in an overall yield of 80%.

$$\underset{\text{II}}{RCOCH_2SOCH_3} + NaNO_2 \xrightarrow{HCl} \underset{\text{III}}{RCOC(Cl)=NOH}$$

Table 1. Formation of α-chloro-α-isonitroso ketones (III)

Compound	R	Yield, %
IIIa	C_6H_5	80
IIIb	$C_6H_5CH_2CH_2$	84
IIIc	n-C_3H_7	82

The IR and NMR spectra of III were in accordance with the assigned structures. For example, IIIa showed an absorption due to the carbonyl group at 1660 cm^{-1} in the IR spectrum and an absorption due to an extremely acidic proton of the hydroxyl group at τ −3.68 in the NMR spectrum.

However, when the α-substituted β-keto sulfoxide IIe was nitrosated in a similar manner, a mixture of isonitrosopropiophenone (IV) and 1-phenylpropane-1,2-dione (V) was obtained. The relative yields of IV and V depended upon the reaction conditions employed.

1) A part of the results of this investigation was presented at the 19th Symposium on Organic Reaction Mechanisms, Yamagata, October, 1968.

2) E. J. Corey and M. Chaykovsky, *J. Amer. Chem. Soc.*, **86**, 1639 (1964); *ibid.*, **87**, 1345 (1965).

3) H.-D. Becker, G. J. Mikol, and G. A. Russell, *ibid.*, **85**, 3410 (1963).

4) G. A. Russell and G. J. Mikol, *ibid.*, **88**, 5498 (1966).

5) G. A. Russell, E. Sabourin, and G. J. Mikol, *J. Org. Chem.*, **31**, 2854 (1966).

6) Y. Otsuji, H. Yabune, and E. Imoto, This Bulletin, **41**, 1745 (1968).

$$\text{IIe} + NaNO_2 \xrightarrow{HCl} C_6H_5COC(CH_3)(NOH) + C_6H_5COCOCH_3$$
IV V

Under conditions where the reaction was conducted at 0—5°C using an excess of sodium nitrite, IV was isolated only when the reaction time was 15 min; an extension of the reaction time to 2 hr gave only V as an isolable product.

In order to explain these observations, the hydrolysis of IV to V was studied in some detail. When IV was subjected to hydrolysis in dilute hydrochloric acid and in the presence of sodium nitrite at 0—5°C, V was obtained in a high yield. However, the treatment of IV with hydrochloric acid in the absence of sodium nitrite under identical conditions resulted in the recovery of the starting material. These results clearly indicate that the hydrolysis of IV is assisted by nitrous acid. Brooks and his co-workers[7] have previously found that steroidal ketoximes can readily be hydrolyzed to the corresponding ketones in the presence of nitrous acid, and they have proposed the following mechanism for the action of nitrous acid:

$$RR'C{=}\overset{\curvearrowright}{N}{-}O{-}H \longrightarrow RR'C{=}\overset{+}{N}{-}O^- \longrightarrow RR'CO + N_2O$$
$$\searrow NO^+ \qquad\qquad | NO$$

The hydrolysis of IV in hydrochloric acid in the presence of nitrous acid must proceed by a mechanism similar to that shown above.

The structure of IV was confirmed by comparing it with an authentic sample prepared by the nitrosation of propiophenone.[8] The structure of V was established by converting it to its disemicarbazone.

Becker and Russell[9,10] have recently found that the treatment of dimethyl phthalate (VIa) with 2 equiv. of the methylsulfinyl carbanian, followed by the acidification of the reaction mixture with hydrochloric acid, yields 2-chloro-2-methylthio-1,3-indanedione (VIIIa) through the intermediate (VIIa), which is analogous in structural type to IIe, *i.e.*, α-substituted β-keto sulfoxide. In the light of their investigations, VIa was treated with 2 equiv. of the methylsulfinyl carbanion, and the resulting mixture was nitrosated with sodium nitrite and hydrochloric acid. As expected, the reaction took place in a manner similar to that for IIe to give 2-nitroso-1,3-indanedion (IXa) in a 37% yield.[6] In a similar manner, dimethyl 4-methoxyphthalate (VIb) was converted to 5-methoxy-2-nitroso-1,3-indanedione (IXb) in a 66% yield.[6]

The structure of IXa was confirmed by comparing it with an authentic sample prepared by the nitrosation of 1,3-indanedione,[11] its IR and NMR spectra (see Experimental section) showed that IXa exists predominantly in the form of IX'a. The structure of IXb was established by comparing it with an authentic sample obtained by a method previously reported.[12] However, the predominant form among the possible isomeric structures for IXb remains unestablished.

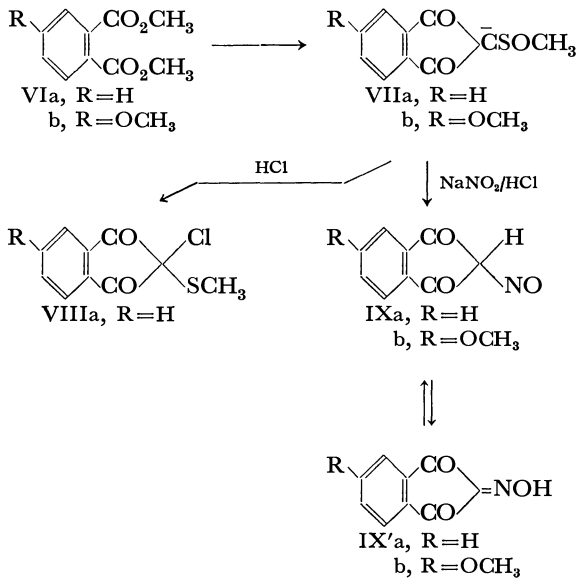

Mechanistic Studies. Inspection of the structures of the products obtained above suggests that two reactions, the Pummerer rearrangement of the sulfoxide group and the nitrosation of the active methylene group, may somehow be involved in the nitrosation of the β-keto sulfoxide. Which reaction takes place first? In order to solve this question, the following experiments were undertaken.

Compound VIIIa, prepared by the method of Becker and Russell,[9] was subjected to nitrosation under conditions similar to those employed for the nitrosation of β-keto sulfoxides. This experiment resulted in the recovery of the starting material, implying that the nitrosation takes place in advance of the Pummerer rearrangement. Futher evidence was obtained by the isolation of a plausible intermediate of the reaction.

The treatment of IIa with isoamyl nitrite in ethanol, using sodium ethoxide, gave ω-nitroso-ω-(methylsulfinyl) acetophenone (X). The IR and NMR spectra (see Experimental section) showed again that X exists predominantly in the form of X'. Upon refluxing X' in hydrochloric acid for 5 hr, IIIa was isolated from the reaction mixture.

$$\text{IIa} + i\text{-AmONO} \xrightarrow{C_2H_5ONa} C_6H_5COCH(NO)SOCH_3$$
X

$$\rightleftharpoons C_6H_5COC(=NOH)SOCH_3 \xrightarrow{HCl} \text{IIIa}$$
X'

These results suggest that the reaction proceeds through the pathways represented in Scheme 1:

7) S. G. Brooks, R. M. Evans, G. F. H. Green, J. S. Junt, A. G. Long, B. Mooney, and L. J. Wyman, *J. Chem. Soc.*, **1958**, 4614.
8) W. H. Hartung and F. Crossley, "Organic Syntheses," Coll. Vol. II, p. 363 (1948).
9) H.-D. Becker and G. A. Russell, *J. Org. Chem.*, **28**, 1896 (1963).
10) H.-D. Becker, *ibid.*, **29**, 1358 (1964).
11) W. Wislicenus, *Ann. Chem.*, **246**, 347 (1888).
12) Y. Otsuji, H. Yabune, and E. Imoto, This Bulletin, **42**, 732 (1969).

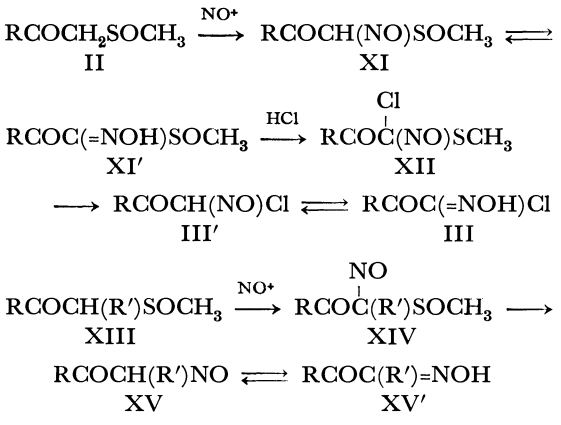

Scheme 1

For the β-keto sulfoxides (II), the nitrosation takes place first to produce XI, which would be in equilibrium with XI'. The Pummerer rearrangement of XI[13] gives XII, which then affords the final product, III, by an unusual cleavage of the C–S bond. The driving force of this cleavage might be an accumulation of the electronegative groups on the α-carbon which stabilizes the carbanion. Thus, upon the hydrolysis of XII, the sulfur bore a positive charge and was removed as methylsulfenic acid. The other plausible mechanism of the cleavage of XI would be a direct nucleophilic attack of the chloride ion on the α-carbon of XI to form III:

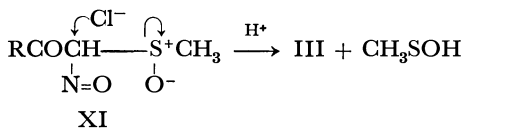

However, the above both mechanisms remained undiscriminated in this investigation.

For the α-substituted β-keto sulfoxides, XIII, the nitrosation gives XIV, which then produces the final product, XV or XV'. A possible mechanism of this final conversion would be:

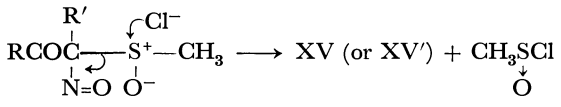

Although this kind of nucleophilic substitution on the sulfoxide sulfur is very rare, the electronegative groups at the α-position may force it to take place.

Experimental

The melting points are uncorrected. The IR spectra were recorded on a Hitachi EPI-S2 infrared spectrophotometer. The NMR spectra were obtained on a Hitachi H-60 high-resolution NMR spectrometer, with TMS as the internal standard. The elemental analyses were performed with a Yanagimoto MT-1 CHN Corder.

13) It is necessary, if the Pummerer rearrangement is to take place, that β-keto sulfoxides have an acidic hydrogen at the α-position. Thus, the rearrangement of the β-keto sulfoxides must occur from the form of XI (not from the form of XI'). In the rearrangement of the isolated X, relatively vigorous conditions were required for the reaction; this supports the idea that the favorable form of the compound is X (not X').

Reagents. DMSO was purified by two distillations over calcium hydride under reduced pressure. A commercial sodium nitrite (97% purity) was used without further purification. Unless otherwise noted, the methylsulfinyl carbanion in DMSO was prepared by the method of Corey and Chaykovsky[2] from sodium hydride and DMSO.

Preparation of β-Keto Sulfoxides. General Procedure: A 1.5 to 2 M solution of the methylsulfinyl carbanion in DMSO was prepared and diluted with an equal volume of dry tetrahydrofuran (THF). A solution of the carboxylic ester (0.5 equiv. based on 1 equiv. of the carbanion) in THF was stirred, over a period of 30 min, into the solution of the carbanion under cooling in an ice bath. The ice bath was then removed, and stirring was continued for 1 hr; the reaction mixture was then poured into three times its volume of water, acidified with hydrochloric acid to a pH of 3—4, and thoroughly extracted with chloroform. The combined chloroform extracts were washed four times with water, dried over anhydrous sodium sulfate, and evaporated to dryness to yield the crude β-keto sulfoxide. The crude product, if solid, was triturated with cold ether or isopropyl ether and collected by filtration to give the product, which was generally in a good state of purity and which could be used for the successive reactions without further purification. The crude product, if liquid, was distilled under reduced pressure to give the pure product.

The reaction of the methylsulfinyl carbanion with ethyl phenylacetate under similar conditions did not afford the corresponding β-keto sulfoxide, but it did give the hydrolysis product, phenylacetic acid, in an almost quantitative yield.

ω-(Methysulfinyl)acetophenone (IIa).[2] The treatment of 15 g (0.1 mol) of ethyl benzoate (Ia) with 0.2 mol of the methylsulfinyl carbanion yielded 14.4 g (79%) of IIa as a white crystalline solid after the trituration of the crude product with ether; mp 86—87°C (lit,[2] mp 86—86.5°C).

Methylsulfinylmethyl β-Phenethyl Ketone (IIb). The treatment of 8.9 g (0.05 mol) of ethyl dihydrocinnamate with 0.1 mol of the methylsulfinyl carbanion yielded 8.7 g (88%) of IIb as a white crystalline solid after recrystallization from isopropyl ether; mp 64—65°C.

Found: C, 62.74; H, 6.81%. Calcd for $C_{11}H_{11}O_2S$: C, 62.86; H, 6.67%.

IR (KBr): 1700 (C=O), 1360, 1020 cm^{-1} (SO). NMR ($CDCl_3$): τ 6.30 (2H, *s*, $COCH_2SO$), 7.10(4H, *s*, CH_2CH_3), 7.44 (3H, *s*, $SOCH_3$).

Methylsulfinylmethyl n-*Propyl Ketone (IIc).* The treatment of 5.8 g (0.05 mol) of ethyl butyrate (Ic) with the methylsulfinyl carbanion yielded a brown liquid. The distillation of the liquid gave 4.0 g (54%) of IIc as a yellow liquid; bp 114—115°C/2 mmHg.

Found: C, 48.38; H, 8.24%. Calcd for $C_6H_{12}O_2S$: C, 48.64; H, 8.16%.

IR ($CHCl_3$): 1720 (C=O), 1310, 1030 cm^{-1} (SO). NMR (CCl_4): τ 6.22 (2H, *s*, $COCH_2SO$), 7.4 (3H, *s*, $SOCH_3$), 8.22—9.20 (7H, *m*, $CH_3CH_2CH_2$).

Methylsulfinylmethyl n-*Pentyl Ketone (IId).*[2] The treatment of 7.2 g (0.05 mol) of ethyl caproate (Id) with 0.1 mol of the methylsulfinyl carbanion yielded 6.8 g (72%) of IId after the recrystallization of the crude product from 1 : 1 isopropyl ether-petroleum ether; mp 44—45°C (lit,[2] mp 45—46.5°C).

ω-Methyl-ω-(methylsulfinyl)acetophenone (IIe).[5] This compound was prepared by the method of Russell, Sabourin, and Mikol[5] from IIa and methyl iodide. The crude product, obtained as a yellow oil, was cooled in an ice bath to give a solid which was a diasteroisomer. The crude solid was then washed with ether to afford a white solid which melted

at 74—75°C and which was used for the successive reactions without further purification.

Nitrosation of β-Keto Sulfoxides with Sodium Nitrite in Hydrochloric Acid. General Procedure. Into a mixture of the β-keto sulfoxide (0.01 mol) and sodium nitrite (0.02 mol) in water (25 m*l*), we stirred, drop by drop, an equal volume of a concentrated hydrochloric acid with cooling in an ice bath. After the ice bath had then been removed, stirring was continued for 2 hr at room temperature. The solid thus obtained was separated by filtration and recrystallized to yield the nitroso compound.

The nitrosation of methylsulfinylmethyl *n*-pentyl ketone (IId) by this procedure gave a brown oil which could not be solidified and which was decomposed upon distillation under reduced pressure.

ω-Chloro-ω-isonitrosoacetophenone (IIIa). **A.** The treatment of 1.5 g (0.008 mol) of IIa with 1.2 g (0.016 mol) of sodium nitrite and hydrochloric acid immediately gave the crude product as a white precipitate. Recrystallization from chloroform afforded 1.23 g (84%) of IIIa as white needles; mp 132—133°C (lit,[14] 131—132°C).

Found: C, 52.40; H, 3.29; N, 7.76%. Calcd for $C_8H_6O_2NCl$: C, 52.33; H, 3.29; N, 7.63%.

IR (KBr): 3350 (OH), 1660 cm^{-1} (C=O). NMR (DMSO-d_6): τ −3.68 (1H, *s*, OH), 1.95—2.46 (5H, *m*, aromatic).

This compound was identical in every respect with the authentic sample prepared by the method of Rheinbodt and Dumont.[14]

B. A similar treatment of 3.8 g (0.025 mol) of IIa and 1.8 g (0.025 mol) of sodium nitrite and hydrochloric acid gave 3.4 g (80%) of IIIa. Thus, no appreciable change in the yield of IIIa was observed upon using equal molar quantities of IIa and sodium nitrite.

1-Chloro-1-isonitroso-4-phenylbutanone-2 (IIIb). The treatment of a mixture of 3 g (0.014 mol) of IIb and 2 g of sodium nitrite in 50 m*l* of water with 50 m*l* of hydrochloric acid for 2.5 hr yielded a yellow solid which was collected by filtration and washed with water. The recrystallization of the solid from carbon tetrachloride gave 2.5 g (84%) of IIIb as white needles; mp 98°C.

Found: C, 56.74; H, 4.67; N, 6.69%. Calcd for $C_{10}H_{10}O_2NCl$: C, 56.73; H, 4.73; N, 6.62%.

IR (KBr): 3230 (OH), 1695 cm^{-1} (C=O). NMR ($CDCl_3$): τ 0.73 (1H, *s*, OH), 2.30—3.25 (5H, *m*, aromatic), 6.64—7.16 (4H, *m*, CH_2CH_2).

1-Chloro-1-isonitrosopentanone-2 (IIIc). The treatment of a mixture of 3 g (0.02 mol) of IIc and 3 g of sodium nitirte in 50 m*l* of water with 50 m*l* of hydrochloric acid for 2 hr, after which the mixture was allowed to stand overnight, yeilded a brown solid. The recrystallization of the solid from carbon tetrachloride gave 2.5 g (82%) of IIIc as white crystals; mp 65—67°C.

Found: C, 39.98; H, 5.42; N, 9.31%. Calcd for $C_5H_8O_2NCl$: C, 40.14; H, 5.39; N, 9.37%.

IR (KBr): 3250 (OH), 1680 cm^{-1} (C=O). NMR ($CDCl_3$): τ 2.65 (1H, *s*, OH), 7.1 (2H, *t*, J=7.0 Hz, $CH_3CH_2\mathbf{CH_2}CO$), 7.98—8.73 (2H, *m*, $CH_3\mathbf{CH_2}CH_2CO$), 9.05 (3H, *t*, J=7.0 Hz, $CH_3\mathbf{CH_2}CH_2CO$).

Formation of Isonitroso Compounds from Esters. ω-Chloro-ω-isonitrosoacetophenone (IIIa). A solution of the methylsulfinyl carbanion in DMSO was prepared by the method of Becker and Russell[3] from 2 g (0.05 g-atom) of potassium, 50 m*l* of *t*-butyl alcohol, and 40 m*l* of DMSO. To this mixture 3.8 g (0.025 mol) of ethyl benzoate were added in a stream of nitrogen at room temperature. We continued to agitate the reaction mixture by a stream of nitrogen for 2 hr, then most of the solvent was evaporated under reduced pressure on a water bath, with the temperature kept bellow 60°C. A solution of 5.2 g (0.075 mol) of sodium nitrite in 30 m*l* of water was then added to the residue, and the mixture was extracted with 30 m*l* of ether. The aqueous layer was acidified with 40 m*l* of 6N hydrochloric acid to give yellow oil, which solidified on standing overnight. The recrystallization of the solid from chloroform gave 3.6 g (80%) of IIIa.

Nitrosation of ω-Methyl-ω-(methylsulfinyl)acetophenone (IIe). **A.** Into a solution of 1.0 g (0.005 mol) of IIe and 0.6 g (0.0065 mol) of sodium nitrite in 30 m*l* of 50% aqueous dioxane, 20 m*l* of concentrated hydrochloric acid were stirred at 0—5°C. Stirring was continued for 15 min, and then the reaction mixture was extracted with ether. The ether layer was washed with 10% sodium carbonate and then with water. The ether was dried over sodium sulfate and then evaporated. The brown residue was chromatographed on a column packed with silica gel. The development was carried out by using two different solvents. Methylene chloride was used first, and then 95% ethanol. The evaporation of the first solvent, methylene chloride, and the subsequent distillation of the residue afforded 1-phenylpropane-1,2-dione (V); bp 101—102°C/7 mmHg (lit,[15] 123°C/22 mmHg). IR ($CHCl_3$): 1700, 1660 cm^{-1} (C=O).

The disemicarbazone formed from the above residue by the usual manner melted at 230°C (lit,[15] mp 229—230°C) and was identical in every respect with the disemicarbazone prepared from the authentic sample of V.

The evaporation of ethanol and the recrystallization of the residue from toluene gave 400 mg (48%) of isonitrosopropiophenone (IV); mp 111—113°C (lit,[8] 112—113°C).

B. The same reaction was carried out under similar conditions, but stirring was continued for 2 hr instead of for 15 min. A similar work-up of the reaction mixture gave 0.53 g (70%) of V. In this case, IV was not obtained.

Hydrolysis of Isonitrosopropiophenone (IV) in the Presence of Sodium Nitrite in Hydrochloric Acid. Into a stirred mixture of 1 g (0.006 mol) of IV and 0.42 g (0.006 mol) of sodium nitrite in 30 m*l* of 50% aqueous dioxane, we added 20 m*l* of concentrated hydrochloric acid over a period of 30 min at 0—5°C. The reaction mixture was then extracted with ether. The ether layer was washed with water, dried over sodium sulfate, and then evaporated. The IR spectrum of the residue was identical with that of V. Furthermore, the treatment of the residue with an excess of semicarbazide gave the disemicarbazone of V; mp 231—232°C.

The treatment of IV with hydrochloric acid under the same conditions in the absence of sodium nitrite resulted in the recovery of the starting material in a 90% yield.

2-Nitroso-1,3-indanedione (IXa). A suspension of 2.7 g (0.05 mol) of sodium methoxide in 30 m*l* of DMSO was stirred for 15 min at room temperature in a stream of nitrogen. To this suspension we then added, drop by drop, a solution of 2.5 g (0.0125 mol) of dimethyl phthalate (VIa) in 10 m*l* of DMSO. We continued to stir the reaction mixture, which soon turned yellow, for 3 hr in a stream of nitrogen, and then most of the solvent was evaporated at 1 mmHg on a water bath at 60°C. The residue was mixed with a solution of 1.8 g (0.025 mol) of sodium nitrite in 25 m*l* of ice water, and the mixture was extracted with ether. The aqueous layer was acidified by striring in 50 m*l* of 6N hydrochloric acid with cooling in an ice bath. The precipitated solid was collected by filtration and recrystallized from acetic acid to

14) H. Rheinbodt and O. S. Dumont, *Ann. Chem.*, **444**, 113 (1925).

15) D. Vom Dorp, *Ber.*, **36**, 3187 (1906); *ibid.*, **50**, 1612 (1917).

give 800 mg (37%) of IXa; mp 196—198°C (decomp) (lit,[11] 197—198°C).

Found: C, 61.56; H, 2.73; N, 7.98%. Calcd for $C_9H_5O_3N$: C, 61.72; H, 2.88; N, 8.00%.

IR (KBr): 3500 (OH), 1738, 1705 cm^{-1} (C=O).

This compound was identical in every respect with the authentic sample prepared by the nitrosation of 1,3-indanedione by the method of Wislicenus.[11]

5-Methoxy-2-nitroso-1,3-indanedione (IXb). A solution of the methylsulfinyl carbanion in DMSO was prepared from 0.8 g (0.02 g-atom) of potassium, 20 m*l* of *t*-butyl alcohol, and 15 m*l* of DMSO. Into this solution we then stirred a solution of 1.0 g (0.0045 mol) of dimethyl 4-methoxyphthalate (VIb) in 5 m*l* of DMSO in a stream of nitrogen at room temperature. Stirring was continued for 2.5 hr, and then most of the solvent was evaporated under reduced pressure. To the residue 10 m*l* of ice water were added, and the mixture was extracted with 10 m*l* of ether. The aqueous layer was separated, poured into an aqueous saturated solution containing 0.8 g of sodium nitrite, and then acidified with 40 m*l* of 6N hydrochloric acid. The solid thus precipitated was recrystallized from ispropyl alcohol to yield 0.65 g (70%) of IXb; mp 204—206°C (decomp).

This compound was identical in every respect with the sample prepared by the method previously reported.[12]

Nitrosation of ω-(Methylsulfinyl)acetophenone (IIa) with Isoamyl Nitrite. To a solution of 0.25 g (0.011 mol) of sodium in 50 m*l* of absolute ethanol, we added 2 g (0.011 mol) of IIa. Isoamyl nitrite (2 g, 0.017 mol) was then stirred in at room temperature. Stirring was continued for 2 hr, and the solvent was evaporated. The residue was poured into 50 m*l* of ice water, and subsequently extracted with 50 m*l* of ether. The aqueous layer was acidified with hydrochloric acid to pH 4—5 to yield a yellow solid. Recrystallization from ethanol gave 1.2 g (40%) of ω-nitroso-ω-(methylsulfinyl)acetophenone (X) as a white solid; mp 124°C.

Found: C, 51.85; H, 4.49; N, 6.66%. Calcd for $C_9H_9O_3NS$: C, 51.28; H, 4.30; N, 6.63%.

IR (KBr): 1640 (C=O), 1040 cm^{-1} (SO). NMR (DMSO-d_6): τ −3.96 (1H, *s*, OH), 1.87—2.41 (5H, *m*, aromatic), 6.92 (3H, *s*, $SOCH_3$).

Pummerer Rearrangement of ω-Nitroso-ω-(methylsulfinyl)acetophenone (X). A suspension of 1 g of X in 30 m*l* of concentrated hydrochloric acid was refluxed for 5 hr and then cooled to room temperature. The solid separated was collected by filtration and recrystallized from chloroform to yield 0.3 g of IIIa; mp 131—133°C.

BULLETIN OF THE CHEMICAL SOCIETY OF JAPAN, VOL. 44, 223—226(1971)

The Preparation and Reactions of Benzoylnitrile Oxide from Dimethylphenacylsulfonium Bromide[1]

Yoshio Otsuji, Yasuhiro Tsujii, Akihiko Yoshida, and Eiji Imoto

Department of Applied Chemistry, College of Engineering, University of Osaka Prefecture, Sakai-shi, Osaka

(Received August 3, 1970)

The nitrosation of dimethylphenacylsulfonium bromide (I) with sodium nitrite and hydrochloric acid in water gave 3,4-dibenzoyl-1,2,5-oxadiazole 2-oxide (II) in a 76% yield. The nitrosation of I in a similar manner in 1 : 1 dioxane-water afforded ω-chloro-ω-isonitrosoacetophenone (III) in an 80% yield. The treatment of III with triethylamine produced II through benzoylnitrile oxide (IX). 1,3-Dipolar cycloadditions of IX generated from III were conducted, using methyl methacrylate, styrene, acrylonitrile, and ethyl chloroformate as dipolarophiles, to yield the expected cycloadducts. The mechanisms of these reactions are discussed.

The α-hydrogen in β-keto sulfonium compounds is extremely acidic and is readily removed by bases such as triethylamine or sodium hydroxide to yield the corresponding sulfonium ylides. The ylides thus formed can be subjected to such electrophilic substitutions as acylation and sulfonation at the α-carbon.[2] The α-hydrogen in β-keto sulfoxides is of a similar character, and such electrophilic substitutions as alkylation and bromination take place at the α-carbon of the sulfoxides.[3,4]

In a previous paper,[5] we have reported that β-keto sulfoxides are nitrosated at the α-position with nitrous acid in hydrochloric acid, and that, at the same time, the sulfoxide group is eliminated; thus, β-keto sulfoxides with no substituent at the α-position are converted to the α-chloro-α-nitroso (or isonitroso) ketones, and α-substituted β-keto sulfoxides, to the α-nitroso ketones.

Recently we found that the nitrosation of dimethylphenacylsulfonium bromide (I) with nitrous acid in hydrochloric acid affords 3,4-dibenzoyl-1,2,5-oxadiazole 2-oxide (II) or ω-chloro-ω-isonitrosoacetophenone (III) in high yields, the yields depending on the reaction conditions employed. In the present paper we will describe the results of a detailed study of this reaction. We will also report on some 1,3-dipolar

1) A part of this investigation was presented at the 19th Symposium on the Organic Reaction Mechanisms, Yamagata, October, 1968.

2) H. Nozaki, *Yuki Gosei Kagaku Kyokai Shi*, **27**, 125 (1965), and the references cited therein.

3) G. A. Russel and G. J. Mikol, *J. Amer. Chem. Soc.*, **88**, 5498 (1966).

4) G. A. Russel, E. Sabourin, and G. J. Mikol, *J. Org. Chem.*, **31**, 2854 (1966).

5) Y. Otsuji, Y. Tsujii, A. Yoshida, and E. Imoto, This Bulletin, **44**, 219 (1971).

cycloaddition reactions of benzoylnitrile oxide (IX), which is readily derived from III and which would constitute a new type of reactive 1,3-dipole.

Results and Discussion

Nitrosation of Dimethylphenacylsulfonium Bromide (I). The treatment of a mixture of I and sodium nitrite in water with hydrochloric acid gave 3,4-dibenzoyl-1,2,5-oxadiazole 2-oxide (II) in a 76% yield, plus a small amount of ω-chloro-ω-isonitrosoacetophenone (III). However, the similar treatment of the same mixture in a 1:1 dioxane-water mixture afforded III in an 80% yield, along with a small amount of II.

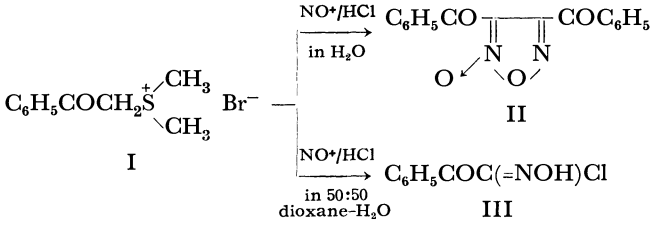

The structure of II was established by the elemental analysis, by a molecular-weight determination (302, calcd 294), and by a study of its spectra data. The IR spectrum (KBr) showed two carbonyl absorptions around 1660 cm^{-1} as a doublet. The NMR spectrum ($CDCl_3$) showed only multiplet absorptions due to aromatic protons at τ 1.75—2.35. The assigned structure for II was also supported by the fact that II could be obtained by the treatment of III with bases, as will be discussed later. The structure of III was confirmed by comparing it with the sample prepared in the previous paper,[4] they were identical in every respect.

One of the most significant features of the nitrosation of the sulfonium salt is its remarkable solvent effect on the proportions of the products formed. How can this solvent effect be explained?. The first step of the reaction, both in water and an aqueous dioxane, is no doubt an attack of the nitrosonium ion at the α-carbon of the sulfonium salt to produce the nitroso sulfonium bromide (IV), which might be unstable under the reaction conditions.[6] We assumed that the configurations of IV in the solvents determined the proportions of the products, and we chose α-nitroso-propiophenone (V) as a model compound of IV. Its configurations were then studied in the mixed solvents of dioxane and water. The UV spectrum of V in dioxane and in dioxane-water (1:1) showed, respectively, absorption maxima at 250 mμ ($\varepsilon=1.1\times10^4$) and 255 mμ ($\varepsilon=1.2\times10^4$); these values are very close to that of benzene in the same solvent (255 mμ). On the other hand, the spectrum of V in water showed a maximum at 280 mμ ($\varepsilon=9\times10^3$), a value which is very close to that of benzaldehyde in the same solvent. These results suggest that V exists predominantly in the form of VI in dioxane-water and in the form of VII in water. In VI the keto and hydroxyimino groups form a stabilized, six-membered ring system by means of intramolecular hydrogen bonding; hence, the conjugation between the benzene ring and carbonyl group would be considerably reduced by the loss of the coplanarity between them. Thus, the UV spectrum of VI resembles that of benzene. On the other hand, an intermolecular hydrogen bonding between water and the keto and/or nitroso groups would dominate the intramolecular hydrogen bonding which is realized in VI. Therefore, the keto group conjugates with the benzene ring and the UV spectrum of VII resembles that of benzaldehyde.

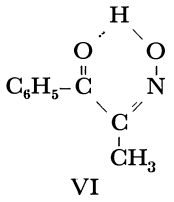

VI

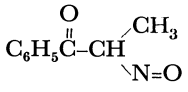

VII

On the basis of the above considerations, we propose the tentative mechanisms represented in Scheme 1 for the nitrosation of the sulfonium salt I.

The intermediate IV is stabilized in water by the elimination of a proton to form VIII, which in turn produces benzoylnitrile oxide (IX). The nitrile oxide, IX, then dimerizes to afford II. However, IV is stabilized in an aqueous dioxane by forming an intramolecularly-hydrogen-bonded X, which then produces III.

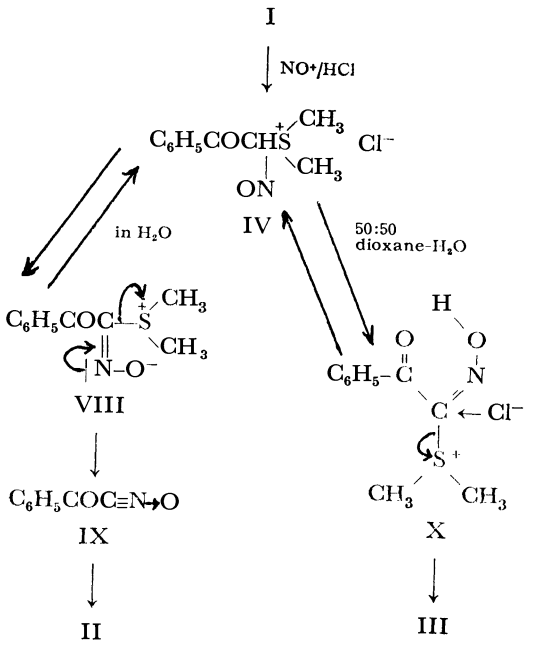

Scheme 1

Reaction of ω-Chloro-ω-isonitrosoacetophenone (III) with Bases. The treatment of III with one equiv. of triethylamine in ethanol afforded II in a quantitative yield. The compound, II, thus produced was identical

6) M. Mukaiyama, N. Takei, and K. Saigo (Abstract of the papers presented at the 23rd Meeting of the Chemical Society of Japan, III, Tokyo (1970) p. 1516) have found that the nitrosation of I with isopropyl nitrite in methylene dichloride gives ω-bromo-ω-isonitrosoacetophenone in a 77% yield. They could not isolate a plausible intermediate, IV, because of its unstability, even in an organic medium.

with the sample obtained in the previous paragraph. The similar treatment of III with a sodium hydroxide solution also yielded II, but in a low yield. Considering that the formation of a 1,2,5-oxadiazole 2-oxide ring system (furoxan) is characteristic of the nitrile oxides,[7] it is apparent that the nitrile oxide, IX, is an intermediate of the above reactions; the reaction can feasibly be regarded as a 1,3-dipolar cycloaddition of one molecule of the nitrile oxide onto the CN bond of the other.

1,3-Dipolar Cycloadditions of Benzoylnitrile Oxide (IX). Since the above results indicated that IX can be liberated from III, the 1,3-dipolar cycloadditions of IX were studied using four unsaturated compounds as dipolarophiles. During the studies it was found that, in order to avoid the interfering dimerization of the reactive nitrile oxide, IX, to the furoxan II, the reaction must be carried out with low stationary concentrations of IX. The slow addition of a dilute solution of triethylamine to an alcoholic solution of III and a dipolarophile at a low temperature (−5—0°C) favored the cycloaddition.

The treatment of III with an equiv. of methyl methacrylate in this manner afforded 3-benzoyl-4-methyl-4-methoxycarbonyl-Δ^2-isoxazoline (XI) in a 91% yield.

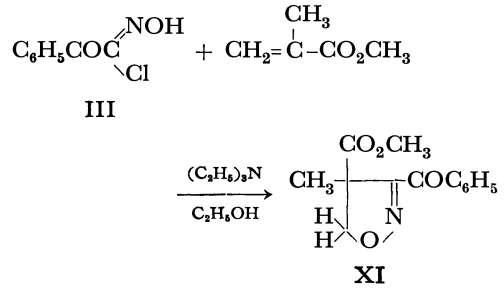

III XI

Similar treatments of III with styrene, acrylonitrile, and ethyl chloroformate produced 3-benzoyl-5-phenyl-Δ^2-isoxazoline (XII), 3-benzoyl-4-cyano-Δ^2-isoxazoline (XIII), and 3-benzoyl-5-chloro-5-ethoxy-1,4,2-dioxazole (XIV) in yields of 61%, 51%, and 26% respectively.

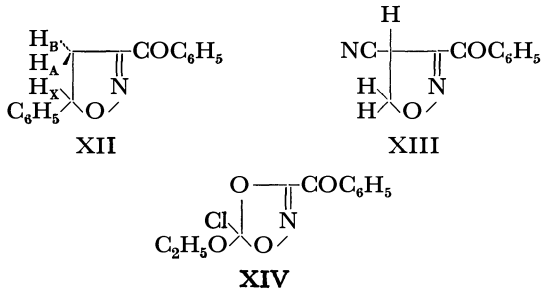

XII XIII XIV

The structures of XI, XII, XIII, and XIV were derived from their analytical and spectral data. The results of the elemental analyses, the molecular-weight determinations, and the IR spectra for these compounds were consistent with the assigned structures, as will be described in the "Experimental" section. However, the structures of these compounds were finally established by their NMR spectra. The NMR spectrum of XI in carbon tetrachloride exhibited a multiplet at τ 1.75—2.25 (5H, C_6H_5CO), two singlets at τ 6.22 (3H, $COOCH_3$) and 8.36 (3H, CH_3 at 4-C), and an AB quartet at τ 6.85 (2H, J=17 Hz, 5-CH_2). These signals, especially the chemical shift and the spectral pattern of the AB quartet, support the assigned structure for XI. The NMR spectrum of XII in carbon tetrachloride showed a multiplet at τ 1.70—2.72 (10H, C_6H_5CO at 3-C and C_6H_5 at 5-C) and an ABX pattern due to H_A, H_B, and H_X protons. The signals of this ABX system appeared at τ 6.27 and 6.76 (2H, H_A and H_B of 4-C) and at τ 4.35 (1H, H_X of 5-C). The coupling constants were as follows: J_{AB}=17.8 Hz, J_{AX}=11.2 Hz and J_{BX}=9.7 Hz. These data strongly support the assigned structure for XII. The NMR spectrum of XIII in carbon tetrachloride was relatively simple in its pattern as compared with that of XII. The spectrum showed a multiplet at τ 1.69—2.72 (5H, C_6H_5-CO), a triplet at τ 4.60 (1H, J=9.0 Hz, 4-CH), and a doublet at τ 6.25 (2H, J=9.0 Hz, 5-CH_2). The chemical shifts of the triplet and doublet signals indicate that the assigned structure for XIII is correct and that no other structures can be derived from these spectral data. Finally, the NMR spectrum of XIV in carbon tetrachloride showed a multiplet at τ 1.78—2.55 (5H, C_6H_5CO), a quartet at τ 5.36 (2H, J=7.5 Hz, OCH_2CH_3), and a triplet at τ 8.59 (3H, J=7.5 Hz, OCH_2CH_3). These data are again in agreement with the assigned structure for XIV.

As can be seen from these examples, the nitrile oxide, IX, undergoes 1,3-dipolar cycloadditions onto the C=C and C=O double bonds. It also adds preferentially to the C=C rather than to the C≡N bond in acrylonitrile, as is commonly observed with such aromatic nitrile oxides as benzonitrile oxide.[7] The orientation of the cycloaddition can be interpreted in a manner similar to that proposed for benzonitrile oxide;[7] *i. e.*, the resonance structures of IX would be XV, XVI, and XVII, and its principal polarized formula would be XVII:

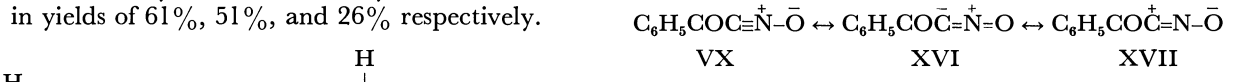

VX XVI XVII

Experimental

The melting points are uncorrected. The IR spectra were recorded on a Hitachi EPI-S2 infrared spectrometer. The NMR spectra were obtained on a Hitachi H-60 high-resolution NMR spectrometer, with TMS as the internal standard. The UV spectra were recorded on a Hitachi EPU-2V recording spectrophotometer. The elemental analyses were performed with a Yanagimoto MT-1 CHN Corder. The molecularweight determinations were carried out with a Hitachi-Perkin Elmer 115 molecular-weight apparatus, using benzene as the solvent.

Reagents. A commercial sodium nitrite (97% purity) was used without further purification. The α-isonitropropiophenone was prepared by the method of Hartung and Crossley.[8] The other chemicals were of commercial origin and

7) R. Huisgen, *Angew. Chem., Int. Ed. Engl.*, **2**, 565 (1963).

8) W. H. Hartung and F. Crossley, "Organic Syntheses," Coll. Vol. II, p. 363 (1948).

were used after purification by distillation or recrystallization.

Dimethylphenacylsulfonium Bromide (I)[9]. A solution of 80 g (0.4 mol) of phenacyl bromide and 25 g (0.4 mol) of dimethyl sulfide in 250 m*l* of methanol was refluxed for 10 hr, and then the solvent was evaporated to dryness to give a white solid. Recrystallization from ethanol afforded 73 g (70%) of the pure sulfonium bromide (I); mp 142—143°C.

Nitrosation of I in Water. Into a solution of 10 g (0.04 mol) of I and 3.5 g (0.05 mol) of sodium nitrite in 100 m*l* of water, 100 m*l* of concentrated hydrochloric acid were stirred over a period of 1 hr at room temperature. Stirring was continued for 2 hr to yield a yellow solid, along with a small amount of an orange solid. Both solids were precipitated on the bottom of the flask. The orange solid was picked out from a mixture of the solids by a spatula. The recrystallization of the yellow solid from isopropyl alcohol gave 4.3 g (76%) of 3,4-dibenzoyl-1,2,5-oxadiazole (II) as white crystals; mp 78—80°C.

Found: C, 65.55; H, 3.45; N, 9.81%. Calcd for $C_{16}H_{10}O_4N_2$: C, 65.30; H, 3.43; N, 9.52%.

The orange solid was recrystallized from benzene to yield 120 mg of ω-chloro-ω-isonitrosoacetophenone (III) as white crystals; mp 130—132°C.

Nitrosation of I in an Aqueous Dioxane. Into a solution of 10 g (0.04 mol) of I and 3.5 g (0.05 mol) of sodium nitrite in 50 m*l* of water and 50 m*l* of dioxane, 100 m*l* of concentrated hydrochloric acid were stirred over a period of 1 hr at room temperature. Stirring was continued for 2 hr to produce a white solid, along with a small amount of a yellow solid; these solids were then separated by filtration. The yellow solid was picked out from a mixture of the solids by a spatula. The recrystallization of the white solid from chloroform afforded 6 g (80%) of III as white crystals; mp 130—132°C.

The yellow solid was recrystallized from isopropyl alcohol to yield 60 mg of II as white crystals, the IR spectrum of which was completely identical with that of the authentic sample of II obtained above.

Reaction of ω-Chloro-ω-isonitrosoacetophenone (III) with Bases. A. With Triethylamine. A solution of 2 g (0.02 mol) of triethylamine in 50 m*l* of ethanol was stirred into a solution of 3 g (0.016 mol) of III in 50 m*l* of ethanol under cooling in an ice bath over a period of 30 min. Stirring was continued for 2 hr, and then the solvent was evaporated to dryness. The residue was recrystallized from isopropyl alcohol to yield II as white crystals in an almost quantitative yield; mp 78—80°C. The material thus obtained was identical with the sample prepared above in every respect.

B. With Sodium Hydroxide. Into a suspension of 2 g of III in 40 m*l* of benzene, we stirred, drop by drop, 12 m*l* of a 14% aqueous sodium hydroxide solution at 0°C. After stirring for 1 hr, the benzene layer was separated, dried over calcium chloride, and then evaporated to yield a white solid. The recrystallization of the solid from isopropyl alcohol gave about 200 mg of II; mp 78—80°C.

Formation of 3-Benzoyl-4-methyl-4-methoxycarbonyl-Δ^2-isoxazoline (XI). Into a solution of 3 g (0.016 mol) of III and 1.6 g (0.016 mol) of methyl methacrylate in 50 m*l* of absolute ethanol, we stirred, at −5—0°C, a solution of 2 g (0.02 mol) of triethylamine in 50 m*l* of absolute ethanol over a period of 2 hr. The mixture, which soon turned yellow, was stirred for 3 more hr at the same temperature, concentrated to half its volume under reduced pressure, and then poured onto 100 m*l* of water. The aqueous mixture was extracted several times with methylene dichloride. The organic layer was washed with water and dried over sodium sulfate, and the solvent was evaporated. The distillation of the residue afforded 3.6 g (91%) of XI as a pale yellow oil; bp 190—191°C/7 mmHg.

Found: C, 62.84; H, 5.05; N, 5.87%. Calcd for $C_{13}H_{13}O_4N$: C, 63.15; H, 5.30; N, 5.67%.

Molecular weight: 252 (calcd 247). IR (KBr): 1740, 1655 cm^{-1} (C=O).

Formation of 3-Benzoyl-5-phenyl-Δ^2-isoxazoline (XII). A solution of 3 g (0.016 mol) of III and 1.7 g (0.016 mol) of styrene in 50 m*l* of absolute ethanol was treated with a solution of 2.02 g (0.02 mol) of triethylamine in 50 m*l* of absolute ethanol as has been described above. After stirring for 3 hr under cooling in an ice bath, the reaction mixture was concentrated to half its volume under reduced pressure and then poured onto 100 m*l* of water. The aqueous mixture was extracted several times with methylene dichloride. The organic layer was washed with water and dried over sodium sulfate, and then the solvent was evaporated. The distillation of the residue gave 2.5 g (61%) of XII as a yellow oil; bp 185°C/3.5 mmHg.

Found: C, 75.87; H, 5.33; N, 5.93%. Calcd for $C_{16}H_{13}O_2N$, C, 76.47; H, 5.22; N, 5.57%.

Molecular weight: 250 (calcd 246). IR ($CHCl_3$): 1700, 1660 cm^{-1} (C=O).

Formation of 3-Benzoyl-4-cyano-Δ^2-isoxazoline (XIII). A solution of 3 g (0.016 mol) of III and 0.85 g (0.016 mol) of acrylonitrile in 50 m*l* of absolute ethanol was treated with 2.02 g (0.02 mol) of triethylamine in 50 m*l* of absolute ethanol as has been described above. A similar work-up of the reaction mixture produced a brown oil after the evaporation of the methylene dichloride. The oil solidified upon cooling in a dry ice-acetone mixture. The solid was separated by filtration and recrystallized from water-ethanol to afford 1.7 g (52%) of XIII as pale yellow crystals; mp 70—71°C.

Found: C, 66.40; H, 4.13; N, 14.09%. Calcd for $C_{11}H_8O_2N_2$: C, 66.02; H, 4.03; N, 13.99%.

Molecular weight: 203 (calcd 200). IR (KBr): 1770 cm^{-1} (C=O).

Formation of 3-benzoyl-5-chloro-5-ethoxy-1,4,2-dioxazole (XIV). A solution of 3 g (0.016 mol) of III and 1.7 g (0.016 mol) of ethyl chloroformate in 50 m*l* of absolute ethanol was treated with 2.02 g (0.02 mol) of triethylamine in 50 m*l* of absolute ethanol as has been described above. A similar work-up of the reaction mixture and evaporation of the solvent (methylene dichloride) produced a brown oil which solidified upon cooling in a dry ice-acetone mixture. The solid was separated by filtration and recrystallized from ethanol to yield 1 g (26%) of a white solid; mp 56—59°C.

Found: C, 51.96; H, 4.08; N, 5.61%. Calcd for $C_{11}H_{10}O_4NCl$: C, 51.66; H, 3.91; N, 5.48%.

Molecular weight: 256 (calcd 256). IR (KBr): 1800, 1680 cm^{-1}.

9) K. W. Ratts and A. Yao, *J. Org. Chem.*, **31**, 1185 (1966).

Nitration of Pentamethylnitrobenzene, Pentamethylbenzoic Acid and Its Methyl Ester, Pentamethylacetanilide, and Pentamethylphenol and Its Methyl Ether. Orienting Effect of the Substituents for the Side-chain Nitrooxylation[1]

Hitomi SUZUKI and Kiyomi NAKAMURA

Department of Chemistry, Faculty of Science, Kyoto University, Sakyo-ku, Kyoto

(Received August 3, 1970)

The nitration of a series of the titled pentamethylbenzene derivatives has been investigated in order to know the orienting effect of substituent groups for the side-chain nitrooxylation. The nitrooxylation was found to occur almost exclusively at the methyl groups adjacent to the electron-withdrawing substituents (NO_2, COOH, and $COOCH_3$), while with the compounds containing electron-donating groups (OH and OCH_3) the main reaction led to the conversion into cyclohexadienone, with the concomitant formation of small amounts of meta-nitrooxylated product. Pentamethylacetanilide underwent side-chain nitrooxylation along with some deacetylation. The location of the nitrooxymethyl group seems to be most likely ortho and meta, the latter being predominant.

Polyalkylated aromatic compounds often suffer side-chain substitution to give benzyl nitrates when they are treated with fuming nitric acid at low temperature. A particularly important feature of this unusual reaction is the peculier orientation and high positional selectivity. Nitration of pentamethylbenzene, for example, gives 2,3,4,5-tetramethylbenzyl nitrate as the major product,[2] while halopentamethylbenzenes yield comparable amounts of 5-halo-2,3,4,6-tetramethylbenzyl nitrate and 6-halo-2,3,4,5-tetramethylbenzyl nitrate.[3] Other isomeric products were never formed in any significant amounts. Such high positional selectivity seems to make this reaction an attractive pathway for the synthesis of the otherwise with difficulty accessible polysubstituted aromatic compounds, because the nitrooxymethyl group is known to be quite versatile for various transformations. To obtain a further information about the character of this reaction, especially the orienting effect of substituent groups, the action of fuming nitric acid upon pentamethylnitrobenzene (I), pentamethylbenzoic acid (II) and its methyl ester (III), pentamethylphenol (IV) and its methyl ether (V), and pentamethylacetanilide (VI) has been studied.

Pentamethylnitrobenzene (I) was comparatively stable towards nitric acid, and remained essentially unchanged under the conditions successfully employed for halopentamethylbenzenes. However, by treating with a large excess of fuming nitric acid at somewhat elevated temperature, it gave a light yellow half-crystalline solid with infrared bands characteristic of nitrobenzyl nitrates, at 876, 1277, 1535, and 1636 cm^{-1}. This was shown by TLC and PMR spectroscopy to contain five components, the principal of which was readily identified as 6-nitro-2,3,4,5-tetramethylbenzyl nitrate (VII) by the comparison of its infrared spectrum with that of an authentic specimen, prepared by the chloromethylation of 5-nitro-1,2,3,4-tetramethylbenzene and the subsequent treatment of the benzyl chloride with silver nitrate in acetonitrile. A close spectroscopic inspection confirmed the formation of some 5-nitro-2,3,4,6-tetramethylbenzyl nitrate (VIII, less than 5% of the total nitrate), but 4-nitro-2,3,5,6-tetramethylbenzyl nitrate (IX) could not be detected. The products were usually accompanied by some dinitroprehnitene. The anisotropic effect of the adjacent nitro group makes the methylene protons of VII to absorb considerably at high-field (4.68 τ) as compared to VIII (4.32 τ) and IX (4.30 τ). A minor peak at 4.70 τ which might arise from 6-nitro-2,3,4,5-tetramethylphenylnitromethane was also observed. VII could be isolated from the reaction mixture by chromatography on a short alumina column, followed by fractional crystallization from light petroleum. When refluxed with excess of dilute hydrochloric acid, the reaction product was converted into a light brown solid, from which 6-nitro-2,3,4,5-tetramethylbenzyl alcohol was obtained as a light yellow prisms.

An ortho-directing effect of electron-attracting groups for side-chain nitrooxylation was further evidenced by the nitration of pentamethylbenzoic acid (II) and its methyl ester (III). II was nitrated with fuming nitric acid in dichloromethane at 0—5°C to yield a white crystalline solid, TLC and PMR spectroscopy of which indicated that it was almost a single compound. Crystallization of the product from dichloromethane - light petroleum mixture gave white fine needles, mp 150—152°C, which had a molecular formula $C_{12}H_{15}NO_5$; PMR peaks at 7.66 (2 Me), 7.72 (2 Me), 4.38 (CH_2), and 2.28 τ (OH, broad); infrared bands at 863, 1272, 1617 (ONO_2), and 1685 cm^{-1} (COOH), consistent with it being a nitrooxymethyltetramethylbenzoic acid. A quite similar result was obtained by the nitration of III. The product was white needles, mp 104—105°C, with a composition $C_{13}H_{17}NO_5$; PMR peaks at 7.84 (Me), 7.77 (2 Me), 7.72 (Me), 6.16 (COOMe), and 4.60 τ (CH_2); infrared bands at 877, 1279, 1613 (ONO_2), 1193, and 1718 cm^{-1} (COOMe), and was readily formulated as methyl nitrooxymethyltetramethylbenzoate. When both products from II and III were heated with concentrated hydrochloric acid, it gave a light brown solid, from which the identical product was obtained as white needles in high yield. This compound, of formula $C_{12}H_{14}O_2$, exhibited PMR peaks at 7.78

1) The Reaction of Polysubstituted Aromatics. XX. Part XIX: H. Suzuki, This Bulletin, **43**, 3299 (1970).

2) H. Suzuki and K. Nakamura, *ibid.*, **43**, 473 (1970).

3) L. I. Smith and J. W. Horner, *J. Amer. Chem. Soc.*, **62**, 1349 (1940); H. Suzuki, This Bulletin, **43**, 481 (1970).

(Me), 7.70 (2 Me), 7.37 (Me), and 4.92 τ (CH_2); infrared bands at 1123, 1262, and 1735 cm^{-1} ($CO\cdot OCH_2$). No absorption due to hydroxyl group was observed. It did not dissolve into aqueous sodium hydrogen carbonate, but on prolonged heating with dilute sodium hydroxide it slowly went into solution and was again precipitated on acidification. From its mode of reaction and spectral data, therefore, the product was formulated as 3,4,5,6-tetramethylphthalide, the identity of which was further confirmed by preparing the authentic specimen in low yield from the condensation of chloromethyl methyl ether with 2,3,4,5-tetramethylbenzoic acid in the presence of anhydrous zinc chloride. When a methylol or chloromethyl group is located ortho to a carboxyl group, a loss of water or hydrogen chloride usually occurs to produce a phthalide.[4] Since the ortho relationship of carboxyl and methylol groups was established, the original nitrooxylated products were identified as 6-nitrooxymethyl-2,3,4,5-tetramethylbenzoic acid (X) and methyl 6-nitrooxymethyl-2,3,4,5-tetramethylbenzoate (XI), respectively. Further supporting evidence for the predominant ortho substitution was obtained by reducing the product mixtures with lithium aluminum hydride to bis-hydroxymethyl-tetramethylbenzenes, which, after conversion into bis-acetoxymethyl compound, was gas-chromatographed to prove 1,2-bis(acetoxymethyl)-3,4,5,6-tetramethylbenzene as the sole main product.

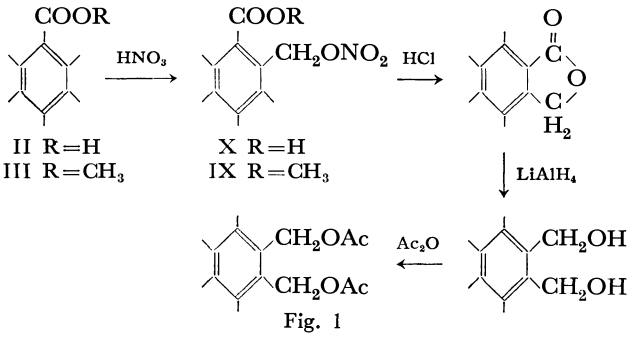

Fig. 1

In a previous paper of this series, directing effect of halogen atoms for the side-chain nitrooxylation of halopentamethylbenzenes has been shown to be a comparable extent of ortho and meta.[3] With highly electron-withdrawing nitro and carboxyl groups, the nitrooxylation was found to occur almost exclusively at ortho methyl groups. From the electronic points of view, therefore, the orientation exhibited by the electron-releasing groups is of special interest. Thus, pentamethylphenol (IV) and its methyl ether (V), and pentamethylacetanilide (VI) were treated with nitric acid. Since fuming nitric acid was found to react with these highly activated aromatic systems destructively under ordinary conditions,[5] the nitration was carried out cautiously in a very dilute methylene chloride solution at −10——5°C with a limited reaction time. Both IV and V reacted actively with nitric acid to give light brown oil of almost identical composition. The methyl group bonded to the oxygen atom of V was completely cleaved during nitration. These products showed a very weak PMR peak at 4.79 τ (CH_2ONO_2) and infrared bands at 845, 1270, and 1630 cm^{-1} (ONO_2), indicating the formation of a benzyl nitrate only as a minor product. When stored at cool place, the syrupy product partly solidified to a sticky, half-crystalline mass, which could be separated into white prisms (mp 138—140°C) by fractional crystallization from light petroleum and diethyl ether. However, a considerable part of it was lost as a non-crystallizable syrup during recrystallization. The PMR spectrum of the carbon tetrachloride solution showed three methyl signals at 8.63, 8.16, and 7.96 τ of relative intensities 1 : 2 : 2. Its infrared spectrum contained strong bands for unsaturated ketones and hydroxyl group, at 1084, 1613, 1662, and 3390 cm^{-1}, and its ultraviolet spectrum produced a single intense band at 242 mμ ($\log \varepsilon = 4.20$) which is characteristic of cross-conjugated cyclohexadienones.[6] The analysis and spectral data are in agreement with the structure of 4-hydroxy-2,3,4,5,6-pentamethylcyclohexa-2,5-dienone, $C_{11}H_{16}O_2$. The isolation of hydroxycyclohexadienone and the numerous examples of parallel reactions of polysubstituted phenolic systems[7] are, therefore, consistent with the formulation of the major component of the original mixture as 4-nitro-2,3,4,5,6-pentamethylcyclohexa-2,5-dienone (XII). Trituration of the pasty mixture in cold ethanol gave small amounts of white powder, melting with decomposition up to *ca.* 260°C, which had an elemental analysis (C, 64.6; H, 7.4; N, 4.5%) and showed a complicated PMR spectral pattern. It was probably a secondary product from the cyclohexadienone and no further attempt was made to elucidate the structure.

In view of the supposed instability of 2- and 4-hydroxytetramethylbenzyl nitrates and their possible degradation product, quinomethide, the accumulation of these nitrates to any significant amount in the reaction mixture seems very unlikely.[8] Therefore, a small amount of benzyl nitrate found in the nitration product is probably 3-hydroxy isomer. With the aim to confirm this, attempts were made to prepare the authentic 3-hydroxy-2,4,5,6-tetramethylbenzyl nitrate (XIII) from the reaction of the corresponding benzyl chloride with silver nitrate in acetonitrile. The product was unfortunately a yellow to light brown syrupy mixture of several substances, although the nitrate appeared still to be the main component. Since the

4) C. A. Buehler, T. A. Powers, and J. G. Michels, *J. Amer. Chem. Soc.*, **66**, 417 (1944); C. A. Buehler, J. O. Harris, C. Shacklett, and B. P. Block, *ibid.*, **68**, 574 (1946); J. C. Overeen and G. J. M. van der Kerk, *Rec. Trav. Chim. Pays-Bas*, **83**, 1023 (1946).

5) Kolka and Vogt claimed the unusual chemical stability of V, which was recovered according to their experiment after heating with fuming nitric acid and concentrated sulfuric acid for two hours on a water bath.[15] However, their V was recently proved to be 2,3,4,4,5,6-hexamethylcyclohexa-2,5-dienone.[16]

6) H. H. Jaffé and M. Orchin, "Theory and Application of Ultraviolet Spectroscopy," Wiley, New York (1962), p. 204.

7) G. M. Sharma and P. R. Burkholder, *Tetrahedron Lett.*, **1967**, 4147; D. H. R. Barton, A. K. Ganguly, R. H. Hesse, S. N. Loo, and M. M. Rechet, *Chem. Commun.*, **1968**, 806; G. Antinori, E. Baciocchi, and G. Illuminati, *J. Chem. Soc., B*, **1969**, 373; J. C. Richer and A. Rossi, *Can. J. Chem.*, **47**, 3935 (1969).

8) The synthesis and property of these polysubstituted benzyl nitrates will be described in detail in a later paper. For quinomethide, *cf.* A. B. Turner, *Quart. Rev.* (London), **28**, 347 (1964).

amount was very small, the identity of this nitrooxy compound was inferred by indirect means of spectral comparison of the product mixture with the above impure reference compound. It revealed, in fact, that all the major peaks belonging to the impure XIII were contained in the spectra of the nitration products from IV and V. When the syrupy product from IV was treated with cold concentrated hydrochloric acid for some days, a pale yellow pasty solid was obtained, PMR spectrum of which showed several new prominent peaks in the methylene protons region (4.32, 4.72, and 5.25 τ).

Pentamethylacetanilide (VI) underwent the nitration under similar condition much more smoothly than did IV and V. A light brown gummy product with ordor of acetic acid showed prominent PMR peaks due to $-CH_2ONO_2$ at 4.48 and 4.43 τ; infrared bands at 876, 1280, 1613 (ONO_2), 1645 (CONH), and 3220 cm^{-1} (NH), indicating the formation of benzyl nitrate and the partial deacetylation. Several crystallization of the product from dichloromethane - light petroleum mixture gave the major component as white needles, which was identified by analysis, infrared and PMR spectroscopy as a nitrooxymethyltetramethylacetanilide. The minor nitrate with the benzylic protons signal at lower field of 4.43 τ could not be isolated. Because of the difficulty involved in the preparation of the authentic samples, a firm structural assignment for these nitrooxy compounds has not been made yet. However, it is expected that the acetamido group will exhibit anisotropic deshielding effect on the benzylic protons at the ortho positions, but will exert a net shielding effect on these at meta and para positions. Considering the appearance of the methylene protons signal of the minor nitrate at lower field, the orientation of these nitrate seems most likely to be ortho and meta substituted, the latter outweighing the former in its amount.

The nitration of acetanilides has been known to involve the interaction of p- or π-electron on nitrogen or carbonyl oxygen with the nitrating species, leading to the formation of XIV as the most readily accessible σ-complex (Fig. 2). The observed partial deacetylation would probably arise from such interaction. When this special effect was superimposed with ordinary ortho and para activating and somewhat meta deactivating effect of acetamido group, the most favored intermediates will be ions XIV and XV, which, according to the previously suggested cyclic process for side-chain nitrooxylation,[2] will form the meta substituted nitrate as the most preferred isomeride. The minor nitrate is probably ortho-substituted and would be derived from the less important contributor XVI (Fig. 2), in which the preferred proton release will occur from the methyl groups adjacent to the acetamido group ($X=NHCOCH_3$), because the protons of these groups are more positively polarized and the transition state for the migration of the nitro group to the neighboring side-chain will be stabilized more effectively, as in XVII (Fig. 3), through the electron supply from the methyl group meta to the attacking site as well as through the polar interaction between the p-electrons on carbonyl oxygen and the leaving hydrogen atom.

In the case of para substitution, the conjugative electron release from the acetamido group is greatly disturbed by the methyl groups on both sides, and so the former group will act in an opposite way during the electron-redistribution, by increasing the electron deficit at the attacking site and thus rendering the departure of the nitro group with its unshared electron pair more difficult, as depicted in XVIII (Fig. 3). In view of the almost exclusive ortho substitution for I, II and III, and a comparable extent of ortho and meta substitution for halopentamethylbenzenes, this interpretation seems quite reasonable.

Predominant ortho directing effect of nitro, carboxyl and methoxyl groups probably involves a similar mechanism. Strongly electron-attracting nitro group or carboxyl group will direct the entering nitronium ion at the meta position to yield the benzenonium ion XVI ($X=NO_2$ or COOH) as the most stable intermediate species, which has three methyl groups at the most favorable position to delocalize the positive charge. Methyl protons next to the nitro or carboxyl group are subject to the further activation due to the nitronium ion introduced at the another neighboring position. Hyperconjugative proton release from this highly activated methyl group, followed by the migration of the nitro group to this side-chain according to the outlined sequence will result in the expected ortho-substitution (Figs. 2 and 3).

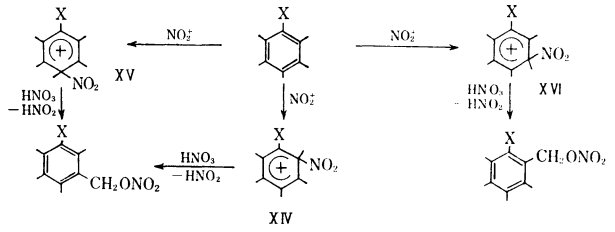

Fig. 2

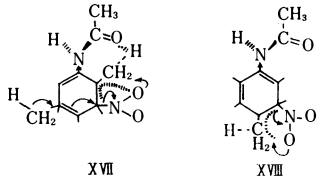

Fig. 3

A small amount of meta-substituted product would arise from the less stabilized ion XIV, in which only two methyl groups can contribute to the stabilization.

The methoxyl cleavage and subsequent meta-nitrooxylation observed in the nitration of pentamethylanisole (V) may be rationalized on a similar basis:

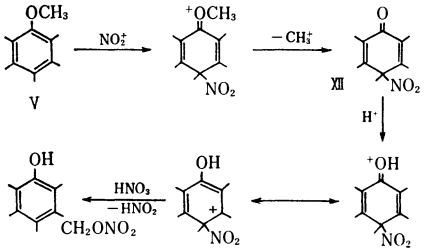

XIII Fig. 4

Initial step of the reaction would be the attachment of nitro group at 4-position, and the methyl group is rapidly cleaved from the oxygen atom to form a dienone XII, which will be partly protonated on the oxygen atom to give the hydroxybenzenonium ion and then transformed into meta-substituted benzyl nitrate XIII (Fig. 4).

Experimental

Melting points were determined on a hot stage apparatus and were uncorrected. Infrared spectra were measured with a KBr disc on a Jasco DS-402 G spectrophotometer, and ultraviolet spectra were recorded in methanol solution with a Shimadzu QV-50 spectrophotometer. PMR spectra were obtained in carbon tetrachloride and deuteriochloroform with a Varian A-60A spectrometer and with a Jeolco 3H-60 spectrometer against internal TMS.

Materials. Pentamethylnitrobenzene (I, mp 158—159°C),[2] pentamethylbenzoic acid (II, mp 210—211°C) and its methyl ester (III, mp 68—69°C),[9,10] and pentamethylacetanilide (VI, mp 212—214°C)[11] were prepared as described in the literatures.

Most of the previously reported synthetic methods for pentamethylphenol (IV) were found to be not entirely satisfactory as a simple laboratory procedure, owing to a difficult access for the material, low yield, or the laborious procedure involved in the synthesis and purification processes.[11,12] A simple and rapid synthesis of pure IV (mp 126—128°C) was accomplished by reducing 3,5-bis(chloromethyl)-2,4,6-trimethylphenol,[13] readily prepared from mesitol by chloromethylation in acetic acid, with lithium aluminum hydride in anhydrous tetrahydrofuran, followed by the purification through steam-distillation. *O*-Methylation of IV required quite long time and was still incomplete.

Pentamethylanisole (V, mp 62—63°C)[14] was similarly prepared by the reduction of the bischloromethylation product from 2,4,5-trimethylanisole. Direct methylation of anisole with boron trifluoride - methanol complex according to the Kolka and Vogt's procedure[15] was found unsatisfactory since the major product of the reaction was not the expected V, but the 2,3,4,4,5,6-hexamethylcyclohexa-2,5-dienone,[16] although some V could be isolated from the reaction mixture. The reaction could hardly be controlled to stop at the stage of pentamethylation, and it always went too far to yield the dienone as the final stable product.

Tetramethylbenzyl nitrates used as a reference compound were prepared in 70—85% yield by treating the corresponding benzyl chlorides[17] with silver nitrate in acetonitrile, and recrystallized from *n*-hexane.

6-Nitro-2,3,4,5-tetramethylbenzyl Nitrate (VII): mp 102—103°C. IR, 707, 758, 842, 876, 974, 1277 (ONO_2), 1535 (NO_2), and 1637 cm^{-1} (ONO_2); PMR, 7.84 (Me), 7.72 (2 Me), 7.67 (Me), and 4.68 τ (CH_2).

Found: C, 52.0; H, 5.8%. Calcd for $C_{11}H_{14}N_2O_5$: C, 52.0; H, 5.6%.

5-Nitro-2,3,4,6-tetramethylbenzyl Nitrate (VIII): mp, 132—134°C. IR, 705, 756, 838, 871, 967, 1281 (ONO_2), 1528 (NO_2), and 1638 cm^{-1} (ONO_2); PMR, 7.67 (Me), 7.58 (2 Me), 7.50 (Me), and 4.32 τ (CH_2).

Found: C, 52.0; H, 5.6%. Calcd for $C_{11}H_{14}N_2O_5$: C, 52.0; H, 5.6%.

4-Nitro-2,3,5,6-tetramethylbenzyl Nitrate (IX): mp, 157—158°. IR, 713, 757, 848, 867, 966, 1274 (ONO_2), 1531 (NO_2), and 1633 cm^{-1} (ONO_2); PMR, 7.76 (2 Me), 7.55 (2 Me), and 4.30 τ (CH_2).

Found: C, 52.2; H, 5.6%. Calcd for $C_{11}H_{14}N_2O_5$: C, 52.0; H, 5.6%.

Bis(acetoxymethyl)tetramethylbenzenes were obtaind in 80—90% yield from the bis(chloromethyl)tetramethylbenzenes[18] by treatment with silver acetate in gently refluxing glacial acetic acid, and crystallized from ethanol.

1,2-Bis(acetoxymethyl)-3,4,5,6-tetramethylbenzene: mp, 117—118°C. IR, 906, 954, 1025, 1235 (CO·O, broad), and 1731 cm^{-1} (CO·O); PMR, 7.94 (O·$COCH_3$), 7.68 (Me), 7.65 (Me), and 4.67 τ (CH_2).

Found: C, 69.2; H, 8.2%. Calcd for $C_{16}H_{22}O_4$: C, 69.1; H, 8.0%.

1,3-Bis(acetoxymethyl)-2,4,5,6-tetramethylbenzene: mp, 114—115°C. IR, 912, 958, 979, 1031, 1243 (CO·O, broad), and 1731 cm^{-1} (CO·O); PMR, 7.93 (O·$COCH_3$), 7.68 (Me), 7.62 (2 Me), 7.55 (Me), and 4.82 τ (CH_2).

Found: C, 69.0; H, 8.1%. Calcd for $C_{16}H_{22}O_4$: C, 69.1; H, 8.0%.

1,4-Bis(acetoxymethyl)-2,3,5,6-tetramethylbenzene: mp, 191—192°C. IR, 917, 962, 1027, 1239 (CO·O, broad), and 1732 cm^{-1} (CO·O); PMR, 7.81 (O·$COCH_3$), 7.52 (Me), and 4.68 τ (CH_2).

Procedure for Nitration of Pentamethylnitrobenzene (I), Pentamethylbenzoic Acid (II) and Methyl Pentamethylbenzoate (III). Fuming nitric acid (d=1.50, 6.3 g) was added over a period of 30 min to a vigorously stirred solution of II (3.8 g) or III (4.1 g) in dichloromethane (30 m*l*). During the addition, the temperature of the system was kept at −5—0°C. Since I (3.9 g) was recovered mostly unchanged under the same condition, it was treated with a large excess of fuming nitric acid (12.6 g) in dichloromethane (20 m*l*) at somewhat elevated temperature (30—32°C). The mixture was poured into water and the organic layer was washed thoroughly with water. Removal of the solvent left a solid, which was directly subjected to the infrared and PMR spectral determinations.

The nitration product from I showed PMR peaks at 7.76, 7.73, 7.68, and 4.68 τ along with a minor peak at 4.70 τ; infrared bands at 708, 760, 878, 976, 1277, 1535, and 1636 cm^{-1}. On hydrolysis with hydrochloric acid and subsequent recrystallization from ligroin, it gave 6-nitro-2,3,4,5-tetramethylbenzyl alcohol as light yellow prisms, mp 175—176°C. The same compound was obtained from the unsuccessful

9) H. Suzuki, *Nippon Kagaku Zasshi*, **91**, 179 (1970).
10) H. Suzuki, *ibid.*, **91**, 484 (1970).
11) A. W. Hofmann, *Ber.*, **18**, 1821 (1885).
12) O. H. Hey, *J. Chem. Soc.*, **1931**, 1581; R. W. Cripps and O. H. Hey, *ibid.*, **1943**, 14; D. E. Winkler and S. A. Ballard, U. S. 2440036, 2448942 (1948); A. Burawoy and J. T. Chamberlain, *J. Chem. Soc.*, **1944**, 624, 626; B. R. M. Monnenberg, A. Ova, and U. Lehmuskoskii, *Paperi ja Puu*, **35**, 8 (1953); *Svensk Paperstidn.*, **56**, 46 (1954); B. R. M. Monnenberg, Swed. 145389 (1953); N. P. Buu-Hoï, G. Lejeune, and M. Sy, *Compt. Rend.*, **240**, 224 (1955); B. V. Gregorovich, K. S. Y. Liang, D. M. Clugston, and S. F. MacDonald, *Can. J. Chem.*, **46**, 3291 (1968).
13) R. Wegler and E. Regel, *Makromol. Chem.*, **9**, 1 (1952).
14) G. Vavon, J. Bolle, and J. Calin, *Bull. Soc., Chim. Fr.*, **6**, 1025 (1939).
15) A. J. Kolka and R. R. Vogt, *J. Amer. Chem. Soc.*, **61**, 1463 (1939).
16) H. Hart and O. W. Swatton, *ibid.*, **89**, 1874 (1967); B. I. Mokrousov, P. Adomenas, and V. A. Koptyug, *Zh. Org. Khim.*, **3**, 2255 (1967).
17) H. Suzuki, This Bulletin, **43**, 3299 (1970).
18) M. J. Rhoad and P. J. Flory, *J. Amer. Chem. Soc.*, **72**, 2216 (1950); M. S. Newman, J. R. LeBlanc, H. A. Karnes, and G. Axelrad, *ibid.*, **86**, 868 (1964).

synthesis of 6-nitro-2,3,4,5-tetramethylphenylnitromethane by treating 6-nitro-2,3,4,5-tetramethylbenzyl chloride with silver nitrite in acetonitrile. PMR, 7.78 (Me), 7.68 (2 Me), 7.56 (Me), and 5.59 τ (CH_2).

Found: C, 63.0; H, 7.3%. Calcd for $C_{11}H_{15}NO_3$: C, 63.2; H, 7.2%.

The yields of crude products from the nitration of II and III were 70—80% and a single crystallization was usually enough to purify them.

6-Nitrooxymethyl-2,3,4,5-tetramethylbenzoic Acid: mp, 150—152°C.

Found: C, 57.2; H, 5.9; N, 5.3%. Calcd for $C_{12}H_{15}NO_5$: C, 56.9; H, 6.0; N, 5.5%.

Methyl 6-Nitrooxymethyl-2,3,4,5-tetramethylbenzoate: mp, 104—105°C.

Found: C, 58.3; H, 6.6%. Calcd for $C_{13}H_{17}NO_5$: C, 58.4; H, 6.4%.

3,4,5,6-Tetramethylphthalide: mp, 233—235°C.

Found: C, 75.5; H, 7.1%. Calcd for $C_{12}H_{14}O_2$: C, 75.8; H, 7.4%.

Procedure for Nitration of Pentamethylphenol (IV), Pentamethylanisole (V) and Pentamethylacetanilide (VI). A solution of fuming nitric acid (d=1.50, 2.0 g) in dichloromethane (10 m*l*) was added dropwise to a magnetically stirred solution of IV (3.3 g) or V (3.6 g) in the same solvent (25 m*l*) over a period of 20 min. The temperature was cautiously kept at −10—−5°C during the addition. The solution rapidly yellowed, and the color intensified to orange to light brown. VI (4.1 g) reacted less vigorously under the same condition. After the end of the addition, the mixture was diluted with water and the organic part was thoroughly washed with water. After drying over anhydrous sodium sulfate, the solvent was evaporated to give a yellow syrup or a light brown pasty cake, on which infrared, ultraviolet and PMR spectroscopic inspections were performed.

The nitration products (*ca.* 3.5—3.8 g) from IV and V both showed almost identical infrared and PMR spectral pattern. IR: 852, 1002, 1024, 1083, 1272, 1340, 1374, 1445, 1540—1550, 1617—1635, and 1735 cm^{-1}; PMR, 8.79, 8.69, 8.66, 8.88—8.30, 6.58, 5.40, and 4.79 τ. When the syrupy product was dissolved in a minimum amount of light petroleum - ether mixture and set aside in a refrigerator for weeks, it slowly separated crystalline solid of wide melting range (70—90°C), which was purified through fractional crystallization from a mixture of light petroleum and ether to give white prisms (mp 138—140°C) and was formulated as 4-hydroxy-2,3,4,5,6-pentamethylcyclohexa-2,5-dienone on the basis of analysis, infrared, ultraviolet and PMR spectral data.

Found: C, 72.4; H, 8.9%. Calcd for $C_{11}H_{16}O_2$: C, 73.3; H, 8.9%.

A white powder obtained from the above syrup by trituration in cold ethanol melted at up to 260°C with decomposition. It showed infrared bands at 1020, 1074, 1345, 1372, 1540—1545, 1630, and 3420 cm^{-1}, and PMR peaks at 8.79, 8.61, 7.90—8.20 (complicated multiplet), and 6.52 τ.

Found: C, 64.6; H, 7.4, N, 4.5%.

The nitration product (*ca.* 4.2 g) from VI exhibited PMR peaks at 8.73, 8.31, 7.97, 7.86—7.67, 4.48, and 4.43 τ; IR bands at 876, 1280, 1365—1380, 1510, 1613, 1645, 1725, 2900, and 3218 cm^{-1}. Upon crystallization from a mixture of light petroleum and methylene chloride, it gave a nitrooxymethyltetramethylacetanilide, mp 126—127°C, which had PMR peaks at 7.83 (Me), 7.75 (3 Me), 7.66 (COMe), and 4.45 τ (CH_2); IR bands at 877 (ONO_2), 1282 (ONO_2), 1368, 1382, 1613 (ONO_2), 1685 (COMe), and 3220 cm^{-1} (NH).

Found: C, 58.4; H, 7.0; N, 10.3%. Calcd for $C_{12}H_{17}NO_4$: C, 58.6; H, 6.8; N, 10.5%.

A New Phosphorylating Reagent. III.[1] Preparation of Mixed Diesters of Phosphoric Acid by the Use of an Activatable Protecting Group

Yoshitaka MUSHIKA, Tsujiaki HATA, and Teruaki MUKAIYAMA

Department of Chemistry, Tokyo Institute of Technology, Ookayama, Meguro-ku, Tokyo

(Received August 4, 1970)

A novel method for the preparation of mixed diesters of phosphoric acid has been investigated. It was found that mixed diesters of phosphoric acid were prepared by the reaction of alkyl 2-chloromethyl-4-nitrophenyl hydrogen phosphates with alcohols in dry pyridine. On the other hand, these diesters were also obtained from dialkyl 2-chloromethyl-4-nitrophenyl phosphates on hydrolysis under mild conditions. By using both of these methods, analytically pure samples of mixed diesters of phosphoric acid could be obtained in high yields.

In a previous paper,[2] it has been reported that highly pure samples of alkyl dihydrogen phosphates (**3**) were prepared in high yields under mild conditions by treating alkyl 2-chloromethyl-4-nitrophenyl hydrogen phosphates (**1**) with aqueous pyridine.

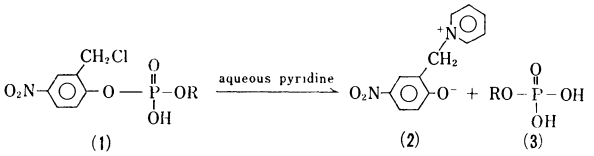

(1) (2) (3)

This result shows that 2-chloromethyl-4-nitrophenyl group functions to facilitate the elimination of this group through an intermediate, inner salt of 1-(2-alkyl hydrogen phosphoroxy 5-nitrobenzyl)pyridinium hydroxide (**4**), formed by an attack of pyridine on the chloromethyl group of **1** as sketched below. Therefore, it can be expected that mixed diesters of phosphoric acid would be successfully synthesized when **1** is treated with alcohols in dry pyridine.

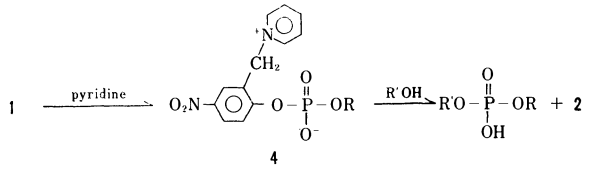

4

When a mixture of one equiv. of **1** and two equiv. of *n*-pentyl alcohol in five equiv. of pyridine was allowed to stand at room temperature for two days and then was heated at 90°C for 6 hr, ethyl *n*-pentyl hydrogen phosphate (**5a**) was obtained in 81% yield along with inner salt of 1-(2-hydroxy-5-nitrobenzyl)pyridinium hydroxide (**2**).

In a similar manner, various mixed diesters of phosphoric acid were obtained in high yields as shown in Table 1.

In the cases of *n*-hexadecyl derivatives (**5b**, **5i**, **5j**, **5k**, and **5l**), it is necessary to carry out the reaction by using ten equiv. of pyridine because *n*-hexadecyl derivatives are less soluble in pyridine than the other

TABLE 1. PREPARATION OF DIALKYL HYDROGEN PHOSPHATES (**5**)

Compd.	R	R′	Yield[a] (%)	Mp (°C)	$n_D^{°C}$	R_f[b]	Formula	Calcd C	Calcd H	Found C	Found H
5a	Ethyl	*n*-Pentyl	81		1.4250^{26}	0.83	$C_7H_{17}O_4P$	42.85	8.73	42.91	8.90
5b		*n*-Hexadecyl	74	54—55		0.90	$C_{18}H_{39}O_4P$	61.69	11.22	62.31	11.21
5c		Cyclohexyl	58		1.4552^{26}	0.83	$C_8H_{17}O_4P$	46.15	8.23	46.50	8.51
5d		Bornyl	69		1.4717^{25}	0.87	$C_{12}H_{23}O_4P$	54.95	8.84	54.50	8.78
5e		Benzyl	60		[c]	0.81	$C_9H_{13}O_4P$	50.00	6.06	50.64	5.84
5f	*n*-Pentyl	*p*-Tolyl	57		1.4891^{25}	0.91	$C_{12}H_{19}O_4P$	55.81	7.42	55.62	7.17
5g		*p*-Chlorophenyl	61		1.4933^{25}	0.91	$C_{11}H_{16}ClO_4P$	47.41	5.79	47.27	5.62
5h		*p*-Nitrophenyl	55	61—62		0.91	$C_{11}H_{16}NO_6P$	45.68 (N=4.84)	5.58	46.30 (N=4.69)	5.62
5b	*n*-Hexadecyl	Ethyl	97	54—55		0.90					
5i		*n*-Pentyl	92	45—47		0.94	$C_{21}H_{45}O_4P$	64.25	11.55	63.95	11.90
5j		Cyclohexyl	87		1.4717^{25}	0.92	$C_{22}H_{45}O_4P$	65.31	11.21	65.73	10.96
5k		Bornyl	89		1.4782^{24}	0.94	$C_{26}H_{51}O_4P$	68.09	11.21	68.37	11.60
5l		Benzyl	86	58—60		0.94	$C_{23}H_{41}O_4P$	66.96	10.02	66.99	10.36
5f	*p*-Tolyl	*n*-Pentyl	72		1.4893^{25}	0.91					

a) Yields are based on the phosphate **1**.
b) Paper chromatography was carried out by ascending technique using Toyo Roshi No. 50 paper. Solvent system used was: isopropyl alcohol, conc. ammonium hydroxide, water (7 : 1 : 2 v/v).
c) The compound **5e** is pale yellowish oil.

1) Paper II: T. Hata, Y. Mushika, and T. Mukaiyama, *Tetrahedron Lett.*, **1970**, 3505.

2) T. Hata, Y. Mushika, and T. Mukaiyama, *J. Amer. Chem. Soc.*, **91**, 4532 (1969).

derivatives.

It was also found that phenols are successfully phosphorylated to give the corresponding alkyl aryl hydrogen phosphates. When *n*-pentyl 2-chloromethyl-4-nitrophenyl hydrogen phosphate (**1f**) was treated with *p*-cresol, *n*-pentyl *p*-tolyl hydrogen phosphate (**5f**) was obtained in 57% yield as a major product and a small amount of P^1,P^2-di-*n*-pentyl pyrophosphate (**6f**) was detected as a by-product.

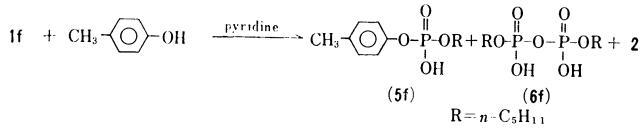

The formation of **6f** would be explained by considering the competitive reaction of **1f** with **4f** (R=*n*-C_5H_{11}). In order to avoid the undesirable formation of **6f**, *p*-tolyl 2-chloromethyl-4-nitrophenyl hydrogen phosphate (**1m**), prepared from lithium phenoxide and 2-chloromethyl-4-nitrophenyl phosphorodichloridate (**7**), was chosen with the consideration that **5f** would be exclusively produced because alcohols can react with **1m** much faster than phenols.

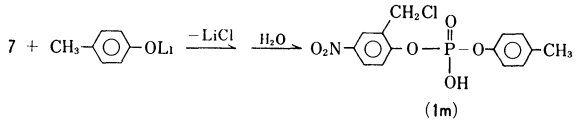

When the phosphate **1m** was treated with *n*-pentyl alcohol in dry pyridine, *n*-pentyl *p*-tolyl hydrogen phosphate (**5f**) was isolated in 72% yield without accompanying the formation of the pyrophosphate.

$$\mathbf{1m} + n\text{-}C_5H_{11}OH \xrightarrow{\text{pyridine}} \mathbf{5f} + \mathbf{2}$$

The reaction of thiols with **1** proceeded very sluggishly even when they were refluxed in dry pyridine. Similar to the cases of phenols mentioned above, *O*,*S*-di-*n*-pentyl hydrogen phosphorothioate (**8**) could be prepared in 42% yield starting from *S*-*n*-pentyl *O*-2-chloromethyl-4-nitrophenyl hydrogen phosphorothioate (**9**) by the treatment with *n*-pentyl alcohol in dry pyridine as shown in the following equation.

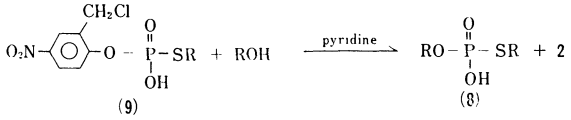

In the next place, the preparation of mixed diesters of phosphoric acid from 2-chloromethyl-4-nitrophenyl phosphorodichloridate (**7**) and two different kinds of alcohols was investigated.

It was established that one of the two chlorine atoms of **7** reacts selectively with one equiv. of an alcohol in the presence of exactly one equiv. of pyridine to afford the corresponding alkyl 2-chloromethyl-4-nitrophenyl phosphorochloridate (**10**). The phosphorochloridate **10** was further, without isolating, treated with one equiv. of another alcohol in the presence of one equiv. of pyridine. The triester, dialkyl 2-chloromethyl-4-nitrophenyl phosphate (**11**) was obtained in high yield and it was purified by silica-gel column chromatography in order to remove **1**, formed by hydrolysis of **10**.

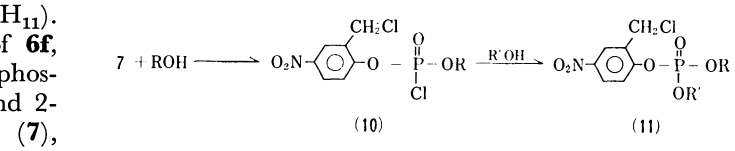

The structure of **11** was confirmed by elemental analysis as well as infrared and ultraviolet spectra. Several triesters **11** were obtained by this method as shown in Table 2.

Table 3. Preparation of dialkyl hydrogen phosphates (**5**) from dialkyl 2-chloromethyl-4-nitrophenyl phosphates (**11**)

Compd.[a]	R	R′	Yield[b] (%)	Appearance
5p	Ethyl	Ethyl	81	colorless oil
5a	Ethyl	*n*-Pentyl	85	colorless oil
5b	Ethyl	*n*-Hexadecyl	79	white powder (mp 54—55°C)
5c	Ethyl	Cyclohexyl	56	colorless oil
5n	*n*-Pentyl	Cyclohexyl	86	colorless oil

a) The compounds were identified with authentic samples listed in Table 1.
b) Yields are based on the phosphates **11**.

The triester **11** was smoothly hydrolyzed in aqueous pyridine to the corresponding dialkyl hydrogen phosphate (**5**). These results are summarized in Table 3.

The assumed intermediate, a pyridinium derivative (**12p**) could be isolated when diethyl 2-chloromethyl-

Table 2. Preparation of dialkyl 2-chlorometyl-4-nitrophenyl phosphates (**11**)

Compd.	R[a]	R′[a]	R′OH (mol ratio)	Yield[b] (%)	R_f[c]	Formula	Calcd C	Calcd H	Calcd N	Found C	Found H	Found N
11p	Ethyl	Ethyl	1/1	64	0.94	$C_{11}H_{15}ClNO_6P$	40.82	4.67	4.35	41.02	4.98	4.64
11a	*n*-Pentyl	Ethyl	1/1	57	0.96	$C_{14}H_{21}ClNO_6P$	45.97	5.79	3.83	46.07	5.89	3.92
			5/1	93								
11b	*n*-Hexadecyl	Ethyl	2/1	81	0.96	$C_{25}H_{43}ClNO_6P$	57.74	8.33	2.69	57.99	8.08	2.78
11c	Cyclohexyl	Ethyl	2/1	91	0.95	$C_{15}H_{21}ClNO_6P$	47.69	5.60	3.71	48.01	5.82	3.88
11d	*n*-Pentyl	Cyclohexyl	1/1	46	0.96	$C_{18}H_{27}ClNO_6P$	51.49	6.48	3.34	51.26	6.31	3.56

a) The phosphorodichloridate **7** was allowed to react with ROH and then with R′OH.
b) Yields are based on the phosphorodichloridate **7**.
c) Paper chromatography was carried out by ascending technique using Toyo Roshi No. 50 paper. Solvent system used was: isopropyl alcohol, conc. ammonium hydroxide, water (7 : 1 : 2 v/v).

4-nitrophenyl phosphate (**11p**) was treated with one equiv. of pyridine in the absence of alcohol. The compound **12p** was very hygroscopic pale yellow prisms and melted at 191°C.

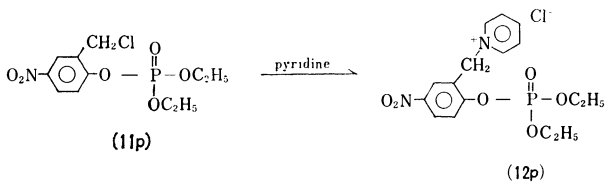

(11p) (12p)

Experimental

Reagents. Alcohols, mercaptans, phenols and pyridine were purified and dried by ordinary procedures. 2-Chloromethyl-4-nitrophenyl phosphorodichloridate (**7**) and alkyl 2-chloromethyl-4-nitrophenyl hydrogen phosphates (**1**) were prepared as described in a previous publication.[2]

Paper Chromatography. Paper chromatography was carried out by ascending technique using Toyo Roshi No. 50 paper. Solvent system used was: isopropyl alcohol, concentrated ammonium hydroxide, water (7 :1 : 2 v/v).

*Preparation of Dialkyl Hydrogen Phosphates (**5**) from Alkyl 2-Chloromethyl-4-nitrophenyl Hydrogen Phosphates (**1**).* *General Procedure*: Alkyl 2-chloromethyl-4-nitrophenyl hydrogen phosphate (**1**) (0.01 mol) and an alcohol (0.02 mol) were dissolved in 4-8 m*l* of dry pyridine. The mixture was allowed to stand at room temperature for 2 days and then heated at 90°C for 6 hr. After addition of 30 m*l* of ethanol, a pale yellowish precipitate, inner salt of 1-(2-hydroxy-5-nitrobenzyl)pyridinium hydroxide separated. It was removed by filtration and washed with 30 m*l* of ethanol. The combined filtrate and washings were concentrated to dryness. Dialkyl hydrogen phosphate was isolated from the oily residue by means of either *Method A* or *Method B*. The compounds (see Table 1), **5d**, **5f**, and **5g** were prepared by *Method A-1*. The compounds, **5a**, **5b**, **5c**, **5e**, and **5h** were obtained by *Method A-2*. The other compounds, **5i**, **5j**, **5k**, and **5l** were isolated by *Method B*.

The results are summarized in Table 1.

Method A: The oily residue was dissolved in 50 m*l* of water containing 1.7 g (0.02 mol) of sodium hydrogencarbonate and the solution was washed with ether. The aqueous layer was acidified with hydrochloric acid and extracted with three 30 m*l* portions of petroleum ether (*Method A-1*) or ether (*Mothod A-2*). The combined extracts were washed with three 10 m*l* portions of water and dried over anhydrous sodium sulfate. After removal of the solvent, pure sample of dialkyl hydrogen phosphate (**5**) was obtained without further purification.

Method B: After complete removal of the solvent under high vacuum, the residue was dissolved in 100 m*l* of petroleum ether (bp 45—60°C). The solution was washed with dilute hydrochloric acid and then three 10 m*l* portions of water. After drying the solution over anhydrous sodium sulfate, petroleum ether was removed by evaporation. Highly pure sample of dialkyl hydrogen phosphate (**5**) was obtained as white powder (**5i** and **5l**) or colorless oil (**5j** and **5k**).

S-n-*Pentyl* O-*2-Chloromethyl-4-nitrophenyl Hydrogen Phosphorothioate (**9**).* A suspension of lithium *n*-pentyl mercaptide, which was prepared from 2.42 m*l* (0.02 mol) of *n*-pentyl mercaptan in 20 m*l* of tetrahydrofuran (THF) and 12 m*l* (0.02 mol) of 10% solution of *n*-butyllithium in *n*-hexane, was slowly added at −20°C to a solution of 6.08 g (0.02 mol) of 2-chloromethyl-4-nitrophenyl phosphorodichloridate (**7**) in 30 m*l* of tetrahydroquran. The stirring was continued at −20——10°C for 3 hr and further at room temperature for 2 hr. The mixture was poured into 50 m*l* of water containing 1.6 m*l* (0.02 mol) of pyridine at a temperature below 20°C and then stirred for 30 min. THF was removed and the solution was extracted with three 50 m*l* portions of benzene. The extract was washed with three 10 m*l* portions of water and dried over anhydrous sodium sulfate. After removal of benzene, *S-n*-pentyl *O*-2-chloromethyl-4-nitrophenyl hydrogen phosphorothioate (**9**) (3.30 g, 49%) was obtained as reddish oil; R_f: 0.92; $\lambda_{max}^{H_2O}$ 290 mμ (ε: 8400).

Found: C, 39.89; H, 4.77; N, 4.22%. Calcd for $C_{12}H_{17}ClNO_5PS$: C, 40.74; H, 4.84; N, 3.96%.

O,S-*di*-n-*Pentyl Hydrogen Phosphorothioate (**8**).* A solution of 3.40 g (0.01 mol) of *S-n*-pentyl *O*-2-chloromethyl-4-nitrophenyl hydrogen phosphorothioate (**9**) and 2.16 m*l* (0.02 mol) of *n*-pentyl alcohol in 4 m*l* (0.05 mol) of dry pyridine was allowed to stand at room temperature for 2 days and further heated at 90°C for 6 hr. Thirty m*l* of ethanol was added and pale yellowish precipitate, inner salt of 1-(2-hydroxy-5-nitrobenzyl)pyridinium hydroxide (1.76 g, 66%) separated and was filtered off. The filtrate was concentrated and the residue was dissolved in 30 m*l* of water containing 1.7 g of sodium hydrogencarbonate. The aqueous solution was washed with ether and acidified with hydrochloric acid and then extracted with three 30 m*l* portions of petroleum ether. The combined extracts were washed with three 10 m*l* portions of water and dried over anhydrous sodium sulfate. After decolorizing with charcoal, the solvent was removed by evaporation. *O,S*-di-*n*-pentyl hydrogen phosphorothioate (**8**) (1.19 g, 47%) was obtained as yellowish oil; R_f 0.92; n_D^{20} 1.4762.

Found: C, 47.67; H, 8.91, S. 13.50%. Calcd for $C_{10}H_{23}O_3PS$: C, 47.22; H, 9.12; S, 12.61%.

Formation of P^1,P^2-*di*-n-*Pentyl Pyrophosphate (**6f**).* A solution of *n*-pentyl 2-chloromethyl-4-nitrophenyl hydrogen phosphate (**1f**) (3.38 g, 0.01 mol) in 4 m*l* (0.05 mol) of pyridine was allowed to stand at room temperature for 2 days and further heated at 90°C for 6 hr. Ethanol (30 m*l*) was added to the solution. Pale yellowish precipitate, inner salt of 1-(2-hydroxy-5-nitrobenzyl)pyridinium hydroxide (2.25 g, 84%) separated and was filtered off. The filtrate was evaporated and the residue was dissolved in 30 m*l* of water. The solution was acidified with hydrochloric acid and extracted with four 30 m*l* portions of ether. The extracts were combined and dried over anhydrous sodium sulfate. After removal of ether, the residual oil was dissolved in 20 m*l* of ether and then 3.0 g of aniline was added. The mixture was kept standing in a refrigerator overnight. A white precipitate separated and was collected by filtration. The precipitate was recrystallized from a mixture of ethanol and acetone. Di-anilinium salt of P^1,P^2-di-*n*-pentyl pyrophosphate (**6f**) (0.93 g, 37%) was obtained as white prisms; mp 134°C; R_f 0.78.

Found: C, 51.78; H, 7.67; N, 5.57%. Calcd for $C_{22}H_{35}N_2O_7P_2$: C, 52.38; H, 7.59; N, 5.55%.

*Preparation of Dialkyl 2-Chloromethyl-4-nitrophenyl Phosphates (**11**).* *A Typical Procedure*: To a solution of 6.01 g (0.02 mol) of 2-chloromethyl-4-nitrophenyl phosphorodichloridate (**7**) in 30 m*l* of THF was added slowly a solution of cyclohexanol (2.00 g, 0.02 mol) and pyridine (1.60 g, 0.02 mol) in 20 m*l* of THF with stirring at a temperature below −10°C. The mixture was stirred for 4 hr and further at room tem-

perature for 2 hr. A solution of ethanol (2.33 m*l*, 0.04 mol) and pyridine (1.6 m*l*, 0.02 mol) in THF (20 m*l*) was then added under cooling. Stirring was continued for 2 hr and further at room temperature for 5 hr. After concentrating the mixture, the residue was poured into water (30 m*l*) and extracted with benzene (80 m*l*). The benzene was washed with water and dried over anhydrous sodium sulfate. After removal of the solvent, the syrupy residue was passed through a column of Wakogel C-200 (100—200 mesh) (20 mm × 500 mm) by using benzene for elution. The eluent was concentrated to dryness. Ethyl cyclohexyl 2-chloromethyl-4-nitrophenyl phosphate (**11d**) (6.9 g, 91%) was obtained as a pale yellowish syrup. In a similar manner, the triesters (**11**), such as **11p**, **11b**, **11c**, and **11e** were obtained in high yields as shown in Table 2.

*Preparation of Dialkyl Hydrogen Phosphates (**5**) from Dialkyl 2-Chloromethyl-4-nitrophenyl Phosphates (**11**). A Typical Procedure*: A solution of *n*-pentyl cyclohexyl 2-chloromethyl-4-nitrophenyl phosphate (**11e**) (4.20 g, 0.01 mol) in 12 m*l* of aqueous pyridine (30% solution) was allowed to stand at room temperature for 2 days and then heated at 90°C for 3 hr. The reaction mixture was concentrated to dryness. Ethanol (30 m*l*) was added and pale yellowish precipitate, inner salt of 1-(2-hydroxy-5-nitrobenzyl)pyridinium hydroxide (2.35 g, 88%) separated and was filtered off. The filtrate was concentrated and the residue was dissolved in 30 m*l* of water. The aqueous solution was acidified with hydrochloric acid and extracted with three 30 m*l* portions of petroleum ether (bp 45—60°C). The extracts were combined and washed with three 10 m*l* portions of water and dried over anhydrous sodium sulfate. After removal of petroleum ether, *n*-pentyl cyclohexyl hydrogen phosphate (**5n**) (2.15 g, 86%) was obtained as colorless oil, R_f 0.85; n_D^{22} 1.4552.

Found: C, 53.30, H, 8.61%. Calcd for $C_{11}H_{23}O_4P$: C, 52.79; H, 9.26%.

In a similar manner, the other dialkyl hydrogen phosphate (**5**), such as **5p**, **5a**, **5b**, and **5c** were prepared as shown in Table 3.

*Isolation of an Intermediate 1-(2-Diethyl Phosphoroxy 5-Nitrobenzyl)pyridinium Chloride (**12p**).* A solution of diethyl 2-chloromethyl-4-nitrophenyl phosphate (**11p**) (3.24 g, 0.01 mol) in 8.0 m*l* of dry pyridine was allowed to stand at room temperature for 3 days. After addition of acetone (40 m*l*), yellowish precipitate, **12p** was separated and was collected by filtration. It was recrystallized from a mixture of ethanol (4 m*l*) and acetone (15 m*l*) to afford a pure sample (1.65 g, 43%) as pale yellowish prisms; mp 191°C dec., $\lambda_{max}^{H_2O}$ 262 mμ (ε: 10700), 267 mμ (ε: 10700), 289 mμ (ε: 10500); R_f 0.61.

Found: C, 50.03; H, 5.65; N, 7.46%. Calcd for $C_{16}H_{21}N_2O_7P$: C, 50.00; H, 5.51; N, 7.29%.

We wish to thank Mr. Masaru Koezuka for his help with elemental analysis.

BULLETIN OF THE CHEMICAL SOCIETY OF JAPAN, VOL. 44, 235—239 (1971)

Synthesis and Elimination Reaction of *O*-Methyl Derivatives of Methyl (Methyl α-D-Glucopyranosido)uronate

Hironobu HASHIMOTO, Takeshi SEKIYAMA, Hideo SAKAI, and Juji YOSHIMURA

Laboratory of Chemistry for Natural Products, Faculty of Science, Tokyo Institute of Technology, Ookayama, Meguro-ku, Tokyo

(Received August 4, 1970)

Several methyl ethers [2,3,4-tri-*O*-methyl- (**1**), 4-*O*-methyl- (**2**), 3-*O*-methyl- (**3**), and 2-*O*-methyl- (**4**)] of methyl (methyl α-D-glucopyranosido)uronate were used as model compounds for the examination of β-elimination reaction. **1** was purely synthesized from methyl α-D-glucopyranoside and both **3** and **4** were newly synthesized *via* the corresponding methyl ethers of methyl α-D-glucopyranoside. The condition of β-elimination reaction was examined using **1** as a model compound. It was shown that β-elimination reaction occurred only when an alkoxide was used as a base. The yield of the unsaturated product, *i. e.*, methyl (methyl 4-deoxy-2,3-di-*O*-methyl-β-L-*threo*-hex-4-enopyranosido)uronate (**13**) was about 40—50% by sodium methoxide in methanol at 60—70°C, and 70—80% by potassium *t*-butoxide in *t*-butyl alcohol even at room temperature. In both cases the reaction was completed within several minutes. The β-elimination reaction was followed by UV spectra using the molecular extinction coefficient of purely isolated **13**, and the reaction products were examined by gas-liquid chromatography. The β-elimination product of **2** was also obtained in good yield, but that of **3** in very poor yield.

The selective cleavage of a certain glycosidic bond in heteropolysaccharides is essential for the sequential elucidation of compositional monosaccharides. For this the enzymatic cleavage is often used, but the desired enzyme is not easily available. The development of some chemical method has for long been a subject of interest.

Recently the selective cleavage of glycosidic bonds around uronic acid residues has been investigated in polyuronides and polysaccharides containing uronic acids. One investigation was carried out on the selective cleavage of glycosidic bonds by utilizing the β-elimination reaction in alkali.[1,2] Another was carried out on the selective cleavage of glycuronosyl bonds by acid hydrolysis after the Hofmann degradation of uronic

1) C. W. McCleary, D. A. Rees, J. W. B. Sammel, and I. W. Steele, *Carbohyd. Res.*, **5**, 492 (1967).

2) C. J. Lawson, C. W. McCleary, H. I. Nakada, D. A. Rees, I. W. Sutherland, and J. F. Wilkinson, *Biochem. J.*, **115**, 947 (1969).

acid amide residues, derived from uronic acid esters.[3]

It is well known that polyuronides such as pectin depolymerize in neutral or alkaline solution,[4] and this was applied to obtain a few depolymerized polysaccharides.[5] Thus, the β-elimination reaction seems to be useful for the structural analysis of naturally occurring uronic acid-containing polysaccharides. However, in aqueous solution the reaction proceeds only slightly owing to competing de-esterification, and the cleavage of the glycosidic bonds might occur only when they are 1→4 linkages to hexopyranuronoside structure.

Heim and Neukom[6] reported that methyl (methyl α-D-galactopyranosido)uronate and methyl 4-*O*-(methyl α-D-galactopyranosyluronate)-(methyl α-D-galactopyranosido)uronate underwent the elimination reaction when treated with sodium methoxide in methanol, but details of the reaction were not presented. This reaction was applied by McCleary *et al.*[1] to partial depolymerization of 2-hydroxyethyl alginate, and recently by Lawson *et al.*[2] to structural analysis of colanic acid. On the other hand, Fujinaga and Matsushima[7] reported the degradation of methyl 4′,6′-*O*-ethylidene-β-pseudocellobiouronoside methyl ester by the treatment of hydrazine, conceivably due to β-elimination reaction.

For more efficient application of this β-elimination reaction to structural elucidation of uronic acid-containing polysaccharides, we examined the β-elimination reaction using several synthesized methyl ethers [2,3,4-tri-*O*-methyl- (**1**), 4-*O*-methyl- (**2**), 3-*O*-methyl- (**3**), and 2-*O*-methyl- (**4**)] of methyl (methyl α-D-glucopyranosido)uronate as model compounds. Possibility of a further cleavage of 1→2 glycosidic bond by δ-elimination reaction of once formed unsaturated compounds as shown in the case with picroclocin[8] was also examined.

Results and Discussion

Methyl (methyl 2,3,4-tri-*O*-methyl-α-D-glucopyranosido)uronate (**1**) was synthesized by the method of Jones[9] from D-glucurono-6,3-lactone. This was fairly contaminated with β-anomer, which was ascertained by gas-liquid chromatography and NMR spectrum. **1** was synthesized purely from methyl α-D-glucopyranoside by catalytic oxidation and methylation in the usual manner.

Methyl (methyl 4-*O*-methyl-α-D-glucopyranosido)-uronate (**2**) was synthesized by the method of Wacek.[10] Methyl (methyl 3-*O*-methyl-α-D-glucopyranosido)uronate (**3**) newly synthesized as shown in Fig. 1. 1,2:

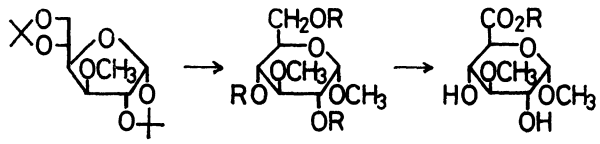

5 6, R = H 8, R = H
7, R = Ac 3, R = CH3

Ac=acetyl

Fig. 1

5,6-Di-*O*-isopropylidene-3-*O*-methyl-α-D-glucofuranose (**5**)[11] was converted to syrupy methyl 3-*O*-methyl-α-D-glucopyranoside (**6**) by refluxing in methanolic hydrogen chloride for 20 hr. In order to purify by distillation, acetylation of **6** was performed, and deacetylation and catalytic oxidation were carried out in one step.

Methyl (methyl 2-*O*-methyl-α-D-glucopyranosido)-uronate (**4**) was also newly synthesized from 3-*O*-benzyl-1,2:5,6-di-*O*-isopropylidene-α-D-glucofuranose,[12] which was methanolized by refluxing in methanolic hydrogen chloride to give syrupy methyl 3-*O*-benzyl-α-D-glucopyranoside. This was converted to 4,6-*O*-benzylidene derivative (**9**), and then to 2-*O*-methyl derivative (**10**) in the usual manner. **10** was debenzylidenated and debenzylated by catalytic hydrogenolysis to give syrupy methyl 2-*O*-methyl-α-D-glucopyranoside (**11**),[13] and **11** gave methyl 2-*O*-methyl-α-D-glucopyranosidouronic acid (**12**) by catalytic oxidation, which was converted to its methyl ester (**4**) with diazomethane (Fig. 2). The

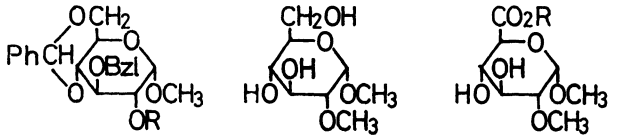

9, R = H 11 12, R = H
10, R = CH3 4, R = CH3

Ph=phenyl Bzl=benzyl

Fig. 2

anomeric configuration of all synthesized *O*-methyl derivatives of methyl (methyl D-glucopyranosido)uronate was ascertained to be α by NMR spectra and optical rotations. However, in the case of **3** and **4** slight contamination with β-anomer was observed (*ca.* 10%), because the glycosidation products could not be crystallized.

First of all, the condition of the β-elimination reaction was examined using **1** as a model compound in some basic mediums, *i. e.*, aqueous solutions containing sodium hydroxide or sodium carbonate, or alcoholic solutions containing sodium hydroxide or sodium methoxide. The expected elimination reaction was observed only when sodium methoxide was used as a base. In other cases it was observed by thin-layer chromatography

3) N. K. Kochetkov, O. S. Chizhov, and A. F. Sviridov, *Carbohed. Res.*, **4**, 362 (1967); N. K. Kochetokov, O. S. Chizhov, and A. F. Sviridov, *Izv. Akad. Nauk SSSR, Ser. Khim.*, **1968**, 2089.

4) P. Albersheim, H. Neukom, and H. Deuel, *Arch. Biochem. Biophys.*, **90**, 46 (1960).

5) R. W. Stddart, A. J. Barrett, and D. H. Northcote, *Biochem. J.*, **102**, 194 (1967).

6) P. Heim and H. Neukom, *Helv. Chim. Acta*, **45**, 1735, 1737 (1962).

7) M. Fujinaga and Y. Matsushima, This Bulletin., **40**, 1706 (1967).

8) R. Kuhn and I. Löw, *Ber.*, **74**, 219 (1941).

9) W. J. G. Jones, L. N. Owen, and S. Peat, *J. Chem. Soc.*, **1941**, 339.

10) A. Wacek, *Monatsh. Chem.*, **90**, 562 (1957).

11) I. E. Muskat, *J. Amer. Chem. Soc.*, **56**, 2449 (1934).

12) R. Kuhn, I. Löw, and H. Trischmann, *Chem. Ber.*, **90**, 203 (1957).

13) W. N. Hawarth, E. L. Hirst, and E. G. Teece, *J. Chem. Soc.*, **1931**, 2858.

that methyl uronate were converted to the corresponding sodium uronates and no elimination was observed.

The elimination reaction was followed by measurement of the NMR and UV spectra at suitable intervals. As the elimination reaction proceeded, in NMR spectra measured in CD_3ONa/CD_3OD a signal assigned to the vinyl proton appeared, whose intensity increased to a certain maximum value and then decreased slowly. This is attributed to the exchange between hydrogen and deuterium. Thus the intensity of the vinyl proton was unsuitable for quantitative discussion. In UV spectra, the absorption of α,β-unsaturated ester appeared at 235—240 mμ, and the optical density at this wavelength increased. The elimination reaction was followed by UV spectra in a suitable solvent.

In order to determine the molecular extinction coefficient of the elimination product, *i. e.*, methyl (methyl 4-deoxy-2,3-di-*O*-methyl-β-L-*threo*-hex-4-enopyranosido)uronate (**13**), its isolation was attempted. **1** was treated with sodium methoxide in methanol and refluxed for 45 min. The reaction mixture was treated with a strongly acidic resin (Amberlite IR-120 H-form) and evaporated to give a slightly yellowish syrup. **13** was obtained in about 35% yield by distillation of the syrup. The structure was ascertained by UV, IR and NMR spectra (Fig. 3).

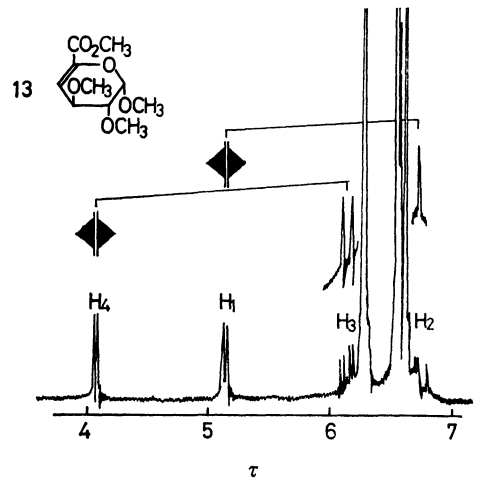

Fig. 3. NMR spectrum of **13** (100 MHz, in CCl_4).

The elimination reaction was carried out with sodium methoxide in methanol at 60—70°C and the optical density at 238 mμ was measured after partial neutralization of the reaction mixture with ethanolic hydrogen chloride. The amount of **13** was then calculated by using the molecular extinction coefficient of **13** (ε_{max}= 5500). Under these conditions the yield of **13** was about 40% (Fig. 4, curve 1). However, this increased to about 55% by direct addition of sodium to a methanol solution of **1** (Fig. 4, curve 2). The yield of the elimination product of **2** was also 50% under the same conditions (Fig. 4, curve 3). In these cases the reaction proceed to completion within 5 min. The yield could not be increased by elongation of the reaction time and elevation of the reaction temperature.

A more effective and moderate reaction condition was sought by using a stronger base, potassium *t*-

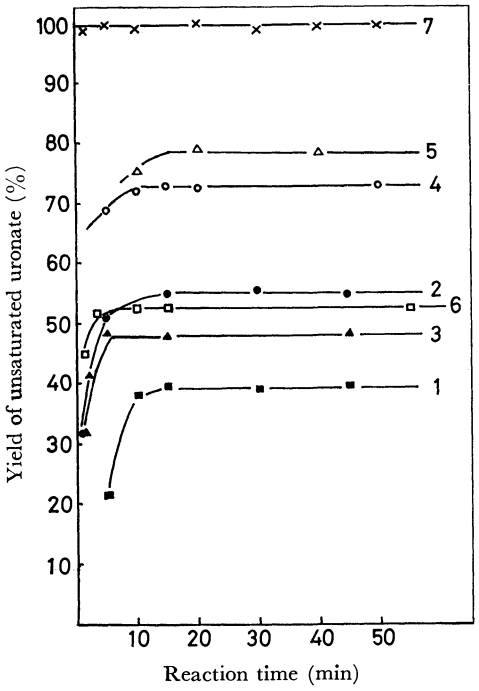

Fig. 4. Elimination reaction of **1**, **2**, and **13**.
1: **1**, CH_3ONa, 70°C
2: **1**, Na, 64°C
3: **2**, Na, 64°C
4: **1**, *t*-C_4H_9OK
5: **1**, *t*-C_4H_9OK
6: **1**, *t*-C_4H_9OK (stored *t*-butyl alcohol was used.)
7: **13**, *t*-C_4H_9OK

butoxide. The reaction was carried out with freshly prepared potassium *t*-butoxide in freshly distilled *t*-butyl alcohol and the amount of **13** formed by the elimination reaction was determined by the optical density at 238 mμ after neutralization with ethanolic hydrogen chloride and dilution with ethanol. As shown in Fig. 4, the elimination reaction proceeded instantaneously even at room temperature and in a few minutes reached about 70—80% (curves 4 and 5). This reaction limit was not altered by elongation of the reaction time and heating. It is noteworthy that the yield decreased in about 40—50%, when stored *t*-butyl alcohol for a few days after distillation was used (curve 6). In order to investigate the nature of the reaction in detail, the reaction mixture was examined by gas-liquid chromatography after neutralization. As shown in Fig. 5, three peaks appeared in the chromatogram. The first and smallest peak was identified as the starting material (**1**),

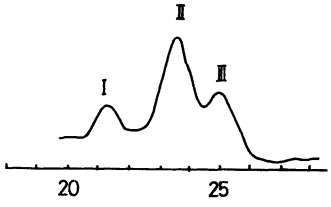

Fig. 5. Gas-liquid chromatogram of reaction mixture of **1**.
I: **1**
II: de-esterified **1** and **13**
III: **13**

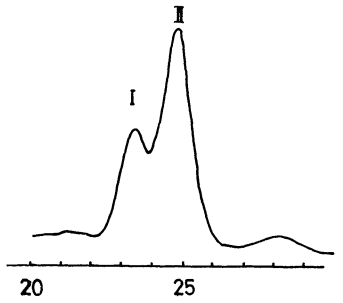

Fig. 6. Gas-liquid chromatogram of reaction mixture of **13**.
I: de-esterified **13**
II: **13**

the second and largest one as a mixture of methyl 2,3,4-tri-*O*-methyl-α-D-glucopyranosidouronic acid and methyl 4-deoxy-2,3-di-*O*-methyl-β-L-*threo*-hex-4-enopyranosidouronic acid (de-esterified **1** and **13**), and the last as **13**. It is remarkable that the ester groups of both the unchanged starting material and reaction product were partially hydrolyzed during the reaction. Comparing the result of the treatment of **13** with potassium *t*-butoxide in *t*-butyl alcohol (Fig. 6), it is suggested that the elimination reaction did not proceed completely, because of hydrolysis of a certain part of the starting material. Such hydrolysis took place probably by the moisture introduced during the operation.

No marked peak, other than the above mentioned three peaks, was detected, which suggests that the δ-elimination reaction did not occur. Both at room and elevated temperature no component other than **13** and its de-esterified derivative was detected in the reaction mixture by gas-liquid chromatography (Fig. 6). This was also ascertained by the fact that the optical density at 238 mμ of **13** was not altered by treatment with potassium *t*-butoxide (Fig. 4, straight line 7).

The elimination reaction of the synthesized model compound **2** and **3** was then attempted. It is predicted that water liberated as the reaction proceeds inhibits the elimination reaction by de-esterification. After treatment with potassium *t*-butoxide in *t*-butyl alcohol for 10 min at room temperature the reaction solution was passed through the column packed with an acidic resin. The syrup obtained by evaporation of the solvent was purified once or twice on an alumina column. However, a small amount of impurity detected in NMR spectra was involved in both products. Although methyl (methyl 4-deoxy-β-L-*threo*-hex-4-enopyranosido)uronate (**14**) was obtained from **2** in very good yield (80%), from **3** de-esterified methyl 4-deoxy-3-*O*-methyl-β-L-threo-hex-4-enopyranosidouronic acid (**15**) was obtained in every low yield (a few %). The low yield of **15** will be attributed to adsorption on the alumina column, since its formation in about 20—30% was estimated by UV spectra.

Experimental

Melting points are uncorrected. Specific rotations were measured with a Carl Zeiss LEP Al polarimeter and a 0.2 dm tube. The IR spectra were recorded with a Hitachi Model EPI-GS grating IR spectrophotometer. The NMR spectra were recorded at 100 MHz with a Japan Electron Optics JNM 4H-100 spectrometer for solutions in suitable solvents such as $CDCl_3$, CCl_4, and CD_3OD containing tetramethylsilane as the internal standard. The UV spectra were recorded with a Hitachi Perkin-Elmer 139 spectrophotometer and a Hitachi Model EPS-3T recording spectrophotometer. Thin-layer chromatography was performed with Wako gel G-O and the solvent system [A: ethyl acetate - acetic acid - formic acid - water (18 : 3 : 1 : 4), B: *n*-butanol - acetic acid - water (4 : 1 : 5), C: chloroform - methanol - acetic acid (9 : 1 : 1)]. Gas-liquid chromatography was performed with a Hitachi Model K-53 gaschromatograph using a column (1 m) packed with butanediol succinate (20%) on Chromosorb WAW (60—80 mesh) at 150—190°C.

General Method of Methylation. Methylation was carried out by the methods of Purdue and Irvine,[14] and Kuhn *et al.*[15] To a solution of starting material in chloroform or dimethylformamide was added silver oxide (1.2 parts), Drierite (15—20 g/100 m*l* of solvent), and finally methyl iodide dropwise under stirring and cooling in an ice-bath. Stirring was continued at room temperature for 2—4 days in the dark and the undissolved materials were filtered off. Evaporation of the filtrate gave methylated derivative.

General Method of Catalytic Oxidation. Into a suspended solution of starting material and the same amount of 10% platinum-charcoal or palladium-charcoal in water was bubbled oxygen (1.5—2.0 atm) at 80—100°C under vigorous stirring. The pH-value of the solution was maintained between 6 and 8 by addition of a sodium hydrogencarbonate solution during the reaction. After disappearance of the spot of the starting material on thin-layer chromatography, *i.e.*, after 20—30 hr, the catalyst was filtered off and the filtrate was evaporated to give the corresponding sodium uronate. The free uronic acid derivative was obtained by treatment of this salt on a column packed with Amberlite IR-120 or Dowex 50 W×8 (H-form).

Methyl (Methyl 2,3,4-Tri-O-methyl-α-D-glucopyranosido)uronate (1). *Method (A)*: This compound was synthesized by the method of Jones *et al.*[9] from D-glucurono-6,3-lactone. Bp 88—90°C/0.05 mmHg, $[\alpha]_D^{23}$ +87° (*c* 1.0, methanol); lit,[9] bp 120°C/0.02 mmHg, $[\alpha]_D$ +84° (*c* 1.0, methanol).

Method (B): Methyl α-D-glucopyranoside (12.4 g) was catalytically oxidized to give methyl α-D-glucopyranosidouronic acid, which was methylated by the method of Kuhn *et al.*[15] to give **1** in 35% yield (5.6 g). Bp 94—97°C/0.18 mmHg, $[\alpha]_D^{23}$ +140° (*c* 1.2, methanol).

Found: C, 50.33; H, 7.46%. Calcd for $C_{11}H_{20}O_7$: C, 49.99; H, 7.63%.

Methyl (Methyl 4-O-Methyl-α-D-glucopyranosido)uronate (2). This compound was synthesized by the method of Wacek.[10] Bp 140°C/0.15 mmHg, $[\alpha]_D^{23}$ +135° (*c* 1.0, methanol); lit,[10] bp 130—140°C/0.6 mmHg, $[\alpha]_D$ +145° (methanol).

Methyl (Methyl 3-O-Methyl-α-D-glucopyranosido)uronate (3). Methyl 2,4,6-tri-*O*-acetyl-3-*O*-methyl-α-D-glucopyranoside[16] (**7**, 5.0 g) was converted by catalytic oxidation to syrupy methyl 3-*O*-methyl-α-D-glucopyranosidouronic acid (**8**), which was treated with methanolic hydrogen chloride overnight. After evaporation of the solvent, the residual syrup was distilled to give **3** in 68% yield (2.4 g). Bp 137°C/0.07 mmHg,

14) T. Purdue and J. C. Irvine, *J. Chem. Soc.*, **83**, 1021 (1903).
15) R. Kuhn, H. Trischmann, and I. Löw, *Angew. Chem.*, **67**, 32 (1955).
16) R. W. Jeanloz and M. Gut, *J. Amer. Chem. Soc.*, **76**, 5793 (1954).

$[\alpha]_D^{23}$ +98.5° (*c* 1.1, methanol).

Found: C, 45.97; H, 7.09%. Calcd for $C_9H_{16}O_7$: C, 45.76; H, 6.83%.

Methyl 3-O-Benzyl-4,6-O-benzylidene-α-D-glucopyranoside (9). 3-*O*-Benzyl-1,2:5,6-di-*O*-isopropylidene-α-D-glucofuranose[12] (30 g) was dissolved in methanol containing 3% hydrogen chloride (200 m*l*) and the solution was refluxed for 20 hr. After neutralization with barium carbonate, undissolved material was filtered off and the filtrate was evaporated to dryness. The resulting syrup was benzylidenated with benzaldehyde and anhydrous zinc chloride in the usual manner. The crude product was crystallized from ethanol. Yield, 9.2 g (29%), mp 172—174°, $[\alpha]_D^{23}$ +30.4° (*c* 1.1, methanol).

Found: C, 67.55; H, 6.58%. Calcd for $C_{21}H_{24}O_6$: C, 67.73; H, 6.50%.

Methyl 3-O-Benzyl-4,6-O-benzylidene-2-O-methyl-α-D-glucopyranoside (10). **9** (9.0 g) was methylated by the method of Purdue and Irvine.[14] Yield, 7.8 g (83%), mp 103—104°C, $[\alpha]_D^{28}$ +16.7° (*c* 1.5, ethanol).

Found: C, 68.63; H, 7.00%. Calcd for $C_{22}H_{26}O_6$: C, 68.63; H, 6.78%.

Methyl (Methyl 2-O-Methyl-α-D-glucopyranosido)uronate (4). Methyl 2-*O*-methyl-α-D-glucopyranoside[13] (**11**, 4.4 g), which was obtained by catalytic hydrogenolysis of **10**, was catalytically oxidized in the presence of platinum-charcoal to give syrupy methyl 2-*O*-methyl-α-D-glucopyranosidouronic acid (**12**). **12** was esterified with diazomethane in ether - methanol. After evaporation of the solvent the residual syrup was distilled to give **4** in 33% yield (1.6 g). Bp 152°C/0.095 mmHg, $[\alpha]_D^{28}$ +98° (*c* 1.0, methanol).

Found: C, 45.17; H, 6.69%. Calcd for $C_9H_{16}O_7$: C, 45.76; H, 6.83%.

Methyl (Methyl 4-Deoxy-2,3-di-O-methyl-β-L-threo-hex-4-enopyranosido)uronate (13). **1** (5.2 g) was dissolved in methanol containing 1.5 N sodium methoxide (30 m*l*). After refluxing for 45 min the reaction mixture was treated with Amberlite IR-120 (H-form) and evaporated to dryness. The residual syrup was distilled to give **13** in 35% yield (1.6 g). Bp 75—82°C/0.03 mmHg, $[\alpha]_D^{28}$ +189° (*c* 1.0, methanol), IR (NaCl, cm^{-1}): 2940, 1725, 1645, UV (ethanol, mμ): 238 (ε=5500), NMR (CCl_4, τ): 4.07 (d, H_4), 5.13 (d, H_1), 6.13 (q, H_3), 6.68 (q, H_2), 6.27 (s, CO_2CH_3), 6.54, 6.55, 6.61 (three s, OCH_3), $J_{1,2}$ 2.0 Hz, $J_{2,3}$ 7.5 Hz, $J_{3,4}$ 2.5 Hz (see also Fig. 3).

Found: C, 51.24; H, 6.84%. Calcd for $C_{10}H_{16}O_6$: C, 51.72; H, 6.94%.

Methyl (Methyl 4-Deoxy-β-L-threo-hex-4-enopyranosido)uronate (14). To a solution of **2** (3 g) in *t*-butyl alcohol (20 m*l*) was added quickly potassium (680 mg) in *t*-butyl alcohol (50 m*l*) under nitrogen stream. After being shaken gently for 10 min the reaction mixture was neutralized with methanolic hydrogen chloride and evaporated under reduced pressure at room temperature. The residual syrup was dissolved in a small amount of methanol and evaporated. The resulting syrup was then dissolved in ethanol and undissolved potassium chloride was filtered off. Evaporation of the filtrate gave crude **14**. Purification was performed on an alumina column (30 g) by elution with petroleum ether - ethanol (95 : 5, 400 m*l*) and then with methanol - water (7 : 3, 50 m*l*). Evaporation of the latter eluate gave **14** in about 80% yield (2.2 g). $[\alpha]_D^{28}$ +184° (*c* 1.0, methanol), IR (NaCl, cm^{-1}): 3400, 1725, 1645, UV (ethanol, mμ): 238 (ε=4600), NMR ($CDCl_3$, τ): 3.97 (d, H_4), 4.97 (d, H_1), 6.22 (s, CO_2CH_3), 6.51 (s, OCH_3).

Found: C, 46.73; H, 6.14%. Calcd for $C_8H_{12}O_6$: C, 47.06; H, 5.92%.

Methyl 3-O-Methyl-4-deoxy-β-L-threo-hex-4-enopyranosidouronic Acid (15). To a solution of **3** (5 g) in *t*-butyl alcohol (20 m*l*) was added potassium (160 mg) in *t*-butyl alcohol (6 m*l*) under nitrogen stream. After standing at room temperature for 10 min the reaction mixture was treated with Amberlite IR-120 (H-form) to remove potassium ions. The syrup obtained by evaporation of the solvent was purified on an alumina column (100 g) by elution with petroleum ether - ethanol (95 : 5, 300 m*l*). Evaporation of the eluant gave crude **15** (40 mg), which was purified once more on the alumina column to give **15** in very low yield (22 mg). Elemental analysis could not be carried out but the structure was ascertained by spectral data. $[\alpha]_D^{28}$ +170° (*c* 1.0, ethanol), IR (NaCl, cm^{-1}): 3450, 1725, 1645, UV (ethanol, mμ): 238 (ε=4100), NMR ($CDCl_3$, τ): 3.97 (d, H_4), 5.03 (d, H_1), 6.42, 6.51 (two s, OCH_3).

Examination of β-Elimination Reaction in Some Basic Mediums. 1) By UV Spectra: The following three kinds of alkali solution of **1** were heated in sealed tubes at 60—95°C for about 1 hr. (a) 0.02N and 2.0N sodium carbonate aqueous solution, 0.02N, 0.5N and 2.0N sodium hydroxide aqueous solution, (b) 1.3N sodium hydroxide in ethanol, (c) 1.5N sodium methoxide in methanol. After neutralization with 1N hydrochloric acid or ethanolic hydrogen chloride the UV spectrum of the reaction solution was measured.

2) By NMR spectra: NMR spectrum was measured only in the case of (c). The reaction was carried out in an NMR measuring tube using CD_3ONa in CD_3OD as a base.

β-Elimination Reaction of 1. 1) By Sodium Methoxide in Methanol: The elimination reaction was carried out in two different ways. *Method (A)*: A solution of **1** (1.6×10^{-2}mol/*l*) and sodium methoxide (2.7N) in methanol were prepared separately. 1 m*l* of each solution was mixed in a glass tube and sealed quickly. After heating in a water bath at 70°C the tube was cooled with tap water and the reaction solution was acidified and diluted to exactly 5 m*l* with ethanolic hydrogen chloride (about 0.4N). The solution was centrifuged with 7000—8000 rpm for 10 min at 0°C and the optical density at 238 mμ was measured after dilution of the supernatant with ethanol (Fig. 4, curve 1).

Method (B): To 1 m*l* of a methanol solution of **1** (1.6×10^{-2} mol/*l*) in a glass tube (0.8×20 cm), which was previously heated at 60°C in a mantle heater, a piece of sodium (18 mg) was added. While the piece of sodium dissolved in the methanol, the reaction solution was refluxed. The reaction temperature was then maintained at 64°C by refluxing in an open tube or by heating in a sealed tube. The UV spectra were measured in the same manner as above mentioned.

2) By Potassium t-Butoxide in t-Butyl Alcohol: A solution of **1** and **13** (1.4×10^{-1} mol/*l*) and potassium *t*-butoxide (0.37N; curves 4, 6 and straight line 7 and 0.56N; curve 5) in *t*-butyl alcohol were prepared separately. The same amount of each solution was mixed as quickly as possible. 0.01 m*l* of the reaction solution was pipetted at suitable intervals and the UV spectra were measured after dilution with ethanolic hydrogen chloride to 5 m*l*.

Financial assistance from the Naito Memorial Science Promotion Foundation is gratefully acknowledged.

The Ruthenium-Catalyzed Hydrogenation of Aromatic Amines Promoted by Lithium Hydroxide

Shigeo NISHIMURA, Yutaka KONO, Yoshiharu OTSUKI, and Yoshio FUKAYA

Department of Industrial Chemistry, Tokyo University of Agriculture and Technology, Koganei-shi, Tokyo

(Received August 6, 1970)

The effects of the addition of various alkaline substances on the ruthenium-catalyzed hydrogenation of aromatic amines have been investigated at raised temperature and pressure. The addition of lithium hydroxide was shown to be the most effective for rapid and selective hydrogenation of aromatic amines. The effect of various solvents on the hydrogenolysis of carbon-nitrogen bonds has also been studied in the hydrogenation of *m*-xylene-α,α′-diamine and *N*,*N*-dimethyl-*p*-phenylenediamine. Generally, the hydrogenation was fast and the amount of the hydrogenolysis was small in secondary alcohols. Typical examples of the syntheses of alicyclic amines are given.

It was previously shown that the ruthenium-catalyzed hydrogenation of aniline is promoted by the addition of small amounts of alkalies which not only depress the formation of dicyclohexylamine but also eliminate a strong inhibitory action of the ammonia produced along with the secondary amine.[1]

Subsequently, the effect of the addition of various alkaline substances has been compared in the hydrogenation of some aromatic amines over ruthenium catalysts, and it has been found that the addition of lithium hydroxide in fairly large amounts is the most effective for rapid and selective hydrogenation of aromatic amines. The effect of solvents on the hydrogenolysis of carbon-nitrogen bonds has also been studied in the hydrogenation of *m*-xylene-α,α′-diamine and *N*,*N*-dimethyl-*p*-phenylenediamine which are both known liable to the hydrogenolysis rather readily.[2,3]

Experimental

Materials. The aromatic amines hydrogenated were carefully purified by distillation at reduced pressure, if necessary, under the atmosphere of nitrogen. Aniline, bp 79°C/20 mmHg; *o*-toluidine, bp 90°C/18 mmHg; *N*,*N*-dimethylaniline, bp 85°C/19 mmHg; *N*,*N*-dimethyl-*p*-phenylenediamine, bp 143.5—144.5°C/21 mmHg, mp 36—37°C; *m*-xylene-α,α′-diamine, bp 130—131°C/4 mmHg, n_D^{20} 1.5707; *p*-xylene-α,α′-diamine, bp 157°C/21.5 mmHg, mp 52—54°C; 4,4′-methylenedianiline, bp 170—172°C/6 mmHg, mp 92—93°C. These amines were of commercial preparations except *p*-xylene-α,α′-diamine.

p-Xylene-α,α′-diamine was prepared by hydrogenation of terephthalonitrile (25 g) with rhodium hydroxide catalyst (0.3 g) and lithium hydroxide (0.4 g) in 100 m*l* ethanol at 85°C under the hydrogen pressure of 70—100 kg/cm² for 1.5 hr (70% yield).

Catalysts. The ruthenium hydroxide catalyst was prepared by adding a slight excess of lithium hydroxide solution to a hot aqueous ruthenium chloride. The ruthenium-carbon catalyst (5% Ru) was obtained from the Nippon Engelhard Co.

Hydrogenation. All hydrogenations were carried out in stainless steel bombs with stirrers driven magnetically. The catalyst, the additive, the substrate, and then the solvent, if necessary, were put into the bomb. Sodium and potasssium hydroxides were added in a 10% solution. The other alkaline substances were added in fine powder. The reaction temperature was controlled within 0.5°C by immersing the bomb in an oil bath maintained at a constant temperature.

Analysis of the Products. The hydrogenation product was analyzed directly by gas chromatography (column: PEG 6000-KOH on Chromosorb W). The product was also isolated by distillation after removing most of the catalyst by filtration, if necessary with addition of ether to the reaction mixture.

Results and Discussion

The effect of the addition of three alkalies is compared in Table 1 in the hydrogenation of aniline with ruthenium hydroxide catalyst. It is seen from the Table that aniline is hydrogenated most rapidly when lithium hydroxide was added in the amounts more than 30 mg (as monohydrate) to 65 mg of the catalyst. The stronger alkalies, sodium and potassium hydroxides, greatly depressed the rate of the hydrogenation even when added in the amount less than 10% of the weight of the catalyst. Aniline was hydrogenated fairly rapidly even when no alkali was added. This is probably due to the promotion by a small amount of the alkali which was contaminated into the catalyst during its preparation.[4]

Table 1. Effect of added alkalies on the hydrogenation of aniline[a]

Alkali added	mg	Reac. time (hr)	Aniline hydrogenated (%)
None	—	2.5	90
$LiOH \cdot H_2O$	10	2.5	94
$LiOH \cdot H_2O$	30	2.5	99
$LiOH \cdot H_2O$	50	2.5	100
$LiOH \cdot H_2O$	100	2.5	99
NaOH	3	2.5	90
NaOH	6	2.5	73
KOH	6	2.5	30

a) Aniline (65 g) was hydrogenated with 65 mg of the ruthenium hydroxide catalyst at 110°C under the hydrogen pressure of 70—100 kg/cm².

1) S. Nishimura, T. Shu, T. Hara, and Y. Takagi, This Bulletin, **39**, 329 (1966).

2) I. Hashimoto and M. Tashiro, *Yuki Gosei Kagaku Kyokai Shi*, **25**, 144 (1967).

3) a) L. C. Behr, J. E. Kirby, R. N. MacDonald, and C. W. Todd, *J. Amer. Chem. Soc.*, **68**, 1296 (1946). b) M. Freifelder and G. R. Stone, *J. Org. Chem.*, **27**, 3568 (1962).

4) Analysis of a specimen of the ruthenium hydroxide catalyst by the atomic absorption spectrophotometric method indicated that 0.45% of lithium (as metal) was contained in the catalyst.

Table 2. Effect of added alkali and alkaline-earth metal hydroxides and sodium carbonate on the hydrogenation of *o*-toluidine

Catalyst, mg	Additive, mg	Reac. time (hr)	*o*-Toluidine hydrogenated (%)	Secondary amine formed (%)[b]
Ru hydroxide, 30	None, —	4[c]	79.4	6.7
Ru hydroxide, 30	$LiOH \cdot H_2O$, 30	6	99.8	0.7
Ru hydroxide, 30	NaOH, 1.5	6	85.1	2.3
Ru hydroxide, 30	NaOH, 3.0	6	55.0	—
Ru hydroxide, 30	Na_2CO_3, 100	6	94.4	1.9
Ru hydroxide, 30	$Ca(OH)_2$, 80	6	96.4	2.4
Ru hydroxide, 30	$Ba(OH)_2 \cdot 8H_2O$, 100	6	90.6	2.7
5% Ru-carbon, 360	None, —	10.5	46.8	7.4
5% Ru-carbon, 360	$LiOH \cdot H_2O$, 120	10.5	99.7	0.3
5% Ru-carbon, 360	$LiOH \cdot H_2O$, 360	10.5	97.8	trace

a) *o*-Toluidine (25 g) was hydrogenated at 110°C under the hydrogen pressure of 70—100 kg/cm².
b) Based on the *o*-toluidine converted.
c) The hydrogenation almost stopped.

In Table 2 the effects of the addition of alkali and alkaline-earth metal hydroxides and sodium carbonate are compared in the hydrogenation of *o*-toluidine where differences in the effect are more clearly seen than in the case of aniline. The hydrogenation was also the most rapid in the presence of lithium hydroxide. The addition of lithium hydroxide is also the most effective to suppress the formation of secondary amine and accordingly 2-methylcyclohexylamine is formed in the highest yield under the promotion of lithium hydroxide. When other bases or no base were added, it was difficult to complete the hydrogenation within a reasonable time and the formation of secondary amine increased. The addition of lithium hydroxide was also effective in the hydrogenation over a ruthenium-carbon catalyst as seen in Table 2.

Table 3. Effect of added alkalies on the hydrogenation of *m*-xylene-α,α′-diamine (*m*-XD)[a]

Expt. No.	*m*-XD (g)	Alkali added, mg	Time for complete hydrogenation (hr)	Proportion of hydrogenolysis (mol%)[b]
1	4	None, —	1.8	10.2
2	4	$LiOH \cdot H_2O$, 6	0.7	8.3
3	4	$LiOH \cdot H_2O$, 20	0.7	2.1
4	4	$LiOH \cdot H_2O$, 50	0.7	1.3
5	4	$LiOH \cdot H_2O$, 100	0.6	2.8
6	4	NaOH, 0.75	1.7	2.3
7	4	NaOH, 1.5	1.0	3.3
8	4	NaOH, 3.0	1.3	1.9
9	4	NaOH, 6.0	1.5	1.4
10	4	KOH, 0.75	0.6	9.0
11	4	KOH, 1.5	0.6	2.4
12	4	KOH, 3.0	1.0	3.2
13	4	KOH, 6.0	1.6	3.1
14	12	$LiOH \cdot H_2O$, 50	2.0	2.1
15	12	KOH, 1.5	4.8	11.1

a) *m*-Xylene-α,α′-diamine was hydrogenated with 30 mg of the ruthenium hydroxide catalyst in 10 m*l* of isopropyl alcohol at 120°C under the hydrogen pressure of 70—100 kg/cm².
b) Given by mol (*m*-methylbenzylamine + 1-aminomethyl-3-methylcyclohexane + 2 × *m*-xylene) × 100/mol (*m*-XD converted).

The effect of three alkalies added in various amounts on the hydrogenation of *m*-xylene-α,α′-diamine (*m*-XD) is shown in Table 3. In contrast to the hydrogenation of aniline and *o*-toluidine, the addition of a small amount of potassium hydroxide was more effective in this hydrogenation than the addition of sodium hydroxide. The same tendency was also observed in the hydrogenation of benzylamine.[5] Figure 1 illustrates the decrease in the rate during the course of hydrogenation of *m*-XD as a function of conversion, when each alkali was added in its optimum amount. It is clearly seen that the decrease in the rate is the least in the presence of lithium hydroxide. This result becomes important when the hydrogenation is performed in a larger substrate to catalyst ratio (see Expts. 14 and

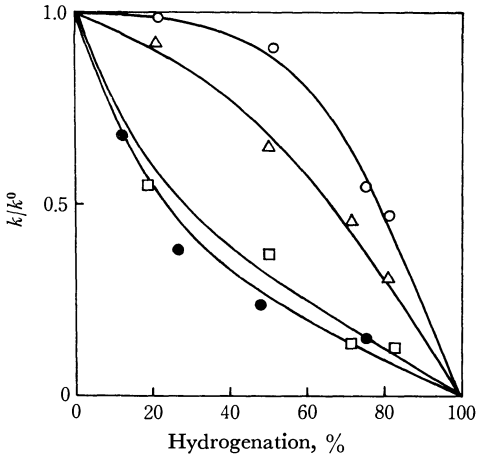

Fig. 1. Decrease in the rate during the hydrogenation of *m*-xylene-α,α′-diamine (*k*: rate at a given hydrogenation; k^0: rate at the initiation).
○: with addition of 50 mg $LiOH \cdot H_2O$
△: with addition of 1.5 mg KOH
□: with addition of 1.5 mg NaOH
●: without addition of alkali
(For reaction conditions, see Table 3)

5) unpublished observation.

and 15 in Table 3). The hydrogenation of *m*-XD may be accompanied by the hydrogenolysis of the benzyl-nitrogen bond, with formation of *m*-methylbenzylamine, 1-aminomethyl-3-methylcyclohexane and *m*-xylene.[2] The addition of alkalies was found also effective to suppress the hydrogenolysis as seen from the results shown in Table 3. In particular, the addition of lithium hydroxide is seen very effective for this purpose, since the amount of the hydrogenolysis was only 2.1% even in the hydrogenation of a larger amount of the substrate (Expt. 14 in Table 3). *N,N*-Dimethyl-*p*-phenylenediamine (DMP) is also known to be liable to an extensive hydrogenolysis of the dimethylamino group on hydrogenation.[3] Since the nature of the solvent may have a profound effect on the hydrogenolysis of a polar bond, as shown previously in the hydrogenation of *p*-anisidine,[6] the effect of various solvents on the hydrogenolysis of carbon-nitrogen bond has been studied on the hydrogenation of *m*-XD and DMP. The results are summarized in Table 4. It will be seen from the

TABLE 4. EFFECT OF SOLVENTS ON THE HYDROGENOLYSIS OF *m*-XYLENE-α,α'-DIAMINE (*m*-XD) AND *N,N*-DIMETHYL-*p*-PHENYLENEDIAMINE (DMP)[a]

Solvent	Hydrogenation of *m*-XD			Hydrogenation of DMP	
	React. time (hr)	Half-hydrogenation time (hr)	Amount of hydrogenolysis (mol %)	Reac. time (hr)	Amount of hydrogenolysis (mol %)
MeOH	3.5	0.38	9.5	4.3	29.3
EtOH	4.6	0.42	8.8	3.3	35.8
PrOH	2.8	0.17	5.4	3.7	15.4
i-PrOH	2.4	0.23	5.1	2.7	13.4
BuOH	—	—	—	3.0	14.7
s-BuOH	2.1	0.20	5.6	2.7	13.3
t-BuOH	2.6	0.23	7.0	3.0	15.9
t-PeOH	2.4	0.17	4.4	—	—
THF[b]	—	—	—	4.7	36.1
$i\text{-Pr}_2O$	6.2	0.47	11.7	4.3	18.3
Bu_2O	5.6	0.85	9.6	—	—
MCH[c]	3.0	0.23	5.7	3.3	10.1

a) *m*-XD and DMP (0.03 mol) were hydrogenated with 30 mg of the ruthenium hydroxide catalyst and 6 mg of $LiOH\cdot H_2O$ under 70—100 kg/cm² hydrogen pressure, in 20 m*l* solvent at 120°C for *m*-XD and in 10m*l* solvent at 130°C for DMP.
b) Tetrahydrofuran
c) Methylcyclohexane

results in the table that the proportion of the hydrogenolysis is smaller in higher primary alcohols, secondary and tertiary alcohols and methylcyclohexane. Among these solvents, secondary alcohols appear the most preferred ones, as the rate of hydrogenation is in most cases larger in secondary alcohols than in the other solvents mentioned. In Fig. 2 initial rates of the formation of hydrogenolysis products[6] in the hydrogenation of *m*-XD are plotted *versus* the reciprocal of the dielectric constant of the solvents in which hydrogenations were carried out. A similar dependence of the rates on the polarity of the solvents as observed in the hydrogenation of *p*-anisidine can be seen also in this hydrogenation, but the effect is much less pronounced than in the case of *p*-anisidine. Since differences in the rates of hydrogenolysis are rather small among the solvents, the proportion of hydrogenolysis seems to depend more on the variation of the rates of the hydrogenation with the solvents as shown in Fig. 3.

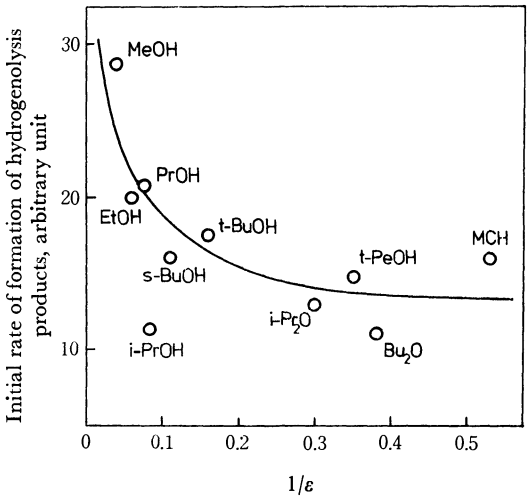

Fig. 2. Effect of solvents on the initial rates of formation of hydrogenolysis products as a function of the reciprocal of the dielectric constant of solvents (ε at 80°C) in the hydrogenation of *m*-xylene-α,α'-diamine with ruthenium hydroxide catalyst.

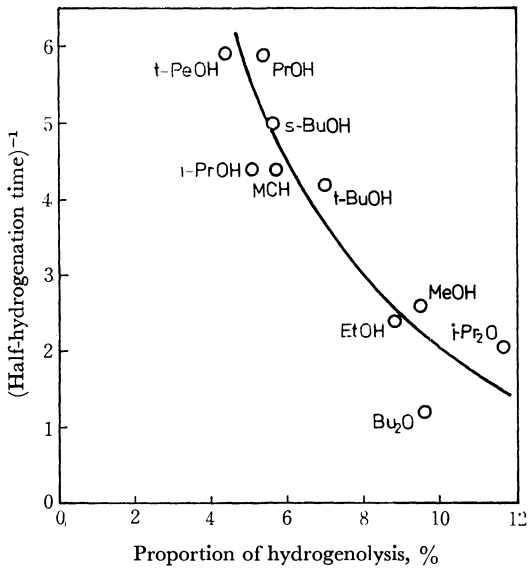

Fig. 3. Relation between proportion of hydrogenolysis and the rate of hydrogenation in the hydrogenation of *m*-xylene-α,α'-diamine with ruthenium hydroxide catalyst.

The results shown in Tables 1—3 and in Fig. 1 indicate that lithium hydroxide is the most effective promotor of the alkaline substances investigated in the ruthenium-catalyzed hydrogenation of aromatic amines. Since ruthenium is one of the most effective metals for the hydrogenation of aromatic amines,[7] the present im-

6) S. Nishimura and H. Yoshino, This Bulletin, **42**, 499 (1969).

7) P. N. Rylander, "Catalytic Hydrogenation over Platinum Metals," Academic Press, Inc., New York (1967), p. 352.

Table 5. Hydrogenation of aromatic amines with ruthenium hydroxide catalyst promoted by lithium hydroxide[a)]

Compound, g	Catalyst (mg)	$LiOH \cdot H_2O$ added (mg)	Solvent, ml	Reac. temp. (°C)	Reac. time (hr)	Yield of alicyclic amine (%)	
						By glpc.	By distil.
Aniline, 65	65	50	—	110	2.5	99.8	93[b)]
o-Toluidine, 43	50	50	—	110	4.5	99.2	93[c)]
N,N-Dimethylaniline, 61	61	50	—	110	2.0	99.7	97[d)]
N,N-Dimethyl-*p*-phenylenediamine, 14	100	160	*i*-PrOH, 25	120	4.0	95.5	83[e)]
m-Xylene-α,α'-diamine, 12	30	50	*i*-PrOH, 10	120	2.0	96.9	87[f)]
p-Xylene-α,α'-diamine, 12	30	50	*i*-PrOH, 10	120	6.3	89.0	73[g)]
4,4′-Methylenedianiline, 30	100	160	*i*-PrOH, 50	120	7.5	—	84[h)]

a) Aromatic amines were hydrogenated under the hydrogen pressure of 70—100 kg/cm².
b) Bp 134.5—135.5°C; n_D^{25} 1.4558.
c) Bp 153—154°C; n_D^{25} 1.4564.
d) Bp 163—164°C.
e) Bp 98.5—100°C/22 mmHg; n_D^{25} 1.4785 [reported: bp 200—205°C/755 mmHg; n_D^{25} 1.4795, Ref. 3b].
f) Bp 120—121°C/17 mmHg; n_D^{20} 1.4939 [reported: bp 110.4°C/8 mmHg; n_D^{20} 1.4950 (*trans*); bp 85—86°C/2 mmHg; n_D^{20} 1.4917 (*cis*), J. C. Dubin, Fr. Pat. 1408314 (1965); *Chem. Abstr.*, **65**, 5637 (1966)].
g) Bp 140°C/34 mmHg; n_D^{20} 1.4919 [reported: bp 98—99°C/5 mmHg; n_D^{20} 1.4890 (*trans*); bp 79—79.5°C/2 mmHg; n_D^{20} 1.4959 (*cis*), A. Bell, J. G. Smith, and C. J. Kibler., *J. Polym. Sci., Part A-3*, 19 (1965)].
h) Bp 140°C/5 mmHg; n_D^{25} 1.5037 [reported: bp 128°C/1.2 mmHg; n_D^{25} 1.5051, A. E. Barkdoll, D. C. Engl, and H. W. Gray, W. Kirk, Jr., and G. M. Whitman., *J. Amer. Chem. Soc.*, **75**, 1156 (1953)].

provement of the hydrogenation by the addition of lithium hydroxide offers a very useful general method of the synthesis of alicyclic amines from aromatic amines. Typical examples of the hydrogenation in preparative scales are listed in Table 5. It is seen that in most cases hydrogenations were completed within a few hours with use of only small portions of the catalyst to the substrate (0.1—0.7% as Ru hydroxide or 0.06—0.4% as Ru metal) and the corresponding alicyclic amines were obtained in excellent yields.[8)]

The authors are indebted to the Mitsubishi Chemical Industries Co., Ltd., for the analysis of the lithium in the catalyst and also for providing some of the aromatic amines and terephthalonitrile.

8) Lithium hydroxide added to or contained in the catalyst was shown also effective in the rhodium-catalyzed hydrogenation of nitriles and aromatic amines.[1,9,10)] However, the simple addition of lithium hydroxide appears not always effective as noticed in the hydrogenation of *p*-anisidine.[10)]

9) Y. Takagi, S. Nishimura, K. Taya, and K. Hirota, *Sci. Pap. Inst. Phys. Chem. Res.* (Tokyo), **61**, 114 (1967).
10) S. Nishimura, H. Uchino, and H. Yoshino, This Bulletin, **41**, 2194 (1968).

Cyclopropenones. IV. The Reactions of Diphenylcyclopropenone with Water, Carboxylic Acid, Phenol, and Amide

Fumio Toda, Toshiaki Kataoka, and Katsuhiko Akagi
Department of Industrial Chemistry, Faculty of Engineering, Ehime University, Matsuyama
(Received August 7, 1970)

The pyrolysis of diphenylcyclopropenone monohydrate (II) at 150°C afforded α-phenyl-*trans*-cinnamic anhydride (VI). It was proved that the reaction consists of two main steps, the nucleophilic attack of water on I to yield α-phenyl-*trans*-cinnamic acid (IV), and the reaction of I with IV, thus finally yielding VI. The same type of reaction as that of I with IV was also observed when I was heated in phenol to afford phenyl α-phenyl-*trans*-cinnamate (XII). The reaction of I with the weak nucleophilic reagent, α-phenyl-*trans*-cinnamamide (XIV), afforded a monoimino derivative of VI (XVI), which is believed to be produced by the nucleophilic attack of the amide-oxygen of XIV on the carbonyl-carbon of I.

Since the first preparation of diphenylcyclopropenone (I) in 1959 by Breslow and his co-workers[1] and by Vol'pin and his co-workers,[2] independently, many reactions of I have been reported.[3] Because of the strongly polarized nature of the ketone,[4] to which the contribution of the IA and IB structures is considerable, the carbonyl carbon and the double bond of I cause a nucleophilic attack by various reagents. Although the reaction of I with a base such as aqueous sodium hydroxide,[4] hydroxylamine,[4] liquid ammonia,[5,6] aqueous ammonia,[7] primary amine,[6] aziridine,[8] and alkyllithium[9] has been reported, no reaction with acid has yet been done except the case in which I forms hydrobromide in crystalline forms.[2] The salt, however, can be decomposed by heating or by weak bases to give I again.[2]

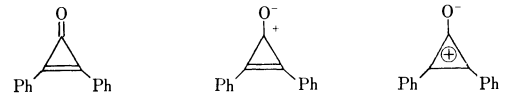

(I) (IA) (IB)

We have found that I reacted with such acids as α-phenyl-*trans*-cinnamic acid (IV) and phenol at 150°C to give α-phenyl-*trans*-cinnamic anhydride (VI) and phenyl α-phenyl-*trans*-cinnamate (XII) respectively. We have also found that I reacted with a weak nucleophilic reagent, α-phenyl-*trans*-cinnamamide, and *N*-methylacetamide to afford a monoimino derivative of VI (XVI) and *N*-methyl-α-phenyl-*trans*-cinnamamide (XVII) respectively.

The heating of the monohydrate (II)[10] at 150°C for 32 hr afforded the anhydride VI, the cyclic dimer VII, and tolan (VIII) in 12.6, 14.1, and 23.9% yields respectively. The structure of VI (mp 117—118.5°C) was determined by a comparison of its electronic, infrared, and NMR spectral data with those reported in the literature for the anhydride (mp 113—117°C).[11] The spectral data of VII were identical with those recorded for the cyclic dimer[4] obtained in 40%, together with VIII (20%), by the pyrolysis of I at 145—150°C for 36 hr, to this dimer the structure VII has been assigned[4] provisionally. Since the heating of an equimolar mixture of I and IV at 150°C for 3 hr and 10 hr afforded VI in 25.4 and 55.5% yields respectively, IV must be the intermediate of the pyrolysis of II. The formation of IV from II can be interpreted in terms of the ketonization of the III initially produced by the attack of water on the carbonyl-carbon of I. The reaction of I with IV, of the same fashion as that of I and water, would give V as an intermediate.

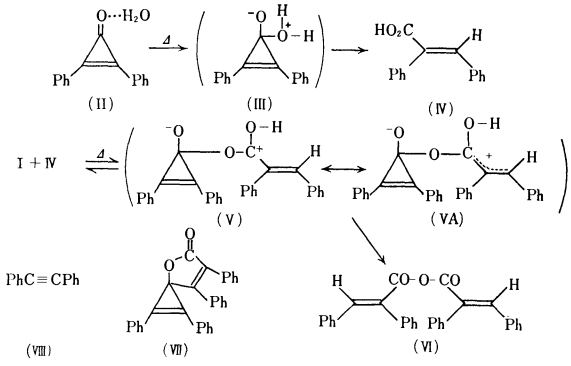

Scheme 1

The ketonization and the ring-openning of V afford VI (Scheme 1). The contribution of the cation-delocalized structure (VA) to V, and the reversibility of the process of the formation of V from I and IV, are considerable, judging from the following observations. The heating of an equimolar mixture of I and α-phenyl-*cis*-cinnamic acid (IX) at 150°C for 27 hr afforded VI and the *trans*-acid IV in 35.4 and 31.6% yields respectively, but no recovered IX or *cis*-isomer of VI was detected. Since it is known that[12] the *trans*-acid

1) R. Breslow, R. Haynie, and J. Mirra, *J. Amer. Chem. Soc.*, **81**, 247 (1959).
2) M. E. Vol'pin, Yu. D. Koreshkov, and D. N. Kursanov, *Izv. Akad. Nauk USSR, Otd, Khim. Nauk.*, **3**, 560 (1959).
3) For a recent review, see A. W. Krebs, *Angew. Chem. Int. Ed. Engl.*, **4**, 10 (1965).
4) R. Breslow, T. Eicher, A. Krebs, R. A. Peterson, and J. Posner, *J. Amer. Chem. Soc.*, **87**, 1320 (1965).
5) F. Toda, T. Mitote, and K. Akagi, *Chem. Commun.*, **1969**, 228.
6) F. Toda, T. Mitote, and K. Akagi, This Bulletin, **42**, 1777 (1969).
7) E. V. Dehmlow, *Ann. Chem.*, **729**, 64 (1969).
8) E. V. Dehmlow, *Tetrahedron Lett.*, **1967**, 5177.
9) J. Ciabattoni, P. J. Kocienski, and G. Melloni, *ibid.*, **1969**, 1883.
10) F. Toda and K. Akagi, *ibid.*, **1968**, 3735.
11) K. G. Krachanov and B. I. Kurtev. *ibid.*, **1965**, 3085.
12) L. F. Fieser, "Experiments in Organic Chemistry," 3rd ed., D. C. Heath and Company, Boston (1957), p. 183.

IV is more stable than *cis*-acid IX because of the much greater steric interaction between the phenyl and carboxylic group in IX than that between the two phenyls in IV, and since the heating of IX at 150°C for 34 hr gave recovered IX in almost a quantitative yield, the isomerization of IX into IV probably occurs during the course of the reaction of I and IX.

The above complete isomerization of the geometry around the carbon-carbon double bond both in the product, VI, and in the acid, IV, can be reasonably interpreted by assuming a reversible process and the contribution of the cation-delocalized structure (VA or XA), as has been described above. The intermediate, X, initially produced by the reaction of I and IX can be rearranged to V *via* the cation-delocalized structure, XA, in which a rotation around the carbon-carbon bond of the diphenylethylene part is possible for its increased single-bond nature, as is shown in Scheme 2.

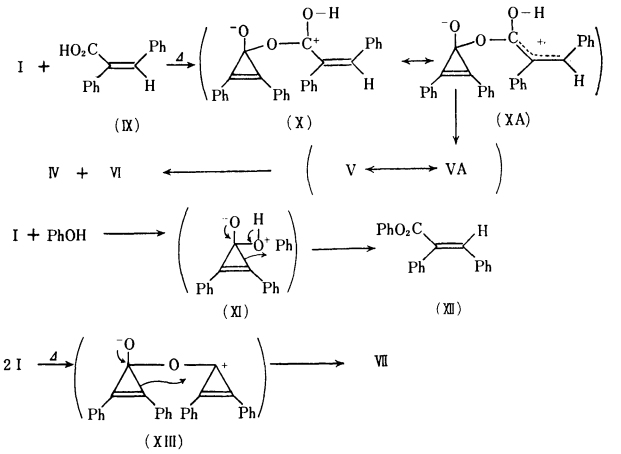

Scheme 2

The reaction of I with another carboxylic acid, such as *trans*-cinnamic acid or benzoic acid, gave no any acid anhydride. However, I reacted with phenol at 150°C for 26 hr to afford the ester XII in a 42% yield. The structure of XII was determined by a comparison of its spectral data with those of an authentic sample prepared according to the previously reported method.[13] The reaction probably proceeds *via* XI, which corresponds to V or X. Therefore, XIII is a possible intermediate of the thermal dimerization of I.

The observation that the oxygen of water, carboxylic acid (IV), and phenol react with I prompted us to investigate the reaction of I with several amides. Our attention was focussed on the question of which it was, the oxygen or the nitrogen of amide, which reacts with I. The heating of a mixture of I and an equimolar amount of the amide XIV at 150°C for 33 hr afforded XVI in a 4.2% yield, together with VIII (17.6%), recovered XIV (45%), and a small amount of an unidentified product, $C_{15}H_{13}ON$. The structure of XVI was determined by means of a study of the spectral data and by a base-catalyzed hydrolysis, which gave IV only. The electronic spectrum of XVI, 225 and 312 nm in ethanol, was comparable to that of VI, 223 and 300 nm in ethanol. The infrared spectrum of XVI in chloroform showed ν_{NH} $\nu_{C=O}$, and $\nu_{C=N}$ and/or $\nu_{C=C}$ at 3380, 1735, and 1615 cm^{-1} respectively, in addition to the strong ester absorption band at 1145 cm^{-1}. Since no absorption band of amide-II appeared in the 1600—1500 cm^{-1} region, and since the $\nu_{C=O}$ appeared at the field of frequencies higher than 1700 cm^{-1}, there is no possibility that XVI is amide or urea. The NMR spectral data, 1.88 (s, =CH, 1H), 2.10 (s, =CH, 1H), 2.86 (m, Ph, 20H), and 8.03 τ (s, =NH, 1H), which disappeared upon shaking with D_2O, also supported the structure of XVI.

The formation of XVI in the reaction of I with XIV shows that the reaction site of XIV is oxygen, not nitrogen, as is shown in Scheme 3. This result is reasonable, since the electron density on the oxygen of amide is higher than that of nitrogen because of the resonance, $-\overset{|}{N}-\overset{|}{C}=O \longleftrightarrow -\overset{|}{N}^{+}=\overset{|}{C}-O^{-}$. This result is also consistent with the fact that the protonation of amide in a solution occurs on its oxygen.[14-16] The *N*-alkyl derivative of XIV, however, did not react with I.

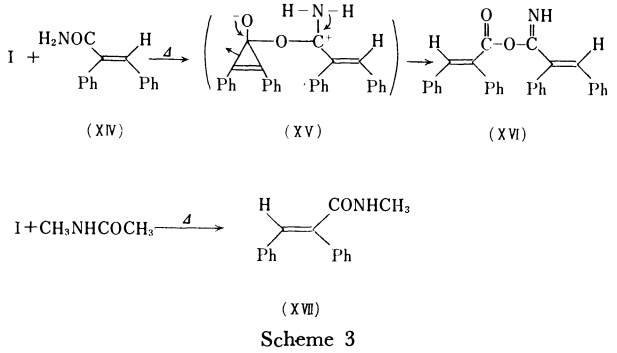

Scheme 3

Nevertheless, the reaction of I with *N*-methylacetamide under the same conditions as those employed for the above reaction showed a widely different mode, and the reaction product was *N*-methyl-α-phenyl-*trans*-cinnamamide (XVII). The structure of XVII was determined by a comparison of its spectral data with those of an authentic sample prepared from IV by the method described in the Experimental section. The product XVII can be derived formally by the attack of the methylamino group produced by the fission of the amide-bond of *N*-methylacetamide on I, in the same fashion as that shown in Schemes 1—3.

Experimental

All the melting points are uncorrected. The electronic spectra were measured on a Hitachi spectrophotometer, model 124. The infrared spectra were recorded on a spectrophotometer, IR-E, of the Japan Spectroscopic Co. The NMR spectra were recorded in deuteriochloroform on a Japan Electron Optics Laboratory H-100 spectrometer, TMS being used as the internal standard.

Materials. Diphenylcyclopropenone (I) was prepared according to the reported procedure;[4] mp 119—120°C (lit,[4] mp 119—121°C). Diphenylcyclopropenone monohydrate (II)

13) R. A. Nicolaus, *Ann. Chim. Applicata*, **39**, 542 (1949).

14) G. Fraenkel, A. Loewenstein, and S. Meiboom, *J. Phys. Chem.*, **65**, 700 (1961).

15) R. L. Gillespie and T. Birchall, *Can. J. Chem.*, **41**, 148 (1963).

16) S. J. Kuhn and J. S. Mclntyne, *ibid.*, **43**, 997 (1965).

was prepared according to the previously-reported method;[10] mp 87.5°C (lit,[10] mp 87.5°C). α-Phenyl-*trans*-cinnamic acid (IV) and α-phenyl-*cis*-cinnamic acid (IX) were prepared by the reported method.[12]

Pyrolysis of II. In an oil bath, II (2.2 g, 10 mmol) was heated at 150°C for 32 hr. After cooling, the crude product which had solidified was dissolved in ethanol (20 m*l*). An alcohol-insoluble crystalline solid was collected by filtration and recrystallized from ethanol to yield VI as colorless needles; yield, 0.27 g (12.6%); mp 117—118.5°C (lit,[11] mp 113—117°C). λ_{max}^{EtOH}: 223 (13400) and 300 nm (ε, 16000), IR (Nujol): 1715 and 1750 cm^{-1} (C=O), NMR: 2.23 (s, =CH, 2H) and 2.80 τ (m, Ph, 20H). The spectral data were identical with those reported for VI in the literature.[11]

The ethanol mother liquor remaining after the separation of VI was concentrated to dryness, and the residue was recrystallized from cyclohexane to afford VII; yield, 0.29 g (14.1%); mp 180—181°C (lit,[4] mp 181—182°C). The infrared and electronic spectra of VII thus obtained were identical with those of an authentic sample.[4] The evaporation of the solvent of the cyclohexane solution remaining after the removal of VII afforded tolan (yield, 0.45 g (23.9%)) after recrystallization from petroleum ether.

Reaction of I with IV. A mixture of I (0.5 g, 2.5 mmol) and IV (0.56 g, 2.5 mmol) was heated at 150°C for 3 hr. After cooling, the reaction mixture was recrystallized from ethanol to afford VI; yield, 0.28 g (25.4%). When the above mixture was heated at 150°C for 10 hr, 0.61 g (55.5%) of VI was isolated.

Reaction of I with IX. A mixture of I (0.7 g, 3.4 mmol) and IX (0.76 g, 3.4 mmol) was heated at 150°C for 27 hr. After cooling, the reaction mixture which had solidified was fractionated into the following two components by fractional recrystallization from ethanol: VI, 0.53 g (35.4%), and IV, 0.24 g (31.6%).

Reaction of I with Phenol. A mixture of I (2 g, 10 mmol) and phenol (2.8 g, 30 mmol) was heated at 150°C for 26 hr. After cooling, the crude product which had crystallized was recrystallized from cyclohexane to give XII; 1.68 % (42%); mp 138.5—139.5°C (lit,[13] mp 142—143°C). The infrared spectrum of the XII thus obtained in Nujol mull, 1725 (C=O), 1620 (C=C), and 1235, 1200, 1170, and 1155 cm^{-1} (ester), was identical with that of an authentic sample prepared according to the literature.[13]

Reaction of I with XIV. A mixture of I (3.0 g, 15 mmol) and XIV (3.36 g, 15 mmol) was heated at 150°C for 33 hr. After the mixture had cooled, cyclohexane (10 m*l*) was added. The crystals which separated out were collected by filtration and recrystallized from ethanol to afford XVI as colorless needles; 0.27 g (4.2%); mp 199—200°C. λ_{max}^{EtOH}: 225 (13000) and 312 nm (ε, 19500), IR ($CHCl_3$): 3380 (NH), 1736 (C=O), and 1145 cm^{-1} (ester), NMR: 1.88 (s, =CH, 1H), 2.10 (s, =CH, 1H), 2.86 (m, Ph, 20H), and 8.03 τ (s, =NH, 1H).

Found: C, 84.04; H, 5.34; N, 3.74%. Calcd for $C_{30}H_{23}O_2N$: C, 83.89; H, 5.40; N, 3.26%.

The heating of a solution of XVI in acetone-aqueous potassium hydroxide afforded IV.

The cyclohexane solution which remained after the removal of XVI was concentrated to dryness. Then the residue was chromatographed on alumina, using carbon tetrachloride as the solvent. From the fraction eluted with carbon tetrachloride, tolan (0.47 g (17.6%)) was obtained. From the fraction eluted with benzene, an unidentified product, $C_{15}H_{13}ON$, was isolated, 0.1 g; mp 161—163°C. From the fraction eluted with benzene - chloroform (1:1), XIV (1.51 g (45%)) was recovered.

Reaction of I with N-*Methylacetamide.* A mixture of I (1.5 g, 7.5 mmol) and *N*-methylacetamide (1.1 g, 15 mmol) was heated at 150°C for 40 hr. The crude product which solidified upon cooling was chromatographed on alumina, using carbon tetrachloride as the solvent. The fraction eluted with carbon tetrachloride was concentrated by distillation to afford tolan (0.38 g (28%)). From the fraction eluted with chloroform, XVII (0.14 g (7.9%)) was isolated, mp 166—167°C. λ_{max}^{EtOH}: 223 (8500) and 289 nm (ε, 12300), IR (Nujol): 1630 (C=O), 1610 (C=C), and 1540 cm^{-1} (amide-II), NMR: 2.68 (m, Ph, 10H), 3.13 (s, =CH, 1H), 4.06 (s, NH, 1H), and 7.23 τ (d, CH_3, 3H).

Found: C, 80.92; H, 6.30%. Calcd for $C_{16}H_{15}ON$: C, 80.98; H, 6.37%.

The spectral data of XVII were identical with those of an authentic sample (mp 165.5—167°C) prepared by the reaction of methylamine and α-phenyl-*trans*-cinnamoyl chloride derived from IV.

The authors wish to express their thanks to Mr. Kunio Ishibashi and Mr. Shoichi Kato for their elemental analyses, and to Miss Toshiko Matsutomo for her measurement of the electronic spectra.

Reactions of Metal Alkyl–Active Methylene Chelate Compounds with α,β-Unsaturated Carbonyl Compounds

Yusuke KAWAKAMI and Teiji TSURUTA

Faculty of Engineering, The University of Tokyo, Bunkyo-ku, Tokyo

(Received August 10, 1970)

The method of the preparation of zinc (or aluminum) alkyl-active methylene chelate compounds was studied. The chelate compounds were identified mainly by NMR, IR, and component analysis. Zinc alkyl-active methylene chelate compounds were found to cause a Michael-type addition reaction with α,β-unsaturated esters or nitriles. Aluminum alkyl-active methylene chelate compounds exhibited lower reactivities than the zinc chelate compounds toward α,β-unsaturated carbonyl compounds. Kinetic studies of the addition reaction revealed that the reaction proceeded according to a first-order rate law with respect to both the metal compound and the α,β-unsaturated carbonyl compound. The effects of substituents on the metal atom as well as on the chelate ring were also studied. The intercorrelation among the chemical shift of the methine proton of the chelate ring, σ_p of the subsituents and the reactivity of metal alkyl-active methylene chelate compounds suggested that the rate of the addition reaction was governed mainly by the stability of the chelate ring.

In previous papers,[1-5] a series of studies of the reaction modes of metal alkyls, such as *n*-BuLi, *n*-BuMgBr, *n*-Bu_2Zn, and *n*-Bu_3Al, with α,β-unsaturated carbonyl compounds was reported. The reactivities of both metal alkyls and α,β-unsaturated carbonyl compounds were quantitatively determined. These studies were undertaken in order to elucidate the initiation mechanism in the anionic polymerization of α,β-unsaturated carbonyl compounds. In the course of our studies, we noticed some characteristic chemical behavior of the metal alkyl-active methylene compound system; this promoted us to study in more detail the structure and the reactivity of the metal alkyl-active methylene compound system in the reaction with α,β-unsaturated carbonyl compounds, and to compare them with those of simple metal alkyls in the reaction.

This paper will be concerned with studies of the method of the preparation of chelate compounds from the metal alkyls and active methylene compounds and of their structure identification, mainly by the use of nuclear magnetic resonance spectra (NMR) and infrared spectra (IR). The results of kinetic studies of the reactions between the metal alkyl-active methylene chelate compound and the α,β-unsaturated carbonyl compound are also included in this paper. Dimethyl malonate was mainly used as the active methylene component.

Experimental

Reagents. Benzene, *p*-cymene, and *n*-hexane were distilled over sodium wire.[6] Tetrahydrofuran was distilled after refluxing over potassium hydroxide, and again distilled over sodium wire.[6] Dimethyl malonate, dimethyl methylmalonate, dimethyl chloromalonate, ethyl acetoacetate, methyl cyanoacetate, and malononitrile were distilled after refluxing over calcium hydride. Methanol was dehydrated by magnesium methoxide.[6] Diethylamine was distilled after refluxing over potassium hydroxide and distilled again over calcium hydride.[6] *n*-Butyl mercaptan was distilled over calcium hydride.[6] Methyl isopropenyl ketone (MIPK) and methyl propenyl ketone (MNPK) were synthesized from the corresponding ketones and aldehydes[7,8] respectively. Commercial methyl acrylate (MA), methyl methacrylate (MMA), methyl crotonate (MCr), acrylonitrile (AN), and crotononitrile (CrN) were distilled over calcium hydride. Commercial methyl vinyl ketone (MVK) was dried by means of a molecular sieve and distilled. Methacrylonitrile (MAN) was synthesized according to the literature.[9] Di-*n*-butylzinc and triethylindium were synthesized according to the literature.[10,11] *n*-Butylzinc chloride was synthesized by Noltes' method[12] and was purified by recrystallization from *n*-hexane. Commercial triethylaluminum, triisobutylaluminum, and diethylaluminum chloride were distilled under reduced pressure.

Preparation of Metal Alkyl-Active Methylene Chelate Compounds. *n*-Butyl(dimethyl malonato)zinc was prepared by a hydrogen-abstraction reaction between *n*-Bu_2Zn and dimethyl malonate in the molar ratio of 1 : 1, in benzene and at room temperature. After the solvent had been dried up, *n*-butyl(dimethyl malonato)zinc was obtained in the form of a white solid. Diethyl(dimethyl malonato)aluminum was prepared from Et_3Al and dimethyl malonate in a malor ratio of 1 : 1, in benzene and at room temperature. It was distilled under reduced pressure after distilling off the solvent. Colorless liquid; bp 53°C/0.15 mmHg. Other metal alkyl-active methylene chelate compounds were prepared in a similar way. The preparation method is tabulated in Table 1.

The abbreviations of the names of the metal alkyl-active methylene chelate compounds are as follows:

n-Butyl(dimethyl malonato)zinc: *n*-BuZnDMM, (Dimethyl malonato)zinc chloride: ClZnDMM, (Dimethyl malonato)-

1) N. Kawabata and T. Tsuruta, *Makromol. Chem.*, **86**, 231 (1965).
2) N. Kawabata and T. Tsuruta, *ibid.*, **98**, 262 (1966).
3) Y. Yasuda, N. Kawabata, and T. Tsuruta, *J. Macromol. Sci.*, **A1**, 669 (1967).
4) T. Tsuruta and Y. Yasuda, *ibid.*, **A2**, 943 (1968).
5) Y. Kawakami, Y. Yasuda, and T. Tsuruta, *ibid.*, **A3**, 205 (1969).
6) A. Weissberger, E. Proskauer, J. Riddick, and E. Toops, Jr., "Technique of Organic Chemistry," Vol. VII, Organic Solvents. Wiley(Interscience), New York (1955).
7) E. F. Landau and F. P. Irany, *J. Org. Chem.*, **12**, 422 (1947).
8) A. L. Wilds and D. Djerassi, *J. Amer. Chem. Soc.*, **68**, 1718 (1946).
9) D. Gotkis and J. B. Cloke, *ibid.*, **56**, 2710 (1934).
10) R. C. Krug and P. J. C. Tang, *J. Amer. Chem. Soc.*, **76**, 2262 (1954).
11) F. Runge, W. Zimmermann, H. Pfeiffer, and I. Pfeiffer, *Z. Anorg. Allg. Chem.*, **267**, 39 (1951).
12) J. Boersma and J. G. Noltes, *Tetrahedron Lett.*, **1966**, 1521.

TABLE 1. PREPARATIVE METHOD OF METAL ALKYL-ACTIVE METHYLENE CHELATE COMPOUNDS[a)]

Compound	Compound A	Compound B	Reaction temp.	State of product
n-BuZnDMM[b)]	*n*-Bu_2Zn	$CH_2(CO_2Me)_2$	r.t.	Colorless solid
ClZnDMM[b)]	*n*-BuZnCl	$CH_2(CO_2Me)_2$	r.t.	Colorless solid
MeOZnDMM[b)]	*n*-BuZnOMe	$CH_2(CO_2Me)_2$	40°C	Colorless solid
n-BuSZnDMM[b,c)]	*n*-BuZnSBu	$CH_2(CO_2Me)_2$	40°C	Colorless solid
$Et_2NZnDMM$[b)]	*n*-BuZnDMM	Et_2NH	60°C	Solid
n-BuZnDMMM[b)]	*n*-Bu_2Zn	$CH_3CH(CO_2Me)_2$	r.t.	Colorless solid
n-BuZnDMCM[b)]	*n*-Bu_2Zn	$ClCH(CO_2Me)_2$	r.t.	Colorless solid
n-BuZnEAA	*n*-Bu_2Zn	$CH_3COCH_2CO_2Et$	r.t.	Glassy state
Et_2AlDMM	Et_3Al	$CH_2(CO_2Me)_2$	r.t.	bp 53°C/0.15 mmHg
EtClAlDMM	Et_2AlCl	$CH_2(CO_2Me)_2$	r.t.	bp 70°C/0.20 mmHg
EtMeOAlDMM	Et_2AlDMM	MeOH	r.t.	Glassy state
i-$BuEt_2NAlDMM$	*i*-Bu_2AlNEt_2	$CH_2(CO_2Me)_2$	60°C	—
$Et_2AlDMMM$	Et_3Al	$CH_3CH(CO_2Me)_2$	r.t.	bp 66°C/0.30 mmHg
$Et_2AlDMCM$	Et_3Al	$ClCH(CO_2Me)_2$	r.t.	mp *ca.* 30°C, bp 83°C/0.40 mmHg
Et_2AlMCA	Et_3Al	$CNCH_2CO_2Me$	r.t.	Glassy state
EtClAlMCA	Et_2AlCl	$CNCH_2CO_2Me$	r.t.	Glassy state
Et_2AlEAA	Et_3Al	$CH_3COCH_2CO_2Et$	r.t.	bp 45°C/0.20 mmHg
Et_2InDMM	Et_3In	$CH_2(CO_2Me)_2$	r.t.	Colorless solid

a) All reactions were carried out by adding B into a benzene solution of A.
b) All zinc alkyl-active methylene chelate compounds were purified by washing with *n*-hexane or recrystallization from *n*-hexane.
c) *n*-BuZnSBu was prepared from *n*-Bu_2Zn and *n*-BuSH in benzene.

TABLE 2. COMPONENT ANALYSIS OF ZINC ALKYL-ACTIVE METHYLENE CHELATE COMPOUNDS

Compound	*n*-Bu	Cl	MeO	Et_2N	*n*-BuS	Zn	DMM	DMMM	DMCM	EAA
n-BuZnDMM	0.97	—	—	—	—	1.00	1.02	—	—	—
ClZnDMM	—	a)	—	—	—	1.00	1.00	—	—	—
MeOZnDMM	—	—	1.01	—	—	1.00	0.97	—	—	—
n-BuSZnDMM	—	—	—	—	0.98	1.00	0.99	—	—	—
$Et_2NZnDMM$	—	—	—	0.96	—	1.00	1.00	—	—	—
n-BuZnDMMM	1.02	—	—	—	—	1.00	—	0.98	—	—
n-BuZnDMCM	0.98	—	—	—	—	1.00	—	—	0.97	—
n-BuZnEAA	0.99	—	—	—	—	1.00	—	—	—	1.01

a) Chlorine was not determined.

TABLE 3. COMPONENT ANALYSIS OF ALUMINUM ALKYL-ACTIVE METHYLENE CHELATE COMPOUNDS

Compound	Et	Cl	MeO	Al	DMM	DMMM	DMCM	EAA
Et_2AlDMM	2.02	—	—	1.00	1.00	—	—	—
EtClAlDMM	1.00	a)	—	1.00	1.02	—	—	—
EtMeOAlDMM	1.02	—	0.98	1.00	0.96	—	—	—
$Et_2AlDMMM$	1.98	—	—	1.00	—	0.99	—	—
$Et_2AlDMCM$	2.00	—	—	1.00	—	—	1.00	—
Et_2AlEAA	2.01	—	—	1.00	—	—	—	1.02

a) Chlorine was not determined.

TABLE 4. DEGREE OF ASSOCIATION OF ZINC ALKYL-ACTIVE METHYLENE CHELATE COMPOUNDS

Compound	Concn. (mol/*l*)	Degree of association
n-BuZnDMM	0.188	2
MeOZnDMM	0.206	4—6
$Et_2NZnDMM$	0.250	1
n-BuZnDMMM	0.300	1—2
n-BuZnDMCM	0.305	1—2
n-BuZnEAA	0.206	2

TABLE 5. DEGREE OF ASSOCIATION OF ALUMINUM ALKYL-ACTIVE METHYLENE CHELATE COMPOUNDS

Chelate compound	Concn. (mol/*l*)	Degree of association
Et_2AlDMM	0.105	1
EtMeOA1DMM	0.197	1
EtClAlDMM	0.164	1
$Et_2AlDMCM$	0.175	1
$Et_2AlDMMM$	0.180	1
Et_2AlEAA	0.193	1

TABLE 6. NMR DATA OF METAL ALKYL - ACTIVE METHYLENE CHELATE COMPOUNDS

Compound	No. of peak	Assignment	Chemical shift[a]	Area ratio
Dimethyl malonate	1	$-CO_2CH_3$	6.65	6
	2	CH_2	6.89	2
Dimethyl chloromalonate	3	$-CO_2CH_3$	6.72	6
	4	Cl-CH	5.40	1
Dimethyl methylmalonate	5	CO_2CH_3	6.63	6
	6	-CH	6.84	1
	7	CH_3-C-	8.80	3
Methyl cyanoacetate	8	$-CO_2CH_3$	6.69	3
	9	CN-CH_2	7.23	2
Ethyl acetoacetate	10	$-OCH_2-$	6.09	2
	11	$-CH_2-$	6.97	2
	12	$CH_3C(=O)-$	8.21	3
	13	CH_3	9.03	3
n-BuZnDMM	1	MCH	5.57	1
	2	$-CO_2CH_3$	6.67	6
	3	$-CH_2-CH_2-$	—	4
	4	CH_3	8.90	3
	5	M-CH_2-	9.22	2
ClZnDMM[b]	6	MCH	5.27	1
	7	$-CO_2CH_3$	6.52	6
MeOZnDMM	8	MCH	5.19	1
	9	CH_3O	6.04	3
	10	$-CO_2CH_3$	6.54	6
Et_2NZnDMM	11	MCH	5.26	1
	12	$-CO_2CH_3$	6.54	6
	13	CH_2-N	7.80	4
	14	CH_3	9.17	6
n-BuZnDMCM	1	$-CO_2CH_3$	6.59	6
	2	$-CH_2-CH_2-$	—	4
	3	CH_3	8.93	3
	4	M-CH_2-	9.42	2
n-BuZnDMMM	5	$-CO_2CH_3$	6.51	6
	6	CH_3-CM	8.01	3
	7	$-CH_2-CH_2-$	—	4
	8	CH_3	8.96	3
	9	M-CH_2-	9.27	2
n-BuZnEAA	10	MCH	5.05	1
	11	$-OCH_2$	6.08	2
n-BuZnEAA	12	CH_3-C(=O)-	8.02	3
	13	$-CH_2CH_2$	—	4
	14	CH_3	8.95	3
	15	$OCH_2C\underline{H}_3$	8.98	3
	16	M-CH_2-	9.34	2
Et_2AlDMM	1	MCH	5.36	1
	2	$-CO_2CH_3$	6.81	6
	3	CH_3	8.67	6
	4	M-CH_2	9.70	4
EtClAlDMM	5	MCH	5.47	1
	6	$-CO_2CH_3$	6.92	6
	7	CH_3	8.70	3
	8	M-CH_2	9.60	2
EtMeOAlDMM	9	MCH	5.18	1
	10	CH_3O	6.48	3
	11	$-CO_2CH_3$	6.64	6
	12	CH_3	8.60	3
	13	M-CH_2-	9.70	2
i-BuEt_2NAlDMM	14	MCH	5.08	1
	15	CO_2CH_3	6.58	6
	16	N-CH_2	7.35	4
	17	-CH	—	1
	18	CH_3	8.92	6
	19	N-$CH_2-C\underline{H}_3$	9.15	6
	20	M-CH_2	9.76	2
Et_2AlDMCM	1	$-CO_2CH_3$	6.80	6
	2	CH_3	8.72	6
	3	M-CH_2	9.80	4
Et_2AlDMMM	4	$-CO_2CH_3$	6.78	6
	5	CH_3-CM	8.23	3
	6	CH_3	8.63	6
	7	M-CH_2	9.57	4
Et_2AlEAA	8	MCH	5.18	1
	9	$-C(=O)-O-CH_2$	6.20	2
	10	$CH_3C(=O)$	8.37	3
	11	M-CH_2-CH_3	8.63	6
	12	$-C(=O)-O-CH_2-C\underline{H}_3$	9.13	3
	13	M-CH_2	9.68	4

a) τ-value, tetramethylsilane as internal standard.
b) Mixed solvent (THF: Benzene = 1 : 1) was used.

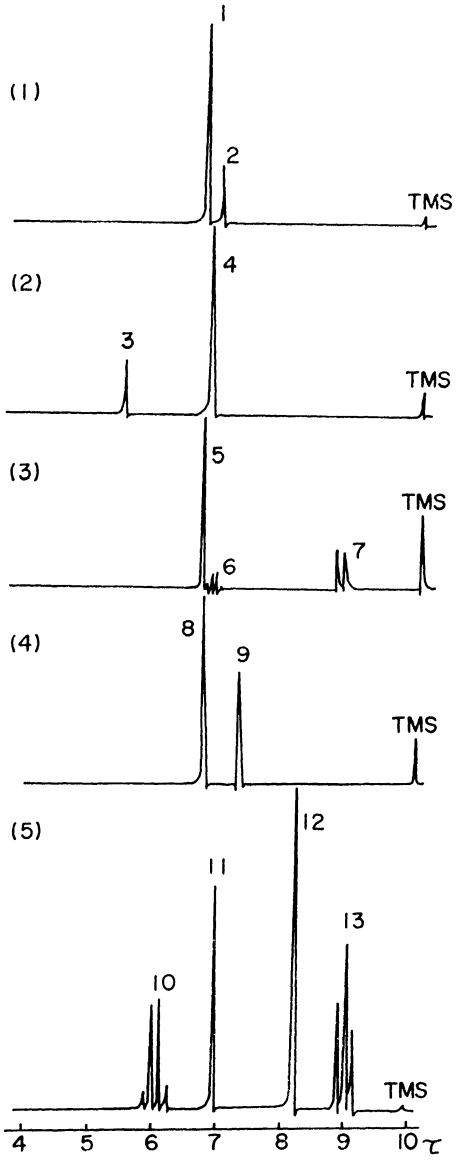

Fig. 1. NMR spectra of active methylene compounds (in benzene).
(1) Dimethyl malonate (2) Dimethyl chloromalonate
(3) Dimethyl methylmalonate (4) Methyl cyanoacetate
(5) Ethyl acetoacetate

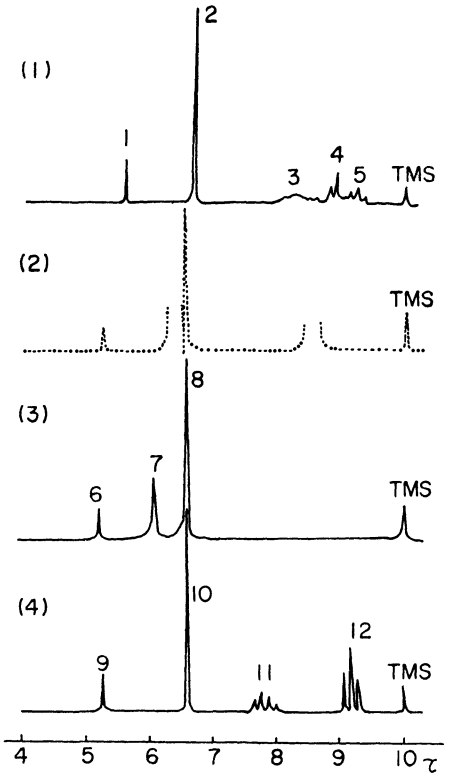

Fig. 2. NMR spectra of XZnDMM (in benzene).
(1) *n*-BuZnDMM (2) ClZnDMM (in THF)
(3) MeOZnDMM (4) $Et_2NZnDMM$

zinc methoxide: MeOZnDMM, (Dimethyl malonato)zinc butylmercaptide: *n*-BuSZnDMM, (Dimethyl malonato)zinc diethylamide: $Et_2NZnDMM$, *n*-Butyl(dimethyl methylmalonato)zinc: *n*-BuZnDMMM, *n*-Butyl(dimethyl chloromalonato)zinc: *n*-BuZnDMCM, *n*-Butyl(ethyl acetoacetato)zinc: *n*-BuZnEAA, Diethyl(dimethyl malonato)aluminum: Et_2AlDMM, Ethyl(dimethyl malonato)aluminum chloride: EtClAlDMM, Ethyl(dimethyl malonato)aluminum methoxide: EtMeOAlDMM, Isobutyl(dimethyl malonato)aluminum diethylamide: *i*-$BuEt_2NAlDMM$, Diethyl(dimethyl methylmalonato)aluminum: $Et_2AlDMMM$, Diethyl(dimethyl chloromalonato)aluminum: $Et_2AlDMCM$, Diethyl(methyl cyanoacetato)aluminum: Et_2AlMCA, Ethyl(methyl cyanoacetato)aliminum chloride: EtClAlMCA, Diethyl(ethyl acetoacetato)aluminum: Et_2AlEAA, Diethyl(dimethyl malonato)indium: Et_2InDMM.

Analyses of Metal Alkyl-Active Methylene Chelate Compounds. The analyses of the metal alkyl-active methylene chelate compounds were performed by chelate titration, NMR, IR, and vapor-phase chromatography(VPC). The degree of association was measured in benzene by the cryoscopic method. The results obtained are shown in Tables 2—6 and in Figs. 1—5.

These results show that one alkyl group of every metal alkyl derivative, *e. g.*, RZnX, was quantitatively reacted with an active methylene compound, while alkane was eliminated, as follows:

$$RZnX + CH_2(CO_2Me)_2 \longrightarrow \underset{(XZnDMM)}{XZnCH(CO_2Me)_2} + RH$$

Procedure for Reactions with α,β-Unsaturated Carbonyl Compounds. Into a magnetic-stirred solution of a metal alkyl-active methylene chelate compound in a 30-m*l*, one-necked flask fitted with a three-way cock, an α,β-unsaturated carbonyl compound was added through the three-way cock from a syringe. After a given time interval, the reaction was stopped by adding acetic acid and the reaction products were determined by VPC. All the procedures described above were carried out under a dried nitrogen atmosphere. The NMR spectra were obtained by the use of a Japan Electron Optics Lab. Co., model C-60, high-resolution spectrometer using a 10 mol% benzene solution of a metal alkyl-active methylene chelate compound. The τ-values were determined by the use of tetramethylsilane as the internal standard. The IR spectra were obtained by the use of a Hitachi IR spectrometer, model EPI-G3, between KBr plates.

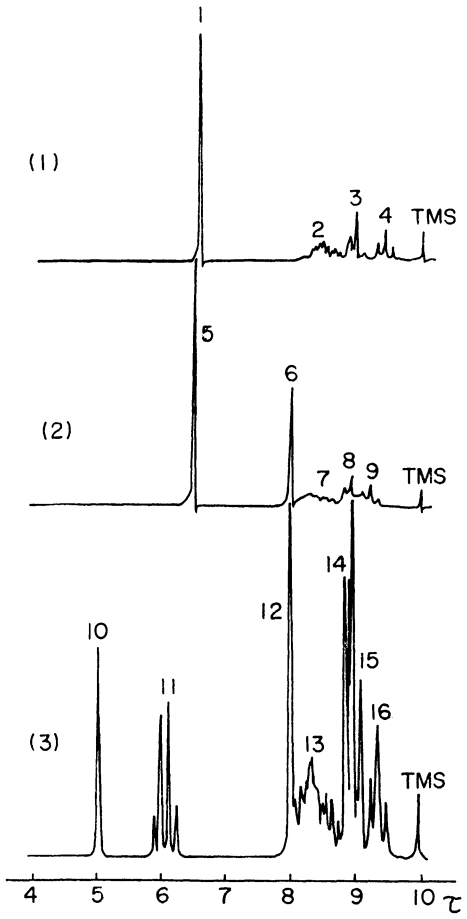

Fig. 3. NMR spectra of *n*-BuZnC(X)(Y)CO_2Me (in benzene).
(1) *n*-BuZnDMCM (2) *n*-BuZnDMMM (3) *n*-BuZnEAA

Results and Discussion

1. Structure of Meta Alkyl - Active Methylene Chelate Compounds. As is shown in Figs. 2—5 and in Tables 2, 3, and 6, each of the products from the metal alkyl - active methylene compound systems is a stoichiometric compound. The IR spectra of the carbonyl region is shown in Fig. 6.

The frequency of >C=O stretching is shifted to a region lower by 100—150 cm^{-1}, a fact which seems to indicate a chelating structure produced through the oxygen atom of the carbonyl group. Most of the chemical shifts of the methine proton in the NMR data are observed in the vicinity of 5.3 τ, which shows that the methine carbon is not linked directly with the metal atom. In order to elucidate the structure of the aluminum alkyl - active methylene chelate compound more clearly, the coupling constant, J^{13}_{C-H} at the methine proton was measured by using a neat sample. The results are shown in Table 7.

The value of J^{13}_{C-H} is regarded as a measure of the *s*-character of the carbon atom.[13] As is shown in the table, the value is about 170 cps for the aluminum

Table 7. Coupling constant $J_{^{13}C-H}$ at C–H

Compound	$J_{^{13}C-H}$(cps)
Et_2AlDMM	170
EtClAlDMM	168
Et_2AlEAA	168
DMM	130

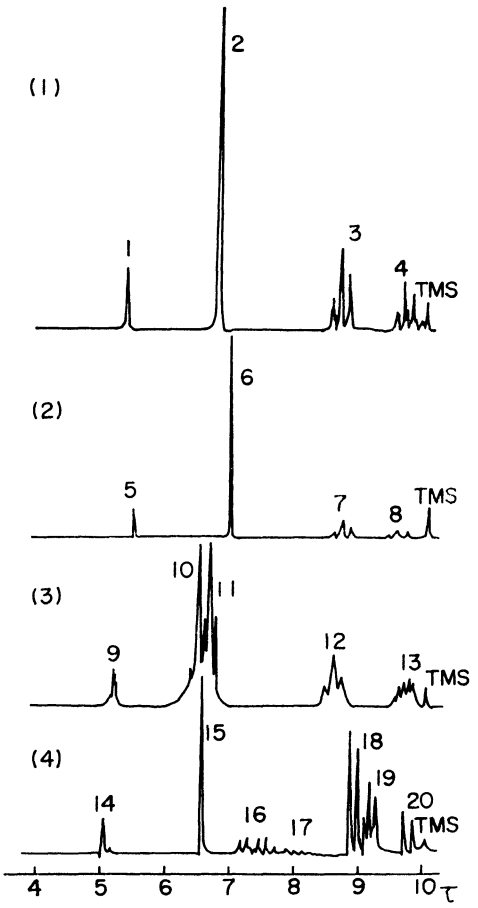

Fig. 4. NMR spectra of EtXAlDMM (in benzene).
(1) Et_2AlDMM (2) EtClAlDMM
(3) EtMeOAlDMM (Sample only dried up was used.)
(4) *i*-BuEt_2NAlDMM

chelate, a fact which indicates that the central carbon of the active methylene compound in the aluminum chelate compound is in the sp^2 valence state. Kroll and Naegele[14] reported that diethyl(acetylacetonato)-aluminum has the following chelating structure:

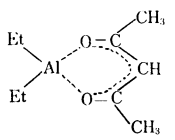

13) a) N. Muller and D. E. Pritchard, *J. Chem. Phys.*, **31**, 768, 1471 (1959). b) J. N. Shoolery, *ibid.*, **31**, 1427 (1959). c) C. Juan and H. S. Gutowsky, *ibid.*, **37**, 2198 (1962).

14) W. R. Kroll and W. Naegele, *J. Organometal. Chem.*, **19**, 439 (1969).

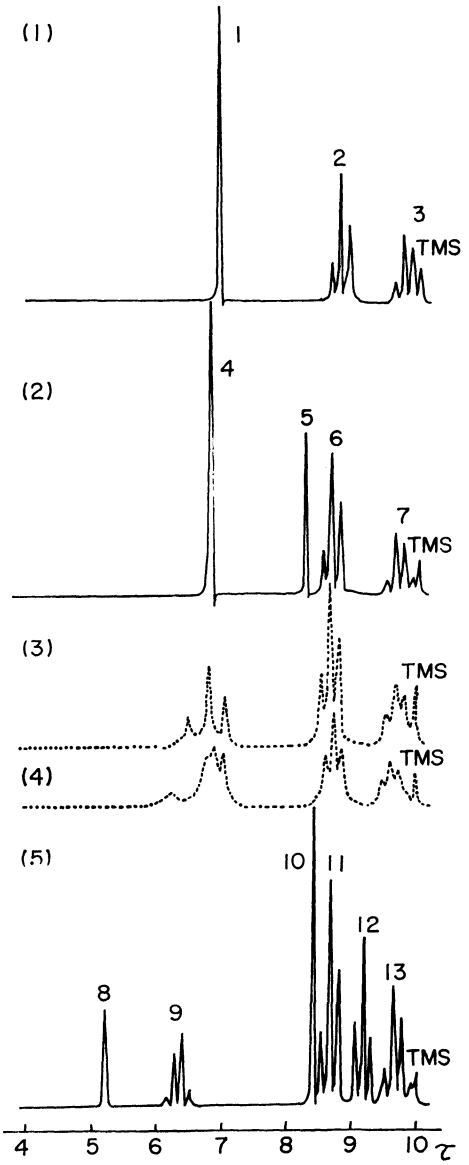

Fig. 5. NMR spectra of $Et_2AlC(X)(Y)CO_2Me$ (in benzene).
(1) $Et_2AlDMCM$ (2) $Et_2AlDMMM$
(3) Et_2AlMCA (Sample only dried up was used.)
(4) EtClAlMCA (Sample only dried up was used.)
(5) Et_2AlEAA

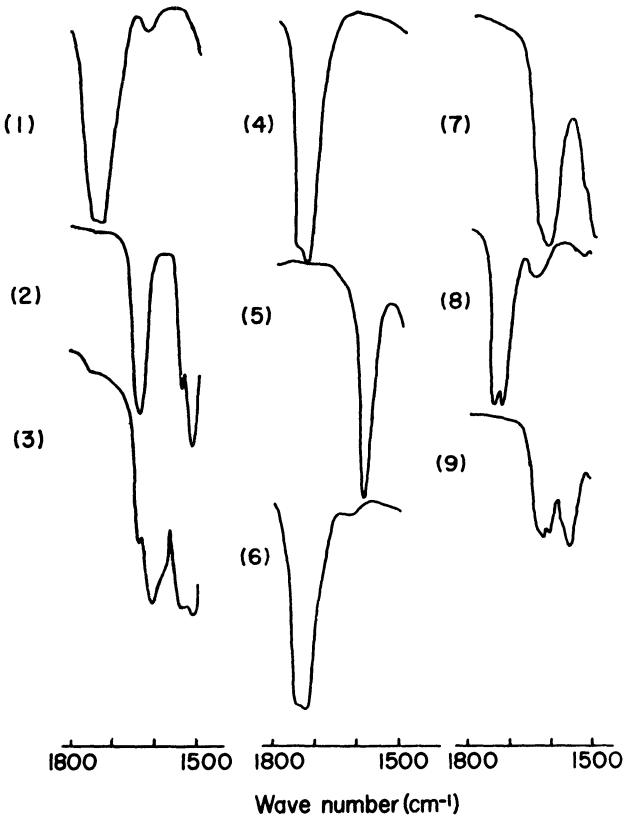

Fig. 6. IR spectra of aluminum alkyl chelate compounds in carbonyl region.
(1) Dimethyl malonate (2) Et_2AlDMM (3) EtClAlDMM
(4) Dimethyl chloromalonate (5) $Et_2AlDMCM$
(6) Dimethyl methylmalonate (7) $Et_2AlDMMM$
(8) Ethyl acetoacetate (9) Et_2AlEAA

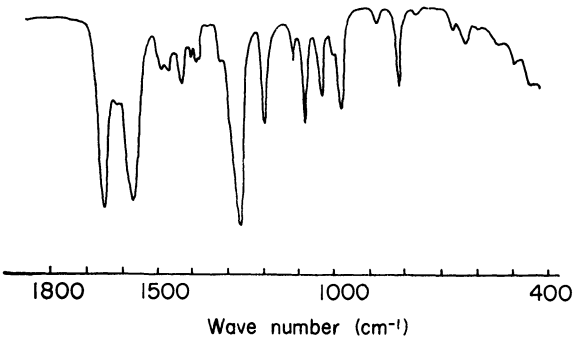

Fig. 7. IR spectrum of *n*-BuZnEAA.

Judging from Figs. 4—6 and Table 7, the products from aluminum alkyl-active methylene compound systems can reasonably be concluded to have a similar structure of the chelate ring.

Measurements of J^{13}_{C-H}, however, were not possible for the zinc alkyl-active methylene compound system, because all of the zinc compounds prepared, *e.g.*, XZnDMM, were solid. We may, though, suppose the structure of the zinc compound to be similar to the aluminum chelate from the NMR data (Figs. 2 and 3) as well as the IR data (Fig. 7).

2. Reaction Mode of Zinc (or Aluminum) Alkyl-Active Methylene Chelate Compounds with α,β-Unsaturated Carbonyl Compounds. In the reaction of *n*-BuZnDMM with methyl acrylate (MA), dimethyl malonate was found to decrease in the course of the reaction, ultimately almost disappearing, a fact which shows that no hydrogen abstraction by DMM occurred, and an addition product, $(MeOOC)_2CHCH_2CH_2CO_2Me$, of DMM to MA was detected by VPC. Since the formation of methanol in the reaction mixture was not detected, the possibility of the carbonyl addition reaction can be excluded. The addition product, fractionated by VPC, was identified by a comparison of its IR spectrum with that of an authentic sample.

These results show the only elementary reaction in this case to be a Michael-type 1,4 addition reaction. Reactions with α,β-unsaturated ketones and nitriles were also studied. The reactivity of the aluminum alkyl-active methylene chelate compound is rather lower than that of the zinc chelate, no addition reactions to α,β-unsaturated esters or nitriles being observed at 30°C

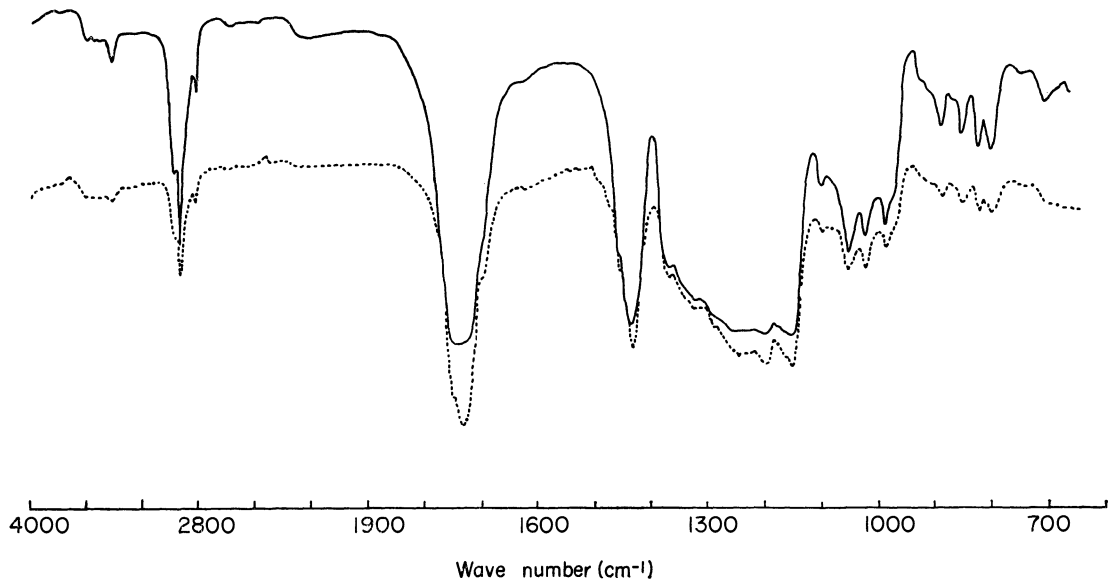

Fig. 8. IR spectra of the reaction products of BuZnDMM with MA and authentic sample (---).

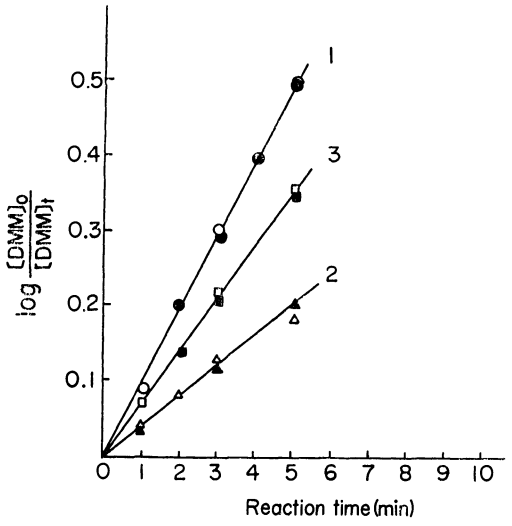

Fig. 9. Reaction of *n*-BuZnDMM with α,β-unsaturated carbonyl compounds.

(1) MIPK (2) MA (3) AN

○ [Zn]=0.20 mol/*l* △ [Zn]=0.23 mol/*l*

□ [Zn]=0.20 mol/*l* ● [Zn]=0.10 mol/*l*

▲ [Zn]=0.12 mol/*l* ■ [Zn]=0.10 mol/*l*

in benzene. The reactivity of EtClAlDMM, however, was found to be high enough to add to the α,β-unsaturated ester or nitrile under the same conditions. The mode of the addition reaction was confirmed to be also a Michael-type reaction in the case of the aluminum chelate just as with the zinc-chelate compound.

3. Reaction-rate Analysis. The rate of the addition reaction was determined by measuring the quantities of dimethyl malonate recovered after the interruption of the reaction. To ascertain the effect of substituents on the metal atom, the reaction of XZnDMM (X=*n*-Bu, Cl, MeO, *n*-BuS, Et_2N) with MA was kinetically studied in detail. Substituent effects on the central carbon of DMM were also studied. Besides dimethyl malonate, ethyl acetoacetate, and methyl cyanoacetate were examined for the sake of comparison. In all

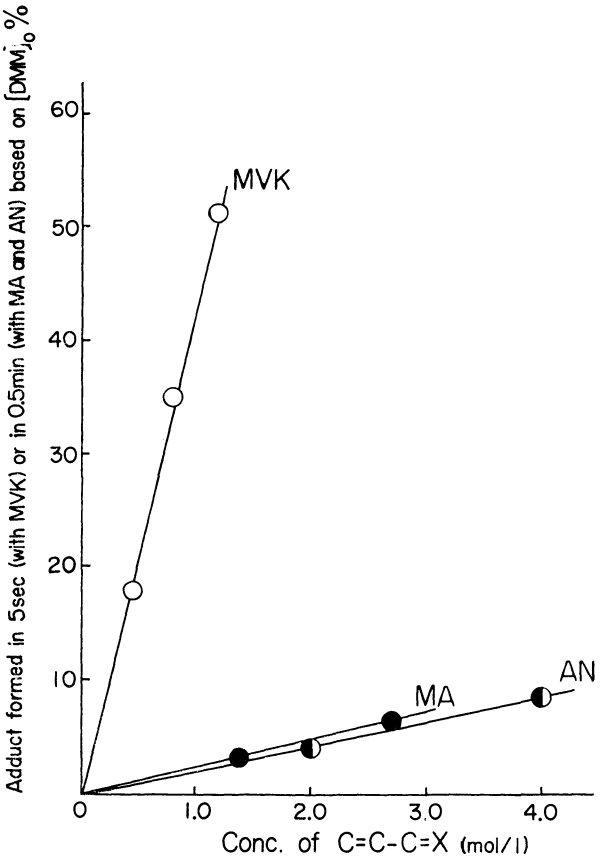

Fig. 10. Dependence of rate on the concentration of α,β-unsaturated carbonyl compound in the reaction with *n*-BuZnDMM (0.1 mol/*l*).

cases, the Michael-type addition of an active methylene compound to an α,β-unsaturated carbonyl compound was confirmed to take place. The results are tabulated in Tables 8, 9, 10, and 11.

The data in Tables 8—11 were found to fit the first-order rate law with respect to the metal alkyl-active methylene chelate compound. This was confirmed also by the further experiments shown in Fig. 9,

TABLE 8. REACTION OF ZXnDMM WITH α,β-UNSATURATED CARBONYL COMPOUND[a)]

Carbonyl compd.	X	Reaction time (min)	X[b)] Recovered (%)	Dimethyl malonate (%)
MVK	*n*-Bu	0	100	100
		0.083	100	5.0
		5	100	0
MIPK	*n*-Bu	0	100	100
		1	100	66.4
		3	99	29.5
		5	101	13.6
		10	98	10.5
		20	100	6.7
MNPK	*n*-Bu	0	100	100
		2	100	28.9
		5	98	3.7
		10	102	1.0
MA	*n*-Bu	0	100	100
		1	100	91.0
		2	98	81.9
		3	99.4	74.0
		5	100	67.3
		10	—	44.6
		1200	100	3.5
MMA	*n*-Bu	0	100	100
		60	99	98
		120	102	96
		1440	100	58.8
MCr	*n*-Bu	0	100	100
		60	—	96.5
		120	—	93.5
		240	99	87.7
AN	*n*-Bu	0	100	100
		1	—	83.7
		3	—	59.6
		5	—	43.1
		10	100	17.7
MAN	*n*-Bu	0	100	100
		60	—	98.3
		120	—	94.6
		300	—	87.0
		600	100	76.0
CrN	*n*-Bu	0	100	100
		30	—	98.0
		60	—	93.5
		120	—	87.5
		300	—	71.8
		600	100	50.0
MVK	MeO	0	100	100
		0.5	—	52.2
		1	—	27.2
		2	—	7.4
MIPK	MeO	0	100	100
		0.5	—	85.5
		1	—	79.6
		2	—	63.7
		3	—	50.8
		5	100	32.2
MNPK	MeO	0	100	100
		1	—	94.3
		2	—	89.0
		3	—	84.0
		5	—	74.8
		10	100	56.2
MA	MeO	0	100	100
		60	—	64.3
		120	—	45.0
		180	—	29.9
		300	102	17.4
AN	MeO	0	100	100
		60	—	—
		120	—	29.7
		1200	100	3.7
MVK	Cl	0	—	100
		1/2	—	42.2
		1/6	—	17.5
		5	—	0
MA	Cl	0	—	100
		0.5	—	93.2
		1	—	87.1
		2	—	75.9
		5	—	51.9
MA	*n*-BuS	0	100	100
		180	—	88.7
		420	—	75.6
		720	—	61.4
		1260	100	44.4
MA	Et_2N	0	100	100
		420	—	80.4
		1260	100	68.4

a) All reactions were carried out in benzene at 30°C. [MVK] 0.4 mol/*l*, [MIPK] 1.5 mol/*l*, [MNPK] 1.5 mol/*l*, [MA] 1.4 mol/*l*, [MMA] 2.44 mol/*l*, [MCr] 2.44 mol/*l*, [Nitrile] 2.0 mol/*l* for BuZnDMM; [MVK] 0.56 mol/*l*, [MIPK] or [MNPK] 2.0 mol/*l*, [MA] 2.4 mol/*l*, [AN] 1.6 mol/*l* for MeOZnDMM; [MA] 2.0 mol/*l*, 1.0 mol/*l* and 2.0 mol/*l* for ClZnDMM, *n*-BuSZnDMM, and $Et_2NZnDMM$ respectively. [MVK] 0.48 mol/*l* for ClZnDMM. The concentration of zinc compounds was 0.1 mol/*l*.

b) Recovered X: *n*-BuH, MeOH, *n*-BuSH, and Et_2NH, respectively. Chlorine was not measured.

Table 9. Reaction of n-BuZnC(XY)CO_2Me with methyl acrylate[a]

X	Y	Reaction time (min)	Recovered C(XY)CO_2Me (%)
Cl	CO_2Me	0	100
		1	88.0
		2	78.0
		3	68.7
		5	55.0
		10	33.0
CH_3	CO_2Me	0	100
		1	60.8
		2	37.2
		3	24.1
		5	14.3
		10	9.9
H	CH_3CO[b]	0	100
		300	66.6

a) MA 2.0 mol/l: Zinc compound 0.1 mol/l
b) Ethyl acetoacetate was used.

Table 10. Reaction of EtXAlDMM with α,β-unsaturated carbonyl compound[a]

Compound	X	Reaction time (min)	Recovered DMM (%)
MVK	Et	0	100
		2	95.2
		5	88.4
		10	77.5
		30	52.7
MVK	Cl	0	100
		0.333	5
MA	Cl	0	100
		10	87.5
		20	77.0
		30	67.3
		60	45.4
		120	20.7
MVK	MeO	0	100
		2	98.2
		5	96.8
		10	93.7
		30	82.5
MVK	Et_2N[b]	0	100
		60	93.0
		120	87.0
		180	80.5
		600	71.2
		1230	23.8

a) MVK 2.56 mol/l, 0.5 mol/l, 2.0 mol/l, and 4.0 mol/l for X=Et, Cl, MeO, and Et_2N, respectively.
MA 1.5 mol/l
Aluminum compound 0.1 mol/l
b) i-BuEt_2NAlDMM was used.

in which the concentration of the metal component is a half of that in Table 7.

The straight line in Fig. 9 shows that the addition reaction is a first-order one with respect to the metal compound. The dependence of the reaction rate on the concentration of the α,β-unsaturated carbonyl compound was also examined, as is shown in Fig. 10.

Table 11. Reaction of $Et_2AlC(XY)CO_2Me$ with α,β-unsaturated carbonyl compound[a]

Carbonyl compound	X	Y	Reaction time (min)	Recovered C(XY)CO_2Me (%)
MVK	Cl	CO_2Me	0	100
			30	68.6
			60	46.5
			150	14.8
MVK	CH_3	CO_2Me	0	100
			120	78.7
			1440	10.1
MVK	H	CN	0	100
			0.5	13.6
MA	H	CN	0	100
			10	61.2
			20	37.6
			30	23.0
			60	12.0
MVK	H	CH_3CO[b]	0	100
			1440	100

a) Carbonyl compound 1.0 mol/l
Aluminum compound 0.1 mol/l
b) Ethyl acetoacetate was used.

From the above data, the rate expression for the addition reaction can be given as Eq. (1):

$$\frac{d[DMM]}{dt} = k[M][\text{carbonyl compound}] \qquad (1)$$

Table 12. Rate constants[a] of addition reaction of Et(X)Al-Y with methyl vinyl ketone and methyl acrylate

X	Y	MVK	MA
Et	DMM	9.7×10^{-3}	b)
Cl		3.0	8.8×10^{-3}
MeO		3.2×10^{-3}	b)
Et_2N		4.0×10^{-4}	b)
Et	DMMM	2.0×10^{-3}	b)
	DMCM	1.3×10^{-2}	b)
	MCA	16	4.9×10^{-2}

a) l/mol·min
b) No reaction occurred.

Table 13. Rate constants[a] of addition reaction of X-Zn-Y with α,β-unsaturated carbonyl compound

X	Y	MVK	MIPK	MNPK	MA
n-Bu	DMM	44	0.28	0.44	6.9×10^{-2}
Cl		21.5	—	—	6.9×10^{-2}
MeO		2.6	0.12	0.029	2.9×10^{-3}
Et_2N		—	—	—	2.6×10^{-4}
n-BuS		—	—	—	6.7×10^{-4}
n-Bu	DMMM	—	—	—	4.7×10^{-1}
	DMCM	—	—	—	6.2×10^{-2}
	EAA	0.64	—	—	6.8×10^{-4}

a) l/mol·min

where [M] is the concentration of the metal compound. Equation (1) was found to be true for all the reactions examined between metal alkyl-active methylene chelate compounds and α,β-unsaturated carbonyl compounds. The rate constants of the second-order reaction are listed in Tables 12 and 13.

4. Reactivity of Metal Alkyl-Active Methylene Chelate Compounds. It can be seen from the preceding sections that RZnDMM exhibits much higher reactivity than ZnR_2 in the addition reaction to α,β-unsaturated esters or nitriles. As we reported previously, ZnR_2 or AlR_3 can add to α,β-unsaturated ketones,[5] but not to the unsaturated esters (*e. g.*, methyl acrylate, methyl methacrylate, and methyl crotonate) or nitriles (*e. g.*, acrylonitrile, methacrylonitrile, and crotononitrile). Contrary to RZnDMM, the reactivity of R_2AlDMM was not enough to result in the addition reaction with the unsaturated esters or nitriles, though the latter chelate compound adds easily to more reactive double bonds of α,β-unsaturated ketones.

Since significant effects were noticed in the reactivity of XZnDMM or EtXAlDMM (X: R, Cl, RO, RS, R_2N) in the addition reactions to α,β-unsaturated carbonyl compounds, systematical studies of the substituent effect were undertaken. From Tables 12 and 13, the main features of the reactions of metal alkyl-active methylene chelate compounds can be listed as follows:

i) The reactivity of XZnDMM or EtXAlDMM increases in the order, X: $Et_2N<$*n*-BuS$<$MeO$<$*n*-Bu(or Et)$\leqq$Cl, which is in accordance with the order of the methine proton chemical shift from a lower to a higher field.

ii) The more stable chelate ring seems to have a more diminished reactivity.

iii) The substituent effect on the central carbon atom of *n*-BuZn[$XC(CO_2Me)_2$] is the reverse of that of $Et_2Al[XC(CO_2Me)_2]$. The reactivity of *n*-BuZn-[$XC(CO_2Me)_2$] increases in the order; X: Cl$<$H$<CH_3$, while the reactivity of $Et_2Al[XC(CO_2Me)_2]$ decreases in this order.

An electron-withdrawing substituent, X, in EtXAl-DMM causes the chemical shift of the methine proton to a higher field. This could be interpreted in terms

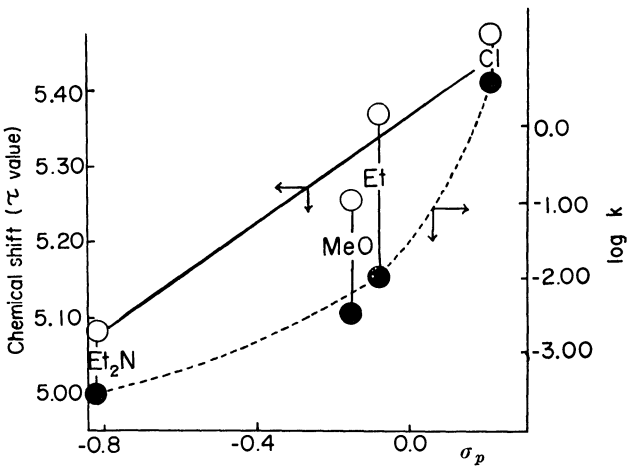

Fig. 11. Correlation among Hammett's σ_p, the chemical shift of methine proton in EtXAlDMM and reactivity.

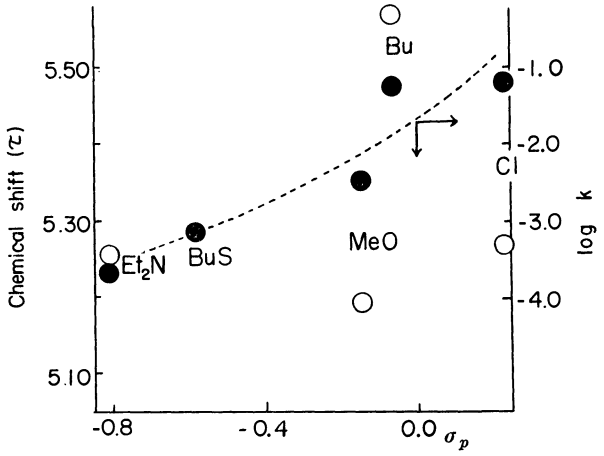

Fig. 12. Correlation among Hammett's σ_p, the chemical shift of methine proton in XZnDMM and reactivity.

of the decrease in the ring current, because of the electron-withdrawing nature of X, in the pseudo-aromatic system of the aluminum chelate compound. A linear relationship is observed between Hammett's substituent constants, $\sigma_{p,x}$ and the chemical shift of the methine proton in EtXAlDMM, as is shown in Figs. 11 and 12. It is assumed from the above data that the reactivity of the EtXAlDMM system is governed by the stability of the chelate ring. For instance, an electron-withdrawing substituent, Cl, attached to methine or aluminum, decreases the electron density (or ring current) of the chelate ring, meaning the loss of the aromaticity of the chelate ring. Therefore, the more diminished ring current (or the lower aromaticity) is closely related to the higher reactivity of EtXAlDMM.

In the case of XZnDMM, no linear relationship was observed; between $\sigma_{p,x}$ and the chemical shift of methine proton in XZnDMM this might be ascribed at least partly to the association of the zinc compound or to the intrinsic nature of the zinc atom. The correlation between the reactivity, log *k*, and the σ_p of XZnDMM was, however, found to be similar to that in EtXAlDMM.

On the other hand, an electron-donating substituent (*e. g.*, CH_3), attached to the active methylene group, was found to increase the reactivity of *n*-BuZn[$XC(CO_2Me)_2$], a situation which is in contrast with the substituent effect in $Et_2Al[XC(CO_2Me)_2]$. An electron-withdrawing substituent such as halogen in *n*-BuZn-[$XC(CO_2Me)_2$] also exerts an effect opposite to that in $Et_2Al[XC(CO_2Me)_2]$.

It seems not to be easy to draw a consistent interpretation of the reactivities of the chelate complexes of aluminum and of zinc. We are inclined to consider, however, that the opposite substituent effects can be understood if we assume two steps [(i) and (ii)] in determining the rate of the addition reaction of the chelate complexes to the unsaturated carbonyl compounds.

For instance,

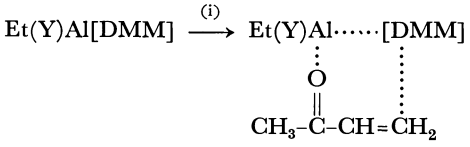

$$\xrightarrow{\text{(ii)}} \text{Et(Y)Al-O-}\overset{\overset{CH_3}{|}}{C}\text{=CH-CH}_2\text{-DMM}$$

The chelate ring is probably loosened (Step (i)) before the β-carbon atom of the unsaturated carbonyl compound is attacked by [DMM] at Step (ii). We have discussed the reactivity of $Et(Y)Al[C(X)(CO_2Me)_2]$ in terms of the stability of the chelate ring, which means the rate-determining step is probably Step (i).

In the light of the stability constants of metal acetylacetonates, according to Block *et al.*,[15-17] the chelate ring of the zinc alkyl complex system can be assumed to be much more unstable than the aluminum alkyl complex.

Table 14. Stability constants of metal acetylacetonates

Metal	Stability constant (log k)	Ion strength
Zn	9.11 (k_1)	75% dioxane[15]
	4.98 (k_1)	0[16]
	8.09 (k_2)	75% dioxane[15]
	3.83 (k_2)	0
Al	8.6 (k_1)	0[16]
	7.9 (k_2)	0[17]
	5.8 (k_3)	0[17]

Therefore, it is not unreasonable to deduce that the rate-determining step is Step (ii) with the zinc alkyl complex, the reactivity of which is governed, rather, by the reactivity of the active methylene component itself. For example, the chlorine substituent on the central carbon stabilized the [DMCM] anion, resulting in a decrease in the reactivity of the malonate anion. The methyl substituent has a reverse effect. It should be pointed out at this stage that the substituent effect in dimethyl malonato sodium in the Michael reaction[18] is in the same direction as with the zinc alkyl complex, a fact which is consistent with the above discussion, because the ability of chelate-ring formation should be extremely small in dimethyl malonato sodium in comparison with the case of the aluminum chelate.

5. *Vinyl Polymerization with Metal Alkyl - Active Methylene Chelate Compounds.* The possibility of polymerization was examined with several α,β-unsaturated carbonyl compounds by the use of the metal alkyl - active methylene chelate as the initiator, but high polymers were not formed in benzene at 30°C. When dimethyl sulfoxide or hexamethylphosphoric triamide was used as the solvent, MA was polymerized, as is shown in Table 15. When malononitrile was used instead of dimethyl malonate, the metal alkyl complex was also able to initiate the polymerization of MA. The anionic character of the polymerization was confirmed by the copolymerization method with styrene.

Table 15. Polymerization of α,β-unsaturated esters by the metal alkyl - active methylene chelate compound as catalyst

Monomer	Catalyst[a]	Solvent	Temp. (°C)	Time (day)	Yield (%)
MA	*n*-BuZnDMM	DMSO	20	4	5
MA	*n*-BuZnDMM	HMPA	20	4	10
MMA	*n*-BuZnDMM	HMPA	20	4	11
MCr	*n*-BuZnDMM	DMSO	20	4	0
MA	Et_2AlDMM	DMSO	20	4	0
MA	*i*-Bu_2Al·MN	Bz	20	1	20

a) 5 mol% to monomer.

The authors are grateful to Dr. Yasukazu Saito, the University of Tokyo, for his advice in the interpretation of the NMR data. The authors are also indebted to Dr. Tsuneo Hirano, this laboratory, for discussions referring to his own results on some organoaluminum chelate compounds.[19]

15) L. G. Van Vitert, W. C. Farnelius, and B. E. Douglas, *J. Amer. Chem. Soc.*, **75**, 457, 2736 (1953).
16) R. M. Izatt, C. G. Haas, Jr., B. P. Block, and W. C. Fernelius, *J. Phys. Chem.*, **58**, 1133 (1954).
17) R. M. Izatt, W. C. Fernelius, C. G. Haas, Jr., and B. P. Block, *ibid.*, **59**, 170 (1955).
18) A. Kishi, Y. Yasuda, and T. Tsuruta, unpublished data.
19) T. Hirano, H. Fukushima, M. Ikeda, and T. Tsuruta, unpublished data.

The Preparation of Fukinane, A New Skeletal Sesquiterpenic Hydrocarbon[1]

Keizo NAYA and Masakazu KOBAYASHI

Department of Chemistry, Faculty of Science, Kwansei Gakuin University, Uegahara, Nishinomiya, Hyogo

(Received August 12, 1970)

A novel skeletal sesquiterpenic hydrocarbon, fukinane (I), has been prepared by conversion from an eremophilane type, fukinone (VIII), *via* fukinan-8-ol (IX). A rearrangement of the fukinane skeleton into an eremophilane type through fukinan-8-ol tosylate (X) has been studied.

We have previously reported the isolation and stereochemistry of several new sesquiterpenoids with a fukinane (I) skeleton (fukinanolide (II),[2] fukinolide (III),[2] *S*-fukinolide (IV),[2] homofukinolide (V),[3] and dihydrofukinolide (VI))[3] from *Petasites japonicus* Maxim. The absolute configurations of these compounds were established by correlation with fukinone (VIII) through fukinan-8-ol (IX).[4] The absolute configuration of fukinone (VIII) had already been settled.[5]

Now we have an interest in preparing a new type of sesquiterpene hydrocarbon, fukinane (I); the present paper will report the results of the following three routes for synthesizing fukinane (I) from fukinan-8-ol (IX).

For the purpose of removing the oxygen function at C-8, we attempted the following three routes: (i) the reduction of fukinan-8-ol tosylate (X) with lithium aluminum hydride, (ii) the Wolff-Kishner reduction of fukinan-8-al semicarbazone (XVI), and (iii) the reduction of fukinan-8-al ethylene thioacetal (XVIII) with Raney nickel.

From Tosylate (X). Fukinan-8-ol (IX),[4] $C_{15}H_{28}O$, mp 38—39°C, was treated with three equivalents of tosyl chloride to give the tosylate (X) quantitatively. An attempt at the further purification of the tosylate (X) by chromatography on silica gel involved a Wagner-Meerwein-type rearrangement[6] to produce a mixture of hydrocarbons XI, XII and XIII. The glc pattern is illustrated in Fig. 2, while the relative ratio of the yield is shown in Table 1. The mixture reacted positively to a tetranitromethane-test and was exclusively converted to eremophilane (XIV) by hydrogenation with Adams' catalyst in acetic acid. Those facts suggest that the rearrangement proceeded stereoselectively, involving the migration of the C-9 methylene to the

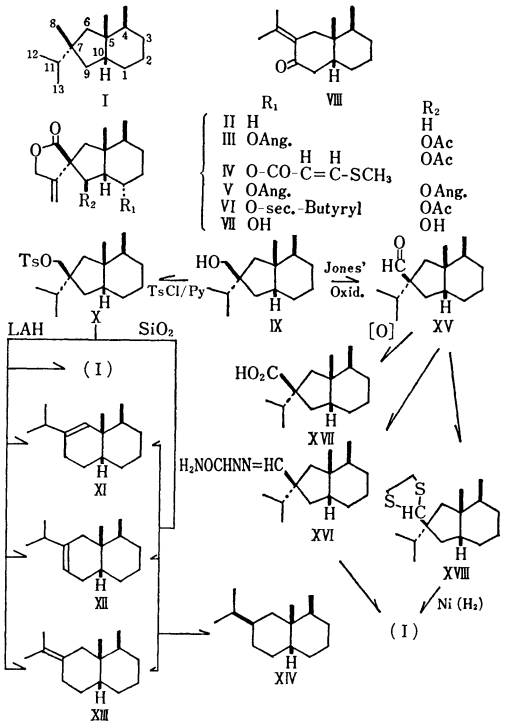

Fig. 1.

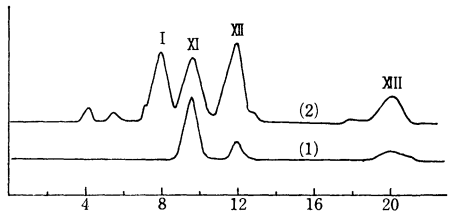

Fig. 2. Glc of hydrocarbons I, XI, XII, and XIII.
(1) Rearrangement of the tosylate (X) through SiO_2
(2) $LiAlH_4$ reduction of the tosylate (X)
(PEG 6000, 2.6 m. 170°C, H_2: 54.5 ml/min)

TABLE 1. RELATIVE RATIO OF HYDROCARBONS I, XI, XII, AND XIII

Run	Product			
	I	XI	XII	XIII
1	—	5	1.4	1
2	1.9	1.9	2.4	1

Run 1) Rearrangement of the tosylate (X) through SiO_2
Run 2) $LiAlH_4$ reduction of the tosylate (X)

1) This report is dedicated to Professor Munio Kotake for his 75th birthday, "Kiju".

2) K. Naya, I. Takagi, M. Hayashi, S. Nakamura, and M. Kobayashi, 11th Symposium on the Chemistry of Natural products, Symposium Papers (1967), p. 88; N. Abe, R. Onoda, K. Shirahara, T. Kato, M. C. Woods, and Y. Kitahara, *ibid.*, p. 96; N. Abe, R. Onoda, K. Shirahara, T. Kato, M. C. Woods, and Y. Kitahara, 11th Symposium on the Chemistry of Terpenes, Essential Oils and Aromatics, Symposium Papers (1967), p. 147; K. Naya, I. Takagi, M. Hayashi, S. Nakamura, M. Kobayashi, and S. Katsumura, *Chem. Ind.* (London), **1968**, 318.

3) M. Hayashi, S. Katsumura, I. Takagi, and K. Naya, 18th Annual Meeting of Chemical Society of Japan (1968), Collective Papers, Vol. 3, p. 2152.

4) K. Naya and M. Kobayashi, *ibid.*, p. 1836.

5) K. Naya, I. Takagi, Y. Kawaguchi, Y. Asada, N. Shinoda, and Y. Hirose, *Tetrahedron*, **24**, 5871 (1968).

6) W. G. Dauben and J. B. Rogan, *J. Amer. Chem. Soc.*, **79**, 5002 (1957).

electron-deficient C-8, but not to the C-6. Each hydrocarbon was isolated by preparative glc. The structures of the hydrocarbons XI, XII, and XIII, were determined as will be described below.

The NMR spectrum[7] of the compound XI shows a singlet at 5.03, suggesting a C=CH–C– grouping. The structure was settled as in formula XI from the MS fragmentation shown in Fig. 3.

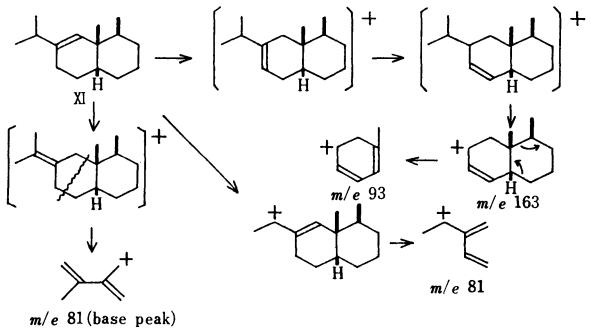

Fig. 3. Mass fragmentation of hydrocarbon XI.

The NMR spectrum of the compound XII shows a multiplet signal centered at 5.24 which was presumed to be the result of the long-range coupling between the vinyl proton at C-8 and the protons at C-6 and C-11. In the MS spectrum, the base peak at *m/e* 110 was derived from a retro-Diels-Alder rupture of the molecular ion. The structure was, then, represented by the stereoformula XII, based on the MS fragmentation, shown in Fig. 4.[8]

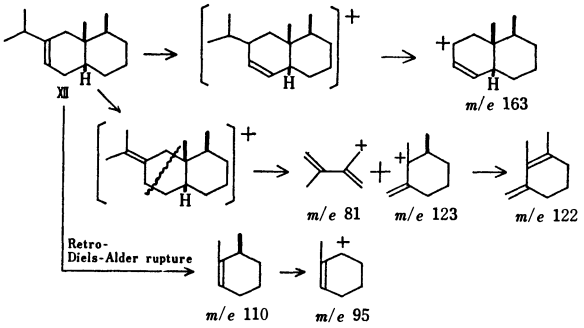

Fig. 4. Mass fragmentation of hydrocarbon XII.

The hydrocarbon XIII shows a singlet at 1.62 (6H) due to an isopropylidene group in its NMR spectrum. The structure XIII was established with the aid of the MS fragmentation shown in Fig. 5.[8]

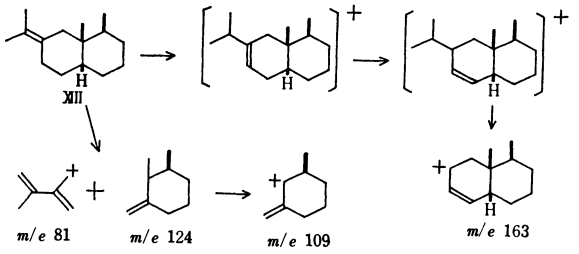

Fig. 5. Mass fragmentation of hydrocarbon XIII.

7) All NMR spectra were taken in CCl_4 on a JEOL C-60 spectrometer, otherwise mentioned, with TMS as an internal reference. The values are reported in ppm.

8) H. Budzikiewics, C. Djerassi, and D. H. Williams, "Mass Spectrometry of Organic Compounds," Holden-Day Inc., San Francisco (1967), p. 71.

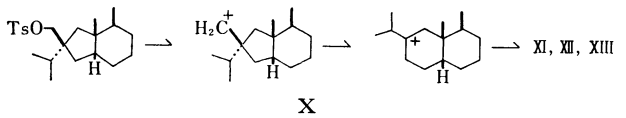

X

Fig. 6. The scheme of rearrangement of the tosylate (X).

The rearrangement should occur by means of the scheme shown in Fig. 6.

Because the tosylate (X) yielded predominantly migration products with an eremophilane sekeleton when submitted to chromatography over silica gel, the tosylate (X) was submitted to lithium aluminum hydride reduction without further purification. The glc pattern of the hydrocarbons obtained by the reduction is shown in Fig. 2. The products proved to include mainly the migration hydrocarbons, plus a small amount of fukinane (I).

From Fukinan-8-al Semicarbazone (XVI). Fukinan-8-al (XV) was obtained in a comparatively good yield by Jones' oxidation[9] under controlled conditions. The product XV was appreciably air-oxidized to the carboxylic acid (XVII), mp 125.5—126.0°C, by leaving it overnight in the air at room temperature, or by preparative tlc. The crude aldehyde (XV) was, therefore, quickly transformed to the semicarbazone (XVI). The product XVI was submitted to Wolff-Kishner reduction to afford fukinane (I) (10% yield; 3.7% overall yield from fukinan-8-ol). We turned to an alternate approach to produce fukinane (I) in a good yield.

From Fukinan-8-al Ethylene Thioacetal (XVIII). The third route involved the reduction of the ethylene thioacetal of fukinan-8-al (XVIII). The condensation of fukinan-8-al (XV) with ethanedithiol afforded the ethylene thioacetal (XVIII) in a 70.2% yield. Its reduction with Raney nickel proceeded readily to give fukinane (I) (yield, 79%), which was identical with the sample prepared by the other routes described

Table 2. Physical properties of fukinane (I)

n_D^{17}	n_D^{20}	$n_D^{24.5}$	d_4^{20}	$[\alpha]_D^{23a)}$
1.4761	1.4750	1.4734	0.89077	+41.8°

a) (*c*, 1.42, CCl_4)

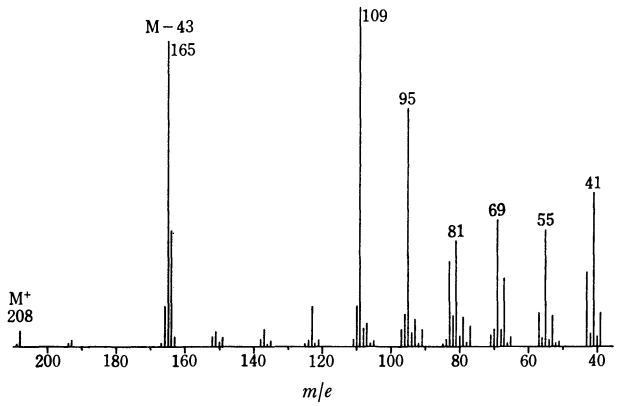

Fig. 7. Mass spectrum of fukinane (I).

9) K. Bowden, I. M. Heilbron, E. R. H. Jones, and B. C. L. Weedon, *J. Chem. Soc.*, **1946**, 39.

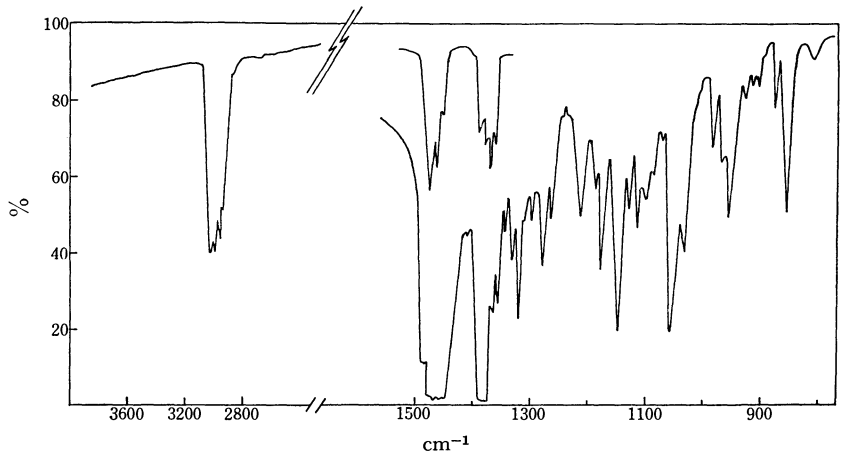

Fig. 8. IR spectrum of fukinane (I).

above. The physical properties of fukinane (I) are listed in Table 2. The MS spectrum is shown in Fig. 7, and the IR spectrum, in Fig. 8.

Experimental

All the melting points are uncorrected. The MS spectra were measured with a Hitachi RMU-6 MS spectrometer: ion-source temperature 250°C; evaporation temperature, 150°C. The IR spectra were recorded with a JASCO DS-402G spectrophotometer, and the optical rotations were measured with a Hitachi EPU-2A spectrophotometer. Glc was carried out using a Shimadzu GC-1C apparatus on a stainless steel column (ϕ=3 mm).

Fukinan-8-ol (IX)[4] was prepared from fukinolidol (VII),[2] which had been derived by alkaline hydrolysis from fukinolide (III),[2] *S*-fukinolide (IV),[2] homofukinolide (V),[3] and dihydrofukinolide (VI),[3] and also from fukinanolide (II)[2] and fukinone (VIII).[5]

Tosylate of Fukinan-8-ol (IX). To a solution of fukinan-8-ol (IX) (346 mg, 1.54 mmol) in dry pyridine (6.8 m*l*), was added tosyl chloride (909 mg, 4.8 mmol); the reaction mixture was then left at room temperature for 19 hr. Subsequent working up in the usual manner yielded the tosylate (X) (560 mg, yield 95.2%); almost one spot by tlc analysis with R_f=0.35 (light petroleum: benzene=3 : 1). IR (film): 1600, 1379, 1190, 1100, 960, 845, 820 cm^{-1} (characteristic of a tosylate).

Rearrangement of Tosylate (X) by Silica Gel. Fukinan-8-ol tosylate (X) (1.21 g, 3.45 mmol) was chromatographed on silica gel (30 g). The light petroleum-benzene (5 : 1) eluates were combined to give a mixture of the hydrocarbons XI, XII, and XIII (457 mg, 70%). Their pure specimens were furnished by preparative glc (PEG-20M on Celite 545; 2.6 m; H_2 37 m*l*/min; column temperature, 160°C).

Compound XI, $[\alpha]_D^{23}$ +23.1° (*c*, 0.91, CCl_4); n_D^{15} 1.4901; NMR: 0.78 (d, 3H, J=6 Hz), 0.86 (s, 3H), 1.02 ppm (d, 6H, J=6.6 Hz); MS: M$^+$ *m/e* 206, base peak *m/e* 81.

Found: C, 87.41; H, 12.54%. Calcd for $C_{15}H_{26}$: C, 87.30; H, 12.70%.

Compound XII, $[\alpha]_D^{23}$ −16.4° (*c*, 1.70, CCl_4); $n_D^{15.5}$ 1.4919; NMR: 0.85 (s, 3H), 0.89 (d, 3H, J=4.5 Hz), 0.98 (d, 6H, J=6.6 Hz), 5.24 ppm (br. s, 1H); MS: M$^+$ *m/e* 206, base peak *m/e* 110.

Compound XIII, $n_D^{15.5}$ 1.5060; NMR: 0.78 (d, 3H, J=6 Hz), 0.85 (s, 3H), 1.62 ppm (s, 6H); MS: M$^+$ *m/e* 206, base peak *m/e* 81.

Catalytic Reduction of the Hydrocarbons XI, XII, and XIII. A mixture of the hydrocarbons XI, XII, and XIII (99.4 mg) was hydrogenated in glacial acetic acid (3 m*l*) with Adams' catalyst (22 mg) at room temperature and at atmospheric pressure. After the hydrogen uptake had ceased, the catalyst was filtered. The filtrate was diluted with aqueous sodium hydrogen carbonate, and the product was extracted with benzene. The evaporation of the solvent *in vacuo* then gave a hydrocarbon (88 mg) which was found to be identical with eremophilane (XIV) in glc analysis; retention time, 6.1 min; PEG-6000 on Celite 545 (2.5 m, 60—80 mesh); carrier gas, H_2, flow rate, 120 m*l*/min; column temperature, 160°C.

Lithium Aluminum Hydride Reduction of Tosylate (X). To a stirred and refluxed mixture of lithium aluminum hydride (147 mg, 3.87 mmol) in absolute ether (10 m*l*), a solution of the tosylate (X) (289 mg, 0.76 mmol) in absolute ether (7 m*l*) was added, drop by drop over a 45 min period. The mixture was then maintained at that temperature for an additional 7 hr. After being cooled to room temperature, the reaction mixture was treated with moist ether and aqueous 10% hydrochloric acid, and then washed thoroughly with water. The ethereal extract was dried over anhydrous sodium sulfate. The evaporation of the solvent gave an oily residue (163 mg), which was then chromatographed over silica gel (7 g). Elution with light petroleum afforded a mixture of hydrocarbons (30 mg, 19%), which was proved by glc analysis to be a mixture of fukinane I, XI, XII, and XIII. Further elution with benzene-ethyl acetate (40 : 1) afforded fukinan-8-ol (IX) (104 mg; yield, 60%).

Semicarbazone of Fukinan-8-al (XV). Into a solution of fukinan-8-ol (IX) (334 mg, 1.5 mmol) in acetone (7.6 m*l*), 0.57 m*l* of Jones' reagent (containing 157 mg of chromium trioxide) was stirred in a single portion at −16°C. The mixture was kept for 30 min, methanol (4 m*l*) was added, and the solvent was removed under reduced pressure. The residue was then extracted with ether, and the ethereal extract was washed with aqueous sodium hydrogen carbonate and then with water. The ethereal solution was dried over anhydrous sodium sulfate, after which the solvent was evaporated to give a crude aldehyde, fukinan-8-al (XV); positive to tetrazolium test; IR (film): 1720 cm^{-1}. The residual oil was treated in ethanol (2 m*l*) with semicarbazide hydrochloride (400 mg) and freshly-fused sodium acetate (60 mg) as soon as possible. The reaction mixture was then left at room temperature for 16 hr to afford crystalline semicarbazone

(XVI) (208 mg, 49%); mp 189—190°C (decomp.). Recrystallization from aqueous methanol gave a pure semicarbazone; mp 206.0—206.5°C (decomp.); $[\alpha]_D^{23}$ +19.1° (*c*, 1.1, $CHCl_3$); IR (KBr disk): 3500, 3300 (sh), 3240, 3180, 1695, 1625 (sh), 1580, 1565 (sh), 1143, 1045, 1008, 948, 772 cm^{-1}; NMR:[10] 0.79 (d, 3H, J=6.1 Hz), 0.89 (d, 6H, J=6.0 Hz), 0.89 (s, 3H), 5.53 (br. s, 2H, $-CO-NH_2$), 7.01 (s, 1H, -CO-NH-N=), 8.96 ppm (s, 1H, -N=CH).

Found: C, 68.92; H, 10.42; N, 15.39%. Calcd for $C_{16}H_{29}N_3O$: C, 68.77; H, 10.46; N, 15.04%.

Wolff-Kishner Reduction of Semicarbazone (XVI). The semicarbazone (XVI) (325 mg, 1.17 mmol) and powdered potassium hydroxide (233 mg, 4.2 mmol) were heated under reflux for 9 min to give a brownish-yellow syrup. After being cooled, the reaction mixture was diluted with water and extracted with ether. Then the solvent was removed. The IR spectrum of the residue (219 mg) showed an absorption band at 1640 cm^{-1}, presumably due to the C=N group. The residual oil was heated under reflux again with potassium hydroxide (197 mg, 3.5 mmol). After the evolution of the gas had subsided, the solution was diluted with water and extracted with ether, and the ethereal solution was dried over anhydrous sodium sulfate. The evaporation of the solvent gave a crude oil (188 mg), which was then chromatographed on preparative tlc to give fukinane (I) (24 mg, 10%; total yield from IX, 4.9%).

Ethylene Thioacetal of Fukinan-8-al (XV). Fukinan-8-ol (IX) (574 mg, 2.6 mmol) was treated with 1.3 m*l* of Jones' reagent (containing 364 mg of chromium trioxide) at −13°C for 7 min to give a crude aldehyde (XV). After being dried throughly by azeotropic evaporation with dry benzene, the aldehyde (XV) was dissolved in ethanedithiol (1 m*l*) and to this a catalytic amount of BF_3-etherate was added. The reaction mixture was then left at room temperature for 1.5 hr. Methanol (2 m*l*) was added, and the mixture was diluted with 5% aqueous potassium hydroxide, extracted with ether, washed with water and dried over anhydrous sodium sulfate. The evaporation of the solvent gave an oil (1.24 g), which was chromatographed over silica gel (10 g) and eluted with light petroleum to afford fukinan-8-al ethylene thioacetal (XVIII) (536 mg, yield, 70.2%); $[\alpha]_D^{23}$ +22.5° (*c*, 1.1, CCl_4); $n_D^{18.5}$ 1.5544; IR (film): 1392, 1386, 1376, 1315, 1280, 1185, 1165, 1125, 1107, 1023, 944, 860, 840, 783 cm^{-1}; NMR; 0.78 (d, 3H, J=6 Hz), 0.92 (s, 3H), 0.99 (d, 6H, J=6.9 Hz), 3.11 (fine splitting, s, 4H, $-S-CH_2-CH_2-S-$), 4.81 ppm (s, 1H, -S-CH-S-); glc: retention time, 9 min; Thermol-3 (1.1 m) on Shimalite (60—80 mesh); carrier gas, H_2; flow rate, 200 m*l*/min; column temperature, 170°C.

Found: C, 68.72; H, 10.13: S, 21.30%. Calcd for $C_{17}H_{30}S_2$: C, 68.39; H, 10.13; S, 21.48%.

Raney Nickel Reduction of Ethylene Thioacetal (XVIII). A solution of the ethylene thioacetal (XVIII) (534 mg, 1.8 mmol) in ethyl acetate (3 m*l*) was stirred drop by drop into a suspension of Raney nickel (10 g) in ethyl acetate (10 m*l*) over a 12-min period. The reaction mixture was then refluxed for an additional hour, and subsequently filtered. The filtrate was evaporated *in vacuo* to give fukinane (I) (303 mg, 79%); single peak by glc analysis; retention time, 4.1 min; PEG-20M (2.6 m) on Celite 545 (60—80 mesh); carrier gas, H_2; flow rate, 37.3 m*l*/min; column temperature, 168°C. The pure specimen was obtained by preparative glc. MS: M^+ *m/e* 208, base peak *m/e* 109; NMR; 0.70—0.91 (15H, five methyls).

Found: C, 86.90; H, 13.26%. Calcd for $C_{15}H_{28}$: C, 86.46; H, 13.54%. The physical properties are listed in Table 2. The MS spectrum is shown in Fig. 7, and the IR spectrum, in Fig. 8.

The authors wish to thank the Shionogi Research Laboratory, Shionogi & Co., Ltd., for the microanalysis and the Institute of Food Chemistry for the measurements of the MS and NMR spectra.

10) This spectrum was taken in $CDCl_3$ on H-6013 (Hitachi) spectrometer.

Effects of *para*-Substituents on the Rates of Inversion of Biphenyl Derivatives. I. 5,7-Dihydrodibenzo[*c*,*e*]thiepins

Michinori Ōki, Hiizu Iwamura, and Gaku Yamamoto

Department of Chemistry, Faculty of Science, The University of Tokyo, Bunkyo-ku, Tokyo

(Received August 22, 1970)

Several 3,9-disubstituted 5,7-dihydrodibenzo[*c*,*e*]thiepins were synthesized and temperature dependence of their NMR spectra was examined. All the substituted derivatives showed a lower energy barrier to inversion than the unsubstituted one. The effects of the substituents on the energy barrier may be interpreted in terms of resonance stabilization and/or out-of-plane bending of the axis bond at the transition state.

Many earlier works have revealed that the major part of the origin of energy barrier to inversion in biphenyl derivatives is the steric strain at the transition state due to non-bonded interactions between atoms or groups at the *ortho* positions.[1] Westheimer and his coworkers[2] successfully calculated the enthalpy of activation for racemization of 2,2′-dibromobiphenyl and 2,2′-diiodobiphenyl, assuming a planar transition state with deformation within the plane only and completely neglecting electronic factors.

In contrast, the influence of electronic factors on the energy barrier has been left unclarified. The gain in resonance energy in the transition state may contribute in lowering the activation energy, but Westheimer's success in calculation can be taken as suggesting the existence of some compensating factors.

Although the assumption that the transition state is coaxial and coplanar has generally been accepted, some authors[3,4] suggested that bending of the axis bond out of plane of the benzene ring may decrease the non-bonded interactions and that the energy barrier to inversion is affected by the relative ease of the bending. Harris and Cheung King Ling[4] studied the racemization rates of optically active 4,4′-symmetrically substituted 2,2′-diiodobiphenyls and found that the energy barrier to inversion is considerably affected by the *para* substituents. They have claimed that in the transition state the two benzene rings are neither coaxial nor coplanar, but distorted out of the plane to each other, and the *para* substituents affect the ease of bending of the axis bond and thus the energy barrier. They also suggested that in this system *ortho* substituents are so bulky that even at the ground state it has a distorted non-coaxial conformation. It is then considered that with the extreme bulkiness of the *ortho* groups the biphenyl system experiences the distorted transition state.

From the above discussion, it will be interesting to known whether the out-of-plane bending of the axis bond is operating or not in biphenyl systems with less bulky *ortho* substituents. Such systems necessarily possess very low optical stability and polarimetric study may become impossible.

However, with dynamic NMR technique it is possible to obtain information on intramolecular motions with a specific rate of 1 to 10^3 sec^{-1}.[5] Energy barrier to inversion in several biphenyl systems has been studied by applying NMR technique.[6–10] Kurland and his coworkers[6] reported the temperature dependent NMR spectra of 5,7-dihydrodibenzo[*c*,*e*]thiepin (I). Methylene protons of I showed an AB quartet signal at low temperature, which coalesced at 43°C into a singlet. This change of spectra was correlated with the rate of inversion. The free energy of activation was calculated to be 16.1 kcal/mol with the entropy of activation less than 2 eu. This system seemed to be suitable for the present purpose because of synthetic ease and convenience in measurement and analysis of the NMR spectra.

Thus five 3,9-disubstituted derivatives of I (II—VI) were synthesized and their NMR spectra were measured over a wide range of temperature to find out the effects of substituents on the energy barrier to inversion.

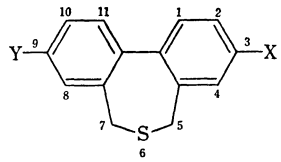

I: X=Y=H
II: X=OCH_3, Y=NO_2
III: X=Y=OCH_3
IV: X=Y=F
V: X=Y=Br
VI: X=Y=CO_2CH_3

Results

Compounds II—VI were synthesized by benzylic bromination of 4,4′-substituted *o*,*o*′-bitolyl followed by ring closure with sodium sulfide (Scheme).

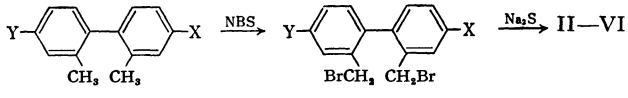

1) R. Adams and H. C. Yuan, *Chem. Rev.*, **12**, 261 (1933).
2) F. H. Westheimer, "Steric Effects in Organic Chemistry," ed. by M. S. Newman, Wiley, New York, N. Y. (1956), pp. 542—555.
3) G. Baddeley, *Nature*, **157**, 694 (1946).
4) M. M. Harris and C. Cheung King Ling *J. Chem. Soc.*, **1964**, 1825.
5) G. Binsch, "Topics in Stereochemistry," Vol. 3, ed. by E. L. Eliel and N. L. Allinger, Interscience Publishers, New York, London, Sydney (1968), p. 97.
6) R. J. Kurland, M. B. Rubin, and W. B. Wise, *J. Chem. Phys.*, **40**, 2426 (1964).
7) W. L. Meyer and R. B. Meyer, *J. Amer. Chem. Soc.*, **85**, 2170 (1963).
8) M. Ōki, H. Iwamura, and N. Hayakawa, This Bulletin, **37**, 1865 (1964).
9) I. O. Sutherland and M. V. J. Ramsay, *Tetrahedron*, **21**, 3401 (1965).
10) M. Ōki and H. Iwamura, *ibid.*, **24**, 2377 (1967).

Table 1. NMR Spectral parameters of 5,7-dihydrodibenzo[*c*,*e*]thiepins

Compound	Solvent	Frequency (MHz)	T_c (°C)	δ_{AB} (Hz)	J_{AB} (Hz)	Ref
I	CS_2	60	43±1	13.1	12.4	6)
	$CDCl_3$	60	45	12.7	12.6	9)
II	$CHCl_2CHCl_2$	100	20±5	10.0[b]	13.5[b]	a)
				13.0[c]	12.7[c]	a)
III	$CHCl_2CHCl_2$	60	24±2	15.6	12.6	a)
IV	$CHCl_2CHCl_2$	60	38±2	10.3	12.9	a)

a) The present work.
b) Represents the quartet at higher field.
c) Represents the quartet at lower field.

Table 2. Kinetic parameters of the inversion of 5,7-dihydrodibenzo[*c*,*e*]thiepins

Compound	Solvent	$\Delta G_c^{\ddagger}$ (kcal/mol)	$\Delta H^{\ddagger}$ (kcal/mol)	$\Delta S^{\ddagger}$ (eu)	Ref
I	CS_2	16.1±0.3		<2	6)
	$CDCl_3$	16.0			9)
II	$CHCl_2CHCl_2$	14.6±0.3	13.6±1.0	−3±4	a)
III	$CHCl_2CHCl_2$	15.2±0.3	13.1±1.0	−7±4	a)
IV	$CHCl_2CHCl_2$	16.1±0.3	16.0±0.5	0±2	a)

a) The present work.

In NMR spectra, the protons of each methylene group of compounds II, III and IV showed an AB quartet signal at low temperature due to the non-equivalence of protons, indicating slow inversion. The quartet signal coalesced into a single broad line at about room temperature, then gradually sharpened with increasing temperature. The obtained spectral parameters are summarized in Table 1. For compound II, two AB quartets due to 5- and 7-methylenes overlapped each other, and this made the determination of the coalescence temperature (T_c) somewhat inaccurate.[11]

The inversion rate k_c at T_c was calculated using the equation[10]

$$k_c = \frac{\pi}{\sqrt{2}}(\delta_{AB}^2 + 6J_{AB}^2)^{1/2} \quad (1)$$

From the line width W of the coalesced singlet, the approximate inversion rate k at various temperatures could be obtained by means of

$$k = \frac{\pi\delta_{AB}^2}{2(W - W_0)} \quad (2)$$

where W_0 is the extrapolated line width for $k=\infty$. Arrhenius plots gave parameters E_a and $\log A$. Eyring parameters, $\Delta G^{\ddagger}$, $\Delta H^{\ddagger}$ and $\Delta S^{\ddagger}$ could be derived from the following equations.

$$\Delta G^{\ddagger} = -RT\ln\frac{hk}{k_B T} \quad (3)$$

$$\Delta H^{\ddagger} = E_a - RT \quad (4)$$

$$\Delta S^{\ddagger} = \frac{\Delta H^{\ddagger} - \Delta G^{\ddagger}}{T} \quad (5)$$

The results are summarized in Table 2.

The methylene protons of V and VI were observed as a singlet down to the lowest attainable temperature (−50°C). Slight broadening was observed with lowering temperature. This seems to be due to the increased viscosity of the sample solution, because reference signals also showed broadening. Although this might be interpreted in terms of rapid inversion down to the lowest temperature, it is unreasonable to think that substitution at *para* positions caused such a large lowering of coalescence temperature. An alternative and more probable interpretation is that the lack of splitting is due to accidental magnetic equivalence of the methylene protons although the inversion is slow on the NMR time scale. Several examples have been reported in which diastereotopic protons show magnetic equivalence. Sometimes aromatic solvents give rise to magnetic non-equivalence of the protons which are equivalent in non-aromatic solvents such as chloroform and carbon tetrachloride. However, attempts to measure the NMR spectra of V and VI in pyridine and *o*-dichlorobenzene failed because of the low solubility of the samples in these solvents.

Discussion

The lack of full line shape analysis of the NMR spectra of these compounds and the essential tendency of the data of enthalpy and entropy of activation to include rather large systematic errors as pointed out by Gutowsky[12] prevent a direct comparison of the $\Delta H^{\ddagger}$ values obtained and the delicate quantitative discussions about the transition state of inversion. Qualitatively, however, we might conclude from these data (Table 2) that the barrier to inversion decreases in the order I≈IV>III≥II.

11) Theoretically two T_c's corresponding to the two kinds of methylene should exist, but could not be detected separately.

12) A. Allerhand, H. S. Gutowsky, J. Jones, and R. A. Meinzer, *J. Amer. Chem. Soc.*, **88**, 3185 (1966).

Fluorine atom is known to exert no large electronic effect on the *para* position, and it may be reasonable for compounds I and IV to have nearly the same value of activation parameters.

Several factors can be considered by which the substituents at *para* positions influence the energy barrier to inversion in this system. It may be reasonably assumed that the effects of the substituents on the ground state energy of this system are negligible, and only those on the transition state energy should be considered.

In 3,9-unsymmetrically substituted derivatives such as II with an electron-withdrawing group at one *para* position and an electron-releasing group at the other, resonance stabilization as represented by the canonical structure VII should contribute in lowering the energy level of the transition state. A farily large decrease in ΔH^* value of II agrees with this prediction.

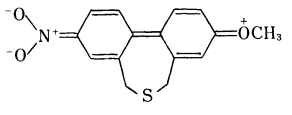

VII

It has been suggested[13] that the large contribution of VII in the resonance hybrid would increase the double bond character of the axis bond, causing a shortening of the bond which would result in the increase of the nonbonded interaction. That is, the energy barrier would be heightened in contrast to the effect of the resonance stabilization. The present data show that the effect of bond shortening is rather unimportant. Here, the two benzene rings may be considered to be coaxial and coplanar at the transition state and the release of steric strain by the out-of-plane bending of the axis bond is much less important.

In 3,9-symmetrically substituted derivatives (III—VI), large resonance stabilization as observed in II can not be expected. Ultraviolet spectroscopic studies of 4,4′-disubstituted biphenyls[14] showed that all the substituents, irrespective of their nature, increase conjugation between the two rings to some extent. If such conjugation really contributes to stabilize the transition state for inversion, all the derivatives III—VI should have lower barriers than unsubstituted I.

In the coaxial and copolanar transition state (VIII), nonbonded interactions involving internal strains of the seven-membered ring would be the greatest, causing the barrier to inversion. These interactions would be considerably released if the axis bond could be bent out of the plane of the benzene rings as schematically shown in IX. The higher the π-electron density at the 1,1′-positions of the biphenyl skeleton, the easier will be the bending motion of the axis bond.[15]

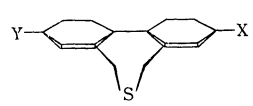

VIII

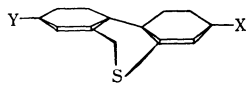

IX

Derivative III, with methoxyl groups at 3- and 9-positions, shows a lower barrier to inversion than I, which can be explained by either of two factors. On one hand, the methoxyl group will lower the energy barrier because of the contribution of resonance structure through the two benzene rings. On the other hand, the same group will make it easy to take the transition state IX because of electron-releasing tendency.

The lack of data on the effect of electron-withdrawing substituents prevents us from determiniing which of these factors is more important. Considerable drop in ΔH^* value in III relative to I does not seem to be explained only in terms of resonance stabilization, and the out-of-plane bending is likely to contribute in lowering the barrier of III.

Further study is necessary for a definite conclusion on the ratio of contribution of these factors, but we may tentatively conclude as follows. In the case of compounds in which a strong resonance interaction is expected, the planar transition state is important, whereas in the case in which no strong resonance interaction is expected, both the planar and bent transition state must be considered.

Experimental

Spectra. The NMR spectra of II were obtained on a JNM 4H-100 spectrometer operating at 100 MHz, and those of III and IV on a JNM C-60H spectrometer at 60 MHz. Temperatures were read with methanol or ethylene glycol sample and are accurate to ± 2°C. Approximately 10% (w/w) solutions in 1,1,2,2-tetrachloroethane were employed.

Materials.[19] *4-Methoxy-4′-nitro-2,2′-bitolyl*: 2-Bromo-5-nitrotoluene[18] (43 g, 0.2 mol) and 2-iodo-5-methoxytoluene[17] (50 g, 0.2 mol) were heated with copper bronze (100 g) at 220—230°C over a period of 5 hr. The reaction mixture was extracted with acetone and distilled *in vacuo*. Repeated recrystallization of the fraction boiling at 158—163°C/1 mmHg from methanol gave yellowish white crystals; yield 3.2 g (6%), mp 91—92°C.

Found: C, 70.35; H, 5.88; N, 5.44%. Calcd for $C_{15}H_{15}O_3N$: C, 70.02; H, 5.88; N, 5.44%.

4,4′-Difluoro-2,2′-bitolyl: *m*-Tolidine hydrochloride (114 g, 0.4 mol), prepared according to Wenner's method[20] was suspended in 20% hydrochloric acid (400 m*l*) and tetrazotized with aqueous solution of sodium nitrite (61 g, 0.88 mol). The reaction mixture was filtered and treated with a saturated aqueous solution of sodium fluoroborate. The tetrazonium fluoroborate was filtered, washed with saturated solution of sodium fluoroborate and cold water, dried in a vacuum desiccator, pyrolyzed and distilled with steam. Yellow oil boiling at 100—102°C/1.2 mmHg was obtained, which crystallized on cooling; yield 25 g (29%), mp 25—26°C (from methanol).

13) M. Calvin, *J. Org. Chem.*, **4**, 256 (1939).
14) B. Williamson and W. H. Rodebush, *J. Amer. Chem. Soc.*, **63**, 3018 (1941).
15) The correlation of the electron density and the ease of the out-of-plane bending has been observed. In IR spectra, the absorption due to out-of-plane bending of C–H bonds of monosubstituted benzenes appears in 750 cm^{-1} region and electron-withdrawing groups shift the absorption to higher wave number. These phenomena were interpreted in terms of "orbital following".[16]
16) R. D. Kross, V. A. Fassel, and M. Margoshes, *J. Amer. Chem. Soc.*, **78**, 1332 (1956).
17) All the melting points are uncorrected.
18) C. S. Gibson and J. D. A. Johnson, *J. Chem. Soc.*, **1929**, 1229.
19) T. Sato and M. Ōki, This Bulletin, **30**, 857 (1957).
20) W. Wenner, *J. Org. Chem.*, **17**, 523 (1952).

Found: C, 76.87; H, 5.56%. Calcd for $C_{14}H_{12}F_2$: C, 77.04; H, 5.54%.

4,4'-Dibromo-2,2'-bitolyl: Tetrazotization of *m*-tolidine hydrochloride (71 g, 0.25 mol) with 48% hydrobromic acid (350 m*l*) and sodium nitrite (39 g) followed by decomposition with copper bronze (5 g) gave an oil boiling at 170—175°C/3 mmHg. Recrystallization of the distillate from acetone - methanol (1 : 1) afforded white crystals; yield 11 g (13%), mp 57—58°C.

Found: C, 49.50; H, 3.47%. Calcd for $C_{14}H_{12}Br_2$: C, 49.45; H, 3.56%.

Dimethyl 2,2'-Bitolyl-4,4'-dicarboxylate: 4,4'-Dicyano-2,2'-bitolyl, propared according to the method of Theilacker[21] was hydrolyzed with alkali. The crude carboxylic acid was suspended in ether and treated with the ether solution of diazomethane. The solvent and excess diazomethane were evaporated and the residue was recrystallized from methanol affording white crystals, mp 98—99°C.

Found: C, 72.61; H, 6.07%. Calcd for $C_{18}H_{18}O_4$: C, 72.47; H, 6.08%.

2,2'-Bisbromomethyl-4-methoxy-4'-nitrobiphenyl: 4-Methoxy-4'-nitro-2,2'-bitolyl (5.1 g, 0.02 mol), *N*-bromosuccinimide (7.1 g, 0.04 mol) and benzoyl peroxide (0.2 g) were heated under reflux in carbon tetrachloride (150 m*l*) for 2.5 hr. Succinimide was filtered off and the filtrate was evaporated. Chromatography of the residual oil on alumina gave the desired compound by elution with petroleum ether - benzene (1 : 1); mp 115—116°C (from acetone - methanol (1 : 1)).

Found: C, 43.02; H, 3.22; N, 3.36%. Calcd for $C_{15}H_{13}O_3NBr_2$: C, 43.40; H, 3.16; N, 3.38%.

Elution of the column with benzene gave yellow crystals melting at 148—150°C, which were identified as 3-methoxy-9-nitro-5,7-dihydrodibenz[*c,e*]oxepin. The oxepin was inferred to be formed by the reaction of the dibromide with a trace of water existing in the column under the catalysis of alumina.

Found: C, 66.16; H, 4.97; N, 5.49%. Calcd for $C_{15}H_{13}O_4N$: C, 66.41; H, 4.83; N, 5.16%.

3-Methoxy-9-nitro-5,7-dihydrodibenzo[c,e]*thiepin (II)*: 2,2'-Bisbromomethyl-4-methoxy-4'-nitrobiphenyl (2.1 g, 0.005 mol) and sodium sulfide nonahydrate (1.4 g, 0.0055 mol) in methanol (300 m*l*) were heated under reflux for 10 hr. A major portion of the solvent was evaporated. The residue was poured into water and extracted with benzene. The combined extracts were dried with anhydrous sodium sulfate, evaporated and chromatographed on an alumina column. The eluate with petroleum ether - benzene (1 : 1) gave pale yellow crystals; mp 140—141°C (from methanol).

Found: C, 62.28; H, 4.72; N, 4.98%. Calcd for $C_{15}H_{13}O_3NS$: C, 62.70; H, 4.56; N, 4.88%.

3,9-Dimethoxy-5,7-dihydrodibenzo[c,e]*thiepin (III)*: 4,4'-Dimethoxy-2,2'-bitolyl[22] (9.7 g, 0.04 mol), *N*-bromosuccinimide (16.0 g, 0.09 mol) and benzyol peroxide (0.2 g) in carbon tetrachloride (200 m*l*) were heated under reflux for 2 hr. Filtration of succinimide and evaporation of the solvent gave an oily residue, which without purification was heated with sodium sulfide nonahydrate (10 g) in methanol for 8 hr. The product was recrystallized from acetone to afford white crystals, mp 141—142°C.

Found: C, 70.20; H, 6.38%. Calcd for $C_{16}H_{16}O_2S$: C, 70.55; H, 5.92%.

3,9-Difluoro-5,7-dihydrodibenzo[c,e]*thiepin (IV)*: 4,4'-Difluoro-2,2'-bitolyl was similarly treated with *N*-bromosuccinimide to give the dibromide which boiled at 155—156°C/1 mmHg and was heated with sodium sulfide. The product was distilled at 134—135°C/1.5 mmHg and recrystallized from methanol, affording colorless crystals melting at 88—89°C.

Found: C, 67.82; H, 4.13%. Calcd for $C_{14}H_{10}F_2S$: C, 67.72; H, 4.06%.

3,9-Dibromo-5,7-dihydrodibenzo[c,e]*thiepin (V)*: A similar treatment of 4,4'-dibromo-2,2'-bitolyl with *N*-bromosuccinimide and then with sodium sulfide afforded white crystals, mp 184.5—185°C (lit,[23] 191—192°C), after recrystallization from acetone.

Dimethyl 5,7-Dihydrodibenzo[c,e]*thiepin-3,9-dicarboxylate (VI)*. Dimethyl 2,2'-bitolyl-4,4'-dicarboxylate, treated similarly with *N*-bromosuccinimide followed by sodium sulfide, yielded the desired compound, mp 107—108°C, on recrystallization from ethanol - acetone (1 : 1).

Found: C, 65.77; H, 5.19%. Calcd for $C_{18}H_{16}O_4S$: C, 65.84; H, 4.91%.

21) W. Theilacker and W. Ozegowski, *Ber.* **73B**, 33 (1940).

22) Y. Osawa, *Nippon Kagaku Zasshi*, **84**, 140 (1963).

23) W. E. Truce and D. D. Emrick, *J. Amer. Chem. Soc.*, **78**, 6130 (1956).

Effects of *para*-Substituents on the Rates of Inversion of Biphenyl Derivatives. II. 2-Isopropyl-2′-methoxybiphenyls

Michinori Ōki and Gaku Yamamoto

Department of Chemistry, Faculty of Science, The University of Tokyo, Bunkyo-ku, Tokyo

(Received August 22, 1960)

Nine 4,4′-substituted 2-isopropyl-2′-methoxybiphenyls were synthesized and temperature dependence of the NMR spectra of these compounds was examined. The effects of the substituents on the energy barrier to inversion of the biphenyl skeleton can be interpreted in terms of both resonance stabilization and out-of-plane bending of the axis bond at the transition state. In the latter, an electron-donating substituent makes the bond bendig easier and lowers the barrier, whereas an electron-withdrawing group raises the barrier.

In a preceding paper[1] we reported that, in an *o,o′*-bridged biphenyl system where dynamic NMR technique (DNMR) could be applied, the energy barrier to inversion was really affected by the *para*-substituents. We postulated that the effects of the substituents on the barrier might be interpreted in terms of resonance stabilization and out-of-plane bending of the axis bond at the transition state. However, no definite conclusion could be given, because of the limited number of examples due to synthetic and other difficulties.

In this paper we wish to report on a study of the effects of *para*-substituents on the energy barrier to inversion of the non-bridged biphenyl system. There has been only one case where the energy barrier to inversion of non-bridged biphenyl is examined using DNMR. Meyer and Meyer[2] reported on the DNMR of 2,2′-bis(acetoxymethyl)biphenyl (I), where methylene protons showed AB quartet signal ($\delta_{AB}=3.5$, $J_{AB}=12.6$ Hz, in CS_2) at room temperature, and coalesced

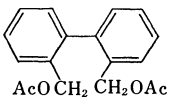

I

at 94°C into a singlet, the result indicating the activation energy of about 13 kcal/mol. A small chemical shift difference seemed to prevent precise line-shape analysis, hence this system did not seem suitable for our purpose.

o,o′-Diisopropylbiphenyl (II), possessing geminal dimethyl groups instead of methylene groups in *ortho* positions, was considered. The NMR spectrum of II at room temperature showed double doublets corresponding to the methyl protons of isopropyl groups, indicating that the inversion is slow on the NMR time scale. That the double doublets neither broadened nor coalesced up to 180°C (in hexachloro-1,3-butadiene) indicated that the free energy of activation for rotation about the axis bond is higher than 27 kcal/mol, and that this system also was unsuitable for DNMR study.

2-Isopropyl-2′-methoxybiphenyl (III), derived by replacement of one of the isopropyl groups in II by a less bulky methoxyl group, was considered for study

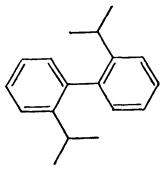

II

by means of DNMR. Replacement by methoxyl was chosen considering the synthetic ease. III and its 4,4′-substituted derivatives (IV—XI) were thus synthesized and their NMR spectra were examined over a wide range of temperature.

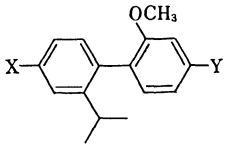

III: X=Y=H
IV: X=H, Y=OCH_3
V: X=H, Y=NO_2
VI: X=OCH_3, Y=H
VII: X=Y=OCH_3
VIII: X=OCH_3, Y=NO_2
IX: X=NO_2, Y=H
X: X=NO_2, Y=OCH_3
XI: X=Y=NO_2

Results and Discussion

Nine derivatives of 2-isopropyl-2′-methoxybiphenyl were synthesized by the Ullman reaction, *viz.*, the coupling of 2-iodocumenes (XII—XIV) and 2-iodoanisoles (XV—XVII) in the presence of copper bronze (Scheme 1).

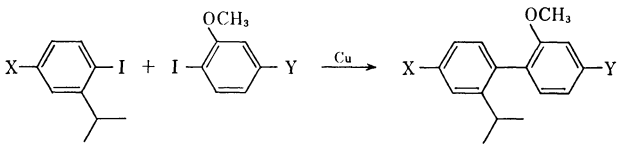

XII: X=H
XIII: X=OCH_3
XIV: X=NO_2
XV: X=H
XVI: X=OCH_3
XVII: X=NO_2
III—XI

Scheme 1

The desired unsymmetrical biphenyls were isolated by distillation and/or column-chromatography. Nine biphenyls (III—XI) as well as two 2-iodocumenes (XIII and XIV) are new compounds. Elementary analyses and NMR spectra of these compounds were consistent with the expected ones.

5-Methoxy- (XIII) and 5-nitro-2-iodocumene (XIV)

1) M. Ōki, H. Iwamura, and G. Yamamoto, This Bulletin, **44**, 262 (1971).

2) W. L. Meyer and R. B. Meyer, *J. Amer. Chem. Soc.*, **85**, 2170 (1963).

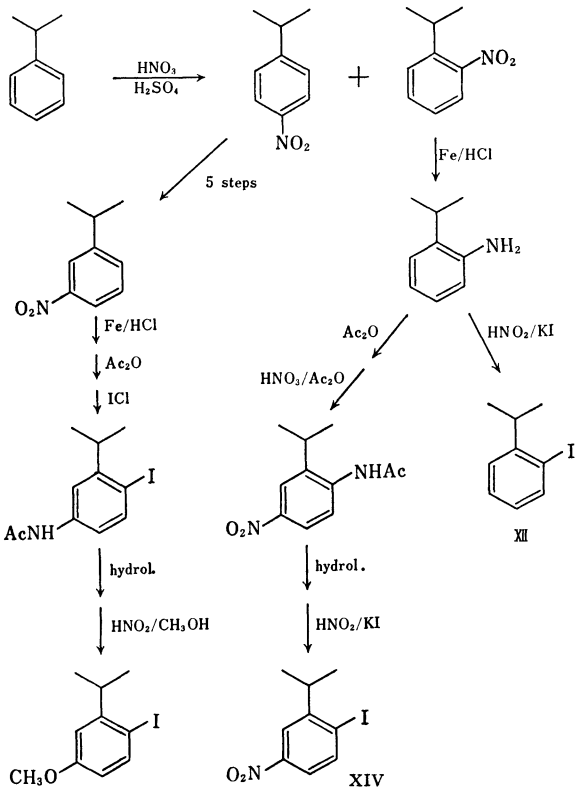

Scheme 2

were synthesized from cumene as described in Scheme 2. The positions of the introduced iodine in XIII and of the nitro group in XIV were confirmed by analysis of the aromatic proton signals in their NMR spectra, and further by comparison of the spectra with those of the corresponding toluene derivatives; XIII *vs.* 2-iodo-5-methoxytoluene and XIV *vs.* 2-iodo-5-nitrotoluene, each pair of spectra showing the same pattern of the aromatic proton signals.

The NMR spectra were measured as 15% solutions in 1,1,2,2-tetrachloroethane over a range from −10 to +150°C. Methyl protons of each compound showed a pair of doublets ($J\sim7$ Hz), with a separation of about 10 Hz at room temperature. This magnetic nonequivalence of the two methyls of the isopropyl groups indicated that inversion of the biphenyl skeleton is slow on the NMR time scale.

As the temperature was raised, the double doublet signal gradually broadened accompanying the gradual decrease in apparent chemical shift difference. The signal then became a broad single peak. The temperature at which this line shape was attained was regarded as the coalescence temperature T_c. With a further rise of temperature the signal split into two peaks, which gradually sharpened. At 150°C a sharp doublet was observed indicating fast inversion. A typical example, the case of V, is shown in Fig. 1.

The apparent chemical shift difference of the two methyl groups below T_c changed as shown in Fig. 2. The "intrinsic" chemical shift difference without exchange varied almost linearly with temperature. This phenomenon may be explained as follows. The "intrinsic" chemical shift difference is a weighed average of the chemical shift differences in conformations arising

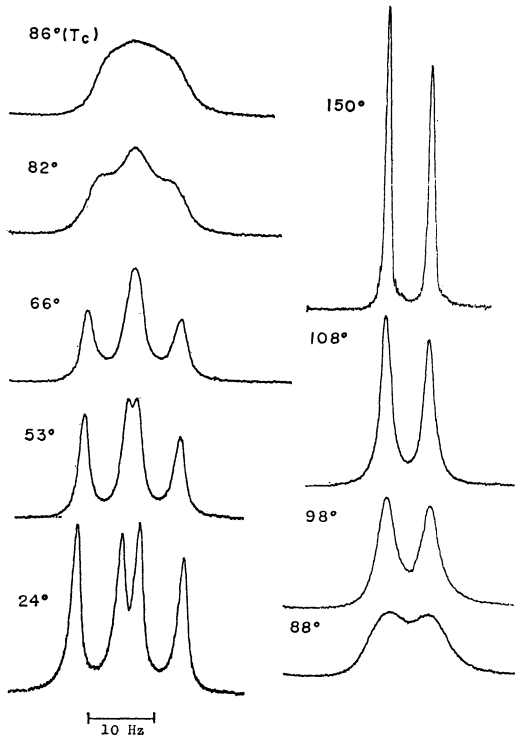

Fig. 1. The temperature dependence of the methyl proton signal of V.

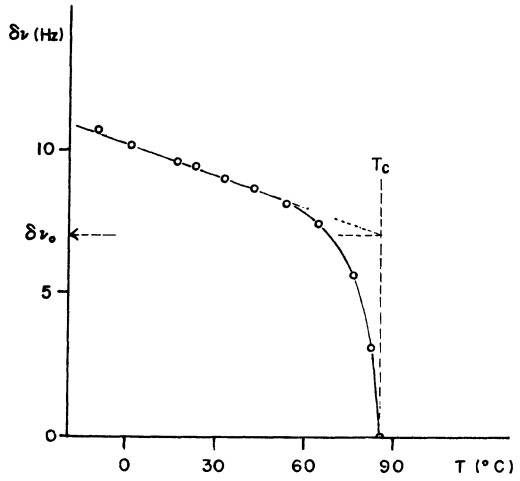

Fig. 2. The temperature dependence of the apparent chemical shift difference of the methyl protons of III.

from rotation about the bond between the isopropyl group and the benzene ring. The relative populations of these conformations may change with temperature because of the difference in potential energies, and this causes the observed change in chemical shift difference.

The same phenomenon was observed in the NMR spectra of *o,o′*-diisopropylbiphenyl (II). The methyl protons of II showed a chemical shift difference of 5.2, 4.9 and 4.5 Hz at 80, 120 and 180°C, respectively, at 60 MHz.

In order to obtain the kinetic parameters for inversion, these spectral changes were analyzed regarding them as two overlapping doublets, each coalescing into a singlet.

Inversion rate, k_c, at T_c was calculated using the

equation[3]

$$k_c = \frac{\pi\delta\nu_0}{\sqrt{2}} \quad (1)$$

where $\delta\nu_0$ represents the chemical shift difference of the two methyl groups without exchange. $\delta\nu_0$ was obtained by extrapolating the chemical shift differences at various temperatures to T_c.

Approximate inversion rate k at temperatures above T_c was calculated following the fast exchange approximation

$$k = \frac{\pi(\delta\nu_0)^2}{2(W - W_0)} \quad (2)$$

where W and W_0 are the signal width at half height at a given temperature and at a free exchange on the NMR time scale, respectively. W value at the highest temperature was used as W_0. The same numerical value as was used for the $\delta\nu_0$ in Eq. (1) was used for the $\delta\nu_0$ in Eq. (2). Uncertainty of the value inevitably gives rise to a considerably large error in k values.

The k values were plotted against the reciprocal temperature, which gave fairly good linearity. The inversion rate at 86°C was obtained graphically from this plot and $\Delta G_{86}^{\ddagger}$, the free energy of activation at 86°C, was calculated for each compound. The results are given in Table 1.

Table 1. Kinetic parameters of the inversion of 2-isopropyl-2′-methoxybiphenyls

Compound	X	Y	T_c (°C)	$\delta\nu_0$[a] (Hz)	$\Delta G_c^{\ddagger}$[b] (kcal/mol)	k_{86} (sec^{-1})	$\Delta G_{86}^{\ddagger}$[b] (kcal/mol)
III	H	H	86	7.2	19.2	16	19.2
IV	H	OCH_3	74	7.8	18.5	33	18.7
V	H	NO_2	86	7.1	19.2	16	19.2
VI	OCH_3	H	70	7.5	18.3	53	18.3
VII	OCH_3	OCH_3	61	7.3	17.9	82	18.0
VIII	OCH_3	NO_2	65	7.8	18.0	65	18.2
IX	NO_2	H	79	7.2	18.8	23	18.9
X	NO_2	OCH_3	58	8.0	17.6	80	18.0
XI	NO_2	NO_2	82	6.6	19.0	19	19.1

a) Extrapolated value to T_c.
b) The maximum errors for $\Delta G_c^{\ddagger}$ and $\Delta G_{86}^{\ddagger}$ are estimated to be ±0.1 and ±0.3 kcal/mol, respectively.

Enthalpy and entropy of activation derived from NMR line shape analysis, particularly by use of approximate equations were noted to involve serious errors.[4] Thus, in our case it seemed risky to discuss quantitatively using the obtained values of $\Delta H^{\ddagger}$ and $\Delta S^{\ddagger}$. We will rather discuss assuming that there is no large variation in $\Delta S^{\ddagger}$ values among the compounds in question, that is, the relative order of $\Delta G_{86}^{\ddagger}$ values corresponds to the relative order of the energy barrier to inversion. $\Delta G_{86}^{\ddagger}$ is considered to be reliable within the error of 0.3 kcal/mol.

Low barriers in 4-methoxy-4′-nitro- (VIII) and 4′-methoxy-4-nitro- (X) derivatives are in accordance with the results in 5,7-dihydrodibenzo[*c*,*e*]thiepin system[1] and may be explained in terms of resonance stabilization of the transition state, due to the contribution of canonical structures XVIII and XIX.

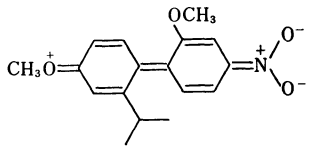

XVIII

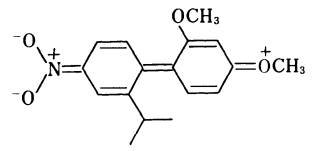

XIX

Comparison of the data for compounds IV and V is of interest. The contribution of resonance stabilization by the through conjugation in these compounds is thought to be of the same order. The difference may then be attributed to the difference in the extent of release of steric interactions by the out-of-plane bending of the axis bond. The electron-donating methoxyl group increases the π-electron density at 1,1′-positions, and according to the orbital following theory[5] this makes the out-of-plane bending of the axis bond easier. This means that the steric interactions between the *ortho* positions in the coplanar transition state are more easily released and thus the energy barrier to inversion is lowered.

Decrease in the $\Delta G_{86}^{\ddagger}$ values for IV relative to that for III may be interpreted to be due to the sum of the small conjugation effect and the bond bending effect.

The ease of the bond bending is reasonably expected to increase with the increasing number of the methoxyl groups: 2′-(III)<2′,4′-(IV)<4,2′-(VI)<4,2′,4′-(VII). The obtained data clearly agree with this prediction. It is interesting that the 4,4′-dimethoxy derivative (VII) has almost the same barrier as the 4-methoxy-4′-nitro one (VIII), which indicates that the bond bending factor is as important as the resonance stabilization factor in lowering the barrier.

On the other hand, the orbital following theory predicts that the electron-withdrawing nitro group lowers the π-electron density at 1,1′-positions and makes the out-of-plane bending of the axis bond less easy. The reason why V has the same barrier as III is ascribed to two compensating factors, *viz.*, resonance stabilization and destabilization due to the difficulty of the out-of-plane bending at the transition state. A small decrease in the barrier for IX relative to that for III may be interpreted as the conjugation effect represented

3) H. S. Gutowsky and C. H. Holm, *J. Chem. Phys.*, **25**, 1228 (1956).
4) A. Allerhand, H. S. Gutowsky, J. Jonas, and R. A. Meinzer, *J. Amer. Chem. Soc.*, **88**, 3185 (1966).
5) R. D. Kross, V. A. Fassel, and M. Margoshes, *J. Amer. Chem. Soc.*, **78**, 1332 (1956). J. M. Linnett and P. J. Wheatley, *Trans. Faraday Soc.*, **45**, 33 (1949).

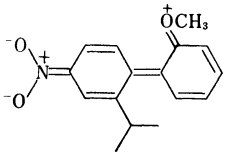

XX

by the canonical structure XX exceeding the destabilization effect of the nitro group. It seems that an *o*-quinoid structure such as XX is much less important in stabilizing the transition state than *p*-quinoid structures such as XVIII and XIX. Increased double bond character of $C_{2'}$-O bond makes the in-plane bending of this bond difficult, which otherwise could release the non-bonded interactions at the transition state. In compound XI an almost complete compensation of the two factors is observed.

Of course, the bond bending factor may be operating also in compounds VIII and X, but here the resonance stabilization factor may be far more important in lowering the energy barrier.

Harris and Cheung King Ling[6] have proposed that the dependence of the racemization rates of optically active 2,2′-diiodobiphenyls on the *para*-substituents could be interpreted on the assumption that the axis bond bent out of the plane of the benzene rings at the transition state.

The possibility of such bond bending could be attributed to the extreme bulkiness of the *ortho* substituents. But the present study seems to show that out-of-plane bending of the axis bond contributes in lowering the energy barrier to inversion in biphenyl systems possessing as low a barrier as can be studied by DNMR.

Experimental

Spectra. NMR spectra were obtained on a JNM C-60H or a Hitachi R-20A spectrometer both operating at 60 MHz. The temperatures were read with ethylene glycol sample and are accurate to ±2C°. Approximately 15% (w/w) solutions in 1,1,2,2-tetrachloroethane were employed.

Materials.[7] o-*Iodocumene (XII)*: *o*-Isopropylaniline, prepared by reduction of *o*-nitrocumene, was diazotized and treated with potassium iodide. Slightly colored oil was obtained; bp 116—117°C/12 mmHg (lit,[8] 84—85°C/2 mmHg).

3-Isopropyl-4-iodoacetanilide: Freshly prepared iodine monochloride (16.2 g, 0.1 mol) in acetic acid (10 m*l*) was added to a stirred solution of *m*-isopropylacetanilide (13.5 g, 0.1 mol) in acetic acid (15 m*l*) at room temperature over a period of 1 hr. The reaction mixture was poured into water containing a small amount of sodium bisulfite. The solidified mass, after recrystallization from methanol - water (5 : 1), gave colorless plates; yield 20 g (60%), mp 130—131°C.

Found: C, 43.40; H, 4.58; N, 4.68%. Calcd for $C_{11}H_{14}ONI$: C, 43.58; H, 4.66; N, 4.62%.

3-Isopropyl-4-iodoanisole (XIII): 3-Isopropyl-4-iodoacetanilide (18.2 g, 0.06 mol) was hydrolyzed with alcoholic potassium hydroxide. The resulting aniline was dissolved in 100 m*l* methanol containing sulfuric acid (15 m*l*), diazotized with sodium nitrite (5 g) in minimal amount of water with ice-cooling. The diazotized solution was warmed on a water bath until boiling and finally heated under reflux for 15 min. After evaporation of the major portion of methanol, the residue was poured into water and extracted with ether. The ethereal solution was shaken with dilute sodium hydroxide solution to separate the phenol from the anisole. The aqueous layer was treated with dimethyl sulfate and the resulting oil was extracted with ether. The two ethereal solutions were combined, washed with dilute alkali and water, and dried with potassium carbonate. Vacuum distillation gave colorless oil; yield 14 g (80%), bp 110—111°C/2 mmHg.

Found: C, 43.36; H, 4.72%. Calcd for $C_{10}H_{13}OI$: C, 43.50; H, 4.74%.

2-Isopropyl-4-nitroacetanilide: *o*-Isopropylaniline (40.5 g, 0.3 mol), dissolved in acetic anhydride (300 m*l*), was cooled down to −50°C with dry ice-alcohol, and freshly distilled nitric acid (specific gravity 1.51) was added dropwise during the course of 3 hr. Stirring was continued further 4 hr during which period the temperature was kept below −40°C. The reaction mixture was poured onto ice-water affording an oil. Repeated recrystallizations from methanol gave colorless needles; yield 12 g (18%), mp 159—161°C.

Found: C, 59.28; H, 6.65; N, 12.74%. Calcd for $C_{11}H_{14}O_3N_2$: C, 59.45; H, 6.35; N, 12.60%.

2-Iodo-5-nitrocumene (XIV). 2-Isopropyl-4-nitroacetanilide (22.2 g, 0.1 mol) was heated under reflux with sulfuric acid (30 m*l*) in water (100 m*l*) for 3 hr. The solution was cooled with ice-bath, and diazotized with sodium nitrite (8 g) solution. After decomposition of excess nitrous acid with urea, aqueous potassium iodide (20 g, 0.12 mol) was added. The reaction mixture was kept at room temperature for 10 min, at 60°C for 15 min and cooled to room temperature. After extraction with ether, the ether layer was washed successively with sodium bisulfite solution, dilute sodium hydroxide solution and water and dried with potassium carbonate. Distillation gave 19.5 g (67%) of an oil, bp 128—129°C/2 mmHg.

Found: C, 37.21; H, 3.59; N, 4.82%. Calcd for $C_9H_{10}O_2NI$: C, 37.14; H, 3.46; N, 4.81%.

General Procedure of the Ullman Reaction. *o*-Iodocumene (or its 4-substituted derivative) and 1 to 5 molar equivalent of *o*-iodoanisole (or its 4-substituted derivative) were mixed and heated at 150°C. Approximately the same weight of copper bronze as the iodine compounds was added to the mixture, which was then gradually heated up to 220—250°C and kept for 1 to 2 hr. The reaction mixture was cooled to room temperature and extracted with acetone. The evaporated extract contained symmetrically substituted biphenyls, 2,2′-dimethoxybiphenyl and 2,2′-diisopropylbiphenyl, as well as the decomposition products of low molecular weight, in addition to the desired unsymmetrical biphenyl. In most cases the desired product was isolated by distillation under reduced pressure and/or column chromatography followed by repeated recrystallizations.

2-Isopropyl-2′-methoxybiphenyl (III) was obtained after recrystallization from methanol as colorless crystals, mp 36°C.

Found: C, 84.93; H, 8.31%. Calcd for $C_{16}H_{18}O$: C, 84.91; H, 8.02%.

2-Isopropyl-2′,4′-dimethoxybiphenyl (IV) was collected as a fraction boiling at 142—145°C/2 mmHg which resisted crystallization. Repeated distillation gave a colorless oil.

Found: C, 79.82; H, 7.65%. Calcd for $C_{17}H_{20}O_2$: C, 79.65; H, 7.86%.

2-Isopropyl-2′-methoxy-4′-nitrobiphenyl (V) was obtained as pale

6) M. M. Harris and C. Cheung King Ling, *J. Chem. Soc.*, **1964**, 1825.

7) All the melting points and boiling points are uncorrected.

8) H. C. Brown, J. D. Brady, M. Grayson, and W. H. Bonner, *J. Amer. Chem. Soc.*, **79**, 1897 (1957).

yellow crystals, mp 101—102°C (from methanol).

Found: C, 70.98; H, 6.50; N, 5.04%. Calcd for $C_{16}H_{17}O_3N$: C, 70.83; H, 6.32; N, 5.16%.

2-Isopropyl-4,2'-dimethoxybiphenyl (VI) was obtained as a colorless oil, bp 142—145°C/2.5 mmHg.

Found: C, 79.70; H, 7.68%. Calcd for $C_{17}H_{20}O_2$: C, 79.65; H, 7.86%.

2-Isopropyl-4,2',4'-trimethoxybiphenyl (VII) crystallized from methanol as colorless granules, mp 56—57°C.

Found: C, 75.35; H, 7.95%. Calcd for $C_{18}H_{22}O_3$: C, 75.49; H, 7.74%.

2-Isopropyl-4,2'-dimethoxy-4'-nitrobiphenyl (VIII) was recrystallized from petroleum ether (bp 50—60°C) affording yellow orange granules, mp 73.5—74.5°C.

Found: C, 67.63; H, 6.40; N, 4.44%. Calcd for $C_{17}H_{19}O_2N$: C, 67.76; H, 6.36; N, 4.65%.

2-Isopropyl-2'-methoxy-4-nitrobiphenyl (IX) was obtained by recrystallization from methanol as pale yellow crystals, mp 72—73°C.

Found: C, 70.84; H, 6.61; N, 5.09%. Calcd for $C_{16}H_{17}O_3N$: C, 70.83; H, 6.32; N, 5.16%.

Chromatography of the reaction mixture also afforded 2,2'-diisopropyl-4,4'-dinitrobiphenyl as orange crystals, mp 172—174°C (from methanol).

Found: C, 65.93; H, 6.20; N, 8.45%. Calcd for $C_{18}H_{20}O_4N_2$: C, 65.84; H, 6.14; N, 8.53%.

2-Isopropyl-2',4'-dimethoxy-4-nitrobiphenyl (X) was obtained by repeated recrystallizations from ethanol as yellow crystals, mp 108—110°C.

Found: C, 68.06; H, 6.84; N, 4.66%. Calcd for $C_{17}H_{19}O_4N$: C, 67.76; H, 6.36; N, 4.65%.

2-Isopropyl-2'-methoxy-4,4'-dinitrobiphenyl (XI) was obtained by repeated recrystallizations from acetone as orange yellow plates, mp 139—140°C.

Found: C, 60.56; H, 5.25; N, 8.75%. Calcd for $C_{16}H_{16}O_5N_2$: C, 60.76; H, 5.10; N, 8.86%.

NOTES

BULLETIN OF THE CHEMICAL SOCIETY OF JAPAN, VOL. 44, 271—272 (1971)

Studies of the *N*-Oxides of *N,N*-Dialkylamino Acids. IV. The Decarboxylation of *N,N*-Dimethylamino Acid *N*-Oxides with *p*-Toluenesulfonyl Chloride in Pyridine

Yoshikazu IKUTANI

Department of Chemistry, Osaka Kyoiku University, Tennoji-ku, Osaka

(Received December 30, 1969)

Though many investigations have been made of the reactions between heteroaromatic tertiary amine *N*-oxides and acylating reagents, little attention has been paid to the similar reactions of aliphatic tertiary amine *N*-oxides especially *N,N*-dialkylamino acid *N*-oxides.

In the previous papers of this series, the preparations of *N*-oxides of *N,N*-dimethyl neutral amino acids,[1] *N,N*-dialkylglycine,[2] and *N,N*-dimethyl acidic amino acids[3] were investigated. In the present study, the decarboxylations of *N,N*-dimethylamino acid *N*-oxides with *p*-toluenesulfonyl chloride in pyridine and the hydrolysis of the reaction products have been investigated.

The evolution of carbon dioxide was observed immediately when *N,N*-dimethylamino acid *N*-oxide was treated with an equivalent amount of *p*-toluenesulfonyl chloride in pyridine at 5°C or below. The mixture, when allowed to stand for about a half an hour with shaking, turned a light red-brown. The carbon dioxide generated was collected as barium carbonate and weighed. The results thus obtained are shown in Table 1.

Table 1. The decarboxylation of *N,N*-dimethylamino acid *N*-oxide with *p*-toluenesulfonyl chloride in pyridine

Parent amino acid	Yields of carbon dioxide (%)
Gly	80
DL-Ala	33
DL-Val	16
L-Glu	57
L-Phe	74

In the reaction of *N,N*-dimethylglycine *N*-oxide with *p*-toluenesulfonyl chloride, the reaction mixture was concentrated to remove the excess pyridine; the residue was then treated with hot acetone to remove the pyridine hydrochloride and the pyridine hydro-*p*-toluenesulfonate. All attempts to obtain any crystalline product from the dark red-brownish sticky residue failed, but the following experiments confirmed the syrup to be a mixture of *N,N*-dimethyl-methyleneimmonium chloride and *p*-toluenesulfonate. The acid hydrolysis of the syrup gave formaldehyde and dimethylamine.

Further experiments with ion-exchange resin were performed in order to confirm the structure of the reaction product. The decarboxylation was performed much as has been described above, and the residue was dissolved in water. A half of the resulting solution was deposited on an ion-exchange column (Amberlite IRA-410, OH-form); it was then eluted with water. The eluate was hydrolysed much as has been described above. Formaldehyde as 2,4-dinitrophenylhydrazone and dimethylamine as *p*-toluenesulfonamide were obtained in almost quantitative yields. Another half of the resulting solution was deposited on an ion-exchange column (Amberlite IR-120, H-form), and subsequently eluted with water. The eluate included *p*-toluenesulfonic acid and hydrochloric acid. A part of the effluent was titrated directly, and another part was dried up in order to remove the hydrochloric acid, dissolved in water, and titrated. The value of the former was 2.02 equivalents of the corresponding *N*-oxide, while the value of the latter was 0.98. These results indicate that the formation of the immonium salts and the reaction mechanism shown in Fig. 1 may be postulated.

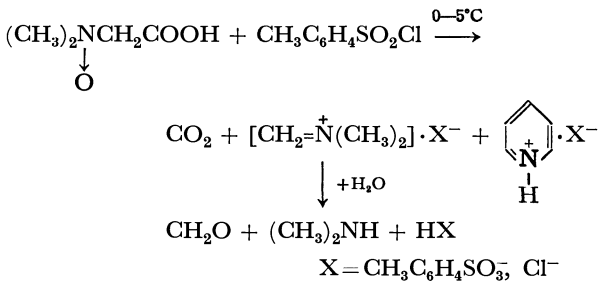

Fig. 1

Experimental

The Decarboxylation of N,N-*Dimethylglycine* N-*Oxide with* p-*Toluenesulfonyl Chloride in Pyridine.* In a flask, 3.5 g of *N,N*-dimethylglycine *N*-oxide were placed, the flask was cooled in an ice bath to 5°C or below, and then 5.7 g of *p*-toluenesulfonyl chloride in 20 m*l* of pyridine were added, drop by drop with shaking, over a period of approximately 15 min, after which the mixture was shaken for more than 15 min. At the end of the reaction, the evolution of carbon dioxide ceased. The carbon dioxide generated was led into

1) Y. Ikutani, This Bulletin, **41**, 1679 (1968).
2) Y. Ikutani, *ibid.*, **42**, 2330 (1969).
3) Y. Ikutani, *ibid.*, **43**, 3602 (1970).

a solution of barium hydroxide with nitrogen gas; 4.7 g of barium carbonate were thus obtained. The reaction mixture was concentrated under reduced pressure to remove the excess pyridine. The residue was then extracted with three 20 m*l* portions of hot acetone. The combined extract was concentrated under reduced pressure and stored in a refrigerator overnight. Pyridinium *p*-toluenesulfonate (5.1 g) was thus obtained as a precipitate. The filtrate was then dried up under reduced pressure; 1.2 g of pyridine hydrochloride were obtained. The extracted remnant was washed with ether several times and dried under reduced pressure. It was then dissolved in 100 m*l* of water, controlled to pH 2 with hydrochloric acid. To a half of the resulting solution, a mixture of 3.0 g of 2,4-dinitrophenylhydrazine, 15 g of concentrated sulfuric acid, 20 m*l* of water, and 70 m*l* of ethanol was added; the solution was then allowed to stand at room temperature for a few days. The yield of 2,4-dinitrophenylhydrazone of formaldehyde thus obtained was 3.1 g. To the other half of the solution, 15 m*l* of 2N hydrochloric acid were added, and the mixture was allowed to stand at room temperature for 5 days. To the resulting solution 5.0 g of *p*-toluenesulfonyl chloride were added, and then 2N aqueous sodium hydroxide was added with vigorous stirring to keep the mixture in a weak alkaline condition overnight. The precipitates were then collected by filtration, washed with water, and dried under reduced pressure to yield 2.2 g of *N*,*N*-dimethyl-*p*-toluenesulfonamide.

In another experiment, the decarboxylation of 2.4 g of *N*,*N*-dimethylglycine *N*-oxide and 3.8 g of *p*-toluenesulfonyl chloride in 15 m*l* of pyridine was performed in a manner similarly to that described above. After the completion of the reaction, 30 m*l* of water were added. A half of the resulting solution was deposited on an ion-exchange column of Amberlite IRA-410 (OH-form), and then eluted with water. The eluate was collected until it became neutral. To a half of the effluent, 25 m*l* of 2N hydrochloric acid, and then a mixture of 2.0 g of 2,4-dinitrophenylhydrazine, 10 g of concentrated sulfuric acid, 15 m*l* of water, and 50 m*l* of ethanol, were added. The mixture was allowed to stand at room temperature, and then it was heated at 80°C for 6 hr. 2,4-Dinitrophenylhydrazone of formaldehyde (1.0 g) was thus obtained. To one half of the effluent, 25 m*l* of 2N hydrochloric acid were added. When the mixture was treated much as has been described above, 0.90 g of *N*,*N*-dimethyl-*p*-toluenesulfonamide was obtained. The other half of the resulting solution was deposited on a column of Amberlite IR-120 (H-form) and then eluted with water. The effluent was diluted to 250 m*l* with water. The titration of 25 m*l* of the resulting solution with 0.1N (f=1.14) aqueous sodium hydroxide, using phenolphthalein as an indicator, required 17.93 m*l*. Another 25 m*l* portion of the resulting solution was dried up under reduced pressure and dissolved in 20 m*l* of water. The titration required 8.50 m*l* of 0.1N (f=1.14) aqueous sodium hydroxide.

The author is indebted to Professor Eizo Matsumura for his constant guidance in the course of the work, and to Professor Yoshiharu Izumi of Osaka University for his valuable advice and encouragement.

BULLETIN OF THE CHEMICAL SOCIETY OF JAPAN, VOL. 44, 272—273 (1971)

The Dipole Moment of the Trimethylamine-iodine Complex

Hiroaki MIHONO and Koichi TOYODA

Department of Chemistry, Faculty of Science, Kumamoto University, Kurokami-machi, Kumamoto

(Received April 30, 1970)

One of the present authors[1] reported last year that his experimental measurements of the dipole moment of the triethylamine-iodine(Et_3N-I_2) complex confirmed the value, 5.5—5.7D, previously reported by Boule[2] in a cyclohexane solution. Furthermore, the dipole moment of the Et_3N-I_2 complex in a benzene solution was found to increase with the time after the two solutions had been mixed. These experimental values of the dipole moment show a much lower value than the value,[3] 12D, obtained in a dioxane solution. One of the present authors[3] has recently reported that his experimental dipole moment of the trimethylamine-iodine(Me_3N-I_2) complex shows the very large value, 10D, in a dioxane solution. We have reinvestigated the dipole moment of the Me_3N-I_2 complex in cyclohexane and in benzene; the importance of the complex as a typical example is so great that extra efforts to obtain accurate data are justified.

Experimental

The cyclohexane, benzene, and iodine were purified and stored by the method reported previously.[1] Trimethylamine generated from its aqueous solution by adding concentrated aqueous alkali was dried by potassium hydroxide. The dry trimethylamine thus obtained was led into cyclohexane to prepare the stock solution. The I_2 and Me_3N solutions were both made up by weight. The Me_3N solutions were prepared by the use of Le Fèvre's method.[4] The apparatus for the measurements of dielectric constants and the picnometer for the measurements of densities have been reported on previously.[1] The temperature was kept constant within 25.00 ± 0.05°C throughout the series of measurements. The dipole moment of nitrobenzene obtained by means of this apparatus was 4.06D in a benzene solution at 25°C. In each series of measurements, benzene or cyclohexane solutions containing a fixed concentration of Me_3N and various concentrations of iodine were used. The latter concentrations ranged from 0 to 8.0×10^{-3} mol/l in benzene solutions and from 0 to $3.5\times$

1) A. Funatsu and K. Toyoda, This Bulletin, **43**, 279 (1970).
2) P. Boule, *J. Amer. Chem. Soc.*, **90**, 517 (1968).
3) K. Toyoda and W. B. Person, *ibid.*, **88**, 1629 (1966).
4) R. J. W. Le Fèvre and P. Russell, *Trans. Faraday Soc.*, **43**, 374 (1947).

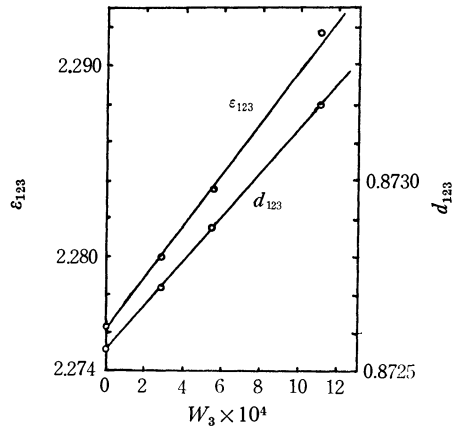

Fig. 1. In a benzene solution, the relations between the dielectric constants of solutions (ε_{123}) or the densities of solutions (d_{123}) and the weight fractions of complexes (W_3).
These straight lines are able to express
$\varepsilon_{123}=2.2763+13.3174W_3$, $d_{123}=0.87256+0.58852W_3$.

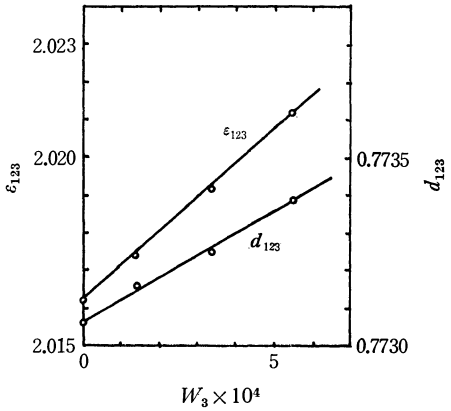

Fig. 2. In a cyclohexane solution, the relations between ε_{123} or d_{123} and W_3. These straight lines are able to express
$\varepsilon_{123}=2.0163+8.6538W_3$, $d_{123}=0.77308+0.57333W_3$.

10^{-3} mol/l in cyclohexane solutions; they never exceeded one-fifteenth that of amine in the solution. The dipole moments of the complex increased with an increase in the amine concentration in a mixed solvent containing benzene or cyclohexane and an amine. The dipole moments of the complexes were obtained by the use of the Kobinata-Nagakura method[5] as well as by that of a previous article.[1]

Results and Discussion

The Et_3N-I_2 complex was unstable in a benzene solution, but we have found that the Me_3N-I_2 complex is stable in a benzene solution. The relations between the experimentally-observed dielectric constants or the densities of the solutions and the weight fractions of the complexes for each series of measurements are shown in Fig. 1 for benzene solutions, and in Fig. 2 for cyclohexane solutions, as examples of the measurements. The dipole moments of the complex were calculated from the slopes of these straight lines by the use of only the first term of the Kobinata-Nagakura equation.[5] In a benzene solution, the experimental values of the dipole moment of the complex thus obtained are 6.31, 6.20, 6.12, 6.63, and 6.30D; in a cyclohexane solution, they are 5.31, 4.75, 5.42, 5.53, and 5.26D. We believe these values are reasonable as compared with the values of the Et_3N-I_2 complex in a benzene or cyclohexane solution. From the dipole moment thus obtained, the contribution of the dative structure in the present complex can be estimated at 29%.

5) S. Kobinata and S. Nagakura, *J. Amer. Chem. Soc.*, **88**, 3905 (1966).

BULLETIN OF THE CHEMICAL SOCIETY OF JAPAN, VOL. 44, 273—275 (1971)

An ESR Study of Radicals Produced in γ-Irradiated Allyl Alcohol Glass and Their Photochemical Reaction at 77°K

Shoji NODA, Keizo TORIMOTO, Kenji FUEKI, and Zen-ichiro KURI

Department of Synthetic Chemistry, Faculty of Engineering, Nagoya University, Chikusa-ku, Nagoya

(Received May 15, 1970)

The ESR spectrum of γ-irradiated allyl alcohol glass is a composite of four-line and five-line spectra.[1] The four-line spectrum has been assigned to the α-hydroxy allyl radical[1-3] (I), which disappears with UV-irradiation.[1] The five-line spectrum has been assigned to the allyl radical[1-3] (II). Neither coloration nor the ESR spectrum due to the trapped electron has been observed in this system, in contrast with the cases of γ-irradiated alkyl alcohol glasses.[4] In this work we have investigated the fate of the thermal electron, and also the photolysis and thermal behavior of the radicals in allyl alcohol glass.

Experimental

Allyl alcohol and triethylamine (TEA) were purified by fractional distillation. The γ-irradiation and ESR and optical measurements were described previously.[5] Thermal

1) M. C. Chachaty, *C. R. Acad. Sci., Paris*, **259**, 2219 (1964).
2) K. A. Mass and D. H. Volman, *Trans. Faraday Soc.*, **60**, 1202 (1960).
3) M. Fujimoto and D. J. Ingram, *ibid.*, **54**, 1304 (1958).
4) A. Ekstrom and J. E. Willard, *J. Phys. Chem.*, **72**, 4599 (1968).
5) S. Noda, K. Fueki, and Z. Kuri, *J. Chem. Phys.*, **49**, 3287 (1968).

annealing experiments were carried out at various temperatures in the range of 90—140°K by keeping the sample tube in a JES variable-temperature quartz Dewar insert. Photolysis experiments were performed with UV light from a high-pressure mercury lamp. Cut-off filters were employed if necessary.

Results and Discussion

The ESR spectrum of γ-irradiated allyl alcohol glass at 77°K is shown in Fig. 1. The trapped-electron

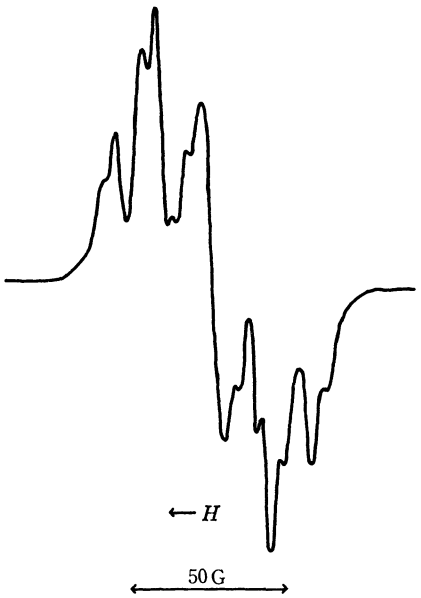

Fig. 1. ESR spectrum of γ-irradiated allyl alcohol glass at 77°K.

signal was not observed in this system, although ESR measurements were made at microwave powers low enough to avoid power saturation[6,7] and in the dark. Upon γ-irradiation, TEA glass produces a blue color and gives an ESR spectrum consisting of a sharp singlet due to the trapped electron and a broad unresolved signal due to the solvent radical.[7] The ESR spectrum of the γ-irradiated TEA containing 1 mol% of allyl alcohol is shown in Fig. 2a. The five-line spectrum appears with a decrease in the intensity of the central sharp singlet. The illumination of infrared light bleached the trapped-electron signal and increased the intensity of the five-line spectrum (see Fig. 2b). This five-line spectrum is ascribed to the radical(II) on the basis of its ESR parameters. These facts indicate that allyl alcohol reacts with the thermal electron dissociatively to produce the radical(II) and the hydroxy anion:

$$CH_2{=}CH{-}CH_2OH + e^- \longrightarrow CH_2{=}CH{-}\dot{C}H_2(II) + OH^-$$

Making use of the competitive reaction, the cross section, σ(R–OH), for electron capture by allyl alcohol relative to biphenyl was determined. Optical measurements were made in order to determine the yield of the

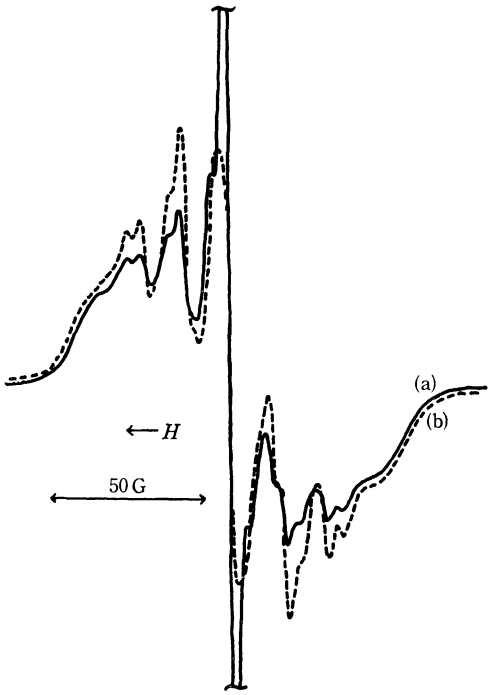

Fig. 2. ESR spectra of γ-irradiated TEA glass containing 1 mol% of allyl alcohol at 77°K, a) before bleaching, b) after bleaching with infrared light.

biphenyl anion (410 nm[8]). The observed ratio, σ(R–OH)/σ(biphenyl), was about 0.3. This agrees with that given by Habersbergerová *et al.*,[9] the ratio of the electron-capture efficiency of allyl alcohol to that of naphthalene in methanol glass being about 0.25. We have also found that other allylic compounds, such as allyl acetate, allyl formate, and allyl nitrile, react with thermal electron dissociatively to produce the radical(II) and the corresponding anion, although detailed studies on these compounds were not carried out.

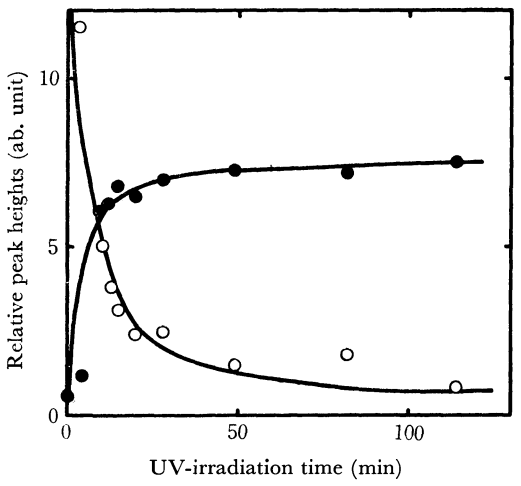

Fig. 3. The plots of relative ESR peak heights against the UV-irradiation time, ●, allyl radical; ○, α-hydroxy allyl radical.

6) D. R. Smith and J. S. Pieroni, *Can. J. Chem.*, **43**, 876 (1965).
7) H. Tsujikawa, K. Fueki, and Z. Kuri, *J. Chem. Phys.*, **47**, 256 (1967).
8) W. H. Hamill, "Radical Ion," ed. by. E. T. Keiser and L. Kevan, Interscience Publishers, New York (1968), p. 321.
9) A. Habersbergerová, Lj. Josimović, and J. Teplý, *Trans. Faraday Soc.*, **66**, 656 (1970).

When the γ-irradiated allyl alcohol glass was warmed to 118°K, the ESR spectrum changed to the pure four-line spectrum.[1] Moreover, UV-irradiation, following the γ-irradiation, caused the ESR spectrum of pure allyl alcohol glass to change from a composite of the four-line and five-line spectra into the five-line spectrum.[1] On warming this sample characterized by only a five-line spectrum, a weak four-line spectrum appeared with the decay of the five-line one. When the same sample was kept in the dark for a few days at 77°K, the spectrum changed to a composite of the four-line and five-line spectra. These facts seem to suggest that the radical(II) abstracts an α-H from allyl alcohol to produce the radical(I) at 77°K as well as at 118°K, but the evidence for this is not conclusive.[2]

Until now it has not been clear whether or not the radical(I) produces the radical(II) by UV-irradiation. The pure four-line spectrum remaining at 118°K was changed into a composite of the four-line and five-line spectra by UV-irradiation at 77°K, while prolonged UV-irradiation caused the composite spectrum to change completely into the five-line spectrum. The relative ESR peak heights of the four-line and five-line spectra are plotted against the UV-irradiation time in Fig. 3. From these results, it is apparent that the radical(I) decomposes upon UV-irradiation to produce the radical(II). As the mechanism of this photochemical conversion in allyl alcohol, the following process may be proposed:

$$CH_2{=}CH{-}CH_2OH + CH_2{=}CH{-}\dot{C}HOH\ (I) \xrightarrow{UV}$$
$$CH_2{=}CH{-}\dot{C}H_2\ (II) + CH_2{=}CHCOH + H_2O$$

A spot test[10] of the sample which had been UV-irradiated after γ-irradiation gave evidence of the presence of aldehyde, but we could not identify the aldehyde with acrolein because of the detection limit. Therefore, the scheme proposed above should be regarded as only tentative.

The relative primary yields of radicals in γ-irradiated allyl alcohol glass were obtained. The primary yield of the radical(II) was estimated to be about twice that of the radical(I). Since the radical yields of I and II must be the same if the ionic processes play an important role, the excitation process may also be concerned with the radiolysis of allyl alcohol glass. However, further product analysis is required for a complete understanding of the mechanism of the radiolysis and photolysis of allyl alcohol.

10) F. Feigel, "Spot Tests in Organic Analysis," Elsevier Publishing Company, Amsterdam (1960), p. 223.

BULLETIN OF THE CHEMICAL SOCIETY OF JAPAN, VOL. 44, 275—277 (1971)

Distribution of Aqueous Sodium Perchlorate into Some Polar Organic Solvents

Yuko HASEGAWA, Teruhiko ISHII, and Tatsuya SEKINE

Department of Chemistry, Science University of Tokyo, Kagurazaka, Shinjuku-ku, Tokyo

(Received June 3, 1970)

As sodium ions or perchlorate ions are usually believed to form only very weak complexes, sodium perchlorate has often been used in order to control the activity coefficients of ionic species in aqueous solutions.

However, in the systems where anionic species are extracted as ion pairs with sodium ions into an organic phase, the sodium concentration in the aqueous phase should be taken into account, and if the extracted ion pairs dissociate in the organic phase, the sodium-ion concentration in the organic phase is also important. In the extraction of mercury(II) complexes with halide or thiocyanate ions into polar solvents, some part of the complexes is assumed to consist of ion pairs of mercury(II) complex anions with sodium ions,[1] and the extraction of indium(III) halides or thiocyanate into polar solvents is very much effected by the aqueous sodium concentrations,[2] an effect which can also be explained in terms of the extraction of ion pairs of anionic indium complexes with sodium ions.

The present study has been carried out in order to obtain further, more detailed information about the liquid-liquid distribution behavior of sodium perchlorate as ion pairs.

Experimental

Reagents. The sodium-24 radioactive tracer was obtained as a sodium chloride solution. This was diluted with a large amount of water in order to prepare the stock tracer solution. The sodium perchlorate was prepared from perchloric acid and sodium carbonate and was recrystalized three times from water. The TBP(tributylphosphate), MIBK-(methylisobutylketone), methylisobutylcarbinol, and nitromethane were obtained from the Tokyo Kasei Co. They were washed with perchloric acid, water, and aqueous sodium hydroxide successively, and then several times with water. The hexane used was of a reagent grade and was used without further purification.

Procedures. All of the procedures were carried out in a thermostatted room at 25°C. Stoppered glass tubes (volume, 20 ml) were always used for the equilibration of the two phases. Sodium perchlorate solutions labelled by a radio-

1) T. Sekine and T. Ishii, This Bulletin, **43**, 2422 (1970).
2) Y. Hasegawa, H. Takeuchi, and T. Sekine, to be published.

active tracer and the organic solvent were placed in the tubes. The initial volume of the two phases was always 5 m*l*. The two phases were agitated mechanically for thirty minutes and then centrifuged. The γ-radioactivity of both phases was measured with a well-type (NaI) scintillation counter, and the distribution ratio of sodium was calculated as;

$$D = \frac{[\mathrm{Na(I)}]_{org,\ total}}{[\mathrm{Na(I)}]_{total}} = \frac{\gamma\text{-count rate per m}l\text{ of the org. phase}}{\gamma\text{-count rate per m}l\text{ of the aq. phase}}$$

Results and Discussion

In an aqueous phase, sodium salt could usually be assumed to dissociate. In an organic phase, on the other hand, the extracted ion pairs of the sodium ion and a large univalent anion, A^-, could dissociate completely or partially, or they could remain in the associated form. The distribution of sodium ion pairs from an aqueous phase to an organic phase can be described as:

$$Na^+ + A^- \rightleftarrows Na^+A^-(org) \quad (1)$$

$$K = \frac{[Na^+A^-]_{org}}{[Na^+][A^-]} \quad (2)$$

When the dissociation occurs in the organic phase:

$$Na^+A^-(org) \rightleftarrows Na^+(org) + A^-(org) \quad (3)$$

$$K^o_{diss} = \frac{[Na^+]_{org}[A^-]_{org}}{[Na^+A^-]_{org}} \quad (4)$$

The distribution ratio of sodium(I) can be described as:

$$D = \frac{[Na^+A^-]_{org} + [Na^+]_{org}}{[Na^+]} \quad (5)$$

When only one kind of sodium salt is present in the system, it is assumed that the concentration of the sodium ions is equal to that of the total number of anions, and that, consequently, $[Na^+]=[A^-]$ and $[Na^+]_{org}=[A^-]_{org}$. Then, by introducing Eqs. (2) and (4) into Eq. (5), the following equation is obtained:

$$D = K^{1/2}(K^{1/2}[Na^+] + (K^o_{diss})^{1/2}) \quad (6)$$

As no control of the activity of the chemical species in the two phases was made in the present study, only a qualitative discussion can be made of the results.

Figure 1 gives the distribution ratio of sodium between TBP, nitromethane, MIBK, or methylisobutylcarbinol and aqueous sodium perchlorate solutions as a function of the initial aqueous salt concentration. It was observed during the experiments with nitromethane that the organic volume decreases, and the aqueous volume increases remarkably, in the highest-salt-concentration region. In such systems, the aqueous salt concentration should decrease upon the volume change and also upon extraction. However, as the correction for these factors will not be easy, the sodium perchlorate concentration in the figures is given by their initial values. The extraction with these solvents is much higher than that with nitrobenzene ($D \simeq 10^{-4}$ at 0.1~5M $NaClO_4$[3]).

It may be seen from Fig. 1 that the distribution ratio of sodium in the nitromethane system is almost constant in the lower-salt-concentration region (below 1M). Equation (6) shows that if the extracted salt dissociates completely, the distribution ratio is independent of the concentration. As the activity coefficients in both the phases may be changed by the changes in the salt concentration, no definite conclusion should be introduced without information about the activities. However, it is probable that the extracted salt is almost dissociated in this organic solvent with a very high dielectric constant (ε=34.82 at 25°C[4]), at least when the salt concentration is low. However, as the extraction depends somewhat on the salt concentration in the other three solvents, the ions in them should associate to some extent. The increase in the distribution ratio in the higher-salt-concentration region (above 1M) could be due to the association of the sodium and perchlorate ions in the organic phase (*cf.* Eq. (6)) and/or to the change in the activity coefficients of the ionic species.

Figure 2 shows the extraction of sodium into undiluted, 50% (v/v), and 1M TBP in hexane as a function of the aqueous sodium perchlorate concentration. The decrease in the extraction upon the dilution of TBP is to be expected from the law of mass action, but it could also be due to the change in the nature of the organic phase (the polarity, the dielectric constants, the activity coefficients of TBP and ionic species, *etc.*).

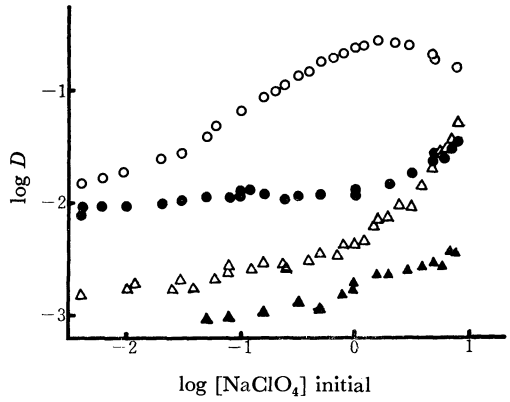

Fig. 1. Distribution of sodium(I) between TBP (○), nitromethane (●) MIBK (△) or methylisobutylcarbinol (▲) and aqueous sodium perchlorate solutions. The aqueous salt concentrations are the intial values.

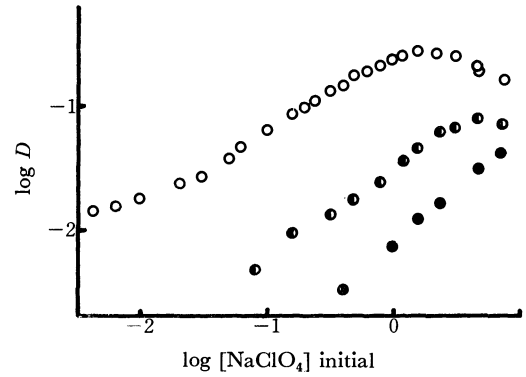

Fig. 2. Distribution of sodium(I) between undiluted TBP (○) 50% (v/v) TBP (◐) or 1M TBP (●) in hexane and aqueous sodium perchlorate solutions. The aqeuous concentrations are the initial values.

3) T. Sekine and D. Dyrssen, *Anal. Chem. Acta*, **45**, 433 (1969).
4) A. A. Maryott and E. A. Smith, "Table of Dielectric Constant of Pure Liquids" NBS Circular 514, Aug. 10, 1951.

It is remarkable that the shape of the extraction curve is changed by the dilution, as may be seen from Fig. 2.

The extractions of sodium perchlorate with these solvents are not very low; for example, when the aqueous phace is 1M Sodium perchlorate solution, 1—10 mM sodium perchlorate is present in all the organic solvents except TBP, and more than 0.1M is contained in TBP; as a dissociation of the extracted salt in the organic phase is assumed in these polar solvents, these organic phases can be regarded as constant ionic media for a small amount of other solutes in these organic phases, such as, for example, an aqueous sodium perchlorate solution at a constant concentration.

These facts should be taken into account when the extraction of ion pairs of sodium with anionic complexes occurs; they are especially important when the extracted ion pairs undergo dissociation in the organic phase.

BULLETIN OF THE CHEMICAL SOCIETY OF JAPAN, VOL. 44, 277—278 (1971)

Anion Radicals Produced by the Non-aqueous Polarographic Reduction of Several Benzonitrile *N*-Oxides[1]

Hiroshi MIYAZAKI, Koichi NISHIKIDA, and Tanekazu KUBOTA
Shionogi Research Laboratory, Shionogi & Co., Ltd., Fukushima-ku, Osaka

(Received July 14, 1970)

Anion and cation free radicals and their structures, produced by the controlled potential electrolysis of heterocyclic amine *N*-oxides, have been extensively studied in our laboratory.[2] It has usually been found that the anion[2a-d] or cation[2e] free radical of the mother compound is produced at the first reduction or oxidation wave respectively. We have now extended this kind of study to several benzonitrile *N*-oxides whose electronic structures and physicochemical properties[3] have also been investigated in detail in comparison with such other amine oxides as pyridine *N*-oxide and nitrone. The experimental results obtained here, however, are somewhat different from those previously reported.[2] In this note we will report on the non-aqueous polarographic behaviour of the substituted benzonitrile *N*-oxides listed in Table 1, and on the electron-spin-resonance (ESR) spectra and their analyses of anion radicals produced by the controlled potential electrolysis of the nitrile *N*-oxides.

Of the samples, the 4-nitro-2,6-dimethyl-benzonitrile *N*-oxide (**5**) was prepared by the well-known Grundmann method[4] from 4-nitro-2,6-dimethylbenzoaldoxime and NaOBr, the corresponding nitrile (**10**) (see Table 1) being obtained by the deoxygenation of the above nitrile *N*-oxide with $(CH_3O)_3P$.[4] The other samples used and the experimental techniques were the same as those described in our previous papers.[2,5] As a typical example, in Fig. 1 we show the polarograms of 2,4,6-trimethylbenzonitrile *N*-oxide (**2**) and the corresponding nitrile (**7**) and the ESR spectrum obtained by electrolysis at the second wave of **2**. All the other experimental data are included in Table 1. We can see from Fig. 1 that the wave height of the first reduction wave of the DC polarogram of **2** is substantially larger than that of the second wave. For the case of the AC polaro-

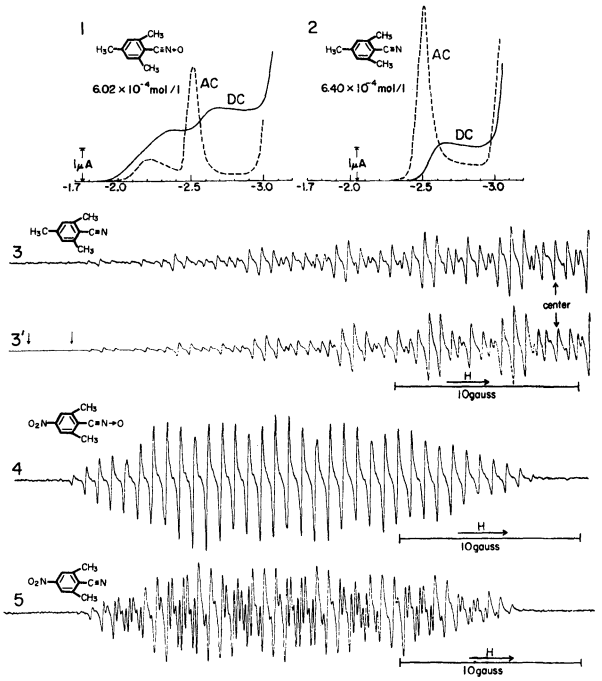

Fig. 1. ESR spectra of the anion radicals and non-aqueous polarograms of the compounds given in this figure. Simulated half spectrum for the observed one (3) is shown in the spectral number 3′ where vertical arrows indicate that the weak signals (1 : 2 : 1 triplet) also appear at these positions (hfc constant values used are listed in Table 1).

1) Presented in part at the 21st Annual Meeting of the Chemical Society of Japan, Osaka, April, 1968.

2) a) T. Kubota, H. Miyazaki, and Y. Mori, *Rev. Polarog.* (Kyoto), **14**, 313 (1967). b) T. Kubota, K. Nishikida, H. Miyazaki, K. Iwatani, and Y. Ōishi, *J. Amer. Chem. Soc.*, **90**, 5080 (1968). c) T. Kubota, Y. Ōishi, K. Nishikida, and H. Miyazaki, This Bulletin, **43**, 1622 (1970). d) K. Ezumi, H. Miyazaki, and T. Kubota, *J. Phys. Chem.*, **74**, 2397 (1970). e) K. Nishikida, T. Kubota, H. Miyazaki, and S. Sakata, Presented at the 8th Symposium of Electron Spin Resonance held by the Chemical Society of Japan, Hiroshima, Nov., 1969, to be published.

3) See M. Yamakawa, T. Kubota, and H. Akazawa, *Theor. Chim. Acta*, **15**, 244 (1969) as a leading reference.

4) C. Grundmann and J. M. Dean, *Angew. Chem. Int. Ed. Engl.*, **3**, 585 (1964); *J. Org. Chem.*, **30**, 2809 (1965); C. Grundmann and H. D. Frommeld, *ibid.*, **30**, 2077 (1965). The authors wish to express their thanks to Mrs. H. Ishida (née Akazawa) for preparing these samples.

5) M. Yamakawa, T. Kubota, and H. Akazawa, This Bulletin, **40**, 1600 (1967).

Table 1. Non-aqueous polarographic data, observed hyperfine coupling constants of produced anion radicals, and their assignments of the compounds shown in this Table

Compound	R	No.	Mp °C	$-E_{1/2}$: V *vs.* SCE (Lingane's constant)[a]		AC peak-height[a] μmhos/mmol		Hyperfine coupling constants (absolute value) of the corresponding anion radicals[a]
				1st wave	2nd wave	1st wave	2nd wave	
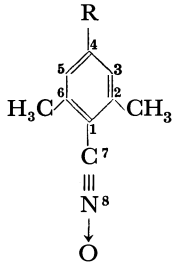	H	1	79.5—81.0	1.95[b] (1.68)	2.38 (1.31)	12	134	[c]
	CH_3	2	110.0	2.12[b] (2.64)	2.52 (1.32)	20	125	[c]
	Br	3	100.0—101.5	1.90[b] (2.43)	2.39 (0.99)	27	49	[c]
	OCH_3	4	69.0—71.0	2.24[b] (2.01)	2.62 (1.73)	14	69	—
	NO_2	5	130.0—131.0	0.915 (1.04)	1.132 (0.44)	213	85	6.02(4-NO_2), 3.71(3,5), 1.52(8), 0.74(2,6-CH_3)
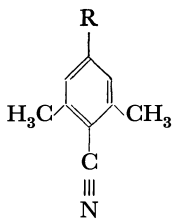	H	6	88.5—89.0	2.403 (2.22)	—	195	—	8.49(4), 3.87(2,6-CH_3), 2.41(8), 0.40(3,5)
	CH_3	7	50.0—51.5	2.505 (2.15)	—	189	—	9.52(4-CH_3), 4.10(2,6-CH_3), 2.38(8), 0.66(3,5)
	Br	8	69.0—70.0	1.849 (3.97)	2.367 (2.29)	52	223	[c]
	OCH_3	9	70.0—71.5	2.592 (3.39)	—	92	—	—
	NO_2	10	120—122	0.879 (2.14)	1.706 (1.86)	406	289	6.46(4-NO_2), 2.96(3,5), 0.82(8), 0.63(2,6-CH_3)

a) All measurements were made in dimethylformamide containing tetra-*n*-propylammonium perchlorate 0.1 mol/*l*. Here, Lingane's constant, I, was calculated by the equation $I(=607n\sqrt{D})=i_d/(cm^{2/3}t^{1/6})$, were i_d and c are wave height (μA) of diffusion current and sample concentration (mM), respectively. m (mg/sec) and t (sec/1 drop) are well-known characteristics of dropping mercury electrode. The t value was measured at the potential of diffusion current, but the m value in open circuit was approximately adopted.

b) The shape of the first wave is quite far from that of a normal one electron reduction wave as is seen in Fig. 1-1. Especially, for R=H the first wave seems to be divided into two waves. The former value is in this Table and the latter would be $E_{1/2}\approx-2.13$ V (0.90) and AC peak-height ≈6.

c) See discussions in the text.

gram, however, the above relationship between the first and second waves is just the reverse, the second peak height being considerably higher. In addition, the half-wave reduction potential values, $E_{1/2}$, of **2** and **7** are in almost the same order if a comparison is made between the second wave of **2** and the first wave of **7**. When controlled potential electrolysis has been made at the second reduction wave of **2**, one can obtain the well-resolved ESR spectrum shown in Fig. 1, which has the same pattern as that obtained by the electrolysis at the first wave of **7**. Therefore, we see that the anion radical of 2,4,6-trimethylbenzonitrile is produced there. On the other hand, no ESR signal was observed when the electrolysis was made at the first wave of **2**. Behaviour similar to the above was also found in the compound **1** (see Table 1).

All of the experimental facts mentioned above suggest the conclusion that the first wave of nitrile *N*-oxides is due to the deoxygenation process of the $-C\equiv N\rightarrow O$ group, which is behaviour similar to that observed in an aqueous medium,[2a] and that the second wave may be due to the anion-radical formation of the deoxygenated nitrile compound. This fact is quite different from the case of heterocyclic amine *N*-oxides, where the first reduction wave is due to the anion-radical formation of mother compounds, as is often the case. In the case of compound **3**, it was observed that the deoxygenation and debromination occur at the same time at the first reduction wave. The assignment of the hyperfine coupling (hfc) constants given in Table 1 is straightforward from the point of view of the molecular symmetry and the number of atoms which are in the same chemical environment, and seems to be reasonable in terms of theory.

The only exceptional compound in the present experiments is 2,6-dimethyl-4-nitrobenzonitrile *N*-oxide (**5**), whose anion radical was observed at the first reduction wave. The ESR spectrum obtained is well resolved, but is quite different from that of the anion radical of the corresponding nitrile (**10**). These spectra are shown in Fig. 1.[6] The fact that the oxygen atom of the nitrile-oxide group is very reactive[5,7] may be responsible for the deoxygenation process at the first wave. For the molecule **5**, however, the large intramolecular charge-transfer effect[3,5] from the nitrile-oxide group oxygen atom to the nitro group may stabilize the $\equiv N\rightarrow O$ bond more effectively; thus, the anion radical of the mother compound **5** is produced.

The authors wish to express their thanks to Professors Soichiro Musha and Makoto Munemori of the College of Engineering, University of Osaka Prefecture, for their useful discussions.

6) Detailed discussions of all the hfc constant values in this case (see Table 1) will be made in a separate paper, where they will be compared with the anion radical data of nitrones having a nitro group, *etc.*

7) R. Huisgen, *Angew. Chem. Int. Ed. Engl.*, **2**, 565 (1963).

BULLETIN OF THE CHEMICAL SOCIETY OF JAPAN, VOL. 44, 279—280 (1971)

Non-aqueous Polarogrophic Behavior of the Anion Radical Itself of 4-Nitropyridine *N*-Oxide[1]

Hiroshi MIYAZAKI and Tanekazu KUBOTA

Shionogi Research Laboratory, Shionogi & Co., Ltd., Fukushima-ku, Osaka

(Received July 16, 1970)

Although many reports have been published on the non-aqueous polarography of organic substances, there have been only a few reports on the polarographic behaviour of the anion radical itself, prepared macroscopically,[2] because of the instability of the radicals. However, a comparison of the non-aqueous polarogram for the neutral molecule (mother compound) with that of the anion radical formed from the mother compound also seems to be important in elucidating the reduction mechanism. From this point of view, we tried to make polarographic measurements of the anion radical itself of 4-nitropyridine *N*-oxide (4NPO) and of 4,4′-dinitrobiphenyl, whose polarograms usually show two waves: the first wave is due to the anion-radical formation of the mother compound,[3] while the second one may be caused by dianion formation.[3,4] In this note we would like to report our experimental results, and also our findings on the electrolysis cell, which may be very convenient for carrying out the measurement in a non-aqueous medium in which the contamination of water, *etc.* diffusing from the saturated calomel electrode (SCE) has been completely eliminated.

Experimental

The controlled potential electrolysis cell employed here is illustrated in Fig. 1. The cathode potential of either one of two electrolysis cells of almost the same size is controlled *versus* the SCE. The other cell is then in a parallel connection to the first one, as may be seen in Fig. 1. Now, it can easily be understood that the cathode potential of the second cell is also automatically controlled so as to operate at the cathode potential of the first cell. Since no reference cell is necessary for the second cell, any contamination originating from the reference cell is completely removed. Operation under a vacuum system or at a higher or a lower temperature is also very easy by making a little modification to satisfy this experimental purpose. In the present experiments, dimethylformamide was employed as the solvent, the supporting electrolyte being 0.1 mol/*l* tetra-*n*-propylammonium perchlorate. The capillary used for the dropping mercury

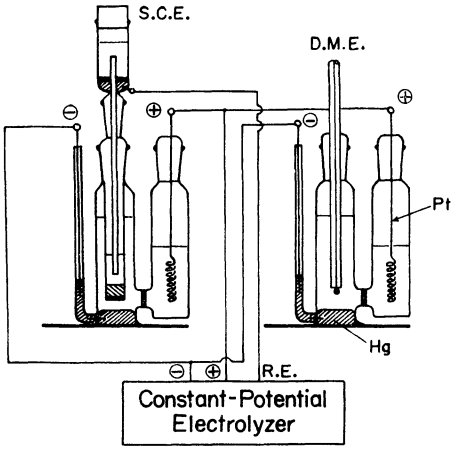

Fig. 1. Cells employed for recording the polarogram of anion radical itself (D.M.E.: dropping mercury electrode). The inlet part of N_2 gas for removing the dissolved oxygen is omitted in this figure for simplicity (see Fig. 1 of the reference 3a in text).

electrode had the following open circuit values in distilled water: $m=1.00$ mg/sec and $t=9.55$ sec at $h=70$ cm. When we measured the polarogram of the anion radical produced in the second cell, first the cell circuit was made free from the constant-potential electrolyzer, and then the anode of the cell (right-hand side in Fig. 1) was quickly replaced with SCE in a nitrogen atmosphere. The polarogram was subsequently recorded *versus* SCE. The other experimental procedure was just the same as in previous papers.[3,4]

Results and Discussion

The polarograms recorded for 4NPO are shown in Fig. 2 as typical examples. The observed constant values, such as the half reduction (or oxidation) potential, $E_{1/2}$, the DC wave height, i_{DC}, and the AC peak height, i_{AC}, are listed in Table 1. It was previously

Table 1. Polaroglaphic data of 4-nitropyridine *N*-oxide and its anion radical[a]

4-Nitropyridine *N*-oxide	$-E_{1/2}$[b] (V)	i_{DC} (μA)	i_{AC} (μmhos)	$-E_{1/2}$[b] (V)	i_{DC} (μA)	i_{AC} (μmhos)
	1st reduction wave			2nd reduction wave		
Neutral species	0.80	1.66	294	1.69	2.10	172
	Oxidation wave			Reduction wave		
After electrolysis at −1.10 V	0.77	1.38	228	1.66	1.88	128

a) See text for the meaning of each notation, and Fig. 2 for experimental conditions.

b) $-E_{1/2}$ values are *versus* SCE and corrected for so called *IR*-drop term.

1) Presented at the 14th Symposium of Polarography, Hiroshima, Oct. 7, 1968.

2) a) K. S. V. Santhanam and A. J. Bard, *J. Amer. Chem. Soc.*, **88**, 2669 (1966). b) J. L. Sadler and A. J. Bard, *J. Electrochem. Soc.*, **115**, 343 (1968). c) J.-P. Billon, *Bull. Soc. Chim. Fr.*, **1961**, 1923.

3) a) T. Kubota, K. Nishikida, H. Miyazaki, K. Iwatani, and Y. Ōishi, *J. Amer. Chem. Soc.*, **90**, 5080 (1968); b) K. Nishikida, H. Miyazaki, T. Kubota, S. Katsumata, and S. Nagakura, Presented at the 22nd Annual Meeting of the Chemical Society of Japan, Tokyo, April, 1969.

4) T. Kubota, Y. Ōishi, K. Nishikida, and H. Miyazaki, This Bulletin, **43**, 1622 (1970).

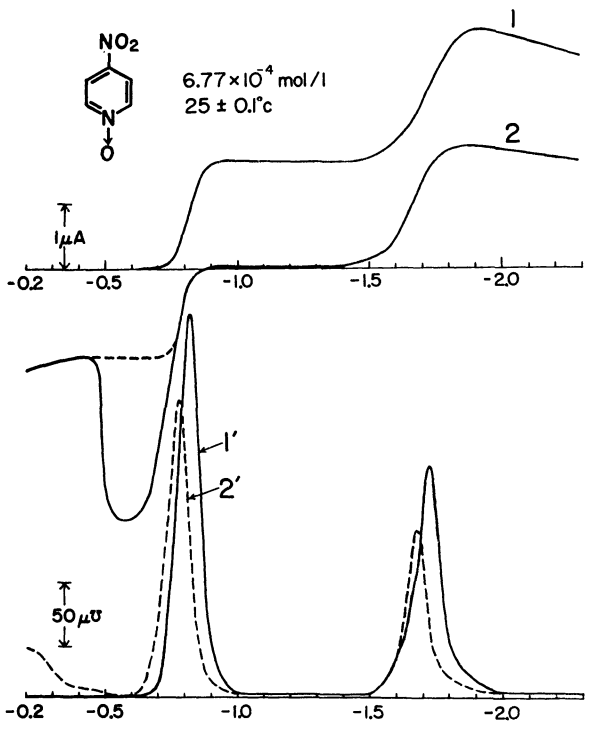

Fig. 2. DC (upper part) and AC (lower part) polarograms of 4-nitorpyridine *N*-oxide (1 and 1′) and its anion radical (2 and 2′).

shown that the first wave of the 4NPO neutral species is caused by the formation of the anion radical, which is quite stable,[5] and that the second wave may be due to the dianion formation, since: (i) DC wave-heights of the first and the second waves are almost the same and (ii) controlled potential electrolysis at the second wave gives the ESR signal of the 4NPO anion radical, perhaps because of a rapid electron exchange between neutral and dianion species. The results in Fig. 2 now give additional evidence for the interpretation of the reduction wave. That is, in the polarogram (curve 2) taken after reduction at -1.10 V for 60 min,[6] we see that the first wave disappears almost completely and that the oxidation wave appears at a potential close to that of the first wave of the polarogram 1.[7] In addition, (i) the second wave of the polarogram 1 decreases in wave height an amount corresponding to a one-electron reduction, so that the wave height of the polarogram 2 at ~ -2.0 V is almost the same as that of the first wave of the polarogram 1, and (ii) the AC peak-height (curve 2′) after reduction is also quite high in both the oxidation and reduction waves. These experimental results may indicate that the anion radical (A^-) formed at the first wave of the neutral species (N) is in an oxidation and reduction equilibrium like $N \rightleftarrows A^- \rightleftarrows A^=$, where $A^=$ stands for the dianion of the N species. Of course, the reversibility of the equilibrium between A^- and $A^=$ is less than that between N and A^-, since the reactivity of the $A^=$ species is quite high.[6] A polarographic behaviour of the anion radical similar to that described above was also observed in 4,4′-dinitrobiphenyl.[7]

In the case of 4-methylpyridine *N*-oxide, whose first reduction wave is not responsible for the anion radical formation, *i. e.*, in which the succeeding reaction also occurs at the first wave,[3a] no oxidation wave such as is seen in Fig. 2 could be observed in the polarogram of the substance produced after electrolysis at the first wave. This result seems to be reasonable because there is no good equilibrium between the A^- and N species.

The authors wish to express their thanks to Professors Soichiro Musha and Makoto Munemori of the College of Engineering, University of Osaka Prefecture, for their useful discussions.

5) K. Ezumi, H. Miyazaki, and T. Kubota, *J. Phys. Chem.*, **74**, 2397 (1970).

6) The color of the solution varied from pale yellow to pale blue→deep blue→and finally deep blue-greem, which again changed to pale yellow upon the introduction of dry air. In addition, polarographic measurements after reduction at -2.0 V (second wave: see Fig. 2) showed that the polarogram is somewhat complicated and time-dependent, indicating that the dianion generated macroscopically is not so stable as, and more reactive than, the monoanion radical.

7) Here, one remarkable point is that a quite strong maximum wave is superposed on the oxidation wave of the anion raidcal (see Fig. 2). This phenomenon seems to be generally observed in the experiments by us and by Bard *et al.*[2] The later authors explained it in terms of a pronounced streaming mechanism occurring on the dropping mercury electrode during the oxidation of the A^- species.

BULLETIN OF THE CHEMICAL SOCIETY OF JAPAN, VOL. 44, 281—283 (1971)

Direct and Sensitized Photoreactions of Allyl Phenyl Ether

Nakako SHIMAMURA and Akira SUGIMORI

Department of Chemistry, Faculty of Science and Technology, Sophia University, Kioi-cho, Chiyoda-ku, Tokyo

(Received August 4, 1970)

It has been reported that UV irradiation of allyl phenyl ether gives rearrangement products (*o*- and *p*-allylphenol) and phenol.[1-4] Although the mechanism of the photo-rearrangement has been proposed,[4] little investigation has been carried out on the excited states responsible for the formation of photo-rearrangement products and phenol. The present work deals with the effects of solvents and additives (sensitizers and quenchers) for the elucidation of the character of the excited states in the photoreaction.

Results and Discussion

Unsensitized photoreaction of allyl phenyl ether in transparent solvents is explained by reaction paths a,b,c,d, and e in Scheme 1.

The formation of a radical pair in a solvent cage is concluded from the effect of the viscosity of the solvents. Cage reactions are dependent on the viscosity (η) of solvent. The following equation was presented:[5]

$$\frac{\phi_1 + \phi_2}{\phi_1} = K_1 + \frac{K_2}{\eta} \qquad (1)$$

where ϕ_1 and ϕ_2 are the quantum yields of the reaction within and outside a solvent cage, and K_1 and K_2 are constants. In the unsensitized photoreactions of allyl phenyl ether, the equation was satisfied when allylphenols and phenol were taken as the products within and outside a solvent cage, respectively (Fig. 1).

As shown in Table 1, the quantum yields of the reactions within and outside a cage were almost independent of the presence of 1,3-pentadiene (a triplet quencher). This suggests that the unsensitized photoreaction occurs *via* excited singlet state. Photo-Fries rearrangement has been reported to proceed from excited singlet state of aryl esters.[6,7]

In the photosensitized reaction it was observed that aromatic hydrocarbons acted as sensitizers in a different way from carbonyl compounds. The photoreaction of allyl phenyl ether in aromatic hydrocarbons such as benzene and toluene satisfies Equation (1) as shown in Fig. 1. Addition of naphthalene to the cyclohexane solution of ether slightly affected the ratio of the quantum yields of the reactions within and outside a solvent cage. The reaction in benzene solution was not quenched by the addition of 1,3-pentadiene. Thus, sensitization by aromatic hydrocarbons should proceed through singlet-singlet energy transfer.

In contrast to aromatic hydrocarbons, the presence of carbonyl sensitizers (benzaldehyde, acetophenone, benzophenone and substituted benzophenones) increased the formation of phenol.

Carbonyl compounds are photo-reactive and undergo photo-induced reactions such as hydrogen abstraction

TABLE 1. EFFECTS OF ADDITIVES

Additive (mol/*l*)		E_t kcal/mol	Solv.[a]	Irr. time (hr)	ϕ_{PhOH}[b]	ϕ_o[b]	ϕ_p[b]	$\frac{\phi_o+\phi_p}{\phi_{PhOH}}$
—	—	—	C	2	0.058	0.061	0.055	2.0
—	—	—	B	5	0.045	0.036	0.038	1.7
Acetophenone	5.5×10^{-2}	74	C	2	0.054	0.0057	0.0025	0.13
Acetophenone	5.9×10^{-2}	74	B	2	0.049	0.0070	0.0064	0.28
Benzaldehyde	5.6×10^{-2}	72	C	2	0.051	0.0055	0.0029	0.17
Benzophenone	5.1×10^{-2}	69	C	2	0.026	+	+	<0.1
Benzophenone	5.0×10^{-2}	69	B	2	0.042	0.012	0.012	0.57
p,*p*′-Dimetoxybenzophenone	2.5×10^{-2}	70	B	2	0.076	0.019	0.012	0.41
p-Hydroxybenzophenone	1.0×10^{-1}	68	B	2	0.044	0.021	0.017	0.86
Michler's ketone	2.5×10^{-2}	61	B	2	0.027	0.0058	0.0053	0.42
Naphthalene	5.1×10^{-2}	61	C	5	0.012	0.0088	0.0089	1.5
1,3-Pentadiene	2.5×10^{-1}	59	C	5	0.033	0.028	0.030	1.8
1,3-Pentadiene	2.5×10^{-1}	59	B	5	0.043	0.032	0.028	1.4
Oxygen	—	—	C	5	0.011	0.012	0.011	2.0

a) B: 0.1M Benzene solution, C: 0.1M Cyclohexane solution

b) ϕ_{PhOH}, ϕ_o and ϕ_p represent the quantum yields of phenol, *o*-allylphenol and *p*-allylphenol, respectively.

1) M. S. Kharasch and G. Stampa, Science, **116**, 309 (1952).
2) K. Schmid and H. Schmid, *Helv. Chim. Acta*, **36**, 687 (1953).
3) D. P. Kelly and J. T. Pinhey, *Tetrahedron Lett.*, **1966**, 5953.
4) G. Koga, N. Koga, and N. Kikuchi, This Bulletin, **41**, 745 (1968).
5) D. Booth and R. M. Noyes, *J. Amer. Chem. Soc.*, **82**, 1868 (1960).
6) H. Shizuka, T. Morita, Y. Mori, and I. Tanaka, This Bulletin, **42**, 1831 (1968).
7) H. J. Hagman, *Tetrahedron*, **25**, 6015 (1969).

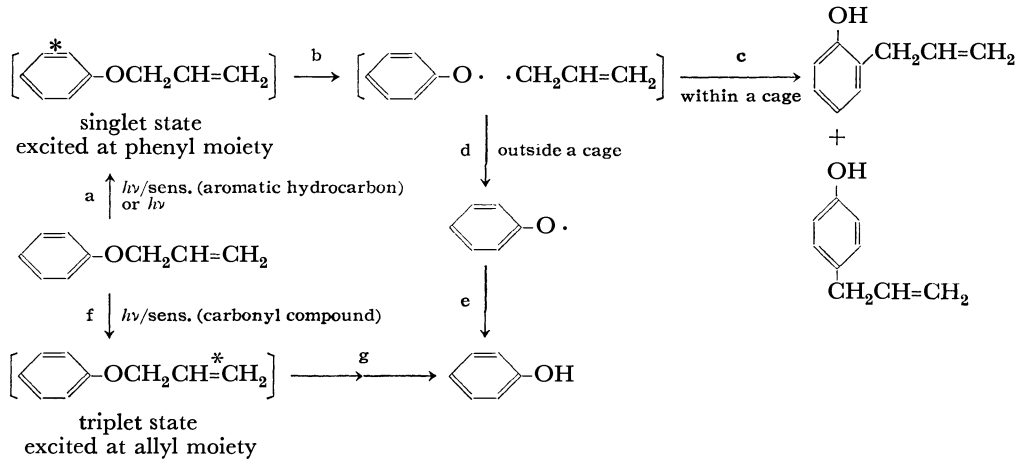

Scheme 1

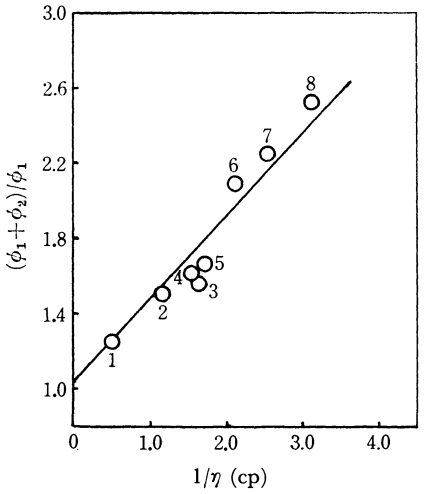

Fig. 1. Effect of viscosity on cage reaction $\phi_1=\phi_C+\phi_P$, $\phi_2=\phi_{PhOH}$. 1. 2-Propanol, 2. Cyclohexane, 3. Cyclohexene, 4. Benzene, 5. Toluene 6. Isooctane 7. *n*-Heptane, 8. *n*-Hexane

and oxetane formation. These reactions might induce phenol formation from allyl phenyl ether. (In this case the consumption of sensitizers is expected.) However, this sort of "sensitization" is not probable: (i) UV absorption and gas-chromatographic examination of the acetophenone and benzophenone sensitized reactions in benzene revealed that no sensitizer was consumed in the course of the reaction; (ii) sensitization was observed with Michler's ketone and *p*-hydroxybenzophenone which are known to be photo-unreactive; (iii) thermal decomposition of benzoyl peroxide in benzene containing allyl phenyl ether did not give allylphenols or phenol.

The results can be interpreted by the mechanism of energy transfer from *n*-π^* triplet state of carbonyl compounds to olefins proposed by Yang, Cohen, and Shani.[8] The mechanism consists of two steps: (i) addition of excited carbonyl compounds to olefinic double bonds; (ii) elimination of ground state carbonyl compounds to give excited olefins. This suggests that the triplet energy of carbonyl compounds can be transferred selectively to the double bond of allyl moiety rather than phenyl moiety of allyl phenyl ether, while the excess energy of aromatic hydrocarbons is transferred to phenyl moiety of the ether. Excitation of allylic double bond would bring about phenol formation, the mechanism of which is still unknown.

The photoreactions of allyl phenyl ether are summarized in Scheme 1.

8) N. C. Yang, J. I. Cohen, and A. Shani, *J. Amer. Chem. Soc.*, **90**, 3264 (1968).

Experimental

Materials. Ally phenyl ether was synthesized from phenol and allyl bromide and purified by distillation, bp 92°C/25 mmHg. The purity determined by gas-chromatography was 98.6%. Benzophenone, *p,p'*-dimethoxybenzophenone, 3,4-dimethylphenol (G.R. grade of Tokyo Kasei Co.), *p*-hydroxybenzophenone, Michler's ketone (E.P. grade of Tokyo Kasei Co.), naphthalene (E.P. grade of Showa Kagaku Co.), and benzoyl peroxide (T.G. grade of Wako Junyaku Co.) were used without further purification. Benzaldehyde, acetophenone (E.P. grade of Yoneyama Yakuhin Co.), and 1,3-pentadiene (T.G. grade of Tokyo Kasei Co.) were purified by distillation.

Solvents. Commercially available *n*-hexane, *n*-heptane, and isooctane of spectral quality (Dotite Spectrosol) were used without further purification. Benzene, toluene, and 2-propanol (each E.P. grade of Junsei Kagaku Co.) were purified by fractional distillation. Cyclohexane was purified by treatment with nitric acid, followed by treatment with a silica gel column. Cyclohexane, *n*-hexane, *n*-heptane, and isooctane used had no or a slight absorption at 254 nm.

UV Irradiation. Degassed 0.1 M solution of ally phenyl ether in a quartz tube was irradiated externally with a low pressure mercury lamp (16W spiral type lamp made by Taika Kogyo Co.) with or without sensitizers and quenchers. The solution was stirred with a magnetic stirrer. The reaction vessel and the mercury lamp were immersed in a thermostat kept at 25°C. Up to 5 hours the products increased nearly in proportion to irradiation time. Prolonged irradiation caused a decrease in the quantum yields of the products probably because of the contamination of the wall of the vessel by photolysis products.

Analysis of the Products. The reaction products were analyzed gas-chromatographically with Yanagimoto Gas Chromatograph Model GCG 550 F (column, 1.2 m, 20% Carbowax on Celite; temperature, 180°C).

In the experiment of photosensitization by carbonyl compounds, the quantities of carbonyl compounds after irradiation were estimated by UV absorption spectroscopy and gas-chromatography. Absorption of acetophenone at 320 nm and absorption of benzophenone at 345 nm were used for the estimation.

Actinometry. Actinometry was performed with potassium ferrioxalate actinometer.[9] In the reaction condition above, the intensity of light was 2.9×10^{17} quanta/sec for 20 m*l* of solution.

9) C. G. Hatchard and C. A. Parker, *Proc. Roy. Soc.* (London), **A 235**, 518 (1956).

BULLETIN OF THE CHEMICAL SOCIETY OF JAPAN, VOL. 44, 283—285 (1971)

Asymmetric Reactions. V. Homogeneous Hydrogenation of Unsaturated Compounds Catalyzed by Bis-(dimethylglyoximato)cobalt(II)[1]

Yoshiaki OHGO, Seiji TAKEUCHI, and Juji YOSHIMURA

Laboratory of Chemistry for Natural Products, Tokyo Institute of Technology, Meguro-ku, Tokyo

(Received August 4, 1970)

Schrauzer and Windgassen[2] reported that stable metal-alkyl complexes are formed in the reaction of bis(dimethylglyoximato)cobalt(II) complex and certain olefines under hydrogen atmosphere, and that in some cases reduction products are obtained concurrently. Reductive methylation of amines and mercaptanes with formaldehyde and hydrogen catalyzed by bis(dimethylglyoximato)cobalt(II) was also reported by the same investigators.[3]

As a part of studies on the asymmetric reduction using optically active metal complexes,[4,5] we have tried to obtain a suitable metal-alkyl complex by the reaction of bis(dimethylglyoximato)cobalt(II) with several unsaturated compounds under hydrogen atmosphere. However, no metal-alkyl complex but the reduction product could be obtained.

We wish to report that bis(dimethylglyoximato)-cobalt(II) is a useful catalyst for reduction of activated olefines, unsaturated nitrogen compounds, α-diketones and α-keto acid esters.

Experiments were carried out under atmospheric pressure of hydrogen at room temperature, and the products were confirmed by mixed melting point and/or IR and NMR spectra. The results are summarized in Tables 1 and 2.

It can be considered that both steric and electronic

Table 1. Hydrogenation of olefines catalyzed by bis(dimethylglyoximato)cobalt

Run	Substrate	S/Co[b]	Reaction time[c]	Products (Yield)
1	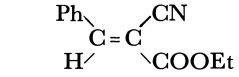	2	7 hr	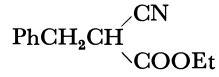 (89%)[a]
2	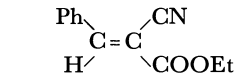	10	8 hr	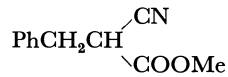 (80%)
3	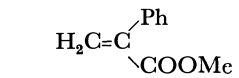	1	1 hr	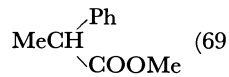 (69%)
4	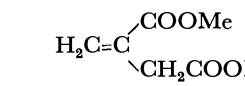	4	1 hr	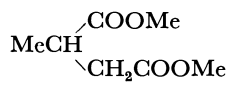 (100%)
5	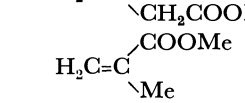	10	2 hr	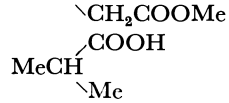 (98.5%)
6	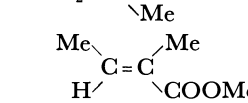	3	1 day	recovered
7	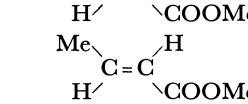	10	4 days	recovered

1) This work was presented at the 23rd Annual Meeting of the Chemical Society of Japan, April., 1970.

2) G. N. Schrauzer and R. J. Windgassen, *J. Amer. Chem. Soc.*, **89**, 1999 (1967); G. N. Schrauzer, *Accounts Chem. Res.*, **1**, 97 (1968).

3) G. N. Schrauzer and R. J. Windgassen, *Nature*, **214**, 492 (1967).

4) Asymmetric Reactions. IV., Y. Ohgo, S. Takeuchi, and J. Yoshimura, This Bulletin, **43**, 505 (1970).

5) S. Takeuchi, Thesis for M.Sc., Tokyo Institute of Technology, March, 1969.

8	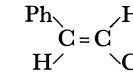	2	4 days	recovered
9	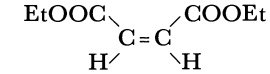	4	3 days	$EtOOCCH_2CH_2COOEt$ (69%)[a]
10	$H_2C{=}CHPh$	4	3 days	recovered
11	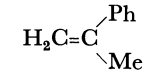	5	3 days	recovered
12	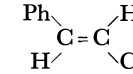	7	4 days	recovered
13	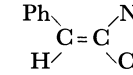	1	2 days	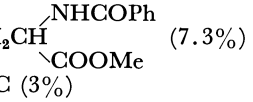 (7.3%) MBAC (3%)
14	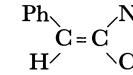 (MBAC)	1	1 day	recovered
15	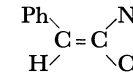 [d]	1	3 days	recovered

a) Solvent; ethanol, in systems except for a) methanol was used.
b) S/Co; molar ratio of substrate to catalyst (Co).
c) Time required for the completion of reaction for the reaction mixture to be left standing.
d) C_6H_{11}=cyclohexyl

Table 2. Hydrogenation of unsaturated compounds containing hetero atoms catalyzed by bis(dimethylglyoximato)cobalt (II)

Run	Substrate	S/Co[a]	Reaction time[b]	Products (yield)
16	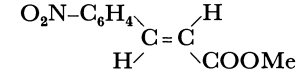	2	1 hr	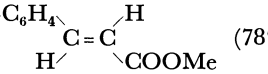 (78%)
17	$PhNO_2$ (2.4 g)	7	5 days	PhNHNHPh, $PhNH_2$ (1.5 g)
18	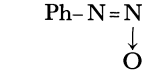	3	45 min	Ph-N=N-Ph (76%)
19	Ph-N=N-Ph	5	29 min	PhNHNHPh (99%)
20	PhCOCOOEt	10	80 min	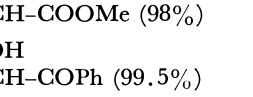 (98%)
21	PhCOCOPh	10	35 min	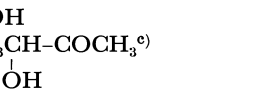 (99.5%)
22	$CH_3COCOCH_3$	10	24 hr	 [c]

a) S/Co: molar ratio of substrate to catalyst (Co).
b) Time required for the completion of reaction or for the reaction mixture to be left standing.
c) Biacetyl adsorbed a theoretical amount of hydrogen, but only a small amount of acetoin was obtained because of an unsuitable isolation procedure.

factors have an effect on the reactivity. As shown in Table 1, olefines which have electron defficient double bond were catalytically reduced by hydrogen. However, the olefines having no electron-withdrawing group were not reduced. Steric factors do not seem to be so important as electronic ones. From this viewpoint, methyl *p*-nitrocinnamate was considered to be catalytically reducible. However, it was found that the C–C double bond of this compound was not reduced, but the nitro group was reduced to give amino group contrary to anticipation (Table 2). Nitrobenzene was also reduced to give aniline and hydrazobenzene. Azobenzene and azoxybenzene gave hydrazobenzene, but a prolonged treatment for isolation and purification afforded azobenzene. This implies that hydrazobenzene is catalytically oxidized by oxygen during the course of isolation. Nitroalkanes were not reduced under mild conditions. α-Diketones and α-keto acid esters were also reduced easily. Studies on the reduction mechanism are now in progress.

Experimental

$CoCl_2 \cdot 6H_2O$ (0.708 g, 0.03 mol) was dissolved in 50 m*l* of methanol or ethanol, and to the solution was added 0.690 g of dimethylglyoxime (0.06 mol) with stirring under nitrogen atmosphere for 5 min. To this solution was added a solution of 0.28 g of sodium hydroxide (0.07 mol), pyridine (0.23 g)

and substrate (1—10 equivalent to cobalt) successively. Stirring was then stopped. The vessel containing the solution was purged with hydrogen, and the solution was again stirred under hydrogen atmosphere at room temperature. After absorption of the theoretical amount of hydrogen, the reaction mixture was diluted with water containing a small amount of acetic acid and extracted with ether or methylene chloride. The organic layer was washed with water, dried over anhydrous sodium sulfate and concentrated *in vacuo*. The resulting products were confirmed by mixed melting point (incase of crystals) and/or IR and NMR spectra. The results are shown in Tables 1 and 2.

BULLETIN OF THE CHEMICAL SOCIETY OF JAPAN, VOL. 44, 285—286 (1971)

Electronic Spectra of Amino-substituted Pteridines

Mamoru KAMIYA
Shizuoka College of Pharmacy, Oshika, Shizuoka

(Received August 26, 1970)

Several SCF-MO calculations have been reported for the π-electronic structure of pteridines, chiefly of the parent molecule,[1-6] but little is known about a systematic calculation for a series of substituted pteridines forming fundamental structures of complicated biopteridines. Here, the semiempirical VESCF-MO-CI[7-9] calculations on pteridines and all its monoamino derivatives and a few of its diamino derivatives have been performed in making a systematic survey of amino-substitution effects upon electronic spectra. The elements of the F matrix are usually evaluated by adopting the zero differential overlap approximation. On the basis of the atomic spectroscopic data reported by Pritchard and Skinner,[10] the equations representing

TABLE 1. COMPARISON BETWEEN CALCULATED AND OBSERVED SPECTRA

Compound	Calculated $\Delta E^{a)}$	($f^{b)}$)	$\alpha^{0\,c)}$	Observed $\Delta E^{a)}$ ($\varepsilon_{max}\times 10^{-3}$)
Pteridine	4.417	(0.253);	16	4.12 (7.5)[11]
	4.937	(0.051);	70	5.27 (2.9)
	5.897	(0.280);	−35	5.90 (11.0)
	6.250	(0.039);	−40	
	6.645	(0.562);	−49	
2-Amino	3.582	(0.304);	25	3.35 (6.6)[12]
	4.341	(0.106);	−22	
	5.064	(0.018);	−72	
	5.535	(0.542);	−24	5.51 (24.0)
	6.032	(0.003);	60	
4-Amino	3.818	(0.281);	48	3.70 (6.6)[12]
	4.353	(0.008);	−70	
	5.177	(0.379);	−36	5.08 (15.8)
	5.376	(0.202);	21	
	5.749	(0.048);	33	
6-Amino	3.509	(0.333);	22	3.42 (5.6)[13]
	4.482	(0.135);	−15	4.81 (10.2)
	5.028	(0.004);	79	
	5.730	(0.190);	−35	5.56 (19.9)
	6.145	(0.973);	−38	
7-Amino	3.655	(0.288);	14	3.71 (10.7)[13]
	4.489	(0.029);	−12	4.73 (6.3)
	5.282	(0.040);	59	
	5.779	(0.478);	32	5.44 (18.2)
	5.918	(0.654);	33	
2,4-Diamino	3.370	(0.296);	27	3.41 (6.3)[14]
	4.064	(0.019);	−15	
	4.966	(0.426);	−49	4.86 (17.8)
	5.194	(0.422);	−13	
	5.503	(0.019);	−87	
4,6-Diamino	3.404	(0.329);	32	3.31 (6.5)[15]
	4.138	(0.084);	18	
	4.754	(0.369);	−43	4.71 (15.1)
	5.159	(0.157);	−11	
	5.314	(0.122);	64	
4,7-Diamino	3.532	(0.244);	5	3.66 (11.2)[15]
	4.052	(0.091);	84	
	4.968	(0.184);	−17	
	5.044	(0.420);	66	5.14 (24.0)
	5.289	(0.121);	−15	

a) Singlet π-π^* transition energy in eV.
b) Oscillator strength.
c) Polarization direction measured counterclockwise to the x-axis.

1) G. Favini, I. Vandoni, and M. Simonetta, *Theor. Chim. Acta*, **3**, 418 (1965).
2) B. Tinland, *ibid.*, **8**, 361 (1967).
3) R. D. Brown and B. A. W. Coller, *ibid.*, **7**, 259 (1967).
4) R. L. Flurry, E. W. Stout, and J. J. Bell, *ibid.*, **8**, 203 (1967).
5) A. Hincliffe, M. A. Ali, and E. Farmer, *Spectrochim. Acta*, **23**, 501 (1967).
6) M. Kamiya, *Nippon Kagaku Zasshi*, **90**, 769 (1969).
7) R. Pariser and R. G. Parr, *J. Chem. Phys.*, **21**, 466, 767 (1953).
8) J. A. Pople, *Trans. Faraday Soc.*, **49**, 1357 (1953).
9) R. D. Brown and M. L. Heffernan, *ibid.*, **54**, 757 (1958).
10) H. O. Pritchard and H. A. Skinner, *Chem. Rev.*, **55**, 745 (1955).
11) S. F. Mason, *J. Chem. Soc.*, **1955**, 2336.
12) A. Albert, D. J. Brown, and G. Cheeseman, *ibid.*, **1951**, 474.
13) A. Albert. D. J. Brown, and H. C. S. Wood, *ibid.*, **1954**, 3832.
14) M. F. Mallete, E. C. Taylor, Jr., and C. K. Cain, *J. Amer. Chem. Soc.*, **69**, 1814 (1947).
15) A. Albert, J. H. Lister, and C. Pederson, *J. Chem. Soc.*, **1956**, 4621.

the parabolic dependence of the valence-state ionization potential (I_r) and one-center repulsion integral (γ_{rr}) upon the effective nuclear charge (Z_r) are taken to be as follows:

for =C– and –$\overset{|}{\text{N}}$– ($sxyz$, V_4)

$$I_r = 3.390Z_r^2 - 7.899Z_r + 1.157,$$
$$\gamma_{rr} = -0.432Z_r^2 + 9.164Z_r - 14.527,$$

for =N– (sx^2yz, V_3)

$$I_r = 3.455Z_r^2 - 10.594Z_r + 3.256,$$
$$\gamma_{rr} = -0.415Z_r^2 + 9.912Z_r - 19.435.$$

The two-center repulsion integrals (γ_{rs}) and the core-resonance integrals (β_{rs}) of all the atomic pairs were recalculated after each SCF iteration process according to the Pariser-Parr method[7] and the equation of $\beta_{rs} = -1/2S_{rs}(I_r + I_s)$, respectively. S_{rs} is the theoretically calculated overlap integral between the Slater-type atomic orbitals. The molecular orbitals became self-consistent to five-decimal places in fifteen interations, on the average. Full-configuration interaction is included between all singly-excited configurations. The molecular geometry of the pteridine ring is obtained from the X-ray analysis data by Hamor and Robertson,[16] and the bond-length of the C-NH_2 bond is assumed to be 1.34 Å and the direction of the bond is assumed to bisect the intra-ring angle around the substituted position. Actual numerical calculations were performed with the HITAC 5020-E computer at the University of Tokyo.

Table 1 shows that the two lowest transitions in the calculated spectrum of pteridine are polarized in agreement with the experimental data by Mason.[11] This fact suggests that the first and second π–π^* bands are polarized along the long-axis and the short-axis respectively. The calculated (observed) lowest π–π^* transition energy of the monoamino derivatives is in the increasing order of: $6 \leqq 2 < 7 < 4$ ($2 < 6 < 4 \leqq 7$). This indicates that the amino-group substituted parallel to the long-axis, especially to the 2- and/or 6-position, exerts a large bathochromic effect on this transition. The corresponding oscillator strength is in the increasing order of: $4 \leqq 7 < 2 < 6$, while the observed intensity is mostly enhanced by the 7-substitution. Furthermore, on all monoamino-substitutions except that to the 4-position, the polarization direction of the second π–π^* transition is also turned to the long-axis, and a weak theoretical transition appears between the two transitions correlated with the observed second and third π–π^* bands. The calculated spectra of the diamino derivatives are in fairly good agreement with those observed for the 2,4-, 4,6-, and 4,7-substituted derivatives. In this case also, it can be predicted that the substitution to the 7- and 4-positions causes the lowest π–π^* transition to be polarized quite close to the long-axis.

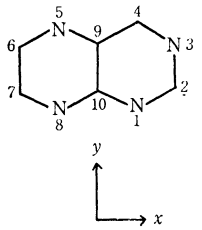

Fig. 1. The numbering of pteridine ring.

16) T. A. Hamor and J. M. Robertson, *J. Chem. Soc.*, **1956**, 3586.

BULLETIN OF THE CHEMICAL SOCIETY OF JAPAN, VOL. 44, 286—287 (1971)

The Resolution of *t*-Butyloxycarbonyl-DL-α-phenylsarcosine

Hideki KINOSHITA, Masaki SHINTANI, Tomoo SAITO, and Hiroshi KOTAKE

Faculty of Science, Kanazawa University, Kanazawa

(Received August 26, 1970)

α-Phenylsarcosine was first found in nature by Sheehan *et al.* from the hydrolysate of etamycin and was proved to belong to the L-series.[1] Although Sheehan *et al.*[1] reported that the amino acid isolated from etamycin showed $[\alpha]_D^{31}$ +118° (in N hydrochloric acid), this value seemed to show not the actual value, but that of partially racemized α-phenylsarcosine. Since the actual specific rotation values of this amino acid has not yet been established as far as we know, we attempted to obtain optically pure components. In this paper the resolution of DL-α-phenylsarcosine using ephedrines is described. The usefulness of these substances for the resolution of amino acids has reported in a previous paper.[2]

t-Butyloxycarbonyl-DL-α-phenylsarcosine (I), which was prepared by the *t*-butyloxycarbonylation of DL-α-phenylsarcosine,[3] following a procedure of Sakakibara *et al.*,[4] was mixed with (−)-ephedrine (molar ratio 1:1.1) in benzene - hexane to give crystalline *t*-butyloxycarbonyl-L-α-phenylsarcosine·(−)-ephedrine salt (II).

1) J. C. Sheehan, H. G. Zachau, and W. B. Lawson, *J. Amer. Chem. Soc.*, **80**, 3349 (1958).

2) K. Oki, K. Suzuki, S. Tuchida, T. Saito, and H. Kotake; This Bulletin **43**, 2554 (1970).

3) T. Araga, T. Saito, and H. Kotake, *Nippon Kagaku Zasshi*, **86**, 111 (1965).

4) S. Sakakibara, I. Honda, and K. Takada, This Bulletin, **42**, 809 (1969).

The filtrate from this salt was treated with (+)-ephedrine in benzene - hexane at room temperature to give *t*-butyloxycarbonyl-D-α-phenylsarcosine·(+)-ephedrine salt (III). The salt II was treated with hydrochloric acid to give *t*-butyloxycarbonyl-L-α-phenylsarcosine (IV) ($[\alpha]_D^{24}$ +134.8°), which was then treated with formic acid[5] to give L-α-phenylsarcosine (VI), $[\alpha]_D^{34}$ +169.3° (in N hydrochloric acid). By a similar procedure, III was converted to *t*-butyloxycarbonyl-D-α-phenylsarcosine (V)($[\alpha]_D^{29}$ −134.1°),which was then treated with formic acid to give D-α-phenylsarcosine (VII), $[\alpha]_D^{34}$ −170.7° (in N hydrochloric acid). These values of L- and D-phenylsarcosine were supported by the results of an alternative method of resolution. The resolution of benzyloxycarbonyl-DL-α-phenylsarcosine with brucine, followed by the removal of the benzyloxycarbonyl group by means of catalytic reduction, gave L-α-phenylsarcosine, $[\alpha]_D^{34}$+169.9° (in N hydrochloric acid).

Experimental

All the melting points are uncorrected. The optical rotation values were measured with a Jasco DIP-SL-type polarimeter.

t-Butyloxycarbonyl-DL-α-phenylsarcosine (I). A stock solution of *t*-butyl chloroformate was added to a solution of 7.59 g (0.03 mol) of DL-α-phenylsarcosine in ethanol containing 3.89 g of potassium hydroxide, and then 10 m*l* of dimethylformamide was added with stirring at 0—−3°C. The reaction mixture was agitated vigorously during the addition over a period of about half an hour. The stirring was continued for a further 2 hr at 0°C, and then for an additional hour at room temperature. The reaction mixture was subsequently adjusted to pH 2—3 with N hydrochloric acid, and the product was extracted with ethyl acetate. The ethyl acetate layer was washed with a saturated solution of sodium chloride and dried over anhydrous sodium sulfate. The ethyl acetate was evaporated to dryness to afford 4.4 g of *t*-butyloxycarbonyl-DL-α-phenylsarcosine (55.3%). Recrystallization from benzene-petroleum ether gave 4.0 g of I with a melting point of 122—123°C (50.2%).

Found: C, 63.30; H, 7.35; N, 5.26%. Calcd for $C_{14}H_{19}O_4N$: C, 63.38; H, 7.22; N, 5.28%.

t-Butyloxycarbonyl-L-α-phenylsarcosine·(−)-Ephedrine Salt (II) and t-Butyloxycarbonyl-D-α-phenylsarcosine·(+)-Ephedrine Salt (III). 1.060 g (0.004 mol) of I and (−)-ephedrine hemihydrate (750 mg, 0.0043 mol) were dissolved in 2 m*l* of hot benzene, and then 7 m*l* of hexane were added. The mixture was then allowed to stand for 24 hr at room temperature. The deposited crystals were filtered off and washed with 4 m*l* of benzene - hexane (1 : 3) to afford 830 mg (92.6%) of II, mp 84—88°C. Two recrystallizations from ethyl acetate-petroleum ether gave 680 mg (75.9%) of the pure material with a melting point of 91—93°C. $[\alpha]_D^{27}$ +65.2° (*c* 0.951; absolute ethanol).

Found: C, 64.23; H, 8.10; N, 6.37%. Calcd for $C_{24}H_{34}O_5N_2\cdot H_2O$: C, 64.26; H, 8.09; N, 6.25%.

The mother liquor obtained after the removal of II was evaporated to dryness to give an oily material. This oily material was dissolved in 6 m*l* of ethyl acetate, and the ethyl acetate layer was washed with 3 m*l* of N hydrochloric acid and water. The organic layer was dried over anhydrous sodium sulfate and then evaporated to dryness to give 530 mg of an oily product. This product and (+)-ephedrine hemihydrate (375 mg, 0.0022 mol) were dissolved in 1.3 m*l* of hot benzene, and then 7 m*l* of hexane were added. The deposited crystals were filtered off to afford 560 mg (65.2%, mp 84—89°C) of III. Two recrystallizations from ethyl acetate-petroleum ether gave 500 mg (55.8%) of an optically pure material with a melting point of 91—93°C. $[\alpha]_D^{28}$ −65.2° (*c* 0.605; absolute ethanol).

Found: C, 63.85; H, 8.17; N, 5.93%. Calcd for $C_{24}H_{34}O_5N_2\cdot H_2O$: C, 64.26; H, 8.09; N, 6.25%. A mixed-melting-point determination of (−) and (+) salt was depressed to 80—85°C.

t-Butyloxycarbonyl-L-α-phenylsarcosine (IV). To a suspension of 600 mg (0.0014 mol) of II in 7 m*l* of ethyl acetate, there were added 2.3 m*l* of N hydrochloric acid; the mixture was then shaken effectively in a separatory funnel. After washing with water (three 1-m*l* portions), the ethyl acetate layer was dried over anhydrous sodium sulfate. The ethyl acetate was evaporated to dryness to give 370 mg of crude crystals (quantitative, mp 110—112°C). Recrystallization from benzene-petroleum ether gave 312 mg (84.3%) of pure crystals with a melting point of 111.5—112.5°C. $[\alpha]_D^{24}$ +134.8° (*c* 0.804, absolute ethanol).

Found: C, 63.73; H, 7.23; N, 5.60%. Calcd for $C_{14}H_{19}O_4N$: C, 63.38; H, 7.22; N, 5.28%.

t-Butyloxycarbonyl-D-α-phenylsarcosine (V). Following the method used for the preparation of IV, from 600 mg (0.0014 mol) of III, 340 mg of crude crystals were obtained (91.9%, mp 110—111°C). Recrystallization from benzene-petroleum ether gave 300 mg (80.1%) of pure crystals with a melting point of 112—112.5°C. $[\alpha]_D^{29}$ −134.1° (*c* 0.682, absolute ethanol).

Found: C, 63.25; H, 7.32; N, 5.18%. Calcd for $C_{14}H_{19}O_4N$: C, 63.38; H, 7.22; N, 5.28%.

L-α-Phenylsarcosine (VI). 150 mg (0.566 mmol) of IV were dissolved in 7.5 m*l* of formic acid, and the mixture was allowed to stand for 1.5 hr at 22°C. The formic acid was evaporated to dryness at 22°C to afford 87 mg of VI (93.7%). Recrystallization from water - acetone gave 80 mg of a pure material (86.2%). $[\alpha]_D^{34}$ +169.3° (*c* 0.655, N hydrochloric acid), mp 245° (sublime).

Found: C, 65.45; H, 6.72; N, 8.18%. Calcd for $C_9H_{11}O_2N$: C, 65.44; H, 6.71; N, 8.43%.

D-α-Phenylsarcosine (VII). Following the method used for the preparation of L-α-phenylsarcosine, 88 mg of VII was obtained from 150 mg of V (94.8%). Recrystallization from water - acetone gave 80 mg of a pure material (86.2%). $[\alpha]_D^{34}$ −170.7° (*c* 0.571, N hydrochloric acid), mp 244°C (sublime).

Found: C, 65.68; H, 6.84; N, 8.34%. Calcd for $C_9H_{11}O_2N$: C, 65.44; H, 6.71; N, 8.43%.

5) B. Halpern and D. E. Nitecki, *Tetrahedron Lett.*, **1967**, 3031.

BULLETIN OF THE CHEMICAL SOCIETY OF JAPAN, VOL. 44, 288 (1971)

Hydrogenation of Acid Anhydrides with Cobalt Carbonyl Catalyst

Hachiro WAKAMATSU, Junko FURUKAWA, and Nobuyuki YAMAKAMI
Central Research Laboratories, Ajinomoto Co., Inc., Suzuki-cho, Kawasaki

(Received August 31, 1970)

Various carboxylic acid derivatives such as acid chlorides, imidochlorides, *N*-alkylamides, thioesters, hydrazides, and nitriles are known to give aldehydes on hydrogenation. However, little is reported[1] on the selective hydrogenation of carboxylic acid anhydrides to give aldehydes. Carboxylic acid anhydrides were found to be catalytically hydrogenated to give corresponding aldehydes and acids. Intermolecular anhydrides gave acids and aldehydes in comparable amount, whereas intramolecular anhydrides gave aldehydic acids. The new hydrogenation reaction is catalyzed by cobalt carbonyl and takes place at elevated temperatures under pressure of hydrogen and carbon monoxide. No effort was made to improve yields of the aldehydes in the experiments. The results are given in Table 1. Benzoic, acrylic, and maleic anhydrides gave anomalous results.

$$(RCO)_2O + H_2 \longrightarrow RCO_2H + RCHO$$

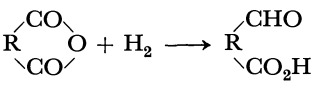

The solvent effect is greater on the rate of reaction than on the hydroformylation of olefins. At 130°C, the reaction carried out in acetone gives pseudo first order rate constant five times larger than that in diethyl ether. The rate is about the same for the reaction in acetone at 130°C, that in acetic acid at 160°C, and that in benzene or cyclohexane at 175°C. When toluene was used as a solvent, the main products from acetic anhydride were reported to be acetic acid and ethyl acetate.[2] Addition of a catalytic amount of pyridine accelerates the hydrogenation reaction and thus makes the reaction possible at lower temperatures (~130°C) even in benzene and cyclohexane. Sodium iodide has an accelerating effect on the hydrogenation reaction in diethyl ether. The effect of partial pressure of carbon monoxide and hydrogen on the rate of hydrogenation of acetic anhydride is quite the same as that reported for hydroformylation and cobalt carbonyl catalyzed hydrogenation of aldehydes.[3]

When hydrogen cobalt tetracarbonyl was dissolved in acetic anhydride at −40°C and brought to −15°C, acetic acid, acetaldehyde and dicobalt octacarbonyl were obtained.

TABLE 1. HYDROGENATION OF ACID ANHYDRIDES

Acid anhydride	Reaction conditions	Product
Acetic anhydride 530 mmol	$Co_2(CO)_8$ 300 mg † H_2 100, CO 100 1 hr, 20 min	Acetic acid 225 mmol Acetaldehyde 180 mmol
Propionic anhydride 230 mmol	$Co_2(CO)_8$ 300 mg † H_2 100, CO 100 2 hr, 40 min	Propionic acid 170 mmol Propionaldehyde 114 mmol
Stearic anhydride 44 mmol	$Co_2(CO)_8$ 450 mg Acetone 75 m*l* † H_2 100, CO 100 1 hr, 45 min	Stearic acid 43 mmol Stearaldehyde 25 mmol
Succinic anhydride 100 mmol	$Co_2(CO)_8$ 300 mg Dioxane 43 m*l* Pyridine 3 mmol † H_2 170, CO 30 41 hr	β-Formylpropionic acid 26 mmol
Glutaric anhydride 100 mmol	$Co_2(CO)_8$ 300 mg Dioxane 43 m*l* Pyridine 3 mmol † H_2 170, CO 30 4 hr, 30 min	γ-Formylbutyric acid 32 mmol

Reaction temperature, 130°C
A 100 m*l* capacity autoclave was used.
† Initial gas pressure in kg/cm², at room temperature.

1) H. Musso and K. Figge, *Chem. Ber.*, **95**, 1844 (1962).
2) I. Wender, S. Friedman, W. A. Steiner, and R. B. Anderson, *Chem. Ind.* (London), **1958**, 1694.
3) L. Marko, *Proc. Chem. Soc.*, **1962**, 67.

SHORT COMMUNICATIONS

The Synthesis of 2′,3′,4,4′,6′-Pentahydroxychalcone[1]

Heitaro OBARA, Jun-ichi ONODERA, and Yuji KURIHARA
Department of Applied Chemistry, Faculty of Engineering, Yamagata University, Yonezawa
(Received September 21, 1970)

The structure of carthamin, the coloring matter of the flowers of *Carthamus tinctorius*, has been identified as a glucoside of 2′,3′,4,4′,6′-pentahydroxychalcone (III).[2,3]

The hydrolysis of carthamin gave the corresponding flavanones, *i. e.*, carthamidin and isocarthamidin. However, the aglycon (III) has not been isolated as a chalcone form because of its instability.[2] This uncertain behavior of III has prompted the present authors to attempt the synthesis of III according to the following scheme:

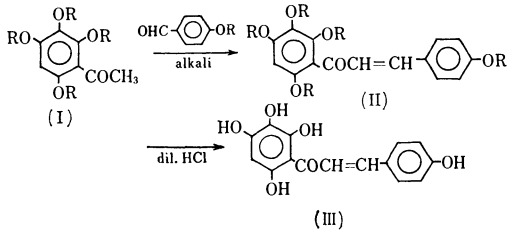

(R:CH_3OCH_2-)

The condensation of 2,3,4,6-tetrakis(methoxymethoxy)acetophenone (I), which had been prepared by the methoxymethylation of 2,3,4,6-tetrahydroxyacetophenone[4] with *p*-methoxymethoxybenzaldehyde, afforded 2′,3′,4,4′,6′-pentakis(methoxymethoxy)chalcone (II) as a pale yellow, viscous oil. The subsequent cautious hydrolysis of II with dilute hydrochloric acid in methanol gave III as yellow crystals; mp 180—182°C: UV; λ_{max}^{EtOH} 375 mμ (log ε=4.47).

The structure of this compound was identified by elemental analysis, by a study of the IR spectrum, and, furthermore, by its conversion into 2′,3′,4,4′,6′-pentamethoxychalcone, mp 92—93°C, which was identified by a comparison of the melting point and the UV and IR spectra with those of an authentic sample.[6]

The overall yield of III from 2,3,4,6-tetrahydroxyacetophenone was 25%. The IR spectrum of the new chalcone (III) is shown in Fig. 1.

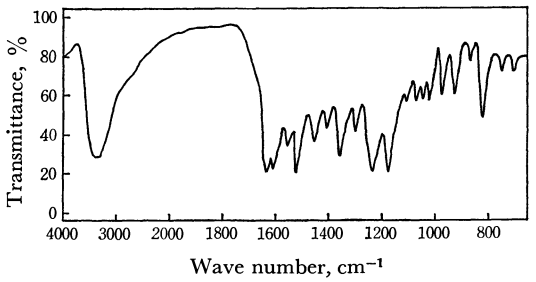

Fig. 1. The IR spectrum of 2′,3′,4,4′,6′-pentahydroxychalcone (III).

1) Presented at the 23rd Annual Meeting of the Chemical Society of Japan, Tokyo, April, 1970.
2) C. Kuroda, *Nippon Kagaku Zasshi*, **51**, 237 (1930); *J. Chem. Soc.*, **1930**, 752.
3) T. R. Seshadri and R. S. Thakur, *Curr. Sci.*, **29**, 54 (1960).
4) This compound was prepared from 1,2,3,5-tetrahydroxybenzene by a Hoesch reaction, mp 236—238°C (lit,[5] mp 204—205°C); tetramethylether, mp 55—56°C (lit,[2] mp 53—54°C).
5) M. Nierenstein, *J. Chem. Soc*, **1917**, 4.
6) This sample was prepared by the condensation of 2,3,4,6-tetramethoxyacetophenone with *p*-methoxybenzaldehyde according to Kuroda's method,[2] and the structure was confirmed by elemental analysis and by a study of the IR and NMR spectra; mp 92—93°C (lit,[2] mp 112°C).

Isopiestic Studies of Non-Aqueous Solutions of Quaternary Ammonium Halides. Comparison of the Degree of Solvations in Methanol and in Acetonitrile

Takeki MATSUI, Fumiyoshi YAMAUE, and Niichiro TOKURA
Department of Applied Chemistry, Faculty of Engineering, Osaka University, Suita, Osaka
(Received April 13, 1970)

We wish to report on the result of an application of isopiestic vapor pressure method to estimate the relative stability of halide ions in non-aqueous solvents, methanol and acetonitrile, the former being hydroxylic and the latter a dipolar aprotic solvent. The static data is used to explain the solvent effects on the following equilibrium constant K.

$$CH_3Br + I^- \underset{k_r}{\overset{k_f}{\rightleftharpoons}} CH_3I + Br^- \qquad (I)$$

$$K = k_f/k_r$$

Two partially contrary views have been proposed with respect to the effects of solvents on both reactivities and nucleophilic activities for this type of reaction. The views are: (1) anions are "desolvated" in dipolar aportic solvents,[1] (2) small anions are also solvated in these solvents as in protic solvents.[2] A different set of extrathermodynamic assumptions may lead to this contrary conclusion. These assumptions have been used to determine the relative stability of single anions. We wished to provide a conclusion to the subject through an independent method.

For the isopiestic study tetra-*n*-butylammonium bromide and iodide were taken for their relatively large solubilities in the solvents. We used similar apparatus and procedure to those of Davies and Thomas.[3] The time required for an equilibration process was about ten days. The equilibrium concentrations of these two solutions result in the isopiestic ratio R which is here defined as the ratio of equilibrium molarity of iodide solution to that of bromide solution. Figure 1 shows the plot of R *vs.* equilibrium concentration of bromidesolution.

An attempt to correlate the static data with the rate or eqiulibrium data for reaction (I) is quantitatively made through the activity B coefficient according to the expression of activity coefficient. The difference in B values among two ions I^- and Br^- is obtained by the limiting derivative of R with respect to m, *viz.*,

$$\lim_{m\to 0} \partial R/\partial m = 2.303/2(B_{Br^-} - B_{I^-}) = 2.303/2\Delta B$$

Figure 1 gives the ΔB values of 0.76 and 0.04, in methanol and in acetonitrile, respectively. The rate

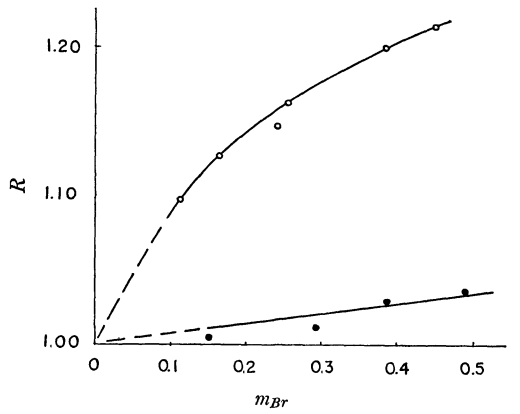

Fig. 1. Relationship between isopiestic ratio, R and molarity of bromide solution. ○, in methanol; ●, in acetonitrile

TABLE 1. RATE DATA FOR REACTION (I) AND STATIC DATA IN METHANOL AND IN ACETONITRILE AT 30°C

	in CH_3OH[a]	in CH_3CN[b]
k_f, $M^{-1}\cdot sec^{-1}$	13.7×10^{-4}	0.091
k_r, $M^{-1}\cdot sec^{-1}$	13.8×10^{-5}	0.292
K	9.9	0.31
ΔB, M^{-1}	0.76	0.04

a) The rate data are taken from E. A. Moelwyn-Hughes. *J. Chem. Soc.*, **1939**, 368.
b) The rate data are taken from K. Uosaki and N. Tokura, unpublished result.

data for reaction (I) are shown in Table 1 together with the ΔB values.

K is split into two terms, *i. e.*, intrinsic (denoted by superscript 0) and solvent-dependent terms, *viz.*,

$$\log K = \log K^0 + \log r_{I^-}/r_{Br^-}$$

where r_i is the solvent activity coefficient of i species. A plot of log K *vs.* ΔB for the changes in solvent results in the intrinsic nucleophilicity K^0. Log K^0 is obtained as the value on the ordinate of this plot at a point where $\Delta B=0$. The result shows that K^0 is smaller than 1.0, which in turn suggests the rate data in acetonitrile may reflect the intrinsic property of the reaction.

From the situations for ΔB and K we conclude as follows. The stability of halide ions is in the order $Br^- > I^-$ in both solvents, but these ions are more stabilized in protic solvents than in dipolar aprotic solvents. The latter explains the solvent effects on k_r or k_f.

1) A. J. Parker, *Quart. Rev.* (London), **16**, 613 (1962).
2) R. F. Rodewald, K. Mahendran, J. L. Beare, and R. Fuchs, *J. Amer. Chem. Soc.*, **90**, 6698 (1968).
3) M. Davies and D. K. Thomas, *J. Phys. Chem.*, **60**, 41 (1956).

Direct Observation of Catalytic Activity Change in Nickel Metal Deformed in Torsion During Reaction

Eizo MIYAZAKI, Takakazu FUKUSHIMA, Kiyoshi KAWASAKI, and Kazuo NAKADA
Department of Chemical Engineering, Niigata University, Nagaoka
(Received September 24, 1970)

There have been many experimental investigations on the role of defect structure in the catalytic activity of metals. Some investigations[1] show that the defect plays an important role in heterogeneous catalysis; others[2] show that the effect of defect is minimal. The former proposal is, however, based mainly on the parallelism between the change in catalytic activities of cold-worked, quenched and irradiated metals during annealing. The purpose of this paper is to show more explicitly the influence of the defect on catalytic activity by a method in which metal was *in situ* cold-worked during reaction.

The main parts of the apparatus consist of a reaction tube and a manometer. In the center of the reaction tube a nickel sheet (0.1 mm thick, 3 mm wide and 130 mm long), washed in acetone and subsequently annealed in hydrogen at 700°C, was fixed to a pyrex glass rod with one end connected to a ground glass joint. The sheet was treated afresh in hydrogen at 600°C in order to remove the oxidized layer on surface before reaction, and the sheet was deformed in torsion during reaction up to a definite number of turns with the aid of the joint. The reaction was followed by continuously recording the total pressure change with a newly-devised glass made manometer.[3] The small surface areas of the catalysts were measured by the BET method using xenon vapor at 78°K.[4] The surface areas before and after deformation in torsion up to 6 turns were 10.1 cm^2 and 13.1 cm^2 per catalyst, respectively. A full description of the apparatus will be given in a later publication.

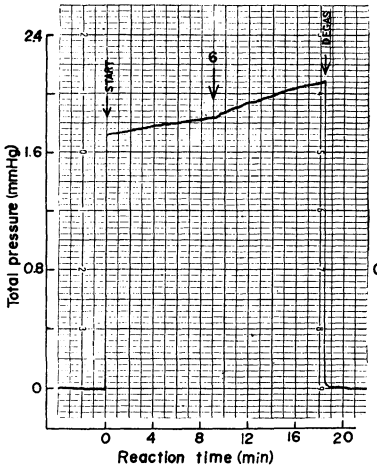

Fig. 1

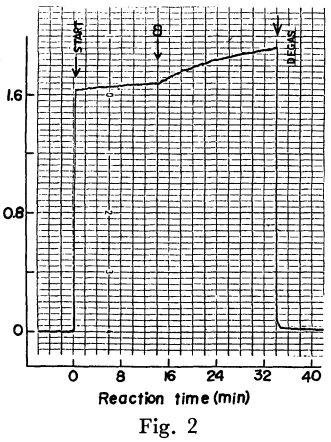

Fig. 2

Figs. 1 and 2. Changes in total pressure with reaction time at 194°C(Fig. 1) and 182°C (Fig. 2). Deformations in torsion were made at the points given by arrows up to 6 and 8 turns, respectively.

Figure 1 shows a typical curve obtained in the change of total pressure for the decomposition of formaldehyde ($H_2CO=CO+H_2$) over nickel sheet at 194°C, where deformation by torsion was carried out up to 6 turns at the point given by arrow. The discontinuity or sudden increase in total pressure was observed at the point of deformation, *i. e.*, deformation elevated the activity (slope of the curve). A similar result was obtained when the torsion was made up to 8 turns at 182°C as shown in Fig. 2, in which the increase in activity by deformation was found to be more drastic. However, such deformation-induced activities were found to practically disappear after the catalysts were annealed at 400°C. In addition, the reaction was confirmed to be kinetically first order with respect to formaldehyde pressure regardless of deformation range. Integral forms of the first order reaction before and after deformation during reaction are shown respectively as follows: $2.3\log(P_0/P)=kt$ and $2.3\log(P_0'/P)=k'(t-t_0')$, where k and k' are rate constants and P_0 or P_0' is formaldehyde pressure at $t=0$ or $t=t_0'$ (reaction time when deformation was made), respectively. The ratio of k' to k for the case shown in Fig. 1 was 2.1, *i. e.*, the activity was enhanced by 110% due to the deformation in torsion up to 6 turns during formaldehyde decomposition at 194°C. Increase in activity, however, might be due to the increase in surface area accompanying deformation in torsion. The actual surface areas were therefore measured for the catalysts only annealed and deformed in torsion up to 6 turns. The result was 29.8% increase; the residual increase in activity (110−30=80%) due to the deformation should be therefore attributed to other origins such as lattice imperfections which are known to be produced when nickel is subjected to deformation in torsion.[5] This can be also supported from the result of the annealing effect.

1) I. Uhara, S. Yanagimoto, K. Tani, and G. Adachi, *Nature*, **192**, 867 (1961); Y. Inoue and I. Yasumori, *J. Phys. Chem.*, **73**, 1618 (1969); K. B. Keating, A. G. Rozner, and I. Youngston, *J. Catal.*, **4**, 608 (1965).

2) J. Bagg, H. Jaeger, and J. V. Sanders, *J. Catal.*, **2**, 449 (1963); H. Jaeger, *ibid.*, **9**, 237 (1967); E. M. A. Willhoft, *Chem. Commun.*, **1968**, 146.

3) I. Yasumori, S. Ohno, and E. Miyazaki, This Bulletin, **40**, 769 (1967).

4) P. Chenebault, *J. Phys. Chem.*, **69**, 2300 (1965); T. Kabe, T. Mizuno, and I. Yasumori, This Bulletin, **40**, 2047 (1967).

5) L. M. Clarebrough, M. E. Hargreaves, and G. W. West, *Proc. Roy. Soc.* (London), **A232**, 252 (1955).

Synthetic Studies of Carbohydrate Derivatives with Photochemical Reaction. II.[1] Photochemistry of Benzylidene Sugar Derivatives

Kazuo MATSUURA, Sadao MAEDA, Younosuke ARAKI, and Yoshiharu ISHIDO
Department of Chemistry, Tokyo Institute of Technology, Ookayama, Meguro-ku, Tokyo
(Received September 26, 1970)

The acetone-sensitized photochemical conversion of cyclic acetals to the corresponding carboxylic esters[2] suggests the possibility that the reaction may serve as an unique procedure for the preparation of deoxy sugars from cyclic acetals of sugars. A study on the photochemistry of sugar cyclic acetals has been carried out and part of the results will be described in the present communication.

A solution of methyl 2,3-*O*-benzylidene-β-D-ribofuranoside[3] (I)(0.02M) in a mixture of *t*-butyl alcohol and acetone (9:1) was irradiated[4] at room temperature under nitrogen atmosphere[5] for 60 hr, and the volatiles were evaporated *in vacuo*. The residue was subsequently chromatographed on a silica gel column by elution with benzene - acetone (95 : 5) to give I (recovery : 34%) as the first fraction and methyl 2(or 3)-*O*-benzoyl-β-D-ribofuranoside (II)[6] (58% yield) as the second

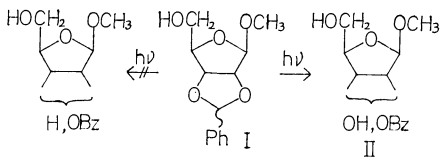

fraction. Contrary to expectation, the corresponding deoxy sugar was not produced. Variation of the molar concentration of I to 0.08 and 0.40 resulted in a stepwise decrease of the yield of II, and in an increase of that of recovered I. These results are summarized in Table 1. The correlation between the molar concentration of I and the results is now under investigation especially with respect to the effect of oxygen[7] which is slightly

Table 1. PHOTOCHEMICAL REACTION OF METHYL 2,3-*O*-BENZYLIDENE-β-D-RIBOFURANOSIDE (I)

Run	Conc. of I[a] (mol)	Recovery of I		Yield of II (%)
		Yield (%)	*exo*-H/*endo*-H	
1	0.02	34	0.25,[b] 0.20[c]	58[c]
2	0.08	67	0.27[c]	28[c]
3	0.40	100	0.75[c]	—

All the reactions were carried out in *t*-butyl alcohol - acetone (9 : 1) for 60 hr under irradiation.[4]

a) *exo*-H/*endo*-H of the isomers in the starting material was NMR spectroscopically 1.5, and gas chromatographically 2.0, and also refers to b and c.

b) Calcd by NMR[*exo*-H 4.29 τ, *endo*-H 4.03 τ ($CDCl_3$)]; These assignments were done by reference to 8).

c) Calcd by glc[Column: SE 30 1% on Chromosorb W, injection temp. 270°C, column temp. 200°C, carrier gas: N_2 150 ml/min, retention time (min): *exo*-H-I 5.2, *endo*-H-I 5.6 and II 9.8].

contained in commercial nitrogen. It is of interest that the content ratios of *endo*- and *exo*-benzylic proton isomers in each recovered I were considerably varied as compared with that of I applied as the starting material. This leads to the conclusion that *endo-exo* photoisomerization of the isomers actually took place along with the unexpected photooxygenation reaction of I. The reaction may be generalized to proceed *via* the benzylic radical(III) which is convertible into all the species mentioned above as follows:

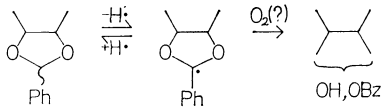

III

A similar treatment of 3,5-*O*-benzylidene-1,2-*O*-isopropylidene-α-D-xylofuranose[6] also gave the corresponding 3- and 5-*O*-monobenzoate of 1,2-*O*-isopropylidene-α-D-xylofuranose[6] in good yield. Detailed results with other sugar derivatives will be published elswhere.

1) K. Matsuura, S. Maeda, Y. Araki, and Y. Ishido, *Tetrahedron Lett.*, **1970**, 2869.
2) D. Elad and R. D. Youssefyeh, *ibid.*, **1963**, 2189.
3) G. R. Baker and T. M. Noone, *J. Chem. Soc.*, **1955**, 1327.
4) A Pyrex-glass mercury lamp (450 W) of Ushio Electric Inc. was used.
5) Commercial nitrogen was used without further purification.
6) Analytical, NMR, and mass spectral data were consistent with the expected structure.
7) H. E. Seyfarth, A. Rieche, and A. Hesse, *Chem. Ber.*, **100**, 624 (1967).
8) N. Baggett, K. W. Buck, A. B. Foster, and J. W. Webber, *J. Chem. Soc.*, **1965**, 3401 and the preceding papers.

The Oxyhydration of Olefin over Transition Metal Oxide Catalysts

Yoshihiko MORO-OKA, Yusaku TAKITA, and Atsumu OZAKI
Tokyo Institute of Technology, Ohokayama, Meguro-ku, Tokyo
(Received October 9, 1970)

A number of catalytic oxidations of olefin have been developed on the transition metal oxide catalysts. Though the mechanisms of these oxidations have been extensively studied by the tracer technique with regard to the behavior of olefin,[1] little work has been done on the behavior of active oxygen. In this communication, we wish to report evidence which demonstrates that the oxygen atom is introduced into the oxidized product of olefin in two different ways, depending on the type of product. One is the case where the oxygen atom is introduced from molecular oxygen, and another is where the atom is introduced from the water molecule:

$$A + \frac{1}{2}O_2 \longrightarrow AO \quad (1)$$

$$A + \frac{1}{2}O_2 + H_2O^* \longrightarrow AO^* + H_2O \quad (2)$$

where A is the olefin to be oxidized.

TABLE 1. $H_2{}^{18}O$ TRACER IN THE OXIDATION OF PROPYLENE TO ACROLEIN OVER MoO_3–Bi_2O_3 CATALYST

Run	Reaction temp. (°C)	C_3' conv. (%)	Selectivity to acrolein (%)	^{18}O content (%)	
				H_2O[a]	CH_2=CHCHO
1	360	2.50	73.0	3.92	0.26±0.2
2	385	4.35	65.5	3.84	0.00±0.2
3	433	9.45	55.0	3.73	0.16±0.2
4	460	14.80	51.0	3.40	0.18±0.2

a) Average of the values for input (4.00) and output gas.
GHSV: 600 m*l*-STP/m*l*-cat·hr
Gas composition; C_3H_6 20 vol%, O_2 30%, H_2O 30%, N_2 20%.

A typical example of Eq. (1) is the oxidation of propylene to acrolein over the MoO_3-Bi_2O_3 catalyst. The oxidation of propylene was done in the presence of the water vapor, 4% of which was $H_2{}^{18}O$. As can be seen in Table 1, the concentrations of ^{18}O in acrolein are far lower than those in water in the reactant gas. It can be concluded that the oxygen atom in acrolein comes from molecular oxygen, not from the water molecule, although it is well known that the presence of water vapor in the reactant gas mixture increases the selectivity to acrolein.

An example of Eq. (2) is the oxidation of propylene to acetone, which was previously reported by the present authors.[2] Propylene was oxidized to acetone in the presence of $H_2{}^{18}O$ vapor on the SnO_2-MnO_3 catalyst at two different temperatures. The experimental results are summarized in Table 2. As is shown in Table 2, the concentrations of ^{18}O in acetone are almost equal to those in water in the reactant gas. The exchange reaction of the oxygen atom between molecular oxygen and water:

$$^{16}O_2 + H_2{}^{18}O \rightleftarrows {}^{16}O{}^{18}O + H_2{}^{16}O \quad (3)$$

did not occur under the reaction conditions adopted in this experiment. These results clearly show that the oxygen atom in acetone comes from water, not from molecular oxygen. It has been suggested, regarding the mechanism of this oxidation, that acetone is formed *via* the hydration of propylene to form an alcoholic intermediate, followed by oxydehydrogenation.[3] The results obtained in this work present strong evidence for this proposed mechanism of acetone formation.

It has been proved that there are two different ways of oxygen introduction in the heterogeneous oxidations of olefin over metal oxide catalysts. It seems interesting that these two paths of the introduction of oxygen atoms to oxidized products correspond to two typical enzymatic oxidations, *i. e.*, oxidations by oxygenase[4] and oxidase.

TABLE 2. $H_2{}^{18}O$ TRACER IN THE OXIDATION OF PROPYLENE TO ACETONE OVER SnO_2–MoO_3 CATALYST

Run	Reaction temp. (°C)	GHSV (m*l*-STP/ m*l*-cat·hr)	C_3' conv. (%)	Selectivity to acetone (%)	^{18}O content (%)		
					H_2O (input)	H_2O (output)	CH_3COCH_3
1	125	600	3.99	93.7	5.48	4.62	5.35
2	125	600	3.99	93.7	5.48	4.91	5.26
3	225	2000	1.67	68.1	8.60	—	8.39

Gas composition is same with Table 1.

1) H. H. Voge and C. R. Adams, *Advan. Catal.*, **17**, 151 (1967).
2) Y. Moro-oka, S. Tan, Y. Takita, and A. Ozaki, This Bulletin, **41**, 2820 (1970).
3) S. Tan, Y. Moro-oka, and A. Ozaki, *J. Catal.*, **17**, 132 (1970).
4) O. Hayaishi, Proc. 6th Intern. Congr. Biochem., New York 1964.

Separation of Semi-Xylenol Orange from Xylenol Orange by Thin-Layer Chromatography with Solvents Giving Stepwise pH Change on the Plate

Mutsuo YAMADA and Masatoshi FUJIMOTO
Department of Chemistry, Faculty of Science, Hokkaido University, Sapporo
(Received October 12, 1970)

Semi-Xylenol Orange (SXO) is a very suitable reagent as compared with Xylenol Orange (XO) for interpreting the kinetic behavior for complex formation. The *n*-butanol - water - acetic acid solvents reported for the separation of XO and SXO with a cellulose column[1,2] often cause serious tailing and cross-contamination. In the present communication we propose a new procedure with solvents giving stepwise pH change on the plate, whereby the clear-cut separation of SXO from XO is effectively performed by thin-layer chromatography with sandwich technique.

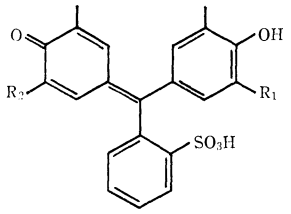

XO · $R_1 = R_2 = CH_2N(CH_2COOH)_2$
SXO · $R_1 = CH_2N(CH_2COOH)_2$, $R_2 = H$

A slurry for one plate (10×20 cm) was made by mixing 6 g of pretreated cellulose powder (Toyo, 300 mesh) with 18 m*l* of water. Developing solvents were prepared shortly before use from various amounts of 28% ammonia and 12 m*l* of *n*-butanol saturated with 10% acetic acid. The solvents formed regions I and II divided by a distinct boundary directly visible (Fig. 1). Region II gave an intense and uniform positive test with the Nessler reagent and a basic color (bluish green) with Bromothymol Blue (BTB), whereas region I showed an almost negative Nessler test and an acid color (orange) with BTB. Uniformity of the sensitive coloration indicates that the development with the given solvent automatically forms two distinct zones with different pH values, region I (*n*-butanol - acetic acid - water) and region II (*n*-butanol - ammonia - ammonium acetate - water).

In Fig. 1 the chromatograms for SXO and XO

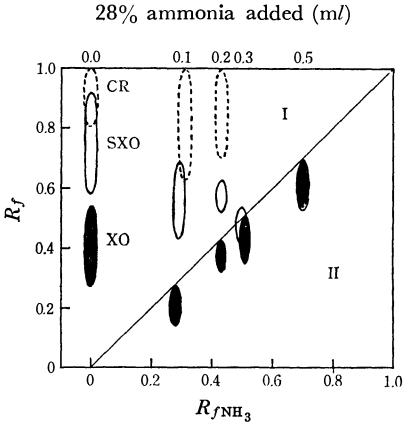

Fig. 1. Chromatograms for SXO and XO as a function of the R_{fNH_3}.
Spot solutions: 0.5 μl of 1×10^{-3} mol/*l* CR, SXO, or XO in *n*-BuOH satd. with 10% HOAc.
The straight line gives the ammonia front.

after 10 cm's development are plotted against R_{fNH_3}, the R_f values of the so-called ammonia front. XO lies always in region II beneath the boundary, whereas SXO is in region I for the R_{fNH_3} values lower than 0.5. When R_{fNH_3} is about 0.4, the cross-contamination of SXO and Cresol Red (CR), one of the raw materials, also disappears. In any case ammonia is very effective to prevent tailing. It is thus concluded that the solvent, 12 m*l* of *n*-butanol saturated with 10% acetic acid and 0.2 m*l* of 28% ammonia (R_{fNH_3}=0.43), gives the best separation of SXO from XO within only 1 hr. Preparative thin-layer chromatography for SXO of high purity using the present procedure is now in progress.

The solvent systems as mentioned above would be useful for the chromatographic separation of other series of substances of similar structure, where the subtle differences in charge type and its pH-dependence may be the primary factors for the sharp separation.[3] Further details for such systems will be reported elsewhere.

1) D. C. Olson and D. W. Margerum, *Anal. Chem.*, **34**, 1299 (1962).
2) M. Murakami, T. Yoshino, and S. Harasawa, *Talanta*, **14**, 1293 (1967).
3) With the given solvents the disubstituted commercial specimen such as GCR, GTB, MTB, and MXB gave at least three distinct spots corresponding to the raw material, mono- and di-substituted derivatives.

Charge-Transfer Interaction between *N,N,N',N'*-Tetramethyl-*p*-phenylenediamine and Chloranil

Takashi NOGAMI, Keitaro YOSHIHARA, and Saburo NAGAKURA
The Institute for Solid State Physics, The University of Tokyo, Roppongi, Minato-ku, Tokyo
(Received October 12, 1970)

As an extension of a series of studies[1] of charge-transfer (CT) interactions between aromatic amines and chloranil, we measured temperature and concentration dependencies of an electronic absorption spectrum for a system including *N,N,N',N'*-tetramethyl-*p*-phenylenediamine (TMPD) and chloranil in an ethyl ether-isopropyl alcohol (3 : 1) mixed solvent.

The system showed spectra due to two different kinds of complexes. One is greenish yellow and exhibits an absorption peak at 830 mμ. This band was identified by Foster and Thomson[2] as the CT band of the outer complex. The other is reddish brown and has absorption peaks at 1100, 635, 520, and 434 mμ. The 1100 mμ band corresponds to a reverse CT band ($D \cdot A \leftarrow D^+A^-$) of the inner (ion-pair or ionic EDA) complex observed by Sato *et al.*[3] for the solid TMPD-chloranil. We studied the behaviors of these two specimens in the solution by measuring their absorption spectra at room temperature, 193°K and 77°K. In Table 1, the observed

TABLE 1. TEMPERATURE AND CONCENTRATION DEPENDENCIES OF THE CT COMPLEXES BETWEEN TMPD AND CHLORANIL

[D][a]	[A][a]		
	20	5	1.25
160	A	B	C
80			
40	B		
20		C	
10			
5	C		D
2.5			
2			
1.75	D	D	E
1.25			
1	E	E	
0.75			

a) [D] and [A] are the concentrations (in the unit of 10^{-4} mol/*l*) of TMPD and chloranil, respectively.

results, A, B, C, D, and E denote the following phenomena. A: Immediately after mixing the TMPD and chloranil solutions at room temperature, the outer complex is formed and converted gradually into the inner complex. B: Only the outer complex is formed at room temperature, and the inner-complex formation starts by lowering the temperature of the solution to 193°K. C: Only the outer complex is formed in the temperature range from room temperature to 193°K, and the inner-complex formation starts at 77°K. D: The component molecules which are almost completely free at room temperature start to form the outer complex at 193°K. This process is reversible. By raising the solution temperature to 193°K after once having lowered it to 77°K, the inner complex is formed. By raising the temperature further, the solution returns to the initial stage at room temperature. E: Only the outer complex is formed in the range of 193°K to 77°K, and the inner complex is not formed.

The present results of the outer-complex formation are reasonable and can be explained by the equilibrium-shift toward the outer-complex formation caused by the lowering of temperature. The results concerning the inner complex, though rather complicated, suggest that its formation can not occur unless the outer-complex concentration exceeds some limited values. This seems to show that the inner-complex formation needs environmental cooperation; in particular, that there must be a clustering of donor-acceptor pairs before the inner-complex formation begins.[4] In this connection, phenomenon D is particularly interesting as showing the following color cycle with temperature:

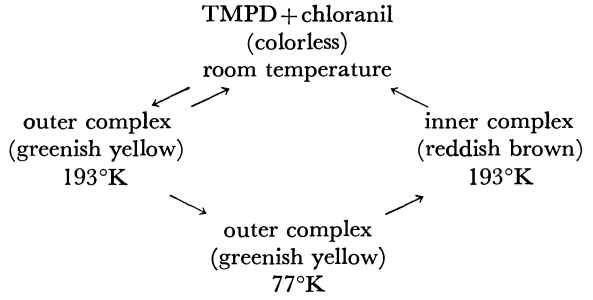

The colorless solution at room temperature turns greenish yellow at 193°K and the color becomes deeper by decreasing the temperature to 77°K. The solution changes from greenish yellow to reddish brown by raising the temperature from 77°K to 193°K.[5] By raising further the temperature, the solution returns to the initial colorless state. The color cycle occurs regardless of the lowering and raising rates of temperature and can be repeated many times. Although the mechanism of the inner-complex formation in this cycle is not clear at the present stage, the phenomenon seems to support the opinion that the outer complex is a precursor to the inner-complex formation in the reaction path.

1) T. Nogami, K. Yoshihara, H. Hosoya, and S. Nagakura, *J. Phys. Chem.*, **73**, 2670 (1969); T. Yamaoka and S. Nagakura, This Bulletin, **43**, 355 (1970); T. Nogami, T. Yamaoka, K. Yoshihara, and S. Nagakura, *ibid.*, to be published.

2) R. Foster and T. J. Thomson, *Trans. Faraday Soc.*, **58**, 860 (1962).

3) Y. Sato, M. Kinoshita, M. Sano, and H. Akamatu, This Bulletin, **43**, 2370 (1970).

4) Mulliken presented a similar view for the formation of $NH_4^+Cl^-$ crystals from NH_3 and HCl gases (R. S. Mulliken, *J. Phys. Chem.*, **56**, 801 (1952)).

5) This process is irreversible.

Electrophilic Substitutions on 8-Cyanoheptafulvene

Masaji ODA and Yoshio KITAHARA*
Department of Chemistry, Faculty of Science, Tohoku University, Katahira, Sendai
(Received October 26, 1970)

We wish to report here the first examples of electrophilic substitutions on 8-cyanoheptafulvene (**I**)[1] which is a moderately stable and the simplest derivative of heptafulvenes. The compound **I** is unstable to acids, however, basic conditions were found to be best for obtaining successful results.

Bromination. The addition of one equivalent of bromine to a solution of **I** and a small excess of triethylamine in methylene chloride at 0°C gave, by silica gel chromatography, 8-bromo-8-cyanoheptafulvene (**II**) as orange needles, mp ~50°C decomp., in a 87% yield. The compounds **II** is unstable and is liable to decompose at room temperature. When a mass of **II** was heated at *ca.* 40°C, it decomposed explosively and an evolution of hydrogen bromide was observed. Therefore, we could not obtain successful elemental analytic data. However, the structure was established by means of the spectral data given in the table.

Nitration. When **I** was treated with tetranitromethane in pyridine - ethanol at 10°C for one hour, it gave 8-cyano-8-nitroheptafulvene (**III**) as fine yellowish-brown needles, mp 168°C decomp., in a 16.5% yield. With other nitrating reagents, only polymeric materials were obtained.

Formylation. The Vilsmeyer reaction of **I** was successful in giving 8-cyano-8-formylheptafulvene (**IV**)[2] as red prisms, mp 181—182°C, in a 47% yield.

Trifluoroacetylation. The treatment of **I** with trifluoroacetic anhydride in methylene chloride at 4°C gave 8-cyano-8-trifluoroacetylheptafulvene (**V**) as orange red prisms, mp 213—214°C, in a 20% yield.

The structures of **III**, **IV**, and **V** were established by their elemental analyses and by their spectral data (see Table 1). The selectivity of the substitution position (C-8) is in accord with the polar character of **I**, which has a high electron density at C-8. The chemical shift of the ring protons of **II** (6.08 ppm) is close to that of **I** (6.13 ppm),[1] however, those of **III**, **IV**, and **V** are 1—1.5 ppm lower, suggesting their larger polar character because of the introduction of electron-withdrawing groups.

From these results, we can say that 8-cyanoheptafulvene (**I**) has an aromatic character.

Table 1. Spectral data

Compd.	ν_{max} (KBr) cm^{-1}			λ_{max} nm (log ε)		δ ppm (J Hz)[a]	
II	2210	1644	1586	246	(*ca* 4.0)[b]	6.61br.d (12)	1H[c]
	1547	1512	753	356	(*ca* 4.3)	6.08	5H
				444sh	(*ca* 2.5)		
				484sh	(*ca* 2.4)		
				525sh	(*ca* 2.3)		
				570sh	(*ca* 2.0)		
III	2205	1625	1527	228	(4.20)[d]	7.70—7.25m[e]	
	1496	1303	1228	256	(4.01)		
	762			280sh	(3.84)		
				438	(4.38)		
IV	2205	1642	1620	219	(4.18)[d]	9.78s	1H[e]
	1520	1490	1270	256	(4.01)	8.87br.d (12)	1H
	1190	756		413	(4.31)	7.63br.d (12)	1H
						7.40—7.00m	4H
V	2205	1648	1618	224	(4.33)[d]	9.02br.d (12)	1H[e]
	1505	1492	1390	255	(4.02)	8.20br.d (12)	1H
	1231	1187	1138	267	(4.03)	7.93—7.50m	4H
	1047	775		436	(4.40)		

a) TMS as internal standard, b) in CH_2Cl_2, c) in acetone, d) in EtOH, e) in $CDCl_3$

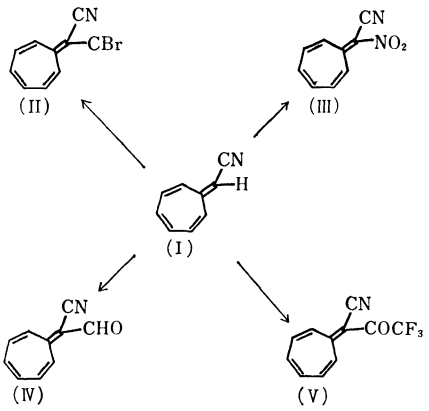

* To whom all communications should be addressed.

1) M. Oda and Y. Kitahara, *Chem. Commun.*, **1969**, 352.

2) This compound has also been synthesized by an other method in our laboratory; *cf.* T. Machiguchi, Ph. D. Dissertation, Tohoku University, 1970.

Four New Flavonoids Isolated from *Alnus sieboldiana*[1]

Yoshinori ASAKAWA, Fumihide GENJIDA, and Takayuki SUGA
Department of Chemistry, Faculty of Science, Hiroshima University, Hiroshima
(Received October 26, 1970)

Isolation of two new ketols having a phenyl-propane skeleton from *Alnus sieboldiana* has been reported.[2] We now wish to report the isolation of four new flavonoids with an unsubstituted B-ring from the phenolic portion of the benzene extract of the same plant. These substances were readily separated by their solubility difference in ether and methanol and purified by means of preparative thin-layer chromatography using a mixture of benzene, dioxane, and acetic acid.

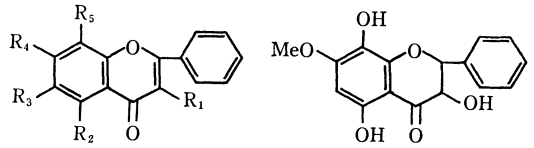

R_1=R_2=R_4=OH R_3=OMe R_5=H (I) (IV)
R_1=R_3=R_4=OMe R_2=OH R_5=H (II)
R_1=H R_2=OH R_3=R_4=R_5=OMe (III)

3,5,7-Trihydroxy-6-methoxyflavone (I). Compound I (a main flavonoid of the plant), $C_{16}H_{12}O_6$, M+ 300, mp 239.0—241.0°C, exhibited positive coloration with $FeCl_3$ and Mg-HCl tests and the spectral properties as follows: *m/e* 285 (M-15), 282 (M-H_2O), 257 (M-43, base), 105, 77, 69; λ_{max}^{EtOH} mμ (log ε) 270 (4.25), 325 (4.26), 362$_{sh}$ (4.20), $\lambda_{max}^{EtOH+AcONa}$ 271 (4.39), 328 (4.15), 368 (4.20), $\lambda_{max}^{EtOH+AlCl_3}$ 278 (4.38), 350 (4.25), 415 (4.26); ν_{max}^{Nujol} 3350, 3300 (OH), 1640 (C=O), 762, 680 cm^{-1} (monosubst. benzene ring); $\delta_{ppm}^{CD_3COCD_3}$ (60 MHz) 3.89 (s, 3H, OMe), 6.68 (s, 1H, C_8-H), 7.60, 8.20 (m, 5H, B-ring), 9.25 (s, 1H, OH), 12.23 (s, 1H, C_5-OH). No bathochromic shifts in the UV spectrum on addition of H_3BO_3 and AcONa indicated the absence of *o*-dihydroxy group.[3] The results suggested that the structure of I is 3,5,7-trihydroxy-6-methoxy- or 3,5,7-trihydroxy-8-methoxyflavone. The strong fragment peak at *m/e* 285 (M-15) indicated the presence of the OMe group at C-6 position.[4] Methylation of I gave 3,5,6,7-tetramethoxyflavone[5] (mp 112.0—112.5°C), which was converted into benzoic acid and 2-hydroxy-ω,4,5,6-tetramethoxyacetophenone with alkali. Thus, compound I was determined to be 3,5,7-trihydroxy-6-methoxyflavone.

5-Hydroxy-3,6,7-trimethoxyflavone (II). Compound II possessed the following physical properties: mp 175.0—176.0°C; λ_{max}^{EtOH} 271 (4.30), 317 (4.09), $\lambda_{max}^{EtOH+AlCl_3}$ 286 (4.29), 337 (4.08), 392 (4.01); ν_{max}^{Nujol} 1660 (C=O), 765, 695 cm^{-1} (monosubst. benzene ring); $\delta_{ppm}^{CDCl_3}$ 3.89, 3.94, 3.97 (s, 9H, 3 OMe), 6.54 (s, 1H, C_8-H), 7.56, 8.10 (m, 5H, B-ring), 12.58 (s, 1H, C_5-OH). Methylation gave 3,5,6,7-tetramethoxyflavone. The results indicated the structure of II to be 5-hydroxy-3,6,7-trimethoxyflavone.

5-Hydroxy-6,7,8-trimethoxyflavone (III). Compound III, mp 100.0—101.0°C, showed the NMR signals at $\delta_{ppm}^{CDCl_3}$ 3.95, 3.97, 4.10, (s, 9H, 3 OMe), 6.69 (s, 1H, C_3-H), 7.56, 7.95 (m, 5H, B-ring), 12.45 (s, 1H, C_5-OH). Methylation gave 5,6,7,8-tetramethoxyflavone[6]: mp 112.0—113.0; λ_{max}^{EtOH} 270 (4.34), 305 (4.08); $\delta_{ppm}^{CDCl_3}$ 3.98 (s, 6H, 2 OMe), 4.04 (s, 3H, OMe), 4.10 (s, 3H, OMe), 6.70 (s, 1H, C_3-H), 7.57, 7.95 (m, 5H, B-ring). Thus, the structure of III was established to be 5-hydroxy-6,7,8-trimethoxyflavone.

3,5,8-Trihydroxy-7-methoxyflavone (IV). Compound IV, $C_{16}H_{14}O_6$, M+ 302, mp 175.0—177.0°C, showed positive coloration with $FeCl_3$, Mg-HCl, Zn-HCl, and Pachcós tests and the following spectral properties: *m/e* 273, 91 (M-CHO and 120-CHO, characteristic for flavanonol), 195, 183 (base), 167, 156, 120, 91, 77; λ_{max}^{EtOH} 215 (4.58), 226$_{sh}$ (4.48), 290 (3.87), $\lambda_{max}^{EtOH+AlCl_3}$ 313 (4.74), $\lambda_{max}^{EtOH+AcONa}$ and $\lambda_{max}^{EtOH+AcONa+H_3BO_3}$ no bathochromic shifts[2]; ν_{max}^{Nujol} 3480, 3460, 3340 (OH), 1635—1654 cm^{-1} (C=O); $\delta_{ppm}^{CDCl_3}$ 3.86 (s, 3H, OMe), 4.40, 4.97 (d, J= 12 Hz, C_3-H and C_2-H), 5.99 (s, 1H, C_6-H), 7.33 (s, 5H, B-ring), 11.34 (s, 1H, C_5-OH). The small fragment peak at *m/e* 301 (M-1) indicated the absence of OH and OMe groups at C_6 position.[4] The spectral data as well as the specific color reaction thus indicated that IV is 3,5,8-trihydroxy-7-methoxyflavone.

1) The plant name "*Alnus firma* Sieb. et Zucc." has been given in our previous papers.[2a-c] We wish to correct it to "*Alnus sieboldiana*."

2) a) Y. Asakawa, F. Genjida, S. Hayashi, and T. Matsuura, *Tetrahedron Lett.*, **1969**, 3235. b) Y. Asakawa, This Bulletin, **43**, 575 (1970). c) Y. Asakawa, *ibid.*, **43**, 2223 (1970).

3) T. A. Geissman, "The Chemistry of Flavonoid Compounds," Pergamon Press, New York (1962), p. 127.

4) J. H. Bowie and D. W. Cameron, *Aust. J. Chem.*, **19**, 1627 (1966).

5) A. C. Jain, T. R. Seshadri, and K. R. Sreenivasan, *J. Chem. Soc.*, **1955**, 3908.

6) H. H. Lee and C. H. Tan, *ibid.*, **1965**, 2743.

Molecular Complex between the Cation Radicals of Perylene and Tetracene

Tomoko YAMAZAKI and Katsumi KIMURA

Physical Chemistry Laboratory, Institute of Applied Electricity, Hokkaido University, Sapporo

(Received October 27, 1970)

A spectroscopic study of a molecular complex formed between two kinds of Würster's cations in solution has been reported by Takemoto *et al.*[1] Recently, Kimura *et al.*[2] have studied the reversible dimerizations of (perylene)$^+$ and (tetracene)$^+$ in concentrated sulfuric acid from an electronic-absorption study. In the present work, we have first established, spectroscopically, the existence of an interesting 1 : 1 complex between the cation radicals of cata-condensed hydrocarbons in concentrated sulfuric acid. The (perylene)$^+$-(tetracene)$^+$ complex may be one of the typical examples of radical-radical complexes.

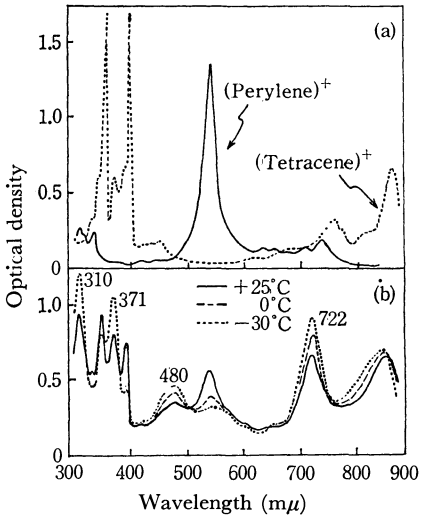

Fig. 1. (a) Electronic absorption spectra of (perylene)$^+$ (2.38×10^{-5}M) and (tetracene)$^+$ (2.21×10^{-5}M) in concentrated sulfuric acid at room temperature.
(b) Temperature dependent spectra of a mixed solution containing the two cations, whose concentrations are almost the same as above.

Perylene and tetracene are readily soluble in concentrated sulfuric acid; they thus form stable cation radical.[3] The absorption measurements were carried out under conditions in which none of the cations dimerized in a dilute concentrated-sulfuric acid solution. In Fig. 1, the electronic absorption spectra of the mixed solutions of (perylene)$^+$ and (tetracene)$^+$ measured at room temperature and also at lower temperatures are shown. Upon the mixing of the two cations, new several absorption bands appear at 264, 310, 371, 480, and 722 mμ, in addition to their own absorption bands, which become weak upon the mixing; several isosbestic points also exist.

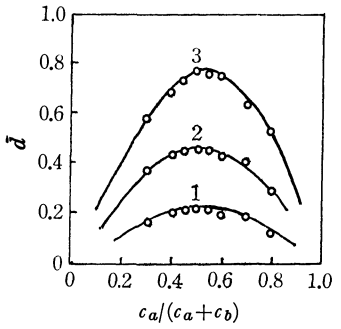

Fig. 2. Plots of $\bar{d}$ against $c_a/(c_a+c_b)$ in the continuous-variation method for different wavelengths.
Curve 1: 310 mμ, 2: 371 mμ, and 3: 538 mμ.
$c_a+c_b=5.0\times10^{-5}$M.

In order to identify this new species, we attempted to analyze the changes in the absorption intensity by using a method of continuous variation, in which concentrations of the two cations were selected so as to be constant. In Fig. 2, the increments of the optical densities, $\bar{d}=d-(c_a\varepsilon_a+c_b\varepsilon_b)$, are plotted aganst $c_a/(c_a+c_b)$ for three different wavelengths. Here, d is the optical density; c_a and c_b are the concentrations of (perylene)$^+$ and (tetracene)$^+$ respectively and ε_a and ε_b are the molar extinction coefficients of the absorption peaks of (perylene)$^+$ and (tetracene)$^+$ respectively. From Fig. 2 it can be seen that the maximum of each curve is located at 0.5. Therefore, it may reasonably be concluded that the (perylene)$^+$ and (tetracene)$^+$ in the solutions are in equilibrium with the 1:1 complex. This result was also supported by another analysis of the present absorption data by using the mole-ratio method, in which c_b was changed from 1.0×10^{-5} to 4.5×10^{-5}M, while c_a was kept constant (3.0×10^{-5}M). Furthermore, it was confirmed that the observed electronic absorption spectrum of the mixed solution can not be explained in terms of a mixture of (perylene)$^{2+}$ and tetracene, or of perylene and (tetracene)$^{2+}$; no absorption bands due to these species appear upon the mixing of the two cations.

The electronic absorption spectra were measured by a Cary Model 15 spectrophotometer, quartz cells with a pathlength of 1 cm being used. Commercial materials of perylene and tetracene were purified by vacuum sublimation. Concentrated sulfuric acid of a high purity ("Wako" 98.08%) was used without further purification.

1) K. Takemoto, S. Nakayama, K. Suzuki, and Y. Ooshika, This Bulletin, **41**, 1974 (1968).
2) K. Kimura, T. Yamazaki, and S. Katsumata, to be published.
3) W. I. Aalbersberg, G. J. Hoijtink, E. L. Mackor, and W. P. Weijland, *J. Chem. Soc.*, **1959**, 3049.

On the Structure of *Trans* Ethyl Methyl Ether and the W Form of Diethyl Ether

Michiro HAYASHI, Hisae IMAISHI, Keiichi OHNO, and Hiromu MURATA

Department of Chemistry, Faculty of Science, Hiroshima University, Higashi-sendamachi, Hiroshima

(Received November 4, 1970)

We have measured the microwave spectra of ethyl methyl ether and its isotopically substituted species. Since the measurements have not been finished for ^{18}O and one of ^{13}C species, the r_s structure can not be obtained at present.

We found many weak spectra around the expected regions for the spectra of the ^{18}O and one of three ^{13}C species. Some of these spectra may be assigned to those of the vibrationally excited states of the molecule. Since these spectra are confusing, it is preferable to assign them before the assignments of the spectra are undertaken for the ^{18}O and the ^{13}C species. However, we have tried to determine a tentative structure of *trans* ethyl methyl ether which reproduces the observed rotational constants for the parent and nine isotopic species.

In Table 1 are shown the observed rotational constants and the differences between the observed and the calculated rotational constants which were calculated using the obtained structural parameters given in Table 2. Work is in progress with respect to both the *trans* and the *gauche* isomers on the electric dipole moment, the internal rotation of the CH_3CH_2 and OCH_3 groups and the skeletal torsion and spectra due to the vibrationally excited states.

We have also tried to measure the microwave spectra of diethyl ether based on the trial calculation for the rotational constants of four possible molecular forms of diethyl ether using the structural parameters given in Table 2. We could find a set of spectra assigned to the W form (or the *trans-trans* form) of the molecule. In order to reproduce the observed rotational constants, we have adjusted only the structural parameters of the skeleton. The best agreement is obtained when we reduce the ∠COC angle by about 1° from the values for *trans* ethyl methyl ether. The results are given in Table 1.

TABLE 1. THE OBSERVED ROTATIONAL CONSTANTS (MHz) AND THE DIFFERENCES BETWEEN THE OBSERVED AND PREDICTED ROTATIONAL CONSTANTS

Species		$A(\Delta A)$[a]	$B(\Delta B)$[a]	$C(\Delta C)$[a]
trans ethyl methyl ether				
$CH_3CH_2OCH_3$		27992.03 (13.96)	4159.61 (4.61)	3891.11 (0.06)
$CH_3CH_2OCH_2D$	sym[b]	27218.96 (5.98)	3956.97 (4.21)	3699.99 (−0.74)
	asym[b]	26194.77 (0.52)	4009.66 (6.49)	3765.02 (2.23)
$CH_3CHDOCH_3$		25040.20 (10.71)	4131.86 (4.86)	3843.20 (0.18)
$CH_3CD_2OCH_3$		22669.17 (10.70)	4095.93 (5.23)	3804.65 (0.05)
$CH_2DCH_2OCH_3$	sym[b]	27505.31 (7.36)	3937.57 (−0.39)	3683.49 (0.02)
	asym[b]	26057.29 (18.57)	4008.84 (4.44)	3760.41 (0.20)
$CH_3CH_2OCD_3$		23838.31 (0.85)	3704.12 (7.48)	3491.59 (3.02)
$^{13}CH_3CH_2OCH_3$[c]		27951.36 (17.20)	4041.94 (6.71)	3787.16 (2.23)
$CH_3CH_2O^{13}CH_3$[c]		27978.56 (16.60)	4051.52 (6.66)	3796.06 (2.16)
the W form of diethyl ether				
$(CH_3CH_2)_2O$		17955.83 (6.87)[d]	2244.15 (2.71)[d]	2101.73 (0.12)[d]
		(−114.65)[e]	(−0.27)[e]	(−4.15)[e]

a) $\Delta R = R_{calctd} - R_{obsd}$, $R = A, B, C$

b) "sym" and "asym" refer to the symmetric and asymmetric forms, respectively with respect to the molecular plane.

c) Since the Q branches of the transitions have only been measured at present for two ^{13}C species, the rotational constants are determined on the assumption that the difference of $I_a+I_b-I_c$ between the parent and the isotopic species is the same as that found in CH_3CH_2Br and $(CH_3)_2O$, respectively.

d) The difference between the observed and predicted rotational constants calculated from the adjusted structural parameters.

e) The difference between the observed and predicted rotational constants calculated from the structural parameters obtained for *trans* ethyl methyl ether.

TABLE 2. STRUCTURAL PARAMETERS OBTAINED FOR *trans* ETHYL METHYL ETHER

CH_3O		CH_3C		CH_2		Skeleton	
$r(CH_s)$	1.091Å	$r(CH_s)$	1.083Å	$r(CH)$	1.097Å	$r(CC)$	1.540Å
$r(CH_a)$	1.097Å	$r(CH_a)$	1.087Å			$r(CH_3O)$	1.412Å
$\angle H_aCH_a$	109°24′	$\angle H_aCH_a$	108°48′	∠HCH	107°30′	$r(CH_2O)$	1.412Å
$\angle H_aCH_s$	110°10′	$\angle H_aCH_s$	109°45′	∠HCC	110°51′	∠COC	111°23′
$\angle H_sCO$	107°13′	$\angle H_sCC$	109°30′	∠HCO	109°50′	∠OCC	107°57′
$\angle H_aCO$	110°5′	$\angle H_aCC$	109°30′				

locked angles for: CH_3O, 1°55′; CH_2O, 1°15′

The Methylation of the Mercuric Ion by Methylcobaloximes

Jong-Yoon KIM, Nobumasa IMURA, Tyunoshin UKITA, and Takao KWAN
Faculty of Pharmaceutical Sciences, The University of Tokyo, Hongo, Tokyo
(Received November 7, 1970)

Cobaloximes and certain other cobalt complexes have recently been of interest as model compounds of vitamin B_{12}, and the chemistry involving the Co–C bond has been extensively investigated, particularly in connection with cobaloximes.[1]

It has been reported that Hg^{2+} is alkylated by alkylcobalamin, in the presence of a reducing agent, both enzymatically and nonenzymatically, to produce monoalkyl and dialkyl mercury.[2] Recently, Ukita *et al.*[3] found that the methylation of Hg^{2+} to afford monomethyl and/or dimethyl mercury took place by means of methylcobalamin in the absence of a reducing system. In view of the stability of the alkyl-cobalt bond,[4,5] the facile cleavage of the bond by Hg^{2+} to form alkyl mercurials is worthy of note.

Prompted also by the previous report that methylpentacyanocobalt complex can transfer its methyl group to Hg^{2+},[6] we were led to simulate the nonenzymatic reaction with methylcobaloximes and $HgCl_2$ in the absence of reducing agent and in a phosphate buffer solution. As a result, we found that the expected methylation took place although only methylmercuric chloride was formed.[7] The transmethylation may be represented by

$$CH_3\text{–(Co)–B} + HgCl_2 \xrightarrow[pH=7.0]{37^\circ, \text{dark}} CH_3HgCl + HO\text{–(Co)–B} + Cl^-$$

where (Co)-B denotes the cobaloxime moiety, with B representing an axial base such as H_2O or imidazole. Figure 1 shows the yield of the product with the time.

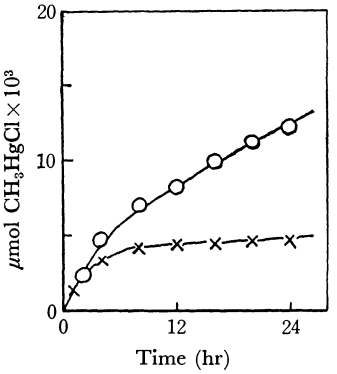

Fig. 1. The time course for the formation of CH_3HgCl in the dark at 37°C under an aerobic condition.
The reaction contained 0.1 μmol methylcobaloxime and 0.05 μmol $HgCl_2$ in 0.25M phosphate buffer at pH 7.0.
—○— methyl(imidazole)cobaloxime
—×— methyl(aquo)cobaloxime

It is apparent from Fig. 1 that the imidazole-coordinated cobaloxime is more reactive than the aquo-complex. This phenomenon is in accord with the kinetic data on the similar reaction between methylcobalamin or methylcobinamide and Hg^{2+}.[8] Also, it is to be noted that the methylcobaloxime is less reactive than the methylcobalamin, as is demonstrated by the formation of dimethyl mercury with the cobalamin. The difference in reactivity between the cobaloxime and the cobalamin is consistent with their electronic nature.[9] It is obvious, however, that the methylcobaloximes are reactive enough to methylate Hg^{2+} to yield monomethyl mercury.

1) G. N. Schrauzer, *Accounts Chem. Res.*, **1**, 97 (1968), and the references therein.
2) J. M. Wood, P. S. Kennedy, and C. G. Rosen, *Nature*, **220**, 173 (1968).
3) T. Ukita, E. Sukegawa, J. Y. Kim, N. Imura, and T. Kwan, in preparation.
4) G. N. Schrauzer and R. J. Windgassen, *J. Amer. Chem. Soc.*, **88**, 3738 (1966).
5) G. N. Schrauzer and J. W. Sibert, *ibid.*, **92**, 3509 (1970).
6) J. Halpern and J. P. Maher, *ibid.*, **86**, 2311 (1964).
7) The product was confirmed by means of both thin-layer chromatography and gas chromatography.
8) H. A. O. Hill, J. M. Pratt, S. Ridsdale. R. F. Williams, and R. J. P. Williams, *Chem. Commun.*, **1970**, 341.
9) G. N. Schrauzer, L. P. Lee, and J. W. Sibert, *J. Amer. Chem. Soc.*, **92**, 2997 (1970).

Effect of Phase on the Primary Process of the Formation of Butyl Radicals in the Radiolysis of Solid Isobutane-2-d_1

Yoshiyuki SAITAKE, Terunobu WAKAYAMA, Toyoaki KIMURA, Tetsuo MIYAZAKI, Kenji FUEKI, and Zen-ichiro KURI

Department of Synthetic Chemistry, Faculty of Engineering, Nagoya University, Chikusa-ku, Nagoya

(Received November 10, 1970)

We have studied the radiolysis of organic compounds in the solid state and have proposed that two important problems must be solved in order to elucidate the mechanism of the solid-phase radiolysis. One is the problem of the extent to which the formation of an exciton plays an important role;[1] the other is how the condition of the solid matrix affects the reaction of the exciton.[2,3] It was recently reported that the i-C_4H_9 radical is formed in the radiolysis of isobutane in the crystalline state, while the t-C_4H_9 radical is formed in the glassy state.[2] The possibility that the phase effect may be attributed to an isomerization of butyl radicals, such as i-$C_4H_9 \rightleftarrows t$-$C_4H_9$, was not completely excluded in the previous study.

In order to determine whether or not the phase change affects the primary process of the C–H bond rupture or the isomerization of butyl radicals, the radiolysis of $(CH_3)_3CD$ has been investigated by ESR spectroscopy at 77°K. $(CH_3)_3CD$ was prepared by the reaction of t-butyl magnesium bromide with D_2O. The ESR spectrum of γ-irradiated isobutane, which is polycrystalline at 77°K, is shown in Fig. 1a. The spectrum can be assigned to the $(CH_3)_2CHCH_2\cdot$ radical. The ESR spectrum of γ-irradiated pure $(CH_3)_3CD$ in the polycrystalline state is shown in Fig. 1b. The spectrum in Fig. 1b is quite different from that in Fig. 1a; it consists of three broad lines, with a splitting constant of 22.7G. The splitting constants of the α-proton and the β-proton of the $(CH_3)_2CHCH_2\cdot$ radical have been reported to be 22 and 35 G respectively.[4] Since the splitting due to a deuteron is about 15% of that due to a proton, it is expected that the spectrum of the $(CH_3)_2CDCH_2\cdot$ radical is split into three lines by two α-protons, with a slitting constant of 22 G, and that each line is then split further into three lines by a β-deuteron with a splitting constant of 5 G. Since the splitting due to a deuteron is, however, very small, the poorly-resolved spectrum in the solid state may consist of three broad lines with a splitting constant of 22 G. Thus, the spectrum in Fig. 1b coincides well with the spectrum expected for the $(CH_3)_2CDCH_2\cdot$ radical. An $(CH_3)_3$-CD sample containing methylcyclohexane (5.7 mol%) can be frozen to a clear glass by rapid cooling at 77°K. Upon the γ-irradiation of the mixture in the glassy state, the ESR spectrum shown in Fig. 1c was obtained. The spectrum is the same as that[2] obtained in the radiolysis of isobutane in the glassy state at 77°K; it can be assigned to the $(CH_3)_3C\cdot$ radical. Therefore, the bond rupture in the radiolysis of $(CH_3)_3CD$ in the solid state may be represented as follows:

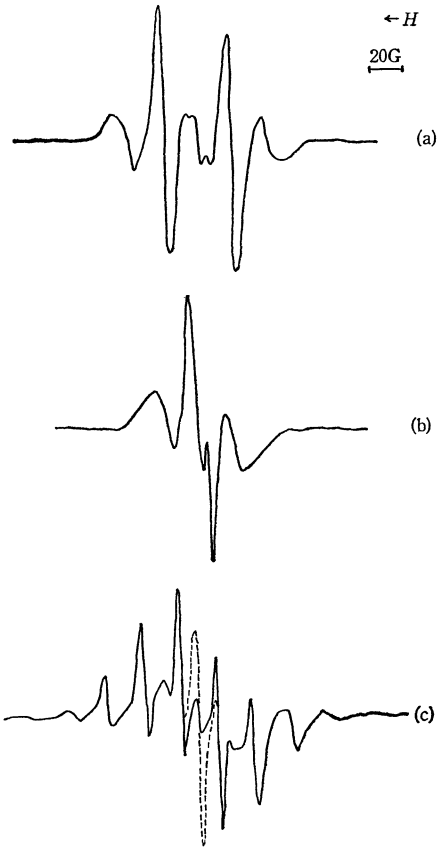

Fig. 1. (a) ESR spectrum of γ-irradiated i-C_4H_{10} in the polycrystalline state.
(b) ESR spectrum of γ-irradiated $(CH_3)_3CD$ in the polycrystalline state.
(c) ESR spectrum of γ-irradiated $(CH_3)_3CD$ containing methylcyclohexane (5.7 mol%) in the glassy state.
A dotted line represents the spectrum of trapped electron which is easily bleached by the illumination with visible light.
Irradiation dose: 2×10^5 rad.
Irradiation temperature: 77°K

$$(CH_3)_3CD \xrightarrow[\text{polycrystal}]{\sim\sim} (CH_3)_2CDCH_2\cdot + H \quad (1)$$

$$(CH_3)_3CD \xrightarrow[\text{glass}]{\sim\sim} (CH_3)_3C\cdot + D \quad (2)$$

It can be concluded that the phase change affects the primary process of the C–H bond rupture.

1) a) T. Wakayama, T. Miyazaki, K. Fueki, and Z. Kuri, This Bulletin, **42**, 1164 (1969). b) T. Wakayama, T. Kimura, T. Miyazaki, K. Fueki, and Z. Kuri, *ibid.*, **43**, 1017 (1970). c) T. Miyazaki, T. Yamada, T. Wakayama, K. Fueki, and Z. Kuri, to be published.

2) a) T. Miyazaki, T. Wakayama, K. Fueki, and Z. Kuri, This Bulletin, **42**, 2086 (1969). b) T. Wakayama, T. Miyazaki, K. Fueki, and Z. Kuri, *J. Phys. Chem.*, **74**, 3584 (1970).

3) a) T. Miyazaki, S. Okada, T. Wakayama, K. Fueki, and Z. Kuri, This Bulletin, **43**, 1907 (1970). b) T. Miyazaki, Y. Fujitani, T. Wakayama, K. Fueki, and Z. Kuri, to be published.

4) R. W. Fessenden and R. H. Schuler, *J. Chem. Phys.*, **39**, 2147 (1963).

The Reduction of Enamines and the Reductive Alkylation of *sec*-Amines with Potassium Hydridotetracarbonylferrate

Take-aki MITSUDO, Yoshihisa WATANABE, Masato TANAKA,
Kazuo YAMAMOTO, and Yoshinobu TAKEGAMI
Department of Hydrocarbon Chemistry, Faculty of Engineering, Kyoto University, Sakyo-ku, Kyoto
(Received November 13, 1970)

Enamines have been recognized to have elegant and broad utility in organic synthesis.[1] On the other hand, little attention has been paid to the reactions of enamines with organotransition metal complexes. The present communication will deal with the reaction of enamines with potassium hydridotetracarbonylferrate, $KHFe(CO)_4$[2] (I), under carbon monoxide.

We have found that enamines react with the alcoholic ferrate (I) at 30°C, with a rapid absorption of carbon monoxide, to give the corresponding saturated amines.[3] No carbonylated product of the enamines was detected, however. The ferrate (I) also reacts with a binary system, consisting of a *s*-amine and a carbonyl compound, from which an enamine can be prepared, to give a *t*-amine in a fairly good yield.

The results of the typical reactions are shown in Table 1. To 11 mmol of the ferrate (I) in 50 m*l* of ethanol, was added 33 mmol of 1-morpholino-1-cyclohexene at 30°C under one atmosphere of carbon monoxide. Twenty mmol of carbon monoxide was absorbed in 1.5 hr, giving 15 mmol of *N*-cyclohexylmorpholine. The reaction also proceeded under nitrogen, but the yield of the product was lower. The yield of the *N*-cyclohexylmorpholine was improved by the addition of excess potassium hydroxide. 1-Piperidino-1-isobutene was readily reduced to the isobutane derivative. The ferrate (I) reacted with an equimolar mixture of morpholine and cyclohexanone, with a slow absorption of carbon monoxide, to give *N*-cyclohexylmorpholine. Neither morpholine and cyclohexanone, however, reacted separately with the ferrate (I). Pyrrolidine and acetophenone gave *N*-(1-phenylethyl)pyrrolidine. The iminium salt of 1-morphorino-1-cyclohexene, *N*-cyclohexylidenemorpholium perchlorate, also reacted with the ferrate (I) to give *N*-cyclohexylmorpholine.

The facts that iron pentacarbonyl is not effective for this type of reduction of enamines, and that the reductive alkylation of *s*-amines with a potassium hydroxide-carbon monoxide system is very slow, show that the ferrate (I) is essential for this reaction. Hydrogenation catalysts, such as Raney nickel[4] and derivativ of formic acid,[5] are effective for the reductive alkylation of amines, but both reactions require some more drastic reaction conditions than does the present reaction. It is plausible that the reduction of enamines and the reductive alkylation of *s*-amines with the ferrate (I) proceeds *via* iminium salt, which has been shown to be an intermediate in the reduction of enamines by formic acids.[6] Studies of the mechanism of this reaction and some of the extension fields of this system will be reported in more detail in the near future.

TABLE 1. THE REDUCTION OF ENAMINES AND REDUCTIVE ALKYLATION OF AMINES BY $KHFe(CO)_4$[a]

Exp. No.	Reagent[b]	Reaction time, hr	CO absorbed	Max. Rate of CO absorption	Product	Yield
1	1-Morpholino-1-cyclohexene	1.5	1.8[c]	13[d]	*N*-Cyclohexylmorpholine	1.4[c]
2	1-Morpholino-1-cyclohexene	1.5	—[e]	—	*N*-Cyclohexylmorpholine	0.9
3[f]	1-Morpholino-1-cyclohexene	5.0	2.0	10	*N*-Cyclohexylmorpholine	2.4
4	1-Piperidino-1-isobutene	48	1.9	0.8	*N*-Isobutylpiperidine	1.5
5	Morpholine-Cyclohexanone	48	1.7	1.0	*N*-Cyclohexylmorpholine	1.4
6	Pyrrolidine-Acetophenone	48	1.5	1.0	*N*-(1-Phenylethyl)pyrrolidine	1.1

a) $KHFe(CO)_4$ 11 mmol in 50 m*l* ethanol, at 30°C.
b) 3.0 mol/mol-$KHFe(CO)_4$ of reagent was used.
c) mol/mol-$KHFe(CO)_4$.
d) m*l*/min.
e) Nitrogen atmosphere.
f) Excess KOH (11 mol) was added.

1) For a review of enamines see, for example, A. G. Cook, "Enamines: Synthesis, Structure and Reaction," Marcel Dekker, New York (1969).
2) $KHFe(CO)_4$ is formed by the following equation. $Fe(CO)_5+3KOH\rightarrow KHFe(CO)_4+K_2CO_3+H_2O$
3) The products in each case were identified by IR, NMR, Mass and vpc analysis.
4) W. S. Emerson, *Organic Reactions*, **4**, 174 (1949).
5) M. L. Moore *ibid.*, **5**, 301 (1949); P. L. DeBenneville and J. H. Macartney, *J. Amer. Chem. Soc.*, **72**, 3073 (1950).
6) N. J. Leonald and R. R. Sauers, *J. Amer. Chem. Soc.*, **79**, 6210 (1957).

Anomalous Products Obtained by Nitration of Some Polyalkylnaphthalenes

Hitomi SUZUKI and Kiyomi NAKAMURA

Department of Chemistry, Faculty of Science, Kyoto University, Sakyo-ku, Kyoto

(Received November 16, 1970)

Polyalkylbenzenes react with fuming nitric acid in an unusual way to yield benzyl nitrate as the main product. The reaction has an electrophilic feature and is characterized for its peculiar orientation and high positional selectivity.[1] Our studies on the anomalous nitration are now extended to include naphthalene series. Among various polyalkylnaphthalenes investigated, anomaly was observed only with those systems in which both 1 and 4 positions were occupied by alkyl groups. In contrast to the results obtained with polyalkylbenzene derivatives, the major product in this case was not nitrooxymethylnaphthalene but nitromethylnaphthalene.

1,4-Dimethylnaphthalene (I) was treated with fuming nitric acid in dilute methylene chloride solution at −5—0°C for 0.5 hr to give a pale yellow oily mixture, which was found to contain besides 4-methyl-1-nitromethylnaphthalene (V) some amounts of a methylene compound, presumably 1-methylene-4-nitro-4-methyl-1,4-dihydronaphthalene (III), and addition products on the basis of infrared, ultraviolet and PMR spectra as well as by spectral comparison with the anomalous nitration product from 9,10-dimethylanthracene.[2] Our result differs somewhat from both an earlier report by Robinson and Thompson[3] who isolated V, and from the recent comment by Davies and Warren[4] who obtained 1,4-dimethyl-5-nitronaphthalene (VI).

With the use of excess of nitric acid, 1,2,4-trimethylnaphthalene readily underwent side-chain nitration at less hindered methyl group to give 3,4-dimethyl-1-nitromethylnaphthalene (mp 92—95°C) as the principal product. However, 1,2,3-trimethylnaphthalene was only nitrated at ring position to give 1,2,3-trimethyl-4-nitronaphthalene (mp 148—149°C) in good yield. No side-chain attack was observed. 1,2,3,4-Tetramethylnaphthalene showed a similar anomaly to give 2,3,4-trimethyl-1-nitromethylnaphthalene (mp 99.5—101.5°C). The orientation of these side-chain substituted products has been established by treatment of the corresponding polymethylnaphthylmethyl chlorides with silver nitrite in acetonitrile, followed by purification of the resulting nitro compounds through repeated precipitations from alkaline solution.

Davies and Warren[4] recently suggested that the nitromethyl compound V can be derived from an acid-catalysed rearrangement of VI. Although the nitro group at the hindered position is known to be subjected to migration in some cases,[5] there seems so far to be no analogy of such rearrangement. More probable reaction sequences which account for side-chain nitration might be as shown in Scheme 1

Nitronium ion attaches to 1-position of the higher alkylated ring to form arenonium ion II, in which steric strain due to the interaction between alkyl group and peri-hydrogen is partly relieved and the positive charge is more effectively delocalized when the alkyl groups are located at 1- and 4-positions. Loss of proton from the alkyl side-chain, followed by electrophilic attack of nitronium ion at the terminal methylene group of III, redistribution of electrons to regain the naphthalene ring system, and the concomitant departure of the nitro group from the ring will lead to the formation of side-chain nitro compound. An alternative reaction scheme involves intermediate formation of addition product. The methylene compound III may undergo 1,4-addition of dinitrogen pentoxide to form IV which, on further removal of dinitrogen pentoxide from the ring, will lead to side-chain nitration.

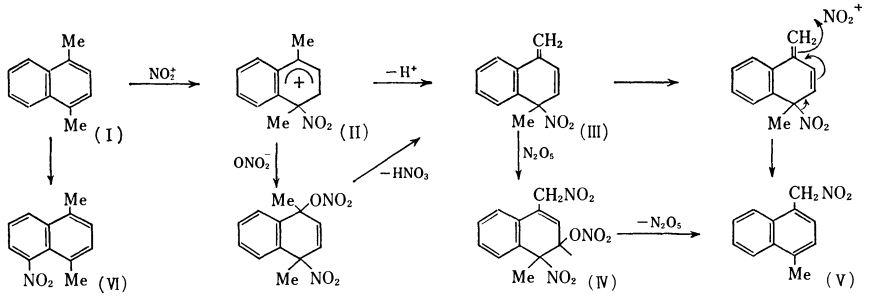

Scheme 1

1) H. Suzuki and K. Nakamura, This Bulletin. **43**, 473 (1970); H. Suzuki, *ibid.*, **43**, 481 (1970); H. Suzuki, *ibid.*, **43**, 879 (1970); K. Nakamura, *ibid.*, **44**, 133 (1971); K. Nakamura and H. Suzuki, *ibid.*, **44**, 227 (1971).

2) Unpublished result.

3) R. Robinson and H. W. Thompson, *J. Chem. Soc.*, **1932**, 2015.

4) G. Davies and K. D. Warren, *ibid.*, *B*, **1969**, 873.

5) K. H. Pausacker and J. G. Scroggie, *ibid.*, **1955**, 1897; P. H. Gore, *ibid.*, **1957**, 1436.

Photosensitized Electrolytic Oxidation of Iodide Ions on Cadmium Sulfide Single Crystal Electrode[1]

Akira FUJISHIMA, Eiichi SUGIYAMA, and Kenichi HONDA

Institute of Industrial Science, The University of Tokyo, Roppongi, Minato-ku, Tokyo

(Received November 2, 1970)

The semiconductor electrode reactions have been studied by a number of research workers[2]; they exhibit interesting behavior different from that of metal electrodes. The present authors[3] have studied mainly the effect of the irradiation with light on the semiconductor electrode reactions and have learned that the oxidation reactions, such as oxygen evolution from water or the oxidation of halogen ions, occur at more negative potentials than the standard oxidation potential on a TiO_2 or ZnO single crystal electrode.[4]

The behavior of the CdS semiconductor electrode, which has a band gap of 2.4 eV, has been reported only by Williams,[5] who especially studied the mechanism of its photo-voltaic effect.

In the present paper, it is concluded that the photosensitized electrolytic oxidation does occur on the CdS electrode in the same way as on the TiO_2 and ZnO electrodes. It will also be reported that the mechanism of this photosensitized electrolytic reaction can be determined by using the method of a rotating ring-disk electrode, in which the disk electrode consists of a cadmium sulfide single crystal and the ring electrode gold or amalgamated gold.

The anodic current of the CdS electrode does not flow in the dark, but under irradiation it flows in proportion to the intensity of light at potentials more positive than -0.68 V (*vs.* SCE) and depends on the wavelength of light (the greatest anodic current is found to flow at 520 mμ, *i.e.*, 2.4 eV). The anodic reaction is related to the holes formed by the irradiation in the valence band and is rate-controlled by the supply of the holes to the surface of the electrode.

When the anodic reaction occurs on the CdS disk electrode, the reduction current on the ring amalgamated electrode is found to begin to flow from -0.6 V towards the negative potential and then to appear in the limiting reduction current region. The half-wave potential of this reduction corresponds to the reduction of Cd^{2+} to Cd. The ratio of the disk electrode current to the ring electrode current nearly agrees with the calculated collection efficiency. After the anodic disk current flows for several minutes, the surface of CdS is observed to become white-yellow because of some adhered substance, which is found to be sulfur from its high solubility into CS_2. These facts indicate that the anodic reaction of the CdS electrode under irradiation is the anodic dissolution of the electrode, as expressed by the following reaction (1):

$$CdS + 2p^+ \rightarrow Cd^{2+} + S. \quad (1)$$

When the electrolyte solution contains iodide ions, the apparent anodic behavior is similar to that in the electrolyte not containing iodide ions from the viewpoint of the current-voltage curves of the CdS electrode. However, the anodic current can be attributed to the oxidation of iodide ions:

$$2I^- + 2p^+ \rightarrow I_2 \quad (2)$$

as revealed from the behavior of the ring electrode, which shows an increase of the reduction current at a more negative potential than 0.3 V, indicating the formation of iodine on the CdS surface. In this case, the change of the CdS surface can scarcely be detected after the anodic oxidation.

The fact that the starting potential of the oxidation of iodide ions is -0.68 V, which is much more negative than its reversible potential, indicates that photosensitized electrolytic oxidation occurs even on CdS.

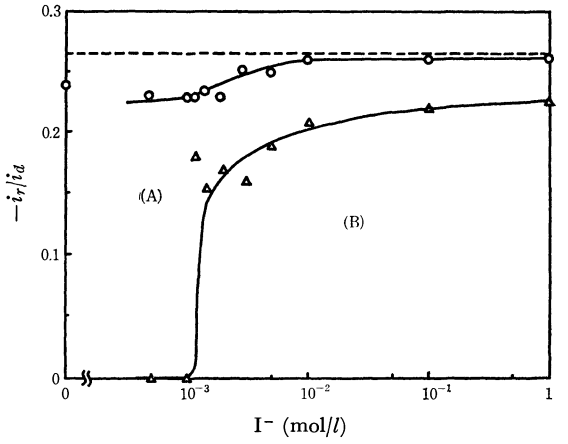

Fig. 1. Competition between dissolution of CdS and oxidation of iodide ions against the concentration of iodide ions.
Potential of the disk electrode (V_d): 1.0 V
△: Potential of the ring electrode, -0.40 V, at which iodine can be detected.
○: Potential of the ring electrode, -1.00 V, at which both iodine and cadmium ions can be detected.

In Fig. 1, the ratio of the current of the amalgamated ring electrode to the disk current against the concentration of iodide ions is shown. The collection efficiency of this electrode is calculated to be 0.265 from the geometric dimensions of the electrode. When the concentration of iodide ions is lower than 10^{-3} mol/l, the dissolution of CdS occurs ((A) in Fig.1); on the other hand, when it is higher than 10^{-3} mol/l, the oxidation of iodide ions occurs in competition with the dissolution of CdS ((B)). The degree of the competition between the reaction (1) and (2) may depend on the amount of iodide ions adsorbed on the CdS surface.

The results will be reported in detail in due course.

1) Studies on Photosensitive Electrode Reactions. IV.

2) For example, H. Gerischer, *J. Electrochem. Soc.*, **113**, 1174 (1966).

3) A. Fujishima, K. Honda, and S. Kikuchi, *Kogyo Kagaku Zasshi*, **72**, 108 (1969).

4) This behavior has previously been termed "photosensitized electrolytic oxidation" by the present authors.[3]

5) R. Williams, *J. Chem. Phys.*, **32**, 1505 (1960).

The Separation of Copper Isotopes by Ion-exchange Chromatography

Tadao KANZAKI[1] and Hidetake KAKIHANA

Research Laboratory of Nuclear Reactors, Tokyo Institute of Technology, Ookayama, Meguro-ku, Tokyo

(Received May 14, 1970)

A break-through experiment on the separation of copper isotopes was carried out through the use of a cation-exchange resin column. By analysing the experimental results, the approximate values of the single-stage (elementary) separation factors, S^{63}_{65}, were determined. The copper sulphate and copper chloride systems gave significant separation factors ($S^{63}_{65}=1.0000_3-1.0004_2$), but the copper nitrate system gave no isotope separation. These data were analysed in terms of the theory of the two-phase distribution of isotopes previously proposed by one of the present authors (Kakihana). The equilibrium coefficient for isotopic-exchange reaction by complex formation in an external solution ($K_1=1.0001_5$ for the copper sulphate system, and $K_1=1.0005$ for the copper chloride systems) was estimated.

Since the first experiment on isotope separation by ion-exchange chromatography was carried out by Taylor and Urey[2] in 1938, many experiments have been done on the separation of isotopes using the same method. Some results, especially these for nitrogen[3–5] and uranium[6–8] isotopes, were not, however, the results of a simple ion-exchange reaction, but those of the effects combining with some other chemical reactions, *e.g.*, complex formation and an electron-exchange reaction.

In order to explain these results, the theory of the two-phase distribution of isotopes was proposed by one of the present authors (Kakihana);[8–12] the isotope effects caused by complex formation and electron-exchange reaction have been analysed using this theory in connection with experiments on lithium,[8,13] nitrogen,[8] and uranium[7,8] isotopes.

In this paper, for the further extension of these studies, copper, which forms various well-known complexes, was selected and studied.

Experimental

The 0.1 M copper solutions shown in Table 1 were passed very slowly through an ion-exchange column of Dowex 50W-X12 in the H^+ form (100—200 mesh) (about 100 cm in height and 1 cm in diameter). In the case of the experiments IV, V, VI, and VII, an acetone-water mixed solvent of the same acid concentration and acetone content as the copper solution had been passed through the column beforehand. Each fraction of the effluent copper solutions from the column was collected and analysed in the following way.

The copper concentrations were determined by chelatometric titration with ethylenediaminetetraacetic acid (EDTA).[14]

The abundance ratios of the copper isotopes were determined on a copper nitrate sample by means of a Nier-type 60° mass spectrometer, Atlas CH 4, using the surface ionization method.[15] Copper nitrate samples were obtained from the effluent by the following procedure. For the experiment I, the effluent copper solutions were evaporated to dryness directly. For the other experiments, a small amount of 2 M hydrochloric acid was added to the effluent solution (for the experiments VI and VII, the effluents were evaporated to dryness to remove the acetone before the addition of the hydrochloric acid), the copper was deposited from the unstirred solution onto a small platinum electrode by adjusting the voltage so that the current was 0.2 to 0.3 A and by allowing the electrolysis to continue more than 8 hr (the yield of copper was above 99.9%). After the cathode had been rinsed with deionized water, the copper was stripped from the electrode with dilute nitric acid; the copper nitrate sample was then obtained by the evaporation of the solution. The reagents used in this experiments were all of an analytical grade except for the copper reagent. Copper nitrate was prepared by dissolving copper metal of a high purity (above 99.99%) with dilute nitric acid and then recrystallizing it. Copper chloride and copper sulphate were prepared by passing the copper nitrate solution through a column of the cation-exchange resin, Dowex 50W-X12, in the H^+ form, and by eluting the copper ions adsorbed on the column using dilute hydrochloric acid or sulfuric acid, and by recrystallizing them.

Results

The elution curves obtained for each experiment are shown in Fig. 1-1—1-7. Sample numbers of the mass-spectrometric analysis are also shown in Fig. 1. The total amounts of copper isotopes adsorbed in the ion-exchanger, Q, were estimated from these curves (Table 2).

The results of the mass-spectrometric analysis are given in Table 3. In Table 3, the significant values are underlined (the accuracy of the mass-spectrometric analysis is within ±0.0007 for the R_o–R_t value). The

1) Present address: Department of Chemistry, Tokyo Institute of Technology, Ookayama, Meguro-ku, Tokyo.

2) T. I. Taylor and H. C. Urey, *J. Chem. Phys.*, **6**, 429 (1938).
3) F. H. Spedding, J. E. Powell, and H. J. Svec, *J. Amer. Chem. Soc.*, **77**, 6125 (1955).
4) T. Ishimori, This Bulletin, **33**, 516 (1960).
5) H. Kakihana, T. Nomura, and K. Kodaira, *J. Atomic Energy Soc. Japan*, **3**, 519 (1961).
6) H. Kakihana, Y. Mori, H. Sato, and T. Kanzaki, *ibid.*, **4**, 857 (1962).
7) H. Kakihana, K. Gonda, H. Sato, and Y. Mori, *ibid.*, **5**, 990 (1963).
8) H. Kakihana, *J. Chim. Phys.*, **60**, 81 (1963).
9) H. Kakihana and K. Kurisu, *Nippon Kagaku Zasshi*, **84**, 470 (1963).
10) H. Kakihana, K. Kurisu, and M. Hosoe, *ibid.*, **84**, 784 (1963).
11) H. Kakihana and K. Kurisu, *ibid.*, **86**, 151 (1965).
12) H. Kakihana, K. Takahashi, and Y. Yato, *J. Nucl. Sci. Tech. Japan*, **5**, 93 (1968).
13) H. Kakihana, T. Nomura, and Y. Mori, *J. Inorg. Nucl. Chem.*, **24**, 1145 (1962).
14) K. Ueno, "Chelatometry," Nankodo, Tokyo (1962), p. 253.
15) T. Kanzaki, S. Yokozuka, and H. Kakihana, *Japan Analyst*, **16**, 7 (1967).

TABLE 1. EXPERIMENTAL CONDITIONS

Experiment No.	Copper salt	Solvent	Copper concentration mol/l	Hydrochloric acid concentration mol/l	Average flow rate ml/hr
I	$Cu(NO_3)_2$	water	0.101_4	0.000	22.4
II	$CuSO_4$	water	0.0983_3	0.000	18.0
III	$CuCl_2$	water	0.102_3	$0.007^{a)}$	19.5
IV	$CuCl_2$	HCl	0.0973_6	0.477_7	21.6
V	$CuCl_2$	HCl	0.0978_7	0.964_7	20.8
VI	$CuCl_2$	20 vol% acetone	0.100_0	$0.007^{a)}$	15.0
VII	$CuCl_2$	40 vol% acetone	0.100_4	$0.007^{a)}$	14.6

a) For prevention of hydrolysis of copper salt a small amounts of hydrochloric acid was added to the solution

TABLE 2. TOTAL AMOUNTS OF COPPER ISOTOPES ADSORBED IN THE ION-EXCHANGER, Q

Experiment No.	Q mol
I	0.0917_3
II	0.0937_0
III	0.0877_0
IV	0.0556_0
V	0.0335_1
VI	0.0875_3
VII	0.0845_0

Total capacity of ion-exchanger is 0.198 equivalent in all experiments.

D values were calculated from these values by a method which will be described below.

Discussion

The single-stage (elementary) separation factors can be calculated from the results in Tables 2, and 3 by means of the following equation:[16]

$$S_{65}^{63} = \frac{\text{Total amount of } {}^{63}\text{Cu in the ion-exchanger phase}}{\text{Total amount of } {}^{65}\text{Cu in the ion-exchanger phase}} \times \frac{\text{Total amount of } {}^{65}\text{Cu in the external solution phase}}{\text{Tatal amount of } {}^{63}\text{Cu in the external solution phase}} = 1 + \frac{D}{Q-D} \cdot \frac{1}{R_o} \quad (1)$$

where Q is the total amount of copper isotopes adsorbed in the ion-exchanger (mol), R_0 is the mole fraction of the ^{63}Cu isotope in the feed solution, and D is the amount of the ^{63}Cu isotope enriched in the ion-exchanger (mol).

$$D = \frac{1}{(1-R_o)} \sum_{i=1}^{n} (R_o - R_i) \cdot f_i \quad (2)$$

where f_i and R_i denote the sum of the copper isotopes, ^{63}Cu and ^{65}Cu (mol), and the mole fraction of the ^{63}Cu isotope in the effluent fraction i, respectively.

The results calculated by means of Eq. (1) are given in Table 4; they lead to the following conclusions:

16) H. Kakihana and T. Kanzaki, *Bull. Tokyo Inst. Tech. Japan*, **1969**, 77.

TABLE 3. RESULTS OF MASS SPECTROMETRIC ANALYSIS

Experiment No.	Sample No.	Amounts of copper in fraction i, f_i, mol	Mole fraction of lighter isotope ^{63}Cu, R_i	$R_0^{a)} - R_i$	$D^{b)} \times 10^7$ mol
I	1	0.000901	0.692_4	-0.000_4	0
	2	0.00113_5	0.691_8	$+0.000_2$	
	3	0.00113_0	0.691_3	$+0.000_7$	
	4	0.00113_0	0.692_5	-0.000_5	
	5	0.00113_0	0.692_9	-0.000_9	
	6	0.00113_0	0.692_2	-0.000_2	
II	1	0.000314	0.688_6	$+0.003_4$	80.5
	2	0.000875	0.690_5	$+0.001_5$	
	3	0.000894	0.691_1	$+0.000_9$	
	4	0.000894			
	5	0.000894	0.692_6	-0.000_6	
	6	0.000894	0.691_7	$+0.000_3$	
III	1	0.000280	0.690_2	$+0.001_8$	16.4
	2	0.000857	0.691_1	$+0.000_9$	
	3	0.000973	0.692_1	-0.000_1	
	4	0.000973	0.691_1	$+0.000_9$	
	5	0.000973	0.691_7	$+0.000_3$	
	6	0.000973	0.691_2	$+0.000_8$	
IV	1	0.000237	0.693_1	-0.001_1	66.2
	2	0.000705	0.692_9	-0.000_9	
	3	0.00104_6	0.692_6	-0.000_6	
	4	0.00104_9	0.690_9	$+0.001_1$	
	5	0.00104_9	0.690_9	$+0.001_1$	
	6	0.00104_9	0.692_1	-0.000_1	
V	1	0.000224	0.692_5	-0.000_5	98.3
	2	0.000818	0.690_5	$+0.001_5$	
	3	0.00100_2	0.690_2	$+0.001_8$	
	4	0.00100_7	0.691_9	$+0.000_1$	
	5	0.00110_8	0.692_0	0.000_0	
VI	1	0.000699	0.691_3	$+0.000_7$	97.4
	2	0.00103_5	0.689_1	$+0.002_9$	
	3	0.00103_8	0.691_7	$+0.000_3$	
	4	0.00104_3	0.691_5	$+0.000_5$	
	5	0.00104_5	0.692_0	0.000_0	
VII	1	0.00125_4	0.691_7	$+0.000_3$	130.8
	2	0.00118_6	0.688_6	$+0.003_4$	
	3	0.00120_8	0.692_0	0.000_0	
	4	0.00120_8	0.691_8	$+0.000_2$	
	5	0.00120_8	0.692_7	-0.000_7	

a) Mole fraction of lighter isotope, ^{63}Cu in the feed solution: 0.692_0.

b) Amounts of isotope, ^{63}Cu enriched in the ion-exchanger.

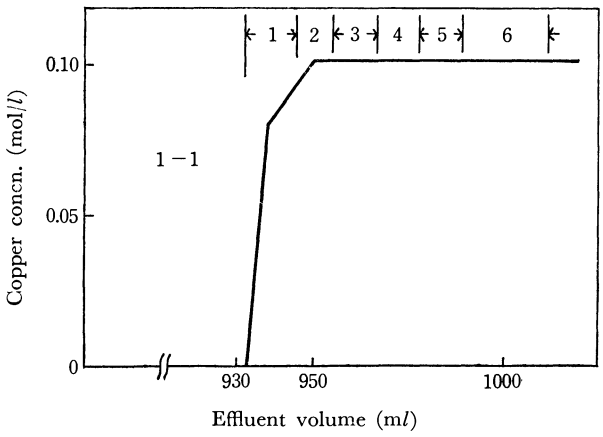

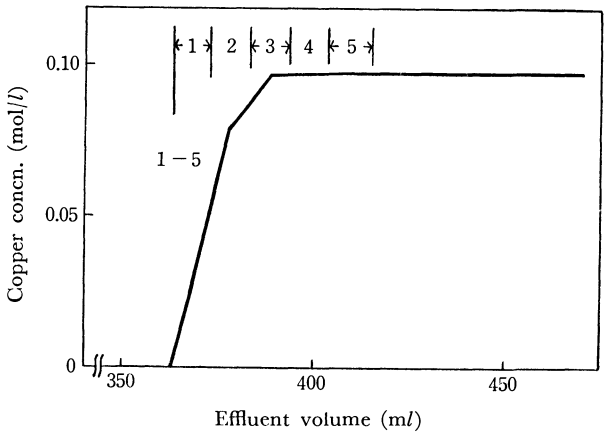

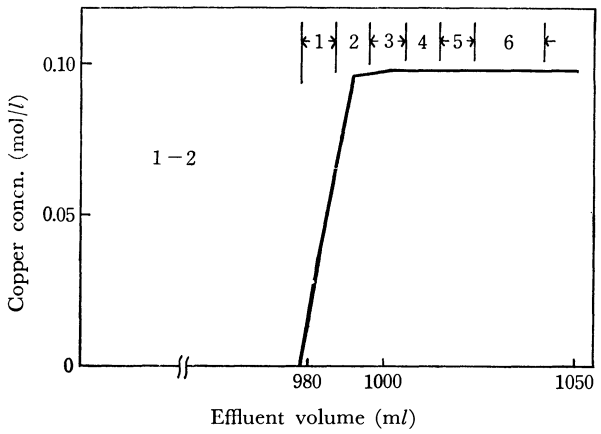

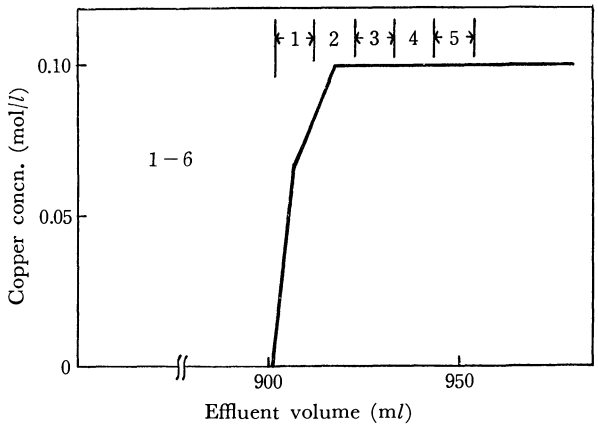

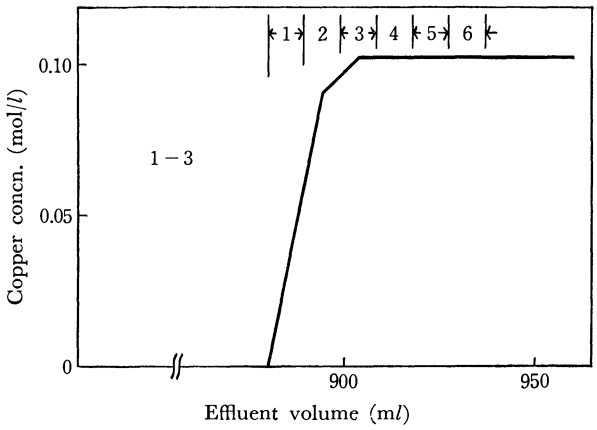

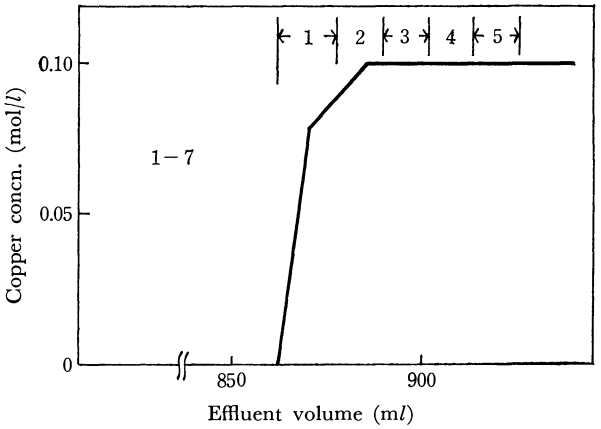

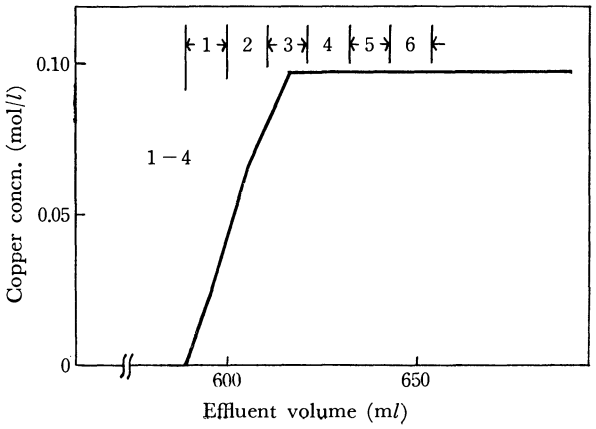

Fig. 1. Elution curves.
1—1. Experiment I. 1—2. Experiment II. 1—3. Experiment III. 1-4. Experiment IV. 1—5. Experiment V. 1—6. Experiment VI. 1—7. Experiment VII.

(a) For all systems, the lighter isotope, ^{63}Cu, is enriched in the ion-exchanger.

(b) For the copper nitrate system (experiment I), scarcely no isotope effect is found within our limits of experimental accuracy, while for the copper sulphate and copper chloride systems, significant isotope effects are found.

(c) The value of the single-stage (elementary) separation factor obtained for the $CuSO_4$-water system (experiment II) is larger than that for the $CuCl_2$-water (experiment III).

TABLE 4. SINGLE STAGE (ELEMENTARY) SEPARATION FACTOR, S_{65}^{63}

Experiment No.	Copper salt	Solvent	S_{65}^{63}
I	$Cu(NO_3)_2$	water	1.0000_0
II	$CuSO_4$	water	1.0001_2
III	$CuCl_2$	water	1.0000_3
IV	$CuCl_2$	0.5 M HCl	1.0001_7
V	$CuCl_2$	1.0 M HCl	1.0004_2
VI	$CuCl_2$	20 vol% acetone	1.0001_6
VII	$CuCl_2$	40 vol% acetone	1.0002_2

(d) For the $CuCl_2$–HCl system, the values of the single-stage separation factor become larger with an increase in the concentration of hydrochloric acid.

(e) For the $CuCl_2$-acetone-water mixed solvent system, the values of the single-stage separation factor become slightly larger with an increase in the acetone content.

The four facts (b), (c), (d), and (e) can be explained by the isotope effects in complex-formation reactions.

Since copper nitrate dissociates nearly completely in an aqueous solution, the isotope effects for the $Cu(NO_3)_2$-water system can be said to result from a simple ion-exchange reaction only: that is, they represent the isotope difference in the hydrated copper ion between the aqueous-solution and the ion-exchanger phases.[17]

On the other hand, in the cases of the $CuSO_4$ and $CuCl_2$ systems, such complexes as $(CuSO_4)$, $(CuCl^+)$, and $(CuCl_2)$ are formed in the solution. Therefore, the isotope effects of the systems result from the combination of these complex formation reactions with the simple ion-exchange reaction. It has been suggested by Kakihana, in his theory of the two-phase distribution of isotopes, that, for the cation exchange system, the greater the amounts of complex species formed in the external solution, the larger the single-stage separation factors obtained. The four experimental facts, (b), (c), (d), and (e) agree with this suggestion, as will be described below. As will be discussed below, in an aqueous solution the amount of the copper sulphate complex $(CuSO_4)$ is one hundred times as much as that of the chlorocomplexes of copper $(CuCl^+)$, $(CuCl_2)$. This may be the reason why the isotope effect of the copper sulphate system (experiment II) is higher than that of the copper chloride system (experiment III). In the hydrochloric acid solution, the amounts of the chlorocomplexes increase with the increase in the concentration of hydrochloric acid, which has a higher isotope effect in a higher hydrochloric acid system (experiment V) than in a dilute hydrochloric acid system (experiment IV) or in an aqueous solution system (experiment III). In the acetone-water mixed solution, the amount of the chlorocomplexes is much more than in the aqueous solution because of the decrease in the dielectric constant of the solvent. This gives the higher isotope effect in the acetone-water mixed systems (experiments VI and VII).

From the results in Table 4, we can estimate the equilibrium coefficients for the isotopic-exchange reactions involved in the external solution by applying the theory of the two-phase distribution of isotopes.

The single-stage separation factors, S, obtained from the abundance ratios of copper isotopes in the two phases (external-solution and ion-exchanger phases) can be expressed by the following equation:

$$\begin{aligned}\ln S_A^B = {} & \ln {}_A^B K_z \\ & - \ln \Big[1 + \sum_{n=0}^{z-1}\sum_{t=0}^{T} x_{nt}\Big(\prod_{n+1}^{z} K_n \cdot \prod_{1}^{t} K_{nt}^{-1} - 1\Big) \\ & \quad + \sum_{n=z}^{r}\sum_{t=0}^{T} x_{nt}\Big(\prod_{z+1}^{n} K_n^{-1} \cdot \prod_{1}^{t} K_{nt}^{-1} - 1\Big)\Big] \\ & + \ln \Big[1 + \sum_{n=0}^{z-1}\sum_{s=0}^{S} \bar{x}_{ns}\Big(\prod_{n+1}^{z} \bar{K}_n \cdot \prod_{1}^{S} \bar{K}_{ns}^{-1} - 1\Big) \\ & \quad + \sum_{n=z}^{r}\sum_{s=0}^{S} \bar{x}_{ns}\Big(\prod_{z+1}^{n} \bar{K}_n^{-1} \cdot \prod_{1}^{S} \bar{K}_{ns}^{-1} - 1\Big)\Big] \qquad (3)^{12)}\end{aligned}$$

Since only one ligand, Cl^- or SO_4^{2-} in our case, exists, Eq. (3) can be reduced to:

$$\begin{aligned}\ln S_{65}^{63} = {} & \ln {}_{65}^{63}K_z - \ln\Big[1 + \sum_{n=0}^{z-1} x_n\Big(\prod_{n+1}^{z} K_n - 1\Big) + \sum_{n=z}^{r} x_n\Big(\prod_{z+1}^{n} K_n^{-1} - 1\Big)\Big] \\ & + \ln\Big[1 - \sum_{n=0}^{z-1} \bar{x}_n\Big(\prod_{n+1}^{z} \bar{K}_n - 1\Big) + \sum_{n=z}^{r} \bar{x}_n\Big(\prod_{z+1}^{n} \bar{K}_n^{-1} - 1\Big)\Big]\end{aligned} \qquad (4)$$

where x and $\bar{x}$ are the mole fraction of each chemical species in the external-solution phase and in the ion-exchanger phase respectively. ${}_{65}^{63}K_z$ is the equilibrium coefficient for an isotopic exchange reaction between the two phases (the external-solution and ion-exchanger phases) of the chemical species, CuX_z, which are contained in both phases (X is the ligand). K_n and $\bar{K}_n$ are the equilibrium coefficients for an isotopic-exchange reaction by complex formation in the external-solution and the ion-exchanger phases respectively, and $\prod_1^0 K_n = 1$.

The equations for the copper sulphate and copper chloride systems are derived from Eq. (4) as follows.

Copper Sulphate System (Experiment II). In this system, the chemical species existing in the external solution are Cu^{2+} and $CuSO_4$, and in the cation-exchange resin only Cu^{2+} can be adsorbed in appreciable amounts. These facts indicate that, in Eq. (4), z is zero (which means that Cu^{2+} exists in both phases), $r=1$ (which means that only Cu^{2+} and $CuSO_4$ exist in the external solution) and $\bar{x}_0=1$ (which means that only Cu^{2+}, not $CuSO_4$, is adsorbed in the cation-exchange resin). Therefore, Eq. (4) becomes:

$$\begin{aligned}\ln S_{65}^{63} = {} & \ln {}_{65}^{63}K_0 - \ln\Big[1 + x_0\Big(\prod_{1}^{0} K_n^{-1} - 1\Big) + x_1(K_1^{-1} - 1)\Big] \\ & + \ln\Big[1 + \bar{x}_0\Big(\prod_{1}^{0} \bar{K}_n^{-1} - 1\Big)\Big],\end{aligned} \qquad (5)$$

where $\prod_1^0 K_n^{-1}$ equals to 1 in our definition, and:

17) H. Kakihana, T. Nomura, H. Fukutomi, H. Ōtaki, and K. Yamazaki, *J. Atomic Energy Soc. Japan*, **1**, 46 (1959).

$$\ln S_{65}^{63} = \ln {}_{65}^{63}K_0 - \ln [1+x_1(K_1^{-1}-1)] . \quad (6)$$

K_1 is the equilibrium coefficient for isotopic-exchange reaction by complex formation in the external solution:

$$^{65}Cu^{2+} + {}^{63}CuSO_4 \overset{K_1}{\rightleftarrows} {}^{65}CuSO_4 + {}^{63}Cu^{2+}, \quad (7)$$

or the ratio of the stability constants of the sulphate complexes of isotopes:

$$^{65}Cu^{2+} + SO_4^{2-} \overset{\beta^{65}}{\rightleftarrows} {}^{65}CuSO_4 \quad (8)$$

$$^{63}Cu^{2+} + SO_4^{2-} \overset{\beta^{63}}{\rightleftarrows} {}^{63}CuSO_4 \quad (9)$$

and:

$$K_1 = \frac{\beta^{65}}{\beta^{63}} . \quad (10)$$

Copper Chloride System (Experiments III, IV, V, VI, and VII). In these systems, the chemical species existing in the external solution are Cu^{2+}, $(CuCl^+)$, and $(CuCl_2)$, and in the cation-exchange resin only Cu^{2+} can be adsorbed in appreciable amounts. Therefore, in Eq. (4), $z=0$, $r=2$, $\bar{x}_0=1$, and:

$$\ln S_{65}^{63} = \ln {}_{65}^{63}K_0 - \ln [1+x_1(K_1^{-1}-1)+x_2(K_1^{-1}\cdot K_2^{-1}-1)], \quad (11)$$

where x_1 and x_2 are the mole fractions of the $(CuCl^+)$ and $(CuCl_2)$ complexes respectively in the external solution. K_1 and K_2 are the equilibrium coefficients for an isotopic-exchange reaction by complex formation:

$$^{65}Cu^{2+} + {}^{63}CuCl^+ \overset{K_1}{\rightleftarrows} {}^{65}CuCl^+ + {}^{63}Cu^{2+} \quad (12)$$

$$^{65}CuCl^+ + {}^{63}CuCl_2 \overset{K_2}{\rightleftarrows} {}^{65}CuCl_2 + {}^{63}CuCl^+ \quad (13)$$

or the ratios of the stability constants chlorocomplexes of isotopes:

$$^{65}Cu^{2+} + Cl^- \overset{\beta_1^{65}}{\rightleftarrows} {}^{65}CuCl^+ \quad (14)$$

$$^{63}Cu^{2+} + Cl^- \overset{\beta_1^{63}}{\rightleftarrows} {}^{63}CuCl^+ \quad (15)$$

$$^{65}CuCl^+ + Cl^- \overset{\beta_2^{65}}{\rightleftarrows} {}^{65}CuCl_2 \quad (16)$$

$$^{63}CuCl^+ + Cl^- \overset{\beta_2^{63}}{\rightleftarrows} {}^{63}CuCl_2 \quad (17)$$

and:

$$K_1 = \frac{\beta_1^{65}}{\beta_1^{63}}, \quad K_2 = \frac{\beta_2^{65}}{\beta_2^{63}} . \quad (18)$$

The values of the stability constants of copper sulphate and chloride complexes in an aqueous solution obtained by Davies and McConnell are shown in Table 5. Since the stability constants of copper chloride complexes have not yet been measured in an acetone-water mixture, the values are approximately estimated by assuming that the logarithm of the stability constants is proportional to the reciprocal of the dielectric constant of the solution. Two sets of values of the stability constants are used for the calculation on the monochlorocopper complex: (a) the stability constants in pure water[19] and in pure acetone,[20] and (b) the stability constants in pure water and in a 5 vol% acetone-water mixture which has previously been measured by the present authors by means of spectrophotometry[19] using an EPS-3T type Hitachi Automatic Recording spectrophotometer with a quartz cell 1 mm thick. The values obtained by the use of these two bases are shown in Table 5. In the case of the dichlorocopper complex, only the first set of stability constants is used because of the insufficient accuracy of our stability constants.

Table 5. Stability constant (25°C)

Copper salt	Solvent	Logarithm of stability constant		
		$\log\beta$	$\log\beta_1$	$\log\beta_2$
$CuSO_4$	Water	2.3[18],*		
$CuCl_2$	Water (contains HCl)		0.11[19],**	−0.64[19],**
	20 vol%		0.30[a],**	−0.45[a],**
	Acetone		0.40[b],**	
	40 vol%		0.60[a],**	−0.17[a],**
	Acetone		0.80[b],**	

* Conductometric data.
** Spectrophotometric data: a) the first set of the values of stability constant is used, b) the second set of the values of stability constant is used.

Table 6. Mole fraction of copper complexes in the external solution

Experiment No.	Copper salt	Solvent	Mole fraction of copper complex, x_n		
			$(CuSO_4)$	$(CuCl^+)$	$(CuCl_2)$
II	$CuSO_4$	water	0.80		
III	$CuCl_2$	water		0.19_1	0.00_9
IV	$CuCl_2$	0.5 M HCl		0.42_2	0.05_9
V	$CuCl_2$	1.0 M HCl		0.50_9	0.12_5
VI	$CuCl_2$	20 vol% acetone		0.26[a] 0.30[b]	0.01_6[a] 0.01_8[b]
VII	$CuCl_2$	40 vol% acetone		0.37[a] 0.47[b]	0.04_0[a] 0.05_0[b]

a) and b) correspond to a) and b) in Table 5, respectively.

Table 7. Equilibrium coefficient for isotopic exchange reaction by complex formation K_1 and K_2

Experiment No.	Copper salt	Solvent	K_1	K_2
II	$CuSO_4$	water	1.0001_5	
III	$CuCl_2$	water	1.0001_6	
IV	$CuCl_2$	0.5 M HCl	1.0004_0	
V	$CuCl_2$	1.0 M HCl	1.0005_2*	1.0007_2
VI	$CuCl_2$	20 vol% acetone	1.0006_2[a] 1.0005_3[b]	
VII	$CuCl_2$	40 vol% acetone	1.0005_9[a] 1.0004_7[b]	

* The value is the mean value of that obtained for experiment IV, VI, and VII.
a) and b) correspond to a) and b) in Table 5, respectively.

18) C. W. Davies, *J. Chem. Soc.*, **1938**, 2093.
19) H. McConnell and N. Davidson, *J. Amer. Chem. Soc.*, **72**, 3164 (1950).
20) J. Gažo, *Chem. Zvesti.*, **10**, 509 (1956).

The mole fractions of copper complexes in the external solution (x_n) were estimated by using the values of the total concentration of copper described in Table 1 and the stability constants described in Table 5; they are shown in Table 6. The values of the equilibrium coefficients for an isotopic-exchange reaction (K_1, K_2) were estimated by means of Eqs. (6) and (11) (Table 7). The values in Table 6 were used for x_1 and x_2 in Eqs. (6) and (11), while the value for S_{65}^{63} of the copper nitrate system (no complex formation) in Table 4 was used for ${}_{65}^{63}K_0$ in Eqs. (6) and (11). In the cases of the experiments III, IV, VI, and VII, the values of x_2, the mole fraction of the $CuCl_2$ complex in the external solution, were so small that it was impossible to estimate the values for K_2. However, the values for K_1 could be calculated with good accuracy. In the case of the experiment V, the value of K_2 was estimated by means of Eq. (11) using with the mean value of K_1 obtained in the experiments IV, VI, and VII. The results in Table 7 indicate that the values of the equilibrium coefficient for isotopic-exchange reactions by complex formation for copper chloride systems are larger than the value for the copper sulphate system, and that there is a good agreement of the values of K_1 for all the copper chloride systems except in experiment III.

Conclusion

The conclusions of our break-through experiment on the separation of copper isotopes and for our analysis based on the theory of the two-phase distribution of isotopes are as follows:

(a) The ion-exchange chromatography through a cation-exchange resin column proves that the lighter isotope, ^{63}Cu, is enriched in the ion-exchanger phase.

(b) The isotope effect caused by the simple ion-exchange reaction, that is, by the distribution of the hydrated copper ion between the external solution and the ion-exchanger phase, is very small (experiment I).

(c) Significant isotope effects ($S_{65}^{63}-1.0000_3$—1.0004_2) were found for the systems with the complex formation in the external solution. Moreover, the values of the equilibrium coefficient for isotopic-exchange reaction by the complex formation of copper, $K_1=1.0001_5$ for the copper sulphate system and $K_1 \fallingdotseq 1.0005$ for the copper chloride systems, were estimated. These values are the first ones obtained for the equilibrium coefficients for isotopic-exchange reactions by means of the complex formation of copper.

BULLETIN OF THE CHEMICAL SOCIETY OF JAPAN, VOL. 44, 310—312 (1971)

Group Interactions in Polyelectrolytes. IV. Kinetics of the Alkaline Hydrolysis of Polymethyl Acrylate (Part II)

Hiroshi KAWABE and Masaya YANAGITA

The Institute of Physical and Chemical Research, Yamato-machi, Saitama

(Received May, 28 1970)

Rate equations which express the over-all kinetics of the alkaline hydrolysis of polymethyl acrylate in the presence of a large excess of alkali were derived. The over-all course of this reaction was calculated by using the rate constants given in the previous paper, which were derived from the kinetic data obtained by the reaction in a 29% (*v*/*v*) aqueous acetone solution with a slight excess of sodium hydroxide at 55°C. The partially-hydrolyzed polymethyl acrylate (30.6% hydrolyzed) was hydrolyzed by the addition of about sixteen times as much sodium hydroxide as the amount of the ester group; the kinetic data thus obtained were found to be in good agreement with the calculated values.

In the previous study,[1] the rate equations of a polymer reaction which proceeds in more than two steps were derived and applied to the alkaline hydrolysis of polymethyl acrylate. Upon the examination of the published kinetic data,[2] the reaction in a 29% (*v*/*v*) aqueous acetone solution with a slight excess of sodium hydroxide was found to proceed in four steps, and the corresponding four rate constants were determined.

In the present study, rate equations which express the over-all kinetics have been derived in a simple case; that is, the over-all rate of a reaction with a large excess of alkali has been calculated by using the rate constants at 55°C given previously. It is the purpose of the present study to confirm the validity of the assumptions, adopted in the derivation of these rate equations, by comparing the calculated values with the experimental values. For this reason, the alkaline hydrolysis of polymethyl acrylate in the presence of a large excess of sodium hydroxide has been carried out in a 29% aqueous acetone solution at 55°C.

Experimental

Materials. Polymethyl acrylate was prepared and purified as previously.[1] It was dissolved in acetone and partially hydrolyzed by carefully adding a limited amount of an aqueous sodium hydroxide solution over a long period so as to keep the solution homogeneous. The volume ratio of acetone to water in the solution was finally adjusted to 2/5. The solution was kept at 40°C until the alkalinity of the solution almost disappeared; this solution was then used for the kinetic measuremtns. The degree of hydrolysis was deter-

1) H. Kawabe and M. Yanagita, This Bulletin, **42**, 3109 (1969).
2) I. Sakurada, Y. Sakaguchi, and S. Fukui, *Kobunshi Kagaku*, **13**, 355, 361, 408 (1956).

mined by the usual titration method; it was found to be 30.6%.

Determination of the Degree of Hydrolysis. Partial and complete hydrolyses of polymethyl acrylate were carried out in aqueous acetone solutions containing the necessary amount and a slight excess of sodium hydroxide respectively. The degree of hydrolysis was determined by pouring an aliquot of the solutions into water containing an excess of hydrochloric acid and by then titrating the mixture with 0.1 N sodium hydroxide. In kinetic runs, since a large excess of sodium hydroxide (about sixteen times as much as the moles of the ester group) was used, it was necessary before titration to remove sodium ions in the solution by Dowex-50. This method has already been described with respect to low-molecular esters;[1] also in the present study it was found to be effective for polymethyl acrylate. Five grams of Dowex-50 (X-8, 50—100 mesh), which had previously been half-neutralized and which had an effective capacity of 0.668 meq/g-wet, were added to a 50-m*l* aqueous solution containing 0.104 meq of polyacrylic acid and 1.074 meq of sodium hydroxide. The mixture was stirred, and its pH was measured by the use of Beckman's model G pH meter. The results are shown in Table 1. After removing the resin, the solution was titrated with 0.1 N sodium hydroxide in the presence of sodium chloride in order to determine the original amount of polyacrylic acid.

Table 1. Removal of sodium ions from an aqueous solution containing polyacrylic acid and sodium hydroxide by dowex 50

Time, sec	0	30	45	60	600
pH	12.39	4.91	3.95	3.92	3.99

Kinetic Measurement. The alkaline hydrolysis of the 30.6% hydrolyzed polymethyl acrylate was carried out in an aqueous acetone solution (acetone/water=2/5) containing a large excess of sodium hydroxide. During the course of this reaction, the temperature was kept at 55±0.1°C. The total concentration of sodium hydroxide in the solution, including that used for preliminary partial hydrolysis, was 0.0905 mol/*l*, and the concentration of the total carboxylate groups was 0.0055 mol/*l*. At appropriate intervals, aliquots of the solution were taken out and poured into water containing Dowex-50, after which the mixture was stirred for a few minutes in order to remove sodium ions. After removing the resin, the carboxylic acid content was determined by titration.

Rate Equations

In the previous paper,[1] the rate equations for a polymer reaction which proceeds in σ steps was derived on the model of the reaction of a low-molecular compounds containing σ groups whose reactivity altered when one of the groups was changed.

$$X_{n-1}Y_{\sigma-(n-1)} \xrightarrow{k_n} X_nY_{\sigma-n} \xrightarrow{k_{n+1}} X_{n+1}Y_{\sigma-(n+1)}$$

where X represents a changed group in a compound; Y, an unchanged one; n, the number of the changed group, and σ, the total number of groups. The over-all kinetics in the presence of a large excess of reagent was also expressed by a pair of rate equations in the case when $\sigma=3$. The derivation of the equations was based on the assumption that the reaction at nth and $(n+1)$th steps was controlled by the two rate constants, k_n and k_{n+1}.

When $\sigma=4$, the corresponding equations can similarly be derived on the same assumption. When $n=1$, the rate is thus controlled by k_1 and k_2 in the range of fractional conversion (β) from 0 to 1/2 and can be expressed by the following equation:

$$dx/dt = a[k_1b - (4k_1 - 6k_2)x_1 - 3k_2x] \quad (1)$$

where a and b are the initial concentration of a reagent and that of the group in the compound respectively, and where x_1 and x are the concentration of the first changed group and that of the total changed groups in the compound, again respectively, at the time t. Moreover, x_1 is given by:

$$x_1 = (1 - e^{-4k_1at})b/4 \quad (2)$$

Upon integration, Eq. (1) becomes:

$$\beta = \frac{1}{2} - \frac{2k_1 - 3k_2}{2(4k_1 - 3k_2)}e^{-4k_1at} - \frac{k_1}{4k_1 - 3k_2}e^{-3k_2at} \quad (3)$$

where $\beta=x/b$. When $n=2$, the rate, which is controlled by k_2 and k_3 in the 1/4—3/4 range of β, is given by:

$$dx/dt = a[(3k_2 + 2k_3)b/4 - (3k_2 - 4k_3)x_2 - 2k_3x] \quad (4)$$

where x_2 is the concentration of the secondly-changed group in the compound and is given by:

$$x_2 = (1 - e^{-3k_2a(t-t_{1/4})})b/4 \quad (5)$$

Upon integration, Eq. (4) yields:

$$\beta = \frac{3}{4} - \frac{3k_2 - 4k_3}{4(3k_2 - 2k_3)}e^{-3k_2(t-t_{1/4})} - \frac{3k_2}{4(3k_2 - 2k_3)}e^{-2k_3a(t-t_{1/4})} \quad (6)$$

where $t_{1/4}$ is the time where β is 1/4. Similarly, when $n=3$, the following equations can be derived in the β range from 1/2 to 1:

$$dx/dt = a[(k_3 + k_4)b/2 - 2(k_3 - k_4)x_3 - k_4x] \quad (7)$$

$$x_3 = (1 - e^{-2k_3a(t-t_{1/2})})b/4 \quad (8)$$

where x_3 is the concentration of the thirdly-changed group in the compound and where $t_{1/2}$ is the time when β is 1/2. Upon integration, Eq. (7) becomes:

$$\beta = 1 - \frac{k_3 - k_4}{2(2k_3 - k_4)}e^{-2k_3a(t-t_{1/2})} - \frac{k_3}{2(2k_3 - k_4)}e^{-k_4a(t-t_{1/2})} \quad (9)$$

Results and Discussion

The alkaline hydrolysis of the partially-hydrolyzed polymethyl acrylate (30.6% hydrolyzed) was carried out in a 29% aqueous acetone solution at 55°C. Since a large excess of sodium hydroxide was used in this experiment (a=0.0905 mol/*l*, b=0.0055 mol/*l*, and a/b=16.5), the over-all course of the reaction is given by Eqs. (3), (6), and (9). In the previous paper,[1] the rate constants were given on the basis of Sakurada's data[2] for the reaction in a 29% aqueous acetone solution containing a slight excess of sodium hydroxide at 55°C. They were $k_1=8.02\times10^{-1}$, $k_2=1.66\times10^{-1}$, $k_3=4.04\times10^{-2}$, and $k_4=3.31\times10^{-3}$ *l*/mol min. The values of β were first computed on the basis of Eq. (3) and plotted against t as is shown by the full line in Fig. 1 (Curve I), from which $t_{1/4}$ was determined to be 6.5 min. The plots obtained by means of Eq. (6)

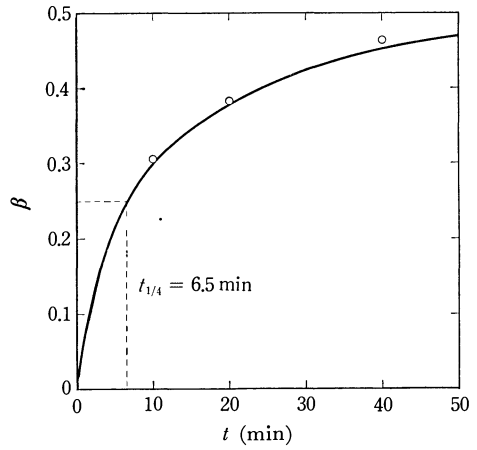

Fig. 1. Alkaline hydrolysis of polymethyl acrylate. Calculated curve I.

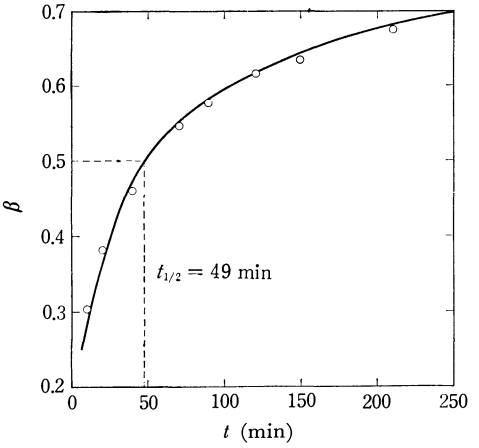

Fig. 2. Alkaline hydrolysis of polymethyl acrylate. Calculated curve II.

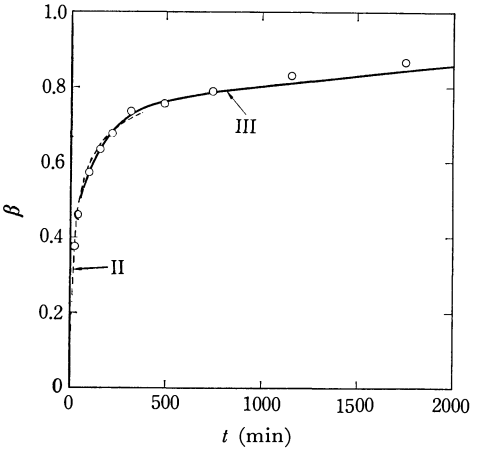

Fig. 3. Alkaline hydrolysis of polymethyl acrylate. Calculated curves II and III.

are shown in Fig. 2 (Curve II); $t_{1/2}$ was determined to be 49 min. Finally, the plots fitting Eq. (9) are shown in Fig. 3 (Curve III).

In Figs. 1, 2, and 3, the white circles indicate the values observed in the present experiment. Since polymethyl acrylate used in this experiment was preliminarily 30.6% hydrolyzed, and since this value of β corresponds to the reaction time of 10 min, as may be seen in Figs. 1 and 2, the observed values of β are plotted against the corrected time, namely, the actual reaction time plus 10 min. A fairly good agreement is shown between the calculated and observed values. Although the conditions in this experiment and those in Sakuradas' are different except for the temperature and the composition of the medium, the agreement is remarkable; this justifies deriving the rate equations on the basis of the assumption adopted in the previous paper, the assumption that the reactivity of ester groups in a polymethyl acrylate molecule is electrostatically affected mainly by the first and second neighboring groups when the reaction is carried out in a water-rich system.

In the previous paper, it was also shown that the plot of the logarithmic term of the simple second-order rate equation (Eq. (10)) against the time could be divided into four lines:

$$k_{\mathrm{app}} = \frac{1}{(a-b)t} \ln \frac{b(a-x)}{a(b-x)} \tag{10}$$

where k_{app} is the apparent rate constant. This is also true of the present experiment, as is shown in Fig. 4,

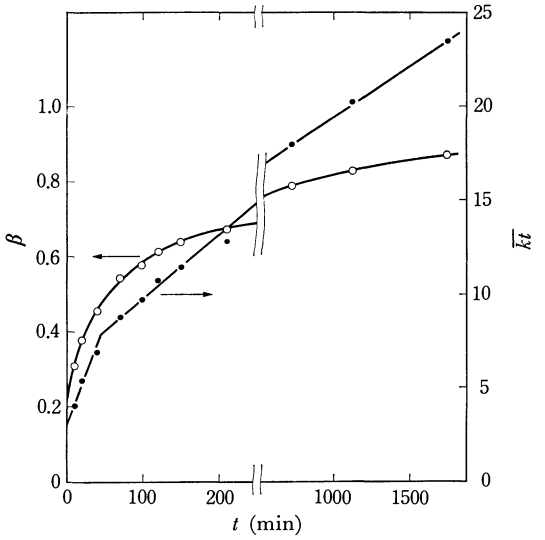

Fig. 4. Plot of $\overline{kt}$ *viz.* t in the alkaline hydrolysis of polymethyl acrylate.

where $\overline{kt} \equiv [1/(a-b)]\ln[b(a-x)/a(b-x)]$, and where the white and black circles represent the observed values of β and $\overline{kt}$ respectively. The approximate value of the rate constant, k_n', as estimated in terms of the slope, can be expressed thus:

$$k_n' = \Delta\overline{kt}/\Delta t \tag{11}$$

The values are shown in Table 2, in which those values obtained from Sakurada's data in the previous paper are also given for comparison.

TABLE 2. APPROXIMATE VALUES OF THE RATE CONSTANTS

n	k_n' (l/mol min)	
	present experiment	Sakurada's data
1		3.99×10^{-1}
2	1.10×10^{-1}	1.40×10^{-1}
3	2.75×10^{-2}	3.07×10^{-2}
4	5.40×10^{-3}	3.31×10^{-3}

The authors wish to express their thanks to Mr. N. Sato and Mr. M. Hayashi for their helpful assistance in preparing the sample and in carrying out the measurements.

The N-H Stretching Absorption Band Intensities in Secondary Amides, Secondary Thioamides, and Anilides

P. Usha BAI

Department of Physics, College of Science, Osmania University, Hyderabad-7, India

and K. Venkata RAMIAH

Department of Physics, Post-Graduate Centre, Osmania University, Warangal (A. P.), India

(Received January 5, 1970)

The intensities of the N–H stretching absorption bands of a number of *N*-methylamides, *N*-methylthioamides and anilides have been measured in a solution of carbon tetrachloride. It was observed that the intensities of the N–H stretching absorption bands of *N*-methylacetamide and *N*-methylpropionamide are considerably higher than those of the same band in the corresponding anilides. On the other hand, the intensity of the N–H stretching absorption band of *N*-methylformamide is of the same order as that of formanilide. The pattern of variation of the intensity of the N–H streching absorption bands in these compounds is similar to that of the C=O stretching absorption bands of the same compounds, but the variation in their frequencies is different. It was also observed that the intensities of the N–H stretching bands of *N*-methylthioamides are considerably higher and their frequencies are lower than those of the corresponding secondary amides.

Variations in the position and integrated absorption intensities of the carbonyl band in aldehydes, ketones, esters, and amides have received considerable attention.[1-8] They have been generally interpreted in terms of changes in resonance contribution or the variation in the interaction of the orbitals in these molecules.[7,8] Some authors[3,6] have taken the mesomeric, inductive, and steric effects as well as the environmental factors into consideration to account for the variation in the integrated intensities of the carbonyl band. Huggins and Pimentel[9] measured the intensities of OH and NH stretching absorption bands of methanol, phenol, and pyrrole and found that the intensity of the OH stretching band in phenol is considerably higher than that of methanol. Stone and Thompson[10] discussed the variation in frequencies and intensities of the OH stretching bands of phenols with the electron-withdrawing or electron-donating substituents. Elliott and Mason[11] have shown that the frequencies and the intensities of the N–H stretching bands, the HNH bond angle and the N–H bond dipole gradient increase in monocyclic *N*-heteroaromatic amines relative to the values for aniline. Russel and Thompson,[12] and Kreuger and Thompson[13] measured the intensities of several characteristic absorption bands including those of O–H and N–H stretching absorption bands. From the studies of the position of the N–H stretching absorption bands of anilides and thioanilides Suzuki *et al.*[14] discussed the nature of *cis* or *trans* structure of the molecules. The authors report in this paper the intensities of N–H stretching absorption bands of a number of secondary amides, secondary thioamides, and anilides and correlate the results with those of C=O stretching absorption bands of some of the same compounds measured by earlier workers.[8]

Experimental

The infrared spectra of the N–H stretching absorption bands of the amides and the anilides were recorded with Perkin Elmer Model 221 infrared spectrophotometer using matched quartz cells of 3 cm thickness. The gear combinations were so chosen as to spread the spectrum to 100 cm^{-1}=10 cm^{-1}. The operating conditions of the spectrophotometer were: slit programme=947, gain=2.3, attenuator speed=1100, expansion=XI and scale factor 4. *N*-methylthioacetamide was synthesised. The rest of the chemicals used were of British Drug Houe and Eastman Organic Chemicals. They were purified by conventional methods and dried before use. The functional groups responsible for H bond in amides, anilides and thioamides are the N–H and the C=O or C=S bond and therefore very dilute solutions of these amides and anilides in solutions of CCl_4 were used so as to eliminate intermolecular association. This is indicated by the presence of only one absorption band in the region of 3450 cm^{-1} arising from the stretching vibration of free N–H group in all compounds except for formanilide wherein one observes two absorption bands with a difference of about 20 cm^{-1} as shown in Fig. 1. On the other hand, the N–H stretching absorption band in acetanilide and the *N*-methylthioamides is a single absorption band as shown in Figs. 2 and 3. The concentrations of the amides and the anilides chosen were such that Beer's Law holds as given in Fig. 4 by the linear relationship between the absorbance and the corresponding molar concentration.

A point by point measurement of the molecular extinction

1) G. M. Barrow, *J. Chem. Phys.*, **21**, 2008 (1953).
2) H. W. Thompson and D. Jameson, *Spectrochim. Acta*, **13**, 236 (1959).
3) T. L. Brown, J. F. Regan, R. D. Schuetz, and J. C. Strernberg, *J. Phys. Chem.*, **63**, 1324 (1959).
4) *Ibid.*, **64**, 1956 (1960).
5) S. Pinchas, D. Samuel, and M. Weiss-Brody, *J. Chem. Soc.*, **1961**, 3063
6) R. N. Jones, W. F. Forbes, and W. A. Mueller, *Can. J. Chem.*, **35**, 504 (1957).
7) M. St. C. Flett, *Spectrochim. Acta*, **18**, 1537 (1962).
8) V. V. Chalapathi and K. V. Ramiah, *J. Mol. Spectrosc.*, **26**, 444 (1968).
9) C. M. Huggins and G. C. Pimentel, *J. Phys. Chem.*, **60**, 1615 (1956).
10) P. J. Stone and H. W. Thompson, *Spectrochim. Acta*, **10**, 17 (1957).
11) J. J. Elliott and S. F. Mason, *J. Chem. Soc.*, **1959**, 1275.
12) R. A. Russel and H. W. Thompson, *ibid.*, **1955**, 483.
13) P. J. Kreuger and H. W. Thompson, *Proc. Roy. Soc.* (London), **A243**, 173 (1958).
14) I. Suzuki, M. Tsuboi, T. Shimanouchi, and S. Mizushima, *Spectrochim. Acta*, **16**, 471 (1960).

coefficient ε of the band was made at intervals of 5—10 cm^{-1} and plotted against ν in cm^{-1}. The area under the curve was measured for an interval of $\nu-\nu_m=60$ cm^{-1} on either side of the band maximum by planimeter. ν_m is the frequency at the maximum absorption. As there is some overlapping of the two N–H stretching absorption bands in formanilide (Fig. 1), the total area of the two bands has been obtained by drawing symmetrical curves with respect to the maximum absorption of each curve and then substracting the area common to both the absorption bands from the sum of the two areas. The intensity of the bands for each compound was measured at three to four concentrations and the average values were calculated. The halfband width of all these absorption bands is in the neighbourhood of 15 cm^{-1}. Wings correction was not applied.

Results

The intensities of the N–H stretching absorption bands of the secondary amides, secondary thioamides, and anilides measured in the solution of carbon tetrachloride are given in Table 1. The integrated intensities of the carbonyl band of some of these compounds obtained by the earlier workers[8] are also given in Table 1 for comparison. The existence of two bands in the N–H stretching region of formanilide is due to the co-existence of *trans* and *cis* structures because of the steric repulsion between the carbonyl group and phenyl group of *trans* form of formanilide. This makes the *trans* structure in formanilide less stable compared to that in the other anilides, since the steric repulsion is overcome by strong repulsion between the CH_3 group and the phenyl group in an anilide like acetanilide.

It is seen from Table 1 that as in the case of C=O stretching absorption bands, the intensities of the N–H stretching absorption bands of *N*-methylacetamide and *N*-methylpropionamide are higher than those of the corresponding anilides, whereas the intensity of the same band of *N*-methylformamide is of the same order as that of formanilide (in case of formanilide, the intensity given is the sum of the intesnsities of the N–H stretching absorptions of *trans* and *cis* structures). The result is similar to that obtained by the earlier workers[8]

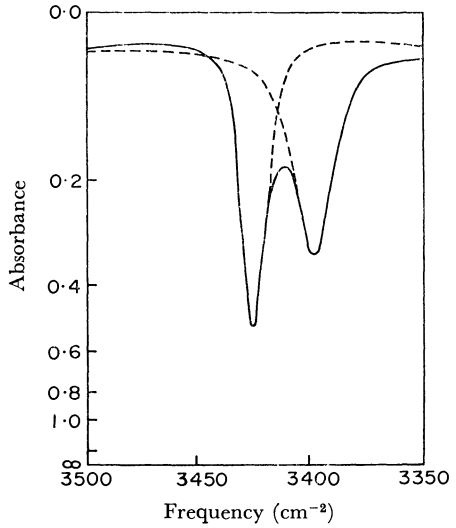

Fig. 1. N–H stretching band of formanilide in dilute solution of carbon tetrachloride. (Molar concentration = 0.0020)

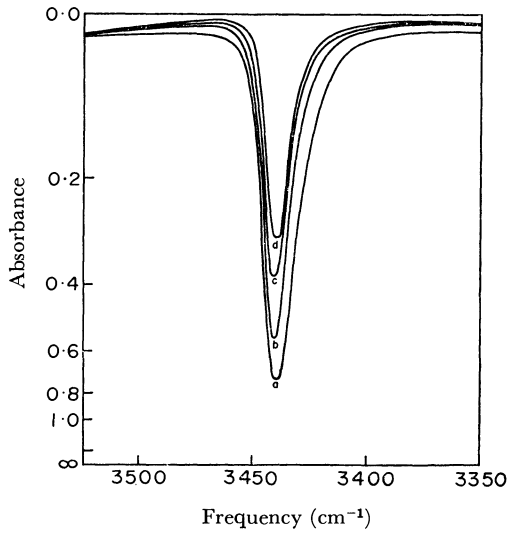

Fig. 2. N–H stretching band of acetanilide in dilute solutions of carbon tetrachloride at various concentrations.

(a) 0.0021 molar (b) 0.0015 molar
(c) 0.0010 molar (d) 0.0008 molar

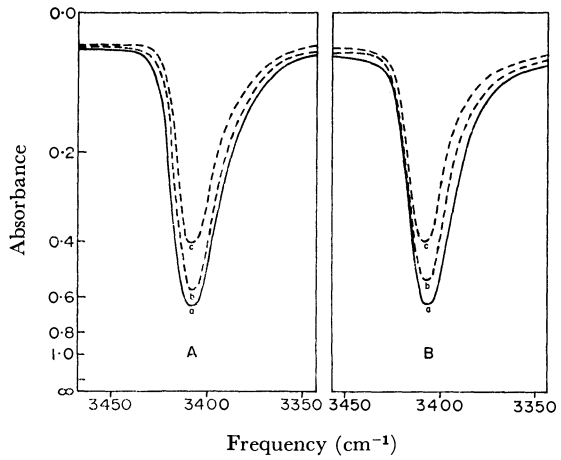

Fig. 3. A: N–H stretching band of *N*-methylthioacetamide in dilute solution of carbon tetrachloride at various concentrations.
(a) 0.0020 molar (b) 0.0015 molar (c) 0.0010 molar
B: N–H stretching band of *N*-methylthiopropionamide in dilute solution of carbon tetrachloride at various concentrations.
(a) 0.0020 molar (b) 0.0015 molar (c) 0.0010 molar

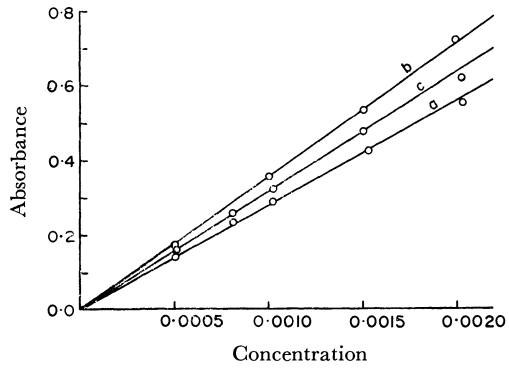

Fig. 4. Plot of absorbance *versus* molar concentration of:

(a) *N*-methylformamide
(b) *N*-methylacetamide
(c) *N*-methylpropionamide

Table 1. Integrated intensities of the N–H and C=O stretching absorption bands in secondary amides and anilides

Amide or anilide	N–H Stretching absorption band		C=O Stretching absorption band	
	Frequency	Intensity A ($mol^{-1} \cdot l \cdot cm^{-2} \times 10^4$ in solution of CCl_4)	Frequency	Integrated absorption intensity A ($mol^{-1} \cdot l \cdot cm^{-2} \times 10^4$ in solution of CCl_4)
N-Methylacetamide	3470	0.52	1691	3.5
Acetanilide	3440	0.42	1710	2.6
N-Methylpropionamide	3467	0.55	1688	3.6
Propionilide	3436	0.32	1701	2.4
N-Methylformamide	3460	0.55	1698	3.9
Formanilide	3420 3400	0.58	1704 (a doublet with a frequency difference of 5 cm^{-1})	4.0
N-Methylthioacetamide	3408	0.73	—	—
N-Methylthiopropionamide	3407	0.73	—	—

as regards the integrated intensities of the carbonyl band of the same compounds as shown in Table 1. The pattern of variation in intensities of N–H and C=O stretching bands of these compounds is similar, but it is different with respect to their frequencies. While the frequencies of the carbonyl bands of anilides are higher than those of the corresponding *N*-methylamides, the frequencies of the N–H stretching absorption bands of the same anilides are lower than those of the corresponding secondary amides. It is also seen from Table 1 that the intensities of the N–H stretching absorption bands of *N*-methylthioacetamide and *N*-methylthiopropionamide are considerably higher than those of *N*-methylacetamide and *N*-methylpropionamide. On the other hand, the frequencies of the N–H stretching absorption bands of the same secondary thioamides are lower than those of the corresponding ordinary secondary amides.

Discussion

In amides and anilides, no single valence bond structure is consistent with all their properties. Two possible structures contribute to the resonance hybrid in the molecules, with the dipolar resonance structure making substantial contribution to the ground state of the molecules giving partial single and double bond characters to the C=O and C–N linkages. Cannon[15,16] discussed this problem in terms of interaction and mixing of the π orbitals of C=O group and $2P_z$ orbitals of nitrogen atom in the sp^2 hybrid configuration. The π–p orbitals mixing lengthens the bond length of C=O and shortens that of C–N bond relative to the normal valence bond structure. This may explain the high values of the intensities of N–H stretching absorption bands of secondary amides and anilides compared to those of amines reported by Elliott and Mason.[11] The important factor responsible for the difference in the positions and intensities of the N–H stretching absorption bands of *N*-methylamides and anilides may be due to the delocalisation of the lone pair of electrons of the amino group over the aromatic nucleus of the anilides.

The C–N stretching frequencies of primary and tertiary amides and thioamides and the stretching frequencies of the amide III bands in secondary amides and secondary thioamides are given in Table 2.

Table 2

Amide	Mode of vibration and Frequencies (in cm^{-1})	
	Mode	(Frequency in cm^{-1})
Formamide	ν (C–N)	1309
Thioformamide	ν (C–N)	1325
N-Methylformamide	Amide III	1248
N-Methylthioformamide	Amide III	1297
N-Methlacetamide	Amide III	1300
N-Methylthioacetamide	Amide III	1360
Dimethylformamide	ν (C–N)	1502
Dimethylthioformamide	ν (C–N)	1540
Dimethylacetamide	ν (C–N)	1494
Dimethylthioacetamide	ν (C–N)	1510

As seen from Table 2, the C–N stretching frequencies of primary and tertiary thioamides are higher than those of the corresponding ordinary amides. Similarly the frequencies of the amide III band in secondary thioamides, to which the contribution of C–N stretch is considerable, have higher values than those in the corresponding secondary amides. The higher values of the C–N stretching frequencies in the thioamides may thus be due to (i) the difference in the contribution of various modes of vibrations to this absorption frequency and/or (ii) higher double bond character of the C–N bond with the dipolar resonance structure making greater contribution to the ground state of the molecules than in the case of ordinary amides. These factors may be responsible for the high values of the intensity of the N–H stretching absorption bands in *N*-methylthioamides.

One of us (P. U. B.) expresses her sincere thanks to the University Grants Commission for financial assistance.

15) C. G. Cannon, *J. Chem. Phys.*, **24**, 491 (1956).
16) C. G. Cannon, *Microchim. Acta*, **2**, 555 (1955).

Infrared Spectra and Normal Vibrations of *N,N*-Dimethylformamide and *N,N*-Dimethylthioformamide*

G. DURGAPRASAD, D. N. SATHYANARAYANA, and C. C. PATEL

Department of Inorganic and Physical Chemistry, Indian Institute of Science, Bangalore-12, India

(Received May 27, 1970)

The infrared spectra of *N,N*-dimethylformamide (DMF) and *N,N*-dimethylthioformamide (DMTF) have been investigated in the range 4000—250 cm^{-1}. Assignment of the frequencies of DMF has been made on the basis of normal coordinate analysis for DMF, DMF-^{15}N, and DMF-d_7 using Urey-Bradly, modified Urey-Bradley, and symmetrized valence force fields. Calculations have been extended to *N,N*-dimethylthioformamide and *N,N*-dimethylselenoformamide, using the Urey-Bradley and symmetrized valence force fields. The assignments for DMF from the modified Urey-Bradley field are found to be more satisfactory. The frequency shifts on isotopic substitution and on complexation have been explained. The results of the calculations are discussed in comparison with other related molecules.

The infrared spectra of amides have been subjected to many studies.[1-5] Detailed assignments are available in literatures for primary and secondary amides.[1-4,6-8] In these amides, the characteristic infrared frequencies are due to highly coupled vibrations and the N–H bending mode is mixed extensively with the other vibrations. However, in the case of tertiary amides, the C–N stretching mode appears in the region of C–H bending vibration, rendering its identification difficult.

The simplest tertiary amide is *N,N*-dimethylformamide (DMF). While there has been no difficulty in assigning some of its frequencies, a satisfactory and complete assignment of the infrared spectrum has not been possible. The valence bond approach to assign a few important bands from the frequency changes in metal complexes of DMF has not been helpful. The different earlier assignments for a few important bands have been summarized by Randall *et al.*[9]

Kaufman and Leroy[10] have carried out a force constant calculation for DMF and made assignments which follow largely those of *N*-methylformamide by Suzuki[2] and those of DMF by Jones.[3] Chalapathi and Ramaiah[11] have made a normal vibration calculation for the DMF skeleton. Their assignments comply generally to the earlier assignments. The different assignments[9-11] for DMF have not been substantiated and doubts regarding the assignment of some of the bands still exist. For example, the band at 1395 cm^{-1} in DMF has been assigned to C–H bending vibration, which appears to be incorrect, since the same band is present in DMF-d_1.[12] Moreover, the frequency shifts are now available from the spectrum of DMF-^{15}N which could be used to test the validity of a potential field employed. This tempted us to undertake a fresh normal coordinate treatment to make a reasonable and complete assignment for DMF. As the assignments are known to be somewhat sensitive to the force fields, the three commonly employed potential fields were tried. The study includes related *N,N*-dimethylthioformamide (DMTF) and *N,N*-dimethylselenoformamide (DMSeF) for understanding the nature of the vibrations in the simplest thioamides and selenoamides.

Experimental

Dimethylformamide used was a product of Riedel De Haen AG which was redistilled at reduced pressure, after keeping over KOH pellets for four days. Dimethylthioformamide was obtained through the courtesy of Prof. W. Walter, Institute of Organic Chemistry, Hamburg.

The infrared spectra of DMF and DMTF as thin films were recorded on a Carl-Zeiss UR 10 Spectrophotometer in the range 4000—400 cm^{-1} and on a Perkin-Elmer 521 Grating Spectrophotometer in the range 400—250 cm^{-1}. The spectra in the range 400—1800 cm^{-1} are given in Fig. 1. The infrared spectra of DMF-d_7 and DMF-^{15}N were kindly supplied by Dr. T. H. Siddall, III,[13] Savannah River Laboratory, E. I. du Pont de Nemours & Co., Aiken, South Carolina and Dr. J. J. Zuckerman,[9] Department of Chemistry, State University of New York at Albany, respectively.

Normal Coordinate Treatment

The vibrational problem was set up in internal coordinates, using GF matrix method.[14] The secular

* Presented at the Tenth European Congress on Molecular Spectroscopy, Liege (Belgium), 1969.

1) T. Miyazawa, T. Shimanouchi, and S. Mizushima, *J. Chem. Phys.*, **24**, 408 (1956).
2) I. Suzuki, This Bulletin **35**, 540, 1279, 1286, 1449, 1456 (1962).
3) R. L. Jones, *J. Mol. Spectrosc.*, **11**, 411 (1963).
4) J. E. Katon, W. R. Feairheller, Jr., and J. V. Pustinger, Jr., *Anal. Chem.*, **36**, 2126 (1964).
5) V. V. Chalapathi and K. V. Ramaiah, *Curr. Sci.*, **34**, 12 (1965).
6) T. Miyazawa, T. Shimanouchi, and S. Mizushima, *J. Chem. Phys.*, **29**, 611 (1958).
7) R. D. McLachlan and R. A. Nyquist, *Spectrochim. Acta*, **20**, 1397 (1964).
8) E. M. Bradbury and A. Elliott, *ibid.*, **19**, 995 (1963).
9) E. W. Randall, C. M. S. Yoder, and J. J. Zuckerman, *Inorg. Chem.*, **5**, 2240 (1966), and the relevant references therein.
10) G. Kaufman and M. J. F. Leroy, *Bull. Soc. Chim. Fr.*, **1967**, 402.
11) V. V. Chalapathi and K. V. Ramaiah, *Proc. Indian Acad. Sci.*, **68A**, 109 (1968).
12) A. Castelli and D. J. Cragle, "Developments in Applied Spectroscopy," Vol. 4, ed. by E. N. Davis, Plenum Press, New York (1965), p. 187.
13) K. L. Dorris, T. H. Siddall, III, W. E. Stewart, and M. L. Good, *Spectrochim. Acta*, **23A**, 1657 (1967).
14) E. B. Wilson, Jr., J. C. Decius, and P. C. Cross, "Molecular Vibrations," McGraw-Hill Book Company, New York (1955).

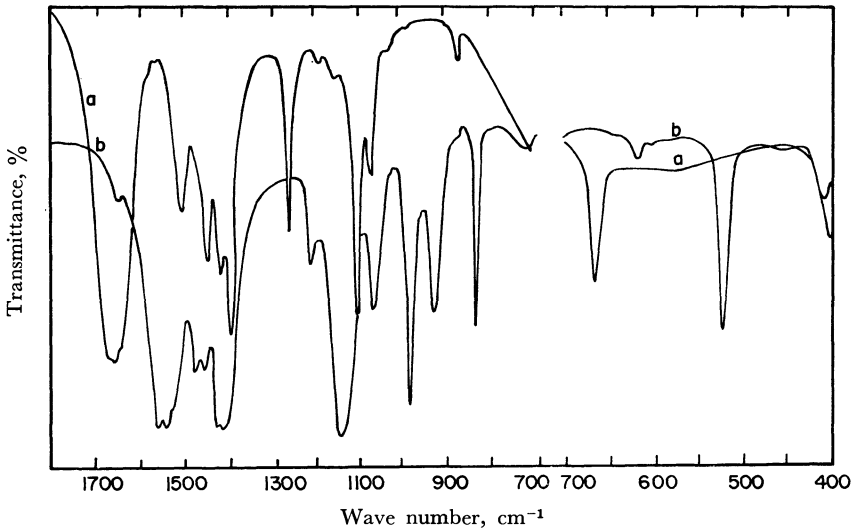

Fig. 1. Infrared spectra of (a) DMF and (b) DMTF.

equation was solved using Miyazawa's method[15,16] on a National Elliott 803 computer. The least squares adjustment of the frequencies has not been made because of the small computer at hand. The high frequency C–H stretching modes were split off from the lower vibrations for the same reason.

Dimethylformamide belongs to the point group C_S and its 30 fundamental vibrations are split into $19A'$ and $11A''$ vibrations. The calculations have been made for the A' vibrations only, since the assignment of frequencies in question belong to this species. The internal coordinates are defined in Fig. 2 and the symmetry coordinates are given in Table 1.

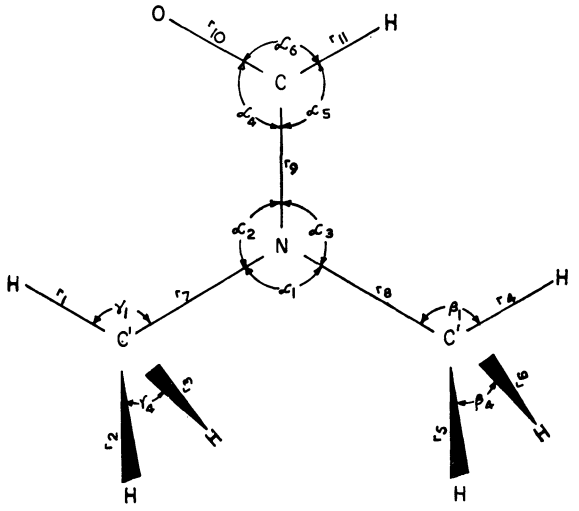

Fig. 2. Internal coordinates for DMF.

The structural parameters of DMF are taken from the electron diffraction data,[17] except for the angles around carbonyl carbon which are from the microwave data of formamide.[18] The C=S bond length is taken as in thioformamide[2] while C=Se distance is from the covalent radii. The other parameters for DMTF and DMSeF are the same as those of DMF. The structural parameters are listed in Table 2.

The final sets of force constants, for DMF and DMTF, obtained after several trials, are given in Tables 3 and

Table 1. Symmetry coordinates

Symmetry coordinate	Description[a]
$S_1=(2\Delta r_1-\Delta r_2-\Delta r_3+2\Delta r_4-\Delta r_5-\Delta r_6)/\sqrt{12}$	$\nu_a(CH_3)$
$S_2=(2\Delta r_1-\Delta r_2-\Delta r_3-2\Delta r_4+\Delta r_5+\Delta r_6)/\sqrt{12}$	$\nu_a(CH_3)$
$S_3=(\Delta r_1+\Delta r_2+\Delta r_3+\Delta r_4+\Delta r_5+\Delta r_6)/\sqrt{6}$	$\nu_s(CH_3)$
$S_4=(\Delta r_1+\Delta r_2+\Delta r_3-\Delta r_4-\Delta r_5-\Delta r_6)/\sqrt{6}$	$\nu_s(CH_3)$
$S_5=\Delta r_{11}$	ν(CH)
$S_6=(\Delta r_7+\Delta r_8)/\sqrt{2}$	ν_s(C'N)
$S_7=(\Delta r_7-\Delta r_8)/\sqrt{2}$	ν_a(C'N)
$S_8=\Delta r_9$	ν(CN)
$S_9=\Delta r_{10}$	ν(CO)
$S_{10}=(2\Delta\alpha_1-\Delta\alpha_2-\Delta\alpha_3)/\sqrt{6}$	δ(C'NC')
$S_{11}=(\Delta\alpha_2-\Delta\alpha_3)/\sqrt{2}$	r(C'NC')
$S_{12}=(2\Delta\alpha_4-\Delta\alpha_5-\Delta\alpha_6)/\sqrt{6}$	δ(OCN)
$S_{13}=(\Delta\alpha_5-\Delta\alpha_6)/\sqrt{2}$	δ(CH)
$S_{14}=(2\Delta\gamma_4-\Delta\gamma_5-\Delta\gamma_6+2\Delta\beta_4-\Delta\beta_5-\Delta\beta_6)/\sqrt{12}$	$\delta_a(CH_3)$
$S_{15}=(2\Delta\gamma_4-\Delta\gamma_5-\Delta\gamma_6-2\Delta\beta_4+\Delta\beta_5+\Delta\beta_6)/\sqrt{12}$	$\delta_a(CH_3)$
$S_{16}=(-\Delta\gamma_1-\Delta\gamma_2-\Delta\gamma_3+\Delta\gamma_4+\Delta\gamma_5+\Delta\gamma_6$ $-\Delta\beta_1-\Delta\beta_2-\Delta\beta_3+\Delta\beta_4+\Delta\beta_5+\Delta\beta_6)/\sqrt{12}$	$\delta_s(CH_3)$
$S_{17}=(-\Delta\gamma_1-\Delta\gamma_2-\Delta\gamma_3+\Delta\gamma_4+\Delta\gamma_5+\Delta\gamma_6$ $+\Delta\beta_1+\Delta\beta_2+\Delta\beta_3-\Delta\beta_4-\Delta\beta_5-\Delta\beta_6)/\sqrt{12}$	$\delta_s(CH_3)$
$S_{18}=(2\Delta\gamma_1-\Delta\gamma_2-\Delta\gamma_3+2\Delta\beta_1-\Delta\beta_2-\Delta\beta_3)/\sqrt{12}$	$r(CH_3)$
$S_{19}=(2\Delta\gamma_1-\Delta\gamma_2-\Delta\gamma_3-2\Delta\beta_1+\Delta\beta_2+\Delta\beta_3)/\sqrt{12}$	$r(CH_3)$
$S_{20}=(\Delta\alpha_1+\Delta\alpha_2+\Delta\alpha_3)/\sqrt{3}$	Redundant
$S_{21}=(\Delta\alpha_4+\Delta\alpha_5+\Delta\alpha_6)/\sqrt{3}$	Redundant
$S_{22}=(\Delta\gamma_1+\Delta\gamma_2+\Delta\gamma_3+\Delta\gamma_4+\Delta\gamma_5+\Delta\gamma_6$ $+\Delta\beta_1+\Delta\beta_2+\Delta\beta_3+\Delta\beta_4+\Delta\beta_5+\Delta\beta_6)/\sqrt{12}$	Redundant

a) ν, δ, r, a, and s mean stretching, bending, rocking, asymmetric, and symmetric, respectively.

15) T. Miyazawa, *J. Chem. Phys.*, **29**, 246 (1958).
16) J. H. Schachtschneider and R. G. Synder, *Spectrochim. Acta*, **19**, 117 (1963).
17) L. V. Vilkov, P. A. Akishin, and V. M. Presnyakova, *Zh. Strukt. Khim.*, **3**, 5 (1962); *Chem. Abstr.*, **58**, 7455e (1963).
18) C. C. Costain and J. M. Dowling, *J. Chem. Phys.*, **32**, 158 (1960).

Table 2. Structural parameters of DMF, DMTF, and DMSeF

Bond length		Bond angle	
C-H	1.08 Å	HC'N	109°28′
C'-N	1.45	C'NC'	117°30′
C-N	1.34	C'NC	121°15′
C=O	1.22	NCO	123°
C=S	1.713	HCO	
C=Se	1.91		

4, respectively. The observed and calculated frequencies for DMF, DMF-^{15}N and DMF-d_7 along with their assignments from the modified Urey-Bradley field (MUBF) are given in Table 5. The frequencies for DMTF and their assignments from Urey-Bradley field (UBF) are given in Table 6. Finally, the present assignments for DMF are compared with the previous assignments in Table 7.

Results and Discussion

Dimethylformamide. Lower Vibrations: The lowest frequency in the spectrum at 319 cm^{-1} is assigned to C'NC' rocking vibration, instead of a band at 350 cm^{-1} as assigned by Kaufman and Leroy.[10] Katon *et al.*[4] favour the band near 350 cm^{-1} to a similar wagging mode in amides. The 350 cm^{-1} band may, therefore, be assigned to C'NC' wagging vibration. The bands at 405 and 660 cm^{-1} need no comment since their

Table 3. Force constants for DMF (md/Å, md/rad, md Å/rad^2)

	Stretching		Bending		Repulsive		Interactions[a]	
MUBF	K(C'-N)	4.30	H(HCH)	0.512				
	K(C-N)	5.66	H(HC'N)	0.787				
	K(C=O)	8.85	H(C'NC)	0.734	F(C'C)	0.6269	C'N with HC'N	0.4264
			H(C'NC')	0.526	F(C'C')	0.26	HC'N with H_0C'N	−0.017
			H(NCO)	0.955	F(NO)	1.154	H_0C'N with H_0C'N	
			H(NCH)	0.268	F(NH)	0.72	C'NC with HC'N	0.2078
			H(OCH)	0.270	F(OH)	0.92	C'NC with H_0C'N	0.06

	Stretching		Bending		Repulsive		Intramolecular tension	
UBF	K(C'-N)	3.24	H(HCH)	0.502	F(HH)	0.05	k	−0.04
	K(C-N)	6.11	H(HC'N)	0.439	F(HC'N)	0.52		
	K(C=O)	8.565	H(C'NC)	0.905	F(C'C)	0.42		
			H(C'NC')	0.505	F(C'C')	0.30		
			H(NCO)	0.726	F(NO)	1.50		
			H(NCH)	0.253	F(NH)	0.72		
			H(OCH)	0.257	F(OH)	0.92		
SVF	F_{66}	5.35	F_{1212}	1.38	F_{1818}	0.85	F_{89}	1.20
	F_{77}	4.58	F_{1313}	0.63	F_{1919}		F_{812}	0.45
	F_{88}	6.40	F_{1414}	0.52	F_{616}	−0.35	F_{813}	0.25
	F_{99}	10.85	F_{1515}	0.51	F_{711}	0.42	F_{912}	0.40
	F_{1010}	0.90	F_{1616}	0.59	F_{717}	−0.35	F_{913}	−0.25
	F_{1111}	1.06	F_{1717}					

a) H and H_0 denote hydrogen atom lying in and out-of-plane of the molecule.

Table 4. Force constants for DMTF (md/Å, md/rad, md Å/rad^2)

	Stretching		Bending		Repulsive		Intramolecular tension	
UBF	K(C'-N)	3.04	H(HCH)	0.478	F(HH)	0.06	k	−0.05
	K(C-N)	6.20	H(HC'N)	0.493	F(HC'N)	0.50		
	K(C=S)	4.18	H(C'NC)	0.777	F(C'C)	0.46		
			H(C'NC')	0.746	F(C'C')	0.30		
			H(NCS)	0.404	F(NS)	0.92		
			H(NCH)	0.278	F(NH)	0.65		
			H(SCH)	0.263	F(SH)	0.60		
SVF	F_{66}	5.58	F_{1212}	0.86	F_{1818}	0.89	F_{89}	0.65
	F_{77}	4.44	F_{1313}	0.61	F_{1919}	0.87	F_{812}	0.25
	F_{88}	6.45	F_{1414}	0.51	F_{616}	−0.30	F_{813}	0.20
	F_{99}	5.05	F_{1515}		F_{711}	0.41	F_{912}	0.30
	F_{1010}	1.05	F_{1616}	0.58	F_{717}	−0.30	F_{913}	−0.25
	F_{1111}	1.00	F_{1717}					

Table 5. Calculated and observed frequencies (cm^{-1}) and potential energy distribution for DMF, $DMF^{15}N$, and DMF-d_7

	Calculated			Observed[a]	Approx. PED. (MUBF)
	MUBF	UBF	SVF		
DMF	318	319	318	319 m	$r(C'NC')+0.52\delta(OCN)$
	405	405	406	405 m	$\delta(C'NC')$
	660	662	669	660 s	$\delta(OCN)+0.54\nu_s(C'N)+0.42\nu_a(C'N)+0.36r(C'NC')$
	872	856	855	870 m	$\nu_s(C'N)$
	1059	1017	1069	1067 m	$r(CH_3)+0.38\nu_a(C'N)$
	1085	1046	1095	1099 vs	$r(CH_3)$
	1264	1293	1279	1268 s	$\nu_a(C'N)$
	1376	1397	1397	1395 vs	$\delta_s(CH_3)+0.67\nu(CN)+0.34\nu_s(C'N)$
	1409	1414	1406	(1410)	$\delta(CH)$
	1430	1418	1409	1410 s	$\delta_s(CH_3)$
	1454	1432	1435	1450 m	$\delta_a(CH_3)+0.61\delta_s(CH_3)$
	1460	1473	1465	1460 w	$\delta_a(CH_3)$
	1493	1504	1508	1512 m	$\delta_s(CH_3)+0.91\delta_a(CH_3)+0.76\nu(CN)+0.74r(CH_3)$
	1690	1683	1677	1685 vs	$\nu(CO)+0.41\nu(CN)+0.31\delta(CH)$
$DMF-^{15}N$	317	318	317	[b]	$r(C'NC')+0.51\delta(OCN)$
	404	406	405	[b]	$\delta(C'NC')$
	659	661	668	653 w	$\delta(OCN)+0.51\nu_s(C'N)+0.41\nu_a(C'N)+0.37r(C'NC')$
	870	854	854	862 w	$\nu_s(C'N)$
	1056	1016	1063	1059 w	$r(CH_3)+0.47\nu_a(C'N)$
	1084	1046	1094	1081 vs	$r(CH_3)$
	1239	1267	1258	1234 m	$\nu_a(C'N)$
	1362	1396	1395	1369 s	$\nu(CN)+0.95\delta_s(CH_3)+0.44\nu_s(C'N)$
	1408	1413	1399	1395 vw	$\delta(CH)$
	1430	1416	1409	1404 w	$\delta_s(CH_3)$
	1452	1419	1426	1432 m	$\delta_s(CH_3)+0.96\delta_a(CH_3)$
	1460	1472	1464	1451 w	$\delta_a(CH_3)$
	1481	1493	1497	1493 m	$\delta_a(CH_3)+0.69\delta_s(CH_3)+0.53r(CH_3)+0.38\nu(CN)$
	1686	1676	1675	1684 vs	$\nu(CO)+0.37\nu(CN)+0.3\delta(CH)$
DMF-d_7	293	291	290	288 vs	$r(C'NC')+0.49\delta(OCN)+0.3\delta(C'NC')$
	352	350	351	344 m	$\delta(C'NC')$
	623	615	618	619 vs	$\delta(OCN)+0.57\nu_s(C'N)+0.37\nu_a(C'N)+0.3r(C'NC')$
	771	747	760	765 s	$\nu_s(C'N)+0.7r(CH_3)$
	823	793	845	834 s	$r(CH_3)$
	862	840	865	890 vs	$r(CH_3)+0.3\delta(CH)$
	1045	1044	1042	1035 s	$\delta_a(CH_3)$
	1047	1050	1053	1046 s	$\delta_a(CH_3)$
	1060	1055	1058	1052 s, sh	$\delta_s(CH_3)$
	1074	1076	1076	1068 s, sh	$\delta(CH)+0.54\delta_s(CH_3)$
	1107	1127	1119	1120 s	$\delta_s(CH_3)+0.32\nu_s(C'N)$
	1263	1298	1264	1258 vs	$\nu_a(C'N)$
	1402	1437	1428	1385 vs, b	$\nu(CN)$
	1670	1666	1654	1645 vs, b	$\nu(CO)+0.42\nu(CN)$

a) s, m, w, v, b, and sh mean strong, medium, weak, very, broad, and shoulder, respectively.
b) spectrum in this region was not obtained.

assignments are undoubted.

Methyl Rocking Vibrations: The bands at 1067 and 1099 cm^{-1} are assigned to methyl rocking vibrations of the *A'* type while the methyl rocking mode of the *A''* type is observed as a weak band at 1150 cm^{-1}. The 1099 cm^{-1} band in DMF increases by about 25 cm^{-1} in metal complexes and was assigned to C–N stretching mode since the double bond character of C–N is expected in increase on theoretical grounds with the decreasing bond order of C=O in metal complexes.[9] However, that this correlation is misleading may be judged from: (a) the infrared spectra of compounds containing gem dimethyl groups [includes $-N(CH_3)_2$] show strong bands in the region 1000—1200 cm^{-1} for CH_3 rocking modes,[19-23] and hence the assignment of frequencies at 1067, 1099, and 1150 cm^{-1}

19) F. B. Brown and W. H. Fletcher, *Spectrochim. Acta*, **19**, 915 (1963).
20) W. H. Fletcher and W. B. Barish, *ibid.*, **21**, 1647 (1965).
21) R. G. Snyder and G. Zerbi, *ibid.*, **23A**, 391 (1967).
22) H. A. Szymanski, "Theory and Practice of Infrared Spectroscopy," Plenum Press, New York (1964), pp. 213, 222, 227.
23) P. Cossee and J. H. Schachtschneider, *J. Chem. Phys.*, **44**, 97 (1966).

Table 6. Calculated and observed frequencies (cm^{-1}) and potential energy distribution for DMTF

Calcd UBF	Calcd SVF	Obsd	Approx. PED (UBF), %
220	215	a)	δ(SCN) 58, r(C'NC') 37
407	406	405 m	δ(C'NC') 65, r(C'NC') 16, ν(CS) 8
527	529	521 s	δ(C'NC') 23, δ(SCN) 21, r(C'NC') 21, ν(CS) 12, ν_s(C'N) 9, ν_a(C'N) 9
816	810	828 s	ν_s(C'N) 68, ν(CN) 8, δ(SCN) 9
974	975	975 vs	ν(CS) 50, $r(CH_3)$ 17, ν_s(C'N) 10
1024	1064	1058 s	$r(CH_3)$ 64, ν_a(C'N) 19, $\delta_a(CH_3)$ 14
1091	1123	1140 vs	$r(CH_3)$ 49, ν(CS) 20, $\delta_a(CH_3)$ 12, ν(CN) 11
1238	1236	1212 m	ν_a(C'N) 45, δ(CH) 15, r(C'NC') 14, $r(CH_3)$ 11
1392	1395	1405 vs	δ(CH) 39, $\delta_a(CH_3)$ 21, ν(CN) 12
1417	1406	1410 vs, sh	$\delta_s(CH_3)$ 95
1421	1424	1420 vs	$\delta_s(CH_3)$ 92
1449	1455	1450 m	$\delta_a(CH_3)$ 64, δ(CH) 16
1464	1469	1472 m	$\delta_a(CH_3)$ 62, $r(CH_3)$ 17, δ(CH) 11
1561	1561	1560 vs	ν(CN) 53, δ(CH) 13, $r(CH_3)$ 12

a) Spectrum was not scanned in this region.

to CH_3 rocking vibrations is reasonable, (b) rocking frequencies are sensitive and are known to shift on complex formation[22]; thus the frequency rise of the CH_3 rocking mode in DMF metal complexes is not unexpected, and (c) the 1099 cm^{-1} band does not show any change in the infrared spectrum[9] of DMF-^{15}N, thus ruling out any major C–N stretching contribution in the 1099 cm^{-1} band. Only about 10% C–N character is indicated by the calculation. The assignment of 1099 cm^{-1} to methyl rocking mode is in accord with these facts.

C=O *and* C'–N *Stretching Vibrations*: There is complete agreement over the assignment of the bands at 1685, 1268, and 870 cm^{-1} to C=O stretching, C'–N asymmetric and symmetric stretching vibrations, respectively. The carbonyl band has contributions from C–N stretching and C–H bending modes, as also expected by others.[10,11] From the band shapes of the vapor phase spectrum, Jones[3] has supported the assignment of C'–N symmetric and asymmetric stretching, OCN bending and CH_3 rocking vibrations and these agree with the present assignments.

C–N *Stretching Vibration*: The weak to medium band at 1512 cm^{-1} is a highly coupled vibration and has a complex character. This band is due to a CH_3 deformation vibration with contributions from CH_3 rocking and C–N stretching vibrations. The mixing of CH_3 deformation modes with skeletal vibrations has been found in other similar molecules containing gem dimethyl groups.[20,23] The 1512 cm^{-1} band of DMF is absent in diethylformamide (DEF).[5] It could, therefore, be expected that the coupling of CH_3 deformation vibrations with C–N stretching mode, present in DMF, does not occur in DEF. The band assignable to C–N stretching motion in DEF appears in the region 1420—1370 cm^{-1}.

The 1512 cm^{-1} band hardly shifts by 5 cm^{-1} in metal complexes. In the spectrum of DMF-^{15}N, the 1512 cm^{-1} band is lowered by 7 cm^{-1}, while the calculated shifts are -11 to -12 cm^{-1}.

C–H *Bending and* CH_3 *Deformation Vibrations*: The assignments in the region 1395—1450 cm^{-1} were found to be very sensitive to the force fields employed. In the UBF, the 1397, 1414, and 1418 cm^{-1} and in the symmetrized valence field (SVF), the 1397, 1409, and 1406 cm^{-1} bands have approximately the same assignments as the bands at 1409, 1430, and 1376 cm^{-1} in the MUBF (Table 5).

The MUBF calculations indicate that the 1376 and 1430 cm^{-1} bands are due to CH_3 symmetric deformation vibrations, and the band at 1409 cm^{-1} to C–H

Table 7. A comparison of the assignments for DMF in the range 300—1700 cm^{-1} a)

Obsd, cm^{-1}	J[3]	KL[10]	RYZ[9]	CR[11]	Present work (PED, %)
319				r(C'NC')	r(C'NC') 56, δ(OCN) 29, δ(C'NC') 11
350		δ(C'NC)		τ(CN)	r(C'NC') $\perp$
405		δ(C'NC')		δ(C'NC')	δ(C'NC') 78, r(C'NC') 14
660	δ(OCN)	δ(OCN)		δ(OCN)	δ(OCN) 36, ν_s(C'N) 19, ν_a(C'N) 15, r(C'NC') 13
870	ν_s(C'N)	ν_s(C'N)		ν_s(C'N)	ν_s(C'N) 65, δ(OCN) 14, ν_a(C'N) 10
1067		$r(CH_3)$ $\perp$		δ(CH) $\perp$	$r(CH_3)$ 66, ν_a(C'N) 16
1099	$r(CH_3)$	$r(CH_3)$	δ(CH)	$r(CH_3)$	$r(CH_3)$ 75, ν(CN) 9
1150	$r(CH_3)$ $\perp$			$r(CH_3)$ $\perp$	$r(CH_3)$ $\perp$
1268	ν_a(C'N)	ν_a(C'N)	ν_a(C'N)	ν_a(C'N)	ν_a(C'N) 49, r(C'NC') 12
1395	δ(CH)	δ(CH)ν(CO)ν(CN)	ν(CN)	δ(CH)	$\delta_s(CH_3)$ 35, ν(CN) 24, ν_s(C'N) 12
1410	$\delta_s(CH_3)$	$\delta_s(CH_3)$		$\delta_s(CH_3)$	δ(CH) 64, ν(CO) 15, $\delta_s(CH_3)$ 12
1410[b]					$\delta_s(CH_3)$ 84, δ(CH) 9
1450					$\delta_a(CH_3)$ 56, $\delta_s(CH_3)$ 34
1460	$\delta_a(CH_3)$	$\delta_a(CH_3)$		$\delta_a(CH_3)$	$\delta_a(CH_3)$ 82, $r(CH_3)$ 13
1512	ν(CN)	ν(CN)ν(CO)δ(CH)		ν(CN)	$\delta_s(CH_3)$ 23, $\delta_a(CH_3)$ 21, ν(CN) 18, $r(CH_3)$ 17
1685	ν(CO)	ν(CO)ν(CN)δ(CH)	ν(CO)	ν(CO)	ν(CO) 55, ν(CN) 23, δ(CH) 17

a) See footnote to Table 1. τ: Torsion, $\perp$: Out-of-plane
b) Not resolved.

bending vibration. The CH_3 asymmetric deformation vibrations are easily located at 1450 and 1460 cm^{-1}.

The 1395 cm^{-1} band is a coupled vibration with major contributions from CH_3 deformation (~35%) and C–N stretching (~24%) modes. It is lowered by 20 to 40 cm^{-1} in metal complexes and this shift may be understood from the major components of the band. It is also known that the CH_3 symmetric deformation vibration is more sensitive to the atom adjacent to the methyl group than the asymmetric vibration.[22]

The 1395 cm^{-1} band in DMF was observed to shift by −13 cm^{-1} in the spectrum[9] of DMF-^{15}N, which is in good agreement with the calculated value of −14 cm^{-1} in the MUBF. It should be noted that the calculated frequencies for DMF-^{15}N in the UBF and SVF indicate no shift for 1395 cm^{-1} band, which is contradictory to the experimental data. On the other hand, the calculations showed shifts for 1432 cm^{-1} frequency in the UBF and 1406 and 1435 cm^{-1} frequencies in the SVF, which is again contradictory to the observed data, since these bands remain unaffected in the infrared spectrum of DMF-^{15}N. This piece of evidence suggests that the assignments from the MUBF are to be preferred.

Some of the earlier investigators had favoured the assignment of the 1395 cm^{-1} band to C–H bending mode.[3,10,11] That this band is not due to C–H bending vibration also finds support from the spectrum of DMF-d_1.[24] Castelli and Cragle[12] have recorded the infrared spectra of DMF and DMF-d_1 as liquids. It is found that (a) a shoulder at 1400 cm^{-1} in DMF (corresponding to 1410 cm^{-1} of the present work) is absent in the spectrum of DMF-d_1, and is observed at ~1010 cm^{-1} as expected with the replacement of hydrogen by deuterium, indicating that this band can be assigned to C–H bending vibration, and (b) the band at 1380 cm^{-1} (this work, 1395 cm^{-1}) is present both in DMF and DMF-d_1, showing that this band is not due to aldehydic C–H bending vibration. These expected assignments are realised only in the results of MUBF. Notably, the 1395 cm^{-1} band has the assignment as C–H bending vibration in UBF and SVF, which is incorrect as discussed above.

Out-of-plane Vibrations: A brief mention is made here of the out-of-plane vibrations for completeness, although no calculations were made to aid the assignments. In the region under study, seven A'' vibrations are expected. Since the spectrum is of the liquid, some of the methyl group modes may overlap. Further, since some of the out-of-plane vibrations are weak, it may not be possible to observe them.

The band at 350 cm^{-1} is assigned to C'NC' wagging mode (may also be associated with C–N torsional mode). The C=O wagging vibration is expected near 550—600 cm^{-1}; but no band is observed in this region. Similarly, the C–H wagging mode expected at 900—1100 cm^{-1} is not observed. The intensities of these bands are probably too weak to be observed or the bands might have merged with the neighbouring absorptions. The weak band at 1150 cm^{-1} is assigned to CH_3 wagging mode.[3] Another out-of-plane rocking mode expected for A'' species may be too weak to be observed or may be taken to have merged with 1067 cm^{-1} band belonging to A' vibrations.[10] The CH_3 deformation vibrations may be taken to have overlapped with 1460 and 1410 cm^{-1} bands of the A' vibrations. These features are commonly encountered in other similar molecules.[19,20,23]

Dimethylformamide-^{15}N. The observed and calculated frequencies for DMF-^{15}N are given in Table 5 along with their assignments. It is interesting to observe the changes in the assignments as compared to those of DMF, particularly with respect to C–N stretching mode.

Dimethylformamide-d_7. The calculated frequencies obtained for DMF-d_7 using the same force constants as those of DMF are given in Table 5 along with the observed frequencies. Two points worth noting are: the absence of 1512 cm^{-1} frequency in the infrared spectrum of DMF-d_7 and the appearance of pure C–N stretching vibration at 1385 cm^{-1}. A detailed picture of the changes due to complete deuteration of DMF can be obtained from the same Table .

Force Fields. The UBF force constants of formamide and *N*-methylformamide,[2] and MUBF force constants of *N*-methylacetamide[24] formed the starting point for UBF and MUBF calculations of DMF.

There is considerable difference between the observed and the calculated frequencies due to methyl rocking modes in the UBF. The difficulties of reproducing the rocking frequencies in this force field are well known.[2,23] Some unacceptable assignments in the UBF and SVF (where a number of interaction constants are neglected) may reflect upon the inadequacies of these force fields. The frequency-fit alone cannot be a criterion in judging the suitability of a force field and therefore, while making a choice among the force fields, the reproducibility of the data from the frequency shifts in isotopic molecules should be kept in view. Such data could be useful in making correct assignments.[25] The results of the MUBF for DMF are in good agreement, as discussed before, with the frequency shifts from the isotopic species, DMF-^{15}N, DMF-d_1 and DMF-d_7; whereas the results from the other two force fields are not. Only the assignments from MUBF are, therefore, given (Table 5).

Dimethylthioformamide. The UBF force constants for DMTF are transferred from thioformamide,[2] *N*-methylthioformamide[2] and DMF. The appropriate SVF force constants are taken from DMF. The assignments for DMTF are very nearly the same both in UBF and SVF. Frequency shifts from isotopic substitution are not available for DMTF to test the validity of the force fields, and the MUBF was not attempted in this case.

The assignments from the calculations are discussed here briefly. The symmetric and asymmetric C'–N stretching at 828 and 1212 cm^{-1} compare well with

24) The authors are not in possession of the spectrum of DMF-d_1.

25) J. Jakes and B. Schneider, *Coll. Czech. Chem. Commun.*, **33**, 643 (1968).

26) L. H. Jones, L. B. Asprey, and R. R. Ryan, *J. Chem. Phys.*, **47**, 3371 (1967).

those of DMF. In DMTF complexes of cobalt(II) and nickel(II) chlorides,[27] the bands at 1560 and 521 cm^{-1} in DMTF shift to higher frequencies to around 1580 and 535 cm^{-1}, respectively and the band at 975 cm^{-1} shifts to lower frequencies to 950 cm^{-1}. These shifts agree with the assignments made for the bands at 1560, 521, and 975 cm^{-1} to C–N stretching, coupled C=S bending and C=S stretcing vibrations, respectively. The band at 1130 cm^{-1} is due to a CH_3 rocking vibration coupled with C=S and C–N stretching vibrations. This mode, being sensitive, shifts to higher frequencies in metal complexes and on *S*-methylation.[28]

Jensen and Nielsen[28] have studied the infrared absorption bands of a series of thioamides and located the characteristic bands. Recently, Indirachary and Ramaiah[29] have made a normal coordinate analysis of DMTF, treating the methyl groups as point masses. In particular, the bands at 970, 915, and 518 cm^{-1} have been assigned to C–H out-of-plane bending, C=S stretching and C'NC' bending vibrations, respectively.[29] These assignments differ from the present ones. The band at 922 cm^{-1} can be assigned to the out-of-plane bending mode of C–H.

Dimethylselenoformamide. In a series of thioamides and related selenoamides, Jensen and Nielsen[28] observed that the substitution of sulphur with selenium behaves like 'isotopic substitution' and shifts the C=S stretching by 30—100 cm^{-1} towards lower frequencies, while the other frequencies are generally unaltered. Employing the force constants of DMTF, approximate calculations have been made for DMSeF. The calculated frequencies show the expected trend. The C=Se stretching and bending are expected around 930 and 497 cm^{-1} respectively, according to the present calculations.

The authors wish to thank Professor M. R. A. Rao for his keen interest in the work.

27) G. Durgaprasad and C. C. Patel, unpublished data.

28) K. A. Jensen and P. H. Nielsen, *Acta Chem. Scand.*, **20**, 597 (1966).

29) C. A. Indirachary and K. V. Ramaiah, *Proc. Indian Acad. Sci.*, **69A**, 18 (1969).

BULLETIN OF THE CHEMICAL SOCIETY OF JAPAN, VOL. 44, 322—324 (1971)

Dielectric Relaxation of 1,2-Dichloroethane and 1,2-Dibromoethane in the Liquid State

Abul HASAN, Arati PAL, and Alpana GHATAK

Optics Department, Indian Association for the Cultivation of Science, Calcutta 32, India

(Received July 14, 1970)

The activation energies for dielectric relaxation (ΔH_τ) of the gauche rotational isomers of 1,2-dichloroethane and 1,2-dibromoethane in the liquid state have been determined from the dielectric relaxation data obtained from the absorption in 1.62 cm and 3.20 cm microwave regions at different temperatures. The activation energies (ΔH_τ) in both the liquids obtained in the present investigation agree fairly well with the values of electrostatic self energy of the polar isomers in the liquid state calculated theoretically by Wada.

It is well known that the energy differences between the *trans*- and *gauche*-rotational isomers of the molecules of 1,2-dichloro- and 1,2-dibromoethanes in the gaseous state are 1.27 kcal/mol and 1.7 kcal/mol respectively and in the liquid state this energy difference in the former molecules is almost zero while in the latter molecules about 800 cal/mol.[1-3]

Wada[4] explained the observed decrease in the values of energy difference in the pure liquids to be due to the electrostatic energy of the polar gauche molecules embedded in a continuous dielectric medium and the results of his calculations seem to agree with the experimental results.

Since measurements on the temperature dependence of relaxation times of the molecules of polar liquids afford a method for determining the activation energy of the molecules *i. e.* the potential energy of the molecules in the liquid state due to the various intermolecular forces in the liquid, it was intended to study the relaxation times of 1,2-dichloroethane and 1,2-dibromoethane molecules in the liquid state at different temperatures by the method of microwave absorption.

The experimental results and discussions of the results are presented in this paper.

Experimental

Chemically pure samples of 1,2-dichloroethane and 1,2-dibromoethane obtained from E. Merck were first dehydrated with fused calcium chloride and then fractionated. The proper fractions were then distilled under reduced pressure and used in the experiment.

The dielectric constant (ε') and dielectric loss (ε'') values of the two liquids at different temperature were measured by

1) Y. Morino, I. Watanabe, and S. Mizushima, *Sc. paper J.P.C.R.* (Tokyo), **39**, 396 (1941).
2) D. H. Rank, R. E. Kagrise, and D. W. E. Axford, *J. Chem. Phys.*, **17**, 1354 (1949).
3) N. Sheppard, *Advan. in Spectry.*, **1**, 298 (1959).
4) A. Wada, *J. Chem. Phys.*, **22**, 198 (1954).

Surber's method[5] at 1.62-cm and by Poley's method[6] at 3.2-cm microwaves. The values of the static dielectric constants (ε_0) were determined at 1 MHz while the refractive indices (n) were measured with an Abbe Refractometer. The temperature in all the measurements were kept constant within $\pm 1/2$°C by means of a thermostat.

Results

The values of ε' and ε'' determined experimentally at different temperatures and at the two microwave frequencies in the case of liquid 1,2-dichloroethane and 1,2-dibromoethane are given in Tables 1 and 2. Each of the tables also contains the measured values of ε_0 and n at the corresponding temperatures.

Table 1. Values of ε', ε'', ε_0, and n of 1,2-dichloroethane at different temperatures

Temp. °C	$\lambda=1.62$ cm		$\lambda=3.20$ cm		ε_0	n
	ε'	ε''	ε'	ε''		
31.5	7.01	3.19	8.65	2.50	9.80	1.437
50	7.11	2.74	8.31	2.23	9.35	1.428
65	7.17	2.42	7.94	1.82	8.55	1.420

Table 2. Values of ε', ε'', ε_0, and n of 1,2-dibromoethane at different temperatures

Temp. °C	$\lambda=1.62$ cm		$\lambda=3.20$ cm		ε_0	n
	ε'	ε''	ε'	ε''		
30	3.44	0.802	4.01	0.185	4.67	1.533
50	3.53	0.869	4.16	0.805	4.65	1.520
65	3.64	0.922	4.21	0.712	4.62	1.512
80	3.76	0.873	4.25	0.656	4.55	1.511

The values of ε' and ε'' for the two liquids at different temperatures have been fitted into the Cole-Cole arc plots, some of which are shown in Figs. 1 and 2. The values of τ, ε_∞ and the distribution parameters α determined from these plots are shown in Tables 3

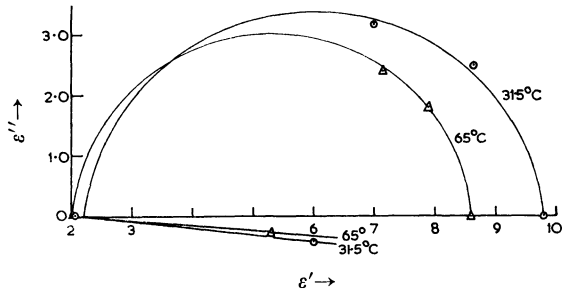

Fig. 1. Cole-Cole arc plot of 1,2-dichloroethane at 31.5°C and 65°C.

Table 3. Relaxtion time τ, Cole-Cole parameter α, ε_∞, and activation energies of 1,2-dichloroethane

Temp. °C	$\tau\times10^{12}$ sec	α	ε_∞	ΔH_τ kcal/mol	ΔH_η kcal/mol
31.5	6.05	0.07	2.20		
50	5.07	0.06	2.10	1.29	2.30
65	4.44	0.05	2.05		

5) W. H. Surber, Jr., *J. Appl. Phys.*, **10**, 534 (1948).
6) J. Ph. Poley, *Appl. Sci. Res.*, **B4**, 337 (1955).

Table 4. Relaxation time τ, Cole-Cole parameter α, ε_∞, and activation energies of 1,2-dibromoethane

Temp. °C	$\tau\times10^{12}$ sec	α	ε_∞	ΔH_τ kcal/mol	ΔH_η kcal/mol
30	8.60	0.19	2.36		
50	7.36	0.13	2.33	1.09	2.55
65	6.44	0.12	2.32		
80	5.63	0.10	2.29		

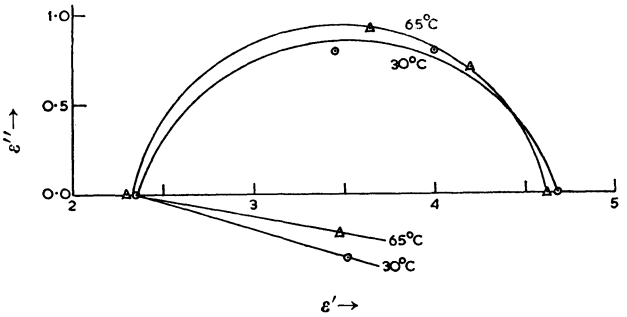

Fig. 2. Cole-Cole arc plot of 1,2-dibromoethane at 30°C and 65°C.

and 4. The values of activation energy (ΔH_τ) for dielectric relaxation obtained from the usual plots of $\log(T\tau)$ *vs.* $1/T$ (Fig. 3) and the activation energy (ΔH_η)-values for viscous flow obtained from the plots of $\log(T\tau)$ *vs.* $1/T$ are given in Tables 3 and 4 respectively. The viscosity values at different tempera-

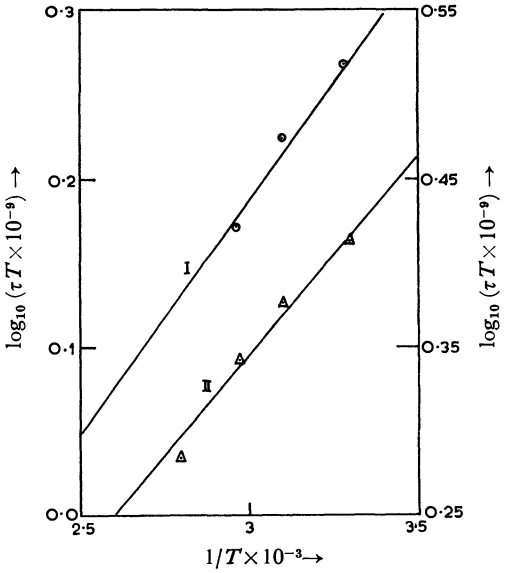

Fig. 3. Plot of log ($T\tau$) versus $1/T$
Curve I: 1,2-dichloroethane Ordinate to the left.
Curve II: 1,2-dibromoethane Ordinate to the right.

tures are taken from standard literatures.[7]

The accuracy of the τ values so determined is 3% in the case of 1,2-dichloroethane and in the case of 1,2-dibromoethane it is about 5%.

7) *Int. Critical Tables*, **7**, 213 (1930).

Discussions

It is seen from Tables 3 and 4 that the relaxation time of 1,2-dibromoethane at any temperature is larger than that of 1,2-dichloroethane which is consistent with the larger size of the former molecule. The τ value 6.15 p·sec of 1,2-dichloroethane at 31°C is compatible with the value 5.6 p·sec at 25°C for a solution of 1,2-dichloroethane in *p*-xylene as reported by Crossley and Walker[8] but is somewhat larger than the value 4.53 p·sec for the same solution at 20°C given by Chitoku and Higasi.[9] However the value of relaxation time for the pure liquid has not been apparently reported in the literature. In this connection it may be noted that from the measurements of spin-lattice relaxation of a solution of 1,2-dichloroethane in 1,2-dichloroethane-d_4 Bock and Tomchuk[10] derived a value of 8.62 p·sec for the relaxation time of 1,2-dichloroethane at 20°C. This value seems to be slightly higher than the value obtained in the present investigation.

The value of 0.07 for the distribution parameter (α) obtained in this investigation for the pure liquid at 31°C is near the value of 0.08 reported by Crossley and Walker[8] and is much smaller than the value 0.19 obtained by Chitoku and Higasi.[9] It is seen from Table 3 that the α-values for the pure liquid decreases with the increase of temperature as is generally observed. The α value for 1,2-dibromoethane (Table 4) is somewhat larger than that of 1,2-dichloroethane and also decreases with increasing temperature as in the case of 1,2-dichloroethane.

It is seen from Tables 3 and 4 that the values for the activation energy for dielectric relaxation (ΔH_τ) of 1,2-dichloroethane and 1,2-dibromoethane are both smaller than the respective values of the activation energy for viscous flow (ΔH_η) for both the liquids as are generally observed with other polar liquids.

The activation energy (ΔH_τ) of 1.3 kcal/mol in the case of 1,2-dichloroethane in liquid state as determined in the present investigation is almost equal to Wada's calculated value 1.22 kcal/mol[4] representing the electrostatic self energy of the polar gauche molecule in the liquid state. In the case of 1,2-dibromoethane in the liquid state the activation energy (ΔH_τ) is found to be 1.09 kcal/mol while according to Wada's calculation[4] the electrostatic self energy in this case is about 800 cal/mol.

Thus though the observed value of ΔH_τ in the case of 1,2-dichloroethane closely agrees with the value calculated by Wada, in the case of 1,2-dibromoethane the calculated value is somewhat lower than the observed one. It need be noted that Wada considered only the electrostatic energy of the polar gauche molecules in the liquid but did not take into account other types of intermolecular forces within the liquid which will further lower the energy of the gauche isomers. The small difference in ΔH_τ in the case of 1,2-dibromoethane may arise from this cause.

Considering the accuracy of the determination of the τ-values in the present investigation it may be concluded that the values of the activation energy determined experimentally are in agreement with the values calculated by Wada and that the greater part of the potential energy of the gauche isomers of the molecules of 1,2-dichloroethane and 1,2-dibromoethane in the liquid state arises from the electrostatic self energy of the polar molecules.

The authors are grateful to Dr. S. B. Roy for his guidance and to Professor G. S. Kastha, D. Sc. for his continued interest during the progress of the work.

8) J. Crossley and S. Walker, *J. Chem. Phys.*, **48**, 4742 (1968).
9) K. Chitoku and K. Higasi, This Bulletin, **40**, 773 (1967).
10) E. Bock and E. Tomchuk, *Can. J. Chem.*, **47**, 4635 (1969).

The Hydrogenation of Aniline over Supported Rhodium-Palladium Alloy Catalysts

Kazue IKEDATE and Sadao SUZUKI

Research Laboratory of Resources Utilization, Tokyo Institute of Technology, Ookayama, Meguro-ku, Tokyo

(Received July 3, 1970)

The hydrogenation of aniline was investigated in the temperature range from 30° to 50°C over Rh-Pd alloy catalysts supported on activated carbon. The reactions were mainly carried out in acetic acid at an atmospheric pressure of hydrogen. The activity per unit weight of the catalysts was measured and plotted for the alloy composition. It showed a maximum at 75—85 wt% Rh. However, the activity per unit of surface area showed a maximum at about 25 wt% Rh, and the minimum activation energy of this reaction was observed at the same composition. The relationship between the selectivity and the alloy composition was also studied. The maximum selectivity to dicyclohexylamine was observed at 20—30% Rh, while the maximum formation of *N*-phenylcyclohexylamine appeared at 50—60% Rh. However, the selectivity to cyclohexylamine showed a minimum at about 25% Rh. The initial rates of the formation of cyclohexylamine and *N*-phenylcyclohexylamine were measured and plotted for the catalyst composition. The maximum activity was observed at about 85 wt% Rh for the formation of cyclohexylamine and at 50—60% Rh for the formation of *N*-phenylcyclohexylamine. Then the ratios of the two simple reaction rates were calculated. At a higher Rh content, (above about 25% Rh), the selectivity increased as the ratio increased. The reaction over the catalysts prepared by different methods and the hydrogenation of aniline in cyclohexane were also investigated.

Recently some interesting work with respect to the binary alloy catalysts of the platinum group metals have been reported.[1-7] However, there have been only a few reports on the Rh-Pd alloy system, and, moreover, these reports have shown two different tendencies for the catalytic activity change in this alloy series; on the one hand, a maximum activity was found for the hydrogenation of nitrobenzene and ethyl methyl ketone[4] at each certain Rh content, and on the other hand, the activity for CH_4+D_2 exchange and propane cracking [3a] changed smoothly with an increase in the Rh content.

Then we investigated the activity change for the hydrogenation of aniline with Rh-Pd alloy catalysts supported on activated carbon, in order to consider the contribution of any unpaired *d* electrons present in the metal and concerned with its magnetic susceptibility. The structure of the catalyst was studied by X-ray diffraction, and the surface area of the metal on the catalyst was measured by the CO adsorption method. The selectivity change in this series was of as much interest as the activity change. However, this subject was scarcely investigated. There has been one report showing that on Rh-Pt alloys of the Adams type, the catalysts containing 70 to 90 wt% Rh were the most active and selective for the hydrogenation of acetophenon.[1] In that report, however, the selectivity was not referred to any detail beyond the above description. Therefore in this report the selectivity change for the hydrogenation of aniline and the relationship between the selectivity and the activity were investigated with respect to the composition of the binary alloy catalyst.

Moreover, we studied how the activity and selectivity depended upon the catalysts obtained by the different method of preparation. The hydrogenation of aniline in a cyclohexane solvent with Rh-Pd alloy catalysts was also investigated.

Experimental

Procedure of Catalyst Preparation. The catalysts were prepared by the reduction of a solution of mixed Rh and Pd chlorides with formaldehyde, and by co-precipitation followed by reduction with hydrogen gas. Activated carbon was used as the carrier, and 5 wt% metal was supported on it.

Catalyst Preparation by Reduction with Formaldehyde: The method used as almost the same as that proporsed by Willstätter.[8] A given amount of the solution of mixed metal chlorides was added to the activated carbon. Then the metal chlorides were reduced with formaldehyde and sodium hydroxide at room temperature for 30 min and next at 100°C for 1 hr. It was left to stand overnight and then, after filtration, dilute hydrochloric acid was added until the pH of the solution went below about 3. After one day, it was washed fully with ion-exchanged water; a catalyst dried in the vacuum system was used directly for the reaction.

Catalyst Preparation by Co-precipitation: A given amount of the solution of the mixed metal chlorides was added at a stretch to the activated carbon, which was stirred at 40°C in a solution containing the calculated amount of sodium hydroxide. Then the metal hydroxide co-precipitated on the carrier was reduced to the metal by bubbling hydrogen gas into the solution and washed fully with ion-exchanged water. The dried catalyst in the vacuum system was used directly for the reaction.

Hydrogenation of Aniline. The hydrogenation experi-

1) S. Nishimura, This Bulletin, **34**, 1544 (1961).
2) D. W. Mckee and F. J. Norton, *J. Phys. Chem.*, **68**, 418 (1964).
3) a) D. W. Mckee and F. J. Norton, *J. Catalysis*, **3**, 252 (1964); b) *ibid.*, **4**, 510 (1965).
4) G. C. Bond and D. E. Webster, *Platinum Metals Rev.*, **9**, 12, (1965); *ibid.*, **10**, 10 (1966).
5) K. Yoshida, *Shokubai*, **10**. 2 (1968).
6) D. W. Mckee and F. J. Norton, *Trans. Faraday. Soc.*, **64**, 2200 (1968).
7) R. L. Moss, H. R. Gibbens, and D. H. Thomas, *J. Catalysis*, **16**, 117 (1970).
8) R. Willstätter and E. Waldschmidt-Leitz, *Ber.*, **54**, 113 (1921).
9) K. Ikedate, T. Suzuki, and S. Suzuki, *Nippon Kagaku Zasshi*, **88**, 972 (1967).

ments were carried out in the liquid phase at an atmospheric pressure of hydrogen in the apparatus described in a previous paper.[9] The rates of the hydrogenation of aniline were measured 2 or 3 times. When almost the same value was obtained in two measurements, that value was taken as the activity of the used catalyst. The method of the analysis of the reaction samples was the same as that already reported.[10] The surface area of the metal on the carrier was measured by the ordinary CO adsorption method.

Results and Discussion

X-Ray Diffraction of Rh-Pd Alloy Series. In order to examine whether or not, the catalysts prepared by reduction with formaldehyde were homogeneous, they were subjected to a X-ray diffraction. The X-ray diffraction angles observed for the Rh-Pd alloy catalysts are shown in Fig. 1. Since a linear relationship between these angles and the composition was observed, we considered that the catalysts prepared by this method formed homogeneous alloys.

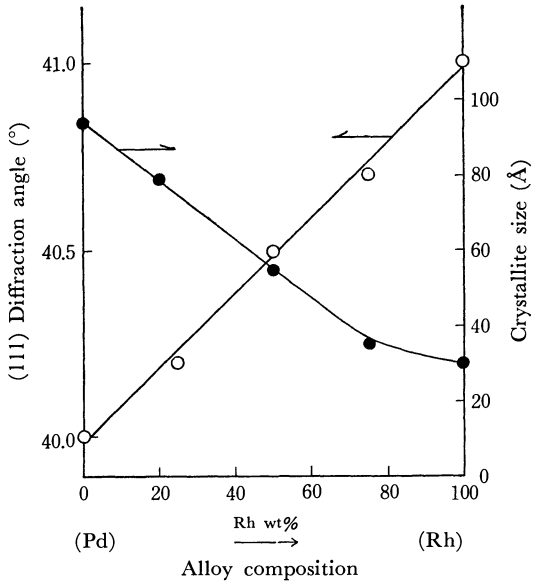

Fig. 1. X-ray diffraction angle and crystallite size of Rh-Pd supported on activated carbon.

The particle size, which was calcuated by the X-ray line-broaden method, changed smoothly in the range of about 30—100 Å. These catalysts were then used for the hydrogenation of aniline.

Hydrogenation of Aniline in Acetic Acid. The reaction was carried out in acetic acid at an atmospheric pressure of hydrogen in the temperature range from 30° to 50°C. The hydrogenation of aniline in this solvent over palladium supported on activated carbon, as has already been reported,[9] proceeded under a zero order of aniline concentration and one order of hydrogen pressure.

The influences of the hydrogen pressure on the reaction rates were investigated over a catalyst with a 15 wt% Rh content and over one with a 100% Rh content. The results are shown in Fig. 2. From this figure, it may be seen that over these catalysts the

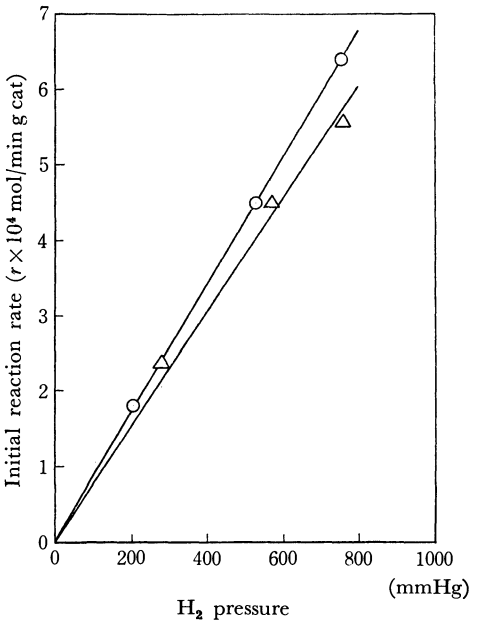

Fig. 2. Influence of the hydrogen pressure to the initial reaction rate.
—○— 15% Rh (at 50°C) —△— 100% Rh (at 40°C)

initial reaction rate was first order with respect to the hydrogen pressure. Since, in an initial reaction period, the aniline was consumed almost lineary for the reaction time, we consider that the reaction proceeds with zero order of the aniline concentration. Hence, we concluded that, over the Rh-Pd alloy series, the initial reaction rate may be expressed by the following equation, as on the Pd catalyst, when the constant weight of the catalyst is used: $V=kP_{H_2}$ Here, k denotes the rate constant.

Then the initial reaction rate of the hydrogenation

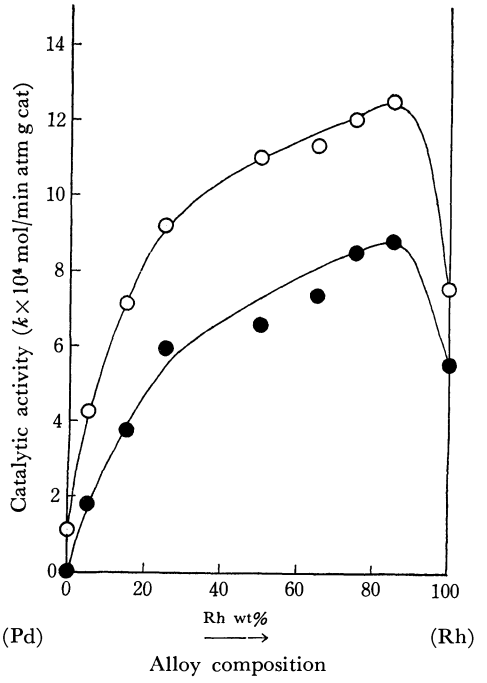

Fig. 3. Catalytic activity per g catalyst for the hydrogenation of aniline in acetic acid.
—○— at 50°C —●— at 40°C

10) K. Ikedate, T. Suzuki, and S. Suzuki, *Nippon Kagaku Zasshi*, **89**, 304 (1964).

was measured; the rate constant as a function of the alloy composition is shown in Fig. 3. In this alloy series the activity per unit of weight of the catalyst has a maximum at a 75—85% Rh content.

Since, in the last section, it was shown that the particle size of the metal on the carrier varied with the composition of the catalysts, it can be easily presumed that the active surface areas of the catalysts also vary with the composition. Therefore, the metal surface area on the carrier was measured by the CO adsorption method and the catalytic activity per unit surface area of the metal was calculated. The results, plotted in Fig. 4, show that the catalytic activity curve changed. The maximum of the activity shifted to about a 25 wt% Rh content, at that point the activation energy observed for this reaction had its minimum value.

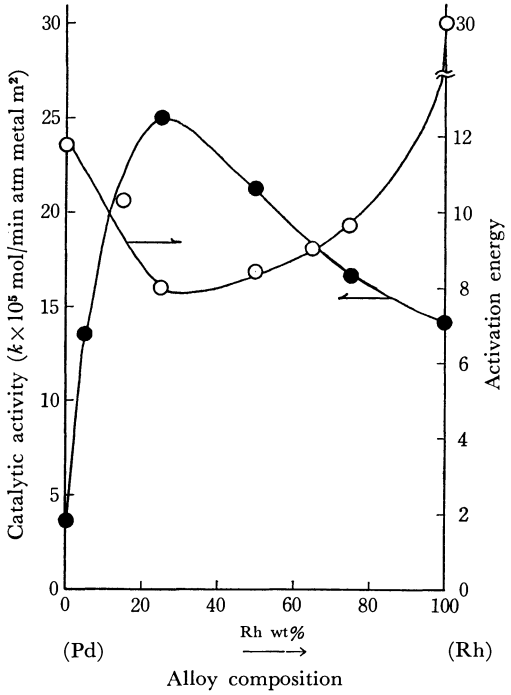

Fig. 4. Catalytic activity per unit surface area of metal on the carrier —●— and activation energy —○—.

Since the magnetic susceptibility of the Rh-Pd alloys has a maximum value at 5 atm% Rh, as has been reported in the literature,[11,12] we considered that the unpaired *d* electrons concerned with the magnetic susceptibility might influence the activity of the catalysts, as Yoshida also pointed out in his report[5,13] on Rh-Pt catalysts. However, the composition at the maximum in the magnetic susceptibility of the Rh-Pd alloy series did not completely agree with that at the maximum activity observed in this reaction, and also in his data,[5] the composition at the maximum of the magnetic susceptibility of the Rh-Pt alloy series does not coincide exactly with that at the catalytic activity maximum based on the unit of the metal surface area for the hydrogenation of phenol and benzoic acid. Therefore, it may be considered that the catalytic activity could not be explained only in terms of the magnetic susceptibility of the metal used as the catalyst.

The Reaction Mechanism on Rh-Pd Alloys in Acetic Acid. Over the catalysts of the platinum-group metals, the hydrogenation of aniline proceeds through the reaction mechanism illustrated in Fig. 5, as has been shown in our previous reports.[10,14] When acetic acid was used as the solvent, over the Rh-Pd alloy catalysts dicyclohexylamine was formed from *N*-phenylcyclohexylamine (hereafter descrived as NPC) much as over other platinum metals,[14] and the hydrogenation of the NPC formed did not occur at the same time the hydrogenation of aniline was progressing. The hydrogenation of NPC began when almost all the aniline had been consumed. In acetic acid, then, the selectivity for the formation of cyclohexylamine in the hydrogenation of aniline was influenced by two steps in the reaction mechanism: namely by k_2 and k_3, and by k_5 and k_6. The former is named the first step, and the latter, the second step (Fig. 5).

Selectivity. The reaction was investigated in acetic acid at 50°C. Since the hydrogenation of aniline was finished, the yields of the cyclohexylamine and dicyclohexylamine formed express the selectivities for the respective amines. The selectivities at the end point of the reaction are plotted as a function of the alloy composition in Fig. 6. The maximum yield of the NPC formed, an intermediate, in the course of the reaction is also plotted. In this experiment the Pd-C catalyst prepared by the adsorption method reported previously[10] was used, because the palladium catalyst which was prepared by the reduction with formaldehyde was almost inactive and so, on this catalyst, the reaction proceeds scarcely not at all. A maximum of the formation of dicyclohexylamine was shown at 20—30

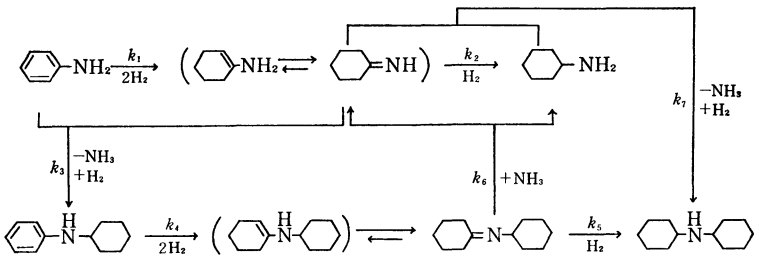

Fig. 5. Mechanism of the hydrogenation of aniline.[10]

11). E. Vogt, E. Oeholer, and W. Treutmann, *Ann. Phys.*, **18**, 168 (1966).
12) A. J. Manvel and J. M. P. St. Quintion, *Proc. Roy. Soc.*, (*Ser.*), *A*, **273**, 412 (1963).
13) K. Yoshida, *Nippon Kagaku Zasshi*, **88**, 222 (1967).
14) K. Ikedate and S. Suzuki, *ibid.*, **90**, 91 (1969).

wt% Rh. Then it greatly decreased beyond about 50% Rh. The formation curve of NPC showed a maximum at 50—60% Rh, but in the formation curve of cyclohexylamine a maximum was not found, while a minimum was shown at about 25% Rh.

The quantity of dicyclohexylamine formed was somewhat decreased when the reaction temperature went down. However, the formation curve observed at 40°C had a maximum at 20—30% Rh and showed almost the same shape as that observed at 50°C. Of course, the selectivity of the catalyst is influenced by the reaction temperature, but the formation curves may show almost the same tendency near 50°C.

From Fig. 6 it may be considered that the deviation between the curve of dicyclohexylamine and NPC shows the variety in the activity of each catalyst for the hydrogenating decomposition of NPC. This activity of the catalyst contributes to the second step and influences the selectivity. However, the change in the selectivity to cyclohexylamine can not be explained only this deviation.

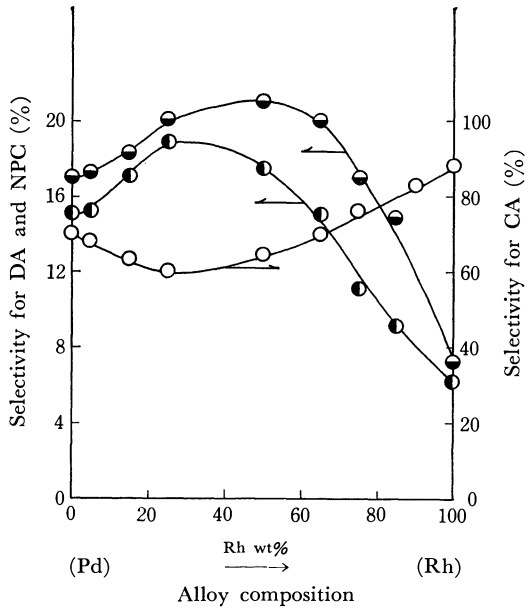

Fig. 6. Selectivity change for cyclohexylamine (CA) —○—, dicyclohexylamine (DA) —◑—, *N*-phenylcyclohexylamine (NPC) —◒— in acetic acid at 50°C.

The rates of the formation of cyclohexylamine and NPC, which influenced the first step, were measured. They are plotted in Fig. 7. The activity per unit weight of the catalyst for cyclohexylamine formation showed a sharp peak at about 85% Rh, while the activity for NPC formation showed a peak near 60% Rh and decreased in the region of Rh contents more than 75—85%. The activity per unit of weight of the catalyst for aniline had a maximum at 75—85% Rh, and it almost coincided with the maximum activity per unit of weight for the cyclohexylamine formation. Therefore, it was considered that, in this system, the total activity of this reaction depended mainly on the activity of the direct hydrogenation of aniline to cyclo-

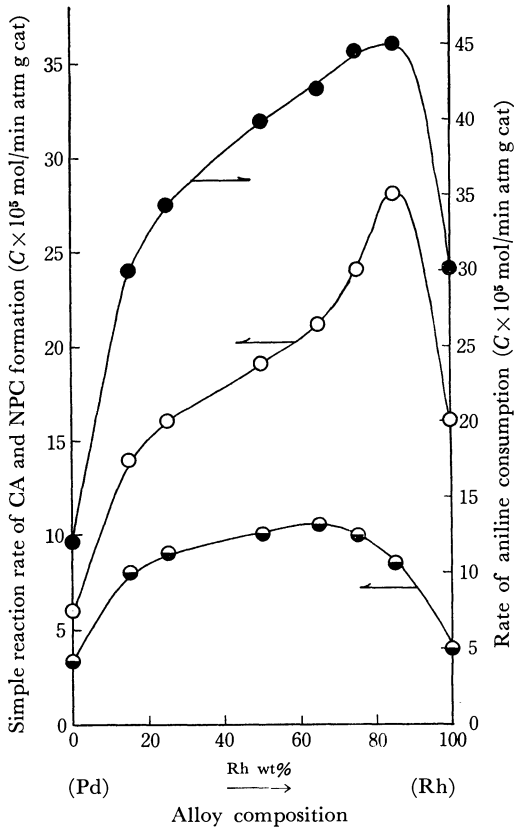

Fig. 7. Simple reaction rates of formation of cyclohexylamine —○—, *N*-phenylcyclohexylamine —◒—, and rate of aniline consumption —●— at 50°C, in acetic acid.

Table 1. Relationship between ratio of simple reaction rates and selectivity for cyclohexylamine

Catalyst Ph–Pd–C (Rh content wt%)	$-\frac{dA^{b)}}{dt}\times10^4$ mol/min atm gcat	$\frac{dNPC}{dt}\times10^4$ mol/min atm gcat	$\frac{dCA}{dt}\times10^4$ mol/min atm gcat	Ratio $\frac{CA}{NPC}$	Selectivity CA %
0% Rh (100% Pd)	1.2	0.33	0.60	1.8	70
15% Rh	3.0	0.80	1.4	1.8	64
25% Rh	3.4	0.90	1.6	1.8	60
50% Rh	4.0	1.0	1.9	1.9	64
65% Rh	4.2	1.05	2.1	2.0	70
75% Rh	4.4	1.0	2.4	2.4	74
85% Rh	4.5	0.85	2.8	3.3	80
100% Rh	2.4	0.40	1.6	4.0	88

a) The catalyst was prepared from H_2PdCl_4 adsorption on activated carbon.[9]
b) A: aniline

hexylamine.

In the Rh-Pd alloy series the selectivity to cyclohexylamine did not have a maximum and showed a minimum at about 25% Rh, as is shown in Fig. 6. Here, the selectivity can not be interpreted only on the basis of the activity of the catalyst. The ratios between the simple reaction rate of cyclohexylamine formation and that of NPC were then calculated; they are collected in Table 1. In Table 1 the rate of the formation of each substance is shown as an activity per unit of weight of the catalyst, but the ratio between the simple reaction rates does not have an order with respect to the catalyst. Therefore, it should be the same if it is obtained from the rates per unit of the surface area of the metal on the catalyst.

Beyond 25% Rh to 100% Rh the value of this ratio increased gradually with the increase in the Rh content. Between the selectivity to cyclohexylamine and this ratio, a good proportional relationship was observed. It was considered that, on these catalysts, the selectivity to cyclohexylamine was governed mainly by the first step under the present reaction conditions. For example, in spite of the lower activity over 100% Rh than over the other alloy catalyst, a better selectivity to cyclohexylamine was shown at 100% Rh. This can be explained on the basis of the fact that in the first step, the ratio for rhodium is the largest in the Rh-Pd alloy series. Therefore, it is clear that the selectivity did not depend only on the simple catalytic activity for the hydrogenation, but was also determined by the relative activity for the simple reactions which were concerned with the selectivity.

From 0% Rh (*viz.*, 100% Pd) to 25% Rh, the ratios between the rate of cyclohexylamine and NPC formation were almost constant. This signifies that, over catalyst in this composition range, the rate of the formation of cyclohexylamine increased to the same degree as that of NPC. However, the selectivity to cyclohexylamine decreased. Hence, it was considered that, in this composition range, the catalytic activity which was connected with the second step, mainly influenced the selectivity.

Influence of the Different Method of Catalyst Preparation. Changes in the selectivity and the activity were investigated over Rh-Pd catalysts prepared by two different methods: one was prepared by reduction with formaldehyde, and the other by the co-precipitation of these metals. A catalyst with a 25% Rh content was used, and the reaction carried out under the conditions described above.

The results are shown in Table 2. The total activity of the catalyst prepared by reduction with formaldehyde for the hydrogenation of aniline was higher than that of the catalyst prepared by the co-precipitation. Further, the activity for the hydrogenation of benzene had the same tendency as that described above. Hence, we expected that the former catalyst would have the higher activity for the benzene nucleous of aniline and would give the better selectivity to cyclohexylamine. However, the amount of NPC formed was almost the same in both cases; if anything, that of cyclohexylamine was somewhat lower on the former than on the latter. That the same amount of NPC was formed shows that, in the first step, the ratio between the simple reaction rates (*viz.*, k_2 and k_3) was almost the same over both the catalysts. Judging from the small difference in the amount of dicyclohexylamine formed, it was considered that, in this case, the preparation of the catalyst influenced the hydrogenating decomposition rate of NPC, although the difference between them in the amount of cyclohexylamine formed was not very large (about 6%).

Therefore, it may be said that the selectivity of the catalyst does not differ much when the composition of the catalyst is the same. That is, this suggests that,

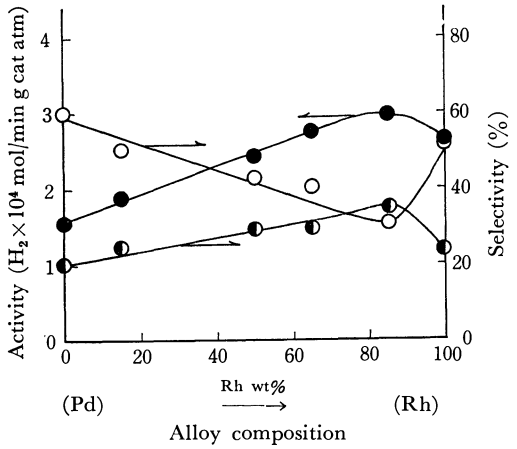

Fig. 8. Hydrogenation of aniline in cyclohexane at 50°C.
—●— rate of hydrogenation, —○— cyclohexylamine, —◐— dicyclohexylamine.

Table 2. Hydrogenation of aniline and benzene over the supported Rh–Pd catalysts prepared by the different method at 50°C in acetic acid

Catalyst	Method of preparation	Rate of hydrogenation: Benzene H_2 adsorbed $\times 10^4$ mol/min atm g cat	Rate of hydrogenation: Aniline H_2 adsorbed $\times 10^4$ mol/min atm g cat	Products in the hydrogenation of aniline: Intermediate[b] NPC (%)	Final products[a] DA (%)	Final products[a] CA (%)
25 wt% Rh	Reduction with formaldehyde	5.0	8.7	20	19	62
	Co-precipitation hydroxide	3.0	6.0	21	16	68

a) Mol. percent of DA and CA based on the moles of aniline consumed at the end point of the reaction.
b) Mol. percent of the maximum amount of NPC formed in the course of hydrogenation.

at a given composition of the catalyst, the ratios of the simple reaction rates are almost the same.

Hydrogenation of Aniline in a Cyclohexane Solvent. With the intention of considering the hydrogenation of free aniline over Rh-Pd catalysts, the reaction was carried out in a cyclohexane solvent. The results are shown in Fig. 8. The catalyst prepared by the reduction with formaldehyde was used. The catalysts were inhibited rapidly by the amine formed in the hydrogenation. The catalytic activity was then obtained from the initial reaction rate. The activity per g of catalyst showed a maximum at 75—85% Rh, the same composition as that observed in acetic acid.

The curves of the selectivity to dicyclohexylamine and cyclohexylamine in the non-polar solvent were different from those in acetic acid. The selectivity to dicyclohexylamine showed a maximum at the activity maximum. On the whole, the formation of dicyclohexylamine in cyclohexane was higher than that in acetic acid.

On the other hand, in a cyclohexane solvent the formation of NPC was extremely small as compared with that in an acetic acid solvent; at 15% Rh, the NPC formed was about 5 mol% of the material; at 85% Rh, NPC was barely perceived by gas chromatography with a thermal conductivity detector, and, as was reported in a previous paper,[14] at 100% Rh it was not found at all. Hence, it was clear that, in the hydrogenation of free aniline, dicyclohexylamine was formed mainly by the combination of imine and cyclohexylamine; this process is shown as k_7 in Fig. 5.

Thus, over the Rh-Pd alloy catalysts the process of the formation of dicyclohexylamine in cyclohexane was different from that in acetic acid. Therefore, the curves of the selectivity to dicyclohexylamine are different in the two solvents. From this, it was considered that the amine and imine which were formed in the hydrogenation, were in different adsorption states over the catalysts in the two solvents.

BULLETIN OF THE CHEMICAL SOCIETY OF JAPAN, VOL. 44, 330—334 (1971)

A Nuclear Magnetic Relaxation of ^{139}La in Ionic Aqueous Solutions

Keikichi NAKAMURA and Kazutaka KAWAMURA

National Research Institute for Metals, Nakameguro, Meguro-ku, Tokyo

(Received July 7, 1970)

The nuclear magnetic relaxation rates of the ^{139}La ion in aqueous solutions of halides, nitrate, sulfate, and perchlorate have been measured. The observed relaxation rates increased as the concentration of the salts increased. However, in the low concentration range, the relaxation rate divided by the relative viscosity, $\Delta\nu/\eta_r$, increased only in the cases of nitrate and sulfate, while it decreased in the cases of halides and perchlorate. It was found that the formation of inner-sphere complexes is a satisfactory explanation of the increase in the $\Delta\nu/\eta_r$ of nitrate and sulfate solutions in the low to middle concentration range. With the fact, proved by various authors, that the lanthanide ions have several coordination numbers, the decrease in the $\Delta\nu/\eta_r$ of halide and perchlorate solutions in the same concentration range can be explained in terms of the existence of an equilibrium between two hydrated species, such as:

$$La(H_2O)_9^{3+} \rightleftharpoons La(H_2O)_8^{3+} + H_2O$$

and the symmetrical species, $La(H_2O)_8^{3+}$, contributes to the decrease in $\Delta\nu/\eta_r$. At a high nitrate concentration, after reaching the maximum value $\Delta\nu/\eta_r$ decreases, demonstrating that a symmetrical trinitrato species may be formed in the solution.

It has been shown that, in solution, lanthanide ions have no definite coordination number, being in an equilibrium between several possible coordination numbers.[1-4] The coordination numbers for the lanthanides vary through the lanthanide series, a higher coordination number is favourable for the lighter lanthanides, while a lower coordination number is favourable for the heavier lanthanides. Because ^{139}La ($I=7/2$) is diamagnetic and has a relatively large quadrupole moment (0.5×10^{-24} cm^2), which interacts with the electric field gradient, a nuclear magnetic relaxation study of ^{139}La should provide various information concerning the symmetry of the molecule and the distribution of anions outside the first coordination sphere.

Abragam[5] has derived the following relation for the relaxation of a quadrupole nucleus in solution:

$$T_1^{-1} = \frac{3\cdot(2I+3)}{40I^2\cdot(2I+1)}\cdot\left(1+\frac{1}{3}\xi\right)\cdot\left(\frac{e^2qQ}{\hbar}\right)^2\tau_c \qquad (1)$$

where eQ is the nuclear quadrupole moment, where eq

1) L. O. Morgan and A. W. Nolle, *J. Chem. Phys.*, **31**, 365 (1959); L. O. Morgan, *ibid.*, **38**, 2788 (1963).

2) F. H. Spedding, D. A. Csejka, and C. W. Dekock, *J. Phys. Chem.*, **70**, 2423 (1966); F. H. Spedding, M. J. Pikal, and B. O. Ayers, *ibid.*, **70**, 2430 (1966); F. H. Spedding, M. J. Pikal, and B. O. Ayers, *ibid.*, **70**, 2440 (1966); F. H. Spedding and K. C. Jones, *ibid.*, **70**, 2450 (1966).

3) D. G. Karraker, *Inorg. Chem.*, **7**, 473 (1968).

4) K. Nakamura, This Bulletin, **41**, 1254 (1968); K. Nakamura, *J. Inorg. Nucl. Chem.*, **31**, 455 (1969); **32**, 2265 (1970).

5) A. Abragam, "Principles of Nuclear Magnetism," Oxford Univ. Press, London (1961), p. 314.

is the z principal component of the electric field gradient tensor, where ξ is the assymmetry parameter, and where τ_c is the correlation time for the quadrupole interaction and is given by:[6]

$$\tau_c = \frac{4\pi a^3}{3KT}\eta \qquad (2)$$

assuming that the molecule can be regarded as a rigid sphere with a radium of a.

However, to evaluate eq and τ_c in ionic solutions, two different models can be used. One is that the water molecules or anions in the first coordination sphere move uncorrelatively; *i.e.*, the correlation time for the individual motion of water or an anion is shorter than the correlation time for the Brownian motion of the entire water-metal or metal-anion complex. In this case, the observed relaxation rate[7] is z (z: coordination number) times the relaxation rate for the quadrupole interaction due to the fluctuating field of one water molecule or one anion coordinated to the metal ion. Moreover, the observed relaxation rate will increase monotonously as the concentration of the salts increases. This is because of the additional electric field gradient due to ions.

However, when the mean resident time of water molecules or anions in the first coordination sphere is sufficiently longer than the correlation time for the entire complex motion, the field gradient at the metal ion will depend strongly on the symmetry of the molecule. In this case, the observed relaxation rate will not increase monotonously with the concentration increase, but will strongly depend on the kind of species existing in the solution. If the coordination fluctuates between different configurations, the observed relaxation rate will be a weighted average of the relaxation rates of different configurations.

The purpose of this paper is to obtain information on the hydration number change and the complex formation with the anion through the quadrupole interaction of ^{139}La.

Experimental

The NMR spectra were obtained with a Varian VF-16 wide-line spectrometer operating at 6.012 MHz. The magnetic fields were controlled with a "Fieldial Mark II" with a stability of 5×10^{-7}. The frequency were monitored with a Matsushita VP-437 A electronic counter. Distortion due to the finite modulation width were corrected by using different modulation widths and by extrapolating to zero amplitude. Since the observed line shape is Lorenzian, the line width (cycles/sec) is related to the relaxation time thus;

$$T_1^{-1} = \sqrt{3}\pi\Delta\nu \qquad (3)$$

The relative viscosities were measured by using an Ostwald-type viscometer in a thermostat bath at 23.0±0.1°C. To check the accuracy of the method used, the relative viscosities of the $LaCl_3$ solutions were compared with the literature value[2] and found to agree within ±1%.

Reagent. The lanthanum nitrate, sulfate, perchlorate, and halide solutions were obtained by dissolving lanthanum oxide (99.95%) purchased from Michigan Chemical Corporation with these acids. All these acids were of a reagent grade and were used without further purification.

Results and Discussion

The concentration dependence of the line width can be separated into two contributions. One is the correlation time, which increases with the viscosity increase of the solution according to Eq. (2). Spedding *et al.*[2] have shown that the concentration dependence of the relative viscosity of a lanthanide chloride solution at a moderate or high concentration can be described in terms of a modification of Vand's equation in this form:

$$\ln(\eta/\eta_0) = A_3C/(1 - Q''C) \qquad (4)$$

where $\eta/\eta_0=\eta_r$ is the relative viscosity of the solution, where C is the molar concentration, and where A_3 and Q'' are adjustable parameters. According to Spedding, the success of Eq. (3) suggests that the major contribution of a lanthanide chloride solution at a moderate or high concentration arises from the interference of large hydrated ions with the stream of the solvent. This implies that the lanthanide ions are firmly coordinated with one row of water molecules; *i.e.*, the correlation time for the reorientational motion of the hydrated lanthanide ion is sufficiently short compared with the mean resident time of water molecules in the first coordination sphere.

Another is the change in the field gradient due to the changes in the molecular environment. These changes may involve both the change in the first hydration sphere and the change in the charge distribution around it. Figure 1 shows the concentration dependence of the ^{139}La line widths. An examination of the figure

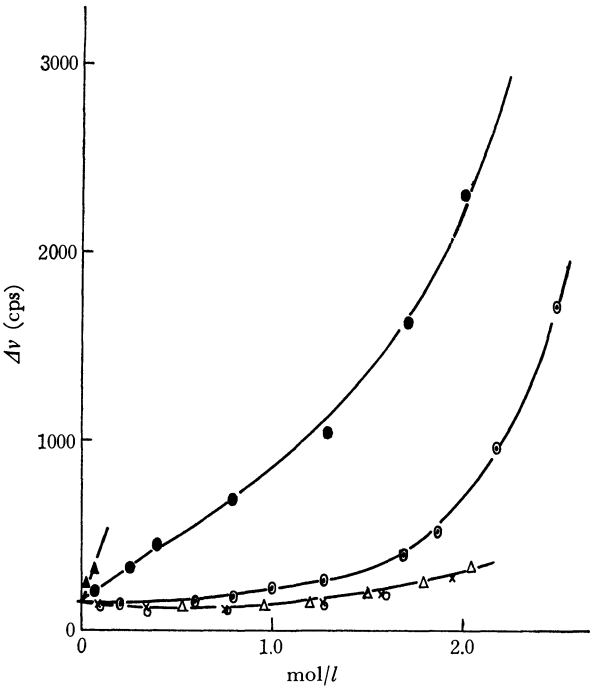

Fig. 1. The concentration dependence of ^{139}La line widths.
▲ $La_2(SO)_3$, △ $LaCl_3$, ● $La(NO_3)$, × LaBr
⊙ $La(ClO_4)_3$, ○ LaI_3

6) N. Bloembergen, E. M. Purcell, and R. V. Pound, *Phys. Rev.*, **73**, 697 (1948).
7) H. G. Hertz, *Electrochem.*, **65**, 20 (1961).

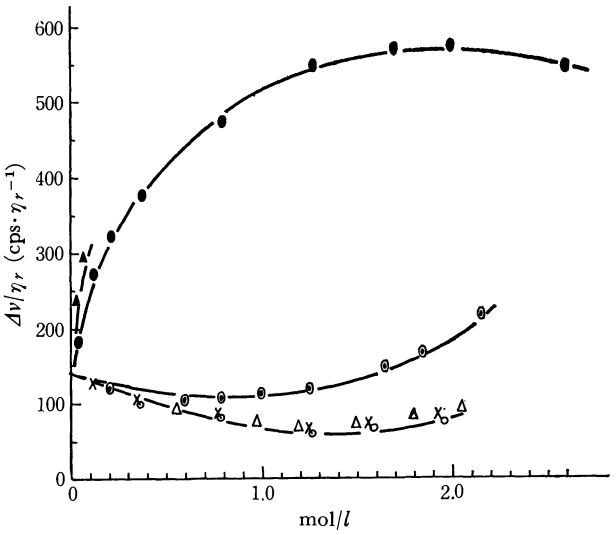

Fig. 2. The concentration dependence of ^{139}La line width/relative viscosity ($\Delta\nu/\eta_r$).
▲ $La_2(SO_4)_3$, △ $LaCl_3$, ● $La(NO_3)_3$, × $LaBr_3$
⊙ $La(ClO_4)_3$, ○ LaI_3

will show that the line widths increase with the concentration increase in the salts due to the increase in the viscosity and the change in the molecular environment. However, to ascertain the change in the molecular environment, it is necessary to divide the line width by the relative viscosity of the solution.[8] The results are shown in Fig. 2, which shows a marked difference in the concentration dependence.

Line Width at an Infinite Dilution. Since the electric field gradient at an infinite dilution is solely determined by the water molecules, the line widths at an infinite dilution are independent of as the anions, as is shown in Figs. 1 and 2. To discuss the line width at an infinite dilution, it is necessary to know the mean resident time of the coordinated water molecules, the coordination number, and the symmetry of the entire lanthanum-water complex.

As has been described previously, a relative viscosity of the $LaCl_3$ solution has shown the existence of a firmly-coordinated lanthanum ion. Recently, Reuben and Fiat[9] have calculated the water-exchange rate constants from ^{17}O NMR. Their calculated rates ranged from 2.6×10^7 to 3×10^6 sec^{-1} as the ionic-radii change from Tb to Tm. If we extraporate these rate constants to the ionic radius of La^{3+}, we obtain 2×10^9 sec^{-1}. This rate is about one-tenth of the reciprocal of the correlation time for the reorientational motion of the hydrated lanthanum ion;[10] moreover, this rate is considerably larger than the observed relaxation rates (100—1000 cps) and the chemical shift (<100 cps).[11]

The coordination numbers of hydrated lanthanide ions have been investigated by various authors. Proton NMR study[1] has shown that the coordination numbers vary in the lanthanide series, being 9 for lighter lanthanides and 6 for heavier lanthanides. On the other hand, the apparent molar volume, the heat capacity, the heat of dilution, and relative viscosity studies[2] have shown that the lanthanide ions in water exist in an equilibrium between two possible coordination numbers; *i.e.*, the coordination number of 9 is favourable for from La^{3+} to Nd^{3+}, while 8 is favourable for from Tb^{3+} to Yb^{3+}. Karraker's spectrometric study[3] of an Nd^{3+} aqueous solution supports this conclusion. He concluded that Nd^{3+} has two coordination numbers, 9 for a dilute and 8 for a concentrated aqueous solution.

The mean resident time and the existence of the two coordination numbers mentioned above indicate that the observed line width is determined by the rapid exchange condition[12] according to:

$$\Delta\nu/\eta_r = P_9\Delta\nu_9^0 + P_8\Delta\nu_8^0 \quad (5)$$

where P_9 and P_8 are the fractional populations of the species and where $\Delta\nu_9^0$ and $\Delta\nu_8^0$ are the line widths of $La(H_2O)_9^{3+}$ and $La(H_2O)_8^{3+}$ respectively at $\eta_r=1$. When 8 coordinated species is symmetrical, the observed line width will be determined only by the fraction of the 9 coordinated species by;

$$\Delta\nu/\eta_r = P_9\Delta\nu_9^0 \quad (6)$$

Effect of Anion Concentration. The change in $\Delta\nu/\eta_r$ due to the anion concentration increase may be interpreted in terms of the following several reasons:

1) Some kinds of the anions can replace the water molecules in the first coordination sphere of La^{3+}. This changes the symmetry of the molecule and, hence, the field gradient.

2) The activity of water decreases as the anion concentration increases. This has the effect of reducing the coordination number.

3) So far as the ions outside the first coordination sphere can be treated as point charges, fluctuations from a spherical Debye-Hückel charge distribution also contribute to the relaxation process.

Among the above three reasons, 2) and 3) do not depend strongly upon the difference in the anions of the same charge. At least, they can be considered to have similar concentration dependences. Therefore, the large difference in the concentration dependence between NO_3^- and X^- ions shown in Figs. 1 and 2 is caused primarly by 1).

Only a few studies have been made of the formation constants of lanthanum halide and nitrate. Spectrometric study[13] has shown that K_1 for $LaCl^{2+}$ is −0.2, while that for $La(NO_3)^{2+}$ is 0.26, which is smaller than that for $LaCl^{2+}$. On the other hand, ion-exchange study[14] has shown that K_1 and K_2 for $La(NO_3)^{2+}$ and $La(NO_3)_2^{1+}$ are 0.25 and 0.18 respectively. Depending on the experimetal method used, these values differ. However, even if we compare the formation constants derived from the same method, the large difference between the $\Delta\nu/\eta_r$ of nitrate and

8) R. E. Richard and B. A. Yorke, *Mol. Phys.*, **6**, 289 (1963).
9) J. Reuben and P. Fiat, *J. Chem. Phys.*, **51**, 4918 (1969).
10) With a=4.0 Å,[2] $\eta=10^{-2}$ poise, and T=300°K, Eq. (2) yields $\tau_c=6.8\times10^{-11}$ sec.
11) The largest observed chemical shift in this experimental series, corresponding to that of the $La(NO_3)_3$ concentrated aqueous solution relative to the diluted aqueous solution, is about 100 cps.
12) J. A. Pople, W. G. Shneider, and H. J. Bernstein, "High Resolution Nuclear Magnetic Resonance Spectroscopy," Chap. 10, McCraw Hill, London (1959).
13) K. L. Mattern, UCRL-1407 (1951).
14) R. E. Kriss and Z. A. Sheka, *Radiokhimiya*, **4**, 312 (1962).

halides can not be explained. Two probable explanations for the above discrepancy are that NO_3^- acts as a bidentate ligand[15] and that halide ions can not form an inner-sphere complex.[16]

If the line width of each species were known, the successive formation constants could be obtained by successive approximation and least-square fitting, using the observed line width, the total metal amount, and the anion concentration. Unfortunately, we have obtained no information about the line widths except for the line width at an infinite dilution. However, at a very low concentration where only the mononitrato complex is a dominant species, the $\Delta\nu/\eta_r$ for the mononitrato complex can be obtained by using the K_1 value (0.25) and the line width at an infinite dilution (141 cps$\cdot\eta_r^{-1}$). The calculated value for $La(NO_3)^{2+}$ is about 600 cps$\cdot\eta_r^{-1}$. It is confirmed that the highest $\Delta\nu/\eta_r$ is about 600 cps$\cdot\eta_r^{-1}$ at 1.9 M $La(NO_3)_3$ and that $\Delta\nu/\eta_r$ decreases above this concentration. Assuming that it is capable of forming an inner-sphere complex up to three NO_3^- ions, and considering the above confirmation, it may be concluded that the $\Delta\nu/\eta_r$ of $La(NO_3)_2^{1+}$ is above 600 cps$\cdot\eta_r^{-1}$, while that of $La(NO_3)_3$ is smaller than that of $La(NO_3)_2^{1+}$ due to the symmetrical configuration of the complex.

Effect of Coordination-number Change.[17] It has been shown in coordination chemistry that perchlorate ions do not form any complexes with metal ions in the low-concentration range. The ^{17}O NMR study[9] also supports this fact. As has been described previously, halide ions also form no inner-sphere complexes with lanthanide ions in the low-concentration range. Therefore, the decrease in the $\Delta\nu/\eta_r$ values of these salts can be explained in terms of the change in the hydration number of the lanthanum ion according to the following equilibrium:

$$La(H_2O)_9^{3+} \rightleftharpoons La(H_2O)_8^{3+} + H_2O \qquad (7)$$

The thermodynamic stability constant can be expressed as:

$$^tK_{8,9} = \frac{a_9}{a_8 \cdot a_{H_2O}} = \frac{y_9}{y_8 \cdot y_{H_2O}} \cdot {}^cK_{8,9} \qquad (8)$$

$$\left({}^cK_{8,9} = \frac{C_9}{C_8 \cdot C_{H_2O}}\right)$$

where the subscripts 9 and 8 indicate $La(H_2O)_9^{3+}$ and $La(H_2O)_8^{3+}$ species and where a, y, and C mean the activity, the molar activity coefficient, and the molar concentration respectively. The activity coefficient of H_2O in a ionic solution is measurable. However, the meaning of the activity coefficient of $La(H_2O)_9^{3+}$ and $La(H_2O)_8^{3+}$ is not known. The measured activity coefficient may be the averaged value of these two species.

If we assume that the 8 coordinated species is a symmetrical species and has a zero field gradient, the observed line width can be, from Eqs. (5) and (7), expressed as;

$$\Delta\nu = P_9 \cdot \Delta\nu_9 = {}^tK_{8,9} \cdot \frac{y_8 \cdot y_{H_2O}}{y_9} C_{H_2O} \Big/ \left(1 + {}^tK_{8,9} \frac{y_8 \cdot y_{H_2O}}{y_9} \cdot C_{H_2O}\right) \qquad (9)$$

Figure 3 shows the calculated concentration dependence of $\Delta\nu/\eta_r$ for various values of ${}^cK_{8,9}$ assuming a constant activity coefficient. However, this assumption is a very rough approximation; the activity coefficient ratio, $y_8 \cdot y_{H_2O}/y_9$ may strongly depend on the lanthanum salt concentration.

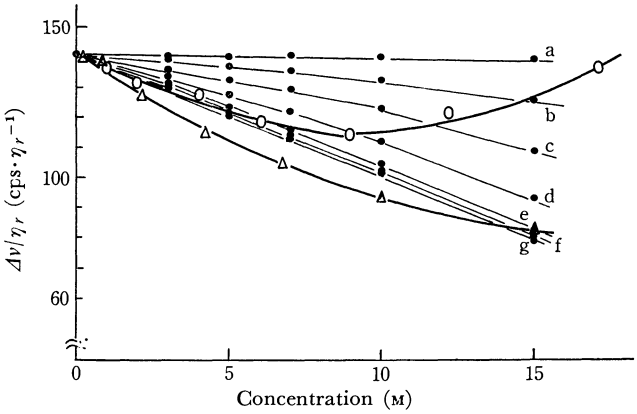

Fig. 3. The calculated concentration dependence of $\Delta\nu/\eta_r$ for various values of ${}^cK_{8,9}$

	${}^cK_{8,9}$		${}^cK_{8,9}$		${}^cK_{8,9}$		${}^cK_{8,9}$
a	1	c	0.03	e	0.003	g	0.0001
b	0.1	d	0.01	f	0.001		

The observed concentration dependence of $\Delta\nu/\eta_r$ for $LaCl_3$ △ and $La(ClO_4)_3$ ○ are also shown in the figure.

Figure 4 shows the concentration dependence of the fraction of $La(H_2O)_9^{3+}$ for various values of ${}^cK_{8,9}$. $\Delta\nu/\eta_r$ values calculated by using Eq. (8) are also given in the figure. The calculated $\Delta\nu/\eta_r$ values range from 140 to 25700 cps$\cdot\eta_r^{-1}$ as ${}^cK_{8,9}$ changes from 1 to 0.0001. However, considering the experimental facts that the highest $\Delta\nu/\eta_r$ observed in this experimental series is about 1000 cps$\cdot\eta_r^{-1}$ and that the change to 8 coordination takes place in the high-concentration range, such low formation constants as 0.01 to 0.0001 and such high formation constants as 1.0 are thought to be unlikely.

Even if we take the values of ${}^cK_{8,9}$ ranging from 0.1 to 0.01, as plausible constants, there are still large deviations from the observed values. However, these deviations may be compensated for if we take into account errors due to the decrease in y_{H_2O} with the concentration increase and due to the change in y_8/y_9. The differences in the kind of anions shown in Fig. 4 may come from the different dependencies of $y_8 \cdot y_{H_2O}/y_9$ on the salt concentration.

Effect of an Additional Electric Field due to Ions. $\Delta\nu/\eta_r$ values for the halides and perchlorate, after reaching the minimum value, increase in the middle to high concentration range. According to Hertz,[7] these increases can be explained as the result of an

15) C. C. Addison and N. Logan, "Advance in Inorganic and Nuclear Chemistry," Vol. 6, Academic Press, New York (1964), p. 72, 136.

16) G. W. Brady, *J. Chem. Phys.*, **33**, 1079 (1960).

17) There still exists a possibility that the hydrolysis changes the line width. To check this, we measured the effect of the acid ($HClO_4$) concentration on $\Delta\nu/\eta_r$, but found no significant change other than the experimental error.

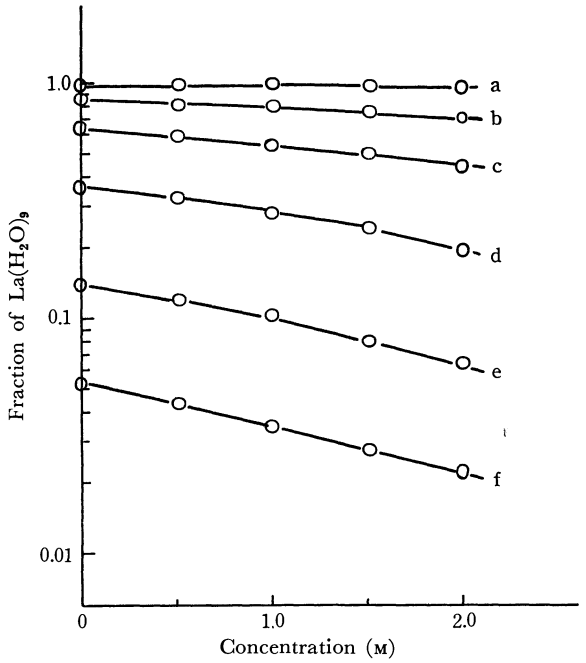

Fig. 4. The calculated concentration dependence of the fraction of $La(H_2O)_9$ and $\Delta\nu_9/\eta_r$ for various values of ${}^cK_{8,9}$.

	${}^cK_{8,9}$	$\Delta\nu_9/\eta_r$ (cps·$\eta_r{}^{-1}$)		${}^cK_{8,9}$	$\Delta\nu_9/\eta_r$ (cps·$\eta_r{}^{-1}$)
a	1	143.8	d	0.01	396.9
b	0.1	166.7	e	0.001	2,691
c	0.03	226.1	f	0.0001	25,691

additional electric field due to other ions which are spherically distributed around the central ion. He treated ions as point charges which are in a uniform distribution outside of the central ion with a radius of a. However, in strongly dissociated dilute electrolytes, the Debye-Hückel charge distribution is valid. Eisenstadt and Friedman[18] treated them by means of this distribution. In either case, such a relaxation mechanism due to the additional electric field is considered to be the same for both anions and cations. The ratio of the relaxation rate of the cation to that of the anion is, from by modifying Eqs. (31)—(36) of Ref. 7 and Eq. (5.11) of Ref. 18, approximately given by:

$$\frac{\Delta\nu_{\text{anion}}^{\text{ion-ion}}}{\Delta\nu_{\text{cation}}^{\text{ion-ion}}} = A\left(\frac{Q_{\text{anion}}}{Q_{\text{cation}}}\right)^2\left(\frac{(1-\gamma_\infty)_{\text{anion}}}{(1-\gamma_\infty)_{\text{cation}}}\right)^2 \qquad (10)$$

where A is $((2I+3)/I^2(2I+1))_{\text{anion}}/((2I+3)/I^2(2I+1))_{\text{cation}}$, where $(1-\gamma_\infty)$ is the Sternheimer antishielding factor.

To understand whether the relaxation mechanism proposed by Hertz is predominant in this case for both ions, the relaxation rate for ${}^{79}Br$ in the $LaBr_3$ solution has been measured and compared with the theoretical value calculated by using Eq. (10). With the value of $eQ_{La}=0.5e\times10^{-24}$ cm^2, $eQ_{Br}=0.34e\times10^{-24}$ cm^2, $(1-\gamma_\infty)_{La}=69.0$,[19] $(1-\gamma_\infty)_{Br}=98.0$,[20] and A=9.8,

18) M. Eisenstadt and H. Friedman, *J. Chem. Phys.*, **44**, 1407 (1966).
19) R. E. Watson and A. J. Freeman, *Phys. Rev.*, **135**, 1209 (1964).
20) E. G. Wikner and T. P. Dass, *ibid.*, **109**, 360 (1958).

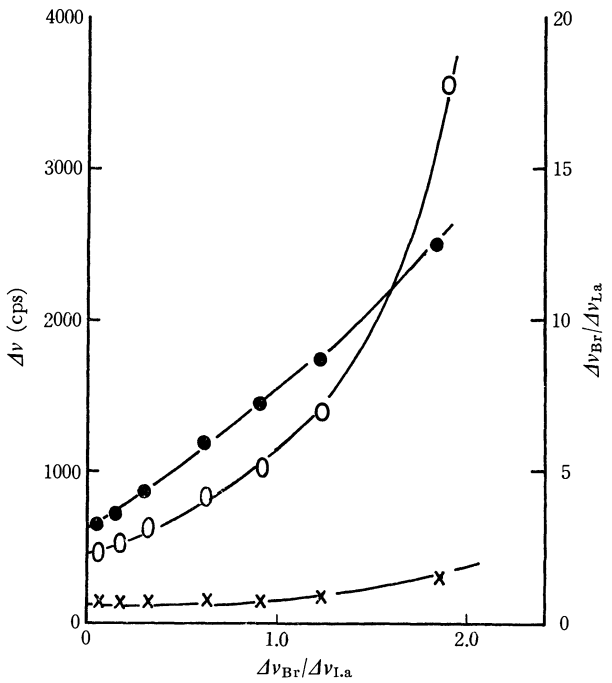

Fig. 5. The concentration dependence of ${}^{139}La$ and ${}^{79}Br$ line widths and $\Delta\nu_{Br}/\Delta\nu_{La}$.
○ ${}^{79}Br$, × ${}^{139}La$, ● $\Delta\nu_{Br}/\Delta\nu_{La}$

the calculated value of Eq. (10) is 10.9. However, it is very hard to obtain an accurate $\Delta\nu_{Br}^{\text{ion-ion}}/\Delta\nu_{La}^{\text{ion-ion}}$ ratio experimentally, since the observed relaxation rate of ${}^{139}La$ consists of two parts:

$$\Delta\nu_{Br}/\eta_r = \Delta\nu^0{}_{Br} + \Delta\nu_{Br}^{\text{ion-ion}} \qquad (11)$$

$$\Delta\nu_{La}/\eta_r = P_8\Delta\nu_8{}^0 + P_9\Delta\nu_9{}^0 + \Delta\nu_{La}^{\text{ion-ion}} \qquad (12)$$

where $\Delta\nu^0{}_{Br}$ is the line width of ${}^{79}Br$ at an infinite dilution. To obtain an accurate $\Delta\nu_{Br}^{\text{ion-ion}}/\Delta\nu_{La}^{\text{ion-ion}}$ ratio experimentally by using Eqs. (11) and (12), it is necessary to ascertain the value of $P_8\Delta\nu_8{}^0+P_9\Delta\nu_9{}^0$; however, this can not be obtained accurately in the present investigation.

Conclusions. Through the study of the ${}^{139}La$ relaxation times, we can draw the following conclusion: a) The line width at an infinite dilution is determined by the rapid exchange of two hydrated species; symmetrical $La(H_2O)_8{}^{3+}$ and unsymmetrical $La(H_2O)_9{}^{3+}$ are the most probable in the solution;
b) In the solutions of nitrate and sulfate, the formation of inner-sphere complexes is thought to be a main reason for the increase in $\Delta\nu/\eta_r$. This explanation is consistent with the result of ${}^{17}O$ NMR study of lanthanide aqueous solutions;[9]
c) The change in the hydration number is found to be the most probable explanation for the decrese in the $\Delta\nu/\eta_r$ of halide and perchlorate solutions, and
d) The effect of an additional electric field gradient due to anions is found to be present, but to be less effective than the other relaxation mechanisms.

The authors wish to express their deep gratitude to Professors Shizuo Fujiwara and Yoji Arata of the University of Tokyo and to Dr. Tadashi Yanagihara for their interest and encouragement during this work.

Four Radical Species Produced Photochemically in the Solid Mixture of Acridine and Acridan

Shigeya NIIZUMA, Hiroshi KOKUBUN, and Masao KOIZUMI

Department of Chemistry, Faculty of Science, Tohoku University, Katahira, Sendai

(Received August 11, 1970)

It has been established from measurement of the fusion curve that a 1 : 1 complex of acridine and acridan is formed in the solid state. The complex has an absorption band at 400—500 nm and is considered to be of C-T character although hydrogen bonding plays a role in complexing. Excitation of this complex gives rise to four radical species which display the corresponding characteristic ESR signals *a*, *b*, *c*, and *d*. The line width of *a* (α) and the line separations of *b*, *c*, *d* (β, γ, δ) are $\alpha=18.0\pm3.5$, $\beta=112\pm2$, $\gamma=137\pm5$, $\delta=212\pm6$ gauss. Studies on the dependence of the relative intensities of *a*, *b*, *c*, and *d* upon the acridine-acridan ratio and upon the length of irradiation have led to the conclusion that *a* and *b* are due to C- and N-radicals (the latter, triplet with separation of 44 gauss) and *c* and *d* are two kinds of radical pair. Detection of $\Delta M=\pm2$ transition at 1670 gauss (with 9337.4 MHz) also confirmed the above assignment of *c* and *d*. It is likely that the mutual transformation occurs only during irradiation. It is concluded that C-radical is more stable than N-radical in agreement with the result in fluid state. An interesting decay feature of signal *a* was found and was given a plausible interpretation.

The photoreduction of acridine in the fluid state has been extensively investigated and four main features in the reaction have been elucidated. 1) Photoreduction in alcohols occurs mainly at singlet excited state but a higher $T(n\text{-}\pi^*)$ can participate in the reaction to some extent in methanol and to a very little extent in ethanol.[1-3] 2) Although the lowest $T(\pi\text{-}\pi^*)$is not a reactive state in alcohol, it can be in some cases, for example in tetrahydrofuran.[7] 3) Reaction occurs in general *via* two mechanisms; *viz.*, a molecular mechanism in which no intermediate can be detected by the usual flash technique, and a radical one in which half reduced radical can be captured in a free state.[1,2,8] 4) Two types of radical are produced generally,[9,10] *i.e.*, C-radical and N-radical, with an unpaired electron on 9-C-atom and on N-atom, respectively. Only C-radical is produced in the photoreduction in alcohols,[9]while in the reaction between acridine and acridan, the former yields C-radical and the latter, N-radical. We have been continuing ESR studies on the radical anions[12] and neutral radical species[14] related to acridine and acridan. However, the information obtained on the neutral radical species is still very scanty. We have only succeeded in detecting an ESR spectrum of radical species originating from acridine or acridan in the crystalline medium of benzene, tetrahydrofuran or of t-butanol at 77°K. In these media, the ESR spectrum appeared upon irradiation of acridan (except benzene) or by excitation of acridine in the acridine-acridan mixture. During the course of this work, we found that the mixture of acridine and acridan is colored yellow at 77°K, suggesting the formation of a certain molecular complex.

The present paper deals with an extension of the above work. By irradiating at 430—600 nm, the mixture of acridine and acridan in crystalline benzene medium at 77°K, or by irradiating the mixture with no medium, obtained either by distilling off the solvent or by fusing the mixture of two components, we could detect four types of ESR signal, two of which are due to radicals in the free state, most likely C- and N-radical, and the other two kinds of radical pair. The study on the fused sample was particularly successful and it has been established that a molecular complex, perhaps of C-T type, consisting of 1 acridine and 1 acridan is formed in the solid state having an absorption band ~450 nm. The excitation in this band region produced four different radical species, the behavior of which was studied under various conditions.

Experimental

Materials. Acridine, ethanol, and tetrahydrofuran were purified as described previously.[13] Preparation and purification of acridan were carried out in the same way. Benzene of Wako Junyaku G.R. was used without further purification. *N*-methylacridan was prepared by reducing *N*-methylacridinium iodide (obtained from acridine and

1) M. Koizumi, Y. Ikeda, and T. Iwaoka, *J. Chem. Phys.*, **43**, 1869 (1968).
2) M. Koizumi, Y. Ikeda, and H. Yamashita, This Bulletin, **41**, 1056 (1968).
3) According to Kellmann and Dobois,[4] singlet excited state and $T(n-\pi^*)$ are reactive in methanol, while Vander Donkt and Porter[5] concluded that only singlet excited state is reactive in isopropanol. Wilkinson and Dubois[6] claimed that singlet excited state mainly participates in the reaction in ethanol. All these statements are essentially consistent with our data.
4) A. Kellmann and J. T. Dubois, *J. Chem. Phys.*, **42**, 2518 (1965).
5) E. Vander Donkt and G. Porter, *ibid.*, **46**, 1173 (1967).
6) F. Wilkinson and J. T. Dubois, *ibid.*, **48**, 2651 (1968).
7) Y. Miyashita, S. Niizuma, H. Kokubun, and M. Koizumi, This Bulletin, **43**, 3435 (1970).
8) V. Zanker and G. Prell, *Ber. Bunsenges. phys. Chem.*, **73**, 791 (1969).
9) A. Kira and M. Koizumi, This Bulletin, **42**, 625 (1969).
10) V. Zanker and his collaborators observed the formation of C- and N-radicals in the photooxidation of acridan derivatives and some other reactions.[11,12]
11) V. Zanker, E. Erhardt, and H. H. Mantsch, *Z. Phys. Chem. N. F.*, **58**, 1 (1968).
12) V. Zanker and E. Erhardt, *Ber. Bunsenges. Phys. Chem.*, **72**, 267 (1968).
13) S. Niizuma and M. Koizumi, This Bulletin, **41**, 795 (1968).
14) S. Niizuma and M. Koizumi, *ibid.*, **41**, 1090 (1968).

methyliodide) by $NaBH_4$. It was recrystallized from ethanol. mp 94.5—95.5°C.

Apparatus and Procedures. As a light source for UV irradiation, an Ushio USH-500 mercury lamp or a Toshiba SHL-100 UV was used and for the visible light irradiation, a tungsten lamp of Kondo 1 kW or 500 W was used. The filters used for visible light, $CuSO_4$ aq. solution—Toshiba VY-43 (or VY-45 or VY-48), for the UV irradiation, Hoya crystal U-2—Toshiba L-1A—water, 1 cm. The former transmits 430 (or 450 or 480) ~600 nm while the latter only 365 nm. In the case of irradiation at shorter wavelengths, the light from a mercury lamp was passed through 1 cm layer of water. Samples were prepared as follows. Removal of the solvent from benzene or tetrahydrofuran solution of acridine and acridan, was performed in a sample tube for ESR by distillation *in vacuo*. The fused sample was prepared by keeping a ESR capillary cell containing a mixture of acridine and acridan in an electric furnace, after having been evacuated and sealed, at temperatures higher than melting point by 5—15°C for 1—5 min. It was then cooled rapidly with water. A JEOL P-10-type ESR spectrometer (X-band 100 Kc modulation) was used for the measurement of $\Delta M=\pm 1$ transition, and a Hitachi Model 771-ESR spectrometer for that of $\Delta M=\pm 2$.[15] Electronic spectra were taken with a Hitachi EPS-3T spectrophotometer.

Results and Assignment of Radical Species

Experiment Using a Sample in a Benzene Medium. A solution of acridine and acridan in benzene colored yellow when frozen. Upon irradiation by 365 nm at 77°K, it turned brown and gave an ESR spectrum. The signal intensity grew rapidly in a few minutes irradiation and then the increase became much more gradual. Figures 1a and b give two examples of ESR signals for acridine: acridan=1 : 2 and 1 : 5, respectively. All the spectra are characterized by four peaks (or shoulders) *a*, *b*, *c*, *d* as shown in the figure. The line width of *a* (ΔH_{msl}) and the line separations of *b*, *c*, and *d* are denoted by α, β, γ, and δ, respectively. Although the relative intensities

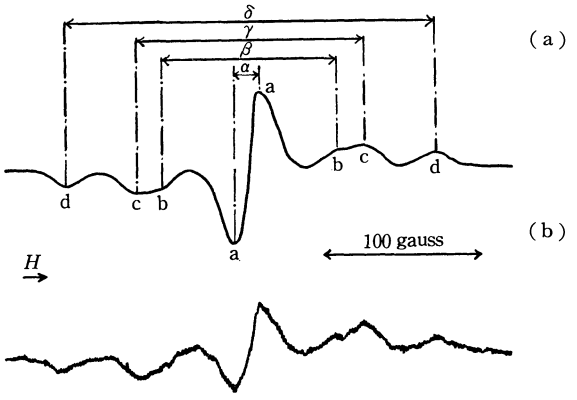

Fig. 1. ESR signals of the mixtures of acridine and acridan in benzene media.
(a) acridine : acridan=1 : 2
(b) acridine : acridan=1 : 5

15) Thanks are due to Dr. Y. Ikegami and Dr. M. Iwaizumi of Chem. Res. Inst. of Non-Aqueous Solution for use of their instrument.

a, *b*, *c*, and *d* varied according to experimental conditions (for instance, *b* which exists as a shoulder in this figure becomes a peak in some other cases), the values of α, β, γ, and δ remained almost the same. The mean values determined from a number of experiments are

$$\left.\begin{aligned}\alpha &= 18.0 \pm 3.5 \text{ gauss}\\ \beta &= 106 \pm 2 \text{ gauss}\\ \gamma &= 135 \pm 2 \text{ gauss}\\ \delta &= 226 \pm 9 \text{ gauss}\end{aligned}\right\} \quad (1)$$

The g-value of peak *a* was 2.004. As a general tendency, peak *a* becomes stronger with the increase in the mole ratio of acridine to acridan, $[A]/[AH_2]$. An over-all survey of the results leads us to the conclusion that these four peaks (or shoulders) are ascribed to different radical species.

Figure 2 shows the effect of irradiation time upon the intensity ratio (evaluated from the peak to peak height of the differential curve) of *a* and *c* for a sample for which $[A]/[AH_2]=1$.[16] A remarkable change in

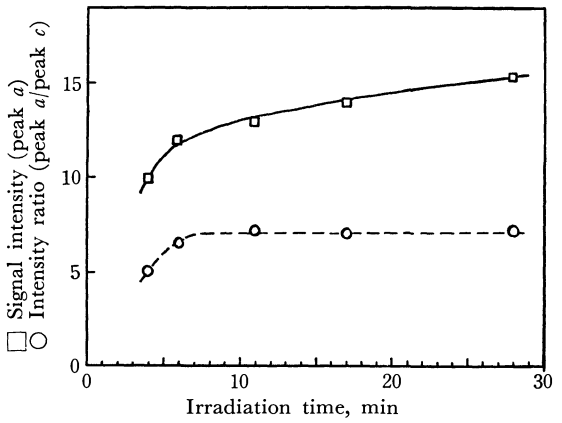

Fig. 2. Effect of irradiation time upon intensity ratio of *a* to *c*. ($[A]/[AH_2]=1$).

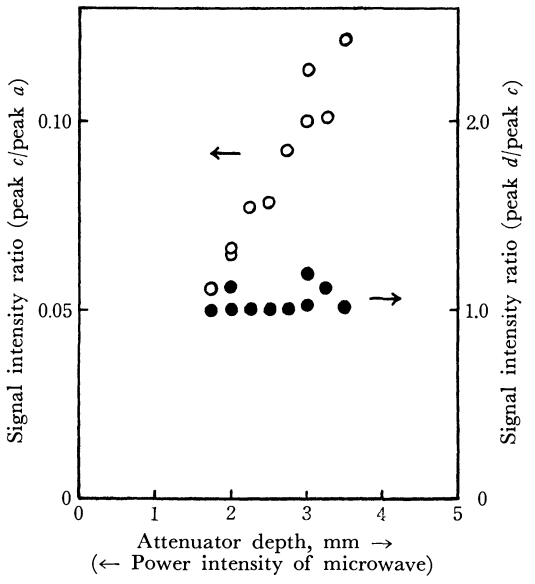

Fig. 3. Effect of microwave intensity upon intensity ratio of *c* to *a* and that of *d* to *c*.

16) It is thought that *b* contributes to the intensity of *c* to some extent.

this ratio during the first seven minutes clearly indicates that *a* and *c* are different species. Figure 3 shows the effect of microwave intensity upon the intensity ratio of *c* and *a* and that of *c* and *d* for the sample, $[A]/[AH_2]=1/2$. It is evident that the former changes remarkably while the latter remains almost constant. This again shows that *a* and *c* are different species.

Although at 77°K the signals are quite stable and the intensity scarcely decreases after being kept for a night in the dark, they decay more rapidly with rising temperature. The temperature effecton the signal shape and the decay rate was examined from −27 to −158°C using the sample for which $[A]/[AH_2]=1$. Since the signal intensities are so weak at higher temperatures that the peaks other than *a* are almost comparable with the noise, the decay could be measured only at peak *a*. It is remarkable that all the decays in the whole temperature region could be analysed as a sum of two first order terms. As an example a decay at −57°C is shown Fig. 4. Furthermore, moderately good Arrhenius plots were obtained for the two rate constants k_S (short lived species) and k_L (long lived species) as shown in Fig. 5. The activation energies obtained are for the former 3.3 and for the latter 3.9 kcal/mol. The values of k_S and k_L at various temperatures are listed in Table 1. It should be noted that the point at 114°K deviates a great deal from the linear plot. Since the second order transition point of benzene exists at 110°K[17] the above anomaly can be ascribed to the different state of benzene medium, if the error in temperature measurement is taken into account. The ratios of the quantity of short lived and long lived species immediately after the interruption of irradiation, which were evaluated by extrapolating the linear part in the later stage (decay of a long lived species), to the time origin, are plotted against the temperature in Fig. 6. There is a clear tendency for a relative yield of short lived species to increase with the rise of temperature. The temperature effect strongly suggests that there are two independent species (or states) with different stability and that the four radical species do not mutually transform thermally. If this were to occur such a simple behavior as obtained would not be expected.

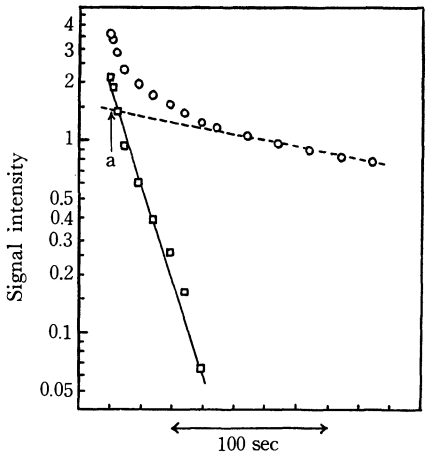

Fig. 4. Decay of signal intensity measured at peak *a*.

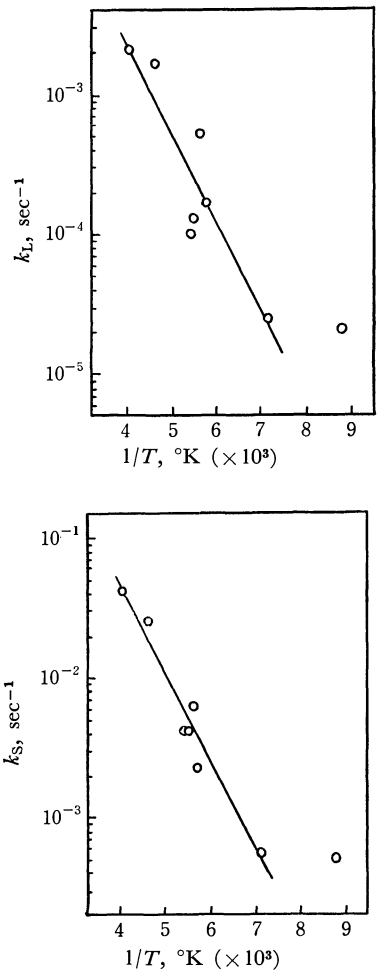

Fig. 5. Arrhenius plots for the decay constants of long lived (k_L) and short lived species (k_S).

Table 1. Decay constants of short-lived (k_S) and long-lived species (k_L) at various temperatures

Temp., °C	Irrad. time	k_S (sec^{-1})	k_L (sec^{-1})
−158—−160	12 min 4 sec	5×10^{-4}	$2.2_2 \times 10^{-5}$
−131—−134	24 min 40 sec	5.5×10^{-4}	$2.5_0 \times 10^{-5}$
−95— −97	26 min 20 sec	$2.2_4 \times 10^{-3}$	$1.6_7 \times 10^{-4}$
−95	ten several min	6.17×10^{-3}	$5.2_4 \times 10^{-4}$
−89— −92	5 min 35 sec	4.21×10^{-3}	1.02×10^{-4}
−85— −89	15 min 11 sec	4.16×10^{-3}	1.29×10^{-4}
−57	several min	2.50×10^{-2}	1.67×10^{-3}
−27	several min	4.17×10^{-2}	$2.1_7 \times 10^{-3}$

The results obtained for the solid mixture of acridine and acridan prepared by evaporating the solvent (benzene or tetrahydrofuran) were essentially the same as above. The sample was deep yellow at room temperature, suggesting again the strong interaction between the two components. The ESR signals obtained upon 365 nm irradiation at 77°K showed similar spectral feature and spectral change during irradiation.

17) N. N. Semenov, "XVIIIth International Congress of Pure and Applied Chemistry. Special Lectures," Butterworths, London (1962), p. 353.

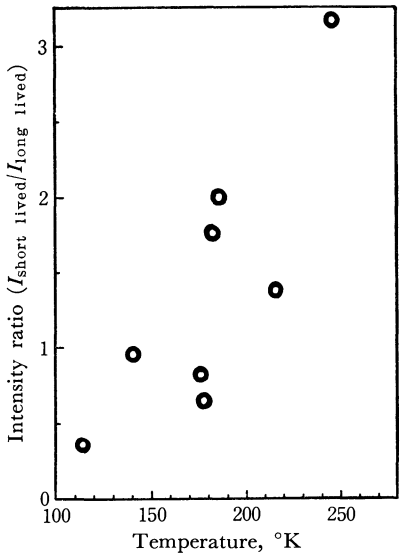

Fig. 6. Ratio of the quantity of short lived and long lived species plotted against temperature.

Experiments Using the Solid Sample prepared by Fusing the Mixture of Acridine and Acridan. The ESR signals obtained in this sample had better S/N ratios than the preceeding ones and the spectral feature could be studied more satisfactorily.

First, the electronic spectrum of the sample was taken by the following procedure. A mixture of acridine and acridan 1 : 1 in ratio was placed between two cover glasses (for melting point determination), and was fused on a hot plate. The liquefied deep yellow mixture spread as a thin film and remained almost transparent after being solidified. The spectrum obtained is shown in Fig. 7. An acridine film prepared similarly as above is shown by a broken line and the two cover glasses by a dotted line. An absorption band is clearly observed in the region 400—500 nm.

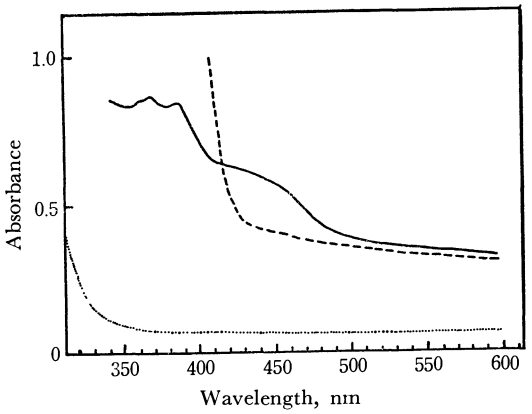

Fig. 7. Absorption spectrum of the mixture of acridine and acridan, 1 : 1 in ratio.

In order to confirm the existence of a molecular complex if any, and determine its composition, melting points of the mixture of acridine (mp 110°C) and acridan (mp 172°C) in various composition were measured. The phase diagram obtained is given in Fig. 8. It is seen that a clear peak exists at a mole fraction of

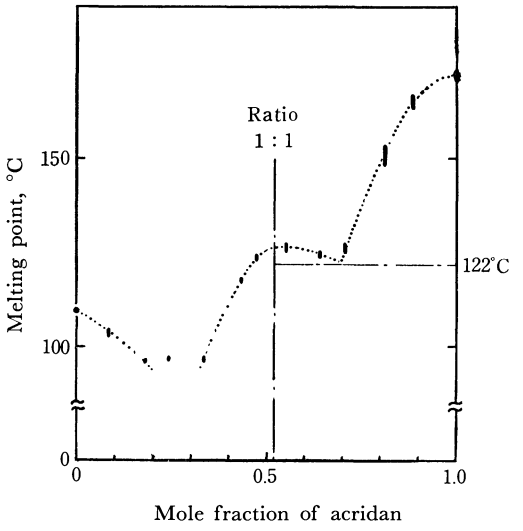

Fig. 8. Fusion curve for the mixture of acridine and acridan.

~0.52 corresponding to 1 : 1 complex. It appears that another peak exists near 0.25 which suggests the formation of 3 : 1 complex.

The ESR signals obtained upon irradiation were found to change considerably in their spectral shape according to the composition, and the assignment of the four species could be made on the basis of these spectral changes. In spite of the change in shape, the values of parameters β, γ, and δ were almost the same as those obtained for the sample in a benzene medium.

$$\left.\begin{aligned}\beta &= 112 \pm 2 \text{ gauss}\\ \gamma &= 137 \pm 5 \text{ gauss}\\ \delta &= 212 \pm 6 \text{ gauss}\end{aligned}\right\} \quad (2)$$

Figure 9 shows a typical example of the spectral change depending on the composition. Mixing ratio [A]/[AH_2] is written on the left, and the exciting light and irradiation time on the right side. Similar signals were obtained by 365 nm- and 480—600 nm-irradiations. From a number of experiments, we could conclude as follows. 1) The relative intensity of peak *a* compared with other peaks increases with [A]/[AH_2]. 2) It increases with the length of irradiation time. 3) The intensity ratio of peak *d* to *c* is scarcely affected by the irradiation time and depends largely on the composition. As a general tendency, it increases with [A]/[AH_2]. 4) Generally the sum of *c* and *d* is relatively large in the low [A]/[AH_2] region and becomes quite small in the high region. Hence in the former case, peak *b* tends to be hidden in peak *c*, while in the latter case it becomes difficult to be observed. 5) The resolution of peak *a* becomes worse whenever peak *b* is prominent.

From 3), there is no doubt that *c* and *d* are due to different species and the spectral shape of *c* and *d* have been made quite clear from (a)—(c) in Fig. 9. If separately drawn, they are certainly of types C and D in Fig. 10. From the line shapes and large line separations, there is scarcely any doubt that they are due to $\Delta M = \pm 1$ transitions of certain radical pairs. If so, the signal due to transition $\Delta M = \pm 2$ should exist at the magnetic field of about half strength. In fact,

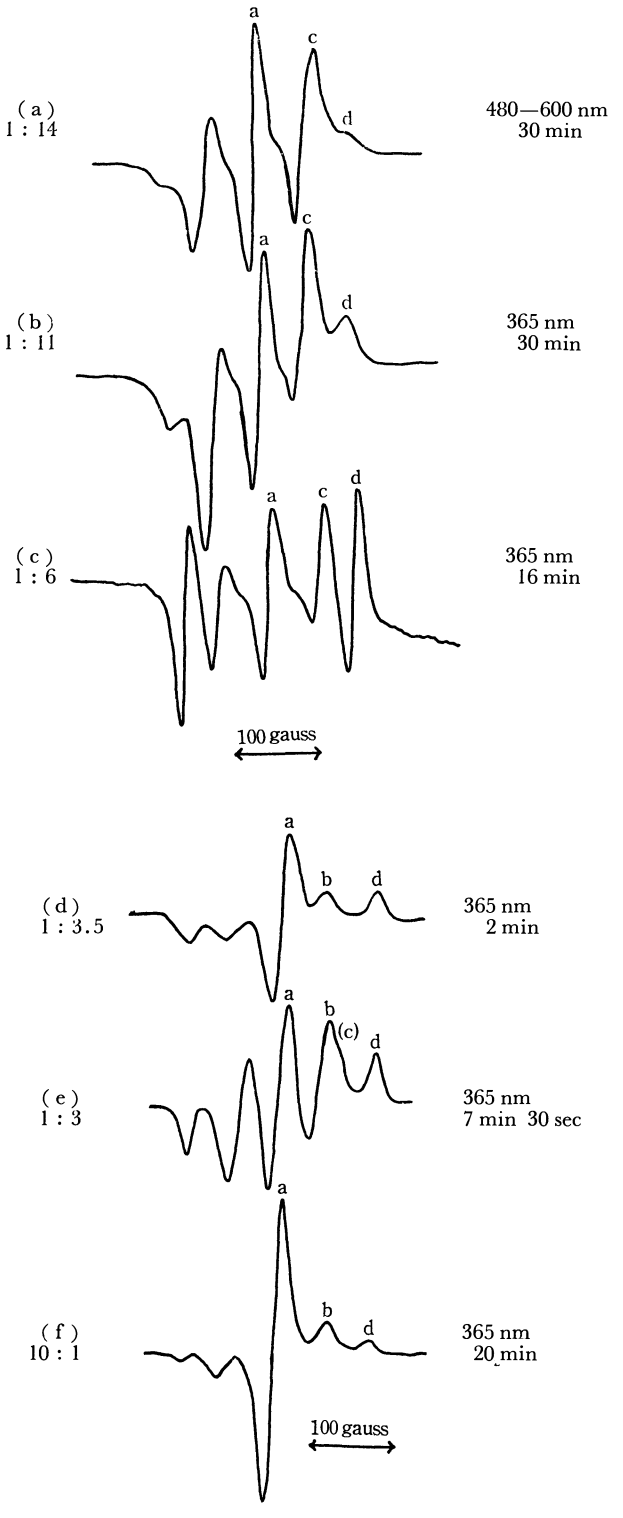

Fig. 9. Some examples of ESR spectrum.

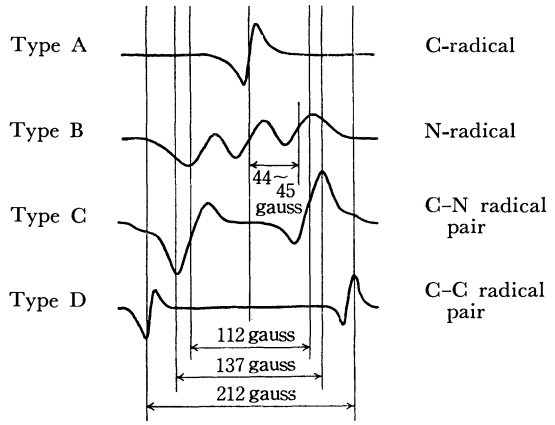

Fig. 10. ESR signal for each radical species.

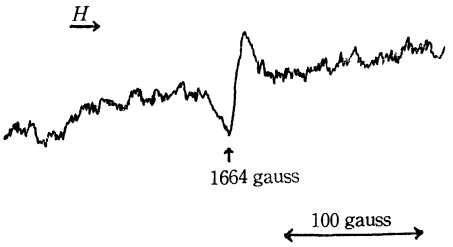

Fig. 11. ESR signal of radical pair due to $\Delta M = \pm 2$ transition.

we could succeed in detecting a signal at 1670 gauss (with 9337.4 MHz) as shown in Fig. 11. The sample composition was acridine : acridan=1 : 5.4. The irradiation was performed for 50 min with no filter, using a 1 kW superhigh pressure mercury lamp. The signals at higher magnetic field in this sample, consisted of peaks *a*, *b*, and *d*. Peak *c* was observable only in a certain period of irradiation. For the measurement of $\Delta M = \pm 2$ transition, the sensitivity was raised 22 times that for the $\Delta M = \pm 1$ measurement. In spite of the above success, it is not certain whether this signal corresponds to type C or D. However, if the two species were to be captured at the same time, they would appear at about the same position and could not be discriminated.

c- and *d*-species now having been identified as radical pairs, unpaired electron distances for *c*- and *d*-species were evaluated by the usual method[18] as 6.0 and 5.1 Å, respectively, from the zero field splitting constant $D=$ 137 and 212 gauss (assuming $E=0$).

a- and *b*-species were assigned as follows. From 5), it can be judged that peak *b* has its component in peak *a*. That the decay for the sample in a benzene medium consists of two first order terms also supports the superposition of the two species. Hence the spectral shape of A and B can be drawn as shown in Fig. 1 . Type A with g=2.004 and $\Delta H_{msl}=18$ gauss always appears under various conditions. Type B is a triplet with a separation of 44 gauss and is easily observed in the high $[A]/[AH_2]$ region. There is scarcely any doubt that *a* and *b* are due to C- and N-radical, respectively, the existence of which has already been fully established in the previous works.[9,11,19] The value of coupling constant 44 gauss is reasonable for ^{14}N taking anisotropy into account.[20]

18) Y. Kurita, H. Ohigashi, and M. Kashiwagi, *Bussei*, **9**, 87 (1968).
19) T. Shida and A. Kira, This Bulletin, **42**, 1197 (1967).
20) Isotropic and anisotropic hyperfine coupling constants of N-radical in *t*-butyl chloride are (private communication from Dr. T. Shida) $A_{iso}=34.6$ $A_{aniso}=6.80$ gauss.

Discussion

Now that the ESR signals of the solid mixture of acridine and acridan have been successfully analysed and the four radical species, N-radical, C-radical and two kinds of radical pair have been identified, the problems to be considered are 1) the primary step for the formation of these species and 2) the nature and behavior of these radical species. They may be answered to some extent on the ground of the present results.

It is most likely that the molecules of acridine and acridan in a solid state interact in such a way that a molecular complex is formed by hydrogen bonding and that the formation of radical species is intimately connected with it. The formation of 1 : 1 complex in a solid state has been fully established by the L-S phase diagram of acridine and acridan in addition to a new band observed in the region 400—500 nm. That the hydrogen bond plays a role in this complex formation, is supported by the following facts. The formation of a similar 1 : 1 complex takes place between 9,9-dimethylacridan having N-H hydrogen and acridine (or 9-methylacridine),[21] whereas according to our experiment, *N*-methylacridine is not colored when it is fused with acridine, and furthermore, a mixture of various compositions (deaerated) never gives the ESR signal upon irradiation at 365 nm at 77°K. Thus it is reasonable to say that the hydrogen bond of N···H-N type is involved in the complex formation.

It is well known, however, that in a fluid state acridine and acridan show no sign of such hydrogen bonding. For instance, the electronic spectrum of a mixture of acridine and acridan is a mere superposition of the spectrum of two separated components.[22] In addition, it has been established from the fluorescence quenching experiment that acridan does not form a hydrogen bond with triethylamine which is a most powerful H-acceptor. In view of these facts, the hydrogen bond between acridine and acridan in a solid state must be very weak. Furthermore, the appearance of a new band at 400—500 nm strongly suggests the C-T character of the complex.

The formation of radical species was achieved only by irradiation, but the fact that the light of 480—600 nm is as equally effective as 365 nm implies that excitation of the complex leads to the radical formation in question. Thus we have schematically

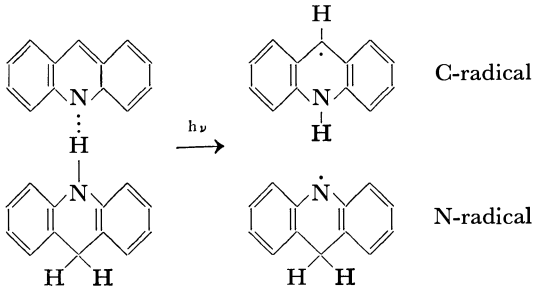

The radical species primarily produced are considered to be a radical pair consisting of C-radical and N-radical and also the equimolar separated C- and N-radicals. During the course of irradiation, however, mutual transformation occurs, and this is the reason why the spectral shape varies according to the experimental conditions.

For the nature and behavior of radical species, we have to be content with a speculative discussion in present stage. Generally the formation of radical pair is considered to depend on the diffusibility of the produced radicals, which in turn is determined by the magnitude of kinetic energy associated with the radicals and also by the rigidity of the medium. In the present case, however, we are tempted to consider the problem in terms of C- and N-radical. Assuming that the mutual transformation occurs only during irradiation, the increase in the yield of C-radical (*a*-species) and also the increase in the ratio of C-radical (*a*-species) to *c*-species both with the increase in irradiation time (finding 2) and Fig. 2) indicates that C-radical is produced efficiently from other species photochemically. The finding 1) that the yield of C-radical increases with the higher $[A]/[AH_2]$ may then be interpreted to be due to the fact that the reaction

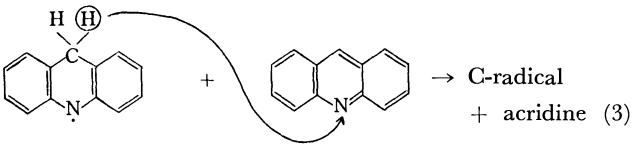

occurs photochemically not but the reaction

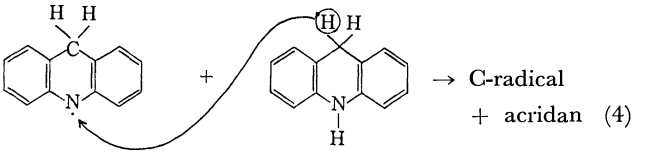

This is reasonable from the thermodynamic stability of acridine and acridan.

Finding 4) (the yield of N-radical (*b*-species) is small when $[A]/[AH_2]$ is very small) can be interpreted that under such a condition it is difficult for process (3) to occur, and N-radical chiefly exists as a radical pair. This will be supported again from another point of view. The above statements are consistent with Zanker's view as well as ours, *i.e.*, C-radical is more stable than N-radical in the fluid state[7] or in the rigid solvents.[11]

It is most remarkable that the decay of *a* species is reproduced by the superposition of the two first order processes. Since the disappearance of radical occurs only by recombination or disproportionation process, the first order decay may require that radicals exist in pairs and in such neighborhood to each other that mutual attraction favors their encounter but not close enough for the ESR signal of the radical pairs to become observable. As such radical pairs lying apart, the following two are conceivable, *i.e.*, C-C radical pair (apart) and C-N radical pair (apart) (N-N radical pair does not exist appreciably since N-radical cannot exist in excess). If such a hypothesis be admitted,

21) W. L. Semon and D. C. Craig, *J. Amer. Chem. Soc.*, **58**, 1278 (1936); D. C. Craig, *ibid.*, **60**, 1458 (1938).

22) S. Niizuma, Y. Ikeda, and M. Koizumi, This Bulletin, **40**, 2249 (1967).

then a short-lived species may be assigned as C-C radical pair (apart) and long-lived species as C-N radical pair (apart). The higher yield of a short-lived species at higher temperatures is consistent with this assignment, because the N-radical→C-radical process may more easily occur at higher temperatures.

Finally the radical pairs *c* and *d* may be assigned as follows. From the finding that *d* increases with the larger $[A]/[AH_2]$ as compared with *c*, *d*-species may be assigned as C-C radical pair and in consequence *c*-species as C-N radical pair. Finding 4) (*c*-species mainly exists in very low $[A]/[AH_2]$ and the non-appearance of N-radical in this region, *cf. a*, *b*, and *c* in Fig. 9) can be understood by the above assignment, because it is difficult for reaction (3) to occur under such a condition.

BULLETIN OF THE CHEMICAL SOCIETY OF JAPAN, VOL. 44, 341—347 (1971)

Mechanistic Studies on the Photochemical Oxidation of Phenothiazine with Oxygen in Ethanol

Teiki IWAOKA, Hiroshi KOKUBUN, and Masao KOIZUMI

Department of Chemistry, Faculty of Science, Tohoku University, Katahira, Sendai

(Received September 3, 1970)

It has been established that phenothiazine (PTH) undergoes photooxidation, $PTH+O_2 \xrightarrow{h\nu} PT\cdot+HO_2$ in the aerated ethanol (dehydrated!) yielding a neutral radical as a stable product. The reaction is a one photon process and the reactive state is triplet PTH. It has further been established that the reaction occurs *via* a molecular complex (PTH-O_2) most likely of C-T type, which has the absorption at ~385 nm and decays with the first order rate constant of 1.6×10^2 sec^{-1}. A similar transient C-T complex has been found to be produced from triplet PTH and dimethylisophthalate (weak electron acceptor) (absorption ~385 nm, decay constant 2×10^3 sec^{-1}) with almost the diffusion controlled rate constant, although the eventual reaction does not occur. Thus in case of (PTH-O_2), reaction (PTH-O_2)→PT·+HO_2 occurs while in case of (PTH-DMIP), the analogous reaction does not. Behavior of radical species (containing radical cation and (PTH-O_2)) produced in the rigid aerated ethanol at 77°K has also been studied. The present C-T complex is interesting in the point that it is produced *via* triplet state of donor and has a rather long lifetime.

The oxidation reaction of phenothiazine has long been attracting much attention owing to the interest in the pharmacological properties of its substituted derivatives. As Lhoste *et al.* have pointed out,[1] this compound having π-electrons in number differing from $4n+2$ as a result of two heteroatoms in the central ring, is very liable to be oxidized photochemically as well as chemically. It is seen in literature that phenothiazine (PTH) (I) converts by one step oxidation to radical cation (II) or neutral radical (III) according to the experimental conditions, and by the additional oxidation to diamagnetic phenazothionium ion (IV).

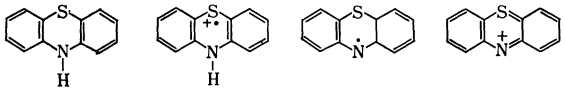

(I) (II) (III) (IV)

Shine and Mach[2] who have made systematic studies on the related compounds, observed that I in the aqueous acetic acid transforms to II photochemically but they proposed on the ground of the difference in ESR signals that in 95% aqueous ethanol, III instead of II is produced photochemically. Gilbert *et al.*[3] reported on the other hand, that by oxidation with perchlorate in acetonitrile, II is produced as a perchlorate salt, and in the reaction of II with water in acetonitrile, III is produced as a primay product. According to them, III is also obtained from II by treating it with triethylamine or D_2O. Although it is possible to capture IV electrochemically, for instance by anodic oxidation of I in acetonitrile,[4] II and III are extremely stable under the ordinary conditions. However, reactions of these species have been reported in some systems, for instance, III produced in DMSO-Ac_2O mixture (deaerated) gradually converts to two types of dimer and certain higher polymers.[5] Even at liquid nitrogen temperature, PTH is photooxidized rather easily. For instance, Kasha[6] reported that upon irradiation of PTH in EPA (perhaps aerated), a new absorption peak at 19300 cm^{-1} with another weak band ~22900 cm^{-1} appeared, indicating the formation of II. In addition, ESR studies on II were reported by Odiot and Tonnard,[7] and those of II and III by Shine *et al.*[2] and also by Gilbert *et al.*[3]

In spite of all these observations, there is still no detailed kinetic work made on this photooxidation reaction as far as we know. The purpose of the present investigation is to confirm that the photochemical

1) J. M. Lhoste, C. Helene, and M. Ptak in Proceedings of the International Symposium of Triplet States, Beirut, 1967 (Cambridge Univ. Press, New York, 1967).
2) H. J. Shine and E. E. Mach, *J. Org. Chem.*, **30**, 2130 (1964).
3) B. C. Gilbert, P. Hanson, R. O. C. Norman, and B. J. Sutcliffe, *Chem. Commun.*, **1966** (6), 161.
4) J. P. Billon, *Bull. Soc. Chim. Fr.*, **1960**, 1784.
5) Y. Tsujino, *Tetrahedron Lett.*, **38**, 4111 (1968).
6) B. R. Henry and M. Kasha, *J. Chem. Phys.*, **47**, 3319 (1967).
7) S. Odiot and F. Tonnard, *J. Chim. Phys.*, **61**, 382 (1964).

oxidation of phenothiazine with oxygen yields III in *pure et hanol* and to elucidate the detailed mechanism of the reaction, by the steady light experiment and by the flash technique. ESR studies on the radical species produced at 77°K have also been made.

Experimental

Materials. Phenothiazine of Tokyo Kasei E.P. grade was recrystallized two times from ethanol. Ethanol of Wako Junyaku G.R. grade was used without further purification unless otherwise described. DMIP of Tokyo Kasei E.P. grade was purified by recrystallization from ethanol, carbon tetrachloride and finally from G.R. grade ethanol. It was then dried *in vacuo* for one day.

Procedures and Apparatus. The 253.7 nm irradiation was made using a Toshiba 6 W low pressure germicidal lamp and the 313 nm irradiation by a Toshiba 100W high pressure mercury lamp using, as a filter, potassium chromate 1×10^{-3} M, 0.05 N NaOH in a quartz cell of 5 mm thickness. The reaction was followed by a Hitachi EPS-3T spectrophotometer. A JEOL P-10-type ESR spectrometer (X-band, 100 kc modulation) was used for the ESR measurement. Apparatus and procedures for the flash experiment are the usual ones employed in our laboratory.

Results and Discussion

Steady Light Experiments. General Feature of the Steady Light Photooxidation: When the aerated solution of PTH in ethanol was irradiated by 253.7 nm or 313 nm, photoreaction of a simple type occurred as shown in Fig. 1. Isosbestic points are observed clearly at 241

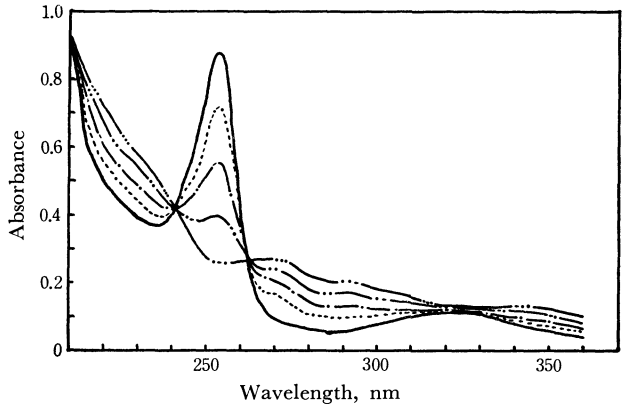

Fig. 1. Spectral change upon illumination (253.7 nm) of the phenothiazine solution in the aerated ethanol; —— 0 sec, ---- 75 sec, —·— 184 sec, —··— 340 sec, —···— 700 sec.
[PTH] = 2.6×10^{-5} M

and 263 nm. The spectrum obtained ultimately kept its shape for a few days. When the solution was degassed, practically no reaction occurred; irradiation for more than an hour caused the decrease of only 0.5% or so in optical density. It was checked that there is no essential spectral difference between the deaerated and aerated solution. The photoproduct was identified as a neutral radical by taking its ESR spectrum; thus the spectrum obtained was almost the same as that of a neutral radical reported by Gilbert *et al.*[3] and was quite different from that of radical cation which for the purpose of comparison, was produced in the concentrated sulfuric acid. It was ascertained further, that the hfs constants obtained by a simulation method agrees aproximately with those reported by Gilbert *et al.*[3] Thus our results have reconfirmed Shine and Mach's statement[2] and that reaction,

$$PTH + O_2 \xrightarrow{h\nu} PT\cdot + HO_2 \qquad (1)$$

occurs in ethanol. We thought however, that it is necessary to examine the effect of the presence of a small quantity of water in view of the experimental conditions employed by the previous workers. For instance, Shine and Mech[2] used 95% aqueous ethanol while Gilbert *et al.*[3] prepared a neutral radical by treating a radical cation (obtained by oxidizing PTH with perchloric acid in acetonitrile) with the buffered aqueous solution of pH 7. We therefore purified ethanol and removed a trace of water with much care and repeated the experiment with the so purified ethanol. The result was essentially the same, except that the kinetic feature of the reaction became a bit simpler (see below) and the quantum yield became a little larger. This may be due to the removal of impurities of aldehyde type, and the possibility of the scheme

$$\left.\begin{aligned} PTH + O_2 &\rightarrow PTH\cdot^+ + O_2^- \\ PTH\cdot^+ + H_2O &\rightarrow PT\cdot + H_3O^+ \end{aligned}\right\} \qquad (2)$$

is rejected.

Effect of Light Intensity: The runs for reaction were satisfactorily reproduced by linear $\ln(e^{\alpha cd}-1)$ *vs.* t plots when the inner-filter effect of photoproduct was taken into account.[8] It is to be noted that purification of ethanol does not alter the feature of the run except a little better linearity of the plot with a little larger slope. As is shown in Fig. 2, the rate of disappearance of PTH (evaluated from the initial slope of the run) is proportional to the light intensity. Thus the main reaction is a one photon process.

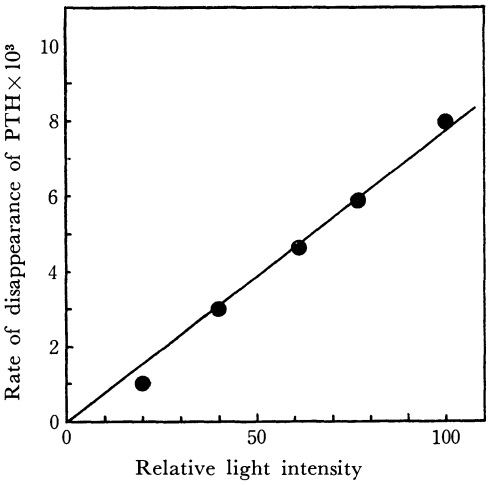

Fig. 2. Dependence of the rate of disappearance of phenothiazine on the light intensity; relative light intensity 100 corresponds to 8.8×10^{-9} M/cm² sec.

8) T. Iwaoka, S. Niizuma, and M. Koizumi, This Bulletin, **43**, 2786 (1970).

The Effect of Oxygen Concentration on the Rate: The overall reaction having been established (except for the reactions induced by HO_2) as

$$PTH + O_2 \rightarrow PT\cdot + HO_2 \quad (1)$$

the effect of oxygen concentration on the rate was examined in order to know the reactive state of PTH. For the system containing $\sim 10^{-6}$ M of oxygen, the rate decreased gradually but recovered by redissolving the oxygen through shaking the sample cell. It is to

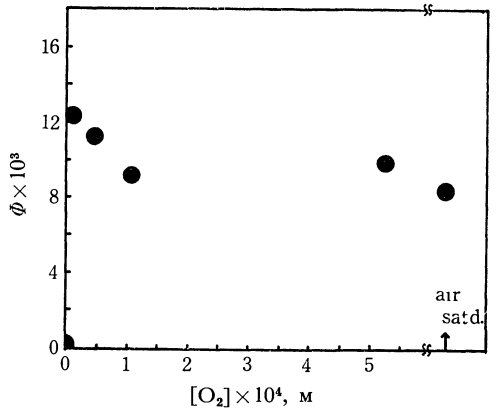

Fig. 3. Effect of oxygen concentration on the quantum yield of phenothiazine disappearance in ethanol; [PTH]= 3×10^{-5} M.

be added that a slight recovery of absorption was observed when the irradiation was stopped. This suggests the existence of very long lived intermediate (see below). Figure 3 gives the plot of quantum yield *vs.* the oxygen concentration. Although a little larger values were obtained at lower concentrations of oxygen, the reason for which is unknown, the quantum yields were almost constant when the concentration of oxygen was larger than 10^{-4} M. This strongly suggests that the triplet state is a reactive one.

The Effect of PTH Concentration on the Quantum Yield: Table 1 gives the quantum yields at various PTH concentrations. Since there is no concentration effect, we may conclude that the participation of the ground state PTH in the later stage of reaction does not occur in any sense.

Table 1. The effect of PTH concentration on the quantum yield, Φ

[PTH]	$\Phi \times 10^3$
$1.2_3 \times 10^{-5}$	6.6
$1.8_1 \times 10^{-5}$ a)	6.9
$2.6_0 \times 10^{-5}$ b)	8.6
$3.7_6 \times 10^{-5}$	6.4
$2.2_3 \times 10^{-4}$	6.4
$3.6_9 \times 10^{-4}$	6.2

a) G.R. grade ethanol was used.
b) Sample solution was prepared in the dried box, immediatetly after the purification of ethanol.
Other data were for the ethanol purified previously.

Studies on the Reaction Mechanism by the Flash Technique. Now that the overall reaction has been established to be very simple, the next problem is to make clear whether the reaction occurs as a real simple reaction or a complex one, and in the latter case to know the composing processes, in particular the primary one. Reasonable schemes other than a simple reaction are

$$\left.\begin{aligned} &PTH + O_2 \rightarrow PTH\cdot^+ + O_2^- \text{ (electron transfer)} \\ &PTH\cdot^+ + O_2^- \rightarrow PT\cdot + HO_2 \end{aligned}\right\} \quad (3)$$

$$\left.\begin{aligned} &PTH + O_2 \rightarrow (PTH\text{-}O_2) \text{ (formation of molecular complex)} \\ &(PTH\text{-}O_2) \rightarrow PT\cdot + HO_2 \end{aligned}\right\} \quad (4)$$

To solve the problem, the behaviors of transient species have been studied by the flash technique.

The Behaviors of Transient Species Produced in a PTH-O_2 System. Figure 4 shows the transient spectra for degassed PTH solutions in ethanol. These are assigned as T–T absorption on the ground that the peak (465

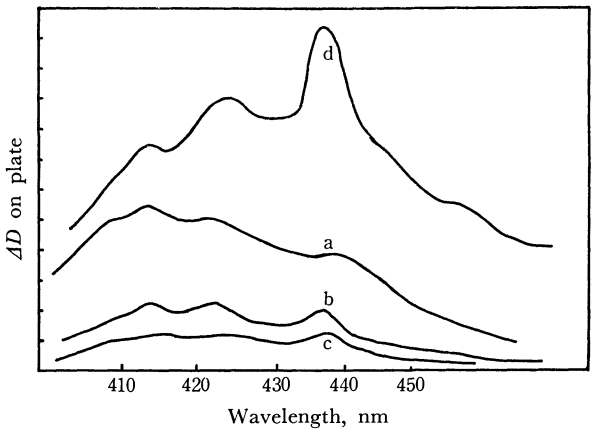

Fig. 4. Transient absorption spectra obtained by the flash photolysis of the degassed phenothiazine solution in ethanol (plate, orthochromatic): [PTH] = 2.2×10^{-4} M.
a: 82 μsec, b: 150 μsec, c: 780 μsec after flashing. d is a transient absorption at 82 μsec taken with a panchromatic plate.

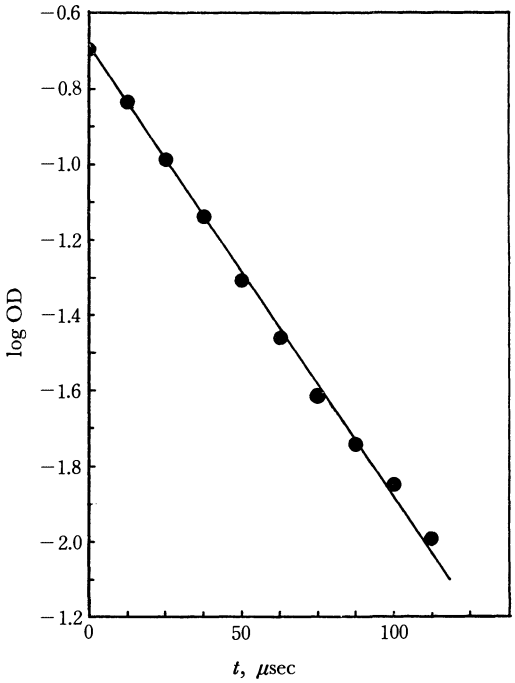

Fig. 5. First order decay of phenothiazine triplet state in deaerated ethanol (470 nm); [PTH] = 1.1×10^{-4} M.

nm) agrees with the peak of T–T absorption (467 nm) (77°K, EPA) reported by Kasha and Henry[6] and that the decay is first order with the rate constant of $1.5\pm 0.4\times10^{4}$ sec^{-1}. This is shown in Fig. 5. The decay curve suggests the existence of a small amount of another long lived species ($\tau_{1/2}$ a few sec) which might be a PTH$\cdot^{+}$ the reason for which will be described later.

In the aerated solutions, the T–T absorption did not appear at all and a new absorption band of small intensity was observed near 385 nm. A principal photoproduct obtained after several flashings was identified as a neutral PT$\cdot$, because the spectral shape was similar to that obtained by the steady light irradiation. A slight difference might be due to the reaction product originating from radical cation. This band (hereafter designated as a X-band and a species giving rise to this band as X-species) decays as a first order process with the rate constant of 1.6×10^{2} sec^{-1}. Figure 6 gives the spectrum drawn from the decay curves at different wavelengths. In parallel with the decay at 385 nm, the absorption increased at 290 nm where the absorption of both photoproduct and the initial PTH exist. This indicates that X-intermediate converts to PT$\cdot$ or reconverts to PTH. When 0.1 N HCl was added to the solution, X-band did not appear and a new band was observed near 510 nm (perhaps radical cation, see below). Thus there is no doubt that X-intermediate is a precursor of reaction PTH$+O_2\rightarrow$ PT$\cdot+HO_2$.

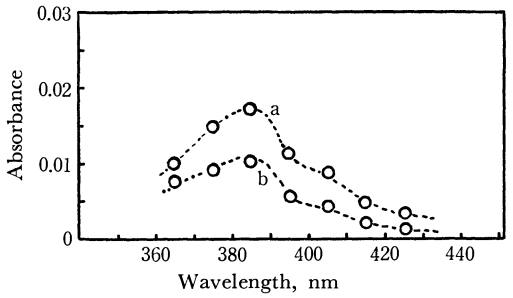

Fig. 6. Absorption of X-species in the aerated ethanol solution of phenothiazine; [PTR]$=1.9\times10^{-5}$ M.
a, immediately after flashing
b, 5 msec after flashing

Experiment using DMIP as an Electron Acceptor. We have now reached to the step to elucidate the nature of X-species. To confirm more definitely that it is a molecular complex with oxygen, we have studied the transient species when DMIP instead of oxygen was used as an acceptor. DMIP is a weak electron acceptor[9] and it was expected to act just like oxygen as far as electron transfer is concerned, but not to produce a stable neutral radical because reaction (PTH^{+}-DMIP^{-})$\rightarrow$PT$\cdot+$DMIPH$\cdot$ is not likely to occur. Another reason for performing such an experiment was that the intensity of X-band in the case of oxygen was considered to be too weak to make accurate quantitative studies. This way of attacking the problem has proved to be very successful.

The transient spectra were measured varying the concentrations of DMIP from 10^{-6} to 10^{-2} M at a fixed PTH concentration of 1.14×10^{-4} M. It was established that the eventual reaction does not occur by a number of flashing. As Fig. 7 shows, the transient spectrum

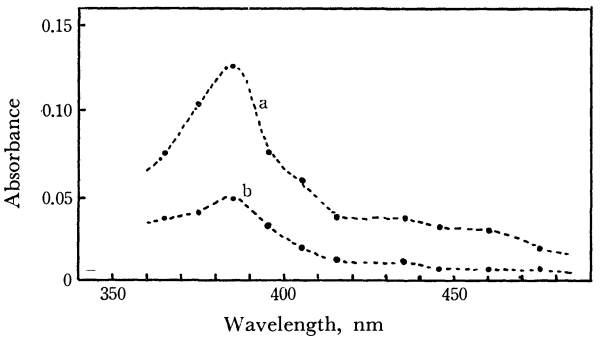

Fig. 7. Transient absorption spectra obtained upon flashing the degassed ethanol solutions of PTH-DMIP; [PTH]$=1.1\times10^{-4}$ M, [DMIP]$=1\times10^{-2}$ M.
a, immediately after flashing
b, 5 msec after flashing

is very much like X-band in the case of oxygen. The decay is first order and the rate constant obtained is 1.7×10^{3} sec^{-1} independent of wavelengths. When the concentration of DMIP was lower than 5×10^{-5} M, T–T absorption of PTH was observed at 420—470 nm. The triplet PTH decayed faster with the increasing DMIP concentration. Figure 8 gives the plot of the

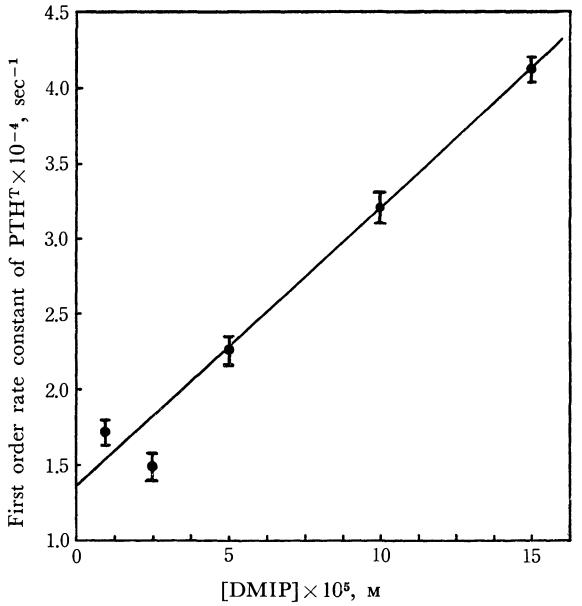

Fig. 8. Dependence of the apparent first order rate constant of phenothiazine triplet state upon the concentration of dimethylisophthalate; [PTH]$=1.1\times10^{-4}$ M.

apparent first order decay constant against [DMIP]. From the slope, the second order rate constant for the disappearance reaction of PTH^{T}, PTH$^{T}+$DMIP$\rightarrow$ was evaluated as 1.9×10^{9} M^{-1}sec^{-1}. The yield of X-intermediate increases with the increases in [DMIP]. Assuming that the interaction between triplet PTH

9) M. Koizumi and H. Yamashita, *Z. Physik. Chem. N. F.*, **57**, 103 (1968); H. Yamashita, H. Kokubun, and M. Koizumi, This Bulletin, **41**, 2312 (1968).

and DMIP consists only of reaction $PTH^T + A \xrightarrow{k_r} X$ (A stands for DMIP), the following equation can easily be derived.

$$[OD_{PTH^T}]_0/[OD_X]_\infty = (\varepsilon_{PTH^T}/\varepsilon_X)(1 + k_d/k_r[A]) \quad (5)$$

where $[OD_{PTH^T}]_0$, optical density of triplet PTH immediately after flashing, $[OD_X]_\infty$, optical density of X immediately after disappearance of PTH^T, and k_d, the decay constant of triplet PTH.

As shown in Fig. 9 the plot of $[OD_{PTH^T}]_0/[OD_X]_\infty$ against 1/[DMIP] gives a straight line as is expected from (5). The rate constant k_r as evaluated from the slope and the intercept, is 1.3×10^9 M^{-1}sec^{-1}. Thus

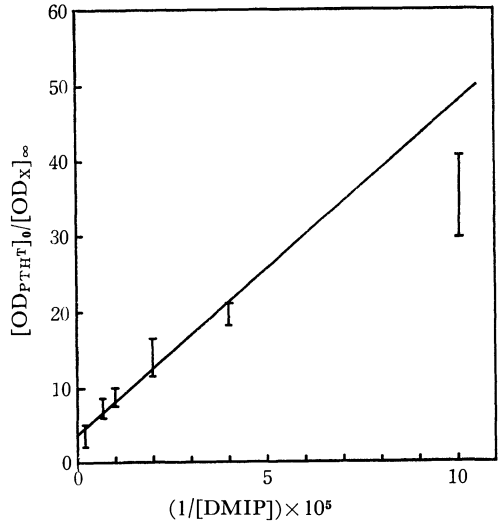

Fig. 9. Plot of $[OD_{PTH^T}]_0/[OD_X]_\infty$ against 1/[DMIP], as obtained at 470 nm; $[PTH] = 1.1 \times 10^{-4}$ M.

it has been verified that the reaction between triplet PTH and DMIP occurs with an almost diffusion controlled rate and produces intermediate X.

Intermediate X in the present system also decays as first order independent of the concentration of DMIP. Table 2 gives the results. It is to be added that a small quantity of a very long lived species ($\tau \sim$sec) is suspected to exist from the decay feature of X. This species appears to decay as second order and may perhaps be a radical cation.

Figure 10 shows the transient spectrum for the PTH solution in the degassed acidic ethanol (0.1 N HCl) containing 2.5×10^{-6} M of DMIP. This agrees with the spectrum of cation radical obtained in *s*-butylchloride by γ-radiolysis[10] and that in H_2SO_4 reported by Shine and Mach.[2] There is no sign of X-band. The decay is second order with the rate constant of $k/\varepsilon = 2.8 \times 10^5$. Thus in an acidic medium intermediate X is not produced and only the formation of radical cation occurs.

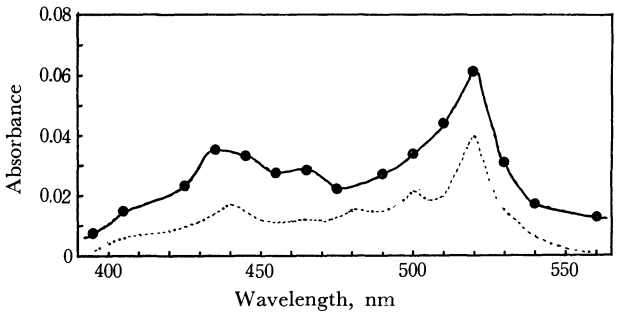

Fig. 10. Transient absorption spectrum immediately after flashing the solution of phenothiazine in the degassed acidic ethanol (0.1 N HCl) containing 2.5×10^{-6} M DMIP; $[PTH] = 1.1 \times 10^{-4}$ M.
----: cation radical produced by γ-radiolysis in *s*-butylchloride[10] at 77°K (1/20 of the measured absorbance)

We may now conclude that X-species is a molecular compound most likely of C–T character. Although there is a possibility that this is a triplet exciplex, it may perhaps be a C–T complex in the ground state which is unstable as compared with the two separated components. If this is true, the peak position of X-band should be well related with those of other stable complexes. It is well known that the wave number of C–T absorption is linearly related with the electron affinity of the acceptor. Phenothiazine with very low ionization potential of 6.96 eV,[11] forms stable

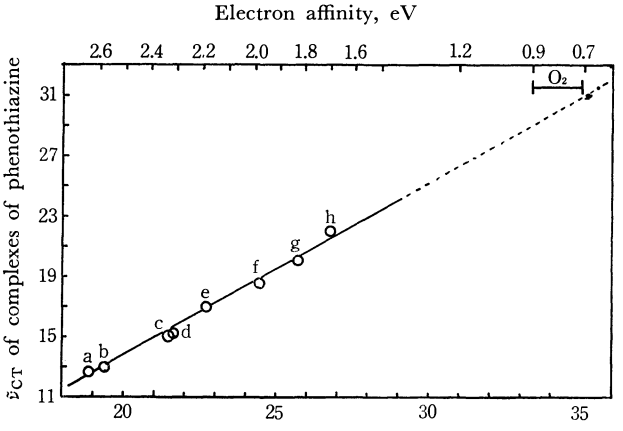

Fig. 11. Plots of $\tilde{\nu}$ for complexes of phenothiazine with various acceptors against $\tilde{\nu}$ for the corresponding hexamethylbenzene complexes; Acceptor; a: bromanil, b: chloranil, c: 2,6-dichloro-*p*-benzoquinone, d: 2,5-dichloro-*p*-benzoquinone, e: monochloro-*p*-benzoquinone, f: *p*-benzoquinone, g: 1,3,5-trinitrobenzene, h: 2,4,6-trinitrotoluene, cited from Ref. 12. Electron affinity scales were added by the authors.

Table 2. Decay constant of X

[DMIP]	1.0×10^{-6}	2.5×10^{-6}	5×10^{-6}	1.0×10^{-5}	1.5×10^{-5}	5.0×10^{-5}	1.0×10^{-4}	1×10^{-2}
Rate const. $\times 10^{-3}$	2.1	2.3	1.8	2.0	2.3	2.7	2.2	1.7

10) We are grateful to Dr. T. Shida of Inst. of Phys. and Chem. Res. Tokyo for presenting this spectrum.

11) A. Fulton and L. E. Lyons, *Aust. J. Chem.*, **21**, 873 (1968).

C–T complexes with a large number of electron acceptors. According to Foster and Hanson,[12] a good linear relation exists between $\tilde{\nu}_{CT}$ and the electron affinity of acceptor. This is shown in Fig. 11. The electron affinity of oxygen is 0.7—0.9 eV and that of DMIP is considered to be a little less than 1.5 eV (the value for phthalic anhydride). The peak position of 385 nm for oxygen and DMIP does not appear to deviate so much from the linear relation of Foster and Hanson as shown in Fig. 11.

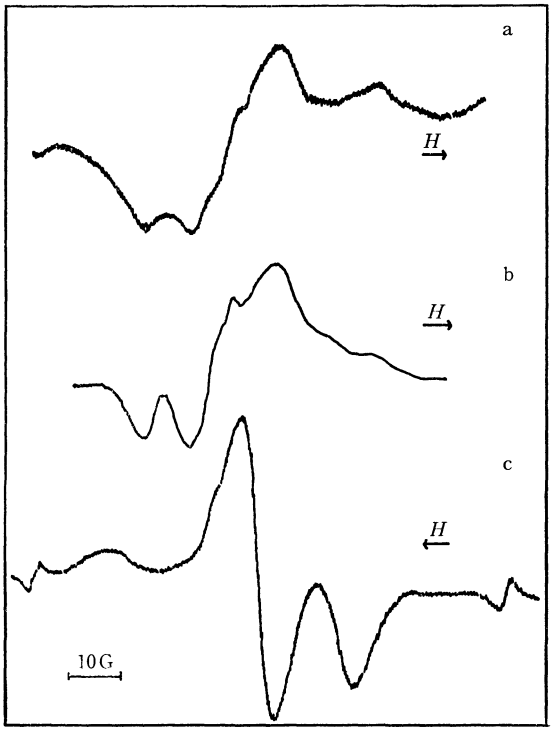

Fig. 12. ESR spectra at 77°K for a) photoproduct obtained upon illumination of the aerated ethanol solution of phenothiazine, b) phenothiazine radical cation in concentrated H_2SO_4, and c) phenothiazine neutral radical produced at room temperature.

Behavior of the Radical Species Produced when the Aerated Solution of PTH in Ethanol was Irradiated at 77°K. To get further information on the radical species related to the present reaction, ESR studies have been made on the photoproduct obtained by irradiation at 77°K. Upon irradiation of the PTH solution in ethanol at 77°K by the light 250—400 or >340 nm, the solution gradually colored from yellow to light brown and the absorption spectrum of the resultant rigid solution displayed peaks at 385 and ~520 nm. This implies that both X-intermediate and the radical cation are formed at 77°K. The ESR spectra observed were of a simple shape independent of the exciting wavelength. Figure 12 shows the ESR spectra for a) the photoproduct, b) the radical cation produced in a concentrated sulfuric acid solution and c) the neutral radical produced at room temperature, all measured at 77°K. The agreement of a) and b) leads to the conclusion that the main radical species produced at 77°K is the radical cation. The colors of the solution for a) and b) were both light brown while that for c) colored pink with a tint of violet. This also supports the above assignment. The formation of the radical cation at 77°K agrees with the observation of Henry and Kasha[6] in EPA. From the above findings, we may conclude that X-intermediate is diamagnetic and reaction (PTH^+-O_2^-)→$PT\cdot+HO_2$ does not occur photochemically.

It is to be added that in the degassed medium, 313 or 365 nm irradiation produces mainly ethanol radical which could be identified by comparing the ESR signals with those reported by Niizuma and Koizumi.[13]

Next, the sample irradiated at 77°K was brought to room temperature. The ESR spectrum showed a complicated structure and was quite different from that of the neutral radical. This sample upon cooling to 77°K, showed the ESR spectrum which clearly showed the coexistence of the neutral and cation radicals. This is very natural since X-species converts quickly to the neutral radical at room temperature. An interesting conclusion which we can draw from this experiment is that the radical cation is rather stable and can coexist with the neutral radical, because it took more than an hour to carry through the above experiment. The radical cation once formed does not seem to transform to the neutral radical so easily.

The results obtained by further irradiation are also interesting. Irradiation by 395 nm for more than two hours at 77°K caused very little formation of the neutral radical. This again indicates the stability of X-species against irradiation. When the radical cation obtained at 77°K was brought to room temperature and was irradiated by the $\lambda>395$ nm light, then the color turned from light brown to pink violet. The ESR spectrum at room temperature clearly showed three peaks due to ^{14}N and at 77°K it consisted mainly of the neutral radical (with a very small contribution of the radical cation). We may conclude that the radical cation when excited, transforms to the neutral radical while the neutral radical is rather stable against irradiation.

General Discussion and Some Future Problems. The present work has established that the final photoproduct for the aerated PTH solution in ethanol at room temperature, is the neutral radical III. On the other hand, a large quantity of radical cation II was produced in the rigid ethanol at 77°K. The reason for this difference may be as follows. The formation of C–T type X-species may require the reorientation of the solvent molecules surrounding donor and acceptor to a higher extent, which is easy to occur at room temperature but not at 77°K. For radical cation II to be formed on the other hand, a pair of radical ions produced, must diffuse apart from each other utilizing the excess energy as the kinetic one of the two components prior to its dissipation to the surrounding medium. This may be more feasible in the rigid medium. The formation of II or III may also depend upon the solvent polarity and also on the acidity and basicity of the medium. For instance, the formation of II may be fovored by the high polarity of the solvent.

12) R. Foster and P. Hanson, *Biochem. Biophys. Acta*, **112**, 482 (1966).

13) S. Niizuma and M. Koizumi, This Bulletin, **41**, 1090 (1968).

As to the stability of radical species, it is easy to understand that III is stable, because the HO_2 radical produced by reaction, $PTH+O_2 \rightarrow PT\cdot+HO_2$ may quickly disappear in the succeeding reactions leaving only PT·. But the finding that radical cation II produced at 77°K can coexist with III for more than an hour, seems somewhat curious; O_2^- produced by reaction, $PTH+O_2 \rightarrow PTH\cdot^+ + O_2^-$ is expected to react according to $PTH\cdot^+ + O_2^- \rightarrow PT\cdot + HO_2$, if HO_2 is more stable than O_2^- in pure ethanol. That II remains stable might be due to reaction $O_2^- + H_3O^+ \rightarrow HO_2 + H_2O$, because the experiment was not performed in the purified ethanol.

Turning to the mechanism for the formation of III, it has been established on the basis of the experiments on PTH-O_2 and PTH-DMIP systems that intermediate X of C–T type is a precursor of the reaction. Further it has been concluded that X reacts as follows in the aerated solution,

$$(PTH^+\text{-}O_2^-) \begin{cases} \nearrow PTH + O_2 \\ \searrow PT\cdot + HO_2 \end{cases}$$

HO_2 disappearing in the succeeding reactions and thus leaving PT· as a stable radical. The reason why DMIP does not give the neutral radical is that reaction

$$(PTH^+\text{-}DMIP^-) \rightarrow PT\cdot + DMIPH\cdot$$

does not eventually occur, because even if it occurs the backward reaction $PT\cdot + DMIPH\cdot \rightarrow PTH + DMIP$ will soon ensue. The effect of environmental medium on the stability of this complex is again an interesting problem. By the analogy of exciplex, the stability may perhaps increase from nonpolar to weakly polar solvents and further, the molecular compound might gradually turn into the ion pair and finally to the separated ions as the solvent becomes from medium to highly polar. In this respect, we have made some preliminary experiments using acetonitrile and cyclohexane as solvents. In these solvents the photooxidation of PTH with oxygen occurred in the same way as in ethanol, $PTH+O_2 \rightarrow PT\cdot+HO_2$, and the transient spectra observed were very much like that of X in ethanol. Table 3 gives the comparison of the quantum yields of reaction (Φ) and the first order rate constant for the disappearance of X-spesies (k) in the three solvents. The results are understandable from the general nature of C–T complex. Thus in moderately polar solvents the complex becomes more stable than in nonpolar solvents. In addition, reaction $(PTH^+\text{-}O_2^-) \rightarrow PT\cdot + HO_2$ may occur more easily in nonpolar solvents. This causes the increase in Φ and may contribute to the increase in the k-value for cyclohexane.

Table 3.

	DK	Φ	k
Ethanol	24.3	6.5×10^{-3}	1.6×10^{2}
Acetonitrile	37.5	1.4×10^{-3}	1.4×10^{2}
Cyclohexane	2.02	2.4×10^{-2}	too fast to be measured

Studies on the solvent effects in the wider scope are desirable.

Studies on the present C–T type molecular complex from various view points will be interesting. Although X-species is most likely a C–T complex in the ground state, still a possibility of triplet exciplex may not be excluded altogether. It is desirable to develop the similar studies using acceptors of various strength including those constituting stable C–T complexes and to investigate their absorption and emission spectra (if any).

Admitting that the present C–T complex is an unstable ground state one, it can be said that it is a very novel type of reaction intermediate. A few years ago we proposed the formation of a somewhat similar molecular complex between eosine and oxygen in the aqueous solution,[14] but it was considered to be a solvent-shared ion pair ($D^+\cdots O_2^-$) having almost the same absorption band as that of free D^+. The present complex is produced in moderately polar solvents and has a quite different absorption band from that of free cation. Moreover, it has quite a long lifetime of more than msec. We believe that this is the first example of a molecular complex in the points that it is produced *via* triplet donor and acceptor and has such significant characteristics. It will be instructive to investigate the general nature of the intermediate of this type.

14) Y. Usui and M. Koizumi, This Bulletin, **40**, 440 (1967); Y. Usui, C. Iwanaga, and M. Koizumi, *ibid.*, **42**, 1231 (1969).

The Electronic Structure of Zeise's Salt, $[PtCl_3C_2H_4]^-$

Hajime KATÔ

Department of Chemistry, Faculty of Science, Kobe University, Nada-ku, Kobe

(Received August 13, 1970)

A semiempirical SCF MO method including all the valence electrons in a molecule has been applied to Zeise's salt, which is one of the most simple metal-olefin π-complexes. The electron-repulsion integrals are included explicitly in the present method. The results agree well with the available experimental data, indicating that the C-C bond order is equal to 1.545 and that the ethylene is tightly bound to platinum. An attempt to assign the observed bands to particular electron transitions has been made on the basis of a calculation of the transition energies and transition moments. We identify the band at 40700 cm^{-1} as the charge-transfer band corresponding to the electronic transition from ethylene to platinum. Several properties of Zeise's salt are calculated, and much information on the bonding is obtained.

Since Zeise isolated the first olefin complex, $K^+[PtCl_3(C_2H_4)]^-\cdot H_2O$, known as Zeise's salt,[1,2] a very large number of olefin complexes of platinum and other metals have been reported. Many reviews of the research of metal-olefin complexes have been reported by many investigators.[3–6] Zeise's salt is one of the most simple metal-olefin π-complexes. The research into the structure and bonding mechanism is interesting and important. The X-ray structure determination has shown that the ethylene molecule forms an approximately symmetrical π-type bond with the platinum atom and that the C–C bond length is 1.44(3) Å.[7] Infrared studies of Zeise's salt have been reported by many investigators.[8–14] Recently, Raman and infrared spectra have been obtained by Hiraishi.[15] He identified the C–C stretching frequency as a strong, polarized Raman line at 1243 cm^{-1}, while the two Pt-C stretches were thought to be at 405 cm^{-1} (symmetric) and 493 cm^{-1} (antisymmetric). He concluded that the C_2H_4 group has many similarities to the C_2H_4 group in ethylene oxide and that the ethylene is tightly bound to the Pt(II) atom.

Various electronic structures have been proposed to explain the bonding scheme between the ethylene molecule and platinum, but that scheme was not satisfactorily explained until 1953. Chatt and Duncanson[8] then applied Dewar's description[16] of the bonding in silver-olefin complexes to Zeise's salt. The σ-type bond is formed by the overlap of a $5d6s6p^2$ hydrid orbital of the platinum atom with the filled π-orbital of the ethylene molecule. The π-type bond is formed by the overlap of a $5d6p$-hydrid orbital of the platinum atom with the vacant anti-bonding π-orbital of the ethylene molecule; this is referred to as "back-bonding." This interpretation of the bonding is now generally accepted for metal-olefin π-complexes.[5]

This paper will describe the results of a molecular orbital investigation of the electronic structure and bonding mechanism in Zeise's salt. The electronic spectra of Zeise's salt have been reported,[17–21] and three attempts have been made to assign the observed bands to particular transitions,[19–21] but in their molecular orbital treatment the electron repulsion integrals have not been considered explicitly. The electron-repulsion integrals are considered explicitly in the present semiempirical self-consistent molecular orbital calculation for all the valence electron systems. A new assignment based on the calculation of the excitation energies and on the calculation of the transition moments is proposed in this article. The C–C bond order, the dipole moments, and H-^{195}Pt coupling constant are also discussed.

Method of Calculation

A semiempirical LCAO-MO-SCF method including electron repulsion for all valence electrons is presented. The valence electrons are represented by LCAO molecular orbitals, as given by:

$$\Phi_i = \sum_\nu C_{i\nu}\chi_\nu \qquad (1)$$

where χ_ν's are valence atomic orbitals. We take as a χ_ν Slater-type AO (atomic orbital)[22] centered on each atom:

$$\chi_\nu(n, l, m) = Nr^{n-1}\exp(-\zeta r)\, Y_l^m(\theta, \varphi) \qquad (2)$$

where n is the principal quantum number. We use orbital exponents, ζ's which have been preferably

1) W. C. Zeise, *Pogg. Ann.*, **9**, 632 (1827); **21**, 497 (1831).
2) W. C. Zeise, *Mag. Pharm.*, **35**, 105 (1830).
3) R. N. Keller, *Chem. Rev.*, **28**, 229 (1941).
4) M. A. Bennett, *ibid.*, **62**, 611 (1962).
5) R. Jenes, *ibid.*, **68**, 785 (1968).
6) F. R. Hartley, *ibid.*, **69**, 799 (1969).
7) M. Black, R. H. B. Mais, and P. G. Owston, *Acta Cryst.*, **B25**, 1753 (1969).
8) J. Chatt and L. A. Duncanson, *J. Chem. Soc.*, **1953**, 2939.
9) H. B. Jonassen and J. E. Field, *J. Amer. Chem. Soc.*, **79**, 1257 (1957).
10) D. B. Powell and N. Sheppard, *Spectrochim. Acta*, **13**, 69 (1958); *J. Chem. Soc.*, **1960**, 2519.
11) A. A. Babushkin, L. A. Gribiv, and A. D. Geliman, *Dokl. Akad. Nauk SSSR*, **123**, 461 (1958).
12) D. M. Adams and J. Chatt, *Chem. Ind.* (London), **1960**, 149.
13) M. J. Grogan and K. Nakamoto, *J. Amer. Chem. Soc.*, **88**, 5454 (1966); **90**, 918 (1968).
14) J. Pradilla-Sorzano and J. P. Fackler, Jr., *J. Mol. Spectrosc.*, **22**, 80 (1967).
15) J. Hiraishi, *Spectrochim. Acta*, **25A**, 749 (1969).
16) M. J. S. Dewar, *Bull. Soc. Chim. Fr.*, **18**, C79 (1951).
17) S. J. Lokken and D. S. Martin, Jr., *Inorg. Chem.*, **2**, 562 (1963).
18) R. G. Denning and L. M. Venanzi, *J. Chem. Soc.*, **1963**, 3241.
19) S. I. Shupack and M. Orchin, *J. Amer. Chem. Soc.*, **86**, 586 (1964).
20) J. W. Moore, *Acta Chem. Scand.*, **20**, 1154 (1066).
21) R. G. Denning, F. R. Hartley, and L. M. Venanzi, *J. Chem. Soc., A*, **1967**, 1322.

determined by a variational procedure.[23] For a molecule with a closed-shell configuration, the variational treatment of the orbital coefficients, $C_{\nu i}$, leads to the Roothaan equations:[24]

$$\sum_{\nu} F_{\mu\nu}C_{i\nu} = E_i C_{i\mu}$$

where $F_{\mu\nu}$ are matrix elements of the Hartree-Fock Hamiltonian. The eigenvalues, E_i, are roots of the secular equation:

$$|F_{\mu\nu} - E\delta_{\mu\nu}| = 0$$

Using zero differential overlap approximation, we approximate the matrix elements, $F_{\mu\nu}$, as:

$$F_{\mu\mu} = H_{\mu\mu}^{\text{core}} - 1/2P_{\mu\mu}(\mu\mu|\mu\mu) + \sum_{\nu} P_{\nu\nu}(\mu\mu|\nu\nu), \quad (3)$$

$$F_{\mu\nu(\mu\neq\nu)} = H_{\mu\nu}^{\text{core}} - 1/2P_{\mu\nu}(\mu\mu|\nu\nu), \quad (4)$$

$$H_{\mu\mu}^{\text{core}} = -I_p(\mu) - (N_\mu - 1)(\mu\mu|\mu\mu) - \sum_{\nu(\neq\mu)} N_\nu(\mu\mu|\nu\nu), \quad (5)$$

$$H_{\mu\nu(\mu\neq\nu)}^{\text{core}} = 0.25S_{\mu\nu}[2(\mu\mu|\nu\nu) - (\mu\mu|\mu\mu) - (\nu\nu|\nu\nu) + (\mu|\nu\nu) + (\nu|\mu\mu) - (\mu|\mu\mu) - (\nu|\nu\nu)] \quad (6)$$

where I_p is the valence-state ionization potential, where N_μ is the number of valence electrons occupying χ_μ, where $S_{\mu\nu}$ is the overlap integral between χ_μ and χ_ν, and where $P_{\mu\nu}$ is the charge-density and bond-order matrix:

$$P_{\mu\nu} = 2\sum_{i}^{occ} C_{i\mu}C_{i\nu} \quad (7)$$

The one-center Coulomb repulsion integrals $(\mu\mu|\mu\mu)$ are semiempirically estimated by:

$$(\mu\mu|\mu\mu) = I_p(\mu) - E_A(\mu) \quad (8)$$

The valence-state electron affinities, E_A, are assumed to be equal to the experimental values, and the valence-state ionization potential, I_p, is assumed to be equal to the values of the valence orbital ionization potential (VOIP).[25,26] The required term energies and ionization potentials are taken from Moore's table.[27] The values of I_p and E_A are summarized in Table 1.

Table 1. Valence orbital ionization potential (I_p) and valence state electron affinity (E_A) of AO's

Atom	AO	I_p (eV)	E_A (eV)
H	1s	13.60	0.85
C	2s	21.01	8.91
	2p	11.27	0.34
Cl	3s	24.02	14.45
	3p	15.03	3.73
Pt	6s	8.74	0.1
	6p	4.59	0.1
	5d	8.61	0.1

22) B. J. Ransil, *Rev. Mod. Phys.*, **32**, 245 (1960).
23) E. Clementi and D. L. Raimondi, *J. Chem. Phys.*, **38**, 2686 (1963); **47**, 1300 (1967).
24) C. C. J. Roothaan, *Rev. Mod. Phys.*, **23**, 69 (1951).
25) H. Basch, A. Viste, and H. B. Gray, *J. Chem. Phys.*, **44**, 10 (1966).
26) H. Basch, A. Viste, and H. B. Gray, *Theor. Chim. Acta*, **3**, 458 (1965).
27) C. E. Moore, "Atomic Energy Levels," Natl. Bur. Std. Circ, No. 467 (1958), Vols. 1, 2, and 3.

The one-center and two-center Coulomb repulsion integrals are calculated by:[28]

$$(\mu\mu|\nu\nu) = \frac{14.3986}{R + a} \quad (9)$$

$$a = \frac{28.7972}{(\mu\mu|\mu\mu) + (\nu\nu|\nu\nu)} \quad (10)$$

where R is the distance between the centers, μ and ν, with R represented in Å units, and $(\mu\mu|\nu\nu)$, in eV's. The molecular integrals, $(\mu|\nu\nu)$, are evaluated by means of the product of the effective nuclear charge and $(\mu\mu|\nu\nu)$.

The calculated results obtained by this procedure do not vary with respect to an orthogonal transformation of the atomic orbital basis function. This can easily be proved by the invariance of the F-matrix under the unitary transformation.

The molecular dipole moments, μ_{total}, are obtained as a sum of two parts:[29]

(1) A contribution from the net atomic charge densities, Q_A,

$$\mu_{point}(\text{debyes}) = 4.803 \sum_{A}^{atom} Q_A r_A \quad (11)$$

(2) A contribution from atomic polarizations, μ_{atom}(debyes)

$$= 4.803 \sum_{A}^{atom} P_{ns(A),np(A)} \int \chi^A{}_{ns} \boldsymbol{r} \chi^A{}_{np} d\tau \quad (12)$$

where $\boldsymbol{r}$ is the vector of the appropriate cartesian coordinate in units of Å.

Calculations on the $[PtCl_3C_2H_4]^-$ Ion and Results

In order to apply this method of calculation, it is necessary to know the coordinates of the atoms in the molecule. The molecular structure of Zeise's salt in the crystal was determined by X-ray diffraction;[7] it was found that the deviations from ideal symmetry (C_{2v}) are small. The Raman and infrared spectra of an aqueous solution of $K^+[PtCl_3(C_2H_4)]^-$.

H_2O[15] were measured, and it was concluded that the $[PtCl_3C_2H_4]^-$ ion has C_{2v} symmetry, whether the C_2H_4 group is planar or whether the CH_2's are bent

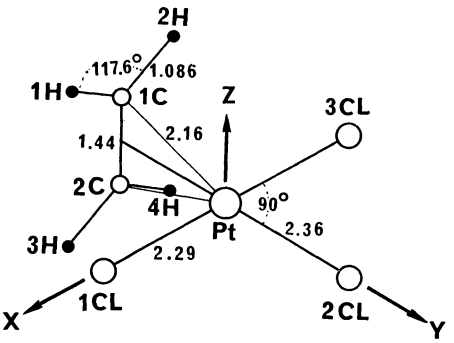

Fig. 1. A molecular orbital coordinate system and structure for $[PtCl_3C_2H_4]^-$ ion, and numbering convention.

28) N. Mataga and K. Nishimoto, *Z. Phys. Chem. N. F.*, **13**, 140 (1957).
29) J. A. Pople and G. A. Segal, *J. Chem. Phys.*, **43**, S136 (1965).

symmetrically toward or away from the Pt atom. The high-resolution proton magnetic resonance spectrum[10] of the $[PtCl_3C_2H_4]^-$ ion in deuterium oxide is in agreement with a symmetrically-co-ordinated ethylene molecule. On the basis of these results, it is reasonable to assume the C_{2v} symmetry for the $[PtCl_3C_2H_4]^-$ ion as the base of the molecular orbital calculations. The spatial arrangement is taken to be as is shown in Fig. 1. The C_2H_4 group is assumed to be planar, and the C–H bond distance and ∠HCH-bond angle are assumed to be equal to that of the free ethylene molecule.

The values of VOIP used in this calculation are as follows, in units of eV: 13.595 for $(1s)_H$, 23.384 for

TABLE 2. CALCULATED ORBITAL ENERGIES AND ORBITAL SYMMETRIES

	Molecular orbital	Symmetry representation	Orbital energy (in eV)		Molecular orbital	Symmetry representation	Orbital energy (in eV)
Occupied MO	Φ_1	a_1	−40.03		Φ_{18}	a_2	− 9.56
	Φ_2	b_2	−28.24		Φ_{19}	a_2	− 7.70
	Φ_3	a_1	−26.79		Φ_{20}	a_1	− 7.65
	Φ_4	b_1	−24.84		Φ_{21}	b_2	− 7.64
	Φ_5	a_1	−21.54		Φ_{22}	b_1	− 6.40
	Φ_6	b_2	−16.21	Vacant MO	Φ_{23}	b_1	− 0.33
	Φ_7	a_1	−13.53		Φ_{24}	b_2	1.08
	Φ_8	b_2	−13.43		Φ_{25}	a_1	1.29
	Φ_9	a_1	−13.33		Φ_{26}	b_1	2.23
	Φ_{10}	b_1	−13.27		Φ_{27}	a_1	3.34
	Φ_{11}	a_1	−12.15		Φ_{28}	b_1	4.22
	Φ_{12}	a_2	−10.98		Φ_{29}	a_1	5.74
	Φ_{13}	b_2	−10.59		Φ_{30}	a_2	7.52
	Φ_{14}	b_1	−10.02		Φ_{31}	b_1	8.07
	Φ_{15}	a_1	− 9.75		Φ_{32}	b_2	9.48
	Φ_{16}	b_2	− 9.67		Φ_{33}	a_1	10.90
	Φ_{17}	a_1	− 9.57				

TABLE 3a. MOLECULAR ORBITALS[a] FOR $[PtCl_3C_2H_4]^-$ ION: OCCUPIED MO

$\Phi_1 = -0.29s+0.39y-0.10(Cl_s^1+Cl_s^3)+0.05(Cl_y^1+Cl_y^3)+0.06Cl_s^2-0.50(C_s^1+C_s^2)-0.05(C_y^1+C_y^2)$
$+0.11(C_z^1-C_z^2)-0.21(H1+H2+H3+H4)$

$\Phi_2 = 0.54x+0.56(Cl_s^1-Cl_s^3)-0.10(Cl_x^1+Cl_x^3)+0.09Cl_x^2+0.10(C_x^1+C_x^2)$

$\Phi_3 = 0.37s+0.32y+0.35(Cl_s^1+Cl_s^3)-0.06(Cl_x^1-Cl_x^3)+0.06(Cl_y^1+Cl_y^3)+0.68Cl_s^2-0.13Cl_y^2$

$\Phi_4 = -0.44z+0.05yz-0.11(Cl_z^1+Cl_z^3)-0.08Cl_z^2-0.43(C_s^1-C_s^2)-0.24(C_z^1+C_z^2)-0.25(H1+H2-H3-H4)$

$\Phi_5 = 0.08y-0.54(Cl_s^1+Cl_s^3)+0.55Cl_s^2+0.16(C_s^1+C_s^2)-0.06(C_y^1+C_y^2)$

$\Phi_6 = 0.12xy+0.13(Cl_s^1-Cl_s^3)+0.11(Cl_x^1+Cl_x^3)+0.13(Cl_y^1-Cl_y^3)-0.52(C_x^1+C_x^2)-0.29(H1-H2+H3-H4)$

$\Phi_7 = -0.10s-0.33y+0.05zz+0.05(Cl_s^1+Cl_s^3)+0.11(Cl_x^1-Cl_x^3)-0.36(Cl_y^1+Cl_y^3)+0.33Cl_s^2$
$+0.54Cl_y^2-0.15(C_s^1+C_s^2)+0.24(C_y^1+C_y^2)+0.06(C_z^1-C_z^2)$

$\Phi_8 = -0.38x-0.60xy+0.29(Cl_s^1-Cl_s^3)+0.47(Cl_x^1+Cl_x^3)-0.09(Cl_y^1-Cl_y^3)-0.37Cl_x^2+0.11(H1-H2+H3-H4)$

$\Phi_9 = 0.28s-0.08zz-0.17(Cl_s^1+Cl_s^3)-0.36(Cl_x^1-Cl_x^3)-0.07(Cl_y^1+Cl_y^3)-0.12Cl_s^2-0.27Cl_y^2$
$-0.17(C_s^1+C_s^2)+0.38(C_y^1+C_y^2)+0.22(C_z^1-C_z^2)+0.08(H1+H2+H3+H4)$

$\Phi_{10} = 0.46z+0.45(Cl_z^1+Cl_z^3)+0.38Cl_z^2-0.26(C_s^1-C_s^2)+0.12(C_y^1-C_y^2)-0.08(C_z^1+C_z^2)-0.07(H1+H2-H3-H4)$

$\Phi_{11} = -0.13xxyy-0.21zz-0.07(Cl_x^1-Cl_x^3)-0.09Cl_y^2+0.25(C_y^1+C_y^2)-0.54(C_z^1-C_z^2)-0.21(H1+H2+H3+H4)$

$\Phi_{12} = -0.27xz-0.57(Cl_z^1-Cl_z^3)-0.22(C_x^1-C_x^2)-0.20(H1-H2-H3+H4)$

$\Phi_{13} = 0.08x-0.22xy-0.16(Cl_x^1+Cl_x^3)-0.59(Cl_y^1-Cl_y^3)-0.34Cl_x^2-0.12(C_x^1+C_x^2)-0.09(H1-H2+H3-H4)$

$\Phi_{14} = 0.06yz-0.37(Cl_z^1+Cl_z^3)+0.84Cl_z^2$

$\Phi_{15} = -0.05y-0.35xxyy+0.16zz+0.38(Cl_x^1-Cl_x^3)+0.35(Cl_y^1+Cl_y^3)+0.35(C_y^1+C_y^2)+0.08(C_z^1-C_z^2)$

$\Phi_{16} = -0.07x+0.22(Cl_x^1+Cl_x^3)-0.31(Cl_y^1-Cl_y^3)+0.82Cl_x^2$

$\Phi_{17} = -0.10y+0.26xxyy-0.27(Cl_x^1-Cl_x^3)+0.45(Cl_y^1+Cl_y^3)+0.59Cl_y^2$

$\Phi_{18} = -0.05xz-0.36(Cl_z^1-Cl_z^3)+0.37(C_x^1-C_x^2)+0.33(H1-H2-H3+H4)$

$\Phi_{19} = 0.96xz-0.18(Cl_z^1-Cl_z^3)$

$\Phi_{20} = 0.13s+0.94zz-0.10(C_x^1-Cl_x^3)-0.13(C_z^1-C_z^2)-0.05(H1+H2+H3+H4)$

$\Phi_{21} = 0.96xy-0.14(Cl_y^1-Cl_y^3)-0.12Cl_x^2$

$\Phi_{22} = 0.42z-0.49yz-0.31(Cl_z^1+Cl_z^3)-0.24Cl_z^2-0.19(C_s^1-C_s^2)+0.34(C_y^1-C_y^2)$

a) The contributions from the atomic orbitals whose AO coefficients are smaller than 0.05 are neglected in this table. s, x, y, z, xz, yz, xy, $xxyy$, and zz denote the atomic orbital 6s, 6p_x, 6p_y, 6p_z, 5d_{xz}, 5d_{yz}, 5d_{xy}, 5$d_{x^2-y^2}$, and 5d_{z^2} of platinum respectively. (Cl_s^i, Cl_x^i, Cl_y^i, Cl_z^i), (C_s^i, C_x^i, C_y^i, C_z^i), and Hi denote the atomic orbital (3s, 3p_x, 3p_y, 3p_z) of i-chlorine, (2s, 2p_x, 2p_y, 2p_z) of i-carbon, and 1s of iH proton respectively.

Table 3b. Molecular orbitals[a] for $[PtCl_3C_2H_4]^-$ ion: vacant MO

$\Phi_{23}=0.35z+0.81yz-0.16(Cl_z^1+Cl_z^3)-0.21Cl_z^2-0.19(C_s^1-C_s^2)+0.08(H1+H2-H3-H4)$
$\Phi_{24}=-0.47z-0.05xy+0.20(Cl_s^1-Cl_s^3)-0.36(Cl_x^1+Cl_y^3)+0.13Cl_x^2-0.28(C_x^1+C_x^2)+0.24(H1-H2+H3-H4)$
$\Phi_{25}=-0.06y+0.87xxyy-0.05(Cl_s^1+Cl_s^3)+0.23(Cl_x^1-Cl_x^3)+0.07Cl_s^2-0.23Cl_y^2+0.13(C_y^1+C_y^2)$
$\Phi_{26}=-0.30z-0.16yz+0.07(Cl_z^1+Cl_z^3)+0.09Cl_z^2-0.38(C_s^1-C_s^2)-0.08(C_y^1-C_y^2)+0.15(C_z^1+C_z^2)$
$+0.35(H1+H2-H3-H4)$
$\Phi_{27}=0.06s-0.22y+0.07(Cl_y^1+Cl_y^3)+0.06Cl_s^2-0.09Cl_y^2-0.39(C_s^1+C_s^2)-0.16(C_y^1+C_y^2)-0.29(C_z^1-C_z^2)$
$+0.30(H1+H2+H3+H4)$
$\Phi_{28}=0.42z-0.23yz-0.08(Cl_z^1+Cl_z^3)-0.08Cl_z^2-0.10(C_s^1-C_s^2)-0.59(C_y^1-C_y^2)$
$\Phi_{29}=0.37s+0.64y+0.05xxyy-0.07zz-0.09(Cl_s^1+Cl_s^3)+0.15(Cl_x^1-Cl_x^3)-0.11(Cl_y^1+Cl_y^3)$
$-0.28Cl_s^2+0.40Cl_y^2+0.07(C_y^1+C_y^2)-0.11(C_z^1-C_z^2)+0.11(H1+H2+H3+H4)$
$\Phi_{30}=-0.55(C_x^1-C_x^2)+0.31(H1-H2-H3+H4)$
$\Phi_{31}=0.09(C_s^1-C_s^2)-0.63(C_z^1+C_z^2)+0.20(H1+H2-H3-H4)$
$\Phi_{32}=0.55x-0.16(Cl_s^1-Cl_s^3)+0.18(Cl_x^1+Cl_x^3)-0.34(C_x^1+C_x^2)+0.28(H1-H2+H3-H4)$
$\Phi_{33}=0.71s-0.34y-0.06zz-0.12(Cl_s^1+Cl_s^3)+0.15(Cl_x^1-Cl_x^2)+0.06Cl_y^2-0.10(C_s^1+C_s^2)-0.20(C_y^1+C_y^2)$
$+0.09(C_z^1-C_z^2)-0.19(H1+H2+H3+H4)$

a) See references under Table 2a.

Table 4. Valence electron distributions of $[PtCl_3C_2H_4]^-$ ion

Atom	Orbital	Charge distribution	
		on AO	on atom
Pt	$6s$	0.684	10.558
	$6p_x$	0.927	
	$6p_y$	0.810	
	$6p_z$	1.204	
	$5d_{xz}$	2.000	
	$5d_{yz}$	0.511	
	$5d_{xy}$	1.993	
	$5d_{x^2-y^2}$	0.453	
	$5d_{z^2}$	1.976	
1Cl, 3Cl	$3s$	1.804	7.141
	$3p_x$	1.461	
	$3p_y$	1.956	
	$3p_z$	1.920	
2Cl	$3s$	1.814	7.171
	$3p_x$	1.952	
	$3p_y$	1.529	
	$3p_z$	1.876	
1C, 2C	2s	1.251	4.235
	$2p_x$	0.990	
	$2p_y$	1.083	
	$2p_z$	0.911	
1H, 2H 3H, 4H	$1s$	0.880	0.880

$(2s)_C$, 13.032 for $(2p)_C$, 25.272 for $(3s)_{Cl}$, 13.708 for $(3p)_{Cl}$, 8.619 for $(5d)_{Pt}$, 8.749 for $(6s)_{Pt}$, and 4.600 for $(6p)_{Pt}$.

The basic set of atomic orbitals used in this calculation is: platinum; $5d$, $6s$, and $6p$; chlorline; $3s$ and $3p$; carbon; $2s$ and $2p$, and hydrogen; $1s$. The initial electron configurations of the atoms in the $[PtCl_3C_2H_4]^-$ ion used in the calculation of the F-matrix are. $(5d)^9(6s)^1$ for platinum, $(3s)^2(3p)^5$ for chlorine, $(2s)^1(2p)^3$ for carbon, and $(1s)^1$ for hydrogen.

Table 5. Overlap integral and bond order between ethylene π-orbital and Pt atomic orbitals

Pt/C	Overlap integral		Bond order		
	$2p_y^{C1}$	$2p_y^{C2}$	$2p_y^{C1}$	$2p_y^{C2}$	
$6s$	0.184	0.184	0.253	0.253	σ-type bond
$6p_x$	0.0	0.0	0.0	0.0	
$6p_y$	−0.193	−0.193	−0.299	−0.299	
$6p_z$	0.137	−0.137	0.432	−0.432	π-type bond
$5d_{xz}$	0.0	0.0	0.0	0.0	
$5d_{yz}$	−0.060	0.060	−0.345	0.345	
$5d_{xy}$	0.0	0.0	0.0	0.0	σ-type bond
$5d_{x^2-y^2}$	−0.066	−0.066	−0.281	−0.281	
$5d_{z^2}$	−0.023	−0.023	−0.005	−0.005	
Overlap integral	$(2p_y^{C1}2p_y^{C2})=0.249$		Bond order	$(2p_y^{C1}2p_y^{C2})=0.545$	

The calculated orbital energies and the orbital symmetry representations in C_{2v} symmetry are given in Table 2, while the molecular orbitals are given in Table 3*a* and 3*b*.

We present, in Table 4, the valence electron distributions on each atomic orbital and on each atom in the $[PtCl_3C_2H_4]^-$ ion. In order to show the bonding mechanism between platinum and ethylene, we present in Table 5 the overlap integrals and the bond orders between the ethylene π-orbital and the Pt atomic orbitals, as well as those between the π-atomic orbital in 1C and that of in 2C.

Ultraviolet and visible spectra have been reported for the solution and the crystal of Zeise's salt,[17-20] and molecular orbital calculations have been carried out in an attempt to assign the observed bands to particular electronic transitions within the complex.[19-21] In our molecular orbital calculations, the excitation of an electron from the MO Φ_i to the MO Φ_j give rise to the excitation energies, δE_{i-j}, relative to the ground state. These energies are given by:

$$\delta E_{i-j}=\varepsilon_j-\varepsilon_i-J_{ij}+2K_{ij} \quad (13)$$

where ε_i is the orbital energy of Φ_i, and the J_{ij} and K_{ij} are the Coulomb and exchange integrals respec-

TABLE 6. TRANSITION ENERGIES (δE) AND OSCILLATOR STRENGTHS (f)

Calcd. Transition	δE(cm^{-1})	$f\times10^2$	Polariz.	Exptl.[a] δE(cm^{-1})	$f\times10^2$
$\Phi_{22b_1}-\Phi_{23b_1}$	15198	0.11	y		
$\Phi_{22b_1}-\Phi_{25a_1}$	20385	0.12	z		
$\Phi_{20a_1}-\Phi_{24b_2}$	34784	0.70	x	34400	1.0
$\Phi_{21b_2}-\Phi_{24b_2}$	34994	0.37	y		
$\Phi_{22b_1}-\Phi_{26b_1}$	35018	3.83	y	37700	1.9
$\Phi_{22b_1}-\Phi_{27a_1}$	42101	0.60	z		
$\Phi_{18a_2}-\Phi_{23b_1}$	44448	6.99	x	41600	6.6
$\Phi_{19a_2}-\Phi_{26b_1}$	47022	0.68	x		

a) From Ref. 21.

tively. The calculated excitation energies and oscillator strengths are given in Table 6.

Calculation of H-^{195}Pt Nuclear Spin-spin Coupling Constant

The high-resolution proton magnetic resonance spectrum of the $[PtCl_3C_2H_4]^-$ ion in deuterium oxide[10] shows a strong singlet attributed to the ethylenic protons with a weak side band, 34 Hz apart, produced by the spin-spin coupling with ^{195}Pt.[30] The most important term giving nuclear spin-spin coupling is the term due to the Fermi contact interaction.[31,32] The Fermi contact coupling is also likely to be the principal contributor to the coupling constant between the hydrogen atom and ^{195}Pt in Zeise's salt, because the electrons on a hydrogen atom are represented by a 1s atomic orbital. By substituting the LCAO MO wave functions in the general Ramsey formulae, the following molecular orbital expression for the Fermi contact spin-spin coupling constant between a particular pair of nuclei, N and N', has been given by Pople and Santry:[33]

$$J_{NN'} = -\frac{64}{9}h\gamma_N\gamma_{N'}\beta^2\sum_i^{occ}\sum_j^{vac}({}^3\delta E_{i\to j})^{-1} \sum_{\lambda\mu\nu\sigma} C_{i\lambda}C_{j\mu}C_{j\nu}C_{i\sigma}\langle\chi_\lambda|\delta(\boldsymbol{r}_N)|\chi_\mu\rangle\langle\chi_\nu|\delta(\boldsymbol{r}_{N'})|\chi_\sigma\rangle \quad (14)$$

where γ_N and $\gamma_{N'}$ are the nuclear magnetic ratios, where β is the Bohr magneton, and where the other notations are in accordance with those in Ref. 32.

Using the results of the above MO calculations, we have calculated the H-^{195}Pt coupling constant on the basis of Eq. (14). The formula involves the value of the valence $(6s)_{Pt}$ atomic orbital at platinum: the magnitude at the center is important in the calculation of the H-^{195}Pt coupling constant. Accordingly, it is necessary to use a $(6s)_{Pt}$ atomic orbital accurate at the center of platinum in order properly to evaluate the molecular integrals, $\langle x_\nu|\delta(\boldsymbol{r}_N)|x_\mu\rangle$. The analytical wavefunctions accurate at the inner part have been calculated for a number of atoms.[34-36] However, so far these calculations have not been reported for platinum. Accordingly, we have employed an approximate analytical (6s) wavefunction for radon as (6s). The values of the atomic orbitals at platinum and at the proton (1H) are given in Table 7. It can easily be seen that the values of $\langle(1s)_H|\delta(\boldsymbol{r}_H)|(1s)_H\rangle$ and $\langle(6s)_{Pt}|\delta(\boldsymbol{r}_{Pt})|(6s)_{Pt}\rangle$ are dominant over the other molecular integrals, $\langle\chi_\lambda|\delta(\boldsymbol{r}_H)|\chi_\mu\rangle$ and $\langle\chi_\nu|\delta(\boldsymbol{r}_{Pt})|\chi_\sigma\rangle$ respectively. Thus, we have obtained -40.4 Hz as the calculated value of the H-^{195}Pt coupling constant; this indicates that the ethylene is firmly bound to

TABLE 7. VALUES OF THE ATOMIC ORBITALS AT PLATINUM AND PROTON (1H) (in atomic unit)

Atomic orbital	Values of radial part[a] of AO at proton (1H),	at platinum
$(5d)_{Pt}$	0.000	0.000
$(6s)_{Pt}$	0.081	(-7.344)[b]
$(6p)_{Pt}$	0.081	0.000
$(3s)_{1Cl}$	0.001	0.006
$(3p)_{1Cl}$	0.003	0.014
$(3s)_{2Cl}$	0.000	0.004
$(3p)_{2Cl}$	0.000	0.011
$(3s)_{3Cl}$	0.000	0.006
$(3p)_{3Cl}$	0.000	0.014
$(2s)_{1C}$	0.286	0.021
$(2p)_{1C}$	0.292	0.024
$(2s)_{2C}$	0.019	0.021
$(2p)_{2C}$	0.021	0.024
$(1s)_{1H}$	2.000	0.028
$(1s)_{2H}$	0.059	0.028
$(1s)_{3H}$	0.015	0.028
$(1s)_{4H}$	0.005	0.028

a) The radial part is $R_n(\zeta)=\frac{(2\zeta)^{\frac{2n+1}{2}}}{\sqrt{(2n)!}}r^{n-1}\exp(-\zeta r)$.

b) This is the value of $(6s)_{Rn}$-analytical wavefunction, see Ref. 36.

30) S. Maricic, C. R. Redpath, and J. A. S. Smith, *J. Chem. Soc.*, **1963**, 4905.
31) N. F. Ramsey, *Phys. Rev.*, **91**, 303 (1953).
32) J. A. Pople, W. G. Schneider, and H. J. Bernstein, "High Resolution Nuclear Magnetic Resonance," Chapter 8, McGraw Hill, New York (1959).
33) J. A. Pople and D. P. Santry, *Mol. Phys.*, **8**, 1 (1964).
34) J. W. Richardson, W. C. Nieuwpoort, R. R. Rowell, and W. F. Edgell, *J. Chem. Phys.*, **36**, 1057 (1962).
35) E. Clementi, *J. Chem. Phys.*, **38**, 996, 1001 (1963); **41**, 295, 303 (1964).
36) M. Synek and G. E. Stungis, *J. Chem. Phys.*, **42**, 3068 (1965).

platinum. This calculated value is in very good agreement with the observed value of 34 Hz. The sign of the experimental coupling constant is not known, but the theoretical calculation shows it to be negative.

Discussion

The signs and magnitudes of molecular orbital coefficients (Table 2*a* and 2*b*) indicate that the ethylene π^*(anti-bonding) orbital is included in the highest occupied orbital, Φ_{22}. This is consistent with the π-type bond which is referred to as "back-bonding." The ethylene π(bonding) orbital is included in the Φ_{15} and Φ_{19} orbitals. This is consistent with the σ-type bond.[8] The form of the molecular orbitals, Φ_{22} and Φ_{15}, are shown schematically in Figs. 2 and 3. These results show essentially the same bonding mechanism as when Chatt and Duncanson[8] applied Dewar's[16] description to Zeise's salt, but it should be pointed out that the mixing of the ligand chlorine atomic orbitals with these molecular orbitals is considerably large. It should also be pointed out that the ethylene π^* orbital is included in the vacant molecular orbital, Φ_{28}.

The importance of the *trans*-effect caused by ethylene should also be noted. A review[37] of the *trans*-effect favored the π-bonding mechanism for the *trans*-effect of olefins,[38] in which a ligand olefin which can form π-bonds will with draw some of the electron density of the d_{yz} orbital from the ligand in the *trans* position. Moreover, it was pointed out that this should weaken the Pt-X(*trans*) bond. Certainly it does (see Fig. 2) but we should also note that the σ-type bonding (see Fig. 3) strengthens the Pt-Cl(*cis*) bond, but not the Pt-Cl(*trans*) bond.

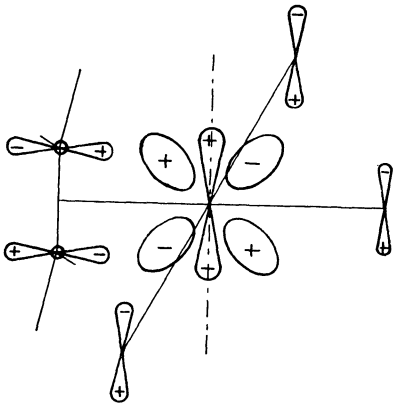

Fig. 2. Shematic scheme of MO Φ_{22}, illustrating the π-type bonding.

The ionization potential of a molecule should, according to Koopmans' theorem,[39] be approximately equal to the calculated orbital energy of the highest occupied orbital multiplied by -1. We can see in Table 1 that the calculated ionization potential of the $[PtCl_3C_2H_4]^-$ ion is equal to 6.40 eV. The experimental ionization potential of this salt has not been reported, but this calculated value seems to be reasonable with respect to the ionization potential of platinum. The orbital energy of the lowest vacant orbital, Φ_{23}, is slightly negative. Nevertheless, the over-all picture of orbital energies is very encouraging in comparison with the negative values of the vacant molecular orbitals in the calculation of many sorts of metallic compounds.[40-42]

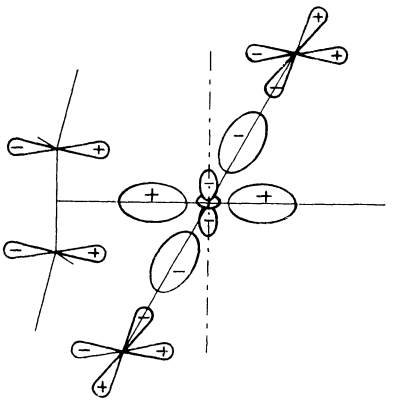

Fig. 3. Shematic scheme of MO Φ_{15}, illustrating the σ-type bonding.

Let us now consider the valence electron distributions obtained from the calculations (Table 3). The electrons of the protons in ethylene are redistributed to the carbons. The excess charge, (-e), is redistributed to platinum and chlorines. It should be noted that the electrons in the 5*d* orbitals in platinum are largely redistributed to the 6*p* orbitals. This redistribution can be considered to be due to the large contribution of 6*p* orbitals to the bonding of platinum with the ethylene molecule, as can easily be seen from the form of the molecular orbitals in Tables 2*a* and 2*b*. Our method predicts the dipole moment of $\mu_{total}=2.772$ debyes for the $[PtCl_3C_2H_4]^-$ ion, where $\mu_{point}=2.035$ debyes and $\mu_{atom}=0.737$ debyes. From the experimental dipole moments of compounds of the C_2H_4, amine, $PtCl_2$ type, Chatt and Duncanson[8] estimated that the dipole moment of the C_2H_4-Pt bond has a value of about 4 debyes. Our calculated result is in good agreement with their estimated value.

Let us next consider the data on the overlap integrals and bond orders between the ethylene π-orbital and platinum atomic orbitals (Table 4). From the signs and magnitudes of the overlap integrals and bond orders, we can understand the bonding mechanism due to the formation of the σ-type bond and the π-type bond. As can easily be seen, the total σ-type bond order is equal to 0.833, while the total π-type bond order is equal to 0.777. Accordingly, the bonding between ethylene and platinum is found to be through both the σ- and the π-type bonds. The calculated

37) F. Basolo and R. G. Pearson, *Prog. Inorg. Chem.*, **4**, 381 (1962).
38) J. Chatt, L. A. Duncanson, and L. M. Venanzi, *J. Chem. Soc.*, **1955**, 4456.
39) T. A. Koopmans, *Physica*, **1**, 104 (1933).
40) H. Basch and H. B. Gray, *Inorg. Chem.*, **6**, 365 (1967).
41) F. A. Cotton and C. B. Harris, *ibid.*, **6**, 369 (1967).
42) I. H. Hillier and R. M. Canadine, *Discuss. Faraday Soc.*, **47**, 27 (1969).

ethylene π-bond order is reduced from 1.0 to 0.545 by forming a bond with $PtCl_3$. Thus, the C–C bond order is reduced from 2.0 to 1.5. This is consistent with the experimental results.

Let us now consider the assignment of the electronic spectra. We will not, in contrast to previous authors,[19,20] discuss the assignment on the basis only of the arrangement of the electronic energy levels (see Eq. (13)). Since the $[PtCl_3C_2H_4]$ ion is a molecule of low symmetry (C_{2v}), there are many group theoretically-allowed transitions. In spite of this fact, the number of probable transitions is reduced to a relatively small number by calculating the transition moments and neglecting the small ones. The transitions given in Table 5 are those which satisfy the following conditions: 1) the calculated oscillator strength (f) is larger than 10^{-3}, and

2) the excitation energy is smaller than 50000 cm^{-1}. Considering the intensities of the absorption spectrum and the calculated oscillator strengths, we can identify the band at 40700 cm^{-1} as $\Phi_{18a_1}-\Phi_{23b_1}$ ($^1A_1-^1B_1$), that is, the charge-transfer band corresponding to the transition from ethylene to platinum. The band at 37450 cm^{-1} may also be identified as $\Phi_{22b_1}-\Phi_{26b_1}$ ($^1A_1-^1A_1$) and the band at 33450 cm^{-1}, as $\Phi_{20a_1}-\Phi_{24b_1}$ ($^1A_1-^1B_1$). The calculated excitation energies for these transitions are 44448 cm^{-1}, 35018 cm^{-1}, and 34784 cm^{-1} respectively, showing good agreement with the experimental results. Previously, three attempts[19,20] have been made to assign the observed bands to particular electron transitions within the complex, but the three assignments are different. The present assignment is also different from previous ones and indicates that there is considerable mixing of the component atomic orbitals.

The magnitude of the spin-orbit interaction is given by ζ.[43] For the platinum $(5d)^9(6s)^1-^3D$ multiplet, the ζ-value is calculated to be [27] $\zeta=388$ cm^{-1}. In this molecular orbital treatment we do not consider the effect of spin-orbit coupling, although this effect is indefinably included through the evaluation of the VOIP's. However, this effect should be precisely considered if one wants to assign the small intensity bands of the polarized spectrum of crystal Zeise's salt.

The author wishes to thank Professor Hiroshi Kato for a very instructive discussion of this article. He also wishes to thank Professor Teijiro Yonezawa for his generous support of this work.

43) E. U. Condon and G. H. Shotley, "The Theory of Atomic Spectra," Cambridge University Press, Cambridge (1967), p. 199.

BULLETIN OF THE CHEMICAL SOCIETY OF JAPAN, VOL. 44, 354—360 (1971)

ESR and Optical Studies on the EDA Complexes of Di-*t*-butyl-*N*-oxide Radical

Yoshifumi MURATA and Noboru MATAGA[1]

Faculty of Engineering Science, Osaka University, Toyonaka, Osaka

(Received August 20, 1970)

It has been confirmed that di-*t*-butyl-*N*-oxide (DTBNO) forms EDA complexes with various electron acceptors, and the resulting complexes show CT (charge transfer) absorption bands. Wave-numbers of the CT bands agreed satisfactorily with theory. Charge distributions in the EDA complexes of DTBNO, including hydrogen bonded complexes with proton donors, have been investigated by means of ESR. From the effect of the EDA complex formation upon the hyperfine coupling constant of ^{14}N of DTBNO, contribution of electrostatic forces to complex formation has been demonstrated. However, in the case of complexes with strong acceptors such as tetracyanoethylene, the values of the hyperfine coupling constant have indicated a significant contribution of CT interaction to complex formation.

The structures and properties of the EDA complexes have been studied extensively and are being subjected to active investigation. Among organic molecular complexes, there are numerous EDA complexes consisting of molecules with closed shell ground state.[2] However, little investigation has been carried out on the complexes in solution which have unpaired spins in the electronic ground state.

Studies on the ground state of molecular complexes have supported the CT theory,[2] but there are still some questions concerning the extent to which the classical electrostatic forces contribute to the binding energy and dipole moments of EDA complexes, especially in the case of weak complexes.[3-5] For example, Hanna[4] has shown that quadrupole-induced dipole forces may be comparable to CT forces in importance in explaining the stability of benzene-iodine and of similar complexes. Other authors have also insisted that the multipole-multipole and multipole-induced multipole interactions are important for the stability of π–π type EDA complexes.[3] Nevertheless, it seems

1) To whom correspondence should be addressed.

2) See for example, G. Briegleb, "Elektronen-Donator-Acceptor Komplexe," Springer-Verlag, Göttingen, 1961; R. S. Mulliken and W. B. Person, "Molecular Complexes," A Lecture and Reprint Volume, John Wiley and Sons, New York, 1969.

3) H. O. Hooper, *J. Chem. Phys.*, **41**, 599 (1964); M. J. S. Dewar and C. C. Thompson, Jr., *Tetrahedron, Suppl.*, **7**, 97 (1956).

4) M. W. Hanna, *J. Amer. Chem. Soc.*, **90**, 285 (1968); M. W. Hanna and D. E. Williams, *ibid.*, **90**, 5358 (1968); J. L. Lippert, M. W. Hanna, and P. J. Trotter, *ibid.*, **91**, 4035 (1969).

5) R. S. Mulliken and W. B. Person, *ibid.*, **91**, 3409 (1969).

that there is no direct evidence for the predominant contributions of the electrostatic forces to the interactions in the complexes.

Elucidation of the above problem and CT interactions can be achieved by measurement of the ESR spectra of complexes which have unpaired spins in the ground state.

Since almost all radicals with doublet ground state are unstable, ESR studies are possible only for some complexes involving exceptionally stable radicals. We have found that DTBNO forms stable complexes with some electron acceptors, and studied the complexes by means of optical as well as ESR spectral measurements.

Experimental

The absorption spectra were measured with a Cary 15 spectrometer and a Shimadzu MPS-50L spectrophotometer. ESR spectra were recorded by a JES-3BX spectrometer of Japan Electron Optics using X-band.

DTBNO was synthesized according to the method given in literature,[6] and was purified by repeated distillation under reduced pressure. The purified sample was distilled in a vacuum and sealed off in parts. Tetracyanoethylene (TCNE) was recrystallized several times from monochlorobenzene and was sublimed in vacuum. Purified sample of 2,3-dichloro-5,6-dicyano-*p*-benzoquinone (DDQ) was kindly supplied by Dr. Y. Sato of this institute. Chloranil was recrystallized twice from benzene. 2,5-Dichloro-*p*-benzoquinone (DQ) and phthalic anhydride (PA) were sublimed under reduced pressure. Phenol was carefully distilled. Pyromellitic dianhydride (PMDA) was recrystallized twice from ethylacetate. *s*-Tetracyanobenzene (TCNB) was the same sample as used before.[7] It was recrystallized several times from ethanol and sublimed in a vacuum before use.

Cyclohexane and *n*-hexane were passed through a column of activated silica gel twice, dried over metallic sodium, and distilled. Toluene and benzene were shaken with sulfuric acid, neutralized, and distilled. The distillate was passed through a column of activated silica gel, dried over metallic sodium and distilled. Tetrahydrofurane (THF) was refluxed over metallic sodium fifty hours, and distilled. Other solvents were purified by the methods described in literature.[8]

For ESR measurements, solutions in the sample tube were carefully deaerated by an ordinary procedure with an evacuating system equipped with a rotary and oil diffusion pump.

Results and Discussion

A. Optical Absorption Spectra. The visible absorption spectrum of DTBNO in *n*-hexane is given in Fig. 1. This absorption band can be assigned to the n–π^* transition.[9] When amines which can act as electron donors in the complex formation, are added to the solution of DTBNO, or when they are used as solvents for DTBNO, the absorption spectrum of DTBNO does not change. As will be discussed later in detail, the hyperfine coupling (hfc) constant due to

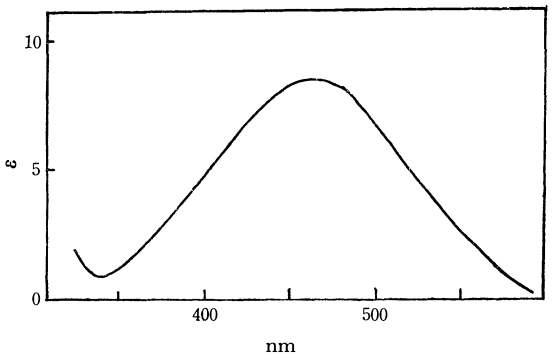

Fig. 1. Visible absorption spectrum of DTBNO in *n*-hexane at room temperature (~23°C).

the nitrogen atom of DTBNO dissolved in *N,N*-dimethylaniline (DMA) is almost the same as when it is dissolved in monochlorobenzene. The ionization potential of DMA is much smaller than that of monochlorobenzene while their dipolemoments or static dielectric constants are almost equal. Thus, it seems certain that DTBNO hardly works as an electron acceptor.

On the other hand, when a strong electron acceptor such as TCNE or DDQ is added to the DTBNO solution, we can observe a new absorption band as indicated in Fig. 2. In a sufficiently polar solvent such as acetonitrile, we can observe clearly that the DTBNO-TCNE

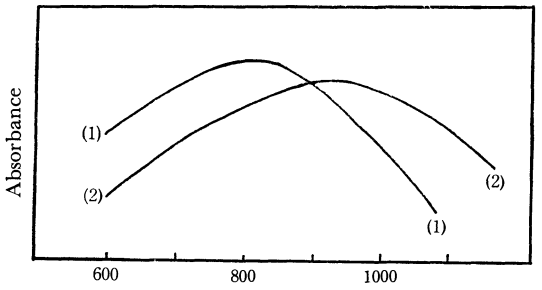

Fig. 2. Absorption spectra of DTBNO complexes in ether solution at room temperature (~23°C). Acceptors: (1) TCNE, (2) DDQ.

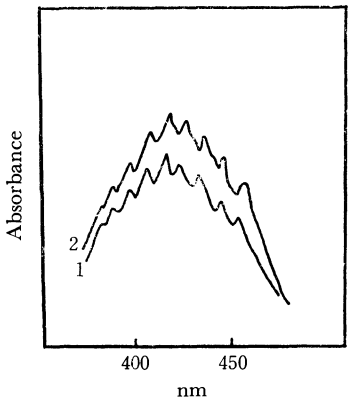

Fig. 3. Absorption band of TCNE anion observed for DTBNO-TCNE-acetonitrile system at room temperature (~23°C).
1. Immediately after mixing of DTBNO and TCNE solutions.
2. 10 min after the mixing.

6) A. K. Hoffman, *ibid.*, **86**, 641 (1964).
7) N. Mataga and Y. Murata, *ibid.*, **91**, 3144 (1969).
8) A. Weissberger, ed., "Technique of Organic Chemistry," Vol. VII, Interscience Publishers, New York, N. Y. (1955).
9) T. Kawamura, S. Matsunami, and T. Yonezawa, This Bulletin, **40**, 1111(1967).

system undergoes ionic dissociation and there arises the anion radical of TCNE (Fig. 3). The reaction of ion radical formation is not very rapid, and the produced TCNE anion is fairly stable even in the air.

We have examined the origin of the new absorption band in Fig. 2 by the method frequently used for usual EDA complexes. Application of the Benesi-Hildebrand equation[10] to the three component system, TCNE-DTBNO-diethylether, gives a good linear relation as shown in Fig. 4, from which the equilibrium constant for the complex formation has been evaluated to be 4.0 *l*/mol. Thus it is certain that DTBNO forms 1 : 1 complex with TCNE.

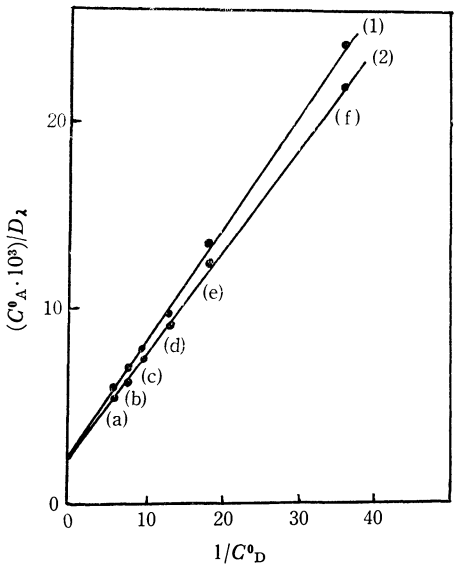

Fig. 4. Benesi-Hildebrand plot for DTBNO-TCNE system in ether at room temperature (~23°C). C^0_A and C^0_D are analytical concentrations of TCNE and DTBNO, respectively.
$C^0_A = 2.57 \times 10^{-3}$ M.
C^0_D: (a) 1.6×10^{-1} M, (b) 1.3×10^{-1} M, (c) 1.0×10^{-1} M, (d) 7.7×10^{-2} M, (e) 5.6×10^{-2} M, (f) 2.8×10^{-2} M.
1. at 850 nm, 2. at 790 nm.

The wavelengths of the new absorption bands which appeared when various electron acceptors are added to the solution are listed in Table 1. We see that the

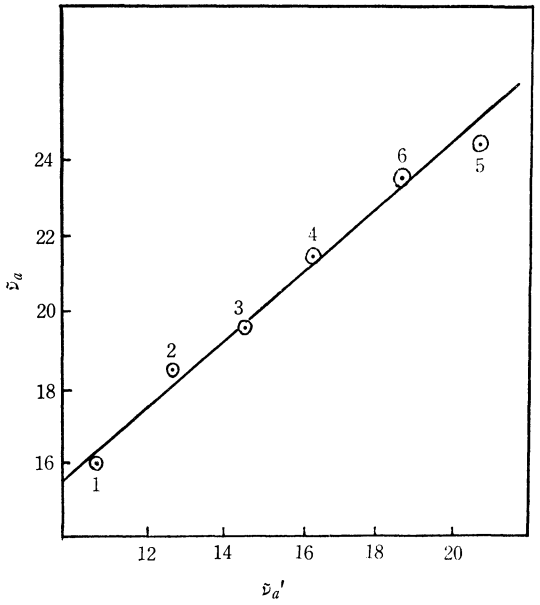

Fig. 5. Relation between the band maxima of the hexamethylbenzene complexes ($\tilde{\nu}_a$) and those of the DTBNO complexes ($\tilde{\nu}'_a$) for the common acceptors. See Table 1 for the numbering of the points in the figure.

larger the electron affinity of the acceptor, the longer the wavelength of the absorption band. Furthermore, we have compared the wavenumbers of the absorption bands of DTBNO-acceptor systems with those of the CT absorption bands of hexamethylbenzene complexes with the same acceptors. As shown in Fig. 5, we have a linear relation which can be written approximately as

$$\tilde{\nu}'_a = \tilde{\nu}_a + \text{Const.} \quad (1)$$

For ordinary EDA complexes, the energy of the CT absorption band is approximately given by

$$h\nu_{CT} = I_D - E_A + C \quad (2)$$

where I_D, E_A, and C are ionization potential of the donor, electron affinity of the acceptor, and the interaction term including the coulomb energy between the ion-pair, respectively. The corresponding equation for the DTBNO complexes may be written as

TABLE 1. WAVELENGTHS OF ABSORPTION BAND MAXIMA OF DTBNO COMPLEXES WITH ELECTRON ACCEPTORS IN SEVERAL SOLVENTS (wavelength in nm)

Solvent	Acceptor					
	1. DDQ	1. TCNE	3. Chloranil	4. 2.5-Dichloro-*p*-benzoquinone	5. PMDA	6. TCNB
Ether	925	790	(a)	(a)	(a)	(a)
THF	925	790	685	610	480	—
Acetonitrile	(b)	anion	(a)	605	(a)	530
Electron affinity of acceptor (c)	1.9	1.80	1.3	1.1	0.8	0.4

(a) Because of the small solubilities of the acceptor and the small equilibrium constant of the complex formation, the new absorption band could not be detected.
(b) Immediately after the preparation of the solution, some chemical changes occured and the new absorption band of the complex was not observable.
(c) In units of electron volts. The numerical values were taken from G. Briegleb, Angew. Chem. International Ed., 3, 617 (1964).

10) H. A. Benesi and J. H. Hildebrand, *J. Amer. Chem. Soc.*, **71**, 2703 (1949).

Table 2. Solvent shifts of absorption band maxima of DTBNO

	Solvent	n	ε	$\left(\frac{\varepsilon-1}{\varepsilon+2}-\frac{n^2-1}{n^2+2}\right)$	λ_{max} (nm)
1	n-Hexane	1.375	1.89	0.000	466
2	Toluene	1.49413	2.379	0.022	461
3	Monochlorobenzene	1.5248	5.621	0.300	456
4	THF	1.4040	7.6	0.443	457
5	Benzonitrile	1.5282	25.20	0.582	454
6	Acetonitrile	1.3441	38.8	0.715	454
7	Ethanol	1.3614	24.30	0.664	441
8	Acetic acid	1.3716	6.15	0.405	428
9	Water	1.3330	81.0	0.758	421
10	m-Cresole	1.5438	11.8	0.467	418

$$h\nu_{CT}' = I_D' - E_A + C' \quad (3)$$

where I_D' is the ionization potential of DTBNO. Thus we have

$$\tilde{\nu}'_{CT} \approx \tilde{\nu}_{CT} + \text{Const.} \quad (4)$$

From the above arguments, it has been confirmed that DTBNO forms EDA complexes with various electron acceptors and the new absorption band due to the complex can be ascribed to the CT transition.

In connection with the CT interaction, we have examined the hydrogen bonding of DTBNO with several proton donors. The solvent effect upon the wave number of the visible absorption band of DTBNO is indicated in Table 2 and Fig. 6. In Fig. 6, the wave number is plotted against the factor $[(\varepsilon-1)/(\varepsilon+2)-(n^2-1)/(n^2+2)]$, where ε and n are the static dielectric constant and the refractive index of the solvent, respectively. The solvent shift of the electronic spectrum, when the short range interactions such as molecular complex formations are absent, can be given as a function of ε and n. As an example, the equation given by McRae[11] is

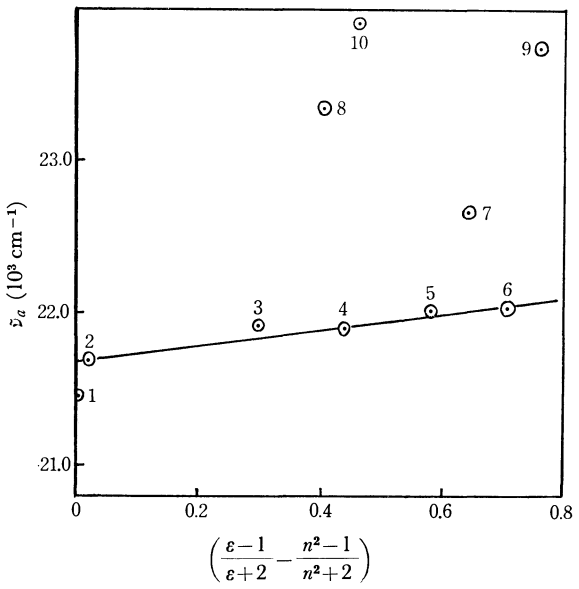

Fig. 6. Solvent shift of the absorption band of DTBNO. See Table 2 for the numbering of the points.

$$hc\Delta\tilde{\nu}_a \approx (AL_0+B)\frac{(n^2-1)}{(2n^2+1)} + C\left(\frac{\varepsilon-1}{\varepsilon+2}-\frac{n^2-1}{n^2+2}\right) + D\left(\frac{\varepsilon-1}{\varepsilon+2}-\frac{n^2-1}{n^2+2}\right)^2 \quad (5)$$

The second term on the right hand side of Eq. (5) comes from the permanent dipole-permanent dipole interaction between the solute and solvent molecules. The contribution of this term will be predominant in the present case, since DTBNO has a large dipolement (3.08D) in the ground state. As we see from Fig. 6, $\tilde{\nu}_a$ is approximately linear with respect to $[(\varepsilon-1)/(\varepsilon+2)-(n^2-1)/((n^2+2)]$ when the solvent is not likely to form the hydrogen bond with DTBNO (from this linear relationship, we have estimated the dipole-moment of DTBNO in the lowest excited state to be 2.6D.). In the case of the solvent which seems to form hydrogen bond with DTBNO, the blue shift of the spectrum is large and the deviation from the linear relation is remarkable. The spectral behaviors in the hydrogen bonding solvents are quite similar to those of the n–π^* transitions of ordinary closed shell molecules. Of course, the hydrogen bonding interaction may also affect the distribution of the unpaired electron of DTBNO.

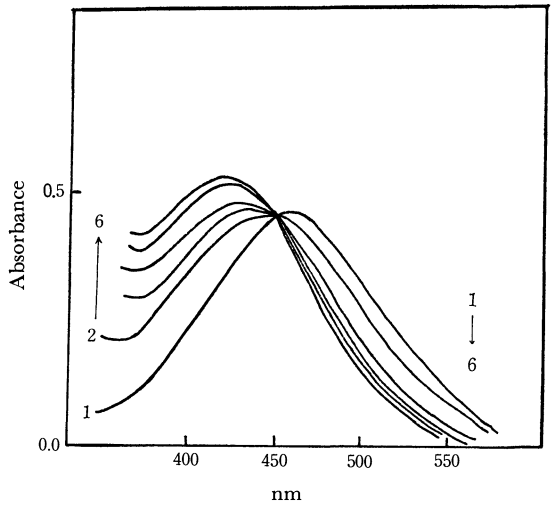

Fig. 7. Change of the absorption spectrum of DTBNO in toluene caused by the added phenol at room temperature (~23°C).
Concentration of DTBNO: 5.85×10^{-2} M.
Concentration of phenol: (1) 0, (2)—(6) 8.5×10^{-2} M—2.02M.

11) E. G. McRae, *J. Phys. Chem.*, **61**, 562 (1957).

In order to make a more detailed study of the hydrogen bonding effect on the absorption spectrum, we have examined the three component system DTBNO-phenol in toluene. It is evident from Fig. 7 that there arises 1 : 1 hydrogen complex. We have evaluated equilibrium constant to be 6.4 *l*/mol at room temperature.

When trifluoroacetic acid, a strong proton donor, was added to the benzene solution of DTBNO, the visible absorption band of DTBNO vanished completely and a new absorption band with a maximum at *ca.* 700 nm appeared. In contrast to the case of DTBNO-phenol-toluene system, this benzene solution showing the new absorption band does not show any ESR signal. We have observed the absorption band at 700 nm also for the acetic acid solution of DTBNO when a small amount of concd. sulfuric acid is added to the solution. Although the origin of this long wavelength absorption band is not clear, it may be due to some product of unknown reaction occurring in a strongly acidic media.

B. ESR Spectra. The ESR spectrum of DTBNO in toluene solution at room temperature is shown in Fig. 8. It is possible that, in a highly concentrated

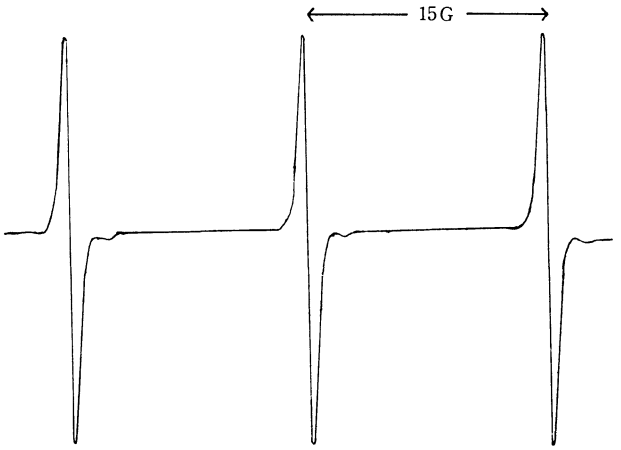

Fig. 8. ESR spectrum of DTBNO in toluene. Concentration of DTBNO: 10^{-4} M.

solution, DTBNO forms a cluster which has a spin multiplicity greater than doublet. However, the ESR spectrum due to triplet or higher multiplet state could not be observed at room temperature. At 77°K the mixtures of DTBNO and cyclohexane (volume ratio 1 : 1 and 1 : 10) showed ESR spectrum due to triplet state ($\Delta m=2$ transition). From the spectrum we can evaluate the dipole-dipole interaction parameter D, which is directly related to the separation between two unpaired electrons. D/hc was found to be 0.0370 $cm.^{-1}$ By using the equation[12]

$$\tilde{r}_{12}=(2|D|/3\,g^2\beta^2)^{1/3} \tag{6}$$

the average separation $\tilde{r}_{12}$ between two unpaired electrons was evaluated as 4.2 Å.

Hirota[12] measured D/hc and $\tilde{r}_{12}$ for some ion radical pairs. For the anion radical of hexamethylacetone with lithium cation as gegen ion: $D/hc=0.0210$ cm^{-1} and $\tilde{r}_{12}=5.0$ Å. For the same radical with sodium cation: $D/hc=0.0155$ cm^{-1} and $\tilde{r}_{12}=5.6$ Å. Since these radical pairs are ion-pair dimers, *i.e.* the gegen ion is placed between the two radical ions, their $\tilde{r}_{12}$ values are a little larger than that of DTBNO dimer. Though DTBNO molecules have bulky *t*-butyl groups which can more or less hinder the interactions between unpaired electrons, they can approach each other to form a triplet state dimer.

Let us examine the effect of the EDA complex formation on the ESR spectrum.

$$A + \dot{D} \rightleftarrows (A\dot{D}) \tag{7}$$

According to Gendell *et al.*,[13] when the complex formation and dissociation reaction of Eq. (7) is very rapid, the observable hfc constant $\bar{a}$ is given by

$$\bar{a}=\frac{1}{2}(a_D+a_{AD})+\frac{1}{2}(K[A]-1)/(K[A]+1)\,(a_{AD}-a_D) \tag{8}$$

where a_D and a_{AD} are the coupling constants of $\dot{D}$ and $A\dot{D}$, respectively, and K is the equilibrium constant of complex formation.

Equation (8) can be rewritten as[13]

$$\bar{a}=a_{AD}-\left(\frac{1}{K}\right)(\bar{a}-a_D)/[A]. \tag{9}$$

Validity of Eqs. (8) and (9) for the hydrogen bonded complex formation has been examined by several workers and it has been proved that these equations

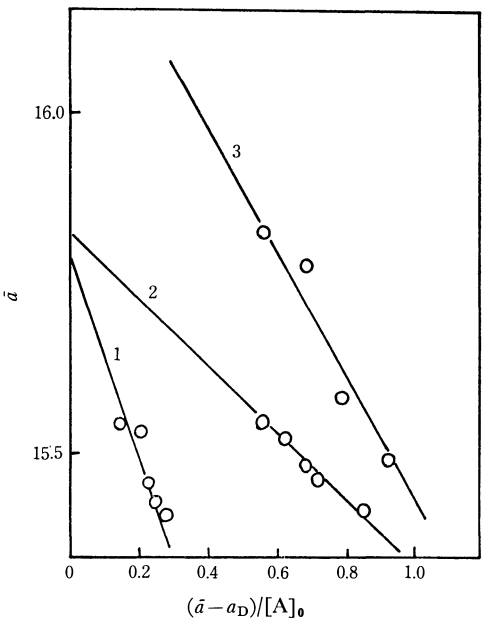

Fig. 9-a. $\bar{a}$ *vs.* $(\bar{a}-a_D)/[A]_D$ relation for DTBNO-electron acceptor systems. ($\bar{a}$ is the observed nitrogen hfc constant of DTBNO.)

	A	Solvent
1	PA	THF
2	TCNE	Toluene
3	PMDA	THF

12) N. Hirota, *J. Amer. Chem. Soc.*, **89**, 32 (1967).

13) J. Gendell, J. H. Freed, and G. K. Frenkel, *J. Chem. Phys.*, **37**, 2832 (1962).

Table 3. Equilibrium constant of complex formation obtained by optical and ESR measurements and the values of nitrogen hfc constant of DTBNO complexes

	Optical spectra			ESR spectra		
	λ_{max} (nm)	K (M^{-1})	Solvent	$a_N(G)$	K (M^{-1})	Solvent
TCNE	790	4.0	Ether	15.82	5.0	Toluene
PMDA	480	—	THF	16.34	1.1	THF
PA	—	—	—	15.80	0.6	THF
Benzonitrile	—	—	—	15.9	0.1	Toluene
Acetonitrile	—	—	—	15.9	0.1	Toluene
Phenol	423	6.4	Toluene	16.80	6.7	Toluene

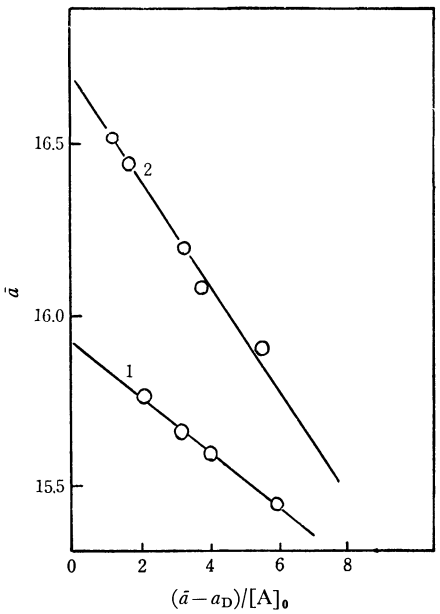

Fig. 9-b. $\bar{a}$ *vs.* $(\bar{a}-a_D)/[A]_0$ relation for
1. DTBNO-phenol-toluene system,
2. DTBNO-acetonitrile-toluene system.

are useful.[14,15] We have applied Eq. (9) to our systems, since the interactions between the partners are rather weak leading to rapid formation and dissociation reactions.

The results of measurements are given in Fig. 9 and Table 3. Since [A] is much larger than the concentration of DTBNO in our present systems, we can use the analytical concentration $[A]_0$ instead of [A], and we can evaluate K and a_{AD} from the plot of $\bar{a}$ against $(\bar{a}-a_D)/[A]_0$. As can be seen from Table 3, agreement between the K value obtained by optical spectral measurement and that estimated by ESR measurement is satisfactory. For some systems where optical measurement was not possible, K values were determined by means of ESR.

The interactions between the halves in the EDA complexes, which seem to affect the ESR spectra, will be the CT interaction and the electrostatic one, because both can affect the spin densities on DTBNO.

According to the theory of Karplus and Frenkel,[16] the hfc constant of DTBNO nitrogen can be written as

$$a_N = Q_1\rho_N + Q_2\rho_O \quad (10)$$

in terms of the spin densities on nitrogen and oxygen. As an example, Ayscough and Sargent[17] show that, for diphenyl-*N*-oxide, $a_N = 36.65\rho_N + 1.38\rho_O$ when Hückel MO was used for the spin density calculation, and $a_N = 35.61\rho_N - 0.93\rho_O$ if the McLachlan spin densities were used. Furthermore, Vasserman and Buchechenko[18] have used the formula $a_N = Q\rho_N$ for some nitric oxide derivatives. According to the SCF calculation by Kikuchi[19] with CNDO/2 approximation, the unpaired electron is almost completely localized on the $2p\pi$ AO's of nitrogen and oxygen of nitric oxide derivatives.

In the case of CT interaction with an electron acceptor, both of ρ_N and ρ_O of DTBNO will decrease. Since $|Q_1| \gg |Q_2|$ and $Q_1 > 0$ in Eq. (10), the CT interaction may cause the decrease of a_N.

The electrostatic interaction seems to polarize the charge distribution on the NO group, thus affecting the densities. Namely, when DTBNO is put in a polar environment or if some polar group approaches the NO group, the polarization in the sense $>N^{+\delta}-O^{-\delta}$ will occur, leading to the enhancement of the spin density on nitrogen. We assume that the spin densities change respectively to $\rho_N + \delta\rho_N$ and $\rho_O - \delta\rho_O$ by electrostatic interaction. Thus, the change of a_N can be written as $\Delta a_N = Q_1\delta\rho_N + Q_2\delta\rho_O$. As $\delta\rho_N - \delta\rho_O = 0$ (no intermolecular charge transfer), $\Delta a_N = (Q_1 - Q_2)\delta\rho_N = (Q_2 - Q_1)\delta\rho_O$. Since $\delta\rho_N > 0$ and $Q_1 \gg Q_2$ as mentioned above, a_N may increase by electrostatic interaction.

In the case of the hydrogen bonding interaction with proton donors such as ethanol and phenol, the σ-type lone pair electrons on oxygen of DTBNO will be mainly concerned with the bonding. Owing to the short range interaction, the electrostatic polarization $>N^{+\delta}-O^{-\delta}$ will be more extensive in the hydrogen bonding interaction than in the case of the non-hydro-

14) T. Kubota, Y. Oishi, K. Nishikida, and H. Miyazaki, This Bulletin, **43**, 1622 (1970).
15) A. H. Maki and E. W. Stone, *J. Amer. Chem. Soc.*, **87**, 454 (1965).
16) M. Karplus and G. K. Frenkel, *J. Chem. Phys.*, **35**, 1312 (1961).
17) P. B. Ayscough and F. P. Sargent, *J. Chem. Soc., B*, **1966**, 907.
18) A. M. Vasserman and A. L. Buchechenko, *J. Struct. Chem., USSR*, **7**, 633 (1966).
19) O. Kikuchi, This Bulletin, **42**, 1187 (1969).

gen-bonding electrostatic interaction. Moreover, the electron delocalization in the hydrogen bond as indicated by $>N^{+}-O-H\cdots O^{-}-$ will contribute to the enhancement of the spin density on nitrogen. Thus, the hydrogen bonding interaction will increase a_N a great deal.

Summarizing the above arguments, the hfc constant of nitrogen decreases by the charge transfer from the highest occupied π-orbital of DTBNO in the EDA complex formation, while it increases by the non-hydrogen-bonding electrostatic interaction as well as by the hydrogen bonding interaction.

Deguchi[20] pointed out that the increase of the hfc constant of some stable radicals in non-hydrogen-bonding polar solvents was approximately proportional to the dipole moment μ of the solvent molecule. The solvent effects on the hfc constant of DTBNO nitrogen is shown in Fig. 10 and Table 4. We see from Fig. 10, that there is an approximately linear relation between the a_N value of DTBNO and the μ value of the non-hydrogen-bonding solvent. The relation between a_N and μ values might be ascribed to the fact that the

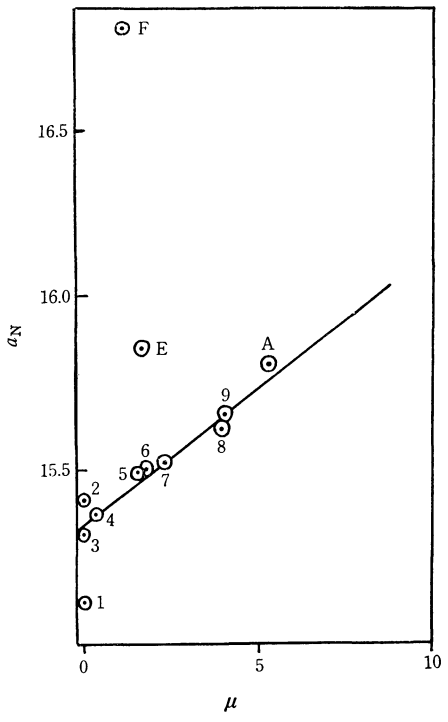

Fig. 10. The relation between the nitrogen hfc constant of DTBNO and the dipole moment of the solvent. See Table 4 for numberings 1—9 in the figure.
A: the value for DTBNO-PA complex in toluene.
E: the a_N value in ethanol solution.
F: the a_N value of DTBNO-phenol complex in toluene.

20) Y. Deguchi, This Bulletin, **35**, 260 (1962); K. Mukai, H. Nishiguchi, K. Ishizu, and Y. Deguchi, *ibid.*, **40**, 2731 (1967).

TABLE 4. SOLVENT EFFECT ON THE ^{14}N hfc CONSTANT OF DTBNO

	Solvent	ε	$\lvert\mu\rvert$	$a_N(G)$
1	Cyclohexane	2.023	0	15.15
2	Benzene	2.284	0	15.41
3	Mesitylene	2.27	0	15.31
4	Toluene	2.379	0.39	15.36
5	Monochlorobenzene	5.621	1.56	15.49
6	DMA	5.29	1.61	15.49
7	*o*-Dichlorobenzene	9.93	2.26	15.51
8	Nitrobenzene	34.82	3.99	15.62
9	Benzonitrile	25.20	4.05	15.65

ESR spectra reflect the short range molecular interactions more sensitively than the optical spectra.

The a_N value of the DTBNO-phenol hydrogen bonded complex in toluene and that of DTBNO in ethanol are given in Fig. 10. The a_N values are much larger than those expected from the $a_N \sim \mu$ linear relation in the non-hydrogen-bonding solvents. This is in accordance with the above argument.

It can be seen from Tables 3 and 4 that the EDA complex formation of DTBNO with electron acceptors such as TCNE, PMDA, and PA leads to the increase of a_N. Several workers argued that electrostatic interaction between the partners in the EDA complex seems to make an important contribution to the stability of the complex, particularly in the case of weak π-π complexes. Our results indicate that the electrostatic forces play important roles also in the case of π–π complexes of DTBNO. Although TCNE as well as PMDA molecules do not have dipole moment as a whole, they have large local dipole moment. The local electric moment seems to cause the increase of a_N in the molecular complex formation. However, we cannot conclude even for these weak π–π complexes that the electrostatic interaction is predominant (or exclusive) in the ground state. If the electrostatic interaction is predominant, we can expect that the a_N value of TCNE-DTBNO complex is larger than or at least nearly equal to that of PMDA-DTBNO complex, since TCNE seems to have larger local dipole moments than those of PMDA. Contrary to this, the observed a_N value of the former complex is significantly smaller than the value of the latter. Thus, in the case of the TCNE-DTBNO complex, the CT interaction seems to play an important role. This is in accordance with the ordinary CT concept in view of the fact that the electron affinity of TCNE is 1.8 eV compared with 0.8 eV of PMDA.

The authors express their cordial thanks to Dr. T. Kubota of Shionogi Research Laboratory for his helpful discussions.

Diffuse Reflection Spectra of Filter Papers Dyed with 1-Arylazo-2-naphthols

Yoshio MATSUNAGA and Nobuhiko MIYAJIMA

Department of Chemistry, Faculty of Science, Hokkaido University, Sapporo

(Received August 21, 1970)

The diffuse reflection spectra of filter papers dyed with sixteen 1-arylazo-2-naphthols were examined in the range from 350 to 700 mμ. The absorption bands due to both the azo and hydrazone tautomers were observed in this state. Appreciable changes in the hue of the dyed papers caused by moisture were attributed to the deviation from the Kubelka-Munk theory due to the increased regular reflection; however, the movement of the tautomeric equilibrium caused by moisture was also clearly demonstrated in many cases. The direction was found to depend upon the kind and position of the substituents, *e.g.*, towards the azo tautomer in the case of the *p*-Cl and *o*-NO_2 derivatives and towards the hydrazone tautomer in the case of the *m*-Cl and *o*-MeO derivatives.

Spectroscopic studies of 1-arylazo-2-naphthols have indicated that these compounds exist in solution and also in the solid state as mixtures of the azo and hydrazone tautomers, I and II.[1-5]

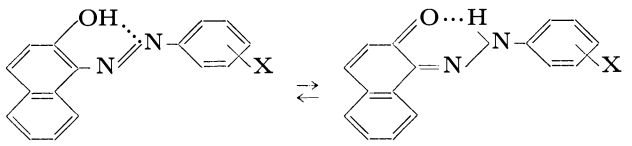

(I) (II)

In a previous paper, we demonstrated that diffuse reflection spectra of 1-phenylazo-2-naphthol and its fifteen derivatives diluted with sodium chloride consist of absorption bands which can be assigned to both the azo and hydrazone tautomers.[6] In addition, we disclosed that the equilibrium moves by dilution towards the hydrazone tautomer, regardless of the kind and position of the substituents. As the compounds are prototypes of azo dyestuffs, it seemed that it would be interesting to examine the possible tautomerism in the compounds deposited on various substrates, *e.g.*, cotton, silk, wool *etc.*, by the same technique. We wish to report in this paper, the first of our attempts along this line, the results of our spectral measurements of filter papers dyed with 1-arylazo-2-naphthols. As we noticed that the hue of the dyed papers is sensitive to moisture, the effects of this on the spectra were also studied.

Experimental

Materials. The samples of 1-arylazo-2-naphthols were the same as those used in our previous work.[6] The derivatives carried one of the following substituents in the *o*-, *m*-, and *p*-positions on the phenyl ring: methyl, chloro, hydroxy, methoxy, and nitro.

Measurements. Toyo filter papers, No. 2, 5.5 cm in diameter, were wetted as uniformly as possible with an acetone solution of one of the 1-arylazo-2-naphthols, dropped from a 1-m*l* pipette with graduations. The concentration and volume were adjusted to achieve 3—6 μg of the dye per cm^2 of the paper. After the solvent had been evaporated at room temperature, the papers were dried at 100°C for 10 min and then cooled in a desiccator over silica gel. The difference in reflectance between the filter paper and the dyed paper, which is generally in the range from 0 to 60%, was recorded in the visible region by means of a Beckman DK 2A spectroreflectometer. When this measurement was finished, both the dyed paper and the reference were left overnight in a desiccator containing distilled water; then the difference in reflectance was measured in order to obtain the spectrum affected by moisture. To check the reproducibility, the papers were dried again and the measurements were repeated. The spectra were plotted using the Kubelka-Munk function, $f(R)=(1-R)^2/2R$, where R is the reflectance. The absorption spectra of the 1-arylazo-2-naphthols dissolved in *n*-hexane, ethanol, and chloroform were measured by means of a Beckman DK 2A spectrophotometer. The concentrations were in the order of 10^{-5} mol/*l*. In all the figures in this paper, the reflection and absorption spectra are plotted taking the maxima arbitrarily as 1.00.

Results and Discussion

1-Phenylazo-2-naphthol (Figs. 1 and 2). As is shown in Fig. 1, the spectrum of the dried dyed paper consists of a broad band located in the region between 350 and 440 mμ and a sharp strong band with a maximum at 490 mμ. This spectrum closely resembles that measured in the chloroform solution (see curve *c* in Fig. 2). The former band, which dominates in the spectrum observed in a hexane solution, has been assigned to the azo tautomer, and the latter, to the hydrazone tautomer.[1] When the dyed paper is moistened, the relative intensity in the region from 350 to 440 mμ is much increased. However, the correlation between the spectral change and the movement of the equilibrium is not straightforward. Examining the solution spectra presented in Fig. 2, we reach the conclusion that the movement of the equilibrium towards the azo tautomer is probably not accompanied by an increase in the relative intensity in the region above 500 mμ. This is in serious disagreement with the finding in Fig. 1. The apparent change of the spectrum by moisture may be mostly caused by the deviation from the Kubelka-Munk theory due to the increased regular reflection. In accordance with this view, the absolute intensity at the absorption maximum

1) A. Burawoy, A. G. Salem, and A. R. Thompson, *J. Chem. Soc.*, **1952**, 4793.
2) D. Hadzi, *ibid.*, **1956**, 2143.
3) K. J. Morgan, *ibid.*, **1961**, 2151.
4) I. Saito, Y. Bansho, and A. Kakuta, *Kogyo Kagaku Zasshi*, **70**, 1715 (1967).
5) H. Rau, *Ber. Bunsenges. Phys. Chem.*, **72**, 637 (1968).
6) C. Dehari, Y. Matsunaga, and K. Tani, This Bulletin, **43**, 3404 (1970).

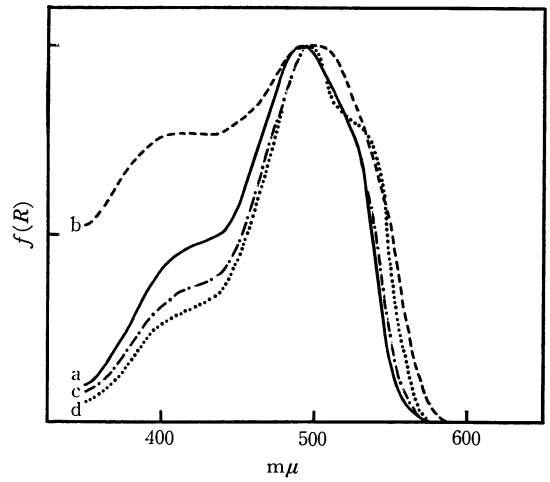

Fig. 1. Spectra of filter papers dyed with 1-phenylazo-2-naphthol; (a) dried and (b) moistened, and with 1-(*o*-tolylazo)-2-naphthol; (c) dried and (d) moistened.

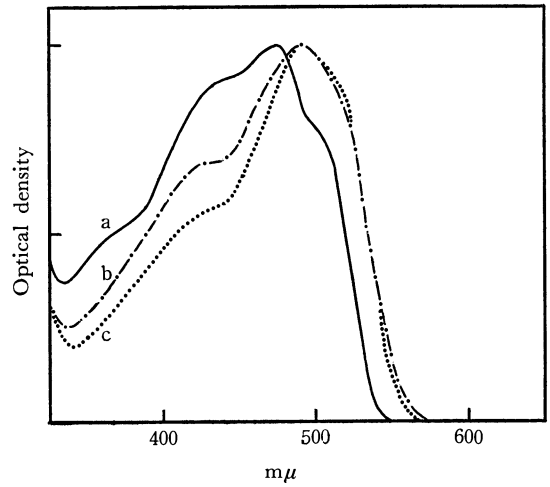

Fig. 2. Spectra of 1-phenylazo-2-naphthol dissolved in (a) *n*-hexane, (b) ethanol, and (c) chloroform.

observed with the moist dyed paper is only one eighth of that observed with the dried paper.

1-Tolylazo-2-naphthols (Fig. 1). When the papers are dried, all the Me derivatives show essentially the same spectrum. In the case of the *o*-Me derivative shown in Fig. 1, the spectrum is only slightly flattened by moisture (see Table 1). It is easy to see that the relative intensity decreases in the region from 350 to 490 mμ and increases in the region from 520 to 580 mμ upon this treatment. A shoulder due to the hydrazone tautomer can be clearly seen around 530 mμ. As the azo tautomer has an absorption maximum around 430 mμ, the whole change may be considered as an indication of a slight movement of the equilibrium towards the hydrazone tautomer. In the other two derivatives, marked decreases in the absolute intensity were observed upon moistening; however, no movement of the equilibrium could be detected. The relative intensity in the region from 350 to 450 mμ, which has been considered a measure of the amount of the azo tautomer by Burawoy and also by Bansho, increases in the order of substituents: *o*-Me<*m*-Me≲H≲*p*-Me. This is in accordance with the order found

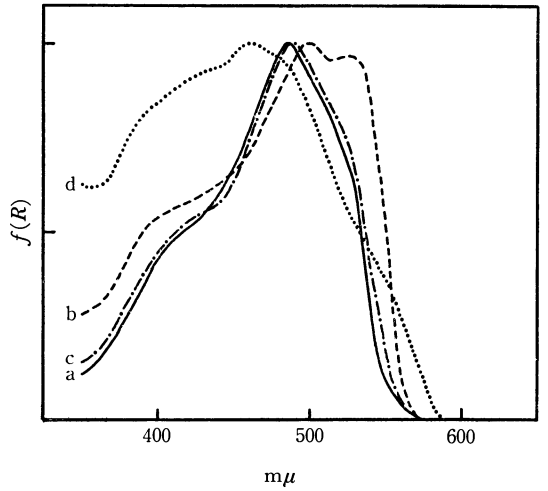

Fig. 3. Spectra of filter papers dyed with 1-(*m*-chlorophenylazo)-2-naphthol; (a) dried and (b) moistened, and with 1-(*p*-chlorophenylazo)-2-naphthol; (c) dried and (d) moistened.

in an ethanolic solution by Burawoy *et al.*

1-Chlorophenylazo-2-naphthols (Fig. 3). The spectra of the dried papers dyed with these derivatives are very close to each other; however, large differences can be found when they are moistened. The spectrum of the *o*-Cl derivative is least affected by moisture. A relatively slight flattening and the appearance of a shoulder around 525 mμ can be noted. The spectrum of the moistened paper dyed with the *m*-Cl derivative presented in Fig. 3 has a well-resolved doublet, located at 500 and 525 mμ, indicating the movement of the equilibrium towards the hydrazone tautomer. This spectrum is similar to that of the same compound highly diluted with sodium chloride.[6] Not only a flattening by a factor of ten by moisture, but also a drastic change in the spectrum, was observed in the case of the *p*-Cl derivative. The relative intensity is very much increased in the region from 350 to 480 mμ and is decreased in the region from 490 to 540 mμ. This change may be attributed to the movement of the equilibrium towards the azo tautomer. It may be pointed out that the spectrum thus obtained looks like the spectrum of the same compound diluted with sodium chloride at a concentration of 1%.[6] As may be noticed in Fig. 3, the relative intensities in the region from 350 to 450 mμ are little different from each other in the dry state.

1-Hydroxyphenylazo-2-naphthols (Figs. 4 and 5). When the dyed papers are dry, the *o*-OH and *m*-OH derivatives exhibit spectra similar to that of 1-phenylazo-2-naphthol. Upon moistening, the spectrum of the *o*-OH derivative shows a decrease in its relative intensity in the region between 500 and 550 mμ. As a result, a shoulder appears around 550 mμ. The equilibrium seems to move a little towards the azo tautomer upon the addition of moisture. As is shown in Fig. 4, the effect of moisture on the spectrum of the *m*-OH derivative is somewhat strange. The whole spectrum seems to be simply shifted to wavelengths shorter by 30 mμ. However, from a comparison with the spectra measured in various solvents shown in Fig. 5, we may conclude that the observed change arises from

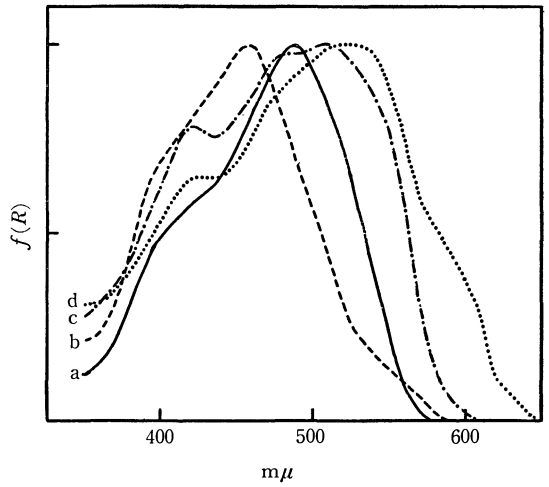

Fig. 4. Spectra of filter papers dyed with 1-(*m*-hydroxyphenylazo)-2-naphthol; (a) dried and (b) moistened, and with 1-(*p*-hydroxyphenylazo)-2-naphthol; (c) dried and (d) moistened.

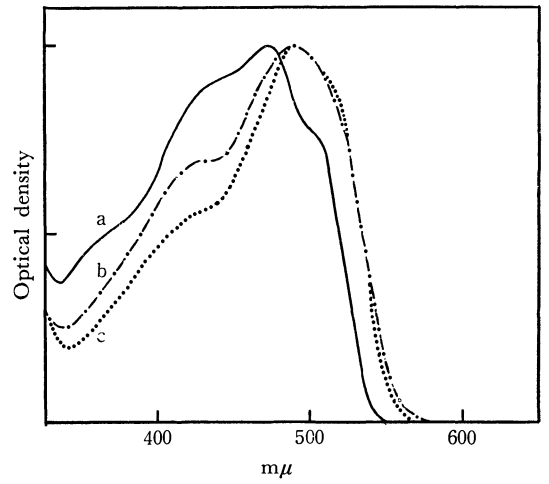

Fig. 5. Spectra of 1-(*m*-hydroxyphenylazo)-2-naphthol dissolved in (a) *n*-hexane, (b) ethanol, and (c) chloroform.

the movement of the equilibrium towards the azo tautomer. The *p*-OH derivative shows a spectrum very different from those of the other two, even in the dry state. The high relative intensity of the absorption around 420 mμ indicates that a fairly large amount of the azo tautomer is present. The spectral change caused by moisture may be attributed to an increase in the amount of the hydrazone tautomer.

1-Anisylazo-2-naphthols (Fig. 6). The spectra of the *o*-MeO and *m*-MeO derivatives are of the same kind. The only difference is in the relative intensity in the region from 350 to 450 mμ; it is much higher in the *m*-MeO derivative than in the *o*-MeO derivative. The same tendency is also observed in various solvents. Both of them are flattened by moisture. The doublet appearing at 525 and 560 mμ and assignable to the hydrazone tautomer can be distinctly seen in the case of the *o*-MeO derivative. The spectral change caused by moisture found in the case of the *m*-MeO derivative is less pronounced here. Nevertheless, the appearance of a shoulder at 525 mμ is undoubtedly a sign of the movement of the equilibrium towards

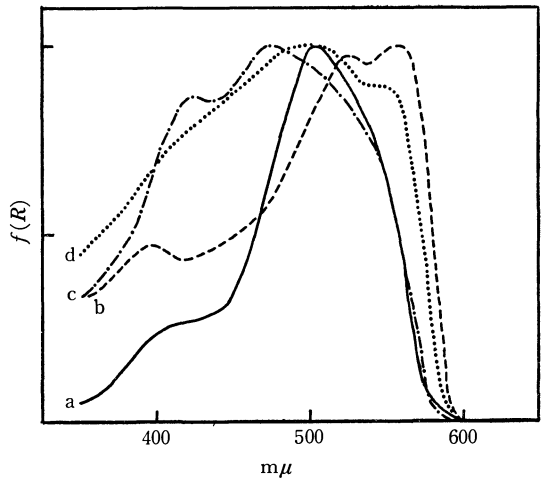

Fig. 6. Spectra of filter papers dyed with 1-(*o*-anisylazo)-2-naphthol; (a) dried and (b) moistened, and with 1-(*p*-anisylazo)-2-naphthol; (c) dried and (d) moistened.

the hydrazone tautomer. The spectrum of the *p*-MeO derivative is rather similar to that of the *p*-OH derivative. For these two compounds, the equilibria in solution very much favor the azo tautomer. The presence of strong maxima at 420 and 480 mμ to be assigned to the azo and hydrazone tautomers respectively indicates that the amounts of the two are comparable in the dry state. When the dyed paper is moistened, the above-mentioned maxima are replaced by those at 500 and 550 mμ assignable to the hydrazone tautomer. The former maximum apparently corresponds to the one at 480 mμ in the dry state. The relative intensities in the region from 350 to 450 mμ are in the order: *o*-MeO<*m*-MeO<H<*p*-MeO; this order is in good agreement with the order found in ethanolic solutions.[1)]

1-Nitrophenylazo-2-naphthols (Figs. 7 and 8). Although the spectra of these derivatives look alike in the dry state, the effects of moisture are not the same. In the case of the *o*-NO_2 derivative, the sharp peak at 490 mμ disappears and a broad band with a maximum at 440 mμ becomes dominant. The tautomeric

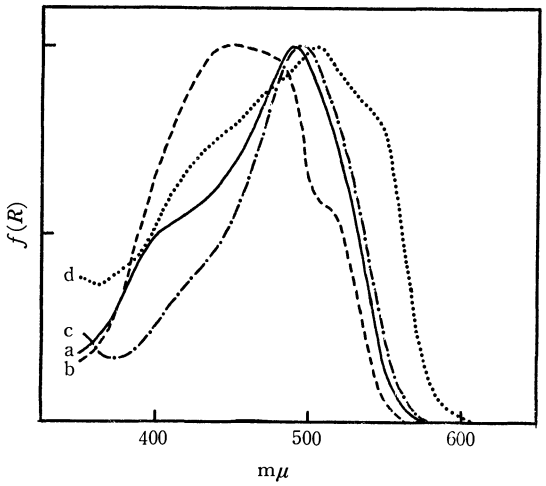

Fig. 7. Spectra of filter papers dyed with 1-(*o*-nitrophenylazo)-2-naphthol; (a) dried and (b) moistened, and with 1-(*p*-nitrophenylazo)-2-naphthol; (c) dried and (d) moistened.

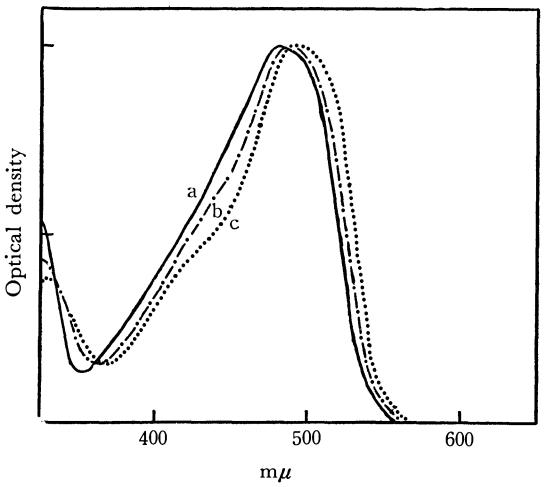

Fig. 8. Spectra of 1-(*p*-nitrophenylazo)-2-naphthol dissolved in (a) *n*-hexane, (b) ethanol, and (c) chloroform.

equilibrium moves drastically towards the azo tautomer. The spectrum of the *m*-NO_2 derivative is most flattened by moistening; nonetheless, the movement of the equilibrium is clear. The sharp peak at 480 mμ observed in the dry state is replaced by a broad one at 510 mμ on moistening. It must be added that these absorption bands are shifted to wavelengths longer by 50 mμ compared to those observed in solution.

Although the spectrum of the *p*-NO_2 derivative looks similar to those of the other two, comparison with the spectra observed in the solid, two-component system with sodium chloride suggests that the peak located at 495 mμ is due to the azo tautomer. The shoulder appearing at 540 mμ on moistening is to be assigned to the hydrazone tautomer. These assignments are supported by our measurements of the absorption spectra. This compound has been considered to exist nearly exclusively as a hydrazone tautomer in solution; however, a close examination of the spectra presented in Fig. 8 shows that the two tautomers exhibit absorption maxima only 40—50 mμ apart. Compared to these spectra, the bands in the spectrum of the dyed paper appear to be shifted by as much as 70 mμ.

General Remarks. On the basis of the spectrum, we may conclude that 1-arylazo-2-naphthol exists, in general, as a mixture of the azo and hydrazone tautomers when deposited on filter paper. As is summarized in Table 1, the spectrum plotted using the Kubelka-Munk function is flattened by moisture, mostly by a factor between two and ten. This phenomenon, attributed to the deviation from the theory due to the increased regular reflection, suggests a drastic change in the state of the dispersion of the dye molecules caused by moisture. As cellulose, the substrate in the present work, is a kind of polyhydric alcohol, and as the dyestuff is less soluble in water than in alcohol, it is very likely that the molecules of the dyestuff deposited on filter paper are segregated on moistening. Of course,

Table 1. The intensity ratio of the absorption maximum in the spectrum of moistened dyed paper to that in the spectrum of the corresponding dried paper and the direction of the movement of the equilibrium by moisture; towards the azo tautomer (+) or the hydrazone tautomer (−)

Substituent	Position		
	ortho	*meta*	*para*
None		0.12 (±)	
Methyl	0.8 (−)	0.1 (±)	0.2 (±)
Chloro	0.45 (−)	0.3 (−−)	0.1 (++)
Hydroxy	0.3 (+)	0.5 (+)	0.5 (−)
Methoxy	0.25 (−−)	0.35 (−)	0.2 (−)
Nitro	0.4 (++)	0.2 (−)	0.3 (−)

the extent of the segregation may depend upon the strength of the interaction between the dye molecule and the substrate, which, in turn, depends upon the nature of the substituent carried on the dye molecule.

It has been noted by Burawoy *et al.* that the relative stabilities of the hydrazone tautomer increase in this order of the solvents: hexane<alcohol<chloroform<water.[1] Therefore, the movement of the equilibrium of the dyestuff deposited on filter paper towards the hydrazone tautomer on moistening is reasonable if we consider the chemical constitution of cellulose. However, our observations, summarized in Table 1, indicate that this is not necessarily the case. Such a disagreement may be accounted for if we take into consideration the effect of moisture on the state of dispersion. In our previous work on the dyestuff-sodium chloride system, the spectral changes by dilution were attributed, at least in part, to the movement of the equilibrium towards the hydrazone tautomer.[6] The segregation of dye molecules deposited on filter paper by moisture must, therefore, favor the azo tautomer. These two effects of moisture oppose each other, but their magnitudes appear to be comparable. As is observed in our present study, the total effects depend on the kind and position of the substituent carried on the phenyl ring. As a matter of fact, the *o*-NO_2 derivative, which exhibits an exceptionally pronounced spectral change caused by moisture, is known to be one of those compounds which have solid-state spectra dominated by the absorption which is to be assigned to the azo tautomer.[6] In conclusion, the whole phenomenon is determined not only by the nature of the dyestuff itself, but also by the interaction between the dye molecule and the substrate. The results of the spectral measurements of the same compounds deposited on various fabrics made of both natural and synthetic fibers are in good accordance with this conclusion; the semeasurements will be the subject of forthcoming papers.

Infrared Absorption Spectra and Normal Coordinate Analysis of Metal-DL-α-Serine Chelates

Yoshie INOMATA, Tadaaki INOMATA, and Takao MORIWAKI

Department of Chemistry, Faculty of Science and Technology, Sophia University, Chiyoda-ku, Tokyo

(Received September 1, 1970)

The infrared absorption spectra of DL-α-serine and four metal-DL-α-serine chelates have been investigated from 4000 to 200 cm^{-1}. A normal coordinate analysis has been accomplished for the metal chelates as a 27-body problem and an approximate description of the vibrational mode has been assigned to the observed frequencies. The frequency separation between carboxylate antisymmetric and symmetric stretching vibrations and values of the bond-stretching force constants for the metal-nitrogen bonds have been found to decrease in the order Pt(II)>Pd(II)>Cu(II)>Ni(II). These facts show that the hydroxy group in the β-position of DL-α-serine has no influence on the order of metal-ligand bond strength, which order has been already found in aliphatic α-amino acids chelates having no hydroxy group in the β-position. Two species of copper chelates have been prepared. Though the infrared spectrum of one of them is similar to that of the nickel(II) chelate, that of the other species is different. This fact may be explained by assuming that the copper ion has been coordinated with the hydroxy group in the latter.

The infrared absorption spectra and the normal coordinate analysis for aliphatic α-amino acid chelates have already been studied by Lane[1] and Walter[2-4]. However, DL-α-serine having hydroxy group in the β-position and its metal-chelates have not been studied yet in detail. Nakamura[5] has made some empirical assignments for DL-α-serine copper(II) chelate in the region 1700 to 400 cm^{-1}. Nakamoto[6] have demonstrated that in amino acid chelates the frequency separation between carboxylate stretching vibrations increases in the order Ni(II)<Cu(II)<Pd(II)<Pt(II) regardless of the nature of the ligand, if the comparison is made in the same physical state. They have concluded that this fact is based on the increase of the covalent character in metal-oxygen bond. Nakagawa *et al.*[2] showed in DL-α-valine chelates that the metal-nitrogen bond-stretching force constants vary in the order Ni(II)<Cu(II)<Pd(II)<Pt(II) which indicates a relative strength of the interaction of metal-nitrogen bond and that the NH_2 stretching and the NH_2 rocking frequencies follow the same order.

In this investigation, the infrared spectra of four metal-serine chelates have been studied. The bond-stretching force constants for the metal-nitrogen bond have been calculated. In addition, we discuss how the hydroxy group in β-position influences the relation mentioned above. The problem of whether the hydroxy group coordinates with metal ion or not is also taken up.

Experimental

Preparation of Compounds. Bis(DL-α-serino)-platinum-(II) was prepared by stirring 2.6 g (0.025 mol) of DL-α-serine and 1.3 g (0.0031 mol) of potassium tetrachloroplatinate(II) in water (50—100 m*l*) at room temperature for several days. The white crystals separated were recrystallized from hot water and dried at room temperature *in vacuo* for several hours.

Found: C, 18.13; H, 2.85; N, 6.80%. Calcd for Pt-$C_6H_{12}N_2O_6$: C, 17.87; H, 3.00; N, 6.95%.

Bis(DL-α-serino)-palladium(II) was prepared by employing essentially the same procedure as that used above for the platinum(II) chelate.

Found: C, 22.38; H, 3.68; N, 8.75%. Calcd for Pd-$C_6H_{12}N_2O_6$: C, 22.91; H, 3.85; N, 8.91%.

Two species of Bis(DL-α-serino)-copper(II) were prepared. Elementary analysis of each of these two species gives the same results, but the absorption spectra and the color of these two chelates are different. One of them which gives a similar spectrum to the nickel(II) chelate was named "A chelate" and the other was named "B chelate".

The A chelate was prepared by stirring 5.3 g (0.05 mol) DL-α-serine and 2.8 g (0.013 mol) of basic copper carbonate in hot water at 70°C for 15 min, then condensing the filtrate to 25 m*l* after filtering. The blue crystal formed was filtered at hot stage. By cooling the filtrate, the sky blue B chelate was obtained. Both precipitates were washed by water and dried for several hours at 50°C *in vacuo*.

These chelates will be discussed in detail below.

A chelate. Found: C, 26.81; H, 4.23; N, 10.29%. Calcd for $CuC_6H_{12}N_2O_6$: C, 26.52; H, 4.45; N, 10.31%.

B chelate. Found: C, 26.89; H, 4.29; N, 10.30%. Calcd for $CuC_6H_{12}N_2O_6$: C, 26.52; H, 4.45; N, 10.31%.

Bis(DL-α-serino)-nickel(II) was prepared from 5.3 g (0.05 mol) of DL-α-serine and 3.0 g (0.008 mol) of nickel carbonate by the same procedure used above for the copper A chelate.

Found: C, 23.74; H, 5.39; N, 9.29%. Calcd for Ni-$C_6H_{12}N_2O_6 \cdot 2H_2O$: C, 23.79; H, 5.32; N, 9.25%.

Deuteration of Compounds. The deuterated DL-α-serine and metal chelates were prepared by dissolving the DL-α-serine and each chelate in 99.75 atom% deuterium oxide at 80°C and drying them *in vacuo*. The NH and OH groups were deuterated by this method.

Thermal Analysis of Chelates. Thermal analysis was performed with Rigaku Denki DTA-8001 from room temperature to 400°C in air and at the same time, the decrease of weight accompanying an endothermic reaction was measured. It was found that only the nickel(II) chelate had two molecules of water.

1) T. J. Lane, C. S. C., J. A. Durkin, and R. J. Hooper, *Spectrochim. Acta*, **20**, 1017 (1964).

2) I. Nakagawa, R. J. Hooper, and J. L. Walter, C. S. C., *ibid.*, **21**, 1 (1965).

3) J. F. Jackovitz and J. L. Walter, C. S. C., *ibid.*, **22**, 1393 (1966).

4) J. F. Jackovitz, J. A. Durkin, and J. L. Walter, C. S. C., *ibid.*, **23A**, 67 (1967).

5) K. Nakamura, *Nippon Kagaku Zasshi*, **80**, 113 (1959).

6) K. Nakamoto, "Infrared Spectra of Inorganic and Coordination Compounds," John Wiley & Sons, Inc., New York (1963), p. 201.

Absorption Measurement. The infrared absorption spectra from 4000 to 200 cm^{-1} were obtained with Hitachi EPI-G_2 and EPI-L spectrophotometers and were calibrated with polystylene, 1.2.4-trichlorobenzene and atmospheric water vapor. Samples were prepared as potassium bromide discs and nujol mulls. The spectra are shown in Figs. 1 and 2. The observed absorption frequencies and assignments for DL-α-serine and the metal chelates are listed in Table 1.

Discussion

The assignments of observed frequencies were made by comparison with metal-glycine,[1] -valine,[2] -leucine,[3] and -alanine[4] chelates and DL-α-amino-*n*-butyric acid[7] which had been thoroughly studied.

The spectra of DL-α-serine chelates are similar to the spectra of those which have *trans* configurations. The observed frequencies of DL-α-serine chelates have been reasonably assigned.

Assignment of Observed Frequencies. *DL-α-serine*: The spectrum of DL-α-serine shows the bands of NH_3^+ and COO^- which are characteristic of a zwitter ion as shown in Fig. 1. The strong broad bands at about 2900 cm^{-1} are assigned to the OH, CH and NH_3^+ stretching vibrations. On deuteration, the CH stretching vibration band is not shifted and is assigned easily.

The bands at 1662, 1633, 1513 and 1166 cm^{-1} which shift on deuteration are due to NH_3^+ deformation vibrations, since no corresponding bands appear in the metal chelates.

In addition there are bands at 1250 and 729 cm^{-1} which disappear on deuteration. Primary alcohols in the bonded state have diffuse association bands near 1420 and 1330 cm^{-1} (OH deformation and CH_2 wagging).[8] All alcohols show very broad bands in the range 750—650 cm^{-1}, which are assigned to out-of-plane bonded OH deformation vibrations.[9] It has been generally known that the frequencies of OH deformation vibrations can be affected by structures and hydrogen bond.[9] Therefore, it is reasonable to assign these two bands respectively to the OH in plane and out-of-plane deformation vibrations, considering that these bands appear at the same region also in the metal chelates and that the force constants of OH deformation vibrations calculated by normal coordinate analysis are approximately equal to that already reported for alcohol.

The assignments for COO^- stretching and deformation vibrations and CH and CH_2 deformation vibrations are easily made as shown in Table 1. The bands of CH and CH_2 deformation vibrations appear in the same region as DL-α-amino-*n*-butyric acid.[7] The hydroxy group is thought not to have affected these deformation vibrations. CN and CC stretching and skeletal deformation vibrations are assigned by comparison with the spectra of the metal chelates. The band at 1030 cm^{-1} is assigned to CO stretching vibration as in methyl alcohol.[9]

Metal-chelates: The spectra of the metal chelates shown in Figs. 1 and 2 are similar to each other except for that of copper(II) B chelate.

3400 to 2800 cm^{-1}: Although the bands above 3000 cm^{-1} are due to NH_2 antisymmetric and symmetric stretching and OH stretching vibrations, it is difficult to assign them separately, since all bands shift on deuteration.

1700 to 500 cm^{-1}: In this region the NH_2 deformation vibration appears instead of NH_3^+ deformation vibration of the ligand. They are assigned in view of the shift in deuterated compounds. The COO^- antisymmetric stretching vibration is observed in higher frequencies and deformation vibrations are at lower frequencies than those of the ligand. The OH in plane deformation vibration occurs at the same region (1250 cm^{-1}) as in the ligand and the OH out-of-plane

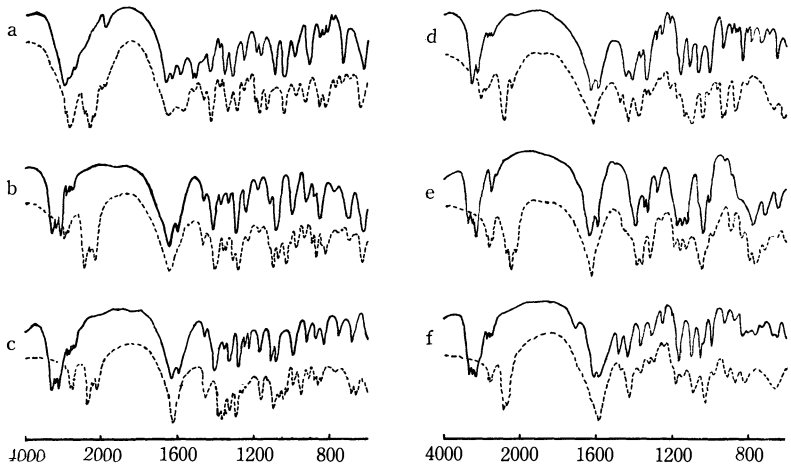

Fig. 1. Infrared absorption spectra of DL-α-serine, its chelates (——) and these deuterated compounds (----) in KBr disks.
a=DL-α-serine, b=Pt(II), c=Pd(II), d=Cu(II) A, e=Cu(II) B, f=Ni(II)

7) N. B. Colthup, L. H. Daly, and S.E. Wiberley, "Introduction to Infrared and Raman Spectroscopy," Academic Press, New York and London (1964), p. 275.
8) L. J. Bellamy, "The Infrared Spectra of Complex Molecules," John Wiley & Sons, Inc., New York (1958), p. 108.
9) M. Tsuboi and T. Takenishi, "Kagaku no Ryoiki," Zokan 37, Nanko-do, Tokyo (1959), p. 41.

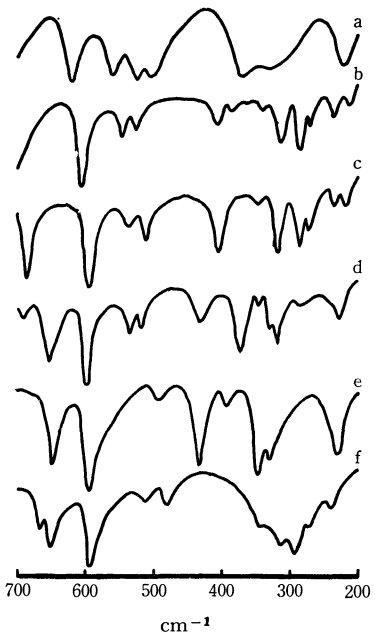

Fig. 2. Infrared absorption spectra of DL-α-serine and its metal chelates in nujol.
a=DL-α-serine, b=Pt(II), c=Pd(II), d=Cu(II) A, e=Cu(II) B, f=Ni(II)

deformation vibration shifts to lower frequencies.

500 to 200 cm^{-1}: In this region the absorption bands which cannot be observed in the ligand appear at 404 cm^{-1} for platinum(II) chelate, 407 cm^{-1} for palladium(II) chelate, 373 cm^{-1} for copper(II) A chelate, 394 cm^{-1} for copper(II) B chelate and 350 cm^{-1} for nickel(II) chelate. They are assigned to metal-nitrogen stretching vibration. The bands at 217 cm^{-1} for platinum(II) chelate and 218 cm^{-1} for palladium(II) chelate are assigned to metal-oxygen stretching vibration. Nakamura[5] has assigned the bands at 588 cm^{-1} for DL-α-serine copper(II) chelate and 581 cm^{-1} for DL-α-alanine copper(II) chelate to copper-nitrogen stretching vibration, and the bands at about 420 cm^{-1} to COO^- rocking vibration. These assignments are different from ours. If the band at about 590 cm^{-1} is assigned to metal-nitrogen stretching vibration, the force constant of metal-nitrogen stretching vibration has the value of 1.8—2.0 mdyn/Å by the calculation, which is much larger than that for glycine[1] and valine[2] chelates. In addition NH_2 vibrations for serine chelate are at the same region as those for valine chelate.[2] Therefore it is doubtful to assign the band at about 590 cm^{-1} to metal-nitrogen stretching vibration. The metal-nitrogen stretching vibration was observed in the region from 400 to 360 cm^{-1} and the NH_2 stretching vibration in the region from 3300 to 3100 cm^{-1} for valine chelate, for which the covalent character of the metal-nitrogen bond has been established.[2] Since the NH_2 stretching vibrations for the serine chelates are observed in the same region as those for valine chelates, the metal-nitrogen bonds of serine chelates must be fairly covalent and metal-nitrogen stretching vibrations for serine chelates should be in the region 400 to 360 cm^{-1}. Therefore the bands in this region of the chelates can be assigned to metal-nitrogen stretching vibration.

The carboxylate stretching vibrations are not shifted considerably on chelation, which indicates that the covalent character of metal-oxygen bond is weak. Consequently, metal-oxygen stretching vibration should be in the lower region than metal-nitrogen stretching vibration. Therefore the new bands at 217 cm^{-1} for platinum(II) chelate and 218 cm^{-1} for palladium(II) chelate can be assigned to metal-oxygen stretching vibration.

The skeletal deformation vibrations are assigned to the same range as those in the ligand by comparison with DL-α-leucine chelates.[3]

Copper Chelate. The spectra of the two species differ in many points as shown in Figs. 1 and 2. The principal difference is that the bands at 1250 and 686 cm^{-1} assigned to OH in plane and out-of-plane deformation vibrations respectively in copper(II) A chelate and in the ligand, disappear in copper(II) B chelate. In the far infrared region, the spectrum of B chelate is not similar to either those of A chelate or of any metal chelate. The copper(II) chelate studied by Nakamura[5] has no band to be assigned to OH deformation vibrations like the copper(II) B chelate. In addition, the X-ray spectra of copper(II) A chelate and copper (II) B chelate are different from each other. The infrared spectrum of the copper(II) chelate prepared from L-α-serine or D-α-serine does not coincide with either those of copper(II) A chelate or of copper(II) B chelate of DL-α-serine. It has been frequently discussed that the hydroxy group is coordinated with metal without changing its shape. The stability constants of metal-amino polycarboxylic acids chelates with hydroxy groups are higher than those without hydroxy groups. From this result it has been concluded that the hydroxy groups are coordinated to metals by forming chelate rings and that the chelates become stable.[10]

In the copper(II) B chelate, it may be assumed that the hydroxy group is coordinated with copper ion and becomes stable, since the basic character of the nitrogen atom of the amino group decreases from the inductive effect of the hydroxy group and since the copper ion can take on a distorted octahedral structure. Because the results of elementary analysis show the same values for both copper(II) A and copper(II) B chelates, it is doubtful whether the hydroxy group is coordinated to metal removing its hydrogen atom. In addition, it is hardly possible for the copper(II) B chelate to take the structure in which the hydroxy group forms a chelate ring, considering the bond distances and the bond angles of DL-α-serine studied by X-ray diffraction method.[11] Therefore copper(II) B chelate probably has the structure in which the hydroxy group bonds to another copper ion.

Thus, DL-α-serine chelates are found to be coordinated with metal through nitrogen and oxygen as well as other aliphatic α-amino acids, and the hydroxy group

10) T. Sakaguchi and K. Ueno, "Kinzoku Kireito," Vol. 1, Nanko-do, Tokyo (1965), p. 126.
11) D. P. Shoemaker, R. E. Burieau, J. Donohue, and Chia-Si Lu, *Acta Crystallogr.*, **6**, 241 (1957).

TABLE 1. OBSERVED FREQUENCIES AND ASSIGNMENTS FOR DL-α-SERINE AND METAL-DL-α-SERINE CHELATES (cm^{-1})

RH	PtR_2	PdR_2	CuR_2 A	CuR_2 B	NiR_2	Assignments
				3330 s		
	3268 s	3285 s	3285 vs	3311 sh	3310 s	
	3203 m	3202 m		3244 s	3249 s	N-H str. and O-H str.
	3097 s	3108 s	3139 s	3140 sh	3181 s	
2938 vs, b						
	2967 w	2961 w	2982 w		2980 w	
	2950 w	2944 w	2930 w	2945 sh	2953 w	C-H str.
	2919 w	2925 w		2929 w	2920 w	
	2891 w	2885 w	2870 w	2893 sh	2902 w	
					1713 m	H_2O
1662 vs						NH_3^+ deg. def.
1633 s						
1583 vs	1640 vs	1623 s	1621 vs	1628 s	1603 vs	COO^- asym. str.
	1598 m	1589 s	1589 vs	1583 s	1581 s	NH_2 scissors
1513 vs						NH_3^+ symm. def.
1506 vs						
1455 sh	1457 w	1458 w	1444 s		1481 s	CH_2 scissors
1435 s	1402 m	1404 s	1408 s	1397 s	1428 s	COO^- symm. str.
1377 w	1372 w	1377 w	1373 vw	1358 m	1372 s	CH_2 twisting
1355 vs	1331 w	1334 m	1359 m	1337 m		CH bending
1313 vs	1291 s	1287 s	1287 w	1288 m	1307 m	CH_2 wagging
1250 s	1242 s	1252 w	1250 w		1249 w	OH in plane def.
1186 m		1220 m	1206 w			
1166 m	1189 w	1172 m	1160 s	1153 s	1165 s	NH_2 wagging and CH bending for metal complexes
1154 m				1131 s		NH_3^+ rocking for DL-α-serine
	1102 m	1105 s	1108 s	1110 m	1108 s	NH_2 twisting
1098 s	1082 s	1080 m	1060 s	1057 sh	1062 s	C-N str.
				1040 s		
1030 vs	991 m	992 m	1000 s	1001 m	997 m	C-OH str.
988 m						
902 m	922 m	919 m	917 m	915 w	921 w	
851 w	874 w	868 m	890 w	885 w	867 w	C-C str.
			868 w			
			851 w			
830 w	850 m	831 m	831 m	829 vw	829 m	COO^- scissors and C-C str.
816 w			809 vw			
782 vw	776 w	756 m	786 w	784 m	762 m	CH_2 rocking
			731 w	728 m	701 vw	
729 m	698 m	687 m	686 w		667 m	OH out-of-plane def.
			651 m	647 m	652 m	NH_2 rocking
620 s	607 s	596 s	596 m	593 m	592 s	COO^- wagging
561 m	549 m	535 w	535 m	534 w	512 vw	COO^- rocking
526 m	521 w	513 w	519 m	494 vw	476 m	
503 m			438 w	434 m		
	404 w	407 m	373 m	394 vw	350 sh	M-N str.
375 mb		347 vw	347 w	348 m		
328 mb	335 vw	320 m	328 m	328 m		CCCN asym. def.
			319 m		317 sh	
	315 w	303 vw				
	284 w	283 m	285 w		293 m	CCCN symm. def.
225 mb	235 w	235 w	220 wb	230 m	240 w	CCCN def.
	217 w	218 w				MO str.

Abbreviations: RH=DL-α-serine, s=strong, m=medium, w=weak, sh=shoulder, b=broad

probably does not participate in coordination except in the case of copper(II) B chelate.

Normal Coordinate Analysis. A normal coordinate analysis for a metal chelate was performed as a 27-body problem using the model illustrated in Fig. 3. The calculations were carried out on HITAC 5020E[12] and IBM 1130 computers.

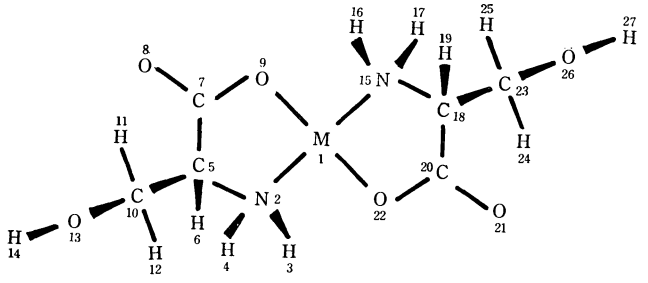

Fig. 3. Structure of DL-α-serine chelates.

The model adopted has M_1 as a center of symmetry. In the left side of the model, M_1, N_2, C_5, C_7, and O_9 form a planar five membered chelate ring and O_8 is on the same plane. The atoms C_5, C_{10}, O_{13}, and H_{14} are on the same plane which is perpendicular to this chelate ring and H_{11}, C_{10}, and H_{12} are on the same plane which is parallel to this chelate ring. Since no X-ray data for metal-DL-α-serine chelate is available, the bond lengths and bond angles listed in Table 2 were used in the calculation. They were taken from Refs. 4, 11, and 13.

Table 2. Bond lengths and bond angles used in the calculation for DL-α-serine chelate

Bond lengths (Å)					
1.	M_1–N_2	1.86	8.	O_9–M_1	1.916223
2.	N_2–H_3	1.01	9.	C_5–H_6	1.09
3.	N_2–H_4	1.01	10.	C_5–C_{10}	1.513
4.	N_2–C_5	1.491	11.	C_{10}–H_{11}	1.09
5.	C_5–C_7	1.528	12.	C_{10}–H_{12}	1.09
6.	C_7–O_8	1.261	13.	C_{10}–O_{13}	1.425
7.	C_7–O_9	1.252176	14.	O_{13}–H_{14}	0.956
Bond angles (°)					
O_9–M_1–N_2		90	O_8–C_7–O_9		120
C_5–C_7–O_8		120	C_7–O_9–M_1		$330-2\theta$
C_5–C_7–O_9		120			

θ: 190°28′

All other angles are assumed to be 109°28′. The same bond lengths and bond angles are used for second chelate ring.

The frequencies of infrared active species were calculated using the symmetry coordinates listed in Table 3. Wilson's *GF* matrix method[14] was used and all results were obtained using FORTRAN program designed by Shimanouchi.[15] The potential field employed was the following modified Uray-Bradley type,

$$2V = \sum_i \boldsymbol{K}_i(\Delta r_i)^2 + \sum_{i<j} \boldsymbol{H}_{ij}(r_0\Delta\alpha_{ij})^2 + \sum_{i<j} \boldsymbol{F}_{ij}(\Delta q_{ij})^2 + \sum_{i<j} \boldsymbol{F'}_{ij}\mathbf{Y} + \boldsymbol{P}(\Delta\omega)^2 + \sum_{i<j} \boldsymbol{T}_{ij}(\Delta\tau_{ij})^2$$

$$\Delta q_{ij} = S_{ij}\Delta r_i + S_{ji}\Delta r_j + (t_{ij}t_{ji})^{1/2}(r_0\Delta\alpha_{ij})^2$$

$$\mathbf{Y} = t_{ij}{}^2(\Delta r_i)^2 + t_{ji}{}^2(\Delta r_j)^2 - S_{ij}S_{ji}(r_0\Delta\alpha_{ij})^2 - 2t_{ij}t_{ji}(\Delta r_i)(\Delta r_j) + 2t_{ij}S_{ji}r_i(\Delta r_i)(\Delta\alpha_{ij}) + 2t_{ji}S_{ij}r_i(\Delta r_j)(\Delta\alpha_{ij})$$

$$r_0 = (r_ir_j)^{1/2}, \quad S_{ij} = (r_i - r_j\cos\alpha_{ij})/q_{ij},$$

$$t_{ij} = r_j\sin\alpha_{ij}/q_{ij}$$

where r_i is a bond length and α_{ij} is the angle between bonds r_i and r_j at an equilibrium position. q_{ij} is the distance between atoms i and j which are bonded to a common atom. ω is the angle between the C–C-(ring) bond and the COO^- plane. τ_{ij} is the torsion about the axis connecting atoms i and j. These torsions are C–C(ring), C–C, and C–OH.

The force constants are given by $\boldsymbol{K}$(stretching), $\boldsymbol{H}$ (bending), $\boldsymbol{F}$(repusion), $\boldsymbol{P}$(out-of-plane wagging) and $\boldsymbol{T}$(torsion). $\boldsymbol{F'}$ is introduced as a force constant associated with the linear terms of the repulsion energy and remains in this equation as an internal tension. The value of $\boldsymbol{F'}$ is estimated to be $-0.1\boldsymbol{F}$. Table 4 shows the observed and calculated frequencies, poten-

Table 3. Symmetry coordinates of the infrared active species for DL-α-serine chelates

	Description of coordinate		Description of coordinate
S_1	OH str.	S_{23}	CH_2 rocking
S_2	NH_2 asym. str.	S_{24}	COO^- scissors
S_3	NH_2 sym. str.	S_{25}	MO bending
S_4	CH_2 asym. str.	S_{26}	COO^- rocking
S_5	CH_2 sym. str.	S_{27}	MN str.
S_6	CH str.	S_{28}	CCCN asym. def.
S_7	NH_2 scissors	S_{29}	CCCN asym. def.
S_8	CH_2 scissors	S_{30}	CCCN sym. def.
S_9	COO^- asym. str.	S_{31}	CCO def.
S_{10}	COO^- sym. str.	S_{32}	MO str.
S_{11}	CO str.	S_{33}	MNC def.
S_{12}	OH in plane def.	S_{34}	COM def.
S_{13}	NH_2 wagging	S_{35}	MN bending
S_{14}	CH_2 wagging	S_{36}	COO^- wagging
S_{15}	NH_2 twisting	S_{37}	COO^- twisting
S_{16}	CH_2 twisting	S_{38}	C-CH_2 torsion
S_{17}	CN str.	S_{39}	OH torsion
S_{18}	NC-COO^- str.	S_{40}	redundancy N
S_{19}	CH_2–CH str.	S_{41}	redundancy C_5
S_{20}	CH bending	S_{42}	redundancy C_{10}
S_{21}	CH bending	S_{43}	redundancy C_7
S_{22}	NH_2 rocking		

The contents of symmetry coordinates are the same as those of Ref. (4) except OH vibrations.

12) These calculations are performed at Computer Centre, The University of Tokyo.

13) "Kagaku Binran Kiso hen II," Maruzen Inc., Tokyo (1966), p. 1163.

14) E. B. Wilson, *J. Chem. Phys.*, **7**, 1047 (1939); **9**, 76 (1941).

15) T. Shimanouchi, "Computer Programs for Normal Coordinate Treatment of Polyatomic Molecules," The University of Tokyo, Tokyo (1968).

TABLE 4. OBSERVED AND CALCULATED FREQUENCIES AND POTENTIAL ENERGY DISTRIBUTIONS AMONG SYMMETRY COORDINATES AND FORCE CONSTANTS FOR THE INFRARED ACTIVE VIBRATIONS OF THE PLATINUM(II) CHELATE

Obsd cm^{-1}	Calcd cm^{-1}	PED in symmetry coordinates %	PED in force constants %	Description
3268	3259	S_2 (100)	$\boldsymbol{K}$(N-H) 96	NH_2 asym. str.
3203	3213	S_3 (100)	$\boldsymbol{K}$(N-H) 95	NH_2 symm. str.
3097	3103	S_1 (99)	$\boldsymbol{K}$(O-H) 94	OH str.
2967	2978	S_4 (100)	$\boldsymbol{K}$(C-H) 82, $\boldsymbol{F}(HCO_{13})$ 14	CH_2 asym. str.
2950	2948	S_5 (97)	$\boldsymbol{K}$(C-H) 79, $\boldsymbol{F}(HCO_{13})$ 16	CH_2 symm. str.
2919				
2891	2878	S_6 (101)	$\boldsymbol{K}$(C-H) 87	CH str.
1640	1641	S_9 (85), S_{26}(15)	$\boldsymbol{K}(C-O_8)$ 55, $\boldsymbol{K}(C-O_9)$ 28	COO^- asym. str.
1598	1600	S_7 (99)	$\boldsymbol{H}$(HNH) 81	NH_2 scissors
1457	1458	S_8 (47), S_{14}(41)	$\boldsymbol{F}(HCO_{13})$ 39, $\boldsymbol{H}$(HCH) 32	CH_2 scissors
1402	1408	S_{10}(93), S_{24}(28)	$\boldsymbol{K}(C-O_9)$ 40, $\boldsymbol{K}(C-O_8)$ 20	COO^- symm. str.
1372	1374	S_{16}(64), S_{12}(16)	$\boldsymbol{F}(HCO_{13})$ 47, $\boldsymbol{H}(HCO_{13})$ 18	CH_2 twisting
1331	1332	S_{21}(54), S_{20}(18)	$\boldsymbol{H}$(NCH) 36, $\boldsymbol{F}$(NCH) 21	CH bending
1291	1292	S_{14}(61), S_8 (55)	$\boldsymbol{H}$(HCH) 38, $\boldsymbol{H}(C_{10}C_5H_6)$ 26	CH_2 wagging
1242	1244	S_{12}(73), S_{16}(21)	$\boldsymbol{H}(CO_{13}H)$ 42, $\boldsymbol{F}(CO_{13}H)$ 29	OH in plane def.
1189	1193	S_{13}(44), S_{20}(39)	$\boldsymbol{H}$(MNH) 17, $\boldsymbol{H}$(HNC) 16	NH_2 wagging
	1148	S_{13}(52), S_{21}(25)	$\boldsymbol{H}$(MNH) 22, $\boldsymbol{H}$(HNC) 17	NH_2 wagging
1102	1116	S_{15}(77)	$\boldsymbol{H}$(HNC) 33, $\boldsymbol{F}$(HNC) 25	NH_2 twisting
1082	1069	S_{17}(48), S_{23}(12)	$\boldsymbol{K}$(N-C) 31, $\boldsymbol{F}$(NCH) 11	CN str.
991	995	S_{11}(45), S_{24}(17)	$\boldsymbol{K}$(C-OH) 20, $\boldsymbol{F}$(OCO) 14	CO str.
	978	S_{11}(52), S_{24}(26)	$\boldsymbol{K}$(C-OH) 22, $\boldsymbol{F}$(OCO) 20	CO str.
922				
874	893	S_{19}(37), S_{23}(29)	$\boldsymbol{F}(C_{10}C_5H_6)$ 20, $\boldsymbol{K}(C_5-C_{10})$ 16	CC str.
850	835	S_{23}(18), S_{19}(18)	$\boldsymbol{F}(C_5C_{10}O_{13})$ 18, $\boldsymbol{F}(C_{10}C_5H_6)$ 15	CC str.
776	768	S_{23}(37), S_{22}(13)	$\boldsymbol{H}(C_{10}C_5H_6)$ 18, $\boldsymbol{F}(C_{10}C_5H_6)$ 13	CH_2 rocking
698	698	S_{39}(100)	$\boldsymbol{T}(C_{10}-O_{13})$ 100	OH out of plane def.
	688	S_{22}(67), S_{19}(10)	$\boldsymbol{H}$(MNH) 33, $\boldsymbol{H}$(HNC) 15	NH_2 rocking
607	607	S_{36}(100),	$\boldsymbol{P}(O_8C_7O_9)$ 100	COO^- wagging
	592	S_{31}(38), S_{18}(20)	$\boldsymbol{H}(C_5C_{10}O_{13})$ 17, $\boldsymbol{F}(CCO_9)$ 14	CCO def.
549	533	S_{26}(42), S_{17}(18)	$\boldsymbol{F}(CCO_8)$ 20, $\boldsymbol{H}(CCO_8)$ 18	COO^- rocking
521				
404	406	S_{27}(54), S_{28}(17)	$\boldsymbol{K}$(M-N) 40, $\boldsymbol{F}$(MNH) 11	MN str.
335	323	S_{29}(41), S_{31}(9)	$\boldsymbol{H}(C_7C_5C_{10})$ 44, $\boldsymbol{F}(C_7C_5C_{10})$ 19	CCCN asym. def.
315				
284	265	S_{30}(45), S_{29}(15)	$\boldsymbol{H}(NC_5C_{10})$ 15, $\boldsymbol{F}(NC_5C_{10})$ 7	CCCN symm. def.
235				
217	217	S_{32}(35), S_{28}(23)	$\boldsymbol{H}(NC_5C_{10})$ 22, $\boldsymbol{K}$(O-M) 27	OM str.

tial energy distributions to symmetry coordinates and force constants with an approximate description of the vibrational mode for the platinum(II) chelate. The force constants used in this calculation are listed in Table 5. They were evaluated so as to obtain the best fit between the calculated and the observed frequencies by a trial and error method guided by the values of a Jacobian matrix.

Metal-ligand Bonds. A similar calculation was accomplished for the palladium(II), copper(II) A, and nickel(II) chelates and good agreement was obtained between the observed and calculated frequencies for these chelates as well as for those of the platinum(II) chelate. In Table 6 the important frequencies related to the metal-ligand bonds are summarized for each chelate. The force constants used in these calculations are given in Table 7.

As seen in Table 6, the frequency separation of COO^- antisymmetric and symmetric stretching vibrations increases from the nickel(II) chelate to the platinum (II) chelate except for the copper(II) B chelate. The values of $\boldsymbol{F}_{dia}$(M-O) and $\boldsymbol{K}$(M-O) for platinum(II) chelate are larger than those of palladium(II) chelate as seen in Table 7. Therefore, the covalent character of the metal-oxygen bond can be considered to increase in the order Ni(II)<Cu(II)<Pd(II)<Pt(II). This same order has already been reported for glycine,[1] alanine,[4] and other aliphatic α-amino acids chelates.[2,3] A similar trend is observed in the COO^- rocking vibration. Although the metal-nitrogen stretching frequencies increase in the order Ni(II)< Cu(II)<Pt(II)<Pd(II), the force constants of the metal-nitrogen stretching vibration and the frequencies of the NH_2 scissors increase in the order Ni(II)<

TABLE 5. FORCE CONSTANTS USED IN THE CALCULATION FOR THE PLATINUM(II) CHELATE (mdyn/Å)

Streching		Bending		Repulsion	
K(M–N)	0.75	H(MNH)	0.19	F(MNH)	0.09
K(N–H)	5.55	H(MNC)	0.05	F(MNC)	0.10
K(N–C)	2.50	H(HNH)	0.57	F(HNH)	0.06
K(C_5–C_7)	1.50	H(HNC)	0.20	F(HNC)	0.40
K(C–O_8)	7.90	H(NCH)	0.285	F(NCH)	0.54
K(C–O_9)	6.80	H(NC_5C_7)	0.20	F(NC_5C_7)	0.20
K(O–M)	0.42	H(NC_5C_{10})	0.20	F(NC_5C_{10})	0.20
K(C–H)	3.96	H($C_7C_5H_6$)	0.19	F($C_7C_5H_6$)	0.36
K(C_5–C_{10})	1.50	H($C_7C_5C_{10}$)	0.40	F($C_7C_5C_{10}$)	0.30
K(C–O_{13})	2.30	H($H_6C_5C_{10}$)	0.187	F($H_6C_5C_{10}$)	0.36
K(O–H)	5.13	H(CCO_8)	0.50	F(CCO_8)	0.70
		H(CCO_9)	0.50	F(CCO_9)	0.70
		H(OCO)	0.65	F(OCO)	2.50
		H(COM)	0.05	F(COM)	0.10
		H(OMN)	0.05	F(OMN)	0.05
		H($C_5C_{10}O_{13}$)	0.45	F($C_5C_{10}O_{13}$)	1.20
		H(HCH)	0.37	F(HCH)	0.05
		H(HCO_{13})	0.16	F(HCO_{13})	1.288
		H($CO_{13}H$)	0.325	F($CO_{13}H$)	0.598
		H($O_{22}MN$)	0.05	F($O_{22}MN$)	0.05

Out-of-plane wagging
P(COO^-) 0.54 mdyn·Å

Torsion
T(C_5–C_7) 0.15 mdyn·Å, T(C_5–C_{10}) 0.065 mdyn·Å, T(C_{10}–O_{13}) 0.194 mdyn·Å

TABLE 6. OBSERVED AND CALCULATED FREQUENCIES RELATED TO THE METAL-LIGAND BOND (cm^{-1})

Vib. Mode	Pt(II)		Pd(II)		Cu(II) A		Cu(II) B		Ni(II)	
	Obsd	Calcd	Obsd	Calcd	Obsd	Calcd	Obsd	Calcd	Obsd	Calcd
NH_2 asym. str.	3268	3259	3285	3260	3285	3286	3311		3310	3294
NH_2 symm. str.	3203	3213	3202	3217		3239	3244		3249	3246
COO^- asym. str.	1640	1641	1623	1627	1621	1621	1628		1603	1606
NH_2 scissors	1598	1600	1589	1590	1589	1577	1583		1581	1580
COO^- symm. str.	1402	1408	1404	1388	1408	1408	1397		1428	1421
OH in plane def.	1242	1244	1252	1254	1250	1249			1249	1248
NH_2 wagging	1189	1193	1172	1178	1160	1168	1153		1165	1165
OH out of plane def.	698	698	687	688	686	686			667	665
COO^- wagging	607	607	596	595	596	596	593		592	592
COO^- rocking	549	533	535	524	535	524	534		512	515
MN str.	404	406	407	410	373	374	394		350	351
MO str.	217	217	218	222						

TABLE 7. VALUES OF FORCE CONSTANTS AND F_{dia} RELATED TO THE METAL-LIGAND BONDS

Force constant (mydn/Å)	Pt(II)	Pd(II)	Cu(II)A	Ni(II)	Force constant	Pt(II)	Pd(II)	Cu(II)A	Ni(II)
K(MN)	0.75	0.70	0.40	0.22	T(CO) mdyn·Å	0.19	0.19	0.19	0.18
K(NH)	5.55	5.55	5.65	5.68	P(OCO) mdyn·Å	0.54	0.52	0.52	0.52
K(CO_{ring})	6.80	6.80	6.80	6.70	F_{dia}(NH_2 asym. str.) mdyn/Å	5.78	5.78	5.87	5.90
K(CO)	2.30	2.40	2.44	2.50					
K(OH)	5.13	5.17	5.26	5.45	F_{dia}(COO^- asym. str.) mdyn/Å	7.72	7.67	7.62	7.52
K(MO)	0.42	0.35							
H(HNH)	0.57	0.56	0.56	0.56	F_{dia}(MN str.) mdyn/Å	1.01	0.98	0.65	0.45
H(CCO_{ring})	0.50	0.45	0.45	0.40	F_{dia}(MO str.) mdyn/Å	0.55	0.48		
H(OCO)	0.65	0.50	0.71	0.55	F_{dia}(NH_2 rocking) mdyn·Å	0.47	0.46	0.43	0.43
H(COH)	0.33	0.34	0.34	0.33	F_{dia}(CO torsion) mdyn·Å	0.19	0.19	0.19	0.18
H(MNH)	0.19	0.17	0.15	0.15					

F_{dia}=the diagonal elements of the symmetrized F matrix

Cu(II)<Pd(II)<Pt(II). The frequencies of the NH_2 wagging vibration show a slightly different trend. This fact can be explained by considering how little the metals affect this vibration, since the NH_2 wagging vibration is closely coupled with other vibrations as seen in Table 4. The calculated frequency of metal-nitrogen stretching vibration agrees fairly well with the observed frequency, and the force constant takes a reasonable value for each chelate. Therefore, considering the value of $\boldsymbol{K}$(M–N) and $\boldsymbol{F}_{\text{dia}}$(M–N), it is reasonable to conclude that the strength of the metal-nitrogen bond increases in the order Ni(II)<Cu(II)<Pd(II)<Pt(II). This trend is the same as that in many aliphatic α-amino acids chelates.[1–4] From these facts it might be asserted that the hydroxy group in the β-position of DL-α-serine has no influence on the order of the metal-ligand bond strength, which has been already found in aliphatic α-amino acid chelates having no hydroxy group in the β-position.

BULLETIN OF THE CHEMICAL SOCIETY OF JAPAN, VOL. 44, 372—374 (1971)

Low Frequency Infrared Absorption Bands of Water of Crystallization at Low Temperature

Kunio FUKUSHIMA

Department of Chemistry, Faculty of Science, Shizuoka University, Oya, Shizuoka

(Received September 3, 1970)

The low temperature infrared absorption spectra of water of crystallization of $BaCl_2 \cdot 2H_2O$, $CuCl_2 \cdot 2H_2O$ and $K_2C_2O_4 \cdot H_2O$, which have water of crystallization in different bound states, were measured and compared with the room temperature spectra. Corresponding to the change of temperature of the samples, remarkable change in frequencies and intensities was observed for the bands due to the lattice vibrations associated with water of crystallization.

Water of crystallization is classified into several types on the basis of its type of bonding with surrounding ions, electron acceptor or donor groups.[1] The infrared spectra of water of crystallization in the low frequency region vary with the difference of its bound state in the crystals, and they were investigated for aquo complexes by Nakagawa and Shimanouchi[2] and for several inorganic hydrates by van der Elsken and Robinson,[3] respectively. The author carried out calculations of optically active lattice vibrations of $BaCl_2 \cdot 2H_2O$, $BaCl_2 \cdot 2D_2O$,[4] $K_2C_2O_4 \cdot H_2O$, $K_2C_2O_4 \cdot D_2O$,[5] $CuCl_2 \cdot 2H_2O$ and $CuCl_2 \cdot 2D_2O$[6] crystals, which are different from each other in the type of bonding of water of crystallization, and obtained information about the bound state of the water of crystallization. A remarkable change in the far infrared spectra of certain kinds of water of crystallization with change of temperature has been reported.[7] In the present investigation, this change of infrared spectra with change of temperature has been studied for the crystals containing water of crystallization in different bound states.

Experimental

The samples were prepared by recrystallization of $BaCl_2 \cdot 2H_2O$ of Wako Pure Chemical Industries. Ltd., $CuCl_2 \cdot 2H_2O$ of Koso Chemicals Co., Ltd., and $K_2C_2O_4 \cdot H_2O$ of Koso Chemicals Co., Ltd. from their aqueous solutions, respectively. The infrared spectra of the samples in Nujol mull in the 700—60 cm^{-1} region were measured at low temper-

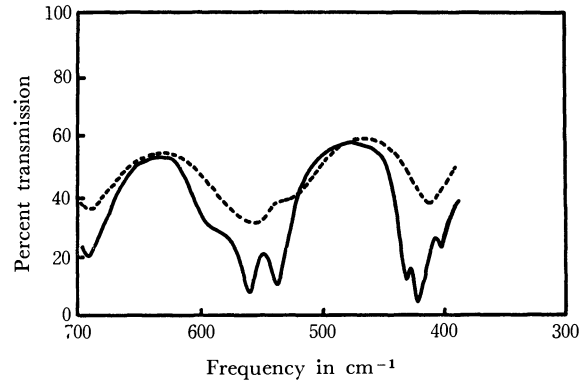

Fig. 1. Infrared spectra of $BaCl_2 \cdot 2H_2O$ at −150°C (solid line) and at room temperature (dotted line).

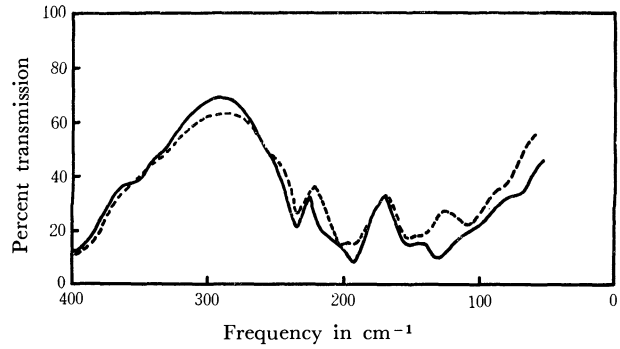

Fig. 2. Far infrared spectra of $BaCl_2 \cdot 2H_2O$ at −100°C (solid line) and at room temperature (dotted line).

1) R. Chidambaram, A. Sequeira, and S. K. Sikka, *J. Chem. Phys.*, **41**, 3616 (1964).
2) I. Nakagawa and T. Shimanouchi, *Spectrochim. Acta*, **20**, 429 (1964).
3) J. van der Elsken and D. W. Robinson, *ibid.*, **17**, 1249 (1961).
4) K. Fukushima and H. Kataiwa, This Bulletin, **43**, 690 (1970).
5) K. Fukushima, *ibid.*, **43**, 1313 (1970).
6) K. Fukushima, to be published.
7) Y. Kuroda, M. Nagasaki, and M. Kubo, presented at Symposium on Molecular Structure, Fukuoka, Japan (1969).

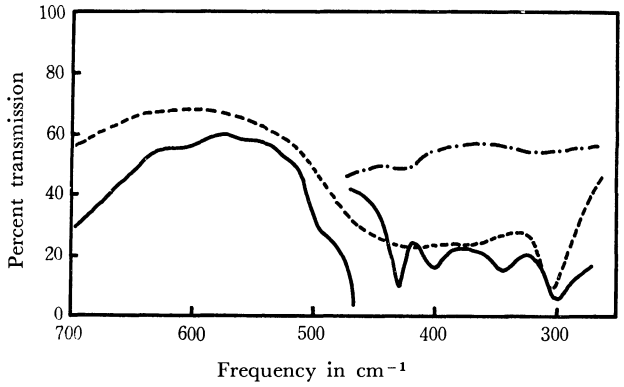

Fig. 3. Infrared spectra of $CuCl_2 \cdot 2H_2O$ at $-95°C$ (solid line) and at room temperature (dotted line); (broken line, Nujol placed between polyethylene plates at $-95°C$).

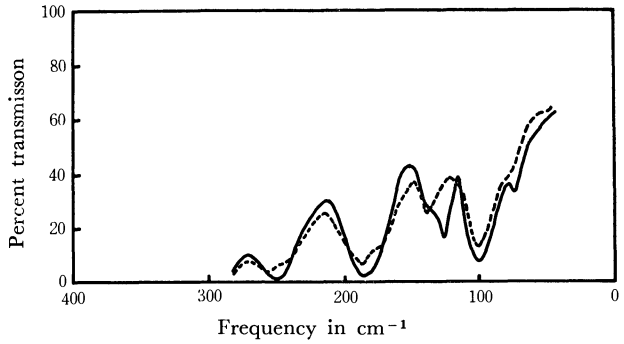

Fig. 4. Far infrared spectra of $CuCl_2 \cdot 2H_2O$ at $-100°C$ (solid line) and at room temperature (dotted line).

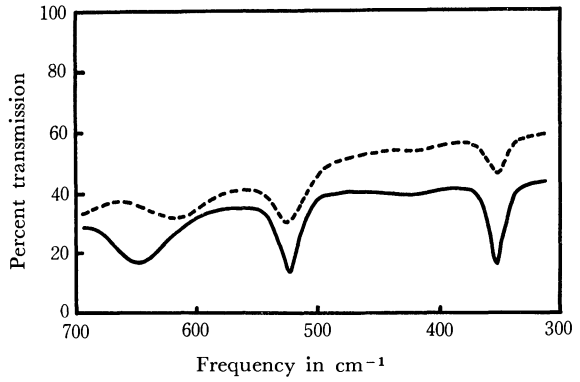

Fig. 5. Infrared spectra of $K_2C_2O_4 \cdot H_2O$ at $-75°C$ (solid line) and at room temperature (dotted line).

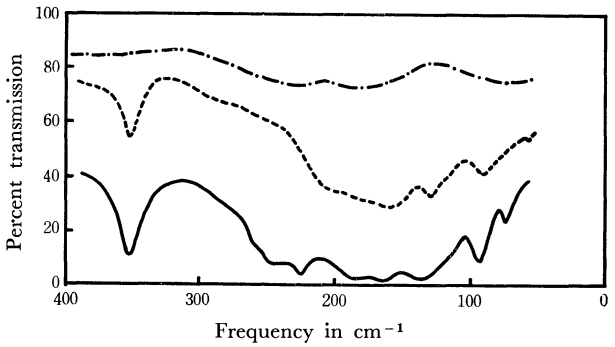

Fig. 6. Far infrared spectra of $K_2C_2O_4 \cdot H_2O$ at $-100°C$ (solid line) and at room temperature (dotted line); (broken line, Nujol placed polyethylene at $-100°C$).

ature. The measurements were made using low temperature cells cooled with liquid nitrogen. The Nujol mull was placed between two CsI plates for the measurements of the infrared spectra of $BaCl_2 \cdot 2H_2O$ and $K_2C_2O_4 \cdot H_2O$ in the 700—400 cm^{-1} region, while it was placed between two polyethylene plates for the measurements of these samples in the 400—60 cm^{-1} region and of $CuCl_2 \cdot 2H_2O$ in the 700—400 cm^{-1} region, respectively. By means of a copper-constantan thermocouple recording system the temperature of the samples was found to be constant within $\pm 2°C$ through the measurements. The infrared spectra were recorded with a Hitachi EPI-L spectrophotometer for the 700—400 cm^{-1} region and with a Hitachi FIS-3 far infrared spectrophotometer for the 400—60 cm^{-1} region. In the measurements of the low temperature spectra with the latter spectrophotometer, the effect of radiation of the samples and the low temperature cell was removed by the double chopping devices in the spectrophotometer. The spectra are shown in Figs. 1—6.

Results and Discussion

(A) $BaCl_2 \cdot 2H_2O$. The infrared spectra at low temperature are shown in Figs. 1 and 2, compared with those at room temperature. Among the bands in the room temperature spectra, which were concluded to be due to water of crystallization on the basis of frequency shift associated with deuteration,[4] those at 684 cm^{-1}, 555 cm^{-1} and 525 cm^{-1} become sharp at low temperature, but do not change their frequencies markedly. On the other hand, at low temperature the bands at 405 cm^{-1} and 330 cm^{-1} increase their frequencies and two other new bands appear at 432 cm^{-1} and 400 cm^{-1}. According to the results of the lattice vibration calculation[4] for the crystal structure (space group, $P2_1/n\text{-}C^5_{2h}$) determined by Padmanabhan,[8] four H_2O rocking vibrations are expected to appear in the infrared absorption spectra in the 400—300 cm^{-1} region (calculated frequencies, 398 cm^{-1}, 328 cm^{-1} (A_u species); 401 cm^{-1}, 334 cm^{-1}. (B_u species). Therefore, the appearance of the four bands is expected, and the fact that the bands in the room temperature spectra have lower frequencies than those of corresponding bands in the low temperature spectra suggests increase of the hindering potential for rocking motion of water of crystallization (the hindering potential about the C axis of H_2O molecule) at low temperature.

(B) $CuCl_2 \cdot 2H_2O$. As are shown in Figs. 3 and 4, three sharp bands appear at 425 cm^{-1}, 400 cm^{-1} and 340 cm^{-1} in the low temperature spectra instead of the one broad band in the room temperature spectra, which has been assigned as due to water of crystallization.[6] According to the calculation of the optically active lattice vibrations[6] for the crystal structure determined by Petersen and Levy,[9] three bands (one B_{1u}, one B_{2u} and one B_{3u} species) due to the rotational lattice vibrations associated with water of crystallization are expected to appear in the infrared absorption spectra. The three sharp bands seem to correspond

8) V. M. Padmanabhan, W. R. Busing, and H. A. Levy, *Acta Crystallogr.*, **16**, 13 (1963).

9) S. W. Petersen and H. A. Levy, *J. Chem. Phys.*, **26**, 220 (1957).

to the above-mentioned three vibrations. The bands at 250 cm^{-1}, 180 cm^{-1} sharpen and one at 125 cm^{-1} increase its intensity at low temperature. The calculation showed presence of optically active lattice vibrations primarily associated with translational lattice modes of water of crystallization, whose frequencies correspond well to the frequencies of the bands.[6]

(C) $K_2C_2O_4 \cdot H_2O$. The bands at 624 cm^{-1} and 524 cm^{-1} in Figs. 5 and 6 in the room temperature spectra were interpreted as due to water of crystallization on the basis of frequency shift on deuteration and neutron scattering data.[5,10] At low temperature, the former band shifts to higher frequency, while the latter does not change its frequency. According to the calculation of the optically active vibrations,[5] the former band is assigned to a rotational lattice vibration primarily associated with H_2O rocking and wagging modes, and the latter to one primarily associated with an H_2O twisting mode. Therefore, it may be concluded that the degree of hindering around the principal axes, B and C, of the H_2O molecule increase at low temperature, while that around the A axis does not change. At low temperature the bands at 230 cm^{-1} and 244 cm^{-1} increase their intensities. The calculated frequencies, 224 cm^{-1} (A_u species) 208 cm^{-1} (B_u species) of the lattice vibrations associated with the translational lattice modes of water of crystallization[5] suggest an assignment of these bands to the above-mentioned vibrations.

In the crystal of $CuCl_2 \cdot 2H_2O$, the H_2O molecule is bound to Cl^-'s and Cu^{2+} as is shown in Fig. 7B, and the $Cu^{2+} \cdots O$ bond is considered to be strong, as the ion-atom distance is short (1.925 Å). On the other hand, in the crystal of $BaCl_2 \cdot 2H_2O$, the H_2O molecule is bound to Cl^-'s and Ba^{2+}'s as is shown in Fig. 7A. The Ba^{2+}'s are located almost in the direction of the lone-pair orbitals of the O atom (assuming sp^3 hybridization) and thus are in favorable bonding position, although the $Ba^{2+} \cdots$ O distances are rather long (2.7—3.0 Å). In the case of $K_2C_2O_4 \cdot H_2O$, the K^+'s are located off the direction of the lone-pairs of the O atoms and the $K^+ \cdots O$ distance is long (2.933 Å). Therefore, the H_2O molecules are differenlty bound in these crystals. Although it is very difficult to interpret the difference between the room temperature spectra and the low temperature spectra, the following comments will be made here in the present paper. In the case of $CuCl_2 \cdot 2H_2O$, the

10) K. Fukushima, This Bulletin, **43**, 39 (1970).

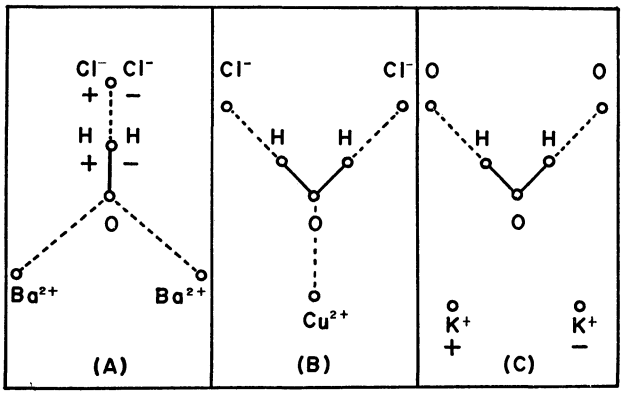

Fig. 7. Schematic representation of water of crystallization in crystals.
(+, above the paper plane; −, below the plane).

water of crystallization is so-called "coordinate water", and two H_2O molecules and two Cl^-'s are bound to Cu^{2+} by covalent type bonds. They altogether form one "molecule", $CuCl_2 \cdot 2H_2O$. Therefore, it is expected that in the room temperature spectra the bands due to H_2O molecules may be better described as ones of $CuCl_2 \cdot 2H_2O$ "molecules" arranged in the crystal. At low temperature, however, the interactions between $CuCl_2 \cdot 2H_2O$ "molecules" increase, and the state of H_2O molecules becomes similar to that of so-called "lattice water". The observed spectral change of sharpening of band width and shift of bands as a whole to lower frequency with temperature depression (see Fig. 3) may be considered as due to change of the bound state of H_2O molecule from "coordinate water" to "lattice type water". On the other hand, in the case of $BaCl_2 \cdot 2H_2O$ and $K_2C_2O_4 \cdot H_2O$, the water of crystallization is so-called "lattice water". The spectral change of the crystals with temperature depression is the increase of frequencies and intensities of some bands along with sharpening of bands. This may be caused by change of the degree of interactions between H_2O molecules and surrounding atoms and ions.

The author wishes to express his gratitude to Professor T. Miyazawa of Osaka University for allowing him to use the Hitachi EPI-L spectrophotometer and the Hitachi FIS-3 far infrared spectrophotometer, and also to Dr. T. Kitagawa and Miss M. Tsuchida of Professor Miyazawa's laboratory for their kind assistance through the measurements.

The Recombination of Iodine Atoms Generated by a C. W. Argon Ion Laser

Naohiko HARADA, Yuji MORI, and Ikuzo TANAKA

Department of Chemistry, Tokyo Institute of Technology, Ookayama, Meguro-ku, Tokyo

(Received September 8, 1970)

The rate constants of iodine-atom recombination in various foreign gases were determined by measuring the relative concentrations of iodine atoms in the photostationary state, through irradiation by a c.w. argon-ion laser at 4880 Å. The relative concentration has been obtained from the absorption intensity for the emission line from an iodine discharge lamp at 1830 Å. The rate constants have been given for the diffusion of iodine atoms and for the second-order recombination of iodine atoms. The values of the diffusion rate constants in various foreign gases have been compared with the calculated values. The logarithmic second-order rate constants in various gases were plotted against their ionization potentials. The plot yielded a straight line, indicating that the formation of the charge-transfer complex between iodine atoms and foreign gas molecules is important in the recombination process, as has been suggested by Porter *et al.*

The gas-phase iodine-atom recombination reaction in the presence of third-body gases has already been studied by several methods. Some of the earliest measurements have been made by Rabinowitch and Wood,[1] using the photostationary state method, by measuring the change in the absorbance of molecular iodine.

The flash-photolysis technique has been applied to iodine-atom recombination by numerous investigators.[2–12] Christie, Harrison, Norrish, and Potter,[3] measuring the decrease of iodine molecules, have pointed out that there is a rapid termolecular reaction, $I+I+I_2 \rightarrow I_2+I_2$.

Porter and Smith[10] have found that the second-order recombination rate constant for iodine atoms shows a negative activation energy which decreases as the chaperon efficiency increases. This was explained by the existence of intermediate complexes, as has been suggested by Rabinowitch and Wood,[1] where the complexes resulted not from normal van der Waals-type interactions but from charge-transfer interactions between the third body (M) and the iodine atom.[9,10,13]

$$I + M \rightleftarrows IM$$

$$IM + I \rightarrow I_2 + M.$$

Strong *et al.*[6] have observed the same rate of recombination at different wavelengths for photolytic initiation; they have concluded that excited atoms ($^2P_{1/2}$) either recombine at the same rate as ground-state atoms or are deactivated to the ground state ($^2P_{3/2}$) before measurements are made.

The present study has been planned in order to investigate the recombination reaction of iodine atoms, a reaction initiated by the intense light from a c.w. argon-ion laser at 4880 Å. This method enables us to detect the iodine atoms directly by absorption.

In this study the recombination rate was measured by monitoring the concentration of the atomic iodine in the ground state, which absorbs the resonance lines of iodine atoms, not by monitoring the concentration of iodine molecules. Under our experimental conditions, the measurements by the former will be more accurate than those by the latter, because only a very small proportion of iodine molecules decreases upon irradiation.

Experimental

1. *C. W. Argon-ion Laser.* An argon-ion laser has been constructed in our laboratory. The maximum output power with a single line at 4880 Å was 810 mW at the discharge current of 28 Å and with a magnetic field of about 600 gauss. The output power from the laser was controlled by changing the discharge current.

2. *Reaction Cell and the Optical System for the Detection of Iodine Atoms.* Figure 1 is a schematic diagram of the optical system used in the present measurements. The monochromatic light beam at 4880 Å from the argon-ion laser entered the quartz reaction cell and induced the photodissociation of iodine molecules into atoms. In order to increase the dissociation rate, a concave mirror with a focal length of 80.2 cm was put behind the cell to reflect the laser beam into the cell. The reaction cell had four windows and a small tube at the bottom. The small tube contained a small amount of iodine crystals and was immersed in a water bath at 22°C (iodine vapor pressure was 0.25 Torr at 22°C).

The 1830 Å light beam from an iodine discharge lamp entered the reaction cell, crossed the laser beam at a right angle, and fell on the incident slit of a monochromator after passing through the cell. The iodine lamp, which was powered by microwave. was made of a quartz tube 20 mm in outer-diameter, and had a side arm immersed in a water-ice bath in order to maintain a constant iodine vapor pressure and to give narrow, unreversed lines. The carrier gas of the lamp was 2 Torr He. The monochromator with a 1440 lines/mm grating was set at 1830 Å with a slit width of 0.5

1) E. Rabinowitch and W. C. Wood, *J. Chem. Phys.*, **4**, 497 (1936).
2) M. I. Christie, R. G. W. Norrish, and G. Porter, *Proc. Roy. Soc., Ser. A*, **216**, 152 (1953).
3) M. I. Christie, A. J. Harrison, R. G. W. Norrish, and G. Porter, *ibid., Ser. A*, **231**, 446 (1955).
4) R. Marshall and N. Davidson, *J. Chem. Phys.*, **21**, 659 (1953).
5) K. E. Russell and J. Simons, *Proc. Roy. Soc., Ser., A*, **217**, 271 (1953).
6) R. L. Strong, J. C. W. Chien, P. E. Graf, and J. E. Willard, *J. Chem. Phys.*, **26**, 1287 (1957).
7) D. L. Bunker and N. Davidson, *J. Amer. Chem. Soc.*, **80**, 5085, 5090 (1958).
8) R. Engelman, Jr., and N. Davidson, *ibid.*, **82**, 4770 (1960).
9) S. J. Rand and R. L. Strong, *ibid.*, **82**, 5 (1960).
10) G. Porter and J. A. Smith, *Proc. Roy. Soc. Ser. A*, **261**, 28 (1961).
11) T. A. Gover and G. Porter, *ibid., Ser. A*, **262**, 476 (1961).
12) G. Porter, Z. G. Szabo and M. G. Townsend, *ibid., Ser. A*, **270**, 493 (1962).
13) G. Porter, *Discuss. Faraday Soc.*, **33**, 198 (1962).

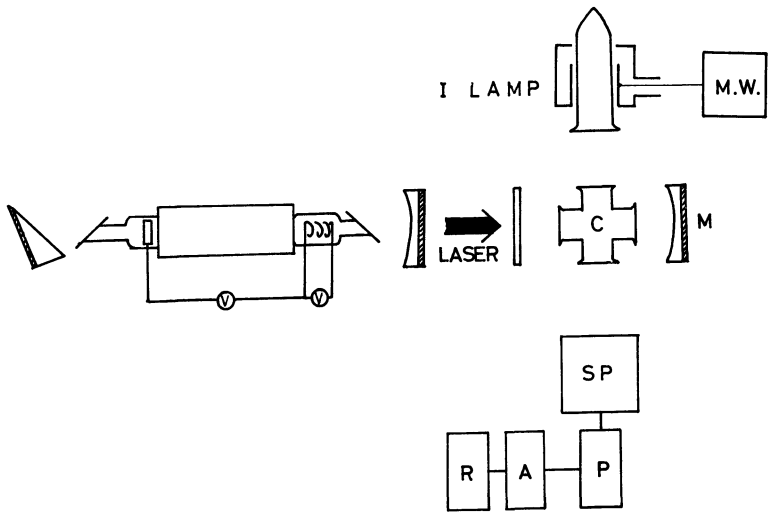

Fig. 1. Schematic diagram of apparatus.

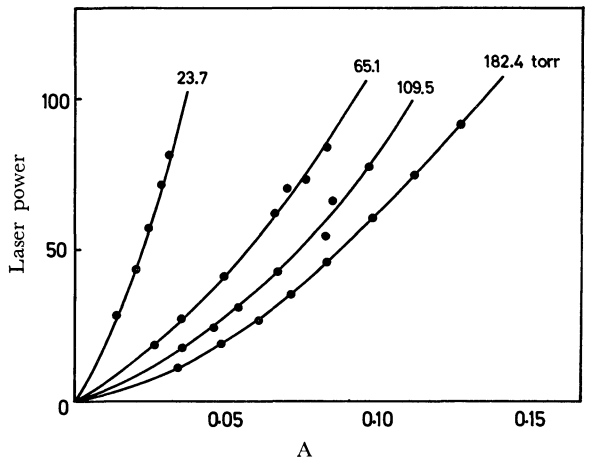

Fig. 2. Plots of the laser output power (P_0) to absorbance of iodine atoms (A) at various pressure of argon.

mm. The intensity of the exit beam from the monochromator was measured and recorded on a chart paper with a conventional photomultiplier-D.C. amplifier-recorder combination. Since the atmospheric oxygen absorbs the light below 1900 Å, nitrogen streamed between the iodine lamp and the cell, in the monochromator and also in the photomultiplier casing.

3. *Materials.* Commercially-available reagent-grade iodine crystals were used after purification by sublimation three times. The foreign gases used in the present study, He, Ne, Ar, Xe, H_2, N_2, NO, CO, CO_2, and C_3H_8, were supplied by the Takachiho Chemical Industry Co. and were used without further purification.

4. *Procedure.* The iodine atoms in the cell were detected by measuring the absorbance for a resonance line of iodine atoms. At first, upon closing the shutter for the laser light, the intensity of the analyzing light at 1830 Å, I_0, was measured. Then, the shutter was opened and the intensity, I, was measured again. The absorbance at 1830 Å, log I_0/I, gives the relative concentration of iodine atoms.

The absorbance by molecular iodine of the laser light was independent of the laser output power and of the pressure of foreign gases, and it remained constant during the reaction, within the limits of experimental error. Thus, it can be said that the production rate of iodine atoms is proportional to the laser output power and that iodine molecules decompose to only a small extent.

The effect of the light absorption at 1830 Å due to molecular iodine on the determination of the iodine-atom concentration can be ignored because of the weak absorption of molecular iodine. Much care was taken in adjusting the optical system so that the analyzing light beam crossed the laser light beam exactly.

Results

Figures 2, 3, and 4 illustrate the results obtained in argon as a foreign gas. Figure 2 shows that the laser output power increases with an increase in the absorbance of iodine atoms at 1830 Å, and the slope

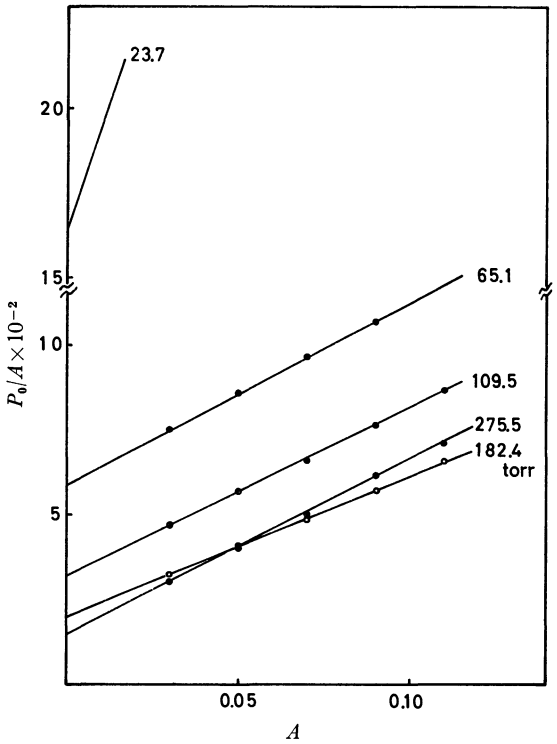

Fig. 3. Plots of P_0/A against A.

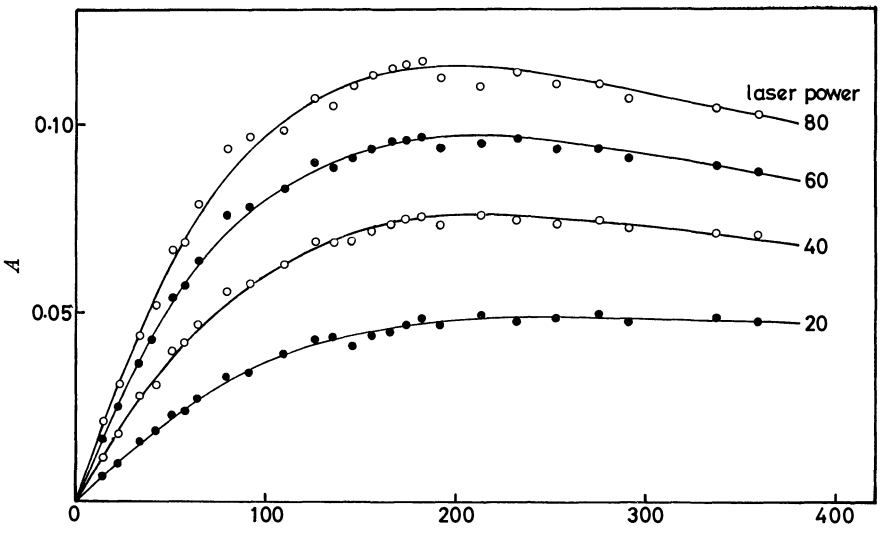

Fig. 4. Variation of absorbance of iodine atoms with the change in argon pressure.

gradually becomes steeper at high absorbances. This is clearly shown in Fig. 3, where the ratio of the laser-output power (P_o) to the absorbance at 1830 Å (A; relative concentration of iodine atoms) increases linearly with the absorbance. This indicates that the participation of the second-order iodine atom recombination becomes important at high concentrations of iodine atoms. The pressure effect of a foreign gas on the iodine-atom recombination is demonstrated in Fig. 4, where the absorbance at 1830 Å may be seen to increase at low foreign-gas pressures, while at high pressures it decreases with an increase in the foreign-gas pressure after it reaches a maximum. This can be interpreted in terms of the decreasing rate of the diffusion of iodine atoms to the wall at low pressures and by the increasing rate of iodine-atom recombination in the gas phase because of the increased second-order rate constant at high pressures of foreign gases.

The absorption of the laser light at 4880 Å by iodine molecules induces the decomposition of iodine molecules into atoms, a half of the atoms in the ground state ($^2P_{3/2}$) and the rest in the excited state ($^2P_{1/2}$):

$$I_2 + h\nu(4880\,\text{Å}) \xrightarrow{I_a} I(^2P_{3/2}) + I^*(^2P_{1/2}) \quad (1)$$

The excited iodine atoms are, however, subjected to fast quenching collisions with molecules before recombination[14,15]:

$$I^*(^2P_{1/2}) + M \longrightarrow I(^2P_{3/2}) + M \quad (2)$$

and have little effect on the recombination reaction.[4]

The mechanisms of the iodine-atom recombination in the gas-phase are believed to involve the following reactions:

1) recombination to form iodine molecules after the diffusion of iodine atoms to the wall of the reaction vessel:

$$I + \text{wall} \xrightarrow[k_3]{\text{(diffusion)}} 1/2\ I_2 + \text{wall} \quad (3)$$

2) recombination of iodine atoms through collisions with foreign-gas molecules:[1]

$$I + I + M \xrightarrow[k_4]{} I_2 + M \quad (4)$$

3) recombination of iodine atoms through collisions with iodine molecules:[3]

$$I + I + I_2 \xrightarrow[k_5]{} 2I_2 \quad (5)$$

Reaction (3) plays an important role in the recombination of iodine atoms at low foreign-gas pressures, while, at higher pressures, reaction (4) predominates over reaction (3). Reaction (5) can not be ignored in spite of the very low concentration of iodine molecules, for the rate constant of reaction (5) has a much larger value than that of reaction (4).[13]

A photostationary-state treatment leads to the next equation for the mechanism of the iodine-atom recombination:

$$\frac{d[I]}{dt} = 2I_a - k_3[I] - (k_4[M] + k_5[I_2])[I]^2 = 0 \quad (6)$$

where [I] is the concentration of iodine atoms, which is proportional to the absorbance of iodine atoms at 1830 Å, [M], the concentration of foreign-gas molecules, and [I_2], that of iodine molecules. Since I_a is proportional to the laser output power (P_o), the next equation can be obtained from Eq. (6):

$$\alpha P_0 = k_3[I] + (k_4[M] + k_5[I_2])[I]^2 \quad (7)$$

and:

$$\frac{\alpha P_0}{[I]} = k_3 + (k_4[M] + k_5[I_2])[I] \quad (8)$$

where α is a constant. This equation can explain the linear relationship between P_o/A and A in Fig. 3, because A gives the relative concentration of iodine atoms. The intercept in the figure gives the relative value of k_3 for a pressure of a foreign gas, and the slope of the linear plot gives the relative value of $k_4[M]+k_5[I_2]$. Since k_3 is inversely proportional to the pressure of a foreign

14) R. J. Donovan and D. Husain, *Nature*, **206**, 171 (1965).
15) R. J. Donovan and D. Husain, *Trans. Faraday Soc.*, **62**, 11 (1966).

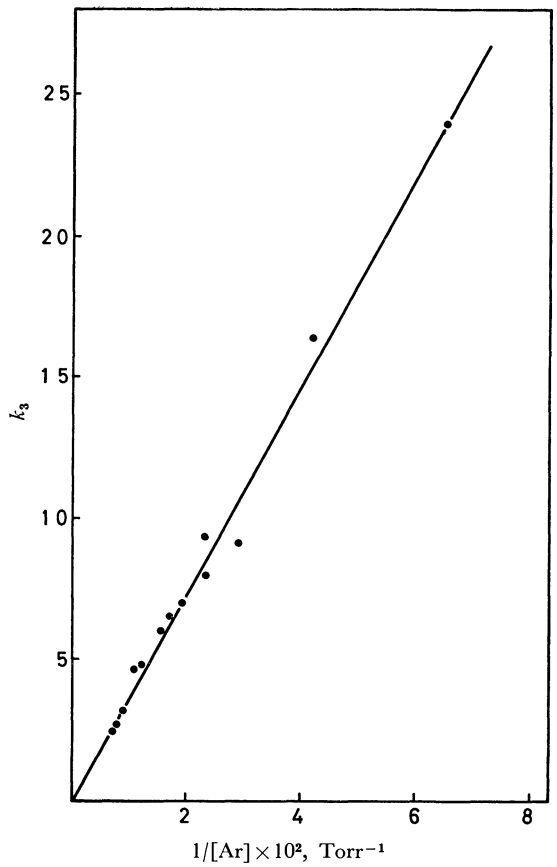

Fig. 5. Plots of k_3 against 1/[Ar].

gas, as is shown in Fig. 5, the relative value of the diffusion-rate constant, β, can be obtained by using the relation:

$$k_3 = \frac{\beta}{[M]} \tag{8'}$$

The plots of the values of $k_4[M]+k_5[I_2]$ for various foreign-gas pressures give the straight line in Fig. 6. From the intercept in the figure, the relative value of the rate constant, k_5, can be obtained, while from the slope of the linear plots, the relative value of k_4 can be obtained. The relative values of β for various foreign gases are listed in Table 1, and those of k_4 and that of k_5 are listed in Table 2.

TABLE 1. RELATIVE VALUE OF THE DIFFUSION RATE CONSTANT OF IODINE ATOMS IN VARIOUS GASES

Gas	β	D'(calculated)
He	5.1	4.0
Ne	1.7	1.7
Ar	1	1
Xe	0.81	0.52
H_2	5.1	4.8
N_2	1.2	1.2
CO	0.95	1.1
CO_2	0.95	0.92
C_3H_8	0.80	0.60

TABLE 2. RELATIVE VALUE OF k_4 IN VARIOUS FOREIGN GASES

Gas	This work	Other work
He	0.5	0.4[a]
Ne	0.4	0.5[a]
Ar	1	1
Kr		1.3[a]
Xe		1.6[a]
H_2	0.8	1.9[b]
N_2	0.4	
CO	3.8	
CO_2	6.8	4.5[b]
C_3H_8	27	
n-C_4H_{10}		12[b]
I_2	4×10^2	260[a], 530[b]

a) M. I. Christie *et al.*[3]
b) G. Porter.[13]

Discussion

Diffusion-rate Constant. Helium and hydrogen offer the least resistance to the diffusion of iodine atoms, as is shown in Table 1. Xenon shows the slowest diffusion among rare gases. The rates in carbon dioxide and in propane had to be less accurately measured because of the fast rates of the recombination of iodine atoms in these gases. Since there have been no available data of the diffusion coefficient of iodine atoms in various gases, we have calculated the diffusion-rate constant, which can be compared with β.

The diffusion coefficient of iodine atoms in a gas is given by the next equation, based on a simple gas kinetic theory:

$$D = \frac{3}{16}\frac{1}{p\sigma_{12}^2}kT\left(\frac{1}{m_1}+\frac{1}{m_2}\right) \tag{9}$$

where p is the total pressure of the system, σ_{12} is the collision diameter between the iodine atom and the molecule, and m_1 and m_2 are the masses of the iodine atom and the foreign gas molecule respectively. Since this equation involves pressure, we define the diffusion-rate constant by the next expression:

$$D' = \frac{3}{16}\frac{1}{\sigma_{12}^2}kT\left(\frac{1}{m_1}+\frac{1}{m_2}\right) \tag{10}$$

where the total pressure, p, has been approximated by the pressure of a foreign gas. In the calculation, the value of the collision diameter, σ_{12}, has been obtained as a sum of the radius of iodine atoms and the kinetic collision radius of the molecule. The calculated values of D' for various foreign gases are shown in the right column of Table 1.

The relative values of the diffusion-rate constant observed in various foreign gases are plotted against the relative values of D' in Fig. 7. The relation between β and D' is approximately linear; this indicates that the diffusion of iodine atoms can be understood by the usual gas kinetic theory.

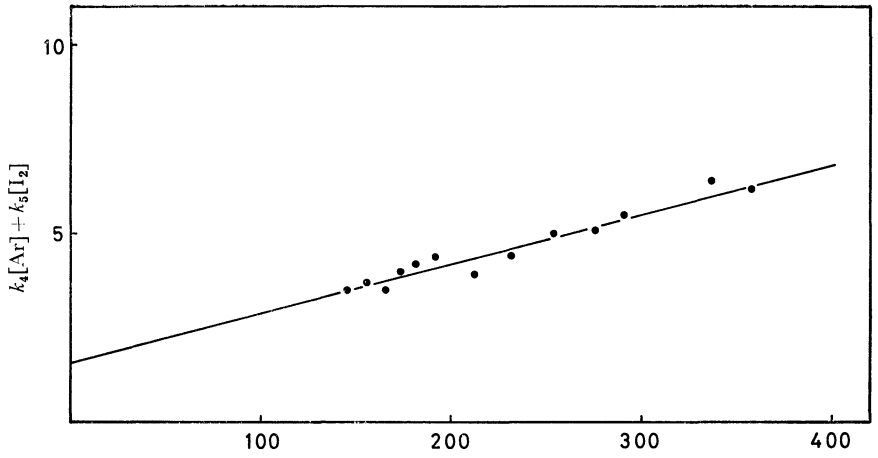

Fig. 6. Plots of $k_4[Ar]+k_5[I_2]$ against [Ar].

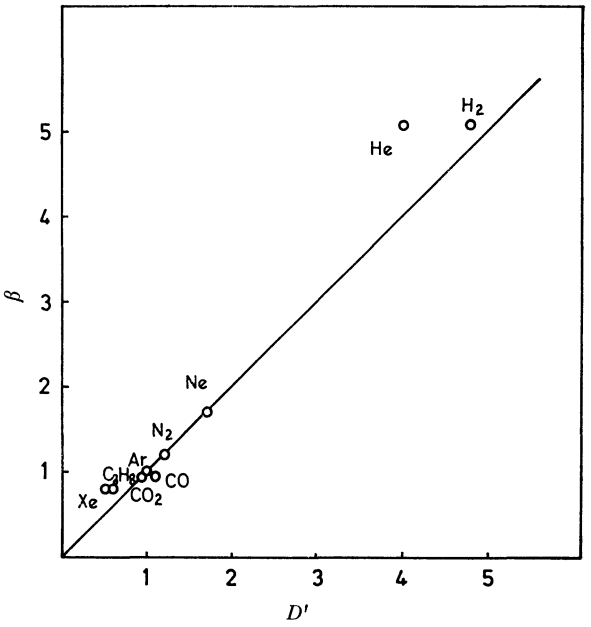

Fig. 7. Relation between β and D'.

Recombination-rate Constant. The obtained rate constants, though relative, are found to be qualitatively in good agreement with those obtained by other methods[3,13] (Table 2). The efficiency in the recombination process as a third body is smaller in the case of mono-atomic gases (He, Ne, and Ar) and is larger in the case of polyatomic gases, because the additional degrees of the freedom of internal motion make the energy transfer from the atom to the molecule easier.

The exceptionally high rate constant in the case of iodine molecules as the third body, which can not be explained by the van der Waals interaction, may imply the formation, and the considerable stability, of the I_3 molecule.[3] The complex mechanism may also be applied to the iodine atom decay in propane.

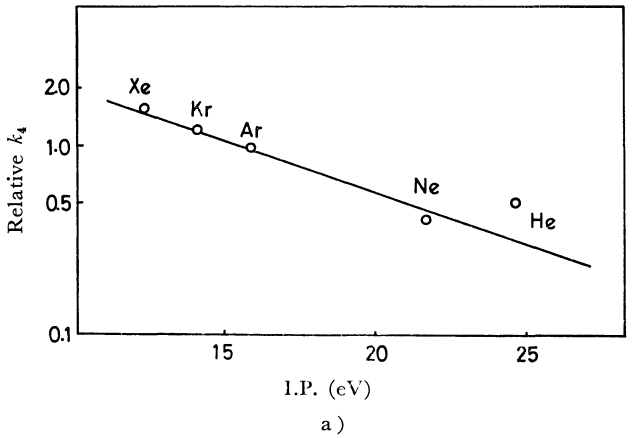

a)

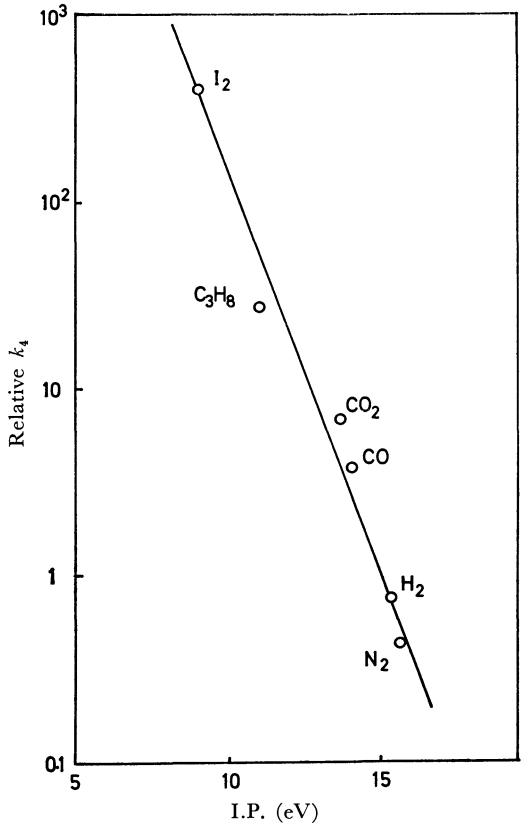

b)

Fig. 8a, 8b. Relative values of k_4 for various foreign gases as a function of ionization potential of foreign gases.
a) for mono-atomic gases
b) for molecules.

Callear and Wilson[16,17] have suggested the existence of $I...C_3H_8$ as an intermediate complex in the recombination reaction of iodine atoms.

Porter and Smith[10,13] have suggested that a charge-transfer complex is responsible as an intermediate complex and that the recombination rates increase with decrease in the ionization potential of the third-body gas which acts as a donor. We have plotted the logarithmic relative recombination rate constants against the ionization potentials of added gases in Figs. 8a and 8b, where the values for krypton and xenon are those of Cristie *et al.*[3] The plots yield two straight lines, with different slopes, one for rare gases and another for polyatomic gases. The difference in the slope between mono- and poly-atomic gases is due to the stability of IM in the following elementary reactions.

$$I + M \rightarrow IM \quad (11)$$

$$IM + I \rightarrow I_2 + M \quad (12)$$

The intermediate complex, IM, is more stable for the polyatomic gases than for the monoatomic, because, in the case of polyatomic gases, the excess energy in the complexes will be distributed over the increased internal degrees of freedom.

Detection of $I^*(^2P_{1/2})$. Attempts to detect iodine atoms in the excited state have met with failure, even in a rare gas, because of the low concentration due to the short life of $I^*(^2P_{1/2})$. The rare gases are inefficient quenchers of excited iodine atoms, but iodine molecules are efficient quenchers of excited iodine atoms. The concentration of iodine molecules in the system is sufficient to quench $I^*(^2P_{1/2})$ in a short time. The life time of excited iodine atoms is estimated to be of the order of 10^{-3} sec, using the value of the quenching rate for $I^*(^2P_{1/2})$ by I_2, $k_q=3.0\times10^9$ l $mol^{-1}sec^{-1}$.[14] Since the stationary concentration of excited iodine atoms is estimated to be of the order of 10^{14} atoms/cm^3, the excited iodine atoms can probably be detected with the present apparatus with an improved sensitivity.

We would like to thank Mr. Y. Izumisawa for his assistance with the measurements.

16) A. B. Callear and J. F. Wilson, *Trans. Faraday Soc.*, **63**, 1357 (1967).
17) A. B. Callear and J. F. Wilson, *ibid.*, **63**, 1983 (1967).

BULLETIN OF THE CHEMICAL SOCIETY OF JAPAN, VOL. 44, 380—386 (1971)

Charge Transfer Interaction and Chemical Reaction. III. Reactions of *m*-Phenylenediamine and Related Compounds with Chloranil

Takashi NOGAMI, Tsuguo YAMAOKA,* Keitaro YOSHIHARA, and Saburo NAGAKURA

The Institute for Solid State Physics, The University of Tokyo, Roppongi, Minato-ku, Tokyo

(Received September 11, 1970)

The interactions of chloranil with several aromatic amines were studied by measuring visible and ultraviolet absorption spectra at various temperatures between 70°K and 300°K, *m*-aminophenol, *m*-phenylenediamine, *N*,*N*-dimethyl-*m*-phenylenediamine, 1,3,5-triaminobenzene, and 1-methyl-2,4,6-triaminobenzene being taken as electron donors. The *m*-phenylenediamine-chloranil system was studied in detail and outer and inner complexes were found to exist as reaction intermediates. The structure and stability of the inner complex were discussed. Kinetic studies were made for the *m*-phenylenediamine-chloranil and 1,3,5-triaminobenzene-chloranil systems. The enthalpy change, ΔH, for the formation of the outer complex was determined from the temperature dependence of the equilibrium constant. The activation energies, ΔE_1 and ΔE_2, for the processes from the outer complex to the inner complex and from the inner complex to the succeeding intermediate, respectively, were determined by analysing the time dependence of the absorption-peak intensity of the inner complexes measured at several temperatures. The results are as follows: $\Delta H=-3.7$, $\Delta E_1=10$, and $\Delta E_2=22$ (kcal/mol) for the *m*-phenylenediamine-chloranil system; $\Delta H=-2.6$, $\Delta E_1=16$, and $\Delta E_2=14$ (kcal/mol) for the 1,3,5-triaminobenzene-chloranil system.

The aromatic substitution reaction has hitherto been extensively studied.[1] There still remain, however, some important problems unsolved. For instance, the role of the outer (π) and inner (σ) complexes has been discussed by many authors, but is still in dispute.[2]

One of the present authors (S. N.) previously presented the charge-transfer mechanism of the aromatic substitution reaction[3] on the basis of Mulliken's concept[4] on the electron donor-acceptor interaction. In order to clarify further this problem from the experimental point of view, we have carried out several

* Permanent address: Department of Printing, Faculty of Engineering, Chiba University, Yayoi-cho, Chiba.

1) R. O. C. Norman and R. Taylor, "Electrophilic Substitution in Benzenoid Compounds," Elsevier Publishing Co., Amsterdam (1965); "Organic Reaction Mechanism," An International Symposium, The Chemistry Society, London (1965); S. D. Ross, "Progress in Physical Organic Chemistry," Vol. I, ed. by S. G. Cohen, A. Streitwieser, Jr., and R. W. Taft, Interscience Publishers, New York, N. Y. (1963), p. 1; E. Berliner, *ibid.*, Vol. II (1964), p. 253; E. Baciocchi and G. Illuminati, *ibid.*, Vol. V (1967), p. 1.

2) H. C. Brown and J. D. Brady, *J. Amer. Chem. Soc.*, **74**, 3570 (1952); G. A. Olah and J. D. Brady, *ibid.*, **83**, 4571 (1961); R. Nakane, O. Kurihara, and A. Natsubori, *ibid.*, **91**, 4528 (1969).

3) S. Nagakura, *Tetrahedron*, **19**, Supl. 2, 361 (1963).

4) R. S. Mulliken, *J. Phys. Chem.*, **56**, 801 (1952); R. S. Mulliken and W. B. Person, "Molecular Complexes," John Wiley & Sons, Inc., New York (1969).

experimental studies, taking benzoquinone and its halo-derivatives as electron acceptors. In previous papers of this series, the reactions of aniline[5a] and 1,3,5-triaminobenzene[5b] with chloranil were studied, special attention being paid to the roles of the outer (π) and inner (σ) complexes in the reaction. The present paper is concerned with several systems containing meta-substituted derivatives of aniline and chloranil. The *m*-phenylenediamine-chloranil system was studied in particular detail in order to clarify the reaction mechanism and to determine the potential energy curve for the reaction.

Experimental

Materials. 1,3,5-Triaminobenzene, 1-methyl-2,4,6-triaminobenzene, and *N,N*-dimethyl-*m*-phenylenediamine were synthesized by reducing the corresponding nitro compounds catalytically.[6] They were purified by vacuum sublimation. Commercially-available *m*-aminophenol and *m*-phenylenediamine (abbreviated to *m*-PD) were also purified by the same method. Chloranil was purified by repeated recrystallizations from acetone.

Measurements. A Cary recording spectrophotometer model 14 M was used for the measurements of ultraviolet and visible absorption spectra, a quartz cell of 1 cm path length being used. The donor and acceptor solutions, which were separately prepared, were mixed with each other immediately before the absorption measurements. For the measurements at low temperatures, a sample cell was cooled with dry ice-acetone in a quartz dewar vessel designed for the spectroscopic measurements.

The temperature dependence of the equilibrium constant of the outer complex was measured in the range from −84°C to −93°C.[7] For this purpose, a sample cell was immersed in the dewar vessel and was cooled with cold nitrogen gas. The temperature was regulated by the nitrogen-flow velocity. The rate constants for the reaction processes from the outer complex to the inner complex and from the inner complex to the succeeding intermediates, were measured in the temperature range from 9.5 to 25.5°C. The temperature of a sample cell in the dewar vessel was regulated by circulating thermostated water.

Results and Discussion

Temperature or Time Dependence of the Electronic Absorption Spectrum of the m-*PD-chloranil System.* After mixing the acetone solution of *m*-PD with that of chloranil at −80°C (*m*-PD, 2.0×10^{-3} M; chloranil, 1.0×10^{-3} M), the reaction process was studied by measuring the absorption spectra at various stages. The results are shown in Fig. 1. A band at 680 mμ (curve 1) measured immediately after mixing at low temperatures is assigned to the outer complex for the following reasons. The peak position is consistent with the value expected for the *m*-PD-chloranil system from a comparison with the CT band positions observed for the chloranil and trinitrobenzene complexes with several aromatic amines. Furthermore, the band intensity below −80°C changes reversibly with increasing and decreasing temperature, and the equilibrium constant for the 1 : 1 complex formation can be obtained, as will be described later, from the concentration dependence of the absorption intensity of the 680 mμ band. This means that the band is due to the outer 1 : 1 complex.

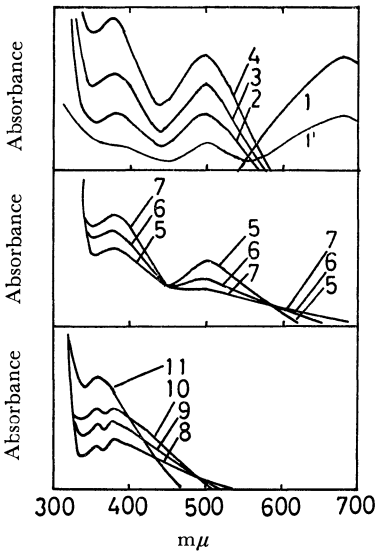

Fig. 1. The absorption spectra of the system containing *m*-PD (2.0×10^{-3} M) and chloranil (1.0×10^{-3} M).
Curve 1: measured at 77°K, immediately after mixing in ethyl ether-isopropyl alcohol (3:1) mixed solvent.
Curve 1': measured at ~200°K, 10 min after mixing in acetone.
Curves 2—11: measured at room temperature for the acetone solution with the following time intervals after mixing:
6, 14, 25, 32, 46, 62, 90, 217, 374 min, and 28 hr, respectively.

The outer complex is stable below −80°C, but at room temperature it is unstable and the 680 mμ band decreases in intensity. Parallel with the intensity decrease of the 680 mμ band, two new absorption bands appear at 500 mμ and 380 mμ. These two bands increase in intensities for 30 min after the mixing, thereafter, the intensity of the 500 mμ band decreases gradually. This band is assigned to the inner (σ) complex between *m*-PD and chloranil for a reason to be described later.

Even when the 500 mμ band starts to decrease in intensity, the 380 mμ band continues to increase. As may clearly be seen from curves 8—11 in Fig. 1, a new band appears at 355 mμ, parallel with the decrease in the intensity of the 380 mμ band. This new band is due to the final product, the 2(*m*-PD) : 1 (chloranil) substitution product, as will be described later. This experimental result shows that the 380 mμ band is due to the reaction intermediate (P_1) between the inner (σ) complex and the final reaction product,

5a) T. Nogami, K. Yoshihara, H. Hosoya, and S. Nagakura, *J. Phys. Chem.*, **73**, 2670 (1969) (Part I of this series).
5b) T. Yamaoka and S. Nagakura, This Bulletin, **43**, 355 (1970) (Part II of this series).
6) T. Yamaoka, H. Hosoya, and S. Nagakura, *Tetrahedron* **24**, 6203 (1968).
7) The temperature range is limited by the instability of the outer complex and also by the solidification of the acetone solution. In order to obtain accurate results within these limitations, we took as many points as possible in the range from −84°C to −93°C.

2,5-dichloro-3,6-di-*m*-aminoanilino-*p*-benzoquinone (P_2). A similar phenomenon was observed for the triaminobenzene-chloranil system.[5b] In this system, the intermediate corresponding to P_1 was isolated as a pure crystal and was identified as the 1 : 1 substitution product, 2,5,6-trichloro-3-triaminobenzo-*p*-benzoquinone from the elemental analysis and also from the NMR spectrum. By an analogy with this P_1 in the present case may be identified as 2,3,5-trichloro-6-*m*-aminoanilino-*p*-benzoquinone (see Fig. 2). The mixture of *m*-PD and chloranil with the concentration ratio of *m*-PD: chloranil = 1 : 5 exhibits the 380-mμ band even after it has been kept for 24 hours at room temperature. This supports the above assignment, because the reaction from the 1 : 1 species (P_1) to the 2 : 1 species (P_2) may be expected to proceed hardly at all in this case where the concentration of chloranil is much larger than that of *m*-PD. The P_1 species has another weak and broad absorption band extending over nearly the whole range of the visible region and with its absorption peak at 630 mμ.

After 28 hours the reaction has almost completely finished, producing the final reaction product with its absorption peak at 355 mμ. It is identified as 2,5-dichloro-3,6-di-*m*-aminoanilino-*p*-benzoquinone ($C_{18}H_{14}Cl_2N_4O_2$) from the elemental analysis[8] and the NMR spectrum.[9]

An absorption spectrum due to the inner (σ) complex similar to the 500 mμ band observed for the *m*-PD-chloranil system was found for several systems containing chloranil and meta-derivatives of aniline, such as *m*-aminophenol, *N*,*N*-dimethyl-*m*-phenylenediamine and 1-methyl-2,4,6-triaminobenzene. Furthermore, the temperature and time dependencies of the absorption spectra observed for these systems are similar to those for the *m*-PD-chloranil system. This seems to mean that the above reaction mechanism holds for the systems containing *m*-derivatives of aniline as electron donor.

The Spectrum and Structure of the Inner (σ) Complex. For all the systems containing chloranil and the *m*-derivatives of aniline studied here, the absorption peak appears at ~500 mμ in the intermediate stage between the outer (π) complex and the 1 : 1 species corresponding to P_1. By an analogy with the corresponding intermediate in other ring-substitution reactions like the nitration, alkylation, and sulfonation of aromatic hydrocarbons, the intermediate with the peak at 500 mμ may be identified as the inner (σ) complex shown in Fig. 2. In this complex, one of the ring-carbon atoms of chloranil taking the sp^3 hybridization forms a new bond with an aromatic amine and is excluded from the conjugated system. Therefore, we can explain the finding that aromatic amines attached to this carbon have hardly any influence on the absorption spectra of the inner complexes.

Benzoquinone also forms inner complexes with several meta-substituted derivatives of aniline in ethanol, and their absorption peaks (λ_{max} = 490 mμ) are almost the same as those for the chloranil complexes. We calculated lower transition energies for the inner (σ) complex between aromatic amine and benzoquinone, assuming the structure shown in Fig. 2. The details of the calculation will be described in the Appendix. The calculated transition energies are 2.14, 4.57, 5.19, 6.55, 6.59, and 7.55 eV. The observed value, 2.53 eV, coincides well with the lowest transition energy calculated. This seems to support the assignment of the 500 mμ band.

Another tentative structure of the inner complex is that an aromatic amine combines with chloranil on one of its ring carbon atoms (see σ' in Fig. 2). This structure, however, may be excluded for the following reason.

The electronic absorption spectrum of the inner complex has no band in the position expected for the benzenium ion-type species of the respective donors. Table 1 shows the peak positions of the ring-protonated and amino-protonated aromatic amines.[10] The ring-protonated aromatic amines exhibit a characteristic band at ~360 mμ. Since the σ' species in Fig. 2 consists of the π-electron system, which is similar to the corresponding ring-protonated aromatic amine, it may be expected to have the characteristic band at ~360 mμ. In actuality, however, the absorption spectrum of the inner complex has no band in the expected position. Therefore, we can exclude the possibility that the inner complex has the structure of σ' in Fig. 2. The fact that P_2 is obtained as the final product also supports the above conclusion as to the structure of the inner (σ) complex.

Contribution of the Outer Complex to the Reaction. Electrophilic aromatic substitution reactions are known to involve both the outer and inner complexes as reaction intermediates.[11] However, it is not well establish-

Table 1. The peak positions of the ring and amino protonated aromatic amines

Amine	Position of protonation	Peak position (mμ)		
1,3,5-Triaminobenzene	ring	365	272	220
	amino	290	220	
N,*N*-Dimethyl-*m*-phenylenediamine	ring	360		
	amino	290	240	
m-Phenylenediamine	ring	360		
	amino	290	240	

8) Found: C, 58.26; H, 4.43; Cl, 18.96; N, 14.41%. Calcd for $C_{18}H_{14}Cl_2N_4O_2$: C, 55.53; H, 3.59; Cl, 18.25; N, 14.39%. The discrepancy between the results of the elemental analysis and the calculated values is due to the existence of small amounts of impurities, for example, the 1 : 1 species and HCl salt of *m*-PD. We tried to purify the sample by chromatography and recrystallization techniques, but we were not successful mainly because of the very small solubility of the sample.

9) The NMR spectrum of the reaction product shows a signal due to the proton of the secondary amine (τ_H = 3.05 ppm). This fact shows that the substitution reaction occurs on the amino group.

10) T. Yamaoka, H. Hosoya, and S. Nagakura, *Tetrahedron*, **26**, 4125 (1970).

11) R. O. C. Norman and R. Taylor, "Electrophilic Substitution in Benzenoid Compounds," Elsevier Publishing Company, New York (1965).

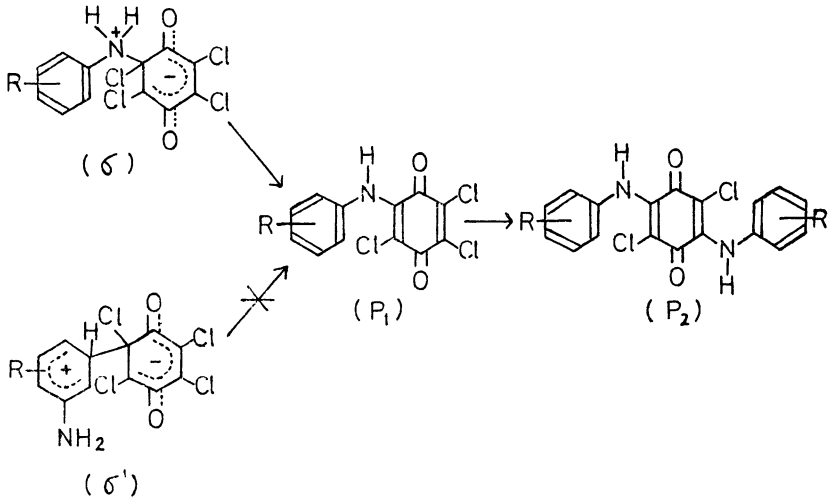

Fig. 2. The structures of the inner complexes ((σ) and (σ')) and the reaction products (P_1 and P_2).

ed whether the outer complex takes part in the main reaction as an intermediate or in a side reaction. The former and latter cases are referred to as "Reaction 1" and "Reaction 2", respectively.

Reaction 1:

$$D + A \underset{k_2}{\overset{k_1}{\rightleftharpoons}} \pi \xrightarrow{k_3} \sigma \xrightarrow{k_4} \cdots \rightarrow P$$

Reaction 2:

$$\pi \underset{k_1'}{\overset{k_2'}{\rightleftharpoons}} D + A \xrightarrow[k_3']{} \sigma \xrightarrow[k_4']{} \cdots \rightarrow P$$

Here, D,A,π,σ, and P denote aromatic amine, chloranil, the outer complex, the inner complex, and the final reaction product, respectively. The rate constant for each process is indicated by k_i or k_i'. The ΔH, ΔE_1, and ΔE_2 values are the enthalpy change for the formation of the outer complex, the activation energy from π to σ, and that from σ to the succeeding reaction intermediate, respectively. These notations are used throughout this paper.

Since $k_1[D]_0$ ($[D]_0$ is the initial concentration of the donor) and since k_2 are generally much larger than k_3 and k_4 (or $k_1'[D]_0$, $k_2' \gg k_3'[D]_0$, k_4'), it is difficult to determine which of Reaction 1 or Reaction 2 actually occurs. In connection with this, experimental studies of the Friedel-Crafts reaction are worthy of notice.[12] The reaction was found to occur only when the outer complex is formed; *o*-xylene, which forms the outer complex with t-C_4H_9Cl–BF_3, causes the butylation reaction, but *p*-xylene, which does not form it, is insusceptible to the Friedel-Crafts reagent. These facts show that the outer complex takes part in the Friedel-Crafts reaction.

Another suggestive fact concerning this problem was found by us for the *N*,*N*,*N'*,*N'*-tetramethyl-*p*-phenylenediamine(TMPD)-chloranil system in an ether-isopropyl alcohol (3 : 1) mixed solvent.[13] We can not detect the inner complex when the system of appropriate concentrations of the component molecules, for which the outer complex formation is negligibly small at room temperature, is cooled directly to the temperature of dry ice-acetone. However, the inner complex is formed by raising the temperature of the system to the dry ice-acetone temperature after it has once been cooled to the liquid nitrogen temperature, at which a considerable amount of the outer complex is formed. This seems to indicate that the inner complex can not be formed directly from the component molecules, but only *via* the outer complex. This finding suggests that Reaction 1 is more probable than Reaction 2. Therefore, we carry out kinetic study taking the path of Reaction 1.

Kinetic Study of the Reaction. The rate equations for Reaction 1 are as follows:

$$\frac{d[A]}{dt} = k_2[\pi] - k_1[D][A] \quad (1)$$

$$\frac{d[\pi]}{dt} = k_1[D][A] - (k_2+k_3)[\pi] \quad (2)$$

$$\frac{d[\sigma]}{dt} = k_3[\pi] - k_4[\sigma] \quad (3)$$

These equations are solved under the following two reasonable conditions;

(a) The concentration of D, [D], is much larger than that of A, [A],[14] and is considered to be approximately equal to the initial concentration, $[D]_0$, throughout the reaction.

(b) Since

$$k_1[D]_0,\ k_2 \gg k_3,\ k_4, \quad (4)$$

a preliminary equilibrium exists between the component molecules and the outer complex with the equilibrium constant, K;

$$K = \frac{[\pi]}{[D][A]} \approx \frac{k_1}{k_2} \quad (5)$$

From Eqs. (1), (2) and condition (a), the following differential equation for [π] is derived:

12) G. A. Olah, S. H. Flood, and M. E. Moffat, *J. Amer. Chem. Soc.*, **86**, 1060 (1964); R. Nakane, A. Natsubori, and O. Kurihara, *ibid.*, **87**, 3597 (1965); R. Nakane and A. Natsubori, *ibid.*, **88**, 3011 (1966); R. Nakane, T. Oyama, and A. Natsubori, *J. Org. Chem.*, **33**, 275 (1968).

13) The details will be published in near future.

14) In our experiment, [D]=40[A].

$$\frac{d^2[\pi]}{dt^2} + (k_1[D]_0 + k_2 + k_3)\frac{d[\pi]}{dt} + k_1k_3[D]_0[\pi] = 0 \quad (6)$$

Considering the boundary condition $(d[\pi]/dt)_{t=0} = k_1[D]_0[A]_0 - (k_2+k_3)[\pi]_0$, we can obtain the equation for $[\pi]$:[15]

$$[\pi] = pe^{-\alpha t} + qe^{-\beta t} \quad (7)$$

Here,
$$p = \frac{k_1[D]_0[A]_0 - (k_2+k_3-\beta)[\pi]_0}{\beta-\alpha}$$
$$q = \frac{(k_2+k_3-\alpha)[\pi]_0 - k_1[D]_0[A]_0}{\beta-\alpha}$$
$$\binom{\alpha}{\beta} = \frac{1}{2}\left\{k_1[D]_0 + k_2 + k_3 \mp \sqrt{(k_1[D]_0+k_2+k_3)^2 - 4k_1k_3[D]_0}\right\} \quad (8)$$

By substituting Eq. (7) into Eq. (3) and considering $[\sigma]_0=0$, we can obtain the equation for $[\sigma]$:

$$[\sigma] = \frac{pk_3}{k_4-\alpha}(e^{-\alpha t} - e^{-k_4 t}) + \frac{qk_3}{k_4-\beta}(e^{-\beta t} - e^{-k_4 t}) \quad (9)$$

The approximate forms of Eqs. (7), (8), and (9) can be derived by adopting Eqs. (4) and (5) as follows:[16]

$$\alpha \approx \frac{k_3K[D]_0}{K[D]_0+1} \quad (8)'$$
$$\beta \approx k_1[D]_0 + k_2$$
$$[\pi] \approx pe^{-\alpha t} \quad (7)'$$
$$[\sigma] \approx \frac{pk_3}{k_4-\alpha}(e^{-\alpha t} - e^{-k_4 t}) \quad (9)'$$

Eqs. (8)′ and (9)′ are used to obtain the activation energies, ΔE_1 and ΔE_2. Furthermore, we can derive the following equation from Eq. (9);

$$\int_0^\infty I_\sigma dt = \frac{k_1[D]_0[A]_0 + (\alpha+\beta-k_2-k_3)[\pi]_0}{k_1k_4[D]_0} \times \varepsilon_\sigma L \approx \frac{\varepsilon_\sigma L[A]_0}{k_4} \quad (10)$$

Here, ε_σ and I_σ denote the molar extinction coefficient and absorbance observed with the inner complex, respectively, and L is a light-path length. Equation (10) shows that ε_σ is obtained by measuring the time dependence of I_σ for the inner complex, the I_σ-t curve.

Potential Energy Curve of the Reaction. The *m*-PD-chloranil and TAB-chloranil systems were taken up for the purpose of determining the potential energy curve of the reaction, because the inner complexes in these systems are fairly stable, even at room temperature,[5b] and because the changes in their concentrations with the time can be easily followed by electronicabsorption measurements. We chose the acetone solution for the purpose of determining the potential energy curves, because the main reaction product in this solvent consists of only one species, 2,5-dichloro-3,6-di-*m*-aminoanilino-*p*-benzoquinone, when there is much more *m*-PD than chloranil. On the other hand, at least two main reaction products were found in such solvents as ethyl ether, ethanol, and an ether-isopropyl alcohol mixed solvent, and the reaction mechanism in these solvents seems to be more complicated than that in acetone.

Let us start from the determination of the enthalpy (ΔH) and entropy (ΔS) changes for the outer-complex formation. The absorbance values at the peak position (680 mμ) of the CT band of the outer complex were measured for acetone solutions including various concentrations of *m*-PD and chloranil. The peak molar extinction coefficient, ε_{max}, was determined to be 3120 $M^{-1}cm^{-1}$ from the Benesi-Hildebrand plot[17] measured at −80°C. Assuming ε_{max} to be independent of temperature, the temperature dependence of the equilibrium constant of the outer complex was determined in the range from −84°C to −93°C in the same way as has been described previously.[5a] The ΔH and ΔS for the *m*-PD-chloranil system in acetone were determined to be −3.7 kcal/mol and −13.7 cal/mol·deg, respectively.

The outer complex of the TAB-chloranil system has its absorption peak at 660 mμ in acetone.[5b] The complex is unstable even at temperature of dry ice-acetone, and it is difficult to obtain ε_{max} from the Benesi-Hildebrand plot at a low temperature. Therefore, ε_{max} of the outer complex for this system was estimated to be 2770 $M^{-1}cm^{-1}$ from the reasonable relation: $(I_{max})_{m\text{-PD}}/(I_{max})_{TAB} = (\varepsilon_{max})_{m\text{-PD}}/(\varepsilon_{max})_{TAB}$. Here, $(I_{max})_{m\text{-PD}}$ and $(I_{max})_{TAB}$ are, respectively, the maximum absorbances of the outer complexes measured at −196°C for the *m*-PD-chloranil and TAB-chloranil systems with equal concentrations of chloranil. Since chloranil is almost completely complexed in both solutions, the concentrations of the outer complexes are expected to be almost equal to each other. By the aid of this value, ΔH and ΔS for the TAB-chloranil system in acetone were determined to be −2.6 kcal/mol and −5.4 cal/mol·deg, respectively.

Immediately after mixing acetone solution of each electron donor with that of chloranil ([*m*-PD]=[TAB]=2.0×10^{-2} M, [chloranil]=5.0×10^{-4} M), we started the measurement of I_σ and obtained the I_σ-t curves at several temperatures. Both the systems gave curves which fit in well with Eq. (9)′. Figure 3 shows the result observed at 15.8°C for the *m*-PD-chloranil system. By analysing the experimental results by the aid of Eq. (9)′, the temperature dependences of α and k_4 were obtained. Furthermore, k_3 was obtained from

15) An initial concentration is represented by attaching the suffix 0.

16) The rate equations for Reaction 2 can be solved definitely by the same procedures as have been described above. The final approximate forms are as follows:

$$[\pi] \approx p'e^{-\alpha' t} \quad (11)$$
$$[\sigma] \approx \frac{k_3'[D]_0q'}{k_4'-\alpha'}(e^{-\alpha' t} - e^{-k_4' t}) \quad (12)$$
$$\alpha' \approx \frac{k_3'[D]_0}{1+K[D]_0} \quad (13)$$
$$\beta' \approx (k_1'+k_3')[D]_0 + k_2'$$
Here, $p' = \frac{k_1'[D]_0[A]_0 + (\beta'-k_2')[\pi]_0}{\beta'}$
$$q' = \frac{k_2'[\pi]_0 - (k_1'[D]_0 + k_3[D]_0 - \beta')[A]_0}{\beta'}$$

17) H. A. Benesi and J. H. Hildebrand, *J. Amer. Chem. Soc.*, **71**, 2703 (1949).

α by the aid of Eq. (8)', K being estimated by extrapolating the log K-1/T relation obtained at low temperatures. The values of k_3 and k_4 thus obtained are tabulated in Table 2. From the Arrhenius plot of these results, ΔE_1 and ΔE_2 were determined; the results are given in Table 3.[18]

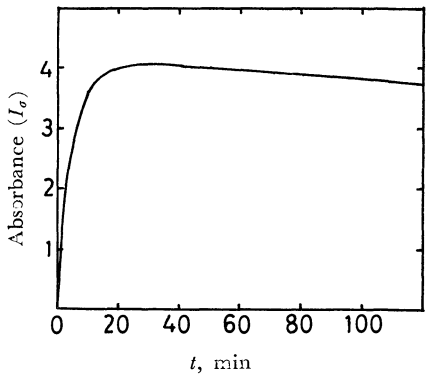

Fig. 3. The time-dependence of the absorption peak intensity observed at 15.8°C for the inner complex between *m*-phenylenediamine and chloranil.

Table 2. Temperature dependence of k_3 and k_4 (in sec^{-1}) for the *m*-phenylenediamine-chloranil and 1,3,5-triaminobenzene-chloranil systems

m-PD-Chloranil	15.8°	20.8°	25.5°
$k_3 \times 10$	2.55	3.33	4.65
$k_4 \times 10^5$	3.52	5.93	12.20
TAB-Chloranil	9.5°	17.7°	22.5°
k_3	1.07	1.69	3.91
$k_4 \times 10^5$	1.92	5.27	6.06

Table 3. The ΔH, ΔE_1 and ΔE_2 values (in kcal/mol) for the *m*-phenylenediamine-chloranil and 1,3,5-triaminobenzene-chloranil systems

	m-PD-Chloranil	TAB-Chloranil
ΔH	−3.7	−2.6
ΔE_1	10	16
ΔE_2	22	14

Figure 4 shows schematically the potential energy curves of the reactions for the *m*-PD-chloranil and TAB-chloranil systems. The structures of P_1 and P_2 are shown in Fig. 2; σ_1 corresponds to σ in the same figure. σ_2, the inner (σ) complex between P_1 and *m*-PD, is tentatively assumed to exist as an intermediate between P_1 and P_2, though it has not yet been observed. The potential energy curves from P_1 to P_2, the parts drawn by broken lines in Fig. 4, are difficult to be investigated for the following two reasons: (1) The σ_2 can not be detected by an electronic absorption measurement, and (2) the absorption bands due to P_1 and P_2 overlap with each other, so the time depenedenc of the absorption peak intensity is difficult to be obtained separately for each band.

18) These values are estimated by assuming a diffusion-controlled reaction.

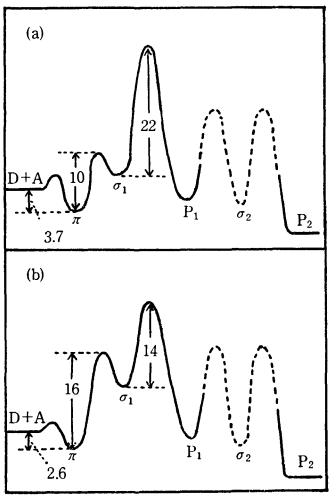

Fig. 4. Experimentally determined potential energy curves for the reactions: (a) between *m*-phenylenediamine and chloranil, (b) between 1,3,5-triaminobenzene and chloranil (unit, kcal/mol).
In both systems, the potential energy curves from P_1 to P_2 could not be determined.

None of the inner complexes formed between aromatic amines under consideration and chloranil can be isolated stably, and their molar extinction coefficients (ε_{max}'s) can not be determined directly. The ε_{max}'s value of the *m*-PD-chloranil system was estimated to be 8600 $M^{-1}cm^{-1}$ by applying Eq. (10) to the I_o-t curve measured at 25°C.

Rate-determining Step of the Reaction. In the *m*-PD-chloranil and TAB-chloranil systems, the rate for the outer-complex formation ($k_1[D]_0$) is probably 10^7 (sec^{-1}) or larger.[18] On the other hand, k_3 and k_4 are 10^0 and 10^{-5} (sec^{-1}), respectively. In actuality, the outer-complex formation is very fast in the reactions under consideration, and it is clear that the inner (σ) complex plays an important role in the rate-determining step. Therefore, it is concluded that Brown's view is the more appropriate to the present systems.

Stability of the Inner Complex. A parallel relationship exists between the electron-donating ability of the meta-substituent group of aniline and the stabilities of the inner complexes; *i.e.*, the following order of the stabilities of the inner complex was found:

m-anisidine(a few seconds)<*m*-aminophenol (a few minutes)<*m*-PD≈*N*,*N*-dimethyl-*m*-PD≈*s*-TAB≈1-methyl-2,4,6-TAB (a few hours)≪*N*,*N*,*N*',*N*'-tetramethyl-*m*-PD (about five days). Here, the time in parentheses indicate the approximate duration of existence for the corresponding inner complex at room temperature.

These facts can be explained as follows. With the increasing electron-donating ability of the meta-substituent, the electron-migration from the amino group to the benzene ring decreases and the nonbonding electron density on the nitrogen atom increases. Thus, chloranil may be expected to form a more stable inner complex with the meta-derivatives of aniline with stronger electron-donating groups.

We should like to express our sincere gratitudes to Dr. Ichiro Hanazaki, The Institute of Physical and

Chemical Research and Dr. Renji Okazaki, The University of Tokyo for their helpful discussions. Thanks are also due to Dr. Fumihiko Hirota of our laboratory for his help in the SCF MO calculation.

Appendix

Calculation of the Electronic Structure of the Inner Complex. We studied theoretically the π-electron structures of the inner complex between benzoquinone and aromatic amine by method combining the CI procedure with the Pariser-Parr-Pople type SCF MO,[19] taking a model of the negative ion in which one of the six ring carbon atoms of benzoquinone is excluded from the conjugated system. In actual calculation, the bond lengths of the ion were taken to be equal to those of benzoquinone.[20] The transition energies were evaluated by the aid of a HITAC 5020E electronic computer at the Computer Centre, The University of Tokyo. The ionization potentials, I_p's, and electron affinities, E_a's of carbon, nitrogen. and oxygen in their valence states were taken from Pilcher-Skinner's table.[21] The core resonance integral, β_{x-y}, was considered only for the nearest neighbours. These quantities are taken to be as follows:

$I_C = 11.2$ eV, $I_N = 28.88$ eV, $I_O = 17.25$ eV,

$E_C = 0.6$ eV, $E_N = 12.25$ eV, $E_O = 2.58$ eV,

$\beta_{C-C} = -2.39$ eV. $\beta_{C-N} = -2.60$ eV, $\beta_{C=O} = -2.60$ eV.

19) R. Pariser and R. G. Parr, *J. Chem. Phys.*, **21**, 466, 767 (1953); J. A. Pople, *Trans. Faraday Soc.*, **49**, 1375 (1953).

20) M. Kimura and S. Shibata, This Bulletin, **27**, 163 (1954).

21) G. Pilcher and H. A. Skinner, *J. Inorg. Nucl. Chem.*, **24**, 937 (1962).

BULLETIN OF THE CHEMICAL SOCIETY OF JAPAN, VOL. 44, 386—391 (1971)

Molecular Structure of Diacetylene as Studied by Gas Electron Diffraction

Mitsutoshi TANIMOTO,* Kozo KUCHITSU, and Yonezo MORINO*

Department of Chemistry, Faculty of Science, The University of Tokyo, Hongo, Bunkyo-ku, Tokyo

(Received September 28, 1970)

The molecular structure of diacetylene has been studied by gas electron diffraction. Thermal-average bond distances are determined to be: r_g(C–C) = $1.383_7 \pm 0.001_9$ Å, r_g(C≡C) = $1.217_6 \pm 0.001_4$ Å, and r_g (C–H) = $1.093_5 \pm 0.010$ Å. The C–C single bond is about 0.007 Å shorter than that in cyanogen, while the C≡C triple bond is about 0.005 Å longer than that in acetylene. The observed mean amplitudes are slightly larger than the parallel amplitudes based on harmonic calculations. A suggestion has been made to account for the discrepancies by the use of empirical constants representing the interaction between bending and bond-stretching vibrations, which makes the bond distances slightly longer, on the average, in a momentary bent structure than in a linear structure. This interaction also seems to account for a slight difference between the rotational constant B_0 estimated from the above r_g distances and those derived from spectroscopic experiments.

At an early stage of the structure studies by modern methods, Herzberg *et al.*[1] and Pauling *et al.*[2] remarked that a C–C single bond adjacent to a triple bond was shorter than that in saturated hydrocarbons. Subsequently, systematic analyses of experimental data led Stoicheff *et al.*[3] to an empirical rule that a C–C bond distance increases linearly with the number of adjacent atoms. According to Stoicheff,[4] this rule was applicable to most of the C–C distances reported up to 1962 within the uncertainty of 0.005 Å.

There are, however, a number of basic molecules which require further experimental studies. By the use of the recent technique of gas electron diffraction, the structure of some of the molecules studied previously can be determined with somewhat higher accuracy. Thus, from the studies of a number of conjugated aliphatic hydrocarbons with or without heteroatoms, a significant heteroatom effect on the C–C bond distance has been observed.[5–7] As for the molecules with a C–C bond between two triple bonds (the *sp-sp* system), the structure of cyanogen (N≡C–C≡N) was determined by electron diffraction[8] in combination with the rotational constant obtained from high-resolution infrared spectroscopy.[9] The r_g, C–C bond distance, was found to be about 0.01 Å larger than the value expected from the Stoicheff rule.

On the other hand, none of the previous studies of the diacetylene (HC≡C–C≡CH) structure by means of electron diffraction,[2] infrared,[10,11] and rotational

* Present address: Sagami Chemical Research Center, 3100 Ohnuma, Sagamihara, Kanagawa.

1) G. Herzberg, F. Patat, and H. Verleger, *J. Phys. Chem.*, **41**, 123 (1937).

2) L. Pauling, H. D. Springall, and K. J. Palmer, *J. Amer. Chem. Soc.*, **61**, 927 (1939).

3) G. Herzberg and B. P. Stoicheff, *Nature*, **175**, 79 (1955); C. C. Costain and B. P. Stoicheff, *J. Chem. Phys.*, **30**, 777 (1959).

4) B. P. Stoicheff, *Tetrahedron*, **17**, 135 (1962).

5) K. Kuchitsu, T. Fukuyama, and Y. Morino, *J. Mol. Structure*, **1**, 463 (1968).

6) K. Kuchitsu, T. Fukuyama, and Y. Morino, *ibid.*, **4**, 41 (1969).

7) T. Fukuyama and K. Kuchitsu, *ibid.*, **5**, 131 (1970).

8) Y. Morino, K. Kuchitsu, Y. Hori, and M. Tanimoto, This Bulletin, **41**, 2349 (1968).

9) A. G. Maki, *J. Chem. Phys.*, **43**, 3193 (1965).

10) A. V. Jones, *ibid.*, **20**, 860 (1952).

11) G. D. Craine and H. W. Thompson, *Trans. Faraday Soc.*, **49**, 1273 (1953).

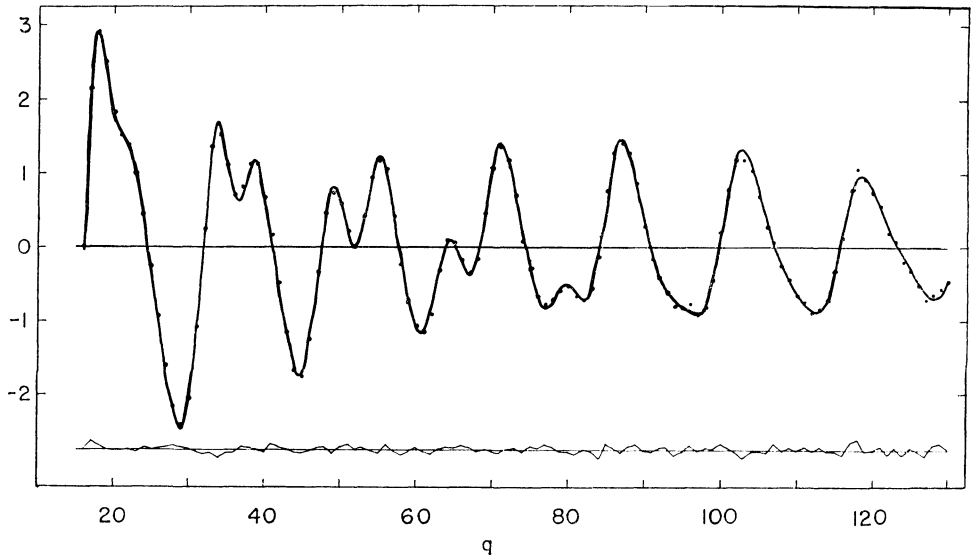

Fig. 1. Molecular intensity curves (dots for observed values and the solid curve calculated from the best-fit model) and the residuals (below).

Raman spectroscopy[12] were of comparable accuracy, nor were they free from the ambiguity due to the assumptions about the structural parameters. The present study aims to determine the structure of this molecule by electron diffraction in order to compare the C–C and C≡C bond distances with those in cyanogen and acetylene, respectively.

Experimental

The sample of diacetylene (95% pure) purchased from Tokyo Kagaku Seiki Co. Ltd. was purified by vacuum distillation. An electron beam of the wavelength of about 0.06 Å, calibrated with reference to the r_a(C=O) distance of carbon dioxide[13] (1.1646 Å), was used to take diffraction photographs at room temperature (23°C) with the camera lengths of 107.79±0.02 mm and 243.23±0.02 mm. Photographic densities measured by a digital microphotometer were converted into electron intensities, from which reduced molecular intensities (Fig. 1) were obtained by a standard technique.[14] Other experimental details have been described elsewhere.[8,13] The radial distribution curve is shown in Fig. 2.

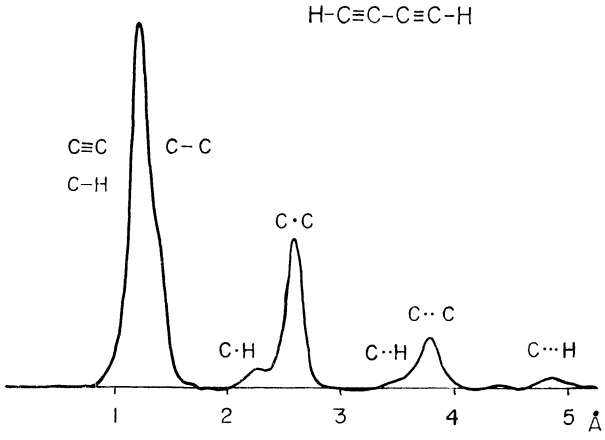

Fig. 2. Observed radial distribution curve.

Analysis

The reduced molecular intensities were fitted to a theoretical expression using a least-squares method[15] with a diagonal weight function estimated from past experience. The κ parameters representing asymmetric probability distributions for bonded pairs (2.0×10^{-5} Å^3 for C–H and 7×10^{-7} Å^3 for C–C and C≡C) were estimated by a diatomic approximation.[16] The κ parameters for nonbonded pairs were ignored. The mean amplitude and the distance for the H–H were fixed to their estimated values, because the contribution of this pair to the molecular intensity is insignificant. Tables 1, 2, and 3 list the r_g distances,

Table 1. Observed internuclear distances[a] (in Å units)

	r_g		r_g
C—H	$1.093_5\pm0.010$	C · C	$2.587_4\pm0.002_5$
C≡C	$1.217_6\pm0.001_4$	C··H	$3.63_0\pm0.03_3$
C—C	$1.383_7\pm0.001_9$	C··C	$3.788_7\pm0.006_3$
C · H	$2.27_8\pm0.01_5$	C···H	$4.83_6\pm0.02_4$

a) Dots represent the number of atoms intervening each nonbonded atom pair. The uncertainties are estimated limits of error.

12) J. H. Callomon and B. P. Stoicheff, *Can. J. Phys.*, **35**, 373 (1957).
13) Y. Murata, K. Kuchitsu, and M. Kimura, *Japan. J. Appl. Phys.*, **9**, 591 (1970).
14) Numerical experimental data of the leveled total intensity, the background function and the error matrix have been deposited with the Chemical Society of Japan (Document No. 7103). A copy may be secured by citing the document number and by remitting, in advance, ¥250 for photoprints. Payment by check or money order payable to: Chemical Society of Japan.
15) Y. Morino, K. Kuchitsu, and Y. Murata, *Acta Crystallogr.*, **18**, 549 (1965).
16) K. Kuchitsu, This Bulletin, **40**, 498, 505 (1967).

TABLE 2. OBSERVED AND CALCULATED MEAN AMPLITUDES (in Å units)

	l_{obsd}	l_{calcd}[a]		
		(a)	(b)	(c)
C≡C	$0.039_8 \pm 0.001_0$	0.0368	(0.0368)	0.0389
C—C	$0.045_5 \pm 0.001_3$	0.0419	(0.0419)	0.0455
C · C	$0.049_8 \pm 0.002_0$	0.0467	0.0569	0.0501
C··C	$0.061_3 \pm 0.004_5$	0.0514	0.0700	0.0579
C—H	$0.085_5 \pm 0.005_5$	0.0741	(0.0741)	0.0855
C · H	$0.09_7 \pm 0.01_2$	0.0794	0.0852	—
C··H	$0.10_7 \pm 0.03_3$	0.0840	0.0965	—
C···H	$0.07_7 \pm 0.03_6$	0.0866	0.1060	—

a) Calculated values based on models (a), (b), and (c) discussed in the text: (a) harmonic parallel amplitudes, $\langle \Delta z^2 \rangle^{1/2}$, (b) rod model without bending-stretching interactions, (c) rod model with bending stretching interactions.

TABLE 3. OBSERVED AND CALCULATED SHRINKAGES (in Å units)

	δ_{gobsd}	δ_{gcalcd}	
		(a)	(b)
C · H	$0.03_3 \pm 0.03$	0.020	0.021
C · C	$0.014_1 \pm 0.002$	0.011	0.011
C··H	$0.06_4 \pm 0.03$	0.035	0.036
C··C	$0.030_2 \pm 0.006$	0.027	0.027
C···H	$0.07_6 \pm 0.03$	0.054	0.056

(a), (b) See footnote a) of Table 2.

mean amplitudes and linear shrinkages, respectively, derived from the analysis.[14] The uncertainties were estimated as 2.5 times the standard deviations with allowance for systematic errors (particularly, those in the scale factor for the distances and in the extraneous background for the mean amplitudes).[17]

Discussion

Comparison of Bond Distances. C-C Single Bond: The C–C bond distance (r_g) in diacetylene has been determined to be $1.387_7 \pm 0.001_9$ Å, about 0.007 Å shorter than in cyanogen[8] ($1.390_8 \pm 0.002$ Å).[18] This difference is analogous to, but much smaller than, that observed between the C–C distances in butadiene and glyoxal, 1.465±0.003 Å and 1.526±0.003 Å, respectively.[6] As in that case, it seems possible to account for the observed difference at least qualitatively in terms of the difference in π bond orders. According to a semiempirical estimate by the use of the Pariser-Parr-Pople method,[19] the C-C π bond order for diacetylene (0.4—0.5) appears to be slightly (of the order of a few hundredths) larger than that for cyanogen. The absolute magnitude of the estimated bond orders depends so sensitively on the empirical parameters assumed[7] that a more elaborate treatment is necessary for a fully quantitative discussion. The C–C distance in diacetylene conforms to the Stoicheff rule,[4] which predicts a "normal" ≡C–C≡ distance to be 1.379 Å.

C≡C Triple Bond: A significant difference has been observed between the C C bonds (r_g) in diacetylene ($1.217_6 \pm 0.001_4$ Å) and that in acetylene[20] ($1.212_2 \pm 0.001_0$ Å). There seems to be no previous experimental study in which confirmative evidence is given for a change in the triple-bond distance due to conjugation, whereas such a difference of the order of 0.005 Å or less is not unexpected[21] from those in the π bond orders (theoretical) and those in the C C stretching force constants (experimental). For instance, Julg and Pellégatti[22,23] calculated the bond order of the diacetylene C C bond to be 1.906 or 1.888, which, together with their estimates of the gradient $\Delta r/\Delta p$, results in the difference in the C≡C bond distances of $0.122 \times (2-1.906) = 0.011_4$ Å or $0.130 \times (2-1.888) = 0.014_6$ Å, apparently larger than the experimental r_g difference (~0.005 Å) given above.

C–H Bond: The C–H bond distance derived here ($r_g = 1.093_5 \pm 0.010$ Å) has much larger experimental error than those in the C–C distances. While this distance appears to be somewhat larger than those in acetylene[20] ($r_g = 1.083_5 \pm 0.005_0$ Å) and in cyanoacetylene[12,24,25] ($r_s = 1.0574$ Å, $r_0 = 1.057$ Å or 1.069 Å), the differences may be spurious, since they are within the limits of error; moreover, C–H distances are the most sensitive to the difference in the definition of distances.[26]

Effect of Bending Vibrations on Mean Amplitudes. Harmonic Parallel Amplitudes: The observed mean amplitudes are compared in Table 2 with the mean parallel amplitudes, $\langle \Delta z^2 \rangle^{1/2}$, calculated by a conventional method[27,28] (column a) using the quadratic force constants determined by Abe and Shimanouchi.[29] For both bonded and nonbonded pairs the calculated parallel amplitudes are consistently smaller than the observed values. In particular, the observed CC amplitudes seem to have sufficient accuracy to investigate the origin of the "significant" discrepancies.

17) The experimental errors in the distances and mean amplitudes have been estimated with particular caution, since appreciable differences were recognized between the observed and calculated mean amplitudes and rotational constants, as described in the discussion section.

18) The r_g(C–C) distance for cyanogen observed by electron diffraction, $1.392_5 \pm 0.002_2$ Å,[8] has here been revised according to the recalibration of the scaler factor by the use of the infrared rotational constant, as described in Ref. 8.

19) R. Pariser and R. G. Parr, *J. Chem. Phys.*, **21**, 767 (1953); J. A. Pople, *Trans. Faraday Soc.*, **49**, 1375 (1953).
20) Y. Morino, K. Kuchitsu, T. Fukuyama, and M. Tanimoto, *Acta Crystallogr.*, **A25**, S127 (1969); Y. Morino, K. Kuchitsu, and M. Tanimoto, to be published.
21) D. R. Lide, Jr., *Tetrahedron*, **17**, 125 (1962).
22) A. Julg and A. Pellégatti, *Theor. Chim. Acta*, **2**, 202 (1964).
23) A. Pellégatti, Thesis, Marseille (1967).
24) A. A. Westenberg and E. B. Wilson, *J. Amer. Chem. Soc.*, **72**, 199 (1950).
25) C. C. Costain, *J. Chem. Phys.*, **29**, 864 (1958).
26) K. Kuchitsu, *ibid.*, **49**, 4456 (1968).
27) Y. Morino, K. Kuchitsu, and T. Shimanouchi, *ibid.*, **20**, 726 (1952).
28) S. J. Cyvin, "Molecular Vibrations and Mean Square Amplitudes", Universitetsforlaget, Oslo and Elsevier, Amsterdam (1968).
29) K. Abe and T. Shimanouchi, to be published.

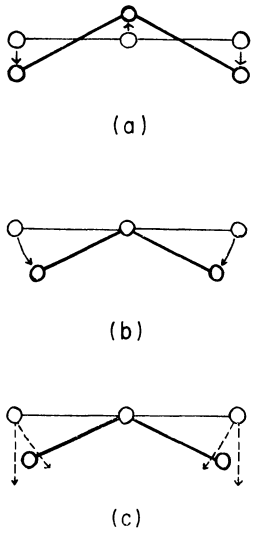

Fig. 3. The loci of the atoms in the bending vibration of a triatomic system: (a) normal coordinates of bending, (b) rod model without bending-stretching interaction, (c) bending-stretching interaction with a positive α parameter is included.

The conventional method ignores the effect of bending vibrations (perpendicular to the equilibrium molecular axis, Fig. 3a) on the displacements of internuclear distances, and the bond-stretching vibrations (parallel to the axis) are assumed to be "harmonic" (here called model a). However, since the present molecule has a low-frequency bending vibration (ν_9=222 cm^{-1}),[30] the stretching displacements should depend appreciably on the bending displacements, and the above approximations may not be valid.

Effect of Bending without Bend-Stretch Interaction: A simple approach to this problem is to assume model b, where the bonds retain their "average" distances in the bending displacements[31-33] (Fig. 3b). The potential function is assumed to have no third-order term proportional to $\Delta r \cdot \phi^2$, which represents the interaction between the stretching and bending displacements. Accordingly, the probability distribution function of a bond distance, $P(r)$, which has a Gaussian form with a slight distortion due to the stretching anharmonicity, is assumed to be independent of the bending displacements.[34]

If one expands an instantaneous distance r (bonded or nonbonded) in terms of the Cartesian displacements parallel and perpendicular to the equilibrium molecular axis, Δz and $\Delta\rho$, respectively, one gets[16,35]

$$r = r_e + \Delta r = r_e + \Delta z + \frac{\Delta\rho^2}{2r_e} - \frac{\Delta z\Delta\rho^2}{2r_e^2} + \frac{\Delta z^2\Delta\rho^2}{2r_e^3} - \frac{\Delta\rho^4}{8r_e^3} + \cdots \quad (1)$$

where $\Delta\rho^2=\Delta x^2+\Delta y^2$. The mean-square amplitude reckoned from the r_g distance is given by

$$l_g^2 = \langle r^2\rangle - \langle r\rangle^2 = \langle \Delta z^2\rangle - \langle \Delta z\rangle^2 + \frac{1}{r_e}(\langle \Delta z\Delta\rho^2\rangle - \langle \Delta z\rangle\langle \Delta\rho^2\rangle) + \frac{1}{r_e^2}\left[\frac{1}{4}(\langle \Delta\rho^4\rangle - \langle \Delta\rho^2\rangle^2) - (\langle \Delta z^2\Delta\rho^2\rangle - \langle \Delta z\rangle\langle \Delta z\Delta\rho^2\rangle) + \cdots \right. \quad (2)$$

where the carets denote thermal averages. Since the molecule is linear in equilibrium, the Cartesian displacements for a nonbonded pair are simply the sums of the corresponding displacements for the component bonded pairs. For instance, a parallel displacement for a nonbonded i-k pair in a linear i-j-k arrangement is given by

$$\Delta z_{ik} = \Delta z_i - \Delta z_k = \Delta z_{ij} + \Delta z_{jk} \quad (3)$$

The parallel displacement for a bonded pair, on the other hand, is related to the bond-stretching displacement, Δr, and the perpendicular displacement,

$$\Delta z(\text{bond}) = \Delta r - \frac{\Delta\rho^2}{2r_e} + \frac{\Delta r\Delta\rho^2}{2r_e^2} - \frac{\Delta\rho^4}{8r_e^3} - \frac{\Delta r^2\Delta\rho^2}{2r_e^3} + \cdots \quad (4)$$

Since the contribution from the second (negative) term is important, the mean projected displacement $\langle \Delta z$ (bond)$\rangle$ is usually much smaller than $\langle \Delta r\rangle$ and is sometimes negative.[16,36]

According to the present assumption, Δr and $\Delta\rho^2$ are independent of each other, and the Δr for a bond is equal to the Δz for a linear structure without bending displacements. The latter can be expressed as a linear combination of the Σ-type normal coordinates (Q_1 through Q_5) with their coefficients a_i determinable from a conventional normal-coordinate analysis,[37]

$$\Delta r = \sum_{i=1}^{5} a_i Q_i \quad (5)$$

The perpendicular displacement, $\Delta\rho^2$, can be calculated in a similar way from the Δx and Δy, which are linear functions of the π-type coordinates, Q_6 through Q_9.

The mean amplitudes for nonbonded pairs calculated by this model, listed in column b of Table 2, are appreciably larger than those based on model a, where all the $\Delta\rho$ displacements in Eqs. (2) and (4) are equal to zero. The observed CC amplitudes lie between a and b, indicating that the latter model overestimates the effect of bending vibrations. Hence, a bending-stretching interaction ought to be introduced in order to attain a better agreement. (See next subsection.)

Shrinkage Effects: The shrinkage[35] calculated by the models a and b are nearly equal, as listed in Table 3. The shrinkage depends essentially on the perpendicular displacements alone and is independent of whether the atoms take rectilinear or curvilinear loci shown in Fig. 3a and 3b, respectively.[35]

Rotational Constants: The r_g distances determined in the present study have been converted into the r_α^0 distances by the equation, which is based on model b,[26,38]

30) F. A. Miller, D. H. Lemmon, and R. S. Witkowski, *Spectrochim. Acta*, **21**, 1709 (1965).
31) L. S. Bartell, *J. Chem. Phys.*, **38**, 1827 (1963).
32) M. A. Pariseau, I, Suzuki, and J. Overend, *ibid.*, **42**, 2335 (1965).
33) K. Kuchitsu and Y. Morino, This Bulletin, **38**, 805 (1965).
34) M. Tanimoto, K. Kuchitsu, and Y. Morino, *ibid.*, **43**, 2776 (1970).
35) Y. Morino, J. Nakamura, and P. W. Moore, *J. Chem. Phys.*, **36**, 1050 (1962).
36) K. Kuchitsu, This Bulletin **44**, 96 (1971).
37) E. B. Wilson, Jr., J. C. Decius and P. C. Cross, "Molecular Vibrations," McGraw-Hill, New York (1955).
38) K. Kuchitsu and S. Konaka, *J. Chem. Phys.*, **45**, 4342 (1966).

TABLE 4. AVERAGE STRUCTURE AND ROTATIONAL CONSTANTS

		Obsd	Calcd[a] (b)	Calcd[a] (c)
$r_g-r_\alpha^0$ (Å)	C—H	—	0.0038	0.0113
	C≡C	—	0.0062	0.0078
	C—H	—	0.0288	0.0328
B_0 (cm^{-1})		0.14638±0.0001[b]	0.1453±0.0003	0.1464
		0.14641±0.00013[c]		
		0.14689±0.00004[d]		

a) Calculated by models (b) and (c) respectively. See text and footnote a) of Table 2.
b) Infrared, Ref. 10. c) Infrared, Ref. 11. d) Rotational Raman, Ref. 12.

$$r_\alpha^0=r_g-\frac{3}{2}a(\langle\Delta z^2\rangle_T-\langle\Delta z^2\rangle_0)-\langle\Delta\rho^2\rangle_0/2r_e-\delta r \qquad (6)$$

where the centrifugal corrections,[39] δr, are less than 10^{-4} Å for all the bonded pairs. The corrections for the r_g to r_α^0 conversion[40], listed in Table 4 column b, are significant, since they exceed the experimental error of r_g.

The rotational constant for the ground vibrational state, B_0, has been calculated from the r_α^0 parameters on the assumption that the correction from B_z ($\approx B_\alpha^0$)[37] to B_0 conforms to the ordinary second-order formula[41,42] based on infinitesimal vibrational amplitudes. This correction, being proportional to B^2, is trivial for this molecule (-8×10^{-5} cm^{-1}).

The rotational constant estimated in this way, B_0(ED)=0.1453±0.0003 cm^{-1}, is significantly different from any of the spectroscopic values given in Table 4. The infrared values are presumably more accurate than the Raman value, since in the latter experiment the rotational analysis may have been biased by overlapping hot bands, as was pointed out by Maki[9] in the case of cyanogen.

The discrepancy is probably originated, at least in part, in the B_0(ED), which is based on model b for the r_g to r_z conversion. A possible systematic error due to this model has not been counted in the uncertainty given above. A further study in this regard is made in the next subsection.

While the basic scheme of coordinating the average structure derived from electron diffraction and spectroscopy seems to work for a number of nonlinear polyatomic molecules with small vibrational amplitudes,[26,38] a special formalism is required for a calculation of the ground-state rotational constant for a molecule with large-amplitude vibrations (in particular, for a quasi-linear molecule) from a given set of thermal-average distances.[43] None of such a treatment has been made in the present study.

Bend-Stretch Interactions. The discrepancies observed in the mean amplitudes and in the rotational constant discussed above indicate the presence of appreciable contributions from bending-stretching interactions left out in the calculations. Suppose a displacement Δr in Eq. (4) increases with the bending displacement $\Delta\rho^2$ so as to partially compensate for the second term, $-\Delta\rho^2/2r_e$, and the atoms take loci shown in Fig. 3c. Then the mean amplitude should fall in between (a) and (b) of Table 2, and the effective B_0 (ED) should increase. One may thus assume a model c, where the displacement of a bond j is given, in place of Eq. (5), as

$$\Delta r_j=\sum_{i=1}^{5}a_iQ_i+\alpha_j(\phi_j^2+\phi_j'^2) \qquad (7)$$

where α_j is a positive constant. The angles of bending from π on both ends of the bond j, ϕ_j and ϕ_j', can be expanded in terms of the normal coordinates Q_6 through Q_9.

The physical significance of a positive parameter α_j is to introduce into the potential function a negative third-order term, $-\alpha_jf_j\Delta r_j(\phi_j^2+\phi_j'^2)$, where f_j is a second-order force constant for the bond stretching. For a number of linear molecules (CO_2,[32,33] CS_2,[32,33] OCS,[44] HCN(DCN),[45] NNO,[46] C_2H_2(C_2D_2)[47]), where precise values of third-order potential constants are known from spectroscopic experiments, the constants representing the bending-stretching interaction of this sort are all *negative* (of the order of a few tenths of one mdyn). Furthermore, the π bond order of the C–C single bond in diacetylene is expected to decrease with the C≡C–C bending displacements as a result of the decrease in the degree of conjugation, and this effect should make an appreciable positive contribution to α_{C-C}. The corresponding (probably negative) contribution to $\alpha_{C\equiv C}$ seems to be much less important, since the difference in the C≡C bond distances in diacetylene and acetylene is found in the present study to be only about 0.005 Å.

It has been shown, on an empirical basis, that the following set of bending-stretching interactions makes the bonded and nonbonded CC mean amplitudes agree with the observed values as listed in Table 2, column (c):

39) M. Iwasaki and K. Hedberg, *J. Chem. Phys.* **36**, 2961 (1962).
40) Y. Morino, K. Kuchitsu, and T. Oka, *ibid.*, **36**, 1108 (1962).
41) D. R. Herschbach and V. W. Laurie, *ibid.*, **37**, 1668 (1962).
42) M. Toyama, T. Oka, and Y. Morino, *J. Mol. Spectrosc.* **13**, 193 (1964).
43) J. T. Hougen P. R. Bunker, and J. W. C. Johns, *ibid.*, **34**, 136 (1970).
44) T. Nakagawa and Y. Morino, *ibid.*, **26**, 496 (1968).
45) T. Nakagawa and Y. Morino, This Bulletin, **42**, 2212 (1969).
46) I. Suzuki, *J. Mol. Spectrosc.* **32**, 54 (1969).
47) I. Suzuki and J. Overend, *Spectrochim. Acta*, **25A**, 977 (1969); I. Suzuki, private communication, 1970.

$\alpha_{C-C}=0.352$ Årad^{-2}, $\alpha_{C\equiv C}=0.152$ Årad^{-2},

and $\alpha_{C-H}=0.599$ Årad^{-2}.

In addition, the $r_g-r_\alpha^0$ corrections based on this set are shown to result in the B_0 (ED) in excellent accord with the B_0(infrared) as listed in Table 4.

The present model c should be taken with reservation, in spite of the above virtual success, since the bending-stretching interactions given above seem to be larger than those expected for ordinary linear molecules, even if the influence of the conjugation in diacetylene is taken into account. The above α parameters are subject to a further examination with suspicion of systematic errors.

Such a strong bending-stretching interaction, if present, poses a problem in the comparison of bond distances in different molecules. A usual scheme of comparison in terms of the average bond distances, where the difference in the r_g distances is regarded as a good representation of that in the r_e distances,[26] is no longer valid for a group of molecules with very different α parameters. Future systematic studies of the structures of linear conjugated molecules will present a clue to the solution of this problem.

BULLETIN OF THE CHEMICAL SOCIETY OF JAPAN, VOL. 44, 391—395 (1971)

Inclusion Compounds of Some Charge-Transfer Complexes

Masatake OHMASA*, Minoru KINOSHITA, and Hideo AKAMATU
Department of Chemistry, Faculty of Science, The University of Tokyo, Hongo, Tokyo

(Received October 3, 1970)

The charge-transfer complex of benzidine and tetracyano-*p*-quinodimethane has been shown to form an inclusion compound with certain molecules such as dichloromethane, dibromomethane and acetone. The molecular volumes of these guest substances are all smaller than 75 cm^3/mol, while the substances which are not included have a molecular volume larger than 80 cm^3/mol. Besides the size, the molecular shape is also considered to be a primary factor for the formation of the inclusion compound. The heat of formation of the inclusion compound with dichloromethane as a guest was determined to be 11.1 ± 1 kcal per mole of the guest substance by the thermochemical measurements. Similar inclusion compounds were also obtained, when 3,3′-diaminobenzidine, 3,3′-dichlorobenzidine and *o*-tolidine were used in place of benzidine.

In a previous paper,[1] we have reported that benzidine (BD) and tetracyanoquinodimethane (TCNQ) form two types of complexes, the type being determined by the solvent used in the preparation. One is the complex which contains solvent molecules in addition to BD and TCNQ, (BD·TCNQ·S)[2], and the other is the complex which does not contain solvent molecules, BD·TCNQ(n). The amount of the solvent contained in the BD·TCNQ·S complex is as much as those of BD and TCNQ, and several solvents which are different in chemical properties form this type of complexes. In the present paper, the BD·TCNQ·S complex will be shown to possess the characteristics of the inclusion compounds.

A variety of inclusion compounds have been studied[3,4] and are known to possess the following common features.[5] They are composed of two components, host and guest, and the host lattice has cavities to include the guest molecules. Although many kinds of molecules are to be included in the cavity of the same host lattice, the formation of an inclusion compound is normally controlled by the size and shape of a guest molecule. The force binding the guest molecules is intermolecular one and the heats of formation of the inclusion compounds fall usually in the range of 5—12 kcal per mole of the guest substance.

The compounds studied here, whose host lattice is comprised by the organic charge-transfer complexes, are found to possess these characteristics.

Experimental

Chemicals. Benzidine, *o*-tolidine (TL), 3,3′-diaminobenzidine (DABD), and 3,3′-dichlorobenzidine (DCBD) were obtained from commercial sources, and used after purification by recrystallization from ethanol or carbon tetrachloride. Synthesis and purification of TCNQ were described previously.[6]

Complex Preparation. BD·TCNQ·S(CH_2Cl_2): To a solution of 35 mg of BD in 80 m*l* of dichloromethane was added a solution of 44 mg of TCNQ in 120 m*l* of dichloromethane at room temperature, and shiny dark green crystals thus formed were collected.

BD·TCNQ(n) (from Chloroform): Dark green polycrystals were obtained by mixing a solution of 16 mg of BD in 10 m*l* of chloroform with a solution of 23 mg of TCNQ in

* Present address: The Institute of Physical and Chemical Research, Wakō, Saitama.

1) M. Ohmasa, M. Kinoshita, and H. Akamatu, This Bulletin, **42**, 2402 (1969).

2) For simplicity, the complex of BD with TCNQ which contains solvent molecules will be abbreviated as BD·TCNQ·S, and if the solvent is required to be specified, the notation BD·TCNQ·S (chemical formula of the solvent)is used, *e.g.*, BD·TCNQ·S(CH_2Cl_2).

3) L. Mandelcorn, *Chem. Rev.*, **59**, 827 (1959).

4) F. Cramer, *Angew. Chem.*, **68**, 115 (1956).

5) J. H. van der Waals and J. C. Platteeum, *Advan. Chem. Phys.*, **2**, 1 (1959).

6) M. Ohmasa, M. Kinoshita, M. Sano, and H. Akamatu, This Bulletin, **41**, 1998 (1968).

60 ml of chloroform at room temperature.

Other complexes including TL, DABD, and DCBD complexes were prepared in a similar manner.

Measurement of X-Ray Diffraction Patterns. X-Ray diffraction patterns of powdered samples were measured at room temperature with a diffractometer, Rigaku Denki Geigerflex.

Calorimetric Measurement. A conductive twin microcalorimeter made by Oyodenki Co. was used to determine the heats of reaction, $(-\Delta H_2)$ and $(-\Delta H_3)$, for the reactions defined by Eqs. (2) and (3) in the following section. The heats were measured at constant temperature, 25°C and at 1 atm.

The procedures of the measurement are as follows. (i) About 400 mg of the powdered sample was sealed in a thin-wall glass tube. The saturated solution of BD·TCNQ complex in dichloromethane was placed in the reaction vessel and in the reference vessel. The volume of the solution in each vessel was set at 50 ml.

(ii) The glass tube containing the sample was placed in the reaction vessel and the vessels were laid in the heat resservoir overnight to achieve the thermal equilibrium.

(iii) The glass tube was then broken and the reaction was started. The difference of the temperature between the reaction vessel and the reference vessel was recorded until the reaction was completed and the temperature of the reaction vessel became constant. It took about 3 hr.

(iv) A certain amount of heat was then generated on the side of the reaction vessel by the standard heater and the difference of the temperature was recorded again.

(v) The areas below the recorded curves for the heat of the reaction and the reference heat were measured and the former heat was calculated by using these areas and the latter heat.

(vi) The heat of reaction calculated in this way was then corrected for the heat generated by breaking the glass tube, which was measured in a blank test.

For this experiment, the BD·TCNQ(n) complex was prepared from chloroform. The special grade dichloromethane from Wako-junyaku Co. was used.

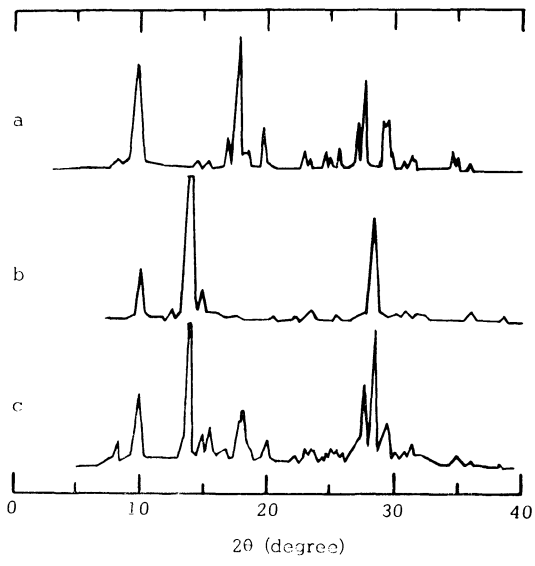

Fig. 1. The X-ray diffraction patterns of powders of BD·TCNQ complexes.
a) BD·TCNQ·S(CH_2Cl_2)
b) BD·TCNQ(n)
c) BD·TCNQ(n) which was exposed to dichloromethane vapor overnight and then placed in a vacuum for several hours (see the text).

Thermogravimetric Analysis (TGA). Thermogravimetric analysis was performed using thermobalance made by Tokyo Koki Seizosho. The heating rate was about 0.75°C/min. Nitrogen gas was slowly streamed about the sample during the measurement.

Differential Thermal Analysis (DTA). The differential thermal analysis for the freshly prepared sample of BD·TCNQ·S(CH_2Cl_2) complex was made with a Rigakudenki DTA apparatus in the air. The heating rate was 2.5°C/min.

Characterization of BD·TCNQ System. To know whether the complex prepared in a solvent contains the solvent molecules or not, the infrared absorption spectrum of the complex was examined. As was described in the previous paper,[1] the spectra of BD·TCNQ·S complexes are similar to one another and are quite different from that of BD·TCNQ(n) complex. In the former spectra are observed the absorption bands which are assigned to the vibrational modes of the solvent molecule contained in the complex, while the bands of the solvent molecule are not observed in the latter. These features are employed as criteria for the characterization of the BD·TCNQ complexes.

Composition of Complexes of TCNQ with TL, DABD, and DCBD. The ratios, (donor) : (acceptor) : (solvent), of the complex of TL, DABD, and DCBD were calculated from the results of elementary analysis of the complex.

Results and Discussion

X-Ray Diffraction Patterns. The X-ray diffraction patterns for powders of BD·TCNQ system are shown in Fig. 1. The pattern for BD·TCNQ·S(CH_2Cl_2) (Fig. 1a) is quite different from that of BD·TCNQ(n) (Fig. 1b). It is therefore concluded that these two complexes have different crystal structures.

The BD·TCNQ(n) and BD·TCNQ·S complexes readily change their structures to each other. When a sample of BD·TCNQ·S(CH_2Cl_2) is heated on a thermobalance, the weight of the sample begins to reduce at about 50°C and becomes constant at about 120°C. When the heated sample is cooled to the room temperature, its X-ray diffraction pattern becomes identical with that for the BD·TCNQ(n) complex. On the other hand, when a sample of BD·TCNQ(n) is exposed to the vapour of dichloromethane at about 200 mmHg and is laid overnight at room temperature, the X-ray diffraction pattern becomes identical with that for BD·TCNQ·S (CH_2Cl_2).

The X-ray diffraction pattern illustrated in Fig. 1c was obtained for the sample of BD·TCNQ(n) which was exposed to the vapour of dichloromethane in the manner described above and then sealed in a vacuum for several hours at room temperature. This pattern is well interpreted as a superposition of the pattern for BD·TCNQ·S(CH_2Cl_2) complex and that for the BD·TCNQ(n) complex.

These facts show that the solvent molecules contained in the complex are very weakly bound in the crystal lattice. Therefore, it is plausible to conclude that the BD·TCNQ·S(CH_2Cl_2) complex is a kind of inclusion compounds. If so, this complex is a new family of the inclusion compounds in the sense that its host lattice is composed of a charge-transfer complex.

Thermodynamic Properties. The heat of formation of the inclusion compound is rather small, because the guest molecule is bound to the host lattice by the intermolecular force. Many inclusion compounds show the value in the range of 5—12 kcal per mole of the guest molecule.[7-10]

The heat of formation ($-\Delta H_f$) of BD·TCNQ·S(CH_2Cl_2) in the following reaction was measured by the calorimetric method.

$$\text{BD·TCNQ(n)(s)} + 1.8\ CH_2Cl_2(g) = \text{BD·TCNQ·S(s)};\ \Delta H_f \quad (1)$$

where (s) and (g) denote that the substance is in the solid state and in the gaseous state, respectively. It was assumed that one mole of BD·TCNQ·S(CH_2Cl_2) contains 1.8 mole of dichloromethane.[11]

Equation (1) is considered to be equivalent to the combination of the following thermochemical equations (2)—(4) according to Hess' law.

$$\text{BD·TCNQ(n)(s)} + 1.8\ CH_2Cl_2(l) = \text{BD·TCNQ·S(sol)};\ \Delta H_2 \quad (2)$$

$$\text{BD·TCNQ·S(sol)} = \text{BD·TCNQ·S(s)};\ \Delta H_3 \quad (3)$$

$$1.8\ CH_2Cl_2(g) = 1.8\ CH_2Cl_2(l);\ \Delta H_4 \quad (4)$$

$$\Delta H_f = \Delta H_2 + \Delta H_3 + \Delta H_4 \quad (5)$$

Here, (l) denotes that the substance is in the liquid state and (sol) shows that the solid substance is placed in the saturated solution of BD·TCNQ complex in dichloromethane.

The heats of reactions, ($-\Delta H_2$) and ($-\Delta H_3$), were measured calorimetrically. The heat of condensation, ($-\Delta H_4$), was calculated from the value given in a literature.[12] In the measurement, the sample of BD·TCNQ(n) or BD·TCNQ·S complex was dropped into the saturated solution of BD·TCNQ complex in dichloromethane in order to avoid the effect of dissolution of the solid. The values of ΔH_f, ΔH_2, ΔH_3, ΔH_4 obtained are given in Table 1.

The heat of formation of BD·TCNQ·S(CH_2Cl_2) per mole of dichloromethane is thus estimated as 11 kcal/mol. This value is reasonable in comparison with that for ordinary inclusion compounds.

Table 1. Heat of formation of BD·TCNQ·S(CH_2Cl_2) complex from BD·TCNQ(n) complex and dichloromethane gas

A)	Heat of formation per one mole of the complex	
	$-\Delta H_2$:	9.1±1 kcal/mol
	$-\Delta H_3$:	−1.2±1 kcal/mol
	$-\Delta H_4$:[a]	12.0 kcal
	$-\Delta H_f$:	19.9±2 kcal/mol
B)	Heat of formation per one mole of dichloromethane	11.1±1 kcal/mol

a) This value was calculated from the value given in Ref. 12.

The TGA curve and the differential thermogram for freshly prepared sample of BD·TCNQ·S(CH_2Cl_2) are presented in Figs. 2 and 3, respectively. The amount of the weight loss of the sample shows that the solvent molecules are completely desorbed from the sample during the heating. This was further confirmed by the fact that, as was mentioned before, the X-ray diffraction pattern of the sample after TGA measurement became identical with that of BD·TCNQ(n).

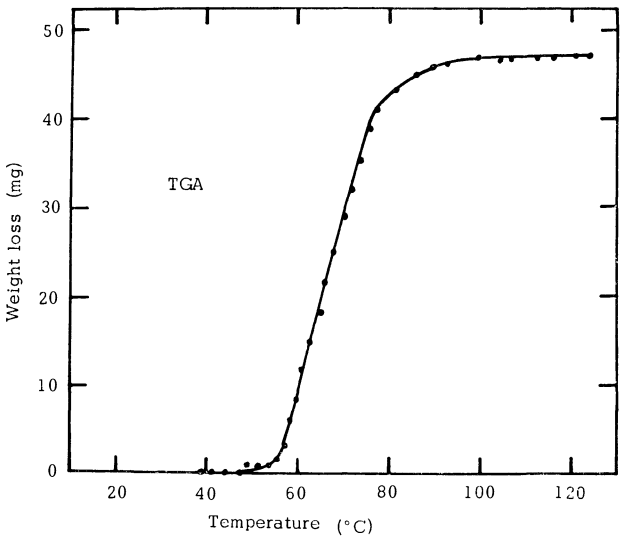

Fig. 2. The thermogravimetric analysis (TGA) curve for BD·TCNQ·S (CH_2Cl_2) complex.
Heating rate was about 0.75°C/min. The weight of the sample was 165 mg before the measurement and 118 mg after the measurement.

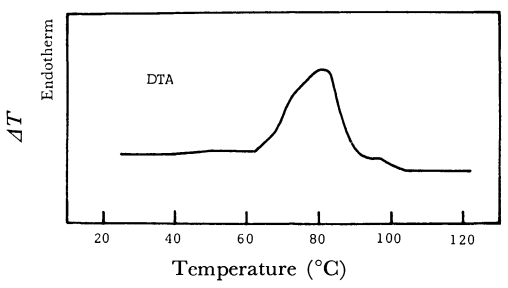

Fig. 3. The differential thermogram of BD·TCNQ·S (CH_2Cl_2) complex.
Heating rate was about 2.5°C/min. The weight of the sample was 136 mg before the measurement and 97 mg after the measurement.

7) R. M. Barrer and A. V. J. Edge, *Proc. Roy. Soc., Ser. A*, **300**, 1 (1967).
8) S. A. Allison and R. M. Barrer, *Trans. Faraday Soc.*, **64**, 549 (1968).
9) R. D. Whitaker, A. J. Barreiro, P. A. Furman, W. C. Guida, and E. S. Stallings, *J. Inorg. Nucl. Chem.*, **30**, 2921 (1968).
10) E. E. Aynsley, W. A. Campbell, and R. E. Dodd, *Proc. Chem. Soc.*, **1957**, 210.
11) The solvent molecules contained in the complex escape slowly from the complex in air at room temperature, so that the composition of the complex changes with time.
As was reported in Ref. 1, the composition of BD·TCNQ·S (CH_2Cl_2) determined spectroscopically was (BD) : (TCNQ) : (CH_2Cl_2) = 1.0 : 1.1 : 1.6. But this composition is not so accurate, because evaporation of dichloromethane from the solid was not strictly considered.
To find the reliable value of the solvent content, TGA measurement of a freshly prepared sample of BD·TCNQ·S(CH_2Cl_2) was carried out. The composition of the complex was then calculated from the result of the measurement and was found as (donor) : (acceptor) : (solvent) = 1 : 1 : 1.8. This result is adopted here.
12) "Landolt-Börnstein, Zahlenwerte und Funktionen," Vol. II, part 4, Springer, Berlin (1961), p. 292.

The curves shown in Figs. 2 and 3 indicate that the included dichloromethane molecules were evaporated in one step, which means that all the solvent molecules are bound equivalently in the crystal of BD·TCNQ·S (CH_2Cl_2).

Inclusion of Solvent Molecules in BD·TCNQ System. It seems that the formation of the BD·TCNQ·S complex is mainly determined by the structural requirement, that is, by the size and the shape of the solvent molecule used in the preparation of the complex. This also indicates that the BD·TCNQ·S complexes are inclusion compounds.

The intermolecular forces between the solvent molecule and the host lattice are not considered to be the determining factor of the formation of the BD·TCNQ·S complex. The molecular volume, the molecular polarizability and the dipole moment of the solvent molecules used in the experiment are compared in Table 2. The type of the complex (solvent contained or not) is also given in the table. The molecular polarizability and the dipole moment are closely related to the dispersion force[13,14] and the electrostatic force which act on the solvent molecule, but these two quantities of the solvents examined so far do not seem to be related to the formation of BD·TCNQ·S complexes. For example, chloroform and 1,1-dichloroethane which give BD·TCNQ(n) complexes have larger molecular polarizability than dichloromethane and ethyl bromide which give BD·TCNQ·S complexes, and the dipole moment of 1,1-dichloroethane is also larger than that of dichloromethane.

Table 2. Molecular volume, molecular polarizability and dipole moment of the solvent used in preparation of BD·TCNQ complexes

Solvent	Type of complex[a]	Molecular volume[b]	Molecular polarizability[c]	Dipole moment[d]
$CHCl_3$	n	80.5	85.2	1.01
CH_3CHCl_2	n	84.1	85.2	2.06
CH_2Cl_2	s	64.0	65.0	1.60
CH_3CH_2Br	s	74.6	75.6	2.03
CH_2Br_2	s	69.6	87.2	1.43
CH_3COCH_3	s	73.6	64.5	2.88
CH_3NO_2	s	53.7	49.8	3.46
CH_3CN	s	52.2	44.1	3.92
CH_2ClCH_2Cl	(s)[e]	80.1	86.0	1.47

a) The type of BD·TCNQ complex prepared in the solvent. n: BD·TCNQ(n), s: BD·TCNQ·S
b) The value in the unit of cm^3/mole at 20°C.
c) These values are calculated by the equation, $(4/3)\pi N\alpha=[(n^2-1)/(n^2+2)](M/d)$ where n is refractive index, M is molecular weight, d is density, N is Avogadro's number and α is molecular polarizability. The value of α at 20°C in the unit of 10^{-25} cm^3 is listed here.
d) debye unit.
e) The complex prepared in this solvent is considered to include solvent molecules partially, because the infrared absorption spectrum of this complex is a superposition of the spectra of BD·TCNQ(n) and BD·TCNQ·S complexes.

13) F. London, *Z. Phys. Chem.*, **B11**, 222 (1930).
14) D. F. Evans and R. E. Richards, *Proc. Roy. Soc., Ser. A*, **223**, 238 (1954).

The presence of some functional groups in the solvent molecule is not again the determining factor for the formation of BD·TCNQ·S complexes, because 1,1-dichloroethane gives a BD·TCNQ(n) complex, although dichloromethane and ethyl bromide give BD·TCNQ·S complexes.

Unlike the factors mentioned above, there is a close correlation between the molecular volume of the solvent molecule and the formation of BD·TCNQ·S complexes. As is seen in Table 2, the molecular volumes of chloroform and 1,1-dichloroethane which give BD·TCNQ(n) complexes are larger than those of the solvents which are found to be included in BD·TCNQ system. Therefore it is likely that the formation of the BD·TCNQ·S complex is controlled by the size of the solvent molecule on the one hand.

On the other hand, the molecular shape of chloroform and 1,1-dichloroethane is pyramidal, while that of dichloromethane is regarded as a triangle, if the van der Waals' radius of hydrogen atom is neglected. The shape of other solvent molecules which form BD·TCNQ·S complexes can also be regarded as triangular. Acetonitrile molecule is the only exception which is a linear one. Although both chloroform and dichloromethane molecules are composed of carbon, hydrogen and chlorine atoms and are methane type molecules, chloroform molecule is not included in the BD·TCNQ system, while dichloromethane gives a BD·TCNQ·S complex. This shows that the molecular shape of the solvent is another important factor, which determines the formation of the BD·TCNQ·S complex. 1,2-Dichloroethane whose molecular volume is as large as that of chloroform is partially included in the BD·TCNQ system as is shown in Table 2. This fact also indicates the importance of the molecular shape of the solvent.

Complexes of TCNQ with TL, DABD, and DCBD. The charge-transfer complexes of TL, DABD, and DCBD with TCNQ were expected to form inclusion compounds with certain solvents such as dichloromethane, because the molecular structures of these donors are similar to that of BD. Some of these complexes were prepared using dichloromethane or chloroform as a solvent. Their compositions were determined by analyzing the results of elementary analysis. The results are presented in Table 3. As is seen in the table, the system of TL·TCNQ contains a considerable amount of dichloromethane or chloroform and these complexes are considered to be inclusion compounds. The complex of DABD·TCNQ prepared in dichloro-

Table 3. Composition of the complexes of TCNQ with TL, DABD and DCBD

Donor	Solvent used in preparation	Mole ratios[a]
TL	CH_2Cl_2	1 : 1.00 : 1.23
TL	$CHCl_3$	1 : 1.07 : 0.52
DABD	CH_2Cl_2	1 : 1.00 : 0.45
DCBD	CH_2Cl_2	1 : 0.80 : 0.16

a) (Donor) : (Acceptor) : (Solvent)

methane is also regarded as an inclusion compound for the same reason. The complex of DCBD·TCNQ, however, contains a small amount of dichloromethane, and it is questionable that the complex is an inclusion compound. As is shown in Table 3, the amount of TCNQ is less than that of DCBD by a small amount which is nearly the same as the amount of the included solvent. The solvent molecules in this complex, therefore, may be trapped in the vacancies of the TCNQ molecules.

Tolidine·TCNQ system forms an inclusion compound with chloroform in contrast to the BD·TCNQ system. The physical properties of TL·TCNQ·S($CHCl_3$) are similar to those of BD·TCNQ·S(CH_2Cl_2).[15] It seems, therefore, that the structure of the donor molecule is also an important factor for the formation of the inclusion compounds of this type.

The authors wish to thank Professor Nobufusa Saito for the use of his laboratory thermal analysis facilities and Mr. Kenji Nakada for his kind help in the DTA experiments.

15) M. Ohmasa, M. Kinoshita, and H. Akamatu, This Bulletin, **44**, 395 (1971).

BULLETIN OF THE CHEMICAL SOCIETY OF JAPAN, VOL. 44, 395—400 (1971)

Electronic Properties of Benzidine·TCNQ System

Masatake OHMASA,* Minoru KINOSHITA, and Hideo AKAMATU

Department of Chemistry, Faculty of Science, The University of Tokyo, Hongo, Tokyo

(Received October 7, 1970)

The benzidine·tetracyano-*p*-quinodimethane (TCNQ) system forms two types of charge-transfer complexes; one (I) containes some sort of solvent molecules, while the other (II) does not. The electronic properties of I have been found to be unusual in many respects compared to II which shows the properties expected from those of ordinary charge-transfer complexes. I and II did not exhibit ESR absorption, if they were well-grown crystals. However, when they were pulverized to fine powder, I showed a strong absorption while II did not. The visible range absorption spectra of I and II consisted of three main bands, but all the bands of I were found to be shifted to longer wavelengths compared to those of II. In addition to these bands, two shoulders were found in the spectrum of I. The shoulders were considered to be due to the ion radicals produced from benzidine and TCNQ. The electrical resistivities are again quite different from one another. The resistivity of I was found to be 10^3—10^5 ohm cm at room temperature, the value being dependent on the kind of the solvent molecules included, while that of II was 2×10^9 ohm cm. The activation energy for conduction was smaller for I (0.1—0.2 eV) than for II (0.34 eV).

The electronic properties of charge-transfer complexes of tetracyanoquinodimethane (TCNQ) with a series of aromatic diamines were examined in the previous paper.[1] It was found that the complex of benzidine (BD) with TCNQ which was prepared in dichloromethane showed unusual properties compared with the other complexes studied. The electrical resistivity of the BD·TCNQ complex was very low and its infrared absorption spectrum was not explained either by a superposition of the spectra of ionic components or that of neutral components.

Later study revealed that BD and TCNQ form two types of complexes[2]: one is the complex which contains solvent molecules [BD·TCNQ·S][3] and the other is the complex which does not contain solvent molecules [BD·TCNQ(n)]. The former complex was proved to be a kind of inclusion compound.[4] Preliminary examination has revealed that the electronic properties of these two types of complexes are quite different from each other. It was the BD·TCNQ·S complex which was observed previously to show unusual properties.

Several authors[5-9] have studied the effect of the occluded solvent molecules on the electronic properties of charge-transfer complexes and on the difference in the electronic properties of the complexes which are composed of the same donor and acceptor and are prepared from different solvents. Ottenberg *et al.*[7] studied electrical and ESR properties of the *p*-phenylenediamine·*p*-chloranil complex. They observed no significant effect of entrapped solvent molecules on these properties. Cairns and McGeer[8] prepared diaminodurene·TCNE complex in chloroform and tetrahydrofurane and obtained two types of complexes which have different colors. Among these works, the study on polymorphic forms of diaminopyrene·chloranil system by Matsunaga[5,6] is parti-

* Present address: The Institute of Physical and Chemical Research, Wakō, Saitama.

1) M. Ohmasa, M. Kinoshita, M. Sano, and H. Akamatu, This Bulletin, **41**, 1998 (1968).

2) M. Ohmasa, M. Kinoshita, and H. Akamatu, *ibid.*, **42**, 2402 (1969).

3) As for the notation of the complex, see Ref. 4.

4) M. Ohmasa, M. Kinoshita, and H. Akamatu, This Bulletin, **44**, 391 (1971).

5) Y. Matsunaga, *Nature*, **211**, 183 (1966).

6) Y. Matsunaga, *Nippon Kagaku Zasshi*, **89**, 905 (1968).

7) A. Ottenberg, C. J. Hoffman, and J. Osiecki, *J. Chem. Phys.*, **38**, 1898 (1963).

8) T. L. Cairns and E. G. McGeer, *Chem. Abstr.*, **62**, 1775f (1965).

9) M. Batley and L. E. Lyons, *Mol. Cryst.*, **3**, 357 (1968).

cularly interesting. He observed that electronic properties of this complex precipitated from benzene were greatly changed by compressing the sample in the presence of benzene. After the compression, electrical resistivity of the sample was greatly reduced and its infrared absorption spectrum was entirely changed. These facts indicate that the occluded solvent has an important effect on the electronic properties of the diaminopyrene·chloranil system. However, the cause of the effect of the occluded solvent is not clear at present.

The benzidine·TCNQ system is similar to the diaminopyrene·chloranil system in some respects, and is considered to be suited for the study of the effect of the occluded solvent, because both BD·TCNQ(n) and BD·TCNQ·S complexes can be prepared individually, and many kinds of solvents are found to form the BD·TCNQ·S complex. In the present study, the electronic properties of BD·TCNQ·S and BD·TCNQ(n) complexes are described in detail and are compared with each other.

Some of the electronic properties of the complexes of TCNQ with *o*-tolidine, 3,3′-diaminobenzidine and 3,3′-dichlorobenzidine were also examined in brief.

Experimental

Complex Preparation. The BD·TCNQ·S and BD·TCNQ(n) complexes were prepared by the method previously.[4]

Infrared Absorption Measurement. To determine the character of the complex, infrared absorption spectra of the complex and related compounds were examined with a Hitachi infrared spectrophotometer in the range of 4000—400 cm^{-1}. The method of Nujol mull was adopted in the measurement.

ESR Absorption Measurement. Electron spin resonance (ESR) absorptions were measured as described in the previous paper.[1]

Visible and Near Infrared Absorption Measurement. Absorption spectra in the visible and infrared regions were measured for the solid samples using the method of Nujol mull.

Electrical Resistivity. Electrical resistivity of a complex was measured in a form of compressed pellet by a DC-method. Measurements on single crystals were also made for BD·TCNQ·S(CH_2Cl_2) at room temperature.

Results and Discussion

Infrared Absorption Spectra. The infrared absorption spectra of BD·TCNQ(n) and BD·TCNQ·S(CH_3COCH_3) are shown in Fig. 1 together with the spectra of BD, BD bromide, TCNQ and lithium salt of TCNQ. The spectra of the complexes containing other solvent molecules are similar to that of BD·TCNQ·S(CH_3COCH_3) complex except for the bands due to the solvent molecules.

The spectra of TCNQ[10,11] and TCNQ anion radical (lithium salt of TCNQ) are clearly different in the following points. Firstly, the C≡N stretching vibration of TCNQ appears at 2223 cm^{-1} and is very sharp, but the corresponding band of TCNQ anion radical appears at 2203 cm^{-1} and is broadened and split.[1] Secondly, a strong absorption band which is located at 1540 cm^{-1} in TCNQ is considered to be a superposition of the ring C=C stretching mode and the ethylenic C=C stretching mode. In the spectrum of TCNQ anion radical, however, no strong band appears at 1540 cm^{-1} and new bands are located at 1580 cm^{-1} and 1507 cm^{-1}. This is considered to be due to the difference in bond lengths of the ring and ethylenic C=C bonds in TCNQ and its anion radical. Thirdly, a strong absorption band is observed at 1183 cm^{-1} for the anion radical, whereas no strong band is observed for TCNQ in this region.

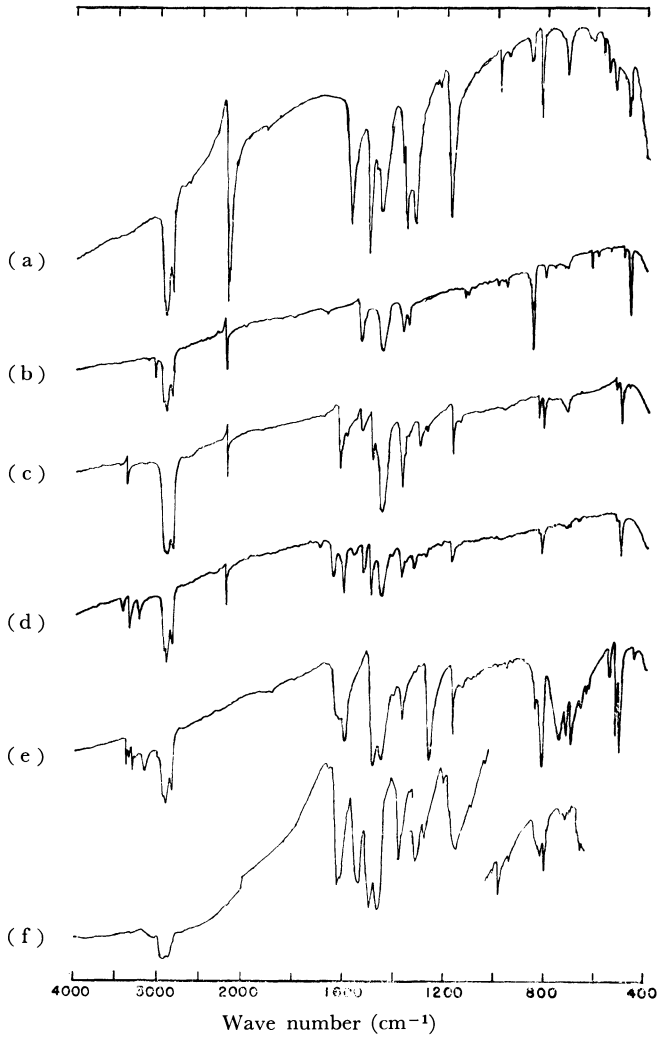

Fig. 1. Infrared absorption spectra of BD·TCNQ complexes and related compounds.
(a) LiTCNQ, (b) TCNQ, (c) BD·TCNQ(*n*), (d) BD·TCNQ·S(CH_3COCH_3), (e) BD, (f) BD·bromide.

The absorption spectra of BD and BD cation radical (BD bromide) are also very different in many respects.[12] In the spectrum of BD cation radical was

10) T. Takenaka, Preprint of Symposium on Molecular Electronic States, October, 1969, Fukuoka, Japan.
11) B. Lunelli and C. Pecile, *J. Chem. Phys.*, **52**, 2375 (1970).
12) The infrared absorption spectrum of BD is very similar to that of aniline and the vibrational modes were assigned according to the assignments of aniline by Evans.[13]
13) J. C. Evans, *Spectrochim. Acta*, **16**, 428 (1960).

observed a fairly intense band at 1545 cm^{-1}, but no intense band was observed around this wave number for BD. The ring stretching mode involving considerable C–N stretching appears at 1268 cm^{-1} for neutral BD, but in the spectrum of BD cation radical, no strong absorption is located in this region and a new band appears at 1318 cm^{-1}. The bands at 1176 cm^{-1} and 1140 cm^{-1} for BD are assigned to the in-plane CH bending modes. For BD cation radical, a fairly broad band is located at 1160 cm^{-1}, but the shape of this band is clearly distinguishable from the shape of the CH bending modes.

(a) BD·TCNQ(n) Complex: In the spectrum of BD·TCNQ(n) complex, the C≡N stretching frequency is slightly shifted to lower values compared with that of neutral TCNQ (from 2223 cm^{-1} to 2205 cm^{-1}), but the band is neither broadened nor split. The C=C ring stretching mode of TCNQ of the complex is observed at the same frequency as that of neutral TCNQ. As for the amine part, the ring stretching mode which is located at 1490 cm^{-1} in neutral BD is observed at 1498 cm^{-1} in the complex, and the bands at 1176 cm^{-1} and 1146 cm^{-1} for the complex are found to be clearly resembling in the frequency and in the shape to the in-plane CH bending modes of neutral BD. Furthermore, no band of the complex is found to correspond to the ring stretching band at 1545 cm^{-1} for BD bromide. From these, it is concluded that BD·TCNQ(n) complex is essentially of non-bonding type.

In the ground state, however, the dative structure seems to contribute to somewhat large extent in this complex, because the ring stretching mode involving considerable C–N stretching is shifted to 1308 cm^{-1} in the complex and the position is close to the band at 1318 cm^{-1} for BD bromide.

(b) BD·TCNQ·S(CH_3COCH_3) Complex: In the BD·TCNQ·S(CH_3COCH_3) complex, the C≡N stretching mode of TCNQ appears at 2210 cm^{-1}, and is neither broadened nor split. The fact suggests that the complex is of non-bonding type.

The following observations, however, show fairly large contribution of the dative structure to the ground state of the complex. The C=C stretching bands which appear at 1540 cm^{-1} in neutral TCNQ are shifted to 1528 cm^{-1} in the complex. The band at 1180 cm^{-1} of the complex shows almost the same frequency and shape as the band at 1183 cm^{-1} of lithium salt of TCNQ. In this complex, the in-plane CH bending mode of neutral BD at 1140 cm^{-1} disappears and a shoulder is located at 1160 cm^{-1} where a band of BD bromide lies. The ring stretching mode involving considerable C–N stretching of BD is observed to be shifted to 1330 cm^{-1} and is found to be rather near the band of BD bromide at 1318 cm^{-1}. Moreover, a new band appears in the complex at 1560 cm^{-1}, where no band is observed in the spectra of BD, BD bromide, TCNQ, and lithium salt of TCNQ. This band may correspond to the band at 1545 cm^{-1} of BD bromide or to the band at 1580 cm^{-1} of lithium salt of TCNQ.

From these observations, it is concluded that BD·TCNQ·S(CH_3COCH_3) complex is neither of non-bonding type nor of ionic type and that its electronic character may be considered to lie in the intermediate between the non-bonding and the ionic characters. The same conclusion is also drawn for BD·TCNQ containing other solvent molecules.

For BD·TCDQ·S complexes, the band characteristic of the solvent included is also observable. For example, the C=O stretching mode of acetone is seen at 1705 cm^{-1} in the spectrum of BD·TCNQ·S(CH_3COCH_3).

Magnetic Properties. The magnetic properties of BD·TCNQ·S complexes are very different from those of BD·TCNQ(n) complex. BD·TCNQ(n) is diamagnetic and exhibit no ESR absorption, whether the sample is in the form of crystal or in the form of finely ground powder. The well-grown crystals of BD·TCNQ·S show no (or sometimes very weak) ESR absorption, but when they are ground to fine powder, they exhibit a strong ESR absorption signal. When the pulverized sample of BD·TCNQ(n) is exposed to the vapor of dichloromethane overnight, it becomes to show a strong ESR absorption. The fact is consistent with the observed change in the X-ray diffraction pattern described in Ref. 4.

The unpaired electrons in BD·TCNQ·S are produced by the following three ways. (i) The spin concentration of a crystalline sample of BD·TCNQ·S complex increases greatly when the sample is ground. For example, when the crystals of BD·TCNQ·S(CH_2Cl_2) were ground in a vacuum at room temperature, the ESR absorption intensity of the sample increased by a factor of 270.

(ii) The spin concentration of freshly prepared samples of BD·TCNQ·S is dependent on conditions of the sample preparation. The sample which was prepared in a concentrated solution of the components and was not composed of well grown crystals showed a larger spin concentration than the complex which was prepared in a dilute solution and was composed of well-grown crystals. The results of the experiments on BD·TCNQ·S (CH_2Cl_2) are shown in Table 1, where relative intensities of the ESR absorption are listed as a measure of spin concentrations.

Table 1. Relation between ESR absorption intensity of BD·TCNQ·S (CH_2Cl_2) complex and the condition of its preparation

Sample	Initial concentration of components[a]		Relative intensity of ESR absorption[b]
1	TCNQ	2.6×10^{-3} mol/l	4.50
	BD	7.6×10^{-3}	
2	TCNQ	2.7×10^{-3}	1.90
	BD	2.5×10^{-3}	
3	TCNQ	9.2×10^{-4}	0.32
	BD	8.3×10^{-4}	

a) These values show the initial concentration of each component in the solution from which the complex is precipitated.
b) ESR absorption intensity is measured within a several hours after filtration of the sample.

(iii) The ESR intensity of BD·TCNQ·S increases gradually when it is exposed to the air.

The facts (i) and (ii) show that the unpaired electrons are produced at the lattice defect and/or on the surface

of the crystals.

The temperature dependence of the ESR intensity of BD·TCNQ·S (CH_2Cl_2) is given in Fig. 2. The ESR intensities of both samples, ground and not ground, increase in proportion to $1/T$ as the temperature is lowered down to 77°K. The fact indicates that the interaction between the unpaired electrons is very weak in the complex. The line shape of the ESR absorption, however, is very much narrowed and asymmetric in a vacuum. For example, the width between the points of half maximum of the absorption curve ($\Delta H_{1/2}$) was 1.1G for BD·TCNQ·S (CH_2Cl_2) in a vacuum. The narrow line width seems to be due to the motional narrowing, because the interaction between unpaired electrons is very weak.

The ESR absorption signal is sensitively changed by an introduction of air. In the air, the absorption line is almost symmetric and Lorentzian, whereas it is symmetric in a vacuum. The line width in the air is greater than that in a vacuum. The width $\Delta H_{1/2}$ of BD·TCNQ·S(CH_2Cl_2) is 3.1G in the air. This behavior suggests that the unpaired electron is produced near the surface. The integrated ESR absorption intensity, however, is not affected so sensitively by the introduction of air, although the intensity increases gradually in the air. The value of g-factor for BD·TCNQ·S(CH_2Cl_2) is 2.0027±0.0004.

The ESR behavior of the unpaired electrons generated by grinding and by the interaction with the air was identical. Therefore, both kinds of the unpaired electrons are considered to belong to the same paramagnetic species.

Visible and Near Infrared Absorption Spectra. The visible and near infrared absorption spectra of solid BD·TCNQ(n), BD·TCNQ·S (CH_2Cl_2) and BD·TCNQ·S(CH_3CN) complexes are shown in Fig. 3. The absorption peaks for the solutions of BD, BD·bromide,[14] TCNQ,[15] lithium salt of TCNQ[16] and BD·TCNQ complex are also shown in this figure. The spectrum of BD·TCNQ·S(CH_2Cl_2) is essentially identical with that reported by T. Amano *et al.*[17]

These spectra are composed of three main bands. The bands for BD·TCNQ·S complexes, however, are shifted to longer wave lengths compared with those of BD·TCNQ(n) complexes.

The bands of BD·TCNQ(n) at 1300 mμ and 520 mμ are assigned to the first and the second charge-transfer band; respectively, because of the following reasons. Firstly, the solution spectra of both BD and TCNQ[15] show individually no absorption peak in the region longer than 450 mμ. Since BD·TCNQ (n) is essentially of non-bonding type as was described before, these two bands of BD·TCNQ(n) are considered to be charge-transfer bands. Secondly, the positions of these two bands are near to the first and the

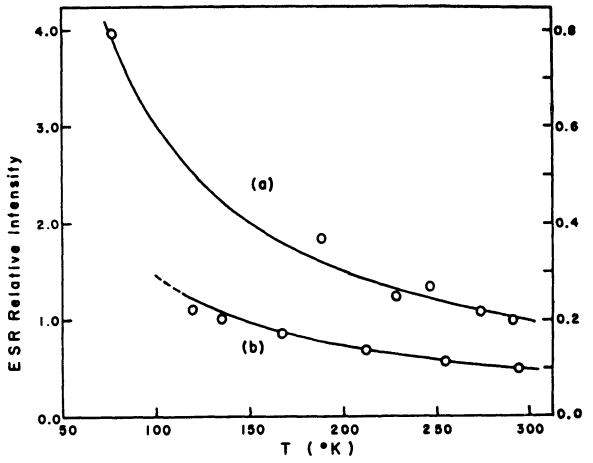

Fig. 2. Plots of relative ESR absorption intensities as a function of temperature for BD·TCNQ·S(CH_2Cl_2); (a) the sample which was ground mechanically, and (b) the sample which was not ground.
The scale for (a) is indicated on the left, while for (b) on the right.

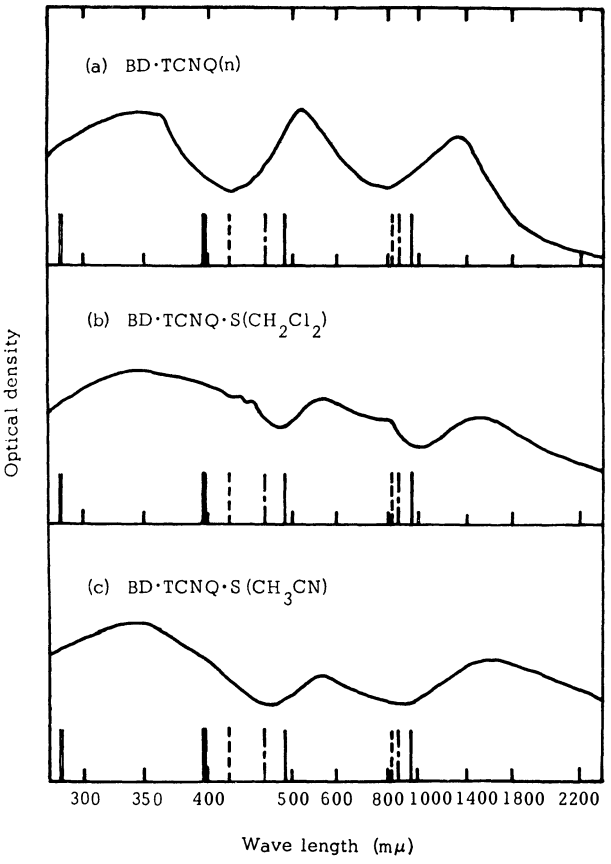

Fig. 3. Visible and near infrared absorption spectra of the solid complexes; (a) BD·TCNQ(n), (b) BD·TCNQ·S(CH_2Cl_2), and (c) BD·TCNQ·S(CH_3CN).
In the figure are also shown the positions of absorption peaks for solutions of TCNQ (——), BD (═══), Li^+TCNQ^- (- - -) and BD bromide (—·—), and of charge-transfer absorption maxima of chloroform solution of BD·TCNQ complex (——).

14) K. Takemoto, H. Matsusaka, S. Nakayama, K. Suzuki, and Y. Ooshika, This Bulletin, **41**, 764 (1968).
15) D. S. Acker and W. R. Hertler, *J. Amer. Chem. Soc.*, **84**, 337 (1962).
16) L. R. Melby, R. J. Harder, W. R. Hertler, W. Mahler, R. E. Benson, and W. E. Mochel, *ibid.*, **84**, 3374 (1962).
17) T. Amano, H. Kuroda, and H. Akamatu, This Bulletin, **42**, 671 (1969).

second charge-transfer bands for the solution of BD·TCNQ, respectively. Thirdly, as is shown in Table 2, the difference in the energies for the peaks at 520 mμ and 1300 mμ of BD·TCNQ(n) is nearly equal to the difference in the energies of the second and the first charge-transfer bands for the solution of BD·TCNQ.

The broad band at about 360 mμ for BD·TCNQ(n) considered to be related to the intramolecular transitions of BD and TCNQ.

As is shown in Fig. 3, the three main bands of BD·TCNQ·S complexes are almost independent of the kind of the solvent contained and their peaks are observed at 1500—1600, 550—560 and ~340 mμ. The lowest energy and the second lowest energy transitions can be assigned to the first and the second charge-transfer bands, respectively, because they are near to the first and the second charge-transfer bands of of BD·TCNQ(n), and because the energy difference in the former bands is equal to that in the latter bands (Table 2).

Table 2. Energies of charge-transfer transitions of BD·TCNQ system

	First C-T band[a)]	Second C-T band[a)]	Difference[b)]
Chloroform solution	1.29 eV	2.56 eV	1.27 eV
BD·TCNQ(n)	0.95	2.38	1.43
BD·TCNQ·S (CH_3CN)	0.78	2.22	1.44

a) The energy at the charge-transfer absorption maximum.
b) The energy difference between the second and the first charge-transfer bands.

Besides the three main bands just discussed, the weak absorption bands were observed in the spectra of BD·TCNQ·S complexes. These bands appear at 430 and 820 mμ as shoulders of the main bands, and their wave lengths are very close to those of the absorption peaks of TCNQ anion radical[16] and BD cation radical.[14] The intensity of these weak bands are dependent on the kind of the solvent included. In fact, as is seen in Fig. 3, these bands are clearly observed in BD·TCNQ·S(CH_2Cl_2), but they are very weak and are scarcely observed in BD·TCNQ·S(CH_3CN). On the other hand, the effect of grinding on the ESR intensity is more remarkable in the former complex than in the latter.[18] By considering these facts, it is concluded that the weak bands at 430 and 820 mμ are due to TCNQ anion radical and BD cation radical which are formed at the lattice defects or on the surface.

It may be pertinent to note here that the complex, which was prepared by grinding carefully an equimolar mixture of BD and TCNQ in an agatemortar, showed similar optical and magnetic properties to those of the BD·TCNQ·S complexes, although the complex thus obtained does not contain solvent molecules. For example, a rather intense ESR absorption was observed with this complex, and its infrared absorption spectrum showed the bands characteristic of BD·TCNQ·S complexes, although the bands characteristic of BD·TCNQ(n) complex were very also weakly observable. In Fig. 4 is shown the optical absorption spectrum in the visible and near infrared region for the complex prepared under the dry condition. The location and the shape of the main bands in the spectrum are very similar to those observed in the spectrum of BD·TCNQ·S complexes shown in Fig. 3.

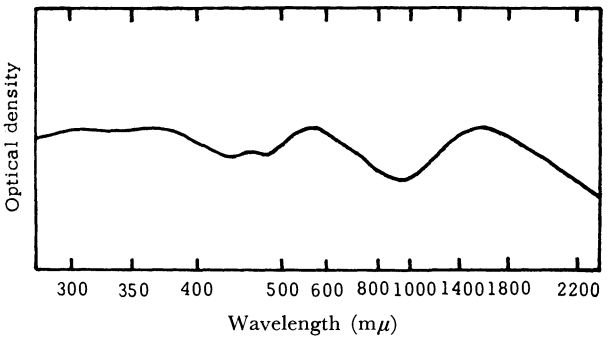

Fig. 4. Optical absorption spectrum of BD·TCNQ complex which was prepared by grinding a mixture of TCNQ and BD powders.

Table 3. Specific resistivities of BD·TCNQ complexes

Solvent included	$\rho_{18°C}$ (Ω·cm)	E (eV)
CH_2Cl_2	7×10^3	0.10
C_2H_5Br	6×10^3	0.12
CH_3CN	7×10^4	0.16
CH_3COCH_3	4×10^5	0.21
no solvent	2×10^9	0.34

Electrical Properties. The electrical resistivities of polycrystalline samples of BD·TCNQ(n) and BD·TCNQ·S complexes were found to follow the equation, $\rho=\rho_0\exp(E/kT)$. The values of E and $\rho_{18°C}$ observed are listed in Table 3. Both E and $\rho_{18°C}$ are lower for BD·TCNQ·S complexes than for BD·TCNQ(n) complex. The resistivities of BD·TCNQ·S complexes are small compared with most of other nonionic molecular complexes.[19,20]

The resistivities of the single crystals of BD·TCNQ·S(CH_2Cl_2) were measured several times. The crystal of the complex was a thin needle and its typical dimension was 2.5 mm × 0.10 mm × 0.06 mm. The resistivity was measured along the long axis at room temperature. The average of the results obtained is $1.4\times10^3\Omega$cm. This value is several times lower than the value for the polycrystalline sample listed in Table 3.

In order to eliminate the possibility that the observed low resistivity be due to ionic conduction, the following experiment was carried out. A pellet of BD·TCNQ·S(CH_2Cl_2) was pressed at 165 kg/cm² and the

18) After grinding in an agatemortar, the spin concentration of BD·TCNQ·S(CH_2Cl_2) increased to 6×10^{22} per mole, while that of BD·TCNQ·S(CH_3CN) to 1×10^{22} per mole.

19) Y. Matsunaga, *Nature*, **205**, 72 (1965).
20) M. M. Labes, R. Sehr, and M. Bose, *J. Chem. Phys.*, **33**, 868 (1960).

current was run through it at room temperature until the amount of charge passed had exceeded the amount expected from the Faraday's law by 3 times. No significant decrease was observed in conductivity. The conduction was thus concluded to be electronic in character.

Complexes of TCNQ with o-Tolidine, 3,3'-Diaminobenzidine and 3,3'-Dichlorobenzidine. The electronic properties of these complexes are dependent on the kind of the donor. Thus, 3,3'-dichlorobenzidine (DCBD) which is the weakest of the three donors gives a diamagnetic complex. DCBD·TCNQ complex does not show any ESR absorption whether the sample is ground or not. This behavior is similar to that of BD·TCNQ(n) complexes.

On the other hand, the complex of 3,3'-diaminobenzidine (DABD), which is the strongest of the three donors, shows a strong ESR absorption. No significant effect of grinding on the ESR absorption intensity was observed. These facts indicate that the complex is ionic in character.

The magnetic properties of the complex of *o*-tolidine (TL) and TCNQ which contains dichloromethane or chloroform are similar to those of BD·TCNQ·S complexes. The spin concentration of the sample of TL·TCNQ·S(CH_2Cl_2) was found to be 8×10^{21} per mole before grinding and was found to increase by 16 times after grinding. The line width (ΔH_{msl}) of a sample was observed to be 0.93 G in vacuo, while it became 1.70G in the air. From these observations, it is concluded that TL·TCNQ·S complexes have a similar electronic character to that of BD·TCNQ·S complex. This conclusion was further supported by the fact that the characteristics of the infrared absorption spectra for the former complexes are very similar to those for the latter.

BULLETIN OF THE CHEMICAL SOCIETY OF JAPAN, VOL. 44, 400—403 (1971)

Paper Electrophoresis and Polarography of the Reaction Product between the Chromium(III) Ion and Potassium Hexacyanoferrate(II)[1]

Michiko SHIRAI

Department of Chemistry, Faculty of Hygienic Science, Kitasato University, Minato-ku, Tokyo

(Received September 30, 1969)

In continuation of the previous work (Y. Matsumoto and M. Shirai, Bunseki kagaku, **12**, 608 (1963); Y. Matsumoto and M. Shirai, This Bulletin, **39**, 59 (1966).), results of a study of the colored products resulting from the reaction between the chromium(III) ion and potassium hexacyanoferrate(II) by paper electrophoresis and polarography will be presented in this paper. Paper-electrophoretical experiments illustrated that the negatively-charged complexes containing both Cr and Fe were gradually formed by reaction. In the presence of excess potassium hexacyanoferrate(II), the resulting complexes were constant in color and situation in the electrophoretical patterns, regardless of the molar ratio of reactants. On the other hand, in the case of a reactant molar ratio ($Fe(CN)_6^{4-}$ to Cr^{3+}) below 2.5, the patterns varied with the ratio. The product, sampled either in the form of a reaction mixture or as isolated state (Y. Matsumoto, M. Shirai, and H. Saito, This Bulletin, **41**, 2542 (1968).), was found to present no reduction wave of Cr^{3+} on polarography at the dropping mercury electrode.

The chromium(III) ion slowly reacts with potassium hexacyanoferrate(II) in an aqueous solution to form an orange-yellow to reddish-brown complex which is very soluble in water; this is in contrast with most heavy metal ions, which react rather quickly with the same reagent to form insoluble product.

This contrast, as well as the characteristic coloration, has attracted attention to the nature of the reaction product, especially to its structure in an aqueous solution, so that a number of approaches have been made[2-9] during the last ten years or so.

In the present work, the nature of the product in its aqueous solution, especially of the ion which composes the major moiety of this colored product, was studied using paper electrophoresis and polarography.

Experimental and Results

Electrophoresis was conducted on filter papers (2×40 cm, Toyoroshi Co., No. 51A), each saturated with a 0.1 M KCl solution, for 2 hr under an applied voltage of 200 V in a horizontal-type apparatus. The location of the chromium complex was detected by means of the diphenylcarbazide method.

One milliliter of a chrome alum solution (2 mg/m*l*

1) This work was partly presented at the 15th and 16th Symposia on Co-ordination Chemistry (1965 and 1966), and at the 19th and 20th Annual Meetings of the Chemical Society of Japan (1966 and 1967).

2) Y. Matsumoto and M. Shirai, *Bunseki kagaku*, **12**, 608 (1963).

3) Y. Matsumoto and M. Shirai, This Bulletin, **39**, 55 (1966).

4) Y. Matsumoto, M. Shirai, and H. Saito, This Bulletin, **41**, 2542 (1968).

5) Y. Matsumoto, M. Shirai, H. Saito, T. Kawashima, and Y. Sakabe, Proceedings of the 18th Symposium on Co-ordination Compounds (1968).

6) W. U. Malik, *J. Sci. Ind. Res.*, **18B**, 463 (1959).

7) W. U. Malik, *ibid.*, **20B**, 213 (1961).

8) W. U. Malik, *J. Indian Chem. Soc.*, **38**, 297 (1961).

9) W. U. Malik and J. Singh, This Bulletin, **39**, 2541 (1966).

for Cr^{3+}) was mixed with 3.2 m*l* of a potassium hexacyanoferrate(II) solution (50 mg/m*l* for $K_4Fe(CN)_6 \cdot 3H_2O$), the molar ratio of hexacyanoferrate(II) to Cr^{3+} being 10 : 1; the chromium concentration in the mixed solution was found to be about 10^{-2} M (reaction mixture 1). This yellow-colored reaction solution gave, on electrophoretical separation, two yellow spots (A and B), both located in the direction toward the positive electrode (Fig. 1). Extracts from both the spots, obtained with distilled water, were decomposed by (1+1) sulfuric acid, and then tested for the presence of Cr and Fe. The spot A proved to contain both Cr and Fe, while the spot B contained Fe alone. Upon the coloration test with diphenylcarbazide, the spot A turned purple, and the spot B, a grayish blue.

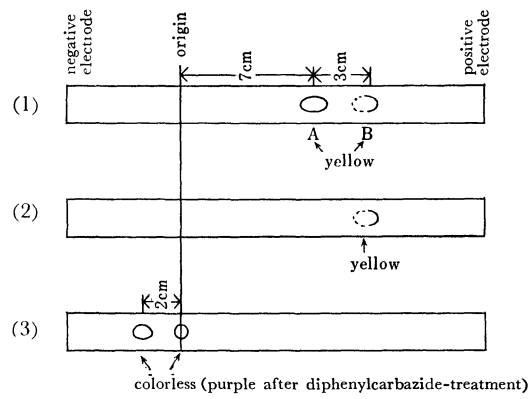

Fig. 1. Paper electrophoresis with (1) yellow-colored reaction mixture, (2) $K_4Fe(CN)_6$ soln, and (3) Cr^{3+} soln.

For reference, a potassium hexacyanoferrate(II) solution and a chrome alum solution of the same final concentrations as the corresponding concentrations in the sample solution were charged individually on other papers and then subjected to electrophoresis. On the reference paper charged with potassium hexacyanoferrate(II), one yellow spot was found in the position as far from the origin as the position B on the paper charged with the sampled solution, while Fe was not found at the position corresponding to A. On the reference paper for the Cr^{3+} solution, were observed two spots which proved to contain Cr by the diphenylcarbazide test; one of them was in the direction toward the negative electrode, and the other was at the point of origin. On the other hand, no chromium-containing spot other than A was observed on the electrophoretical pattern for the sample solution which had stood for an adequate reaction period.

The paper-electrophoretical study thus confirmed that the yellowish-orange-colored and negatively-charged complex ion, which contained both chromium and iron, existed predominantly in the reaction mixture resulting from the reaction between the chromium(III) ion and excess potassium hexacyanoferrate(II).

The process of the gradual formation of the chromium-containing complex from the chromium(III) ion, characterized in terms of the change to a negative species from a positive one, was successfully visualized by paper-electrophoretical patterns varying in the course of the progress of the reaction. A chrome alum solution of 2.5 m*l* (20 mg/m*l* for Cr^{3+}) was mixed with a potassium hexacyanoferrate(II) solution of 10 m*l* (200 mg/m*l* for $K_4Fe(CN)_6 \cdot 3H_2O$), the molar ratio of hexacyanoferrate(II) to Cr^{3+} being 5 to 1 (reaction mixture 2). The concentrations of the reactants in this reaction mixture were made larger than those in the foregoing one (reaction mixture 1) in order that the evidence for any transition state of chromium(III) ion from its free state to any other coordinated state could be observed distinctly; the reactant ratio of 5 : 1 was adopted after it had been confirmed that the reaction solution resulting from this reactant ratio gave qualitatively the same paper-electrophoretical pattern as was given by the solution with a reactant ratio of 10 : 1. The mixed solution of this reactant ratio were allowed to stand for varying periods of time (0, 2, 4 hr and 1 and 2 days) at room temperature after mixing; then they were subjected to paper electrophoresis. The coloration was done by means of the diphenylcarbazide method (Fig. 2).

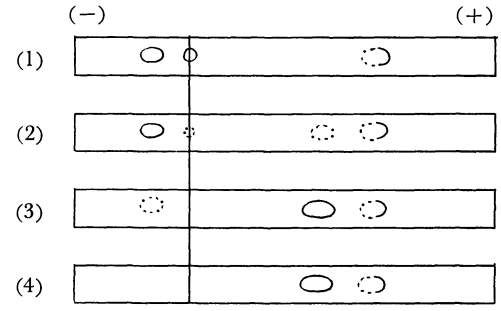

Fig. 2. Paper-electrophoretical patterns of the reaction mixture, altering in the course of the proceeding of the reaction: (1) immediately, (2) 2 hr, (3) 4 hr, and (4) 2 days after mixing reactants.

The results were as follows: (1) with the solution tested immediately after mixing, no colored chromium-containing spot was found, but two chromium-containing spots were detected by means of diphenylcarbazide coloration, one on the original point and another one at a distance from the point of origin in the direction of the negative electrode.

(2) With the solution which had stood for 2 hr after mixing, a yellow chromium-containing spot was found to appear in the direction of the positive electrode in addition to the visually colorless chromium-containing spots still present in the negative electrode direction and on the original point.

(3) With the solution allowed to stand for 4 hr after mixing, there appeared a chromium-containing yellow spot in the positive electrode direction, more intense in color, and a diphenylcarbazide-test-positive spot in the negative electrode direction, weaker in color, than in the foregoing case, *i.e.*, the case of the shorter reaction time. The former kind of spot became the more intense in color, and the latter kind became the weaker, the longer the time which elapsed after mixing. On the point of origin, no chromium-containing spot remained.

(4) Two days later after mixing, all the chromium was contained in the yellow complex which, on electro-

phoresis, is located in the positive electrode direction.

In order to study the properties of the reaction products produced at varying reactant ratios, the solutions were also prepared by mixing 2.5 m*l* of a chromium(III) solution with the Cr^{3+} concentration of 20 mg/m*l* and 10-m*l* portions of potassium hexacyanoferrate(II) solutions with the salt concentrations of 200, 100, 80, 60, 40, and 20 mg/m*l* so that the resulting solutions contained potassium hexacyanoferrate(II) in ratios of 5, 2.5, 2, 1.5, 1, and 0.5 mol respectively to 1 gram ion of the Cr^{3+} ion. After having stood for two days, each colored reaction solution was centrifuged for 15 min at 3000 rpm; the supernatant was then subjected to paper electrophoresis.

The results are shown in Fig. 3. The products of the reaction at the reactant ratios (hexacyanoferrate(II) to Cr^{3+}) below 2.5 were visually similar to, but electrophoretically different from, those of the reactant ratios above 2.5. The lower the ratio of hexacyanoferrate(II) to Cr^{3+} the shorter the distance the corresponding chromium complex was shifted, and the more greenish became the color of the complex.

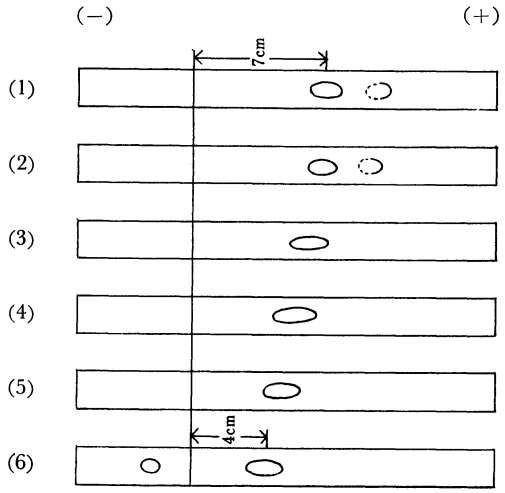

Fig. 3. Paper-electrophoretical patterns along with a variety of reactants ratios: (1) 5, (2) 2.5, (3) 2, (4) 1.5, (5) 1, and (6) 0.5 mol of $K_4Fe(CN)_6$ respectively to 1 gram ion of Cr^{3+}.

The remaining activity of Cr(III) in the reaction solution was further examined by polarography. The reaction mixture at the reactant ratio of 10 : 1 (chromium concentration 10^{-2} M), in which KCl had been added to 1 M, after which N_2 gas had been bubbled through the mixture, was examined by polarography *vs.* a saturated calomel electrode. The characteristic wave for Cr(III) was found to have disappeared, whereas, in the presence of the same concentration KCl, the solution of Cr^{3+} (chrome alum) gave the wave corresponding to $Cr^{3+} \rightarrow Cr^{2+}$, which was proportional in height to the concentration of Cr^{3+} salt in the range from 10^{-2} M (this concentration gave a wave having the reduction current of 18 μA and the $E_{1/2}$ of −0.9 V) to 10^{-3} M, indicating that the diffusion-controlled conditions hold for this concentration range of Cr^{3+}.

Malik reported[6] the disappearance of the reduction wave in these reaction mixtures at the same electrode, without giving interpretation about it.

In order to observe from what reactant ratio chromium(III) wave appears, solutions in molar ratios varying from 0.1 to 1 of potassium hexacyanoferrate(II) per Cr(III) ion were prepared, while the concentration of Cr^{3+} was kept at a constant value (10^{-2} M); the solutions were then allowed to react at 47°C for 2 hr. The reduction wave for Cr^{3+} diminished in height with an increase in the reactant ratio (hexacyanoferrate(II) to the Cr(III) ion) of the reaction solution and almost disappeared when the reactant ratio was raised to 0.5 : 1 (Fig. 4-a).

This depression of the reduction wave took place even immediately after mixing the reactants. The aqueous solutions of chrome alum and of potassium hexacyanoferrate(II) to which KCl had been added were both bubbled through with N_2 gas, and then they were mixed with each other to make a solution containing Cr^{3+}, $Fe(CN)_6^{4-}$, and KCl in concentrations of 10^{-2} M, 10^{-1} M and 1 M respectively; immediately afterwards, this mixed solution was subjected to polarography. The reduction wave could not be observed unless the molar ratio of hexacyanoferrate(II) to Cr(III) decreased to 0.8 : 1 (Fig. 4-b).

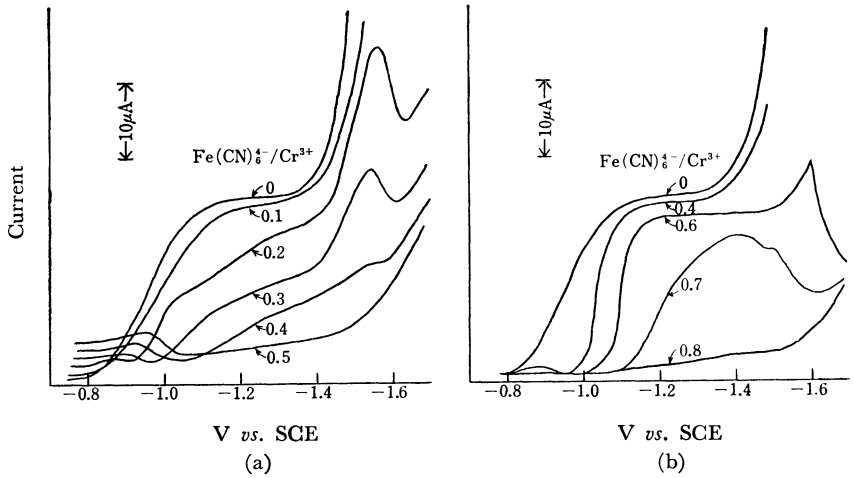

Fig. 4. The gradual disappearance of polarographical reduction wave for Cr^{3+} (10^{-2} M) with the increasing molar ratio of $K_4Fe(CN)_6$ to Cr^{3+} in two cases, (a) after the reaction time of 2 hr at 47°C, and (b) soon after mixing the reactants.

The solution containing the Cr^{3+} ion (10^{-2} M) and potassium hexacyanoferrate(II) (0.5 M), but not potassium chloride, lacked the reduction wave for Cr(III), too.

This disappearance of the reduction wave for Cr(III) was not, however, observed on the polarography of such other chromium(III) complexes, as potassium hexacyanochromate(III), even in the presence of excess potassium hexacyanoferrate(II). An aqueous solution of potassium hexacyanochromate(III) containing 0.5 M potassium hexacyanoferrate(II) as a supporting electrolyte was made using crystals of potassium hexacyanochromate(III) prepared[10] from chromium acetate and potassium cyanide. On polarography, the solution presented a very clear reduction wave corresponding to Cr(III) (Fig. 5).

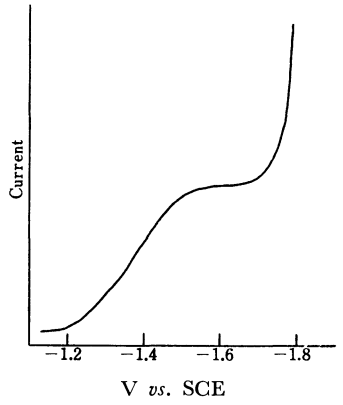

Fig. 5. Polarography of $K_3Cr(CN)_6$ in the presence of 0.5 M $K_4Fe(CN)_6$.

These waves were proportional in height to the Cr concentrations in the range from 10^{-2} to 10^{-3} M.

Recently, it was reported[4] that a reddish-yellow compound could be isolated in a pure form from the reaction mixture by Sephadex G-25 column chromatography. The Cr(III)-hexacyanoferrate(II) complex purified as has been described above was confirmed by paper electrophoresis to be free from the unreacted potassium hexacyanoferrate(II), and it showed no reduction wave on its polarogram.

It was surprising at first glance that even in the reaction mixture which stood only a short time after the mixing of the reactants and which was confirmed on paper electrophoresis still to contain many free Cr^{3+} ions, there was no reduction wave.

The paper-electrophoretical results indicate that this lack of a reduction wave can not be accounted for by presuming a particularly stabilized state of the chromium(III) ion coordinated with hexacyanoferrate(II), but it might well be attributed to the current-insulating effect of the deposition of an insoluble complex, the chromium(II)-hexacyanoferrate(II) complex, produced on the electrode surface by the polarographic reduction of Cr(III).

The insoluble film of the deposition, Cr(II)-hexacyanoferrate(II), would be formed either by the reduction of free Cr(III) ions in the presence of hexacyanoferrate(II) ions or by the reduction of the Cr(III)-hexacyanoferrate(II) complex already formed.

The author is grateful to Professor Yoshio Matsumoto for his help and advice throughout this work.

10) J. H. Bigelow and J. C. Bailar, Jr., "Inorganic Syntheses," Vol. 2, p. 203 (1946).

Distribution of Nickel across the Thickness of Al Anodic Oxide Films Sealed in Nickel Sulphate Solutions

Luigi CAMPANELLA

Italian National Researches Council, Rome, Italy

Institute of Analytical Chemistry, University Rome, Italy

(Received February 23, 1970)

The distribution of nickel across the thickness of Al anodic oxide films, produced in 15.5% w/v H_2SO_4 as electrolyte and sealed in nickel sulphate solutions, is determined and an approximate confirmation of the conical shape of pores is obtained.

As is well known, anodizing of Al in sulphuric acid electrolyte yields porous films of oxide which are usually sealed before being used. On being sealed, anhydrous oxide is hydrated, swells and fills up the hollow of its pores by the transformation into boehmite ($Al_2O_3 \cdot H_2O$), a less dense phase than the preexisting anhydrous alumina. The usual technique of sealing includes immersion in boiling distilled water, hot water vapour, boiling solutions of chromates, dichromates and salts, such as Ni or Co acetate or sulphate, or capillary active organic compound.[1] The use of nickel and cobalt salts is particularly convenient as they prevent the harmful action of silicates and phosphates, always contained in tap water, so that it can be used in place of distilled water as a sealing medium.[2] Nickel and cobalt salts are adsorbed in the film, where they are hydrolized and precipitated as almost colourless hydroxides. This technique of sealing is also very useful for dyed layers. In this case, according to Speiser,[3] three different reactions occur: 1) hydration of films, as in the case of sealing in boiling distilled water, 2) precipitation of the hydroxide in the pores with consequent blocking-in of the dye, 3) chemical reaction between the nickel (or cobalt) compound and the dye to form a new metal complex.

However, the functions of nickel (or cobalt) in the sealing process are not very clear and need further investigation. This paper deals with the distribution of nickel across the full thickness of Al anodic oxides sealed in nickel sulphate solutions.

The study was performed with the aim of improving the knowledge of sealing mechanism, particularly concerning the functions of nickel salts in sealing solutions and the shape of the pores present in the anodic oxide.

Experimental

a) 99.99% Al samples ($5 \times 10 \times 0.1$ cm) were freed from grease with toluene and polished both mechanically and chemically (in 20 g/*l* NaOH solutions), then rinsed successively in distilled water, 1 : 1 HNO_3 solution, and distilled water again. After drying they were anodized in 15.5% w/v H_2SO_4 solution, at 25.0 ± 0.5°C, 1.3 A/dm^2, for 40 min. Stirring and symmetry of the electrolytic bath were warranted by means of rotating anode and the presence of two bored cathodes, larger than the anodized samples (surface area ratio 1 : 3), equidistant from the central anode.

b) Sealing: The anodized samples were washed with running distilled water and immersed for 30 min in boiling $NiSO_4 \cdot 7H_2O$ 15 g/*l* solution.

c) Cationic exchanger Dowex 50-X 8 (100—200 mesh), H^+ form, medium porosity, total capacity approximately 5.0 ± 0.3 meq/g dry, moisture content 50—56% by weight.

Anionic exchanger Dowex 1-X 4 (100—200 mesh), Cl^- form, high porosity, total capacity approximately 3.3 ± 0.3 meq/g dry, moisture 54—60% by weight.

The two ionic exchangers were contained in columns each 30 cm long and 20 mm internal diameter, which were washed before use: the cationic one with 12M HCl and distilled water (flux rate 2 ml/min) and the anionic one with only distilled water (flux rate as above).

d) Spectrophotometer Beckman DU

e) Amel, mod. 461, polarograph.

The anodized sample is kept for a long time in a solution which can dissolve the oxide and nickel is determined in the corroding solution. In order to get consistent information, we assume that chemical attacks proceed uniformly from a layer to the next inner one and that no localized pitting corrosion takes place. The at tacking solutions were Edwards mixture (35 ml/*l* H_3PO_4 85% and 20 g/*l* CrO_3) acting for 0—20 min and 1.5M HCl acting for a prolonged time.

Quantitative determination of nickel was performed by four different methods for nickel solutions in the presence of aluminium.

1) After having acted for the specified time, the Edwards mixture was passed on an anionic exchanger in order to eliminate phosphate and chromate anions. In this operation a reduction of Cr(VI) to Cr(III) by the resin was observed and a green solution resulted at the end of the column, the intensity of this colour not being possible to be accounted for by the presence of Ni(II) ions. Al(III) was separated by passage through the cation exchanger and elution with 1.5M HCl.[4] Nickel was determined gravimetrically by dimethylglyoxime, having masked Cr(III) by adding citrate.[5]

2) After the necessary lapse of time for the dissolution reaction the 1.5M HCl solution was evaporated to dryness and the residue was dissolved in distilled water. Nickel was determined in the resulting solution a) spectrophotometrically by complexing it with α-furildioxime[6–8] and extraction

1) S. Wernick and R. Pinner, "Les traitements de surface et la finition de l'aluminium et de ses alliages," Eyrolles, Paris (1962), p. 378.

2) H. Richaud, Conference on Anodising, University of Nottingham, Session VI, paper XVI, 12—14 Sept. (1961).

3) C. T. Speiser, Electropl. and Met. Finishing, 9, n.4, 109—116, 128 (1956).

4) C. Michaelis, N.S. Tarlano, J. Clune, and R. Yolles, *Anal. Chem.*, **34**, 1425 (1962).

5) A. J. Vogel, "A Text-book of Quantitative Inorganic Analysis," Longmans, London (1961), p. 479.

6) E. N. Pollock and L. P. Zopatti, *Anal. Chim. Acta*, **28**, 68 (1963).

7) J. S. Forrester and L. J. Jones, *Anal. Chem.*, **32**, 1443 (1960).

8) G. C. Taylor, *Analyst*, **81**, 369 (1959).

of the complex with $CHCl_3$, having previously masked Al(III) by citrate or tartrate; b) by back-titration at pH=10 with EDTA and standard Zn(II) solution, using NET as indicator and masking Al by fluoride;[9-11] c) amperometrically in deoxygenated 0.1M NH_4Cl and 0.5M NH_4OH as supporting electrolyte at −1.7 V *vs.* SCE, using dimethylglyoxime as titrating agent: as both nickel and dimethylglyoxime give diffusion currents, a sharp V shaped titration curve was obtained;[12,13] Al was eliminated by the technique described in 1), just above.

Each measurement was carried out for at least three different samples. The results are given by mean values.

Results

In Table 1 the data of the gravimetric determination are given. In Fig. 1 the calibration curve used for the spectrophotometric titration with α-furildioxime is reported: 2, 2.5, 3, 3.5, 4 m*l* of a standard solution of $NiSO_4 \cdot 7H_2O$, *at concentration 14.6 μg Ni/ml, were* taken, put into a volumetric flask and diluted to 25m*l* with distilled water, so obtaining concentration values 29.2, 36.5, 43.8, 51.1, 58.4 μg Ni/25 m*l*, for which the respective optical densities were measured at 435 mμ (Table 2). In Table 3 the results of the spectrophotometric determination are given; they are determined on the basis of the calibration curve previously drawn. In order to calculate the values of the last column, the dilution ratios must also be considered. This ratio was controlled in the different experiments in order to bring optical densities in the range observed during calibration, thus avoiding extrapolating approximations.

Table 1. Data of gravimetric analysis

Time of acting of Edwards mixture (min)	Weight of nickel-dimethylglyoxime (mg/dm²)	weight of nickel (mg/dm²)
3	5.41	1.10
5	6.99	1.42
8	8.81	1.79
10	9.45	1.92
15	9.60	1.95
20	10.00	2.03

Table 2. Data of the calibration curve

m*l* of standard solution diluted to 25 m*l*	Optical density (at 435 mμ)
2.0	0.395
2.5	0.495
3.0	0.600
3.5	0.695
4.0	0.790

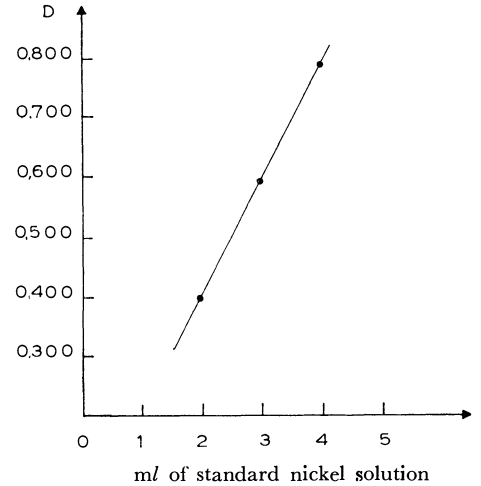

Fig. 1.

Table 3. Data of spectrophotometric analysis

Time of acting of 1.5M HCl (hr)	Optical density	Volume (m*l*)	Dilution ratio	Weight of nickel (mg/dm²)
9.5	0.600	25	1:25	1.1
16	0.710	25	1:25	1.3
24	0.435	25	1:50	1.6
36	0.515	25	1:50	1.9
48	0.545	25	1:50	2.0

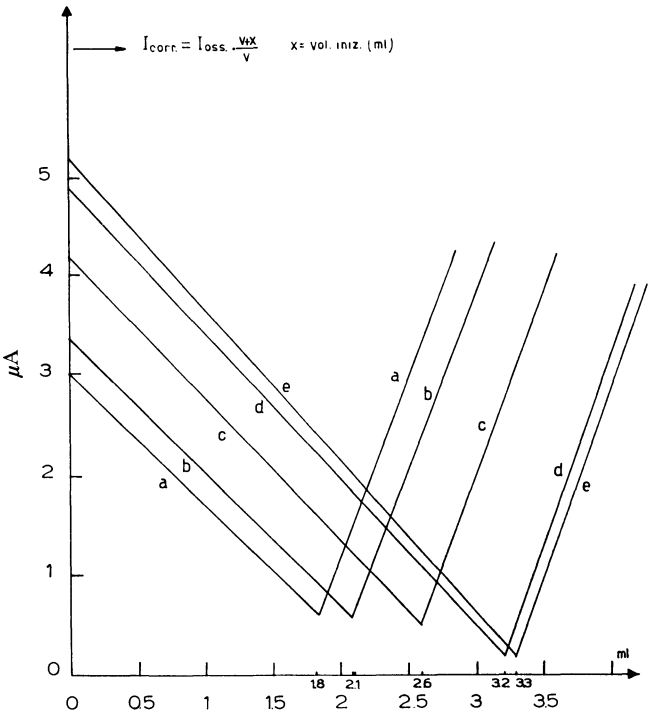

Fig. 2 Curves of amperometric titrations of nickel solutions with ethanolic solution of dimethylglyoxime in ammonia solutions. Nickel content results from the corroding action of HCl 1.5 M for the following times:

curve a: 9.5 hr
curve b: 16 hr
curve c: 24 hr
curve d: 36 hr
curve e: 48 hr

9) F. J. Welcher, "The Analytical Uses of EDTA," Van Nostrand, New Jersey (1964), p. 234.
10) H. A. Flascka, "EDTA Titrations," Pergamon Press, London (1964), p. 81.
11) D. H. Williams and L. E. Hibbs, *Anal. Chim. Acta*, **18**, 372 (1958).
12) I. M. Kolthoff and A. Langer, *J. Amer. Chem. Soc.*, **62**, 211 (1960).
13) J. A. Barnard and R. Chayen, "Modern Methods of Chemical Analysis," McGraw Hill, London (1965), p. 45.

TABLE 4. DATA OF AMPEROMETRIC ANALYSIS

Time of acting of 1.5M HCl (hr)	Volume of reactive solution added at the end point (m*l*)	Weight of nickel-dimethylglyoxime equivalent to m*l* given in the last column (mg/dm²)	Weight of nickel (mg/dm²)
9.5	1.8	5.4	1.1
16	2.1	6.4	1.3
24	2.6	7.9	1.6
36	3.2	9.3	1.9
48	3.3	9.8	2.0

TABLE 5. DATA OF COMPLEXOMETRIC ANALYSIS

Time of acting of 1.5M HCl (hr)	Volume of EDTA solution added (m*l*)	Volume of $ZnSO_4$ solution at the end point (m*l*)	Weight of nickel (mg/dm²)
9.5	4.0	1.88	1.10
16	4.0	1.67	1.31
24	4.0	1.35	1.60
36	4.0	1.04	1.90
48	4.0	0.95	2.01

In Table 4 and Fig. 2 the results of the amperometric determinations of nickel by dimethylglyoxime (609.05 mg in 250 m*l* 95% ethanol) are reported. In Table 5 the results of the complexometric titration of nickel with 0.0125M EDTA and 0.0170M $ZnSO_4$ are recorded as a function of the time of acting of the corroding solution.

Discussion

By considering the amounts of nickel found in the corroding solution as function of the attacking time, the distribution curve of nickel across the thickness of the oxide layer can be deduced, assuming that

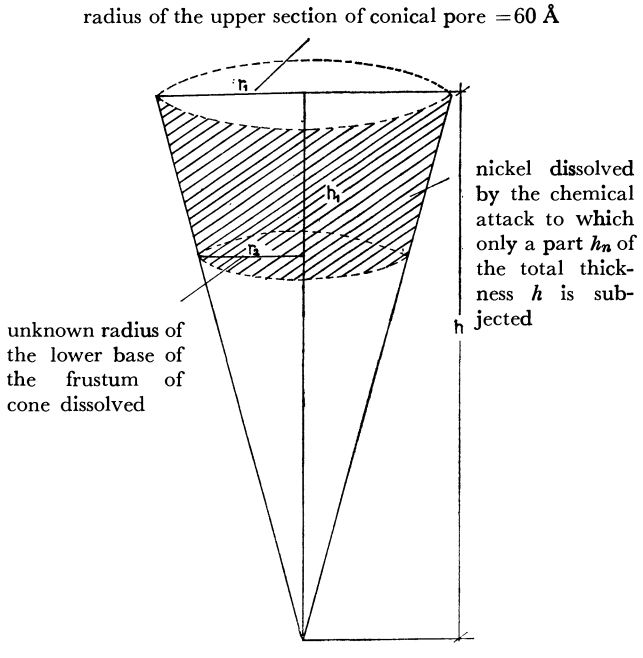

Fig. 3

oxide layers nearer to the basis metal are successively subjected to uniform dissolution. Nickel turns out to be mostly concentrated in the outer portion of the anodic film and the rate of decrease of its concentration through the depth of the oxide supports the conical shape of the pores, as shown in Fig. 3, where nickel content is plotted against percentage of the total thickness (measured by Dermitron, an eddy-currents instrument, manufactured by Unit Process Assemblies Inc., New York).

Considering that the nickel amounts taken off during each attack are those contained in the volumes of the frusta of the cone, which are successively dissolved, and that 2 mg/dm² of nickel are found for the total dissolution of the oxide, a pore can be drawn, taking 120 Å as base diameter[14] and applying the following two equations:

$$r_1^2 h/3 = k m_{tot}$$

$$(r_1^2 + r_n^2 + r_1 r_n) h_n/3 = k m_n$$

where:

- k = a constant term
- r_1 = upper base radius = 60 Å
- r_n = lower base radius
- h = height of the cone, taken approximately as 13 μ, that is, the thickness of the oxide layer, measured by Dermitron, neglecting the thickness of the barrier layer which should be subtracted
- h_n = height of the frusta of the cones successively dissolved
- m_n = nickel content of the corroding solution
- m_{tot} = 2 mg nickel/dm²

The above system must be applied to each conical frustum equivalent to the varying times of chemical attack. All the frusta have the same upper base. Several values for r_n are calculated, by which Fig. 4 can be

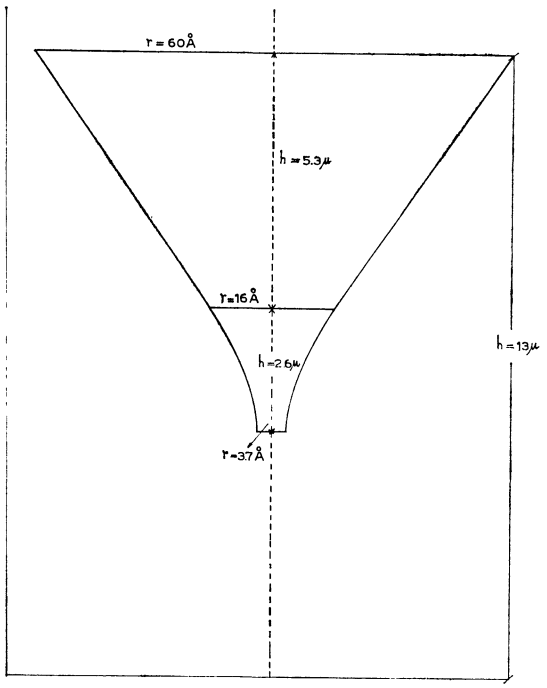

Fig. 4

14) F. Keller, M. S. Hunter, and D. L. Robinson, *J. Electrochem. Soc.*, **100**, 411 (1953); **101**, 335 (1954).

drawn, as representing a pore of the oxide film. The approximations introduced can account for the wider angle we found than ISML researchers.[15]

The present work was carried out with the aid of the Italian National Researches Council.

15) F. Sacchi and G. Paolini, "Indagine sulla struttura fine di strati di ossido anodico su alluminio mediante misure di adsorbimento, micrografia elettronica ed esame gravimetrico," Report of I. S. M. L. (Istituto Sperimentale Metalli Leggeri: Experimental Institute of Light Metals), Novara, Italy (1962—1963).

BULLETIN OF THE CHEMICAL SOCIETY OF JAPAN, VOL. 44, 407—408 (1971)

N-Benzenesulphonyl β-Alanine as a Masking Agent for Hg(II)

Nripendra Nath Ghosh and Anjali Bhattacharyya
Department of Inorganic Chemistry, University College of Science, Acharyya Prafulla Chandra Road, Calcutta-9, India

(Received June 16, 1970)

N-Benzenesulphonyl glycine and *N*-benzenesulphonyl α-alanine form water soluble complexes with Hg(II), Cu(II), and Ag(I). But *N*-benzenesulphonyl β-alanine ($R_b^{\beta}H_2$) gives only stable complex ion $Hg(R_b^{\beta})_2^{2-}$, showing that $R_b^{\beta}H_2$ is a highly selective masking agent for Hg(II). Utilising this masking property, methods for detection and determination of Hg(II) have been developed. $R_b^{\beta}H_2$ reacts with Hg(II) at pH≈8, yielding the ion $Hg(R_b^{\beta})_2^{2-}$ and on subsequent treatment with KI, two equivalents of alkali are liberated. On titrating the alkali liberated with a standard acid, the amount of Hg(II) may be calculated. Interferences due to diverse ions have been studied; Br^- and I^- interfere. The spot test of Hg(II) based on the same principle has been developed and it appears to be specific under specified condition. The limit of identification is 0.5 μg with a dilution limit of 1:100000.

A rapid and accurate method for determination of Hg(II) has been described using *N*-benzenesulphonyl glycine (R_bH_2).[1] *N*-Benzenesulphonyl glycine forms water soluble complexes[2] $K_2Hg(R_b)_2$, $Na_2Cu(R_b)_2$, and $KAg(R_b)$ which are stable at pH≈8 or higher. The comparable results are also obtained with the ligand *N*-benzenesulphonyl α-alanine ($R_b^{\alpha}H_2$);[3] the Ag(I) compound could not be isolated in the pure state. But *N*-benzenesulphonyl β-alanine ($R_b^{\beta}H_2$) gives at higher pH only stable complex[3] $K_2Hg(R_b^{\beta})_2$ showing that $R_b^{\beta}H_2$ is highly selective masking agent for Hg(II). Utilising this masking property of $R_b^{\beta}H_2$, detection as well as determination of Hg(II) is possible in presence of various commonly associated cations and anions such as Ag(I), Cu(II), Be(II), Mg(II), Zn(II), Cd(II), Pb(II), Al(III), Fe(III), Cr(III), Bi(III), Zr(IV), Th(IV), U(VI), chloride, sulphate, acetate, phosphate, molybdate, and vanadate.

The compound $R_b^{\beta}H_2$ is a monobasic acid but the dissociation of the hydrogen attached to the nitrogen increases so much on complex formation that it becomes possible to titrate with an alkali in the case of $H_2Hg(R_b^{\beta})_2$, affording complex salts. Thus when Hg(II) solution is titrated with a standard alkali solution in presence of $R_b^{\beta}H^-$ ($R_b^{\beta}H_2$ made neutral to phenolphthalein with KOH), then there occurs the following reaction:

$$Hg^{2+} + 2R_b^{\beta}H^- + 2OH^- = Hg(R_b^{\beta})_2^{2-} + 2H_2O$$

In presence of other metal ions stated above, during this titration Hg(II) gives water soluble $Hg(R_b^{\beta})_2^{2-}$ anion and the other metal cations are precipitated mostly as their hydrous oxides. On adding excess of KI to the neutralised solution, $Hg(R_b^{\beta})_2^{2-}$ reacts according to the following equation:

$$Hg(R_b^{\beta})_2^{2-} + 4I^- + 2H_2O = HgI_4^{2-} + 2R_b^{\beta}H^- + 2OH^-$$

The moles of alkali liberated are equivalent to twice those of Hg(II) present. Therefore

$$1\ ml\ of\ (N)\ H_2SO_4 \equiv 100.3\ mg\ of\ mercury$$

Based on the same principle a virtually specific spot test has been developed for Hg(II).

Experimental

Reagents and Solutions. All solutions were prepared with carbon dioxide free water and the reagents used were of A. R. quality except in a few cases where they were properly purified. The reagent $R_b^{\beta}H_2$ was prepared and purified in the laboratory following the method stated in the literature.[4]

A standard alkali solution was prepared by dissolving pure KOH in water and standardised against $KH(IO_3)_2$ using phenolphthalein as indicator.

A standard dilute sulphuric acid solution was prepared by standardising against above alkali using phenolphthalein as indicator.

For preparing stock solution of $R_b^{\beta}H_2$, it was suspended in water and titrated with KOH solution to phenolphthalein end point and diluted so that the strength was about 3.5%.

Stock mercuric nitrate solution was prepared by dissolving pure HgO in nitric acid, free from nitrous fumes. This solution was standardised gravimetrically[5] as HgS and volumetrically with *N*-benzenesulphonyl glycine[1] along with free as-

1) N. N. Ghosh and M. N. Majumdar, *J. Indian Chem. Soc.*, **41**, 286 (1964).
2) N. N. Ghosh and M. N. Majumdar, *ibid.*, **40**, 945 (1963).
3) N. N. Ghosh and A. Bhattacharyya, *ibid.*, **46**, 1040 (1969).
4) H. V. Pechmann, *Ann. Chem.*, **264**, 289 (1891).
5) A. I. Vogel, "A Text Book of Quantitative Inorganic Analysis," Longmans, Green and Co., Ltd., London (1968), p. 487.

Table 1. Determination of Hg(II)

Hg(II) soln. taken in m*l*	Hg present in mg	Alkali reqd. in m*l* (0.04139N KOH soln.)	Acid reqd. in m*l* (0.04458N H_2SO_4)	Concentration of free acid found	Hg found in mg	Error %
4	35.58	13.85	7.95	0.05469N	35.55	−0.10
5	44.48	17.30	9.95	0.05448N	44.49	+0.02
6	53.38	20.75	11.95	0.05440N	53.44	+0.11
8	71.17	27.70	15.90	0.05469N	71.11	−0.09
10	88.96	34.60	19.95	0.05424N	89.21	+0.28

sociated acid. Concentrations of Hg(II) and free acid were found to be 0.04435M and 0.05450N, respectively.

Spot Test for Hg(II). *Procedure*: The solution of Hg-(II) nitrate containing some other ions was treated with excess of $R_b{}^{\beta}H^-$ and slight excess of alkali using phenolphthalein (one drop of 1% ethanolic solution) till it became pink in colour. It was boiled for one minute, whereby other metals completely precipitated as oxide, just decolourised with dil H_2SO_4 solution and centrifuged. To one drop of the colourless test solution on a spot plate, one drop of 1% KI solution was added. A pink colour appeared due to liberation of alkali, confirming the presence of Hg(II). The limit of identification was found to be 0.5 μg of Hg(II) with a dilution limit of 1 : 100000.

Interferences: The spot test described above was highly selective and appeared to be specific under specificed conditions. Interferences were not found with Ag(I), Cu(II), Be(II), Mg-(II), Zn(II), Cd(II), Pb(II), Al(III), Cr(III), Bi(III), Ti(IV), Th(IV), Zr(IV), U(VI), phosphate, molybdate, and vanadate. Chloride in small concentration did not interfere. Bromide and iodide interfered. However by adding excess of $AgNO_3$, the interference due to chloride, bromide, and iodide for identification of Hg(II) may be eliminated. But there was a decrease in sensitivity particularly in presence of iodide.

Volumetric Determination of Hg(II). *Procedure*: A known volume of the standard Hg(II) solution was taken in a flask, treated with excess [about 3 to 4 times the amount of Hg(II) present] of the prepared reagent ($KR_b{}^{\beta}H$). The volume at this stage was kept about 50 m*l*. After adding two drops of 1% ethanolic solution of phenolphthalein, it was titrated with a standard alkali solution till a pink colour appeared. The amount of alkali consumed was equivalent to the sum of the free acid and twice the moles of Hg(II) present. To this solution excess of KI ($\approx$2 g) was added, when colour of the solution changed to deep pink due to liberation of alkali. This was titrated with a standard acid solution. The amounts of Hg(II) and free acid, taken and found by estimation, are shown in Table 1.

For determination of Hg(II) when associated with other metal ions the method was modified as follows: the solution was titrated with an alkali solution till a pink colour appeared and a slight excess was added. The volume at this stage was 50—60 m*l*. This mercury solution with the precipitated oxides of other metals was boiled for 2 min. The excess of alkali was then just neutralised, cooled and the volume was made upto 100 m*l*. The precipitates were then allowed to settle for about 1 hr. Fifty milliliters of the clear supernatant liquid was pipetted out and Hg(II) was estimated. The determination of Hg(II) at this stage was made to confirm that the extraction of Hg(II) as water soluble complex ion $Hg(R_b{}^{\beta})_2{}^{2-}$ was quantitative or not. In typical cases titrations, 5 m*l* of standard Hg(II) nitrate solution [containing 44.48 mg of Hg-(II)] was taken along with other metal salt solutions. Foreign ions with the amounts in the parentheses that were tolerated are stated in Table 2.

Table 2. Effect of foreign ions

Cations	Ag^+(37.6 mg), Cu^{2+}(35.52 mg), Pb^{2+}(64.0 mg) Be^{2+}(5.0 mg), Mg^{2+}(12.1 mg), Cd^{2+}(54.4 mg), Zn^{2+}(24.0 mg) Al^{3+}(7.2 mg), Fe^{3+}(10.4 mg), Cr^{3+}(10.5 mg), Bi^{3+}(64.0 mg) Zr^{4+}(10.6 mg), Th^{4+}(21.8 mg), $UO_2{}^{2+}$(45.6 mg)
Anions	Cl^-(25 mg), Cl^- with excess of $AgNO_3$(37.5 mg), $SO_4{}^{2-}$(560 mg) CH_3COO^-(780.0 mg), $HPO_4{}^{2-}$(43.04 mg), $MoO_4{}^{2-}$(41.5 mg), $VO_3{}^-$(46.2 mg)

Interferences: All cations which were precipitated as hydrous oxides gave low results when present in large amounts due to adsorption. Anions-acetate, sulphate, chloride in small concentration, phosphate, molybdate, and vanadate did not interfere, but chloride in large concentration, bromide and iodide interfered. However by adding excess of $AgNO_3$ to the original solution, the interferences due to chloride could be eliminated.

One of the authors (A.B.) is thankful to University Grants Commission for award of a research followship.

Transition-metal Complexes of Pyrrole Pigments. III. Copper(II) and Zinc(II) Complexes of 1,19-Dideoxy-8,12-dicarbethoxy-1,3,7,13,17,19-hexamethylbiladiene-ac[1]

Yukito MURAKAMI, Yoshihisa MATSUDA, and Yukiko KANAOKA

Department of Organic Synthesis, Faculty of Engineering, Kyushu University, Hakozaki, Fukuoka

(Received June 22, 1970)

The copper(II) and zinc(II) complexes of 1,19-dideoxy-8,12-dicarbethoxy-1,3,7,13,17,19-hexamethylbiladiene-ac were synthesized and investigated by near-ultraviolet, visible, near-infrared, infrared, NMR, and ESR measurements as well as X-ray diffraction measurements of powdered samples. The ligand-field bands appeared at 701 and 752 mμ for the copper complex provided information on its geometry around the central metal atom. Namely, the copper atom is subjected to the square-planar ligand-field in the complex. Infrared bands characteristic of asymmetric stretching vibration of the carbethoxy groups at 8 and 12, and X-ray powder diffraction pattern gave another support to this structure by referring to the corresponding data for the nickel complex. ESR measurements also provided the spin Hamiltonian parameters consistent with the square-planar coordination. The most plausible structure for the zinc complex was concluded to be the binuclear form with tetrahedral coordination in conformity with that for the cobalt complex, which was revised in this work. Infrared bands in the 1100—1300 cm^{-1} range due to asymmetric vibration of the ester groups at 8 and 12, and X-ray powder pattern provided the evidence for this structure in reference to the corresponding data for the cobalt complex. The up-field shift of proton signals due to the methyl groups at 1, 7, 13, and 19, the 10-methylene group, and to the ethyl moiety of carbethoxy groups at 8 and 12 upon coordination are consistent with the tetrahedral coordination with dimeric structure. The molecular weight determination also confirmed the dimeric nature of the zinc complex.

Bilirubin and mesobilirubin are the typical biochemical compounds possessing a saturated methylene bridge at the center of a linear tetrapyrrolic structure, each of the four pyrrole rings of which are linked by a single carbon atom. These biladienes-ac are the members of so called bile pigments and have been extensively studied from biochemical point of view. Meanwhile, these biladienes (I) in general may behave as tetradentate ligands and produce various complex metal chelate compounds. In our previous work,[2] the cobalt and nickel complexes of 1,19-dideoxy-8,12-dicarbethoxy-1,3,7,13,17,19-hexamethylbiladiene-ac (II) were synthesized and investigated by means of various spectroscopic methods. As a result, a dimeric structure was assigned to the cobalt complex in which each cobalt atom attained approximately a tetrahedral configuration (III). On the other hand, the nickel atom was found to be subjected to the square-planar ligand-field in the complex of monomeric type (IV).

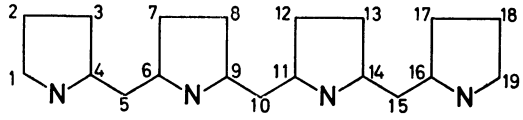

I

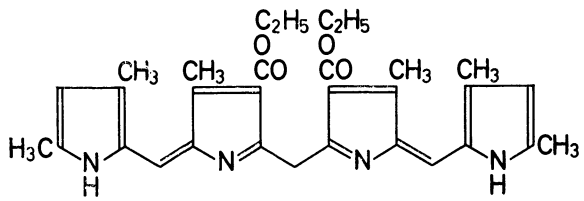

II

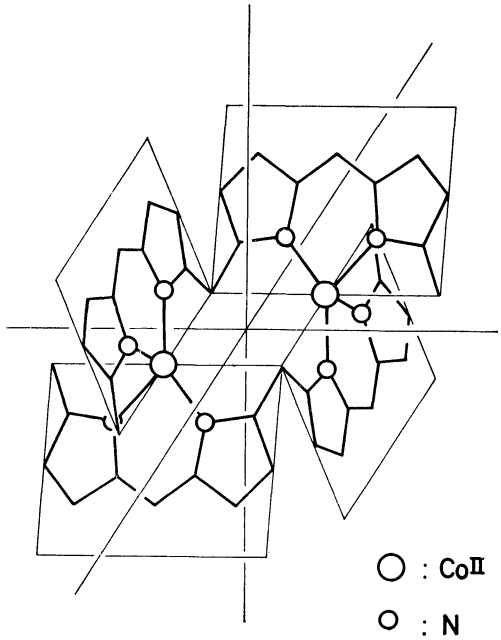

III

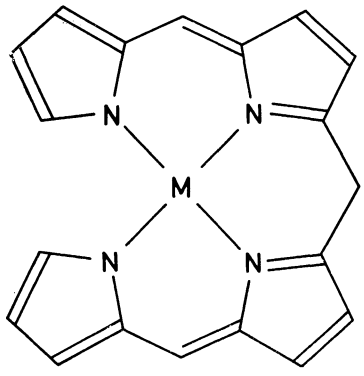

M : Ni^{II}, Cu^{II}

IV

1) Contribution No. 196 from the Department of Organic Synthesis, Faculty of Engineering, Kyushu University.

2) Y. Murakami, Y. Kohno, and Y. Matsuda, *Inorg. Chem. Acta*, **3**, 671 (1969).

This paper reports the synthesis and the structural properties of copper(II) and zinc(II) complexes of the above biladiene pigment, as examined by visible, near-infrared, infrared, NMR, and ESR measurements as well as X-ray diffraction measurements of powdered samples. Since copper and zinc tend to assume square-planar and tetrahedral configurations, respectively, coordination configurations of the present metal complexes are to be discussed in reference to the corresponding nickel and cobalt complexes already reported.[2]

Experimental

Spectral Measurements. Visible and near-infrared spectra in chloroform (10^{-3}—10^{-5} M) were recorded on a Hitachi Model EPS-2 spectrophotometer at room temperature. Infrared and far-infrared spectra covering the range 4000—200 cm^{-1} were measured with a JASCO Model DS-403G grating spectrophotometer at room temperature, where both KBr disc and Nujol mull techniques were adopted. A Varian A-60 spectrometer was used to obtain NMR spectra in chloroform-d (3×10^{-2} M) at room temperature. Chemical shifts were reported in ppm from internal tetramethylsilane (TMS) and calibrated by the use of chloroform signal as the secondary reference. ESR spectra were taken on a JEOL JES-ME-3X X-band spectrometer using 100 kHz field modulation, where the copper-doped crystals (~1 wt%) of the isomorphous nickel complex and the xylene-benzene solution of the copper complex at room temperature as well as the frozen sample of the copper complex in xylene-benzene at 77°K were used as samples. X-Ray diffraction patterns of the powdered solid samples were measured with a Norelco X-ray diffractometer.

Zinc Complex. A 300 mg sample of zinc acetate dihydratein 10 m*l* of methanol was added to a suspension of 300 mg of 1,19-dideoxy-8,12-dicarbethoxy-1,3,7,13,17,19-hexamethylbiladiene-ac[2] (abbreviated as BLD hereafter) (free base) and 400 mg of sodium acetate trihydrate in 50 m*l* of methanol while heating on a water-bath. After refluxing for one hour, the mixture was allowed to cool down to room temperature. Reddish violet crystals were recovered and recrystallized from acetone: yield 250 mg (74.4%). Further recrystallization was performed from chloroform-methanol: 200 mg; mp>250°C(decomp.).

Found: C, 62.88; H, 5.93; N, 9.29%;[3] mol wt (osmometric method[4]), 1230. Calcd for $C_{62}H_{68}N_8O_8Zn_2$: C, 62.89; H, 5.79; N, 9.46%; mol wt, 1184.05.

Copper Compex. A 500 mg sample of copper acetate monohydrate in 30 m*l* of methanol was added to a mixture of 300 mg of the free base of BLD, 600 mg of sodium acetate trihydrate and 120 m*l* of methanol, and refluxed for 40 min. The dark crystalline precipitate was recovered and washed several times with methanol. The chloroform solution of this material was applied to the top of a chromatographic column of silica gel (60—80 mesh, Kanto Chemical Co., Inc.) and eluted with chloroform. The initial effluent was concentrated *in vacuo* and the product was recovered by reprecipitation with methanol: dark crystalline solid of metallic luster; yield 150 mg (44.3%). Further recrystallization was performed from chloroform-methanol: 120 mg; mp 214—217°C (decomp.).

Found: C, 62.76; H, 5.84; N, 9.35%; mol wt (osmometric method), 603. Calcd for $C_{31}H_{34}N_4O_4Cu$: C, 63.09; H, 5.81; N, 9.49%; mol wt, 590.18.

Results and Discussion

Electronic Spectra. The near-ultraviolet, visible, and near-infrared spectra for the BLD free base and the corresponding zinc and copper complexes in chloroform are shown in Fig. 1. The biladiene shows two intense absorption bands at 425 and 495 mμ, whose absorption coefficients are 27700 and 14800 respectively. These are attributed to the $\pi\rightarrow\pi^*$ transition.[5] Other broad bands located in the near-ultraviolet region may be due to the transitions to higher π energy levels.

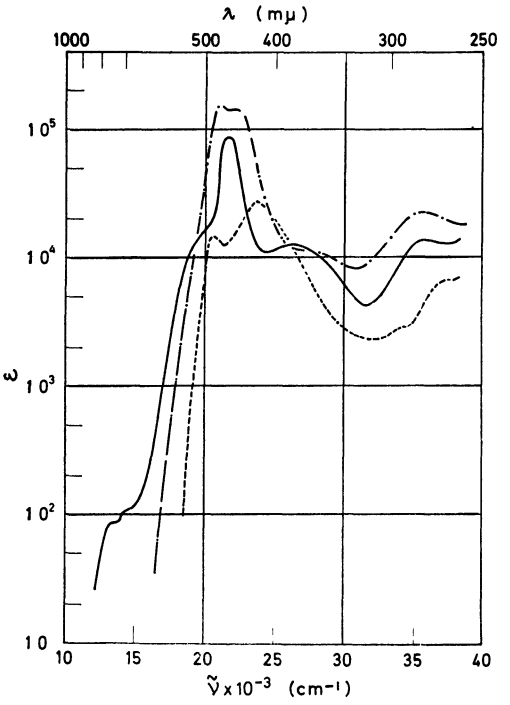

Fig. 1. Electronic absorption spectra in chloroform: ----, BLD free base; —·—·—, the zinc complex; ——, the copper complex.

The zinc complex shows four absorption bands in the 260—1000 mμ range. The bands in a higher energy region—282 mμ (ε=22800) and 356 mμ (ε=11400)—are considered to be due to the $\pi\rightarrow\pi^*$ transitions for which the ligand part is responsible. Both of the quite intense bands appearing at 454 mμ (ε=146000) and 475 mμ (ε=153000) are tentatively assigned to the metal to ligand charge transfer transitions, judging from their intensity and location. In the longer wavelength region beyond 620 mμ, there observed no significant absorption bands whose intensity is higher than 0.1.

The copper complex demonstrates six absorption bands in the 260—1000 mμ range, among which the

3) The elemental analyses were performed at the Microanalysis Center of Kyushu University.

4) A Hitachi Model 115 vapor pressure osmometer was used to measure the molecular weight of a sample dissolved in chloroform.

5) The spectrum of the BLD free base has been shown in our previous paper.[2] Its absorption intensity indicated in Fig. 1 of the previous paper is twice as large as the real value as a matter of fact. The correction has to be made for this mis-presentation of the spectrum.

higher energy bands observed at 280 mμ (ε=13700) and 380 mμ (ε=12700) are attributed to the $\pi \rightarrow \pi^*$ transitions of the ligand part. The most intense band appearing at 461 mμ (ε=97800) is assignable to the metal to ligand charge transfer transition, while the weaker bands at 701 mμ (ε=103) and 752 mμ (ε=85) in a lower energy region of the present study is due to the $d \rightarrow d$ transitions of the metal atom. When the copper atom is placed in the square-planar ligand-field, a $d \rightarrow d$ ($d_{z^2}, d_{xy}, d_{xz}, d_{yz} \rightarrow d_{x^2-y^2}$) absorption band has been known to appear in the 500—700 mμ range. In the case that the copper ion is subjected to a strong ligand-field perturbation produced by the four nitrogen donor atoms, such a $d \rightarrow d$ band can be found in general near the 500 mμ range.[6] The corresponding absorption intensity varies from several tens to a few hundreds, depending upon the structure of the ligand part.[7] When the copper complex assumes approximately a tetrahedral configuration around the central metal atom, no significant absorption bands originated from $d \rightarrow d$ transitions are seen in a shorter wavelength region lying below 1000 mμ.[8] If the coordination configuration is something between these two typical cases or the symmetry property of the ligand-field is lowered below D_{4h}, the multi-absorption bands tend to appear in the intermediate wavelength range with significant energy separation.[9,10] The above consideration leads to the conclusion that the copper atom in the BLD complex attains primarily the square-planar coordination without much distortion.

Vibrational Spectra. The infrared spectra in the 1000—1600 cm^{-1} range for the BLD free base and its zinc and copper complexes are shown along with those for the corresponding cobalt and nickel complexes in Fig. 2. The vibrational character of a family of tetrahedral complexes is found to be different from that of square-planar complexes particularly in the 1100—1300 cm^{-1} range in the present study. These characteristic bands are attributed to the asymmetric stretching modes of the ester group situated at positions 8 and 12 in the ligand part.[11]

The cobalt complex, where the metal atom has been shown to assume a tetrahedral coordination,[2] shows two absorption bands of equal intensity and a shoulder band in between in this range as shown in Fig. 2 by arrows. The present zinc complex demonstrates vibrational characteristics quite similar to those of the corresponding cobalt complex.

On the other hand, two strong bands of nearly equal intensity are located closely in the higher frequency part of the 1100—1300 cm^{-1} range and another band of medium intensity is found in the lower frequency part for the nickel complex which assumes a square planar configuration around the metal atom, as seen in Fig. 2. The present copper complex also shows vibrational bands of similar trend in the same frequency range. The infrared spectrum of the BLD free base appears to bear a resemblance to those of the cobalt and zinc complexes rather than those of the corresponding copper and nickel complexes. Outside this region some minor differences between these two types of complexes can be noticed around 1400 and 1550 cm^{-1}.

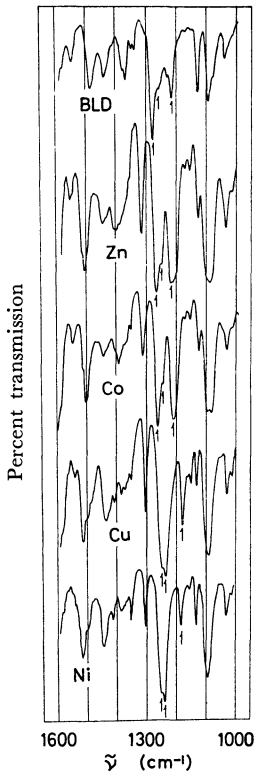

Fig. 2. Infrared spectra of the BLD complexes of bivalent metals (KBr disc method). Arrows refer to the characteristic bands due to asymmetric stretching vibration of the carbethoxy group (see text).

The above results indicate that the carbethoxy groups located at positions 8 and 12 of the ligand part in the cobalt and zinc complexes of tetrahedral configuration

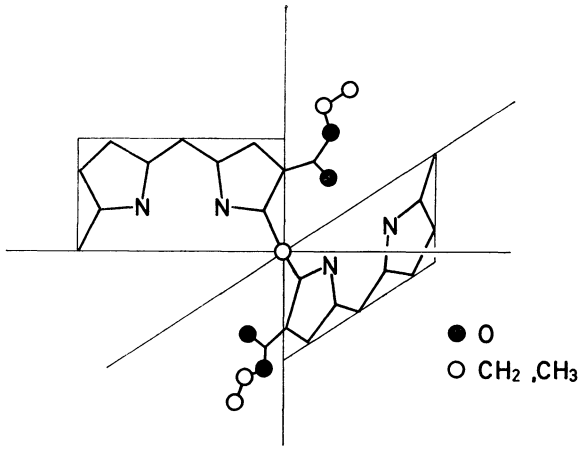

Fig. 3. Plausible geometrical structure for the BLD free base.

6) R. E. Clarke and J. H. Weber, *J. Inorg. Nucl. Chem.*, **30**, 1837 (1968).
7) R. L. Belford and W. A. Yeranos, *Mol. Phys.*, **6**, 121 (1963).
8) A. B. P. Lever, "Inorganic Electronic Spectroscopy," Elsevier Publishing Co., Amsterdam (1968), p. 359.
9) M. Goodgame and L. I. B. Haines, *J. Chem. Soc., A*, **1966**, 174.
10) F. A. Cotton and J. J. Wise, *Inorg. Chem.*, **6**, 915 (1967).
11) N. B. Colthup, L. H. Daly, and S. E. Wiberley, "Introduction to Infrared and Raman Spectroscopy," Academic Press, New York (1964), p, 249.

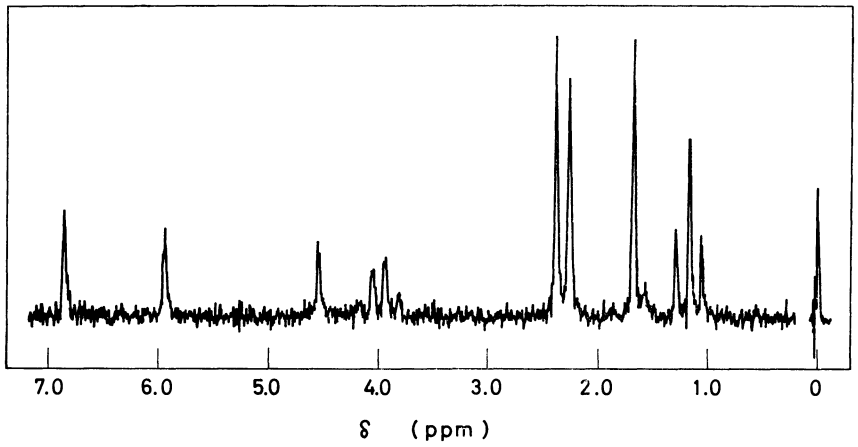

Fig. 4. NMR spectrum of the Zn(II)-BLD complex in chloroform-*d*; TMS as an internal reference.

Table 1. Proton chemical shifts for BLD and the metal complexes

	Solvent	δ, ppm								Ref.
BLD	CCl_4	1.32	2.08	2.18	2.42	4.26	4.69	5.85	6.65	2
Ni complex	$CDCl_3$	1.39	1.98	2.18	2.57	4.33	4.87	5.93	7.00	2
Zn complex	$CDCl_3$	1.19	1.70	2.25	2.40	4.01	4.55	5.94	6.86	This work
Assignment		a	b	c	d	e	f	g	h	

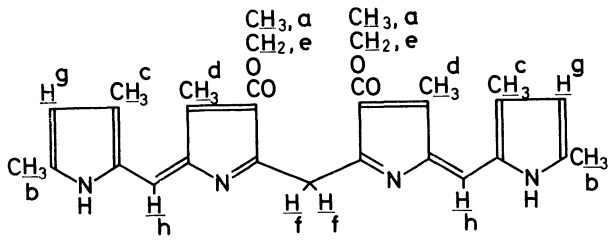

are free from steric strain as expected in the ligand free base, a plausible structure for which is depicted in Fig. 3.

By inference from the far-infrared study on the dipyrromethene complexes,[12,13] absorption bands due to metal-nitrogen stretching modes are expected to appear in the 300—400 cm^{-1} range. Nevertheless, any reasonable assignments of empirical nature were not possible at present due to the complexity of these spectra caused by vibrational modes of the ligand part.

NMR Spectrum of the Zinc Complex. The NMR spectrum for the zinc complex is shown in Fig. 4 and the assignments are listed in Table 1 together with those for the BLD free base and the corresponding nickel complex. The proton signals due to the 3- and 17-methyl groups, the 2- and 18-protons, and the 5- and 15-methine groups shifted down-field upon coordination with zinc. All other proton signals, on the other hand, shifted up-field. The electron density around methine-carbon atoms at positions 5 and 15 seems to be decreased through delocalization caused by chelate ring formation, and the protons attached to these carbon atoms are deshielded as a result. This electronic effect for the zinc complex is smaller than that for the nickel complex. The similar explanation may be given to other proton signals which demonstrate down-field shift as mentioned above. The signal for protons of the 10-methylene group in the zinc complex is found in the highest field among the corresponding signals for the three compounds listed in Table 1. This is most likely due in part to the fact that the 10-methylene group is not involved in a chelate ring through coordination, while this group becomes a member of the chelate ring in the corresponding nickel complex of square-planar configuration. The similar trend was also observed for the proton signals due to the ethyl moiety of carbethoxy groups at positions 8 and 12, as well as for the signal due to the 7- and 13-methyl groups. Placement of these groups in the shielding zones of near-by pyrrole rings of another BLD molecule and the corresponding chelate rings in the same complex seems to result in such up-field shifts of the corresponding proton signals. This situation can be visualized by Fig. 5, where the zinc atoms are bound to pyrrolic nitrogens by assuming a tetrahedral configuration at a 2 : 2 molar ratio of ligand to metal. The ligand molecule attains a conformation entirely similar to that expected in the free base state

12) Y. Murakami and K. Sakata, *Inorg. Chem. Acta*, **2**, 273 (1968).

13) Y. Murakami, K. Sakata, and Y. Matsuda, unpublished results.

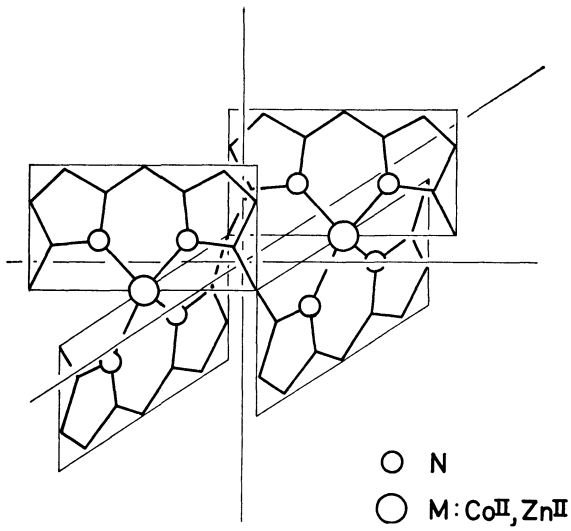

Fig. 5. The most plausible structure for the Co(II)- and Zn(II)-BLD complexes; the binuclear structure with tetrahedral coordination of metal atoms.

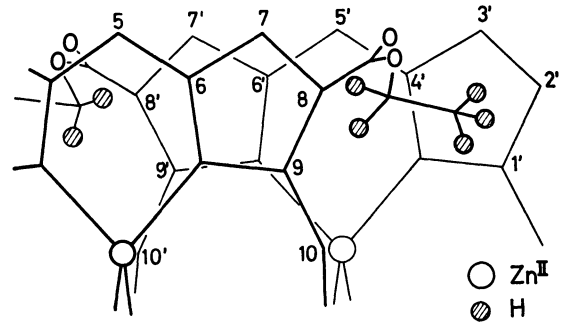

Fig. 6. Plausible geometrical configuration of the 8-carbethoxy group in the Zn(II) complex of binuclear structure.

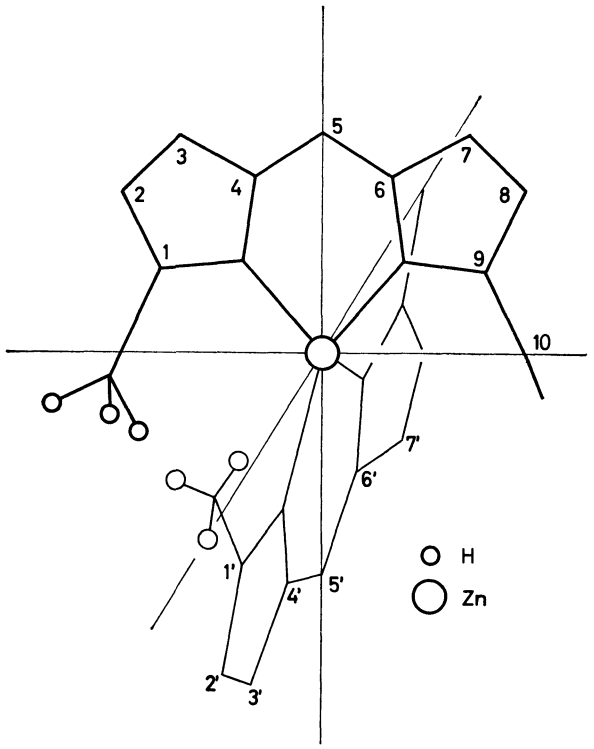

Fig. 7. Plausible geometrical configuration of the 1-methyl group in the Zn(II) complex of binuclear structure.

(Fig. 3) and the least steric interaction between the carbethoxy groups at positions 8 and 12 seems to be secured as a result. The state of affair around the 8- and 12-carbethoxy groups is shown in more understandable manner in Fig. 6. This is in agreement with the conclusion derived from the infrared data. A significant up-field shift of the proton signal due to the 1- and 19-methyl groups may also be caused by the shielding effect of pyrrole rings and metal chelate rings as shown in Fig. 7. The situation would be somewhat different in the nickel complex. A steric interaction between the 1- and 19-methyl groups in the monomeric nickel complex of square-planar coordination seems to result in a slight twist of these groups from the plane of each pyrrole ring. This effect would place these methyl groups in an edge of the shielding zone of each pyrrole ring.

ESR Spectra of the Copper Complex. The ESR spectra for the copper complex in xylene-benzene at room temperature and at 77°K as well as that doped in the isomorphous nickel complex at room temperature are shown in Fig. 8. The general feature of spectra B and C is consistent with the square-planar coordination. In these two spectra, the hyperfine lines due

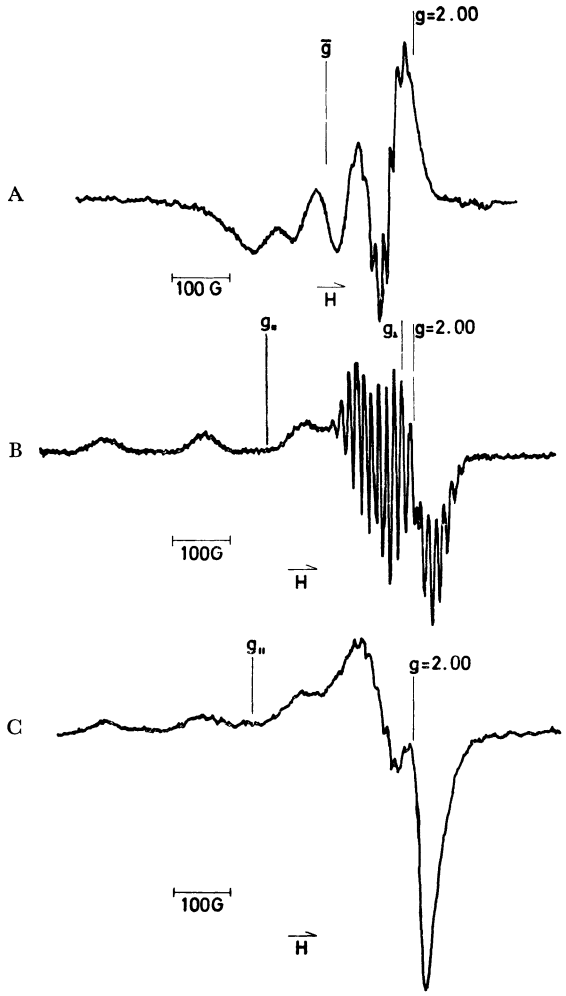

Fig. 8. ESR spectra of the Cu(II)-BLD complex: A, in xylene-benzene (6 : 4) at room temperature; B, in xylene-benzene (6 : 4) at 77°K; C, doped in the Ni(II)-BLD complex at room temperature.

to the copper nucleus can be observed on the $g_{\parallel}$ positions while such splittings are not obvious on the $g_{\perp}$ positions. Super-hyperfine lines due to the nitrogen nuclei, from which A_N values were evaluated, appear on the $g_{\perp}$ positions. The solution spectra (A) also shows four hyperfine lines due to the copper atom and additional splittings caused by the nitrogen nuclei in the upper field. The $g_{\perp}$ and $A_{\perp}$ values for the frozen sample were evaluated by the simulation method of hyperfine structure appeared in the upper field. The spin Hamiltonian parameters obtained in this work are almost comparable with the data for the phthalocyanine and porphyrin complexes taken from the literature, as shown in Table 2.

One of the σ-molecular orbitals for coordination in D_{4h} symmetry can be represested as follows:

$$\Psi_{B_{1g}} = \alpha d_{x^2-y^2} - 1/2\,\alpha' [-\sigma_x^{(1)} + \sigma_y^{(2)} + \sigma_x^{(3)} - \sigma_y^{(4)}]$$

The sigma-bonding parameter α^2 can be calculated by the following equation given by Kivelson and Neiman:[14]

$$\alpha^2 = -(A_{\parallel}/P) + (g_{\parallel} - 2) + 3/7\,(g_{\perp} - 2) + 0.04$$

where 0.036 was given to P. Judging from α^2 values, the coordinate bond character seems to be comparable to those in the phthalocyanine and porphyrin complexes.

X-Ray Powder Diffraction Patterns. The X-ray powder diffraction patterns for the copper, zinc, nickel, and cobalt complexes of BLD are shown in Fig. 9. The general feature of the diffraction pattern for the copper complex has a close resemblance to that for the nickel complex although the careful comparison reveals some minor difference in their relative intensity. On the other hand, the powder pattern for the zinc complex is found to be almost identical with that for the corresponding cobalt complex. As a result, stacking manner of the copper complex in crystalline state is close to or almost identical to that of the nickel complex; so is the zinc complex to the cobalt complex.

These results provide another evidence for the structural properties of the present complexes: the copper complex involves the coordinate bonds of square-planar orientation in a monomeric form, while the zinc complex consists of tetrahedrally coordinated bonds in a binuclear form.

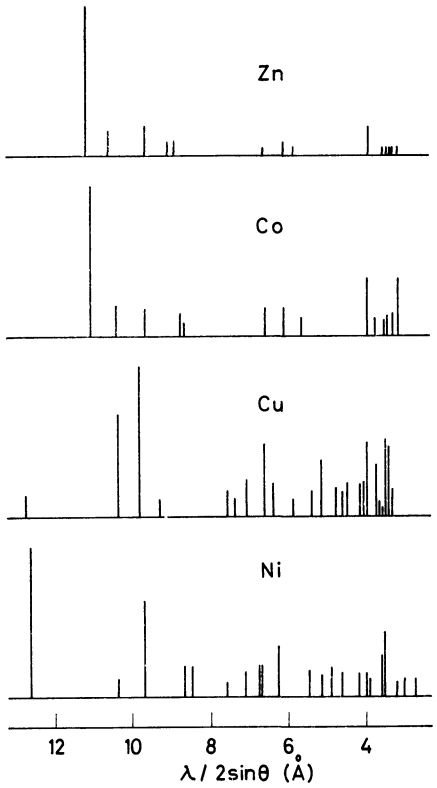

Fig. 9. X-Ray powder diffraction patterns of the BLD complexes of bivalent metals. The relative diffraction intensity at a Bragg angle θ is represented by the height of vertical lines.

Structure of the Metal Complexes. The elemental analysis of the copper complex is consistent with a ligand to metal ratio of 1 : 1 with no additional ions or species. The molecular weight determination by means of vapor pressure osmometer indicates this complex is monomeric. The infrared bands characteristic of asymmetric stretching vibration of the carbethoxy groups at positions 8 and 12 are different in their positions from those observed for the BLD free base and the corresponding zinc and cobalt com-

TABLE 2. SPIN HAMILTONIAN PARAMETERS FOR THE COPPER COMPLEXES

Ligand[a]	Diluent	Temp.[b]	g_0	$g_{\parallel}$	$g_{\perp}$	$A_0\times10^4$, cm^{-1}	$A_{\parallel}\times10^4$, cm^{-1}	$A_{\perp}\times10^4$, cm^{-1}	$A_N\times10^4$, cm^{-1}	α^2	Ref.
BLD	xylene-benzene[c] (6 : 4)	R	2.102			76.2			13.5		This work
BLD	xylene-benzene[c] (6 : 4)	77°K		2.197	2.042		177	48.1	14.2	0.75	This work
BLD	Ni-BLD	R		2.212			180		13.5		This work
PHC	H_2SO_4	G		2.174	2.045		202			0.78	14
PHC	H_2SO_4	136°K		2.180	2.037					0.72	16
EPP	Caster oil, benzene		2.097	2.169	2.061		188	39		0.74	15

a) BLD, the present biladiene-ac; PHC, phthalocyanine; EPP, ethioporphyrin II.
b) R, room temperature; G, frozen to glass state.
c) Concentration of the complex; $\sim10^{-4}$ mol/l at room temperature.

14) D. Kivelson and R. Neiman, *J. Chem. Phys.*, **35**, 150 (1961).
15) E. M. Roberts and W. S. Koski, *J. Amer. Chem. Soc.*, **82**, 3006 (1960).
16) E. M. Roberts and W. S. Koski, *ibid.*, **83**, 1865 (1961).

plexes, but in conformity with those for the nickel complex of square-planar coordination. The appearance of the ligand-field bands at 701 and 752 mμ also indicates that the copper atom is placed approximately in a square-planar ligand-field. The overall feature of the ESR spectrum and spin Hamiltonian parameters obtained therefrom ($g_{\parallel}$, $g_{\perp}$ and A values) are consistent with the square-planar coordination. Since the X-ray diffraction pattern of the powdered sample is closely related to that of the nickel complex, this data may give another support to the structure. In conclusion, these experimental facts as a whole are consistent with the square-planar coordination of the copper atom with the pyrrolic nitrogens of BLD in a monomeric manner (IV).

By referring to the elemental analysis and the molecular weight measurement of the zinc complex, the complex is binuclear with a ligand to metal ratio of 2 : 2. The infrared bands due to asymmetric stretching vibration of the ester groups provide an evidence that the carbethoxy groups at positions 8 and 12 are free from steric strain to an extent expected in the BLD free base and in the corresponding cobalt complex of tetrahedral coordination as explained in the previous section. The dimeric nature of the complex was also demonstrated by NMR spectroscopy. All the upfield shifts of proton signals through coordination can be predicted on the basis of binuclear complex formation. Although a dimeric form with tetrahedral coordination shown by structure III was put forward previously for the cobalt complex,[2] this turns out to be unsatisfactory for explaining the experimental data reported in this work and deserves an appropriate revision as depicted in Fig. 5. The X-ray powder diffraction pattern was indentical with that of the cobalt complex which assumes tetrahedral configuration around the central metal atom with dimeric structure. As a result, the most plausible structure for the zinc complex is the binuclear form with tetrahedral coordination of the metal atom, identical with the corresponding cobalt complex, as depicted in Fig. 5.

BULLETIN OF THE CHEMICAL SOCIETY OF JAPAN, VOL. 44, 415—417 (1971)

Chloropentakis(trichlorostannato)ruthenate(II)

Hisateru OKUNO, Tatsujiro ISHIMORI, Kunihiko MIZUMACHI, and Haruhiko IHOCHI*

Department of Chemistry, College of Science, Rikkyo (St. Paul's) University, Nishi Ikebukuro, Tokyo

(Received June 26, 1970)

The cesium and triethylammonium salts of chloropentakis(trichlorostannato)ruthenate(II), $Cs_4[RuCl(SnCl_3)_5]\cdot CsCl$ and $(Et_3NH)_4[RuCl(SnCl_3)_5]$, were prepared. Their IR absorption bands near 210 cm^{-1} are thought to be due to the Ru–Sn stretching vibration. The electronic spectra of dilute hydrochloric acid solutions of the complex salts were the same as the spectrum of a single crystal of the cesium salt. This suggests the presence of the complex ion, $[RuCl(SnCl_3)_5]^{4-}$, in acid solutions. A hydrolysis product of the complex ion contained ruthenium, tin and chlorine in the atom ratio of 1 : 5 : [$\alpha(<1)$], and the cesium salt was yielded from a dilute hydrochloric acid solution of the hydrolysis product. The observations show the presence of the Ru–Sn bonds in the complex ion.

. Complexes of platinum metals with the coordinating $(SnCl_3)^-$ groups have recently been studied.[1-7] As for the ruthenium complexes of this kind, $M^I_2[RuCl_2(SnCl_3)_2]$,[3] $[Ru_2Cl_3(SnCl_3)(CO)_2(PPh_3)_3(Me_2CO)_2]$, $[Ru_2Cl_3(SnCl_3)(CO)_2(PPh_3)_4]$ (PPh_3=triphenylphosphine)[6] and $[Me_4N][RuX_2(CO)_2(SnCl_3)_2]$ (X=Cl or Br)[6,7] have been reported. In the present work salts of chloropentakis(trichlorostannato)ruthenate(II), $[RuCl(SnCl_3)_5]^{4-}$ were prepared, and their chemical properties were investigated. A hydrolysis product of the complex ion was also isolated.

Experimental

Ruthenium(III and IV) in a hydrochloric acid solution was prepared from the distillate of ruthenium(VIII) tetroxide passed into an alcoholic hydrochloric acid solution. All the other reagents were of analytical grade. IR-spectra were measured in Nujol mull over the region of 700—200 cm^{-1} on JASCO IR-F.

Preparation of $[RuCl(SnCl_3)_5]^{4-}$ Complex Ion. Sufficient tin(II) chloride dihydrate (1.13 g) was added to 40 mg of ruthenium(III and IV) in 50 m*l* of 2—3 M hydrochloric acid solution, and the solution was digested in a boiling water bath for 45—60 min. The yellowish red solution obtained was passed through an anion-exchange column of Dowex 1, X-16 (20 m*l* of the chloride form), yielding a hydrochloric acid solution of the complex ion. This ion-exchange procedure is to remove tin(IV) and an excess of tin(II), and, if present, any small anionic ruthenium species

* Present address: Department of Chemistry, University of Arkansas, Fayetteville, Ark., U. S. A.

1) R. D. Cramer, E. L. Jenner, R. V. Lindsey, Jr., and U. G. Stolberg, *J. Amer. Chem. Soc.*, **85**, 1691 (1963).

2) A. G. Davies, G. Wilkinson, and J. F. Young, *ibid.*, **85**, 1692 (1963).

3) J. F. Young, R. D. Gillard, and G. Wilkinson, *J. Chem. Soc.*, **1964**, 5176.

4) R. D. Cramer, R. V. Lindsey, Jr., C. T. Prewitt, and U. G. Stolberg, *J. Amer. Chem. Soc.*, **87**, 658 (1965).

5) R. V. Lindsey, Jr., G. W. Parshall, and U. G. Stolberg, *Inorg. Chem.*, **5**, 109 (1966).

6) T. A. Stephenson and G. Wilkinson, *J. Inorg. Nucl. Chem.*, **28**, 945 (1966).

7) J. V. Kingston and G. Wilkinson, *ibid.*, **29**, 2709 (1967).

in the reaction mixture. However, no complex ion of a large size was adsorbed appreciably by the anion-exchanger with a high crosslinkage.

Preparation of $Cs_4[RuCl(SnCl_3)_5]\cdot CsCl$ and $[(C_2H_5)_3NH]_4[RuCl(SnCl_3)_5]$. Addition of acid cesium chloride solution to the complex ion in 2—3 M hydrochloric acid solution yielded a yellow salt, which was washed with a mixture of ethanol and hydrochloric acid (5 : 1). Crystals 0.5 to 1.5 mm in length were prepared by introducing 0.2 M cesium chloride solution slowly from a capillary into a 2—3 M hydrochloric acid solution of the complex ion; the solution was covered with ligroin during the addition of cesium chloride and the formation of the crystals.

Found: Ru, 5.0; Sn, 30.4; Cs, 33.8; Cl, 30.7%. Calcd for $Cs_5RuSn_5Cl_{17}$: Ru, 5.15; Sn, 30.25; Cs, 33.87; Cl, 30.72%.

Addition of a large excess of a concentrated acid triethylammonium chloride solution yielded an orange salt. The salt was washed with an acid triethylammonium chloride solution and then with the mixture of ethanol and hydrochloric acid (5 : 1). The triethylammonium salt was much more soluble in dilute hydrochloric acid than the cesium salt.

Found: Ru, 5.94; Sn, 35.2; Cl, 33.0; N, 3.46; C, 17.82%. Calcd for $[(C_2H_5)_3NH]_4[RuCl(SnCl_3)_5]$: Ru, 6.05; Sn, 35.52; Cl, 33.96; N, 3.35; C, 17.26%.

The tetramethylammonium salt was prepared in a similar way. It was less soluble in dilute hydrochloric acid than the triethylammonium salt.

Preparation of Hydrolysis Product of the Complex. When a 2—3 M hydrochloric acid solution of the complex ion was diluted 40-fold with water, a yellow hydrolysis product was obtained. This product was washed with water several times by centrifuging or by decantation; the chloride ion was gradually removed from the hydrolysis product by successive washings. The product turned brown when it was washed with ethanol and then ether or when it was dried over tetraphosphorus decaoxide. The brown product contained 10.6% Ru, 61.5% Sn and 0.4—3.1% Cl; the chloride content varied with the extent of the washing.

Results and Discussion

Complex Salts. The compositions of the cesium and triethylammonium salts were consistent with $Cs_5RuSn_5Cl_{17}$ and $(Et_3NH)_4RuSn_5Cl_{16}$, respectively. These compounds were diamagnetic. They are thought to be complex salts of ruthenium(II). Six-coordination is a very strong inherent tendency of ruthenium(II) complexes, and the only exceptions may be some complexes[6,8] with triphenylphosphine or triphenylstibine such as $RuCl_2(PPh_3)_3$. However, X-ray study on $RuCl_2(PPh_3)_3$[9] has shown that the complex is quasi-octahedral. From geometrical consideration, it is seen that covalent radii of ruthenium(II), tin(II), and Cl(-I) make an octahedral arrangement as $[RuCl(SnCl_3)_5]^{4-}$ possible for the complex ion presented here, and its complex salt can be represented as $Cs_4[RuCl(SnCl_3)_5]\cdot CsCl$ or $(Et_3NH)_4[RuCl(SnCl_3)_5]$. The equivalent conductivity, Λ_e, of the tetramethylammonium salt in nitromethane was 102.9, 104.1, and 106.1 $ohm^{-1}cm^2$ at 6.03×10^{-5}, 4.06×10^{-5}, and 2.05×10^{-5} eq/l, respectively, at 25°C. The data were compared with those of (3 : 1), (2 : 1) and (1 : 1) electrolytes by the method of Feltham and Hyter.[10] The value of $(\Lambda_0-\Lambda_e)/\sqrt{c}$, where Λ_0 is Λ_e at infinite dilution and c equivalent concentration, was 1.66×10^3, while the values for $Na[BPh_4]$, $[Ni(phenan)_3](ClO_4)_2$, and $[Co(bipy)_3](ClO_4)_3$ have been reported to be 216, 465, and 1020 respectively. The results of the comparison indicate that the tetramethylammonium salt is an electrolyte of the (4 : 1) type. The electronic absorption spectra of the tetramethylammonium and triethylammonium salts in nitromethane were the same as those of the salts in a dilute hydrochloric acid solution, which in turn are the same as the spectrum of the cesium salt single crystal. Thus, both cesium and triethylammoniun salts contain an identical complex anion, $[RuCl(SnCl_3)_5]^{4-}$.

The properties of the cesium salt were as follows: yellow for fine crystals and orange for crystals of length of the order of millimeters, insoluble in ethanol and ether; cubic system with the well developed (1, 1, 1) plane; lattice constant, $a=15.66\pm0.22$ Å; number of chemical units in an unit cell, $Z=4$; density=3.37 g/cm^3 at 25°C; refractive indices, $n_{700m\mu}=1.758\pm0.005$, $n_{589m\mu}=1.765\pm0.004$ at 23°C.

The electronic absorption spectrum of the crystal shown in Fig. 1 was measured by a photoelectric spectrometer equipped with a special microphotometric attachment.[11,12] Since the crystal used did not have completely planar surfaces, its thickness was not measured. A decrease in absorption was observed on irradiation with ultraviolet rays. This seems to be caused by a partial decomposition of the complex salt during the course of irradiation.

The infrared spectrum of the cesium salt has absorption bands at 324, 288(shoulder), 211, and 205 (shoulder) cm^{-1} as shown in Fig. 2. The spectrum of

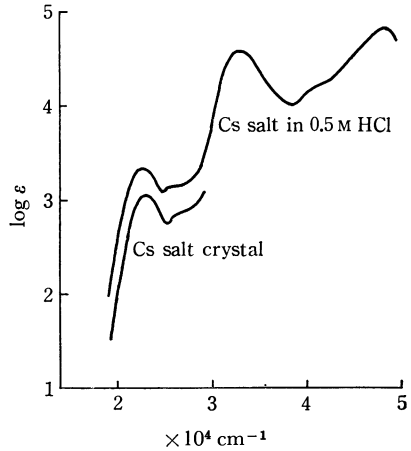

Fig. 1. Electronic Spectra of $Cs_4[RuCl(SnCl_3)_5]\cdot CsCl$.
The ordinate is not to scale for the spectrum of the crystal.

8) D. Evans, J. A. Osborn, F. H. Jardine, and G. Wilkinson, *Nature*, **208**, 1203 (1965).

9) S. J. La Placa and J. A. Ibers, *Inorg. Chem.*, **4**, 778 (1965).

10) R. D. Feltham and R. G. Hayter, *J. Chem. Soc.*, **1964**, 4588.

11) The crystal absorption spectum was kindly measured by Professor Y. Kondo of Rikkyo University.

12) Y. Kondo, *Science of Light*, **11**, 76 (1962).

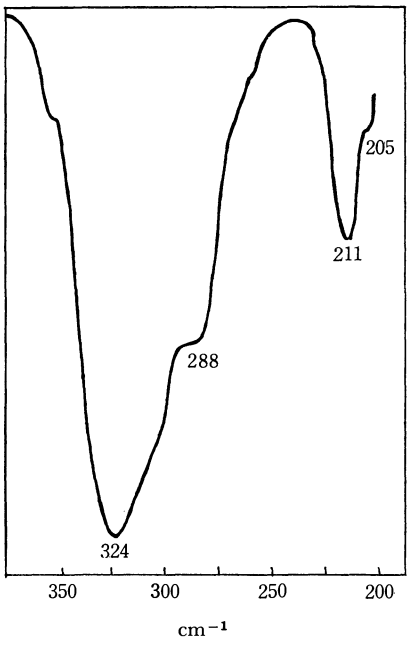

Fig. 2. Infrared spectrum of $Cs_4[RuCl(SnCl_3)_5]\cdot CsCl$ in Nujol mull.

the triethylammonium salt was the same as that of the cesium salt: the absorptions were at 318, 294(shoulder), 212, and 205(shoulder) cm^{-1}. The absorption bands in the region 350—275 cm^{-1}, including unresolved shoulders, are thought to be due to the stretching vibrations of Sn–Cl and Ru–Cl. Infrared absorptions[13] due to the platinum metal-tin bonds have been found near 200 cm^{-1} for $[Rh_2Cl_2(SnCl_3)_4]^{4-}$ and $[Pt(SnCl_3)_5]^{3-}$. The absorption bands at 210 cm^{-1} observed here can be assigned to the Ru–Sn stretching vibration.

Complex Ion in a Hydrochloric Acid Solution. The solution of the complex ion was prepared by use of an anion exchange column, and the Ru : Sn ratio in the solution was 1 : 5. When tin(II) chloride was added to this complex ion solution and the mixture again treated with the anion exchange column, the Ru : Sn ratio in the effluent was still 1 : 5. The results suggest that the complex ion in a dilute hydrochloric acid solution contains ruthenium and tin in the ratio of 1 : 5, and further that the coordinating $(SnCl_3)^-$ groups do not greatly dissociate and the rate of dissociation is not fast. The electronic absorption spectrum of the cesium salt in 0.5 M hydrochloric acid is shown in Fig. 1 ($\log \varepsilon = 3.34$, 4.58, and 4.83 at 22520, 32890, and 48540 cm^{-1} respectively). It is the same as that of the crystals of the cesium salt in the region 1.9×10^4—2.9×10^4 cm^{-1}. The spectrum of the complex ion prepared as a dilute hydrochloric acid solution was also identical with that of the cesium salt solution. Thus, the complex ion, $[RuCl(SnCl_3)_5]^{4-}$, is thought to be present in a dilute hydrochloric acid solution. However, the complex ion in an acid solution slowly fades.

Hydrolysis Product. The Ru : Sn : Cl ratio in the hydrolysis product was 1 : 5 : [$\alpha(<1)$]. The infrared absorption bands due to the Ru–Sn stretching vibrations were observed for the complex salts, but the corresponding bands were not found for the hydrolysis product. This is probably due to a polymer structure of the hydrolysis product. However, when the hydrolysis product was dissolved in 1 M hydrochloric acid, the electronic absorption spectrum of the solution was the same as that of the cesium salt in a hydrochloric acid solution ($\log \varepsilon = 3.0$ and 4.5 at 22520 and 34130 cm^{-1}). The slight differences in $\log \varepsilon$ and the wave numbers at the maximum absorptions are thought to be caused by the decomposition of a small part of the hydrolysis product. The cesium salt was prepared from a dilute hydrochloric acid solution of the hydrolysis product in a reasonable yield; decomposition products in the hydrolysis product, if any, were previously removed from the solution by the anion exchange technique. The cesium salt prepared was identified by means of electronic and infrared spectra. Thus, the skeleton of "$RuSn_5$" remains in the hydrolysis product, and the presence of direct metal-metal bonds in the complex ion is shown in terms of chemical reactions, the formation of the hydrolysis product from the complex ion and the reformation of the complex ion from the hydrolysis product. Incidentally, any hydrolysis product with metal-metal bonds other than that described above has not been reported yet.

Young *et al.*[3] have reported the preparation of $(Me_4N)_2[RuCl_2(SnCl_3)_2]$, and we tried to prepare this complex salt following their directions. However, the Ru : Sn ratio in the product was 1 : 5, not 1 : 2. The infrared spectrum was the same as that of $(Et_3NH)_4[RuCl(SnCl_3)_5]$.

The authors wish to express their appreciation to Professors Yukio Kondo and Masayoshi Nakahara of Rikkyo University for many helpful discussions, and to Miss Noriko Okazaki for her technical assistance. This work was made possible by the support of the Scientific Research Fund of the Ministry of Education.

13) D. M. Adams and P. J. Chander, *Chem. Ind.* (London), **1965**, 269.

The Formation of κ- and κ'-Al_2O_3 from the Dehydration of Tohdite $5Al_2O_3 \cdot H_2O$

Masataro Okumiya, Goro Yamaguchi, Osamu Yamada, and Shuichiro Ono*

Department of Industrial Chemistry, Faculty of Engineering, The University of Tokyo, Hongo, Tokyo

** Government Chemical Industrial Research, Tokyo, Shinjuku-ku, Tokyo*

(Received August 3, 1970)

The dehydration of tohdite $5Al_2O_3 \cdot H_2O$ is well followed by means of the single-crystal electron-diffraction patterns, the X-ray powder patterns, differential thermal analysis, and the measurement of the density. Thermogravimetric measurements were also performed, both under a normal atmosphere and in a high vacuum. Just after the dehydration, an unstable intermediate phase was obtained; it was denoted as κ'-Al_2O_3 (from tohdite). The mechanism of the transformation series:

$$\text{tohdite} \rightarrow \kappa'\text{-}Al_2O_3 \rightarrow \kappa\text{-}Al_2O_3 \rightarrow \alpha\text{-}Al_2O_3$$

was discussed, and some basic data to serve as clues to elucidate the crystal structure of κ'- and κ-Al_2O_3 were obtained.

In 1966, Krischner reported an investigation into the thermal dehydration of tohdite $5Al_2O_3 \cdot H_2O$ (Al_2O_3-K1, according to his notation) by the electron-diffraction method.[1] In his work, fine-grained hexagonal plates of tohdite, with a particle size of about 1 micron, which had been obtained by the hydrothermal treatment of bayerite, were heated by means of an electron beam in an electron microscope, and electron-diffraction patterns were obtained at various reaction stages. Since the incident beam was parallel to the *c*-axis, all the patterns obtained in his work represent the reciprocal *a-b* plane. No experimental results to elucidate the atomic arrangement along the *c*-axis were obtained in his work. Therefore, it is difficult to determine the crystal structure of dehydration products of tohdite from his experimental results only.

Furthermore, Krischner's experimental results were insufficient to elucidate the transformation mechanism, because his experiment was limited to the method of comparing the electron-diffraction patterns of the materials heated by an electron beam at uncertain temperature.

The present study has aimed at elucidating the thermal dehydration and transformation mechanism in more detail, and at obtaining basic data to serve as clues to elucidate the atomic arrangement of dehydration products. For this purpose, differential thermal analysis, thermogravimetric measurements under both a normal atmosphere and in a high vacuum, an X-ray powder diffraction experiment, and density measurements were performed. A single-crystal electron-diffraction experiment was also performed for the needle-like crystals in order to obtain information on the atomic arrangement along the *c*-axis as well as for the hexagonal-plate crystals.

Experimental Procedure

Specimen Preparation. In previous paper,[2,3] detailed conditions for tohdite formation were discussed. It was established that the addition of certain mineralizers favers the formation of tohdite. The specimen of tohdite used in this experiment was prepared as follows.

(a) A sample of η-Al_2O_3 obtained from the dehydration of bayerite at 800°C in air was inverted to tohdite by heating it hydrothermally at 460°C, 300 atm, without any mineralizer. The tohdite thus obtained was in the form of hexagonal plates with a particle size of about 1 micron and will be denoted as "tohdite(η)."

(b) Gibbsite was heated hydrothermally at 480°C, 800 atm in the presence of aluminium fluoride. The tohdite thus obtained was in the form of hexagonal plates with a particle size of about 1 micron and will be denoted as "tohdite(F)." It contains about 0.3% fluorine ion in the crystal structure.

(c) Gibbsite was heated under hydrothermal conditions of 500°C, 1000 atm, by adding $Ti(SO_4)_2$ as a 3—4% aqueous solution. The tohdite thus obtained was in the form of needle-like crystals about 10 micron in size and will be denoted as "tohdite(Ti)."

Differential Thermal Analysis and Thermogravimetric Measurements. The differential thermal analysis and thermogravimetric measurements were performed simultaneously under a normal atmosphere and at a heating rate of 5°C/min using a simultaneous thermobalance analyser.

Thermogravimetric measurements in a high vacuum (10^{-4} mmHg) were also performed using a silica spring thermobalance (Fig. 1).

Electron-diffraction Procedure. Single-crystal electron-diffraction patterns were obtained by means of a Hitachi electron microscope, Type HU-11DS. All the specimens were dispersed with water on a folmbar film attached to the sample grid and were observed at a 100 kV accelerating potential.

X-Ray Powder Measurements. X-Ray powder diffraction patterns were obtained by means of a Rigaku-Denki diffractometer using Ni-filtered Cu$K\alpha$ radiation.

Density Measurements. The density of the dehydrated materials of tohdite was measured using the Archimedian principle. The buoyance of the materials (about 1 g) in toluene was measured with a highly-sensitive ($\pm$0.01 mg) microbalance, and the density was calculated. In order to increase the accuracy of measurement, the specific gravity of toluene (about 0.89) was checked at every measurement with a standard material of a piece of pure gold (99.99%).

1) H. Krischner, *Ber. Deut. Keram. Ges.*, **39**,1366 (1966).

2) G. Yamaguchi, H. Yanagida, and S. Ono, *J. Ceram. Assoc. Japan*, **74**, 84 (1966).

3) S. Ono, G. Yamaguchi, and H. Yanagida, *ibid.*, **77**, 126 (1969).

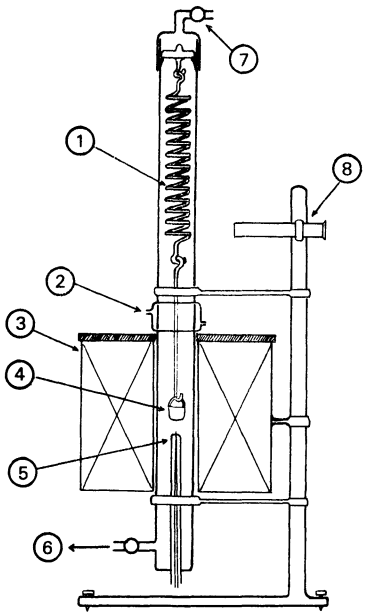

Fig. 1. High vacuum TGA instrument.

1 silica spring
2 water jacket
3 heater
4 sample holder (silica basket)
5 thermo couple
6 diffusion pump
7 leak valve
8 cathetometer

Experimental Results

Differential Thermal Analysis and Thermogravimetric Data. The DTA and TGA curves at a normal atmosphere are shown in Fig. 2. A single endotherm was observed in the temperature range of 700—800°C, and there was a large weight loss. As can be seen in Fig. 2, the dehydration of tohdite is completed in a single step at this temperature range. After dehydration, no further change in DTA and TGA curves occurred until about 1000°C.

At about 1000°C an exotherm was observed ((a), (c) diffuse, (b) sharp). The X-ray powder diffraction patterns of the materials after exothermic reaction are the same as that of α-Al_2O_3.

The X-ray powder diffraction pattern of the material heated in the 700—1000°C temperature range, which corresponds to the temperature range between the endothermic and exothermic peaks, is very similar to the pattern of κ-Al_2O_3, which is one of the dehydration products of gibbsite. Therefore, this material will be denoted as "κ-Al_2O_3 (from tohdite)."

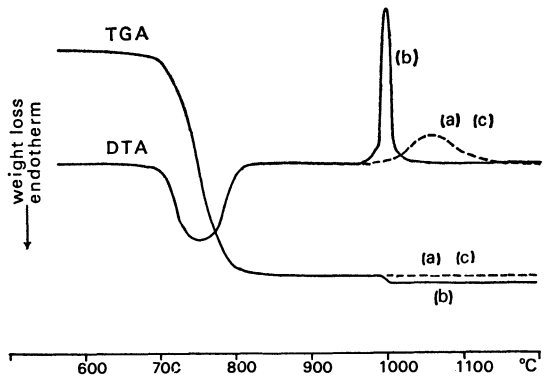

Fig. 2. DTA and TGA curves of tohdite.
(a) tohdite(η), (b) tohdite(F), (c) tohdite(Ti).

The dehydration of tohdite in a high vacuum also proceeded in a single step. Dehydration was observed at a lower temperature range (650—750°C) because of the rapid water loss in a high vacuum, the X-ray diffraction pattern of the dehydrated material is unlike the pattern of κ-Al_2O_3 (from tohdite) and this material will be denoted as "κ'-Al_2O_3 (from tohdite)." As κ'-Al_2O_3 (from tohdite) is an unstable intermediate phase, it can easily be transformed into κ-Al_2O_3 (from tohdite) by further heating both in a high vacuum and under a normal atmosphere. The stabilities of κ'-Al_2O_3 are, however, slightly different according to their starting materials, tohdite(η), tohdite(F), and tohdite(Ti). The κ'-Al_2O_3 obtained from tohdite(η) is more unstable than the κ'-Al_2O_3(from tohdite(F)) and the κ'-Al_2O_3 (from tohdite(Ti)); therefore, it is not easy to obtain κ'-Al_2O_3 (from tohdite(η)) crystal as as single phase without κ-Al_2O_3 crystals.

X-Ray Powder Data. The X-ray powder patterns of tohdite and its dehydration products κ'-Al_2O_3 (from tohdite) and κ-Al_2O_3 (from tohdite) are shown in Fig. 3. An important feature of the pattern of κ'-Al_2O_3 is that it resembles the pattern of tohdite itself, though it is rather more simple.

The tohdite reflections to which the oxygen atoms do not contribute decrease in intensity, while the reflections due mainly to the oxygen atoms remain to form the main part of the κ'-Al_2O_3 (from tohdite) pattern. The contribution of oxygen atoms to the intensity of the tohdite reflections was calculated; it is illustrated in Fig. 3, with sign + and −.

The reflections of κ'-Al_2O_3 (from tohdite) can be well indexed on the basis of the hexagonal unit cell of tohdite, which contains 5⅓ formulas of Al_2O_3. The propriety of employing this unit cell will be discussed later. The unit-cell dimensions of κ'-Al_2O_3 (from tohdite(F)) calculated from the X-ray data are shown in Table 1.

Table 1. Cell dimensions (in Å)

Tohdite(η)	$a=5.575$,	$c=8.761$
Tohdite(F)	$a=5.577$,	$c=8.774$
κ'-Al_2O_3 (from tohdite(F))	$a=5.544$,	$c=9.024$
κ-Al_2O_3 (from tohdite(F))	$a=9.599$,	$c=9.015$

The similarity between κ'- and κ-Al_2O_3 (from tohdite) was also seen (Fig. 3). The additional reflections of κ-Al_2O_3 (from tohdite) are probably caused by the distribution of aluminium atoms. The reflections are indexed on the basis of hexagonal unit cell with $a \approx \sqrt{3}a$ of tohdite, $c \approx c$ of tohdite. These cell dimensions were calculated from the X-ray data; they are also listed in Table 1.

Electron-diffraction Data. Electron-diffraction patterns were obtained for the following specimen series (the dehydration products have the same particle size and shape as the starting tohdite):

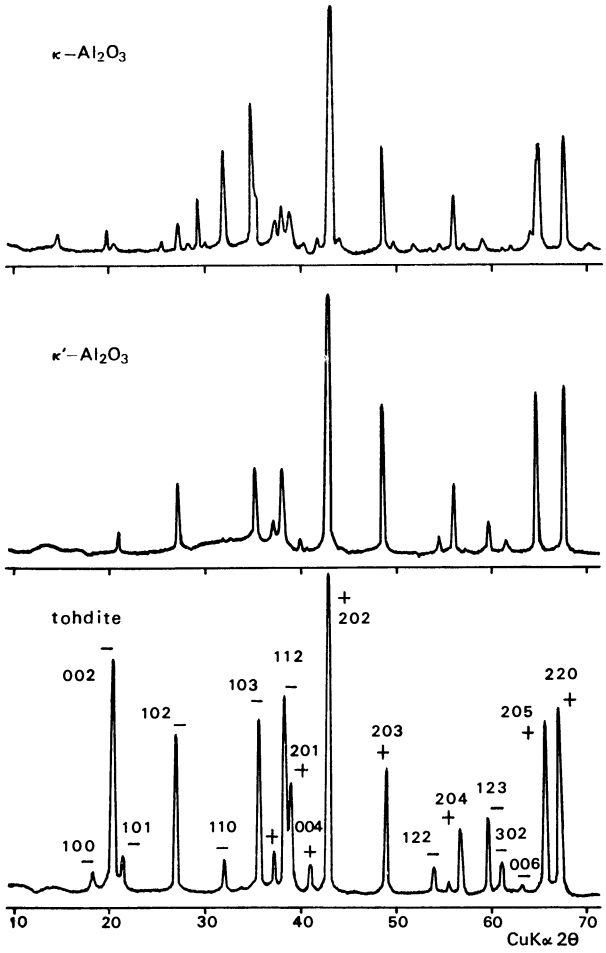

Fig. 3. X-Ray diffraction pattern of tohdite(F), κ'-Al_2O_3 (from tohdite(F)) and κ-Al_2O_3 (from tohdite(F)). The contribution of oxygen atoms on the intensity of tohdite is calculated.
+: reflection which is due mainly to the oxygen atoms
−: reflection for which oxygen atoms do not contribute

(a) tohdite(η) $\xrightarrow{900°C \text{ in air}}$ κ-Al_2O_3 (from tohdite(η))

These specimens correspond to the KI and KII of Krischner's study.

(b) tohdite (F) $\xrightarrow[(10^{-4} \text{ mmHg})]{750°C \text{ in vacuum}}$ κ'-Al_2O_3 (from tohdite(F))
$\xrightarrow{900°C \text{ in air}}$ κ-Al_2O_3 (from tohdite (F))

(c) tohdite (Ti) $\xrightarrow[(10^{-4} \text{ mmHg})]{750°C \text{ in vacuum}}$ κ'-Al_2O_3 (from tohdite(Ti))
$\xrightarrow{900°C \text{ in air}}$ κ-Al_2O_3 (from tohdite(Ti))

Patterns:

(a) The electron diffraction pattern of κ-Al_2O_3 (from tohdite(η)) agrees with that of KII described by Krischner. As has also been described by Krischner, this pattern agrees with the pattern, "(D)," of the dehydration product of gibbsite described by Brindley and Choe.[4]

(b) The electron-diffraction patterns of this series specimen are shown in Figs. 4, 5, and 6. The pattern of κ-Al_2O_3 (from tohdite(F)) is the same as that of κ-Al_2O_3 (from tohdite(η)).

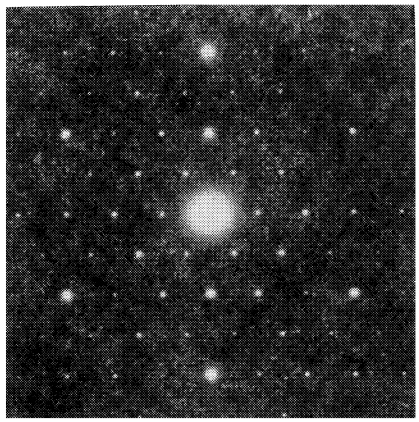

Fig. 4. Electron diffraction pattern of tohdite(F).

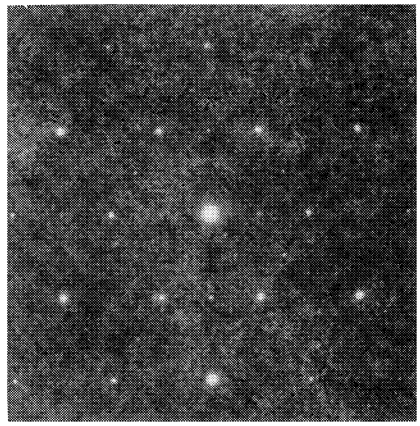

Fig. 5. Electron diffraction pattern of κ'-Al_2O_3 (from tohdite(F)).

Fig. 6. Electron diffraction pattern of κ-Al_2O_3 (from tohdite(F)).

The pattern of κ'-Al_2O_3 (from tohdite(F)) resembles that of tohdite, though the intensity distribution is different. Therefore, the reflections of this pattern are indexed on the basis of the unit cell of tohdite.

(c) The electron-diffraction patterns of needle-like crystals evaporated with aluminium metal were also obtained (Figs. 7—10). These patterns represent $(h, k, \overline{h+k}, l)$ reflections of the materials, where h and k are integers which should be determined from the

4) G. W. Brindley and J. O. Choe, *Amer. Mineral*, **46**, 771 (1961).

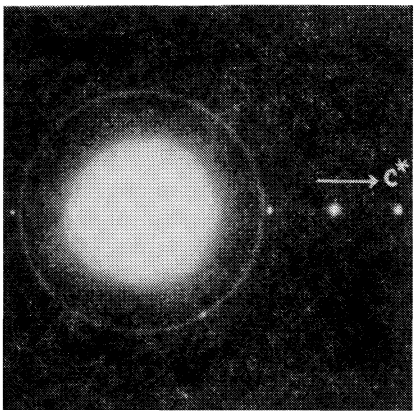

Fig. 7. The electron diffraction pattern of needle like crystal tohdite(Ti). (The electron beam $\perp$ c-axis.)
The strongest ring is that of the 111 reflection of aluminium metal (d=2.338 Å).

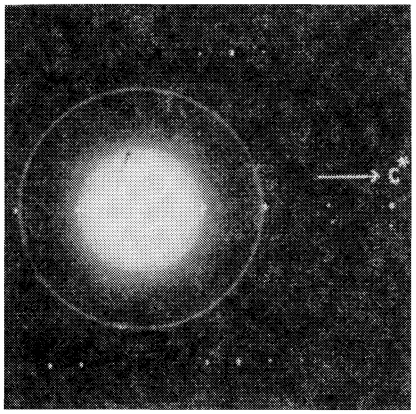

Fig. 8. The electron diffraction pattern of needle like crystal κ'-Al_2O_3 (from tohdite(Ti)).

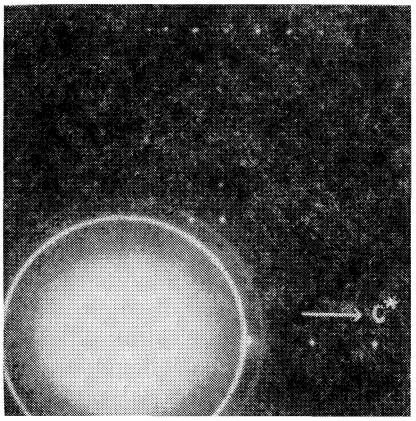

Fig. 9. The electron diffraction pattern of needle like crystal κ-Al_2O_3 (from tohdite(Ti)).

atomic netplane parallel to the electron beam. Whatever value h and k may have, a row of (000l) reflection spots can be found in the pattern. The interval between the (000l) spots of tohdite was calculated as 4.4 Å from the pattern. This agrees with the values of $c/2$=4.38 Å calculated from the X-ray data; the spots are indexed as (0002), (0004), *etc.* This indexing can also be expected from the crystal structure of tohdite,

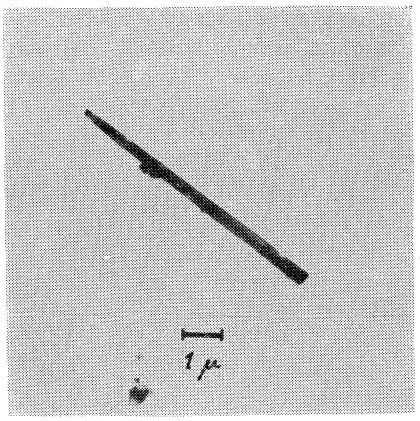

(a)

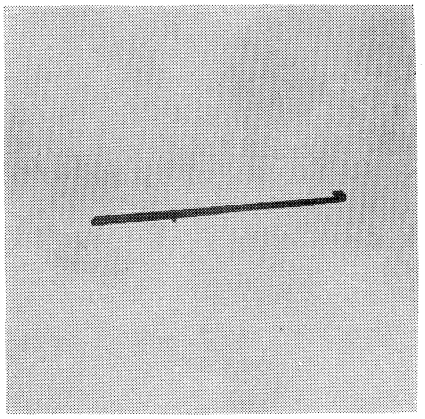

(b)

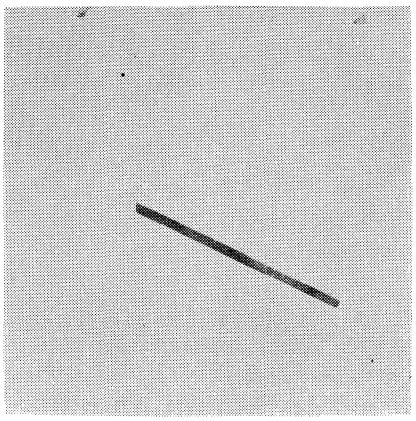

(c)

Fig. 10. Needle like crystal. (a) tohdite(Ti), (b) κ'-Al_2O_3 and (c) κ-Al_2O_3 (from tohdite(Ti)).

which was determined from the X-ray powder data.[5,6] However, in some patterns of tohdite(Ti), the (000l) l=odd reflections were observed to have a very weak intensity, indicating a small deviation from the ideal structure of tohdite ($P6_3mc$). This deviation may be caused by the impurity titanium atoms contained in tohdite(Ti) (about 3%).

5) G. Yamaguchi, H. Yanagida, and S. Ono, *ibid.*, **37**, 752 (1964).
6) G. Yamaguchi, M. Okumiya, and S. Ono, *ibid.*, **42**, 2247 (1969).

By comparing the pattern of κ-Al_2O_3 (from tohdite (Ti)) with the pattern of tohdite(Ti), the following results are obtained. The row of (000l) spots is of the same type as that of tohdite(Ti), and the interval between the spots is 4.5 Å. From this value, the c-axis of κ-Al_2O_3 (from tohdite(Ti)) is calculated as 9.0 Å. In some patterns of κ-Al_2O_3 (from tohdite (Ti)), very weak (000l) l=odd reflections were also observed as in the case of tohdite(Ti), but no evidence was found that the c-axis of κ-Al_2O_3 (from tohdite (Ti)) was twice as large as that of tohdite(Ti).

The pattern of κ'-Al_2O_3 (from tohdite(Ti)) resembles that of κ-Al_2O_3 (from tohdite(Ti)). The cell dimension of c=9.0 Å which was calculated from the electron-diffraction patterns agrees with that of c= 9.015 Å calculated from the X-ray powder diffraction data.

Density Measurements. It is difficult to obtain the absolute value of the density of the fine-grained materials with a high accuracy. In the present work, it is important to compare the density of the dehydration products with that of the starting tohdite. For this purpose, the specimen series (b) was used, because the specimens of this series were easily obtained in a large amounts as a single phase. The average values of five measurements and their standard deviation are shown in Table 2. The measured valued of the density are as follows:

tohdite(F)<κ'-, κ-Al_2O_3 (from tohdite(F))<α-Al_2O_3

Table 2. Density of tohdite, κ'-, and κ-Al_2O_3 (from tohdite)

	Measured density with their standard deviations	Calculated density[a)]
Tohdite(F)	3.63 (0.006)	3.72
κ'-Al_2O_3 (from tohdite(F))	3.68 (0.002)	3.76
κ-Al_2O_3 (from tohdite(F))	3.67 (0.008)	3.77
α-Al_2O_3 (from tohdite(F))	3.96 (0.008)	4.00

a) These value are calculated from unit cell dimensions listed in Table 1 and formula unit per unit cell. The formula units are assumed as follows.
tohdite(F): $5Al_2O_3 \cdot H_2O$
κ'-Al_2O_3 (from tohdite(F)): $5\frac{1}{3}Al_2O_3$
κ-Al_2O_3 (from tohdite(F)): $16Al_2O_3$

Discussion

Krischner concluded, on the basis of their experimental results on electron diffraction, that the basic lattice of oxygen atoms is preserved during the transformation from tohdite to κ-Al_2O_3 (from tohdite), while the cations move to make the symmetry of κ-Al_2O_3 (from tohdite). However, their conclusion for the crystal structure of κ-Al_2O_3 (from tohdite) was that 30 formulas Al_2O_3 exist in a hexagonal unit cell with the cell dimensions of a=9.71 Å, and c=17.86 Å. This indicates a non-close-packed oxygen arrangement. He said that the measured density of 3.5 g/cm^3 agrees well with the value calculated from this unit cell and 30 formulas Al_2O_3. However the experimental results of the present work show that the measured density of κ-Al_2O_3 (from tohdite) (the value for κ-Al_2O_3 (from tohdite(F)), 3.67 g/cm^3), which has a close-packed oxygen arrangement in the crystal structure. Therefore, the present authors consider that the oxygen arrangement of κ-Al_2O_3 (from tohdite) is a close-packed one, as is that of κ'-Al_2O_3 (from tohdite) (the measured density for κ'-Al_2O_3 (from tohdite(F)) is 3.68 g/cm^3).

However, his experimental results on electron diffraction seem important in support the idea of the preservation of the oxygen lattice. This was confirmed by various methods in the present work. We will now consider the mechanism of the transformation and the crystal structure of the dehydration products on the basis of this idea.

Just after the 100% water loss, aluminium atoms are distributed at random in octahedral and tetrahedral positions between the oxygen layers, which are unchanged during the transformation. This atomic arrangement may give the X-ray and electron diffraction pattern of κ'-Al_2O_3 (from tohdite). The impurity atoms which are considered to distributed at random in the crystal structure of the starting tohdite stabilize the κ'-phase. As κ'-Al_2O_3 is an unstable intermediate phase, the κ'-Al_2O_3 (from tohdite) obtained by quenching has a "freezed" crystal structure.

The experimental results can be explained well by this consideration. Therefore, it is proper to employ a unit cell with cell dimensions of a=5.544 Å, and c= 9.024 Å, and which contains a non-integer unit formula of 5⅓ Al_2O_3 and an ABAC stacking sequence of oxygen layers for κ'-Al_2O_3 (from tohdite).

The electron-diffraction pattern of the material identified as "Bild 7" in the Krischner paper is very similar to that of κ'-Al_2O_3 (from tohdite) (Fig. 6). The cell dimensions calculated from "Bild 7" have been reported to include a=from 5.56 to 5.54 Å. This value agrees well with the cell dimension of κ'-Al_2O_3 (from tohdite), a=5.54 Å, calculated from the X-ray powder diffraction data. Therefore, the material, "Bild 7", which was obtained by heating tohdite quickly by an electron beam in an electron microscope may correspond to κ'-Al_2O_3 (from tohdite).

At higher temperatures aluminium atoms are allowed to move more freely and are distributed in a symmetry which gives the X-ray and electron-diffraction patterns of κ-Al_2O_3 (from tohdite). Though the oxygen position may deviate from the ideal position of tohdite, it is proper to assume that the oxygen arrangement of κ-Al_2O_3 (from tohdite) is an ABAC-type closed packing and that the unit cell dimensions are a=9.60 Å, and c=9.02 Å.

Over a temperature of 1000°C, a large-scale oxygen rearrangement takes place and the ABAC stacking sequence changes into the ABAB of α-Al_2O_3. The sharp exothermic peak for the specimen series (b) (Fig. 2) can be explained as follows. Since tohdite (F) is obtained by hydrothermal treatment with aluminium fluoride as a miniralizer, it is expected that this specimen will contain fluorine ions as impurities in

the crystal of tohdite. Furthermore, it can be assumed that fluorine ions, the ion radius of which is comparable to that of oxygen, exist in the oxygen sub-lattice of tohdite and remain in the oxygen sub-lattice of κ-Al_2O_3 (from tohdite(F)). The transformation reaction to α-Al_2O_3, which takes place through the rearrangement of oxygen stacking, is accelerated by the dissociation of the impurity fluourine ions from the oxygen sub-lattice, causing a sharp exotherm (Fig. 2). The dissociation of fluourine ions, which was observed as a slight weight loss (about 0.3%) in the thermogravimetric measurements (Fig. 2), was confirmed by the following analysis. The fluorine gas dissociated from the crystal was captured by a wet nitrogen flow which was introduced into a NaOH aqueous solution, and the photometric determination was performed with an alizarin complexon.

Conclusions

(1) The transformation series:

tohdite $\rightarrow$ κ'-Al_2O_3 (from tohdite)
$\rightarrow$ κ-Al_2O_3 (from tohdite) $\rightarrow$ α-Al_2O_3

was confirmed.

(2) Density measurements and electron-diffraction and X-ray diffraction experiments showed that the oxygen arrangements of both κ'- and κ-Al_2O_3 (from tohdite) are close-packed ones, with the oxygen sub-lattice kept unchanged. No evidence was found that the c-axis was twice as large as that of tohdite, in spite of Krischner's assumption. Therefore, it is proper to assume that the stacking sequence of oxygen layers is ABAC and a close-packed one.

(3) For κ'-Al_2O_3 (from tohdite), the hexagonal unit cell containing $5\frac{1}{3}$ Al_2O_3 non-integer unit formulas was employed. The cell dimensions were $a=5.544$ Å, and $c=9.015$ Å. The unit cell of κ-Al_2O_3 (from thodite) is hexagonal, with cell dimensions of $a=9.599$ Å, and $c=9.024$ Å.

On the basis of this conclusion, a crystal structure analysis of κ'- and κ-Al_2O_3 (from tohdite) is now being perfomed. The results will be published later.

BULLETIN OF THE CHEMICAL SOCIETY OF JAPAN, VOL. 44, 423—426 (1971)

The Effect of Consecutive Complex Formation on the Separation of Rare Earths by Electromigration

Emiko Ohyoshi

Department of Chemistry, Faculty of Science, Kumamoto University, Kurokami-machi, Kumamoto

(Received August 24, 1970)

The effect of a complexing agent with which rare earths consecutively form complexes on the separation of an adjacent pair of rare earths by electromigration was investigated. By assuming the complexes ML and ML_2 to be formed, the relation of the separation factor, the difference in the zone mobility of the two rare earths, to the ligand-ion concentration was derived and examined for the separation of the La-Ce and Ce-Pr pairs by using nitrilotriacetic acid (NTA), which is known to form the ML and ML_2 complexes with rare earths. It is found that the separation factor is affected not only by the difference in the first (k_1) or the second (k_2) consecutive formation constant of the two elements to be separated, but also by the value of the k_1/k_2 ratio.

In a previous paper,[1] it was reported that the separation of an adjacent pair of rare earths by using a complexing agent in electromigration is considerably influenced by the ligand-ion concentration and that when only one complex, ML, is assumed to be formed, the optimum ligand-ion concentration for their separation can be predicted from the values of the formation constants of the complexes. It was also suggested that, in the case where the consecutive formation of complexes, ML, ML_2,$\cdots$, ML_n, takes place, the range of ligand concentrations suitable for separation becomes wider compared with the case where only one complex is formed. However, the previous work was not extended beyond qualitative discussions. It appears to require further investigation for verification.

This paper will deal with the effect of a complexing agent with which rare earths consecutively form complexes on the separation of an adjacent pair of rare earths by electromigration. When two complexes, ML and ML_2, are assumed to be formed, the relation of the separation factor to the ligand-ion concentration has been derived and examined for the separation of the La-Ce and Ce-Pr pairs by using nitrilotriacetic acid (NTA), which is known to form the ML and ML_2 complexes with rare earths.

The Separation Factor for Two Kinds of Rare Earths. When the ML and ML_2 complexes are consecutively formed, the equilibria in solution can be expressed as follows:

$$M + L = ML \quad (1)$$

$$ML + L = ML_2 \quad (2)$$

where the charges are omitted for the sake of simplicity. The equilibrium constant of each process, *i.e.*, the first (k_1) and second (k_2) consecutive formation constants, are given by $k_1=[ML]/([M][L])$ and $k_2=[ML_2]/([ML][L])$. When the two species, M and ML, are equilibrated, the equation expressing the zone

1) E. Ohyoshi, This Bulletin, **43**, 1387 (1970).

mobility has previously been derived.[1,2] From a similar point of view, the following equations can be given for the system of the above equilibria, the attainment of which is rapid:

$$u([M] + [ML] + [ML_2]) = u_M[M] + u_{ML}[ML] + u_{ML_2}[ML_2] \quad (3)$$

$$u = \frac{u_M + u_{ML}k_1[L] + u_{ML_2}k_1k_2[L]^2}{1 + k_1[L] + k_1k_2[L]^2} \quad (4)$$

where u, u_M, u_{ML}, and u_{ML_2} are the mobilities of the zone, M, ML, and ML_2 respectively.

Since the charge of the complex tends to become more and more negative with the progress of the consecutive complex formation, the difference in the zone mobility of the two elements should be taken as the separation factor, S:

$$\begin{aligned} S &= u - u' \\ &= \{(u_M - u_{ML})(k_1' - k_1)(L) \\ &\quad + (u_M - u_{ML_2})(k_1'k_2' - k_1k_2)[L]^2 \\ &\quad + (u_{ML} - u_{ML_2})k_1k_1'(k_2' - k_2)[L]^3\}/ \\ &\quad \{(1 + k_1[L] + k_1k_1[L]^2)(1 + k_1'[L] + k_1'k_2'[L]^2)\} \end{aligned} \quad (5)$$

where it is assumed that $u_M = u'_M$, $u_{ML} = u_{ML}$, and $u_{ML_2} = u'_{ML_2}$. Equation (5) suggests that the greater the difference in the mobility of M, ML, and ML_2, or the greater the difference in the first or the second consecutive formation constants of the two elements, the larger the value of S.

When the values of k_1 and k_1' are much larger than those of k_2 and k_2', Eq. (5) can be simplified to Eq. (6) or (7) in a range of either low or high ligand concentrations.

$$S_{(1)} = \frac{(u_M - u_{ML})(k_1' - k_1)[L]}{(1 + k_1[L])(1 + k_1'[L])} \quad (6)$$

$$S_{(h)} = \frac{(u_{ML} - u_{ML_2})(k_2' - k_2)[L]}{(1 + k_2[L])(1 + k_2'[L])} \quad (7)$$

Equations (6) and (7) exhibit only two species, either M and ML or ML and ML_2, present in the respective range. As was shown by the relation of S to [L] expressed by Eq. (6) presented in the previous paper,[1] $S_{(1)}$ has its maximum at:

$$[L] = \{1/(k_1k_1')\}^{1/2} \quad (8)$$

An expression of Eq. (7) similar to that of Eq. (6) indicates that if $k_2' > k_2$, $S_{(h)}$ also has its maximum at:

$$[L] = \{1/(k_2k_2')\}^{1/2} \quad (9)$$

where $dS_{(h)}/d[L] = 0$. Hence, when $k_1 \gg k_2$ and $k_1' \gg k_2'$, S takes two maxima in a range of low or high ligand concentrations.

Experimental

The sample solution was prepared as has been described previously.[1] The concentration of La^{3+}, Ce^{3+}, or Pr^{3+} was 3×10^{-4} M. The electrolyte solutions were prepared as follows. Nitrilotriacetic acid (Dotite NTA), plus a small amount of NaOH, was dissolved in solutions of different pH's (1.86—4.80) to give concentrations from 10^{-3} to 10^{-2} M. Mixtures of 0.05 M HCl and 0.05 M NaCl (pH<2.1), biphthalate buffer solutions (pH 2.2—3.0), and acetate buffer solutions (3.5—4.8) were used to prepare solutions of various concentrations of the nitrilotriacetate ion, $[L^{3-}]$ ranging from 10^{-12} to 10^{-8} M. Considering the dissociation of NTA, the ionic strength of the solutions was finally adjusted so as to maintain them at 0.05. The chemicals used were of a G. R. grade.

The procedure for paper electromigration was essentially the same as that described previously.[1] In this experiment, the sample was spotted at the center of the paper strip, since the zone may migrate toward either the cathode or the anode, depending on the degree of complex formation. The migrating zone was detected by studying the color reaction with Arsenazo III.

Results and Discussion

The Concentration of NTA. For the rapid attainment on the paper strip of the equilibria expressed by Eqs. (1) and (2), an amount of a complexing agent sufficient to enable us to neglect the amount bound to the metal must be used. By using solutions of the same concentration of the ligand ion, obtained by adjusting the pH, the zone mobility was measured as a function of the total NTA concentration. From the results it was found that, at concentrations above 2.5×10^{-3} M, the mobility was almost constant, but it was lowered at 1.25×10^{-3} M. Hence, NTA concentrations ranging from 2.5×10^{-3} to 1.0×10^{-2} M were used.

Determination of u_M, u_{ML}, and u_{ML_2}. Since there is an appreciable difference between the first and the second consecutive formation constants of rare earth-NTA complexes (the value of k_1/k_2 is of the order of 10^3), Eqs. (6) and (7) can be applied in the ranges of both low and high ligand concentrations. The rearrangement of Eqs. (6) and (7) leads to these expressions:

$$u = \frac{1}{k_1[L] + 1}(u_M - u_{ML}) + u_{ML} \quad (6')$$

$$u = \frac{1}{k_2[L] + 1}(u_{ML} - u_{ML_2}) + u_{ML_2} \quad (7')$$

Hence, by plotting u *vs.* $1/(k_1[L]+1)$ or $1/(k_2[L]+1)$, the values of u_M, u_{ML}, and u_{ML_2} can be obtained from the intercept and slope. The plots of u *vs.* $1/(k_1[L^{3-}]+1)$ and $1/(k_2[L^{3-}]+1)$ for lanthanum, cerium, and praseodymium are shown in Figs. 1 and 2, where k_1 and k_2[3] are the first and second consecutive formation constants of the La(III)-, Ce(III)-, and Pr(III)-NTA complexes. The concentration of L^{3-} is calculated by dividing the total concentration of NTA by the α coefficient,[4] which is a function of the pH. The linear relationship obtained in both Figs. 1 and 2, proves that Eqs. (6) and (7) can be applied to these ranges of $[L^{3-}]$. From the intercept and slope of the lines, the values of u_M, u_{ML}, and u_{ML_2} are given as 0.014, 0, and -0.011 cm²/V min respectively. The value of 0 given for u_{ML} is consistent with the fact that the ML

2) V. P. Shvedov and A. V. Stepanov, *Radiokhimiya*, **1**, No. 2, 62 (1959).

3) T. Moeller, and R. Ferris, *Inorg. Chem.*, **1**, 49 (1962).

4) A. Ringbom, "Complexation in Analytical Chemistry," Translated ed. by N. Tanaka and H. Sugi, Sangyo Tosho Pub. Co., Ltd., Tokyo (1965), p. 35.

complex is a neutral species.

Effect of the Ligand-ion Concentration on the Separation Factor. To verify Eq. (5), the separation of the La-Ce and the Ce-Pr pairs was carried out at various concentrations of the nitrilotriacetate ion, L^{3-}. In Fig. 3, the separation factor, S, the difference in the zone mobilities of lanthanum and cerium or of cerium and praseodymium observed (points) and calculated from Eq. (5) (the solid or dotted line) is given as a function of $[L^{3-}]$. From the fact that the points obtained experimentally are observed to be close to the lines, Eq. (5) is found to be verified. As has been described above, when $k_1 \gg k_2$ as in this case, the plots of S *vs.* $[L^{3-}]$ for both the La-Ce and the Ce-Pr pairs yield curved with two maxima at $[L^{3-}]=2.51\times10^{-11}$ and 2.72×10^{-8} M for the La-Ce pair, and at $[L^{3-}]=1.12\times10^{-11}$ and 8.92×10^{-9} M for the Ce-Pr pair, as calculated by Eqs. (8) and (9) (Fig. 3). These curves show that S varies with the degree of complex formation, that is, as M forms ML, S reaches the first peak and then decreases with a subsequent increase in the fraction of ML; after passing through the minimum where almost all of the metal exists in the form of ML, S again increases with the formation of ML_2, reaches a second peak, and then decreases with the completion of the formation of ML_2.

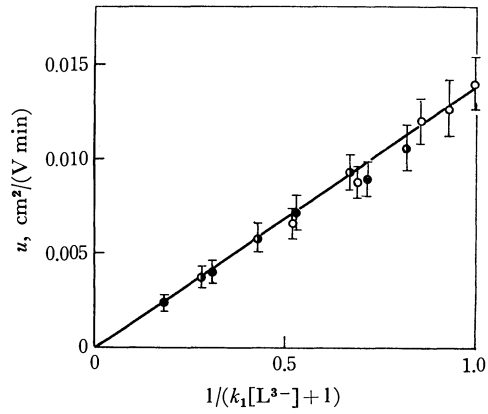

Fig. 1. A plot of u *vs.* $1/(k_1[L^{3-}]+1)$ for La ○, Ce ◑, and Pr ●.
L^{3-}=nitrilotriacetate ion

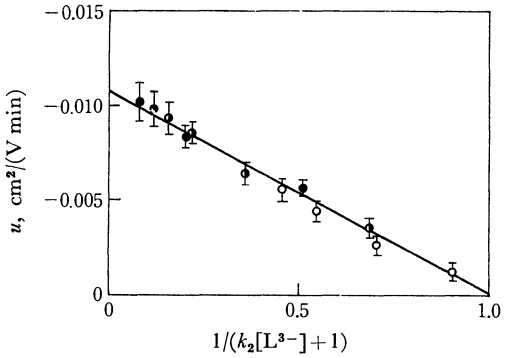

Fig. 2. A plot of u *vs.* $1/(k_2[L^{3-}]+1)$ for La ○, Ce ◑, and Pr ●.
L^{3-}=nitrilotriacetate ion

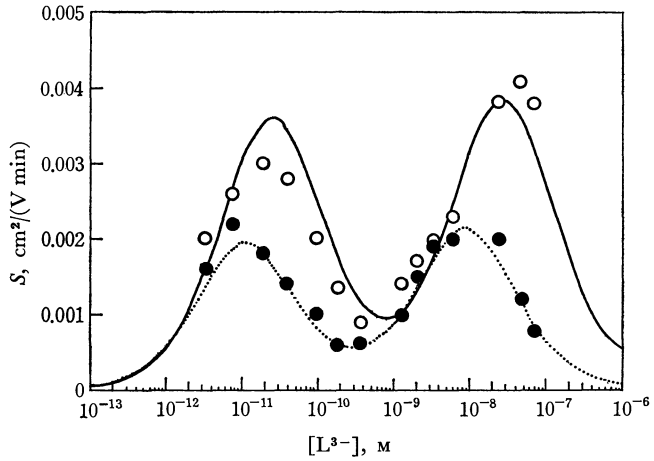

Fig. 3. Plots of S *vs.* $[L^{3-}]$, L^{3-}=nitrilotriacetate ion.
Observed values for the La-Ce pair ○ and the Ce-Pr pair ●; Theoretical curves given by Eq. (5) for the La-Ce pair — and Ce-Pr pair ·····.

In seeking for the effect of the consecutive formation of complexes on the separation factor, we attempt to plot S *vs.* [L], assuming various conditions, in Fig. 4. Curve 1 is a plot of the relation given by Eq. (5) by assuming that $u_{ML}/u_M=0.2$, $u_{ML_2}/u_M=-0.5$, $k_1=10^3$, $k_1'=2k_1$, $k_2=10$, and $k_2'=1.5\,k_2$. Curves 2 and 3 plot the relations given by the simplified equations (6) and (7) by using the values assumed in curve 1. When we compare these curves, we find that in the range on the lower side of $[L]=\{1/(k_1k_1')\}^{1/2}$ and the higher side of $[L]=\{1/(k_2k_2')\}^{1/2}$ curve 1 agrees well with curves 2 and 3, indicating that only two species, M and ML or ML and ML_2 are present in such ranges. It is noted that, in the range between two maxima where three species M, ML, and ML_2, are coexisting, curve 1 always gives a higher value than those given by curves 2 and 3. This clearly indicates that the formation of both ML and ML_2 serves to enhance the separation factor. To make the three species, M, ML, and ML_2, all present, the value of k_1 must be close to that of k_2. Under the condition assumed in curve 1, if only the k_1/k_2 ratio is varied from 10^2 to 10, the plot

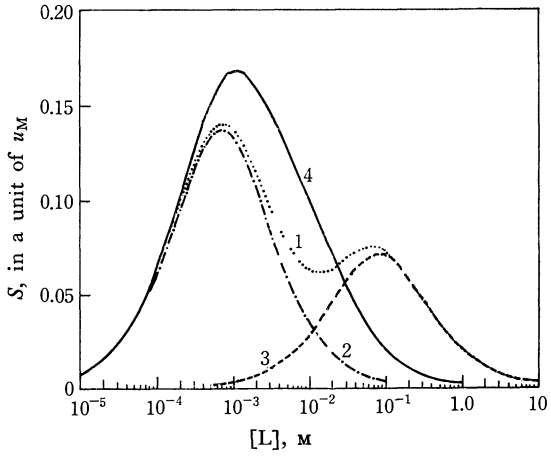

Fig. 4. Effect of the consecutive complex formation on the separation factor.
Curve 1, 4: Plots of S (in a unit of u_M) *vs.* [L] given by Eq. (5) assumed to be $u_{ML}/u_M=0.2$, $u_{ML_2}/u_M=-0.5$, $k_1=10^3$, $k_1'=2\,k_1$, $k_2'=1.5\,k_2$, and $k_2=10$ for curve 1 or $k_2=10^2$ for curve 4. Curve 2,3: A plot of $S_{(l)}$ (curve 2) or $S_{(h)}$ (curve 3) *vs.* [L] by using the same values as those in curve 1.

gives curve 4. When we compare curve 1 with curve 4, we find that even when the same difference in the k_1 or k_2 value of two elements is given, the S value is appreciably affected by the ratio of k_1 to k_2. With a reduction in the k_1/k_2 ratio, the two maxima become one, the value of which is considerably enhanced. This suggests that, when the further formation of ML_3, ML_4, $\cdots$, ML_n occurs and when their consecutive formation constants are not very different from each other, the high separation factor may be maintained over a wide range of ligand concentrations.

The above discussion was based on the assumption that $k_1' > k_1$, $k_2' > k_2, \cdots$, $k_n' > k_n$. Hence, when $k_1' > k_1$, $k_2' \simeq k_2, \cdots$, $k_n' \simeq k_n$, we can obtain only the same results as those in the cases when only one complex, ML, is formed.

BULLETIN OF THE CHEMICAL SOCIETY OF JAPAN, VOL. 44, 426—431 (1971)

Circular Dichroism of Mixed Biguanide Ethylenediamine Cobalt(III) Complexes

Kozo Igi, Takaji Yasui,* Jinsai Hidaka, and Yoichi Shimura
Department of Chemistry, Faculty of Science, Osaka University, Toyonaka, Osaka

(Received September 7, 1970)

Two kinds of mixed biguanide ethylenediamine complexes, $[Co(bgH)_2(en)]Cl_3 \cdot 3H_2O$ and $[Co(bgH)(en)_2]Cl_3 \cdot 2H_2O$, have been resolved into their optically active isomers. The circular dichroism spectra of a complete series of the mixed complexes, $(-)_{589}$-$[Co(bgH)_3]^{3+}$, $(+)_{589}$-$[Co(bgH)_2(en)]^{3+}$, $(+)_{589}$-$[Co(bgH)(en)_2]^{3+}$, and $(+)_{589}$-$[Co(en)_3]^{3+}$, have been investigated in neutral and alkaline aqueous solutions. In alkaline solutions, the circular dichroism and absorption curves of the biguanide complexes shift to longer wavelengths than those in neutral solutions; this may be caused by the change of the coordinated biguanide (bgH) to the uninegative ligand (bg^-) by deprotonation. A mixed guanylurea complex, $[Co(guH)(en)_2]Cl_3 \cdot 2H_2O$, has been newly prepared and optically resolved.

Biguanide, $NH\{C(NH_2)NH\}_2$=bgH,[1] combines with many kinds of transition metal salts to give a variety of coordination compounds with six-membered chelate rings,[2–4] of which cobalt(III) and chromium(III) complexes have recently been noted in terms of the circular dichroism (CD) spectra and absolute configuration.[5,6] Michelsen,[5] for example, suggested that $(-)_{589}$-$[Co(bgH)_3]^{3+}$ and $(-)_{589}$-$[Cr(bgH)_3]^{3+}$ have an absolute configuration Λ,[7] comparing the CD behavior of the complexes in the so-called first absorption band region with that of $\Lambda(+)_{589}$-$[Co(en)_3]^{3+}$, whose absolute configuration was unequivocally determined by an X-ray technique.[8] Recently, Brubaker and Webb[6] determined the absolute configuration of the $(-)_{589}$-$[Cr(bgH)_3]^{3+}$ to be Λ on the basis of X-ray analysis of the *d*-10-camphorsulfonate and suggested that the $(-)_{589}$-$[Co(bgH)_3]^{3+}$ should have Δ configuration, from the comparison of the ultraviolet CD spectra of the cobalt(III) and chromium(III) complexes. Thus, the conclusions from the CD of *d–d* absorption band region and of ultraviolet ligand absorption band region completely contradict each other for the tris-biguanide complex of cobalt(III).

In these circumstances, it is thought to be desirable to study more systematically the CD spectra of mixed complexes of ethylenediamine and biguanide, namely, $[Co(bgH)_3]^{3+}$, $[Co(bgH)_2(en)]^{3+}$, $[Co(bgH)(en)_2]^{3+}$, and $[Co(en)_3]^{3+}$. In the present paper, preparations and optical resolutions of such complexes and their absorption and CD spectra are reported. In the course of this study, a new guanylurea cobalt(III) complex, $[Co(guH)(en)_2]^{3+}$, happened to be obtained, where guH stands for a guanylurea molecule $NH(NH_2)CNHCO(NH_2)$.

Experimental

Preparation and Optical Resolution. *$[Co(bg)_3] \cdot 2H_2O$ and $[Co(bgH)_3]Cl_3$*: These complexes were prepared by the method of Ray and Dutt.[9]

Found: C, 18.82; H, 5.76; N, 54.08%. Calcd for $C_6H_{18}N_{15}Co \cdot 2H_2O = [Co(bg)_3] \cdot 2H_2O$: C, 18.23; H, 5.62; N, 53.15%.

Found: C, 15.95; H, 4.70; N, 44.97%. Calcd for $C_6H_{21}N_{15}Cl_3Co = [Co(bgH)_3]Cl_3$: C, 15.37; H, 4.53; N, 44.84%.

$(-)_{589}$-$[Co(bgH)_3]Cl_3$: The optical resolution was carried out by the method of Ray and Dutt.[10] $[\alpha]_{589}^{13} = -450°$, $[M]_{589}^{13} = -2110°$.

$[Co(bgH)_2(en)]Cl_3 \cdot 3H_2O$: The chloride was obtained

* Present address: Faculty of Literature and Science, Kochi University, Asakura, Kochi.

1) The abbreviations, bgH and bg, represent a biguanide molecule and a deprotonated biguanide (uninegative ion), respectively.

2) P. Ray, *Chem. Rev.*, **61**, 313 (1961).

3) D. Sen, *J. Chem. Soc.*, *A*, **1969**, 2900.

4) R. L. Dutta, *J. Indian Chem. Soc.*, **44**, 863 (1967).

5) K. Michelsen, *Acta Chem. Scand.*, **19**, 1175 (1965).

6) G. R. Brubaker and L. E. Webb, *J. Amer. Chem. Soc.*, **91**, 7199 (1969).

7) The symbols Δ and Λ are used for absolute configurations of the tris or bis chelate type metal complexes, according to a tentative proposal by the Commission on the Nomenclature of Inorganic Chemistry of the IUPAC: *Inorg. Chem.*, **9**, 1 (1970).

8) Y. Saito, *Pure Appl. Chem.*, **17**, 21 (1968).

9) P. Ray and N. K. Dutt, *J. Indian Chem. Soc.*, **16**, 621 (1939).

10) P. Ray and N. K. Dutt, *ibid.*, **18**, 289 (1941).

by converting the known sulfate[11] with barium chloride. This complex was also prepared by the reaction of K[Co-$(CO_3)_2$(en)][12] and biguanide sulfate monohydrate. The complex is very soluble in water.

Found: C, 15.11; H, 5.97; N, 34.61%. Calcd for $C_6H_{22}N_{12}Cl_3Co\cdot 3H_2O$=[Co(bgH)$_2$(en)]$Cl_3\cdot 3H_2O$: C, 14.96; H, 5.87; N, 34.90%.

(−)$_{589}$- and (+)$_{589}$-[Co(bgH)$_2$(en)]$Cl_3\cdot H_2O$: To a solution containing 4.3 g of (±)-[Co(bgH)$_2$(en)]$Cl_3\cdot 3H_2O$ in 20 m*l* of hot water (70°C) was added with stirring a solution of 5.0 g of potassium di-μ-L-tartrato(4-)diantimonate-(III) trihydrate, $K_2[Sb_2(d\text{-}C_4H_2O_6)_2]\cdot 3H_2O$, in 30 m*l* of hot water (70°C). After the solution had been kept at room temperature for about an hour, the diastereomer deposited was filtered (the filtrate was used for the isolation of (+)$_{589}$ isomer) and washed with ice-water, ethanol and then ether. The diastereomer which was obtained in yellow crystals was recrystallized from hot water. $[\alpha]_{589}^{20}=+100°$.

To a suspension of 2.0 g of the diastereomer in 20 m*l* of water was added 3.5 g of powdered barium chloride dihydrate with vigorous stirring, and then 100 m*l* of ethanol was added to the resulted solution. After the solution had been kept in an ice-bath, the resulted precipitate was filtered off. The filtrate was evaporated to dryness in a vacuum evaporator at room temperature. The orange-colored residue was recrystallized from a small amount of water by adding ethanol-acetone (1 : 1) mixture and then acetone, and dried in air. $[\alpha]_{589}^{20}=-93°$, $[M]_{589}^{20}=-415°$.

(+)$_{589}$-[Co(bgH)$_2$(en)]$Cl_3\cdot H_2O$ was obtained from the filtrate described above.

Found: C, 16.33; H, 5.58; N, 37.43%. Calcd for $C_6H_{22}N_{12}Cl_3Co\cdot H_2O$=(+)$_{589}$-[Co(bgH)$_2$(en)]$Cl_3\cdot H_2O$: C, 16.17; H, 5.44; N, 37.72%. $[\alpha]_{589}^{20}=+93°$, $[M]_{589}^{20}=+415°$.

[Co(bgH)(en)$_2$]$Cl_3\cdot 2H_2O$: The preparation of this complex was carried out by a modified procedure of Dutta's method.[4] A solution containing 7.6 g of biguanide sulfate monohydrate in 200 m*l* of water was added to 150 m*l* aqueous solution of 11.1 g of barium hydroxide octahydrate. After the resulted barium sulfate had been filtered off, the filtrate was added to a solution containing 10 g of *trans*-[Co(Cl)$_2$-(en)$_2$]Cl in 100 m*l* of water. The solution was heated on a water bath for 8 hr at 55°C. The color of the solution changed from purple to orange red. When the solution was concentrated to about 80 m*l* with a vacuum evaporator at 33°C, the orange crystals, [Co(bgH)$_3$]Cl_3, began to appear. After the solution was kept in an ice-bath for about an hour, the crystals were removed by filtration. The filtrate was concentrated to 25 m*l* in a vacuum evaporator and allowed to stand at room temperature for several days. The crude orange red complex was filtered and washed with ethanol and then ether. Yield: 5.7 g. The crude product was recrystallized from hot water by adding ethanol-acetone (1 : 1) mixture.

Found: C, 17.01; H, 6.73; N, 29.89%. Calcd for $C_6H_{23}N_9Cl_3Co\cdot 2H_2O$=[Co(bgH)(en)$_2$]$Cl_3\cdot 2H_2O$: C, 17.05; H, 6.45; N, 29.83%.

(−)$_{589}$-[Co(bgH)(en)$_2$]$Cl_3\cdot 3H_2O$: The racemate, (±)-[Co(bgH)(en)$_2$]$Cl_3\cdot 2H_2O$, (2.0 g), was dissolved in 15 m*l* of hot water. To this solution was added a solution containing 2.37 g of potassium di-μ-L-tartrato(4-)diantimonate(III) trihydrate in 25 m*l* of hot water with stirring. The mixed solution was kept at room temperature for a few min to complete the crystallization. The less soluble diastereomer was obtained in light orange powder. $[\alpha]_{589}^{15}=-96°$.

One gram of the diastereomer, 3 g of barium chloride dihydrate and 10 m*l* of water was triturated in a mortar. The white precipitate resulted was filtered off. Fifty milliliters of ethanol was added to the filtrate and the white precipitate was filtered off again. After the filtrate had been concentrated to 4 m*l* in a vacuum evaporator at 28°C, 2 m*l* of ethanol-acetone (1 : 1) mixture was added to it. The white precipitate was filtered off once again. Then the filtrate was concentrated to 3 m*l* in the same way. After 12 m*l* of ethanol-acetone (1 : 1) mixture had been added to the solution, the orange red crystals desired were separated by filtration. Recrystallization of this complex was carried out from 2 m*l* of water by adding ethanol-acetone (1 : 1) mixture. The complex obtained was washed with ethanol and ether.

Found: C, 16.60; H, 6.45; N, 28.81%. Calcd for $C_6H_{23}N_9Cl_3Co\cdot 3H_2O$=(−)$_{589}$-[Co(bgH)(en)$_2$]$Cl_3\cdot 3H_2O$: C, 16.34; H, 6.64; N, 28.61%. $[\alpha]_{589}^{15}=-352°$, $[M]_{589}^{15}=-1551°$.

[Co(guH)(en)$_2$]Br_3 and [Co(guH)(en)$_2$]$Cl_3\cdot 2H_2O$: The suspension of 10 g of [Co(CO_3)(en)$_2$]ClO_4 and 6.5 g of biguanide sulfate monohydrate in 20 m*l* of water was heated on a water bath for about 30 min. To the hot solution was added 15 m*l* of perchloric acid (20%) with constant stirring and the solution was heated on a water bath for 2 hr. After cooling the resulted solution to room temperature, 16 g of powdered sodium bromide was dissolved into it. The orange crystals deposited were collected by filtration, and washed with water-ethanol (1 : 1) mixture, ethanol and then ether. The crude complex was recrystallized from hot water. As described in the Results and Discussion section, it was shown that during the reaction, the biguanide employed was hydrolyzed and changed into a guanylurea.

Found: C, 13.83; H, 4.31; N, 21.48%. Calcd for $C_6H_{22}N_8OBr_3Co$=[Co(guH)(en)$_2$]Br_3: C, 13.83; H, 4.26; N, 21.51%.

This bromide was converted to the chloride by treating it with silver chloride.

Found: C, 17.05; H, 6.38; N, 26.53%. Calcd for $C_6H_{22}N_8OCl_3Co\cdot 2H_2O$=[Co(guH)(en)$_2$]$Cl_3\cdot 2H_2O$: C, 17.01; H, 6.20; N, 26.45%.

(−)$_{589}$-[Co(guH)(en)$_2$]$(HO_3)_3$: Twenty and eight-tenths grams of (±)-[Co(guH)(en)$_2$]Br_3 was dissolved in 40 m*l* of warm water. To this solution was rapidly added a solution containing 20 g of potassium di-μ-L-tartrato(4-)diantimonate(III) trihydrate in 60 m*l* of hot water (70°C) with vigorous stirring. After the solution had been chilled in an ice-bath, the light orange needle crystals deposited were filtered, and washed with cold water, ethanol and then ether. Recrystallization was carried out from hot water. The diastereomer obtained was sparingly soluble in water. $[\alpha]_{589}^{20}=-142°$.

A mixture of the diastereomer (10 g), silver nitrate (10 g) and warm water (30 m*l*) was ground enough in a mortar. The resulted precipitate was filtered off and washed twice with a small amount of water. The combined washings and filtrate was evaporated to dryness with a vacuum evaporator at room temperature. The orange-colored residue was recrystallized from hot water. The orange needle crystals deposited were filtered, and washed with a little amount of ice-water, water-ethanol (1 : 1) mixture, absolute ethanol and then ether, and dried in air.

Found: C, 15.37; H, 4.81; N, 33.19%. Calcd for $C_6H_{22}N_{11}O_{10}Co$=(−)$_{589}$-[Co(guH)(en)$_2$]$(NO_3)_3$: C, 15.42; H, 4.75; N, 32.98%. $[\alpha]_{589}^{20}=-480°$, $[M]_{589}^{20}=-2243°$.

Measurements. The electronic absorption spectra were measured by Shimadzu spectrophotometer QR-50. The CD spectra were recorded with a Roussel-Jouan dichrograph

11) R. L. Dutta and S. Sarkar, *Sci. Cult.* (Calcutta), **30**, 549 (1964).

12) M. Mori, M. Shibata, E. Kyuno, and K. Hoshiyama, This Bulletin, **31**, 291 (1958).

and the optical rotatory dispersions were checked with Yanagimoto Recording spectropolarimeter model-185. The CD measurements were made in aqueous and 0.10 N and 0.25 N NaOH aqueous solutions. In 0.25 N NaOH aqueous solutions, $(+)_{589}$-$[Co(bgH)_2(en)]^{3+}$ and $(-)_{589}$-$[Co(bgH)(en)_2]^{3+}$ were not racemized and the racemization of $(-)_{589}$-$[Co(bgH)_3]^{3+}$ in 0.10 N NaOH aqueous solution was negligible during the CD measurement. The CD curves and data for the $(-)_{589}$-$[Co(bgH)(en)_2]^{3+}$ and $(-)_{589}$-$[Co(guH)(en)_2]^{3+}$ and of their deprotonated species are presented in reverse signs in Results and Discussion Section, Table 2, and Figs. 1—4, for the convenience of comparison with those of the other complexes; therefore the CD curves and data are refered as those for the $(+)_{589}$ isomers.

Results and Discussion

1. The Absorption and CD Spectra of Ethylenediamine-Biguanide Cobalt(III) System. The first absorption bands of the biguanide complexes are shifted to the longer wavelength side and are more intense than that of $[Co(en)_3]^{3+}$ (Fig. 1 and Table 1). In this region, $(+)_{589}$-$[Co(bgH)_2(en)]^{3+}$ and $(-)_{589}$-$[Co(bgH)_3]^{3+}$ in water exhibit two CD bands, one negative and another positive listing from the longer wavelength side, whereas $(+)_{589}$-$[Co(bgH)(en)_2]^{3+}$ shows only a positive CD band which is more intense than the positive E_a CD component of $(+)_{589}$-$[Co(en)_3]^{3+}$ (Table 2). In the second absorption band region, all the biguanide complexes show negative CD bands in contrast to the $(+)_{589}$-tris(ethylenediamine) complex which shows a positive one. In the shorter wavelength region, the absorption spectra of the present complexes are similar to each other on the whole (Fig. 1 and Table 1). In the tris- and bis-biguanide complexes, it seems that the intense absorption bands which locate at the shorter wavelength than 250 mμ are due to π–π^* transitions of the coordinated biguanide ligand; the CD spectra in the corresponding region show two oppositely signed CD bands, and these are very intense only when two or three biguanide ligands coordinate to a cobalt(III)

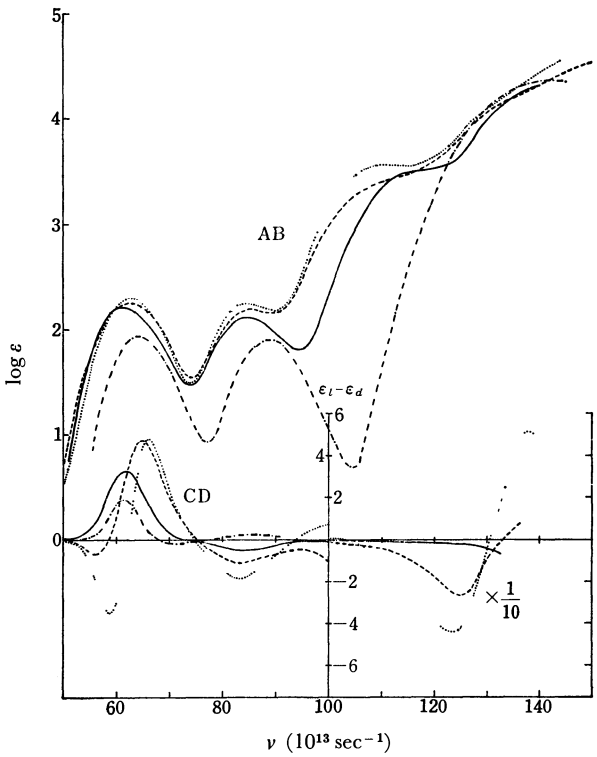

Fig. 1. Absorption (AB) and CD curves of $(-)_{589}$-$[Co(bgH)_3]^{3+}$ (……), $(+)_{589}$-$[Co(bgH)_2(en)]^{3+}$ (----), $(+)_{589}$-$[Co(bgH)(en)_2]^{3+}$ (——), and $(+)_{589}$-$[Co(en)_3]^{3+}$ (—·—·—).

ion (Figs. 2 and 3, and Table 2). Brubaker and Webb suggested that such CD band splitting in this region may be interpreted as the excition splitting, of which a theory has been recently developed mainly by Mason,[13] Bosnich,[14] and others,[15] and that the $(-)_{589}$-$[Co(bgH)_3]^{3+}$ complex which exhibits a negative CD component at lower energy has Δ configuration. This suggestion, however, seems to contradict with a conclusion from the behavior in the *d–d* absorption band region (see later section 3). The absorption bands

Table 1. Absorption data of the complexes in aqueous solutions: ν_{max}[a] (log ε_{max})

Complex	First band	Second band	Charge transfer band
$[Co(bgH)_3]^{3+}$	62.8 (2.30)	84.8 (2.25)	110.0 (3.56)
$[Co(bg)_3]$	62.2 (2.40)	*ca.* 84 (2.38)	*ca.* 102 (3.26)
$[Co(bg)_3]$[b]	62.2 (2.38)	*ca.* 84 (2.31)	*ca.* 103 (3.27)
$[Co(bgH)_2(en)]^{3+}$	62.5 (2.25)	85.7 (2.19)	*ca.* 110 (3.37)
$[Co(bg)_2(en)]^{+}$[b]	62.5 (2.30)	*ca.* 85 (2.40)	*ca.* 102 (3.14)
$[Co(bgH)(en)_2]^{3+}$	61.2 (2.21)	84.5 (2.11)	*ca.* 116 (3.50)
$[Co(bg)(en)_2]^{2+}$[b]	58.8 (2.27)	83.3 (2.25)	*ca.* 103 (3.04)
$[Co(guH)(en)_2]^{3+}$	61.8 (2.21)	*ca.* 78 (1.72)	*ca.* 115 (3.34)
		87.0 (1.93)	
$[Co(gu)(en)_2]^{2+}$[b]	60.8 (2.26)	*ca.* 79 (1.82)	*ca.* 106 (2.98)
		ca. 86 (2.06)	
$[Co(en)_3]^{3+}$	64.0 (1.94)	88.8 (1.90)	

a) In the unit of 10^{13} sec^{-1}.
b) Measured in NaOH aqueous solutions using the corresponding bgH or guH complex.

13) S. F. Mason, *Inorg. Chim. Acta Rev.*, **2**, 89 (1968).
14) B. Bosnich, *Accounts Chem. Res.*, **2**, 266 (1969); *Inorg. Chem.*, **7**, 2379 (1968).
15) J. Ferguson, C. J. Hawkins, N. A. P. Kane-Maguire, and H. Lip, *Inorg. Chem.*, **8**, 771 (1969).

TABLE 2. CD DATA OF THE COMPLEXES IN AQUEOUS SOLUTIONS: ν_{ext}[a] $(\varepsilon_l - \varepsilon_d)$

Complex	First band	Second band	Charge transfer band	Ligand band
$(-)_{589}$-$[Co(bgH)_3]^{3+}$	58.8 (−3.52)	83.3 (−1.84)	100.0 (+0.75)	123.5 (−44)
	66.2 (+4.76)			137.6 (+51)
$(-)_{589}$-$[Co(bg)_3]$[b]	57.4 (−3.11)	82.9 (−3.19)		114.5 (−36)
	64.9 (+8.03)			137.6 (+81)
$(+)_{589}$-$[Co(bgH)_2(en)]^{3+}$	56.2 (−0.70)	83.8 (−1.09)		125 (−26.2)
	64.9 (+4.73)			
$(+)_{589}$-$[Co(bg)_2(en)]^{+}$ [b]	55.3 (−1.66)	84.5 (−2.62)		117.6 (−36)
	64.1 (+7.97)			132.7 (+17.3)
$(+)_{589}$-$[Co(bgH)(en)_2]^{3+}$	61.6 (+3.24)	84.5 (−0.48)		
$(+)_{589}$-$[Co(bg)(en)_2]^{2+}$ [b]	60.7 (+4.18)	82.2 (−1.28)		120.0 (− 6.8)
$(+)_{589}$-$[Co(guH)(en)_2]^{3+}$	*ca.* 59 (+2.0)	*ca.* 78 (−0.16)		
	ca. 65 (+1.6)	85.5 (−0.59)		
$(+)_{589}$-$[Co(gu)(en)_2]^{2+}$ [b]	59.8 (+3.40)	*ca.* 77 (−0.25)		
		84.4 (−0.93)		
$(+)_{589}$-$[Co(en)_3]^{3+}$	61.5 (+1.90)	85.7 (+0.26)		
	70.6 (−0.14)			

a) In the unit of 10^3 sec^{-1}.
b) Measured in NaOH aqueous solutions using the corresponding bgH or guH complex.

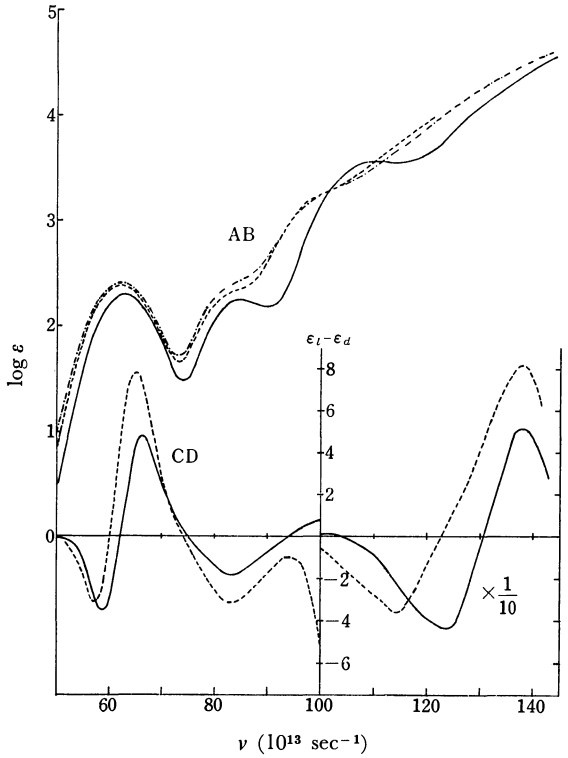

Fig. 2. Absorption (AB) and CD curves of (a) $(-)_{589}$-$[Co(bgH)_3]^{3+}$ and (b) $[Co(bg)_3]$: (a) in water (——), (a) in 0.10 N NaOH aq. soln. (----), and (b) in water (—·—·—).

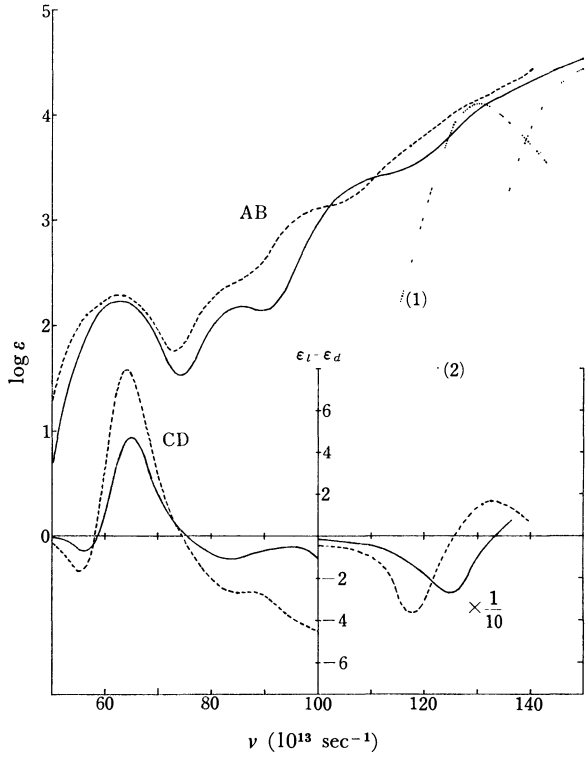

Fig. 3. Absorption (AB) and CD curves of $(+)_{589}$-$[Co(bgH)_2(en)]^{3+}$: in water (——) and in 0.25 N NaOH aq. soln. (----); and AB of biguanide sulfate monohydrate ($bgH \cdot H_2SO_4 \cdot H_2O$): in 0.10 N NaOH aq. soln. (1) (……) and in 0.10 N H_2SO_4 aq. soln. (2) (……).

which locate at about 270 mμ are not so contributed to CD that these bands may be considered to be charge transfer ones (or other kinds of inter ligand absorption bands).

The CD and absorption curves in NaOH aqueous solutions shift to the longer wavelength side on the whole than those in water, especially the bands which locate at the shorter wavelengths shift remarkably as seen in Figs. 2, 3, and 4. A similar red shift was also observed for the absorption curve of the free ligand biguanide (Fig. 3). The absorption curve of $(-)_{589}$-$[Co(bgH)_3]^{3+}$ in NaOH aqueous solution coincides well with that of $[Co(bg)_3]$ in water (Fig. 2). This fact points out that in 0.10 N NaOH aqueous solution, each of the three ligands of $(-)_{589}$-$[Co(bgH)_3]^{3+}$ is deprotonated and consequently $(-)_{589}$-$[Co(bgH)_3]^{3+}$ changes to optically active $[Co(bg)_3]$. It may be suggested that in the

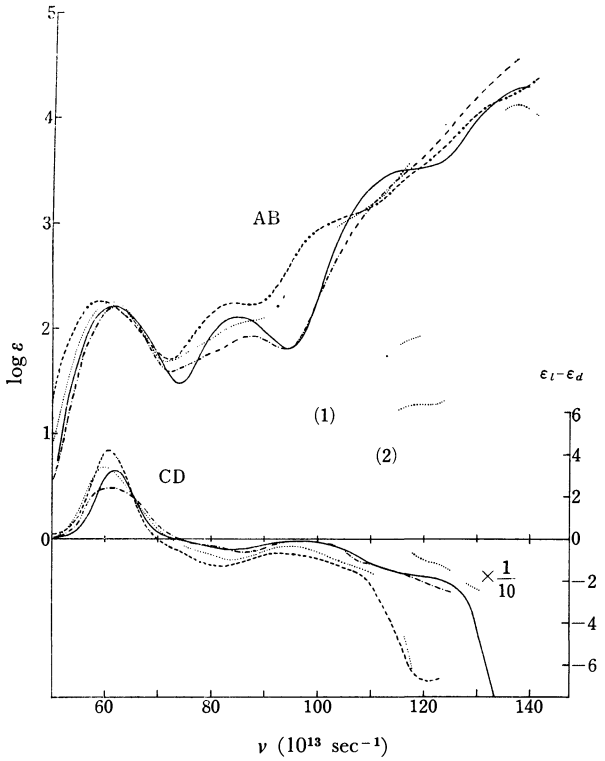

Fig. 4. Absorption (AB) and CD curves of (a) $(+)_{589}$-$[Co(bgH)(en)_2]^{3+}$ and (b) $(+)_{589}$-$[Co(guH)(en)_2]^{3+}$: (a) in water (——), (a) in 0.25 N NaOH aq. soln. (----), (b) in water (—·—·—), and (b) in 0.25 N NaOH aq. soln. (·····); and AB of guanylurea sulfate dihydrate ($(guH)_2\cdot H_2SO_4\cdot 2H_2O$): in 0.10 N NaOH aq. soln. (1) (·····) and in 0.10 N H_2SO_4 aq. soln. (2) (·····).

cases of $(+)_{589}$-$[Co(bgH)(en)_2]^{3+}$ and $(+)_{589}$-$[Co(bgH)_2(en)]^{3+}$ also the corresponding optically active bg^- complexes are formed in the alkaline solutions. Shift or intensification of the CD bands by such deprotonation occurred in the d-d absorption band region and these are also the case of the addition of sodium phosphate or selenite; then it was impossible to use the socalled "ion-paring criterion" proposed by Mason *et al.*,[16] for the component assignment of these biguanide complexes. Thus the assignment proposed by Brubaker and Webb[6] for the CD components of the first absorption band of $(-)_{589}$-$[Cr(bgH)_3]^{3+}$ from this criterion may be meaningless.

2. The Characterization of the Guanylurea Complex. As described in Experimental section, the analytical results suggest that the complex which was derived from $[Co(Cl)_2(en)_2]Cl$ and biguanide is $[Co(bgH)(en)_2]^{3+}$ and that the one from $[Co(CO_3)(en)_2]Cl$ and biguanide sulfate is $[Co(guH)(en)_2]^{3+}$. In the latter case, the biguanide is hydrolyzed into the guanylurea in the course of the reaction with $[Co(CO_3)(en)_2]Cl$.

The first absorption band of $[Co(guH)(en)_2]^{3+}$ is similar to that of $[Co(bgH)(en)_2]^{3+}$ as is shown in Fig. 4. Considering the fact that the effective symmetry of the former is much lower than that of the latter, it is expected that the first band of the former splits into two or more components. This consideration is realized in the CD spectra; namely, $[Co(guH)(en)_2]^{3+}$ exhibits an overlapped pattern of two positive CD bands, whereas $[Co(bgH)(en)_2]^{3+}$ shows only one positive (Fig. 4). Contrary to the first absorption band region, the second absorption band of $[Co(guH),(en)_2]^{3+}$ differs remarkably from that of $[Co(bgH)(en)_2]^{3+}$. The second band of the former splits into two components at 345 mμ and *ca.* 385 mμ, though the CD spectra of both the complexes are similar to one another in the corresponding region. It should be noted that the guanylurea complex is a rather rare example which shows the apparent splitting in the second absorption band. The CD and absorption curves shift to the longer wavelengths in alkaline solutions than those in water, especially in the region of the ultraviolet ligand absorption band; the absorption curve of the free ligand also shift to red in alkaline solution.

From the data presented in Table 1, it has been concluded that the spectrochemical series of the ligands concerned in this paper is

$$en > guH > bgH > gu^- > bg^-.$$

It is unknown which of the O and N atoms of the urea part in the guanylurea ligand is coordinated to the central cobalt(III) ion. This is also the case of a tris-guanylurea complex of cobalt(III).[2]

3. Absolute Configuration. Currently there have been encountered some difficulties in the attempt to make an inference of the absolute configuration of a tris-chelate type cobalt(III) or chromium(III) complex from the comparison of its CD signs in the region of the *d-d* or the ultraviolet ligand absorption bands to those of a reference complex, whose absolute configuration has been determined conclusively.

It is well known that MaCaffery and Mason[17] assigned a strong positive CD component at 61.5 (10^{13} sec^{-1}) of $(+)_{589}$-$[Co(en)_3]^{3+}$, whose absolute configuration was unequivocally determined by an X-ray technique by Saito *et al.*[8,18,19] to the transition $^1A_1$-^1E_a of the first absorption band from the CD measurement of a single crystal of $Na(+)_{589}$-$[Co(en)_3]_2Cl_7\cdot 6H_2O$; therefore another weak negative CD component at 70.6 (10^{13} sec^{-1}) of this complex should be assigned to a $^1A_1$-$^1A_2$ or to any other origin. Recently, Judkins and Royer[20] measured the single crystal CD spectra of $\Delta(+)_{589}$-$[Co(tn)_3]Cl_3\cdot 4H_2O$ containing trimethylenediamine (tn), whose absolute configuration was determined by Nomura *et al.*,[21] and reported that the relative positions of the A_2 and E_a components are reversed in this complex as compared with those found in $[Co(en)_3]^{3+}$; this means the E_a and the A_2 components of the Δ isomer of trimethylenediamine complex have positive and negative signs, respectively. Jud-

16) S. F. Mason and B. J. Norman, *Proc. Chem. Soc.*, **1964**, 339; *J. Chem. Soc., A*, **1966**, 307; R. Larsson, S. F. Mason, and B. J. Norman, *ibid.*, **1966**, 301.

17) A. J. McCaffery and S. F. Mason, *Mol. Phys.*, **6**, 359 (1963).

18) K. Nakatsu, M. Shiro, Y. Saito, and H. Kuroya, This Bulletin, **30**, 795 (1957).

19) K. Nakatsu, *ibid.*, **35**, 832 (1962).

20) R. R. Judkins and D. J. Royer, *Inorg. Nucl. Chem. Lett.*, **6**, 305 (1970).

21) T. Nomura, F. Marumo, and Y. Saito, This Bulletin, **42**, 1016 (1969).

kins and Royer explained this contradiction between the ethylenediamine and trimethylenediamine complexes on the line of Piper's prediction[22,23] that stated, if the N–M–N angle in the chelate ring, α, is greater than 90°, the sign of the Cotton effects will reverse with respect to the complex with α less than 90°; the angle α of the $[Co(en)_3]^{3+}$ and $[Co(tn)_3]^{3+}$ have been reported to be 87.4°[19] and 94.5°,[21] respectively.

Unfortunately, Brubaker, and Webb reported that all three angles α of $[Cr(bgH)_3]^{3+}$ are 90° within experimental error, though this is for a chromium(III) and not for the cobalt(III) complex. In the meanwhile, the $\Lambda(-)_{589}$-$[Cr(bgH)_3]^{3+}$ has almost identical CD pattern in the *d–d* absorption band region to that of the $(-)_{589}$-$[Co(bgH)_3]^{3+}$. Accordingly, as far as we concern the *d–d* absorption band region, the $(-)_{589}$-$[Co(bgH)_3]^{3+}$ may be assigned to have the absolute configuration Λ, and the correspondency which is seen in Fig. 1 may suggest that all the isomers presented in Fig. 1 have the same absolute configuration Λ.

22) T. S. Piper and A. G. Karipides, *Mol. Phys.*, **5**, 475 (1962).
23) T. Bürer, *ibid.*, **6**, 541 (1963).

Nevertheless, a serious difficulty comes from the ultraviolet CD spectra as mentioned in Section 1 above; the criterion from the so-called exciton splitting shows reverse assignment, Δ, at least for the $(-)_{589}$-$[Co(bgH)_3]^{3+}$ and $(+)_{589}$-$[Co(bgH)_2(en)]^{3+}$ and their deprotonated species. A similar case has been found for $[Co(dip)_3]^{3+}$ (dip=2,2′-dipyridyl); the $(-)_{589}$ isomer has positive sign in the main CD component of the first absorption band and the negative and positive exciton splitting CD components, at longer and shorter wavelengths respectively, in the ultraviolet ligand absorption band region.[15] Clearly further studies are needed for these anomalies.

The overlapped positive CD components of the $(+)_{589}$-$[Co(guH)(en)_2]^{3+}$ in the first absorption band region suggest that this $(+)_{589}$ isomer has an absolute configuration Λ. It may be noticed that all the isomers containing biguanide or guanylurea, which were suggested to have absolute configuration Λ from the behavior in the first absorption band, have commonly negative CD bands in the second absorption band region.

BULLETIN OF THE CHEMICAL SOCIETY OF JAPAN, VOL. 44, 431—433 (1971)

The Characterization of $CdFe(CO)_4$ and $HgFe(CO)_4$ by Infrared and Mössbauer Spectroscopy and X-Ray Diffractometry

Tetsuo TAKANO and Yukiyoshi SASAKI

Department of Chemistry, Faculty of Science, The University of Tokyo, Hongo, Tokyo

(Received September 8, 1970)

Two compounds, $MFe(CO)_4$ (M=Cd or Hg), were investigated by the use of infrared and Mössbauer spectroscopy and X-ray diffractometry. The infrared data suggested that the M atoms link $Fe(CO)_4$ units to form infinite zig-zag chains; these metal atoms are attached to the iron atom at *cis*-positions and form an octahedron with four carbonyl groups. The Mössbauer spectra and infrared data indicate that the Cd–Fe and Hg–Fe bonds are not ionic but covalent, that they are as strong as C–Fe bonds in iron carbonyls. The isomorphism of the two compounds was confirmed by the X-ray diffractometry.

Among the compounds with metal-metal bonds, those with the simplest composition, $MFe(CO)_4$ (M= Cd, Hg), are interesting for their structures. They have been thought to have a polymeric structure formed by means of direct Cd–Fe or Hg–Fe bonds. Wells[1] proposed an endless structure of $HgFe(CO)_4$ in which the iron and mercury atoms are alternatively bonded to form a straight, linear chain. Adams *et al.*[2] and Beck and Noak[3] suggested that two cadmium or two mercury atoms and four carbonyl groups form an octahedral *cis*-configuration around the central iron atom of $CdFe(CO)_4$ or $HgFe(CO)_4$. However, so far no attempts have been made to provide precise structural information about these compounds. In this paper, their electronic states and structures will be discussed on the basis of infrared and Mössbauer spectroscopy and X-ray diffraction data.

Experimental

The sample of $HgFe(CO)_4$ was prepared by treating iron carbonyl with mercuric sulphate.[4] The corresponding cadmium compound was synthesized by the method of Feigl and Krumholtz,[5] yellow needle-like crystals of $CeFe(CO)_4$ being obtained after heating voluminous precipitates of $Cd(NH_3)_2Fe(CO)_4$ in an aqueous solution at 50°C for three days. The results of elemental analyses were satisfactory with regard to the above compositions. Thermal decomposition was carried out in a nitrogen stream over the temperature range of 15—300°C, using a Shimadzu Thermal Balance and a Rigaku Denki DTA apparatus. The infrared spectra were recorded with Nihon-Bunko DS402G (4000—700 cm^{-1}), Hitachi EPI-L02 (700—200 cm^{-1}), and Hitachi FIS-1 (300—60 cm^{-1}) spectrometers as Nujol mulls and as dispersion in fused polyethylene, at room temperature and at the temperature of

1) A. F. Wells, "Structural Inorganic Chemistry," 3rd ed. Oxford University Press, London (1962), p. 723.
2) D. M. Adams, D. J. Cook, and R. D. W. Kemmit, *Nature*, **205**, 589 (1965).
3) W. Beck and K. Noak, *J. Organometal. Chem.*, **10**, 307 (1967).
4) H. Stuhlman and H. Hock, *Ber.*, **62**, 431 (1929).
5) F. Feigl and P. Krumholtz, *Z. Anorg. Allg. Chem.*, **215**, 242 (1933).

liquid nitrogen. The Mössbauer spectra were measured with a constant-velocity drive-type spectrometer with a source of ^{57}Co diffused onto a Pt-foil. The powder X-ray diffraction patterns were recorded with Rigaku-Denki and Norelco X-ray diffractometers. Filtered Cu$K\alpha$ and Fe$K\alpha$ radiations were used. Weissenberg cameras were used to obtain oscillation photographs of single crystals.

Results and Discussion

IR Spectra. The observed infrared absorption frequencies (measured as Nujol mulls at room temperature) are listed in Table 1a. The use of polyethylene as the dispersion media gave essestially the same results. In the far-infrared region, there appeared to be some discrepancies between our results and those of previous workers.[2,3] In the carbonyl region, four prominent stretching bands were observed for both compounds. This characteristic is just like that found for *cis*-$M(CO)_4L_2$ molecules of the C_{2v} symmetry with regard to the central metal atom, M. The four carbonyl stretching modes, assigned as is shown in Table 1a, and their force constants, calculated according to the Cotton-Kraihanzel model,[6] are listed in Table 1b, where K_1 is the stretching force constant of C–O *trans* to Hg or Cd, and where K_2 is the stretching force constant of C–O *cis* to Hg or Cd. The agreement between these values and the calculated frequencies of the A_1^1 mode support the present assignments. The fact that the frequency of each CO stretching band for $CdFe(CO)_4$ is lower than that of the corresponding band of $HgFe(CO)_4$ is consistent with the observations for $M[Co(CO)_4]_2$, where M refers to Cd or Hg.[7] In both cases, the order of frequencies may be associated with the difference in electronagativity and in atomic size between Cd and Hg.

Thus, it may be concluded that Cd is poorer π-electron acceptor than Hg in these molecules; in other words, the p orbitals of cadmium are less facile than those of mercury in forming $d\pi$–$p\pi$ bonds with the d-orbitals of iron.

The bands due to metal-metal vibrations are expected to appear in the region of the far-infrared spectra, where no band due to the M–CO group except those due to CMC bending vibrations is likely to appear.[8,9] Accordingly, the bands clearly observed at 217 cm^{-1} and 196 cm^{-1} can most reasonably be assigned to the Cd–Fe and Hg–Fe stretching modes; the other mode, A_1^1, could not be detected, presumably because this skeletal vibration frequency is lowered when molecules are polymeric,[10] as in the present cases. By assuming that a cadmium or mercury atom links $Fe(CO)_4$ groups to form a zig-zag chain, the force constants are calculated to be 2.1 and 1.9 md/Å for $HgFe(CO)_4$ and $CdFe(Co)_4$ respectively. These values, although rather rough, are still acceptable.[11] As for the above-mentioned cobalt carbonyl compounds, $M[Co(CO)_4]_2$ (M=Cd, Hg), the K(Cd–Co) and K(Hg–Co) values were reported to be 2.33 and 2.61 md/Å respectively by Stammreich, Kawai, and Sala.[7] These four bonds seem to be stronger than the Sn–Mn bonds in $Cl_3SnMn(CO)_5$ or $(CH_3)_3SnMn(CO)_5$, for which the values of 1.00 and 0.67 md/Å were obtained.[12]

The strength of the metal-metal bond in the compounds in question may be estimates to be comparable with those covalent metal-carbon bonds in neutral metal carbonyls. By comparing the K_1, K_2, and K_i values with those of iron carbonyl derivatives containing various ligands and Fe(0), the oxidation number of the iron atom in the present compounds was estimated to be nearly zero.

Mössbauer Spectra. The Mössbauer spectra data are given in Table 2 and in Fig. 1, along with those for the related compounds containing metal-metal bonds between different elements (these later values being taken from the literature).[13,14] In $HgFe(CO)_4$ the

Table 1a. Infrared frequencies (cm^{-1})

$CdFe(CO)_4$	$HgFe(CO)_4$	Assignments	
2031 m	2047 m	A_1^1	(C–O) str.
2010 w sh	2012 w sh		
1960 s	1979 s	A_1^2	
1941 w sh			
1921 s	1952 s	B_1	
1871 s	1917 s	B_2	
1829 w sh			
632 vw			(MCO) bend. or (M–C) str.
604 vs br[a]	596 vs br[a]		
550 m	550 m		
524 m	533 m		
500 w	516 w		
454 s	443 s		
432 s	427 m		
412 w	419 w		
408 vw	413 vw		
217 s	196 s	B_1^1	(M–M) str.
88 w			(CMC) bend.

a) The splitting of both bands could not be detected at the temperature of liquid nitrogen.
vs very strong, s strong, m medium, w weak, vw very weak, br broad, sh shoulder,str str. stretching, bend. bending.

Table 1b. Force constants for carbonyl stretching frequencies

	K_1	K_2	K_i md/Å	Calcd. freq. of A_1^1 mode cm^{-1}
$CdFe(CO)_4$	14.17	15.84	0.53	2025
$HgFe(CO)_4$	15.26	16.22	0.42	2044

6) F. A. Cotton and C. S. Kraihanzel, *J. Amer. Chem. Soc.*, **84**, 4432 (1962).
7) H. Stammreich, K. Kawai, and O. Sala, *J. Chem. Phys.*, **35**, 2175 (1963).
8) P. N. Brier, A. A. Chalmers, and S. B. Wild, *J. Chem. Soc. A*, **1967**, 1889.
9) N. A. D. Carey and H. C. Clark, *Chem. Commun.*, **1967**, 293.
10) S. Mizushima and T. Shimanouchi, *J. Amer. Chem. Soc.*, **71**, 1320 (1947).
11) H. M. Gager, J. Lewis, and M. J. Ware, *Chem. Commun.*, **1966**, 616.
12) S. Onaka, private communication.
13) N. E. Erickson and A. W. Fairfall, *Inorg. Chem.*, **4**, 1320 (1965).
14) M. T. Jones, *Inorg. Chem.*, **6**, 1249 (1967).

Table 2. Mössbauer effect data

Absorber	Temp. °K	I.S. (mm/sec)	Q.S. (mm/sec)	Ref.
$CdFe(CO)_4$	79	0.190±0.03	0.20±0.05	
	123	0.140±0.03	0.10±0.05	
	292	0.136±0.03	0.10±0.05	
$Na_2Fe(CO)_4$	298	0.110	0	12
$Me_4SnFe_4(CO)_{16}$	298	0.16	0.30	14
$Me_4SnFe_2(CO)_8$	298	0.15	0.16	14
n-$Bu_4Sn_2Fe_2(CO)_8$	78	0.24	0.12	14

I.S. Isomer shift measured relative to the midpoint of the spectrum of $[Na_2Fe(CN)_5NO]\cdot 2H_2O$.
Q.R. Quadrupole splitting.

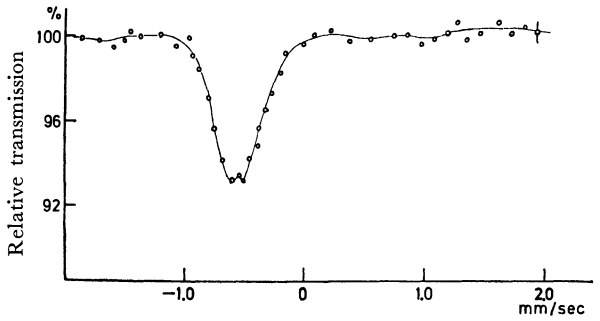

Doppler velocity (*vs.* S.S. 310)

Fig. 1. Mössbauer spectrum of $CdFe(CO)_4$ at 292°K.

Mössbauer effect could not be measured because of the large non-resonant absorption of mercury nuclides. The spectra of $Cd(NH_3)_2Fe(CO)_4$ which is the starting material for preparing $CdFe(CO)_4$ were too weak to be registered even at the temperature of liquid nitrogen. The large, negative isomer shift of $CdFe(CO)_4$ indicates that the charge on the iron atom is only slightly negative or is almost neutral.

The observed absorption, which is intense even at room temperature, suggests a rigid poymeric structure. Consequently, the polymeric structure containing the Cd(0)–Fe(0) covalent bond seems to be preferable to the ionic form, Cd^{2+}–$Fe(CO)_4^{2-}$, in the present complex.

It can be seen from the data that the compounds with the Sn–Fe–Sn bond, which also have a *cis*-configuration around the iron atoms,[14] closely resemble $CdFe(CO)_4$ in the valence state of the iron atom.

Two remarkable features of the Mössbauer spectra of $CdFe(CO)_4$ are the small value of the quadrupole splitting and its small temperature dependence. This fact may reflect a high-electric-field gradient symmetry around the iron atom, which can be interpreted in terms of the hybrid orbitals of the iron.

In six octahedral hybrid orbitals of these carbonyl compounds of iron in the low-valency state, the *d*-orbitals are so occupied as to complete the inert gas structure. The resulting electronic configuration reduces the angular dependency of the expanded *d*-electron clouds to some degree,[15] so that the field gradient at the iron nucleus becomes smaller, even in the present case, where a *cis*-configuration of the C_{2v} symmetry is suggested by the infrared data.

Considering the nature of the metal-metal bonds in terms of force constants, the results of our infrared and Mössbauer spectroscopy are compatible with regard to the electronic environment of the central iron atom.

Thermal Decomposition. On heating under nitrogen, $CdFe(CO)_4$ suddenly began to decompose at 245°C, while releasing just four CO per chemical unit. The residue burned violently on exposure to air. On its DTA curve, a sharp and huge endothermic-peak corresponding to the sudden decomposition appeared at 260°C. The stability of $CdFe(CO)_4$ against thermal decomposition up to 245°C seems unique among the metal carbonyl compounds of this type. On the other hand, $HgFe(CO)_4$ began to decompose gradually, releasing both carbon monoxide and mercury vapor.

Crystal Structure. The polarizing microscopic observations of the crystals of these compounds supported the idea that they belong to either a triclinic or a monoclinic system. The twenty-two diffraction lines observed for each compound were examined by Ito's method,[16] and it could be concluded that both compounds are triclinic and isomorphous, with the following lattice parameters:

$CdFe(CO)_4$ $a=11.8$, $b=9.4$, $c=9.3$ Å,
$\alpha=111.5$, $\beta=124.5$, $\gamma=106.0°$
Vol. $=748.2$ Å^3, $D_{calcd.}=2.48$ g/cm^3,

$HgFe(CO)_4$ $a=12.9$, $b=10.8$, $c=10.3$ Å,
$\alpha=108.5$, $\beta=121.5$, $\gamma=106.0°$
Vol. $=782.6$ Å^3, $D_{calcd.}=3.03$ g/cm^3.

Their densities, measured pycnometrically in benzene, gave the values of 2.5 and 3.1 g/cm^3, values which agreed with $Z=4$, for $CdFe(CO)_4$ and $HgFe(CO)_4$ respectively.

Although we have not been able to determine their precise structures from these results, there should be no significant differences in the crystal and molecular structures between the cadmium and mercury compounds. From the site symmetry about the iron atoms of C_{2v}, as estimated from the infrared data, one of the most probable structures is given in Fig. 2.

The weakness of the Mössbauer spectra of $Cd(NH_3)_2$-$Fe(CO)_4$ suggests that the metal-metal links are absent

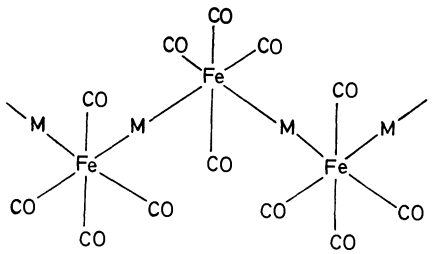

Fig. 2. Probable structure for $MFe(CO)_4$ (M=Cd, Hg).

in this compound and that they formed on the heat decomposition of this complex to yield $CdFe(CO)_4$.

15) T. C. Gibbs and N. N. Greenwood, *J. Chem. Soc.*, **1966**, 43.

16) T. Ito, *Nature*, **164**, 755 (1947).

The Syntheses and Properties of Some 2,4-Dimethyl-1,5-benzodiazepinium Halogenometalates

Akira Ouchi, Toshio Takeuchi, Mitsuhisa Nakatani, and Yoshiaki Takahashi

Department of Chemistry, College of General Education, The University of Tokyo, Komaba, Meguro-ku, Tokyo

(Received September 21, 1970)

When 2,4-dimethyl-1,5-benzodiazepinium halide was reacted with a metal halide in ethanolic media, crystalline products, $M(C_{11}H_{13}N_2)_xX_y$ (where X=Br, Cl; M=Co(II), Mn(II), Zn(II), Cd(II), Sb(III) (chloride), Cu(II) (chloride), and Cu(I) (bromide)), were obtained. They are all new compounds. Their electronic and infrared spectra resemble those of the sarting chloride or bromide. The infrared band at about 1639 cm^{-1} of the chloride shifts to the lower-wave-number side when it is turned into a halogenometalate. On the other hand, the characteristic ν(M–X) bands were found in the far-infrared spectra of the halogenometalates, These compounds are likely to be ionic compounds consisting of the halogenometalato anion and the 2,4-dimethyl-1,5-benzodiazepinium cation.

Although tropolone and its derivatives were used as the ligands of the metal chelates, comparatively little investigation has been made of the metal compounds containing seven-membered ring components. Diazepines are relatively easily synthesized by the condensaion of diamine with diketones, as has been studied by Thiele[1] and Lloyd,[2-6] and these compounds have the seven-membered ring. From *o*-phenylenediamine and acetylacetone, for example, 2,4-dimethyl-3*H*-1,5-benzodiazepine is obtained. This compound forms a salt, deep violet in color, with hydrochloric acid. The salt is stable in the solid state, and it can be kept in the open air at room temperature without decomposition. There have been several discussions about the bonding structure of the salt,[4,7,8] but at any rate it is clear that the salt contains the 2,4-dimethyl-1,5-benzodiazepinium cation and that, therefore, the seven-membered ring was kept and not destroyed. When the salt was mixed with the anhydrous metal halides in an ethanolic medium, crystalline precipitates were obtained. These products are as deeply colored as the original dimethyl-benzodiazepinium salt. Repeated syntheses and elemental analyses gave reproducible results. Therefore, these products seem to be a new species containing the seven-membered ring.

Experimental

Instruments. The infrared spectra were obtained by the Nujol or hexachloro-1,3-butadiene mull procedure, using a 403G-type infrared spectrophotometer of Japan Spectroscopic Co., Ltd. The electronic spectra were obtained with a Hitachi EPS-2-type automatic recording spectrophotometer. The magnetic moments were measured with a Gouy balance at room temperature.

The Syntheses of the Compounds: *The Synthesis of the 2,4-Dimethyl-1,5-benzodiazepinium Chloride Dihydrate*: This compound was synthesized from *o*-phenylenediamine and acetylacetone according to the Thiele or Lloyd method.[1,4]

The bromide was obtained by almost the same method, but using hydrobromic acid in place of hydrochloric acid. The bromide obtained was the dihydrate as the chloride.

The Synthesis of 2,4-Dimethyl-1,5-benzodiazepinium Tetrachlorocobaltate(II) Monohydrate: Five-tenths of a gram (2.1 mmol) of cobalt(II) chloride hexahydrate was heated, and the crystalline water was removed. A 99% ethanolic solution of the blue anhydrous salt (about 5 m*l*) and a 99% ethanolic solution of the 2,4-dimethyl-1,5-benzodiazepinium chloride dihydrate (0.5 g (2.0 mmol) in 5 m*l* of the solvent) were mixed and stirred. A crystalline precipitate appeared. The product was filtered off after it had stayed one night in a refrigerator. It was washed with 99% ethyl alcohol and then with ethyl ether. The recrystallization of the products has not yet been successful.

The other compounds were synthesized by almost the same method from the 2,4-dimethyl-1,5-benzodiazepinium chloride or bromide and the metal halides of the same halogen element.

In the case of the copper salt, the product from the chloride is paramagnetic and divalent, but the product from the bromide is diamagnetic and probably univalent. The analytical results support the results.

Some metal salts, nickel(II) halides, for example, do not give the precipitate by this method. Probably this is because of the instability of the halogeno complexes of these metals.

Results and Discussion

The elemental analyses, the chemical formula, and the magnetic moments of the compounds thus obtained are shown in Table 1. As the table shows, these compounds have the formula of ML_xX_y (where L^+ is the 2,4-dimethyl-1,5-benzodiazepinium ion and where X is Cl or Br). The oxidation number of the L is always+1. Although these compounds are all synthesized in the 99% ethanol medium, some of them contain crystalline water.

From the magnetic moments of cobalt complexes, it is possible to infer how the central cobalt ion is surrounded by ligands—either octahedrally or tetrahedrally. Due to the spin-orbit interaction, the magnetic moments of the cobalt complexes are higher than the spin-only value; if the magnetic moment is 4.7—

1) J. Thiele and G. Steimmig, *Ber.*, **40**, 955 (1907).
2) D. Lloyd and D. R. Marshall, *J. Chem. Soc.*, **1956**, 2597.
3) D. Lloyd and D. R. Marshall, *ibid.*, **1958**, 118.
4) D. Lloyd, R. H. McDougall, and D. R. Marshall, *ibid.*, **1965**, 3785.
5) C. Barnett, H. P. Cleghorn, G. E. Cross, D. Lloyd, and D. R. Marshall, *ibid.*, *C*, **1966**, 93.
6) D. Lloyd, R. H. McDougall, and D. R. Marshall, *ibid.*, *C*, **1966**, 780.
7) I. L. Finar, *ibid.*, **1958**, 4094.
8) J. A. Barltrop, C. G. Richards, D. M. Russell, and G. Ryback, *ibid.*, **1959**, 1132.

TABLE 1. THE ANALYSES AND THE MAGNETIC MOMENTS OF COMPOUNDS
(Figures are given in % for analyses and B.M. for magnetic moments)

		Metal	Halogen	C	H	N	Magnetic moments
$LCl \cdot 2H_2O$	Calcd		14.49	53.99	7.00	11.45	
	Found		14.30	53.78	6.46	11.59	
$LBr \cdot 2H_2O$	Calcd		27.63	45.69	5.93	9.69	
	Found		28.50	45.58	6.17	9.68	
$CoL_2Cl_4 \cdot H_2O$	Calcd	10.43	25.09	46.75	4.99	9.91	
	Found	10.47	24.78	46.73	5.15	9.87	4.77
CoL_2Br_4	Calcd	8.13	44.08	36.45	3.62	7.73	
	Found	8.66	44.45	36.48	3.65	7.73	4.98
$CuL_2Cl_4 \cdot H_2O$	Calcd	11.15	24.88	46.37	4.95	9.83	
	Found	11.31	24.38	46.37	4.87	9.81	1.82
$CuLBr_2$	Calcd	16.02	40.30	33.31	3.30	7.06	
	Found	16.80	39.88	33.04	2.91	6.99	(dia)
ZnL_2Cl_4	Calcd	11.81	25.61	47.73	4.73	10.12	
	Found	11.52	25.80	47.35	4.72	9.94	(dia)
ZnL_2Br_4	Calcd	8.94	43.70	36.13	3.58	7.66	
	Found	8.99	44.10	36.29	3.39	7.65	(dia)
$CdLCl_3$	Calcd	28.67	27.13	33.70	3.34	7.15	
	Found	28.50	27.00	33.87	3.28	7.14	(dia)
CdL_2Br_4	Calcd	14.44	41.06	33.94	3.37	7.20	
	Found	14.60	41.00	34.10	3.46	7.20	(dia)
MnL_2Cl_4	Calcd	10.11	26.11	48.64	4.82	10.31	
	Found	10.41	26.45	48.37	4.63	10.26	6.11
MnL_2Br_4	Calcd	7.62	44.33	36.65	3.63	7.77	
	Found	7.21	45.30	36.61	3.73	7.78	6.10
$SbLCl_4$	Calcd	27.87	32.47	30.25	3.00	6.41	
	Found	27.50	32.27	30.22	2.60	6.43	(dia)

$L^+ = C_{11}H_{13}N_2^+$ (2,4-dimethyl-1,5-bezodiazepinium ion)

5.2 B.M., it is in the octahedral form, while if it is 4.4—4.8 B.M., it is in the tetrahedral form. The observed magnetic moments of the products are 4.77 B.M. and 4.98 B.M., as the table shows. The dithiolium halogenometalates which contain CoX_4^{2-} ions have magnetic moments of 4.6—4.8 B.M.,[9-11] this value is a little high, though it is expected, as in the tetrahedral configuration. Therefore, although the magnetic moments of these complexes are a little higher than that expected for the tetrahedral form, the central ion is probably surrounded tetrahedrally by four halogen atoms in these complexes. A deformed octahedral form, including additional coordination of the halogen atoms of other complex molecules or the halogen-bridging structure, is also probable. However, a strong coordination of the 2,4-dimethyl-1,5-benzodiazepinium cation to the central metal ion is less probable.

In the cases of copper compounds, only the Cu(I) compound was obtained from copper(II) bromide, while only the Cu(II) compound was obtained from copper(II) chloride. The stability of the copper(I)-compounds depends very strongly on the nature of the counter-anion or the ligand present, while the stabilities of Cu(I) halides are in the order of CuI > CuBr > CuCl; CuF is yet unknown. On the other hand, the dimethyl-benzodiazepinium salt seems to have a little reducing ability. Consequently, it reduced the copper(II) bromide to the stable copper(I) salt, while it is not a strong enough reagent as to produce the less stable copper(I) chloride.

The electronic absorption spectra of the ethanolic solution of these products were also examined. These metal compounds show spectra almost identical with those of the 2,4-dimethyl-1,5-benzodiazepinium halides. The main peaks (in kK) and their intensities (in $\log \varepsilon$ shown in parentheses) are as follows: 44.5 (4.1), 38.3 (4.4), 37.2 (4.4), ~30 (~3) 28.4 (3.0), 19.6 (2.9), 16.4 (2.5). As the absorption coefficients of the bands of the ion are too high, the peaks of the *d-d* bands of metals as well as the specific bands of the halogenometalates are not identified. Moreover, the halogenometalato ion may be decomposed into metal and halogen ions in such a dilute ethanolic solution.

The infrared spectra of these compounds were also examined. The general pattern of the spectra of the metal compounds resembles that of the 2,4-dimethyl-1,5-benzodiazepinium chloride in the finger-print region.

The exact assignments of the peaks are not easy, as the vibrations of the dimethylbenzodiazepinium ion

9) A. Furuhashi, T. Takeuchi, and A. Ouchi, This Bulletin, **41**, 2049 (1968).
10) Y. Takahashi, M. Nakatani, and A. Ouchi, *ibid.*, **42**, 274 (1969).
11) A. Ouchi, H. Eguchi, T. Takeuchi, and A. Furuhashi, *ibid.*, **42**, 2259 (1969).

conjugate with each other and they can be separated into group vibrations only with difficulty. However, bands in the region of 1350—1650 cm^{-1} are likely to consist of ν(C=N), ν(C=C) or a mixture of them; at least, the contribution of these vibrations to these bands is probably important.

In the far-infrared region, there are some bands which are characteristic of the metal compounds and which are not observed in the spectra of the chloride of the ligand. Although no exact assignments were easily obtained, their ν(M–X) bands were tentatively assigned. The maxima of these bands are shown in Table 2.

Table 2. The wave numbers of some infrared spectrum bands of the compounds (cm^{-1})

	ν(C=N), ν(C=C) or the mixture of them		ν(M–X)
$LCl \cdot 2H_2O$	1639 s	1595 s	
$LBr \cdot 2H_2O$	1643 sh 1630 s	1594 s	
$CoL_2Cl_4 \cdot H_2O$	1625 m	1598 s	291 s
CoL_2Br_4	1621 s	1598 s	223 s
$CuL_2Cl_4 \cdot H_2O$	1622 m	1600 s	254 s
$CuLBr_2$	1630 s	1587 s	<200
ZnL_2Cl_4	1627 s	1595 s	297 s
ZnL_2Br_4	1622 s	1597 s	200 s
$CdLCl_3$	1627 s	1597 s	266 s
CdL_2Br_4	1621 s	1597 s	<200
MnL_2Cl_4	1629 s	1598 s	282 s
MnL_2Br_4	1622 s	1597 s	218 s
$SbLCl_4$	1618 s	1600 s	280 s

s: strong, sh: shoulder, m: medium.

The wave numbers of the ν(M–X) bands of these compounds are very similar to the values observed in the spectra of other halogenometallates.[12-14] The ν(M–X) bands of bromocuprate and bromocadmate compounds are not observed above 200 cm^{-1}. However, as the edge absorption appears near 200 cm^{-1}, they are expected to be found in the lower wave number region.

The band of the chloride at 1639 cm^{-1} shift to the lower wave number side, about 10—20 cm^{-1}, when the metal compounds are formed, as is shown in Table 2. This is probably caused by a slight change in the bonding states in the seven-membered-ring system of the cation—a prohibition of the tautomerism transition, for example. Thus, however, difficult as it is for a strong bond between the cation and metal ion to exist, some kind of interference between the cation and halogenometalato ion, such as was shown in the case of 3,5-dimethyl-1,2-dithiolium tetrachloroferrate(II), is to be expected in this case, too.[15]

Consequently, these metal compounds probably consist of the 2,4-dimethyl-1,5-benzodiazepinium cation and halogenometalato anion.

The authors wish to express their appreciation to Professors Yukichi Yoshino and Kunihiko Watanuki and their colleagues of this laboratory for their helpful discussions.

12) K. Nakamoto, "Infrared Spectra of Inorganic and Coodination Compounds," 2nd Ed., Wiley & Sons, New York (1969), p. 214.
13) G. E. B. Y. Ahlija and M. Goldstein, *Chem. Commun.*, **1968**, 359.
14) R. J. H. Clark and T. M. Dunn, *J. Chem. Soc.*, **1963**, 1198.
15) G. H. Hearth, R. L. Martin, and I. M. Stewart, *Aust. J. Chem.*, **22**, 83 (1969).

The Dehydration of *N*-Benzyloxy and *N*-Hydroxymaleamic Acid and the Isomerization of *N*-Benzyloxyisomaleimide

Mitsuaki NARITA, Masayasu AKIYAMA,* and Makoto OKAWARA

Research Laboratory of Resources Utilization, Tokyo Institute of Technology, Ookayama, Meguro-ku, Tokyo

(Received July 17, 1969)

The dehydration of *N*-benzyloxy and *N*-hydroxymaleamic acids and the isomerization of *N*-benzyloxyisomaleimide were carried out under various conditions to obtain *N*-benzyloxyisomaleimide, *N*-hydroxyisomaleimide, and *N*-benzyloxymaleimide. *N*-substituents, such as benzyloxy, hydroxy, and acetoxy groups, depress the reactivity of nitrogen electronically and facilitate the formation of isomaleimides in the dehydration of *N*-substituted maleamic acids. The thermal isomerization of *N*-benzyloxyisomaleimide to the maleimide has been successful only in *N*,*N*-dimethylformamide. Further the conversion of isomaleimide to maleimide was performed *via* the addition of hydrogen bromide to isomaleimide followed by isomerization and dehydrobromination.

In peptide syntheses, *N*-hydroxysuccinimide has been frequently used as a convenient component for activation of carboxyl group of amino acids. In our early works, we reported the preparation of polymer (*e.g.* V) having the *N*-hydroxyimide structure in the chain and the activation of carboxylic acid group by use of such polymers.[1,2] During the course of these works, it was found[2] that the dehydrocyclization product of *N*-benzyloxymaleamic acid (I) with thionyl chloride was not the expected *N*-benzyloxymaleimide but *N*-benzyloxyisomaleimide (II), and that *N*-benzyloxy- (IV) or *N*-hydroxysuccinimide (V) structure was obtained by successive isomerization and hydrolysis of polymer (III). In this paper, we wish to report

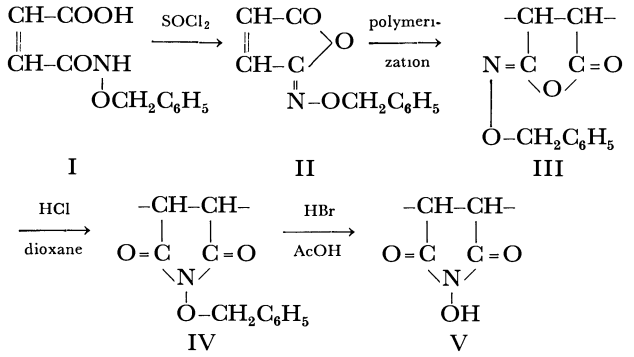

the result of the further investigation on cyclization reactions of *N*-benzyloxy- and *N*-hydroxymaleamic acids with various dehydrating agents and also on the possibility of direct isomerization of *N*-benzyloxyisomaleimide to *N*-benzyloxymaleimide.

Results and Discussion

The Dehydration of N-*Benzyloxymaleamic Acid.* The dehydration of *N*-substituted amic acids, especially *N*-substituted maleamic and phthalamic acids, produces the corresponding imides[3–5] or isoimides[5–9] depending on the nature of amic acids and the reaction condition employed. One would postulate that *N*-substituted maleamic acid would be in equilibria with the tautomer of iminohydrine structure which is strongly stabilized by conjugation with the double bond and that the iminohydrine tautomer will produce the corresponding isoimide by treatment with dehydrating agents under certain condition as shown in Scheme 1.[8]

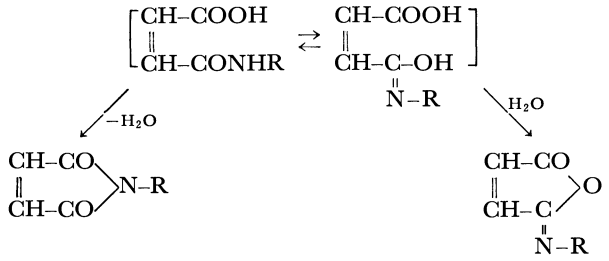

Scheme 1

Cotter[6] and Roderick[7] investigated on the reagents used for the dehydration of amic acids and classified the reagents which employed most commonly to effect the dehydration of amic acids to imides and isoimides. The effect of *N*-substituents in amic acids on the direction of the dehydration, however, has not been investigated systematically.

Ames reported[10] the formation of *N*-benzyloxymaleimide by treating *N*-benzyloxymaleamic acid (I) with thionyl chloride. We reported that the product obtained by Ames's procedure was *N*-benzyloxyisomaleimide (II).[2] In this paper, the action of phosphorus pentoxide, dicyclohexylcarbodiimide

* Present address: Department of Industrial Chemistry, Tokyo University of Agriculture and Technology, Koganei, Tokyo.

1) M. Akiyama, M. Narita, and M. Okawara, *J. Polym. Sci., Part A-1*, **7**, 1299 (1969).

2) M. Akiyama, Y. Yanagisawa, and M. Okawara, *ibid., Part A-1*, **7**, 1905 (1969).

3) a) P. O. Tawney, R. H. Snyder, C. E. Bryan, R. P. Conger, F. S. Dovell, R. J. Kelly, and C. H. Stiteler, *J. Org. Chem.*, **25**, 56 (1960). b) D. E. Bublitz, U. S. 3394145 (1968); *Chem. Abstr.*, **69**, 76972p (1968). c) H. Schmalz, German 1269126 (1968); *Chem. Abstr.*, **69**, 35498v (1968).

4) V. S. Ivanov, V. K. Smirnova, A. E. Semenova, and Tsao Yure, *J. Org. Chem., USSR*, **1**, 1729 (1965); *Chem. Abstr.*, **64**, 586g, (1966).

5) M. Yamada, I. Takase, K. Hayashi, K. Hashimoto, and Y. Komiya, *Yuki Gosei Kagaku Kyokai Shi*, **23**, 166 (1965).

6) R. J. Cotter, C. K. Sauers, and J. M. Whelan, *J. Org. Chem.*, **26**, 10 (1961).

7) W. R. Roderick and P. L. Bhatia, *ibid.*, **28**, 2018 (1963).

8) E. Hedaya, R. L. Hinman, and S. Theodoropulos, *ibid.*, **31**, 1311; 1317 (1966).

9) A. Le Berre and B. Dumaite, *C. R. Acad. Sci., Paris, Ser. C*, **226**, 334 (1968); *Chem. Abstr.*, **69**, 19103g (1968).

10) D. E. Ames and T. F. Grey, *J. Chem. Soc.*, **1955**, 631.

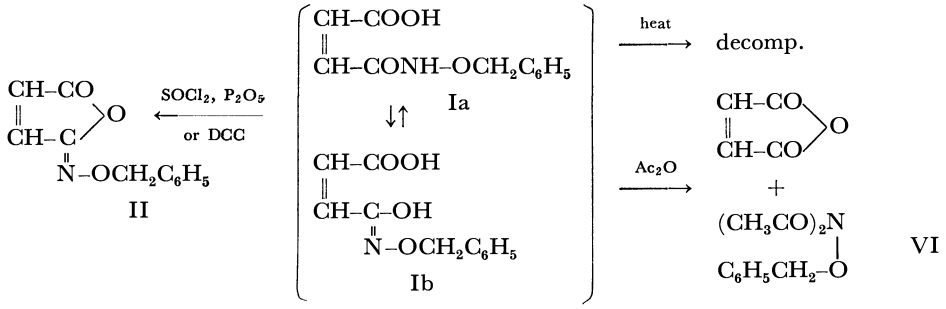

Sheme 2

TABLE 1. THE ISOMERIZATION OF *N*-BENZYLOXYISOMALEIMIDE (II)[a] TO THE CORRESPONDING IMIDE (XIII)

No.	Solvent[b] (10 m*l*)	Catalyst (g)	Reaction temp. (°C)	Reaction time (hr)	Yield of XIII (recovered II) (%)
1	DMSO[e]		170~180	4	(60)
2	NB[f]	—	150~160	10	(90)
3	—	—	140~150	4	(61)
4	DMF[g]	—	reflux	10	40
5	AAn[h]	CH_3COONa (0.4)	reflux	10	(60)
6	DMF	Pyridine (1.0)	100	6	(90)
7	NB	Quinoline (0.5)	150~160	10	(72)
8	Dioxane	CF_3COOH (0.3)	reflux	20	(88)
9	Dioxane	$BF_3 \cdot OEt_2$ (0.3)	reflux	10	(78)
10	CH_3COOH	HBr (2.0)	r. t.	5	85[c]
11	Dioxane	I_2 (0.1)	reflux	5	(75)
12	Dioxane	TsOH (0.2)	reflux	5	28[d]

a) One gram of II was used for the reaction in every case. b) In the case of No. 5, 20 m*l* of the solvent was used. c) The product was α-bromo-*N*-benzyloxysuccimide(XV). d) The product was the mixture of II and XIII which was identified by IR spectrum. e) DMSO; dimethylsulfoxide. f) NB; nitrobenzene. g) DMF; *N*,*N*-dimethylformamide. h) AAn; acetic anhydride.

(DCC), acetic anhydride as well as thionyl chloride will be reported. Treatment of I with these dehydrating agents produced various compounds as shown in Scheme 2. The dehydration was carried out with thionyl chloride in benzene, phosphorus pentoxide in *N*,*N*-dimethylformamide(DMF) and DCC in DMF or dioxane. In every cases, the product was only the isoimide (II) in about 70% yield. The compound (I) decomposed at about 145°C and so the thermal dehydration failed to produce the imide. Treatment of I with acetic anhydride at room temperature gave maleic anhydride and *N*,*N*-diacetyl-*O*-benzylhydroxylamine (VI) probably due to the following way (Scheme 3).

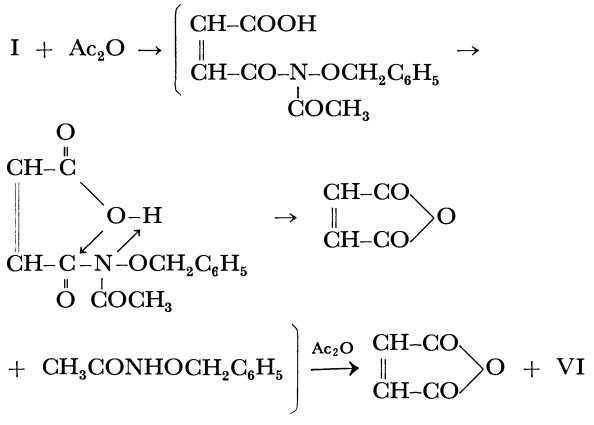

Scheme 3

The Dehydration of N-*Hydroxymaleamic Acid.* We attempted the dehydration of *N*-hydroxymaleamic acid (VII) with phosphorus pentoxide, thionyl chloride, acetic anhydride, *p*-toluenesulfonic acid (TsOH), DCC and acetyl chloride-in-pyridine. These results are shown in Scheme 4. Ivanov *et al.*[4] reported that they obtained *N*-hydroxymaleimide by treatment of VII with phosphorus pentoxide. However, *N*-

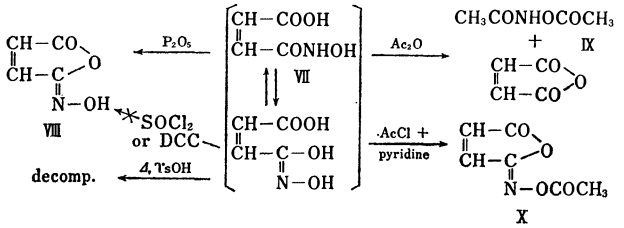

Scheme 4

hydroxyisomaleimide(VIII) was obtained instead of the corresponding maleimide by the dehydration of VII with phosphorus pentoxide as shown in Scheme 4. Using thionyl chloride and DCC as dehydrating agents, neither *N*-hydroxymaleimide nor *N*-hydroxyisomaleimide was obtained. The compound(VII) decomposed at *ca.* 130°C and the thermal dehydration failed. The compound (VII) decomposed at 100°C by treatment with TsOH. The reaction of VII with acetic anhydride yielded *N*,*O*-diacetylhydroxyamine (IX) and maleic anhydride. With excess acetyl chloride

Table 2. Physical and spectral data of II, VIII, X, and XIII

Compd.	Formula	Mp (°C)	Anal. (Calcd) % C	H	N	IR data[a] (cm^{-1})
II	$C_{11}H_9O_3N$	80~80.5	64.93 (65.02)	4.60 (4.46)	6.91 (6.89)	1795 (C=O) (s) 1630 (C=N) (m)
VIII	$C_4H_3O_3N$	145 (dec.)	42.81 (42.49)	2.45 (2.67)	12.49 (12.39)	1770 (C=O) (s) 1700 (?) (s) 164~20 (C=N) (s)
X	$C_6H_5O_4N$	115~116.5	46.06 (46.46)	3.02 (3.25)	9.02 (9.03)	1786 (C=O) (s) 1662 (C=N) (m) 1808 (C=O of $=N-OCOCH_3$) (s)
XIII	$C_{11}H_9O_3N$	89~90.5	64.45 (65.02)	4.13 (4.46)	6.86 (6.89)	1730 10 (C=O) (s)

a) Absorption intensity is expressed; s=strong, m=medium

in pyridine, VII gave *N*-acetoxyisomaleimide (X) probably through XI as shown in Scheme 5. Struc-

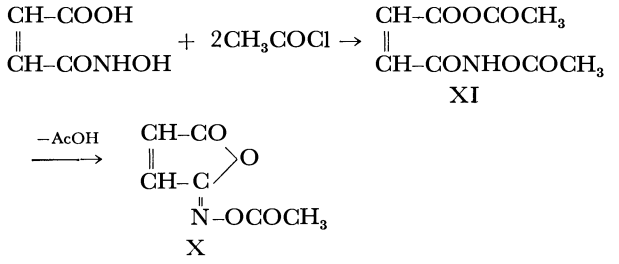

Scheme 5

tural evidences (IR and NMR spectra) of these compounds are shown in Tables 2 and 3.

Table 3. NMR data[a] of II, VIII, X, XIII, and XVI

Compd.	Chemical shift (δ)	Multiplicity[b] (J, Hz)	Number of protons	Assignment
II[c]	5.13	S	2	Methylenic H
	6.30	D (9)	1	Olefinic H_b[d]
	7.20	D (9)	1	Olefinic H_a[d]
	7.28	S	5	Aromatic H
VIII	5.62	D (8)	1	Olefinic H_b
	7.66	D (8)	1	Olefinic H_a
X	2.24	S	3	$OCOCH_3$
	6.61	D (6)	1	Olefinic H_b
	7.55	D (6)	1	Olefinic H_a
XIII	5.06	S	2	Methylenic
	6.53	S	2	Olefinic H
XVI[17]	7.36	M	5	Aromatic H
	2.32	S	3	$OCOCH_3$
	6.75	S	2	Olefinic H

a) NMR spectra were measured in deuteriochloroform solution.
b) S=singlet, D=doublet, M=multiplet.
c) Carbon tetrachloride was used for the solvent.
d) H_a and H_b are indicated in XVII.

The Isomerization of N-*Benzyloxyisomaleimide (II) to the Corresponding Maleimide (XIII).* Isomerization of many cyclic isoimides to imides can be found in the literatures.[6-8,11-14] This reaction proceeds by basic or acidic catalyst and also thermally. For example, *N*-arylisomaleimide,[6,14] *N*-methoxyisophthalimide[11] and *N*-phenylisophthalimide[12] isomerize to the corresponding imides in the presence of sodium acetate in acetic anhydride, hydrogen bromide in nitromethane and thermally in chlorobenzene, respectively.

We carried out the attempted isomerization of *N*-benzyloxyisomaleimide (II) to *N*-benzyloxymaleimide (XIII) under certain conditions. The results are shown in Table 1. The thermal isomerization of II to XIII did not occur in dimethylsulfoxide (DMSO), nitrobenzene or by heating without solvent (Nos. 1—3). In DMF, however, II isomerized to XIII in a 40% yield when refluxed for ten hours (No. 4). In this case, basic impurities in DMF might act as an acyl group transfer agent by attacking the carbonyl group to give the intermediate (XII) as shown in Scheme 6. To confirm this, sodium acetate, pyridine, and quinoline were used as basic components, but the isomerization of II to XIII did not occur (Nos. 5—7). On the other hand, the isoimide (II) reacted with aniline in DMF at 100°C to give the ring opening product (XIV) in a 91% yield. In these reactions, it is most plausible

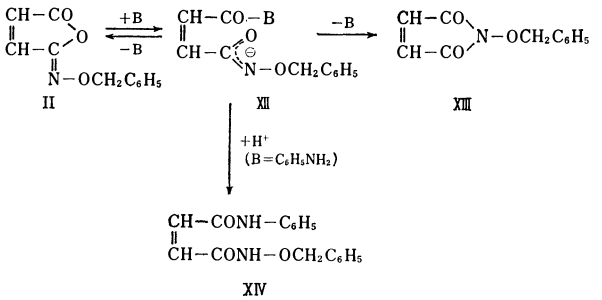

Scheme 6

11) L. A. Carpino, *J. Amer. Chem. Soc.*, **79**, 98 (1957).
12) A. E. Kretov, N. E. Kyl'Chitskaya, and A. J. Mal'nev, *Zh. Obshch. Khim.*, **31**, 2415 (1961).
13) D. Y. Curtin and L. L. Miller, *J. Amer. Chem. Soc.*, **89**, 637 (1967).
14) C. K. Sauers, *J. Org. Chem.*, **34**, 2275 (1969).

that the base attacks first the carbonyl group to form the intermediate (XII) from which the starting isomaleimide (II), maleimide (XIII) or the ring opening product (XIV) is produced according to the kinds of bases. Trifluoroacetic acid and boron trifluoride etherate were uneffective on the isomerization of II to XIII (Nos. 8 and 9).

On the other hand, *N*-substituted saturated amic acids are known to produce only the corresponding imides. Therefore the use of the compound which can add to double bond and easily leave to regenerate double bond is thought to be an alternate method to obtain intended compound (XIII). In order to verify this expectation, the reaction of II with hydrogen bromide was carried out in acetic acid at room temperature. As expected, the reaction yielded α-bromo-*N*-benzyloxysuccinimide (XV). (No. 10, Table 1) as shown in Scheme 7. The compound (XV) was easily dehydrobrominated with base to give XIII. Iodine and TsOH, which are known as effective catalysts for the isomerization of maleic acid derivatives, were not effective on the isomerization of II to XIII.

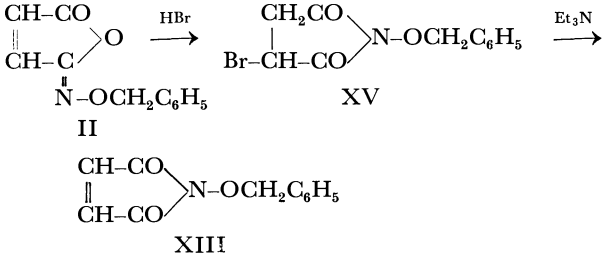

Scheme 7

Curtin and Miller[14] indicated that the electron-withdrawing substituents on Ar ring retarded the O→N migration of benzoyl group (*i.e.* ρ in Hammett rule was negative) in the following example. On

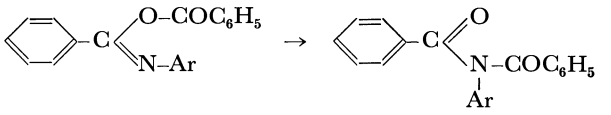

the other hand, Yamada *et al.*[5] examined the dehydrocyclization of *N*-β- or *N*-γ-hydroxypropylmaleamic acid with acetic acid and suggested the formation of maleimide or isomaleimide depended on the steric factor in the intermediates. These works and our results lead to the following conclusion.

The electron-withdrawing substituents such as hydroxy, acetoxy, and benzyloxy reduced the nucleophilic reactivity of nitrogen in *N*-substituted maleamic acids resulting the formation of isomaleimides in either the dehydration or the isomerization process shown below. Isomaleimide obtained by the dehydrocyclization of maleamic acid was isomerized to maleimide by heating in DMF, while the reason of effectiveness of DMF was not enough explained. Further, an indirect method was indicated to obtain maleimide in which the double bond of isomaleimide was saturated once with HBr to facilitate the isomerization.

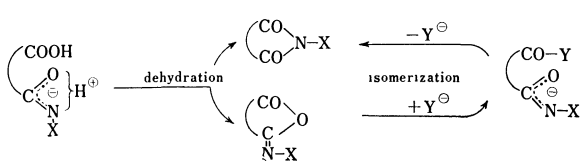

Proof of Structure of N-*Substituted Isoimides and Imides.* Proof of the structures of II, VIII, X, and XIII were derived from the elemental analyses, IR and NMR spectra. Physical properties and spectral evidence were summarized in Tables 2 and 3. To compare with X, *N*-acetoxymaleimide (XVI)[16] was put in Table 3. Isomaleimides generally have two sharp bands in the infrared at *ca.* 1780 (strong) and 1670 (medium) cm^{-1}. These absorptions can be associated with the anhydride-like carbonyl and the >C=N–bonds present in the isomaleimide ring.[8] In contrast, maleimides have characteristic broad carbonyl bands in the infrared with maxima near 1720 cm^{-1}.[8] Infrared data of the compounds II, X, and XIII agree with these infrared data. The compound (VIII) have three bands of almost the same intensity at 1770, 1700, and 1630 cm^{-1}. We could not assign the band at 1700 cm^{-1}. In comparison with X, *N*-acetoxymaleimide have three bands at 1813 (strong, acetoxy carbonyl), 1780 (medium, imide), and 1741 (strong, imide) cm^{-1}.

The NMR spectra of isoimides show two doublets due to unsymmetrical nature of olefinic hydrogen. In contrast, maleimides have only one singlet due to symmetrical nature of olefinic hydrogen. The NMR data of the compounds II, VIII, and X show two doublets due to H_a and H_b which are shown in XVII. On the other hand, those of the compounds XIII and XVI show only one singlet due to symmetrical nature of olefinic hydrogen.

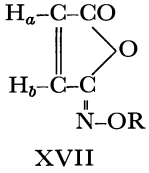

XVII

Experimental

All melting and boiling points are uncorrected. Infrared spectra were measured as potassium bromide disks or in liquid state using a Hitachi Infrared Photometer Model EPI-S2. NMR spectra were obtained with a Japan Electron Optics C-100 spectrometer in deuteriochloroform solution with tetramethylsilane as an internal standard. All solvents used for reactions were purified by usual methods.

Dehydration of N-*Benzyloxymaleamic Acid (I). Treatment of I with Thionyl Chloride*: According to Ames's procedure, the amic acid (I) was treated with thionyl chloride in benzene at refluxing temperature followed by working up of the reaction mixture to give the isoimide (II). Recrystallization from *n*-hexane gave colorless needles, mp 80—80.5°C (lit,[10] mp 80—81°C). Yield 72%.

Treatment of I with Phosphorus Pentoxide: Phosphorus pentoxide (1.7 g) was suspended in 10 m*l* of DMF. The amic acid (I), 2.2 g, was dissolved in 10 m*l* of DMF and the latter was combined with the suspension of P_2O_5 with cooling in

16) M. Narita, T. Teramoto, and M. Okawara, This Bulletin, **44** (1971), in press.

ice-cold water. After the exothermal reaction ended, the mixture was kept for 6 hr at room temperature and was poured into 100 m*l* of water. The precipitate was collected on filter and washed with water to give 1.4 g of the product (II), mp 73—76°C. Recrystallization from *n*-hexane gave colorless needles, mp 80—80.5°C.

Treatment of I with Dicyclohexylcarbodiimide: The amic acid (I), 1.0 g, was added to a solution of 1.1 g of dicyclohexylcarbodiimide in 10 m*l* of DMF. The reaction mixture was kept for 5 hr at room temperature. Dicyclohexylurea began to precipitate immediately. It was filtered off and the filtrate was poured into 100 m*l* of water to give precipitates which was collected by filtration and washed with water. The product was recrystallized from *n*-hexane, yield 0.73 g, mp 79—80.5°C. The same reaction was carried out in 10 m*l* of dioxane instead of DMF, yield 0.7 g, II, mp 79—80.5°C.

Treatment of I with Acetic Anhydride: The amic acid (I), 5.0 g, was suspended in 20 m*l* of acetic anhydride. It took 20 hr at room temperature till all the compounds dissolved in acetic anhydride. At the end of this time, acetic anhydride was distilled off under reduced pressure. The residue was dissolved in *n*-hexane and cooled. The product (VI) crystallized and was collected by filtration with suction, yield 0.23 g, mp 98—101°C. Repeated recrystallization of the product from *n*-hexane afforded needles of *N*,*N*-diacetyl-*O*-benzylhydroxylamine, mp 101—102°C (lit,[10] mp 101—102°C). The filtrate was distilled under reduced pressure to give three fractions. Fraction I, bp 63—65°C/3.5 mmHg (1.35 g), was maleic anhydride, fraction II, bp 120—5°C/0.4 mmHg (0.93 g), was the product (VI) and fraction III, bp 125—135°C/0.4 mmHg (1.96 g), was a mixture of VI and undefined product. These products were identified by IR spectra.

Dehydration of N-*Hydroxymaleamic Acid (VII). Treatment of VII with Phosphorus Pentoxide*: Phosphorus pentoxide, 6.0 g, was suspended in 7 m*l* of DMF and a solution of 2.6 g of the amic acid in 8 m*l* of DMF was mixed with it and the mixture was cooled in ice-cold water. When the heat ceased to evolve from the reaction mixture, it was kept for 5 hr at room temperature and poured into 80 m*l* of water. The solution was kept in a refrigerator for several days until the crystals appeared. Yield 0.24 g, mp 145°C (dec.). Further recrystallization from benzene-ethanol furnished pure *N*-hydroxyisomaleimide, mp 148°C (dec.).

Treatment of VII with Acetic Anhydride: The amic acid (VII), 5.0 g, was suspended in 20 m*l* of acetic anhydride. It took 20 hr at room temperature till all the compounds dissolved in acetic anhydride. At the end of this time, acetic anhydride was distilled off under reduced pressure. The residue was dissolved in 40 m*l* of hot benzene and cooled. The product, *N*,*O*-diacetylhydroxylamine (IX), crystallized and was collected by filtration with suction, yield 1.4 g, mp 86—90°C. Repeated recrystallisation of the product from benzene furnished colorless needles, mp 88.5—90°C (lit,[15] mp 91°C). IR (KBr disks): 3350, 3150 cm^{-1} (NH), 1795 cm^{-1} (–CO–O–N), 1655 cm^{-1} (–CO–NH–).

Found: C, 41.23; H, 6.14; N, 11.93%. Calcd for $C_4H_7NO_3$: C, 41.02; H, 6.03; N, 11.96%.

The filtrate (benzene solution) was distilled under reduced pressure to give maleic anhydride, bp 91—93°C/16 mmHg, (4.25 g). Maleic anhydride was identified by infrared spectrum. The pot residue was found to be *N*,*O*-diacetylhydroxylamine (0.65 g).

Treatment of VII with Acetyl Chloride and Pyridine: The amic acid (VII), 6.5 g, and 10 g of pyridine was dissolved in 50 m*l* of DMF. To this solution, a solution of 10 g of acetyl chloride in 50 m*l* of DMF was added with stirring under cooling with ice-cold water to maintain the temperature below 20°C. After the exothermal reaction ended, the mixture was kept for 6 hr at room temperature. DMF was distilled off under reduced pressure and the viscous residue was poured into 200 m*l* of water to give a precipitate, which was collected and washed with water, yield 2.9 g, mp 99—114°C. Recrystalization from carbon tetrachloride gave *N*-acetoxyisomaleimide, mp 115—116.5°C.

Isomerization of N-*Benzyloxyisomaleimide (II) to the Corresponding Imide (XIII).* Nos. 1—4 (see Table 1). The isoimide (II), 1.0 g, was dissolved in 10 m*l* of the solvent and the reaction was continued under the conditions described in Table 1. The solvent was distilled off under a reduced pressure and the residue was recrystallized from *n*-hexane. The respective products were characterized by mixed melting point with authentic sample and IR spectra. In the case of No. 4, the product was *N*-benzyloxymaleimide (XIII).

Nos. 5—9, No. 11, and No. 12 (see Table 1). The reaction was carried out under the condition shown in Table 1. After the reaction was over, the mixture was poured into 100 m*l* of water and the precipitate was collected and washed with water. The precipitates were recrystallized from *n*-hexane. The product was identified by mixed melting point with authentic sample and IR spectrum.

Reaction of N-*Benzyloxyisomaleimide (II) with Hydrogen Bromide and Dehydrobromination of the Product (XV).* No. 10 (see Table 1). The isoimide (II) was dissolved in 10 m*l* of 20% hydrogen bromide in acetic acid. The reaction mixture was kept for 5 hr at room temperature and then poured into 70 m*l* of water. The precipitate was collected and washed with ethanol, yield 1.2 g, mp 73—91°C. Repeated recrystallizations, from ethanol gave colorless needles, α-bromo-*N*-benzyloxysuccinimide (XV), mp 96—96.5°C. The product has characteristic bands at 3100—3050 cm^{-1}, 1500 cm^{-1} (–C_6H_5) and 1797 (weak), 1740 cm^{-1} (strong) (imide).

Found: C, 47.27; H, 3.43; N, 5.03; Br, 28.45%. Calcd for $C_{11}H_{10}NO_3Br$: C, 46.51; H, 3.55; N, 4.93; Br, 28.10%.

The imide (XV) (1.5 g) was suspended in 8 m*l* of triethylamine and allowed to stand for 3 hr at room temperature and poured into 80 m*l* of water. The precipitate was filtered off and washed with water to give 0.44 g of *N*-benzyloxymaleimide (XIII), yield 41%, mp 78—90°C. It was recrystallized from *n*-hexane to give light yellow crystals, mp 89.5—91°C.

Reaction of N-*Benzyloxyisomaleimide (II) with Aniline.* The isoimide (II), 1.02 g, was combined with 1.0 g of aniline in 10 m*l* of DMF and heated for 6 hr at 100°C. The mixture was cooled and poured into 50 m*l* of water to give precipitates, which were collected and washed with water to give 1.35 g of the product (XIV). The product was recrystallized from ethanol, mp 139.5—140.5°C. It has characteristic bands at 3320 cm^{-1} (NH), 1660, 1620 cm^{-1} (CO) and 1545 cm^{-1} (NH).

Found: C, 69.76; H, 5.72; N, 9.45%. Calcd for $C_{17}H_{16}N_2O_3$: C, 68.90; H, 5.44; N, 9.45%.

15) O. Exner and M. Horák, *Collect. Czech. Chem. Commun.*, **24**, 2992 (1959).

The Reaction of Azoxybenzene with Acetic Anhydride[1]

Shigeru OAE, Tetsuya MAEDA, and Seizi KOZUKA

Department of Applied Chemistry, Faculty of Engineering, Osaka City University, Sumiyoshiku, Osaka

(Received December 7, 1970)

When azoxybenzene was allowed to react with equimolar amount of acetic anhydride, a mixture of azobenzene, acetanilide, and acetic acid was obtained along with such gaseous products as carbon dioxide, carbon monoxide and methane. In the reaction of azoxybenzene with an excess acetic anhydride, however, azobenzene was not isolated, and only acetanilide was obtained. Acetanilide and acetic acid were also obtained in the reaction of azobenzene with acetic anhydride. The results suggest the initial formation of azobenzene which is eventually converted to acetanilide in the subsequent reaction with an excess acetic anhydride. The formation of acetanilide was inhibited by the addition of such radical scavengers as iodine, hydroquinone, and nitrobenzene. A free radical mechanism is suggested for the reaction. Phenazine *N*-oxide also apparently undergoes similar reaction.

The reactions of tertiary amine *N*-oxides such as pyridine or picoline *N*-oxides with acetic anhydride have been investigated extensively by means of product analyses,[2] kinetics,[3] and tracer studies.[4] The first step of the reactions are considered to proceed throughout initial acylation of oxygen of the *N*-oxides.[5] Thus, the reactivity of *N*-oxide in the reaction with acetic anhydride depends primarily on the basicity of the *N*-oxide oxygen. Dimethylaniline *N*-oxide, a more basic *N*-oxide (pK_a=4.21[6]), reacts smoothly with acetic anhydride even below 0°C[7]), while the reaction of pyridine *N*-oxide, a less basic *N*-oxide (pK_a=0.56[8]), requires a few hours of refluxing for the completion of the reaction with the same reagent. Very little study has been made on the reaction of azoxybenzene with acetic anhydride,[9] presumably due to its poor reactivity. The reaction, however, did occur under prolonged heating at relatively high temperatures to give an unusual product, acetanilide, as the main product. This paper deals with the details of preliminary investigation of the reaction studied mainly by means of product analysis.

Results and Discussion

Reaction of Azoxybenzene with Acetic Anhydride. Since the basicity of azoxybenzene is very small (pK_a=6.45[10]), the reaction of azoxybenzene with acetic anhydride is considered to be sluggish. Thus, the reaction was carried out at 190°C in an autoclave under nitrogen atmosphere, and a mixture of azobenzene and acetanilide was obtained. The yield of acetanilide was less than 100% based on the amount of azoxybenzene used. That is, only a half of azoxybenzene used is apparently converted to acetanilide. Under the same conditions, azoxybenzene underwent no thermal deoxygenation. Gaseous components were analyzed by means of gas chromatography. Carbon dioxide, carbon monoxide, and methane were detected as the main gaseous products. When *N*-oxide was treated with an excess acetic anhydride, no detectable amount of azobenzene was found, whereas acetanilide was obtained along with acetic acid and gaseous products. The reaction conditions and the yield of the products are listed in Table 1.

Table 1. Reaction of azoxybenzene with acetic anhydride under N_2 atmosphere in autoclave

Reaction system	Reaction condition Molar ratio	Product (%)
PhN=NPh + Ac_2O ↓ O	190°C, 15 hr 1 : 1	PhN=NPh (60) $PhNHCOCH_3$(13) CH_3CO_2H(63) CO_2(95), CH_4(2) CO(14)
PhN=NPh + Ac_2O ↓ O	190°C, 15 hr 1 : 5	$PhNHCOCH_3$(78) CH_3CO_2H(70)
PhN=NPh + AcOH ↓ O	190°C, 15 hr 1 : 1	no reaction

The first step of the reaction is considered to be the formation of the *N*-acetoxyammonium salt (A) as in the

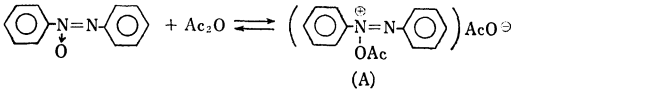

(A)

reactions of pyridine- and the related *N*-oxides with acylating agents.[5] No oxygen exchange reaction was found between the *N*-acyloxy compound of pyridine

1) Part XXVI on Rearrangement of *t*-Amine Oxides.

2) a) M. Katada, *Yakugaku Zasshi*, **67**, 51 (1947). b) S. Okuda, *Pharm. Bull.*, **3**, 316 (1955). c) V. Bockelheide and W. Linn, *J. Amer. Chem. Soc.*, **76**, 1286 (1954).

3) a) T. H. Markgraf, H. B. Brown, Jr., S. C. Morre, and R. G. Peterson, *J. Amer. Chem. Soc.*, **85**, 958 (1963). b) J. H. Markgraf and M. K. Ahn, *ibid.*, **86**, 2699 (1964).

4) a) S. Oae, T. Kitao, and Y. Kitaoka, *Tetrahedron*, **19**, 827 (1963). b) S. Kozuka, S. Tamagaki, T. Negoro, and S. Oae, *Tetrahedron Lett.*, **1968**, 923.

5) C. W. Muth and R. S. Darlak, *J. Org. Chem.*, **30**, 1909 (1965).

6) M. Colonna, *Boll. Sci. Fac. Chim. Ind. Bologna*, **15**, 1 (1957).

7) R. Huisgen, F. Bayerleine, and W. Heydkamp, *Chem. Ber.*, **93**, 363 (1960).

8) T. Kubota and H. Miyazaki, *Nippon Kagaku Zasshi*, **79**, 924 (1958).

9) M. M. Shemyakin, T. E. Agadzhanyan, V. I. Maimind, R. V. Kudryavtsev, and D. N. Kursanov, *Proc. Nat. Acad. Sci, U.S.*, **135**, 1295 (1960).

10) Chi-Sun Harn and H. H. Jaffe, *J. Amer. Chem. Soc.*, **84**, 949 (1962).

bases such as (B) in our earlier ^{18}O-tracer experiments,[11]

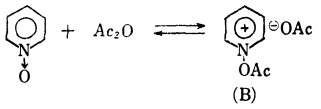

but a somewhat different oxygen exchange could be expected in this case through the following five membered cyclic migration. This supposition is based on

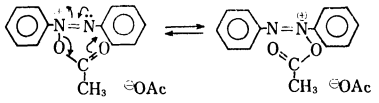

the observation with ^{15}N-labeled azoxybenzene by Shemyakin *et al.*[12] who showed that there is an intramolecular oxygen migration within the Wallach rearrangement. In order to examine the possible oxygen equilibration during the reaction, azoxybenzene was treated with equimolar amount of ^{18}O-labeled acetic anhydride and recovered when the reaction was about half completed . If the migration of the acetoxy group from one nitrogen atom to the other occurs during the reaction, a substantial incorporation of ^{18}O in the recovered *N*-oxide is expected. However, no noticeable amount of ^{18}O was found in the recovered *N*-oxide. Thus, the possibility of such a migration can be ruled out. For further insight into the nature of the reaction, the effect of atmosphere on the reaction was examined and the results are tabulated in Table 4. In view of the large amounts of carbon dioxide, carbon monoxide and methane, the mechanism of the reaction seems to involve the homolytic fission of the N–O bond of the *N*-acyloxy compound at the initial stage of the reaction. Acetanilide obtained in the reaction with an excess acetic anhydride is considered to be

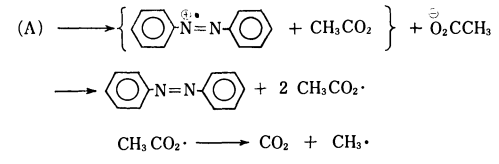

formed *via* azobenzene. A similar reaction involving the formation of the salt (A) and subsequent homolytic fission of the N–O bond seems to take place with phenazine *N*-oxide which in the presence of acetic anhydride

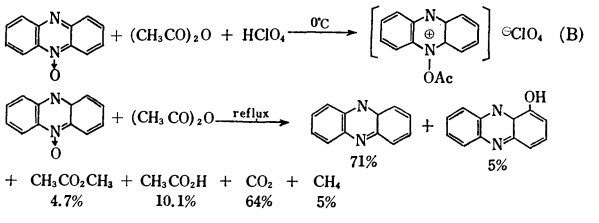

gives salt (B) of perchloric acid, and generates large amounts of methane and carbon dioxide yielding mainly the reduced compound, phenazine, under refluxing with acetic anhydride.

Reaction of Azobenzene with Acetic Anhydride. Examination of the data shows that the reaction of an equimolar amount of azoxybenzene and acetic anhydride gives azobenzene along with a small amount of acetanilide while the reaction with excess acetic anhydride gave only acetanilide in a better yield. In order to examine the formation of the intermediate,

Table 2. Reaction of azobenzene with acetic anhydride under N_2 atmosphere in autoclave

Reaction system	Reaction condition Molar ratio	Product (%)
PhN=NPh+Ac_2O	190°C, 15 hr 1 : 1	$PhNHCOCH_3$(83) CH_3CO_2H(60) CO_2(29), CO(7)
PhN=NPh+AcOH	200°C, 15 hr 1 : 1	no reaction
p-$CH_3C_6H_4N$=NPh +Ac_2O	200°C, 12 hr 1 : 1	*p*-$CH_3C_6H_4N$=NPh (30 recovered) *p*-$CH_3C_6H_4NHCOCH_3$ (13) $PhNHCOCH_3$(15)

Table 3. Reaction of azobenzene with acetic anhydride under N_2 atmosphere Effect of radical acceptors

Reaction system	Reaction condition Molar ratio	Yield of $PhNHCOCH_3$
PhN=NPh+Ac_2O	200°C, 15 hr 1 : 5	83%
PhN=NPh+Ac_2O +*p*-hydroquinone	200°C, 15 hr 1 : 5 : 0.2	40%
PhN=NPh+Ac_2O+I_2	200°C, 15 hr 1 : 5 : 0.2	42%
PhN=NPh+Ac_2O +$PhNO_2$	200°C, 15 hr 1 : 5 : 0.1	0%

Table 4. Effect of atmosphere in autoclave

Reaction system	Reaction condition	Yield of $PhNHCOCH_3$
PhN=NPh+Ac_2O	200°C, 15 hr, 1 : 5 under N_2 atm.	83%
PhN=NPh+Ac_2O	200°C, 19 hr, 1 : 5 under H_2 atm.	68%
PhN=NPh+Ac_2O	200°C, 15 hr, 1 : 5 under O_2 atm.	70%
PhN=NPh+Ac_2O ↓ O	200°C, 15 hr, 1 : 5 under N_2 atm.	78%
PhN=NPh+Ac_2O ↓ O	200°C, 15 hr, 1 : 5 under air	47%

11) Unpublished work from our laboratory.
12) M. M. Shemyakin, V. I. Maimind, and B. K. Vaichunaite, *Zh. Obshch. Khim.*, **28**, 1708 (1958).

azobenzene, the reaction of azobenzene with acetic anhydride was studied. As was expected, acetanilide was obtained in good yield from the reaction mixture along with moderate amounts of acetic acid and gaseous products. Acetic acid was found to undergo no reaction with azobenzene. The effects of radical scavengers and atmosphere in an antoclave were also examined, the results of which are in Tables 2—4. The reaction with an unsymmetrical azobenzene, 4-methylazobenzene, gave nearly the same amount of both acetanilide and 4-methylacetanilide. No symmetrical azobenzene was found in the recovered reaction mixture in which only 4-methylazobenzene was found. The results clearly rule out the possibility of crossover and the return of the fragments to the original compound. The yield of acetanilide was apparently decreased not only by the presence of oxygen but also by the addition of radical scavengers such as hydroquinone, iodine and, nitrobenzene, suggesting a free radical mechanism for the reaction. The mechanism of the reaction of azobenzene with acetic anhydride to give acetanilide may be formulated as follows.

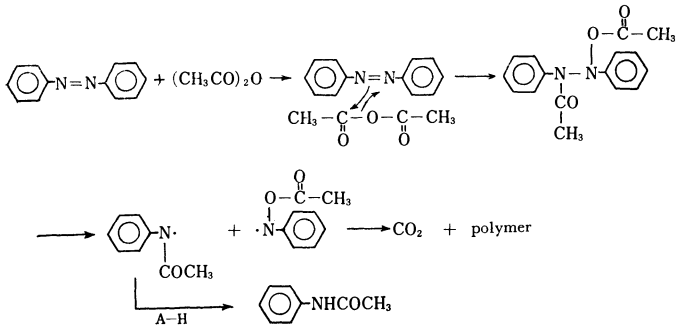

Experimental

Materials. Azoxybenzene was prepared by the reduction of nitrobenzene[13] (mp 35—36°C from methanol). Azobenzene was prepared by the usual method[14] (mp 66—67.5°C from ethanol). 4-Methylazobenzene was prepared by the process reported by Godger[15] (mp 71—72°C from ethanol). Preparation of ^{18}O-labeled acetic anhydride and the method of its isotope analysis were described previously.[16] Phenazine *N*-oxide was synthesized from aniline and nitrobenzene with sodium hydroxide.[17]

The reaction of Azoxybenzene with Acetic Anhydride. A mixture of azoxybenzene (7.0 g, 0.035 mol) and acetic anhydride (3.8 g 0.037 mol) was heated in an autoclave at 190°C for 15 hr under N_2 atmosphere. Distillation of the reaction mixture gave acetic acid (1.4 g). The residue was extracted first with *n*-hexane three times and then with benzene three times. From the hexane layer, azobenzene (3.8 g, 66—68°C) was obtained along with a small amount of acetanilide (0.04 g). Separation was performed by recrystallization from *n*-hexane. Acetanilide (0.6 g, mp 114—115°C) was obtained from the benzene layer. The residue which did not dissolve in these solvents, was chromatographed through an active alumina column with chloroform as an eluent. A small amount of acetanilide (0.05 g) was obtained. The gaseous components were directly transferred from the autoclave into a gas sampler and analyzed by gas chromatography (H_2 carrier, temp.: 60°C, active carbon 4 m); carbon dioxide, methane and carbon monoxide were detected. These compounds were identified by comparing their retention times with those of the corresponding authentic samples. Quantitative analysis of carbon dioxide was performed by the measurement of the amount of barium carbonate absorbed in saturated $Ba(OH)_2$ aq. solution. Carbon monoxide and methane were determined by comparing the peak areas with that of carbon dioxide, taking the relative intensities of the respective gaseous products into consideration hydrogen being used as a carrier gas.

Reaction of Azoxybenzene with ^{18}O-Labeled Acetic Anhydride. A mixture of azoxybenzene (2.0 g, 0.01 mol) and ^{18}O-labeled acetic anhydride (1.1 g, 0.01 mol, 0.89 atom% ^{18}O) was heated in an autoclave at 175°C for 10 hr under N_2 atmosphere. Distillation under reduced pressure gave crude azoxybenzene (1.2 g, bp 195—200°C/16 mmHg) along with small amounts of azobenzene (0.13 g) and acetanilide (trace). The recovered *N*-oxide was then purified by recrystallization from ethanol (mp 34—35°C). No incorporation of any excess ^{18}O was found in the recovered azoxybenzene (0.20 atom% ^{18}O).

Reaction of Phenazine N-Oxide with Acetic Anhydride. A mixture of phenazine *N*-oxide (5.0 g, 0.026 mol) and acetic anhydride (14.0 g, 0.14 mol) was refluxed for 5 hr. The low boiling point fractions trapped in acetone - dry ice bath and gaseous products were analyzed by gas chromatography. After any residual acetic anhydride was driven off, the residue was chromatographed on active alumina with methylene chloride as an eluent. The eluent was evaporated and the residue was hydrolyzed with 20% NaOH aq. solution. The precipitate was collected and recrystallized from ethanol (mp 171—172°C). This compound was identified as phenazine (3.3 g). The filtrate was acidified with HCl and the precipitate was recrystallized from isopropyl alcohol. Thus 1-hydroxy phenazine (0.25 g, mp 155—157°C) was obtained. All these compounds were determined by comparison with the authentic samples.

The isolation of N-Acetoxyphenazinium Perchlorate. The compounds was prepared by the process reported by Muth and Daolak[5] An ice cold solution of 0.7 g of 70% $HClO_4$ in 3 m*l* acetic anhydride was added dropwise to a stirred, ice-cold solution of 0.5 g of phenazine *N*-oxide in 5 m*l* of acetic acid and 10 cc of acetic anhydride. Orange colored crystals were separated by filtration. The crystals of *N*-acetoxyphenazinium perchlorate (mp 274—275°C, dec.) weighed 0.6 g. Found: C, 49.97; H, 3.38; N, 8.12%. Calcd for $C_{14}H_{11}ClN_2O_6$: C, 49.71; H, 3.26; N, 8.29%.

Reaction of Azobenzene with Acetic Anhydride. A mixture of azobenzene (6.4 g, 0.035 mol) and acetic anhydride (17.5 g, 0.175 mol) was heated at 190°C for 15 hr in an autoclave under N_2 atmosphere similarly and both acetanilide (3.88 g, 0.029 mol) and acetic acid (1.3 g) were isolated. Through gas-chromatographic analysis of the gaseous products, carbon dioxide and carbon monoxide were detected but not methane. The reaction 4-methylazobenzene (2.0 g, 0.013 mol) with acetic anhydride (1.1 g, 0.011 mol) was also carried out similarly and a mixture (0.41 g) of acetanilide and 4-methylacetanilide was obtained. The ratio of the mixture components was determined by integrating the NMR chemical shifts of methyl protons, *i.e.*, the 4-methyl signal of N-acetyl-*p*-toluidine *vs.* acetyl methyl protons of acetanilide. The results are given in Table 2. All the other experiments were carried out under corresponding conditions.

13) A. Lachman, *J. Amer. Chem. Soc.*, **24**, 1180 (1902).
14) "Organic Syntheses," Vol. 22, p. 28, ed by H. Blatt.
15) G. M. Gadger, R. T. Drewer, and G. E. Lewis, *Aust. J. Chem.*, **16**, 1047 (1963).
16) S. Oae and S. Kozuka, *Tetrahedron*, **20**, 2691 (1964).
17) C. Whol and . Aue, *Ber.*, **34**, 2446 (1910).

The Tracer Study of the Reaction of Diphenyl Sulfone-1-^{14}C with Elemental Sulfur Using a Convenient Degradative Method

Shigeru OAE, Mamoru NAKAI,* Yoshiyuki TSUCHIDA, and Naomichi FURUKAWA

Department of Applied Chemistry, Faculty of Engineering, Osaka City University, Sumiyoshiku, Osaka

(Received June 23, 1970)

The reaction of diphenyl sulfone with elemental sulfur to give diphenyl sulfide and sulfur dioxide at above 300°C was investigated using diphenyl sulfone-1-^{14}C. By the degradation of the product, diphenyl sulfide-*x*-^{14}C, it was found that no migration of sulfide group took place. *β*-Naphthyl phenyl sulfone was also subjected to the same reaction, and not only *β*-naphthyl phenyl sulfide but also di-*β*-naphthyl sulfide and diphenyl sulfide were found among the products. These observations appear to indicate the reaction to be a rather simple displacement reaction that involves the initial attack of polymeric sulfur radical chain at C-1 bearing sulfonyl function.

Krafft and Vorster[1] showed that diphenyl sulfone reacts with elemental sulfur to form diphenyl sulfide and sulfur dioxide at elevated temperature. The mechanism of this reaction was recently investigated using ^{35}S-labeled compounds.[2] It was shown to involve the initial S–C bond cleavage of the sulfone and the subsequent replacement of sulfone group by elemental sulfur as shown by Eq. (1). The reaction of diphenyl sulfoxide with elemental sulfur proceeds through a simple reduction involving the cleavage of S–O bond as shown by Eq. (2). The difference between the above two reactions seem to be due to the fact that the force constant of the S–O bond of the sulfoxide is appreciably lower than that of the sulfone.[3]

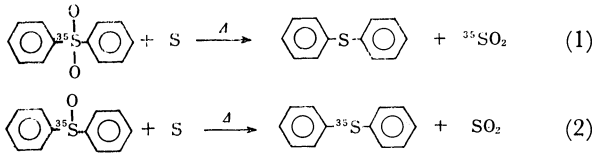

(1)

(2)

We have extended the reaction with elemental sulfur to dibenzyl[4] and dibutyl[5] sulfones or sulfoxides. We have also studied the reaction of diphenyl sulfone and sulfoxide with diphenyl disulfide,[6] and found that in each case the weakest bond of the respective compound is cleaved by elemental sulfur radical chain at the initial stage of the reaction. An important remaining question is if there is any cross-over of phenyl group between diphenyl sulfone or sulfide during the reaction. If there is any cross-over of the phenyl group, the possibility of migration of the sulfide group arises, since the attack of polymeric sulfur radical chain at *o*- or *p*-position of diphenyl sulfone could eventually give rise to the sulfide.

Thus, we have carried out a few critical experiments such as cross-over and ^{14}C tracer, by allowing *β*-naphthyl phenyl sulfone and diphenyl sulfone-1-^{14}C to react with elemental sulfur. We also examined the possibility of using the photolysis of diphenyl sulfone for a convenient method of degradation. This paper gives a detailed account and implications of these observations.

Results and Discussion

Reaction of β-Naphthyl Phenyl Sulfone with Sulfur. In order to examine the possibility of intermolecular cross-over of phenyl group in the reaction of diphenyl sulfone with sulfur, *β*-naphthyl phenyl sulfone was employed for the reaction. The reaction was carried out with equimolar amounts of the sulfone and elemental sulfur at a high temperature. The identification and analysis of the products were performed by means of gas chromatography.

If the reaction proceeded *via* an intermolecular process involving complete rupture of aryl-sulfur bonds, both diphenyl sulfide and *β*-dinaphthyl sulfide should be obtained among the products. If it proceeded without any cross-over of two aryl groups, *β*-naphthyl phenyl sulfide would be the sole product. (Eq. (3)).

Actually, from the product analysis, both diphenyl and di-*β*-naphthyl sulfides were obtained in 8% and 10% yields, respectively, along with *β*-naphthyl phenyl sulfide in 21% yield. Apparently the result indicates that there is some cross-over of aryl groups during the reaction, though the non-cross-over process is the predominant one.

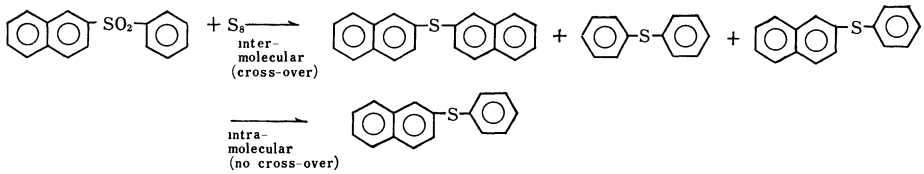

(3)

* Ube Industries Ltd., Ube, Yamaguchi-ken.

1) F. Krafft and W. Vorster, *Ber.*, **26**, 2813 (1893).
2) S. Oae and S. Kawamura, This Bulletin, **36**, 163 (1963).
3) C. C. Price and S. Oae, "Sulfur Bonding," Ronald Press Inc., New York (1962), p. 66.
4) W. Tagaki, S. Kiso, and S. Oae, This Bulletin, **38**, 414 (1965).
5) S. Kiso and S. Oae, *ibid.*, **40**, 1722 (1967).
6) S. Oae, Y. Tsuchida, and H. Nakai, *ibid.*, **44**, 451 (1971).

TABLE 1.

Activity of diphenyl sulfone	Condition	Sulfide[a] formed	Sulfone recovered	% of rearrangement[b]
3020 cpm/mg	310°C, 1 hr	38.2%	26.6%	4.7%
3540 cpm/mg	320°C, 1 hr	45.7%	20.6%	5.7%

a) Assayed by transformation into diphenylsulfone. The yield was determined by means of the isotope dilution technique.
b) Calculated by Eq. (6).

TABLE 2.

Activity of diphenyl sulfone	Condition	Yield of biphenyl	Activity of biphenyl	Activity of benzoic acid	% of rearrangement
4.62×10^5 dpm/mmol	15 hr, r.t. 0.3 g in 100 ml of benzene	27%	4.65×10^4 dpm/mmol	3.70×10^4 [a] dpm/mmol	0.6%

a) Employed diphenyl sulfone the activity of which was originally placed in 80.2% at 1-position.

Reaction of Diphenyl Sulfone-1-^{14}C with Sulfur. The synthesis of diphenyl sulfone-1-^{14}C is outlined below.

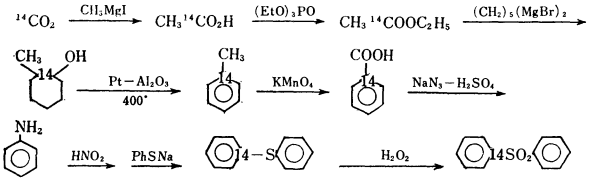

Diphenyl sulfone-1-^{14}C thus obtained was reacted with an equimolar amount of elemental sulfur at 310—320°C in nitrogen stream. Both the yield of diphenyl sulfide-*x*-^{14}C formed and diphenyl sulfone-*x*-^{14}C recovered were determined by the isotope dilution method. The degradation of diphenyl sulfide-*x*-^{14}C was carried out by the covenient process mentioned below (Eq. (4)). The results are shown in Table 1.

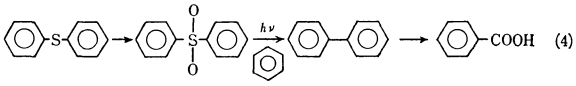

(4)

The result reveals that the amount of the ^{14}C rearrangement remains nearly the same in spite of the change of the reaction condition, though a slight difference is observed in the yield of diphenyl sulfide formed. Thus, the reaction of diphenyl sulfone with elemental sulfur appears to be a direct displacement reaction of the sulfone group by elemental sulfur, since the ratio of the rearrangement remains only about 5%. Besides diphenyl sulfide, a small amount of diphenyl disulfide and polymeric substance were formed in the reaction. Both the tracer experiments and previous results, suggest that the replacement of the sulfone group with sulfur atom involves the initial attack of sulfur biradical[7] on the carbon atom bearing sulfone group, followed by the cleavage of C–S bond of the sulfonyl radical and the subsequent attack on another sulfone by polymeric sulfur chain biradical, giving rise to diphenyl sulfide and diphenyl disulfide. Thus a rough sketch of the overall reaction may be illustrated as shown below. (Eq. (5)).

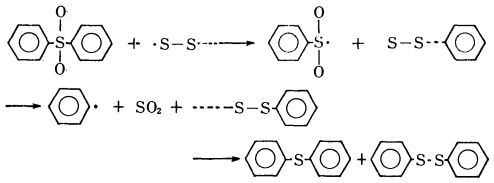

(5)

Previously, the degradation of ^{14}C-labeled diphenyl sulfone was carried out by means of a rather tedious way of the initial alkaline fusion of the sulfone,[8] followed by subsequent cleavage of phenol obtained.

Recently, it has been reported by Kharasch and Khodair that the photolysis of diphenyl sulfone in benzene at room temperature gave biphenyl in a good yield upon irradiation with 2537 Å light.[9]

In order to test the possibility of using this reaction for a simple convenient degradation, diphenyl sulfone-1-^{14}C was subjected to photolysis to see whether or not the original activity at ^{14}C remains at the same position. The result of the degradation reveals that all the activity remains at the carboxyl carbon of benzoic acid (corresponding to 1-position of diphenyl sulfone) as shown in Table 2. The low yield of biphenyl appears to be caused by the use of low efficient irradiation. Biphenyl formed by the photolysis was diluted with an aliquot of inactive biphenyl and then oxidized by CrO_3 in acetic acid. The activity of benzoic acid thus obtained was compared with that of biphenyl. The percentage rearrangement of the activity at 1-position of the sulfide or the sulfone was calculated by the following equation.

$$\left(1-\frac{\text{Activity of benzoic acid}}{\text{Activity of biphenyl}}\right)\times 100 \qquad (6)$$

Thus, the photolysis of diphenyl sulfone in benzene was found to proceed through the mechanistic route proposed earlier by Kharasch and Khodair[9] as shown by

7) It is known that elemental sulfur behaves as a biradical chain at high temperatures and diphenyl sulfide is obtained together with by-products such as diphenyl disulfide, when a mixture of benzene and sulfur is heated at 350°C. W. A. Pryor, "Mechanism of Sulfur Reactions," McGraw-Hill Book Co., Inc., New York (1962), p. 8; H. B. Glass and E. E. Reid, *J. Amer. Chem. Soc.*, **51**, 3428 (1929).

8) S. Oae and N. Furukawa, This Bulletin, **39**, 2260 (1966).
9) N. Kharasch and A. I. A. Khodair, *Chem. Commun.*, **1967**, 98.

Eq. (7).

$$RC_6H_4SO_2C_6H_4R \longrightarrow RC_6H_4\cdot + RC_6H_4SO_2\cdot$$

$$RC_6H_4\cdot + C_6H_6 \longrightarrow RC_6H_4(H)\text{-}C_6H_5 \quad (A)$$

$$(A) + RC_6H_4SO_2\cdot \longrightarrow RC_6H_4C_6H_5 + RC_6H_4SO_2H \quad (?)$$

(or $RC_6H_4\cdot$) (or RC_6H_5)

(where R=H or CH_3) (7)

According to this mechanism no rearrangement of the activity at 1-position should take place during photolysis of the sulfone. Therefore, the photolysis of diphenyl sulfone is a quite suitable and convenient method for the degradation.

Experimental

Preparation of Diphenyl Sulfone-1-^{14}C. Diphenyl sulfone-1-^{14}C was synthesized through 9 steps starting from barium carbonate-^{14}C. The synthetic method was described elsewhere.[10]

Reaction of Diphenyl Sulfone-1-^{14}C with Sulfur. The reaction was carried out in the same way as for the previous cases:[2] diphenyl sulfone-1-^{14}C, (0.005 mol), was thoroughly mixed with 0.005 g atom of elemental sulfur in a Claisen-flask, which was quickly placed in a pre-heated metal-bath, nitrogen gas being passed through the reaction flask. The reaction started at 310 or 320°C (metal-bath temperature) and sulfur dioxide evolved was trapped in several traps cooled with dry-ice - acetone. After the reaction mixture was kept at around 310 or 320°C for 1 hr, it was dissolved in benzene into which known amount of inactive diphenyl sulfide and the sulfone was added in order to determine their yields by means of the isotope dilution method. When a clear benzene solution was concentrated, crystals of the sulfone deposited and were recrystallized from *n*-hexane - benzene two or three times. Diphenyl sulfide obtained was also repeatedly distilled until it became transparent, then was converted into diphenyl sulfone for ^{14}C-counting.

Reaction of β-Naphthyl phenyl Sulfone with Sulfur. The reaction was carried out in the same way as in the reaction of diphenyl sulfone-1-^{14}C with sulfur. Identification of the products was performed by means of gas chromatography (High Vacuum Silicon at 250 or 300°C).

The Degradation of Diphenyl Sulfide-x-^{14}C. Photolysis of the sulfone in benzene was carried out in the same way as that by Kharasch and Khodair:[9] photolysis of the sulfone (0.3 g) was carried out in 100 m*l* of benzene at room temperature for 15 hr, and gave biphenyl in 27% yield together with tarry by-products. The reaction mixture was treated with carbon disulfide, and a part dissolved in it was diluted with 0.5 g of inactive biphenyl. An aliquot (about 0.1 g) of the crude biphenyl was purified by sublimation and the rest was dissolved in 5 m*l* of acetic acid. To this solution was added a solution of 5 g of anhydrous chromic acid in 2 m*l* of water and 5 m*l* of acetic acid dropwise with stirring at 70—75°C. Carbon dioxide evolved during the oxidation. After the addition was complete, the contents of the flask was stirred for 1/2 hr at 70—75°C. The reactant was then quenched into 40 m*l* of water and extracted with ether. The ether layer was washed with water three times to remove acetic acid and then re-extracted with 5% alkali solution. The crude benzoic acid thus obtained was purified by sublimation. The benzoic acid was obtained in about 20% yield. Both benzoic acid and biphenyl were employed for counting of ^{14}C activity.

Measurement of the Activities. All the compounds were counted by a liquid scintillation counter (TEN), in toluene solution using POPOP as a scintilator.

We wish to thank Dr. M. Hamada and Dr. T. Nakabayashi of the Radiation Center of Osaka Prefecture for their advice, and for affording facilities for the measurement of the activities.

10) S. Oae, N. Furukawa, M. Kise, and M. Kawanishi, This Bulletin, **39**, 1212 (1966).

The Mechanism of Silver Perchlorate Catalyzed Solvolysis Reaction of 2-Chlorocyclohexanone-1-^{14}C

Taketoshi MASUIKE, Naomichi FURUKAWA, and Shigeru OAE

Department of Applied Chemistry, Faculty of Engineering, Osaka City University, Sumiyoshiku, Osaka

(Received July 2, 1970)

Silver perchlorate assisted solvolysis of 2-chlorocyclohexanone-1-^{14}C in ethanol-water solution gives 2-ethoxycyclohexanone-*x*-^{14}C. Successive degradation of the product reveals that the ^{14}C activity is distributed in both the carbonyl carbon and the α-carbon of ethoxyketone. The ^{14}C distribution pattern suggests that a part of the reaction proceeds *via* an epoxide intermediate which is formed by the initial attack of ethanol on the carbonyl carbon, followed by the migration of carbonyl oxygen to the α-carbon of 2-chlorocyclohexanone.

In the silver or mercury ion-catalyzed solvolytic reactions of haloketones, a carbonyl group, attached to either γ or δ position of the leaving group, is known to accelerate remarkably the rate of the reaction despite the fact that the carbonyl group is expected to retard it by its strong electron-withdrawing property. These results suggest that the carbonyl group participates in the solvolysis reaction. The rate enhancement and neighboring group participation of the carbonyl group were in fact confirmed by both kinetic study[1,2] and isolation of the products[2,3] such as **1** which undoubtedly results from the participation of carbonyl oxygen. Further, Ward and Sherman, Jr. recently isolated the intermediate **2** as a hexachloroantimonate.[4] More recently, Gassman and his coworkers demonstrated that the enol form of the ketone, which exists in a small amount in an equilibrium with the keto form, participates in the solvolysis reaction, by showing that the rate of solvolysis of anti-7-hydroxynorbornane-2-one-*p*-toluenesulfonate is 2×10^7 times larger than that of 7-hydroxynorbornane-*p*-toluenesulfonate.[5] Although participation of the carbonyl group in the solvolytic reaction has been well established in the case of halo-ketones, in which the carbonyl group is separated at least one methylene group away from the cationic center, evidence supporting the interaction of the carbonyl group with the adjacent cation center is also available. As an example of such interaction, Bergmann obtained the compound **3** from the methanolysis of 2-bromocyclohexanone.[6] The product **3** is probably formed by the dimerization of the epoxide **4**. Silver perchlorate-catalyzed solvolysis of 2-chlorocyclohexanone-1-^{14}C was carried out, to make this interaction clearer. This paper describes briefly the partial migration of carbonyl oxygen of 2-chlorocyclohexanone to the α-position of the product and the probable mechanism of the whole reaction.

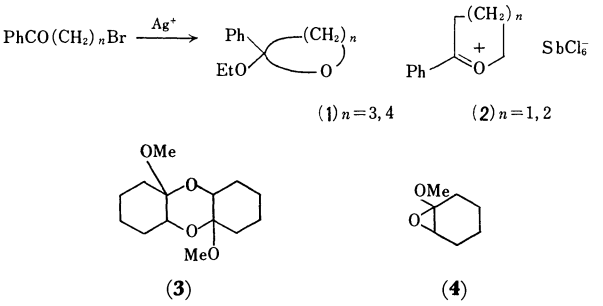

(1) $n=3,4$ (2) $n=1,2$

(3) (4)

2-Chlorocyclohexanone-1-^{14}C was synthesized, and a series of successive degradations of the product was carried out as shown below (Fig. 1).

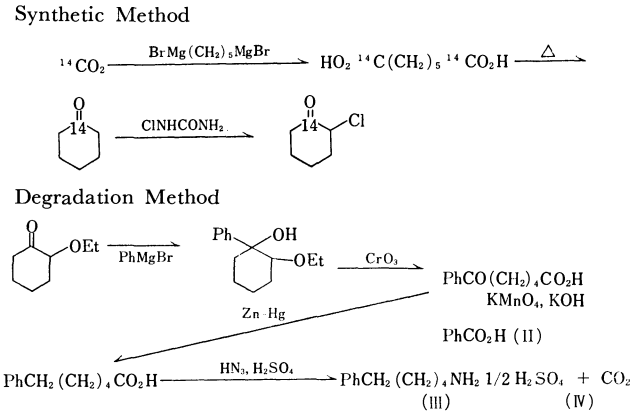

Fig. 1.

Experimental

Preparation of 2-Chlorocyclohexanone-1-^{14}C[7]. Pimeric acid-1,7-^{14}C was obtained by carbonation of the Grignard reagent prepared from 0.9 g of magnesium and 4.0 g of pentamethylene dibromide, with $^{14}CO_2$ generated from 7.0 g (5 mCi) of barium carbonate. The crude product was recrystallized from benzene: yield was 1.8 g (64.9%), mp 104°C.

A mixture of 1.8 g of pimeric acid-1,7-^{14}C and 0.1 g of barium carbonate was gradually heated in a metallic bath to about 320°C and the distillate was collected. The crude cyclohexanone-1-^{14}C (1.0 g), was diluted by adding 10 g of ordinary cyclohexanone and purified by distillation (bp 154—155.5°C). Four grams of the cyclohexanone-1-^{14}C was stirred gently overnight in a water bath at room temperature with 2 g of acetic acid and 20 m*l* of chlorourea solution, which was prepared by absorbing 35 g of chlorine in a stirred suspension of 50 g of calcium carbonate and 300 g of urea in 50 m*l* of water. The solution was then filtered with suction and the filtrate was finally diluted with water to 200 m*l*.

1) S. Oae, *J. Amer. Chem. Soc.*, **78**, 4030 (1956).
2) G. Baddley, E. K. Baylis, B. G. Heaton, and J. W. Rasburn, *Proc. Chem. Soc.*, **1961**, 451.
3) D. J. Pasto, K. Graves, and M. M. Serve, *J. Org. Chem.*, **32**, 774 (1967).
4) H. R. Ward and P. D. Sherman, Jr., *J. Amer. Chem. Soc.*, **90**, 3812 (1968).
5) P. G. Gassman and J. L. Marshall, *ibid.*, **88**, 2599 (1966); P. G. Gassman, J. L. Marshall, and J. M. Hornback, *ibid.*, **91**, 5811 (1969); P. G. Gassman and J. M. Hornback, *ibid.*, **91**, 5817 (1969).
6) M. Bergmann and M. Gierth, *Ann. Chem.*, **448**, 48 (1926).
7) R. B. Loftfield, *J. Amer. Chem. Soc.*, **73**, 4707 (1951).

The reaction mixture was then extracted with benzene. The benzene solution was dried over anhydrous sodium sulfate. After removing the solvent, the residue was distilled to give 4 g of 2-chlorocyclohexanone-1-^{14}C, bp 159—159.5°C (74%).

Solvolysis of 2-Chlorocyclohexanone-1-^{14}C and Isolation of the Products. 2-Chlorocyclohexanone-1-^{14}C was solvolyzed in 12.5 m*l* of 80% aqueous ethanol containing 3.1 g of silver perchlorate at 70°C in a water bath for 18 hr. After completion of the reaction, the reaction mixture was neutralized with aqueous sodium carbonate solution. In order to determine the yield of the products by isotopic dilution method, the following non-radioactive compounds were added to the solution, *i.e.*, 1.113 g of 2-ethoxycyclohexanone, 1.086 g of 2-hydroxycyclohexanone, and 0.798 g of ethyl cyclopentanecarboxylate. After the precipitated silver chloride was filtered off, the filtrate was extracted with ether and then with methylene chloride. Both extracts were dried over sodium sulfate. The ether extract gave 2.7 g of yellow oily product (bp *ca.* 88°C/22.5 mmHg) from which 2-ethoxycyclohexanone (0.750 g) and ethyl cyclopentanecarboxylate (0.460 g) were identified and separated with gas liquid chromatography. 2-Hydroxycyclohexanone (0.340 g) was obtained from the methylene chloride extract by removing the solvent and keeping the residue in an ice-box for a few days, mp 110—113°C. The products thus obtained were identified by comparing their NMR, IR spectra and melting points with those of the authentic samples. The yield of the products is shown in Table 1.

Table 1. Yield of products[a)]

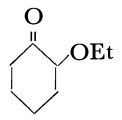	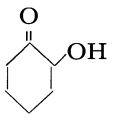	
31%	23%	1%

a) The yields were determined by the isotopic dilution method.

Degradation of 2-ethoxycyclohexanone-x-^{14}C. 2-Ethoxycyclohexanone-*x*-^{14}C (0.75 g) was mixed with 2.00 g of ordinary 2-ethoxycyclohexanone and dissolved in 30 m*l* of dry ether. This etheral solution was added with stirring to the Grignard reagent prepared from 4.13 g of bromobenzene and 0.64 g of magnesium in 30 m*l* of dry ether. The solution was kept at room temperature overnight, and then acidified with dilute hydrochloric acid. The ether layer was separated and the aqueous layer was extracted with ether. The combined ether extract was washed with aqueous sodium bisulfite solution, neutralized with aqueous sodium carbonate solution, washed with water, and finally dried over sodium sulfate. After removal of ether, 3.8 g, of crude 1-phenyl-2-ethoxycyclohexanol was obtained in 70% yield (bp 114.5—116.0°C/1.5 mmHg). Found: C, 76.07; H, 9.03%. Calcd for $C_{14}H_{20}O_2$: C, 76.32; H, 9.15%.

A mixture of crude 1-phenyl-2-ethoxycyclohexanol-*x*-^{14}C (3.8 g) and chromic acid (1 g) was vigorously stirred. When the temperature reached 25°C, another 9 g of chromic acid was added during a period of one hour keeping the temperature at around 30°C. After the addition of chromic acid, the mixture was diluted with an equal amount of water and was extracted with ether several times. The ether extract was washed with water. The etheral solution was extracted with 300 m*l* of aqueous 5% sodium hydroxide solution. The alkali extract was warmed on a water bath to remove excess ether. After cooling, the solution was acidified with 100 m*l* of concentrated hydrochloric acid. The precipitates were filtered and recrystallized from benzene-*n*-hexane. Thus, 5-benzoylvaleric acid (1.01 g) was obtained in 31% yield; mp 75—76°C. A mixture of 0.35 g of 5-benzoylvaleric acid-*x*-^{14}C, 2.8 g of potassium permanganate, and 1.45 g of potassium hydroxide was dissolved in 50 m*l* of water and refluxed for 4 hr. After the reaction, the precipitates were filtered off and washed with *ca.* 100 m*l* of boiling water. The filtrate was bubbled with sulfur dioxide, acidified with dilute hydrochloric acid and then extracted with ether. The extract was dried over sodium sulfate. After removal of ether, benzoic acid was obtained in 71% yield, mp 120—121°C (recrystallized from *n*-hexane). 5-Benzoylvaleric acid-*x*-^{14}C (1.38 g) was reduced by Martin and Clemmensen's method.[8)] Thus, 6-phenylcaproic acid-*x*-^{14}C (0.81 g) was obtained in 62% yield, bp 150—151.5°C, mp 16—21°C. 6-Phenylcaproic acid-*x*-^{14}C (0.81 g), dissolved in 1.7 m*l* of concentrated sulfuric acid, was decarboxylated with 6.5 m*l* of 1.6 N hydrazoic acid in chloroform solution and the carbon dioxide generated was trapped with

Table 2. The ^{14}C counting data

Run	Method of[a)] Measurement	$PhCO(CH_2)_4CO_2H$ (I)	$PhCO_2H$ (II)	$Ph(CH_2)_5NH_2 1/2H_2SO_4$ (III)	CO_2[b)] (IV)
I	(A) cpm/mmol	2.84×10^5	2.10×10^5		
	(B) cpm	11388			2855
(^{14}C distribution)		(100 %)	(74.9 %)		(25.1 %)
II	(B) cpm	5170		4182	1122
(^{14}C distribution)		(100 %)		(80.9 %)	(21.7 %)

a) (A) liquid scintillation counter, (B) G. M. Counter (Van Slyke method)
b) Counted as barium carbonate.
All runs were repeated at least twice.

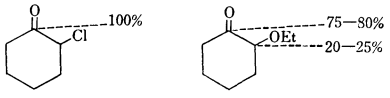

^{14}C-Distribution

8) "Organic Reaction," Vol. 1, John Wiley & Sons, New York, p. 155; L. D. Freedman and G. O. Doak, *J. Amer. Chem. Soc.*, **71**, 779 (1949).

9) S. Oae, N. Furukawa, M. Kise, and M. Kawanishi, This Bulletin, **39**, 1212 (1966).

0.25 N aqueous barium hydroxide solution. After completion of the reaction, chloroform and excess hydrazoic acid were removed *in vacuo*. The residue, to which a small amount of water was added, was filtered, washed with acetone-ether, and recrystallized from water. 5-Phenylamylamine-*x*-^{14}C 1/2 H_2SO_4 (0.673 g) was thus obtained in 75.2% yield, mp 325—330°C (decompd.).

Measurement of the Activities. The activities of the samples were measured both with a 2π-gas flow G.M. counter using Q gas and with a liquid scintillation counter using POP and POPOP as scintillators in toluene solution. 5-Benzoylvaleric acid-*x*-^{14}C was used as the standard sample of the total activity. The activity measurement with 2π-gas flow G.M. counter was described precisely in a previous paper.[9] An aliquot of each sample was thoroughly oxidized by the Van Slyke-Folch method, and all the carbon dioxide formed was converted to a barium carbonate tablet which was then subjected to measurement of its ^{14}C activity. The results are shown in Table 2.

Results and Discussion

The products were isolated and identified by the ordinary method and their yields were determined by isotope dilution technique. The result is shown in Table 1. The usual synthetic procedures were used for the ^{14}C compounds. Degradation of 2-ethoxy cyclohexanone was also carried out by a well-known procedure involving no skeltal rearrangement. 5-Benzoylvaleric acid was used as the standard sample of the total activity. The ^{14}C total activities and those of the respective degradative products were calculated from the specific activities of the corresponding samples. The result of the degradation is listed in Table 2. We see that 5-benzoylvaleric acid carries 75—80% of the total activity in carbonyl carbon and the rest is found in carboxylic carbon. This means that 75—80% of the total ^{14}C activity is in the carbonyl carbon atom and 20—25% is in the carbon atom bearing ethoxy group in 2-ethoxycyclohexanone. Namely, around 25% carbonyl oxygen migrates to the α-carbon attached to chlorine. The product analysis seems to rule out both the Wagner Meerwein type rearrangement mechanism, in which the carbon-carbon bond migrates to the cation center as in the case of the deamination of 2-amino cyclohexanone[10] and the Favorskii type mechanism[11] involving the initial formation of cyclopropanone *via* the participation of enolizable carbon-carbon double bond. If the reaction proceeds through one of these routes, cyclopentanecarboxylic acid derivatives would be the major products. Thus, both product analysis and ^{14}C tracer experiments suggest the following mechanism (Fig. 2). Namely, silver ion assists the abstraction of chlorine anion following the migration of carbonyl oxygen to the α carbon atom bearing chlorine atom.

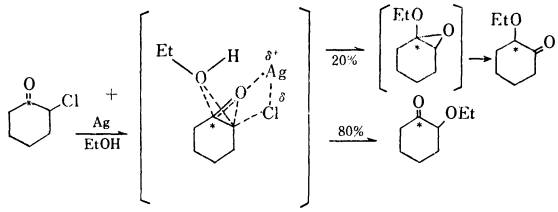

Fig. 2. Mechanism of the reaction.

The authors wish to express their appreciation to Dr. M. Hamada of the Radiation Center of Osaka Prefecture for the measurement of ^{14}C activities.

10) M. Nakai, N. Furukawa, and S. Oae, This Bulletin, **42**, 2917 (1969).
11) R. B. Loftfield, *J. Amer. Chem. Soc.*, **72**, 632 (1950).

Tracer Study of the Reactions of Diphenyl Sulfone and Diphenyl Sulfoxide with Diphenyl Disulfide[1]

Shigeru OAE, Yoshiyuki TSUCHIDA, and Mamoru NAKAI

Department of Applied Chemistry, Faculty of Engineering, Osaka City University, Sumiyoshiku, Osaka

(Received August 22, 1970)

Diphenyl sulfoxide and diphenyl sulfone were found to react with diphenyl disulfide at elevated temperatures, forming in both reactions diphenyl sulfide and sulfur dioxide. On the basis of ^{35}S and ^{14}C tracer experiments, these reactions were found to proceed through quite different mechanistic routes, *viz.*, S–O bond fission in the case of sulfoxide and C–S bond fission in sulfone. The reactions apparently proceed through the attack of the thiyl radical on the sulfoxide and sulfone functions. Further mechanistic details of the reactions are discussed.

Diphenyl sulfoxide[2] and diphenyl sulfone[3] are known to react with elemental sulfur at elevated temperatures to yield diphenyl sulfide and sulfur dioxide.

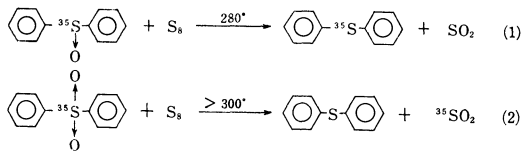

We found through radio-active sulfur-35 tracer experiments that these two reactions, though yielding the same products, proceed through different mechanistic routes (Eqs. (1) and (2)).[2] In the case of sulfoxide the reaction is a straightforward reduction to give sulfide by the abstraction of labile oxygen atom with elemental sulfur. In the reaction of diphenyl sulfone, however, the sulfur atom of the sulfonyl group is replaced by that of elemental sulfur, apparently initiated by the attack of biradical chain of polymeric sulfur to cleave the C–S bond followed by the extrusion of sulfur dioxide and the formation of the sulfide (Eq. (3)).

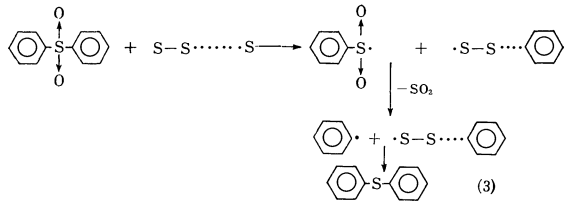

These different reaction paths are ascribed to the weaker bond strength of the S–O bond of the sulfoxide than that of sulfone. However, further mechanistic details of these reactions are not well understood, mainly because of the complicated nature of elemental sulfur at elevated temperatures.

Diphenyl sulfone is known to react with diphenyl disulfide at elevated temperatures to form diphenyl sulfide and sulfur dioxide.[3] We found that diphenyl sulfoxide also reacts with disulfide similarly. The reactions appear to serve as simple model reactions for making detailed mechanistic study of the reactions with elemental sulfur.

1) Paper XXXV on Sulfoxide.
2) S. Oae and S. Kawamura, This Bulletin, **36**, 163 (1963).
3) F. Kraft and W. Vorster, *Ber.*, **26**, 2813 (1893).

We have investigated the reactions of diphenyl sulfoxide and sulfone with diphenyl disulfide and present in this paper a detailed account of our investigation.

Results and Discussion

Diphenyl sulfoxide reacts nearly explosively with diphenyl disulfide at 250°C under nitrogen atmosphere giving diphenyl sulfide, sulfur dioxide, and a small amount of benzenesulfonic acid as shown in the following equation.

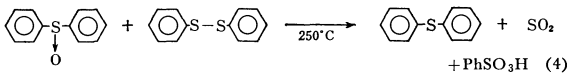

The reaction of diphenyl sulfone with diphenyl disulfide was shown by Kraft and Vorster to give diphenyl sulfide and sulfur dioxide in about 75% yield at about 300°C, a higher temperature than that for the reaction with sulfoxide.

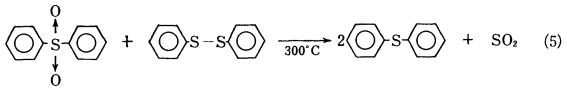

^{35}S-Tracer Experiments. ^{35}S-tracer technique was very useful for showing that the reactions of sulfoxide and sulfone with elemental sulfur proceed through different mechanistic routes, and we have examined the reactions of sulfoxide and sulfone with diphenyl disulfide using sulfur-35 labeled diphenyl sulfoxide and diphenyl sulfone. The specific activities

Table 1. Tracer experiments

	Reactant cpm/mg	Product cpm/mg	Product / Reactant	Condition
I	8844[b]	7677[a]	86.8%	250°C (about 5 min)
II	22100[c]	481[a]	2.2%	310°C (30 min)
III	5250[a]	11[d]	0.0%	250°C (1 hr)
IV	2647[c]	507[a]	19.2%	310°C (30 min)

I: $Ph^{35}SOPh + PhSSPh$, II: $Ph^{35}SO_2Ph + PhSSPh$
III: $PhSOPh + Ph^{35}SPh$, IV: $PhSO_2Ph\text{-}^{14}C + PhSSPh$

a) Activity of formed sulfide (counted after being converted to sulfone).
b) Sulfoxide (counted after being converted to sulfone).
c) Sulfone.
d) Recovered sulfoxide.

of the reactants and the products were then counted, and the results are tabulated in Table 1.

Inspection of the data reveals that replacement of sulfur atom does not take place in the reaction of the sulfoxide (Eq. (6)) and the reaction is a reduction proceeding through the S–O bond fission.

In the case of the sulfone, the activity of the sulfide formed was only 2.2% of that of the original sulfone. As will be shown later, 19.2% of the sulfide resulted from the sulfone and the rest from diphenyl disulfide under this reaction condition. Nevertheless, these results suggest that replacement of sulfur atom occurs during the reaction, and not the S–O bond but the C–S bond of the sulfone is cleaved in the main path.

The results from the two tracer experiments are similar to those obtained from the reactions with elemental sulfur.

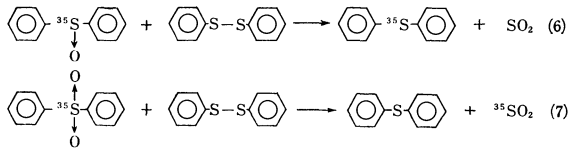

These different modes of reaction can be interpreted in terms of the difference of the bond strengths of the S–O linkages of the respective compounds. It is known that the force constant of the S–O bond in the sulfone calculated from the infrared data, 9.5×10^5 dyne/cm,[4a] is appreciably higher than that of the sulfoxide (7.0×10^5 dyne/cm). Thus, unlike the sulfoxide group, the sulfur-oxygen bond in the sulfone group is not easily cleaved.[4b]

Mechanism of the Reaction of Diphenyl Sulfoxide with Diphenyl Disulfide. Two mechanisms are conceivable for the relatively facile S–O bond cleavage of sulfoxide as shown in Fig. 1, the homolytic reductive cleavage of the sulfoxide bond induced by the benzenethiyl radical formed by the thermal dissociation of the sulfur-sulfur bond of diphenyl disulfide (path A), and the nucleophilic reaction between the sulfoxide and the disulfide (path B). The fact that the reaction temperature (250°C) is high enough to dissociate diphenyl disulfide into the corresponding radical[5] and that the reaction proceeds nearly explosively suggests the free radical chain mechanism to be more favorable.

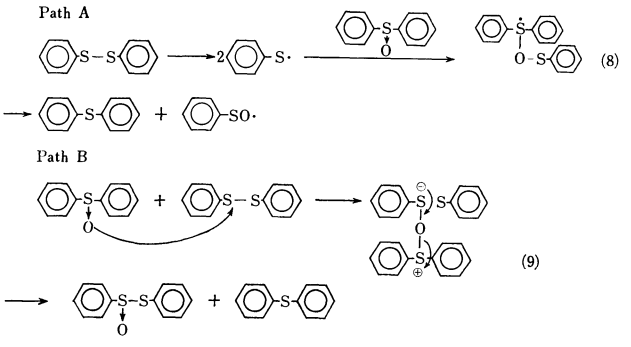

Fig. 1

4) a) These values are of alkyl sulfoxides and sulfones, C. C. Price and S. Oae, "Sulfur Bonding," Ronald Press, Inc., New York (1962), p. 66. b) *ibid.*, p. 132.

Evidence to support path A may be found in the following observations. (1) Apparently, oxygen acts as an inhibitor. When nitrogen gas was not passed through the reaction system to sweep oxygen before heating, either a prolonged induction period was observed for this reaction or the reaction did not occur at all. (2) If the reaction proceeds through path B, it is reasonable to consider that an oxygen exchange reaction takes place between diphenyl sulfoxide and diphenyl sulfide as in the case with disulfide. However, by the ^{35}S tracer experiment no such exchange reaction was found to take place (Table 1). (3) A free radical

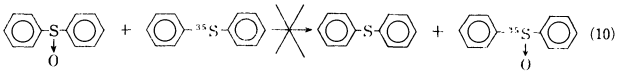

induced reductive cleavage of semi-polar *N*-oxide bond has been reported.[6]

In view of these observations, the cleavage of the sulfoxide seems to proceed through the former path (path A) involving the attack of the benzenethiyl radical on the sulfoxide oxygen.

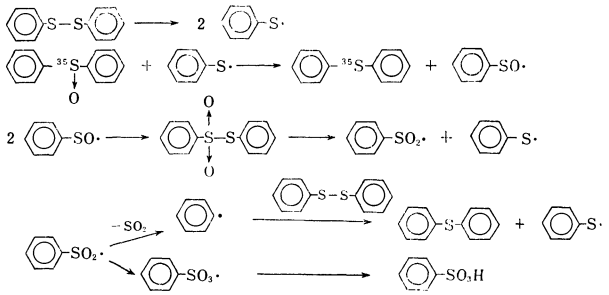

Fig. 2

The overall mechanism of the reaction is thus illustrated in Fig. 2. Phenylsulfinyl radical, PhSO·, has been considered to be rather long-lived[7] and known to undergo dimerization to give the corresponding thiolsulfonate.[7,8] However, thiolsulfonate thus formed would dissociate into $PhSO_2\cdot$ and PhS· radicals at these reaction temperatures. Desulfonylation[9] and disproportionation[10] of $PhSO_2\cdot$ radical have been known to occur readily. Desulfonylation of phenylsulfonyl radical leads to the formation of SO_2 and phenyl radical which would immediately be converted to diphenyl sulfide by the chain transfer reaction with diphenyl disulfide. By disproportionation both $PhSO_3\cdot$ and PhSO· radicals would result. Formation of a small amount of benzenesulfonic acid in the products may be rationalized on the basis of hydrogen abstraction with $PhSO_3\cdot$ radical.

According to this mechanism, the first step of the

5) a) G. Leandri and A. Tundo, *Ann. Chim.* (Rome), **44**, 63 (1954); *Chem. Abstr.*, **49**, 4563 (1955). b) J. G. D. Brandt and J. R. Davidson, *J. Chem. Soc.*, **1956**, 15.

6) N. Inamoto, *Yuki Gosei Kagaku Kyokai Shi*, **17**, 174 (1959).

7) S. Oae and K. Ikura, This Bulletin, **38**, 58 (1965).

8) R. M. Topping and N. Kharasch, *Chem. Ind.* (London), **1961**, 178.

9) For the decomposition of phenyl benzenthiolsulfonate; F. Kraft and O. Steiner, *Ber.*, **34**, 564 (1901).

10) J. L. Kice and N. A. Favstritsky, *J. Org. Chem.*, **35**, 114 (1970).

reaction in Fig. 2 will afford radioactive sulfide, and the subsequent desulfonylation of thiolsulfonate will afford the nonactive sulfide. Thus, the specific activity of diphenyl sulfide formed will be reduced substantially as compared to the activity of the original sulfoxide. This is consistent with our experimental result (Table 1).

Mechanism of the Reaction of Diphenyl Sulfone with Dephenyl Disulfide. It is known that at these temperatures for the reaction of sulfone (300°C) diphenyl disulfide dissociates into a pair of benzenethiyl radicals, which then attack the original diphenyl disulfide, eventually giving rise to diphenyl sulfide and elemental sulfur in several steps.[11]

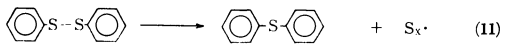

(11)

Since the reaction occurs nearly spontaneously at higher temperatures than that with diphenyl sulfoxide, the reaction of the sulfone with the disulfide is considered to proceed through a free radical process.[2] The following three paths involving the C–S bond fission are conceivable for the initial step of the reaction of diphenyl sulfone and diphenyl disulfide (Fig. 3), A) the attack of benzenethiyl radical formed from diphenyl disulfide at the sulfone function, B) the initial decomposition of diphenyl disulfide into the sulfide and polymeric sulfur, which in the subsequent step attacks the sulfone, C) both mechanisms occur concurrently.

Path A

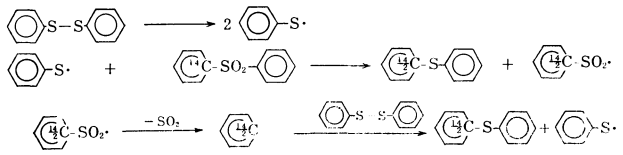

Path B

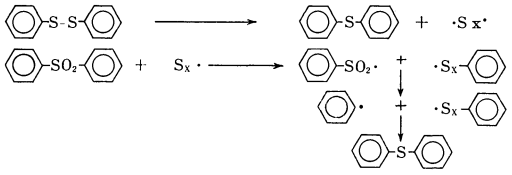

Path C A and B in parallel

Fig. 3

In order to examine the possibility of the three conceivable mechanistic pathways, we first tried the reaction of diphenyl sulfone with bis(*p*-chlorophenyl)-disulfide, but this procedure was unsuccessful because of unexpected side reactions giving rise to many complicated products including chlorobenzene *etc.* Thus we adopted the reaction of carbon-14 labeled diphenyl sulfone with the disulfide. If the reaction proceeds through path A, the specific activity of the sulfide formed should be one half of that of the original sulfone at any time during the course of the reaction.

11) C. Graebe, *Ann. Chem.*, **174**, 189 (1874).

The result given in Table 1 reveals that the sulfide formed has an activity corresponding to 19.2% of the original sulfone. This indicates that the mechanism A can be excluded. Of the two mechanisms B and C, the latter seems to be adequate on the basis of the following observations.

$$\underset{1.0}{PhSSPh} \xrightarrow[21\ min]{302^\circ C} \underset{0.45}{PhSPh} + \cdot Sx\cdot \qquad (12)$$

$$\underset{1.0}{PhSO_2Ph} + \underset{1.0}{\cdot Sx\cdot} \longrightarrow \underset{0.10}{PhSPh} + SO_2 \qquad (13)$$

$$\underset{1.0}{PhSO_2Ph} + \underset{1.0}{PhSSPh} \longrightarrow \underset{0.68}{PhSPh} + \underset{(\times 10^{-3}\ mol)}{SO_2} \qquad (14)$$

Diphenyl disulfide, 1.0×10^{-3} mol, gave 0.45×10^{-3} mol of the sulfide and elemental sulfur at 302°C for 21 min, and equimolar (1.0×10^{-3} mol) amounts of the sulfone and elemental sulfur gave 0.10×10^{-3} mol of the sulfide under the same condition. If the reaction of the sulfone with the disulfide were to proceed through path B, the total amount of the sulfide formed should be less than $(0.45+0.1)\times10^{-3}=0.55\times10^{-3}$ mol, when equimolar (1.0×10^{-3} mol) amounts of the sulfone and the disulfide were reacted. However, 0.68×10^{-3} mol of the sulfide is actually formed.

The results cannot be explained on the assumption that the reaction proceeds through path B. Thus, it is reasonable to consider that both mechanisms A and B exist, namely, the attack of both benzenethiyl radical and the radical chain of elementary polymeric sulfur take place on the sulfone. Thus, the reaction of the sulfone proceeds through mechanism C.

Experimental

Diphenyl sulfide-^{35}S was prepared by Friedel-Crafts' reaction of benzene with radioactive sulfur in the presence of aluminium chloride according to the method[2] previously reported.

Diphenyl sulfoxide-^{35}S was prepared by the usual bromine oxidation of ^{35}S-labeled diphenyl sulfide.[12] From 4.6 g of the sulfide, the sulfoxide-^{35}S (mp 70.5°C) was obtained in 66% yield after repeated recrystallization from benzene-hexane.

Diphenyl sulfone-^{35}S was prepared by oxidizing diphenyl sulfide-^{35}S with potassium permanganate in glacial acetic acid. From 2.0 g of the sulfide, the sulfone-^{35}S (mp 123°C) was obtained in 80% yield.

Diphenylsulfone-1-^{14}C was prepared according to the procedure described elsewhere.[13]

Reaction of Diphenyl Sulfoxide with Diphenyl Disulfide. Diphenyl sulfoxide, 2.02 g, was thoroughly mixed with 1.09 g of diphenyl disulfide in a Claisen-flask and heated to about 100°C in order to melt the reactants. Dry nitrogen gas was bubbled through the liquid reaction mixture to remove any residual air. Then the flask was quickly put in a preheated silicon bath. In ten minutes the reaction took place nearly explosively and dark colored solution was formed with evolution of sulfur dioxide which was trapped in a few traps cooled with methanol - dry ice. The products were distilled *in vacuo*, and the distillate and the residue thus obtained were analyzed

12) S. Oae, Y. Ohnishi, S. Kozuka, and W. Tagaki, This Bulletin, **39**, 364 (1966).

13) S. Oae and N. Furukawa, *ibid.*, **39**, 2260 (1965).

by gas-liquid and column-elution chromatography, respectively. The distillate was found to be diphenyl sulfide alone. From the residue benzenesulfonic acid and a small amount of tarry substance were separated. Benzenesulfonic acid was identified as its thiouronium salt which has the same melting point and infrared spectrum as that of the authentic sample. The ^{35}S-tracer experiment was carried out similarly. The original sulfoxide having the specific activity of 8844 cpm/mg (converted to the sulfone) was treated with ordinary diphenyl disulfide. Diphenyl sulfide obtained was distilled repeatedly, usually two or three times, and then converted to diphenyl sulfone by the usual method (7677 cpm/mg).

Exchange Reaction of Diphenyl Sulfide-^{35}S and Diphenyl Sulfoxide. A mixture of diphenyl sulfide-^{35}S (5250 cpm/mg, converted to the sulfone), 1.03 g, and ordinary diphenyl sulfoxide, 1.12 g, was treated in the same way as in sulfoxide with disulfide. The reaction time was prolonged to 1 hr. After cooling the sulfide was distilled and the recovered sulfoxide was washed with *n*-hexane and recrystallized twice and the activity was counted (1.0 cpm/mg).

Reaction of Diphenyl Sulfone-^{35}S with Diphenyl Disulfide. Diphenyl sulfone-^{35}S (22100 cpm/mg), 1.09 g, was mixed with ordinary diphenyl disulfide, 1.09 g, in a Claisen flask and was put in a preheated air bath while nitrogen gas was passed through the reaction flask. After about 30 min, the flask was cooled down to room temperature and diphenyl sulfide formed was distilled *in vacuo* three times, and then converted to diphenyl sulfone by the usual method (481 cpm/mg).

Reaction of Diphenyl Sulfone-1-^{14}C with Diphenyl Disulfide. The reaction was carried out in the same way as in diphenyl sulfone-^{35}S. Diphenyl sulfone-1-^{14}C and diphenyl sulfide formed (converted into the sulfone) was found to have the activities of 2647 cpm/mg and 507 cpm/mg, respectively.

Estimation of the Conversions. The decomposition reaction of diphenyl disulfide was carried out at 302°C in degassed sealed tube in which 1.0×10^{-3} mol of the disulfide was placed with no solvent. A sealed tube was taken out from the silicon oil bath and cooled down to room temperature. The contents were then diluted with benzene to 10m*l* and the amount of diphenyl sulfide was determined by gas-liquid chromatography with biphenyl as an internal standard.

Conversion of the reactions of diphenyl disulfide (1.0×10^{-3} mol) and elemental sulfur (1.0×10^{-3} g atom) with diphenyl sulfone (1.0×10^{-3} mol) was determined similarly.

Counting of Radioactivities. The activities of all the compounds were counted by Packard Tri-Carb liquid scintillation counter, in toluene solution using POPOP as scintillator.

We are grateful to Dr. S. Kawamura of the Radiation Center of Osaka Prefecture, who kindly performed the counting of specific activities.

Study of Acidity Constants of 3-, 4-, 5-, and 6-Chloro-*o*-toluidinium Ions in Aqueous Solution and Related Thermodynamic Quantities. I

A. H. GANDHI and S. R. PATEL
Department of Chemistry, Sardar Patel University, Vallabh Vidyanagar, India
(Received April 13, 1970)

The acidity constants of anilinium, simple and 3-, 4-, 5-, and 6-chloro-*o*-toluidinium ions have been studied at seven different temperatures by pH metry in aqueous solution and correlated using the relation $\ln K=A+BT+CT^2$. The values of ΔG, ΔH, ΔS, and ΔC_p have been calculated at different temperatures. The possibility of the additivity in the thermodynamic quantities of these disubstituted anilinium ions has been examined. Hammett type equation has been developed to correlate the acidity constant of these ions at 25°C. Attempt has been made to explain the trends in the thermodynamic quantities of these ions in terms of polar, steric, and solvent effects.

Acidity constants of anilinium, *o*-, *m*-, and *p*-toluidinium and *o*-, *m*-, and *p*-chloroanilinium ions have been reported by Biggs at different temperatures.[1] The heats of ionization of the isomeric xylidinium and toluidinium ions have been determined by Laidler and co-workers by calorimetric method.[2] The present communication deals with the study of the acidity constants of 3-, 4-, 5-, and 6-chloro-*o*-toluidinium ions by pH metry at equally spaced seven temperatures ranging from 15 to 45°C. The acidity constant of each of these ions is correlated with temperature using a three constant equation, $\ln K=A+BT+CT^2$. This equation is used to calculate thermodynamic functions ΔG, ΔH, ΔS, and ΔC_p at all the seven temperatures. The thermodynamic quantities of the ionization of anilinium and *o*-toluidinium ions were required to check the possible additivity in the corresponding thermodynamic quantities of chlorotoluidinium ions. For examining such an additivity, it was desirable to study the acidity constants of these two ions at the corresponding temperatures under the conditions under which the acidity constants of the isomeric chloro-*o*-toluidinium ions were determined. Hence the acidity constants of these two ions were redetermined and the thermodynamic quantities were calculated by the application of the above mentioned equation. Modified Hammett relation is derived and applied to correlate the acidity constants of these *o*-substituted anilinium ions with Hammett σ and ρ constants. Attempt has also been made to interpret the values of the thermodynamic quantities ΔG, ΔH, and ΔS in terms of the polar, steric, and solvent effects.

Experimental

Reagents. Anilinium chlorides were prepared by the following method starting with laboratory grade chemicals. Each aniline derivative was distilled in an all-glass apparatus and the fraction boiling at constant boiling point was collected. The fraction was then redistilled over zinc dust. The liquid thus purified was dissolved in 10 times its weight of dry ether. Dry hydrogen chloride prepared from AR grade chemicals was passed through this solution and the white solid which separated was filtered and washed with ether. The white solid was crystallized from pure ethanol. The crystalline solid was dried over anhydrous calcium chloride in a vacuum desiccator. It was preserved in a dry coloured bottle kept in a vaccum desiccator. The boiling points of the aniline derivatives and the melting points of their anilinium chlorides were in accordance with those reported in literature.[3] The equivalents weights of the anilinium salts agreed within 0.2% of the calculated value.

Apparatus. The pH metric titrations were carried out using Metrohm pH meter E300 with an expanded scale on which pH could be conveniently read up to 0.005 pH units. A Metrohm dosigraph E364 micrometer syringe type burette capable of delivering volume of 0.001 m*l* was used. Metrohm glass electrode EA 100 X and calomel electrode with saturated potassium chloride solution were used. A 100 m*l* pyrex beaker was covered at the top with a special bakelite cork with four wholes, two of which were for the electrodes, one for thermometer and one for admitting the tip of the burette. The solution was stirred magnetically.

Temperature Control. The acidity constants were determined at equally spaced seven different temperatures from 15 to 45°C. The cell temperature was maintained by circulating water from a constant temperature bath into a jacket around the cell. The temperature of the cell was controlled within 0.1°C of the reported value.

Standardization of pH Meter. As pH of the reagent-solutions were found to lie in the range from 3 to 4, 0.05M aqueous solution of potassium hydrogen phthalate and saturated aqueous solution of potassium hydrogen tartarate were considered as suitable buffer solutions for the standardization of the pH meter. The pH values of NBS standard of these buffer solutions at various temperatures were followed while standardizing pH meter at the respective temperatures.[4]

Procedure. A stock solution, 0.01M with respect to the required anilinium chloride and 0.005M with respect to potassium chloride was prepared in distilled water. The three sets of solutions, 0.002, 0.003, and 0.004M, for the actual titration were prepared by diluting 10, 15, and 20 m*l* of the stock solution to 50.0 m*l* by adding ditilled water. The titrations were carried out at these three concentrations at each temperature. Standard potassium hydroxide solution, was prepared using carbonate free potassium hydroxide in triple distilled water. Its strength was adjusted to an exact value around 0.15M. The amount of titrant added each time was so adjusted that pH changes by about 0.05 to 0.10 units for each addition. The titration was carried out almost up to the point of neutrali-

1) A. I. Biggs, *J. Chem. Soc.*, **1961**, 2572.
2) T. W. Zawidzki, H. M. Papee, W. J. Canady, and K. J. Laidler, *Trans. Faraday Soc.*, **55**, 1738 (1959).
3) I. Heilborn and H. M. Bunbury (Editors in Chief), "Dictionary of Organic Compounds," Eyer and Spottiswoode, London.
4) R. G. Bates, "Electrometric pH Determinations," John Wiley and Sons, Inc., New York, p. 74.

zation.

As it was not possible to prepare a clear solution of 6-chloro-*o*-toluidinium ion in water, the procedure for titration of this ion was modified. Three solutions which were 0.002, 0.003, and 0.004M with respect to HCl and three other solutions which were 0.002, 0.003, and 0.004 both with respect to HCl and 6-chloro-*o*-toluidinium ion were prepared. They were titrated against the same standard alkali solution.

The pH meter readings for the titration of blank HCl solution and of solution containing both the reagent and HCl of the corresponding strength were plotted against the amount of alkali added on the same graph paper. The readings from the middle portion of graph were selected for calculation.

Results and Discussion

Calculations. At constant ionic strength, the thermodynamic acidity constant K_a^T for the reaction

$$BH^+ + H_2O \rightleftharpoons B + H_3O^+ \quad (1)$$

is given by the relation:

$$K_a^T = \frac{[B](H_3O^+)}{[BH^+]} \cdot \frac{1}{f_{BH^+}} = K_a^M \cdot \frac{1}{f_{BH^+}} \quad (2)$$

$$\therefore \quad pK_a^T = pK_a^M + \log f_{BH^+} \quad (3)$$

where K_a^M is called the mixed constant because out of the three terms in the equilibrium expression, [B] and [BH] are concentration terms and (H_3O^+) is an activity term.

Seven to eight titration readings were selected from the middle portion of the titration data in order to evaluate K_a^T. The activity term (H_3O^+) was calculated from the measured pH of the solution at a given stage in the titration. If $[K^+]$, [B], and $[BH^+]$ are the concentrations of the bracketed terms at the same stage in titration, and if $[BH_0^+]$ is the original concentration of the solution, it can be proved[5] that

$$[B] = [K^+] + [H_3O^+] \quad (4)$$

$$[BH^+] = [BH_0^+] - [B] \quad (5)$$

The concentration of OH^-, which is extremely low in acidic solution, is neglected. The activity coefficient f_{BH^+} was calculated using the Debye-Hückel limiting law,[6]

$$\log f_i = AZ_i^2\sqrt{I_m} \quad (6)$$

where $A = -1.823 \times 10^6/(DT)^{3/2}$, $Z_i = 1$ and I_m is the ionic strength at the stage of half neutralization. It has been recommended that for titration at low concentrations, the value of the ionic strength at the stage of half neutralization may be used in deriving the DHLL correction.[6] The DHLL corrections were not applied to 6-chloro-*o*-toluidinium ion as the observed scatter in the values of pK_a of this ion was of the order of the correction to be applied.

The method of calculation of acidity constant for ionization of 6-chloro-*o*-toluidinium chloride was slightly different. The concentration term [B], was obtained by subtracting the hydrogen ion concentration of blank HCl titration at a given stage of titration from the hydrogen ion concentration at the corresponding stage of titration of the solution of the anilinium chloride in HCl of the same strength. $[BH^+]$ is calculated using relation (5).

The values of pK_a^T for anilinium, *o*-toluidinium and 3-, 4-, 5-, and 6-chloro-*o*-toluidinium ions at all the seven temperatures are reported in Table 1. The values of pK_a^T agree within ± 0.01 pK units except for 6-chloro-*o*-toluidinium ion. For the latter ion the scatter is found to be about ± 0.02 pK unit.

Table 1. pK values of anilinium ions

	Temperature °C						
	15	20	25	30	35	40	45
Anilinium	4.78	4.70	4.615	4.51	4.425	4.345	4.27
o-Toluidinium	4.58	4.495	4.45	4.345	4.28	4.20	4.12
3-Cl-*o*-T	3.745	3.67	3.62	3.52	3.455	3.385	3.32
4-Cl-*o*-T	3.98	3.92	3.85	3.78	3.705	3.62	3.57
5-Cl-*o*-T	3.55	3.48	3.385	3.34	3.265	3.20	3.15
6-Cl-*o*-T	2.59	—	2.49	2.39	—	2.23	—

Correlation of Acidity Constants and Temperature. Out of the many empirical equations proposed by various workers to correlate acidity constants with temperature,[7-11] the equation

$$\ln K = A + BT + CT^2 \quad (7)$$

is employed to correlate the experimental data reported in the present communication and to evaluate the thermodynamic quantities. This equation was empolyed by Ives and Pyror[10] to correlate successfully the variation of ionization constants of monohalogenoacetic acids with temperature. The selection of the equation is justified by the fact that the equation represents the experimental data within the limits of experimental error. The constants of the equations are evaluated by the application of the method of least squares.

From Eq. (7), the following equations are derived:

$$G = -RAT - RBT^2 - RCT^3 \quad (8)$$

$$H = RBT^2 + 2RCT^3 \quad (9)$$

$$S = 2RBT + 3RCT^2 + RA \quad (10)$$

$$C_p = 2RBT + 6RCT^2 \quad (11)$$

It has been reported that more than one equations may represent the same experimental data almost equally well and that there may be a fair agreement in the values of ΔH and ΔS calculated by the application of each of the equations. However, the values of ΔC_p are found to be different.[12] From this point of view, the values of ΔC_p evaulated by the appli-

5) H. Freiser and Q. Fernando, "Ionic Equilibria in Analytical Chemistry," John Wiley and Sons, Inc., New York, Ch. IV.

6) A. Albert and E. P. Serjeant, "Ionization Constants of Acids and Bases," Methuen and Co., Ltd., London.

7) a) D. H. Everett and W. F. K. Wynne-Jones, *Trans. Faraday Soc.*, **35**, 1380 (1939). b) *ibid.*, *Proc. Roy. Soc.* (London), **A169**, 190 (1938).

8) H. S. Harned and R. A. Robinson, *ibid.*, **36**, 973 (1940).

9) H. S. Harned and N. D. Embree, *J. Amer. Chem. Soc.*, **56**, 1042, 1050 (1934).

10) D. J. G. Ives and J. H. Pyror, *J. Chem. Soc.*, **1955**, 2104.

11) F. S. Feates and D. J. G. Ives, *ibid.*, **1956**, 2798.

12) David T. Y. Chen and K. J. Laidler, *Trans. Faraday Soc.*, **58**, 480 (1962).

Table 2. Thermodynamic quantities of anilinium ions
Constants of equation $\ln K = A + BT + CT^2$

Ion	Equation	Ion	Equation
Anilinium	$\ln K = -31.5851 + 0.099798T - 0.00009868T^2$	5-Cl-*o*-T	$\ln K = -35.8960 + 0.155257T - 0.00020504T^2$
o-Toluidinium	$\ln K = -13.6471 - 0.0113382T + 0.00007675T^2$	*o*-Chloro-anilinium[a]	$\ln K = -8.1393 - 0.0127182T + 0.00006579T^2$
3-Cl-*o*-T	$\ln K = -20.1652 + 0.04635506T - 0.00002193T^2$	*m*-Chloro-anilinium[a]	$\ln K = -35.4502 + 0.1505216T - 0.0001974T^2$
4-Cl-*o*-T	$\ln K = -15.0409 + 0.0092946T + 0.00003838T^2$	*p*-Chloro-anilinium[a]	$\ln K = -25.8009 + 0.075349T - 0.00006579T^2$

a) pK values at five temperatures from Ref. 1.

Temperature T	Anilinium ion	*o*-Toluidinium ion	3-Cl-*o*-T	4-Cl-*o*-T	5-Cl-*o*-T	6-Cl-*o*-T	*o*-Chloro-anilinium ion	*m*-Chloro-anilinium ion	*p*-Chloro-anilinium ion
ΔG kcal·mol^{-1}									
288.16	6.31	6.04	4.94	5.25	4.68	—	—	—	—
293.16	6.29	6.04	4.93	5.25	4.66	—	3.62	4.83	5.45
298.16	6.28	6.04	4.91	5.25	4.64	3.36	3.60	4.81	5.44
303.16	6.26	6.04	4.90	5.24	4.62	—	3.58	4.79	5.42
308.16	6.25	6.03	4.87	5.22	4.60	—	3.56	4.78	5.40
313.16	6.23	6.02	4.85	5.20	4.59	—	3.53	4.77	5.38
318.16	6.21	5.99	4.83	5.18	4.58	—	—	—	—
ΔH kcal·mol^{-1}									
288.16	7.08	5.43	5.56	5.18	6.12	—	—	—	—
293.16	7.16	5.75	5.72	5.43	5.98	—	4.41	5.94	6.28
298.16	7.23	6.08	5.88	5.68	5.82	2.62	4.68	5.79	6.38
303.16	7.30	6.43	6.04	5.94	5.65	—	4.96	5.63	6.47
308.16	7.35	6.78	6.20	6.22	5.45	—	5.25	5.44	6.56
313.16	7.40	7.16	6.36	6.49	5.23	—	5.55	5.24	6.65
318.16	7.44	7.54	6.52	6.78	4.98	—	—	—	—
ΔS cal·deg^{-1}·mol^{-1}									
288.16	2.68	−2.11	2.16	−0.25	4.99	—	—	—	—
293.16	2.95	−1.01	2.70	0.60	4.52	—	2.71	3.79	2.81
298.16	3.20	0.12	3.24	1.47	3.99	2.48	3.62	3.30	3.15
303.16	3.41	1.27	3.76	2.34	3.40	—	4.55	2.76	3.47
308.16	3.59	2.44	4.28	3.22	2.75	—	5.49	2.15	3.77
313.16	3.75	3.64	4.80	4.12	2.04	—	6.46	1.49	4.04
318.16	3.88	4.86	5.31	5.02	1.26	—	—	—	—
ΔC cal·deg^{-1}·mol^{-1}									
298.16	13.7	67.9	31.7	51.7	−33.3	—	54.6	−30.9	19.5

cation of Eq. (8) have been reported at 25°C and no attempt has been made to attach any significance to the calculated value.

The calculated values of thermodynamic quantities for anilinium, *o*-toluidinium, 3-, 4-, and 5-chloro-*o*-toluidinium ions at all temperatures are given in Table 2. The thermodynamic quantities for the ionization of *o*-, *m*-, and *p*-chloroanilinium in aqueous solutions at 25°C were required for examining the possible additivity in the corresponding thermodynamic quantities of isomeric chloro-*o*-toluidinium ions. They were calculated by the application of Eq. (7) to the acidity constants of these ions reported by Biggs[1] at five different temperatures.

The scatter in evaluated acidity constants of 6-chloro-*o*-toluidinium ion was found to be of the order of DHLL correction. Hence it was throught improper to apply this correction to the calculated pK_a. For the same reason it was considered improper to apply Eq. (7) to the data for the purpose of correlating the values of acidity constants with temperature. The values are correlated using the following simplified equation[7b]

$$\log K = A - B/T \qquad (12)$$

The thermodynamic quantities of this ion at 25°C are reported in Table 2.

Additivity of Thermodynamic Quantities. According to Laidler the prediction of thermodynamic quantities for disubstituted anilinium ions from the changes produced when single substituents are introduced sepa-

TABLE 3. THERMODYNAMIC QUANTITIES OF $R_1(R_2)C_6H_3NH_3^+ + C_6H_5NH_2 \rightleftharpoons R_1(R_2)C_6H_3NH_2 + C_6H_5NH_3^+$ AT 25°C

Acid	pK_a	ΔG kcal·mol^{-1}	ΔH kcal·mol^{-1}	ΔS cal·deg^{-1}·mol^{-1}	ΔG kcal·mol^{-1} (estimated)	ΔH kcal·mol^{-1} (estimated)	ΔS cal·edg^{-1}·mol^{-1} (estimated)
Anilinium	4.615	0.00	0.00	0.00	—	—	—
o-Toluidinium	4.45	−0.24	−1.15	−3.08	—	—	—
o-Chloroanilinium	2.64	−2.68	−2.55	+0.42	—	—	—
m-Chloroanilinium	3.52	−1.47	−1.44	+0.10	—	—	—
p-Chloroanilinium	3.98	−0.84	−0.85	−0.05	—	—	—
3-Cl-*o*-T	3.62	−1.37	−1.35	+0.04	−1.71	−2.59	−2.98
4-Cl-*o*-T	3.85	−1.03	−1.55	−1.73	−1.08	−2.00	−3.13
5-Cl-*o*-T	3.386	−1.64	−1.41	+0.79	−1.71	−2.59	−1.98
6-Cl-*o*-T	2.49	−2.92	−4.61	−5.68	−2.92	−3.70	−2.66

rately in anilinium ion is referred to as additivity.[13] Laidler has analysed the role of polar, steric, and solvent effects in deciding the additivity of thermodynamic quantities. Laidler has also indicated that interpretation of the thermodynamic quantities has proved to be complicated because the above-mentioned effects do not operate independently.[13]

With a view to examining the additivity in the thermodynamic quantities of disubstituted anilinium ions, ionization of anilinium ion in aqueous solution is considered as a reference reaction. The increments in each of the thermodynamic quantities due to introduction of a single substituent is calculated by deducting the value of the particular thermodynamic quantity for the ionization of the mono-substituted anilinium ion (say $RC_6H_4NH_3^+$) from that of the corresponding quantity for the ionization of anilinium ion. The increments in the value of ΔG, ΔH, and ΔS thus calculated may be considered to be the corresponding thermodynamic quantities of the following reaction

$$ArNH_3^+ + PhNH_2 \rightleftharpoons ArNH_2 + PhNH_3^+ \qquad (13)$$

These values are shown in Table 3.

The increments in a particular thermodynamic quantity due to introduction of each of the substituents separately in the required position in anilinium ion are added up to calculate the increments due to the introduction of the two substituents in their respective positions in disubstituted anilinium ion.

Examination of the values shown in Table 3 indicates that additivity is observed in ΔG values of 4-, 5-, and 6-chloro-*o*-toluidinium ions. It is not observed in ΔG value of 3-chloro-*o*-toluidinium ion.

The additivity is not observed in ΔH and ΔS values of 3-, 4-, 5-, and 6-chloro-*o*-toluidinium ions. The predicted and the experimental values differ appreciably. However, the fact that the additivity is observed in ΔG values for the ionization of 4-, 5-, and 6-chloro-*o*-toluidinium ions, suggests that through the variations in ΔH and ΔS appear to be quite random, their variations have occurred in a compensating manner as suggested by Laidler.[13]

Linear Free Energy Relationships. The acidity constants of *m*- and *p*-substituted anilinium ions are correlated by the application of Hammett type equation.[14] The value of the reaction constant for the ionization of anilinium ions in aqueous solution at 25°C is reported by Jáffe to be 2.767.[15] The substituent constants for ortho substituents are not obtainable mainly because of the variable nature of steric and conjugation effects of such group in different reactions. According to Clark and Perrin,[14] apparent σ-ortho constants which are valid only for the given reaction conditions under which they are determined can be used satisfactorily in conjunction with the normal σ-meta and σ-para constants for prediction. The method suggested by Clark and Perrin[14] is used in arriving at the following equation on the basis of the values of acidity constants reported in Table 4 for *o*-substituted anilinium ions at 25°C.

$$pK_a = 4.615 - 2.85\sum\sigma \qquad (14)$$

TABLE 4. LINEAR FREE ENERGY RELATIONS IN *o*-TOLUIDINIUM IONS AT 25°C. IN AQUEOUS SOLUTION
$pK_a = 4.615 - 2.85\sum\sigma$

Acid	pK_a Reported at 25°C	$\sum\sigma$	pK_a Estimated
o-Toluidinium	4.45	+0.06[a]	4.44
2:3-Xylidinium	4.70[16]	−0.01	4.64
2:4-Xylidinium	4.89[16]	−0.11	4.93
2:5-Xylidinium	4.53[16]	−0.01	4.645
2:6-Xylidinium	3.95[16]	+0.12	4.27
o-Chloroanilinium	2.64[1]	+0.71[b]	2.59
3-Cl-*o*-T	3.62	+0.43	3.39
4-Cl-*o*-T	3.85	+0.29	3.785
5-Cl-*o*-T	3.386	+0.43	3.39
6-Cl-*o*-T	2.49	+0.77	2.42

a) *o*-Me = +0.06, *m*-Me = −0.07,[14] *p*-Me = −0.17[14]
b) *o*-Cl = +0.71, *m*-Cl = +0.37,[14] *p*-Cl = +0.23[14]

The apparent σ-ortho constants for methyl and chlorine are calculated for ionization of *o*-substituted anilinium ions in aqueous solution at 25°C. The normal Hammett equation was used for this purpose.

$$\log (K/K_0) = \rho \cdot \sigma \qquad (15)$$

The value of ρ was taken to be equal to 2.767.[15]

13) K. J. Laidler, *Trans. Faraday Soc.*, **55**, 1725 (1959).
14) J. Clark and D. D. Perrin, *Quart. Rev.*, **28**, (3) 295 (1954).
15) H. H. Jáffe, *Chem. Rev.*, **53**, 191 (1953).
16) R. N. Beale, *J. Chem. Soc.*, **1954**, 4494.

The value of pK for anilinium ion was taken to be 4.615 (pK_o) at 25°C. The reported σ-meta and σ-para constants of methyl and chlorine groups were used.

A comparison of the experimental and estimated pK values indicates that except for 2:6-xylidinium and 3-chloro-*o*-toluidinium ion, there is a good agreement. As reported in the preceding section additivity is not observed in ΔG values of 3-chloro-*o*-toluidinium ions.

Interpretation of the Results

The fact that *o*-toluidinium ion is a stronger acid than anilinium ion is contrary to expectation on the basis of the inductive effect of methyl group ortho to NH_3^+ group. As compared to the ionization of anilinium ion, the ionization of *o*-toluidinium ion is less endothermic and less random. The contribution of the entropy effect to the ΔG values of *o*-toluidinium is very small. ($T\Delta S=0.036$ kcal·mol^{-1})

Molecular model for *o*-toluidinium ion constructed using Catalin Molecular Models showed that the CH_3 and NH_3^+ groups could be just accommodated in the ortho positions only in certain conformations. In such a situation, the interaction between the two groups through the π-electron system of benzene may not be completely restricted. However, the space around NH_3^+ is partly occupied in its immediate vicinity by the ortho methyl groups. Therefore, the extent of solvation will be reduced proportionately. The interaction between the electron releasing methyl group and the positive charge on the nitrogen atom of NH_3^+, will disperse this positive charge on the nitrogen atom. This will reduce the extent of solvation of the *o*-toluidinium ion and make the *o*-toluidinium ion more random. Hence, the process of ionization of *o*-toluidinium ion will proceed with a smaller entropy change. This explains why ΔS is smaller for ionization of this ion than that of anilinium ion.

The fact that ionization of *o*-toluidinium ion is less endothermic than that of anilinium ion suggests that the steric and solvent effects play a more important role than the polar effect. Such a view is also expressed by Brown and co-workers.[17]

The isomeric chloroanilinium ions are stronger acids than anilinium ion. This seems to be due to the presence of electron attracting chlorine atom which makes the release of protons easier. The entropy changes for the ionization of all the three chloroanilinium ions are very nearly the same as they do not differ much from that of the ionization of anilinium ion. Therefore the extent of solvation and hence stability induced by solvation will most probably be the same for all these ions. Hence the difference in ΔH values may possibly be due to the difference in the polar effects operating in bare chloroanilinium ions.

The trends in the thermodynamic quantities of the isomeric 3-, 4-, 5-, and 6-chloro-*o*-toluidinium ions are not explicable simply from the knowledge of the manner in which a particular property is affected by the introduction of a single substituent, methyl or chlorine, in the required position in anilinium ion. It is difficult and perhaps impossible to predict the nature of the possible interactions between the methyl and chlorine substituents in a chlorine substituted *o*-toluidinium ions.

It is also not reasonable to assume that each one of these groups will influence the reaction site independently. Hence no attempt is made to explain the trends in the thermodynamic quantities of these ions. The question of 3-chloro- and 6-chloro-*o*-toluidinium ions is considered because of their peculiar structures.

The molecular model for 3-chloro-*o*-toluidinium ion shows that it is possible to accommodate the three groups respectively in three consecutive positions on the benzene nucleus if NH_3^+ and CH_3 groups take up certain conformations. The methyl and chlorine substituents which are placed in ortho position with respect to each other have opposite polarities. It is quite possible that the methyl group may be pushed nearer to the chlorine atom and away from the NH_3^+ group. Due to this it will make the space around the NH_3^+ group roomier and its interaction with NH_3^+ group weaker. This may explain why ionization of 3-chloro-*o*-toluidinium ion is more random than that of *o*-toluidinium ion.

6-Chloro-*o*-toluidinium ion is the strongest acid of all the four isomeric chloro-*o*-toluidinium ions. The steric and solvent effects are likely to play a prominent role in the ionization of this ion. The space around the NH_3^+ group in this ion is occupied by the methyl and chlorine substituents placed in ortho position to NH_3^+ group. This will reduce the number of water molecules that can associate with NH_3^+ group and will increase the randomness of the ion. It is likely that under the given situation its randomness exceedes that of the hydronium ion. The ionization of 6-chloro-*o*-toluidinium ion may then proceed with decrease in randomness as has been observed. The decreased solvation of this ion will increase its enthalpy. Therefore, the ionization of this ion will be less endothermic than that of *o*-toluidinium or anilinium ion.

The authors thank Professor Dr. R. D. Patel and Dr. C. K. Patel for taking keen interest in the work and making helpful suggestions.

17) H. C. Brown and A. Cahn, *J. Amer. Chem. Soc.*, **72**, 2939 (1950).

Studies of Phosphorylation. V.[1] The Synthesis of Inosine-5′-thiophosphates

Kazuko HAGA, Masatsune KAINOSHO, and Masaharu YOSHIKAWA
Central Research Laboratories, Ajinomoto Co., Inc., Kawasaki
(Received April 20, 1970)

Two isomers of inosine-5′-thiophosphates, inosine-5′-phosphorothionate and 5′-deoxy-5′-thioinosine-5′-phosphorothioate, were synthesized by the direct phosphorylation of inosine with phosphorus thiochloride, and by the treatment of 5′-deoxy-5′-iodoinosine with trisodium phosphorothioate, respectively. The structure of the thiophosphate residues was identified by means of ^{31}P NMR. The flavoring activities of these thiophosphates were measured as the synergistic strength with monosodium glutamate; it was found that the strength of each compound was lower than that of inosine-5′-phosphate.

The nucleoside-5′-thiphosphates are of interest in connection with the relationship of the flavoring activity of the 5′-nucleotide to the structure of the phosphate residues. The present authors have attempted to prepare inosine-5′-thiophosphates and have obtained two isomers: inosine-5′-phosphorothionate (I) and 5′-deoxy-5′-thioinosine-5′-phosphorothioate (II). The other possible isomer, inosine-5′-phosphorothiolate (III), was not detected in the product. The synergistic flavoring strengths[2] of the nucleoside thiophosphates with monosodium glutamate were compared with that of inosine-5′-phosphate; the relative strengths of I and II were shown to be one-half and one-fortieth respectively. This paper will deal with the synthesis of the two isomers of inosine-5′-thiophosphates and with their structural identification by ^{31}P NMR.[3]

Results and Discussion

Synthesis of Inosine-5′-thiophosphates. The pyrimidine nucleoside phosphorothionates have been synthesized by the treatment of 3′-*O*-acetylthymidine and 2′,3′-*O*-dimethoxybenzylidene uridine with triimidazoyl-1-phosphinsulfide in only 25—30% yields.[4] In our previous report,[5] it has been shown that nucleosides were phosphorylated with phosphoryl chloride in trialkyl phosphate to give, selectively, the 5′-phosphates in good yields. This method was successfully applied to the phosphorylation of inosine with phosphorus thiochloride; inosine-5′-phosphorothionate (I) was obtained after the hydrolysis of the phosphorylation mixture. The product (I) was isolated by column chromatography and was identified by elemental analysis and by ^{31}P NMR spectroscopy, as will be

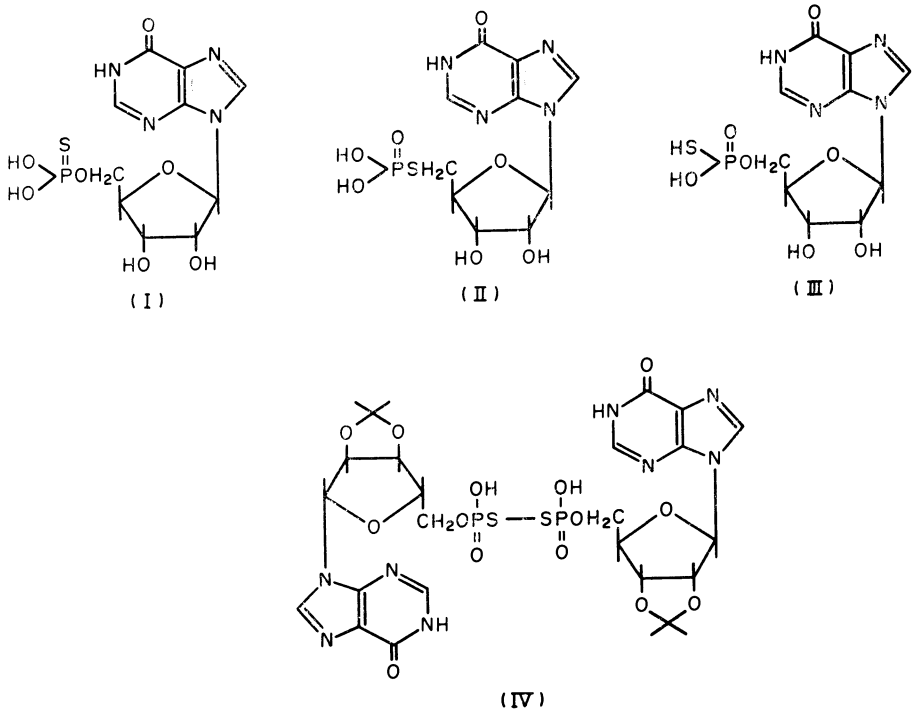

(I) (II) (III) (IV)

1) Part IV: M. Yoshikawa, M. Sakuraba, and K. Kusashio, This Bulletin, **43**, 456 (1970).

2) M. Ohara, T. Ninomiya, S. Ikeda, S. Yamaguchi, and T. Yoshikawa, *J. Agr. Chem. Soc. Jap.*, **40**, 69 (1966).

3) The synthesis of nucleoside-5′-thiophosphates in similar manners was reported by A. Hampton *et al.* (*Biochemistry*, **8**, 2303 (1969)) and by A. W. Murray *et al.* (*Biochemistry*, **7**, 4023 (1968)) while we were making our structural investigation.

4) F. Eckstein, *J. Amer. Chem. Soc.*, **88**, 4292 (1966).

5) M. Yoshikawa, T. Kato, and T. Takenishi, This Bulletin, **42**, 3505 (1969).

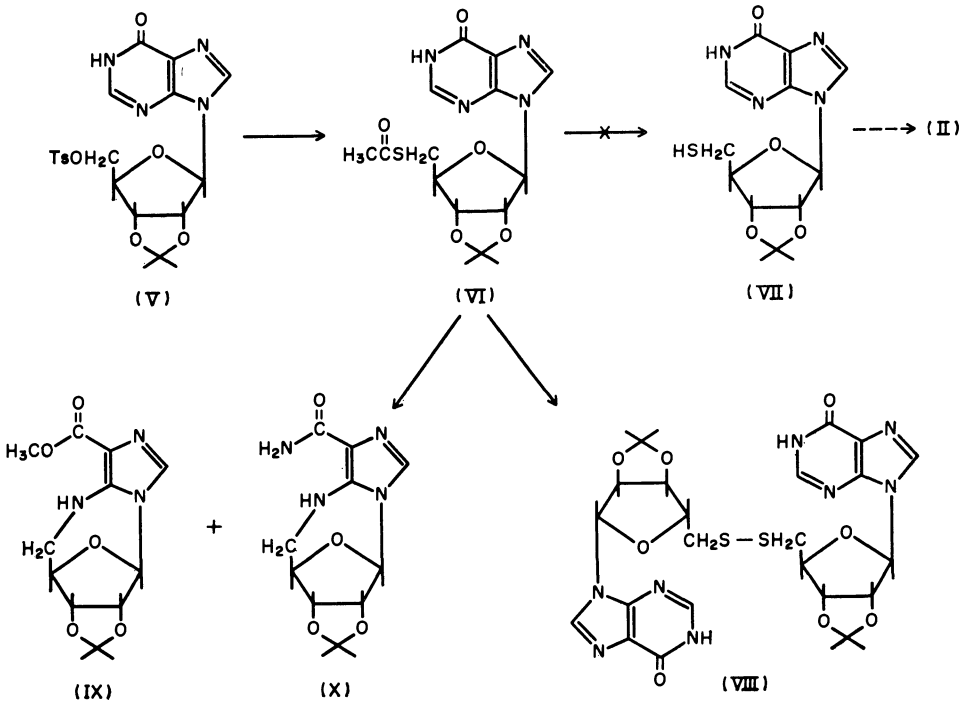

described later. The phosphorothionate was completely desulfurized to give inosine-5'-phosphate by being left for a few hours in an aqueous solution of pH 1—5, but it was stable in a neutral or mildly alkaline medium. When the phosphorothionate (I) was treated with active charcoal in order to purify it, the I was observed by paper chromatography to be entirely transformed into a different compound. The product was positive in sulfur analysis and was reduced quantitatively to I by the treatment of sodium in liquid ammonia. It can be concluded, from these results and from those of the ^{31}P NMR, that the oxidized compound was P^1,P^2-bis(inosine-5'-phosphoryl) disulfide (IV).

For the preparation of 5'-deoxy-5'-thioinosine-5'-phosphorothioate (II), we attempted to prepare 5'-deoxy-5'-thio-2',3'-*O*-isopropylideneinosine (VII) as an intermediate. The acetylthio derivative of inosine (VI) was prepared by heating 2',3'-*O*-isopropylidene-5'-*O*-(*p*-toluenesulfonyl)inosine (V) with sodium thioacetate using a modification of the method reported by Baddiley and Jamieson.[6] However, the treatment of the product with methanolic ammonia for deacetylation produced 5',5'-bis(5'-deoxy-2',3'-*O*-isopropylideneinosyl) disulfide (VIII), contrary to our expectations. The structure of disulfide was confirmed by its positive test with a Grote reagent[7] only after the treatment with potassium cyanate. The interesting result was observed, in the course of the preparative investigation of the acetylthio derivative, that two kinds of cyclonucleosides were produced by the self-exothermic degradation when the reaction has carried out without cooling. These products were isolated by alumina column chromatography. The PMR spectrum of one of the products has two peaks at 8.65 τ due to the isopropylidene group, a single peak at 6.19 τ due to the methyl ester, and a single peak at 3.91 τ due to the C_1'-proton, the latter of which is a typical signal of a cyclonucleoside group. The spectral results and the results of the elemental analysis prove that the product is 5-amino-4-methoxycarbonyl-N^5,5'-cyclo-1-β-D-(2',3'-*O*-isopropylideneribofuranosyl)imidazole (IX). The other product was confirmed to be 5-amino-4-carbamoyl-N^5,5'-cyclo-1-β-D-(2',3'-*O*-isopropylideneribofuranosyl)imidazole (X) by a comparison with an authentic sample.[8]

Some *S*-phosphoric esters have been synthesized by the treatment of halo-compounds with trisodium phosphorothioate.[9] When the 5'-deoxy-5'-iodoinosine was treated with trisodium phosphorothioate in water at room temperature, 5'-deoxy-5'-thioinosine-5'-phosphorothioate (II) was produced quantitatively; it was then isolated from the reaction mixture by means of cellulose-column chromatography. The phosphorothioate was extremely labile in acidic media and was completely hydrolyzed, in less than one minute, to produce 5'-deoxy-5'-thioinosine and orthophosphoric acid under the acidic conditions of pH 3 at 60°C. The compound, however, was relatively stable in neutral or alkaline media.

^{31}P NMR Spectra of Inosine-5'-thiophosphates. In order to clarify the ambiguities of inosine-5'-thiophosphates, the ^{31}P NMR spectra were determined at 40.5 MHz; the results are summarized in Table 1. The ^{31}P signal of I in aqueous ammonia appeared as a rather broad triplet (caused by the spin-coupling with the two protons at *C*-5') at 2812 Hz upfield from the locked P_4O_6. This chemical shift is approximately equal to that of −43.1 ppm downfield from 85%

6) J. Baddiley and G. A. Jamieson, *J. Chem. Soc.*, **1955**, 1085.
7) J. W. Grote, *J. Biol. Chem.*, **93**, 25 (1931).
8) K. Kusashio and M. Yoshikawa, This Bulletin, **41**, 142 (1968).
9) S. Akerfeldt, *Acta Chem. Scand.*, **13**, 1479, 1897 (1959).

TABLE 1. PARAMETERS OF THE ^{31}P NMR SPECTRA[a)]

Compound	Solvent	Chemical shifts[b)] (multiplicity; J[c)])
I	NH_4OH aq.	−43.1 (broad triplet; $J\simeq4.5$ Hz)
II	H_2O	−16.1 (triplet; $J\simeq10$ Hz)
IV	H_2O	−17.3 (broad singlet)
5'-IMP 2Na	H_2O	−3.9 (triplet; $J\simeq4.5$ Hz)
S=P(OEt)$_2$ | ONa (XI)	—	−56 −59
O=P(OEt)$_2$[d)] | SH (XII)	—	−24
O=P(OEt)$_2$ | ONa (XIII)	—	−3.8

a) All spectra were measured at room temperature (34°C).
b) Chemical shifts (ppm) are represented from 85% H_3PO_4 signal which is assumed to appear 4556 Hz upfield from P_4O_6.
c) Multiplicities and coupling constants are estimated based on the first order approximations.
d) "^{31}P Nuclear Magnetic Resonance," M. M. Crutchfield, C. H. Dungen, J. H. Letcher, V. Mark, and J. R. Van Wazer, Interscience Publishers, New York (1967).

H_3PO_4 which shows the phosphorothionate type (P=S), as is also supposed from the ^{31}P NMR spectrum of sodium diethyl phosphorothionate (XII). On the other hand, the ^{31}P NMR spectra of II and IV showed well-resolved triplets (J 10 Hz) at −16.1 and −17.3 ppm from 85% H_3PO_4 respectively. By comparing the chemical-shift data with those of the acyclic analogues, diethyl phosphorothiolate (XII), II and IV can be easily identified as thiophosphates which have a P–S single bond. The considerable differences encountered are attributable to the differences in the monoesters and diesters. Disodium inosine-5'-phosphate showed a triplet at −3.9 ppm downfield from 85% H_3PO_4, which is quite similar to that of sodium diethyl phosphate (XIII).[10)]

Experimental

Measurement of the ^{31}P NMR Spectra of Thiophosphates. The 100 MHz PMR spectra were recorded on a Varian HA-100 spectrometer by the frequency-sweep mode. The 40.5 MHz phosphorus-31 NMR spectra were also measured by the frequency-swept HA-mode, using a Varian HA-100 apparatus. A moltein P_4O_6 (supplied by Gallard-Schlesinger Co.) in a co-axial capillary held in the usual 5 mm sample tube offered a stable lock signal for the field/frequency control. A modulation frequency for the lock signal was generated by a Hewlett-Puckard 4204A audio-oscillator, and the chemical shifts from the lock signal were determined by a Hewlett-Puckard 5512A digital counter.

Paper Chromatographies of the Thio-compounds. The paper chromatographies were carried out by the ascending technique on Toyo Roshi No. 51 paper (40×40 cm), using the following solvent systems: Solv. A, *n*-propanol - concentrated ammonium hydroxide - water, 20 : 12 : 3; Solv. B, *n*-butanol - acetic acid - water, 4 : 1 : 1; Solv. C, isopropanol-saturated ammonium sulfate - water, 2 : 79 : 19. The R_f values of the thio-compounds are listed in Table 2.

TABLE 2. R_f VALUES OF THE THIO-COMPOUNDS

Compound	R_f Value		
	A	B	C
5'-Deoxy-5'-thionosine	0.43	0.38	0.30
5',5'-Bis(5'-deoxyinosyl)disulfide	0.39	0.08	0.01
5',5'-Bis(5'-deoxy-2',3'-*O*-isopropylideneinosyl)disulfide (VIII)	0.86	0.88	0.01
Inosine-5'-phosphorothionate (I)	0.30	0.02	0.54
5'-deoxy-5'-thioinosine-5'-phosphorothioate (II)	0.25	0.02	0.58
5'-acetylthio-5'-deoxy-2',3'-*O*-isopropylideneinosine (VI)	0.83	0.74	0.01
P',P^2-Bis(inosine-5'phosphoryl)-disulfide (IV)	0.32	0.02	0.29

Disodium Salt of Inosine 5'-Phosphorothionate (I). To a solution of phosphorus thiochloride (24 m*l*, 0.12 mol) in cold trimethyl phosphate (100 m*l*), inosine (10 g, 0.04 mol) was added, and then the solution was stirred for 8—9 hr at 0°C. The reaction mixture was poured into ice water, and the aqueous solution was adjusted to pH 3 with sodium hydroxide. The acidic solution was passed through a column of decolorizing resin (Resinous Adsorbent of Hokuetsu Tanso Kogyo Co.). The column was then washed well with water and eluted with a large volume of 0.5 N ammonium hydroxide. The eluate was concentrated and adjusted to pH 9—10 with concentrated ammonium hydroxide. The solution was then passed through a column of Dowex 1×2 ($HCOO^-$ form). After having been washed with water, the phosphorylated product was eluted with a large volume of 2—4 N formic acid. The eluate was evaporated to dryness *in vacuo*. Pure inosine 5'-phosphorothionate was obtained by means of cellulose (Toyo Roshi) column chromatography, which was developed in *n*-propanol-concentrated ammonium hydroxide-water (20 : 12 : 3). Ammonium salt of inosine 5'-phosphorothionate was converted to sodium salt and then recrystallized from water-methanol to give 9.5 g of the product, mp 205°C (dec.).

Found: C, 29.94; H, 3.56; N, 13.46%. Calcd for $C_{10}H_{11}N_4O_7SPNa_2$: C, 29.42; H, 2.72; N, 13.72%.

Disodium Salt of 5'-Deoxy-5'-thioinosine-5'-phosphorothioate (II). Trisodium phosphorothioate (7 g, 40 mmol) and 5'-deoxy-5'-iodoinosine (3.78 g, 10 mmol) were dissolved in water (100 m*l*), and then the solution was stirred for 7 hr at 40°C. The reaction mixture was evaporated *in vacuo* below 30°C, and the residual oil was dissolved in concentrated ammonium hydroxide (20 m*l*). After standing for 30 min, the precipitate was filtered off; the filtrate was then passed through a cellulose column (Toyo Roshi) which was developed in *n*-propanol-concentrated ammonium hydroxide-water (20 : 12 : 3). The fraction of II was evaporated to dryness *in vacuo* at 30°C, and the residue was dissolved in water. After filtration, ethanol was added to the filtrate and the resulting precipitate was recrystallized from water-ethanol to yield 3.5 g of the product, mp 208°C (dec).

Found: C, 27.22; H, 3.18; N, 12.68%. Calcd for $C_{10}H_{11}N_4O_7SPNa_2\cdot1.5\,H_2O$: C, 27.59; H, 3.24; N, 12.87%.

5'-Acetylthio-5'-deoxy-2',3'-O-isopropylideneinosine (VI). To a solution of sodium (2.9 g, 0.13 mol) in anhydrous methanol (75 m*l*), thioacetic acid (8.8 m*l*, 0.13 mol) was added with

10) Detailed accounts of the ^{31}P NMR spectra of nucleotides will be published elsewhere (M. Kainosho, A. Nakamura, and M. Tsuboi).

cooling on an ice bath; acetone (75 m*l*) and 2',3'-*O*-isopropylidene-5'-*O*-(*p*-toluenesulfonyl)inosine (V) (11.5 g, 0.025 mol) were then added. The reaction mixture was refluxed for 3 hr and evaporated to dryness at 40°C. The residue was dissolved in chloroform (150—200 m*l*), and the insoluble material was filtered off. The filtrate was evaporated to dryness, and the residue was dissolved in methanol (100 m*l*). After standing at room temperature for a few hours, the precipitate was separated and recrystallized from methanol to yield 8.5 g of the product, mp 241°C.

Found: C, 48.96; H, 4.69; N, 15.53%. Calcd for $C_{15}H_{18}N_4O_5S$: C, 49.17; H, 4.96; N, 15.29%.

5-Amino-4-methoxycarbonyl-N^5*,5'-cyclo-*1-*β*-D-*(2',3'-*O-isopropylideneribofuranosyl)imidazole (IX).* V was treated without cooling in the same manner as in the preceding paragraph. The reaction products soluble in chloroform were dissolved in a small amount of methanol and then passed through a column of alumina. The column was eluted with 5% methanolic-ether. The eluate was concentrated and ether was added to the residue to crystallize IX, mp 155°C.

Found: C, 52.37; H, 5.65; N, 13.98%. Calcd for $C_{13}H_{17}N_3O_5S$: C, 52.87; H, 5.80; N, 14.23%.

X was isolated by eluting the column with 50% methanolic ether.

*5',5'-Bis-(5'-deoxy-2',3'-*O*-isopropylideneinosyl)Disulfide (VIII).* 5'-Acetylthio-5'-deoxy-2',3'-*O*-isopropylideneinosine (VI) was dissolved in methanol, and the solution was saturated with anhydrous ammonia at 0°C. After standing overnight, the solution was concentrated and methanol was added to the residue. The resulting precipitate was recrystallized from water to give 5.5 g of the product, mp 235°C.

Found: C, 47.76; H, 5.04; N, 17.26; S, 9.89%. Calcd for $C_{26}H_{30}O_8N_8S_2$: C, 48.28; H, 4.67; N, 17.33; S, 9.92%.

The authors wish to thank Dr. Tetsuya Kato of Ajinomoto Co., Inc. for his valuable advice.

BULLETIN OF THE CHEMICAL SOCIETY OF JAPAN, VOL. 44, 463—467 (1971)

Thermal and Photolytic Decompositions of Azobis(2-phenylthio)-2-propane

Atsuyoshi OHNO, Noboru KITO, and Yutaka OHNISHI
Sagami Chemical Research Center, Ohnuma, Sagamihara-shi, Kanagawa

(Received May 18, 1970)

Thermal and photolytic decompositions of azobis(2-phenylthio)-2-propane have been studied. The reaction mechanisms have been discussed on the basis of products. Almost all reactions of 2-phenylthioprop-2-yl radicals produced from the azo compound photolytically proceed with in-cage processes. The ratio, disproportionation/dimerization, predicts qualitatively that the radical center of the free radical is more electronegative than that of the corresponding oxygen analog.

In a study on the effect of a heteroatom on a radical center, we reported preliminary results on the rates of decomposition of azo compounds that have sulfur or oxygen atoms at α-positions.[1] We consider it worthwhile studying the reactions of free radicals produced from the azo compounds, since this will help to shed light on the nature of the interaction between a heteroatom and a radical center. The photolyses of azo compounds are often used as potential sources of free radicals, but their secondary reaction products have been scarcely studied.

The present study was carried out to see what information the product distribution would give on the mechanism of decomposition of azo compounds. In this paper, we wish to report thermal and photochemical reactions of 2-phenylthioprop-2-yl (**1**) and discuss the mechanism.

$$PhS\text{–}\dot{C}(CH_3)_2$$

1

Results

When a 0.25 M solution of azobis(2-phenylthio)-2-propane (**2**) in *p*-xylene was subjected to thermolysis, **2** decomposed completely over a period of 20 hr at 160°C. Products identified from the reaction mixture were 2-phenylthiopropane (**3**), 2-phenylthiopropene (**4**), 2,3-diphenylthio-2,3-dimethylbutane (**5**), diphenyl disulfide (**6**), 2-phenylthio-2-*p*-methylbenzylpropane (**7**), and 4,4′-dimethylbibenzyl (**8**) along with two minor unidentified compounds and polymeric material. On the other hand, the photolysis of the same solution in a pyrex flask at 25°C for 6 hr with the light from a 400 W high-pressure mercury lamp (principal wavelength, 3150 and 3660 Å) led to the complete decomposition of **2** and afforded 2,2-diphenylthiopropane (**9**), propylene (**10**), and 1,2-diphenylthiopropane (**11**) in addition to **3**, **4**, **5**, and polymeric material. Reaction conditions and yields are summarized in Table 1. The results of photolysis of azobis(2-benzyl)-2-propane, a methylene analog of **2**, in benzene are listed in Table 2 for comparison.

Yields were based on the free radical, two species of which had been produced from one molecule of the azo compound, and were determined by combination of vpc and NMR. As **5** and **14** could not be detected by vpc and their NMR spectra are quite similar to those of parent azo compounds, the yields of these compounds were determined by isolation from column chromatograms. For the analyses of gaseous products, mass spectroscopy and vpc were employed.

The free radical **1** can be generated by an alterna-

1) A. Ohno and Y. Ohnishi, *Tetrahedron Lett.*, **1969**, 4405.

Table 1. Products from thermolysis and photolysis of **1** in various conditions

Run		1	2	3	4	5	6	7	8	9
Mode of Decomposition		hν	hν	hν	hν	hν	hν	hν	Δ	Δ
Temperature, °C		25	25	25	80	120	160	160	120	160
Time, hr		6	15	40	20	15	10	20	40	20
Product						Yield, %				
$PhSCH(CH_3)_2$	**3**	35.2	33.2	31.4	34.1	37.9	34.5	38.0	29.8	27.5
$PhSC(CH_3)=CH_2$	**4**	14.2	9.9	5.9	7.8	7.5	7.3	6.9	3.6	8.5
$[PhSC(CH_3)_2]_2$	**5**	+	+	13.0[a]	+	+	+	+	+	9.0[a]
PhSSPh	**6**	.....	.....	Trace	.....	.....	2.6	4.0	3.9	6.5
$PhSCMe_2CH_2C_6H_4CH_3$-*p*	**7**	0	0	0	Trace	0.8	5.2	5.5	5.7	7.8
$(PhS)_2C(CH_3)_2$	**9**	7.8	10.3	12.4	8.7	3.8	4.7	3.9	0	0
$CH_3CH=CH_2$	**10**[b]	+	+	+	+	+	+	+	0	0
$PhSCHMeCH_2SPh$	**11**	1.9	3.4	4.6	+	+	+	+	Trace	Trace

a) Isolated yields. b) Qualitatively analyzed.

Table 2. Products from photolysis of azobis-(2-benzyl)-2-propane in benzene at 25°C

Product		Yield, %
$PhCH_2CH(CH_3)_2$	**12**	50.7
$PhCH_2C(CH_3)=CH_2$	**13**	37.8
$[PhCH_2C(CH_3)_2]_2$	**14**	11.5

Table 3. Products from photolysis of a mixture of **3** and DTBP at 25°C

Product		Yield, %[a]
$PhSC(CH_3)=CH_2$	**4**	Trace
$PhS(CH_2)_2CH_3$	**15**	3.5
PhSSPh	**6**	9.7
$CH_3CH=CH_2$	**10**[b]	+
$(PhS)_2C(CH_3)_2$	**9**	Trace

a) DTBP : **3** = 1 : 1 in mol ratio. Conversion = 11.6%
b) Qualitatively analyzed.

tive method. A mixture of **3** and di-*t*-butylperoxide (DTBP) (1 : 1 in mole ratio) was irradiated in the same way as described above, which resulted in no products expected from bimolecular reactions of **1** (except for trace of **4**) being found (see Table 3). Instead, a considerable amount of **6** and **10** with a small amount of phenyl *n*-propyl sulfide (**15**) were isolated.

Discussion

The products could be divided into several groups according to the reactions for their formation, *via*, disproportionation, dimerization and hydrogen abstraction of **1**. The former two proceed by either thermal or photolytic conditions, while hydrogen abstraction takes place only at elevated temperatures. All the reactions give important information and it will be convenient to discuss them separately.

Disproportionation and Dimerization. The presence of **3**, **4**, and **5** in the reaction mixture invokes unequivocally that both thermal and photolytic decompositions of **2** proceed with a radical mechanism.

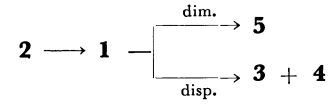

Although yields of disproportionation products **3** and **4** are not counterbalanced, this is mainly due to their further decomposition or polymerization. As seen in Table 1, the longer the reaction time and the higher the temperature, the lower their yields, It is apparent that disproportionation is not the only route to **3** at least for thermolysis (*vide infra*). for This also seems true for photolysis, because the yields of **12** and **13** are unbalanced in spite of the fact that 100% of products have been identified. It is noteworthy that the ratio of yields, (**3**+**4**)/**5** or disproportionation/dimerization, is considerably smaller than the corresponding values with the methylene and oxygen analogs.[2] These ratios do not represent exactly the relative ratios of disproportionations and dimerizations. However, this tendecy indicates, at least qualitatively, that the electron density at the radical center decreases by a substituent at an α-position with the order $O \gg CH_2 \gtrsim S$.[3-5] This seems to imply that a canonical form **16** is more important for the oxygen analog than for the sulfur one.[1]

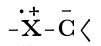

16

The photolytic decomposition of **2** produces almost all these compounds by "in-cage" reactions, since the reaction of **3** with DTBP does not afford them in a measurable amount. In the latter reaction, **1** is not paired by a partner and has difficulty in encountering one.

2) A. Ohno, N. Kito, and Y. Ohnishi, This Bulletin, **44**, 467 (1971).
3) S. W. Benson, *Advan. Photochem.*, **2**, 1 (1964).
4) a) J. R. Shelton, C. K. Liang, and P. Kovacic, *J. Amer. Chem. Soc.*, **90**, 354 (1968); b) P. Kovacic, R. R. Flynn, J. F. Gormish, A. H. Kappelman, and J. R. Shelton, *J. Org. Chem.*, **34**, 3312 (1969).
5) P. J. Wagner and H. N. Schott, *J. Amer. Chem. Soc.*, **91**, 5383 (1969).

Another interesting phenomenon, seen in Table 2, is that the olefin formed by disproportionation was only **13** and no **17** was detected, contrary to expecta-

$$PhCH{=}C(CH_3)_2$$

17

tion from the reactivities of hydrogen.[6] There are few such examples of high selectivity in radical reactions. Steric effects seem to play an important role for hydrogen abstraction.[7]

Hydrogen Abstraction from the Solvent. Since **7** and **8** are formed only at elevated temperatures, the

reaction might require a certain amount of activation energy. Taking into account the lifetime of **1**,[8] it is reasonable to attribute a "cage-wall" reaction for the formation of **7**.

Photochemical Reactions. Formation of **9** and **10** presents an interesting photochemistry. Since these compounds are not afforded by thermal reactions (runs 8 and 9 in Table 1) and since the experiment shown in run 7 in Table 1 confirms that they are not consumed by further reactions under the present thermal conditions, it is apparent that these compounds have been formed by a photochemical process.

A control experiment revealed that they were formed from olefin, **4**, photochemically. The increase of the yield of **9** with prolonged irradiation (runs 1 to 3 in Table 1 and Experimental) can be attributed to this reaction. The mechanism may be as follows.

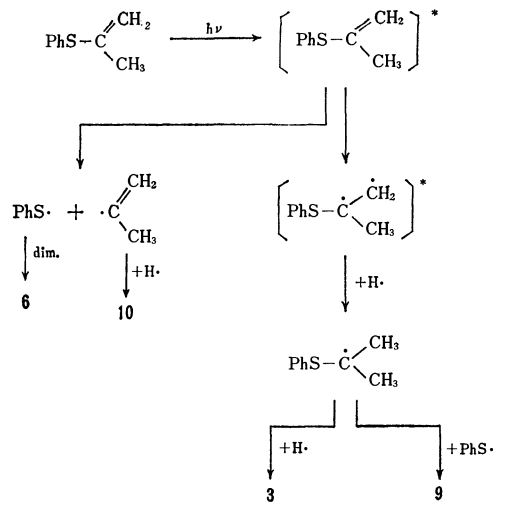

The olefin is known to undergo photocyclization yielding a benzothiophene derivative.[9] However, this mode of photodissociation has not been reported. It is interesting to note the formation of a vinyl radical.

Although **11** is formally afforded by the addition of thiophenol to **4**, there is an alternative pathway: the migration of **9** to **11**.[10,11] However, a control experiment showed that such a reaction does not take place under the present conditions both photochemically and thermally.

We claimed thermal carbene-formation from the fact that thermolysis of **2** in *p*-tolylmercaptan affords *p*-tolyl isopropyl sulfide (**18**).[1] However, we now believe that the mechanism of this reaction can be better ascribed to the addition-elimination process:

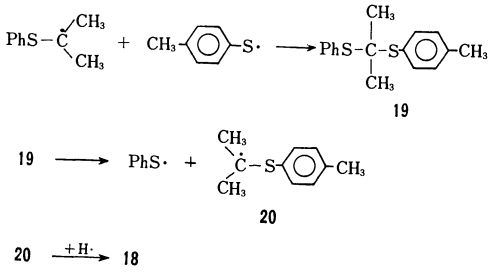

When a solution of **9** in *p*-tolylmercaptan was kept at 160°C for 20 hr, 2,2-(*p*-tolylthio)propane was isolated in good yield.

Experimental

Materials. Azobis(2-phenylthio)-2-propane (**2**) was prepared according to Benzing[12]; mp 90—90.5°C (lit, 90—90.5°C).

Azobis(2-benzyl)-2-propane was synthesized by the oxidation of 1,1-dimethyl-2-phenylethyl amine with IF_5;[13] 120 m*l* of CH_2Cl_2, 18 m*l* of pyridine, and more than 5 m*l* of IF_5 were placed in a 1*l* three-necked flask equipped with a mechanical stirrer, a dropping funnel, and a refluxing condenser, and cooled to about −10°C with a dry ice—CCl_4 bath. A solution of 1,1-dimethyl-2-phenylethyl amine (14 g)[14] in CH_2Cl_2 (10 m*l*) was then added slowly through dropping funnel. The whole mixture was stirred further for 1 hr at −10°C and 2 hr at 0°C. After excess IF_5 had been decomposed with water, the organic layer was washed with water, dilute aq-HCl, and 5% aq-$Na_2S_2O_3$, and dried over Drierite. Evaporation of the solvent under reduced pressure left a dark-brown oil, which was extracted with ether giving crystalline material. Recrystallization from methanol gave 2.5 g of the azo compound (mp 68—70°C).

Found: C, 81.70; H, 8.98; N, 9.61%. Calcd for $C_{20}H_{26}N_2$: C, 81.58; H, 8.90; N, 9.52%.

Authentic samples were prepared according to refer-

6) W. A. Pryor, "Free Radicals," McGraw-Hill Book Co., New York, N. Y. (1966), pp. 149—175.

7) W. D. Totherow and G. J. Gleicher, *J. Amer. Chem. Soc.*, **91**, 7150 (1969).

8) A. Ohno, N. Kito, and Y. Ohnishi, This Bulletin, **44**, 470 (1971). The ESR signal could not be obtained by photolysis of **2** at room temperature, though its oxygen and methylene analogs gave signals. This fact indicates that the lifetime of **1** is fairly short, which is also evidenced by the distribution of products from the reaction of **3** with DTBP.

9) S. H. Groen, R. M. Kellogg, J. Buter, and H. Wynberg, *J. Org. Chem.*, **33**, 2218 (1968).

10) R. Kh. Freidlina, A. B. Terent'ev, and R. G. Petrova, *Dokl, Akad. Nauk SSSR*, **149**, 860 (1963); *Chem. Abstr.* **59**, 7411b (1963).

11) R. Kh. Freidlina, *Advan. Free-Radical Chem.*, **1**, 211 (1965).

12) E. Benzing, *Ann. Chem.*, **631**, 1 (1960).

13) S. F. Nelsen and P. D. Bartlett, *J. Amer. Chem. Soc.*, **88**, 137 (1966); T. E. Stevens, *J. Org. Chem.*, **26**, 2531 (1961).

14) J. J. Ritter and J. Kalish, *J. Amer. Chem. Soc.*, **70**, 4048 (1948).

ences.[15-19]

Photolysis. General Procedure: Unless otherwise indicated, all photolyses were carried out in pyrex tubes (15 mm o.d.) using a 400 W high-pressure mercury lamp (Riko-Kagaku Sangyo), which was placed in a water-cooled quartz immersion well.

All the solutions (0.25 M in purified *p*-xylene) were degassed under reduced pressure at 10^{-4} mmHg by the freeze-thaw method to exclude air and oxygen, and then were sealed in the usual manner. Sample tubes were placed 40 mm from the source of light.

Photolyses at elevated temperatures were performed by using a two-necked quartz tube; a sample tube was inserted from one side with the thermometer and hot air was introduced from the other. Temperatures were maintained within ±3°C.

Photolysis of **2**: Run 3 of Table 1 will be described in detail as a typical example. Photolysis of **2** (825 mg) was performed at 25°C for 40 hr. Compounds **3** and **4** were identified by retention time with those of authentic samples on vpc and by IR and NMR spectra. After elimination of excess solvent, **3**, and **4** under reduced pressure, the concentrated mixture was chromatographed on a column of silica gel (200 mesh) packed in petroleum ether. Elution of the column with a mixture of petroleum ether and benzene (90 : 10) yielded 98 mg (13%) of **5**, a trace of **6**, and an oil. Compound **5** was recrystallized from ethanol, mp 126—127°C, whose NMR spectrum had signals at (δ from TMS in CCl_4) 1.41 (s, 12H) and 7.02—7.35 (m, 10H).

Found: C, 71.27; H, 7.32; S, 21.07%. Calcd for $C_{18}H_{22}S_2$: C, 71.50; H, 7.33; S, 21.17%.

An oil was rechromatographed on a column of silica gel with petroleum ether - benzene (85 : 15) mixture as an eluent. Purified oil was identified to be **9** by comparing IR, NMR and mass spectra with those of the authentic sample as well as elemental analyses. Compound **11** was also obtained as an oil on column chromatographic separation on silica gel, IR, NMR, and mass spectra of which were identical with those of the authentic compound.

Formation of **10** was carefully examined by an independent photolysis of **2** in a breakable-sealed tube. Gas analyses on mass spectrometry and gas chromatography showed the presence of **10** in a considerable amount.

Thermolysis. General Procedure: Aliquots prepared as described above were placed in an oil bath of 160°C. Temperature was maintained within ±1°C.

Thermolysis of **2**: Run 9 of Table 1 will be described in detail as a typical example. Thermolysis of **2** (825 mg) was undertaken at 160°C for 20 hr. After the decomposition of **2** had been completed, **3**, **4**, and **6** were analyzed by VPC quantitatively. The reaction mixture was chromatographed on a column of silica gel packed in petroleum ether after the elimination of the solvent and **3** under reduced pressure. Elution of the column with a mixture of petroleum ether and benzene (90 : 10) gave white crystals and **6**. The crystals were identified to be **7** by the following evidence: NMR (δ from TMS in CCl_4) 1.15 (s, 6H), 2.28 (s, 3H), 2.76(s, 2H), 6.94(s, 4H), and 7.08—7.60 (m, 5H). Mass spectrum showed a parent peak at *m/e* 256 and a base peak at *m/e* 151 $(PhSCMe_2)^+$.

Found: C, 79.79; H, 7.87; S, 12.51%. Calcd for $C_{17}H_{20}S$: C, 79.65; H, 7.86; S, 12.48%.

Compound **8** was collected by vpc and was rechromatographed on a column of silica gel and its identity was confirmed with the authentic compound.

The presence of **10** in a mixture of thermolysis products was examined independently. There was no indication of the formation of this compound.

Thermolysis and Photolysis of **3**. Thermolysis (160°C) and photolysis (25°C) of **3** in *p*-xylene (0.25 M) were carried out in degassed tubes for 20 hr. It was found that no reaction had taken place.

Photolysis of **4**. A solution of **4** in *p*-xylene was irradiated as described above. Reaction conditions and results are summarized in Table 4.

Table 4. Products from photolysis of **4** in *p*-xylene at 25°C

Irrad. Time, hr		20	40
Conversion, %		62.1	89.0
Product		Yield, %[a]	
$PhSCH(CH_3)_2$	**3**	Trace	Trace
PhSSPh	**6**	6.5	5.9
$CH_3CH{=}CH_2$	**10**[b]	+	+
$(PhS)_2C(CH_3)_2$	**9**[c]	16.2	11.5

a) Based on consumed **4**. b) Qualitatively analyzed. c) Contaminated by a trace of **11**.

Thermal and Photochemical Additions of Thiophenol to **4**. Equimolar mixtures of thiophenol and **4** in benzene (4.0 ml, 0.25 M) and in *p*-xylene (4.0 ml, 0.25 M) were subjected to photochemical (25°C) and thermal (160°C) reactions, respectively. No quantitative analysis on products was carried out. However, anti-Markownikoff addition product **11** was obtained, along with **6** and unreacted **4**, from both reactions.

Thermal and Photochemical Rearrangements of **9**. Thermolysis (160°C) and photolysis (25°C) of **9** in *p*-xylene (5.0 ml, 0.5 M) were performed in evacuated sealed tubes for 20 hr. Most of the starting material was recovered along with small amounts of **6**, **4**, and an unidentified material. It is apparent that the thermal and photochemical rearrangements from **9** to **11** did not occur. No formation of **10** took place.

Thermal Decomposition of **5**. Compound **5** (148 mg) was thermally decomposed in *p*-xylene (2.0 ml) at 160°C for 20 hr. Most of **5** was found to be recovered, but was detected the formation of 2,3-dimethylbutene-2 by vpc and mass spectrometry along with **6**.

Thermal and Photochemical Decompositions of **11**. Thermolysis (160°C, 40 hr) and photolysis (25°C, 40 hr) in *p*-xylene (5.0 ml, 0.25 M) were carried out in a degassed sealed tube. No definite change took place in both reactions. Original **11** was mostly recovered. Propylene **10** was detected by analyses of gaseous products.

The Reaction of **3** *with DTBP*. An equimolar mixture of **3** and DTBP was degassed thoroughly and sealed in a pyrex tube. Photoirradiation was carried out at 25°C for 20 hr. Product analysis was carried out as described before. Compound **12** was collected by vpc and was rechromatographed on a column of silica gel. Identity of its structure with that of the authentic compound was confirmed by

15) $PhSCH(CH_3)_2$, bp 110.5—111.5°C/40 mmHg (lit, 260.5—207.5°C): V. N. Ipatieff, H. Pines, and B. S. Friedman, *J. Amer. Chem. Soc.*, **60**, 2731 (1938).

16) $PhSC(CH_3){=}CH_2$, bp 79—84°C/10 mmHg (lit, 97—98°C/20 mmHg): W. H. Muller and K. Griesbaum, *J. Org. Chem.*, **32**, 856 (1967).

17) $(CH_3)_2C(SPh)_2$, bp 162°C/0.25 mmHg (lit, 146°C/0.1 mmHg): A. Schonberg and K. Praefcke, *Chem. Ber.*, **100**, 778 (1967).

18) $PhSCH(CH_3)(CH_2SPh)$, 176—179°C/4 mmHg (lit, 166—167°C/2 mmHg): Ref. 11.

19) $PhCH{=}C(CH_3)_2$, collected by vpc: R. N. Castle and C. F. Poe, *J. Amer. Chem. Soc.*, **66**, 1438 (1944).

spectral data.

The Reaction of **9** *with* p-*Tolylmercaptan.* In a degassed and sealed tube, 0.1303 g (5×10^{-4} M) of **9** and 5.0 g (4×10^{-2} M) of *p*-tolylmercaptan were placed. The mixture was kept at 160°C for 20 hr. Excess *p*-tolylmercaptan was eliminated from a reaction mixture under reduced pressure, bp 72—74°C/12 mmHg. The residue was chromatographed on silica gel with petroleum ether-benzene (90 : 10) mixture as an eluent, yielding 0.133 g (92%) of 2,2-(*p*-tolylthio)propane: mp 65—66°C (lit,[20] mp 66°C).

We wish to thank Dr. G. Tsuchihashi of Sagami Chemical Research Center for useful discussion.

20) E. Fromm and G. Raiziss, *Ann. Chem.*, **374**, 90 (1910).

BULLETIN OF THE CHEMICAL SOCIETY OF JAPAN, VOL. 44, 467—470 (1971)

Thermal and Photolytic Decompositions of Azobis(2-phenoxy)-2-propane

Atsuyoshi OHNO, Noboru KITO, and Yutaka OHNISHI
Sagami Chemical Research Center, Ohnuma, Sagamihara-shi, Kanagawa

(Received May 18, 1970)

Thermal and photolytic decompositions of azobis(2-phenoxy)-2-propane have been studied. More than half of the 2-phenoxyprop-2-yl radicals thus produced thermally cause the phenyl group to migrate from oxygen to the carbon, followed by elimination of the methyl group. Most of the remaining radicals abstract hydrogen from the solvent. When phenyl ether is employed as a solvent, homolytic aromatic substitution takes place yielding isopropylbenzene derivatives. It is shown by mechanistic consideration, although not completely decisively, that this is a new type of reaction in the sense that a part of the leaving group constitutes a part of the entering group.

In contrast to the ionic species, little has been studied on the effect of heteroatoms in free radicals. In a previous paper concerning kinetics of decompositions of azo compounds which have heteroatoms at α-positions, we reported that an α-oxygen atom exerts very minor, if any, effect on the stabilization of a carbon radical in comparison to an α-methylene group, while a sulfur atom stabilizes it extensively.[1] On the other hand, it is known from the study on ESR spectroscopy that a free radical which has an α-oxygen atom has much longer lifetime than its methylene or sulfur analog under the irradiation of light.[2] These facts indicate that the oxygen-containing radical is less reactive than others at least under the condition of photolysis. This prompted us to study the mechanism of thermal and photochemical decompositions of azobis(2-phenoxy)-2-propane (**1**) and of secondary reactions involving 2-phenoxyprop-2-yl (**2**).

$$PhO\text{–}\dot{C}(CH_3)_2$$

2

This paper deals with the analyses of final products of these reactions. The results are discussed in comparison to those obtained with sulfur and methylene analogs of **2**.[3]

Results

A 0.25 M solution of **1** in *p*-xylene was subjected to thermolysis at 160°C for 20 hr. Identified products were 2-phenoxypropane (**3**), 2-phenoxypropene (**4**), 2,3-diphenoxy-2,3-dimethylbutane (**5**), acetophenone (**6**), and methane (**7**) along with a considerable amount of *p*,*p*′-dimethylbibenzyl (**8**). Irradiation of light from a 400 W high-pressure mercury lamp to the same solution in a pyrex flask at 25°C for 6 hr (principal wavelength 3150 and 3660 Å) gave **3**, **4**, **5**, and phenol (**9**). Results are summarized in Table 1. Yields were based on the free radical **2**, two species of which had been produced from one molecule of the azo compound, and were determined by using vpc and NMR except for **5**. Since **5** has identical NMR signals to those of **1** and it decomposes in a column of vpc, the yield of this compound was obtained by isolation from a column chromatogram.

Irradiation of light to a mixture of **3** and di-*t*-butylperoxide (DTBP) also affords the same free radical, **2**. Products obtained were **4**, **5**, **9**, and a mixture of

TABLE 1. PRODUCTS FROM THERMOLYSIS AND PHOTOLYSIS OF **1** IN VARIOUS CONDITIONS

Run		1	2	3	4	5
Mode of decomposition		hν	hν	hν	hν	Δ
Temperature, °C		25	25	80	120	160
Time, hr		6	40	20	15	20
Product		Yield, %				
$PhOCH(CH_3)_2$	**3**	39.2	42.2	43.4	38.8	45.1
$PhOC(CH_3)=CH_2$	**4**	31.8	28.7	24.9	20.1	4.2
$[PhOC(CH_3)_2]_2$	**5**[a]	1.3	1.5	1.1	1.2	Trace
$PhCOCH_3$	**6**	0	0.4	2.7	4.7	50.7
CH_4	**7**[b]	—	—	—	—	+
$[p\text{-}CH_3C_6H_4CH_2]_2$	**8**[c]	Trace	2.1	5.6	10.9	64.0
PhOH	**9**	8.1	8.5	8.6	8.8	0

a) Isolated yields.
b) Qualitatively analyzed.
c) Calculated by assuming the formation of one species of *p*-methylbenzyl radical from one species of **2**.

1) A. Ohno and Y. Ohnishi, *Tetrahedron Lett.*, **1969**, 4405.
2) A. Ohno, N. Kito, and Y. Ohnishi, This Bulletin, **44**, 470 (1971).
3) A. Ohno, N. Kito, and Y. Ohnishi, *ibid.*, **44**, 463 (1971).

isomers of isopropoxycymenes. Since the last mixture consisted of more than 95% of *o*-isomer, we will refer to this as *o*-isopropoxycumene (**10**). The results are listed in Table 2.

Table 2. Products from photolysis of a mixture of **3** and DTBP at 25°C

Mol Ratio (**3**/DTBP)		2	1
Conversion, %		4.0	25.4
Product		Yield, %	
$PhOC(CH_3)=CH_2$	**4**	Trace	24.2
o-Isopropoxycumene	**10**	51.5	7.2
PhOH	**9**	42.5	5.4
$[PhOC(CH_3)_2]_2$	**5**	Trace	12.4

Azobis(*p*-tolyloxy)-2-propane (**11**) was also decomposed in *p*-xylene at 160°C under irradiation of light for 15 hr. Products identified were *p*-methyl derivatives of **3**, **4**, **6**, and **9**. Neither *o*,*o*'-dimer nor *o*,*p*'-dimer of cresol (Pummerer's ketone)[4] was detected.

In isopropoxybenzene, **1**, **11**, and azobis(*p*-chlorophenoxy)-2-propane (**12**) decomposed photolytically. Yields of *o*-isopropoxycumene are listed in Table 3 together with the result of thermolysis of **1** in the same solvent.

Table 3. Yields of *o*-isopropoxycumene

Azo compound	Yield, %	
	$h\nu$[a]	Δ[b]
1	21.3	19.4
11	1.2	—
12	2.8	—

a) At 25°C. b) At 160°C.

Discussion

In view of the product distribution, marked difference can be seen between thermal and photolytic decompositions of **1**. Acetophenone is formed as a main product of thermolysis, while it is absolutely absent in the photolysis mixture. On the other hand, phenol is produced only by photolysis. Furthermore, as seen in the reaction of **3** with DTBP, homolytic aromatic substitution takes place when a reasonable amount of phenyl ether is present, which is not the case with phenyl sulfides or with aromatic hydrocarbons. These and other observations will be discussed respectively under separate titles.

Migration. The presence of acetophenone and methane suggests clearly that the reaction takes place

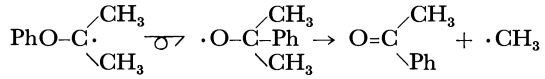

in the solution. Although this type of rearrangement is known in gas phase,[5-7] this is the first example of migration in a solution. The second step of the reaction takes place easily in solution and has been studied both kinetically[8-10] and spectroscopically.[11] Activation energy is estimated to be about 8 kcal/mol.[8] Cumyloxy radicals generated by the photolysis of dicumyl peroxide in benzene have too short a life for ESR detection at a room temperature.[11] However, 2-phenoxyprop-2-yl radicals generated by the photolysis of **1** in *p*-xylene have enough lifetime for detection after the irradiation of light has been stopped.[2] From the results, migration seems to require activation energy of more than 8 kcal/mol.

The fact that the same reaction with **11** affords *p*-methylacetophenone solely, seems to suggest that migration proceeds through a transition state expressed by **13**.

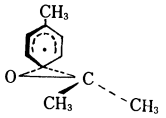

13

Homolytic Aromatic Substitution. When a mixture of **3** and DTBP is irradiated with light, a large amount of **9** and **10** is formed at the sacrifice of **4**.[12] The aromatic substitution of the same type also takes place when **1**, **11**, and **12** are decomposed in **3**. Several mechanisms are possible for this substitution:

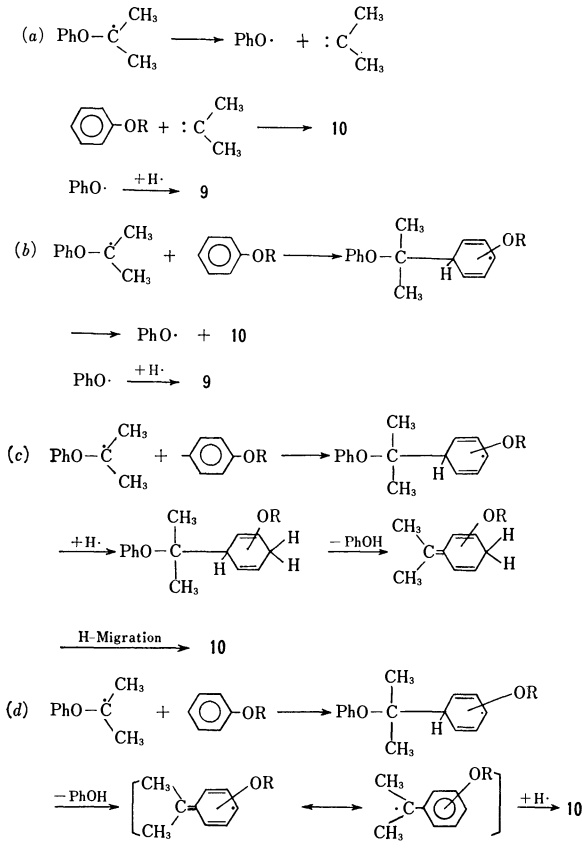

4) R. Pummerer, H. Puttfarcken, and P. Scopflocker, *Ber.*, **58**, 1811 (1925).
5) J. A. Berson, *J. Amer. Chem. Soc.*, **76**, 4060 (1954).
6) M. F. R. Mucahy, B. G. Tucker, D. J. Williams, and J. R. Wilmshurst, *Chem. Commun.*, **1965**, 609.
7) I. N. Nazarov and L. D. Bergel'son, *Zh. Obshch. Khim.*, **27**, 1540 (1957); *Chem. Abstr.*, **52**, 3660g (1958).
8) C. Walling and A. Padwa, *J. Amer. Chem. Soc.*, **85**, 1593 (1963).
9) a) C. Walling and P. J. Wagner, *ibid.*, **85**, 2333 (1963); b) C. Walling and P. J. Wagner, *ibid.*, **86**, 3368 (1964).
10) A. A. Zavitsas and S. Seltzer, *ibid.*, **86**, 3836 (1964).
11) J. J. Zwolenik, *J. Phys. Chem.*, **71**, 2464 (1967).

where R stands for an isopropyl group and many other canonical forms are neglected for simplicity.

Mechanism *a* is highly implausible, since almost exclusive formation of the *o*-isomer cannot be explained by this mechanism.[13] In addition, there is no indication of carbene-formation during the reaction.[14] On the other hand, the predominancy of *o*-attack is well established in free-radical aromatic substitution.[15]

Although mechanism *b* seems reasonable, it involves free-radical 1,2-hydrogen shift. Despite much effort to find such a type of migration, nothing has been achieved.[16] This reduces the possibility of this mechanism greatly. Furthermore, it is important to consider the formation of phenol. If a phenoxy radical is a precursor of a phenol, we might expect coupling products at least in a detectable amount. However, no such compound was found. This implies that phenol results not from phenoxy radicals but from something which can eliminate it directly. Thus, mechanisms *c* and *d* remain as plausible pathways.

The difference between these mechanisms lies on the timing of hydrogen abstraction. The former mechanism involves abstraction of a hydrogen by a cyclohexadienyl radical before a phenol departs from it. This type of reaction is well known.[17-20] On the other hand, the latter mechanism consists of the elimination of a phenol followed by hydrogen abstraction at a benzyl position. Although it is impossible to decide which mechanism is correct without further information, we believe that mechanism *d* is more plausible than the others. In mechanism *d*, the driving force for the elimination of phenol could be attributed to the aromatization of a cyclohexadienyl radical. No such energy gain can be found in the step of phenol elimination in mechanism *c*.

It is noteworthy that this type of substitution is greatly reduced when **2** has a substituent at the *p*-position (Table 3) and that no reaction takes place when phenyl isopropyl sulfide is employed as a solvent. These facts suggest considerable contribution of electronic effect(s) for this reaction.[21] Even though mechanism *d* is plausible, some variations must be considered in this mechanism to elucidate giving *o*-isomer predominantly.

It should be noted anyhow that the reaction is of a new type of homolytic aromatic substitution in the sense that the entering group itself keeps a part of the leaving group.

Hydrogen Abstraction from the Solvent. The result of run 5 in Table 1 shows that about 40% of **2** thermally produced abstracts hydrogen from the solvent. At lower temperatures, discrepancies of yields of **3** and **4** are much smaller or almost comparable indicating disproportionation is much more important than hydrogen abstraction from the solvent. The corresponding value for the sulfur analog of **2** is at most 15%.[3] Uneyama and co-workers have reported that the relative reactivity of thioanisole and anisole toward hydrogen abstraction by *t*-butoxy radicals is only 1.5 : 1.0.[22] Although the present result is far from quantitative and cannot be compared to kinetic data precisely, longer life of **2** than its sulfur analog seems to play an important role for such a great facility of **2** in hydrogen abstraction. Thus, **2** has many chances to escape from a solvent-cage or from its counterpart and to react with the solvent in "out-of-cage" process. Since the sulfur analog of **2** is short-lived, the only chance for it to react with the solvent is a process of "cage-wall" reaction. According to this scheme, it is understandable why the sulfur analog of **2** affords 2-phenylthio-2-*p*-methylbenzylpropane and **2** does not afford the corresponding oxygen compound: when a *p*-methylbenzyl radical is formed at "cage-wall", as being the case of the sulfur compound, it is easily captured by a radical in "cage", while a *p*-methylbenzyl radical produced at out of "cage" has little chance to find such a counterpart.

Experimental

Materials. Azobis(2-phenoxy)-2-propane (**1**) was prepared after Benzing[23] from the corresponding chloride and phenol. For this reaction, however, ethanol was not a useful solvent and *N,N'*-dimethylformamide was employed (yield, 40%): mp 91—92°C.

Found: C, 72.80; H, 7.40; N, 9.43%. Calcd for $C_{18}H_{22}N_2O_2$: C, 72.45; H, 7.43; N, 9.39%.

Azobis(2-*p*-tolyloxy)-2-propane (**11**) was also prepared with 25% yield as described above: mp 76—78°C.

Found: C, 73.42; H, 8.11; N, 8.73%. Calcd for $C_{20}H_{26}N_2O_2$: C, 73.59; H, 8.03; N, 8.58%.

Azobis(2-*p*-chlorophenoxy)-2-propane (**12**) was prepared with the same procedure: mp 95—96°C.

Found: C, 58.88; H, 5.51; N, 7.82; Cl, 19.31%. Calcd or $C_{18}H_{20}Cl_2N_2O_2$: C, 58.87; H, 5.49; N, 7.63; Cl, 19.31%.

Photolysis and Thermolysis of Azo Compounds. A general procedure has been described previously.[3] All products except for **4** were identified by comparing their IR, NMR, and mass spectra and retention times of vpc with corresponding authentic compounds. Compound **4** was isolated from a column chromatogram of silica gel (200 mesh) and its structure was confirmed by the following data: mp 103—103.5°C. NMR (δ from TMS in CCl_4) 1.42 (s).

12) A. Ohno and N. Kito, This Bulletin, **43**, 1272 (1970).
13) H. Meerwein, H. Disselnkotter, F. Rappen, H. v. Rintelen, and H. van de Vloed, *Ann. Chem.*, **604**, 151 (1957).
14) Propylene was isolated from the reaction mixture of the sulfur analog of **2** under the photolytic condition. For detail, see Ref. 2.
15) R. Ito, T. Migita, N. Morikawa, and O. Simamura, *Tetrahedron*, **21**, 955 (1965).
16) J. March, "Advanced Organic Chemistry: Reactions, Mechanisms, and Structure," McGraw-Hill Book Co., New York, N. Y. (1968), p.p. 790—793 and references cited therein.
17) a) D. H. Hey, M. J. Perkins, and G. H. Williams, *Tetrahedron Lett.*, **1963**, 445; b) D. H. Hey, M. J. Perkins, and G. H. Williams, *J. Chem. Soc.*, **1965**, 110.
18) D. F. DeTar and R. A. J. Long, *J. Amer. Chem. Soc.*, **80**, 4742 (1958).
19) a) E. L. Eliel, M. Eberhardt, O. Simamura, and S. Meyerson, *Tetrahedron Lett.*, **1962**, 749; b) Inukai, K. Kimura, O. Simamura, and T. Suehiro, This Bulletin, **35**, 129 (1960).
20) J. F. Garst and R. S. Cole, *Tetrahedron Lett.*, **1963**, 679.
21) G. H. Williams, "Homolytic Aromatic Substitution," Pergamon Press, New York, N. Y. (1960), pp. 45—79.
22) K. Uneyama, H. Namba, and S. Oae, This Bulletin, **41**, 1928 (1968).
23) E. Benzing, *Ann. Chem.*, **631**, 1 (1960).

Found: C, 79.77; H, 8.29%. Calcd for $C_{18}H_{22}O_2$: C, 79.96; H, 8.20%.

The Reaction of **3** *with DTBP.* The procedure and the method of product analyses were the same as described above. Compound **10** was collected by vpc and its NMR spectrum was found to be nearly the same as that of the authentic sample of *o*-isopropoxycumene: bp 93—93.5°C/13.5 mmHg (lit,[24] 223—240°C).

We thank Prof. T. Suehiro of Gakushuin University and Dr. G. Tsuchihashi of Sagami Chemical Research Center for useful discussion.

24) E. A. Goldsmith, M. J. Schlatter, and W. G. Toland, *J. Org. Chem.*, **23**, 1871 (1958).

BULLETIN OF THE CHEMICAL SOCIETY OF JAPAN, VOL. 44, 470—474 (1971)

Studies on Electron Spin Resonance Spectra of 2-Substituted Prop-2-yl Radicals

Atsuyoshi Ohno, Noboru Kito, and Yutaka Ohnishi
Sagami Chemical Research Center, Ohnuma, Sagamihara-shi, Kanagawa

(Received May 18, 1970)

Electron spin resonance spectra of 2-substituted prop-2-yl radicals have been obtained. The substituents reported herein are phenylthio, phonoxy, benzyl, ethylthio, ethoxy, and *n*-propyl groups. Spectra were not obtained for phenylthio- and ethoxy-substituted radicals. It has been elucidated that α-heteroatoms greatly delocalize the odd electron. The mechanism of heteroatom-participation is discussed. Time dependency of intensities of signals in ESR spectra has revealed a qualitative order of the lifetime of these free radicals.

Kinetic studies on decompositions of 2-substituted azobis-2-propane (**1** and **2**) have revealed that the stability of a free radical increases in the order $CH_2 \leq O < S$, and the results have been discussed in view of the effect of heteroatoms on the radical center.[1] The argument was based on enthalpies of activation of decompositions. Thus, in order to elucidate the absolute order of stabilities of these free radicals, we must know the quantitative order of ground-state stabilities of azo compounds. This involves difficulties, since we need data on heats of formations of solutions.

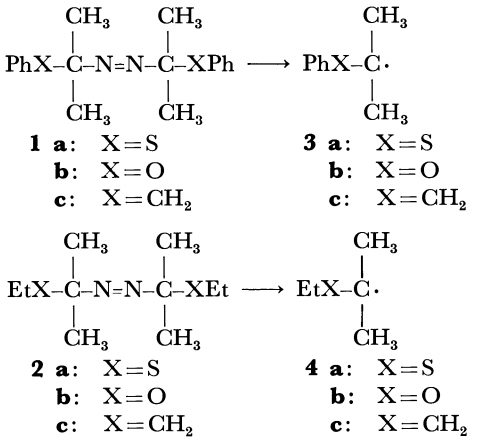

Another problem exists in the assumption that activation parameters of decompositions of azo compounds exemplify the effect of stabilities of free radicals being produced.[2]

It is well known that hyperfine splitting constants (a_H^i) in ESR spectra of free radicals are well correlated to spin densities of the unpaired π-electrons (ρ_c^i) on carbon atoms by means of McConnell's equation[3]

$$a_H^i = Q\rho_c^i \quad (1)$$

where Q is almost constant for similar radicals. Since the degree of delocalizations of π-electrons is a very important measure of stabilities of free radicals, a_H^i would present valuable information.

This paper deals with a discussion on the effect of heteroatoms on a carbon-radical center from the viewpoint of ESR spectroscopy. Qualitative discussion is given on lifetimes (or more precisely, reactivities) of free radicals under a certain condition.

Results

A 0.25 M solution of an azo compound in benzene was irradiated with light from a 100 W high-pressure mercury lamp (principal wavelength 3150 and 3660 Å) at room temperature in a cavity of ESR spectrometer. This technique is essentially suitable for generating free radicals. It produces free radicals in high concentration which makes it possible to detect them at elevated temperatures and free radicals of unequivocal and desired structure can be generated, which is an advantage over the technique of hydrogen abstraction. As an example, free radical **3c** cannot be generated predominantly by hydrogen abstraction reaction, because a benzylic hydrogen is more reactive than (or at least comparable to) the tertiary hydrogen.

The ESR spectrum of 2-phenoxyprop-2-yl (**3b**) was obtained with a good signal-to-noise ratio (Fig. 1) and showed a septet of intensity ratios 1 : 6 : 15 : 20 : 15 : 6 : 1. Other spectra so far obtained had signals attributable to structures **3** and **4**. However, none of them showed splittings due to aromatic protons or ethyl protons.[4]

1) A. Ohno and Y. Ohnishi, *Tetrahedron Lett.*, **1969**, 4405.
2) W. Pryor, "Free Radicals," McGraw-Hill Book Co., New York, N. Y. (1966), p. 128.
3) H. M. McConnell and D. B. Chesnut, *J. Chem. Phys.*, **28**, 107 (1958).
4) Similar results have been reported: J. K. Kochi and P. J. Krusic, *J. Amer. Chem. Soc.*, **91**, 3940 (1969).

No signal from **3a** was obtained when a solution of **1a** was subjected to measurement. Neither a change of solvent nor the lowering of temperature ($\geqslant -100°C$) could achieve the detection of signals. This suggests that the fade of **3a** is much faster than that of **3b** under the condition. Similarly, we could not obtain signals from a solution of **2b** at room temperature, but ethyl radical was detected at $-196°C$.[5,6] The results are summarized in Table 1.

It has been demonstrated that a free radical **3b** is fairly long-lived. As seen in Fig. 2, the most intense signal from this radical remains detectable after the irradiation with light has stopped. Signals from **3c** and **4c** are detectable only during irradiation. In contrast, the intensities of signals from **4a** decreases in prolonged irradiation, indicating rapid fade of this radical (Fig. 3).

Table 1. Hyperfine splitting constants and *g*-values of 2-substituted prop-2-yl radicals

Radical	a, G		*g*-Value	No. of Signals	
	CH_3	CH_2		Found	Theoret.
3a	—	—	—	—	—
3b	20.20		2.00324	7	7
3c	23.12	18.26	2.00263	17	21
4a	19.50		2.00359	7	7
4b	—	—	—	—	—
4c	22.2	17.8	2.0025	17	21

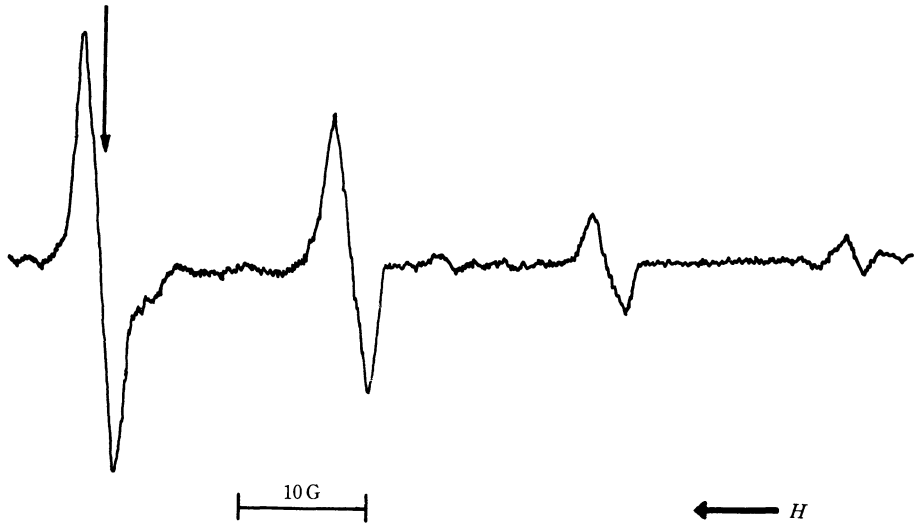

Fig. 1. ESR spectrum of 2-phenoxyprop-2-yl radical at room temperature. The arrow points to the center of the spectrum.

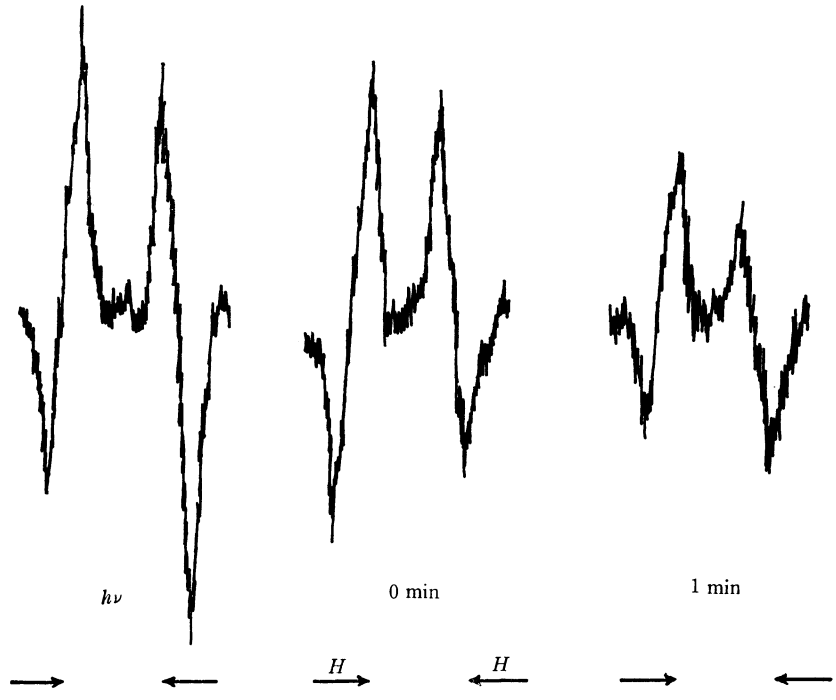

Fig. 2. Time-dependency of intensity of the most intense signal from **3b**.

5) C. Walling and M. J. Mintz, *ibid.*, **89**, 1515 (1967).
6) S. -O. Lawesson and C. Berglund, *Acta Chem. Scand.*, **15**, 36 (1961).

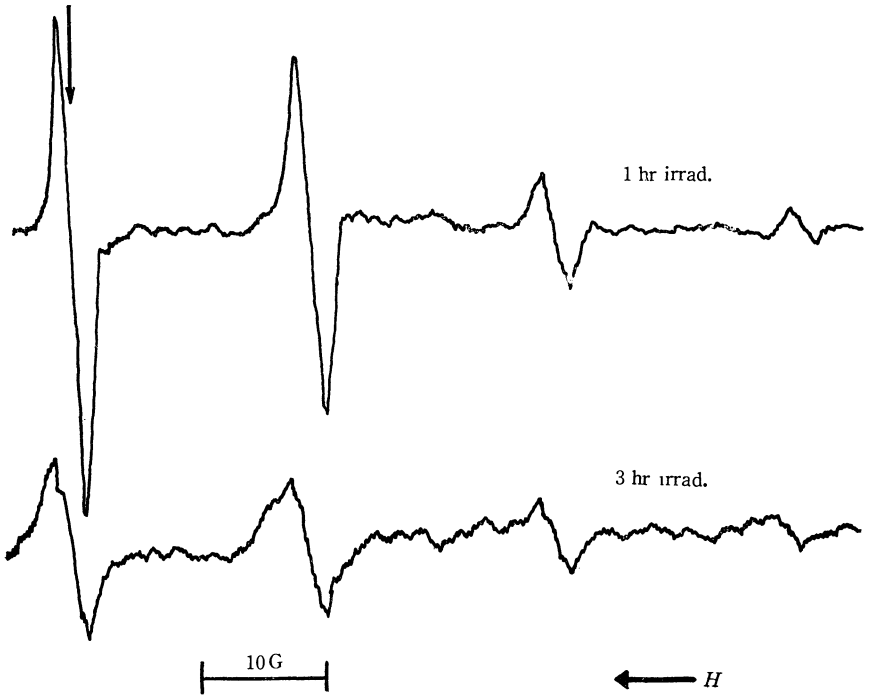

Fig. 3. ESR spectrum of 2-ethylthioprop-2-yl radical at room temperature. The arrow points to the center of the spectrum.

Discussion

As seen in Table 1, there exists a good agreement between hyperfine splitting constants and g-values for **3c**, **4c**, and t-butyl radical (22.7 gauss)[7] as well as for **3b** and 2-hydroxyprop-2-yl radical (20.0 gauss).[8] This enables us to compare the effect of heteroatoms on radical centers by using hyperfine splitting constants due to β-hydrogens in the absence of data on **3a** and **4b**. However, this situation does not hold, at least with an α-hydrogens (Table 2).

Table 2. Hyperfine splitting constants of substituted methyl radicals

Radical	a_α, G	Ref.
$PhS\dot{C}H_2$	16.5	10
$PhO\dot{C}H_2$	17.7	10
$PhCH_2\dot{C}H_2$	22.0	4
$HS\dot{C}H_2$	19	9
$HO\dot{C}H_2$	17.2	8
$HCH_2\dot{C}H_2$	22.4	7

It has been also established that, as far as hyperfine splitting constants due to β-hydrogen are concerned, the value of Q in Eq. (1) is not affected by α-substituents.[11] Thus, we can use hyperfine splitting constants directly as a measure of spin delocalization, which increases in the order $S \gtrsim O > CH_2$ with the present series of free radicals. The corresponding g-values also support this order.[11,12]

The fact that, despite the large difference in spin-orbit coupling constants ($\zeta_s = -382$ cm^{-1}, $\zeta_o = -152$ cm^{-1}),[13] g-values of **3b** and **4a** do not differ a great deal suggests larger σ-character for the orbital containing an odd electron in **4a** than that in **3b**.[14] An alternative interpretation is, of course, possible: Smaller delocalization of an odd electron in **4a** than that in **3b**. However, the latter cannot explain results of kinetics[1] and others.[15]

It is interesting to compare the order of stabilities of radicals from the viewpoint of spin delocalization ($S > O \gtrsim CH_2$) with that obtained from activation parameters of decomposition of parent azo compounds ($S \gtrsim O > CH_2$). Although qualitative orders are the same for both cases, semi-quantitative orders are somewhat different with respect to positions of the oxygen-containing radical. We believe that this is attributable to larger electronegativity of oxygen than that of sulfur and methylene group. If the resonance effects of oxygen and sulfur were the same, the spin density on the carbon atom is expected to be smaller in the oxygen-containing radical than in its sulfur analog, because a larger inductive effect of oxygen than sulfur reduces more spin density on the former through a

7) R. W. Fessenden and R. H. Schler, *J. Chem. Phys.*, **39**, 2147 (1963).
8) W. T. Dixon and R. O. C. Norman, *J. Chem. Soc.*, **1963**, 3119.
9) D. H. Volman, J. Wlostenholme, and S. Hadley, *J. Phys. Chem.*, **71**, 1798 (1967).
10) A. Hudson and H. A. Hussain, *J. Chem. Soc., B*, **1969**, 793.
11) H. Fischer, *Z. Naturorsch., A*, **18**, 866 (1964): *A*, **20**, 428 (1965).
12) R. O. C. Norman and R. J. Pritchett, *Chem. Ind.* (London), **1965**, 2040.
13) D. S. McClure, *J. Chem. Phys.*, **20**, 682 (1952); **17**, 905 (1949).
14) R. O. C. Norman, *Chem. Brit.*, **6**, 66 (1970).
15) A. Ohno, N. Kito, and Y. Ohnishi, This Bulletin, **44**, 463 (1971).

σ-bond.[14] This in turn, predicts larger resonance effect for sulfur than for oxygen from the fact that these radicals have nearly equal hyperfine splitting constants. Since free radicals generated here are essentially neutral, the inductive effect of a heteroatom does not change significantly, from the starting azo compounds to the transition states of the decompositions. Thus, activation parameters hardly reflect inductive effects of heteroatoms. It has been reported that the substituent effect in decompositions of substituted azobiscumenes is correlated to the Hammett relationship with σ_R.[16] Consequently, kinetic order represents stabilization by resonance participation, while spectral order that by net electronic effect. The larger σ-character of the sulfur-containing radical than its oxygen analog does not contradict this conclusion, since potential *d-sp*^{3} overlapping is suggested for sulfur-carbon π-bonding.[17-19]

In addition, the time-dependency of signal intensities predicts qualitative order of life-times of free radical as

$$\mathbf{3b} > \mathbf{3c} \approx \mathbf{4c} > \mathbf{4a} (> \mathbf{3a})$$

Thus, we have found that reactivities of these radicals under photolytic conditions are quite different from their thermodynamic stabilities.

Experimental

Materials. Compounds **1a**, **1b**, **1c**, and **2a** were prepared as described previously.[15,20,21]

Azobis(2-ethoxy)-2-propane (**2b**): Into a 300 m*l* round-bottomed flask equipped with a condenser and a stirrer were placed 150 m*l* of anhydrous ethanol and 5.1 g (0.22 g-atom) of sodium metal. Azobis(2-chloro)-2-propane (18.2 g, 0.1 mol) was added slowly to sodium ethoxide at the temperature of ice-water. Exothermic reaction occurred gradually in 2 hr, and the reaction mixture then turned to milky white. The mixture was stirred for additional 2 hr to complete the reaction. Excess ethanol was evaporated under reduced pressure. After filtration, the filtrate was poured into ice-water, and organic material was then extracted with ether. Careful distillation under reduced pressure yielded 2.5 g (11% yield) of pure **2b**, bp 70.5—71.0°C/12 mmHg.

Found: C, 59.06; H, 10.73; N, 15.72%. Calcd for $C_{10}H_{22}N_2O_2$: C, 59.37; H, 10.96; N, 15.82%.

Azobis(2-propyl)-2-propane (**2c**): 2-Methylpentylamine (bp 100—104°C) was prepared from the corresponding alcohol according to Ritter and Kalish.[22] Sulfuryl chloride (13 g) in 10 m*l* of dry *n*-hexane was added dropwise to the amine (21 g) in *n*-hexane at the temperature of ice-water. After the addition had been completed, the organic layer was washed with water several times and dried over Drierite. Resulting crude sulfone amine (7.0 g) was used for the foregoing reaction without further purification. A mixture of the sulfone amine (7.0 g) in 50 m*l* of *n*-hexane and 150 m*l* of sodium hypochlorite (10% efficiency) was continuously stirred for 35 hr at room temperature. The organic layer was washed with water and dried over Drierite. Distillation under reduced pressure yielded 2 g (38% yield) of **2c**, bp 76—80°C/15 mmHg.

Found: C, 72.45; H, 13.40%. Calcd for $C_{12}H_{26}N_2$: C, 72.66; H, 13.21%.

Spectrometry. A 0.25 M solution of an azo compound in benzene was placed in 5 mm-o.d. quartz tube, which was thoroughly degassed by the thawing and freezing method. The sample tube was then sealed. The light from a 100 W high-pressure mercury lamp was focused on the sample in the cavity of the ESR spectrometer.

ESR spectra of generated radicals were measured at room temperature with a X-band, JES-3BX type spectrometer (Japan Electron Optics Laboratory Co., Ltd.) with 100 KHz field modulation. Magnetic-field-calibration markers were placed directly on the recorded spectrum by noting the occurrence of the proton resonance at a particular oscillator frequency which was then measured with a Hewlett-Packard frequency counter, Model 5245L.

2-Phenylthioprop-2-yl (**3a**): No signal was detected when a solution of **1a** in benzene, toluene, tetrahydrofuran or acetonitrile was subjected to measurement at various temperatures ($\geqslant -100$°C). An unidentified broad signal was observed at −196°C only when 2-methyltetrahydrofuran was used as a solvent. The signal is due to neither a benzenethiyl radical, nor a radical from the solvent, since the obtained *g*-value was 2.0026.

2-Phenoxyprop-2-yl (**3b**): After a few minutes irradiation with light, signals appeared on the first run of the spectrum. Signal intensities increased with prolonged irradiation period and a well-resolved spectrum was obtained within 2 hr. The spectrum showed a septet of relative intensity ratios 1.4 : 5.9 : 15.5 : 20.0 : 15.7 : 5.8 : 1.2, which were in good agreement with thoeretical values. The most intense signal from the radical remained detectable even after irradiation with light had been stopped. This kind of observation was obtained exclusively when 2-phenoxyprop-2-yl was applied in these studies.

2-Benzylprop-2-yl (**3c**): A spectrum resulting from the irradiation for 2 hr consisted of 17 lines of relative intensity ratios from the center of the spectrum to the wing; 20 : 9.3 : 9.7 : 14.3 : 3.6 : 7.5 : 5.7 :— : 3.6 : 1.8 : —. No resolvable hyperfine interaction was observed with the aromatic hydrogens in **3b** and **3c** with a modulation of 1 gauss.

2-Ethylthioprop-2-yl (**4a**): A spectrum obtained by irradiation for 2 hr exhibited a septet of relative intensity ratios close to the theoretical ones. Signal intensities decreased with a prolonged irradiation period. Splittings due to ethyl protons were not detected in the radical with a modulation of 0.5—1.0 gauss.

2-Ethoxyprop-2-yl (**4b**): When a solution of **2b** in *n*-pentane or isopentane was subjected to measurement, no signal was investigated at temperatures above −80°C. A well-resolved spectrum consisting of 12 lines (triplets of quartets) was obtained at −196°C, which was attributable to ethyl radical rather than **4b**. Observed hyperfine coupling constants ($a_\alpha = 22.4$ and $a_\beta = 26.7$) and *g*-value (2.0026) were in good agreement with those of previous studies.[4,7]

2-Methylpent-2-yl (**4c**): A similar type of spectrum with **3c** was obtained when **2c** was irradiated with light in benzene. No resolvable hyperfine interaction with 7-hydrogens was observed with a modulation of 0.5 gauss.

16) J. R. Shelton, C. K. Liang, and P. Kovacic, *J. Amer. Chem. Soc.*, **90**, 354 (1968).

17) D. J. Gram, "Fundamentals of Carbanion Chemistry," Academic Press, New York, N. Y. (1965), pp. 71—84.

18) C. C. Price and S. Oae, "Sulfur Bonding," The Ronald Press Co., New York, N. Y. (1962), pp. 26—55.

19) Only $2p$–$2p$ π-overlapping or a canonical form of $-\ddot{\underset{\cdot\cdot}{O}}^{+\cdot}-\overline{C}<$ is possible for the oxygen analog.

20) A. Ohno, N. Kito, and Y. Ohnishi, This Bulletin, **44**, 467 (1971).

21) E. Benzing, *Ann. Chem.*, **631**, 1 (1960).

22) J. J. Ritter and J. Kalish, *J. Amer. Chem. Soc.*, **70**, 4048 (1948).

A part of this work has been carried out with a spectrometer at the Department of Chemistry, Faculty of Science, The University of Tokyo. We are grateful to Prof. S. Fujiwara and Mrs. N. Watanabe for their kind assistance. We also wish to thank Drs. Y. Morino and H. Uehara of Sagami Chemical Research Center for helpful discussion.

BULLETIN OF THE CHEMICAL SOCIETY OF JAPAN, VOL. 44, 474—477 (1971)

The Reaction of α-Oxo Acids with *N*-Phenyltriphenylphosphinimine[1)]

Chung-gi SHIN,* Hiroaki ANDO, and Juji YOSHIMURA

Laboratory of Chemistry for Natural Products, Faculty of Science, Tokyo Institute of Technology, Ookayama, Meguro-ku, Tokyo

(Received May 25, 1970)

The reaction between ethyl α-oxocarboxylate and *N*-phenyltriphenylphosphinimine gave a mixture of ethyl α-phenyliminocarboxylate (IVa—f) and the tautomeric isomers (Va—f) in good yield. IVa and Va derived from ethyl pyruvate was converted gradually into 3-anilino-5-ethoxycarbonyl-5-methyl-1-phenyl-Δ^3-pyrrolin-2-one (VIIa) on standing at room temperature. The free acid of IVa and Va prepared by the same method could not be purified, but a small amount of 3-anilino-5-methyl-1-phenyl-Δ^3-pyrrolin-2-one (IX) was obtained from the reaction mixtures. In the reaction of aniline and pyruvic acid, α,γ-dianilino-γ-carboxy-α-methyl-γ-butyrolactone (XII) was obtained in the neutral reaction condition and 4-anilino-2-phenyliminopentanoic acid (XIV) in basic condition. The structure of the products was proved by NMR and IR spectrum, and the reaction courses were discussed.

In the previous paper, one of the authors reported the isolation of a primary enamine (ethyl α-amino-β-methylcrotonate (II)) by the reduction of the corresponding α,β-unsaturated α-nitrocarboxylic ester, and the tautomeric imine (ethyl 2-imino-3-methylbutanoate (III)) by the reaction of the corresponding α-oxocarboxylic ester (Ic) with triphenylphosphinimine (Scheme 1). The acylation of both II and III yielded the same enamine derivative,[2-4)] and the isomerization between II and III was not reached.

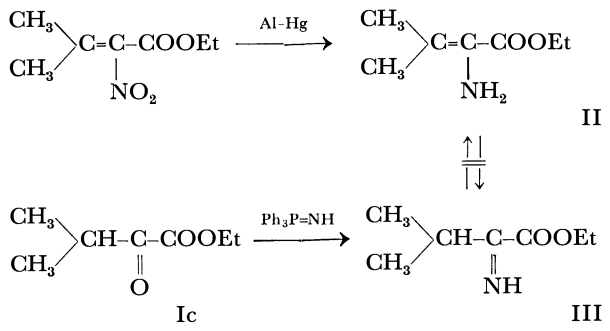

Scheme 1

On the other hand, Wieland *et al.*[5)] have reported that a treatment of pyruvic acid (Ia′) with aniline[6,7)] did not yield any amount of α-phenyliminopropionic acid (IVa′). However, it was expected from our previous result that the reaction of *N*-phenyltriphenylphosphinimine with α-oxocarboxylic acids would give the homologue of IVa′ and/or the tautomeric isomers.

In the present paper, the reactions of α-oxocarboxylic acid (Ia′) or α-oxocarboxylic esters (Ia—f) with *N*-phenyltriphenylphosphinimine or aniline were described.

Results and Discussion

Ethyl pyruvate (Ia) was treated with *N*-phenyltriphenylphosphinimine[8)] in anhydrous acetonitrile under reflux. Triphenylphosphine oxide precipitated quantitatively was removed by filtration and the filtrate was distilled under the reduced pressure to afford pale yellow oil in a 66% yield, which was a mixture of the corresponding imine (IVa) and enamine (Va) (Scheme 2). The infrared spectrum of the mixture of IVa and Va showed absorption bands at 3350 (NH), 1730—1720 (two COOEt), 1650 (C=N) and 1590 (C=C) cm^{-1}, while the NMR spectrum showed peaks at τ2.55—3.40 (m, two C_6H_5 and vinyl protons, *ca.* 10.9H), 5.62 (two q, $-CH_2-$, 4H), 7.58 (s, NH in Va, *ca.* 0.3H), 7.92 (s, $-\overset{\|}{C}-CH_3$ in IVa, *ca.* 2.2H), and 8.62 (two t, $-CH_3$ in IVa and Va, 6H). From the intensity of $-\overset{\|}{C}-CH_3$ proton signal of IVa and $-\overset{|}{C}=CH_2$ proton signal of Va, the yield was determined to be 47.4 and 18.6%, respectively. α-Oxocarboxylic esters (Ib—f), on being treated with *N*-phenyltriphenylphosphinimine, afforded similarly the corresponding mixtures (IVb—f and Vb—f). In other cases, these

1) This paper was presented at the 22nd Annual Meeting of the Chemical Society of Japan, Tokyo, April, 1969.

* Present Address: Laboratory of Organic Chemistry, Faculty of Technology, Kanagawa University, Rokkakubashi, Kanagawa-ku, Yokohama. To whom inquires should be addressed.

2) C. Shin, M. Masaki, and M. Ohta, This Bulletin, **39**, 858 (1966).

3) C. Shin, M. Masaki, and M. Ohta, *J. Org. Chem.*, **32**, 1860 (1967).

4) M. Masaki, C. Shin, H. Kurita, and M. Ohta, *Chem. Commun.*, **1968**, 1447.

5) T. Wieland, G. Ohnacker, and R. K. Rothhaupt, *Chem. Ber.*, **88**, 633 (1955).

6) L. Simon, *Ann. Chem.*, **188**, 336 (1877); *C. R. Acad. Sci., Paris*, **118**, 1342 (1894).

7) C. Böttinger, *Ber.*, **10**, 818 (1877); *Ann. Chem.*, **188**, 366 (1877).

8) R. Appel and A. Hauss, *Z. Anorg. Chem.*, **311**, 290 (1961).

Table 1. The mixtures of ethyl α-phenylimino (IVa-f) and α-anilino (Va-f) carboxylates

Compd. IV+V	R	R′	Bp °C/mmHg	Yield (%)	Formula	Found, %			Calcd, %		
						C	H	N	C	H	N
a	H	H	94—96/1	66	$C_{11}H_{13}NO_2$	69.28	6.93	7.51	69.09	6.85	7.33
b	H	CH_3	89—93/1.5	55	$C_{12}H_{15}NO_2$	70.37	7.07	6.43	70.22	7.37	6.82
c	CH_3	CH_3	91—94/2	53	$C_{13}H_{17}NO_2$	71.22	7.49	6.61	71.20	7.82	6.39
d	H	CH_2CH_3	98—101/1.5	66	$C_{13}H_{17}NO_2$	71.68	7.43	6.49	71.20	7.82	6.39
e	H	$CH_2CH_2CH_3$	100—101/1	53	$C_{14}H_{19}NO_2$	72.08	8.11	6.41	72.07	8.21	6.00
f	H	$CH(CH_3)_2$	106—109/2	52	$C_{14}H_{19}NO_2$	71.97	7.92	6.29	72.07	8.21	6.00

Table 2. The IR spectrum of the mixture of IVa-f and Va-f

Compd. IV+V	R	R′	IR Spectrum (cm^{-1}, in NaCl)				
			NH	COOEt		C=N	C=C
a	H	H	3350	1720	1730	1650	1590
b	H	CH_3	3400	1720	1730	1650	1590
c	CH_3	CH_3	3400	1720	1730	1660	1600
d	H	CH_2CH_3	3400	1720	1730	1650	1595
e	H	$CH_2CH_2CH_3$	3400	1720	1730	1650	1595
f	H	$CH(CH_3)_2$	3400	1730	1740	1650	1600

Table 3. The NMR spectrum of the mixture of IVa-f and Va-f (τ-Value, in $CDCl_3$)

Compd. IV+V	R	R′	R′ | R-C-	R′ | R-C=	-NH-	Composition (%)	
						IV[e]	V[e]
a	H	H	7.92(s)	2.55—3.40[b]	7.58(s)	47.4	18.6[g]
b	H	CH_3	7.40(q)	3.58(q)	4.55(bs)[c]	33	22[h]
c	CH_3	CH_3	7.15(sp)[a]	—	5.79(bs)[c]	10.4	42.6[f,i]
d	H	CH_2CH_3	7.45(t)	3.73(t)	4.32(bs)[c]	52.8	13.2[i]
e	H	$CH_2CH_2CH_3$	7.29(t)	3.65(t)	2.30—3.50[b]	23.3	28.7[j]
f	H	$CH(CH_3)_2$	7.57(d)	3.80(d)	4.57(s)[d]	27.5	25.5[k]

a) sp=Septet. b) Overlap in benzene ring protons. c) bs=Broad singlet. d) In CCl_4. e) Evaluated from the intensity of methylene and vinyl protons in the β-position of IV and V. f) Evaluated from the intensity of methylene protons in the β-position and NH proton. g) Standing for 3 days at 5°C. h) Standing for 1 day at room temperature. i) Standing for 3 days at room temperature. j) Standing for 5 days at 5°C. k) Redistilled after standing for 4 days at room temperature.

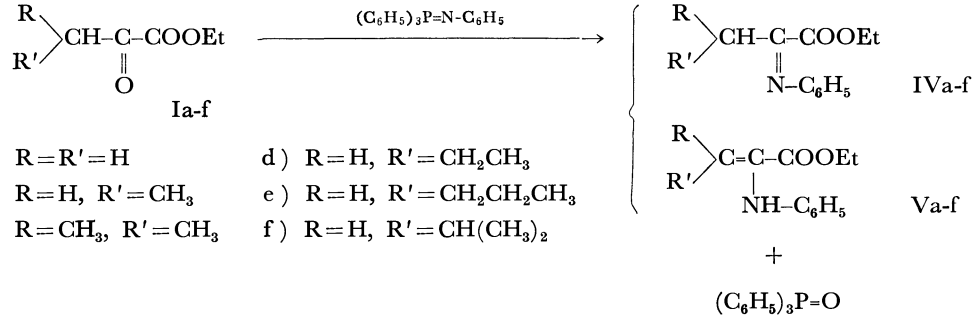

a) R=R′=H d) R=H, R′=CH_2CH_3
b) R=H, R′=CH_3 e) R=H, R′=$CH_2CH_2CH_3$
c) R=CH_3, R′=CH_3 f) R=H, R′=$CH(CH_3)_2$

Scheme 2

ratios were evaluated from that of methylene and vinyl protons in the β-position of IV and V. The yields and some spectral data of the mixtures are summarized in Tables 1, 2 and 3.

On standing for a week at room temperature, the mixture (IVa and Va) became viscous and colored gradually, and then a part of the oil crystallized. This crystalline compound (VIIa) was identified as the same product obtained from Ia and aniline, and assigned as 5-ethoxycarbonyl-5-methyl-3-phenylimino-2-pyrrolidinone (VIII) by Simon.[9] However, VIIa showed the peaks at τ2.55—3.09 (m, tow C_6H_5 and NH, 11H), 4.03 (s, vinyl proton, 1H), 5.85 (q, $C\underline{H}_2$-CH_3, 2H), 8.36 (s, CH_3, 3H) and 8.80 (t, $CH_2C\underline{H}_3$), while the infrared spectrum showed the absorption bands of NH at 3270, of ester at 1720, of carbonyl at

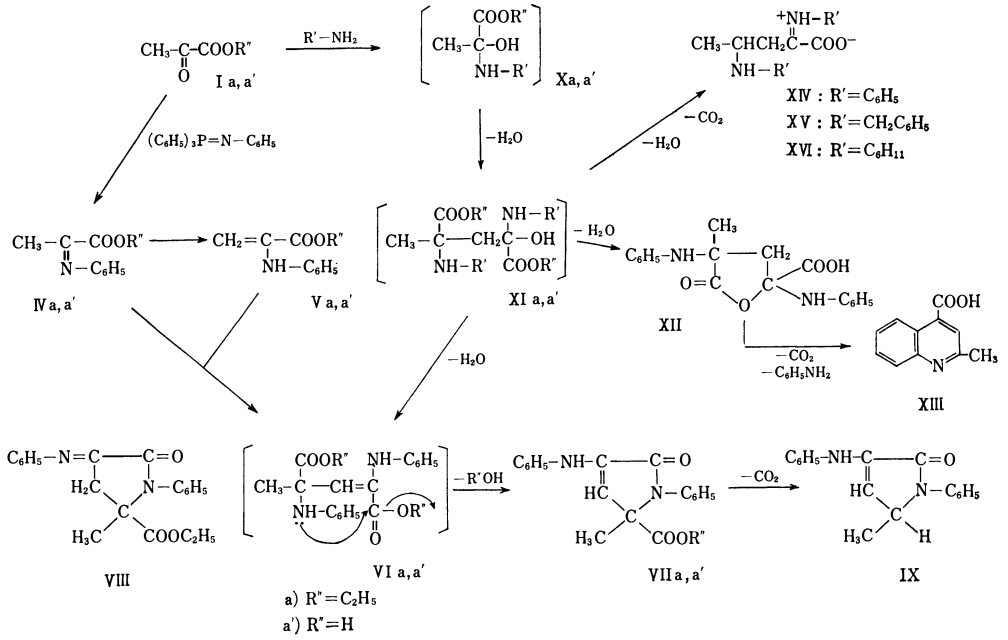

Scheme 3.

1680, and of carbon-carbon double bond at 1640 cm^{-1}. The presence of one vinyl proton, and NH and C=C absorption in the above data indicates that VIIa is 3-anilino-5-ethoxycarbonyl-5-methyl-1-phenyl-Δ^3-pyrrolin-2-one, the enamine form of VIII. In order to explore the intermediate step for the formation of VIIa, the conversion of viscous and colored oil into VIIa was followed spectrometrically. The appearance of two NH (τ6.15, s) and new vinyl proton signal (τ5.15, s) indicates that the reaction of IVa and Va proceeds through the formation of ethyl 2,4-dianilino-4-ethoxycarbonyl-2-pentenoate (VIa).

Simon has reported the treatment of Ia′ with aniline in ether gave a small amount of 4-anilino-2-phenyliminopentanoic acid (XIV) and α,γ-dianilino-γ-carboxy-α-methyl-γ-butyrolactone (XII),[9] which was converted into 4-carboxy-2-methylquinoline (XIII).[6] This reaction was reinvestigated in detail under various condition. The treatment of Ia′ with amines (aniline, benzylamine and cyclohexylamine) in the presence of triethylamine gave 4-(substituted-amino)-2-(substituted-imino)pentanoic acids (XIV—XVI), while in the absence of triethylamine the treatment of Ia′ with aniline afforded XII, which was qantitatively converted into XIII by heating in water, accompanying with the liberation of CO_2 and aniline. It was assumed that an intermediate (XIa′) formed *via* α-hydroxy-α-alkylaminopropionic acid (Xa′) was subjected to decarboxylation, β-elimination and isomerization in a basic media to give XIV—XVI, but in neutral condition XIa′ yielded XII by intramolecular dehydration. The infrared spectrum of XIV—XVI showed the absorption bands of NH (3250—3273), carbon-nitrogen double bond (1620—1625) and carboxylate group ($-COO^-$) (1520—1540 cm^{-1}), and the structures of XIV—XVI were assigned on the basis of these spectral data.

In order to obtain IVa′ and Va′, the mixture of IVa and Va was hydrolysed with 10% potassium hydroxide at room temperature, but pyruvic acid (Ia′) was obtained. Ia′ was treated with *N*-phenyltriphenylphosphinimine to give a viscous syrup (IVa′ and Va′) in a good yield and triphenylphosphine oxide in almost quantitative yield. Attempts to purify the resultant syrup were unsuccessful. The crude syrup was esterified, which, on being allowed to stand for few weeks at room temperature, gave a small amount of VIIa. This fact indicates that IVa′ and Va′ are certainly formed by reaction of Ia′ with *N*-phenyltriphenylphosphinimine. Moreover, the above assumption was supported by the fact that 3-anilino-5-methyl-1-phenyl-Δ^3-pyrrolin-2-one (IX) is gradually precipitated from the mixture of IVa′ and Va′ in 50% ethanol on standing for 2 days at room temperature.

Experimental

All boiling and melting points are uncorrected. The IR spectrum was recorded with a Hitachi EPI-S2 Spectrometer. The NMR spectrum was measured with a JNM-4H-100 Spectrometer (Japan Electron Optics Laboratory Co., Ltd.) at 100 MHz.

Materials. *N*-Phenyltriphenylphosphinimine was prepared by the reaction of triphenylphosphine dibromide with aniline in the presence of triethylamine by the method reported.[10] Mp 126—128°C (lit, mp 128—130°C). The acetonitrile used was distilled from phosphorous pentoxide and dried over calcium hydride.

Reaction of Ethyl α-Oxocarboxylate with N-Phenyltriphenylphosphinimine. To a solution of ethyl α-oxocarboxylate (0.02 mol) in anhydrous acetonitrile (30 m*l*), *N*-phenyltriphenylphosphinimine (0.02 mol) was added and then the mixture was refluxed for 1 hr. On concentrating the resulting solution, a brown syrup remained, to which dry ether (30 m*l*)

9) L. Simon, *C. R. Acad. Sci., Paris*, **134**, 1063 (1902); *ibid.*, **144**, 140 (1907); *ibid.*, **147**, 126 (1908).

10) L. Hornor and H. Oediger, *Ann. Chem.*, **627**, 142 (1959).

Table 4. Physical constants of XIV-XVI

Compd.	R′	Mp °C	Yield (%)	Formula		Elemental analysis (%) C	H	N	IR Spectrum (cm^{-1}, in KBr) NH	C=N+	COO^-
XIV	C_6H_5	195—197[a,c]	70	$C_{17}H_{18}N_2O_2$	Found	72.36	6.68	9.91	3273	1620	1540
					Calcd	72.32	6.43	9.92			
XV	$CH_2C_6H_5$	205—208[b,c]	46	$C_{19}H_{22}N_2O_2$	Found	73.51	7.02	9.91	3270	1620	1520
					Calcd	73.52	7.14	9.03			
XVI	C_6H_{11}	260>[a,c]	60	$C_{17}H_{30}N_2O_2$	Found	69.19	9.73	9.92	3250	1625	1520
					Calcd	69.37	10.27	9.54			

a) Recrystallized from methanol. b) Recrystallized from ethanol. c) Colorless needles.

was added, and then triphenylphosphine oxide precipitated was filtered off. The ethereal solution was concentrated to one third of its volume and then allowed to stand overnight in a refrigerator. The further triphenylphosphine oxide precipitated was filtered off. After concentrating the ethereal solution, dry petroleum ether (20 m*l*) was added to the residual syrup and the small amount of triphenylphosphine oxide was filtered off, and then finally the solvent was removed by evaporation. Distillation of the resulting syrup afforded a pale yellow oil. The results are summarized in Tables 1, 2 and 3.

Confirmation of Ethyl 2,4-Dianilino-4-ethoxycarbonyl-2-pentenoate (VIa) as Intermediate. When the mixture of IVa and Va, or the reaction mixture of ethyl pyruvate (Ia) with aniline, was allowed to stand for few days at room temperature, the oil became colored and viscous gradually. This syrup was subjected to the measurements of IR abosrption in NaCl and of NMR absorption in $CDCl_3$ using tetramethylsilane as an internal standard. The results are described in the former section.

3-Anilino-5-ethoxycarbonyl-5-methyl-1-phenyl-Δ^3-pyrrolin-2-one (VIIa). A) From Mixture of IVa and Va: When the above intermediate (VIa, 1 g) was allowed to stand for several days, the viscous syrup crystallized gradually. To the resulting product, a small quantity of dry ether was added, and then crystals precipitated were collected on a filter. Recrystallization from ethanol gave colorless prisms (0.5 g, 32%), mp 146—147°C.

Found: C, 71.62; H, 6.28; N, 8.29%. Calcd for $C_{20}H_{20}N_2O_3$: C, 71.41; H, 5.99; N, 8.33%.

B) From Ia and Aniline: A mixture of Ia (1.16 g) and aniline (0.93 g) was allowed to stand at room temperature for 3 days, during which water separated gradually in the reaction mixture, and crystalline product was obtained from the dark brown syrup. Recrystallization from petroleum ether (bp 70—120°C) gave colorless prismatic needles (0.62 g, 37%), mp 144—146°C. The melting point of this compound was not depressed on admixture with the compound obtained from procedure *A*.

Reaction of Pyruvic Acid and Amines (Aniline, Benzylamine, and Cyclohexylamine) in the Presence of Triethylamine. To a solution of pyruvic acid (0.025 mol) in dry ether (25 m*l*) with the presence of triethylamine (0.025 mol), amine (0.025 mol) was added drop by drop with stirring below 5°C. After standing for 2 hr in a refrigerator, the reaction mixture was kept overnight at room temperature. A red syrup in the bottom crystallized upon addition of water. Recrystallization from methanol or ethanol afforded colorless needles. results are summarized in Table 4.

Reaction of Pyruvic Acid and N-Phenyltriphenylphosphinimine. A) Esterification of the Reaction Product: To a solution of pyruvic acid (1.1 g) in dry acetonitrile (40 m*l*), *N*-phenyltriphenylphosphinimine (4.5 g) was added and then the mixture was refluxed for 1 hr. Triphenylphosphine oxide was removed out of the reaction mixture by the similar way to that for the reaction of ethyl α-oxocarboxylate. Thus obtained syrup was dissolved in ethanol (50 m*l*) and heated under reflux for 3 hr in the presence of *p*-toluenesulfonic acid (0.5 g) and concentrated sulfuric acid (0.5 m*l*). The solution was concentrated under a reduced pressure to give residual oil, which was extracted with ether. The ethereal extract was washed with water and dried over anhydrous sodium sulfate and then the solvent was evaporated. This oil, without further purification, was allowed to stand for few weeks at room temperature to yield a small amount of crystals. This compound was the same as VIIa. Yield 0.08 g.

B) 3-Anilino-5-methyl-1-phenyl-Δ^3-pyrrolin-2-one (IX). In the above procedure *A*), the final syrup (4.8 g) after removal of triphenylphosphine oxide was diluted with 50% ethanol (50 m*l*). On standing for 2 days at room temperature, crystals precipitated. Recrystallization from ethanol gave pale yellow needles (1.1 g), mp 175—178°C. IR (KBr): 3350 (νNH), 1680 (νC=O) and 1660 (νC=C) cm^{-1}. NMR ($CDCl_3$): 3.44 (broad s, NH, 1H), 3.95 (d, vinyl proton, 1H), 5.74 (double q, methine proton, 1H), and 8.74 (d, methyl protons, 3H)τ.

Found: C, 77.23; H, 6.27; N, 10.43%. Calcd for $C_{17}H_{16}N_2O$: C, 77.25; H, 6.10; N, 10.60%.

The authors are indebted to Mr. Kiyofumi Fukukawa of our Laboratory for the NMR measurement.

Studies on Seven-Membered Heterocyclic Compounds Containing Nitrogen. XI. The Schmidt Reaction of 1-Benzyl-1-azacycloheptan-4-one, Menthone, and 2-Methyl-4,5,6,7-tetrahydrobenzo[*b*]thiazol-7-one[1]

Yoshifumi SAKAKIDA,[2] Anthonius Sina KUMANIRENG,[3] Heizan KAWAMOTO, and Akira YOKOO

Department of Chemistry, Faculty of Science, Okayama University, Tsushima, Okayama

(Received June 17, 1970)

The Schmidt reaction of 1-benzyl-1-azacycloheptan-4-one afforded a mixture of 1-benzyl-1,4-diazacyclooctan-5-one (IV) and a tetrazole derivative (V). The treatment of menthone (VIII) was found to give a lactam (IX), plus a tetrazole derivative (X) as a minor product. 2-Methyl-4,5,6,7-tetrahydrobenzo[*b*]thiazol-7-one (XII) was subjected to the Schmidt reaction to give a lactam XIIIa; it did not afford a tetrazole derivative. The structures of these products were determined on the evidence of the NMR spectra.

As a part of our investigation of the syntheses and reactions of seven-membered nitrogen heterocycles leading to azepine compounds, we studied the Schmidt reaction of the compounds named in the title. Dickermann and his co-workers[4] have reported that the Schmidt reaction of 1-methyl- and 1-benzylpiperid-4-one (Ia and b) gave the corresponding 1,4-diazacycloheptan-5-ones (IIa and b respectively) in reasonable yields.

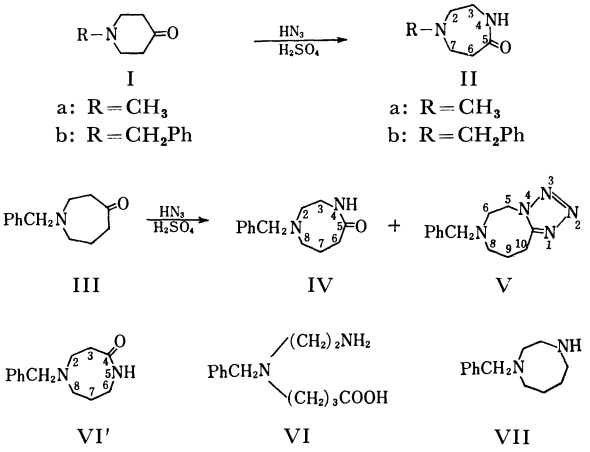

Scheme 1

The treatment of 1-benzyl-1-azacycloheptan-4-one[5] (III) was found to give a mixture of 1-benzyl-1,4-diazacyclooctan-5-one (IV) and a tetrazole derivative (V) on the evidence of the NMR spectra. The main product, IV, gave a single spot on a paper chromatogram and showed the presence of an amido group in the IR spectrum. The assignment of the NMR signals (Table 1) was made by comparing them with those of 2-pyrrolidone[6] and the diazacycloheptanone, IIb. Deuterium exchange in the spectrum of IV caused the disappearance of the multiplet at τ 2.4 and the simultaneous collapse of the multiplet at 6.8 to a broad triplet. On the irradiation of the deuterium-exchanged solution at τ 8.45, the multiplet at 7.7 and the triplet at 7.43 collapsed to broad singlets, while the broad triplet at 6.8 remained unchanged. This observation eliminated the possibility of an isomeric structure (IV') for IV, because if IV' were present, the broad triplet at τ 6.8 due to the methylene protons adjacent to the lactam nitrogen in the structure IV' would have collapsed to a singlet upon irradiation. The ring opening of the lactam IV with 5% sulfuric acid gave an amino acid (VI), and reduction with lithium aluminum hydride afforded 1-benzyl-1,4-diazacyclooctane (VII). The assignment of the NMR signals of the tetrazole derivative (V) is shown in Table 1. The lower chemical shift of the triplet at τ 5.50 indicated the presence of a methylene group adjacent to the tetrazole nitrogen. A reinvestigation of Dickermann's work gave no tetrazole derivative other than the lactam.

The Schmidt reaction of a carbocyclic six-membered ketone, menthone (VIII), afforded a lactam (IX), plus a tetrazole derivative (X) as a minor product. The NMR signals at τ 6.97 [CH(7) adjacent to the seven-membered ring nitrogen] for the lactam and at 5.65 for the tetrazole, and also the possible mode of formation, led to the assignment of the structure IX

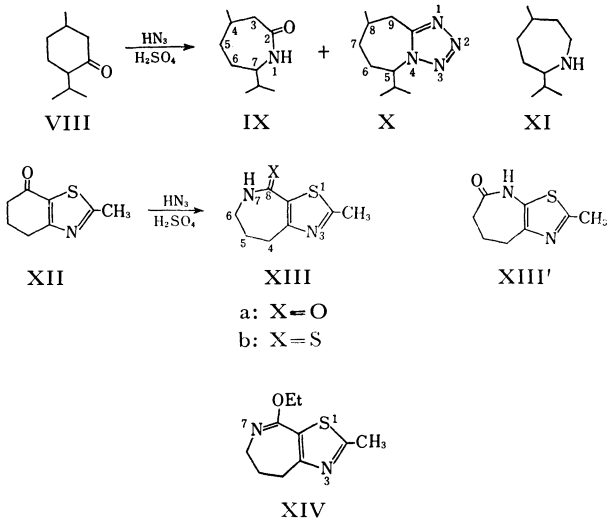

Scheme 2

1) Presented in part at the Local Meeting of the Chemical Society of Japan, Okayama, October, 1967.

2) Present address: Morishita Seiyaku Co., 4-29 Doshomachi, Higashi-ku, Osaka.

3) Department of Chemistry, Faculty of Science, Tohoku University, Sendai.

4) S. C. Dickermann and G. Lindwall, *J. Org. Chem.*, **14**, 530 (1949); S. C. Dickermann and A. J. Beozzi, *ibid.*, **19**, 1855 (1954).

5) A. Yokoo and S. Morosawa, This Bulletin, **29**, 631 (1956).

6) Frank A. Bovey, "NMR Data Table for Organic Compounds," Vol. 1, John Wiley & Sons, New York (1967), p. 70.

Table 1. Assignment of NMR signals

Series of compounds	τ Values[a] for					
1[b,d] 2[c,d] 3[e]	CH_2(2)(6)	CH_2(3)(5) CH(7)(5) CH_2(6)	NH(4) NH(1) NH(7)	CH_2(6)(10) CH_2(3)(9)	CH_2(7)(9) CH_2(5, 6)(6, 7) CH_2(5)	CH_2(8)(8) CH(4)(8) CH_2(4)
2-Pyrrolidone[f,g]	—	6.63 t	—	7.77 t	—	—
IIb[h]	7.34 bs	6.68 bq	2.25 bm	7.40 m	7.34 bs	—
IV[g]	7.43 bt	6.80 m	2.40 bm	7.70 m	8.45 m	7.43 bt
V[h]	7.40 m	5.50 t	—	7.00 bt	8.25 m	7.40 m
IX[g]	—	6.97 bqn	—	7.82 bd	8.35 m	8.35 m
X[g]	—	5.65 bqn	—	6.95 m	8.00 m	7.62 m
XIIIa[h]	—	6.54 bq	2.35 m	—	7.80 m	6.81 t
XIIIb[h]	—	6.45 bq	0.80 m	—	7.85 m	6.82 t

a) TMS as an internal standard. Suffixes: b, broad; s, singlet; d, doublet; t, triplet; q, quartet; qn, quintet; m, multiplet. b) Compounds, IIb, IV, and V. c) Compounds, IX and X. d) Figures in the former parentheses are for the compounds of the lactam type. e) Compounds, XIIIa and b. f) Values are from Ref. 6. g) In CCl_4. h) In $CDCl_3$.

and X for these products. The assignment of the signals is shown in Table 1. The treatment of IX with lithium aluminum hydride yielded the azacycloheptane (XI). The tetrazoles V and X were not formed from IV and IX under the same conditions as in the reaction of III or VIII. Therefore, the lactam can not be an intermediate of the tetrazole formation under these conditions.

2-Methyl-4,5,6,7-tetrahydrobenzo[*b*]thiazol-7-one (XII), which had been prepared according to the literature,[7] was subjected to the Schmidt reaction to give a lactam (XIIIa) in a 68% yield, but not a tetrazole derivative. It showed amido absorption in the IR spectrum. The assignment of the NMR signals is given in Table 1. On deuterium exchange, the multiplet at τ 2.35 disappeared and the broad quartet at 6.54 simultaneously became a more complex multiplet, while the other signals remained unchanged. This fact, as well as the lower chemical shift of the quartet at τ 6.54, indicated the presence of a methylene group adjacent to the lactam nitrogen, supporting the idea of the structure XIIIa for the reaction product. The alternative isomeric form (XIII') was eliminated on the grounds that such a compound would give the signal of CH_2(6) at about τ 7.7—7.8 (*cf.* the signals of 2-pyrrolidone, IV, and IX in Table 1) and that the deuterium exchange could not affect any signals of the compound. The complexity of the signal of CH_2(6) at τ 6.54 after deuterium exchange can be explained in terms of the unequivalency of the methylene hydrogens. The carbonyl group in XIIIa resisted reduction with lithium aluminum hydride even when refluxed for 15 hr in tetrahydrofuran. However, treatment with phosphorus pentasulfide gave the thio lactam, XIIIb, the structure of which was confirmed by a study of the NMR spectrum (for the assignment, see Table 1). The deuterium exchange caused the disappearance of the broad multiplet at τ 0.8, with a simultaneous change in the broad quartet at 6.45 to a more complicated multiplet, as in the case of XIIIa.

On the reaction of XIIIa with triethyloxonium fluoroborate,[8] the ethoxy compound XIV was obtained in a 78% yield.

Experimental

Elementary analyses were carried out using a Yanagimoto C.H.N. Corder, MT-1. The NMR spectra were recorded by means of a Hitachi High-resolution NMR Spectrometer, R-20A, and the IR spectra, by means of a Nihon-Bunko IR-S Spectrophotometer. Each analytical sample gave a single spot on a paper chromatogram (Toyo Roshi No. 51) developed with 3% aqueous ammonium chloride or 5 N acetic acid / 1-butanol (29 : 71 v/v) and examined under ultraviolet light at 365 and 254 mμ in turn.

1-Benzyl-1,4-diazacyclooctan-5-one (IV) and 7-Benzyl-5,6,7-8,9,10-hexahydrotetrazolo[4,5-d][1,4]diazocine (V). To a stirred solution of 9.6 g (0.04 mol) of III hydrochloride in 34 m*l* of concentrated sulfuric acid were added, in small portions, 4.2 g (0.065 mol) of sodium azide over a period of 6 hr at room temperature. After having been stirred for an additional 22 hr at the same temperature, for 9 hr at 30°C, and for 6 hr at 50—55°C, the reaction mixture was poured onto 50 g of ice and made alkaline with a saturated solution of sodium hydroxide under ice cooling. The sodium sulfate was filtered off, and the filtrate was extracted with ether and chloroform successively. The combined and dried (over anhydrous potassium carbonate) extract was evaporated, and the residue was distilled *in vacuo* to give two kinds of oily products. The first fraction (IV) amounted to 5.3 g (64%) (colorless; bp 155—156°C/0.14 mmHg, R_f=0.6).

Found: C, 71.64; H, 8.16; N, 13.20%. Calcd for $C_{13}H_{18}N_2O$: C, 71.52; H, 8.31; N, 12.84%.

The second fraction (V), 0.4 g (7%), was a viscous, light yellow oil, bp 177—180°C/0.1 mmHg, R_f=0.4.

Found: C, 63.96; H, 6.63; N, 28.41%. Calcd for $C_{13}H_{17}N_5$: C, 64.17; H, 7.04; N, 28.78%.

4-Methyl-7-isopropyl-1-azacycloheptan-2-one (IX) and 5-Isopropyl-8-methyl-5,6,7,8-tetrahydro-9H-tetrazolo[4,5-a]azepine (X). To a stirred, ice-cooled solution of 20 g (0.13 mol) of VIII in 50 m*l* of concentrated sulfuric acid were added 18 g (0.28 mol) of sodium azide over a period of 18 hr. The reaction mixture was stirred for an additional 50 hr at room temperature and then poured onto 100 g of ice and made alkaline

7) G. Lehmann, B. Luecke, H. Schick, and G. Hilgetag (Deut. Akad. Wiss., Berlin), *Z. Chem.*, **7** (11), 422 (1967); *Chem. Abstr.*, **68**, 39529h (1968).

8) V. G. Granik and R. G. Glushkov., *Khim.-Farm. Zh.*, **1**, 21 (1967); *Chem. Abstr.*, **68**, 12942a (1968).

with a saturated solution of sodium hydroxide. The sodium sulfate thus formed was filtered off, and the filtrate was extracted with ether. The ether layer was dried over anhydrous potassium carbonate and evaporated to give a mixture of an oil and crystals. The mixture was dissolved in ethanol, and water was added. The solid was collected and recrystallized from dilute ethanol to give 10.6 g (70%) of IX as white needles, mp 118—119°C.

Found: C, 71.08; H, 11.00; N, 7.92%. Calcd for $C_{10}H_{19}NO$: C, 70.96; H, 11.31; N, 8.28%.

The original filtrate was concentrated, and the residue was distilled *in vacuo* to give 4.3 g (16%) of X as a colorless oil, bp 142—143°C/0.20 mmHg.

Found: C, 61.99; H, 9.28; N, 29.11%. Calcd for $C_{10}H_{18}N_4$: C, 61.82; H, 9.29; N, 28.84%.

N-Benzyl-N-(2-aminoethyl)-4-aminobutanoic Acid (VI). A solution of 3.0 g of IV in 60 m*l* of 5% sulfuric acid was refluxed for 10 hr. After cooling, the solution was adjusted to pH 7.0—7.2 with a 5% barium hydroxide solution. The excess barium hydroxide was removed by saturating the the solution with carbon dioxide, followed by filtration. The filtrate was evaporated to dryness under reduced pressure, and the residue was dissolved in a small amount of methanol (*ca.* 5 m*l*); ether was then added in small portions until precipitation began. The separation of the precipitate and two recrystallizations from methanol gave 1.3 g (58%) of VI as white prisms, mp 173°C (decomp.). The drying of an aliquot of the prisms at 70°C for 2 hr gave the analytical sample.

Found: C, 65.86; H, 8.52; N, 11.82%. Calcd for $C_{13}H_{20}N_2O_2$: C, 66.07; H, 8.53; N, 11.85%.

Picrate: VI combined with two molecules of picric acid to form yellow plates, mp 183°C (from ethanol). The analytical sample was dried at 70°C for 2 hr.

Found: C, 44.10; H, 4.17; N, 16.10%. Calcd for $C_{13}H_{20}N_2O_2 \cdot 2C_6H_3N_3O_7$: C, 43.83; H, 3.83; N, 16.36%.

2-Methyl-8-oxo-4,5,6,7-tetrahydro-8H-thiazolo[5,4-c]azepine (XIIIa). To a stirred solution of 3 g (0.018 mol) of XII in 15 m*l* of concentrated sulfuric acid, maintained at 0—5°C, were carefully added 2.5 g (0.038 mol) of sodium azide. After the mixture had been stirred for 10 hr, 100 m*l* of ice-cold water were added. The mixture was adjusted to pH 5 by adding a saturated solution of sodium hydroxide, and then it was repeatedly extracted with chloroform. The combined chloroform solution was dried over anhydrous magnesium sulfate and evaporated under reduced pressure. The residual solid was recrystallized from a mixture of acetone and chloroform to afford 2.1 g (67.5%) of XIIIa as colorless crystals, mp 174—175°C, which sublimed at 120°C/0.2 mmHg.

Found: C, 52.69; H, 5.54; N, 15.15%. Calcd for $C_8H_{10}N_2OS$: C, 52.72; H, 5.53; N, 15.37%.

2-Methyl-8-thioxo-4,5,6,7-tetrahydro-8H-thiazolo[5,4-c]azepine (XIIIb). A mixture of 1 g (0.0051 mol) of XIIIa, 1.4 g (0.0061 mol) of phosphorus pentasulfide, and 15 m*l* of pyridine was heated under reflux for 1 hr. The reaction mixture was treated with a small amount of water, evaporated to dryness under reduced pressure, and sublimed at 160°C/0.2 mmHg to give 0.9 g (83%) of XIIIb as light yellow crystals, mp 176—178°C.

Found: C, 48.34; H, 4.79; N, 14.20%. Calcd for $C_8H_{10}N_2S_2$: C, 48.45; H, 5.08; N, 14.13%.

2-Methyl-8-ethoxy-5,6-dihydro-4H-thiazolo[5,4-c]azepine (XIV). To a stirred solution of triethyloxonium fluoroborate[9] (freshly prepared from 5 m*l* of borontrifluoride etherate, 15 m*l* of dry ether, and 5 m*l* of epichlorohydrin), was added a solution of 1 g (0.0055 mol) of XIIIa in 20 m*l* of dichloromethane at room temperature. The mixture was stirred for 30 hr and then made alkaline by adding an aqueous solution of potassium carbonate. Extraction with dichloromethane, followed by the evaporation of the solvent and vacuum distillation, gave 0.9 g (78%) of XIV as a colorless oil, bp 94—95°C/0.22 mmHg.

Found: C, 57.88; H, 7.12; N, 12.17%. Calcd for $C_{10}H_{14}N_2OS$: C, 57.11; H, 6.71; N, 13.32%.

The *picrate* formed as yellow crystals, mp 149—150°C (from ethanol).

Found: C, 43.56; H, 3.76; N, 15.79%. Calcd for $C_{10}H_{14}N_2OS \cdot C_6H_3N_3O_7$: C, 43.73; H, 3.90; N, 15.94%.

The authors wish to thank Dr. S. Morosawa and Dr. H. Yamamoto for their valuable advice and encouragement.

9) L. A. Paquette, *J. Amer. Chem. Soc.*, **86**, 4096 (1964).

Studies on Microbial Utilization of Petroleum. I. Separation and Characterization of Carotenoids Produced by a Species of *Brevibacterium* in Hydrocarbon Media

Hyoichiro SAKURAI, Kenji KATO, Toshio SAKAI, Yoshiro MASUDA, and Tohoru KURIYAMA

Central Research Laboratory, Mitsubishi Petrochemical Company Limited, Ami-machi, Inashiki-gun, Ibaraki

(Received June 22, 1970)

Ten pigment fractions were separated from a *Brevibacterium* sp. KY-4313 in hydrocarbon fermentation. The pigments were extracted from cell with a mixture of petroleum ether and acetone, and purified by column and thin-layer chromatography. The principal carotenoid of this organism was identified as canthaxanthin (4,4′-dioxo-β-carotene) by using visible, IR, NMR, and mass spectra of the pigment. Three other pigments were characterized as β-carotene, echinenone (4-oxo-β-carotene), and 15-*cis*-4,4′-dioxo-β-carotene. Three carboxylic carotenoids and three other carotenoids were also separated but their structures were left unidentified. Quantitation of the pigments showed that canthaxanthin represented 53% and its *cis*-isomer 20% of the pigments separated from extracts. β-Carotene derivatives comprise more than 80% of the pigments. Canthaxanthin and echinenone have not previously been reported as bacterial pigments in hydrocarbon fermentation.

Studies on carotenoid production by hydrocarbon fermentation have been reported regarding *Mycobacterium lacticola*,[1,2] *Nocardia lutea*,[3] *N. corallina*,[3] *Pseudomonas methanica*,[4] *Rhodotorula aurantiace*,[5] *R. glutinis*,[5] *Mycobacterium smegmatis*,[6] and *M. lacticolum*.[7]

Recently Iizuka and Nishimura[8] have reported that *Brevibacterium* strain No. 103 essentially produces astacin and astaxanthin when cultured on several *n*-alkanes.

Kato *et al.*[9] reported the cultural conditions for carotenoid production by a *Brevibacterium* sp. KY-4313 in *n*-alkane media and suggested that the bacterium seemed to produce xanthophylls extractive with petroelum ether.

The present authors reexamined the carotenoid pigments produced by *Brevibacterium* sp. KY-4313 cultivated on the different hydrocarbon medium, and established the presence of canthaxanthin among other carotenoids, as the main component.

Canthaxanthin has been isolated from mushroom *Cantharellus cinnabarinus*,[10] the feathers and the skin of the lesser flamingo *Phoeniconias minor*,[11] *Cyclops strenuus*,[12] and *Micrococcus roseus*[13] and *Corynebacterium michiganense*[14] in non hydrocarbon media.

Experimental

Measurements. Hitachi EPS-3, Perkin Elmer 225, Varian HA 100D, and Hitachi RMU-6 spectrometer were used for the measurements of visible, IR, NMR, and mass spectrum, respectively.

Reduction of Carbonyl Group. Carbonyl groups in carotenoids were reduced by sodium borohydride in 95% ethanol solution.

Detection Test for Carboxylic Group. Carboxylic groups were detected by the formation of ferric hydroxamates (brown).

Microorganism. The microorganism used was a *Brevibacterium* sp. KY-4313. The organism was maintained on a meat extract agar slant.

Media and Cultural Conditions. A meat extract agar slant was used as an inoculum. For sub-inoculum a portion of 100 m*l* conventional natural nutrient medium in a 500 m*l* Erlenmeyer flask was used. Mass cultures were grown for 7 days in fifty 500 m*l* Erlenmeyer flasks containing 200 m*l* of medium shown in Table 1 at 30°C on a rotary shaker running at 220 rpm describing a circle of 70 mm diameter.

Harvesting of Cells. The pale yellow culture was poured into a separatory funnel, allowed to stand for 1 hr, and the green aqueous layer was discarded. The yellow supernatant was centrifuged at 7000 rpm at 0°C for 10 min.

Extraction of Pigments from the Medium. Experiments

Table 1. Composition of hydrocarbon medium

$NH_4H_2PO_4$	2.5 g
KH_2PO_4	2.0 g
$Na_2HPO_4 \cdot 12H_2O$	3.0 g
$MgSO_4 \cdot 7H_2O$	0.2 g
$CaCl_2 \cdot 2H_2O$	0.01 g
$FeSO_4 \cdot 7H_2O$	0.005 g
$MnSO_4 \cdot 4\text{–}6H_2O$	0.005 g
Vitamin B_{12}	100 γ
n-C_{14-16} mixture	20 m*l*
Distd. water	1000 m*l*
pH	7.0

1) H. F. Haas, M. F. Yantzi, and L. D. Bushnell, *Trans. Kansas Acad. Sci.*, **44**, 39 (1941).
2) H. F. Haas and L. D. Bushnell, *J. Bacteriel.*, **48**, 219 (1944).
3) T. Nagasaki, K. Fujii, A. Tanaka, and S. Fukui, *Bitamin*, **34**, 146 (1966).
4) M. Dworkin and J. W. Foster, *J. Bacteriol.*, **72**, 646 (1956).
5) E. M. Dikanskaya, N. L. Kudinova, and A. P. Kryuchova, *Chem. Abstr.*, **70**, 46194q (1969).
6) A. Tanaka, T. Nagasaki, and S. Fukui, *J. Ferment. Technol.*, **46**, 477 (1966).
7) N. N. Grechushkina, M. B. Yakovleva, and I. L. Rabotnova, *Mikrobiologiya*, **37**, 799 (1968), *cf. Chem. Abstr.*, **70**, 17694x (1969).
8) H. Iizuka and Y. Nishimura, *J. Gen. Appl. Microbiol.* (Tokyo), **15**, 127 (1969).
9) K. Kato, A. Tanaka, and S. Fukui, Presented at the Annual Meeting of the Agricultural Chemical Society of Japan, Fukuoka, April 4, 1970.
10) F. Haxo, *Botan. Gaz.*, **112**, 228 (1950).
11) H. Thommen and H. Wackernagel, *Biochem. Biophys. Acta*, **69**, 387 (1963).
12) B. Czeczuga and R. Czerpak, *Comp. Biochem. Physiol.*, **26**, 101 (1966).
13) J. J. Cooney, H. W. Jr. Marks, and A. M. Smith, *J. Bacteriol.*, **92**, 342 (1966).
14) S. Saperstein, *Biochem. J.*, **57**, 273 (1954).

TABLE 2. CHROMATOGRAPHIC SEPARATION OF THE CAROTENOIDS AND THEIR CONTENTS

Column chromatog.[a]		Thin-layer chromatography				Per cent[b] content
Fraction	System of solvents	Layer	System of solvents	Fraction	R_f value	
1	PE-Ac (9.5+0.5, v/v)	Silica gel	PE-Bz (85+15)	1-1	0.67	6.2
				1-2	0.53	
				1-3	0.49	
				1-4	0	
2	(98+2)	$MgHPO_4$	CCl_4	2	0.57	7.4
3	(50+50)	Silica gel-$Ca(OH)_2$ (1+2)	Bz-Me (98+2)	3-1[c]	0.21	52.8
				3-2	0.12	20.2
4	Ac	Silica gel	PE-Ac (30+70)	4-1	0.71	7.0
				4-2	0.49	4.1
				4-3	0	2.3

a) Silica gel (200 mesh, 0.8×48 cm) was used for adsorbent.
b) The content was determined spectrophotometrically as β-carotene ($E^{1\%}_{1cm}$: 2580 in PE).
c) The main pigment was also isolated from Fr. 3 in PE at −20°C in the form of a fine deep red plate, which was found pure by thin-layer chromatography.
PE: petroleum ether, Ac: acetone, Bz: benzene, Me: methanol.

were carried out throughout under dim light and N_2 atmosphere. A portion of 2.5 *l* of petroleum ether and the same volume of acetone were added to about 200 g of orange yellow harvest. The hole mixture was washed with 5 *l* of distd. water. The procedure was repeated twice. The collected orange petroleum ether layer was evaporated to dryness in a vacuum and pigments were then dissolved in acetone. The carotenoid solution in acetone was allowed to stand at −20°C overnight, and the waxy substances separated were removed by filtration. The pigments were again transferred from the acetone solution into petroleum ether. The solution was passed through a silica gel column (0.8×48 cm, 200 mesh) to remove residual hydrocarbon, the column being washed with petroleum ether, and the adsorbed pigments were eluted with acetone.

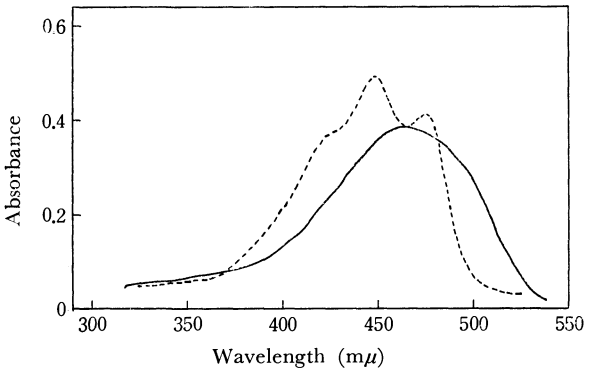

Fig. 1. The change of the absorption spectrum of Fr. 3-1 by $NaBH_4$ reduction.
Solvent: *n*-Hexane, (——): Fr. 3-1, (- - -): Reduced Fr. 3-1.

Saponification of the pigments was carried out in a 10% methanolic potassium hydroxide solution for 30 min at 40°C with continuous stirring in N_2 atmosphere, and the unsaponifiable matters were extracted with petroleum ether.

Separation of Pigments. Separation procedures are summarized in Table 2. Thin-layer chromatographic purification by different adsorbents was carried out.

Results and Discussion

The content of the pigments and their absorption maxima are shown in Tables 2 and 3, respectively.

The main carotenoid (Fr. 3-1, Fr. is used for fraction instead hereinafter) was identified with canthaxanthin. Three carotenoids were characterized as β-carotene, echinenone, and canthaxanthin *cis*-isomer. Hydroxy-carotenoid, a presumable precursor in oxocarotenoid biosynthesis, was not obtained.

From the fact that reduction of the pigment makes a 17 mμ hypsochromic shift in the visible spectra (Table 3, Fig. 1), the main pigment is considered to have two conjugated carbonyl groups on its ionone

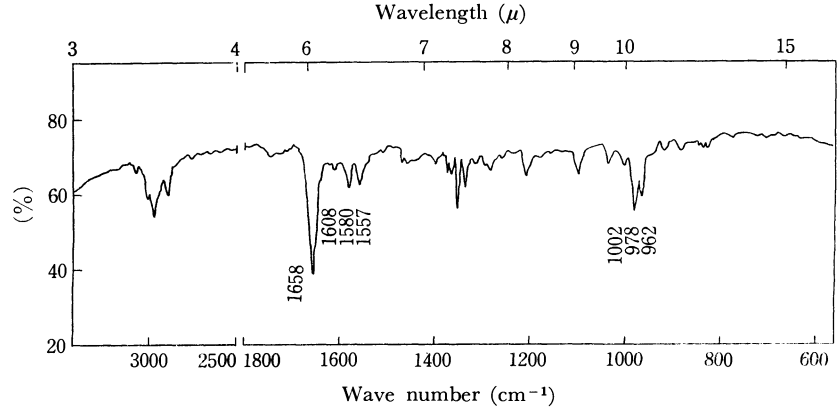

Fig. 2. IR spectrum of Fr. 3-1 (KBr: 0.3 g, Sample: 0.5 mg).

Table 3. Absorption maxima and identification of carotenoids

Carotenoid	Absorption maxima (mμ)	Solvent	R_f Value	Identification
Fr. 1-1	425 446 473	PE	0.67[g]	β-Carotene[a]
Fr. 1-3	439 466 496	PE		Unknown[b]
Fr. 2	458	*n*-Hexane	0.85[h]	Echinenone[c]
Reduced Fr. 2	426 450 478	*n*-Hexane	0.76[h]	
Fr. 3-1	466	*n*-Hexane	0.83[h]	Canthaxanthin[d]
Reduced Fr. 3-1	426 449 476	*n*-Hexane	0.51[h]	
Fr. 3-2	356 460	*n*-Hexane		*cis*-Isomer of canthaxanthin[e]
Reduced Fr. 3-2	332 422 445 472	*n*-Hexane		
Fr. 4-1	348 435 457 483	Chloroform		Carboxylic carotenoids[f]
Fr. 4-2	435 459 482	Chloroform		
Fr. 4-3	433 455 482	Chloroform		
β-Carotene[i]	425 447 475	PE	0.67[g]	
Echinenone[15]	458	PE		
Isocryptoxanthin[16]	426 451 479	*n*-Hexane		
Canthaxanthin[15]	467	*n*-Hexane		
Isozeaxanthin[15]	426 450 478	*n*-Hexane		

a) Identified with β-carotene from the R_f values and spectrum.
b) This pigment is neither carbonyl, hydroxy, nor carboxylic carotenoid from TLC behavior and result of $NaBH_4$-reduction.
c) Identified with echinenone from results of the maximum absorption shift and the change of R_f value on reduction, and by agrrement with the absorption maxima given in literature (Fig. 4).
d) The main pigment was identified with canthaxanthin from the results of visible absorption, IR, NMR and mass spectrum.
e) Identified with canthaxanthin *cis*-isomer (15-*cis*-) from the position of *cis*-peak[17] (Fig. 5).
f) Positive to the detection test of carboxylic group.
g) Layer: Silica gel, Solvent system: PE-Bz (85+15).
h) Layer; Silica gel, Solvent system: CH_2Cl_2-AcOEt (90+10).
i) β-Carotene (E. Merck, for biochemistry grade) used after being purified on TLC.

Table 4. IR absorption of Fr. 3-1 and canthaxanthin

Carotenoid	Frequencies in cm^{-1}						
	Conjug. C=O	Conjug. C=C			CH out-of-plane of conjug. *trans*-CH=CH		
Fr. 3-1	1658 vs	1608 w	1580 m	1557 m	1002 w	978 s	962 m
Canthaxanthin[18]	1658 vs	1608 w	1581 m	1555 s		998 m	966 s
Canthaxanthin[19]	1640 vs		broad (m)			*ca.* 960 s broad	

vs: very strong, s: strong, m: medium, w: weak. KBr discs were used.

Table 5. NMR absorption of Fr. 3-1 and canthaxanthin

Carotenoid	Solvent	*gem*-Me	Me on C adjacent to C=O	Me on polyene chain	*Vicinal* CH_2					
					α position to C=O			β position to C=O		
Fr. 3-1	C_6D_6-$CDCl_3$ (3+1)	8.99	7.98	8.12 8.14[a]	7.53	7.60	7.67	8.36	8.42	8.49[b]
Fr. 3-1	$CDCl_3$	8.79	8.12	7.99	7.42	7.48	7.55	8.08	8.15	8.22
Canthaxanthin[19]	CCl_4	8.81	8.21	7.89 7.99						
Relative intensity[c]		6	3	6		2			2	

a) The bands at 8.12 and 8.14 arise from 9,9'-Me and 13,13'-Me groups, respectively.
b) These two sets of triplet due to the vicinal CH_2 groups were confirmed by spin-spin decoupling technique.
c) The ratio was calculated from the spectrum measured in C_6D_6-$CDCl_3$.

15) F. J. Petracek and L. Zechmeister, *J. Amer. Chem. Soc.*, **78**, 1427 (1956).
16) L. Wallcave and L. Zechmeister, *ibid.*, **75**, 4495 (1953).
17) L. Zechmeister and A. Polgár, *ibid.*, **65**, 1522 (1943).
18) C. K. Warren and B. C. L. Weedon, *J. Chem. Soc.*, **1958**, 3986.
19) O. Isler, R. Rüegg, and P. Shudel, *Chimia*, **15**, 208 (1961).
20) M. S. Barber, J. B. Davis, L. M. Jackman, and B. C. L. Weedon, *J. Chem. Soc.*, **1960**, 2870.

rings. As shown in Table 4 and Fig. 2, the IR spectrum gives more information than the spectra reported heretofore, that is, we may conclude that the splitting of the region (960—1002 cm^{-1}) is due to the conjugation of ω,ω'-carbonyl groups through the trans polyene chain.

The NMR spectrum measured in a C_6D_6-$CDCl_3$ solution provides more useful information for complete assignment of bands than the ones measured in $CDCl_3$, or in CCl_4 (Table 5, Fig. 3). In the measurement in a C_6D_6-$CDCl_3$ solution, a band at 7.98 (τ value, Me on C adjacent to C=O) and a triplet at 8.42 (*vicinal* CH_2) can be completely separated by magnetic anisotropy effect of C_6D_6, while it is observed as an overlapping spectrum in $CDCl_3$.

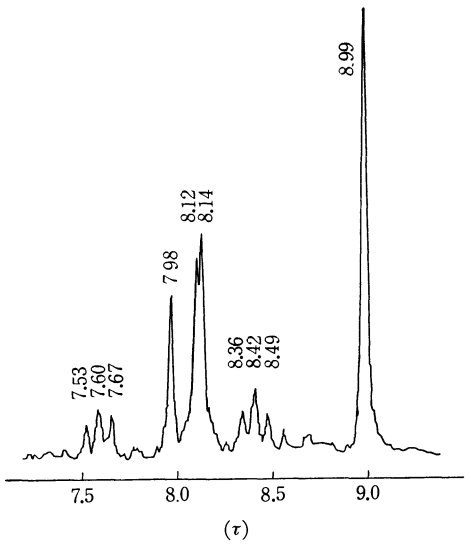

Fig. 3. NMR spectrum of Fr. 3-1. 0.5 mg/0.01 m*l* C_6D_6-$CDCl_3$ (3 : 1) at 100 MHz.

In the mass spectrum of Fr. 3-1, M^+ shows 564 mu (Calcd for $C_{40}H_{52}O_2$: mol wt, 564.4). The intensity ratio of M^+-92 to M^+-106 is 2.6, which agrees well with that of canthaxanthin (2.56) reported by Enzell *et al.*[21]

From the results, we identify Fr. 3-1 with canthaxanthin (4,4'-dioxo-β-carotene) (I).

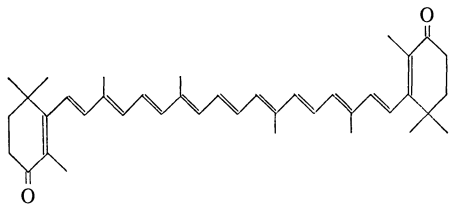

(I) Canthaxanthin

Fr. 3–1 exposed to sunlight shows the same absorption spectrum as that of Fr. 3–2. Canthaxanthin is considered to have been converted to its *cis*-isomer during the cultivation of bacterium.

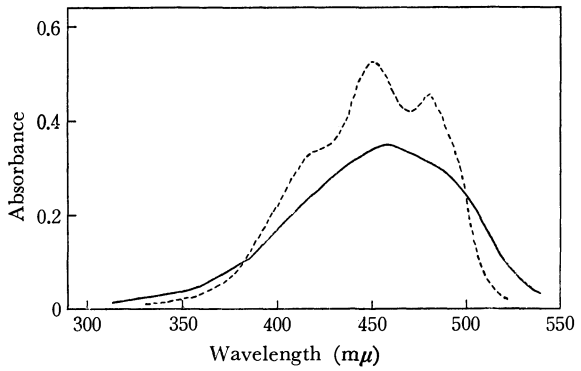

Fig. 4. The change of the absorption spectrum of Fr. 2 by $NaBH_4$ reduction. Solvent: *n*-Hexane. (——): Fr. 2, (- - -): Reduced Fr. 2.

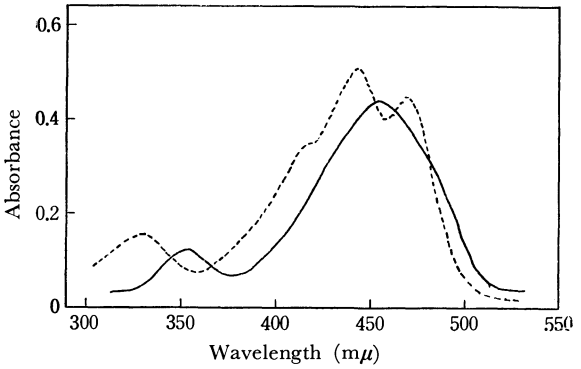

Fig. 5. The change of the absorption spectrum of Fr. 3-2 by $NaBH_4$ reduction. Solvent: Petroleum ether. (——): Reduced Fr. 3-2, (- - -): Reduced Fr. 3-2.

Brevibact. sp. KY-4313 and *B.* strain No. 103[8] differ in the carotenoid formation. While the former produces mainly mono- and dioxo-carotenoids, the latter gives dihydroxy-dioxo- and tetraoxo-carotenoids almost exclusively.

Mycobact. smegmatis[6] was reported to produce oxo- and hydroxy-oxo-carotenoids as main components in hydrocarbon media, but no hydroxy-carotenoid has been isolated so far.

In non-hydrocarbon medium *Micrococcus roseus*[13] has been found to produce a trace of isozeaxanthin as a precursor for canthaxanthin which is the main component.

From these facts, it seems that the organisms such as *Brevibact.* sp. KY-4313, *N.* strain No. 103, *Mycobact. smegmatis*, and *Micrococcus roseus* readily oxidize the hydroxyls of precursors to ketones.

We wish to thank Professor S. Fukui of Kyoto University for a gift of the specimen of *Brevibacterium* sp. KY-4313 and his helpful discussion, and also the technical assistants of our laboratory. We also wish to thank Mr. J. Fukuda, Director of Central Research Laboratory, Mitsubishi Petrochemical Co., Ltd., for permission to publish this paper.

21) C. R. Enzell, G. W. Francis, and S. Leaaen Jensen, *Acta Chem. Scand.*, **22**, 1054 (1968).

Optical Rotatory Dispersion and Circular Dichroism of the Osmate Esters of Cyclic Mono-olefins[1,2]

Naokazu SAKOTA and Shunsaku TANAKA

Department of Industrial Chemistry, Faculty of Engineering, Ehime University, Bunkyo-cho, Matsuyama

(Received July 3, 1970)

The osmate esters (as the di-pyridine adducts) of optically active mono-, di- and tricyclic mono-unsaturated terpenes were prepared for measurements of optical rotatory dispersion (ORD) and circular dichroism (CD). All the osmate esters of the cyclic olefins examined exhibited a strong Cotton effect in 470 mμ regions and a weak Cotton effect near 600 mμ regions, which were similar to those of the osmate esters of the open chained olefins reported in our previous paper. The sign of CD maximum in 470 mμ regions was found to be correlated to the chirality of gauche structure of the chelate ring containing an osmium chromophore. Furthermore, their absolute configurations were deduced from the data of circular dichroism of two diastereoisomers of *cis*-α-pineneglycol.

An effective method has been reported by Bunnenberg and Djerassi[3] to introduce an appropriate chromophore to an ethylenic bond of optically active mono-unsaturated compound and to give rise to a Cotton effect in the relatively longer wavelength regions for the convenience of the measurement of ORD. They reported that the steroidal olefins reacted with osmium tetroxide to form the osmate esters, which exhibited a multiple Cotton effect in visible spectrum regions.

We have already mentioned that the sign of the Cotton effect of the osmate esters of optically active acryloyl esters,[4] α-olefins,[4] acryloyl-L-amino acids[5] and 1,2-glycols[6] can be associated with the configurations of these olefins. We measured ORD and CD curves of the osmate esters of optically active cyclic mono-unsaturated terpenes and tried to account for the correlation between the conformational structure of the osmate esters and the sign of CD maximum in 470 mμ regions.

Experimental

Menthene Isomers. (+)-*1-Menthene* [*1*]. The crude (+)-l-menthene supplied by Nippon Terpene Chem. Co., was subjected in batches to preparative gas chromatography (Silicone DC 550, 2.6 m×10 mmφ, 160°C), α^{17}_{589} +82.8° (neat).

(+)-trans-*2-Menthene* [*2*][7]. *l*-Menthyl toluene-*p*-sulphonate obtained by the reaction of *p*-toluenesulfonyl chloride with *l*-menthol was added to a solution of sodium in absolute ethanol. The mixture was refluxed for 6 hr in dry nitrogen. After ether extraction, the product was purified by preparative gas chromatography as above, α^{21}_{589}+109° (neat). The resulting product was found to contain (+)-*trans*-2-menthene (92%) and (+)-3-menthene (8%) by analytical gas chromatography (Dinonylphthalate, 3.7 m×3 mmφ, 145°C).

(−)-trans-*2-Menthene* [*3*]: The product obtained from α-menthyl tosylate by the method as above was found to contain (−)-*trans*-2-menthene (91%) and (−)-3-menthene (9%), α^{21}_{589} −108° (neat).

(+)-*3-Menthene* [*4*].[8] *l*-Menthol was added to metallic sodium in dry toluene and refluxed for 20 hr. To the reaction mixture was added ether solution of carbon disulfide and methyliodide. The yielded methyl (−)-menthyl xanthate was pyrolyzed to [*4*], which was purified by preparative gas chromatography. From the result of the analytical gas chromatography, it was found to contain (+)-*trans*-2-menthene (31%), α^{17}_{589} +83.2° (neat).

Dicyclic mono-terpenes.

The purity of the following compounds was determined by analytical gas chromatography (PEG 6000, 3 m×3 mmφ, 130°C).

(+)-α-*Pinene* [*5*][9]: $[\alpha]^{11}_{D}$ +21.5° (neat), purity 97%.
(−)-α-*Pinene* [*6*][9]: $[\alpha]^{11}_{D}$ −26.5° (neat), purity 97%.
(−)-β-*Pinene* [*7*][9]: $[\alpha]^{11}_{D}$ −19.9° (neat), purity 97%.
(−)-*Camphene* [*8*][9]: $[\alpha]^{21}_{D}$ −28.3° (*c* 8, ethanol), purity 92.5%.
(+)-*Bornylene* [*9*][9]: $[\alpha]^{21}_{D}$ +8.3° (*c* 6, benzene), purity 87%.

Patchoulene Isomers.

α- *and* γ-*Patchoulene* [*10*], [*12*].[10] Phosphorus oxychloride was added into a solution of patchouli alcohol ($[\alpha]^{22}_{D}$ −120°, *c* 5, chloroform) in pyridine. The resulting patchoulene was separated into two components by preparative gas chromatography (PEG 6000, 2.6 m×10 mmφ, 160°C). α-Patchoulene [*10*]; α^{22}_{589} −45.10° (neat), purity 99%. γ-Patchoulene [*12*]; purity 87% (containing 12% α-patchoulene).

β-*Patchoulene* [*11*].[10] This was prepared by dehydration of patchouli alcohol in concd. sulfuric acid and purified by preparative gas chromatography (PEG 6000, 2.6 m×10 mmφ). α^{22}_{589} −37.8° (neat). Purity 99%.

α-*Pineneglycols.* (+)-(*1R:2R:3R:5R*)-trans- *and* (−)-(*1R:2R:3S:5R*)-cis-α-*Pineneglycol* [*13*], [*14*]. (+)-2-Hydroxypinocamphone prepared by oxidation of chromic acid anhydride from (−)-α-pinene ($[\alpha]_D$ −26.9°) was reduced by lithium aluminum hydride. The mixture gave crude glycols which were chromatographed on silica

1) Studies on Optical Rotatory Dispersion Part VII. Part VI: N. Sakota, S. Tanaka, K. Okita, and N. Koine, *Nippon Kagaku Zasshi*, **91**, 265 (1970).

2) Presented at the 13th Symposium on the Chemistry of Terpenes, Essential Oils and Aromatics, held at Kagoshima in 1969.

3) I. Bunnenberg and C. Djerassi, *J. Amer. Chem. Soc.*, **82**, 5953 (1960).

4) N. Sakota, T. Tanigaki, K. Okita, and N. Koine, *Nippon Kagaku Zasshi*, **90**, 593 (1969).

5) N. Sakota and N. Koine, *ibid.*, **88**, 1087 (1967).

6) N. Sakota, S. Tanaka, K. Okita, and N. Koine, *ibid.*, **91**, 265 (1970).

7) W. Hückel and W. Tappe, *Ann. Chem.*, **543**, 191 (1940).

8) L. Tschugaeff, *Ber.*, **32**, 3332 (1899).

9) The samples were supplied by the Nippon Terpene Chem. Co., Ltd. except for (−)-α-pinene, which was supplied by the Yoneyama Chemical Co., Ltd.

10) G. Büchi, R. E. Erickson, and N. Wakabayashi, *J. Amer. Chem. Soc.*, **83**, 927 (1961).

gel column with the mixture of ethyl acetate and *n*-hexane into *cis*- and *trans*-α-pineneglycol. The homogeneity of these glycols separated was checked by chromatostrip analysis. *cis*-Glycol 〔*14*〕, $[\alpha]_{589}^{11}$ −0.40° (*c* 5, chloroform). Lit[11] $[\alpha]_D^{25}$ −0.890° (*c* 7.91, chloroform), from (−)-α-pinene ($[\alpha]_D^{25}$ −39.9°). *trans*-Glycol 〔*13*〕, $[\alpha]_{589}^{26}$ −20.5° (*c* 1.5, ethanol), mp 153—156°C. Lit[8] $[\alpha]_D^{25}$ −33.1° (*c* 4.8, ethanol), mp 159—160°C, from (−)-α-pinene ($[\alpha]_D^{25}$ −39.9°).

(−)-(*1R*:*2S*:*3R*:*5R*)-cis-α-*Pineneglycol* 〔*15*〕.[12] Pinocarbonoxide mixture prepared from (−)-α-pinene (optical purity 71%, kindly supplied by Mr. Katsuhara), was reduced by lithium aluminum hydride. The resulting mixture was separated as shown above into two *cis*-α-pineneglycols and a *trans*-α-pineneglycol. The *trans*-glycol and the *cis*-glycols were identified to be 〔*13*〕, 〔*14*〕, and 〔*15*〕 respectively by the R_f values of thin-layer chromatography.

Measurements of ORD, CD and Visible Absorption Spectrum. Olefin (3—5 mg) was treated with two molar equivalents of pyridine dissolved in 1 m*l* of dichloromethane and one equivalent of osmium tetroxide. After standing for a certain time at room temperature, ORD, CD and visible absorption spectra were recorded on a Jasco Optical Rotatory Dispersion, Model UV-5 with an attached CD recorder using 1 mm and 2 mm cells. In the case of α-pineneglycol, 0.4% (v/v) pyridine - methanol was used as a solvent.

Results and Discussion

It has been reported[13] that the mono-unsaturated compounds react with one equivalent of osmium tetroxide and two equivalents of pyridine yielding the osmate esters (as di-pyridine adducts) as follows.

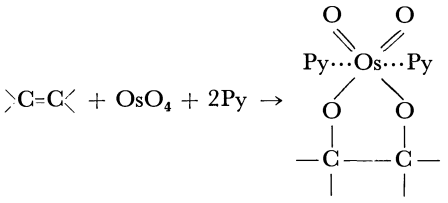

The ORD, CD and visible absorption spectra of the osmate esters of mono-unsaturated terpenes differ markedly from each other in amplitude, fine structure and position of the extrema according to their chemical structures. However, general features of these spectra resemble each other. As two examples, the spectra of the osmate esters of monocyclic terpene, (+)-1-menthene and dicyclic terpene, (−)-β-pinene are shown in Figs. 1 and 2, respectively. When these terpenes are treated with pyridine and OsO_4 in dichloromethane, the maximum absorption is always obtained only after standing for 1—2 days at room temperature, and the spectra at the maximum absorption are shown in these figures. As shown in Fig. 1, the osmate esters of (+)-1-menthene 〔*1*-Os〕 exhibit a strong negative CD maximum at about 465 mμ with the corresponding Cotton effect. Because of the strong absorption exhibited below 410 mμ, the visible absorption band corresponding to the CD maximum at 465

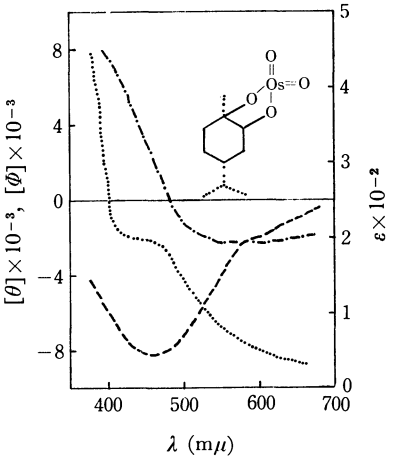

Fig. 1. CD (----), ORD (—·—) and visible absorption spectrum (·····) of osmate ester of (+)-1-menthene in dichloromethane.

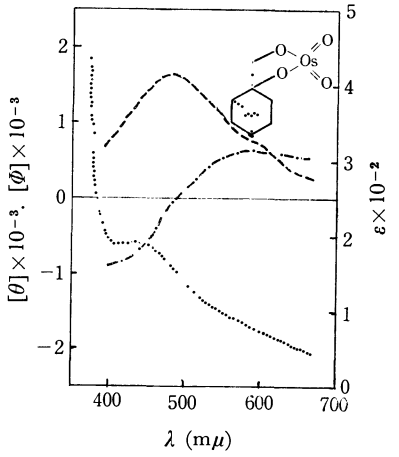

Fig. 2. CD(----), ORD(—·—) and visible absorption spectrum(·····) of osmate ester of (−)-β-pinene in dichloromethane.

mμ regions reveals itself merely as a shoulder, which is shifted to the shorter wavelength. In Fig. 2, the osmate ester of (−)-β-pinene 〔*7*-Os〕 exhibits a similar CD curve of opposite sign.

The molar elipticities at maximum wavelength ($[\theta]_{max}$) of the osmate esters of mono-, di- and tricyclic mono-unsaturated terpenes are summarized in Fig. 3. The general features of the CD curves are similar to those of the osmate esters of the open chained mono-unsaturated compounds[4-6] and also to those of the osmate esters of steroidal olefins.[3] Notable results are obtained from Fig. 3 as follows. The osmate esters of monocyclic terpene, 1-, 2- and 3-menthene exhibit fairly large $[\theta]_{max}$ values compared to those of di- and tricyclic terpenes. Menthene reacts with osmium tetroxide, when a pair of diastereoisomers of the osmate esters are produced owing to the direction of the *cis*-addition. The ratio of the formation of these two stereoisomers might differ according to the stereoselectivity of the menthene to osmium tetroxide. As an example, the use of OsO_4 for (±)-*trans*- and (±)-*cis*-2-menthene is reported to take place in the

11) T. Suga, T. Shishibori, T. Hirata, and T. Matsuura, This Bulletin, **41**, 1180 (1968).
12) J. Katsuhara, *ibid.*, **41**, 2700 (1968).
13) R. Criegee, B. Marchand, and H. Wannowius, *Ann. Chem.*, **550**, 107 (1942).

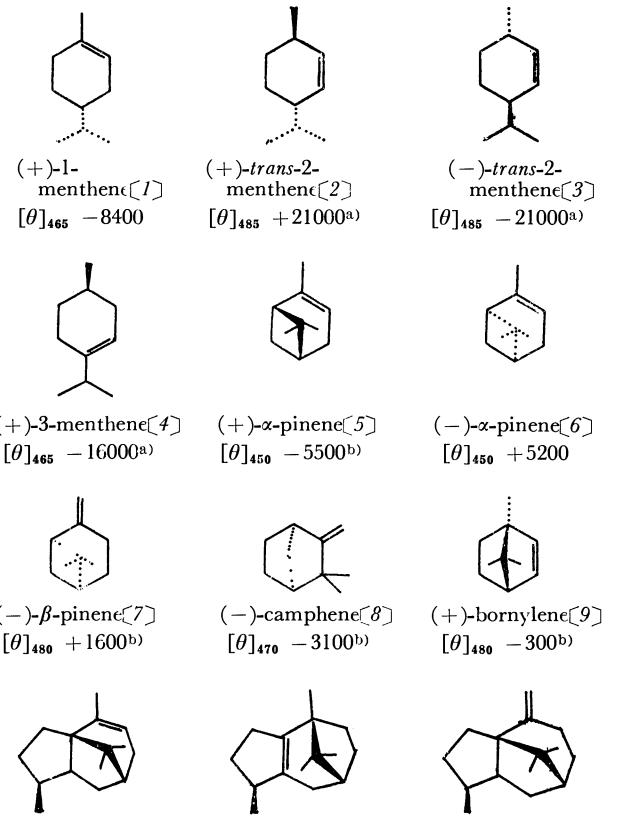

Fig. 3. The absolute configuration of cyclic terpenes and the $[\theta]_{max}$ in CD curves of their osmate esters.

a) $[\theta]_{max}$ values of *trans*-2-menthene and 3-menthene are calculated from $[\theta]_{max}$ values of the two mixtures having different proportions of 〔2〕 or 〔3〕 to 〔4〕.

b) These $[\theta]_{max}$ values show the corrected ones to the optical pure compounds. The specific rotations of optical pure terpenes are postulated as follows.
(+)-α-pinene $[\alpha]_D^{20}+51.8°$,[14]
(−)-α-pinene $[\alpha]_D-51.5°$,[14]
(−)-β-pinene $[\alpha]_D-22.1°$,[15]
(−)-camphene $[\alpha]_D^{20}-99.4°$,[16]
and
(+)-bornylene $[\alpha]_D^{17}+23.9°$.[17]

formation of a single epimer in each case.[18] In these cases, the stable conformation of the osmate esters must be the one in which cyclohexane ring takes one of the two possible chair forms.

The molecular model shows that the five membered ring containing an osmium chromophore is twisted and forms gauche structures, which seem to be more stable than the plain one with respect to the O–C–C–O angle. If the two gauche structures are defined as δ- and λ forms as shown in Fig. 4, it is reasonable to consider that the stable conformation of 〔3-Os〕 is the

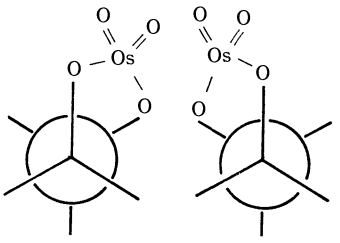

Fig. 4. The gauche structures of the osmium chromophore.

δ form and 〔2-Os〕 is the λ form. Experimental results show that the sign of CD maximum at 470 mμ is negative for 〔3-Os〕 and positive for 〔2-Os〕. This suggests that the sign of CD maximum at 470 mμ can be correlated to the gauche structure of the five membered ring. In contrast, the chiralities of 〔1-Os〕 and 〔4-Os〕 are so little effected by the stereoselectivity of 1- and 3-menthene to osmium tetroxide that the predominant twisted conformation is not easy to predict. However, if the above mentioned rule is applicable for 〔1-Os〕 and 〔4-Os〕, the negative sign of the Cotton effect of their osmate esters is ascribed to the predominance of δ form in the chirality of their five membered ring.

Bunnenberg and Djerassi[3] measured the ORD spectra of the osmate esters of four steroidal cholestenes which have a more rigid and twisted conformation than those of menthene isomers. Their results also show that λ- and δ structure of five membered ring exhibit the positive and negative Cotton effect near 470 mμ, respectively. In previous papers, it was suggested that the sign of the 460 mμ CD maximum in osmate esters of open chained (S)-1,2-glycols CH_2-(OH)CH(OH)R[6] and open chained (S)-α-olefins CH_2=CHR[4,5] was affected by the conformation of the five membered ring. It is well known that the metal complexes of ethylenediamine and propylenediamine have gauche structures.[19] Dwyer *et al.*[20] also showed that the stable conformation of the propylenediamine-cobalt complex is the gauche structure, in which the conformation of the methyl group is equatorial. The stable conformation of the osmate esters of (S)-open chained compounds is suggested to be δ structure in which R group is equatorial, and can explain the negative CD maxima.

Thus the chiral structure of five membered ring of the osmate esters can be correlated to the sign of the CD maximum near 470 mμ. A similar conclusion has been reported by Djerassi *et al.*,[21] who showed that the sign of the Cotton effect attributed to π–π* and n–π* transition of the steroidal trithiocarbonate depends upon the chirality of the trithiocarbonate chromophoric ring. In dibenzoate compounds, the

14) F. H. Thurber and R. C. Thielke, *J. Amer. Chem. Soc.*, **53**, 1030 (1931).
15) G. Dupont, J. Allard, and R. Dulou, *Bull. Soc. Chim. Fr.*, [**4**], **53**, 602 (1933).
16) Golbev, *J. Russ. Phys. Chem. Soc.*, **36**, 1107 (1904).
17) I. M. McAlpine, *J. Chem. Soc.*, **1932**, 545.
18) A. Killen Macbeth and W. G. P. Robertson, *ibid.*, **1953**, 895.
19) K. Nakatsu, M. Shiro, Y. Saito, and T. Kuroya, This Bulletin, **30**, 795 (1957).
20) F. P. Dwyer, T. E. MacDermott, and A. M. Sargeson, *J. Amer. Chem. Soc.*, **85**, 2913 (1963); F. P. Dwyer, A. M. Sargeson, and L. B. James, *ibid.*, **86**, 590 (1964).
21) C. Djerassi, H. Wolf, D. A. Lightner, E. Bunnenberg, K. Takeda, T. Komeno, and K. Kuriyama, *Tetrahedron*, **19**, 1547 (1963).

same consideration was reported by Harada and Nakanishi.[22] For the octahedral metal complexes, the possibility of a correlation between the octant sign and the sign of the Cotton effect for identified transitions within certain symmetry groups is mentioned.[23]

However, the molecular structure of the osmate esters of dicyclic monoterpenes, α-pinenes and bornylene, [5-Os], [6-Os] and [9-Os] are more rigid than those of the monocyclic terpenes, and their gauche structures of the chelate ring are less twisted. Thus, it is difficult to predict whether their stable chiral structure is to be λ or δ. In the case of the osmate esters of β-pinene [7-Os] and camphene [8-Os], not only the skeleton of the terpene moiety but also the whole molecular structure of the osmate ester should be taken into account for the evaluation of the stability of the five membered ring since the double bond is situated in exo position. Thus, for these osmate esters, the existence of a puckered conformation as mentioned above is difficult to predict. It is well established that in general the puckered chromophore contributes much more to the amplitude of the CD maximum than the plain chromophore. In Fig. 3, the molecular elipticities at CD maximum of the osmate esters of dicyclic terpenes are recognized to be smaller than those of monocyclic terpenes. This suggests the puckered conformation for the osmate esters of monocyclic terpenes. In the case of the osmate esters of patchoulene isomers, the situation seems to be more complicated.

Criegee *et al.*[13] has reported that glycols as well as α-olefins react with osmium tetroxide and pyridine to produce the osmate esters which resemble those from α-olefins:

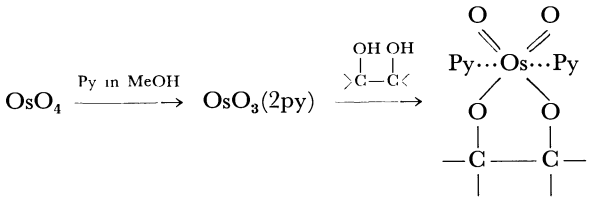

In order to gain further insight into the osmate esters of (−)-α-pinene [6-Os], a *trans-* and two *cis*-α-pineneglycols, in which the configuration differs from each other only at C_2 and C_3 positions, were synthesized and the CD of these osmate esters was measured. Addition of osmium tetroxide to *trans*-α-pineneglycol [13] does not exhibit the CD maximum at 470 mμ, which denies the possibility of the trans addition of OsO_4 to olefins. The absolute configuration of *cis*-α-pineneglycol [14] obtained from (+)-2-hydroxypinocamphone was assigned to be [C] in Fig. 5 by Suga *et al.*,[11] but Schmidt[23] and Katsuhara[12] assigned [D] to it. Another *cis*-α-pineneglycol [15] having the opposite configuration at C_2 and C_3 was obtained from (−)-pinocarbonoxide. The CD curves of these two osmate

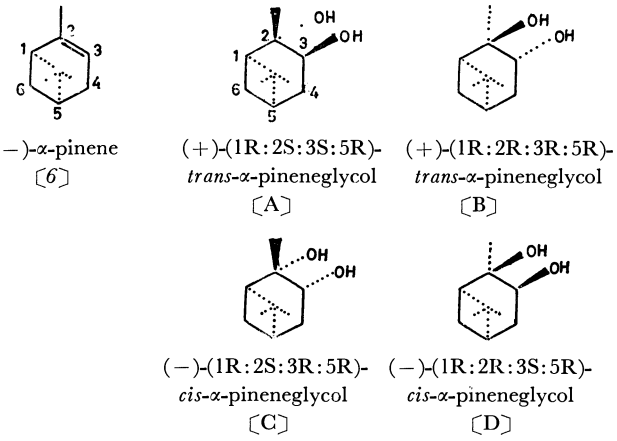

Fig. 5. The absolute configuration of (−)-α-pinene and *trans-*, *cis*-α-pineneglycols.

TABLE 1. THE $[\theta]_{max}$ IN CD CURVES OF THE OSMATE ESTERS OF α-PINENEGLYCOLS

Osmate ester	$[\theta]_{max}$[a]
[13-Os]	0
[14-Os]	+6400
[15-Os]	−12000
[6-Os]	+5200

a) These values are the corrected ones in relation to the optical pure compounds.

esters were measured, and the $[\theta]_{max}$ values were obtained as +6400 and −12000, respectively (Table 1). The osmate ester of (−)-α-pinene [6-Os] consists of two isomeric esters of *cis*-α-pineneglycols [C-Os], [D-Os]. The fraction of [D-Os] is considered to be larger than that of [C-Os], because the cis addition of osmium tetroxide to the double bond should be affected by the steric hinderance of the geminate dimethyl. The results in Table 1 show that [6-Os] mainly consists of [14-Os], and the absolute configurations of [14] and [15] should be assigned to [D] and [C], respectively. The trans glycol [13] obtained from (+)-2-hydroxypinocamphone should also be assigned to [B].

If we supposed that the sign of CD is dependent only upon the twisting of the five membered ring affected by the inherent α-pinene skeleton, both the CD maximum of [14-Os], and [15-Os] should have the same sign. However, the experimental results show different signs for them. This means that when osmium tetroxide reacts with (−)-α-piene from upper side or lower, the twisting of the chromophoric five membered ring might be reversed, *viz.*, the stable conformation of (−)-α-pinene skeleton is reversed. Accordingly, the chromophore in [14-Os] and [15-Os] should be a twisted five membered ring, whose conformation should be affected by the steric effects not only from the terpene moiety but also from the whole molecule.

We acknowledge the generosity of Mr. Katsuhara of Sun Star Research for providing the samples. We also wish to thank the Nippon Terpene Chem., Ltd. and the Yoneyama Chemical Industry Co., Ltd. for gifts of samples.

22) N. Harada and K. Nakanishi, *J. Amer. Chem. Soc.*, **91**, 3991 (1969).
23) C. J. Hawkins and E. Larsen, *Acjta Chem. Scand.*, **19**, 185 (1965).
24) H. Schmidt, *Chem. Ber.*, **93**, 2485 (1960).

Studies of the Synthesis of Furan Compounds. XXII.[1] Synthesis and Antibacterial Activity of 5-[2-(5-Nitro-2-furyl)-1-(2-furyl)vinyl]-2-amino-1,3,4-thiadiazole and Its Related Compounds[2]

Yasuhiko KATO

Laboratory of Organic Synthesis, Department of Chemical Engineering, Kyushu Institute of Technology, Tobata-ku, Kita-kyushu

(Received July 6, 1970)

In continuing our study of the relationship between structures and antibacterial activity, 5-[2-(5-nitro-2-furyl)-1-(2-furyl)vinyl]-2-amino-1,3,4-thiadiazole and related derivatives have been synthesized. Their structures were confirmed by their chemical reactions and by their UV, IR, and NMR spectra. 1,3,4-Thiadiazole and its related derivatives show significant antibacterial activity.

In 1944 Dodd and Stillman[3] reported their finding that furan derivatives with a nitro group in the 5-position possess antibacterial activity; since then, extensive studies of the syntheses of 5-nitrofurans for an antibacterial substance have been undertaken. The substituents at the 2-position of the furan nucleus may be grouped into two types; one is –C=N–N–C=, as proposed by Dodd *et al.*,[4] and the other is –C=C, which has been investigated mainly by Japanese researchers.[5] In comparing the antibacterial activity of these two types, the latter is generally more effective than the former *in vitro*, but less effective *in vivo*. Therefore, the compounds which contain both these two atomic arrangements may be expected to retain a high activity both *in vitro* and *in vivo*. An example is the analog of 5-[2-(5-nitro-2-furyl)vinyl]-1,3,4-oxadiazole, in which the –C=C– system connects the furan nucleus with a heterocycle involving a –C=N–N=C– system; this has been studied in our laboratory.[6] The syntheses of two groups of such compounds, the 5-[2-(5-nitro-2-furyl)-1-(2-furyl)vinyl]-2-amino-1,3,4-thiadiazoles and -1,3,4-oxadiazoles, will be described in this paper.

Results and Discussion

1-[3-(5-Nitro-2-furyl)-2-(2-furyl)acryloyl]thiosemicarbazide(IIa) and hydrazide (III) were, respectively, prepared from thiosemicarbazide and hydrazine hydrate with chloride of acid (Ia)[7] (Chart 1). 5-[2-(5-Nitro-2-furyl)-1-(2-furyl)vinyl]-2-amino-1,3,4-thiadiazole (IV) was obtained from IIa by the method described in a previous report.[8a] In a similar manner, when IIa was treated with phosphoryl chloride at 90—95°C, an isomer (V) of IV was obtained, along with a small amount of its 2-phosphoric amide compound (VI). Compound VI was easily converted to V by heating with water. The *cis-trans* conformations[9] of IV and V were confirmed on the basis of their UV, IR, and NMR spectra (Fig. 1—3) and the chemical reactions of their mother acid and esters.

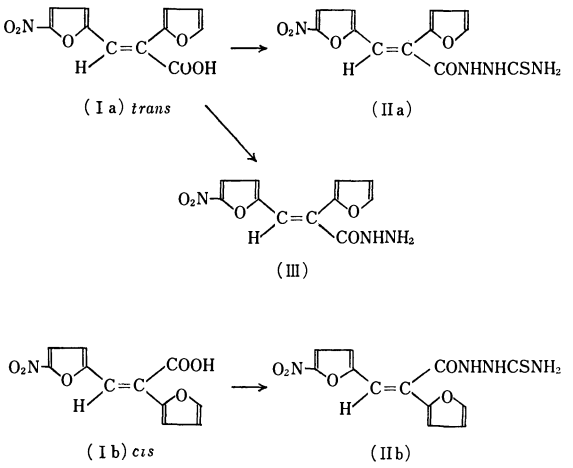

Chart 1

In our previous paper, an unknown isomer (VIIb) of methyl 3-(5-nitro-2-furyl)-2-(2-furyl)acrylate (VIIa) was isolated by the treatment of VIIa with hydrazine hydrate in methanol.[6d] It seems that the hydrazine serves as an isomerization catalyst much like the secondary amines. Thus, the isomerization reactions of the mother acid, Ia, and its esters with ahydrazine catalyst were attempted under several conditions (Table 1). The isomerization was involved in the conversion of the mother acid, Ia, and its benzyl ester (VIIIa) to their isomers (Ib[10] and VIIIb) in rather good yields,

1) Part XXI of this series: Y. Kitamura, M. Yamashita, M. Kashihara, and I. Hirao, *Nippon Kagaku Zasshi*, **90**, 713 (1969).

2) Presented at the 22nd Annual Meeting of the Chemical Society of Japan, Tokyo, April, 1969.

3) M. C. Dodd, W. B. Stillman, M. Roys, and C. Crosby, *J. Pharmacol. Exptl. Therap.*, **82**, 11 (1944).

4) M. C. Dodd, D. L. Cramer, and W. C. Ward, *J. Amer. Pharm. Assoc.*, **39**, 313 (1950).

5) See for example, H. Saikachi and H. Ogawa, *J. Amer. Chem. Soc.*, **80**, 3642 (1958).

6) a) I. Hirao and Y. Kato, *Nippon Kagaku Zasshi*, **85**, 693 (1964). b) Y. Kato, Y. Hara, and I. Hirao, *ibid.*, **86**, 957 (1965). c) Y. Kato and I. Hirao, *ibid.*, **87**, 1336 (1966). d) Y. Kato, N. Nakajima, and I. Hirao, *ibid.*, **89**, 955 (1968).

7) H. Saikachi and A. Tanaka, *Yakugaku Zasshi*, **83**, 147 (1963).

8) a) I. Hirao, *Nippon Kagaku Zasshi*, **89**, 713 (1968). b) *ibid.*, **88**, 574 (1967).

9) The *cis* and *trans* conformation were determined on the basis of the structures assigned[7] as follows.

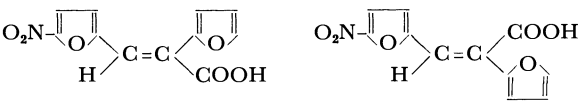

trans acid (Ia) *cis* acid (Ib)

In this case, *trans* isomer (IV) means that 1,3,4-thiadiazole ring is on opposite side of 5-nitrofuran ring toward the ethylene double bond, and *cis* isomer (V) is both of the two rings being on a side.

10) This product did not agree with the compound already reported by Saikachi and Tanaka[7] dealing with the mp, UV, and IR spectrum.

TABLE 1. ISOMERIZATION OF 3-(5-NITRO-2-FURYL)-2-(2-FURYL)ACRYLIC ACID AND ITS ESTERS WITH HYDRAZINE HYDRATE

trans Compound (mp°C)	Reaction conditions			Products			
	Hydrazine hydrate/ *trans* Comp. (mol/mol)	Temp. (°C)	Time (hr)	Reaction mixture[a] (%)	Recovered *trans* comp.[b] (%)	*cis* Isomers[b] (%)	(mp °C)
Acid (Ia)	1.0	65	3	80.0	50.0	50.0(Ib)	(183—184)[d]
(177—178)[c]	1.3	65	3	75.4	28.1	71.9	
	1.5	65	3	72.3	0	100[e]	
	2.0	65	3	trace			
	2.0	40	3	75.6	82.6	17.4	
Methyl ester (VIIa)	1.0	10	4	100	100[e]	0	
(98—99)[f]	1.0	20	4	44.4	58.1	0.5(VIIb)	(134—135)[f]
	1.0	24	4	40.6	41.9	4.9	
	1.0	40	1	39.0	52.3	trace	
Benzyl ester(VIIIa)	1.0	40	2.5	37.4	46.0	3.7(VIIIb)	(109—110)
(99—100)	1.0	60	1	48.6	0	53.8	
	1.0	65	1	45.5	0	63.8	
Ethyl ester(IXa)	1.0	25	2.5	38.0	100[e]	0 (IXb)	(152—153)[g]
(68—70)[h]	1.0	50	1.5	23.0	100[e]	0	

a) Yields of crude materials. b) Pure yields, calculated on the basis of crude reaction mixture. c) Lit, mp 177—178°C.[7] d) Lit, mp 176—177°C, reddish plates.[7] e) Purity was satisfactory without purifications. f) Lit, mp 98—99°C and 134—135°C.[6d] g) Prepared from *cis* acid. h) Lit, 68—70°C.[7]

TABLE 2. SPECTROSCOPIC DATA FOR THE GEOMETRICAL ISOMERS OF 3-(5-NITRO-2-FURYL)-2-(2-FURYL)ACRYLIC ACID AND ITS METHYL ESTER

	Acid		Methyl ester	
	Ia	Ib	VIIa	VIIb
mp (°C)	177—178	183—184	98—99	134—135
NMR (δ) in DMSO-d_6				
Vinyl proton	7.42(1H, s)	6.98(1H, s)	7.47(1H, s)	7.06(1H, s)
Nitrofuran ring proton				
-4-H	7.67(1H, d, J=4.0 Hz)	7.71(1H, d, J=4.0 Hz)	7.65(1H, d, J=4.0 Hz)	7.70(1H, d, J=4.0 Hz)
-3-H	6.98(1H, d, J=4.0 Hz)	7.02(1H, d, J=4.0 Hz)	6.97(1H, d, J=4.0 Hz)	7.02(1H, d, J=4.0 Hz)
Furan ring proton				
-3-H	6.97(1H, m)	6.81(1H, m)	6.97(1H, m)	6.75(1H, m)
Other proton				
COOH[a]	*ca.* 7.00	*ca.* 7.81		
$COOCH_3$			3.83(3H, s)	3.99(3H, s)
UV mμ (ε)[b]	307 (9580)	302(12240)	305(10751)	301(10783)
	401(16100)	412(26020)	396(15204)	401(18632)
IR (cm^{-1}) with KBr				
C=O	1693	1705	1712	1730

a) The signal was overlapped with ring protons and disappeared by treating with deuterium oxide.
b) The spectra of Ia and Ib were recorded in methanol, and of VIIa and VIIb were in ethanol previously reported[6d] by the author *et al.*

except for the cases of the methyl (VIIa) and ethyl esters (IXa); the methyl ester, VIIa, was isomerized to its isomer (VIIb) in a lower yield but the ethyl ester (IXa)[7] was not. Furthermore, the author confirmed this reaction to be irreversible (Ib, VIIb, and VIIIb–⤫→Ia, VIIa, and VIIIa). The isomerization reaction of Ia also took place with sodium hydroxide, but those of the acids (Ia and Ib) and their esters (VIIa, b, VIIIa, b, and IXa) did not occur by means of an acid catalyst such as hydrochloric acid.

The structures of the acids (Ia and Ib) and their methyl esters (VIIa and VIIb) were determined by means of a study of their NMR spectra (Table 2); in the spectra, the chemical shift of the vinyl proton of Ia appeared at a lower magnetic field than that of Ib (Δ_{tc} 0.44 ppm), and also, in the case of the two methyl esters (VIIa and VIIb), the vinyl proton of VIIa revealed a signal lower than that of VIIb (Δ_{tc}

0.41 ppm). The conclusions may be reached from these results that both Ia and VIIa are *trans* and that the other two (Ib and VIIb) are *cis*. A similar conclusion may be reached as to the conformation of the other esters (VIIIa, b, and IXa). The structures of the *cis* esters were further confirmed by the treatment of chloride of the *cis* acid Ib with alcohols to afford the same *cis* esters. Thus, the *cis* isomer (IXb) of the ethyl ester, which could not be obtained by the isomerization of IXa, was prepared (Chart 2). Similarly, the 1,3,4-thiadiazole V was also produced from the *cis* acid Ib *via* its acyl thiosemicarbazide (IIb).

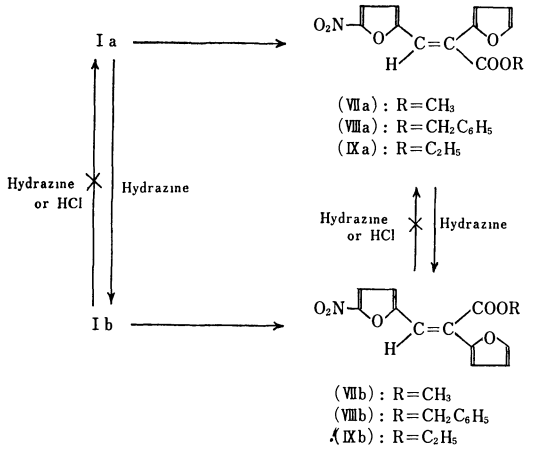

Chart 2

In conclusion, the conformation of V was determined to be *cis* and the compound, IV, which was derived from the *trans* acid, Ia, *via* its acyl thiosemicarbazide, IIa, was determined to be *trans*, since the posibility of the acid-catalytic isomerization of the starting acids (Ib and Ia) during the synthetic routes could be ruled out. The spectral data of these compounds (IV and V) also supported the above conclusion. In the UV spectra, the absorption maximum of V was observed at a slightly shorter wavelength and the extinction coefficient was larger than that of IV (Fig. 1). The IR spectrum of IV contained two medium NH_2 bands, at 3360 and 3300 cm^{-1}, and a medium C=N band at 1645 cm^{-1} due to the thiadiazole ring vibration. However, in the spectrum of V, a medium band (3400 cm^{-1}), a weak band (3300 cm^{-1}), and two medium C=N bands (1640 and 1615 cm^{-1}) were observed (Fig. 2). In comparison with the NMR spectra between IV and V (Fig. 3), the chemical shift of the NH_2 proton of IV was observed at a slightly lower magnetic field than that of V.

IV and V afforded the 2-acylamino (IVa—c and Va—c) and 2-hydroxymethylamino (IVd and Vd) derivatives respectively, when treated with acid anhydrides and 37% formaldehyde respectively in the usual way. 2-Methylamino (Xa), 2-ethylamino (Xb), and 2-anilino-5-[2-(5-nitro-2-furyl)-1-(2-furyl)vinyl]-1,3,4-thiadiazole (Xc) were prepared by the treatment of the corresponding 4-substituted 1-[3-(5-nitro-2-furyl)-2-(2-furyl)acryloyl]thiosemicarbazides (IIIa—c)[1] with phosphoryl chloride.

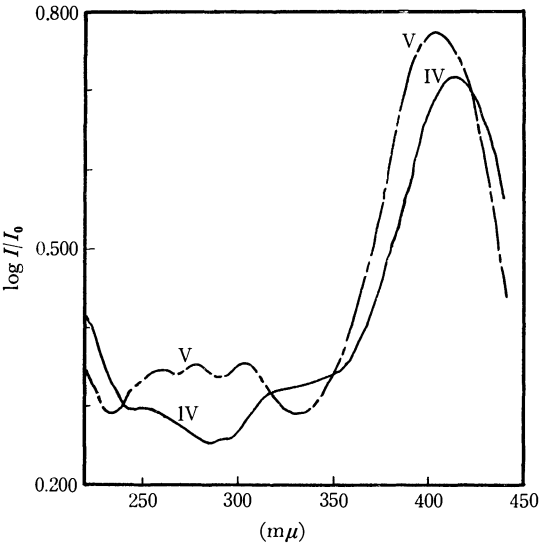

Fig. 1. UV spectra of IV and V (EtOH).

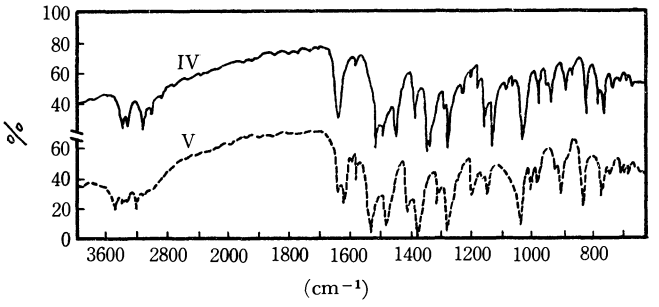

Fig. 2. IR spectra of IV and V (KBr).

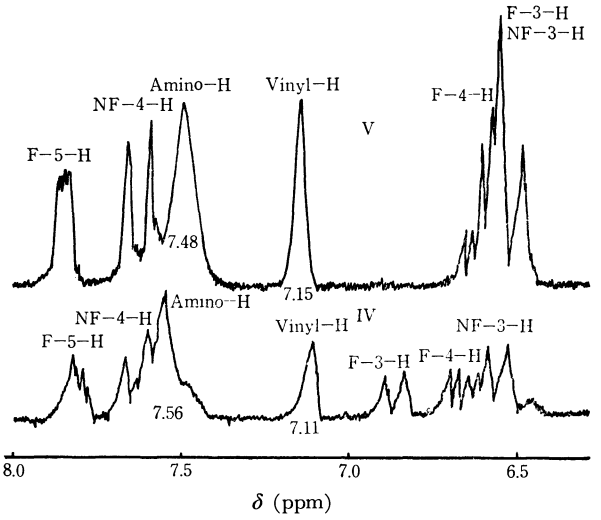

Fig. 3. NMR spectra of IV and V (DMSO-d_6).

F-5-H: C_5-H of furan ring

NF-4-H: C_4-H of 5-nitro-2-furan ring

5-[2-(5-Nitro-2-furyl)-1-(2-furyl)vinyl]-2-amino-1,3,4-oxadiazole (XI) was prepared according the method of a previous paper.[8b] Two monoacetyl derivatives, XIa and XIIa, were isolated on the treatment of XI with acetic anhydride in refluxing dioxane.

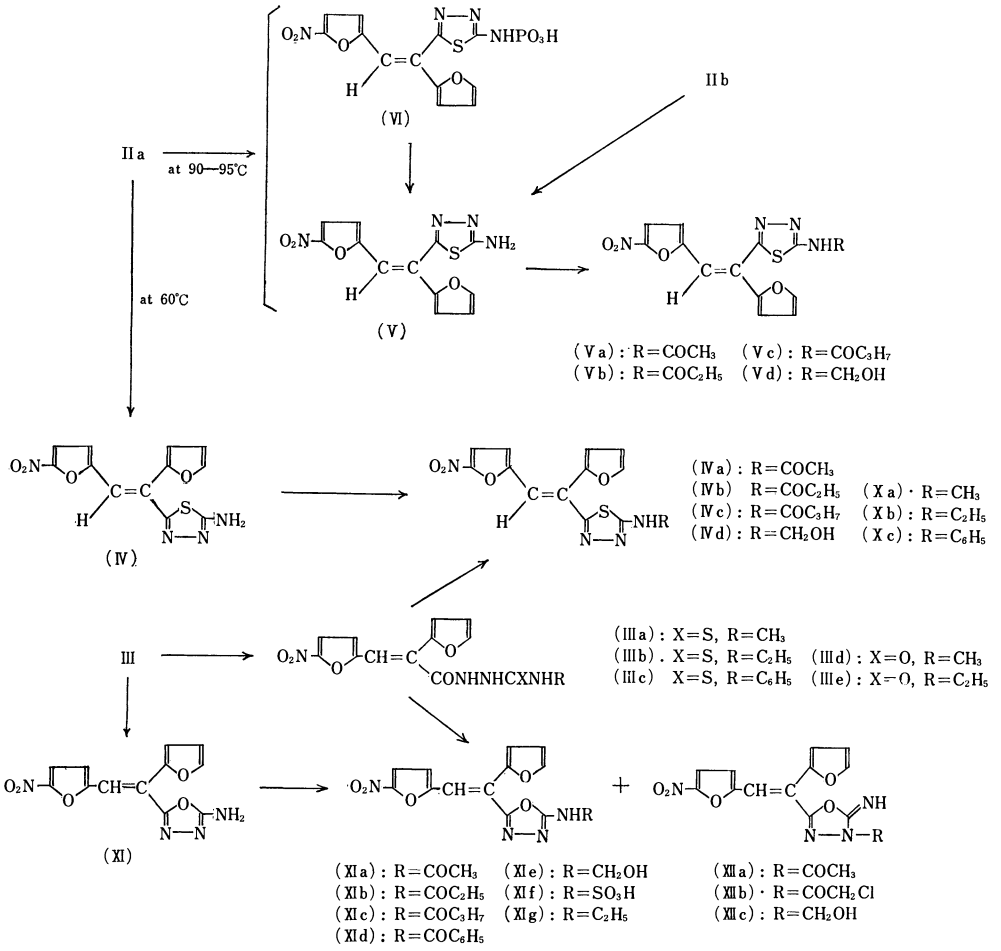

Chart 3

When XI was treated with boiling acetic anhydride without dioxane, XIIa was obtained as the main product. The compound XIa was a normal 2-acetylamino derivative, and the structure of XIIa was confirmed to be that of a ring acetyl compound, 5-[2-(5-nitro-2-furyl)-1-(2-furyl)vinyl]-3-acetyl-1,3,4-oxadiazol-2-imine, on the basis of the analytical and spectral data. In the IR spectra, both the C=O and C=N stretching frequencies of XIIa were moved, the former to higher frequencies, and the latter to lower, in the order of 20 cm^{-1} compared with those of XIa. A ring-acylated XIIa-type compound, 5-[2-(5-nitro-2-furyl)-1-(2-furyl)vinyl]-3-chloroacetyl-1,3,4-oxadiazol-2-imine (XIIb), was also produced by the reaction of XI with chloroacetic anhydride in a similar manner. By the reaction of XI with propionic and butyric anhydrides and benzoyl chloride, the corresponding 2-acylamino-type compounds, XIb, XIc, and XId respectively, were obtained. The hydroxymethylation of XI was carried out by treating it with 37% formaldehyde in *N*,*N*-dimethylformamide; this afforded two products, 5-[2-(5-nitro-2-furyl)-1-(2-furyl)vinyl]-2-hydroxymethylamino-1,3,4-oxadiazole (XIe) and 5-[2-(5-nitro-2-furyl)-1-(2-furyl)vinyl]-3-hydroxymethyl-1,3,4-oxadiazol-2-imine (XIIc).

When XI was treated with chlorosulfonic acid in refluxing ethyl acetate, 5-[2-(5-nitro-2-furyl)-1-(2-furyl)-vinyl]-2-hydrosulfoamino-1,3,4-oxadiazole (XIf) was obtained as its monohydrate. The IR spectrum had a strong absorption band at 1740 cm^{-1} due to the ring C=N stretching frequency, which was moved to abnormally higher frequencies by the interaction of a SO_3H group.

An attempt to prepare 2-substituted amino derivatives from the corresponding 4-substituted 1-[3-(5-nitro-2-furyl)-2-(2-furyl)acryloyl]semicarbazide (IIId, e) by the use of phosphoryl chloride was unsuccessful except for 2-ethylamino-5-[2-(5-nitro-2-furyl)-1-(2-furyl)vinyl]-1,3,4-oxadiazole (XIg).

Microbiological Assays.[11] The antibacterial activities of the 5-nitrofuran compounds in response to ten microorganisms were examined (Table 3). The minimum amounts necessary for the complete inhibition of growth were determined by the dilution method, using the usual bouillon agar medium. As is shown in Table 3, *cis* and *trans* 5-[2-(5-nitro-2-furyl)-1-(2-furyl)vinyl]-2-amino-1,3,4-thiadiazole (V and IV) and -1,3,4-oxadiazole (XI) were found to exhibit strong antibacterial activity against most of the microorganisms employed. The antibacterial activity showed little difference between the *cis* and *trans* isomers of 1,3,4-thiadiazole and its 2-acylamino derivatives. 2-Hydroxymethylamino derivatives (Vd and

11) The author is indebted to Dr. R. Ueno and his staff of Ueno Pharmaceutical Company, Ltd., for the assay.

Table 3. Inhibitory activity of twenty-one compounds on microorganisms

Minimum inhibitory concentration, μg/ml

Compound		*Di. pneumoniae* Dp-1	*Str. haemolyticus* Group A 089	*St. aureus* 209P	*B. subtilis* PCI-219	*Sal. enteritidis* 1891	*Sal. pullorum* Chuyu 114	*E. coli* O-55	*Kle. pneumoniae* ST-101	*Pr. vulgaris* HX 19	*Ps. aeruginosa* Iijima
2-Amino-1,3,4-thiadiazole	(IV) *t*	<0.15	<0.15	0.8	<0.2	0.8	0.8	3	0.8	3	0.8
	(V) *c*	<0.15	0.3	0.8	<0.2	1.5	1.5	1.5	0.4	1.5	1.5
2-Phosphoric amide-	(VI) *c*	>0.15	>0.15	0.8	<0.2	0.8	3	3	0.8	1.5	1.5
2-Acetylamino-	(IVa) *t*	2.5	1.2	1.5	<0.2	>12.5	>12.5	>12.5	>12.5	>12.5	>12.5
	(Va) *c*	5	0.6	1.5	0.8	6	25	25	12.5	25	>25
2-Propionylamino-	(IVb) *t*	>5	1.2	>6	0.8	>6	>6	>6	>6	>6	>6
	(Vb) *c*	20	2.5	3	0.4	>25	>25	>25	25	>25	>25
2-Butyrylamino-	(IVc) *t*	>5	>5	>6	0.4	>6	>6	>6	>6	>6	>6
	(Vc) *c*	>20	20	>25	0.4	>25	>25	>25	>25	>25	>25
2-Hydroxymethylamino-	(Vd) *c*	0.3	<0.15	0.8	<0.2	0.8	1.5	1.5	0.4	1.5	1.5
2-Methylamino-	(Xa)	3	1.5	0.8	<0.2	1.5	6	12.5	1.6	1.6	25
2-Ethylamino-	(Xb)	12.5	6.25	3.13	1.56	25	>25	25	6.25	12.5	>25
2-Phenylamino	(Xc)	>1.2	>1.2	>1.5	0.4	>1.5	>1.5	>1.5	>1.5	>1.5	>1.5
2-Amino-1,3,4-oxadiazole	(XI)	<0.15	0.6	0.4	<0.2	1.5	0.8	3	3	1.5	<0.2
2-Acetylamino-	(XIa)	0.31	0.62	0.78	1.56	6.25	3.13	6.25	25	3.13	3.13
2-Propionylamino-	(XIb)	1.2	0.6	0.8	0.4	1.5	3	12	15	6	25
2-Butyrylamino-	(XIc)	5	2.5	1.5	0.4	3	6	12	3	6	12
2-Hydroxymethylamino-	(XIe)	1.2	1.2	0.8	0.4	1.5	6	3	1.5	6	3
2-Hydrosulfoamino-	(XIf)	20	20	>25	6	>25	>25	>25	>25	>25	>25
3-Acetyl-1,3,4-oxadiazol-2-imine	(XIIa)	0.6	0.6	0.8	<0.2	0.8	3	12	1.5	3	3
3-Hydroxymethyl-	(XIIc)	2.5	1.2	3	0.4	1.5	6	6	12	12	25
Contrast[a]		10	0.6	1.5	0.4	0.8	1.5	3	0.4	6	3

a) 3-(5-Nitro-2-furyl)-2-(2-furyl)acrylic amide was employed in the test.

XIe) still retain the high antibacterial activity of the mother compounds (V and XI). 3-Substituted 1,3,4-oxadiazol-2-imine-type compounds (XIIa and XIIc) slightly lowered the activity of XI. The substituted amino derivatives showed decreasing activity in the order: $R=CH_2OH \gg CH_3 \geq COCH_3 \approx C_2H_5 > COC_2H_5 > COC_3H_7$, SO_3H. This decreasing tendency of the activity is parallel with the increase in the carbon number of the substituent, R. These results suggest that the free amino group may be one of the dominant factors in antibacterial activity and that the long carbon chain blocks the reactivity of the amino group by steric hindrance.

Experimental

All the melting and decomposing points are uncorrected. Microanalyses were carried out with a Yanagimoto C. H. N. Corder, MT-2 type. The ultraviolet absorption spectra (UV) were recorded on a Shimadzu photoelectric spectrophotometer, Model QV-50. The infrared absorption spectra (IR) were obtained with a Shimadzu IR-27 S spectrophotometer. The nuclear magnetic resonance spectra (NMR) were determined by means of a Nihon-Denshi NMR spectrometer, JMN C-60HL (60 MHz). All the spectra were measured in dimethylsulfoxide, with tetramethylsilane as the internal standard; the peak positions were expressed in δ-values.

trans-*5-[2-(5-Nitro-2-furyl)-1-(2-furyl)vinyl]-2-amino-1,3,4-thiadiazole (IV).* This product was prepared according to a procedure described before.[8a] Red needles (recrystallized from methanol); mp 169—170°C; decomposition. The yield was 55%. UV: λ_{max}^{EtOH} mμ(ε) 252sh(8652), 317sh (9284), 414(21104).

cis-*5-[2-(5-Nitro-2-furyl)-1-(2-furyl)vinyl]-2-amino-1,3,4-thiadiazole (V) and Its 2-Phosphoric Amide Compound (VI). From 1-[3-(5-nitro-2-furyl)-2-(2-furyl)acryloyl]thiosemicarbazide (IIa):* A mixture of 16.1 g (50 mmol) of IIa[8a] and 50 ml of phosphoryl chloride was heated for 2 hr on a steam bath, cooled, and then poured onto ice with agitation. The solidified material was filtered off and washed with hot water. The crude product was purified by recrystallization from methanol to afford 5.75 g (37.8%) of yellow plates (V): mp 178—179°C dec. UV: λ_{max}^{EtOH} mμ(ε) 261(10126), 278(10617), 303(10757), 405(22750).

Found: C, 47.60; H, 2.90; N, 17.90%. Calcd for $C_{12}H_8N_4O_4S$: C, 47.36; H, 2.65; N, 18.41%.

A small amount of an oily substance was separated during the recrystallization of V; it solidified on standing and was crystallized from methanol to give 0.85 g (4.4%) of orange needles (VI), mp 160°C dec. Compound VI was easily converted to V by boiling it with water for several minutes. UV: λ_{max}^{EtOH} mμ(ε) 258(10754), 280(10934), 303(10756), 405(24272). IR: (KBr) cm^{-1} 3300(N–H), 1640(C=N). Qualitative analyses: Cl(−), S(+), and P(+).

Found: C, 37.16; H, 2.64; N, 14.19%. Calcd for $C_{12}H_8N_4O_7SP$: C, 37.50; H, 2.34; N, 14.60%.

From cis-*1-[3-(5-Nitro-2-furyl)-2-(2-furyl)acryloyl]thiosemicarbazide (IIb):* The method used here was virtually identical with that described for IV,[8a] but 9.8 g (30 mmol) of IIb were used instead of IIa; a 23% yield of V was obtained. Mp 178—179°C dec, undepressed upon admixture with a sample prepared by the above method.

Compound IIb was obtained by treating *cis* acid chloride

(mp 111—113°C dec) with thiosemicarbazide in dioxane according to a previously-established procedure;[8a] mp 179—180°C dec; yellow needles (methanol). The yield was 67.3%.

Found: C, 44.97; H, 3.61; N, 17.03%. Calcd for $C_{12}H_{10}N_4O_5S$: C, 44.72; H, 3.12; N, 17.39%.

trans-5-[2-(5-Nitro-2-furyl)-1-(2-furyl)vinyl]-2-acetylamino-1,3,4-thiadiazole (IVa). Compound IV (0.9 g, 3 mmol) was covered with acetic anhydride (10 m*l*) and warmed on a steam bath for 1 hr. On cooling, the separated product was collected and washed with water, thus affording 1.0 g (99%) of orange-yellow needles; mp 231—234°C dec. Recrystallization from methanol raised the melting point to 239—239.5°C dec. IR: (KBr) cm^{-1} 1703(C=O).

Found: C, 48.65; H, 3.04; N, 16.20%. Calcd for $C_{14}H_{10}N_4O_5S$: C, 48.56; H, 2.91; N, 16.18%.

cis-5-[2-(5-Nitro-2-furyl)-1-(2-furyl)vinyl]-2-acetylamino-1,3,4-thiadiazole (Va). A similar treatment of 0.9 g (3 mmol) of V instead of IV (0.9 g) afforded 0.93 g (94%) of Va; mp 241°C dec. Crystallization from methanol gave yellow needles; mp 243°C dec. IR: (KBr) cm^{-1} 1709(C=O).

Found: C, 48.48; H, 2.77; N, 15.92%. Calcd: same value as the IVa above.

trans-5-[2-(5-Nitro-2-furyl)-1-(2-furyl)vinyl]-2-propionylamino-1,3,4-thiadiazole (IVb). This was prepared in the same way as was IVa, but using propionic anhydride (8 m*l*). In this way, 1.05 g (quantitative) of IVb were obtained; mp 244—245°C dec. Crystallization from 2-methoxyethanol gave orange needles; mp 248—249°C dec. IR: (KBr) cm^{-1} *ca.* 2920—2800(CH_3, CH_2), 1702(C=O).

Found: C, 50.13; H, 3.72; N, 15.57%. Calcd for $C_{15}H_{12}N_4O_5S$: C, 50.00; H, 3.53; N, 15.55%.

cis-5-[2-(5-Nitro-2-furyl)-1-(2-furyl)vinyl]-2-propionylamino-1,3,4-thiadiazole (Vb). This was prepared by the method used for IVa, using 0.3 g (1 mmol) of V and 3 m*l* of propionic anhydride. Work-up as above afforded 0.29 g (84.2%) of Vb as orange needles; mp 230°C dec (from 2-methoxyethanol). IR: (KBr) cm^{-1} *ca.* 2900—2780(CH_3, CH_2), 1700(C=O).

Found: C, 49.87; H, 3.19; N, 15.14%. Calcd: same value as the IVb above.

trans-5-[2-(5-Nitro-2-furyl)-1-(2-furyl)vinyl]-2-butyrylamino-1,3,4-thiadiazole (IVc). Yellow needles; mp 217.5—218°C dec (2-methoxyethanol). The yield was 91%. IR: (KBr) cm^{-1} *ca.* 2800(CH_3, CH_2), 1696(C=O).

Found: C, 51.56; H, 3.44; N, 14.66%. Calcd for $C_{16}H_{14}N_4O_5S$: C, 51.33; H, 3.77; N, 14.79%.

cis-5-[2-(5-Nitro-2-furyl)-1-(2-furyl)vinyl]-2-butyrylamino-1,3,4-thiadiazole (Vc). Orange needles; mp 186°C dec (2-methoxyethanol). Yield: 72.5%. IR: (KBr) cm^{-1} *ca.* 2900(CH_3, CH_2), 1700(C=O).

Found: C, 51.24; H, 3.66; N, 15.35%. Calcd: same value as the IVc above.

trans-5-[2-(5-Nitro-2-furyl)-1-(2-furyl)vinyl]-2-hydroxymethylamino-1,3,4-thiadiazole (IVd). A mixture of IV (0.3 g, 1 mmol) and 37% formaldehyde (3 m*l*) was warmed at 60°C for 1 hr. After cooling, 6 m*l* of water were added. The solidified product was collected and washed with water, ether, and ethanol successively. The product was obtained as an orange powder, mp 121°C dec., weighing 0.27 g (80.5 %). Recrystallization was unsuccessful because of the instability.

Found: C, 46.31; H, 2.57; N, 16.91%. Calcd for $C_{13}H_{10}N_4O_5S$: C, 46.70; H, 2.99; N, 16.80%.

cis-5-[2-(5-Nitro-2-furyl)-1-(2-furyl)vinyl]-2-hydroxymethylamino-1,3,4-thiadiazole (Vd). A similar treatment of V instead of IV afforded 0.23 g (72.1%) of an orange powder, Vd; mp 168°C dec.

Found: C, 46.49; H, 3.03; N, 16.77%. Calcd: same value as the IVd above.

5-[2-(5-Nitro-2-furyl)-1-(2-furyl)vinyl]-2-methylamino-1,3,4-thiadiazole (Xa). 4-Methyl-1-[3-(5-nitro-2-furyl)-2-(2-furyl)acryloyl]thiosemicarbazide (IIIa)[1] (1.8 g, 5.4 mmol) and phosphoryl chloride (10 m*l*) were heated together under reflux for 2 hr. After cooling, the mixture was poured onto crushed ice, and the precipitate was filtered, washed with water, and extracted with hot ether (*ca.* 4 *l*). On the concentration of the extracts, a red-colored residue was obtained; mp 120—155°C; 0.7 g. Recrystallization from benzene gave red prisms; mp 179—180°C dec. The yield was 0.31 g (18%).

Found: C, 49.41; H, 3.17; N, 17.92%. Calcd for $C_{13}H_{10}N_4O_4S$: C, 49.06; H, 3.14; N, 17.61%.

5-[2-(5-Nitro-2-furyl)-1-(2-furyl)vinyl]-2-ethylamino-1,3,4-thiadiazole (Xb). This was prepared in a way similar to that used for Xa above, using IIIb ($R=C_2H_5$)[1] (2 g, 5.7 mmol) and phosphoryl chloride (5 m*l*). Red prisms; mp 171°C (benzene). Yield, 26%.

Found: C, 51.06; H, 3.57; N, 16.33%. Calcd for $C_{14}H_{12}N_4O_4S$: C, 50.60; H, 3.61; N, 16.87%.

5-[2-(Nitro-2-furyl)-1-(2-furyl)vinyl]-2-anilino-1,3,4-thiadiazole (Xc). A mixture of 1.5 g (20 mmol) of acetyl chloride and IIIc ($R=C_6H_5$) (2 g, 5 mmol) was heated at 45—55°C for 20 min, and then it was poured into water. Cooling gave a crude product; mp 168—178°C dec. Crystallization from benzene provided 0.45 g (23.7%) of red crystals; mp 209.5—211°C dec.

Found: C, 55.74; H, 3.17; N, 14.45%. Calcd for $C_{18}H_{12}N_4O_4S$: C, 55.68; H, 3.16; N, 14.74%.

Compound IIIc was obtained as follows: the hydrazide III[6d] (5.2 g, 20 mmol) and phenyl isothiocyanate (3.24 g, 24 mmol) were heated under reflux in 100 m*l* of methanol for 1.5 hr. Cooling provided 6.34 g (79.7%) of the product, IIIc; mp 163—164°C dec. Recrystallization from ethanol gave orange-yellow prisms; mp 166—167°C dec.

Found: C, 54.10; H, 3.69; N, 14.38%. Calcd for $C_{18}H_{14}N_4O_5S$: C, 54.27; H, 3.52; N, 14.07%.

5-[2-(5-Nitro-2-furyl)-1-(2-furyl)vinyl]-2-amino-1,3,4-oxadiazole (XI). This was obtained according to a procedure previously described.[8b] Deep red needles; mp 224—225°C dec (dioxane). Yield, 90%. The product, XI, was shown to be the same by a study of its IR spectrum and by its failure to depress the melting point when mixed with an authentic sample. UV: λ_{max}^{EtOH} mμ(ε) 246(12733), 407(25933). IR: (KBr) cm^{-1} 3420 and 3280(NH_2), 1655(C=N).

5-[2-(5-Nitro-2-furyl)-1-(2-furyl)vinyl]-2-acetylamino-1,3,4-oxadiazole (XIa) and 5-[2-(5-Nitro-2-furyl)-1-(2-furyl)vinyl]3-acetyl-1,3,4-oxadiazol-2-imine (XIIa). A solution of 4.32 g (15 mmol) of XI and 2.04 g (20 mmol) of acetic anhydride in 200 m*l* of dioxane was heated under reflux for 5 hr. The solvents and the excess acid anhydride were then removed under reduced pressure. The residual crude product was purified by recrystallization from methanol to give a mixture (XIa and XIIa) as light orange-small needles, mp 218—219°C dec, weighing 4.9 g (almost quantitative). IR: (KBr) cm^{-1} 3240(N–H), 1735—1730(C=O), 1660 sh and 1640 (C=N).

Found: C, 51.37; H, 3.10; N, 17.00%. Calcd for $C_{14}H_{10}N_4O_6$(XIa and XIIa): C, 50.91; H, 3.03; N, 16.98%.

This mixture was extracted with 100 m*l* of hot benzene. On the cooling of the benzene extracts, the precipitates were filtered and then they were combined with the solid residue. Two recrystallizations from toluene afforded the pure material of XIa as light brown prisms, mp 189—190°C dec., weighing 0.3 g (6%). The benzene filtrate was taken to dryness under

reduced pressure. The residue and 200 ml of toluene were boiled, filtered, and then recrystallized from 2-methoxyethanol and then from dioxane to give XIIa as orange needles; mp 233—234°C dec. The yield was 0.54 g (11%). IR: (KBr) cm^{-1} XIa; 3240(N–H), 1720(C=O), 1660(C=N). XIIa; 3240(N–H), 1740(C=O), 1640(C=N).

Found: XIa; C, 51.14; H, 3.19; N, 17.11%. XIIa: C, 51.06; H, 2.94; N, 16.99%. Calcd for $C_{14}H_{10}N_4O_6$: C, 50.91; H, 3.03; N, 16.89%.

The 3-acetyl derivative, XIIa, was obtained by the following procedure. Compound XI (4.32 g, 15 mmol) was covered with acetic anhydride (6—10 ml) and heated under a reflux for 10 min. Cooling provided 2.92 g (59.1%) of the product; mp 221—223°C dec. Subsequent crystallization from dioxane gave orange needles; mp 233—234°C dec. The melting point of this product was not depressed by admixture with the sample of XIIa described above. From the mother filtrate small amounts of XIa and XIIa were obtained.

5-[2-(5-Nitro-2-furyl)-1-(2-furyl)vinyl]-3-chloroacetyl-1,3,4-oxadiazol-2-imine (XIIb). The procedure outlined above for XIa was followed using chloroacetic anhydride (3.4 g, 20 mmol). The product was obtained as fine yellow crystals; mp 213—214°C dec (dioxane). Yield: 4.74 g (86.8%). IR: (KBr) cm^{-1} 3240(N–H), 1749(C=O), 1640(C=N).

Found: C, 44.51; H, 2.38; N. 15.57%. Calcd for $C_{14}H_9N_4O_6Cl$: C, 44.26; H, 2.55; N, 15.89%.

5-[2-(5-Nitro-2-furyl)-1-(2-furyl)vinyl]-2-propionylamino-1,3,4-oxadiazole (XIb). A mixture of 1.44 g (5 mmol) of XI and 30 ml of propionic anhydride was heated at 95—100°C for 2 hr. The excess acid anhydride was removed *in vacuo*, and the residue was washed with water to afford a yellow powder, mp 215—217°C dec, weighing 1.74 g (quantitative). Subsequent recrystallization from methanol gave yellow needles; 216—217°C dec. IR: (KBr) cm^{-1} 2900(CH_2), 1725(C=O), 1630(C=N).

Found: C, 52.33; H, 3.53; N, 16.45%. Calcd for $C_{15}H_{12}N_4O_6$: C, 52.33; H, 3.49; N, 16.28%.

5-[2-(5-Nitro-2-furyl)-1-(2-furyl)vinyl]-2-butyrylamino-1,3,4-oxadiazole (XIc). The procedure described above for XIb was employed using butyric anhydride (0.87 g, 5.5 mmol) in 50 ml of dioxane. A work-up as above afforded 1.1 g (58.5%) of ochreous needles; mp 177—178°C dec (dichloroethane). IR: (KBr) cm^{-1} 2900(CH_2), 1725(C=O), 1630(C=N).

Found: C, 53.60; H, 4.09; N, 15.45%. Calcd for $C_{16}H_{14}N_4O_6$: C, 53.63; H, 3.93; N, 15.64%.

5-[2-(5-Nitro-2-furyl)-1-(2-furyl)vinyl]-2-benzoylamino-1,3,4-oxadiazole (XId). The procedure outlined above for XIb was followed using benzoyl chloride (1.06 g, 7.5 mmol) in 50 ml of dioxane. Ochre-colored needles; mp 218—219°C dec (methanol). Yield: 1.1 g (69.4%).

Found: C, 57.86; H, 3.18; N, 14.16%. Calcd for $C_{19}H_{12}N_4O_6$: C, 58.16; H, 3.06; N, 14.29%.

5-[2-(5-Nitro-2-furyl)-1-(2-furyl)vinyl]-2-hydroxymethylamino-1,3,4-oxadiazole (XIe) and 5-[2-(5-Nitro-2-furyl)-1-(2-furyl)-vinyl]-3-hydroxymethyl-1,3,4-oxadiazol-2-imine (XIIc). A mixture of XI (1.44 g, 5 mmol), 37% formaldehyde (0.75 g, 9.3 mmol), and 50 ml of *N,N*-dimethylformamide was heated at 60°C for 2 hr. The resulting solution was taken to dryness *in vacuo*, and the residue was washed with ether and methanol. Subsequent reprecipitation from methyl acetate-ether gave 0.21 g of a dark yellow powder XIIc; mp 148—152°C dec. Repeated similar treatment raised the melting point to 163—165°C dec. Yield: 0.12 g (7.6%). On the concentration of the mother methyl acetate - ether filtrate, the product was separated as a dark brown powder, mp 128—130°C, weighing 0.39 g (24.6%). Reprecipitation from methyl acetate - ether brought the melting point to 134—135°C; orange powder; XIe.

Found: XIe; C, 49.50; H, 3.00; N, 17.93%. XIIc; C, 49.36; H, 2.89; N, 17.72%. Calcd for $C_{13}H_{10}N_4O_6$: C, 49.06; H, 3.17; N, 17.61%.

5-[2-(5-Nitro-2-furyl)-1-(2-furylvinyl]-2-hydrosulfoamino-1,3,4-oxadiazole (XIf). To a stirred, ice-cooled suspension of XI (1.44 g, 5 mmol) in 50 ml of ethyl acetate, we added, drop by drop, a solution of chlorosulfonic acid (10 ml) in 50 ml of ethyl acetate. After the addition, the suspension was heated under reflux for 5 hr and cooled, and the product was collected by filtration; the product was then washed with cold ethyl acetate and crystallized from methanol to give 0.42 g (22.4%) of XIf as yellow needles; mp 190°C (darkened) (depressed to 160—163°C on admixture with the sulfate of XI of mp 174—175°C dec). IR: (KBr) cm^{-1} 1740(C=N), 1205 and 1042(SO_2), 640(S–O).

Found: C, 37.29; H, 2.68; N, 14.01%. Calcd for $C_{12}H_8N_4O_8S \cdot H_2O$: C, 37.31; H, 2.59; N, 14.51%.

5-[2-(5-Nitro-2-furyl)-1-(2-furyl)vinyl-2-ethylamino-1,3,4-oxadiazole (XIg).[1] A suspension of 4-ethyl-1-[3-(5-nitro-2-furyl)-2-(2-furyl)acryloyl]semicarbazide (IIIe) (0.67 g, 2 mmol) in phosphoryl chloride (30 ml) was heated gently at 70°C for 4 hr. The resulting solution was taken to dryness *in vacuo*, and the residue was dissolved in 200 ml of ethanol. On cooling, orange needles precipitated; mp 194—195°C dec; weight, 0.53 g (84.1%).

Found: C, 53.11; H, 3.95; N, 17.70%. Calcd for $C_{14}H_{12}N_4O_5$: C, 53.16; H, 3.95; N, 17.72%.

Compounds IIIe and IIId were prepared as follows: the hydrazide III (2.63 g, 10 mmol) and ethyl (or methyl) isocyanate (10 mmol) were heated together at 60—65°C in 50 ml of ethanol (100 ml of methanol) for 2 hr. Cooling provided a crude product, and then recrystallization was carried out. IIIe; yellow needles (ethanol); mp 157—158°C dec. Yield: 2.4 g.

Found: C, 50.44; H, 4.08; N, 16.57%. Calcd for $C_{14}H_{14}N_4O_6$: C, 50.29; H, 4.19; N, 16.76%. IIId (R=CH_3); yellow needles (methanol); mp 161.5—162°C dec. Yield: 2.1g.

Found: C, 48.68; H, 3.59; N, 17.32%. Calcd for $C_{13}H_{12}N_4O_6$: C, 48.75; H, 3.75; N, 17.50%.

Isomerization of 3-(5-Nitro-2-furyl)-2-(2-furyl)acrylic Acid and Its Esters with Hydrazine Hydrate. A mixture of 10 mmol of *trans* acid (or esters) and 80% hydrazine hydrate in 100 ml of methanol was stirred under the reaction conditions indicated in Table 1. The resulting mixture was neutralized with concentrated hydrochloric acid and then taken to dryness *in vacuo*. The residue was washed with cold water to afford a crude reaction mixture. Fractional crystallization from methanol gave pure isomers; the yields are shown in Table 1.

cis *Acid (Ib)*: yellow needles (50% aqueous methanol); mp 183—184°C dec. Found: C, 52.98; H, 3.26; N, 5.44%. Calcd for $C_{11}H_7NO_6$: C, 53.01; H, 2.83; N, 5.62%.

cis *Benzyl Ester (VIIIb)*: yellow-ochre plates (aq. methanol), mp 109—110°C. Found: C, 64.05; H, 3.84; N, 4.02%. Calcd for $C_{18}H_{13}NO_6$: C, 63.72; H, 3.86; N, 4.13%.

The *cis* acid and its esters were not converted to *trans* isomers under the same reaction conditions.

Another isomerization reaction of each *trans* (or *cis*) acid and its esters was carried out in the presence of hydrochloric acid (1/20 fold mol) in refluxing methanol. No isomerization of these *trans* and *cis* isomers was observed.

Preparation of Esters of 3-(5-Nitro-2-furyl)-2-(2-furyl)acrylic Acid. From Chloride: The esters were prepared in a way similar to that described by Saikachi and Tanaka[7] for

the preparation of the *trans* ethyl ester (IXa). Crystallization from aqueous methanol gave pure esters. Yield: 40—75%.

From Sodium Salt: To a warmed (45°C), stirred suspension of acid (10 mmol), alkyl halide (13 mmol) in 100 m*l* of ethanol, we added, drop by drop, a solution of sodium (10 mg atom) in ethanol (50 m*l*). Then the mixture was heated under reflux for 2 hr. On the concentration of the solution, the product separated along with an inorganic salt was washed with water and subsequently dried. Work-up as above afforded pure esters. Yield: 70—90%.

trans Benzyl ester (VIIIa); orange prisms (aq. methanol); mp 99—100°C. Found: C, 63.78; H, 4.01; N, 4.16%. Calcd for $C_{18}H_{13}NO_6$: C, 63.72; H, 3.86; N, 4.13%. *cis* Ethyl ester (IXb); orange-yellow plates (aq. methanol); mp 152—153°C. Found: C, 56.40; H, 4.01; N, 5.08%. Calcd for $C_{13}H_{11}NO_6$: C, 56.32; H, 3.97; N, 5.05%.

The author wishes to thank Dr. I. Hirao, Professor of Kyushu Institute of Technology, for his many helpful discussions and suggestions.

BULLETIN OF THE CHEMICAL SOCIETY OF JAPAN, VOL. 44, 496—505 (1971)

Optical Activity of Bis-1,1′-spiroindanes. I. Optical Resolution and Absolute Configuration

Sanji HAGISHITA and Kaoru KURIYAMA
Shionogi Research Laboratory, Shionogi & Co., Ltd., Sagisu, Fukushima-ku, Osaka
and
Masanori HAYASHI, Yasuko NAKANO, Keiji SHINGU, and Masazumi NAKAGAWA
Department of Chemistry, Faculty of Science, Osaka University, Toyonaka, Osaka

(Received July 8, 1970)

The resolutions of 6,6′-dihydroxy-3,3,5,3′,3′,5′-hexamethyl-bis-1,1′-spiroindane (IIIa), 3,3,3′,3′-tetramethyl-bis-1,1′-spiroindane-6,6′-dicarboxylic acid (IIIc), and 5,5′-dihydroxy-bis-1,1′-spiroindane (VIII) are reported. The circular dichroism and absorption spectra of these optically active compounds and their derivatives were measured. The spectra were analysed by means of a coupled oscillator model. The relative frequencies and signs of the rotational strengths associated with the *p*-band transition calculated for the (S)-configuration of 6,6′-disubstituted-bis-1,1′-spiroindanes agree with the positions and signs of the CD bands observed for the compounds derived from (−)-IIIc, establishing the absolute configuration of this series. The result was confirmed by the X-ray diffraction study of (−)-7,7′-dibromo-derivatives prepared from (+)-IIIa. It was found that these spiro compounds having the (S)-configuration showed a negative CD band in the longest wavelength region, except for the case in which the effect of the charge transfer between two aromatic chromophores overwhelmed that of the dipole-dipole interaction.

It is well known that, in the chiral molecules with the same two ligands at the tetragonal central atom, $X(A_2B_2)$, there are two types of structures, spiro types I and II[1] (Fig. 1). Several molecules of these types have already been resolved[2] and the absolute configuration of some of them has been determined by chemical methods.[3] It is interesting to study the relations between the structure and the CD spectrum of the molecule having C_2 symmetry like spiro type II bearing the aromatic chromophore at positions A or B, from the standpoint of the determination of the absolute configuration and the origin of the optical rotatory power.

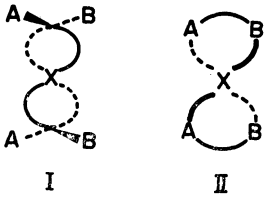

Fig. 1. Chiral molecules of the spiro type.

Curtis and his coworker[4] proved that Barnes's tetrahydroindenoindane derivatives, which were obtained from the reaction of 4-methyl-4-phenylpentane-2-one with acid,[5] had the structures of 3,3,3′,3′-tetramethyl-bis-1,1′-spiroindane. Later the mechanisms of the above reaction were proposed by others.[6] Other bis-1,1′-spiroindane derivatives have also been prepared by Baker and his coworkers and other group[7] by the reaction of phenols and acetone in the presence of acid.

These compounds have rigidly fixed conformation and it is interesting to investigate the spectrum arising from an interaction of the transition dipoles of the same two aromatic chromophores.

1) R. S. Cahn, C. Ingold, and V. Prelog, *Angew. Chem.*, **78**, 413 (1966).

2) a) W. H. Mills and C. R. Nodder, *J. Chem. Soc.*, **117**, 1407 (1920). b) G. Haas and V. Prelog, *Helv. Chim. Acta*, **52**, 1202 (1969).

3) a) G. Krow and R. K. Hill, *Chem. Commun.*, **1968**, 430. b) H. Gerlach, *Helv. Chim. Acta*, **51**, 1587 (1968). c) J. H. Brwester and R. S. Jones, Jr., *J. Org. Chem.*, **34**, 354 (1969).

4) a) R. F. Curtis, *Chem. Ind.* (London), **1960**, 928. b) R. F. Curtis and K. O. Lewis, *J. Chem. Soc.*, **1962**, 418.

5) a) A. Hoffman, *J. Amer. Chem. Soc.*, **51**, 2542 (1929). b) R. A. Barnes and B. D. Beitchman, *ibid.*, **76**, 5430 (1954).

6) L. R. C. Barclay and R. A. Chapman, *Can. J. Chem.*, **42**, 25 (1964).

7) a) W. Baker, *J. Chem. Soc.*, **1934**, 1678. b) C. H. Fisher, R. W. Furlong, and M. Grant, *J. Amer. Chem. Soc.*, **58**, 820 (1936). c) W. Baker and J. C. McGown, *J. Chem. Soc.*, **1938**, 347. d) W. Baker and D. M. Besly, *ibid.*, **1939**, 1421. e) R. F. Curtis, *ibid.*, **1962**, 415.

Chart 1

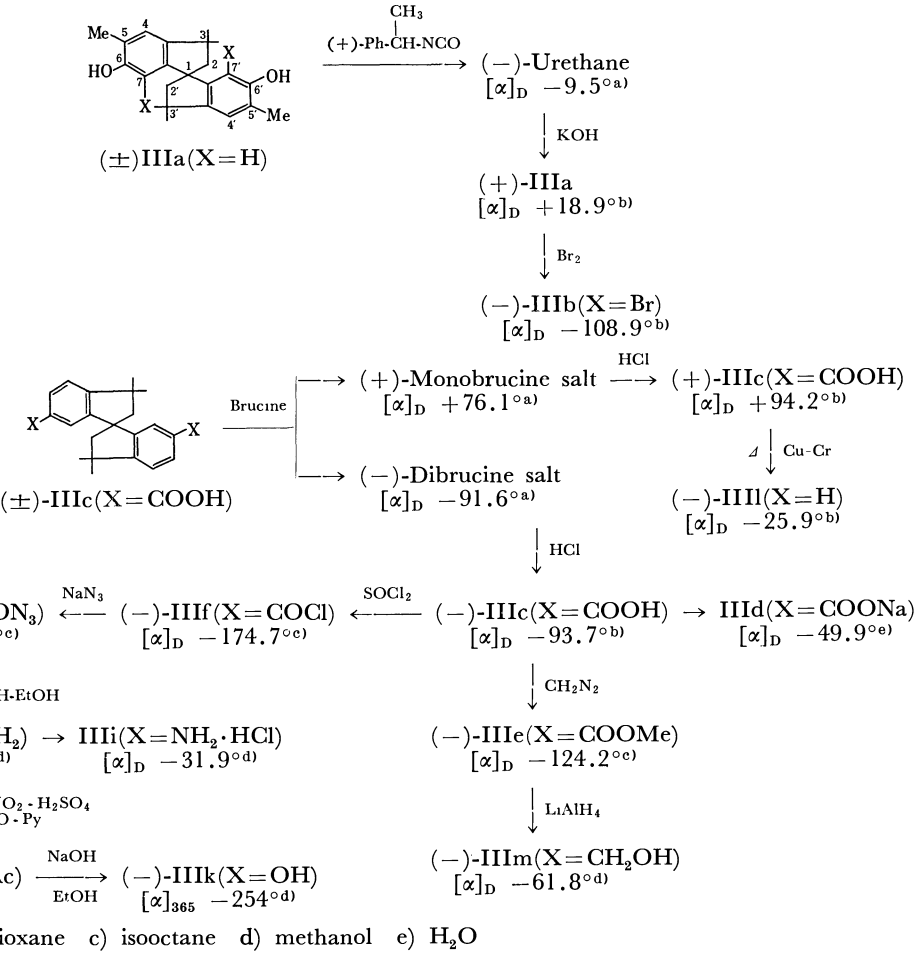

a) $CHCl_3$ b) dioxane c) isooctane d) methanol e) H_2O

We wish to report the resolution and CD spectrum of this type of compound and the theoretical assignments of absolute configurations on some of them.

Resolution of 6,6'-dihydroxy-3,3,5,3',3',5'-hexamethyl-bis-1,1'-spiroindane, IIIa, which was prepared according to the direction of Baker and Besly,[7] was accomplished after a number of experiments[8] by using (+)-phenethylisocyanate.[9] The optically pure (−)-urethane, $[\alpha]_D$ −8.6° ($CHCl_3$), obtained by fractional recrystallization, was hydrolysed with KOH-EtOH (10%) to give (+)-IIIa, $[\alpha]_D$ +19.4° (dioxane), from which (−)-IIIb, $[\alpha]_D$ −108.9° (dioxane), was prepared by the action of bromine in chloroform.

Meanwhile, (−)-isomer of 6,6'-dicarboxylic acid derivative IIIc, $[\alpha]_D$ −93.7° (dioxane), was obtained by the decomposition of (−)-dibrucine salt, $[\alpha]_D$ −91.6° (MeOH), and also another antipode, (+)-IIIc, $[\alpha]_D$ +94.2° (dioxane), was prepared by the decomposition of (+)-monobrucine salt, $[\alpha]_D$ +76.1° (MeOH).

Optically active diamino derivative, (−)-IIIh, $[\alpha]_D$ −144.1° (MeOH), diacetoxy derivative, (−)-IIIj, $[\alpha]_{365}$ −301° (isooctane) and dihydroxy derivative, (−)-IIIk, $[\alpha]_{365}$ −254° (MeOH) were prepared from (−)-IIIc, and also non-substituted deriv-

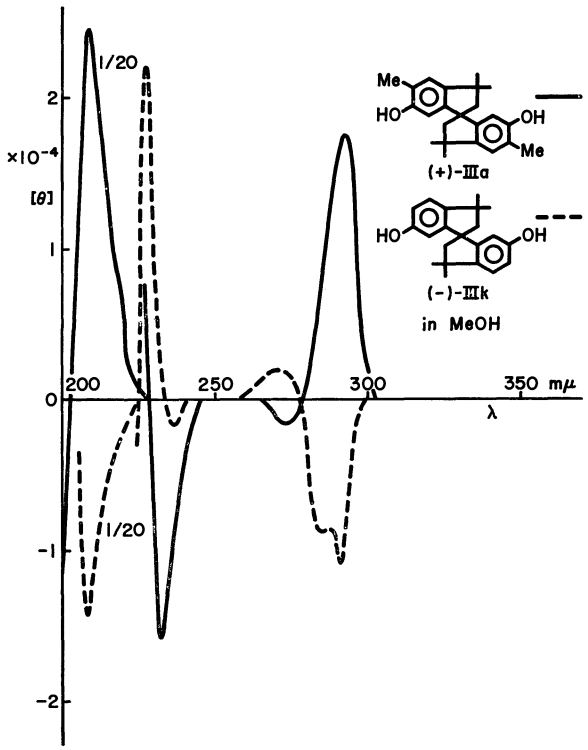

Fig. 2. CD spectra of (+)-IIIa and (−)-IIIk in methanol.

8) All attempts to resolve IIIa employing (+)-10-camphorsulfonic acid chloride, (−)-menthoxyacetic acid chloride and, (+)-α-phenchocomphorone-1-isocyanate failed.

9) T. L. Cairns, *J. Amer. Chem. Soc.*, **63**, 871 (1941).

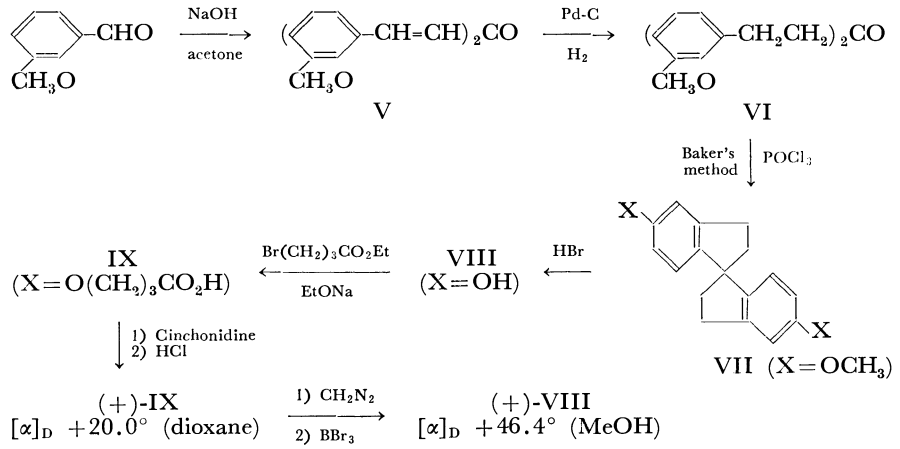

Chart 2

ative, (−)-IIIl, $[\alpha]_D$ −25.9° (dioxane) from (+)-IIIc, according to procedures similar to those used in the racemic ones described in literature.[4] We also obtained di-acid chloride, (−)-IIIf, $[\alpha]_D$ −174.7° (isooctane), and diazide, (−)-IIIg, $[\alpha]_D$ −246.3° (isooctane), stepwisely by applying the Curtius reaction to (−)-IIIc. Dicarbinol, (−)-IIIm, $[\alpha]_D$ −61.8° (MeOH), was prepared by the reduction with $LiAlH_4$ of diester, (−)-IIIe, $[\alpha]_D$ −124.2° (*n*-hexane), which was obtained by the esterification of (−)-IIIc with diazomethane. Configurational correlation among these compounds is shown in Chart 1. In connection with these 6,6′-disubstituted spiroindanes, optically active 5,5′-dihydroxy derivative IX was synthesized by the route described in Chart 2.

Comparing IIIa with IIIk, the aromatic chromophore can be regarded as the same from the viewpoint an electronic transition because the methyl group gives little perturbation effects to phenol chromophore. Thus, we considered that if optically active IIIa and IIIk had the same absolute configuration, these two derivatives would give almost the same Cotton effects. In fact, the CD spectrum of (+)-IIIa appears almost opposite to that of (−)-IIIk as shown in Fig. 2. An empirical rule can be obtained from Chart 1 and Table 1, that the compounds, (−)-IIIc—(−)-IIIm, including non-substituted spirane, (+)-IIIl, show negatively signed CD in the longest wave length [It should be noted that (−)-IIIl was derived from (+)-IIIc and hence (+)-IIIl must be correlated to the same configuration as (−)-IIIc. But even in this case, the above empirical rule was found to be valid.]. (+)-IIIa shows positively signed CD in the longest wave length. From the above observations, it was decided that the absolute configuration of (+)-IIIa and (−)-IIIb is opposite to that of the other derivatives, (−)-IIIc—(−)-IIIm, cited in Table 1.

The CD and UV spectra of these derivatives are shown in Table 1. Accessible CD spectra of these compounds consist of three bands which are termed α, p and β, from the longer wavelength according to the classification of Clar. From this Table it seems that the intensity and the polarization direction of the electronic transition or each aromatic chromophore

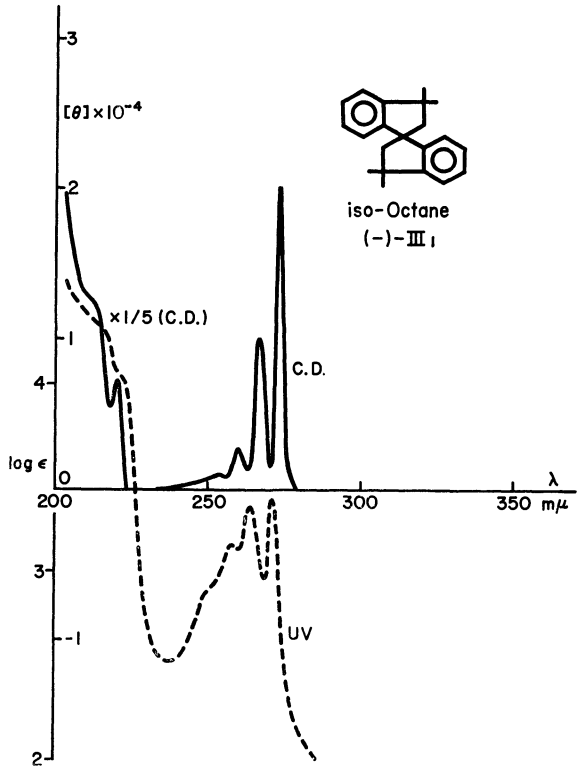

Fig. 3. CD and UV spectra of (−)-IIIl in isooctane.

have direct influence on CD spectra. For polysubstituted benzenes, a quantity called the spectroscopic monent has been assigned to each group by Platt.[10] Employing the spectroscopic moment, the absorption intensities and the transition moment directions may be calculated by the vector addition formula. The spectroscopic moment is considered to be useful for interpreting the CD of these derivatives. Following the value of the spectroscopic moment and the origin of the Cotton effect, we divided the derivatives into classes, I, II, III, and IV.

In class I, the substituent groups at the position 6

10) J. R. Platt, *J. Chem. Phys.*, **19**, 263 (1951); J. Petruska, *ibid.*, **34**, 1111, 1120 (1961).

Table 1. UV and CD spectra of the examined spiro compounds

Compd	Solv.	UV $\lambda_{m\mu}$ ($\varepsilon \times 10^3$)			CD $\lambda_{m\mu}$ ([θ]) $\times 10^3$)		
		α	P	β	α	P	β
(+)-IIIa	MeOH	286 (8.90)	223[i] (16.5)	202.3 (66.7)	292 (+17.6)	231 (−15.8)	209 (+250)
					274 (−1.65)	223[i] (+14.6)	
(−)-IIIb	Dioxane	293 (8.84)			293 (−5.25)	245 (−11.2)	211 (+100)
		286 (7.77)				231 (−5.18)	
(−)-IIIc	MeOH	288 (2.43)	240 (23.4)	202.5 (55.2)	289 (−19.4)	249 (−95.0)	217 (−337)
		278 (2.78)			283 (−7.76)	232 (+65.0)	
					275 (+2.55)		
(−)-IIId	0.1 N NaOH	284 (2.01)	236 (19.4)		285 (−23.8)	245 (−66.0)	219 (−137)
		274 (2.59)			277 (−13.3)	232 (+64.7)	208[i] (+169)
(−)-IIIe	MeOH	288 (2.69)	241 (21.8)	216 (38.8)	290 (−23.4)	251 (−97.3)	218 (−288)
		279 (3.05)		202 (50.8)	282 (−9.14)	234 (+60.1)	209 (−336)
		270 (2.52)			275 (+3.23)		198[i] (+366)
(−)-IIIf	Isooctane	299 (3.83)	262[i] (44.0)	222.7 (52.3)	300 (−18.2)	264 (−198)	223 (−175)
		289 (4.98)	256.5 (46.5)	206 (50.8)	291 (−10.2)	248 (+72.9)	212 (−278)
(−)-IIIg	Isooctane	298 (4.82)	263 (37.5)	223 (40.7)	299 (−25.4)	267 (−173)	222[i] (−175)
		287 (6.41)	258 (37.5)	206 (41.3)	290 (−17.6)	246 (+34.3)	214 (−268)
(−)-IIIh	MeOH	296 (5.57)	236 (17.0)	207 (72.5)	299 (−14.1)	244 (−25.7)	220 (−607)
						233 (+62.7)	
(−)-IIIi	HCl - MeOH	275 (2.99)	225[i] (10.2)		275 (−58.4)	227 (+39.3)	210[i] (−266)
		268 (2.44)	220[i] (16.6)		269 (−35.3)	221[i] (−82.2)	
		266 (2.47)	215[i] (19.7)		261 (−10.6)		
		261 (1.77)			247 (−5.14)		
(−)-IIIj	Isooctane	276 (2.79)	217[i] (17.2)		279 (−15.2)	237 (−2.71)	208[i] (−246)
		270 (2.69)			271 (−10.8)	226 (+28.1)	
		262[i] (1.87)					
(−)-IIIk	MeOH	289 (6.24)	220[i] (16.5)		290 (−10.9)	236 (−1.98)	209 (−289)
		284 (6.58)			284 (−8.05)	229 (+18.6)	
					270 (+1.98)		
(−)-IIIl	Isooctane	272 (2.59)	223 (11.0)	213[i] (22.0)	273 (+20.3)	221 (+36.6)	
		265 (2.24)	218[i] (18.2)		267 (+10.4)	213[i] (+62.0)	203[i] (+99.0)
		257 (1.43)			260 (+2.97)		
					253 (+0.99)		
(−)-IIIm	MeOH	277 (2.58)	222[i] (19.6)		277 (−25.7)	228 (+37.1)	210[i] (−383)
		268 (2.15)	217[i] (22.0)		271 (−12.4)	223[i] (−32.2)	
		263 (1.46)			263 (−1.90)		
(+)-VIII	MeOH	289[i] (4.33)	231.8 (12.5)		289.5 (+19.2)	232.5 (−30.7)	
		282.5 (5.12)			271.5 (−0.89)		

!: last reading. i: inflection.

and 6′ of III influence the absorption spectrum of benzene to a lesser extent. (−)-IIIi, (−)-IIIl and (−)-IIIm belong to this class. They have very sharp Cotton effects in all transitions. In α-band, the Cotton effects attributable to the vibrational transition are all of negative sign, but in p-band, two oppositely signed Cotton effects are observed except for (−)-IIIl. In (−)-IIIl as shown in Fig. 3, the sign of all Cotton effects in the region accessible with the apparatus (205 mμ), is positive, but that of specific rotation at D-line is negative, from which it is deduced that there are very strong negatively signed Cotton effects in far-UV region.

In class II, the substituents have a comparatively large value in Platt's spectroscopic moment. In this class, (+)-IIIa, (−)-IIIc—g, and (−)-IIIj—k are included and the CD spectra seem to split into oppositely signed pair centered at each absorption region. That is, (−)-IIIk has the oppositely signed pair of Cotton effects centered at α- and p-bands, as shown in Fig. 2, although the rotational strengths are not the same. IIIa with the opposite absolute configuration gives negative and positive CD bands at longer and shorter wavelengths, respectively, in the region of the p-band.

A more typical example is observed in (−)-IIIc and (−)-IIIe (as shown in Fig. 4 on (−)-IIIc). Their Cotton effects in p-band are oppositely signed and almost similar in rotational strength, although in α-band they are not the same in magnitude.

(−)-IIIc was measured in a number of solvents but no remarkable solvent effect was observed. Moreover, the CD spectrum of (−)-IIId is similar to that of (−)-IIIc except for a small positively signed Cotton

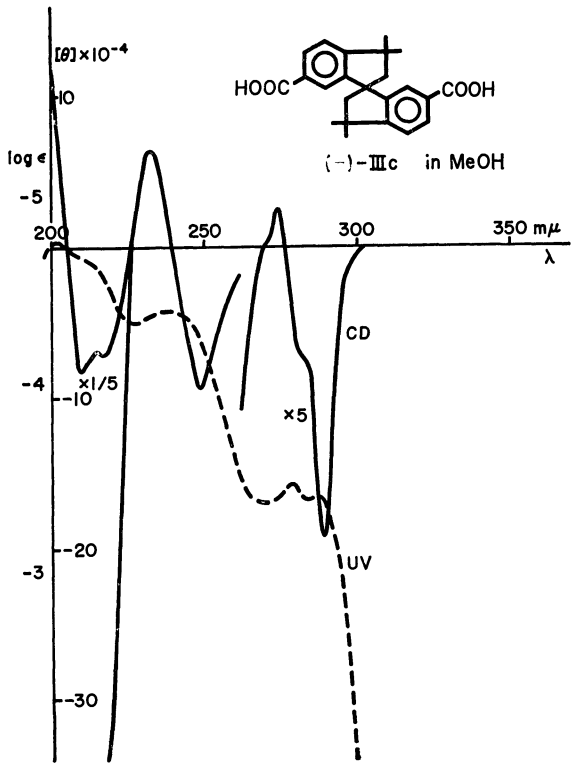

Fig. 4. CD and UV spectra of (−)-IIIc in methanol.

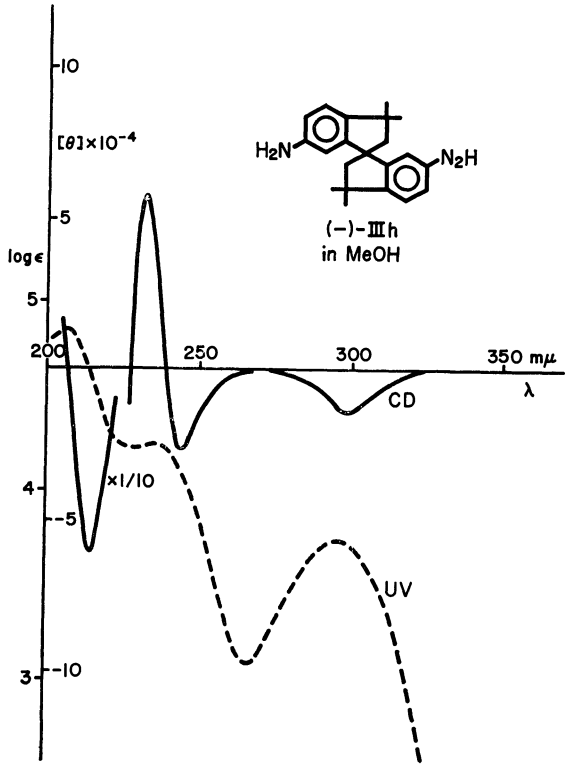

Fig. 5. CD and UV spectra of (−)-IIIh in methanol.

effect observed in α-band of (−)-IIIc.[11] (−)-IIIf and (−)-IIIg show the shift to a higher wavelength, but the curve is similar to that of (−)-IIId. From the similarlity in CD of the derivatives with COX group, it can be said that the polarization direction of the transition in the benzoyl chromophore is not affected so much, even if the group X is changed.

In class III, the substituent group interacts very strongly with the benzene ring. (−)-IIIh alone is contained in this class. Its spectrum (shown in Fig. 5) is also a typical example of splitting, as Mason and his coworkers[12] have pointed out in two-fold rotation axis molecules with aniline chromophore. But the α-band shows only negatively signed Cotton effect.

In class IV, the splitting of the CD band could not be observed, as shown in Fig. 6. (−)-IIIb is the only one example. In this molecule the bromo substituent of one aromatic chromophore is placed just over the other within the region where the exchange integral has a large value, as shown in X-ray crystallography.[13] Therefore one aromatic chromophore interacts with the other owing rather to the exchange force than the dipole-dipole interaction.

In these dissymmetrically situated dimers of aromatic chromophore, a given monomer excitation is doubly

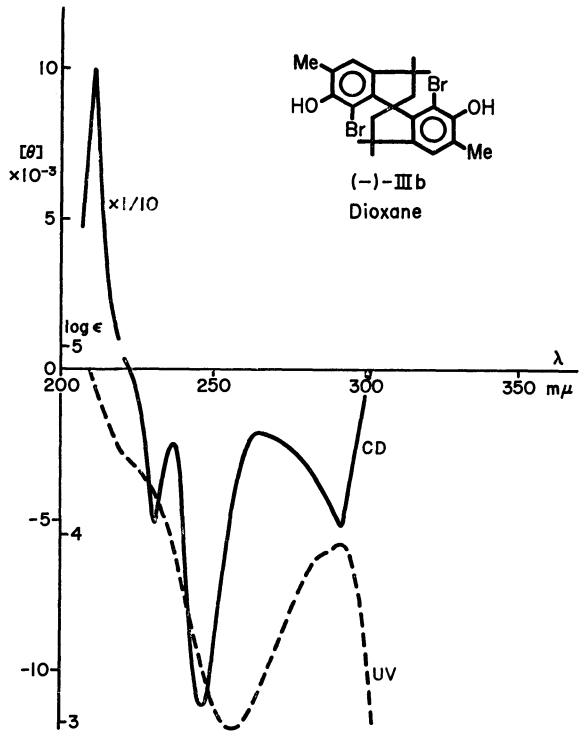

Fig. 6. CD and UV spectra of (−)-IIIb in dioxane.

degenerated to a zero-order, but dipole-dipole interaction between the two excitation monents splits the degeneracy and gives two optically active resultant transitions, one with A and the other with B symmetry in the point group C_2.[12,14]

11) We found that CD spectra of 11 (*endo*), 12 (*endo*)-dicarbomethoxy-9,10-dihydro-9,10-ethanoanthracene-1,5-dicarboxylic acid and its sodium salt show a remarkable difference at around 230 mμ. The details will be reported in the near future.

12) a) S. F. Mason and G. W. Vane, *J. Chem. Soc., B*, **1966**, 370. b) S. F. Mason, K. Schofiels, R. J. Wells, J. S. Whitehurst, and G. W. Vane, *Tetrahedron Lett.*, **1967**, 137. c) S. F. Mason, G. W. Vane, and J. S. Whitehurst, *Tetrahedron*, **23**, 4087. (1967).

13) M. Shiro, S. Hagishita, and K. Kuriyama. Details will be published in a subsequent paper.

14) J. G. Kirkwood, *J. Chem. Phys.*, **5**, 479 (1937).

From the assumption that an excitation moment of the benzenoid chromophore is a point dipole located at the center of the benzene ring, the rotational strengths R of the two transitions are given by

$$R_A = -R_B = \pi\bar{\nu}d\rho^3 \cos v \cos t \quad (1)$$

and the separation $\Delta\bar{\nu}$ between the two resultant transition frequencies by

$$\Delta\bar{\nu} = \bar{\nu}_A - \bar{\nu}_B = 2\rho^2(\cos^2 v - \cos^2 t + 2\cos^2 r)/hcd^3 \quad (2)$$

In these expressions ρ is the transition dipole moment of the transition in the isolated chromophore which occurs at a wave number frequency of $\bar{\nu}$ and d is the distance between the centres of the two benzene rings. Each of the two excitation dipoles ρ have components directed parallel to the Cartesian axes of the dimeric system, and the magnitudes of the components are determined by the cosines of the vertical, tangential and radial angles, v, t, and r, respectively, between the excitation dipole and the local Cartesian axes, in which the x-axis is definied by the line joining the centres of the two benzene rings and z is the C_2 symmetry axis.

The stereochemical parameters d, v, t, and r necessary for the calculation of rotational strengths and the frequency intervals between the transitions depend upon the orientation of the excitation dipole within the benzenoid chromophore as well as the mutual stereochemical disposition of the two chromophores.

In the present case the values of the spectroscopic moments listed by Platt and an other[10] are applicable and the direction of the transition moment of each monomer is obtained by the vector addition of the spectroscopic moments induced by each substituent. The alkyl bridge which makes up the spiro skeleton is also regarded as a substituent and the value of t-butyl group was adopted. However, NH_2 group interacts so strongly with benzene that we neglected the effect of the alkyl bridge in (−)-IIIh and used the direction of the α- and p-bands of aniline. In other cases the following values were used for calculation: COOH(−28); OH(34); t-butyl(2); CH_2OH (−7); methyl(7).

Values of the parameters, d, v, t, and r are determined not only by the transition moment directions in the benzenoid chromophore but also by the spatial relations between the two chromophores. The stereochemical parameters have unique values in the rigid dimeric systems, but they have a range of values in the case of spiro indanes, owing to the conformational lability of the molecule. Models indicate that the extreme forms of the five membered ring in indanes are the planar (IVa) and the envelope conformation (IVb), in which the carbon atom at position 2 is moved out of the plane of the other four carbon atoms by 0.285 Å and the carbon atom at the position 2' is quasi-axial.

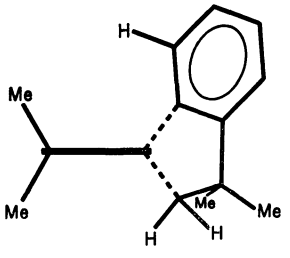

IVa

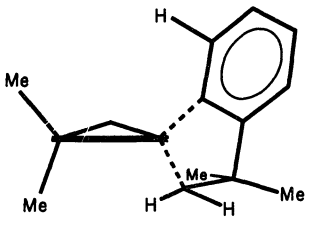

IVb

It has been reported[15] that the puckering of the cyclopentene ring having an atom out of the plane by an amount up to about 0.3 Å gave no change on the potential energy of the system. If we consider the 1,3-di-quasiaxial interactions between one of the gem-dimethyl group at position 3 and the methylene group at position 2', the planar conformation (IVa) would be probably more stable. In the cases of (−)-IIIh and (−)-IIIl (Table 2), the qualitative forms of the theoretical CD spectra depend only upon the configuration and are independent of the conformation. Therefore, the sets of stereochemical parameters, v, t, and r for the planar conformation of (S)-configuration are calculated from the coordinates provided by the X-ray diffraction study of 5,6-dibromoindane,[16] and are listed in Table 2. The theoretical and experimental results indicate that for (−)-IIIl and (+)-IIIm which belong to Class I, the absolute configurations can not be predicted. The following may be one of the main reaons. We approximated the alkyl bridge to the t-butyl group, but as the value of the spectroscopic moment of the substituent at positions 6 and 6' is small, the small change is value of position 1 should exert great influence on the direction of the excitation moment. Therefore the sign of rotational strength and/or the separation of frequencies might be changed.

An amino group interacts so strongly with the benzene ring that the contribution of other substituents can be neglected as compared to that of the amino group. Therefore, the direction of the transition dipole moment in the isolated chromophore of (−)-IIIh is independent of the change in the value of the spectroscopic moment of other substituents. In the case of (−)-IIIh, the calculated rotational strengths and separation indicate that the signs of the two CD bands associated with the p-band should be negative and then positive, from longer to shorter wavelength for (S)-configuration (Table 2). Although the CD in the α-band region shows only a negative sign, the observed CD bands in the region of the absorption maximum at 236 mμ lie clearly in the expected order (Fig. 5). Thus it is deduced that (−)-IIIh has (S)-configuration. The consistency between the calculated and experimental signs of the rotational strengths associated with the p-band for the derivatives in class II supports the assignment of (S)-configuration to the compounds derived from (−)-IIIc.

In class II and III the theoretical CD spectra for (S)-configuration lie in the order positive and then negative to lower wavelength in the region of the α-band, but the sequence of signs of the observed CD bands is opposite except in (−)-IIIh which shows only negative CD spectrum.

15) C. W. Beckett, N. K. Freeman, and K. S. Pitzer, *J. Amer. Chem. Soc.*, **70**, 4227 (1948).

16) A. Kossiakoff and H. D. Springall, *J. Amer. Chem. Soc.*, **63**, 2223 (1941).

Table 2. Rotational strengths and frequency intervals of (S)-configuration

Compd	Band	Component	Found				Theoretical				
			D (10^{-36} cgs)	λ mμ	R (10^{-40} cgs)	$\lvert\nu_A-\nu_B\rvert$ (cm^{-1})	cos r	cos t	cos v	R (10^{-40} cgs)	$\nu_A-\nu_B$ (cm^{-1})
(+)-IIIa^E	α	B	2.70	286	−5.30	2250	−.908	+.278	−.314	+13.2	+340
		A			+0.41					−13.2	
	P	A	5.00	223	+3.71	1553	+.031	+.769	+.638	+178	−68.6
		B			−1.94					−178	
(−)-IIIc	α	B	1.08	278	−4.18	1409	−.861	+.498	−.109	+3.36	+101
		A			+0.26					−3.36	
	P	B	10.0	240	−34.3	2944	+.385	+.594	+.706	−281	+334
		A			+16.9					+281	
(−)-IIIh	α	B	2.97	296	−7.23	—	−.878	+.454	−.154	+12.3	+305
		A								−12.3	
	P	B	8.60	236	−8.70	1935	+.248	+.677	+.693	−274	+92.7
		A			+14.6					+274	
(−)-IIIk	α	B	2.61	285	−4.30	2554	−.888	+.419	−.189	+11.6	+283
		A			+0.63					−11.6	
	P	B	4.20	224	−0.02	2470	+.201	+.701	+.684	−145	+18.0
		A			+2.38					+145	
(+)-IIIl^E	α	B	0.64	270	−3.06	—	+.648	+.358	+.672	−9.16	+56.4
		A								+9.16	
	P	B	6.38	217	−17.1	—	−.645	+.734	+.210	−73.0	+163
		A								+73.0	
(−)-IIIm	α	B	0.83	277	−4.67	—	−.798	+.603	+.014	−0.40	+57.0
		A								+0.40	
	P	B	5.45	220	+3.51	3089	+.448	+.547	+.707	−153	+247
		A			−1.86					+153	
(−)-IIIh*	α	B	2.97	296	−7.23	—	−.908	+.412	−.078	+4.97	+360
		A								−4.93	
	P	B	8.60	236	−8.70	1935	+.198	+.584	+.787	−261	+250
		A			+14.6					+261	
(+)-IIIl^E*	α	B	0.64	270	−3.06	—	+.626	+.300	+.720	−8.00	+63.3
		A								+8.00	
	P	B	6.38	217	+17.1	—	−.687	+.649	+.327	−97.7	+328
		A								+97.7	
(−)-VIII^E	α	A	1.50	288	−6.17	2290	+.282	−.822	−.485	+34.3	−30.6
		B			+0.10					−34.3	
	P	B	5.62	232	−9.77	—	+.866	+.016	−.500	+3.01	+741
		A								−3.01	

* Envelope conformation. E: enantiomer is measured.
Theoretical values were obtained from equations 1 and 2.

The ambiguity of the assignment of the absolute configuration due to the inconsistency between the theoretical and the experimental CD spectra in the α-band is avoided by the X-ray analysis of (−)-7,7′-dibromo-6,6′-dihydroxy-derivative, (−)-IIIb, which has the (R)-configuration. Thus, the inconsistency in α-band comes from the use of the point dipole approximation and the neglect of configurational interaction between transitions of the same symmetry. But even if the exciton theory cannot explain the CD in α-bands satisfactorily, it should be noted that all these spiro compounds having (S)-configuration except for class IV show the CD of negative sign in the longest wavelength. This means that the sign of the CD in the longest wavelength region is always determined by the configuration of spiro atom, *i.e.* the spatial arrangement of the two benzene rings.

In relation to the above consideration, it was observed that the CD of 5,5′-dihydroxyspiroindane, (+)-VIII, is similar to that of the corresponding 6,6′-derivatives, particularly in the region of α-band. The sign of the CD band was, from the longest wavelength to shorter, positive and negative in α-band, and negative in p-band (Fig. 7). From the feature of the CD curve (+)-VIII is considered to have (R)-configuration.

Applying the exciton theory to (R)-VIII, the calculated value of the CD should have the sign in the order negative and positive both in α-band and in p-band. This is contrary to the observed result. But the sign of the CD band in α-band may be reversed by a small change in the value of the parameters as in the case of spiroindane (−)-IIIl where the width of the splitting is small (−31 cm^{-1}).

The fact that the observed rotational strength in the p-band is greater than that calculated from exciton

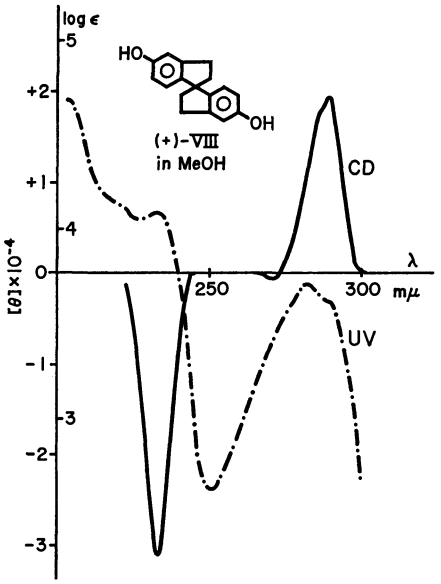

Fig. 7. CD and UV spectra of (+)-VIII in methanol.

theory may be considered to reflect the contribution from the mixing of other local transitions.

At any rate, exciton theory is not effective for deciding the absolute configuration of (+)-VIII, which should be confirmed by its correlation with other spiro compounds.

Experimental

All melting points were uncorrected. Optical rotations were measured on a Perkin Elmer polarimeter Model 141 using a 1-dm quartz cell. CD spectra were taken with a JASCO Model ORD/UV-6 and a Roussel-Jouan Dichrograph Type B. The UV spectra were run on a Hitachi Model EPS-3T spectrometer. The NMR spectra were taken at 60 Mc with a Varian A-60 spectrometer using TMS as internal standard. The IR spectra were measured on a JASCO Model DS 402G doublemonochromatic spectrophotometer in $CHCl_3$ solution. The mass spectra were measured on a Hitachi RMU-6 Single Focus Mass spectrometer.

Resolution of 6,6'-Dihydroxy-3,3,5,3',3',5-hexamethy-bis-1,1'-spiroindane (+)-IIIa. The mixture of (+)-IIIa (1.07 g), which was prepared according to the procedure of Baker and Besly,[7d] (+)-α-phenethylamine[9] (0.95 g), $[\alpha]_D$ +1.96° (*c* 1.890, benzene), and one drop of pyridine in dry toluene (10 m*l*) was heated under reflux for 25 hr. The solvent was distilled off and the residue was crystallized from toluene: *n*-hexane (405 mg). The (−)-diurethane was recrystallized from benzene three times to afford pure diastereomer (216 mg), mp 218—219°C. $[\alpha]_D$ −9.5° (*c* 0.200, $CHCl_3$). IR ν_{max} 3445, 1738 cm^{-1}.

Found: C, 78.22; H, 7.26; N, 4.17%. Calcd for $C_{41}H_{46}N_2O_4$: C, 78.06; H, 7.35; N, 4.44%.

(−)-Diurethane (216 mg) obtained above, and KOH-EtOH (10%, 5 m*l*) were heated under reflux for 6.5 hr. After cooling, the solution was acidified with 4 N HCl and crystalline product was collected, washed with H_2O and dried (100.6 mg). Recrystallization from benzene: *n*-hexane gave colorless leaflet (20.9 mg), mp 220—221°C. $[\alpha]$ +19.4° (*c* 0.194, dioxane). The IR spectrum in $CHCl_3$ was identical with that of racemic compound.

(−)-7,7'-Dibromo-6,6'-dihydroxy-3,3,5,3',3',5'-hexamethyl-bis-1,1'-spiroindane (−)-IIIb. Bromine (1.0 g) in $CHCl_3$ (20 m*l*) was dropped in to a solution of (+)-IIIa (150 mg) in $CHCl_3$ (5 m*l*) with stirring until the color did not fade any more. After further stirring for 20 min, EtOH was added. Crystals were filtered (138 mg), and then recrystallized from $CHCl_3$: EtOH to give prisms, mp 273—273.5°C. $[\alpha]_D$ −108.0°C (*c* 0.213, dioxane). NMR (in $CDCl_3$) τ: 8.69 (s, 6H), 8.63 (s, 6H), 7.82 (d, J=13.0 Hz, 2H), 7.69 (s, 6H), 7.50 (d, J=13.0 Hz, 2H), 4.47 (s, 2H), 3.14 (s, 2H). Mass spectrum: *m/e* 496, 492 (molecular ion). IR ν_{max} 3515 cm^{-1}.

Found: C, 55.92; H, 5.29; Br, 33.04%. Calcd for $C_{23}H_{26}Br_2O_2$: C, 55.89; H, 5.30; Br, 32.34%.

Resolution of 3,3,3',3'-Tetramethyl-bis-1,1'-spiroindane-6,6'-dicarboxylic Acid (−)-IIIc and (+)-IIIc. (±)-IIIc was prepared according to the procedure of Curtis.[7e] Mass spectrum: m/e 364 (parent peak).

Found: C, 76.40; H, 6.74%. Calcd for $C_{23}H_{24}O_4$: C, 75.80; H, 6.64%.

(±)-IIIc (12.0 g) and brucine·$2H_2O$ (28.4 g) in 99.5% EtOH (15 m*l*) were heated under reflux for 2 hr and then left to stand overnight at room temperature. The crystals were collected, washed with EtOH, dried *in vacuo* and then recrystallized from EtOH three times (6.3 g). $[\alpha]_D$ −91.6° (*c* 0.32, $CHCl_3$).

From the mother liquor of the reaction, EtOH was distilled off under reduced pressure. The residue was crystallized from acetone. The crude diastereomer was purified by recrystallization from MeOH: $CHCl_3$ five times (1.96 g). $[\alpha]_D$ +76.1° (*c* 0.551, $CHCl_3$).

(−)-Salt (6.3 g) was shaken with 6 N HCl (50 m*l*) at 50°C for 30 min. Crystals were filtered, washed with H_2O, dried *in vacuo*, and recrystallized from dioxane: acetone (1.57 g). $[\alpha]_D$ −93.7° (*c* 0.206, dioxane). (+)-Salt (1.25 g) was treated as above to give (+)-IIIc (476 mg). $[\alpha]_D$ +94.2° (*c* 0.243, dioxane).

(−)-Dimethyl-3,3,3',3'-tetramethyl-bis-1,1'-spiroindane-6,6'-dicarboxylate (−)-IIIe. A solution of diazomethane in ether was added to a solution of (−)-IIIc (200 mg) until the yellow color still remained. Ether was distilled off. The residue was chromatographed on Al_2O_3 (6.0 g, Woelm Co., Act. II) in benzene and then crystallized from *n*-hexane to give prisms (99.8 mg), mp 170.5—171°C. $[\alpha]_D$ −124.2° (*c* 0.233, *n*-heptane). Mass spectrum: *m/e* 392 (molecular ion). IR ν_{max} 1717 cm^{-1}.

Found: C, 76.79; H, 7.44%. Calcd for $C_{25}H_{28}O_4$: C, 76.50; H, 7.19%.

(−)-3,3,3',3'-Tetramethyl-bis-1,1'-spiroindane-6,6'-dicarboxylic Acid Chloride (−)-IIIf. (−)-IIIc (1.0 g) and thionylchloride (3.3 g) in abs. THF (5.0 m*l*) were heated under reflux for 1 hr. THF and excess thionylchloride were evporated under reduced pressure. The residue was crystallized from *n*-hexane and then recrystallized further two times (773 mg), mp 175—177°C. $[\alpha]_D$ −174.7°C (*c* 0.314, isooctane). IR ν_{max} 1755 cm^{-1}. Mass spectrum: *m/e* 400, 404 (molecular ion).

Found: C, 68.70; H, 5.63; Cl, 17.86%. Calcd for $C_{23}H_{22}O_2Cl_2$: C, 68.83; H, 5.53; Cl, 17.67%.

(−)-3,3,3',3'-Tetramethyl-bis-1,1'-spiroindane-6,6'-dicarboxylic Acid Azide (−)-IIIg. Sodium azide (230 mg) in H_2O was added in one portion to a solution of (−)-IIIf (718 mg) in acetone (5 m*l*) under cooling with vigorous stirring. After stirring for 15 min, oily precipitate was extracted with CH_2Cl_2 at 0°C. CH_2Cl_2 layer was washed with ice-water and dried with Na_2SO_4. CH_2Cl_2 was distilled under reduced pressure at room temperature. The residue was crystallized from *n*-hexane (271 mg), mp 92—93°C

(dec). $[\alpha]_D$ −246.3° (*c* 0.166, isooctane). IR ν_{max} 2143, 1691 cm^{-1}.

(−)-6,6'-Diamino-3,3,3',3'-tetramethyl-bis-1,1'-spiroindane (−)-IIIh. (1) (−)-IIIg (265 mg) in dry benzene (10 m*l*) was heated under reflux for 6 hr. Benzene was distilled off under diminished pressure. The IR spectrum showed N : C : O stretching absorption at 2270 cm^{-1}. This isocyanate was used for the next hydrolysis without further purification. The oily residue and 10% KOH-EtOH (10 m*l*) were heated under reflux for 2 hr. After cooling, H_2O (20 m*l*) was added and the mixture was extracted with benzene. The benzene solution was washed with H_2O and dried on Na_2SO_4. Benzene was distilled off. The residue was crystallized from benzene: *n*-hexane and then further sublimated at 170°C/2 mmHg (136 mg), mp 165—167°C. $[\alpha]_D$ −144.1° (*c* 0.270, MeOH). Mass spectrum: *m/e* 306 (molecular ion). IR ν_{max} 3380, 3458 cm^{-1}.

Found: C, 82.08; H, 8.56; N, 8.75%. Calcd for $C_{21}H_{26}N_2$: C, 82.30; H, 8.55; N, 9.14%.

(2) (−)-IIIc (370 mg) was treated according to the procedure of Curtis[7e] to give (−)-IIIh (236 mg), mp and the IR spectrum were identical with those of the above product.

(−)-6,6'-Diacetoxy-3,3,3',3'-tetramethyl-bis-1,1'-spiroindane, (−)-IIIj. This was prepared according to the procedure of Curtis,[7e] and recrystallized twice from *n*-hexane, mp 152—154°C. $[\alpha]_{365}$ −301 (*c* 0.00803, isooctane).

(−)-6,6'-Dihydroxy-3,3,3',3'-tetramethyl-bis-1,1'-spiroindane, (−)-IIIk. (−)-IIIj was hydrolyzed by the methods of Curtis,[7e] mp 96—98°C. $[\alpha]_{365}$ −254 (*c* 0.01284, MeOH). Mass spectrum: *m/e* 308 (parent peak). IR ν_{max} 3605 cm^{-1}.

Found: C, 79.07; H, 7.98%. Calcd for $C_{21}H_{24}O_2 \cdot 1/2H_2O$: C, 79.45; H, 7.94%.

(−)-3,3,3',3'-Tetramethyl-bis-1,1'-spiroindane (−)-IIIl. Decarboxylation of (+)-IIIc was performed by using copper chromite catalyst according to literature,[7e] mp 122.0—122.5°C. $[\alpha]_D$ −25.9° (*c* 0.315, dioxane). Mass spectrum *m/e* 276 (molecular ion). IR ν_{max} 1600 cm^{-1}.

Found: C, 91.26; H, 8.79%. Calcd for $C_{21}H_{24}$: C, 91.26; H, 8.79%.

(−)-6,6'-Dihydroxymethyl-3,3,3',3'-tetramethyl-bis-1,1'-spiroindane (−)-IIIm. $LiAlH_4$ (30 mg) in abs. ether (10 m*l*) was added to a solution of (−)-IIIe (86.2 mg) at room temperature. The reaction mixture was made to boil and then stirred for 1.5 hr. Excess $LiAlH_4$ was decomposed by dropping AcOEt and then HCl under cooling. The mixture was extracted with ether and ether layer was washed with $NaHCO_3$ - H_2O and H_2O and then dried on Na_2SO_4. Solvent was distilled off and the residue was crystallized from *n*-hexane (54.1 mg). $[\alpha]_D$ −61.8° (*c* 0.647, MeOH), mp 144—145°C. Mass spectrum: *m/e* 336 (molecular ion). IR ν_{max} 3600, 3440 cm^{-1}.

Found: C, 82.02; H, 8.45%. Calcd for $C_{23}H_{28}O_2$: C, 82.10; H, 8.39%.

Bis-(3-methoxybenzal)-acetone (V). A mixture of 50.0 g of *m*-methoxybenzaldehyde and 10.7 g of acetone in 25 m*l* of ethanol was added dropwise with stirring to the water-cooled alkaline solution (36.6 g of sodium hydroxide, 25 m*l* of ethanol and 370 m*l* of water). After stirring for 2 hr, the water layer was extracted with ether, the organic layers were combined and washed with water. Working up as usual furnished yellow oil, 60.1 g, which was chromatographed on a column of 90 g of Al_2O_3 (act. III). Benzene-petroleum ether and benzene eluate furnished 40.8 g oil, which solidified on standing. 2,4-Dinitrophenylhydrazone, mp 175.5—176.8°C.

Found: C, 62.90; H, 4.72; N, 11.77%. Calcd for $C_{25}H_{22}O_6N_4$: C, 63.28; H, 4.67; N, 11.81%.

Bis-(3-methoxybenzyl)-acetone (VI). 10 g of dienone (V) in 500 m*l* of acetone was hydrogenated on 1.0 g palladium-charcoal (10%). The uptake of hydrogen amounted to 110% of the theory in 90 min. After addition of a few drops of methanol, the catalyst was removed by filtration and the solvent was evaporated. The residual oil was taken in benzene and filtered on 20 g of Al_2O_3 (act. III).

Six runs from the total amount of 89.4 g of dienone in analogous procedure gave 85.3 g of crude oil, which was dissolved in 300 m*l* acetic acid and treated with a chromic acid solution (19.0 g of chromic trioxide, 18 m*l* of water and 150 m*l* of acetic acid). After the usual procedure the obtained oil, 72.2 g, was dissolved in benzene eluate ketone (VI) as yellow oil, 45.4 g (50%).

5,5'-Dimethoxy-bis-1,1'-spiroindane (VII). 5.2 g Bis-(3-methoxybenzyl)-acetone (VI) and 22 m*l* of freshly distilled phosphorus oxychloride dissolved in 57 m*l* of benzene were refluxed 4 hr. The reaction mixture was poured into ice-water and treated as usual. The obtained brown oil dissolved in petroleum ether was filtered on Al_2O_3 (act. III), and crystallized from petroleum ether, Yield 2.75 g (56.8%), mp 67—78°C. Recrystallisation raised the melting point to 83—85°C.

Found: C, 81.47; H, 6.61%. Calcd for $C_{18}H_{18}O_2$: C, 81.17; H, 6.81%.

5,5'-Dihydroxy-bis-1,1'-spiroindane (VIII). A mixture of 14.5 g of dimethoxy compound (VII), 120 m*l* of concentrated hydrobromic acid (d=1.48) and 120 m*l* of acetic acid was refluxed for 5 hr. After cooling, the reaction mixture was poured into 800 m*l* of water, extracted with ether and treated as usual. The obtained viscous oil was dissolved in benzene - acetone (6 : 1) and filtered on 20 g Al_2O_3 (act. III). Crystallisation from benzene yielded 7.4 g (57%) crystals, mp 175—178°C.

Found: C, 81.04; H, 6.29%. Calcd for $C_{17}H_{16}O_2$: C, 80.92; H, 6.39%.

Bis-1,1'-spiroindane-5,5'-dioxybutyric Acid (IX). 3.00 g of dihydroxyspiroindane (VIII) in 8.3 m*l* of absolute ethanol was added under reflux into a sodium ethoxide solution (1.1 g of sodium, 20 m*l* of abs. ethanol). To the mixture was added 18.0 g of ethyl - bromobutyrate. After refluxing for 90 min, a sodium ethoxide solution (0.54 g of sodium in 5.7 m*l* of absolute ethanol) and subsequently 6.07 g of bromo ester were added again. Refluxing was continued for 6 hr and the mixture was allowed to stand overnight. 40 m*l* of 30% aqueous sodium hydroxide was added and the mixture was boiled for 1 hr. Ethanol was evaporated under reduced pressure, water was added and the solution was acidified with hydrochloric acid. After working up as usual, the viscous oil was crystallized from aqueous methanol. Yield, 2.93 g (57%), mp 208—218°C. After drying at 140°C *in vacuo* the melting point was 213—216°C.

Found: C, 70.84; H, 6.63%. Calcd for $C_{25}H_{28}O_6$: C, 70.74; H, 6.65%.

Resolution of the Dicarboxylic Acid (IX). 500 mg of the carboxylic acid (IX) dissolves in 11 m*l* of methanol was mixed with 678.8 mg of cinchonidine in 22 m*l* of methanol and allowed to stand overnight. Evaporation of the solvent gave viscous oil, which was crystallized from 47 m*l* of methanol and 59 m*l* of water. Recrystallisation from aqueous methanol was repeated 4 times. Decomposition with 1 N hydrochloric acid and recrystallisation from aqueous methanol gave optically active dicarboxylic acid, 67.5 mg, $[\alpha]_D^{20}$ +23.2° (*c* 0.25, dioxane).

872 mg of the carboxylic acid (IX) treated with cinchonidine in acetone as above gave salt, mp 91—99°C.

Found: C, 71.67; H, 7.33; N, 5.21%. Calcd for $C_{63}H_{72}O_8N_4 \cdot 2H_2O$: C, 72.10; H, 7.32; N, 5.34.

Recrystallisation of the salt six times and decomposition with hydrochloric acid gave 39 mg of dicarboxylic acid, $[\alpha]_D^{20}$ +19.2° (*c* 0.13, dioxane).

Dealkylation of the Dicarboxylic Acid. 181.5 mg of the racemic dicarboxylic acid suspended in 76 m*l* of ether was treated with excess diazomethane in ether. The obtained homogeneous solution, after evaporating, gave 200 mg of ester, which was dissolved in 25 m*l* of toluene and treated with 0.18 m*l* of boron tribromide at −10°C. After 1 hr the reaction mixture was poured into water and treated as usual. The obtained amorphous product, 71 mg, was treated with charcoal in methanol, giving 60.5 mg of dihydroxy compound. The active dicarboxylic acid, 150 mg, treated analogously gave 15 mg of active acid, mp 164—172°C.

Found: C, 78.63; H, 6.71%. Calcd for $C_{17}H_{16}O_2 \cdot 1/2H_2O$: C, 78.13; H, 6.57%.

BULLETIN OF THE CHEMICAL SOCIETY OF JAPAN, VOL. 44, 505—508 (1971)

Studies of Compounds Related to Azines. VII.[1] The Pyrorlysis of 2-Acetylthiophene- and 2-Acetylfuranketazine

Otohiko TSUGE, Haruyuki WATANABE, and Kozo HOKAMA*

Research Institute of Industrial Science, Kyushu University, Hakozaki, Fukuoka

** Department of Chemistry, Faculty of Science and Engineering, Ryukyu University Naha, Okinawa*

(Received July 15, 1970)

As part of a study attempting to elucidate the relation between the chemical structure of an azine and its pyrolysate, the pyrolyses of 2-acetylthiophene- (I) and 2-acetylfuranketazine (II) have been investigated. The pyrolysis of I at 270°C afforded principally nitrogen, ammonia, and 7-methyl-5-(2-thienyl)-thieno[2,3-*c*]pyridine (III), plus lesser quantities of thiophenecarbonitrile and 2-acetylthiophene. The reductive desulfurization of III, followed by oxidation, afforded pyridine 2,4,6-tricarboxylic acid *via* 5-*n*-butyl-7-methyl-thieno-[2,3-*c*]pyridine and 2-*n*-butyl-4-ethyl-6-methylpyridine. On the other hand, II was pyrolyzed to give nitrogen, ammonia, and tars as the major products, together with furan, furancarbonitrile, 2-acetylfuran, 5-(2-furyl)-7-methyl-furo[2,3-*c*]pyridine, and 2,4,6-tri(2-furyl)pyridine.

In order to elucidate the relation between the chemical structure of an azine and its pyrolysate, pyrolyses of various azines have been investigated,[2–6] and it has been found that aromatic ketazines are decomposed by a free-radical process, giving the corresponding Piloty-Robinson's reaction product as the main product in many cases.[3–5]

In this paper we wish to report the formation of novel products from the pyrolyses of 2-acetylthiophene-(I) and 2-acetylfuranketazine (II).

When I was pyrolyzed at 270°C for 1 hr, nitrogen, ammonia, and colorless crystalline compound III, mp 103—104°C, were obtained as major products, accompanied by lesser quantities of thiophenecarbonitrile and 2-acetylthiophene.

Although the compound III was in agreement with the expected molecular formula, $C_{12}H_9NS_2$, which corresponded to that of the Piloty-Robinson's reaction product, 2,5-dithienylpyrrole, its IR spectrum did not show any bands ascribed to the NH group, while it did show the C=N band at 1570 cm^{-1}. The NMR spectrum had signals at τ 7.48 (3H, CH_3, *s*) and 2.3—3.2 (6H, aromatic protons, *m*), while the mass spectrum exhibited the parent ion peak (M^+) at *m/e* 231, together with major peaks at *m/e* 216 (M^+–Me), 205 (M^+–C_2H_2), 186 (M^+–CHS), 148 (186^+—C_3H_2), and 133 (148^+–Me). On the basis of these spectral data and the following chemical transformations, it seems reasonable to assume that III is a methyl-thienyl-substituted thienopyridine.

The relative desulfurization of III with Raney nickel catalyst was carried out. Treatment with Raney nickel catalyst (W-1 type) gave pale yellow oil IV and colorless oil V. On the further treatment of IV with Raney nickel catalyst (W-4 type), IV was transformed into V in a good yield.

The compound IV ($C_{12}H_{15}NS$) was assumed, by spectral studies as well as by elemental analysis, to be *n*-butyl-methyl-substituted thienopyridine, whose structure corresponded to that which will be derived from III under the reductive desulfurization of the thienyl group in III to the *n*-butyl group. The NMR spectrum exhibited signals at τ 9.1 (3H, $C\underline{H}_3$–$(CH_2)_3$–, *t*), 8.0—9.3 (4H, Me–$(C\underline{H}_2)_2$–CH_2–, *m*), 7.5 (3H, CH_3, *s*), 7.25 (2H, Me–$(CH_2)_2$–$C\underline{H}_2$–, *t*), 3.2 (1H, pyridine ring proton, *s*), 2.6 and 2.43 (each 1H, thieno ring proton, *dd*). In the mass spectrum, the parent ion peak (M^+) appeared at *m/e* 205, together with major peaks at *m/e* 190 (M^+–Me), 176 (M^+–Et), 163 (M^+–$MeCH{=}CH_2$), 148 (163^+–Me) and 122 (163^+–MeCN).

1) Part VI of this series: O. Tsuge, M. Tashiro, and K. Hokama, *Nippon Kagaku Zasshi*, **90**, 572 (1969).
2) O. Tsuge, M. Tashiro, and K. Hokana, *Kogyo Kagaku Zasshi*, **71**, 1293 (1968).
3) O. Tsuge, M. Tashiro, K. Hokama, and K. Yamada, *ibid.*, **71**, 1667 (1968).
4) O. Tsuge, K. Hokama, and H. Watanabe, *ibid.*, **72**, 1107 (1969).
5) O. Tsuge, K. Hokama, and H. Watanabe, *Yakugaku Zasshi*, **89**, 783 (1969).
6) O. Tsuge, K. Hokama, and M. Koga, *ibid.*, **89**, 789 (1969).

On the other hand, the compound V ($C_{12}H_{19}N$) was presumed, by spectral studies and chemical transformation, to be 2,4,6-trialkyl (*n*-butyl, ethyl, and methyl)pyridine. The IR and UV spectra of V were very similar to those of 2,4,6-collidine, while the NMR spectrum had signals at τ 9.1 (3H, $C\underline{H}_3$–$(CH_2)_3$–, *t*), 8.8 (3H, $C\underline{H}_3$–CH_2–, *t*), 8.0—9.3 (4H, Me–$(C\underline{H}_2)_2$–CH_2–, *m*), 7.8 (3H, CH_3, *s*), 7.1—7.6 (4H, Me–$(CH_2)_2$–$C\underline{H}_2$– and Me–$C\underline{H}_2$–, *m*) and 3.4 (2H, pyridine ring protons, *s*). The mass spectrum showed the parent ion peak (M^+) at *m/e* 177, together with major peaks at *m/e* 162 (M^+–Me), 148 (M^+–Et), 135 (M^+–MeCH=CH_2), 120 (135^+–Me), and 107 (135^+–C_2H_4).

Furthermore, V was oxidized with selenium dioxide in pyridine to give pyridine 2,4,6-tricarboxylic acid, which was identical with an authentic specimen prepared by the oxidation of 2,4,6-collidine.

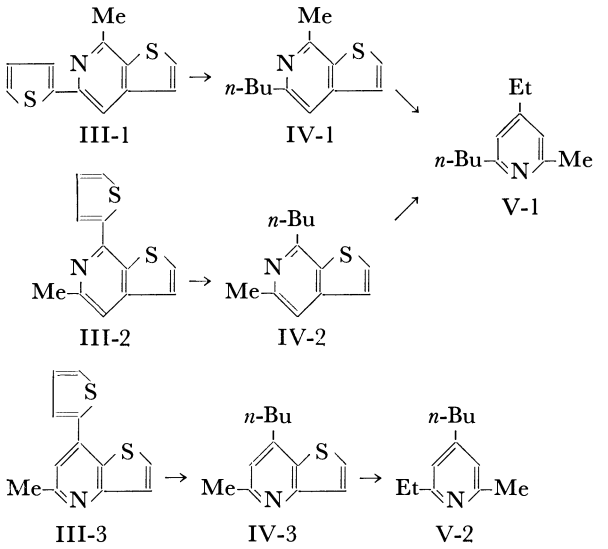

On the basis of the chemical shift of methyl protons in the respective NMR spectrum of III, IV, or V, it is evident that the methyl group is located at the α-position of the pyridine ring in the respective compound. Consequently, 2-*n*-butyl-4-ethyl-6-methyl- (V-1) and 4-*n*-butyl-2-ethyl-6-methylpyridine (V-2) are both possible structures for V.

It should be deduced that the compounds III and IV are 7-methyl-5-(2-thienyl)- (III-1) or 5-methyl-7-(2-thienyl)- (III-2) and 5-*n*-butyl-7-methyl- (IV-1) or 7-*n*-butyl-5-methylthieno[2,3-*c*]pyridine (IV-2) from the structure of V-1, and 5-methyl-7-(2-thienyl)- (III-3) and 7-*n*-butyl-5-methyl-thieno[2,3-*b*]pyridine (IV-3) from the structure of V-2. Unfortunately, it is very difficult to determine from spectral data which isomers would be more reasonable for III and IV.

It has previously been found that the main pyrolytic pathway of aromatic ketazines is that through the homolysis of the N–N bond of ketazines.[3–5] For the formation of III-2 or III-3 from the ketazine I, anomalous homolyses of I and complicated reactions must take place.

In analogy with the pathway of the formation of 2,5-diphenylpyrrole from acetophenoneketazine,[4] however, the formation of III-1 from I can be illustrated by the homolytic dissociation of the N–N bond of I, followed by the rearrangement and recombination of the formed radicals and the subsequent elimination of ammonia.

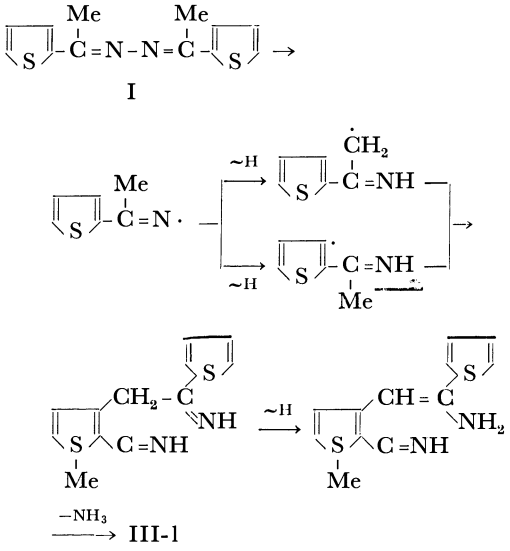

On the basis of the spectral data and considerations of the pyrolytic pathway, it seems reasonable to conclude that III, IV, and V are 7-methyl-5-(2-thienyl)- (III-1), 5-*n*-butyl-7-methyl-thieno[2,3-*c*]pyridine (IV-1), and 2-*n*-butyl-4-ethyl-6-methylpyridine (V-1) respectively.

A similar pyrolysis of II gave 5-(2-furyl)-7-methyl-furo[2,3-*c*]pyridine (VI) and 2,4,6-tri(2-furyl)pyridine (VII) in low yields, accompanied by other products and intractable tars. The structure of VI was assumed on the basis of spectral studies as well as the elemental analysis. The UV spectrum of VI was similar to that of III, while the parent ion peak (M^+) appeared at *m/e* 199, together with major peaks at *m/e* 184 (M^+–Me), 170 (M^+–CHO), 142 (184^+–CH_2C=O) and 132 (170^+–C_3H_2) in the mass spectrum. On the other hand, the compound VII was identified by

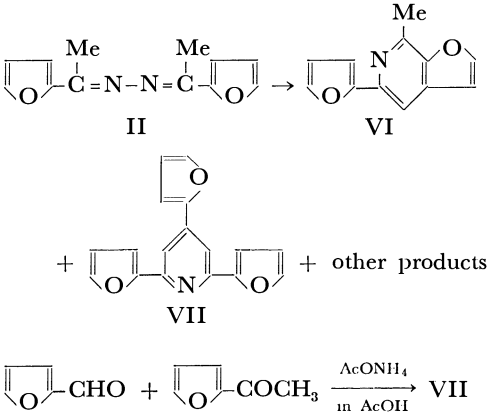

comparing its IR spectrum with that of an authentic sample prepared by the reaction of furfural with 2-acetylfuran in the presence of ammonium acetate according to the improved Chichibabin pyridine synthetic method.[7]

7) M. Weiss, *J. Amer. Chem. Soc.*, **74**, 200 (1952).

Experimental[8]

Materials. The 2-Acetylthiophene- (I) and 2-acetylfuranketazine (II) were prepared by the reaction of the corresponding 2-acetyl compound with hydrazine hydrate in acetic acid; each was then recrystallized from ethanol. The yield was quantitative.

I: mp 95—96°C (lit,[9] 93°C).

II: mp 102—103°C. Found: C, 66.62; H, 5.52; N, 13.07%. Calcd for $C_{12}H_{12}O_2N_2$: C, 66.65; H, 5.59; N, 12.96%.

Procedure. After the pyrolysis had been carried out in an apparatus similar to one described previously,[3] the products were analyzed by the following methods. The products were divided into three fractions: gaseous material (nitrogen, ammonia), a lower-boiling fraction, and a residual fraction.

The analyses of nitrogen and ammonia were carried out by the reported method.[3] The lower-boiling fraction was analyzed by gas chromatography. The conditions for the gas chromatography were as follows: column, 30% high-vacuum silicon grease (HVSG) (3 m) and 20% PEG - 0.5% adipic acid (0.75 m); temperature, 200°C; carrier gas, hydrogen 30 ml/min. From the areas of the individual peaks, mol% figures were calculated for each product after determining the relative response data by the internal standard method using *o*-chloronitrobenzene. Individual peaks were identified by means of the retention times of pure samples.

After the residual fraction had been extracted with benzene, the benzene extract was chromatographed on alumina, giving pure crystalline compounds. The quantitative estimation of the compounds was carried out by the gas-chromatographic internal standard method using 1-benzylnaphthalene. The conditions for the gas chromatography were as follows: column, 30% HVSG (0.75 m); temperature, 300°C; carrier gas, hydrogen 147 ml/min.

Pyrolysis of I. Five grams of I were pyrolyzed at 270°C for 1 hr. The respective yields (mol%) of products obtained from the average values of three runs under the same conditions were as follows: nitrogen, 12.3; ammonia, 96.7; thiophenecarbonitrile, 2.6; 2-acetylthiophene, 3.1; 7-methyl-5-(2-thienyl)-thieno[2,3-*c*]pyridine (III), 50.5 mol%.

III: mp 103—104°C, colorless prisms. UV λ_{max}^{EtOH} mμ (log ε): 276 (4.3), 304 (4.0), 324 (4.0). Found: C, 62.15; H, 4.02; N, 5.91%. Calcd for $C_{12}H_9NS_2$: C, 62.34; H, 3.92; N, 6.06%.

Reductive Desulfurization of III with Raney Nickel Catalyst (W-1). A solution of III (10.0 g) in ethanol (800 ml) was stirred with a freshly-activated W-1 Raney nickel catalyst (100 g) under reflux for 60 hr. After the reaction mixture had then been filtered, the filtrate was concentrated, leaving a brown oil. The oil was divided by distillation into the fraction F_1 (bp 60—70°C/5 mmHg, colorless oil, yield 0.9 g), F_2 (bp 140—144°C/5 mmHg, pale yellow oil, yield 3.0 g), and a residue (yield 2.1 g). The fractions F_1 and F_2 were then both submitted to gas chromatography: from each fraction 2-*n*-butyl-4-ethyl-6-methylpyridine (V) and 5-*n*-butyl-7-methylthieno[2,3-*c*]pyridine (IV) were obtained in the pure state.

IV: UV λ_{max}^{EtOH} mμ (log ε): 231 (3.4), 273 (2.9), 298 (2.8). Found: C, 70.26; H, 7.26; N, 6.78%. Calcd for $C_{12}H_{15}NS$: C, 70.22; H, 7.37; N, 6.82%.

V: UV λ_{max}^{EtOH} mμ (log ε): 265 (3.7), 272 (3.7). Found C, 81.19; H, 10.82; N, 7.61%. Calcd for $C_{12}H_{19}N$: C, 81.30; H, 10.80; N, 7.90%.

A benzene solution of the residue was chromatographed on alumina, giving 1.2 g of III.

Reductive Desulfurization of IV with Raney Nickel Catalyst (W-4). A solution of IV (0.6 g) in ethanol (150 ml) was stirred with a freshly-activated W-4 Raney nickel catalyst (10 g) under reflux for 11 hr. After the reaction mixture had then been treated in a manner similar to that described above, a pale yellow oil (0.45 g) which was found to be composed of 70.6% of V by the gas-chromatographic estimation was obtained.

Oxidation of V. A solution of V (1.0 g) in pyridine (20 ml) was stirred with selenium dioxide (15.2 g) under reflux for 15 hr. The reaction mixture was filtered, and the filtrate was subjected to steam distillation. After active charcoal and chips of filter paper had then been added to the residue, the mixture was refluxed and then filtered. The filtrate was concentrated to about 20 ml and then allowed to stand overnight, giving pyridine 2,4,6-tricaraoxylic acid, mp 227°C (decomp.) (lit,[10] 227°C (decomp.)), as colorless crystals. Yield, 0.6 g (50%). This compound was identical the authentic sample prepared by the oxidation of 2,4,6-collidine.

Pyrolysis of II. Five grams of II were pyrolyzed under several conditions; the results are shown in Table 1.

5-Furyl-7-methyl-furo[2,3-*c*]pyridine (VI); mp 68—69°C, colorless prisms. NMR: τ 7.4 (3H, CH_3, *s*), 3.5 (1H, *m*), 3.0 (2H, *m*), 2.5 (2H, *m*), 2.2 (1H, *d*). UV λ_{max}^{EtOH} mμ (log ε): 241 (4.2), 268 (4.0), 277 (3.9), 320 (4.1). Found:

Table 1. Pyrolysis of II[a]

Conditions		Products, mol%							
Temp. (°C)	Time (min)	N_2	NH_3	F[b]	N[b]	A[b]	VI	VII	II
240	75	48.2	57.8	1.0	1.0	6.2	0	3.3	22.4
250	50	no determined		1.5	0.8	8.7	1.2	4.6	3.3
275	20	37.0	68.0	3.0	3.0	9.8	1.5	5.2	0

a) Intractable tars were formed in a large amount.
b) F: furan, N: furancarbonitrile, A: 2-acetylfuran.

8) All the melting points are uncorrected. The IR spectra were recorded on a Nippon Bunko IR-S spectrophotometer, while the UV spectra were measured in ethanol with a Shimadzu SV-50A spectrophotometer. The NMR spectra were determined in a carbon tetrachloride solution at 60 MHz with a Hitachi R-20 NMR spectrometer, using TMS as the internal reference. The multiplicity of signals is indicated in abbreviated form; *s*: signlet, *d*: doublet, *dd*: double doublet, *t*: triplet, *m*: multiplet. The mass spectra were obtained on a Hitachi RMS-4 mass spectrometer using a direct inlet and an ionization energy of 70 eV.

9) H. H. Szmant and H. J. Planinrek, *J. Amer. Chem. Soc.*, **72**, 4981 (1950).

10) R. Craf and F. Zelle, *J. Prakt. Chem.*, [2], **1937**, 148.

C, 72.61; H, 4.42; N. 6.95%. Calcd for $C_{12}H_9O_2N$: C, 72.37; H, 4.55; N, 7.07%.

2,4,6-Tri(2-furyl)pyridine (VII). A mixture of 2-2-acetylfuran (3.3 g), furfural (1.5 g), and ammonium acetate (15 g) in acetic acid (38 m*l*) was refluxed for 1 hr. After the reaction mixture had been extracted with benzene (100 m*l*), the benzene-extract was washed with water, dried over sodium sulfate, and then concentrated. A benzene solution of the residue was chromatographed over alumina, giving VII, mp 128—129°C, as colorless needles. Yield, 0.6 g (14 %).

Found: C, 73.73; H, 3.94; N, 5.00%. Calcd for $C_{17}H_{11}O_3N$: C, 73.64; H, 4.00; N, 5.05%.

This compound was identified by comparing its IR spectrum with that of the product melting at 128—129°C obtained in the pyrolysis of II.

BULLETIN OF THE CHEMICAL SOCIETY OF JAPAN, VOL. 44, 508—513 (1971)

Stoichiometric Carbonylation of Aryl Halide with Nickel Tetracarbonyl in the Presence of Potassium Acetate

Mikitake NAKAYAMA and Tsutomu MIZOROKI

Gevernment Chemical Industrial Research Institute, Tokyo, Mita, Meguro-ku, Tokyo

(Received July 30, 1970)

In the stoichiometric reaction of aryl halide with $Ni(CO)_4$ in methanol to form the corresponding ester, it has been found that the carbonylation is effectively promoted by adding potassium acetate to the starting materials, and that four moles of the ester are obtained from one mole of $Ni(CO)_4$ without any appreciable side reactions. From the inhibition by gaseous carbon monoxide and the IR measurements during the carbonylation, it has been concluded that nickel tricarbonyl, $Ni(CO)_3$, is the initiator of the carbonylation and that its regeneration is the rate-determining step. The present results provide a basis on which the course of the carbonylation of aryl halide with carbon monoxide catalyzed by $Ni(CO)_4$ under high temperatures and pressures may be reasonable explained.

Nickel tetracarbonyl is highly reactive in the carbonylation of organic halide, especially for aryl[1,2] and allyl halide.[3] They give the corresponding esters in a methanol solution. The yield of the ester is highly increased by adding an acceptor of hydrohalogenic acid formed during the carbonylation, though the role of the acceptor is not yet understood well.

In our previous paper dealing with the carbonylation of aryl bromide catalyzed by nickel carbonyl under high temperatures and pressures, it was reported that the carbonylation is promoted by adding a sufficient amount of carboxylic salt; this yields a quantitative amount of the corresponding carboxylic acid[4] as follows:

$$C_6H_5Br + CO + H_2O + AcOK \xrightarrow{Ni(CO)_4} C_6H_5COOH + AcOH + KBr \quad (1)$$

The role of the added carboxylic salt has been considered to reduce the concentration of hydrobromic acid, which inhibits the regeneration of nickel carbonyl. A similar effect was also observed in the stoichiometric reaction of aryl iodide with $Ni(CO)_4$ in methanol at a low temperature. That is, the carbonylation rate is effectively increased by adding carboxylic salt. It is to be noticed in this reaction that about four moles of the carboxylic ester are obtained from one mole of $Ni(CO)_4$, without any appreciable side reaction; this novel result is similar to that claimed by Reppe in the stoichiometric carbonylation of acetylene with $Ni(CO)_4$,[5] $Ni(CO)_4 + 4CH{\equiv}CH + 4ROH + 2HX \rightarrow 4CH_2{=}CHCOOR + NiX_2 + H_2$ ($R = CH_3$, C_2H_5, *etc.*; $X = Cl$, Br, CH_3CO_2, *etc.*). During the course of this study, it was reported by Corey and Hegedus[6] that the treatment of organic halide, RX, with several equivalents of nickel carbonyl in an alcoholic medium (R'OH) containing 2—3 equivalents of the corresponding sodium or potassium alkoxide (strongly basic medium) also results in the formation of the RCOOR' ester, while the reaction path of the coordinated carbon monoxide is still obscure.

The present study has been undertaken in order to investigate the reaction path of coordinated carbon monoxide in the stoichiometric reactions of aryl iodides with nickel tetracarbonyl in a methanol solution. On the basis of the results of this study, the course of catalytic carbonylation with nickel carbonyl has been discussed.

Results

The results of the stoichiometric reaction of iodobenzene with nickel tetracarbonyl in methanol under a nitrogen atmosphere at 50°C are summarized in Table 1. Iodobenzene, which has been known to react with nickel tetracarbonyl in methanol at re-

1) N. L. Bauld, *Tetrahedron Lett.*, **1963**, 1841.
2) E. Yoshisato, M. Ryang, and S. Tsutsumi, *J. Org. Chem.*, **34**, 1500 (1969).
3) F. Guerrieri and G. P. Chiusoli, *J. Organometal. Chem.*, **15**, 209 (1968).
4) M. Nakayama and T. Mizoroki, This Bulletin, **42**, 1124 (1969).
5) J. W. Copenhaver and M. H. Bigelow, "Acetylene and Carbon Monoxide Chemistry," Reinhold Publishing Corp., New York (1949), p. 246.
6) E. J. Corey and L. S. Hegedus, *J. Amer. Chem. Soc.*, **91**, 1233 (1969).

Table 1. Mass balance of the carbonylation of iodobenzene with $Ni(CO)_4$

(mol ratio) $Ni(CO)_4$[a] : C_6H_5I : AcOK			Ni^{0} [b] (mmol)	Ni^{2+} (mmol)	total Ni (mmol)	I^- (mmol)	I^- (%)[c]	$C_6H_5COOCH_3$ (mmol)	$C_6H_5COOCH_3$ (%)[c]
1	4	0	0	0.8	0.8	0.3	0	0	0
1	4	2	2.84	8.2	11.0	33.7	306	23.6	214
1	4	4	3.98	5.98	9.97	40.6	407	32.1	321
1	4	6	3.42	6.72	10.1	38.6	382	31.0	307
1	6	6	0.50	10.9	11.4	49.7	436	41.0	367

a) $Ni(CO)_4$, 11.6 mmol; CH_3OH, 2.0 mol
b) Metallic nickel isolated.
c) Based on the amount of total nickel.

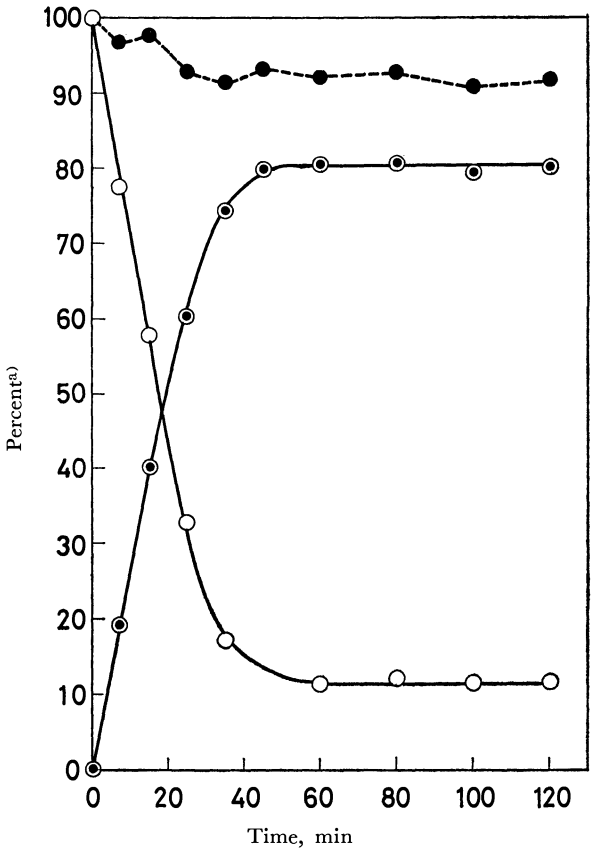

Fig. 1. Reaction rate of iodobenzene with nickel tetracarbonyl at 50°C under nitrogen. The rates illustrated are for iodobenzene, ○, methyl benzoate, ⊙, and mass balance of iodobenzene, ●.
C_6H_5I, 0.046 mol; $Ni(CO)_4$, 0.012 mol; AcOK, 0.046 mol; CH_3OH, 2.0 mol
a) The percentage was based on the amount of iodobenzene used.

flux to form methyl benzoate, was unchanged in the absence of potassium acetate under the conditions specified in Table 1, while it was vigorously changed by the addition of potassium acetate. It is highly soluble in methanol (more than 33 g/100 g methanol at 25°C). This is why potassium acetate and methanol were used preferably in this study. As soon as the temperature of the solution reached 50°C, its color changed from almost colorless to a reddish brown; this change was followed by the deposition of a black precipitate within half an hour. In the final stage, the solution turned green because of the Ni(II) ion.

In the absence of aryl halide, no reaction of nickel tetracarbonyl with potassium acetate was observed. The variations in the amounts of iodobenzene and methyl benzoate during the reaction were followed by gas chromatography; the results are shown in Fig. 1. The reaction was practically finished within 1 hr. The black precipitation did not show any absorption in the NaCl region of the IR spectrum, and it was easily dissolved in a dilute aqueous nitric acid solution, while some gas was evolved. The precipitate was found, by elementary analysis, to be metallic nickel, which has been partially oxidized by air during the separation. As is shown in Table 1, the mole ratio of the iodide ion to the total nickel[7] in the product ($[I^-]$/[Total Ni]), and that of methyl benzoate to the total nickel in the product ($[C_6H_5COOCH_3]$/[Total Ni]), are both approximately four. Practically no carbon monoxide was evolved during the carbonylation. From these results, we may conclude that all the carbon monoxide involved in nickel tetracarbonyl is consumed in the carbonylation of iodobenzene, as is represented by Eq. (2):

$$Ni(CO)_4 + 4C_6H_5I + 4CH_3OH + 4AcOK \longrightarrow Ni + 4C_6H_5COOCH_3 + 4AcOH + 4KI \quad (2)$$

That the $[C_6H_5COOCH_3]$/[Total Ni] ratio was smaller than 4 seems to be caused by the formation of smaller amounts of benzene and anisole. Neither free benzoic acid nor phenyl acetate could be detected.

Under a nitrogen atmosphere the carbonylation of iodobenzene took place smoothly, as has been described above; no carbonylation was, however, observed at all under a carbon monoxide atmosphere, and the solution remained colorless for at least 3 hr at 50°C, despite our expectation that the carbonylation might take place catalytically even under these mild conditions. This means that the reaction was completely inhibited by an atmospheric pressure of carbon monoxide. It was found that the carbonylation really started, even at room temperature (20°C), when a trace amount of carbon monoxide in the gas phase was removed by means of a nitrogen gas stream.

The IR absorption during the reaction with iodobenzene and with α-iodonaphthalene is shown in Figs. 2 and 3. As soon as the solution turned a reddish brown, four new bands are observed, at 1993, 1963,

7) "Total nickel" means the sum of the Ni^{2+} and the metallic nickl formed.

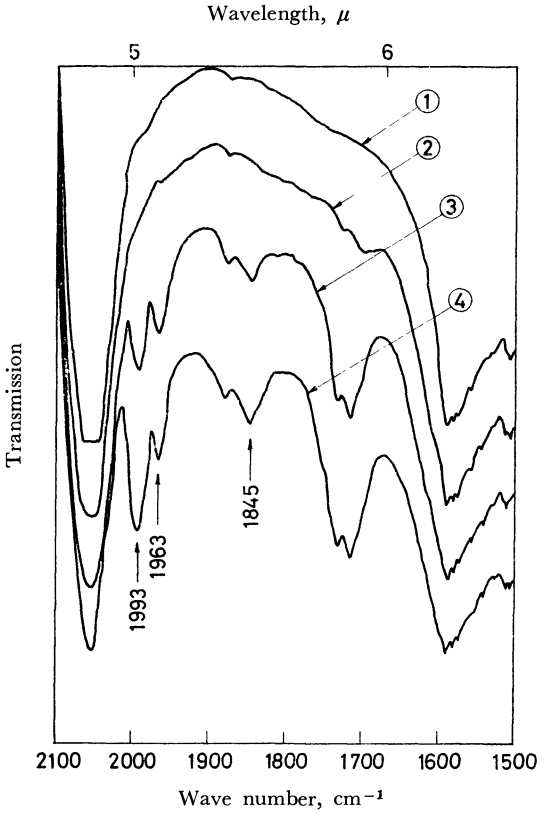

Fig. 2. IR absorption during the reaction of iodobenzene with nickel tetracarbonyl in methanol at 30—40°C under nitrogen.
① starting solution
②—④ during the reaction

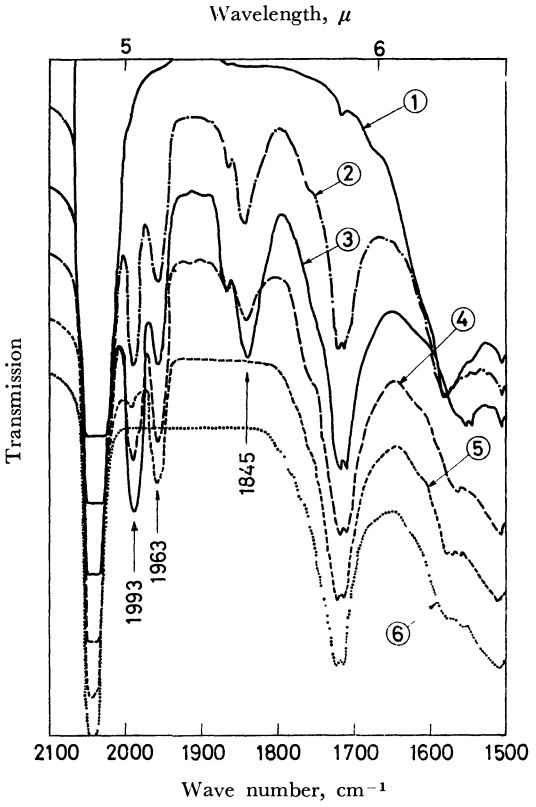

Fig. 3. IR absorption during the reaction of α-iodonaphthalene with nickel tetracarbonyl in methanol at 20—25°C under nitrogen.
① starting solution
②—⑤ during the reaction
⑥ after the reaction finished

1845, and about 1720 cm^{-1}, in the range of the CO stretching vibration. The last one consisted of two absorptions due to the methyl esters formed and acetic acid; these absorptions were checked by authentic samples. Figure 3 shows that the intensities of the former three absorptions gradually decrease with the consumption of α-iodonaphthalene in the carbonylation, and that they disappear when the reaction is almost finished. In fact, α-iodonaphthalene is more reactive than iodobenzene, resulting in an almost quantitative formation of α-methyl naphthoate under the reaction conditions cited in Fig. 3. It should be noticed here that the absorptions at 1993 and 1845 cm^{-1} disappear more rapidly than that at 1963 cm^{-1}.

Aryl bromides, such as bromobenzene, α-bromonaphthalene or *p*-bromoanisole, did not undergo carbonylation under even more forced conditions than those cited in Table 1, while both α- and ω-bromostyrene were much more reactive than aryl iodides; in the cases of α- and ω-bromostyrene, methyl α-phenyl acrylate, and methyl cinnamate were selectively formed respectively.[8] Most of the carbon monoxide involved in nickel tetracarbonyl was found to be also consumed in their carbonylations. These carbonylations too rapidly, even at room temperature, and they were accompanied by the formation of much potassium bromide precipitation; this prevented the taking of the IR absorption spectrum during their reactions. Such alkyl halides as ethyl-, *t*-butyl-, *n*-amyl-, *t*-amyl, and cyclohexyl halides, including iodides, were treated with $Ni(CO)_4$ by the same procedure; however, no carbonylation was observed, only dehalogenation products as the corresponding alcohols and methyl ethers from ethyl-, *t*-butyl-, *n*-amyl-, or *t*-amyl halides and cyclohexene from cyclohexyl halide. On the other hand, allyl halide reacted vigorously with $Ni(CO)_4$ in methanol, even at 0°C, to form methyl 3-butenoate, plus considerable amounts of such by-products as 1,5-hexadiene, methyl allyl ether, and diallyl ether. The amount of methyl 3-butenoate was also increased by adding potassium acetate, whereas only half the amount of the carbon monoxide involved in $Ni(CO)_4$ could be used for the carbonylation of allyl halide, where no inhibition by gaseous carbon monoxide was observed. In this respect, the carbonylation of aryl halide was quite different from that of allyl halide, which has been studied in detail by Guerrieri and Chiusoli.[3]

8) α-Phenylacrylic acid and cinnamic acid, besides their esters, were isolated from the respective products.

Discussion

It is known that nickel tetracarbonyl forms unstable substitution products with such relatively weak bases as pyridine in a methanol solution and that they are

present in solution in equilibrium[9] with such polynuclear carbonyl anion as $[Ni_2(CO)_6]^{2-}$, $[Ni_3(CO)_8]^{2-}$, *etc.*[10,11] In a strong basic solution, as in potassium hydroxide solution, $[Ni_2(CO)_6]^{2-}$ or $[Ni_3(CO)_8]^{2-}$ is preferably formed. If these nickel carbonyl anions were reactive species in the carbonylation of aryl halide, a stronger basic solution would be more favorable for the carbonylation. However, carbonylation takes place more readily in a weak basic solution, as in the presence of potassium acetate, than in a strong basic solution, though no interaction between $Ni(CO)_4$ and potassium acetate is observed in the absence of aryl iodide.

From the following considerations, it has been concluded that nickel tricarbonyl is an active species in the carbonylation.

The Inhibition by Carbon Monoxide. The fact that iodobenzene does not undergo carbonylation at all under an atmospheric pressure of carbon monoxide, as has been described in the preceding section, can be understood on the basis of the following scheme:

$$Ni(CO)_4 \underset{k_2}{\overset{k_1}{\rightleftarrows}} Ni(CO)_3 + CO \quad (k_1 \ll k_2) \tag{3}$$

$$Ni(CO)_3 + C_6H_5I \xrightarrow{k_3} (C_6H_5I)Ni(CO)_3 \quad (k_3 \ll k_2) \tag{4}$$

It is well known that the exchange reaction between $Ni(CO)_4$ and ^{14}CO proceeds *via* S_N1 ($k_2 \gg k_1$) and that its rate is very large under a normal temperature and pressure (the half-value period of ^{14}CO radioactivity in the gas phase is less than 4 min in a toluene solution[9]). Accordingly, the coordination of iodobenzene to nickel tricarbonyl is in competition with the rapid recombination of carbon monoxide, where k_3 must be much smaller than k_2. The carbonylation starts practically when the former rate becomes larger than the latter. Accordingly, the lower the pressure of carbon monoxide, the more favorable for the coordination of iodobenzene to nickel tricarbonyl. It can be understood why no carbonylation is observed when $Ni(CO)_3(PPh_3)$ or $Ni(CO)_2(PPh_3)_2$ ($Ph = C_6H_5$) is used instead of $Ni(CO)_4$, since the dissociation rates of carbon monoxide from these carbonyls are extremely small.[12]

IR Absorption Spectrum During the Course of Reaction. Figures 2 and 3 show that the IR absorptions at 1845, 1963, and 1993 cm^{-1} during the carbonylation of iodobenzene are identical with those observed during the reaction of α-iodonaphthalene. These absorptions can not be regarded as due to some acyl complex such as $RCO\text{-}Ni(CO)_nI$, nor due to some σ-complex such as $R\text{-}Ni(CO)_nI$ ($R = C_6H_5$ or α-$C_{10}H_7$), because absorptions of acyl metal carbonyls are usually observed in the range between 1700—1750 cm^{-1}. If they correspond to aryl σ-complexes, the IR absorption of the phenyl σ-complex will probably be different from that of the naphthyl complex.

As was pointed out in the preceding section, the absorptions at 1993 and 1845 cm^{-1} disappear more quickly than that at 1963 cm^{-1}. This suggests that there are two kinds of intermediates present during the carbonylation. One has two absorptions, at 1993 and 1845 cm^{-1}, while the other has only one, at 1963 cm^{-1}. In the neutral binary carbonyls, the higher frequencies (2050—1900 cm^{-1}) are regarded as being due to terminal carbonyl groups, and the lower frequencies (1900—1800 cm^{-1}), as due to the bridging carbonyl groups, whose molar extinction coefficients are smaller than those of terminal carbonyls.[13] Accordingly, one of the intermediates can be ascribed to a binuclear nickel complex[14] with both bridging and terminal carbonyls, and the other, to a mononuclear nickel complex with only terminal carbonyls.

Reaction Path. From the considerations described above and the fact that all the carbon monoxide in $Ni(CO)_4$ are used for the carbonylation of aryl iodide, the reaction path can be represented as follows:

$$Ni(CO)_4 \rightleftarrows Ni(CO)_3 + CO \tag{3}$$

$$Ni(CO)_3 + RI \longrightarrow (RI)Ni(CO)_3 \tag{4}$$

$$(RI)Ni(CO)_3 + CH_3OH \longrightarrow (HI)Ni(CO)_2 + RCOOCH_3 \tag{5}$$

$$(HI)Ni(CO)_2 + AcOK \longrightarrow Ni(CO)_2 + AcOH + KI \tag{6}$$

$$Ni(CO)_2 + Ni(CO)_4 \rightleftarrows Ni_2(CO)_6 \tag{7}$$

$$3Ni(CO)_2 \rightleftarrows Ni + Ni_2(CO)_6 \tag{7'}$$

$$Ni_2(CO)_6 \longrightarrow 2Ni(CO)_3 \tag{8}$$

($R = C_6H_5$ or α-$C_{10}H_7$)

The reaction (5) proceeds rapidly, probably through steps analogous to those reported in the carbonylation using *cis*-$Rh(PPh_3)_2(CO)Cl$,[16] namely: $(C_6H_5I)Ni(CO)_3 \rightarrow C_6H_5\text{-}Ni(CO)_3I \rightarrow C_6H_5CO\text{-}Ni(CO)_2I \xrightarrow{+CH_3OH} (HI)Ni(CO)_2 + C_6H_5COOCH_3$. The reaction (6) means that the acetate anion effectively takes proton from $(HI)Ni(CO)_2$. In the absence of potassium acetate, $(HI)Ni(CO)_2$ will be rapidly decomposed and $Ni(CO)_3$ will not be supplied smoothly, with the result that practically no carbonylation is observed. The two intermediates expected from the IR absorptions observed during the carbonylation can be regarded as: 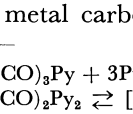 ($Ni_2(CO)_6$) and $Ni(CO)_2$.[17] These

9) Namely: $3Ni(CO)_3Py + 3Py \rightleftarrows [NiPy_6][Ni_2(CO)_6] + 3CO$
$3Ni(CO)_2Py_2 \rightleftarrows [NiPy_6][Ni_2(CO)_6]$
$[NiPy_6][Ni_2(CO)_6] + Ni(CO)_3Py \rightleftarrows [NiPy_6][Ni_3(CO)_8] + Py + CO$

10) F. Calderazzo, R. Ercoli, and G. Natta, "Organic Syntheses *via* Metal Carbonyls," Vol 1, ed. by I. Wender and P. Pino, Interscience Publishers, New York (1968), p. 67.

11) W. Hieber, J. Ellermann, and E. Zahn, *Z. Naturforsch.*, *B*, **18**, 589 (1963).

12) F. Basolo and A. Wojcicki, *J. Amer. Chem. Soc.*, **83**, 520 (1961).

13) E. W. Abel, *Quart. Rev.* (London), **17**, 133 (1963).

14) The hexacarbonyldinickelate anion, $[Ni_2(CO)_6]^{2-}$, has four absorptions, at 1978, 1968, 1927, and 1870 cm^{-1}, in a potassium hydroxide methanol solution; these are all different from the absorptions observed during the carbonylation. This anion was prepared according to the method described in Ref. 15.

15) W. Hieber, W. Kroder, and E. Zahn, *Z. Naturforsch.*, **B**, **15**, 325 (1960).

16) J. Tsuji and K. Ohno, *Tetrahedron Lett.*, **1966**, 4713.

17) The solvent molecule or iodide ion probably coordinates to these intermediates.

intermediates can be accumulated sufficiently to be observed by IR absorption when the reaction (8) (the regeneration of $Ni(CO)_3$) is rate-determining. The formation of a considerable amount of metallic nickel[18] can also be explained by the reaction (7'). The stoichiometric equation (2), showing that all the carbon monoxide involved in $Ni(CO)_4$ is used for the carbonylation of aryl iodide, can be derived by combining the reaction path described above.

The catalytic carbonylation of aryl bromide under high temperatures and pressures can be reasonably explained by this reaction path, with Br and H_2O replacing I and CH_3OH respectively. The catalytic carbonylation of α-bromonaphthalene with carbon monoxide and water in the presence of $Ni(CO)_4$ is highly promoted by adding a sufficient amount of potassium acetate, resulting in the quantitative formation of α-naphthoic acid, as has been reported in the preceding paper.[19] That is, its rate increasing with an increase in the amount of $Ni(CO)_4$ and also with that of potassium acetate, while it depends on neither the amounts of α-bromonaphthalene and water, nor on the pressure of carbon monoxide under 60—150 kg/cm² at 200°C, though the rate decreases with an increase in the pressure to more than 200 kg/cm². Lower pressures should favor the equilibria of the reactions (3) and (4) inclining much toward the right, and the rate of the reaction (5) must be sufficiently large at this temperature. Accordingly, the rate of carbonylation will be determined by either the reaction (6) or the regeneration of nickel tricarbonyl. In this catalytic reaction, nickel tricarbonyl must be regenerated, preferably by the coordination of carbon monoxide to the $Ni(CO)_2$ formed by the reaction (6) instead of that formed by the reactions (7) and (8). Since the carbonylation rate of α-bromonaphthalene under lower pressures is independent of the pressure of carbon monoxide, the reaction (6) must be rate-determining.

On the other hand, a different kinetics has been observed for the carbonylation of bromobenzene under pressures of more than 150 kg/cm² at 250°C, where the rate is proportional to the amounts of $Ni(CO)_4$, bromobenzene, water, and the reciprocal of the pressure of carbon monoxide, and is independent of the amount of potassium acetate when its amount is more than that of the bromobenzene used, as has been reported in a previous paper.[4] In this case, bromobenzene is less reactive than α-bromonaphthalene and the catalyst must be present predominantly in the form of $Ni(CO)_4$ because of the high pressures of carbon monoxide. The carbonylation rate of bromobenzene can, accordingly, be explained by the same reaction path, assuming that the reactions (3) and (4) are in equilibrium and that (5) is rate-determining.

From the above discussion, it can be concluded that nickel tricarbonyl is the active species in the carbonylation of aryl halide with nickel tetracarbonyl in the presence of potassium acetate in methanol, and that the course of its catalytic reaction can reasonably be explained by the reaction path derived from the stoichiometric reaction.

Experimental

Materials. The iodobenzene and *trans*-ω-bromostyrene were commercial products. They were distilled before use. Iodobenzene especially was carefully purified by fractional distillation (Podbielniak 4500; glass concentric-tube column), because a trace amount of nitrobenzene strongly inhibited the carbonylation of iodobenzene. The *trans*-ω-bromostyrene might contain a small amount of *cis*-ω-bromostyrene, which was difficult to separate by distillation. The α-iodonaphthalene was freshly prepared by the iodination of naphthalene using $AgClO_4$, according to the method described in the literature.[20] The α-bromostyrene was prepared by drawing out hydrobromic acid with a potassium hydroxide ethanol solution from the α,ω-dibromoethylbenzene obtained by the bromination of styrene.[21] All these substances were purified by distillation under a vacuum. The nickel tetracarbonyl, potassium acetate, and other compounds employed in this study were obtained from commercial sources.

Carbonylation of Iodobenzene. A methanol solution of iodobenzene and potasssium acetate was placed in a two-necked flask (100 m*l* in vol.) equipped with a reflux condenser. A given amount of distilled nickel tetracarbonyl was condensed into the flask, which had been cooled by immersing it in solid carbon dioxide - methanol; then the flask was warmed up to 50°C while being vigorously stirred under an atmospheric pressure of nitrogen, with the temperature being kept constant. After 2 hr, the residual nickel tetracarbonyl was completely evacuated; then the solution was filtered to separate a black precipitate (metallic nickel). Sufficient amounts of ether and water were added to the filtrate to extract and separate organic compounds from the Ni^{2+} and I^- formed. The amounts of methyl benzoate and iodobenzene in the ether solution were determined by gas chromatography. The black precipitate was dissolved in aqueous nitric acid; its quantity was determined by the ordinary EDTA method. These results are summarized in Table 1.

Carbonylation of α-Iodonaphthalene. The reaction of α-iodonaphthalene (0.023 mol) with $Ni(CO)_4$ (0.0056 mol) was carried out at 30°C for 6 hr in methanol(2.0 mol) containing potassium acetate (0.023 mol) under an atmospheric pressure of nitrogen. By treating the product according to the same procedure described above, I^- (0.0177 mol) and total nickel (0.0049 mol; metallic nickel 0.0017 mol and Ni^{2+} 0.0032 mol) were separated from the organic compounds, where $[I^-]/[\text{Total Ni}]$ was 3.64. The amount of α-methylnaphthoate could be estimated from the amount of I^- formed, because no other organic compounds, such as naphthalene or ketones, were detected.

Carbonylation of Bromostyrene. Under the same reaction conditions and using the same procedure as those used for iodobenzene, ω-bromostyrene (0.046 mol) reacted with $Ni(CO)_4$ (0.012 mol) in methanol (2.0 mol) containing potassium acetate (0.046 mol) to give methyl cinnamate and cinnamic acid. In this case, the amounts of Br^- and Ni^{2+} were 0.046 mol and 0.0095 mol respectively. From an ethereal

18) The Ni^{2+} ion is presumably formed by the reaction of metallic nickel with the acetic acid formed, namely: $Ni + 2\,AcOH \rightarrow Ni(AcO)_2 + H_2\uparrow$.

19) M. Nakayama and T. Mizoroki, This Bulletin, **43**, 569 (1970).

20) L. Birckenbach and J. Goubeau, *Ber.*, **65**, 395 (1932).

21) F. Ashworth and G. N. Burkhardt, *J. Chem. Soc.*, **1928**, 1801.

solution, free cinnamic acid (0.0054 mol) beside its ester (0.0271 mol) were isolated, though no free carboxylic acid was isolated from the carbonylation product of iodobenzene or α-iodonaphthalene. α-Bromostyrene (0.046 mol) also gave methyl α-phenyl acrylate and α-phenylacrylic acid (atropic acid) (Found: C, 72.6; H, 5.4%. Calcd for $C_9H_8O_2$: C, 73.0; H, 5.4%. mp 108—9°C), and a small amount of styrene (0.0059 mol) was observed on their gas chromatograms. The total amount of α-phenylacrylic acid formed could be estimated from that of Br^- (0.0441 mol).

Analytical Procedure. Most of the organic compounds were quantitatively determined by gas chromatography. A 1.5-m stainless steel column (3 mmϕ) with silicone DC 11 was used at a temperature of 160 or 190°C, with a hydrogen carrier and a gas-flow rate of 40 ml/min. In this procedure, naphthalene was used as the internal standard for determining the amounts of iodobenzene and methyl benzoate, and α-bromonaphthalene was used for bromostyrene and their corresponding esters. Free carboxylic acids (cinnamic acid and α-phenylacrylic acid) were precipitated by adding an aqueous hydrochloric acid solution to their potassium salts, and their amounts were titrated with an aqueous potassium hydroxide solution. The compounds were identified by means of the IR absorption spectrum, the melting points, a comparison of their gas chromatograms with those of authentic samples, or the results of elementary analysis, if necessary. The halide ion (Br^- or I^-) and the nickel(II) ion were determined by the Volhard and EDTA methods respectively.

IR Absorption Spectra during the Carbonylation. To record the IR absorption spectrum during the course of the reaction with iodobenzene or α-iodonaphthalene, the carbon monoxide present in the gas phase had been excluded by a nitrogen-gas stream before the reaction was carried out at room temperature. A part of the solution was drawn out from the vessel about once an hour by means of a small cylinder and put into a KRS-5 cell under nitrogen in order to record the variation in the IR absorption spectra during the carbonylation.

The authors wish to acknowledge the enthusiastic assistance of Mr. Masao Ichinose in carrying out this work.

BULLETIN OF THE CHEMICAL SOCIETY OF JAPAN, VOL. 44, 513—519 (1971)

Polarography of Halides in Dimethylformamide. VI. The Formation of the Benzhydryl Radical from Benzhydryl Bromide and Its Subsequent Reduction at the Dropping Mercury Electrode

Yoshihisa MATSUI, Takashi SOGA, and Yoshio DATE

Department of Agricultural Chemistry, Shimane University, Nishikawazu-cho, Matsue

(Received August 6, 1970)

The polarographic behavior of benzhydryl bromide at the dropping mercury electrode was investigated in dimethylformamide at 25°C. It gives three waves, with half-wave potentials at about +0.19, −0.15, and −1.00 V *vs.* SCE. The first wave is anodic, while the others are cathodic. It was concluded that benzhydryl bromide, prior to being electrolytically reduced, rapidly reacts with the mercury of the cathode according to the following equation:

$$3(C_6H_5)_2CHBr + Hg \longrightarrow 2(C_6H_5)_2CH\cdot + (C_6H_5)_2CH^+ + HgBr_3^-$$

The first wave given by the bromide was ascribed to the oxidation of $HgBr_3^-$ to $HgBr_2$; the second, to the reduction of $HgBr_3^-$ to Hg and Br^-, and the third, to the reduction of $(C_6H_5)_2CH\cdot$ to $(C_6H_5)_2CH^-$. The cation, $(C_6H_5)_2CH^+$, was found to give no wave. Such behavior of benzhydryl bromide was discussed in comparison with that of the corresponding chloride, which gives a single wave with a usual two-electron transfer.

Organic halides are not always electrolyzed in a usual two-electron reduction, followed by the uptake of the hydrogen ions to yield the corresponding hydrocarbons. For example, when an organic halide reacts rapidly with the mercury used as the indicator electrode, the electrode process can differ from those of usual halides which are reduced in two-electron steps. Thus, Keller *et al.*[1] have polarographically shown that the mercury may remove two chlorine atoms from 1,1-di-*p*-chlorophenyl-1,2,2,2-tetrachloroethane before the electron transfer occurs and thus form 1,1-di-*p*-chlorophenyl-2,2-dichloroethylene, which in turn is electrolytically reduced. Wawzonek *et al.*[2] have shown that benzyl iodide in acetonitrile, prior to being electrolytically reduced, reacts with the mercury of the indicator electrode to yield benzylmercuric iodide, which is then reduced to toluene, mercury, and the iodide ion. Similar examples can also be seen in benzotrichloride,[3] diphenyldichloromethane,[3] and triphenylmethyl chloride.[4] These indicate that polarography with the dropping mercury electrode is a useful means of elucidating the mechanisms of the reactions between mercury and the organic species which are reactive to mercury.

In the present paper, we will examine the polarographic behavior of benzhydryl bromide in dimethylformamide (DMF). The bromide was found to give unusual polarographic waves as a result of its reaction with mercury preceding the electrolytic reduction. The mechanism of the chemical and electrochemical reactions of the bromide at the dropping mercury

1) H. Keller, M. Hochweber, and H. von Halban, *Helv. Chim. Acta*, **29**, 761 (1946).

2) S. Wawzonek, R. C. Duty, and J. H. Wagenknecht, *J. Electrochem. Soc.*, **111**, 74 (1964).

3) S. Wawzonek and R. C. Duty, *ibid.*, **108**, 1135 (1961).

4) P. J. Elving and J. M. Markovitz, *J. Phys. Chem.*, **65**, 686 (1961).

electrode will be discussed in detail on the basis of the results of DC polarography and large-scale electrolysis at a controlled potential.

Results and Discussion

Polarographic Behavior of Benzhydryl Bromide. The polarographic behavior of benzhydryl bromide at the dropping mercury electrode was investigated in DMF containing 0.10 M tetraethylammonium perchlorate at 25°C. The bromide gives three waves; the first wave is anodic,[5] while the others are cathodic (Fig. 1). The ratio of the heights of these waves is approximately 1 : 2 : 2. However, the height of the third wave decreases with the time, while those of the first and second waves remain constant (Table 1). The decrease in the height of the third wave can be accelerated by stirring the cell solution, but it is appreciably

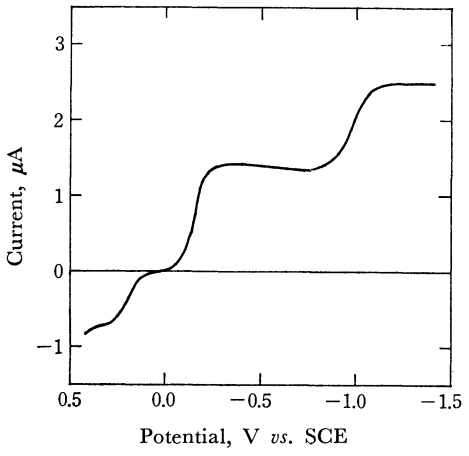

Fig. 1. Polarogram of 0.75 mM $(C_6H_5)_2CHBr$ in DMF containing 0.1 M Et_4NClO_4 at 25°C.

Table 1. Change of the heights of the waves given by benzhydryl bromide[a] with the time (25°C)

Time[b] (min)	i_d (μA)		
	1st wave	2nd wave	3rd wave
2	1.20	2.38	2.11
120	1.18	2.39	1.87
180	1.22	2.47	1.30
260	1.17	2.13	1.00

a) 1.0 mM.
b) The time was measured after the addition of mercury to the test solution.

5) When the solution of the bromide in DMF was fresh enough, the first wave was cathodic in part; it then turned anodic in time. The change did not stop until the first wave became completely anodic. It seems that this change is closely related to the simultaneously-occurring increase in the specific conductance of the bromide solution, as will be shown in Fig. 5. Thus, it is evident that the bromide undergoes ionization in DMF to form the ion-pair intermediate, and that the polarographic behavior of the resulting ionic species is different from that of the bromide in a covalently-bonded initial state. In the present study, the bromide was always allowed to stand in DMF for at least 3 hr before being used. Accordingly, most of the bromide might have been ionized by the time it was examined.

suppressed by using the platinum foil as the anode instead of the mercury pool. So far as the test solution is allowed to stand without contact with mercury, the height of the third wave does not decrease. These facts indicate that benzhydryl bromide reacts with mercury to form at least two electroactive species, one of which must be labile. Accordingly, the measurement of the polarogram of this depolarizer was always started as soon as possible after the test solution had come into contact with the mercury.

The polarographic characteristics of the bromide at various concentrations are given in Table 2. The height of each wave is practically proportional to the concentration of the depolarizer and to the square root of the height of the mercury reservoir; these facts indicate that each wave is diffusion-controlled. The diffusion coefficient of the bromide, calculated from the Ilkovic equation on the assumption that the third wave is due to a one-electron reduction, is equal to 3.3×10^{-6} cm²/sec; this value is too small to be regarded as the true value. We will discuss this question again later. It was also found that the half-wave potential of the third wave is practically independent of the concentration of the depolarizer, whereas that of the second wave shifts to the more negative potentials with an increase in the concentration. Because of the considerable irregularity of the plots given, no trends were obtained as to the change in the half-wave potential of the first wave with the concentration.

Table 2. Polarographic characteristics of benzhydryl bromide at various concentrations (25°C)

Concn. (mM)	$E_{1/2}$ (V vs. SCE)			I_d[a]		
	1st wave	2nd wave	3rd wave	1st wave	2nd wave	3rd wave
0.10	+0.171	−0.114	−0.977	0.56	1.32	1.18
0.25	+0.193	−0.120	−0.962	0.56	1.03	0.86
0.50	+0.188	−0.129	−0.967	0.52	1.04	1.07
0.75	+0.210	−0.131	−0.964	0.58	1.08	0.95
1.00	+0.166	−0.153	−1.000	0.56	1.04	1.10
1.50	+0.185	−0.176	−1.009	0.53	0.99	1.11
2.00	+0.212	−0.162	−1.009	0.56	1.08	1.01
2.50	+0.193	−0.195	−1.067	0.61	1.14	1.14

a) $I_d=i_d/Cm^{2/3}t^{1/6}$.

Comparison of the Polarographic Behavior of Benzhydryl Bromide with That of the Corresponding Chloride. The polarogram of benzhydryl chloride is in clear contrast to that of the corresponding bromide. The former gives only a single reduction wave (Fig. 2), although a maximum appears at depolarizer concentrations higher than 0.8 mM. The polarographic characteristics of the chloride at various concentrations are shown in Table 3. The height of the wave is virtually proportional to the concentration of the depolarizer; this indicates that the wave is diffusion-controlled. The diffusion coefficient of the chloride, calculated from the Ilkovic equation on the assumption that the wave is due to a two-electron step, is equal to 11.3×10^{-6} cm²/sec; this value is fairly appropriate for this molecule. The marked difference in the polaro-

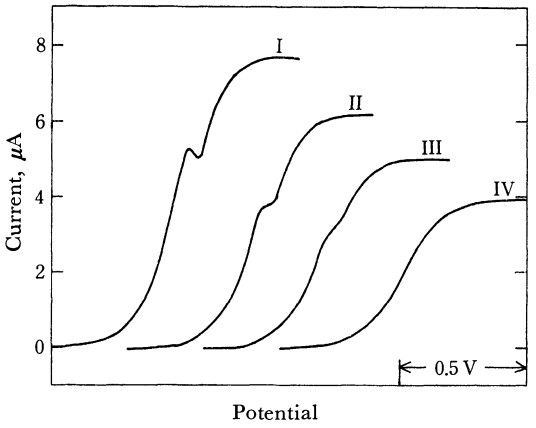

Fig. 2. Polarograms of $(C_6H_5)_2CHCl$ in DMF containing 0.1 M Et_4NClO_4 at 25°C. Each recording was started from −1.20 V *vs.* SCE.
I, 1.2 mM; II, 1.0 mM; III, 0.8 mM; IV, 0.6 mM

TABLE 3. POLAROGRAPHIC CHARACTERISTICS OF BENZHYDRYL CHLORIDE AT VARIOUS CONCENTRATIONS (25°C)

Concn. (mM)	$E_{1/2}$ (V *vs.* SCE)	I_d[a)]
0.10	−1.642	5.16
0.30	−1.675	4.07
0.50	−1.664	4.16
0.60	−1.679	4.07
0.80	b)	4.03
1.00	b)	4.07
1.20	b)	4.06
2.00	b)	4.00

a) $I_d = i_d/Cm^{2/3}t^{1/6}$.
b) Impossible to measure owing to the maximum.

graphic behavior between the chloride and the bromide may be related to the difference in their reactivities with mercury. As has been described above, benzhydryl bromide in DMF reacts rapidly with mercury. It seems that the rate of the reaction is determined by the diffusion of the bromide. On the other hand, benzhydryl chloride in DMF reacts very slowly with mercury. When a solution of the chloride in DMF was stirred with mercury at 25°C, the height of the polarographic wave resulting from the reduction of the chloride decreased very slowly with the time (Fig. 3). At the same time, two new waves appeared in the less negative potential region, and they increased with the time. The new waves were closely similar in characteristics to the first and second waves of benzhydryl bromide; the first was anodic, the second was cathodic, and the ratio of the wave heights was about 1 : 2.

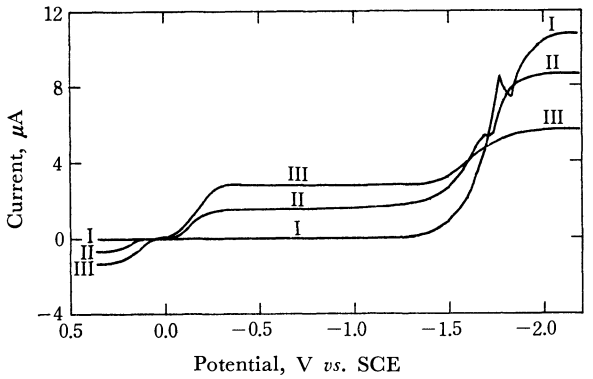

Fig. 3. Change of the polarogram of $(C_6H_5)_2CHCl$ (1.68 mM) in DMF at 25°C with the time.
I, 0 min; II, 2.0 days; III, 10.0 days after the addition of mercury to the test solution

The First and the Second Waves of Benzhydryl Bromide. It was noticed that the first and the second polarographic waves of benzhydryl bromide, as well as those of the reaction mixture of benzhydryl chloride with mercury, are very similar to the waves of the trihalogenomercurate ion. As has been shown in previous papers,[6,7] the trihalogenomercurate ion gives two waves, at about +0.2 and −0.15 V *vs.* SCE; the first is anodic, the second is cathodic, and the ratio between the heights of the waves is approximately equal to 1 : 2. This suggests that benzhydryl bromide and chloride react with mercury to form the tribromo- and trichloromercurate ions respectively. The reaction of benzhydryl bromide with mercury may be so rapid that it precedes the electrolytic reduction. Hence, the bromide gives the waves due to the electrolysis of the tribromomercurate ion instead of those due to the electrolysis of benzhydryl bromide itself.

This conclusion was substantiated by the analysis of the waves given by benzhydryl bromide. The electrode reactions of the tribromomercurate ion at the dropping mercury electrode can be expressed in terms of the following equations:[6]

$$\text{1st wave: } 2\,HgBr_3^- + Hg \rightleftarrows 3\,HgBr_2 + 2\,e \quad (1)$$

$$\text{2nd wave: } 2\,HgBr_3^- + 4\,e \rightleftarrows 2\,Hg + 6\,Br^- \quad (2)$$

If the first and the second waves of benzhydryl bromide are due to the depolarization by the tribromomercurate ion, the following relations between current and potential, which have shown to hold for the waves of the latter,[6] should hold for those of the former:

$$\text{1st wave: } E = C_1 + (RT/2F)\ln i^3/(i_d - i)^2 \quad (3)$$

$$\text{2nd wave: } E = C_2 - (RT/2F)\ln i^3/(i_d - i) \quad (4)$$

The results of the analyses of these waves, as well as that of the third wave, are given in Fig. 4. A nearly linear relation was obtained for each of these waves; this means that the presumption presented above is valid. From Eqs. (3) and (4) we can easily derive the relation between the half-wave potential and the concentration of the depolarizer,[6] which shows that the half-wave potential of the first wave should shift to more positive potentials, and that of the second wave, to more negative potentials, with an increase in the depolarizer concentration. The results in Table 2 show that this speculation is also valid, although the data for the first wave show considerable scatter.

The Third Wave of Benzhydryl Bromide. It was found that the height of each of the waves given by 1.0 mM of the tribromomercurate ion (I_d's=1.95 and

6) Y. Matsui, R. Kawakado, and Y. Date, This Bulletin, **41**, 2913 (1968).
7) Y. Matsui, Y. Kurosaki, and Y. Date, *ibid.*, **43**, 2046 (1970).

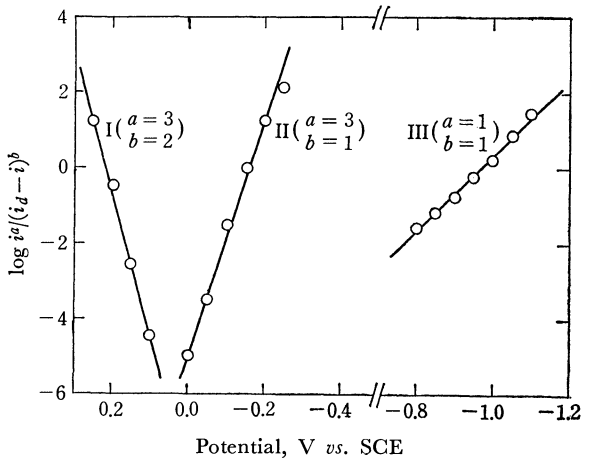

Fig. 4. Analysis of the polarograms of 0.75 mM $(C_6H_5)_2CHBr$ in DMF.
Reciprocal slopes: I, 0.029 V; II, −0.031 V; III, −0.098 V

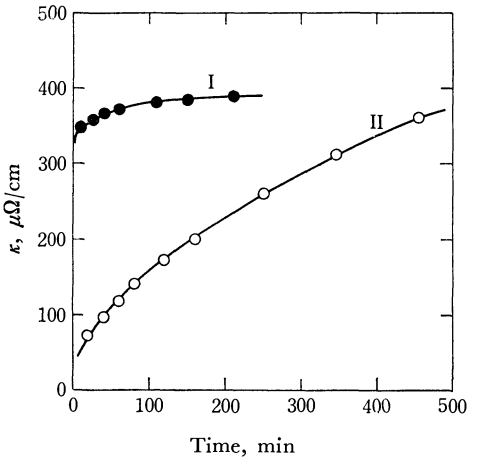

Fig. 5. Plots of the conductance *vs.* the time.
I: $(C_6H_5)_2CHBr$ (44.4 mM) + $HgBr_2$ (44.4 mM) in DMF
II: $(C_6H_5)_2CHBr$ (83.4 mM) in DMF

3.54 for the first and the second waves respectively[6]) is about three times that of the corresponding waves given by 1.0 mM of benzhydryl bromide; this indicates that three moles of benzhydryl bromide react with one gram-atom of mercury to yield one mole of the tribromomercurate ion. Hence, the following stoichiometric equation seems the most probable:

$$3\,(C_6H_5)_2CHBr + Hg \longrightarrow 2\,(C_6H_5)_2CH\cdot + (C_6H_5)_2CH^+ + HgBr_3^- \qquad (5)$$

Provided that the reaction expressed by Eq. (5) precedes the electrolytic reduction of benzhydryl bromide itself, the third wave of the bromide may be ascribed either to the reduction of the benzhydryl radical or to that of the benzhydryl cation. In order to make this point clear, we examined the polarographic behavior of an equimolar solution of benzhydryl bromide and mercuric bromide in DMF. The reaction between them is fairly rapid, as is shown by the rapid increase in the conductance of the solution (Fig. 5), while the conductance of the DMF solution containing only benzhydryl bromide shows a slower increase with the time. The polarogram of the equimolar solution is shown in Fig. 6. Although the two waves corresponding to the electrolyses of the tribromomercurate ion appeared, no wave arose in the potential region where the third wave of benzhydryl bromide appeared. This shows that benzhydryl bromide reacts with mercuric bromide and yields the tribromomercurate ion, together with the benzhydryl cation; the latter, however, gives no polarographic wave. The cation thus formed may be so labile that it may rapidly react either with the solvent or with the moisture in the solution to form electrolytically-inert species, such as the strongly solvated benzhydryl cation or benzhydrol. Accordingly, the third wave of benzhydryl bromide can be ascribed to the reduction of the benzhydryl radical (Eq. (6)). This is substantiated by the identification of the reaction products, to be described later.

$$\text{3rd wave: } (C_6H_5)_2CH\cdot + e \rightleftarrows (C_6H_5)_2CH^- \qquad (6)$$

It is evident that we can explain, in terms of the

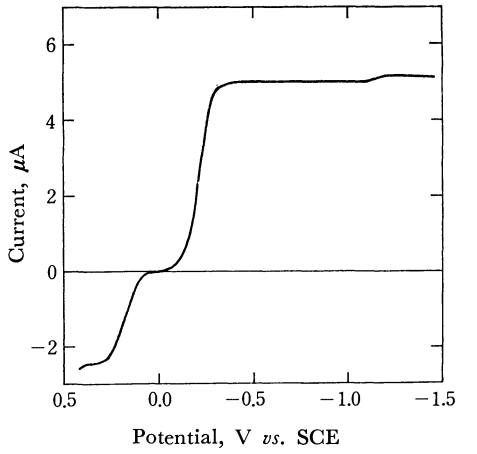

Fig. 6. Polarogram of the equimolar solution (0.83 mM) of $(C_6H_5)_2CHBr$ and $HgBr_2$ in DMF at 25°C.

chemical reaction expressed by Eq. (5) and the subsequent electrochemical reactions expressed by Eqs. (1), (2), and (6), the fact that the ratio among the three waves of the bromide is approximately 1 : 2 : 2. Moreover, the diffusion coefficient of the bromide calculated on the basis of this mechanism equals 7.4×10^{-6} cm²/sec; this value seems appropriate for the depolarizer. The decrease in the height of the third wave of benzhydryl bromide with the time can also be explained in terms of the above mechanism. During repeated measurements of the polarograms, benzhydryl bromide reacts with mercury, mainly that of the mercury pool. The resulting benzhydryl radical is so unstable that it dimerizes to form *sym*-tetraphenylethane, which is electrolytically inert. Since the decrease in the concentration of benzhydryl bromide in the cell solution is accompanied by no increase in the concentration of the benzhydryl radical, the height of the third wave decreases with the time. On the other hand, the decrease in the concentration of benzhydryl bromide is accompanied by an increase in the concentration of the tribromomercurate ion. Therefore, the heights of the first and the second waves scarcely change at all with the time.

The logarithmic plot of the third wave is shown in Fig. 4. A nearly linear relation was obtained between the potential and $\log i/(i_d-i)$ with the reciprocal slope of 0.098 V, indicating that the electrode reaction is irreversible.

It is noteworthy that the half-wave potential of the labile benzhydryl radical is less negative by 0.67 V than that of benzhydryl chloride. The polarographic reduction of organic halide is usually expressed in terms of the following reactions:[8]

$$RX + e \rightleftarrows R\cdot + X^- \quad (7)$$

$$R\cdot + e \longrightarrow R^- \quad (8)$$

$$R^- + \text{solvent} \longrightarrow RH \quad (9)$$

Among these reactions, the one expressed by Eq. (7) is considered to be the potential-determining step, for the radical, R·, may be more reducible than the starting halide. Thus, once the halide is electrolytically reduced to the corresponding radical, the latter may immediately be reduced to the corresponding carbanion at the same potential. However, the half-wave potential of such an unstable organic radical had never actually been measured until, in the present experiment, it was shown that the half-wave potential of the benzhydryl radical is less negative than that of the corresponding chloride.

Identification of Reaction Products. Benzhydryl bromide in DMF containing 0.10 M tetraethylammonium perchlorate was reacted with mercury in an atmosphere of nitrogen. From the reaction mixture, *sym*-tetraphenylethane, benzophenone, and benzhydrol were isolated by chromatography in 46, 6, and 34% yields respectively, based on the starting bromide (see the Experimental section). It seems that the *sym*-tetraphenylethane is formed by the dimerization of the benzhydryl radical. It might be considered that the benzophenone is an impurity contained in the starting bromide. However, it is known[9] that the radicals with α-hydrogens, such as the benzhydryl radical, react with oxygen and form the corresponding ketones, together with the corresponding alcohols, according to the following reactions (see also the subsequent paragraph):

$$R_2CH\cdot + O_2 \longrightarrow R_2CHOO\cdot \quad (10)$$

$$2\ R_2CHOO\cdot \longrightarrow R_2CO + R_2CHOH + O_2 \quad (11)$$

Thus, it seems that at least a part of the benzophenone, as well as a part of the benzhydrol, may be formed by the reaction of the benzhydryl radical with the small amount of oxygen contained in the nitrogen. The main part of the benzhydrol may be formed by the hydrolysis of the solvated benzhydryl cation. Thus, the reaction products can be classified into two groups, *i.e.*, the products obtained *via* the benzhydryl radical and those obtained *via* the benzhydryl cation; it is evident that the number of the moles of the former is approximately twice that of the latter. Furthermore, it was found that in this reaction *ca.* 1.0 g-atom of mercury is consumed per three moles of the benzhydryl bromide. These results indicate that Eq. (5) is valid.

When benzhydryl bromide was allowed to react with mercury in a stream of dry air, the yield of *sym*-tetraphenylethane based on the starting bromide decreased to 18%, whereas those of benzophenone and benzhydrol increased significantly, to 24 and 45% respectively. Dibenzhydryl ether, which may be produced by the reaction of the benzhydryl cation with benzhydrol, was also obtained in an 8% yield. These results agree well with those to be expected from Eqs. (10) and (11).

In order to examine the effect of the solvent on the present reaction, benzhydryl bromide was allowed to react with mercury in benzene. It was found that *sym*-tetraphenylethane is formed quantitatively, while benzophenone and benzhydrol are scarcely formed at all. It was also found that mercurous bromide is quantitatively formed at the same time. These results indicate that the solvent plays an important role in the present reaction. It is known[6] that the tribromomercurate ion, as well as mercuric bromide, is extremely stable in DMF, while mercurous bromide is insoluble in DMF and decomposes in part to form mercury and mercuric bromide. Hence, benzhydryl bromide in DMF reacts with mercury to yield the most stable species of the brominated mercurys, *i.e.*, the tribromomercurate ion, together with the benzhydryl radical and the benzhydryl cation. On the other hand, in benzene mercurous bromide may be more stable than either mercuric bromide or the tribromomercurate ion. Thus, the benzhydryl bromide in benzene reacts with mercury to form mercurous bromide and the benzhydryl radical, but the benzhydryl cation may not be formed in this case.

When benzhydryl bromide in DMF was electrolyzed with the Hg cathode at the controlled potential of −0.60 V *vs.* SCE, where the limiting current corresponding to the second polarographic wave of the bromide flows, an almost quantitative yield (89%) of *sym*-tetraphenylethane was obtained. The quantity of electricity (n) required for the reduction of one mole of the depolarizer was found to be 1.10 Faradays. These results can be explained in terms of the following mechanism:

$$3\ (C_6H_5)_2CHBr + Hg \longrightarrow 2\ (C_6H_5)_2CH\cdot + (C_6H_5)_2CH^+ + HgBr_3^-$$

$$HgBr_3^- + 2\ e \rightleftarrows Hg + 3\ Br^-$$

$$(C_6H_5)_2CH^+ + Br^- \longrightarrow (C_6H_5)_2CHBr \quad (12)$$

$$2\ (C_6H_5)_2CH\cdot \longrightarrow (C_6H_5)_2CHCH(C_6H_5)_2 \quad (13)$$

The bromide ion, formed by the reduction of the tribromomercurate ion at −0.60 V *vs.* SCE, may react with the solvated benzhydryl cation, thus regenerating the original benzhydryl bromide. Thus, none of the products expected to be formed *via* the benzhydryl cation are obtained. Furthermore, it can also be explained in terms of the above mechanism that the value of n is virtually equal to 1.0 Faraday rather than to the 0.67 Faraday which is to be expected from the results of the DC polarography.

8) P. J. Elving and B. Pullman, "Advances in Chemical Physics," Vol. III, ed. by I. Prigogine, Interscience Publishers, New York, N. Y. (1961), p. 1.

9) C. Walling, "Free Radicals in Solution," John Wiley & Sons, New York, N. Y. (1957), p. 423.

The electrolytic reduction of benzhydryl bromide with the Hg cathode at the controlled potential of −1.40 V *vs.* SCE, where the limiting current of the third polarographic wave of the bromide flows, resulted in the formation of 38% of diphenylmethane and 51% of *sym*-tetraphenylethane, based on the original bromide. The value of n was measured to be 1.13 Faradays. These results can be explained by the following mechanism:

$$3\,(C_6H_5)_2CHBr + Hg \longrightarrow$$
$$2\,(C_6H_5)_2CH\cdot + (C_6H_5)_2CH^+ + HgBr_3^-$$
$$HgBr_3^- + 2\,e \rightleftarrows Hg + 3\,Br^-$$
$$2\,(C_6H_5)_2CH\cdot + 2\,e \rightleftarrows 2\,(C_6H_5)_2CH^-$$
$$(C_6H_5)_2CH^- + \text{solvent} \longrightarrow (C_6H_5)_2CH_2 \quad (14)$$
$$(C_6H_5)_2CH^- + (C_6H_5)CH^+ \longrightarrow (C_6H_5)_2CHCH(C_6H_5)_2 \quad (15)$$

Since diphenylmethane has never been obtained until the present run, it is obvious that the substance is formed *via* the benzhydryl anion. About a half of the benzhydryl anion generated may react with the solvated benzhydryl cation to form *sym*-tetraphenylethane. According to the above mechanism, the value of n should equal 1.33 Faradays; this value agrees roughly with that observed.

The electrolytic reduction of benzhydryl chloride at the controlled potential of −2.13 V *vs.* SCE, where the limiting current corresponding to the single polarographic wave of the chloride flows, resulted in the formation of 46% of diphenylmethane and 6% of *sym*-tetraphenylethane. *It is remarkable that the yield* of diphenylmethane is much higher than that of *sym*-tetraphenylethane, unlike the case of benzhydryl bromide. This indicates that the benzhydryl anion has reacted with the solvent to form diphenylmethane before it reacts with the benzhydryl chloride diffusing toward the electrode to form *sym*-tetraphenylethane. On the other hand, when benzhydryl bromide is the depolarizer, the formation of the benzhydryl cation by the chemical process, together with that of the benzhydryl anion by the electrochemical process, occurs on the electrode surface. Hence, the yield of the product due to the combination of the anion with the cation, *i.e.*, the yield of *sym*-tetraphenylethane, increases significantly.

Experimental

Materials. The DMF used as a solvent was purified as has been described previously.[10] The tetraethylammonium perchlorate used as a supporting electrolyte was prepared according to the directions of Fujinaga *et al.*[11] The benzhydryl bromide was prepared by the reaction of bromine with diphenylmethane[12] (bp 148—150°C/5 mmHg). The benzhydryl chloride was prepared by the reaction of thionyl chloride with benzhydrol[13] (bp 131—133.5°C/7 mmHg). Mercuric bromide obtained commercially was purified by recrystallizing it from ethanol.

Procedure. DC polarography, large-scale electrolysis at a controlled potential, and conductivity measurements were carried out as has been described previously.[6] All the potential measurements were done with reference to an aqueous saturated calomel electrode connected with the cell solution by a DMF-agar salt bridge.[14] The dropping mercury electrode used had the following characteristics in a 0.10 M solution of tetraethylammonium perchlorate in DMF (open circuit): $m=1.540$ mg/sec and $t=6.4$ sec for $h=66$ cm. Benzhydryl bromide was always allowed to stand in DMF for at least 3 hr before being used. The oxygen dissolved in the solution was expelled by passing a stream of dry nitrogen through the cell solution for about 20 min prior to each electrolysis.

The Reaction of Benzhydryl Bromide with Mercury in a Degassed DMF Solution. A 0.10 M solution (50 ml) of tetraethylammonium perchlorate in DMF was degassed for 1 hr with nitrogen. To the solution, mercury (68.73 g, 342.6 mg-atom) and benzhydryl bromide (1.30 g, 5.26 mmol) were then added; the mixture was subsequently held at 25°C under a nitrogen atmosphere for 22.5 hr. The mercury was then separated from the reaction mixture, washed with water, dried *in vacuo*, and found to weigh 68.40 g (341.0 mg-atom). Hence, 1.6 mg-atom of mercury was consumed for its reaction with 5.26 mmol of the bromide. The DMF solution was concentrated by vacuum distillation, and the residue was taken up with benzene. The resulting solution was washed with water, dried with calcium chloride, and evaporated. The residue was recrystallized from *n*-hexane - benzene (4 : 1 by volume) to afford 0.366 g of *sym*-tetraphenylethane (mp 207—210°C; lit,[15] mp 211°C), the infrared spectrum of which was identical with that of an authentic sample. The mother liquor from the recrystallization was evaporated *in vacuo*, and the residue was chromatographed on alumina. Elution with *n*-hexane - benzene (9 : 1 by volume) afforded 0.033 g of additional *sym*-tetraphenylethane, mp 205—207°C (its identity was established by the infrared spectrum). The benzene fractions gave 0.062 g of benzophenone (mp 46—48°C; lit,[16] mp 49°C), which was identified by comparing its infrared spectrum with that of an authentic sample. The ether fractions afforded 0.326 g of benzhydrol (mp 65—67°C; lit,[16] mp 69°C), the infrared spectrum of which was identical with that of an authentic sample. From these results, the yields of *sym*-tetraphenylethane, benzophenone, and benzhydrol were estimated to be 46, 6, and 34% respectively.

The Reaction of Benzhydryl Bromide with Mercury in a DMF Solution Saturated by Oxygen. Dry air was bubbled into a mixture of 3.00 g (12.1 mmol) of benzhydryl bromide, 93.50 g of DMF, and 80.60 g of mercury for 280 min at room temperature. A white precipitate appeared. The reaction mixture was then filtered, and the filtrate was concentrated by vacuum distillation. When benzene was added to the residue, *ca.* 1 ml of insoluble liquid appeared; this was then separated. The benzene solution was washed with water, dried with magnesium sulfate, and evaporated *in vacuo*. By the recrystallization of the residue from methanol, 0.34 g

10) Y. Matsui, Y. Kurosaki, and Y. Date, This Bulletin, **43**, 1707 (1970).
11) T. Fujinaga, K. Izutsu, K. Umemoto, T. Arai, and K. Takaoka, *Nippon Kagaku Zasshi*, **89**, 105 (1968).
12) J. F. Norris, R. Thomas, and B. M. Brown, *Chem. Ber.*, **43**, 2959 (1910).
13) H. Gilman and J. E. Kirby, *J. Amer. Chem. Soc.*, **48**, 1735 (1926).
14) K. Takaoka, *Rev. Polarography*, **14**, 63 (1966).
15) P. Sabatier and M. Murat, *C. R. Acad. Sci., Paris, Ser. C*, **157**, 1497 (1900).
16) W. J. Hickinbottom, "Chemistry of Carbon Compounds," Vol. III, ed. by E. H. Rodd, Elsevier Publishing Co., New York, N. Y. (1956), pp. 1055—1063.

of *sym*-tetraphenylethane was obtained (mp 206—208°C). The combined filtrates were evaporated *in vacuo* to give 1.97 g of an oily material, of which 0.96 g was chromatographed on alumina. *n*-Hexane fractions gave 0.10 g of crystals, which were fractionally recrystallized from ethanol to give 0.009 g of *sym*-tetraphenylethane (mp 195—201°C) and 0.079 g of dibenzhydryl ether (mp 101—105°C; lit,[17] mp 110°C; its identity was established by a study of the infrared spectrum). The benzene fractions gave 0.235 g of benzophenone (mp 44—48°C). The ether fractions gave 0.492 g of benzhydrol (mp 66—68°C). From these results, the yields of *sym*-tetraphenylethane, dibenzhydryl ether, benzophenone, and benzhydrol were estimated to be 18, 8, 24, and 45% respectively.

The Reaction of Benzhydryl Bromide with Mercury in a Benzene Solution. To a solution of 1.505 g (6.09 mmol) of benzhydryl bromide in 50 m*l* of benzene, 5 m*l* of mercury was added, and the resultant mixture was boiled under reflux for 9 hr. Gray solids precipitated. After the separation of the mercury, the reaction mixture was filtered. The residue was washed several times with hot benzene, and the combined benzene solution was evaporated *in vacuo* to give a viscous oil containing some white crystals; these crystals were recrystallized from benzene to give 0.659 g of *sym*-tetraphenylethane (mp 202—207°C). The mother liquor was evaporated *in vacuo*, and the residue was chromatographed on alumina. Elution with *n*-hexane gave 0.287 g of *sym*-tetraphenylethane (mp 205—207°C; total yield, 93%). The benzene fractions gave 0.001 g (0.1% yield) of benzophenone, and the ether fraction gave a trace of benzhydrol. Each of these products was identified by means of its infrared spectrum.

The gray solids precipitated from the reaction mixture were practically insoluble in DMF, too. However, when they were added to the solution of 2.56 g (12.2 mmol) of tetraethylammonium bromide in 100 m*l* DMF, they dissolved and the mercury was separated. The polarographic measurement of the resulting solution indicated that it contained 2.70 mmol of the tribromomercurate ion. This behavior of the gray solids is identical with that of mercurous bromide, which has been studied in the previous paper.[6] Hence, the yield of mercurous bromide was estimated to be 89%, based on the original bromide.

The Controlled Potential Electrolysis of Benzhydryl Bromide in DMF at −0.60 V vs. SCE. In a 1-*l* electrolytic cell, 300 m*l* of DMF, 6.87 g of tetraethylammonium perchlorate, and 50 m*l* of mercury were placed; the mixture was cooled to 2—4°C and degassed with nitrogen. Immediately after 0.366 g (1.48 mmol) of benzhydryl bromide had been added to the mixture, controlled potential electrolysis was started at −0.60 V *vs.* SCE. The quantity of electricity required for the complete electrolysis was estimated graphically from the current-time curve to be 0.00163 Faraday. The polarogram of the resulting catholyte agreed virtually completely with that of the bromide ion. The catholyte was concentrated by vacuum distillation and the residue was taken up in benzene. The benzene solution was washed with water, dried with calcium chloride, and evaporated. From the residue, 0.221 g (89% yield) of *sym*-tetraphenylethane (mp 205—206.5°C) and 0.029 g (8% yield) of benzophenone were isolated by fractional recrystallization and chromatography on alumina. Identity was established by a study of the infrared spectrum.

The Controlled Potential Electrolysis of Benzhydryl Bromide in DMF at −1.40 V vs. SCE. In a 1-*l* electrolytic cell, 300 m*l* of DMF, 6.87 g of tetraethylammonium perchlorate, and 50 m*l* of mercury were placed; the mixture was cooled to 2—4°C and degassed by a stream of nitrogen for 2 hr. Immediately after 0.344 g (1.39 mmol) of benzhydryl bromide had been added to the mixture, the resulting solution was electrolyzed at −1.40 V *vs.* SCE for 130 min. The quantity of electricity required for the complete electrolysis was estimated to be 0.00157 Faraday. The polarogram of the resulting catholyte agreed closely with that of the bromide ion. The catholyte was worked up exactly as in the previous experiment; 0.119 g (51% yield) of *sym*-tetraphenylethane (mp 210—212°C), 0.088 g (38% yield) of diphenylmethane (mp 25—26°C; lit,[16] mp 27°C) (identity established by a study of the infrared spectrum), and 0.012 g (5% yield) of benzophenone were thus obtained.

The Controlled Potential Electrolysis of Benzhydryl Chrolide in DMF at −2.13 V vs. SCE. A solution of 300 m*l* of DMF, 6.89 g of tetraethylammonium perchlorate, and 5.70 g (28.1 mmol) of benzhydryl chloride was degassed for 2 hr with pure nitrogen, and then electrolyzed at a controlled potential of −2.13 V *vs.* SCE. The current started at 7.5 A and fell to 0.026 A after 42.5 hr. The resulting catholyte was worked up exactly as in the previous experiment; 2.182 g (46% yield) of diphenylmethane (mp 25—26°C), 0.270 g (6% yield) of *sym*-tetraphenylethane (mp 206.5—207.5°C), 0.164 g (3% yield) of benzophenone, and 0.308 g (6% yield) of benzhydrol were thus obtained. Identity was established by a study of the infrared spectrum.

17) J. U. Nef, *Ann. Chem.*, **298**, 232 (1897).

The Mechanism of the Reaction of Quinolines with Organolithium Compounds[1]

Yoshio Otsuji, Kiyohiko Yutani, and Eiji Imoto

Department of Applied Chemistry, College of Engineering, University of Osaka Prefecture, Sakai-shi, Osaka

(Received August 12, 1970)

The treatment of lepidine (IV) with phenyllithium in ether afforded 2-phenyl-4-methylquinoline (V) along with small amounts of 2-phenylquinoline (VI) and 2-methyl-4-phenylquinoline (VII). The similar treatment of IV with phenyllithium and then with ethyl chloroformate gave 1-ethoxycarbonyl-4-methyl-4-phenyl-1,4-dihydroquinoline (VIIIa). The alkaline hydrolysis of VIIIa produced a mixture of V, VI, and VII. Similar experiments were carried out on the reactions between IV and *n*-butyllithium and between quinoline and phenyllithium. On the basis of these results and other observations, a new mechanism involving an addition-rearrangement-elimination was proposed for the reaction of quinolines with organolithium compounds.

Many investigations have already been made into the mechanism of the reactions of quinolines with organometallic compounds.[2] However, the mechanism still seems not to be well established. For example, quinoline reacts with phenyllithium,[3] butyllithium,[4] and phenylmagnesium bromide[5] to give mainly the 2-substituted products, *i.e.*, 2-phenyl- or 2-butylquinoline, along with only a small amount of the corresponding 4-substituted product. On the other hand, the treatment of quinoline with the methylsulfinyl carbanion in DMSO undergoes the substitution reaction exclusively at the 4-position of quinoline to produce lepidine in a quantitative yield.[6,7]

Throughout a whole series of these reactions between quinolines and organometallic reagents, it has always been assumed that the reactions proceed *via* the intermediate I or II. However, no conclusive evidence

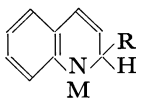

I

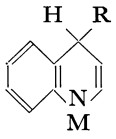

II

for the existence of these intermediates has yet been appeared in the literature.[8] Furthermore, the factors which cause the difference in the orientation of the reactions (1,2- or 1,4-additions) remain unexplained.

In this paper we wish to report our findings on the isolation and characterization of the intermediates in the reactions of quinolines with organolithium compounds. We will also propose a new mechanism of the reactions based on the chemical properties of these intermediates.

Results and Discussion

Products of the Reaction of Lepidine with Phenyllithium. The treatment of lepidine (IV) with phenyllithium in ether at −70°C for 30 min produced a yellow precipitate. After the hydrolysis of the precipitate with water, the mixture was analyzed by the vpc. The analysis revealed that the mixture contained 2-phenyl-4-methylquinoline (V), 2-phenylquinoline (VI) and 2-methyl-4-phenylquinoline (VII) in a ratio of 96.5 : 3.0 : 0.5 respectively.

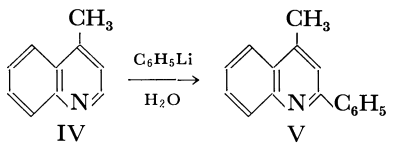

IV V

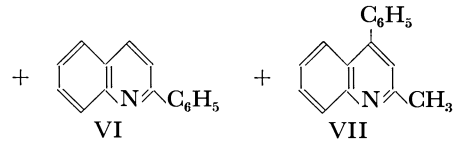

VI VII

Isolation and Characterization of the Intermediates in the Reactions of Quinolines with Organolithium Compounds. When an ethereal solution of ethyl chloroformate was added to the suspension of the yellow precipitate in ether which had been produced by the reaction of lepidine with phenyllithium, the precipitate disappeared and a homogeneous solution was obtained. From this solution, 1-ethoxycarbonyl-4-methyl-4-phenyl-1,4-dihydroquinoline (VIIIa) was isolated as white crystals in a 51% yield, along with small amounts of V and VII. The similar treatment of lepidine with *n*-butyllithium and then with ethyl chloroformate gave 1-ethoxycarbonyl-4-*n*-butyl-4-methyl-1,4-dihydroquinoline (VIIIb) as a pale yellow liquid in a 45% yield.

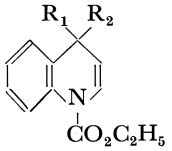

VIII a, $R_1=CH_3$ $R_2=C_6H_5$
b, $R_1=CH_3$ $R_2=n\text{-}C_4H_9$
c, $R_1=H$ $R_2=C_6H_5$

1) A part of this work was presented at the 2nd Symposium on the Chemistry of Heterocyclic Compounds, Nagasaki, November, 1969.

2) K. Blaha and O. Cervinka, "Advances in Heterocyclic Chemistry," Vol. 6, ed. by A. R. Katritzky, Academic Press, New York, N. Y. (1966), p. 147; R. G. Shepherd and J. L. Fedrick, *ibid.*, Vol. 4 (1965), p. 145; *cf.* the references cited therein.

3) K. Ziegler and G. Zeiser, *Ann. Chem.*, **485**, 174 (1931).

4) H. Gilman and G. C. Gainer, *J. Amer. Chem. Soc.*, **69**, 877 (1947).

5) F. W. Bergstrom and S. H. McAllister, *ibid.*, **52**, 2845 (1930).

6) H. Nozaki, Y. Yamamoto, and R. Noyori, *Tetrahedron Lett.*, **1966**, 1123.

7) G. A. Russell and S. A. Weiner, *J. Org. Chem.*, **31**, 248 (1966).

8) Recently, G. Fraenkel and J. C. Cooper (*Tetrahedron Lett.*, **1968**, 1825), in studying the reaction of pyridine with butyllithium, and C. S. Gian and J. L. Stout (*Chem. Commun.*, **1969**, 142), in studying the reaction of pyridine with phenyllithium, have characterized the intermediate of the type III on the basis of the NMR data.

III

The structures of VIIIa and VIIIb were established by a study of the results of their elemental analyses and spectral data, which are summarized in Table 1. The absorptions due to the C=C double bond in the IR spectra partly support the assigned structures; the comparison of the IR spectra of 1,4-dihydroquinolines and those of 1,2-dihydroquinolines suggests that the C=C double bond of the former absorbs at higher wave numbers than that of the latter compounds, which appears at $<1630\ cm^{-1}$, probably because the C=C bond in the latter is in conjugation with the benzene ring.[9] However, the final confirmation of the structures was attained from the NMR spectra, shown in Figs. 1 and 2. The spectra for the protons of the hetero-ring were readily analyzed as of the AB and AX types.

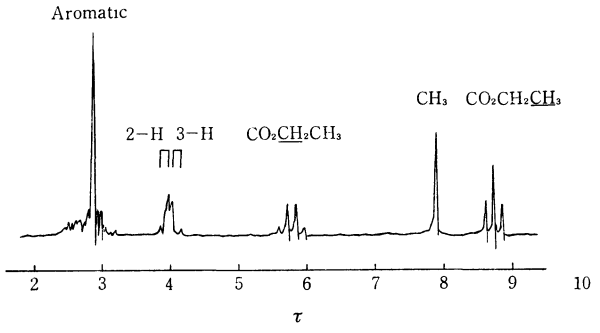

Fig. 1. NMR spectrum of 1-ethoxycarbonyl-4-methyl-4-phenyl-1,4-dihydroquinoline (VIIIa) in CCl_4.

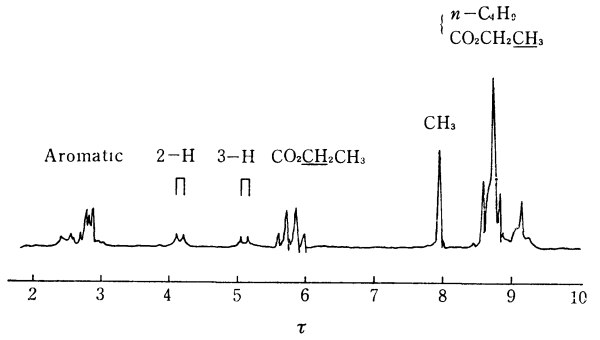

Fig. 2. NMR spectrum of 1-ethoxycarbonyl-4-*n*-butyl-4-methyl-1,4-dihydroquinoline (VIIIb) in CCl_4.

The chemical shifts for 2-H and 3-H, and the coupling constants, $J_{2,3}$ listed in Table 1, clearly indicate that they are of the olefinic protons in the hetero-ring; therefore, the structures identified as VIIIa and VIIIb are correct. It is now worthwhile to point out that the $J_{2,3}$ values obtained in this investigation are very close to those found by Bramley and Johnson[10] for the majority of 1,4-dihydroquinolines.

When quinoline was treated in ether with phenyllithium and then with ethyl chloroformate in a manner similar to that described above, a pale yellow liquid was obtained in a 59% yield. The structure of this liquid was supposed to be 1-ethoxycarbonyl-4-phenyl-1,4-dihydroquinoline (VIIIc). Though the IR spectrum supported the assigned structure, showing absorptions at 1695 and 1650 cm^{-1} (shoulder) due, respectively, to the C=O and C=C double bonds, the NMR spectra in CCl_4 exhibited a complex pattern which could not be readily analyzed; τ 2.5—3.2 (9H, multiplet, aromatic), 3.25—3.98 (3H, multiplet, 2-H, 3-H, 4-H), 5.78 (2H, quartet, $J=7.0$ Hz, $CO_2\mathbf{CH_2}$-CH_3), 8.72 (3H, triplet, $J=7.0$ Hz, $CO_2CH_2\mathbf{CH_3}$). However, further suport for the structure was secured by the experiments to be described below.

Hydrolysis of 1-Ethoxycarbonyl-1,4-dihydroquinolines. Surprisingly, VIIIa, VIIIb, and VIIIc were all unable to hydrolyze with hydrochloric acid or sodium hydroxide in an aqueous ethanol even when the mixtures were refluxed for 2 hr; all were recovered in quantitative yields. The hydrolysis of these compounds was satisfactorily performed with sodium hydroxide in DMSO-water (5 : 1) by heating on a water bath. The vpc analysis of the reaction mixtures after almost complete hydrolysis gave the following products in the molar ratios shown in the parentheses:

VIIIa → V(87.5%) + VI(7.5%) + VII(5%)

VIIIb → 2-*n*-butyl-4-methylquinoline(IX)(100%)

VIIIc → VI(74.5%) + VII(25.5%)

The hydrolysis of VIIIc yielded an unexpected product, VII. The reason for this result was, however, soon clarified. The treatment of VIIIc with the dimethylsulfinyl carbanion in DMSO, followed

Table 1. Spectral data

Compd.	NMR			Others[a,b]	IR, cm^{-1}		UV, mμ
	2-H[a]	3-H[a]	$J_{2,3}$[b]		C=O	C=C	$\lambda_{max}^{n\text{-hexane}}$
VIIIa	3.85	4.00	7.5	Aromatic: 2.41—2.98(m) $CO_2CH_2CH_3$: 5.76 (q, $J=7.5$) $CO_2CH_2CH_3$: 8.72 (t, $J=7.5$) CH_3: 7.85(s)	1686[c]	1660[c]	267 ($\varepsilon=5\times10^3$) 307 ($\varepsilon=2\times10^3$)
VIIIb	4.14	5.12	6.5	Aromatic: 2.41—3.10(m) $CO_2CH_2CH_3$: 5.78 (q, $J=7.5$) $CO_2CH_2CH_3$, n-C_4H_9: 8.62—9.17(m) CH_3: 7.95(s)	1695[d]	1660[d]	270 ($\varepsilon=2\times10^3$) 305 ($\varepsilon=2\times10^3$)

a) Chemical shifts are represented as τ-values. b) Coupling constants are represented in the Hz unit. c) in KBr. d) in liquid film. The absorption at 1660 cm^{-1} appeared as a shoulder.

9) H. Ahlbrecht and F. Kröhnke, *Ann. Chem.*, **717**, 96 (1968).

10) R. Bramley and M. D. Johnson, *J. Chem. Soc.*, **1965**, 1372.

by the hydrolysis, resulted in an increase in the yield of VII to 38.4%. A plausible explanation of these results is that VII is produced by the attack of the carbanion on the 2-position of VIIIc. Thus, the above results support the structure VIIIc.

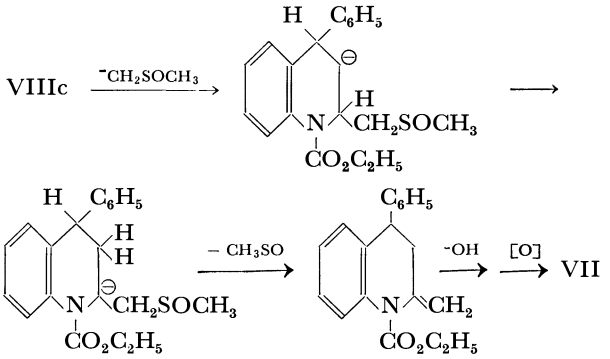

Rate of the Hydrolysis of 1-Ethoxycarbonyl-4-methyl-4-phenyl-1,4-dihydroquinoline (VIIIa). The hydrolysis of VIIIa was carried out with sodium hydroxide in DMSO-ethanol-water (60 : 15 : 15) at 72°C. The rate of the reaction was followed by analyzing the amounts of the products by means of vapor-phase chromatography. The results are depicted in Fig. 3. The amount of V produced reached a maximum after about 3 hr and then gradually decreased. On the other hand, the amount of VI increased with the decrease in the amount of V.

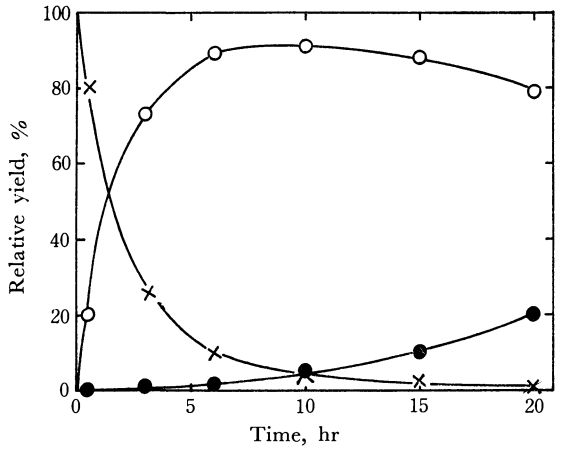

Fig. 3. Rate of the hydrolysis of 1-ethoxycarbonyl-4-methyl-4-phenyl-1,4-dihydroquinoline (VIIIa) in DMSO-H_2O-C_2H_5OH (60 : 15 : 15) at 72±1°C.
—×—, VIIIa; —○—, 2-phenyl-4-methylquinoline (V); —●—, 2-Phenylquinoline (VI)

Reaction of 2-Phenyl-4-methyl-1,2-dihydroquinoline (X). Since the rate profile of the hydrolysis of VIIIa described in the preceding paragraph suggested that VI is produced from X which is a precursor of V, the chemistry of X was studied; V itself was stable under the reaction conditions used for the hydrolysis of VIIIa.

It is well known that quinolines can be reduced to 1,2-dihydroquinolines by the action of $LiAlH_4$, though with some difficulty.[11] Hence, V was treated with $LiAlH_4$ in boiling ether. However, no reaction took place, and the starting material was recovered unchanged. This is probably because of a steric hindrance due to the phenyl group at the 2-position. The methiodides of quinolines are, however, readily reduced to the corresponding 1,2-dihydro derivatives with $LiAlH_4$.[12] In view of these facts, V was treated in ether with BF_3-etherate and then with $LiAlH_4$. After hydrolysis, the vpc analysis of the reaction mixture revealed that the mixture consisted of 31% of V and 69% of VI. This result suggests that VI is produced from X. A probable mechanism of this reaction is as follows:

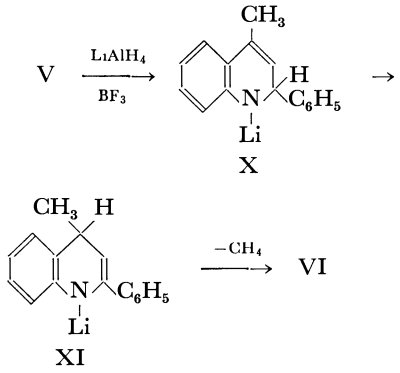

Mechanism. On the basis of the observations presented earlier, we propose a new mechanism, involving addition-rearrangement-elimination(or-oxidation), for the reaction of quinolines with organolithium

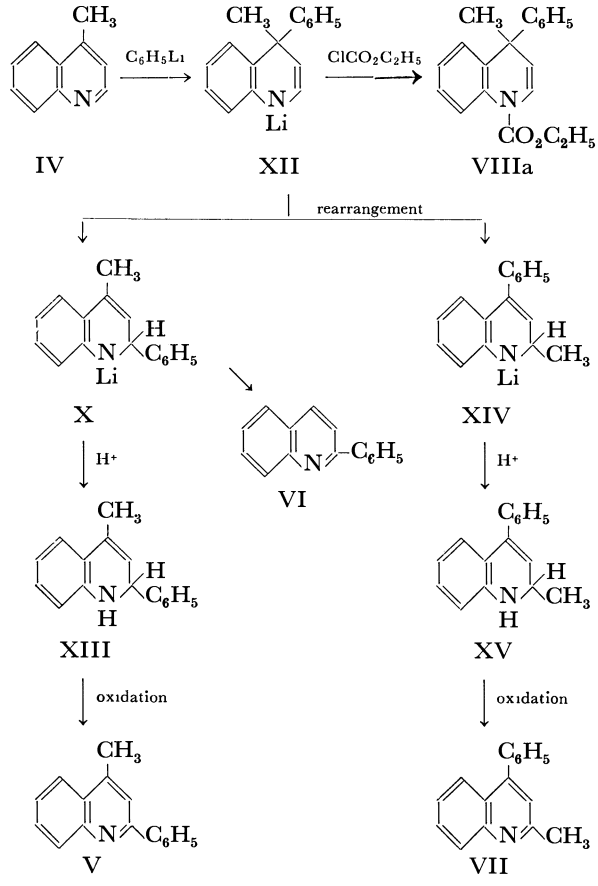

Scheme 1

11) K. W. Rosenmund, *Chem. Ber.*, **87**, 1229 (1954).

12) R. C. Elderfield and B. H. Wark, *J. Org. Chem.*, **27**, 543 (1962).

compounds. The mechanism is represented Scheme 1, taking as an example the reaction of lepidine with phenyllithium. A similar mechanism would operate for the other reactions.

The possibility of the rearrangement of XII to X and XIV can be explained by the Woodward-Hoffmann rule for the sigmatropic reactions.[13] In this rearrangement, the transition state could be envisaged as being made up by the combination of the orbital of the phenyl or methyl radical with those of the quinoline radical anion, which contains eleven π electrons. The highest occupied orbital of the radical anion possesses the symmetry shown in Fig. 4.[14] Since the migrating group, the phenyl or methyl radical, can possess an accessible π orbital, the appreciable positive overlap between the framework orbital and that of the migrating group can be maintained in the transition state (Fig. 5). Hence, the rearrangement is possible. Furthermore, the overlap of the above sort would be larger between C_4 and C_2 than between C_4 and C_3, since the coefficients of the component π AO's on the highest occupied MO are larger at C_2 than at C_3. The migration can, therefore, be expected to take place from C_4 to C_2 rather than from C_4 to C_3. The migratory aptitudes of the migrating groups would be proportional to the availability of the π orbital on the groups in the transition state of the rearrangement. Thus, the phenyl migration is favored over the methyl migration in the rearrangement of XII to X and XIV.

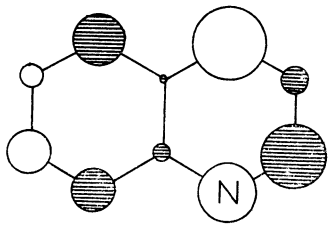

Fig. 4. HO MO of the quinoline radical anion. The phase of π AO's on the one side of the molecular plane are depicted: the shaded circle represents the positive phase and the unshaded one the negative phase.

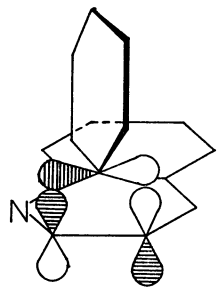

Fig. 5. Transition state of the phenyl migration.

The existence of the dihydro species, XIII and XV, although their structures were not unambiguously confirmed, was inferred from the facts that the NH absorption appeared in the IR spectra of the initially-isolated products and that this absorption disappeared upon the oxidation of the products with air or nitrobenzene.

Experimental

The melting points are uncorrected. The IR spectra were recorded on a Hitachi EPI-S_2 infrared spectrophotometer. The UV spectra were determined on a Hitachi EPU-2U recording spectrophotometer. The NMR spectra were obtained on a Hitachi H-60 high-resolution NMR spectrometer, with TMS as the internal standard. The elemental analyses were performed with a Yanagimoto MT-1 CHN Corder. The vpc analyses were carried out with a Yanagimoto GCG 5DH chromatograph, employing a stainless steel column (2 m×6 mm o.d.) packed with 25% PEG-20 M or 25% Apiezon N on chromosorb (80 mesh). The column temperature was generally maintained at 300°C with a helium flow rate of 30 m*l*/min. For quantitative analyses, the respective authentic samples were used as the internal standards.

Materials. Lepidine (IV) was prepared from methyl vinyl ketone and aniline hydrochloride by the method of Campbell and Schaffner,[15] bp 86—88°C/1 mmHg. 2-Phenyl-4-methylquinoline (V) was prepared from benzylideneacetone and aniline hydrochloride by the method of John and Noziczka,[16] mp 58—59°C. 2-Phenylquinoline (VI) was prepared from quinoline and phenyllithium by the method of Ziegler,[17] mp 81—82°C. 2-Methyl-4-phenylquinoline was prepared, starting with paraldehyde, acetophenone, and aniline, by the method of Knövenagel and Goos,[18] mp 98—99°C. The other chemicals were of commercial origin and were used after purification by distillation or recrystallization.

Reaction of Lepidine and Phenyllithium. A solution of 5.3 g (0.034 mol) of bromobenzene in 25 m*l* of ether was stirred, drop by drop and over a period of 30 min, into a suspension of 0.47 g (0.067 mol) of small pieces of lithium foil in 100 m*l* of ether under nitrogen and at room temperature. Stirring was continued for 30 min to complete the reaction, during which time the reaction mixture was refluxed. During this period the lithium dissolved completely and lithium bromide was precipitated. The mixture was cooled in a dryice - acetone bath, and a solution of 4.0 g (0.0167 mol) of lepidine in 25 m*l* of ether was stirred, drop by drop, into this mixture under a nitrogen atmosphere. A yellow solid soon started to precipitate. After stirring for 30 min, the reaction mixture was hydrolyzed by adding 25 m*l* of water under cooling in a dry ice - acetone bath. The yellow precipitate disappeared, and a homogeneous mixture was obtained. The ether layer was separated, and the aqueous layer was extracted with ether. The combined ether solution was washed with water, dried over sodium sulfate, and then evaporated to produce 6.1 g (almost quantitative) of a yellow oil. The oil was directly subjected to the vpc analysis, which revealed that the oil consisted of a mixture of V, VI, and VII.

13) R. B. Woodward and R. Hoffmann, "The Conservation of Orbital Symmetry," Verlag Chemie, GmbH, Weinheim/Bergstr. (1970), Chapter 7.

14) The highest occupied MO of the quinoline radical anion was calculated by the Hückel method, using as parameters $\alpha_N=\alpha+\beta$ and $\beta_{CN}=\beta$. The coeffcients of the component π AO's were: N=−0.39354, C_2=0.42401, C_3=0.20559, C_4=−0.51515, C_5=0.36108, C_6=−0.18282, C_7=−0.28004, C_8=0.30696, C_9=0.14397, and C_{10}=0.02276. The size of each π AO in Fig. 4 is so dipicted as to reflect the above coefficients.

15) K. N. Campbell and I. J. Schaffner, *J. Amer. Chem. Soc.*, **67**, 86 (1945).

16) H. John and F. Noziczka, *J. Prakt. Chem.*, [2], **111**, 68, 73 (1897).

17) K. Ziegler, *Ann. Chem.*, **479**, 147 (1930); *ibid.*, **483**, 185 (1931).

18) E. Knövenagel and O. Goos, *Ber.*, **55**, 1934 (1922).

The oil was distilled under reduced pressure to give again a pale yellow oil; bp 175—179°C/2 mmHg. The IR spectrum (liquid film) of this oil showed absorptions at 3400 and 1650 cm^{-1} due, respectively, to the NH and C=C bonds. These results indicate that the species initially produced by the reaction are the dihydro derivatives of V, VI, and VII (see Mechanism) and that they are oxidized to V, VI, and VII themselves in a column during the vapor-phase chromatography.

To isolate 2-phenyl-4-methylquinoline (V), 10.0 g (0.07 mol) of lepidine were treated with phenyllithium in ether, which had been prepared from 1.4 g (0.2 mol) of lithium and 15.7 g (0.1 mol) of bromobenzene, in a manner similar to that described above. The yellow oil obtained after the evaporation of the ether was refluxed in 60 m*l* of nitrobenzene for 3 hr. A 6 N sulfuric acid was added to the reaction mixture to yield a solid (sulfate of the bases), which was then filtered and washed with three 10-m*l* portions of ether. The filtrate was extracted with ether, and the organic layer was separated. The aqueous layer and the solid were combined, made alkaline with aqueous sodium hydroxide and sodium carbonate solutions, and then extracted with ether. The ether solution was washed with water, dried over sodium sulfate, and evaporated to yield 14 g (82%) of a crude V. Recrystallization from water-ethanol gave pure V as white needles; mp 58—59°C.

The IR spectrum (KBr) of the V thus obtained showed an absorption at 1600 cm^{-1} and was identical with that of the authentic sample, lacking absorptions due to the NH and C=C bonds.

The hydrochloride, mp 212—213°C, and the picrate, mp 208—209°C, were all identical with those of the authentic sample in every respect and gave satisfactory elemental analyses.

Isolation of 1-Ethoxycarbonyl-4-methyl-4-phenyl-1,4-dihydroquinoline (VIIIa). A suspension of phenyllithium in 170 m*l* of ether was prepared from 1.4 g (0.02 mol) of lithium and 15.7 g (0.1 mol) of bromobenzene as described above. Into this suspension we stirred, drop by drop, a solution of 14.3 g (0.1 mol) of lepidine in 20 m*l* of ether at room temperature under nitrogen. The mixture soon turned green and then started to precipitate a yellow solid. After stirring for 1 hr, a solution of 10.9 g (0.1 mol) of ethyl chloroformate in 50 m*l* of ether was added, drop by drop, to the above mixture. The yellow solid gradually dissolved with the evolution of heat. When stirring was continued for 1 hr, the yellow solid disappeared completely. The mixture was cooled in an ice bath, and then 50 m*l* of water was added. The ether layer was separated, and the aqueous layer was extracted with ether. The combined ether solution was washed with water, dried over sodium sulfate, and evaporated to yield 26.3 g of a yellow oil. The recrystalliation of the oil from water-ethanol gave 14.9 g (51%) of VIIIa as white needles; mp 74—75°C. No picrate was formed.

Found: C, 77.67; H, 6.34; N, 4.87%. Calcd for $C_{19}H_{19}O_2N$: C, 77.79; H, 6.53; N, 4.77%.

Isolation of 1-Ethoxycarbonyl-4-methyl-4-butyl-1,4-dihydroquinoline (VIIIb). A suspension of 0.1 mol of *n*-butyllithium in 170 m*l* of ether was prepared by the reaction between a suspension of 1.4 g (0.2 mol) of lithium in 150 m*l* of ether and a solution of 13.8 g (0.1 mol) of *n*-butyl bromide in 20 m*l* of ether in a manner similar to that described for the preparation of phenyllithium. Into this suspension we then stirred a solution of 14.3 g (0.1 mol) of lepidine in 40 m*l* of ether at room temperature. A yellow solid soon started to precipitate. Stirring was continued for 30 min at room temperature, and then a solution of 10.9 g (0.1 mol) of ethyl chloroformate in 50 m*l* of ether was added to the reaction mixture. By the time the mixture has been stirred for 1 hr, the yellow solid had completely disappeared. The mixture was cooled in an ice bath, and then a 50-m*l* portion of water was added. The ether layer was separated, dried over sodium sulfate, and evaporated to yield 23.8 g of a pale yellow oil. Two distillations gave 12.3 g (45%) of VIIIb; bp 125—128°C/0.2 mmHg. No picrate was formed.

Found: C, 74.34; H, 8.59; N, 4.96%. Calcd for $C_{17}H_{23}O_2N$: C, 74.69; H, 8.47; N, 5.12%.

Isolation of 1-Ethoxycarbonyl-4-phenyl-1,4-dihydroquinoline (VIIIc). A suspension of 0.1 mol of phenyllithium in 170 m*l* of ether was prepared as has been described above. Into this suspension we then stirred a solution of 13 g (0.1 mol) of quinoline in 25 m*l* of ether at room temperature. A yellow solid precipitated. Stirring was continued for 1 hr at room temperature, and then a solution of 10.9 g of ethyl chloroformate in 50 m*l* of ether was added. The yellow solid disappeared, and the reaction mixture was worked up in a manner similar to that described above. The evaporation of the ether yielded 23.4 g of an oil. The distillation of this oil gave 12.6 g (59%) of VIIIc; bp 172—174°C/1 mmHg. No picrate was formed.

Found: C, 77.57; H, 5.87; N, 5.19%. Calcd for $C_{18}H_{17}O_2N$: C, 77.39; H, 6.13; N, 5.01%.

Hydrolysis of VIIIa. *A. Acid hydrolysis*: A mixture of 4.40 g (0.015 mol) of VIIIa in 20 m*l* of 95% ethanol and 30 m*l* of 2 N hydrochloric acid was heated on a boiling-water bath for 5 hr. The mixture was made alkaline with an aqueous sodium carbonate solution and then extracted with ether. The ether solution was washed with water, dried over sodium sulfate, and then evaporated to give 4.3 g of the starting material.

The heating of VIIIa in a mixture of acetic acid and concentrated hydrochloric acid(1 : 1) on a boiling-water bath for 5 hr resulted in the recovery of the starting material in a quantitative yield.

B. Alkaline Hydrolysis in an Aqueous Ethanol: A mixture of 1.7 g (0.0058 mol) of VIIIa in 30 m*l* of ethanol and 1.0 g (0.018 mol) of sodium hydroxide in 5 m*l* of water was refluxed for 2 hr. The work-up of the mixture resulted in the recovery of the starting material in an almost quantitative yield.

C. Alkaline Hydrolysis in an Aqueous DMSO: A mixture of 2.5 g (0.0085 mol) of VIIIa in 25 m*l* of DMSO and 1.5 g (0.027 mol) of sodium hydroxide in 5 m*l* of water was warmed at 72°C for 27 hr and then extracted with ether. The ether layer was washed thoroughly with water, dried over sodium sulfate, and evaporated to yield 2.0 g of an oil. When the oil thus obtained was subjected to the vpc analysis, the oil was found to be a mixture of V, VI, and VII.

The picrate formed from this oil was recrystallized from methanol; it melted at 208—209°C and was identical in every respect with that of the authentic sample of V.

Hydrolysis of VIIIb. *A*: The acid hydrolysis of VIIIb with a mixture of acetic acid and concentrated hydrochloric acid, and alkaline hydrolysis with an aqueous sodium hydroxide solution, were carried out under conditions similar to those described for VIIIa. In each case, the starting material was recovered in an almost quantitative yield.

B: A mixture of 1.0 g (0.0037 mol) of VIIIb in 25 m*l* of DMSO and 0.6 g (0.01 mol) of sodium hydroxide in 5 m*l* of water was heated on a boiling-water bath for 3 hr and then extracted with ether. The ether layer was washed thoroughly with water, dried over sodium sulfate, and evaporated to give an oil. The vpc analysis of the oil revealed that the oil consisted of only one compound. The distillation of the oil

gave 0.5 g (68%) of 2-*n*-butyl-4-methylquinoline (IX); bp 115—117°C/mmHg.

Found: C, 84.01; H, 8.72; N, 7.25%. Calcd for $C_{14}H_{17}N$: C, 84.37; H, 8.60; N, 7.03%.

IR($CHCl_3$): 1605, 1563, 1510, 1452 cm^{-1}. NMR(CCl_4): τ 1.98—3.00 (5H, *m*, aromatic), 7.12(2H, *t*, J=7.0 Hz, $\mathbf{CH_2}CH_2CH_2CH_3$), 7.39(3H, s, CH_3), 7.95—9.04(7H, *m*, $CH_2\mathbf{CH_2CH_2CH_3}$).

This compound did not form the picrate, probably due to bulky butyl substituent at the 2-position. The spectral data and the above result support the structure IX.

Hydrolysis of VIIIc. A mixture of 4.4 g (0.016 mol) of VIIIc in 30 m*l* of DMSO and 2.5 g (0.045 mol) of sodium hydroxide in 6 m*l* of water was heated on a boiling-water bath for 3 hr, and then the reaction mixture was worked up as has been described above. The evaporation of the ether extract produced 3.0 g of a yellow oil which was then analyzed by vapor-phase chromatography. The oil contained 2-phenylquinoline (VI) as the main product, along with a small amount of VII. The oil formed a pictrate which melted at 187—188°C after recrystallization from methanol and which was identical in every respect with that of the authentic sample of VI.

Reaction of VIIIc with the Dimethylsulfinyl Carbanion. The dimethylsulfinyl carbanion in DMSO was prepared from 0.02 mol of sodium hydride and 80 m*l* of DMSO by the method of Corey and Chaykovsky.[19] Into this solution we stirred, drop by drop, a solution of 2.7 g (0.01 mol) of VIIIc in 50 m*l* of DMSO over a period of 30 min at room temperature under nitrogen. The mixture, which soon turned red and then deep blue, was stirred for a further 3 hr at 50°C under nitrogen. A 20-m*l* portion of water was added, after which the reaction mixture was heated on a boiling-water bath for 2 hr while a white solid precipitated. The mixture was poured onto 200 m*l* of water and extracted with ether. The ether layer was washed thoroughly with water, dried over sodium sulfate, and then evaporated to give 2.2 g of an oil. The vpc analysis of this oil revealed that the oil consisted of 61.6% of VI and 38.4% of VII.

Rate of Hydrolysis of VIIIa. A homogeneous mixture was prepared by mixing a solution of 1.0 g (0.0034 mol) of VIIIa, 0.80 g (0.014 mol) of sodium hydroxide in 15 m*l* of water, and 15 m*l* of 95% ethanol (the ethanol was necessary to obtain a homogeneous mixture). Fourteen-m*l* portions of the mixture were pipetted into six 30-m*l* test tubes. The test tubes were then sealed and immersed into a constant-temperature bath at 72±1°C. The six tubes was withdrawn after 0.5-, 3-, 6-, 10-, 15-, and 20-hr intervals, respectively, and the contents were extracted with 50 m*l* of ether. The ether solution was washed twice with 20-m*l* portions of water, dried over sodium sulfate, and then concentrated. The residue was directly subjected to the vpc analysis. The proportion of the components in the mixture was calculated from the corresponding peak areas on the chromatogram; the peak areas for the components had been calibrated with the corresponding authentic samples.

Reaction of 2-Phenyl-4-methylquinoline (V) with $LiAlH_4$-BF_3. Into a solution of 1.0 g (0.0056 mol) of V in 50 m of ether we stirred 6.5 g of BF_3-etherate (47%) at room temperature under nitrogen. A pale yellow solid soon precipitated, after which the mixture was stirred for an additional 30 min. To this mixture 1.0 g (0.026 mol) of powdered $LiAlH_4$ was added in portions. Stirring was continued for 24 hr at room temperature, and then 10 m*l* of ice water were added, drop by drop, to the reaction mixture, which had been cooled in an ice bath. The mixture was filtered, and the filtrate was extracted with ether (when the filtrate was diluted with ethanol, the BF_3-salt of V precipitated as white needles). The evaporation of the ether yielded 0.5 g of an oil. The vpc analysis of the oil revealed that the oil was 69% 2-phenylquinoline (VI) and 31% V.

19) E. J. Corey and M. Chaykovsky, *J. Amer. Chem. Soc.*, **87**, 1345 (1965).

Rotatory Dispersion and Stereochemistry of Organic Compounds. XVI.[1] Carbonylphenyl Glucosides

Yojiro TSUZUKI, Shintaro KATAOKA, Minako FUNAYAMA, and Koko SATSUMABAYASHI*

Department of Chemistry, Science University of Tokyo, Kagurazaka, Shinjuku-ku, Tokyo

(Received August 17, 1970)

Rotatory dispersion, circular dichroism and ultraviolet absorption of six kinds of carbonylphenyl tetraacetyl glucoside (carbonyl=*o*- and *p*-CHO, *o*- and *p*-$COCH_3$, *o*- and *p*-COC_2H_5) and their deacetylation products were measured, and the optical rotatory contributions of carbonyl groups were investigated, especially with respect to the effect of the bulk and position of the substituent. This led to the conclusion that all the absorption bands due to the $n\rightarrow\pi^*$ and $\pi\rightarrow\pi^*$ transitions are optically active. Anomaly was also observed in the *o*-substitution products, thus making the general effect of electrophilic substituents on optical rotation definite, *viz.*, that all the Cotton effects of the longer wavelength (due to the $n\rightarrow\pi^*$ transition) are negative in *p*-carbonylphenyl β-glucosides, and in good accordance with the optical contribution of C_1-configuration, but optical anomaly was invariably observed with the *o*-isomers which displayed positive Cotton effects. This rule in rotatory dispersion holds with the deacetylated compounds, in contrast to the deacetylated *o*-nitrophenyl glucosides (in this sense *o*-nitro group is anomalous). Some regularities were found with the Cotton effects due to the $\pi\rightarrow\pi^*$ transition and the effect of the bulk of the carbonyl groups was discussed.

The anomalous specific rotation of *o*-nitrophenyl glycosides was elucidated by studying the rotatory dispersion of various nitrophenyl glycosides, and it was found that the sign of the Cotton effects became inverted by deacetylation of acetyl-*o*-nitrophenyl glycosides, which is contrary to the corresponding *p*-substituted derivatives.[1]

The present paper deals with a similar study on phenyl glucosides containing three types of carbonyl group situated at the ortho and para positions, in order to investigate whether the anomaly[1,2] is characteristic of the nitro group. For this purpose the twelve compounds shown in Fig. 1 were studied. They are all β-glucosides with aglycones, such as *o*- and *p*-formylphenyl, *o*- and *p*-acetylphenyl as well as *o*- and *p*-propionyl phenyl (compounds Ib—VIb) and their acetyl derivatives (compounds Ia—VIa).

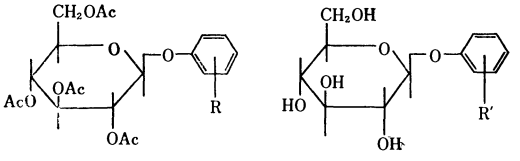

(Ac=$COCH_3$)

Compound	R	Compound	R'
Ia	*o*-CHO	Ib	*o*-CHO
IIa	*p*-CHO	IIb	*p*-CHO
IIIa	*o*-$COCH_3$	IIIb	*o*-$COCH_3$
IVa	*p*-$COCH_3$	IVb	*p*-$COCH_3$
Va	*o*-COC_2H_5	Vb	*o*-COC_2H_5
VIa	*p*-COC_2H_5	VIb	*p*-COC_2H_5

Fig. 1. Twelve β-phenylglucosides studied.

Measurements were made with these compounds on their rotatory dispersion (RD), circular dichroism (CD), ultraviolet absorption (UV) and NMR spectra. Some considerations will be given on the effect of the bulk of the substituents affecting the optical rotation.

Results and Discussion

The RD, CD, and UV curves of *o*-formylphenyl tetraacetyl-β-D-glucoside (Ia) are shown in Fig. 2. The RD curve exhibits complex Cotton effects. The CD curve shows a positive peak at 340 mμ, a negative CD_{max} at 300 mμ and a positive CD_{max} below 260 mμ, from which the signs of the Cotton effects are clearly determined. That the RD and CD curves have fine structures near the absorption regions is evidenced by the UV curve, which shows a slight anomaly near 350 mμ and two absorption maxima at 304 mμ and 250 mμ. Hence, the positive Cotton effects (CD_{max} at 340 mμ) show that the $n\rightarrow\pi^*$ transition due to the *n*-electron resonance between the phenyl group and the carbonyl group is optically active, although it is not clearly seen from the UV curve. It became evident that the absorption bands around 304 mμ and 250 mμ are also optically active, and are attributed to the $\pi\rightarrow\pi^*$ transition brought about by the resonance

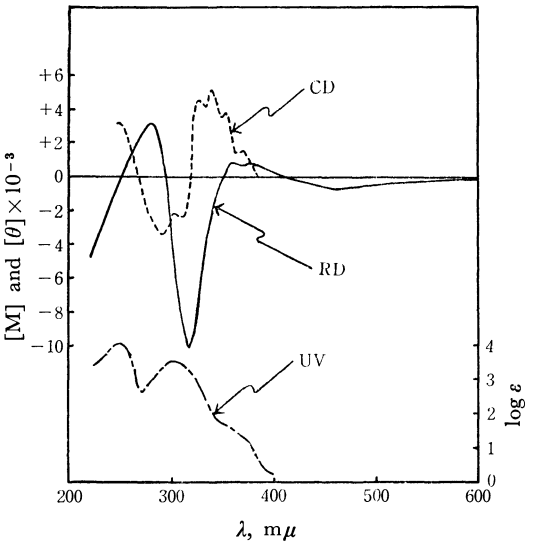

Fig. 2. RD, CD, and UV of compound Ia.

1) Y. Tsuzuki, M. Koyama, K. Aoki, T. Kato, and K. Tanabe, This Bulletin, **42**, 1052 (1969).

* née Tanabe.

2) Y. Tsuzuki, M. Koyama, and K. Tanabe, *ibid.*, **41**, 1008 (1968).

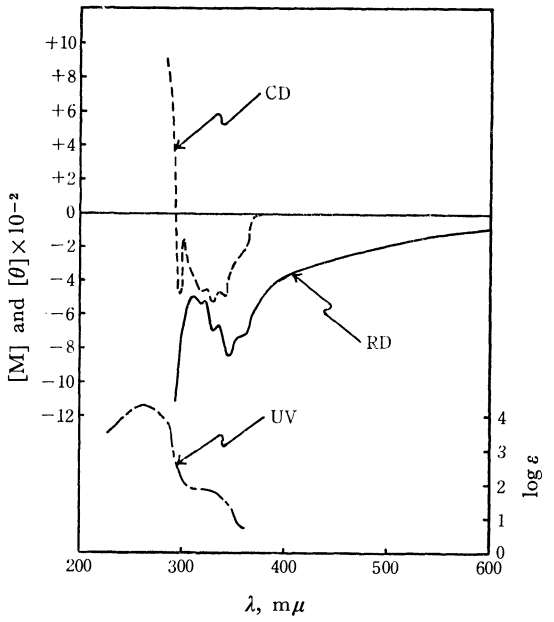

Fig. 3. RD, CD, and UV of compound IIa.

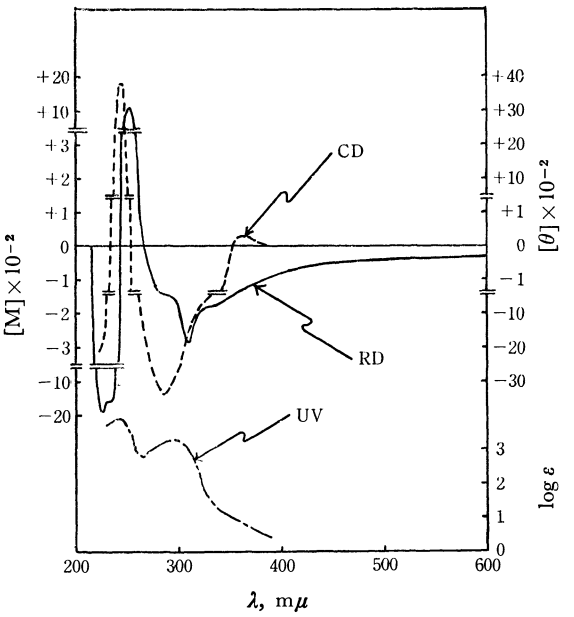

Fig. 4. RD, CD, and UV of compound IIIa.

electron of the phenyl-carbonyl group. This is evident in the UV curve.

In the NMR spectrum of *o*-formylphenyl glucoside (Ia) is observed the proton of an aromatic aldehyde as a singlet, which is in agreement with the signal of the proton of aromatic *o*-aldehydes.

In the RD, CD, and UV spectra of *p*-formylphenyl tetraacetyl-*β*-D-glucoside (IIa), given in Fig. 3, the RD curve exhibits a negative Cotton effect evidenced by the CD curve, which shows a CD_{max} near 330 mμ, and a positive Cotton effect can be expected to appear below 290 mμ from the CD curve. The UV spectrum has an absorption maximum at 264 mμ and a shoulder around 310—330 mμ. Like compound Ia this indistinct absorption due to the $n\rightarrow\pi^*$ transition is optically active, and the positive Cotton effect expected to appear on the shorter wavelength region from the CD curve may be attributed to the $\pi\rightarrow\pi^*$ transition around 264 mμ.

By comparing the RD of Ia and IIa, it is apparent that the Cotton effect near 330—340 mμ is positive in the ortho-aldehyde of the glucoside and negative in the para isomer, thus exhibiting a distinct difference in the two compounds. The NMR spectrum of IIa exhibits a singlet near $\delta=10$ ppm as a signal of the proton of *p*-aldehydes.

The RD, CD, and UV spectra of *o*-acetylphenyl tetraacetyl-*β*-D-glucoside (IIIa) and those of *o*-propionyl tetraacetyl-*β*-D-glucoside (Va) are shown in Figs. 4 and 5, respectively. They exhibit similar curves of complex Cotton effects, both RD curves exhibiting no clear Cotton effect in the longer wavelength region, where a small positive CD_{max} appears. Compound IIIa shows a more or less red- shifted CD_{max} of positive sign, due to the $n\rightarrow\pi^*$ transition, as compared with compound Va, but the CD_{max} and the Cotton effects due to the $\pi\rightarrow\pi^*$ transition in these two compounds are both negative at 285 mμ and positive at 240 mμ and again negative below 220 mμ, the values being

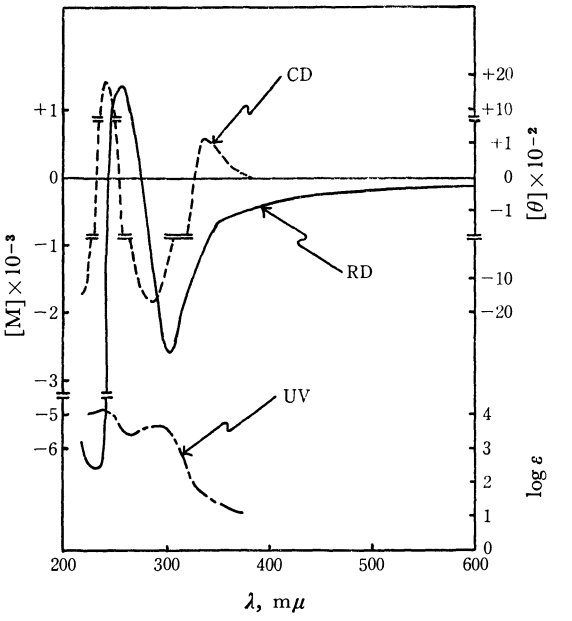

Fig. 5. RD, CD, and UV of compound Va.

also of the magnitude of the same order. In the UV curves of IIIa and Va, both absorption maxima appear at 290 mμ and 240 mμ[3] but no absorption bands corresponding to the CD_{max} at 335 mμ (Va) and 360 mμ (IIIa).

The RD, CD, and UV curves of *p*-acetylphenyl tetraacetyl-*β*-D-glucoside (IVa) are shown in Fig. 6. The RD curve exhibits complex Cotton effects, which can be evidenced, however, by the CD curve with maxima at 320 mμ and 265 mμ. The RD curve is similar in pattern to that of compound IIa which con-

3) These absorption bands are red-shifted by 3—4 mμ in polar solvents, which can be explained by presuming that $\pi\rightarrow\pi^*$ transition is subjected to the conjugation effect between the carbonyl group and the benzene ring. See S. Nagakura and K. Kuboyama, *J. Amer. Chem. Soc.*, **76**, 1003 (1954).

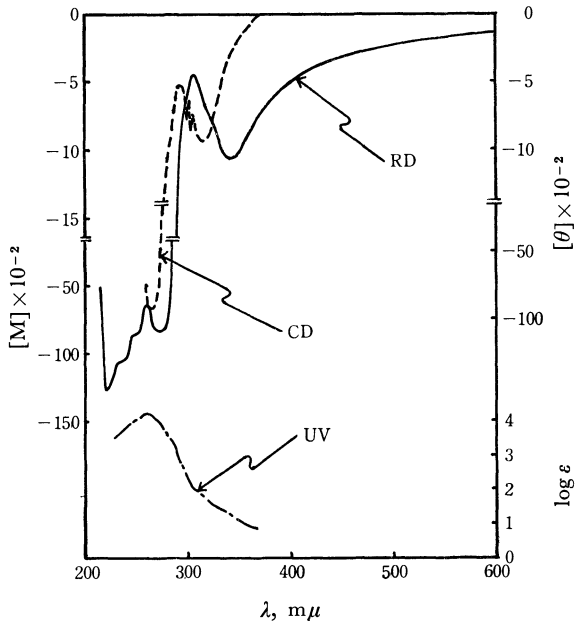

Fig. 6. RD, CD, and UV of compound IVa.

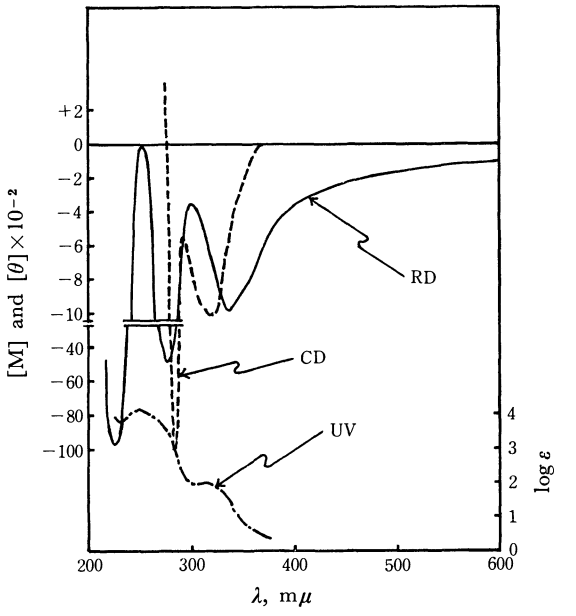

Fig. 7. RD, CD, and UV of compound VIa.

tains an aldehyde group at the *p*-position, but a difference can be seen, *viz.*, the CD_{max} of IVa at 265 mμ is negative while the CD_{max} expected from the CD curve of IIa is positive.

The RD curve of *p*-propionylphenyl tetraacetyl-β-D-glucoside (VIa) shown in Fig. 7 together with CD and UV spectra is also similar in pattern to those of *p*-compounds IIa and IVa. The CD curve of VIa has a negative maximum at 320 mμ like IIa and is expected to have a large positive maximum below 280 mμ. The UV curve of VIa exhibits absorption bands due to the $\pi \rightarrow \pi^*$ transition around 312 mμ and 252 mμ, and the absorption band attributed to the $n \rightarrow \pi^*$ transition is optically active, though it is not apparent in the curve. Thus the *p*-substituted phenyl glucosides exhibit no singularity due to the carbonyl group, having curves similar to those of *p*-NO_2 derivatives.[1] These facts suggest that the compounds with electrophilic substituents have common properties in rotatory contribution.

The RD, CD, and UV curves of the deacetylated products of the above mentioned acetylated phenyl glucosides are shown in Figs. 8—13.

Figure 8 gives the RD, CD, and UV spectra of *o*-formylphenyl β-D-glucoside (Ib). The spectra are complex, the CD_{max} at 340 mμ being positive, those at 306 mμ and 250 mμ both negative, and that below 220 mμ expected to be negative. The UV spectrum shows absorption bands around 310 mμ and 256 mμ. These bands as well as the Cotton effects evidenced by the CD_{max} can be interpreted in a similar way as in the case of the corresponding acetylated compound

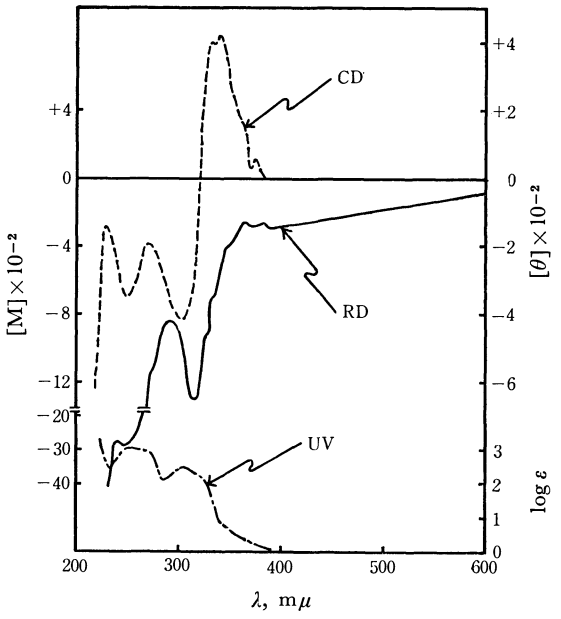

Fig. 8. RD, CD, and UV of compound Ib.

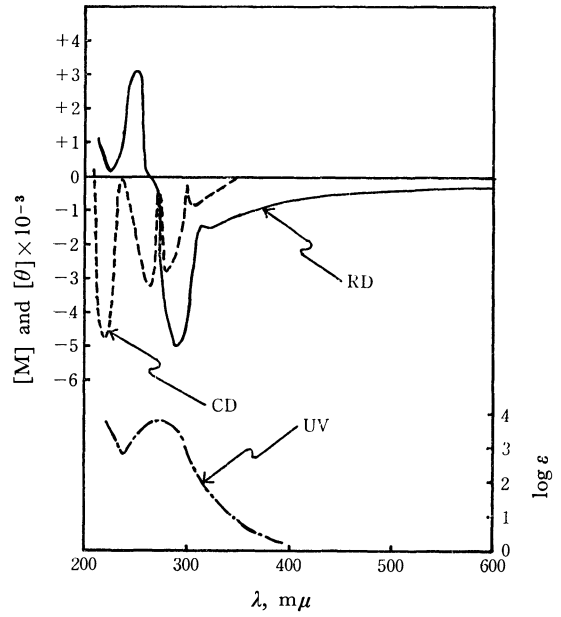

Fig. 9. RD, CD, and UV of compound IIb.

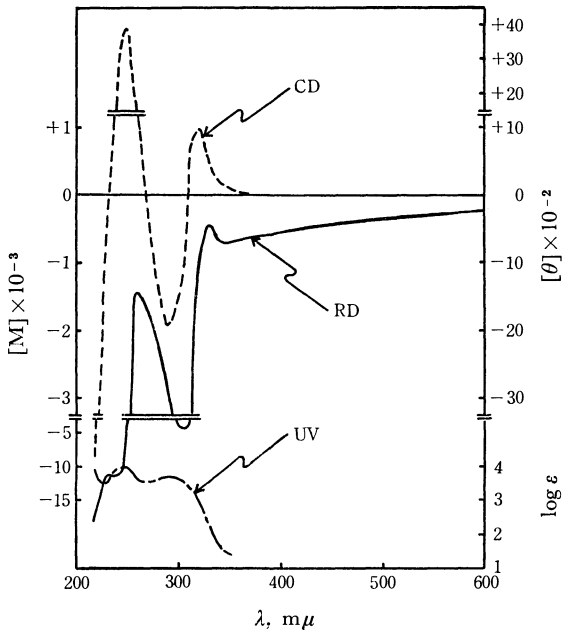

Fig. 10. RD, CD, and UV of compound IIIb.

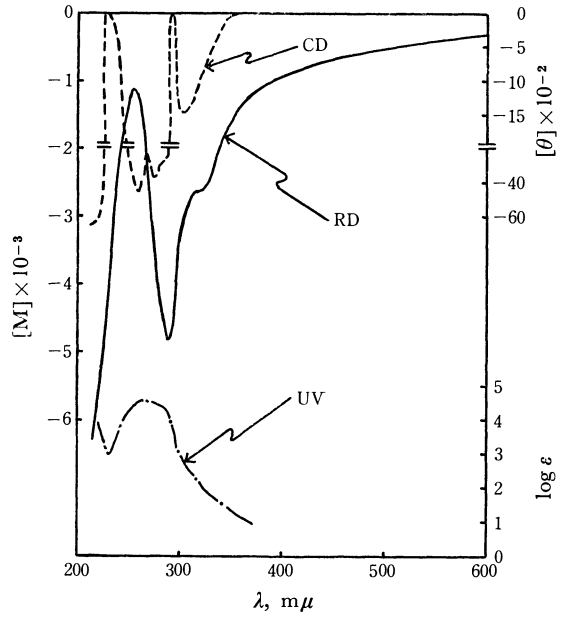

Fig. 11. RD, CD, and UV of compound IVb.

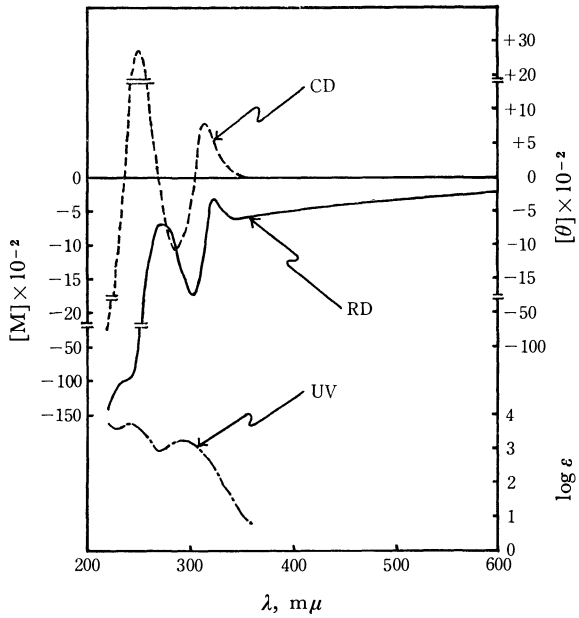

Fig. 12. RD, CD, and UV of compound Vb.

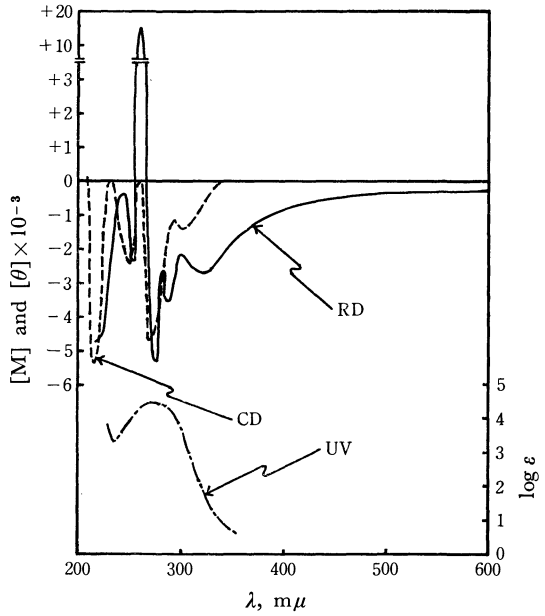

Fig. 13. RD, CD, and UV of compound VIb.

Ia (Fig. 2). However, it should be noted that the Cotton effect centered at 250 mμ due to the $\pi\rightarrow\pi^*$ transition is inverted in sign, that is, a positive Cotton effect is expected in Ia, whereas a negative Cotton effect appears in Ib. This is the greatest difference between the acetylated and deacetylated products.

Figure 9 shows the RD, CD, and UV curves of *p*-formylphenyl β-D-glucoside (IIb). The RD curve has a shoulder around 310—320 mμ, suggesting a weak Cotton effect which was confirmed to be negative by the CD_{max} at 303 mμ. The CD_{max} due to the $\pi\rightarrow\pi^*$ transition which appears at 264—280 mμ is split, but the UV spectrum is observed to have a single absorption band centered at 270 mμ. It should be noted however, that a negative CD_{max} was observed at 219 mμ.

Figure 10 shows the RD, CD, and UV curves of *o*-acetylphenyl β-D-glucoside (IIIb). The Cotton effects appearing at 320 mμ and 290 mμ in the RD curve can be decided by the RD curve to be positive and negative, respectively, and those around 250 mμ and below 220 mμ respectively positive and negative. The CD curve is similar to that of the corresponding, acetylated compound IIIa (Fig. 4), and attribution to the absorption bands may be made in a similar fashion excepting that the CD_{max} attributable to the $n\rightarrow\pi^*$ transition is of $[\theta]_{320}=965°$ in IIIb, and $[\theta]_{360}=28.2°$ in IIIa, indicating that the position as well as the intensity of the Cotton effect is affected by acetylation.

Figure 11 shows the RD, CD and UV curves of *p*-acetylphenyl β-D-glucoside (IVb). The RD curve exhibits no distinct Cotton effect above 300 mμ, indicating a shoulder around 310—220 mμ. This is sup-

ported by the negative CD_{max} appearing at 300 mμ, suggesting that the Cotton effect must be negative in contrast to the positive Cotton effect of the *o*-substituted product (IIIb), and although the UV curve shows no distinct absorption bands except at 268 mμ, the absorption due to the $n\rightarrow\pi^*$ transition must be hidden as in the case of IVa (Fig. 6), but is proved to be optically active. By comparing the RD curves of *p*-acetyl substitution product (IVb) and *p*-formyl derivative (IIb) it is seen that the signs of the Cotton effects are the same and their position nearly the same, although the optical rotation of IIb below 260 mμ appears in the positive region. This is due to the difference of the substituents, but the fact that the CD curves of IVb and IIb are almost the same can be attributed to similar absorptions.

The RD, CD, and UV curves of *o*-propionylphenyl β-D-glucoside (Vb) are given in Fig. 12. The CD curve exhibits a positive peak at 315 mμ, a negative maximum at 285 mμ, again a positive peak at 250 mμ and a negative maximum below 220 mμ. These curves are almost the same as those of the acetylated product of substituted phenyl glucoside (IIIb), indicating that the acetyl and propionyl groups at the ortho position in these glucosides hardly influence the RD at all either sterically or electronically.

The RD, CD and UV curves of *p*-propionylphenyl β-D-glucoside (VIb) in Fig. 13 show a slight, but distinct negative Cotton effect due to the $n\rightarrow\pi^*$ transition in the RD curve unlike IIb (Fig. 9) and IVb (Fig. 11). The UV curve only shows an absorption band at 277 mμ, but the absorption due to the $\pi\rightarrow\pi^*$ transition is not apparent. It should be noted, however, that two negative Cotton effects corresponding to the split CD_{max} due to the K-band were observed around 245—283 mμ in VIb. As stated above, deacetylated *p*-substituted products show no distinct Cotton effects above 300 mμ in the RD curves.

It has thus been found that the $n\rightarrow\pi^*$ transition as well as the $\pi\rightarrow\pi^*$ transition become optically active in carbonylphenyl glucosides.

It is concluded by the wavelength of the absorption band that the $n\rightarrow\pi^*$ transition is caused by the *n*-electron as the result of resonance between the carbonyl and phenyl groups, and becomes optically active irrespective of the sort and the substitution position of the carbonyl groups. However, the optical rotatory contributions are different, that is, the Cotton effect is positive with *o*-substituted products, and negative with *p*-isomers. This experimental rule holds irrespective of the presence of acetyl groups, which shows that the inversion of the sign of Cotton effect due to the $n\rightarrow\pi^*$ transition on deacetylation on acetyl *o*-nitrophenyl glycosides is an anomaly observable only with the nitro group.[1]

The question arises as to the reason for the difference in sign of Cotton effect between the *o*- and *p*-substituted products. With *o*-carbonylphenyl glucosides a certain steric effect of the carbonyl group on the sugar moiety causes one of the possible rotational isomers (due to the rotation of the aglycone) to be stable or fixed making the rotatory contribution positive in sign.[1] On the other hand the optical activity of the *p*-compound is mainly determined by the configuration of C_1 to be laevorotatory in accordance with the β-configuration of the glucoside, since the *p*-substituent is free from steric hindrance.

We shall next consider the $\pi\rightarrow\pi^*$ transition due to the resonance between the phenyl and carbonyl groups. *o*-Carbonylphenyl glucosides show two peaks in the UV spectra and *p*-compounds only one high peak. These peaks are all closely related to the optically active chromophores corresponding to the maxima of the CD curves.

According to the studies of Burawoy *et al.*,[4] and Plott,[5] the UV absorption due to the $\pi\rightarrow\pi^*$ transition observed with *o*-substituted products gives two peaks (B- and K-bands), while with *p*-substituted products a larger K-band (of a shorter wavelength) covers the B-band (of a longer wavelength) and thus a wide UV maximum appears. When this assignment is applied to the carbonylphenyl glucosides, we have the results given in Table 1, which shows the signs of the Cotton effects due to the bands. As can be seen from Table 1, the R-band (due to the $n\rightarrow\pi^*$ transition) signs are all positive in the *o*-substituted products and negative in the *p*-substituted products. Furthermore, all the B-bands contribute to negative Cotton effects, while the K-bands appear complicated. The solvent effect on the $n\rightarrow\pi^*$ transition should be mentioned. The blue-shift by polar solvents can be observed in the RD as well as CD curve of IVb (in ethanol) in contrast to that of IVa (in 1,2-dichloroethane), where the role of conjugation effect is clearly displayed.[3] In addition, strong negative optical rotations may be expected by some CD curves below 220 mμ, which should, however, be attributed to the CT bands.[6]

Table 1. Cotton effects due to UV absorption band

Glucoside	Carbonyl group	K-band	B-band	R-band
Ia	*o*-CHO (acetylated)	+	−	+
Ib	*o*-CHO	−	−	+
IIIa	*o*-$COCH_3$ (acetylated)	+	−	+
IIIb	*o*-$COCH_3$	+	−	+
Va	*o*-COC_2H_5 (acetylated)	+	−	+
Vb	*o*-COC_2H_5	+	−	+
IIa	*p*-CHO (acetylated)	+	−	−
IIb	*p*-CHO	−		−
IVa	*p*-$COCH_3$ (acetylated)	−	(−)[a]	−
IVb	*p*-$COCH_3$	−		−
VIa	*p*-COC_2H_5 (acetylated)	+	−	−
VIb	*p*-COC_2H_5	−		−

a) ( ) unstable.

4) A. Burawoy, M. Cais, J. T. Chamberlain, F. Liversedge, and A. R. Thompson, *J. Chem. Soc.*, **1955**, 3721, 3727.
5) J. R. Plott, *J. Chem. Phys.*, **17**, 484 (1949).
6) K. Kimura, H. Tsubonuma, and S. Nagakura, This Bulletin, **37**, 1336 (1964).

We will next consider the effects of the bulk of the carbonyl group and of the acetyl group on the optical rotation.

The CD_{max} values due to the R-band in the *o*-carbonylphenyl glucoside are shown in Table 2. The

Table 2. [θ]-Values of CD_{max} due to R-band

Carbonyl group	Acetylated glucoside		Deacetylated glucoside	
CHO	Ia	5090°	Ib	433°
$COCH_3$	IIIa	28.2°	IIIb	965°
COC_2H_5	Va	114°	Vb	815°

acetylated derivative Ia with an aldehyde group solely exhibits an incomparably higher value, since the aldehyde group being small in bulk may exert only a slight steric hindrance as compared with that of larger carbonyl groups (IIIa and Va) and thus the resonance between the carbonyl and the phenyl group may be unhindered to such a degree that it may influence mainly the C_1-atom of the glucoside. The difference in bulk between the acetyl group (IIIa) and the propionyl group (Va) is regarded to have little effect on C_1-atom, so that they are nearly equal in rotatory contribution. This effect is more evident in the deacetylated glucosides (IIIb and Vb). As is shown in Table 2, the rotatory contribution of C_1 is increased ([θ]-value is enhanced) because of resonance effect between the phenyl group and the acetyl group (IIIb), or the propionyl group (Vb) being increased by removal of the steric hindrance between the carbonyl group and the acetyl groups of the glucose moiety. A weak bond between the free OH group and the more bulky carbonyl group is possible in view of the increase of the [θ]-value and accordingly fixation of the flexible conformation is conceivable. On the other hand it is seen that the [θ] value falls by deacetylation, due to the small bulk of the formyl group (Ib). With the *p*-substituted-carbonylphenyl glucosides such a steric hindrance is inconceivable, and the Cotton effect due to the $n\rightarrow\pi^*$ transition is not affected much by the kind of substituents and by the presence of the acetyl groups on the side of the sugar moiety.

Experimental

The rotatory dispersion and circular dichroism were measured in 1,2-dichloroethane, water, and ethanol at 25°C in the wavelength region from 210 to 600 mμ with a JASCO optical rotatory dispersion recorder of the ORD/UV-5 type. The ultraviolet absorption was measured in 1,2-dichloroethane, ethanol, and water with a self-recording spectrophotometer of Hitachi EPS-3T type. The NMR spectra were measured with a Varian A-60 spectrometer.

o-*Formylphenyl Tetra*-O-*acetyl*-β-D-*glucopyranoside (Ia)*.[7,8] A solution of salicyl aldehyde (0.03 mol), anhydrous potassium carbonate (5 g) and tetra-*O*-acetyl-α-D-glucopyranosyl bromide (0.025 mol) in anhydrous acetone (100 m*l*) was refluxed for 3 hr. The product was precipitated by adding water and cooling to 0°C. Recrystallization from ethanol gave needles; mp 142°C. The RD was measured at 25°C in 1,2-dichloroethane (*c* 0.990). $[\alpha]_{600}$ −25.0°, $[\alpha]_{589}$ −25.0°, $[\alpha]_{500}$ −33.0°, $[\alpha]_{400}$ +22.0°, $[\alpha]_{360}$ +197° (peak), $[\alpha]_{316}$ −2270° (trough), $[\alpha]_{280}$ +707° (peak), $[\alpha]_{220}$ −1210°. The CD was measured at 25°C in 1,2-dichloroethane (*c* 0.990). $[\theta]_{370}$ +138°, $[\theta]_{340}$ +5090° (peak), $[\theta]_{310}$ −2750° (trough), $[\theta]_{250}$ +3160°. The UV spectrum was measured at 25°C 1,2-dichloroethane. ε_{304} 3420 (max), ε_{250} 11500 (max).

p-*Formylphenyl Tetra*-O-*acetyl*-β-D-*glucopyranoside (IIa)*.[9] The compound was prepared according to the method of Ia. Colorless needles; mp 143.5—144°C. The RD was measured at 25°C in 1,2-dichloroethane (*c* 1.000). $[\alpha]_{400}$ −88.0°, $[\alpha]_{346}$ −188° (trough), $[\alpha]_{312}$ −108° (peak), $[\alpha]_{300}$ −162°. The CD was measured at 25°C in 1,2-dichloroethane (*c* 1.018). $[\theta]_{360}$ −205°, $[\theta]_{330}$ −586° (trough), $[\theta]_{280}$ +1320°. The UV spectrum was measured at 25°C in 1,2-dichloroethane. ε_{264} 18100 (max).

o-*Acetylphenyl Tetra*-O-*acetyl*-β-D-*glucopyranoside (IIIa)*.[10] The compound was prepared by cooling and triturating a mixture of tetra-*O*-acetyl-α-D-glucopyranosyl bromide (0.025 mol), *o*-hydroxyacetophenone (0.03 mol), silver oxide (0.025 mol), and quinoline (0.08 mol), standing for half an hour on anhydrous calcium chloride with stirring every ten min. The mixture was extracted with glacial acetic acid (40 m*l*). The product was precipitated by pouring the extract into water (450 m*l*) at 0°C and recrystallized from ethanol to give yellowish needles; mp 151°C. The RD was measured at 25°C in 1,2-dichloroethane (*c* 0.512). $[\alpha]_{600}$ −52.7°, $[\alpha]_{589}$ −55.7°, $[\alpha]_{309}$ −615° (trough), $[\alpha]_{252}$ +2440° (peak), $[\alpha]_{226}$ −19100° (trough), $[\alpha]_{215}$ 0°. The CD was measured at 25°C in 1,2-dichloroethane (*c* 0.980). $[\theta]_{380}$ +6.28°, $[\theta]_{360}$ +28.2° (peak), $[\theta]_{285}$ −3390° (trough), $[\theta]_{243}$ +3770° (peak), $[\theta]_{225}$ −1880°. The UV spectrum was measured at 25°C in 1,2-dichloroethane. ε_{293} 2220(max), ε_{241} 8940(max).

p-*Acetylphenyl Tetra*-O-*acetyl*-β-D-*glucopyranoside (IVa)*. The compound was prepared according to the method for IIIa. Yellowish needles; mp 168—169°C. The RD was measured at 25°C in 1,2-dichloroethane (*c* 0.530). $[\alpha]_{600}$ −32.7°, $[\alpha]_{589}$ −34.6°, $[\alpha]_{342}$ −237°(trough), $[\alpha]_{307}$ −100° (peak), $[\alpha]_{270}$ −1830°(trough), $[\alpha]_{260}$ −1440°(peak), $[\alpha]_{220}$ −2790°(trough), $[\alpha]_{214}$ −4940°. The CD was measured at 25°C in 1,2-dichloroethane (*c* 0.520). $[\theta]_{360}$ −65.0°, $[\theta]_{323}$ −945°(trough), $[\theta]_{265}$ −9450°(trough), $[\theta]_{260}$ −8860°. The UV was measured at 25°C in 1,2-dichloroethane. ε_{250} 15800(max).

o-*Propionylphenyl Tetra*-O-*acetyl*-β-D-*glucopyranoside (Va)*.[9] The compound was prepared according to the method for IIIa. Colorless plates; mp 162°—162.5°C. The RD was measured at 25°C in 1,2-dichloroethane (*c* 0.440). $[\alpha]_{600}$ −30.0°, $[\alpha]_{589}$ −31.0°, $[\alpha]_{302}$ −545°(trough), $[\alpha]_{258}$ +273° (peak), $[\alpha]_{230}$ −1360°(trough), $[\alpha]_{220}$ −1250°. The CD was measured at 25°C in 1,2-dichloroethane (*c*, 0.530). $[\theta]_{370}$ +18.0°, $[\theta]_{338}$ +114°(peak), $[\theta]_{285}$ −2690°(trough), $[\theta]_{240}$ +1790°(peak), $[\theta]_{220}$ −2540°. The UV was measured at 25°C in 1,2-dichloroethane. ε_{290} 4200(max), ε_{240} 14000 (max).

p-*Propionylphenyl Tetra*-O-*acetyl*-β-D-*glucopyranoside (VIa)*.[9] The compound prepared according to the method for IIIa. Colorless needles; mp 158°—159.5°C. The RD was measured at 25°C in 1,2-dichloroethane (*c* 0.450). $[\alpha]_{600}$ −20.0°, $[\alpha]_{589}$ −21.5°, $[\alpha]_{336}$ −203°(trough), $[\alpha]_{304}$ −74.0°(peak), $[\alpha]_{224}$ −2230°(trough), $[\alpha]_{220}$ −1340°, The CD was measured at 25°C in 1,2-dichloroethane (*c* 1.000). $[\theta]_{350}$ −28.3°,

7) F. Michael, *Amer. Chem. J.*, **1**, 309 (1879).
8) H. Schiff, *Ann. Chem.*, **154**, 19 (1870).
9) L. Reichel and R. Schickle, *ibid.*, **553**, 98 (1942).
10) B. Capon, W. G. Overend, and M. Sobell, *J. Chem. Soc.*, **1961**, 5172.

$[\theta]_{320}$ −1100°(trough), $[\theta]_{286}$ −1730°(trough), $[\theta]_{280}$ +471°. The UV was measured at 25°C in 1,2-dichloroethane. ε_{312} 120(max), ε_{258} 19100(max).

o-*Formylphenyl β-*D*-Glucopyranoside (helicin) (Ib).*[7,8] The acetate Ia was dissolved in 10 m*l* of dry methanol, to which was added 3 m*l* of a freshly prepared solution of sodium methoxide (0.5 g of sodium dissolved in 100 m*l* of methanol) with stirring at room temperature. When the reaction was complete (20 min), a few drops of water were added and the sodium was removed by stirring with a slight excess of the ion-exchange resin (H^+) until the solution became neutral. The resin was filtered and the solution was evaporated to a sirup under reduced pressure. The sirup was crystallized from ethanol or water to give colorless needles; mp 179°—180°C. The RD was measured at 25°C in ethanol (*c* 1.000). $[\alpha]_{400}$ −99.0°, $[\alpha]_{364}$ −93.0°(peak), $[\alpha]_{314}$ −455°(trough), $[\alpha]_{294}$ −297°(peak), $[\alpha]_{248}$ −1050°(trough), $[\alpha]_{240}$ −989°(peak), $[\alpha]_{230}$ −1390°. The CD was measured at 25°C in ethanol (*c* 1.000). $[\theta]_{380}$ +43.3°, $[\theta]_{340}$ +433° (peak), $[\theta]_{306}$ −416°(trough), $[\theta]_{250}$ −347°(trough), $[\theta]_{220}$ −628°. The UV was measured at 25°C in ethanol. ε_{256} 1140(max), ε_{310} 291(max).

p-*Formylphenyl β-*D*-Glucopyranoside (IIb).*[9] The compound was prepared according to the method for Ia. Colorless crystals; mp 154°—155°C. The RD was measured at 25°C in water (*c* 0.450). $[\alpha]_{600}$ −78.9°, $[\alpha]_{589}$ −82.2°, $[\alpha]_{316}$ −523°(trough), $[\alpha]_{310}$ −467°(peak), $[\alpha]_{290}$ −1780° (trough), $[\alpha]_{254}$ +1110°(peak), $[\alpha]_{226}$ 0°(trough), $[\alpha]_{220}$ +556°. The CD was measured at 25°C in water (*c* 0.450). $[\theta]_{320}$ −500°, $[\theta]_{303}$ −812°(trough), $[\theta]_{280}$ −2830°(trough), $[\theta]_{264}$ −3250°(trough), $[\theta]_{219}$ −4790°(trough), $[\theta]_{210}$ 0°. The UV was measured at 25°C in ethanol. ε_{270} 6600(max).

o-*Acetylphenyl β-*D*-Glucopyranoside (IIIb).*[10] The compound was prepared according to the method for Ib. Colorless crystals; mp 146°C. The RD was measured at 25°C in water (*c* 0.508). $[\alpha]_{600}$ −84.5°, $[\alpha]_{589}$ −86.5°, $[\alpha]_{350}$ −236°(trough), $[\alpha]_{330}$ −157°(peak), $[\alpha]_{310}$ −1570°(trough), $[\alpha]_{260}$ −492° (peak), $[\alpha]_{220}$ −5700°. The CD was measured at 25°C in water (*c* 0.508). $[\theta]_{380}$ +3.86°, $[\theta]_{320}$ +965° (peak), $[\theta]_{290}$ −1930°(trough), $[\theta]_{250}$ +3860°(peak), $[\theta]_{220}$ −7720°. The UV was measured at 25°C in ethanol. ε_{245} 9080(max), ε_{290} 4530(max).

p-*Acetylphenyl β-*D*-Glucopyranoside (IVb).* The compound prepared according to the method for Ib. Colorless needles; mp 191°C. The RD was measured at 25°C in water (*c* 0.488). $[\alpha]_{600}$ −117°, $[\alpha]_{589}$ −121°, $[\alpha]_{290}$ −1640° (trough), $[\alpha]_{260}$ −410°(peak), $[\alpha]_{220}$ −2050°. The CD was measured at 25°C in water (*c* 0.488). $[\theta]_{340}$ −142°, $[\theta]_{300}$ −1510°(trough), $[\theta]_{275}$ −4020°(trough), $[\theta]_{260}$ −4820° (trough), $[\theta]_{220}$ −6050°. The UV was measured at 25°C in ethanol. ε_{268} 33200(max).

o-*Propionylphenyl β-*D*-Glucopyranoside (Vb).*[10] The compound was prepared according to the method for Ib. Colorless needles; mp 105°C. The RD was measured at 25°C in water (*c* 0.482). $[\alpha]_{600}$ −64.3°, $[\alpha]_{589}$ −66.4°, $[\alpha]_{340}$ −191°(trough), $[\alpha]_{323}$ −104°(peak), $[\alpha]_{305}$ −560° (trough), $[\alpha]_{270}$ −228°(peak), $[\alpha]_{240}$ −3010°, $[\alpha]_{220}$ −4360°. The CD was measured at 25°C in water (*c* 0.482). $[\theta]_{360}$ +21.5°, $[\theta]_{316}$ +815°(peak), $[\theta]_{258}$ −1070°(trough), $[\theta]_{250}$ +2750° (peak), $[\theta]_{220}$ −6860°. The UV was measured at 25°C in water. ε_{245} 5700(max), ε_{295} 1700(max).

p-*Propionylphenyl β-*D*-Glucopyranoside (VIb).*[11] The compound was prepared according to the method for Ib. Colorless needles; mp 160°C. The RD was measured at 25°C in water (*c* 0.438). $[\alpha]_{600}$ −91.3°, $[\alpha]_{589}$ −95.9°, $[\alpha]_{320}$ −868°(trough), $[\alpha]_{300}$ −709°(peak), $[\alpha]_{287}$ −1160°(trough), $[\alpha]_{261}$ +3350°(peak), $[\alpha]_{254}$ −774°(trough), $[\alpha]_{245}$ −129° (peak), $[\alpha]_{220}$ −1470°. The CD was measured at 25°C in water (*c* 0.438). $[\theta]_{320}$ −729°, $[\theta]_{300}$ −1400°(trough), $[\theta]_{270}$ −4700°(trough), $[\theta]_{250}$ −2490°(trough), $[\theta]_{216}$ −5410° (trough), $[\theta]_{210}$ 0°. The UV was measured at 25°C in ethanol. ε_{277} 30800(max).

The authors are very grateful to Mr. T. Takakuwa of the Japan Spectroscopy Co., Ltd. for the RD and CD measurements.

11) G. Wagner, *Arch. Pharm.* (Weinheim), **290**, 625 (1957).

The Formation of Triaryl-*s*-triazine in the Chemiluminescence Reaction of Triarylimidazole and in the Photo-oxygenation of Triarylimidazole in the Presence of Ammonia[1)]

Koko MAEDA* and Taro HAYASHI**

* *Department of Chemistry, Faculty of Science, Ochanomizu University, Bunkyo-ku, Tokyo*

** *The Institute of Physical and Chemical Research, Yamato-machi, Kitaadachi-gun, Saitama*

(Received August 19, 1970)

2,4,6-Triphenyl-*s*-triazine (II) is formed either in the chemiluminescence reaction of 2,4,5-triphenylimidazole (I) in the presence of oxygen and a strong base or in the photolysis of I in alcohol in the presence of ammonia and oxygen. II is also formed in the sensitized photo-oxygenation of I in alcohol containing ammonia. It was found that II was produced by the reaction between the lophyl hydroperoxide (V), which was prepared from I and was known to be one of the intermediates in chemiluminescence reaction of I, and ammonia. Chemical and spectroscopic evidence that II is produced from V and not *via* the dioxetane-type peroxide (VI) nor *N,N'*-dibenzoylbenzamidine (IV), is given. II and several other 2,4,6-triaryl-*s*-triazines were found to be easily prepared from the corresponding triarylimidazoles by the sensitized photo-oxygenation in methanol in the presence of ammonium acetate and this provides a new method for the synthesis of triaryl-*s*-triazine.

We found[2)] that after the chemiluminescence of 2,4,5-triphenylimidazole (I) was exhibited by oxygen for about 1 day in 1 N ethanolic solution of potassium hydroxide at room temperature, a small amount (lower than 5%) of 2,4,6-triphenyl-*s*-triazine (II) was isolated as alkali-insoluble fine crystals, besides the major products, benzoic acid and ammonia.[3)] Formation of II was also found to occur in a photolysis of I in alcohols in the presence of oxygen and ammonia at room temperature (16% yield) and in a sensitized photo-oxygenation of I in the presence of ammonia at about 0°C (22% yield). In this paper we will report the results of the study on the species involved in the transformation of I into II which led to a new synthetic method of triaryl-*s*-triazine.

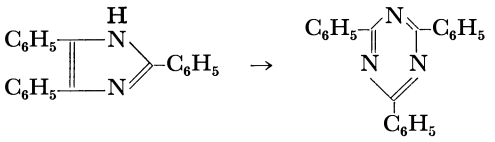

I II

Results and Discussion

Compound II obtained in the chemiluminescence reaction of I was considered to be formed by the ring expansion of I by insertion of one nitrogen atom between C-4 and C-5 of the imidazole ring. The yield of II decreases with rise of the reaction temperature and increases slightly by addition of ammonia to the solution. These facts suggested that the inserted nitrogen atom is supplied by ammonia which is one of the major products of the chemiluminescence reaction of I. Therefore, the photolysis of I in the presence of ammonia was investigated in some detail. When a methanolic solution of I containing ammonia was irradiated by a high-pressure mercury lamp under bubbling of oxygen, II separated from the solution in 16% yield, and from the filtrate 4,5-(9',10'-phenanthryl)-imidazole (9%), benzamide (25%) and *N*-benzoylbenzamidine (III) (45%) were isolated. When the photo-oxygenation of I was carried out in a methanolic solution of ammonia containing methylene blue as sensitizer at about 0°C by an incandescent lamp, a considerable change in UV absorption of the solution was observed and after the irradiation was shut off II gradually separated from the solution in 22% yield. From the filtrate, III (33%) and benzamide (12%) were obtained. 4,5-(9',10'-Phenanthryl)imidazole could not be detected in this case. White and Harding[4)] isolated III and IV from the reaction products of the chemiluminescence reaction of I and found that the observed luminescence is the fluorescence emission of IV which was suggested to be formed from the anion of lophyl hydroperoxide (V) through the anion of the dioxetane-type peroxide (VI). In view of their work and our present results, we assumed that IV, V or VI and ammonia were involved in the formation of triphenyl-*s*-triazine.

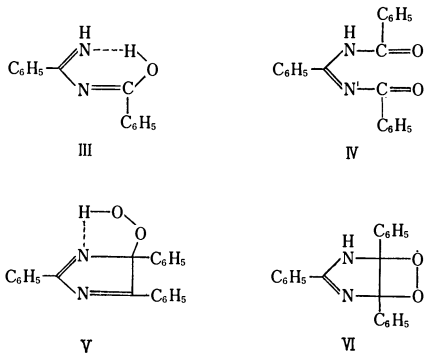

III IV V VI

In order to clarify the mechanism involved in the ring expansion, reactions of IV and V with ammonia were investigated. When V which was prepared[5)] by the photo-oxygenation of I was dissolved in a metha-

1) Presented in part at the Symposium on Photochemistry, Tokyo, October, 1969.

2) T. Hayashi and K. Maeda, Presented at the 12th Annual Meeting of the Chemical Society of Japan, Kyoto, April, 1959.

3) B. Radziszewski, *Ber.*, **10**, 70 (1877).

4) E. H. White and M. J. C. Harding, *Photochem. Photobiol.*, **4**, 1129 (1965).

5) J. Sonnenberg and D. M. White, *J. Amer. Chem. Soc.*, **86**, 5685 (1964).

nolic solution of ammonia at room temperature, II separated from the solution within about 15 min (20% yield based on V) and from the filtrate I (13%), a small amount of III, and benzamide (65%) were isolated. II was also obtained by dissolving V in solutions of ammonia in ethanol, 2-propanol or dimethyl sulfoxide when the yield of II was lower than that obtained in alcoholic solutions. When V was dissolved in ether, acetone or benzene containing ammonia, II was not isolated. On the other hand, when IV was dissolved in a methanolic solution of ammonia at room temperature, II was not obtained, but III and benzamide were isolated. These facts showed that the ring expansion proceeds through V (probably its anion) and IV is not involved in the reaction. In order to elucidate whether VI is involved in the ring expansion or not, the following experiments were carried out. When V (0.026 g) was dissolved in a methanolic solution of potassium hydroxide (1 N, 20 m*l*), the solution exhibited chemiluminescence and showed an absorption band (λ_{max} 245 nm) coinciding with that of IV. The band disappeared within about 20 min with appearance of absorption bands (λ_{max} 247, 279 nm) which coincided with those of III and gradually changed to that of benzamide (λ_{max} 225 nm). On the other hand, when V (0.026 g) was dissolved in a methanolic solution of ammonia (0.45 g in 20 m*l*), the solution did not exhibit chemiluminescence and an absorption spectrum gradually changed to that of III without appearance of the absorption

TABLE 1. 2,4,6-TRIARYL-*s*-TRIAZINE OBTAINED FROM 2,4,5-TRIARYLIMIDAZOLE AND AMMONIUM ACETATE

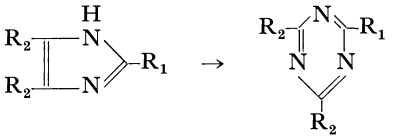

Triaryl-*s*-triazine R_1	Triaryl-*s*-triazine R_2	Mp (°C) (lit.)	λ_{max}^{EtOH} (nm) ($\varepsilon \times 10^{-3}$)			Yield (%)
p-$(CH_3)_2N$-C_6H_4-	C_6H_5-[a]	225—226		263 (18)	369 (15.5)	49
p-CH_3O-C_6H_4-	C_6H_5-*	161—162 (157.5—158.5)[6]	228 (sh)	270 (8)	300 (sh)	39
p-OH-C_6H_4-	C_6H_5-[b]	291—291.5	231 (sh)	268 (10)	303 (7)	30
o-OH-C_6H_4-	C_6H_5-*	257—257.5 (245)[7]	213 (sh)	273 (60)	340 (9.5)	56
p-CH_3-C_6H_4-	C_6H_5-*	206—208 (182—183)[8]	212 (sh)	272 (50)		33
o-CH_3-C_6H_4-	C_6H_5-[c]	121—122		268 (19.5)		25
3′,4′-CH_2<O,O>C_6H_3-	C_6H_5-[d]	184—185	246	269 (9)	328 (4)	30
p-Cl-C_6H_4-	C_6H_5-*	200—201 (197.2—197.8)[9]	211 (11)	272 (30)		47
p-Br-C_6H_4-	C_6H_5-[e]	204—205	212 (sh)	275 (14)		28
C_6H_5-	C_6H_5-*	238—239 (232)[9]		268 (41)		35
C_6H_5-	3′,4′-CH_2<O,O>C_6H_3[f]	195—196	240 (28)	277 (22)	330 (25)	33
p-CH_3-C_6H_4-	*p*-CH_3-C_6H_4-*	285—286 (280—281)[10]	214 (18)	283 (46.5)		30
p-Cl-C_6H_4-	*p*-Cl-C_6H_4-*	336—337 (335)[10]	216 (5)	283 (14)		32

* Satisfactory C, H, and N analyses were obtained for the corresponding formulas. sh: shoulder

a) Found: C; 78.38, H; 5.65, N; 15.93%. Calcd for $C_{23}H_{20}N_4$: C; 78.40, H; 5.68, N; 15.90%.
b) Found: C; 77.31, H; 4.62, N; 12.72%. Calcd for $C_{21}H_{15}N_3O$: C; 77.54, H; 4.62, N; 12.92%.
c) Found: C; 81.48, H; 5.18, N; 12.78%. Calcd for $C_{22}H_{17}N_3$: C; 81.78, H; 5.26; N; 13.00%.
d) Found: C; 74.68, H; 4.28, N; 11.70%. Calcd for $C_{22}H_{15}N_3O_2$: C; 74.78, H; 4.25, N; 11.89%.
e) Found: C; 65.18, H; 3.60, N; 10.68, Br; 20.60%. Calcd for $C_{21}H_{14}N_3Br$: C; 64.96, H; 3.60, N; 11.08, Br; 20.60%.
f) Found: C; 69.32, H; 3.83, N; 10.41%. Calcd for $C_{23}H_{15}N_3O_4$: C; 69.52, H; 3.70, N; 10.57%.

6) E. F. Silversmith, *J. Org. Chem.*, **28**, 3568 (1963).
7) A. Pinner, *Ber.*, **23**, 2934, 3820 (1890); A. W. Titherley and E. C. Hughes, *J. Chem. Soc.*, **99**, 1493 (1911).
8) M. Kung, K. Koherle, and E. Berthold, US 1989042 (1932).
9) R. D. Spencer and B. H. Beggs, *Anal. Chem.*, **35**, 1633 (1963).
10) D. Davidson, M. Weiss, and M. Jelling, *J. Org. Chem.*, **2**, 319 (1937).

band of IV, and then gradually changed to that of benzamide. Considering these facts together with the conclusion of White and Harding[4] it seems that in a methanolic solution of ammonia, II is formed directly from V and ammonia and VI is not involved in the ring expansion.

When ammonium salts (acetate, chloride, and carbamate) were used in place of ammonia, it was found that II was obtained from V in yields higher than those in the case of ammonia. When V was dissolved in a methanolic solution of ammonium acetate at room temperature, II precipitated in 35% yield after a few minutes. From the filtrate, a large amount of I (64%) was recovered, but III, IV, and benzamide were not obtained.

2-*p*-Chlorophenyl-4,6-diphenyl-*s*-triazine was obtained by the reaction of hydroperoxide of the corresponding imidazole with ammonia or ammonium acetate in methanol at room temperature. 2-*m*-Nitrophenyl-4,5-diphenylimidazole which did not give a hydroperoxide by the sensitized photo-oxygenation did not produce the corresponding *s*-triazine in the presence of oxygen and ammonia. The results are compatible with our finding that lophyl hydroperoxide is an immediate precursor in the ring expansion.

II was also obtained in relatively high yield (35%) by a sensitized photo-oxygenation of I in a methanolic solution of ammonium salts. Other substituted triphenyl-*s*-triazines shown in Table 1, were obtained from the corresponding substituted triphenylimidazole by the similar method. This is a new synthetic method of triaryl-*s*-triazine. This method has an advantage over other procedures since the triazines are obtained in an almost pure state even without recrystallization.

Experimental

Materials. Triarylimidazoles shown in Table 2 were prepared according either to the method of Davidson, Weiss, and Jelling[10] or that of Cook and Jones.[11]

Hydroperoxides of triarylimidazole were prepared according to the method of Sonnenberg and White.[5] A chloroform solution of triarylimidazole (0.20 g and 100 m*l*) containing methylene blue (0.015 g) as sensitizer was irradiated by an incandescent lamp (300 W) for 20 min under cooling with ice-water until an absorption spectrum of the hydroperoxide was observed. After methanol was removed under reduced pressure at room temperature, the residue was dissolved in ether to remove methylene blue. After removal of ether under reduced ressure, the hydroperoxide was obtained as an oily product which was crystallized from methanol.

2,4,5-Triphenyl-4-hydroxy-4*H*-isoimidazole (V) decomposed at 235—245°C, producing I. λ_{max}^{EtOH}: 225 nm (ε: 1.5×10^4), 280 nm (ε: 1.6×10^4). IR (KBr and $CHCl_3$): 2820, 1620, and 850 cm^{-1}. NMR ($CDCl_3$): Signals were observed at 7—9 ppm, but no signal was observed at 10—15

Table 2.

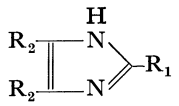

Triarylimidazole[a] R_1	Triarylimidazole[a] R_2	Mp (°C) (lit.)	Method of preparation
p-$(CH_3)_2N$-C_6H_4-	C_6H_5-	261—262 (259.5—260[12])	10
p-CH_3O-C_6H_4-	C_6H_5-	238—239 (233.7—233.9[12])	10
p-OH-C_6H_4-	C_6H_5-	270—271 (268—268.5[12])	10
o-OH-C_6H_4-	C_6H_5-	214—215 (214—215[12])	10
p-CH_3-C_6H_4-	C_6H_5-	239—240 (237—237.5[12])	10
o-CH_3-C_6H_4-	C_6H_5-	249—250 (244—246[13])	10
3′,4′-CH_2(O,O)C_6H_3-	C_6H_5-	262—263.5 (246—247[13])	10
p-Cl-C_6H_4	C_6H_5-	261—262 (284—286 (d)[14] 256—257[12])	10
p-Br-C_6H_4-	C_6H_5-	268—269 (260—261 (d)[14] 253—254[13])	10
C_6H_5-	C_6H_5-	286—287 (273.5—274[4])	10
C_6H_5-	3′,4′-CH_2(O,O)C_6H_3-	269—270 (monohydrate)[b]	10
p-CH_3-C_6H_4-	*p*-CH_3-C_6H_4-	285—286 (280—281[11])	11
p-Cl-C_6H_4-	*p*-Cl-C_6H_4-	336—337 (335[11])	11

a) Satisfactory C, H, and N analyses were obtained for the corresponding formulas

b) Found: C; 68.46, H; 4.94, N; 6.76%. Calcd for $C_{23}H_{18}N_2O_5$: C; 68.66, H; 4.48, N; 6.96%.

11) A. H. Cook and D. G. Jones, *J. Chem. Soc.*, **1941**, 278.

12) D. M. White and J. Sonnenberg, *J. Org. Chem.*, **29**, 1926 (1964).

13) S. Kori and S. Narisawa, *Asahi Garasu Kenkyu Hokoku*, **12**, 55 (1962).

14) G. E. Philbrock, M. A. Maxwell, R. E. Taylor, and J. R. Totter, *Photochem. Photobiol.*, **4**, 1175 (1965).

ppm.

Found: C, 76.80; H, 4.91; N, 8.53%. Calcd for $C_{21}H_{16}N_2O_2$: C, 76.82; H, 4.48; N, 8.53%.

2-*p*-Chlorophenyl-4,5-diphenyl-4-hydroxy-4*H*-isoimidazole decomposed at 235—245°C, producing 2-*p*-chlorophenyl-4,5-diphenylimidazole. λ_{max}^{EtOH}: 230 nm (ε: 1.5×10^4), 290 nm (ε: 1.7×10^4). IR (KBr): 2810, 1620, 840 cm^{-1}.

Found: C, 69.83; H, 4.70; N, 7.51; Cl, 9.83%. Calcd for $C_{21}H_{15}N_2O_2Cl$: C, 69.52; H, 4.13; N, 7.72; Cl, 9.79%.

N,N'-Dibenzoylbenzamidine (IV) was prepared according to the method of Dufraisse and Martel,[15] mp 141.5—142.5°C. Satisfactory C, H, and N analyses were obtained for $C_{21}H_{16}N_2O_2$.

Photolysis of I in Methanol in the Presence of Oxygen and Ammonia. A methanolic solution of I (0.5 g in 500 m*l*) containing ammonia (0.5 g) was irradiated at room temperature by a 100 W high-pressure mercury lamp under bubbling of oxygen, until a crystalline precipitate of II began to separate after about 2 hr. Absorption spectrum and thin-layer chromatogram of the solution showed the absence of I and suggested the presence of 4,5-(9',10'-phenanthryl)imidazole, III, and benzamide in the solution. II (mp 238—239°C) was collected by filtration (0.083 g 16%) which was proved to be identical with an authentic sample. The filtrate was evaporated to leave a yellow oil which deposited a white crystalline precipitate upon standing overnight. A small amount of benzene was added and the crystalline precipitate (about 0.15 g) was filtered. The precipitate (A) was shown to consist of benzamide and III by thin-layer chromatography and UV spectrum. An oily residue obtained by evaporation of the solvent from the yellow filtrate was dissolved in methanol and a small amount of water was added to produce a crystalline precipitate, The precipitate collected was identified to be 4,5-(9',10'-phenanthryl)imidazole (0.050 g, 9%) by mixed-melting with an authentic sample. After removal of the solvent, the oily residue was shown to contain III and benzamide by thin-layer chromatography and UV spectrum. The oily residue and the precipitate (A) were dissolved in benzene-acetone (4 : 1) and chromatographed on a column of alumina (20 g), using the same solvent system for elution. The early fractions collected were evaporated and the oily residue obtained was crystallized from *n*-hexane to give colorless crystals of III (0.181 g, 45%) which was proved to be identical with an authentic sample. From the later fractions collected benzamide (mp 124—125°C, 0.190 g, 25%) was obtained by evaporation of the solvent.

Sensitized Photo-oxygenation of I in Methanol in the Presence of Ammonia. A methanolic solution of I (0.10 g in 100 m*l*) containing ammonia (0.1 g) and methylene blue (0.015 g) was irradiated by a 300 W incandescent lamp for 15 min under bubbling of oxygen at about 0°C. Thin-layer chromatogram and UV spectrum of the resultant solution showed the absence of I and formation of lophyl hydroperoxide (V). When the solution was allowed to stand at room temperature for about 1 hr, a crystalline precipitate of II separated from the solution. II (mp 238—239°C) was collected by filtration (0.023 g, 22%). The filtrate was evaporated to dryness, and the residue was dissolved in ether to remove methylene blue. The yellow filtrate was evaporated to obtain a yellow residue (about 0.05 g) showing the presence of III and benzamide by UV spectrum and thin-layer chromatography. A benzene-acetone (4 : 1) solution of the residue was chromatographed on a column of alumina (5 g) using the same solvent system for elution. III (0.024 g, 33%) and benzamide (0.010 g, 12%) were obtained from the early and later fractions, respectively.

Reaction of V with Ammonium Acetate in Methanol. When V (0.20 g) was dissolved in a methanolic solution of ammonium acetate (1.0 g in 10 m*l*) at room temperature, a crystalline precipitate appeared within about 5 min. It was proved to be identical with an authentic sample of II. After the solution was allowed to stand overnight at room temperature, the precipitate of II (mp 238—239°C) was collected by filtration (0.066 g, 35%). The filtrate was shown by thin-layer chromatography and UV spectrum to consist largely of I. After the filtrate was concentrated to about one-half, water was added to yield a precipitate of I. The precipitate of I collected was washed with water and recrystallized from ethanol (mp 272—273°C, 0.107 g, 64%).

Preparation of II by Sensitized Photo-oxygenation of I in a Methanolic Solution of Ammonium Acetate. A methanolic solution of I (0.20 g in 100 m*l*) containing ammonium acetate (5.0 g) and methylene blue (0.015 g) was irradiated by a 300 W incandescent lamp at about 0°C under bubbling of oxygen. On irradiation for 10—20 min, the absorption spectrum of I changed to that of V and only a spot of V on a thin-layer chromatogram was obtained. After shutting off the irradiation the solution was heated (about 50°C) until the absorption band of II appeared with diminishing of that of V (about 3 hr). When the solution was allowed to stand at room temperature, II gradually separated from the solution. II (mp 238—239°C) was collected by filtration (0.073 g, 35%). The filtrate was shown to consist largely of I by thin-layer chromatography and UV spectrum. The filtrate was concentrated by evaporation and water was added to the residue to give a precipitate of I and to remove methylene blue. The precipitate of I collected was washed with water and recrystallized from ethanol (mp 272—273°C, 0.10 g, 50%). The yield of II did not increase when the solution was allowed to stand at room temperature or lower after shutting off the irradiation.

The authors wish to express their gratitude to Professor Ikuzo Tanaka of Tokyo Institute of Technology and Dr. Hiroshi Midorikawa of the Institute of Physical and Chemical Research for their kind help. This research was supported in part by a Grant for Co-operative Research from the Ministry of Education.

15) C. Dufraisse and J. Martel, *Compt. Rend.*, **244**, 3106 (1957).

The Cationic Polymerization of Methallyl Vinyl Ether

Heimei YUKI, Koichi HATADA, Tomoyuki EMURA, and Kazuhiko NAGATA

Department of Chemistry, Faculty of Engineering Science, Osaka University, Toyonaka, Osaka

(Received August 25, 1970)

The polymerization of methallyl vinyl ether was carried out in toluene by means of $BF_3 \cdot OEt_2$. The reaction proceeded through the vinyl double bond, giving a polymer containing one methallyl double bond per monomeric unit. The polymer obtained below −78°C was a white powder and had an isotactic configuration. The molecular weight of the polymer decreased with an increase in the polymerization temperature, and the polymer obtained at 0°C was a viscous liquid. In *n*-heptane, the yields of the polymer decreased and a part of the polymer obtained was insoluble in usual organic solvents, probably because of the cross-linking which occurred during the polymerization reaction. In *n*-heptane - toluene mixtures, the yields were much higher than those in toluene or *n*-heptane alone. The NMR spectra of the polymer were measured in CCl_4, benzene, pyridine, and quinoline at various temperatures in order to investigate the polymer-solvent interaction; the π-complex formation between the monomeric unit of the polymer and the aromatic solvent molecule was suggested.

A number of papers have been published on the stereospecific polymerization of vinyl ethers.[1-6] However, there have been only a few reports[7-9] on the cationic polymerization of vinyl ether with an unsaturated substituent. In a previous work,[9] we studied the polymerization of allyl vinyl ether by $BF_3 \cdot OEt_2$. In the present work we investigated the polymerization of methallyl vinyl ether (MAVE) by $BF_3 \cdot OEt_2$; the polymerization was found to proceed through the vinyl double bond, giving a polymer containing one methallyl double bond per monomeric unit. At low polymerization temperatures, the polymer produced was a white powder with a predominantly isotactic configuration.

Experimental

Reagents. MAVE was prepared from methyl vinyl ether and methallyl alcohol by the vinyl transetherification catalyzed by mercuric acetate in the presence of molecular sieves.[10] The monomer obtained was refluxed over lithium aluminum hydride under a nitrogen atmosphere and was then fractionally distilled. Bp 90.0°C. The purified MAVE was sealed in ampoules under dry nitrogen and was stored at −20°C.

The toluene and *n*-heptane were purified in the usual manner, dried, and stored over calcium hydride. They were then dried further with a small amount of *n*-butyllithium and distilled under a high vacuum just before use.

Methylene chloride, nitroethane, and diethyl ether were purified as usual, dried with calcium hydride, and distilled under a high vacuum just before use.

$BF_3 \cdot OEt_2$ was purified by distillation under a reduced nitrogen pressure and was used as a toluene solution.

Nitrogen gas was purified by being passed through a column packed with molecular sieves 4A cooled at −78°C in a dry ice - acetone bath.

Polymerization. A vessel equipped with a three-way stop-cock was flushed with dry nitrogen. The monomer and a solvent were added with hypodermic syringes, and cooled at a given temperature. The polymerization was initiated by introducing the catalyst drop by drop with a syringe, and was stopped by adding a small amount of ammoniac methanol which had been cooled to the same temperature as the reaction mixture. The mixture was then poured into a large amount of methanol containing a small amount of phenyl-β-naphthylamine. The precipitated polymer was collected by filtration, washed throughly with methanol, and dried *in vacuo* at room temperature for three days. The filtrate was concentrated to dryness under a high vacuum. The resultant methanol-soluble fraction was redissolved in benzene to free it from inorganic materials and then dried by the freeze-drying technique. The polymer was stored under reduced nitrogen pressure at −20°C in order to avoid the formation of a cross-linked insoluble polymer.

Measurements of NMR Spectra. The NMR spectra were obtained with a JEOL JNM-4H-100 spectrometer at 100 MHz by using a 10 w/v% solution containing a small amount of tetramethylsilane as an internal standard. The spectra of the polymer and MAVE were measured in carbon tetrachloride at 60°C and in chloroform at 22.5°C respectively. The spectra using a spin-decoupling technique were measured in pyridine at 100°C.

The temperature dependence of the spectrum of the polymer was investigated in several solvents, using hexamethyldisilane as an external standard, in precision coaxial tubing (Wilmad Glass Co.). A correction of the chemical shift involving the difference between the bulk diamagnetic susceptibilities of the reference compound and the sample solution was applied. The volume magnetic susceptibilities, χ_v, were taken from the literature.[11,12] The χ_v value of the neat solvent was used instead of that of the sample solution.

Viscosity Measurements. The solution viscosity of the polymer was measured on its toluene solution (0.7—1.0 g/dl) at 30.0±0.03°C using Ostwald's viscometer.

1) C. E. Schildknecht, S. T. Gross, H. R. Davison, J. M. Lambert, and A. O. Zoss, *Ind. Eng. Chem.*, **40**, 2104 (1948).
2) G. Natta, G. Dall'Asta, G. Mazzanti, U. Giannini, and S. Cesca, *Angew. Chem.*, **71**, 205 (1959).
3) T. Higashimura, K. Suzuoki, and S. Okamura, *Makromol. Chem.*, **86**, 259 (1965).
4) E. J. Vandenberg, *J. Polymer Sci.*, **C1**, 207 (1963).
5) H. Yuki, K. Hatada, K. Ohta, I. Kinoshita, S. Murahashi, K. Ono, and Y. Ito, *J. Polymer Sci.*, *A*-1, **7**, 1517 (1969).
6) S. Murahashi, S. Nozakura, M. Sumi, and K. Matsumura, *Polymer Lett.*, **4**, 59 (1966).
7) R. Paul, G. Roy, M. Fluchaire, and G. Collardeau, *Bull. Soc. Chim. Fr.*, **1950**, 121.
8) J. Lal, *J. Polymer Sci.*, **31**, 179 (1958).
9) H. Yuki, K. Hatada, K. Ohta, and T. Sasaki, This Bulletin, **43**, 890 (1970).
10) H. Yuki, K. Hatada, K. Nagata, and K. Kajiyama, *ibid.*, **42**, 3546 (1969).
11) J. W. Emsley, J. Feeney, and L. H. Sutcliffe, "High Resolution Nuclear Magnetic Resonance Spectroscopy," Pergamon Press, London (1965), p. 605.
12) K. Hatada, Y. Terawaki, and H. Okuda, This Bulletin, **42**, 1781 (1969).

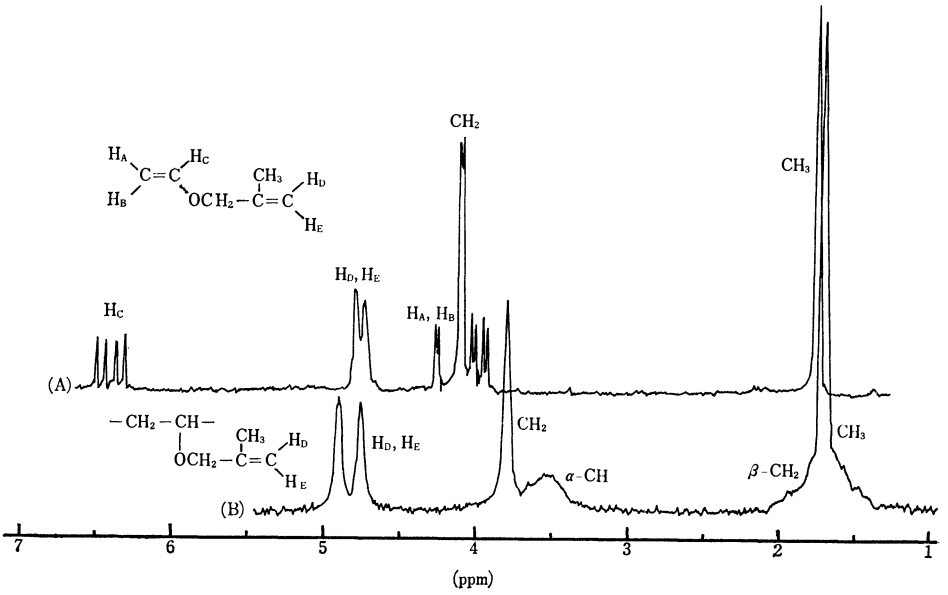

Fig. 1. NMR spectra of methallyl vinyl ether (A) and poly(methallyl vinyl ether) (B) obtained in toluene at −78°C by $BF_3 \cdot OEt_2$

Measurements of Molecular Weight. The molecular weight of the polymer was measured on its benzene solution (10 g/*l*) at 37°C using a Mechrolab 301 A Vapor Pressure Osmometer.

Results and Discussion

Structure and Tacticity of PMAVE. Figure 1 shows the NMR spectrum of PMAVE obtained at −78°C in toluene by $BF_3 \cdot OEt_2$, together with the spectrum of MAVE. The spectrum of the polymer consisted of four groups of peaks, which correspond to the methyl-proton signal overlapping with that of the β-methylene protons, α-methine proton signal, methallyl methylene proton signal, and the terminal methylene proton signals with decreasing magnetic field. The intensity ratio of these groups of peaks was 5.3 : 1.1 : 2.0 : 2.0. There were no resonances due to the protons of the vinyl group, which were observed at about 3.9—4.3 and 6.4 ppm in the spectrum of the MAVE. These facts show that MAVE polymerized exclusively through the vinyl double bond, leaving the methallyl double bond unaffected by the polymerization.

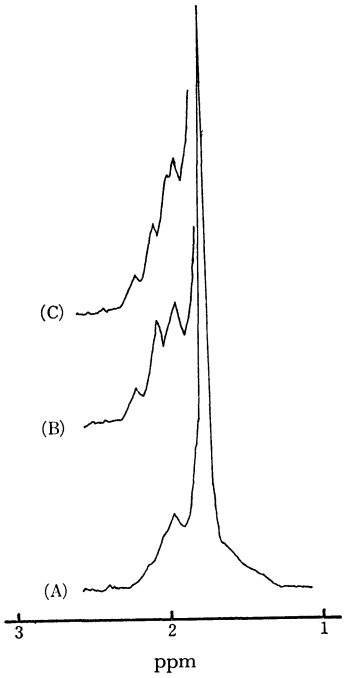

Fig. 2. β-Methylene and methyl protons resonances of PMAVE obtained in toluene at −78°C (20 w/v% pyridine solution, 100°C).
A: Undecoupled.
B: Decoupled from α-methine proton.
C: PMAVE obtained in toluene at 0°C. Decoupled from α-methine proton.

In the CCl_4 solution the β-methylene-proton resonance of PMAVE overlapped with methyl-proton resonance, but in the pyridine solution it was partially separated from it as is shown in Fig. 2 (A). The β-methylene-proton resonance decoupled from the α-methine proton split into three peaks, at 1.96, 2.08, and 2.21 ppm (B in Fig. 2). These splittings are considered to be three of the four peaks of a typical AB quartet, which originated from the meso methylene protons of an isotactic polymer. The fourth peak at the highest field, must overlap with the methyl signal. These results suggest that the polymer obtained at −78°C was highly isotactic. On the other hand, the decoupled β-methylene resonances of the polymer obtained at 0°C in toluene (C in Fig. 2) was somewhat different, showing that the polymer was less isotactic and that the singlet due to the syndiotactic methylene protons overlaps with the peak at 1.96 ppm, one of the signals of the meso methylene quartet. However, no quantitative determination of the tacticity could be made because of the poor resolution of the decoupled spectrum.

NMR Spectra of PMAVE in Various Solvents. The NMR spectra of PMAVE obtained at −78°C in toluene were taken at 22.5°C on a 10 w/v% solution in various solvents. The results are shown in Table 1. All the signals shifted to a higher field on going from a CCl_4

Table 1. NMR spectra of PMAVE in various solvents at 22.5°C

Solvent	Chemical shift (ppm)					
	$-CH_2-\underset{\underset{O}{|}}{C}-$	$-\underset{\underset{O}{|}}{C}-CH-$	$\overset{O}{\overset{|}{CH_2}}\overset{|}{C}$	$\overset{|}{C}-CH_3$	$\overset{|}{C}-$	$\overset{\|}{CH_2}$
Carbon tetrachloride	2.12	3.98	4.30	2.24	5.29	5.42
Benzene	1.54	3.56	3.67	1.49	4.64	4.91
Pyridine	1.56	3.54	3.66	1.43	4.57	4.82
Quinoline	1.96	3.87	3.95	1.69	4.86	5.16

solution to the solutions in aromatic solvents. The extent of the shift is almost the same in the benzene and pyridine solutions. The quinoline solution showed a smaller shift than the above two solutions did. While pyridine and quinoline have nearly the same dielectric constant and dipole moment, those of benzene are considerably smaller. The above results clearly indicate that the shifts are not caused by the different dielectric constants and dipole moments of the solvents, but by the interaction of the polymer with the solvents. The interaction may be the π-complex formation between the monomeric unit in PMAVE and the solvent molecule, as was reported in connection with the benzene solution of poly(methyl methacrylate).[13]

The temperature dependences of the chemical shifts were investigated in CCl_4 and quinoline solutions. In the CCl_4 solution the chemical shifts of all the protons were scarcely dependent at all upon the temperature. On the other hand, in the quinoline solution all the signals shifted to a low field with an increase in the temperature (Fig. 3). In the benzene and pyridine solutions, nearly the same changes in the chemical shifts were observed. These results may support the idea of the formation of a π-complex in these aromatic solvents.

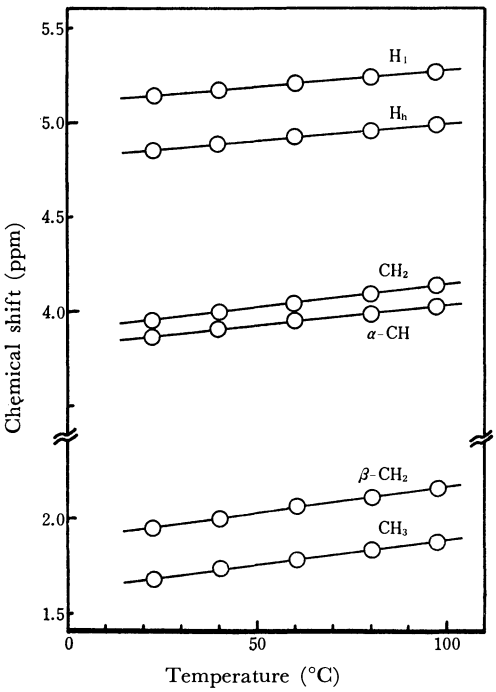

Fig. 3. Temperature dependences of the chemical shifts of all protons in PMAVE obtained in toluene at −78°C. ——Quinoline solution—— H_l and H_h denote the protons of vinyl methylene ones which give the signals at the lower and the higher field, respectively.

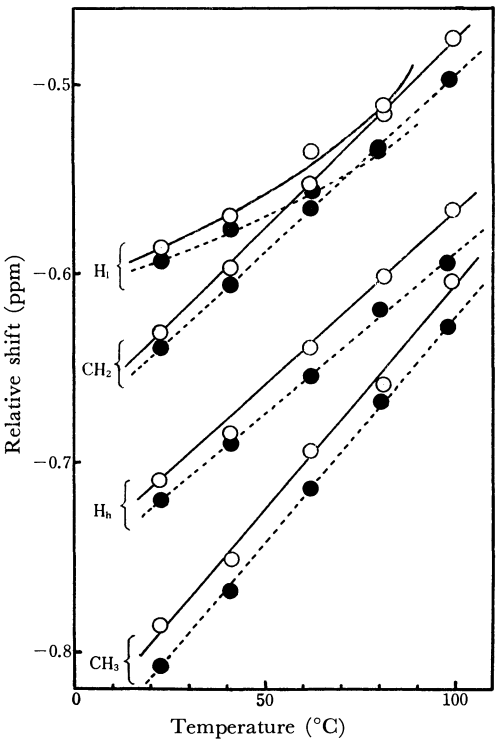

Fig. 4. Relative shifts of the protons in PMAVEs obtained in toluene at 0°C (○) and at −78°C (●) ——Pyridine solution——.

In Figs. 4 and 5 the relative shifts of the protons of the PMAVEs obtained at −78°C and 0°C in toluene are plotted against the temperature, where the relative shift is defined as the difference between the chemical shifts of each particular group in an aromatic solvent and in CCl_4. In both the pyridine (Fig. 4) and quinoline (Fig. 5) solutions, the relative shifts became smaller with an increase in the temperature. Small but significant differences were observed between the relative shifts of the PMAVE obtained at −78°C and those of the PMAVE obtained at 0°C in both the solutions. Liu[14] has revealed, by NMR spectroscopy, that

13) M. Nagai and A. Nishioka, *J. Polymer Sci.*, *A*-1, **6**, 1655 (1968).

14) K. J. Liu, *J. Polymer Sci.*, *A*-2, **5**, 1199 (1967).

TABLE 2. POLYMERIZATION OF MAVE IN VARIOUS SOLVENTS BY $BF_3 \cdot OEt_2$
MAVE 16.8 mmol, $BF_3 \cdot OEt_2$ 0.2 mmol, Solvent 18 m*l*
Temp. −78°C, Time 24 hr.

No.	Solvent	Polymer yield (%)		
		Total	MeOH sol.	MeOH insol.
141	Toluene	56.9	5.8	51.1
68	CH_2Cl_2	13.7	13.7	trace
173	$EtNO_2$	trace	trace	0
145	Et_2O	0	0	0
169	Heptane + Toluene (2 : 7)[b]	58.1	8.6	49.5
165	Heptane + Toluene (1 : 1)[b]	76.3	15.6	70.7
168	Heptane + Toluene (7 : 2)[b]	81.5	14.0	67.5
166	Heptane	35.7	16.8	18.9[a]

a) Insoluble in usual organic solvent b) Volume ratio

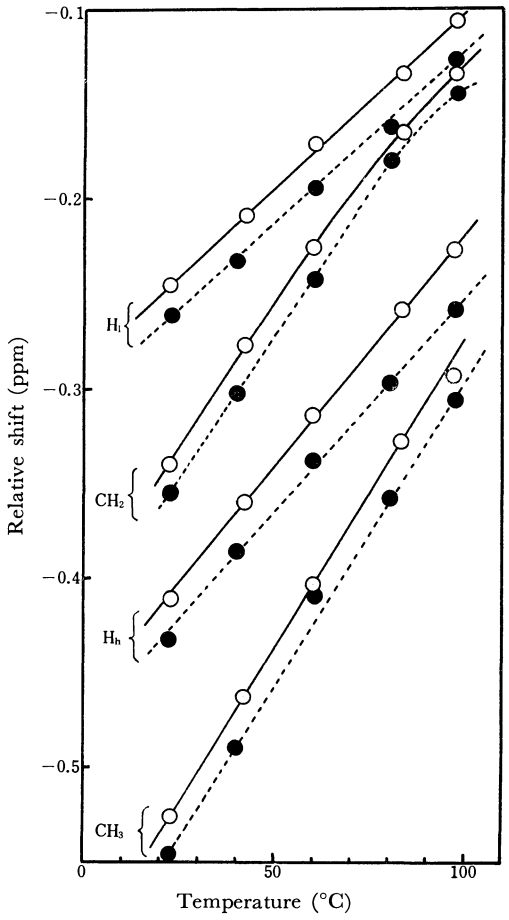

Fig. 5. Relative shifts of the protons in PMAVEs obtained in toluene at 0°C (○) and at −78°C (●) ——Quinoline solution——.

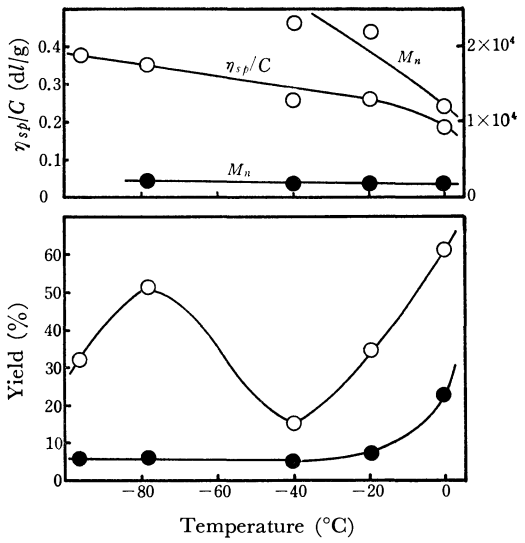

Fig. 6. Polymerization of MAVE in toluene by $BF_3 \cdot OEt_2$ for 24 hrs at various temperatures.
○: Methanol insoluble polymer, ●: Methanol soluble polymer. MAVE 16.8 mmol, toluene 18 m*l*, $BF_3 \cdot OEt_2$ 0.20 mmol.

the tacticity variation affects the polymer-solvent interaction in a benzene solution of poly(methyl methacrylate). Therefore, the results presented above indicate that the tacticity of PMAVE obtained at −78°C in toluene is different from that of PMAVE obtained at 0°C, as has been suggested above.

Effect of the Polymerization Temperature. The polymerizations were carried out in toluene at various temperatures. The results are shown in Fig. 6. The yield of the methanol-soluble polymer was constant below −20°C and increased remarkably at 0°C. However, the molecular weight was almost constant, regardless of the polymerization temperature.

The yield of the methanol-insoluble polymer had its minimum at −40°C. The solution viscosity and the molecular weight of the methanol-insoluble polymer decreased slightly with the elevation of the polymerization temperature. The polymer obtained below −78°C was a white powder which had an isotactic configuration, as has been mentioned above. The polymer obtained at 0°C was a viscous liquid which had a molecular weight of 12000. The rate of the termination or chain-transfer reaction in the polymerization may increase, and a polymer with a lower molecular weight may be obtained with an increase in the polymerization temperature.

Polymerization in Various Solvents. The polymerizations were carried out in various solvents at −78°C. The results are listed in Table 2. The yield of the polymer was lowered in polar solvents, and no methanol-insoluble polymer was obtained.

In *n*-heptane-toluene mixtures, the yields of the methanol-insoluble polymer were much higher than in toluene or *n*-heptane alone. In *n*-heptane, the yield of the polymer decreased and a part of the polymer obtained was insoluble not only in methanol but also in usual organic solvents, probably because of cross-linking during the polymerization reaction.

The authors wish to express their thanks to Mr. Y. Terawaki for the NMR experiments and to Mrs. F. Yano for her clerical assistance in preparing the manuscript.

BULLETIN OF THE CHEMICAL SOCIETY OF JAPAN, VOL. 44, 541—545 (1971)

Condensation Reactions of Sulfonylcarbanion

Yasusi YAMAMOTO, Tetuya NISIMURA, and Hitosi NOZAKI

Department of Industiral Chemistry, Kyoto University, Yoshida, Kyoto

(Received September 5, 1970)

Phenylsulfonylcarbanion $PhSO_2CH_2^-$ reacts with anthracene and acridine in HMPA to afford methylated products much as does methylsulfinylcarbanion $MeSOCH_2^-$ in DMSO. The reaction mechanism is examined by following the change in the D-content during the reaction of 9-deuterioanthracene. The transformation of the negatively-charged σ-complex into the methylated product involves the concerted occurrence of a hydride shift and the elimination of the sulfinate anion. Meanwhile, the reaction of this carbanion with anthracene at a higher temperature yields the ethylated products of 9-ethyl-10-methyl- and 9,10-diethylanthracene besides 9,10-dimethylanthracene. Other condensation reactions of the carbanion investigated are those with (a) $Ph_2C{=}CH_2$, (b) $PhC{\equiv}CPh$, (c) Ph_2CO, (d) PhCOCOPh, and (e) 2-aminobenzophenone, the main products being (a) $Ph_2CHCH_2\text{-}CH\text{-}CPh_2$ (cyclopropane ring), (b) $Ph_2C{=}C(Ph)Me$, (c) $Ph_2C(OH)CH_2CH_2SO_2Ph$ and $Ph_2C{=}CHCH_2SO_2Ph$, (d) $PhCOCH_2SO_2Ph$ and PhCOOH, and (e) 3-phenylindole respectively.

Synthetic reactions by means of methylsulfinylcarbanion were explored by Corey,[1] Russell,[2] and their co-workers.[3] Previously, we recorded the attainment of the nucleophilic methylation of condensed aromatic rings with this carbanion,[4,5] this reaction was reported independently by several other groups at almost the same time. The condensation reactions of sulfonylcarbanions were documented equally well[6] and our previous communication[7] was concerned with aromatic methylation involving the carbanion produced from methyl phenyl sulfone and sodium hydride in HMPA. The present paper will present (a) a summary of our investigations of the aromatic methylation and (b) a comparison of the behavior of sulfinyl- and sulfonylcarbanions in relation to aryl-conjugated olefinic and acetylenic bonds as well as compounds containing a benzoyl group.

Table 1 summarizes the methylation of anthracene and acridine with sulfonylcarbanions. The reaction can be effected by means of the carbanion derived from *N,N*-dimethyl(methylsulfonamide) equally well, and the solvent HMPA can be replaced with DMF. Phenanthrene, quinoline, and isoquinoline failed to be methylated with sulfonylcarbanions, whereas the reaction of these substrates with methylsulfinylcarbanion proceeded smoothly. The mechanism of the methylation with sulfinylcarbanion was outlined in the previous communication.[5a] Analogous investigations have now been extended to the methylation of anthracene with sulfonylcarbanions. Scheme 1 shows two possible reaction paths, A and B. The path A implies that a concerted hydride shift and the elimination of the sulfinate anion are involved in the transformation of the negatively-charged σ-complex (IIa or IIb) into the methylated product. The other path, B,[5a] assumes proton abstraction by IIa or IIb, followed by the elimination of sulfinic acid and, finally aro-

1) a) E. J. Corey and M. Chaykovsky, *J. Amer. Chem. Soc.*, **84**, 866 (1962). b) *Ibid.*, **87**, 1345 (1965) and Refs. cited. c) *Ibid.*, **87**, 1353 (1965).

2) a) G. A. Russell, E. G. Janzen, H. D. Becker, and F. S. Smentowski, *ibid.*, **84**, 2652 (1962). b) G. A. Russell and H.-D. Becker, *ibid.*, **85**, 3406 (1963). For β-keto sulfoxides see: c) H.-D. Becker, G. J. Mikol, and G. A. Russell, *ibid.*, **85**, 3410 (1963). d) G. A. Russell and L. A. Ochrymowycz, *J. Org. Chem.*, **34**, 3618 (1969).

3) For detailed account see: T. Durst, "Advances in Org. Chem. Methods and Results," Vol. 6, ed. by E. C. Taylor and H. Wynberg, Interscience Publishers, New York (1969), p. 285.

4) Ordinarily a paper such as this should contain experimental details on the nucleophilic aromatic methylation with methylsulfinylcarbanion reported in our previous communication (Ref. 5a), but this will not be done. The reason is that independent reports by Russell, Argabright, and their co-workers have made such a description meaningless. Though the reaction of D-labelled aromatics was recorded only in Ref. 5a, the experimental procedure was almost the same as the methylation reaction with phenylsulfonylcarbanion in HMPA described in the "Experimental" section.

5) a) H. Nozaki, Y. Yamamoto, and R. Noyori, *Tetrahedron Lett.*, **1966**, 1123. b) P. A. Argabright, J. E. Hofmann, and A. Schriesheim, *J. Org. Chem.*, **30**, 3233 (1965). c) G. A. Russell and S. A. Weiner, *ibid.*, **31**, 248 (1966). d) For aromatic methylation by means of dimethyloxosulfonium methylide see: H. König, H. Metzger, and K. Seelert, *Chem. Ber.*, **98**, 3712 (1965); V. J. Traynelis and Sr. J. V. McSweeney, O. P., *J. Org. Chem.*, **31**, 243 (1966); B. M. Trost, *Tetrahedron Lett.*, **1966**, 5761.

6) a) H.-D. Becker and G. A. Russell, *J. Org. Chem.*, **28**, 1896 (1963). b) H. O. House and J. K. Larson, *ibid.*, **33**, 61 (1968). c) D. F. Tavares and P. F. Vogt, *Can. J. Chem.*, **45**, 1519 (1967). d) J. M. McFarland and D. N. Buchanan, *J. Org. Chem.*, **30**, 2003 (1965).

7) H. Nozaki, Y. Yamamoto, and T. Nisimura, *Tetrahedron Lett.*, **1968**, 4625.

TABLE 1. METHYLATION OF ANTHRACENE AND ACRIDINE BY MEANS OF RSO_2CH_2Na

Aromatics	R	Solvent[a]	(Aromatic/Base) Mole ratio	Reaction Temp. (°C)	Reaction Time (hr)	Products (Yield %)[b]
Anthracene	Ph	HMPA	3	60	15	9-Methylanthracene (55) 9,10-Dimethylanthracene (10)
Anthracene	NMe_2	HMPA	2.1	30	20	9-Methylanthracene (35)[c]
Acridine	Ph	HMPA	1.5	25	4	9-Methylacridine (60)
Acridine	Ph	HMPA	2	80	4	9-Methylacridine (33) 9-Methylacridane (4)
Acridine	Ph	DMF	3	30	4	9-Methylacridine (67)
Acridine	NMe_2	HMPA	3	22	4	9-Methylacridine (40)

a) HMPA stands for hexamethylphosphoric triamide and DMF for *N,N*-dimethylformamide.
b) All reaction products were identified with authentic samples.
c) Yields are based on the substrates initially added, as the recoveries of unchanged materials have not determined accurately.

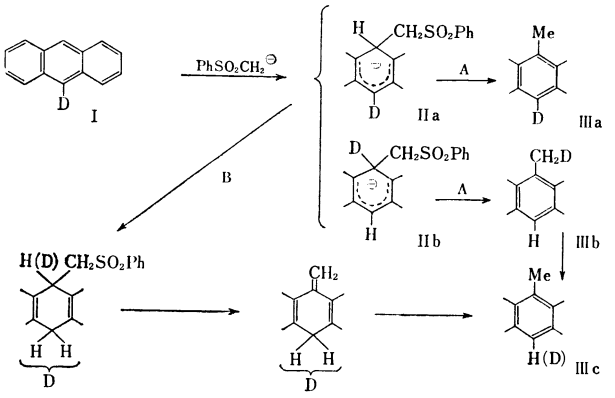

Scheme 1

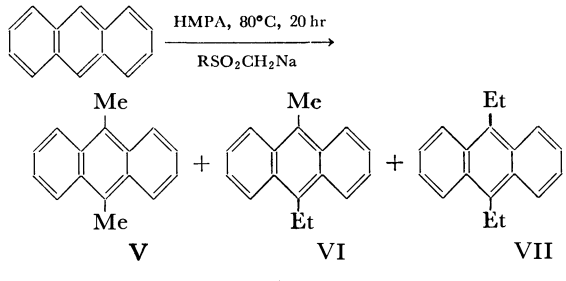

Scheme 2[8]

matization. A choice between the two is made by examining the change in the D-content in the reaction of 9-deuterioanthracene (I). As the CH_2D group (IIIb) attached to the aromatic ring is rapidly changed into the CH_3 group (IIIc) under the reaction conditions, the path A gives a 50% retention, and the path B, a 25% retention, in the absence of a primary isotope effect. Mass spectrometric analyses have indicated that the original D-content (82%) is unchanged in the recovered I. In contrast, the 9-methylanthracene produced retains 45% of its D-content; therefore, nearly 50% of the deuterium is lost by methylation.

The path A is also supported by another experimental fact, the fact that the reaction of acridine with ethyl phenyl sulfone gives 9-(α-phenylsulfonylethyl)-acridane (IV). This indicates that the hydride shift in the σ-complex is slower than the protonation in this case, possibly because of the presence of a methyl substituent in the S_N center.

A remarkable feature of aromatic substitution by means of sulfonylcarbanion is the formation of ethylated by-products, as is shown in Scheme 2. *A priori*, we can not exclude the possibility of the initial formation of ethyl phenyl sulfone. However, all attempts either to detect ethyl phenyl sulfone among the recovered sulfone or to confirm the formation of monoethylated anthracene were unsuccessful. In contrast, the treatment of V under the conditions of Scheme 2 gave a 53% yield of VI and a 24% yield of VII, besides a 46% recovery of V. The ethylation would thus conceivably involve the preliminary formation of arylcarbanion by proton-abstraction from the C-methyl group.

Other condensation reactions of sulfinylcarbanion with 1,1-diphenylethylene (VIII),[9,10] tolan (XV),[11] benzophenone (XVII),[9,10] and with benzil (XXI)[12] in DMSO were recorded previously. We have examined the condensation of phenylsulfonylcarbanion with these substrates in HMPA in order to observe closely the several remarkable points of difference.

8) As the three products could not be sharply separated, the yields were calculated as follows. On the basis of a comparison of the products with authentic samples by GLC (Apiezon L 30%), we could detect the presence of 9,10-dimethyl-, 9-ethyl-10-methyl-, and 9,10-diethylanthracene (not isolated). 9-Methylanthracene was absent. The NMR spectra indicated that the substituents of anthracene were either methyl- or ethyl-groups and that the substitution had occurred at C-9 and C-10 exclusively (This is the AA′BB′-pattern of aromatic protons). Accordingly, we calculated the yields of 9,10-dimethylanthracene and 9-ethyl-10-methylanthracene from the integral ratio of the NMR signals of the mixture, while a small amount of diethylanthracene was detected by observing the parent peak in the mass spectra.

9) M. Chaykovsky and E. J. Corey, *J. Org. Chem.*, **28**, 254 (1963).

10) C. Walling and L. Bollyky, *ibid.*, **28**, 256 (1963).

11) I. Iwai and J. Ide, *Chem. Pharm. Bull.* (Tokyo), **13**, 663 (1965).

12) a) J. C. Trisler, C. S. Aaron, J. L. Frye, and J. Y. Park, *J. Org. Chem.*, **33**, 1077 (1968). b) J. C. Trisler, J. K. Doty, and J. M. Robinson, *ibid.*, **34**, 3421 (1969).

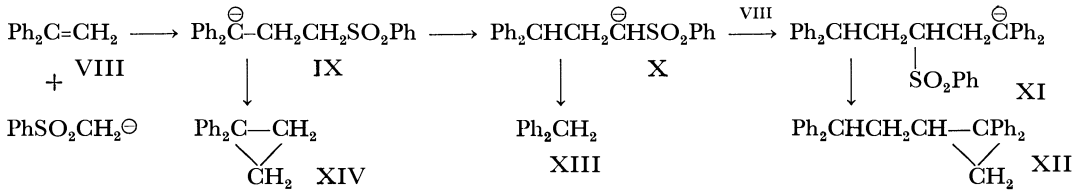

Scheme 3

The reaction of phenylsulfonylcarbanion (15 mmol) with VIII (10 mmol) yielded mainly XII (60%), besides XIII (34%) and XIV (1%) (Scheme 3); these results are in contrast with those of methylsulfinylcarbanion, which afforded XIII (64%) and XIV (36%) only. The present reaction is, therefore, characterized by the facile isomerization of the carbanion IX into the sulfonylcarbanion X.

The reaction of XV with methylsulfinylcarbanion is known to produce 2,3-diphenyl-1,3-butadiene.[11] Meanwhile, the reaction with phenylsulfonylcarbanion proceeded according to Scheme 4 to give 1,1,2-triphenylpropene (XVI) (21%), possibly *via* Truce-Smiles rearrangement.[13]

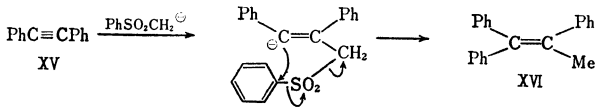

Scheme 4

Scheme 5 shows the reactions of XVII with phenylsulfonylcarbanion, affording XIX (21%) and XX (22%). The condensation of XVII with methylsulfinylcarbanion[9,10] gives mainly VIII (47%), in addition to such by-products as XIII (30%), XIV (3%), and diphenylacetaldehyde (20%). The aldehyde may be ascribed to intermediary 2,2-diphenyloxirane (XVIII) (not isolated). In contrast, the reaction of phenylsulfonylcarbanion with XVIII gave XIX (44%), whose dehydration with trifluoroacetic acid afforded XX.

The reaction of phenylsulfonylcarbanion with benzil (XXI) afforded mainly phenacyl phenyl sulfone (XXII) (22%) and benzoic acid (XXIII) (26%), besides desoxybenzoin (XXIV) (17%) and the Kostanecki compound (XXV) [14] (11%). This is in contrast to that of methylsulfinylcarbanion, which has been recorded to produce 2,4,5-triphenyl-3-benzoylfuran and XXIII.[12] The condensation of phenylsulfonylcarbanion with 2-aminobenzophenone (XXVI) yielded 3-phenylindole (XXVII) (59%), while that with salicylaldehyde (XXVIII) gave not benzofuran, but *o*-hydroxystyryl phenyl sulfone (XXIX) (73%).

On the basis of these observations, we may summarize the points of difference between sulfinyl- and sulfonylcarbanions as follows: the sulfinylcarbanion has a higher reactivity than the sulfonylcarbnion, as is evident from the comparison of the methylation reaction of condensed aromatics and from the reaction temperature required for the condensation with olefinic and acetylenic compounds. It is also to be noticed that higher temperatures are generally required for the reaction of sulfonylcarbanion and that products retaining the sulfonylgroup are obtained more frequently, although it has often been demonstrated that sulfinic acid is a better leaving group than the sulfenic acid.[16] The reason for this remains to be clarified.

Experimental

All the mps are uncorrected. The microanalyses were performed at the Elemental Analyses Center of Kyoto University and by Mrs. K. Fujimoto at Prof. K. Sisido's Laboratory. The NMR spectra were obtained in $CDCl_3$, CCl_4, or D_3CSOCD_3 on a 60 MHz instrument (JEOL C-60H spectrometer). The mass spectra were obtained on a Hitachi RMU-6E or RMU-6D spectrometer, lent by the Sagami Chemical Research Center and the Toray Co. respectively.

Reaction of Phenylsulfonylcarbanion with Anthracene. A solution of sodium phenylsulfonylcarbanion was prepared under N_2 from sodium hydride (0.41 g, 16.8 mmol) and methyl phenyl sulfone (5.3 g, 33.6 mmol) in HMPA (30 m*l*). Into this solution, at room temperature, anthracene (1.0 g, 5.6 mmol) in HMPA (30 m*l*) was stirred over a period of

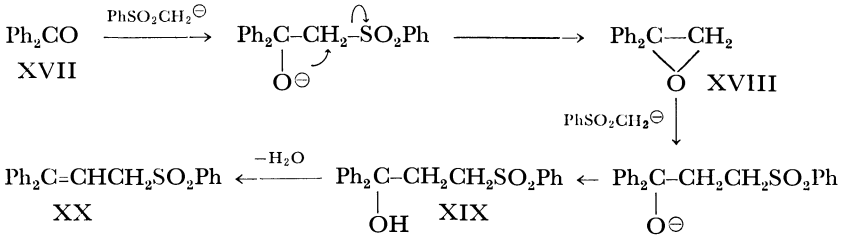

Scheme 5

13) a) G. P. Crowther and C. R. Hauser, *ibid.*, **33**, 2228 (1968). b) W. E. Truce, C. R. Robbins, and E. M. Kreider, *J. Amer Chem. Soc.*, **88**, 4027 (1966).

14) This is 1,2,3-tribenzoylpropene (and tautomers). For details see: Y. Yamamoto and H. Nozaki, The 23rd Annual Meeting of Chem. Soc. Japan, No. 14305, Tokyo (1970), and Ref. 15.

15) a) P. Yates, D. G. Farnum, and G. H. Stout, *Chem. & Ind.*, **1956**, 821. b) P. E. Devitt, E. M. Philbin, and T. S. Wheeler, *Ibid.*, **1956**, 822.

16) J. L. Kice, *Accounts Chem. Res.*, **1**, 58 (1968) and Refs. cited.

2 min. The dark-brown reaction mixture was then stirred at 65°C for 15 hr. The products were isolated and confirmed by chromatography on a silica-gel column and GLC (Apiezon L 30%). 9-Methylanthracene was obtained in a 55% yield as prisms; mp and mixed mp 81°C (EtOH) (lit,[17] 81°C). The recovery of anthracene was 4%.[18] GLC of the mother liquor indicated the presence of 9,10-dimethylanthracene (*ca.* 10%).

An equimolar mixture of 9-deuterioanthracene (I) (D-content 82%, obtained by the treatment of the Grignard reagent of 9-bromoanthracene with D_2O), and phenylsulfonylcarbanion in HMPA was allowed to react at 65°C for 15 hr. The reaction mixture was separated by preparative GLC (Apiezon L 30%). The D-contents of the recovered anthracene and 9-methylanthracene were estimated to be 82% and 45% respectively, on the basis of the molecular peaks in the mass spectra.

Meanwhile, the reaction of anthracene (1.0 g, 5.6 mmol) in HMPA (30 m*l*) with the phenylsulfonylcarbanion obtained from sodium hydride (0.4 g, 17 mmol) and methyl phenyl sulfone (5.25 g, 34 mmol) in HMPA (40 m*l*) yielded 0.59 g of a mixture of 9,10-dimethylanthracene (13%) and 9-ethyl-10-methylanthracene (43%) as yellow needles; mp 145—146°C upon chromatography on a silica-gel column. The yields were calculated by the method described in the footnote.

The Reaction of Phenylsulfonylcarbanion with 9,10-Dimethylanthracene. 9,10-Dimethylanthracene (0.52 g, 2.5 mmol), dissolved in HMPA (30 m*l*), was added to a solution of carbanion prepared from sodium hydride (0.24 g, 10 mmol) and methyl phenyl sulfone (1.56 g, 10 mmol) in HMPA (30 m*l*); the mixture was then allowed to react at 85°C for 24 hr. A subsequent work-up gave 53% of 9-ethyl-10-methylanthracene and 24% of 9,10-diethylanthracene, besides 46% of the recovered 9,10-dimethylanthracene.

The Reaction of Phenylsulfonylcarbanion with Acridine. Acridine (2.0 g, 11 mmol), dissolved in HMPA (10 m*l*), was added to a solution of carbanion prepared from sodium hydride (0.40 g, 17 mmol) and methyl phenyl sulfone (2.6 g, 17 mmol) in HMPA (30 m*l*); the mixture was then allowed to react at 25°C for 4 hr. A subsequent work-up and isolation by chromatography on a silica-gel column gave 9-methylacridine (1.3 g, 60%); mp 118—119°C (lit,[19] 117—118°C) (EtOH).

The heating of a solution of the same components (2 : 2 : 1 ratio) at 80°C for 4 hr gave 9-methylacridine (33%) and 9-methylacridane (4%); mp 123—125°C (lit,[19] 124—125.5°C). IR (Nujol): 3400 cm^{-1} (NH). NMR (CCl_4): δ 1.34 (d, 3H, Me), 4.02 (q, 1H, -CH-), 5.83 (s (broad), 1H, NH) and 6.43—7.25 (m, 8H, aromatic protons).

9-(α-Phenylsulfonylethyl)acridane (IV). Acridine (2.0 g, 11 mmol), dissolved in HMPA (10 m*l*), was treated with a solution of carbanion obtained from ethyl phenyl sulfone (3.0 g, 18 mmol) and sodium hydride (0.41 g, 17 mmol) in HMPA (40 m*l*) under N_2 at 50°C for 4 hr. A subsequent work-up gave IV (2.11 g, 54%). The analytical sample crystallized from benzene as colorless prisms; mp 209—212°C (dec.). IR (Nujol): 3300 cm^{-1} (NH), 1300, 1140 cm^{-1} (SO_2). NMR (CD_3SOCD_3 at 72°C using hexamethyldisilane as an internal standard): δ 0.82 (d, 3H, Me, J=8 Hz), 3.16 (d of q, 1H, -C*H*(Me)SO_2-, J=2 and 8 Hz), 4.94 (d, 1H, -C*H*-CH(Me)SO_2-, J=2 Hz), 6.7—8.0 (m, 13H, aromatic protons) and 8.60 (s (broad), 1H, NH).

Found: C, 72.1; H, 5.2%. Calcd for $C_{21}H_{19}NO_2S$: C, 72.2; H, 5.5%.

The Reaction of Phenylsulfonylcarbanion with 1,1-Diphenylethylene (VIII). A solution of phenylsulfonylcarbanion was prepared under N_2 with sodium hydride (0.36 g, 15 mmol) and methyl phenyl sulfone (2.3 g, 15 mmol) in HMPA (40 m*l*). A solution of VIII (1.6 g, 9 mmol) in HMPA (10 m*l*) was stirred into this carbanion solution at room temperature over a period of 5 min. After subsequent stirring at 85°C for 20 hr, the mixture was separated from the recovered sulfone by chromatography on an alumina column and was distilled at 70—90°C/2.5 mmHg. The distillate was isolated by GLC (Apiezon L 30%) and was identified as being composed of diphenylmethane (XIII) and 1,1-diphenylcyclopropane (XIV). The yields were 34% and 1% respectively. A work-up of the mother liquor gave 1.01 g (60%) of 1,1-diphenyl-2-(β,β-diphenylethyl)cyclopropane (XII) as white prisms; mp 109—110°C. IR (Nujol): 1030 cm^{-1} (cyclopropane). NMR ($CDCl_3$): δ 1.00—2.35 (m, 5H, cyclopropane hydrogens and those of ring-attached methylene), 3.95 (t, 1H, Ph_2CH-) and 6.99, 7.06, 7.12 and 7.28 (four s, total 20 H, aromatic protons). Mass *m/e* (rel intensity): 374 (M^+), 296 (trace), 270 (7), 207 (17), 194 (33), 180 (26), 167 (15) and 91 (100).

Found: C, 92.9; H, 6.9%. Calcd for $C_{29}H_{26}$: C, 93.0; H, 7.0%.

The Reaction of Phenylsulfonylcarbanion with Tolan (XV). A solution of XV (0.90 g, 5 mmol) in HMPA (20 m*l*) was stirred into a carbanion solution prepared from sodium hydride (0.35 g, 15 mmol) and methyl phenyl sulfone (1.95 g, 13 mmol) in HMPA (30 m*l*). After stirring at 95°C for 18 hr, the reaction mixture was treated as above. 1,1,2-Triphenylpropene (XVI) (0.28 g, 21%) was thus obtained as white crystals; mp 85—86°C (lit,[20] 86—89°C). NMR ($CDCl_3$): δ 2.12 (s, 3H, Me), 6.95, 7.12, 7.28 (three s, 15H, aromatic protons). Mass *m/e*: 275 (M^+).

Found: C, 93.0; H, 6.7%. Calcd for $C_{21}H_{18}$: C, 93.3; H, 6.7%.

The Reaction of Phenylsulfonylcarbanion with Benzophenone (XVII). The treatment of benzophenone (1.82 g, 10 mmol) with a solution of carbanion prepared from sodium hydride (0.36 g, 15 mmol) and methyl phenyl sulfone (2.34 g, 15 mmol) in HMPA (20 m*l*) at 60°C for 20 hr gave a mixture of 3,3-diphenyl-3-hydroxypropyl phenyl sulfone (XIX) and 3,3-diphenyl-2-propenyl phenyl sulfone (XX). XIX (0.73 g, 21%), mp 200—201°C, was isolated as a product which did not resolve in benzene. IR (Nujol): 3500 cm^{-1} (OH), 1300, 1150 cm^{-1} (SO_2).

Found: C, 71.9; H, 5.8%. Calcd for $C_{21}H_{20}O_3S$: C, 71.6; H, 5.7%.

XX (0.73 g, 22%), isolated from the mother liquor by chromatography on a silica-gel column (benzene), showed a mp of 109—110°C. IR (Nujol): 1300, 1140 cm^{-1} (SO_2). NMR ($CDCl_3$): δ 3.90 (d, 2H, -CH_2-), 6.14 (t, 1H, =CH-) and 6.53—7.80 (m, 15H, aromatic protons).

Found: C, 75.3; H, 5.6%. Calcd for $C_{21}H_{18}O_2S$: C, 75.5; H, 5.4%.

The Reaction of Phenylsulfonylcarbanion with 2,2-Diphenyloxirane (XVIII). The treatment of XVIII (2.76 g, 15 mmol) with a solution of carbanion prepared from sodium hydride (0.72 g, 30 mmol) and methyl phenyl sulfone (4.64 g, 30 mmol) in HMPA (20 m*l*) at 60°C for 20 hr gave XIX (2.32 g, 44%).

17) A. Sieglitz and R. Marx, *Ber.*, **56**, 1619 (1923).

18) All the yields are based on the starting materials consumed unless otherwise stated.

19) O. Blum, *ibid.*, **62**, 881 (1929).

20) J. Bornstein and F. Nunes, *J. Org. Chem.*, **30**, 3324 (1965).

The Reaction of Phenylsulfonylcarbanion with Benzil (XXI). To a solution of carbanion prepared from sodium hydride (0.72 g, 30 mmol) and methyl phenyl sulfone (4.7 g, 30 mmol) in HMPA (30 m*l*), we added XXI (3.15 g, 15 mmol) in HMPA (10 m*l*) at room temperature; the mixture was then allowed to react at 85°C for 20 hr. The reaction mixture was treated with water and extracted with benzene. A subsequent work-up of the benzene solution gave the Kostanecki compound (XXV) (11%) and desoxybenzoin (XXIV) (17%) upon chromatography on a silica-gel column. The water solution was neutralized with acetic acid and extracted with benzene. Phenacyl phenyl sulfone (XXII) (22%) and benzoic acid (XXIII) (26%) was obtained upon chromatography on a silica-gel column. Sulfone XXII showed a mp of 92—93.5°C (lit,[21] 93—94°C). IR (Nujol): 1670 cm^{-1} (CO), 1300, 1150 cm^{-1} (SO_2). NMR ($CDCl_3$): δ 4.30 (s, 2H, $-CH_2-$) and 7.20—8.15 (m, 10 H, aromatic protons). The Kostanecki compound, XXV, showed a mp of 122—123°C (lit,[15] 120°C) and was identical with the authentic sample.

The Reaction of Phenylsulfonylcarbanion with 2-Aminobenzophenone (XXVI). The reaction of carbanion, prepared from sodium hydride (0.96 g, 40 mmol), and the sulfone (6.2 g, 40 mmol) in HMPA (30 m*l*) with XXVI (2.23 g, 11 mmol) in HMPA (10 m*l*) was carried out at 110°C for 48 hr. Chromatography on a silica-gel column (hexane) gave 3-phenylindole (XXVII) (1.25 g, 59%); mp 88—89°C (lit,[22] 88—89°C).

Found: C, 87.0; H, 5.7; N, 7.1%. Calcd for $C_{14}H_{11}N$: C, 87.0; H, 5.7; N, 7.3%.

The Reaction of Phenylsulfonylcarbanion with Salicylaldehyde (XXVIII). The reaction of carbanion, prepared from sodium hydride (0.72 g, 30 mmol), and the sulfone (4.68 g, 30 mmol) in HMPA (25 m*l*) with salicylaldehyde (2.64 g, 22 mmol) in HMPA (10 m*l*) gave *o*-hydroxystyryl phenyl sulfone (XXIX) (4.17 g, 73%); mp 171—172°C. IR (Nujol): 3350 cm^{-1} (OH), 1280, 1130 cm^{-1} (SO_2) and 965 cm^{-1} (-CH=CH-). NMR (CD_3SOCD_3 using sodium 3-(trimethylsilyl)propylsulfonate as the internal standard): 6.70—8.31 (m, 11H, aromatic and olefinic protons) and 10.65 (s (broad), 1H, OH).

Found: C, 64.6; H, 4.7%. Calcd for $C_{14}H_{12}O_3S$: C, 64.6; H, 4.7%.

The authors are indebted to Professor K. Sisido for his help and encouragement. This work was partially supported by the Scientific Research Fund of Ministry of Education, Japanese Government. Financial support from Toray Science Foundation is acknowledged with pleasure.

21) E. H. Holst and W. C. Fernelius, *ibid.*, **23**, 1881 (1958).

22) E. Fischer and T. Schmidt, *Ber.*, **21**, 1811 (1888).

BULLETIN OF THE CHEMICAL SOCIETY OF JAPAN, VOL. 44, 545—550 (1971)

Reaction of Aromatics with Thallic Salts——Preparation of Arylthallic Compounds[1]

Katsuhiko Ichikawa, Sakae Uemura,* Takeshi Nakano, and Eizo Uegaki

Department of Hydrocarbon Chemistry, Faculty of Engineering, Kyoto University, Yoshida, Kyoto

**Institute for Chemical Research, Kyoto University, Uji, Kyoto*

(Received September 8, 1970)

Arylthallic acetate perchlorate monohydrates, Ar-Tl(OAc)(ClO_4)·H_2O, were obtained as the major products of the reaction between thallic acetate and aromatics in acetic acid containing perchloric acid. As the minor products, various types of oxidation products including oxidative coupling were obtained. Reactivity order of the aromatics and the isomer distributions in the products were the same as those in the usual electrophilic aromatic substitution. With thallic nitrate, sulfate, and chloride, no arylthallic compounds could be obtained.

Aromatic mercuration has been well known as one of the family of electrophilic aromatic substitution.[2,3] Davidson and Triggs reported the possibilities of aromatic substitution with heavy metals such as thallation, plumbation, auration, palladation, and platination.[4] Since aromatic heavy metal compounds are not always stable, isolation of the compounds from direct substitution products was successful only in the case of thallation.[4] We have also studied the aromatic thallation under the similar conditions independently and wish to present our results, since our experiments were to develope a synthetic method of preparation of arylthallic compounds and different from those by Davidson and Triggs which were rather for mechanistic study.

So far, several methods of preparation of aromatic thallium compounds (using no metal exchange reaction) have been reported, for example, the reaction of thallic chloride with dibenzofuran[5] and the reaction of thallic isobutyrate with benzene and alkoxybenzenes.[6,7] Very recently, McKillop *et al.* found that thallic trifluoroacetate reacts with various aromatics to give arylthallic di-trifluoroacetates in good yields at room temperature.[8]

1) Presented partly at the 21st Annual Meeting of the Chemical Society of Japan, Osaka, April 1968 and at the 22nd Annual Meeting, Tokyo, April 1969.

2) H. C. Brown and C. W. McGary, *J. Amer. Chem. Soc.*, **77**, 2300 (1955).

3) W. Kitching, *Organometal. Chem. Rev.*, **3**, 35 (1968).

4) J. M. Davidson and C. Triggs, *J. Chem. Soc., A*, **1968**, 1324.

5) H. Gilman and R. K. Abbott, *J. Amer. Chem. Soc.*, **65**, 122 (1943).

6) V. P. Glushkova and K. A. Kocheshkov, *Izv. Akad. Nauk SSSR, Otd. Khim. Nauk*, **1957**, 1186.

7) V. P. Glushkova and K. A. Kocheshkov, *Dokl. Akad. Nauk SSSR*, **103**, 615 (1955); **116**, 233 (1957).

8) A. McKillop, J. S. Fowler, M. J. Zelesko, J. D. Hunt, E. C. Taylor, and G. McGillivray, *Tetrahedron Lett.*, **1969**, 2423.

Results and Discussion

Aromatic compounds were added to acetic acid solutions of various thallic salts such as acetate, sulfate, nitrate, and chloride at various temperatures. The mixtures were homogeneous except in the case of thallic sulfate. As the reaction proceeded, formation of insoluble thallous salts was observed. Product distribution depends on the several factors such as the structure of aromatics, the kind of thallic salt used, the addition of mineral strong acid, and the conditions. Structures of the identified products are shown in Chart 1.

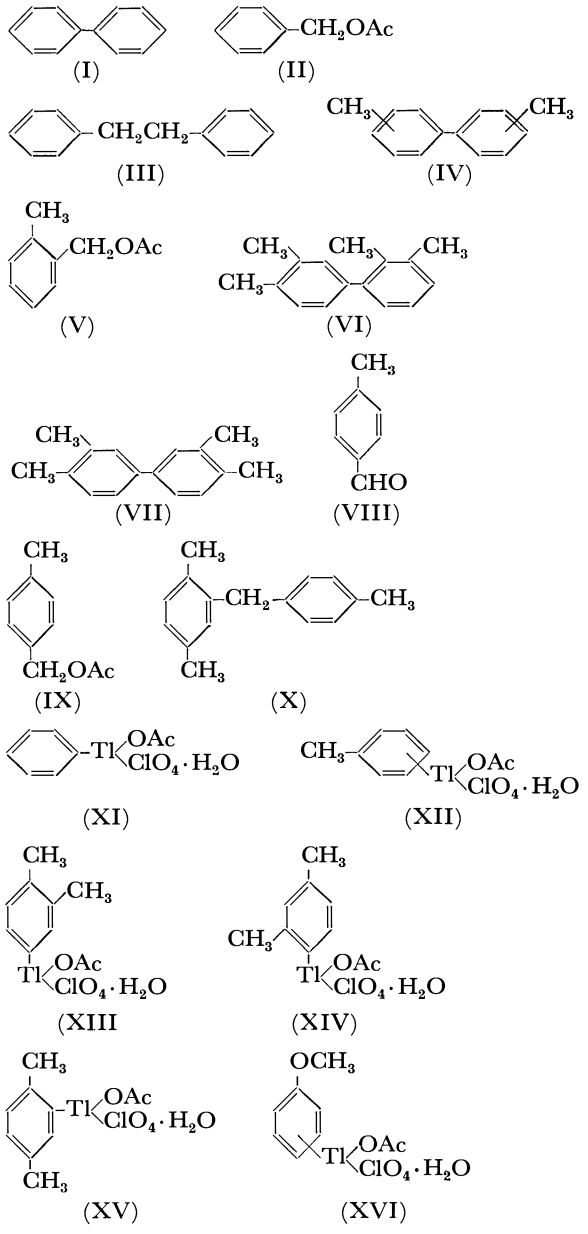

Chart 1. Structures of products.

Reaction with Thallic Acetate. In Table 1, the experimental results are summarized. Sluggish reactions between aromatics and thallic acetate were accelerated remarkably by the addition of perchloric acid to the reaction mixtures. Sulfuric acid, nitric acid and boron trifluoride showed the same effect, but were not so effective. The main products were arylthallic acetate perchlorate monohydrate, $ArTl(OAc)(ClO_4)\cdot H_2O$. Oxidative coupling products were also obtained along with small amounts of oxidation products of side chain. The yields were calculated according to the following equations on the basis of thallic acetate used.

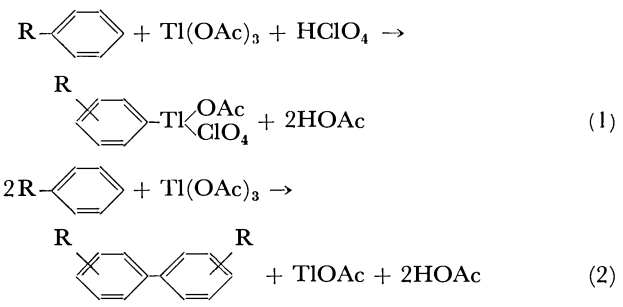

Material balance of oxidation-reduction by Eq. (2) was very poor, probably because acetic acid was oxidized with thallic acetate, particularly in the presence of perchloric acid. In fact, 97% of thallic acetate (0.35 M) dissolved in acetic acid containing perchloric acid (0.6 M) were reduced to thallous salt after refluxing for 7 hr. It has been reported also that the yield of thallic acetate was poor when thallic oxide was dissolved in refluxing acetic acid.[9]

Fairly good yields of arylthallic compounds have been obtained by the reaction of benzene, toluene, xylenes, and anisole. Prolonged reactions at higher temperature resulted in the decrease in the yields of arylthallic compounds and in the increase of the oxidation products. No quantitative relationship, however, appears to exist between the two types of the reaction. It was also noted that some of the arylthallic salts oxidize acetic acid as solvent at refluxing temperature gradually and form thallous salt without giving oxidative coupling products.

Anisole reacted readily even at lower temperature to give anisylthallic derivative. At refluxing temperature, however, no organothallium and only a trace of oxidation products could be obtained even after short reaction time, despite that thallic salt was reduced to thallous state completely. With mesitylene the same phenomenon was observed. Aromatic compounds with electron withdrawing group such as nitro and chloro did not react at all. Therefore, the reactivity order of aromatics appears to be similar to that in the usual electrophilic aromatic substitution.

The structures of arylthallic compounds were identified to be arylthallic acetate perchlorate monohydrate by the results of elemental analyses and IR and NMR spectra measurements. IR spectra (KBr disc) showed strong absorption at 1570—1530 and 1420—1380 cm^{-1} due to carboxylate group and at 1150—1080 cm^{-1} due to perchlorate anion. As a typical example, in Figs. 1 and 2, are shown the spectra of XI together with that of thallic acetate for a con-

9) A. South and R. J. Ouellette, *J. Amer. Chem. Soc.*, **90**, 7064 (1968).

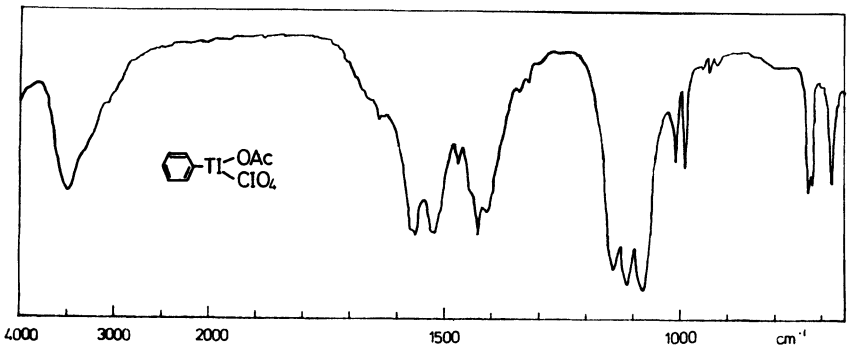

Fig. 1. IR spectrum of XI.

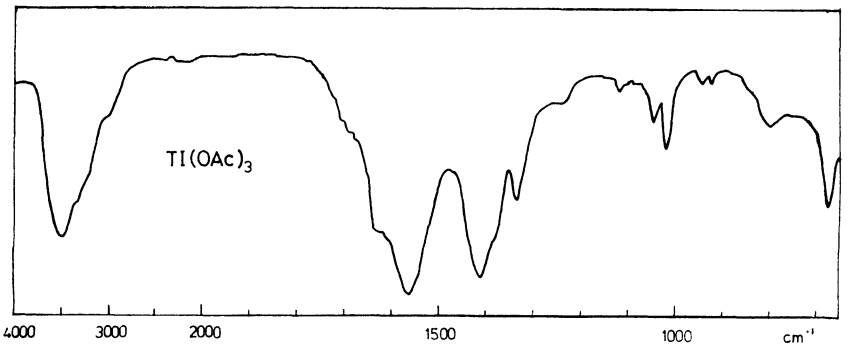

Fig. 2. IR spectrum of thallic acetate.

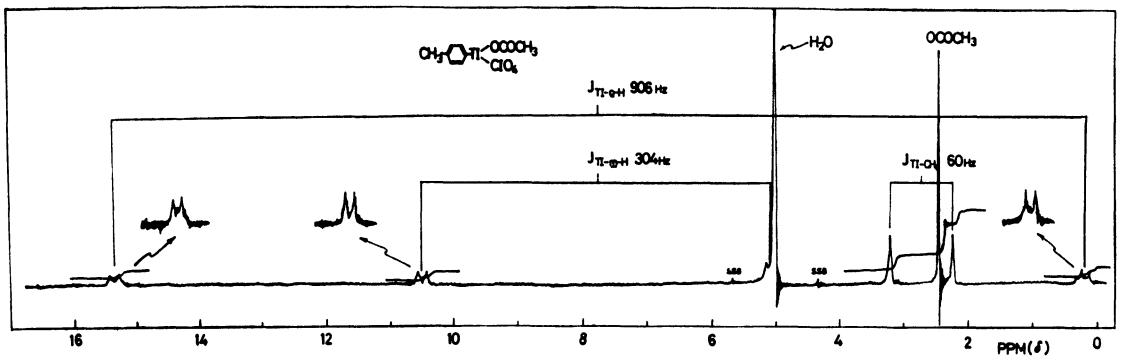

Fig. 3. NMR spectrum of *p*-isomer of XII (solvent D_2O)

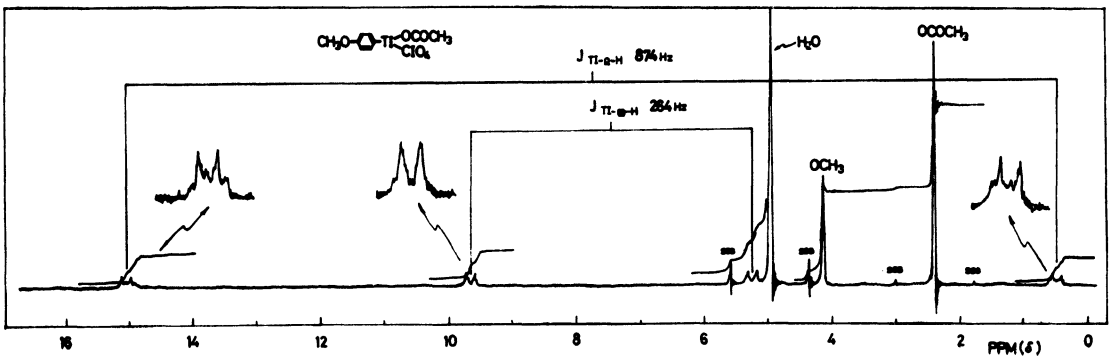

Fig. 4. NMR spectrum of *p*-isomer of XVI (solvent D_2O).

Table 1. Reaction of aromatics with $Tl(OAc)_3$

Aromatic (mol)	$Tl(OAc)_3$ (mol)	HOAc (ml)	$HClO_4$ (mol/l)	React. temp. (°C)	React. time (hr)	Product (yield[a]%)
Benzene 0.25	0.05	80	0.5	90	6	I (2.0) XI (54.9)
Benzene 0.10	0.05	100	0.5	105	13	I (13.0)
Toluene 0.10	0.05	60	0.5	115	3	II (2.8) III (2.0) IV (1.3) XII (47.4)
Toluene 0.24	0.05	80	0.5	115	14	II (4.3) III (4.2) IV (1.8)
Toluene 0.10	0.02	40	0.5	115	2	XII (73.1)
Toluene 0.10	0.02	40	0.5	80	8.5	XII (67.0)
Toluene 0.10	0.05	65	—	112	18	II, III, IV (trace)
o-Xylene 0.10	0.05	80	0.5	112	2	V (trace) VI (1.2) VII (0.6) XIII (38.4)
o-Xylene 0.10	0.05	100	0.5	110	14	V (4.1) VI (5.0) VII (5.7)
m-Xylene 0.10	0.05	80	0.5	114	2	XIV (51.3)
p-Xylene 0.10	0.056	80	0.5	112	2	VIII, IX (trace) X (6.5) XV (22.6)
p-Xylene 0.10	0.034	100	0.5	115	13	VIII (6.0) IX (trace) X (21.8)
p-Xylene 0.10	0.05	60	—	115	23	VIII (4.2) IX (1.5)
Anisole 0.05	0.012	50	0.5	35	1	XVI (44.0)

a) Calculated on the basis of used thallic acetate

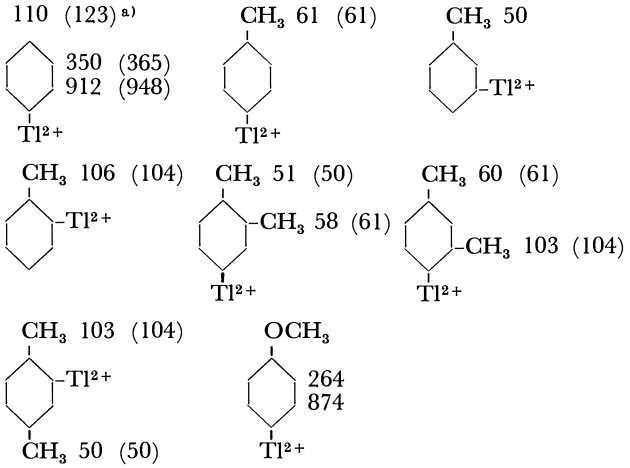

Chart 2. $J_{Tl^{205}-H}$ and $J_{Tl^{205}-CH_3}$ of arylthallic compounds.

a) The values reported by Maher and Evans are in parenthesis.

venience of comparison. Absorptions at about 3500 cm^{-1} due to water were observed in all of XI—XVI. Elemental analyses show that they are monohydrated. NMR spectra (in D_2O) shows the presence of aromatic protons and acetyl protons. From the comparison of the intensities of the two types of protons, it is concluded that ratio of aromatic nucleus and acetyl group is 1 : 1. In Figs. 3 and 4, the NMR spectra of *p*-isomers of, XII and XVI are given as typical examples. $J_{Tl^{205}-H}$ and $J_{Tl^{205}-CH_3}$ values (Chart 2), which agreed well with those reported by Maher and Evans,[10] were useful for determining the substituted position of thallium and rough isomer distribution. For example, crude tolylthallic compound from toluene was found to be mixture of *o*-/*m*-/*p*-isomers of 12/6/82 in one run and 16/6/78 in the other run.

The arylthallic compounds are stable in air, soluble in water, acetone, methanol, ethanol, pyridine, DMF, and DMSO, insoluble in ether, ligroin, and benzene, and can be recrystallized from acetic acid to give white crystalline products. All of them reacted with bromine in carbon tetrachloride to give corresponding bromobenzenes.[11] XI gave diphenylthallic chloride (mp >300°C) upon treating with excess of aqueous sodium chloride and phenylthallic acetate bromide with one mole of aqueous potassium bromide.

Concerning the oxidation products according to Eq. (2), the following remarks should be added to the data shown in Table 1. Throughout the experiments no acetoxylated products of aromatic nucleus could be detected. NMR data showed that IV from toluene

10) J. P. Maher and D. F. Evans, *J. Chem. Soc.*, **1965**, 637.
11) S. Uemura, K. Sohma, M. Okano, and K. Ichikawa, Presented at the 23rd Annual Meeting of the Chemical Society of Japan, Tokyo, April 1970.

contained unidentified Ar–CH_2–Ar′ type product other than those in Table 1 (NMR τ 6.15, methylene protons). In the case of *p*-xylene, fairly good yield of X was obtained. This type of oxidative coupling of *p*-xylene has been reported by Kovacic and Wu[12] as a side reaction in the preparation of *p*-tolyl-di-*p*-xylylmethane by the reaction of *p*-xylene with ferric chloride.

Reaction of Other Thallic Salts than Acetate with Aromatics. Several attempts to obtain arylthallic compounds by the reaction of aromatics with other thallic salt than acetate were unsuccessful. Under the conditions similar to those with thallic acetate in Table 1, the yields of organic products containing no thallium were also low.

With 50 mmol of thallic nitrate (at 105—115°C, 12 hr) the following products were isolated: From benzene (0.1 mol); nitrobenzene (1.6 mmol) and I (trace). From toluene (0.1 mol); benzaldehyde (trace), II (4.7 mmol), IV (trace), *o*-nitrotoluene (7.0 mmol). and *p*-nitrotoluene (5.9 mmol). From *p*-xylene (0.1 mol); VIII (7.5 mmol), IX (10.6 mmol), *p*-toluic acid (16.2 mmol), and nitro-*p*-xylene (6.1 mmol). All amounts of thallic salt were reduced to thallous salt.

With thallic sulfate (at 110—114°C, 1 hr) the following products were obtained: From benzene; I (trace). From toluene; IV (6.4%, calculated on the basis of thallic salt used). From *p*-xylene; X (9.3%). The amount of reduced thallic salt was 70—80%.

With thallic chloride, the reaction was very slow and only 22—27% of thallic salt was reduced at refluxing temperature in 14 hr. The following products were obtained: From benzene; nothing. From toluene; III (2.0%) and IV (0.3%). From *p*-xylene; VIII (1.8%) and X (1.6%). Addition of perchloric acid gave little effect on the reaction.

Experimental

Materials. All starting organic materials were used after distillation. Thallic acetate was prepared by dissolving thallic oxide into acetic acid at 60°C in 20 hr, collecting white crystals after cooling and drying over P_2O_5 (purity by iodometry was more than 98%). Thallic chloride and nitrate were commercial products. Thallic sulfate was prepared by dissolving the oxide into hot aqueous sulfuric acid.

Reaction of Alkylbenzene with $Tl(OAc)_3$: Formation of Organothallium Compounds. The following example shows a typical experimental procedure. Toluene (200 mmol) was added to a solution of thallic acetate (45.5 mmol) in 80 m*l* of acetic acid containing 8 g of 70% perchloric acid (*ca.* 0.5 M) at refluxing temperature (115°C). The reaction mixture was kept at 110°C under stirring. The color of the mixture turned from pale yellow to purple red. After 3 hr's duration the hot mixture was filtered off from white precipitates formed (4.78 g). When the filtrate was allowed to stand at room temperature, the same precipitates(0.60 g) were obtained again. These precipitates (5.38 g, 17.7 mmol) were identified as thallous perchlorate ($TlClO_4$) by the IR spectrum. Distillation of most part of acetic acid from the filtrate under reduced pressure gave 7.40 g of pale yellow crystals which were identified as XII (decomposed at 126°C 15.7 mmol, 34.6%). The residue from which XII was filtered off was diluted with water and extracted with benzene. The benzene extract was washed with saturated aqueous $NaHCO_3$ and dried over Na_2SO_4. Upon removal of benzene, there was obtained 0.66 g of residue, which was found to be consisted of benzene, toluene, benzaldehyde (trace), II (5%), III (68%), and IV (14%, mainly *p,p′*-isomer) by gas chromatographic analysis. The yields of II, III, and IV were calculated to be 0.2 mmol (0.4%), 2.5 mmol (5.4%), and 0.5 mmol (1.1%), respectively. Recrystallization of XII three times from acetic acid gave white crystals which were pure *p*-isomer. XII was stable in air, soluble in water, methanol, ethanol, acetone, pyridine, DMF, DMSO, and hot acetic acid, and insoluble in ether, ligroin, benzene, and chloroform. IR spectrum of XII is very similar to that of XI (Fig. 1). NMR spectrum of XII (*p*-isomer) in D_2O is shown in Fig. 3.

XI, XIII, XIV, and XV were obtained similarly by the method described above. They all decomposed without melting and showed almost the same solubility as those of XII. The IR spectra were similar to that of XI, showing the strong absorption bands due to carboxylate group and perchlorate ion. Coupling constants of Tl^{205}–H in NMR determination (D_2O solvent) are summarized in Chart 2. Analytical data are as follows:

	Dec. p. (°C)	Calcd for $ArTl(OAc)ClO_4 \cdot H_2O$		Found	
		C	H	C	H
XI	174	20.98	2.20	21.06	2.25
XII	145	22.88	2.56	22.79	2.40
XIII	165	24.71	2.90	24.72	2.91
XIV	175	24.71	2.90	24.52	2.47
XV	176	24.71	2.90	24.40	2.87

Reaction of Anisole with $Tl(OAc)_3$: Formation of XVI. Anisole (50 mmol) was added to a solution of thallic acetate (12 mmol) in 50 m*l* of acetic acid containing 4 g of 70% perchloric acid (*ca.* 0.5 M) at 35°C. The reaction mixture was kept at 35°C for 1 hr under stirring. The color of the mixture changed from white to red brown. White precipitates thus formed (0.30 g, 1 mmol) were filtered off and acetic acid was evaporated from the filtrate to give brownish crystals of XVI (2.60 g, 5.33 mmol, 44.0%). NMR spectra showed that main constituent of XVI was para-isomer. Recrystallization from acetic acid gave 2.20 g of pure *p*-isomer of XVI which decomposed slightly at 157°C and completely at 177°C. (Found: C, 22.15; H, 2.48%. Calcd for $C_9H_{12}O_8TlCl$: C, 21.89; H, 2.42%.)

Reaction of Benzene with $Tl(OAc)_3$: Formation of I. Benzene (100 mmol) was added to a solution of thallic acetate (50 mmol) in 100 m*l* of acetic acid containing 8 g of 70% perchloric acid (*ca.* 0.5 M) at 117°C. The reaction mixture was kept at 105°C (refluxing temp.) for 10 hr under stirring. After cooling to room temperature white precipitates thus formed ($TlClO_4$, 13.0 g, 42.9 mmol) were filtered off. The fitrate was diluted with water and extracted with benzene. The extract was washed with saturated aq. $NaHCO_3$ and dried over Na_2SO_4. After removing benzene white crystals of I (1.0 g, 13%) were obtained as residue. Recrystallization from ethanol gave pure I, mp 69—70°C.

Reaction of p-*Xylene with $Tl(OAc)_3$: Formation of X.*

12) P. Kovacic and C. Wu, *J. Org. Chem.*, **26**, 762 (1961).

Reaction between *p*-xylene (100 mmol) and thallic acetate (34 mmol) was carried out in 100 m*l* of acetic acid at 117°C for 13 hr. Yellowish white precipitates thus formed ($TlClO_4$, 9.0 g, 29.7 mmol) were filtered off from the resulting black solution. The filtrate was treated as mentioned above. There was obtained a mixture which was analyzed to contain *p*-xylene, VIII (0.23 g, 5.8%), and X (1.47 g, 20.7%). Distillation of the mixture gave pure X (bp 128—131°C/2.5 mmHg, $n_D^{20}=1.5678$). NMR ($CDCl_3$) τ 3.0—3.20 (m.) 7H, 6.17 (s.) 2H, 7.75 (s.) 6H, and 7.85 (s.) 3H. (Found: C, 91.62; H, 8.93%; Calcd for $C_{16}H_{18}$: C, 91.37; H, 8.63%.)

Reaction of XV with p-*Xylene in Acetic Acid.* A mixture of XV (2.14 mmol) and *p*-xylene (10 mmol) dissolved in 40 m*l* of acetic acid containing 70% perchloric acid (2.3 g, *ca.* 0.4 M) was stirred at 110°C for 2 hr. The color of the reaction mixture turned from clear pale yellow to purple red and white precipitates were formed. After removing the precipitates ($TlClO_4$, 0.50 g, 76%) the filtrate was treated as described above. Gas chromatographic analysis showed that the products were VIII (4.3%), X (1.6%), and unidentified material (3.5 times as large as X in peak area). Any amount of xylenyl acetate could not be detected.

Reaction of Toluene with $Tl_2(SO_4)_3 \cdot 7H_2O$: Formation of IV. Toluene (100 mmol) was added to a milky suspension of thallic sulate (22 mmol) in 100 m*l* of acetic acid at 114°C under stirring. After 10 hr the black reaction mixture was cooled to room temperature and white precipitates were filtered off. The precipitates were found to be consisted of 33.4 mmol of thallous salt and 13.7 mmol of thallic salt. The filtrate was treated as mentioned above and 0.51 g (2.8 mmol, 15.2%) of IV (mainly *p,p'*-isomer) was obtained. Distillation gave almost pure *p,p'*-isomer of ditolyl, bp 100—115°C/3mmHg, mp 110—115°C. Recrystallization from ether gave pure *p,p'*-isomer of IV, mp 120°C.

Authentic Samples for Gas Chromatography. I, II, III, V, VIII, nitrobenzene, *o*- and *p*-nitrotoluenes, and benzaldehyde were commercial products. VI and VII were prepared by the reaction of palladium chloride and sodium acetate with *o*-xylene.[13] Nitro-*p*-xylene was prepared by the method reported in the literature,[14] bp 109°C/9 mmHg. IX (bp 104—108°C/13 mmHg) was prepared by acetylation of *p*-methylbenzyl alcohol (mp 58°C) with acetic anhydride at 50°C for 1 hr in the presence of zinc chloride catalyst.

Spectral Measurements. IR spectra were obtained by Hitachi EPI-2 and EPS-3T. NMR spectra were determined by JEOL-3H-60 and Varian A-60 using TMS as internal standard in $CDCl_3$ in the case of organic products and in D_2O (without internal standard) in the case of organothallium compounds. Gas chromatographic analyses were carried out on Hitachi K-53 using Apiezon-L 1 m and PEG 20 M 1 m columns and Shimadzu 4APT using the similar 3 m colunns.

13) R. van Helden and G. Verberg, *Rec. Trav. Chim. Pays-Bas*, **84**, 1263 (1965).

14) H. R. Snyder and F. J. Pilgrim, *J. Amer. Chem. Soc.*, **70**, 3787 (1948).

BULLETIN OF THE CHEMICAL SOCIETY OF JAPAN, VOL. 44, 550—553 (1971)

4-Acetylierung der 5-Hydroxy-indol-Derivate

Tadashi SUEHIRO und Machiko NIITSU
Chemisches Institut der Gakushuin Universität, Mejiro, Tokio

(Eingegangen am 16, September, 1970)

5-Hydroxy-4-acetyl-2-äthoxycarbonyl-indol und 5-Hydroxy-2-methyl-4-acetyl-indol wurden durch die Friedel-Crafts-Acetylierung oder durch die Fries-Umlagerung in Gegenwart von Lewis-Säure bzw. unter Belichtung hergestellt. Die Acetylierung wird stark von dem sterischen Faktor des 3-Subtituenten beeinflusst und bei 5-Hydroxy-2-methyl-3-äthoxycarbonyl-indol läuft die 6-Acetylierung ab. Wenn kein 3-Substituent vorhanden ist, wird es eher an der 4-Stellung als an der 6-Stellung acyliert. Der Strukturbeweis wurde aus den NMR-Spektren geführt. 5-Hydroxy-4-acetyl-2-äthoxycarbonyl-indol lässt sich in Dimethylformamid durch Natriumhydrid und Alkylhalogenid an den *O*- und *N*-Stellungen alkylieren.

Aus synthetischen Interessen haben wir die 4-Acylierung von 5-Hydroxy-indol-Derivaten unternommen. Die Friedel-Crafts-Acetylierung von 5-Hydroxy-2-methyl-3-äthoxycarbonyl-indol (Ia) in Nitrobenzol bei 50°C führt zu einer Acetyl-Verbindung vom Schmp. 229—235°C (II) in 19% Ausbeute. Dieselbe Verbindung erhält man bei der Fries-Umlagerung von 5-Acetoxy-2-methyl-3-äthoxycarbonyl-indol (Ib) bei 70°C in Gegenwart von zweifachen Mengen Aluminiumchlorid in 6% Ausbeute. NMR-Spektrum von II mit zwei Singuletts bei τ 2.04 (H^7) und 2.30 (H^4) in Trifluoressigsäure hatte zur Folge, dass die Acetyl-Gruppe in die 6-Stellung eingeführt wurde. Die Belichtung einer äthanolischen Lösung von Ib mit Hoch- bzw. Niederdruckbrenner ergab wieder II in 7% Ausbeute.

Es war also nicht gelungen, bei I durch die Friedel-Crafts-Reaktion oder durch die Fries-Umlagerung, selbst unter photolytischen Bedingungen, die Acetyl-Gruppe in die 4-Stellung einzuführen. Dass die 3-Äthoxycarbonyl-Gruppe so sehr gegen die Aufnahme des Acetyl-Restes an die 4-Stellung wirkt, ist bemerkenswert, wenn man die leichte 4-Benzylierung[1,2] und 4-Allylierung[1,2] von Ia berücksichtigt.

5-Hydroxy-2-äthoxycarbonyl-indol (IIIa) lässt sich in Nitrobenzol bei 50°C in 42% Ausbeute an der 4-Stellung acetylieren, und 5-Hydroxy-4-acetyl-2-äthoxycarbonyl-indol (IVa) vom Schmp. 235—239°C (Zers) wird erhalten. Die 4-Acetyl-Struktur von IVa wird durch die NMR-Signale von zwei Dubletts bei τ 2.17 (H^7) und 2.87 (H^6) jede mit J=9 Hz unterstützt.

Aus der Nitrobenzol-Lösung der Friedel-Crafts-

1) T. Suehiro, *Chem. Ber.*, **100**, 905 (1967).
2) T. Suehiro und S. Sugimori, Dieses Bulletin, **40**, 2925 (1967).

Reaktion isoliert man nebenbei eine Verbindung vom Schmp. 123—124°C (V) in 11% Ausbeute, dessen Struktur aufgrund der Mikroanalyse und NMR-Spektren zu der *O*,3-Diacetyl-Verbindung von IIIa kommt; es zeigt sich hier, dass die 5-Acetoxy-indol-Verbindung an die 3-Stellung acetyliert werden kann, wie es in der Mannich-Base Darstellung der Fall ist.

IVa lässt sich auch in Kohlendisulfid durch Acetylieren von 5-Benzyloxy-2-äthoxycarbonyl-indol (IIIb) in kleiner Ausbeute (1.4%) erhalten, dabei entsteht ein Acetyl-Derivat, 5-Benzyloxy-3-acetyl-Verbindung vom Schmp. 177—180°C (IVb) (0.7%).

Die 4-Acetylierung von IIIa und IIIb durch die Friedel-Crafts-Reaktion läuft in Nitrobenzol in mässiger Ausbeute ab, nebenbei entstehen aber manche andere Acetyl-Derivate. In diesem Sinne verläuft die Fries-Umlagerung einfach: Der Acetyl-Rest von 5-Acetoxy-2-äthoxycarbonyl-indol (IIIc) wandert in die 4-Stellung beim 67 Stunden Belichten einer äthanolischen Lösung von IIIc, und das Produkt IVa wird in 11% Ausbeute isoliert. Die Umlagerung des Acetyl-Restes in die 6-Stellung verlief in kleinerem Masse (0.4%), diese Isomere konnte man leicht abtrennen.

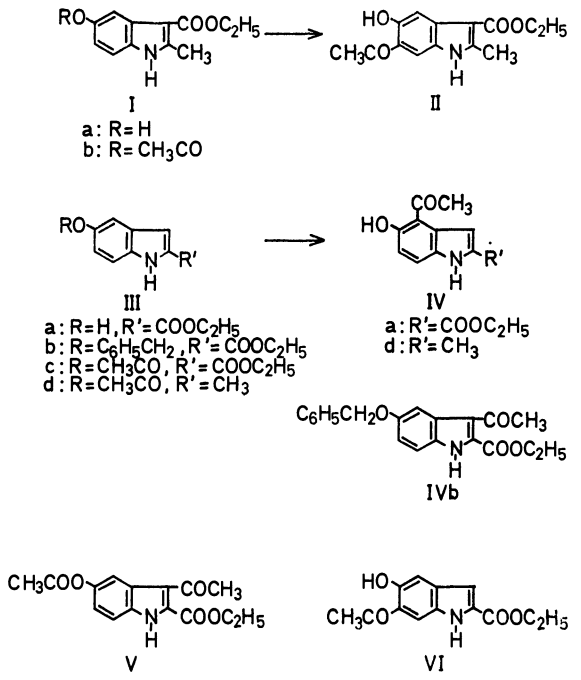

Formelschema 1.

Die Zuordnung der Substituenten an die 4- bzw. 6-Stellung lässt sich durch die Deutung der Proton-Signale von IIIc erleichtern. Die Spektren von IIIc in Deuteroaceton bei Ab- und Anwesenheit von Deuteriumoxyd sind in Abbild. 1 wiedergegeben. Durch H-D-Austausch an N-H gehen die doppelten Dubletts von H^3 [3] (2.3 Hz und 0.9 Hz) bei 431 Hz in ein Dublett mit J=0.9 Hz über, und die doppelte Tripletts bei 445 Hz gehen in die doppelte Dubletts mit J=0.7 Hz und 2.3 Hz über. Die doppelte Dubletts bei 422 Hz mit J=9.0 Hz und 2.3 Hz und die doppelte Tripletts bei 452 Hz mit J=9.0 Hz und 0.8 Hz bleiben beim H-D-Austausch unverändert. Die beiden Signale sollten von H^6 und H^7 stammen aufgrund der Grösse von J=9.0 Hz. Die Signale bei 445 Hz mit J=0.7 Hz und 2.3 Hz gehören dann zu dem H^4-Atom ($J_{4,7}$= 0.7 Hz und $J_{4,6}$=2.3 Hz). Weiter folgt die Zuordnung der Signale bei 452 Hz mit J=9.0 Hz und 0.8 Hz dem H^7. Das Wasserstoffatom H^7 koppelt ferner noch mit H^3 mit J=*ca.* 0.8 Hz. Hier ist zu bemerken, dass H^7 nicht mit N-H koppelt und H^4 nicht mit H^3 koppelt. Diese Reihenfolge von H^6 und H^7 ist umgekehrt der von Thomas und anderen[4] gedeuteten.

Die Fries-Umlagerung von 5-Acetoxy-2-methyl-indol (IIId) läuft in Gegenwart von Lewis-Säure nicht glatt, aber beim Belichten doch in mässiger Ausbeute (26%) ab, und 5-Hydroxy-2-methyl-4-acetyl-indol (IVd) vom Schmp. 188—189°C wird gebildet. Die Beweisführung der 4-Acetyl-Struktur von IVd erfolgte aus dem Spektrum, in dem zwei Dubletts bei τ 2.65 und 3.30 jede mit J=9 Hz auftreten.

IVa lässt sich sehr schwer unter alkalischen Bedingungen alkylieren, weil die Verbindung wie 1-Acetyl-2-naphthol im alkalischen Medium sehrunbeständig ist.[5] Doch gelingt die Alkylierung in einer Ausbeute von 10% in Tetrahydrofuran bei 50°C mittels Natriumhydrid und Benzyljodid bzw. Bromessigester. Besser, d.h. in 16% Ausbeute, verläuft die Allylierung in Dimethylformamid bei Raumtemperatur mittels Natriumhydrid und Allylbromid, wobei auch *N*,*O*-Diallylierung zu VIId in 4% Ausbeute mitlief. Jedenfalls findet die Alkylierung nur an der *O*- oder *N*-Stellung statt, und keine C^4-Alkylierung unter Bildung von 5-Oxo-4,4-dialkyl-4,5-dihydro-indol-Derivat VIII wie bei der Benzylierung von Ia[1] war zu finden.

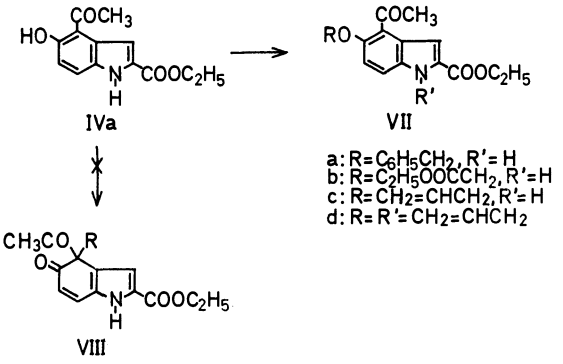

Formelschema 2.

Beschreibung der Versuche[6]

5-Hydroxy-2-methyl-3-äthoxycarbonyl-indol (II). a) Friedel-Crafts-Reaktion: Zu einer Suspension von 5 g (22.8 mMol)

3) Die Signale können nicht von H^6 oder H^7 sondern von H^3 oder H^4 herkommen, weil die Koppelung klein ist. Wenn es H^4 ist, so muss es nach H-D Austausch noch mit H^6 und H^7 Koppelung und doppelte Dubletts zeigen.

4) D. W. Thomas, H. Achenbach, und K. Biemann, *J. Amer. Chem. Soc.*, **88**, 1537 (1966).

5) O. N. Witt und O. Braun, *Ber.*, **47**, 3230 (1915).

6) Die Schmelzpunkte sind nicht korrigiert. Die Aufnahme der NMR-Spektren erfolgte mit eimem Gerät von Varian A60 Spektrometer. Der innere Standard war Tetramethylsilan.

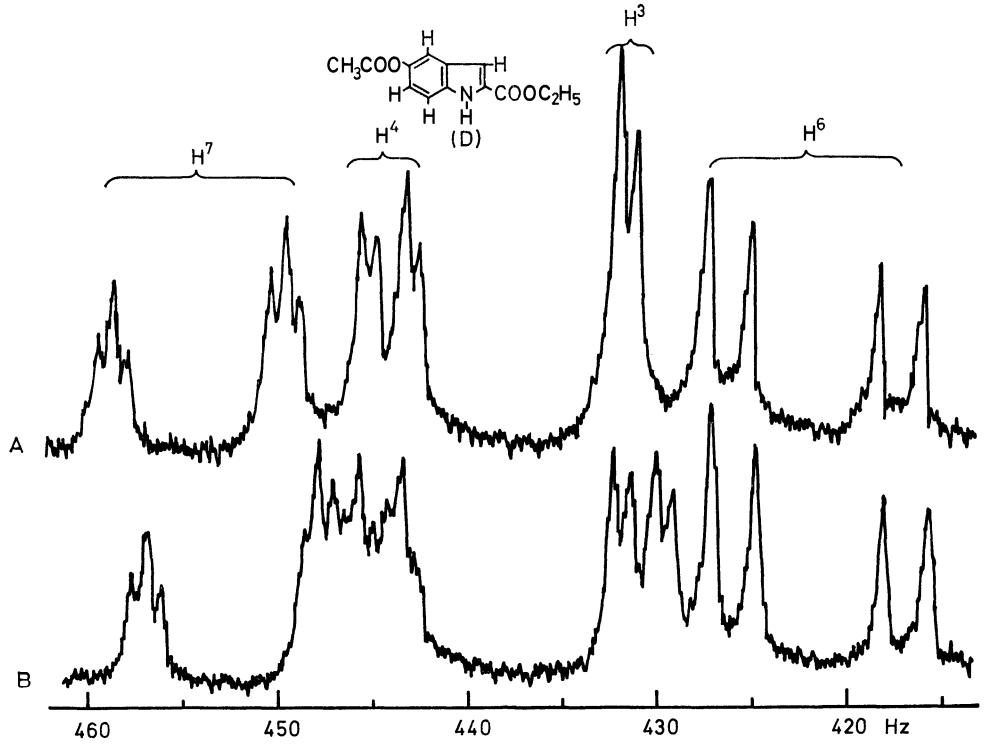

Abbild. 1. NMR-Spektren von 5-Acetoxy-2-äthoxycarbonyl-indol (IIIc) in Deuteroaceton in (A) An- und (B) Abwesenheit von Deuteriumoxyd (Hz aus Tetramethylsilan als innerem Standard)

5-Hydroxy-2-methyl-3-äthoxycarbonyl-indol (Ia) in 200 m*l* Nitrobenzol fügt man 9.23 g (68.4 mMol) Aluminiumchlorid ein, wobei die Suspension in die Lösung geht. Dazu gibt man 2.7 g (34.2 mMol) Acetylchlorid unter Eiskühlung und erwärmt die Mischung 3 Stunden bei 50°C. Nach dem Zersetzen der Reaktionmischung durch verd. Salzsäure destilliert man das Nitrobenzol mit Wasserdampf ab, kristallisiert den Rückstand aus Äthanol um und erhält 1.11 g (19%) feine gelbe Nadeln vom Schmp. 229—233°C. Diese Verbindung stimmt im Schmp. und im IR-Spektrum mit denen vom Produkt nach der Fries-Umlagerung überein.

b) Fries-Umlagerung: Man löst 1.00 g (3.85 mMol) 5-Acetoxy-2-methyl-3-äthoxycarbonyl-indol (Ib) vom Schmp. 150—151.5°C[1] in 15 m*l* Nitrobenzol und versetzt mit 1.00 g (6 mMol) Aluminiumchlorid und lässt die Mischung 48 Stunden bei Raumtemperatur stehen. Nach Aufarbeitung wie üblich erhält man 60 mg (6%) feine gelbe Nadeln vom Schmp. 227—232°C (zers.). IR-Bande (KBr) bei 3450 1665, 1645, 1625/cm. NMR-Spektrum (Trifluoressigsäure) bei τ 0.37 (NH), 2.04 s (H^7), 2.30 breites s (H^4), 5.41 quartett, 7.15 s, 8.40 t.

Gef.: C, 64.44; H, 5.36; N, 5.57%. Ber. für $C_{14}H_{15}O_4N$: C, 64.36; H, 5.79; N, 5.36%.

c) Photolytische Fries-Umlagerung: Man belichtet 96 Stunden eine Lösung von 6.53 g (25 mMol) Ib in 850 m*l* Äthanol bei Raumtemperatur unter Stickstoffatmosphäre mit Niederdruckbrenner. Beim Einengen der Lösung bis zu *ca.* 100 m*l* kommen hellbraune Blättchen aus. Umkristallisieren aus wässr. Äthanol gibt 0.47 g (7.2%) IIa vom Schmp. 234—237°C.

Gef., C, 64.64; H, 5.57; N, 5.29%.

5-Hydroxy-4-acetyl-2-äthoxycarbonyl-indol (IVa). a) Friedel-Crafts-Reaktion.: Man versetzt eine Suspension von 2.00 g 5-Hydroxy-2-äthoxycarbonyl-indol (IIIa)[7] vom Schmp. 151—152°C in 50 m*l* Nitrobenzol mit einer Lösung von 4.00 g (30 mMol) Aluminiumchlorid in 50 m*l* Nitrobenzol und erwärmt die Mischung nach Zugabe von 1.26 g (15 mMol) Acetylchlorid 3 Stunden bei 50°C. Beim Zersetzen mit verd. Salzsäure fällt ein hellgelber Niederschlag aus, welcher nach Umkristallisieren aus Essigester 1.03 g (42%) gelbe Nadeln vom Schmp 235—239°C, (Zers.) gibt. Der Schmelz punkt und das IR-Spektrum stimmen mit denen von nach b) hergestelltem Produkt IVa überein.

Man treibt Nitrobenzol mit Wasserdampf ab, und den Rückstand kristallisiert man mehrmals aus verd. Äthanol bzw. Benzol um, und man isoliert 0.27 g (11%) hellbraune Kristalle vom Schmp 123—124°C. IR-Bande (KBr) bei 3250, 1755, 1715, 1545/cm. NMR-Spektrum (Deuterochloroform) bei τ 0.16 breites s (NH), 2.22d (2 Hz, H^4), 2.78d (9 Hz, H^7), 3.08 doppelte d (9 Hz, 2 Hz, H^6), 5.58q (OCH_2CH_3), 7.32s (CH_3CO), 7.68s (CH_3CO), 8.63t (OCH_2-CH_3).

Gef.: C, 62.63; H, 5.18; N, 4.82%. Ber. für $C_{15}H_{15}O_5N$ 5-Acetoxy-3-acetyl-2-äthoxycarbonyl-indol (V): C, 62.28; H, 5.23; N, 4.84%.

Man acetyliert 3.00 g (10 mMol) 5-Benzyloxy-2-äthoxycarbonyl-indol[8] (IIIb) in Suspension in einer Mischung von 60 m*l* Kohlendisulfid und 60 m*l* Benzol 3 Stunden bei 50°C mittels 1.2 g (15 mMol) Acetylchlorid in Gegenwart von Aluminiumchlorid. Nach dem Zersetzen mit verd. Salzsäure trennt man die unlöslichen Kristalle ab (0.33 g), kristallisiert aus verd. Äthanol um und erhält 31 mg IVa vom Schmp. 220—230°C. Das IR-Spektrum stimmt mit dem vom Produkt nach b) überein.

Aus der Kohlendisulfid-Benzol-Lösung isoliert man 26 mg (0.7%) farblose Nadeln vom Schmp. 177—180°C. IR-Bande (KBr) bei 3370, 1760, 1700/cm. NMR-Spektrum (Trifluoressigsäure) bei τ 2.55 breites s (H^4), 2.80s (C_6H_5), 2.95d (9 Hz, H^6), 2.60d (teilweise überlagert von H^4, 9 Hz,

7) Hergestellt aus IIIb durch katalytische Hydrierung über Pd/C nach F. Bergel und A. L. Morrison, *J. Chem. Soc.*, **1943**, 49.

8) W. R. Boehme, *J. Amer. Chem. Soc.*, **75**, 2502 (1953).

H^7), 5.45q, 5.75s ($PhCH_2$), 7.70s (CH_3CO), 8.51t.

Gef.: C, 71.21; H, 5.78; N, 4.38%. Ber. für $C_{20}H_{19}O_4N$ 5-Benzyloxy-3-acetyl-2-äthoxycarbonylindol (IVb), C, 71.20; H, 5.68; N, 4.15%.

b) Fries-Umlagerung: *5-Acetoxy-2-äthoxycarbonyl-indol (IIIc)*: Man acetyliert IIIa in Pyridin mit Acetanhydrid. Farblose Nadeln vom Schmp. 148—150°C. Die NMR-Spektren (Deuteroaceton) von Ring-Protonen sind in Abbild. 1 gezeigt.

Gef.: C, 63.65; H, 5.20; N, 5.65%. Ber. für $C_{13}H_{13}O_4N$: C, 63.15; H, 5.30; N, 5.67%.

Man äelichtet 11.3 g (48 mMol) IIIc in 1 *l* Äthanol 67 Stunden unter Stickstoffatmosphäre bei Raumtemperatur mit Niederdruckbrenner. Beim Einengen bis zu 100 m*l* fallen 1.27 g (11%) gelbe Nadeln vom Schmp. 230—237°C (zers), aus. IR-Bande (KBr) bei 3350, 1695, 1610, 1520, 1260, 1240, 1020/cm. NMR-Spektrum (Trifluoressigsäure) bei τ 2.17d (9 Hz, H^7), 2.42 breites s (H^3), 2.87d (9 Hz, H^6).

Gef.: C, 63.42; H, 5.29; N, 5.47%. Ber. für $C_{13}H_{13}O_4N$: C, 63.15; H, 5.30; N, 5.67%.

Die Mutterlauge dampft man ab, und den Rückstand chromatographiert man an Aluminiumoxyd mit Essigester, wobei man 39 mg gelbe Nadeln vom Schmp. 193—196°C aus 66% Äthanol erhält. IR-Bande (KBr) bei 3330, 1710, 1640, 1610/cm. NMR-Spektrum (Trifluoressigsäure) bei τ 1.77 breites s (H^4), 2.65s (H^7), 2.70 breites s (H^3).

Gef.: C, 62.97; H, 5.21; N, 5.47%. Ber. für $C_{13}H_{13}O_4N$ 5-hydroxy-6-acetyl-2-äthoxycarbonyl-indol (IV): C, 63.15; H, 5.30; N, 5.67%.

5-Acetoxy-2-methyl-indol (IIId): Man kocht 2.0 g (9.1 mMol) Ia mit 20%iger Salzsäure 2 Stunden unter Stickstoffatmosphäre. Nach Neutralisieren bis zu Kongo-Rot sauer zieht man mit Essigester aus. Man dampft die Lösung ab, kristallisiert den Rückstand aus *n*-Hexan - Methylenchlorid um und erhält 5-Hydroxy-2-methyl-indol vom Schmp. 131—134°C in 52% Ausbeute. Man acetyliert 2.0 g von dem Indol in Pyridin mit Acetanhydrid. Farblose Nadeln vom Schmp. 129—131°C aus Äthanol. Ausbeute 1.5 g (58%). IR-Bande (KBr) bei 3430, 1730, 1240/cm.

Gef.: C, 69.32; H, 5.33; N, 7.22%. Ber. für $C_{11}H_{11}O_2N$: C, 69.82; H, 5.86; N, 7.40%.

5-Hydroxy-2-methyl-4-acetyl-indol (IVd). a) Man lässt 1.00 g (5.3 mMol) IIId in 15 m*l* Nitrobenzol 24 Stunden bei Raumtemperatur mit 1.4 g (11 mMol) Aluminiumchlorid stehen. Man erhält nur die Ausgangssubstanz zurück. Wenn man die Mischung von IIId und Zinkchlorid 5 Stunden auf 150—160°C erhitzt, so isoliert man 6 mg in Benzol unlösliche gelbe Kristalle vom Schmp. 165—172°C, deren IR-Spektrum mit dem vom Produkt nach b) übereinstimmt.

b) Man belichtet eine Lösung von 2.00 g (11 mMol) IIId in 100 m*l* Äthanol 48 Stunden unter Stickstoffatmosphäre mit Hochdruckbrenner. Beim Einengen fällt ein gelblich braunes Produkt aus. Umkristallisieren aus wässr. Äthanol gibt 0.51 g (26%) gelbe Nadeln vom Schmp. 188—189°C. IR-Bande (KBr) bei 3350, 1610, 1235/cm. NMR-Spektrum (Deuterochloroform) bei τ 2.65d (9 Hz, H^7), 3.30d (9 Hz, H^6), 3.66 breites s (H^3), 7.24s, 7.54s.

Gef.: C, 70.22; H, 5.91; N, 7.45%. Ber. für $C_{11}H_{11}O_2N$: C, 69.82; H, 5.86: N, 7.40%.

5-Benzyloxy-4-acetyl-2-äthoxycarbonyl-indol (VIIa). Man versetzt unter Stickstoffatmosphäre 0.52 g (2.2 mMol) IVa in 50 m*l* Tetrahydrofuran - Benzol bei Raumtemperatur mit 0.105 g (2.2 mMol) 50% Natriumhydrid, wobei ein rotes Natriumsalz ausfällt. Man gibt dazu 0.477 g (2.2 mMol) Benzyljodid in 10 m*l* Tetrahydrofuran und erwärmt 3 Stunden bei 50°C. Man filtriert 0.33 g Niederschlag ab, und gewinnt daraus 0.20 g Ausgangssubstanz zurück. Man dampft die Tetrahydrofuran-Lösung ab, chromatographiert den Rückstand an Aluminiumoxyd mit Essigester und erhält 65 mg (9%) farblose Nadeln (aus Äthanol) vom Schmp. 152—153°C. IR-Bande (KBr) bei 3370, 1680, 1650, 1520/cm. NMR-Spektrum (Deuterochloroform) bei τ 2.29 doppelte d (2 Hz, H^3), 1.3 breites s (NH), 2.45d (9 Hz, teils überlagert von C_6H_5, H^7), 2.85d (9 Hz, H^6), 2.55s (C_6H_5), 4.79s ($PhCH_2$), 5.55q, 7.31s, 8.58t.

Gef.: C, 71.35; H, 5.29; N, 4.00%. Ber. für $C_{20}H_{19}O_4N$: C, 71.20; H, 5.68; N, 4.15%.

5-Äthoxycarbonylmethoxy-4-acetyl-2-äthoxycarbonyl-indol (VIIIb). Wie bei VIIa versetzt man 0.52 g (2.2 mMol) IVa mit 0.105 g (2.2 mMol) Natriumhydrid in Tetrahydrofuran und dann mit 0.365 g (2.2 mMol) Bromessigester bei 50°C. Man isoliert durch Chromatographie an Aluminiumoxyd-Essigester 0.27 g rohes Produkt, welches beim Umkristallisieren aus Tetrachlorkohlenstoff 55 mg (10%) farblose Nadeln vom Schmp. 157—158.5°C gibt. UV (Äthanol) λ_{max} (nm) (ε) bei 252 (10100), 265 (Schulter), 332 (14300). IR-Bande (KBr) bei 3450, 1750, 1710, 1650, 1530/cm. NMR-Spektrum (Deuterochloroform) bei τ 2.36 doppelte d (2 Hz, 1 Hz, H^3), 2.51 doppelte d (9 Hz, 1 Hz, H^7), 3.06d (9 Hz, H^6), 5.27s (OCH_2COO), 5.66 (zwei Quartetts machen ein Quintett, OCH_2CH_3), 7.22s, 8.65 (zwei Tripletts machen ein Quartett, OCH_2CH_3).

Gef.: C, 61.20; H, 5.52; N, 4.08%, Ber. für $C_{17}H_{19}O_6N$: C, 61.25; H, 5.75; N, 4.20%.

5-Allyloxy-4-acetyl-2-äthoxycarbonyl-indol (VIIc). In 60 m*l* Dimethylformamid versetzt man 2.1 g (8.9 mMol) IVa mit 0.43 g (10 mMol) 50% Natriumhydrid unter Stickstoffatmosphäre und Eiskühlung. Nach 2 Stunden Umrühren gibt man 2.58 g (17.8 mMol) Allylbromid dazu und lässt 20 Stunden bei Raumtemperatur und zum Schluss 2 Stunden bei 50°C reagieren. Nach dem Eindampfen nimmt man den Rückstand in Essigester auf und chromatographiert an Aluminiumoxyd-Essigester, wobei man 0.40 g (16%) farblose Kristalle vom Schmp. 145—147°C erhält. IR-Bande (KBr) bei 3350, 1680, 1640/cm. NMR-Spektrum (Deuterochloroform) bei τ 2.30 doppelte d (2 Hz, 1 Hz, H^3), 2.48 doppelte d (9 Hz, 1 Hz, H^7), 2.98d (9 Hz, H^6), 7.23s (CH_3CO).

Gef.: C, 66.51; H, 5.90; N, 4.77%. Ber. für $C_{16}H_{17}O_4N$: C, 66.88; H, 5.96; N, 4.88%.

Aus der Mutterlauge der Umkristallisierung isoliert man unreines *N,O*-Diallyl-4-acetyl-2-äthoxycarbonyl-indol (VIId) vom Schmp. 87—90°C in 4% Ausbeute.

Gef.: C, 69.06; H, 6.17; N, 4.40%. Ber. für $C_{19}H_{21}O_4N$: C, 69.70; H, 6.47; N, 4.28%.

NOTES

BULLETIN OF THE CHEMICAL SOCIETY OF JAPAN, VOL. 44, 554—555 (1971)

Spectrophotometric Determination of Iodide Ions by Solvent Extraction with Neutral Red[1)]

Masahiro TSUBOUCHI
Faculty of Education, Tottori University, Tottori
(Received April 27, 1970)

Many investigations have been made on the spectrophotometric determination of iodide ions. Although the catalytic method[2)] and diphenylcarbazone-mercury(II) method[3)] are sensitive, they are influenced by the changes in temperature or the presence of bromide ions.

This paper deals with a new spectrophotometric method for iodide ions, which is based on a solvent extraction of the ion-pair formed between the colored neutral red cation and colorless iodide ion. The method has a greater sensitivity than that in which methylthymol blue - mercury(II),[4)] diethyldithiocarbamate-silver(I)[5)] or 1,10-phenanthroline-iron(II)[6)] complex, are employed.

Experimental

Apparatus and Reagents. Absorbance measurements were made with a Shimadzu Beckman Model QR-50 spectrophotometer with matched 1 cm quartz cells. An Iwaki Model KM shaker was used for extraction.

Potassium iodide of guaranteed grade was dissolved in deionized water; it was then standardized according to Volhard's method. The working standard solutions were obtained by diluting this solution. The neutral red (NR) solution of 2×10^{-3}M was prepared by dissolving NR (guaranteed grade) in 0.01N sulfuric acid. The citrate buffer solution of 0.2M was made from sodium citrate and dilute sulfuric acid.

Procedure. 2—10 m*l* of sample solutions containing less than 5×10^{-5}M of iodide ions were placed in separatory funnels. 5 m*l* of the buffer solution (pH 3) and 5 m*l* of the NR solution were then added. The solution was diluted to 25 m*l* with water. After adding 10 m*l* of nitrobenzene, the contents were mixed thoroughly by means of a shaker for about 2 min. The nitrobenzene layer were drawn off into glass tube equipped with a glass stopper containing about 1 g of anhydrous sodium sulfate, and shaken to remove droplets of water. The absorbance of the extract was measured at 552 mμ against a reagent blank.

Results

Figure 1 shows the obtained visible absorption spectra of extracts. The absorbance maximum of the extracts was at 552 mμ. From pH 7 to 11 the red color was not formed in the nitrobenzene layer. The optimum pH was 2—4. Of the solvents such as chloroform, isoamyl alcohol, nitrobenzene, methyl isobutyl ketone *n*-hexane, ethyl acetate, benzene, and ether, only nitrobenzene can extract the ion-pair consisting of NR and iodide ion. 0.01—0.08M citrate used as a buffer had no influence on the absorbance of the extract. Maximum

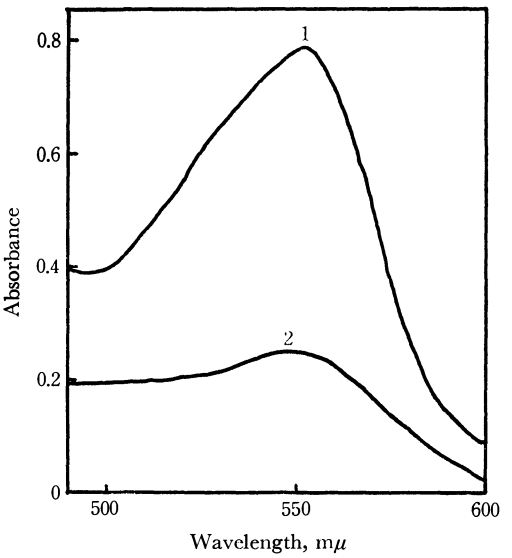

Fig. 1. Absorption spectra
1: Spectrum of organic phase extracted from the aqueous solution (25 m*l*) contained 1.6×10^{-5}M iodide.
2: Reagent blank
Reference: Nitrobenzene

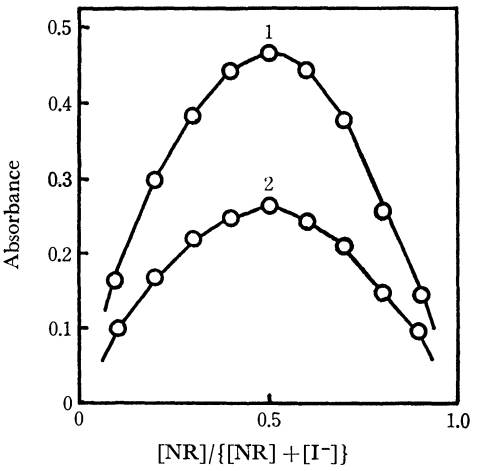

Fig. 2. Continuous variations plots.
[NR]+[I⁻]: 8×10^{-5}M
1: 552 mμ, 2: 510 mμ
Reference: Reagent blank

1) Presented at the 23rd Annual Meeting of the Chemical Society of Japan, Tokyo, April, 1970.
2) I. Iwasaki, S. Utsumi, and T. Osawa, This Bulletin, **26**, 108 (1953).
3) T. Okutani, *Nippon Kagaku Zasshi*, **88**, 737 (1967).
4) T. Nomura and S. Komatsu *ibid.*, **90**, 168 (1969).
5) S. Komatsu and T. Nomura, *ibid.*, **88**, 1164 (1967).
6) Y. Yamamoto and S. Kinuwaki, This Bulletin, **37**, 434 (1964).

color development in the nitrobenzene layer required about a 10-fold molar excess of NR to iodide ion. Variation of room temperature 14—24°C had no measurable effect. Full color development took about 1 min shaking. The red color of the extract remained stable for 2 hr.

In order to investigate the structure of the extracted species the method of continuous variations was employed. As shown in Fig. 2, the resulting curves have a maximum at 0.5 mol fraction of NR, indicating a 1 to 1 NR - iodide ion ratio.

Calibration and Foreign Ions. The system followed Beer's law over the range of 4×10^{-6}—2×10^{-5}M of iodide ions, with molar absorptivity of 3.25×10^{4} $mol^{-1}\cdot cm^{-1}$ liter in the aqueous solution. Experiments with ten identical samples, each with a final iodide concentration of 1.6×10^{-5}M, gave the mean absorbance 0.520, with a standard deviation of 0.005 absorbance unit.

The effect of foreign anions was studied by adding solutions of their sodium or potassium salts. Tolerance for a foreign ion was taken as the largest amount that could be present and give an absorbance differing by no more than 0.025 from that produced by iodide alone. Tolerances are shown in Table 1. Halogens and cyanide did not interfere.

Table 1. Effect of foreign ions

Ion	Tolerance(M)	Ion	Tolerance(M)
Br^-	5×10^{-3}	HCO_3^-	5×10^{-3}
BrO_3^-	1×10^{-3}	$H_2PO_4^-$	5×10^{-3}
Cl^-	5×10^{-3}	IO_3^-	1×10^{-6}
ClO_3^-	1×10^{-6}	NO_2^-	5×10^{-5}
ClO_4^-	1×10^{-7}	NO_3^-	2×10^{-5}
CN^-	5×10^{-3}	SCN^-	2×10^{-7}
CH_3COO^-	5×10^{-3}	SO_4^{2-}	5×10^{-3}
F^-	5×10^{-3}	$S_2O_3^{2-}$	1×10^{-4}

Iodide ion: 1×10^{-5}M

The author would like to thank Professor Yuroku Yamamoto of Hiroshima University for valuable advice.

BULLETIN OF THE CHEMICAL SOCIETY OF JAPAN, VOL. 44, 555—556 (1971)

The Photoreaction of Dehydroacetic Acid

Noboru SUGIYAMA, Toshiaki SATO, Hiroshi KATAOKA and Choji KASHIMA
Department of Chemistry, Tokyo Kyoiku University, Otsuka, Tokyo

(Received May 14, 1970)

Since dehydroacetic acid (DHA)[1] shows strong antifungal and antibacterial activity, it has been widely used as a fungicide and bactericide in food. The present authors are interested in the photoreaction of DHA in the solid state from the points of view of photochemistry and biochemistry.

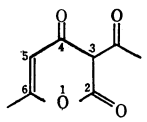

1

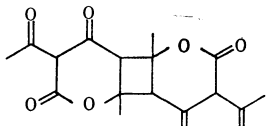

2

DHA (**1**) was irradiated for a week in the solid state in thin layers by means of a high-pressure mercury lamp. After removing the cold, acetone-soluble fraction from the irradiated material, the residue was recrystallized from acetone to give colorless needles (**2**) in a yield of 4%. The elemental analysis, the thermal decomposition to a monomer at the melting point, and the mass spectrum fragment (*m/e* 239 M^+-COCH_3 and *m/e* 168, which is equivalent to a monomer) all show a dimeric structure. The UV,[2] IR,[2] and NMR spectra supported the idea of the presence of the $(2+2)\pi$ dimer at the 5 and 6-positions. The NMR spectrum, which showed a singlet signal at τ 6.60, indicated a cyclobutane methine proton instead of a vinyl proton in a monomer. The head-to-tail form was suggested by the following reactions. The hydrolysis of the dimer **2** with aqueous sodium hydroxide gave 2-acetyl-3,5-xylenol (**5**) and 2,6-diacetyl-3,5-xylenol (**6**) in a yields of 46 and 42% respectively. The formation of **5** and **6** may be explained by assuming the intermediates **3** and **4**, which have been postulated by Yates[3] in the hydrolytic formation of 2-acetyl-1,8-dihydroxy-3,6-dimethylnaphthalene from the 2,6-dimethyl-4-pyrone cage dimer. In the case of the hydrolysis of **2**, the reaction conditions are stronger than these of the cage dimer of Yates, so two deacetyl-

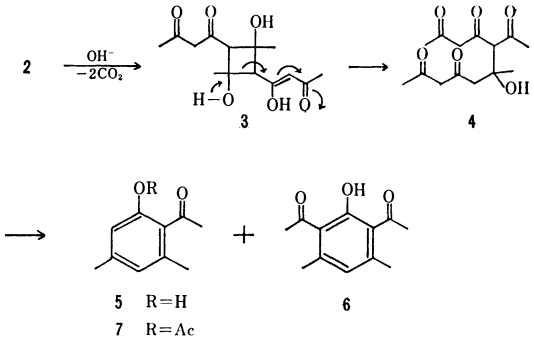

3 **4**

5 R=H
7 R=Ac

6

1) Physical data are listed in E. E. Royals and J. C. Leffingwell, *J. Org. Chem.*, **30**, 1255 (1965).

2) Methyl 2-acetylacetoacetate has a closely similar structure. IR: 1711(s), 1559(braod), 1441(s) 1240, 1086(s), 918 cm^{-1}. UV: 277 nm (log ε, 4.08). T. Motoda and Y. Yoshida, *Kogyo Kagaku Zasshi*, **68**, 1669 (1965).

3) P. Yates and M. J. Jorgenson, *J. Amer. Chem. Soc.*, **85**, 2956 (1963).

ated compounds, **5** and **6**, might be produced. The compound **5** was identical with the authentic specimen of 2-acetyl-3,5-xylenol,[4] while **6** was identical with the authentic specimen of 2,6-diacetyl-3,5-xylenol prepared by the Fries rearrangement of the acetate **5** (**7**).

Although whether the structure of **2** is of a syn or anti form is at present uncertain, the formation of this head-to-tail, four-membered dimer is the first such example in any photodimer of 4-pyrones[3,5] and 2-pyrones[6,7] except for the case of 2,6-diphenyl-4*H*-thiopyran-4-one.[8]

Experimental

Photoreaction of Dehydroacetic Acid (**1**). The inner surface of the wall of the irradiation vessel (cylindrical, 10×25 cm) was covered with solid DHA film by rotating and warming the vessel. In the vessel we placed a concentrated acetone solution of 1 g of DHA. The DHA film thus formed was irradiated with a 125-W, high-pressure mercury lamp at room temperature for a week. After irradiation, the solid was triturated with acetone to dissolve the unchanged starting material. The sparingly-soluble, colorless solid was collected and washed with cold acetone. This material, the crude photodimer (**2**), was obtained in a yield of about 4%. Recrystallization from acetone gave colorless needles; mp 214.5—215.5°C.

Found: C, 57.39; H, 4.90%. Calcd for $C_{16}H_{16}O_8$: C, 57.14; H, 4.80%. Mass: *m/e* 293(4%), 169(82%, base), 153(base), 125(33%), 85(62%), 69 (33%), 43(118%). UV: λ_{max}^{EtOH} nm (ε) 279 (27800). IR (KBr): 1706(s), 1555 (broad), 1445(s), 1240, 1080(s), 910 cm^{-1}. NMR (in $CDCl_3$): τ 8.46 (s, 6H), 7.31(s, 6H), 6.60(s, 2H), −7.91(s, 2H).

The irradiation of 1-g protions of DHA solutions in 5 m*l* of acetone, 6 m*l* of benzene, or 20 m*l* of methanol in a Pyrex tube under a nitrogen atmosphere with a high-pressure mercury lamp for 5 days showed no change.

Hydrolysis of the Dimer **2** *to 2-Acetyl-3,5-xylenol* (**5**) *and 2,6-Diacetyl-3,5-xylenol* (**6**). A mixture of 40 mg of **2**, 12.5 m*l* of saturated aqueous sodium bicarbonate, and 2.5 m*l* of aqueous 5% sodium hydroxide was heated under reflux for 4.5 hr. After cooling, the reaction mixture was extracted with chloroform. The aqueous layer was acidified with dilute sulfuric acid and then again extracted with chloroform. Treating both chloroform extracts separately in the usual manner gave **5** (9 mg; 46%) and **6** (10 mg; 42%) respectively; they were purified by silica-gel-column chromatography using benzene. No change was observed upon the same treatment of DHA.

Preparation of 2-Acetyl-3,5-xylenol (**5**) *and 2,6-Diacetyl-3,5-xylenol* (**6**). Compound **5** was prepared by Smith's method[4]; mp 56—58°C (lit, 57—58.5°C). To a pyridine solution of 290 mg of **5** we added an excess of acetic anhydride. After the reaction mixture had stood overnight, it was poured into cold water and extracted with chloroform. Treating the chloroform extract in the usual manner gave 2-acetoxy-4,6-dimethylacetophenone (**7**) (370 mg; 100%); bp 164—167°C /13 mmHg.

Found: C, 69.81; H, 6.95%. Calcd for $C_{12}H_{14}O_3$; C, 69.88; H, 6.95%. UV: λ_{max}^{EtOH} nm(ε) 246(20600), 285(3000) sh. IR (KBr): 1770, 1695 cm^{-1}. NMR(in $CDCl_3$): τ 7.77, 7.74, 7.70, 7.58 (all s, 3H each), 3.23 (s, 1H), 3.12 (s, 1H).

A mixture of 370 mg of **7** and 720 mg of anhydrous aluminum chloride was heated on a steam bath for 2.5 hr, and then it was mixed with *ca.* 5 m*l* of water. The mixture was extracted with chloroform. The chloroform extract was treated in the usual manner, the chloroform was evaporated, and the residue was chromatographed on silica gel. The fraction which was eluted with benzene gave **5** (96 mg; 33%) and **6** (175 mg; 42%), mp 108—109.5°C.

Found: C, 69.87; H, 6.97%. Calcd for $C_{12}H_{14}O_3$; C, 69.88; H, 6.84%. UV: λ_{max}^{EtOH} nm 243 (12900), 267 (9500) sh. IR (KBr): 1687, 1615 cm^{-1}. NMR (in $CDCl_3$): τ 7.60(s, 6H), 7.41(s, 6H), 3.42(s, 1H), −2.10(s, 1H).

4) L. I. Smith and J. W. Opie, *J. Org. Chem.*, **6**, 427 (1941).
5) P. Yates and D. J. Macgregor, *Tetrahedron Lett.*, **1969**, 453.
6) P. de Mayo and R. W. Yip, *Proc. Chem. Soc.*, **1964**, 84.
7) W. H. Pirkle and L. H. Mckendry, *Tetrahedron Lett.*, **1968**, 5279.
8) N. Sugiyama, Y. Sato, H. Kataoka, C. Kashima, and K. Yamada, This Bulletin, **42**, 3005 (1969).

BULLETIN OF THE CHEMICAL SOCIETY OF JAPAN, VOL. 44, 557—558 (1971)

Kinetics of the Reaction of Imidazole with Acrylonitrile by Using NMR

Fukiko YAMADA and Yasuyoshi FUJIMOTO

Department of Applied Chemistry, Faculty of Engineering, Kansai Universtiy, Senriyama, Osaka

(Received June 6, 1970)

Imoto and his co-workers[1] recently reported that acrylonitrile (AN) polymerized in the system of imidazole (Im) and carbon tetrachloride (CCl_4) and that the polymerization proceeded through the radical mechanism. On the other hand, Sawa and Okamura[2] confirmed that, in the presence of the catalyst, potassium hydroxide, the Im derivatives reacted with AN at 100°C to give the corresponding 1-(β-cyanoethyl)-imidazoles. In the latter case, the cyanoethylation appears to proceed through the following ionic mechanism:

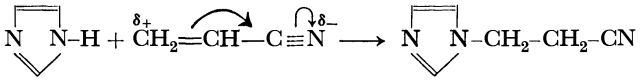

The work reported here was carried out in order to study the kinetics of the ionic reaction and to ascertain how the polymerization can be initiated when CCl_4 is present in the reaction system.

Experimental

Measurements. The NMR spectra were obtained at 60 MHz with a Japan Electron Optics Model JNM 3H-60 spectrometer. The chemical shifts are reported in ppm downfield from the internal TMS (δ). A constant-temperature water bath was employed; it was equipped with an immersion heating element that afforded a temperature control of ± 0.1°C.

Materials. The AN, Im, and CCl_4 were purified by the reported methods.[1,3] All the reagents used were of an analytical grade.

The Reactions. (*1*) *Cyanoethylation*: The reaction between Im and AN with or without CCl_4 was carried out in sealed tubes. The rate of the disappearance of Im was followed by the NMR method. After the reaction had been completed, the evaporation of the remaining AN at room temperature afforded an oily product that was then purified by means of column chromatography on silica-gel, using methylene chloride as the eluent; this yielded pure 1-(β-cyanoethyl)imidazole (CEIm). NMR, δ, (in CH_2Cl_2): 7.6 (singlet, 1H), 7.0 (doublet, 2H), 4.2 (triplet, 2H), and 2.8 (triplet, 2H). IR absorption (C≡N) at 2258 cm^{-1}. Mol wt (by mass spectrometry), 121. Picrate, mp 121°C (lit,[2] mp 120—121°C), Found N, 23.76%; Calcd for $C_{12}H_{10}N_6O_7$: N, 24.00%.

(2) *Polymerization*: The polymerization of AN in the system of Im and CCl_4 was carried out in sealed tubes in the dark. Definite amounts of AN, Im, and CCl_4 were charged in separate test tubes, cooled in a bath of dry ice and methanol, and sealed in a vacuum. The sealed tubes were then shaken at 25°C for a given time. The rate of the disappearance of Im was followed by the NMR method. After the polymerization had been initiated, the polymer produced was precipitated in the system. Each ingredient was then freed from the precipitate, and the filtrate was examined by the NMR method. The precipitate was washed with methanol. The molecular weight of the polymer obtained for 29 hr at 25°C was found to be 7.20×10^7 by the viscometric method in the dimethylformamide solution.[3]

Results and Discussion

Cyanoethylation. In the reaction between Im and AN with CCl_4, the changes in the NMR spectra with the reaction time are shown in Fig. 1. The one-proton

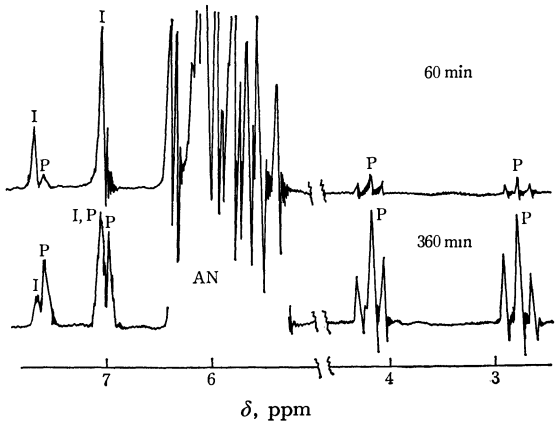

Fig. 1. Changes of the NMR spectra with reaction time at 25°C. Peaks marked AN, I, and P belong to acrylonitrile, imidazole, and the product, respectively.

and two-proton singlets due to the ring protons of Im appear at 7.7 and 7.1 ppm respectively. In the earlier period of the reaction, the new methylene signals due to the reaction product, CEIm, began to appear at 4.2 and 2.8 ppm respectively, and their intensities increased with the reaction time. The proton numbers of the methylene signals can be evaluated by comparing the data of the integrated signals with those of the signals due to the Im ring protons, which were unchanged by the reaction. The conversion of the cyanoethylation based on the initial concentration of Im can, therefore, be obtained by means of the integrated data of these signals. The time-conversion curve is shown in Fig. 2. From these data, the reactions between Im and AN with or without CCl_4 were found to follow a second-order rate equation:

$$dx/dt = k(a-x)(b-x)$$

giving;

$$\log_{10} b(a-x)/a(b-x) = kt(a-b)/2.303$$

where;

1) M. Imoto, K. Takemoto, T. Otsuki, N. Ueda, S. Tahara, and H. Azuma, *Makromol. Chem.*, **110**, 37 (1967).

2) N. Sawa and S. Okamura, *Nippon Kagaku Zasshi.*, **90**, 704 (1969).

3) M. Imoto, K. Takemoto, and H. Sutoh, *Makromol. Chem.*, **110**, 31 (1967).

a=the initial concentration of AN
and b=the initial concentration of Im

The values of the second-order rate constants, k, were obtained graphically by plotting $\log_{10}b(a-x)/a(b-x)$ against t, the slope of the line being $k(a-b)/2.303$. The points obtained fell on good straight lines. The rate constants for the reactions between Im and AN with or without CCl_4 at 25°C are presented in Table 1.

Table 2 shows the rate constants for the reaction at different temperatures, along with the values of the activation energy as evaluated from the slope of the Arrhenius plots.

Table 1. Second-order rate constants for the reaction of Im with AN at 25°C

Run	(AN/Im), mol ratio	CCl_4, mol/l	$k\times10^4$, l/mol·min
1	6.8	0.88	3.7
2	8.2	2.00	3.7
3	9.2	2.01	3.7
4	6.0	3.65	3.6
5	5.7	4.12	3.7
6	3.4	——	5.2
7	6.9	——	4.6, 4.9, 5.0
8	9.8	——	4.9
9	13.4	——	4.6

Table 2. Reaction rates and the energy of activation for the reaction of Im with AN in CCl_4

Temperature °C	10	20	25	30	40
$k\times10^4$, l/mol·min	1.2	2.8	3.6	4.6	9.0
E, kcal/mol			12.0		

As is shown in Table 1, in the absence of CCl_4 the rates were slightly increased over those of the reactions in CCl_4. In runs 1 and 5, the mol ratios of Im : AN : CCl_4 are 1 : 7 : 0.5 and 1 : 6 : 3. When the CCl_4 content in the system exceeds the latter ratio, they do not blend with each other. Under the conditions shown in Table 1, the rate is unaffected by the concentration of CCl_4.

Polymerization of AN. As can be seen in Fig. 2, the polymerization of AN was carried out at 25°C in the system of Im and CCl_4. The cyanoethylation of

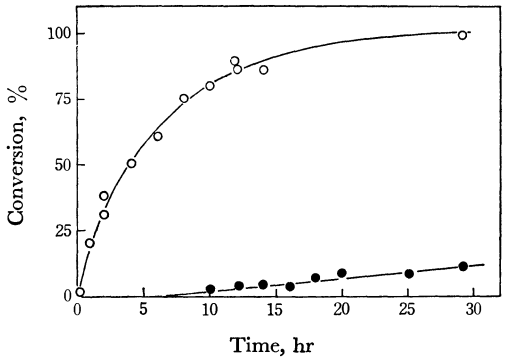

Fig. 2. Time-conversion curves in the system of Im-AN-CCl_4 (mol ratio, 1:6:2.5) at 25°C.
○: Conversion of cyanoethylation is based on the initial concentration of Im.
●: Conversion of polymerization is based on the initial concentration of AN.

Im had also occurred in the reaction system before the radical polymerization, and the rate constant of the cyanoethylation was found to be 3.7×10^{-4} l/mol·min, which was the same as that of the reaction without polymerization in the presence of air.

Possible Formation Mechanism. On the basis of the results mentioned above and other considerations,[1-3] a possible reaction mechanism for the polymerization and the cyanoethylation can be described as follows:

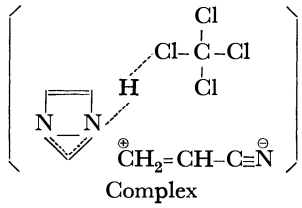

Complex

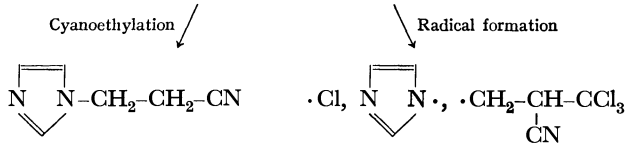

The above complex may be expected to be formed by the participation of Im, AN, and CCl_4 in the initial step of the reaction.

We wish to thank the Toho Rayon Co. Ltd., for the supply of imidazole.

BULLETIN OF THE CHEMICAL SOCIETY OF JAPAN, VOL. 44, 559—560 (1971)

Simple Relationship between Entropy Change upon Fusion or Sublimation at Melting Point, Electronic Polarizability and the Interatomic Distance for Alkali Halides

Hitoshi KANNO

Department of Chemistry, The University of Tokyo, Bunkyo-ku, Tokyo

(Received June 24, 1970)

It has been previously reported[1] that in alkali halides there is almost a linear relation between $\Delta S(m)/\alpha^{1/3}$ and r^+/r^- for a sequence LiX, NaX, KX, and RbX (X=F, Cl, Br, and I). Here $\Delta S(m)$, α, and r^+/r^- are the entropy change upon fusion, electronic polarizability of the salt, and the ionic radius ratio of cation to anion, respectively. Thus the entropy change upon melting can be given by

$$\Delta S(m) = \alpha^{1/3}\left(\frac{A}{r^-}+B\right) \qquad (1)$$

where A and B are the constants for the system.

The present author would like to point out that a similar relation also exists between the entropy change upon sublimation at melting point $\Delta S(s)$, α, and, r^+/r^-. As shown in Fig. 1, a good linear relationship between $\Delta S(s)/\alpha^{1/3}$ and r^+/r^- is obtained for the sequence LiX, NaX, KX, RbX, and CsX with exceptions of KF, RbF, and CsF.

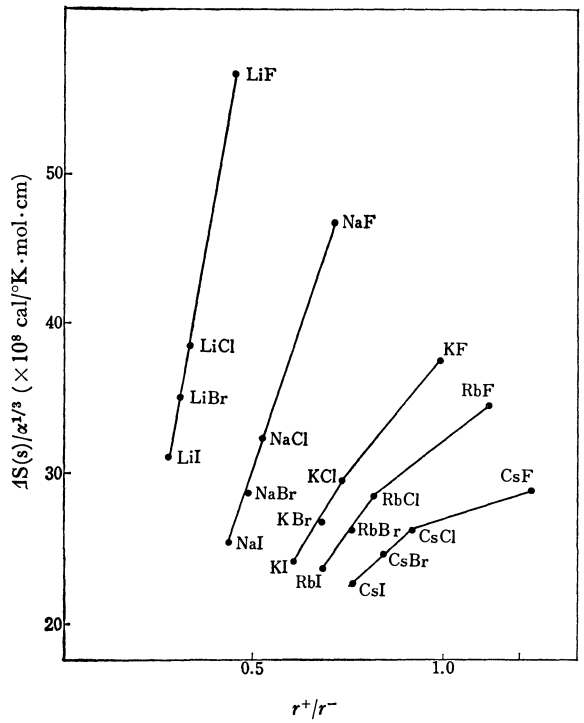

Fig. 1. Linear relationship of $\Delta S(s)/\alpha^{1/3}$ against r^+/r^- for alkali halides.
Sources of data: Heat of sublimation; S. H. Bauer and R. F. Porter, "Molten Salt Chemistry," ed. by M. Blander, Interscience Publishers, New York, N. Y. (1964), p. 627, Melting point: L. Brewer and E. Brackett, *Chem. Rev.*, **61**, 425 (1961), Electronic polarizability; J. R. Tessman, A. H. Kahn and W. Schockley, *Phys. Rev.*, **92**, 890 (1953), Ionic Radius: L. Pauling, "The Nature of the Chemical Bond," third ed., Cornell Univ. Press, Ithaca, N. Y., (1960), p. 527.

1) H. Kanno, *Nature*, **218**, 765 (1968).

Irregular variances of KF, RbF, and CsF are also observed in the case of fusion. A posssible explanation may be found in the data obtained by Pistorius,[2] in which he found that the change of volume upon fusion is considerably smaller for the fluorides of potassium and rubidium than for other halides of potassium and rubidium. He also stated that while chloride, bromide, and iodide of both potassium and rubidium have remarkably similar melting curves, the fluorides of potassium and rubidium behave differently from the other halides. It is of interest to note that the point of CsCl falls on the extrapolated line connecting the points of CsCl and CsI. In the case of fusion, the $\Delta S(m)/\alpha^{1/3}$ value of CsCl is much lower than that expected from the extrapolation of the straight line of CsBr and CsI (Fig. 2). This may be ascribed to the fact that solid CsCl

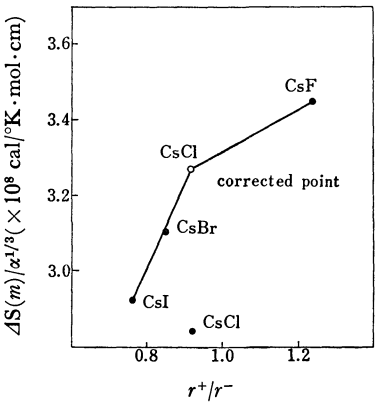

Fig. 2. Regular variation of the corrected $\Delta S(m)/\alpha^{1/3}$ of CsCl

shows phase transformation from the P_m3_m (CsCl) structure to F_m3_m (NaCl) structure at 446°C with an entropy change of 0.807 cal/deg mol.[3] As shown in Fig. 2, the point corrected by including the entropy of phase transformation into the entropy change upon melting nearly falls on the extrapolated line of CsBr and CsI. On the other hand, it is considered that in the case of sublimation a small change of entropy gives little effect upon regularity.

Another interesting aspect in Fig. 1 is the linear relation of $\Delta S(s)/\alpha^{1/3}$ with r^+/r^- for the halides having same anion except for lithium halides which behave

2) C. W. F. T. Pistorius, *J. Chem. Phys.*, **43**, 1557 (1965).

3) K. J. Rao, G. N. R. Rao, and C. N. R. Rao, *Trans. Faraday Soc.*, **63**, 1013 (1967).

differently. It has been experimentally shown that many thermodynamic properties of simple ionic salts, such as alkali halides and alkaline earth oxides, vary in regular fashion with change in interatomic distance.[4,5] Concurrently, much effort has been made to understand these thermodynamic properties on the basis of models.[6,7] Of the many suggested models, the most simple one is the reduced equation of state for ionic salt obtained by Reiss, Mayer, and Katz.[6] They noted that the potential function for the system can be characterized by a single distance scale factor, namely $r^+ + r^-$ $(=r)$. They postulated that the melting point of alkali halides is represented by

$$T_m = \frac{10^5}{3.19 \cdot r} \text{ °K} \tag{2}$$

In this connection, some improvements can be made by replacing r^+/r^- with $1/r$ in Eq. (1):

$$\Delta S = \alpha^{1/3}\left(\frac{A'}{r} + B'\right) \tag{3}$$

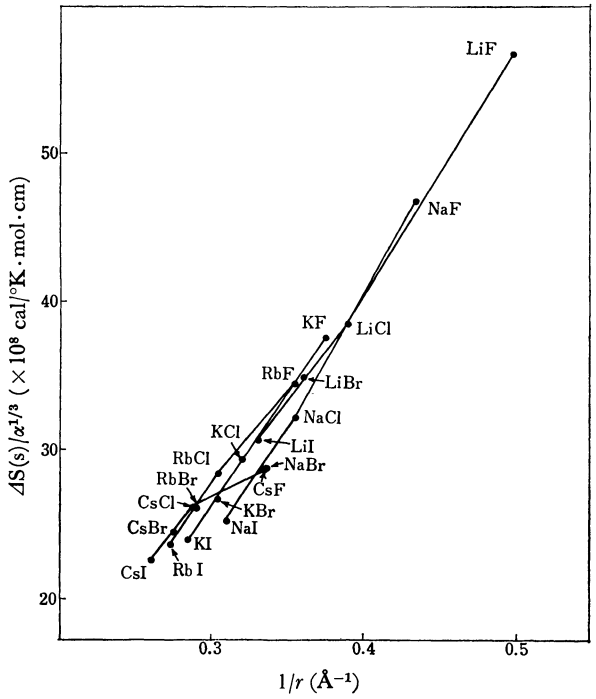

Fig. 3. Relationship of $\Delta S(s)/\alpha^{1/3}$ against $1/r$ for alkali halides. Interatomic distance; L. Pauling, "The Natune of the Chemical Bond", third ed., Cornell Univ. Press, Ithaca, N. Y., (1960), p. 527.

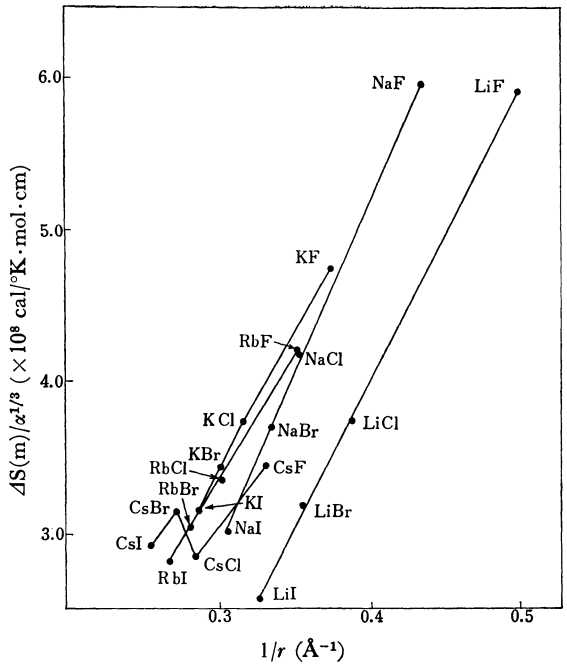

Fig. 4. Relationship of $\Delta S(m)/\alpha^{1/3}$ against $1/r$ for alkali halides. Heat of fusion; A. S. Dworkin and M. A. Bredig, *J. Phys. Chem.*, **64**, 269 (1960).

Substituting Eq. (2) into Eq. (3), we have

$$\Delta S = \alpha^{1/3}(A'' T_m + B'') \tag{4}$$

where A', B', A'', and B'' are the constants for the system.

The relationship between $\Delta S(s)/\alpha^{1/3}$ or $\Delta S(m)/\alpha^{1/3}$ and $1/r$ is shown in Figs. 3 and 4.

We see that all points of alkali halides are approximately represented by a linear function of the reciprocal of the interatomic distance. A significant feature of Fig. 3 is that nearly the same value of $\Delta S(s)/\alpha^{1/3}$ is given for the salts having the same value of $1/r$. Thus it is concluded that the interatomic distance is the better correlating parameter than the ionic radius ratio.

Let $\Delta S(v)$ represent the entropy change of vaporization for alkali halides at a specified temperature and we obtain the following relation at the melting point

$$\Delta S(s) = \Delta S(v) + \Delta S(m) \tag{5}$$

Thus it is expected that the linear relation also holds between $\Delta S(v)/\alpha^{1/3}$ and $1/r$.

In conclusion, we might say that the entropy change upon phase transformation is well characterized by the interatomic distance and the electronic polarizability of the salt.

4) O. J. Kleppa and L. S. Hersh, *J. Chem. Phys.*, **34**, 351 (1961).
5) Y. P. Varshni and R. C. Shukla, *ibid.*, **35**, 582 (1961).
6) H. Reiss, S. W. Mayer, and J. L. Katz, *ibid.*, **35**, 820 (1961).
7) E. Blomgren, *Ann. N. Y. Acad. Sci.*, **79**, 781 (1960).

BULLETIN OF THE CHEMICAL SOCIETY OF JAPAN, VOL. 44. 561—562 (1970)

Conductometric Studies of the Reaction of Pyridine and 3-Picoline with Iodine in Methanol

J. P. SAXENA, B. K. JOSHI, and G. D. MENGHANI
Chemical Laboratories, University of Jodhpur, Jodhpur, India

(Received July 17, 1970)

Saxena and Gelra[1] investigated the reaction of some heterocyclic tertiary bases (pyridine, 3-picoline, quinoline, *etc.*) with acetone in methanolic medium; an extension of King's keto-alkylation reaction[2] to aliphatic ketones. They reported the formation of *N*-acetonylpyridinium and *N*-acetonyl-3-picolinium iodides in good yields. An immediate formation of the di-iodide[3] of the heterocyclic tertiary bases was first observed on mixing the base with iodine and acetone in methanol. The crystals of the di-iodide gradually disappeared on keeping for 2—3 days and crystals of the quaternary β-ketoalkyl iodide appeared. This prompted us to investigate the mechanism of formation of the di-iodides of the heterocyclic tertiary bases (pyridine and 3-picoline) and their subsequent reaction with methyl ketones resulting in the formation of quaternary β-ketoalkyl iodides. In the present investigation only the first part of the reaction, *i. e.* the reaction of pyridine and 3-picoline with iodine in methanol, has been studied through conductivity measurements. The latter part of the reaction with the methyl ketones will be reported elsewhere.

Experimental

Reagents Used. Analytical grade reagents were used. They were purified before use by standard methods. Every care was taken to use reagents in the reaction in the complete absence of moisture.

Procedure. A stock solution of iodine in absolute methanol was prepared. No change in conductivity values of this solution was observed the solution was preserved in a flask tightly stopped with ground glass. Fresh slutions of pyridine or 3-picoline in methanol containing 5—15% of the desired tertiary base were made in different flasks. This particular range was selected because in concentration of the base below 5%, the reaction was found to be very slow and the conductivity keeps on changing for more than 24 hr, whereas in concentrated solutions (base above 15%), the reaction becomes extremely fast and the conductivity changes are negligible after 15 min. Selected volumes of the solutions of iodine and the desired base were mixed in a tightly stoppered conductance cell, with the platinum electrodes immeresed in the reaction mixture. The cell was thermostated and the conductance values were recorded at temperatures 25, 30, 35, and 45°C. As the time of measurement was nearly 2 hr, no appreciable effect of the platinum electrodes on the resistance values was observed. Philips conductivity bridge was used for conductivity measurements.

The results are summarized in Tables 1—4.

Table 1. Effect of variation in concentration of pyridine on rate of reaction

$[I_2]=2.3425\times10^{-4}$M Temperature=303°K

No.	[Pyridine] M	$k'\times10^9$ sec^{-1}	Sp. rate constant $k'/[Py]\times10^9$ $l\cdot mol^{-1}\cdot sec^{-1}$
1	1.24	4.866	4.248
2	1.86	7.884	4.239
3	2.48	10.530	4.246

Table 2. Effect of variation in concentration of 3-picoline on rate of reaction

$[I_2]=2.5\times10^{-3}$M Temperature=303°K

No.	[3-Picoline] M	$k'\times10^9$ sec^{-1}	Sp. rate constant $k'/[3\text{-Pic}]\times10^9$ $l\cdot mol^{-1}\cdot sec^{-1}$
1	0.537	3.282	6.112
2	0.860	5.244	6.098
3	1.290	7.881	6.109

Table 3. Effect of variation in concentration of iodine on rate of reaction

[3-Picoline]=1.29M Temperature=303°K

No.	[Iodine], M	$k'\times10^9$, sec^{-1}
1	2.5×10^{-3}	7.881
2	3.5×10^{-3}	7.858
3	4.5×10^{-3}	7.846

Table 4. Effect of variation in temperature on rate of the reaction

$[I_2]$ in case of 3-picoline$=2.5\times10^{-3}$M
$[I_2]$ in case of pyridine$=2.3425\times10^{-4}$M

No.	Temperature °K	[3-Picoline]=1.29M $k'\times10^9$, sec^{-1}	[Pyridine]=1.24M $k'\times10^9$, sec^{-1}
1	298	4.995	2.966
2	303	7.881	4.866
3	308	10.353	7.416
4	318	15.777	11.544

Discussion

Neglecting the change of equivalent conductance with ionic strength, the reciprocal of resistance (R) was assumed to be proportional to the ionic concentration,[4] and a plot of $1/R$ against time gave a straight line. This linear relationship showed a zero-order of reaction with respect to iodine. The change in con-

1) J. P. Saxena and M. R. Gelra, *Aust. J. Chem.*, **20**, 1771 (1967).
2) L. C. King, *J. Amer. Chem. Soc.*, **66**, 894 (1944).
3) J. P. Saxena and M. R. Gelra, *Ind. J. Chem.*, **6**, 562 (1968).
4) R. G. Pearson, *J. Amer. Chem. Soc.*, **69**, 3100 (1947).

centration of the base resulted in a corresponding change in the slope, thereby showing that the reaction is first order with respect to the base.

Saxena and Gelra[5] studied the reaction of pyridine with iodine in methanol and proposed the following mechanism:

$$MeOH \cdot I_2 + Py \overset{K_1}{\rightleftharpoons} Py \cdot I_2 + MeOH \quad \text{(fast)} \qquad (1)$$

$$Py \cdot I_2 \overset{K_2}{\rightleftharpoons} [Py \cdot I]^+ + I^- \quad \text{(slow)} \qquad (2)$$

We have studied the reactions of both pyridine and 3-picoline with iodine in methanol at different temperatures and have found that the general behavior of both the reactions is identical, and in the case of 3-picoline also the dissociation of 3-Pic$\cdot I_2$ is the rate determining step, as suggested in the case of pyridine.

$$3\text{-Pic} \cdot I_2 \overset{K_3}{\rightleftharpoons} [3\text{-Pic} \cdot I]^+ + I^- \quad \text{(slow)} \qquad (3)$$

The thermodynamic data also confirm the identity of the behavior of the di-iodides of the two bases. From the specific rate constants obtained in the case of pyridine-iodine system, the activation energy was calculated to be 14.97 kcal/mol and the entropy change was evaluated as −8.69 e.u. In the case of 3-picoline-iodine system the activation energy was found to be 11.67 kcal/mol and the entropy change was evaluated as −10.4 e.u. This negative value of entropy change lends additional support to the proposed rate determining step, because as expected the dissociation would lower the entropy change appreciably in both cases. In the case of 3-picoline the hyperconjugative effect of the 3-CH_3 group is operative, due to which the dissociation of I^- ions from 3-Pic$\cdot I_2$ takes place with greater ease and gives rise to the decrease in the entropy change (ΔS^* −10.4) as compared with pyridine (ΔS^* −8.69). With the existence of $[Py \cdot I]^+$ as $[Py_2 \cdot I]^+$ apparently through solvation,[6] and of I^- ions as I_3^- ions, a negative entropy change is anticipated. This also holds true in the case of 3-picoline, and subscribes to the mechanistic step (3).

We are thankful to Professor R. C. Kapoor for providing facilities for work.

5) J. P. Saxena and M. R. Gelra, *Proceedings of the Symposium on Electrode Processes*, Jodhpur Univ., Nov. 1966, p. 157.

6) I. Haque and J. L. Wood, *Spectrochim. Acta, Part A*, **23**(4), 959 (1967).

BULLETIN OF THE CHEMICAL SOCIETY OF JAPAN, VOL. 44, 563—564 (1971)

Diels-Alder Reactions of Benzoquinone. I. Reactions of Methoxybenzoquinone with Styrene and *o*-Methylstyrene[1]

Yoshinobu INOUYE and Hiroshi KAKISAWA
Department of Chemistry, Tokyo Kyoiku University, Otsuka, Tokyo

(Received July 9, 1970)

The Diels-Alder reactions of substituted benzoquinones with vinyl aromatics were mainly examined by Lora-Tamayo.[2] The characteristic features of substituted benzoquinones when compared with those of aliphatic dienes[3,4] are as follows: i) the addition occurs only at the non-substituted ethylene linkage of benzoquinone, and no addition occurs if subtituents are present on both ethylene linkages such as in *p*-xyloquinone and 4-methoxytoluquinone[5]; ii) the reaction generally accompanies tetradehydrogenation[2] to give a phenanthrenequinone derivative. The orientation of the quinone is not clarified except the reaction between styrene (I) and methoxybenzoquinone (III) to afford 2-methoxyphenanthrene-1,4-quinone (IVb) exclusive ly.[2]

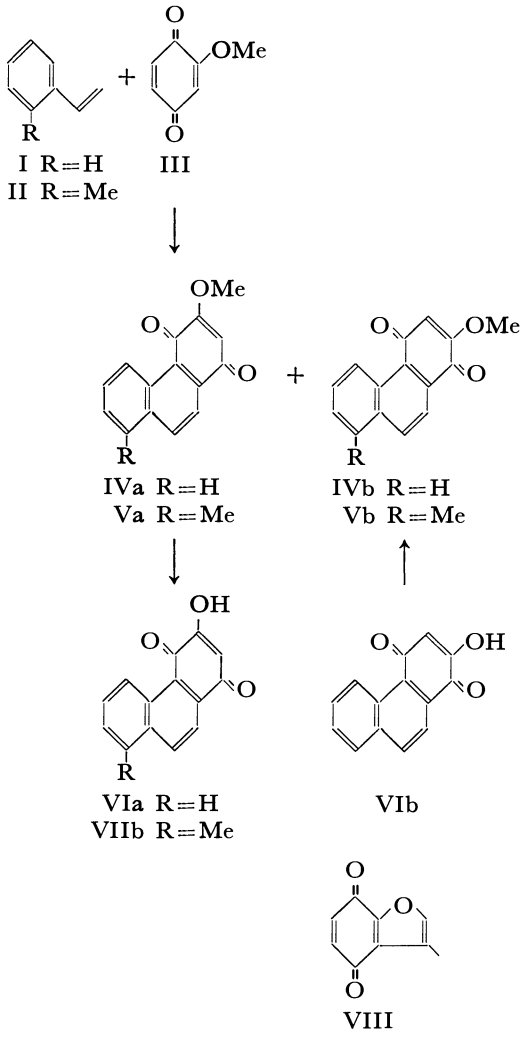

During the course of our studies on the Diels-Alder reaction of 3-methylbenzofuran-4,7-quinone (VIII),[4] we found that the orientation (namely of the oxygen function) of VIII to the aliphatic diene was identical with that of methoxybenzoquinone (III), and that the reaction of VIII with *o*-methylstyrene (II) gave 3,7-dimethylphenanthro[3,2-*b*]furan-4,11-quinone as a main product.

These results throw doubt upon Lora-Tamayo's experiments.[2] Firstly we examined the Diels-Alder reaction between *o*-methylstyrene (II) and methoxybenzoquinone (III) to clarify the difference between III and VIII in the behavior to vinyl aromatics.

The mixture of II and III was heated at 100—110°C for 10 hr and the phenanthrenequinone parts were isolated through silicic acid column in 42% yield. Recrystallization from benzene afforded a pure quinone Va (or Vb), $C_{16}H_{12}O_3$, mp 243—245°C (dec), although the melting point was slightly lower than that of the reported, mp 253°C (dec).[2] The quinone Va (or Vb) was hydrolyzed with ethanolic potassium hydroxide to the corresponding hydroxyquinone VIIa (or VIIb), $C_{15}H_{10}O_3$, mp 219—224°C (dec), which was identified as 3-hydroxy-8-methylphenanthrene-1,4-quinone (VIIa) by mixed melting point and by comparison of IR spectra with the authentic sample.[6]

As Lora-Tamayo has not clarified the position of the methoxyl group, the difference in melting points seemed to be due to the positional isomer. However, the isomer VIIb could never be characterized in the present work.

Determination of the methoxyl position in the reaction of *o*-methylstyrene (II) prompted us to reinvestigate the reaction of styrene (I) itself. The reaction between I and III was carried out under the same condition as before. The phenanthrenequinone fractions were obtained in 26% yield, from which pure 3-methoxyphenanthrene-1,4-quinone (IVa),[7] mp 168—169°C was isolated by recrystallization from methanol. Melting point of IVa was similar to but IR spectrum was quite different from that of the authentic isomer IVb[8] (see

1) Presented at the 23rd Annual Meeting of the Chemical Society of Japan, Tokyo, April, 1970.

2) M. Lora-Tamayo, *Tetrahedron*, **4**, 17 (1958) and references cited therein.

3) M. F. Ansell, B. W. Nash, and D. A. Wilson, *J. Chem. Soc.*, **1963**, 3012.

4) a) Y. Inouye and H. Kakisawa, This Bulletin, **42**, 3318 (1969). b) H. Kakisawa and Y. Inouye, *Tetrahedron Lett.*, **1969**, 1929.

5) C. de Corral, *Rev. real acad. cienc. exact., fis. y nat. Madrid*, **51**, 103 (1597); *Chem. Abstr.*, **52**, 7257b (1958).

6) A. C. Baillie and R. H. Thomson, *J. Chem. Soc., C*, **1968** 48.

7) L. F. Fieser, *J. Amer. Chem. Soc.*, **51**, 940 (1929).

8) L. F. Fieser, *ibid.*, **51**, 1896 (1929).

experimental). By careful chromatographic separation, IVb was isolated in low yield. The ratio of IVa to IVb was 12.

Lora-Tamayo's confidence to 2-methoxyl structure has been based on comparison of the physical properties and the products formed on alkaline hydrolysis with those of the authentic samples,[7,8] although details were not reported. Alkaline hydrolysis of IVa gave 3-hydroxyphenanthrene-1,4-quinone (VIa), $C_{14}H_8O_3$, mp 194—196°C (dec), to which Fieser[7] reported the melting point to be 230°C (dec).

In conclusion, the position of methoxyl group in the main product in the Diels-Alder reaction of methoxybenzoquinone and vinyl aromatics is not at C_2, but at C_3 in contrast to Lora-Tamayo's assignment.[2]

Finally, the influence of the molar ratio of methoxybenzoquinone (III) to styrene (I) on the yield of adducts was investigated and the results are summarized in Table 1. Apparently, the yield depends on the molar ratio when it is below 3, but does not when it is above 3. This might correspond to the fact that two moles of the quinone act as the acceptor of hydrogen from the adduct.

Table 1. Reactions between sytrene (I) and methoxybenzoquinone (III)

Run	Styrene (I) mg	Quinone (III) mg	Molar ratio of III/I	Solvent ml	Reaction time hr	Yield[a] mg	Yield[a] %
1	65	85	1	—	10	20	13.4
2	58	154	2	—	10	34	26
3	30	120	3	—	10	21	31
4	—	50	0	0.15 benzene	40	[b]	
5	65	87	1	0.25	40	18	12.1
6	58	154	2	0.2	40	35	26
7	23	92	3	0.2	40	18	34
8	27	180	5	0.2	40	20	32

a) mixtures of IVa and IVb
b) 100% recovery of the quinone (III)

Experimental

Diels-Alder Reaction between o-*Methylstyrene (II) and Methoxybenzoquinone (III).* a) A mixture of 53 mg of *o*-methylstyrene (II) and 124 mg (two equivalents to the diene) of methoxybenzoquinone (III) in a sealed tube was heated at 100—110°C for 10 hr.[2] The resulting dark red oil was chromatographed on silicic acid (10 g) and phenanthrenequinone fractions (47 mg, 42%) were collected from chloroform eluates. Repeated recrystallization from benzene afforded 3-methoxy-8-methylphenanthrene-1,4-quinone (Va), mp 243—245°C(dec).[9] IR(KBr): 1668, 1643, 1620 cm^{-1}. UV(EtOH): 227(logε=4.62), 287.5(4.36), 320 (3.70), 376 mμ(3.54).

Found: C, 76.06; H, 4.93%. Calcd for $C_{16}H_{12}O_3$; C, 76.18; H, 4.80%.

b) A suspension of 55 mg of II and 129 mg of III in 0.2 m*l* of benzene was heated at 100—110°C in a sealed tube for 40 hr. Working up as in a) afforded 50 mg (42%) of phenanthrenequinones.

Hydrolysis of 3-Methoxy-8-methylphenanthrene-1,4-quinone (Va). To a suspension of 30 mg of Va in 3 m*l* of ethanol was added *ca.* 200 mg of powdered potassium hydroxide. After standing overnight, water was added and the solution was acidified with 6 N hydrochloric acid. Precipitates were collected and purified through silicic acid column. Recrystallization from benzene gave 3-hydroxy-8-methylphenanthrene-1,4-quinone (VIIa), mp 219—224°C (dec). IR (KBr): 3320, 1653, 1632, 1587 cm^{-1}. UV (EtOH): 225, 290, 331, 380 mμ. Mass: *m/e* 238 (M^+), 210 (M^+-CO). Found: C, 75.25; H, 4.12%. Calcd for $C_{15}H_{10}O_3$: C, 75.62; H, 4.23%.

The IR spectrum of VIIa was identical with that of Thomson's[6] and mixed melting point was 217—220°C (dec) although the original Thomson's sample had somewhat different melting point (~213°C (dec)).

2-Hydroxyphenanthrene-1,4-quinone (VIb). Following the known procedure,[6,10] 2-hydroxyphenanthrene[11] was converted into 2-hydroxyphenanthrene-1,4-quinone *via* 1,2-phenanthrenequinone. Pure VIb, mp 184—185°C (dec) (from benzene). (Lit,[8] mp 190°C (dec)). IR (KBr): 3370, 1660sh, 1647, 1640sh cm^{-1}.

2-Methoxyphenanthrene-1,4-quinone (IVb). To a solution of 25 mg of 2-hydroxyphenanthrene-1,4-quinone (VIb) in 3 m*l* of ether was added 10 m*l* of ethereal diazomethane (prepared from 300 mg of nitrosomethylurea) and the mixture was left for 30 min. The ether solution was washed with dilute alkali, dried through anhydrous sodium sulfate layer and was evaporated to give solid (25 mg). Recrystallization from methanol afforded pure 2-methoxyphenanthrene-1,4-quinone (IVb), mp 168—169°C. (Lit,[8] mp 172.5°C). IR (KBr): 1675, 1640, 1620 cm^{-1}. UV (EtOH): 223 (4.59), 282 (4.38), 374 mμ (3.31).

Found: C, 75.28; H, 4.17%. Calcd for $C_{15}H_{10}O_3$: C, 75.62; H, 4.23%.

Diels-Alder Reaction between Styrene (I) and Methoxybenzoquinone (III). a) The reaction was carried out with or without benzene as in the case of *o*-methylstyrene and the phenanthrenequinone was obtained in 26% yield in both reactions. Recrystallization from methanol gave 3-methoxyphenanthrene-1,4-quinone (IVa), mp 168—169°C. (Lit,[7] mp 170°C). IR (KBr): 1670, 1648, 1623 cm^{-1}. UV (EtOH): 226 (4.58), 282.5 (4.33), 316 (3.82), 371 mμ (3.51). Mass: *m/e* 238 (M^+), 223.

Found: C, 75.14;H, 4.12%. Calcd for $C_{15}H_{10}O_3$: C, 75.62; H, 4.23%.

The crude mixture (69 mg) was recrystallized from methanol to give 48 mg of IVa and the residue was chromatographed on silicic acid (10 g) to afford further 10 mg of IVa and 5 mg IVb. The latter, purified by recrystallization from methanol, melted at 169°C and showed identical IR spectrum with that of the authentic sample.

b) A mixture of styrene and methoxybenzoquinone in a different molar ratio was heated at 100—110°C in a sealed tube. The results are summarized in Table 1.

Hydrolysis of 3-Methoxyphenanthrene-1,4-quinone (IVa). As in the case of Va, IVa was hydrolyzed in ethanolic potassium hydroxide to afford 3-hydroxyphenanthrene-1,4-quinone (VIa) in 93% yield. Recrystallization from benzene gave the pure sample, mp 194—196°C (dec). (Lit,[7] mp 230°C (dec)). IR(KBr): 3200, 1650, 1627 cm^{-1}.

Found: C, 74.90; H, 3.60%. Calcd for $C_{14}H_8O_3$: C, 74.99; H, 3.60%.

We are deeply indebted to Professor Thomson for a gift of 3-hydroxy-8-methylphenanthrene-1,4-quinone.

9) Lora-Tamayo[2] reported the melting point of the adduct to be 253°C (dec), though the position of methoxyl group has not been clarified.

10) L.F. Fieser, "Organic Syntheses," Coll. Vol. II, p. 35, 430 (1943).

11) This substance was derived from 7-methoxy-4-oxo-1,2,3,4-tetrahydrophenanthrene[12] by successive reactions: sodium borohydride reduction, hydrogenolysis, DDQ oxidation and hydrolysis.

12) M. Ghosal, *J. Org. Chem.*, **25**, 1856 (1960).

BULLETIN OF THE CHEMICAL SOCIETY OF JAPAN, VOL. 44, 565—566 (1971)

The Dipole Moment of Halogenobenzotropones

Takashi SHIMOZAWA, Shigekazu KUMAKURA, Masamatsu HOSHINO, and Seiji EBINE

Department of Chemistry, Saitama University, Shimo-Okubo, Urawa

(Received July 17, 1970)

The dipole moments of three bromobenzotropones and a chlorobenzotropone were measured in benzene solutions, and the positions of halogen atoms on the tropone ring were determined by comparing the observed and calculated values of their dipole moments. The bond moments of C=O and C–X (X=halogen) bonds were examined through an analysis of their dipole moments. The dipole moment of 4,5-benzotropone was also measured, and the derived bond moment of the corbonyl group suggested that the carbonyl group is affected by the conjugation of the benzene ring through the double bonds of the tropone ring.

Experimental and Results

a) Samples. The synthesis of the samples has been described elsewhere.[1] The samples were used for the observations without any further purification.

b) Dipole Moment Measurements. The dipole moment (μ) was observed by the solution method using benzene as a solvent. The dielectric constant (ε) was measured by the heterodyne beat method, and the density (d) was obtained using a pycnometer. The details of the measurements of the dipole moments were the same as in a previous report of one of the authors (T.S).[2]

The observed values of the total polarization (P), the summation of the electronic and the atomic polarization and the dipole moments are listed in Table 1. The electronic polarizations (P_E) are computed from the table of atomic refraction; and the atomic polarization (P_A) was taken as 5% of the electronic polarization. Each value of the observed dipole moment includes an inaccuracy of $\pm$ 0.01 D.

TABLE 1. OBSERVED VALUES OF DIPOLE MOMENTS

Compound	P	P_E+P_A	μ(D)
5-Bromobenzotropone (I)	215.52cc	56.70cc	2.79
5-Chlorobenzotropone (II)	200.91	53.66	2.68
4,7-Dibromobenzotropone (III)	263.04	64.85	3.08
5,7-Dibromobenzotropone (IV)	326.67	64.85	3.53
4,5-Benzotropone (V)	535.44	48.54	4.88

Calculation of Dipole Moments

a) Bond Angles. The bond angles of these compounds were assumed to be such as would result if the tropone ring and the benzene ring are connected with each other holding their skeletal angles. Figure 1 shows the bond angles of the benzotropone ring.

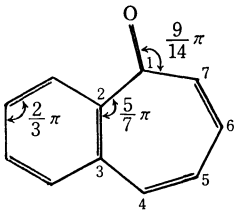

Fig. 1. The bond angle of benzotropone.

b) Bond Moments. The bond moments of C=O and C–X (C–Cl and C–Br), were assumed to be 4.0 and 1.4 D, respectively, which are the values of halogenotropones.[3,4]

c) Monosubstituted Compounds (Compounds I and II). The calculated values of dipole moments for monohalogenobenzotropones are listed in Table 2, where the bond moments of C=O and C–X assumed in (b) are used.

TABLE 2. CALCULATED VALUES OF DIPOLE MOMENTS FOR MONOSUBSTITUTED BENZOTROPONES

Position of halogen atom	4	5	6	7
μ calcd (D)	2.80	2.80	3.93	4.99

d) Disubstituted Compounds (Compounds III and IV). The disubstituted compounds have six possible structures, as listed in Table 3, in which the corresponding values of dipole moments calculated using the bond moments assumed in (b) are shown.

TABLE 3. CALCULATED VALUES OF DIPOLE MOMENTS FOR DISUBSTITUTED BENZOTROPONES

Position of halogen atoms	(4,5)	(4,6)	(4,7)	(5,6)	(5,7)	(6,7)
μ calcd (D)	1.48	2.54	3.64	3.13	3.99	5.18

Discussion

1) Monosubstituted Benzotropones. Compounds I and II (Table 1) have dipole moments of 2.7—2.8 D; therefore, the position of the halogen atom in each of these compounds could be chosen from either the 4 or 5 position by a comparison of the observed (Table 1) and calculated (Table 2) values of their dipole moments. However, the position of the halogen substituent in compound I has been determined to be 5, by NMR study of this compound and its Diels-Alder adduct with maleic anhydride.[5,6] Thus the possibility of substitution

1) S. Ebine and M. Hoshino, This Bulletin, **41**, 2942 (1968).
2) T. Shimozawa, *ibid.*, **38**, 1046 (1965).
3) Y. Kurita and M. Kubo, *ibid.*, **27**, 364 (1954).
4) D. J. Bertelli and T. G. Andrews, Jr., *J. Amer. Chem. Soc.*, **91**, 5280 (1969).
5) S. Ebine, to be published.
6) W. E. Parham, D. A. Bolon, and E. E. Sweizer, *J. Amer. Chem. Soc.*, **83**, 603 (1961).

at the 4-position is eliminated.

For compound II, two kinds of substitution reactions can be considered, namely, 5 or 7.[6] The dipole moment measurements excluded the possibility of 7-bromobenzotropone for this compound II. Thus, compound II is determined to be 5-chlorobenzotropone by the dipole moment measurement.

2) Disubstituted Compounds (III and IV). The calculated values of dipole moment in Table 3 are thought to be accurate within the range of ± 0.7 D, so the comparison of the observed and the calculated values results in three possibilities for compound III: (4,6), (4,7), or (5,6). However, it is not possible that compound III has a halogen atom at the 6-position, considering the chemistry of III.[1] Therefore, compound III is determined to be 4,7-dibromobenzotropone which has no halogen atom at the 6-position.

The possible structures of compound IV are (4,7), (5,6), or (5,7), for which the calculated values of dipole moments are in agreement with the observed within ± 0.7 D. It has also been reported that in the case of compound IV, the halogen atom could not be at the 6-position.[1] Therefore, there remain two possibilities, (4,7) or (5,7) for compound IV through a consideration of the dipole moment.

Fortunately, compound III is uniquely determined as the 4,7-disubstituted compound. Since compound III is different from compound IV, the latter should be 5,7-dibromobenzotropone. Although the calculated values for monosubstituted compounds are in agreement with those observed, there are substantial differences between the calculated and observed values of the disubstituted series. These discrepancies can be explained using the so-called ortho effect. Both of these compounds have a halogen atom at the 7-position which is an ortho position to the carbonyl group, and because of negative groups adjacent to each other, the values of the bond moments of both C=O and C–X bonds should decrease.

By bringing the calculated and the observed values of compounds III and IV into agreement through repeated calculations, the bond moments for C=O and C_7–X were finally obtained as 3.6 and 1.2 D, respectively. The decreases in the C=O bond moment of 0.4 D and that in the C–X of 0.2 D are thought to be reasonable, on considering the ortho effect of compounds such as *o*-dichlorobenzene, where 10—20% decreases in C–Cl bond moment from that of chlorobenzene are known.[7]

3) 4,5-Benzotropone (V). The observed value of compound V, 4.88 D, is larger than that of tropone which was used for the estimation of the C=O bond moment (4.0 D) of the benzotropone series. The difference of 0.8 D in those bond moments might be the induction moment resulting from the conjugation between the carbonyl bond and the benzene ring (Fig. 2), provided that the intrinsic bond moment of the C=O group has the same magnitude in both 4,5-benzotropone and 2,3-benzotopone.

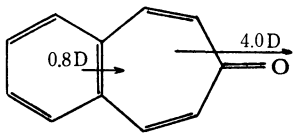

Fig. 2. Dipole moment of 4,5-benzotropone μ(C=O) and μ(induction)

Summary

The dipole moments of 5-bromo-, 5-chloro-, 4,7-dibromo-, and 5,7-dibromobenzotropones and 4,5-benzotropone were reported; and the positions of the substituents were determined and the bond moments of the carbon-halogen bonds and the carbonyl bonds were estimated.

The authors wish to express their gratutide for a Scientific Research Grant provided by the Ministry of Education.

7) A. L. McClellan, "Table of Experimental Dipole Moments," W. H. Freeman and Company, San Francisco, Calif. (1963).

BULLETIN OF THE CHEMICAL SOCIETY OF JAPAN, VOL. 44, 567 (1971)

Rearrangements in the Palladium-Catalyzed Dehydrogenation of Cyclohexylphenols to Phenylphenols

Hisashi MATSUMURA, Kimiaki IMAFUKU, Izumi TAKANO,[1] and Senjiro MATSUURA
Department of Chemistry, Faculty of Science, Kumamoto University, Kurokami-machi, Kumamoto
(Received August 10, 1970)

Although allyl phenyl ether is well known to rearrange to *o*-allylphenol upon heating to a high temperature,[2] diphenyl ether does not rearrange to phenylphenols. Photochemically, however, diphenyl ether rearranges not only to *o*- and *p*-phenylphenols[3,4] but also to dibenzofuran.[5]

In the dehydrogeation of cyclohexylphenols to phenylphenols, we found the formation of diphenyl ether as a rearrangement product and dibenzofuran as a cyclization product.

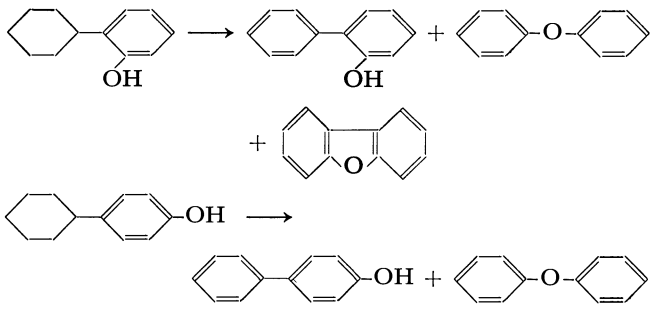

Experimental

Materials. *Cyclohexylphenols*: *o*- and *p*-Cyclohexylphenols were prepared by Friedel-Crafts type condensation of phenol with cyclohexyl chloride in the presence of ferric chloride hexahydrate,[6] and were purified by fractional recrystallization. The purity of each cyclohexylphenol was checked by gas-chromatography.

Palladium Catalyst: Five per cent palladium-charcoal catalyst, manufactured by Kawaken Fine Chemical Co. Ltd., Tokyo, was used without purification.

Dehydrogenation of Cyclohexylphenols. A mixture of 1 g of *o*- or *p*-cyclohexylphenol and 200 mg of palladium catalyst was heated at 300°C (bath temperature) for 4 hr under nitrogen atmosphere. The reaction mixture was dissolved in benzene, and the catalyst was filtered off. The filtrate was analyzed gas-chromatographically for the determination of reaction products.

Identification and Determination of the Products. Identification and quantitative determination of each product were performed gas-chromatographically on a Shimadzu Model GC-1C (column packing: XE-60) with authentic materials.

1) Present address: Shokubai Kasei Kogyo Co. Ltd., Wakamatsu, Kitakyushu.

2) A. A. Shamshurin and R. A. Ibadulin, *Zh. Obshch. Khim.*, **19**, 1669 (1949); *Chem. Abstr.*, **44**, 1443[f] (1950).

3) M. S. Kharasch, *Science*, **116**, 309 (1952).

4) D. P. Kelley, J. T. Pinkey, and R. D. Rigby, *Tetrahedron Lett.*, **1966**, 5953.

5) H. Stegemeyer, *Naturwissenschaften*, **53**, 582 (1966).

6) A. R. Abdurasuleva and K. N. Akhemov, *Uzb. Khim. Zh.*, **1964** (5), 31.

Results and Discussion

Gas-chromatographical analysis of the dehydrogenation products gave results given in Table 1.

TABLE 1. DEHYDROGENATION PRODUCTS FROM CYCLOHEXYLPHENOLS (in %)

Starting material	Phenylphenol	Diphenyl ether	Dibenzofuran
o-Cyclohexylphenol	72	23	3
p-Cyclohexylphenol	79	17	—

Although the main products are *o*- and *p*-phenylphenols, respectively, a considerable amount of diphenyl ether is found in both cases. Formation of diphenyl ether on dehydrogenation of cyclohexylphenols involves a novel rearrangement, containing C–C bond fission between the two benzene nuclei and the new C–O bond formation. It is not clear, however, whether the formation of diphenyl ether results by intramolecular or intermolecular rearrangement.

Cyclization to dibenzofuran also occurred in the dehydrogenation of *o*-cyclohexylphenol. Under the same condition, *o*-phenylphenol also cyclizes to give dibenzofuran (5%) and diphenyl ether (trace), but *p*-phenylphenol and diphenyl ether do not give dibenzofuran. Changes in the yields of dibenzofuran from *o*-cyclohexylphenol and *o*-phenylphenol with the reaction time were very similar to those shown in Fig. 1.

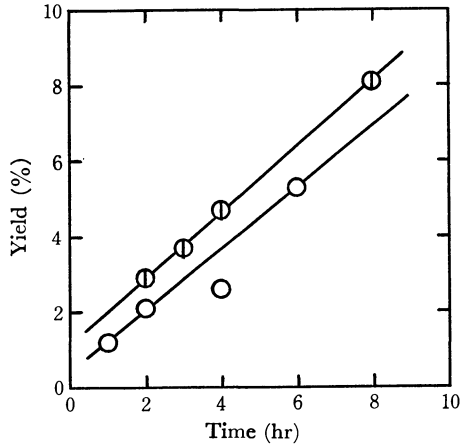

Fig. 1. Dibenzofuran from *o*-cyclohexylphenol(○) and *o*-phenylphenol (ⓘ).

From these results, it is concluded that diphenyl ether is directly formed in the dehydrogenation of the *o*- and *p*-cyclohexylphenols, and dibenzofuran is produced *via* *o*-phenylphenol.

BULLETIN OF THE CHEMICAL SOCIETY OF JAPAN, VOL. 44, 568—569 (1971)

Abstraction of Methyl Hydrogen of Organosilicon Compounds by *t*-Butoxy Radicals

Hideki SAKURAI,[1] Akira HOSOMI, and Makoto KUMADA

Department of Synthetic Chemistry, Faculty of Engineering, Kyoto University, Sakyo-ku, Kyoto

(Received August 11, 1970)

It has been known that in photochlorination of organosilicon compounds with chlorine in the liquid phase a large amount of dichloromethyl derivatives is produced as a by-product, along with the chloromethyl compounds.[2] On the other hand, although 1,2-phenyl migration readily takes place in the system of $Ph_3CCH_2\cdot$,[3] the similar migration does not occur for $Ph_3SiCH_2\cdot$,[4] instead triphenylmethylsilane being formed. Such differences in the chemical behavior of silicon- and carbon-substituted radicals may be attributed to the former being larger in size than the latter, the electronegativity being lower for silicon as compared with carbon, and the availability of empty *d*-orbitals in silicon, which are absent in carbon.

In this connection, it seemed interesting to investigate the relative reactivity of organosilicon compounds towards free radicals in solution. Studies of the radical chemistry of organosilicon compounds are not ample and most of the reported investigations are related to synthesis.[5] Recently, a kinetic information in the gas phase has been reported in this field.[6] Nagai *et al.* also reported the relative reactivities of some alkylsilanes in the liquid phase photochlorination.[7] The reactions described here were concerned with reactivities of *t*-butoxy radicals in hydrogen abstraction of methylsilicon compounds.

TABLE 1. RELATIVE REACTIVITIES OF ONE METHYL HYDROGEN OF ORGANOSILICON COMPOUNDS TOWARDS *t*-BUTOXY RADICALS AT 45.0°C IN 1,1,2-TRICHLOROTRIFLUOROETHANE

Substrate	k_a/k_d	Substrate	k_a/k_d
$Si(CH_3)_4$	0.29	$C_6H_5C(CH_3)_3$	0.21
$C_6H_5Si(CH_3)_3$	0.27	$(C_6H_5)_3CCH_3$	0.52
$(C_6H_5)_2Si(CH_3)_2$	0.33	$C_6H_5OCH_3$	1.99
$(C_6H_5)_3SiCH_3$	0.54	$C_6H_5SCH_3$	8.66
p-$ClC_6H_4Si(CH_3)_3$	0.29	$C_6H_5N(CH_3)_2$	very large
m-$ClC_6H_4Si(CH_3)_3$	0.33	$C_6H_5CH_3$	2.19
$(CH_3)_3SiSi(CH_3)_3$	0.60		
$Ph(CH_3)_2SiSi(CH_3)_2Ph$	0.52		

By the application of the quantitative method described in the previous papers,[8,9] the reactivities of one methyl hydrogen atom of methylsilanes towards the abstraction by *t*-butoxy radicals have been investigated in 1,1,2-trichlorotrifluoroethane (Freon 113) at 45.0°C. Di-*t*-butyl peroxyoxalate[10] was used as a source of *t*-butoxy redicals. The results are given in Table 1 along with the reactivities of compounds of the type of C_6H_5-$M(CH_3)_n$, in which M stands for a carbon atom or a heteroatom, O, N, and S. It is apparent that, for the attack by the *t*-butoxy radicals, the relative reactivities (k_a/k_d), which show the ratio of rate constant of hydrogen abstraction to that of decomposition of *t*-butoxy radicals to acetone and methyl radicals, are identical within an experimental error, for the substituted phenyltrimethylsilanes.

$$(Me_3COOC)_2 \longrightarrow 2Me_3CO\cdot + 2CO_2$$

$$Me_3CO\cdot \xrightarrow{k_d} Me\cdot + Me_2CO$$

$$Me_3CO\cdot + R\text{-}CH_3 \xrightarrow{k_a} Me_3COH + R\text{-}CH_2\cdot$$

The reactivities of methyl hydrogen in organosilicon compounds are little larger than those of the corresponding carbon analogs. Since the transition state of hydrogen abstraction, especially by electrophilic radicals such as *t*-butoxy radicals, resembles the initial state of the reaction, the polar effect is exerted mainly on the reactivities of abstraction, unless overthrowing strong conjugation effect is present. Therefore, the fact that the reactivities of organosilicon compounds do not differ considerably from those of the corresponding carbon analogs shows that the free redical formed by hydrogen abstraction is little stabilized by vacant 3*d*-orbitals of silicon, but the reactivities depend on the electron density of the C–H bond. It may be concluded also that pentamethyldisilanyl group is more electron-releasing than trimethylsilyl group.[11]

It might be considered that the reactivities of the compounds containing one of the other hetero-atoms such as O, S, and N are very large, since these atoms have the electron-releasing effect due to lone pair electrons.

In conclusion, the α-silyl radicals formed by hy-

1) To whom all correspondence should be directed at the Department of Chemistry, Faculty of Science, Tohoku University, Sendai.

2) J. L. Speier, Jr., *J. Amer. Chem. Soc.*, **71**, 273 (1949).

3) a) W. Rickatson and T.S. Stevens, *J. Chem. Soc.*, **1963**, 3960; b) D. Y. Curtin and M. J. Hurwitz, *J. Amer. Chem. Soc.*, **74**, 5381 (1952); c) D. Y. Curtin and J. C. Kauer, *J. Org. Chem.*, **25**, 880 (1960); d) D. Y. Curtin and J. C. Miller, *ibid.*, **25**, 885 (1960).

4) J. W. Wilt, O. Kolewe, and J. F. Kraemer, *J. Amer. Chem. Soc.*, **91**, 2624 (1969).

5) C. Eaborn, "Organosilicon Compounds," Butterworths, London (1960).

6) E. R. Morris and J. C. J. Thynne, *J. Organometal. Chem.*, **17**, 93 (1969).

7) Y. Nagai, N. Machida, H. Kono, and T. Migita, *J. Org. Chem.*, **32**, 1194 (1967).

8) H. Sakurai and A. Hosomi, *J. Amer. Chem. Soc.*, **89**, 458 (1967).

9) H. Sakurai, A. Hosomi, and M. Kumada, *J. Org. Chem.*, **35**, 993 (1970).

10) P. D. Bartlett, E. P. Benzing, and R. E. Pincock, *J. Amer. Chem. Soc.*, **82**, 1762 (1960).

11) H. Sakurai, S. Deguchi, M. Yamagata, S. Morimoto, M. Kira, and M. Kumada, *J. Organometal. Chem.*, **18**, 285 (1969).

drogen abstraction is little stabilized by a conjugation between 3*d*-orbitals on silicon and an odd electron on carbon.

Experimental

Materials. Di-*t*-butyl peroxyoxalate was prepared by the method of Bartlett *et al.*[10] Freon-113 was commercially available and used after distillation. *t*-Butylbenzene, anisole, thioanisole, dimethylaniline, and toluene were commercial samples and were used after purification by the usual way. All of the organosilicon compounds and 1,1,1-triphenylethane were prepared by the Grignard reaction.

Procedure for Kinetic Runs. The procedure for kinetics was carried out in a similar way to that described previously[8,9] at 45.0°C in Freon-113. *t*-Butyl alcohol/acetone ratios were determined by glc on a column packed with polyethylene glycol 1500 using helium as a carrier gas at 90.0°C. The ratios of *t*-butyl alcohol/acetone *vs.* concentration of the substrates were calculated by the method of least squares.

BULLETIN OF THE CHEMICAL SOCIETY OF JAPAN, VOL. 44, 569—570 (1971)

The Photolysis of 1,3-Cyclootadiene Vapor. Vibrationally Excited Molecules Produced by the Photoelimination of Ethylene

Setsuo TAKAMUKU and Hiroshi SAKURAI

The Institute of Scientific and Industrial Research, Osaka University, Suita, Osaka

(Received August 25, 1970)

Photochemical initiation has often been used as a method of studying vibrationally-excited molecules.[1] The primary step in many systems is followed by a sequence of steps, which may include conventional unimolecular processes of species with excess energy. In a previous paper of this series,[2] it has been observed that a vibrationally-excited molecule (**1**) was produced by the elimination of ethylene in the mercury-photosensitized decomposition of 1,5-cyclooctadiene (1,5-COD) vapor:

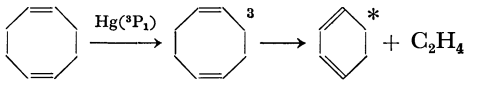

(**1**)

The vibrationally-excited molecule (**1**) may decompose to benzene and hydrogen, may be collisionally stabilized to 1,3-cyclohexadiene(CHD), or may isomerize to 1,3,5-hexatriene(HT). In the present study, it has been observed that the mercury-photosensitized decomposition of 1,3-cyclooctadiene (1,3-COD) also causes an elimination of ethylene, leading to the formation of a vibrationally-excited 1,3,5-hexatriene molecule which gives final products similar to those from 1,5-COD.

Experimental

The experimental procedures were essentially the same as those reported previously in the photolysis of 1,5-COD.[2] The vapor of 1,3-COD, which had been obtained commercially and which had been shown to be 99.8% pure by gas-chromatographic analysis, was irradiated in a quartz reaction vessel (5-cm in diameter and 5 cm long) with light from a low-pressure mercury resonance lamp in the presence of a small amount of mercury vapor. Most of the runs were at temperatures between 20 and 22°C.

The product gases volatile at −196°C were collected by means of a Toepler pump in a gas buret in a greaseless vacuum system, and then subjected to a Pd thimble heated at 300°C for hydrogen measurements. The other products were analyzed mainly gas chromatographically. A 3-m silica gel column at 100°C was used for the gases volatile at −120°C (C_2 fraction), and a 7.5-m squalane column at 80°C was used for the liquid components. Quantitative determinations were based on the calibrations of peak areas using measured amounts of certain hydrocarbon standards (propane and benzene respectively).

The quantum yields were determined by comparison with those of the mercury-photosensitized decomposition of propane at 300 mmHg, in which the hydrogen yield was assumed to be unity at a low conversion (0.06%).[3]

Results and Discussion

In the mercury-photosensitized reaction of 1,3-COD vapor, ethylene and *cis*-and *trans*-1,3,5-hexatriene were

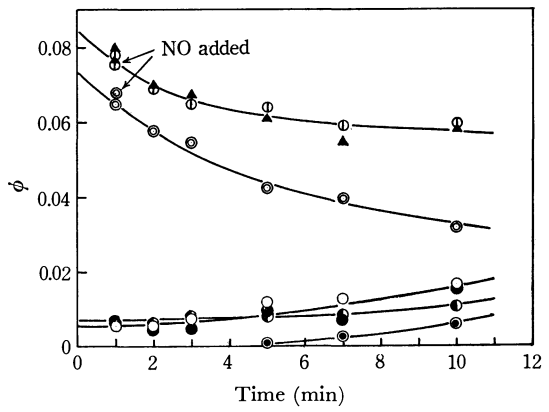

Fig. 1. Quantum yields *vs.* exposure time in the mercury-photosensitized decomposition of 1,3-COD (pressure 3 mmHg); ○, H_2; ⊙, C_2H_2; ⓘ, C_2H_4; ●, benzene; ◐, 1,3-cyclohexadiene; ◎, 1,3,5-hexatriene; ▲, total C_6 (benzene+1,3-CHD+1,3,5-HT).

1) T. F. Thomas, C. I. Sutin, and C. Steel, *J. Amer. Chem. Soc.*, **89**, 5107 (1967).

2) S. Takamuku and H. Sakurai, *J. Phys. Chem.*, **73**, 1171 (1969); S. Takamuku, M. Utsunomiya, and H. Sakurai, *Chem. Commun.*, **1969**, 173.

3) R. A. Back, *Can. J. Chem.*, **37**, 1834 (1959); K. Yang, *J. Amer. Chem. Soc.*, **86**, 3941 (1964).

found to be the major initial products, together with small amounts of hydrogen, benzene, and 1,3-cyclohexadiene. Figure 1 gives the dependence of the quantum yields on the exposure time at relatively low conversions (less than 5%). The yields of these main products decreased with an increase in the irradiation time, while the minor products increased gradually. The plot also clearly shows that acetylene is newly produced by prolonged irradiation. These observations may be explained satisfactorily on the basis of the further photolysis of the main products (ethylene and 1,3,5-hexatriene), which forms hydrogen, acetylene, and 1,3-cyclohexadiene, as has been pointed out in discussing the photolyses of ethylene[4] and hexatriene[5] respectively. Thus, acetylene was not assumed to be a primary product.

The yields of the main products were unaffected by the addition of 15 mole% nitric oxide, as is shown in Figure 1, and the minor products were also essentially unaffected. These results strongly suggest an intramolecular mechanism, to the exclusion of a free radical path, for the formation of these products.

The mercury-photosensitized decomposition of 1,3-COD was studied as a function of the pressure (0.4—4.3 mmHg) in order to obtain some information on the active intermediates of this reaction. When the 1,3-COD pressure was increased, the yields of the main products increased; they showed a maximum at a pressure about 2 mmHg and then gradually decreased, probably because of the collisional deactivation of a triplet 1,3-COD molecule, while the yields of hydrogen and benzene homogeneously decreased with the pressure. Further, the pressure dependence of a path producing hydrogen and benzene seemed to be different from those of paths forming 1,3,5-hexatriene or 1,3-cyclohexadiene (the kinetic plots are shown in Fig. 2), suggesting the competing processes shown in the following scheme:

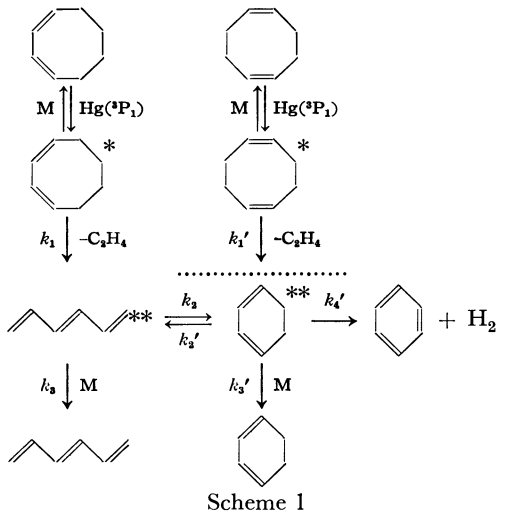

Scheme 1

An excited 1,3-COD molecule with a relatively long lifetime, probably a triplet state, may produce a vibrationally-excited 1,3,5-hexatriene by the simultaneous ruptures of two allylic C–C bonds in the molecule, *i. e.*, the molecular elimination of ethylene. It has been observed by Lossing[6] and by Cvetanovic[7] that, in the mercury-photosensitized decomposition of olefin, an initial rupture of the weak allylic bond occurs. The vibrationally-excited 1,3,5-hexatriene thus formed isomerizes to vibrationally-excited 1,3-cyclohexadiene, which is then subjected to collisional deactivation or dissociates to benzene and hydrogen. The pathway for the photolysis of 1,5-COD, which was proposed previously,[2,8] is also presented in the scheme (above the dotted line). It can be seen that very similar photolysis products were observed in 1,3- and in 1,5-COD.

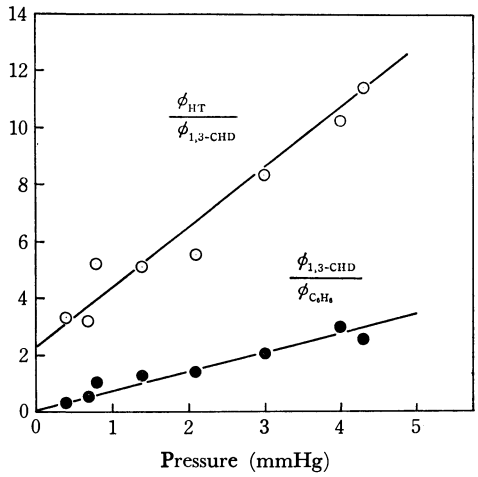

Fig 2. Kinetic plots of $\phi_{HT}/\phi_{1,3\text{-CHD}}$ and $\phi_{1,3\text{-CHD}}/\phi_{C_6H_6}$ *vs.* pressure of 1,3-COD (irradiated for 1 min); $\phi_{HT}/\phi_{1,3\text{-CHD}}$, intercept=2.4, slope=2.0 $mmHg^{-1}$; $\phi_{1,3\text{-CHD}}/\phi_{C_6H_6}$, slope=0.71 $mmHg^{-1}$.

The satisfactory material balances shown in Eqs. (1) and (2) were observed to hold under a wide variety of conditions (Fig. 1):

$$\phi_{C_2H_4} = \phi_{HT} + \phi_{1,3\text{-CHD}} + \phi_{C_6H_6} \quad (1)$$

$$\phi_{C_6H_6} = \phi_{H_2} \quad (2)$$

A steady-state treatment of the reaction scheme for 1,3-COD gives:

$$\frac{\phi_{HT}}{\phi_{1,3\text{-CHD}}} = \frac{k_3}{k_2}\left(\frac{k_4'+k_2'}{k_3'}+M\right) \quad (3)$$

$$\frac{\phi_{1,3\text{-CHD}}}{\phi_{C_6H_6}} = \frac{k_3'}{k_4'}\cdot M \quad (4)$$

Although there is some scatter in the data shown in Figure 2, satisfactory trends are apparent. The kinetic parameter deducible from such a treatment may permit a precise discussion of the excess energy if it is compared with that obtained from the 1,5-COD system, in which a similar reaction mechanism has been observed. In addition, such a photoelimination process of ethylene has also been found in the mercury-photosensitized decomposition of cyclooctene;[9] it seems to be characteristic of cyclic olefins.

4) R. J. Cvetanovic and A. B. Callear, *J. Chem. Phys.*, **23**, 1182 (1955).

5) R. Srinivasan, *J. Amer. Chem. Soc.*, **83**, 2806 (1961).

6) F. P. Lossing, D. G. H. Marsden, and J. B. Farmer, *Can. J. Chem.*, **34**, 701 (1956).

7) R. J. Cvetanovic and L. C. Doyle, *J. Chem. Phys.*, **37**, 543 (1962).

8) In the photolysis of 1,5-COD, a biradical intermediate  was proposed for the elimination process of C_2H_4 (see Ref. 2). However, the main dissociation process was also allylic C–C bond rupture forming two 1,3-butadiene molecules.

9) S. Takamuku, K. Moritsugu, and H. Sakurai, to be published.

BULLETIN OF THE CHEMICAL SOCIETY OF JAPAN, VOL. 44, 571—572 (1971)

The Reaction of Bis(methoxycarbonyl)carbene with Allyl Chloride. "Solvent Effect"

Wataru Ando, Shuji Kondo, and Toshihiko Migita
Department of Chemistry, Gunma University, Kiryu, Gunma

(Received August 31, 1970)

We have recently reported that the bis(methoxycarbonyl)carbene generated by the photochemical decomposition of dimethyl diazomalonate reacts with allyl halides to give addition products to the carbon-carbon double bond, cyclopropane derivatives (I) and the carbon–halogen insertion product, allylhalogenomalonate (II).[1] We have also indicated that only singlet bis(methoxycarbonyl)carbene is capable of affording the insertion product through an allylic rearrangement of the halonium ylide intermediate, and that the triplet carbene produced by a benzophenone-photosensitized decomposition is added to olefin rather than interacts with the halogen atom.[2]

A carbene in a singlet excited state has been reported to be transformed into the triplet state by collision with inert solvents,[3,4] particularly with those possessing heavy atoms.[5] The effect of such a collisional transformation may be expected to affect the ratio of the insertion and the addition products if the reactions of bis(methoxycarbonyl)carbene with allyl halides are carried out in such solvents. In this paper, we wish to repot on the ratio of the insertion and the addition products in the photochemical reactions of dimethyl diazomalonate with allyl chloride in methylene halides and cyclohexane as the solvents, these data will give some evidence of transformation into the deactivated bis(methoxycarbonyl)carbene produced by the collision of singlet bis(methoxycarbonyl)carbene with solvent molecules. The results are compiled in Table 1.

We can immediately see that the ratio of the insertion and addition products (II/I) decreases with dilution with methylene halides, and it tends toward the value obtained in the benzophenone-sensitized reaction. We take this to indicate that the reacting carbene species are partly triplet in these solvents and that almost they are exclusively triplet in the system highly diluted with CH_2Br_2. Furthermore, in 10% methylene halides, the ratio of the insertion and addition products is highest in CH_2Cl_2 and lowest in CH_2I_2. These tendencies are in agreement with the findings that the singlet-triplet interconversion is more effective when the reaction solvents possess heavier halogen atoms.[6] The overall yields (I+II) decreased as the concentration of methylene halides increased. This is probably because of the reaction of the singlet carbene with the solvent to give halogenomalonate as well as the insertion product into the carbon–halogen bond of the solvent.[7]

$$N_2C(CO_2CH_3)_2 + CH_2X_2 \xrightarrow{h\nu} CH_2XCX(CO_2CH_3)_2 + CHX(CO_2CH_3)_2$$

Table 1. The effects of solvents on the photochemical decomposition of dimethyl diazomalonate in allyl chloride

Solvent	Concn.[a] %	II/I	Overall yield %
none	0	2.35	76
none+$Ph_2C=O$	0	0.056	93
C_6H_{12}	10	3.39	64
C_6H_{12}	50	2.52	26
C_6H_{12}	90	1.95	5
CH_2Cl_2	10	2.38	60
CH_2Cl_2	50	2.20	35
CH_2Cl_2	90	1.17	10
CH_2Br_2	10	2.19	36
CH_2Br_2	50	1.60	14
CH_2Br_2	90	0.06	4
CH_2I_2	10	1.94	27

a) Mole per cent of solvents.
b) Yield of a mixture of the insertion and the addition products based on used diazomalonate.

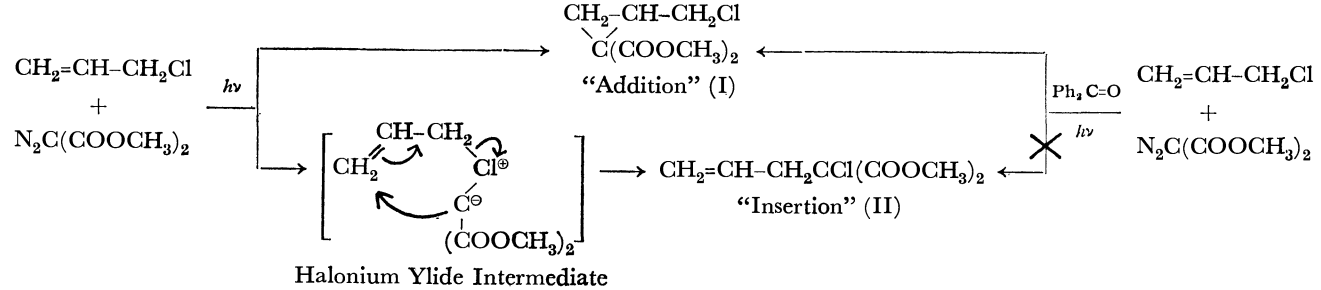

Halonium Ylide Intermediate

1) W. Ando, S. Kondo, and T. Migita, *J. Amer. Chem. Soc.*, **91**, 6516 (1969).
2) W. Ando, K. Nakayama, K. Ichibori, and T. Migita, *ibid.*, **91**, 5164 (1969).
3) M. Jones, Jr., and K. R. Rettig, *ibid.*, **87**, 4013 (1965).
4) E. Ciganek, *ibid.*, **88**, 1979 (1966).
5) W. H. Pikle and G. F. Koser, *Tetrahedron Lett.*, **1968**, 3959.
6) C. P. McClynn, R. Sunseri, and N. Christodouleas, *J. Chem. Phys.*, **37**, 1818 (1962).
7) T. Migita, W. Ando, S. Kondo, H. Matuyama, and M. Kosugi, *Nippon Kaguku Zasshi*, **91**, 374 (1970).

Therefore, an alternative explanation might be advanced: perhaps the singlet carbene is trapped preferentially by the solvent, thus giving a higher proportion of the triplet in the solution and leading to more of the addition product. Unfortunately, the reaction mechanism of the carbene with methylene halides is not yet clear.

The addition of cyclohexane to the irradiation mixture results in initially increased yields of the insertion products. This can presumably be explained in terms of the deactivation of a part of the excited singlet carbenes formed by photolysis to the lowest singlet state in which it can react more selectively. A similar dilution effect has previously been reported, that is, dilution with hexafluorobenzene increased the stereospecificity of the addition of bis(methoxycarbonyl)carbene to a olefin.[8]

On the basis of the data presented here, we may conclude that the singlet carbene formed by the photolysis of dimethyl diazomalonate can be readily deactivated, through collisions with methylene halides, to the triplet carbene, which is incapable of ylide formation with allyl chlorides.

Experimental

General. Samples of dimethyl diazomalonate were placed in clean 10×100 mm Pyrex tubes. The tubes were then corked(nondegassed) and placed in a water-cooled bath in order to irradiate them. The light source was a Rikosha 400-W high-pressure mercury lamp with maximum out-put at 3650—3660Å. Photolyses were carried out until the diazo band in the infrared spectra disappeared. The solutions were analyzed on an Ohkura gas-liquid partition chromatography with a calibrated 2 m×4 mm stainless steel column of 10% DC-710 and 10% Carbowax 20M on C-22 Firebrick.

Preparation of Dimethyl Diazomalonate. A solution of dimethyl diazomalonate(26.4 g) and tosyl azide (39.4 g) in diethyl ether (200 m*l*) was treated at 0°C with dry diethylamine (20 m*l*). The mixture was stirred for 1 hr at 0°C, and then for a further hour at room temperature. When a solid has been deposited, the mixture was treated with petroleum ether (bp below 60°C) and the solid was filtered off. The removal of solvent from the filtrate and the distillation of the residue gave dimethyl diazomalonate; bp 60—61°C/2mmHg (50% yield), (lit,[9] 63°C/1 mmHg).

Reaction of Dimethyl Diazomalonate in Allyl Choride. In a typical run, 0.218 g (0.0013 mol) of diazomalonate in 1 m*l* of allyl chloride was irraidated in a Pyrex tube for 5 hrs. Dimethyl allylchloromalonate and bis(methoxycarbonyl)cyclopropane were observed as the major products in yields of 53 and 23% respectively. Dimethyl allylchloromalonate showed infrared bands at 1752, 1645, and 950 cm^{-1}, and its NMR spectrum showed at 1.92 (doublet, 2-H), 3.78 (singlet, 6-H), and 5.24 ppm(multiplet, 3-H). Found: C, 46.71; H, 5.49%. Calcd for $C_8H_{11}O_4Cl$: C, 46.48; H, 5.32%.

The cyclopropane showed an infrared band at 1725 cm^{-1}, and its NMR spectrum showed bands at 1.43 (doublet, 1-H), 1.55 (singlet, 1-H), 2.12 (multiplet, 1-H), 3.50 (doublet, 2-H), 3.71 (singlet, 3-H), and 3.75 ppm (singlet, 3-H). Found: C, 46.49; H, 5.43%. Calcd for $C_8H_{11}O_4Cl$: C, 46.48; H, 5.32%.

Photosensitized Decomposition of Dimethyl Diazomalonate in Allyl Chloride. A solution of 0.325 g of diazomalonate and 1.74 g of benzophenone was irradiated in 2 m*l* of allyl chloride. The usual work-up yielded 88% of bis(methoxycarbonyl)-cyclopropane and 5% of the insertion product, dimethyl allylchloromalonate.

8) M. Jones, Jr., A. Kulczycki, Jr., and K. F. Hummel, *Tetrahedron Lett.*, **1967**, 183.

9) E. Ciganek, *J. Org. Chem.*, **30**, 4366 (1965).

BULLETIN OF THE CHEMICAL SOCIETY OF JAPAN, VOL. 44, 572—573 (1971)

The Syntheses of 5,5′-, 6,6′-, and 5,6′-Diformyl-2,2′,3,3′-tetramethoxybiphenyls

Yoshimori Omote, Yoshimori Fujinuma, and Noboru Sugiyama
Department of Chemistry, Tokyo Kyoiku University, Otsuka, Bunkyo-ku, Tokyo

(Received September 2, 1970)

Very recently Chapman and Swan[1] have reported the syntheses of biphenyls and related compounds, which are possible intermediates in the melanogenesis of 3,4-dihydroxyphenylalanine (DOPA). They have synthesized three DOPA dimers, one of which had already been reported by us.[2] In relation to the DOPA dimers, three kinds of veratrumaldehyde dimers, 5,5′-, 6,6′-, and 5,6′-diformyl-2,2′,3,3′-tetramethoxybiphenyl (I, II, and III), are of interest.

Among these, I and II are known. The dimer I was obtained by the oxidative coupling of vanillin with ferric chloride,[3] or by that of sodium persulfate catalyzed by ferrous sulfate,[4] followed by methylation. The dimer II was obtained by an Ullmann reaction on 2-iodo-3,4-dimethoxybenzaldehyde.[5] Chapman and Swan,[1] however, found it more convenient to use the 2-bromo-compound, which is easier to prepare. They prepared I and II, but did not give any spectral data.

Now we wish to report on the synthesis of the unknown head-to-tail dimer (III), and present the spectra of I, II, and III. The dimer III was obtained by the Ullmann reaction of 2- and 5-iodo-veratraldehyde. The molecular models of these dimers suggest that two benzene rings

1) R. F. Chapman and G. A. Swan, *J. Chem. Soc., C*, **1970**, 865.
2) a) Y. Omote, Y. Fujinuma, and N. Sugiyama, *Chem. Commun.* **1968**, 190; This Bulletin, **42**, 1752 (1969); b) Y. Omote, Y. Fujinuma, and N. Sugiyama, *Nippon Kagaku Zasshi*, **89**, 94 (1968).
3) F. Tiemann, *Ber.*, **18**, 3493 (1885).
4) K. Elbs and H. Lerch, *J. Prakt. Chem.*, **93**, 1(1916).
5) M. Nilsson, *Acta Chem. Scand.*, **12**, 1830 (1958).

of each dimer are perpendicular to each other. The UV data support this suggestion, because the spectra of the dimers roughly coincide with that of veratraldehyde.

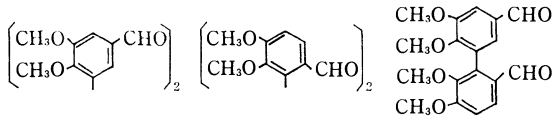

I II III

Experimental

Attempted Synthesis of the Dimer I by an Ullmann Reaction. It was examined if 5-bromoacetylvanillin gives its dimer by an Ullmann reaction.[6] Reactions at fusion or in various solvents, such as nitrobenzene, dimethylformamide, or methyl benzoate, were tested. In spite of many attempts under various conditions, the dimer was not obtained.

Attempted Synthesis of II by an Oxidative Coupling. The dimerization of isovanillin in the presence of sodium persulfate or ferric chloride was examined, but the formation only of black, intractable materials was observed. This result is consistent with the consideration that isovanillin can behave as a bifunctional compound to give polymeric pigments.

2-Iodo-and 5-Iodo-veratraldehyde. The former was prepared from vanillin by the route of acetylation, nitration, reduction, halogenation, and methylation,[7] while the latter was prepared by the same route except for acetylation. We found that 2-nitrovanillin was reduced smoothly to 2-aminovanillin with ferrous sulfate, but not with stannous chloride,[8] while 5-nitrovanillin was reduced only with stannous chloride.[7]

5,5′-Diformyl-2,2′,3,3′-tetramethoxybiphenyl (I). By the oxidative coupling of vanillin with sodium persulfate, followed by methylation with dimethyl sulfate, I was obtained nearly quantitatively. Colorless needles; mp 136°C, IR (KBr) cm^{-1} 2930(CH), 2840(CH), 1685(CHO), 1575(aromatic), 1450 (CH), 1388(CH), 1265(COC), and 1135(COC); UV λ_{max}^{EtOH} nm (ε) 228(34900), 275(18600), and 313(12000); NMR($CDCl_3$) δ 9.92(2H, s, CHO), 7.51(2H, d, J=2.5Hz, 6,6′-H), 7.32 (2H, d, J=2.5 Hz, 4,4′-H), 4.00(6H, s, 3,3′-OCH_3), and 3.80 (6H, s, 2,2′-OCH_3).

6,6-Diformyl-2,2′,3,3′-tetramethyoxybiphenyl (II). A mixture of 1 g of 2-iodo-3,4-dimethoxybenzaldehyde and 7 g of copper powder was heated in a pressure tube at 180—190°C for 1 hr. The reaction mixture was then extracted with chloroform. After the removal of the solvent, the residue was extracted with ether. The extract was evaporated to dryness and recrystallized from ethanol to afford 0.25 g (37.6%) of II as colorless prisms; mp 134—135°C; sublimed at 130—140°C/10^{-3}—10^{-4} Torr. When the reaction period was extended to 4 hr, the yield was 9.4%; when it was shortened to 30 min at 170—185°C, the yield was 63.4%. IR(KBr) cm^{-1} 2930, 2840, 1675, 1585, 1450, 1386, 1250, and 1135; UV λ_{max}^{EtOH} nm(ε) 232(28200) and 287(21500); NMR($CDCl_3$) δ 9.56 (2H, s, CHO), 7.82(2H, d, J=8.4Hz, 5,5′-H), 7.11(2H, d, J= 8.4Hz, 4,4′-H), 4.00(6H, s, 3,3′-OCH_3 and 3.61(6H, s, 2,2′-OCH_3).

5,6-Diformyl-2,2′,3,3′-tetramethoxybiphenyl (III). From a solution of 5 g of 2-iodo-3,4-dimethoxybenzaldehyde and 5 g of 5-iodo-3,4-dimethoxybenzaldehyde in benzene, the solvent was evaporated. The residual mixture was heated with 50 g of copper powder in a pressure tube at 180—187°C for 30 min. The reaction mixture was then worked up as has been described above to give 4.5 g of the product, which was chromatographed on silica gel with benzene-ethyl acetate (20:1 v/v). Each dimer, I, II, and III, was eluted, in that order. The yields of the dimers in a pure form were 27.8, 20.4, and 18.6% respectively. We attempted to improve the yield of III by changing the ratio of the 2-iodo- and 5-iodo-compounds. When a mixture of 2 g of coper powder was heated under the above conditions, the yields of I, II, and III, were 15.3, 37.1, and 13.5% respectively. The dimer III; colorless prisms from ethanol; mp 126—127°C. (Found: C, 65.22; H, 5.67%. Calcd for $C_{18}H_{18}O_6$; C, 65.44; H, 5.49%.; IR (KBr) cm^{-1} 2930, 2840, 1685, 1580, 1455, 1385, 1250, and 1135; UV λ_{max}^{EtOH} nm(ε) 229(31800) and 280(19100); NMR($CDCl_3$) δ 9.92(1H, s, 5-CHO), 9.61 (1H, s, 6′-CHO), 7.82(1H, d, J=8.4Hz, 5′-H), 7.55(1H, d, J=2.5Hz, 6-H), 7.35(1H, d, J=2.5Hz, 4-H), 7.11(1H, d, J=8.4Hz, 4′-H), 4.01(6H, s, 3,3′-OCH_3), 3.76(3H, s, 2-OCH_3), and 3.66(3H, s, 2′-OCH_3).

6) a) P. H. Gore and G. H. Hughes, *J. Chem. Soc.*, **1959**, 1615; b) W. Davey and R. W. Latter, *ibid.*, **1948**, 264; c) N. Kornblum and D. L. Kendall, *J. Amer. Chem. Soc.*, **74**, 5782 (1952); d) S. Kobayashi, M. Azekawa, and H. Morita, *Chem. Pharm. Bull.* (Tokyo), **17**, 89 (1969).

7) L. C. Raiford and E. H. Wells, *J. Amer. Chem. Soc.*, **57**, 2500 (1935).

8) L. C. Raiford and W. C. Storesser, *ibid.*, **50**, 2556 (1928).

BULLETIN OF THE CHEMICAL SOCIETY OF JAPAN, VOL. 44, 574—576 (1971)

The γ-Radiolysis and Mercury-Photosensitized Decomposition of Ethylbenzene Vapor

Yukio YAMAMOTO, Setsuo TAKAMUKU, and Hiroshi SAKURAI

The Radiation Laboratory, The Institute of Scientific and Industrial Research, Osaka University, Suita, Osaka

(Received September 10, 1970)

Previously we reported that, in the gas-phase radiolyses of toluene, ethylbenzene, and *m*-xylene, the benzylations of the aromatic nuclei of the parent alkylbenzene molecules were commonly observed as the main processes of the product formations.[1] These reactions have been attributed to the electrophilic substitutions by $C_7H_7^+$ ions,[2] which are well known to be the most abundant ions in the mass spectra of these alkylbenzenes.[3] Furthermore, in a preceding paper on the gas-phase radiolysis of toluene the overall product formation was studied and compared with that of the mercury-photosensitized decomposition.[4] In order to investigate the specific mode of the gas-phase radiolyses of alkylbenzenes, where ionic species and various excited molecules play important roles, we felt it was of some significance to compare those results with those of photolytic studies. In the present paper we wish to call attention to the radiolysis and mercury-photosensitized decomposition of ethylbenzene vapor at room temperature.

Experimental

The radiolysis was carried out in Pyrex cylinders approximately 120 m*l* in volume with γ-rays from a 5000 Ci cobalt-60 source. The dose rate to ethylbenzene was 4.3×10^{15} eV/hr·μmol, and the total dose, 3.1×10^{17} eV/μmol.

The photolysis of ethylbenzene containing a small amount of mercury vapor at 2537 Å was studied using cylindrical quartz cells (5 cm in diameter and 5 cm long) and a low-pressure mercury lamp.[5] The relative yields of the products were not appreciably affected by the use of a filter, Toshiba UV-25, which does not transmit below about 2000 Å; therefore, the contribution of 1849 Å light from the low-pressure mercury lamp may be neglected. The analysis of the products was the same as that described previously.[4]

Results and Discussion

Mercury-Photosensitized Decomposition. A few papers have been published on the mercury-photosensitized decomposition of ethylbenzene vapor at 2537 Å,[6,7] though these have dealt exclusively with the gaseous products. The products reported by Takase *et al.*[7] are ethane and relatively small yields of hydrogen and methane. They concluded that the major bond scission in the primary process occurs at the C–C bond β to the ring as follows:

$$\text{EB(Ethylbenzene)} \xrightarrow[\text{Hg}]{h\nu} \text{EB}^* \quad (1)$$

$$\text{EB}^* \longrightarrow C_6H_5CH_2\cdot + CH_3\cdot \quad (2)$$

and that ethane is formed almost exclusively by the combination of methyl radicals, judging from the results of the photolysis of ethylbenzene-β-d_1 vapor.

Table 1. The product yields of the Hg-sensitized photolysis and γ-radiolysis of ethylbenzene vapor at room temperature

Product	Photolysis, μmol	Radiolysis, *G* value		
	Pressure, mmHg			
	4	4	4 with NO[b]	7.6[a]
H_2	0.046	0.71	n.d.[c]	0.76
CH_4	0.10	0.54	n.d.[c]	0.51
C_2H_2	n.d.[d]	0.46	0.50	0.56
C_2H_4	n.d.[d]	0.32	0.35	0.40
C_2H_6	0.84	0.99	0	0.92
C_3H_8	0.018	0.10	0	—
Benzene	0.022	0.41	0.28	0.38
Toluene	0.22	0.34	0.11	0.34
i-PB[e]	0.16	0.03	0	0.11
Bibenzyl	0.34	0.05	0	—
1,2-DPP[f]	0.30	0.06	0	—
2-EDPM[g]	n.d.[d]	0.06	0.06	—
3-EDPM	n.d.[d]	0.82	0.85	—
4-EDPM	n.d.[d]	0.10	0.09	—

a) Data of Wiltzbach and Kaplan (Ref. 9). The *G* values of the other products such as xylenes and ethyltoluenes are also determined.
b) The mol% of NO was 10.
c) Not determined owing to the interference with added NO.
d) Not detectable.
e) Isopropylbenzene.
f) Diphenylpropane.
g) Ethyldiphenylmethane.

The product yields of our study are presented in Table 1, together with the results of the radiolysis. The formation of large yields of the products, such as ethane and bibenzyl, which is attributable to the reactions of the radicals formed by the β C–C bond scission, the reaction (2), was also observed in our study. As is shown in Table 1, small amounts of benzene and propane,

1) Y. Yamamoto, S. Takamuku, and H. Sakurai, *J. Amer. Chem. Soc.*, **91**, 7192 (1969).
2) The question of whether the $C_7H_7^+$ ions, which attack aromatic rings, are tropylium ions, as has been suggested in the mass-spectrometric studies (see Ref. 3), or benzyl ions still remains.
3) H. M. Grubb and S. Meyerson, "Mass Spectrometry of Organic Ions," ed. by F. W. McLafferty, Academic Press, New York (1963), p. 453.
4) Y. Yamamoto, S. Takamuku, and H. Sakurai, *J. Phys. Chem.*, **74**, 3325 (1970).
5) The direct photolysis may also occur to some extent, since ethylbenzene absorbs light in the 2537 Å region.
6) R. R. Hentz and M. Burton, *J. Amer. Chem. Soc.*, **73**, 532 (1951).
7) A. Takase, M. Murano, H. Mikuni, and M. Takahashi, International Conference on Photochemistry, Tokyo (1965).

the latter of which is thought to be formed by the combination of methyl and ethyl radicals, were formed in almost equivalent yields; it is indicated that the scission of the α C–C bond occurs in the primary process, though to a relatively small extent.

$$EB^* \longrightarrow C_6H_5\cdot + C_2H_5\cdot \quad (3)$$

In previous studies,[6,7] the possibility of the formation of styrene has been pointed out. However, in our study styrene was not found to be produced in a detectable yield; the only primary process leading to the formation of hydrogen suggested by our results is as follows:[8]

$$EB^* \longrightarrow C_6H_5\dot{C}HCH_3 + H \quad (4)$$

In our experiment at room temperature, the predominant reactions of the radicals formed by the primary processes, (2), (3), and (4), are considered to be combinations and α hydrogen abstractions from ethylbenzene with relatively small activation energies. Thus, we can write the processes of the formation of the observed products as follows:

$$R\cdot + EB \longrightarrow RH + C_6H_5\dot{C}HCH_3 \quad (5)$$

$$R\cdot + R\cdot \longrightarrow R\text{–}R \quad (6)$$

where R· represents any radical produced in the primary processes or by the hydrogen abstractions from ethylbenzene.

Neglecting the combinations of the radicals and hydrogen atoms, the yield of the $C_6H_5\dot{C}HCH_3$ radicals formed by the hydrogen abstractions (5) may be approximately represented by the sum of the yields of hydrogen, methane, benzene, and toluene. Such a yield, 0.39 μmol, was smaller than the sum of the yields of the products from $C_6H_5\dot{C}HCH_3$ radicals, isopropylbenzene (*i*-PB) and 1,2-diphenylpropane (1,2-DPP), 0.46 μmol, supporting the view that $C_6H_5\dot{C}HCH_3$ radicals are formed by the process (4) as well as by the hydrogen abstractions (5).

Radiolysis. The *G* values of the products of the gas-phase radiolysis of ethylbenzene were obtained in the presence and in the absence of a radical scavenger, nitric oxide; they are presented in Table 1, together with the results of the previous study.[9] As new products which were not detected in the photolysis, acetylene, ethylene, and three isomers of ethyldiphenylmethane (EDPM) were formed in the radiolysis.

When 10 mol% NO was added, ethane, propane, *i*-PB, bibenzyl, and 1,2-DPP disappeared; it may be that these products are formed through radicals as are some benzene and toluene substances, whose yields were partially reduced by the addition of 10 mol% NO (to be discussed below). The appreciable yields of ethane and propane indicate that methyl radicals are largely formed in the primary process of the radiolysis; this is analogous with the photolysis.

The remarkable difference between the radiolysis and the photolysis was observed in the formation of dimeric products; that is, the main dimeric products in the radiolysis were EDPM's, whose yields were not appreciably affected by the addition of 10 mol% NO, while the main products in the photolysis were bibenzyl and 1,2-DPP. As has been previously reported,[1] the formation of EDPM's may be attributed to the ion-molecule reaction of the $C_7H_7^+$ ions with ethylbenzene, as is shown by the following scheme:[10]

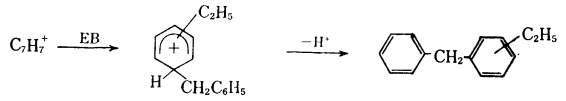

On the basis of these results, it may be concluded that the major bond scission in the primary process of the gas-phase radiolysis of ethylbenzene occurs at the β C–C bond *via* ionization, resulting in the formation of a methyl radical and the $C_7H_7^+$ ion as follows:

$$EB \rightsquigarrow EB^{+*} \quad (7)$$

$$EB^{+*} \longrightarrow C_7H_7^+ + CH_3\cdot \quad (8)$$

The formation of the $C_7H_7^+$ ions is the most important process observed in the mass spectrometry of ethylbenzene as well as in those of toluene and xylenes.[3]

When 10 mol% of NO was added, ethylene and acetylene were not appreciably affected, indicating that these products are formed through intermediates unscavengeable with NO. In our study of the gas-phase radiolysis of toluene,[4] the yield of ethylene was negligible over the pressure range studied (2 to 19 mmHg); the fact that the *G* value of ethylene from ethylbenzene is much larger than that from toluene seems to indicate that a great portion of ethylene is formed from the side chain, the ethyl group, of ethylbenzene, probably through an excited ethyl radical.[11] On the other hand, the *G* value of acetylene from ethylbenzene was of the almost same order as that from toluene; the processes of the acetylene formation suggested in the gas-phase radiolysis of toluene,[4] that is, the fragmentations of the $C_7H_7^+$ ions and aromatic rings, is probable for the ethylbenzene radiolysis.

The dependence of the yields of benzene and toluene on the NO concentration was studied. These yields were partially reduced by the addition of 10 mol% NO (Table 1); it was also observed that both were almost constant above about 6 mol% NO, indicating the presence of the unscavengeable benzene and toluene. The mechanism of the formation of these unscavengeable products is uncertain, though the possible mechanisms might be thought to involve the reactions of $C_6H_5^+$ ions[12] and $C_7H_7^+$ ions.

8) The dissociation of this bond might also occur by means of the reaction of the excited mercury atoms and ethylbenzene molecules.

9) K.E. Wiltzbach and L. Kaplan, *Advances in Chemistry Series*, No. 82, American Chemical Society, Washington, D. C., (1968), p. 134.

10) In a previous paper (Ref. 1), the isomer distribution of EDPM's has been accounted for by the isomerization of the intermediate complexes, $C_{15}H_{17}^+$ ions; the precise mechanism of such an electrophilic substitution of aromatic rings by $C_7H_7^+$ ions has also been discussed in a previous paper on the gas-phase radiolysis of toluene (Ref. 4).

11) The formation of ethylene by the decomposition of the excited ethyl radicals has been proposed in the vacuum ultraviolet photolysis of saturated hydrocarbons [J. R. McNesby and H. Okabe, "Advances in Photochemistry," Vol. 3, ed. by W. A. Noyes, Jr., G. S. Hammond, and J. N. Pitts, Jr., Interscience Publishers, New York, N. Y. (1964), p. 204].

12) The $C_6H_5^+$ ions are the product ions in the mass spectra of toluene and ethylbenzene (see Ref. 3); the formation of unscavengeable benzene was also observed in the gas-phase radiolysis of toluene (see Ref. 4).

The most interesting result obtained in these experiments was that the β bond scissions are the major primary process in both the γ-radiolysis and the mercury-photosensitized decomposition of ethylbenzene vapor. However, in the former, the $C_7H_7^+$ ions result, while the latter results in benzyl radicals. A similar result was also obtained in the study of toluene vapor, as has previously been reported.[4]

BULLETIN OF THE CHEMICAL SOCIETY OF JAPAN, VOL. 44, 576—577 (1971)

Application of Proton NMR Shift Reagents to the Stereochemical Analysis of Nicotine

Mamoru OHASHI, Isao MORISHIMA, and Teijiro YONEZAWA

Department of Hydrocarbon Chemistry, Faculty of Engineering, Kyoto University, Sakyo-ku, Kyoto

(Received September 10, 1970)

Recently the proton NMR contact shift has received considerable attention.[1-4] In previous papers[5,6] we have discussed the proton paramagnetic shifts of piperidines using nickel and cobalt diacetylacetonate (Ni(AA)$_2$ and Co(AA)$_2$), as well as their application to the stereochemical analysis of some tropane alkaloids. This communication will deal with the application of these paramagnetic shifts to the 220 MHz-NMR-spectrum analysis of nicotine and to the determination of its conformation.

In contrast to the case of the 60 MHz NMR spectrum,[7] this high-frequency NMR technique demonstrated the presence of two triplet signals at δ 3.27 (J=8Hz) and 3.11 (J=8Hz) ppm and a quartet peak at δ 2.34 (J=8Hz) ppm (Fig. 1). These signals can unquestionably be assigned to the methine and methylene protons positioned alpha to the nitrogen in the pyrrolidine ring. In order to assign these signals to particular hydrogens, the contact and pseudocontact shifts of these signals with Co(AA)$_2$, Ni(AA)$_2$, and tris(benzoylacetonato)europium Eu(BA)$_3$ were used effectively. Since the proton magnetic resonance of a particular proton was found to shift from its normal value in proportion to the concentration of the added

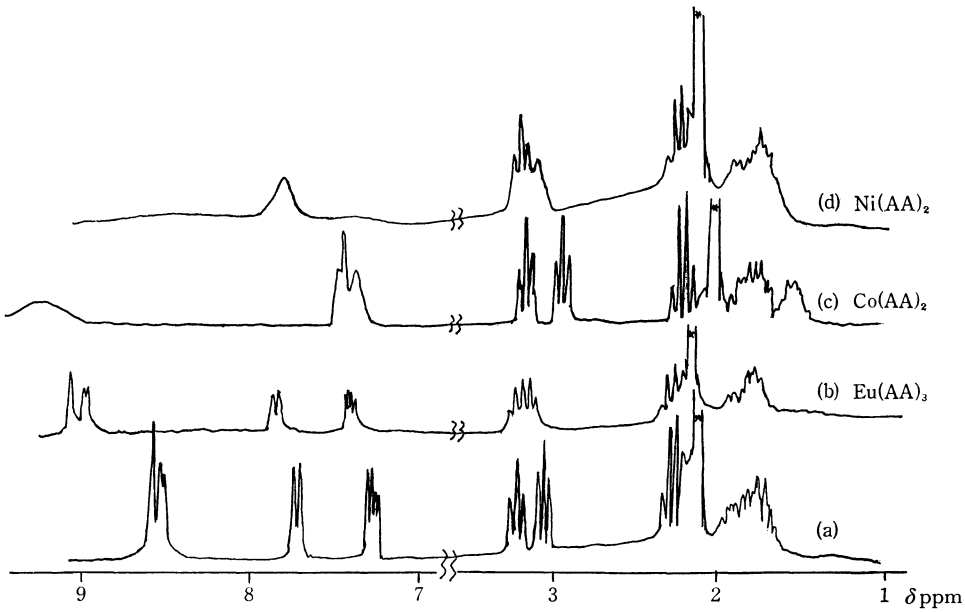

Fig. 1. Proton spectra of nicotine at 220 MHz.
(a) normal diamagentic spectrum in $CDCl_3$ with TMS reference. Same system but with (b) Eu(BA)$_3$, 0.1 mol, (c) Co(AA)$_2$, 0.03 mol, (d) Ni(AA)$_2$, 0.02 mol added.
* *N*-methyl signal.

1) C. C. Hinckley, *J. Amer. Chem. Soc.*, **91**, 5160 (1969); *J. Org. Chem.*, **35**, 2834 (1970).
2) J. K. M. Sanders and D. H. Williams, *Chem. Commun.*, **1970**, 422.
3) J. Brigs, G. H. Frost, F. A. Hart, C. P. Moss, and M. L. Staniforth, *ibid.*, **1970**, 749.
4) W. A. Szarek and M. C. Baird, *Tetrahedron Lett.*, **1970**, 2097.
5) T. Yonezawa, I. Morishima, and Y. Ohmori, *J. Amer. Chem. Soc.*, **92**, 1267 (1970).
6) I. Morishima, K. Okada, M. Ohashi, and T. Yonezawa, *Chem. Commun.*, **1971**, 32; M. Ohashi, I. Morishima, K. Okada, T. Yonezawa, and T. Nishida, *ibid.*, **1971**, 34.
7) Varian NMR Spectra Catalog, No. 269, Varian Assoc., Palo Alto, (1962).

Table 1. Chemical shifts and relative contact shifts[a] for nicotine coordinated with the metal chelates

(+ and − mean up- and downfield shifts respectively, in CDCl, internal standard TMS at 220 MHz)

	2′	4′	5′	6′	2	5ax	5eq	3	NCH_3
δ ppm	8.53	7.70	8.47	3.11	3.11	2.34	3.27	−1.8[b]	2.16
$Ni(AA)_2$	−[c]	−10.0	−[c]	−[c]	−5.4	0	0	0	0
$Co(AA)_2$	−10.0	+ 3.5	−1.5	−10.0	+1.8	+0.8	+0.7	+2.6	+1.5
$Eu(BA)_3$	−10.0	− 3.1	−3.1	− 9.1	−1.9	−0.5	−0.5	−1.6	−1.3

a) The observed shifts are normalized to give a value of 10.0 for the largest proton shift.
b) Signals are overlapped one another and the exact chemical shift can not be determined.
c) Line broadening is so great that the exact position is not obvious.

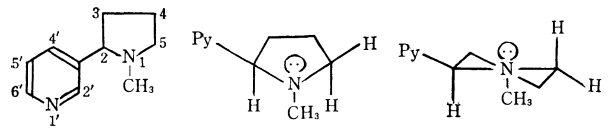

(1) (2) (3)

Scheme. 1

metal chelates,[5,8] we are interested only in the relative shifts for various protons. The results are summarized in Table 1.

From these data the following conclusions were drawn: i) Since the 2, 5′ and 6′-hydrogens were shifted dramatically, the nitrogen lone-pair of pyridine, not that of pyrrolidine, is the binding site of the metal chelates. ii) On the addition of $Ni(AA)_2$ or $Co(AA)_2$, the triplet signal at δ 3.11 ppm shifted downfield or upfield respectively. This behavior is similar to that of the methyl in the β-picoline spectrum;[8] the signal was, consequently, assigned to 2-hydrogen. iii) On the basis of the coupling features, a triplet signal at δ 3.27 ppm and a quartet at δ 2.34 ppm were analyzed to be quasi-equatorial and -axial protons respectively at C_5 position. iv) As far as energy is concerned, two conformers, an envelope form (**2**) and a half-chair form (**3**), are conceivable for the pyrrolidine ring.[9] In **2**, the quasi-equatorial and -axial protons are in *cis* and *trans* relationships to the pyridyl group respectively, while in **3** the relationships are the reverse. It is well known that the observed paramagnetic shift using $Co(AA)_2$ is the sum of the isotropic contact shift and the anisotropic pseudocontact shift, which is proportional to the geometric factor, $f=(3\cos^2\theta-1)/r^3$, where r is the distance between the resonating proton and the Co atom and where θ is the angle between the Co–N axis and the r vector.[10] Since the contact shift with $Ni(AA)_2$ was not observed on the protons attached to the pyrrolidine ring, and since the ratios of the spin densities at the various protons would be the same for the Co(II) and Ni(II) systems,[5] the upfield shifts of *N*-methyl, C_3, and C_5-protons must be due only to the anisotropic pseudocontact shift caused by the cobalt t_{2g} orbital.[8] It is also known that, in the case of the rare earth chelates of Eu(III), the observed downfield shifts are probably caused by the predominant pseudocontact term and that, therefore, they depend upon the geometric factor.[10,11] Assuming the nitrogen-metal length to be 2 Å,[5] the molecular model of nicotine indicates that the amount of the geometric factor is qualitatively in the order of: the C_3-quasi-axial proton > *N*-methyl protons > C_5-quasi-axial ≈ -equatorial protons in the case of **2**, while it is: the C_3-quasi-axial proton > *N*-methyl ≈ C_5-quasi-axial protons > the C_5-quasi-equatorial proton in the case of **3**. The fact that the observed relative amount of the paramagnetic shift of each proton is in accord with the case of **2** and not of **3** indicates that the conformation of the pyrrolidine ring is in an envelope form.

It is well established that the chemical shift of a proton positioned at the *cis* configuration to the nitrogen lone-pair is in a lower field than that of *trans*.[12] The fact that the chemical shift of the quasi-equatorial proton (δ 3.27 ppm) is in a lower field than that of the quasi-axial proton (δ 2.34 ppm) is consistent with the case of **2** and supports the aforementioned conclusion.

The above discussion is an example of the usefulness of contact and pseudocontact shifts with $Ni(AA)_2$, $Co(AA)_2$ and $Eu(BA)_3$ in analyzing complex spectra and in solving stereochemical problems. Further applications of these phenomena to alkaloids as well as to natural-product chemistry are now in progress.

Experimental

All the materials used in this study except $Eu(BA)_3$ were commercially available ones. The $Ni(AA)_2$ and $Co(AA)_2$ were dried at 60°C *in vacuo* overnight before use. The $Eu(BA)_3$ was supplied by Dr. T. Suzuki of this department.[13]

The spectra were observed with a Varian HR-220 spectrometer for $CDCl_3$ solutions containing varying amounts of nicotine and $Co(AA)_2$, Ni(AA), or $Eu(BA)_2$. The proton-resonance shifts were measured relative to the internal TMS. The spectra were recorded after each of the successive additions of a few milligrams of the metal chelates.

8) J. A. Happe and R. L. Ward, *J. Chem. Phys.*, **39**, 1211 (1963).
9) E. L. Eliel "Stereochemistry of Carbon Compounds," McGraw-Hill Book Co. Inc., New York (1968), p. 215.
10) R. W. Kluiber and W. D. Horroks, Jr., *J. Amer. Chem. Soc.*, **87**, 5350 (1965).
11) D. R. Eaton, *ibid.*, **87**, 3097 (1965).
12) M. Uskokovic, H. Bruderer, C. von Planta, T. Williams, and A. Brossi, *ibid.*, **86**, 3364 (1964) and references therein.
13) We wish to thank Dr. T. Suzuki for his generous supply of samples of $Eu(BA)_3$. For the synthesis of this compound, see S. Y. Tyree, Jr. (ed.), "Inorganic Synthesis," Vol. 9, McGraw-Hill Book Co., New York (1967), p. 37.

BULLETIN OF THE CHEMICAL SOCIETY OF JAPAN, VOL. 44, 578—579 (1971)

Aromatic Substitution of Olefins XV. The Steric Course of the Reaction

Ichiro MORITANI,* Sadao DANNO,** Yuzo FUJIWARA,* and Shiichiro TERANISHI*

* *Faculty of Engineering Science, Osaka University, Machikaneyama, Toyonaka, Osaka*

** *Polymer Research Laboratory, Ube Industries Ltd., Goi, Chiba*

(Received September 25, 1970)

In previous papers, we have reported that aromatic compounds react smoothly with olefins in the presence of palladium acetate to produce aryl-substituted olefins (Eq. (1))[1] and that the reaction proceeds through a different mechanism from that of the Wacker process,[2] for no hydride shift occurs in the course of the aromatic substitution reaction of olefins.

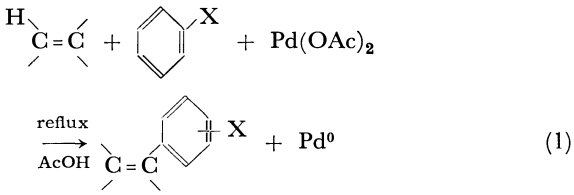

(1)

It has been reported that, in the Wacker process,[3] a σ-complex (I) may be formed after the nucleophilic attack of an anion on the olefin-Pd π-complex, followed by the π-electron transfer:

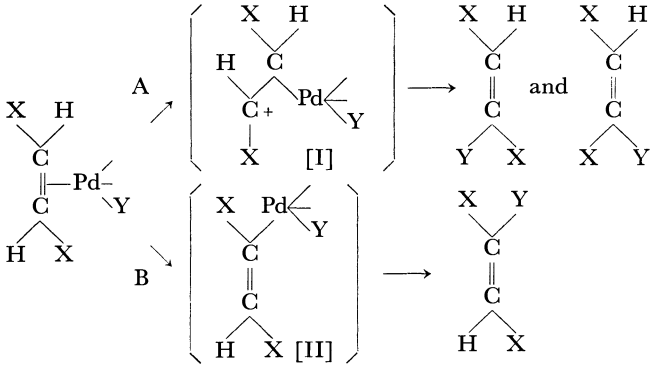

In the aromatic substitution of olefins, we have proposed a mechanism in which an olefin-palladium σ-complex (II) is formed through hydrogen abstraction from the olefin.[4]

If the aromatic substitution reaction proceeds *via* an intermediate (I) according to the path A, a free rotation about the C–C axis becomes possible, for the electronic configuration changes from sp^2 to sp^3 hybridization, and the products will be a mixture of *cis*- and *trans*-isomer.

Contrary to this, in the case of the path B, olefinic carbon atoms will remain in the intermediate (II), so the reaction will proceed with a retention of the configuration.

Thus, it is possible to determine the reaction path if the olefins which do not isomerize under the reaction conditions are allowed to react with benzene, and the stereochemistry of the product can be investigated.

Therefore, *trans*-stilbene, *cis*- and *trans*-dichloroethylenes were selected as olefins, for they do not isomerize in the course of the reaction.

The reaction of *trans*-dichloroethylene with benzene proceeded in acetic acid in the presence of palladium acetate. Phenyl-*trans*-dichloroethylene was obtained in a 42% yield (based on pallaium), but no phenyl-*cis*-dichloroethylene was detected (Eq. (2)). Similary, *cis*-dichloroethylene reacted with benzene and produced phenyl-*cis*-dichloroethylene.

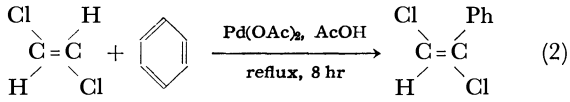

(2)

Moreover, the *trans*-stilbene was reacted with benzene to produce *p*-tolyl-*trans*-stilbene. The reaction of *cis*-stilbene with toluene was not the same, however, because it is isomerized to the *trans*-isomer when treated under the same conditions for two hours.

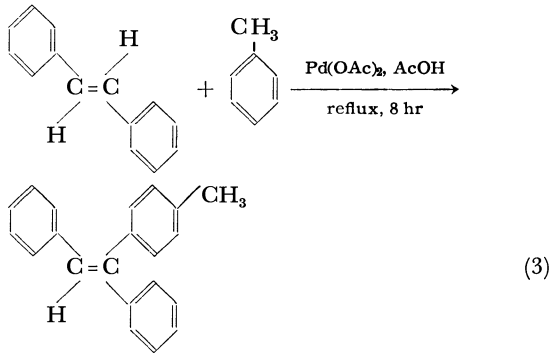

(3)

These results strongly demonstrate that the substitution reaction proceeds with a retention of the configuration of the olefins, and the path B is favored for the aromatic substitution reaction of olefins. Moreover, it is reasonable to assume the existence of an olefin-palladium σ-bonded intermediate in the reaction.

Experimental

All the boiling points are uncorrected. The infrared spectra recorded by means of a Hitachi EPI-S2 IR spectrophotometer, while the ultraviolet spectra were obtained on a Hitachi-EPS-2U spectrophotometer. The NMR spectra were obtained by the use of a Japan Electron Optics JNM-4H-100 or JNM-C-60HL spectrometer, using tetramethylsilane as the internal standard. Chemical shifts are given on the τ-scale, together

1) For example, Y. Fukiwara, I. Moritani, S. Danno, R. Asano, and S. Teranishi, *J. Amer. Chem. Soc.*, **91**, 7166 (1969).

2) S. Danno, I. Moritani, and Y. Fujiwara, *Chem. Commun.*, **1970**, 610; S. Danno, I. Moritani, Y. Fujiwara, and S. Teranishi, *J. Chem. Soc., B*, in press.

3) J. Smidt, W. Hafner, R. Jira, R. Sieber, and J. Sedlmeier, *Angew. Chem. Internat. Edn.*, **1**, 80 (1962); P. M. Henry, *J. Amer. Chem. Soc.*, **86**, 3242 (1964); *ibid.*, **88**, 1596 (1966); I. I. Moiseev, M. N. Vargaftik, and Ya. K. Syrkin, *Dokl. Akad. Nauk SSSR*, **153**, 140 (1963).

4) S. Danno, I. Moritani, and Y. Fujiwara, *Tetrahedron*, **25**, 4819 (1969).

with the splitting patterns and the relative integrated area.

General Procedure for the Reaction. A mixture of the palladium acetate, an equivalent amount of the olefin, acetic acid, and the aromatic compound was stirred for 8 hr at reflux. The reactions were carried out with an excess of the aromatic compound, which behaved as both a reactant and a solvent. The resulting mixture was filtered to remove the palladium metal, and then the filtrate was poured into water and the organic layer was separated. The organic layer was treated with an aqueous sodium bicarbonate solution, washed with water to free it from acetic acid, and then dried over anhydrous magnesium sulfate. After the evaporation of the solvent, the products were isolated by gas chromatography. Analyses of the products were carried out by the use of a Yanagimoto GCG-3 gas chromatograph, using an Apiezon L, Carbowax 20M, or SE-30 column. Identities with the products formed were proved by IR, UV, or NMR comparison with authentic samples.

Reaction of trans-*Stilbene with Toluene.* In a solution of dry toluene (300 m*l*) and dry acetic acid (100 m*l*), we dissolved palladium acetate (28.8 mmol, 6.47 g) and *trans*-stilbene (28.8 mmol, 5.25 g). The mixture was then refluxed for 8 hr. The resulting mixture was filtered to remove the reduced palladium metal and the filtrate was poured into water. The organic layer was treated with an aqueous sodium bicarbonate solution, washed with water, and then dried over $MgSO_4$. After the evaporation of the solvent, the products were separated by vpc to give 1.79 g of *p*-tolyl-*trans*-stilbene; UV spectrum: $\lambda_{max}^{EtOH}=312$ mμ (ε: 2.08×10^4); NMR spectrum (in CCl_4): 2.8(m,14H), 3.17(s,1H), and 7.65τ (s, 3H).

Preparation and Separation of p-*Tolyl*-cis *and* trans-*Stilbenes.* *p*-Methylbenzophenone (10 g) dissolved in absolute ether (30 m*l*) was added, drop by drop, to the Grignard reagent prepared from freshly distilled benzyl chloride (8.3 g) and magnesium shoot (1.6 g). After having been refluxed for 1.5 hr, the reaction mixture was hydrolysed with cold water. The residual oil was refluxed for 2 hr with 20% sulfiic acid (70 m*l*) to dehydrate the alcohol thus produced. *p*-Tolylstilbene, (175—182°C/2.5 mmHg[5]) was obtained in a 94% yield. Found: C, 93.10; H, 6.82%. Calcd for $C_{21}H_{18}$: C, 93.29; H, 6.71%.

The *p*-tolyl-*cis* and *trans*-stilbenes prepared by the above described method were separated by VPC (10% SE-30 on Celite 545, 2 m$\times$6 mm, 260°C, 30 m*l* He/min). *p*-Tolyl-*cis*-stilbene; UV spectrum: $\lambda_{max}^{EtOH}=314$mμ(ε: 4.45×10^4); NMR spectrum (in CCl_4): 2.9(m, 14H), 3.19(s, 1H), and 7.62 τ (s, 3H). *p*-Tolyl-*trans*-stilbene; the UV and NMR spectra have been described above.

Preparation of cis-*Dichlorostyrene.* This compound was prepared by the methods described by Dycherhoff.[6] A mixture of ω-chloroacetophenone (8 g) and phosphorus pentachloride (10.8 g) were heated at 135°C for 2 hr, and the product was distilled in a boiling range of 225—234°C. The distillate was dried over $MgSO_4$ and then redistilled (bp 221—224°C). This product was separated and purified by VPC. NMR Spectrum (in CCl_4): 3.0 (m, 5H) and 3.16τ (s, 1H). Also, *trans*-dichlorostyrene was prepared by the method of Koenig and Wolf.[7] Bp 90—93°C/10 mmHg; IR spectrum (direct): 695, 760 (monosub. benzene), and 1660 cm^{-1}; NMR spectrum in CCl_4): 2.58 (m, 5H) and 3.33 τ (s, 1H).

5) B. Hoei, *Bull. Soc. Chim. Fr.*, **1946**, 117.
6) R. Dycherhoff, *Ber.*, **10**, 120 (1877).
7) J. Koenig and V. Wolf, *Tetrahedron Lett.*, **1970**, 1629.

SHORT COMMUNICATIONS

The Effect of the Krypton Moderator on the Isomeric Transition-induced Reactions of ^{80}Br with CH_4

Masuo YAGI, Kenjiro KONDO, and Takaaki KOBAYASHI*1

Laboratory of Nuclear Science, Tohoku University, Sendai

(Received October 22, 1970)

In a previous paper[1] we studied the reactions of isomeric transition-activated ^{80}Br in the CH_4-$^{80m}BrBr$ system and found that the $CH_3{}^{80}Br$ yields were much higher than the $CH_2{}^{80}BrBr$ yields over the whole range of mole fractions of the $^{80m}BrBr$ additive. In this paper, we will report on our investigation of the effect of the Kr moderator in the same system in order to elucidate further the chemical behavior of the isomeric transition-activated ^{80}Br.

Nicholas and Rack[2] studied the effects of rare gas moderators on the total organic yields in the CH_4-$^{82m}BrBr$ system and suggested that one-half of the organic products are formed *via* the excess kinetic-energy processes, while the others are formed *via* the thermal ionic (kinetic-energy-independent) processes. Tachikawa[3] and his co-workers[4,5] also studied the influence of the moderator gases, such as He, Ar, and Xe, on the individual product yields in the CH_4-$^{80m}BrBr$ and the CH_4-$^{82m}BrBr$ systems, they concluded that the radioactive $CH_3{}^*Br$ is formed *via* both the excess kinetic-energy and the thermal ionic processes, while the radioactive $CH_2{}^*BrBr$ is formed *via* only the thermal ionic processes.

Since the Br_2 additive is an efficient moderator of the bromine hot atoms, it is necessary to use the smallest pressure of Br_2. Therefore, in our experiments, the mole fraction of the $^{80m}BrBr$ additive to CH_4 was kept constant at 0.029 and the individual product yields were determined in the presence of pressures of Kr gas sufficient to remove the excess kinetic-energy of the ^{80}Br atoms. The experimental methods may be found elsewhere.[1]

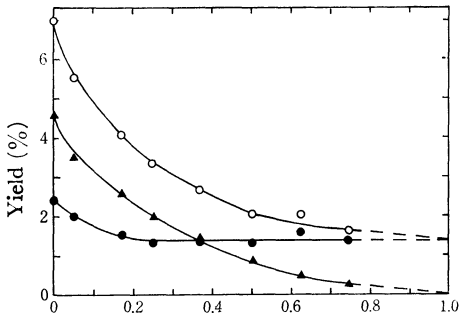

Fig. 1. Effect of the Kr moderator on the product distribution in the reaction of (I.T.)-activated ^{80}Br with CH_4. ($^{80m}BrBr/CH_4=0.029$, total pressure: 400—700 mmHg)
○: ^{80}Br as organic, ▲: $CH_3{}^{80}Br$, ●: $CH_2{}^{80}BrBr$

The effects of the Kr moderator on the total organic and the individual product yields are shown in Fig. 1. Extrapolations of the presented values to the zero mole fraction of the Kr moderator gave the limiting $CH_3{}^{80}Br$ yield of $4.6\pm0.2\%$ and the $CH_2{}^{80}BrBr$ yield of $2.4\pm0.1\%$ respectively. On the other hand, at one mole fraction of the Kr moderator, the data are $0.0\pm0.1\%$ for the $CH_3{}^{80}Br$ and $1.4\pm0.1\%$ for the $CH_2{}^{80}$ BrBr respectively. Our value of 1.4% for the total organic yield at one mole fraction of the Kr moderator was agreed very well with that of 1.6% reported by Tachikawa[3] and his co-workers[4,5] for the ^{80}Br and ^{82}Br systems. However, it was significantly lower than that of 3.7% reported by Nicholas and Rack[2] for the ^{82}Br. It is not immediately obvious why our value is lower than their value.

Under our experimental conditions, $CH_3{}^{80}Br$ may be seen to be formed *via* only the excess kinetic-energy processes. On the contrary, it is clear that the $CH_2{}^{80}BrBr$ yield of 2.4% minus 1.4% is derived from the excess kinetic-energy processes and that of 1.4% is derived from the thermal ionic processes. These facts indicate that about 80% of the organic products are formed principally *via* the excess kinetic-energy processes, while the rest are formed principally *via* the thermal ionic processes under the present conditions.

*1 Present address: Department of Chemistry, Faculty of Science, Tohoku University, Sendai.

1) M. Yagi and K. Kondo, *Radiochem. Radioanal. Lett.*, **5**, 75 (1970).
2) J. B. Nicholas and E. P. Rack, *J. Chem. Phys.*, **48**, 4085 (1968).
3) E. Tachikawa, This Bulletin, **42**, 2404 (1969); **43**, 63 (1970).
4) E. Tachikawa and T. Kahara, *ibid.*, **43**, 1293 (1970).
5) E. Tachikawa and J. Okamoto, *Radiochim. Acta*, **13**, 159 (1970).

Arylation of Olefin with Aryl Iodide Catalyzed by Palladium

Tsutomu Mizoroki, Kunio Mori, and Atsumu Ozaki

Research Laboratory of Resources Utilization, Tokyo Institute of Technology, Ohokayama, Meguro-ku, Tokyo

(Received October 20, 1970)

The arylation of olefin with aromatic hydrocarbon[1] or arylmercuric compound[2] by the reaction with palladium(II) compound has been reported, where the reaction consumes almost stoichiometric amount of the palladium(II) compound, forming metallic palladium. In this communication we wish to report that the arylation of olefin with iodobenzene in the presence of a catalytic amount of palladium(II) dichloride takes place smoothly when potassium acetate is added as an acceptor of hydrogen iodide formed. A characteristic feature of this reaction is that the arylation of olefin is effectively catalyzed by palladium or palladium(II) compounds without accompanying polymerization of the corresponding styrene derivatives formed, as long as the amount of potassium acetate added is greater than that of iodobenzene used. The reaction can be represented as follows:

$$C_6H_5I + CH_2{=}CHX + CH_3COOK \longrightarrow C_6H_5CH{=}CHX + CH_3COOH + KI$$
(X=H, C_6H_5, CH_3, and $COOCH_3$)

This can be compared with the carbonylation of aryl halide with carbon monoxide catalyzed by nickel carbonyl in the presence of sufficient amount of potassium acetate in methanol ($C_6H_5X + CO + CH_3OH + CH_3COOK \longrightarrow C_6H_5COOCH_3 + CH_3COOH + KX$, X=I, Br).[3]

The catalyst in the present case was initially palladium dichloride, but most of the palladium was found to be reduced to metal in the course of the reaction. As shown in Table 1, metallic palladium has also high catalytic activity for the arylation of olefin (No. 5). This differs considerably from the stoichiometric arylation of olefin with palladium(II) compounds. Pyridine, triethylamine, or potassium benzoate was also used as the acceptor of hydrogen iodide formed, potassium acetate being the most effective. Ethylene, propylene, styrene, and methyl acrylate were used as olefin. The corresponding styrene derivatives (styrene, α- or β-methylstyrene, *trans*-stilbene and methyl cinnamate, respectively) were produced in high yields. The results are summarized in Table 1.

The experimental procedure is illustrated by the arylation of ethylene with iodobenzene. Iodobenzene (50 mmol), potassium acetate (60 mmol), palladium dichloride (0.5 mmol), and methanol (1.0 mol) were placed in a titanium-alloy autoclave (100 m*l*) equipped with a magnetic stirrer. The gas phase in the autoclave was displaced by nitrogen stream, and ethylene from commercial sources was then introduced up to 8 kg/cm² at room temperature. The autoclave was heated up to 120—125°C within 1 hr and kept at this temperature for 3 hr. The decrease in pressure was observed during the first 1 hr (from 16 to 9 kg/cm²). After the reaction, all materials were taken out from the autoclave by using methanol and acetone and the products were quantitatively determined by gas chromatography.

Table 1. Arylation of olefin with iodobenzene

$PdCl_2$ 0.50 mmol, CH_3OH 0.8—1.0 mol, Temp. 120°C

No.	C_6H_5I (mmol)	CH_3COOK (mmol)	Olefin introduced	React. time (hr)	Arylation product (mmol) (%)[c]	
1	50	0	C_2H_4, 8 kg/cm² [b]	3	$C_6H_5CH{=}CH_2$	trace(0)
2	50	15	C_2H_4, 8 kg/cm²	3	$C_6H_5CH{=}CH_2$	13 (26)
3	50	30	C_2H_4, 8 kg/cm²	3	$C_6H_5CH{=}CH_2$	24 (48)
4	50	60	C_2H_4, 8 kg/cm²	3	$C_6H_5CH{=}CH_2$	37 (74)[d]
5[a]	50	60	C_2H_4, 8 kg/cm²	3	$C_6H_5CH{=}CH_2$	36 (72)[d]
6	50	60	$C_6H_5CH{=}CH_2$ 100 mmol	2	*trans*-Stilbene 1,1-Diphenylethylene	45 (90) 6.0 (12)
7	30	48	C_3H_6, 3.5 kg/cm² [b]	2	α-Methylstyrene β-Methylstyrene	8.1 (27) 22 (73)
8	30	48	$CH_2{=}CHCOOCH_3$ 60 mmol	2	Methyl cinnamate	29 (97)[e]

a) Palladium black (54 mg) obtained by reducing $PdCl_2$ was used as a catalyst.
b) The methanol solution was saturated with the olefin at room temperature.
c) Based on the amount of iodobenzene used.
d) *trans*-Stilbene and 1,1-diphenylethylene were detected in the product.
e) No methyl atropate was detected.

1) Y. Fujiwara, I. Moritani, S. Danno, R. Asans, and S. Teranishi, *J. Amer. Chem. Soc.*, **91**, 7166 (1969).
2) R. F. Heck, *ibid.*, **91**, 6709 (1969).
3) M. Nakayama and T. Mizoroki, This Bulletin, **42**, 1124 (1969).

Diiodo-π-cyclopentadienyliridium and Its Derivatives

Hiroshi YAMAZAKI

The Institute of Physical and Chemical Research, Wako-shi, Saitama

(Received October 28, 1970)

Recently formation of dihalo-π-(pentamethylcyclopentadienyl)iridium from the reaction of iridium chloride hydrate with hexamethyl (Dewar benzene) was reported.[1] However, simple dihalo-π-cyclopentadienyliridium is not known as yet in spite of its ability to prepare complexes having a π-cyclopentadienyliridium group. We wish to report the preparation of diiodo-π-cyclopentadienyliridium and some derivatives thereof.

Cyclooctatetraene-π-cyclopentadienyliridium[2] [mp 114—116°C. IR(KBr): $\nu_{C=C}$ 1635 cm^{-1}. NMR(*p*-xylene): 4.27τ (singlet, –CH=CH–), 5.21τ (singlet, C_5H_5), 5.77τ (singlet, coordinated –CH=CH–).] was treated with equimolar amount of iodine in methylene chloride at room temperature to give insoluble brown crystals of diiodo-π-cyclopentadienyliridium (I) in almost quantitative yield. The infrared spectrum of I is very similar to that of the rhodium analogue.[4] A similar treatment of 1,5-cyclooctadiene-π-cyclopentadienyliridium did not give I but insoluble brown crystals having a combined composition of the reactant, $C_{13}H_{17}I_2Ir$, which was deduced on the basis of elemental analysis.

Similar to the rhodium analogue,[5] I reacted with triphenylphosphine in methylene chloride giving air-stable orange red crystals of diiodo-triphenylphosphine-π-cyclopentadienyliridium (II) [Yield 90%. Mp ~310°C (decomp). NMR($CDCl_3$): 2.2—2.7τ (C_6H_5), 4.57τ (doublet, J_{PH} 1.5 Hz, C_5H_5).]. Methyldiphenylphosphine and carbon monoxide also gave diiodo-methyldiphenylphosphine-π-cyclopentadienyliridium [Orange red crystals. Yield 82%. Mp 209—211°C. NMR($CDCl_3$): 2.1—2.7τ (C_6H_5), 4.57τ (doublet, J_{PH} 1.5 Hz, C_5H_5), 7.26τ (doublet, J_{PH} 11 Hz, CH_3).] and diiodo-carbonyl-π-cyclopentadienyliridium [Red crystals. Yield 93%. Mp>180°C (decompn without melting). IR(KBr): ν_{CO} 2040 cm^{-1} (with a shoulder at 2020 cm^{-1}). NMR($CDCl_3$): 3.99τ (singlet, C_5H_5).] respectively.

The reaction of II with methylmagnesium iodide in tetrahydrofuran-benzene mixture gave air-stable orange red crystals of iodo-triphenylphosphine-π-cyclopentadienylmethyliridium [Yield 80%. Mp 233—236°C (decomp). NMR($CDCl_3$): 2.4—2.7τ (C_6H_5), 4.89τ (doublet, J_{PH} 1.5 Hz, C_5H_5), 8.37τ (doublet, J_{PH} 7 Hz, CH_3).]. The reaction of II with isopropylmagnesium bromide in the presence of carbon monoxide afforded triphenylphosphine-carbonyl-π-cyclopentadienyliridium[6] [Yellow crystals. Yield 18%. Mp 180—183°C. IR(Nujol): ν_{CO} 1925 cm^{-1}. NMR($CDCl_3$): 1.9—3.1τ (C_6H_5), 5.03τ (singlet, C_5H_5).] and in the presence of triphenylphosphine, ionic hydridoiridium complex of the formula, $[C_5H_5Ir(PPh_3)_2H]^+I^-$ [Colorless crystals. Yield 47%. Mp 194—198°C (decomp). IR(KBr): ν_{IrH} 2150 cm^{-1}. NMR($CDCl_3$): 2.4—3.0τ (C_6H_5), 4.60τ (singlet, C_5H_5), 24.4τ (triplet, J_{PH} 26 Hz, Ir–H).]. The last reaction differs from the cases of cobalt and rhodium analogues which gave bis(triphenylphosphine)-π-cyclopentadienyl-cobalt and -rhodium.[7]

1) J. W. Kang, K. Moseley, and P. M. Maitlis, *J. Amer. Chem. Soc.*, **91**, 5970 (1969).

2) This compound was prepared by a procedure similar to that for the preparation of 1,5-cyclooctadiene-π-cyclopentadienyliridium.[3] Satisfactory results have been obtained for the analysis of all the compounds described in this communication.

3) S. D. Robinson and B. L. Shaw, *J. Chem. Soc.*, **1965**, 4997.

4) R. J. Angelici and E. O. Fischer, *J. Amer. Chem. Soc.*, **85**, 3733 (1963).

5) A. Kasahara, T. Izumi, and K. Tanaka, This Bulletin, **40**, 699 (1967).

6) This compound was prepared in a higher yield from the reaction of Vaska's complex with sodium cyclopentadienide.[7]

7) H. Yamazaki and N. Hagihara, "Symposium of Organometallic Compounds," Osaka, October 16, 1968; Preprints, p. 123.

Asymmetric Hydrogenation Catalyzed by Bis(dimethylglyoximato)cobalt(II)-Optically Active Amine Complex

Yoshiaki OHGO, Seiji TAKEUCHI, and Juji YOSHIMURA

Laboratory of Chemistry for Natural Products, Tokyo Institute of Technology, Meguro-ku, Tokyo

(Received November 11, 1970)

We reported that cyanocobalt - optically active amine complexes catalyze asymmetric hydrogenation.[1] It has been concluded that rigid conformational fixation and proximity of asymmetric grouping to the reaction center result in higher optical yield, but at the same time there is the drawback that the close and rigid grouping prevents coordination of substrate.

In order to overcome this, we sought a system in which a polyfunctional asymmetric substance bound to ligand could draw the substrate into the reaction center with a weakly attractive force.

On the other hand, it has previously been reported that bis(dimethylglyoximato)cobalt(II) complex, Co(DMG)$_2$, catalyzes hydrogenation of activated olefins, nitro-, azoxy-, and azo-benzenes, α-diketones, and α-keto carboxylic esters.[2,3] This complex has polar groups around the metal which are suitable for the binding of asymmetric substances. Thus we used this complex with quinine (polyfunctional, optically active substance) in the hydrogenation of benzil.

Catalytic hydrogenation was carried out at room temperature under atmospheric pressure of hydrogen. The reaction mixture was poured into water and extracted with benzene or ether. The organic layer was successively washed with water, hydrochloric acid, sodium hydroxide solution and water. The organic layer was concentrated *in vacuo* to give crystals which were characterized as benzoin by IR and NMR spectra. It was shown by gas-liquid chromatography and thin layer chromatography that the crystals contained no substantial contaminant. Optical yield was calculated from the specific rotation of the product and that of the optically pure benzoin. The results are shown in Table 1. In every case S(+)-benzoin was predominant.

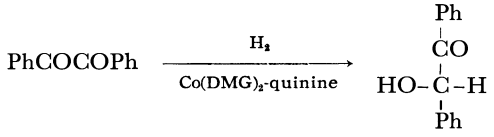

From the Table 1 it can be seen that increase in the molar ratio of substrate to cobalt or base causes no decrease in optical yield. The benzoin recovered after the treatment of racemic benzoin under the same conditions as in run 6 was found to be optically inactive. This indicates that the asymmetric synthesis is not due to a quinine-catalyzed isomerization(favored in S(+)-isomer) of racemic benzoin, but to the asymmetric induction at the stage of catalytic hydrogenation. Stereoselectivity of the asymmetric hydrogenation was sensitive to the polarity of the solvent. The reaction in benzene afforded maximum optical yield(61.5%). So far, this optical yield is the highest for homogeneous metal complex-catalyzed asymmetric syntheses.[4] However, the asymmetric induction seems to occur through a mechanism different from our initial idea, *i. e.*, one equivalent of optically active amine is enough to bring about maximum asymmetric yield, and alkylcobalt complexes produced by the reaction of olefins with Co(DMG)$_2$-Base and hydrogen have trans structure.[2] Provided that the reduction of benzil proceeds through the same reaction mechanism as that of olefins, the reaction must take place at the trans site which can not interact directly with asymmetry of the base. This asymmetric reaction would be considered to be due to an induced asymmetry on the bis-dimethylglyoxime ring.

TABLE 1. ASYMMETRIC HYDROGENATION OF BENZIL CATALYZED BY Co(DMG)$_2$-QUININE[a]

Run	S/Co[b]	B/Co[c]	Solvent (ratio)[d]	Yield (%)	$[\alpha]_D$[e]	Optical Yield (%)
1	5	3	M	98.5	+10.3	8.7
2	20	3	M/B(1.4)	99	+27.8	23
3	50	3	M/B(1.07)	85	+33.5	28
4	20	1	M/B(1.4)	96.5	+29.7	25
5	20	2	M/B(1.4)	99	+30.2	25.5
6	20	2	M/B(0.43)	96.5	+50.1	42
7	20	2	THF	95.5	+42.6	36
8	20	2	THF/B(0.6)	97	+59	50
9	10	2	B	98	+72.7	61.5

a) In this series of experiments a solution of quinine containing 0.48 molar equivalent HCl was used.
b) Molar ratio of substrate to cobalt.
c) Molar ratio of base (quinine) to cobalt.
d) Ratio of solvents in volume; M = methanol; B = benzene.
e) Solvent; acetone, $c = 2$—5. Specific rotation of optically pure isomer, $[\alpha]_D$, ±118.5 (acetone, $c = 1$).[5]

1) Y. Ohgo, K. Kobayashi, S. Takeuchi, and J. Yoshimura, presented at the 23rd Annual Meeting of Chemical Society of Japan, Tokyo, April, 1970; Y. Ohgo, S. Takeuchi, and J. Yoshimura, This Bulletin, **43**, 505 (1970).

2) G. N. Schrauzer, *Accounts Chem. Res.*, **1**, 97 (1968).

3) Y. Ohgo, S. Takeuchi, and J. Yoshimura, presented at the 23rd Annual Meeting of Chemical Society of Japan, Tokyo, April, 1970; S. Takeuchi, M. Sc. Dissertation, Tokyo Institute of Technology, March, 1969.

4) H. Nozaki, H. Takaya, S. Moriuti, and R. Noyori, *Tetrahedron*, **24**, 3655 (1968); L. Horner, H. Büthe, and H. Siegel, *Angew. Chem.*, **80**, 1034 (1968); W. S. Knowles and M. J. Sabacky, *Chem. Commun.*, **1968**, 1445 and references therein; P. Abley and F. J. McQuillin, *ibid.*, **1969**, 477.

5) I. V. Hopper and F. J. Wilson, *J. Chem. Soc.*, **1928**, 2483.

Hydrolysis of *p*-Nitrophenyl(deoxyguanylyldeoxyguanosine Succinate) by Deoxyguanylyldeoxyguanosine *N*-Acetylhistidate on Polycytidylic Acid

Takeo SHIMIDZU* and Robert L. LETSINGER**

*Faculty of Engineering, Kyoto University, Kyoto

**Department of Chemistry, Northwestern University, Evanston, Illinois, U.S.A.

(Received December 4, 1970)

For a study of a chemical reaction on a macromolecule, it is important to make clear a shape of the interaction of a reactant onto the macromolecule. The interaction between polyribonucleotide and oligodeoxyribonucleotide is specific and selective, although the magnitude of the interaction varies with its condition. In the present study, the shape of the interaction was investigated through the hydrolysis of *p*-nitrophenyl (deoxyguanylyldeoxyguanosine succinate) (I) by deoxyguanylyldeoxyguanosine *N*-acetylhistidate (II) on polycytidylic acid, Poly C, (III).

I and II were synthetized from di-*p*-methoxytrityldeoxyguanosine dimer.[1] I contained 1.2 *p*-nitrophenyl group per molecule and II contained 0.9 imidazolyl group per molecule.

Figure 2 shows the hydrolyses of I by II with poly C and without poly C. The hydrolysis rate, R, was

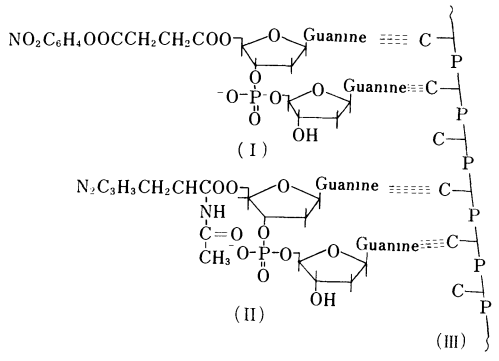

Fig. 1. Schematic diagram showing the hydrolysis of I by II on III.

1) T. Shimidzu and R. L. Letsinger, *J. Org. Chem.*, **33**, 708 (1968).

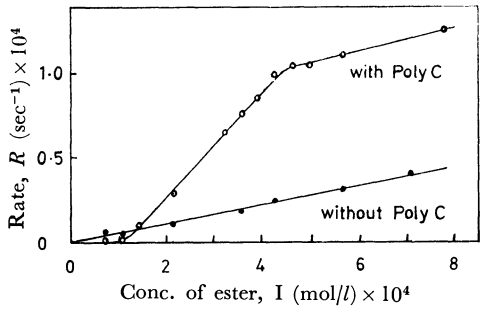

Fig. 2. Hydrolysis rates of I by II with and without Poly C.
○: presence of Poly C; 0.35×10^{-3} mol/l
●: absence of Poly C
0.01 M $MgCl_2$, 0.0001 M $Mg(OAc)_2$ pH=7.9; 5°C;
EtOH : H_2O = 1 : 100
I and II are the same concentrations.

defined as the increase of the hydrolyzed *p*-nitrophenol residue concentration per unit concentration of histidyl group, at the initial stage of the hydrolysis; R= [*p*-nitrophenol]/[*N*-acetylhistidine in II]·t.

The hydrolysis does not occur when the ratio of I and II to poly C is less than 0.2, but it increases linearly with the ratio exceeding 0.3. When the ratio is over 1.3, the rate increasing with I in the presence of poly C is parallel to that in the absence of poly C.

It can be concluded that the interaction between the dinucleotide derivatives and poly C is statistically homogeneous at lower concentrations, so that the distance of two dinucleotide derivatives widens and no reaction takes place, and also that the shape of the interaction becomes heterogeneous with increase of the concentration of the dinucleotide derivatives so that the reaction takes place because of a successive lining up.

Photochemical Reactions of Phenanthraquinone with Hydrogen Donors. An Investigation of the Reaction by CIDNP Method

Kazuhiro MARUYAMA, Heisaburo SHINDO,* and Tetsuo MARUYAMA*

Department of Chemistry, College of Liberal Arts and Science, Kyoto University, Kyoto

**Japan Electron Optics Laboratory, Akishima, Tokyo*

(Received December 5, 1970)

The rate of hydrogen abstraction by α-dicarbonyl compounds in triplet state is usually too fast for the observation of intermediate radicals by means of ESR technique. In order to make direct confirmation of the contribution of radicals in the photochemical reaction between phenanthraquinone and hydrogen donors, CIDNP (chemically induced dynamic nuclear polarization) technique[1] was applied. During the course of irradiation a strongly enhanced proton NMR absorption signal was observed at the methylene group region of photo-adduct. This is due to the secondary recombination process of two different intermediate radicals resulting from the primary hydrogen abstraction reaction by photo-excited phenanthraquinone triplet state as shown in the following:

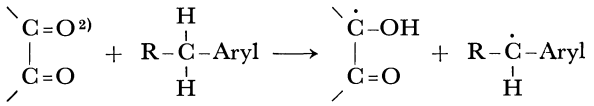

(primary hydrogen abstraction process)

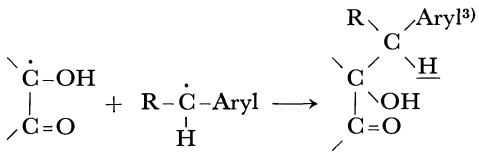

(secondary recombination process)

Phenomena of such an enhanced NMR absorption signal were observed during the course of irradiation in the following systems: phenanthraquinone and toluene (enhanced signal at τ: 7.10), phenanthraquinone and ethylbenzene (enhanced signal at τ: 7.10), and phenanthraquinone and diphenylmethane (enhanced signal at τ: 5.92). When irradiation was stopped, the enhanced signal disappeared immediately. Thus, the contribution of radical species in the hydrogen abstraction reaction of photo-excited α-dicarbonyl compounds was directly confirmed.

General procedures: Phenanthraquinone, dissolved into a hydrogen donor as solvent, was irradiated in a rotating NMR sample tube fitted with a light guide with a 500 W high pressure Hg lamp from above. Light was collected by a quartz lens before irradiation, and focused at the light guide. The light guide is a simple quartz tube coated on the in ner side with an aluminum metal. Oxygen dissolved into a sample was expelled by passing nitrogen. Assignment of a signal observed to the photo-adduct was carried out by comparison with that of the authentic sample, prepared by photochemical reaction of phenanthraquinone with a hydrogen donor on a larger scale. 60 MHz NMR spectrometer manufactured by JEOL was used.

1) G. L. Closs and L. E. Closs, *J. Amer. Chem. Soc.*, **91**, 4549 (1969); G. L. Closs, *ibid.*, **91**, 4550, 4552 (1969); G. L. Closs and A. D. Trifunac, *ibid.*, **91**, 4554 (1969); *ibid.*, **92**, 2183, 2186 (1970); G. L. Closs, C. E. Doubleday, and D. R. Paulson, *ibid.*, **92**, 2185 (1970); R. Kaptein and J. L. Oosterhoff, *Chem. Phys. Lett.*, **4**, 195, 214 (1969).

2) Photo-excited triplet state.

3) Enhanced signal is due to the underlined proton.

The Crystal Structure of *cis*-Dichlorobis(2,2′-dipyridyl)cobalt(III) Tetrachlorocobaltate(II), *cis*-[Co Cl_2 dip_2]$_2$[Co Cl_4]

Masayuki HINAMOTO, Shun'ichiro OOI, and Hisao KUROYA

Department of Chemistry, Faculty of Science, Osaka City University, Sugimoto-cho, Sumiyoshi-ku, Osaka

(Received December 10, 1970)

In 1936 Jaeger prepared a green-colored cobalt(III) complex,[1] [Co Cl_2 dip_2]Cl, whose cation has been believed to have a structure analogous to that of *trans*-[Co Cl_2 en_2]$^+$,[2] the two dipyridyl molecules being coplanar. A coplanar disposition of dipyridyl molecules, however, has never yet been found, not even for any of the bis-dipyridyl copper(II) complexes,[3-6] in which the dipyridyl molecules are most likely to be on a plane. This is attributable to the steric interference between the two dipyridyl molecules in this arrangement. Therefore, the structure of Jaeger's green cobalt complex is of much interest with respect to the disposition of the chelating ligands.

The crystals obtained by Jaeger's method[1] were too thin for X-ray work. Vlček found another way of preparing this compound.[7] The crystals of a suitable size were obtained following the latter method. However, none of the definite formulae, such as [Co Cl_2-dip_2]Cl, were compatible with the values of elemental analyses (C, 43.31; N, 10.00; H, 3.19%).

The crystal data were as follows: monoclinic, $a=21.22$, $b=14.11$, $c=7.36$ Å, and $\beta=98.3°$; the space group was $P2/n$. Z was assumed to be four. Multiple-film equi-inclination Weissenberg photographs, $hk0$-$hk5$, were taken with Ni$K\alpha$ radiation. The intensities of 1684 reflections were estimated visually, and the usual corrections were applied. The crystal structure was determined by the conventional Patterson and Fourier techniques and refined to an R factor of 0.136 by block-diagonal least-squares method, using isotropic thermal parameters.

It was established that the green crystal does not contain the *trans*-[Co Cl_2 dip_2]$^+$, but is composed of *cis*-[Co Cl_2 dip_2]$^+$ and [Co Cl_4]$^{2-}$ in a ratio of 2:1. The results of elemental analyses are consistent with the formula of *cis*-[Co Cl_2 dip_2]$_2$[Co Cl_4].[8] The crystal structure is shown in the figure. The geometry around the Co(III) atom is similar to that in *cis*-[Co Cl_2 en_2]$^+$[9] and in *cis*-[Co Cl_2 $phen_2$]$^+$.[10]

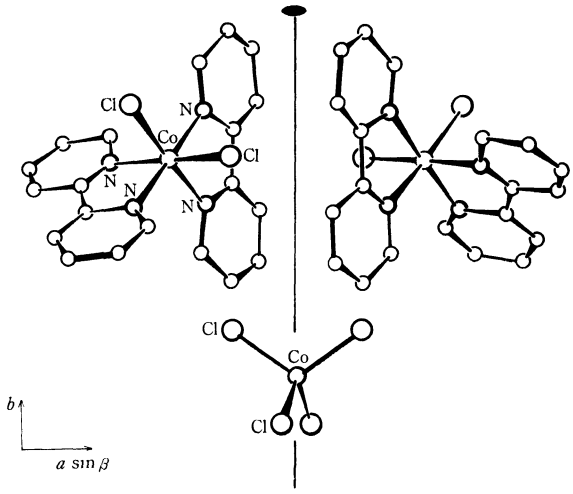

Figure. The crystal structure viewed along the c-axis.

The corresponding bond lengths and angles agree well with one another within the limits of experimental error; the values used below are averages. The Co(III)–Cl bond, 2.23 Å, compares well with those in the above complexes. In the chelate ring, ∠N–Co–N and ∠Co–N–C are 81.3° and 122.7° respectively. Both of the dipyridyl molecules are almost planar, the two pyridine rings twisting slightly to each other (~5°).

[Co Cl_4]$^{2-}$ is almost tetrahedral. Co(II)–Cl is 2.28 Å, which is consistent with that found in [$N(CH_3)_4$]$_2$[Co-Cl_4] (2.280 Å).[11]

1) F. M. Jaeger and J. A. van Dijk, *Z. Anorg. Allg. Chem.*, **227**, 273 (1936).
2) A. Nakahara, Y. Saito, and H. Kuroya, This Bulletin, **25**, 331 (1952).
3) G. A. Barclay, B. F. Hoskins, and C. H. L. Kennard, *J. Chem. Soc.*, **1963**, 5691.
4) H. Nakai, S. Ooi, and H. Kuroya, This Bulletin, **43**, 577 (1970).
5) I.M. Procter and F.S. Stephens, *J. Chem. Soc., A*, **1969**, 1248.
6) H. Nakai, private communication on the crystal structure of [Cu dip_2 (ClO_4)] (ClO_4).
7) A. A. Vlček, *Inorg. Chem.*, **6**, 1425 (1967).
8) The Vlček's green complex has been reexamined by J. G. Gibson, R. Laird, and E. D. McKenzie (*J. Chem. Soc., A*, **1969**. 2089); they concluded that it should be denoted as *cis*-[Co Cl_2-dip_2]$_2$ [Co Cl_4] on the basis of the studies of magnetic property, reflectance spectra and X-ray powder diffraction pattern. However, we have been unware of their work until recently.
9) K. Matsumoto, S. Ooi, and H. Kuroya, *Nippon Kagaku Zasshi*, **89**, 167 (1968).
10) A. V. Ablov, A. Yu. Kon, and T. I. Malinovskii, *Dokl. Akad. Nauk. SSSR*, **167**, 1051 (1966).
11) J. R. Wiesner, R. C. Srivastava, C. H. L. Kennard, M. DiVaira, and E. C. Lingafelter, *Acta Crystallogr.*, **23**, 565 (1967).

The X-Ray Emission Spectra of the Compounds of Third-period Elements. I. The *K* Spectra of Chlorine in Compounds

Yoshihito TAKAHASHI

Government Industrial Development Laboratory, Hokkaido, Higashi-Tsukisamu, Sapporo

(Received March 15, 1970)

On chlorine gas and several oxysalts of chlorine, the values of the wavelength shift of Cl$K\alpha_{1,2}$ lines and the spectra of Cl$K\beta$ lines were measured. We thus verified our assumption that the $K\beta'$ line results from the bias of valence electrons from the atom of the third-period element to the oxygen atom in the oxyanion; this can be explained in terms of the relationship between the chemical structure and the Cl$K\beta$ spectrum of the hypochlorite ion. The relationship between the relative intensity of the $K\beta'$ line and the wavelength shift of the $K\alpha_{1,2}$ lines was linear, just as in the cases of oxygen-sulfur compounds.

In previous papers, we reported our studies of the wavelength shifts of S$K\alpha_{1,2}$ lines and the shapes of the S$K\beta$ band spectra in many sulfur compounds.[1-3] It was found that a linear relation exists between the relative intensity of the S$K\beta'$ satellite line and the wavelength shift of the S$K\alpha_{1,2}$ lines in the spectra of oxygen-sulfur compounds. We think that this relationship offers a key for the assignment of the $K\beta'$ satellite line, which we have not yet been able to decide clearly. Therefore, in order to ascertain the generality of this relationship, we intend to extend our investigation to other elements of the third-period. In this paper, we will report on the $K\beta$ spectra of several chlorine compounds, particularly on the character of the $K\beta'$ line.

Recently, Best investigated the Cl$K\beta$ spectra of some oxysalts of chlorine.[4] Schnell measured the Cl$K\beta$ spectra on several chlorine compounds.[5] LaVilla and Deslattes measured the $K\beta$ spectra on some gaseous chlorine compounds.[6] On hypochlorite and chlorine gas, though, the *K* spectra have not yet been examined.

Experimental

The apparatus was the same as that described in previous papers.[1,3] A Machlett Wolfram target X-ray tube OEG-50 was operated at 40 kV, 40 mA. A flat, germanium analyzing crystal (2d: 6.53272 Å) was used. The helium path was maintained using a flow of 1.5 *l*/min at ordinary pressure. For the measurement of the spectrum of chlorine gas, a gas-sample cell was used.[7]

The wavelengths of the $K\alpha_{1,2}$ lines were measured as follows: the X-ray intensities were counted for a minute at intervals of $1'(2\theta)$; then, after drawing the spectral curve, the position of the line was decided as the maximum intensity position (the average of triplicates). In actual measurement, the wavelength shifts from the Cl$K\alpha_{1,2}$ lines of sodium chloride were measured. The absolute wavelength value of the Cl$K\alpha_{1,2}$ lines of sodium chloride was decided by comparison with the third-order line (4.62150 Å) for Cu$K\alpha_1$. The spectrum of the $K\beta$ lines was obtained as follows: the X-ray intensities were measured of a minute at intervals of $3'(2\theta)$, and then, after the substraction of the background (X-ray intensity at 4.54 Å), these intensities were plotted against the wavelength. Each spectrum was made on the same scale at the maximum intensity.

The separation of the $K\beta$ spectrum into several peaks was done as follows: 1) assuming that the $K\beta$ spectrum of sodium chloride can be taken as the standard shape of the C peak in Fig. 1, 2) to separate the C peak from each spectrum, this curve was superposed on the highest peak of each spectrum; 3) the A and D peaks were separated by the subtraction of C peak from the original spectrum. By the way, Best had reported in his paper the presence of a $K\beta_x$ satellite line at the short-wavelength side of the $K\beta_1$ line in the spectrum of sodium chloride,[4] but we could not separate them. Therefore, the present method might have a chance of mistakes in the separation of the D peak from the spectrum, but for the A peak ($K\beta'$ line) there can be no mistake.

A solution sample of sodium hypochlorite was prepared as follows: 1) to eliminate impurities (mainly chloride), a mixture of some higher bleaching powder and a small amount of cooled water was slowly stirred for ten or more minutes, and subsequently filtered. 2) The precipitate was dispersed into water and then, after about 30 min, filtered. 3) The filtrate was converted into a solution of sodium salt. The sample prepared by this method contained 0.80M hypochlorite and 0.09N chloride (impurity). After X-ray irradiation for two hours, the sample lost 5 percent of the hypochlorite and the equivalent amount of chloride was increased.

Results

In Fig. 1a—f, we show the Cl$K\beta$ spectra of the element and five compounds. The shapes of the spectra are similar to those of sulfur compounds which show a corresponding chemical structure, *i. e.*, chloride to inorganic sulfide, chlorate to sulfite, and perchlorate to sulfate, respectively. The characteristic values of the Cl$K\alpha_{1,2}$ lines and Cl$K\beta$ lines of the element and five compounds are listed in Table 1. In order to compare these data with the data of sulfur compounds, the directly-measured values of the energy shift in the $K\alpha_{1,2}$ lines of sodium chloride were converted to those of the element (Cl_2 gas). The intensity ratio of the $K\beta'$ line is defined as the ratio of the area of the $K\beta'$ line (the A peak in Fig. 1) to the total area of the $K\beta$ lines in the spectrum. A linear relationship exists between the

1) T. Sato, Y. Takahashi, and K. Yabe, This Bulletin, **40**, 298 (1967).
2) Y. Takahashi, K. Yabe, and T. Sato, *ibid.*, **42**, 2707 (1969).
3) Y. Takahashi and K. Yabe, *ibid.*, **42**, 3064 (1969).
4) P. E. Best, *J. Chem. Phys.*, **49**, 2797 (1968).
5) E. Schnell, *Monatsh. Chem.*, **93**, 1383 (1962).
6) R. E. LaVilla and R. D. Deslattes, *J. Chem. Phys.*, **45**, 3446 (1966).
7) The details of the gas-sample cell will be given by T. Sato *et al.*, in another paper.

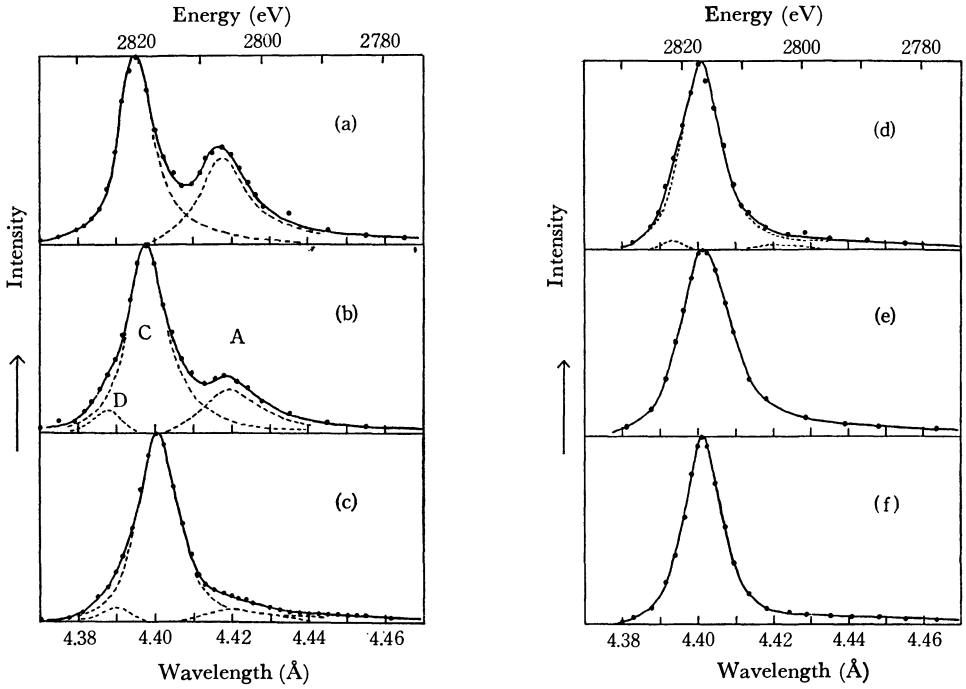

Fig. 1. a—f. $K\beta$ spectra of chlorine in compounds.
a: sodium perchlorate, b: sodium chlorate, c: sodium chlorite, d: sodium hypochlorite, e: chlorine gas, f: sodium chloride. A: $K\beta'$ line, C: $K\beta_1$ line.

TABLE 1. THE CHARACTERISTIC VALUES ABOUT THE Cl$K\alpha_{1,2}$ AND Cl$K\beta$ LINES

	$K\alpha_{1,2}$		$K\beta$			
				Intensity Ratio		
	λ (Å)	ΔE(eV)	λ(Å) C	A	C	D
NaCl	4.72949	−0.22	4.4015	0.00	1.00	0.00
Cl_2	909	±0.00	4.4005			
NaOCl	909	±0.00	4.4005	0.01	0.98	0.01
$NaClO_2$	872	+0.22	4.4000	0.09	0.86	0.05
$NaClO_3$	753	+0.87	4.3983	0.23	0.71	0.06
$NaClO_4$	660	+1.38	4.3955	0.37	0.63	0.00
Error		±0.07		±0.02		±0.02

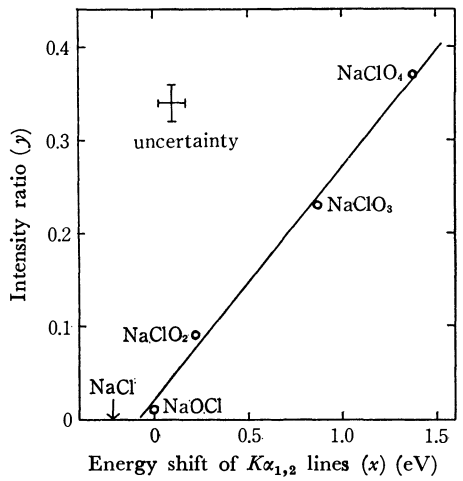

Fig. 2. Relationship between the intensity ratio and the energy shift of $K\alpha_{1,2}$ lines about chlorine compounds.
$y = 0.25x + 0.02$

intensity ratio of the $K\beta'$ line and the energy shift of the $K\alpha_{1,2}$ lines,[8] as is shown in Fig. 2.

Discussion

On the intensity ratio of the Cl$K\beta'$ line of the perchlorate, our value (sodium salt) is 0.37, but Best's (potassium salt) is 0.225,[4] in terms of the present definition. Under X-ray irradiation, potassium per-

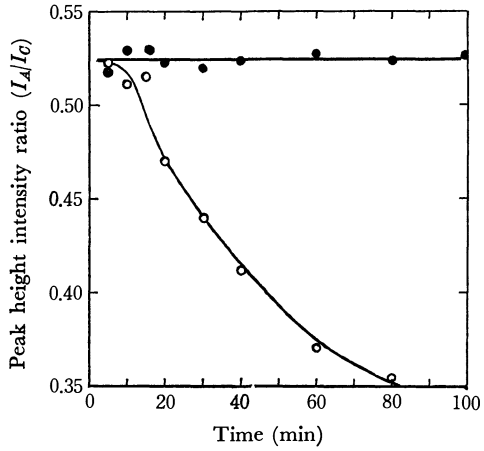

Fig. 3. Variation of the intensity ratio ($K\beta'/K\beta_1$) about perchlorates.
● $NaClO_4$ ○ $KClO_4$

8) The energy shift of the $K\alpha_{1,2}$ lines relates to the effective charges of the chlorine atom in a compound.[9-11]
9) E. Clementi, *Table of Atomic Functions, Suppl. to IBM J. Research and Development*, No. 1 (1965).
10) W. S. Urusof, *Dokl. Akad. Nauk SSSR*, **166**, 660 (1966).
11) W. I. Nefedow, *Phys. Status Solidi*, **2**, 904 (1962).

chlorate was decomposed to chloride,[12] and so its $K\beta'$ ratio was rapidly lowered, as is shown in Fig. 3. Moreover, his sample was placed in a vacuum; this might have caused the more rapid decomposition in his measurements. We adopted only the value of sodium salt.

In the previous paper,[3] we reported that the relative intensity of the $K\beta'$ line increased as the number of the valence electrons of the sulfur atom decreased. Therefore, we now presume that the $K\beta'$ line occurs as a result of the bias of valence electrons from the atom of the third-period element to the oxygen atom in the oxyanion. In the Cl$K\beta$ spectrum of a hypochlorite solution, the $K\beta'$ line is little observed; nevertheless, the oxygen atom is present in its molecule (see Fig. 1d). This result is explainable on the basis of the chemical structure of the hypochlorite ion ($Cl-O^-$) and our presumption relating to the occurrence of the $K\beta'$ line. That is, in this oxyanion, 1) the chlorine atom is combined with a oxygen atom by a single bond. The electron-inductive effect of the oxygen atom in a single bond is less than that of the oxygen atom in a double bond, and 2) the difference in the electronegativity between the oxygen atom (3.5) and the chlorine atom (3.0) is small. Moreover, the force of the electron attraction of the oxygen atom becomes weakened as a result of the acceptance of electrons from the sodium atom to the oxygen atom. Therefore, the valence electrons of the chlorine atom will be little attracted by the oxygen atom (indeed, the energy shift of Cl$K\alpha_{1,2}$ lines of this sample was small, if present at all). Consequently, from the above presumption, it may be concluded that the $K\beta'$ line occurs to only a small extent in the spectrum of hypochlorite. The above explanation serves to verify the assumption relating to the occurrence of the $K\beta'$ line.

For further discussion, we show the relationship between the relative intensity of the $K\beta'$ line and the energy shift of the $K\alpha_{1,2}$ lines for chlorine compounds in Fig. 2, and that for sulfur compounds,[3] in Fig. 4. To our surprise, the two relationships are expressed by the same straight line. From the fact that the straight line runs near the point of origin, there might be no other dominant factor which contributes to the occurrence of the $K\beta'$ line other than the energy shift of the $K\alpha_{1,2}$ lines, namely, the effective charges of the atom. From the equality of the gradient of the two lines, we cannot but think that the gradient of the line is determined by neither the sulfur atom nor the chlorine atom, but only by the oxygen atom, in oxygen-compounds. Nefedow claimed in his paper that, on the compound of the third-period element having second-period elements, the $K\beta'$ line was related to the electron transition from the molecular orbital to the $1s$ state of the third-period element, that this molecular orbital could virtually be regarded as the $2s$ orbital of the second-period element.[13] Our results seem to be consistent with his deduction.

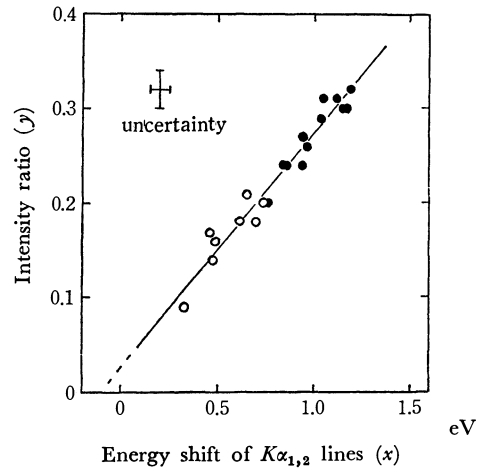

Fig. 4. Relationship between the intensity ratio and the energy shift of $K\alpha_{1,2}$ lines about sulfur compounds.
●: sulfate or sulfone ○: sulfite or sulfoxide
$y = 0.25x + 0.02$

The author wishes to thank Mr. K. Yabe for his considerable assistance and Dr. T. Sato and Mr. T. Takahashi for lending me the gas sample cell.

12) We detected the presence of a little chloride in the X-ray irradiated sample which had discolored to a yellow-brown upon titration with silver nitrate.

13) W. I. Nefedow, *Zh. Struk. Khim.*, **8**, 686, 1037 (1967).

The Chemisorption of Nitric Oxide and Nitrogen on Rhenium

Teijiro TAMURA

Department of Chemistry, Faculty of Industrial Arts, Kyoto Technical University, Matsugasaki, Sakyo-ku, Kyoto

(Received May 16, 1970)

The chemisorption of nitric oxide and nitrogen on a polycrystalline rhenium filament was studied using flash-desorption mass spectroscopy. For the chemisorption of nitric oxide, the initial sticking probability was found to be close to unity, with a saturation coverage of 5.2×10^{14} molecules/cm^2 at room temperature. Nitric oxide adsorbs nondissociatively, and dissociation occurs at an elevated temperature. The rate of the desorption of nitrogen from the nitric oxide layer is roughly proportional to θ^2. The majority of the oxygen in the nitric oxide layer was presumed to be liberated as rhenium oxide. The nitrogen adsorption was investigated in order to compare it with the nitric oxide adsorption. The saturation coverage and the initial sticking probability were 1.08×10^{14} molecules/cm^2 and 0.003 respectively.

Studies of the chemisorption of gases on metal surfaces are useful in deducing the mechanism of chemical reactions between gas and metal. Many studies in this field have been reported, and, recently, more useful information has been provided by such modern techniques as the method of flash filament, isotopic mixing, F.E.M., F.I.M., and L.E.E.D.[1-3]

Extensive studies of the chemisorption of gases on tungsten have been made,[4-19] but there have been only a few studies of rhenium.[20-26]

Although there is a general similarity between the physical properties of tungsten and rhenium, particularly in their very high melting points, there are some marked differences in their chemical properties;[27] for example, tungsten can form stable carbides and nitrides, while rhenium can not.

It is of interest to determine whether or not chemisorbed nitric oxide molecules are dissociated to form adsorbed atomic species, and what changes occur by flash desorption.

In the present investigations, the chemisorption of nitric oxide on rhenium has been studied using flash desorption mass spectroscopy. The saturation coverage of nitric oxide on rhenium was about one-third of that on tungsten, but the initial sticking probability was very high compared with that of other gases (its value was close to unity). The desorption of nitric oxide as molecules was negligibly small; the majority of the nitric oxide was decomposed and evaporated as nitrogen, oxygen, and rhenium oxide molecules when the rhenium temperature was raised.

Apparatus

The apparatus is shown schematically in Fig. 1. The reaction system, including the omegatron mass spectrometer, the Bayard-Alpert ionization gauge (B–A gauge), and the Pirani gauge, was all made of glass. The reaction vessel with a volume of $V=0.8\ l$ contained a rhenium filament with a geometrical area of $A=0.6$ cm^2. The rhenium filament was analyzed spectroscopically. (Found; Si:0.02%, Fe:0.008%, Mg: 0.005%.) The system was pumped through a greaseless valve with an ion pump. After a rigorous outgassing of all parts of the system, the ultimate pressure, as read with the B–A gauge, was 3×10^{-10} Torr. The omegatron mass spectrometer was operated in a magnetic field of 3600G with a variable r. f. generator driven by a synchronous motor. The ion currents were measured with a high-sensitivity electrometer (TAKEDA RIKEN TR-81). The mass spectrum was recorded on a chart recorder with a 0.8 sec full-scale response. Under the conditions employed, the 28—30 masses were completely resolved, the sensitivities were taken to be 12 Torr^{-1} for N_2 (mass 28) and 11.8 Torr^{-1} for NO (mass 30). The omegatron was also used to measure the partial pressure as a function of the time in slow-flash experiments. This was done by recording the

1) J. A. Becker "Advances in Catalysis," Vol. 7, ed. by W. G. Frankenburg, V. I. Komarewsky, and K. E. Rideal, Academic Press, New York (1955), p. 135.
2) G. Ehrlich "Advances in Catalysis," Vol. 14, ed. by D. D. Eley, H. Pines, and P. B. Weisz, Academic Press, New York (1963), p. 255.
3) D. O. Hayward and B. M. W. Trapnell, "Chemisorption," 2nd ed., Butterworths, London (1964).
4) J. Eisinger, *J. Chem. Phys.*, **29**, 1154 (1958).
5) T. W. Hickmott and G. Ehrlich, *J. Phys. Chem. Solids*, **5** 47 (1958).
6) J. Eisinger, *J. Chem. Phys.*, **30**, 412 (1959).
7) J. A. Becker, E. J. Becker, and R. G. Brandes, *J. Appl. Phys.*, **32**, 411 (1961).
8) G. Ehrlich, *J. Chem. Phys.*, **34**, 29 (1961).
9) G. Ehrlich, *ibid.*, **34**, 39 (1961).
10) P. A. Redhead, *Trans. Faraday Soc.*, **57**, 641 (1961).
11) T. Oguri, *J. Phys. Soc. Japan*, **18**, 1280 (1963).
12) L. J. Rigby, *Can. J. Phys.*, **42**, 1256 (1964).
13) L. J. Rigby, *ibid.*, **43**, 532 (1965).
14) T. E. Madey, J. T. Yates, Jr., and R. C. Stern, *J. Chem. Phys.*, **42**, 1372 (1965).
15) J. T. Yates, Jr., and T. E. Madey, *ibid.*, **43**, 1055 (1965).
16) T. E. Madey and J. T. Yates, Jr., *ibid.*, **44**, 1675 (1966).
17) J. T. Yates, Jr., and T. E. Madey, *ibid.*, **45**, 1623 (1966).
18) J. L. Robins, W. K. Warburton, and T. N. Rhodin, *ibid.*, **46**, 665 (1967).
19) B. McCarroll, *ibid.*, **46**, 863 (1967).
20) M. D. Scheer and J. D. McKinley, *Surface Sci.*, **5**, 332 (1966).
21) R. P. H. Gasser and R. Thwaites, *Vacuum*, **17**, 265 (1967).
22) R. P. H. Gasser, R. Thwaites, and J. Wilkinson, *Trans. Faraday Soc.*, **63**, 195 (1967).
23) R. P. H. Gasser, K. Roberts, and R. Thwaites, *ibid.*, **63**, 2765 (1967).
24) T. Hamamura and G. Tomita, This Bulletin, **40**, 1066 (1967).
25) K. F. Poulter and J. A. Pryde, *Brit. J. Appl. Phys. Ser., 2*, **1**, 169 (1968).
26) J. T. Yates, Jr., and T. E. Madey, *J. Chem. Phys.*, **51**, 334 (1969).
27) C. T. Sims "Rhenium," ed. by B. W. Gonser, Elsevier, New York (1962), p. 27.

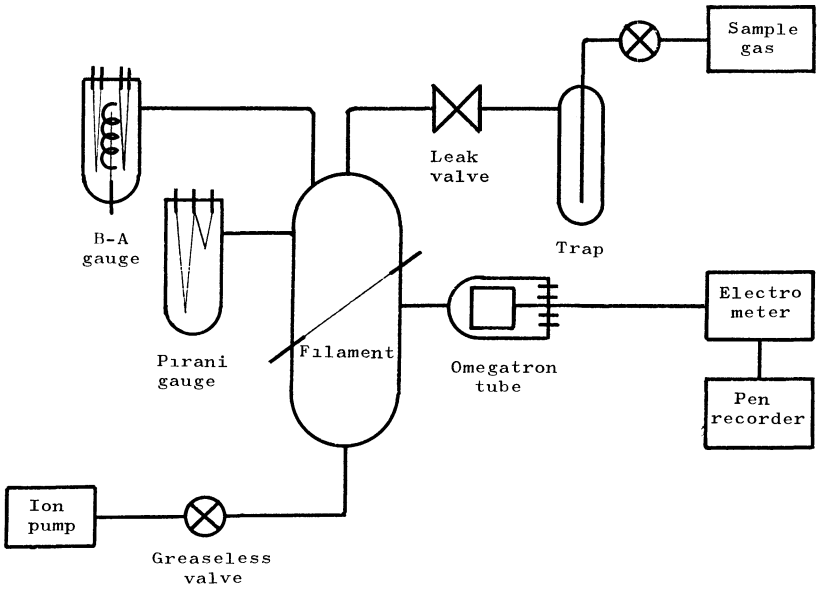

Fig. 1. Schematic drawing of the apparatus for flash desorption mass spectroscopy.

time variation of the ion current at a constant r.f. corresponding to a particular mass peak.

The Pirani gauge was used to measure the total pressure; it has a sensitivity of 7.2×10^{-8} Torr/μV for N_2 and NO. The B–A gauge was used only to measure the ultimate pressure; it was not operated during the actual experiments.

The rhenium filament could be flashed rapidly (within 1 sec) to 2200°K for rapid desorption experiments or slowly to 2000°K, with an approximately linear sweep rate of 20°/sec, for slow desorption experiments, by means of a controllable DC power supply. The temperature of the filament was determined from the resistance using the published values of the resistance-temperature relationship for rhenium,[28] above 1000°K, its temperature was also measured with a micro optical pyrometer.

The nitric oxide was prepared by dropping sulfuric acid into a mixed solution of potassium nitrate and potassium iodide. The gas thus evolved was passed through a concentrated caustic potash solution and a dry ice trap, was purified by liquid nitrogen trap-to-trap distillations, and was finally stored in a 1 *l* gas reservoir.

The nitrogen was prepared by the thermal decomposition of barium azide, labeled extra pure, and was introduced into a gas reservoir through the liquid nitrogen trap and stored there without further purification. No impurities up to mass 200 were detected by means of the omegatron mass spectrometer.

Procedure

Amount of Adsorption. In order to burn off any possible carbonaceous surface contamination prior to the adsorption experiments, the rhenium filament was heated to about 2000°K in oxygen of 1×10^{-6} Torr for several hours. When the rhenium filament is heated at high temperature in a nitric oxide atmosphere, rhenium oxide is formed on the surface. Therefore, the conventional flash-filament method[1,2,5,10] can not be used. To avoid this difficulty, the rhenium filament was flashed in a vacuum to clean it and then allowed to cool to room temperature. The leak-valve was opened to give a suitable exposure of the nitric oxide, and the pressure was recorded, by means of the omegatron or Pirani gauge, as a function of the exposure time. The number of nitric oxide molecules that strike the filament during the exposure can be calculated from the pressure-*vs.*-time curve. After the leak-valve was closed, the system was evacuated until the nitric oxide pressure dropped to 5×10^{-9} Torr. The system was then separated from the evacuating system by means of the greaseless valve, and the rhenium filament was flashed at 2200°K in the closed system. The amount of molecules desorbed can be calculated from the pressure and the volume of the system. In the case of the adsorption of nitric oxide, the number of molecules adsorbed is twice the number of molecules desorbed, because the desorbed gas is nitrogen.

Desorption Spectra. Nitric oxide or nitrogen, at a desired pressure, was streamed over the rhenium filament by adjusting the leak-valve. After the desired exposure time had passed, the leak-valve was closed and the system was evacuated. When the pressure dropped to 5×10^{-9} Torr, the slow desorption runs were initiated by using a controllable DC power supply. At that time, ion currents of the omegatron mass spectrometer for each mass were recorded on the chart recorder as a function of the time. The desorption spectra were obtained for each chemical species; they are shown in Fig. 6.

Results and Discussion

Sticking Probability and Amount of Adsorption. The number of molecules of nitric oxide that strike

28) C. T. Sims, C. M. Craighead, R. I. Jaffee, D. N. Gideon, E. N. Wyler, F. C. Todd, D. M. Rosenbaum, E. M. Sherwood, and I. E. Campbell, "Investigations of Rhenium," Battle Memorial Institute, Wright Air Development Center Technical Report 54—371, June (1954), p. 47.

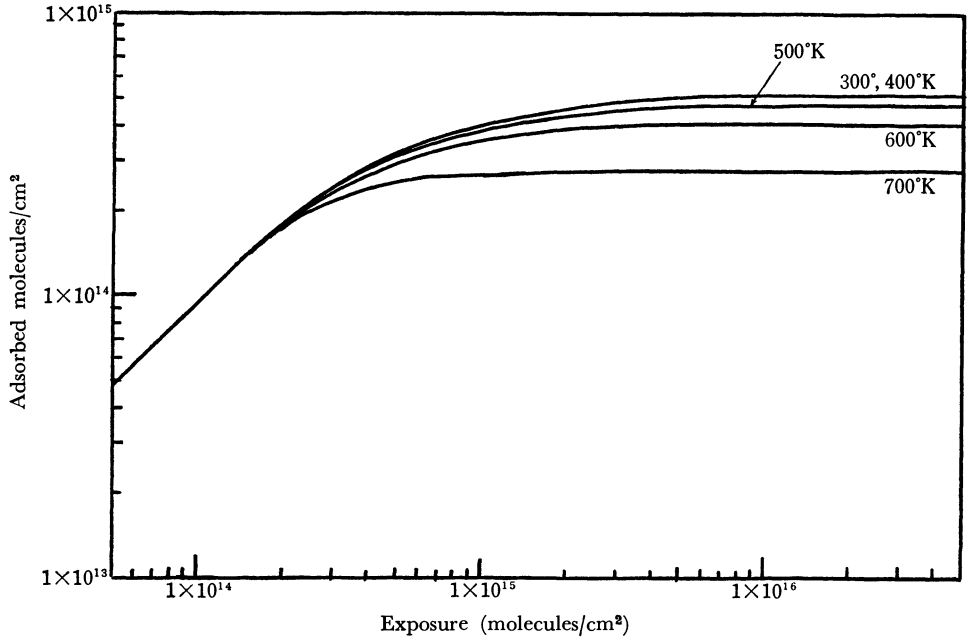

Fig. 2. Surface coverage as a function of exposure.

the filament during the adsorption process, $N_{(e)}$, is calculated from the recorder trace of the omegatron, while the number of molecules adsorbed, N, is obtained by rapid flashing into the closed system, as has been described above. The relation between the number of molecules colliding with the filament at various temperatures and those adsorbed is shown in Fig. 2. The saturation coverage (θ=1) of nitric oxide was 5.2×10^{14} molecules/cm² at 300°K, about one-third of that on tungsten (1.4×10^{15} molecules/cm²).[17] When the rhenium temperature was increased, the saturation coverage of nitric oxide decreased, as Fig. 2 shows. Assuming that the number of metal surface atoms is 1.5×10^{15} atoms/cm², these are equivalent to a Re: NO ratio of about 3:1 and to a W:NO ratio about 1:1. It seems that a considerable number of bare sites exist on rhenium, even for the full coverage of the nitric oxide adsorption.

From the curve in Fig. 2, the sticking probability, s, can be calculated by means of the following equation:

$$s = \mathrm{d}N/\mathrm{d}N_{(e)}.$$

The dependence of the sticking probability on the coverage at various temperatures is shown in Fig. 3. The initial sticking probability is close to unity. Such a high value has not been seen for other gases.[20-22,25,26] Therefore, the Re-N_2 system was studied by the same method for the sake of comparison. The saturation coverage of nitrogen on rhenium was 1.08×10^{14} molecules/cm², this value agreed well with the previously-reported values, 1.5×10^{14} molecules/cm² at 291°K,[21] 7×10^{13} molecules/cm² at 300°K,[20] and 8.9×10^{13} molecules/cm² at 300°K.[26] The initial sticking probability was 0.003; this also agreed well with the previously-reported values of 0.0024[21] and 0.0022,[26] but it differed from that of 0.009.[20] This difference can be accounted for by differences in the polycrystalline wires used.

The results obtained by the usual method, using the flash desorption at a constant flow rate,[10] also agreed well with those of the present method.

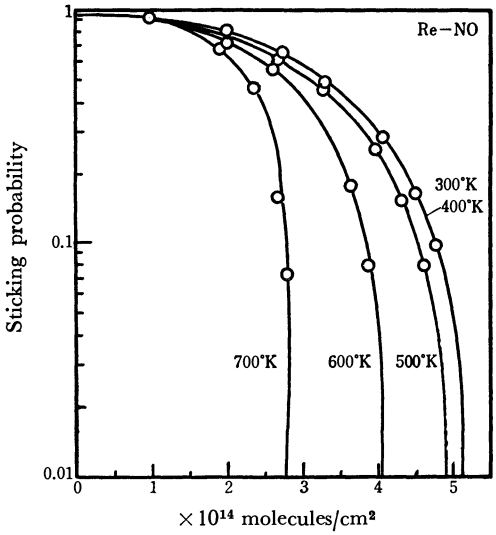

Fig. 3. Sticking probability as a function of surface coverage.

The saturation coverage of nitric oxide is 4.8 times as much as that of nitrogen on the same rhenium. This ratio agrees well with that on tungsten.[17] However, the saturation coverage on rhenium is smaller than that on tungsten.

The initial sticking probability of the nitric oxide adsorption is very high compared with the nitrogen adsorption on rhenium. We consider that one of the reasons for such a high value is probably that the electron in the nitric oxide molecule transfers easily to the vacant *d*-orbital in rhenium, because the ionization potential of nitric oxide (9.5 eV) is lower than that of nitrogen (~16 eV).[29]

29) R. B. Heslop and P. L. Robinson "Inorganic Chemistry," Elsevier Pub., Co., New York (1960), p. 319.

Rates of Adsorption and Desorption. At various combinations of the pressure of nitric oxide and the exposure time needed to obtain the same exposure, it was found that the amounts of adsorptions were always the same. These results show that the rate of adsorption depends on the first-power of the pressure. The rate of adsorption at a constant pressure and temperature may, then, be expressed as:

$$dN/dt = K \cdot P(1-\theta)^n,$$

where K and n are constants and where P is the nitric oxide pressure.

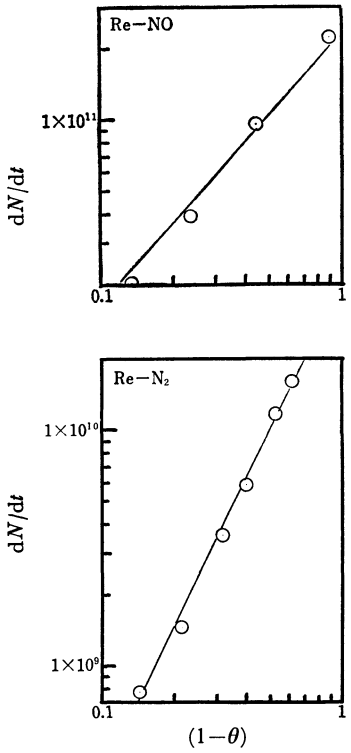

Fig. 4. The relation between the rate of adsorption and $(1-\theta)$.

For the nitric oxide and the nitrogen adsorption at a constant pressure and 300°K, the dependence of the rate of adsorption on the vacant site, $(1-\theta)$, is shown in Fig. 4. On the nitric oxide adsorption, it was found that the rate of adsorption was proportional to $(1-\theta)$ for surface coverages between 0.1 and 0.8. This indicates that the nitric oxide molecules are adsorbed non-dissociatively on rhenium. On the nitrogen adsorption, it is shown that the adsorbed nitrogen exists dissociatively, because the rate of adsorption was proportional to $(1-\theta)^2$.

When the adsorbed nitric oxide or nitrogen is desorbed at a definite temperature in the closed system, the rate of desorption may be simply written as:

$$-dN/dt = K'\theta^{n'},$$

where K' is a rate constant of the $K'=\nu\exp(-E/\boldsymbol{R}T)$ form and where n' is the order of the desorption. In the Re-NO system, the nitric oxide is decomposed with a rise in the rhenium temperature and is desorbed as nitrogen. The relation between the rate of desorption and the surface coverage is shown in Fig. 5. As

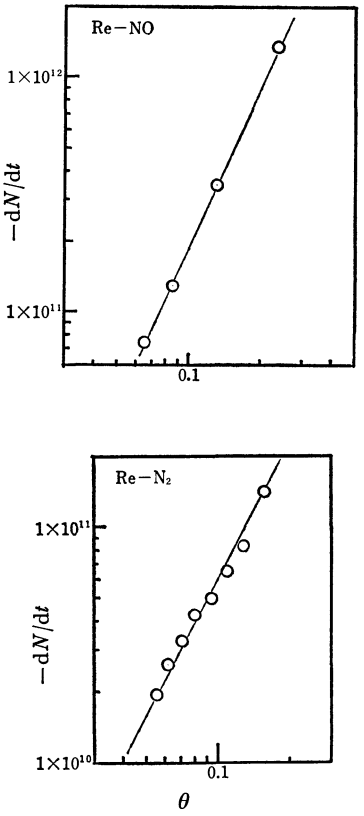

Fig. 5. The relation between the rate of nitrogen desorption and θ.

can be seen, the rate of the desorption of nitrogen from both nitric oxide and nitrogen layers is roughly proportional to θ^2. At such high temperatures, the re-adsorption can be neglected.

Desorption Spectra. *1) Desorption from a Nitric-oxide Monolayer on Rhenium*: For the saturation coverage of nitric oxide, the desorption spectra are shown in Fig. 6. The evolution of nitric oxide (mass 30) begins at about 350°K. The temperature of the desorption-peak maximum was about 450°K, and above 900°K no further desorption of nitric oxide was observed. The amount of nitric oxide desorbed corresponds to about 0.5% of the total amount of nitric oxide at saturation coverage.

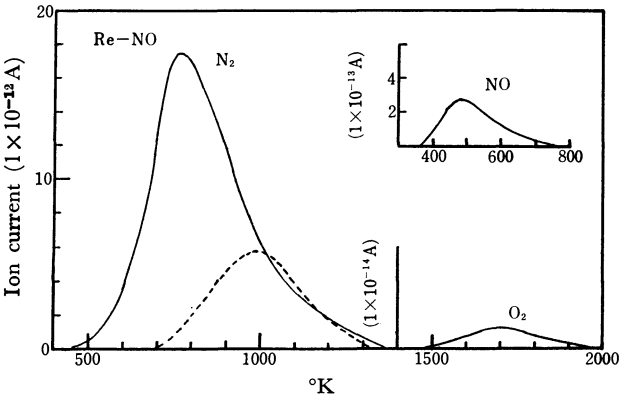

Fig. 6. The desorption spectra from a nitric oxide monolayer on rhenium.
Dashed curve denotes nitrogen from nitrogen monolayer.

For the desorption of nitrogen from a nitric oxide monolayer, the temperature at which the desorption rate was at its maximum, T_p, was 775°K, and the greater part of the nitrogen was desorbed before the temperature reached to 1300°K. The T_p of nitrogen desorption from a nitric oxide monolayer is lower than that from a nitrogen monolayer by about 200°K.

The oxygen desorption was seen at a considerably high temperature, and the T_p of oxygen was about 1700°K. The amount of oxygen desorbed was relatively small. From these results, it seems that the majority of the oxygen from nitric oxide evaporates as rhenium oxide.

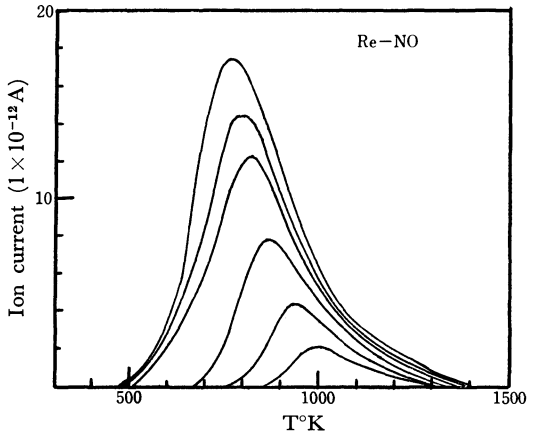

Fig. 7. The desorption spectra from various initial coverages of nitric oxide.

2) Desorption of Nitrogen from a Partial Coverage of Nitric Oxide on Rhenium: The nitrogen desorption spectra for various initial coverages of nitric oxide ($\theta\simeq0.1$—1.0) at 300°K are shown in Fig. 7. The T_p of the nitrogen desorption monotonously shifts to higher temperatures with a decrease in the coverage. On the chemisorption of nitric oxide on tungsten, a retrograde behavior of T_p above $\theta=0.8$ was observed in the nitrogen desorption spectra, and two ω mode peaks (ω_1, ω_2) were observed in the desorption spectrum.[17] However, no such behavior was observed for the nitric oxide adsorption on rhenium. Yates *et al.*[17] state that vacant sites are necessary for the decomposition of nitric oxide on tungsten. If this assumption is true, the fact that a retrograde T_p behavior was not found on rhenium at a high coverage can be understood from the fact that the vacant sites already existed on the rhenium surface, as has been mentioned above.

The desorption spectra from the very low coverages of nitric oxide on rhenium resemble those from the very low coverages of nitrogen. This behavior is reasonable, since the dissociation of nitric oxide at a very low coverage and at an elevated temperature would produce a dilute layer of adsorbed nitrogen and oxygen; the desorption of nitrogen should, under these conditions, be uninfluenced by the small oxygen coverage. Therefore, the processes of adsorption, dissociation, and desorption may be simply expressed as follows:

$$NO_{(g)} \longrightarrow NO_{(a)} \quad (1)$$

$$NO_{(a)} \longrightarrow N_{(a)} + O_{(a)} \quad (2)$$

$$2N_{(a)} \longrightarrow N_{2(g)} \quad (3)$$

Equations (2) and (3) show the reactions during the heating process. We consider that the rate of the process (2) is faster than that of the process (3), since the rate of nitrogen desorption is roughly proportional to θ^2.

3) Desorption of Nitrogen from a Nitrogen Layer on Rhenium: Although studies of the nitrogen adsorption of rhenium had previously been made,[20,21,26] the present experiments were carried out to compare it with the nitric oxide adsorption. An α state was not found in the nitrogen desorption spectra from the nitrogen layer. This result agreed with that of Yates *et al.*[26] Although the β state from nitrogen layer on tungsten was separated into two states, β_1 and β_2,[11,13,15,16] the β state from the nitrogen layer on rhenium was only one state (corresponding to β_2); this finding agreed with those of other papers.[20,21,26] Since the desorption energy of nitrogen on rhenium is lower than that on tungsten, the binding force with rhenium may be said to be weaker than that with tungsten.[26] Therefore, it seems that the β_1 (weaker than β_2) adsorption may not occur; the lack of a β_1 state may be a reason why many vacant sites remain on rhenium for the nitric oxide adsorption compared with those on tungsten.

Summary

1) The saturation coverage of nitric oxide on rhenium is 5.2×10^{14} molecules/cm^2, and the sticking probability is close to unity in the initial stage of adsorpion at room temperature.

2) Nitric oxide adsorbs nondissociatively on rhenium at room temperature. The rate of adsorption is proportional to $(1-\theta)$.

3) As the rhenium temperature is increased, the saturation coverage of nitric oxide decreases.

4) The evolution of nitric oxide (mass 30) begins at about 350°K, and the amount of nitric oxide corresponds to about 0.5% of the saturation coverage.

5) The rate of the desorption of nitrogen from a nitric oxide layer is proportional to θ^2.

6) The T_p of nitrogen desorption from a nitric oxide monolayer is lower than that from a nitrogen monolayer by about 200° as a result of the interactional effect in the adsorbed layer of oxygen.

7) A small fraction of the oxygen from the nitric oxide layer desorbs above 1500°K as molecules; it seems that the rest of the oxygen evaporates as rhenium oxide.

8) At a high coverage of nitric oxide, the retrograde behavior of T_p for nitrogen desorption is not observed.

9) At a very low nitric oxide coverage, the desorption spectra resemble those from a very low coverage of nitrogen.

10) The saturation coverage of nitrogen on rhenium is 1.08×10^{14} molecules/cm^2, and the initial sticking probability is 0.003 at room temperature.

11) Nitrogen adsorbs dissociatively at room temperature. The rate of adsorption is proportional to $(1-\theta)^2$.

12) For nitrogen adsorption at room temperature, an α state is not found, and the β state is only one state.

The author wishes to express his deep thanks to Professor Takuya Hamamura of this Institute, to Professor Kumasaburo Kodera and Dr. Masaru Onchi of Kyoto University for their kind discussion and encouragement, and to Dr. Minoru Ozasa of the Matsushita Electronics Corporation, who made the spectroscopic analysis of rhenium.

BULLETIN OF THE CHEMICAL SOCIETY OF JAPAN, VOL. 44, 595—599 (1971)

Inter and Intramolecular Charge and Excitation Transfer Observed in Irradiated Polyvinyl Chloride Particles with Surface-coated Additives

Hisashi UEDA and Dairokuro YASHIRO

Government Chemical Industrial Research Institute, Tokyo, Mita, Meguro-ku, Tokyo

(Received May 27, 1970)

Particles of polyvinyl chloride were coated with small amounts of various aromatic compounds from benzene solutions and were then irradiated in a vaccum. The ESR spectra of the specimen thus obtained were recorded. Though the amount of the coated additives, in the ratio of 1 molecule for 100 monomer units of PVC, was small, strong effects on the ESR spectra were observed. The additives coated on the surface affect the ESR spectra in two ways. They cause a decrease in the total ESR absorption intensity; this was observed with all the additives studied. They also often transform the ESR spectrum; this was observed with several additive compounds, such as *p*-benzoquinone, tetramethylphenylenediamine-2·HCl, chrysene, hydroquinone, nitrosonaphthol, perylene, and diphenylpicrylhydrazine. Only the conduction of the excitations, holes and electrons formed in the bulk particles, to the surface of the particle can explain these results. On the surface of the particle, the excitation or the electric charge is transferred to the additive by means of an intermolecular interaction with it. The possibilities for the mechanism of the conduction of the excitation and the electric charges, and the ionization processes are discussed.

Ueda and his co-workers studied the ESR spectra of γ-irradiated polyvinyl chloride (to be abbreviated as PVC) and their trans-formations in the presence of various gases.[1-5] Some of the anomalies observed in these transformations were ascribed to free radical transformations. In the past decade, much evidence for ionic processes has been found for the systems including alkyl halide-aromatic hydrocarbon solutions in both the solid and liquid phases.[6-10] It seems quite obvious, however, that free radical interpretations do not wholly account for the observed phenomena.[5] Therefore, it is necessary to reinvestigate the ESR of irradiated PVC from a different point of view.

The results of the kinetic studies of the pulse radiolysis of the alkyl halide-aromatic hydrocarbon solutions showed that only the "conduction theory" of the ions and possibly their precursors explains the kinetic data obtained. Therefore, it seems desirable to test further the possibilities of the conduction of the radiation-induced activated species across a particle of PVC.

The transient species generated in radiation-chemical systems are observed either by a quick-detection method or by trapping them in some stable forms. Many experiments have been done by trapping them in frozen rigid glass.[9,10] It has also been possible to trap them on porous solid surfaces. For this reason, we expected to find some stable ionic species on the surface of PVC which are trapped and stabilized at room temperature.

Experimental

The PVC powder used in this study was Vinychlon 4000L of the Mitsui Toatsu Chemical Co.; it contained no additives. The particle were all below 50 mesh in size. 0.500 g of PVC (8 mmol of $-CH_2CHCl-$ equivalent) and 0.08 mmol of additive were mixed, and then 2.0 m*l*, or more if needed, of benzene was poured onto it in order to dissolve the additive completely. The mixture thus prepared was kept in the air at room temperature under a dust cover to evaporate the solvent. The sample thus obtained, *i. e.*, the PVC particles coated with an additive, was placed in a spectrosil ESR sample tube; the tube was evacuated to 10^{-4} mmHg and then sealed off. Irradiation was made with 1.5 kCi ^{60}Co source to the dose of 6.65×10^4 rad (referred as D_1) and 7.315×10^5 rad (referred as D_2) at 20°C.

In this work, the number of unpaired electrons trapped in the specimen must be determined, together with their physical states. For this reason, the quantitative measurements were carried out as follows. A microwave output of 9V54 was attenuated to exactly 1/10, thus maintaining the same incident powder. The crystal current of the detector, 1N23C, was always adjusted to the same value, 0.08 mA, by adjusting the dielectric rod in one of the arms of the magic

1) Z. Kuri, H. Ueda, and S. Shida, *Isotopes and Radiation*, **2**, 496 (1959).
2) Z. Kuri, H. Ueda, and S. Shida, *J. Chem. Phys.*, **32**, 371 (1960).
3) Z. Kuri and H. Ueda, *J. Polymer Sci.*, **50**, 349 (1961).
4) H. Ueda and Z. Kuri, *J. Appl. Polymer Sci.*, **5**, 478 (1961).
5) H. Ueda and S. Shida, *Kogyo Kagaku Zasshi*, **69**, 1527 (1966).
6) H. Ueda, This Bulletin, **41**, 2578 (1968).
7) H. Ueda, *ibid.*, **43**, 297 (1970).
8) H. Ueda, *J. Phys. Chem.*, **71**, 3084 (1967).
9) T. Shida and W. H. Hamill, *J. Chem. Phys.*, **44**, 2375 (1966).
10) T. Shida and W. H. Hamill, *ibid.*, **44**, 4372 (1966).

tee. 100 kHz phase-sensitive amplifier was allowed to stand for at least three hours prior to use. The overall signal intensity was checked and calibrated by using standard specimens, such as dispersed charcoal in alumina powder sealed in a vacuum, and Mn^{2+} ions diluted with MgO.

Results

The intensities of the ESR absorption for D_1 are listed in Table 1. The paramagnetic species, which is observed in the PVC without any additive and which shows the ESR spectrum of Fig. 1a when irradiated to D_1 in a vacuum, is written as S·. The S· has been described as a free radical in the early literature,[1,2] but its true nature has not been known exactly. Its observed amount is written as r_0. The amount of S· obtained with the PVC with an additive at the same dose is written as r. The r/r_0 ratio is shown in Table 1. The amount of the species which is obtained at the dose of D_1, and which shows the ESR spectra shown in Figs. 1b and 1c, is written as r_+. The r_+/r_0 ratio is also shown in Table 1. The same values for D_2 are listed in Table 2. In Table 2, the spin concentration (divided by r_0) due to the species, which was unaffected by bleaching the sample in air, A^+-left, is also shown. In Figs. 1—3, the ESR spectra obtained from the PVC-perylene, PVC-hydroquinone, PVC-*p*-benzoquinone, PVC-α-nitroso-β-naphthol, and PVC-β-nitroso-α-naphthol specimens are shown. Figure 1b′ indicates that there are eight almost equivalent protons which interact with the unpaired electron. Figure 1c indicates that at the dose of D_2, the spectrum resembles Fig. 1a more than Fig. 1b (see Tables 1 and 2) with respect to r_+/r_0. The same tendencies may be found in Fig. 2. In Fig. 3b, the hyperfine splitting is better resolved than in Fig. 3a because the absorption due to S· had been bleached by

Table 1. The concentrations of various species after irradiation to D_1

Additive	r/r_0	r_+/r_0	$1-r/r_0$	$\frac{1-r_+/r_0}{-r/r_0}$
p-Benzoquinone	0.000	0.793	1.000	0.207
Tetramethylphenylenediamine -2·HCl	0.000	0.377	1.000	0.622
Chrysene	0.000	0.179	1.000	0.821
Fluorene	0.008	0.092	0.992	0.901
2,3-Benzophenanthrene	0.106	0.008	0.894	0.887
3-Methylcholanthrene	0.113	0.000	0.887	0.887
Dibenzoanthracene	0.191	0.153	0.809	0.656
Hydroquinone	0.202	0.462	0.798	0.336
α-Nitroso-β-naphthol	0.216	0.195	0.784	0.588
trans-Stilbene	0.271	0.000	0.729	0.729
o-Terphenyl	0.281	0.000	0.719	0.719
Anthracene	0.292	0.000	0.708	0.708
β-Nitroso-α-naphthol	0.304	0.127	0.696	0.569
Styrene	0.306	0.000	0.694	0.694
Triphenylbenzene	0.318	0.034	0.682	0.648
Perylene	0.324	0.173	0.676	0.503
Phenanthrene	0.333	0.000	0.667	0.667
Pyrene	0.333	0.000	0.667	0.667
m-Terphenyl	0.370	0.000	0.630	0.630
Triphenylethylene	0.380	0.000	0.620	0.620
Naphthalene	0.385	0.000	0.615	0.615
p-Terphenyl	0.401	0.000	0.599	0.599
Diphenylpicrylhydrazine	0.406	0.497	0.594	0.097
Anthrone	0.412	0.013	0.588	0.575
Phenylacetylene	0.428	0.000	0.572	0.572
α-Naphthylamine	0.434	0.000	0.566	0.566
Thio-β-naphthol	0.441	0.000	0.559	0.559
Biphenyl	0.458	0.000	0.542	0.542
Tetraphenylethylene	0.449	0.070	0.551	0.481
Diphenylamine	0.463	0.000	0.537	0.537
Benzoine	0.486	0.000	0.513	0.513
α-Nitronaphthalene	0.499	0.000	0.501	0.501
Triphenylamine	0.510	0.000	0.490	0.490
Triphenylene	0.544	0.000	0.456	0.456
Anthraquinone	0.573	0.000	0.426	0.426
Azobenzene	0.595	0.000	0.404	0.404
α-Naphthoquinone	0.662	0.000	0.338	0.338
α-Naphthol	0.691	0.000	0.309	0.309

Table 2. The concentrations of various species after irradiation to D_2

Additive	r/r_0	r_+/r_0	$\frac{1-r_+/r_0}{-r/r_0}$	A^+-left
p-Benzoquinone	0.138	0.315	0.545	0.088
Tetramethylphenylenediamine -2·HCl	0.000	0.346	0.653	0.072
Chrysene	0.000	0.120	0.879	0.027
Fluorene	0.017	0.039	0.942	0.006
2,3-Benzophenanthrene	0.083	0.000	0.916	0.000
3-Mehtylcholanthrene	0.123	0.006	0.870	0.000
Dibenzoanthracene	0.130	0.044	0.825	0.010
Hydroquinone	0.390	0.067	0.541	0.012
α-Nitroso-β-naphthol	0.446	0.169	0.383	0.068
trans-Stilbene	0.266	0.000	0.733	0.000
o-Terphenyl	0.288	0.000	0.711	0.000
Anthracene	0.281	0.000	0.718	0.000
β-Nitroso-α-naphthol	0.531	0.230	0.237	0.099
Styrene	0.430	0.000	0.569	0.000
Triphenylbenzene	0.415	0.000	0.584	0.000
Perylene	0.156	0.089	0.753	0.045
Phenanthrene	0.391	0.000	0.608	0.000
Pyrene	0.391	0.036	0.572	0.036
m-Terphenyl	0.430	0.000	0.569	0.000
Triphenylethylene	0.402	0.000	0.597	0.000
Naphthalene	0.452	0.000	0.547	0.000
p-Terphenyl	0.401	0.000	0.598	0.000
Diphenylpicrylhydrazine	0.190	0.177	0.631	0.142
Anthrone	0.539	0.003	0.457	0.010
Phenylacetylene	0.670	0.000	0.329	0.000
α-Naphthylamine	0.437	0.028	0.534	0.028
Thio-β-naphthol	0.539	0.000	0.460	0.000
Biphenyl	0.474	0.000	0.529	0.000
Tetraphenylethylene	0.345	0.000	0.654	0.000
Diphenylamine	0.468	0.051	0.531	0.051
Benzoine	0.562	0.000	0.437	0.000
α-Nitronaphthalene	0.395	0.000	0.604	0.000
Triphenylamine	0.639	0.000	0.360	0.000
Triphenylene	0.601	0.000	0.398	0.000
Anthraquinone	0.554	0.014	0.430	0.014
Azobenzene	0.663	0.000	0.336	0.000
α-Naphthoquinone	0.464	0.000	0.535	0.000
α-Naphthol	0.566	0.021	0.412	0.021

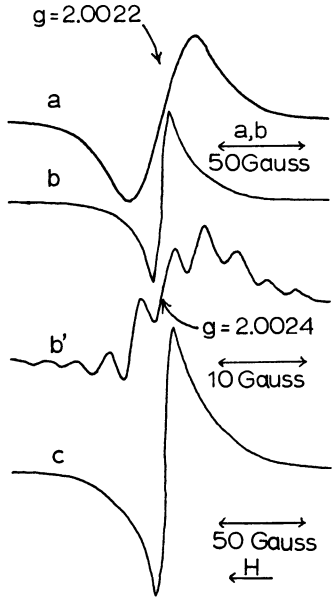

Fig. 1. a; PVC without additive irradiated to D_1.
b; PVC with perylene irradiated to D_1.
b'; the sample same as (b) but modulation width was 0.46 gauss.
c; PVC with perylene irradiated to D_2.
In all the spectra, modulation width employed was 8.0 gauss unless otherwise indicated.

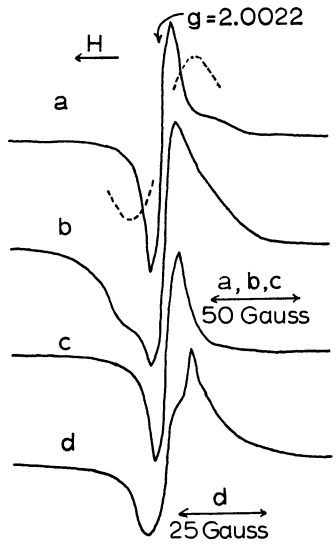

Fig. 2. a; PVC with hydroquinone irradiated to D_1. The dotted curve indicates a part of the spectrum same as Fig. 1a.
b; same as (a) irradiated to D_2.
c; PVC with *p*-benzoquinone irradiated to D_1.
d; same as (c) but modulation width was 0.5 gauss.

air before this spectrum was taken. Figures 3a and 3c indicate that, in these two isomers of nitrosonaphthol, the isotropic hyperfine splittings are somehow different.

Discussion

The primary radiation-chemical process in PVC is undoubtedly either an ionization or the formation of an excited state. Until now, the thermal-molecular and the thermal-segmental motions have generally been

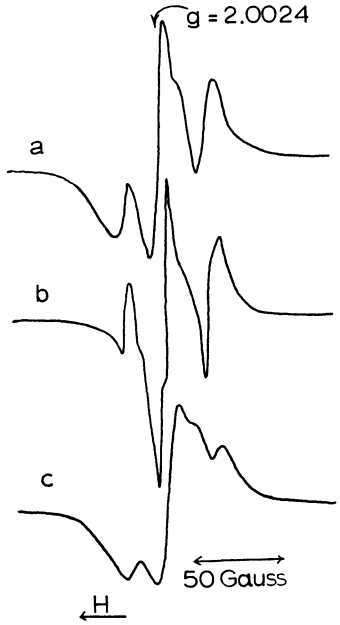

Fig. 3. a; PVC with α-nitroso-β-naphthol irradiated to D_1.
b; same as (a) but irradiated to D_2 and then bleached in air. The modulation width was 0.9 gauss.
c; PVC with β-nitroso-α-naphthol irradiated to D_1.

used to interpret the transporation of the excitation and the ionization in condensed phases as well as in the gas phase, and the kinetics governed by them. If, in some cases, the molecular motion-transportation theory was unsuccessful in explaining the kinetic data obtained, some inhomogeneous distribution of the primary, activated species, *e. g.*, a spur-like distribution, or some unknown impurities were assumed in order to solve such difficulties. In the present work it was found that the ESR of PVC can be totally converted to something else, or some 90% of it does not appear at all, if the PVC particles are coated with an aromatic additive. Benzene, used as the solvent for the additive, is not a solvent of PVC, and so it is very unlikely that additive molecules as large as 3-methylcholanthrene (5 rings with a methyl side chain) can uniformly penetrate into the segments of PVC. The additives are adsorbed only on the surface of polymer particles, probably by van der Waals adsorption. Therefore, it is definitely impossible to interpret the results obtained in this work if we limit the mechanism of the charge and excitation transporations to the molecular and the segmental motions.

The radiation-chemical studies of alkyl halides and the systems in which an alkyl halide is the matrix or the solvent have almost established that an aromatic compound is converted to its cation, not to its anion, when it is supported in the alkyl halide matrix and irradiated by ionizing radiation.[6-10] In the present work, therefore, the most likely species for explaining the ESR spectra in Figs. 1, 2, and 3 are the cations of the additive molecules which coated the surface of PVC particles. Free radicals can be ruled out from the possible species for interpreting the spectra. If PVC $\rightsquigarrow$ PVC'$\cdot$+H$\cdot$ (or Cl$\cdot$), which is a bond scission, occurs and if the atomic species formed jumps out of the PVC particle and adds to the aromatic hydrocarbon on the surface

of the particle, A, to form AH·, both PVC'· (which should be identical with S·) and AH· will be observed in most of the cases studied. The hyperfine structure of the perylene-PVC spectrum in Fig. 1 also leads us to reject the idea of the existence of AH·. Since AH· has 13 hydrogen atoms, two of which are in the $>CH_2$ form, there cannot be any set of eight nearly-equivalent pairs of protons interacting with the unpaired electron.

Two effects of the additives adsorbed on the surface have been observed. One is the transformation of S· to the additive cation, and the other is the quenching of the precursors of S·, which otherwise generates S·. In the cases of diphenylpicrylhydrazine and *p*-benzoquinone, at the dose of D_1 most of the unpaired electrons were observed in the form of the additive cation. In the cases of fluorene, 2,3-benzophenanthrene, and 3-methylcholanthrene, the number of unpaired electrons observed was reduced to some 10% of the value obtained without an additive.

These results indicate that the activated species (ionic or excited) can conduct through a PVC particle. On the surface, this activation is transferred to the additive molecule by intermolecular interaction. After the transfer, the activated additive molecule can either be ionized or lose its energy by a radiative or a nonradiative deactivation to its ground state.

If the primary activated state of PVC described above is an excited state, to be written as P**, it moves to the surface to become a surface excited species, P_s**;

$$P^{**} \longrightarrow P_s^{**},\ P_s^{**} + A \longrightarrow P_s + A^* \qquad (1)$$

which then may react with the adsorbed additive, A, to be deactivated to P_s. The P_s** may also produce S·, whose nature is not yet known exactly. The excited additive, A*, thus formed will be deactivated or ionized to A^+ and e^-, depending on the nature of the additive molecule:

$$A^* \longrightarrow A^+ + e^- \qquad (2)$$

$$A^* \longrightarrow A + (h\nu) \qquad (3)$$

Along with (2), the electron capture by PVC, P, takes place: $e^- + P \rightarrow P^-$. The amounts of S· and A^+ are shown in Table 1 and Table 2. The amount of (3) is equal to $(1-r_+/r_0-r/r_0)$ in the tables. $(1-r/r_0)$ in the tables indicates, then, the sum of the amounts of (2) and (3). In other words, $1-r/r_0$ in Table 1 indicates the total amount of energy going out of a PVC particle to the surface additives. $1-r/r_0-r_+/r_0$ in both tables indicates the total amount of energy which is dissipated by A* by a radiative (with $h\nu$ in (3)) or by a non-radiative relaxation to the ground state. An alternate scheme, postulated by Ueda,[7] is also possible; in it (1) and (2) are replaced by the equation: $P_s^{**} + A \rightarrow P_s^- + A^+$.

A hole-conduction may also explain the phenomena. By irradiation, an excited ion, P+*, may be formed. The P+*, an energy-rich hole, may then move to the surface to form P_s^{+*}, which may then be transferred to the additive molecule:

$$P \rightsquigarrow P^{+*} + e^-$$

$$P^{+*} \longrightarrow P_s^{+*},\ P_s^{+*} + A \longrightarrow P_s + A^+ \qquad (1')$$

P_s^{+*} may also form S·;

$$P_s^{+*} \longrightarrow S\cdot \qquad (2')$$

The electron, which conducts more slowly than P+* in this system,[6] will gradually come to the surface of the particle to recombine with A^+, which will create an excited state of A, which may then go to the ground state; on the other hand, if the electron affinity of A^+ is not larger than P, A^+ will stay stable on the surface. According to this scheme;

$$A^+ + e^- \longrightarrow A^* \longrightarrow A + (h\nu) \qquad (3')$$

$1-r/r_0$ in the tables is equal to the amount of (1'). So far as the present paper is concerned, there is no way to judge which is true, (1) or (1'), or whether or not both are true.

As is shown in Table 2, oxygen does not much affect the unpaired electrons found in additive molecules (see (A^+-left) in Table 2). This is good evidence that these species are cations and not anions, because an anion is very vulnerable to O_2. The unpaired electron left in pure (meaning without an additive) PVC after irradiation has been believed to be in the form of a free radical. However, the electric conductivity studies of irradiated PVC by Barnes *et al.*[11] have indicated that the unpaired electrons formed in irradiated PVC can be squeezed out if an electrostatic field and some thermal gradient is applied. Therefore, it is proper to say that no definite structure has been established for the paramagnetic species formed in irradiated PVC at room temperature.

Though the carbon atom has $2s2p^3$ sigma bonds, there can be $3s3p^3$ sigma orbitals and so on. Normally these additional "sigma orbitals" are not occupied by any electrons. However, if the 1*s* electron of a carbon atom is knocked off by a γ-photon, it may occupy the $3s3p^3$-sigma orbital, which is extended throughout the molecule. This excited state, P**, $1s^1(2s2p^3)^{8/2}(3s3p^3)^{1/n}$, where 8/2 signifies the shared covalent bond and where $1/n$ signifies a bond extended to *n*-carbon atoms, would move quite quickly throughout the molecule or the polymer particles. Also, the P+*, $1s^1(2s2p^3)^{8/2}$ hole can be expected to conduct. Though the 1*s* orbital radius of carbon atom is considerably smaller than the $2s2p^3$ sigma-bond radius, which decides the adjacent C–C bond distance in PVC, some overlap of adjacent 1*s* orbitals is possible if one of them includes only one electron. Therefore, the 1*s* unpaired spin (hole) may be exchanged between two adjacent carbon atoms.

It may be concluded that the cation or the excitation of PVC formed inside a particle penetrates through the particle toward the surface to form P_s^{+*} or P_s^{**}. Otherwise, 90% of the quenching of the unpaired electrons on the surface is impossible. Inside a particle, the molecular orbital or the unpaired electron will show some repulsive interactions with the normal sigma orbitals of other polymer segments or other molecules. On the surface, no such interaction exists; the ionized species can thus be said to be more stable than inside the particle.

In the present experiments, it seemed that the surfaces of PVC particles were saturated with the additive molecules. The overall efficiency of an additive, therefore, may be determined by the following four conditions:

11) J. E. Barnes, F. E. Hoeker, and L. Kevan, *Rad. Res.*, **40**, 235 (1969).

(a) the concentration of the additive on the surface (which is almost saturated with the additive) of the PVC particle; (b) the overlap integral between the wave functions of the additive orbitals and that of the surface of a PVC particle in the excited or the ionized state; (c) the energies required for the ionization or the excitation of the additive molecule, and (d) the relaxation rate constants of the excited states of the additive molecule on the surface of PVC. The values of (a) and (b) are not yet known, while those of (c) and (d) have been partly tabulated in several books.[12,13] There is an experimental method for ascertaining the values of (a), but the values of (b) will not easily be found. For this reason, at the present stage of our research, it is not possible to interpret the data in Table 1 and Table 2 in terms of the physical properties of each of the 38 additive compounds listed. It is hoped that the data presented in the tables nevertheless open a new possibility for the study, both in experiment and in theory, of the conduction and stabilization processes of the radiation-induced active centers in the condensed phases.

The authors wish to express their thanks to Dr. Sachiyuki Tominaga of the Mitsui Toatsu Chemical Co. for his kind suggestions in connection with this work.

12) J. G. Calvert and J. N. Pitts, Jr., "Photochemistry," John Wiley & Sons, New York, N. Y. (1967), p. 308.
13) A. Streitwieser, Jr., "Molecular Orbital Theory for Organic Chemists," John Wiley & Sons, New York, N. Y. (1962), p. 178.

BULLETIN OF THE CHEMICAL SOCIETY OF JAPAN, VOL. 44, 599—603 (1971)

The Electrodeposition of Aluminum from a Solution of Aluminum Bromide in *N,N*-Dimethyl Aniline

Takeo HISANO, Toshio TERAZAWA, Ichiro Takeuchi, Shinzo INOHARA, and Hiroshi IKEDA

Department of Applied Chemistry, Faculty of Engineering, Tokushima University, Minami-Josanjima-cho, Tokushima

(Received June 4, 1970)

This paper will describe that metallic aluminum was deposited electrolytically from a solution of aluminum bromide in dimethyl aniline with a current efficiency of 95% or more under optimum conditions. The superposition of a sinusoidal alternating current (AC) on the electrolysis direct current (DC) affected the properties of coatings and the throwing power of solutions to a great extent. A smooth, white-bright, ductile, and adherent coating was obtained under such appropriate conditions as that the frequency of AC was 60 Hz, the AC to DC ratio of 2 to 3. Aluminum dissolved anodically, and it was deposited at the cathode. The freezing temperature-composition diagram indicated the occurrence of two stoichiometric molecular complexes, $AlBr_3 \cdot C_6H_5N(CH_3)_2$ and $AlBr_3 \cdot 2C_6H_5N(CH_3)_2$, and the former was isolated.

Aluminum has not been deposited electrolytically from any aqueous solutions, probably because of the preferential discharge of hydrogen ions. For that reason, the electrodeposition of the metal from organic solutions containing no hydrogen ion has attracted considerable attention during the last about 20 years. The history has been well reviewed in the papers of Brenner[1-3] and other authors.[4] Several baths for the electroplating have been proposed by various investigators, but most of the baths are easily deteriorated by moisture and/or are difficult to operate. Of these, the lithium-aluminum-hydride-type bath, which was developed by Brenner and his co-workers,[5] would probably be the most excellent one for commercial use at present. The bath, however, seems not to be entirely perfect, because the solvent, diethyl ether, is inflammable and the aluminum dissolved at the anode does not deposit at the cathode. In order to improve this type of bath, Ishibashi and his co-workers[6] have proposed the use of tetrahydrofuran instead of ether as the solvent.

A variety of organic solvents has been examined by various authors in the studies of the electrodeposition of aluminum as well as of other metals, but *N,N*-dimethyl aniline (DMA) seems never to have been referred to. The present paper will describe that metallic aluminum was electroplated from the solution of aluminum bromide in DMA with a current efficiency of 95% or more under optimum conditions. When an alternating current (AC) was superimposed on the direct current (DC) in the electrolysis, a bright, ductile, and adherent coating was obtained.

Though preliminary experiments showed that aluminum chloride could be used as an alternative to the bromide, the latter was here chosen simply because its anhydride can be more easily prepared.

1) D. E. Couch and A. Brenner, *J. Electrochem. Soc.*, **99**, 234 (1952).

2) A. Brenner, *ibid.*, **106**, 148 (1959).

3) Ed. by P. Delahay and C. W. Tobias, "Advances in Electrochemistry and Electrochemical Engineering," Vol. 5, J. Wiley/Interscience, N. Y. (1967), p. 205.

4) I. A. Menzies and D. B. Salt, *Trans. Inst. Metal Finish.*, **43**, 186 (1965).

5) J. H. Conner and A. Brenner, *J. Electrochem. Soc.*, **103**, 657 (1956).

6) N. Ishibashi, Y. Hanamura, M. Yoshio, and T. Seiyama, *Denki-Kagaku* (A Journal published by The Electrochemical Soc. of Japan), **37**, 73 (1969).

In an electrochemical sense, DMA seems to be a moderately active solvent, having in the molecule a nitrogen atom capable of coordinating with a solute. On account of this property, DMA and its related compounds are worthy of study as non-aqueous solvents in the electrodeposition of metals, particularly of metals that have never been electrodeposited from aqueous solutions.

Experimental

Aluminum Bromide. Its preparation and subsequent purification were carried out in an all-glass apparatus capable of evacuation. The bromide was synthesized by heating alminum turnings (99.5% pure) in a current of purified bromine vapor. The bromide thus formed, without being exposed to the air, was purified by successive sublimation through a series of vessels, and finally sealed off in glass ampules, each of which was fitted with a breakable joint for subsequent use *in vacuo*. Colorless and anhydrous aluminum bromide was thus obtained.

N,N-*Dimethyl Aniline.* Care was taken to remove aniline, monomethylaniline, and water from a commercial DMA. When mixed with a suitable amount of acetic anhydride, it was submitted to fractional distillation. After the removal of the remaining acetic anhydride by washing with water, and the removal of the water by standing over potassium hydroxide, the distillate was further distilled fractionally under reduced pressure of nitrogen in the presence of metallic sodium.

Electrolysis Cells, Ancillary Apparatus, and Procedures. The cells and the procedures used here for the electrolyses were virtually identical with those of Menzies and others.[4,7] In brief, care was taken so as to prevent the contamination of the solution with atmospheric oxygen and moisture during both the mixing of the constituents and the electrolysis. About 40 m*l* of the solution was used in each run. The quantity of electricity (60—200 coulombs usually) passed through an electrolysis cell was measured with a water coulometer when an DC only was applied. The superposition of a sinusoidal AC on the DC was carried out by the usual method. The currents over a frequency range of 20—2,000 Hz were supplied from an audio-frequency generator. The net quantity of electricity participating in the cathodic process at the cathode was calculated from the area of a wave in an oscillogram of the resultant electrolysis current. In the expression for the ratio between the amount of superimposed AC and that of DC, the former was described by a root mean-square value.

Preparation of Electrodes. An aluminum spiral ribbon was generally used as the anode; at its center a cathode was placed. The aluminum was 99.5% pure, containing Fe, Cu, and Si as the main impurities. When the anodic dissolution of aluminum was studied, an aluminum wire anode (99.999% pure) was used. They were cleaned before use with a sodium hydroxide solution, dil hydrochloric acid, water, and finally with methanol. As the cathode a copper plate or a platinum wire was mainly used; its widest surface area was about 2 cm^2. They were cleaned in a mixture of hydrochloric, nitric, and sulfuric acids, as recommended by Graham.[8]

The aluminum deposited at a cathode was determined in two ways. One was a volumetric method, while the other was the measurement of the volume of the hydrogen generated by the addition of 8N hydrochloric acid. These two methods always gave concordant results, within the limits of experimental errors, which was a support for the idea of the deposit being completely metallic.

Adherence of Coating to Base Metal. This was estimated simply on the basis of the number of times at which a specimen was bent at right angles with pincers until the coating showed signs of flaking.

Freezing Temperature-Composition Diagram for the Solution System. The freezing points were determined on the basis of the cooling curves. The successive dilution of a solution with DMA was carried out in the presence of dry nitrogen (1 atmospheric pressure) in a vessel equipped with a magnetic stirrer.

Preparation of 1 : 1 Molecular Complex. After the dissolution of aluminum bromide in excess amounts of DMA with the aid of gentle heating, the excess DMA was permitted to distill off. The residue was then distilled at a higher temperature and collected in ampules. All the operations were carried out under a reduced pressure of nitrogen.

Results and Discussion

Appearance of Solutions. *In vacuo* or in an atmosphere of dry nitrogen free from oxygen, a newly-prepared solution of aluminum bromide in DMA was colorless at any temperature lower than about 100°C and at any concentration. At an elevated temperature above 100°C, the solutions gradually developed a color between light yellow and reddish orange *in vacuo* or in nitrogen, except for a solution with an equimolar composition, which was colorless irrespective of the temperature. In the air, the solutions containing less than 50 mol% of bromide turned blue. Even in the absence of oxygen, sunlight or ultraviolet rays also turned the solution blue. Sato[9] has shown that the reaction of DMA with aluminum chloride *in vacuo* gives a blue solution, the electronic spectrum of which displays an absorption maximum at 600—610 mμ, and that the maximum is the same as crystal violet in the same solvent gives. In the present case of an aluminum bromide-DMA solution that was colored by virtue of oxygen or

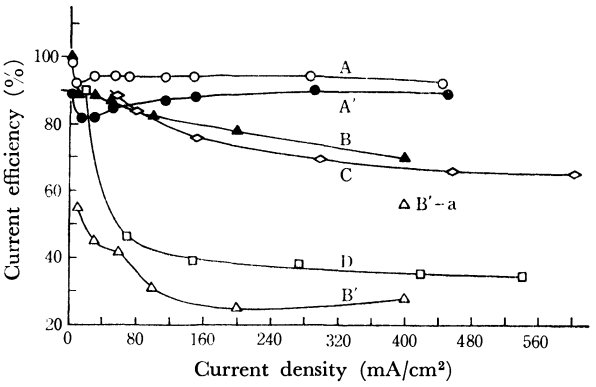

Fig. 1. Variation of cathode current efficiency with current density.

Curve	A	A′	B	B′	C	D
Concn. (mol %)	82.6	82.6	35.0	35.0	60.1	56.4
Temp. (°C)	120	150	120	80	120	120

7) I. A. Menzies and L. W. Owen, *Electrochimica Acta*, **11**, 251 (1966).

8) A. K. Graham, *Trans. Amer. Electrochem. Soc.*, **52**, 289 (1927).

9) H. Sato, This Bulletin, **38**, 1719 (1965).

ultraviolet rays, a maximum was also found at about 605 mμ. In the air, the solutions containing the bromide more than 50 mol% turned light brown; this was perhaps an alkaline color of crystal violet.

When electrolyzed, these solutions exhibited various colors, from blue to reddish violet, according to the experimental conditions. The coloring during electrolysis was partly attributed to unknown reactions at the anode.

Cathode Current Efficiency. The first run of electrolyses of freshly-prepared solutions occasionally yielded an unusually low current efficiency and a poorly adherent deposit. This is perhaps due to the trace amounts of water remaining in the solvent. The experimental datum of every first run was, therefore, discarded, or solutions were preliminarily electrolyzed for a while.

Figure 1 shows some examples of the effects of current density (CD) on the cathode current efficiency. At any concentration of aluminum bromide, the efficiency varied remarkably within a range of relatively low CDs; then it remained almost constant over a wide range of higher CDs. Again, the rise of the temperature decreased the efficiency rather slightly for concentrated solutions (curves A and A'), while it affected the efficiency for dilute solutions in the other direction (B and B').

The variation in the efficiency with the concentration of aluminum bromide is illustrated in Fig. 2, which shows the case when the CD was 50 mA/cm² at 120°C. The efficiency varied unusually with the concentration,

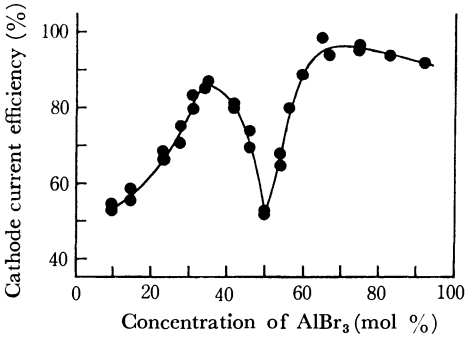

Fig. 2. Variation of cathode current efficiency with bath composition (120°C, 50 mA/cm²).

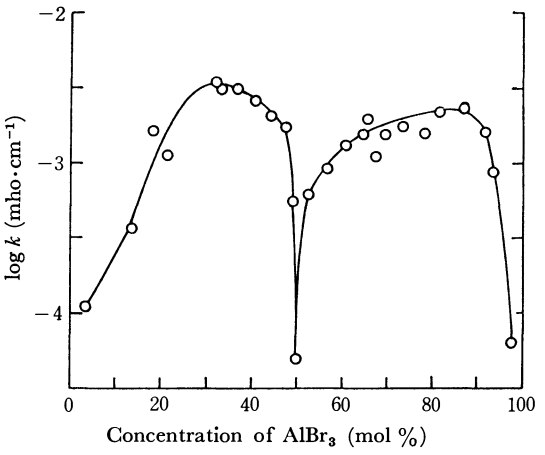

Fig. 3. Variation of specific conductivity (k) with composition at 110°C.

exhibiting maximum values of about 85 and 95% at concentrations around 35 and 65 mol% respectively. For the solution with an equimolar composition, the efficiency dropped unexpectedly, irrespective of the CD, to a value of about 50—60%. As is illustrated in Fig. 3, the curve for specific conductivity plotted against the composition of the solution also passed through a minimum at the equimolar composition, regardless of the temperature. It is of interest to note that the curve of Fig. 2 is, to some extent, similar in shape to that of Fig. 3; it is difficult at present to explain this.

Improvement of the Properties of Coating by Superimposing AC. The deposits were metallic aluminum with no organic contaminants. They were, however, generally grey or sometimes black. Moreover, a nodular or dendritic growth of the deposit was often observed, particularly when the concentration of aluminum bromide was less than about 50 mol%. At higher concentrations these irregular growths diminished considerably, but were favored by high CDs. The adhesion of the coating to the substrate (copper or steel) was not very good, so pealing or blistering of the coating occasionally occurred, even when it was bent only once.

In order to improve the properties of the coating,

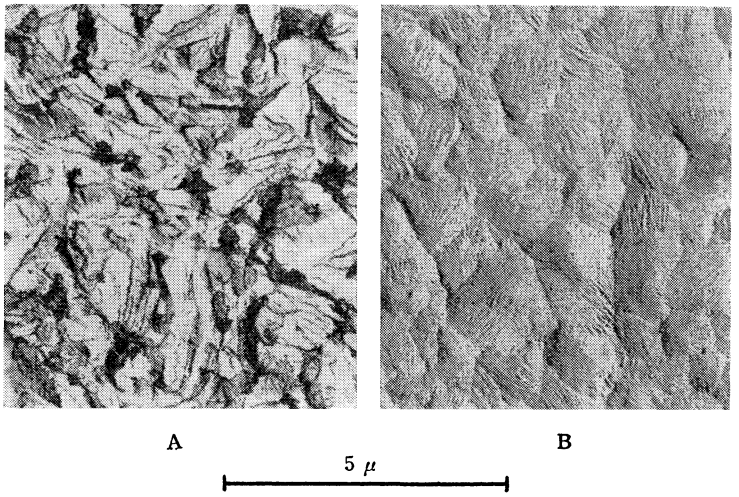

Fig. 4. Electron microphotograph (carbon replica) of surface of Al deposited (100 mA/cm², 58.5 mol%, 160°C).
A: DC only B: AC was superimposed (AC/DC = 3)

each of the following substances was added to the bath in various amounts of 10 to 1,500 mg/*l*. The attempt, however, was unsuccessful. The appearance and the adhesion were more inferior than ever. The tested substances were polyvinyl chloride, thiourea, sulfamic acid, benzoic acid, and sodium 2,7-dinaphthalen sulfonate. For the same purpose, a sinusoidal AC was superimposed on the DC for the electroplating. It affected the properties of coating to a great extent. The superposition, when the conditions were appropriate, yielded a smooth, white-bright, ductile and adherent coating, improving the throwing power of the bath, though the estimation of its extent was qualitative. Figure 4 (electron microphotographs) may be sufficient to illustrate that the superposition effectively smoothed the surface of the coating. Clean, white-bright electroplates as thick as 0.05 mm, which was not the maximum value possible, were easily obtained.

The frequency of a superimposed AC had appreciable effects on the properties of the coating and the throwing power of the bath. Generally, the favorable effects were observed at frequencies from roughly 60 to 200 Hz. At frequencies of 300 and 20 Hz, the coatings obtained were of a dull appearance and the throwing power was very poor. At frequencies above 300 Hz, grey coatings were obtained. At above 1,000 Hz, the coatings were black and less adherent than ever. The ratio of the amount of AC to that of DC was also one of the influential factors. The irregular growth was prevented when the ratio was more than 2. The current with an AC–DC ratio more than 4, however, generally yielded a poor cathode throw and a rough surface was deposited, particularly when the CD was high. The current efficiency decreased with an increase in the ratio. Some examples are shown in Fig. 5.

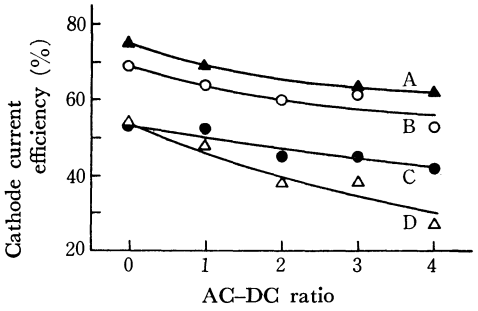

Fig. 5. Variation of current efficiency with AC–DC ratio (150°C, 60 Hz).

Curve	A	B	C	D
Concn. (mol %)	58.5	30.5	18.6	18.6
CD (mA/cm²)	100	100	25	100

Anodic Behavior of Aluminum in the Solution. An aluminum anode dissolved electrolytically into the solution. Figure 6 shows the variation in the anodic current efficiency with anode CD. These efficiencies were computed for the formation of trivalent ions. At higher concentrations (above 55 mol%) of aluminum bromide, the efficiency was practically constant and was 100% over the whole range of CD observed; moreover, its change with the temperature was very small. Figure 7 shows the variation in the efficiency with the composition of the solution at 120°C and at a CD of 90—100 mA/cm². The efficiency decreased markedly as the concentration decreased below 50 mol%, and the solution adjacent to the anode turned blue or violet, seemingly because of the deposition of bromine.

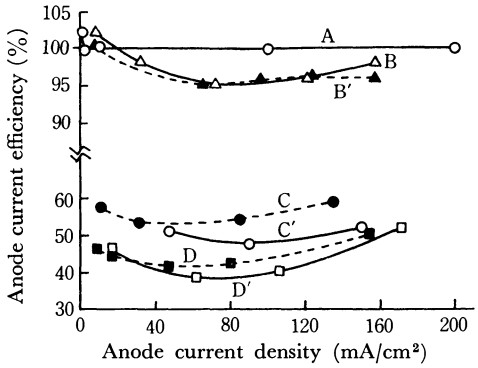

Fig. 6. Current efficiency for anodic dissolution of Al.

Curve	A	B	B′	C	C′	D	D′
Concn. (mol %)	92	48	48	35	35	22	22
Temp. (°C)	120	150	110	80	120	55	120

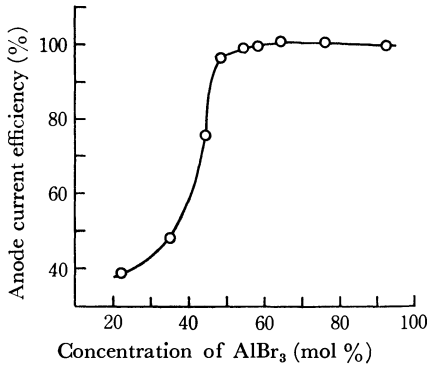

Fig. 7. Variation of anode current efficiency with composition (120°C, 90—100 mA/cm²).

Conner and Brenner[5] have reported that the aluminum dissolved at the anode did not deposit at the cathode in their Li-Al-hydride-type bath, probably because of the formation of a new ionic species. On the contrary, the following experimental facts suggested that the aluminum dissolved anodically could deposit at the cathode in the present bath. A solution of 6 m*l*, initially containing 68.5 mg of aluminum, was electrolyzed with an DC of 5 mA/cm² of CD for 72 hr; 198 mg of aluminum were thus deposited on the cathode. Similar results were obtained when an AC was superimposed.

Molecular Complexes between Aluminum Bromide and DMA. Figure 8 shows the freezing diagram of the system. An open circle represents the freezing point that was observed by cooling a solution from a temperature 10—20°C higher than the point. There were some cases in which the freezing point shifted slightly after the same solution had once been heated to about 150°C. The closed circles in the figure represent such cases. The curve connecting the open circles passes through one maximum and two minima; the latter are the freezing points of eutectic mixtures. The maximum at the equimolar composition suggests the occurrence of a molecular complex, the simplest formula of which is expected to be $AlBr_3 \cdot C_6H_5N(CH_3)_2$. Koblukow and

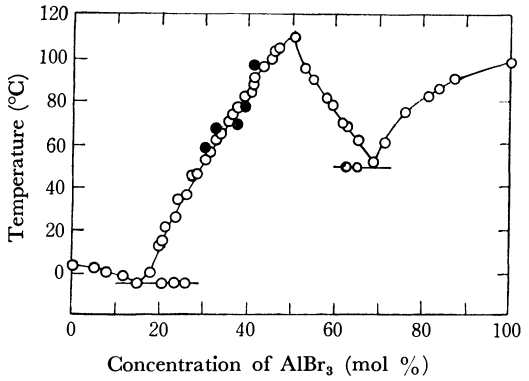

Fig. 8. Freezing temperature-composition diagram for $AlBr_3$-DMA system.

Ssachanow[10] have already reported a complex as being a dimeric molecule $Al_2Br_6 \cdot 2C_6H_5N(CH_3)_2$ on the basis of their thermometric data. Its melting point (mp) was 95°C. On the other hand, the compound isolated by the present authors had a mp of 108—110°C. It seems likely, however, that these two compounds are the same. The difference in mp may be ascribable to the difference in purity between the two. The compound obtained here was colorless, crystalline, and somewhat hygroscopic; it was decomposed by water, but not so easily as aluminum bromide. It was colored blue by sunlight, but not by dry air. Found: Al, 6.92; Br, 61.4; C, 24.61; H, 3.52; N, 3.60%. Calcd for $AlBr_3 \cdot C_6H_5N(CH_3)_2$: Al, 6.96; Br, 61.80; C, 24.77; H, 2.86; N, 3.61%. The apparent molecular weight of the complex in benzene was 402, while the calculated value for the monomeric molecule was 388.

The curve connecting the closed circles exhibits a discernible shoulder at the composition of about 33 mol%. This seems to indicate the presence of another complex, possibly $AlBr_3 \cdot 2C_6H_5N(CH_3)_2$, though attempts at its isolation have not yet succeeded. Considering that the cathode-current efficiency exhibited a maximum around this composition, as may be seen in Fig. 2, this anticipated complex appears to be closely related to the behavior in electrolysis and to the conductivity of the solutions. An example is seen in Fig. 1. The curve B′ represents the current efficiency for a 35 mol% solution at 80°C; the solution had never been heated above this temperature. On the other hand, the point B′-a is for the same conditions except that the solution was once heated to 120°C. The difference in efficiency is remarkable. Again, the specific conductivity of any solution with a concentration of lower than 50 mol% was essentially changed and never returned to its initial value, after the solution had been submitted to a certain higher temperature. For example, the conductivity of the 33% solution was initially $10^{-3.7}$ $(ohm.cm)^{-1}$ at 80°C; it finally became $10^{-2.6}$ at the same temperature after the solution had once been heated to 150°C.

The results described above are, of course, insufficient to establish the mechanism of the cathode reaction. The solution system displayed very intricate changes in conductivity as functions of the composition, the temperature, and the time of heating; the details will be reported at a later date. Throughout this study, the efficiencies were calculated for convenience on the basis of the reaction $Al^{3+} \rightarrow Al$. Considering the complicated change in the conductivity, together with that of the cathode-current efficiency, however, one can doubt whether the number of electrons, or the ionic species, participating in the cathode process would be the same throughout the whole range of aluminum-bromide concentrations. Further work, therefore, such as electrode-potential and transport-number measurements, will be required.

10) I. Koblukow and A. Ssachanow, *Chem. Zentr.*, **1910 Bd. I**, 912 (1910).

Electronic Structure of Lone Pairs. II.[1] Disulfides and Acyl Thiol

Hiroko YAMABE, Hiroshi KATO,[2] and Teijiro YONEZAWA

Department of Hydrocarbon Chemistry, Faculty of Engineering, Kyoto University, Sakyo-ku, Kyoto

(Received July 4, 1970)

The electronic structure and the electronic transition of three cyclic disulfides, $(CH_2)_3S_2$, $(CH_2)_4S_2$, and $(CH_3)_2S_2$, are calculated by the semi-empirical ASMO SCF method in order to study the interaction of the neighbouring lone pairs of the S–S bond in connection with the ability of reductive scission. It is concluded that the absorption at 2500—3000 Å is the transition of n—σ^* and that the variation in the maximum for the various cyclic disulfides and the chain disulfide are induced by the change in the dihedral angle that a molecule can take. The electronic structure and the reactivity of $(CH_3)_2S_2$, CH_3SSH, and CH_3SCOCH_3 are then discussed on the basis of an extended Hückel calculation. It is suggested that there is the possibility of an interaction between two molecules, R_2S_2, through the S–S bond of each molecule, in the HO of one molecule and in the LV of another.

The compounds containing sulfur atoms have some characteristic properties in organic and biological reactions. The S–S bond between two divalent sulfur atoms has a particular role in retaining the tertiary structure of polypeptide as a weak chemical bond. Also, 6,8-thioctic acid is a coenzyme for the decarboxylation of pyruvate to active groups, which through CoA feed carbon atoms into the Krebs cycle; a reductive scission of the S–S linkage of 6,8-thioctic acid to form a dithiol is also involved in the mechanism.[3] Acetyl CoA, $CoASCOCH_3$, is an important biological acetylating reagent, and its C–S bond is a so-called high-energy bond. Though many experimental investigations have been made, there have been only a few discussions of their electronic structures.[4]

Previously we calculated the electronic structure and the electronic interaction of the lone pairs of some azine compounds and quinones.[5] In this connection, in the earlier part of the present paper the electronic structures and electronic transitions of several disulfides, trimethylene-disulfide $(CH_2)_3S_2$ (a model compound of 6,8-thioctic acid), tetramethylene-disulfide $(CH_2)_4S_2$, and dimethyl disulfide $(CH_3)_2S_2$ were investigated by the semi-empirical ASMO SCF method[6] for valence electron systems in order to study the interaction of the neighbouring lone pairs of S–S linkage in connection with the ease of reductive scission. In the later part, the electronic structures of $(CH_3)_2S_2$, CH_3SSH, and CH_3SCOCH_3 (a model compound of $CoASCOCH_3$) are calculated by the extended Hückel method[7] in order to establish the properties of these molecules, based upon the MO theory, and to discuss the reactivity in relation to the lone pair.

I. Dimethyl Disulfide and Cyclic Disulfides

The normal value for the dihedral angle for the S–S bonds of such compounds as S_8, S_2Cl_2,[8] and $(CH_3)_2S_3$[9] is known to be approximately equal to 100° from the X-ray analysis, the measurement of the dipole moment, the IR spectrum, and so on. The dihedral angle of $(CH_3)_2S_2$,[9,10] too, is approximately 90°. On the other

Table 1. Observed transition energies[12] of some disulfides

	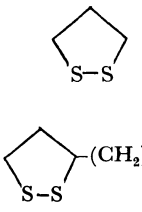	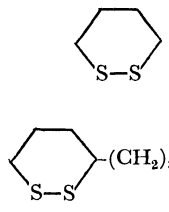	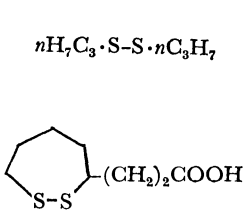	H_3C-S-S-CH_3[9]
λ_{max}(eV)	3.76	4.28	4.96	4.96
Oscillator strength			increase	0.031
ϕ°	~0	~40	~90	90

1) Presented at the Annual Meeting of the Chemical Society of Japan, April, 1968.

2) Present address: Department of General Education, Nagoya University, Chikusa-ku, Nagoya.

3) P. W. Sadler, *Chem. Rev.*, **60**, 575 (1960); J. D. Watson, "Molecular Biology of the Gene," W. A. Benjamin Inc., New York (1965).

4) B. Pullman and A. Pullman, "Quantum Biochemistry," Interscience publishers, New York, London (1963): VII.

5) T. Yonezawa, H. Yamabe, and H. Kato, This Bulletin, **42**, 76 (1969).

6) H. Konishi, H. Kato, and T. Yonezawa, Symposium of the electronic structure of molecules, Hokkaido, October, 1967; This Bulletin, **42**, 933 (1969).

7) R. Hoffmann, *J. Chem. Phys.*, **39**, 1397 (1963).

8) L. Pauling, *Proc. Nat. Acad. Sci.*, **35**, 495 (1949).

9) S. D. Thompson, D. G. Carroll, F. Watson, M. O. Donnel, and S. P. McGlynn, *J. Chem. Phys.*, **45**, 1367 (1966).

10) S. P. Stevenson and J. Y. Beach, *J. Amer. Chem. Soc.*, **60**, 2872 (1938).

hand, only a few investigations[9,11] have been performed on the electronic structures and configurations of these compounds in relation to the electronic spectrum. Calvin *et al.*[12] observed the UV spectrum of some cyclic disulfides and *n*-propyl disulfides out of their biological interest in 6,8-thioctic acid (see Table 1). They discussed the variation in the absorption spectra in the 2500—3000Å range of these compounds qualitatively in relation to the ring strain, which may come from the interaction of the two lone pairs of the sulfurs and the shift of the dihedral angle from its stable value of about 90°. Later, Bergson[11] made an attempt to interpret the above observation in terms of a simple molecular orbital theory. That is, he explained it by considering only the interaction between two lone pairs constructed by the $3p$ electrons of the neighbouring sulfur atoms.

Including all the valence electrons, and also taking into account the conformations of these molecules, our calculation in this paper was carried out by the semi-empirical ASMO SCF method for valence electron systems previously proposed by the present authors.[6]

Calculations. By estimating on the base of the molecular model, the dihedral angles of the above cyclic disulfides seem to be in the neighbourhood of 0°, 40°, and 90° for the five-, six-, and seven-membered rings respectively. In order to establish the relation between the dihedral angle and the absorption maximum, shown in Table 1, the electronic structures of dimethyl disulfide with the dihedral angles of 0°, 45°, and 90°

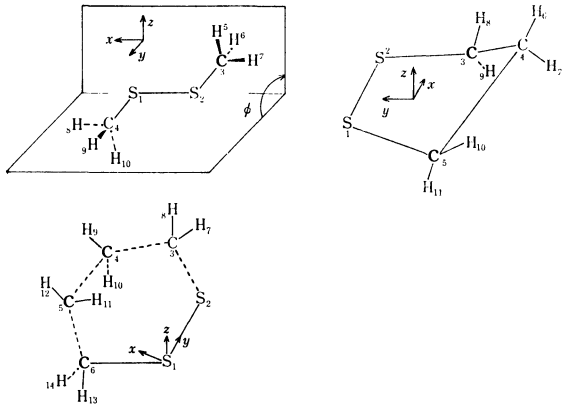

Fig. 1. Models employed for the calculation, coordinate axes and dihedral angle ϕ.

Table 2. Bond lengths (in Å) and bond angles (in degree)

$(CH_3)_2S_2$	S–S	2.04	$(CH_2)_4S_2$	S–S	2.10
	S–C	1.78		S–C	1.78
	C–H	1.09		C–C	1.54
	∠SSC	1.07		C–H	1.09
$(CH_2)_3S_2$	S–S	2.10	CH_3S_2H	S–S	2.04
	S–C	1.84		S–H	1.33
	C–C	1.54		C–H	1.09
	C–H	1.09		∠SSH	95
	∠SSC	97	CH_3SCOCH_3	S–C	1.78
	∠CCC	116.5		C–C	1.54
	∠SCC	109.7		C–O	1.22
dihedral angle[a]		10		∠CCS	120
				∠CSC	107
			C_2H_6	C–C	1.54
				C–H	1.09

a) Dihedral angle between the x–y plane and the C_3–C_4–C_5 plane (see Fig. 1).

are calculated. It is the purpose of these calculations not only to reveal the ϕ dependency (see Fig. 1) of the absorption spectra, but also to carry out a simplified model calculation for the cyclic disulfides. The validity of this simplification is confirmed by the calculation of tri- and tetra-methylene disulfide for the assumed structure of Fig. 1. The bond lengths and bond angles of dimethyl disulfide and the five-membered ring are referred to the compilation by Sutton.[13] They are shown in Table 2. The structure of the six-membered ring is assumed by taking the S–S, S–C, and C–C bond lengths as 2.10Å, 1.78Å, and 1.54Å respectively and the hybridization for all carbon atoms as sp^3. However, the resulting dihedral angle becomes approximately 10°, which is considerably smaller than the expected value.[14] The numberings of the atoms of the five- and six- membered rings are shown in Fig. 1, in which the S_1, S_2, C_3, and C_4 atoms and the S_1, S_2, and C_6 atoms are assumed to be on the same x–y planes. The calculation was carried out by the semi-empirical ASMO SCF method for valence electron systems,[6] in this method the approximation of the zero differential overlap is adopted, and the contribution of $3d$ and $4s$ orbitals of the sulfur atom is neglected.

Table 3. Some calculated results of $(CH_3)_2S_2$, $(CH_2)_3S_2$, and $(CH_2)_4S_2$

	$(CH_3)_2S_2$			$(CH_2)_3S_2$	$(CH_2)_4S_2$
	$\phi°=0$	$\phi°=45$	$\phi°=90$		
Difference of the total energy (eV)	1.99	0.64	0.00	—	—
Transition energy (eV)	4.08	4.19	4.81	3.79	4.01
Oscillator strength	0.039	0.043	0.084	0.015	0.034
p_{sr}^{LV} of the S–S p_σ bond	—0.777	—0.772	—0.770	—0.831	—0.762

a) First $n_1 \rightarrow \sigma^*$ transition

11) G. Bergson, *Arkiv Für Kemi.*, **12**, 233 (1958).
12) J. A. Barltrop, P. M. Hayes, and M. Calvin, *J. Amer. Chem. Soc.*, **74**, 6153 (1952); *ibid.*, **76**, 4343 (1954).
13) L. E. Sutton, "Interatomic Distances of Molecules and Ions," The Chemical Society, London (1958).
14) The dihedral angle of the six-membered ring is considered to be about 40°, assuming a molecular model with somewhat deformed angles of the carbon atom from the sp^3 hybridization. This value (~40°) seems to be reasonable in view of the UV spectrum (see Table 1). when the sp^3 hybridization is assumed, for convenience in the calculation of the molecular conformation, the dihedral angle becomes about 10°.

Dimethyl Disulfide. The calculated results for the dimethyl disulfide, $(CH_3)_2S_2$, are given in Table 3. The minimum value of the total energy[15] of $(CH_3)_2S_2$ is obtained for the dihedral angle of 90°; this is in accordance with the observation.[10] The calculated transition energies are in good agreement with the experimental values (Table 1). The oscillator strengths increase with the increase in the dihedral angle from 0° to 90°, and run parallel with the experimental values.[12] The lowest vacant orbital (LV) becomes an antibonding orbital of the S–S $p\sigma$ bond. The partial bond orders of the S–S $p\sigma$ bond, p_{sr}^{LV},[6] in the lowest vacant orbital are negative and large, and their absolute values increase in the order of 0°, 45°, and 90°. This means that the ring-opening reaction by the means of the nucleophilic reagent occurs more easilly in this order; the five-, six-, and seven-membered rings, this order may be parallel to that of the ring strain of these compounds.[12,16,17] In fact, the ring-opening reaction to form linear polymers is known to take place in this order.[16] It has been reported[18] that 5- and 4- thioctic acids have, respectively, 0.3% and 0.1% pyruvate oxidation activity relative to 6-thioctic acid.

TABLE 4. ATOMIC-CHARGE DENSITY, AO-CHARGE DENSITY OF $(CH_3)_2S_2$ AND BOND ORDER p_{s,p_i} OF THE SULFUR ATOM

ϕ°(degree)		0	45	90	180
Atomic-charge density	S_1	6.126	6.126	6.128	6.183
	C_3	4.142	4.127	4.123	4.115
	$C_3+H_6+H_7+H_8$	6.874	6.873	6.872	6.862
AO-charge density	S_1s	1.664	1.664	1.665	1.665
	x	1.109	1.111	1.110	1.108
	y	1.354	1.356	1.363	1.367
	z	1.998	1.994	1.990	1.998
	S_2s	1.664	1.664	1.665	1.665
	x	1.109	1.105	1.109	1.108
	y	1.354	1.683	1.990	1.367
	z	1.998	1.683	1.364	1.998
	C_3s	0.987	0.982	0.981	0.979
	x	1.110	1.110	1.111	1.108
	y	0.916	0.911	0.904	0.899
	z	1.130	1.124	1.126	1.129
	C_4s	0.987	0.981	0.981	0.979
	x	1.110	1.108	1.108	1.108
	y	0.916	1.014	1.130	0.899
	z	1.130	1.016	0.904	1.129
p_{s,p_i}	S_1s-x	0.260	0.262	0.264	0.261
	s-y	−0.336	−0.335	−0.334	−0.333
	s-z	0.000	0.001	0.000	0.000
	S_2s-x	−0.260	−0.259	−0.263	−0.261
	s-y	−0.336	−0.235	0.002	0.333
	s-z	0.000	−0.240	−0.334	0.000

15) The difference of the total energy for 180° is obtained as 0.63 eV.

16) J. G. Affleck and G. Dougherty, *J. Org. Chem.*, **15**, 865 (1950).

17) A. V. Tobolsky, F. Leonard, and G. P. Roeser, *J. Polym. Sci.*, **3**, 604 (1948).

18) M. W. Bullock, J. A. Brockman, Jr., E. L. Patterson, J. V. Pierce, and E. L. R. Stockstad, *J. Amer. Chem. Soc.*, **74**, 3455 (1952).

The atomic orbital (AO) charge densities[6] of the sulfur atom are given in Table 4. For 0°, the electron densities of the p_z AO of the sulfur atom are almost all 2.0; this indicates a lone-pair orbital of the p type. For 90°, the p_z orbital of the S_1 atom (S_1z) and the p_y orbital of the S_2 atom (S_2y) become lone-pair orbitals. That is, the direction of the interacting lone-pair orbitals varies, but almost without changing the absolute value of the population, following the change in the dihedral angle, ϕ. More exactly, one can see in Table 4 that the AO density of the lone pair (S_1z) has a minimum value at 90°, that is, the delocalization of the lone pair is at a maximum. As the dihedral angle increases, the total electron density of the S_1 atom increases and those of the C_3 atom and the CH_3 group, which is a summation of the atomic-charge[6] of the atoms C_3, H_4, H_5, and H_6, decrease. Also, the AO-charge density of S_1y increases and that of C_3y decreases. That is, the electron may migrate from the p_y orbital of the C_3 atom to that of the S_1 atom.[19] The bond orders, s–x and s–y, of the sulfur atom are nearly equal, and that of the s–z is zero for 0°, as is shown in Table 4. The direction of the atomic dipole becomes approximately that of an sp^2-type lone pair. That is, other sp^2-type lone pairs, which result from the delocalization of 3s electrons, are observed. These sp^2-type lone pairs, too, rotate according to the change in the dihedral angle, ϕ.

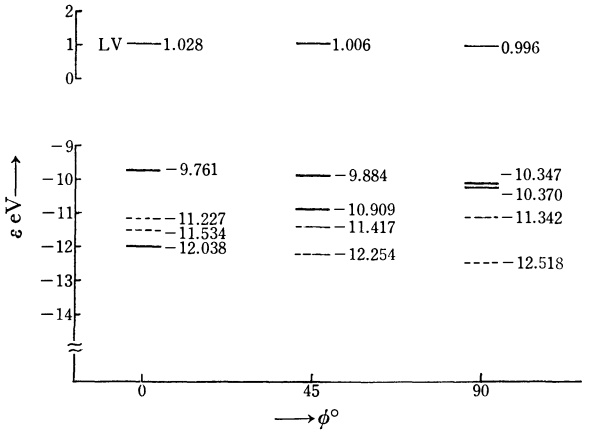

Fig. 2. Lone pair levels and the lowest vacant level of dimethyldisulfide *vs.* dihedral angle ϕ. The heavy lines and the dashed designate the levels of the p-type lone-pair and sp^2-type lone pair, respectively.

The lone-pair levels and the lowest vacant levels of $(CH_3)_2S_2$ for the various ϕ's are illustrated in Fig. 2. The fine line designates the lowest vacant level, while the heavy line and the dashed line designate the lone-pair level of the p type and that of the sp^2 type respectively. It is observed that the splitting of the lone-pair levels of the p type becomes larger in the order of 90°, 45°, and 0°. This may mean that the lone pairs of the p type aligned parallel, as in 0°, have more mutual

19) The same tendency has been observed by Morokuma *et al.* in (Ref. 20) their *ab-initio* calculation of H_2O_2; it may also be seen in the report by Pitzer *et al.* (Ref. 21).

20) L. Pedersen and K. Morokuma, *J. Chem. Phys.*, **46**, 3941 (1967).

21) W. E. Palke and R. M. Pitzer, *ibid.*, **46**, 3948 (1967).

interaction than those in an orthogonal form, as in 90°.

Trimethylene Disulfide and Tetramethylene Disulfide. The calculated results for trymethylene disulfide, $(CH_2)_3S_2$, tetramethylene disulfide, $(CH_2)_4S_2$, are given in Table 3. The transition energies of the n–σ^* of $(CH_2)_3S_2$ show a better agreement with the observed value than in the preceding, simplified calculation, in which the dimethyl disulfide of the dihedral angle 0° corresponds to the observed value of $(CH_2)_3S_2$. The first n–σ^* transition of $(CH_2)_4S_2$ is 4.01 eV; it is the transition from the next highest occupied lone-pair level of a p type to the lowest unoccupied level.[22] As has been mentioned previously, the dihedral angle of the assumed structure is smaller than the expected angle[14] (See Table 1). Therefore, the obtained transition energy should become smaller than the experimental value. The calculated oscillator strength of $(CH_2)_3S_2$ is larger than $(CH_2)_4S_2$, showing a parallelism with the experimental value. Judging from the value of p_{rs}^{LV}, LV is an antibonding orbital of the S–S $p\sigma$ bond. This is compatible with the fact that the scission of the S–S bond of 6,8-thioctic acid is induced by light. The atomic-charge density,[6] the AO charge density,[6] and the partial bond orders of the s–x, s–y, and s–z of the sulfur atom are shown in Table 5. For $(CH_2)_3S_2$, two lone pairs of the p type in the z direction are parallel, and the lone pairs of the sp^2 type lie in a nearly orthogonal form; those of the sp^2 type, too, are approximately orthogonal.

Table 5. Atomic-charge density, AO-charge density and bond order, p_{s,p_i}, of the S_1 atom of $(CH_2)_3S_2$ and $(CH_2)_4S_2$

		$(CH_2)_3S_2$	$(CH_2)_4S_2$
Atomic-charge density		6.148	6.181
AO-charge density	s	1.716	1.679
	x	1.308	1.405
	y	1.126	1.101
	z	1.999	1.996
p_{s,p_i}	S–x	−0.294	−0.330
	S–y	−0.286	−0.238
	S–z	−0.000	0.003

From the results of our calculation, it may be concluded that the absorption of 2500—3000Å is an n–σ^* transition and that the variation in the absorption maximum for various cyclic disulfides and a chain disulfide are induced by the change in the dihedral angle, ϕ, of the molecule.

22) The orbital sequence of the 1 one-pair MO's of $(CH_2)_4S$ is slightly different from that of $(CH_3)_2S_2$, $\phi=45°$, shown in Fig. 2. The highest occupied level (—9.131 eV) of $(CH_2)_3S_2$ is the one connected with the sp^2-type lone pair, which is anomalously high compared to the highest occupied level of $(CH_2)_3S_2$ in various dihedral angles and $(CH_2)_3S_2$. The next highest occupied level (—9.905 eV) becomes the one connected with the p-type lone pair. The transition energies and the oscillator strengths, Osc., of these n(p type)-σ^* and n(sp^2 type)-σ^* transitions of $(DH_2)_4S_2$ are obtained as follows:
n(p type)-σ^* ; 4.01 eV, Osc.=0.034 (See Table 2)
n(sp^2 type)-σ^* ; 4.78 eV, Osc.=0.224

II. Chemical Reactivity of $(CH_3)_2S_2$, CH_3SSH, and CH_3SCOCH_3

It has been noted that the E–H method[17] is a tolerable approximation in some cases for discussing the reactivity.[23] Sometimes, the E–H method gives more reasonable results for use in the interpretation of the reactivity, compared to the semiempirical ASMO SCF method, particularly in the calculation of the interaction of two molecules.[24] Therefore, we employed the E–H method in discussing the chemical reactivity of $(CH_3)_2S_2$, CH_3SSH, CH_3SCOCH_3, and the proton affinity of the S–S bond. It will be established later that a discussion similar to those given by the E–H calculation regarding the reactivity of $(CH_3)_2S_2$ and the cyclic interaction of two $(CH_3)_2S_2$ molecules is also possible on the basis of SCF calculations.

In the E–H calculation,[7] the resonance integral, H_{rs}, is evaluated by $H_{rs}=1/2\ KS_{rs}(H_{rr}+H_{ss})$, putting $K=1.75$, where S_{rs} is the overlap integral between two AO's, X_r and X_s. The Coulomb integrals, H_{rr}'s are given in Table 6.

Table 6. H_{rr}'s in the extended Hückel calculation (eV)

	$1s$	$2s$	$2p$	$3s$	$3p$
H	−13.60	—	—	—	—
C	—	−21.43	−11.42	—	—
O	—	−35.30	−15.45	—	—
S	—	—	—	−20.08	−13.32

$(CH_3)_2S_2$; First we will report the results for $(CH_3)_2S_2$, although the molecular orbital interpretation of the reactivity is carried out analogously to that for H_2O_2, previously reported by the present authors.[23] The highest occupied orbital (HO) and the next highest occupied orbital (NHO) are almost degenerate lone-pair MO's. The AO populations[26] of S_2y and S_1z

Table 7. Some AO populations and partial AO bond populations, p_{rs}^{HO} and p_{rs}^{LV} in HO and LV of $(CH_3)_2S_2$

		HO
AO population	S_2y	1.084
	S_1z	0.289
p_{rs}^{HO}	S_1x–S_2x	−0.013

		LV
AO population	S_1x, S_2x	0.563
	S_1y, S_2z	0.159
p_{rs}^{LV}	S_1x–S_2x	−0.859

23) T. Yonezawa, O. Yamamoto, H. Kato, and K. Fukui, *Nippon Kagaku Zasshi*, **87**, 26 (1966); This Bulletin, **40**, 307 (1967).
24) In the MO calculation of the system composed of NH_3 and HCHO, by changing it the intermolecular distance or the mutual angle, is changed the E-H calculation gives more reasonable results than the SCF method (Ref. 25).
25) H. Yamabe, H. Kato, and T. Yonezawa, "Electronic Structure of Lone Pairs IV. Transannular Interaction of Some Mesocycles," (to be published in This Bulletin)
26) K. Morokuma, H. Kato, T. Yonezawa, and K. Fukui, This Bulletin, **38**, 1263 (1965).

in HO, which are almost equal to those of S_1z and S_2y in NHO respectively, have large values, as is shown in Table 7. This means that a cation attack takes place in the lone-pair direction. LV is an antibonding orbital of the S–S $p\sigma$ bond, and AO populations of S_1x and S_2x are large. This means that the anion attack should takes place at the S atom of the S_2 atom from the outside of the S–S bond[27] and that the S–S $p\sigma$ bond is ready for scission. Then, in the absence of steric hindrance, the molecule having the S–S bond will be able to receive the nucleophilic and the electrophilic interaction from two directions at the same time in a mutually perpendicular way.[26] This property causes the S–S bond to be susceptible to ionic scission.[28] A similar discussion can also be made in the case of the SCF calculation of $(CH_3)_2S_2$, presented in the preceding section.

Possibility of a Cyclic Interaction of two Disulfides. The existence of a O_4 molecule has been known;[30] it seems to be an associated form of two O_2 molecules, in which two O_2 molecules are held together by bonds much weaker than an ordinary covalent bond. In our calculation of $(CH_3)_2S_2$, we notice the possibility of a cyclic interaction between two molecules, R_2S_2, through the S–S bond of each molecule, employing the HO of one molecule and the LV of another.[31] Figures 3(A) and (B) show two kinds of the interaction of $(CH_3)_2S_2$ molecules (I, II); only the atoms S and C are illustrated. Figure 3(A) shows the interaction between the HO of the molecule I and the LV of the molecule II,[32] while Fig. 3(B) shows the interaction between the LV of the molecule I and the HO of the molecule II, which is the reverse of that of Fig. 3(A). The relevant MO coefficients of the p_y orbitals[32] are also shown.[33] The S_1–S_2 and the S_1–C_4 bonds of the I and II molecule are placed in the same plane, and the S_2–C_3 bond is directed upwards from the x–y plane. As has been pointed out by Fukui *et al.*,[31] the most favorable conditions for a cyclic interaction include the same symmetry in the corresponding orbitals of the two molecules. This condition is satisfied in the above case.[34,35]

If a II molecule has a conformation which is a mirror image[36] of that of the I molecule, other forms of the interaction may be constructed.

Furthermore, not only the interactions in the completely-square forms, such as in Figs. 3(A),3(B),3′(A),[34] and 3″(A),[34] but also those in the oblique forms are possible.[37] An example, which is an oblique form of Fig. 3′(A),[34] is shown in Figs. 4(A) and 4(B), where the interaction is denoted by the dotted line. In Fig. 4(A), interaction is assumed between the p_y AO (lone-pair AO) in the HO of one molecule and the p_y AO in the LV of another molecule. At the same time, the inverse interaction, as in Fig. 4(B), is also possible, in which the HO and LV in Fig. 4(A) are replaced by the LV and HO respectively. By the superposition of these two interactions, the interaction between disulfides will become stronger. An interaction of this type may be expected in a crystal of disulfides.[37]

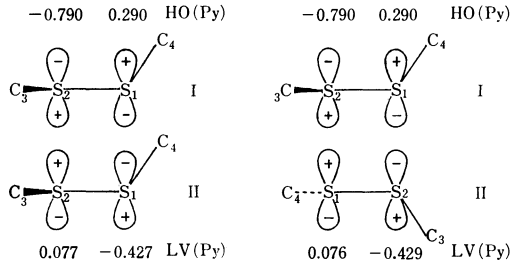

Fig. 3′(A)

Fig. 3″(A)

27) Because, in the inner part of the S–S bond, the mutual signs of the S_1x and S_2x are antagonistic, the AO's largely cancel out and the MO develops to the outside of the S–S bond, as has been pointed out by Fukui *et al.* in their work on H_2O_2 (Ref. 23).

28) In the ionic scission of the S–S bond, the approach of a nucleophile or an electrophile, for the capture of positive or negative scission products, becomes easy (Ref. 29).

29) H. L. Yakel, Jr., and E. W. Hughes, *Acta Cryst.*, **7**, 291 (1954).

30) L. Pauling, "The Nature of the Chemical Bond," 3rd Ed., Cornell University Press, (1960); Chap. 10.

31) K. Fukui and H. Fujimoto, This Bulletin, **39**, 498 (1966).

32) The p_y orbital of the S_2 atom in HO is a lone-pair orbital. The numbering of the atoms and the coordinate axes for each $(CH_3)_2S_2$ molecule are the same as those of Fig. 1.

33) In the preceding section it has been shown that a disulfide such as $(CH_3)_2S_2$, is most stable at the dihedral angle of 90°. It has been pointed out by Fukui (in a private communication) that this stabilization at 90° partially due to the intramolecular interaction between the S_2y AO(lone-pair AO) in the HO and the S_2y AO in the LV.

34) From the point of view of orbital symmetry, another type of cyclic interaction may be expected, as in Fig. 3′(A), as may its inverse form (not shown) constructed in a way similar to that of Fig. 3(B). However, in this case, as the lone pairs of the S_2 atoms of the molecules I and II lie in a line on the same plane, this cyclic form is less probable. The other form of the interaction between the p_y AO(Ref. 33) in the HO of the molecule I and the p_z AO in the LV of the molecule II is also possible, as in Fig. 3″(A) and as in its inverse form. That is, the molecule II of Fig. 3(A) is rotated about its S–S axis. Then, in Fig. 3″(A), the S_1–C_4 bond of the molecule I and the S_2–C_3 bond of the molecule II are placed on the same plane. The S_2–C_3 bond of the molecule I is directed upwards from the plane of the paper, and the S_1–C_4 bond of the molecule II, downward from the plane. However, this type of its interaction is also not very probable, because the lone pairs of the S_1 atoms of the molecules I and II lie on a line.

35) In the case of the SCF calculation, too, there is a possibility of a cyclic interaction when the s orbitals (their NO coefficients are 0.309 and —0.307) are used instead of the p_y AO in the LV of the molecule II of Fig. 3(A) and the molecule I of Fig. 3(B). In this calculation, as a form of cyclic interaction, some rotation about its S–S axis is permited for each molecule, I and II, because the s orbital is spherically symmetric.

36) B. M. Oughton and P. M. Harrison, This Bulletin, **2**, 396 (1959); *ibid.*, **10**, 497 (1957).

37) Yakel *et al.* describe, in their report about the X-ray analysis of *N,N′*-diglycyl-L-cystine dihydrate, that the van der Waals contacts (or the distances) between molecules related by the b-axis repeat are significantly lower than the normal value (Ref. 29). It is to be expected from the discussion in this section that not only the hydrogen bond (Ref. 29), but also the interaction between the S–S bonds may induce the smaller distance of the repeat. Oughton *et al.*, in their study of the structure of hexagonal L-cystine, also pointed out the close van der Waals contacts between each sulfur atom and its non-bonded neighbouring atoms (Ref. 36). Takagi *et al.* have reported that the CD spectrum of L-cystine hydrochloride indicates interaction between the neighbouring S–S bonds (Ref. 38).

38) T. Takagi, N. Ito, and T. Isemura, The 23rd Annual Meeteing of the Chemical Society of Japan, April, 1970.

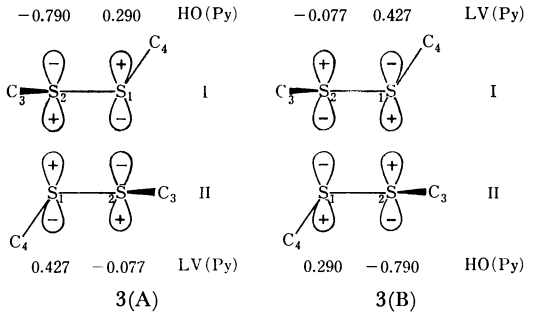

Fig. 3. Cyclic interaction of two disulfides. (A); Interaction between *py* AO in HO of the molecule I and *py* AO in LV of the molecule II. (B); Interaction between *py* AO in LV of the molecule I and *py* AO in HO of the molecule II (Ref. 24).

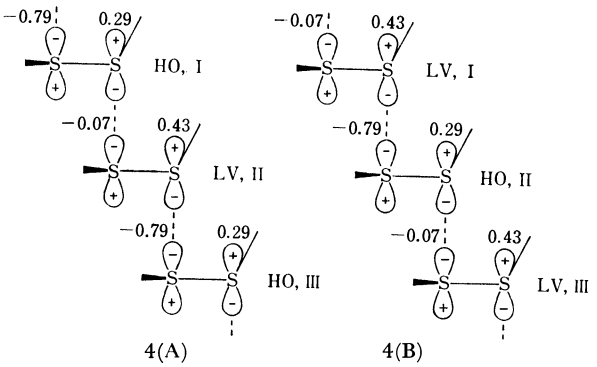

Fig. 4. Interactions in the oblique form.

Proton Affinity of the S–S Bond. Hughes described, in his review,[29] that the outstanding reactive characteristic reactivity of the S–S bond is its ability to undergo ionic (heterolytic) scission in reactions with nucleophilic reagents, and that ionic scission takes place also upon the attack of such electrophilic reagents such as sulfide-forming metal cations and proton. The S–S bond also acts as a chemical bond, are which undergoes ionic scission easily, holding a tertiary structure of polypeptide through a CyS–CyS linkage. Disulfide and dithiol interconversion is a conspicuous property of a S–S bond. In contrast with this, hardly no ionic scission of a C–C bond takes place. These properties of the S–S bond may be due partly to the lone pair of the sulfur and partly to the 3*d* orbitals of the sulfur. In this paper, only the contribution of the lone pair will be discussed.

Table 8. Proton affinity of a S–S bond

	direction of a proton approach	atomic population of proton	Δq[a]	ΔE(eV)[b]
$(CH_3)_2S_2$	case I	0.999	0.966	−4.75
	case II	0.776	0.383	−2.90
C_2H_6	case III	0.525	0.315	−1.72
	case IV	0.526	0.301	−1.85

a) The difference of atomic population, q, between two atoms of Fig. 4.
$\Delta q = q(S_1) - q(S_2)$ for $(CH_3)_2S_2$
$\Delta q = q(S_1) - q(C_2)$ for C_2H_6

b) ΔE is a difference of total energies of two forms, as $\Delta E = E$(protonated form) $- E$(neutral form)

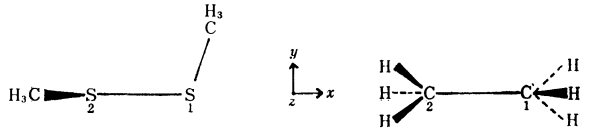

Fig. 5. Conformations and the numbering of the atoms of $(CH_3)_2S_2$ and C_2H_6.

In a case of a proton attack, the following two points must be considered. First, a proton will approach more easily to the S–S bond in a lone-pair direction than to a bond with no lone pairs such as a C–C bond. Second, when a proton approaches one of the lone pairs of the sulfurs, change transfers from the lone pair to the proton and the polarization of the S–S bond will be induced. This polarization may become one step to a heterolytic scission. The protonated form of $(CH_3)_2S_2$ is calculated in Table 8. The calculated results for protonated C_2H_6, in which hardly any ionic scission takes place, are cited in the same table for comparison. In the calculation, the proton is placed 2Å from the S–S bond, first in the lone-pair direction (case I) and then in the z direction to the center of the S–S bond (case II). As for C_2H_6, a proton is placed 2Å from the C–C bond, first in the z direction to the C_1 atom of the C–C bond in Fig. 5 (case III), and then to the center of the C–C bond (case IV). When a proton approaches from a lone-pair direction, the atomic population[26] of the proton is the largest (0.999) and the stabilization energy, ΔE, of the protonated form is the largest (−4.75 eV). The difference in the atomic population[26] between the S_1 atom and the S_2 atom (0.996) is considerably larger than that between the C_1 atom and the C_2 atom (0.315). That is, when a proton approaches the S–S bond, a larger inclination of the charge distribution is induced that in an approach to the C–C bond. The energy of the LV of $(CH_3)_2S_2$ (−0.53 eV) is lower than that of C_2H_6 (3.21 eV), such as in the case of H_2O_2.[23] This means that $(CH_3)_2S_2$ is more apt to accept a nucleophilic attack than C_2H_6, as described before.

Reaction of Aralkyl Hydrodisulfide. Tsurugi *et al.* have given a series of reports[39] about the reaction of

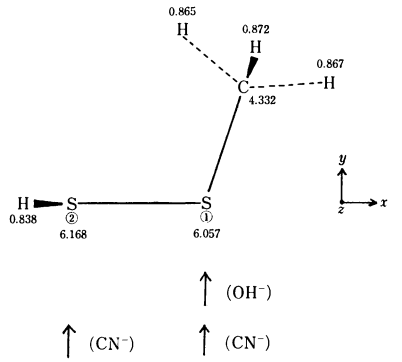

Fig. 6. Conformations and the numbering of the atoms of CH_3SSH are shown together with its atom populations. Arrows show the usual position of an anion attack.

39) "Organic Sulfur Compounds," ed. by N. Kharasch, Pergamon Press New York (1961), Chap. 9, 35, *etc.*; T. C. Bruice, *J. Amer. Chem. Soc.*, **81**, 5444 (1959).

TABLE 9. SOME AO POPULATIONS AND PARTIAL AO BOND POPULATION, P_{sr}^{LV}, IN LV OF CH_3SSH

		LV
AO population	S_1x	0.684
	S_2x	0.531
P_{rs}^{LV}	S_1x-S_2x	0.450

aralkyl hydrodisulfide, RSSH, with various anions. They concluded in one of their papers that, in the absence of steric hindrance, the weaker nucleophiles, such as hydroxide and sulfite ions, attack exclusively the sulfenyl sulfur of benzyl hydrodisulfide. Stronger nucleophiles,[39] such as cyanide and thiolate ions, attack both sulfenyl and sulfhydryl sulfur atoms. We calculated the electronic structure of CH_3SSH, as a model compound. The adopted conformation of the compound is shown in Fig. 6, together with the obtained atomic population. The S_1, S_2, and C_3 atoms are placed on the x–y plane, and the H_7 atom, on the x–z plane, while the dihedral angle is assumed to be 90°. The bond lengths and bond angles are given in Table 2. The AO populations of S_1z and S_2y are 1.996 and 1.989 respectively; they should be lone-pair AO's. The AO populations of S_1x and S_2x in LV are large, as is shown in Table 9, they become antibonding orbitals of the S–S $p\sigma$ bond. That is, an anion attack occurs along the S–S bond from the outside. Furthermore, in LV, the AO population of the S_1x is larger than that of the S_2x, though the difference between them is small. Therefore, the S_1 atom is more susceptible to the anion attack than the S_2 atom. This accounts for the experimental facts that weak nucleophiles attack the S_1 atom, while strong nucleophiles attack both the S_1 and S_2 atoms.

Reactions of Acyl Thiol. There have been several reviews[40,41] about various reactions of acyl thiol and the thiol ester, with particular attention payed to their role in biochemistry. As has been described before, CoAS-$COCH_3$ is an acetylating intermediate and its C–S bond is a high energy bond.[3] We calculated the electronic structure of CH_3COSCH_3, as a model compound. The assumed conformation of the compound is shown in Fig. 7, together with the atomic population. The S_1, C_2, O_3, C_4, and C_5 atoms are all assumed to be on the same x–y plane. The bond lengths and bond angles are given in Table 2. The AO populations are shown in Table 10, while those of the main p orbitals in HO and LV are shown in Table 11. HO(−12.69 eV) is a π-type lone-pair MO, largely localized at the S_1z AO, which is a lone-pair AO of the sulfur atom. This lone-pair level localized at the sulfur atom become higher than that localized at the oxygen atom. Therefore, a cation attack must take place at S_1z AO, this is in agreement with the experimental results The LV is an antibonding π-type MO largely localized at the C_2z AO. The partial AO bond populations of C_2z–O_3z and C_2z–S_1z in LV are −0.352 and −0.276 respectively. Therefore, an anion attack must take place at the C_2z AO in LV. This accounts for the several reactions[42] reviewed by Bruice,[39] in which an inter- or intra-molecular nucleophilic attack on the carbon atom of acyl thiol or the acyl thiol ester by a lone pair of a nitrogen atom or a sulfur atom is often essential. The energy of LV (−8.47 eV)is remarkably lower than those of CH_3SSH (−0.79 eV) and $(CH_3)_2S_2$ (−0.53 eV). This shows that CH_3SCOCH_3 is very apt to accept an anion attack.

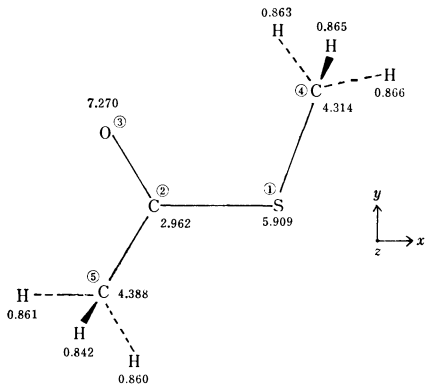

Fig. 7. Conformation and the numbering of the atoms of CH_3SCOCH_3 are shown together with its atom populations.

TABLE 10. AO POPULATION OF CH_3SCOCH_3

AO		AO	
S_1s	1.495	C_4s	1.163
x	1.241	x	1.111
y	1.421	y	0.932
z	1.753	z	1.108
C_2s	1.053	C_5s	1.172
x	0.748	x	1.091
y	0.636	y	1.035
z	0.526	z	1.090
O_3s	1.768		
x	1.906		
y	1.790		
z	1.806		

TABLE 11. SOME AO POPULATIONS IN HO AND LV OF CH_3SCOCH_3

	S_1z	C_2z	O_3z	C_4z	C_5z
LV	0.244	1.465	0.192	0.005	0.009
HO	1.275	0.141	0.078	0.226	0.016

One of the authors(H.Y.) wishes to express her hearty thanks to Professor Kenichi Fukui of Kyoto University for his kind advice in the discussion on the reactivity.

The calculation was carried out on a HITAC 5020 computer at the computation center of the University of Tokyo.

40) S. Kawamura, T. Nakabayashi, T. Kitao, and J. Tsurugi. *et al.*, *J. Org. Chem.*, **31**, 4174 (1966); *ibid.*, **30**, 2707, 2711 (1965); *ibid.*, **31**, 4171 (1966), *etc.*

41) A. L. Parker and N. Kharash, *Chem. Rev.*, **59**, 583 (1959).

42) See Ref. 40; for example, p. 421 (Eq. (1)), p. 430 (Eq. (38)), p. 431 (Eq. (39)), p. 433 (Eq. (43)), p. 437 (Eq. (57)), and p. 438 (Eq. (58)).

Electronic Structure of Lone Pairs. IV.[1] The Transannular Interaction of Several Meso-cycles

Hiroko YAMABE, Hiroshi KATO,[2] and Teijiro YONEZAWA

Department of Hydrocarbon Chemistry, Faculty of Engineering, Kyoto University, Sakyo-ku, Kyoto

(Received June 30, 1970)

The MO calculation of the transannular interaction of eight-membered model systems, containing S,O,N, or C atoms in the position opposed to the C atom of the C=O group, are made by the extended Hückel method and the semi-empirical ASMO SCF method. The relation between the bond order (P_{rs} value or E_{AB} value) and the infrared absorption frequency, $\nu_{C=O}$, is discussed. The electronic absorption maxima in the 221 mμ—235 mμ region are assigned to π–π^* type transitions of intramolecular charge transfer from the interacting atom, X, to the C=O group. The absorptions in the region from 217 mμ to about 190 mμ are n–σ^* type transitions. In the model calculation of the NH_3 and HCHO system, it is shown that the interaction is large, the lone pair being directed to the C atom.

The transannular interaction of diametrically-opposed nitrogen and carbonyl groups in meso-cycles was noticed formerly by Kermack and Robinson[3] in their work on alkaloid. Cromwell *et al.* reported[4] that the presence of an amino group (either substituted or unsubstituted) on the beta carbon atom of an α,β-unsaturated ketone lowers the carbonyl-streching band by 20—80 cm^{-1}. Many subsequent investigations have been performed by Leonard *et al.*[5-8] for the transannular nitrogen-carbonyl interaction in cyclic aminoketones and amino-acyloines of a medium ring size, such as compounds I,[5,6] II,[5,6] and III[5,9] in Fig. 1. They have shown that the

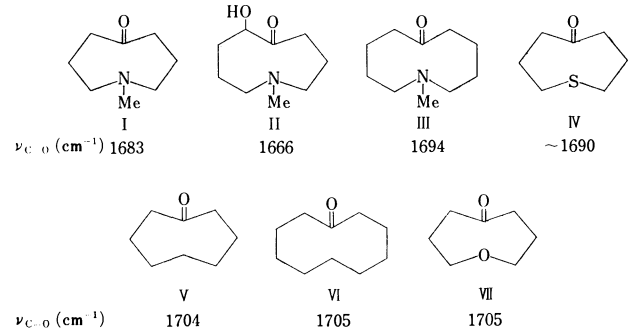

Fig. 1.

occurrence of transannular interaction, $R-\overset{|}{\underset{|}{N}}^{\delta+}: \quad \overset{|}{\underset{|}{C}}=O^{\delta-}$, depends upon the ring size,[6,8,9] the strain,[7,9] and the environmental factors.[5,10] Further, they also established the transannular effects between sulfur or sulfoxide and ketone functions in an eight-membered model systems[11,12] (as IV[5,11] in Fig. 1). Namely, the lone pairs of nitrogen or sulfur atom have a through-space interaction with the carbon atom of the >C=O group (denoted by C_{CO}), which is polarized as $>^{+\delta}C=O^{-\delta}$. The frequencies of the infrared absorption maxima of the C=O stretching, $\nu_{C=O}$, of the compounds (such as I, II, III, and IV in Fig. 1) are abnormally lower than those of the corresponding alkanones[5,11,12] (as V, VI, and VII in Fig. 1). This is probably due to a transannular interaction and may reflect the different bond orders, P_{CO}, of the C=O group in the various compounds in Fig. 1. Note that VII does not show a transannular interaction, in spite of the existence of the lone pair of the oxygen atom.

The UV spectra of these compounds observed by Leonard *et al.*[13] are reproduced in Tables 1A and 1B. In Table 1A, the maxima appear in the ~217 mμ region and ~264 mμ region for the compounds in which no appreciable transannular interaction is expected. On the other hand, the absorption maxima of the molecules in which the transannular interaction is expected appear in the region from 225 mμ to 231 mμ.[14] Similar relations[15] may be seen for the compounds listed in Table 1B. However, the assignments of these transitions have not yet been made.

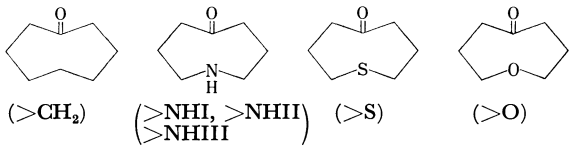

Fig. 2. Model compounds for the calculation and the abbreviated designation for each compound used in this work.

1) Supported in part by a Fellowship of the Japan Society for the Promotion of Science, from October, 1968, to March, 1969.

2) Present address: Department of General Education, Nagoya University, Chikusa-ku, Nagoya.

3) W. O. Kermack and R. Robinson, *J. Chem. Soc.*, **121**, 427 (1922).

4) N. H. Cromwell, F. A. Miller, A. R. Johnson, R. L. Frank, and D. J. Wallace, *J. Amer. Chem. Soc.*, **71**, 3337 (1949).

5) N. J. Leonard and M. Ōki, *Kagaku no Ryoiki*, **10**, 1003 (1956) (in Japanese); K. Mutai, *ibid.*, **21**, 284 (1967); N. J. Leonard, *Rec. Chem. Prog.*, **17**, 243 (1956).

6) N. J. Leonard, R. C. Fox, M. Ōki, and S. Chivarell, *J. Amer. Chem. Soc.*, **76**, 630 (1954).

7) N. J. Leonard and M. Ōki, *ibid.*, **76**, 3463 (1954).

8) N. J. Leonard, R. C. Fox, and M. Ōki, *ibid.*, **76**, 5708 (1954).

9) N. J. Leonard, M. Ōki, and S. Chivarell, *ibid.*, **77**, 6234, 6237 (1955).

10) N. J. Leonard and M. Ōki, *ibid.*, **77**, 241, 6245 (1955).

11) N. J. Leonard, T. W. Milligan, and T. L. Brown, *ibid.*, **82**, 4075 (1960); N. J. Leonard and C. R. Johnson, *ibid.*, **84**, 3701 (1962).

12) Hs. H. Günthard and Th. Bürer, *Helv. Chim. Acta*, **39**, 356 (1956).

13) N. J. Leonard and M. Ōki, *ibid.*, **77**, 6329 (1955).

14) Leonard *et al.* describe how the bands at longer and shorter wavelengths observed for compounds 1 and 6 of Table 1A have disappear or are submerged under the strong 228 mμ band. For compounds 2, 3, 4, and 5, as the interaction between nitrogen and carbonyl is diminished, the intensity of the absorption in the 228 mμ region is decreased and the 217 mμ band becomes evident (Ref. 13).

15) A "red shift" of the maximum at 227 mμ of >S for the polar solvent has been reported (Ref. 11).

TABLE 1A. ULTRAVIOLET ABSORPTION MAXIMA IN DIETHYL ETHER (REF. 13)

	Compound	λ, mμ	log ε	λ, mμ	log ε	λ, mμ	log ε
1	2-Hydroxycyclononanone	217	2.65			264	2.13
II	1-Methyl-1-azacyclononan-5-ol-6-one	*		228	3.77	d	
2	1-Ethyl-1-azacyclononan-5-ol-6-one	*		226	3.62	d	
3	1-Isobutyl-1-azacyclononan-5-ol-6-one	217	3.49			d	
4	1-Isopropyl-1-azacyclononan-5-ol-6-one	218	3.47	~230	3.45	d	
5	1-*t*-Butyl-1-azacyclononan-5-ol-6-one	217	3.43	~231	3.37	d	
6	1-Methyl-1-azacycloheptadecan-9-ol-10-one	216	3.51			~270	1.98
I	1-Methyl-1-azacyclooctan-5-one	*		225	3.80	d	
III	1-Methyl-1-azacyclodecan-6-one	*		221	3.75	d	

d: Weak absorption in this region, no apparent maximum.
*: *cf* Ref. 3.

TABLE 1B. ELECTRONIC ABSORPTION MAXIMA IN CYCLOHEXANE (REF. 11)

	Compound	λ, mμ	log ε	λ, mμ	log ε	λ, mμ	log ε
8	1-Thiacyclooctan-5-one-1-oxide	199	3.38	235	2.78	~290	1.3
IV	1-Thiacyclooctan-5-one	192	3.52	227	3.46	288	1.25
9	Methyl 4-ketopentyl sulfoxide (open chain)	207, ~215	3.46	—	—	275	1.3
10	Methyl 4-ketopentyl sulfide (open chain)	198, ~210	3.4	—	—	278	1.3
V	Cyclooctanone	<185	>2.9	—	—	288	1.18
11	Dimethyl sulfoxide	203	3.4	—	—	—	—

Furthermore, there have been several reports about biochemical interactions; it has reported that a lone pair of a nitrogen or a sulfur atom has a kind of a catalytic action through these transannular interactions[16,17] The important factor in these interactions is a favorable mutual situation of the interacting lone pair and the C=O group, and the maintenance of its situation in time and space, which will be done by the surrounding atoms and groups.[16,17]

The purposes of the present study are three-fold: (i) to ascertain whether the transannular interaction of the molecules can also be seen in the molecular orbital calculation; (ii) to ascertain the role of the lone pair in this interaction, and (iii) to determine the assignment of the main absorption maxima. Fig. 2 shows the electronic structures of some model compounds[20,21] which we investigated in Fig. 2. As a first trial method, the extended Hückel method[22] (abbreviated as E–H) is employed, because the system to be examined is large. Next, in order to ascertain the results by means of E–H calculation and to study the electronic transitions, semi-empirical ASMO SCF calculations[23] (abbreviated as SCF) for the valence electron systems are carried out, neglecting the contribution of the *d* orbitals.

When the molecule has a situation in which the direction of the lone pair to the C_{CO} atom is a ppropriate and the distance between them is one at which their potential energy is about at its minimum, a large transannular interaction may be expected. To show the existence of these critical values, we will make a model calculation of the electronic structure of the NH_3 and HCHO system, varying the mutual angle and distance between the NH_3 molecule and the HCHO molecule. At the same time, the variation in the atomic population,[24] the bond order of the C=O bond, P_{CO}, and the bond order between the C atom and the N atom, P_{CN}, are also studied.

16) There is a report that, with the intramolecular assistance of the imidazole group, the following thiol-ester undergoes solvolysis at 10^6—10^7 times as fast as a normal thiol-ester. Its mechanism may be shown as follows (Refs. 18 and 19):

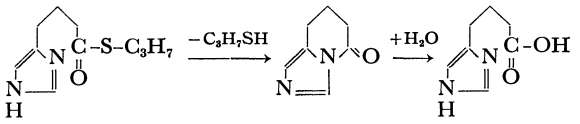

In our E–H calculation of a model compound,

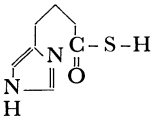

the obtained bond order between the N atom and the opposed C_{CO} atom of the C=O group becomes positive and shows a transannular interaction.

17) An example of the transannular interaction, in the extended sense (through space interaction), is seen in the enzymatic action shown in the following scheme (Ref. 18):

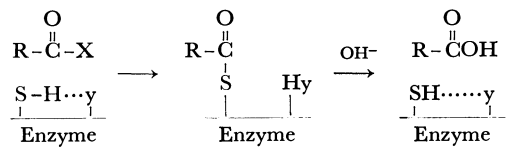

18) "Organic Sulfur Compounds," ed. by N. Kharash, Pergamon Press (1961); Chap. 9 and 35, *etc.*, p 437 (Eq. (57)), p 438 (Eq. (58)).

19) T. C. Burice, *J. Amer. Chem. Soc.*, **81**, 5444 (1959).

20) The abbreviations, such as >CH_2, >NHI, >NHII, >S and >O, used for these compounds are shown in Fig. 2.

21) T. C. Bruice and B. Holmquist, *J. Amer. Chem. Soc* **89**, 4028 (1967).

22) R. Hoffmann, *J. Chem. Phys.*, **39**, 1397 (1963); *ibid.*, **40**, 2745 (1964).

23) T. Yonezawa, H. Konishi, and H. Kato, This Bulletin, **42**, 933 (1969), Symposium of the electronic structure of molecules, Hokkaido, October, 1967.

24) K. Morokuma, H. Kato, T. Yonezawa, and K. Fukui, This Bulletin, **38**, 1263 (1965).

Method of Calculations

Figure 3 shows the conformations used for the MO calculations. The coordinate axes for the conformation of Fig. 3A[25] and the numbering of the atoms are given in Fig. 3C. As no definite conformation of these molecules has been reported, the calculation is carried out for the assumed structure, consulting the literature.[11] The bond lengths[26] and bond angles[26] employed are given in Table 2. With these lengths and angles, the $C_1\cdots X_3$ distance (in Fig. 3A and Fig. 3C) becomes approximately 2.5Å. The y axis is chosen as the line connecting the interacting C_1 atom (C_{CO} atom) and the X_3 atom. The opposed triangle planes, $C_4X_3C_9$ and $C_6C_1C_7$, are parallel to each other, as in Fig. 3C. Namely, the dihedral angle, θ, between these two planes is set as zero.[27]

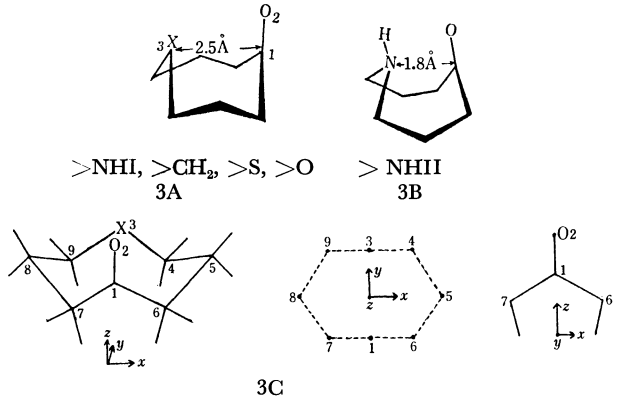

Fig. 3. 3A and 3B show two conformations for the calculation. X denotes the N atom (of NH group), the C atom (of CH_2 group), the S atom or the O atom of each compound (Ref. 26. *cf* Fig. 2).
The coordinate axes for the conformation of 3A, and the numbering of the atoms are given in 3C.

Table 2. bond lengths (in Å) and bond angles

C–H	1.09	∠C (sp^2)	120°
C–C	1.54	∠C (sp^3)	109°28′
C=O	1.22	∠COC	112°
C–O (in C–O–C)	1.44	∠CSC	98°
C–S (in C–S–C)	1.82	∠CNC	107°
C–N (in C–N–C)	1.47		
N–H	1.01		

In this zero conformation the lone pair of the S atom will be approximately directed perpendicularly to the C=O bond.[28] However, the lone pair of the N atom is not directed in the way perpendicular to the C atom, but is directed slightly upwards. Then, for the compound containing the NH group, another limiting conformation, as in Fig. 3B, is calculated. This conformation is referered to as NHII, and the previous one, in Fig. 3A, as >NHI. In >NHII (Fig. 3B), the $C_1\cdots N$ distance becomes shorter, 1.8 Å, and the derection of the lone pair of the N atom is more perpendicular to the plane including the C=O bond than in the case of >NHI.

Results and Discussion

Interaction of NH_3 and HCHO (A Model Calculation). In order to ascertain the interaction of the lone pair and the C=O group more explicitly, we calculated the electronic structure of the system of NH_3 and HCHO. HCHO is assumed to be planar, and the molecular plane is placed on the y–z plane, and the C=O bond, on the z axis, as in Fig. 4. The C···N distance is put

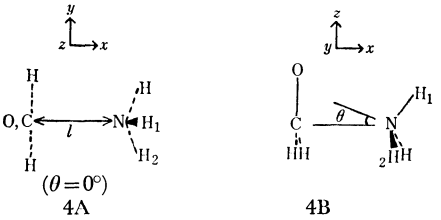

Fig. 4. HCHO and NH_3 system.

as l along the x axis, and the angle between the direction of the sp^2 type lone pair of the N atom and the x axis is put as θ. The angle θ is changed by the rotation of NH_3 on the x–r plane. The calculation of system as a function of θ (from $-10°$ to 30°) and l(from 0.5Å to 3.5Å) is carried out by the E–H method in order to ascertain values of θ and l in which the total energy of the system is at a minimum. The θ dependency of the atomic population[24] is shown in Table 3. The total energy and the bond order of the C–O bond, P_{CO}, and that between the C atom and N atom, P_{CN}, are shown in Table 4. The energy minimum is obtained at $\theta=0°$. The positive P_{CN} value indicates a bonding property between the C atom and the N atom. As θ approaches zero, the charge is transferred from NH_3 to HCHO, the polarization of the C–O bond and the P_{CN} value become large, and the P_{CO} value becomes smaller. Namely, the (transannular) interactions of the two molecules are the largest when the lone pair is directed to the C atom ($\theta=0°$).

As for the l dependency, the energy is decreased monotonically toward a larger l value and the expected energy minimum cannot be obtained by either method. This may be due to a defect in the approximation of the calculation.[29]

Population Analysis. The atomic orbital (AO) population[24] of the X_3 atom calculated by the E–H method and the AO-charge density[23] calculated by the SCF method are shown in Table 5. The AO population

25) In Fig. 3A, X denotes the N atom of the NH group, the C atom of the CH_2 group, and the S atom or the O atom of the NHI, >NHII, $>CH_2$, >S, or >O compounds, respectively. In Fig. 3A, the H atom of the groups and CH_2NH are not shown, for the sake of simplicity.

26) "Tables of Interatomic Distances and Configuration in Molecules and Ions," ed. by L. E. Sutton, The Chem. Soc., London (1956) and (1965).

27) Leonard *et al.* estimated $\theta=21°$ for >O and $\theta=68°$ for >S from the dipole moment (Ref. 11).

28) Actually, as the van der Waals radii of the sulfur atom are large, the molecule may have a larger dihedral angle than zero (Ref 27).

29) In the SCF calculation, the atomic-charge density and the E_{AB} values (E_{CO} and E_{CN}) do not change smoothly with the variation in θ and l.

TABLE 3. θ DEPENDENCY OF ATOMIC POPULATION OF HCHO AND NH_3

$\theta°$	HCHO				NH_3			
	C	O	H	HCHO	N	H_1	H_2	NH_3
−10	3.0609	7.2154	0.8936	12.0635	6.1076	0.6100	0.6088	7.9364
0	3.0615	7.2156	0.8934	12.0640	6.1064	0.6098	0.6099	7.9360
5	3.0610	7.2155	0.8933	12.0631	6.1075	0.6096	0.6101	7.9368
10	3.0599	7.2153	0.8932	12.0616	6.1095	0.6093	0.6101	7.9383
20	3.0563	7.2145	0.8930	12.0568	6.1162	0.6086	0.6097	7.9432
30	3.0512	7.2133	0.8926	12.0498	6.1259	0.6077	0.6089	7.9501
40	3.0505	7.2131	0.8928	12.0493	6.1610	0.5994	0.5909	7.9506
*	3.0351	7.1755	0.8947	12.0000	6.1685	0.6105	0.6105	8.0000

* isolated molecule

TABLE 4. θ DEPENDENCY OF THE TOTAL ENERGY (IN eV) OF A HCHO AND NH_3 SYSTEM, AND BOND ORDER P_{CO} BETWEEN THE C ATOM AND THE O ATOM AND P_{CN} BETWEEN THE C ATOM AND THE N ATOM

$\theta°$	−10	0	5	10	20	30	40
Total energy	−397.214	−397.220	−397.217	−397.210	−397.187	−397.151	−396.863
p_{C-O}	0.8252	0.8250	0.8251	0.8254	0.8262	0.8276	0.8277
$*p_{C\cdots N}$	0.0385	0.0394	0.0390	0.0380	0.0346	0.0296	0.0295

* bond order

TABLE 5. AO POPULATION (E–H) AND AO-CHARGE DENSITY (SCF) OF THE X ATOM

E–H

AO	atom				
	C (>CH_2)	N (>NHI)	S (>S)	O (>O)	N (>NHII)
s	1.198	1.512	1.531	1.782	1.484
x	0.949	1.281	1.072	1.424	1.269
y	1.154	1.717	1.806	1.976	1.248
z	1.035	1.485	1.586	1.852	1.375

SCF

AO	atom				
	C (>CH_2)	N (>NHI)	S (>S)	O (>O)	N (>NHII)
s	1.047	1.412	1.726	1.733	1.506
x	0.961	1.256	1.178	1.222	1.229
y	1.165	1.694	1.958	1.970	1.536
z	1.046	1.459	1.439	1.638	1.354

and the AO-charge density of the p_y AO of the N,S, and O atoms are large. These values of the p_y AO of the C atom are also larger than the p_x AO and the p_z AO. In the extreme case of >NHII, which is revealed to be too extreme, the electron of the p_y orbital flows to the p_y AO of the C_{CO} atom[30] and to the p_y AO of the O atom,[30] compared to the case of >NHI. This trend was also seen in the NH_3 and HCHO system, with a larger transannular interaction.

In the SCF calculation, according to a previous paper,[23] the total electronic energy, E_{AB},[23] of the AB bond is used instead of this bond order:

$$E_{AB} = \sum_{r}^{\text{on A}} \sum_{s}^{\text{on B}} P_{rs}(H_{rs}+F_{rs})$$

where H_{rs} is the core resonance integral,[23] where F_{rs} is the Fock's operator, and where $\sum_{r}^{\text{on A}}$ denotes the summation over all the valence AO's belonging to the A atom. The E_{AB} values obtained by the SCF calculation are listed in Table 6, together with the observed infrared absorption maximum of C=O stretching.[6,8]

TABLE 6. P_{rs} AND E_{AB} VALUES (eV) OF THE C=O BOND AND THE C_{CO}----X INTERACTION OBTAINED BY THE E–H AND THE SCF CALCULATIONS, AND THE OBSERVED CARBONYL FREQUENCY $\nu_{C=O}(cm^{-1})$

compound	E–H		SCF		
	P_{CO}	P_{CX}	E_{CO}	E_{CX}	$\nu_{C=O}$
>CH_2	0.791	0.015	−33.04	−0.36	~1704
>NH I	0.810	0.034	−34.03	−0.46	~1683
>S	0.755	0.149	−33.84	−1.19	~1690
>O	0.816	0.014	−34.04	−0.26	~1705
>NH II	0.455	0.361	−30.72	−7.62	—

The bond orders, P_{CX}'s, between the C_1 atom (or C_{CO} atom) and the X_3 atom (Fig. 3) become positive. This shows the bonding property (the transannular interaction) between the C_{CO} atom and the X atom. In Table 6, a correlation between P_{CO}, P_{CX}, E_{CX}, and $\nu_{C=O}$ may be expected. For the larger transannular interaction and the smaller $\nu_{C=O}$, the P_{CX} value becomes larger, the E_{CX} value becomes more negative, and the P_{CO} value becomes smaller. In the conformation with

30) The AO population of the p_yAO of the C_{CO} and O atoms of >NHI and >NHII are obtained as follows by the E–H calculations:

	>NH I	NH II
C_{CO}	0.405	0.649
O	1.789	1.931

Table 7. Transition energies and transition moments

	Transition	Type of transition	Transition energy Calcd (eV)	Obsd (eV)	Obsd (mμ)	Transition moment M and its component M	M(X)	M(Y)	M(Z)
>CH_2	2→1*	π–π*	5.47	4.31	288 (a)	0.527	0.000	0.286	−0.443
	1→2*	n–σ*	6.89	>6.70	<185 (a)	0.491	0.491	0.000	0.000
	4→1*	n(π̄)–π*	6.72	—	—	0.100	0.000	0.034	0.094
>NHI	2→1*	π–π*	6.30	5.51 (b)	225 (b)	0.374	0.000	−0.207	0.312
	1→3*	n–σ*	6.89	— (c)	— (c)	0.515	0.515	0.000	0.000
	4→1*	n(π̄)–π*	5.55	—	—	0.101	0.000	0.014	0.100
>S	1→1*	π–π*	5.42	5.46	227 (e)	0.512	0.000	−0.386	0.336
	2→4*	n–σ*	6.65	6.46	192	0.485	0.485	0.000	0.000
	5→1*	n(π̄)–π*	6.53	—	—	0.202	0.000	−0.089	−0.181
>O before CI	3→1*	n(π̄)–π*	6.11	—	—	0.262	0.000	−0.107	0.239
	2→1*	π–π*	6.47	—	—	0.238	0.000	−0.095	0.218
	1→3*	n–σ*	6.73	—	—	0.583	0.583	0.000	0.000
after CI	3→1*	n(π̄)–π*	6.08	—	—	0.191	0.000	−0.079	0.174
	2→1*	π–π*	6.50	—	—	0.298	0.000	−0.120	0.273
	1→3*	n–σ*	6.73	—	—	0.583	0.583	0.000	0.000

**: See Table 1A and 1B
(a): Ref. 11.
(b): These values are that of 1-methyl-1-azacyclooctane-5-one (Ref. 13).
(c): Probably the absorption in 217 mμ region will be masked (Ref. 1).
(e): Refs. 11, 2.

Table 8. Energy levels concerning the transition of Table 7 and main orbital coefficients of the C_1, O_2 and X_3 atom

>CH_2

No of levels	4(a′)	2(a′)	1(a″)	1*(a′)	2*(a′)
Energy (eV)	−10.965	−9.757	−9.616	0.955	2.840
Type	n(π̄)	π	σ	π*	σ*
C_1	(Y) −0.094	(Y) 0.145	(X) −0.301	(Y) 0.788	(S) 0.602
	(Z) 0.181	(Z) 0.013		(Z) 0.012	
O_2	(Y) −0.149	(Y) 0.510	(X) 0.576	(Y) −0.489	(S) −0.082
	(Z) −0.277	(Z) −0.047		(Z) −0.006	
C_3	(Y) 0.070	(Y) 0.453	(X) −0.215	(Y) 0.079	(S) −0.050
	(Z) 0.366	(Z) −0.135		(Z) −0.061	

>NHI

No of levels	4(a′)	2(a′)	1(a″)	1*(a′)	2*(a′)
Energy (eV)	−10.962	−9.774	−9.323	1.468	3.270
Type	n(π̄)	π	σ	π*	σ*
C_1	(Y) −0.079	(Y) −0.084	(X) −0.297	(Y) 0.765	(S) 0.573
	(Z) 0.339	(Z) −0.031		(Z) 0.012	
O_2	(Y) −0.150	(Y) −0.332	(X) 0.680	(Y) −0.516	(S) −0.072
	(Z) −0.578	(Z) 0.061		(Z) −0.002	
N_3	(Y) 0.024	(Y) −0.621	(X) −0.104	(Y) 0.058	(S) 0.089
	(Z) 0.106	(Z) 0.282		(Z) −0.030	

>S

No of levels	5(a′)	2(a″)	1(a′)	1*(a′)	3*(a′)
Energy (eV)	−11.425	−9.574	−9.326	1.117	2.886
Type	n(π̄)	σ	π	π*	σ
C_1	(Y) 0.125	(X) −0.274	(Y) −0.112	(Y) 0.715	(S) 0.542
	(Z) 0.250		(Z) −0.011	(Z) 0.035	
O_2	(Y) 0.230	(X) 0.710	(Y) −0.425	(Y) −0.481	(S) −0.054
	(Z) −0.436		(Z) 0.028	(Z) −0.016	
S_3	(Y) −0.241	(X) −0.117	(Y) −0.774	(Y) 0.105	(S) −0.015
	(Z) −0.519		(Z) 0.058	(Z) −0.148	

>O

No of levels	3(a′)	2(a″)	1(a″)	1*(a′)	3*(a′)
Energy (eV)	−10.095	−9.937	−8.949	1.551	3.310
Type	$n(\bar{\pi})$	π	σ	π^*	σ^*
C_1	(Y) −0.095	(Y) −0.042	(X) −0.322	(Y) 0.789	(S) 0.615
	(Z) 0.189	(Z) −0.081		(Z) −0.006	
O_2	(Y) −0.288	(Y) −0.201	(X) 0.540	(Y) −0.523	(S) −0.085
	(Z) −0.257	(Z) 0.109		(Z) 0.007	
O_3	(Y) −0.160	(Y) −0.731	(X) −0.155	(Y) 0.054	(S) 0.040
	(Z) 0.284	(Z) −0.102		(Z) 0.009	

the dihedral angle larger than zero,[27,28] the P_{CX} value of >S becomes smaller and the parallelism with $\nu_{C=O}$ becomes better. When the NHII conformation is adopted (rather than >NHI), the parallelism becomes better. However, the total energy of >NHII is higher than>NHI, and the P_{CX}, E_{CX}, P_{CO}, and E_{CO} values of >NHII deviate too much[31] compared to the values of the other examples (see Table 6). That is, the>NHII conformation is too extreme. It is possible that an actual molecule may have an intermediate conformation[32] between the two, >NHI and >NHII (denoted hereafter by >NHIII), in which the total energy is at a minimum and the parallelism between the P_{rs}, E_{AB}, and $\nu_{C=O}$ values become better. However, since the two methods we employed cannot give an energy minimum for the variation in the distance between the C_{CO} atom and the X atom, it is difficult to determine the actual conformation of >NHIII in these approximations.

Electronic Transitions. The transition energy and the transition moment are calculated by the SCF method. The calculated results are listed in Table 7 and there compared with the observed UV absorpations. As for the π–π^* transition of the oxygen meso-cycles (2→1* and 3→1* of Table 7) the configuration interaction (CI) is carried out. The results are shown in the bottom raws of Table 7. The energy levels concerning these transitions, and the main orbital coefficients of the C_1 or C_{CO}, O_2 and X_3 atoms, are shown in Table 8. The numbering of the levels is made from the highest-occupied level to the lower levels, and from the lowest unoccupied level (denoted by *) to the higher levels.

Though the agreement between the observed and the calculated transition energies is not very good, we tried to obtain some information about the nature of these transitions. The calculated transition with the higher energy is a sort of n–σ^* (A'') transition, the energy of which is equal for $>CH_2$ and >NHI, and does not vary very much for >S and >O. In the n MO, the MO coefficient of the lone pair AO of the O atom of the C=O group is large, and in the σ^* MO the MO coefficient of the s orbital of the C_1 atom is large. That is, it is noted that the n–σ^* transition is not affected very much by the transannular interaction. Therefore, these n–σ^* transitions correspond to the absorption is the 217 mμ region, which shows a comparatively small deviation among the compounds in Table 1A, or to the absorption about the 190 mμ region of the compounds in Table 1B.

The absorption maximum in the 230 mμ region (Tables 1A and 1B) may be a π–π^* (A')-type transition, in which π and π^* MO's are much more affected by the transannular interaction. That is, the π MO (see Table 8) is mainly constituted by the interacting lone pair AO and the π orbital of the C=O group. The π^* MO is considerably localized to the π^* antibonding orbital of the C=O group; the MO coefficient of the C_1 atom is especially large. Thus, these π–π^* transitions are essentially the intramolecular charge transfer from the interacting atom, X, to the C=O group.

In our calcultion, the transition with the third intense transition moment becomes an $n(\bar{\pi})$–π^* type (A′). The orbital, denoted by $n(\bar{\pi})$, has a comparatively large MO coefficient of the lone-pair AO of the O atom of the C=O group. In Table 7, the $n(\bar{\pi})$–π^* transition energy of NHI is smaller than the π–π^*. Possibly, the weak absorption with no detectable maximum in the longer-wavelength (carbonyl) region (shown by d in Table 1A)[13] is due to this $n(\bar{\pi})$–π^*-type transition.

From preceding calculations and discussions, it is found that the P_{CX} value is positive and the E_{CX} value is negative; this indicates the transannular interaction of the bonding type. Because of the larger transannular interaction, the P_{CO} value becomes large. The approximate parallelism between the P_{CO} value and $\nu_{C=O}$ is seen. Furthermore, the πMO, which is mainly constituted by the interacting lone-pair AO and the π orbital of the C=O group, and the π–π^* transition are affected by the transannular interaction.

One of the authors(H.Y) wishes to thank Mr. Hiroshi Nakatsuji for reading the manuscript and for his helpful suggestions.

The calculation was carried out on a HITAC 5020 Computer at the computation center of the University of Tokyo.

31) The P_{CO}, P_{CX}, E_{CO}, and E_{CX} values are sensitively change depending on the interatomic distance between the C_{CO} atom and the X atom.

32) The >NH III contormation has an intermediate $C_{CO}\cdot\cdot X$ distance between the two.

The Optical Activity of Bis-1,1′-spiroindanes. The Direct Calculation of Optical Rotational Strengths

Sanji HAGISHITA and Kaoru KURIYAMA

Shionogi Research Laboratory, Shionogi & Co., Ltd., Sagisu, Fukushima-ku, Osaka

(Received July 8, 1970)

A calculation based on Longuet-Higgins and Murrell's method using the MO's of aniline and phenol obtained by the SCF-MO-CI calculation is carried out for the π-electron structures of (−)-6,6′-diamino-(I) and (−)-6,6′-dihydroxy-bis-1,1′-spiroindane (II). These wave functions are then used to calculate the rotation strengths of these compounds. The circular dichroism curves calculated from the results, assuming a Gaussian curve, are compared with the observed spectra; a quantitative agreement with the experimental value is found. The nature of the transitions and the origin of the optical activity are also discussed.

In a previous paper[1] we reported the resolution, the CD spectra, and, from an analysis of the CD spectra, the determination of the absolute configuration of C_2-symmetrical bis-1,1′-spiroindane derivatives. The previous analysis was based on simple dipole-coupling mechanisms. This treatment has been widely used for the determination of the absolute configuration of the chiral molecules considered to be constructed from two or three groups with electric-dipole-allowed transitions.[2] The determination of the absolute configuration of spiroindanes belonging to the classes II and III[3] was based on the quantitative agreement between the observed and calculated rotational strengths associated with the *p*-band. However, the signs of the Cotton effects associated with the α-band are not in agreement with each other; moreover, there are some derivatives in which only one Cotton effect is associated with the α-band. Therefore, in order to satisfy all the electronic absorption regions, the application of simple dipole-coupling mechanisms seems not to be useful; this may be attributed partly to the fact that the value of the spectroscopic moment and the assumption of a point dipole located on the center of the benzene ring are not suitable.

There are also other shortcomings. The transitions correlated with the α- and the *p*-bands are orthogonal to each other and do not mix; also, it is necessary to adopt the configuration interaction among other transitions of the same symmetry and also, in these spiroindanes, to consider the mixing of the transitions through the repulsion force produced from the interaction between the transitions of one isolated chromophore and that of another chromophore. When two π systems are held in perpendicular planes by a common atom of a tetrahedral geometry, the overlap between the *p* orbitals on atoms bound directly to the insulating atom is considerable. Consequently, exchange interactions may become significant and may also produce charge-transfer transitions and a mixing of the local excitations.

In the present paper, we will report on the analysis of the CD spectra of the 6,6′-diamino-(I) and 6,6′-dihydroxy-bis-1,1′-spiroindane (II) by improved theoretical methods.

Method of Calculation

The σ electron, especially at the C-1 position, will influence the π electron framework;[4] in this calculation, however, only π electrons are considered. Therefore, (−)-I and (−)-II can be approximated to the dimers of two anilines and two phenols respectively, set at the spiro position. The five-membered rings of these spiroindanes may not have the envelope form because of the described in the previous paper.[1] Therefore, we have approximated the planar conformation in which the two systems are held in a perpendicular plane by a carbon atom of a tetrahedral geometry, with the S-configuration depicted in Fig. 1, for we believe that the small difference in geometry will not greatly influence the results of the calculated CD spectra.

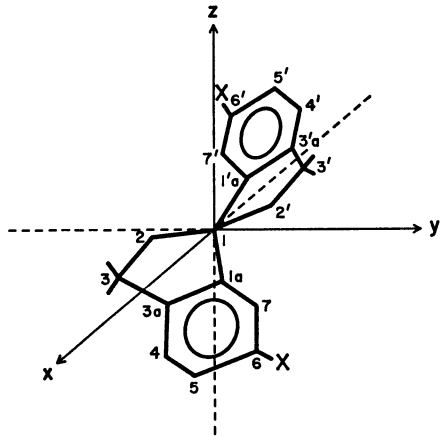

(−)-I : X=NH$_2$ (−)-II : X=OH

Fig. 1. The coordinate system employed. The bond lengths are chosen as follows: the aromatic C–C bond, 1.40 Å; the C–C single bond between C_1 and C_{7a} (and also C_1 and $C_{7a'}$), 1.52 Å, the C–O bond, 1.36 Å; the C–N bond, 1.41 Å. A perfect tetrahedral geometry is taken for C_1.

1) Part I: S. Hagishita, K. Kuriyama, M. Hayashi, Y. Nakano K. Shingu, and M. Nakagawa, This Bulletin, **44**, 496 (1971).

2) J. A. Schellman, *Accounts Chem. Res.*, **1**, 144 (1968); H. Eyring, H-C. Liu, and D. Caldwell, *Chem. Rev.*, **68**, 525 (1968).

3) The spiroindane derivatives were separated into three classes according to the origin of the optical power. In the classes II and III, the contribution of the dispersion force between the two aromatic chromophores is greater than the other effects, and the substituents at the benzene ring have large values in Platt's spectroscopic moment.

4) H. E. Simmons and T. Fukunaga, *J. Amer. Chem. Soc.*, **89**, 5208 (1967).

In this geometry, the resonance integrals between the AO's of the carbon atoms of the two aromatic chromophores must be considered. Assuming appropriate values for the overlap integrals, the wave functions can be obtained for the (−)-I and (−)-II molecules by the SCF–MO treatment. In this calculation, however, the Longuet-Higgins-Murrell formalism[5] is utilized. This method is particularly suitable for the investigation of the nature and origin of the coupling between chromophores and to take account of the configuration interaction effects. Moreover, a fairly well established approximation, such as the SCF-MO-CI method, can be used.

First, it is necessary to obtain the exact wave functions of the local chromophores. Nishimoto and Foster[6] have obtained the wave functions of mono-substituted benzenes by the SCF-CI formalism of the Pariser-Parr-Pople method[7] with variable β approximation. Their results showed that the calculated singlet transition energies and the oscillator strengths of aniline and phenol were in good agreement with the experimental values. Therefore, we adopted these wave functions as the local chromophores (see Appendix 1).

From these wave functions, we took account of only four locally-excited states, from the lowest to the fourth energy level for each chromophore. The resonance integrals between the AO's of the carbon atoms of the two chromophores cannot be neglected, and the energies of the highest occupied and the lowest vacant π MO are very similar to those of the second occupied and the second vacant π MO respectively. Therefore, we took into account an additional eight kinds of charge-transfer configurations, in which an electron is transferred from one aromatic chromophore to another, and *vice versa*. Thus, we considered a total of sixteen configurations for each of the molecules, (−)-I and (−)-II.

Taking the energy of the ground configuration as the standard, the energy values of locally-excited configurations can be directly determined from the results of Nishimoto and Foster.[6]

Neglecting the penetration integrals[8] and assuming a zero differential overlap,[7] the energy for the charge-transfer configuration can be evaluated by the following equation:

$$E_{CT} = I_\mu - A_\nu - \sum_r \sum_s C_r^\mu C_r^\mu C_s^\nu C_s^\nu (rr|ss) \quad (1)$$

where I_μ and A_ν are the ionization potential of μth and the electron affinity of the νth level of the MO of the aromatic chromophore respectively, and where C_r^μ is the coefficient of the rth AO's of the μth level of the MO. Two-center repulsion integrals of the $(rr|ss)$ type are computed from the Ohno approximation:[9]

$$(rr|ss) = \frac{1}{2}\left(1\sqrt{R_{rs}^2 + 1/(rr|rr)^2} + 1\sqrt{R_{rs}^2 + 1/(ss|ss)^2}\right) \quad (2)$$

where the one-center repulsion integrals $(rr|rr)$ are computed from the valence-state ionization potentials, I_r, and the electron affinities, A_r, for carbon, nitrogen, and oxygen by means of Eq. (3):

$$(rr|rr) = I_r - A_r \quad (3)$$

I_r and A_r are taken from Hinze and Jaffé's table.[10]

As the diagonal matrix elements have been evaluated, it is necessary to consider the off-diagonal matrix elements of the total electric Hamiltonian, each of which represents the magnitude of the interaction between two different configurations. The evaluation of the off-diagonal elements is carried out by the formulations by Pople[11] and Longuet-Higgins and Murrell.[5] In these calculations, the values of the two-center core integrals, β_{CX} (X=C, N, or O), at 1.40 Å for a C–C bond, at 1.38 Å for a C–N bond, and at 1.36 Å for a C–O bond are taken as standard from the literature,[6] while the β_{rs} values are evaluated by means of the following equation:

$$\beta_{rs} = (S_{rs}/S_{CX})\beta_{CX} \quad (4)$$

Here, S_{rs}/S_{CX} is the ratio of the overlap integrals at each distance. The two-center repulsion integrals are also calculated by the Ohno approximation.

Solving the secular equations constructed for each molecule by the use of the matrix elements evaluated above, the energy levels and wave functions shown in Table 1 are obtained.

In this calculation, using the Longuet-Higgins-Murrell formalism, the resonance energy between two aromatic chromophores is very small. The mixing of the locally-excited configurations and charge-transfer configurations by this spiro-conjugation contributes only a little. Therefore, in the other methods, the charge-transfer configurations are neglected and the repulsion among the locally-excited configurations is considered only by the formulation by Pople.[11] Moreover, we have taken twenty and sixteen local configurations for the compounds (−)-I and (−)-II respectively. We name this calculation "Method II"; the results are shown in Table 2.

The CD is governed by the rotational strength, R_i, to which Rosenfeld[12] first applied a quantum mechanical theory. The rotational strength is defined as the imaginary part of the scalar product of the molecular electric dipole moment, $\langle\psi_0|\vec{\varepsilon}|\psi_i\rangle$, with the magnetic dipole moment of $\langle\psi_i|\vec{m}|\psi_0\rangle$ for the electric transition under consideration:

$$R_i = Im\langle\psi_0|\vec{\varepsilon}|\psi_i\rangle\langle\psi_i|\vec{m}|\psi_0\rangle \quad (5)$$

where

$$\vec{\varepsilon} = e\sum_k \boldsymbol{r}_k \text{ and } \vec{m} = \frac{eh}{4\pi imc}\sum_k \boldsymbol{r}_k \times \nabla_k$$

The values of the electric and magnetic moments are not formulated on an equal footing; the rotational strength so calculated is origin-dependent. The evaluation of the electric and magnetic dipole moments is

5) H. C. Longuet-Higgins and J. N. Murrell, *Proc. Phys. Soc.*, **A68**, 601 (1955).
6) K. Nishimoto and L. S. Foster, *Theor. Chim. Acta*, **4**, 155 (1966).
7) R. Pariser and R. G. Parr, *J. Chem. Phys.*, **21**, 466 (1953); R. Pariser and R. G. Parr, *ibid.*, **21**, 767 (1953); R. G. Parr and R. Pariser, *ibid.*, **23**, 711 (1955); J. A. Pople, *Trans. Faraday Soc.*, **49**, 1375 (1953).
8) H. Kon, This Bulletin, **28**, 275 (1955).
9) K. Ohno, *Theor. Chim. Acta*, **2**, 219 (1964).
10) J. Hinze and H. H. Jaffé, *J. Chem. Phys.*, **33**, 1834 (1963).
11) J. A. Pople, *Proc. Phys. Soc.*, **A68**, 81 (1955).
12) L. Rosenfeld, *Z. Phys.*, **52**, 161 (1928).

TABLE 1. THE WAVE FUNCTIONS AND ENERGIES OF THE ELECTRONIC STATES OF 6,6′-DIAMINO- AND 6,6′-DIHYDROXY-BIS-1,1′-SPIROINDANE

E(eV)	Symmetry		G	L_1	L_2	L_3	L_4	C_1	C_2	C_3	C_4
						Compound (I)					
−0.010	B	ψ_0^D	+0.999	0	0	0	0	+0.016	−0.022	+0.003	0
4.389	A	ψ_1^D	0	−0.706	−0.018	−0.012	+0.016	−0.006	+0.008	−0.009	+0.024
4.410	B	ψ_2^D	+0.001	−0.706	+0.019	+0.009	−0.014	−0.012	+0.009	−0.019	+0.023
5.363	A	ψ_3^D	0	−0.009	+0.632	+0.044	−0.019	−0.020	+0.020	−0.288	+0.116
5.366	B	ψ_4^D	−0.007	−0.032	−0.571	+0.033	−0.013	+0.099	−0.027	+0.376	−0.141
5.437	A	ψ_5^D	0	−0.021	+0.305	+0.018	+0.039	+0.155	−0.040	+0.601	−0.133
5.504	B	ψ_6^D	−0.007	−0.009	+0.410	−0.026	−0.011	+0.099	−0.029	+0.557	−0.100
5.861	B	ψ_7^D	+0.005	+0.017	−0.062	−0.068	−0.039	+0.039	+0.134	+0.162	+0.666
5.865	A	ψ_8^D	0	−0.021	+0.048	−0.049	+0.022	−0.004	−0.140	−0.181	−0.665
6.155	A	ψ_9^D	0	+0.016	+0.017	−0.566	+0.280	+0.220	−0.194	−0.055	+0.106
6.292	B	ψ_{10}^D	−0.011	−0.005	−0.004	−0.463	−0.342	+0.390	+0.023	−0.105	−0.070
						Compound (II)					
−0.010	B	ψ_0^D	−0.999	0	0	0	0	+0.016	−0.022	0	−0.002
4.650	A	ψ_1^D	0	−0.705	−0.007	+0.009	−0.013	+0.001	−0.047	−0.006	+0.014
4.624	B	ψ_2^D	+0.001	+0.706	−0.006	+0.012	−0.011	−0.014	−0.030	+0.014	−0.017
5.735	A	ψ_3^D	0	−0.003	+0.647	−0.041	+0.032	+0.108	−0.011	−0.247	+0.078
5.754	B	ψ_4^D	+0.004	−0.009	−0.675	−0.038	−0.031	+0.094	−0.004	+0.158	−0.092
5.879	B	ψ_5^D	−0.005	−0.015	+0.156	−0.002	−0.001	−0.099	+0.017	−0.678	−0.079
5.894	A	ψ_6^D	0	−0.010	+0.263	−0.020	−0.014	−0.038	+0.009	+0.651	−0.072
6.230	A	ψ_7^D	0	−0.018	+0.054	+0.021	−0.051	−0.026	+0.088	−0.102	−0.689
6.230	B	ψ_8^D	−0.001	−0.010	+0.075	−0.038	−0.041	+0.005	+0.088	−0.099	−0.688

L_i represents the ith locally excited configuration and
C_i the ith charge transfer configuration.
$L_i=\psi_i^{M_a} \pm \psi_i^{M_b}$
$C_i=\psi_k^a\psi_l^b \pm \psi_k^b\psi_l^a$: $k=3$, $l=5$ for $i=1$; $k=3$, $l=6$ for $i=2$; $k=4$, $l=5$ for $i=3$; $k=4$, $l=6$ for $i=4$, where the minus sign for A symmetry and the plus sign for B symmetry.

TABLE 2. THE WAVE FUNCTIONS AND ENERGIES OF THE ELECTRONIC STATES OF 6,6′-DIAMINO- AND 6,6′-DIHYDROXY-BIS-1,1′-SPIROINDANE, NEGLECTING THE CHARGE TRANSFER CONFIGURATIONS

E(eV)	Sym-metry		G	L_1	L_2	L_3	L_4	L_5	L_6	L_7	L_8	L_9	L_{10}
							Compound (I)						
0.0		ψ_0^D	1.0	0	0	0	0	0	0	0	0	0	0
4.390	A	ψ_1^D	0	−0.706	−0.020	−0.014	+0.017	+0.011	0	+0.002	+0.002	−0.002	0
4.412	B	ψ_2^D	0	+0.707	−0.017	−0.009	+0.014	+0.007	0	+0.002	+0.002	−0.002	0
5.388	A	ψ_3^D	0	−0.022	+0.704	+0.054	−0.015	−0.025	+0.005	+0.005	−0.004	−0.001	+0.022
5.416	B	ψ_4^D	0	−0.016	−0.705	+0.041	0	−0.017	+0.004	+0.005	−0.002	−0.002	−0.002
6.230	A	ψ_5^D	0	+0.019	+0.059	−0.650	+0.254	+0.089	−0.059	−0.028	+0.018	−0.009	+0.006
6.408	B	ψ_6^D	0	+0.003	+0.037	+0.645	+0.286	+0.027	+0.007	+0.013	+0.008	−0.007	−0.001
6.638	A	ψ_7^D	0	+0.012	−0.004	+0.265	+0.650	+0.075	−0.021	−0.024	+0.008	+0.001	+0.008
6.713	B	ψ_8^D	0	+0.015	+0.013	+0.278	−0.638	+0.117	−0.021	−0.021	+0.015	−0.002	+0.008

E(eV)	Symmetry		G	L_1	L_2	L_3	L_4	L_5	L_6	L_7	L_8
						Compound (II)					
0.0		ψ_0^D	1.0	0	0	0	0	0	0	0	0
4.615	A	ψ_1^D	0	−0.707	0.007	+0.015	−0.015	0	+0.005	−0.001	−0.004
4.629	B	ψ_2^D	0	+0.707	−0.006	+0.010	−0.012	0	+0.004	0	−0.003
5.770	A	ψ_3^D	0	−0.008	+0.706	−0.042	+0.006	+0.002	−0.006	+0.003	0
5.785	B	ψ_4^D	0	+0.006	+0.706	+0.029	+0.008	−0.002	+0.003	−0.003	+0.002
6.421	A	ψ_5^D	0	−0.021	−0.039	−0.603	+0.359	+0.014	−0.060	+0.022	+0.030
6.655	B	ψ_6^D	0	+0.004	−0.024	+0.426	+0.564	−0.008	0	−0.017	+0.008
6.851	A	ψ_7^D	0	+0.006	−0.016	−0.362	−0.606	−0.011	+0.010	−0.022	+0.004
7.011	B	ψ_8^D	0	−0.015	−0.017	+0.559	−0.422	+0.020	−0.083	+0.030	+0.032

The symbol G and L_i are used in the same manner as in Table 1.

achieved in the following way:[13]

$$\langle\psi_0|r|\psi_i\rangle = \frac{h}{4\pi^2 m\nu_{i0}}\langle\psi_0|\nabla|\psi_i\rangle \quad (6)$$

where

$$h\nu_{i0} = E_i - E_0$$

The wave functions obtained above can be written in the form:

$$\psi_i^{D} = \sum_i C_i^i\psi_i^{M} + \sum_k C_k^i\psi_k^{CT} \quad (7)$$

where ψ_i^{M} and ψ_k^{CT} represent the ith wave function of the monomer chromophore and the kth wave function of the charge-transfer transition respectively. The monomer wave functions can be rewritten as a linear combination of configurations:

$$\psi_i^{M} = \sum_l\sum_m C^i_{lm}(\psi_l^{-1}\psi_m) \quad (8)$$

Then, the electric dipole moments of the monomer may be approximated as follows:

$$\langle\psi_0^{M}|\nabla|\psi_i^{M}\rangle \doteqdot \sqrt{2}\,C^0_{00}\sum_l\sum_m C^i_{lm}\langle\psi_l|\nabla|\psi_m\rangle \quad (9)$$

Similarly, the magnetic moments are approximated as follows:

$$\langle\psi_i^{M}|\vec{m}|\psi_0^{M}\rangle = \frac{eh}{4\pi imc}\cdot\sqrt{2}\,C^0_{00}\sum_m\sum_l C^i_{ml}\langle\psi_m|r\times\nabla|\psi_l\rangle \quad (10)$$

where $\boldsymbol{r}$ is the radius vector to the electron under consideration. The MO's, ψ_l and ψ_m, are written as linear combinations of AO's (X):

$$\psi_l = \sum_\alpha C_\alpha{}^l\chi_\alpha \quad (11)$$

Therefore,

$$\langle\psi_l|\nabla|\psi_m\rangle = \sum_{\text{all bond}} C^{lm}_{\alpha\beta}\langle\chi_\alpha|\nabla|\chi_\beta\rangle \quad (12)$$

$$\langle\psi_l|r\times\nabla|\psi_m\rangle = \sum_{\text{all bond}} C^{lm}_{\alpha\beta}r_{\alpha\beta}\times\langle\chi_\alpha|\nabla|\chi_\beta\rangle \quad (13)$$

where $C^{lm}_{\alpha\beta}$ is the transitional bond order ($C^{lm}_{\alpha\beta}=C_\alpha{}^lC_\beta{}^m - C_\beta{}^lC_\alpha{}^m$) and where $\vec{r}_{\alpha\beta}$ is the radius vector to the mid-point of the bond. We also made similar calculations on the charge transfer, but the electric and magnetic dipole moments are very small. Therefore, these quantities for the charge-transfer configuration are neglected. By these procedures, we found the rotational strengths which are origin-independent. Using the MO's, the rotational strengths can be calculated on the basis of these formulations.

On the other hand, the rotational strength can be calculated by using Eqs. (5) and (11') for the wave-function of method II:

$$\langle\psi_i|\vec{m}|\psi_0\rangle = \frac{\pi\nu_{i0}}{C}i\sum_k \boldsymbol{R}_k\times\langle\psi_i|e\boldsymbol{r}_k|\psi_0\rangle \quad (11')$$

where $\boldsymbol{R}_k$ is the radius vector to the center of gravity of π-electrons in the ground state of the aromatic chromophore. By this procedure (named method III), we could also find the rotational strengths which are origin-independent.

TABLE 3. COMPARISON OF THE OBSERVED AND CALCULATED SPECTRA OF (S)-6,6'-DIAMINO-(I) AND (S)-6,6'-DIHYDROXY-BIS-1,1'-SPIROINDANE (II)

	Found (in MeOH)				Theoretical							
	UV		CD		Method I			Method II			Method III	
	λ (mμ)	D ($\times 10^{-36}_{cgs}$)	λ (mμ)	R ($\times 10^{-40}_{cgs}$)	λ (mμ)	D ($\times 10^{-36}_{cgs}$)	R ($\times 10^{-40}_{cgs}$)	λ (mμ)	D ($\times 10^{-36}_{cgs}$)	R ($\times 10^{-40}_{cgs}$)	D ($\times 10^{-36}_{cgs}$)	R ($\times 10^{-40}_{cgs}$)
	296	5.95	298.5	−7.23	281.8	1.94	−7.27	282.4	3.20	−7.18	6.91	+28.4
					280.5	0.04	+0.03	281.0	0.11	+0.27	0.27	−21.3
	236	17.2	244.0	−8.70	231.1	7.99	−225.0					
			233.0	+14.6	230.6	3.75	+155.0	230.0	10.1	−262.0	20.8	−812.0
I					226.1	0.99	−27.9	228.9	6.63	+257.0	13.8	+787.0
					224.8	2.13	+90.8					
	207	58.2	220.0	−204.0	211.2	0.05	−1.28	199.0	21.3	+25.3	36.2	+80.4
					211.0	0.11	+0.31	193.5	0.03	+44.3	0.15	+90.5
					201.1	9.90	−52.3	186.8	20.9	−485.0	42.2	−1560.0
					197.7	1.05	+120.0	184.7	14.7	+534.0	29.8	+1640.0
	289	5.22	291.5	−4.30	268.6	1.29	−2.13	268.6	2.06	−2.25	4.16	+31.7
	284		270.0	+0.63	267.6	0.02	−0.02	267.7	0.08	−0.07	0.19	−19.5
	220[t]	8.40	236.0	−0.02	215.8	4.07	−124.0					
			228.0	+2.38	215.0	2.92	+136.0	214.8	4.27	−117.0	9.50	−291.0
					210.5	0.13	+5.18	214.3	2.99	+123.0	6.68	+325.0
II					210.0	0.35	−10.9					
			209.0	−18.6	198.6	0.62	−4.88	193.1	29.4	−27.5	43.7	+288.0
					198.6	~0	−0.10	186.3	4.55	+439.0	10.4	+1263.0
								180.9	35.7	−527.0	69.9	−1588.0
								176.8	16.1	+178.0	33.5	−152.0

13) M. Wolfsberg, *J. Chem. Phys.*, **23**, 793 (1955).

Results and Discussion

From the results of the compounds (—)-I and (—)-II given in Table 1, the contribution of the configurations to the excited states can be estimated, and we can see the nature of the transitions. By method I, the first and the second excited states can be said to be mainly composed of the ψ_1^M configuration (α-band) of the monomer and to have A and B symmetries respectively. In the third and fourth excited states, although the main configuration is the ψ_2^M (p-band) of the monomer, the charge-transfer configuration contributes to these states only to some extent. On the contrary, the main configuration of the fifth and sixth excited states is the charge-transfer configuration. This means that these transitions involve a large amount of electron transfer between the aromatic chromophores.

When the intramolecular charge-transfer configurations are neglected, the results given in Table 2 also show the mixing of the locally-excited configurations and the A and B symmetry of the transitions respectively. The first and the second excited states have mainly the ψ_1^M configuration, while the third and the fourth excited states have again the ψ_2^M configurations; in higher excited states, a mixing of the configurations is clearly observed.

When the excitation energies obtained by the two methods are compared with those of the experiments, the experimental results show still lower energies. This may be explained by the fact that the local excitation energies are adopted from aniline and phenol directly instead of from 6-amino- and 6-hydroxy-indane.

When the observed and the calculated CD spectra are compared, it is important to consider any mutual cancellation or addition of bands in areas where they overlap. The rotational strength, R, of an isolated, optically-active transition can be defined in the terms of directly observable properties, such as the ellipticity, $[\theta]_\lambda$[14]:

$$R = \frac{hc}{48\pi^2 N}\int [\theta]_\lambda \mathrm{d} \ln \lambda \text{ (integration taken through the bond)} \tag{15}$$

If the ellipticity has a Gaussian dependence on the wavelength,

$$[\theta]_\lambda = [\theta]_{max} \exp\left[-\left(\frac{\lambda-\lambda_i}{\Delta_i}\right)^2\right] \tag{16}$$

where $[\theta]_{max}$ is the maximum value of the ellipticity, Δ_i is the half-width, and λ_i is the wavelength corresponding to the maximum ellipticity. Furthermore, one obtains a direct relation between the ellipticity, $[\theta]_\lambda$, and the rotational strengths, R_i:

$$[\theta]_\lambda = \frac{1}{1.233\times 10^{-42}} \sum_i R_i \frac{\lambda_i}{\Delta_i} \exp\left[-\left(\frac{\lambda-\lambda_i}{\Delta_i}\right)^2\right] \tag{17}$$

In this calculation, the values of the half-widths, Δ_i, are different in every transition, but we approximate the λ_i/Δ_i value to a constant. Using this equation and this assumption, we plot the theoretical CD curves in Figs. 2 and 3.

14) W. Moffitt and A. Moscowitz, *J. Chem. Phys.*, **30**, 648 (1959).

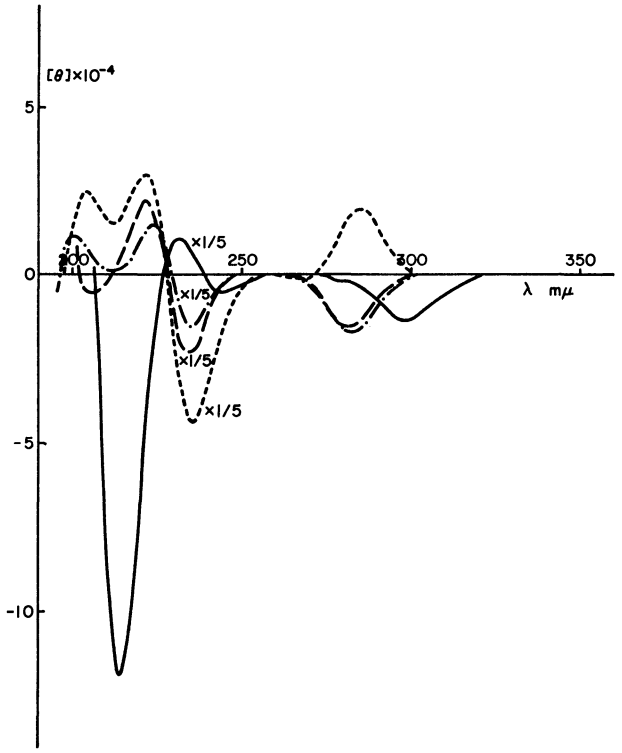

Fig. 2. CD spectra of (—)-3,3,3′,3′-tetramethyl-6,6′-diamino-bis-1,1′-spiroindane. Found (——), method I (----), method II (-·-·-), and method III (·····).

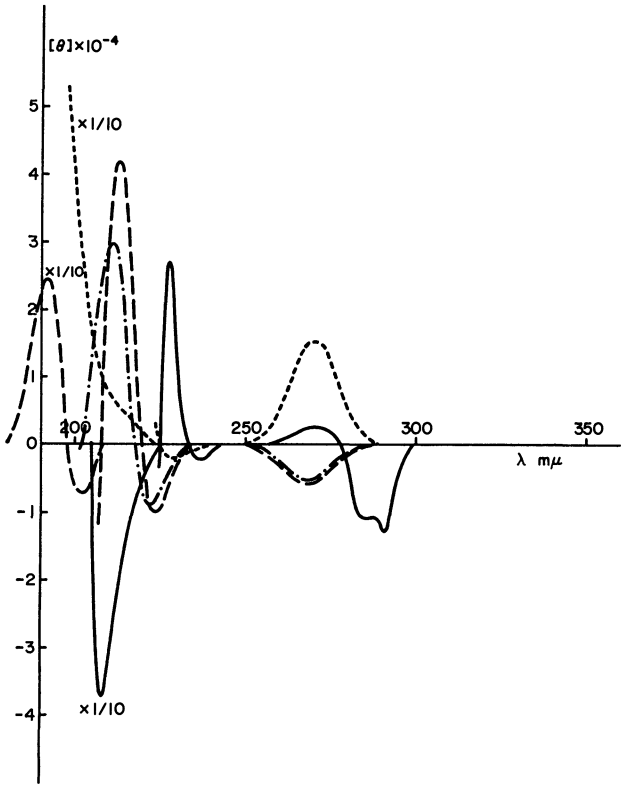

Fig. 3. CD spectra of (—)-3,3,3′,3′,-tetramethyl-6,6′-dihydroxy-bis-1,1′-spiroindane. Found (——), method I (----), method II (-·-·-), and method III (·····).

As has been mentioned above, the calculated excitation energies are higher than the observed ones. By comparing the observed and calculated CD spectra cited in Fig. 2, the calculated Cotton effect centered at

ca. 280 mμ can be considered to be correlated with the observed Cotton effects at *ca.* 300 mμ. Although the simple dipole-coupling mechanisms and method III could not predict the correct signs and magnitudes of the Cotton effect in this region, the results of methods I and II predict almost quantitatively the sign and the magnitude of the Cotton effect.

In (−)-II, we can see two oppositely-signed Cotton effects at 291.5 and 270 mμ, but the CD spectra calculated by methods I and II in Fig. 3 show only the negatively-signed Cotton effect, while that calculated by method III shows only a positively-signed one at *ca.* 269 mμ. Although these methods, I and II, cannot predict the small Cotton effect of a positive sign, the large, negatively-signed Cotton effect corresponds to the results of the calculation. The results are, therefore, not so unsatisfactory, while method III gives an unsatisfactory result from the same point of view.

In the shorter-wavelength regions, the observed rotational strengths at 244 and 233 mμ of (−)-I are correlated with the four calculated strengths at 231.3, 230.6, 226.1, and 224.8 mμ by method I or with the two at 230.0 and 228.9 mμ by the method II, and the calculated magnitudes are much larger than those observed. However, it is considered that many bands overlap with each other in this region, giving rise to a mutual cancellation or addition of band areas; the validity can be judged by means of the calculated CD curves.

From the CD curves depicted in Fig. 2, the observed Cotton effects centered at 244 and 233 mμ of (−)-I can be correlated with those calculated at *ca.* 235 and 225 mμ respectively. Similarly, in Fig. 3 the observed Cotton effects at 236 and 228 mμ of (−)-II can be correlated with those calculated at *ca.* 225 and *ca.* 210 mμ respectively.

In the method I, the charge-transfer configurations are mixed to some extent in the third and fourth excited states; also, the fifth and sixth excited states have the character of a charge-transfer overlap in these band areas, the results calculated by methods I and II, however, show almost the same CD spectra. From these result, the contribution of the charge-transfer transition can be considered to be small. It cannot, however, be denied that the bands in these regions have the character of a mixture of a number of configurations. The signs and the magnitudes of the observed Cotton effects and those calculated by these three methods agree almost quantitatively.

Appendix 1. The wave functions and energies of the electronic states of aniline

	χ_1	χ_2	χ_3	χ_4	χ_5	χ_6	χ_7
ψ_1	+0.45480	+0.55958	+0.36985	+0.27380	+0.23770	+0.27380	+0.36985
ψ_2	+0.58562	+0.25924	−0.10110	−0.39351	−0.50961	−0.39351	−0.10110
ψ_3	0	0	+0.50308	+0.49690	0	−0.49690	−0.50308
ψ_4	+0.60660	−0.33600	−0.36972	+0.14232	+0.45305	+0.14232	−0.36972
ψ_5	0	0	−0.49690	+0.50308	0	−0.50308	+0.49690
ψ_6	+0.24973	−0.57031	+0.23492	+0.30299	−0.56427	+0.30299	+0.23492
ψ_7	+0.14101	−0.42604	+0.40139	−0.39765	+0.40017	−0.39765	+0.40139

	$\psi_4\psi_5$	$\psi_4\psi_6$	$\psi_4\psi_7$	$\psi_3\psi_5$	$\psi_3\psi_6$	$\psi_3\psi_7$	$\psi_2\psi_5$
ψ_1^M	+0.87889	0	0	0	−0.46840	−0.01702	−0.08864
ψ_2^M	0	+0.95475	+0.05865	+0.28526	0	0	0
ψ_3^M	+0.46231	0	0	0	+0.79468	−0.02994	+0.38804
ψ_4^M	0	−0.26055	−0.15385	+0.93659	0	0	0
ψ_5^M	−0.11400	0	0	0	−0.38099	−0.12893	+0.90830
ψ_6^M	0	−0.08423	+0.96971	+0.11769	0	0	0
ψ_7^M	0	−0.11478	+0.10289	+0.16420	0	0	0
ψ_8^M	+0.00337	0	0	0	−0.05146	+0.91400	+0.11491
ψ_9^M	−0.02879	0	0	0	−0.03583	−0.38315	−0.05790
ψ_{10}^M	0	+0.01756	−0.14818	+0.02469	0	0	0

	$\psi_2\psi_6$	$\psi_1\psi_5$	$\psi_1\psi_6$	E(eV)		f	
				Calcd	Found	Calcd	Found
ψ_1^M	0	−0.00342	0	4.404	4.40	0.056	0.028
ψ_2^M	+0.05726	0	−0.01918	5.408	5.39	0.366	0.140
ψ_3^M	0	+0.05734	0	6.379	6.40	0.478	0.510
ψ_4^M	−0.17416	0	−0.03020	6.645	6.88	0.890	0.570
ψ_5^M	0	−0.01493	0	7.614	7.87	0.546	(0.68)
ψ_6^M	0.12418	0	+0.15261	7.651			
ψ_7^M	+0.97291	0	−0.05213	7.973			
ψ_8^M	0	+0.38568	0	8.755			
ψ_9^M	0	+0.92070	0	9.406			
ψ_{10}^M	+0.06642	0	+0.98626	9.744			

Appendix 2. The wave functions and energies of the electronic states of phenol

	χ_1	χ_2	χ_3	χ_4	χ_4	χ_6	χ_7
ψ_1	+0.71851	+0.53215	+0.26534	+0.15244	+0.11526	+0.15244	+0.26534
ψ_2	+0.48242	−0.02488	−0.27207	−0.43389	−0.49202	−0.43389	−0.27207
ψ_3	0	0	−0.50280	−0.49717	0	+0.49718	+0.50280
ψ_4	+0.43788	−0.44910	−0.36616	+0.19584	+0.51159	+0.19584	−0.36616
ψ_5	0	0	−0.49718	+0.50280	0	−0.50280	+0.49718
ψ_6	+0.20913	−0.57444	+0.24199	+0.30393	−0.56958	+0.30393	+0.24193
ψ_7	+0.12469	−0.42957	+0.40366	−0.39721	+0.39811	−0.39721	+0.40366

	$\psi_4\psi_5$	$\psi_4\psi_6$	$\psi_4\psi_7$	$\psi_3\psi_5$	$\psi_3\psi_6$	$\psi_3\psi_7$	$\psi_2\psi_5$
ϕ_1^M	+0.83038	0	0	0	+0.55359	+0.01448	−0.06164
ϕ_2^M	0	+0.89721	+0.01654	−0.43873	0	0	0
ϕ_3^M	−0.55509	0	0	0	+0.81528	−0.02817	−0.16247
ϕ_4^M	0	+0.43146	+0.06106	+0.89498	0	0	0
ϕ_5^M	0	−0.00895	+0.93443	−0.02152	0	0	0
ϕ_6^M	−0.04614	0	0	0	+0.16600	+0.29736	+0.93909
ϕ_7^M	0	−0.09363	+0.35049	−0.07786	0	0	0
ϕ_8^M	−0.01460	0	0	0	−0.03606	+0.95424	−0.29650

	$\psi_2\psi_6$	E(eV)		f	
		Calcd	Found	Calcd	Found
ϕ_1^M	0	4.624	4.59	0.036	0.023
ϕ_2^M	+0.04744	5.780	5.76	0.180	0.175
ϕ_3^M	0	6.718	6.68	0.908	0.585
ϕ_4^M	+0.09550	6.771	6.90	1.125	0.371
ϕ_5^M	−0.35539	8.049			
ϕ_6^M	0	8.050			
ϕ_7^M	+0.92862	8.401			
ϕ_8^M	0	8.905			

In the even-shorter-wavelength regions, the CD bands could not be predicted from these calculations. This may be due to the neglect of the higher energy states in method I and of the π–σ^* transitions, which may contribute to the CD spectra in these regions.

From the quantitative agreement between the experimental and the calculated results obtained by the methods, I and II, these methods can be considered to be suitable for the determination of the absolute configuration and for the estimation of the order of the rotational strengths of compounds with two or more chromophores composed of π-electrons. It must be noted that, for the same good wave-functions, methods II and III give different rotational strengths; method III especially shows incorrect signed Cotton effects in the α-band region. The difference in these results may be caused by the choice of the center of the transition dipole in method III, but the true reason for the failure of method III and for the success of method II does not appear to be understood at present. From our present studies, however, it could be concluded, for π-electron systems, that the rotational strengths calculated by method II are more likely to give a good agreement with the experimental data.

On the Effects of Doubly Excited Configurations in Semi-Empirical Molecular Orbital Calculations on Non-Alternant Hydrocarbons

Hiroshi KASHIWAGI

Department of Chemistry, Faculty of Science, Hokkaido University, Sapporo

(Received July 17, 1970)

Effects of inclusion of doubly excited configurations in semi-empirical SCF-CI calculations are studied for the π-electrons of the four non-alternant hydrocarbons, fulvene, heptafulvene, vinylfulvene, and fulvalene. Transition energies to lower excited states are little affected by inclusion of doubly excited configurations. However, oscillator strengths change substantially and a good agreement with experiment is obtained. Dipole moments of ground states are affected by about 20%.

The importance of configuration interaction (CI) is well known in semi-empirical molecular orbital calculations of π-electron systems. However, often only singly excited configurations are taken into account. Recently, effects of inclusion of doubly or higher excited configurations on calculated molecular properties have been discussed by several authors. Allinger and his coworkers[1-3] treated many unsaturated hydrocarbons by a modified Pariser-Parr-Pople type self-consistent field (SCF)-CI calculation including both singly and doubly excited configurations. They concluded that inclusion of doubly excited configurations has very little effect on transition energies in about 90% of the molecules studied, but it has a substantial effect in certain cases such as *trans*-butadiene. They also found that calculated extinction coefficients become smaller by taking doubly excited configurations into account, but the calculated results are still about 50% too large when compared with the observed values.[2] Eveleth[4,5] and Hirota and Nagakura[6] treated some unsaturated organic hetero-compounds by a similar method. They both found some remarkable changes of transition energies. In some cases, even the order of levels are changed. They also found a large decrease in oscillator strength.

We have studied the effects of doubly excited configurations in semi-empirical SCF-CI calculations. Excitation energies, transition probabilities, and π-electron distributions in a molecule were investigated for four non-alternant hydrocarbons. From our calculations, we hope to find answers to the following questions:

1) Does inclusion of doubly excited configurations lead to a better agreement with experiment. In non-empirical calculations, we believe that bigger CI calculation will yield better wave functions. But this is open to question in semi-empirical calculations.

2) What kind of molecular properties are sensitive to the inclusion of doubly excited configurations?

3) If CI is important, how many configurations should be included to obtain reasonable agreement with experiment?

Fulvene, heptafulvene, vinylfulvene, and fulvalene were chosen because a) only a small number of semi-empirical parameters are necessary, b) π-electron densities on carbon atoms might differ from unity and their values may be sensitive to a small change of wave functions, and c) as many as nine absorptions of singlet π–π transitions are observed for these molecules.

For each molecule, several CI calculations with different dimensions including both singly and doubly excited configurations were carried out. Only basis functions whose energies are below a certain cut-off energy were included in CI. Transition energies, oscillator strengths, π-electron densities, and weights of doubly excited basis functions of excited states were calculated. We investigated the changes of these physical quantities with the cut-off energy. The details of the calculation method is given in the second section. Main features of the results are shown in Figs. 2—9 in the third section.

Method of Calculation

A more or less standard Pariser-Parr-Pople method[7] is followed. Basis wave functions for CI are constructed from SCF molecular orbitals (MO's). For each symmetry type of singlet states, CI matrix elements are calculated and an eigenvalue problem is solved. A FORTRAN program was written. In this program, the number of basic atomic orbitals is not more than 50, and the number of basis wave functions in CI is at most 50 for each symmetry type.

Semi-empirical parameters for carbon $2p\pi$ atomic orbitals are determined as follows: The valence state ionization potential and the one center Coulomb integral are 11.22 eV and 10.60 eV, respectively.[8] Two center Coulomb integrals are evaluated by the quadratic interpolation formula proposed by Pariser and Parr.[7] The effective nuclear charge of the Slater type carbon $2p\pi$ atomic orbital is 3.25. Core resonance integrals between non-nearest neighbors are neglected. For nearest neighbors, core resonance integrals are determined by

$$\beta = -10.59S, \qquad (1)$$

1) N. L. Allinger and J. C. Tai, *J. Amer. Chem. Soc.*, **87**, 2081 (1965).
2) N. L. Allinger, J. C. Tai, and T. W. Stuart, *Theor. Chim. Acta*, **8**, 101 (1967).
3) N. L. Allinger and T. W. Stuart, *J. Chem. Phys.*, **47**, 4611 (1967).
4) E. M. Eveleth, *ibid.*, **46**, 4151 (1967).
5) E. M. Eveleth, *J. Amer. Chem. Soc.*, **89**, 6445 (1967).
6) F. Hirota and S. Nagakura, This Bulletin, **43**, 1010 (1970).
7) P. Pariser and R. G. Parr, *J. Chem. Phys.*, **21**, 767 (1953).
8) G. Pilcher and H. A. Skinner, *J. Inorg. Nucl. Chem.*, **24**, 937 (1962).

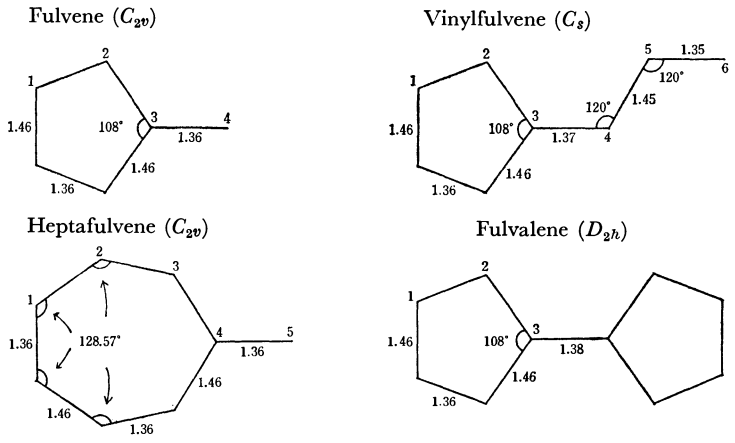

Fig. 1. Molecular geometries. (interatomic distances in Å)

where S is the overlap integral, which is theoretically evaluated from the Slater atomic orbitals. The numerical coefficient in the above formula is fixed by fitting the calculated transition energy $^1A_{1g}-{}^1B_{2u}$ of benzene to the observed value, 4.90 eV. The C–C bond length of benzene is 1.397 Å and the resulting resonance integral is −2.60 eV. It should be noted that the numerical coefficient in Eq. (1) is the only parameter which has been newly determined in this work.

The geometry of the compounds is determined by the following method. The molecular symmetry is assumed as shown in Fig. 1. As for vinylfulvene, it is assumed that the five-membered-ring is symmetric with respect to the axis through the atoms, C_3 and C_4. The values of the marked angles are fixed as shown in Fig. 1. In determining bond lengths and the remaining angles, the following procedure is employed. First bond lengths are assumed, and π-electron wave functions are calculated. From the resulting bond order P, a bond length R is calculated by the formula

$$R = 1.517 - 0.18P. \qquad (2)$$

If there is a difference of more than 0.01 Å between input and output bond lengths, we repeat all the calculation until self-consistency is obtained. The final bond lengths are shown in Fig. 1. All unassumed angles are automatically determined by this procedure.

Results and Discussion

Several calculations with CI are made for each molecule in order to investigate the variation of physical quantities against the number of included configurations. First, only singly excited basis functions are included. We call it S-CI. Other kinds of CI are carried out including both singly and doubly excited basis functions with energies up to certain values, such as 9, 11, 13, 15, and 17 eV. We call these values cut-off energies. The last kind of CI includes the largest number of both singly and doubly excited basis functions for each symmetry type. The largest numbers are 31 ($^1A_1$) and 24 ($^1B_1$) for fulvene. It is 50 for each symmetry type of the other molecules. The CI with the largest number of basis functions is called M-CI.

First Excited States. Transitions to the first excited states of the four molecules are observed at about 3 eV. Their strengths are weak and observed oscillator strengths are about 0.01.

In Fig. 2, transition energies, oscillator strengths, π-electron densities, and weight of doubly excited basis functions are plotted against cut-off energies. The number of doubly excited basis functions and the total number of basis functions included in calculations are also given. The dotted lines show observed values. The calculated transition energies scarcely change

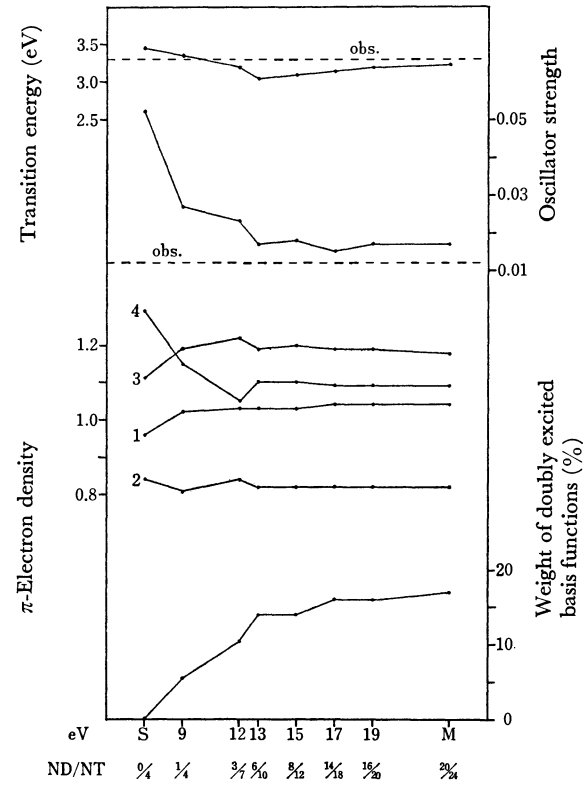

Fig. 2. The first excited state of fulvene ($^1B_1$). Calculated values are plotted against cut-off energies. S and M are abbreviations of CI including only singly excited configurations and CI with the largest number of basis fuctions including both singly and doubly excited functions, respectively. ND is the number of doubly excited basis functions included in CI, and NT is the total number of basis functions included in CI. The numbers of the π-electron density curves correspond to the atomic positions in Fig. 1.

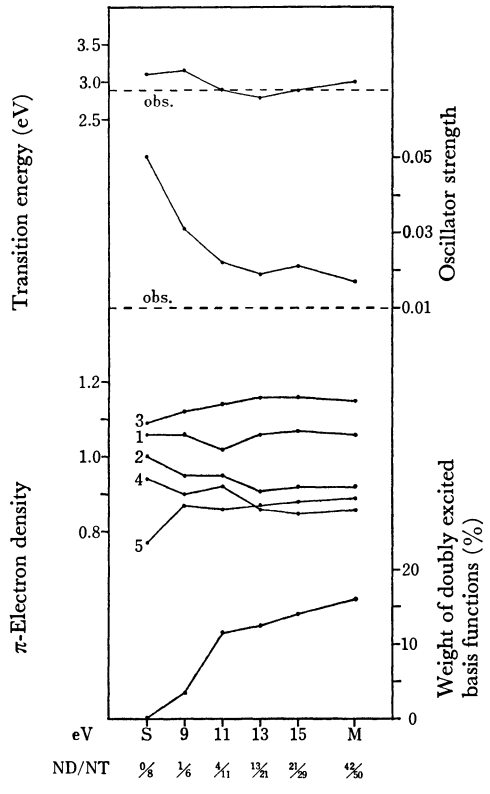

Fig. 3. The first excited state of heptafulvene ($^1B_1$). See legend for Fig. 2.

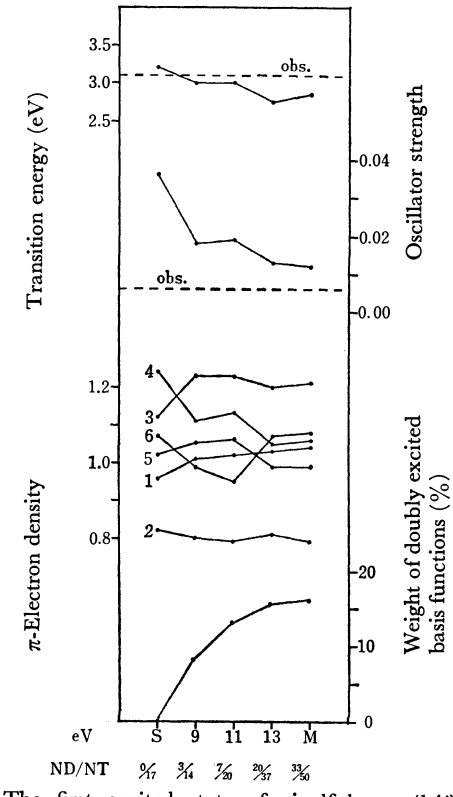

Fig. 4. The first excited state of vinylfulvene ($^1A'$). See legend for Fig. 2.

from S-CI to M-CI. This means that S-CI is good enough to predict the energy of this level. On the other hand, the calculated oscillator strength decreases

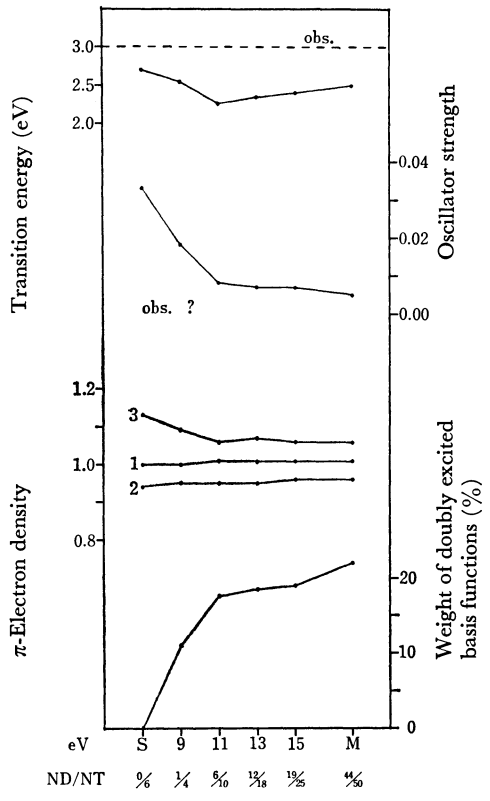

Fig. 5. The first excited state of fulvalene ($^1B_{3u}$). See legend for Fig. 2.

radically from 0.051 of S-CI to 0.017 of a CI with a cut-off energy, 13 eV, where the number of added doubly excited basis function is only six. It then becomes almost a constant, which is close to the observed value. The π-electron densities on the carbon atoms change considerably until the cut-off energy becomes 13 eV, and then none of them markedly change any more. The weight of doubly excited functions also increases until the cut-off energy of 13 eV. On the other hand, in the ground state of fulvene, π-electron densities on the carbon atoms fluctuate by only 0.03 at most, and the weight of the original single determinant is 94.3%. In the case of the other three compounds (Figs. 3—5), almost the same behaviors are obtained. From these four examples, we may conclude that, at a critical point of the cut-off energy, we get an approximate wave function which is good enough to predict not only transition energy but also oscillator strength and probably π-electron distribution as well. The critical value of the cut-off energy is 11—13 eV for the first excited states of the four compounds studied in this paper.

Second Excited States. Second absorptions of the four compounds are observed at about 5 eV. The observed oscillator strengths are 0.2—0.6. In the case of fulvene and heptafulvene (Figs. 6 and 7), the main features of calculated quantities *versus* the cut-off energy are similar to those of the first excited states. Transition energies calculated by S-CI approximately coincide with observed values. They scarcely change by the addition of doubly excited basis functions. But oscillator strengths are greatly improved by inclusion of doubly excited

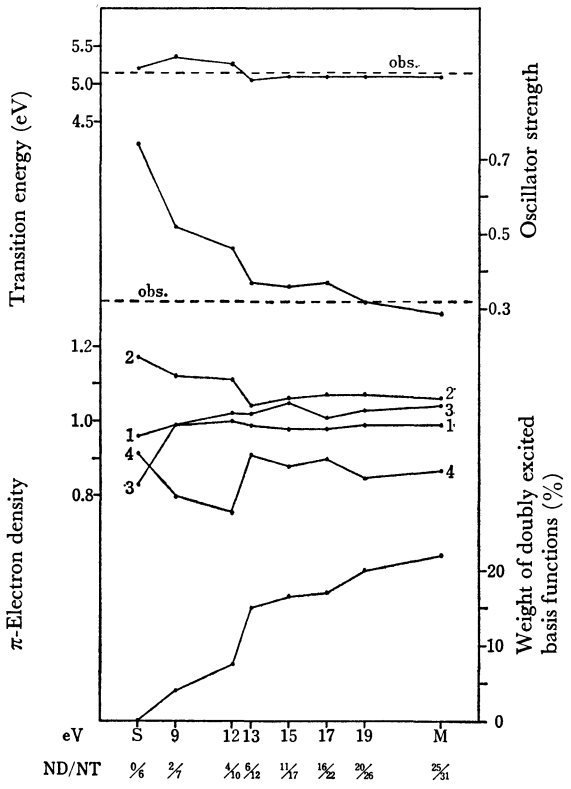

Fig. 6. The second excited state of fulvene ($^1A_1$). See legend for Fig. 2.

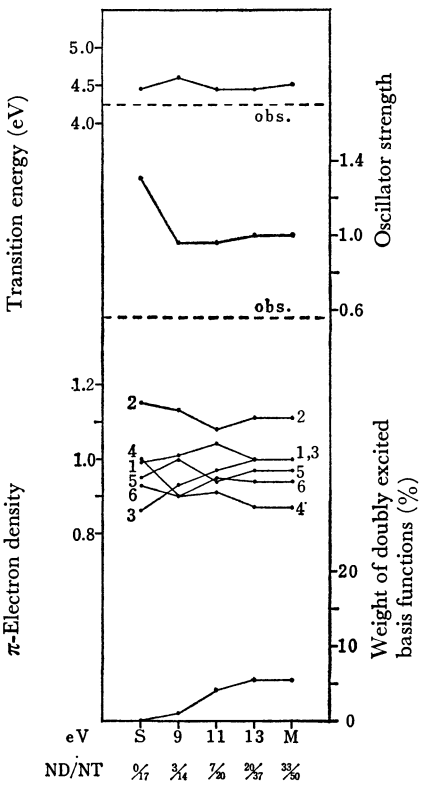

Fig. 8. The second excited state of vinylfulvene ($^1A'$). See legend for Fig. 2.

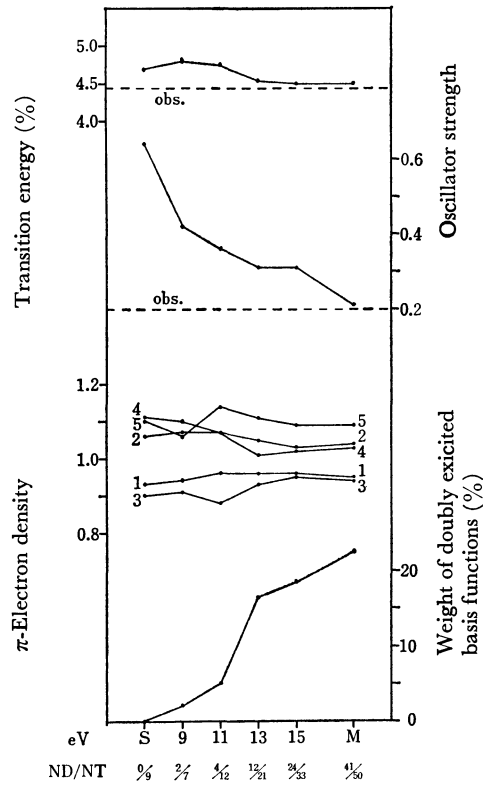

Fig. 7. The second excited state of heptafulvene ($^1A_1$). See legend for Fig. 2.

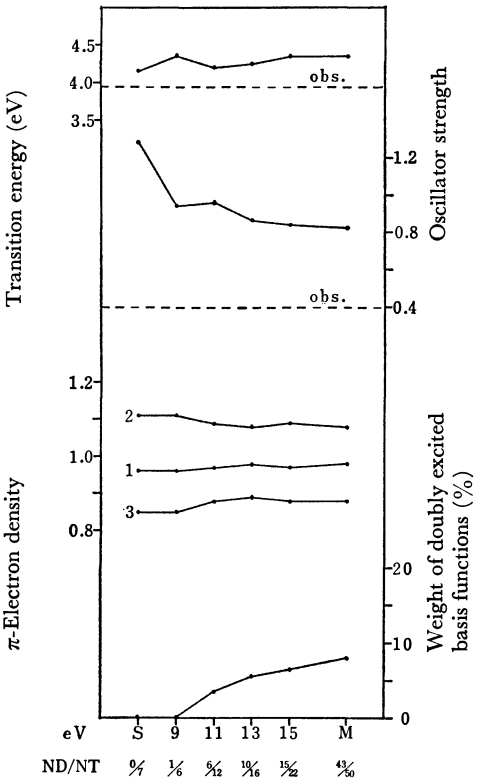

Fig. 9. The second excited state of fulvalene ($^1B_{2u}$). See legend for Fig. 2.

configurations. Their final values are close to the observed values. The curves of π-electron densities on the carbon atoms become flat to some extent when the cut-off energies reach certain values. The critical values are at about 13 eV.

As for the second excited states of vinylfulvene and fulvalene (Figs. 8 and 9), the calculated oscillator strengths of M-CI are closer to the observed values than those of S-CI. But the agreement between the calculated and the observed values is not so good. The weight of doubly excited basis functions is only 5.4% or 8.0% even by M-CI. They are much lower than the weights in the second excited states of fulvene and heptafulvene, which are about 20%. It seems that one must add more basis functions of higher energy or triply excited functions in order to get better results for the second excited states of vinylfulvene and fulvalene.

Higher Excited States. Calculated transition energies and oscillator strengths to excited states, whose transition energies are lower than 7 eV, are listed in Table 1 with experimental data. Most higher excited states appear in the vacuum ultra-violet region, where there is no experimental data. Below this region there are several higher excited states, but many of them have small oscillator strength values. The only exceptions are the two states of heptafulvene, whose energies are 5.48 and 5.99 eV by the M-CI calculation. The observed third peak of heptafulvene corresponds probably to one or both of the two transitions. The calculated oscillator strengths for the two transitions are nearly equal, and are of the same order as the observed value. For all of the four compounds, new π–π absorptions in the vacuum ultra-violet region can be found.

TABLE 1. TRANSITION ENERGIES (IN eV) AND OSCILLATOR STRENGTHS (IN PARENTHESES)

S-CI	M-CI	Obsd
Fulvene		a)
$^1B_1$ 3.44 (0.052)	$^1B_1$ 3.26 (0.017)	3.32 (0.012)
$^1A_1$ 5.22 (0.74)	$^1A_1$ 5.10 (0.29)	5.13 (0.32)
	$^1A_1$ 6.12 (0.20)	
	$^1B_1$ 6.68 (0.085)	
	$^1A_1$ 6.89 (0.12)	
Heptafulvene		b)
$^1B_1$ 3.12 (0.050)	$^1B_1$ 3.01 (0.017)	2.91 (0.01)
$^1A_1$ 4.68 (0.64)	$^1A_1$ 4.50 (0.21)	4.43 (0.2)
$^1B_1$ 6.43 (0.035)	$^1B_1$ 5.41 (0.034)	
$^1A_1$ 6.45 (1.18)	$^1A_1$ 5.48 (0.19)	5.84 (0.4)
	$^1A_1$ 5.99 (0.19)	
	$^1B_1$ 6.09 (0.020)	
	$^1A_1$ 6.83 (0.65)	
	$^1B_1$ 6.88 (0.049)	
Vinylfulvene		c)
$^1A'$ 3.19 (0.036)	$^1A'$ 2.83 (0.012)	3.12 (0.006)
$^1A'$ 4.43 (1.29)	$^1A'$ 4.51 (0.99)	4.27 (0.56)
$^1A'$ 6.38 (0.057)	$^1A'$ 5.12 (0.011)	
$^1A'$ 6.71 (0.22)	$^1A'$ 5.71 (0.048)	
	$^1A'$ 6.26 (0.11)	
	$^1A'$ 6.74 (0.18)	
	$^1A'$ 6.89 (0.009)	
Fulvalene		d)
$^1B_{3u}$ 2.70 (0.033)	$^1B_{3u}$ 2.49 (0.005)	2.98 (?)
$^1B_{2u}$ 4.15 (1.27)	$^1B_{2u}$ 4.35 (0.82)	3.95 (0.4)
	$^1B_{3u}$ 5.56 (0.043)	
	$^1B_{2u}$ 5.63 (0.048)	
	$^1B_{2u}$ 6.51 (0.007)	
	$^1B_{3u}$ 6.88 (0.024)	

S–CI means CI including only singly excited configurations, and M–CI means CI with the largest number of basis functions including both singly and doubly excited functions.
a) Ref. 9. b) Ref. 10. c) Ref. 11. d) Ref. 12.

TABLE 2. CALCULATED QUANTITIES OF GROUND STATES

Molecule	CI	π-electron total-energy (eV)	π-electron dipole-moment (Debye)	Weight of the original single determinant (%)
Fulvene	S–CI	−158.10	1.40	100.0
	M–CI	−158.75	1.11	94.3
Heptafulvene	S–CI	−240.13	0.89	100.0
	M–CI	−240.81	0.80	93.6
Vinylfulvene	S–CI	−235.57	2.04	100.0
	M–CI	−235.96	1.72	96.1
Fulvalene	S–CI	−337.06	0.00	100.0
	M–CI	−337.82	0.00	92.2

S–CI, M–CI: See footnote to Table 1.

Ground States. For the ground states of the four compounds, π-electron total energies, π-electron dipole moments, and weights of the original single determinants are listed in Table 2. The π-electron total energies decrease 0.4—0.6 eV by inclusion of doubly excited configurations. Dipole moments decrease about 20%. As can be seen in the changes of the weights of the original single determinants, the improvement of ground state wave function is smaller than that of excited state wave functions. This is understandable because the calculations are based on SCF MO for the ground state. The improvement of π-electron dipole moments will play non-negligible role in the estimate of the total dipole moments.

Conclusion

The three questions concerning the importance of CI are answered as follows.

1) From the results of the four molecules, we conclude that inclusion of doubly excited configurations leads to a better agreement with experiment for oscillator strengths. For transition energies to lower excited states, the improvement is not so significant.

2) Oscillator strengths and π-electron densities of excited states are sensitive. Transition energies to lower excited states are rather insensitive, but those to higher excited states are sensitive. The properties of ground states are also not so sensitive.

9) J. Thiec and J. Wiemann, *Bull. Soc. Chim. Fr.*, **1956**, 177.
10) W. von E. Doering and D. W. Wiley, *Tetrahedron*, **11**, 183 (1960).
11) M. Neuenschwander, D. Meuche, and H. Schaltegger, *Helv. Chim. Acta*, **47**, 1022 (1964).
12) T. Nakajima and S. Katagiri, *Mol. Phys.*, **7**, 147 (1963—4).

Table 3. The number of basis functions included in CI at the critical points of the cut-off energies (in eV)

Molecule	E (obs.)	CE	ND	NT
Fulvene	3.32	13.0	6	10
	5.13	13.0	6	12
Heptafulvene	2.91	11.0	4	11
	4.42	13.0	12	21
Vinylfulvene	3.12	13.0	20	37
	4.27	—	—	—
Fulvalene	2.98	11.0	6	10
	3.95	—	—	—

The following abbreviations are used in the table:
E(obs.): observed transition energies.
CE: cut-off energies at critical points.
ND: the number of doubly excited basis functions included in CI.
NT: the total number of basis functions included in CI.

3) The number of doubly excited basis functions and the total number of basis functions included in CI at the critical points of the cut-off energies for each state are shown in Table 3. These numbers for vinylfulvene are larger than those for the other molecules, since the CI matrix cannot be separated into two parts because of its lower symmetry. From the table, we see that, in the lower excited states of small molecules, the inclusion of a rather small number of doubly excited basis functions is quite effective in getting better agreement with experiment by the semi-empirical CI calculation.

The author wishes to thank Professor K. Ohno and Dr. F. Hirota, Shizuoka University, for helpful suggestions and discussions. The calculations reported in this paper were carried out on the HITAC 5020E computer in the Computer Center, the University of Tokyo.

BULLETIN OF THE CHEMICAL SOCIETY OF JAPAN, VOL. 44, 629—637 (1971)

Electronic States of Diphenylamine and Its Related Compounds

Tadao HINOHARA,* Seikichi CHO, and Toshifumi MORITA

Department of Chemistry, Faculty of Engineering, Gunma University, Tenjincho, Kiryu

(Received July 27, 1970)

For the analysis of the characteristic nature of the first absorption band of diphenylamine (DPA), calculations of the electronic states of DPA and its analogous compounds, diphenylether (DPE) and diphenylmethane (DPM), were carried out and the solvent effects on the fluorescence spectra of these compounds were investigated. The calculated results show that the first excited states of these three compounds are mainly benzene B_{2u}. However, in DPA, the ionic state (CTs^-) is located very closely to the B_{2u} state. It seems reasonable to say, therefore, that, in solution, the ionic state lowers its energy down to the position of the B_{2u} state and that the first absorption band observed in the solution is a superposed band of two transitions, $G \rightarrow B_{2u}$ and $G \rightarrow CTs^-$. To confirm this assumption, the value of $\Delta\mu$, which is the dipole-moment change between the ground and excited states, is estimated from the solvent effect on the fluorescence spectrum. The observed value of $\Delta\mu$ for DPA is intermediate between the theoretical values for the lowest (B_{2u}) and the second excited state (CTs^-); from this fact it may be inferred that the mixing of CTs^- to the lowest excited state (B_{2u}) is increased in the excited equilibrium state.

The electronic absorption spectra of molecules containing two benzene rings joined by one atom having a lone pair electron (C_6H_5-X-C_6H_5) are expected to differ from that of the corresponding monophenyl compounds (C_6H_5-XH). The observed first absorption bands of diphenylether and diphenylmethane are, however, essentially the same as those of the corresponding monophenyl compounds, phenol and toluene respectively. On the other hand, the first absorption band of diphenylamine is considerably different from that of aniline (see Fig. 1).

The first absorption bands of aniline, phenol, and toluene have been assigned to the B_{2u} band of benzene perturbed by substitution.[1] Therefore, it is probable that the first excited states of diphenylether and diphenylmethane are of a B_{2u} character. On the other hand, the nature of the first excited state of diphenylamine should be different from pure B_{2u}, because the intensity of the first band is too high to attribute it to the B_{2u}-band. In this connection, the chemical reaction in the excited state (photochemical reaction) of diphenylamine has been found to be different from those of diphenylether and diphenylmethane.[2] From these points of view, it seemed that it would be very interesting to clarify the electronic structure of diphenylamine; this is the objective of the present investigation. In this paper, the first absorption band of diphenylamine was mainly treated, because its photochemical reaction is concerned with the first excited state.

Investigations of the electronic absorption spectra of the same type of molecules as are treated in the present investigation have already been published by several authors.[3-8] According to Matsen[6] and Bugai,[7] the

* Present address: Department of Chemistry, Faculty of Engineering, Toyo University, Kawagoe.

1) For example: J. N. Murrell, *Tetrahedron*, **19**, suppl., **2**, 277 (1963).

2) H. Stegemeyer, *Naturwissenschaften*, **53**, 583 (1966).

3) H. H. Jaffe, *J. Chem. Phys.*, **22**, 1430 (1953).

4) J. R. Platt, *ibid.*, **19**, 101 (1951).

5) A. Mangini and C. Zauli, *J. Chem. Soc.*, **1950**, 4960.

6) F. A. Matsen, *J. Amer. Chem. Soc.*, **37**, 5243 (1950).

7) P. M. Bugai, L. M. Bazhenova, A. S. Gol'berkova, V. N. Konel'skaya, and I. I. Naidenova, *Zh. Fiz. Khim.*, **37**, 378 (1963); *Chem. Abstr.*, **58**, 13301c.

8) L. I. Lagutskaya, *Zh. Strukt. Khim.*, **7**, 88 (1966); *Chem. Abstr.*, **63**, 13052a.

first absorption band of diphenylamine is to be attributed to the benzene B_{2u}-band.

In order to clarify the nature of the first excited state, we have measured the solvent effect on the fluorescence spectra of these molecules. We have also made calculations of the energy levels of these molecules in order to obtain more reliable knowledge about the nature of the first excited state.

Experimental

Materials. Commercially-obtained GR-grade diphenylamine and diphenylether were carefully purified by recrystallization from ethanol. GR-grade diphenylmethane was used without further purification. Cyclohexane was purified by passing it through a silica-gel column and by subsequent distillation. The other solvents were purified by the ordinary procedures.

Spectroscopy. The ultraviolet-absorption spectra were measured with a Hitachi EPS 3T and 125 model spectrophotometer. The absorption spectrum in the vapor phase was taken by the flow method, using nitrogen gas as the carrier gas. The temperature of the carrier gas was held at about 80°C.

Experimental Results

Electronic Spectra of C_6H_5-X-C_6H_5 and C_6H_5-XH. To compare the spectra of C_6H_5-X-C_6H_5 and C_6H_5-XH-type molecules, it is desirable to remeasure the absorption spectra under the same conditions, so all the absorption spectra were remeasured in cyclohexane. The observed spectra are shown in Fig. 1. The fluorescence spectra of diphenylamine, diphenylether, and diphenylmethane are also shown in Fig. 1; here, mirror-image relationships are observed. In Fig. 1, it may be seen that the band at about 280 mμ of diphenylamine observed in the solution splits into two bands, the peaks of which are at about 265 and 285 mμ, when the experimental condition is changed from a solution to a vapor.

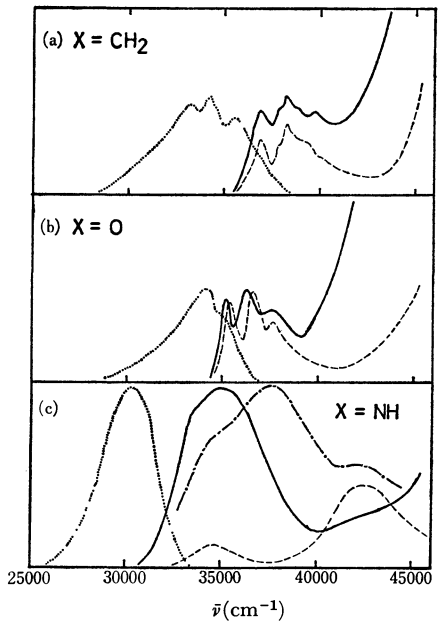

Fig. 1. Absorption and fluorescence spectra of C_6H_5-X-C_6H_5 and C_6H_5-XH. —— absorption in cyclohexane, -·-·- absorption in vapor, ····· fluorescence of C_6H_5-X-C_6H_5, ---- absorption of C_6H_5-XH in cyclohexane. Fluorescence curves are corrected.

Solvent Effects on Fluorescence Spectra. According to Mataga *et al.*[9] and Lippert,[10] the difference between the absorption maximum (σ_a) and the fluorescence maximum (σ_f) is given by the following equation:

$$\sigma_a - \sigma_f = \frac{2\Delta f}{hca^3}(\mu_e - \mu_g)^2 + \text{const.} + \text{smaller terms} \quad (1)$$

where $\Delta f = (D-1)/(2D+1) - (n^2-1)/(2n^2+1)$,
D: dielectric constant of the solvent,
n: refractive index of the solvent,
a: Onsager's cavity radius,
μ_e: dipole moment of the solute in its excited state,
μ_g: dipole moment of the solute in its ground state,
h: Planck's constant, and
c: light velocity.

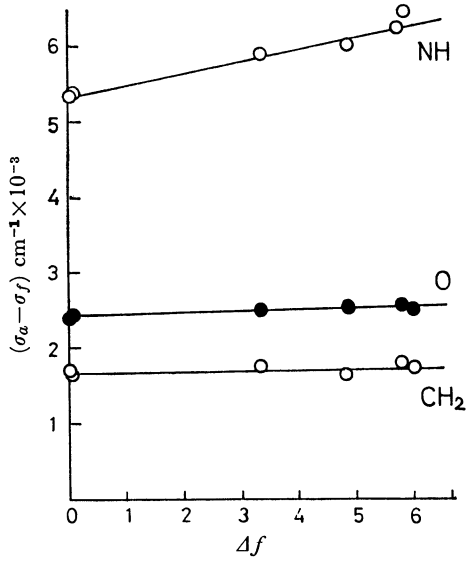

Fig. 2. Difference between absorption and fluorescence maxima, $(\sigma_a-\sigma_f)$, plotted against Δf values.

If the smaller terms in the equation are small enough, the difference, $\sigma_a-\sigma_f$, measured in various solvents should be linear with respect to Δf. The experimental results are shown in Table 1 and Fig. 2. A linear relation between $\sigma_a-\sigma_f$ and Δf is observed in Fig. 2, and from the slopes of these lines, $(\mu_e-\mu_g)^2/a^3$ can be obtained. Assuming that $a=4$ Å[12], and using the value of μ_g given in the literature,[11] the dipole moment in the excited state can be calculated. The results are summarized in Table 2.

9) N. Mataga, Y. Kaifu, and M. Koizumi, This Bulletin, **29**, 465 (1956).

10) E. Lippert, *Z. Naturforsch.*, **109**, 54 (1955); *Z. Elektrochem.*, **61**, 962 (1967).

11) Values of dipole moment in the ground state used here are as follows: 1.0 D for diphenylamine (C. A. Barclay, R. J. W. LeFever, and B. H. Smyth, *Trans. Faraday Soc.*, **47**, 357 (1951)), 1.0 and 0.4 D for diphenylether and diphenylmethane respectively (I. Esterman, *Z. Phys. Chem.*, **B1**, 161 (1928).

12) a is the radius of the equivalent sphere of the molecule, or $(4/3)\pi a^3$=molecular volume. In the present case, however, the same value of a is used for diphenylamine, diphenylether, and diphenylmethane.

TABLE 1. SOLVENT EFFECTS ON ABSORPTION AND FLUORESCENCE MAXIMA

solvent	diphenylamine			diphenylether			diphenylmethane		
	a (Å)	f (Å)	$a-f$ (cm^{-1})	a (Å)	f (Å)	$a-f$ (cm^{-1})	a (Å)	f (Å)	$a-f$ (cm^{-1})
CH	2820	3290	5065	2785	2900	1542	2690	2815	1651
C_6H_6	2860	3380	5380	2785	—	—	—	—	—
$(Et)_2O$	2835	3400	5862	2775	2900	1672	2692	2920	2901
CH_3CN	2820	3470	6642	2773	2910	2357	2682	2820	1825
$C_2H_4Cl_2$	2840	3400	5831	2780	2915	1666	2690	2820	1714
EtOH	2840	3480	6383	2775	2900	1672	2687	2810	2310
H_2O	2780	3800	9862	—	—	—	—	—	—

CH: cyclohexane

TABLE 2. DIPOLE MOMENT OF THE EXCITED STATE OF C_6H_5-X-C_6H_5

X	$(\mu_e-\mu_g)/a^3$ (erg)	$\Delta\mu_{obs}$[a] (D)	μ_e (D)	$\Delta\mu_{cal}$ (D)
NH	3.2×10^{-13}	4.4	5.4	2.9, 7.7[b]
O	1.6×10^{-14}	1.0	2.0	0.9
CH_2	1.0×10^{-14}	0.8	1.0	0.7

a) $\Delta\mu=\mu_e-\mu_g$
b) calculated value for the second excited state

Theoretical

Method. The present method of calculating the electronic structure of C_6H_5-X-C_6H_5-type molecules is essentially based on that presented by Longuet-Higgins and Murrell.[13] In the present case, the interaction between three fragments, consisting of two benzene rings and the central atom, X, are taken into account by configuration interaction among the ground, charge-transfer, and locally-excited configurations. In the present calculation, the doubly-excited configurations were ignored.

The Configuration of C_6H_5-X-C_6H_5. Because of the steric hindrance of two hydrogen atoms at the *o*- and *o'*-positions of two benzene rings, the molecule cannot take the planar configuration. Although several considerations of the configurations of two benzene rings in C_6H_5-X-C_6H_5 molecules have been presented,[14-17] no detailed structural data of these molecule have yet been reported. We assume the nonplanar configuration shown in Fig. 3, where the two rings are twisted around the bond axes, NC_1 and NC'_1, at the angles of φ_1 and φ_2 respectively. When the two benzene rings are twisted in the same direction, the molecule may belong to the point group C_2, and when they are twisted in opposite directions, to C_{1h}. The distance between two hydrogen atoms, H and H', must be equal to or larger than 2.4 Å, because the van der Waals radius of the hydrogen atom is 1.2 Å. Therefore, the twisting angle for diphenylamine, satisfying the above restriction, is as follows:

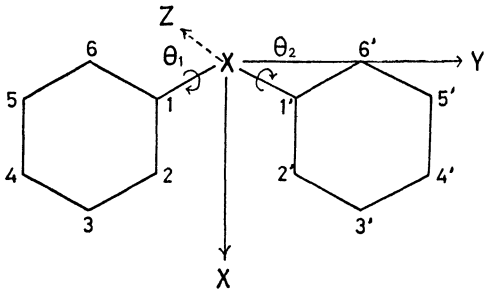

Fig. 3. Configuration of C_6H_5-X-C_6H_5 molecule.

$$\varphi_1 = \varphi_2 = 35° \text{ for } C_2$$
$$\varphi_1 = -\varphi_2 = 88° \text{ for } C_{1h}$$

These values are obtained on the assumptions that the central atom (N) is in the sp^2 hybrid valence state, that the bond length, NC_1, is 1.407 Å,[18] that CC in the benzene ring is 1.397 Å,[10] and that CH is 1.09 Å.[20] Diphenylether and diphenylmethane are assumed to be in the same configuration as diphenylamine.

In the case of the C_{1h} symmetry, the lone-pair orbital of the central atom is almost perpendicular to the pi-electron orbitals of two benzene rings, and the resonance intraction between the central atom and the benzene rings is neglegibly small. The resonance integral, β, can be correlated with the twisting angle, φ, as follows:

$$\beta = \beta_0 \cos\varphi \qquad (2)$$

where β_0 is the resonance integral when the twisting angle is zero.

Local-excitation in a Benzene Ring and the Effect of Excitation Delocalization. Additional effects due to the phenylation of C_6H_5-XH to C_6H_5-X-C_6H_5 may be considerably more complex. Therefore, in the present investigation, our considerations are restricted to the effect necessary for the explanation of the spectral change due to the phenylation, as is shown in Fig. 1.

When the molecules are in a C_{1h} symmetry, the resonance interaction between the central atom and two benzene rings may be ignored, as has been described above, and only the effect of the excitation delocaliza-

13) H. C. Longuet-Higgins and J. N. Murrell, *Proc. Phys. Soc.*, **68A**, 40 (1955); J. N. Murrell, *ibid.*, **68A**, 969 (1955).
14) F. K. Fong, *J. Chem. Phys.*, **40**, 132 (1964).
15) R. J. W. LeFever, A. Sundaram, and K. M. S. Sundaram, This Bulletin, **35**, 690 (1962).
16) K. Higashi, *ibid.*, **35**, 692 (1962).
17) M. Aroney and R. J. W. LeFevre, *J. Chem. Soc.*, **1960**, 3600.
18) T. Sakurai, M. Sundaralingam, and G. A. Jeffery, *Acta Cryst.*, **16**, 351 (1963).
19) K. Kimura and M. Kubo, *J. Chem. Phys.*, **32**, 1776 (1960).
20) B. P. Stoicheff, *Can. J. Phys.*, **32**, 239, 635 (1954); G. Herzberg and B. P. Stoicheff, *Nature*, **175**, 79 (1955).

tion may be taken into account. The singly-excited states of two benzene rings can be written as follows:

$$\begin{aligned}
\Psi(B_{2u}) &= 2^{-1/2}(\phi_3^{-1}\phi_5-\phi_2^{-1}\phi_4),\\
\Psi(B'_{2u}) &= 2^{-1/2}(\phi'_3{}^{-1}\phi'_5-\phi'_2{}^{-1}\phi'_4)\\
\Psi(E_{1u'}) &= 2^{-1/2}(\phi_3^{-1}\phi_5+\phi_2^{-1}\phi_4),\\
\Psi(E'_{1u'}) &= 2^{-1/2}(\phi'_3{}^{-1}\phi'_5+\phi'_2{}^{-1}\phi'_4)\\
\Psi(B_{1u}) &= 2^{-1/2}(\phi_3^{-1}\phi_4+\phi_2^{-1}\phi_5),\\
\Psi(B'_{1u}) &= 2^{-1/2}(\phi'_3{}^{-1}\phi'_4+\phi'_2{}^{-1}\phi'_5)\\
\Psi(E_{1u}) &= 2^{-1/2}(\phi_3^{-1}\phi_4-\phi_2^{-1}\phi_5),\\
\Psi(E'_{1u}) &= 2^{-1/2}(\phi'_3{}^{-1}\phi'_4-\phi'_2{}^{-1}\phi'_5) \qquad (3)
\end{aligned}$$

where the self consistent orbitals, ϕ_t and ϕ'_t, are the same as those used by Pople.[21] The excitation of an electron within a benzene ring will give rise to two singlet states. For instance, if we take the excitation to the B_{2u} state, two singlet states, B_{2u} and B'_{2u}, are possible, and these two will interact with each other in the manner of the exciton interaction.[22] Such interaction produces one set of exciton states, B_{2u}^+ and B_{2u}^-. The wave functions and energy formulae are:

$$\begin{aligned}
&\Psi(B_{2u}^+) = 2^{-1/2}(B_{2u}+B'_{2u}),\ E(B_{2u}^+) = E(B_{2u})+\langle B_{2u}|H|B'_{2u}\rangle\\
&\Psi(B_{2u}^-) = 2^{-1/2}(B_{2u}-B'_{2u}),\ E(B_{2u}^-) = E(B_{2u})-\langle B_{2u}|H|B'_{2u}\rangle
\end{aligned} \qquad (4)$$

where the interaction matrix element is given by:

$$\begin{aligned}
\langle B_{2u}|H|B'_{2u}\rangle &= 2^{-1}\{\langle\phi_3^{-1}\phi_5|H|\phi'_3{}^{-1}\phi'_5\rangle\\
&\quad+\langle\phi_2^{-1}\phi_4|H|\phi'_2{}^{-1}\phi'_4\rangle\}\\
&\quad-\langle\phi_3^{-1}\phi_5|H|\phi'_2{}^{-1}\phi'_4\rangle\\
&= (\phi_3\phi_5|\phi'_3\phi'_5)+(\phi_2\phi_4|\phi'_2\phi'_4)\\
&\quad-2(\phi_3\phi_5|\phi'_2\phi'_4) \qquad (5)
\end{aligned}$$

The two electron integrals were evaluated under the zero-differential overlap approximation, and the two center atomic integrals of the (rr/ss)-type were equated to e^2/R_{rs}. The observed value was used for the local excitation energy in a benzene ring, $E(B_{2u})$. With regard to other local excitations within a benzene ring, E_{1u}, B_{1u}, and E_{1u}, the same type of equations can be derived. The splitting of locally excited states (degenerated) due to exciton delocalization are shown in Fig. 4. The interaction matrix element between B_{2u} and B'_{2u} is zero, and the exciton states, B_{2u}^+ and B_{2u}^-, are degenerated.

Effect of Interaction among the Exciton States. The exciton states can interact with each other. The elements of the matrix for calculating the interaction between the four exciton states are as follows:

For the plus state:

$$\begin{array}{c} \\ B_{2u}^+ \\ E_{1u'}^+ \\ B_{1u}^+ \\ E_{1u}^+ \end{array}\begin{pmatrix} E(B_{2u}^+) & 0 & 0 & 0\\ 0 & E(E_{1u'}^+) & H_{E_{1u'},B_{1u}} & H_{E_{1u'},E_{1u}}\\ 0 & H_{B_{1u},E_{1u'}} & E(B_{1u}^+) & H_{B_{1u},E_{1u}}\\ 0 & H_{E_{1u},E_{1u'}} & H_{E_{1u},B_{1u}} & E(E_{1u}^+) \end{pmatrix}$$

and for the minus state:

$$\begin{array}{c} \\ B_{2u}^- \\ E_{1u'}^- \\ B_{1u}^- \\ E_{1u}^- \end{array}\begin{pmatrix} E(B_{2u}^-) & 0 & 0 & 0\\ 0 & E(E_{1u'}^-) & -H_{E_{1u'},B_{1u}} & -H_{E_{1u'},E_{1u}}\\ 0 & -H_{B_{1u},E_{1u'}} & E(B_{1u}^-) & -H_{B_{1u},E_{1u}}\\ 0 & -H_{E_{1u},E_{1u'}} & -H_{E_{1u},B_{1u}} & E(E_{1u}^-) \end{pmatrix}$$

Diagonal elements are given by Eq. (4) and so on. The off-diagonal elements were evaluated under the same approximation as those used in calculating Eq. (5).

Since all the matrix elements involving $B_{2u}^{\pm}$ are zero, the degeneracy of $B_{2u}^{\pm}$ exciton states is not removed; moreover, $B_{2u}^{\pm}$ does not mix with any of the other exciton states. These results indicate that the B_{2u}-band in the absorption spectrum of C_6H_5-XH will not be essentially changed by the phenylation. This is the case for diphenylether and diphenylmethane, as is shown in Fig. 1 (b) and Fig. 1 (c) respectively. The ground state can not interact with any of the exciton states. The calculated results are shown in Fig. 4 and Table 3.

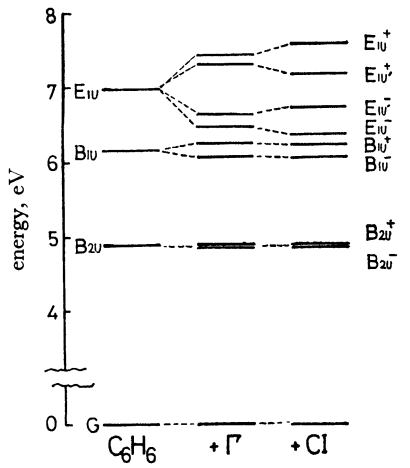

Fig. 4. Change of energy levels due to the exciton interaction (Γ) and configuration interaction (CI).

TABLE 3. THE WAVE FUNCTIONS AND ENERGIES OF C_6H_5-X-C_6H_5 IN C_{1h} SYMMETRY

Energy (eV)	Wave function		
W_1=4.89,	$\Psi_1=B_{2u}^-$		
W_2=4.89,	$\Psi_2=B_{2u}^+$		
W_3=5.86,	$\Psi_3=-0.270B_{1u}^-$	$+0.802E_{1u}^-$	$+0.532E_{1u'}^-$
W_4=6.06,	$\Psi_4=0.998B_{1u}^+$	$+0.041E_{1u}^+$	$+0.041E_{1u'}^+$
W_5=6.29,	$\Psi_5=0.963B_{1u}^-$	$+0.232E_{1u}^-$	$+0.139E_{1u'}^-$
W_6=6.82,	$\Psi_6=-0.012B_{1u}^+$	$-0.552E_{1u}^+$	$+0.834E_{1u'}^+$
W_7=7.17,	$\Psi_7=0.011B_{1u}^-$	$-0.550E_{1u}^-$	$+0.835E_{1u'}^-$
W_8=8.07,	$\Psi_8=-0.057B_{1u}^+$	$+0.833E_{1u}^+$	$+0.550E_{1u'}^+$

Effect of Charge-resonance Interaction. Effect of resonance interaction between the central atom and the two benzene rings must be taken into account if the molecule is in C_2 symmetry, for, in this case, the resonance interaction can not be ignored.

Unlike the benzene excited state, eight ionic states do not interact with each other. However, we can take, for convenience, these ionic configurations in the sym-

21) J. A. Pople, *Proc. Phys. Soc.*, **68A**, 81 (1955).
22) J. N. Murrell, "The Theory of the Electronic Spectra of Organic Molecules," Methuen Co. Ltd., London (1963), p. 135.

metry combination:[23]

$$(CTs^{\pm}) = 2^{-1/2}(\theta^{-1}\phi_5 \pm \theta^{-1}\phi'_5)$$
$$(CTa^{\pm}) = 2^{-1/2}(\theta^{-1}\phi_4 \pm \theta^{-1}\phi'_5)$$
$$(CT_{ij}^{\pm}) = 2^{-1/2}(\phi_i^{-1}\phi'_j \pm \phi'_i{}^{-1}\phi_j) \quad (6)$$

As for CT_{ij}, we take the following four configurations into account: CT_{24}, CT_{25}, CT_{34}, and CT_{35}. The corresponding energies are given by the following equations:

$$E(CTs^{\pm}) = E(\theta^{-1}\phi_5) = (I-A) - Q_s,\ Q_s = (\theta\theta|\phi_5\phi_5)$$
$$E(CTa^{\pm}) = E(\theta^{-1}\phi_4) = (I-A) - Q_a,\ Q_a = (\theta\theta|\phi_4\phi_4)$$
$$E(CT_{ij}^{\pm}) = E(\phi_i^{-1}\phi_j) = (I'-A) - Q_{ij},\ Q_{ij} = (\phi_i\phi_i|\phi_j\phi_j)$$

where A is the electron affinity of benzene and where I and I' the ionization potentials of the central atom, X, and benzene respectively. The $(\phi_i\phi_i/\phi_j\phi_j)$-type integrals were evaluated using the approximation of zero differential overlap and the point charge. Q_s and Q_a may be expanded as follows:

$$Q_s = 3^{-1}\{(C_1C_1|\theta\theta) + 1/2(C_2C_2|\theta\theta) + 1/2(C_3C_3|\theta\theta) + (C_4C_4|\theta\theta)\}$$
$$Q_a = 2^{-1}\{(C_2C_2|\theta\theta) + (C_3C_3|\theta\theta)\} \quad (8)$$

The two center integrals, $(C_jC_j/\theta\theta)$, where C_j indicates the j'th carbon atom of the benzene ring, were calculated by the use of quadratic equations with an interatomic distance of r_{CX}.[24]

The off-diagonal elements of the matrix for calculating the interaction between the exciton states and the electron transfer states are evaluated by the method of Pople[21] and Murrell[13] as follows:

$$H_{G,CTs^{\pm}} = -2/\sqrt{6}(\beta-\beta'),\quad H_{CTs^{\pm},CT_{24}^{\pm}} = \mp 1/\sqrt{3}\beta$$
$$H_{CTs^{\pm},B_{1u}^{\pm}} = -1/\sqrt{6}(\beta+\beta'),\quad H_{CTa^{\pm},CT_{25}^{\pm}} = \mp 1/\sqrt{3}\beta$$
$$H_{CTs^{\pm},E_{1u}^{\pm}} = 1/\sqrt{6}(\beta+\beta') \qquad H_{CT_{ij}^{\pm},CT_{lm}^{\pm}} = -(\phi_i\phi_i|\phi'_j\phi'_m)$$
$$H_{CTa^{\pm},B_{2u}^{\pm}} = 1/\sqrt{6}(\beta+\beta'),$$
$$H_{CTa^{\pm},E_{1u}^{\pm}} = 1/\sqrt{6}(\beta+\beta') \quad (9)$$

where β is the resonance integral between two atomic orbitals belonging to the central atom and adjacent carbon atoms, and where β' is that belonging to the central atom and ortho carbon atoms. β' was originally taken into consideration by Kimura *et al.*[25] in the calculation of the electronic structure of aniline and its related compounds. According to them, β' is correlated with β as follows:

$$\beta' = S'/S \times \beta = 0.116\beta \quad (10)$$

where S and S' are the overlap integrals corresponding to β and β'. In the present investigation, the transition energies and wave functions were calculated by assuming β_0 and I-A as the parameters. The transition energies, ΔW, evaluated by the use of -1.8 eV for β_0 and 35° for φ are plotted against the $(I$-$A)$ values in Fig. 5. In those calculations, the CT_{34} and CT_{35} configurations were ignored, for these configurations were found to be unimportant in interpreting the nautre of the lower energy levels, as is shown in Table 4.

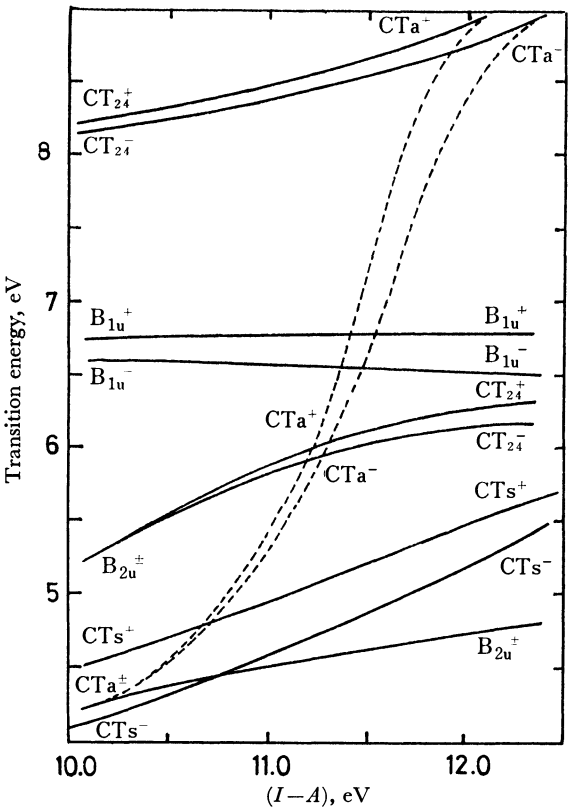

Fig. 5. The calculated transition energies plotted against $(I-A)$ values. ($\beta_0 = -1.8$ eV, $\theta = 35°$)

The results calculated using different β_0 values were essentially the same as those shown in Fig. 5. Therefore, the qualitative nature of the lower excited states of C_6H_5-X-C_6H_5 molecules may be understood from Fig. 5, in which the values of $(I$-$A)$ is assumed to be about 11.0 eV for diphenylamine (X=NH), about 12.0 eV for diphenylether, (X=O), and about 14.0 eV for diphenylmethane ($X=CH_2$). A more detailed comparison of diphenylamine and diphenylether is shown in Fig. 6, in which the relation between the electron configurations used in the present calculation and the energy levels finally obtained is shown.

Table 4 gives the energy levels and wave functions calculated using the following values for $(I$-$A)$ and β_0:

$(I-A) = 11.0$ eV and $\beta_0 = -1.8$ eV for diphenylamine,[26]

$(I-A) = 12.2$ eV and $\beta_0 = -1.64$ eV for diphenylether,[26]

$(I-A) = 14.6$ eV and $\beta_0 = -1.52$ eV for diphenylmethane.[27]

The correlation between the energy levels of diphenylamine and those of aniline is illustrated in Fig. 7 in comparison with the observed spectrum. The oscillator strength was calculated using the following equation:

$$f = 0.0875 \times E\sum_i Q_i^2 \quad (11)$$

23) θ is the nonbonding orbital of the central atom, X.

24) R. Pariser and R. G. Parr, *J. Chem. Phys.*, **21**, 767 (1953).

25) K. Kimura, H. Tsubomura, and S. Nagakura, This Bulletin, **37**, 1336 (1064).

26) Values of $(I$-$A)$ and β_0 used here are taken from the following literature; S. Nagakura and K. Kimura, *Nippon Kagaku Zasshi*, **86**, 1 (1965) and Ref. 23.

27) Ionization potential of CH_3 group and the resonance integral between the central carbon atom and the adjacent carbon atoms are taken as 13.25 and -1.52 eV respectively. (H. Hanazaki, H. Hosoya, and S. Nagakura, This Bulletin, **36**, 1673 (1963)).

TABLE 4. (1) CALCULATED ENERGY LEVELS AND WAVE FUNCTIONS OF DIPHENYLAMINE

Energy, eV	Wave function								
	G	B_{2u}	$E_{1u'}$	B_{1u}	E_{1u}	CTs	CTa	CT_{24}	CT_{25}
$W_{16}=8.46$	0.074	0.057	−0.247	0.185	−0.453	0.485	−0.248	−0.258	0.573
$W_{15}=8.25$	0.040	−0.134	0.454	0.115	−0.116	0.256	0.548	0.530	0.295
$W_{14}=8.24$		−0.074	0.136	−0.170	0.193	−0.451	0.303	−0.373	0.689
$W_{13}=8.15$		−0.137	0.315	0.103	−0.172	0.280	0.546	−0.573	−0.370
$W_{12}=7.53$	−0.003	−0.021	−0.356	0.005	−0.705	−0.019	0.066	0.310	−0.525
$W_{11}=7.17$	0.003	0.018	0.703	0.060	−0.375	0.019	−0.051	−0.524	−0.289
$W_{10}=6.87$		−0.023	0.617	0.069	−0.556	0.120	0.056	0.422	0.331
$W_{9}=6.72$		−0.067	0.505	−0.344	0.507	−0.269	0.150	0.344	−0.390
$W_{8}=6.48$	0.053	0.026	0.044	0.861	0.272	0.267	−0.050	0.039	−0.322
$W_{7}=6.27$		0.048	−0.148	−0.812	−0.496	−0.150	−0.080	−0.131	−0.163
$W_{6}=5.70$	−0.005	−0.586	−0.297	0.053	0.022	−0.022	0.580	−0.478	−0.014
$W_{5}=5.61$		−0.600	−0.433	−0.038	−0.078	0.010	0.526	0.409	0.030
$W_{4}=4.88$	0.201	−0.035	−0.011	−0.451	0.235	0.761	0.000	−0.016	−0.347
$W_{3}=4.54$		0.010	0.022	−0.421	0.339	0.780	0.004	0.014	0.314
$W_{2}=4.33$	−0.005	−0.796	0.149	0.004	−0.013	−0.016	−0.541	0.226	0.013
$W_{1}=4.31$		0.780	−0.195	0.000	−0.019	−0.006	0.549	0.228	0.005
$W_{0}=-0.29$	−0.974	0.000	−0.000	−0.027	0.023	0.219	0.000	0.000	−0.033

(2) CALCULATED WAVE FUNCTIONS OF THE LOWER ENERGY LEVELS OF DIPHENYLAMINE (involving the configurations of CT_{34} and CT_{35})

Energy, eV	Wave function										
	G	B_{2u}	$E_{1u'}$	B_{1u}	E_{1u}	CTs	CTa	CT_{24}	CT_{25}	CT_{34}	CT_{35}
$W_{8}=6.48$	0.053	0.026	−0.042	0.861	0.270	0.266	−0.051	0.038	−0.323	−0.008	−0.038
$W_{7}=6.27$		0.047	−0.143	−0.812	−0.495	−0.150	−0.079	−0.132	−0.164	−0.019	−0.019
$W_{6}=5.70$	0.005	0.586	0.296	−0.053	−0.022	0.022	−0.578	0.479	0.014	0.031	0.009
$W_{5}=5.61$		−0.600	−0.432	−0.038	−0.078	0.010	0.525	0.409	0.030	0.025	0.008
$W_{4}=4.88$	0.201	−0.035	−0.012	−0.451	0.235	0.761	0.000	−0.016	−0.374	−0.004	−0.012
$W_{3}=4.54$		0.010	0.022	−0.421	0.339	0.780	0.004	0.015	0.314	0.003	0.009
$W_{2}=4.33$	0.005	0.795	−0.149	−0.004	0.013	0.016	0.541	−0.227	−0.014	−0.008	−0.002
$W_{1}=4.31$		−0.780	0.195	0.000	0.018	0.006	−0.549	−0.228	−0.005	−0.007	−0.002
$W_{0}=-0.29$	−0.974	0.000	0.000	−0.027	0.023	0.219	0.000	0.000	−0.033	0.000	0.000

(3) CALCULATED WAVE FUNCTIONS OF THE LOWER ENERGY LEVELS OF DIPHENYLETHER

Energy, eV	Wave function								
	G	B_{2u}	$E_{1u'}$	B_{1u}	E_{1u}	CTs	CTa	CT_{24}	CT_{25}
$W_{8}=6.59$	−0.068	−0.046	0.012	−0.714	−0.351	−0.369	0.108	−0.130	0.442
$W_{7}=6.32$		−0.088	0.007	0.707	0.573	0.181	0.172	0.253	0.194
$W_{6}=6.19$	0.002	−0.317	−0.378	0.140	0.066	0.011	0.563	−0.642	−0.062
$W_{5}=6.00$		0.317	0.622	0.160	0.206	−0.007	−0.483	−0.458	−0.038
$W_{4}=5.56$	0.135	−0.021	−0.020	−0.650	0.225	0.622	0.019	−0.036	−0.347
$W_{3}=5.27$		0.009	0.043	−0.579	0.405	0.636	−0.005	0.015	0.305
$W_{2}=4.61$	−0.001	−0.936	0.086	0.000	−0.007	−0.005	−0.315	0.133	0.007
$W_{1}=4.64$		0.929	−0.119	−0.002	−0.012	−0.001	0.322	0.136	0.004
$W_{0}=-0.21$	0.984	0.000	0.000	0.020	−0.016	−0.175	0.000	0.000	0.024

(4) CALCULATED WAVE FUNCTIONS OF THE LOWER ENERGY LEVELS OF DIPHENYLMETHANE

Energy, eV	Wave function								
	G	B_{2u}	$E_{1u'}$	B_{1u}	E_{1u}	CTs	CTa	CT_{24}	CT_{25}
$W_{8}=6.92$		0.045	−0.479	0.018	0.236	−0.016	−0.136	−0.810	−0.196
$W_{7}=6.72$	0.019	−0.106	−0.397	0.112	0.210	0.112	0.286	−0.780	−0.266
$W_{6}=6.57$		0.088	0.598	−0.275	−0.529	−0.126	−0.218	−0.423	−0.191
$W_{5}=6.27$		0.068	0.615	0.369	0.656	0.078	−0.138	−0.152	0.051
$W_{4}=6.07$	−0.045	0.002	−0.010	0.948	−0.088	−0.246	−0.003	0.020	0.175
$W_{3}=5.86$		−0.005	−0.060	0.860	−0.380	−0.285	0.007	−0.009	−0.175
$W_{2}=4.79$	0.000	0.007	−0.039	0.001	0.004	0.001	0.144	0.060	0.003
$W_{1}=4.79$		0.986	−0.054	−0.001	−0.006	0.000	0.146	0.061	0.002
$W_{0}=-0.13$	0.993	0.000	0.000	0.013	−0.011	−0.120	0.000	0.000	0.015

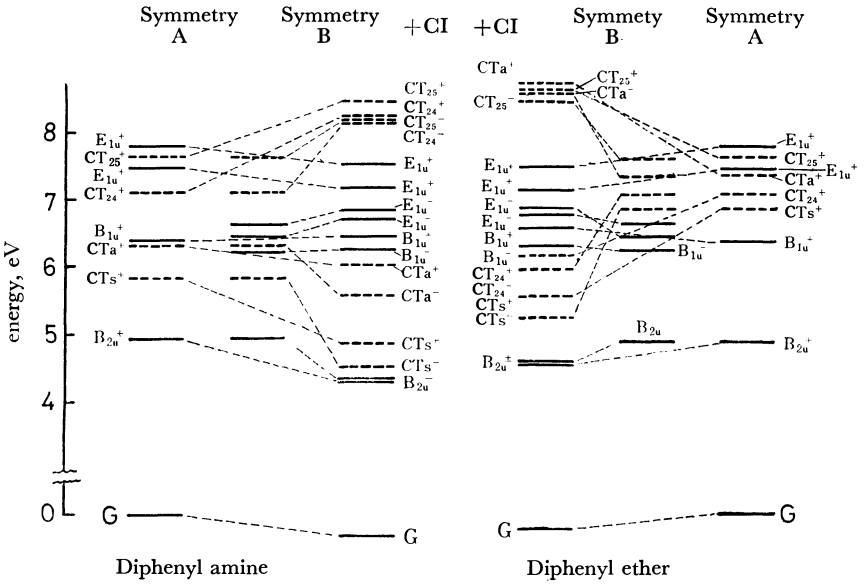

Fig. 6. Energy levels of diphenylamine and diphenylether before and after configuration interaction. (—— locally excited state of benzene; ----- charge transfer state)

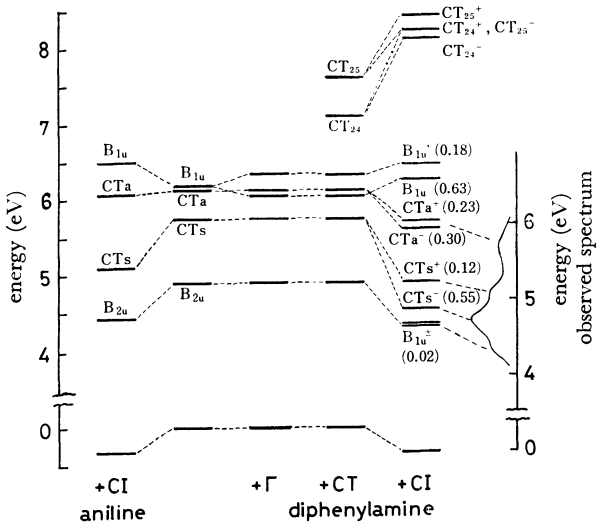

Fig. 7. Correlation among the energy levels of diphenylamine, those of aniline and the observed spectrum. Numbers in parentheses indicate the oscillater strength. The energy levels before and after introduction of excition interaction (Γ), electron transfer interaction (CT) between two benzene rings and configuration interaction (CI) are shown.

where E and Q_i are the transition energy in electron volts and the transition moment in Å respectively.

Theoretical Calculation of $\Delta\mu$ Values. The theoretical expression for $\Delta\mu$ in terms of the state function, Ψ, is given by:

$$\Delta\mu = \langle\Psi_e/M/\Psi_e\rangle - \langle\Psi_g/M/\Psi_g\rangle \qquad (12)$$

where $M = \sum e_t r_t$ and where e_t and r_t are the charge and the position vector of the t'th particle respectively. In the present calculation, Ψ_e for the lowest excited state and Ψ_g are approximated as follows:

$$\Psi_g = \chi_g$$

$$\Psi_e = aB_{2u}^- + bE_{1u'}^- + cCTa^-, \text{ for B symmetry}$$

$$\Psi_e = a'B_{2u}^+ + b'E_{1u'}^+ + c'CTa^+, \text{ for A symmetry}$$

where χ_g is the ground-state configuration. The necessary formulae for the expansion of Eq. (12) have been presented by Pariser[28] and also by Mataga.[29] The Eq. (12) is thereby reduced to the following:

$$\Delta\mu = c^2(M_{44} + M_{4'4'})/2 \text{ for B symmetry}$$

$$\Delta\mu = c'^2(M_{55} + M_{5'5'})/2 \text{ for A symmetry}$$

where $M_{ii} = \langle\phi_i/M/\phi_i\rangle = \sum c_{ij}^2 R_j$. R_j is the position vector of the j'th particle. The calculated values of $\Delta\mu$ for the lowest excited states of diphenylamine, diphenylether, and diphenylmethane are tabulated in Table 2.

Discussion

One of the characteristic features of the calculated results shown in Fig. 5, Fig. 6, and Table 4 is that the lowest excited state of each of the compounds treated here is of a B_{2u} character. Moreover, the exciton states, B_{2u}^+ and B_{2u}^-, are degenerated, and these two states do not interact with any of the other exciton states. These facts indicate that the first absorption band of diphenyl compound, C_6H_5-X-C_6H_5, are essentially the same as that of the monophenyl compound, C_6H_5-XH, in the case of the C_2 symmetry or that of benzene in the case of the C_{1h} symmetry. As may be seen in Fig. 1, the first absorption bands of diphenylether and diphenylmethane are not identical with that of benzene, but they are identical with those of the corresponding monophenyl compounds, phenol and toluene respectively. This clearly indicates that the configurations of the two benzene rings belong to the C_2 symmetry. On the other hand, the first absorption band of diphenylamine can not be attributed solely to the B_{2u} of benzene, for its intensity is too high.

The distinctive feature of diphenylamine observed in Fig. 6 is that the CTs^- state is located very close to the B_{2u}^- states. On the contrary, the finaly CTs^- state of

28) R. Pariser, *J. Chem. Phys.*, **24**, 250 (1956).
29) N. Mataga, This Bulletin, **36**, 654 (1963).

diphenylether obtained after the configuration interaction is located at higher energy and has little effect on the lower-lying energy levels.

Unlike the benzene-excited configurations, the two charge-transfer configurations, $\theta^{-1}\phi_4$ and $\theta^{-1}\phi_4'$, do not interact with each other, and the energy of the charge-resonance state is equal to that of aniline. The origin of the distinction between the observed spectrum of diphenylamine and that of aniline must be attributed to the existence of an interaction between the two benzene rings. Two types of interaction, exciton interaction (Γ) and electron-transfer interaction (CT) between two benzene rings, were considered to explain the distinctive nature of the absorption spectrum of diphenylamine. The effect of the exciton (Γ) and electron-transfer (CT) interactions on the lower energy levels of diphenylamine are illustrated graphically in Fig. 7 and Fig. 8. The energy levels of CTs of aniline split into two levels, CTs^- and CTs^+, upon the introduction of the Γ or CT interaction, while the B_{2u} level is not affected so strongly. The final CTs^- state of diphenylamine obtained after configuration interaction is located at a lower energy than the CTs level of aniline, and the energy gap between CTs^- and B_{2u}^- in diphenylamine is considerably smaller than that in aniline, as may be seen in Fig. 7. This distinction of the calculated energy levels between diphenylamine and aniline can be correlated with that of the observed spectrum between diphenylamine and aniline.

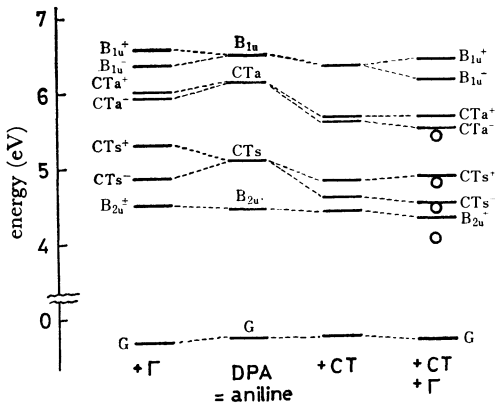

Fig. 8. Comparison of effect of exciton (Γ) and electron transfer (CT) interaction between two benzene rings on stabilizing the CTs^- level of diphenylamine. ○ indicate the observed energy levels.

The mechanism of the stabilization of the CTs^- level due to the introduction of Γ and CT interaction may be illustrated as follows. Firstly, in diphenylamine, the B_{1u} state of benzene, which is located just above the CTs state, splits through the exciton interaction, giving two exciton states, B_{1u}^+ and B_{1u}^-, as may be seen in Fig. 7. The minus state is lower in energy than the plus state, and the energy gap between the CTs^- and B_{1u}^- states is smaller than that between the CTs and B_{1u} states in aniline. Therefore, the configuration interaction will cause more stabilization of the CTs^- level of diphenylamine than the CTs level of aniline. Secondly, the introduction of another benzene ring into aniline at the N-position produces new electron configurations arising from electron transfer between the two benzene rings. One of these configurations, CT_{25}^-, which is located above the CTs^- state, interacts with the CTs^- state; moreover, the interaction matrix element between these two configurations is considerably larger than that between B_{1u}^- and CTs^-. It may be seen in Fig. 8 that the "CT" interaction has a greater effect than the "Γ" interaction in stabilizing the CTs^- level. This result indicates that the electron-transfer interaction between the two benzene rings is important in interpreting the nature of the absorption spectrum of diphenylamine.

The correspondence of the calculated energy levels to the observed absorption spectrum is shown in Fig. 7. The observed band at 260 mμ (4.74 eV) of diphenylamine is reasonably attributed to the Ψ_0—Ψ_3 transition (5.25 eV, f=0.50), and the broad shoulder at 275 mμ (4.49 eV) may be thought to consist of two transitions Ψ_0—Ψ_1 and Ψ_0—Ψ_2 (4.92 eV, degenerated, f=0.016). The nature of the former transition is that of an intramolecular charge transfer, while the later is of a B_{2u} character.

Since the band shift due to the solute-solvent interaction in a solution may be larger in the charge-transfer band than in B_{2u} band,[30] it may be assumed that in solution, these two bands are superposed upon each other, giving one broad intense band. If this assumption is valid, the solvent effects on the wave-number difference between the first absorption and fluorescence bands, $\sigma_a-\sigma_f$, may be expected to be larger than that of diphenylether or diphenylmethane. In Fig. 2, it may be seen that the slope of the straight line for diphenylamine is considerably larger than that of diphenylether or diphenylmethane. As may be seen in Table 2, the values of $\Delta\mu$ obtained from the slope of the straight lines for diphenylether and diphenylmethane are in good agreement with the theoretically-calculated values of $\Delta\mu$. Therefore, it may be said that the lowest excited states (fluorescent state) of diphenylether and diphenylmethane are mainly benzene B_{2u}. In the case of diphenylamine, the situation is somewhat more complicate. As has already been described, the first absorption band of diphenylamine does not consist of one transition, but of two transitions, G→B_{2u} and G→CTs^-. The absorption due to the G→B_{2u} transition appears as a shoulder on the lower-frequency side of the absorption band attributable to the G→CTs^- transition, as may be seen in Fig. 1 (c). Therefore, the effect of the solvent on the shift of the absorption peak should concern the G→CTs^- transition.

It has been known, in general, that the fluorescent state is the lowest excited singlet state. In diphenylamine, the CTs^- state is located very close to the lowest excited singlet state (B_{2u}). However, the possibility that the second excited state (CTs^-) is the emissive state may be eliminated on the basis of the following facts. First, the absorption and fluorescence bands are not in a good mirror-image relation, as may be seen in Fig. 1 (c); the absorption band is broad, while the fluorescence is sharp. Secondly, the energy gap between the first and second excited states is about 1000 cm^{-1}, and the population of the second excited state,

30) E. G. McRae, *J. Phys. Chem.*, **61**, 562 (1957).

as the emissive state, can not be taken into account because of the presence of a rapid internal conversion process and the Boltzman distribution law. Therefore, the observed solvent effect on the fluorescence should be related to the G←B_{2u} transition. However, the observed shift of the fluorescence band due to the change in the solvent polarity is larger than that to be expected from the degree of the CT contribution to the lowest excited state, as may be seen in Table 1 and Table 4. One reasonable explanation for this is the resonance (or mixing) of the first and second excited states. This mixing may arise from the change in the molecular configuration in the excited equilibrium state. The interference effect of two closely-spaced excited states have been discussed by Jano[31] and Bixon.[32] In the present case, also, the fluorescent state may be a mixed state of B_{2u} and CTs^- states. The observed value for $\Delta\mu$ (the dipole-moment change between the ground and excited states) of diphenylamine listed in Table 1 may be explained well as the basis of the above conception.

Summary

As for the configuration of the molecule of the C_6H_5-X-C_6H_5 type, two possibilities may be considered. One belongs to the point group C_2, and the other, to C_{1u}. The first excited states of diphenylether and diphenylmethane, calculated theoretically, are B_{2u}, and theoretical considerations suggest that the first absorption bands of diphenylether and diphenylmethane are identical with that of benzene (in the case of C_{1h}) or those of the corresponding monophenyl compounds, phenol and toluene respectively. The observed spectra clearly indicate that these molecules belong to the C_2 symmetry.

The first absorption band of diphenylamine is quite distinctive compared with those of diphenylether and diphenylmethane. The theoretical analysis of this point indicates that the characteristic feature of the first absorption band of diphenylamine is to be ascribed to its low-lying charge-transfer configuration and to the existence of exciton and electron-exchange interaction between the two benzene rings. The first absorption band of diphenylamine in solution is illustrated by the assumption that the lowest excited state is not pure B_{2u}, but a superposed state of B_{2u} and CTs^-. This assumption is verified experimentally by the solvent effects on the absorption and emission spectra.

The authors wish to express their thanks to Professor Ikuzo Tanaka of the Tokyo Institute of Technology for his valuable suggestions and encouragement during this work.

31) I. Jano, *Chem. Phys. Lett.*, **2**, 643 (1968).
32) M. Bixon and J. Jortner, *Mol. Phys.*, **17**, 109 (1969).

BULLETIN OF THE CHEMICAL SOCIETY OF JAPAN, VOL. 44, 637—641 (1971)

Studies on Salt Solution Aerosols. IV.[1] Droplet Size Determination of Aqueous Sodium Chloride Solution Aerosols by Chemical Spot Method

Yasuo UENO and Isamu SANO

Department of Chemistry, Faculty of Science, Nagoya University, Chikusa-ku, Nagoya

(Received August 11, 1970)

Droplets of aqueous NaCl solution aerosols generated by atomization were collected on an $AgNO_3$ containing film, by measuring microscopically the sizes of the AgCl spots formed on the film, the diameters of the droplets were determined with the aid of the calibration curve between the spot and droplet diameters. It was found that the calibration curve can be expressed by a relation $D_d^3 = Kd_s^2$, where D_d is the volume average diameter of the droplets, d_s the surface average diameter of the spots and K a constant. The meaning of K was considered.

For aerosol investigation it is essential to measure the particle size distribution. This is one of the main tasks of aerosol studies, but it is very difficult to size and count the droplets of volatile aqueous solution that evaporate appreciably during sampling and measurement.

The oil method,[2] in which the collected droplets are suspended in an oil film on a glass slide and observed under a microscope is most frequently used.

There are other methods such as ultramicroscopical measurement of the sedimentation rate of droplets or of their mobility in electric field. Recently photoelectric counters have been available for use, but these are not always applicable for aerosols of volatile droplets as complete elimination of evaporation is very difficult.

As one technique for measuring droplet size with an optical microscope we deal with their spots impressed on a support. Soot-[3] or magnesium oxide-[4] coated glass slides have been utilized widely, though they cannot register spots less than 10 μ in diameter owing to their poor impressions. Because of fragile soot or oxide coating, use of films containing a dye or special reagents

1) Part III: I. Sano, S. Hikita, and Y. Ueno, Nippon Kagaku Zasshi, **90**, 876 (1969).

2) F. Albrecht, *Physik Z.*, **32**, 48 (1931); H. K. Weikmann and H. J. aufm Kampe, *J. Meteor.*, **10**, 204 (1953).

3) L. Strazhevsky, *Tech. Phys. (U. S. S. R.)*, **4**, 978 (1938); R. L. Stoker, *J. Appl. Phys.*, **17**, 243 (1946).

4) K. R. May, *J. Sci. Instr.*, **22**, 187 (1945); H. Maruyama and K. Hama, *J. Meteor. Soc. Japan*, **32**, 49 (1954); E. Uchida, *ibid.*, **44**, 234 (1966).

in gelatine, polyvinyl alcohol, ethyl hydroxycellulose and so on has been introduced.[5] However, these is little information for physicochemical studies both of the spots of aqueous salt solution droplets on these films and of the application to the droplet size measurement, except a few reports on the solid particles of sodium chloride.[6]

Employing an Hg_2SiF_6 or $HgNO_3$ containing gelatine film, Sano *et al.*[7] measured the particle size of NaCl aerosols having an average diameter less than 0.5 μ (prepared by condensation method) and one less than 8 μ (prepared by dispersion method). They assumed the spot of HgCl formed to be hemispherical and found a good agreement between the calculated and observed sizes. Farlow[8] developed a technique making use of an $Ag_2Cr_2O_7$ containing gelatine film. The NaCl particles collected on the film, and dissolved by keeping the film in moist air, reacted with the dichromate to produce the spots of AgCl, which were apparently clear. Assuming that they are cylindrical, he found that the relation $w=0.54\ d^{2/3}$ ($w>20\ \mu$) holds, where w is the particle size represented by the width of one crystal face of a cubic NaCl particle and d the diameter of the spot on the film. This paper will present information on the droplet size determination of aqueous NaCl aerosols.

Experimental

Materials. C_2H_5OH, HNO_3, and $AgNO_3$ used were of the extra pure grade. Polyvinyl alcohol obtained from the Kurashiki Rayon Co. was 1700 in polymerization degree and 85% in saponification.

Preparation of the Reagent Film. An aqueous solution containing 4% by weight of PVA was made by stirring the dry powder into distilled water with strong agitation at room temperature. To 100 g of the solution, 200 m*l* of C_2H_5OH and 1.5 m*l* of 1N HNO_3 were mixed and further, (a) 2 m*l*, (b) 3 m*l*, (c) 5 m*l*, or (d) 7 m*l* of an aqueous 40% $AgNO_3$ solution was added to obtain four NaCl-detecting reagents of different concentrations. The $AgNO_3$ containing PVA solutions so prepared retained their properties for an extended time at room teperature in the dark.

By dropping 10 μl of the $AgNO_3$ containing PVA solution upon a diameter of around 2.1 cm is obtained and the solvent alcohol and water, rapidly evaporate off. The film formed is photosensitive and must be stored in a closed container in the dark.

The glass side used as PVA film carrier was first immersed in chromic acid mixture to remove greasy material and then, thoroughly washed in running water and finally in distilled water. The slides were kept in a desiccator, hanging in a vertical position.

Generation of the Droplets and the Measurement of their Size Distribution. Droplets were generated by using an atomizer filled with an aqueous 5% NaCl solution and introduced into a chamber, where they were dispersed homogeneously and subjected to aging with constant stirring. The chamber is a cylindrical plastic vessel of about 0.23 m^3, the inside of which had been saturated, previous to introduction of the droplets, with water vapor by putting an aqueous 5% NaCl solution on the bottom.

The film carrying glass slides were inserted horizontally, at chamber, the droplets collected on them impressing the spots. In order to know the size of the droplets corresponding to the spots impressed, the oil film technique was applied at the same time, employing glass slides coated on one slide with silicone or the like. Their microphotographs were enlarged and the size reading of both the spots and droplets were made with care, the droplets examined being in the size range of a few tenths of a micron and greater in diameter.

Results

Spots on the Reagent Film. Typical spots impressed on the film are shown in Fig. 1. Influence of the concentration of reagent as well as the exposure to ultraviolet light upon the spot formation is shown in Fig. 2. We see that the smaller spots exhibit more distinct and clear-cut outlines after a 30 min exposure at 10 cm distance from a mercury lamp, the mechanism possibly being that, by photochemical reduction of precipitated AgCl to colloidal silver, spots are given sharp contrast in color, the spots not subjected to the exposure being of somewhat ambiguous image so that they could be observed only when they were of the size above 1 μ in diameter, under a phase-contrast microscope. Figure 3 indicates the microphotographs of the droplets in the oil film.

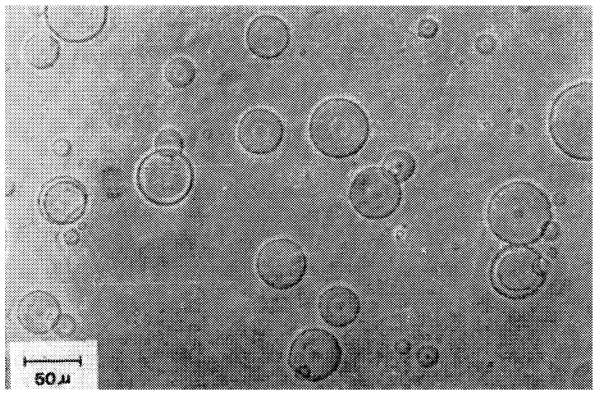

Fig. 1. Spots of 5% NaCl solution droplets (viewed under phase-contrast microscope) on a 5 m*l* $AgNO_3$ solution film.

Construction of the Calibration Curve. The droplets suspending in the oil film and their spots impressed on the reagent film have both their own size distributions, and therefore, taking the volume average diameter (D_d) for the former and the surface average diameter (d_s) for the latter, the calibration curve was drawn for each of the four films, (a), (b), (c), and (d) having different concentrations with respect to the reagent, $AgNO_3$ (Fig. 4). From the figure, it is evident that the spot diameter increases more rapidly than the droplet diameter and that it gets smaller as the reagent concentration in film increases.

Discussion

It has been referred to above that the circular film

5) H. F. Liddel and N. W. Wotten, *Quart. J. Meteor. Soc.*, **83**, 263 (1957); T. Okita, *J. Meteor. Soc. Japan*, **36**, 42 (1958).

6) B. Seely, *Anal. Chem.*, **24**, 576 (1952); N. H. Farlow and F. A. French, *J. Colloid Sci.*, **11**, 184 (1956).

7) I. Sano, Y. Fujitani and T. Sugiyama, Nippon Kagaku Zasshi, **76**, 466 (1955).

8) N. W. Farlow, *Anal. Chem.*, **29**, 883 (1957).

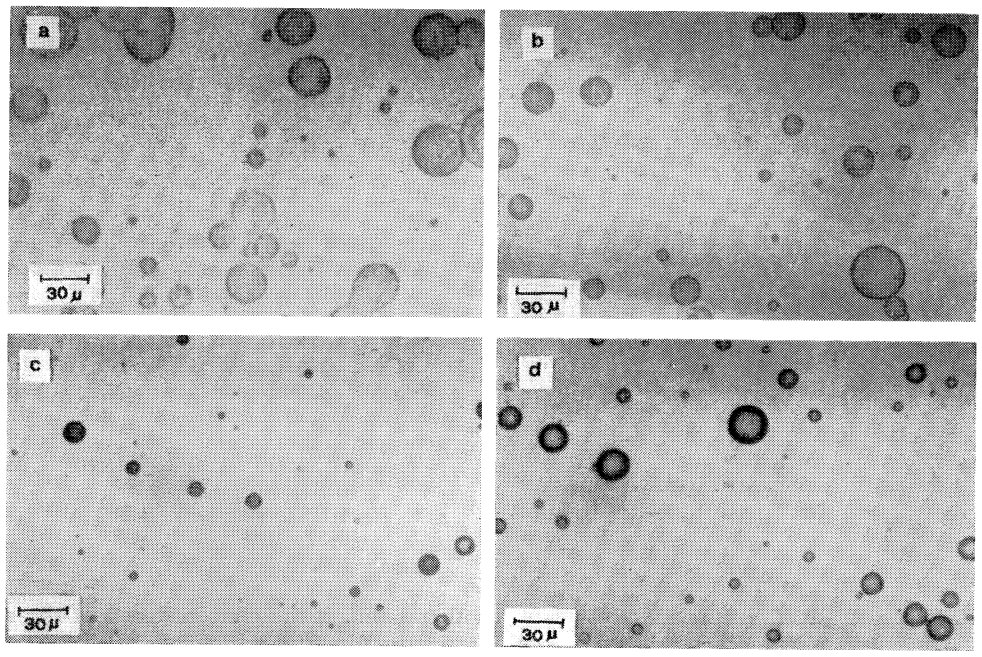

Fig. 2. Spots of 5% NaCl solution droplets after 10 min exposure to ultraviolet light (viewed with ordinary microscope).
(a) on a 2 m*l* $AgNO_3$ solution film (b) on a 3 m*l* $AgNO_3$ solution film
(c) on a 5 m*l* $AgNO_3$ solution film (d) on a 7 m*l* $AgNO_3$ solution film

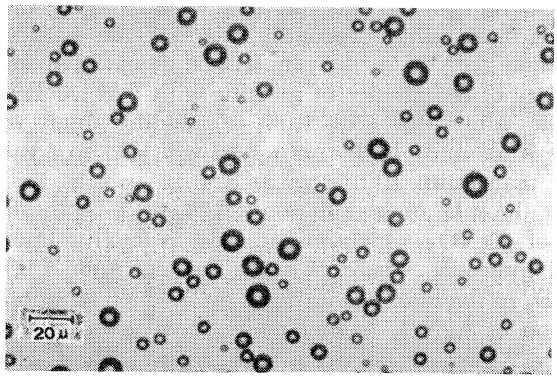

Fig. 3. 5% NaCl solution droplets in oil (viewed under microscope).

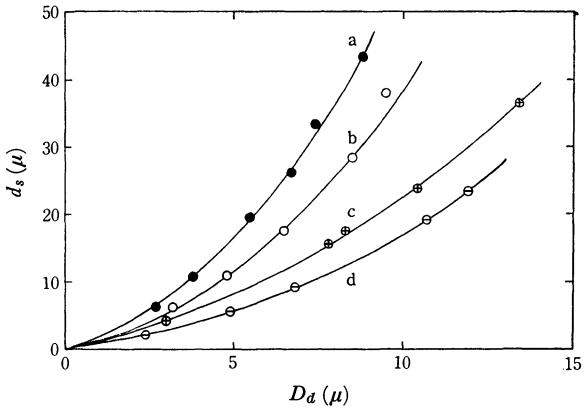

Fig. 4. Plot of the spot diameter (d_s) against the droplet diameter (D_d).
(a): 2 m*l* $AgNO_3$ (b): 3 m*l* $AgNO_3$
(c): 5 m*l* $AgNO_3$ (d): 7 m*l* $AgNO_3$

of PVA–$AgNO_3$ mixture formed on a glass slide is of a constant diameter (2.1 cm) within experimental error, regardless of the reagent concentration in the film. Let us assume as follows:

1) The circular film has a uniform thickness and consists of solid PVA and $AgNO_3$, with a density corresponding to the mixing ratio, 2) the reagent, $AgNO_3$, is distributed homogeneously throughout the film, 3) all the chloride ions in a droplet collected on the film react with silver ions in the film to yield silver chloride, 4) the spots are cylinders which are microscopically viewed and whose heights are equal to the film thickness.

On the basis of these assumptions we obtain the expression

$$D_d^3 = 3/2\rho[\text{Film}]C[AgNO_3]M[\text{NaCl}]/\rho[\text{NaCl}]C[\text{NaCl}]M[AgNO_3]Hd_s^2 \quad (1)$$

ρ[Film]: density of film
ρ[NaCl]: density of aqueous NaCl solution
C[NaCl]: concentration of aqueous NaCl solution (wt%)
C[$AgNO_3$]: concentration of $AgNO_3$ in film (wt%)
M[NaCl]: molecular weight of NaCl
M[$AgNO_3$]: molecular weight of $AgNO_3$
H: thickness of film

Since the concentration of the NaCl solution used is constant throughout the whole range of distribution, we get, in place of Eq. (1),

$$D_d^3 = Kd_s^2 \quad (2)$$

K being a constant which is given by $K=10.0\ \rho[\text{Film}]HC[AgNO_3]$.[9] According to Eq. (2), a plot of log D_d

9) For the values of ρ_{Film}, H and C_{AgNO_3}, *cf.* Table 1. The concentration of the dispersing solution is 5% by weight of NaCl. The term corresponding to $3/2\cdot M_{NaCl}/(\rho_{\text{Film}}\cdot C_{AgNO_3}\cdot M_{AgNO_3})$ is then.

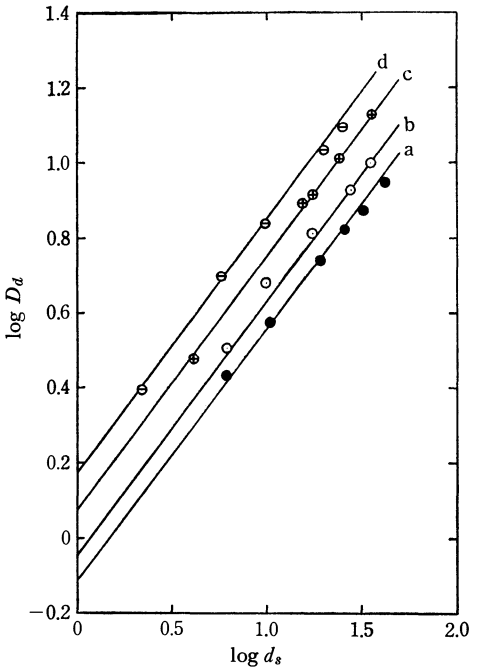

Fig. 5. Plot of log D_d (droplet diameter) against log d_s (spot diameter).
(a): 2 m*l* $AgNO_3$ (b): 3 m*l* $AgNO_3$
(c): 5 m*l* $AgNO_3$ (d): 7 m*l* $AgNO_3$

against log d_s should be linear, and this is found to be actually the case, as is shown in Fig. 5, where the experimental values depicted in Fig. 4 are reproduced as the relation between log D_d and log d_s; these plots are all straight lines parallel with one another and have a slope of 2/3 that might be expected of Eq. (2).

From Eq. (2), we write as follows.

$$D_d{}^3{}_{\text{theor.}} = K_{\text{theor.}} d_s{}^2{}_{\text{theor.}} \quad (3)$$

$$D_d{}^3{}_{\text{exptl.}} = K_{\text{exptl.}} d_s{}^2{}_{\text{exptl.}} \quad (4)$$

It follows from Eqs. (3) and (4), on equating $D_{d\text{exptl.}} = D_{d\text{theor.}}$ that

$$d_{s\ \text{theor.}}/d_{s\ \text{exptl.}} = (K_{\text{exptl.}}/K_{\text{theor.}})^{1/2} = \varepsilon \quad (5)$$

It is to be noted that K's of Eq. (5) can be evaluated either theoretically from Eq. (2) with the known values of ρ[Film], H, and $C[AgNO_3]$ or experimentally as the intercept on the log D_d axis in Fig. 5. Denote the square root of their ratio by ε. It will give us a measure of a theoretical size of a spot relative to a experimental one. The value of ε thus found is represented in Table 1 and it might be considered from the table that ε increases with the increase in the reagent concentration.

If the above assumptions be valid, we should obtain a value of unity for ε. However, this is not the case actually. First, if the concentration of the reagent is small as in the films (a) and (b), a greater part might have been protected by PVA for it to be of lower reactivity, and consequently, the droplets collected would spread to yield larger spots, giving ε values less than unity. In these cases, we have portion of the reagent remaining unreacted in the spot, and in line with this, we have occasionally found a smaller forming on a larger one with the cases of the droplets collected on the film (c) and (d) which contain $AgNO_3$ thickly. On the other hand, if the concentration of the reagent is large as in the films (c) and (d), a greater part would possess reactivity and we will obtain ε values close to unity; for the films of highest concentrations of reagent, it might be very likely that the precipitate of AgCl is formed densely, preventing the NaCl molecules in the droplet from diffusing to react upon $AgNO_3$ molecules outside the spot; in this case, we would have ε values higher than unity. Secondly, there is the possibility that some $AgNO_3$ in the film will be deprived owing to location, of the chance of meeting with NaCl collected on the film; this will vary, depending upon what shape is assumed by the spot, and will lead to ε values other than unity.

Table 1. The estimated values of ρ_{Film}, H, and C_{AgNO_3} and the experimental value of ε

Film	ρ_{Film} (g/cc)[a)]	H (μ)[b)]	C_{AgNO} (%)[c)]	ε
(a)	1.56	0.32	22.7	0.60_6
(b)	1.67	0.33	30.6	0.56_9
(c)	1.86	0.35	42.4	0.80_6
(d)	2.03	0.37	50.7	0.93_0

a), b), c) The values of ρ_{Film}, H, and C_{AgNO_3} are obtained, by the relations:

$$\rho_{\text{Film}} = (W_{\text{PVA}}/\rho_{\text{PVA}} + W_{AgNO_3}/\rho_{AgNO_3})/(W_{\text{PVA}} + W_{AgNO_3})$$
$$H = 4(W_{\text{PVA}}/\rho_{\text{PVA}} + W_{AgNO_3}/\rho_{AgNO_3})/\pi D^2$$
$$C_{AgNO_3} = 100\, W_{AgNO_3}/(W_{\text{PVA}} + W_{AgNO_3})$$

where W and ρ are the weight and density of solid PVA or $AgNO_3$, and D the diameter of the film (2.1 cm). For example, in the case of the reagent concentration of (a),

$$\rho_{\text{Film}} = (1.32\times10^{-4}/1.31 + 3.88\times10^{-5}/4.35)/(1.32\times10^{-4} + 3.88\times10^{-5}) = 1.56$$
$$H = 4(1.32\times10^{-4}/1.31 + 3.88\times10^{-5}/4.35)/3.14\times2.1^2 = 0.32\times10^{-4}$$
$$C_{AgNO_3} = 100\times3.88\times10^{-5}/(1.32\times10^{-4} + 3.88\times10^{-5}) = 22.7$$

For the sake of formulation, let $1-f(C)$ be the fraction of $AgNO_3$ which might hold reactivity upon a NaCl molecule, where C is the concentration (%) of $AgNO_3$ in the film. Concerning $f(C)$ which signifies the fraction of $AgNO_3$ having no reactivity, we have

$$f(C+\mathrm{d}C) = f(C)\cdot(1-\beta \mathrm{d}C)$$

where βdC is the reactivity of an $AgNO_3$ molecule in the range of concentration of dC. It follows that

$$\mathrm{d}f(C) = -f(C)\cdot\beta \mathrm{d}C$$

which, on integrating under the assumption of β being independent of concentration, gives

Table 2. Applicability of Eq. (7), $\varepsilon = K(1-\alpha\, e^{-\beta C})$

C	$\varepsilon_{\text{obsd}}$[a)]	$\varepsilon_{\text{calcd}}$ $K=2.0$[b)]	$K=5.0$[c)]	$K=10.0$[d)]
0.0	—	0.094	0.18	0.19
22.7	0.61	0.52	0.53	0.54
30.6	0.57	0.65	0.64	0.65
42.4	0.81	0.82	0.81	0.83
50.7	0.93	0.92	0.93	0.94
100.0	—	1.38	1.54	1.62

a) *cf.* Table 1.
b) $\alpha = 0.95_3$, $\beta = 0.011_2$
c) $\alpha = 0.96_4$, $\beta = 0.0033_2$
d) $\alpha = 0.98_1$, $\beta = 0.0015_7$

$$f(C) = \alpha e^{-\beta C} \quad (6)$$

where α is a constant determinable by the condition that, $f(C)$ has at $C=100\%$, a value γ, differing from zero since it is probable for some $AgNO_3$ to remain unreacted, so that $\alpha=\gamma\, e^{100\cdot\beta}$. Supposing that the quantity $1/\varepsilon$, which represents the ratio of d_{exptl} to d_{theor} is inversely proportional to the reactivity $1-f(C)$, and is affected by diffusivity composed of lateral (surface) and longitudinal (bulk) components, we obtain

$$\varepsilon = d_{\text{theor}}/d_{\text{exptl}} = k(1-\alpha e^{-\beta C}) \quad (7)$$

where k is a constant relating to diffusivity.

Table 2 indicates the applicability of Eq. (7). We could not carry out experiments for concentrations lower than 20%, because of the difficulty in finding the spots with sharp impression, or for those higher than 60% owing to production of a film with coarse $AgNO_3$ particles deposited, probably due to its decreasing solubility in drying PVA solution.

For a number of years we have been conducting the research on salt solution aerosol droplets and have here reported the size measurement of chloride containing droplets.[10] Extending the technique, we are now making experiments[11] on sulfate containing droplets whose details will be given in near future.

10) I. Sano and Y. Ueno, *Nippon Kagaku Zasshi*, **89**, 102 (1968); *ibid.*, **90**, 47 (1969); I. Sano, S. Hikita, and Y. Ueno, *ibid.*, **90**, 876 (1969).

11) Presented at the 22nd symposium on Colloid- and Interface Chemistry held at Sendai, Japan, on Nov. 11, 1969, under the auspices of the Chem. Soc. of Japan; read before the spring meeting on Cloud Physics held at Nagoya, Japan, on March 6, 1970, under the auspices of the Meteorol Soc. of Japan.

BULLETIN OF THE CHEMICAL SOCIETY OF JAPAN, VOL. 44, 641—643 (1971)

Photosensitive Ionomer. I. Preparation of Mercurous Acrylate and Photosensitive Plates

Shin SUZUKI and Kazuyuki SUGITA

Department of Graphic Engineering, Faculty of Engineering, Chiba University, Yayoi-cho, Chiba

(Received August 14, 1970)

Photographic plates were prepared by coating an emulsion consisting of mercurous acrylate, polyvinyl alcohol and water on glass plates. They were found to be sensitive to light ranging from 250 nm to 340 nm. A dark brown image with density *ca.* 0.6 above the fog was formed by a printing-out process. The latent image could be amplified with the reducing developers such as hydroquinone or metol. Image formation was ascribed to metallic mercury which was isolated by photoreduction and/or reduction of mercurous ion.

On exposure to light, mercurous acetate disproportionates to mercuric acetate and metallic mercury[1] to give dark brown materials as illustrated in Eq. (1). Photoreduction of mercurous ion into metallic mercury is similar to that of silver ion, and mercury is available for photographic image formation.

$$2CH_3COOHg \longrightarrow (CH_3COO)_2Hg + Hg \qquad (1)$$

The ionomer, ionically crosslinked polymer, is well known since 1964. The ionic crosslinkages are $-COO^-\cdots M^+\cdots O^-CO-$ or $-COO^-\cdots M^{2+}\cdots O^-CO-$ formed by adding mono- or divalent metallic ion, respectively, to linear polymer with side chains of carboxyl groups. Though the ionomer has been studied chiefly for the purpose of improving mechanical properties of plastics, no attempt was made for application to photosensitive plastics. As the strength of the ionic crosslinking depends on the valence of metallic ion, the ionomer crosslinked by a metallic ion of variable valence on exposure may become a new type of photosensitive polymer.

Thus, mercuric ion which is produced by photooxidation of mercurous ion, will form crosslinkages, if some linear polymer has side chains of mercurous carboxylate groups. Polymeric mercurous compound is then expected to be a new photosensitive polymer which undergoes hardening by ionic crosslinking, and can be used for lithographic image formation.

We have prepared an emulsion consisting of mercurous acrylate and polyvinyl alcohol which can be regarded as a model emulsion of linear polymer with side chains of mercurous carboxylate and hydroxyl groups, and have studied some photographic properties of the acrylate plate.

Experimental

Materials. Acrylic acid was purified by distillation of a commercial reagent. Polyvinyl alcohol was supplied by Yotsuwa Sangyo K.K. (PVA GL-05, 95% saponified, $\bar{M}n=$ 22000). The other reagents used were chemicals of extra pure grade.

Apparatus. Titration was performed by using a Yokokawa pH Meter KPH-51B. Wedge spectrogram was obtained with a Ushio Xenon Arc Lamp UXL-500D and a Narumi Monochrometer RM-23. Ultraviolet and visible spectra were taken by measuring the reflection of mercurous acrylate plates with a Shimadzu Spectrophotometer QV-50. Photographic plates, which were irradiated by a Ushio Low-pressure Mercury Lamp ULI-309 (chemical lamp) from a distance of 15 cm, were measured for the photographic reflection density by a Macbeth Densitometer RD-100.

1) G. Brauer, "Handbook of Preparative Inorganic Chemistry," Academic Press Inc., London (1965), p. 1120.

Preparation of Mercurous Acrylate. A 10% aqueous solution of sodium hydroxide was exactly neutralized by acrylic acid, and the concentration of sodium acrylate was determined by titration with 0.5N hydrochloric acid. 14 g of mercurous nitrate was dissolved in 80 m*l* of about 6% nitric acid, and concentrations of mercurous ion and nitrate ion were titrated with 0.1N potassium hydroxide. When the mercurous nitrate solution was added to 8 m*l* of the sodium acrylate solution under vigorous stirring in the dark, mercurous acrylate was precipitated as white flakes. In order to prepare white, stable mercurous acrylate, nitrate ion should be equivalent to sodium ion in the sodium acrylate solution. The white flakes were filtered and washed with water. After drying *in vacuo*, mercurous acrylate weighed 1.64 g (yield 87.2%). This compound gradually decomposes above 150°C without fusing.

Preparation of the Photosensitive Plate. White flakes of mercurous acrylate without drying, were uniformly dispersed in 30 m*l* of 20% aqueous solution of polyvinyl alcohol. The emulsion was spread over glass plates and left to dry.

Results and Discussion

Spectral Sensitivity of the Acrylate Plate. The wedge spectrogram (Fig. 1) shows that the mercurous acrylate was sensitive to light 250—340 nm, when the grayish white plate turned dark brown.

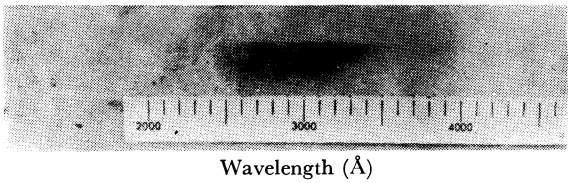

Fig. 1. Wedge spectrogram of a mercurous acrylate plate.

Ultraviolet and Visible Spectra. Reflection spectra were measured for mercurous acrylate plates before and after exposure to ultraviolet light. The results are given in Fig. 2. An absorption below 350 nm, which was found in the ultraviolet spectrum of an unexposed plate, seemed to be closely related with the photosensitivity of the acrylate plate.

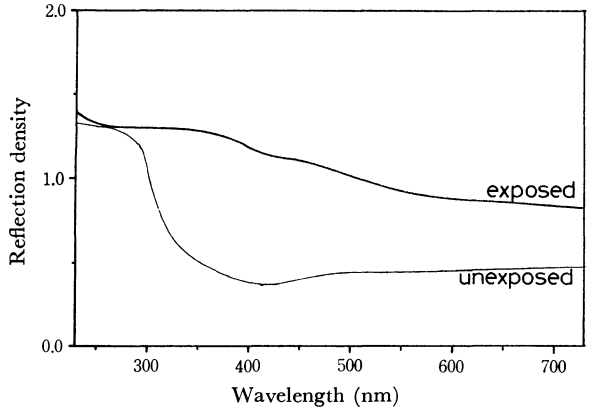

Fig. 2. Reflection UV and visible spectra of mercurous acrylate plates.

Characteristic Curve of the Plate. The plates were placed in a dark box and irradiated by a low-pressure mercury lamp for a certain time and their reflection density was measured. Density was plotted against exposing time. The curve is S-shaped. The maximum density was *ca.* 0.6 above the fog (Fig. 3).

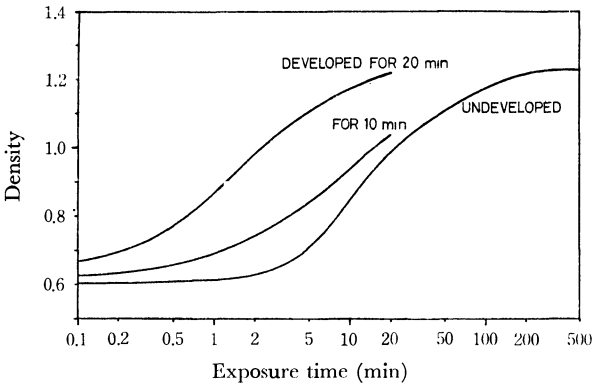

Fig. 3. Characteristic curves of mercurous acrylate plates.

Development of Latent Image. One half of the acrylate plate was irradiated by a low-pressure mercury lamp for two minutes. However, the exposed part was still grayish white and could not be distinguished from the unexposed one. The exposed plate was immersed in an aqueous alcohol solution (water : alcohol=1 : 4, by volume) of hydroquinone. In a few minutes, the exposed part blackened and a distinct difference in color appeared between the exposed and unexposed parts. Fogging was observed on the unexposed part after development for longer than 20 min. Characteristic curves of the acrylate plates, developed in 10 and 20 min respectively, are demonstrated in Fig. 3.

When an aqueous solution of metol or hydroquinone was used for developing, development was completed in 5 min and further development resulted in fogging of the unexposed part. However, the polyvinyl alcohol binder for the mercurous acrylate swelled and the image became detached from the plate when taken out of the developing solution.

Studies on the Preparative Method of the Photosensitive Plate. In the preparation of mercurous acrylate, exact neutralization of sodium hydroxide with acrylic acid was indispensable for excellent photosensitivity of the plate. Otherwise, the plate turned gray while the emulsion was left to dry. Though the density increase smaller because of high fog density, latent images on the gray plate could be developed in the same way as those on a white plate, while no blackening took place in the unexposed part. This may indicate that the gray color was not due to any compounds formed by the disproportionation of mercurous acrylate during the course of drying.

When alkaline solutions such as sodium hydroxide, potassium hydroxide, ammonium hydroxide or hexamethylenetetramine, were used instead of the developing solution, immediate blackening took place on both the unexposed and the exposed parts of the acrylate plate. Blackening caused by alkali may be ascribed to the formation of mercurous hydroxide or mercurous oxide. If the developing solution contains sulfur compounds such as thiourea, sodium thiosulfate, or sodium sulfite, fogging was observed on the unexposed part of the plate. Utilization of gelatin as a binder of the mercurous acrylate gave rise to the fogging of the plate.

The fogging may be due to some dark colored materials formed by the reaction between mercurous ion and the sulfur compounds or basic compounds in gelatin.

Fading and Bleaching of the Image. The black image formed by the developing method as well as the dark brown image formed by the printing-out method were stable and never faded during storage for three months or more.

Treatment of the exposed plate with hydrogen peroxide or nitric acid caused bleaching of the blackened image until no difference in color between the exposed and unexposed parts was observed. Developing by the reducing agent and bleaching by the oxidizing agent suggest that photoreduction of mercurous ion to form metallic mercury, $Hg^{+} \rightarrow Hg$, contributes to the photosensitivity of mercurous acrylate and the formation of image.

The authors wish to thank Professor Takahiro Tsunoda of this University for use of the monochrometer.

BULLETIN OF THE CHEMICAL SOCIETY OF JAPAN, VOL. 44, 643—648 (1971)

The Crystal Structure and Nonstoichiometry of Rare Earth Oxyfluoride

Koichi NIIHARA and Seishi YAJIMA

The Research Institute for Iron, Steel and Other Metals, Tohoku University, Sendai

(Received August 27, 1970)

Oxyfluoride phases for the rare earth Sm, Eu, Gd, Tb, Dy, Ho, Er, Tm, Yb, and Y have been prepared by heating a mixture of lanthanon fluorides, LnF_3, and lanthanon oxides, Ln_2O_3. Three phases were identified. The rhombohedral phases, LnOF, have a stoichiometric composition, and the tetragonal phases, $Ln_4O_3F_6$, have a comparatively large nonstoichiometric composition range. The third cubic phase, with a fluorite-type structure, was observed in the SmOF-$Sm_4O_3F_6$ region after quenching from a high temperature. This establishes that both the rhombohedral SmOF and the tetragonal $Sm_4O_3F_6$ transform to the cubic phase and form a complete solid solution in the high-temperature range. It is postulated that the rhombohedral and tetragonal phases are pseudo-cubic from the fact that the diffraction patterns of these two phases are closely similar to that of the fluorite type.

Relatively few data on the chemical properties of the rare earth oxyfluorides exist in the literature; there is an adequate reason for this. Similar in size to the fluoride ion, the oxide ion may be substituted through a wide concentration range in these heavy metal fluorides. Therefore, the compositional variability of the rare earth oxyfluorides with respect to the anionic ligands is very extensive. Accurate property data are, consequently, very limited. Research problems connected with those materials require mainly information concerning the extent of the oxide-fluoride miscibility before other data may be obtained. If the generally indiscrete composition of the solid phases can be well understood, attempts to obtain other accurate data will be stimulated.

Oxyfluorides of lanthanum, cerium, praseodymium, neodymium, samarium, europium, gadolinium, terbium, dysprosium, holmium, erbium, and yttrium have been prepared using several techniques.[1-6] Zachariasen[1] prepared two types of crystal structures of LaOF and YOF by the hydrolysis of LaF_3 and YF_3 at 900°C and 500°C respectively, one being rhombohedral and the other tetragonal. The rhombohedral phases were observed to have stoichiometric compositions, LaOF and YOF. The tetragonal phases appeared with an increase in the fluorine in the LaO_xF_{3-2x} system ($0.7<x<1$). Zachariasen related all the structures to the fluorite-type structure. He postulated that the rhombohedral and tetragonal forms result from a complete ordering of the oxygen and fluorine atoms into distinct sites of the unit cell.

Hund[2] prepared tetragonal and cubic YOF by heating a mixture of Y_2O_3 and YF_3 in a high vacuum at 900°C for several hr.

Popov[3] and other Russian workers[4] prepared rare earth oxyfluorides (La through Er) by heating their metal fluorides in a muffle furnace in dry air or in a stream of moist air. All the compounds except CeOF, which was cubic, were found to exhibit rhombohedral symmetry.

Thus, there are various structures which have been reported for the rare earth oxyfluorides. The main purpose of this study is to elucidate the relation between the crystal structure and the nonstoichiometric composition of the rare earth oxyfluorides, and to give precise lattice parameters.

Experimental

The anhydrous lanthanon trifluorides, SmF_3, EuF_3, GdF_3, DyF_3, HoF_3, ErF_3, TmF_3, and YbF_3 were prepared by converting the 99.9% pure Ln_2O_3 to fluoride according to the following chemical reaction:

$$Ln_2O_3 + 6NH_4 \cdot HF_2 = 2LnF_3 + 6NH_4 \cdot F + 3H_2O.$$

A mixture containing excess $NH_4 \cdot HF_2$ was heated at 350°C

1) W. H. Zachariasen, *Acta Crystallogr.*, **4**, 231 (1951).
2) F. Hund, *Z. Anorg. Allg. Chem.*, **265**, 62 (1951); *ibid.*, **273**, 212 (1953).
3) A. I. Popov, *J. Amer. Chem. Soc.*, **76**, 4734 (1954).
4) L. R. Batsanona, *Zh. Neorg. Khim.*, **9**(2), 330 (1964).
5) K. S. Vorres, "Rare Earth Research III," ed. by Eyring., Gordon and Breach, New York, N. Y., (1964), p. 521.
6) W. H. Zachariasen, *Z. Krystallogr.*, **80**, 137 (1931).

for 10 hr in a platinum boat, which was placed in an Inconel tube situated in an electric furnace. The resulting water, HF, and NH_4F were evacuated by an aspirator during the reaction. The trifluoride sample thus obtained was degassed in another furnace by careful heating in a high vaccum, *i. e.*, by raising the temperature to 600°C at a rate of 5°C/min and by then maintaining the temperature these for 5 hr.

The lanthanon trifluoride was mixed with lanthanon sesquioxide in various ratios. The fully homogenized mixtures were compacted into pellets, about 10 mm in diameter and 10—30 mm thick. These pellets were reacted in a high vacuum or in an inert gas atmosphere at 1000—1200°C for 5—10 hr, and then quenched or slowly cooled to room temperature. This method of preparing the oxyfluoride is very convenient in studying the nonstoichiometry if enough attention is paid to the weight loss during the reaction and to the anhydrolysis of the rare earth oxides and fluorides.

The nonstoichiometric compositions of the lanthanon oxyfluorides can be expressed as follows:

$$a\mathrm{LnF_3} + b\mathrm{Ln_2O_3} = (a+2b)\mathrm{LnO}_x\mathrm{F}_{3-2x} \quad (x=3b/a+2b)$$

If the amount of either LnF_3 or Ln_2O_3 exceeds the nonstoichiometric composition given by this formula, the excess amount of either LnF_3 or Ln_2O_3 can be determined by X-ray. The pellets thus obtained were pulverized after heat treatment and were examined by X-ray powder diffraction using copper $K\alpha$ radiation and a 114.6 mm-diameter Debye-Scherrer powder camera. Chemical analysis was performed by direct ignition to the oxide.

Experimental Results

The oxyfluorides of samarium, europium, gadolinium, dysprosium, holmium, erbium, thulium, and ytterbium were prepared by the above-described method. The results of the identification of the reaction products cooled slowly in the furnace are shown in Fig. 1; they indicate that there are two oxyfluoride phases. According to the interpretation of the X-ray diffraction patterns, one phase is tetragonal, and the other, rhombohedral. Only in the SmF_3-Sm_2O_3 system, were phases of the fluorite type observed upon quenching from 1200°C. However, in the other system, LnF_3-Ln_2O_3, efforts to obtain a phase of the fluorite type by quenching were unsuccessful.

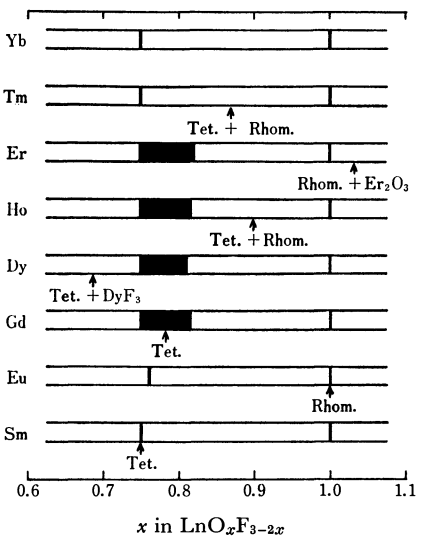

Fig. 1. Phase regions of rhombohedral and tetragonal oxyfluorides.

Rhombohedral-phase LnOF. In all cases, the rhombohedral phases were found to be a single phase only when $x=1$. In the regions of $x>1$ and $x<1$, the diffraction lines of both Ln_2O_3 and the tetragonal oxyfluoride occurred, as well as the rhombohedral phase. No variation in the unit-cell dimensions of this rhombohedral phase was observed. Therefore, it may be concluded that the chemical composition of the rhombohedral phase is sharply defined and corresponds exactly to LnOF. The diffraction data of SmOF and ErOF are shown in Table 1. The diffraction data of EuOF, GdOF, DyOF, HoOF, TmOF, and YbOF are good similar to those of SmOF and ErOF.

Zachariasen[1] found, for LaOF, the space group $R\bar{3}m$ with two molecules in the unit cell; he reported atomic positions which were satisfactory for YOF as well. The data for SmOF, EuOF, GdOF, DyOF, ErOF, TmOF, and YbOF obtained in the present research

Table 1. Diffraction data for rhombohedral SmOF and ErOF

hkl	I (obsd)	SmOF		ErOF	
		$\sin^2\theta$ (obsd)	$\sin^2\theta$ (calcd)	$\sin^2\theta$ (obsd)	$\sin^2\theta$ (calcd)
111	vw	—	0.0141	0.0152	0.0151
100	vvw	—	0.0534	0.0512	0.0571
222	s	0.0567	0.0565	0.0605	0.0605
110	vs	0.0588	0.0581	0.0626	0.0621
211	s	0.0776	0.0770	0.0822	0.0823
221	w	0.0919	0.0911	0.0977	0.0974
333	m	0.1284	0.1273	0.1372	0.1361
322			0.1289		0.1378
33$\bar{2}$	s	0.1527	0.1524	0.1636	0.1629
10$\bar{1}$	s	0.1565	0.1555	0.1674	0.1662
21$\bar{0}$	vvw	—	0.1696	0.1814	0.1813
111	m	0.2087	0.2089	0.2230	0.2232
433			0.2096		0.2234
321	s	0.2129	0.2120	0.2273	0.2266
200			0.2136		0.2283
444	vvw	0.2269	0.2264	0.2419	0.2419
220	m	0.2324	0.2325	0.2487	0.2484
443	w	0.2412	0.2420	0.2581	0.2586
311	vvw	—	0.2466	0.2642	0.2635
432	m	0.2833	0.2828	0.3027	0.3023
331			0.2843		0.3039
422	m	0.3079	0.3079	0.3290	0.3290
544	w	0.3173	0.3175	0.3389	0.3393
555	vw	—	0.3537	0.3775	0.3780
55$\bar{4}$	vw	—	0.3599	0.3826	0.3846
20$\bar{1}$	vw	0.3647	0.3644	0.3883	0.3894
442			0.3645		0.3895
211	m	0.3692	0.3691	0.3948	0.3944
543	w	0.3817	0.3818	0.4077	0.4080
310	w	0.3880	0.3880	0.4146	0.4146
533	vvw	—	0.3975	0.4247	0.4247
320	vvw	—	0.4021	0.4282	0.4297
421	vw	—	0.4398	0.4703	0.4701

SmOF $a=6.863\pm0.002$Å, $\alpha=33.10\pm0.02°$
ErOF $a=6.639\pm0.001$Å, $\alpha=33.10\pm0.01°$

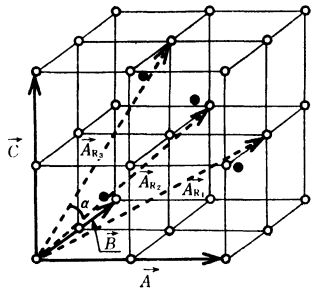

Fig. 2-a. The relation between rhombohedral and fluorite type unit cell.
A, B, C: fluorite type
A_{R_1}, A_{R_2}, A_{R_3},: rhombohedral

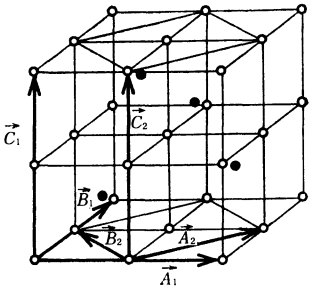

Fig. 2-b. Tetragonal unit cell.
A_1, B_1, C_1,: this research
A_2, B_2, C_2: Zachariasen

can be interpreted in a similar way, as the X-ray diffraction data agree well with those observed by Zachariasen for LaOF and YOF. The structure is a superlattice based upon a slightly distorted CaF_2-type structure. For the undistorted structure, α is 33.56°. The relation between the rhombohedral cell and the fluorite cell is shown in Fig. 2-a. The lattice constants, unit cell volume, and X-ray density obtained are listed in Table 2, where they are also compared with the previous

Table 2. Lattice parameter of rhombohedral rate earth oxyfluorides

Compound	Lattice parameter		Unit cell volume in Å^3	X-Ray density (g/cc)
	a in Å	α in degree		
YOF[a)]	6.697	33.20	79.4	5.18
LaOF[a)]	7.132	33.01	95.9	6.02
PrOF[b)]	7.016	33.03	91.3	6.40
NdOF[b)]	6.953	33.04	88.9	6.69
SmOF	6.863±0.002	33.10±0.02	85.8	7.17
EuOF	6.828±0.002	33.05±0.02	84.3	7.37
GdOF	6.801±0.001	33.05±0.01	83.3	7.67
TbOF[c)]	6.751	33.09	81.6	7.89
DyOF	6.719±0.003	33.02±0.02	80.2	8.18
HoOF	6.687±0.001	33.02±0.02	79.0	8.40
ErOF	6.639±0.001	33.10±0.01	77.7	8.65
TmOF	6.604±0.002	33.06±0.02	76.2	8.93
YbOF	6.569±0.002	33.04±0.02	75.0	9.25

a) Zachariasen, Ref. 1
b) Baenzigh, Ref. 7
c) Templeton, Ref. 8

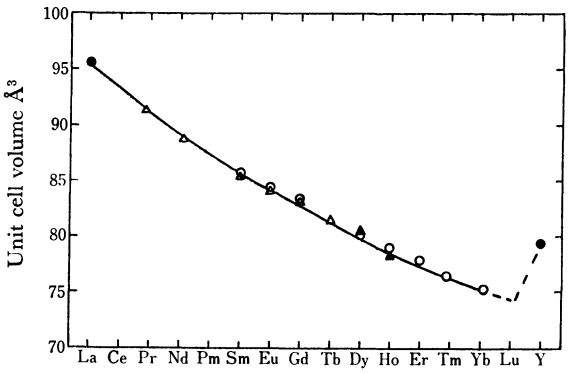

Fig. 3. Unit cell volume of rhombohedral rare earth oxyfluorides, LnOF, as a function of atomic number of rare earth element.
○ this work ○ Zachariasen, Ref. 1
△ Baenziger, Ref. 7 ▲ Vorres, Ref. 9

data.[1,7-9] The change in the molecular volume against the atomic number of rare earth elements plotted in Fig. 3 is characteristic of the well-known lanthanide contraction.

Tetragonal-phase $Ln_4O_3F_6$ ($Ln_2O_3 \cdot 2LnF_3$). The tetragonal phases were observed as mono-phases in the fluorine-rich region. Generally, the chemical composition of the phase throughout its homogeneity range can be expressed by the LnO_xF_{3-2x} formula. As is shown in Fig. 1, the tetragonal phases of Sm, Eu, Gd, Dy, Ho, Er, Tm, and Yb exist as stable mono-phases in the regions of $x=0.75$, $x=0.77$, $0.75<x<0.83$, $0.75<x<0.82$, $0.75<x<0.83$, $0.75<x<0.84$, $x=0.75$, and $x=0.75$ respectively. In the regions of $x<0.75$ and about $x>0.83$, the LnF_3 fluoride and the LnOF rhombohedral oxyfluoride respectively appear as second phases. Therefore, it is resonable to assume that the tetragonal phases have the ideal chemical composition, $LnO_{0.75}F_{1.5}$, that is, $Ln_4O_3F_6(Ln_2O_3 \cdot 2LnF_3)$. The results of the chemical analysis of each $Ln_4O_3F_6$ are summarized in Table 3. The X-ray diffraction data of $Sm_4O_3F_6$ and $Er_4O_3F_6$ are shown in Table 4. The second column lists the indices postulated by Zachariasen. The unit cell of the tetragonal oxyfluoride is illustrated in Fig. 2-b in comparison with the unit cell of Zachariasen. The diffraction data of the tetragonal $Ln_4O_3F_6$ are compara-

Table 3. Composition of $Ln_4O_3F_6$

Ln in $Ln_4O_3F_6$	Observed percentage of metal	Theoretical percentage of metal
Sm	78.50	78.78
Eu	78.45	78.96
Gd	79.36	79.52
Dy	80.01	80.05
Ho	80.26	80.29
Er	80.30	80.52
Tm	80.41	80.89
Yb	81.02	81.04

7) N. C. Baenziger, J. R. Holden, G. E. Knudsen, and A. I. Popov, *J. Amer. Chem. Soc.*, **76**, 4734 (1954).
8) D. H. Templeton and C. H. Dauben, *ibid.*, **76**, 5237 (1954).
9) K. S. Vorres and Richard Rivriells, Proc. Conf. Rare Earth Res., 4th Phoenix, Ariz., (1954), pp. 521—561 (Pub. 1965).

TABLE 4. DIFFRACTION DATA FOR TETRAGONAL $Sm_4O_3F_6$ AND $Er_4O_3F_6$

hkl[a]	hkl[b]	I (obsd)	$Sm_4O_3F_6$ $\sin^2\theta$ (obsd)	$Sm_4O_3F_6$ $\sin^2\theta$ (calcd)	$Er_4O_3F_6$ $\sin^2\theta$ (obsd)	$Er_4O_3F_6$ $\sin^2\theta$ (calcd)
100		vw	0.0189	0.0186	0.0190	0.0194
001	001	w		0.0189	0.0206	0.0205
110	100	vw	0.0370	0.0372	0.0380	0.0389
101		vw		0.0373	0.0400	0.0408
111	101	vs	0.0569	0.0563	0.0595	0.0595
200	110	s	0.0757	0.0747	0.0782	0.0779
002	002	w		0.0757	0.0826	0.0818
201	111	vw	—	0.0936	0.0990	0.0984
112	102	m	0.1134	0.1131	0.1210	0.1211
220	200	s	0.1504	0.1493	0.1564	0.1558
202	112	s		0.1504	0.1604	0.1601
300		w	0.1680	0.1680	0.1777	0.1753
221	201			0.1683		0.1767
003	003	w	0.1707	0.1704	0.1849	0.1845
310	210	w	0.1881	0.1866	0.1977	0.1949
301				0.1890		0.1958
103		vw		0.1887	0.2040	0.2044
311	211	s	0.2065	0.2056	0.2157	0.2153
113	103	m		0.2077	0.2240	0.2239
222	202	m	0.2245	0.2251	0.2380	0.2380
320		vw	—	0.2418	0.2520	0.2522
203	113	m	0.2248	0.2451	0.2630	0.2628
312	212	m	0.2622	0.2628	0.2785	0.2769
400	220	w	0.2978	0.2986	0.3122	0.3116
004	004	w	0.3079	0.3030	0.3293	0.3288
410		vw	0.3189	0.3176	0.3323	0.3322
401	221					
223	203	vw	0.3389	0.3197	0.3409	0.3422
114	104	w		0.3403	0.3683	0.3676
331	301	w	0.3559	0.3549	0.3731	0.3711
313	213	w		0.3571	0.3802	0.3796
420	310	w	0.3737	0.3733	0.3921	0.3895
402	222			0.3744		0.3938
204	114	vvw	—	0.3776	0.4066	0.4066
421	311	vvw	—	0.3922	0.4100	0.4101
332	302	vvw	—	0.4117	0.4342	0.4327
422	312	w	—	0.4492	0.4723	0.4717

a) this work, b) Zachariasen
$Sm_4O_3F_6$ $a=5.643\pm0.003$Å, $c=5.602\pm0.003$Å
$Er_4O_3F_6$ $a=5.524\pm0.001$Å, $c=5.379\pm0.001$Å

tively similar to the data of Zachariasen[1] for the tetragonal YOF and LaOF with respect to the intensities and line structure, compared after the axis transformation. However, the (110) and (103) planes can not be explained by the unit cell of Zachariasen, as is shown in Table 4. On the other hand, all the diffraction planes can be explained by the unit cell used in this research. According to our results, $Ln_4O_3F_6$ is a tetragonal structure containing 4 molecules in the unit cell with $c/a=1$. Thus, our results differ from those of Zachariasen, who assumed 2 molecules in the unit cell with $c/a=\sqrt{2}$. The lattice parameters and X-ray density are given in Table 5. The lattice parameter of the tetragonal $Gd_4O_3F_6$, $Dy_4O_3F_6$, $Ho_4O_3F_6$, and $Er_4O_3F_6$, all of which have a nonstoichiometric composition range, are plotted

TABLE 5. LATTICE PARAMETER OF TETRAGONAL RARE EARTH OXYFLUORIDES

Compound	Lattice paremeter in Å a	c	X-Ray density (g/cc)
YO_xF_{3-2x}[a]	3.910($x=1$)	5.431	
	3.930($x=0.7$)	5.46	
LaO_xF_{3-2x}[a]	4.083($x=1$)	5.825	
	4.098($x=0.7$)	5.840	
$Sm_4O_3F_6$	5.643±0.003	5.602±0.003	7.13
$Eu_4O_3F_6$	5.623±0.002	5.574±0.003	7.28
$Gd_4O_3F_6$	5.595±0.003	5.527±0.003	7.61
$Dy_4O_3F_6$	5.559±0.003	5.456±0.003	8.02
$Ho_4O_3F_6$	5.539±0.002	5.414±0.002	8.23
$Er_4O_3F_6$	5.524±0.001	5.379±0.001	8.43
$Tm_4O_3F_6$	5.513±0.002	5.355±0.002	8.58
$Yb_4O_3F_6$	5.498±0.002	5.323±0.002	8.85

a) Zachariasen, Ref. 1

as a function of the parameter, x, in Fig. 4 and Fig. 5. The variation in the lattice parameters is plotted in Fig. 6 against the atomic number of the rare earth element. The lattice parameters of the tetragonal $Gd_4O_3F_6$, $Dy_4O_3F_6$, $Ho_4O_3F_6$, and $Er_4O_3F_6$ in the homogeneity range vary in such a way that c increases and a decreases. As is shown in Fig. 6, the tetragonal phases show the well-known lanthanide contraction as a function of the atomic number of the rare earth element.

Cubic Phase (Fluorite-type Structure). In the SmF_3-Sm_2O_3 system, the rhombohedral phase and the tetragonal phase were observed, as is shown in Fig. 1. Some of these specimens were reheated to 1200°C and then quenched to room temperature. The crystal structure of these samples was examined by X-ray analysis; it was thus clarified that lines due to a face-

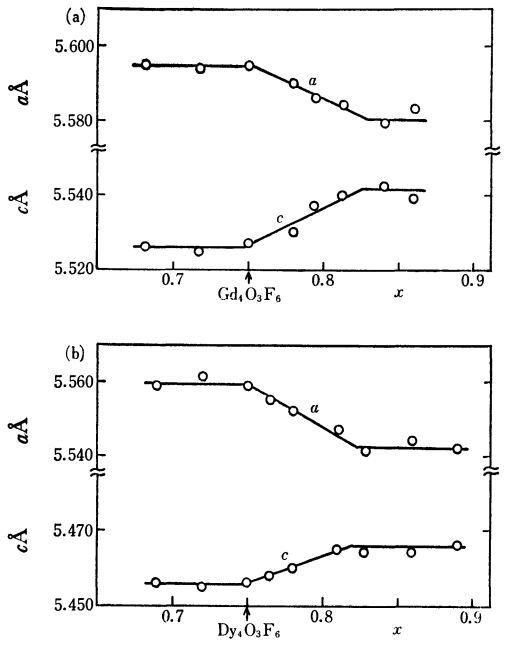

Fig. 4. Lattice parameter of tetragonal oxyfluorides as a function of x in GdO_x F_{3-2x} and DyO_x F_{3-2x}.
(a) gadolinium oxyfluoride (b) dysprosium oxyfluoride

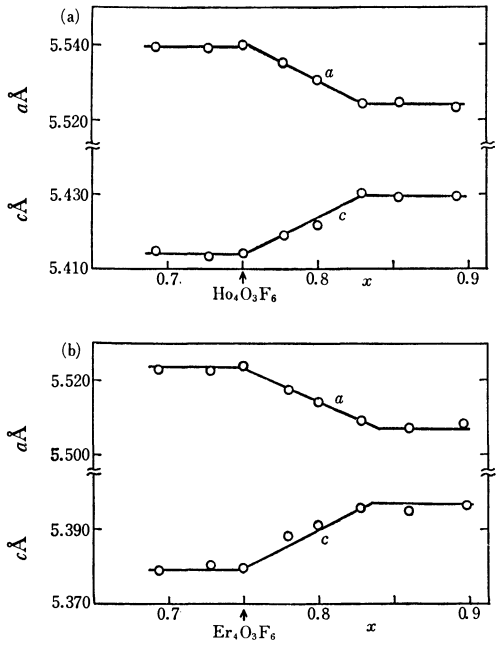

Fig. 5. Lattice parameter of rhombohedral oxyfluorides as a function of x in $HoO_x F_{3-2x}$ and $ErO_x F_{3-2x}$.
(a) holmium oxyfluoride (b) erbium oxyfluoride

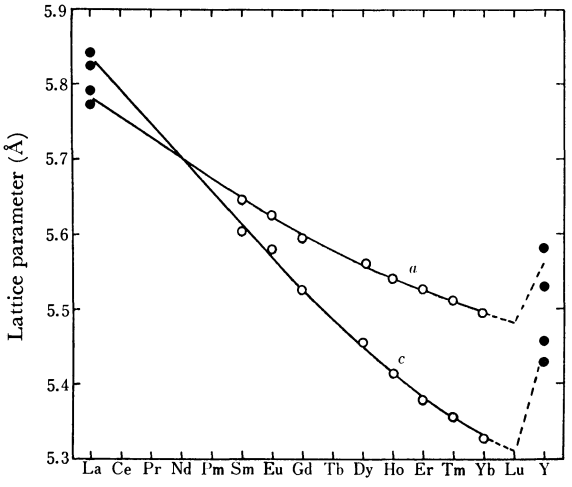

Fig. 6. Lattice parameter of tetragonal oxyfluorides, $Ln_4O_3F_6$, as a function of atomic number of rare earth element.
○ this work, ● Zachariasen, Ref. 1 (The values of a axis are $\sqrt{2}$ times as large as those obtained by Zachariasen.)

centered structure exist, and the relative intensities suggested a fluorite-type structure. In specimens containing only the rhombohedral phase ($x=1$), or only the tetragonal phase ($x=0.75$), or both the rhombohedral and tetragonal phases ($0.75<x<1$), only the fluorite-type phase was obtained by quenching. If two-phase specimens contained the rhombohedral oxyfluoride and Sm_2O_3, or the tetragonal oxyfluoride and SmF_3, quenching produced the fluorite-type phase and left the Sm_2O_3 or SmF_3 respectively unchanged. Consequently, it can be considered that a transformation from the rhombohedral and tetragonal phases to the fluorite-type phase may occur. The correlation between the lattice parameter of the fluorite-type SmO_xF_{3-2x} and the parameter, x, is shown in Fig. 7. This curve

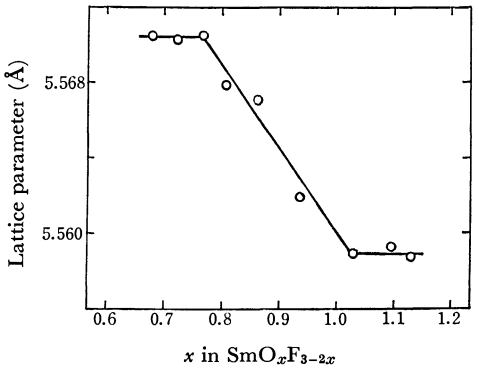

Fig. 7. Variation of the lattice parameter of SmO_xF_{3-2x} with the fluorite type structure.

shows that the lattice parameter decreases linearly with x, *i. e.*, with a decrease in the fluorine content. In all the other systems except SmF_3-Sm_2O_3, the fluorite-type phase was not obtained by quenching. In the $x>1$ region of the SmF_3-Sm_2O_3 system, a strange phenomenon was observed. The Sm_2O_3 used as the starting material had a B-type structure (Sm_2O_3-type, monoclinic), but the Sm_2O_3 found in the quenched products showed a C-type structure (La_2O_3-type, cubic). This means that a transformation of the Sm_2O_3 structure from the B-type to the C-type occurred. According to a previous study,[10] the C-type Sm_2O_3 is stable up to about 950°C and the transition process from the C-type to the B-type is completed within several days at 950°C and within about 1 hr at 1100°C. The transformation had also been found to be irreversible. Therefore, it is conceivable that the C-type Sm_2O_3 obtained in this experiment is stabilized by the presence of small amounts of fluorine.

Discussion

The rare earth oxyfluorides with the rhombohedral-, tetragonal-, and fluorite-type structures were observed in the system of Ln_2O_3-LnF_3. The chemical composition of the rhombohedral structure corresponds to the exact stoichiometric composition, LnOF, and no nonstoichiometric composition range exists in any of the systems. However, two kinds of tetragonal structures could be identified. One is the tetragonal phase, $Ln_4O_3F_6$, with out a nonstoichiometric composition range such as those with Sm, Eu, and Tb. The other type is the tetragonal phase, $Ln_4O_3F_6$ with a comparatively large nonstoichiometric composition range, such as those with Gd, Dy, Ho, and Er. It is very interesting that, in the former type, the rare earth ion is comparatively easy to convert into the divalent ion, but in the latter one this seems to be very difficult.

In the SmF_3-Sm_2O_3 system, the rhombohedral phase, SmOF, was observed at a ratio of 1 : 1, while the tetragonal phase, $Sm_4O_3F_6$, appeared at a ratio of 2 : 1. The fluorite-type phase was observed in the region of SmOF-$Sm_4O_3F_6$ after quenching from a high tempera-

10) S. Stephan, "Phase transformation rates of five rare earth sesquioxides(Series)," U. S. Bureau of Mines Report of investigation 6616 (1965).

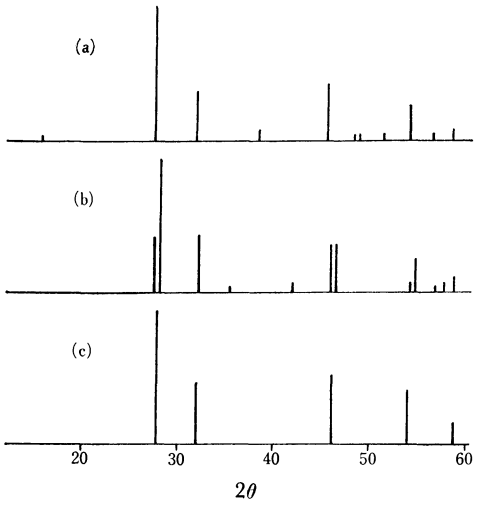

Fig. 8. Typical difraction patterns of samarium oxyfluoride.
(a) Tetragonal, (b) Rhombohedral, (c) Fluorite type

ture. This indicates that both the rhombohedral SmOF and the tetragonal $Sm_4O_3F_6$ are transformed to the cubic phase and form a complete solid solution in the high-temperature range.

Three typical X-ray patterns of the samarium oxyfluorides are illustrated in Fig. 8. The diffraction patterns of the rhombohedral- and tetragonal-type structures are very similar to that of the fluorite type. In view of those results, it is conceivable that the rhombohedral and tetragonal phases are pseudo-cubic.

Zachariasen[1] postulated that both the rhombohedral and tetragonal forms have the LaOF composition and result from a complete ordering of the oxygen and fluorine atoms into distinct sites of the unit cell. He also described the tetragonal unit cell as having the axial ratio of $c/a=\sqrt{2}$ and containing two metal atoms. The present results concerning the rhombohedral phase are in agreement with those of Zachariasen. However, it is concluded that the tetragonal phase has the ideal chemical composition, $Ln_4O_3F_6$, and that the unit cell has the axial ratio of $c/a\fallingdotseq 1$ and contains four metal atoms. Zachariasen also mentions that the tetragonal phase has a wide homogeneity range, LaO_xF_{3-2x} $(0.7<x<1.0)$, but that this phase is unstable relative to the rhombohedral phase at $x=1.0$. Therefore, in the system of LaF_3-La_2O_3 examined by Zachariasen, it is considered that the tetragonal phase, $La_4O_3F_6$, has a large homogeneity range reaching up to LaOF $(x=1)$ by chance.

The relation between the rare earth oxyfluorides, LaOF and $Ln_4O_3F_6$, is similar to that between $NaF\cdot YF_3$ and $5NaF\cdot 9YF_3$[11] in the system of NaF-YF_3, and to that between the uranium oxides, UO_2 and U_4O_9,[12] taking into consideration the fact the fluoride ion is as large as the oxide ion. In the case of the NaF-YF_3 system, two intermediate compounds, $NaF\cdot YF_3$ and $5NaF\cdot 9YF_3$, crystallize from the melt as fluorite-like cubic crystals near the middle of the system, form a continuous series of solid solutions up to the melting temperatre, and are converted to other forms at a low temperature. The $5NaF\cdot 9YF_3$ compound also forms on an ordered phase below 700°C.

As has previously been stated, the fluorite type was observed after quenching only in the SmF_3-Sm_2O_3 system, not in the other Ln_2O_3-LnF_3 systems. However, if more rapid cooling were employed, the fluorite-type structure might appear in all systems.

11) R. E. Thoma and G. M. Hebert, *Inorg. Chem.*, **2**, 1005 (1963).
12) C. A. Alexander and T. A. Shelvin, Paper No. 14, Presented at the Second Conference on Nuclear Reacter Chemistry, Gatlinburg, Tenn., Oct. 10—12, 1961, TID-7622, p. 139.

Intermolecular Forces and Rotational Phase Transition in the C_2H_2 Crystal

Masao HASHIMOTO, Michiko HASHIMOTO, and Taro ISOBE

The Chemical Research Institute of Non-Aqueous Solutions, Tohoku University, Sendai

(Received September 16, 1970)

The potential energy of the acetylene crystal was calculated as a function of the rotational molecular orientations. The potential energy of this crystal has two kinds of minima, not a double minima; one arises from the quadrupole-quadrupole interaction, to which the high-temperature is due, while the other arises from the overlap repulsion interaction with which the low temperature structure is coincident. It was suggested that the mechanism of the phase transition in this crystal is a rotational transition between the two molecular orientations.

Acetylene is known to undergo a phase transition at 133°K. The crystal structure has been determined to be T_h^6-$Pa3$ at 156°K.[1] Below 133°K however, the information given by the X-ray analysis is ambiguous.

From the observed multiplet structure of the infrared-active fundamental vibrations[2,3] of the low-temperature phase, the acetylene molecules were determined to be located at the sites of the C_{2h} symmetry.

Recently, Ito *et al.*[4] have suggested, on the basis of the Laser Raman spectrum, that the low-temperature form has a layer-type orthorhombic structure belonging to the space group D_{2h}^{18}.

In the present article we calculated the intermolecular potential energy of crystalline acetylene in the expectation that the phase transition in this crystal would correspond to the rotational transition between two molecular orientations. The results indicate that there are two stable molecular orientations in this crystal; one of them corresponds to the high-temperature structure, while the other is coincident with the low-temperature structure.

Theoretical

The theoretical foundations for the calculation of the potential energy in the case where intermolecular separations are small enough for the overlap of the molecular wavefunction to be disregarded[5-9] are due mainly to Banerjee and Salem.[10] We will list the main points briefly and apply them to the case of acetylene.

(1) The molecular wavefunction, Ψ, of an acetylene molecule is expressible as an antisymmetrized sum of the products of the one-electron molecular orbitals:

$$\Psi = |\varphi_{C-H}\bar{\varphi}_{C-H}\varphi'_{C-H}\bar{\varphi}'_{C-H}\varphi^{\sigma}_{C-C}\bar{\varphi}^{\sigma}_{C-C}\psi^{\pi 1}_{C-C}\psi^{\pi 1}_{C-C}\psi^{\pi 2}_{C-C}\psi^{\pi 2}_{C-C}|$$

with:

$$\psi_{C-H} = (di_C + 1s_H)/(2+2S_{CH})^{1/2},$$

$$S_{CH} = \int di_C 1s_H d\tau,$$

$$\psi^{\sigma}_{C-C} = (di_C + di_C)/(2+2S)^{1/2},$$

$$S = \int di_C di_C d\tau$$

$$\psi^{\pi}_{C-C} = (\pi_C + \pi_C)/(2+2S_{\pi})^{1/2},$$

and

$$S_{\pi} = \int \pi_C \pi_C d\tau,$$

where di_C and $1s_H$ are the diagonal hybrid and the $1s$ orbital centered on the carbon and hydrogen atoms, respectively. π_C is the $2p\pi$ orbital centered on the carbon atom.

(2) The ionization potential, I and I', appear in terms of the conventional van der Waals energy:

$$W_{disp} = -(3/2)R^{-6}\alpha\alpha' II'/(I+I'), \quad (2)$$

are replaced by quantum mechanically-calculable averages. The results are:

$$W_{disp} = [(A-2B+C)\{\sin\theta\sin\theta'\cos(\phi-\phi') - 2\cos\theta\cos\theta'\}^2 + 3(B-C)\{\cos^2\theta+\cos^2\theta'\} + (2B+4C)]/R^6 \quad (3)$$

with:

$$A = e^2\alpha_{\parallel}\langle(\sum_i q_{\parallel},i)^2\rangle/4,$$

$$B = e^2\alpha_{\parallel}\alpha_{\perp}\langle(\sum_i q_{\parallel},i)^2\rangle\langle(\sum_i q_{\perp},i)^2\rangle/ 2\{\alpha_{\parallel}\langle(\sum_i q_{\perp},i)^2\rangle + \alpha_{\perp}\langle(\sum_i q_{\parallel},i)^2\rangle\},$$

and

$$C = e^2\alpha_{\perp}\langle(\sum_i q_{\perp},i)^2\rangle,$$

where $\langle(\sum_i q,i)^2\rangle$ are called the quantum mechanical averages and where

$$\langle(\sum_i q,i)^2\rangle = \langle\Psi|(\sum_i q,i)^2|\Psi\rangle.$$

$q_{\parallel},i$ and $q_{\perp},i$ are the coordinates of the ith electron along the directions respectively parallel to and perpendicular to the molecular symmetry axis (C–C bond). $\alpha_{\parallel}$ and $\alpha_{\perp}$ are the corresponding components of the polarizability. θ and θ' are the angles which the two molecules, separated by the distance R, make with a line joining their center of gravity. φ and φ' are their azimuthal angles.

(3) The repulsive energy can be expressed as the sum of the interaction energies between individual atoms of the two molecules:

*1 Present address: Department of Pathology, Faculty of Medicine, Tohoku University, Sendai.

1) T. Sugawara and E. Kanda, *Sci. Rept. Res. Inst., Tohoku Unv. Ser.* **A4**, 607 (1952).
2) G. L. Bottger and D. F. Eggers, *J. Chem. Phys.*, **40**, 2010 (1966).
3) A. Anderson and W. H. Smith, *J. Chem. Phys.*, **44**, 4216 (1966).
4) M. Ito, T. Yokoyama, and M. Suzuki, *Spectrochim. Acta*, **26A**, 695 (1969).
5) J. N. Murrel, M. Randic, and D. R. Williams, *Proc. Roy. Soc. (London)*, **A284**, 566 (1965).
6) L. Salem, *Discuss. Faraday soc.*, **40**, 150 (1965).
7) J. I. Musher and L. Salem, *J. Chem. Phys.*, **44**, 2943 (1966); *Mol. Phys.*, **12**, 475 (1967).
8) J. N. Murrel and G. Shaw, *J. Chem. Phys.*, **46**, 1768 (1967).
9) D. A. McQuarrie and J. O. Hirschfelder, *ibid.*, **47**, 1775 (1967).
10) K. Banerjee and L. Salem, *Mol. Phys.*, **11**, 405 (1966).

$$W_{\text{repl}} = \sum_{i>j}\{V(H_i \cdots H_j) + V(H_i \cdots C_j)\} \quad (4)$$

with $V(H_i \cdots H_j)=21.3\times S^2/R$ and $V(H_i \cdots C_j)=49.0\times S^2/R$[11] where $V(H_i \cdots H_j)$ and $V(H_i \cdots C_j)$ are the intermolecular hydrogen-hydrogen and hydrogen-carbon repulsion energies respectively.[11] S is the overlap integral of $1s$ hydrogen atoms separated by the distance R. The C···C repulsion energy may be ignored, as usual.

(4) The pair potential energy between the molecules in the acetylene crystal is made up of Eqs. (3) and (4):

$$W = W_{\text{disp}} + W_{\text{repl}} \quad (5)$$

The potential energy of the crystal is, then, obtained by summing (5) over all the molecules in the crystal.

In this paper, besides the above interactions, we will also consider the following interaction energy and will examine the validity of the pair additivity assumption in the case of the acetylene crystal.

The acetylene molecule has a quadrupole moment of 3.00×10^{-26} c.g.s.e.s.u.;[16] therefore, at least the quadrupole-quadrupole interaction must be considered. This interaction can be expressed as:

$$\begin{aligned}\mathcal{Q}_{ab} = {} & 3qq'[1-5\cos^2\theta-5\cos^2\theta'+17\cos^2\theta\cos^2\theta' \\ & + 2\sin^2\theta\sin^2\theta'\cos(\varphi-\varphi') \\ & + 16\sin\theta\sin\theta'\cos\theta\cos\theta'\cos(\varphi-\varphi')]/4R^5, \quad (7)\end{aligned}$$

where the q's are the observed quadrupole moments of the acetylene molecule and where the θ's and φ's are as defined in Eq. (3).

If the molecules of the polarizabilities, α_a, α_b, and α_c, make an abc triangle, the three-body non-additive force may be expressed as follows:[17,18]

$$E_3 = (9/16)\times I\times\alpha^3\times(3\cos\gamma_a\cos\gamma_b\cos\gamma_c+1)/(R_{ab}{}^3R_{bc}{}^3R_{ca}{}^3), \quad (8)$$

where the γ's are the inner angles of the triangle, the R's are the distances among the three molecules, α is the average polarizability, and I is the mean excitation energy, which can be considered as the ionization potential of the molecules. In the acetylene molecule, $I=11.40$ eV and $\alpha=33.3\times10^{-25}$ cm^3;[19] therefore, for the nearest molecules in the crystal, E_3 is of the order of 10^{-5} kcal/mol; this can be ignored in comparison with the other interaction energies.

Numerical Calculations

If the phase transition of the acetylene crystal corresponds to the transition between the two molecular orientations, the calculated potential energies for various orientations and displacements of the molecules in the crystal should have minima of more than two.

For the displacements of the molecules, no consideration will be made now because there is no drastic structural change which causes a large elongation or

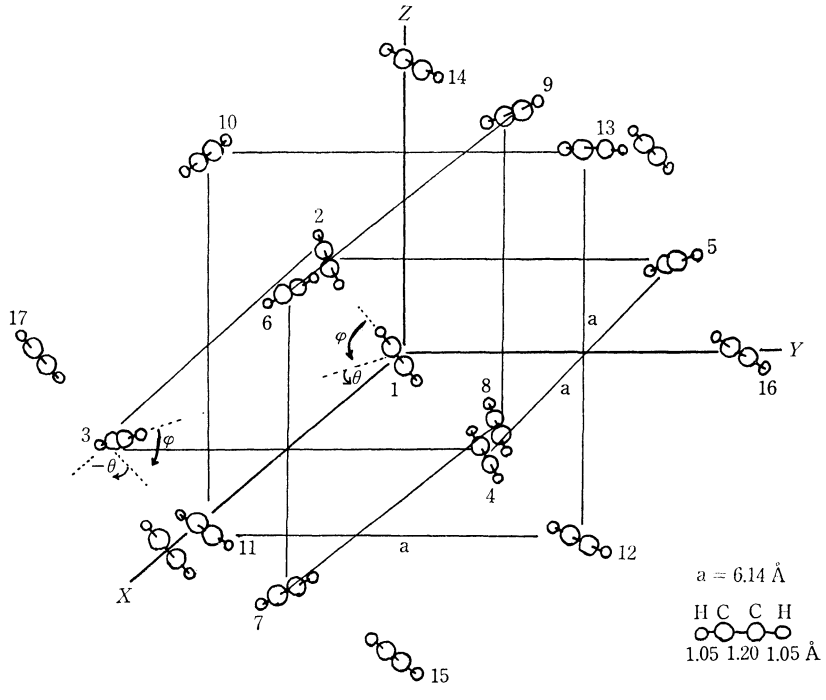

Fig. 1. Face centered position of cubic lattice of C_2H_2 crystal.

11) The coefficient of 21.3 was determined by Banerjee and Salem,[10] so $V(H\cdots H)=k\times S^2/R$ reproduces the H···H potential obtained from the scattering experiments of Amdur *et al.*[12-14] The coefficient of 49.0 was obtained by using the empirical relation due to Adrian,[15] connecting $V(H\cdots H)$ to $V(H\cdots C)$: $V(H\cdots H)=k'\times V(H\cdots C)$.

12) I. Amdur, E. A. Mason, and A. L. Harkness, *J. Chem. Phys.*, **22**, 1071 (1954).

13) I. Amdur and E. A. Mason, *ibid.*, **25**, 632 (1956).

14) I. Amdur, M. S. Longmire, and E. A. Mason, *ibid.*, **35**, 895 (1961).

15) F. J. Adrian, *ibid.*, **28**, 608 (1958).

16) W. Gordy, W. V. Smith, and R. Trambarulo, "*Microwave Spectroscopy*," Wiley, N. Y. (1953), p 345.

17) B. M. Axilrod and E. Teller, *J. Chem. Phys.*, **11**, 299 (1943).

18) B. M. Axilrod and E. Teller, *ibid.*, **19**, 719 (1951).

19) K. L. Wolf, H. Briegleb, and H. A. Stuart, *Z. Physik. Chem.*, **B17**, 429 (1929).

contraction of the lattice during the phase transition.[20] The displacements of the molecules will be discussed in detail in future works of this series.

In the present investigation we have made the calculations on the basis of Eqs. (3), (6), and (7) for various rotational orientations of the molecule.

We start from the structure in which the centers of gravity of the molecules are located on the face-centered position of the cubic lattice, with the unit-cell dimension of $a=6.14$ Å (see Fig. 1).

With respect to the central molecule, 1, at the origin of the coordinate, there are 18 first-neighbour molecules. We calculated the dispersion and quardrupole-quadrupole interaction energies for the molecules from the 1st to 5th nearest neighbours, but the repulsion energy for the 1st neighbours only. The 5th-nearest neighbours are separated from the point of origin by 30 Å.

Two kinds of molecular rotation are considered. One is the rotation measured by the deflection of the molecular axis from the (100) plane, and the other is the rotation measured by the deflection from the (011) plane. The angle of the former is indicated by φ, and the latter, by θ.

The integrals appearing in the quantum-mechanical averages and the overlap integrals are calculated using Simpson's formula.[21] All the computational work in this paper was done at the Computer Center of Tohoku University using the NEAC 2200-500-model Computer System.

Results and Discussion

Figures 2 and 5 indicate the variation in the dispersion energy with φ and θ. In Fig. 2 the values

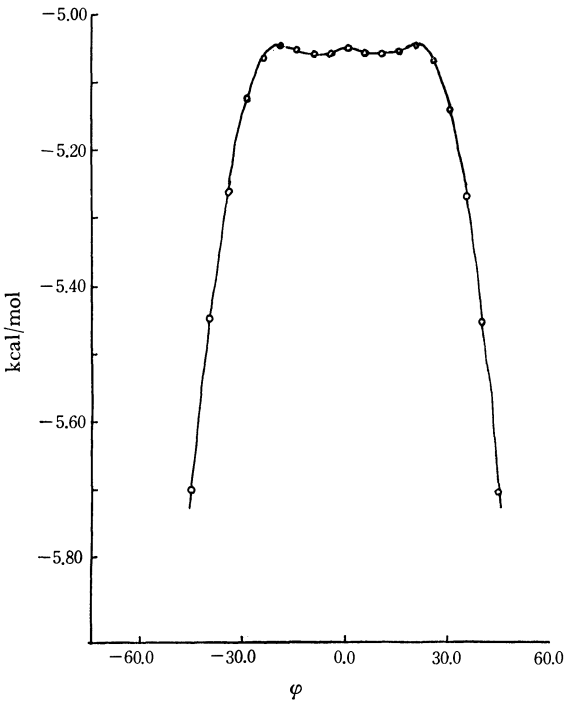

Fig. 2. Dispersion energy of C_2H_2 crystal.

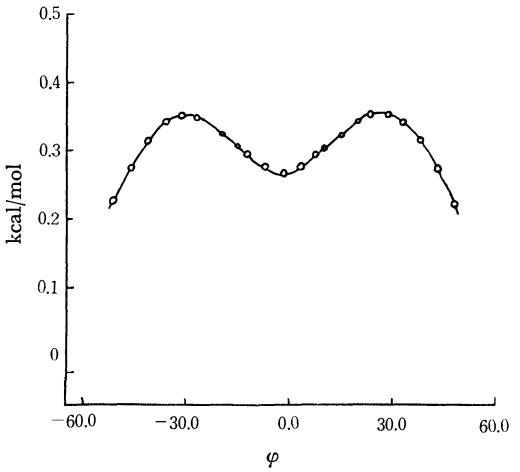

Fig. 3. Quadrupole Interaction energy of C_2H_2 Crystal.

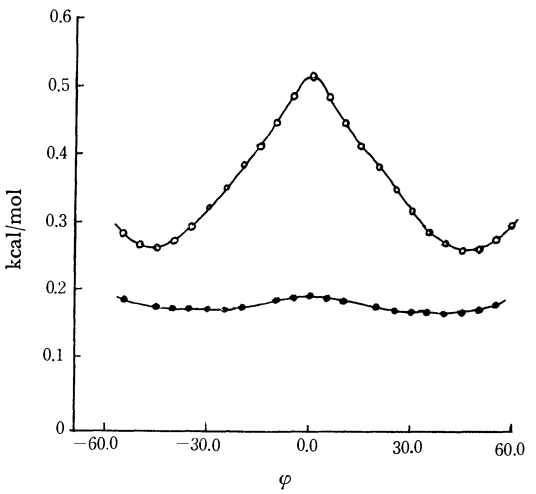

Fig. 4. Overlap repulsion energy of C_2H_2 crystal.
-○-○- H……H, -●-●- C……H

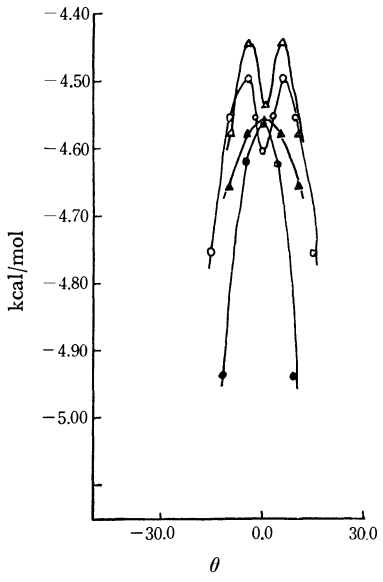

Fig. 5. Dispersion energy of C_2H_2 crystal
-○-○- $\varphi=45.0$ -△-△- $\varphi=30.0$
-▲-▲- $\varphi=15.0$ -●-●- $\varphi=0$

20) Y. A. Schwartz, A. Ron and, S. Kimel, *J. Chem. Phys.*, **51**, 1666 (1969).
21) F. B. Hildebrand, "*Introduction to Numerical Analysis*," McGraw-Hill, (1956).

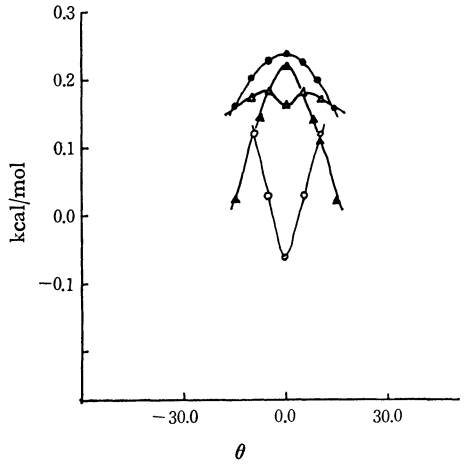

Fig. 6 Quadrupole-quadrupole interaction energy of C_2H_2
-●-●- φ= 0.0 -▲-▲- φ=15.0
-△-△- φ=30.0 -○-○- φ=45.0

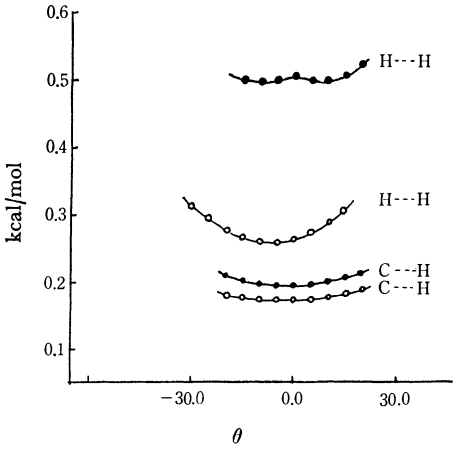

Fig. 7. Repulsion energy of C_2H_2
-●-●- φ=0.0 -○-○- φ=45.0

when θ is zero are indicated. The curves in which θ is different from zero are all more or less similar to the curve in Fig. 2 whenever θ is smaller than ± 10 degrees.

Figure 5 shows that the depth of the potential minimum decreases as φ becomes smaller.

The overlap repulsion energies are indicated in Fig. 4 and in Fig. 7. As we defined the dispersion attraction energy as negative, the repulsive energies are expressed in positive terms. When θ is zero, the curve indicating the variation with the φ has a minimum point at φ= 45°. When φ is constant, the variation with the θ has a minimum when θ is zero, as may be seen from Fig. 7.

The quadrupole interaction energy curves are indicated in Figs. 3 and 6. As in the case of the dispersion energy, the depth of the potential minimum seen in Fig. 6 decreases as the φ becomes smaller and disappears at φ=0.

No one of the above three interaction energies has double potential minimum, contrary to our expectations. However, the potential curves against φ may be worthy of note. In overlap repulsion energy curves the interaction energy has a minimum point at φ=45°, while in quadrupole-quadrupole interaction it has a minimum point at φ=0°. In short, the potential energy of crystalline acetylene has no double minima, but it has two kinds of minima. One arises from the overlap repulsion, and the other, from the quadrupole-quadrupole interaction.

Let us consider which of these two is the more stable. It may be seen from the curves in Figs. 5, 6, and 7 that when φ=0° the quadrupole-quadrupole and dispersion interaction energies reach a maximum at θ=0°, where the repulsion energy for H···H is at a minimum. On the contrary, when φ=45°, not only the repulsion but also the quadrupole-quadrupole and dispersion interaction energies have minima at θ=0°. Therefore, the orientation corresponding to φ=45° is more stable than the molecular orientation corresponding to φ=0°. We have assumed, therefore, that the former molecular orientation will be realized in low-temperature regions. The crystal structure proposed by Ito *et al.* for the low-temperature phase coincides with the structure of φ= 45°.

On the other hand, the molecular orientation corresponding to φ=0° coincides with the structure determined by X-ray analysis by Sugawara *et al.* for the high-temperature form.

The calculated lattice energy of the high-temperature form is 5.1 kcal/mol, while the experimental one[22] is 5.5 kcal/mol. Their coincidence is also quite good.

In conclusion, the potential energy of crystalline acetylene has two kinds of minima, not double minima; one arises from the quadrupole-quadrupole interaction, to which the high-temperature structure is due, and the other, from the overlap repulsion interaction, to which the low-temperature structure corresponds.

22) D. McIntosh, *J. Phys. Chem.*, **11**, 306 (1907).

The Crystal and Molecular Structure of π-Cyclooctenyl-π-cycloocta-1,5-dienecobalt, $Co(C_8H_{13})(C_8H_{12})$

Shigetaka KODA,* Akio TAKENAKA, and Tokunosuké WATANABÉ
Faculty of Science, Kwansei Gakuin University, Nishinomiya
(Received October 9, 1970)

The crystal structure of π-cyclooctenyl-π-cycloocta-1,5-dienecobalt, $Co(C_8H_{13})(C_8H_{12})$, has been established by successive Fourier analyses. The atomic parameters were refined by least-squares techniques using three-dimensional X-ray data to an R factor of 0.125. The complex molecule crystallizes in the space group $P2_1/c$ with four molecules in the unit cell of dimensions: $a=10.78$, $b=7.30$, $c=17.81$ Å, $\beta=104.2°$. The four cobalt atoms lie nearly on the face-centered positions in the unit cell and are sandwiched between the two ligands, cyclooctenyl C_8H_{13} and cyclooctadiene C_8H_{12}. The seven nearest Co···C distances range from 2.02 Å to 2.09 Å. Atoms Co, C(1), C(3) and the respective centers of the two double bonds, C(9)–C(16) and C(12)–C(13), in C_8H_{12} ring are coplanar to within 0.08 Å. The conformation of C_8H_{13} is of the tub form and C_8H_{12} of the boat form. The two lengths of the double bonds in C_8H_{12} are 1.41 Å and 1.39 Å, while those in the allyl part in C_8H_{13} are 1.35 Å and 1.46 Å, respectively. The average distance of the remaining twelve C–C bonds is 1.54 Å.

π-Cyclooctenyl-π-cycloocta-1,5-dienecobalt was prepared by Otsuka and Rossi.[1] They reported the formation of $CoH(dp)_2$ [dp=1,2-bis(diphenylphosphino)-ethane] when this complex was treated with an excess of dp and the release of cyclooctene upon thermal decomposition. The latter is in contrast to the thermal decomposition of bis(cycloocta-1,5-diene)nickel, $Ni(C_8H_{12})_2$ which yields only cyclooctadiene and metallic nickel. On the basis of a NMR and IR study, they proposed two possible molecular structures in each of which two hydrogen atoms on the octenyl ligand are found at exceptionally short distances from the cobalt atom. Thus the reactivity of this complex was attributed to the proximity of the two hydrogen atoms to the cobalt atom. In order to clarify the postulated structures, particular emphasis being laid on the role of the hydrogen atoms, we have undertaken a three-dimensional X-ray crystal analysis of $Co(C_8H_{13})(C_8H_{12})$. A preliminary account of this work has already been reported.[2]

Experimental

Crystals of π-cyclooctenyl-π-cycloocta-1,5-dienecobalt were kindly provided by Professor S. Otsuka. They were recrystallized as brilliant black plates from *n*-hexane solutions. Specimens used in this investigation were sealed in thin-walled glass capillaries and were held below 0°C during experiments to prevent oxidative and thermal decompositions. Oscillation and Weissenberg photographs taken with Fe$K\alpha$ radiation exhibited a monoclinic symmetry with space group $P2_1/c$. The lattice parameters were obtained from ($0kl$) and ($h0l$) Weissenberg photographs superimposed by silicon powder patterns and were refined by a least-squares method. In order to collect the three-dimensional intensity data, equi-inclination integrating Weissenberg photographs were taken with Mn-filtered Fe$K\alpha$ radiation from $0kl$ to $6kl$ and from $h0l$ to $h4l$, using a multiple-film technique. The intensities were visually estimated using a calibrated scale. Thus, 1043 independent non-zero reflections were observed. These relative intensities were corrected for Lorentz and polarization factors and were placed on an absolute scale by Wilson's methods. No absorption correction was applied since $\mu R \simeq 1$. The crystal data are summarized in Table 1.

Table 1. Crystal data of π-cyclooctenyl-π-cycloocta-1,5-dienecobalt, $Co(C_8H_{13})(C_8H_{12})$

Monoclinic	$a=10.78\pm0.03$ Å
	$b=7.30\pm0.02$
	$c=17.81\pm0.04$
	$\beta=104.2\pm0.1°$
U	1361.6 Å^3
Dc	1.35 g/cm^3
Z	4
Space group	$P2_1/c$
μ	30.5 cm^{-1} (for Fe$K\alpha$)

Structure Determination

A three-dimensional sharpened Patterson function showed three large peaks at (1/2, 0, 1/2), (1/2, 1/2, 0), and (0, 1/2, 1/2). This vector set implies that the arrangement of the cobalt atoms is of the face-centered type so that these atoms lie either on the two sets of special positions (centers of symmetry) or on the general positions with $x \fallingdotseq 1/4$, $y \fallingdotseq 0$, $z \fallingdotseq 1/4$. The latter case was chosen because the complex molecule was expected to be noncentro-symmetric. The symbolic addition procedure was applied, but this attempt was not successful owing to a pseudo-symmetry arising from the arrangement of the cobalt atoms.

The positions of the cobalt atom were refined by a diagonal-matrix least-squares method, and a Fourier synthesis phased on the metal atom alone was carried out. All of the sixteen carbon atoms were satisfactorily located by successive Fourier analyses. After several cycles of refinement with isotropic temperature factors for all the atoms, the discrepancy factor R, $R=\sum||F_o|-|F_c||/\sum|F_o|$, dropped to 0.16. The positional and anisotropic thermal parameters were further refined by a block-diagonal-matrix least-squares method to the R value of 0.125. The final atomic coordinates and

* Present address: Department of Chemistry, Faculty of Science, Osaka City University, Sumiyoshi-ku, Osaka.

1) S. Otsuka and M. Rossi, *J. Chem. Soc., A*, **1968**, 2630.
2) S. Koda, A. Takenaka, and T. Watanabé, *Chem. Commun.*, **1969**, 1293.

TABLE 2 (a). THE FINAL ATOMIC COORDINATES WITH ESTIMATED STANDARD DEVIATIONS IN PARENTHESES

Atom	x/a	y/b	z/c	Atom	x/a	y/b	z/c
Co	0.2460(3)	−0.0066(4)	0.2565(2)	C-9	0.2032(22)	−0.0258(34)	0.3606(11)
C-1	0.0896(19)	−0.1571(29)	0.1954(11)	C-10	0.2584(24)	0.1469(33)	0.4125(13)
C-2	0.0944(19)	0.0260(30)	0.1640(10)	C-11	0.3096(29)	0.2925(32)	0.3715(16)
C-3	0.2003(20)	0.0858(30)	0.1435(12)	C-12	0.3491(23)	0.2301(30)	0.2990(14)
C-4	0.2932(24)	−0.0230(38)	0.1031(13)	C-13	0.4320(21)	0.0831(31)	0.2942(12)
C-5	0.2201(25)	−0.1117(34)	0.0247(13)	C-14	0.4996(20)	−0.0285(40)	0.3696(13)
C-6	0.1024(22)	−0.2263(30)	0.0283(11)	C-15	0.4257(20)	−0.1932(34)	0.3855(13)
C-7	0.1186(21)	−0.3753(31)	0.0874(12)	C-16	0.2800(22)	−0.1728(30)	0.3516(11)
C-8	0.1565(22)	−0.3253(27)	0.1745(12)				

TABLE 2 (b). THE ANISOTROPIC TEMPERATURE FACTORS IN THE FORM OF
$\exp\{-(B_{11}h^2+B_{22}k^2+B_{33}l^2+B_{12}hk+B_{23}kl+B_{31}lh)\}$
(Standard deviations in parentheses)

Atom	B_{11}	B_{22}	B_{33}	B_{12}	B_{23}	B_{31}
Co	0.0067(3)	0.0078(5)	0.0016(1)	−0.0006(9)	0.0001(6)	0.0005(3)
C-1	0.0040(23)	0.0078(47)	0.0017(8)	−0.0033(52)	0.0013(31)	−0.0017(21)
C-2	0.0061(23)	0.0088(49)	0.0008(7)	0.0036(59)	−0.0035(32)	−0.0041(19)
C-3	0.0080(27)	0.0054(43)	0.0018(8)	0.0017(57)	−0.0018(32)	−0.0001(24)
C-4	0.0118(31)	0.0169(63)	0.0025(9)	−0.0167(79)	−0.0032(43)	0.0034(27)
C-5	0.0120(33)	0.0137(58)	0.0020(9)	−0.0086(73)	−0.0029(39)	0.0047(27)
C-6	0.0091(28)	0.0075(48)	0.0010(7)	0.0012(60)	0.0018(32)	−0.0023(23)
C-7	0.0050(24)	0.0097(51)	0.0023(8)	−0.0016(56)	−0.0018(34)	−0.0008(23)
C-8	0.0094(28)	0.0002(41)	0.0021(9)	−0.0036(53)	−0.0032(30)	0.0005(25)
C-9	0.0100(27)	0.0132(58)	0.0011(7)	−0.0017(70)	0.0002(36)	0.0008(22)
C-10	0.0095(30)	0.0126(56)	0.0027(9)	−0.0010(66)	−0.0087(38)	0.0037(27)
C-11	0.0178(42)	0.0040(49)	0.0042(12)	−0.0068(75)	−0.0025(41)	0.0060(36)
C-12	0.0100(30)	0.0048(48)	0.0033(10)	−0.0136(63)	−0.0021(37)	−0.0001(27)
C-13	0.0068(27)	0.0088(46)	0.0023(9)	−0.0156(58)	−0.0049(35)	0.0007(24)
C-14	0.0035(22)	0.0270(77)	0.0027(9)	0.0014(71)	0.0079(47)	−0.0030(22)
C-15	0.0032(23)	0.0161(58)	0.0029(10)	0.0049(60)	0.0054(39)	−0.0006(24)
C-16	0.0098(28)	0.0090(48)	0.0009(7)	0.0002(61)	−0.0001(30)	0.0033(23)

anisotropic temperature factors of the form: $\exp\{-(B_{11}h^2+B_{22}k^2+B_{33}l^2+B_{12}hk+B_{23}kl+B_{31}lh)\}$ together with their estimated standard deviations are given in Table 2(a) and (b). The observed and calculated structure factors are listed in Table 3. The scattering factors of Co^{+1} and C were taken from International Tables for X-ray Crystallography (1962). The oxidation state of the cobalt atom will be discussed later. All the numerical calculations were carried out on a FACOM 270-20 computer of this University using the programs written in our laboratory.

Results and Discussion

Figure 1 shows the view of the molecule along the *b*-axis, where the hydrogen atoms are given in positions postulated on the assumption of the conventional bond distances and angles. The numbering scheme for the carbon and hydrogen atoms are also shown. Interatomic bond distances and angles and their estimated standard deviations are summarized in Table 4 (a) and (b).

As is shown in Fig. 1, the cobalt atom is sandwiched between the two ligands, cyclooctenyl C_8H_{13}, and cyclooctadiene C_8H_{12}. Interatomic distances from the metal atom to the seven nearest carbon atoms, C(1), C(2), C(3), C(9), C(12), C(13), and C(16), fall in the range from 2.02 Å to 2.09 Å. Atoms Co, C(1), C(3), and the respective centers of the two double bonds, C(9)–C(16) and C(12)–C(13), in C_8H_{12} ring are coplanar to within 0.08 Å. We shall designate the plane thus described as the Co-plane. The equation of the plane and the deviations of the respective atoms from the plane are listed in Table 5. Figures 2 and 3 represent the geometry around the cobalt atom which are the projections along the directions parallel and normal

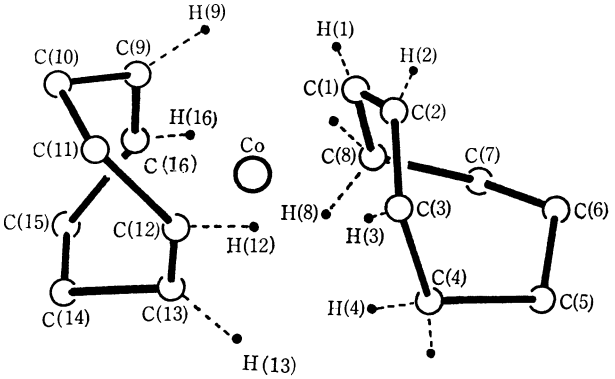

Fig. 1. The molecular structure viewed along the *b* axis.

TABLE 3. OBSERVED AND CALCULATED STRUCTURE FACTORS

H	K	L	FO	FC	H	K	L	FO	FC	H	K	L	FO	FC	H	K	L	FO	FC	H	K	L	FO	FC	H	K	L	FO	FC
0	0	2	92.05	-125.87	6	0	12	16.84	-22.48	-6	0	10	36.15	38.25	1	1	15	28.23	22.32	5	1	12	13.67	-21.38	-3	1	5	97.49	-103.16
0	0	4	38.55	-18.32	8	0	0	38.94	35.16	-6	0	12	49.68	-44.82	2	1	0	91.98	73.67	5	1	13	21.58	-26.71	-3	1	7	76.43	87.91
0	0	6	33.26	-35.88	8	0	2	20.51	-13.36	-6	0	14	30.12	26.76	2	1	1	36.77	-26.01	6	1	0	26.09	-18.86	-3	1	8	12.83	-10.97
0	0	8	90.36	83.90	8	0	4	34.01	36.91	-7	0	4	22.02	-22.72	2	1	2	41.69	-28.14	6	1	1	13.28	-12.49	-3	1	9	52.36	-57.89
0	0	10	57.23	-46.35	8	0	6	32.03	-34.93	-7	0	6	11.16	-9.97	2	1	4	6.53	2.29	6	1	2	11.77	7.82	-3	1	11	51.42	53.18
0	0	12	38.15	32.79	8	0	8	27.54	34.07	-7	0	8	33.95	-27.49	2	1	5	49.90	40.07	6	1	6	16.05	-16.52	-3	1	13	40.39	-47.67
0	0	14	37.83	-31.70	9	0	0	17.47	18.44	-7	0	10	29.66	25.73	2	1	6	14.62	19.62	6	1	7	15.21	-17.57	-3	1	15	20.79	20.50
0	0	16	18.17	12.53	10	0	0	7.63	-7.57	-7	0	12	16.56	-17.26	2	1	7	44.69	-39.88	6	1	9	7.12	7.39	-3	1	17	19.47	-22.36
1	0	2	37.91	31.87	10	0	2	21.79	30.82	-7	0	14	19.77	17.96	2	1	8	19.48	-13.65	6	1	11	5.47	-4.69	-4	1	1	20.80	-20.91
1	0	4	6.15	-6.42	-1	0	4	63.98	61.12	-8	0	2	46.50	-42.21	2	1	9	29.11	-24.03	7	1	0	19.26	-17.18	-4	1	2	37.19	-21.77
1	0	6	20.22	13.79	-1	0	6	49.54	39.05	-8	0	4	47.20	40.23	2	1	10	19.15	16.43	7	1	1	48.97	43.35	-4	1	3	47.04	35.96
1	0	8	67.63	-65.52	-1	0	8	11.42	19.78	-8	0	6	55.66	-46.67	2	1	12	19.35	-17.58	7	1	3	40.14	-43.50	-4	1	4	18.22	11.20
1	0	10	21.21	18.85	-1	0	10	50.55	-48.50	-8	0	8	19.15	13.69	2	1	13	31.06	33.64	7	1	5	21.07	23.43	-4	1	5	17.77	-18.16
1	0	12	23.04	-21.74	-1	0	12	75.77	75.31	-8	0	10	33.12	-32.31	2	1	15	21.51	-22.15	7	1	7	18.96	-18.17	-4	1	6	23.45	-18.90
1	0	16	20.47	-19.37	-1	0	14	16.59	-15.84	-8	0	12	33.47	33.98	3	1	0	52.59	36.12	7	1	9	24.99	34.57	-4	1	7	17.83	14.11
2	0	0	112.95	-161.42	-2	0	2	146.84	186.38	-8	0	14	26.00	-27.26	3	1	1	110.01	99.13	9	1	1	13.01	-11.76	-4	1	9	34.37	-37.57
2	0	2	54.87	-35.65	-2	0	4	83.58	-94.38	-9	0	2	10.45	-9.81	3	1	2	39.77	27.99	9	1	3	20.72	27.40	-4	1	11	23.08	27.63
2	0	4	6.99	-10.17	-2	0	6	93.26	104.11	-9	0	4	25.81	25.36	3	1	3	63.85	-62.42	9	1	5	20.75	-32.64	-4	1	13	12.85	-13.78
2	0	6	27.76	39.76	-2	0	8	78.77	-75.63	-9	0	6	17.94	-22.93	3	1	4	30.01	-26.00	-1	1	1	137.15	191.53	-4	1	15	12.18	8.76
2	0	8	80.99	-84.60	-2	0	10	67.28	70.01	-9	0	8	13.96	11.30	3	1	5	52.24	54.09	-1	1	2	15.43	11.53	-4	1	17	24.90	-29.92
2	0	10	72.68	66.01	-2	0	12	39.73	-38.42	-10	0	2	22.00	22.97	3	1	6	29.34	-24.27	-1	1	3	84.29	-97.09	-5	1	1	102.34	91.96
2	0	12	71.09	-68.48	-2	0	14	31.54	30.42	-10	0	4	26.99	-25.56	3	1	7	85.67	-79.85	-1	1	5	75.33	84.07	-5	1	2	28.60	-16.89
2	0	14	30.17	20.69	-2	0	16	9.28	-6.53	-10	0	6	30.06	29.94	3	1	8	10.19	-11.62	-1	1	6	25.82	-19.75	-5	1	3	41.06	-35.39
2	0	16	20.42	-22.33	-2	0	18	19.93	28.15	0	1	1	17.44	-11.75	3	1	9	71.49	73.59	-1	1	7	52.76	-61.80	-5	1	4	17.49	-13.35
3	0	0	53.70	-51.18	-3	0	2	38.80	43.31	0	1	2	54.18	47.44	3	1	10	25.18	24.62	-1	1	8	12.99	7.29	-5	1	5	55.55	49.01
3	0	2	50.35	-40.16	-3	0	4	16.08	-13.47	0	1	3	42.90	40.62	3	1	11	47.05	-46.82	-1	1	9	76.58	81.78	-5	1	7	44.18	-44.20
3	0	4	37.75	26.12	-3	0	6	10.88	-4.36	0	1	5	14.41	5.00	3	1	12	9.84	-8.38	-1	1	10	13.89	11.76	-5	1	9	36.87	37.49
3	0	6	33.43	-33.82	-3	0	10	20.01	18.64	0	1	6	74.55	64.79	3	1	13	35.10	30.39	-1	1	11	50.73	-52.82	-5	1	11	38.42	-41.01
3	0	8	10.52	-9.47	-3	0	12	42.51	-40.07	0	1	7	41.68	33.74	3	1	14	14.38	-19.78	-1	1	13	28.53	31.95	-5	1	13	41.38	43.00
3	0	10	18.97	15.95	-3	0	14	41.26	37.54	0	1	8	24.62	-17.31	3	1	15	14.28	-13.99	-1	1	14	17.91	16.62	-5	1	15	19.79	-15.85
3	0	12	21.67	20.21	-3	0	16	15.49	-13.93	0	1	9	32.04	-32.92	4	1	0	14.19	-9.52	-1	1	15	18.31	-12.41	-5	1	16	5.94	-5.23
3	0	14	35.21	-32.49	-4	0	2	43.46	-44.50	0	1	11	29.02	29.91	4	1	1	6.93	6.86	-1	1	17	21.83	22.14	-5	1	17	12.21	14.16
4	0	0	75.73	70.70	-4	0	4	54.21	47.21	0	1	12	36.83	33.40	4	1	2	27.57	-26.06	-2	1	1	27.67	-13.09	-6	1	1	6.27	6.93
4	0	2	77.78	-70.83	-4	0	6	69.43	-69.00	0	1	13	26.90	-27.61	4	1	3	22.70	23.82	-2	1	2	13.65	-7.00	-6	1	2	11.54	3.14
4	0	4	46.15	45.37	-4	0	8	63.68	66.02	0	1	16	8.56	7.24	4	1	4	38.56	33.83	-2	1	3	33.17	-24.79	-6	1	4	24.83	-19.64
4	0	6	75.34	-73.42	-4	0	10	66.92	-62.36	0	1	17	12.81	-15.58	4	1	7	11.20	-7.57	-2	1	4	57.84	-50.07	-6	1	5	7.91	5.67
4	0	8	92.33	96.71	-4	0	12	49.14	49.36	1	1	0	43.49	28.71	4	1	8	10.68	-12.34	-2	1	6	9.10	-6.77	-6	1	6	12.74	-12.50
4	0	10	64.05	-60.79	-4	0	14	30.89	-24.92	1	1	1	117.00	-138.62	4	1	11	24.27	29.26	-2	1	7	8.89	-8.43	-6	1	7	28.92	-30.78
4	0	12	23.54	17.21	-4	0	16	20.84	16.43	1	1	2	60.95	45.56	4	1	13	27.04	-31.32	-2	1	8	41.00	39.81	-6	1	9	41.19	44.81
4	0	14	12.18	-12.08	-5	0	2	49.99	-42.16	1	1	3	12.12	17.57	4	1	14	5.07	7.03	-2	1	9	31.82	30.44	-6	1	11	21.25	-24.34
5	0	0	32.28	-27.26	-5	0	4	36.90	33.83	1	1	4	40.22	29.47	5	1	0	17.21	8.37	-2	1	10	23.00	-19.89	-6	1	13	16.52	21.49
5	0	2	25.13	18.18	-5	0	8	34.44	39.59	1	1	5	26.65	-33.61	5	1	1	94.90	-88.25	-2	1	11	29.34	-29.82	-6	1	15	11.41	-13.01
5	0	4	10.27	15.20	-5	0	10	21.56	-22.41	1	1	6	34.63	19.29	5	1	2	28.04	-28.59	-2	1	12	9.65	-9.96	-6	1	16	11.41	-13.73
5	0	12	19.29	-19.21	-5	0	12	17.65	21.01	1	1	7	77.67	77.05	5	1	3	67.09	66.37	-2	1	13	32.13	33.80	-7	1	1	58.55	-55.74
6	0	0	78.18	-80.15	-5	0	14	23.76	-24.03	1	1	8	12.09	9.63	5	1	5	58.71	-64.15	-2	1	15	20.62	-20.17	-7	1	3	56.66	53.35
6	0	2	55.70	53.34	-5	0	16	24.83	26.27	1	1	9	86.26	-76.74	5	1	7	53.14	52.35	-2	1	17	20.09	23.51	-7	1	5	64.34	-59.49
6	0	4	47.74	-52.47	-6	0	2	52.31	46.01	1	1	11	41.46	37.01	5	1	8	11.11	15.15	-3	1	1	64.24	-61.54	-7	1	7	40.28	35.96
6	0	6	51.38	52.86	-6	0	4	58.79	-67.18	1	1	12	19.87	19.65	5	1	9	34.89	-31.32	-3	1	2	20.20	-12.31	-7	1	9	21.72	-25.06
6	0	8	43.26	-36.93	-6	0	6	47.77	51.01	1	1	13	44.15	-40.68	5	1	10	9.70	-7.52	-3	1	3	10.13	9.89	-7	1	11	20.84	24.75
6	0	10	19.79	15.78	-6	0	8	20.60	-21.53	1	1	14	11.30	-7.59	5	1	11	21.85	23.51	-3	1	4	19.64	16.78	-7	1	12	14.03	-13.50
-7	1	13	30.85	-31.37	2	2	4	76.63	-78.28	7	2	0	23.71	-21.63	-4	2	1	8.51	13.11	-8	2	6	43.66	-41.19	2	3	9	15.54	16.96
-7	1	15	21.70	22.70	2	2	6	71.63	76.94	7	2	4	14.53	14.06	-4	2	2	36.64	-39.34	-8	2	7	10.14	11.09	2	3	10	12.55	13.68
-8	1	2	25.67	17.61	2	2	7	12.89	4.16	7	2	5	15.68	-16.80	-4	2	3	16.27	14.88	-8	2	8	32.93	32.72	2	3	11	10.93	-9.85
-8	1	3	18.17	20.33	2	2	8	64.39	-65.93	7	2	6	18.87	-17.90	-4	2	4	37.20	42.35	-8	2	10	18.32	-17.09	2	3	13	10.03	9.84
-8	1	4	16.82	22.88	2	2	9	10.60	-11.60	7	2	7	8.65	-9.92	-4	2	5	10.14	5.31	-8	2	12	20.60	19.47	2	3	14	8.24	-4.02
-8	1	9	19.52	-26.91	2	2	10	61.34	61.16	7	2	9	10.04	11.48	-4	2	6	65.58	-65.56	-8	2	13	11.70	-12.54	3	3	0	33.98	-30.32
-8	1	11	29.12	16.06	2	2	12	28.88	-26.47	8	2	0	32.34	33.92	-4	2	8	56.47	55.92	-8	2	14	15.68	-19.85	3	3	1	88.69	79.86
-8	1	13	18.47	-21.12	2	2	13	11.73	-13.27	8	2	2	36.62	-37.04	-4	2	9	11.04	15.15	-9	2	2	18.27	-20.00	3	3	3	75.90	-72.29
-9	1	1	17.45	20.30	2	2	14	26.22	26.15	8	2	4	15.40	14.91	-4	2	10	36.37	-39.41	-9	2	5	15.88	15.85	3	3	4	17.93	-16.73
-9	1	3	35.69	-36.74	3	2	0	55.67	-42.60	8	2	5	8.21	-10.84	-4	2	11	8.42	-13.18	-9	2	8	11.96	7.84	3	3	5	54.46	54.73
-9	1	5	42.13	42.40	3	2	1	15.27	6.08	8	2	6	20.74	-27.20	-4	2	12	20.07	16.69	-9	2	10	18.14	-21.01	3	3	6	21.18	-22.78
-9	1	7	22.73	-18.13	3	2	2	27.05	22.64	10	2	0	11.66	-12.81	-4	2	13	11.45	10.54	-9	2	11	9.34	10.27	3	3	7	49.79	-51.07
-9	1	9	15.93	14.75	3	2	3	31.72	-21.04	-1	2	2	78.61	18.80	-4	2	14	32.19	-32.49	-9	2	12	15.40	21.09	3	3	9	49.59	51.71
10	1	1	6.67	9.21	3	2	4	34.49	35.64	-1	2	3	101.15	-88.82	-4	2	16	26.80	28.40	-10	2	2	14.93	19.97	3	3	10	10.76	6.76
10	1	2	9.78	-12.41	3	2	5	19.73	16.43	-1	2	5	6.41	2.23	-4	2	17	4.46	-4.73	-10	2	4	27.73	-32.35	3	3	11	26.32	-25.46
10	1	3	14.13	-17.11	3	2	6	9.27	-8.68	-1	2	6	39.32	-41.08	-5	2	1	41.68	-32.36	-10	2	5	10.88	-11.07	3	3	13	19.35	16.81
10	1	6	12.02	11.59	3	2	11	25.64	-24.50	-1	2	7	54.60	52.95	-5	2	3	16.46	13.77	-10	2	6	22.23	22.45	3	3	14	10.26	13.47
10	1	7	12.53	-14.56	3	2	12	34.56	37.56	-1	2	9	21.04	-22.45	-5	2	4	47.82	37.42	-10	2	8	14.44	-17.51	4	3	0	26.21	21.30
10	1	9	10.12	15.89	3	2	14	26.74	-30.08	-1	2	10	28.03	-27.53	-5	2	5	21.04	13.35	0	3	1	9.26	15.23	4	3	1	6.47	3.04
0	2	0	72.32	81.30	3	2	15	14.22	16.25	-1	2	12	31.07	32.52	-5	2	6	21.44	-22.24	0	3	2	11.79	-16.72	4	3	2	24.65	-22.14
0	2	1	9.04	-2.90	4	2	0	97.29	102.45	-1	2	13	13.47	9.42	-5	2	8	34.84	31.64	0	3	3	13.32	-15.48	4	3	4	14.35	-12.69
0	2	2	83.83	-92.55	4	2	1	24.65	24.62	-1	2	14	15.95	-15.72	-5	2	10	33.09	-36.96	0	3	4	30.56	24.16	4	3	5	14.86	-11.74
0	2	4	45.52	55.77	4	2	2	84.47	-91.85	-1	2	16	24.92	16.71	-5	2	11	16.21	-15.96	0	3	5	35.63	-34.15	4	3	6	17.31	12.58
0	2	6	72.48	-74.04	4	2	3	14.15	-14.30	-1	2	17	6.95	7.89	-5	2	12	12.88	15.01	0	3	6	17.83	13.69	4	3	7	16.59	17.99
0	2	8	71.25	75.04	4	2	4	78.16	79.69	-2	2	1	14.75	5.67	-5	2	13	14.41	17.27	0	3	8	28.77	-28.55	4	3	8	8.23	9.49
0	2	9	50.03	40.06	4	2	5	9.64	-10.07	-2	2	2	15.96	24.75	-5	2	16	10.38	10.84	0	3	9	24.64	-27.92	4	3	9	9.50	-9.62
0	2	10	60.48	-63.79	4	2	6	47.65	-45.94	-2	2	3	13.66	-6.97	-6	2	1	21.10	-17.54	0	3	10	12.11	-11.18	4	3	11	11.58	9.48
0	2	11	17.26	15.17	4	2	8	53.69	52.79	-2	2	4	89.17	-83.74	-6	2	2	60.42	53.18	0	3	11	46.43	46.90	4	3	13	12.70	-19.32
0	2	12	52.96	49.26	4	2	9	11.26	8.68	-2	2	5	11.66	-14.66	-6	2	4	57.37	-61.18	0	3	12	13.44	16.01	5	3	0	14.30	-11.84
0	2	14	23.25	-23.34	4	2	10	29.26	-26.63	-2	2	6	77.13	80.49	-6	2	6	65.09	63.14	0	3	13	7.22	-3.42	5	3	1	52.45	-42.91
0	2	15	10.66	-9.32	4	2	12	22.16	22.29	-2	2	7	15.30	-16.10	-6	2	7	14.15	-12.10	1	3	0	15.16	17.49	5	3	2	7.44	3.80
0	2	16	23.00	24.61	4	2	14	25.66	-29.24	-2	2	8	60.11	-64.29	-6	2	8	26.89	-24.94	1	3	1	87.85	-84.13	5	3	3	64.53	62.56
1	2	1	16.07	-11.14	5	2	0	18.54	14.64	-2	2	9	29.82	-28.69	-6	2	10	28.01	31.07	1	3	2	12.61	-12.45	5	3	4	11.09	8.78
1	2	2	57.17	-45.51	5	2	1	9.32	-5.51	-2	2	10	29.85	31.54	-6	2	12	27.67	-29.58	1	3	3	70.89	59.13	5	3	5	36.75	-40.51
1	2	3	19.79	11.57	5	2	2	6.31	-5.01	-2	2	12	47.78	-52.67	-6	2	13	8.26	-7.28	1	3	4	20.17	16.60	5	3	6	9.55	10.88
1	2	4	34.02	-25.98	5	2	3	10.19	10.15	-2	2	13	14.84	10.54	-6	2	14	21.67	21.41	1	3	5	55.03	-53.57	5	3	7	32.73	33.06
1	2	5	51.18	39.95	5	2	4	7.08	2.68	-2	2	14	44.15	44.00	-6	2	15	13.14	14.03	1	3	6	24.33	-20.04	5	3	8	14.93	18.54
1	2	6	44.30	38.87	5	2	5	23.47	20.32	-2	2	16	25.66	-27.10	-6	2	16	12.48	-15.81	1	3	7	76.49	72.61	5	3	9	26.64	-27.30
1	2	7	11.84	-11.82	5	2	6	25.23	26.84	-3	2	1	54.18	37.45	-7	2	4	18.29	12.52	1	3	9	60.65	-61.33	5	3	11	22.76	25.32
1	2	8	9.20	-4.36	5	2	7	21.67	-20.78	-3	2	2	36.23	22.53	-7	2	6	16.77	11.49	1	3	11	56.10	51.80	5	3	12	10.74	14.65
1	2	10	14.22	13.43	5	2	8	14.97	-15.84	-3	2	3	54.98	41.54	-7	2	7	16.77	-8.73	1	3	13	26.92	-25.42	6	3	0	7.72	5.62
1	2	11	30.13	27.09	5	2	10	9.55	7.77	-3	2	4	9.83	-4.68	-7	2	8	35.03	-35.00	1	3	14	8.47	-10.79	6	3	1	12.76	-12.10
1	2	12	13.56	-14.24	5	2	11	7.18	5.99	-3	2	5	62.91	-57.37	-7	2	10	39.42	44.88	1	3	15	26.26	27.52	6	3	2	12.92	-15.27
1	2	13	23.94	-22.47	5	2	12	16.08	-19.35	-3	2	6	9.64	-5.70	-7	2	12	15.87	-15.88	2	3	0	8.25	-12.34	6	3	3	12.41	10.52
1	2	14	22.06	20.63	6	2	0	52.98	-46.17	-3	2	7	17.14	-8.22	-7	2	13	11.82	-10.76	2	3	1	46.29	-33.59	6	3	4	24.68	22.92
1	2	16	14.27	-15.91	6	2	2	69.61	73.79	-3	2	8	34.64	-36.27	-7	2	14	10.30	9.24	2	3	2	16.91	12.76	6	3	5	26.00	28.76
2	2	0	77.23	-75.49	6	2	4	48.51	-50.26	-3	2	10	26.12	26.85	-8	2	2	29.41	-30.00	2	3	4	24.49	-20.55	6	3	6	7.34	8.91
2	2	1	15.63	-11.85	6	2	6	18.26	15.41	-3	2	12	18.70	-19.44	-8	2	3	20.85	-18.53	2	3	5	41.54	33.36	6	3	7	14.66	-14.62
2	2	2	100.99	99.81	6	2	8	22.82	-20.85	-3	2	15	14.45	-14.29	-8	2	4	37.55	37.53	2	3	6	23.71	-20.54	6	3	9	7.76	-9.65
2	2	3	46.22	34.97	6	2	10	25.35	29.94	-3	2	16	29.70	-32.13	-8	2	5	14.66	11.09	2	3	8	7.59	-10.72	7	3	1	46.56	47.97

TABLE 3. Continued

H	K	L	FO	FC	H	K	L	FO	FC	H	K	L	FO	FC	H	K	L	FO	FC	H	K	L	FO	FC	H	K	L	FO	FC
7	3	2	18.63	25.46	-3	3	13	23.98	-21.71	-7	3	13	20.93	-22.95	3	4	8	20.64	-21.35	-2	4	9	20.65	18.71	-7	4	1	14.60	-15.81
7	3	3	47.96	-51.14	-3	3	14	10.14	-7.86	-7	3	14	5.77	-4.74	3	4	10	10.20	-13.83	-2	4	10	29.67	34.64	-7	4	6	12.11	12.85
7	3	4	10.09	-12.13	-3	3	15	40.96	44.27	-8	3	1	10.20	-7.16	3	4	12	14.69	16.70	-2	4	11	17.65	-18.05	-7	4	8	20.36	-17.56
7	3	5	23.36	24.99	-4	3	1	30.53	-21.14	-8	3	4	7.31	8.37	4	4	0	50.05	46.39	-2	4	12	25.48	-24.40	-7	4	10	15.48	15.15
7	3	7	23.34	-28.31	-4	3	2	29.59	18.01	-8	3	7	13.97	15.78	4	4	1	8.24	7.37	-2	4	13	15.50	-20.11	-7	4	11	8.90	-11.38
7	3	8	4.53	-5.23	-4	3	3	44.38	39.83	-8	3	9	22.27	-25.25	4	4	2	64.14	-66.73	-2	4	14	22.12	23.97	-7	4	12	12.23	-14.46
8	3	0	7.08	-6.52	-4	3	4	25.43	17.10	-8	3	11	26.57	29.70	4	4	4	29.29	29.87	-2	4	15	10.70	12.79	-8	4	1	20.95	5.43
8	3	1	6.88	6.18	-4	3	5	15.69	-16.90	-8	3	12	7.35	-7.51	4	4	6	41.09	-41.75	-3	4	1	8.88	-2.93	-8	4	2	12.63	-23.77
8	3	2	6.61	3.77	-4	3	6	15.54	21.14	-9	3	1	19.30	25.26	4	4	8	21.99	20.77	-3	4	3	6.48	-1.32	-8	4	3	26.36	13.87
8	3	5	8.05	-4.02	-4	3	7	13.76	-6.75	-9	3	3	20.99	-27.89	4	4	10	25.60	-26.31	-3	4	4	21.48	-19.22	-8	4	6	18.46	-14.89
8	3	6	4.14	-3.36	-4	3	8	10.10	10.82	-9	3	5	20.81	18.96	4	4	11	8.50	-10.75	-3	4	5	26.10	23.13	-8	4	7	10.85	-14.00
9	3	0	5.56	11.60	-4	3	9	14.13	-16.46	-9	3	7	21.14	-20.68	4	4	12	5.20	26.76	-3	4	6	17.38	19.38	-8	4	8	18.65	15.92
9	3	1	25.51	-29.41	-4	3	10	12.36	-11.02	-9	3	9	15.45	19.74	5	4	0	8.24	-8.23	-3	4	9	21.18	-22.77	-8	4	10	21.13	-17.89
9	3	2	4.71	-4.96	-4	3	11	30.22	31.98	0	4	0	63.60	65.74	5	4	1	8.31	7.13	-3	4	10	45.58	47.09	-9	4	2	7.22	-10.70
9	3	3	23.17	28.94	-4	3	12	18.78	21.21	0	4	1	11.06	-7.67	5	4	2	21.53	-19.24	-3	4	11	13.85	8.43	-9	4	4	8.88	12.95
-1	3	1	82.00	83.74	-4	3	13	13.64	-13.20	0	4	2	59.87	-68.21	5	4	7	11.73	13.95	-3	4	12	19.09	-21.23	-9	4	6	6.87	-10.05
-1	3	3	77.82	-75.87	-4	3	15	13.11	14.31	0	4	3	15.82	-13.21	5	4	9	9.50	8.21	-3	4	14	12.88	17.36	-9	4	7	5.37	-7.27
-1	3	5	34.57	41.55	-4	3	16	6.70	-2.74	0	4	4	48.66	49.22	5	4	10	12.33	17.40	-4	4	1	10.16	10.28	0	5	2	18.01	-17.17
-1	3	6	14.16	9.35	-5	3	1	40.39	33.01	0	4	5	13.14	20.73	6	4	0	31.11	-25.39	-4	4	2	49.14	-45.45	0	5	3	20.22	16.34
-1	3	7	58.64	-57.84	-5	3	2	8.47	-2.87	0	4	6	41.42	-43.01	6	4	2	43.84	42.73	-4	4	4	48.50	45.77	0	5	5	12.80	-11.68
-1	3	8	23.86	-19.41	-5	3	3	61.00	-66.12	0	4	7	12.23	-12.06	6	4	3	21.10	25.67	-4	4	5	35.38	33.46	0	5	10	10.59	11.59
-1	3	9	39.37	39.60	-5	3	4	12.38	-12.10	0	4	8	56.93	61.67	6	4	4	38.08	-40.11	-4	4	6	65.09	-66.74	0	5	11	23.14	23.65
-1	3	10	10.87	-13.10	-5	3	5	62.17	66.10	0	4	10	44.82	-46.87	6	4	5	7.41	-12.64	-4	4	7	30.96	-30.60	1	5	1	51.90	-44.91
-1	3	11	47.74	-46.30	-5	3	6	16.71	12.40	0	4	11	11.49	-9.64	6	4	6	22.55	24.97	-4	4	8	58.52	59.32	1	5	2	13.57	-12.45
-1	3	13	45.22	45.97	-5	3	7	49.11	-51.14	0	4	12	23.67	21.90	6	4	7	8.79	9.54	-4	4	9	8.22	8.60	1	5	3	51.31	46.07
-1	3	15	35.00	-38.31	-5	3	9	44.24	49.34	0	4	13	15.63	16.08	6	4	8	17.38	-20.59	-4	4	10	23.74	-23.63	1	5	4	30.47	27.27
-1	3	16	4.37	-5.33	-5	3	10	24.46	27.19	0	4	14	29.14	-32.68	7	4	0	15.41	-14.70	-4	4	11	17.24	17.84	1	5	5	52.89	-51.30
-2	3	1	19.26	17.89	-5	3	11	28.83	-32.27	1	4	0	9.58	-10.32	7	4	2	14.59	16.13	-4	4	12	20.78	24.73	1	5	6	29.94	-30.34
-2	3	2	12.93	11.38	-5	3	14	8.80	8.41	1	4	1	7.13	6.62	7	4	5	8.32	8.41	-4	4	14	9.03	-11.28	1	5	7	45.24	47.16
-2	3	3	17.69	10.61	-5	3	15	13.70	-15.73	1	4	2	20.36	17.68	8	4	0	22.22	26.18	-4	4	15	6.78	-9.19	1	5	8	21.67	25.41
-2	3	4	28.42	-27.79	-6	3	1	7.69	-4.97	1	4	3	7.80	-4.30	8	4	1	17.26	28.00	-5	4	1	7.98	6.15	1	5	9	28.74	-27.67
-2	3	5	9.50	2.35	-6	3	2	17.75	-14.82	1	4	4	13.85	-8.67	8	4	2	30.70	-40.86	-5	4	4	9.90	8.08	1	5	11	28.00	32.07
-2	3	6	17.58	10.69	-6	3	3	10.18	-6.43	1	4	6	25.95	21.64	8	4	3	15.98	-20.28	-5	4	6	30.70	-25.08	2	5	3	12.46	-10.00
-2	3	8	12.06	-5.28	-6	3	4	9.13	-7.20	1	4	10	17.17	13.03	8	4	4	27.23	32.67	-5	4	7	20.51	15.00	2	5	4	12.41	15.42
-2	3	9	17.02	19.38	-6	3	5	35.05	35.07	1	4	12	15.55	-12.28	-1	4	2	11.95	-13.09	-5	4	10	22.39	-24.85	2	5	5	21.24	17.81
-2	3	10	7.69	-4.43	-6	3	6	11.57	-8.68	2	4	0	63.42	-50.91	-1	4	3	11.07	5.74	-5	4	12	22.53	24.02	2	5	11	14.62	-16.96
-2	3	11	46.35	-49.94	-6	3	7	24.11	-25.18	2	4	1	44.56	-35.82	-1	4	4	36.08	34.46	-5	4	13	7.27	5.09	3	5	0	24.21	-26.93
-2	3	12	12.98	-12.67	-6	3	8	15.20	11.53	2	4	2	87.59	81.65	-1	4	6	10.94	-8.29	-5	4	14	4.80	-6.53	3	5	1	50.88	50.72
-2	3	13	22.03	24.94	-6	3	9	22.08	22.48	2	4	3	30.50	27.18	-1	4	7	17.69	-15.30	-6	4	1	21.35	22.86	3	5	2	48.56	42.28
-2	3	14	13.84	-12.45	-6	3	11	18.16	-20.26	2	4	4	52.15	-51.80	-1	4	8	11.14	10.95	-6	4	2	25.95	22.99	3	5	3	68.86	-65.38
-2	3	15	14.71	-14.00	-6	3	14	12.03	11.31	2	4	5	15.90	-13.69	-1	4	10	36.16	-38.57	-6	4	3	15.50	-15.91	3	5	5	34.69	31.93
-3	3	1	69.16	-62.72	-6	3	15	8.94	-12.14	2	4	6	51.19	51.92	-1	4	12	23.25	23.10	-6	4	4	39.95	-36.36	3	5	7	27.92	-26.19
-3	3	3	68.47	70.50	-7	3	1	13.53	-7.68	2	4	8	55.16	-53.55	-2	4	1	7.19	4.48	-6	4	5	20.27	-18.55	3	5	9	26.06	26.70
-3	3	4	28.48	19.70	-7	3	3	25.95	24.33	2	4	10	24.97	23.37	-2	4	2	71.72	63.64	-6	4	6	34.30	29.23	3	5	11	24.94	-35.32
-3	3	5	71.21	-66.08	-7	3	5	47.74	-46.71	2	4	12	25.48	-26.95	-2	4	3	9.72	-4.04	-6	4	7	23.49	23.68	4	5	1	18.46	-18.47
-3	3	6	12.90	-11.06	-7	3	6	10.98	-11.35	2	4	13	11.05	-12.20	-2	4	4	68.95	-60.19	-6	4	8	47.09	-44.67	4	5	6	7.95	-5.75
-3	3	7	64.03	68.62	-7	3	7	43.07	42.95	3	4	1	11.42	-7.22	-2	4	5	33.82	-30.07	-6	4	9	10.84	-5.72	4	5	7	16.42	-15.92
-3	3	8	28.88	29.07	-7	3	8	7.55	-3.60	3	4	3	10.24	-6.47	-2	4	6	61.03	63.09	-6	4	10	27.96	27.74	5	5	0	11.71	13.16
-3	3	9	38.01	-37.32	-7	3	9	24.33	-24.06	3	4	4	12.98	12.95	-2	4	7	13.60	16.52	-6	4	11	6.75	1.36	5	5	1	57.38	-58.90
-3	3	12	16.46	-17.84	-7	3	11	31.53	31.76	3	4	6	16.07	-17.68	-2	4	8	35.69	-31.56	-6	4	12	28.67	-29.47	5	5	2	8.01	-9.09
5	5	3	39.04	36.91	-5	5	12	6.17	-7.96	-2	6	9	8.95	-11.02																
5	5	5	19.76	-18.11	-6	5	2	12.18	12.24	-2	6	10	14.89	11.61																
5	5	7	18.69	24.23	-6	5	3	7.71	-12.09	-3	6	1	11.91	-10.08																
5	5	8	4.28	-5.19	-6	5	7	9.98	-7.07	-3	6	2	26.58	29.86																
6	5	0	10.67	7.12	-6	5	8	10.54	-10.79	-3	6	4	25.86	-26.66																
6	5	1	7.36	-6.61	-6	5	9	13.88	14.53	-4	6	1	12.21	11.20																
6	5	3	16.89	20.42	-6	5	11	17.05	-18.87	-4	6	2	22.87	-21.79																
6	5	4	6.22	-7.89	0	6	0	56.45	51.97	-4	6	3	14.85	-16.99																
6	5	6	7.06	8.36	0	6	1	13.39	18.38	-4	6	4	30.35	28.84																
-1	5	1	65.25	59.99	0	6	2	44.04	-44.98	-4	6	6	38.21	-42.35																
-1	5	2	23.46	-23.72	0	6	3	13.08	15.01	-4	6	8	28.39	33.02																
-1	5	3	47.06	-44.28	0	6	4	22.16	18.12	-4	6	10	10.89	-17.78																
-1	5	5	41.09	40.76	0	6	6	33.25	-33.15	-5	6	3	10.08	-12.19																
-1	5	6	19.15	20.20	0	6	7	27.15	-30.36	-5	6	4	17.54	18.25																
-1	5	7	31.16	-46.98	0	6	8	28.62	27.39	-5	6	5	9.53	-5.90																
-1	5	9	27.70	29.40	0	6	9	15.34	15.45	-5	6	6	11.04	-12.88																
-1	5	10	16.33	15.12	0	6	10	23.22	-26.71	-5	6	8	7.10	8.83																
-1	5	11	23.34	-25.68	2	6	0	44.02	-44.23	-6	6	2	19.77	23.04																
-1	5	12	8.97	-10.46	2	6	1	12.60	-12.14	-6	6	3	9.82	12.89																
-1	5	13	20.39	24.43	2	6	2	39.26	36.40	-6	6	4	15.51	-14.90																
-2	5	1	12.42	11.10	2	6	3	20.99	15.59	-6	6	5	12.28	-14.66																
-2	5	5	37.35	35.91	2	6	4	30.96	-25.67	-6	6	6	23.99	25.19																
-2	5	11	19.27	-19.29	2	6	5	15.73	-14.05	0	7	1	10.03	-11.77																
-2	5	13	17.18	20.92	2	6	6	35.97	37.50	0	7	2	9.80	-7.98																
-3	5	1	34.87	-29.02	2	6	7	16.30	11.22	0	7	5	10.94	10.11																
-3	5	3	49.45	46.11	2	6	8	31.26	-30.58	1	7	0	21.07	22.76																
-3	5	5	49.88	-47.59	3	6	1	11.69	9.74	1	7	1	39.80	-37.25																
-3	5	6	26.63	-22.93	3	6	4	18.25	20.32	1	7	2	17.37	-18.72																
-3	5	7	59.65	59.11	4	6	0	38.49	38.12	1	7	3	25.05	23.29																
-3	5	9	26.54	-25.35	4	6	1	18.70	20.95	1	7	4	8.61	-9.75																
-3	5	10	10.12	7.80	4	6	2	35.07	-33.76	1	7	5	21.74	-28.78																
-3	5	11	18.35	24.78	4	6	3	7.69	-7.69	2	7	2	8.33	-9.35																
-3	5	12	7.92	8.95	4	6	4	29.36	27.61	3	7	0	14.98	-11.96																
-3	5	13	13.53	-17.23	4	6	6	23.00	-30.47	3	7	1	37.44	38.50																
-4	5	4	9.24	-11.20	5	6	0	9.87	-10.05	-1	7	1	30.85	26.23																
-4	5	5	12.96	-10.92	5	6	1	6.72	-8.39	-1	7	2	23.09	26.37																
-4	5	7	21.62	22.50	5	6	2	8.98	12.83	-1	7	3	28.14	-24.63																
-4	5	9	16.17	-18.29	5	6	3	9.17	-9.00	-1	7	5	23.79	23.12																
-4	5	10	13.00	-17.10	6	6	0	27.87	-32.92	-2	7	1	12.82	14.54																
-4	5	11	20.33	20.53	6	6	1	7.87	-11.69	-2	7	3	25.90	-30.58																
-4	5	13	8.17	-10.73	6	6	2	25.57	33.85	-3	7	1	26.52	-32.03																
-5	5	1	20.92	18.45	-1	6	2	24.39	-25.62	-3	7	3	12.62	16.42																
-5	5	3	23.59	-23.94	-1	6	8	15.62	-15.52	-3	7	5	23.33	-28.94																
-5	5	5	30.18	27.99	-1	6	10	16.20	-17.19																					
-5	5	6	17.21	16.02	-2	6	1	22.05	-22.60																					
-5	5	7	41.36	-45.39	-2	6	2	42.05	41.55																					
-5	5	8	11.79	-11.57	-2	6	4	40.85	-38.85																					
-5	5	9	29.90	31.61	-2	6	6	34.51	33.41																					
-5	5	10	9.07	-8.63	-2	6	7	15.37	14.64																					
-5	5	11	23.41	-27.30	-2	6	8	26.57	-26.13																					

Table 4 (a). Interatomic distances (Å)
(Standard deviations in parentheses)

Co-C(1)=2.08(2)	C(3)-C(4)=1.58(4)
Co-C(2)=2.03(2)	C(4)-C(5)=1.57(3)
Co-C(3)=2.06(2)	C(5)-C(6)=1.54(4)
Co-C(9)=2.02(2)	C(6)-C(7)=1.49(3)
Co-C(12)=2.09(2)	C(7)-C(8)=1.55(3)
Co-C(13)=2.06(2)	C(8)-C(1)=1.52(3)
Co-C(16)=2.04(2)	C(9)-C(10)=1.59(3)
	C(10)-C(11)=1.47(4)
Co-C(4)=2.90(3)	C(11)-C(12)=1.53(4)
Co-C(8)=2.79(2)	C(13)-C(14)=1.59(3)
	C(14)-C(15)=1.51(4)
C(1)-C(2)=1.46(3)	C(15)-C(16)=1.55(3)
C(2)-C(3)=1.35(3)	
C(9)-C(16)=1.39(3)	
C(12)-C(13)=1.41(3)	
C(4)···C(8)=3.09(4)	
C(9)···C(12)=3.89(4)	
C(13)··C(16)=2.84(3)	
C(2)···C(6)=3.06(3)	
C(10)··C(15)=3.17(4)	
C(11)··C(14)=3.12(4)	

Table 4 (b). Bond angles (°).
(Standard deviations in parentheses)

C(1)-Co-C(2)=41.4 (0.8)
C(2)-Co-C(3)=38.6 (0.9)
C(1)-Co-C(3)=72.2 (0.8)
C(9)-Co-C(12)=86.9 (1.0)
C(16)-Co-C(13)=87.5 (0.9)
C(1)-C(2)-C(3)=120.8 (1.9)
C(2)-C(3)-C(4)=129.1 (2.0)
C(8)-C(1)-C(2)=125.8 (1.9)
C(10)-C(9)-C(16)=122.1 (1.9)
C(9)-C(16)-C(15)=127.4 (1.9)
C(11)-C(12)-C(13)=126.2 (2.1)
C(12)-C(13)-C(14)=120.3 (2.1)
C(3)-C(4)-C(5)=112.2 (1.9)
C(4)-C(5)-C(6)=115.4 (2.0)
C(5)-C(6)-C(7)=118.1 (1.7)
C(6)-C(7)-C(8)=119.4 (1.8)
C(7)-C(8)-C(1)=114.4 (1.6)
C(9)-C(10)-C(11)=114.7 (2.0)
C(10)-C(11)-C(12)=114.8 (1.6)
C(13)-C(14)-C(15)=114.5 (1.7)
C(14)-C(15)-C(16)=112.5 (1.8)

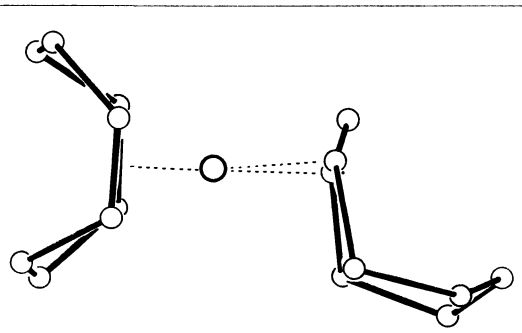

Fig. 2. The molecule viewed along a direction parallel to the Co-plane.

Table 5. Some least-squares planes within the molecule, with deviations (Å) of the atoms from the plane

a) Co-plane	
$0.6827X-0.7107Y-0.3320Z=0.2488$	
distance from this plane	
center of C(9)-C(16)	−0.06 Å
center of C(12)-C(13)	0.06
C(1)	0.07
C(3)	−0.07
Co	0.08
b) Plane C(1)-C(3)-C(4)-C(8)	
$0.5097X+0.0510Y+0.7078Z=2.9196$	
distance from this plane	
C(1)	−0.02 Å
C(3)	0.02
C(4)	−0.02
C(8)	0.02
c) Plane C(9)-C(12)-C(13)-C(16)	
$0.3342X+0.1751Y+0.8159Z=5.9179$	
distance from this plane	
C(9)	0.02 Å
C(12)	−0.02
C(13)	0.02
C(16)	−0.02

In the above equations, X, Y, and Z are the rectangular coordinates in Å unit, where $X=x+z\cos\beta$, $Y=y$, $Z=z\sin\beta$.

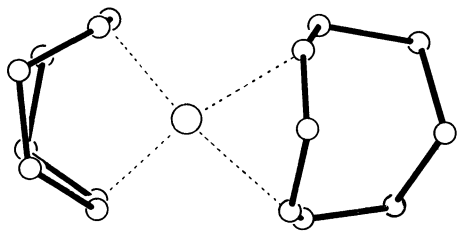

Fig. 3. The molecule viewed along the direction normal to the Co-plane.

to the Co-plane respectively. The planar configuration of the cobalt atom with the allyl part of the cyclooctenyl ligand (C(1)-C(2)-C(3)) and the two double bond centers of the cycloocta-1,5-diene ligand is clearly shown in Figs. 2 and 3. The formal oxidation state of the cobalt atom is suggested to be +1 by the reaction absorbing carbon monoxide to give a carbonyl complex, $Co(CO)(C_8H_{13})(C_8H_{12})$, from which hydridocarbonylphosphine complexes, $CoH(CO)L_3$ ($L=PPh_3$ or $PMePh_2$), are derived.[3] Thus the cobalt atom attains an outer configuration of sixteen electrons by forming the complex with the two ligands. In this case, the allyl part in the octenyl ligand acts as a four-electron bidentate donor.

The two carbon-carbon bond lengths in the allyl part differ somewhat; C(1)-C(2)=1.46 Å and C(2)-C(3)=1.35 Å. On the other hand, the three interatomic distances between the cobalt and the three carbon atoms, C(1), C(2), and C(3), are 2.08 Å, 2.03 Å, and 2.06 Å, respectively. Taking the standard deviations into con-

3) S. Otsuka and M. Rossi, *J. Chem. Soc.*, *A*, **1969**, 497.

sideration, the bonding of the allyl group to the cobalt atom is probably symmetrical. In the NMR spectrum of this complex too, signals of the symmetrical π-allyl group have been found.[1]

The average bond length of the two double bonds, C(9)–C(16) and C(12)–C(13), is 1.40 Å, giving the bond order of 1.5.[4] The remaining twelve C–C interatomic distances in the two ligands are found to be in the range 1.47 Å to 1.59 Å. These are comparable to the reported values of the single bond length in several complexes of this type.[5,6] Some of the bond angles are found definitely larger either than 109.5° for sp^3 or than 120° for sp^2 (Table 4 (a) and (b)).

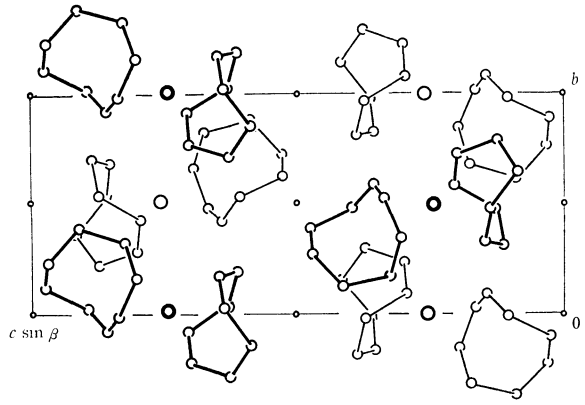

Fig. 4. The crystal structure viewed along the *a* axis.

Atoms C(9), C(12), C(13), and C(16) deviate by only 0.02 Å from a least-squares plane, and atoms C(1), C(3), C(4), and C(8) also approach planarity. The dihedral angles between the Co-plane and plane C(9)–C(12)–C(13)–C(16), plane C(1)–C(3)–C(4)–C(8) and plane C(1)–C(2)–C(3) are 93°, 100°, and 108°, respectively. The equations of these planes and deviations of the respective carbon atoms from the planes are summarized in Table 5.

The cyclooctenyl ring is of the tub form. The two parts of the ligand, C(8)–C(1)–C(2)–C(3) and C(1)–C(2)–C(3)–C(4), deviate from the planar *cis*-conformation. The angles of twist around the two bonds, C(1)–C(2) and C(2)–C(3), are 32° and 38°, respectively. The cycloocta-1,5-diene ring is of the boat form. The conformation of C(9)–C(10)–C(11)–C(12) is incompletely eclipsed; the C(11)–C(12) and C(9)–C(10) groups are skewed around the C(11)–C(12) bond, the dihedral angle between the C(9)–C(10)–C(11) and C(10)–C(11)–C(12) planes being 22°. This twisting probably arises from the repulsion between hydrogen atoms attached to the carbon atoms concerned. The conformation of C(13)–C(14)–C(15)–C(16) is similar to that of C(9)–C(10)–C(11)–C(12). Here, the dihedral angle is 27°.

Positions of the hydrogen atoms attached to all the sixteen carbon atoms were calculated based upon a C–H distance of 1.08 Å and H–C–H bond angles of 120° for sp^2 and 109.5° for sp^3. No abnormally short interatomic distances between Co and H have been found. However, there are two short interatomic distances between hydrogen atoms: H(3)···H(12) and H(4)···H(8) are 1.73 Å and 1.87 Å, respectively, which are comparable to those reported for $Ni(C_8H_{12})_2$.[5]

The arrangement of molecules in the crystal viewed along the *a* and *b* axes is shown in Figs. 4 and 5. The crystal contains discrete molecular units of π-cyclooctenyl-π-cycloocta-1,5-dienecobalt, separated by normal van der Waals distances. The shortest C···C intermolecular distances are 3.84 Å for sp^3–sp^3 and 3.66 Å for sp^2–sp^3.

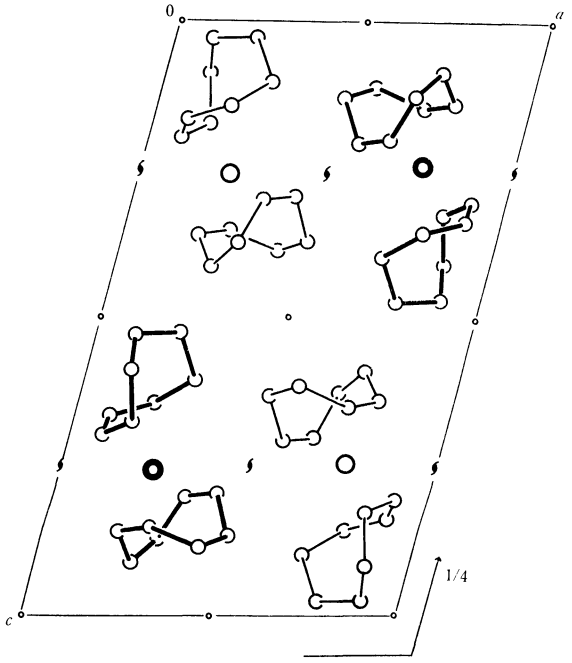

Fig. 5. The crystal structure viewed along the *b* axis.

The authors wish to express their gratitude to Professor S. Otsuka, Faculty of Engineering Science, Osaka University, for providing them with the specimens for this investigation.

4) L. Pauling, "The Nature of the Chemical Bond" 3rd Edition, Cornell University Press, New York (1960), p. 236.

5) H. Dierks and H. Dietrich, *Z. Krist.*, **122**, 1 (1965).

6) J. Coetzer and G. Gafner, *Acta Crystallogr.*, **B26**, 985 (1970).

Emission Spectra Obtained by Low Energy Electron Bombardment of Methane and Chlorinated Methanes

Teiichiro OGAWA,[1] Iwao FUJITA, Motoyoshi HATADA,* and Kozo HIROTA

Department of Chemistry, Faculty of Science, Osaka University, Toyonaka, Osaka

**Osaka Laboratory for Radiation Chemistry, Japan Atomic Energy Research Institute, Mii, Neyagawa, Osaka*

(Received September 4, 1970)

Spectroscopic studies of a molecular beam bombarded by a low energy electron beam were carried out for several simple organic molecules. The collision chamber resembled the ionization chamber of a mass spectrometer, and the electrons were accelerated at about 270 V. The spectrum of methane showed lines of excited hydrogen atoms and bands of excited CH radicals. The spectra of chlorinated methanes showed lines of excited chlorine atoms and bands of excited hydrogen chloride positive ions (HCl^{+}*) in addition. Even the spectrum of a mixture of methane and carbon tetrachloride revealed bands of HCl^{+}*. Dependence of emission intensities on target currents and gas pressures indicated the origin of the excited hydrogen atoms and CH radicals to come from direct fragmentation and the excited HCl^{+} ions from a bimolecular process.

Mass spectrometric studies have provided information on the ionization and fragmentation of electron-bombarded molecules, but it is limited to the ionized species. Though, there are a few studies[2] on the neutral species, little is known on the excitation of molecules and their fragments in the ionization chamber. Thus, spectroscopic studies on the excited species in the ionization chamber would be of use.

The electric discharge method has been used to produce unstable species in combination with their spectroscopic detection in the discharge chamber and on the cathode. Though this method is very effective for analysis, the complicated character of the discharge is a major obstacle for detailed analysis of the mechanism of fragmentation and excitation of the species concerned. Horie, Nagura and Otsuka[3] investigated collisions between molecules and electrons with known velocities and observed an unusual distribution of the rotational energy of the fragment species OH, which was produced by the electron impact of H_2O or H_2O_2. An interpretation by a statistical model was reported.[4] Emission spectra of such simple molecules as N_2, CO, and CO_2 produced by electron bombardment were reported[5] and lifetimes of their excited species were measured by a similar method,[6] though only a few organic molecules were studied.

According to the quasi-equilibrium theory, fragmentation schemes of molecules in a mass spectrometer were interpreted,[7] while by use of a molecular orbital treatment, predictions as to the initial fragmentation were made by Hirota and his co-workers.[8] To clarify the mechanism of bond scissions and to justify the theoretical interpretation, knowledge of possible excited species and their behavior is of vital importance. Thus, we carried out spectroscopic studies of a molecular beam of some simple organic molecules bombarded by electrons.

Experimental

A molecular beam was crossed perpendicularly to collide with an electron beam in a chamber as shown in Fig. 1. A rhenium filament (e) was heated by a regulated DC power supply at about 6V and 3A. Two grids (c, d) were used to push the electron into a collision chamber (a). The collision chamber was kept at 220—270 V above the filament and had a slit of 20×2 mm, through which the electron beam was introduced. A target (b) was kept at 21 V above the chamber to collect the electrons. The sample gas was introduced from the bottom through several pin holes. In order to keep the filament and its surroundings in a high vacuum, a differential pumping system was used. Typical target and chamber currents used were 300 μA and 5 mA, respectively. The rate of molecular beam was estimated to be about 10^{19} molecules/min.

The light emitted perpendicularly both to the molecular beam and to the electron beam through a quartz window (g), 11 mm in diameter, was measured with a Shimadzu GE

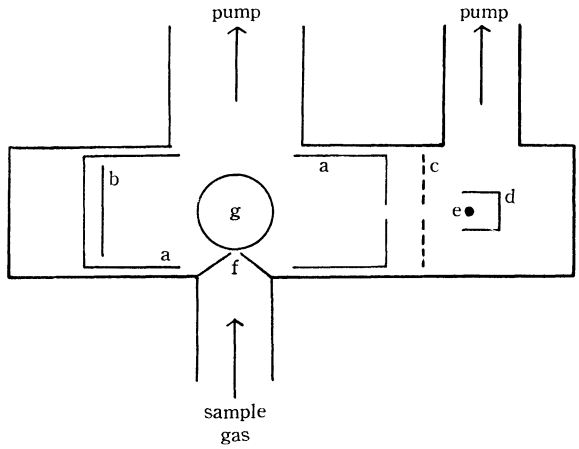

Fig. 1. Schematic diagram of the collision chamber: (a) collision chamber, (b) target. (c) grid 1, (d) grid 2, (e) rhenium filament, (f) pin holes, (g) quartz window.

1) Present address: Faculty of Engineering, Kyushu University, Hakozaki, Fukuoka.

2) D. Beck, *Discuss. Faraday Soc.*, **36**, 56 (1963); R. Clampitt and A. S. Newton, *J. Chem. Phys.*, **50**, 1997 (1969).

3) T. Horie, T. Nagura, and M. Otsuka, *J. Phys. Soc. Japan*, **11**, 1157 (1956).

4) T. Horie and T. Kasuga, *ibid.*, **19**, 1194 (1964), and papers cited therein.

5) For example, R. F. Holland, *J. Chem. Phys.*, **51**, 3940 (1969).

6) For example, T. Sawada and H. Kamada, This Bulletin, **43**, 325 (1970).

7) H. M. Rosenstock and M. Krauss, "Mass Spectrometry of Organic Ions," ed. by F. W. McLafferty, Chapter 1, Academic Press, New York (1963).

8) M. Hatada and K. Hirota, This Bulletin, **38**, 599 (1965); K. Hirota and Y. Niwa, *J. Phys. Chem.*, **72**, 5 (1968); **74**, 410 (1970).

100 grating spectrograph, equipped with a 1200 grooves/mm grating blazed for 5000 Å and with a 1000 mm collimator system. Photographic measurements were carried out with a Kodak Tri-X Pan Film in the 2500—7000 Å region for determination of wavelength and finer details of emission lines. An EMI 6256 B photomultiplier was used for photometric measurements, when the intensities were to be determined in the 2000—6600 Å region.

The wavelength was calibrated by a low pressure mercury lamp. The intensity was calibrated by a Toshiba standard tungsten lamp (1500°C). No features of water or of organic substances were observed in the spectra of nitrogen and of carbon monoxide, which were utilized to see the performance of the instrument. The mass spectrum was recorded on a Hitachi RMU-5 mass spectrometer. Methane used was a Research Grade product from Takachiho Trading Co., and other compounds were of the best grade available from Wako Pure Chemical Ind., except for CH_2Cl_2 which was from Nakarai Chemicals. All the samples were used after repeated degassing in a high vacuum.

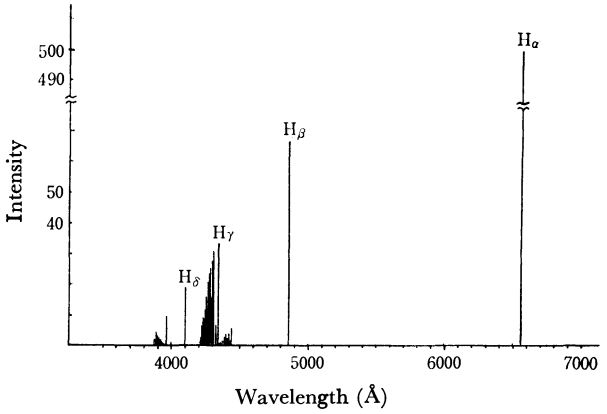

Fig. 2. Emission spectrum of methane bombarded by an electron beam.
260 V impact at 300—400μA.

Results and Discussion

A typical spectrum of methane is shown in Fig. 2. The very intense lines are the hydrogen Balmer series, which are denoted by H_α, H_β,···. Six lines were clearly observed and their relative intensities were close to those in literature,[9] though the intensity of H_α line could not be determined accurately because of the poor sensitivity of the photomultiplier used at 6500 Å. The complicated features in the 3800—4500 Å region were assigned to CH (A→X) and CH (B→X) emission.[10] The detailed spectrum in 4200—4400 Å region is shown in Fig. 3. The assignments of vibrational and rotational bands were carried out with reference to literature.[11] A few very weak lines assignable to nitrogen were found, but no bands of CO.

Dependence of emission intensity on target current is shown in Figs. 4 and 5 for H_β (4861 Å) and for CH (4312 Å), respectively. The linear relationship was found in the region of 10—600 μÅ in both cases. The

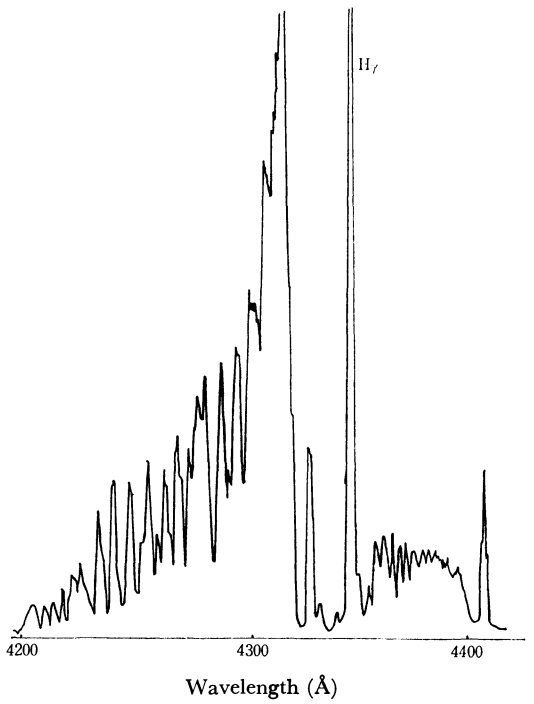

Fig. 3. Emission spectrum of methane in 4200—4400 Å region.
260 V impact at 700 μA. 200 μ slit.

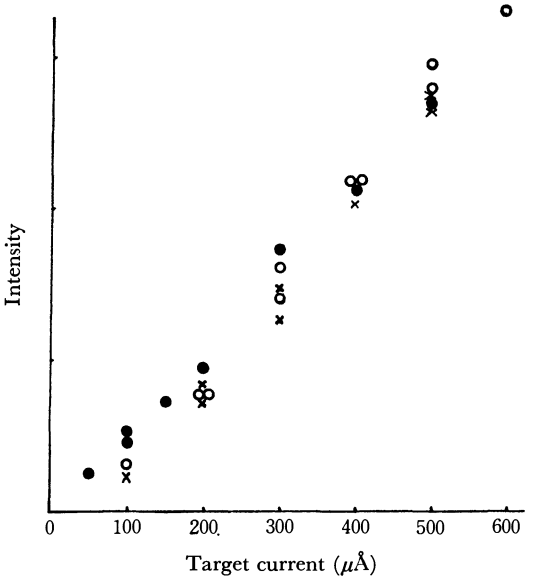

Fig. 4. Emission intensity *vs.* target current. H_β from methane at 4861 Å. For the sake of clarity, ten data were omitted below 50 μA, all of which lay on the same straight line. × 13.5 mm Hg, ● 15 mm Hg and ○ 18.5 mm Hg in the gas reservoir.

production of excited H atoms and excited CH radicals was, therefore, concluded to be a first-order reaction to the incident electrons, if it was assumed to be proportional to the target current. Dependence of emission intensities on gas pressures is shown in Fig. 6 for both H_β (4861 Å) and CH (4312 Å). The gas pressure was measured in the gas reservoir, where the pressure was assumed to be proportional to that in the collision chamber. The intensity of emission lines was in linear relation to pressure at lower pressures but the curves

9) D.A. Vroom and F. J. de Heer, *J. Chem. Phys.*, **50**, 573 (1969).
10) G. Herzberg, "Molecular Spectra and Molecular Structure," Vol. 1. Van Nostrand Reinhold, Princeton, N. J. (1950).
11) L. Gerö, *Z. Phys.*, **118**, 27 (1941).

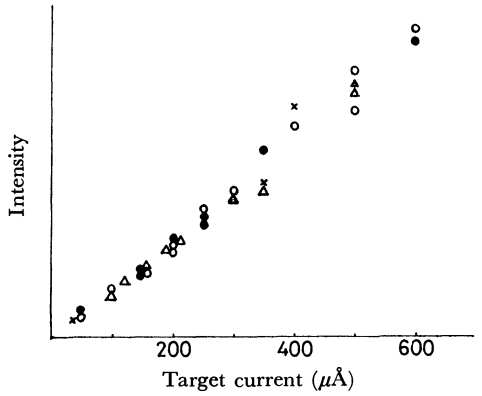

Fig. 5. Emission intensity *vs.* target current. CH* from methane at 4321 Å. For the sake of clarity, eight data were omitted below 60 μA, all of which lay on the same straight line. × 12.5 mmHg, ● 13.5 mmHg, ○ 17 mmHg and △ 21 mmHg in the gas reservoir.

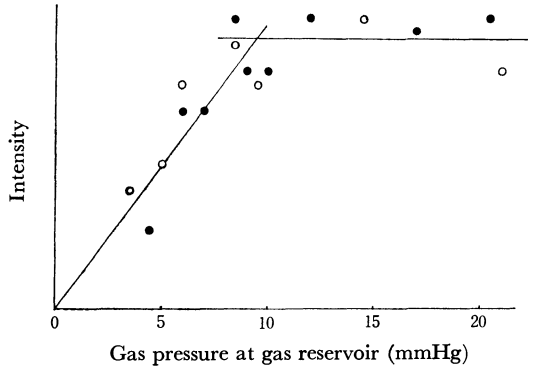

Fig. 6. Emission intensity *vs.* gas pressure. Target current was 10 μA. ○ H_β and ● CH*. Gas pressure indicated was measured not in the collision chamber but in the gas reservoir.

leveled off at a certain pressure, which was common to both H_β and CH and shifted to a lower value when the target current was increased. These results imply that collisional deactivation among excited species plays a dominant role, since the collisional deactivation between excited species and parent molecules should cause a shift to a higher value.

The linear relations lead to the conclusion that the excited hydrogen atoms and the excited CH radicals were produced by a mechanism of direct excitation and fragmentation as follows:

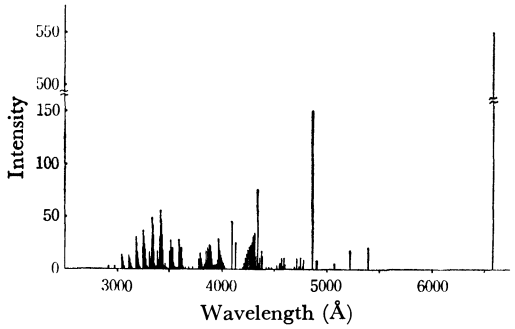

Fig. 7. Emission spectrum of methylene chloride bombarded by an electron beam. 260 V impact at 400—600 μA.

$$CH_4 + e \longrightarrow CH_4^* \longrightarrow H^*, CH^* \cdots$$

The emission spectra of chlorine derivatives of methane bombarded by an electron beam showed some additional features. The spectra of methyl chloride, methylene chloride and chloroform looked alike. A typical spectrum of methylene chloride is shown in Fig. 7. The strongest lines are assigned also to the hydrogen Balmer series, but the relative intensity of H_β to H_α in this case was found to be larger than that of methane. Emission bands of CH radicals (A→X and B→X) were also observed and are similar to those of methane.

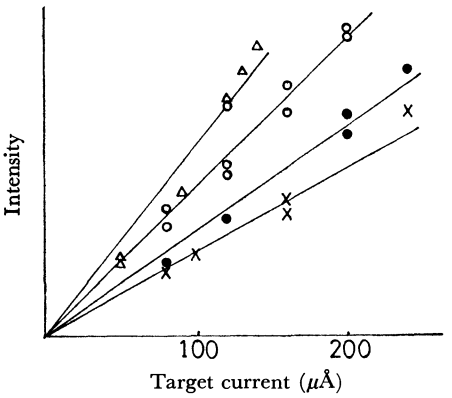

Fig. 8. Emission intensity *vs.* target current. H_β from methylene chloride at 4861 Å. × 5.5 mmHg, ● 10.5 mmHg, ○ 14.5 mmHg and △ 20 mmHg in the reservoir.

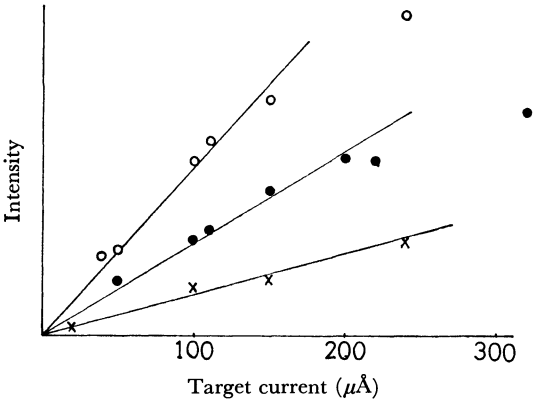

Fig. 9. Emission intensity *vs.* target current. CH* from methylene chloride at 4312 Å. × 6 mmHg, ● 9.5 mmHg and ○ 17.5 mmHg in the gas reservoir.

Dependence of emission intensities on target current is shown in Figs. 8 and 9 for H_β (4861 Å) and for CH (4312 Å), respectively. Since the intensities were in linear relation to target current, the production of excited H atoms and excited CH radicals can be concluded to be of the first order to the incident electrons. The identical argument as for methane could be applied further to the production of H* and CH* from chlorinated methanes, since the behavior of emission intensities was similar.

The most remarkable characteristic in this spectrum is shown by the bands which appear in the 2900—4000 Å region. Doublet splitting of vibrational structures is clearly observed. A detailed spectrum is shown in Fig. 10. The bands, together with vibrational and rotational structures, were assigned to HCl^+ (A→X)

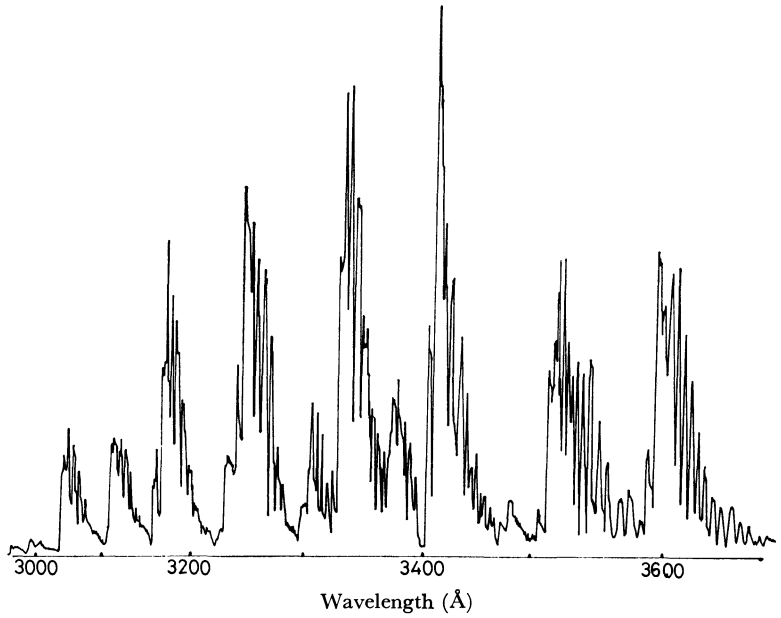

Fig. 10. Emission spectrum of methylene chloride in 3000—3700 Å region. 260 V impact at 400—600 μA.

according to the results by Brice and Jenkins,[12] and Norling.[13] The bands observed were in order of intensity: (1,0) at 3334 Å and 3410 Å, (2,0) at 3180 Å and 3245 Å, (0,0) at 3515 Å and 3595 Å, and (0,1) at 3863 Å and 3965 Å and also the (3,1) and (3,0) bands. The (1,1) (2,1) (2,2) and (4,0) bands could be pointed out. In comparison with the electrical discharge of HCl,[12] HCl^+ was found to be vibrationally excited.

The linear relations between the intensities and the amount of incident electrons as observed in the case of H and CH were not observed for HCl^+. It seems unlikely that H and CH and HCl^+ were produced by a similar mechanism. No strong peak was observed at $m/e=36$ (HCl^+) in the mass spectrum of methylene chloride; the intensity of HCl^+ was 3.5% of that of the strongest CH_2Cl^+. Since the pressure is much lower in the mass spectrometer, this suggests that HCl^{+*} would not be produced by direct fragmentation of methylene chloride, and HCl^{+*} observed in the present study would come from a bimolecular process.

The emission spectra of 1,1,1-trichloroethane and of a one-to-one mixture of methane and carbon tetrachloride were observed by the photographic method. In both cases, the bands of HCl^+ were clearly observed and looked identical to those of CH_2Cl_2. Similarity of the fine structure of HCl^+ suggests that the origins of HCl^+ were common for all parent species. From this and the result of mass spectroscopy on methylene chloride, it can be concluded that the excited hydrogen chloride positive ions were produced by a bimolecular process. Cashion and Polanyi[14] investigated the reaction,

$$H + Cl_2 \longrightarrow HCl + Cl$$

They observed that the product HCl was in vibrationally excited states. In the present study, the vibrationally excited HCl^+ might be produced by a related mechanism.

The authors would like to express their grateful acknowledgement to Professors Shigero Ikeda and Yu Yokoyama for use of their Shimadzu GE 100 monochromator and various accessories. The authors also thank Professors Tadao Horie and Tsuruji Iwai and Dr. Seiji Tsurubuchi for their advice in constructing the collision chamber and calibrating the spectrometer.

12) B. A. Brice and F. A. Jenkins, *Nature*, **123**, 944 (1929).
13) F. Norling, *Z. Phys.*, **104**, 638 (1935).
14) J. K. Cashion and J. C. Polanyi, *Proc. Roy. Soc.*, **A258**, 529 (1960).

The Cation Radical Salts of Phenothiazine and Related Compounds[1]

Yôichi IIDA

Department of Chemistry, Faculty of Science, Hokkaido University, Sapporo

(Received September 10, 1970)

The cation radical salts of phenothiazine bromide, phenothiazine bisulfate monohydrate, and phenothiazine picrate were prepared. The absorption spectra in a dilute hydrochloric acid solution and the solid-state spectra of the salts were examined. The solid-state spectra showed a strong charge-transfer band and blue-shifts of the high-energy bands, unlike the absorption spectra in solution. The magnetic susceptibilities of these salts were measured at room temperature. They were found to be diamagnetic, with values almost corresponding to those of the diamagnetic contribution of the salts, except for that of the picrate. These spectroscopic and magnetic properties were discussed on the basis of the charge-transfer interaction between the phenothiazine cation radicals. The properties of the usual phenothiazine-picric acid charge-transfer complex and the holoquinoid phenothiazine perchlorate were investigated in association with those of the cation radical salts.

In 1913 the cation radical salts of phenothiazine were first prepared by Pummerer and Gassner, and then in 1915 they were prepared again by Kehrmann and Diserens.[2,3] In their articles, however, these cation radical salts were described as "semiquinoid phenazathionium salts," because the concept of "the cation radical salts" had not yet been established.

Much attention has been paid to the cation radical salts of phenothiazine and its derivatives, since (1) the tranquilizer drug, chloropromazine, is a substituted phenothiazine and (2) many dyestuffs, such as methylene blue, are oxidation products of substituted phenothiazines. Although many papers have been written on the ESR of the radical cations of phenothiazine and its derivatives in solution,[4] few attempts have been made to investigate the solid-state properties of the phenothiazine cation radical salts.[5]

In general, solid ion-radical salts have been a matter of great interest, because the ion-radical molecules form, in themselves, a plane-to-plane stacking into columns so as to make a large overlap between their half-filled molecular orbitals.[6] Much knowledge regarding the mutual charge-transfer interaction has been accumulated by measuring the solid-state spectra and the magnetic susceptibilities.[7-10] Hence, the purpose of the present paper is to apply these physical methods to the solid phenothiazine cation radical salts. We shall examine how the charge-transfer interaction contributes to the solid-state properties of these cation radical salts.

On the other hand, the phenothiazine-picric acid charge-transfer complex and the holoquinoid phenothiazine perchlorate were also prepared, since the properties of these compounds are interesting in comparison with those of the phenothiazine cation radical salts.

Experimental

Materials. The cation radical salts of phenothiazine bromide, phenothiazine bisulfate monohydrate,[11] and phenothiazine picrate were prepared according to the methods of Pummerer and Gassner[2] and of Kehrmann and Diserens.[3] Although Pummerer and Gassner reported two polymorphic forms for the picrate,[2] no such polymorphism was found in the present preparation.

The phenothiazine-picric acid charge-transfer complex was precipitated from a benzene solution containing nearly equivalent amounts of phenothiazine and picric acid. The holoquinoid phenothiazine perchlorate was prepared from phenothiazine *S*-oxide, which had been made through the oxidation of phenothiazine with hydrogen peroxide.[3]

The synthetic schemes of these compounds are illustrated in Fig. 1.

Measurements. The absorption spectra of the cation radical salts were measured in a 4.2% aqueous hydrochloric acid solution, while that of the holoquinoid phenothiazine perchlorate was measured in an acetonitrile solution. All the measurements of the absorption spectra were made at room temperature by means of a Beckman DK-2A spectrophotometer.

The diffuse reflection spectra were recorded on a Beckman DK-2A spectroreflectometer in the range from 4.0 to 30.8 kK at room temperature. The solid-state spectra were then obtained by plotting the diffuse reflection spectra using the Kubelka-Munk equation, $f(R)=(1-R)^2/2R$, in which R is the reflectance. The experimental details were the same as those in previous papers.[8-10]

The magnetic susceptibility measurements were made by the Gouy method at room temperature. Water was used in calibrating the cell constant.

1) This work was presented at the Symposium on Molecular Structure, Tokyo, October, 1968.

2) R. Pummerer and S. Gassner, *Ber.*, **46**, 2310 (1913).

3) F. Kehrmann and L. Diserens, *ibid.*, **48**, 318 (1915).

4) G. Vincow, "Radical Ions," ed. by E. T. Kaiser and L. Kevan, Interscience Publishers, New York (1968), p. 188, and the references cited therein.

5) Y. Sato, M. Kinoshita, M. Sano, and H. Akamatu, This Bulletin, **40**, 2539 (1967); **42**, 548 (1969).

6) G. R. Anderson and C. J. Fritchie, Jr., Second National Meeting, Society for Applied Spectroscopy, San Diego, October, 14, Paper 111 (1963); C. J. Fritchie, Jr., *Acta Crystallogr.*, **20**, 892 (1966); C. J. Fritchie, Jr., and P. Arthur, Jr., *ibid.*, **21**, 139 (1966); P. Goldstein, K. Seff, and K. N. Trueblood, *ibid.*, **B24**, 778 (1968); J. Tanaka and N. Sakabe, *ibid.*, **B24**, 1345 (1968).

7) R. G. Kepler, *J. Chem. Phys.*, **39**, 3528 (1963).

8) Y. Iida and Y. Matsunaga, This Bulletin, **41**, 2615 (1968).

9) Y. Iida, *ibid.*, **42**, 71, 637 (1969).

10) Y. Iida, *ibid.*, **43**, 2772 (1970).

11) This compound, although Kehrmann and Diserens described it as phenothiazine sulfate,[3] was found to be bisulfate monohydrate on the basis of our elemental analysis (Calcd for $C_{12}H_{12}NO_5S_2$: C, 45.9; H, 3.9; N, 4.5%. Found: C, 46.7; H, 4.0; N, 5.3%) and the value of the molar extinction coefficient of the absorption spectrum in solution.

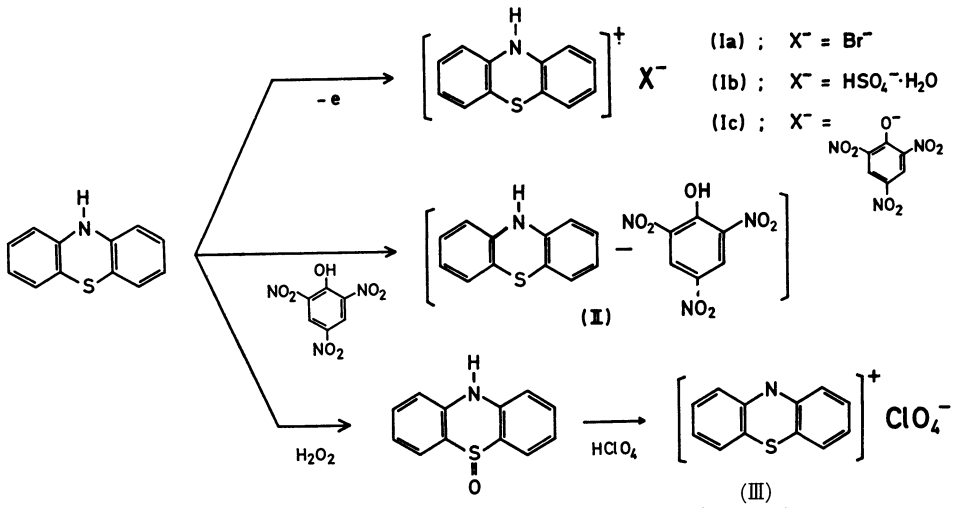

Fig. 1. The synthetic scheme of the compounds used in this study; (Ia) the cation radical salt of phenothiazine bromide, (Ib) the cation radical salt of phenothiazine bisulfate monohydrate, (Ic) the cation radical salt of phenothiazine picrate, (II) the phenothiazine-picric acid charge-transfer complex, and (III) the holoquinoid phenothiazine perchlorate.

The Absorption Spectra in Solution

In order to characterize the solid-state spectra of the phenothiazine cation radical salts, it is necessary to compare them with the absorption spectra of the salts in solution; therefore, we will examine the spectra in this section.

All of the cation radical salts exhibit a golden yellow color in solution and are quite stable in an acidic solution, such as an acetic acid or a dilute hydrochloric acid solution. In other solvents, however, they rapidly decompose to show a green color, the molecular species of which has not yet been ascertained.

Some of the absorption spectra of these cation radical salts in a 4.2% hydrochloric acid solution are reproduced in Fig. 2. In these measurements, the salts seem to be completely dissociated, because the concentrations are as dilute as of $1-2\times10^{-4}$ mol/l. When the counter anions are Br^- and $HSO_4^-\cdot H_2O$, since they have no absorptions in the energy region now under consideration, the absorption spectra of the salts appear to be solely due to the phenothiazine cation radical monomer. The absorption spectrum of the salt of the picrate has extra shoulders around 24.5 kK and 28 kK; these shoulders are assigned to the bands due to the picrate anion.

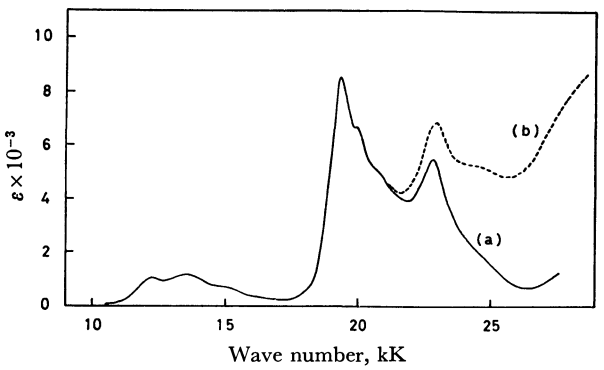

Fig. 2. The absorption spectra of the cation radical salts of (a) phenothiazine bisulfate monohydrate and (b) phenothiazine picrate, in 4.2% aqueous hydrochloric acid solution.

The monomer spectrum of the phenothiazine cation radical has a weak band around 13.5 kK composed of several vibrational structures at 15.0 kK, 13.5 kK, and 12.2 kK, a strong band at 19.3 kK with a shoulder at 19.9 kK, and a band at 22.8 kK. These features are well in accordance with those of the cation radical reported by Shine and Mach,[12] who dissolved phenothiazine in a sulfuric acid solution and then examined the absorption spectrum. Unfortunately, however, no attempt has been made to account for the electronic transitions by means of molecular orbital calculations.

On the other hand, Kagiya *et al.* reported on the temperature variation of the absorption spectrum of the phenothiazine bromide in an ethanol-ether-sulfuric acid solution.[13] They found that, at low temperatures, the monomer absorptions were diminished, while new bands

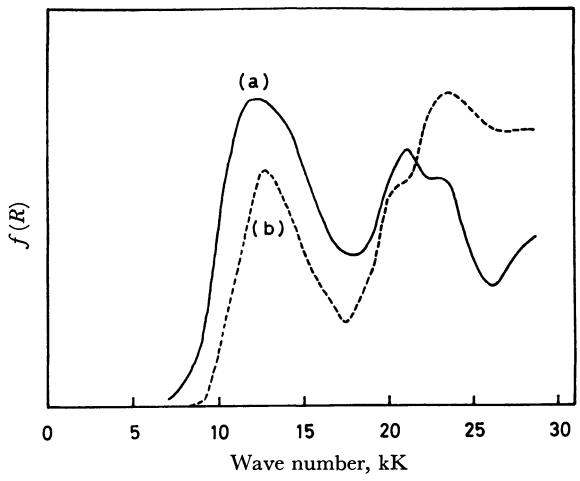

Fig. 3. The solid-state spectra of the cation radical salts of (a) phenothiazine bisulfate monohydrate and (b) phenothiazine picrate.

12) H. J. Shine and E. E. Mach, *J. Org. Chem.*, **30**, 2130 (1965).
13) T. Kagiya, K. Nakai, S. Nakayama, and K. Suzuki, Paper presented at the 23rd Annual Meeting of the Chemical Society of Japan, Tokyo, April, 1970.

appeared at 23.9 kK, 21.3 kK, and 14.5 kK. These bands were assigned to the dimer of the cation radicals on the basis of the concentration dependence on their optical densities. The high-energy bands at 21.3 kK and 23.9 kK seem to be shifted bands of the monomer bands at 19.3 kK and 22.8 kK respectively. On the other hand, the band at 14.5 kK is located in the low-energy region, and it is broad without any vibrational structures. It can not be assigned to the shifted band of the cation radical monomer, since it takes place only when the dimer is formed between the cation radicals. Therefore, the low-energy band at 14.5 kK seems to be attributable to charge-transfer absorption in the dimer.[14]

The Solid-State Spectra

Phenothiazine Bisulfate Monohydrate (Fig. 3, Curve a). The solid-state spectrum of this salt shows a strong low-energy band at 12.0 kK, high-energy bands at 21.1 kK and 23.3 kK, and a shoulder around 28 kK. These spectroscopic features are different from those of the cation radical monomer in solution, but they are similar to those of the cation radical dimer. The high-energy bands at 21.1 kK and 23.3 kK in the solid-state spectrum are coincident with those at 21.3 kK and 23.9 kK respectively in the dimer spectrum. These bands arise mostly from the monomer bands at 19.3 kK and 22.8 kK respectively. This means that in both the solid state and the dimer, when the cation radicals come close enough together for the π orbitals to overlap, the π–π transitions due to the monomer are blue-shifted by the field of the other cation radicals. In accordance with this view, the low-energy band at 12.0 kK of the solid-state spectrum is as much intensified as the charge-transfer band at 14.5 kK of the dimer spectrum.[13] Although the former value is a little bit lower than the latter, the band at 12.0 kK can be assigned to the charge-transfer transition between the phenothiazine cation radicals in the solid state. However, we must keep in mind the fact that the weak absorption due to the monomer spectrum around 13.5 kK should overlap with this charge-transfer band.

Phenothiazine Picrate (Fig. 3, Curve b). The solid-state spectrum of this salt is composed of the charge-transfer band at 12.8 kK and the high-energy bands at 20.7 kK and 23.3 kK. The increased intensity of the absorption at 23.3 kK, compared to that of the bisulfate monohydrate, may arise from the overlap with the band due to the picrate anion. Except for this difference, the situation of the solid state of this salt appears to be very analogous to that of the bisulfate monohydrate.

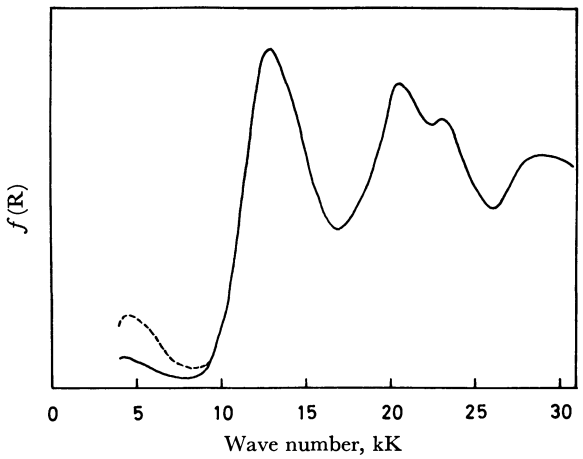

Fig. 4. The solid-state spectrum of the cation radical salt of phenothiazine bromide. The broken line indicates the spectrum of the sample taken from a different batch, as the salt was synthesized repeatedly.

Phenothiazine Bromide (Fig. 4). The solid-state spectrum of this salt shows a weak low-energy band at 4.2 kK, a strong charge-transfer band at 12.9 kK and high-energy bands at 20.5 kK, 23.0 kK, and 28.6 kK. Except for the band at 4.2 kK, these spectroscopic features are quite identical with those for the bisulfate monohydrate. As for the band at 4.2 kK, the intensity, although weak, was found to be not reproducible when the preparation of the salt was repeated. Matsunaga and Shono found that the intensity of this band was very much increased when some iodine was added to this salt.[15] They suggested that the formation of a complex cation radical salt, (Phenothiazine)$^+$ (Phenothiazine)^0 Br_2I^-, might be responsible for the appearance of this band. Therefore, the phenothiazine bromide, which exhibits its band at 4.2 kK, may be contaminated with a small amount of a complex cation radical salt of (Phenothiazine)$^+$ (Phenothiazine)^0 Br_3^-.

Magnetic Susceptibilities

It has been well established that the charge-transfer interaction between the ion radicals leads to a marked decrease in the paramagnetic susceptibilities of ion radical salts.[7–10] The charge-transfer interaction is known to stabilize the antiferromagnetic state where the spins associated with the ion radicals are antiparallel. This is also true of the present phenothiazine cation radical salts. Table 1 shows the observed values of the magnetic susceptibilities at room temperature, together with the estimated diamagnetic contribution.

Solid phenothiazine bromide was found to be diamagnetic at room temperature (-147×10^{-6} emu/mol). After correction had been made for the diamagnetism, the paramagnetic contribution of the salt was found to be as small as 13×10^{-6} emu/mol. It is not clear whether this paramagnetic contribution is due to the intrinsic paramagnetism or to an impurity paramagnetism. However, even if it is attributed to the intrinsic paramag-

14) According to the Hausser and Murrell theory, the ion-radicals in a dimer may be stacked face-to-face, and the spin exchange interaction leads to a singlet ground state and an excited triplet state. Therefore, we must take into consideration the fact that intermolecular charge-transfer may make a significant contribution to stabilizing the ground singlet state of the dimer. The low-energy charge-transfer absorption characteristic of the dimer arises mostly from a transition from the thus-stabilized ground state to an excited singlet state expressed by a combination of the wave functions for charge-transfer structures, R–R^{2+}. See K. H. Hausser and J. N. Murrell, *J. Chem. Phys.*, **27**, 500 (1957).

15) Y. Matsunaga and K. Shono, This Bulletin, **43**, 2007 (1970).

TABLE 1. THE DATA ON THE STATIC MAGNETIC SUSCEPTIBILITIES OF THE PHENOTHIAZINE CATION RADICAL SALTS AT ROOM TEMPERATURE (25°C)

Compound	$\chi_{obs} \times 10^6$ (emu/mol)	$\chi_{dia} \times 10^{6a)}$ (emu/mol)
Phenothiazine Bromide	−147	−160
Phenothiazine Bisulfate Monohydrate	−175	−177
Phenothiazine Picrate	− 56	−205
	− 33	
	− 8	
	+ 18	

a) The values of the calculated diamagnetic contribution of the salts. They were estimated from the value of diamagnetic susceptibility of each component. The experimentally determined value of diamagnetic susceptibility for a neutral phenothiazine was used in place of the cation radical. See Ref. 5.

netism for the bromide, the antiferromagnetic spin exchange interaction between the cation radicals seems to be greater than 0.1 eV. The situation in the bisulfate monohydrate appears to be almost the same as that in the bromide.

In the phenothiazine picrate, the observed value of the magnetic susceptibility was found to increase progressively as the measurements were repeated. This is shown by the multiple values of the susceptibilities listed in Table 1. In this case, the antiferromagnetic spin exchange interaction may be gradually eliminated by the fine pulverization of the sample in the course of the measurements. The population of the free spins may increase accordingly. However, a question still remains of why only the salt of the picrate, as it was ground to a fine powder, shows such a magnetic behavior.

Compounds Related to the Cation Radical Salts

Phenothiazine-Picric Acid Charge-Transfer Complex. The difference in chemical composition between the phenothiazine-picric acid charge-transfer complex and the cation radical salt of the picrate is slight; that is, the former includes the picric acid, while the latter includes the picrate anion. However, there is a marked difference in electronic structure between the two substances. In the cation radical salt, as has been mentioned above, the charge-transfer interaction takes place between the cation radicals, whereas in the charge-transfer complex it takes place between phenothiazine and picric acid. As is shown in the solid-state spectrum (Fig. 5, Curve a), the charge-transfer band in the latter case was found to be located at 18.2 kK.

The magnetic susceptibility for the charge-transfer complex was found to be -197×10^{-6} emu/mol; this value corresponds well to the -205×10^{-6} emu/mol value for the sum of the diamagnetic contribution of the component molecules, and it should be compared with that for the cation radical salt of the picrate.

Holoquinoid Phenothiazine Perchlorate. The phenothiazine cation radical is known to undergo both one-

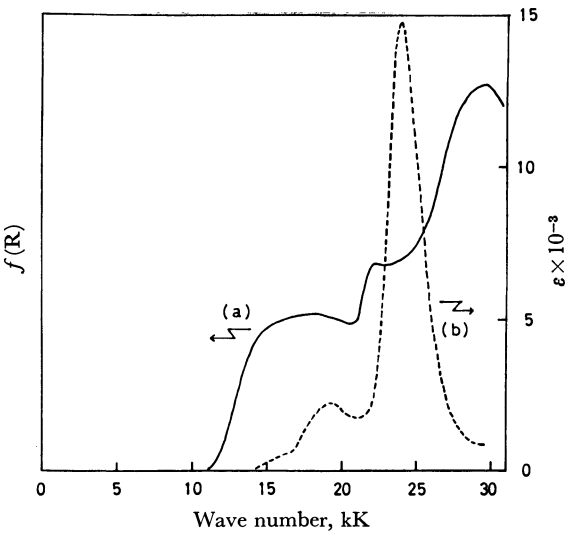

Fig. 5. The solid-state spectrum of the phenothiazine-picric acid charge-transfer complex (a), and the absorption spectrum of the holoquinoid phenothiazine perchlorate in acetonitrile solution (b).

electron oxidation and deprotonation to form the holoquinoid cation;[3] this cation has, therefore, a closed electronic shell and is a univalent cation (see Fig. 1). The holoquinoid cation appears yellow in solution and is stable at room temperature. As is shown by Curve b of Fig. 5, the absorption spectrum of the holoquinoid salt of the perchlorate in an acetonitrile solution[16] consists of a weak band at 19.3 kK and a strong absorption at 23.9 kK. This spectrum seems to be solely due to the holoquinoid cation monomer.

Discussion

The above-mentioned results on the solid-state properties of all the phenothiazine cation radical salts clearly indicate the large values both in an antiferromagnetic spin-exchange interaction and in the intensity of the charge-transfer band. This means that a strong charge-transfer interaction takes place between the phenothiazine cation radicals. Therefore, the cation radical molecules may be expected to be stacked in a face-to-face manner and to form, in themselves, linear chain columns; this feature of the crystal structure has been found in a number of other ion radical

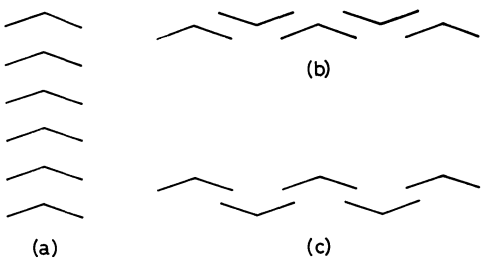

Fig. 6. Three kinds of possible stackings of the phenothiazine cation radical molecules to form linear chain columns in the solid state. A folded figure denotes a phenothiazine cation radical molecule viewed along the direction connecting the nitrogen and sulfur atoms.

16) The concentration of the solution was 8.05×10^{-5} mol/l.

salts.[6] In this case, the charge-transfer absorption may be expressed as a transition of the $\{\cdots P^{+}P^{+}\text{-}P^{+}P^{+}\cdots\} \rightarrow \{\cdots P^{+}P^{2+}P^{0}P^{+}\cdots\}$ type, where P denotes a phenothiazine molecule. As for the spin system, these cation radical salts may be considered to be a linear-chain antiferromagnet.

On the other hand, the molecular structure of neutral phenothiazine is known to be non-planar, but to be of a folded form.[17] It appears that the structure of its cation radical, although it has not yet been ascertained, is also of a folded form. Therefore, unlike planar ion-radical molecules, the stacking manner of the phenothiazine cation radicals seems to be complicated, for the linear chain columns of the cation radicals can be built up not only by the arrangement of (a) but also by that of (b) or (c), as is illustrated in Fig. 6. In this respect, further study of the X-ray diffraction is required to determine by which arrangement the phenothiazine cation radicals are stacked in the present solid salts.

17) J. D. Bell, J. F. Blount, O. V. Briscoe, and H. C. Freeman, *Chem. Commun.*, 1656 (1968).

BULLETIN OF THE CHEMICAL SOCIETY OF JAPAN, VOL. 44, 667—671 (1971)

The Primary Process of the Photochemical Dimerization of Carbostyril

Tetsu YAMAMURO, Ikuzo TANAKA, and Norisuke HATA*

Department of Chemistry, Tokyo Institute of Technology, Ookayama, Meguro-ku, Tokyo

* *Deparment of Chemistry, College of Science and Engineering, Aoyama Gakuin University, Megurisawa-cho, Setagaya-ku, Tokyo*

(Received September 10, 1970)

Carbostyril dimerizes photochemically in ethanol to yield its dimer. In order to clarify the primary process of this photochemical dimerization, studies by means of steady-light irradiation and flash spectroscopy and measurements of the absorption spectrum of the intermediate and of the phosphorescence spectrum at 77°K were carried out under various conditions. The transient absorption was observed around 430 mμ, it was identified as being due to a T–T transition of carbostyril. Experiments on both the decay kinetics of the triplet species and the quantum yield of the carbostyril disappearance under various conditions revealed that the photochemical dimerization of carbostyril proceeded through a bimolecular interaction between the triplet and the unexcited molecules.

Recently, a number of interesting photochemical reactions of heterocyclic *N*-oxides have been reported by several workers.[1,2] In the course of our studies of the primary photochemical process of quinoline *N*-oxide and its derivatives, it was necessary to identify the excited state responsible for the photochemical dimerization of carbostyril, for the carbostyril produced photochemically from the quinoline *N*-oxide in ethanol further absorbs ultraviolet light to yield its dimer. Therefore, in order to clarify the primary process of the photochemical dimerization of carbostyril, the present authors carried out investigations by means of steady-light irradiation and flash spectroscopy and measured the absorption spectrum of the intermediate and also the phosphorescence spectrum at 77°K.

Experimental

Materials. The carbostyril used in this experiment was prepared by ultraviolet irradiation for the quinoline *N*-oxide in ethanol, the product was purified by recrystallization several times.[3] Reagent-grade ethanol and dichloromethane were used without further purification. Reagent-grade piperylene was purified by distillation, while isopentane and liquid paraffin were purified by column chromatography (silica gel). Spectro-grade glycerol and methylcyclohexane were also used.

Steady-light Experiment. The light source employed was a Toshiba high-pressure mercury lamp (H-400P), while for 3130 Å irradiation a filter combination of a nickel sulfate solution with a UV-31 Toshiba filter was used. Two kinds of cylindrical quartz reaction cells were used; one was 5 cm in diameter and 1 cm thick, while the other was 5 cm in diameter and 4 cm thick. In order to determine the quantum yield of the carbostyril disappearance, the light intensity was measured with a potassium ferrioxalate actinometer. The absorption spectra were taken with a Hitachi recording spectrophotometer, EPS-3T.

Flash Spectroscopic Experiment. The absorption spectra of the transient species were taken with a flash-photolysis apparatus described in a previous paper.[4] In the case of the decay kinetic studies of the transient species, a xenon flash lamp used for excitation was operated by discharging a bank of condensers of 2 μF charged to 11 kV, 120 joules of energy being dissipated; the half-width of the discharge time was about 10 μsec.

Results and Discussion

Buchardt[3,5] has reported that the carbostyril (I)

1) G. G. Spence, E. C. Taylor, and O. Buchardt, *Chem. Rev.*, **70**, 231 (1970).

2) P. Beak and W. R. Messer, "Organic Photochemistry," Vol. 2, ed. by O. L. Chapman, M. Dekker Inc., New York, (1969), p. 117.

3) O. Buchardt, *Acta Chem. Scand.*, **17**, 1461 (1963).

4) N. Hata, E. Okutsu, and I. Tanaka, This Bulletin, **41**, 1769 (1968).

5) O. Buchardt, *Acta Chem. Scand.*, **18**, 1389 (1964).

dimerizes, under irradiation by a 3130 Å light in ethanol under bubbling nitrogen to give the carbostyril dimer (II), which is only slightly soluble in the ethanol used as a solvent.

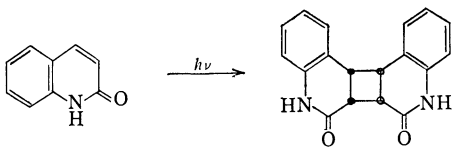

I II

This photochemical dimerization also proceeded in other solvents, such as water, cyclohexane, and dichloromethane, but it was inhibited by the addition of piperylene or the bubbling in of oxygen. As an example of these experiments, Table 1 shows how the photochemical conversion from carbostyril to its dimer in dichloromethane was influenced by the addition of various amounts of piperylene. It is evident from these results that both oxygen and piperylene act as quenchers for the photochemical dimerization of carbostyril.

TABLE 1. EFFECT OF PIPERYLENE ON THE PHOTOCHEMICAL CONVERSION FROM CARBOSTYRIL TO ITS DIMER[a)]

Piperylene (M)	0	0.5×10^{-4}	1.0×10^{-4}	1.8×10^{-4}	7.0×10^{-4}	3.5×10^{-3}
Conversion (%)[b)]	47	38	32	30	25	11

a) Solvent: dichloromethane (under bubbling nitrogen) Concentration of carbostyril: 3.52×10^{-3} M (60 cc) Irradition time: 75 min.
b) Conversion refers to the percentage of carbostyril converted to its dimer.

Figure 1 shows the progressive spectral change of carbostyril on 3130 Å irradiation in ethanol, where it was observed that the absorption of carbostyril decreased progressively with the irradiation time and that a new absorption band appeared around 255 mμ as the irradiation time increased, with isosbestic points at 265 mμ, 283 mμ, and 298 mμ. On the basis of a comparison with the absorption spectrum of the carbostyril dimer in ethanol (Fig. 2), the new absorption band which appeared around 255 mμ on 3130 Å irradiation is considered to be due to a carbostyril dimer.

The phosphorescence spectrum from EPA, ethanol, or methylcyclohexane glass containing approximately 1.0×10^{-4}M carbostyril was measured at 77°K; the spectrum thus obtained is shown in Fig. 3. It was estimated, from the first maximum of the phosphorescence spectrum (434 mμ), that the lowest triplet state of carbostyril has an excitation energy of about 66 kcal·mol^{-1}. Consequently, the addition of piperylene (E_T=57 kcal·mol^{-1}) to the carbostyril in amounts much greater than the molar equivalence led to the complete disappearance of the phosphorescence (Fig. 3). From this result, the radius of the active sphere with the piperylene molecule at its center, where triplet carbostyril molecules outside this sphere were assumed not to be quenched, was estimated to be about 15 Å. The phosphorescence lifetime (τ_p) of carbostyril in EPA at 77°K was also determined to be 0.88 sec (Fig. 9).

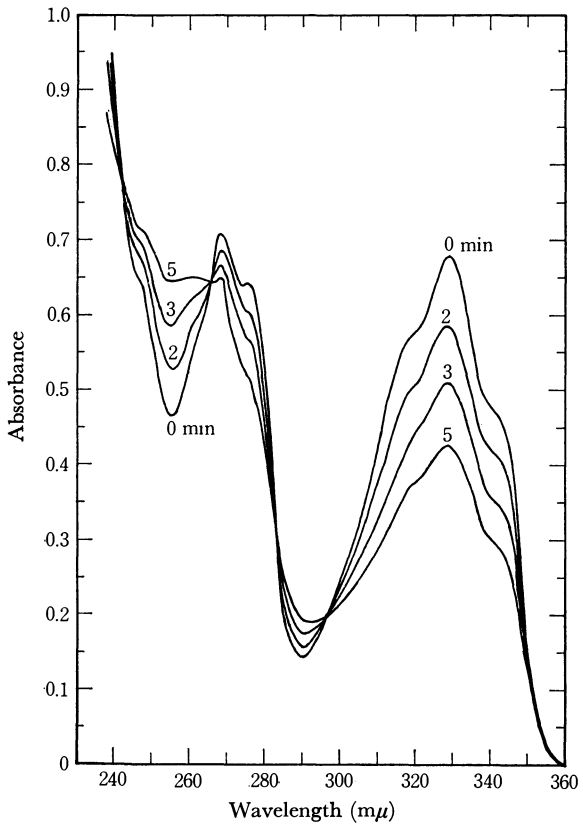

Fig. 1. Spectral change of carbostyril on 3130 Å irradiation in deaerated ethanol (initial concentration of carbostyril: 1.05×10^{-4}M).

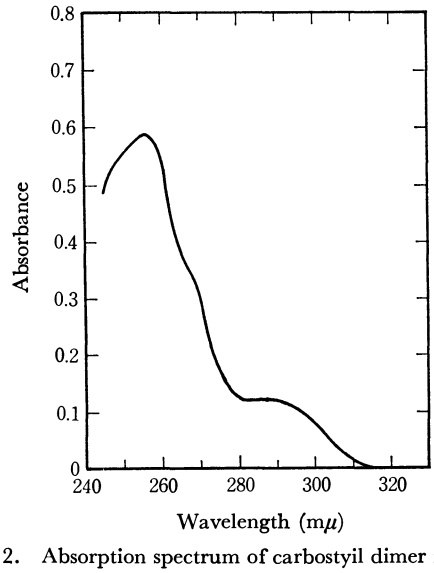

Fig. 2. Absorption spectrum of carbostyil dimer in ethanol.

The quantum yields of the carbostyril disappearance in deaerated ethanol were measured under various conditions. Figure 4 shows the effect of the light intensity on the quantum yield of the carbostyril disappearance, the results indicate that the quantum yield was independent of the light intensity. The quantum yield of the carbostyril disappearance as a function of the concentration was also determined; the results are shown in Fig. 5. As may be seen from Fig. 5, the quantum yield increased with an increase in the con-

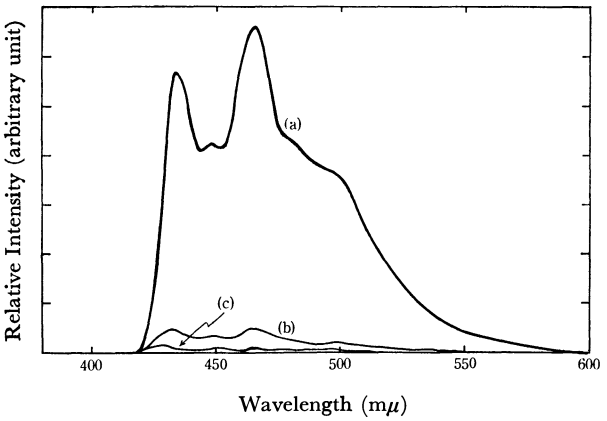

Fig. 3. Phosphorescence spectrum of carbostyril in methylcyclohexane at 77°K (concentration of carbostyril: 1.0×10^{-4}M).
(a) [Piperylene]: 0 M
(b) [Piperylene]: 1.0×10^{-1}M
(c) [Piperylene]: 2.0×10^{-1}M

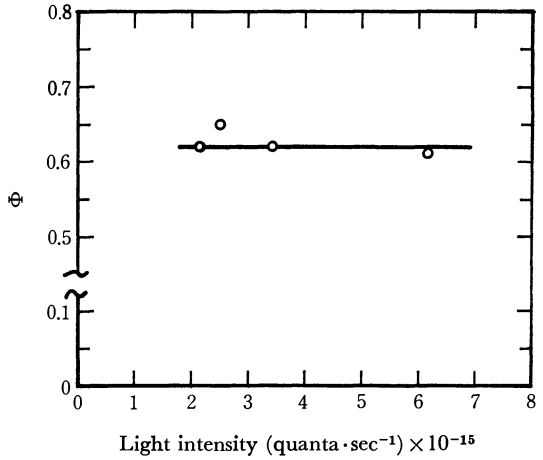

Fig. 4. Quantum yield of carbostyril disappearance *vs.* light intensity in deaerated ethanol at room temperature (concentration of carbostyril: 1.30×10^{-4}M).

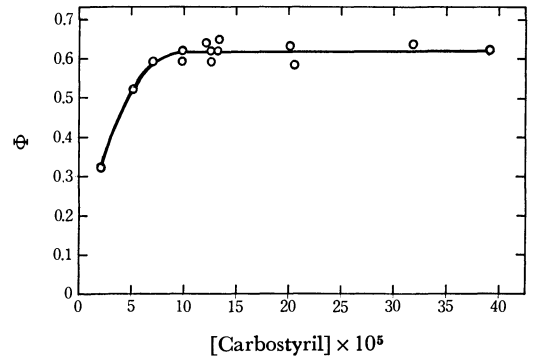

Fig. 5. Quantum yiled of carbostyril disappearance *vs.* concentration in deaerated ethanol at room temperature.

centration, approaching a constant value at concentrations of more than 1.0×10^{-4}M.

Next, in order to characterize the excited state responsible for the photochemical dimerization, the effect of piperylene on the quantum yield of the carbostyril disappearance was investigated, with the piperylene being chosen as the triplet quencher. Figure 6 shows plots of Φ/Φ_Q against the concentration of piperylene

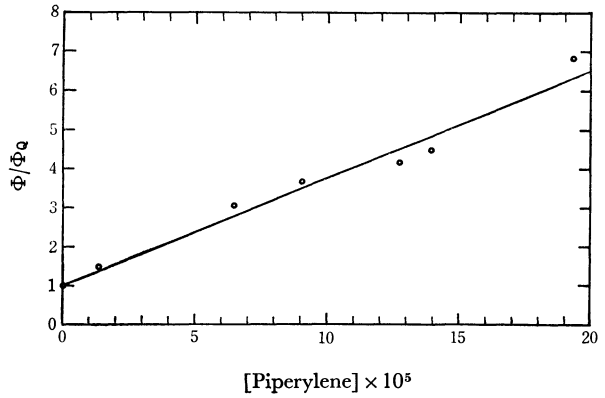

Fig. 6. Stern-Volmer plot for carbostyril dissapearance by piperylene in deaerated ethanol at 20°C (concentration of carbostyril: 1.20×10^{-4}M).

([Q]), where Φ and Φ_Q represent the quantum yield of the carbostyril disappearance in the absence and in the presence of piperylene respectively. It is apparent from Fig. 6 that the simple Stern-Volmer relationship (1):

$$\Phi/\Phi_Q = 1 + K_Q[Q] \tag{1}$$

is followed in this reaction. The quenching constant, K_Q, at $[S_0]=1.20\times10^{-4}$M, $[S_0]$ being the initial concentration of carbostyril, was estimated, from the slope of the curve in Fig. 6, to be $2.76\times10^{4}\ l\cdot\text{mole}^{-1}$. The quenching constant in this photochemical dimerization is represented by Eq. (2):

$$K_Q = \frac{k_8}{k_2 + k_3 + (k_4+k_5)[S_0]} \tag{2}$$

from a consideration of the following reaction scheme, (i)—(viii), to be given below. The observed value of K_Q will be compared with that estimated from a flash-spectroscopic experiment later.

The dependence of the quantum yield on the concentration of carbostyril and the quenching experiment seem to be explained by the following mechanism:

$S_0 + h\nu \longrightarrow S_1 \longrightarrow T_1$	$I_a\phi_{isc}$	(i)
$T_1 \longrightarrow S_0$	k_2	(ii)
$T_1 \longrightarrow$ Decomposition	k_3	(iii)
$T_1 + S_0 \longrightarrow S_0 + S_0$	$k_4[S_0]$	(iv)
$T_1 + S_0 \longrightarrow (T_1S_0)$	$k_5[S_0]$	(v)
$(T_1S_0) \longrightarrow$ Dimer	k_6	(vi)
$(T_1S_0) \longrightarrow S_0 + S_0$	k_7	(vii)
$T_1 + Q \longrightarrow S_0 + Q$	$k_8[Q]$	(viii)

Assuming the photostationary state conditions, the quantum yield of the carbostyril disappearance in the absence of a quencher could be given by the following equation:

$$\Phi = A\left(1-\frac{C}{1+B[S_0]}\right) \tag{3}$$

where:

$$A = \frac{k_5k_6\phi_{isc}}{(k_4+k_5)(k_6+k_7)}$$

$$B = \frac{k_4+k_5}{k_2+k_3}$$

$$C = 1 - \frac{(1+k_4/k_5)(1+k_7/k_6)}{(1+k_2/k_3)}$$

and where ϕ_{isc} represents the efficiency of the S_1—T_1 intersystem crossing. Equation (3) accounts qualitatively for the concentration dependency of the quantum yield.

As has been described above, the photochemical dimerization of carbostyril is considered to proceed through a bimolecular interaction between the triplet and the unexcited molecules. However, another mechanism is also considered to be possible for this reaction. That is, the dimerization might occur from an interaction of the unexcited molecule (S_0) with the intermediate (M) which may be produced from the triplet state of carbostyril as follows:

$$T_1 \longrightarrow M \qquad \text{(ix)}$$

$$M + S_0 \longrightarrow (MS_0) \qquad \text{(x)}$$

$$(MS_0) \longrightarrow \text{Dimer} \qquad \text{(xi)}$$

Therefore, it is necessary to determine which mechanism is most reasonable in accounting for this reaction. If the dimerization proceeds through the processes (v) and (vi), the T–T absorption of carbostyril can possibly be observed. On the other hand, if the processes (ix)—(xi) are involved in the dimerization, the absorption spectrum of the intermediate (M) or, simultaneously, a T–T absorption of carbostyril will probably be obtained. That is, the detection and identification of triplet species and the examination of their kinetic behavior could be important in determining the mechanism of the photochemical dimerization of carbostyril.

Figure 7 shows the absorption spectrum of the transient species produced by a flash excitation of the carbostyril in such solvents as glycerol (room temperature), liquid paraffin (268°K), and EPA (77°K).[6] In each case, the transient absorption was observed in the region between 380 mμ and 500 mμ.

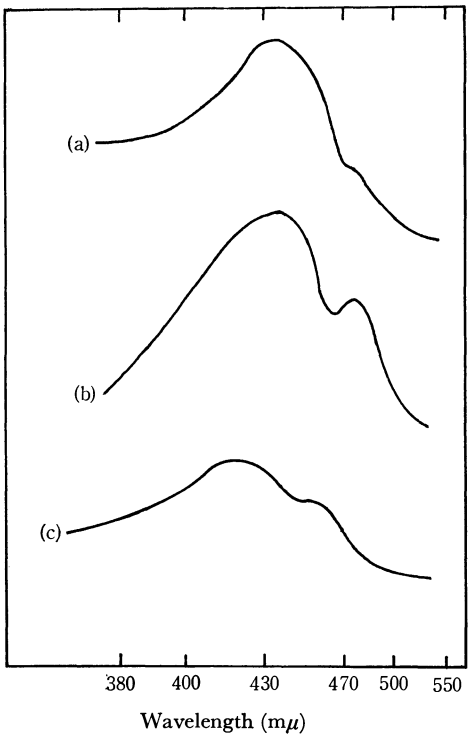

Fig. 7. Transient absorption of carbostyril.
(a) in glycerol (room temperature)
(b) in liquid paraffin (268°K)
(c) in EPA (77°K)

The decay constant of the transient absorption (k_T) was determined at several wavelengths in deaerated ethanol (room temperature), liquid paraffin (268°K), glycerol (room temperature), and EPA (77°K); the results are shown in Figs. 8 and 9. As may be seen from Figs. 8 and 9, the decay obeyed the first-order law and the decay constant was independent of the wavelength. The decay lifetime ($\tau_T = 1/k_T$) in EPA at 77°K was 0.96 sec, very close to the phosphorescence lifetime (τ_p = 0.88 sec) described before. These results suggest that

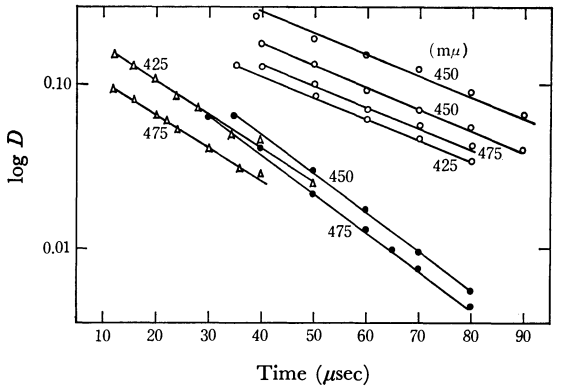

Fig. 8. Decay analysis for the transient species at several wavelengths in various solvents at room temperature.
○ in glycerol ● in liquid paraffin △ in ethanol

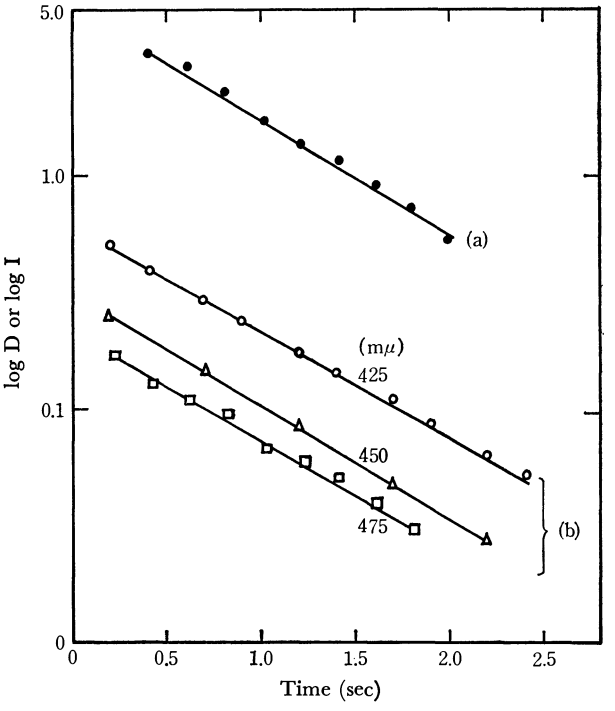

Fig. 9. Decay analysis for the phosphorescence (a) and for the transient species (b) at several wavelength in EPA (1:1:3) at 77°K (concentration of carbostyril: 1.0×10^{-4}M).

6) The absorption spectrum of the transient species in EPA at 77°K was taken by means of a steady-light crossed illumination.

the transient absorption around 430 mμ is due to a T–T transition of carbostyril.

The next problem is to clarify whether or not the triplet species observed is responsible for the photochemical dimerization of carbostyril. If the dimerization proceeds through a bimolecular interaction of the unexcited molecule with the triplet molecule, the decay rate of the triplet species may be given by the following equation:

$$k_T = k_2 + k_3 + (k_4+k_5)[S_0] \quad (4)$$

That is, the decay rate may be expected to vary linearly with the initial concentration of carbostyril. When the piperylene is added to a solution of carbostyril, the decay rate is probably given by the following equation:

$$k_T = k_2 + k_3 + (k_4+k_5)[S_0] + k_8[Q] \quad (5)$$

That is, when $[S_0]$=constant, the rate is considered to increase in proportion to the concentration of the quencher. Therefore, the effects of both the concentration of carbostyril and that of piperylene on the decay rate were examined in deaerated ethanol at room temperature. As is shown in Fig. 10, it was seen that the decay rate of the triplet species was directly proportional to the initial concentration of carbostyril; this was consistent with Eq. (4). k_4+k_5 was evaluated from the slope of the curve, while k_2+k_3 was estimated by extrapolating the concentration of carbostyril to zero. In this manner, the following values were obtained:

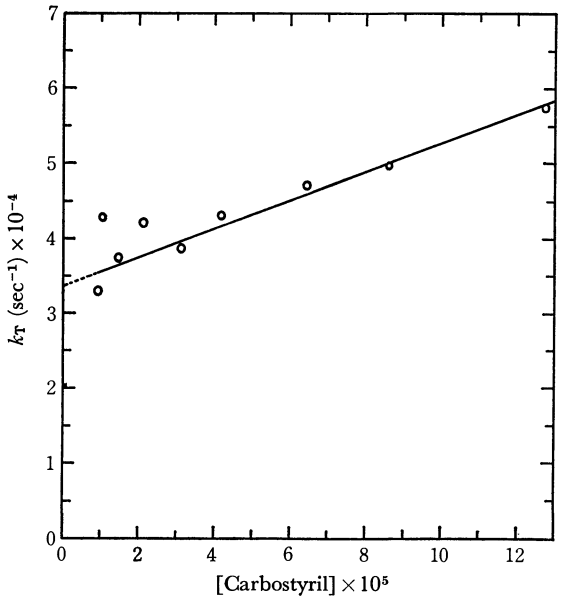

Fig. 10. Decay constant of the triplet species *vs.* concentration in deaerated ethanol at 34°C.

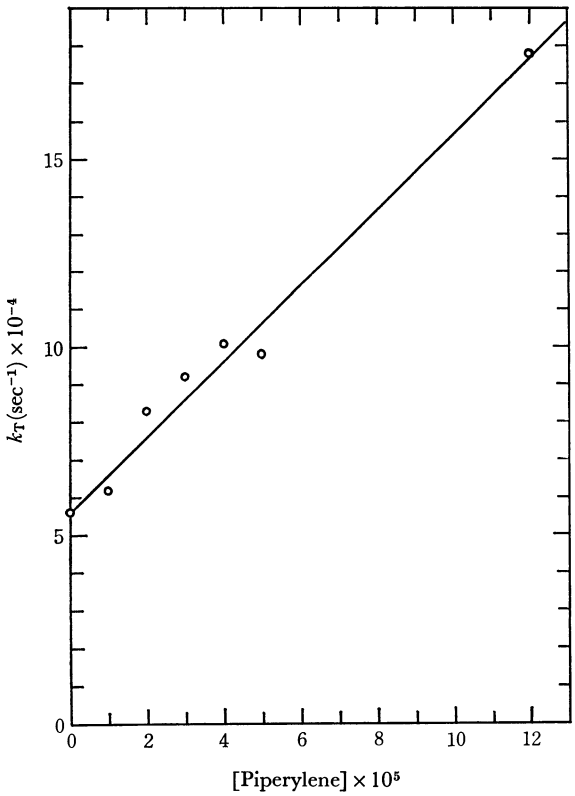

Fig. 11. Quenching of the triplet species by various amounts of piperylene in deaerated ethanol at 35°C (concentration of carbostyril: 1.16×10^{-4}M).

$k_2+k_3=3.36\times10^4$ sec^{-1} and $k_4+k_5=1.92\times10^8$ $l\cdot$mol$^{-1}\cdot$sec^{-1}

The effect of the concentration of the quencher on the decay rate of the triplet species at $[S_0]=1.16\times10^{-4}$M is shown in Fig. 11. As was expected from Eq. (5), a linear relationship between k_T and [Q] was found and the k_8 obtained from the slope was 1.01×10^9 mol^{-1} l sec^{-1}. By substituting the observed values of k_8, k_2+k_3, and k_4+k_5 and $[S_0]=1.20\times10^{-4}$M into Eq. (2), K_Q was obtained as 1.78×10^4 $l\cdot$mol^{-1}; this value agreed closely with that obtained by the steady-light experiment. These facts support the idea that the photochemical dimerization of carbostyril proceeds through a bimolecular interaction between the triplet and the unexcited molecules.

The authors wish to express their hearty thanks to Professor Y. Mori of the Tokyo Institute of Technology for his kind discussions and to Professor S. Matsumoto of Aoyama Gakuin University for his permission to use the flash-photolysis apparatus.

Absorption Spectra of Crystals of Cytosine and Its Derivatives

Masashi TANAKA and Jiro TANAKA
Department of Chemistry, Faculty of Science, Nagoya University, Chikusa, Nagoya
(Received October 16, 1970)

The electronic spectra of cytosine, one of DNA bases, have been studied. The absorption spectra of single crystals of cytosine and its derivatives are presented, and the direction of the transition moment of the first $\pi\rightarrow\pi^*$ band is determined to be inclined at about $+100°$ from the N_1–C_4 line toward the C_5 atom. The second $\pi\rightarrow\pi^*$ band is shown to have polarization direction at $+30°$ inclined to the reference axis.

Cytosine is one of the important base components of DNA and RNA. The electronic structures and spectra of these molecules are significant in studying the conformation and optical properties of polynucleotides since the hypochromism and circular dichroism are mainly governed by the nature of the electronic transitions and the interaction of excited states of these base pairs. The directions of the electronic transition moments are particularly important in considering the exciton type interactions. The polarization measurements of absorptions on the single crystals are most helpful in order to find these directions. Although many investigations[1] have been presented on the spectra of DNA bases in solution, a few works have been connected with the polarization of the excited state. In the subsequent paper[2] we have presented the absorption spectra of the single crystals of thymine and uracil derivatives and discussed on the directions of the transition moments of two lowest $\pi\rightarrow\pi^*$ bands. In the present paper we are presenting the results of the crystal absorption spectra on cytosine and its derivatives with the probable direction of transition moments.

Experimental

Materials. Cytosine and cytidine sulfate were obtained from Wako Pure Chemical Industries, cytidine was purchases from Biochemica Co. Ltd. and 1-methyl cytosine was obtained from Sigma Chemical Company.

Apparatus. The crystal spectra were recorded at room temperature on a specially designed microspectrophotometer consisting of (i) an Olympus polarizing microscope with Zeiss ultrafluar objectives and a quartz Rochon polarizer, (ii) a Zeiss M4Q III monochrometer with tungsten and hydrogen sources and (iii) a 1P28 photomultiplier tube with the standard Zeiss detection system.

Results

1-Methyl Cytosine. The absorption spectrum of the single crystal of 1-methyl cytosine is shown in Fig. 1. The crystals obtained on the quartz plate from the ethanol solution were employed for measurement of the polarized spectra. The developed plane of the crystal is assigned to the (100) plane judging from the paper by Mathews and Rich.[3] In this crystal, the

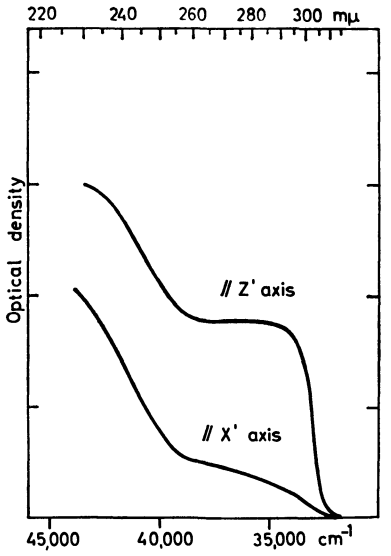

Fig. 1. The polarized absorption spectrum of the single crystal of 1-methyl cytosine.

first $\pi\rightarrow\pi^*$ band is observed in the vicinity of 285 mμ and is shifted to the longer wavelength as compared to the solution and other crystalline spectra. The second band has a peak below 230 mμ for the two perpendicularly polarized light and its position is not firmly ascertained. The direction of the transition moments of these two bands can not be discussed with the crystal since the coordinates of atoms are not reported.[3]

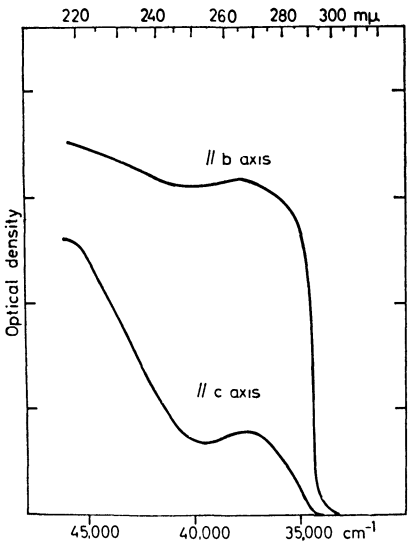

Fig. 2. The polarized absorption spectrum on the plane (100) of the single crystal of cytosine monohydrate.

1) S. F. Mason, *J. Chem. Soc.* (London), **1960**, 219, **1954**, 20; D. Voet, W. B. Gratzer, R. A. Cox, and P. Doty, *Biopolymers*, **1**, 193 (1963); L. B. Clark and I. Tinoco, Jr., *J. Amer. Chem. Soc.*, **87**, 11 (1965).
2) M. Tanaka and J. Tanaka, This Bulletin, to be published.
3) R. S. Mathews and A. Rich, *Nature*, **201**, 180 (1964).

Cytosine. The absorption spectrum of the single crystal of cytosine monohydrate has been measured and is shown in Fig. 2. The crystal structure analysis has been carried out by Jeffrey and Kinoshita[4] and it has been shown that the crystal belongs to the space group of $P2_1/c$ and four molecules are included in a unit cell. The unit cell dimensions are $a=7.80$, $b=9.84$, $c=7.68$ Å, and $\beta=99°42'$. Single crystals of cytosine monohydrate were obtained by slow evaporation from dilute aqueous solution as monoclinic plates tabularly on the (100) plane. The projection of molecules onto this developed plane (100) is pictured in Fig. 3. According to this figure,

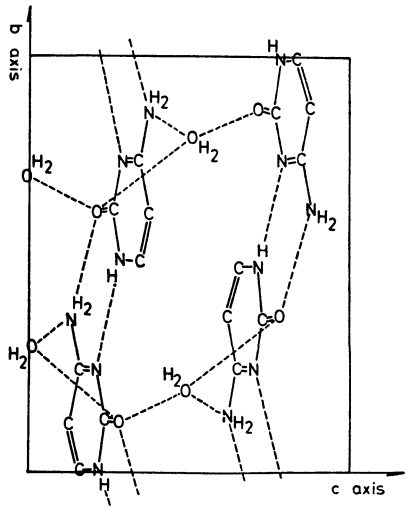

Fig. 3. The projection of cytosine molecules onto the developed plane (100).

the cytosine molecules are hydrogen-bonded into parallel ribbons extending in the *b* axis direction. Adjacent ribbons are related by the *c* glide symmetry and the perpendicular separation of the planes of the ribbons is 3.2 Å. The crystalline absorption spectrum has been measured on the *bc* plane. As shown in Fig. 2, cytosine is a weakly coupled system in this crystal and no large frequency shifts and splitting are observed for the bands in the crystal relative to their positions in the solution spectrum. The first $\pi\rightarrow\pi^*$ band has a peak at 265 mμ in both the *b* and *c* axes spectra. In the second $\pi\rightarrow\pi^*$ bands, only a tail of the band was measured but a peak may be located in the vicinity of 220 mμ in both the *b* and *c* axes spectra. The observed dichloric ratio for the $\pi\rightarrow\pi^*$ band at 265 mμ is determined from the areas under the two perpendicularly polarized absorption curves and (I_b/I_c) may be seen to be equal to $\cot^2\theta$. Here θ is the angle between the transition moment and the *c* axis. From the crystal structure data we may now determine the relation of the molecular frame to the *b* axis and finally the relation of the transition moment to the molecular frame. According to the above method, the transition moment of this band is determined to lie at either $+25°$ or $+100°$ inclined to the reference axis which designates the line joining the nitrogen (N_1) and its para partner (C_4) (clockwise rotation denoted as positive). The dichroic ratio of the second $\pi\rightarrow\pi^*$ band is about 1.5 : 1 (I_b/I_c) judging from the observed

4) G.A. Jeffrey and Y. Kinoshita, *Acta Crystallogr.*, **16**, 20 (1963).

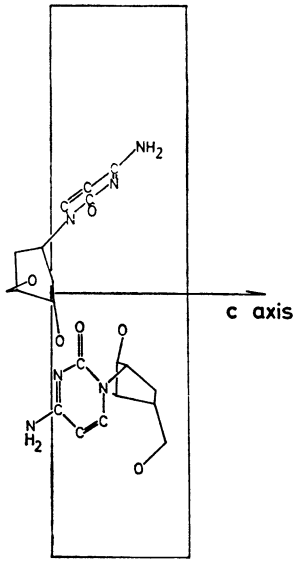

Fig. 4. The projection of cytidine molecules onto the developed plane (110).

region. The angle between the transition moment and the reference axis is determined by the dichroic ratio to be either $+45°$ or $+80°$.

Cytidine. Furberg, Petersen, and Rϕmming[5] analyzed the crystal structure of cytidine and showed that the crystal belongs to the space group of $P2_12_12_1$ and there are four molecules in the unit cell. The unit cell dimensions are $a=13.99$, $b=14.79$, and $c=5.12$ Å. The crystal is obtained by evaporating slowly a solution of cytidine in an alcohol-water mixture and has the shape of prism elongated along the *c* axis. The projection of molecules onto the developed plane (110) is pictured in Fig. 4. Two cytosine rings in the unit cell are nearly parallel to this developed plane and other two cytosine rings are located perpendicularly. The crystalline absorption spectrum has been measured along the directions parallel or perpendicular to the *c* axis on the

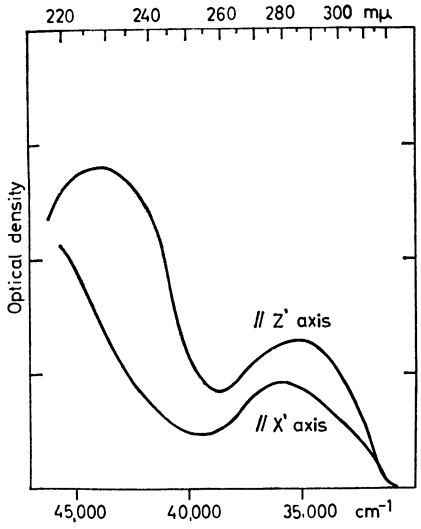

Fig. 5. The polarized absorption spectrum on the plane (110) of the single crystal of cytidine.

5) S. Furberg, C. S. Petersen, and C, Rϕmming, *Acta Crystallogr.*, **18**, 313 (1965).

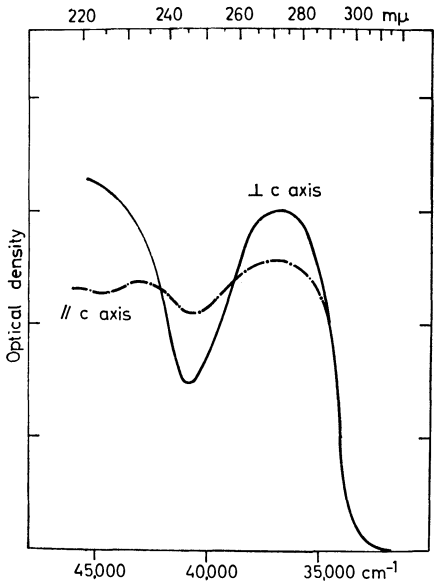

Fig. 6. The polarized absorption spectrum of the single crystal of cytidine sulfate.

plane (110) as shown in Fig. 5. The peak of the first $\pi\rightarrow\pi^*$ band exists at 272 mμ and the observed dichroic ratio is about 1.1 : 1 ($I_{\perp c}/I_c$) and the direction of the transition moment is deduced to be either +15° or +105° to the N_1—C_4 reference axis. The second $\pi\rightarrow\pi^*$ band exists in the 230 mμ region and its dichroic ratio is 1.4 : 1 ($I_{\perp c} : I_c$). By this ratio its transition moment is determined to lie at either +20° or +90° inclined to the reference axis.

Cytidine Sulfate. The absorption spectrum of the single crystal of cytidine sulfate is shown in Fig. 6. In this crystal, Davydov splittings are observed. The first band has a peak at 288 mμ for the light polarized parallel to the *c* axis and at 280 mμ for the light polarized perpendicular to the *c* axis and Davydov splitting is about 1000 cm^{-1}. The second band has a peak at 228 and 220 mμ for the light polarized parallel and perpendicular to the *c* axis, respectively. Davydov splitting of this second band is about 1600 cm^{-1}. Unfortunately the direction of the transition moment can not be discussed with this crystal because the crystal structure has not been analyzed so far.

Discussion

The absorption spectra of single crystals of cytosine and its derivatives show two absorption $\pi\rightarrow\pi^*$ bands corresponding to the 220 and 260 mμ bands in solution in the measured region. The observed dichroic ratios of the 220 and 260 mμ bands of these crystals are summarized in Table 1. There are in general two in-plane directions consistent with a dichroic ratio measured on a single crystal and data from a single crystal face will not in general be sufficient for a unique assignment of polarization directions. Therefore, the spectra of a few of cytosine derivatives were measured in order to determine the directions of the transition moments of

Table 1. Observed dichroic ratios and directions of the transition moments

		First band		Second band	
Cytosine monohydrate	I_b/I_c	7	+ 25° or+100°	1.5	+45° or+80°
Cytidine	$I_{\perp c}/I_c$	1.1	+ 15° or+105°	1.6	+20° or+90°

two $\pi\rightarrow\pi^*$ bands but these directions could not be uniquely assigned from the observed ratios. As shown in Table 1, the transition moment of the first 260 mμ band is determined to be inclined at +20° or +100° from the N_1—C_4 line toward the C_5 atom and that of the second 220 mμ band at +30° or +85°. On the other hand, Nagata *et al.*,[6] Berthod, Giessner, and Pullman[7], and Morita and Nagakura[8] calculated the electronic states of cytosine molecule by the P-P-P method and discussed the directions of the transition moments. Particularly, Berthod, Giessner, and Pullman[7] decided the transition moments of two $\pi\rightarrow\pi^*$ bands to be inclined at +95° and +47° with respects to the N_1–C_4 axis. Accordingly, it is reasonable that the transition moments of the first and second bands are uniquely speculated to be inclined at +100° and +30° from the N_1–C_4 line toward the C_5 atom as shown in Fig. 7.

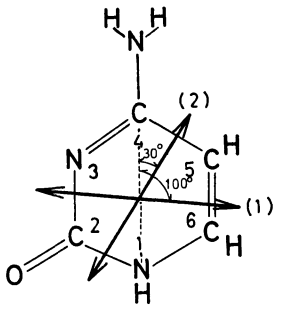

Fig. 7. The directions of the transition moments of the first (1) and second (2) $\pi\rightarrow\pi^*$ bands.

In the polarized absorption spectra of the crystal of thymine and uracil derivatives,[2] an usual absorption band appears at about 285 mμ in addition to the usual $\pi\rightarrow\pi^*$ transition when the crystal has the C=O···H–N hydrogen bond. The direction of the transition moment of this band is along the direction of the hydrogen bond between a pair of C=O···H–N groups. In the crystal of cytosine monohydrate, the cytosine molecules are hydrogen-bonded through N–H···N and C=O···H–N into parallel ribbons extending in the *b* axis direction but no hump was observed in the vicinity of 280 mμ.

6) C. Nagata, A. Imamura, Y. Tagashira, and M. Kodama, This Bulletin, **38**, 1638 (1965).

7) H. Berthod, C. Giessner-Prettre, and A. Pullman, *Theoret. Chim. Acta*, **5**, 53 (1966).

8) H. Morita and S. Nagakura, *Theor. Chim. Acta*, **11**, 279 (1968).

Note added in proof: Recent paper by P. R. Callis and W. T. Simpson, *J. Amer. Chme. Soc.*, **92**, 3593 (1970), discusses the polarization of cytosine absorption bands.

The Effect of Pressure on the Electronic Absorption Spectra of Alkali Metal Cation-Chloranil and -Bromanil Anion Radical Salts, and the Dimerization of the Chloranil Anion Radical in Solution

Nobuko SAKAI, Ichimin SHIROTANI, and Shigeru MINOMURA

The Institute for Solid State Physics, The University of Tokyo, Roppongi, Minato-ku, Tokyo

(Received October 20, 1970)

The pressure dependence, up to 7 kbar, of the electronic absorption spectra of ion-radical salts composed of the alkali metal cation and the chloranil or bromanil anion radical in the crystalline state at room temperature, and the temperature dependence, down to 134°K, of the dimerization of chloranil anions in an ethanol solution at 1 bar have been studied. The absorption band in the visible region shows a blue shift with an increase in the pressure for Li^+ and Na^+ salts, while for K^+ and Rb^+ salts the spectra are insensitive to the pressure. The anion radicals seem to be in the dimeric electronic state for the former and to be in the monomeric state for the latter, in the crystalline state.

The magnetic and electronic properties of the ion-radical salts, such as Würster's blue perchlorate (WBP) and tetracyanoquinodimethane (TCNQ) salts, have attracted interest in connection with the behavior of the unpaired electrons and the characteristic intermolecular interactions in the crystalline state, and their properties under high pressure have been studied in order to get useful information on the electronic structure of ion-radical salts in the crystalline state.[1-6]

The electronic absorption spectra of ion-radical salts have been studied extensively in solution and solid states since Hausser and Murrell[7] pointed out that the new lowest-energy absorption band of the dimer in WBP, which exists in solution at low temperatures, is the charge-transfer band between the half occupied orbitals of component radicals. For example, in the case of Würster's salts, the electronic structures in the crystalline state have been discussed on the basis of the following data; the polarized reflectance spectra of WBP at temperatures above and below the phase transition point,[8] the polarized absorption spectra of some Würster's salts at room temperature,[9,10] and a comparison between the temperature dependence of the charge-transfer band intensity and that of the magnetic susceptibility.[11] On the other hand, Pott and Kommandeur[12] suggested a disproportionation of charges in a crystal which differed from dimerization.

In this paper, the effect of pressure on the electronic absorption spectra of ion-radical salts composed of an alkali metal cation and a chloranil or bromanil anion radical ($M^+(CA)^-$, M:Li, Na, K, and Rb, CA:chloranil, $M^+(BA)^-$, M:Na and K, BA: bromanil) will be investigated in order to determine the influence of the counter ions upon the electronic structures of chloranil or bromanil anion radicals in the crystalline state; also, the dimerization of chloranil anions in an ethanol solution at low temperatures and at 1 bar will be reported.

Experimental

Commercially-available *p*-chloranil and *p*-bromanil synthesized by the method of Torrey and Hunter[13] were purified by recrystallization from benzene and then by sublimation *in vacuo*. Their alkali metal salts were synthesized according to the method of Torrey and Hunter;[13] lithium and rubidium salts were synthesized by a method similar to that used for potassium salt. The ethanol was purified by distillation.

The optical measurements were carried out with a Cary recording spectrophotometer, Model 14M, or with a Shimadzu SV-50A spectrophotometer. The electronic absorption spectra of crystalline powder were measured on samples rubbed on glass plates, because the methods using the KBr disk and liquid paraffin mull, which are usually used for powder samples, were unsuitable for the measurements of the electronic absorption spectra of some ion radical salts because of the influence of the applied force at the time of the disk formation upon their electronic states, and for the measurements of the pressure dependence on the spectra, respectively. The spectra at low temperature were measured by using a Pyrex Dewar vessel and using liquid nitrogen as a refrigerant, the temperature being measured by means of a copper-constantan thermocouple. The spectra under high pressure at room temperature were measured by using a high-pressure optical cell which had two sapphire windows. A hydrostatic pressure up to 7 kbar was applied by means of a pressure-transmitting medium, white gasoline, through a pressure-intensifier. The pressure was determined by a Harwood manganine resistance gauge and a Heise Bourdon tube gauge.

Results and Discussion

A. Absorption Spectra in the Crystalline State. The electronic absorption spectra of four alkali metal cation-chloranil anion-radical salts measured on crystalline

1) A. W. Merkl, R. C. Hughes, L. J. Berliner, and H. M. McConnell, *J. Chem. Phys.*, **43**, 953 (1965).
2) R. C. Hughes, A. W. Merkl, and H. M. McConnell, *ibid.*, **44**, 1720 (1966).
3) R. B. Aust, G. A. Samara, and H. G. Drickamer, *ibid.*, **41**, 2003 (1964).
4) I. Shirotani, T. Kajiwara, H. Inokuchi, and S. Akimoto, This Bulletin, **42**, 366 (1969).
5) I. Shirotani, N. Sakai, H. Inokuchi, and S. Minomura, *ibid.*, **42**, 2087 (1969).
6) N. Sakai, I. Shirotani, and S. Minomura, *ibid.*, **43**, 57 (1970).
7) K. H. Hausser and J. N. Murrell, *J. Chem. Phys.*, **27**, 500 (1957).
8) G. R. Anderson, *ibid.*, **47**, 3853 (1967).
9) Y. Iida and Y. Matsunaga, This Bulletin, **41**, 2615 (1968).
10) J. Tanaka and M. Mizuno, *ibid.*, **42**, 1841 (1969).
11) T. Sakata and S. Nagakura, *ibid.*, **42**, 1497 (1969).
12) G. T. Pott and J. Kommandeur, *J. Chem. Phys.*, **47**, 395 (1967).
13) H. A. Torrey and W. H. Hunter, *J. Amer. Chem. Soc.*, **34**, 702 (1912).

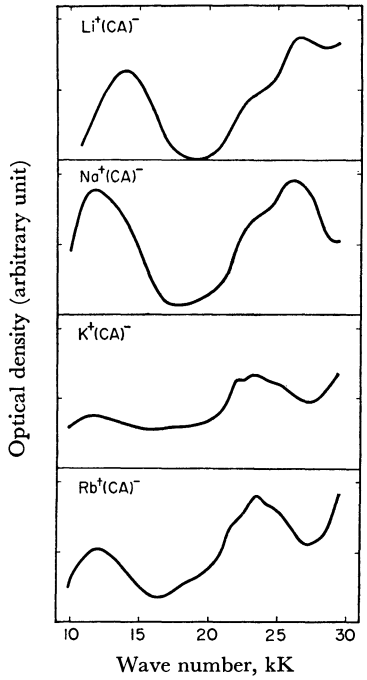

Fig. 1. Electronic absorption spectra of four alkali metal cation-chloranil anion radical salts.

powder samples rubbed on glass plates are shown in Fig. 1.[14] The spectra of $Na^+(CA)^-$ and $K^+(CA)^-$ almost coincide with the recent work of André and Weill.[15] The absorption spectra of $Li^+(CA)^-$ and $Na^+(CA)^-$ show considerable differences from those of $K^+(CA)^-$ and $Rb^+(CA)^-$: that is, in the visible region, the former shows the absorption band around 26 kK, with a shoulder around 23 kK, while the latter shows the band with structures around 22.0, 23.3, and 24.5 kK, and the ratio of the absorption-band intensity in the near-infrared region to that in the visible region is larger for the former than for the latter.[16] The absorption band in the near-infrared region of $Li^+(CA)^-$ is around 14 kK; this energy is 2 kK higher than those of the other salts.

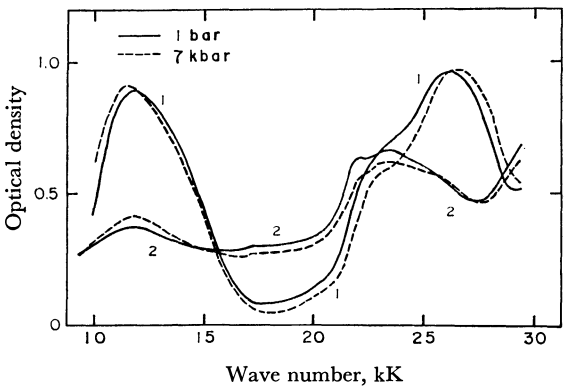

Fig. 2. Pressure dependence of the absorption spectra of crystalline $Na^+(CA)^-$ and $K^+(CA)^-$, curve 1: $Na^+(CA)^-$, curve 2: $K^+(CA)^-$.

The effect of pressures up to 7 kbar on the electronic absorption spectra of these salts was measured at room temperature. The absorption spectra of $Na^+(CA)^-$ and $K^+(CA)^-$ at 1 bar and 7 kbar are shown in Fig. 2. $Li^+(CA)^-$ and $Na^+(CA)^-$ exhibit a blue shift for the visible absorption band and a red shift for the near-infrared band, with an increase in the pressure. The rates of the frequency shift with the pressure are +62 and −58 cm^{-1}/kbar for the 26.2 and 11.8 kK peaks of $Na^+(CA)^-$ respectively, as is shown in Fig. 3 and as has previously been reported briefly[5]; those of $Li^+(CA)^-$ are almost the same. On the other hand, in the cases of $K^+(CA)^-$ and $Rb^+(CA)^-$, the absorption spectra are insensitive to the pressure: that is, no effect of the pressure is observed, at least up to 7 kbar, except for a slight change in the band intensity of $K^+(CA)^-$ (Fig. 2).

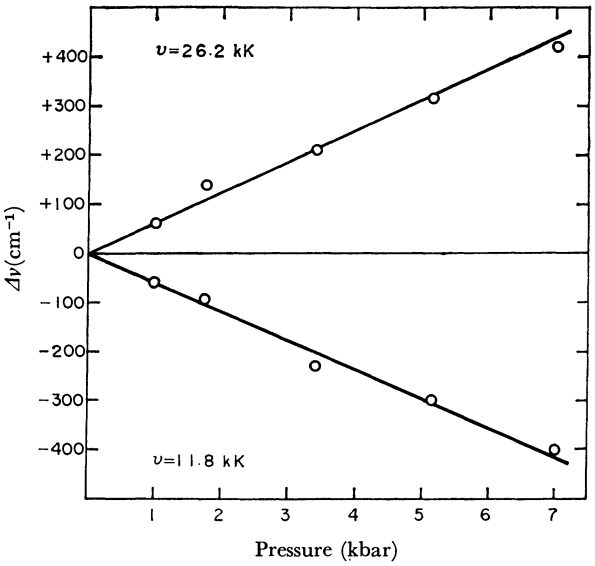

Fig. 3. Frequency shift with pressure for 26.2 and 11.8 kK peaks of $Na^+(CA)^-$.

These pressure effects, in particular, a large pressure-induced blue shift of the band in the visible region, suggest that chloranil anions associate bimolecularly in the crystalline state in $Li^+(CA)^-$ and $Na^+(CA)^-$. This is analogous to the situation with alkali metal cation-TCNQ anion radical salts in the crystalline state, where the absorption spectra are similar to those of the radical dimer $(TCNQ^-)_2$ in an aqueous solution, and where, in the visible region, there is a large blue shift with an increase in the pressure. This shift has been discussed in connection with the stabilization of the electronic-ground state from the characteristic crystalline structure (stacked face-to-face) of TCNQ anions and the crystal-field effect of the metal cations surrounding the TCNQ anions.[6] Therefore, we investigated whether or not the dimerization of the chloranil anion occurs in solutions,

14) As a test of the reliability of this method, the absorption spectra of single crystals of K^+ $(CA)^-$ in the visible region were measured by using a microspectrophotometer. The spectra measured by the present method agree well with those measured on single crystals.

15) J. J. André and G. Weill, *C. R. Acad. Sci., Paris, Ser. B*, **269**, 499 (1969).

16) The spectra of Rb^+ $(CA)^-$ obtained by the method of the KBr disk are similar to those of Na^+ $(CA)^-$ in the visible region; therefore, when the method of the KBr disk is used, some attention should be taken.

as has been observed in a solution of Würster's cation,[17] the *p*-benzosemiquinone anion,[18] and the TCNQ anion;[19] consequently, a monomer-dimer equilibrium for $(CA)^-$ is confirmed in an ethanol solution at low temperatures (see the next section, B).

The absorption spectra of crystalline $Li^+(CA)^-$ and $Na^+(CA)^-$ are similar to those of the dimer in solution, while the spectra of $K^+(CA)^-$ and $Rb^+(CA)^-$ are similar to those of the monomer in solution except for the weak near-infrared absorption band in the crystalline state. Although the dimerization of the chloranil anion in solution is observed in all four alkali metal cation-chloranil anion radical salts, $K^+(CA)^-$ and $Rb^+(CA)^-$ show an electronic structure with the nature of the monomer in the crystalline state.

The X-ray diffraction powder patterns of $Na^+(CA)^-$ and $K^+(CA)^-$ at room temperature, in which slight differences are observed from sample to sample, show a remarkable difference in the crystalline nature between the two salts, as is shown in Fig. 4.

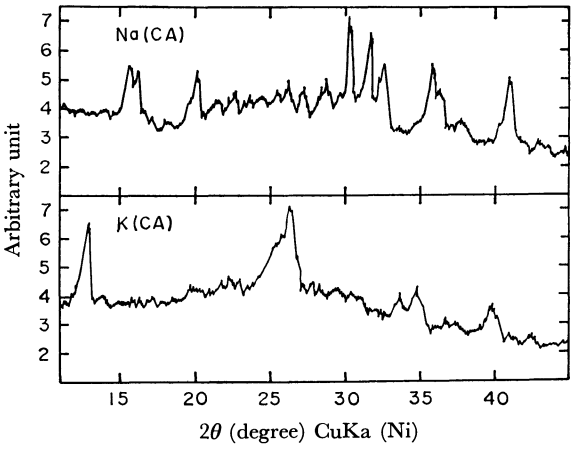

Fig. 4. X-ray diffraction powder patterns of $Na^+(CA)^-$ and $K^+(CA)^-$ at room temperature.

The ionic radii of Li^+, Na^+, K^+, and Rb^+ are 0.78, 0.98, 1.33, and 1.49 Å, respectively, where the increase from Na^+ to K^+ is marked.[20] The polarizing powers, which are equal to Ze/r^2 (Z: number of charge, e: elementary charge, r: ionic radius), are 1.64, 1.04, 0.57, and 0.45 (arbitrary unit) for Li^+, Na^+, K^+, and Rb^+ respectively, where the values for Li^+ and Na^+ are much larger than those for K^+ and Rb^+.[20] That is, Li^+ and Na^+ have a stronger power to distort the opponent electron cloud than K^+ and Rb^+, and the effect of this power cannot be ignored for a molecule with π-electrons. Although alkali metal cation-TCNQ anion radical salts show little difference in the electronic structure of TCNQ anions in the crystalline state, in the case of alkali metal cation-chloranil anion radical salts, the packing and the electronic structure of the chloranil anions in the crystalline state may be considerably affected by the size and the polarizing power of the counter ion; consequently, chloranil anions seem to be dimeric in $Li^+(CA)^-$ and $Na^+(CA)^-$, the alkali metal cations of which have small ionic radii and large polarizing powers.[21] On the other hand, chloranil anions seem to be monomeric, with a weak interaction between anion radicals in $K^+(CA)^-$ and $Rb^+(CA)^-$[21]; it also seems that their absorption spectra are insensitive to the pressure because of the weak inter-radical interaction and seem to be less compressible because of the large ionic radii.

In the case of bromanil salts, the absorption spectra of crystalline $K^+(BA)^-$ are similar to those of crystalline $K^+(CA)^-$, and the effect of pressure on the absorption spectra was not observed, at least up to 7 kbar; the absorption spectra of crystalline $Na^+(BA)^-$ are diffused and are not clear, but they seem to be characteristic of both of the monomer and the dimer of BA^-. The spectra of $Na^+(BA)^-$ obtained by the method of the KBr disk are, however, similar to those of $Na^+(CA)^-$ and behave the same as $Na^+(CA)^-$ under high pressures. The dimerization of the bromanil anion was not observed in an ethanol solution down to the temperature of liquid nitrogen. The X-ray diffraction powder patterns of $Na^+(BA)^-$ and $K^+(BA)^-$ at room temperature resemble each other.

The phase transition accompanying a change in the electronic structure, as has been observed in WBP,[8,11,12,22] should be expected to occur in these chloranil and bromanil anion radical salts in which the intermolecular interaction between anion radicals differs from radical to radical.

B. Dimerization of Chloranil Anion Radical in Ethanol.

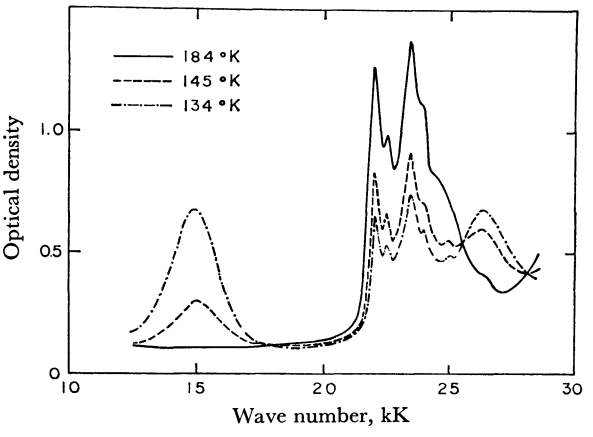

Fig. 5. Temperature dependence of the absorption spectra of $Na^+(CA)^-$ in ethanol.
Stoichiometric concentration: 3.7×10^{-4} mol/*l*. (at 293°K)
Optical path length: 0.40 cm.

17) K. Uemura, S. Nakayama, Y. Seo, K. Suzuki, and Y. Ooshika, This Bulletin, **39**, 1348 (1966).

18) K. Kimura, H. Yamada, and H. Tsubomura, *J. Chem. Phys.*, **48**, 440 (1968).

19) R. H. Boyd and W. D. Phillips, *ibid.*, **43**, 2927 (1965).

20) V. M. Goldschmidt, "Geochemische Verteilungsgesetze der Elemente VII, Die Gesetze der Krystallochemie," Skrifter Norske Videnskap Akad. Oslo. I Mat-Naturv, Kl. (1926).

21) From the temperature dependence of the intensities of the ESR spectra, it has been observed that, in the temperature range from 290°K to 370°K, the singlet-triplet model was approximately followed, with $\delta=0.16$ eV (the singlet-triplet energy separation) for $Na^+(CA)^-$, whereas the Curie-Weiss law was followed for $K^+(CA)^-$. These results would appear to be coincident with the electronic structure of chloranil-anion radical salts assumed from the electronic absorption spectra

22) H. Chihara, M. Nakamura, and S. Seki, This Bulletin, **38**, 1776 (1965).

When an ethanol solution of alkali metal cation-chloranil anion radical salts, a solution which is yellow at room temperature, is cooled to about 145°K, it turns green and new absorption bands appear in the electronic absorption spectra. The temperature dependence of the absorption spectra of $Na^+(CA)^-$ in ethanol is show nin Fig. 5. The absorption band around 22 kK may be attributed to the lowest energy π–π^* transition in the chloranil anion monomer.[23,24] From the concentration dependence (between 10^{-3} and 10^{-4} mol/l) of the absorption intensity of $Na^+(CA)^-$ in ethanol, the monomer and dimer of the chloranil anion radical can be said to be in equilibrium in solution. The thermodynamic quantities of dimerization are obtained by the following procedure.

An equilibrium of the degree of association of n for the anion radical is assumed:

$$n(CA)^- \rightleftarrows (CA^-)_n \qquad (1)$$

The equilibrium constant, K, is given by:

$$K = (1-\alpha)/(nc^{n-1}\alpha^n) \qquad (2)$$

where c is the stoichiometric concentration[25] of $Na^+(CA)^-$ and where α is the fraction of the stoichiometric concentration existing as a monomer. The apparent molar extinction coefficient at a certain wavelength is related to the molar extinction coefficients of the monomer and n-polymer as:

$$\varepsilon = \alpha\varepsilon_m + (1-\alpha)\varepsilon_n \qquad (3)$$

where ε is the apparent molar extinction coefficient, as calculated from the measured optical density and the concentration, where ε_m is the molar extinction coefficient of the monomer, and where ε_n is the molar extinction coefficient of one molecule in the n-polymer. The values of ε_m at several peaks are determined from the optical density measured at higher temperatures (190—170°K), where it seems that no association of the radicals occurred.[26] From the relation of Eqs. (2) and (3), the following equation is obtained:

$$\log\{c(1-\varepsilon/\varepsilon_m)\} = \log(BK) + n\log c(\varepsilon-\varepsilon_n)/\varepsilon_m\} \qquad (4)$$

where:

$$B = n(1-\varepsilon_n/\varepsilon_m)^{1-n}$$

Therefore, assuming $\varepsilon \gg \varepsilon_n$, Eq. (4) leads to:

$$\log\{c(1-\varepsilon/\varepsilon_m)\} = \log(BK) + n\log(c\varepsilon/\varepsilon_m) \qquad (5)$$

When $\log\{c(1-\varepsilon/\varepsilon_m)\}$ is plotted against $\log(c\varepsilon/\varepsilon_m)$ for the monomer band (λ_{max}=427 mμ) at 134°K, the slope of the straight line, n, is about 2. This means that the concentration dependence of the absorption spectra of $Na^+(CA)^-$ in ethanol at low temperatures can be explained by the equilibrium between the monomer and the dimer. The value of ε_d[27] is chosen to give a straight line with a slope of 2 when $\log\{c(1-\varepsilon/\varepsilon_m)\}$ is plotted against $\log\{c(\varepsilon-\varepsilon_d)/\varepsilon_m\}$, as is shown in Fig. 6: using this value of ε_d, the value of K is evaluated from Eq. (4). The ε_d values at other peaks are evaluated using Eq. (3) from the measured ε, ε_m, and α values, calculated from ε, ε_m, and ε_d at 427 mμ using Eq. (3). The molar extinction coefficients at several peaks are shown in Table 1.

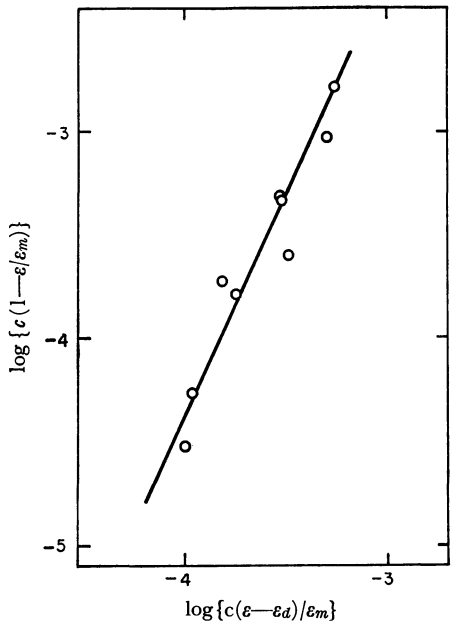

Fig. 6. Plots of $\log\{c(1-\varepsilon/\varepsilon_m)\}$ against $\log\{c(\varepsilon-\varepsilon_d)/\varepsilon_m\}$ for the monomer band (λ_{max}=427 mμ) at 134°K.

Table 1. Molar extinction coefficients of $Na^+(CA)^-$ in ethanol

Absorption peak		ε_m	$2\varepsilon_d$
3800 Å	(26.3 kK)	1700	9700
4270	(23.4 kK)	8500	1800
4545	(22.0 kK)	7700	1300
6700	(14.9 kK)	200	13600

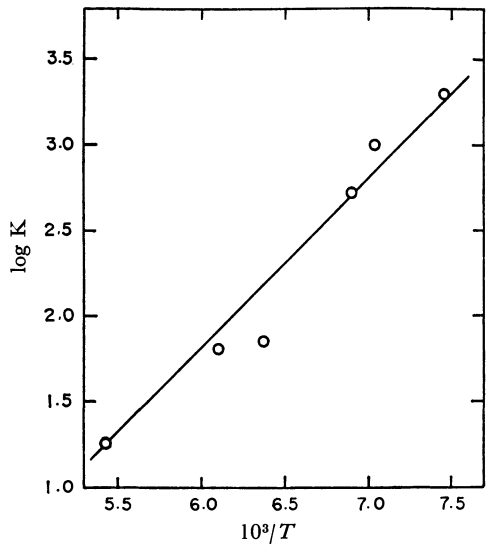

Fig. 7. Plots of $\log K$ against $10^3/T$ (°K)$^{-1}$ for the monomer band.

23) G. Giacometti, P. L. Nordio, and G. Rigatti, *Nuovo Cimento*, **23**, 433 (1962).
24) J. J. André and G. Weill, *Mol. Phys.*, **15**, 97 (1968).
25) Volume changes in solution with the temperature were taken into account.
26) The solution is stable at low temperatures, but it is slowly discolored at room temperature.
27) Here the ε_n in Eq. (4) is rewritten as ε_d.

Table 2. Thermodynamics of dimerization of CA^- at 134°K

K (l/mol)	ΔF (kcal/mol)	ΔH (kcal/mol)	ΔS (cal/mol·deg)
2.0×10^3	−2.0	−4.5	−18.7

A series of spectra at various temperatures on one solution is measured, and the equilibrium constant, K, at each temperature is calculated from α, obtained from the data at 427 mμ, using Eq. (2): in Fig. 7 $\log K$ is plotted against $1/T$. The thermodynamic quantities are shown in Table 2.

The dimerization in ethanol at low temperatures is observed for $Li^+(CA)^-$, $K^+(CA)^-$, and $Rb^+(CA)^-$, too. The thermodynamic quantities for other salts are of interest with regard to the influence of the counter ion upon the dimerization of CA^-.

The dimerization of CA^- is observed in an aqueous solution at room temperature, but it is very unstable in air.[28]

28) R. Foster and T. J. Thomson, *Trans. Faraday Soc.*, **59**, 296 (1963). This fact has been reported together with the absorption maxima of alkali metal salts of chloranil anion in tetrahydrofuran at —50°C.

BULLETIN OF THE CHEMICAL SOCIETY OF JAPAN, VOL. 44, 679—681 (1971)

Spreadability of Ovalbumin Monolayers at Air-water Interface. Effects of Additives to Spreading Solutions

Toshio Ishii* and Mitsuo Muramatsu

Department of Chemistry, Tokyo Metropolitan University, Setagayaku, Tokyo

(Received October 26, 1970)

The effect of additives (urea, potassium chloride, butanol, and thioglycol) to spreading solutions upon spreadability of ovalbumin monolayers has been studied in terms of the rate constants and the limiting areas for intermediate (fast) and final (slow) processes of uncoiling of the protein molecule. It has been found that the addition results in the disappearance of the first (fast) process, which appeared upon spreading without additives. In the second (slow) process, the rate constant is found to be the same as that for the case without additives regardless of the type of the additives. Sodium dodecyl sulfate (SDS) added to the spreading solution is showed a peculiar behavior, which is explained in relation to the interaction between the protein and SDS molecules.

It has been reported that the monolayers of proteins[1-5] and synthetic polypeptides[6-8] are markedly affected by their addition to subphase of various salts, surface-active agents, or other substances which influence the net-work formation involving hydrogen bonding. The increase or decrease thereby observed was interpreted by the interaction between protein and the additive molecules. Most of the interpretations were based on the tacit assumption that the systems were always in the equilibrated states. It has been pointed out in the preceding paper[9] that the properties of protein monolayers should preferably be analysed as a reflection of kinetic processes rather than the equilibrated state. Thus, the isoelectric point was characterized by acidity, when the spreading was achieved instantaneously to give the highest rate of uncoiling of the polypeptide chain. A similar type of instantaneous spreading has also been observed[10,11] when adequate additives are contained in aqueous subphases or in spreading solutions. The present paper deals with the effect of additives to the aqueous solution of ovalbumin on its spreadability at air-water interface, in order to make clear how the mixed solutions of the protein and the additives reveal themselves in the monolayer properties to be studied from the kinetic aspects.

Experimental

Apparatus used was the same as that in the previous work.[9] The surface pressure (F) was determined by means of a Whilhelmy plate balance of ± 0.05 dyn/cm sensitivity. A glass tray contained subphase water, on which ovalbumin monolayers were spread from aqueous solutions of various additives, such as urea, potassium chloride, butanol, thioglycol, and sodium dodecyl sulfate. The aqueous surface prior to the spreading was clean enough to observe $F<5$

* Present address: Chiba Institute of Technology, Narashino-shi, Chiba-ken.

1) K. G. A. Pankhurst, "Surface Phenomena in Chemistry and Biology," ed. by J. F. Danielli, K. G. A. Pankhurst, and A. C. Riddiford, Pergamon Press Inc., London (1958), p. 100.
2) J. H. Schulman and E. K. Rideal, *Proc. Roy. Soc.*, **B122**, 46 (1937).
3) E. G. Cockbain and J. H. Schulman, *Trans. Faraday Soc.*, **35**, 716, 1266 (1939).
4) S. C. Ellis and K. G. A. Pankhust, *Discuss. Faraday Soc.*, **16**, 170 (1954).
5) T. Isemura and K. Hamaguchi, *Ann. Rep. Scient. Works, Fac. Sci. Osaka Univ.*, **5**, 65 (1957).
6) K. Hamaguchi and T. Isemura, This Bulletin, **28**, 9 (1955).
7) T. Isemura, K. Hamaguchi, and H. Kawasato, *ibid.*, **28**, 185 (1955).
8) T. Yamashita and T. Isemura, *ibid.*, **38**, 420 (1965).
9) T. Ishii and M. Muramatsu, This Bulletin, **43**, 2364 (1970).
10) A. Lajtha and E. K. Rideal, *Arch. Biochem. Biophys.*, **33**, 252 (1951).
11) M. Muramatsu and H. Sobotka, *J. Colloid Sci.*, **18**, 625 (1963).

dyn/cm, when it had been compressed to 1/20 area ratio after having been kept standing for 24 hr.

The sample of ovalbumin was the same as that in the previous work.[9] The additives were purified thoroughly by appropriate procedures; recrystallization and/or distillation, followed by ethereal elimination of possible impurities in a Soxhlet extractor. They were all clean enough to recognize appreciable increment in the surface pressure for the protein-free surface, to which their solutions were applied for blank test. All experiments were carried out on subphase of initial pH 5.3±0.1 adjusted with a small amount of hydrochloric acid at 25.0±0.5°C.

Results and Discussion

The surface denaturation processes can quantitatively be expressed as[9]

$$(A_\infty^0 - A^0) = (A_\infty^0 - A_2^0)\exp(-k_2 t) + (A_2^0 - A_1^0)\exp(-k_1 t) \quad (1)$$

where A^0 is the limiting area at a given time, t, elapsed from the spreading, A_∞^0 the area at $t=\infty$, A_1^0 the area for the first process starting at $t=0$, A_2^0 that for the second, and k_1 and k_2 are the rate constants for the two processes, in which the whole denaturation processes are comprised. This is the case of protein monolayer spread from aqueous solution without any additives, appearing as the dotted and dashed lines in Fig. 1. The additives to the spreading solution caused the disappearance of the second term in Eq. (1), as seen in Fig. 1, where the six straight lines for four additives

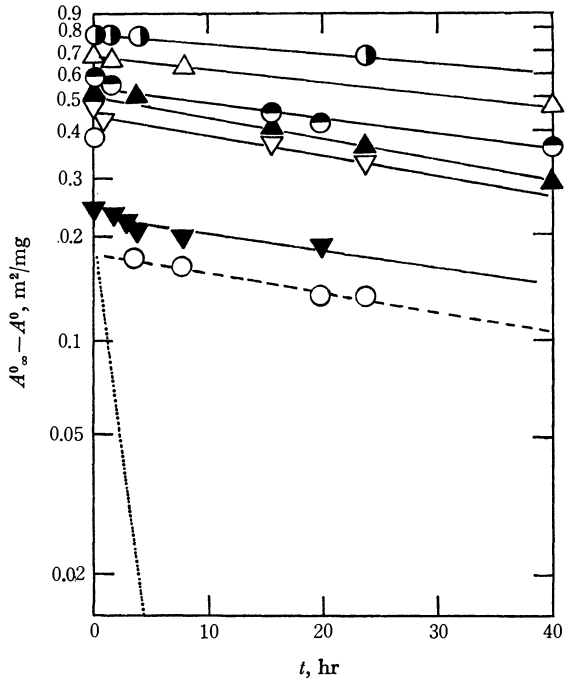

Fig. 1. Time dependences of $(A^0_\infty - A^0)$ for the monolayers of ovalbumin spread from its solutions containing urea (1M, ◑), KCl (1M, △▲), butanol (0.1%, ◓), and thioglycol (0.1%, ▽▼), or without any additives (○). The dashed and dotted lines express the first and second terms, respectively, in Eq. (1) for the case without additives. In the case of KCl and thioglycol, experiments were carried out twice independently and the results are shown as upward and downward triangles, respectively.

run almost in parallel with the dashed line. This means that the k_2 values are not changed by the addition of any of the four additives to the solution, with the $(A_\infty^0 - A_2^0)$ values characteristic of their effect. Such an effect of the additives has been reported for potassium chloride added to the spreading solution of myosin[10] and bovine serum albumin,[11] for which the instantaneous spreading could be understood either as $A_\infty^0 = A_2^0 = A_1^0$ or as $k_1 = k_2 = \infty$.

Differentiation of Eq. (1) gives

$$dA^0/dt = k_2(A_\infty^0 - A_2^0)\exp(-k_2 t) + k_1(A_2^0 - A_1^0)\exp(-k_1 t). \quad (2)$$

For the region,

$$t > \frac{1}{k_1 - k_2}\ln\left(\frac{k_1}{k_2}\cdot\frac{A_2^0 - A_1^0}{A^0 - A_2^0}\right), \quad (3)$$

or for

$$(A_2^0 - A_1^0) = 0, \quad (4)$$

Eq. (1) is simplified as

$$dA^0/dt = k_2(A_\infty^0 - A^0). \quad (5)$$

Eq. (3) is the case of the tailing period of the dashed line, while Eq. (4) corresponds to the disappearance of the dotted line. This means that the addition results in the verified applicability of Eq. (5) to any of the four additives. Taking into account of the conditions, dA^0/dt is plotted in Fig. 2 against A^0. It can be seen from the

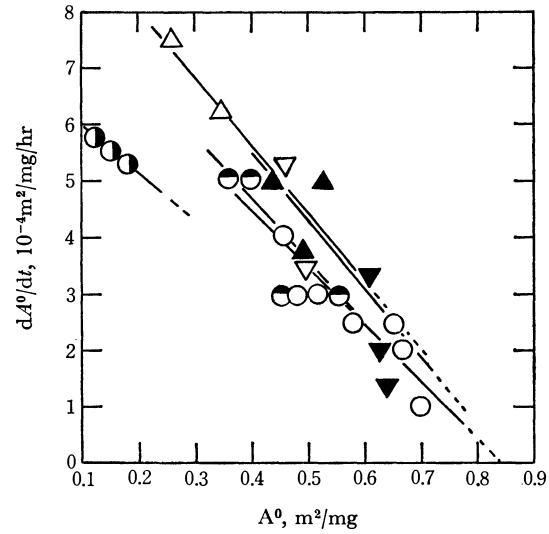

Fig. 2. Relationship of dA^0/dt and A^0 for ovalbumin monolayers spread from aqueous solutions containing urea (1M, ◑), KCl (1M, △▲), butanol (0.1%, ◓), and thioglycol (0.1%, ▽▼), or without any additives (○).

figure that all of the five lines give more or less the same values in their slant and intercept at the abscissa, suggesting the same k_2 and A_∞^0 values in Eq. (5). Thus, the difference in the intercept at the ordinate in Fig. 1 is an indication of the difference in A_2^0 values for individual additives. The additives seem to affect the spreading processes in such a manner as to eliminate one of the two steps involving A_1^0 and to keep the other, starting with individual A_2^0 values and ending at the same A_∞^0 value, which is 0.83 m²/mg or 16.4 Å²/residue, as in the previous report.[9]

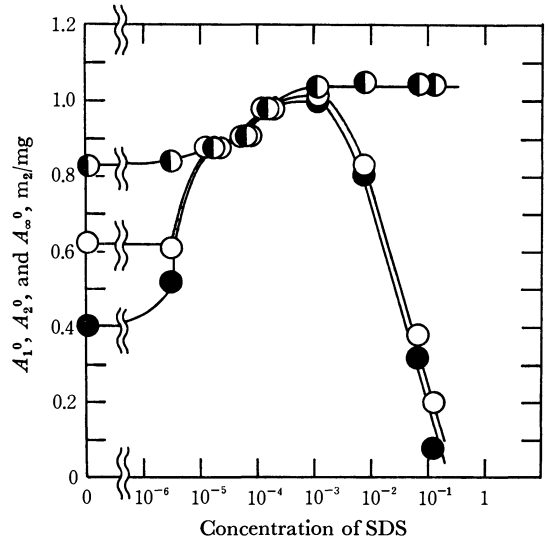

Fig. 3. Effects of SDS concentration in spreading solution on limiting areas, A_1^0 (●), A_2^0 (○), and A_∞^0 (◐) of ovalbumin monolayers.

Similar treatments were applied to the system involving SDS added to the spreading solution. Results are shown in Fig. 3, in which A_i^0's ($i=1$, 2, and ∞) are plotted against SDS concentration in the spreading solution containing protein for monolayer. It can be seen that the addition of SDS to the spreading solution affects in two different stages. For concentrations lower than *ca.* 3×10^{-4}M, it causes increments in A_i^0's with the coincident value of 0.83—1.04 m^2/mg, which is higher than the A_∞^0 value (0.83 m^2/mg) obtained for the protein monolayers without SDS.[9] For concentrations beyond this the addition of SDS results in the constant A_∞^0 value and the marked lowerings in A_1^0 and A_2^0.

These two stages seem to reflect the different fashions in interacting SDS molecules with protein. It should be noted for the first stage that the rate constants, k_1 and k_2, are almost the same as those for the protein without SDS. These phenomena can be interpreted by the attachment of SDS molecules to protein, which causes the increase of limiting area in such a manner as not to influence the easiness of its uncoiling processes.

At the concentration of around 3×10^{-4}M, uncoiling is completed instantaneously. This means that the interaction reaches a critical point, so that the association is made between SDS and protein molecules. A similar association has been proposed for explaining the shifting of optical absorption spectra of a mixed solution of *p*-aminoazobenzene and SDS when bovine serum albumin is added to it.[12] Electrophoretical studies[13] on the mixed solution of SDS and ovalbumin have also shown the appearance of a shift due to the formation of SDS-protein complex at around 10^{-5}M, which is in accord with the threshold value of the coincident region in Fig. 3.

The second stage is characterized by k_2 values 1.4—3.3 times larger than those for the first, with the constant A_∞^0 and the lowering A_1^0 and A_2^0 values. The increment beyond the saturation concentration seems to contribute to the interaction in such a manner as to decrease the A_1^0 and A_2^0 values but not to affect the saturated A_∞^0, which does not much differ from that obtained in the first stage. Probably, the attached SDS is increased by a small amount throughout the second stage. The role of these SDS molecules in the second stage should be different from that in the first. Blei[12] has proposed a solubilizing complex comprised in SDS molecules located to hydropohbic residue of the molecules of bovine serum albumin. A similar structure may be taken into account for elucidating the uncoiling processes of ovalbumin in the second stage of SDS concentration.

12) I. Blei, *J. Colloid Sci.*, **15**, 370 (1960).
13) K. Aoki, This Bulletin, **29**, 369 (1956).

Electronic Structures, Electronic Spectra, and Aromatic Characteristics of Peri-Condensed Tetracyclic Nonbenzenoid Aromatic Hydrocarbons Containing a Naphthalene Nucleus

Hiroyuki YAMAGUCHI and Takeshi NAKAJIMA

Department of Chemistry, Tohoku University, Katahira-cho, Sendai

(Received October 28, 1970)

The ground-state electronic properties and electronic spectra of pyracylene (I), acepleiadylene (II), and dipleiadiene (III) have been studied by using the semi-empirical SCF LCAO-π-MO method, which allows for bond order-bond length correlation at each iteration. It is shown that the I and III molecules do not belong to, respectively, the pentalenoid and heptalenoid systems, as was expected from the HMO energy diagram. The predicted chemical reactivities, diamagnetic anisotropies, and electronic spectra for I and II are in good agreement with the available experimental data. The calculated C–C bond lengths indicate that the I, II, and III molecules are all both aromatic and polyolefinic. The upfield shift of the NMR spectrum and the unusually low value of the first half-wave potential for I can be well explained in terms of, respectively, the diamagnetic anisotropy and the energy of the lowest vacant SCF MO, calculated by using the predicted equilibrium configuration that corresponds to the aromatic model (Ia).

The electronic structures and aromatic characteristics of tetracyclic nonbenzenoid aromatic hydrocarbons containing a naphthalene nucleus have been of theoretical interest since Boekelheide and Vick[1] synthesized acepleiadylene (II) in 1956.

Trost and Bright[2] have recently reported the successful synthesis of pyracylene (I). Theoretical interest in whether I or not is a pentalenoid system was then stimulated. These authors proposed two possible structures, a naphthalene core with two vinyl bridges (Ia) and a cyclododecahexene with a vinyl cross-link (Ib). They concluded, from the upfield shift of the NMR spectrum and the unusually low value of the first half-wave potential, that the peripheral model (Ib) is a better representation for I. Lo and Whitehead[3] have calculated the ground-state electronic properties of I using the LCAO MO SCF PPP ($\pi+\sigma$) method and have concluded that the most stable configuration corresponds to the aromatic model (Ia).

Pullman *et al.*[4] have studied the electronic structures and spectra of II using the Hückel MO method. From the calculated delocalization energy, they have found that II should be aromatic. Koutecký *et al.*[5] have applied the SCF MO method based on the Pariser-Parr-Pople approximation to II and have calculated its transition energies and intensities, but they have not mentioned its aromaticity.

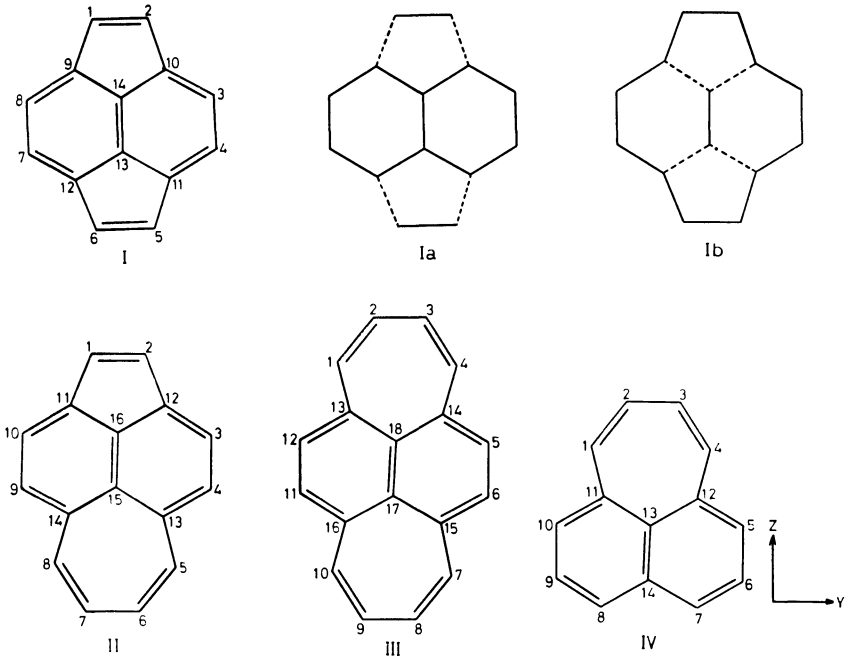

Fig. 1. Co-ordinate system and numbering of atoms.

1) V. Boekelheide and G. K. Vick, *J. Amer. Chem. Soc.*, **78**, 653 (1956).
2) B. M. Trost and G. M. Bright, *ibid.*, **89**, 4244 (1967).
3) D. H. Lo and M. A. Whitehead, *Chem. Commun.*, **1968**, 771.
4) B. Pullman, A. Pullman, G. Berthier, and J. Pontis, *J. Chim. Phys.*, **49**, 20 (1952).
5) J. Koutecký, P. Hochman, and J. Michl, *J. Chem. Phys.*, **40**, 2439 (1964).

Using the HMO method, Zahradnik *et al.*[6] have investigated the electronic structures, electronic spectra, and stability of I, II, and dipleiadiene (III), the last of which is yet unknown. On the basis of a new definition of stability, they have concluded that I and III are unstable, while II is stable. Recently, using the Molecules in Molecules method, Favini *et al.*[7] have calculated the transition energies and intensities for I, II, and III, but they have not considered anything with regard to the stable configurations and aromaticity of these molecules.

It is the purpose of this paper to determine the equilibrium configurations of I, II, and III by using the variable bond-length SCF LCAO-π-MO CI technique and to examine theoretically their ground-state electronic properties and electronic spectra. It should be possible to use the results of such calculations to deepen our understanding of the aromatic characteristics of I, II, and III.

Method of Calculation

The electronic structures and spectra are calculated by using the variable bond-length SCF LCAO-π-MO method, in which the C–C bond lengths and, consequently, the resonance and two-center repulsion integrals are allowed to vary with the bond order at each iteration until self-consistency is reached. The C–C bond lengths, r, are correlated with the bond orders, p, by the following relationship:

$$r(\text{Å}) = 1.520 - 0.186p \quad (1)$$

The two-center repulsion integrals are calculated using the Mataga-Nishimoto formula.[8] The resonance integrals are evaluated using Method 2 of Ref. 9, in which the dependence of the resonance integral on the bond length is assumed to be exponential; the value of the exponent was determined by trying to reproduce as many properties of the ground and excited states as possible in a series of reference molecules. In order to discuss the properties of excited states, a configuration mixing of all the singly-excited states is included.

The diamagnetic susceptibilities are calculated by using the London[10]-Hoarau[11] method in the framework of the Wheland-Mann-type SCF MO approximation.[12] The resonance integral is assumed to be again of the exponential form, the value of the exponent in this case being 4.4 Å^{-1}. This value was determined so as to reproduce the bond lengths, electron densities, and dipole moments, which were obtained from the variable bond-length SCF LCAO-π-MO technique, for butadiene, pentafulvene, heptafulvene, and naphthalene. This method has been applied to a number of benzenoid and nonbenzenoid aromatic hydrocarbons and has been found to produce theoretical values which are in good agreement with the experimental results.[13]

Results and Discussion

Ground-state Symmetries. The HMO energy levels show that, in the I molecule, the lowest unoccupied MO is non-bonding as in pentalene, while in the III molecule the highest occupied MO is non-bonding as in heptalene. In this sense, it has been said that the I molecule belongs to the pentalenoid system, and the III molecule, to the heptalenoid system.[6,14] The energy differences between the highest occupied MO and the lowest unoccupied MO for I and III are almost the same as those of, respectively, the pentalene and heptalene molecules, both of which are pseudo-Jahn-

Table 1. Charge densities, free balence numbers and bond lengths

Molecule	Atom	Charge density	Free valence	Bond	Bond length(Å)
I	1	1.018	0.520	1—2	1.353
	3	0.970	0.439	1—9	1.462
	9	0.991	0.204	3—4	1.412
	13	1.043	0.155	8—9	1.387
				12—13	1.426
				13—14	1.414
II	1	1.033	0.484	1—2	1.362
	3	0.952	0.432	1—11	1.446
	4	1.041	0.434	3—4	1.402
	5	0.978	0.495	4—13	1.397
	6	0.983	0.464	5—6	1.364
	11	1.031	0.175	5—13	1.446
	13	0.973	0.176	6—7	1.440
	15	0.972	0.160	10—11	1.397
	16	1.045	0.159	11—16	1.428
				13—15	1.428
				15—16	1.412
III	1	0.986	0.517	1—2	1.357
	2	0.997	0.488	1—13	1.457
	5	1.019	0.438	2—3	1.452
	13	1.011	0.193	5—6	1.410
	17	0.975	0.155	12—13	1.390
				16—17	1.427
				17—18	1.413
IV	1	0.985	0.514	1—2	1.358
	2	0.993	0.480	2—3	1.449
	5	1.026	0.446	1—11	1.456
	6	0.995	0.402	5—6	1.412
	7	1.016	0.459	6—7	1.380
	11	0.997	0.179	5—12	1.388
	13	0.976	0.159	7—14	1.423
	14	0.998	0.115	11—13	1.427
				13—14	1.413

6) R. Zahradnik, J. Michl, and J. Pancir, *Tetrahedron*, **22**, 1355 (1966).
7) G. Favini, A. Gamba, and M. Simonetta, *Theor. Chim. Acta*, **13**, 175 (1969).
8) N. Mataga and K. Nishimoto, *Z. Phys. Chem.* (Leipzig), **13**, 140 (1957).
9) H. Yamaguchi, T. Nakajima, and T. L. Kunii, *Theor. Chim. Acta*, **12**, 349 (1968).
10) F. London, *J. Chem. Phys.*, **5**, 837 (1937); *J. Phys. Radium*, **8**, 397 (1937).
11) J. Hoarau, *Ann. Chim.* (Paris), **1**, 544 (1956).
12) G. W. Wheland and D. E. Mann, *J. Chem. Phys.*, **17**, 264 (1949).
13) H. Yamaguchi and T. Nakajima, This Bulletin, to be published.
14) G. V. Boyd, *Tetrahedron*, **22**, 3409 (1966).

Teller molecules.[15] Therefore, it may be expected that the I and III molecules will suffer a pseudo-Jahn-Teller effect, which may result in a symmetry reduction from the fully symmetrical configuration.

We thus examined the ground-state symmetries of the I and III molecules, using a method of predicting the energetically most favourable equilibrium configuration of a conjugated hydrocarbon.[16] It turned out that, in both the molecules, the starting bond distortions belonging to irreducible representations, a_g, b_{3g}, b_{1u}, and b_{2u}, of the full symmetry group, D_{2h}, all converge into the unique self-consistent set of bond lengths corresponding to that symmetry group.

Thus, we may conclude that I and III molecules are not pentalenoid and heptalenoid respectively and that neither molecule is a so-called pseudo-Jahn-Teller molecule.

Ground-state π-Electronic Properties. The calculated charge densities, free valence numbers, and bond lengths are summarized in Table 1. The greatest nucleophilic reactivity is predicted to be exhibited by the 3, 4, 7, and 8 atoms in I, by the 3 and 10 atoms in II, and by the 17 and 18 atoms in III. The greatest electrophilic reactivity is expected at the 13 and 14 positions in I, the 16 position in II, and the 5, 6, 11, and 12 positions in III. The results for II do not agree with those of the simple HMO method,[4] which indicate that the highest reactivity for nucleophilic and electrophilic reactions is to be expected at the 5 and 8 positions and at the 1 and 2 positions, respectively. It is hoped that eventually this point can be established experimentally. From the viewpoint of chemical reactivity, it is noteworthy that the free valence values of atoms belonging to the 5- and 7-membered rings of all the molecules examined are significantly larger than those in classical aromatic hydrocarbons. This perhaps provides evidence for the fact that the attempts to isolate the I molecule produce only amorphous yellow polymers.[2]

Next, let us discuss the reactivity for the addition reactions of I, II, and III. It has been known that, in the presence of cyclopentadiene, the 1, 2-dibromo derivative of I gives an addition product[17] at the 5 and 6 positions and that II does not react with maleic anhydride under the same conditions under which maleic anhydride gives Diels-Alder adducts with pleiadiene IV.[1] These facts can be explained by comparing the sum of the free valences for the two positions concerned; $F_5+F_6=1.040$ in I and $F_1+F_4=1.028$ in IV are larger than $F_1+F_2=0.968$ and $F_5+F_8=0.990$ in II. Furthermore, it is expected that III will suffer addition reactions at the 1 and 4 positions, because the sum of the free valences at these positions ($F_1+F_4=1.034$) is comparable to F_1+F_2 for I and F_1+F_4 for IV

As for the bond lengths, it is of interest to note that the bond lengths of the naphthalene core of I, II, and III are almost the same as those of the free naphthalene molecule. There is a marked double-bond fixation in the remainder of the periphery. The I and III molecules show a double-bond fixation in their peripheries to a greater extent than II. In fact, the presence of two isolated vinyl bridges in the periphery of I is confirmed by the experimental fact that hydrogenation occurs only at the 1, 2- and 5, 6-positions to give pyracene.[2] The reason why the equilibrium configurations of I and III show such a double-bond fixation in the periphery may be explained by using a simple perturbational treatment. The I and III molecules have a 4n perimeter which has degenerate nonbonding orbitals, Φ_A and Φ_S, which are antisymmetric and symmetric respectively with respect to the y axis, as is shown in Fig. 2. The antibonding orbital of the vinyl segment located at the center of I interacts with the Φ_A state of the 12-monocyclic system and stabilizes it, as is also shown in Fig. 2. On the other hand, the bonding orbital of the vinyl segment

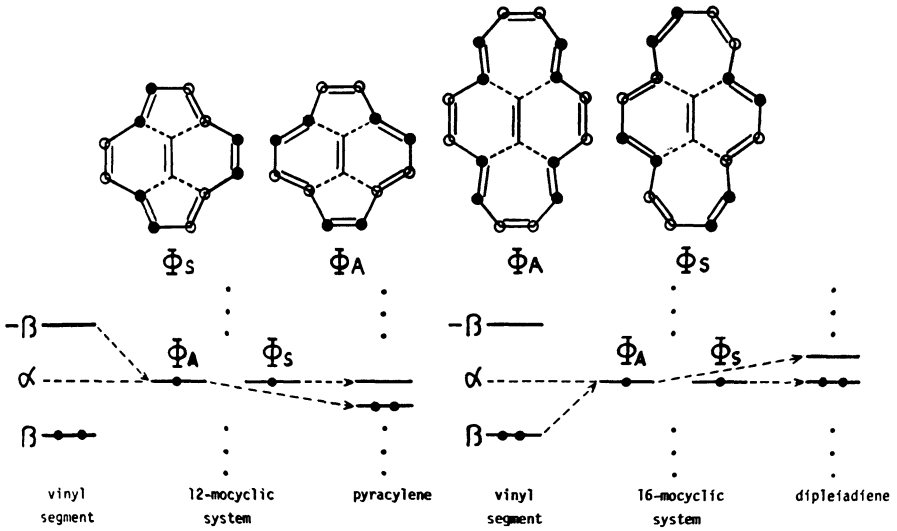

Fig. 2. Wave functions of nonbonding orbitals, Φ_A and Φ_S of 4n monocyclic systems and interaction scheme between vinyl segments and 4n monocyclic systems. The open and dark circles represent plus and minus signs of the LCAO coefficients, respectively.

15) H. A. Jahn and E. Teller, *Proc. Roy. Soc., Ser.* **A161**, 220 (1937).
16) T. Nakajima and A. Toyota, *Chem. Phys. Lett.*, **3**, 272 (1969).
17) B. M. Trost and D. R. Brittelli, *Tetrahedron Lett.*, **1967**, 119.

located at the center of III interacts with the Φ_A state of the 16-monocyclic system and makes it unstable.

Magnetic Properties. The diamagnetic susceptibility of a ring π-electron system is one of the important indications of π-electron delocalization. The calculated molar magnetic anisotropies, ΔK, for I, II, and III are -0.40, 3.92 and -0.34 respectively, in units of $\Delta K_{\text{benzene}}$. The predicted value for II is in good agreement with the experimental exaltation ($\Lambda/\Lambda_{\text{benzene}}=3.87$).[18] It turned out that the magnetically-induced ring currents in I and III are very much impeded. A part of the evidence for this fact is given by the NMR spectrum of I, which consists of two singlets of equal intensity at 3.48 and 3.99τ,[2] which are close to that observed for the olefinic protons of linear conjugated polyenes. The periphery of I and III may give a paramagnetic ring current characteristic of the 4n perimeter.[19] On the other hand, the naphthalene core in I and III may exhibit a diamagnetic ring current to the same extent as that of a free naphthalene molecule. Therefore, it may be expected that the paramagnetic ring current and the diamagnetic ring current cancel out each other to give a small magnetic susceptibility in I and III.

Half-wave Reduction Potentials. It has been shown that there is an excellent correlation between the energy of the first unoccupied molecular orbital and the half-wave reduction potential. Polarographic half-wave reduction potentials for a number of hydrocarbons in aqueous dioxane are summarized in Ref. 20. A plot of these aqueous-dioxane data against m, the energy (in units of eV) of the lowest vacant SCF MO, gives a good linear correlation (see Fig. 3). The least-square correlation line is:

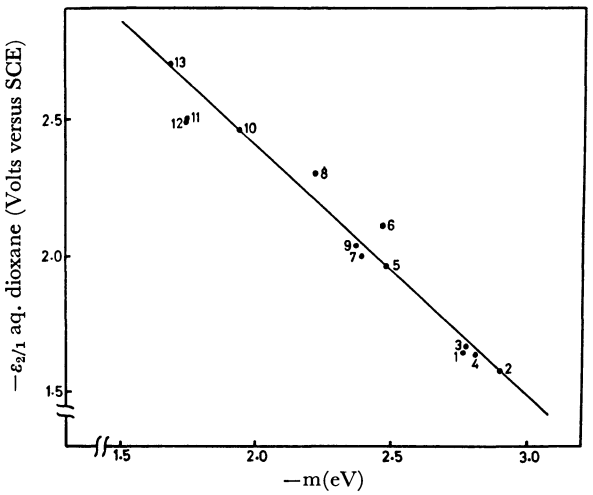

Fig. 3. Plot of half-wave potentials ($-\varepsilon_{1/2}$) in aqueous dioxane against energies ($-m$) of lowest vacant SCF orbitals. (1) Acenaphtylene, (2) Tetracene, (3) Perylene, (4) Azulene, (5) Anthracene, (6) Pyrene, (7) 1,2-Benzanthracene, (8) Chrysene, (9) Coronene, (10) Phenanthrene, (11) Naphthalene, (12) Triphenylene, (13) Biphenyl.

18) H. J. Dauben, Jr., J. D. Wilson, and J. L. Laity, *J. Amer. Chem. Soc.*, **91**, 1991 (1969).
19) J. A. Pople and K. G. Untch, *ibid.*, **88**, 4811 (1966).
20) A. Streitwieser, Jr., "Molecular Orbital Theory for Organic Chemists," John Wiley & Sons. Inc., New York (1961), p. 178.

Table 2. Transition types, energies (ΔE) and intensities (f)

Molecule	Transition type	Theoretical ΔE(eV)	f(cgs)	Experimental ΔE(eV)
I	$B_{3g}\leftarrow A_g$	2.24	forb.	tailing to 2.09[a]
	$B_{2u}\leftarrow A_g$	3.23	0.048	2.91
	$B_{1u}\leftarrow A_g$	3.75	0.33	3.65
	$B_{2u}\leftarrow A_g$	4.09	0.18	3.81
	$A_g\leftarrow A_g$	4.62	forb.	5.23
	$B_{2u}\leftarrow A_g$	5.41	0.008	
	$A_g\leftarrow A_g$	5.97	forb.	5.71
	$B_{2u}\leftarrow A_g$	5.99	2.18	
II	$A_1\leftarrow A_1$	2.98	0.28	2.20[b]
	$B_2\leftarrow A_1$	3.15	0.026	?
	$B_2\leftarrow A_1$	3.32	0.066	3.54
	$B_2\leftarrow A_1$	3.87	0.025	
	$A_1\leftarrow A_1$	4.50	0.96	4.14
	$A_1\leftarrow A_1$	4.67	0.16	
	$B_2\leftarrow A_1$	5.09	0.87	
	$A_1\leftarrow A_1$	5.13	0.010	4.98
	$A_1\leftarrow A_1$	5.26	0.021	
	$A_1\leftarrow A_1$	5.64	0.021	5.90
	$B_2\leftarrow A_1$	5.68	0.40	
III	$B_{3g}\leftarrow A_g$	2.15	forb.	
	$B_{2u}\leftarrow A_g$	3.13	0.014	
	$B_{1u}\leftarrow A_g$	3.30	0.60	
	$B_{2u}\leftarrow A_g$	3.69	0.15	
	$A_g\leftarrow A_g$	4.51	forb.	
	$B_{2u}\leftarrow A_g$	4.70	0.091	
	$A_g\leftarrow A_g$	4.94	forb.	
	$B_{1u}\leftarrow A_g$	5.30	1.17	
	$A_g\leftarrow A_g$	5.46	forb.	
	$B_{2u}\leftarrow A_g$	5.49	1.71	

a) B. M. Trost, personal communication
b) V. Boekelheide and G. K. Vick, *J. Amer. Chem. Soc.*, **78**, 653 (1956).

$$-\varepsilon_{1/2}(\text{aq. diox.}) = -0.919(-m) + 4.240 \qquad (2)$$

The half-wave potentials, $\varepsilon_{1/2}$, predicted using Eq. (2) for I, II, and III are -1.083, -1.716, and -1.935 V *vs.* SCE respectively. The predicted $\varepsilon_{1/2}$ value for I is in good agreement with the experimental value, -1.056 V *vs.* SCE.[2]

Electronic Spectra. The calculated singlet transi-

Tavle 3. Bond lengths of first singlet excited states of I and III

Molecule	Bond	Bond length(Å)
I	1—2	1.390
	1—9	1.430
	3—4	1.394
	8—9	1.411
	12—13	1.439
	13—14	1.399
III	1—2	1.383
	1—13	1.435
	2—3	1.428
	5—6	1.396
	12—13	1.407
	16—17	1.435
	17—18	1.403

tion energies and intensities are summarized and compared with the experimental data in Table 2. The predicted transition energies for I and II are in good agreement with the observed absorption peaks. The spectral results calculated for I, II, and III by Favini *et al.*,[7] who used the aromatic model, are in fairly good agreement with the present results.

The calculated bond lengths of the first singlet excited states for I and III are listed in Table 3. It can be seen that, in both the molecules, the double-bond fixation in the first singlet excited state is considerably more relaxed than that in the ground states. This may be one of the reasons for the appearence of a long tail, extending to 600mμ, on the long-wavelength side of the first absorption band in I.[2]

Aromatic Characteristics. The predicted C–C bond lengths for I, II, and III indicate that, in these molecules, the C–C skeleton is composed of two distinguishable parts: one in which bond lengths are smoothed out and another in which a strong double bond fixation exists. Thus, there are two regions, one aromatic in the sense that π-electrons are highly delocalized and the other polyolefinic, in the peripheries of the I, II, and III molecules. Nevertheless, the II molecule is more aromatic than the I and III molecules.

No definition of aromaticity which is correlated with the global π-electronic properties of a conjugated molecule, such as the delocalization energy and the diamagnetic susceptibility, is sufficient for these molecules, which are essentially both aromatic and polyolefinic.

One of the present authors (T. N.) especially wishes to thank Dr. B. M. Trost for providing him with copies of the ultraviolet absorption spectra of pyracylene.

BULLETIN OF THE CHEMICAL SOCIETY OF JAPAN, VOL. 44, 686—688 (1971)

Studies of the Formation Mechanism of Sodium Tripolyphosphate from Orthophosphates by the Use of Radioisotopes

Takaya IIDA, Nobuharu TAKAI, and Takeo YAMABE

The Institute of Industrial Science, The University of Tokyo, Roppongi, Minato-ku, Tokyo

(Received March 28, 1970)

The reaction process of an equimolar mixture of mono- and disodium orthophosphates was examined to serve as a reference for the considerations of the mechanism of the formation of sodium tripolyphosphate. Differential thermoanalysis, thermogravimetric analysis, X-ray diffraction analysis and thin-layer chromatographic analysis were done. Particularly, the reaction mechanisms (the formation of liquid $Na_3HP_2O_7$, *etc.*) were also examined by the use of the "^{32}P" radioisotope. The reaction process is as follows:

$$\left.\begin{array}{l} NaH_2PO_4 \longrightarrow Na_2H_2P_2O_7 \\ Na_2HPO_4 \longrightarrow Na_4P_2O_7 \end{array}\right\} \rightleftarrows Na_3HP_2O_7\,(liq.) \longrightarrow \left\{\begin{array}{l} Na_2H_2P_2O_7 \\ Na_5P_3O_{10}\,(I) \end{array}\right.$$

$$\longrightarrow Na_5P_3O_{10}\,(I) + Na_5P_3O_{10}\,(II) + NaPO_3\,(II)$$

A feedback phenomenon of $Na_2H_2P_2O_7$ was observed.

Condensed phosphates have interested many investigators as inorganic poly-substances. Among them, sodium tripolyphosphate is industrially most important, because it is used in large quantities as *e. g.*, a builder of synthetic detergents.

In general, sodium tripolyphosphate is prepared from a mixture of orthophosphates with a Na_2O/P_2O_5 mole ratio of 5/3 by thermal dehydration:

$$2Na_2HPO_4 + NaH_2PO_4 \longrightarrow Na_5P_3O_{10} + 2H_2O \quad (1)$$

In the intermediate step, tetrasodium pyrophosphate and sodium acid pyrophosphate are formed at first.[1] T. Seiyama *et al.* proposed that the reaction process of the formation of sodium tripolyphosphate from pyrophosphates mixture was as follows:[2,3]

$$Na_4P_2O_7 + Na_2H_2P_2O_7 \longrightarrow 2Na_3HP_2O_7\,(liq.) \quad (2)$$

$$2Na_3HP_2O_7 \longrightarrow Na_5P_3O_{10}\,(I) + 1/2Na_2H_2P_2O_7 + 1/2H_2O \quad (3)$$

$$1/2Na_2H_2P_2O_7 \longrightarrow 1/4Na_4H_2P_4O_{13} + 1/4H_2O \quad (4)$$

$$1/4Na_4H_2P_4O_{13} + Na_4P_2O_7 \longrightarrow Na_5P_3O_{10}\,(II) + 1/4H_2O \quad (5)$$

In the thermal decomposition of $Na_3HP_2O_7$, reaction (3) takes place at first; then the following reaction occurs:[4]

$$Na_2H_2P_2O_7 \longrightarrow 2NaPO_3\,(II) + H_2O \quad (6)$$

Studies of the thermal reaction of equimolar mixtures of mono- and disodium orthophosphates did not concern the detailed reaction process.[5]

1) J. W. Edwards and A. H. Herzog, *J. Amer. Chem. Soc.*, **79**, 3647 (1957).
2) T. Seiyama, A. Ichikawa, and T. Inoue, *Kogyo Kagaku Zasshi*, **66**, 573 (1963).
3) T. Seiyama, A. Kato, T. Ikeda, and H. Miyazaki, *ibid.*, **68**, 449 (1965).
4) T. Seiyama, A. Ichikawa, and T. Inoue, *ibid.*, **66**, 5 (1963).
5) F. E. Hubbard, *Ind. Eng. Chem.*, **41**, 2908 (1949).

Studies of the thermal reaction of equimolar mixtures of mono- and disodium orthophosphates were also performed; particularly, the reaction mechanisms (the formation of liquid $Na_3HP_2O_7$ from a pyrophosphates mixture, etc.) were investigated by the use of the "^{32}P" radioisotope.

Experimental

Reagents. The Na_2HPO_4 was a commercially available substance (Analytical grade; Wako Pure Chemical Industries, Ltd.); it was dried at 110°C. The NaH_2PO_4 was prepared from commercial $NaH_2PO_4 \cdot 2H_2O$ (Analytical grade; Wako) by thermal dehydration at 110°C.

Differential Thermal Analysis (DTA) and Thermogravimetric Analysis (TGA). DTA and TGA were done simultaneously by the use of a Thermoflex (DG-C1H, Rigaku-Denki Co., Ltd.). Heating rates were 2.5°C/min and 5°C/min, respectively.

As to quenched samples, X-ray diffraction analysis and chromatographic analysis were done. The quenched samples were prepared as follows;

Equimolar mixtures of mono- and disodium orthophosphates were heated to the appointed temperature at the heating rate of 2.5°C/min by the use of the Thermoflex, and then the heated mixtures were rapidly quenched. (Sample No. 1: 223°C, Sample No. 2: 303°C, Sample No. 3: 380°C).

X-Ray Diffraction Analysis. The X-ray diffraction work was done by the use of a Geigerflex (D-9C, Rigaku-Denki Co., Ltd.). The X-ray diffraction analysis was made by the use of the diffraction angles[6] shown in Table 1. Cu$K\alpha$ radiation was used.

Table 1. X-ray diffraction angles used in X-ray diffraction analysis

Phosphates	2θ (°)
$Na_5P_3O_{10}$ (I)	21.8, 29.1
$Na_5P_3O_{10}$ (II)	24.8
$Na_4P_2O_7$	26.4
$Na_3P_3O_9$	26.2
$NaPO_3$ (II)	30.9
$Na_2H_2P_2O_7$	30.5, 25.9

Chromatographic Analysis. The thin-layer chromatographic analysis was done using acidic and basic developing solvents.

Acidic Solvents.[7] Isopropanol-60 m*l*; water-40 m*l*; trichloroacetic acid-4 g; ammonia water(28%)-0.25 m*l*; and acetic acid-1.5 m*l*.

Basic Solvents.[9] Isopropanol-40 m*l*; isobutanol-20 m*l*; ammonia water(28%)-1 m*l* and water-39 m*l*.

The Na_2HPO_4 and NaH_2PO_4 were weighed accurately to make them easy to mix, and then they were enclosed in polyethylene tubes and neutron bombardment was made using JRR-2 ($\phi_n = 8 \times 10^{13}$ n/cm^2·sec; 5 min; reactor temperature) at the Japan Atomic Energy Research Institute, Tokai, Ibaraki.

The formation of phosphorus oxyacids and of polyphosphates other than phosphates is thought to be fairly slight under these conditions,[10] so we did not consider them.

One mole of Na_2HPO_4 was mixed with one mole of neutron applied NaH_2PO_4 (Sample A), and one mole of NaH_2PO_4, with one mole of neutron applied Na_2HPO_4 (Sample B). The two samples were simultaneously heated from room temperature up to the temperature of 380°C at the heating rate of about 3°C/min in quartz tubes in an electric furnace.

Radioactivity Measurements. Sample A and Sample B were dissolved in water, and the undissolved substances were separated by the use of a glass filter. The radioactivity of the undissolved substances was measured using a G.M. counter (SA-30, Ten Kogyo).

Results and Discussion

The DTA and TGA curves of an equimolar mixture of Na_2HPO_4 and NaH_2PO_4 are shown in Fig. 1.

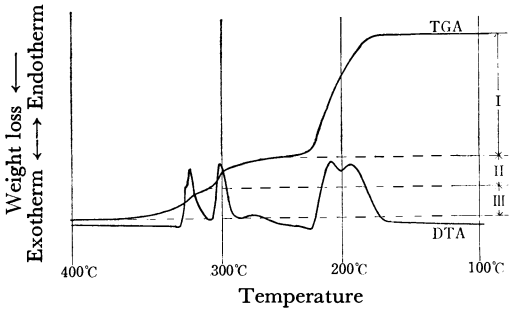

Fig. 1. DTA and TGA curves of equimolar mixture of Na_2HPO_4 and NaH_2PO_4.
Heating rate: 2.5°C/min Sample weight: 389 mg
I: obsd −25.9 mg, calcd −26.7 mg
II: obsd −6.6 mg, calcd −6.7 mg
III: obsd −6.6 mg, calcd −6.7 mg

According to X-ray diffraction analysis and chromatographic analysis, the main substances existing in the quenched samples are as follows:

Sample No. 1: $Na_2H_2P_2O_7$ and $Na_4P_2O_7$

Sample No. 2: $Na_5P_3O_{10}$ (I), and $Na_2H_2P_2O_7$

Sample No. 3: $Na_5P_3O_{10}$ (I), $Na_5P_3O_{10}$ (II), and $NaPO_3$ (II)

We could not separate the endothermic reactions with peaks at 193°C and 210°C. DTA was done on mixtures of orthophosphates in different proportions ($Na_2HPO_4 : NaH_2PO_4 = 2 : 1$, $1 : 1$, and $1 : 2$ (mole ratio)). The results are shown in Fig. 2. It is thought that the endothermic reaction with a peak at 193°C corresponds to the reaction (7), and that the one at 210°C corresponds to the reaction (8):

$$2NaH_2PO_4 \longrightarrow Na_2H_2P_2O_7 + H_2O \quad (7)$$

$$2Na_2HPO_4 \longrightarrow Na_4P_2O_7 + H_2O \quad (8)$$

The endothermic reaction with the peak at 301°C is considered to correspond to this reaction:

$$\left.\begin{matrix} Na_2H_2P_2O_7 \\ Na_4P_2O_7 \end{matrix}\right\} \longrightarrow Na_5P_3O_{10}\,(I) + 1/2Na_2H_2P_2O_7 + 1/2H_2O \quad (9)$$

6) S. Ohashi, ed. "Mukikagaku-Zensho" IV-6, "Phosphorus," Maruzen, Tokyo (1965), p. 49.

7) A solvent slightly modified from the solvent in Ref. 8 was used.

8) E. Thilo and W. Feldmann, *Z. Anorg. Allg. Chem.*, **298**, 316 (1959).

9) E. Karl-Kroupa, *Anal. Chem.*, **28**, 1091 (1956).

10) S. Ohashi *et al.*, "KURRI-TR-52 (Kyoto University Reactor Research Institute Technical Reports)," (1968), p. 23.

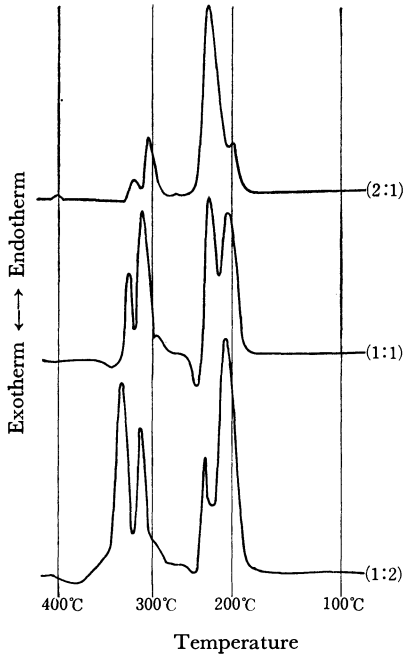

Fig. 2. DTA curves of mixtures of orthophosphates in different proportion (Na_2HPO_4: NaH_2PO_4= 2:1, 1:1, and 1:2 (mole ratio)).
Heating rate: 5°C/min

Further, the endothermic reaction with the peak at 321°C is considered to correspond to this reaction:

$$1/2Na_2H_2P_2O_7 \longrightarrow NaPO_3\,(II) + 1/2H_2O \qquad (10)$$

The final products were sodium tripolyphosphate and sodium metaphosphate (type II). The former is soluble in water, while the latter is insoluble in water. Therefore, these two substances can be separated when the final products are dissolved in water and filtered.

Table 2. Results of radioactivity measurements

Sample	before filtration ($Na_5P_3O_{10}$+$NaPO_3$ (II))	after filtration ($NaPO_3$(II))
A	12150±100 cpm	3374±194 cpm
B	6909±240 cpm	1383± 27 cpm

The results of the radioactivity measurements are shown in Table 2. As for sample A, the ratio of the radioactivity after filtration ($NaPO_3$(II)) to that before filtration ($Na_5P_3O_{10}$+$NaPO_3$(II)) was about 1 : 3.6. As for Sample B, the ratio was about 1 : 5.0.

If all of the $Na_2H_2P_2O_7$ and $Na_4P_2O_7$ react to liquid $Na_3HP_2O_7$ and are then converted to $Na_5P_3O_{10}$(I) and $Na_2H_2P_2O_7$, the ratio should be 1 : 4 (Scheme 1). However, the results do not agree with this value. It is, therefore, better to think of some different processes in this case. Two processes can be considered.

First, it is thought that the decomposition of liquid $Na_2HP_2O_7$ to $Na_2H_2P_2O_7$ and $Na_4P_2O_7$ occurs,[4] but that the ratio should be 1 : 4 if there is no feedback phenomenon of $Na_2H_2P_2O_7$ (this will be discussed below).

Second, it is thought that the formation of liquid $Na_3HP_2O_7$ from $Na_2H_2P_2O_7$ and $Na_4P_2O_7$ is slow, that the conversion to $Na_5P_3O_{10}$(I) and $Na_2H_2P_2O_7$ is fast, and that the feedback phenomenon of $Na_2H_2P_2O_7$ occurs. If only one feedback of $Na_2H_2P_2O_7$ is assumed, it is calculated that about 6.5% of the $Na_2H_2P_2O_7$ is fed back. (For Sample A, the ratio is about 1 : 3.4, and for Sample B, the ratio is about 1 : 4.8 (Scheme 2).)

The $Na_5P_3O_{10}$(II) in Sample No. 3 is thought to be formed by the conversion of the $Na_5P_3O_{10}$(I) in Sample No. 2.[1] The reaction precess is shown in Scheme 3.

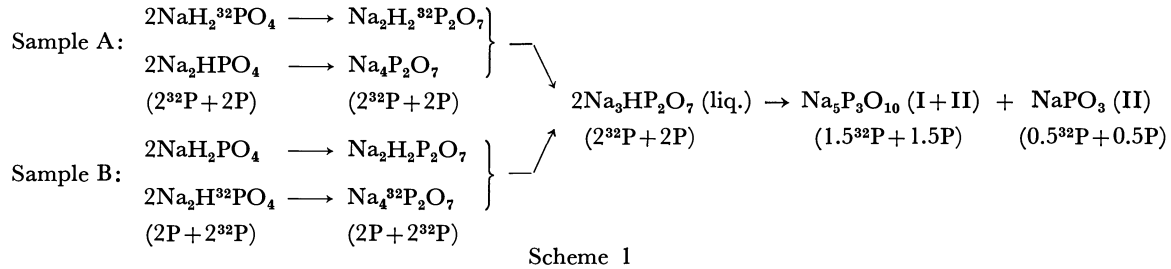

Scheme 1

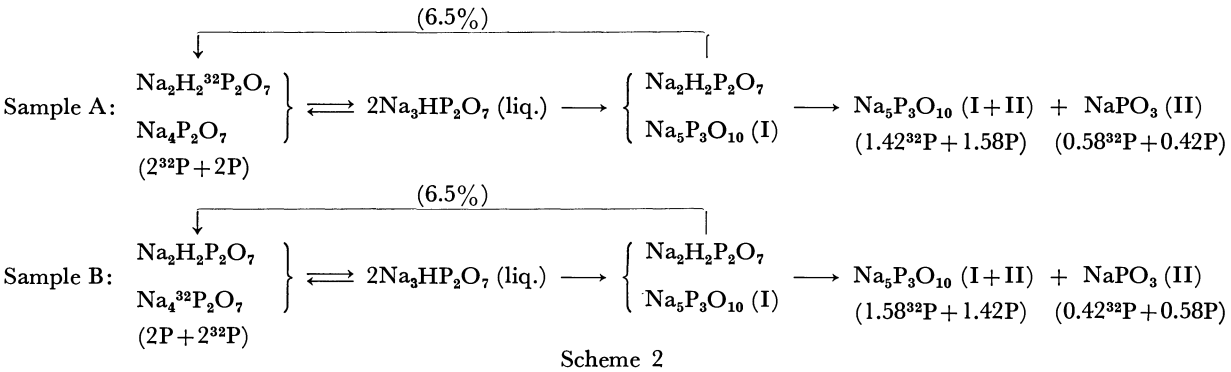

Scheme 2

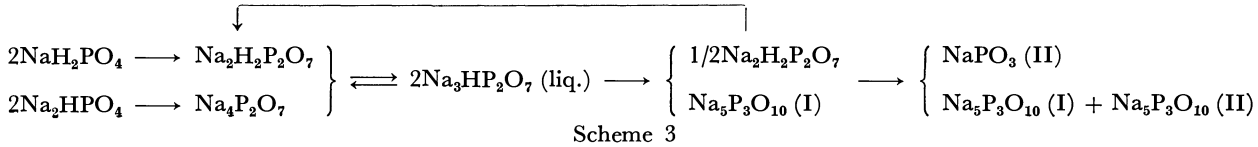

Scheme 3

Study of Hydration and Association of Ions in Solution. I. Chromatographic and Electrophoretic Behaviors of Hexamminetype Cobalt(III) Complexes in Aqueous Solutions of Various Electrolytes

Hayami YONEDA, Masayuki MUTO, Tetsuo BABA,[1] and Takao MIURA
Department of Chemistry, Wakayama University, Masagocho, Wakayama
(Received March 30, 1970)

The dissolved state of ions in solution was investigated through the study of separation mechanism of a series of tervalent hexammine-type cobalt(III) complexes in thin-layer chromatography and in electrophoresis. The results obtained are summarized as follows. In the case of strongly hydrated complexes, a strongly hydrated anion has a greater tendency towards association than a weakly hydrated anion. On the contrary, in the weakly hydrated complexes, a weakly hydrated anion is associated more easily than a strongly hydrated anion. From these findings, ionic association was presumed to occur through direct contact of a complex cation and an anion.

We have been studying the dissolved state of ions by use of inert metal complexes. The reasons for our using inert metal complexes instead of simple salts are as follows: 1) In the case of simple cations, *i. e.*, Mg^{2+}, Fe^{2+}, Ni^{2+}, *etc.*, both direct and solvent-separated associations of anions take place simultaneously around a cation, so that a migrating cationic species changes its structure even at the first coordination sphere. In contrast to this, when inert complex salts are used, only the outer sphere association of anions around a complex cation has to be considered, because the first coordination sphere remains unchanged. Thus, the analysis of the phenomenon is expected to be much simpler. 2) In the case of complex salts, there are a series of related compounds which differ from each other in certain properties, *i. e.*, ionic charge, ionic size, number of N–H bonds, *etc.*, so that the use of such related compounds enables us to find out the effect of the property upon the phenomenon concerned.

In this paper we would like to report the results of experiments with thin-layer chromatography and paper electrophoresis in which a series of tervalent hexammine-type cobalt(III) complexes were used as samples and to discuss the relation between hydration and association of ions in solution.

Results and Discussion

Thin-layer Chromatography on Alumina. The hexammine-type cobalt(III) complexes used in chromatography are $[Co(NH_3)_6]Cl_3$, $[Co(NH_3)_4en]Cl_3$, $[Co(NH_3)_4pn]Cl_3$, $[Co(NH_3)_2en_2]Cl_3$, $[Co\ en_3]Cl_3$, $[Co\ tn_3]Cl_3$, $[Co\ pn_3]Cl_3$, $[Co\ dip_3]Cl_3$, and $[Co\ phen_3]Cl_3$. When these complexes were developed with distilled water, they all remained at the starting point. This is not surprising when we remember that alumina has negatively charged sites on its surface and adsorbs complex cations. However, when aqueous soultions of 0.2M NaCl and $NaClO_4$ were used as a developer, these complexes began to move and showed a regular increase of R_f values in the decreasing order of the number of N–H bonds within the complex. Further, the results from chromatograms developed in 0.2M Na_2SO_4 aqueous solution are worthy of note.

While the spots of the complexes having many N–H bonds show nearly the same R_f values both in NaCl and in Na_2SO_4 developers, the R_f values of $[Co\ dip_3]^{3+}$ and $[Co\ phen_3]^{3+}$ developed with Na_2SO_4 solution are definitely smaller than those developed with the NaCl solution (See Fig. 1).

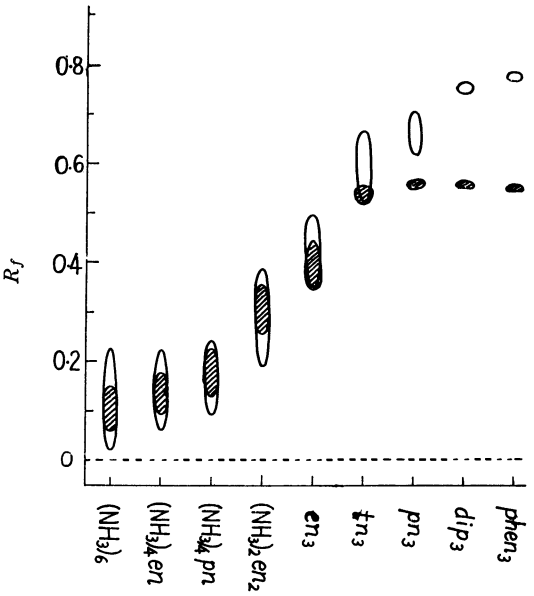

Fig. 1. Chromatogram of hexammine-type cobalt(III) complexes.
○: developed with 2M NaCl
●: developed with 2M Na_2SO_4
adsorbent: alumina

This can be interpreted in terms of ionic association. Through such ionic association, the complex cation reduces its apparent positive charge, which results in the decreased adsorption on alumina and in the increased R_f value. Since hydration of the complex cation is presumed to take place not only by ion-dipole attraction but also through hydrogen bonds between the N–H bonds and solvent water molecules, the degree of hydration is expected to decrease with the decreasing number of N–H bonds within the complex. Thus, the present results are summarized as follows. 1) Ionic association proceeds more easily when the complex has a lower

1) On leave from the Minoshima High School, Arita-shi, Wakayama.
2) T. Baba, M. Muto, and H. Yoneda, This Bulletin, **42**, 2697 (1969).

number of N–H bonds within itself, that is, when the complex is less hydrated.

2) As far as weakly hydrated complexes such as [Co-dip$_3$]$^{3+}$ or [Co phen$_3$]$^{3+}$ are concerned, a univalent anion like Cl^- or ClO_4^- forms an ion-pair more easily than bivalent anion like SO_4^{2-} does.[3] In other words, the more weakly an anion is hydrated, the more easily it forms an ion-pair with a weakly hydrated complex.

Electrophoresis. Although information concerning hydration and association of ions in solution can be obtained through chromatography by use of a simple device, the analysis of the result is not always simple, because adsorption plays an essential role in the process of development. In fact, the above mentioned chromatographic behavior of the complexes can be explained in terms of adsorption also. If we assume that adsorption on alumina is caused not only by the mere electrostatic attraction but also through the Al–O··· H–N–Co type hydrogen bonds to a large extent, it is easily understood that the complex having more N–H bonds is adsorbed more firmly and shows a smaller R_f value than the complex having less N–H bonds. Thus, it may be reasonable to assume that both mechanisms, association and adsorption, work together in the actual development process. In this respect, electrophoresis has an advantage of facilitating the analysis of the result, because adsorption can be eliminated by selecting suitable conditions.

The electrophoresis of tervalent hexammine-type cobalt(III) complexes were studied by Mazzei and Lederer.[4] They measured the mobilities of [Co-(NH$_3$)$_6$]$^{3+}$, [Co en$_3$]$^{3+}$, [Co dip$_3$]$^{3+}$ and [Co phen$_3$]$^{3+}$ in several kinds of salt solutions and showed a marked effect of ionic association upon the mobility of the complex. However, they did not give a detailed discussion of the mechanism of association. We have carried out a similar measurement using a wide variety of background electrolytes in order to find the mechanism of association.

Figure 2 shows a part of the results. Hexammine-type cobalt(III) complexes are represented with their ligands NH_3, en, tn, dip, and phen and arranged in the decreasing order of hydration from left to right. Anions shown at the sides of the curves represent the background electrolytes which were used in electrophoresis. Sodium salts were used in all cases. The ordinate corresponds to the mobility of the complex. (Here the mobility is defined as the relative migrating distance of a complex, when the migrating distance of [Co en$_3$]$^{3+}$ in 0.1 M NaCl is taken to unity.)

Let us consider the behavior of the [Co(NH$_3$)$_6$]$^{3+}$ complex. This complex is presumed to be most highly hydrated through many hydrogen bonds between the coordinating NH_3 and solvent water. In this case, it should be noted that the mobility of the complex is definitely larger in solutions containing univalent anions

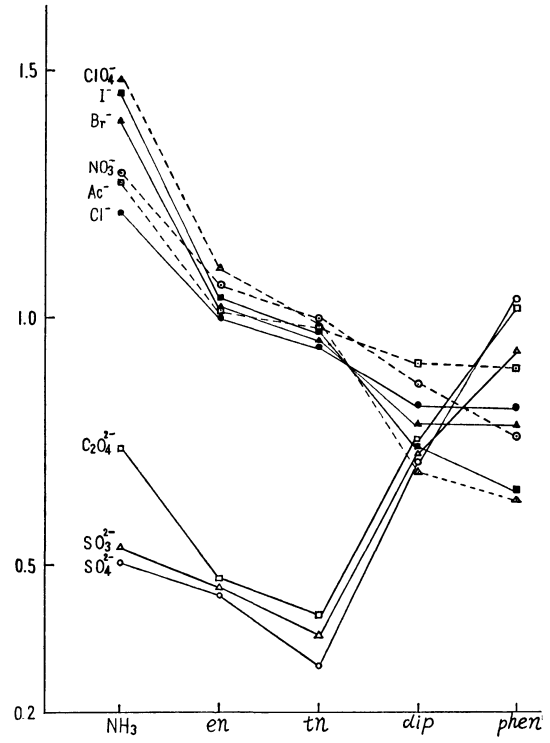

Fig. 2. Electrophoretic migration of hexammine-type cobalt (III) complexes in various background solutions.
potential gradient 500 V/34 cm
time about 1 hour
temperature 25°C
concentration of a background electrolyte 0.1 M

than in solutions containing bivalent anions. In other words, migration of the complex cation is retarded to a greater extent by bivalent anions than by univalent ones. Such difference in mobility is observed also in the cases of [Co en$_3$]$^{3+}$ and [Co tn$_3$]$^{3+}$, though less markedly. However, in the case of [Co dip$_3$]$^{3+}$ and particularly of [Co phen$_3$]$^{3+}$, the situation is the reverse. The complex cation migrates more easily in a solution containing bivalent anions than in a solution containing univalent ones.

Let us next consider the trend of mobilities of the complexes in a certain salt solution from the highly hydrated [Co(NH$_3$)$_6$]$^{3+}$ complex to the poorly hydrated [Co phen$_3$]$^{3+}$ complex. In the case of a salt solution containing univalent anions, the mobility of the complex decreases in the decreasing order of hydration of the complex. On the other hand, a reversed trend is observed in the case of a solution containing bivalent anions, the mobility increasing with the decrease of hydration.

Such a variation of mobility can be attributed to various degrees of the electrostatic withdrawing effect of anions. However, it is more effective to consider the phenomenon in terms of ionic association

$$\text{Complex cation} + \text{anion} \rightleftarrows \text{ion-pair}$$

Through such association, the complex cation reduces its apparent positive charge. This results in the decrease of mobility. Thus, it can be concluded that the more the mobility is decreased, the more the equilibrium can be considered to be shifted towards ion-pair forma-

3) The hydration number of ions can be estimated by various methods. As an example, Padova estimated the hydration number of Cl^-, ClO_4^- and SO_4^{2-} to be 1.1 and 4, respectively, from the amount of Volume decrease of an ionic solution due to hydration (J. Padova, *J. Chem. Phys.*, **39**, 1552 (1963)).

4) M. Mazzei and M. Lederer, *J. Chromatog.*, **31**, 1965 (1967).

tion. The present results can be summarized as follows. In the highly hydrated complex such as $[Co(NH_3)_6]^{3+}$, the bivalent anion is associated with it more easily than the univalent anion is. However, in the weakly hydrated complex such as $[Co\ phen_3]^{3+}$, the situation is reverse. The univalent anion can form an ion-pair more easily than the bivalent anion. In certain salt solution containing univalent anions, the association takes place more easily in a less hydrated complex, and in a certain salt solution containing bivalent anions, association takes place more easily in the more hydrated complex.

The results are in good agreement with the interpretation of the chromatographic behavior of the complexes. As to the hydration of anions, it is reasonably assumed that the bivalent anion is more strongly hydrated than the univalent anion. Thus, we can state as follows. In a strongly hydrated complex, association with a strongly hydrated anion takes place more easily than that with a weakly hydrated anion, and in a weakly hydrated complex, association occurs with a weakly hydrated anion more easily than with a strongly hydrated anion. In either case, ionic association is presumed to take place not in a solvent-separated state but rather by the direct contact of an anion and a complex cation. The strength of hydration is considered to correspond to the tendency towards hydrogen bonding. Thus, a strongly hydrated anion is expected also to form a strong hydrogen bond with the N–H bond of a strongly hydrated complex. This is regarded as the main cause of ionic association in a strongly hydrated complex. In fact, the strength of the hydrogen bonds between the N–H bonds and the outer-sphere anions is estimated from the shift of the N–H stretching frequency of the $[Co(NH_3)_6]^{3+}$ and $[Co\ en_3]^{3+}$ complexes (hydrogen bonding is expected to weaken N–H bond and shift the N–H stretching band to a lower frequency). The infrared data[5] indicate that the strength of the hydrogen bonds is in the order $Cl^->Br^->I^-$. This is in good agreement with the present results.

A weakly hydrated complex has no tendency towards hydrogen bonding. Thus, a strongly hydrated anion has little tendency towards association, because the removal of the solvating water molecules from the anion is not compensated for by the hydrogen bonding with the complex. Thus, a weakly hydrated univalent anion has an advantage for association because the energy required for the removal of the solvating water molecules in less as compared with the case of the more strongly hydrated bivalent anion.[6] This trend is observed not only between the uni- and bivalent anions, but also among univalent anions. Thus, the mobility data indicate that ionic association takes place in the order $I^->Br^->Cl^-$ in the case of a weakly hydrated complex such as $[Co\ dip_3]^{3+}$ and $[Co\ phen_3]^{2+}$. This is just the reverse order of the hydration energies of these halide ions.

Table 1. Mobilities of complex cations in a series of electrolyte solutions

The mobility of the $[Co\ en_3]^{3+}$ complex in 0.1M NaCl solution is taken as standard.

Anion	$[Co(NH_3)_6]^{3+}$	$[Co\ en_3]^{3+}$	$[Co\ tn_3]^{3+}$	$[Co\ dip]^{3+}$	$[Co\ phen_3]^{3+}$
1) In 0.1M electrolyte solutions					
Cl^-	1.21	1.00	0.94	0.82	0.84
Br^-	1.40	1.02	0.95	0.78	0.80
I^-	1.46	1.03	0.96	0.73	0.64
Ac^-	1.29	1.01	0.96	0.90	0.90
ClO_4^-	1.49	1.10	0.98	0.68	0.63
NO_3^-	1.29	1.04	0.99	0.86	0.76
$C_2O_4^{3-}$	0.73	0.45	0.39	0.78	1.03
SO_3^{2-}	0.53	0.43	0.35	0.76	0.93
SO_4^{2-}	0.50	0.43	0.29	0.74	1.03
2) In 0.5M electrolyte solutions					
Cl^-	1.00	0.65	0.64	0.61	0.60
Br^-	1.03	0.72	0.65	0.53	0.52
I^-	1.16	0.75	0.67	0.40	0.34
Ac^-	0.98	0.68	0.67	0.66	0.57
ClO_4^-	1.05	0.73	0.72	0.30	0.27
NO_3^-	0.97	0.77	0.75	0.50	0.48
$C_2O_4^{2-}$	0.55	0.53	0.36	0.62	0.69
SO_3^{2-}	0.35	0.26	0.25	0.55	0.58
SO_4^{2-}	0.33	0.24	0.23	0.61	0.64

The above discussion is based on the mobility data of the complexes in 0.1M electrolyte solutions. The same conclusion can be drawn when 0.5M electrolyte solutions are used as a background, as can be seen in Table 1. However, comparison of the two sets of data obtained in 0.1M and 0.5M solutions revealed that the mobility order of a complex in a series of background solutions in the both cases showed a slight difference from each other. Thus, the mobility of the $[Co(NH_3)_6]^{3+}$ complex in 0.5M solutions decreases in the order

$$I^- > ClO_4^- > Br^- > Cl^- > Ac^- > NO_3^-$$

while the mobility of the same complex in 0.1M solutions decreases in the order

$$ClO_4^- > I^- > Br^- > NO_3^- > Ac^- > Cl^-$$

Therefore, the association tendency in 0.5M solutions is presumed to increase in the order

$$I^- < ClO_4^- < Br^- < Cl^- < Ac^- < NO_3^-$$

while the association tendency in 0.1M solutions is presumed to increase in order

$$ClO_4^- < I^- < Br^- < NO_3^- < Ac^- < Cl^-$$

Thus, the order of association tendency concerning the $[Co(NH_3)_6]^{3+}$ complex in a certain series of electrolyte solutions various with the concentration of an electrolyte solution. This can be explained in the following way. With the increases of the concentration of a solution, the number of the solvating water molecules per one complex cation is presumed to decrease, and the complex is presumed to become poorly hydrated. Owing to such sort of dehydration, the highly hydrated $[Co(NH_3)_6]^{3+}$ in 0.1M background electrolyte solution be-

5) J. Fujita, K. Nakamoto, and M. Kobayashi, *J. Amer. Chem. Soc.*, **78**, 3295 (1956).

6) Among univalent anions, the acetate ion is considered to be strongly hydrated. Thus, the mobility of the $[Co\ dip_3]^{3+}$ and $[Co\ phen_3]^{3+}$ in the acetate solution is fairly large, compared with that in the halide solution.

comes poorly hydrated in the more concentrated background solution, and the hydrated state of the $[Co(NH_3)_6]^{3+}$ becomes similar to that of the less hydrated species like $[Co\ en_3]^{3+}$ and $[Co\ tn_3]^{3+}$ or even to that of the least hydrated $[Co\ dip_3]^{3+}$ and $[Co\ phen_3]^{3+}$ in 0.1M solution. The change in the order of the association tendency with variation of the background electrolyte concentration can thus be understood.

The association constants of the $[Co(NH_3)_6]^{3+}$ and $[Co\ en_3]^{3+}$ with the halide ions are in the order $I^-<Br^-<Cl^-$.[7-9] On the other hand, the solubility of $[Co(NH_3)_6]X_3$ and of $[Co\ en_3]X_3$ (X=Cl, Br, and I) is in the order $I^-<Br^-<Cl^-$. These two trends contradict each other. If we regard the undissolved complex salt which is in equilibrium with the saturated solution, as the final product of ionic association, it is expected from the data of the association constant that the solubility should increase in the order $Cl^-<Br^-<I^-$. However, this is not the case. This apparent discrepancy can be understood by the above consideration. In other words, the hydrated state of $[Co(NH_3)_6]^{3+}$ and $[Co\ en_3]^{3+}$ in the saturated solution is presumed to be similar to that of $[Co\ dip_3]^{3+}$ and $[Co\ phen_3]^{3+}$ in solution, for example in a 0.1M background electrolyte solution. In the latter case, the association constant is presumed to increase in the order $Cl^-<Br^-<I^-$, which is just the same order of decreasing solubility of $[Co(NH_3)_6]X_3$ and $[Co\ en_3]X_3$ (X=Cl, Br, and I).

Concerning the behavior of the perchlorate ion, it is believed that the perchlorate ion has little tendency toward complex formation with a metal ion and also has little associating ability with a complex cation. Consequently, sodium perchlorate is often used to keep the ionic strength of a series of solutions constant in the determination of the formation constant and of the association constant. However, although the tendency of the perchlorate ion toward association with $[Co(NH_3)_6]^{3+}$ and $[Co\ en_3]^{3+}$ is least among univalent anions, it is almost the same as that of the iodide ion as can be seen in Fig. 2. Furthermore, the order of the associating ability of the perchlorate and iodide is reversed in the case of 0.5M background solution. In addition, the association tendency of the perchlorate ion with the hydrophobic complex cations like $[Co\text{-}dip_3]^{3+}$ and $[Co\ phen_3]^{3+}$, is the largest among univalent anions studied. Thus, we must re-examine the validity of the use of the perchlorate for adjustment of ionic strength in the study of an association equilibrium.

Addition of the perchlorate ion to the equilibrium system, *i. e.*,

$$[Co(NH_3)_6]^{3+} + \text{anion } X^- \rightleftarrows \text{ion-pair}$$

gives vise to a new equilibrium

$$[Co(NH_3)_6]^{3+} + ClO_4 \rightleftarrows \text{ion-pair}$$

which causes a big change in the first equilibrium, if the associating ability of the perchlorate ion is comparable to or larger than that of the anion X^-.

The association constants of the $[Co(NH_3)_6]^{3+}$ and $[Co\ en_3]^{3+}$ complexes with the halide and sulfate ions were determined by various methods. For instance Evans and Nancollas[7] determined spectrophotometrically the association constants of the $[Co(NH_3)_6]^{3+}$ with the halide ions, whereas King *et al.*[8] obtained the different values of the association constants of the same ion-pair. Tanaka *et al.*[9] redetermined the association constants of these two complexes with the halide and sulfate ions by the spectrophotometric method under the same ionic strength as by Evans and Nancollas. However, they got quite different values. They attributed this to the inaccurate measurement of optical density by Evans and Nancollas. However, this does not seem to give an explanation. If we assume the big influence of the perchlorate ion upon the equilibrium, the difference can be explained. Although both groups of workers used the same ionic strength, the conditions under which they worked were quite different. Evans and Nancollas worked with very low concentrations and Tanaka *et al.* much higher concentrations of the halide ions as compared with the complex ion. This makes the equilibrium quite different. Thus, it becomes clear that the association constant is of little value unless the disturbing effect of the perclorate ion is taken into consideration.

Experimental

Thin-layer Chromatography on Alumina. As an adsorbent, Merck's aluminum oxide H prepared for thin-layer chromatography was used without further purification. This was spread in 250 μ thickness over a glass plate of 20 cm length. Solutions were applied at a starting point 5 cm above the lower edge of the plate and development was carried out to a distance of 14 cm above the starting point. A sodium sulfate solution was sprayed for visualization of the spot.

Paper Electrophoresis. A migration apparatus with multi-compartment cells was used, so that ten samples could be run at the same time. A paper strip was dipped uniformly in the background electrolyte solution and then the excess of the solution was removed by hanging the strip. After that, about 5 μl of a sample solution was placed on the paper strip (Toyoroshi No. 51 A, 2×40 cm). Samples were run for about one hour under a potential gradient 500 V/34 cm, keeping the temperature of the migrating box at 25°C. The spot of the sample was detected in the same way as in thin-layer chromatography.

The authors wish to express their thanks to Dr. Y. Kiso, Kyoto University, for his kind advice in the electrophoresis experiment.

7) M. G. Evans and G. H. Nancollas, *Trans. Faraday Soc.*, **49**, 363 (1953).

8) E. L. King, J. H. Espenson, and R. E. Visco, *J. Phys. Chem.*, **63**, 755 (1959).

9) N. Tanaka, Y. Kobayashi, and M. Komoda, This Bulletin, **40**, 2839 (1967).

Rapid Extraction of Antimony with Tributyl Phosphate. Direct Photometric Determination with Brilliant Green

A. A. YADAV and S. M. KHOPKAR

Department of Chemistry, Indian Institute of Technology, Bombay-76, India

(Received April 17, 1970)

A new method is developed for the rapid extraction and direct photometric determination of antimony. With 20% TBP-toluene 3 to 15 μg of antimony is extracted from 2M hydrochloric acid containing 1M magnesium chloride. From the organic phase, antimony is directly determined photometrically at 640 nm as its complex with brilliant green. Antimony can be selectively extracted in the presence of a large number of cations and anions. The total operation requires only 20 min.

The methods for the solvent extraction of antimony are best summarised by De, Khopkar[1] in their recent monograph. Tri-dodecylamine,[2] diethyl ether,[3] diisopropyl ether,[4] ethyl acetate,[5] isoamyl acetate,[6] and diisobutyl carbinol[7] were used for the solvent extraction of antimony from mineral acids. The iodocomplex of antimony[8–11] was extracted in benzene from 3—5M sulphuric acid. The complexes of antimony with dyes such as rhodamine B,[12–13] crystal violet;[12–15] methyl violet,[16] pyridylazo compounds[17] malachite green[18] and brilliant green [19–20] were extracted with organic solvents. Bis(2-ethylhexyl) phosphoric acid[21] in heptane was similarly used. However, these methods have certain limitations. They are time consuming, tedious and are neither selective nor applicable at microgram concentrations of antimony.

The method proposed in this paper is rapid, simple and permits clean-cut separation of antimony. 20% TBP-toluene quantitatively extracts antimony from 2M hydrochloric acid with 1M magnesium chloride as the salting-out agent. Antimony from the organic phase is then directly determined photometrically as its complex with brilliant green at 640 nm.

Experimental

Apparatus and Reagents. Type ϕ3KH-57 photoelectric photometer; Type C ϕ8-recording spectrophotometer with matched 10 mm glass cuvettes; Wrist action flask shaker: Cambridge pH indicator.

A stock solution of antimony was prepared by dissolving about 0.27 g of potassium antimonyl tartrate hemihydrate in 10 m*l* of 6N hydrochloric acid.[22] The solution was then made to one liter with water. On standardisation volumetrically with[23] Chloramine-T, it was found to contain 100 μg/m*l* of antimony. The dilute solution was prepared by ten-fold dilution. Tributyl phosphate (B.D.H), bp 143°C.

Brilliant green (B.D.H. Anal R): 0.05% aqueous solution.

General Procedure. An aliquot of solution containing about 10 μg of antimony was taken. In a total volume of 10 m*l*, hydrochloric acid and magnesium chloride were added so that each had a concentration of 2 and 1M respectively. The solution was then transferred to a separatory funnel. Ten milliliters of 20% TBP in toluene (0.73M) was then added. The mixture was vigorously shaken for about three minutes. The two phases were allowed to settle and separate. After withdrawing the aqueous phase, the organic phase was once

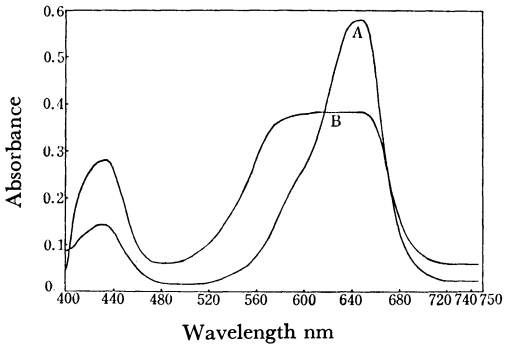

Fig. 1. Absorption spectrum of Sb (III)-brilliant green in 20% TBP toluene.

A = Absorption spectrum of Sb (III)-BG complex in 20% TBP-toluene *VS.* BG 20% TBP-toluene (Sb (III) = 8.22×10^{-6}M)

B = Absorption spectrum of brilliant Green vs 20% TBP-toluene mixture (Brilliant green = 1.19×10^{-4}M)

1) A. K. De, S. M. Khopkar, and R. A. Chalmers, "Solvent Extraction of Metals," Van Nostrand-Reinhold Co., London (1970).
2) A. Alian and W. Sanad, *Talanta*, **14**, 659 (1967).
3) G. K. Schweitzer and L. E. Storm, *Anal. Chim. Acta*, **19**, 154 (1958).
4) J. Bassett and J. C. H. Jones, *Analyst*, **91**, 176 (1966).
5) C. E. White and H. J. Rose, *Anal. Chem.*, **25**, 351 (1953).
6) N. Kosaric and C. Leliaert, *Mikrochim. Acta*, **1961**, 806.
7) R. W. Lowe, S. H. Prestwood, R. R. Rickard, and E. I. Wyatt, *Anal. Chem.*, **33**, 874 (1961).
8) R. W. Ramette, *ibid.*, **30**, 1158 (1958).
9) P. W. West and W. C. Hamilton, *ibid.*, **24**, 1025 (1952).
10) K. Tanaka, *Bunseki Kagaku*, **10**, 1087 (1961).
11) A. P. Grimanis and I. Hadzistelios, *Anal. Chim. Acta*, **41**, 15 (1968).
12) H. Onishi and E. B. Sandell, *ibid.*, **11**, 444 (1954).
13) H. Imai, *Bunseki Kagaku*, **11**, 806 (1962).
14) T. V. Lyashenko, Metallurgi. Khimi Prom. Kazakhstana Nauch Tekhn Sb. 67 (1962); *Anal. Abstr.*, **11**, 942 (1964).
15) K. Studlar and I. Janousek, *Collect. Czech. Chem. Commun.*, **25**, 1965 (1960).
16) M. Cyrankowska and J. Downarowicz, *Chemia Analit*, **12**, 137 (1967).
17) S. I. Gusev, L. V. Poplevina, and A. S. Pesis, *Zh. Anal. Khim.*, **22**, 731 (1967).
18) L. R. Narushkyavichyus, R. M. Kazlauskas and I. B. Marmakaite, *Zavod. Lab.*, **32**, 926 (1966).
19) R. W. Burke and O. Menis, *Anal. Chem.*, **38**, 1719 (1966).
20) L. N. Lapin and V. O. Gein, *Trudy Komissii Anal. Khim Akad. Nauk SSSR. Inst. Geokhim. Anal. Khim.*, **7**, 217 (1956).
21) I. S. Levin, A. A. Shatalova, and I. A. Vorsina, *Izv. Sib. Oldel. Akad. Nauk. SSSR*, 89, (1967); *Anal. Abstr.* **17**, 818 (1969).
22) E. B. Sandell, "Colorimetric Determination of Traces of Metals," Interscience 3rd Ed. (1959), p. 262.
23) A. I. Vogel, "Text Book of Quantitative Inorganic Analysis," Longmans Green 3rd Ed. (1961), p. 392.

again shaken with 2 ml of 0.05% solution of brilliant green for about three minutes. After separating the two phases, the green colored complex[20] of antimony in the organic phase was measured photometrically against a reagent blank at 640 nm.

Results and Discussion

Absorption Spectra. The absorption spectrum of the solution of antimony(III)-brilliant green complex in tributyl phosphate-toluene ($Sb=8.22\times10^{-6}$M) is shown in Fig. 1. The colored complex shows strong absorbance at 640 nm. The reagent blank at this wavelength also shows some absorbance. The difference in absorbance of reagent blank and complex is maximum at 640 nm; hence all absorbance measurements were carried out at this wavelength. The molecular extinction coefficient at 640 nm is 7.3×10^4.

Effect of Acidity and TBP Concentration. The hydrochloric acid concentration was varied from 0.5—5M in the presence of 1M magnesium chloride. The concentration of TBP was varied from 10—100% (0.37—3.66M) with toluene as a diluent. It was observed (Table 1) that quantitative extraction of antimony is possible from 2M hydrochloric acid with 20% TBP-toluene in the presence of 1M magnesium chloride as a salting-out agent. The distribution ratios (D) were

TABLE 1. DISTRIBUTION RATIO AS THE FUNCTION OF ACIDITY
Sb(III)=10 μg; 1M $MgCl_2$ as the salting out agent

TBP, concn. (M)	HCl, M (initial)	Extraction % E	Distribution ratio, D
10% (0.37)	0.5	35.3	0.55
	1.0	47.6	0.91
	1.5	58.8	1.40
	2.0	70.6	2.40
20% (0.73)	0.5	58.8	1.40
	1.0	76.5	3.26
	1.5	94.1	15.95
	2.0—5.0	100	∞
20% (0.73)	0.5	29.4	0.42
(in absence of	1.0	41.2	0.70
1M $MgCl_2$)	1.5	52.9	1.13
	2.0	64.7	1.83
	2.5	85.3	5.86
	3.0—5.0	100	∞
40% (1.46)	0.5	70.6	2.40
	1.0	82.4	4.68
	1.5	94.1	15.95
	2.0—5.0	100	∞
60% (2.19)	0.5	71.8	2.55
	1.0	83.5	5.00
	1.5	95.3	20.28
	2.0—5.0	100	∞
75% (2.74)	0.5	73.5	2.78
	1.0	85.3	5.80
	1.5	97.1	33.48
	2.0—5.0	100	∞
100% (3.66)	0.5	76.5	3.26
	1.0	88.2	7.47
	1.5	97.1	33.48
	2.0—5.0	100	∞

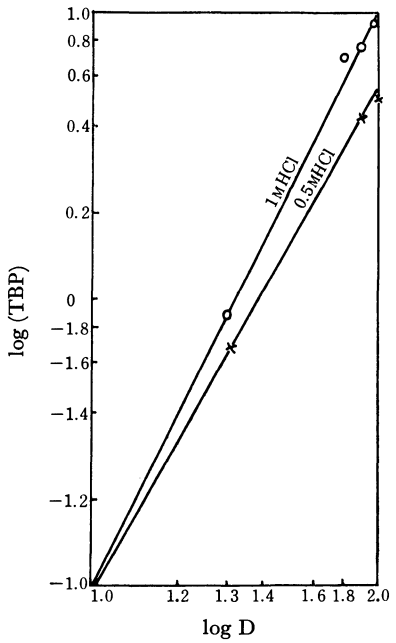

Fig. 2. Extraction as a Function of TBP-Concentration.

calculated as described earlier.[24] An attempt was made to ascertain the probable composition of the extractable species from the plot of log D *vs.* log (TBP) concentration. The slope at 1M hydrochloric acid concentration is 2.14 (Fig. 2). This shows that the probable composition of the extractable species is H [$SbCl_3$ $(TBP)_2$].

TABLE 2. EFFECT OF HYDROCHLORIC ACID CONCENTRATION ON ABSORBANCE
Sb(III)=10 μg; 20% TBP-toluene; in absence of salting out agent.

HCl, M (initial)	Absorbance at 640 nm	Extraction % E	Distribution ratio, D
0.5	0.175	29.4	0.42
1.0	0.245	41.2	0.70
1.5	0.315	62.9	1.13
2.0	0.385	64.7	1.83
2.5	0.510	85.3	5.86
3.0—5.0	0.600	100.0	∞

Effect of Hydrochloric Acid Concentration on Absorbance. Extraction of antimony was carried out with 20% TBP-toluene with varying hydrochloric acid concentration. The results show (Table 2) that the absorbance increases as the acidity is increased. It becomes constant

TABLE 3. BEER'S LAW

Amount of antimony, μg	Absorbance at 640 nm
2.5	0.150
5.0	0.310
7.5	0.450
10.0	0.600
12.5	0.750
15.0	0.880

24) A. V. Rangnekar and S. M. Khopkar, This Bulletin, **41**, 600 (1968).

at 3M hydrochloric acid concentration. With further increase in acidity there is no change in the absorbance. Since these extractions were carried out in the absence of salting-out agent the extraction was quantitative at 3M hydrochloric acid. However, if 1M magnesium chloride is used as the salting-out agent the extraction is complete even at 2M hydrochloric acid.

Beer's Law. Different amounts of antimony were extracted at 2M hydrochloric acid in the presence of 1M magnesium chloride with 20% TBP-toluene (Table 3). They were measured at 640 nm as their complexes with brilliant green. The system conforms to Beer's law over the concentration range of 0.15—15 μg/m*l* of antimony at 640 nm. Sandell's sensitivity was found to be 0.0017 μg/cm^2 of antimony.

Table 4. Effect of salting-out agent
Sb(III)=10 μg; 20% TBP-toluene

Salting-out agent, M		HCl, M (initial)	Extraction % *E*	Distribution ratio, *D*
NH_4Cl	1.0	0.5	35.3	0.55
		1.0	47.6	0.91
		1.5	58.8	1.40
		2.0	70.6	2.40
	2.0	0.5	58.8	1.40
		1.0	70.6	2.40
		1.5	76.5	3.26
		2.0	82.4	4.69
LiCl	0.5	0.5	41.2	0.70
		1.0	52.9	1.13
		1.5	64.7	1.83
		2.0	76.5	3.26
	1.0	0.5	70.6	2.40
		1.0	82.4	4.68
		1.5	91.3	10.58
		2.0	100.0	∞
$MgCl_2$	0.5	0.5	47.6	0.91
		1.0	58.8	1.40
		1.5	70.6	2.40
		2.0	82.4	4.69
	1.0	0.5	36.4	1.40
		1.0	76.5	3.26
		1.5	94.1	15.95
		2.0	100.0	∞
$AlCl_3$	0.5	0.5	52.9	1.13
		1.0	64.7	1.83
		1.5	76.5	3.26
		2.0	88.2	7.48
	1.0	0.5	58.8	1.40
		1.0	70.8	2.40
		1.5	88.2	7.48
		2.0	100.0	∞

Effect of Salting-out Agent. Ammonium, lithium, magnesium, and aluminium chlorides (0.5—2M) were used as the salting-out agents when hydrochloric acid concentration used was 0.5—2M. The results show (Table 4) that ammonium chloride is not a good salting-out agent. 1M lithium, magnesium, or aluminium chloride are effective salting-out agents, at 2M hydrochloric acid concentration. On account of the ease of availability of 1M magnesium chloride, it was preferred as the salting-out agent.

Table 5. Effect of brilliant green concentration
Sb(III)=10 μg; 20% TBP toluene; 2M HCl+1M $MgCl_2$

Reagent concn.	Volume in m*l*	Absorbance at 640 nm
0.001	2	0.010
0.005	2	0.100
0.010	2	0.300
0.02	2	0.450
0.04	2	0.600
0.05	2	0.600
0.05	4	0.600
0.05	5	0.600

Effect of Brilliant Green Concentration. With all other factors kept constant the concentration of brilliant green was varied from 0.001 to 0.05 per cent (Table 5) in the aqueous solution. It was observed that 2 m*l* of 0.05 per cent aqueous solution of brilliant green was quite adequate for color development in 20% TBP toluene media.

Period of Shaking. The period of equilibration during extraction with TBP and during color development with brilliant green was varied from 30 sec to 20 min. In both cases the optimum period of extraction is three minutes.

Table 6. Stability of color of the complex

Time, hr	Absorbance at 640 nm
0.5	0.600
1	0.600
2	0.600
4	0.600
8	0.600
12	0.600
18	0.600
24	0.560
48	0.480

Stability of the Color. The absorbance of the colored complex was measured at lapsed intervals of time (Table 6). The complex decomposes after 18 hr. Therefore, it is recommended to measure the absorbance within the first 12 hr after extraction.

Effect of Diverse Ions. Various ions were studied to observe their effect on the process of extraction (Table 7). The tolerance limit was calculated as the amount to cause $\pm$2% error in antimony recovery. Lead, copper, zinc, cobalt, nickel, zirconium, beryllium, alkali and alkaline earths, thorium, cerium, uranium, selenite, tellurite, phosphate, acetate, and fluoride are tolerated in larger ratios (>1 : 500). Ions like silver, cadmium, bismuth, iron, organic complexing acids, thiocyanate, thiosulphate are tolerated in the ratio of 1 : 100. However, platinum metals, mercury, tin, titanium are tolerated in smaller amounts. Thallium, gold, chromate, bromide, and chlorate interfere. Some interferences can be eliminated by masking ions with EDTA, pyrophosphate, tartaric acid, and sodium fluoride (Table 7).

TABLE 7. EFFECT OF DIVERSE IONS
Sb(III) = 10 μg; 2M HCl + 1M $MgCl_2$; 20% TBP + Toluene

Foreign ion	Added as	Tolerance limit, μg	Foreign ion	Added as	Tolerance limit, μg
Pb^{2+}	$Pb(NO_3)_2$	5000	Sr^{2+}	$SrCl_2 \cdot 6H_2O$	5000
Hg^{2+}	$Hg(NO_3)_2$	500[a]	Ba^{2+}	$BaCl_2 \cdot 2H_2O$	5000
Ag^{+}	$AgNO_3$	1000[a]	Rb^{+}	RbCl	5000
Tl^{+}	$TlNO_3$	None	Cs^{+}	CsCl	5000
Cu^{2+}	$CuSO_4 \cdot 5H_2O$	5000	Ti^{4+}	$TiCl_4 \cdot 4H_2O$	500
Cd^{2+}	$CdCl_2 \cdot 5H_2O$	2500	AsO_4^{3-}	Na_3AsO_4	5000
Sn^{2+}	$SnCl_2 \cdot 2H_2O$	500	Br^{-}	NaBr	None
Bi^{3+}	$Bi(NO_3)_3$	2500	CrO_4^{2-}	K_2CrO_4	None
Ru^{3+}	$RuCl_3 \cdot 3H_2O$	500	ClO_3^{-}	$KClO_3$	None
Rh^{3+}	$RhCl_3 \cdot 3H_2O$	500[c]	F^{-}	NaF	5000
Pd^{2+}	$PdCl_2 \cdot 2H_2O$	500[b]	$Mo_7O_{24}^{6-}$	$(NH_4)_6Mo_7O_{24}$	200
Pt^{4+}	$H_2PtCl_6 \cdot 6H_2O$	500[a]	SeO_3^{2-}	Na_2SeO_3	5000
Au^{3+}	$HAuCl_4 \cdot H_2O$	None	SCN^{-}	NH_4SCN	1000
Fe^{3+}	$FeCl_3 \cdot 6H_2O$	1000[d]	$S_2O_3^{-2}$	$Na_2S_2O_3$	1000
Al^{3+}	$Al(NO_3)_3$	30000	SO_4^{2-}	Na_2SO_4	10000
Zn^{2+}	$ZnSO_4 \cdot 7H_2O$	5000	TeO_3^{2-}	Na_2TeO_3	5000
Mn^{2+}	$MnCl_2 \cdot 4H_2O$	500	VO_3^{-}	NH_4VO_3	1000
Co^{2+}	$CoCl_2 \cdot 6H_2O$	10000	PO_4^{3-}	Na_3PO_4	5000
Ni^{2+}	$NiCl_2 \cdot 6H_2O$	5000	$P_2O_7^{2-}$	$(NH_4)_2P_2O_7$	5000
Th^{4+}	$Th(NO_3)_4 \cdot 4H_2O$	10000	EDTA (disodium salt)		2500
Zr^{4+}	$Zr(NO_3)_4$	5000	Ascorbic acid		2500
Ce^{4+}	$Ce(SO_4)_2$	5000	Citric acid		2500
U^{6+}	$UO_2(NO_3)_2 \cdot 6H_2O$	5000	Malonic acid		1000
Be^{2+}	$Be(NO_3)_2 \cdot 4H_2O$	5000	Oxalic acid		2500
Ca^{2+}	$CaCl_2 \cdot 2H_2O$	5000	Tartaric acid		2500

a) 2500 μg of EDTA was used for masking.
b) 5000 μg of alkali pyrophosphate was used for masking.
c) 2500 μg of Tartaric acid was used for masking.
d) 5000 μg of sodium fluoride was used for masking.

From ten runs with 10 μg of antimony using the general procedure the average recovery is 99.2±0.8%, the relative standard deviation being 1.3%. Each determination took a total of 20 min.

A Polarographic Study of the Complex Formation Equilibria of the Lead(II) Ion with Aspartic and Iminodiacetic Acids

Mutsuo KODAMA and Sozo TAKAHASHI*

Department of Chemistry, Ibaraki University, Bunkyo, Mito, Ibaraki

(Received May 8, 1970)

In this experiment, we studied the complex formation equilibria of the lead(II) ion with aspartic acid and iminodiacetic acid by using the polarographic method. In acetate buffer solutions ($5.80>pH>3.70$), the lead(II) ion forms one normal complex, PbX^0, and two mixed ligand complexes involving the acetate ion, $PbX(Ac)^-$ and $PbX(Ac)_2^{2-}$, with aspartic acid. On the other hand, with iminodiacetic acid, it forms a normal complex, PbX^0, and only one mixed ligand complex, $PbX(Ac)^-$. By observing the effects of the concentrations of the hydrogen ion, the acetate ion, and aspartic acid or iminodiacetic acid on the half-wave potential of the lead(II) ion, their formation constants were determined to be as follows:

$$(K^{Ac}_{PbX})_{Asp} = \frac{[PbX(Ac)^-]}{[PbX^0]\cdot[Ac^-]} = 7.0\times 10, \quad (K^{Ac}_{PbX(Ac)})_{Asp} = \frac{[PbX(Ac)_2^{2-}]}{[PbX(Ac)^-]\cdot[Ac^-]} = 1.3_4,$$

$$(K^{Ac}_{PbX})_{IDA} = \frac{[PbX(Ac)^-]}{[PbX^0]\cdot[Ac^-]} = 3.0, \quad (K_{PbX})_{Asp} = \frac{[PbX^0]}{[Pb^{2+}]\cdot[X^{2-}]} = 1.0_6\times 10^6,$$

$$(K_{PbX})_{IDA} = \frac{[PbX^0]}{[Pb^{2+}]\cdot[X^{2-}]} = 5.7_0\times 10^7, \quad (K^{X}_{PbX})_{Asp} = \frac{[PbX_2^{2-}]}{[PbX^0]\cdot[X^{2-}]} = 1.4_2\times 10^2,$$

$$(K^{X}_{PbX})_{IDA} = \frac{[PbX_2^{2-}]}{[PbX^0]\cdot[X^{2-}]} = 6.0_6\times 10^3$$

In a previous paper,[1] we systematically studied the polarographic behavior of the cadmium(II) ion in an aspartate solution and reported that the cadmium(II) ion can form 1-to-2 as well as 1-to-1 complexes with aspartic acid (Asp). The lead(II) ion can also be expected to form stable complexes with aspartic acid and iminodiacetic acid (IDA). However, few equilibrium studies of the complex formation reaction of the lead(II) ion with these ligand have been conducted. In this connection, it seemed that it would be worthwhile to determine the equilibria between the lead(II) ion and Asp or IDA. In this paper, we will try to determine the solution equilibria between the lead(II) ion and Asp or IDA.

Experimental

Reagents. A standard lead(II) nitrate solution was prepared by dissolving a known amount of pure lead(II) nitrate in redistilled water. Aspartic acid and iminodiacetic acid were recrystallized twice from their aqueous solutions by adding a suitable amount of pure ethanol. The other reagents were of an analytical-reagent grade and were used without further purification. The ionic strength of the sample solution was adjusted by adding an appropriate amount of sodium perchlorate.

Apparatus and Experimental Procedures. All the polarographic studies were conducted in solutions with an ionic strength of 0.30 at 25°C. The DC current-voltage curves were measured by using a manual polarograph similar to that of Kolthoff and Lingane;[2] they were corrected for the residual current and the ohmic drop of the cell circuit. In the pH range from 3.70 to 5.80, an acetate buffer was used to keep the solution's pH constant. In an alkaline medium ($8.30<pH<10.40$), however, no buffer reagent was used, because the sample solution always contains an excess amount of uncomplexed Asp or IDA over the lead(II) ion, hence, it is considered to have a buffer capacity sufficient to keep the solution's pH constant.

Results and Discussion

The lead(II) ion in both Asp and IDA solutions invariably gave a single well-defined wave. As is illustrated by the straight lines in Fig. 1, the plot of $\log(i/(i_l-i))$ against the DC potential, E, gave a straight line with a slope falling in the range from -30 to -32 mV, a line corresponding to the two-electron reversible reduction. Here, i_l and i are the limiting current and the current at E respectively. The limiting current was exactly proportional to the bulk concentration of the lead(II) ion and to the square root of the effective pressure on the dropping mercury electrode (these results are not shown here). Therefore, the electrode reaction is reversible in the usual polarographic sense; hence, the half-wave potentials obtained can be analyzed with the aid of the theoretical relation derived thermodynamically.

In an acid solution, when the other experimental conditions are kept constant, the half-wave potential was shifted to more negative potentials by increasing the concentration of Asp or IDA. It was also shifted to the negative potentials by increasing the acetate-ion concentration. From the thermodynamic point of view, the above findings can be interpreted as resulting from the formation of lead(II) complexes of the acetate ion and Asp or the IDA anion. In a usual complex formation reaction, the coordination number of the lead(II) ion is four or six, and IDA and Asp act as tridentate

* Present address: Department of Chemistry, Ibaraki Technical College, 866, Fukayatsu, Nakane, Katsuta, Ibaraki.

1) M. Shibata, H. Mitsuta, M. Inada, and M. Kodama, *Nippon Kagaku Zasshi*, **85**, 767 (1964).

2) I. M. Kolthoff and J. J. Lingane, "Polarography," Vol. 1, Interscience Publishers, New York (1952), p. 297.

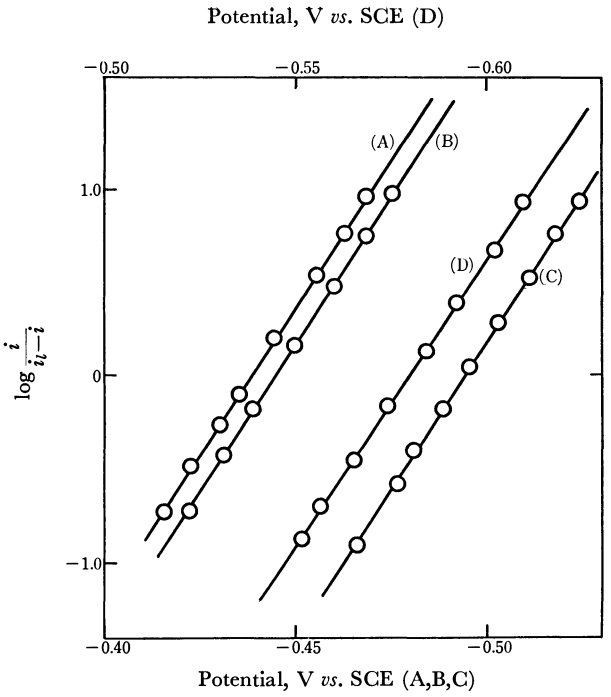

Fig. 1. The plot of log $(i/i_l - i)$ against the *d.c.* potential.
A: Concentration of acetate ion=0.20M
Concentration of lead(II) ion=0.50mM, μ=0.30
Concentration of Asp=70.0 mM, pH=5.62
B: Concentration of acetate ion=0.10M
Concentration of lead(II) ion=0.50mM, μ=0.30
Concentration of IDA=40.0 mM, pH=5.62
C: Concentration of lead(II) ion=0.50 mM
Concentration of Asp=70.0mM, pH=9.33, μ=0.30
D: Concentration of lead(II) ion=0.50 mM
Concentration of IDA=60.0mM, pH=9.50, μ=0.30

ligands. Therefore, as was discussed in connection with the polarography of the copper(II)-GEDTA complex,[3] we can assume the following electrode reaction mechanism for the lead(II) ion in acetate buffer solutions containing Asp or IDA:

$$\begin{array}{ccc} Pb(Ac)_2^0 & \rightleftarrows & Pb(Ac)^+ \\ \uparrow\downarrow & & \uparrow\downarrow \\ PbX(Ac)_2^{2-} & & Pb^{2+} + 2e^- + Hg \rightleftarrows Pb(Hg) \\ \uparrow\downarrow & & \uparrow\downarrow \\ PbX(Ac)^- & \rightleftarrows & PbX^0 \end{array} \quad (1)$$

with the shift of the half-wave potential corresponding to:

$$\Delta E_{1/2} = 0.0296\left[\log\left(1+\frac{K_{PbAc}\cdot[Ac]_f}{(\alpha_H)_{Ac}}+\frac{K_{PbAc}\cdot K^{Ac}_{PbAc}\cdot[Ac]_f^2}{(\alpha_H)^2_{Ac}} + \frac{K_{PbX}[X]_f}{(\alpha_H)_X}+\frac{K_{PbX}K^{Ac}_{PbX}[X]_f\cdot[Ac]_f}{(\alpha_H)_X(\alpha_H)_{Ac}} + \frac{K_{PbX}K^{Ac}_{PbX}K^{Ac}_{PbX(Ac)}\cdot[X]_f[Ac]_f^2}{(\alpha_H)_X(\alpha_H)^2_{Ac}}\right) + \log\frac{k_{PbX}}{k_{Pb^{2+}}}\right] \quad (2)$$

where Ac^- denotes an acetate ion, where X^{2-} denotes Asp or an IDA bivalent anion, where the k's mean the diffusion current constants, and where $[X]_f$ and $[Ac]_f$ are the concentrations of uncomplexed Asp or IDA and of acetic acid respectively. The symbols in Eq. (2) have the following meanings:

$$K_{PbAc} = \frac{[PbAc^+]}{[Pb^{2+}]\cdot[Ac^-]},\quad K^{Ac}_{PbAc} = \frac{[Pb(Ac)_2^0]}{[PbAc^+]\cdot[Ac^-]},$$

$$K_{PbX} = \frac{[PbX^0]}{[Pb^{2+}]\cdot[X^{2-}]},\quad K^{Ac}_{PbX} = \frac{[PbX(Ac)^-]}{[PbX^0]\cdot[Ac^-]},$$

$$K^{Ac}_{PbX(Ac)} = \frac{[PbX(Ac)_2^{2-}]}{[PbX(Ac)^-]\cdot[Ac^-]},$$

$(\alpha_H)_{Ac} = 1 + [H^+]/K_a$ (acetic acid),

$(\alpha_H)_X = 1 + [H^+]/K_2 + [H^+]^2/K_1\cdot K_2$ (Asp or IDA).

Since all the polarographic measurements were conducted in solutions containing large excesses of acetic acid and Asp or IDA over the lead(II) ion, the $[X]_f$ and $[Ac]_f$ in Eq. (2) can be equated with the total concentrations of acetic acid and Asp or IDA respectively. When the acetate-ion concentration and the solution's pH are kept constant, the plot of the antilog-$(\Delta E_{1/2}/0.0296+\log(k_{Pb^{2+}}/k_{PbX}))$ value against $[X]_f$ invariably gives a linear relation (Fig. 2). This clearly

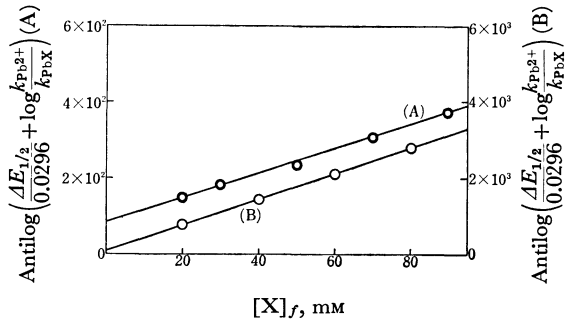

Fig. 2. The plot of antilog$(\Delta E_{1/2}/0.0296 + \log(k_{Pb^{2+}}/k_{PbX}))$ against the concentration of uncomplexed Asp or IDA.
A: Asp system
Concentration of acetate ion=0.15M, pH=5.62
Concentration of lead(II) ion=0.50mM, μ=0.30
B: IDA system
Concentration of acetate ion=0.15M, pH=5.62
Concentration of lead(II) ion=0.50mM, μ=0.30

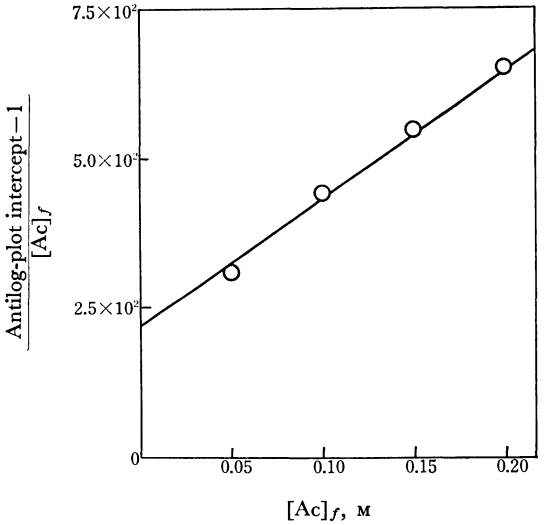

Fig. 3. The plot of (antilog-plot intercept−1)/$[Ac]_f$ against the concentration of acetate ion.
Asp system:
Concentration of lead(II) ion=0.50mM, μ=0.30, pH=5.62

3) M. Kodama and Y. Tominaga, This Bulletin, **42**, 394 (1969).

TABLE 1. EQUILIBRIUM CONSTANTS (μ=0.30, 25°C)

$$K_{PbAc}=\frac{[PbAc^+]}{[Pb^{2+}]\cdot[Ac^-]}=2.1_8\times10^2$$

$$K^{Ac}_{PbAc}=\frac{[Pb(Ac)_2{}^0]}{[PbAc^+]\cdot[Ac^-]}=9.7_0$$

$$(K_{PbX})_{Asp}=\frac{[PbX^0]}{[Pb^{2+}]\cdot[X^{2-}]}=1.0_6\times10^6$$

$$(K_{PbX})_{IDA}=\frac{[PbX^0]}{[Pb^{2+}]\cdot[X^{2-}]}=5.7_0\times10^7$$

$$(K^{X}_{PbX})_{Asp}=\frac{[PbX_2{}^{2-}]}{[PbX^0]\cdot[X^{2-}]}=1.4_2\times10^2$$

$$(K^{X}_{PbX})_{IDA}=\frac{[PbX_2{}^{2-}]}{[PbX^0]\cdot[X^{2-}]}=6.0_6\times10^3$$

$$(K^{Ac}_{PbX})_{Asp}=\frac{[PbX(Ac)^-]}{[PbX^0]\cdot[Ac^-]}=7.0\times10$$

$$(K^{Ac}_{PbX})_{IDA}=\frac{[PbX(Ac)^-]}{[PdX^0]\cdot[Ac^-]}=3.0_9$$

$$(K^{Ac}_{PbX(Ac)})_{Asp}=\frac{[PbX(Ac)_2{}^{2-}]}{[PbX(Ac)^-]\cdot[Ac^-]}=1.3_4$$

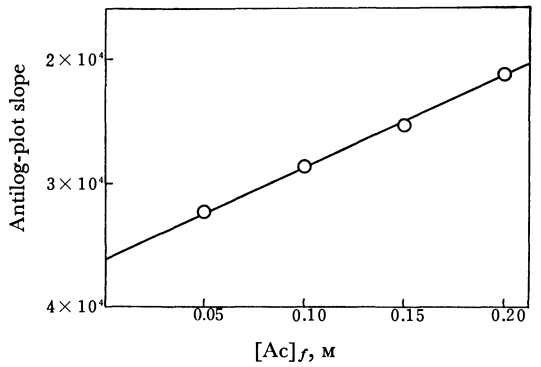

Fig. 4. The plot of antilog-plot slope against the concentration of acetate ion.
IDA system:
Concentration of lead(II) ion=0.50mM, μ=0.30, pH=5.62

indicates that the concentration of the 1-to-2 complex of Asp or IDA is negligible under the present experimental conditions. In the cases of both Asp and IDA systems, the plot of the antilog-plot −1 divided by $[Ac]_f$ *versus* $[Ac]_f$ gives a straight line (Fig. 3). On the basis of Eq. (2), it is very clear that the intercept and the slope of the straight line in Fig. 3 correspond to $K_{PbAc}/(\alpha_H)_{Ac}$ and $K_{PbAc}\cdot K^{Ac}_{PbAc}/(\alpha_H)^2_{Ac}$ respectively. The K_{PbAc} and K^{Ac}_{PbAc} determined from the intercept and the slope of the linear relation in Fig. 3 are given in Table 1. In the case of the IDA system, the plot of the antilog-plot slope *vs.* $[Ac]_f$ gave a linear relation (Fig. 4). This indicates that, with the IDA anion, the lead(II) ion forms a mixed ligand complex, $PbX(Ac)^-$, as well as a normal complex, PbX^0. From the slope and intercept of the above linear relation, the $(K_{PbX})_{IDA}$ and $(K^{Ac}_{PbX})_{IDA}$ values were determined; they are listed in Table 1. On the other hand, in the case of the Asp system, only the plot of the ratio of antilog-plot minus $(K_{PbX})_{Asp}/(\alpha_H)_X$ to $[Ac]_f$ *vs.* $[Ac]_f$ gave a straight line (Fig. 5). This suggests that, in the case of the Asp system, two mixed ligand complexes, $PbX(Ac)^-$ and $PbX(Ac)^{2-}_2$, as well as a normal complex are formed. The K^{Ac}_{PbX} and $K^{Ac}_{PbX(Ac)}$ values determined from the

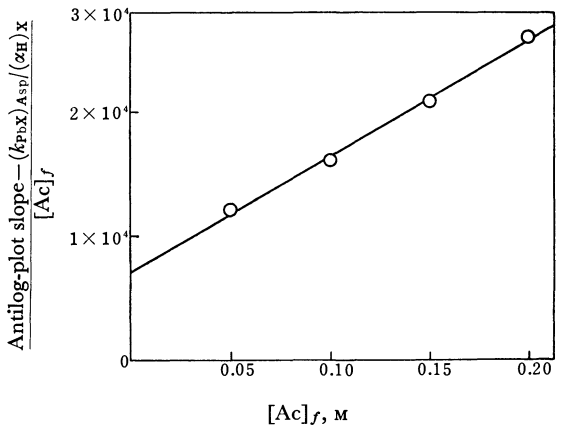

Fig. 5. The plot of (antilog-plot slope $-(k_{PbX})_{Asp}/(\alpha_H)_X$)/$[Ac]_f$ against the concentration of acetate ion.
Asp system:
Concentration of lead(II) ion=0.50mM, μ=0.30, pH=5.62

slope and intercept of the straight line in Fig. 5 are also listed in Table 1. If the above conclusion is correct, the change in the half-wave potential, $\Delta E_{1/2}$, with the change in the hydrogen-ion concentration should be calculable with the aid of Eq. (2). In the case of the IDA system, we used the relation in which the $K_{PbX}\cdot K^{Ac}_{PbX}\cdot K^{Ac}_{PbX(Ac)}\cdot[Ac]^2_f[X]_f/(\alpha_H)^2_{Ac}\cdot(\alpha_H)_X$ in Eq. (2) is not involved. In Table 2, the $\Delta E_{1/2}$ values calculated

TABLE 2. THE RELATION BETWEEN THE HALF-WAVE POTENTIAL AND THE CONCENTRATION OF HYDROGEN ION

Concentration of lead(II) ion=0.5 mM, μ=0.30, 25°C

(A) Asp system
Concentration of Asp=90.0 mM
Concentration of acetate ion=0.05 M

$E_{1/2}$, V *vs.* SCE	pH	$\Delta E_{1/2}$, mV	
		Calcd	Obsd
−0.4015	3.71	0	0
−0.4030	4.60	− 1.9	− 1.9
−0.4112	5.50	−13.0	−12.7

(B) IDA system
Concentration of IDA=40.0 mM
Concentration of acetate ion=0.10 M

$E_{1/2}$, V *vs.* SCE	pH	$\Delta E_{1/2}$, mV	
		Calcd	Obsd
−0.4208	4.50	0	0
−0.4225	4.70	− 4.4	− 4.7
−0.4323	5.01	−11.9	−11.5
−0.4387	5.31	−20.0	−18.0
−0.4443	5.50	−25.2	−23.5

by using the equilibrium constants determined in this study are given, together with those obtained experimentally. The agreement of the calculated $\Delta E_{1/2}$ values with those determined experimentally can be regarded as satisfactory.

In an alkaline medium, in the cases of both Asp and IDA systems, the plot of the antilog $(\Delta E_{1/2}/0.0296+\log(k_{Pb^{2+}}/k_{PbX}))$ value divided by $[X]_f$ *vs.* $[X]_f$ gave

a straight line with an intercept of a definite value. As was discussed in connection with the polarography of the cadmium(II)-EDTP complex,[4] this fact indicates that the lead(II) ions exist in the forms of PbX^0 and PbX_2^{2-}, and that the electrode reactions can be assumed to be:

$$PbX^0 + 2e^- + nH^+ + Hg \rightleftarrows Pb(Hg) + H_nX^{2-n} \quad (3)$$
$$\Updownarrow$$
$$PbX_2^{2-}$$

with the shift of the half-wave potential corresponding to:

$$\Delta E_{1/2} = 0.0296\left[\log\left(\frac{K_{PbX}\cdot[X]_f}{(\alpha_H)_X} + \frac{K_{PbX}\cdot K^X_{PbX}\cdot[X]_f^2}{(\alpha_H)_X^2}\right) + \log\frac{k_{PbX}}{k_{Pb^{2+}}}\right] \quad (4)$$

where H_nX^{2-n} means incompletely-deprotonated Asp or IDA, where PbX_2^{2-} means a 1 : 2 lead(II)-Asp or -IDA complex, and where K^X_{PbX} is the second successive formation constant of the lead(II)-Asp or -IDA complex. From the slopes and intercepts of the straight lines in Fig. 6, the K_{PbX} and K^X_{PbX} values were determined (Table 1). The K_{PbX} values thus determined agreed well with those estimated in an acid solution. If the electrode reaction in an alkaline medium is given by Eq. (3), the K_{PbX} and K^X_{PbX} thus determined should explain satisfactorily the change in the half-wave potential with the change in the hydrogen-ion concentration. The $\Delta E_{1/2}$ values calculated with the aid of Eq. (4) by using the K values in Table 1 and those determined experimentally are listed in Table 3. A good agreement between them could be observed.

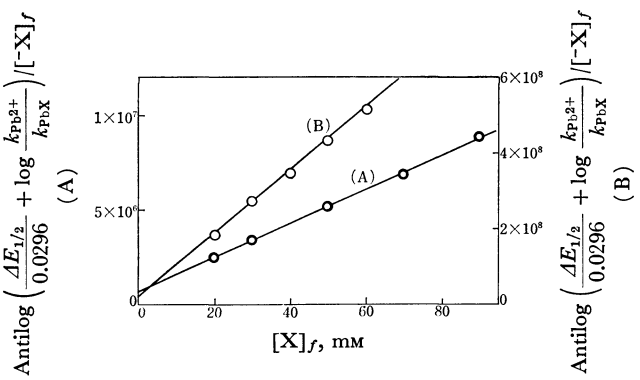

Fig. 6. The plot of antilog $(\Delta E_{1/2}/0.0296 + \log(k_{Pb^{2+}}/k_{PbX}))/[X]_f$ against the concentration of uncomplexed Asp or IDA.
Concentration of lead (II) ion=0.50mM, μ=0.30, 25°C
A : Asp system, pH=9.70
B : IDA system, pH=9.50

The K_{PbAc} and K^{Ac}_{PbAc} values determined in the IDA solution agreed well with those obtained in the Asp solution. They also agree well with those reported by Tanaka and Kato.[5] Here, we can mention that the K^{Ac}_{PbX} and $K^{Ac}_{PbX(Ac)}$ values are all smaller than K_{PbAc} and K^{Ac}_{PbAc}. This is not unreasonable, because the steric and electrostatic effects of coordinated Asp and IDA will reduce the stability of the mixed ligand complexes. The formation constants of the lead(II)-IDA complexes are fairly much larger than those of the Asp complexes. This may be ascribable to the rigid and stable five-membered ring of the IDA complex. It should also be mentioned that, although the Asp anion can from two mixed ligand complexes, the IDA anion can form only one mixed ligand complex, $PbX(Ac)^-$. This fact can be explained well by assuming that the Asp anion acts as a bidentate ligand while the IDA anion acts as a tridentate ligand. As was discussed in the polarographic study of the complex formation reaction of EDTP with the cadmium(II) ion,[4] the assumption that the Asp anion which has a propionate group acts as a bidentate ligand is not unreasonable. Even if the Asp anion acts as a tridentate ligand, from the electronic point of view it can be expected that the lead(II)-Asp complex with a less rigid six-membered ring can be interact with an acetate ion and give a mixed ligand complex more easily than can a rigid IDA complex. In order to describe the properties of the Asp anion as a ligand in detail, further systematic investigations should be conducted.

TABLE 3. THE RELATION BETWEEN THE HALF-WAVE POTENTIAL AND THE CONCENTRATION OF HYDROGEN ION

Concentration of lead(II) ion=0.50 mM, μ=0.30, 25°C

(A) Asp system
Concentration of Asp=70.0 mM

$E_{1/2}$, V *vs.* SCE	pH	$\Delta E_{1/2}$, mV	
		Calcd	Obsd
−0.477	8.35	0	0
−0.494	8.86	−20.3	−17.0
−0.513	8.93	−37.3	−34.0
−0.525	9.70	−47.5	−48.0
−0.537	10.35	−56.4	−60.0

(B) IDA system
Concentration of IDA=50.0 mM

$E_{1/2}$, V *vs.* SCE	pH	$\Delta E_{1/2}$, mV	
		Calcd	Obsd
−0.553	8.76	0	0
−0.562	9.08	− 8.9	− 9.0
−0.577	9.54	−21.9	−24.0
−0.583	9.80	−30.4	−30.0

4) M. Kodama and Y. Tominaga, This Bulletin, **42**, 2267 (1969).

5) N. Tanaka and K. Kato, This Bulletin, **33**, 417 (1960).

Derivatographic Studies on Transition Metal Complexes. IV.[1] Deaquation-Olation of Hydroxoaquo Cobalt(III) Complexes with Aminotricarboxylic Acids.[2]

Ryokichi Tsuchiya, Akira Uehara, and Eishin Kyuno
Department of Chemistry, Faculty of Science, Kanazawa University, Kanazawa
(Received May 13, 1970)

Thermochemical functions of the deaquation-olation on $K[Co(OH)L_4(H_2O)]$ type complexes in the solid phase were determined by means of derivatography and UV spectral measurements and the mechanisms were discussed on the basis of the results. In the above formula, L_4, denotes nitrilotriacetate (nta), nitriloisopropionicdiacetate (nipda), *d,l*-α-amino-*n*-butyric-*N,N*-diacetate (α-abda), *l*-leucine-*N,N*-diacetate (*l*da), *l*-valine-*N,N*-diacetate (vda), *d*-α-phenylglycine-*N,N*-diacetate (pgda), or *d,l*-α-phenylalanine-*N,N*-diacetate (pada) ions. These complexes were found to liberate one mole of coordinating water upon heating and to turn into the olated compound bridged with two OH groups at the same time. From an estimation of enthalpy change and activation energy for the reaction, it was found that the reaction is apt to take place more easily as the structural complexities of chelating agents increase and that the reaction always proceeds in the first order. We might conclude that the evolution of coordinating water is the rate-determining step in the reaction.

In 1907, Werner found that when $[Co(OH)(H_2O)(NH_3)_4]X_2$ type complexes were heated at *ca.* 100°C, the following olation took place.[3]

$$2[Co(OH)(H_2O)(NH_3)_4]X_2 \longrightarrow [(NH_3)_4Co(OH)_2Co(NH_3)_4]X_4 + 2H_2O$$

Wendlandt and Fisher estimated the heats of olation in several complexes of the above type in which only the counter anions are different from each other.[4]

Pfeiffer observed that when the red $[Cr(OH)(H_2O)en_2]Cl_2$ is heated at 120°C, a bluish violet salt is formed.[5] He also suggested that the resulting salt has two bridged OH groups between two metal atoms and the reaction is expressed as follows:[6]

$$2[Cr(OH)(H_2O)en_2]Cl_2 \longrightarrow [en_2Cr(OH)_2Cr\,en_2]Cl_4 + 2H_2O$$

From the fact that the reaction of this type could occur readily, the red salt is considered to have the *cis* configuration with respect to the position of OH and H_2O.

In general, if the quadridentate ligands such as NTA or its analogues reside in the octahedral environment together with OH and H_2O, the latter two are situated at the *cis* position with each other. Therefore, this kind of complex is expected to bring about the olation expressed by

$$2K[M(OH)L_4(H_2O)] \longrightarrow K_2[L_4M(OH)_2ML_4] + 2H_2O.$$

It might be named "Deaquation-olation," because it involves both deaquation of the coordinating water and formation of the olated compound simultaneously. A few examples of such reactions have already been found on the cobalt(III) complexes with the aminotricarboxylic acids.[7–10] However, little thermochemical or kinetic functions of the reaction were reported and no mechanism discussed. Therefore, the present study was undertaken (1) to trace the thermal reaction by means of derivatography, (2) to estimate the enthalpy change (ΔH) and activation energy (E^*) of the respective thermal reactions, and (3) to deduce the mechanisms of the reaction.

Table 1. Structures and abbreviations of the chelating agents and the complexes therewith

Rational formula	R	Abbreviation[a]	Complex
	$-H$	NTA	$K[Co(OH)nta(H_2O)]\cdot H_2O$[7] (I)
R	$-CH_3$	NIPDA	$K[Co(OH)nipda(H_2O)]\cdot 2H_2O$[8] (II)
|	$-C_2H_5$	α-ABDA	$K[Co(OH)\alpha\text{-abda}(H_2O)]\cdot 2H_2O$[10] (III)
/CHCOOH	$-CH(CH_3)_2$	VDA	$K[Co(OH)vda(H_2O)]\cdot 1.5H_2O$[10] (IV)
N—CH_2COOH	$-CH_2\cdot CH(CH_3)_2$	LDA	$K[Co(OH)\,l\text{da}(H_2O)]\cdot H_2O$[9] (V)
\$CH_2$COOH	$-C_6H_5$	PGDA	$K[Co(OH)pgda(H_2O)]$[10] (VI)
	$-CH_2\cdot C_6H_5$	PADA	$K[Co(OH)pada(H_2O)]\cdot 5H_2O$[10] (VII)

a) NTA: Nitrilotriacetic acid
NIPDA: Nitriloisopropionicdiacetic acid
α-ABDA: *d, l*-α-Amino-*n*-butyric-*N,N*-diacetic acid
VDA: *l*-Valine-*N,N*-diacetic acid
LDA: *l*-Leucine-*N,N*-diacetic acid
PGDA: *d*-α-Phenylglycine-*N,N*-diacetic acid
PADA: *d,l*-α-Phenylalanine-*N,N*-diacetic acid

1) Part III of this series: R. Tsuchiya, K. Murai, A. Uehara, and E. Kyuno, This Bulletin, **43**, 1383 (1970).
2) Presented at the 23rd Annual Meeting of the Chemical Scoiety of Japan, Tokyo, April, 1970.
3) A. Werner, *Ber.*, **40**, 4434 (1907).
4) W. W. Wendlandt and J. K. Fisher, *J. Inorg. Nucl. Chem.*, **24**, 1685 (1962).
5) H. Pfeiffer, *Z. Anorg. Allg. Chem.*, **56**, 261 (1907).
6) H. Pfeiffer, *ibid.*, **29**, 107 (1901).

Experimental

Preparation of Starting Complexes. Table 1 gives the rational formulas of the ligands and the chemical formulas of the complexes containing the ligands in the present work. All the ligands are analogues of NTA, and they can form the complexes including the 5,5,5-membered chelate rings when they act as a quadridentate ligand. The complexes were prepared by the methods described in respective references.[7-10]

Derivatographic Measurement. The derivatograms for these complexes were obtained with a Metrimpex Derivatograph Typ-OD-102. All the measurements were carried out in a constant nitrogen stream under the heating rate of 1°C min^{-1}. Five-hundred milligrams of the sample was used in each run. Analysis of derivatograms for each reaction process was carried out in a similar way to that described in part I of this series.[11]

Measurement of Electronic Spectra. The electronic spectra of the complexes were measured with a Hitachi EPU-2A Spectrophotometer in solid state by means of a diffuse-reflection method.

Results and Discussion

Observation on the Thermal Reaction Process by Derivatography. Figure 1 contains the derivatograms for nta- (I), nipda- (II) and *l*da-compleses (V) as the representatives. As seen in this figure, complex II liberates successively two moles and one mole of water at about 100 and 195°C, respectively. The former step is endothermic and the latter exothermic. The color of the sample changed to pink from bluish violet at the latter step. The latter step seems to involve the deaquation of coordinating water and the simultaneous formation of diol complex.

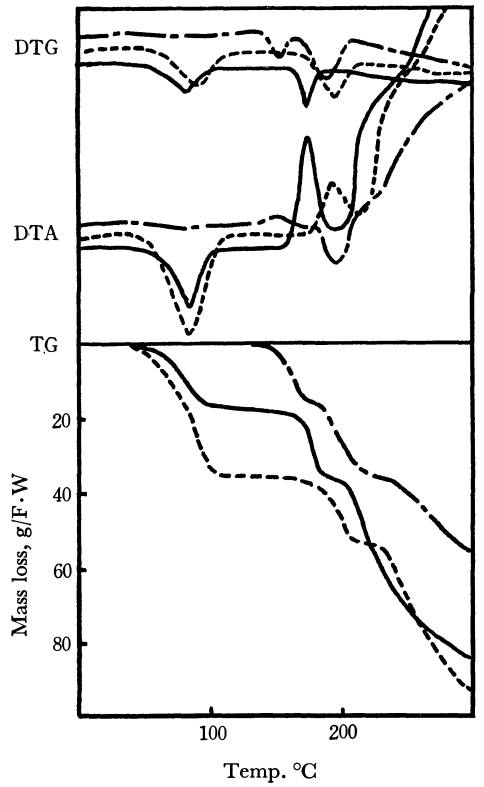

Fig. 1. Derivatograms for nta (·—·—·), nipda (·····) and *l*da (——) complexes.

In complex V, the mass losses corresponding to one mole of crystalline water in an endothermic reaction and then to one mole of coordinating water in an exothermic reaction were found at 100°C and at 180°C, respectively. The color of the sample changed to pink from bluish violet at the latter step as in the case of complex II. Such a change could be observed with all complexes except for complex I.

In complex I, although the two steps of mass losses corresponding to each one mole of water were separately observed at 160°C and 180°C, the color change and the exothermic DTA peak were found only at the former step. The former step is, hence, thought to correspond to the deaquation-olation and the latter, to the liberation of crystalline water alone.

In order to compare the thermal stability of all the complexes with each other, the exothermic DTA peaks alone are sketched in Fig. 2.

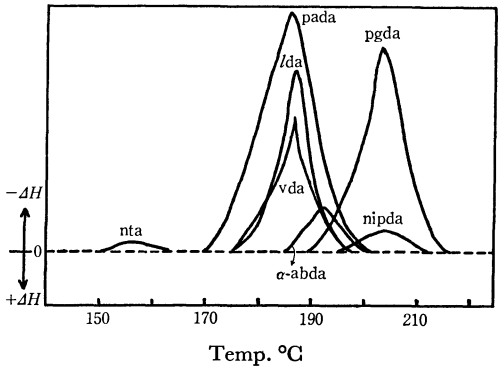

Fig. 2. DTA curves for deaquation-olation of the complexes.

The abscissa shows temperature and the ordinate an arbitrary scale of DTA curves. The dotted line gives the base of DTA curve, and $-\Delta H$ and $+\Delta H$ shows the scales for the exothermic and the endothermic reactions, respectively. As seen from the figure, although the reaction temperature differ with the kinds of the complexes, the peak area becomes larger in the order: nta- < nipda- < α-abda- < vda- < *l*da- < pgda- < pada-complexes.

Electronic Spectra. As an example, the electronic spectra of hydroxoaquo-pada-cobalt(III) complex (VII), of the complex after heating at 190°C and of diol-pada complex prepared in another method[10] are given in Fig. 3. The spectrum for complex VII after heating at 190°C, where the deaquation-olation seems to have taken place, closely resemble that of the diol complex, and the second band (due to *d–d* transition) does not appear distinctly. Similar results are also obtained in all the remaining complexes. They are in line with

7) M. Mori, M. Shibata, E. Kyuno, and Y. Okubo, This Bulletin, **31**, 940 (1958).
8) M. Tachibana, A. Uehara, E. Kyuno, and R. Tsuchiya, *ibid.*, **43**, 1061 (1970).
9) A. Uehara, E. Kyuno, and R. Tsuchiya, *ibid.*, **43**, 414 (1970).
10) To be published elsewhere.
11) R. Tsuchiya, Y. Kaji, A. Uehara, and E. Kyuno, This Bulletin, **42**, 1881 (1969).

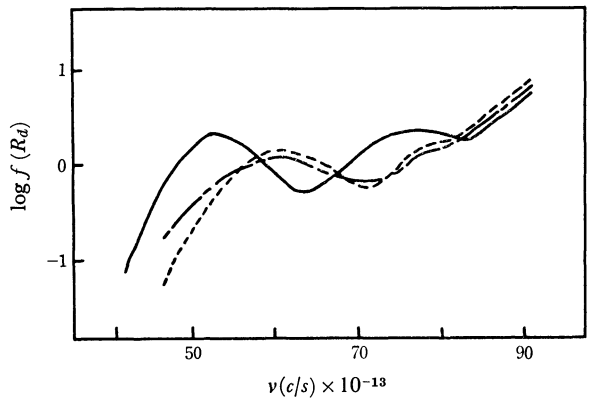

Fig. 3. Electronic spectra for K[Co(OH) pada $(H_2O)]\cdot 5H_2O$ (——), the sample after heating at 190° (·—·—·) and K_2[pada-$Co(OH)_2Co$ pada] (·····).

the electronic spectra for the ol-ammine-cobalt(III)[12] and the diol-nta cobalt(III) complexes.[7]

Enthalpy Change and Activation Energy. The enthalpy changes, ΔH, for each step of the thermal reactions in these complexes were estimated from DTA curves in the same way as described.[11] It was also confirmed by the analyses of DTA curves[13] that both the evolution of the crystalline water and the deaquation-olation proceed in the first order. The Arrhenius plots, log-k *vs.* $1/T$, for both reactions showed a good linearity. Only those for the latter reaction are given in Fig. 4. The activation energies, E^*, of the reactions were

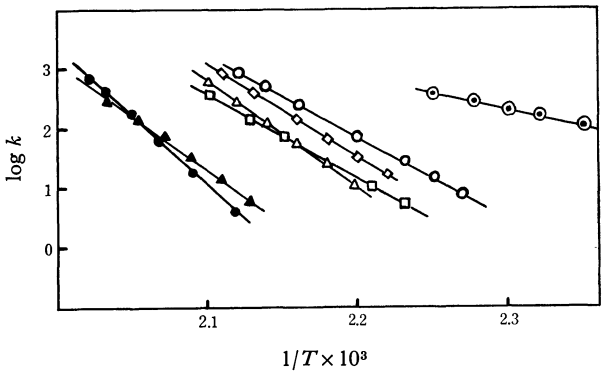

Fig. 4. Arrhenius plots for deaquation-olation of nta-(⊙-⊙), nipda-(▲-▲), α-abda-(△-△), vda-(○-○), *l*da- (□-□), pgda-(●-●), and pada-(○-○) complexes.

calculated from the slope of the respective Arrhenius plots. The values of ΔH and E^* estimated in all the complexes are summarized in Table 2.

The values of ΔH and E^* for the liberation of crystalline water from complexes II, III, IV, and V are close to the values for the reaction $CuSO_4\cdot 5H_2O \rightarrow CuSO_4\cdot 3H_2O + 2H_2O$ ($\Delta H \approx 13.1$ kcal/mol, $E^* \approx 21.3$ kcal/mol). The five moles of crystalline water of complex VII were liberated step by step: first four moles and then one mole. The one mole was more difficult to be liberated than the four. It was found that only in the case of complex I the activation energy for the liberation of crystalline water (38.8 kcal/mol) is greater than that for the deaquation-olation (29.7 kcal/mol). It is thus considered that coordinating water can be more easily lost than crystalline water. This is in good agreement with the fact that the deaquation-olation precedes the evolution of crystalline water as shown by the lower starting temperature in the former process than that in the latter (Table 2).

In the deaquation-olation, the values of ΔH for all the complexes show an increasing trend with the structural complexities of the chelating agents. On the contrary, the inverse trend was found in the values of E^* except complexes I and VI. It is not clear why complexes I and VI show a much lower and higher activation energy respectively. The numerical data in Table 2 indicate that the deaquation-olation takes place in the order: nta-$<$nipda-$<$α-abda-$<$vda-$<$ *l*da-$<$pgda-$<$pada-complexes.

Proposed Thermal Reaction Mechanism. The thermal reaction mechanisms of these complexes will be discussed on the basis of the above results. Figure 5 shows the proposed thermal reaction scheme for complex I and Fig. 6 that for complexes II through VII.

It is reasonable to conclude that for complex I the crystalline water is evolved after deaquation-olation took place. On the other hand, complexes II through VII are considered first to lose the crystalline water, and then to show the deaquation-olation as in Fig. 6.

If the activated complex in the above two figures were assumed to be an intermediate in the deaquation-olation, two mechanisms are possible, *viz.*, the formation of activated complex from the corresponding hydroxoaquo complex is slow or the liberation of coordinating water from the activated complex is slow. However,

Table 2. Thermochemical functions for evolution of crystalline water and deaquation-olation

Complex	Evolution step of crystalline waters			Deaquation-olation step		
	Starting temp (°C)	ΔH(kcal/mol)	E^*(kcal/mol)	Starting temp (°C)	ΔH (kcal/mol)	E^*(kcal/mol)
I	175	8.2	38.8	150	−1.2	29.7
II	40	13.6	19.9	195	−4.8	85.8
III	50	13.5	21.0	185	−6.3	75.4
IV	80	13.3	21.1	175	−12.8	70.8
V	60	13.0	20.3	175	−14.3	65.1
VI				190	−18.8	91.9
VII	40 (4 mol)	12.7	16.3	170	−21.3	62.8
	90 (1 mol)	13.3	24.2			

12) Y. Inamura and Y. Kondo, *Nippon Kagaku Zasshi*, **74**, 627 (1953).

13) H. J. Borchardt and F. Danniels, *J. Amer. Chem. Soc.*, **79**, 41 (1957).

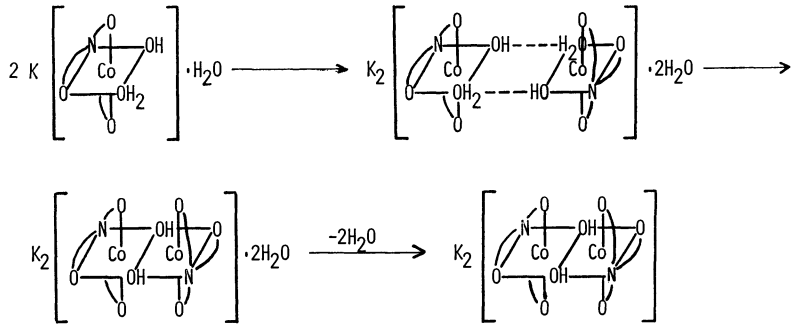

Fig. 5. Proposed thermal reaction scheme for nta-complexes.

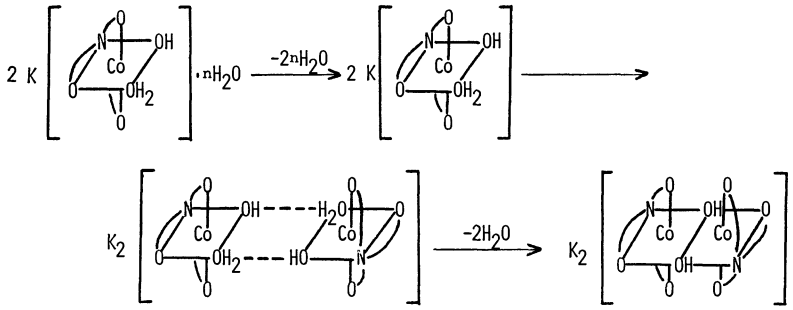

Fig. 6. Proposed thermal reaction scheme for nipda-, α-abda-, vda-, *l*da-, pgda-, and pada-complexes.

the idea that the liberation of coordinating water is slow (the rate-determining step) might be reasonable in the present deaquation-olation. It would be supported by satisfactory linearity in the Arrhenius plots which were plotted from the view point that the reaction proceeds in the first order.

The authors wish to express their appreciation to the Ministry of Education for the financial support granted for this research.

Derivatographic Studies on Transition Metal Complexes. V.[1] Thermal *cis*, *trans*-to-*trans*, *cis* Isomerization of $[CoCl_2(NH_3)_2en]ClO_4$ in Solid Phase[2]

Ryokichi TSUCHIYA, Yasuo NAKATA,[3] and Eishin KYUNO

Department of Chemistry, Faculty of Science, Kanazawa University, Kanazawa

(Received June 27, 1970)

The complex, *cis,trans*-$[CoCl_2(NH_3)_2en]ClO_4$, regardless whether its state is monohydrate or anhydride, was isomerized to *trans,cis*-form by heating in a solid phase. In the kinetic study on perchlorate in a closed system, it was found that the isomerization of the hydrated compound proceeded through a second order reaction with respect to the remaining fraction of the starting compound with the activation energy, $E^*=29.5$ kcal mol^{-1}, while that of the anhydrous one proceeded through a first order reaction with $E^*=51.4$ kcal mol^{-1}. On the other hand, derivatographic analyses showed that the enthalpy change in the dehydration partly including isomerization was $\Delta H=13.9$ kcal mol^{-1} for the monohydrated perchlorate and the activation energy was $E^*=39.9$ kcal mol^{-1}, whereas the enthalpy change of isomerization of the anhydrous perchlorate was $\Delta H=-2.1$ kcal mol^{-1}. From the results, it is believed that the "Aquation-anation" mechanism on the crystal surface is predominant in the isomerization for the hydrate, but it proceeds through some intramolecular reactions for the anhydride.

The isomerization which takes place after complete dehydration has only recently been detected and reported for *trans*-$[CoCl_2(NH_3)_4]IO_3\cdot 2H_2O$.[4,5] Typical examples as the above, where two steps of dehydration and *trans*-to-*cis* isomerization are obviously separated in a solid phase are relatively less in the field of thermochemistry of transition metal complexes. The thermal isomerization of *trans*-$[CoCl_2pn_2](H_5O_2)Cl_2$ to the corresponding *cis*-isomer[6,7] simultaneously gives rise to the loss of one molecule of hydrogen chloride and two molecules of crystalline water. The ammine complex, *trans*-$[CoCl_2(NH_3)_4]Cl$, undergoes partial isomerization accompanied by much decomposition at somewhat higher temperature.[5] In the case of the ethylenediamine complex, *trans*-$[CoCl_2en_2](H_5O_2)Cl_2$,[6] the corresponding isomerization was not detected.

Examples of *cis*-to-*trans* isomerization are much more rare.[8] It is expected in the complexes, *cis,trans*-$[CoCl_2(NH_3)_2en]X$, that, when the two adjacent chloride ions change their coordination sites to the *trans*-position upon heating, the color changes from blue to green.

Three geometrical isomers can be postulated for the above complexes as shown in Fig. 1. Distinct thermochromism from blue to green in a solid phase was observed in our preliminary experiments on the complex *cis,trans*-$[CoCl_2(NH_3)_2en]ClO_4$. A similar phenomenon was also observed for the anhydrous perchlorate. This is considered to correspond to the transformation from *cis,trans*- (a) to *trans,cis*- form (b) as shown in Fig. 1. The present study deals with the thermal isomerization of *cis,trans*-$[CoCl_2(NH_3)_2en]ClO_4\cdot H_2O$ and its anhydride to *trans,cis*-form complex.

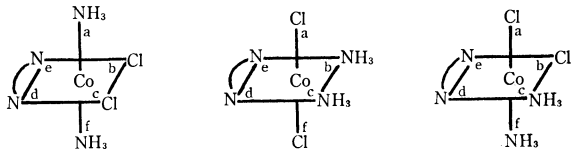

Fig. 1. Three geometrical isomers of $[CoCl_2(NH_3)_2en]X$.
(a) *cis*(dichloro), *trans*(diammine)-form (*cis, trans*-form)
(b) *trans*(dichloro), *cis*(diammine)-form (*trans, cis*-form)
(c) *cis*(dichloro), *cis*(diammine)-form (*cis,cis*-form)

Experimental

Syntheses of Complexes. The complexes *trans,cis*- and *cis,trans*-$[CoCl_2(NH_3)_2en]Cl\cdot nH_2O$ were prepared by the known method.[9] The corresponding perchlorate were obtained from the respective chlorides by saturating their solutions with 60% perchloric acid at room temperature and by putting them to stand in a refrigerator for a while. The blue crystals corresponding to *cis,trans*-form complexes or the green crystals corresponding to *trans,cis*-form complexes deposited out were filtered and washed with a small amount of ethanol-water (2 : 1) and then ethanol-ether (1 : 1) mixtures, and dried over silica-gel in a desiccator for a while.

Found: C, 7.07; H, 4.70; N, 16.51%. Calcd for *cis,trans*-$[CoCl_2(NH_3)_2en]ClO_4\cdot H_2O$: C, 7.03; H, 4.72; N, 16.41%.

Found: C, 7.52; H, 4.40; N, 17.25%. Calcd for *trans,cis*-$[CoCl_2(NH_3)_2en]ClO_4$: C, 7.43; H, 4.36; N, 17.32%.

The corresponding anhydrous *cis,trans*-compound was prepared by standing the monohydrate obtained above over silica-gel in a vacuum desiccator at room temperature for 10 days. The content of the crystalline water in the hydrate was sometimes determined with a thermobalance. In general, complete dehydration of the compound was achieved in a week at room temperature under similar conditions. Complete dehydration was also achieved even at 90°C in a few hours without any detectable isomerization. This was verified by the UV and IR spectral measurements.

1) For part IV in this series: see R. Tsuchiya, A. Uehara, and E. Kyuno, This Bulletin, **44**, 701 (1971).

2) Presented at the 19th Symposium on Coordination Chemistry, Sendai, September, 1969.

3) Present address: Showa Petroleum Industries, Co. Ltd., Yokohama.

4) N. I. Lobanov, *Zh. Neorg. Khim.*, **4**, 344 (1959).

5) H. E. LeMay, Jr., and J. C. Bailar, Jr., *J. Amer. Chem. Soc.*, **89**, 5577 (1967).

6) H. E. LeMay, Jr., *Inorg. Chem.*, **7**, 2531 (1968).

7) R. Tsuchiya, K. Murai, A. Uehara, and E. Kyuno, This Bulletin, **43**, 1383 (1970).

8) J. P. Mathieu and H. Poulet, *J. Chem. Phys.*, **59**, 369 (1962).

9) J. C. Bailar, Jr., and D. F. Pepard, *J. Amer. Chem. Soc.*, **62**, 105 (1940).

Found: C, 7.62; H, 4.40; N, 17.25%. Calcd for $[CoCl_2(NH_3)_2en]ClO_4$: C, 7.43; H, 4.36; N, 17.32%.

Derivatographic Measurement. The derivatograms of these compounds were obtained with a MOM Derivatograph Typ-OD-102.[10] Samples in each run were 0.4 g, finely powdered, 100—200 mesh inch^{-1}. The measurements were carried out under a constant flow of nitrogen stream with the heating rate of 1°C min^{-1} unless otherwise stated. The enthalpy changes, ΔH, and the activation energies, $E^{\neq}$, in the thermal changes concerned were calculated by DTA curve analysis in the derivatograms.[11-13]

Spectral Measurements. Visible and UV absorption spectra of the complexes in solution were measured with a Hitachi R-3 Spectrophotometer. The IR spectral measurements of the complexes were carried out with a JASCO Model IR-E and IR-G Spectrophotometers in a Nujol mull.

Isothermal Measurements. The isothermal rate determination on dehydration was carried out with a Shimadzu TM-1A Thermobalance as a complement to derivatographic determinations. Measurements were carried out at several desired constant temperatures in a static air with the same samples as those used in the derivatographic study.

The rate of isomerization of the complexes was measured by using an Abderhalden apparatus keeping a small sample vessel under constant temperatures in a closed system. The products were taken out from the sample vessel at certain time intervals and the absorption spectra were measured to determine the mole ratio of *cis,trans/trans,cis* in the products.

The complex species, *cis,trans*-$[CoCl_2(NH_3)_2en]ClO_4\cdot H_2O$ and the corresponding *trans,cis*-form anhydride, are fairly soluble in dimethylformamide (DMF) in the original stable form, and the solution is found not to undergo further chemical change at least during the measurement. The absorption obeys Lambert-Beer's law within the concentration range for the determination. The pure complexes as shown in the spectra in Fig. 2, have the following absorption coefficients at 594 and 625 nm in DMF solution:

	ε_{594nm}	ε_{625nm}
cis,trans-$[CoCl_2(NH_3)_2en]ClO_4\cdot H_2O$ and its anhydride	128.8	118.8
trans,cis-$[CoCl_2(NH_3)_2en]ClO_4$	33.8	43.8

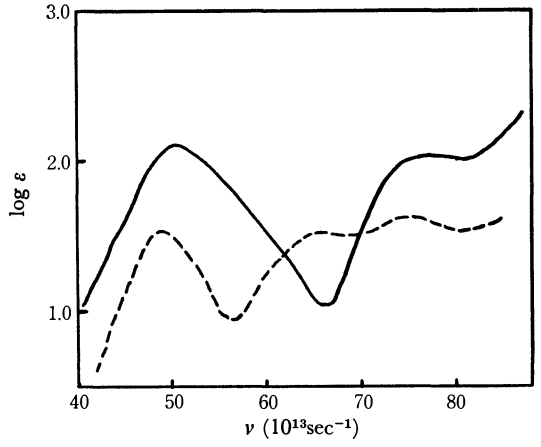

Fig. 2. Electronic spectra of $[CoCl_2(NH_3)_2en]ClO_4$ in DMF.
——, *cis,trans*-isomer; ----, *trans, cis*-isomer

From the results, the mixed mole ratio of two isomers in each product can be calculated spectrophotometrically by means of the equations

$$33.8X + 128.8Y = D_{594}$$
$$43.8X + 118.8Y = D_{625},$$

where X and Y are the concentrations in mol l^{-1} of *trans, cis*-complex and that of *cis,trans*-complex, respectively, and D_{594} and D_{625} the observed absorbancies at 594 nm and at 625 nm, respectively, with a 1.0 cm cell.

Results and Discussion

Dehydration of *cis,trans*-$[CoCl_2(NH_3)_2en]ClO_4\cdot H_2O$ proceeds through one step in TG and DTG curves, but the DTA gives a complicated pattern in the derivatogram as shown in Fig. 3. It is likely that the DTA curve in the derivatogram contains the overlapped heats of the two reactions, dehydration and isomerization. The DTA curve on the corresponding anhydrous complex, however, shows a small exothermic peak at about 160°C, probably due to isomerization, without any detectable mass loss as shown in Fig. 4.

The enthalpy change of the dehydration, including a partial isomerization, and that of the pure isomerization were derivatographically found to be ΔH=13.9 kcal mol^{-1} and −2.1 kcal mol^{-1}, from Fig. 3 and Fig. 4, respectively. Thus, the heat of pure dehydration for the perchlorate is presumed to be about 16 kcal mol^{-1}.

Dehydration containing a partial isomerization of *cis,trans*-$[CoCl_2(NH_3)_2en]ClO_4\cdot H_2O$ is considered to proceed through first order reaction, and the Arrhenius plots obtained on the basis of the above presumption are given in Fig. 5, from which the activation energy is calculated to be 36.6 kcal mol^{-1}.

When the complex, *cis,trans*-$[CoCl_2(NH_3)_2en]ClO_4\cdot H_2O$, was heated in static air by a thermobalance under

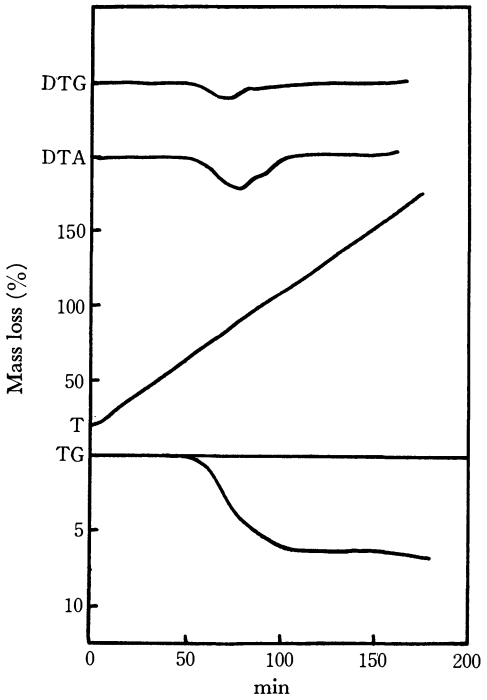

Fig. 3. Derivatogram for *cis,trans*-$[CoCl_2(NH_3)_2en]ClO_4\cdot H_2O$.

10) F. Paulik, J. Paulik, and L. Erdey, *Talanta,* **13**, 1405 (1966).
11) R. Tsuchiya, Y. Kaji, A. Uehara, and E. Kyuno, This Bulletin, **42**, 1881 (1969).
12) N. G. Borchardt and F. Daniels, *J. Amer. Chem. Soc.*, **79**, 41 (1957).
13) N. G. Dave and S. K. Chopra, *Z. Phys.*, **48**, 257 (1966).

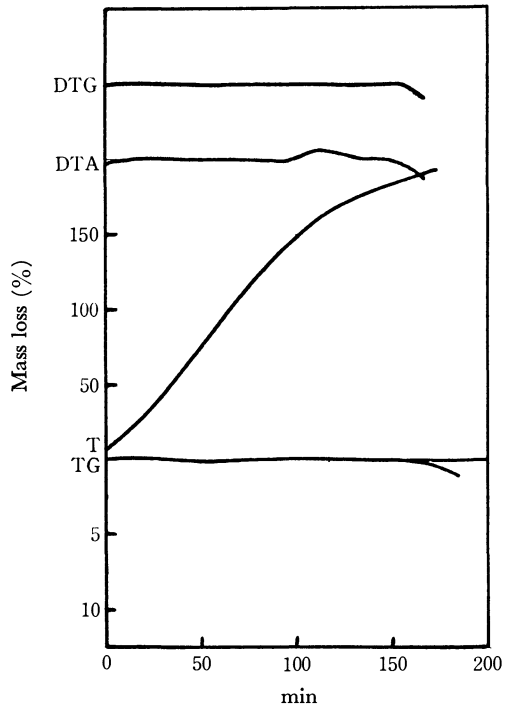

Fig. 4. Derivatogram for *cis,trans*-$[CoCl_2(NH_3)_2en]ClO_4$.

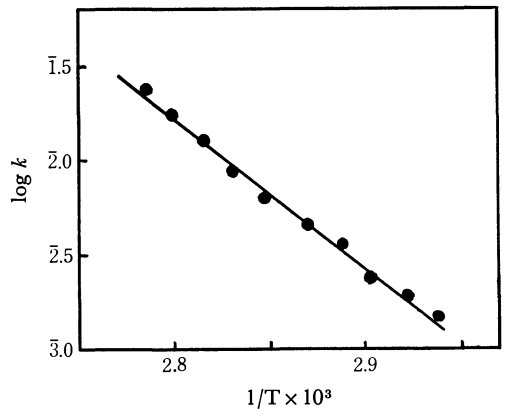

Fig. 5. Arrhenius plots for dehydration containing partial isomerization (derivatography).

the heating rate of 0.5°C min^{-1}, dehydration began at 85°C, and isomerization started at 120°C after complete dehydration. When it was heated at 150°C, the product consisted of about 40% of the *trans,cis*-isomer and the remaining *cis,trans*-isomer. Isomerization was finally completed at 175°C. The IR spectrum for the product obtained at 175°C is shown in Fig. 6, together with those for monohydrated *cis,trans*-isomer and for anhydrous *trans,cis*-isomer directly prepared. The figure verifies that the final heating product is *trans,cis*-$[CoCl_2(NH_3)_2en]ClO_4$. A similar type isomerization was observed in the corresponding anhydrous perchlorate complex.

The rate constants of isomerization for the hydrated and anhydrous *cis,trans*-$[CoCl_2(NH_3)_2en]ClO_4$ in the closed system as well as those of dehydration in the static air were determined in an isothermal condition. The kinetic data are summarized in Table 1.

It is of interest that, in the closed system, isomerization for the hydrated complex was found to proceed in a second order reaction with respect to the remaining complex, and that for the anhydrous complex in first order. The presence of crystalline water might play some important role in the difference described above, but a reasonable explanation could not be obtained.

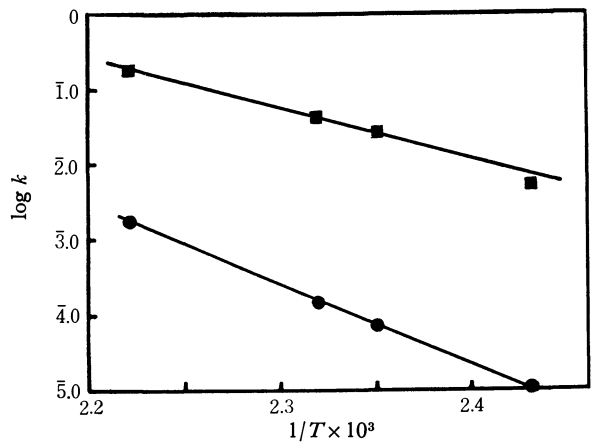

Fig. 7. Arrhenius plots for isomerization (isothermal measurement). -■-■-, *cis,trans*-$[CoCl_2(NH_3)_2en]ClO_4 \cdot H_2O$; -●-●-, *cis, trans*-$[CoCl_2(NH_3)_2en]ClO_4$

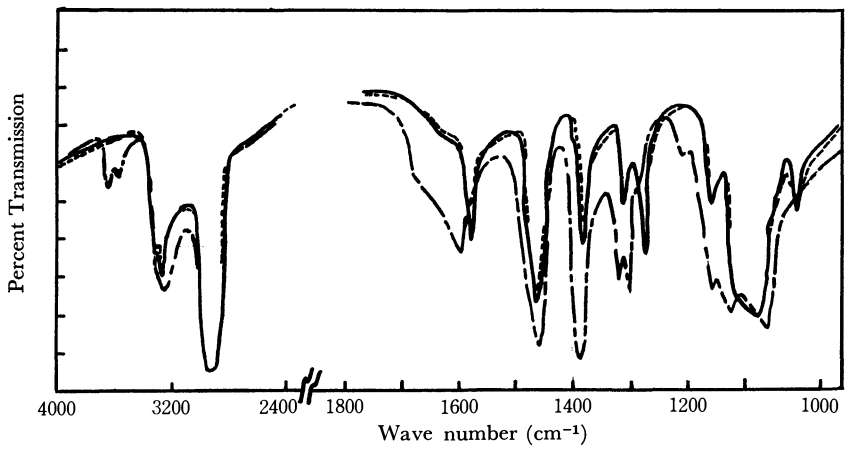

Fig. 6. IR spectra of the complexes. ·—·—·, *cis, trans*-$[CoCl_2(NH_3)_2en]ClO_4 \cdot H_2O$; ·····, *cis, trans*-$[CoCl_2(NH_3)_2en]ClO_4 \cdot H_2O$ after heating at 175 °C; ——, *trans, cis*-$[CoCl_2(NH_3)_2en]ClO_4$.

Table 1. Rate constants for *cis*, *trans*-$[CoCl_2(NH_3)_2en]ClO_4 \cdot H_2O$ and its anhydride

	$[CoCl_2(NH_3)_2en]ClO_4 \cdot H_2O$				$[CoCl_2(NH_3)_2en]ClO_4$	
°C	K_d, sec^{-1}	E_d^*, kcal mol^{-1}	K_i, sec^{-1}	E_i^*, kcal mol^{-1}	K_i, sec^{-1}	E_i, kcal mol^{-1}
70	$(7.9\pm0.3)\times10^{-4}$					
80	$(2.8\pm0.2)\times10^{-3}$					
90	$(5.0\pm0.2)\times10^{-3}$	25.4				
100	$(1.2\pm0.2)\times10^{-2}$					
138			$(2.0+0.2)\times10^{-3}$		$(7.5\pm0.2)\times10^{-6}$	
153			$(2.8\pm0.2)\times10^{-2}$		$(5.2\pm0.2)\times10^{-5}$	
158			$(4.1\pm0.2)\times10^{-2}$	29.5	$(1.2\pm0.2)\times10^{-4}$	51.4
178			$(2.0\pm0.2)\times10^{-1}$		$(1.2\pm0.2)\times10^{-3}$	

k_d and k_i are the rate constants of isomerization and those of dehydration.
E_d^* and E_i^* are the corresponding activation energies.

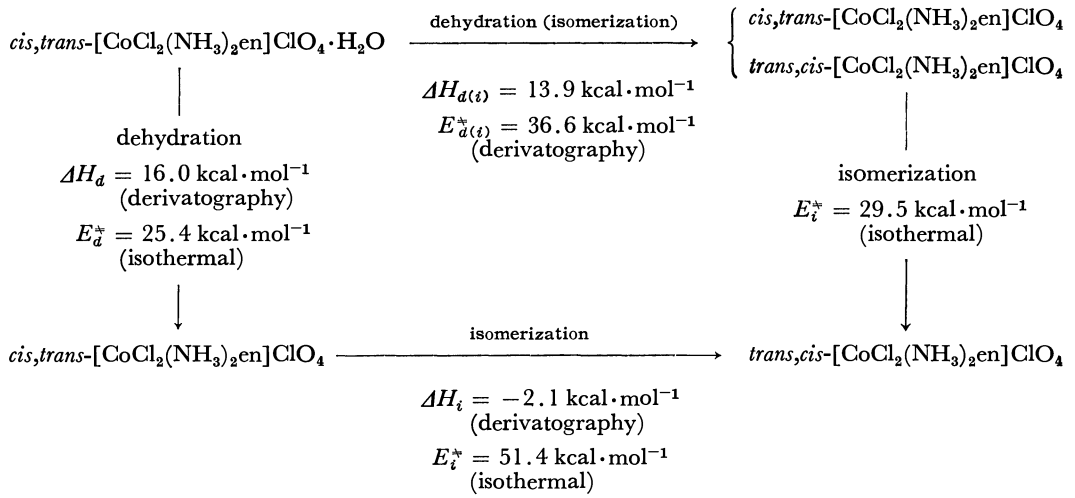

ΔH_d, ΔH_i and $\Delta H_{d(i)}$ represent to enthalphy changes of dehydration, isomerization, and dehydration containing partial isomerization.
$E^*_{d(i)}$ denotes the activation energy of dehydration containing partial isomerization.

Fig. 8. Schematic diagram for thermal reactions on *cis,trans*-$[CoCl_2(NH_3)_2en]ClO_4 \cdot H_2O$.

The Arrhenius plots concerned are shown in Fig. 7, from which the activation energies for isomerization were calculated to be 29.5 kcal mol^{-1} and 51.4 kcal mol^{-1} for the monohydrate and anhydride, respectively.

The thermal reaction pathways concerning *cis,trans*-$[CoCl_2(NH_3)_2en]ClO_4 \cdot H_2O$ and the thermal functions corresponding to the respective steps obtained are summarized schematically in Fig. 8.

The value of activation energy for the isomerization of *cis,trans*-$[CoCl_2(NH_3)_2en]ClO_4 \cdot H_2O$ was found to be of a similar order to that of the *trans*-to-*cis* isomerization of $[CoCl_2pn_2](H_5O_2)Cl_2$ under similar conditions.[7] Thus, the mechanism for the isomerization of the former hydrated complex seems to be explained by that of "aquation-anation" in closed system, as presumed in the latter complex.

Since remarkably higher activation energy is necessitated for the reaction in first order, isomerization of the anhydrous complex suggests an intramolecular reaction mechanism, *e. g.*, "twist" or "chelate ring opening-closing," because a similar mechanism has been also postulated for the isomerization of *trans*-to-*cis* reaction of $[CoCl_2pn_2]Cl$.[7] The difference between the activation energy from the derivatograms and that from the results obtained in a closed system may be due to the fact that the former contains both the data of isomerization and a part of dehydration and the latter that of isomerization only.

Derivatographic Studies on Transition Metal Complexes. VI.[1] Thermal, *cis*, *trans*-to-*cis*, *cis* Exchange-Isomerization[2] of $[CoCl_2(NH_3)_2en]SCN \cdot H_2O$ in Solid Phase[3]

Ryokichi Tsuchiya, Masatatsu Suzuki, and Eishin Kyuno

Department of Chemistry, Faculty of Science, Kanazawa University, Kanazawa

(Received August 27, 1970)

The exchange-isomerization of the complex, *cis*(dichloro), *trans*(diammine)-$[CoCl_2(NH_3)_2en]SCN \cdot H_2O$ to *cis*-(chloro isothiocyanato), *cis*(diammine)-$[CoCl(NCS)(NH_3)_2en]Cl$, was investigated by means of both derivatographic and isothermal methods. The reaction took place immediately after the liberation of crystalline water. The thermochemical functions were obtained to be $\Delta H = (5.5 \pm 1.0)$ kcal/mol and $E^* = (22.8 \pm 2.0)$ kcal/mol for the dehydration, while those for the exchange-isomerization were $\Delta H = (4.8 \pm 1.0)$ kcal/mol and $E^* = (62.3 \pm 3.0)$ kcal/mol, respectively. As a probable reaction mechanism for the exchange-isomerization, a certain seven coordinated intermediate in the reaction pathway was introduced.

Recently, several examples of thermal, *cis*-to-*trans*[1,4] and *trans*-to-*cis*[5–7] isomerization on transition metal complexes in solid phase have been reported. The different mechanisms were proposed between the thermal isomerization including dehydration in the hydrated solid phase and that in anhydrous phase; *i. e.*, "aquation-anation" mechanism was well fitted for the former isomerization and "twisting"[8] or "chelate ring opening-closing" mechanism[9] were mainly applied to the latter.

Although the exchange-isomerization in solid phase on transition metal complexes containing the simultaneous occurrence of the isomerization and exchange reaction between the ligand coordinated and the counter ion in the outer sphere is very rare, it is known that a similar reaction sometimes takes place in the case of using matrix-method[10] for the preparation of the complexes.

When the compound, *cis,trans*-$[CoCl_2(NH_3)_2en]SCN \cdot H_2O$, was heated in solid phase, the following reactions occurred successively:

$$\textit{cis,trans}\text{-}[CoCl_2(NH_3)_2en]SCN \cdot H_2O \longrightarrow \textit{cis,trans}\text{-}[CoCl_2(NH_3)_2en]SCN + H_2O \quad \text{(Dehydration)} \qquad (1)$$

$$\textit{cis,trans}\text{-}[CoCl_2(NH_3)_2en]SCN \longrightarrow \textit{cis,cis}\text{-}[CoCl(NCS)(NH_3)_2en]Cl \quad \text{(Exchange-isomerization)} \qquad (2)$$

The distinct color change, from blue to violet, was found in the reaction (2) at the temperature near 135°C. The present paper is concerned with the dehydration (1) and the exchange-isomerization (2) described above.

Experimental

Preparation of the Complex. The complex, *cis,trans*-$[CoCl_2(NH_3)_2en]Cl$, was prepared by the known method.[11] The corresponding thiocyanate was obtained by saturating the solution of the pure chloride with potassium thiocyanate. The row product was recrystallized in a dilute potassium thiocyanate solution. The blue crystals collected by filtration were washed with small amounts of cold water, ethanol and ether in turn and air-dried.

Found: C, 12.01; H, 5.17; N, 22.97%. Calcd for *cis,trans*-$[CoCl_2(NH_3)_2en]SCN \cdot H_2O$: C, 12.00; H, 5.38; N, 23.48%.

Derivatographic Measurement. The apparatus and techniques used in this work were the same as described in an earlier paper.[6]

Isothermal Measurement by using a Thermobalance. The measurement and analytical method for the experiments were also the same in an earlier paper.[12] Determination of the mixed ratio of two compounds, the starting *cis,trans*-form complex and *cis,cis*-form produced, was made spectrophotometrically.

Results and Discussion

Structural Determination of Reaction Product from the Spectra. The complex, $[CoClX(NH_3)_2en]^+$ is expected to exist in either of the four geometrical isomers as given in Fig. 1.

The infrared absorption spectra of $[CoCl(NCS)(NH_3)_2en]Cl$ produced and of the related compounds the structure of which is clear are shown in Fig. 2. It has been well known that, in general, the cobalt(III) complexes which have the two ammine groups in *cis*-

1) Part V in this series: see R. Tsuchiya, A. Nakata, and E. Kyuno, This Bulletin, **44**, 705 (1971).

2) This was termed for the reaction consisting of both isomerization and ligand-exchange at the same time.

3) Presented at the 23rd Annual Meeting of the Chemical Society of Japan, Tokyo, April, 1970.

4) J. P. Mathieu and H. Poulet, *J. Chem. Phys.*, **59**, 369 (1962).

5) H. E. LeMay, Jr., and J. C. Bailar, Jr., *J. Amer. Chem. Soc.*, **89**, 5577 (1967).

6) R. Tsuchiya, K. Murai, A. Uehara, and E. Kyuno, This Bulletin, **43**, 1383 (1970).

7) Y. Kaji, A. Uehara, E. Kyuno, and R. Tsuchiya, *ibid.*, **43**, 1906 (1970).

8) J. C. Bailar, Jr., *J. Inorg. Nucl. Chem.*, **8**, 165 (1958); P. C. Ray and N. K. Dutt, *J. Indian Chem. Soc.*, **18**, 289 (1941); *ibid.*, **20**, 81 (1943).

9) See, for example, F. Basolo, and R. G. Pearson, "Mechanisms of Inorganic Reactions," 2nd Ed., John Wiley & Sons, Inc., New York (1967) p. 327.

10) W. W. Wendlandt and L. K. Sveum, *J. Inorg. Nucl. Chem.*, **28**, 393 (1966).

11) J. C. Bailar, Jr., and F. Pepard, *J. Amer. Chem. Soc.*, **62**, 105 (1940).

12) R. Tsuchiya, Y. Kaji, A. Uehara, and E. Kyuno, This Bulletin, **42**, 1881 (1969).

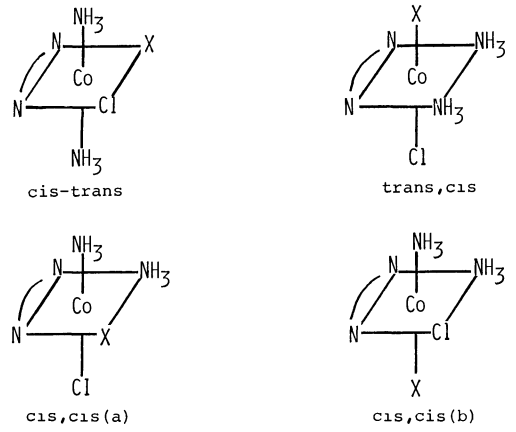

Fig. 1. Four geometrical isomers of $[CoClX(NH_3)_2en]^+$ (X= Cl^- or NCS^-).

position give two peaks assigned to the symmetric deformation, δ_{NH_2}, in the region of 1400—1200 cm^{-1} in the IR spectra, while *trans*-diammine ones have only one peak in this region: *e. g.*, the *cis*-diammine complexes involving organic amine like the ethylenediamine or propylenediamine, *trans,cis*-$[CoCl_2(NH_3)_2en]SCN\cdot H_2O$[13,14] and *trans,cis*-$[CoCl_2(NH_3)_2pn]Cl\cdot H_2O$,[15] show two peaks at 1310 and 1280 cm^{-1}, respectively, while the *trans*-diammine complexes, *cis,trans*-$[CoCl_2(NH_3)_2en]SCN\cdot H_2O$, *cis,trans*-$[CoCl_2(NH_3)_2pn]Cl\cdot H_2O$[16] and *cis,trans*-$NH_4[Co(SO_3)_2(NH_3)_2en]\cdot 2H_2O$,[11] have also two neighboring peaks at 1310 and 1330 cm^{-1} in rather higher wave number region than that given by the *cis*-diammine complexes. It has been understood by the fact that the bands assigned to the symmetric deformation, δ_{NH_2}, of ammonia and of organic amine are overlapped in this region.

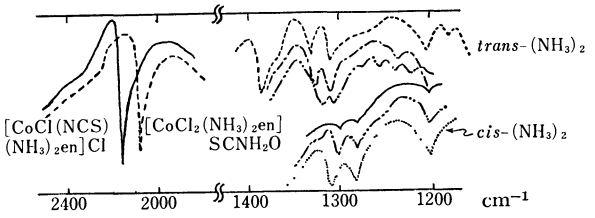

Fig. 2. IR spectra for the complexes.
cis, trans-$[CoCl_2(NH_3)_2en]SCN\cdot H_2O$ (------)
cis, trans-$[CoCl_2(NH_3)_2pn]Cl\cdot H_2O$ (-·-·-·-)
cis, trans-$NH_4[Co(SO_3)_2(NH_3)_2en]\cdot 3H_2O$ (-·-·-)
cis, cis-[CoCl (NCS) $(NH_3)_2en]Cl$ (——)
trans, cis-$[CoCl_2(NH_3)_2pn]Cl\cdot H_2O$ (-·-·-·-)
trans, cis-$[CoCl_2(NH_3)_2en]SCN\cdot H_2O$(·····)

When the complex *cis,trans*-$[CoCl_2(NH_3)_2en]SCN\cdot H_2O$ was heated, the color changed from blue to violet and the two peaks at 1310 and 1330 cm^{-1} of the starting material were shifted to lower wave number side at 1280 and 1310 cm^{-1} in their IR spectra as shown in Fig. 2.

From the above results, it is clearly recognizable that the structural change, from *trans*-diammine to *cis*-diammine, may be involved in the thermal reaction. It has also been found that the band of the starting complex assigned to the stretching vibration, $\nu_{C=N'}$,[17,18] was shifted from 2080 cm^{-1} to 2160 cm^{-1} upon heating it. This shift should include the exchange between chloride coordinated to central metal ion and thiocyanate in counter-ion sphere.

In addition, an interesting information derived from the change in the frequency of the $\nu_{C=N}$ band comes whether or not the linkage isomerism by the coordination of -SCN or -NCS occurs in the exchange reaction. The evidence is not very much clear, but it seems that the ligand coordinates as -NCS toward the central metal atom in this case based on the analysis of IR spectrum.[18]

It has been well known that one of the most available method in determining the geometrical structure of the transition metal complexes is the use of the analysis of electronic spectra. Since a very large difference on the electronic spectra[19] between the complexes involving two negative ligands in the *cis* position and the corresponding ones in the *trans* position has been found clearly, it will be possible to decide whether *cis* or *trans* position is occupied by these ligands coordinated in the unknown geometrical structure. The electronic spectra of $[CoCl(NCS)(NH_3)_2en]Cl$ and of the related complexes are shown in Fig. 3.

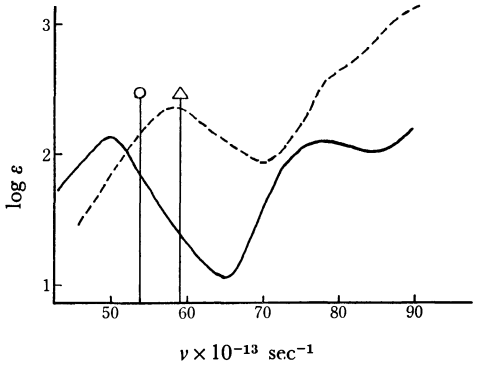

Fig. 3. Electronic spectra for *cis,trans*-$[CoCl_2(NH_3)_2en]SCN\cdot H_2O$(——) and *cis,cis*-$[CoCl(NCS)(NH_3)_2en]Cl$ (·····) (○ and △ indicate the frequencies of absorption maxima for *trans*-$[CoCl(NCS)en_2]Cl$ and *cis*-$[CoCl(NCS)en_2]Cl$, respectively.).

Aside from the appearance of the band splitting tendency[19] when such negative ligands are involved in the *cis* position as in the case of *cis,cis*-$[CoCl(NCS)(NH_3)_2en]Cl$[14] and *cis*-$[CoCl(NCS)en_2]Cl$,[20] the band exists in the rather higher frequency region than that of the corresponding *trans* one, *trans*-$[CoCl(NCS)en_2]Cl$.[14] The first absorption band of bis(ethylenedi-

13) For *cis, trans*- and *trans, cis*-$[CoCl_2(NH_3)_2en]Cl$: E. Kyuno, *Nippon Kagaku Zasshi*, **80**, 722 (1959).
14) M. E. Baldwin, *J. Chem. Soc.*, **1960**, 4369.
15) To be published elsewhere.
16) To be published elsewhere.
17) J. C. Bailar, Jr., and M. M. Chamberlain, *J. Amer. Chem. Soc.*, **81**, 6412 (1959).
18) P. O. H. Mitchell and R. J. P. Williams, *J. Chem. Soc.*, **1960**, 1912.
19) See for examples: K. Nakamoto, J. Fujita, M. Kobayashi, and R. Tsuchida, *J. Chem. Phys.*, **27**, 439 (1957) and H. Yamatera, This Bulletin, **31**, 95 (1956).
20) H. Kuroya and R. Tsuchida, This Bulletin, **15**, 427 (1940).

amine) complexes, in general, appears in slightly higher frequency region than that of diammine-ethylenediamine one, being obeyed on "Spectrochemical Series".[21] The utility of the empirical rule in this case suggests that the product, $[CoCl(NCS)(NH_3)_2en]Cl$ from *cis,trans*-$[CoCl_2(NH_3)_2en]SCN \cdot H_2O$ by the thermal reaction is still held the *cis* structure with respect to two negative ligands coordinated in spite of exchange of one of the ligands.

Kinetic Studies. The derivatogram for *cis,trans*-$[CoCl_2(NH_3)_2en]SCN \cdot H_2O$ is given in Fig. 4. When the complex was heated at the heating rate 1° min^{-1} by using Derivatograph, the loss of crystalline water began at about 75°. The TG curve indicates that the dehydration is completed up to 120° and no further mass loss was detected until about 170°. The DTA curve exhibits two endothermic peaks corresponding to dehydration and the genuine decomposition of the complex, respectively. And one more small exothermic peak appears at about 135° without the change of both TG and DTG curves in the derivatogram, where the color change from blue to violet was, however, found, which is corresponding to the exchange-isomerization, *cis,trans*-$[CoCl_2(NH_3)_2en]SCN \longrightarrow$ *cis,cis*-$[CoCl(NCS)(NH_3)_2en]Cl$. From the situation, it is possible to conclude that the exchange-isomerization proceeds after the dehydration process.

The experimental thermochemical functions calculated from the derivatogram were $\Delta H = (5.5 \pm 1.0)$ kcal/mol and $E^* = (22.8 \pm 2.0)$ kcal/mol for the dehydration, and $\Delta H = (4.8 \pm 1.0)$ kcal/mol and $E^* = (62.3 \pm 3.0)$ kcal/mol for the exchange-isomerization, and the Arrhenius plots for the calculation of the activation energy are shown in Fig. 5.

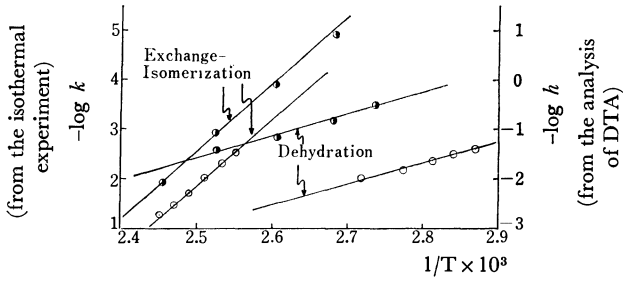

Fig. 5. The Arrhenius plots for *cis, trans*-$[CoCl_2(NH_3)_2en]SCN \cdot H_2O$ from isothermal (◑) and from DTA analysis(○).

The thermal exchange-isomerization of *cis,trans*-$[CoCl_2(NH_3)_2en]SCN \cdot H_2O$ was also studied by means of isothermal method. At a certain constant temperature, the mole ratio of the *cis,trans*-form complex against the *cis,cis*-form complex produced was estimated every after several different times. Since pure *cis,trans*-$[CoCl_2(NH_3)_2en]SCN \cdot H_2O$ and *cis,cis*-$[CoCl(NCS)(NH_3)_2en]Cl$ show the absorption coefficients, 168 and 58.3 at 518 nm, and 65.3 and 121.5 at 598 nm in DMF, respectively, the *cis,trans*/*cis,cis*-ratio in the product in each step can be determined spectrophotometrically by means of the following equations:

$$168X + 58.3Y = D_{518}$$
$$65.3X + 121.5Y = D_{598},$$

where X and Y are the concentrations (in mol l^{-1}) of *cis,trans*- and *cis,cis*-complexes, and D_{518} and D_{598} are the absorbancies at 518 and 598 nm with 1.0 cm cell, respectively. Thus, *cis,trans*/*cis,cis*-ratios are given by X/Y.

From the mole ratio obtained above, the rate constants of dehydration, k_d, and of exchange-isomerization, k_i, were calculated, which are summarized in Table 1.

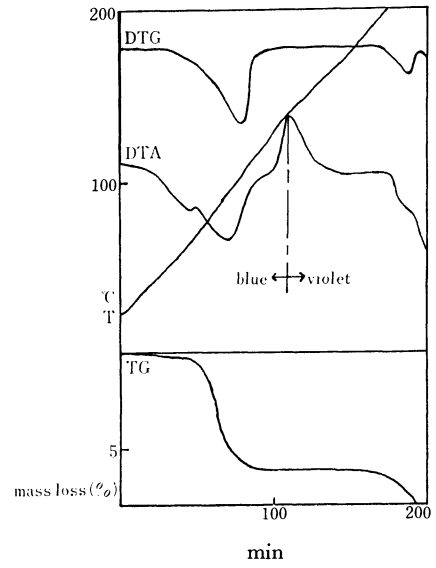

Fig. 4. Derivatogram for *cis,trans*-$[CoCl_2(NH_3)_2en]SCN \cdot H_2O$.

Table 1. The rate constants of dehydration, k_d and of exchange-isomerization, k_i, in isothermal measurements

Temp. (°C)	k_d (sec^{-1})	k_i (sec^{-1})
90	$(1.6 \pm 0.4) \times 10^{-4}$	
100	$(4.9 \pm 0.4) \times 10^{-4}$	$(8.5 \pm 0.3) \times 10^{-6}$
110.8	$(9.2 \pm 0.4) \times 10^{-4}$	$(7.1 \pm 0.3) \times 10^{-5}$
121.1	$(1.5 \pm 0.2) \times 10^{-3}$	$(6.7 \pm 0.3) \times 10^{-4}$
138.3		$(8.0 \pm 0.2) \times 10^{-3}$

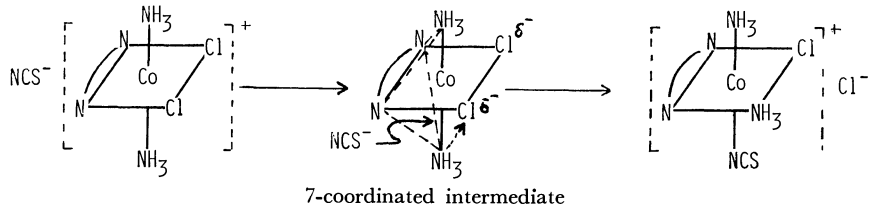

Fig. 6. The possible mechanism for exchange-isomerization of *cis, trans*-$[CoCl_2(NH_3)_2en]SCN \cdot H_2O$ to *cis, cis*-$[CoCl(NCS)(NH_3)_2en]Cl$.

21) Y. Shimura and R. Tsuchida, This Bulltein, **29**, 311 (1956).

The Arrhenius plots are given in Fig. 5, together with those obtained from derivatography. The thermochemical functions calculated from the isothermal measurement were $E^*=(20.1\pm2)$ kcal/mol and (62.3 ± 3.0) kcal/mol for the dehydration and exchange-isomerization, respectively, which are in good agreement with the corresponding data from the derivatography.

The possible reaction mechanism for the exchange-isomerization of *cis,trans*-$[CoCl_2(NH_3)_2en]SCN\cdot H_2O$ to *cis,cis*-$[CoCl(NCS)(NH_3)_2en]Cl$ in the solid phase may be proposed as shown in Fig. 6. It is likely that a a certain intramolecular thermal reaction proceeds through seven coordinated intermediate by the action with SCN^- as the counter ion in the second coordination-sphere. The product by this mechanism should have *cis,cis*-b structure as shown in Fig. 1, if the incoming SCN^- group attacks the *trans* side to the negative coordinated chloride ligand, and as the result, one of Cl^- may be removed from the seven coordinated intermediate by push-effect of NCS ligand.

When the SCN ligand approaches to the central cobalt ion, the linkage: M–NCS will prefer to that of M–SCN. However, there is still no evidence whether the final product is *cis,cis*-a or -b.

BULLETIN OF THE CHEMICAL SOCIETY OF JAPAN, VOL. 44, 712—715 (1971)

The Chemical Structures of Glasses of the $NaPO_3$-Sb_2O_3-Na_2O System

Makoto WATANABE, Kazuo TANABE, Tomoyoshi TAKAHARA, and Tamotsu YAMADA*

Department of Industrial Chemistry, Chubu Institute of Technology, Matsumoto-cho, Kasugai-shi, Aichi

* *Department of Industrial Chemistry, Nagoya Institute of Technology, Gokiso-cho, Showa-ku, Nagoya*

(Received May 15, 1970)

Glassy and crystalline substances of the $NaPO_3$-Sb_2O_3-Na_2O system with P/Sb ratios in the range from 1.0 to 300 were prepared by heating $NaPO_3$, Sb_2O_3, and Na_2CO_3 at 1000°C and by then quenching the melts of the mixtures. Samples with P/Sb ratios smaller than 5.0 were obtained as crystalline substances containing amorphous substances. The chemical compositions of these crystalline substances were estimated from the data obtained by X-ray diffractometry and paper chromatography. Samples with P/Sb ratios larger than 7.0 were obtained as glassy substances. Condensed phosphates were separated by paper-chromatographic analysis, and the average degree of the polymerization of the phosphates was measured by the pH-titration method. It has been found that the crystalline substances in the samples with P/Sb ratios in the range from 1.0 to 5.0 were Sb_2O_5, $NaSbO_3$, and an unknown crystalline substance. Assuming that the glasses have the P-O-P, P-O^-, P-O-Sb, and Sb-O^- linkages, a theoretical treatment of the degree of polymerization of condensed phosphates has been made and compared with the experimental data. It has been concluded that the glasses with P/Sb ratios larger than 7.0 have P-O-P, P-O^-, and P-O-Sb linkages.

Several attempts to prepare condensed phosphates containing oxoacid anions of some elements other than phosphorus have been made. For instance, Thilo and his co-workers investigated arsenate-phosphates,[1] and Ohashi and his co-workers investigated phosphate-silicates,[2] vanadate-phosphates,[3] and borate-phosphates.[4] It has been reported that the condensed compounds of this type have P-O-As, P-O-Si, P-O-V, and P-O-B linkages respectively. All of these oxoacid anions have a tendency to polymerize at a high temperature.

In the present work, glassy and crystalline substances of sodium phosphate-antimonates with various P/Sb ratios have been prepared in order to obtain some information on the chemical compositions and structures of the system. The compositions of the condensed phosphates have been determined by paper-chromatographic analysis of their aqueous solutions, while the structures of the crystals have been estimated by means of a study of their X-ray diffraction patterns. The theoretical treatment of the degree of polymerization of the condensed phosphates has been made and compared with the experimental data. The results reveal that the glasses also have P-O-Sb linkages.

Experimental

Materials. Sodium metaphosphate was prepared by heating monosodium dihydrogen orthophosphate dihydrate in a platinum crucible at 1000°C for 3 hr and by then quenching the melt by pressing it between two stainless steel plates. The average chain length of the glass thus obtained was about 100. The antimony trioxide and sodium carbonate were commercial reagents.

Glassy Substances. After the weight of the glass had been measured, calculated amounts of antimony trioxide and of sodium carbonate were taken on the glass and then mixed in an alumina mortar. The number of moles of sodium carbonate was equal to that of antimony trioxide. The mixture of these three materials was melted at 1000°C for 2 hr and then quenched by the method used in the preparation of sodium metaphosphate. By this procedure, glassy substances of the $NaPO_3$-Sb_2O_3-Na_2O system with P/Sb ratios in the range from 7.0—300 were prepared. All the glasses thus obtained were transparent and colourless.

1) K-H. Jost, H. Worzala, and E. Thilo, *Z. Anorg. Allg. Chem.*, **325**, 98 (1963).
2) S. Ohashi and F. Oshima, This Bulletin, **36**, 1489 (1963).
3) S. Ohashi and T. Matsumura, *ibid.*, **35**, 501 (1962).
4) T. Nakamura and S. Ohashi, *ibid.*, **40**, 110 (1967).

Crystalline Substances. A mixture of sodium metaphosphate, antimony trioxide, and sodium carbonate (with P/Sb ratios of 1.0, 2.0, and 5.0) was heated in a platinum crucible at 1000°C for 2 hr, and then the melts were quenched by placing the crucible in ice water. The crystalline substances with P/Sb ratios of 1.0 and 2.0 were opaque and a weak yellow, and the substances with a P/Sb ratio of 5.0 were transparent and colourless.

Paper Chromatography. The glassy substances were dissolved in water, and the phosphate species in the solution were separated by paper chromatography and then determined colorimetrically. Acidic and basic solvents were used for the paper chromatography. The acidic solvent was made by mixing 70 m*l* of ethyl alcohol, 5 g of trichloroacetic acid, 0.3 m*l* of concentrated aqueous ammonia, and 30 m*l* of water, it was used for the separation of ortho-, di-, tri-, tetra-, and long-chain phosphates. The basic solvent was made by mixing 40 m*l* of isopropyl alcohol, 20 m*l* of isobutyl alcohol, 1 m*l* of concentrated aqueous ammonia, and 39 m*l* of water, it was used for the separation of trimeta- and tetrametaphosphates. A sample solution was made by dissolving 1—2 g of the crystalline or the glassy substance in 150 m*l* of water. About 5 μl of the sample solution was placed on a filter paper of Toyo No. 53 of 2 by 40 cm and developed at room temperature for 20 hr. After the paper had been dried at 75°C for more than 30 min, it was sprayed a perchloric acid-molybdate solution so as to convert the phosphates into molybdophosphates. After it had then been dried again, the paper was exposed to ultraviolet light in order to reduce the molybdophosphates to blue complexes. Each band of the phosphates on the filter paper was identified by the same treatment of the reference solution of known phosphates.

The separated phosphates on the paper chromatograms were determined as follows, the filter paper containing each separated phosphates was cut at the demarcation line, and then immersed in 10 m*l* of a 0.1N aqueous solution of ammonia in a 50-m*l* Erlenmeyer flask. After 1 hr or more, this solution was transferred into a 25-m*l* volumetric flask, and then 10 m*l* of water and 2 m*l* of Lucena-Conde and Prat's reagent[5] were added. The flask was placed in a boiling-water bath for 1 hr, then cooled rapidly by placing it in a bath of cold water, and diluted to the mark with water. The absorbance of the solution was measured with a Shimadzu photoelectric photometer, Spectonic-20, at 800 mμ. The distribution of the phosphate species was calculated from the absorbance data.

The Measurement of the Average Chain Length of Polyphosphates. The average chain length of polyphosphates was measured by the pH-titration method proposed by Van Wazer, Griffith, and McCulough.[6,7] About 2 g of the glassy substance was dissolved in about 100 m*l* of water in a 250-m*l* Erlenmeyer flask. Most of the antimonate in the sample was precipitated and then filtered off. A twenty-five milliliters aliquot of the filtrate was diluted to about 100 m*l* and acidified with 1N hydrochloric acid to about pH 3 and then titrated with 0.1N sodium hydroxide. The volume of the 0.1N sodium hydroxide solution consumed between two inflection points, located at approximately pH 4.5 and 9.5, was measured. Twenty-five milliliters of another aliquot of the filtrate was transferred into a 250-m*l* Erlenmeyer flask, the mixture was diluted to about 80 m*l* with water, and then 10 m*l* of concentrated hydrochloric acid and 1 g of potassium chloride were added. The solution was boiled to dryness in order to hydrolyze completely all the condensed phosphates, the residue was dissolved with 50 m*l* of water and adjusted the pH to about 3 with a 6N carbonate-free sodium hydroxide solution. The solution was titrated by the same method mentioned above. If the volume of the 0.1N sodium hydroxide solution for the first titration is A, and if the volume for the second one is A_h, the average chain length, $\bar{n}$, is given by the $\bar{n}=2A_h/A$ equation, assuming that the only phosphates present in the glass are polyphosphates.

X-Ray Diffractometry. The samples were ground with an agate mortar until they could pass through a 150-mesh screen. Their X-ray diffraction patterns were taken by means of a powder method, using a Toshiba X-ray diffractometer.

Results and Discussion

The ignition loss of the mixture of these three materials was equal to the weight of the CO_2 gas which evolved upon the decomposition of Na_2CO_3. After heating, therefore, the crystalline and the glassy substances formed the $NaPO_3$-Sb_2O_3-Na_2O system. According to the observation of these samples under a polarizing microscope, the samples with the P/Sb ratios of 1.0, 2.0, and 5.0 were composed of an opaque and a transparent portion, and the amounts of the opaque portion decreased when the P/Sb ratio increased. The glasses with P/Sb ratios larger than 5.0 were almost entirely composed of the transparent portion, and the crystalline substances were negligibly small. The crystalline substances in the samples with P/Sb ratios of 1.0, 2.0, and 5.0 can be estimated from the data obtained by X-ray diffractometry. The data for the $NaPO_3$-Sb_2O_3-Na_2O system, with P/Sb ratios of 1.0, 2.0, and 5.0, are given in Table 1. By means of the X-ray diffraction patterns

Table 1. Chemical compositions of substances of the $NaPO_3$-Sb_2O_3-Na_2O system with P/Sb ratios of 1.0—5.0

	X-Ray diffractometry			Paper chromatography Phosphate(P%)				
P/Sb	Sb_2O_5	$NaSbO_3$	Unknown	Ortho	Pyro	Tri	Tri-meta	High poly
1.0	###	###	+	46.5	32.1	1.3		20.1
2.0	##	##	###	41.9	24.2	1.8		32.1
5.0	—	—	+	6.1	34.7	18.2	7.7	33.3

of the samples with P/Sb ratios of 1.0, 2.0, and 5.0, it has been found that there are unknown peaks of a strong intensity at spacings of 7.40 Å and of a medium intensity at spacings of 6.21 Å. Other crystalline substances of the samples with P/Sb ratios of 1.0 and 2.0 are antimony pentoxide and sodium metaantimonate. The antimony pentoxide and sodium metaantimonate were identified by comparing the X-ray patterns of the samples with those of "A. S. T. M. Diffraction Data File." The X-ray diffraction patterns of no phosphate species appear. The antimony pentoxide and sodium metaantimonate contents in these samples decrease with the increase in the P/Sb ratio, while that of the unknown crystalline substance increases with the increase in the P/Sb ratio

5) F. Lucena-Conde and L. Prat, *Anal. Chim. Acta*, **16**, 473 (1957).
6) J. R. Van Wazer, E. J. Griffith, and J. F. McCulough, *Anal. Chem.*, **26**, 1755 (1954).
7) E. J. Griffith, *ibid.*, **28**, 525 (1956).

from 1.0 to 2.0. The crystalline substance of the sample with the P/Sb ratio of 5.0 consists only of the unknown substance, and the contents of the unknown substance are small. From the results of the paper-chromatographic analysis of the samples with P/Sb ratios of 1.0, 2.0, and 5.0, it is found that the quantities of ortho- and pyrophosphate in the samples with the P/Sb ratios of 1.0 and 2.0 are very large, but those of the orthophosphate in the samples decrease rapidly with the increase in the P/Sb ratio from 2.0 to 5.0. When the samples are treated with water, white crystalline substances are deposited. In the X-ray diffraction patterns of the white deposits, there are also unknown peaks of a strong intensity at spacings of 7.40 Å and of a medium intensity at spacings of 6.41 Å, and the peaks of antimony trioxide, antimony pentoxide, and sodium metaantimonate. From these results, it may be concluded that the unknown crystalline substance is not dissolved in water and that all the sodium phosphate species contained in the samples compose an amorphous phase.

TABLE 2. DISTRIBUTION AND AVERAGE CHAIN LENGTH OF PHOSPHATES OF THE $NaPO_3$-Sb_2O_3-Na_2O SYSTEM WITH P/Sb RATIOS OF 7.0—300

	Phosphate (P%)						
P/Sb	Ortho	Pyro	Tri	Tri-meta	Tetra-meta	Higher	$\bar{n}$
7.0	2.7	28.8	21.6	5.4	8.5	33.1	3.6
10	2.0	15.8	7.2	5.6	7.9	61.5	4.7
15	2.0	8.5	7.4	5.6	6.4	70.1	7.0
20	1.9	5.2	5.2	5.0	5.4	77.2	8.4
30	1.8	4.4	4.2	4.3	4.3	80.9	11
50	1.5	4.0	3.9	3.8	4.4	82.3	21
80	1.1	3.3	3.5	3.3	4.1	84.7	29
100	0.8	2.4	3.0	2.6	3.7	87.5	37
150	0.6	1.3	2.5	2.0	3.3	90.3	49
200	0.4	0.9	1.0	1.5	3.4	92.8	52
300	0.4	0.7	0.8	0.8	2.9	94.4	65

When the samples of the glassy substances with the P/Sb ratios larger than 7.0 are treated with water, antimony trioxides are deposited. The compositions of the phosphate species in the sample solutions were determined by paper chromatography. The results for the samples are given in Table 2. When the P/Sb ratio increases, the contents of ortho- and pyrophosphate decrease, and that of high polyphosphate increases. The contents of tripolyphosphate increase with the increase in the P/Sb ratio from 1.0 to 7.0 and decrease with the decrease in the P/Sb ratio from 7.0 to 300. The trimetaphosphate contents indicate the largest value when the P/Sb ratio is 5.0, and decrease with the increase in the P/Sb ratio. The tetrametaphosphate contents decrease with the increase in the P/Sb ratio from 7.0 to 300.

The average chain lengths of the polyphosphates given in Table 2 were measured by the pH titration method, assuming that the phosphates were composed of polyphosphates and did not contain ortho- and ring phosphates. By the results of the paper-chromatographic analysis of the glasses, it is shown that the quantities of orthophosphate and of ring phosphates are less than several per cent. Therefore, the effect of their presence on the calculation of the average chain length of polyphosphates is disregarded in the following discussion.

Between the Na/P ratio and the average chain length, $\bar{n}$, of sodium polyphosphate, there is this relation:

$$\mathrm{Na/P} = (\bar{n}+2)/\bar{n} \qquad (1)$$

where Na/P is the atomic ratio of these two elements. If antimony trioxide does not react with phosphate glass to form P-O-Sb linkages in the melted state, the Na/P ratio is equal to $(x+1)/x$, where x is the P/Sb ratio. By using these relations, Eq. (2) is obtained:

$$\bar{n} = 2x \qquad (2)$$

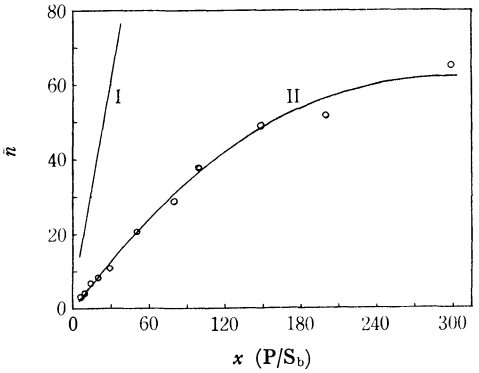

Fig. 1. Variation of average chain length of polyphosphates.
I: Values calculated by Eq. (2)
II: Experimental values

The straight line, I, in Fig. 1 indicates this relation. Curve II in Fig. 1 indicates the relation between the measured average chain length of polyphosphates and the P/Sb ratio, x. The great discrepancy between the straight line, I, and the curve, II, means that the above assumption is not correct. Therefore, the sodium phosphate glass seems to react with antimony trioxide at a high temperature to form P-O-Sb linkages. There are three possible structures containing P-O-Sb and Sb-O$^-$ linkages. Assuming that the hydrolytic scission

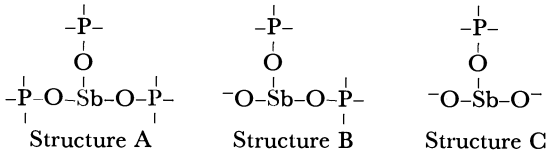

of P–O–Sb linkage occurs rapidly in water, the average chain length, $\bar{n}$, of the polyphosphates in the glass of the $NaPO_3$–Sb_2O_3–Na_2O system is given by Eq. (3):

$$(\bar{n}+2)/\bar{n} = (x+y+1-z)/x \qquad (3)$$

where x, y, and z are the numbers of phosphorus atoms, P-O-Sb linkages, and Sb-O$^-$ linkages per atom of antimony. If the glasses are composed only of Structure A, y is 3 and z is 0, and x is the P/Sb ratio of the glass. The average chain length of the polyphosphate can be calculated by inserting these values into Eq. (3). The calculated values of $\bar{n}$ are given in Table 3. The

Table 3. Average chain length of polyphosphates

x (P/Sb)	$\bar{n}$ Found	Column I $\bar{n}$ calcd by Eq. (3) Structure A (y=3, z=0)	Structure B (y=2, z=1)	Structure C (y=1, z=2)	Column II $\bar{n}$ calcd by Eq. (4) (f=0.02) Structure A (y=3, z=0)	Structure B (y=2, z=1)	Structure C (y=1, z=2)
7.0	3.6	3.5	7.0	∞	3.4	6.5	100
10	4.7	5.0	10	∞	4.8	9.1	100
15	7.0	7.5	15	∞	7.0	13	100
20	8.4	10	20	∞	9.1	17	100
30	11	15	30	∞	13	23	100
50	21	25	50	∞	20	33	100
80	29	40	80	∞	29	44	100
100	37	50	100	∞	33	50	100
150	49	75	150	∞	43	60	100
200	52	100	200	∞	50	67	100
300	65	150	300	∞	60	75	100

underlined values are the average chain length nearest to the measured one. As the column I of Table 3 shows, even the calculated values of the average chain length based on Structure A are considerably larger than the measured values when x is larger than 20.0. The presence of a branching point and impurities in the phosphate-antimonate glasses shortens the chain length of polyphosphates. Representing all these factors by factor f, Eq. (3) is modified into Eq. (4):

$$(\bar{n}+2)/\bar{n} = (x+y+1-z+fx)/x \qquad (4)$$

where f is given with respect to an atom of phosphorus. If f is arbitrarily set at 0.02, the calculated average chain lengths of the glasses shown in column II of Table 3 are given by Eq. (4). If the factor, f, is zero, Eq. (4) is reduced to Eq. (3). As column II of Table 3 shows, the values calculated on the basis of Structure A are close to the experimental values through out the range of P/Sb ratios from 7.0 to 300. According to above discussion, it seems reasonable to conclude that the structural framework of the glasses of condensed phosphate-antimonates is composed of Structure A, and that Structure B and C are not involved in the structural framework.

Summary

Crystalline and glassy substances of phosphate-antimonate systems with P/Sb ratios in the range from 1.0 to 300 were prepared by heating a mixture of sodium metaphosphate, antimony trioxide, and sodium carbonate at 1000°C for 2 hr. The samples with P/Sb ratios in the range from 1.0 to 5.0 were obtained as crystalline substances containing amorphous substances, while those with P/Sb ratios in the range from 7.0 to 300 were obtained as glassy substances. By paper chromatography and X-ray diffractometry, the samples containing crystalline and amorphous substances were found to be composed of Sb_2O_5, $NaSbO_3$, an unknown crystalline substance, and various condensed phosphates. From the results of paper chromatography and the measurement of the average chain length of the phosphates by the pH titration method, it was revealed that the higher the P/Sb ratio, the longer were the chains of the polyphosphates produced; it was concluded that the $NaPO_3$-Sb_2O_3-Na_2O glasses with the P/Sb ratios in the range from 7.0 to 300 had P-O-Sb linkages.

Coexistence States of Iron in Synthesized Iron-bearing Allophane (Al_2O_3-SiO_2-Fe_2O_3-H_2O System)

Joyo OSSAKA,* Shin-ichi IWAI,** Mitsuhiro KASAI,***
Toshiaki SHIRAI,*** and Shuichi HAMADA***

* *Mineralogical Geol. Lab., Faculty of Engineering, Tokyo Institute of Technology, Ookayama, Meguro-ku, Tokyo*
** *Res. Lab. Eng. Materials, Tokyo Institute of Technology, Ookayama, Meguro-ku, Tokyo*
*** *Department of Chemistry, Faculty of Science, Science University of Tokyo, Kagurazaka, Shinjuku-ku, Tokyo*

(Received June, 29, 1970)

A sharp exothermic peak at 980°C, which is found characteristic of allophane in its differential thermal analysis, shifted to the lower-temperature side and broadened as the iron content in the iron-coprecipitated samples increased. In the case of the iron-mixed samples, however, this exothermic peak did not shift, and a new broad exothermic peak, which was ascribed to hydrated ferric oxide, appeared. The crystallization processes in the heat-treated samples were found to depend on the coexistence state and the quantity of the iron. The dimensions of a unit cell of the mullite, crystallized at 1200°C from the iron-coprecipitated samples, varied with the iron content. The iron-mixed samples, however, showed little change in their cell dimensions. It is concluded that there are two states of the coexistence of iron in the allophanes. In one of them, iron ions form solid solutions of the allophane, *i.e.*, as an iron-allophane. In the other, iron is in the mixture as the hydrated ferric oxide. The maximum amount of iron in the solid solution was estimated to be 5 wt% in the iron-allophane.

An allophane is an amorphous or low-crystalline mineral, and its main components are silica, alumina, and water. Its chemical formula may be generally expressed as $1\text{-}2SiO_2 \cdot Al_2O_3 \cdot 5H_2O$. The allophane is considered not to be a simple mixture of a hydrated aluminum oxide gel and a silicic-acid gel.[1,2] The natural allophanes usually contain iron. The natural iron-bearing allophane dose not always show the same properties. It has, therefore, been suggested that there are two states of the coexistence of iron in the soil-allophane.[3]

In this work, the coexistence states of iron in the synthesized iron-bearing allophanes were studied by means of differential thermal analysis and X-ray powder diffractometry on heat-treated samples.

Experimental

Materials. The iron-coprecipitated samples were prepared in the following manner:[4] a mixed solution of aluminum sulfate, sodium silicate,[5] and ferric sulfate was boiled at a specified acidity of pH 5.4—6.0 obtained by adding hexamethylenetetramine. The gel thus coprecipitated was washed by decantation and then air-dried for three weeks. The iron-mixed samples were also prepared by mixing the synthesized allophane, free from iron, and the hydrated ferric-oxide gel in order to compare the properties of the iron-coprecipitated samples. The colors of the iron-coprecipitated and the iron-mixed samples were yellow and light-purplish red respectively.

Procedure. The X-ray powder diffractograms of the samples were taken with a Geigerflex, Model D-3F, Rigaku Denki Company, while the differential thermal analysis was carried out with equipment designed in our laboratory.

The sample, in a quartz tube, was heated for five hrs in an electric furnace at 800, 900, 1000, 1100, and 1200°C respectively. The firing-products were identified and their relative amounts were estimated by using the diffraction peaks at (210) and (120) of the mullite, those at (104) and (110) of the hematite, that at (440) of the silico-alumina spinel, and that at (101) of the cristobalite. The unit-cell dimensions of the mullite, one of the firing products, was calculated by using the diffraction peaks at (230), (121), and (201) of the mullite.

TABLE 1. CHEMICAL COMPOSITIONS OF COPRECIPITATED AND MIXED SAMPLES

Sample		Chemical composition, wt%					Molar ratio	
		SiO_2	Al_2O_3	Fe_2O_3	$H_2O(\pm)$	Total	$\frac{SiO_2}{Al_2O_3}$	$\frac{SiO_2}{Al_2O_3+Fe_2O_3}$
	32[a]	30.04	29.48	tr.	40.66	100.18	1.73	——
Coppted	C32-1[a]	26.00	28.95	1.34	43.32	99.61	1.52	1.48
	C32-2	26.54	27.66	1.98	43.86	100.04	1.63	1.56
	C32-3	25.51	26.89	2.80	44.33	99.53	1.61	1.52
	C32-5	23.74	25.15	5.14	46.25	100.28	1.60	1.42
	C32-8	21.34	23.75	7.93	46.98	99.94	1.55	1.28
	C32-10	21.68	21.62	10.41	46.68	100.39	1.70	1.30
Mixed	M32-3	28.73	28.20	3.05	40.02	100.00[b]	1.73	1.62[b]
	M32-5	27.93	27.41	5.00	39.66	100.00[b]	1.73	1.55[b]
	M32-10	25.84	25.36	10.10	38.71	100.00[b]	1.73	1.38[b]

a) The numerical symbol "32" denotes the rough molar ratio of silica/alumina in the sample to be 3:2, while the numerical postscript "1", for example, denotes the rough iron content in the sample (here, 1 wt%).
b) Calculated.

1) G. Brown, *Clay Mineral Bull.*, **2**, 294 (1955).
2) J. Ossaka, "Advances in Clay Science," Vol. 2, ed. by S. Iwao, Gihodo, Tokyo (1960), p. 339.
3) S. Iwai, J. Ossaka, and M. Kasai, unpublished study.
4) J. Ossaka, S. Iwai, M. Kasai, T. Shirai, and S. Hamada, *Nippon Kagaku Zasshi*, **90**, 1288 (1969).
5) The sodium silicate solution was prepared by dissolving the melt of silica melted with sodium hydroxide.

Results

The chemical compositions of the samples are given in Table 1.

The silica/alumina ratios in the samples did not agree with the original ratios of the components in the solutions. The former were almost always smaller than the latter.[6]

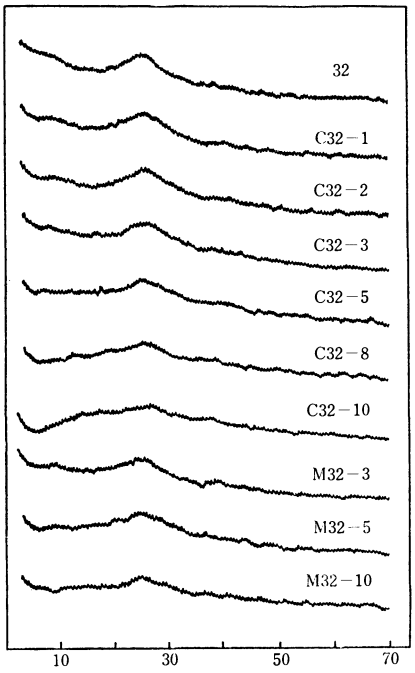

Fig. 1. X-Ray powder diffraction patterns.

The X-Ray Powder Diffractometry and the Differential Thermal Analysis of the Samples. Figure 1 shows the X-ray powder diffraction patterns. All the samples were identified as amorphous or lower crystalline materials, since there were few sharp peaks. However, a very broad peak was observed at approximately 25° (2θ; CuKα) in the iron-coprecipitated samples with a smaller amount of iron.

The DTA curves are shown in Fig. 2. All the samples showed the broad endothermic peak in the range from 100°C to 200°C and the exothermic peak at approximately 900°C, a position which was characteristic of the allophane. The exothermic peak observed in the iron-coprecipitated samples shifted from 980°C to 860°C and broadened as the iron content increased. On the contrary, the exothermic peak observed in the iron-mixed samples did not shift and did not broaden in spite of the change in the iron content, while the very broad exothermic pattern, which was assigned to the hydrated ferric oxide, was observed in the range from 300°C to 500°C. Although the iron-coprecipitated samples containing less than 5 wt% of iron showed only allophane-characteristic DTA curves, the broad exothermic peak due to the hydrated ferric oxide was observed when the iron content was above 5 wt%.

6) J. Ossaka, "Advances in Clay Science," Vol. 3, ed. by S. Iwao, Gihodo, Tokyo (1961), p. 225.

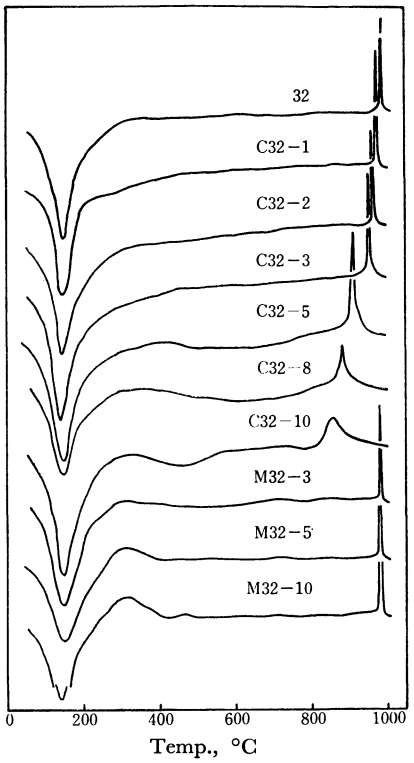

Fig. 2. DTA curves.

The Variation in Firing-products in the Samples during the Heat-treatment. The crystalline phases formed in the heat-treated samples at 800, 900, 1000, 1100, and 1200°C respectively were examined by means of the X-ray powder diffractometer. Although the final product of the heat treatment was the mullite, the crystallization process was found to vary, depending on the condition of the original samples (Fig. 3). The crystal-

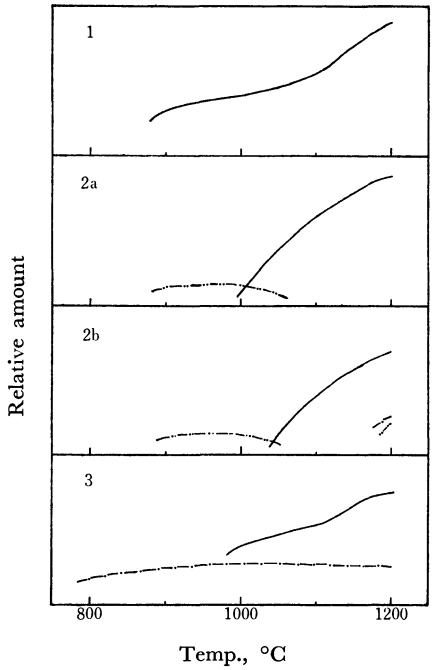

Fig. 3. Types of crystallization processes.
——— Mullite —·—·—·— Silico-alumina spinel
–·–·–·– Hematite ····· Cristobalite

lization processes may be classified into three types, as is shown in Fig. 3. It can be seen from Fig. 3 that the crystallization processes depend on the content and the coexistence state of the iron, while the silica/alumina ratio did not affect the crystallization process. The crystallization of all the iron-mixed samples belonged to the 3-type process, even if the iron content was only 3 wt%. The crystallization process of the iron-coprecipitated samples was found to be of the 1 or 2 type. The crystallization process of the iron-coprecipitated samples with less than 3 wt% iron was the same as that of the iron-free allophane, while those above 3 wt% were transformed into the mullite through the silico-alumina spinel phase. However, the hematite and the cristobalite phases were observed at 1200°C when the samples contained more than 8 wt% of iron. A clear difference between the crystallization processes of the iron-coprecipitated and the iron-mixed samples was also found in the DTA analysis.

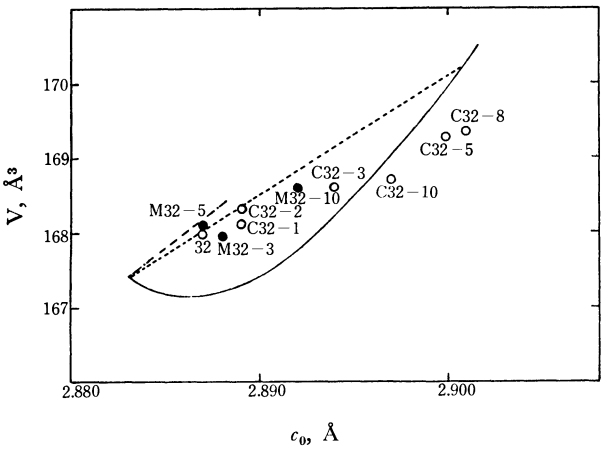

Fig. 4. Relationship between c_0 and V of crystallized mullite at 1200°C.
-·-·-·- iron free mullites[6]
– – – – iron and titanium-bearing mullites.
····· iron bearing mullite[11]

The Unit-cell Dimensions of the Mullite Formed in the Samples. The values of c_0 and the unit-cell volume, V, of the mullite which was formed in the heat-treated samples at 1200°C for five hrs were estimated from the X-ray powder diffractograms. The relationship between c_0 and V is shown in Fig. 4. The c_0 and V values of iron-free mullite varied with the silica/alumina ratios.[7] Therefore, the variation in the cell dimensions in the mullite with the quantity of iron was examined by comparing samples with the same original ratio of silica/alumina. The c_0 and V values of the mullite crystallized from the iron-coprecipitated samples increased with an increase in the iron content, while the c_0 and V values for the iron-mixed samples were nearly equal to those for the iron-free allophane except for the M32-10 sample. A clear difference in the cell dimensions was observed between the two types of samples.

Discussion

The exothermic peak at approximately 900°C in the differential thermal analysis on silica-alumina gel was explained as originating from the formation of γ-alumina[8] or mullite.[9,10] However, the X-ray analysis favored the conclusion that the formation of the mullite was mainly responsible for this peak in the present experiment.

It was found, in the case of the iron-coprecipitated samples with more than 3 wt% of iron, that the transformation to the mullite occurred through the intermediate stage of the formation of the silico-alumina spinel, while the iron-coprecipitated samples with less than 3 wt% of iron were transformed directly into the mullite, as with the iron-free allophane. The existence of the silico-alumina spinel as a metastable phase in the mullite was found in the course of the crystallization of heat-treated kaolinite by Brindley and Nakahira.[11]

The iron-mixed samples were converted into hematite with little change in their cell dimensions. Therefore, it can be said that the silica-alumina gel reacted in some degree with the hydrated ferric oxide, but formed a solid solution only with difficulty. Agrell and Smith,[7] and Murthy and Hummel[12] pointed out that the cell dimensions increased considerably with an increase in the iron content in the solid solution of the mullite, while the silica/alumina ratio in the mullite hardly influenced the cell dimensions. The large change in the cell dimensions of the mullite which was found when the iron content of the sample was varied indicates the formation of a solid solution of the mullite with iron. Agrell and Smith[7] also reported that there was 2 wt% of iron in a solid solution of the mullite, while the hematite was found, besides the solid solution of the mullite, when 5 wt% of iron was present in the sample. In the present study, it can be concluded, as in Fig. 4, that the solid solution of the mullite with iron is formed when the iron content is less than 5 wt%.

These facts support the idea that iron is contained as a solid solution of the allophane, *i.e.*, that it is the iron-allophane, when the amount of iron in the coprecipitated samples, is less than 5 wt%, while a part of the iron takes the form of the hydrated ferric oxide when its quantity is larger than 5 wt%.

7) S. O. Agrell and J. V. Smith, *J. Amer. Ceram. Soc.*, **43**, 69 (1960).

8) H. Insley and R. H. Ewell, *J. Res. Nat. Bur. Stand.*, **14**, 615 (1935).

9) V. J. Wiegman, C. H. Horte, and I. Sücker, *Silikat. Tech.*, **9**, 358 (1958).

10) T. Demadiuk and W. F. Cole, *Nature*, **181**, 1400 (1958).

11) G. W. Brindley and M. Nakahira, *J. Amer. Ceram. Soc.*, **42**, 311 (1959).

12) M. K. Murthy and F. A. Hummel, *ibid.*, **43**, 267 (1960).

Synthesis of Iron-Titanium Oxides under Hydrothermal Conditions

Kiyoshi MATSUOKA

Faculty of Literature and Science, Kôchi University, Kôchi

(Received August 5, 1970)

The solid solutions in the system FeO-Fe_2O_3-TiO_2 were synthesized under hydrothermal conditions up to 700°C and 2.5 kb (P_{H_2O}). The results of X-ray diffraction, chemical and thermomagnetic analyses indicated that the products always consisted of magnetite-ulvöspinel or hematite-ilmenite solid solutions and, in some cases, rutile was also formed. The presence of the solid solutions of magnetite and ulvöspinel indicates a reducing atmosphere during the treatment. When P_{H_2O} increased from 1 kb to 2.5 kb, the FeO contents in the products decreased.

Minerals belonging to the system FeO–Fe_2O_3–TiO_2 are abundant in the earth's crust. Magnetite (Fe_3O_4), a representative mineral, is known to have a spinel structure and to be ferrimagnetic.[1] Ulvöspinel (Fe_2TiO_4) also has a spinel structure but is not ferrimagnetic at room temperature. These two minerals form a continuous solid solution.[2] Hematite (α-Fe_2O_3) has a rhombohedral structure which makes this substance parasitic ferromagnetic.[3] The crystallographic structure of ilmenite ($FeTiO_3$) is analogous to that of hematite, with some differences in magnetic properties.[4] Hematite and ilmenite are the final components of solid solutions, and the relations between chemical composition and cell dimensions have been investigated in detail.[5] Another series of solid solutions is found in the system $FeTi_2O_5$-pseudobrookite (Fe_2TiO_5). These solid solutions have orthorhombic structures and exhibit paramagnetism.[6] Of the three polymorphic forms of TiO_2 (rutile, brookite, and anatase), rutile is the most commonly occurring phase and found to be stable in a wide region of temperature and pressure.[7]

Most investigators have studied the synthesis and stability concerning the FeO–Fe_2O_3–TiO_2 system at atmospheric pressure or below (Ref. 8). In the present investigation, a synthesis of minerals belonging to the above system was attempted in relation to the determination of stable phases under hydrothermal conditions. If this attempt is successful, the results are expected to be useful for explaining the occurrence of these minerals in nature.

Experimental

Starting Materials. A series of solutions containing titanium (IV) chloride and iron (III) chloride in various ratios were mixed with ammonia. The resulting precipitate was washed with ammonia, air-dried, and ground to powder. The powder was confirmed to be amorphous by X-ray diffraction. After ignition, the content of Fe_2O_3 in the powder was determined by the Reinhardt method. The molar ratio of TiO_2 and Fe_2O_3 in the powder was then calculated. The powder was used as the starting material. The chemical compositions of the starting materials are shown in Table 1.

TABLE 1. COMPOSITION (MOL%) OF STARTING MATERIALS

Starting material	TiO_2	Fe_2O_3
A	70.0	30.0
B	59.2	40.9
C	50.9	49.1
D	29.2	70.8
E	15.0	85.0

Apparatus and Procedure of Synthesis. Each starting material was sealed in a gold capsule together with a nearly constant amount of water, and was treated in a test-tube type reactor[9] under various conditions of temperature and pressure from 400° to 700°C and at 1 kb or 2.5 kb (P_{H_2O}). After being kept for 48 to 454 hours, the reactor was quenched to room temperature within three minutes.

Examination of Specimens. *Chemical Analysis*: The FeO content in the quenched specimen was determined by permanganate titration. The molar ratio of TiO_2, Fe_2O_3, and FeO was then calculated.

X-Ray Diffraction: X-Ray powder patterns, obtained with iron-filtered Co-$K\alpha$ radiation, were used for identification of phases and determination of the chemical composition of the solid solutions.

The values of a and c were calculated for the hematite-ilmenite solid solution. The value of c, which is sensitive to variation of the chemical composition, was compared with Lindsley's result[10] to determine the chemical composition. In the case of the magnetite-ulvöspinel solid solution, the chemical composition was also determined by referring to the relation obtained by Lindsley.[10]

Thermomagnetic Analysis: A magnetic balance similar to the apparatus reported by Shimada *et al.*[11] was used for the thermomagnetic analysis at room temperature and above.

Results and Discussion

Synthetic Conditions and Composition of Products. The synthetic conditions and the chemical composition of

1) S. Akimoto, *Buturi*, **14**, 447 (1959).
2) E. Pouillard, *Ann. Chim. (Paris)*, **5**, 164 (1950).
3) L. Néel, *Rev. Mod. Phys.*, **25**, 58 (1953).
4) H. Bizette and B. Tsai, *C. R. Acad. Sci., Paris*, **242**, 2124 (1956).
5) Y. Ishikawa and S. Akimoto, *J. Phys. Soc. Jap.*, **13**, 1110 (1958).
6) S. Akimoto, T. Nagata, and T. Katsura, *Nature*, **179**, 37 (1957).
7) W. A. Deer, R. A. Howie, and J. Zussman, "Rock Forming Minerals," Vol. 5. Longmans, London (1962), p. 34.
8) E. M. Levin, C. R. Robbins, and H. F. McMurdie, "Phase Diagrams for Ceramists," The American Ceramic Society, Columbus, Ohio (1964), p. 62.
9) R. Roy and E. F. Osborn, *Econ. Geol.*, **47**, 717 (1952).
10) D. H. Lindsley, *Carnegie Inst. Year Book*, **64**, 144 (1964—1965).
11) M. Shimada, S. Kume, and M. Koizumi, *J. Amer. Ceram. Soc.*, **51**, 713 (1968).

TABLE 2. SYNTHETIC CONDITIONS AND COMPOSITION OF PRODUCTS

	Starting material		Product composition (mol%)			
		No.	TiO_2	Fe_2O_3	FeO	R*
(a) 1 kb (P_{H_2O})						
700°C 70hr	A	1	55.6	3.5	40.7	0.85
	B	2	44.1	5.0	50.9	0.84
	C	3	39.1	14.6	46.3	0.61
	D	4	21.7	26.6	51.7	0.49
	E	5	11.0	35.2	53.8	0.43
600°C 114hr	A	6	58.5	8.8	32.6	0.65
	B	7	45.7	8.9	45.5	0.72
	C	8	39.9	17.0	43.2	0.56
	D	9	22.3	30.2	47.5	0.44
	E	10	11.4	40.6	48.0	0.37
500°C 168hr	A	11	69.5	29.1	1.4	0.02
	B	12	56.5	34.6	8.9	0.11
	C	13	49.1	44.0	6.9	0.07
	D	14	28.1	64.0	7.9	0.06
	E	15	14.2	73.7	12.2	0.08
400°C 454hr	A	16	69.6	29.3	1.1	0.02
	B	17	58.3	38.8	2.9	0.04
	C	18	49.2	44.2	6.6	0.07
	D	19	28.5	66.5	5.0	0.04
	E	20	14.6	79.3	6.2	0.04
(b) 2.5 kb (P_{H_2O})						
700°C 48hr	A	21	67.2	24.6	8.2	0.14
	B	22	54.1	28.9	17.0	0.23
	C	23	45.0	31.8	23.3	0.27
	D	24	25.2	47.1	27.7	0.23
	E	25	13.5	66.0	20.5	0.13
600°C 212hr	A	26	68.4	27.0	4.5	0.08
	B	27	56.4	34.2	9.4	0.12
	C	28	44.0	29.0	27.0	0.32
	D	29	24.5	43.0	32.5	0.27
	E	30	13.7	68.9	17.4	0.11
500°C 422hr	A	31	68.9	27.9	3.2	0.05
	B	32	56.2	33.8	10.0	0.13
	C	33	47.5	39.2	13.3	0.15
	D	34	27.6	61.3	11.1	0.08
	E	35	14.0	72.4	13.6	0.09

R*: $FeO/(2Fe_2O_3+FeO)$ calculated from composition.

the products are summarized in Table 2. Since no Fe (II) ion was contained in any of the starting materials, the ratio $FeO/(2Fe_2O_3+FeO)$ shows the extent of reduction which occurred during the treatment. Figs. 1 (a) and (b) give ternary diagrams in which the composition of the starting materials and the products are plotted. A comparison of these results with those in Table 2 reveals the following. (1) The extent of reduction increases under conditions of temperature and pressure above 600°C and 1 kb. (2) The extent decreases at 600°C, when P_{H_2O} increases from 1 kb to 2.5 kb.

In the range from 400 to 500°C, hematite-like and

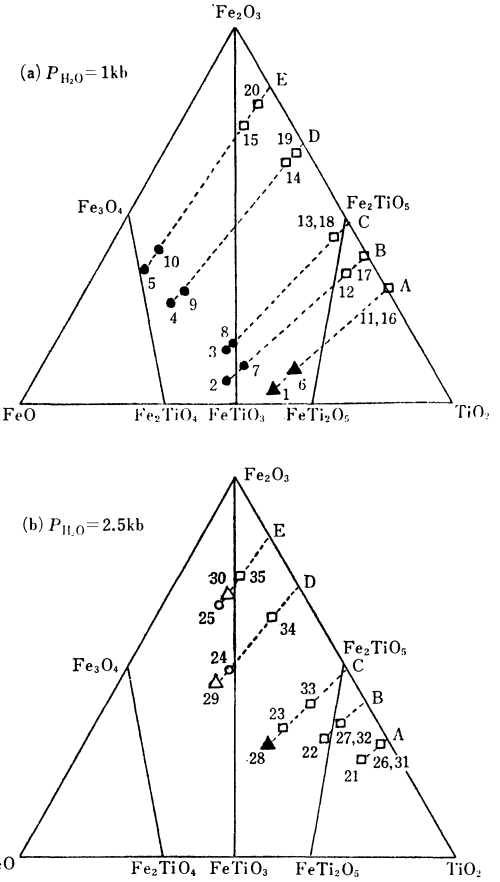

Fig. 1. Ternary diagrams in the system FeO-Fe_2O_3-TiO_2 on which the chemical composition of the starting materials and those of the hydrothermal products are plotted. The letters A, B, *etc.* in the diagrams correspond to those in Table 1. The numbers also correspond to those in Table 2.
●: coexistence of ilmenite-like crystal with magnetite.
○: hematite-like crystal.
□: coexistence of hematite-like crystal with rutile.
△: coexistence of hematite-like crystal with magnetite.
▲: coexistence of ilmenite-like crystal with rutile.

rutile-like crystals are formed regardless of the starting materials. When temperature increases, the composition of the hematite-like crystals approaches that of ilmenite.

X-Ray Diffraction and Composition of Products. The results of X-ray powder diffraction and the composition determined from the cell dimensions are summarized in Table 3. The products consist of one or two phases and each phase corresponds to rutile, hematite, ilmenite or magnetite, although the *d*-spacings of each phase differ from ideal values. The differences are caused by the fact that these phases are not the final components of solid solution series in the FeO–Fe_2O_3–TiO_2 system but those of an intermediate composition.

Figures 2 (a) and (b) show the variation of d_{104} of the hematite-ilmenite solid solutions with the change in reaction conditions. The values of d_{104} of the hematite-ilmenite solid solutions are plotted against the chemical composition in Fig. 3.

Thermomagnetic Analysis. The results of thermomagnetic analysis indicate that the products have the

TABLE 3. X-RAY EXAMINATION OF PRODUCTS

Product No.	Ilmenite-Hematite d_{104}(Å)	I	a (Å)	c (Å)	R_1[a]	Rutile d_{110}(Å)	I	Magnetite-Ulvöspinel d_{220}(Å)	I	a (Å)	R_2[b]
(a) 1 kb (P_{H_2O})											
1	2.750	vs	5.090	14.076	100	3.253	m				
2	2.746	m	5.084	14.051	96			2.984	s	8.441	35
3	2.749	m			98			2.979	vs	8.427	27
4	2.746	m	5.084	14.051	96			2.979	s	8.427	27
5	2.746	s			96			2.991	s	8.460	46
6	2.742	s	5.082	14.019	89	3.249	s				
7	2.740	s			87			2.984	s	8.441	35
8	2.740	s			87			2.971	m	8.404	10
9	2.740	s			87			2.979	s	8.425	26
10	2.740	m			87			2.971	s	8.404	10
11	2.700	m			0	3.251	s				
12	2.702	vs	5.038	13.767	8	3.251	m				
13	2.700	vs	5.034	13.752	0	3.251	m				
14	2.700	vs	5.037	13.747	0	3.249	s				
15	2.704	s	5.039	13.776	10	3.251	s				
16	2.700	m			0	3.251	s				
17	2.700	s			0	?	w				
18	2.704	s			10	3.253	m				
19	2.700	vs	5.034	13.752	0	3.253	m				
20	2.700	vs	5.034	13.752	0	?	w				
(b) 2.5 kb (P_{H_2O})											
21	2.704	m			10	3.251	s				
22	2.712	vs	5.050	13.824	30	3.253	m				
23	2.717	s			47	3.255	s				
24	2.714	vs	5.054	13.840	40						
25	2.706	vs	5.041	13.795	20						
26	2.705	m	5.040	13.786	15	3.251	s				
27	2.709	m	5.042	13.815	26	3.253	s				
28	2.720	m	5.057	13.880	53	3.251	m				
29	2.717	vs	5.056	13.860	47			?	vw		
30	2.709	vs	5.042	13.815	26			?	vw		
31	2.701	m	5.035	13.761	5	3.249	m				
32	2.704	s	5.039	13.776	10	3.253	m				
33	2.704	s			10	3.251	m				
34	2.704	vs	5.039	13.776	10	3.251	m				
35	2.702	vs	5.033	13.767	8	3.253	s				

a) Mole percentage of ilmenite in ilmenite-hematite solid solution.
b) Mole percentage of magnetite in magnetite-ulvöspinel solid solution.
R_1 and R_2 were determined using the cell dimensions and Lindsley's results. When diffraction was weak and the calculation of the cell dimensions was difficult, the composition was estimated by the value of d_{104} with reference to Fig. 3.

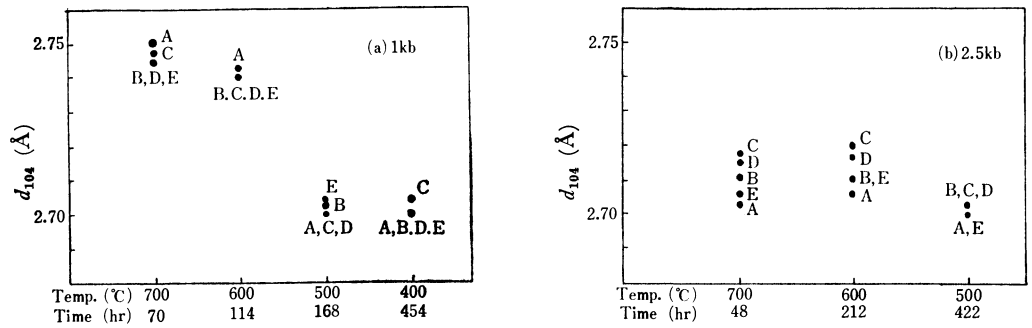

Fig. 2. Variation of d_{104} of hematite-ilmenite solid solutions with change in the reaction conditions. The letters A, B, *etc.* correspond to those in Fig. 1.

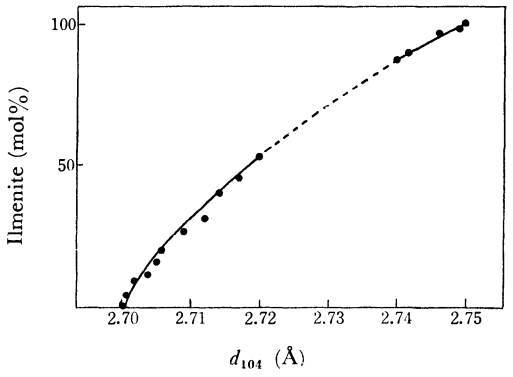

Fig. 3. Relation between the chemical composition and d_{104} in hematite-ilmenite solid solutions.

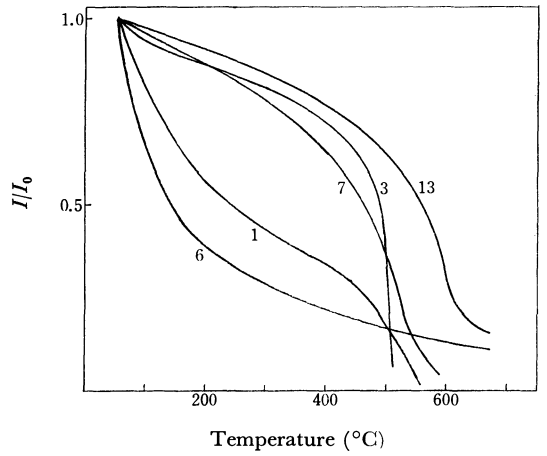

Fig. 4. Magnetization of the products as a function of temperature. The numbers on each curve correspond to those in Table 2. I_0 : Magnetic moment at 50°C.

intermediate composition of solid solution series in the FeO–Fe_2O_3–TiO_2 system. This is in line with the results obtained by X-ray diffraction. In Fig. 4 the curves (3) and (7) show a similar temperature dependency to magnetite. In these cases, the magnetite-ulvöspinel solid solutions are found by X-ray diffraction.

From the curve (13), the presence of a hematite-like crystal is expected which agrees with the result of X-ray diffraction.

It is thought that the decreasing P_{O_2} at elevated temperatures is established either by the dissociation of water or by the reaction of water and the metal wall of the reactor.[12] This has not been clarified in the present experiments.

From the results, the following conclusions are obtained.

(i) All the crystals that belong to the system FeO–Fe_2O_3–TiO_2 and remain stable under hydrothermal conditions up to 700°C and 2.5 kb are classified into rutile, magnetite-ulvöspinel solid solutions and hematite-ilmenite solid solutions.

(ii) Synthesis of a new mineral is unsuccessful under the conditions of the present investigation, when the starting materials belonging to the system Fe_2O_3–TiO_2 are used.

(iii) Atmosphere surrounding the samples under the hydrothermal conditions was reducing to a certain extent. The cause of this reduction is not clearly shown at this stage of investigation, but P_{O_2} acting on the samples at 700°C and 1 kb corresponds to the value of the order of 10^{-8} atm at 1300°C proposed by Taylor.[13]

(iv) The common occurrence of magnetite-ulvöspinel or hematite-ilmenite solid solutions in nature is explained if these minerals remain stable even under hydrothermal conditions as was proved by the present experiments.

The author wishes to thank Professor Mitsue Koizumi and Professor Shoichi Kume of Osaka University for their kind guidance and help. Thanks are also due to Professor Jumei Yamasaki of Kôchi University for his encouragement throughout this work.

12) R. A. Laudise, "Progress in Inorganic Chemistry," Vol. 3, Interscience Publishers, New York, N. Y. (1961), p. 23.

13) R. W. Taylor, Ph. D. Dissertation, Department of Geophysics and Geochemistry, The Pennsylvania State University, 1961.

A Proton Magnetic Resonance Study of Cobalt(III) Complexes Containing 1,10-Phenanthroline and Ethylenediamine

Haruko Ito, Junnosuke Fujita, and Tasuku Ito*

Department of Chemistry, Faculty of Science, Tohoku University, Sendai

* *Department of Chemistry, Faculty of Education, Fukushima University, Fukushima*

(Received August 17, 1970)

The proton magnetic resonance (PMR) spectra of the phenanthroline ligand in $[Co(phen)_3]Cl_3$, $[Co(phen)_2(en)]Cl_3$ (new complex) and $[Co(phen)(en)_2]Cl_3$ were measured in deuterium oxide and analyzed as ABX systems. Significant up-field shifts of signals were observed only for the protons 2 and 9 of $[Co(phen)_3]^{3+}$ and the proton 2 of $[Co(phen)_2(en)]^{3+}$, not for the proton 9 of $[Co(phen)_2(en)]^{3+}$ nor the protons 2 and 9 of $[Co(phen)(en)_2]^{3+}$. The up-field shift was considered to be due to the effect of the ring current of the other phenanthroline ligands, since the protons 2 and 9 of $[Co(phen)_3]^{3+}$ and the proton 2 of $[Co(phen)_2(en)]^{3+}$ lies very close and to above the neighboring aromatic ligand.

The PMR spectra of 1,10-phenanthroline and its diamagnetic tris-complexes of iron(II), ruthenium(II), osmium(II), zinc(II), and cobalt(III) have been well examined.[1,2] Their spectra were analyzed as an ABX system, for the two halves of the ligand are chemically and magnetically equivalent, and no coupling was observed between neighboring protons on different aromatic rings (*e. g.*, H_4 and H_5 in Fig. 1). On the other hand, the spectra of *cis*-$[CoX_2(phen)_2]^{n+}$ were considered to consist of two independent ABX systems (H_2, H_3 and H_4, and H_9, H_8 and H_7) and an AB system (H_5 and H_6).[3] The significant up-field shift of signals corresponding to H_2 and H_9 in $[M(phen)_3]^{n+}$ and to H_2 in $[CoX_2(phen)_2]^{n+}$ was interpreted in terms of a metal-nonbonded hydrogen interaction,[1,2] or the effect of the ring current of the other aromatic ligand.[4,5] In order to clarify the origin of this kind of up-field shift, we have analyzed the PMR spectra of a series of complexes, $[Co(phen)_3]Cl_3$, $[Co(phen)_2(en)]Cl_3$, and $[Co(phen)(en)_2]Cl_3$. These three complexes are ter-positive ions surrounded by six nitrogen atoms in pseudo-octahedral positions. Thus, the effect of solvation on the spectra will not be significantly different among these complexes.

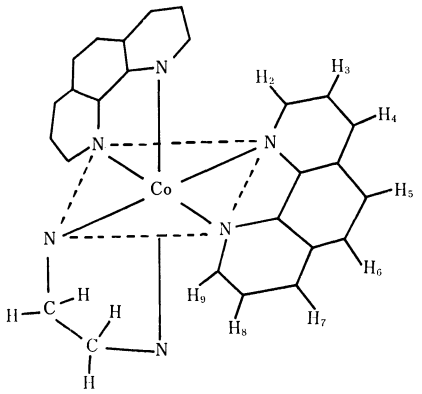

Fig. 1. Numbering of the protons on the phenanthroline ligand.

Experimental

Materials. *Bis(phenanthroline)ethylenediaminecobalt(III) perchlorate,* $[Co(phen)_2(en)](ClO_4)_3$: A mixture of 0.54 g of *trans*-(Cl–Cl)-$[CoCl_2(NH_3)_2(en)]Cl \cdot 0.5H_2O$[6] and 0.78 g of phenanthroline monohydrate in 50 m*l* of water was refluxed at 80°C for about 6 hr. The orange solution was then evaporated on a water bath to about 20 m*l* and cooled to room temperature. A crude complex was precipitated by adding concentrated perchloric acid. The precipitate was filtered off, washed with a small amount of cold water, recrystallized from hot water, and air-dried.

Found: C, 39.36; H, 3.40; N, 10.47%. Calcd for $CoC_{26}H_{24}N_6Cl_3O_{12}$: C, 40.15; H, 3.11; N, 10.80%. For the PMR measurement, the perchlorate was converted into chloride by the anion-exchange method.

The $[Co(phen)_3]Cl_3$ and $[Co(phen)(en)_2]Cl_3$ complexes were obtained by the methods described in the literature.[7,8]

Measurements and Calculation. The PMR spectra were recorded at about 39°C with Varian T 60 and Varian HA 100 spectrometers in a deuterium oxide solution containing sodium trimethylsilylpropanesulfonate (DSS) as the internal standard. The coupling constants, the chemical shifts, and the intensities were calculated with the HITAC 5020E electronic computer at the Computer Center of the University of Tokyo. The Fortran program for Castellano and Waugh's analysis[9] was kindly supplied by Dr. J. Cavanaugh of the Research Department, Socony Mobil Oil Company, Inc., Paulsboro, New Jersey, U.S.A. Since there are some signals which overlap each other, the peak height of the signals was taken as the approximate intensity.

Results and Discussion

The 60 MHz spectra of $[Co(phen)_3]Cl_3$, $[Co(phen)_2(en)]Cl_3$, and $[Co(phen)(en)_2]Cl_3$ in the phenanthroline part are given in Fig. 2.

The spectral pattern of $[Co(phen)(en)_2]^{3+}$ in the

1) J. D. Miller and R. H. Prince, *J. Chem. Soc.*, **1965**, 3185.
2) J. D. Miller and R. H. Prince, *ibid.*, **1965**, 4076.
3) J. D. Miller and R. H. Prince, *J. Chem. Soc., A*, **1969**, 519.
4) S. Castellano, H. Gunther, and S. Ebersole, *J. Phys. Chem.*, **69**, 4166 (1965).
5) R. E. DeSimone and R. S. Drago, *Inorg. Chem.*, **8**, 2517 (1969).
6) J. C. Bailar and D. F. Peppard, *J. Amer. Chem. Soc.*, **62**, 105 (1940).
7) B. R. Baker, F. Basolo, and H. M. Neumann, *J. Phys. Chem.*, **63**, 317 (1959).
8) F. M. Jaeger, *Proc. Roy. Acad. Sci. Amsterdam*, **29**, 559 (1926).
9) S. Castellano and J. S. Waugh, *J. Chem. Phys.*, **34**, 295 (1961).

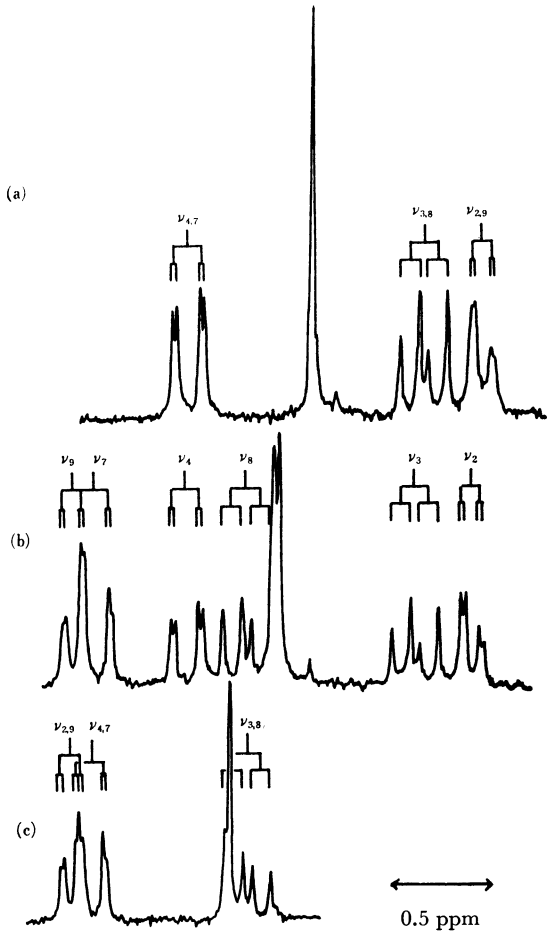

Fig. 2. 60 MHz spectra of $[Co(phen)_3]Cl_3$ (a), $[Co(phen)_2(en)]Cl_3$ (b) and $[Co(phen)(en)_2]Cl_3$ (c) in D_2O. The origin of the abscissa of each complex is arbitrary.

region of the phenanthroline part corresponds well to that of the free ligand,[1] although the chemical shifts are slightly different. The signals of all the protons on the chelate appeared at slightly lower fields than those of the corresponding protons on the free ligand,[1] this may be due to the deshielding effect of the central metal ion. Thus, the $\nu_{2,9}$, $\nu_{3,8}$, and $\nu_{4,7}$ signals in Fig. 2 of $[Co(phen)(en)_2]^{3+}$ were assigned to $H_{2,9}$, $H_{3,8}$, and $H_{4,7}$ respectively. No up-field shift of the signals corresponding to $H_{2,9}$ is observed in this complex.

The chemical environment of half of the phenanthroline part of $[Co(phen)_2(en)]^{3+}$ is similar to that of $[Co(phen)_3]^{3+}$, and that of the other half, to that of $[Co(phen)(en)_2]^{3+}$ (see Fig. 1). Therefore, the spectrum of $[Co(phen)_2(en)]^{3+}$ may be expected to be similar to the sum of those of $[Co(phen)_3]^{3+}$ and $[Co(phen)(en)_2]^{3+}$. As is shown in Fig. 2, the relative positions of ν_2 and ν_3 signals of $[Co(phen)_2(en)]^{3+}$ are very close to those assigned to $H_{2,9}$ and $H_{3,8}$ respectively for $[Co(phen)_3]^{3+}$.[1,2] Thus, these signals can be assigned to the H_2 and H_3 protons respectively (Fig. 1). On the other hand, the resonance of ν_9 and ν_8 appear in the regions of $H_{2,9}$ and $H_{3,8}$ of $[Co(phen)(en)_2]^{3+}$; they are assigned to the H_9 and H_8 signals respectively. The resonances of ν_4 and ν_7 are assigned to H_4 and H_7 respectively for the same reason. These assignments were also confirmed by double-resonance measurements. The 100 MHz spectrum and the double-resonance spectra of $[Co(phen)_2(en)]^{3+}$ are shown in Fig. 3. Upon irradiation at about 9.05 ppm (in the region of H_4), the spectrum in the region of H_2 and H_3 became an AB pattern (Fig. 3(b)), and upon irradiation at about 8.87 ppm (in the region of H_8), the spectrum in the region of H_7 and H_9 changed to a broad doublet (an AB pattern with a small coupling constant) (Fig. 3(c)). In Fig. 3(a), an AB pattern with a coupling constant of 9.1 Hz is observed at 8.73 ppm; this can be assigned to signals of H_5 and H_6.

On the basis of the above assignment, the chemical shifts and the coupling constants were calculated as two independent ABX patterns. Tables 1 and 2 show the calculated values of the chemical shifts and the coupling constants respectively. The calculated and the ob-

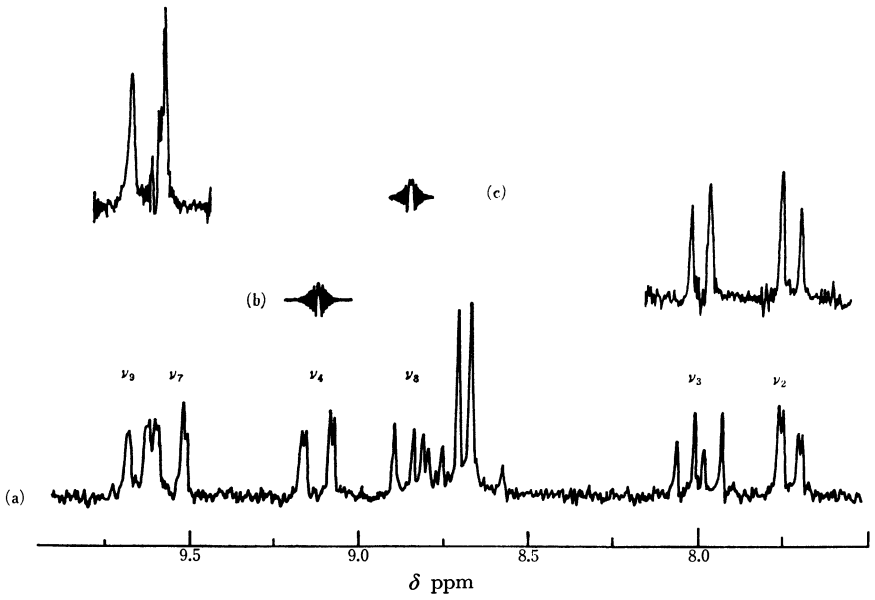

Fig. 3. 100 MHz spectrum of $[Co(phen)_2(en)]Cl_3$ (a), double resonance spectrum irradiated at about 9.05 ppm (b) and double resonance spectrum irradiated at about 8.87ppm (c).

Table 1. Calculated values of the chemical shift (δ in ppm relative to DSS)

	δ_2	δ_9	δ_3	δ_8	δ_4	δ_7	δ_5	δ_6
$[Co(phen)_3]Cl_3$	7.89		8.17		9.35		8.73	
$[Co(phen)_2(en)]Cl_3$	7.75	9.68	8.01	8.85	9.14	9.58	8.73	
$[Co(phen)(en)_2]Cl_3$	9.25		8.39		9.15		8.47	

Table 2. Calculated values of the coupling constant (in Hz)

	J_{23}	J_{89}	J_{24}	J_{79}	J_{34}	J_{78}	J_{56}
$[Co(phen)_3]Cl_3$	5.6_1		1.1_3		8.4_6		
$[Co(phen)_2(en)]Cl_3$	5.2_0	5.6_4	1.1_3	1.0_7	8.1_6	8.5_9	9.1
$[Co(phen)(en)_2]Cl_3$	5.6_2		1.0_5		8.2_0		

Table 3. Calculated and observed intensities

$[Co(phen)_3]Cl_3$[a,c]			$[Co(phen)(en)_2]Cl_3$[a,d]			$[Co(phen)_2(en)]Cl_3$[b]					
Calcd position (Hz)[g]	Intensities		Calcd position (Hz)[g]	Intensities		Calcd position (Hz)[e,g]	Intensities		Calcd position (Hz)[f,g]	Intensities	
	Obsd	Calcd		Obsd	Calcd		Obsd	Calcd		Obsd	Calcd
−70.46	0.0	0.0	−66.28	0.0	0.0	−110.60	0.0	0.0	−104.28	0.0	0.0
−57.70	1.0	0.9	−22.67	0.8	0.8	−88.70	0.9	0.9	−34.37	0.9	0.9
−56.38	1.1	0.9	−21.55	0.9	1.0	−87.50	0.9	0.9	−33.27	1.0	1.0
−49.42	1.2	1.1	−18.47	1.1	0.9	−80.60	1.2	1.1	−28.77	1.0	0.9
−48.10	1.2	1.1	−17.35	0.9	0.7	−79.40	1.1	1.1	−27.67	1.0	1.2
−35.34	0.0	0.0	−17.15	0.9	0.9	−57.50	0.0	0.0	−25.97	1.1	1.0
10.73	0.8	0.8	−16.03	1.3	1.3	22.10	0.8	0.9	−24.87	1.0	0.8
16.33	1.2	1.4	−10.23	1.3	1.4	27.30	1.1	1.3	−17.37	1.4	1.3
19.01	0.6	0.5	−9.11	0.9	0.9	30.20	0.6	0.7	−16.27	0.9	1.0
24.61	1.2	1.3	26.26	1.3	1.3	35.40	1.1	1.1	42.24	0.0	0.0
31.77	1.1	1.3	27.58	0.0	0.0	52.10	1.2	1.2	45.04	1.1	1.2
33.09	1.1	1.3	31.78	1.0	1.0	53.30	1.2	1.2	50.64	1.0	1.0
37.37	0.7	0.7	34.50	0.9	0.9	57.30	0.9	0.8	53.64	0.9	0.9
38.69	0.6	0.6	38.70	0.0	0.0	58.50	0.8	0.8	59.24	0.7	0.8
105.80	0.0	0.0	40.02	0.7	0.7	168.10	0.0	0.0	62.04	0.0	0.0

a) 60 MHz spectrum; b) 100 MHz spectrum; Negative sign indicates that the shift is lower than c) 508 Hz, d) 536 Hz, e) 830 Hz, and f) 937 Hz (DSS is used as an internal standard); g) These are in good argreement with the observed ones.

served intensities are compared in Table 3. The data for $[Co(phen)_3]^{3+}$ and $[Co(phen)(en)_2]^{3+}$ are also listed in these tables.

A large difference in the chemical shifts between H_2 and H_9 was observed for $[Co(phen)_2(en)]^{3+}$ (1.93 ppm). This could not be explained only by the metal-non-bonded hydrogen interaction suggested by Miller and Prince,[1,2] since no significant difference in distances between Co–H_2 and Co–H_9 can be expected. An explanation by the π-bonding effect was also ruled out,[2] and the effect of the solvation[1,2] is considered to be not very significant, as has been discussed earlier.

The molecular model indicates that the proton 2 lies very close above the plane of the pyridine ring of the other phenanthroline ligand. The distance between the proton 2 and this plane is calculated to be about 2.7 Å on the assumption that the bond lengthes of Co–N, C=N, C=C, and C–H are 1.97,[10] 1.39, 1.39, and 1.08 Å respectively, and that all the bond angles in the coordinated ligands are 120°. The nitrogen atoms are also assumed to coordinate in the regular octahedral positions. Accordingly, the large up-field shift can reasonably be explained as being caused by the ring current of the neighboring ligand, as has been suggested by Castellano *et al.* for $[Fe(bipy)_3]^{2+}$.[4]

The differences in the chemical shifts between H_9 and H_2, H_8 and H_3, and H_7 and H_4 of $[Co(phen)_2(en)]^{3+}$ are 1.93, 0.94, and 0.44 ppm respectively. The decrease in the difference in the chemical shift in the above order can be accounted for by the increase in the distances between the proton and the molecular plane of the other phenanthroline ligand.

The authors wish to thank Professor Kazuo Saito for helpful advice and encouragement.

10) D. H. Templeton, A. Zalkin, and T. Ueki, *Acta Cryst.*, **21**, **A154** (supplement) (1966).

^{119}Sn-Mössbauer and ^{1}H- and ^{55}Mn-NMR Spectroscopic Studies of a Series of Compounds, $R_{3-x}X_xSn$-$Mn(CO)_5$

Satoru ONAKA* and Yukiyoshi SASAKI

Department of Chemistry, Faculty of Science, The University of Tokyo, Bunkyo-ku, Tokyo

and Hirotoshi SANO

Department of Chemistry, Faculty of Science, Ochanomizu University, Bunkyo-ku, Tokyo

(Received September 7, 1970)

The electronic configuration around the tin atom for a series of organotin-manganese compounds, $R_{3-x}X_xSn$-$Mn(CO)_5$, has been studied by ^{119}Sn-Mössbauer and ^{1}H- and ^{55}Mn-NMR spectroscopies. All the results obtained from these spectroscopic measurements show that the $Mn(CO)_5$ group is a stronger electron donor than the methyl, phenyl, or halogen group and that the tin-manganese bond prefers the sσ-character whereas the tin-halogen bond prefers the pσ-character. The relationship between the ^{55}Mn-chemical shift and the ^{119}Sn-isomer shift indicates some σ-electron withdrawal from manganese to tin. The phenyl group reduces the magnitude of quadrupole splitting more than the methyl group; this fact may be due to the mesomeric effect of the phenyl group through the π-bond between tin and ligand atoms. The relationship among the ^{119}Sn-isomer shift, the ^{1}H-chemical shift, and the coupling constant $J(^{119}Sn\text{-}^{1}H(CH_3))$ is also shown.

The Mössbauer spectroscopy in ^{119}Sn has been used to study a wide variety of organotin compounds as well as inorganic compounds.[1,2] The two Mössbauer parameters which are common to most studies, the isomer shift and the quadrupole splitting, have been used to elucidate the electronic configuration around the tin atoms, but there are a number of contradictions in these explanations.[3-5] Mössbauer spectroscopic studies of many compounds containing tin-transition-metal bonds, such as tin–iron tin–cobalt, and tin–manganese bonds, have been reported.[2,6-10] Mössbauer and ^{1}H-NMR spectroscopic studies have been published on alkyltin hydrides[11] and a series of compounds, $(CH_3)_{4-x}SnM_x$ (M represents metal carbonyl derivatives).[6,12] In these studies, the two "probe" atoms are used to derive information about the nature of the chemical bond pertaining to a portion of the whole molecule. We have studied a number of organotin compounds by means of Mössbauer spectroscopy,[13-16] and a number of organometallic compounds involving metal-metal bonds by means of IR and NMR spectroscopies.[17] In the present paper, three kinds of atoms, ^{119}Sn, ^{55}Mn, and ^{1}H, were used as probes to get information as to the electronic configuration, especially around the tin atom in the $R_{3-x}X_xSn$-$Mn(CO)_5$ type of compounds, where X is Cl or Br and where R is a methyl or phenyl group.

Experimental

Preparation of Compounds. All the compounds except $Cl_2(CH_3)Sn$-$Mn(CO)_5$, $Br(CH_3)_2Sn$-$Mn(CO)_5$ and $Br_2(CH_3)$-Sn-$Mn(CO)_5$ were prepared by the methods of Gorsich[18] and Graham.[19] Those three compounds were prepared as has previously been reported.[17] Carbon and hydrogen analyses were performed by Mr. Masuda for all the compounds. The purity was also checked by IR, NMR, and/or Mössbauer spectroscopies.

Mössbauer Spectra. Measurements were made as has previously been described.[20] The ^{119}Sn-Mössbauer spectra were obtained against a $Ba^{119m}SnO_3$ source drived at room temperature. The sample was used as an absorber and was kept at 79°K in a cryostat. The pertinent isomer shifts are reported with respect to the centroid of a barium stannate spectrum at room temperature. The velocity scans were calibrated with ^{57}Fe-enriched iron foil and a source of ^{57}Co diffused into copper foil, both kept at room temperature.

NMR Spectra. The ^{1}H-NMR data were obtained on dichloromethane solutions of the samples using a JNM-4H-100 spectrometer at room temperature, where the dichloromethane was used as the internal standard. The ^{1}H-chemical shift values listed in Table 1 were recalculated with respect to tetramethylsilane (TMS). The ^{55}Mn-NMR measurements were made as has been described elsewhere.[17]

* Present address: Chemistry Department, Nagoya Institute of Technology, Showa-ku, Nagoya.

1) "Chemical Applications of Mössbauer Spectroscopy" Chapter 5 and 6, ed. by V. I. Goldanskii and R. H. Herber, Academic Press, New York (1968).
2) V. I. Goldanskii, V. V. Khrapov, and R. A. Stukan, *Organometal. Chem. Rev.*, **A4**, 225 (1969).
3) H. A. Stöckler and H. Sano, *Trans. Faraday Soc.*, **64**, 577 (1968).
4) R. V. Parish and R. H. Platt, *Chem. Commun.*, **1968**, 1118.
5) R. V. Parish and R. H. Platt, *J. Chem. Soc.*, **A**, **1969**, 2145.
6) D. E. Fenton and J. J. Zuckerman, *J. Amer. Chem. Soc.*, **90**, 6226 (1968).
7) D. E. Fenton and J. J. Zuckerman, *Inorg. Chem.*, **8**, 1771 (1969).
8) R. H. Herber and Y. Goscinney, *ibid.*, **7**, 1293 (1968).
9) A. N. Karasev, N. E. Kolobova, L. S. Polak, V. S. Shipnel, and K. N. Anisimov, *Theor. Eksperim. Khim.*, **2**, 126 (1966); R. H. Herber, *Progr. Inorg. Chem.*, **8**, 1 (1967). (References cited from D. E. Fenton and J. J. Zuckerman, *J. Amer. Chem. Soc.*, **90**, 6226 (1969).
10) M. T. Jones, *Inorg. Chem.*, **6**, 1249 (1967).
11) L. May and J. J. Spijkerman, *J. Chem. Phys.*, **46**, 3272 (1967).
12) C. Wynter and L. Chandler, This Bulletin, **43**, 2115 (1970).
13) H. A. Stöckler, H. Sano, and R. H. Herber, *J. Chem. Phys.*, **45**, 1182 (1966).
14) H. A. Stöckler, H. Sano, and R. H. Herber, *ibid.*, **47**, 1567 (1967).
15) H. A. Stöckler and H. Sano, *Phys. Rev.*, **165**, 406 (1968).
16) H. A. Stöckler and H. Sano, *J. Chem. Phys.*, **50**, 3813 (1969).
17) S. Onaka, T. Miyamoto, and Y. Sasaki, This Bulletin, **44**, (1971), in press.
18) R. D. Gorsich, *J. Amer. Chem. Soc.*, **84**, 2486 (1962).
19) W. Jetz, P. B. Simons, J. A. J. Thompson, and W. A. G. Graham, *Inorg. Chem.*, **5**, 2217 (1966).
20) H. A. Stöckler and H. Sano, *Nucl. Instrum. Methods*, **44**, 103 (1966).

Table 1. ^{119}Sn-Mössbauer and NMR (^{55}Mn and ^{1}H) parameters for $R_{3-x}X_xSn-Mn(CO)_5$ compounds

		I.S. (mm/sec)	Q.S. (mm/sec)	^{55}Mn chemical shift (ppm)[a]	^{1}H chemical shift (ppm)[b]	$J(^{119}Sn-^{1}H(CH_3))$ (Hz)
1	$Cl_3Sn-Mn(CO)_5$	1.68	1.57	2024		
2	$Cl_2PhSn-Mn(CO)_5$	1.68	2.36	2278		
3	$Cl_2(CH_3)Sn-Mn(CO)_5$	1.68	2.62	2312	8.65	42.2
4	$ClPh_2Sn-Mn(CO)_5$	1.57	2.49	2460		
5	$Cl(CH_3)_2Sn-Mn(CO)_5$	1.54	2.66	2520	9.02	45.2
6	$Br_3Sn-Mn(CO)_5$	1.79	1.41	2044		
7	$Br_2PhSn-Mn(CO)_5$	1.80	2.63	2252		
8	$Br_2(CH_3)Sn-Mn(CO)_5$	1.69	2.51	2256	8.42	40.3
9	$BrPh_2Sn-Mn(CO)_5$	1.59	2.28	2468		
10	$Br(CH_3)_2Sn-Mn(CO)_5$	1.54	2.54	2485	8.92	45.3
11	$Ph_3Sn-Mn(CO)_5$	1.41	0	2610		
12	$(CH_3)_3Sn-Mn(CO)_5$	1.33	0.61	2660	9.50	48.9

a) ^{55}Mn chemical shift is expressed relative to $KMnO_4$.
b) ^{1}H chemical shift is expressed relative to $(CH_3)_4Si$ (TMS).

Results

A single absorption line was observed in the ^{119}Sn-Mössbauer spectrum of $Ph_3Sn-Mn(CO)_5$, whereas a well-resolved pair of quadrupole split lines was found in the spectra for all the other compounds. A typical Mössbauer spectrum is shown in Fig. 1, while the

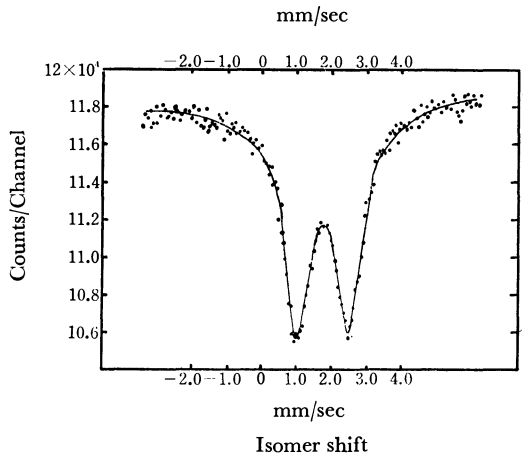

Fig. 1. A typical ^{119}Sn-Mössbauer spectrum ($Br_3Sn-Mn(CO)_5$).

numerical values for the Mössbauer parameters at 79°K are summarized in Table 1. The isomer shifts and quadrupole splittings extracted from the data are in good agreement with those reported by Karasev *et al.*[9] for $Cl_3Sn-Mn(CO)_5$, $Br_3Sn-Mn(CO)_5$, and $Ph_3Sn-Mn(CO)_5$ compounds. The quadrupole splittings are somewhat smaller than those given recently by Wynter and Chandler[12] for $Cl_3Sn-Mn(CO)_5$, $Br_3Sn-Mn(CO)_5$, and $(CH_3)_3Sn-Mn(CO)_5$ compounds, although the isomer shift values are in moderately good agreement. The values for the chemical shift of ^{1}H- and ^{55}Mn-NMR and for the coupling constants of $J(^{119}Sn-^{1}H(CH_3))$ are also listed in Table 1. No splitting of ^{55}Mn-NMR absorption due to the coupling between ^{119}Sn and ^{55}Mn was observed. It may be worth mentioning that both the $^{1}H(CH_3)$ chemical shift and the coupling constant, $J(^{119}Sn-^{1}H(CH_3))$, decrease with a decrease in the number of methyl groups attached to the tin atom.

Discussion

The isomer shift is proportional to the electron density at the Mössbauer nucleus, and it is dependent upon those factors which affect the electron density at the nucleus, for example, the 5s electron density on the tin atom and the extent of the shielding effect on the inner shell s-electron by the 5s, 5p, or 5d electron. It is known that the variation in the 5s electron density influences the isomer-shift value ten times more than the shielding effect in the case of tin compounds.[21] In the present case, therefore, the isomer shift values obatined are interpreted in terms of the 5s electron density.

It is clear from the data shown in Fig. 2 that the isomer shift values of $R_{3-x}X_xSn-Mn(CO)_5$ are higher than those reported previously[3] for the tin compounds, $R_{4-x}X_xSn$, at the same number of x. The isomer shift increases in the $R_{3-x}X_xSn-Mn(CO)_5$ series as the methyl or phenyl groups are successively replaced by halogen atoms. This trend is in contrast to those observed in the $R_{4-x}X_xSn$ series, where the isomer shift attains its maximum at $x=2$. These results suggest that the $Mn(CO)_5$ group is a stronger electron donor either than the methyl or phenyl group, and that the more halogen atoms are attached to tin atom, the more σ-electrons are transferred from the manganese to the tin atom.

Figure 3 illustrates the relationship between the ^{119}Sn-isomer shift and the ^{55}Mn-chemical shift; there is a smooth decrease in the chemical shift with the increase in the isomer shift. A decrease in the ^{55}Mn-chemical shift implies an increased σ-electron with-

21) J. K. Lees and P. A. Flinn, *J. Chem. Phys.*, **48**, 882 (1968).

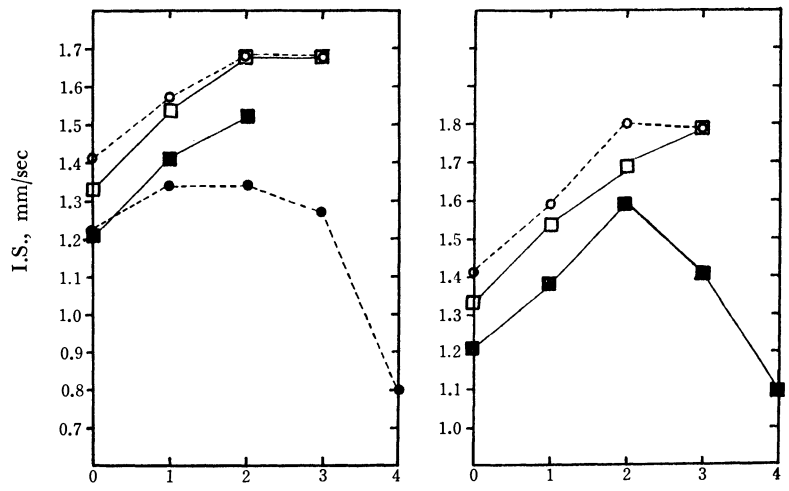

Fig. 2. Relationships between ^{119}Sn-isomer shift and number of halogen on tin atom.
(a). ■—■ represents $(CH_3)_{4-x}Cl_xSn$ compounds, ●···● $Ph_{4-x}Cl_xSn$, □—□ $(CH_3)_{3-x}Cl_xSn$–$Mn(CO)_5$, ○···○ $Ph_{3-x}Cl_xSn$–$Mn(CO)_5$ respectively.
(b). ■—■ represents $(CH_3)_{4-x}Br_xSn$ compounds, □—□ $(CH_3)_{3-x}Br_xSn$–$Mn(CO)_5$, ○—○ $Ph_{3-x}Br_xSn$–$Mn(CO)_5$ respectively.
Isomer shift data except for $R_{3-x}X_xSn$–$Mn(CO)_5$ are cited from the literature.[3)]

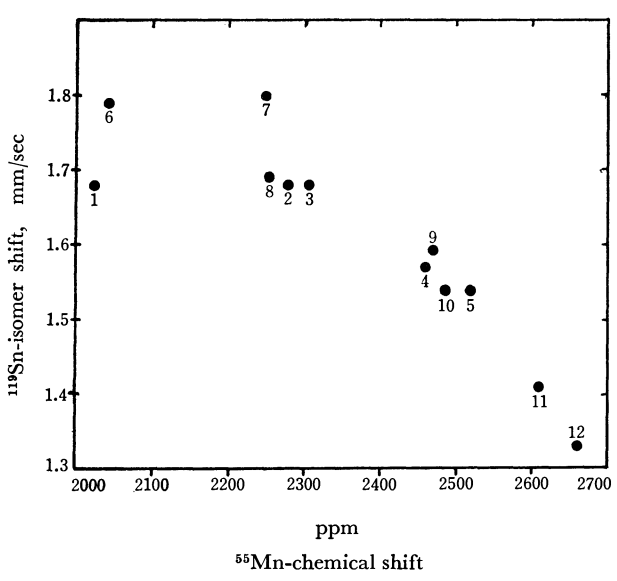

Fig. 3. The relationship between ^{119}Sn-Mössbauer isomer shift and ^{55}Mn-chemical shift. Numbers in the graph represent the compounds in Table 1.

drawal from the manganese atom to the tin atom,[22)] while an increase in the ^{119}Sn–isomer shift implies sσ-electron deposit on the tin atom. This trend may also suggest an electron transfer from the manganese to the tin atom through the σ-bond.

In the series of $(CH_3)_{3-x}X_xSn$–$Mn(CO)_5$, there are linear decreases in the $^1H(CH_3)$-chemical shift and in the coupling constant, $J(^{119}Sn$–$^1H(CH_3))$, with an increase in the ^{119}Sn-isomer shift, as is shown in Fig. 4.

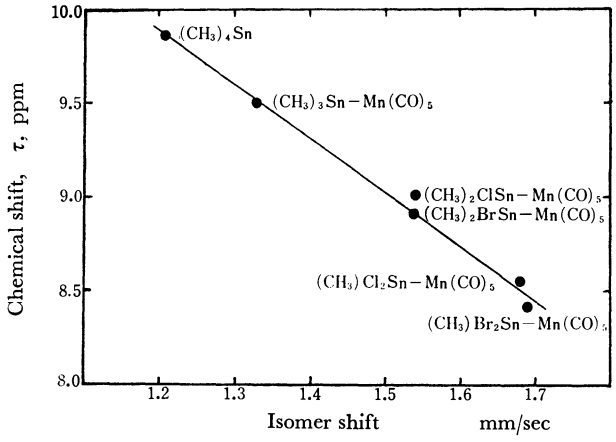

Fig. 4(a). The relationship between ^{1}H-chemical shift and ^{119}Sn-isomer shift.

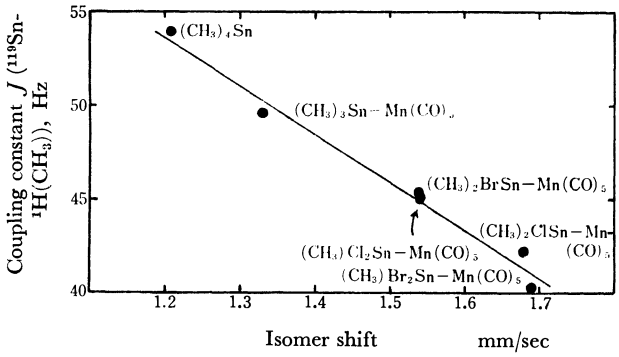

Fig. 4(b). The relationship between coupling constant J (^{119}Sn-^{1}H(CH_3)) and ^{119}Sn-isomer shift. ^{1}H-NMR parameters of $(CH_3)_4Sn$ are cited from the literature.[27)]

22) The detailed discussion in context with CO stretching vibrations will be published elsewhere.

27) N. Flitcroft and H. D. Kaesz, *J. Amer. Chem. Soc.*, **85**, 1377 (1963).

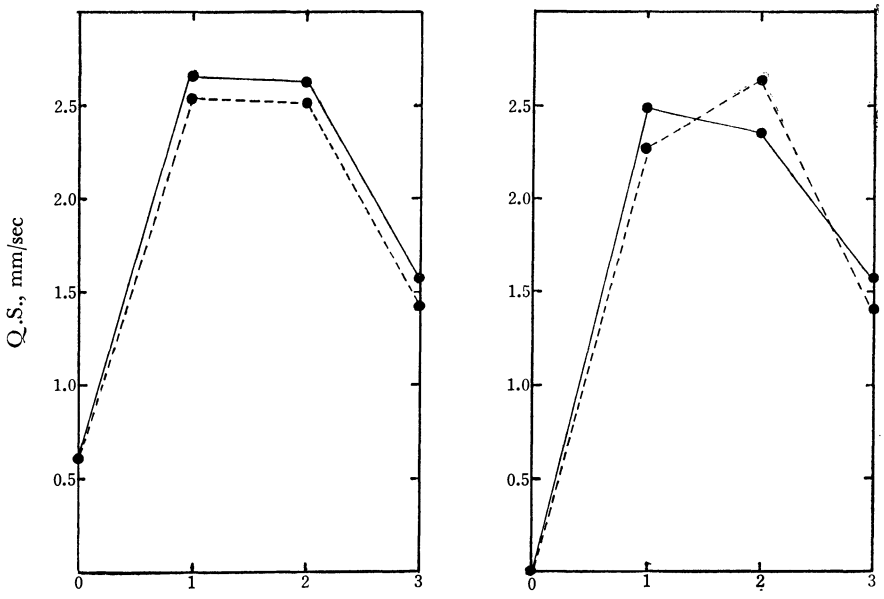

Fig. 5. Relationships between quadrupole splitting and number of halogen on tin atom.
(a). ●—● represents $(CH_3)_{3-x}Cl_xSn$–$Mn(CO)_5$, ●···● $(CH_3)_{3-x}Br_xSn$–$Mn(CO)_5$ respectively.
(b). ●—● represents $Ph_{3-x}Cl_xSn$–$Mn(CO)_5$, ●···● $Ph_{3-x}Br_xSn$–$Mn(CO)_5$ respectively.

Decreases in the coupling constant and increases in the isomer shift with the decrease in the number of methyl group attached to the tin atom may be expected by assuming a higher *p*-character in the tin-halogen bond and a higher *s*-character in the tin-manganese bond than in the other tin-ligand bond.[23,24] The lower coupling constant, $J(^{119}Sn\text{-}^{1}H(CH_3))$, in $(CH_3)_3Sn$–$Mn(CO)_5$ than in $(CH_3)_4Sn$ also indicates that the 5s electron of tin atom is much more localized in the tin-manganese bond than in the tin-carbon bond; *i.e.*, the tin-manganese bond prefers the sσ-character whereas the tin-carbon bond prefers the pσ-character.[25]

The quadrupole splitting of the Mössbauer spectra reflects the electric-field gradient at the tin nucleus. Although the intermolecular interactions might not be negligible in some cases, the dominant origin of the electric-field gradient may be ascribed to the intramolecular bonding around the tin atom as a first approximation. It is found, from the data shown in Fig. 5, that R_2XSn–$Mn(CO)_5$ and RX_2Sn–$Mn(CO)_5$ give the same order of quadrupole splitting values except in the cases of Ph_2BrSn–$Mn(CO)_5$ and $PhBr_2Sn$–$Mn(CO)_5$, and that $R_{3-x}Br_xSn$–$Mn(CO)_5$ gives a lower quadrupole splitting value than the analogous $R_{3-x}Cl_xSn$–$Mn(CO)_5$, while R is the same in both the compounds, again with the exception of $PhBr_2$ Sn–$Mn(CO)_5$. Intermolecular interactions might not be negligible in this compound. The general trend for the quadrupole splitting values to be higher for chloride compounds than for bromide suggests that the *p*-electron imbalance in the 5p-orbital of the tin atom is greater in $R_{3-x}Cl_x$-Sn–$Mn(CO)_5$ than in $R_{3-x}Br_xSn$–$Mn(CO)_5$. As has been mentioned in the previous section, it was found that the *p*-character is highest in the tin-halogen bond and lowest in the tin-manganese bond. This p-electron imbalance in each tin-ligand bond may be considered to be the main origin of the quadrupole splitting. As may be seen in Fig. 6, Ph_3Sn–$Mn(CO)_5$ shows non-resolved quadrupole splitting, whereas $(CH_3)_3Sn$–$Mn(CO)_5$ gives a clearly-resolved spectrum. In general, quadrupole splitting is larger when R is CH_3 than when R is C_6H_5. Cordey-Hayes *et al.*[26] and Stöckler and Sano[3] pointed out that the phenyl groups are more effective in delocalizing π-electrons and, hence, in reducing the magnitude of the quadrupole splitting in the series of $Ph_{4-x}X_xSn$ compounds. Parish and Platt interpreted the fact that the quadrupole splitting is smaller in $Ph_{4-x}X_xSn$ than in $(CH_3)_{4-x}X_xSn$ compounds by assuming a higher electron-withdrawing ability of the phenyl group.[5] However, the ^{119}Sn-isomer shift and the ^{55}Mn-chemical shift data indicate that the $Mn(CO)_5$ group has a stronger σ-electron-donating ability either than the methyl or the phenyl group. The results led us to conclude that the phenyl group reduces the magnitude of quadrupole splitting

23) H. A. Bent, *Can. J. Chem.*, **38**, 1235 (1960); *Chem. Rev.*, **61**, 275 (1961); *J. Inorg. Nucl. Chem.*, **19**, 43 (1961).
24) J. R. Holmes and H. D. Kaesz, *J. Amer. Chem. Soc.*, **83**, 3903 (1961).
25) It has been reported that the *p*-character in tin-halogen bond is larger than in tin-carbon bond in $(CH_3)_{4-x}X_xSn$ compounds. J. R. Holmes and H. D. Kaesz, *J. Amer. Chem. Soc.*, **83**, 3903 (1961); M. M. McGrady and R. S. Tobias, *Inorg. Chem.*, **3**, 1157 (1964); E. V. van der Berghe and G. P. van der Kelen, *Ber. Bunsenges. Phys. Chem.*, **68**, 652 (1964).
26) M. Cordey-Hayes, R. D. Peacock, and M. Vucelic, *J. Inorg. Nucl. Chem.*, **29**, 1177 (1967).

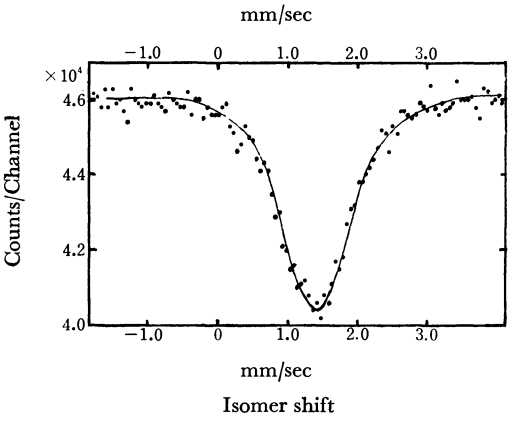

Fig. 6(a). A ^{119}Sn-Mössbauer spectrum of Ph_3Sn–$Mn(CO)_5$.

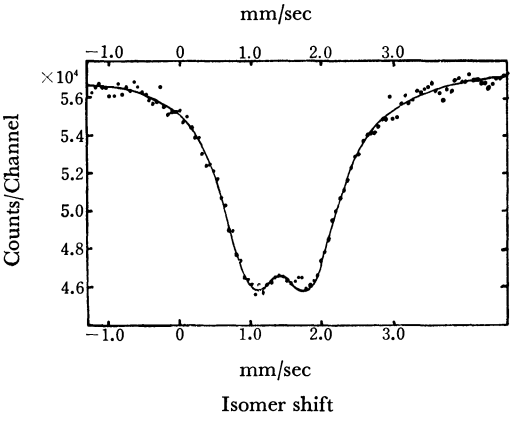

Fig. 6(b). A ^{119}Sn-Mössbauer spectrum of $(CH_3)_3Sn$–$Mn(CO)_5$.

more than the methyl group, whether X is an electronegative or an electropositive group, since the π-backdonation from $Mn(CO)_5$ to Sn in Ph_3Sn–$Mn(CO)_5$ is found not to be stronger than that in $(CH_3)_3Sn$–$Mn(CO)_5$ from the findings on the ^{55}Mn-NMR linewidth.[17] A plausible explanation is the ability of the phenyl group to deposit or withdraw π-electrons through a mesomeric effect and thereby cause a delocalization of π-electrons.

Conclusion

In compounds of the $R_{3-x}X_xSn$–$Mn(CO)_5$ type, where R is (CH_3) or (C_6H_5) and where X is Cl or Br, ^{119}Sn, ^{55}Mn, and ^{1}H were used as probes to derive information as to the electronic configuration. All the results of the ^{119}Sn-isomer shift, the ^{55}Mn-chemical shift, the $^1H(CH_3)$-chemical shift, and the $J(^{119}Sn$-$^1H(CH_3))$ coupling constant indicate that the $Mn(CO)_5$ group is a stronger electron donor than the methyl, phenyl, or halogen group and that the tin-manganese bond prefers the sσ-character, whereas the tin-halogen bond prefers the pσ-character. The σ-electron transfer from the manganese to the tin atom increases with the successive replacement of the organic groups on tin atom by the halogen atoms. The relationship between the ^{55}Mn-chemical shift and the ^{119}Sn-Mössbauer isomer shift shows that the ^{55}Mn-chemical shift values (from $KMnO_4$ standard) become smaller when the degree of $Mn \xrightarrow{\sigma} Sn$-type σ-electron transfer increases.

In general, the phenyl group reduces the magnitude of the quadrupole splitting more than the methyl group, as has been observed in the series of the $R_{4-x}X_xSn$ compound. This behavior can be interpreted as being due to the mesomeric effect of the phenyl group through the π-bond between tin and ligand atoms.

One of the authors (H. S.) especially wishes to thank Dr. H. A. Stöckler and the Nishina Memorial Foundation for financial aid in providing the Mössbauer spectrometer.

Syntheses and Properties of Copper(II), Nickel(II), and Cobalt(II) Complexes of Alkylthioglycolic Acids

Akira OUCHI, Toshio TAKEUCHI, and Yayoi OHASHI

Department of Chemistry, College of General Education, The University of Tokyo, Komaba, Meguro-ku, Tokyo

(Received September, 10, 1970)

Copper(II), nickel(II), and cobalt(II) complexes of alkylthioglycolic acids, $R \cdot S \cdot CH_2COOH$ (where R=ethyl, *n*-propyl, isopropyl, *n*-butyl, isobutyl, and *s*-butyl), were synthesized. Except for some copper complexes, these are new compounds. The attempt to synthesize the solid zinc complexes by the same method has not yet been successful. The relative stabilities of these complexes in the solid state seem to be Zn(II)<Co(II), Ni(II)<Cu(II), considering the yield of the syntheses of the products as well as the solvolizing tendency of the complexes. The nickel and cobalt complexes are expected to be in an octahedral form from the magnetic moments as well as from their electronic spectra. The relation between Taft's substitution constants and the wave numbers of the maxima of the absorption spectra of these complexes in the solid state is not clear.

As a step in the studies of the metal complexes containing sulfur compounds as the ligands, alkylthioglycolato complexes,[1] especially their copper complexes, have been synthesized and studied.[2] As it seems that the structure of the alkylthioglycolato complexes would be more clarified by studying the properties of the complexes of other metals, nickel(II) and cobalt(II) complexes other than the copper(II) complexes were also synthesized. Although the complexes of these metals resemble each other and the solid hydrates are very stable, the nickel and cobalt complexes were a little more difficult to synthesize. The syntheses of zinc(II) complexes were also attempted, but as the complexes were unstable, hardly any solid products were obtained. This fact is understandable referring to the fact that the general stability order of complexes of these metals is: Zn(II)<Co(II), Ni(II)<Cu(II), as has been shown by Mellor and others.[3,4]

As the ligands, ethyl-, *n*-propyl-, isopropyl-, *n*-butyl-, isobutyl-, and secondary butyl- thioglycolic acids were used to investigate the substitution effect of the alkyl groups. Hereafter, they will be abbreviated in this paper as follows: H EtS_1, H *n*-PrS_1, H *i*-PrS_1, H *n*-BuS_1, H *i*-BuS_1, H *s*-BuS_1.

Experimental

Instruments. The infrared spectra were obtained by the Nujol or hexachloro-1,3-butadiene mull procedure, using a 403G-type infrared spectrophotometer of the Japan Spectroscopic Co., Ltd. The electronic spectra were obtained with Hitachi EPS-2-type automatic recording spectrophotometer. The magnetic moments were measured with a Gouy balance at room temperature (20°C).

Syntheses of the Materials. *The syntheses of the Ligands*: H EtS_1, H *n*-PrS_1, H *i*-PrS_1, H *n*-BuS_1, H *i*-BuS_1, and H *s*-BuS_1 were synthesized by Pettit's[5] or Larsson's[6] method from the alkyl halide and thioglycolic acid.

The Syntheses of n-*Propylthioglycolato Cobalt(II) Dihydrate*: An aqueous solution of 1.2 g (5.0 mM) of cobalt(II) chloride hexahydrate was treated with sodium hydroxide, and the cobalt(II) hydroxide thus obtained was washed well with water (by the centrifuge technique). The hydroxide, 5 m*l* of water, 5 m*l* of formalin (37%), and 1.35 g (10 mM) of H *n*-PrS_1 were mixed and stirred. After several minutes, the residue was filtered off and the filtrate was kept overnight in a refrigerator. The product was washed with ice cold water, a little cold ethyl alcohol, and ethyl ether, in that order. The yield was 0.4 g (1.1 mM). If the formalin was not used, a brown by-product, probably the thioglycolate, precipitated when the metal salt was mixed with the ligand and the yield was much lowered.

The other complexes were synthesized by almost the same method. In the case of the copper and nickel complexes, formalin was not used. As was reported previously, in the case of isopropylthioglycolatocopper(II) dihydrate blue and violet isomers were obtained.[2] However, until now this kind of isomerism has not been observed in the cases either of nickel and cobalt complexes or of copper complexes of other alkylthioglycolic acids.

Results and Discussion

The elemental analyses, the chemical formulae of the complexes thus obtained, and the approximate yields of the products are shown in Table 1. From the results, all of these compounds can be said to have the formulae of $ML_2 \cdot 2H_2O$, where HL is an alkylthioglycolic acid.

The magnetic moments of these complexes, as measured by Gouy's balance, are shown in Table 2. Generally, the cobalt and nickel complexes have much higher magnetic moments than the spin-only values. Cobalt complexes have the magnetic moments of about 4.7—5.2 B.M. when they are in the octahedral form and 4.4—4.8 B.M. when in tetrahedral ones.[7] The magnetic moments of nickel complexes are 2.9—3.4 B.M. in the cases of octahedral complexes and 3.5—4.2 B.M. in the cases of tetrahedral complexes.[7] The observed magnetic moments of these products are about 2.9—3.1 B.M. in the cases of nickel complexes and 4.6—5.1 B.M. in the cases of cobalt complexes. Therefore, all of these com-

1) A. Ouchi, Y. Ohashi, T. Takeuchi, and Y. Yoshino, This Bulletin, **43**, 1088 (1970).

2) Y. Ohashi, T. Takeuchi, A. Ouchi, and Y. Yoshino, *ibid.*, **43**, 2845 (1970).

3) D. P. Mellor and L. E. Maley, *Nature*, **159**, 379 (1947).

4) K. Nakamoto and P. J. McCarthy, "Spectroscopy and Structure of Metal Chelate Compounds," Wiley, New York (1968), p. 273.

5) L. D. Pettit and C. Sherrington, *J. Chem. Soc., A*, **1968**, 3078.

6) E. Larsson, *Ber.*, **63**, 1347 (1930).

7) F. A. Cotton and G. Wilkinson, "Advanced Inorganic Chemistry," 2nd Ed., Interscience, New York, (1966), pp. 870, 882.

Table 1. The analyses of complexes (Figures are given in %)

		Metal	C	H	S	Yield
$Cu(EtS_1)_2\cdot 2H_2O$	Calcd	18.81	28.44	5.37	18.98	
	Found	18.16	28.76	5.41	18.40	65
$Ni(EtS_1)_2\cdot 2H_2O$	Calcd	17.63	28.85	5.45	19.25	
	Found	17.91	29.14	5.02	18.75	57
$Co(EtS_1)_2\cdot 2H_2O$	Calcd	17.68	28.83	5.44	19.24	
	Found	17.80	29.09	5.64	18.75	57
$Cu(n\text{-}PrS_1)_2\cdot 2H_2O$	Calcd	17.36	32.82	6.06	17.52	
	Found	17.56	32.95	5.88	17.04	59
$Ni(n\text{-}PrS_1)_2\cdot 2H_2O$	Calcd	16.26	33.26	6.14	17.76	
	Found	16.45	33.40	6.05	17.50	57
$Co(n\text{-}PrS_1)_2\cdot 2H_2O$	Calcd	16.31	33.24	6.14	17.75	
	Found	16.11	33.60	6.29	17.04	52
$Cu(i\text{-}PrS_1)_2\cdot 2H_2O$[a]	Calcd	17.36	32.82	6.06	17.52	
	Found	17.29	33.07	5.96	17.05	42[b]
$Ni(i\text{-}PrS_1)_2\cdot 2H_2O$	Calcd	16.26	33.26	6.14	17.76	
	Found	16.20	33.26	6.07	18.05	42
$Co(i\text{-}PrS_1)_2\cdot 2H_2O$	Calcd	16.31	33.24	6.14	17.75	
	Found	16.75	33.26	5.89	17.51	42
$Cu(n\text{-}BuS_1)_2\cdot 2H_2O$	Calcd	16.13	36.58	6.65	16.27	
	Found	16.27	37.01	6.53	16.80	90
$Ni(n\text{-}BuS_1)_2\cdot 2H_2O$	Calcd	15.08	37.03	6.73	16.48	
	Found	15.23	37.74	6.23	16.53	68
$Co(n\text{-}BuS_1)_2\cdot 2H_2O$	Calcd	15.13	37.01	6.73	16.47	
	Found	14.70	37.28	6.56	16.13	58
$Cu(i\text{-}BuS_1)_2\cdot 2H_2O$	Calcd	16.13	36.58	6.65	16.27	
	Found	16.54	36.74	6.52	15.98	82
$Ni(i\text{-}BuS_1)_2\cdot 2H_2O$	Calcd	15.08	37.03	6.73	16.48	
	Found	14.78	38.07	6.30	16.74	39
$Co(i\text{-}BuS_1)_2\cdot 2H_2O$	Calcd	15.13	37.01	6.73	16.47	
	Found	15.63	36.53	6.26	16.66	39
$Cu(s\text{-}BuS_1)_2\cdot 2H_2O$	Calcd	16.13	36.58	6.65	16.27	
	Found	15.70	36.93	5.95	15.99	76
$Ni(s\text{-}BuS_1)_2\cdot 2H_2O$	Calcd	15.08	37.03	6.73	16.48	
	Found	15.34	37.52	6.89	16.85	58
$Co(s\text{-}BuS_1)_2\cdot 2H_2O$	Calcd	15.13	37.01	6.73	16.47	
	Found	15.65	36.28	6.49	16.32	49

H EtS_1 =ethylthioglycolic acid, H n-PrS_1=n-propylthioglycolic aicd,
H i-PrS_1=isopropylthioglycolic acid, H n-BuS_1=n-butylthioglycolic acid,
H i-BuS_1=isobutylthioglycolic acid, H s-BuS_1=secondary butylthioglycolic acid.

a) blue isomer.

b) optimum yield of the blue isomer (in the run the sum of the blue and the violet complexes was 57%).

Table 2. Magnetic moments (B.M.) of the metal complexes (dihydrate) at 25°C.

Metal	Cu	Ni	Co
H EtS_1	1.73	3.13	4.79
H n-PrS_1	1.85	3.13	4.77
H i-PrS_1	1.84	2.97	4.66
H n-BuS_1	1.83	3.29	4.62
H i-BuS_1	1.95	3.39	5.06
H s-BuS_1	1.64	2.95	4.86

pounds seem to be octahedral complexes.

The water molecules in these products are relatively hard to remove and remain even after overnight drying at room temperature (on silica gel) in a vacuum desiccator. Therefore, the water molecules are probably coordinated with the metal ion, although the linking structure by water molecules is also possible; in any way they occupy two coordination bonds of the metal ion. There are two possibilities of how the alkylthioglycolic acid works as a bidentate ligand; i) two oxygen atoms of a carboxyl group bond to separate two metal ions, and the bridge structure is formed, or ii) one oxygen atom of a carboxyl group and a sulfur atom bond to the metal ion. The thioether-type sulfur does not coordinate to transition-metal ions strongly, and in the cases of some methionine complexes, the sulfur does not coordinate to metal ions.[8] However, at least the copper complexes seem to be S,O-coordinated complexes.[2] The order of the stabilities of various metal complexes of each alkylthioglycolic acid, as expected from the

8) M. V. Veidis and G. J. Palenik, *J. Chem. Soc., D*, **1969**, 1277.

Table 3. The maximum wave numbers and the absorption coefficients of the electronic spectra of some metal complexes

Figures are given in kK for wave numbers and log ε for intensities (in parentheses).

$Cu(n\text{-}PrS_1)_2\cdot 2H_2O$	35 90 (3.48)	28.20 (3.45)	15.15 (2.48)
$Cu(i\text{-}BuS_1)_2\cdot 2H_2O$	35.70 (3.52)	28.00 (3.52)	14.95 (2.35)
$Ni(n\text{-}PrS_1)_2\cdot 2H_2O$	39.50 (3.31)	25.15 (1.63)	14.71 (1.35)
$Ni(i\text{-}BuS_1)_2\cdot 2H_2O$	39.25 (3.28)	25.25 (1.58)	14.93 (1.62)
$Co(n\text{-}PrS_1)_2\cdot 2H_2O$	33.30sh(2.94)	20.20sh(1.62)	
$Co(i\text{-}BuS_1)_2\cdot 2H_2O$	33.30sh(2.95)	20.20sh(1.73)	

yields, the facility of their syntheses, and the resistivity to solvolysis in solution is: Cu>Ni, Co>Zn. Recently the stability constants of ethyl thioglycolates of copper, nickel, and zinc in aqueous solutions were studied; the order of their stabilities was Cu>Ni>Zn.[9] This order is similar to that of a series of complexes where the neutral sulfur atom of the ligand bonds with these metals to form a chelate ring.[10] Consequently, in the nickel and cobalt complexes, the sulfur atom bonds to the central metal less strongly and they are expected to be less stable than the copper complex. Moreover, as the zinc-sulfur bond is weaker, zinc complexes are more unstable and are hard to obtain by this method. As will be shown later, the infrared bands presumably identified as ν(M–S) bands seem to appear in the spectra of these complexes. Therefore, considering also the spectral data, although the possibility of the i) case cannot be completely rejected, the ii) case is more likely, even though the metal-sulfur bonds in these solid complexes are not very strong.

The absorption electronic spectra of ethanolic solutions of several complexes are given in Table 3.

As is shown in the table, when the central metal ion is the same, almost the same patterns of the spectra were obtained, even if different alkylthioglycolic acids are used as the ligands; the wave numbers and the log ε of the complexes of the same metals almost coincide with each other, within the limits of experimental error. The bands at about 15 and 25 kK of the nickel complexes are likely to be $^3A_{2g}\rightarrow{}^3T_{1g}$(F) and $^3A_{2g}\rightarrow{}^3T_{2g}$ (P)re-

Table 4. The wave numbers of the stretching bands of the carboxyl group and the metal-chalcogen bond (cm^{-1})

Ligand	Metal	$\nu(COO)_{asym}$	$\nu(COO)_{sym}$	ν(M–O)	ν(M–S)
	H	1710s	1422s		
H EtS_1	Cu	1614s	1443m	382s	238s
	Ni	1610s	1445w	363s	227s
	Co	1610s	1444m	365s	210m
	H	1708s	1420m		
H n-PrS_1	Cu	1590s	1460m	370s	245,224s
	Ni	1596s	1460m	365s	226s
	Co	1600s	1460s	365m	212s
	H	1710s	1424m		
H i-PrS_1	Cu	1588s	1460s	368s	242,223s
	Ni	1598s	1461,1442m	366s	236s
	Co	1575s	1457m	367s	228s
	H	1707s	1465,1420s		
H n-BuS_1	Cu	1590s	1463m	370s	225s
	Ni	1594s	1465m	362s	227s
	Co	1600s	1463m	360s	210s
	H	1706s	1460s		
H i-BuS_1	Cu	1566s	1460m	360s	223s
	Ni	1565s	1460sh	355s	223s
	Co	1575s	1460m	360s	209m
	H	1707s	1456m		
H s-BuS_1	Cu	1583s	1460,1452m	370s	238s
	Ni	1596s	1460,1452m	363s	227s
	Co	1600s	1460,1452m	365s	210m

s : strong, m: medium, w:weak.

9) A. Sandell, *Acta Chem. Scand.*, **24**, 1561, 1718 (1970).

10) K. Suzuki and K. Yamasaki, *J. Inorg. Nucl. Chem.*, **24**, 1093 (1962).

spectively.[11] The cobalt complexes seem to be solvolized in an ethyl alcohol solution; the solution is brown in color, and the maxima did not appear clearly, only some shoulders being observed. The shoulder near 20 kK is probably the $^4T_{1g}(F) \rightarrow {}^4T_{1g}(P)$ band.[12] Therefore, from the electronic spectra, at least the nickel species, and probably also the cobalt complex species in the solution, which is possibly in a form similar to that of the original complexes, are likely to be in the octahedral form. The bands in the 33—39 kK region seem to be the absorption of the ligand.

The infrared spectra of these compounds were examined. The general feature of the spectra in the fingerprint region (1300—700 cm^{-1}) are almost the same as those of each ligand. The anti-symmetric and symmetric bands of ν (COO) as well as the ν (M–O) and ν (M–S) bands of the complexes are shown in Table 4. The assignments of the bands were obtained with reference to the spectra of the other carboxylato complexes as well as to those of metal complexes of thio compounds.[13–16] Therefore, these assignments are only tentative. The wave numbers of the ν (M–O) and ν (M–S) bands of these complexes are a little lower than those of thioketonato or usual carboxylato complexes.[5,6] This is probably due to the weakness of the bond between the central metal ions and the chalcogen atoms of the ligands; really, the ν (M–S) band of the thiourea complexes, for example, appears in a lower wave-number region.[17]

The effect of the substitution of the alkyl group of alkylthioglycolic acid on the strength of the M–O bond may not be serious, but as the alkyl group is adjacent to the sulfur atom, the M–S bond is likely to be more affected by the substitution. In the case of silver complexes of alkylthioglycolic acids, their stability constants in the solution state are related to the Taft's σ^* functions of the alkyl groups.[5] However, probably because of the restriction from the crystal structure, the wave numbers of the bands of these stretching modes of these solid complexes do not have any clear relation to the σ^* functions of the alkyl groups.

The authors wish to express their appreciation to Professors Yukichi Yoshino and Kunihiko Watanuki, and also to their colleagues in their laboratory, for their helpful discussions.

11) J. R. Perumareddi, *Z. Naturforsch.*, **22**, B, 908 (1967).
12) R. L. Carlin, "Transition Metal Chemistry," Vol. 1, Marcel Dekker Inc., New York (1965), p. 3.
13) K. Nakamoto, "Infrared Spectra of Inorganic and Coordination Compounds," 2nd Ed., Wiley, New York (1969), p. 257, and also the 1st Ed., p. 201.
14) C. G. Barraclough, R. L. Martin, and I. M. Stewart, *Aust. J. Chem.*, **22**, 891 (1969).
15) M. Brierley, W. J. Geary, and M. Goldstein, *J. Chem. Soc., A*, **1969**, 2923.
16) E. J. Duff, M. N. Hughes, and K. J. Rutt, *ibid., A.* **1968**, 2354.
17) D. M. Adams and J. B. Cornell, *ibid., A*, **1967**, 884.

BULLETIN OF THE CHEMICAL SOCIETY OF JAPAN, VOL. 44, 734—737 (1971)

The Determination of Tin in Tin Metal and in Zircaloy by Precise Coulometric Titration

Takayoshi YOSHIMORI, Ikuko MATSUBARA, Tatsuhiko TANAKA, Kazuo YOSHIDA, Kazuo TANAKA, and Toyokazu TANABE

Faculty of Engineering, Science University of Tokyo, Kagurazaka, Shinjuku-ku, Tokyo

(Received October 12, 1970)

The purities of tin metals are determined directly by precise coulometric titration. The sample is dissolved with hydrochloric acid in a nitrogen atmosphere. The solution is then introduced into a hot antimony column. The reduced tin(II) ions are titrated with electrolytically-generated iodine. The titration is accomplished in a special cell by the use of which any disturbance of atmospheric oxygen is avoided. The titration efficiency under these acidic media was decreased when the current density was increased more than several mA/cm^2. The results obtained by two different analysts for the sample of the pure tin metal (5-nine) were 99.996 and 99.991%. The standard deviations of the results were 0.025 and 0.016% respectively. The tin in the other tin metals and in Zircaloy samples was determined satisfactorily without the use of any experimental factor.

The purity of a metal has generally been estimated by analyses of the impurities in the sample and then by the substraction of the sum of their contents from 100%.

In order to distinguish a sample of 99.9% purity from that 99.8% pure by the direct analysis of the bulk constituent, the relative error of the determination must be less than 0.05%. This is, however, less than the maximum accuracy of ordinary analytical methods.

The maximum accuracy of a precise coulometric titration is 0.003% as a standard deviation, while the value of 0.007% is obtained in ordinary laboratories.[1] This method has been used to estimate the purities of several primary standard substances for a volumetric method directly. The accuracy of this method, however, has not been yet used to estimate other metallic

1) T. Yoshimori and I. Matsubara, This Bulletin, **43**, 2800 (1970).

samples, *etc.*

Only one relevant report could be found in the literature; in it the purity of a tin metal was determined directly by the following volumetric method:[2] tetravalent tin was reduced to the divalent state with metallic nickel under a carbon dioxide atmosphere. Most of the tin(II) ions were then oxidized with an accurately-weighed amount of pure potassium iodate, while the remainder were titrated with a standard solution of potassium iodate. Because of the sensitiveness of tin(II) ions to the oxygen in air, this method sometimes gives lower results. A small amount of air on the surfaces of the potassium iodate crystals, and also the oxygen dissolved in the standard solution, may be introduced into the sample solution; they serve to oxidize the tin(II) ions.[3]

Caton and Freund[4] determined the content of tin in Zircaloy by coulometric titration. They used a hot antimony column for the reduction of tetravalent tin to the divalent state, and then titrated the tin(II) ions with electrolytically-generated iodine. Increasing the accuracy for the measurements of the electricity, the present authors determined the purities of several tin metals directly by precise coulometric titration using a biamperometric end-point location. Several improvements of the ordinary analytical treatments were necessary to obtain more accurate results.

Experimental

Apparatus. A sample tin metal was dissolved with hydrochloric acid under an atmosphere of nitrogen. The apparatus is shown in Fig. 1. Figure 2 shows in detail the antimony column used to reduce tin(IV) ions. The column was heated electrically with a flexible heater, while its temperature was controlled by the adjustment of the voltage applied to the heater.

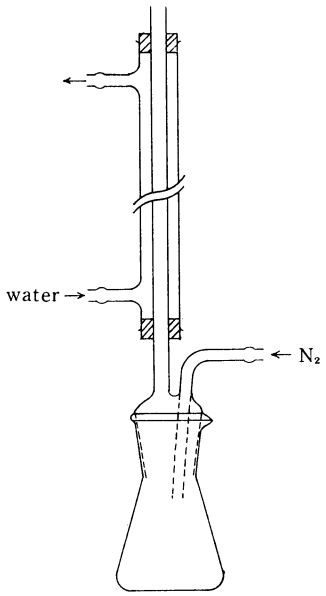

Fig. 1. Decomposition apparatus.

Figure 3 shows the coulometric titration cell. All the steps in the preparation of the electrolyte in the cell and in the washing of the cell could be performed without any disturbance of the atmospheric oxygen.

The chromium(II) chloride solutions were useful for removing traces of the oxygen in nitrogen (Fig. 4). The solutions and the liquid zinc amalgams were stirred continuously

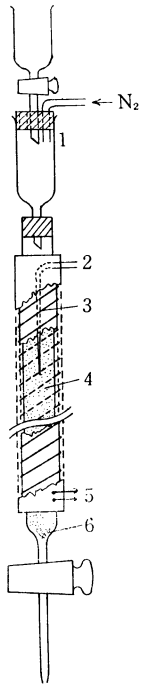

Fig. 2. Reduction column.

1. Funnel 2. Thermocouple 3. Heater
4. Antimony (20—30 Mesh) 5. To variable voltage supply 6. Glass wool

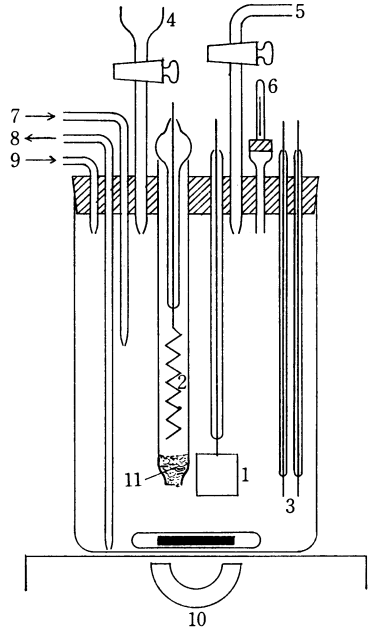

Fig. 3. Titration cell.

1. Generator electrode 2. Auxiliary electrode
3. Indicator electrodes 4. Reductor column
5. 1M KI solution inlet 6. Bunsen valve 7. N_2
8. To aspirator 9. Washing water
10. Magnetic stirrer 11. Silica gel membrane

2) S. Kalimann, *Anal. Chem.*, **22**, 729 (1950).
3) W. F. Hillebrand and G. E. F. Lundell, "Applied Inorganic Analysis," John Wiley, New York (1929), p. 239.
4) R. D. Caton and H. Freund, ASTM Special Technical Publication. No. 272, 207 (1959).

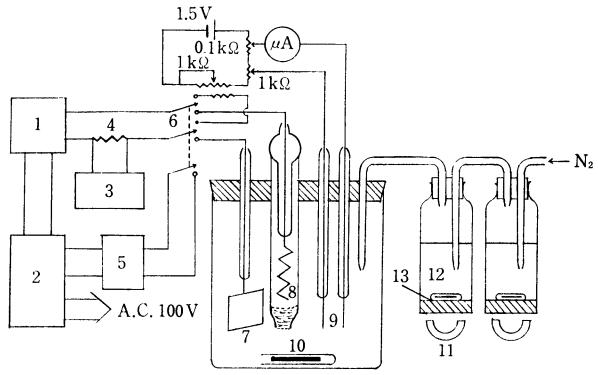

Fig. 4. Whole assembly.
1. Constant current source 2. Constant voltage source 3. Potentiometer 4. Standard resistor 5. Electronic stop watch 6. Switch 7. Generator electrode 8. Auxiliary electrode 9. Indicator electrodes 10. Titration cell 11. Magnetic stirrer 12. $CrCl_2$ solution 13. Liquid Zn amalgam

with magnetic stirrers. This stirring was advisable to keep the chromium ions under the divalent state.

A precise potentiometer and a standard resistor of 1 ohm were used to measure the electrolytic current. Their accuracies had been certified within 0.05% and 0.01% respectively. The constant-current source used here was the same instrument as that shown previously.[1,5] If we consider the errors of the above measuring devices as 3σ, a relative standard deviation of 0.02% may be expected for the measurement of the current, including the reliability of the standard cell used.

An electronic stop watch based on the frequency of a quartz crystal (Nippon Electric Co., Type 102) was used to measure the time of the electrolysis. The relative error, based on the time measurement, did not exceed 0.01%.

The "dead-stop" method using a microammeter (fullscale 10 μA) was used to locate the end-point of the titration. The whole assembly of the apparatus is illustrated in Fig. 4.

The indicator electrodes were frequently washed by dipping them into concentrated nitric acid for 20 minutes. Platinum foil (about 114 cm^2) was used as the generating electrode.

A silica-gel diaphragm[6] was advisable for the present purposes. It was prepared by the following procedure: glass wool was packed tightly at the bottom of the cathode compartment and then soaked in a sodium silicate solution (50%). Hydrochloric acid (3N) was then repeatedly introduced into the compartment until the acid did not leak through the diaphragm. The diaphragm was stored in hydrochloric acid (3N) and could be used several times.

The other precautions in measuring the electricity and the weighing of the sample were the same as those reported previously.[1]

Reagents. All the reagents were of an analytical grade, and all were used without further purification. The antimony metal (20—30 mesh) was washed with boiling 3N hydrochloric acid and then packed in a glass tube (Fig. 2). The purity of the metal was higher than 99.9%.

Procedure. *Dissolution of the Sample*: A sample tin metal was weighed into the decomposition flask (Fig. 1). Nitrogen was allowed to flow through the flask to remove the atmospheric oxygen. Then 20 m*l* of concentrated hydrochloric acid was added; a reflux condenser was necessary to prevent any loss of tin tetrachloride.

The addition of a small piece of an antimony metal to the flask was advisable in order to dissolve the pure samples more quickly. If necessary, the flask was warmed gently. When any black residue was found in the flask, a drop of a hydrogen peroxide solution (30%) was added to the flask and the solution was heated more gently. In this case, the introduction of the nitrogen was unnecessary. Zircaloy samples were placed in a Kjeldahl flask and then dissolved with hot hydrochloric acid and with the drop-by-drop addition of hydrofluoric acid.

After the dissolution of the sample was complete, the solution was cooled to room temperature under an atmosphere of nitrogen.

Preparations of Column and Cell: The solution in the column was boiled for 20 min. Oxygen-free nitrogen was then allowed to flow through the cell. After the temperature of the column had been adjusted to about 100°C, the column was washed with about 50 m*l* of 3N hydrochloric acid. Then the washings in the cell was removed carefully with an aspirator, avoiding any introduction of atmosperic oxygen into the cell. From this period to the end of the titration, the purified nitrogen should be allowed to flow through the cell continuously at a rate of about 150 m*l* per min.

Twenty milliliters of concentrated hydrochloric acid and 50 m*l* of a 1M potassium iodide solution freed from atmospheric oxygen were added to the cell from their reservoirs. Pure nitrogen was introduced into the solution for more than 30 min, and then the gas was allowed to flow over the solution to prevent any spattering of the solution in the cell. If the hydrochloric acid or the potassium iodide solution contained any oxidizing materials (for example, dissolved oxygen or chlorine), some iodine was produced in the mixture. The error based on this iodine could be corrected by reading the indicator current during this period and by continuing the coulometric titration to the point which the indicator current after the end-point was again raised to the same value as in the previous measurement.

Reduction of the Tin(IV) Ion and Coulometric Titration: A sample solution prepared as above was poured into the funnel on the column and then allowed to flow through the column at a rate of 1 ml/min. The flask and the column were washed thoroughly with 150 m*l* of 3N oxygen-free hydrochloric acid.[7] This was done by the introduction of the nitrogen over the solution on the top of the column.[8] From the last period of the washing, the tin(II) ions could be titrated with the coulometrically-generated iodine. During the titration, the generator current was kept constant. This method has already been described elsewhere.[1]

After the end-point, the indicator current began to rise. At this moment, the generator current was stopped; then both the indicator current and the time of the electrolysis were recorded. Again the solution was titrated for a short period, after which both the indicator current and the time were recorded. This short-period titration was repeated several times in order to obtain the titration curve clearly.

Results and Discussion

Dissolution of the Sample. The sample was dissolved in various kinds of glassware. A fairly large loss of tin ions by the spattering or by the vaporization of tin(IV) chloride was found even by the use of a

5) T. Yoshimori, Y. Hino, and T. Takeuchi, *Bunseki Kagaku*, **15**, 1234 (1966).
6) G. Marinenko and J. K. Taylor, *J. Research Natl. Bur. Standards*, **67A**, 453 (1963).
7) M. A. Salam Khan and W. I. Stephen, *Anal. Chim. Acta*, **41**, 43 (1968).
8) C. Yoshimura, *Nippon Kagaku Zasshi*, **74**, 818 (1953).

tall-form beaker or an Erlenmeyer flask. These losses of tin were overcome by the introduction of nitrogen into the flask to prevent the oxidation of the tin(II) ions. The dissolution time for the sample of high purity was shortened considerably by the addition of a piece of an antimony metal to the flask.

Column and Its Use. Instead of the antimony column, several other metals have been used for the reduction of tetravalent tin. Aluminum, iron, and nickel, however, all have relatively low hydrogen overvoltages and produce much hydrogen during the reduction process. Therefore, none of them can be used as the constituent of the column. Lead is sometimes used as the reducing material for the tin(IV) ion. This metal, however, was not adopted for the present purpose because lead ions dissolved in the solution produce lead chloride as a precipitate.[4]

Antimony was thus chosen as the constituent of the column. The flow rate of the sample solution was adjusted between 0.5 m*l*/min and 1 m*l*/min so as to accomplish the complete reduction of the tin(IV) ions.

The ordinary reduction procedure by boiling with metals was not successful because the introduction of air into the tin(II) solution was unavoidable during the process of separating the residual metals from the solution, and also while setting up the cell for the coulometric titration. The residual metals in the solution reduced the excess iodine generated after the endpoint and disturbed the location of the point.

Analysis of Pure Tin Metal (five-nine). A commercially-obtainable tin metal (so-called five-nine) was analyzed by the proposed method. The results of the analysis of the impurities obtained by the authors and by the producer are shown in Table 1. The purities obtained by this method are tabulated in Table 2. The relative standard deviation, as calculated from these results, was less than 0.02%.

Current Efficiency: First, the current density for the generation of the titrant was 13.3 or 8.8 mA/cm^2. In this case, the results obtained were rather high. This indicates that the titration efficiency of tin(II) ions with the electrolytically-generated iodine is less than 100% in this electrolyte.

Marinenko and Taylor[10] measured the current efficiencies for the generation of iodine in various solutions and showed that the efficiencies were somewhat decreased in acidic solutions. Recently Iritani *et al.*, in potentiometrically titrating mixtures of iodide ions and iodine with a potassium iodate standard solution in acidic media, they found that iodine monochloride was formed in the media with more than 3N hydrochloric acid.[11] With the current densities of *ca.* 10 mA/cm^2, some iodine monochloride may perhaps be formed; its current efficiency is unknown.

With reference to the results shown in Table 2, the authors considered that the titration efficiency of tin(II) ions with the electrolytically-generated iodine was 100% when the current density was kept below 1 mA/cm^2.

Oxygen in the Washing Solution: The oxygen in the washings produces hydrogen peroxide by reacting with the antimony in the column[7] and oxidizes the tin(II) ions. This disturbance can be avoided by the introduction of pure nitrogen into the solution on the top of the column.

Coulometric Titration of Several Tin Metals. The purities of the tin metals of various grades were analyzed by the proposed method. The results obtained are shown in Table 3. It can be concluded from these results that the proposed method is satisfactory for estimating the purities of various tin metals directly.

Table 1. Some analytical results of pure tin metals (5-nine) (ppm)

Pb[a]	Cu[a]	O[b]	H[c]	Total sum
1	<1	8	1.1	11

a) Obtained from the producer (spectroscopic method).
b) Obtained in the authors' laboratory by a carrier gas method.
c) The same as b, *cf.* Ref. 9.

Table 2. Direct determination of purity of the pure tin metal (5-nine) (Diaphragm: Silica gel)

Current density (mA/cm^2)	No. of exp.	Purity (%)	σ(%)
1	18	99.945[a]	0.028[b]
13	2	100.055	0.070
9	6	100.028	0.051
0.9	9	99.996[c]	0.025[b]
0.9	6	99.991[c]	0.016

a) Diaphragm was tissur membrane.
b) $\sqrt{V}$ value.
c) Obtained by the different analyst.

Table 3. Analytical results of tin metals and zircaloy samples

Sample	No.of Exp.	Sn Content (%)	σ(%)
Sn (99.7%)[a]	4	99.670	0.034
Sn (99.9%)[a]	3	99.907	0.024
Zircaloy 1	3	1.491	0.004
Zircaloy 2	3	2.148	0.003
Zircaloy 3	3	1.540	0.005
Zircaloy 4	4	0.875	0.005

a) Shown by the producer.

Determination of Tin in Zircaloy. The tin contents in Zircaloy samples were also determined by means of the authors' apparatus. The samples were dissolved in a Kjeldahl flask with hydrochloric and hydrofluoric acids. The results are shown in Table 3. The errors of the results are diminished considerably compared with the case of the value obtained previously.[4]

When the results were compared with those obtained in other laboratories, these values were found to be the highest. The authors believe that the difference shows the effect of the atmospheric oxygen on the tin(II) ions in the other volumetric procedure.[3]

The authors express their sincere thanks to Professor S. Hirano (Toyo University) and Professor T. Takeuchi (Nagoya University) for their valuable suggestion.

9) T. Yoshimori and S. Ishiwari, *Talanta*, **17**, 349 (1970).

10) G. Marinenko and J. K. Taylor, *Anal. Chem.*, **39**, 1568 (1967).

11) N. Iritani, Y. Takino, and N. Kuroda, *Bunseki Kagaku*, **18**, 583 (1969).

Studies on Cobaloxime Compounds. II. Catalytic Activity of Cobaloximes in the Hydrogen Peroxide Decomposition Reaction

Yorikatsu HOHOKABE and Noboru YAMAZAKI

Department of Polymer Science, Faculty of Engineering, Tokyo Institute of Technology, Ookayama, Meguro-ku, Tokyo

(Received October 15, 1970)

Various cobaloximes with the general formula $[CoX(DH)_2B]$ (X: Cl, CN, OH, or CH_3. DH: Dimethylglyoximato monoanion. B: Bases such as water, nicotinamide, pyridine, imidazole, or a low molecular weight copolymer of acrylamide and 4-vinylpyridine, *etc.*) were examined for catalytic activity in the H_2O_2 decomposition reaction. Cyanocobaloximes have less activities than other cobaloximes. The effect of changing the axial bases of cobaloximes was found to be small. When methylcobaloxime was used as a catalyst, the lag time was observed in the dark, while with the irradiation of visible light the reaction proceeded without induction period. An extensive study on chloroaquocobaloxime revealed that the rate is proportional both to the concentration of H_2O_2 and to the concentration of cobaloxime and inversely proportional to $[H^+]$. It was found that the decomposition of H_2O_2 with cobaloximes proceeds with a gradual and partial degradation of cobaloximes.

The decomposition of hydrogen peroxide catalyzed by metal ions has been widely investigated,[1] but the mechanisms have not yet been clarified. A few cobaloximes have been briefly investigated for catalytic activity in the H_2O_2 decomposition reaction by Sasaki and Matsunaga.[2] The catalytic activities decreased in the order $CoCl(DH)_2$P-4VP$>CoCl(DH)_2$Pyr$\gg$Co(CN)-$(DH)_2$P-4VP$>$Co(CN)$(DH)_2$Pyr, where P-4VP means poly-4-vinylpyridine and Pyr pyridine. No study has been reported on the kinetics of the H_2O_2 decomposition reaction catalyzed by cobaloximes.

In this work, the H_2O_2 decomposition reactions with various cobaloximes were investigated and results similar to those of Sasaki[2] were obtained in the case of chloro- and cyano-cobaloximes. Results of other cobaloximes and kinetic studies are also described.

Experimental

Materials. *Preparation of $CoCl(DH)_2$(Copoly—AM-VPy)*: To a hot methanolic solution of 0.39 g (3.4 mmol) of dimethylglyoxime (30 m*l*), 0.40 g (1.7 mmol) of $CoCl_2 \cdot 6H_2O$ in 30 m*l* of methanol was added with stirring. After an hour, an aqueous solution of 1.00 g of a copolymer of acrylamide and 4-vinylpyridine (Copoly—AM-VPy: $\bar{M}n = 1.6 \times 10^3$, AM/VPy molar ratio = 14.3) was added with stirring for an hour. The brown filtrate transparent solution was concentrated under a reduced pressure to precipitate a small amount of unreacted dimethylglyoxime, which was removed by filtration. The brown filtrate was evaporated to dryness in a vacuum. 1.28 g of green residue was obtained. It was dissolved in 20 m*l* of water to yield a brown solution, which was applied on a Sephadex LH-20 column (3.0×37.5 cm). By evaporating the first fraction to dryness, 0.86 g of a polymeric cobaloxime, $CoCl(DH)_2$-(Copoly—AM-VPy) free from monomeric cobaloximes was recovered. From Co analysis, the compound was found to contain 1.8 wt% of Co which corresponds to 41% of the degree of coordination of the pyridine residues in polymeric ligand. The degree of coordination indicates the mole percentage of the cobaloxime moiety per pyridine residue of Copoly—AM-VPy. The brown powder obtained became insoluble after evaporation to dryness. It shows infrared absorption bands at 1238 cm^{-1} (ν_{N-O}), 1090 cm^{-1} (ν_{N-O}), *ca.* 1070 cm^{-1}, 980 cm^{-1}, 860 cm^{-1}, and 512 cm^{-1} (ν_{Co-N}) due to cobaloxime moiety.[3]

Other Materials: The synthesis of other cobaloximes examined in this work was previously reported.[3] The stock hydrogen peroxide was 30% stabilizer-free supplied from Mitsubishi Edogawa Kagaku Co., Ltd. Analytical-grade 0.1N potassium permanganate solution was diluted 10 times to yield 0.01N solution for the titration of the residual hydrogen peroxide in the reaction mixture. Other reagents were obtained from commercial sources and used without further purification.

Methods. A typical procedure is as follows. To an appropriate amount of cobaloxime solution, 5 m*l* of 1M potassium phosphate buffer, a minimal amount of PNE[4] if necessary, and distilled water were added to bring the total volume to 50.0 m*l*. Then, 1.0 m*l* of 3% hydrogen peroxide was added to the mixture. The reaction was usually conducted at 40°C. Aliquots, *e.g.*, 5 m*l*, were taken for analysis at appropriate times. Five milliliters of 9N sulfuric acid was added to the aliquot to stop decomposition, and the residual hydrogen peroxide was titrated with a 0.01N $KMnO_4$ solution. Since there were lag times in some cases as described below, the reaction rates were calculated from the slopes of the time conversion plots at the half-decomposition point.

Spectroscopic Measurements. An aliquot of the reaction mixture was used for the visible spectrum and was diluted 20 times for the ultraviolet spectrum, which was taken with a Shimadzu automatic recording spectrophotometer type SV-50A. Infrared spectrum was taken with a JASCO infrared spectrophotometer, model IR-G.

Results and Discussion

In order to examine the difference in catalytic activity in relation to several axial ligands of cobaloximes, the decomposition reactions of hydrogen peroxide were carried out in the presence of various cobaloximes. Typical time-conversion curves of several cobaloximes are shown in Fig. 1, which shows the presence of a lag time that differs in each case. The decomposition rates were therefore calculated from the slopes of the curves at the half-decomposition point, shown in Table 1. As can be seen in Table 1, cyanocobaloximes have less activities than other cobaloximes in the decomposition

1) J. H. Baxendale, "Advances in Catalysis and Related Subjects," Vol. IV, Academic Press, New York (1952), pp. 31—86.
2) T. Sasaki and F. Matsunaga, This Bulletin, **41**, 2440 (1968).
3) N. Yamazaki and Y. Hohokabe, *ibid.*, **44**, 63 (1971).
4) PNE is a polyoxyethylene nonylphenol ether $P = 10$, known as a non-ionic surface activating reagent.

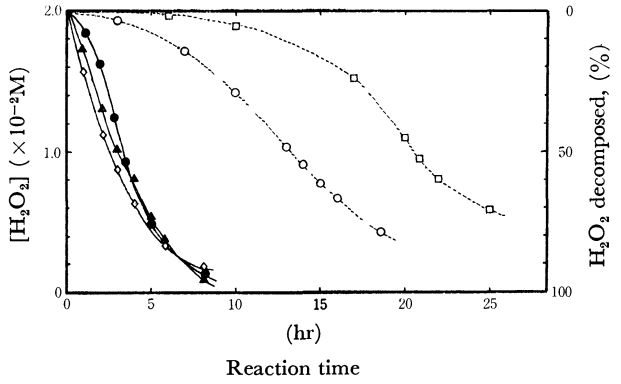

Fig. 1. H_2O_2 decomposition-time profiles catalyzed by several cobaloximes.
$[H_2O_2]_0=2.0\times10^{-2}$ M, $[CoX(DH)_2B]=3.92\times10^{-4}$ M, in 0.1 M potassium phosphate buffer (pH 7.2), 40°C.
[X, B]: —●— (Cl, pyridine); ···○··· (CN, pyridine); —▲— (Cl, H_2O); ···□··· (CN, *p*-toluidine); —◇— ($CoCl_2\cdot6H_2O$).

Table 1. H_2O_2 decomposition rates[a] with various cobaloximes

$[H_2O_2]_0=2.0\times10^{-2}$M, $[Co]=3.92\times10^{-4}$ M, in 0.1M potassium phosphate buffer (pH 7.2), 40°C

$CoX(DH)_2B$ X——B	Decomposition rate ($\times10^{-3}$M/hr)
Cl——pyridine[b]	3.9
Cl——nicotinamide[b]	3.5
Cl——H_2O[b]	3.4
Cl——γ-picoline[b]	3.4
Cl——*p*-toluidine[b]	3.2
Cl——imidazole[b]	3.1
Cl——Copoly—AM-VPy[b]	3.0
OH——H_2O	3.3
OH——Copoly—AM-VPy[b]	3.2
CH_3——γ-picoline[b]	3.3
CH_3——H_2O	3.5(Light[c]), 3.3(Dark)
CN——*p*-toluidine[b]	1.5
CN——pyridine[b]	1.3
$CoCl_2\cdot6H_2O$	3.3

a) At the half-decomposition point, *i. e.*, at the H_2O_2 concentration of 1.0×10^{-2}M.
b) A minimal amount of PNE was added.
c) Irradiated during the course of reaction.

reaction of H_2O_2. Among chlorocobaloximes, the difference in catalytic activity was rather small, and the activity was not in the reasonable order of the axial base such as that of the strength of basicity. The polymeric ligand, Copoly-AM-VPy, *i. e.*, a low molecular weight copolymer of acrylamide and 4-vinylpyridine, exerted little change in the catalytic activity compared with other monomeric bases.

Since chloroaquocobaloxime has greater solubility than other chloro derivatives in aqueous medium, an extensive study on the kinetic behavior of the decomposition reaction was performed in the presence of chloroaquocobaloxime.

First, the dependence on pH (6.0—8.1) was investigated at a constant initial H_2O_2 concentration and a constant cobaloxime concentration. As shown in Fig. 2, the rate was inversely proportional to $[H^+]$, and the reaction order was observed to be −0.98 in $[H^+]$. This suggests that hydrogen peroxide reacts through the ion HO_2^-.

Dependence on the concentration of cobaloxime was then investigated at pH 6.8 and 7.2. The rate was proportional to the concentration of cobaloxime and the reaction order was 0.98 in it at pH 6.8 and 0.88 at pH 7.2 (Fig. 3).

Finally, a study of the dependence on the concentration of H_2O_2 revealed that the rate was 1.28 order in $[H_2O_2]$ at pH 7.2 (Fig. 4).

In another series, the activation energy was determined between 30°C and 45°C, and found to be 17.9 kcal/mol at pH 7.2.

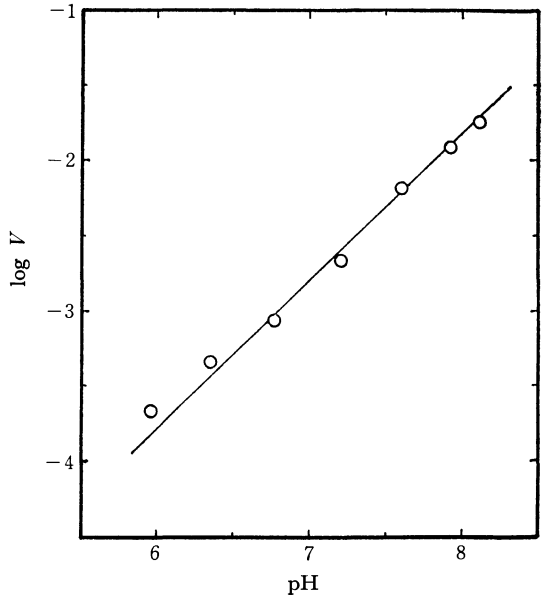

Fig. 2. pH dependence of the H_2O_2 decomposition rate with chloroaquocobaloxime.
$[H_2O_2]_0=2.0\times10^{-2}$M, $[CoCl(DH)_2(H_2O)]=3.92\times10^{-4}$ M, in 0.1 M potassium phosphate buffer, 40°C.
The reaction was so slow at lower pH that the rates at pH 5.96 and 6.35 for 3.92×10^{-4} M of cobaloxime were estimated as half of those at 7.84×10^{-4} M of cobaloxime.

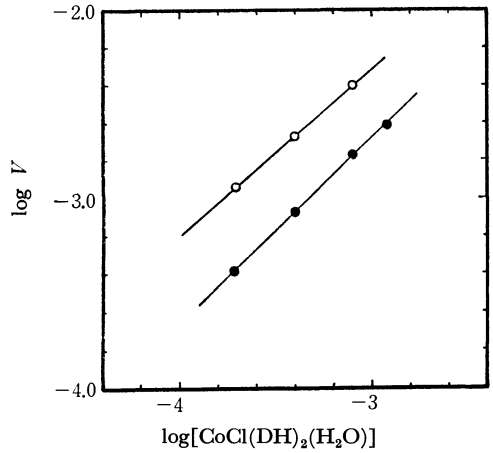

Fig. 3. Dependence of the H_2O_2 decomposition rate upon the concentration of chloroaquocobaloxime.
$[H_2O_2]_0=2.0\times10^{-2}$ M, in 0.1 M potassium phosphate buffer (—○—, pH 7.2; —●—, pH 6.8), 40°C.

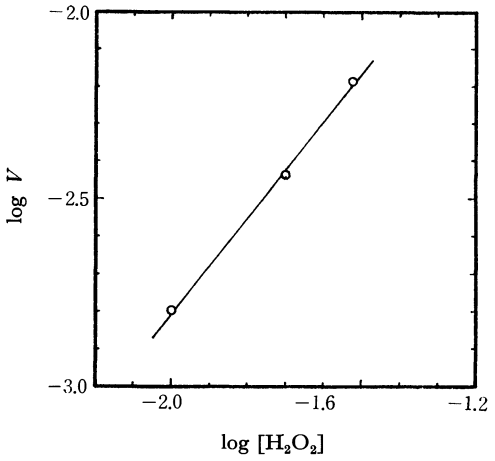

Fig. 4. Dependence of the H_2O_2 decomposition rate upon the concentration of H_2O_2.
$[CoCl(DH)_2(H_2O)]=3.92\times10^{-4}$ M, in 0.1 M potassium phosphate buffer (pH7.2), 40°C.

The results can be summarized in the following equation for the decomposition rate of H_2O_2:

$$V=-\frac{d[H_2O_2]}{dt}=k\cdot\frac{[\text{Cobaloxime}][H_2O_2]}{[H^+]}.$$

A similar rate law was obtained in the reaction of cobaltic ion and H_2O_2 by Baxendale and Wells.[5] Since in our experiments cobaltous chloride which is considered to be oxidized to cobaltic ion in this experimental condition yielded the same rate without lag time as the cobaloximes, the active intermediates in the reaction with cobaloximes are estimated to have more than one free coordination site. Thus the presence of a lag time whose length differs in each case can be explained as follows: The hydroxide or chloride ligand is readily displaced by H_2O_2 or presumably HO_2^-, and hence hydroxo- or chloro-cobaloximes show little lag time, while a strongly coordinated cyano ligand is not readily displaced, resulting in the appearance of lag time.

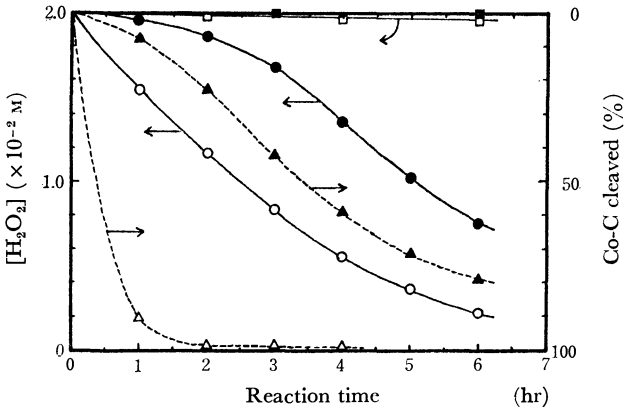

Fig. 5. H_2O_2 decomposition-time profiles with methylaquocobaloxime either in the dark or with irradiation and the Co-C cleavage of methylaquocobaloxime during the course of reactions.
$[H_2O_2]_0=2.0\times10^{-2}$ M, $[CH_3Co(DH)_2(H_2O)]=3.92\times10^{-4}$ M, in 0.1 M potassium phosphate buffer (pH 7.2), 40°C.
—●— H_2O_2 concentration in the dark.
—○— H_2O_2 concentration with irradiation.
—■— H_2O_2 concentration in the absence of cobaloxime in the dark (Blank).
—□— H_2O_2 concentration in the absence of cobaloxime with irradiation (Blank).
···▲··· Co-C cleavage in the dark.
···△··· Co-C cleavage with irradiation.

Methylaquocobaloxime yielded the same rate in the dark as that with the irradiation of visible light, which was performed at a distance of 15 cm with a 100 W tungsten lamp. The decomposition-time profile, however, was distinctly different as shown in Fig. 5. The lag time was observed in the dark, while with irradiation the reaction proceeded without induction period. The degree of the Co–C bond fission at the same time which was determined spectrophotometrically from the decrease in absorption at 443 mμ[6] is also given in Fig. 5. 78% of methyl-Co bond was cleaved by the decomposition reaction of H_2O_2 in the dark. However, the Co–C cleavage step is not considered to be the rate determining step, since the solution of methylaquocobaloxime irradiated prior to the addition of H_2O_2, which exhibits the absorption maximum at 246 mμ due to dimethylglyoximato ligand and is considered to contain hydroxoaquocobaloxime,[6] exerted the same rate in the H_2O_2 decomposition reaction as methylaquocobaloxime in the dark. As the reaction proceeds, the gradual decrease in absorption occurs at a wavelength longer than 230 mμ up to the visible region.

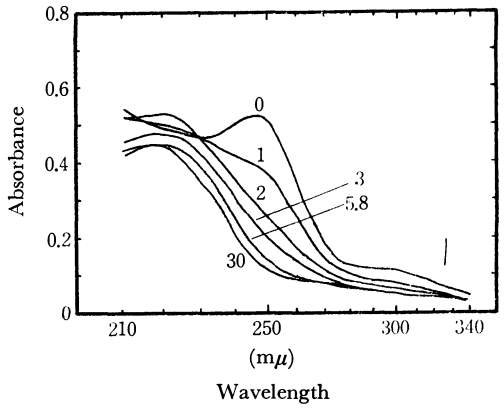

Fig. 6. UV spectral change during the course of the H_2O_2 decomposition reaction by chloroaquocobaloxime.
H_2O_2 decomposition reaction was conducted under the following conditions; $[H_2O_2]_0=2.0\times10^{-2}$ M, $[CoCl(DH)_2(H_2O)]=3.92\times10^{-4}$ M, in 0.1 M potassium phosphate buffer (pH 7.2), at 40°C.
Aliquots were taken after 1, 2, 3, 5, 5.8, and 30 hr, and diluted 20 times to obtain the spectra. At the same time, the percentages of the H_2O_2 decomposed were determined and found to be 14% (1 hr), 35% (2 hr), 49% (3 hr),81% (5.8 hr), and 100% (30 hr), respectively.

There is some indication in the UV spectra that the cobaloxime is transformed or degradated by H_2O_2. The spectral change during the course of the reaction with the preirradiated solution of methylaquocobaloxime as well as with chloroaquocobaloxime solution proceeded quite similarly (Fig. 6): The gradual decrease in ab-

5) J. H. Baxendale and C. F. Wells, *Trans. Faraday Soc.*, **53**, 800 (1957).

6) N. Yamazaki and Y. Hohokabe, "Studies on Cobaloxime Compounds. VI.," submitted to this Bulletin.

sorption occurs at a wavelength longer than 230 mμ up to the visible region with the progress of reaction. The absorption maximum at 246 mμ both in chloro- and hydroxo-aquocobaloximes decreased in intensity and the maximum shifted to *ca.* 220 mμ. Thus, the spectrum of the solution immediately after the addition of H_2O_2 did not differ from that before the addition of H_2O_2, but after an hour when 14—16% of H_2O_2 was decomposed, the absorption maximum at 246 mμ decreased to 65% in intensity and the new absorption maximum appeared at *ca.* 220 mμ. As the reaction further proceeded, the maximum at 246 mμ decreased gradually, but not that at 220 mμ. This seems to show that a partial decomposition of cobaloxime occurs. In fact, by concentrating the solution after the reaction, a trace of blue precipitate was recovered. This seemed to be an inorganic compound whose infrared spectrum is quite different from that of original or typical cobaloximes. The maximum at 220 mμ shifted to 275 mμ when solid alkali was added to the solution. Since dimethylglyoxime which has an absorption maximum at 224 mμ in acidic medium is known to shift the maximum to 265 mμ in alkaline medium,[7] the spectral change in the presence of alkali suggests that the solution contains some substance like oxime which can be dissociated in alkaline medium. This may be some form of cobaloxime or some degradation product.

Thus, it is concluded that cobaloximes catalyze the decomposition of H_2O_2, and they themselves are also gradually and partially degradated during the course of the reaction. The lower activity of cyanocobaloximes than hydroxo-, chloro-, or methyl-cobaloximes can be attributed to higher stability toward the reactant H_2O_2 than other cobaloximes due to stronger interaction of cyano group with Co. A mechanism has been proposed for the decomposition reaction with ferric ion,[8] in which the peroxide concentration was higher than ferric ion concentration. This can be applied to the reactions with cobaloximes. The primary active species reacting with cobaloximes seems to be HO_2^-, but not H_2O_2 as in the case of pentacyanocobaltate(II),[9] since the rate was inversely proportional to $[H^+]$. HO_2^- may coordinate with Co(III) species forming CoOOH by electron transfer from HO_2^- to Co(III). The presence of hydroperoxocobaloxime may be supported by Schrauzer's recent observation of the relative stable mononuclear peroxocobaloxime radicals.[10]

The authors are grateful to Mr. S. Imahashi for performing a part of this work.

7) K. Burger, I. Ruff, and F. Ruff, *J. Inorg. Nucl. Chem.*, **27**, 179 (1965).

8) F. Haber and J. Weiss, *Proc. Roy. Soc. (London)*, **A147**, 332 (1934).

9) P. B. Chock, R. B. K. Dewar, J. Halpern, and L-Y. Wong, *J. Amer. Chem. Soc.*, **91**, 82 (1969).

10) G. N. Schrauzer and L. P. Lee, *ibid.*, **92**, 1551 (1970).

BULLETIN OF THE CHEMICAL SOCIETY OF JAPAN, VOL. 44, 741—744 (1971)

The Preparation and the Structure of (1,9-Diamino-1,4,6,6,9-pentamethyl-3,7-diazanona-3-ene) (*l*-propylenediamine)nickel(II) Perchlorate

Haruko Ito and Junnosuke Fujita

Department of Chemistry, Faculty of Science, Tohoku University, Sendai

(Received October 24, 1970)

A new purple complex of (1,9-diamino-1,4,6,6,9-pentamethyl-3,7-diazanona-3-ene)(*l*-propylenediamine)nickel-(II) perchlorate and the known yellow complex, (octamethyl-1,4,8,11-tetraazacyclotetradecadiene)nickel(II) perchlorate, were obtained by the reaction of tris(*l*-propylenediamine)nickel(II) perchlorate and acetone without any irradiation by ultraviolet light. The structure of the purple complex was estimated from its absorption and circular dichroism spectra in acetonitril and in an aqueous solution, and from its infrared spectrum in the solid state. The complex was found to take an octahedral $[NiN_6]$-type structure in acetonitril and a planar $[NiN_4]$-type structure in aqueous solution. The (1,9-diamino-1,4,6,6,9-pentamethyl-3,7-diazanona-3-ene)nickel(II) perchlorate and (1,9-diamino-1,4,6,6,9-pentamethyl-3,7-diazanona-3-ene)(ethylenediamine)nickel(II) perchlorate complexes were also prepared.

Since it was reported that tris(ethylenediamine)-nickel(II) perchlorate reacts with acetone to form macrocyclic complexes,[1] a number of analogous complexes have been prepared from various metal-amine complexes and ketones or aldehydes.[2] Some of these complexes have geometrical and/or optical isomers, depending on the positions of such substituents as methyl groups. Curtis *et al.* prepared, for example, two non-interconvertible, isomeric (octamethyl-1,4,8,11-tetraazacyclotetradecadien)nickel(II) perchlorates (yellow and orange) by irradiating an acetone solution of tris(*d,l*-propylenediamine)nickel(II) perchlorate with ultraviolet light for several days.[3] Although there are many isomerisms in this ligand, they showed, by X-ray

1) N. F. Curtis, *J. Chem. Soc.*, **1960**, 4409; N. F. Curtis, Y. M. Curtis, and H. K. J. Powell, *J. Chem. Soc. A*, **1966**, 1015.

2) N. F. Curtis, *Coord. Chem. Rev.*, **3**, 3 (1968).

3) M. M. Blight and N. F. Curtis, *J. Chem. Soc.*, **1962**, 1204.

analysis,[4] that both isomers have two imino-groups in *trans* positions, but that the two asymmetric carbon atoms of the yellow isomer are racemic (*d,d* or *l,l*), while those of the orange isomer are meso (*d,l*) (Fig. 1). In fact, only the yellow isomer was produced by the reaction of the optically-active tris (*d* or *l*-propylenediamine)-nickel(II) perchlorate and acetone.

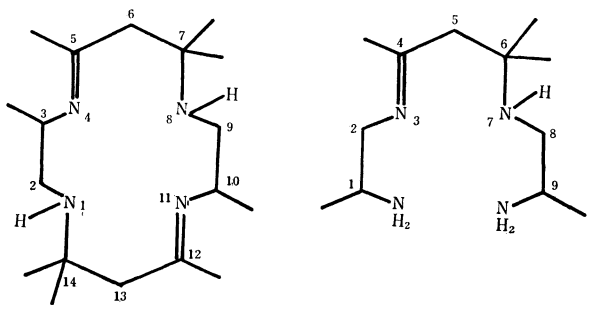

$C_{18}H_{36}N_4$ $C_{12}H_{28}N_4$

Fig. 1.

During our study of the effect of methyl groups on the conformation of five- and six-membered chelate rings of metal complexes,[5] we obtained a new purple complex as well as the above yellow complex from the tris(*l*-propylenediamine)nickel(II) perchlorate and acetone without any irradiation by ultraviolet light. This paper will deal with the chemical properties and structure of this purple complex.

Experimental

Preparations. *l*-Propylenediamine was obtained by resolving its commercial racemate according to Dwyer's method.[6]

(1,9-Diamino-1,4,6,6,9-pentamethyl-3,7-diazanona-3-ene)(l-propylenediamine)nickel(II) perchlorate, $[Ni(C_{12}H_{28}N_4)(l\text{-pn})](ClO_4)_2$: An acetone solution (about 100 m*l*) containing 10 g of $[Ni(l\text{-pn})_3](ClO_4)_2$ was kept at room temperature in a stoppered container. After about two weeks, the purple crystals which had deposited were filtered off and recrystallized from hot water.

The filtrate was kept several more days at room temperature, air-dried until the residue was almost free from acetone, and filtered. A mixture of purple and yellow crystals was then obtained by treating the residue with a small amount of acetone. This mixture can be separated by fractional recrystallization from hot water, because the purple crystals are slightly more soluble in hot water. Recrystallization was effected by adding an aqueous *l*-propylenediamine to the warm aqueous solution from which the yellow crystals had been removed by filtration. Purple complex: Found: C, 31.93; H, 6.76; N, 14.71%. Calcd for $NiC_{15}H_{38}N_6Cl_2O_8$: C, 32.17; H, 6.84; N, 15.00%. The results of the chemical analysis indicated that the yellow complex is the $[Ni(C_{18}H_{36}N_4)](ClO_4)_2$ reported by Curtis *et al.*[4]

(1,9-Diamino-1,4,6,6,9-pentamethyl-3,7-diazanona-3-ene)nickel(II) perchlorate monohydrate, $[Ni(C_{12}H_{28}N_4)](ClO_4)_2 \cdot H_2O$: An aqueous solution of $[Ni(C_{12}H_{28}N_4)(l\text{-pn})](ClO_4)_2$ was passed through a cation-exchange column in the Na-form. The column was washed well with water, and the adsorbed yellow band was eluted with a 12% aqueous sodium perchlorate solution. The eluate was concentrated at 50°C under reduced pressure. Yellow crystals were obtained by cooling the solution in a refrigerator.

Found: C, 28.53; H, 5.70; N, 10.94%. Calcd for $NiC_{12}H_{30}N_4Cl_2O_9$: C, 28.60; H, 6.00; N, 11.11%.

(1,9,-Diamino-1,4,6,6,9-pentamethyl-3,7-diazanona-3-ene)(ethylenediamine)nickel(II) perchlorate, $[Ni(C_{12}H_{28}N_4)(en)](ClO_4)_2$: To a concentrated solution of the above eluate, an aqueous ethylenediamine was added, drop by drop. The purple crystals were recrystallized from hot water.

Found: C, 30.31; H, 6.88; N, 14.79%. Calcd for $NiC_{14}H_{36}N_6Cl_2O_8$: C, 30.79; H, 6.64; N, 15.39%.

Measurements. The absorption (AB) and circular dichroism (CD) spectra in the near-infrared region (1400—700 mμ) were obtained with a Hitachi EPS-3 Recording Spectrophotometer and a Shimadzu QV-50 Spectrophotometer with its CD attachment, respectively. The AB and CD spectra in the visible and ultraviolet region (700—200 mμ) were recorded with a Hitachi 124 Spectrophotometer and a Jasco ORD/UV-5 Spectrophotometer with its CD attachment, respectively. The infrared (IR) spectra in the NaCl region were obtained using a Hitachi EPI-2G Infrared Spectrophotometer. All the measurements were made at room temperature.

Results and Discussion

Figure 2 compares the AB and CD spectra of $[Ni(C_{18}H_{36}N_4)](ClO_4)_2$ (the yellow complex (I)) and

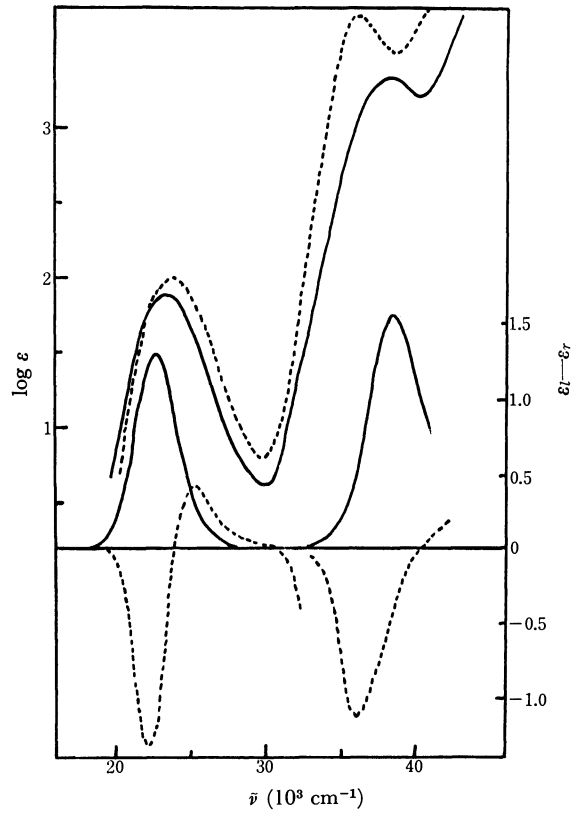

Fig. 2. AB and CD spectra of $[Ni(C_{18}H_{36}N_4)](ClO_4)_2$ (·····) and $[Ni(C_{12}H_{28}N_4)(l\text{-pn})](ClO_4)_2$ (——) in water.

4) N. F. Curtis, D. S. A. Swann, T. N. Waters, and I. E. Maxwell, *J. Amer. Chem., Soc.*, **91**, 4588 (1969).

5) S. Yano, H. Ito, Y. Koike, J. Fujita, and K. Saito, This Bulletin, **42**, 3184 (1969); F. Mizukami, H. Ito, J. Fujita, and K. Saito, *ibid.*, **43**, 3633 (1970).

6) F. P. Dwyer, F. L. Garvan, and A. Shulman, *J. Amer. Chem. Soc.*, **89**, 5780 (1967).

Table 1 (a). AB and CD data in water

Complex[a)]	ν_{max}(log ε)	$\nu_{ext}(\Delta\varepsilon_{ext})$	ν_{max}(log ε)	$\nu_{ext}(\Delta\varepsilon_{ext})$
I	23.7(1.99)	22.5(−1.31) 25.3(+0.41)	35.7(3.72)	36.1(−11)
II	23.2(1.88)	22.7(+1.30)	37.9(3.31)	38.5(+ 1.7)
III	23.2(1.89)	22.7(+1.50)	37.9(3.29)	38.5(+ 1.8)

Table 1 (b). AB and CD data in acetonitril

Complex[a)]	ν_{max}(log ε)	$\nu_{ext}(\Delta\varepsilon_{ext})$	ν_{max}(log ε)	$\nu_{ext}(\Delta\varepsilon_{ext})$	ν_{max}(log ε)	$\nu_{ext}(\Delta\varepsilon_{ext})$
II	10.9(1.06)	9.9(−0.07) 11.5(+0.24)	18.2(0.97)	18.4(−0.04)	29(sh)	29(−)
IV	10.8(0.98)	9.6(−0.06) 11.5(+0.20)	18.1(0.89)	18.5(−0.03)	29(sh)	29(−)
V	11.1(0.84)	10.3(−0.15) 12.2(+0.10)	18.2(0.80)	17.7(−0.02)	28.8(0.94)	29.4(−0.01)

ν in cm^{-1}; sh shoulder

a) Complexes (I) $=[Ni(C_{18}H_{36}N_4)](ClO_4)_2$; (II) $=[Ni(C_{12}H_{28}N_4)(l\text{-pn})](ClO_4)_2$; (III) $=[Ni(C_{12}H_{28}N_4)](ClO_4)_2\cdot H_2O$; (IV) $=[Ni(C_{12}H_{28}N_4)(en)](ClO_4)_2$; (V) $=Ni[(l\text{-pn})_3](ClO_4)_2$

$[Ni(C_{12}H_{28}N_4)(l\text{-pn})](ClO_4)_2$ (the purple complex (II)) in water. The purple complex (II) gives a yellow aqueous solution, and its AB spectrum exhibits a pattern typical of a planar $[NiN_4]$-type complex. The purple complex was formed again by the addition of *l*-propylenediamine to the yellow aqueous solution. When the aqueous solution of the purple complex (II) was passed through a cation-exchange column in the Na-form, a yellow band was adsorbed and the eluate was basic. The yellow band was eluted with a 12% aqueous sodium perchlorate solution, and the eluate was concentrated at 50°C under reduced pressure. On cooling, a yellow complex with the composition of $[Ni(C_{12}H_{28}N_4)](ClO_4)_2\cdot H_2O$ (III) was obtained. The AB and CD spectra of this compound was almost the same as those of the purple complex (II) in water. The addition of aqueous *l*-propylenediamine to the concentrated eluate gave purple crystals which showed the same IR spectrum as that of the original purple complex (II). Purple $[Ni(C_{12}H_{28}N_4)(en)](ClO_4)_2$ (IV) was precipitated by adding aqueous ethylenediamine to the concentrated yellow eluate. These results indicate that the following equilibrium exists in an aqueous solution:

$$[Ni(C_{12}H_{38}N_4)(l\text{-pn})]^{2+} \rightleftarrows [Ni(C_{12}H_{38}N_4)]^{2+} + l\text{-pn}$$

The AB and CD spectra of the purple complex (II) in acetonitril (purple solution) are compared with those of $[Ni(l\text{-pn})_3](ClO_4)_2$ in Fig. 3. The complex (II) exhibits three absorption peaks at 10900, 18200, and about 29000 cm^{-1}; they correspond to those of the latter complex. This result indicates that the purple complex (II) exists as an octahedral $[NiN_6]$-type complex in acetonitril. A weak peak at about 23000 cm^{-1} seems to come from the planar complex (III) partly formed in this solvent. From the intensity of this absorption band, the quantity of the planar complex is estimated to be only several percent. The AB and CD data are summarized in Table 1. The AB and CD spectra of $[Ni(C_{12}H_{28}N_4)(en)](ClO_4)_2$ are quite similar to those of the corresponding *l*-propylenediamine complex.

The strong band around 36000—38000 cm^{-1} of $[Ni(C_{18}H_{36}N_4)](ClO_4)_2$ (I), $[Ni(C_{12}H_{28}N_4)(l\text{-pn})](ClO_4)_2$ (II) (in water), and $[Ni(C_{12}H_{28}N_4)](ClO_4)_2$ (III) can be attributed to the C=N double bond in the ligands.[1] The absorption intensity of the complex (I) in this region is about twice as strong as those of the complexes (II) and (III), indicating that the ligand $C_{12}H_{28}N_4$ has one C=N double bond.

The IR data of the complexes in the 1600-cm^{-1} region are given in Table 2. The bands at 1603 and 1585 cm^{-1} of $[Ni(l\text{-pn})_3](ClO_4)_2$ can be assigned to the NH_2-deformation vibrations and the band at 1653 cm^{-1} of $[Ni(C_{18}H_{36}N_4)](ClO_4)_2$ (I), to the C=N stretching

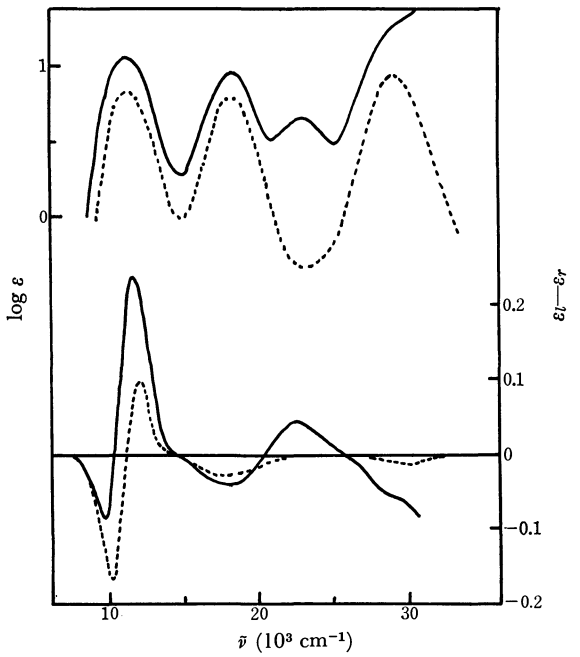

Fig. 3. AB and CD spectra of $[Ni(C_{12}H_{28}N_4)(l\text{-pn})](ClO_4)_2$ (——) and $[Ni(l\text{-pn})_3](ClO_4)_2$(·····) in acetonitril.

Table 2. IR data in 1600 cm^{-1} region (cm^{-1})

Complex	$\gamma_{C=N}$	δ_{NH_2}
I	1653	
II	1653	1603
III	1653	1592
IV	1653	1592
V		1603, 1585

vibration. The complexes (II), (III), and (IV), on the other hand, exhibit two strong bands, at 1653 and around 1600 cm^{-1}, which can be assigned to the C=N stretching and the NH_2–deformation vibrations respectively.

On the basis of these data, we concluded that the ligand $C_{12}H_{38}N_4$ is 1,9-diamino-1,4,6,6,9-pentamethyl-3,7-diazanona-3-ene (Fig. 1), although there are four possible isomers, depending on the positions of the methyl groups of the *l*-propylenediamine residues. Their positions are: (1,8), (1,9), (2,8), and (2,9). Of these, however, the isomer (1,9), in which the methyl groups of the *l*-propylenediamine residues are located far from the six-membered chelate ring, may be expected to be most probable.[7] The reasons for this are as follows: (1) The X-ray analysis[4] of the yellow complex (I) showed that the methyl groups of the propylenediamine residues are on the 3 and 10 carbon atoms (Fig. 1). Thus, the repulsion between these methyl groups and the geminal methyl groups on the 7 and 14 carbon atoms seems to be avoided. (2) The reaction of $[Ni(iso\text{-}bn)_2]^{2+}$ (iso-bn=iso-butylenediamine) and acetone produced only a complex containing 1,9-diamino-1,1,4,6,6,9,9-heptamethyl-3,7-diazanona-3-ene, in which four methyl groups of iso-butylenediamine residues take 1 and 9 positions.[3] (3) $[Ni(bn)_2]^{2+}$ (bn=2,3-diaminobutane) does not react with acetone.[8]

Curtis[8] described an analogous compound, $[Ni(C_{10}H_{24}N_4)(en)](ClO_4)_2$ ($C_{10}H_{24}N_4$ = 1,9-diamino-4,6,6-trimethyl-3,7-diazanona-3-ene), but did not give any details on its structure or chemical properties.

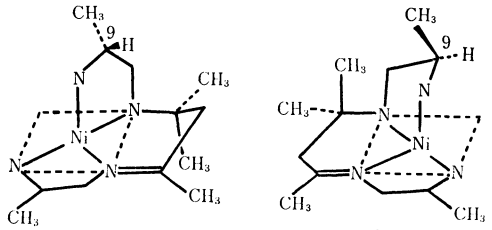

Fig. 4

The quadridentate ligand, $C_{12}H_{28}N_4$, in the $[Ni(C_{12}H_{28}N_4)(ch)]^{2+}$ (ch=en and *l*-pn) should give a *cis*-form complex. Although the *cis* form has two different geometrical arrangements, *cis* α and *cis* β,[9] the present complex is probably *cis* β, since the quadridentate ligand involves an imino-nitrogen. In addition, each geometrical isomer has two optical isomers, Δ and Λ. Since both Δ and Λ isomers involve the same asymmetric carbon atoms in the *l*-propylenediamine residues, they form a pair of diastereoisomers. As Fig. 4 illustrates, the methyl group on the 9-carbon atom of the Δ-*cis* β points away (*exo*) from the central six-membered chelate ring, while that of the Λ-*cis* β points toward (*endo*) the six-membered chelate ring. Since the interaction between the nonbonding atoms is expected to be greater in the endo-Λ-*cis* β isomer, the absolute configuration of the purple complexes, (II) and (IV), could be identified as *exo*-Λ-*cis* β. This assignment is supported further by the facts that the CD spectra in the *d–d* transition region of $[Ni(C_{12}H_{28}N_4)(ch)](ClO_4)_2$ in acetonitril are quite similar to that of Δ-$[Ni(l\text{-}pn)_3](ClO_4)_2$ as is shown in Fig. 3, and that they are enantiomeric to that of *fac*(N)-Λ-$[Ni(L\text{-}prol)_3]^-$.[10] The positional isomers due to the methyl group of *l*-propylenediamine in $[Ni(C_{12}H_{28}N_4)(l\text{-}pn)]^{2+}$ are not clear at present.

As Fig. 2 shows, the CD spectrum of $[Ni(C_{12}H_{28}N_4)]^{2+}$ (III) in water is almost enantiomeric with that of the $[Ni(C_{18}H_{36}N_4)]^{2+}$ (I); the purple complex (II) gives a CD spectrum similar to that of the complex (III) in water, since the former complex liberates the *l*-propylenediamine almost completely in water, as has been stated previously. According to the X-ray analysis,[4] the methyl groups of the *l*-propylenediamine residues in the complex (I) take positions axial to the complex plane. Therefore, the conformation of the *l*-propylenediamine residues in this complex may be described as approximately (pseudo) δ-gauche[5]; the conformation of such five-membered chelate rings involving the imino-nitrogen atom may be somewhat different from the usual gauche structure, as seen in the *l*-propylenediamine chelate. On the other hand, the five-membered chelate rings in the complex (III) may take a pseudo λ- and a usual λ-gauche conformation, since it is known that the methyl group on a puckered chelate ring tends to take an orientation equatorial to the ring unless there is special steric requirement.[11] Therefore the absolute configuration of the secondary amine (7 position) in this complex (III) should become enantiomeric with those of the secondary amines (1, 8 positions) in

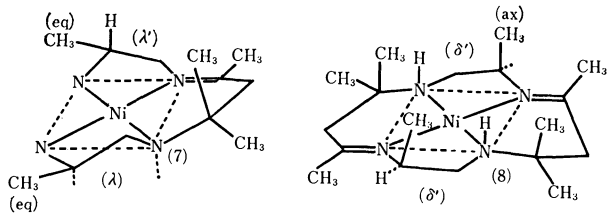

Fig. 5. Schematic drawing of $[Ni(C_{12}H_{28}N_4)]^{2+}$ and $[Ni(C_{18}H_{36}N_4)]^{2+}$.

$[Ni(C_{18}H_{34}N_4)]^{2+}$, as is shown in Fig. 5. The enantiomeric CD curves between the complexes (I) and (III) may be caused by such enantiomeric configurations.

The authors wish to thank Professor Kazuo Saito for his helpful advice and encouragement. They also wish to thank the Ministry of Education for its Grant-in-aid.

7) T. E. MacDermott and D. H. Busch, *J. Amer. Chem. Soc.*, **89**, 5780 (1967).
8) Reference 9 in N. F. Curtis, *Coord. Chem. Rev.*, **3**, 3 (1968).
9) A. M. Sargeson and G. H. Searle, *Inorg. Chem.*, **4**, 45 (1965).
10) J. Hidaka and Y. Shimura, This Bulletin, **43**, 2999 (1970).
11) E. J. Corey and J. C. Bailar, Jr., *J. Amer. Chem. Soc.*, **81**, 2620 (1959).

Studies of the Interaction between the Picrate Ion and Alkali Metal Ions

Mitsuo YAMANE, Tadashi IWACHIDO,* and Kyoji TÔEI

Department of Chemistry, Faculty of Science, Okayama University, Tsushima, Okayama

* *College of Liberal Arts, Okayama University, Tsushima, Okayama*

(Received November 1, 1970)

Alkali metal picrates in an aqueous solution are extractable by nitrobenzene. The investigations of the equilibria in and between the aqueous and organic phases show that the larger the association constants in the aqueous phase and the dissociation constants in the organic phase, the greater the extractability of the salts. The extremely low extractability of alkali metal picrates can be well explained in terms of such equilibrium constants.

The results of earlier works have suggested that an effective extraction of alkali metals can be achieved by the reagents known as the precipitants of these ions. These reagents are all similar in chemical structure—namely, they are all bulky anions. Polyiodide,[1] tetraphenylborate,[2-4] and perchlorate[4] ions are representative reagents, and these salts with alkali metals are extractable into nitrobenzene. In previous papers,[5-8] it has been shown that alkali metals can be effectively extracted by nitrobenzene in the presence of such polynitroamines as hexanitrodiphenylamine.

Considerations of the equilibrium in and between the aqueous and organic phases show that the greater the extractability of these salts, the larger the association in the aqueous phase and the smaller the association in the organic phase. Phenols,[9] especially nitrophenols, have been known as extractants, though the extractability is much less than that of the polynitroamines. In the present paper, it will also be shown that the low extractability of the picrates can be explained by the equilibrium studies.

Experimental

Reagents. Alkali metal picrates were prepared by dissolving picric acid into an aqueous solution containing a slight excess of each alkali metal carbonate or sulfate. The precipitate was filtered and recrystallized two or three times from ethanol or methanol. The crystals were dried at 70°C for 3 to 5 hr under reduced pressure. Nitrobenzene of a guranteed-grade was dried over anhydrous sodium sulfate for two days. The dried nitrobenzene was then distilled under reduced pressure. The fraction boiling at 75°C/5 mmHg was collected and stored in an ampouple in order to protect it from moisture. The distillate has a specific conductance of about 4×10^{-9} Ʊ/cm and is satisfactory enough for the conductivity measurement of these salts.

Extraction Procedures. The aqueous solutions of the picrates (4×10^{-2}, 9×10^{-3}, 2×10^{-3}, and 1×10^{-3} M for Na, K, Rb, and Cs respectively) were prepared, 1- to 10-m*l* aliquots were transferred into separatory funnels and diluted with water to make up the volume to 10 m*l*, and then the same volume of nitrobenzene was added to each. The funnels were shaken at 25°C for 30 min and allowed to stand for half an hour. The alkali metals extracted into the organic phase were determined by an atomic absorption spectrophotometer (Nippon Jarrell Ash, Type AA-1).

Conductance Measurements. The apparatus and the procedures of conductance measurements were the same as those described in an earlier paper.[8]

Theoretical

The dissociation constant, K_d, of alkali metal picrates in nitrobenzene were determined by the method of Shedlovsky.[10] The conductances, Λ, were related with the concentration of electrolytes, C, by the following equation:

$$\frac{1}{\Lambda S}=\frac{1}{\Lambda_\infty}+\frac{C\Lambda S f_o^2}{K_d\Lambda_\infty^2} \tag{1}$$

where Λ_∞ refers to the limiting conductance, and f_0, to the mean activity coefficient. S is a function of Z only.

$$S\equiv\left[\frac{Z}{2}+\sqrt{1+\left(\frac{Z}{2}\right)^2}\right]^2 \tag{2}$$

Z is defined by Eq. (3):

$$Z=\frac{\alpha\sqrt{C\Lambda}}{\Lambda_\infty^{3/2}} \tag{3}$$

where α is the Onsager coefficient. The picrate anion, R^-, associates with alkali metal cations, M^+, to form the ion-pair:

$$M^+ + R^- \overset{K_a^{MR}}{\rightleftharpoons} MR \tag{4}$$

and the association constant in nitrobenzene, K_o^{MR} $(=1/K_d)$, is written as:

$$K_o^{MR}=\frac{[MR]_o}{[M^+]_o[R^-]_o f_o^2} \tag{5}$$

where the subscript o refers to the nitrobenzene phase and the brackets, to the molar concentration of each species.

The values of the mean activity coefficient of the picrates in both the aqueous and organic phases were calculated by means of the following Debye-Hückel limiting law:

1) M. Kyrš and S. Podesva, *Anal. Chim. Acta*, **27**, 183 (1962).
2) K. Haruyama and T. Ashizawa, *Bunseki Kagaku*, **14**, 120 (1965).
3) R. C. Fix and J. W. Irvine, Jr., *MIT Lab. Nuclear Science, Annual Progress Report* (Nov. 30, 1955).
4) T. Sekine and D. Dyrssen, *Anal. Chim. Acta*, **45**, 433 (1969).
5) T. Iwachido and K. Tôei, This Bulletin, **37**, 1276 (1964).
6) H. Ueda, T. Iwachido, and K. Tôei, *Nippon Kagaku Zasshi*, **86**, 865 (1965).
7) T. Iwachido, S. Ukai, and K. Tôei, This Bulletin, **40**, 694 (1967).
8) S. Motomizu, K. Tôei, and T. Iwachido, *ibid.*, **42**, 1006 (1969).
9) W. J. Ross and J. C. White, *Anal. Chem.*, **36**, 1998 (1964).
10) T. Shedlovsky, *J. Franklin Inst.*, **225**, 739 (1938).

$$-\log f^2 = \frac{3.6494\times 10^6\sqrt{I}}{(\varepsilon T)^{3/2}} \quad (6)$$

The association constant of the picrates in the aqueous phase, K_a^{MR}, is also represented as follows:

$$M^+ + R^- \overset{K_a^{MR}}{\rightleftarrows} MR$$

$$K_a^{MR} = \frac{[MR]_a}{[M^+]_a[R^-]_a f_a^2} \quad (7)$$

where the subscript a denotes the aqueous phase. From the atomic absorption measurements, the total quantities of the alkali metal cations in both the aqueous and organic phases, C_a and C_o, were determined.

The ratio of C_o to C_a, or the distribution ratio, is written as follows:

$$q^M = \frac{C_o}{C_a} = \frac{[M^+]_o + [MR]_o}{[M^+]_a + [MR]_a} \quad (8)$$

In considering the $[M^+]_a=[R^-]_a$ relationship, the following equation is derived:

$$\frac{Y}{q^M} = \frac{1}{D^{MR}} + \frac{1}{D^{MR}K_a^{MR}f_a^2[M^+]_a} \quad (9)$$

where D^{MR} refers to the distribution coefficient of an ion-pair.

Y is defined by the following equation:

$$Y = \frac{\sqrt{0.25+C_oK_o^{MR}f_o^2}+0.5}{C_oK_o^{MR}f_o^2} + 1 \quad (10)$$

From a plot of Y/q^M *versus* $1/[M^+]_a f_a^2$, the values of D^{MR} and K_a^{MR} can be determined simultaneously.

Results and Discussion

Association Constants and Limiting Conductances of Alkali Metal Picrates in Nitrobenzene. In order to obtain the association constant from a conductance method, it is necessary to get the limiting conductance of the picrates in nitrobenzene.

At first, Z is calculated by using an approximate value of Λ_∞, which is determined graphically by a plot of Λ *versus* $C^{1/2}$ (Fig. 1); this leads to a first approxima-

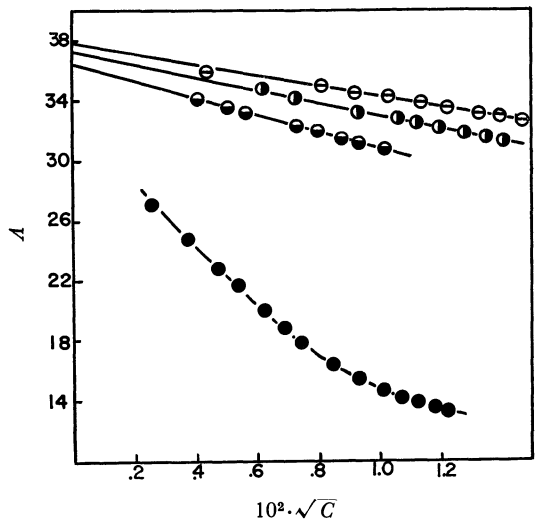

Fig. 1. The Λ-$\sqrt{C}$ curves of alkali metal picrates in dry nitrobenzene.
● Na-Picrate, ◒ K-Picrate, ◑ Rb-Picrate, ⊖ Cs-Picrate

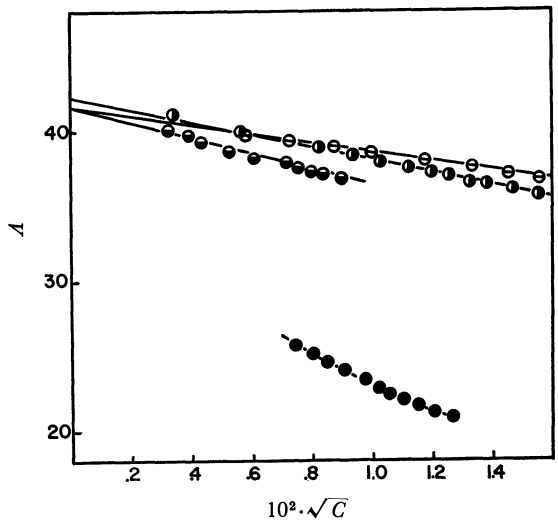

Fig. 2. The Λ-$\sqrt{C}$ curves of alkali metal picrates in nitrobenzene saturated with water.
● Na-Picrate, ◒ K-Picrate, ◑ Rb-Picrate, ⊖ Cs-Picrate

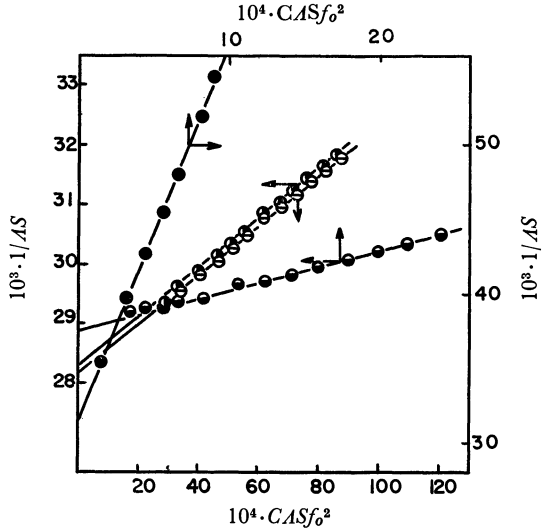

Fig. 3. Shedlovsky plot of the picrates in dry nitrobenzene.
● Na-Picrate, ◒ K-Picrate, ◑ Rb-Picrate, ⊖ Cs-Picrate

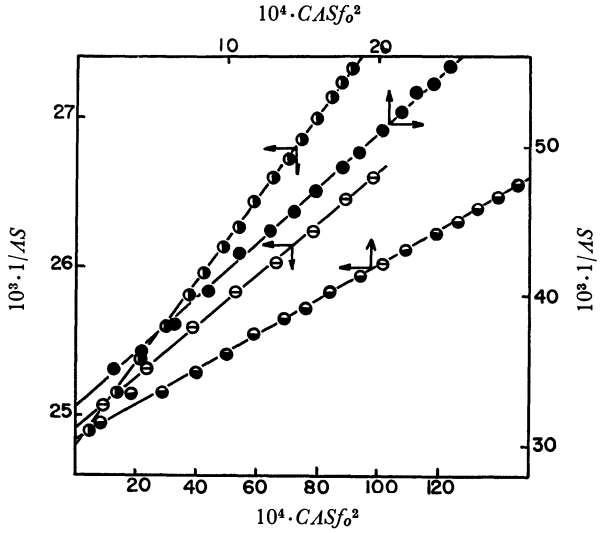

Fig. 4. Shedlovsky plot of the picrates in nitrobenzene saturated with water.
● Na-Picrate, ◒ K-Picrate, ◑ Rb-Picrate, ⊖ Cs-Picrate

tion for S. A first approximation for f_o is calculated from the Debye-Hückel limiting equation (6). These values are applied to Eq. (1) for all the values of C, and the plot of $1/AS$ *versus* $CASf_o^2$ gives the second approximation of Λ_∞. The process is repeated two or three times until Λ_∞ is no longer altered. The constants, Λ_∞ and K_o^{MR}, were calculated from the intercept and the slope of the linear extrapolation by means of the least-squares method (Fig. 3). Association constants in nitrobenzene saturated with water, $K_{o(H_2O)}^{MR}$, are calculated in the same manner by assuming that the dielectric constant and the viscosity of the water-saturated nitrobenzene are equal to those of dry nitrobenzene (Figs. 2 and 4).

The values of Λ_∞, $\Lambda_{\infty(H_2O)}$, K_o^{MR}, and $K_{o(H_2O)}^{MR}$ thus obtained are listed in Table 1. The light alkali metal picrates behave like weak electrolytes; especially is this true for lithium ($K_o^{LiPic} = 10^{7.2}$ after Witschonke and Kraus).[11]

Table 1. The limiting conductances and association constants for alkali metal picrates

MR	Λ_∞	$\log K_o^{MR}$	$\Lambda_{\infty(H_2O)}$	$\log K_{o(H_2O)}^{MR}$
Na-Picrate	33.9	4.48	31.9	3.67
K-Picrate	34.7	3.06	40.3	2.92
Rb-Picrate	35.1	2.81	40.7	2.65
Cs-Picrate	36.4	2.81	40.4	2.43

A plot of log K_o^{MR} *versus* the ionic potential (the ratio of the charge to the crystal radius, z/r) of the alkali metal cation clearly shows that, in both nitrobenzene and the water-saturated nitrobenzene, the larger the radius, the smaller the association constant (Figs. 5 and 6).

Association Constant in an Aqueous Solution. The association constant in an aqueous solution, K_a^{MR}, is

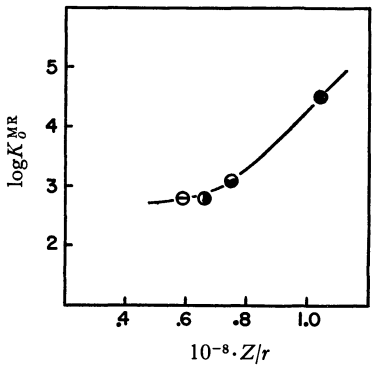

Fig. 5. The plot of log K_o^{MR} *vs.* z/r.
●Na-Picrate, ◒ K-Picrate, ◑ Rb-Picrate, ⊖ Cs-Picrate

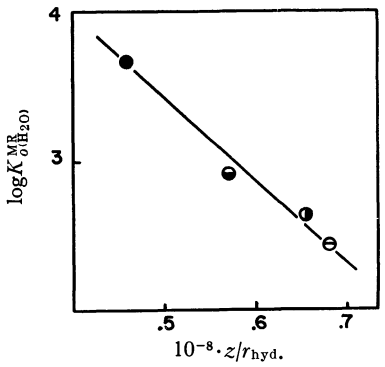

Fig. 6. The plot of $\log K_{o(H_2O)}^{MR}$ *vs.* $z/r_{hyd.}$
● Na-Picrate, ◒ K-Picrate, ◑ Rb-Picrate, ⊖ Cs-Picrate

obtainable by Eq. (9) from the slope of the lines in Fig. (7). First approximate values, K_a^{MR} and D^{MR}, are calculated by substituting the analytical concentration of the alkali metal, C_a, for the concentration of the free metal-cation, $[M^+]_a$. The association constant thus obtained leads to a more accurate value of $[M^+]_a$. These procedures were repeated two or three times until the value of K_a^{MR} did not alter any more upon further refinement. The values of log K_a^{MR} increase gradually in proceeding from Na to Cs, as is shown in Table 2 and Fig. 8.

The Role of Hydration. If the ion-pairing arises from the coulombic force, it will be greatly affected by the radius of the alkali metal cation. An ion of the small effective radius should associate with the oppo-

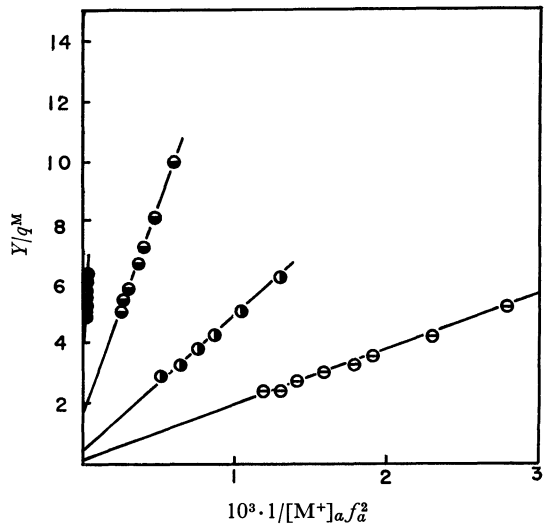

Fig. 7. The plot of Y/q^M *vs.* $1/[M^+]_a f_a^2$.
● Na-Picrate, ◒ K-Picrate, ◑ Rb-Picrate, ⊖ Cs-Picrate

Table 2. The constants of K_a^{MR}, D^{MR}, q^M and $(D^{MR}K_a^{MR}/K_{o(H_2O)}^{MR})^{1/2}$ for alkali metal picrates, along with the ionic radii, r, and the radii of hydrated ions, r_{hyd}

MR	$\log K_a^{MR}$	D^{MR}	q^M	$(D^{MR}K_a^{MR}/K_{o(H_2O)}^{MR})^{1/2}$	r	$r_{hyd.}$
Na-Picrate	1.38	0.0028	0.0035	0.0038	0.97	2.17
K-Picrate	1.64	0.014	0.025	0.027	1.33	1.75
Rb-Picrate	1.94	0.022	0.061	0.066	1.52	1.53
Cs-Picrate	2.07	0.068	0.18	0.17	1.70	1.47

11) C. R. Witschonke and C. A. Kraus, *J. Amer. Chem. Soc.*, **69**, 2472 (1947).

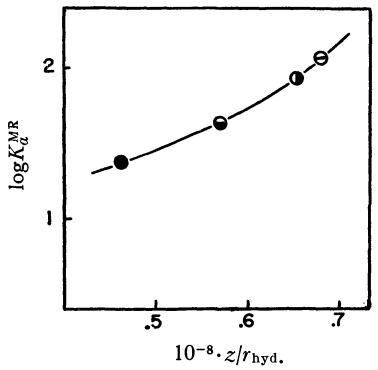

Fig. 8. The plot of $\log K_a^{MR}$ *vs.* $z/r_{hyd.}$
● Na-Picrate, ◒ K-Picrate, ◑ Rb-Picrate, ⊖ Cs-Picrate

sitely-charged ion to form a stable ion pair. Generally, the effective radius of an ion is largely influenced by the hydration. The crystal radius of the alkali metal cation increases gradually from lithium to cesium; the order of the effective radius is completely reversed in an aqueous solution. The sequence of K_o^{MR} in dry nitrobenzene (Table 1) and of K_a^{MR} in an aqueous solution (Table 2) is coincident with the above consideration.

If a hydrated alkali metal cation and a picrate anion form an ion-pair in the water-saturated nitrobenzene, $K_{o(H_2O)}^{MR}$ should increase gradually from sodium to cesium, because the effective radius of the cation decreases from sodium to cesium. However, the sequence of the $K_{o(H_2O)}^{MR}$ values are completely inverse. This implies that the ion pairs formed in the water-saturated nitrobenzene and in the aqueous phase are somewhat different in a hydration state; that is, the hydrated water molecules in the nitrobenzene phase are not effective in the reversal of the order of the crystal radii of cations. It might be attributed to the nature of the picrate anion, which is relatively small and whose charge is not distributed to the whole of the anion, but fairly well to the phenolic oxygen atom.

The sequence of Λ_∞ (Table 1) should decrease from sodium to cesium, because the radius of the ion increases with the atomic weight. However, the results obtained are the inverse of this. It implies that a hydration of ions occurs even in the dry nitrobenzene solution. The evidence proves that the freshly-distilled nitrobenzene contains a small amount of water, the amount determinable by the Karl-Fisher method. The order of the tendency to dissolve the picrates in the dry nitrobenzene is as follows: Cs>Rb>K<Na<Li. The hydrated water molecules loosen the bonding between the cation and the picrate anion, and so enhance the dissociation of the ion pair. Therefore, the unexpected high solubility of sodium and lithium picrates is another evidence of the presence of the hydrated species in the dry nitrobenzene, because they are apt to be hydrated among alkali metal cations.

The values of K_o^{MR} are very consistent with the results of Witschonke and Kraus. They have mentioned that the association constant of lithium picrate in dry nitrobenzene ($10^{7.2}$) is decreased 1/25 fold ($10^{5.8}$) on the addition of 0.03M water. The same tendency was observed in the present case. The water promotes the dissociation of alkali metal picrates, and so $K_{o(H_2O)}^{MR}$ becomes smaller than K_o^{MR}. The tendency decreases from lithium to cesium, and all the $K_{o(H_2O)}^{MR}$ values tend to be convergent.

Distribution Coefficient and Distribution Ratio. The distribution coefficient of the picrate is obtained from the reciprocal of the intercept of the line in Fig. 7. The values of $K_{o(H_2O)}^{MR}$ and K_a^{MR} show the presence of the ion pairs both in the aqueous and nitrobenzene phases, although the amounts of it are not great. Accordingly, the following relation can be obtained by neglecting the formation of the ion pair and the hydrolysis of the picrate ion in both phases:

$$q^M \approx \frac{[M^+]_o}{[M^+]_a} = \sqrt{\frac{D^{MR}K_a^{MR}}{K_{o(H_2O)}^{MR}}} \qquad (11)$$

The distribution ratio of the metal cation, q^M, is expected from Eq. (11) to be constant. Therefore, the ratio of the total concentration of metal in the aqueous phase, C_a ($=[M^+]_a+[MR]_a$), to that in nitrobenzene, C_o ($=[M^+]_o+[MR]_o$), should be constant. The

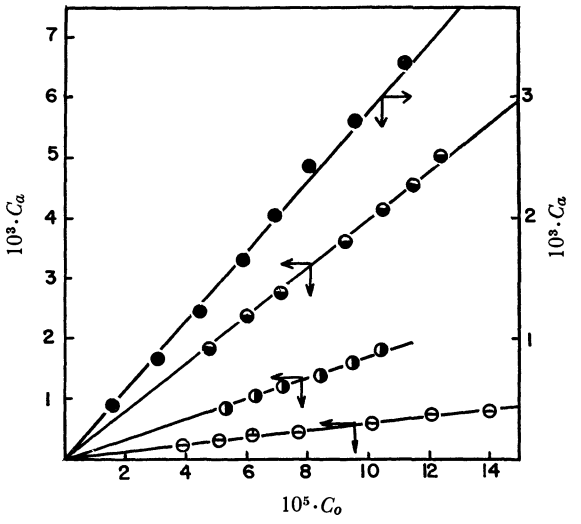

Fig. 9. The plot of concentrations of alkali metal ions in an aqueous phase. C_a, *vs.* those of an organic phase, C_o.
● Na-Picrate, ◒ K-Picrate, ◑ Rb-Picrate, ⊖ Cs-Picrate

circles in Fig. 9 represent the experimental data, while the lines show the experimental mean values of q^M. The calculated values of $(D^{MR}K_a^{MR}/K_{o(H_2O)}^{MR})^{1/2}$ are very coincident with the experimental values of q^M, as is shown in Table 2. If there is a reagent which can be highly dissociated in both phases, namely, $[M^+] \gg [MR]$ and $[M^+]=[R^-]$ in each phase, the extractability could be calculated directly from the values of K_a^{MR}, $K_{o(H_2O)}^{MR}$ and D^{MR}. The complete extraction would be achieved by the use of the reagent with the largest D^{MR} and K_a^{MR} values and the smallest $K_{o(H_2O)}^{MR}$ value.

Conclusion

The extraction of alkali metals by nitrobenzene in the presence of a bulky organic anion may be classified as an ion-association system. However, the present extraction system is somewhat different from the ordinary one in that the ion pair extracted extensively dissociates in the organic phase as well as in the aqueous

phase. The mechanism of the extraction may well be visualized by the following scheme:

$$\begin{array}{lcl} M_{aq}^{+} + R^{-} & \rightleftharpoons & M_{aq}R \quad \text{aqueous phase} \\ \hline & \updownarrow & \\ M_{aq}^{+} + R^{-} & \rightleftharpoons & M_{aq}R \quad \text{organic phase} \end{array}$$

With regard to the number of hydration in the organic phase, there is no direct evidence, but from the analogy with the case of polynitroamine (Hexyl[8]) and from the other indirect evidences, it seems to be reasonable to consider the coextraction of water molecules into nitrobenzene by means of the above scheme.

A high extractability is attainable with a reagent which allows the equilibrium to shift in the direction shown by the bold-faced arrows. From this point of view, the very low extractabilities of the picrates as compared with those of the Hexyl salts can be explained by the facts that the D^{MPic} values are smaller than D^{MHexyl}, and the $K_{o(\text{H}_2\text{O})}^{\text{MPic}}$ values are larger than $K_{o(\text{H}_2\text{O})}^{\text{MHexyl}}$, while the K_a^{MPic} and K_a^{MHexyl} values remain almost the same.

Apart from the equilibrium discussion, it is also of much interest to know with what kind of anions the highest extractability can be obtained. The simple and correct answer is hard to obtain, because the factors affecting the extraction are too complex to elucidate, but it is shown that the size and the charge distribution of anions used may have a great effect on the extractability.

The present work has been supported in part by a Grant for Scientific Research from the Ministry of Education.

BULLETIN OF THE CHEMICAL SOCIETY OF JAPAN, VOL. 44, 749—753 (1971)

The Synthesis of Nitro, Amino, and Acetamino Derivatives of 2,3-Dimethylbenzofuran[1]

Yoshiyuki KAWASE, Setsuko TAKATA, and Etsuko HIKISHIMA

Department of Chemistry, Faculty of Literature and Science, Toyama University, Gofuku, Toyama

(Received February 11, 1970)

Another route to the synthesis of nitro, amino, and acetamino derivatives of 2,3-dimethylbenzofuran was explored. The cyclo-dehydration of 3-(*m*- and *p*-nitrophenoxy)butanones by means of polyphosphoric acid or sulfuric acid afforded 2,3-dimethyl-4- and -5-nitrobenzofurans, which were then converted by reduction to the corresponding 4- and 5-aminobenzofurans. The 4-, 5-, 6-, and 7-aminobenzofurans were prepared by the Hofmann reaction of the corresponding carboxylic amides. The amines thus obtained were converted to 4-, 5-, and 6-acetaminobenzofurans by acetylation. The 5-, 6-,-and 7-acetaminobenzofurans were also prepared by the cyclization of 3-(*p*-, *m*-, and *o*-acetaminophenoxy)butanones. The 7-nitrobenzofuran was prepared by the Sandmeyer reaction of 7-aminobenzofuran. The four aryloxybutanones, 2,3-dimethyl-4- and -7-nitrobenzofurans, 4-amino-2,3-dimethylbenzofuran, and 2,3-dimethyl-4-, -5-, -6-, and -7-benzofurancarboxylic amides are new compounds.

It has previously been reported that the 6-nitro derivative[2] of 2,3-dimethylbenzofuran was prepared by the nitration of the benzofuran, and the 5-nitro derivative[3] was recently prepared by the rearrangement of the *O*-(*p*-nitrophenyl)oxime of butanone, followed by deamino-cyclization, while the 4-, 5-, 6-, and 7-acetamino derivatives[2,4-6] were prepared by the Beckmann rearrangement of oximes of the acetylbenzofurans. The 6-amino derivative[2] was prepared by the reduction of the nitro compound, and the 5-, 6-, and 7-amino

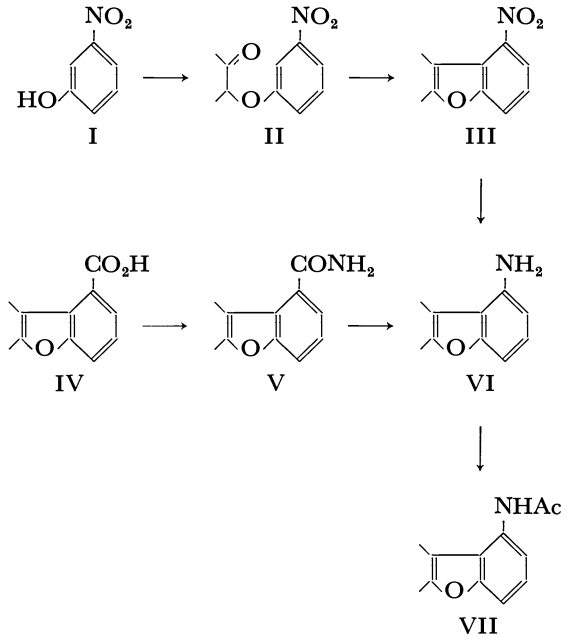

Chart 1

1) The major part of this work was presented at the 22nd Annual Meeting of the Chemical Society of Japan, Tokyo, April, 1969.

2) E. Bisagni, J.-P. Marquet, A. Cheutin, R. Royer, and M.-L. Desvoye, *Bull. Soc. Chim. Fr.*, **1965**, 1466.

3) A. Mooradian, *Tetrahedron Lett.*, **1967**, 407; *cf.* T. Sheradsky, *ibid.*, **1966**, 5225; D. Kaminsky, J. Shavel, Jr., and R. I. Meltzer, *ibid.*, **1967**, 859; A. Mooradian and P. E. Dupont, *ibid.*, **1967**, 2867.

4) E. Bisagni and R. Royer, *Bull. Soc. Chim. Fr.*, **1962**, 925.

5) C. Pène, P. Demerseman, A. Cheutin, and R. Royer, *ibid.*, **1966**, 586.

6) R. Royer, P. Demerseman, C. Pène, and G. Colin, *ibid.*, **1967**, 915.

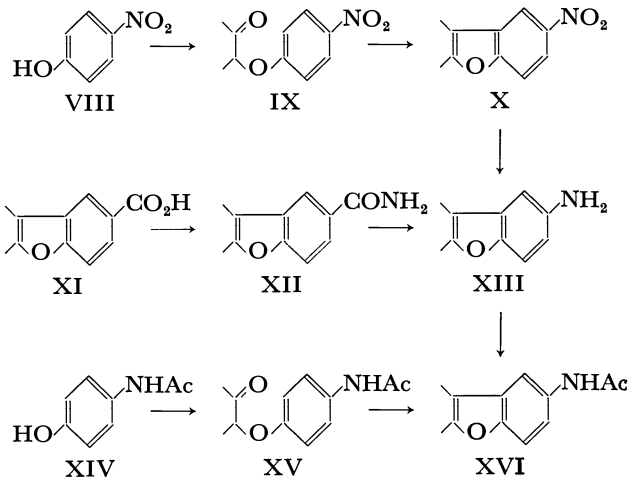

Chart 2

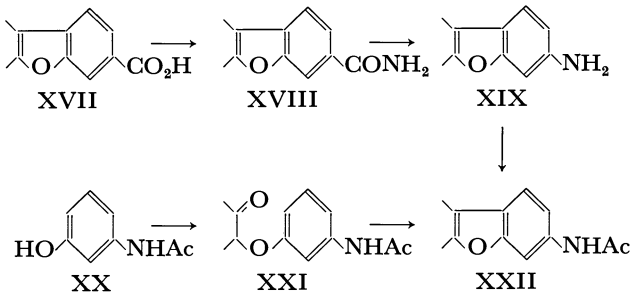

Chart 3

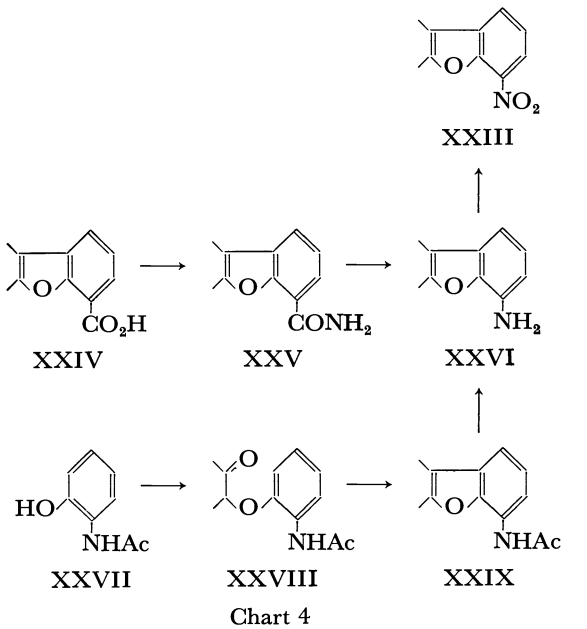

Chart 4

derivatives[4,5] were prepared by the hydrolysis of the acetamino compounds.

In the present paper, the preparation of nitro and acetamino derivatives of 2,3-dimethylbenzofuran by the cyclo-dehydration of 3-(nitro- and acetaminophenoxy)butanones and that of the amino derivatives by the Hofmann reaction of the amides will be described.

The cyclization of 3-(*m*- and *p*-nitrophenoxy)butanones (II and IX) by means of polyphosphoric acid or concentrated sulfuric acid afforded 2,3-dimethyl-4- and -5-nitrobenzofurans (III and X) respectively in good yields. The crude products obtained by the action of polyphosphoric acid on II was found, from a study of its NMR spectrum, to be a mixture of 4- and 6-nitrobenzofurans (97% and 3%); recrystallization afforded a pure compound of 4-nitrobenzofuran (III) (Charts 1 and 2). The analogous cyclization of 3-(*p*-, *m*- and *o*-acetaminophenoxy)butanones (XV, XXI,[7] and XXVIII) with polyphosphoric acid or sulfuric acid afforded 5-, 6-, and 7-acetaminobenzofurans (XVI, XXII, and XXIX) respectively (Charts 2—4). In

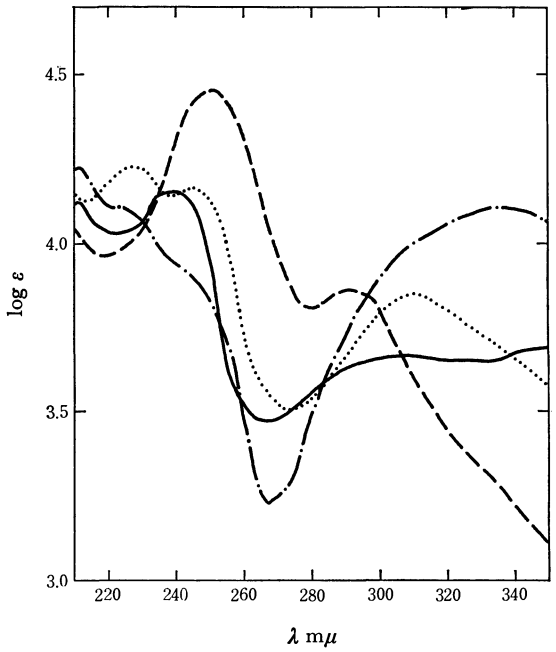

Fig. 1. The UV spectra of nitrobenzofurans:
—— III, —— X, -·-·- 6-nitro-compound, and····· XXIII.

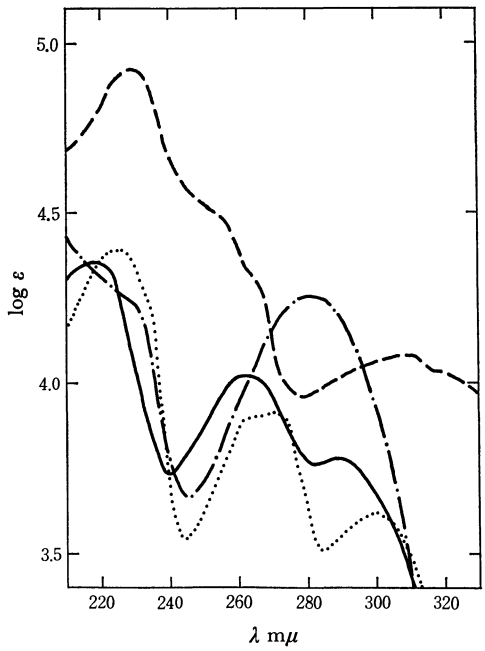

Fig. 2. The UV spectra of acid amides: —— V, ---- XII, -·-·- XVIII, and ····· XXV.

7) This compound was obtained only as an impure sample.

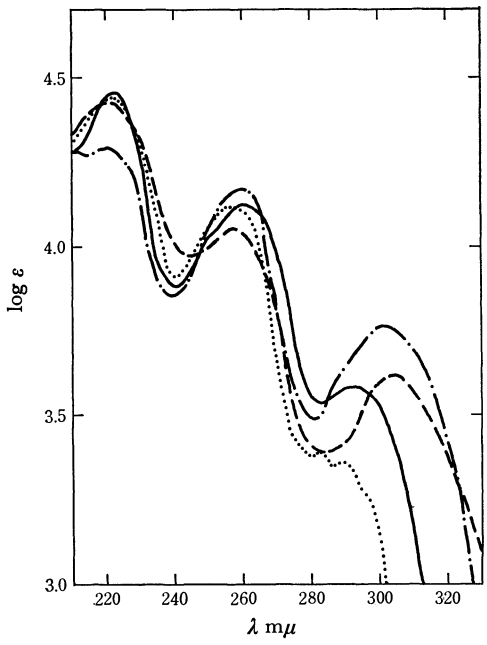

Fig. 3. The UV spectra of aminobenzofurans:
—— VI, —— XIII, -·-·- XIX, and ····· XXVI.

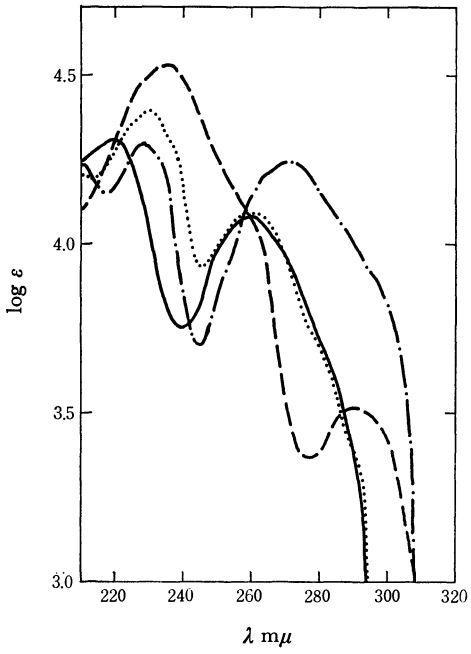

Fig 4. The UV spectra of acetamino compounds:
—— VII, —— XVI, -·-·- XXII, and ····· XXIX.

the case of the cyclization of *m*-substituted aryloxybutanones (II and XXI), it seems notable that the cyclization of II occurred to the *o*-position of the nitro group, while that of XXI occurred to the *p*-position of the acetamino group.[8]

The Hofmann reaction of the amides (V, XII, XVIII, and XXV) of benzofurancarboxylic acids[9,10] (IV, XI, XVII, and XXIV) by the action of sodium hypobromite furnished 4-, 5-, 6-, and 7-amino-2,3-dimethylbenzofurans (VI, XIII, XIX, and XXVI) respectively in low yields (Charts 1—4). The amines VI and XIII were also prepared by the reduction of the corresponding nitrobenzofurans (III and X) with stannous chloride or tin and hydrochloric acid, as has been described in the case of the 6-amino compound[2] XIX, while the acetylation of three amines (VI, XIII, and XIX) with acetic anhydride afforded acetaminobenzofurans (VII, XVI, and XXII). 2,3-Dimethyl-7-nitrobenzofuran (XXIII) was prepared by the Sandmeyer reaction of 7-aminobenzofuran (XXVI) through diazotization and substitution (Chart 4).

It should be mentioned that four aryloxybutanones, II, IX, XV, and XXVIII; two nitrobenzofurans, III and XXIII; the aminobenzofuran VI, and four carboxylic amides, V, XII, XVIII, and XXV, are all new compounds.

In the NMR spectra, the chemical shifts of 3-methyl protons of two 4-substituted benzofurans, III and VI, appeared in a field lower by about 0.1—0.2 ppm than the other isomeric 5-, 6-, and 7-substituted compounds[8] (Table 3).

In the UV spectra, the maximum absorption peaks at 230—250 mμ of 5-nitro-, 5-acetamino-, and 5-carbamoyl-benzofurans have stronger intensities than those of the corresponding 4-, 6-, and 7-substituted isomers. Similarly, 6-nitro-, 6-acetamino-, and 6-carbamoyl-benzofurans showed broader peaks and stronger intensities than those of the 4-, 5-, and 7-substituted ones in the region of 270—335 mμ (Figs. 1—4).

Experimental

All the melting points and boiling points are uncorrected, the NMR spectra were measured on a JEOL JNM-C-60H (60 MHz) spectrometer, and the UV spectra were measured on a Hitachi 139 spectrophotometer. Typical procedures of reactions are described and the detailed data are summarized in the tables.

The Preparation of Aryloxybutanones. Powdered potassium carbonate (168 g) and a small amount (1 g) of potassium iodide were stirred into a solution of *m*-nitrophenol (50 g) and 3-chlorobutanone (47 g) in acetone (400 m*l*), after which the mixture was refluxed for 10 hr. Most of the acetone was distilled off, and the residue was treated with water and extracted with ether. The ethereal solution was concentrated, and the residual product was distilled to give 61 g (81%) of 3-(*m*-nitrophenoxy)butanone (II), bp 154—162°C/6 mmHg. In the case of XXI, it seemed, from the pattern of the IR spectrum, that the product was contaminated by some acetaminobenzofuran (XXII), which was probably formed during distillation.

The Preparation of Nitrobenzofurans. a) By the Cyclization of Aryloxybutanones: i) With H_2SO_4: Concentrated sulfuric acid (12.5 g) was stirred, drop by drop, to the aryloxybutanone IX (5 g) below 50°C, after which the mixture was kept at 50°C for 30 min. After cooling, the mixture was poured into ice and extracted with ether. The ethereal solution was concentrated, and the residual product was crystallized from ethanol to give 3.2 g (70%) of 2,3-dimethyl-5-nitrobenzofuran (X), mp 116—117°C.

8) Preliminary report: Y. Kawase, *Chem. Ind.* (London), **1970**, 687.
9) Y. Kawase and M. Takashima, This Bulletin, **40**, 1224 (1967).
10) Y. Kawase, T. Okada, and T. Miwa, *ibid.*, **43**, 2884 (1970).

ii) With Polyphosphoric Acid (PPA): A mixture of the aryloxybutanone IX (10 g) and PPA (n=2.5,[11] 200 g) was heated at 100°C for 1.5 hr while being stirred. The resulting mixture was treated as has been described above to give

TABLE 1. REACTION CONDITIONS AND THE RESULTS

Starting compound	Reagent	Product	Mp°C (solvent[a]) or bp°C/mmHg	Yield %
	Preparation of Aryloxybutanones			
I	Cl-butanone	II	154—162/6	81
VIII	Cl-butanone	IX	66—67(Et)	72.5
XIV	Cl-butanone	XV	112—113(Et)	68
XX	Cl-butanone	XXI[b]	245—255/17	60
XXVII	Cl-butanone	XXVIII	188—193/6	73
	Cyclo-dehydration of Aryloxybutanones			
II	H_2SO_4	III	80.5—81(Et)	27
II	PPA[c]	III	80.5—81(Et)	46[d]
IX	H_2SO_4	X	116—117[e](Et)	70
IX	PPA	X	116—117[e](Et)	73
XV	H_2SO_4	XVI	174—174.5[f](Et)	55
XV	PPA	XVI	174—174.5[f](Et)	80
XXI[b]	PPA	XXII	181—181.5[g](Et)	55
XXVIII	H_2SO_4	XXIX	134—135.5[h](Et)	29
	Amines from Nitro Compounds			
III	$SnCl_2$-HCl	VI	41—43(Pe)	59
III	Sn-HCl	VI	41—43(Pe)	21.5
X	$SnCl_2$-HCl	XIII	81.5—83[i](Pe)	80
X	Sn-HCl	XIII	81.5—83[i](Pe)	38
	Acid Amides from Acids			
IV	$SOCl_2$-NH_4OH	V	192.5—194(Et)	66.5
XI	$SOCl_2$-NH_4OH	XII	162.5—163(Et)	50
XVII	$SOCl_2$-NH_4OH	XVIII	175—176(Et)	42
XXIV	$SOCl_2$-NH_4OH	XXV	188—189.5(Et)	59
	Amines from Acid Amides			
V	NaOBr	VI	41—43(Pe)	29
XII	NaOBr	XIII	81.5—83[i](Pe)	38
XVIII	NaOBr	XIX	58—58.5[j](Pe)	17
XXV	NaOBr	XXVI	62—63[k](Pe)	25
	Acetamino Compounds from Amines			
VI	Ac_2O-Py	VII	177.5—178[l](Et)	23
XIII	Ac_2O-Py	XVI	174—174.5[f](Et)	31
XIX	Ac_2O-Py	XXII	181—181.5[g](Et)	79.5
	Nitro Compound from Amine			
XXVI	Sandmeyer reaction	XXIII	76.5—77(Et)	4

a) Et: ethanol, Pe: Petroleum ether. b) The crude product. c) Polyphosphoric acid. d) The crude product, mp 73—74°C, 67% yield, contains a 3% of the isomeric 6-nitro compound. e) Mp is not given in the Ref. 3. f) Lit. mp 174—175°C (Ref. 2). g) Lit. mp 182—183°C (Ref. 4). h) Lit. mp 126°C (Ref. 5). i) Lit. mp 79°C (Ref. 2). j) Lit. mp 54°C (Ref. 4). k) Lit. mp 62.5°C (Ref. 5). l) Lit. mp 176°C (Ref. 6).

TABLE 2. THE ANALYSES OF NEW COMPOUNDS

Compd	Formula	Found C%	Found H%	Found N%	Calcd C%	Calcd H%	Calcd N%
	Aryloxybutanones						
II	$C_{10}H_{11}O_4N$	57.92	5.14	6.50	57.41	5.30	6.70
IX	$C_{10}H_{11}O_4N$	57.14	5.08	6.64	57.41	5.30	6.70
XV	$C_{12}H_{15}O_3N$	65.56	7.18	6.17	65.14	6.83	6.33
XXVIII	$C_{12}H_{15}O_3N$	65.23	6.75	6.33	65.14	6.83	6.33
	Nitro Compounds						
III	$C_{10}H_9O_3N$	63.01	4.64	7.04	62.82	4.75	7.33
XXIII	$C_{10}H_9O_3N$	62.79	4.63	7.28	62.82	4.75	7.33
	Amino Compound						
VI	$C_{10}H_{11}ON$	74.51	6.98	8.71	74.51	6.88	8.69
	Acid Amides						
V	$C_{11}H_{11}O_2N$	69.19	5.78	7.18	69.82	5.86	7.40
XII	$C_{11}H_{11}O_2N$	69.61	5.99	7.18	69.82	5.86	7.40
XVIII	$C_{11}H_{11}O_2N$	69.54	5.97	7.17	69.82	5.86	7.40
XXV	$C_{11}H_{11}O_2N$	69.57	5.83	7.39	69.82	5.86	7.40

TABLE 3. THE NMR SPECTRA OF NITRO- AND AMINO-BENZOFURANS[a]

Compd	NH_2	2-Me	3-Me
III		2.46	2.27
X		2.41	2.19
b)		2.44	2.18
XXIII		2.47	2.17
VI	3.69	2.27	2.27
XIII	3.33	2.31	2.05
XIX	3.34	2.27	2.04
XXVI	3.66	2.32	2.07

a) δ-Values (ppm) measured in CCl_4 (*ca.* 5% solution), using TMS as an internal standard.
b) 2,3-Dimethyl-6-nitrobenzofuran.

6.65 g of the nitrobenzofuran X, mp 116—117°C. In the case of the cyclization of II, 6.2 g of a crude product, mp 73—74°C, was obtained after one crystallization. It was found, from the NMR spectrum, to be a mixture of 2,3-dimethyl-4- and -6-nitrobenzofurans; the percentage composition was determined by estimating the areas of the peaks corresponding to the 3-methyl protons (see Table 1). Further recrystallization furnished 4.25 g (46%) of the pure III, mp 80.5—81°C.

b) By the Sandmeyer Reaction: According to the usual manner,[12] the amine XXVI (1.4 g) was diazotized in acetic acid (16 m*l*) with sodium nitrite (1.6 g) and sulfuric acid (8 m*l*); the diazonium compound thus formed was treated with a decomposition mixture which had been prepared from copper sulfate (8 g), sodium sulfite (8 g), and sodium nitrite (20%, 8 g). The product was crystallized from ethanol to give 65 mg (4%) of 2,3-dimethyl-7-nitrobenzofuran (XXIII), mp 76.5—77°C.

The Preparation of Acid Amides. A mixture of 2,3-dimethyl-4-benzofurancarboxylic acid[9] (IV) (4 g) and thionyl chloride (10 g) was refluxed for 1 hr. The excessive reagent was then distilled off, and the residual product was dissolved in dioxane (10 m*l*). A concentrated aqueous ammonia solution (20 m*l*) was added to the solution, and the mixture was treated with water after it had stand for 1 hr. The crystalline

11) Prepared from phosphoric acid (85%) and phosphorus pentoxide (1. 1: 1).

12) H. H. Hodgson, A. P. Mahadevan, and E. R. Ward, "Organic Syntheses," Coll. Vol. 3 (1955), p. 341.

product thus formed was collected and recrystallized from ethanol to give 2.6 g (65.5%) of the acid amide V, mp 192.5—194°C.

The Preparation of Aminobenzofurans. *a) By the Reduction of Nitrobenzofurans*: *i*) With $SnCl_2$-HCl: A mixture of the nitrobenzofuran III (5 g), stannous chloride (20 g), and concentrated hydrochloric acid (20 m*l*) was refluxed for 1 hr. An aqueous sodium hydroxide solution (27%, 123 g) was added to the mixture with cooling, and then the mixture was extracted with ether. The ethereal solution was concentrated; the residual product was distilled at 150—164°C/20 mmHg and then crystallized from petroleum ether to give 2.5 g (59%) of 4-amino-2,3-dimethylbenzofuran (VI), mp 41—43°C.

ii) With Sn-HCl: Concentrated hydrochloric acid (5 m*l*) was stirred into a mixture of the nitrobenzofuran III (1.1 g), ethanol (15 m*l*), and tin (1.4 g), after which the mixture was heated at 45°C for 3 hr while being stirred. After cooling, the mixture was treated as has been described in *i*) to give 0.2 g (21.5%) of the amine VI, mp 41—43°C.

b) By the Hofmann Reaction: A solution of the amide V (2 g) in dioxane (40 m*l*) was stirred into an aqueous sodium hypobromite solution which had been prepared from bromine (2.7 g), sodium hydroxide (4.5 g), water (27 m*l*), and ice (27 g). The mixture was heated at 70°C for 1 hr while being stirred. After the addition of an aqueous sodium hydroxide solution (50%, 13 g), the mixture was heated at 80°C for another hour with stirring and then cooled. The mixture was treated with water and extracted with ether. On treatment as in *a-i*, the ethereal solution gave the amine VI.

The identity of XIII, XIX, and XXVI with the authentic samples prepared independently[2,4,5] was confirmed by a mixed-melting-point determination and by a comparison of their IR spectra.

The Preparation of Acetaminobenzofurans. *a) By the Cyclization of Aryloxybutanones*: Two aryloxybutanones, XV and XXVIII, were treated with sulfuric acid at 40°C to give 5- and 7-acetaminobenzofurans (XVI and XXIX), and XV and crude XXI were treated with PPA to give XVI and 6-acetaminobenzofuran (XXII), as has been described for the nitro compounds.

b) By the Acetylation of Amines: Three amines, VI, XIII, and XIX, were acetylated by the acetic anhydride-pyridine method to give 4-acetaminobenzofuran (VII), XVI, and XXII.

Compounds VII, XVI, XXII, and XXIX were identified by a mixed-melting-point determination and by a comparison of the IR spectra with those of authentic samples.[2,4-6]

The authors are grateful to the members of the Laboratory of Analysis, Faculty of Pharmacology, Toyama University, for their microanalyses and NMR measurements.

BULLETIN OF THE CHEMICAL SOCIETY OF JAPAN, VOL. 44, 753—756 (1971)

Isomerization of Gomberg's Trityl by Protonic Acids in Benzene

Hiroshi TAKEUCHI, Toshikazu NAGAI, and Niichiro TOKURA

Department of Applied Chemistry, Faculty of Engineering, Osaka University, Suita, Osaka

(Received March 10, 1970)

Gomberg's trityl (1-diphenylmethylene-4-trityl-2,5-cyclohexadiene) (I) was isomerized by protonic acids such as HCl and phenol in benzene to form *p*-benzhydryltetraphenylmethane (II). *p*-(Benzhydryl-α-*d*)-tetraphenylmethane (III) was formed by the treatment of I with phenol-*d*. Ph_3CH and Ph_3CCl were treated under the same conditions, but II was not obtained. It was not formed either by the reaction of phenylazotriphenylmethane with phenol. This observation indicates that H^+ adds to the terminal methylene of I to form the cyclohexadienyl cation followed by deprotonation to give II. Similarly, treatment of 1-(phenyl-*p*-tolymethylene)-4-(diphenyl-*p*-tolylmethyl)-2,5-cyclohexadiene (IV) with HCl in benzene afforded α,α,α′-triphenyl-α,α′-(di-*p*-tolyl)-*p*-xylene (V). The results support the view that Gomberg's trityl is not hexaphenylethane but 1-diphenylmethylene-4-trityl-2,5-cyclohexadiene as suggested by Lankamp *et al.* (*Tetrahedron Lett.*, **1968**, 249). 1,1,2,2-Tetraphenylethane and 1,1,2,2-tetra-*o*-tolylethane not having the cyclohexadiene structure could not be isomerized by protonic acids (HCl and PhOH) in benzene. Thus, isomerization of this type is characteristic of the cyclohexadiene structure such as that of Gomberg's trityl.

It is believed that the dimerization of the triphenylmethyl radical discovered by Gomberg leads to hexaphenylethane.

However, Lankamp *et al.*[1] reported in 1968 that the monomer-dimer equilibrium of trityl is not the equilibrium, hexaphenylethane ⇄ 2 triphenylmethyl radicals, and should be represented as: 1-diphenylmethylene-4-trityl-2,5-cyclohexadiene ⇄ 2 triphenylmethyl radicals, by the evidence of UV and NMR spectra.

Guthrie and Weisman[2] reported that the dimer structure suggested by Lankamp *et al.* could be supported from the reaction of Gomberg's trityl toward a base.

During our investigation[3] on the reactivity of Gomberg's trityl toward sulphur dioxide, we found that Gomberg's trityl isomerizes into *p*-benzhydryltetraphenylmethane in the presence of protonic acids. This gives a chemical evidence for the 1-diphenylmethylene-4-trityl-2,5-cyclohexadiene structure as the dimer structure of Gomberg's trityl. We wish to report the de-

1) H. Lankamp, W. Th. Nauta, and C. MacLean, *Tetrahedron Lett.*, **1968**, 249.

2) R. D. Guthrie and G. R. Weisman, *Chem. Commun.*, **1969**, 1316.

3) H. Takeuchi, T. Nagai, and N. Tokura, This Bulletin, **43**, 1747 (1970).

tails of the isomerization of Gomberg's trityl by protonic acids in benzene.

Ullmann and Borsum[4] reported that the reaction of trityl chloride or triphenylcarbinol with Zn-$SnCl_2$ in acetic acid gave a stable hexaphenylethane (mp 225°C). Gomberg[5,6] also reported the formation of hexaphenylethane (mp 225—227°C) by the treatment of the trityl with HCl or acetic acid.

Tschitschibabin[7] synthesized *p*-benzhydryltetraphenylmethane (II) (mp 227°C) by the decomposition of the corresponding diazo compound formed from amino-*p*-benzhydryltetraphenylmethane. He argued against the formation of hexaphenylethane. Schlenk *et al.*[8] postulated the formation mechanism of II (Scheme 1) by the reaction of I with HCl, because II was formed in a 6% yield by the treatment of Ph_3CH with Ph_3CCl.

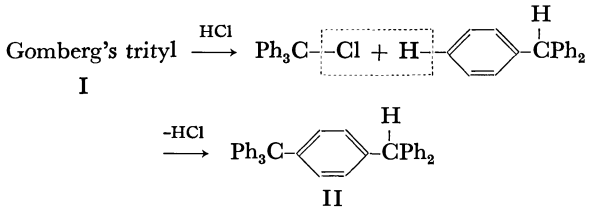

Scheme 1

However, Gomberg's trityl (I), which is not hexaphenylethane but 1-diphenylmethylene-4-trityl-2,5-cyclohexadiene as described by Lankamp *et al.*,[1] reacted with HCl to give II in good yield (82%). Hence the sluggish reaction shown in Scheme 1 can be neglected.

The present study was undertaken in order to explain the reaction mechanism of this type. The present paper deals with the reaction of protonic acids such as HCl and phenol with the derivative of I or tetraarylethanes.

Results and Discussion

Gomberg's trityl (I) reacted with phenol in the presence of SO_2 and O_2 in benzene at 60°C to give *p*-hydroxytetraphenylmethane (VI) as the product.[3] However, in the absence of SO_2 and O_2 in the above system, *p*-benzhydryltetraphenylmethane (II)[3] was formed in a 68% yield. When HCl was used in place of phenol, II was formed (82%). Gomberg *et al.*[4-6] reported the formation of the compound having the same mp (225—227°C) as that of II by the treatment of I with acetic acid, though they characterized this compound as hexaphenylethane.

Schlenk *et al.*[8] proposed the mechanism shown in Scheme 1. Ph_3CH and Ph_3CCl were heated at 60°C for 2 hr in benzene in our experiment, but II was not obtained. Thus, the possibility of the pathway in Scheme 1 could be eliminated.

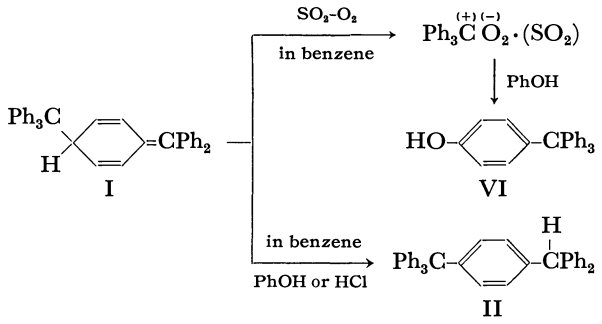

Scheme 2

If the formation of II is characteristic of the trityl radical, it should take place by the reaction of phenylazotriphenylmethane with phenol in benzene at 60°C for 2 hr. However, II was not obtained, which indicates that the reaction dose not occur *via* trityl radical as in the Scheme.

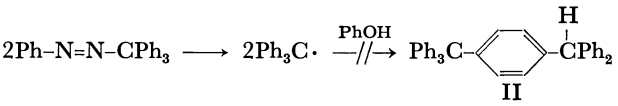

Scheme 3

A detailed investigation was carried out by use of 37 mmol of phenol-*d*[9] (69.5%)—phenol (30.5%) (calculated from mass spectral analysis) and I (4.2 mmol). Formation of *p*-(benzhydryl-α-*d*) tetraphenylmethane (III) was confirmed by IR (ν_{C-D} 2330 cm^{-1}) and mass spectrum (*m/e*; 487(M^+), 410(Ph_3C-C_6H_4-$\overset{+}{C}$DPh) and 168 ($Ph_2\overset{+}{C}D$)). The ratio II: III (36.3: 63.7) was calculated by comparison of the mass spectral molecular peaks of this isotope mixture with those of II. Compound II was treated with the labelled phenol, but the mass spectral analysis showed no peak corresponding to III. This indicates that the isotope scramble of II does not occur. Though the first proton donation step is obscure, the value ($k_H/k_D=1.05\pm0.01$) of the isotope effect was obtained on the assumption that this reaction follows first order of I and second order[10] of phenol.

In such solvents as H_3PO_4 and $POCl_3$,[11] however, $Ph_3C\cdot$ is transformed into $Ph_3\overset{+}{C}$. Phenylazotriphenylmethane[3] or I was also allowed to react with phenol in the presence of SO_2 and O_2 in benzene to give VI by the reaction of PhOH and $Ph_3\overset{+}{C}$ formed in the reaction system such as Scheme 2. Thus, it is plausible that PhOH or HCl in benzene isomerizes I into II more readily than to transform $Ph_3C\cdot$ into $Ph_3\overset{+}{C}$.

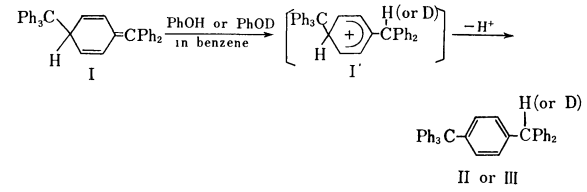

Sheme 4

4) F. Ullmann and W. Borsum, *Ber.*, **35**, 2877 (1902).
5) M. Gomberg, *ibid.*, **35**, 3914 (1902).
6) M. Gomberg, *ibid.*, **36**, 376 (1903).
7) A. E. Tschitschibabin, *ibid.*, **41**, 2427 (1908).
8) W. Schlenk, T. Weickel, and A. Herzenstein, *Ann. Chem.*, **372**, 1 (1910).
9) W. Williams, R. Hofstadter, and R. C. Herman, *J. Chem. Phys.*, **7**, 802 (1939).
10) Y. Pocker and K. D. Stevens, *J. Amer. Chem. Soc.*, **91**, 4205 (1969).
11) T. L. Chu and S. I. Weissman, *J. Chem. Phys.*, **22**, 21 (1954).

The results may indicate that proton or deuteron adds[10] to the terminal methylene of I to form the cyclohexadienyl cation such as I', followed by the deprotonation to give II or III (Scheme 4).[12] From the isotope effect, the protonation step in the reaction of I with phenol does not seem to be rate-determining.[10]

Similarly, the treatment of 1-(phenyl-*p*-tolylmethylene 4-(diphenyl-*p*-tolylmethyl)-2,5-cyclohexadiene (IV) with HCl in benzene afforded α,α,α'-triphenyl-α,α'-(di-*p*-tolyl)-*p*-xylene (V). Confirmation of V was achieved as follows: IR; 810 cm^{-1} (*p*-substituted phenyl). NMR (in CCl_4): τ; 2.5—3.7 (aromatic, multiplet, 27H), 4.6 (methine, singlet, 1H) and 7.7 (methyl, singlet, 6H). Mass: *m/e*; 514(M^+), 437 ($Ph_2(p\text{-}CH_3\text{-}C_6H_4)C\text{-}C_6H_4\text{-}\overset{+}{C}H\text{-}(p\text{-}CH_3\text{-}C_6H_4)$), 257 ($Ph_2(p\text{-}CH_3\text{-}C_6H_4)\overset{+}{C}$), and 181 ($Ph(p\text{-}CH_3\text{-}C_6H_4)\overset{+}{C}H$).

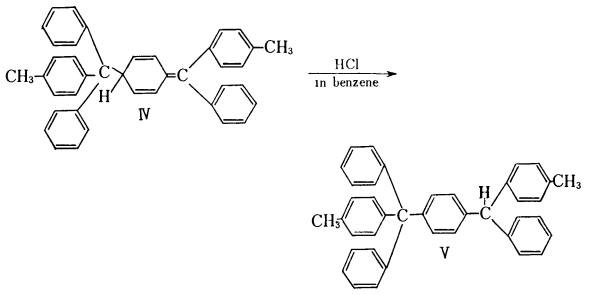

Sheme 5

On the other hand, 1,1,2,2-tetraphenylethane and 1,1,2,2-tetra-*o*-tolylethane were produced by the reaction of the corresponding diarylchloromethanes with Zn in benzene. However, these ethanes without the cyclohexadiene structure could not be isomerized by protonic acids (HCl or phenol). Thus, isomerization of this type is characteristic of the cyclohexadiene structure such as Gomberg's trityl.

$$2Ar_2CHCl \xrightarrow{Zn} Ar_2CH\text{-}CHAr_2$$

$$\xrightarrow[\text{in benzene}]{\text{PhOH or HCl}} Ar_2CH\text{-}C_6H_4\text{-}CHAr$$

Ar; C_6H_5 and $o\text{-}CH_3\text{-}C_6H_4$

The results support the idea that Gomberg's trityl is not hexaphenylethane but 1-diphenylmethylene-4-trityl-2,5-cyclohexadiene as described by Lankamp *et al.*[1]

Experimental

Apparatus. IR spectra were obtained on a EPI-S2 type Hitachi IR spectrometer. NMR spectra were obtained with a Japan Electron Optics Lab. spectrometer. UV spectra were taken with a EPS-3 Hitachi recording spectrometer. Mass spectra were recorded on a Hitachi RMU-6E spectrometer.

Materials. Benzene was purified by the ordinary method. Phenol was obtained commercially. The phenol-*d*-phenol mixture was made by the treatment of phenol with D_2O.[9] Gomberg's trityl (1-diphenylmethylene-4-trityl-2,5-cyclohexadine) (I) was prepared by the method of Gomberg and Cone.[13] Phenylazotriphenylmethane was synthesized by the procedure of Cohen and Wang.[14]

Isomerization of I by Phenol. Compound I (4.7 mmol) and phenol (47 mmol) were dissolved in 60 m*l* benzene and the solution was heated at 60°C for 2 hr in Ar atmosphere. The residual after distillation of benzene was chromatographed over silical gel using petroleum ether-benzene mixture as eluents by changing the polarity of the eluting medium. The following compounds were isolated and identified.

p-*Benzhydryltetraphenylmethane (II)*: Mp 225—227°C (recrystallized from benzene - acetic acid), 68%, IR: 2880 (ν_{C-H}), 840 cm^{-1} (*p*-substituted phenyl). $\lambda_{max}^{cyclohexane}$ 263 mμ (log ε 3.11), shoulder; 255 mμ (log ε 3.15), 269 mμ (log ε 2.99) and 272 mμ (log ε 2.67). NMR (in CCl_4): τ; 2.6—3.1 (aromatic, multiplet, 29H) and 4.6 (methine, singlet, 1H). Mass spectrum: *m/e*; 486 (M^+), 409 ($Ph_3C\text{-}C_6H_4\text{-}\overset{+}{C}HPh$), 243 ($Ph_3\overset{+}{C}$) and 167 ($Ph_2\overset{+}{C}H$).

Found; C, 93.71; H, 6.41%. Calcd for $C_{38}H_{30}$: C, 93.79; H, 6.21%.

Triphenylmethane: Mp 92°C (recrystallized from MeOH) 3%. The compound has same IR spectrum as an authentic specimen and showed no depression of mixed mp.

p-*Hydroxytetraphenylmethane*: Mp 280°C (recrystallized from $CHCl_3$-petroleum ether, 3%. The compound showed no depression of mixed mp and gave an identical IR spectrum with that of an authentic sample.[15]

In order to investigate the isomerization mechanism, I (4.2 mmol) was allowed to react with phenol-*d*[9] (69.5%)-phenol (30.5%) (calculated from mass spectral analysis) in benzene (20 m*l*) at 60°C for 2 hr in Ar. Formation of *p*-(benzhydryl-α-*d*)-tetraphenylmethane (III) was confirmed by IR (ν_{C-D} 2330 cm^{-1}) and mass spectral peaks (*m/e*: 487, 410 and 168). The ratio of II: III (36.3: 63.7) was calculated by comparison of the mass spectral molecular peaks of this isotope mixture with those of II. The above phenol-*d*-phenol mixtre was treated with II under the same conditions, but mass spectral analysis showed no peak corresponding to III. Isotope effect (k_H/k_D) was calculated from the results.

Isomerization of I by HCl. Compound I (2.9 mmol) was dissolved in 15 m*l* benzene saturated with HCl gas, and the solution was made to stand at room temperature for 30 min. The residue obtained after evaporation of benzene was crystallized from ether to give II (82%).

*Isomerization of 1-(Phenyl-*p*-tolymethylene)-4-(diphenyl-*p*-tolylmethyl)-2,5-cyclohexadiene (IV) with HCl.* Diphenyl-*p*-tolylcarbinol[16] was prepared by the interaction of PhMgBr in ether and *p*-toluic acid methylester, and yielded diphenyl-*p*-tolylchloromethane (mp 98—99°C) after treatment with dry HCl in ether.[15] The benzene solution of IV was made by the reaction of diphenyl-*p*-tolylchloromethane (8.5 mmol) with Zn (6 g) in benzene (20 m*l*) at room temperature for 1 hr in Ar, and treated with dry HCl after the solid had been removed by filtration. Compound V was separated by column chromatography over silica gel using benzene-petroleum ether as eluents, mp 77—79°C, 42%, identified as follows. IR: 810 cm^{-1} (*p*-substituted phenyl). NMR (in CCl_4): τ; 2.5—3.7 (aromatic, multiplet, 27H), 4.6 (methine, singlet, 1H), and 7.7 (methyl, singlet, 6H). Mass: *m/e*: 514, 437, 257, and 181.

12) II was not obtained in the experiment using EtOH or Et_3N in place of phenol.

13) M. Gomberg and L. H. Cone, *Ber.*, **37**, 2034 (1904).

14) S. G. Cohen and C. H. Wang, *J. Amer. Chem. Soc.*, **75**, 5504 (1953).

15) M. Busch and R. Knoll, *Ber.*, **60**, 2240 (1927).

16) A. Bistrzycki and J. Gyr, *ibid.*, **37**, 655 (1904).

Found: C, 93.07; H, 6.53%. Calcd for $C_{40}H_{34}$: C, 93.34; H, 6.66%.

Treatment of Tetraarylethanes with Phenol or HCl. 1,1,2,2-Tetraphenylethane (VII) (39%, mp 210°C[17]) and 1,1,2,2-tetra-*o*-tolylethane (VIII) (15%, mp 250°C) were synthesized by the reaction of the corresponding diarylchloromethanes with Zn in benzene. NMR spectra show that VII and VIII are true ethanes: VII in $CDCl_3$: τ; 2.5—3.2 (aromatic, multiplet, 20H) and 5.25 (methine, singlet, 2H), and VIII in $CDCl_3$: τ; 2.6—3.2 (aromatic, multiplet, 16H), 4.9 (methine, singlet, 2H) and 8.55 (methyl, singlet, 12H). These ethanes were not isomerized by phenol or HCl under the conditions for the isomerization of I.

17) F. C. Whitmore and E. N. Thurman, *J. Amer. Chem. Soc.*, **51**, 1491 (1929).

BULLETIN OF THE CHEMICAL SOCIETY OF JAPAN, VOL. 44, 756—761 (1971)

Solvent Effects on ρ Values of the Hammett Equation. II.[1]

Takeki MATSUI and Niichiro Tokura
Department of Applied Chemistry, Faculty of Engineering, Osaka University, Suita, Osaka
(Received April 6, 1970)

The rates of reactions of *N,N*-dimethylbenzylamine or its derivatives with methyl iodide in fourteen nonaqueous solvents at 30°C have been studied. The effects of the solvents on reactivities and Hammett's ρ values have been examined. For establishing the relationship between ρ and solvent polarity, a unique solvent parameter for reactivity ξ_0 was defined, which measures the relative solvent polarity in determining the order of reaction rate with respect to solvent. There is a linear relationship between ρ and ξ_0, but protic and aromatic solvents show deviation from this relation in a particular way. The liner relationship provides a common basis for explaining both substituent and solvent effects. This suggests the importance of solvent reorientation accompanied by an activation process. It is argued that the hydrogen-bonded solvation of reactant amines and solvation of the leaving group are responsible for abnormal behaviors in protic and aromatic solvents.

Since the proposal of Hammett's equation, evidence has accumlated which indicates that the Hammett ρ value is not independent of solvent.[1,2] This indicates the importance of external factors contributing to the transmission of substituent effects. Sufficiently accurate data for a discussion of the effects of solvents on the ρ value have, however, been only recently reported. Wilcox and Leung examined the mode of substituent effects transmission and concluded the dominance of field effects.[3] For esterification of substituted benzoic acids by diphenyl diazomethane, Buckley *et al.* discussed the change of ρ values with solvent in terms of dielectric constant of solvent.[4] At least, the existence of solvent effects on the reaction constant cannot be expected from a purely inductive model.

On the other hand, solvent effects on reactivity have been discussed from some particular aspects by many authors. The classical treatment is based on the assumption that the solvent is a continuous dielectric medium and only provides an electrostatic field where the reaction can take place. The results show that such a classical concept cannot explain the solvent dependence on reactivity. Various ideas have been developed to account for the confusing solvent effects on rates and equilibria.[5] Many attempts have been made to correlate the rate constant with solvent solubility parameters.[6] However, attention has recently been focused on the importance of solvent reorientation which is associated with the activation process.[5,7] We think that in this concept there is a common basis in establishing the simple explanation for both substituent and solvent effects.

In order to gain pertinent information it is necessary to study a reaction system where the mechanism of reaction is least complicated. The change of mechanism accompanied by reactant variation seems to make the problem complicated.[8] Thus, it is of interest to study the solvent effects on ρ values for the reaction of S_N2 type. A method of treatment is given in previous papers.[1,9] In the present paper, we report the results of a study of solvent effects on ρ values for reactions of *N,N*-dimethylbenzylamine, (DMBzA) or its derivatives with methyl iodide. This system was chosen for the need of determining the rate constant in a wider range of solvents than in previous works.

1) Part I: Y. Kondo, T. Matsui, and N. Tokura, This Bulletin, **42**, 1037 (1969).
2) J. E. Leffler and E. Grunwald, "Rates and Equilibria of Organic Reactions," John Wiley & Sons, Inc., New York, N. Y. (1963), p. 178.
3) C. F. Wilcox and C. Leung, *J. Amer. Chem. Soc.*, **90**, 336 (1968).
4) A. Buckley, N. B. Chapman, M. R. J. Dack, J. Shorter, and H. M. Wall, *J. Chem. Soc., C*, **1968**, 631.
5) C. D. Ritchie, G. A. Skinner, and V. G. Badding, *J. Amer. Chem. Soc.*, **89**, 2063 (1967), and references cited.
6) A. P. Stefani, *J. Amer. Chem. Soc.*, **90**, 1694 (1968).
7) G. Kohnstam, "The Transition State," The Chemical Society, Burlington House, London (1962), p. 179.
8) E. Tommila *et al.*, *Ann. Acad. Sci. Fennicae II*, **91**, 10 (1959); A. Kivinen, *ibid.*, **108**, 33 (1961).
9) T. Matsui and N. Tokura, This Bulletin, **43**, 1751 (1970).

Table 1. Rate constants for *N,N*-dimethylbenzylamine derivatives at 30.0°C[a)]

NO.	σ[b)]	*m*-CH_3 −0.069	H 0.000	*m*-Cl +0.373	*m*-NO_2 +0.710	*p*-OCH_3 −0.268	*p*-Cl +0.227	*p*-NO_2 +0.778
1	CH_3CN	230	206	97.0	48.4	311	121	43.6
2	$(CH_3)_2CO$	114	104	46.2	24.0	174	62.1	22.7
3	$C_6H_5NO_2$	145	125	46.6	19.0	223	67.0	20.6
4		24.0	22.2	7.7	3.05	38.2	10.6	2.40
5	THF	24.0	20.8	8.18	3.95	37.8	11.3	3.24
6	C_6H_6	8.13	7.07	2.36	0.751	13.2	3.04	0.595
7	CS_2	0.850	0.628	0.130	0.0288	1.31	0.210	0.0250
8	c-C_6H_{12}	0.0263	0.020	0.0030[c)]	—	0.056	0.00405[c)]	—
9	$C_6H_5CH_3$	5.17	4.31	1.44	0.459	8.10	1.80	0.348
10	C_6H_5Cl	16.0	12.7	3.46	0.939	23.2	5.18	0.888
11	C_6H_5Br	20.5	16.8	4.75	1.27	30.9	7.00	1.22
12	CH_3OH	9.90	9.32	5.40	3.33	12.4	6.71	3.27
13	C_2H_5OH	7.02	6.35	3.41	1.88	10.5	4.23	1.90
14	*i*-PrOH	5.16	4.58	2.17	1.07	7.13	3.00	1.15

a) Average value of rate constants in M^{-1} hr^{-1}.
b) Ref. 11.
c) Rate constant obtained by taking into account autocatalysis of quaternary salt (See Experimental).

Results and Discussion

Rate data for a series of *N,N*-dimethylbenzylamine for quaternisation by methyl iodide in various solvents are given in Table 1. All the rate constants were calculated by the method of least squares and were corrected for thermal expansion of solvent.

It is necessary to compare the unitary term of rate constant k_u in each solvent, instead of rate constant, in order to examine solvent effects on reactivities.[9)] Hammett reaction "constant" is, however, a unitary quantity and independent of solution composition. In order to establish the relationship between ρ and solvent polarity, a solvent parameter for reactivity ξ_0 is defined by

$$\xi_0 = \log k_{u,0}/r_{CH_3I} - \log k_0^0 = \log r_{A0} - \log r_{M^{\neq}0} \quad (1)$$

where r_{CH_3I}, r_{A0} and $r_{M^{\neq}0}$ are the activity coefficients based upon the solvent standard state of methyl iodide, unsubstituted amine and activated complex without substituent, respectively. k_0^0 denotes the hypothetical rate constant in gas phase of the reaction of unsubstituted amine with methyl iodide which is given by[10)]

$$k_0^0 = \kappa \cdot K_0^{\neq}/R \cdot p_{A0}^0 p_{B0}^0/p_{M^{\neq}0}^0 \quad (2)$$

Application of the Hammett equation to the data of Table 1, using σ values given by Brown andMcDaniel[11)] gives the results in Table 2.[12)] There is a discrepancy between ρ^m and ρ^p. Typical plots of the data are shown in Fig. 1. The results of log $k_{u,0}/r_{CH_3I}$ or $\xi_0 + \log k_0^0$ are given in Table 2. The activity coefficient of methyl iodide in various solvents were estimated from regular solution theory.[13)] The r_{CH_3I}-values obtained in this way are compared with those determined experimentally in Table 3. The agreement between the calculated and found values is within the limit of analysis.

Relationship between ρ and ξ_0. The variation in ξ_0 with solvent is required for the changes of ρ values with solvents. Although in all solvents ρ^m is more negative than ρ^p, the mode of variation in ρ with ξ_0 is the same. The situation is illustrated by the plot of ρ against ξ_0 in Fig. 2. With respect to many solvents except for aromatic and alcoholic solvents there is a linear relationship between ρ and ξ_0. There is

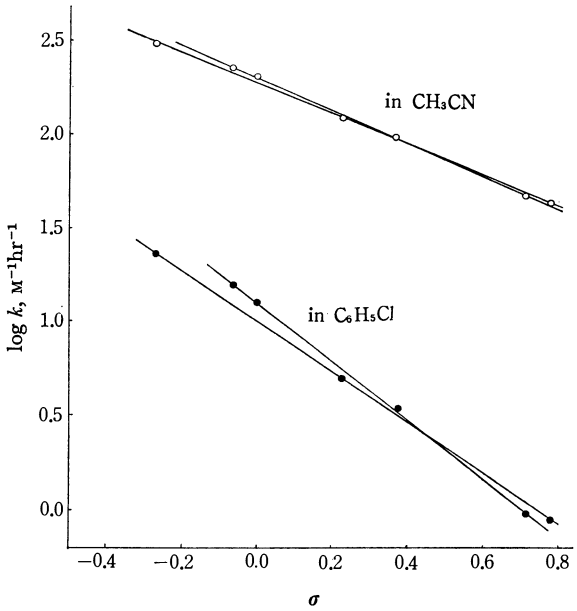

Fig. 1. Hammett plots of the reaction of *N,N*-dimethylbenzylamines with methyl iodide; ○, in CH_3CN; ●, in C_6H_5Cl.

10) S. Glasstone, K. J. Laidler, and H. Eyring, "The Theory of Rate Processes," McGraw-Hill Book Company, Inc., New York, N. Y. (1941), p. 400.
11) H. C. Brown and D. McDaniel, *J. Org. Chem.*, **23**, 420 (1958).
12) The referee commenting on the choice of substituent variables suggested that σ^0 should be chosen rather than σ for the present reaction system. However, the kinetic data correlate better with σ than with σ^0.
13) J. H. Hildebrand and R. L. Scott, "Regular Solutions," Prentice-Hall, Inc., Englewood Cliffs, N. J. (1962), p. 102.

TABLE 2. HAMMETT EQUATION CORRELATIONS

No	Solvent	*meta* substituents				*para* substituents			
		log $k_u^{0a)}$	log k_u^0/r_{CH_3I}	ρ^m	$r^{0b)}$	log $k_u^{0c)}$	log k_u^0/r_{CH_3I}	ρ^p	$r^{b)}$
1	CH_3CN	3.588	3.337	−0.875	−0.9995	3.546	3.296	−0.815	−1.0000
2	$(CH_3)_2CO$	3.144	3.142	−0.886	−0.9985	3.132	3.130	−0.844	−0.9992
3	$C_6H_5NO_2$	3.074	3.017	−1.133	−0.9984	3.061	3.004	−0.987	−0.9994
4	O O	2.387	2.387	−1.175	−0.9990	2.343	2.343	−1.150	−0.9999
5	THF	2.402	—	−1.077	—	2.138	—	−1.019	−0.9996
6	C_6H_6	1.886	1.854	−1.337	−0.9986	1.821	1.789	−1.286	−1.0000
7	CS_2	1.012	1.012	−1.869	−0.9998	0.895	0.895	−1.645	−0.9999
8	c-C_6H_{12}	−0.757	−0.881	−2.15	—	−0.908	−1.032	−2.31	—
9	$C_6H_5CH_3$	1.602	1.563	−1.341	−0.9991	1.525	1.486	−1.307	−1.0000
10	C_6H_5Cl	2.093	2.086	−1.579	−0.9996	1.992	1.985	−1.352	−0.9998
11	C_6H_5Br	2.197	2.196	−1.550	−0.9991	2.111	2.110	−1.342	−0.9998
12	CH_3OH	2.359	1.480	−0.617	−0.9993	2.334	1.455	−0.553	−0.9997
13	C_2H_5OH	2.029	1.681	−0.731	−0.9998	2.037	1.689	−0.706	−0.9959
14	*i*-PrOH	1.766	1.648	−0.874	−0.9996	1.761	1.643	−0.7575	−1.0000

a) Logarithm of unitary term of rate constant for the reaction of unsubstituted amine with methyl iodide.
b) Correlation coefficient of Hammett plot.
c) Logarithm of unitary term of rate constant for hypothetical of "*para*-unsubstituted amine" with methyl iodide.

TABLE 3. ACTIVITY COEFFICIENT OF METHYL IODIDE AT 30°C

Solvent[a)]	1	2	3	4	6	7	8	9	10	11	12	13	14
δ_1[b)]	12.1	9.57	10.9	9.87	8.95	9.87	8.13	8.85	9.40	9.77	14.2	12.6	11.4
log r_{CH_3I} (Experimental[c)])	0.493	0.346	—	—	—	—	—	—	—	—	1.01	—	—
(Calculated[d)])	0.251	0.002	0.06	0.00	0.03	0.00	0.12	0.039	0.007	0.007	0.879	0.348	0.118

a) The numbers in the table correspond to the numbers inTable 1.
b) Solubility parameters of solvent, $cal^{1/2}\ cm^{-3/2}$.
c) Values calculated from the data given by Alexander *et al.* (Ref. 22). The reproducibility seems to be within ±0.2 log unit.
d) Values estimated from equation of RT ln $r_{CH_3I} = V^0_{CH_3I}(\delta_1 - \delta_{CH_3I})^2$ where $V^0_{CH_3I}$ and δ_{CH_3I} are 63.02 cc/mol and 9.780 $cal^{1/2}cm^{-3/2}$, respectively.

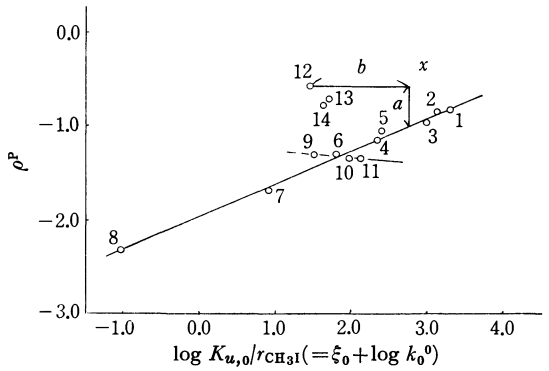

Fig. 2. Correlation of ρ^p with a solvent reactivity parameter. The numbers in the figure correspond to the numbers in Table 1.

a systematic trend that the lower the ξ_0 value the more negative the ρ value becomes.

The quantitative treatment reported previously is applied to the present system. The ρ value in an arbitrary solvent is given by

$$\rho = \rho^o + (\partial\rho/\partial\xi_0)\xi_0 \qquad (3)$$

where ρ^0 is the intrinsic ρ value. Modification of equation (3) shows the ρ value changes with the increase of solvent polarity as

$$\rho = \rho^o\{1 + 1/\rho^o \cdot (\partial\rho/\partial\xi_0)\xi_0\} \qquad (4)$$

The coefficient $1/\rho^0(\partial\rho/\partial\xi_0)$ is termed a leveling coefficient, because the value is in general negative,[14] and the second term in parentheses of Eq. (4) exerts a leveling effect upon substituent effects. For the present reaction the $\partial\rho/\partial\xi_0$ is 0.36, as shown in Fig. 2.

It is of interest to consider a necessary and sufficient condition for constancy of $\partial\rho/\partial\xi_0$. For deriving the condition we make use of the fact that the Hammett equation holds in all solvents. This is expressed in the form

$$\log k_x^o/k_0^o = \rho^o\sigma,\ \log r_{AX}/r_{A0} = \rho_A\sigma,$$
$$\log r_{M^*X}/r_{M^*0} = \rho_{M^*}\sigma \qquad (5)$$

The ξ_0-value is split into ξ_{A0} and ξ_{M^*0}. The contribution of ξ_{A0} and ξ_{M^*0} to ξ_0 is expressed by

$$\xi_0 = \log r_{A0} + (-\log r_{M^*0}) = \xi_{A0} + \xi_{M^*0} \qquad (6)$$

Combination of these equations leads to the following expression for the $\partial\rho/\partial\xi_0$.

$$\partial\rho/\partial\xi_0 = \partial\rho_A/\partial\xi_0 - \partial\rho_{M^*}/\partial\xi_0$$
$$= \partial\rho_A/\partial\xi_{A0} + \partial\rho_A/\partial\xi_{M^*0} - \partial\rho_{M^*}/\partial\xi_{M^*0} - \partial\rho_{M^*}/\partial\xi_{A0} \qquad (7)$$

14) While $\partial\rho/\partial\xi_0$ is positive for reactions in which ρ^0 seems to be negative, negative $\partial\rho/\partial\xi_0$ values are obtained for reactions in which ρ^0 seems to be positive. The former case is observed in S_N2 type reactions, *viz.*, the present system and ionization of phosphines.[9] The latter case is observed in equilibria of proton acids[4] and esterification of benzoic acids.[4]

In general ξ_{A0} is independent of ξ_{M^*0}, and Eq. (7) is modified to be

$$\partial\rho/\partial\xi_0 = \partial\rho_A/\partial\xi_{A0} - \partial\rho_{M^*}/\partial\xi_{M^*0} \quad (8)$$

Let us consider the requirement for constancy of $\partial\rho_A/\partial\xi_{A0}$ or $\partial\rho_{M^*}/\partial\rho_{M^*0}$. We assume that the ξ_x is represented by Eq. (9).

$$\xi_x = g(\xi)f(\sigma_x) \quad (9)$$

where $g(\xi)$ is a function depending upon the solvent, and $f(\sigma_x)$ is a function depending upon the substituent. It is easily shown that the $\partial\rho_A/\partial\xi_{A0}$ or $\partial\rho_{M^*}/\partial\xi_{M^*0}$ becomes independent of solvent. The reverse is also valid; the constancy of $\partial\rho_A/\partial\xi_{A0}$ or $\partial\rho_{M^*}/\partial\xi_{M^*0}$ leads to Eq. (9).

For constancy of $\partial\rho/\partial\xi_0$ the following condition is also required. The effects of solvents on reactivities are attributed to either r_A or r_{M^*}. Uniqueness of $\partial\rho/\partial\xi_0$ which is observed with respect to many solvents (Fig. 2) shows that the conditions are satisfied. We believe that r_{M^*} is an important contributing factor to the changes of reactivities with solvents. Although the value of r_A has not been obtained experimentally, the situation may be valid.[15] Even in such a very non-polar solvent as cyclohexane, r_A may be nearly equal to unity and ρ_A is zero.[16]

It is instructive to consider whether theories proposed previously concerning r are satisfied with the condition expressed by Eq. (9). Kirkwood's first approximation[17] for the stability of dipole molecules in solution seems to fulfil the requirement. A solvent function $g(\xi)$ is a function of dielectric constant of solvent $D-1/2D+1$, and a structural function $f(\sigma_x)$ is a function of dipole moment and radius of molecules μ^2/γ^3. The theory cannot explain, however, the fact that the order of reactivity changes with solvents. In applications of the theory to solvent effects on reaction rates which have been carried out by Hartmann and Schmidt,[18] it is necessary to examine whether the solvents under consideration are satisfied with conditions mentioned by Kirkwood. The same situation holds in the application of regular solution theory to the explanation of solvent effects on reaction rates.[6] We must then consider another explanation of the linear relationship between ρ_{M^*} and ξ_{M^*0}.

The concept that solvent reorientation makes a great contribution to activation thermodynamic parameters, in particular to activation entropies, may give a satisfactory explanation for the phenomenon. The following three considerations are required. First, the existence of Hammett's equation requires the condition that the reaction coordinate of activated complex remains constant within substituent changes. Second, the linear relationship between $\delta_x \log k$ and $\delta_x \log K$ requires that the degree of net charge development in the transition state of all substituted benzyl amines should be the same. Third, the linear correlation of $\delta_\xi \log k_u$ with $\delta_\xi \log K_u$ requires that the mechanism may remain constant within the solvents used.[9] These three requirements lead to the conclusion that the degree of charge distribution accompanied by an activation process varies with substituent, and the Hammett equation holds. Redistribution of electrical charge caused by a substituent affects the entropy change accompanied by solvent reorientation as the consequence of an activation. The situation is more clearly illustrated in Fig. 3. Slopes of the straight line can be determined by the ease of reorientation of solvents accompanied by an activation process. This ease is in the sequence: cyclohexane<carbon disulfide<benzene <dioxane<tetrahydrofuran<nitrobenzene<acetone< acetonitrile. The order is not related to solvent properties such as dielectric constant, solubility parameter.

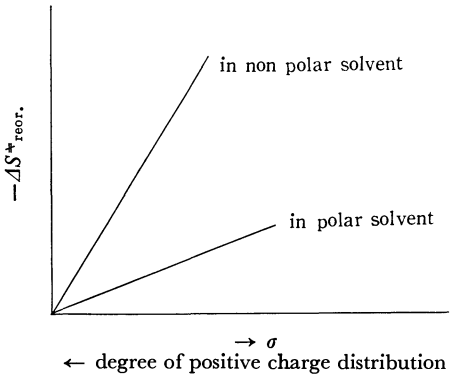

Fig. 3. Scheme for explaining the linear relationship between ρ_{M^*} and ξ_{M^*0}.

Abnormal Behavior of ρ Values in Protic Solvents. Figure 2 shows that ρ values in protic solvents, *i. e.*, methanol, ethanol, and isopropanol, are more positive than expected from the small ξ_0 values in these solvents. Judging from the 1-1 hydrogen-bonded complex formations between alcohols and amines,[19] the first term on the right of Eq. (8) seems to play a still more important role. As a result of these relatively strong interactions, ξ_{A0} in alcohols is more negative than in other solvents. The interaction exercises a more profound influence upon the stability of amines with electron-donating substituents than that with electron-withdrawing substituents. Any deviation with regard to alcohols, as shown in Fig. 2, is thus observed.

The situation is quantitatively treated as follows taking the ρ value in methanol as an example. The method has been adopted to explain the solvent effects on the reaction of pyridine with methyl iodide. The logarithmic ratio of activity coefficient of benzylamine to that of dimethylaniline, $\log r_{Ax}^{CH_3OH}/r_{DMA}^{CH_3OH}$ is determined by a deviation with regard to methanol from a plot of $\log k_u(\text{DMA}+CH_3I)$ *vs.* $\log k_u(\text{X}\cdot\text{DMBzA}+CH_3I)$ values for solvents. The plot of $\log r_{Ax}^{CH_3OH}/$

15) Validity can be judged by volume change experiment for the solution processes. The excess volume of amines in various aprotic solvents is nearly equal to zero. H. Hartmann, H. D. Brauer, H. Kelm, and G. Rinck, *Z. Physik. Chem.*, (*Frankfurt*), **61**, 553 (1968).

16) Dimerization phenomenon is considered to have important effect on activity coefficient of bases. According to Bruckenstein and Untereker (*J. Amer. Chem. Soc.*, **91**, 5741 (1969)), tertiary amines do not dimerize in hexane at the concentration used in the present work.

17) J. G. Kirkwood, *J. Chem. Phys.*, **2**, 351 (1934).

18) H. Hartmann and A. P. Schmidt, *Z. Physik. Chem.*, (*Frankfurt*), **62**, 312 (1968).

19) R. W. Taft, D. Gurka, L. Joris, P. von R. Schleyer, and J. W. Rakshys, *J. Amer. Chem. Soc.*, **91**, 4801 (1969), and the references cited. Data on excess volume of amines in alcohols (ref. 5) also show that amines are very stable in these solvents.

$r_{DMA}^{CH_3OH}$ *vs.* σ results in 0.38 for the value of ρ_A which is given as the distance a in Fig. 2. The deviation of point x in the figure from the straight line of usually accepted $\rho-\xi_0$ relationship is assigned to the log $r_{Ax}^{CH_3OH}$ value and is expressed by the distance b in the figure. The condition expressed by the following equation is required.

$$\log r_{Ax}/r_{A0} = 0.38\sigma_x;\ \log r_{A0} = -1.30 \qquad (10)$$

ρ Values in Aromatic Solvents with Small Dielectric Constant. As shown in Fig. 2, ρ values in aromatic solvents with comparable dielectric constant with that of benzene decrease with increasing reactivities in the solvents. The negative sign of interaction between solvent- and substituent-variable is observed in the solvents. This is in striking contrast to the behavior of ρ values in other solvents. The behavior has also been observed for the reaction of *N,N*-dimethylanilines with methyl picrate.[1] The normal behavior of ρ values result from the important role of a specific solvation of a leaving anion in a transition state. This type of solvation may be closely related to the polarizability of aromatic nucleus in the solvents. The effect is in the sequence: toluene<benzene<chlorobenzene<bromobenzene.[1,20] The susceptibility of a leaving anion I(δ-) to the solvation seems to be dependent on the tightness[21] of developing charge δ-. Accordingly, the demand for solvation stabilization by the various transition states will vary with substituent. In the case of the electron-withdrawing substituents the departing charge δ- will be more localized than in the case of electron-donating substituents. The $I(\delta$-) entity with tight character will have less solvation demand than will that with loose character. Thus the rate of quaternization of benzylamines substituted by electron-withdrawing groups is less sensitive to the effects of solvents in passing from toluene to bromobenzene than those substituted by electron-donating groups, the ρ values decreasing with the ξ_0 values in aromatic solvents.

Our explanation is in marked contrast to the view proposed by Alexander *et al.*[22] that "one cannot concentrate on only one end of a transition state." If it is so and the degree of solvent reorientation changes with only the net value of developing charge in the whole species of a transition state, a single straight line should be observed for $\rho-\xi_0$ relationship.

Experimental

Materials. *N,N*-dimethylbenzylamine and its derivatives were prepared according to Eliel *et al.*[23] from benzyl halide or its derivatives. Reagent grade benzyl chloride was obtained from Wako Pure Chemicals. *p*-Nitro- and *m*-nitrobenzyl bromides were prepared by bromination of *p*-nitro-[24] and *m*-nitrotoluene[25] respectively. *m*-Chlorobenzyl bromide was prepared according to the directions of Jenkins.[26] *p*-Methoxybenzyl chloride was prepared by the reaction of anisyl alcohol with hydrochloric acid.[27] *p*-Chlorobenzyl- and *m*-xylyl chloride were prepared by chlorination of *p*-chlorotoluene and *m*-xylene respectively according to Kharasch and Brown.[28] The prepared amines were dried over KOH pellet and distilled in a vaccum at least three times. The following boiling points were obtained: *N,N*-dimethylbenzylamine, 34—34.5°C/2 mmHg; *p*-methoxy-*N,N*-dimethylbenzylamine, 74—77°C/2.5 mmHg; *m*-methyl-*N,N*-dimethylbenzylamine, 85—85.5°C/19.5 mmHg; *m*-chloro-*N,N*-dimethylbenzylamine, 66—67°C/3 mmHg; *m*-nitro-*N,N*-dimethylbenzylamine, 112—114°C/3.5 mmHg; *p*-chloro-*N,N*-dimethylbenzylamine, 68—73°C/2.5 mmHg; *p*-nitro-*N,N*-dimethylbenzylamine, 125—127°C/6 mmHg. Purity of these samples was ascertained by gas-liquid chromatography, employing a Hitachi K53 gas chromatograph (Z 45 Column).

Methanol, tetrahydrofuran, acetonitrile, acetone, carbon disulfide, benzene, nitrobenzene, and bromobenzene were purified by the method previously described.[1,9] Toluene

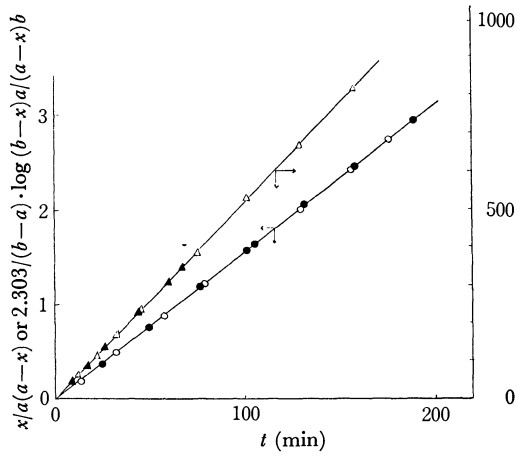

Fig. 4. Second-order rate plots for reactions of methyl iodide with *m*-nitro-*N,N*-dimethylbenzyl amine in chlorobenzene and with *p*-methoxy-*N,N*-dimethylbenzylamine in acetonitrile: in chlorobenzene, ○, $[CH_3I]_0$=0.0147M, $[CH_3I]_0$/[Amine]$_0$=1.00; ●, $[CH_3I]_0$=0.0204M, $[CH_3I]_0$/[Amine]$_0$=2.98; in acetonitrile, △, $[CH_3I]_0$=0.0030lM, $[CH_3I]_0$/[Amine]$_0$=1.00; ▲, $[CH_3I]_0$=0.00188M, $[CH_3I]_0$/[Amine]$_0$=1.64.

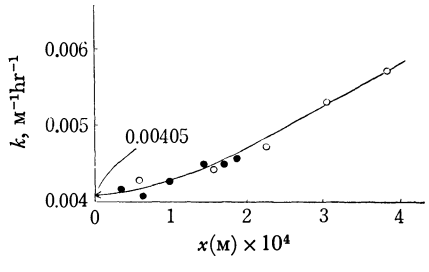

Fig. 5. Plot of second-order rate constants *vs.* concentration of salt produced for reaction of *p*-chloro-*N,N*-dimethylbenzylamine with methyl iodide in cyclohexane: ○, $[CH_3I]_0$=[Amine]$_0$=0.0797M; ●, $[CH_3I]_0$=[Amine]$_0$=0.0623M.

20) J. P. Reinheimer, J. D. Harley, and W. W. Meyers, *J. Org. Chem.*, **28**, 1575 (1963).
21) J. B. Hyne and R. Wills, *J. Amer. Chem. Soc.*, **85**, 3650 (1963),
22) R. Alexander, E. C. F. Ko, A. J. Parker, and T. Broxton, *ibid.*, **90**, 5049 (1968).
23) E. L. Eliel, T. N. Ferdinand, and Sr. M. C. Herrman, *J. Org. Chem.*, **19**, 1693 (1954).
24) G. H. Coleman and G. E. Honeywell, "Organic Syntheses," Coll. Vol. II, p. 443. (1948),
25) R. L. Bent *et al.*, *J. Amer. Chem. Soc.*, **73**, 3100 (1951).
26) S. S. Jenkins, *ibid.*, **55**, 2897 (1933).
27) K. Rorig, J. D. Johnston, R. W. Hamilton, and T. J. Telinski, "Organic Syntheses," Vol. 36, p. 50. (1956),
28) M. S. Kharasch and H. C. Brown, *J. Amer. Chem. Soc.*, **61**, 2142 (1939).

and chlorobenzene were shaken with concentrated sulfuric acid several times and washed with water, aqueous potassium hydroxide, and then with water, dried over calcium chloride, and distilled. The center fraction was further distilled twice from phosphorus pentoxide. Cyclohexane,[29] ethanol,[30] and dioxane[31] were purified as described in literature. Isopropanol was purified by a method similar to that for ethanol.

Kinetic Procedure. The technique of the potentiometric kinetic measurements has been described in detail.[9] Reaction in solvents fitted into second order plots. Typical second order plots are shown in Fig. 4. Comparison was always made by results obtained with a different initial concentration. Reproducibility was mostly within $\pm 1\%$. Initial concentration of each reactant was 0.002—0.02M except for the reaction in cyclohexane where the reactant solutoin of about 0.05M was used for kinetic measurements.

In two cases the second order rate constants increased as the reaction proceeded, a phenomenon reported by Laidler and Hinshelwood[32] and attributed to autocatalysis by quaternary salt. In the reaction of *p*-chloro-*N*,*N*-dimethylbenzylamine with methyl iodide in cyclohexane the increase was bout 50% at 0.5% conversion, and was somewhat larger for the reaction of *m*-chloro-*N*,*N*-dimethylbenzylamine with methyl iodide in the same solvent. In both cases plots of rate constants *vs.* concentrations of salts produced enable us to calculate the rate constant at zero conversion, as shown in Fig. 5. We believe that the constants obtained in this manner are accurate within about $\pm 3\%$.

The reactions of *p*-nitro- and *m*-nitro-substituted amines with methyl iodide in cyclohexane were too slow to determine rate constants of these reactions with reasonable accuracy.

29) R. W. Crowe and C. P. Smith, *ibid.*, **73**, 5406 (1951).
30) F. W. Breivogel, Jr., *J. Phys. Chem.*, **73**, 4203 (1969).
31) A. Rieche, *Angew. Chem.*, **44**, 896 (1931).
32) K. J. Laidler and C. N. Hinshelwood, *J. Chem. Soc.*, **1938**, 838.

BULLETIN OF THE CHEMICAL SOCIETY OF JAPAN, VOL. 44, 761—765 (1971)

A Study of the Catalytic Partial Oxidation of Hydrocarbons. VI. The Effect of Molybdenum Addition to the Vanadium Oxide Catalyst on the Oxidation of Butene to Maleic Anhydride

Mamoru Ai

Research Laboratory of Resources Utilization, Tokyo Institute of Technology, Ookayama, Meguro-ku, Tokyo

(Received March 17, 1970)

In the present work, the vapor-phase partial oxidation of *cis*-2-butene was carried out using V_2O_5-MoO_3 catalysts with different compositions, at 350°C, and at a butene content of 0.65% in air, in order to elucidate the effect of the addition of MoO_3 to the V_2O_5 catalyst on the selectivity and the mechanism for maleic anhydride formation. Two types of catalytic specificities were found, depending upon the Mo content: in the range of less than 20 atom% Mo, the specificity was similar to that of V_2O_5 alone, while in the range of more than 50 atom% Mo, a different specificity was observed, one which gave 1.2 times the yield of maleic anhydride than did V_2O_5 alone or the Mo-poor catalysts. The increase in the selectivity of butene to maleic anhydride which occurred when a large amount of MoO_3 was doped is considered to be caused by the increase in the selectivity of the $C_4H_4O \rightarrow MA$ step, not in that of the $C_4H_8 \rightarrow C_4H_6$ or $C_4H_6 \rightarrow C_4H_4O$ step. The selectivity of the side pathway in the $C_4H_8 \rightarrow C_4H_6$ step was so great that no satisfactory maleic anhydride yield from butene can be expected by the use of the V_2O_5-MoO_3 catalyst.

In previous papers, the mechanism of the catalytic oxidation of butene to maleic anhydride (MA) over V_2O_5 and V_2O_5—P_2O_5 catalysts, and the effect of the addition of P_2O_5 to a V_2O_5 catalysts, have been investigated.[1-3]

Regarding the binary system of V_2O_5–MoO_3, the effect of the catalyst composition on the selectivity and the mechanism of butadiene and furan (C_4H_4O) oxidation have also been reported in a former paper.[4] The results showed that the selectivity of butadiene to maleic anhydride is increased about 20% by the addition of a large amount of MoO_3 to the V_2O_5 catalyst; this increase is considered to be attributable to the increase in selectivity for the $C_4H_4O \rightarrow MA$ step, not to that for the $C_4H_6 \rightarrow C_4H_4O$ step. Nevertheless, the effect of the catalyst composition on butene oxidation is still obscure.

In the present work, we attempted to ascertain how the addition of MoO_3 to the V_2O_5 catalyst affects each reaction step in the step-by-step oxidation of butene to maleic anhydride and to elucidate this effect on the mechanism and the selectivity of the partial catalytic oxidation of butene.

Experimental

The vapor-phase air oxidation of *cis*-2-butene with a large amount of oxygen was carried out over various vanadium-molybdenum oxide catalysts with different compositions, in an ordinary flow-type reaction and at atmospheric pressure, as has been shown in the previous papers.[1-4]

1) M. Ai, K. Harada, and S. Suzuki, *Kogyo Kagaku Zasshi*, **73**, 524 (1970).
2) M. Ai, T. Niikuni, and S. Suzuki, *ibid.*, **73**, 165 (1970).
3) M. Ai, This Bulletin, **43**, 3490 (1970).
4) M. Ai, *Kogyo Kagaku Zasshi.*, **73**, 950 (1970).

The volume concentration of butene was about 0.65% in air, and the flow rate was kept at 1.5 *l*/min. The contact time was varied between 0.002 and 1.6 sec. This was done by changing the amount of the catalysts. The reaction temperature was always kept at 350°C. The experimental and analytic procedures were also the same as those employed in the previous works.[1-4]

The catalysts employed in the experiments were prepared as follows: the required quantities of NH_4VO_3 and $(NH_4)_6Mo_7O_{24}$ were dissolved in hot water by using oxalic acid, after which, pumice, of a mesh size of 10 to 20, was added to the above solution; then the solution was evaporated with constant stirring and finally dried in an oven at 130°C. The amount of pumice was 400 m*l*/g atom of vanadium and molybdenum. The catalyst was calcined under flowing air, at 500°C, for 5 hr.

Results and Discussion

Effect on the Oxidation Activity. Figure 1 shows the total butene conversion (excepting isomerization) at 350°C as a function of the contact time for various compositions of V_2O_5–MoO_3 catalysts. As the plot of log (C_t/C_0), where C_0 and C_t are the concentrations of butene in the charge and the effluent gas respectively, against the contact time gave a straight line, the rate of butene oxidation can be considered to be nearly of the first order for the butene concentration. The rate constants, calculated at 350°C over various V_2O_5–MoO_3 catalysts, were compared with those of butadiene or furan oxidation reported in a previous paper[4] (Fig. 2).

The oxidation of butene, butadiene, and furan were of the same order of magnitude at the same catalyst composition; they formed the sequence; $C_4O_8 < C_4H_6 < C_4H_4O$. The oxidation activity for each reactant increased gradually with the addition of MoO_3 in the range of less than 20 atom%, and then it decreased little by little with an increase in the Mo content in the region over 20 atom% Mo. It thus seems that, in MoO_3-rich compositions, MoO_3 acts only as a diluent. This result was very similar to that of benzene oxidation reported by Ioffe.[5]

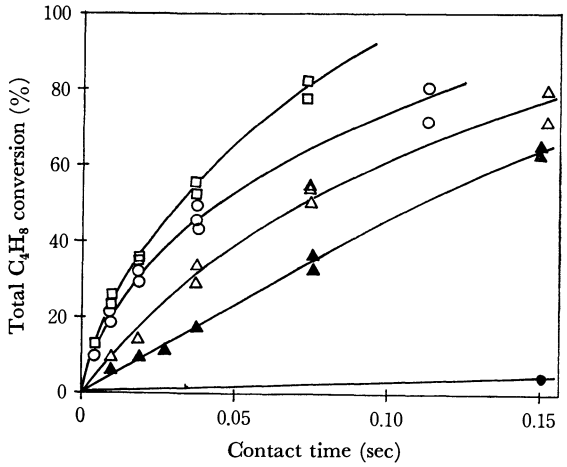

Fig. 1. Total conversion of butene as a function of contact time.
at 350°C, C_4H_8: air=0.65:100, catalyst composition (atomic ratio)
○: Mo/V=0, □: 1/4, △: 1, ▲: 4/1, ●: Mo only

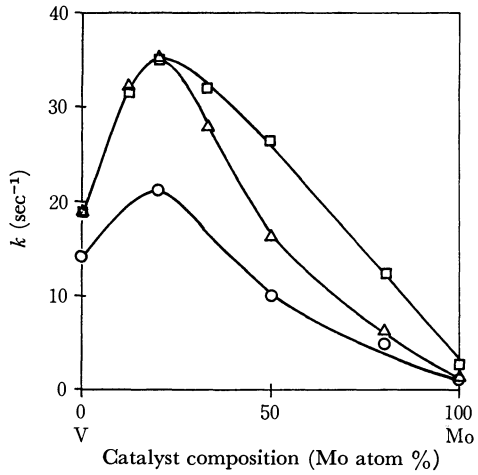

Fig. 2. The relationship of the oxidation activity *versus* the catalyst composition.
at 350°C, reactant: air=0.6—1.0: 100
○: C_4H_8, △: C_4H_6, □: C_4H_4O

Isomerization of Butene. The oxidation of butene was always accompanied by its isomerization. The conversion of *cis*-2-butene to such isomers as *trans*-2-butene and 1-butene is shown as a function of the total *cis*-2-butene conversion in Fig. 3. The results revealed that the formation of the isomers decreased with an increase in the oxidation activity of the catalyst. To clarify the cause of this, the conversion of *cis*-2-butene to *trans*-2-butene and 1-butene was plotted *versus* the contact time at 350°C for each catalyst (Fig. 4). The results suggest that the isomerization activity was independent of the compositions of V_2O_5 and MoO_3, and that only the oxidation activity was affected by the catalyst composition. In the case of a continuous experiment like this, it was observed that, in the absence of oxygen in the charge, neither the isomerization of

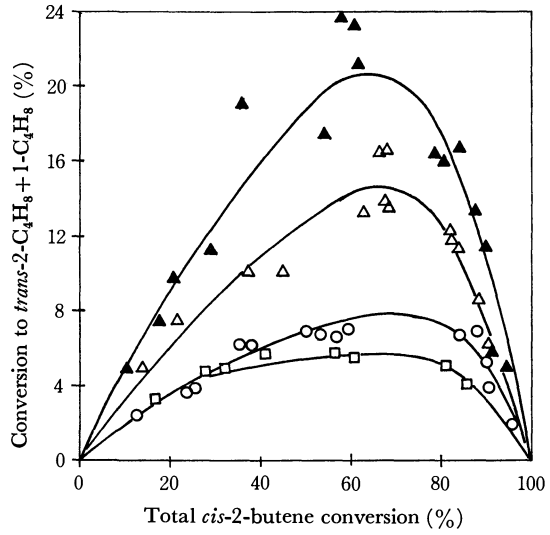

Fig. 3. Formation of isomers of *cis*-2-butene as a function of total *cis*-2-butene conversion.
at 350°C, C_4H_8: air=0.65:100
○: Mo/V=0, □: 1/4, △: 1, ▲: 4/1

5) I. I. Ioffe, *Kinetics and Catalysis (USSR) (Eng. Transl.)*, **3**, 165 (1962); **7**, 670 (1966).

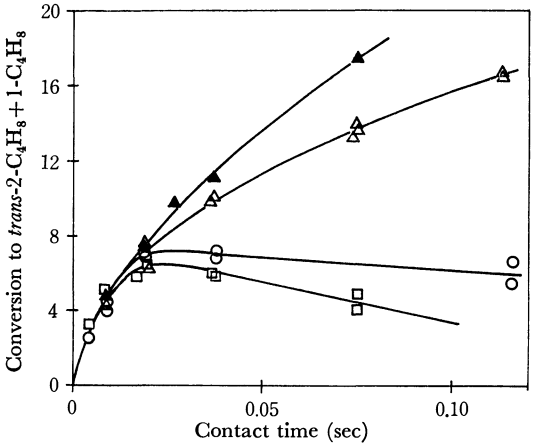

Fig. 4. The relationship of the conversion of *cis*-2-butene to *trans*-2-butene and 1-butene *versus* contact time for each catalyst.
at 350°C, butene: air=0.65:100
○: Mo/V=0, □: 1/4, △: 1, ▲: 4/1

butene nor oxidation occurred over these catalysts; therefore it was considered that the presence of oxygen was necessary even to the isomerization of butene.

Effect on the Maleic Anhydride Formation. The formation of maleic anhydride from butene over V_2O_5–MoO_3 catalysts with different compositions and at 350°C is shown as a function of the total butene conversion in Fig. 5. Selectivity to maleic anhydride was defined thus: conversion to maleic anhydride/total butene conversion. The slopes of these plots, therefore, correspond to the differential selectivity at each butene conversion. These plots of the performance gave two lines, depending upon the Mo content in the catalyst, *i. e.*, Mo-poor (Mo<20 atom%) and Mo-rich (Mo>50 atom%) catalysts. Over the catalysts containing less than 20% Mo, the selectivity to maleic anhydride was less than 20% and did not vary with the Mo content. When the butene conversion was more than 70%, the formation of maleic anhydride decreased, probably because of the destruction of maleic anhydride; therefore, the formation did not exceed 15%. On the other hand, in the case of the Mo-rich catalysts, selectivity to maleic anhydride was also constant with an increase in the Mo content, and the selectivity at

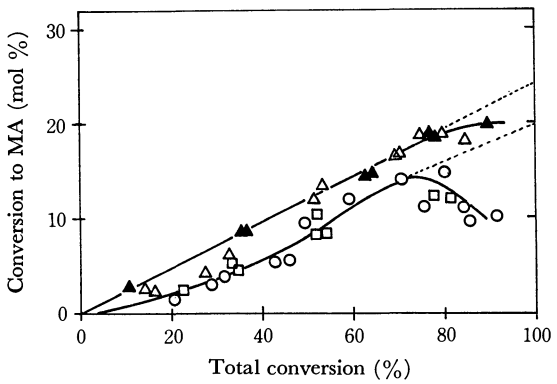

Fig. 5. Effect of catalyst composition on maleic anhydride formation.
at 350°C, C_4H_8: air=0.65:100
○: Mo/V=0, □: 1/4, △: 1, ▲: 4/1

butene conversion of 70% reached 24%. The maximum formation of maleic anhydride reached 20 mol%.

Effect on Intermediate Formation. The formation of butadiene and furan, which may be considered as a primary and a secondary intermediate respectively, in the step-by-step oxidation of butene to maleic anhydride, is shown in Fig. 6. The results reveal that the higher the oxidation activity of the catalyst became, the lower the intermediate formation became, while the maximum conversion to the intermediate always occurred at about 40% butene conversion. However, the amount of intermediate products over the V_2O_5–MoO_3 catalyst was far lower than that obtained over the V_2O_5–P_2O_5 catalyst.[1,3]

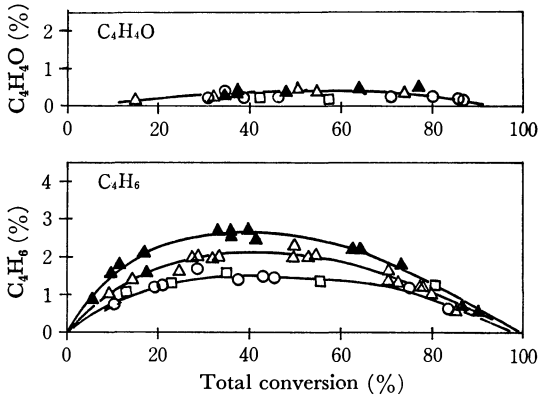

Fig. 6. Effect of catalyst composition on intermediates (butadiene and furan) formation. (Notation as in Fig. 5)

Effect on Side Reactions. A number of by-products have been found in the oxidation of butene over the V_2O_5–P_2O_5 catalyst,[1] while over the V_2O_5 and V_2O_5–MoO_3 catalysts, the major by-products were CO, CO_2, acetaldehyde (AcH), and acetic acid (AcOH); the other products were almost negligible. The conversion to AcH+AcOH (based on the assumption that two moles of AcOH or AcH are formed from one mole of butene, *i. e.*, 1/2 of the real amount of AcH+AcOH) is shown as a function of the total butene conversion in Fig. 7. The results show that the selectivity of butene to AcH and AcOH is almost independent of the catalyst

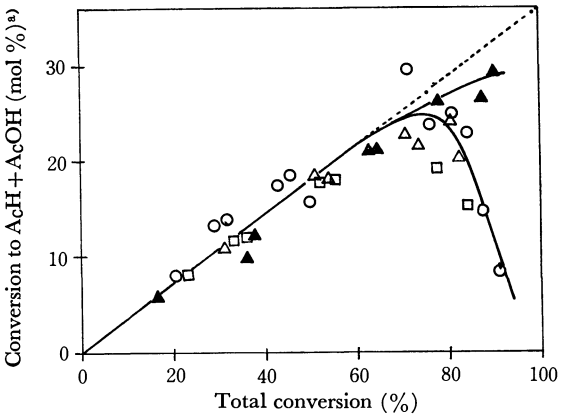

Fig. 7. Conversion to AcH+AcOH[a)] as a function of total butene conversion for various composition of V-Mo catalyst.
a) Basing on the assumption that 2 mol of AcH+AcOH are formed from 1 mol of C_4 compound. (Notation as in Fig. 5)

composition and is about 36% at a butene conversion of less than 70%. The formation of AcH and AcOH decreased, the amount being greatest at a conversion of about 80%, probably because of the destruction of AcH and AcOH.

The conversions to CO and CO_2 are shown as a function of the butene conversion in Figs. 8 and 9. The results reveal that the formation of CO and CO_2 increases rapidly at conversions of above 80%, probably because of the destruction of AcH, AcOH, and maleic anhydride. The CO_2 formation is independent of the catalyst composition, while the CO formation gives one of two lines, depending upon the Mo content, similarly catalyst containing more than 50% Mo showed a low selectivity to CO formation, *i. e.*, the formation was about a half of that obtained by means of the Mo-poor catalyst.

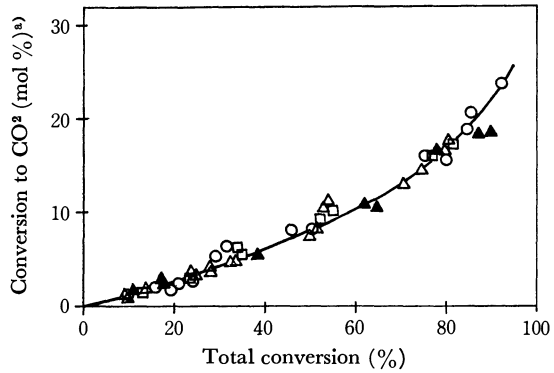

Fig. 8. Conversion[a] to CO^2 as a function of total butene conversion for various composition of V-Mo catalysts.
a) 1/4 of the real amount of the formation.
(Notation as in Fig. 5)

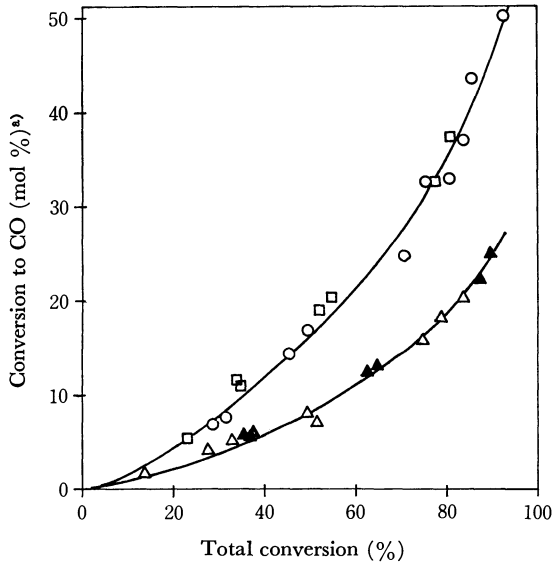

Fig. 9. Conversion[a] to CO as a function of total butene conversion for various composition of V-Mo catalysts.
a) 1/4 of the real amount of the formation.
(Notation as in Fig. 5)

Discussion of the Effect of the MoO_3 Addition. In combination with the data in the previous report,[4] the selectivity to maleic anhydride is summarized in Table 1.

Table 1. Selectibity to maleic anhydride (%)

Catalyst	Reactant		
	C_4H_8	C_4H_6	C_4H_4O
V_2O_5, V_2O_5-MoO_3(Mo<20 %)	20	43	60
V_2O_5-MoO_3 (Mo >50 %)	24	53	73

Table 2. Selectibities of the steps (%)

Catalyst	Step		
	C_4H_8 ↓ C_4H_6	C_4H_6 ↓ C_4H_4O	C_4H_4O ↓ MA
V_2O_2, V_2O_5-MoO_3 (Mo >20 %)	46	72	60
V_2O_5-MoO_3 (Mo >50 %)	46	72	73

Since the amount of the intermediate (butadiene or furan) formed in the oxidation of butene and butadiene[4] to maleic anhydride over the V_2O_5–MoO_3 catalyst was quite small, it is difficult to know exactly how the main reaction pathway for the oxidation of butene proceeds. An assumption has been made that the main reaction proceeds, in the same manner as over the V_2O_5–P_2O_5 catalyst,[1,3] as follows: $C_4H_8 \rightarrow C_4H_6 \rightarrow C_4H_4O \rightarrow MA$. The selectivities towards the main reaction pathway in each consecutive step have been calculated and reported in an earlier paper;[3] they are shown in Table 2. From the above results and the results of butadiene oxidation,[4] the probable scheme of the butene oxidation over Mo-poor (Mo<20 atom%) and Mo-rich (Mo>50 atom%) catalysts may be proposed to be as follows:

V_2O_5, V_2O_5–MoO_3 (Mo<20 atom%)

C_4H_8[100]→C_4H_6[46]→C_4H_4O[33]→MA[20]

AcH+AcOH[36] [18] (54/46) [54] (28/72) [13] (40/60) [13] by-products (CO, CO_2, etc.)

V_2O_5–MoO_3 (Mo>50 atom%)

C_4H_8[100]→C_4H_6[46]→C_4H_4O[33]→MA[24]

AcH+AcOH[36] [18] (54/46) [54] (28/72) [13] (27/73) [9] by-products (CO, CO_2, etc.)

From the results it was found that the addition of less than 20 atom% Mo to V did not affect the catalytic specificity and the Mo-poor catalyst gave the same specificity as V_2O_5 alone, although the doping modified the oxidation activity. On the other hand, the addition of more than 50 atom% Mo to V gave another catalytic specificity, one which was milder and which brought a higher selectivity to maleic anhydride. These two kinds of catalytic specificities may be caused by two different catalytic species. Similar results were observed in toluene oxidation over the V_2O_5–MoO_3 catalyst system.[6] In the range of less than 30 atom% Mo, maleic anhydride was formed mainly, while in the

6) M. Ai, *Kogyo Kagaku Zasshi*, **73**, 946 (1970).

addition of more 40 atom% Mo to V benzaldehyde was the major product.

Many past studies devoted to the physico-chemical properties of the binary system of the V_2O_5–MoO_3 catalyst[5,7-10] have indicated that, in the range of less than 14 atom% Mo, MoO_3 forms a solid solution of the substituted type with V_2O_5, and the active species was considered to be V_2O_5, modified by MoO_3, while the addition of more 33 atom% Mo to V formed a mixture of a new compound (probably $Mo_6V_9O_{40}$) and MoO_3.

Therefore, it may be suggested that, in the Mo-poor catalyst, V_2O_5 acts as an active species, while in the Mo-rich catalyst, the new compound ($Mo_6V_9O_{40}$) acts as the active species and MoO_3 acts only as a diluent. A perusal of the results indicates that the 20% increase (from 20 to 24%) of the selectivity of butene to maleic anhydride which occurred when a large amount of MoO_3 in V_2O_5 was doped may be attributed to the 20% increase (from 60 to 73%) in the selectivity in the $C_4H_4O \rightarrow MA$ step, not in the $C_4H_8 \rightarrow C_4H_6$ or $C_4H_6 \rightarrow C_4H_4O$ step. That is the addition of MoO_3 did not affect the selectivity in the $C_4H_8 \rightarrow C_4H_4O$ step. It may be concluded that, for butene oxidation, satisfactory results cannot be expected by the use of the binary system of V_2O_5–MoO_3.

7) S. Yoshida, *Shokubai*, **10**, 90 (1968).
8) R. Munch and E. D. Pierron, *J. Catal.*, **3**, 406 (1964).
9) K. Tarama, S. Teranishi, and T. Yasui, *Kogyo Kagaku Zasshi*, **60**, 1222 (1955).
10) A. Magneli and B. Oughton, *Acta Chem. Scand.*, **5**, 585 (1951).

BULLETIN OF THE CHEMICAL SOCIETY OF JAPAN, VOL. 44, 765—771 (1971)

Mechanism of The Ullmann Condensation Reaction. II.[1,2] Effects of the Medium, the Additives and the Substituents

Tran Dinh TUONG and Mitsuhiko HIDA

Department of Synthetic Chemistry, Faculty of Engineering, The University of Tokyo, Hongo, Tokyo

(Received May 12, 1970)

The effects of the medium, the additives, and the oxidation state of the copper catalyst on the rate of the Ullmann condensation reaction of sodium 1-amino-4-bromoanthraquinone-2-sulfonate and aniline in an aqueous buffered solution were investigated. The reaction rate was not affected by the ionic strength but depended very largely on the hydrogen-ion concentration. It was also established that the reaction was retarded by the addition of anions which can coordinate to copper; the retarding effect was in the order: $F^- \ll Cl^- < Br^- < I^- < CN^-$. The inhibiting effects of copper-chelating agents and oxygen were also observed. No marked difference, except a slight increase in initial rate, was observed when cuprous chloride was used as the catalyst instead of cupric sulfate. The effect of the substituents of aniline on the reaction rate can be expressed by Yukuwa-Tsuno's equation, in which the parameters, ρ and r, were -2.20 and 0.50 respectively. The experimental results are discussed.

Previous studies[2] of the Ullmann condensation of sodium 1-amino-4-bromoanthraquinone-2-sulfonate (I) and aniline in an aqueous buffered solution, cupric sulfate being used as the catalyst, have shown that the reaction was first order in monomeric aryl halide (I) and first order in amine, while the rate depended hyperbolically on the concentration of cupric sulfate. The reaction was also characterized by a relatively low activation energy (9.14 kcal/mol) and a low frequency factor (10^6). These preliminary results, however, are not sufficient for a discussion of the elementary processes of this Ullmann condensation reaction. This paper will describe some supplemental results which, it is believed, will give more insight into the detailed mechanism.

Results and Discussion

The rate of the reaction (1) was determined under various conditions of the medium. Cupric sulfate was used as the catalyst except when otherwise stated.

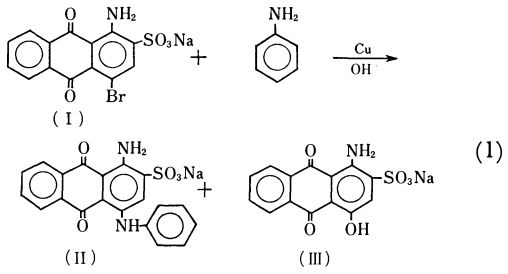

(1)

Effect of The Ionic Strength. The ionic strength of the reaction system was varied by adding an inorganic salt. Sodium sulfate was chosen for this purpose because of its great solubility in water and because of the poor coordinating ability of the sulfate ion.

As is shown in Fig. 1, through a wide range of ionic strength (μ), no marked influence was observed. In view of this fact, it is unlikely that the rate controlling step, or the equilibria preceding it, involve "true" ionic

1) Presented in Part at the Annual Meetings of The Chemical Society of Japan, March, 1968 (Osaka); April, 1969 (Tokyo), and April, 1970 (Tokyo).

2) Part I: T. D. Tuong and M. Hida, This Bulletin, **43**, 1763 (1970).

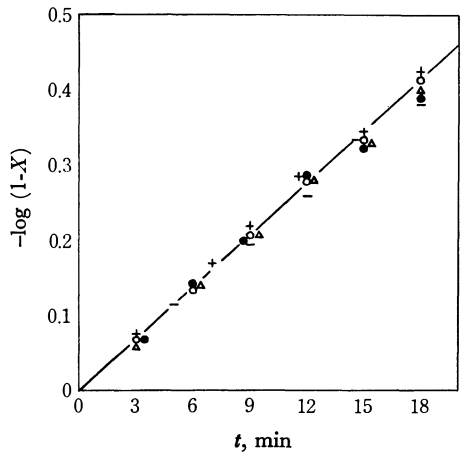

Fig. 1. Effect of ionic strength (X: reaction conversion). [I]= 0.31×10^{-2}mol/l, [$PhNH_2$]=0.30 mol/l, [Cu^{2+}]=2.50×10^{-4} mol/l; pH=9.94, T=70°C. Experiments in nitrogen. μ=0.435 (○), 0.585 (△), 0.885 (—), 1.035 (+), 1.485 (●).

species. This assumption is partly in agreement with the thermodynamical finding that the frequency factor was quite low. This cannot explained by any mechanism involving collisions between oppositely-charged ions in the rate-determining step.[3,4]

Effect of the Hydrogen-ion Concentration. A series of experiments was carried out under various pH conditions (9.37—11.51) which were attained by combining a 0.20M sodium carbonate aqueous solution and a 0.15M borax aqueous solution. The results (Fig. 2) show that no simple relationship exists between the hydrogen-ion concentration and the reaction rate. Because of the absence of the effect of the ionic strength, the behavior observed must be attributed to the action of the hydroxide ion. The presence of an optimum pH can be explained by the assumption that the hydroxide ion acts as both accelerating and retarding species.

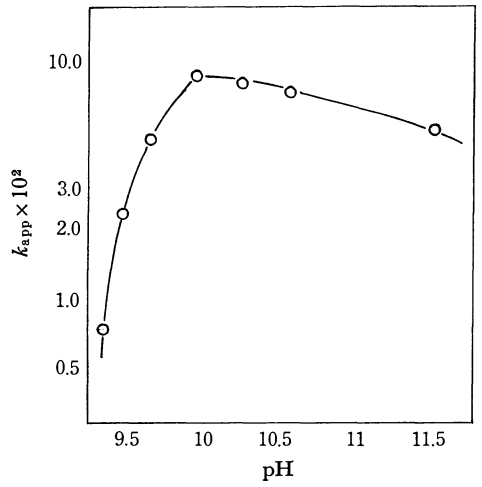

Fig. 2. Semi-logarithmic plots of k_{app} *vs.* pH. [I]=1.25×10^{-2} mol/l, [$PhNH_2$]=0.30 mol/l, [Cu^{2+}]=2.50×10^{-4}mol/l; T=70°C. Experiments in nitrogen.

In the pH range studied, no product other than that described in Eq. (1) was observed; the main product (II) was predominantly produced, along with a 4-hydroxy compound (III) in almost negligible amounts (0—3%). Therefore, the change in the rate could not be attributed to the formation of by-products.

In an aqueous solution, the amine exists as free and protonated species. The equilibrium:

$$PhNH_2 \overset{H^+}{\rightleftharpoons} Ph\overset{+}{N}H_3 \qquad (2)$$

is shifted to the left at a high pH. Since aniline exists as a free base in the pH range used in our experiments, the accelerating effect can be understood by assuming the formation of the $PhNH^-$ which has a greater nucleophilic character and electron-transfer ability to the cupric species than aniline itself. As will be seen later, the process of reducing the divalent metal ion is believed to play an important role in the reaction.

On the other hand, the fact that the rate constant did not vary with the time suggests that the active catalyst is consumed, but then regenerated by a cyclic process. Several results to be described later in this paper suggest that the $Cu^{2+}\rightleftarrows Cu^+$ process is operative. The influence of the alkalinity of the medium on this redox process might be involved. This kind of effect has been observed in several redox equilibria of metal ions in water.[5-7] In our case, it seems reasonable to consider the effect of the pH on the redox potential and to postulate that the coordination to the metal ions of the negative hydroxide ion, OH^-, will favor the removal of one electron from the univalent copper ion by electrostatic repulsion. This argument has been used to explain the influence of charged ligands on the equilibrium of the Fe^{2+}—Fe^{3+} couple in water.[7] If, in the Ullmann condensation, the univalent copper is responsible for the promotion of the reaction, the coordination of the hydroxide ion will result in a decrease in the cuprous concentration, and, thence, in a deceleration of the rate. It has been reported[8] that the Ullmann condensation of bromobenzene with the disodium salt of resorcinol in pyridine was inhibited by the hydroxide ion (generated from added sodium hydroxide or methoxide). The effect may be partly accounted for by the coordination of the hydroxide ion to the catalyst, although the detailed mechanism of deactivation has not yet been made clear.

Finally, it was suggested that the hyperbolic dependence of the reaction rate on the concentration of the catalyst can be explained by postulating the formation of copper clusters.[2] The hydroxide ion, by its ability to act as bridge between the metal ions, may facilitate the process yielding the inactive polynuclear complexes and decrease the rate.

Effect of Molecular Oxygen. When experiments were carried out in air, the reaction rate was markedly

3) A. A. Frost and R. G. Pearson "Kinetics and Mechanism," John Wiley & Sons, 2nd. Ed. (1961), p. 130.
4) R. P. Bell, *J. Chem. Soc.*, **1943**, 629.
5) F. Basolo and R. G. Pearson "Mechanisms of Inorganic Reactions," John Wiley & Sons, 2nd. Ed. (1967), p. 474.
6) B. R. James and R. J. P. Williams, *J. Chem. Soc.*, **1961**, 2007.
7) Ref. 5, p. 76.
8) A. L. Williams, R. E. Kinney, and R. F. Bridger, *J. Org. Chem.*, **32**, 2501 (1967).

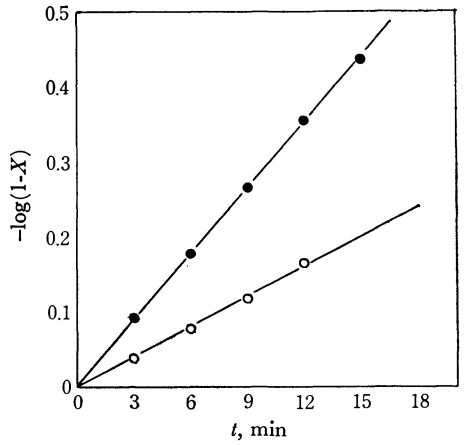

Fig. 3. Effect of oxygen (a): Pseudo-first order plots of the reaction in air (○) and in nitrogen (●). [I]= 1.25×10^{-2} mol/l, [$PhNH_2$]=0.30 mol/l, [Cu^{2+}]=1×10^{-2}mol/l; pH=9.94, T=70°C.

decreased (to about one third) as compared with that in a nitrogen atmosphere. Figure 3 illustrates a typical case. The results suggest that the copper ion behaves as a catalyst in a lower oxidation state.[9] It has been reported in the literature that oxygen retards the reactions which are believed to be catalyzed by cuprous species (formed from cupric salts added initially), such as the reaction of an aromatic diazonium halide with an aliphatic unsaturated compound to give α-halo-β-phenyl alkanes and alkenes (the Meerwein reaction), the Sandmeyer reaction,[10,11] and the hydrolysis of the diphenyliodonium ion.[12,13] The retardation was interpreted in these cases as resulting from the consumption

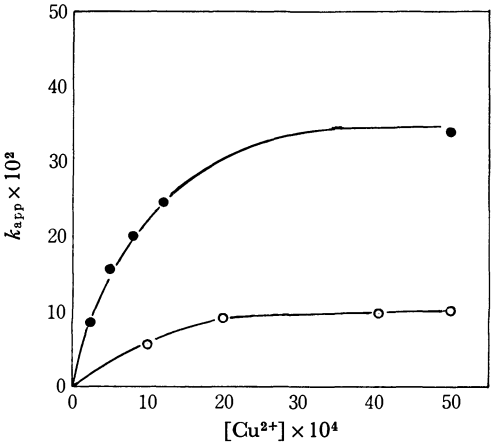

Fig. 4. Effect of oxygen (b): Dependence of the apparent rate constant k_{app} on the initial concentration of cupric catalyst. Experiments in air (○) and in nitrogen (●). [I]=2.50×10^{-2} (○), 1.25×10^{-2} (●) mol/l, [$PhNH_2$]=0.30 mol/l; pH=9.94, T=70°C.

of the univalent copper by oxygen.

An alternative explanation of the inhibiting effect of molecular oxygen may be possible if the reaction is assumed to proceed through a radical (or radicaloid[14]) intermediate which gives the reaction product(s). This point, however, needs further elucidation.

It is noted further that the reaction in the presence of air obeyed the same rate law as the reaction in the case when oxygen was excluded, namely, the reaction was first order in aryl halide (I), and first order in aniline, while the rate increased hyperbolically with the increase in the catalyst concentration (Fig. 4). The effect of oxygen might not be due to the change in the mechanism, but to the decrease in the concentration of the active species.

Effect of Chelating Compounds. The addition of chelating compounds to the reaction system was found to yield some suggestive results.

The apparent rate constants, k_{app},[2] of the reaction in the presence of 8-hydroxyquinoline-5-sulfonic acid (HQS) are summarized in Table 1.[15]

The tendency of the reaction rate to decrease with an increase in the concentration of the chelating agent can reasonably be understood if the added agent is assumed to form thermodynamically stable and unreactive (or less active) complexes. HQS is known to coordinate to cupric copper (β_1=11.9, β_2=21.9 at 25°C).[16]

In order to understand quantitatively the behavior of the chelating agent in the reaction system, we attempted calculations on the assumption that HQS forms an inactive complex:

$$Cu^{2+} + HQS \overset{K_1}{\rightleftharpoons} Cu^{2+}\cdot HQS \qquad (3)$$

From ESR measurements,[2] the catalyst was found to exist mostly in the divalent form. The concentration of cupric copper not bonding to HQS was denoted as c_1, the concentration of HQS not bonding to the metal ion, as L, the equilibrium constant of (3), as K_1, the total concentration of HQS, as l_0, and that of

Table 1. Effects of HQS on the reaction rate[a]

No.	R=[HQS]/[Cu^{2+}]	$k_{app}\times10^2$ l·mol/min	k_R[b]
1	0.00	17.66	1.000
2	0.21	14.20	0.804
3	0.41	10.11	0.570
4	0.82	7.13	0.413
5	1.22	5.14	0.291
6	1.85	3.08	0.174
7	0.00	8.46	1.000
8	0.50	5.85	0.690
9	0.90	3.14	0.370

a) [I]$_0$=0.31×10^{-2} mol/l (Nos. 1—6), 1.25×10^{-2} mol/l (Nos. 7—9); [$PhNH_2$]$_0$=0.30 mol/l; [Cu^{2+}]$_0$=2.50×10^{-4} mol/l; pH=9.94, T=70°C. Experiments in nitrogen.

b) Relative rate constant (see the text).

9) Zero valent copper has been proved to be inactive in the absence of oxygen.[8] See also P. W. Weston and H. Adkins, *J. Amer. Chem. Soc.*, **50**, 859 (1928).

10) J. K. Kochi, *ibid.*, **77**, 5090 (1955); **78**, 1228 (1956); **79**, 2942 (1957).

11) S. C. Dickerman, K. Weiss, and A. K. Ingberman, *ibid.*, **80**, 1904 (1958).

12) M. C. Caserio, D. L. Glusker, and J. D. Roberts, *ibid.*, **81**, 336 (1959).

13) F. M. Beringer, E. M. Gindler, M. Rapoport, and R. J. Taylor, *ibid.*, **81**, 351 (1959).

14) O. Vogl and C. S. Rondestedt, Jr., *ibid.*, **77**, 3067 (1955).

15) The authors are indebted to Mr. H. Inoue of our laboratory for having carried out the experiments Nos. 7, 8, and 9 of Table 1.

16) C. F. Richard, R. F. Gustafson, and A. E. Martell, *J. Amer. Chem. Soc.*, **81**, 1033 (1959).

the catalyst, as c_0. We have:

$$c_1(1+K_1L) = c_0 \quad (4)$$

The mass balance of the chelating agent is represented as:

$$L + K_1c_1L = l_0 \quad (5)$$

or:

$$L = l_0/(1+K_1c_1) = \frac{l_0/c_0}{(1/c_0) + (K_1c_1/c_0)} \quad (6)$$

By combining Eqs. (4) and (6), Eq. (7) is obtained:

$$c_1/c_0 = \left(1+K_1\frac{l_0/c_0}{(1/c_0) + (K_1c_1/c_0)}\right)^{-1} \quad (7)$$

Denoting the c_1/c_0 and l_0/c_0 ratios as x and R respectively, Eq. (7) can be rewritten as:

$$x = \left(1+K_1\frac{R}{(1/c_0)+(K_1x)}\right)^{-1} \quad (8)$$

or:

$$x^2 + ((1/K_1c_0)-1+R)x - 1/K_1c_0 = 0 \quad (9)$$

By solving this equation, x is obtained as a function of R:

$$x = \frac{1}{2}[\sqrt{((1/K_1c_0)-1+R)^2 + 4/K_1c_0} - (1/K_1c_0-1+R)] \quad (10)$$

We postulate further that the apparent rate constant is proportional to the concentration of cupric copper[17] not bonding to HQS, and that the complex Cu^{2+}·HQS is inactive; therefore:

$$x = c_1/c_0 = k_R \quad (11)$$

where k_R is the relative rate constant.

By combining Eqs. (10) and (11), we obtain:

$$k_R = \frac{1}{2}[\sqrt{((1/K_1c_0)-1+R)^2 + 4/K_1c_0} - ((1/K_1c_0)-1+R)] \quad (12)$$

By substituting the numerical values of k_R and R corresponding to Experiment No. 6 in Table 1 into Eq. (9), the value of k_1 was determined to be 1.85×10^4. The values of k_R as calculated from Eq. (12), were plotted against the observed values. The results (Fig. 5) show the validity of the assumptions made above and can be reasonably understood by the assumption that the ligands, such as aniline,[18] with great coordinating power towards the cupric ion, prevent the entering of a second molecule of HQS into the coordination sphere of the metal. Further, the relatively small value of K_1, compared with the stability constant in water at 25°C, is not unreasonable if we consider the presence of the ligands stronger than water and the higher temperature at which the experiments were carried out.

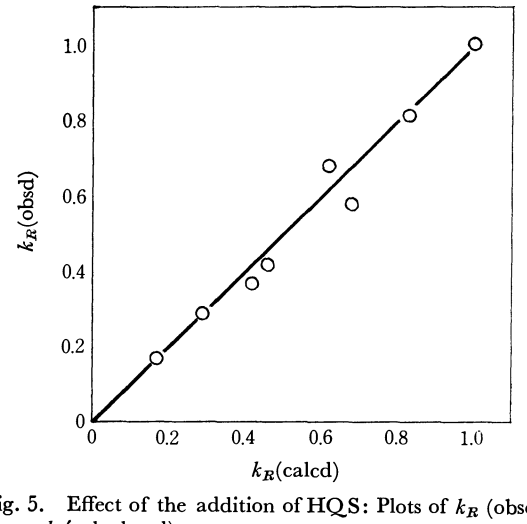

Fig. 5. Effect of the addition of HQS: Plots of k_R (observed) *vs.* $_Rk$ (calculated).

The inhibiting effect of the chelating agents can be interpreted by the assumption that at least three sites of coordination are required for the reaction to be promoted, or that the complexing metal ion is prevented from changing into the univalent state.

Retarding or inhibiting effects were also observed when other chelating agents, such as 2,2′-bipyridyl, 2,2′-biquinolyl, and 2,9-dimethyl-1,10-phenanthroline, were introduced into the reaction system. The effects of these additives are shown in Fig. 6.

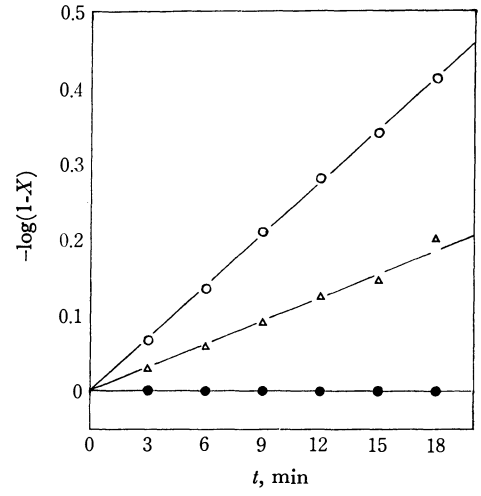

Fig. 6. Effect of chelating compounds (che). [I]$=0.31\times10^{-2}$ mol/l, [$PhNH_2$]$=0.30$ mol/l, [che]$=5.00\times10^{-4}$ mol/l, [Cu^{2+}]$=2.50\times10^{-4}$ mol/l; pH$=9.94$, $T=70$°C.
Experiments in nitrogen.
Control (○), che: cuproin (△), neocuproin, 2,2-dipyridyl (●)

When the mole ratio of the chelating agent to that of the catalyst was 2 : 1, 2,2′-bipyridyl and 2,9-dimethyl-1,10-phenanthroline completely inhibited the reaction, but 2,2′-biquinolyl did so incompletely. The inferiority of the latter in effecting inhibition is presumably due to its poor solubility in the aqueous solution. It was observed that the agent was partly left undissolved and that it floated on the surface of the reaction mixture.

17) Although the rate depended hyperbolically on the initial concentration of the catalyst,[2] linearity between the rate and the concentration of the catalyst could be assumed in the dilute region of the cupric copper.

18) It was observed that cupric copper formed a precipitate with aniline in an aqueous solution. See also: P. Spacu, V. Voicu, and I. Pascaru, *J. Chim. Phys.*, **60**, 368 (1963); I. S. Ahuja, D. H. Brown, R. H. Nuttall, and D. W. A. Snarp, *J. Inorg. Nucl. Chem.*, **27**, 1105 (1965); M. S. Barvinok, I. S. Bukhareva, and Yu. S. Varshavskii, *Zh. Neorg. Khim.*, **10**, 1799 (1965); *Chem. Abstr.*, **64**, 167 (1966).

2,2′-Biquinolyl(cuproin)[19] and 2,9-dimethyl-1,10-phenanthroline(neocuproin)[20] are known as specific chelating agents of cuprous copper and not of cupric species. This specific chelating ability has been used to detect the existence of cuprous copper and, in some cases, to prove its catalytic capacity, especially in systems where the metal is believed to exist in various oxidation states. Thus, the evidence for the presence of Cu^+ intermediate in the cupric-ion-catalyzed oxidation of ascorbic acid[21] or in the solvolysis of diaryliodonium salts in the presence of Cu^{2+} [12] has been afforded by the use of these specific cuprous-ion complexing reagents.

The inhibition of the reaction by cuproin and neocuproin mentioned above likely suggests that the catalyst, initially added as cupric sulfate, is partly reduced to the cuprous state.

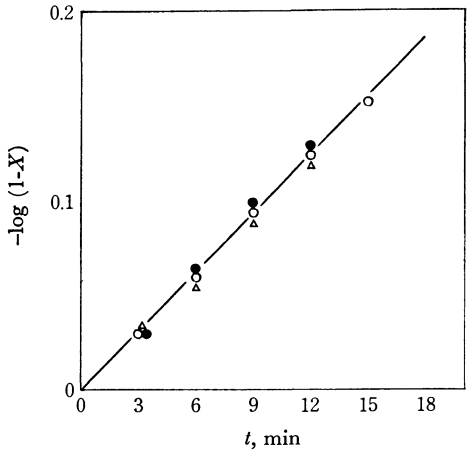

Fig. 7. Effect of anions (a). $[I]=1.25\times10^{-2}$ mol/l, $[PhNH_2]=0.30$ mol/l, $[Cu^{2+}]=2.50\times10^{-4}$ mol/l; pH=9.94, T=70°C.
Experiments in nitrogen.
Catalyst: $CuSO_4$ (○), $CuCl_2$ (●) $CuBr_2$ (△)

Effect of Anions. It was found (Fig. 7) that cupric sulfate, cupric chloride and cupric bromide, when used at equal molar concentrations, all catalyzed the reaction at the same rate. This result can be interpreted by assuming that the anion associated with the cupric ion was readily replaced by other ligands existing in the system.

The situation, however, was different when the anion was added in sufficiently large amounts. Several anions (F^-, Cl^-, Br^-, I^-, CN^-) were introduced in the form of their sodium salts. Their effects are illustrated in Fig. 8, where the pseudo-first order plots of the reaction are represented.

The results show that the fluoride did not exert any marked influence on the reaction, but the other anions decreased the rate. Since the absence of the effect of the ionic strength was confirmed, as has been mentioned above, the retarding effect must be ascribed to the action of the added anions.

Figure 8 reveals that the anions inhibit the reaction

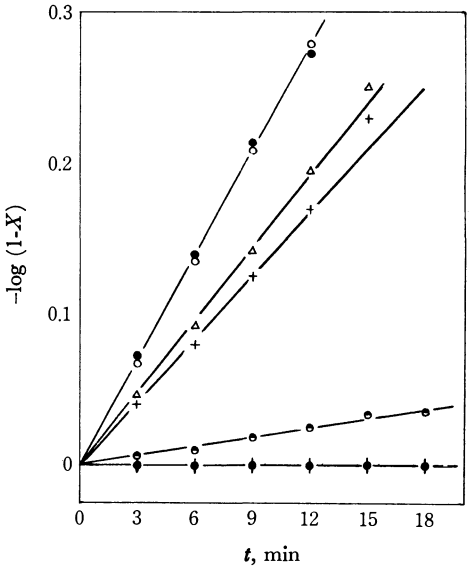

Fig. 8. Effect of anions (b). $[I]=1.25\times10^{-2}$ mol/l, $[PhNH_2]=0.30$ mol/l, $[NaX]=0.20$ mol/l, $[Cu^{2+}]=2.50\times10^{-4}$ mol/l; pH=9.94, T=70°C.
Experiments in nitrogen.
Control (○); X:F (●), Cl (△), Br (+), I (◓), CN (◆)

in this order: $F^-\ll Cl^-<Br^-<I^-<CN^-$. It is well known that both cuprous and cupric copper can form complexes with halides and cyanide, but the reverse order of stability of the complexes has been observed for the two oxidation states.[22] Thus, while the $F^-<Cl^-<Br^-<I^-<CN^-$ order has been reported for the cupric ion, the univalent copper ion forms complexes with the opposite sequence of stabilities: $CN^-<I^-<Br^-<Cl^-<F^-$ (In fact, complex formation from Cu^+ and F^- has not yet been established). The available thermodynamic data[23] also suggest that in an aqueous solution, the cupric complexes with halide and cyanide ions are far more unstable than the corresponding complexes of cuprous copper.

These facts might be interpreted as indicating that cuprous copper is responsible for the promotion of the reaction, and that the retarding effect of the halide and

Table 2. Retarding effects of the Cl^- and Br^- anions[a]

No.	$[X^-]$, mol/l[b]	k_R
1	0.00	1.000
2	0.10	0.805
3	0.20	0.625
4	0.40	0.500
5	0.60	0.415
6	0.10	0.785
7	0.20	0.607
8	0.30	0.430
9	0.40	0.286

a) $[I]_0=0.31\times10^{-2}$ mol/l, $[PhNH_2]_0=0.30$ mol/l, $[Cu^{2+}]_0=2.50\times10^{-4}$ mol/l; pH=9.94, T=70°C.
Experiments in nitrogen.
b) $X^-=Cl^-$ (Nos. 1—5), Br^- (Nos. 6—9)

19) J. Hoste, *Anal. Chim. Acta*, **4**, 23 (1950).
20) W. H. McCurdy and G. F. Smith, *Analyst* (London), **77**, 846 (1952).
21) R. Flitman and E. Frieden, *J. Amer. Chem. Soc.*, **79**, 5198 (1958).
22) S. Ahrland, J. Chatt, and N.R. Davies, *Quart. Rev.* (London), **12**, 265 (1958).
23) "Stability Constants," *Chem. Soc.* (London), Special Pub., No. 17 (1964).

cyanide ions might be described as resulting from the competition between the added anions and the reactants for the metal ion.

The retarding effect of the anions was increasingly pronounced as their concentration increased. The relative rate constants are tabulated in Table 2.

Attempts to derive the quantitative relations between the relative rate constant and the concentration of the anion were, however, unsuccesful, presumably because of the complexities of the manner of action of the anions. Thus, besides their ability of competing with the reactants for the catalyst, the anions might facilitate the formation of polynuclear clusters postulated earlier[2] by bridging. This point is expected to be clarified by further studies.

Catalytic Activity of Cuprous Cloride. The data obtained by investigating the effects of molecular oxygen, cuproin and neocuproin, and added anions suggest that even when the catalyst is introduced as cupric salts, the univalent metal ion might be formed in the reaction system and that this species might play an important role in promoting the reaction. In order to obtain more direct evidence concerning this point, cuprous chloride was used as the catalyst.

The experiments showed that the initial rate was somewhat larger than that of the reaction catalyzed by cupric sulfate, but the steady state was rapidly established (within less than three minutes), and at this steady stage, the rate was found to be almost the same as in the case when cupric copper was used (Table 3).

These results can be explained on the assumptions that cuprous chloride was rapidly converted to cupric species and that the reaction took the same course as when cupric salt was used. The comparatively large rate during the early stage of the reaction might be due to the unconverted univalent copper salt. The reaction during this stage might take place on the surface of the solid catalyst.

Neocuproin exhibited the same inhibiting effect as in the experiments using cupric salt when added in a sufficiently large amount as compared with the concentration of the catalyst, but the reaction did occur (No. 6, Table 3) when the neocuproin: catalyst mole ratio was 1 : 1. This fact can be easily understood if we remember that two molecules of neocuproin can coordinate to one metal ion.[20]

Table 3. Comparison of the activity of cuprous chloride and cupric sulfate[a]

No.	$[Cu^+]_0 \times 10^3$ mol/l	$[Cu^{2+}]_0 \times 10^3$ mol/l	[Che][b] $\times 10^3$ mol/l	$k_{app} \times 10^2$ l·mol/min
1	2.00	0.00	0.00	32.30
2	0.00	2.00	0.00	36.40
3	1.00	0.00	0.00	26.90
4	0.00	1.00	0.00	28.00
5	1.00	0.00	2.00	0.00
6	2.00	0.00	2.00	33.80

a) $[I]_0 = 1 \times 10^{-2}$ mol/l, $[PhNH_2]_0 = 0.30$ mol/l; pH=9.94, T=70°C (Nos. 1—4), 90°C (Nos. 5 and 6). Experiments in nitrogen.
b) Neocuproin.

Although no decisive conclusions as to the activity of cuprous species could be deduced from the above results alone, we have noted that the addition of reducing agents to the system catalyzed by cupric salts enhanced the reaction rate markedly.[2] Detailed results will be reported in a subsequent paper of this series.

Substituent Effect. Six substituted anilines were allowed to react with (I). The reaction rates corresponding to *p*-anisidine, *p*-toluidine, aniline, and *p*-chloroaniline were found to fit Yukawa-Tsuno's equation[24]:

$$\log (k_X/k_H) = \rho(\sigma + r \cdot \Delta\bar{\sigma}_R^+) \qquad (13)$$

in which the reaction parameter, ρ, was found to be -2.20, r, to be 0.50. $\Delta\bar{\sigma}_R^+$ is the difference between the Brown-Okamoto substituent coefficient[25] and the Hammett coefficient.[26] The relation is represented in Fig. 9.

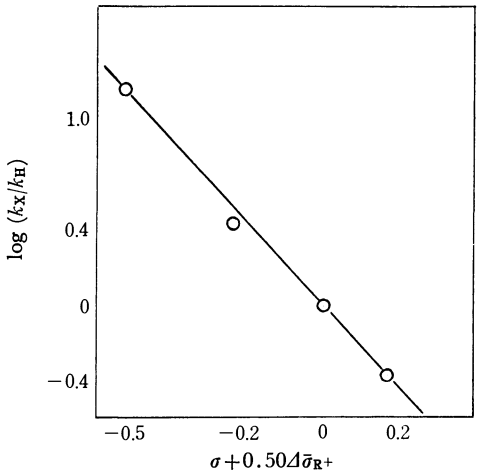

Fig. 9. Substituent effect.

Under the experimental conditions of this work, the reaction rates of *p*-nitroaniline and *p*-aminobenzoic acid with I were too slow to measure.

It has been reported that the yield of the Ullmann condensation reaction of 2-chloro-5-methoxybenzoic acid and anilines increased with an increase in the basicity of the amines[27] but no quantitative correlation has been established.

The basicities of anilines were known to be well correlated by the "normal" Hammett equation,[28] at least when the *para* substituents are not strongly electron-withdrawing. Furthermore, Chapman and Parker have reported that the Hammett relationship was useful in correlating the reactivities of substituted anilines towards activated aryl halides in the absence of a catalytic agent.[29]

The results observed in the Ullmann condensation of I with anilines show that, in the presence of a copper

24) Y. Tsuno, T. Ibata, and Y. Yukawa, This Bulletin, **32**, 960, 965, 971 (1959).
25) H. C. Brown and Y. Okamoto, *J. Amer. Chem. Soc.*, **79**, 1913 (1957); **80**, 4979 (1958).
26) Taken from H. H. Jaffe, *Chem. Rev.*, **53**, 191 (1953).
27) W. G. Dauben, *J. Amer. Chem. Soc.*, **70**, 2420 (1948).
28) A. I. Biggs and R. A. Robinson, *J. Chem. Soc.*, **1961**, 388.
29) N. B. Chapman and R. E. Parker, *ibid.*, **1951**, 3301.

catalyst, the mesomeric effect of the substituents on the reaction center (nitrogen atom) was considerably emphasized. More work must be done in this connection.

Experimental

The experimental technique was described in Part I.[2] The additives were introduced into the reaction system prior to the catalyst.

8-Hydroxyquinoline-5-sulfonic acid, 2,2′-dipyridyl, cuproin, and neocuproin of a guaranteed grade were used without further purification.

Cuprous chloride was prepared by reducing a (cupric sulfate+sodium chloride) system with anhydrous sodium sulfite.[30] Found: Cu, 64.13% (Calcd for CuCl: Cu, 64.18%). This catalyst was added as powder.

This research was supported financially in part by the Asahi Glass Foundation for the Contribution to Industrial Technology.

30) W. C. Ferrelius, "Inorganic Syntheses," Vol. 2, p. 1.

BULLETIN OF THE CHEMICAL SOCIETY OF JAPAN, VOL. 44, 771—777 (1971)

Effective Intramolecular Hydrogen Abstraction by the Sulfonamide Radical

Takehisa OHASHI, Shinichi TAKEDA, Mitsuo OKAHARA, and Saburo KOMORI

Department of Applied Chemistry, Faculty of Engineering, Osaka University, Yamadakami, Suita, Osaka

(Received July 16, 1970)

To study the reactivity of the sulfonamide radical in various reaction systems, the photodecomposition of *N*-*t*-butyl and *N*-methyl-*N*-chloroalkanesulfonamides was investigated. In benzene, the competitive hydrogen abstraction by the chlorine atom occurred to an appreciable extent and the participation of the chlorine atom was retarded with N_2-flow control. In an aqueous solution (AcOH-H_2O, *t*-BuOH-H_2O), the quantitative conversion to γ- and δ-chloroalkanesulfonamide was observed; this was thought to be due to the intramolecular hydrogen abstraction by the sulfonamide radical and to the lowering of the reactivity of the chlorine atom because of the solvation by H_2O. In an acid solution (AcOH-H_2O-H_2SO_4), a higher preference for 1,5 hydrogen transfer was found; this was caused by the protonated sulfonamide radical. The formation ratio of γ- to δ-chloroalkanesulfonamide in several solvents was determined, and the reactivity of the sulfonamide radical was discussed. From the reaction products obtained, several aliphatic sultams were synthesized.

In studies of the free-radical rearrangement of *N*-halo-compounds, the decompositions of *N*-haloamides,[1-4] *N*-haloimides,[5] and *N*-halosulfonamides[6-8] have been reported. These reactions have been reported to proceed in a manner similar to the Hofmann-Löffer reaction,[9] but the rearrangement of these compounds proceeds in the absence of an acid catalyst. It is interesting to study the properties of these nitrogen radicals because intermediates for five and six-membered-ring heterocycles syntheses can be obtained in the reaction of these compounds. In the hydrogen abstraction in these reactions described above, three processes can be assumed; intramolecular hydrogen abstraction by the nitrogen radical, intermolecular hydrogen abstraction by the nitrogen radical, and hydrogen abstraction by the halogen atom.

In previous papers[6] the present authors reported that *N*-alkyl-*N*-chloroalkanesulfonamides, especially *N*-*t*-butyl-*N*-chloroalkanesulfonamides, rearranged to the corresponding chloroalkanesulfonamides and that the reaction proceeded mainly *via* the intramolecular hydrogen abstraction by the sulfonamide radical; the participation of the chlorine atom in the hydrogen abstraction was thought to be relatively small in the decomposition of *N*-*t*-butyl-*N*-chloroalkanesulfonamides. However, in a further investigation of this reaction, the competitive hydrogen abstraction by the chlorine atom was observed to some extent in certain reaction systems, together with intramolecular hydrogen abstraction by the sulfonamide radical, and so a reinvestigation of the mechanism of the hydrogen transfer was necessary. Further, we found that the decomposition of *N*-halosulfonamides in the aqueous solution was a suitable method for effecting intramolecular hydrogen abstraction by the sulfonamide radical.

In the present paper, the properties of intramolecular hydrogen abstraction by the sulfonamide radical were studied in several reaction systems.

1) a) D. H. R. Barton and A. L. J. Beckwith, *Proc. Chem. Soc.*, **1963**, 335. b) D. H. R. Barton, A. L. J. Beckwith, and A. Goosen, *J. Chem. Soc.*, **1965**, 181.

2) A. L. J. Beckwith and J. E. Goodrich, *Aust. J. Chem.*, **18**, 747 (1965).

3) R. S. Neale, N. L. Marcus, and R. G. Schpers, *J. Amer. Chem. Soc.*, **88**, 3051 (1966).

4) Y. L. Chow and T. C. Joseph, *Chem. Commun.*, **1969**, 490.

5) R. C. Petterson and A. Wambsgans, *J. Amer. Chem. Soc.*, **86**, 1648 (1964).

6) a) M. Okahara, T. Ohashi, and S. Komori, *Tetrahedron Lett.*, **1967**, 1629. b) M. Okahara, T. Ohashi, and S. Komori, *J. Org. Chem.*, **33**, 3066 (1968).

7) T. Ohashi, M. Sugie, M. Okahara, and S. Komori, *Tetrahedron*, **25**, 5349 (1969).

8) R. S. Neale and N. L. Marcus, *J. Org. Chem.*, **34**, 1808 (1969).

9) M. E. Wolff, *Chem. Rev.*, **63**, 55 (1963).

TABLE 1. PHOTOREARRANGEMENT[a] OF *N-t*-BUTYL-*N*-CHLORO-*n*-HEXANESULFONAMIDE IN BENZENE OR AcOH

Solvent	N_2 flow rate ml/min	Concn. mol/*l*	Recovery rate[c] %	Composition of reaction product (wt%)		
				Original sulfonamide	*x*-Chlorohexane-sulfonamide[d]	Isomer ratio γ-Cl/δ-Cl/ε-Cl
Benzene	400	0.2	91	12.9	85.0	1.6/1.0/0.1
Benzene	150	0.2	90	22.2	75.1	1.3/1.0/0.5
Benzene	0	0.2	86	22.5	77.0	1.2/1.0/0.8
AcOH	150	0.2	80	38.5	60.0	1.2/1.0/0.6

a) Irradiation with a 150-W high pressure Hg lamp, 28—30°C under nitrogen unless specified otherwise.
b) Determined by glpc
c) The weight of the product obtained/the weight of *N*-chlorosulfonamide ×100.
d) *N-t*-Butyl-γ, δ and ε-chlorohexanesulfonamide.

TABLE 2. PHOTOREARRANGEMENT OF *N-t*-BUTYL-*N*-CHLORO-*n*-BUTANESULFONAMIDE IN BENZENE

Concn. mol/*l*	N_2 flow rate ml/min	Recovery rate %	Composition of reaction product (wt%)			
			Original sulfonamide	γ-Chlorobutane-sulfonamide	δ-Chlorobutane-sulfonamide	Isomer ratio γ-Cl/δ-Cl
0.4	400	93	16.8	71.1	11.3	6.29
0.4	150	92	22.7	62.5	13.3	4.70
0.4	40	90	35.3	52.5	12.2	4.30
0.4	0	90	33.4	53.3	13.0	4.10
Neat	150	90	35.1	51.3	13.2	3.89
0.4 in CCl_4	150	80	55.0	30.0	12.5	2.40

Results and Discussion

The Participation of the Chlorine Atom and the Effect of N_2-Flow Rate. To apply our results, reported in a previous paper[6] and shown in Scheme 1, the photodecomposition of *N-t*-butyl-*N*-chlorohexanesulfonamide was investigated in benzene in a manner similar to that described in the previous paper; the glpc analysis of the products showed the presence of ε-chlorohexanesulfonamide[10] together with γ- and δ-chlorohexanesulfonamides. The formation of ε-chlorohexanesulfonamide can not be explained by the intramolecular hydrogen abstraction; this shows the occurrence of hydrogen abstraction by the chlorine atom or intermolecular hydrogen abstraction by the sulfonamide radical.

Therefore, in order to study the competitive hydrogen abstraction by chlorine and sulfonamide radicals, a series of photodecompositions of *N-t*-butyl-*N*-chloroalkanesulfonamides (C_4–C_6) and *N*-chloro-*N*-methylbutanesulfonamide was investigated, and the isomer ratios of the chloroalkanesulfonamides were determined under various conditions.

$$RCH_2CH_2CH_2CH_2SO_2NClR' \xrightarrow[\text{in benzene}]{h\nu} \begin{cases} RCH_2CHClCH_2CH_2SO_2NHR' \\ RCHClCH_2CH_2CH_2SO_2NHR' \\ RCH_2CH_2CH_2CH_2SO_2NHR' \end{cases}$$

R=H, Me; R'=*t*-Bu, Me

Scheme 1

The results of the photodecomposition of *N-t*-butyl-*N*-chlorohexanesulfonamide in benzene are described in Table 1. As Table 1 shows, the formation of ε-chlorohexanesulfonamide varied with the N_2-flow rate; the isomer ratio of ε-chlorohexanesulfonamide decreased, and the yield[11] of *x*-chlorohexanesulfonamide increased, when the N_2-flow rate was high. These results suggest that chlorine participates in the hydrogen abstraction to an appreciable extent in benzene when the N_2-flow rate is low; *i. e.*, the hydrogen abstraction by the chlorine atom is retarded by the expulsion of chlorine and HCl with the N_2-flow control, and consequently the intramolecular hydrogen abstraction[12] by the sulfonamide radical proceeds mainly. Similar findings, that the yield of conversion and the isomer ratio vary with the N_2-flow rate, were observed in the photodecomposition of *N-t*-butyl-*N*-chlorobutanesulfonamide in benzene (Table 2). As is shown in Table 2, the value of the isomer ratio (γ-Cl/δ-Cl) obtained in the reaction in benzene is higher than that in CCl_4. This seems to show the difference in solvent effect on the chlorine atom between benzene and CCl_4.[13] In the decomposition of *N-t*-butyl-*N*-chlorobutanesulfonamide in benzene, the isomer ratio is larger than that in the reaction of *N-t*-butyl-*N*-chlorohexanesulfonamide, because δ-hydrogen of butanesulfonamide is primary.

It is important to determine whether *N-t*-butyl-δ-chlorobutanesulfonamide is formed as a result of hydrogen abstraction by the sulfonamide radical or by the chlorine atom. Neale[8] has recently reported that no

10) This was identified by comparing the gas chromatogram with that of the photochlorination product of *N-t*-butyl-*n*-hexanesulfonamide, and by the NMR of the reaction mixture, in which the doublet peak of methyl protons (τ, 8.46) was observed.

11) The yield of the conversion to *x*-chloroalkanesulfonamide was thought to be low because of the reaction of *N*-chloroalkanesulfonamide with HCl when the chlorine atom participates in the hydrogen abstraction.

12) The participation in the intermolecular hydrogen abstraction by the sulfonamide radical was thought to be small considering the fact that the yield of the conversion and the isomer ratio vary with the N_2-flow rate.

13) G. A. Russel, *J. Amer. Chem. Soc.*, **80**, 4987 (1958).

N-*t*-butyl-δ-halobutanesulfonamides were observed in the decomposition of *N*-chloro-and *N*-bromo-*N*-*t*-butylbutanesulfonamide. In our investigation, the results of the photodecomposition of *N*-bromo-*N*-*t*-butylbutanesulfonamide agreed with those of Neale, but an appreciable content of δ-chlorobutanesulfonamide was observed in the reaction of *N*-*t*-butyl-*N*-chlorobutanesulfonamide in benzene and CCl_4. The formation of *N*-*t*-butyl-δ-chlorobutanesulfonamide[14] was confirmed by the isolation of butanesultam by the alkali treatment of reaction products, followed by acidification with concentrated HCl, as is shown in Scheme 2.

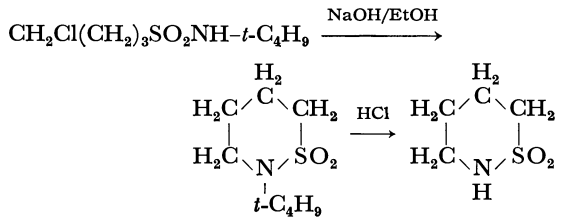

Scheme 2

From these results, it may be concluded that, in the decomposition of *N*-chloroalkanesulfonamide in benzene and CCl_4, competitive hydrogen abstraction by the chlorine atom occurs and that this chlorine atom participation[15] can be somewhat retarded by the expulsion of chlorine and HCl by means of N_2-flow control, and that, in the decomposition of *N*-*t*-butyl-*N*-chlorobutanesulfonamide, the primary hydrogen abstraction by the sulfonamide radical does not occur and *N*-*t*-butyl-δ-chlorobutanesulfonamide is formed *via* hydrogen abstraction by the chlorine atom. This conclusion is supported by the fact that no δ-bromo isomer was observed in the decomposition of *N*-bromo-*N*-*t*-butylbutanesulfonamide; the hypothesis described in our previous paper[6] that *N*-*t*-butyl-δ-chlorobutanesulfonamide is formed by means of the primary hydrogen abstraction by the sulfonamide radical[16] *via* the seven-membered-ring transition state seems thus to be contradicted.

Effective Intramolecular Hydrogen Abstraction in the Aqueous Solution. To cause the selective rearrangement of *N*-chloroalkanesulfonamides, the participation of the chlorine atom must be suppressed; therefore, the photodecomposition of *N*-chloroalkanesulfonamides in aqueous solvents was investigated. Irradiation was carried out with a high-pressure Hg lamp at 28—30°C under N_2 until the active chlorine content was negligible. In every case, a complete loss of active chlorine was observed in 1 hr. The results obtained in aqueous AcOH are listed in Tables 3—6. In the photodecomposition of *N*-*t*-butyl-*N*-chlorobutanesulfonamide (Table 3), the yield of rearranged products and the isomer ratio (γ-Cl/δ-Cl) rose with an increase of the concentration of water, and in the solvents with higher water concentrations ($AcOH/H_2O=1.7$), *N*-*t*-butyl-γ-chlorobutanesulfonamide was obtained almost quantitatively and no δ-chlorobutanesulfonamide was observed. The fact that the formation of *N*-*t*-butyl-δ-chlorobutanesulfonamide is suppressed as well as the reaction of *N*-bromo-*N*-*t*-butylbutanesulfonamide in benzene suggests that a predominant intramolecular hydrogen transfer by the sulfonamide radical occurs and that the participation of the chlorine atom is retarded in the aqueous solution. Similar results were obtained in the reaction of *N*-*t*-butyl-*N*-chloropentane and hexanesulfonamides (Tables 4 and 5), and no appreciable content of ε-chlorohexanesulfonamide was observed in the decomposition of *N*-*t*-butyl-*N*-chlorohexanesulfonamide in a solution with a higher water concentration. This demonstrates the suppression of hydrogen abstraction by the chlorine atom and intermolecular hydrogen abstraction by the sulfonamide radical in the $AcOH–H_2O$ system.

The isomer ratio (γ-Cl/δ-Cl=1.93—1.94) observed in the reaction of *N*-*t*-butyl-*N*-chlorohexanesulfonamide in aqueous acetic acid ($AcOH/H_2O=2.5$—2.1) seems to show that the intramolecular 1,5 hydrogen transfer by the sulfonamide radical occurs in preference to the 1,6 hydrogen transfer because of a quasi-six-membered ring transition state.[18] The isomer ratio (γ-Cl/δ-Cl= 1.10—1.14) determined in the reaction of *N*-*t*-butyl-*N*-chloropentanesulfonamide in aqueous acetic acid is lower than that of *N*-*t*-butyl-*N*-chlorohexanesulfonamide. This result may be due to the stability of the δ-carbon radical resulting from the contribution of the hyperconjugation of the Me group.

This efficient solvent effect could be adapted to the decomposition of *N*-chloro-*N*-methyl-*n*-butanesulfonamide, which has been reprted to proceed less efficiently than the *N*-*t*-butyl analog.[6,8] As is shown in Table 6, *N*-methyl-γ-chlorobutanesulfonamide was obtained in a high yield; this is in accordance with the results obtained in the reaction of the *N*-*t*-butyl analog in the aqueous solution.

To compare the reactivity of the sulfonamide radical in the aqueous AcOH solution with that in a higher acidic solution, the photodecomposition of *N*-*t*-butyl-*N*-chloroalkanesulfonamides in the $AcOH–H_2O–H_2SO_4$ solvent was studied under the same conditions as were used in the $AcOH–H_2O$ system (Tables 3, 4, and 5). Although the conversion to *N*-*t*-butylchloroalkanesulfonamide was rather low because of the decomposition of the intermediate conjugate acid[6,19] to unsubstituted sulfonamides, the isomer ratio (γ-Cl/δ-Cl) was higher than that obtained in the $AcOH–H_2O$ system.

The relative greater facility of 1,5-shifting in H_2SO_4 may be due to the fact that the six-membered transition state is stereochemically more favorable for the protonated sulfonamide radical than for the neutral radical considering the steric repulsions involving non-bonded

14) The NMR of the viscous liquid obtained after the isolation of the γ-chloro isomer and *N*-*t*-butylbutanesulfonamide showed the presence of the δ-chloro isomer (τ, 6.45).

15) In benzene, the chlorine atom would act as the $C_6H_6Cl\cdot$ complex.

16) The absence of the δ-bromo isomer can not be explained by assuming intra- or intermolecular primary hydrogen abstraction by the sulfonamide radical. The high reactivity of the sulfonamide radical towards secondary hydrogens has previously been reported.[17]

17) A. E. Fuller and W. J. Hickinbottom, *J. Chem. Soc.*, **1965**, 3228.

18) Because of its low I strain of cyclohexane-like chair-formed conformation, the six-membered-ring transition state would be more stable than the seven-membered-ring transition state.

19) a) R. E. Buckles, *J. Amer. Chem. Soc.*, **71**, 1157 (1944). b) C. Derbyshire and W. A. Waters, *J. Chem. Soc.*, **1950**, 573.

Table 3. Photorearrangement[a] of *N*-*t*-butyl-*N*-chloro-*n*-butanesulfonamide in aqueous AcOH

Solvent[b]	Concn. mol/*l*	Recovery rate %	Composition of reaction product (wt%)			
			Original sulfonamide	γ-Chloro-butane-sulfonamide	δ-Chloro-butane-sulfonamide	Isomer ratio γ-Cl/δ-Cl
AcOH-H_2O (10.0/1.0)	0.4	85	40.0	50.6	8.3	6.10
AcOH-H_2O (3.4/1.0)	0.4	90	11.4	82.3	5.6	14.70
AcOH-H_2O (2.0/1.0)	0.4	94	2.0	91.0	6.0	15.17
AcOH-H_2O (1.7/1.0)	0.2	94	trace	99.0	trace	—
AcOH	0.4	88	29.0	56.7	14.9	3.80
AcOH-H_2O-H_2SO_4 (3.7/2.7/1.0)	0.4	65	48.4	51.3	trace	—

a) N_2 flow rate is 150 m*l*/min.
b) Values in parentheses are the volume ratio of AcOH to H_2O or H_2O–H_2SO_4.

Table 4. Photorearrangement[a] of *N*-*t*-butyl-*N*-chloro-*n*-pentanesulfonamide

Solvent	Concn. mol/*l*	Recovery rate %	Composition of reaction product (wt%)		
			Original sulfonamide	γ- and δ-Chloro-pentane-sulfonamide	Isomer ratio γ-Cl/δ-Cl
AcOH-H_2O (5.0/1.0)	0.1	90	15.0	83.0	1.10
AcOH-H_2O (2.0/1.0)	0.1	92	6.0	92.0	1.14
AcOH-H_2O-H_2SO_4 (12/4/1)	0.1	80	32.3	66.0	1.29
AcOH-H_2O-H_2SO_4 (7/3/1)	0.1	65	52.6	46.7	1.48
AcOH-H_2O-H_2SO_4 (8.4/5.9/1.0)[b]	0.16	82	32.1	67.7	1.50
AcOH	0.1	80	37.0	58.1	0.94
Benzene	0.1	87	23.0	72.0	0.95—1.00

a) N_2 flow rate is 150 m*l*/min.
b) This result is cited from the previous paper.[6]

Table 5. Photorearrangement[a] of *N*-*t*-butyl-*N*-chloro-*n*-hexanesulfonamide in aqueous solution

Solvent	Concn. mol/*l*	Recovery rate %	Composition of reaction product (wt%)		
			Original sulfonamide	γ- and δ-Chloro-hexanesulfon-amide	Isomer ratio γ-Cl/δ-Cl
AcOH-H_2O (7.0/1.0)	0.2	83	26.5	69.0[b]	1.70[c]
AcOH-H_2O (4.0/1.0)	0.4	90	10.0	88.5	1.80
AcOH-H_2O (3.0/1.0)	0.2	92	7.3	90.3	1.84
AcOH-H_2O (2.5/1.0)	0.2	92	6.5	92.5	1.93
AcOH-H_2O (2.1/1.0)	0.2	95	3.1	95.0	1.93
AcOH-H_2O (2.1/1.0)	0.1	94	1.4	96.5	1.94
t-BuOH-H_2O (1.0/1.0)	0.2	88	trace	98.6	1.89
AcOH-H_2O-H_2SO_4 (13/6/1)	0.1	87	17.0	82.3	2.30
AcOH-H_2O-H_2SO_4 (25/16/1)	0.1	85	22.2	76.0	2.10

a) N_2 flow rate is 150 m*l*/min.
b) The formation of ε-chlorohexanesulfonamide was observed. This value contains the quantity of ε-Cl isomer.
c) γ-Cl/δ-Cl/ε-Cl=1.70/1.00/0.50

Table 6. Photorearrangement[a] of *N*-chloro-*N*-methyl-*n*-butanesulfonamide in aqueous AcOH

Solvent	Concn. mol/*l*	Recovery rate %	Composition of reaction product (wt%)			
			Original sulfonamide	γ-Chloro-butane-sulfonamide	δ-Chloro-butane-sulfonamide	Isomer ratio γ-Cl/δ-Cl
AcOH-H_2O (1.75/1.00)	0.15	89	6.4	89.7	1.0	89.7
AcOH-H_2O (1.40/1.00)	0.15	90	2.5	94.1	trace	—

a) N_2 flow rate is 150 m*l*/min.

Table 7. UV Spectrum of *N*-chlorosulfonamides

RSO_2NCl-*t*-C_4H_9	Solvent[a)]	Max. mμ (ε)
R=C_5H_{11}	Benzene	276 (178)
R=C_5H_{11}	AcOH	269 (115)
R=C_5H_{11}	AcOH-H_2O (7:4)	267 (89)
R=C_6H_{13}	Benzene	279 (172)
R=C_6H_{13}	AcOH-H_2O-H_2SO_4 (3:1:1)	244 (52)

a) Values in parentheses are the volume ratio of AcOH, H_2O, and H_2SO_4.

atoms in the transition state; this is analogous with the case of the aminium radical[20] in the Hofmann-Löffler reaction.

From the result that selective 1,5 and 1,6 hydrogen transfers do not occur in pure AcOH (Table 1), it is clear that the presence of water promotes the intramolecular hydrogen abstraction by the sulfonamide radical; the same result was obtained in the photodecomposition of *N*-*t*-butyl-*N*-chlorohexanesulfonamide in aqueous *t*-BuOH (Table 5).

From the UV spectrum of *N*-chlorosulfonamides, *N*-chlorosulfonamide is evidently protonated in a H_2SO_4 solution, but the absorption in aqueous AcOH is not as characteristic as that in pure AcOH (Table 7).

From these results, it may be considered that the sulfonamide radical is not protonated in aqueous AcOH, but that the reactivity of the chlorine atom is lowered as a result of the solvation by H_2O, and that, consequently, the intramolecular hydrogen abstraction by the sulfonamide radical proceeds predominantly.

Although the solvation of the sulfonamide radical and the solvation of the transition state for rearrangement may be assumed, the evidence is not conclusive at present. From this point of view, the decomposition of *N*-bromoalkanesulfonamides, in which the participation of the halogen atom seems to be small, is under investigation.[21]

Aliphatic Sultams. In a previous paper,[6] we have reported the conversion of *N*-*t*-butyl-γ-chloropentanesulfonamide to *N*-*t*-butyl-3-ethylpropanesultam. In a similar manner, *N*-*t*-butyl-3-methylpropanesultam and *N*-*t*-butylbutanesultam were obtained almost quantitatively from *N*-*t*-butyl-γ-chloro and *N*-*t*-butyl-δ-chlorobutanesulfonamides respectively by the treatment of the rearranged products with ethanolic NaOH. Neale[8] has reported the formation of *N*-*t*-butyl-2-methylcyclopropanesulfonamide, together with *N*-*t*-butyl-3-methylpropanesultam, by various alkali treatments of *N*-*t*-butyl-γ-halobutanesulfonamide, but no evidence of the formation of significant amounts of the cyclopropane isomer was observed upon treatment with ethanolic NaOH, and *N*-*t*-butyl-3-methylpropanesultam was isolated almost quantitatively by distillation. The structure of this sultam was confirmed by NMR and mass spectra. On the other hand, the analogous treatment of *N*-*t*-butyl-δ-chloropentanesulfonamide with ethanolic NaOH gave *N*-*t*-butylpent-3-enesulfonamide almost quantitatively. This suggests that the formation of six-membered-ring sultams containing the *N*-*t*-butyl group and a side chain at the 4-position does not proceed so efficiently as the formation of five-membered-ring sultams and that, consequently, the elimination reaction occurs predominantly. The formation of 4-methylbutanesultam in a high yield from δ-chloropentanesulfonamide demonstrates the lack of a stereochemical barrier of the *N*-*t*-butyl group.

N-*t*-Butyl-γ-chloro (I) and *N*-*t*-butyl-δ-chlorohexanesulfonamides (II) were identified by the fact that 3-propylpropanesultam and 4-ethylbutanesultam were obtained by the alkali treatment of chlorohexanesulfonamides derived by the treatment of I and II with HCl as is shown in Scheme 3:

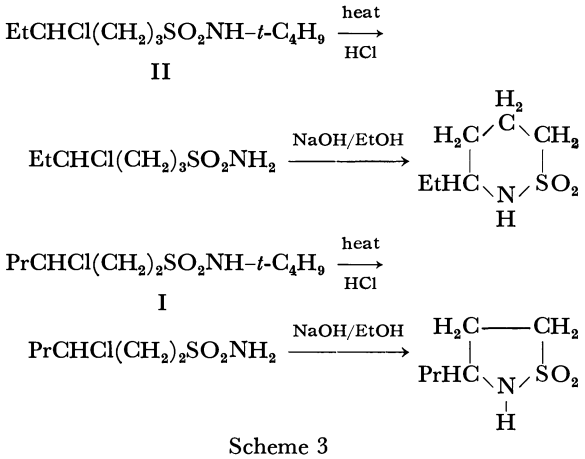

Scheme 3

Table 8. Mass spectrum[a)] of aliphatic sultams

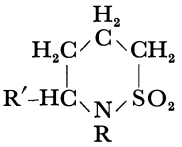	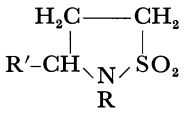	*m/e*
R′=Et, R=H		163 (M^+), 162 (M^+-H), 134 (M^+-Et), 70 (M^+-Et-SO_2)
	R′=Pr, R=H	163 (M^+), 162 (M^+-H), 120 (M^+-Pr), 56 (M^+-Pr-SO_2)
R′=H, R=H		135 (M^+), 134 (M^+-H), 107 (M^+-C_2H_4), 70 (M^+-H-SO_2)
R′=Me, R=H		149 (M^+), 148 (M^+-H), 134 (M^+-Me), 121 (M^+-C_2H_4), 70 (M^+-Me-SO_2)
R′=H, R=*t*-C_4H_9		191 (M^+), 176 (M^+-Me), 136 (M^+-Me-C_3H_4), 112 (M^+-Me-SO_2)
	R′=Me, R=*t*-C_4H_9	191 (M^+), 176 (M^+-Me), 136 (M^+-Me-C_3H_4), 120 (136-CH_4), 112 (176-SO_2)

a) 70 eV.

20) E. J. Corey and W. R. Hertler, *J. Amer. Chem. Soc.*, **82**, 1657 (1960).

21) In contribution, T. Ohashi, M. Okahara, and S. Komori, This Bulletin, **44**, (1971), in prss.

The structure of each five- and six-membered-ring sultam was confirmed by a study of its mass spectrum (Table 8).

Experimental

Apparatus. The IR spectra were run on an IR-E-type Nihon Bunko spectrometer. The NMR spectra were obtained with a Japan Electron Optics Lab. spectrometer (JNM3H-60). The UV spectra were taken on an EPS-3 Hitachi recording spectrometer. The glpc analyses were conducted by a Shimadzu GC-3A apparatus using Apieson L grease 10%, Silicone DC 200 10%, or Silicone oil 550 10% on Diasolid L; 60—80 mesh; 1 m column. The mercury lamp used was an Eikosha 150-W high-pressure mercury lamp.

Materials. The benzene, AcOH, and CCl_4 were purified by an ordinary method.

Titrations for active Cl were conducted by an $Na_2S_2O_3$ assay of the I_2 liberated from 10% aqueous KI acidified with 0.1 N HCl.

Preparation of N-*Halo*-N-*alkyl*-n-*alkanesulfonamides.* *N-t*-Butyl-*N*-chlorobutane, pentanesulfonamides, and *N*-chloro-*N*-methylbutanesulfonamide were prepared as has been described in a previous paper.[6] The *N*-chlorination of *N-t*-butyl-*n*-hexanesulfonamide was done in the same manner, and the *N-t*-butyl-*N*-chlorohexanesulfonamide obtained quantitatively was purified by distillation. Bp 113—115°C/0.2 mmHg, n_D^{20} 1.4730. IR: 2960, 1350, 1150, and 890 cm^{-1}.

Found: Cl, 13.6%. Calcd for $C_{10}H_{22}ClNO_2S$: Cl, 13.86%.

N-*Bromo*-N-t-*butyl*-n-*butanesulfonamide.* *N-t*-Butyl-*n*-butanesulfonamide (0.05 mol) was suspened in water (100 m*l*) in the presence of Na_2CO_3 (21 g); bromine (32 g) was added to the stirred suspension at 10°C, and the solution was stirred for 4 hr. The insoluble oil separated as a lower layer was collected and dissolved in CCl_4. The solution was dried over anhydrous Na_2SO_4, and the solvent was evaporated. Yield, 75%, IR: 2960, 1340, 1145, and 890 cm^{-1}. n_D^{20} 1.4955.

Found: Br, 29.1%. Calcd for $C_8H_{18}BrNO_2S$: Br, 29.36%.

Photodecomposition of N-*Halosulfonamides.* *N*-Alkyl-*N*-halo-*n*-alkanesulfonamides were irradiated at 28—30°C under N_2 with a high-pressure mercury lamp inside a reaction flask until the active halogen content of the solution was negligible. All the reactions were completed in 1 hr. In the reaction in benzene, reaction products were obtained after the evaporation of the benzene, while in the reaction in aqueous solvents the reaction mixture was poured onto ice and the organic layer was extracted with ether.

Isolation and Analyses of Reaction Products. Analyses of the reaction products obtained in the reaction of *N-t*-butyl-*N*-chloro-*n*-butane and pentanesulfonamides were carried out as has been described in a previous paper.[6]

N-t-*Butyl*-n-*hexanesulfonamide.* This was isolated by distillation from the reaction products obtained in the reaction of *N-t*-butyl-*N*-chlorohexanesulfonamide. Bp 118°C/0.2 mmHg. IR: 3280, 2960, 1320, and 1140 cm^{-1}.

Found: C, 54.26; H, 10.45: N, 6.21%. Calcd for $C_{10}H_{23}NO_2S$: C, 54.26; H, 10.47; N, 6.33%.

N-t-*Butyl*-*γ*-*chloro- and δ-chlorohexanesulfonamides.* On the cooling of the hexane solution of the products obtained in the photorearrangement of *N-t*-butyl-*N*-chlorohexanesulfonamide in an AcOH-H_2O solvent to −40°C, a white precipitate was obtained. This precipitate melted at room temperature; glpc and elemental analysis showed it to be a mixture of the two rearranged products. On the cooling of an ether solution of this mixture, *N-t*-butyl-*δ*-chlorohexanesulfonamide was isolated as a white precipitate; it was then recrystallized from ether and hexane. Mp 58°C. IR: 3280, 2960, 1320, and 1130 cm^{-1}. NMR (in $CDCl_3$): τ; 5.45 (1H), 6.10 (multiplet, 1H), 6.80 (triplet, 2H), 7.70—8.55 (multiplet, 6H), 8.65 (singlet, 9H), 8.95 (triplet, 3H).

Found: C, 46.89; H, 8.64; N, 5.40; Cl, 13.6%. Calcd for $C_{10}H_{22}ClNO_2S$: C, 46.95: H, 8.67; N, 5.43; Cl, 13.86%.

The isolation of another rearranged product, *N-t*-butyl-*γ*-chlorohexanesulfonamide, was tried, but it was unsuccessful because of contamination by a small amount of the *δ*-chloro isomer.

N-*Methyl*-*γ*-*chlorobutanesulfonamide.* The liquid obtained from the decomposition of *N*-chloro-*N*-methylbutanesulfonamide in AcOH-H_2O (0.15 mol/*l*, 20 min irradiation) was distilled under reduced pressure. Bp 133°C/0.1 mmHg, n_D^{25} 1.4765. IR: 3300, 2960, 1320, 1140, and 850 cm^{-1}. NMR (in $CDCl_3$): τ; 5.40 (1H), 5.85 (multiplet, 1H), 6.80 (triplet, 2H), 7.20 (doublet, 3H), 7.80 (multiplet, 2H), 8.43 (doublet, 3H).

Found: C, 32.00; H, 6.53; N, 7.49; Cl, 18.8%. Calcd for $C_5H_{12}ClNO_2S$: C, 32.35; H, 6.52; N, 7.55; Cl, 19.09%.

N-t-*Butyl*-*γ*-*bromobutanesulfonamide.* The irradiation of a benzene solution of *N*-bromo-*N-t*-butyl-*n*-butanesulfonamide (0.4 mol/*l*) with a high-pressure mercury lamp produced a viscous liquid (recovery rate, 91%) which was found by glpc to contain 25.0% of *N-t*-butyl-*n*-butanesulfonamide and 74.2% of *N-t*-butyl-*γ*-bromobutanesulfonamide; no formation of the *δ*-bromo isomer was observed. A white precipitate obtained by adding hexane to the reaction mixture was recrystallized from cold ether. Mp 69°C. IR: 3300, 1310, 1130, and 1000 cm^{-1}. NMR (in $CDCl_3$): τ; 5.40 (1H), 5.80 (multiplet, 1H), 6.80 (triplet, 2H), 7.75 (multiplet, 2H), 8.25 (doublet, 3H), 8.63 (singlet, 9H).

Found: C, 35.55; H, 6.94; N, 5.13; Br, 29.2%. Calcd for $C_8H_{18}BrNO_2S$: C, 35.30; H, 6.66; N, 5.15; Br, 29.36%.

Preparation of Sultams. N-t-*Butyl*-3-*methylpropanesultam*: To 50 m*l* of the EtOH solution of *N-t*-butyl-*γ*-chlorobutanesulfonamide[6] (0.01 mol), 0.013 mol of NaOH was added; the solution was then refluxed for 3 hr. The solution was cooled and carefully neutralized with conc. HCl. The salt was filtered off; the residue obtained after the evaporation of EtOH was almost pure, and its IR showed the disappearance of the NH band. It was purified by distillation at reduced pressure. Bp 96—97°C/0.5 mmHg, n_D^{20} 1.4780 (lit,[8] n_D^{25} 1.4733). Yield, 97%. IR: 2960, 1300, 1130, 1020, 980, and 950 cm^{-1}. NMR (in $CDCl_3$): τ; 6.20 (multiplet, 1H), 6.65—7.10 (multiplet, 2H), 7.20—8.30 (multiplet, 2H), 8.60—8.68 (singlet and doublet, 12H).

Found: C, 50.03; H, 9.01%. Calcd for $C_8H_{17}NO_2S$: C, 50.23; H, 8.96%.

N-t-*Butyl*-*butanesultam*: *N-t*-Butyl-*δ*-chlorobutanesulfonamide[6] (0.01 mol) was dissolved in EtOH (50 m*l*). NaOH (0.013 mol) was added, and the solution was refluxed for 3 hr. The salt thus formed was filtered off, and the solvents was evaporated. The residue was extracted with ether (50 m*l*); a white precipitate, which was obtained by adding hexane to the cold ether solution, was then recrystallized from ether and hexane; mp 43°C; yield, 94%. IR: 2960, 1325, 1140, 1020, 920, and 880 cm^{-1}. NMR (in $CDCl_3$): τ; 6.55 (triplet, 2H), 7.00 (triplet, 2H), 7.80 (multiplet, 2H), 8.30 (multiplet, 2H), 8.55 (singlet, 9H).

Found: N, 7.06%. Calcd for $C_8H_{17}NO_2S$: N, 7.33%.

Butanesultam: The reaction mixture (2.8 g) consisting 40% of *N-t*-butyl-*δ*-chlorobutanesulfonamide obtained after the isolation of *N-t*-butyl-*γ*-chlorobutanesulfonamide from the reaction products of *N-t*-butyl-*N*-chlorobutanesulfonamide was treated with ethanolic NaOH (0.5 g) as has been described above and then acidified with conc. HCl. The residue

obtained after the removal of the salt was dissolved in $CHCl_3$ and ether; then hexane was added and cooled. A white precipitate which separated out (0.6 g) was recrystallized from $CHCl_3$ and ether. The same compound was obtained quantitatively by the treatment of *N-t*-butylbutanesultam with conc. HCl in EtOH at room temperature. Mp 115°C (lit.[22] 114—115°C). IR: 3240, 2960, 1320, 1130, 1030, 955, and 770 cm^{-1}. NMR (in $CDCl_3$): τ; 5.70 (1H), 6.60 (multiplet, 2H), 6.90 (triplet, 2H), 7.81 (multiplet, 2H), 8.37 (multiplet, 2H).

Found: C, 35.28; H, 6.83; N, 10.26%. Calcd for $C_4H_9NO_2S$: C, 35.54; H, 6.71; N, 10.36%.

N-t-*Butylpent-3-enesulfonamide*: *N-t*-Butyl-δ-chloropentanesulfonamide[6] (0.01 mol) was dissolved in 50 m*l* of EtOH and then treated with NaOH (0.013 mol) in a manner similar to that described in the synthesis of *N-t*-butyl-3-methylpropanesultam. When the liquid thus obtained was distilled, the corresponding sultam was not obtained, but *N-t*-butylpent-3-enesulfonamide was obtained; bp 120—122°C/1mmHg, n_D^{20} 1.4680; yield, 92%. IR: 3300, 2960, 1320, 1130, and 1000 cm^{-1}. NMR (in $CDCl_3$): τ; 4.57 (multiplet, 2H), 5.40 (1H), 6.90 (triplet, 2H), 7.53 (multiplet, 2H), 8.35 (doublet, 3H), 8.62 (singlet, 9H).

Found: C, 52.31; H, 9.31%. Calcd for $C_9H_{19}NO_2S$: C, 52.65; H, 9.33%.

4-Methylbutanesultam: *N-t*-Butyl-δ-chloropentanesulfonamide (2.4 g) was heated in 40 m*l* of the HCl solution (HCl : H_2O= 3 : 1, ratio of volume) at 90°C for 6 hr. The viscous liquid (1.8 g) obtained after the evaporation of the water was washed with cold hexane and treated with NaOH (0.4 g) in 50 m*l* of EtOH under reflux for 2 hr and then neutralized with HCl. A white precipitate (1.3 g) was obtained by the treatment described in the isolation of butanesultam and was recrystallized from $CHCl_3$ and ether; mp 112°C; yield, 87%. IR: 3280, 2960, 1310, 1130, 950, and 780 cm^{-1}. NMR (in $CDCl_3$): τ; 5.60 (1H), 6.50 (multiplet, 1H), 6.93 (multiplet, 2H), 7.70—8.50 (multiplet, 4H), 8.78 (doublet, 3H).

Found: C, 39.88; H, 7.38; N, 9.33%. Calcd for $C_5H_{11}NO_2S$: C, 40.25; H, 7.43; N, 9.38%.

4-Ethylbutanesultam: *N-t*-Butyl-δ-chlorohexanesulfonamide (2.6 g) was heated in 40 m*l* of a HCl solution in the same manner as has been described in the preparation of 4-methylbutanesultam. The viscous liquid (1.9 g) thus obtained was treated with NaOH (0.4 g) in 50 m*l* of EtOH. A white precipitate (1.4 g) was obtained by the treatment described above and recrystallized from $CHCl_3$ and ether; mp 106°C; yield, 84%. IR: 3230, 2960, 1320, 1130, and 780 cm^{-1}. NMR (in $CDCl_3$): τ; 5.85 (1H), 6.50—7.10 (multiplet, 3H), 7.80 (multiplet, 2H), 8.50 (multiplet, 4H), 9.03 (triplet, 3H).

Found: C, 43.95; H, 7.95; N, 8.33%. Calcd for $C_6H_{13}NO_2S$: C, 44.15; H, 8.02; N, 8.58%.

3-Propylpropanesultam: A mixture (2.6 g) consisting 90% of *N-t*-butyl-γ-chlorohexanesulfonamide and 10% of *N-t*-butyl-δ-chlorohexanesulfonamide was treated with HCl; a white crystal (1.7 g) isolated from the semisolid liquid obtained after the cleavage of the *t*-butyl bond was submitted to the alkali treatment, and the liquid (1.1 g) thus obtained was purified by distillation; bp 115°C/0.1 mmHg; yield, 80%. IR: 3220, 1320, 1130, and 830 cm^{-1}. NMR (in $CCCl_4$): τ; 5.00 (1H), 6.50 (multiplet, 1H), 6.95 (multiplet, 2H), 7.50—8.70 (multiplet, 6H), 9.05 (triplet, 3H).

Found: C, 43.78; H, 7.89; N, 8.49%. Calcd for $C_6H_{13}NO_2S$: C, 44.15; H, 8.02; N, 8.58%.

22) H. Feichtinger, *Chem. Ber.*, **96**, 3068 (1963).

BULLETIN OF THE CHEMICAL SOCIETY OF JAPAN, VOL. 44, 777—780 (1971)

γ-Induced Addition of Trialkyltin Hydrides to Unsaturated Esters

Jitsuo TSURUGI, Masaru IIDA,* Ren NAKAO, Tsugio FUKUMOTO, and Niro MURATA*

Department of Chemistry, Radiation Center of Osaka Prefecture, Shinke-cho, Sakai, Osaka

* *Department of Applied Chemistry, University of Osaka Prefecture, Mozuume-machi, Sakai, Osaka*

(Received July 18, 1970)

γ-Induced hydrostannation of ethyl acrylate, allyl acetate, and vinyl acetate with triethyltin and tri-*n*-butyltin hydrides was attempted. The hydrostannation of ethyl acrylate and allyl acetate gave the corresponding adducts in almost quantitative yield. (2-Acetoxyethyl)-tri-*n*-butyltin expected from hydrostannation of vinyl acetate with tri-*n*-butyltin hydride could not be isolated. However, NMR and IR spectra indicated the formation of the adduct, which was found to decompose into ethylene and tri-*n*-butyltin acetate. The decomposition of the adduct was discussed in comparison with other adducts.

The addition reaction of organotin hydrides to unsaturated bonds is known as hydrostannation and extensively studied.[1,2] However, hydrostannation with γ-irradiation has not been reported so far. In this paper we report the γ-induced hydrostannation of ethyl acrylate, allyl acetate, and vinyl acetate with triethyltin and tri-*n*-butyltin hydrides. The hydrostannation of vinyl acetate and tri-*n*-butyltin hydride was found not to give the expected adduct, (2-acetoxyethyl)-tri-*n*-butyltin, but to yield tri-*n*-butyltin acetate. No successful synthesis of the expected adduct is found in literature. The reason why this adduct cannot be isolated is given.

1) Y. Nagai, *Kagaku no Ryoiki*, **23**, 233 (1969).

2) H. G. Kuivila, "Advances in Organometallic Chemistry," Vol. 1, ed. by F. G. A. Stone and R. West, Academic Press, New York, N. Y. (1964), p. 47.

Results and Discussion

γ-Induced Hydrostannation. A mixture of 1 : 2 molar ratio of tri-*n*-butyltin hydride and vinyl acetate gave a curdy product after being subjected to irradiation. The amount of the product seems proportional

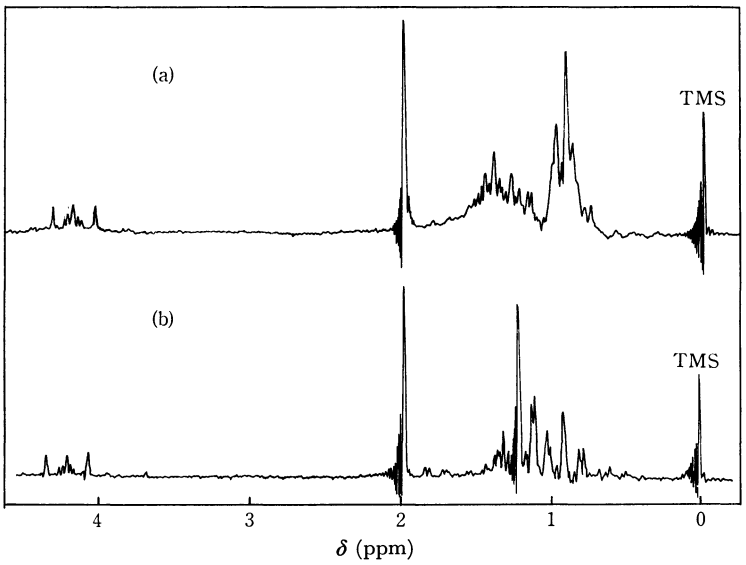

Fig. 1. The NMR spectra in CCl_4 of irradiated mixture of run 4 (a) and of (2-acetoxyethyl)-triethyltin (b).

to irradiation dose in the range 10^5—10^7R. This product was identified as polyvinyl acetate by IR spectrum. An equimolar mixture of trialkyltin hydride and the unsaturated ester was used in the experiments, because the mixture gave no curdy product under irradiation of similar doses. Yields of the 1 : 1 adducts are summarized in Table 1. Table 1 indicates that the hydrostannation proceeds almost quantitatively in runs 1 and 2. From the result we can write the reaction as free radical 1 : 1-β-addition, the detailed mechanims of which has been reviewed.[2] We assume that the equation

$$R_3SnH + CH_2{=}CHR' \rightsquigarrow R_3SnCH_2CH_2R' \quad (1)$$

would still be applicable to runs 3 and 4, and that adduct **4** would decompose completely and **3** partially during separation procedures.

In order to verify this we examined the irradiated mixture of run 4 by NMR and IR methods. Fig. 1a shows the NMR spectrum of irradiated mixture in carbon tetrachloride solution at 60 MHz. In comparison with NMR signals of adduct **3** (Fig. 1b), the superimposed triplet centered at about 0.9 ppm can be assigned to the methylenes bonded to the tin atom, and the remaining multiplet in the high field to butyl methylenes and methyls. The singlet signal at 2.0 ppm is assigned to acetyl protons. In the lower field, complicated signals appear at about 4.2 ppm. From the signal shift and integrated intensity, this is assigned to the methylene protons bonded to the acetyl group. The NMR spectrum of adduct **3** shows similar signals except for the alkyl substituents. Figure 2 shows the IR spectrum of irradiated mixture of run 4. The key bands indicating the existence of the saturated acetylate observed as two strong bands were attributable to the C=O stretching vibration in 1735 cm^{-1} and C–O–C antisymmetrical vibration in 1237 cm^{-1}. The spectrum is devoid of absorption bands due to the carbonyls of tri-*n*-butyltin acetate (1642 cm^{-1}) and vinyl acetate (1760 cm^{-1}). From IR and NMR spectral evidences, hydrostannation is considered to occur also in the case of run 4.

Table 1. γ-Induced hydrostannation of unsaturated esters $CH_2{=}CHR'$ with trialkyltin hydrides R_3SnH in 1:1 molar ratio

Run No.	R in R_3SnH	R′ in $CH_2{=}CHR'$	Dose rate (R/hr $\times 10^5$)	Dose (R $\times 10^7$)	1:1 Adduct No.[a]	1:1 Adduct Yield[b]
1	*n*-C_4H_9	$-COOC_2H_5$	3.0	1.2	1	96
2	*n*-C_4H_9	$-CH_2OCOCH_3$	3.0	1.2	2	98
3	C_2H_5	$-OCOCH_3$	2.5	1.0	3	60
4	*n*-C_4H_9	$-OCOCH_3$	3.0	1.2	4	0

a) adduct 1: (2-carboethoxyethyl)-tri-*n*-butyltin $(n\text{-}C_4H_9)_3SnCH_2CH_2COOC_2H_5$
adduct 2: (3-acetoxypropyl)-tri-*n*-butyltin $(n\text{-}C_4H_9)_3SnCH_2CH_2CH_2OCOCH_3$
adduct 3: (2-acetoxyethyl)-triethyltin $(C_2H_5)_3SnCH_2CH_2OCOCH_3$
adduct 4: (2-acetoxyethyl)-tri-*n*-butyltin $(n\text{-}C_4H_9)_3SnCH_2CH_2OCOCH_3$

b) Gas chromatographic determination for adducts **1** and **2**, and distillation for **3** and **4**. The application of the former to **3** resulted in complete decomposition.

Decomposition of the Adduct 4. Distillation of the irradiated mixture of run 4 gave white needles, bp

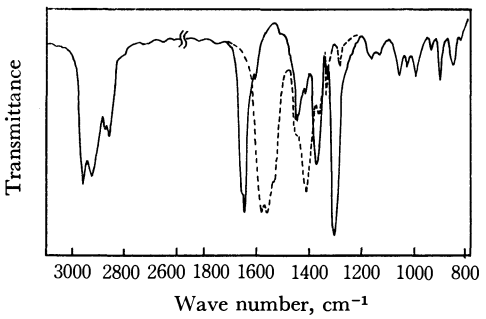

Fig. 2. The IR spectra in CCl_4.
— irradiated mixture of run 4
····· non-irradiated mixture of tri-*n*-butyltin hydride and vinyl acetate

90—100°C/0.001 mmHg, mp 84.8°C (lit,[3] 84.5—85°C), identified as tri-*n*-butyltin acetate by IR and NMR and elemental analysis. Qualitative glpc analysis (at 180°C column temperature) of the irradiated mixture indicates the presence of tri-*n*-butyltin acetate but no other compounds. These results suggest the following equation for the decomposition of adduct **4**.

$$(n\text{-}C_4H_9)_3SnCH_2CH_2OCOCH_3 \longrightarrow (n\text{-}C_4H_9)_3SnOCOCH_3 + CH_2{=}CH_2 \quad (2)$$

Evolution of ethylene was qualitatively observed by gas analysis from the irradiated mixture kept standing for several weeks at room temperature. Addition of acetic acid or anhydride was found effective for the decomposition of adduct **4**. After being kept standing for 24 hr at room temperature in an open vessel, tri-*n*-butyltin acetate was filtered and weighed. The result is shown in Fig. 3.

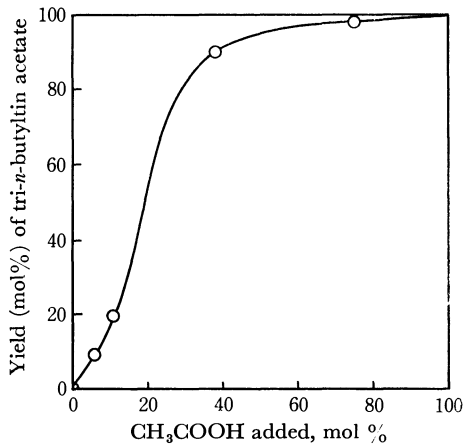

Fig. 3. Effect of the addition of acetic acid to adduct **4**. One mole of adduct **4** was assumed to be produced from irradiated mixture of each one mole of starting materials.

The results in Table 1 indicate that only the adducts resulting from trialkyltin hydride and vinyl acetate decompose during distillation[4] or gas chromatography as compared with almost quantitative yields of the adducts **1** and **2**. Hence, the decomposition can be ascribed to intramolecular formation of cyclic transition state followed by elimination of ethylene and simultaneous formation of Sn–O bond. In a closed vessel

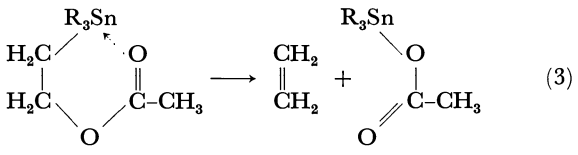

(3)

the presence of ethylene evolved suppresses the decomposition. Distillation, gas chromatography, heating or being left at room temperature in an open vessel allows ethylene to evolve out of the system, and shifts the equilibrium to the right side.

Van der Kerk *et al.*[5] reported that triphenyltin hydride with vinyl acetate yielded the adduct quantitatively. The structure of R in $R_3SnCH_2CH_2OCOCH_3$ seems to play an important role. In the cleavage reaction of tetraalkyltin with chloroacetic acid,

$$(n\text{-}C_3H_7)_4Sn + ClCH_2COOH \longrightarrow (n\text{-}C_3H_7)_3SnOCOCH_2Cl + n\text{-}C_3H_8 \quad (4)$$

$$(i\text{-}C_3H_7)_4Sn + 2ClCH_2COOH \longrightarrow (i\text{-}C_3H_7)_2Sn(OCOCH_2Cl)_2 + 2i\text{-}C_3H_8 \quad (5)$$

Sasin *et al.*[6] interpreted Eqs. (4) and (5) as follows. Stronger electron-releasing effect of *i*-propyl group on the carbon atom of the C–Sn bond is balanced by the substitution of two haloacyloxy groups of strong electron-withdrawing property. In contrast, less electron-releasing effect of *n*-propyl group is sufficient to undergo substitution by only one haloacyloxy group. Alkyl group in (2-acetoxyethyl)-trialkyltin, $R_3SnCH_2CH_2OCOCH_3$, seems to make the adduct susceptible to the decomposition in contrast to phenyl group. In this respect *n*-butyl group is more electron-releasing than ethyl group. Thus, adduct **4** is concluded to be more susceptible than **3**.

Experimental

All melting and boiling points are uncorrected. The IR spectra were obtained by a Perkin-Elmer 221 spectrometer. The NMR spectra were recorded by a Japan Electron Optics 3H-60 spectrometer, using a tetramethylsilane as an internal standard.

Materials. Tri-*n*-butyltin and triethyltin hydrides were prepared by reduction of tri-*n*-butyltin and triethyltin chlorides with lithium alminum hydride,[7] respectively, and distilled just before use. Triethyltin chloride was prepared by disproportionation of tetraethyltin and tin tetrachloride.[8] Commercial products of tri-*n*-butyltin chloride, tin tetrachloride, allyl acetate, vinyl acetate, and ethyl acrylate were used.

Irradiation. An unsaturated ester (0.01 mol), after being degassed by four freeze-thaw processes, was transferred by a vaccum line into an ampul containing degassed trialkyltin hydride (0.01 mol). The ampul, after being fused, was irradiated at room temperature with γ-rays from a ^{60}Co source without agitation.

Separation and Identification of the Products. Gas chromatography was carried out with a Yanagimoto GCG-5DH fitted with a FID detector, using a 2m column containing 25% Silicone DC-200 on Celite 545.

Run 1. The irradiated product was determined by glpc and identified[9] by IR and NMR in a carbon tetrachloride solution. IR (CCl_4): 2950, 2915, 1740, 1450, 1375, 1228, and 1020 cm^{-1}; NMR (CCl_4): δ 4.09 (q, 2H, CH_2), δ 2.47 (t, 2H, CH_2), δ 1.8—0.5 (m, 32H, CH_2 and CH_3).

Run 2. The reaction product was determined by glpc. For identification the product was distilled *in vacuo*, the frac-

3) G. J. M. van der Kerk and J. G. A. Luijten, *J. Appl. Chem.*, **6**, 49 (1956).

4) (2-Acetoxyethyl)-triethyltin was reported to decompose at 70—80°C to yield ethylene and quantitative amount of triethyltin acetate; W. P. Neumann, H. Niermann, and R. Sommer, *Ann. Chem.*, **659**, 27 (1962), and reference therein.

5) J. G. M. van der Kerk, J. G. Noltes, and J. G. A. Luijten, *J. Appl. Chem.*, **7**, 356 (1957).

6) G. S. Sasin, A. L. Borror, and R. Sasin, *J. Org. Chem.*, **23**, 1366 (1958).

7) G. J. M. van der Kerk, J. G. Noltes, and J. G. A. Luijten, *J. Appl. Chem.*, **7**, 366 (1957).

8) K. A. Kozeschkow, *Ber.*, **66**, 1661 (1933).

9) M. Pereyre, G. Colin, and J. Valade, *Bull. Soc. Chim. Fr.*, **1968**, 3358.

tion boiling at 95—100°C/0.001 mmHg being collected. IR (CCl_4): 2950, 2915, 1737, 1450, 1370, 1365, 1233, and 1030 cm^{-1}; NMR (CCl_4): δ 3.94 (t, 2H), δ 2.00 (s, 3H), δ 1.8—0.5 (m, 31H, CH_2 and CH_3).

Run 3. Distillation gave the product boiling at 70—80°C/0.001 mmHg: n_D^{20} 1.4750 (lit,[4] 1.4773). IR (CCl_4): 2950, 2915, 2815, 1740, 1390, 1240, 1055, 1025, and 970 cm^{-1}.

Run 4. A mixture of 1 : 2 molar ratio gave after irradiation curdy products, which were filtered and reprecipitated with petroleum ether from benzene. IR (film): 2950, 1730, 1370, 1240, and 1025 cm^{-1}. In the case of equimolar ratio, tri-*n*-butyltin acetate precipitated in the irradiated mixture was filtered and recrystallized from petroleum ether. IR (KBr): 2950, 2915, 2850, 1575, 1550, 1405, 1340, and 670 cm^{-1}; NMR (CCl_4): δ 1.96 (s, 3H, CH_3), δ 1.8—0.7 (m, 27H, CH_2 and CH_3). Found: C, 47.68; H, 8.82%. Calcd for $C_{14}H_{30}O_2Sn$; C, 48.16; H, 8.66%.

Gas Analysis. Evolution of ethylene from the decomposition of adduct **4** was confirmed as follows. The sample tube fitted with a breakable seal was attached to a vacuum line and the seal was broken. The products noncondensable at −196°C were determined by the Toepler gauge, and analyzed by mass spectrometry (Hitachi RMU-5G) and gc (Hitachi KGL-2A) on a molecular sieves column with N_2 as carrier. The condensable fraction was vaporized with a dry ice-acetone bath, and analyzed by gc using a silica gel column. Ethylene (0.045 mol), *n*-butane (0.009 mol) and hydrogen (0.005 mol) were found. However, tri-*n*-butyltin hydride irradiated under similar conditions gave *n*-butane (0.005 mol) and hydrogen (0.008 mol). Thus, in the case of the decomposition of adduct **4**, *n*-butane and hydrogen can be formed from the irradiation of the starting material (tri-*n*-butyltin hydride) and not from the decomposition of adduct **4**.

BULLETIN OF THE CHEMICAL SOCIETY OF JAPAN, VOL. 44, 780—784 (1971)

Studies of the Synthesis of Furan Compounds. XXIII.[1] Cyclization Derivatives of 5-Nitro-2-furimidoylhydrazine[2]

Ichiro HIRAO, Yasuhiko KATO, Tsunetoshi HAYAKAWA, and Hiromichi TATEISHI

Department of Chemical Engineering, Kyushu Institute of Technology, Tobata-ku, Kita-Kyushu

(Received July 24, 1970)

The reaction of 5-nitro-2-furimidoylhydrazine (I) with diacetyl or furil gave 3-(5-nitro-2-furyl)-5,6-disubstituted-1,2,4-triazine derivatives (IIa, b). Refluxing I in a large excess of ethyl orthoformate afforded 3-(5-nitro-2-furyl)-5-ethoxy-1,2,4-triazoline (III) and bis[3-(5-nitro-2-furyl)-1,2,4-triazolyl]methyl ethyl ether (IV). By heating with ethyl orthoformate, III was converted to IV. When III or IV was heated in diluted sulfuric acid, 3-(5-nitro-2-furyl)-1,2,4-triazole (V) was produced. The reactions of I with cyanogen bromide in refluxing methanol and with nitrous acid in diluted hydrochloric acid gave the corresponding 3-(5-nitro-2-furyl)-5-amino-1,2,4-triazole (VI) or -1,2,4,5-tetrazole (VIII) respectively. When heated in acetic anhydride, the VI afforded monoacetyl compound (VII), while the VIII yielded 5-(5-nitro-2-furyl)-2-methyl-1,3,4-oxadiazole (X). The structures of these compounds were discussed on the basis of their IR and NMR spectra.

In a previous paper[3] the present authors synthesized 5-nitro-2-furimidoylhydrazine (I) by treating 5-nitro-2-furonitrile with hydrazine hydrate. Since the structure of I is analogous to that of aminoguanidine, I is expected to show a reactivity similar to that of aminoguanidine toward various bifunctional compounds. This paper will deal with the preparation of several 5-nitro-2-furyl-heterocycles by the cyclization of I with bifunctional compounds.

Results and Discussion

Erickson[4] has prepared 3-amino-1,2,4-triazine derivatives by the reactions of aminoguanidine carbonate with glyoxal and diacetyl, but Thile *et al.* reported[5] that only bisguanylhydrazone was obtained instead of 1,2,4-triazine by the similar reaction of either aminoguanidine nitrate or the hydrochloride with glyoxal, and Polonovski[6] and Gianturco[7] have investigated this in detail. When I was treated with diacetyl in boiling methanol, an orange crystalline product, mp 212°C, was obtained. An elemental analysis of this product (Found: C, 46.54; H, 3.64; N, 25.42%) did not agree with the calculated value for the desired compound. The IR spectrum of this compound showed N–H absorption at 3250 cm^{-1}, but no C=O absorption was detected. No further determination of the structure of this compound has been undertaken. However, when treated with diacetyl in refluxing methanol containing *N,N*-dimethylformamide, I afforded the desired 3-(5-nitro-2-furyl)-5,6-dimethyl-1,2,4-triazine (IIa). The similar treatment of I with furil in refluxing methanol afforded the desired cyclization product, 3-(5-nitro-2-furyl)-5,6-bis(2-furyl)-1,2,4-triazine (IIb).

1) Part XXII of this series: Y. Kato, This Bulletin, **44**, 489 (1971).

2) Presented at the 20th Annual Meeting of The Chemical Society of Japan, Tokyo, March, 1967.

3) Y. Kato and I. Hirao, *Bull. Kyushu Inst. Tech.*, No. **15**, 57 (1965).

4) J. G. Erickson, *J. Amer. Chem. Soc.*, **74**, 4706 (1952).

5) J. Thile and E. Pralle, *Ann.*, **302**, 275 (1898).

6) M. Polonovski and M. Pesson, *C. R. Acad. Sci., Paris*, **232**, 1260 (1951).

7) M. Gianturco and A. Romeo, *Gazz. Chim. Ital.*, **82**, 429 (1953).

When I was refluxed in a large excess of ethyl orthoformate, two compounds, III (mp 131—132°C (32% yield)) and IV (mp 179—180°C (28.6%)), were produced. Judging from the results of the elemental analysis, III seems to be 3-(5-nitro-2-furyl)-5-ethoxy-1,2,4-triazoline, and IV, bis[3-(5-nitro-2-furyl)-1,2,4-triazolyl]methyl ethyl ether. The presence of a triazole structure in III and IV was supported by the characteristic IR absorption bands in the 3500—2800 cm^{-1} region.[8]

Table 1. Effects of reaction time on the yield and the compound ratio

Reaction time (hr)	Product		
	Total yield (%)	Ratio	
		III	IV
0.25	78.3	92.2	7.8
1	60.6	52.8	47.2
5	58.6	0	100.0

The relation between the reaction time and the product ratio was investigated; the results are shown in Table 1. With an increase in the reaction time, the formation of III as well as the total yields decreased, but that of IV increased. This suggests that III was formed in the initial step and that IV may be produced by the existence of excess ethyl orthoformate.

Compound III was stable to heating in 2-methoxyethanol, but was unstable in diluted sulfuric acid, when it gave 3-(5-nitro-2-furyl)-1,2,4-triazole (V) by eliminating a molecule of ethanol. V was also obtained by heating IV in diluted sulfuric acid. It seems that IV reacts with water under the catalytic action of the acid to afford V by liberating ethyl formate. Compound

Table 2. NMR data of III, IV, and V (at 60 MHz in DMSO-d_6)

	III δ	IV δ	V δ
Triazole ring C–H	8.28 (1H, sharp s)	9.35 (2H, sharp s)	8.82 (1H, sharp s)
Furan ring 4–H	7.78 (1H, sharp d, J=4.1 Hz)	7.86 (2H, sharp d, J=4.2 Hz)	7.85 (1H, sharp d, J=4.2 Hz)
Furan ring 3–H	7.29 (1H, sharp d, J=4.1 Hz)	7.43 (2H, sharp d, J=4.2 Hz)	7.34 (1H, sharp d, J=4.2 Hz)
Triazole ring N–H	6.62 (2H, broad s)		3.62 (1H, very broad s)
Methine (–C(–)–H)		8.17 (1H, sharp s)	
Ethoxy CH_2	4.28 (2H, sharp q, J=7.2 Hz)	4.01 (2H, sharp q, J=7.2 Hz)	
Ethoxy CH_3	1.31 (3H, sharp t, J=7.2 Hz)	1.38 (3H, sharp t, J=7.2 Hz)	

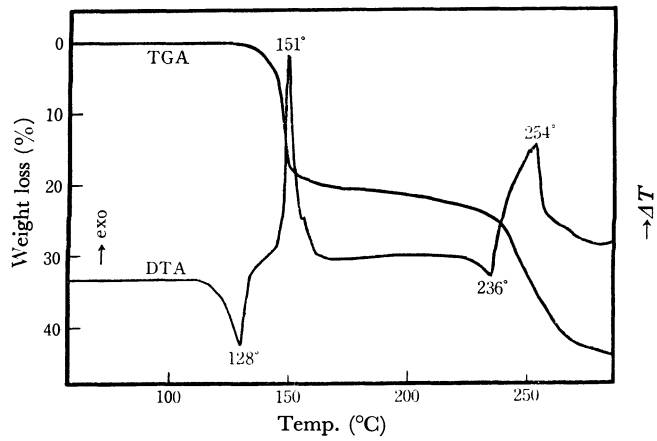

Fig. 1. Thermal analysis of III measured in an argon stream using 21.3 mg of sample at the heating rate of 3°C/min.

V is obviously a 1,2,4-triazole derivative since, in the IR spectrum, characteristic absorptions of C–H in the triazole ring remained, but no more $-OC_2H_5$ was present. III was heated in ethyl orthoformate to give IV, but the V remained unchanged. When an equimolar mixture of ethyl orthoformate and I was heated in 2-methoxyethanol, no formation of IV was observed and the sole product was III. The NMR spectra (shown in Table 2) are compatible with the above structures, III, IV, and V.

Furthermore, the thermostability of III was investigated by thermogravimetric analysis (TGA) and differencial thermal analysis (DTA). In Fig. 1, the DTA curve shows an endothermic peak at 128°C which coincides with the melting point of compound III. Two exothermic peaks, one at 151°C and the other at 254°C, correspond to the initial and the second stages (128—154°C and 236—270°C) respectively of the reduction in weight of the TGA curve. About 20% of the loss of weight occurs in the initial stage; this corresponds to the loss of a molecule of ethanol from III (theoretical 20.3%). The second stage of the reduction in weight agrees with the decomposition point of V during the pyrolysis.

These results show that the releasing of ethanol from III occurred at 128—154°C, but not under the refluxing temperature (110—120°C) in ethyl orthoformate or in 2-methoxyethanol. Therefore, it seems most resonable to conclude that the mechanism of the formation of IV is in the initial step, giving III from I and ethyl orthoformate, and in the following reaction of III with excess ethyl orthoformate, affording IV without the process: III→V→IV.

When acyl hydrazines are treated with cyanogen bromide, 5-substituted 2-amino-1,3,4-oxadiazole is formed.[9] Similarly, 3-(5-nitro-2-furyl)-5-amino-1,2,4-triazole (VI) was obtained by the treatment of I with cyanogen bromide in refluxing methanol. The IR spectrum of VI has characteristic absorptions at 3400, 3295 (νNH_2), 1646 (δNH_2), and 1320 cm^{-1} (νC–N), supporting the amino-triazole structure. A monoacetyl derivative (VII) was obtained by the treatment of VI with hot acetic anhydride, whereas it reverted to the

8) K. T. Potts, *J. Chem. Soc.*, **1954**, 3461.

9) A. Dornow and K. Brunken, *Ber.*, **82**, 121 (1949).

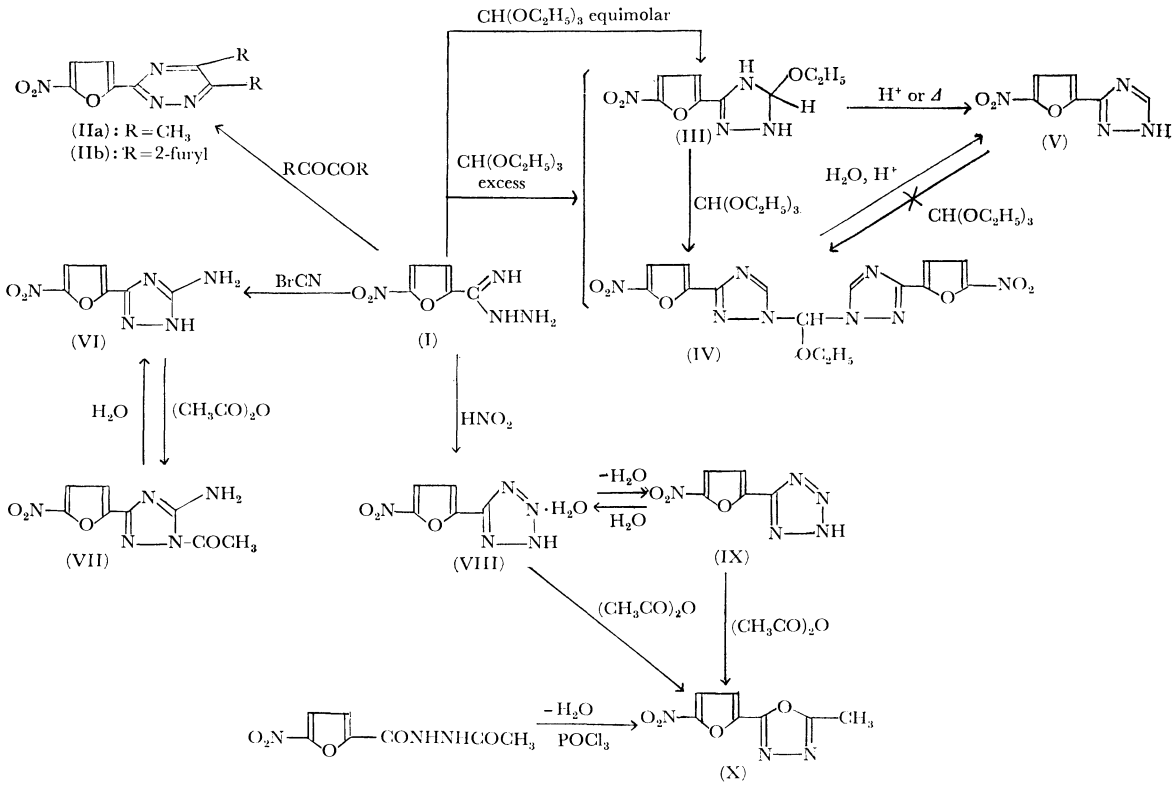

starting material VI upon heating with water. The presence of a carbonyl absorption at 1733 cm^{-1} in the IR spectrum of VII suggests that the acetylation had occurred at the ring imino nitrogen because of a shift to higher frequencies than with the usual amides. The lack of the production of di- or triacetyl derivative is attributable to the low solubility of VII in the given solvent.

In order to prepare the tetrazole derivative, I was treated with nitrous acid in diluted hydrochloric acid according to Pinner's procedure;[10] this afforded the product (VIII), mp 71—72°C. The IR spectrum has an O–H absorption at 3500—3200 cm^{-1}, perhaps due to the water of recrystallization. In fact, the elemental analysis is compatible with the value calculated for the monohydrate of 5-(5-nitro-2-furyl)tetrazole. Water was successfully removed when VIII was heated at 50—55°C *in vacuo* to give 5-(5-nitro-2-furyl)tetrazole (IX), mp 121—122°C, and IX was converted to VIII by heating it in water for several minutes. IX showed no O–H absorption in the infrared spectrum. In order to confirm the above facts, the thermal analysis of VIII was undertaken. As is shown in Fig. 2, two endothermic peaks are observed in the DTA curve, at 57 and 120°C. The initial peak and its shoulder (60°C) are in agreement with a stage of the reduction in weight at 30—70°C (about 8.9% of loss of weight), corresponding to the loss of a molecule of water (9.04%), and with the melting point of VIII of the TGA curve. The second endothermic peak is obviously in good accordance with the melting point of IX for the TGA curve.

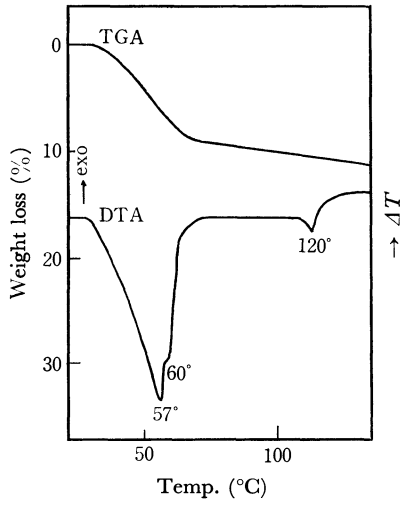

Fig. 2. Thermal analysis of VIII measured in an argon stream using 14.2 mg of sample at the heating rate of 3°C/min.

The IR spectra showed characteristic wide ammonium and immonium absorptions in the 2900—2100 and 2000—1800 cm^{-1} regions for VIII, and in the 3000—2300 cm^{-1} region for IX. These facts, as claimed by Otting,[11] suggest that both VIII and IX participate in an intermolecular association in which the hydrogen atom of the imino group protonates a nitrogen of an adjacent molecule, the two charged particles being stabilized by resonance. The difference between VIII and IX may be presumed to be that VIII can form the structural element $=N^{+}-H$ with greater facility than can IX because of the included water of recrystallization, the hydrogen transfer being thus made easier.

When VIII or IX was heated in acetic anhydride, the product (X) was not the desired *N*-acetyl-tetrazole but 5-(5-nitro-2-furyl)-2-methyl-1,3,4-oxadiazole, which was identified by means of an alternate method of pre-

10) A. Pinner, *Ber.*, **27**, 990 (1894).

11) W. Otting, *Chem. Ber.*, **89**, 2887 (1956).

paration utilizing the dehydration of 1-(5-nitro-2-furoyl)-2-acetylhydrazine with phosphoryl chloride. This reaction might occur much as in the formation of 2,5-disubstituted 1,3,4-oxadiazole from 5-substituted tetrazole and acyl chlorides, as has been reported by Huisgen *et al.*,[12] though Pinner *et al.*[13] obtained a ring-opening *N*-acetyl-*p*-toluamidine on the treatment of 5-*p*-tolyltetrazole with hot acetic anhydride.

Experimental

All the melting and decomposing points are uncorrected. Microanalyses were carried out with a Yanagimoto C.H.N. Corder, MT-2 type. The infrared absorption spectra (IR) were obtained with a Shimadzu IR-27S spectrophotometer by the KBr method. The nuclear magnetic resonance spectra (NMR) were measured with a Nihon-Denshi NMR spectrometer, JNM C-60HL, in DMSO-d_6 and with tetramethylsilane as the internal standard; the peak positions are expressed in δ-values. The thermal analyses were carried out with a Rigaku Denki Thermoflex in an argon stream.

3-(5-Nitro-2-furyl)-5,6-dimethyl-1,2,4-triazine (IIa). A solution of I[3] (3 g, 17.6 mmol) and *N,N*-dimethylformamide (20 m*l*) in 200 m*l* of methanol was stirred slowly into a solution of diacetyl (1.6 g, 18.6 mmol) in 50 m*l* of methanol. The resulting solution was stirred for an additional 2 hr and then heated under reflux for 3 hr. Cooling provided 1.86 g of pale yellow needles (mp 160—161°C). When the mother liquor was concentrated *in vacuo*, a pale yellow powder was obtained, mp 160.5—161°C; weight, 1.61 g. The total yield was 3.47 g. Recrystallization from 30% aqueous methanol gave pale yellow needles, mp 160.5—161°C. The yield was 3.06 g (78.9%).

Found: C, 49.08%; H, 3.52; N, 25.29%. Calcd for $C_9H_8N_4O_5$: C, 49.09; H, 3.64; N, 25.45%.

3-(5-Nitro-2-furyl)-5,6-bis(2-furyl)-1,2,4-triazine (IIb). To a stirred solution of furil (0.19 g, 1 mmol) in 15 m*l* of methanol we added, drop by drop, a solution of I (0.17 g, 1 mmol) in 10 m*l* of methanol. After the addition was over, the resulting solution was refluxed for 3 hr and left to stand overnight; the product was then collected by filtration. Recrystallization from methanol gave yellow needles, mp 159—161°C. The yield was 0.15 g (51.3%).

Found: C, 55.43; H, 2.56; N, 17.53%. Calcd for $C_{15}H_8N_4O_5$: C, 55.56; H, 2.47; N, 17.28%.

3-(5-Nitro-2-furyl)-5-ethoxy-1,2,4-triazoline (III). A mixture of I (1.7 g, 10 mmol), ethyl orthoformate (1.48 g, 10 mmol), and 25 m*l* of 2-methoxyethanol was heated under reflux for 15 min. The resulting solution was concentrated to dryness *in vacuo* below 50°C. The residue was dissolved in hot benzene, and the insoluble material was filtered off. After the solution had been left standing, the precipitates were collected and crystallized from benzene to give 1.31 g (50%) of III as orange needles which melted at 131—132°C. IR: cm^{-1} 3409 and 3310 (N–H), 2980—2870 (CH_3, CH_2).

Found: C, 42.58; H, 4.49; N, 24.83%. Calcd for $C_8H_{10}N_4O_4$: C, 42.47; H, 4.42; N, 24.78%.

Bis[3-(5-nitro-2-furyl)-1,2,4-triazolyl]methyl Ethyl Ether (IV). From I and Ethyl Orthoformate: Compound I (3 g, 17.6 mmol) was suspended in ethyl orthoformate (30 m*l*) and heated under reflux for 5 hr. The solution was then cooled, and the precipitate was collected on a filter, washed with cold benzene, and dried to give a yellow powder. Recrystallization from dioxane-water provided yellow columns; mp 179—180°C. The yield was 2.15 g (58.6%). IR: cm^{-1} 3120 (C–H in triazole ring), 2960—2846 (CH_3, CH_2).

Found: C, 43.30; H, 3.00; N, 26.98%. Calcd for $C_{15}H_{12}N_8O_7$: C, 43.27; H, 2.88; N, 26.92%.

From III and Ethyl Orthoformate: A mixture of III (0.21 g, 1.2 mmol) and 2 m*l* of ethyl orthoformate was heated under reflux for 4 hr. The solution was concentrated *in vacuo* affording 0.23 g of brown crystals; mp 131—161°C. Work-up as above gave 0.11 g (45.5%) of yellow columns, mp 180—181°C. This product was found to be identical with IV by elemental analysis and by a mixed-melting-point determination.

Reaction of I with Excess Ethyl Orthoformate. A mixture of I (1 g, 5.8 mmol) and 10 m*l* of ethyl orthoformate was heated under reflux for a given time (*cf.* Table 1). The ethyl orthoformate was then removed *in vacuo*, and the residue was slurried in boiling benzene to give crude IV. Recrystallization from dioxane-water gave a pure product. The benzene liquor was worked-up as above in order to prepare III. The yields are shown in Table 1.

3-(5-Nitro-2-furyl)-1,2,4-triazole (V). From the Reaction of III in Diluted Sulfuric Acid: A solution of III (0.23 g, 1 mmol) in 15 m*l* of 5% sulfuric acid was heated on a steam bath for 7—10 min. After concentration, the separated product was collected on a filter, washed with ether, and dried. This weighed 0.11 g (61.1%) and melted at 249—251°C with decomposition. Crystallization from water gave pale yellow crystals; mp 254—255°C (dec.). IR: cm^{-1} 3080 (C–H in triazole ring).

Found: C, 40.11; H, 2.00; N, 31.15%. Calcd for $C_6H_4N_4O_3$: C, 40.00; H, 2.22; N, 31.11%.

Decomposition of IV with Sulfuric Acid: A mixture of IV (2.08 g, 5 mmol) and 30 m*l* of 25% sulfuric acid was heated to boiling for 1 hr. On the concentration of the solution to half of the initial volume, the product separated as yellow crystals; mp 249—253°C (dec.); weight, 0.7 g. An additional 1 g was obtained by neutralizing the sulfuric acid solution with solid sodium carbonate. The total yield was 1.7 g (94.4%). Recrystallization as above gave pale yellow crystals; mp 254—255°C (dec.). The melting point of this compound was not depressed upon admixture with an authentic sample.

3-(5-Nitro-2-furyl)-5-amino-1,2,4-triazole (VI). Cyanogen bromide (1.9 g, 17.6 mmol) and I (3 g, 17.6 mmol) were heated together under reflux in 200 m*l* of methanol for 1 hr. The solution was then taken to dryness *in vacuo*, affording a brown residue. Crystallization from water gave yellow plates; mp 273.5—274°C. The yield was 1.8 g (52.4%).

Found: C, 37.21; H, 2.71; N, 35.40%. Calcd for $C_6H_5N_5O_3$: C, 36.92; H, 2.56; N, 35.89%.

3-(5-Nitro-2-furyl)-1-acetyl-5-amino-1,2,4-triazole (VII). Compound VI (0.49 g, 2.5 mmol) was covered with acetic anhydride (5—10 m*l*) and heated on a steam bath for 15 min. Water (50 m*l*) was added to the resulting suspension in order to decompose the surplus acid anhydride. The product was filtered and then slurried in 50 m*l* of boiling methanol. In this way 0.57 g (95.8%) of pure VII was obtained as a fine yellow powder; mp$>$350°C.

Found: C, 40.88; H, 2.90; N, 29.28%. Calcd for $C_8H_7N_5O_4$: C, 40.51; H, 2.95; N, 29.54%.

Hydrolysis of VII. Acetyl compound VII (0.1 g, 0.36 mmol) was heated under reflux in 80 m*l* of water for 4.5 hr. Cooling provided 0.07 g (quantitative) of yellow plates of VI; mp 273°C (dec.) (water). This product was identical in its infrared spectrum with an authentic sample of VI.

5-(5-Nitoro-2-furyl)tetrazole Monohydrate (VIII). To a

12) R. Huisgen, J. Sauer, and H. J. Sturm, *Angew. Chem.*, **70**, 272 (1958).

13) A. Pinner, *Ann.*, **298**, 7 (1897); A. Pinner and N. Caro, *Ber.*, **27**, 3278 (1894).

stirred, ice-cooled solution of I (5.0 g, 29.4 mmol) in a mixture of concentrated hydrochloric acid (5 g) and 50 m*l* of water, we added, portion by portion, 3.24 g (46.9 mmol) of sodium nitrite powder. Stirring was then continued for an additional 2 hr at 3—5°C. The product was filtered and washed with a small amount of water to give 5.1 g of a tan powder. Crystallization from water gave 4.7 g (80.2%) of VIII as yellow plates; mp 71—72°C.

Found: C, 30.67; H, 2.57; N, 35.48%. Calcd for $C_5H_3N_5O_3 \cdot H_2O$: C, 30.15; H, 2.51; N, 35.17%.

5-(5-Nitro-2-furyl)tetrazole (IX). Monohydrate VIII (314.4 mg, 1.58 mmol) was heated at 50—55°C in a vacuum flask for 6 hr. After the loss of 28.4 mg of water, 286 mg of IX were obtained as a pale yellow powder; mp 121—122°C.

Found: C, 33.20; H, 1.59; N, 38.72%. Calcd for $C_5H_3N_5O_3$: C, 33.14; H, 1.65; N, 38.67%.

Hydration of IX. A solution of IX (147 mg, 0.81 mmol) in 1 m*l* of water was heated on a steam bath for 5 min. Cooling gave 163 mg (quantative) of VIII as pale yellow needles; mp 70—71°C, undepressed on admixture with a sample prepared by the method described above for VIII.

5-(5-Nitro-2-furyl)-2-methyl-1,3,4-oxadiazole (X). From the Cyclization of 1-(5-Nitro-2-furoyl)-2-acetylhydrazine: A suspension of 2.13 g (10 mmol) of 1-(5-nitro-2-furoyl)-2-acetylhydrazine in 25 m*l* of phosphoryl chloride was heated on a steam bath for 3 hr. The resulting solution was taken to dryness *in vacuo*, and the residue was washed with water. Crystallization from methanol gave 0.8 g (41%) of X as yellow needles; mp 151—152°C.

Found: C, 42.93; H, 2.67; N, 21.85%. Calcd for $C_7H_5N_3O_4$: C, 43.08; H, 2.56; N, 21.55%.

From the Reacton of VIII or IX with Acetic Anhydride: A mixture of VIII (or IX) (1.5 mmol) and 5 m*l* of acetic anhydride was heated under reflux for 2 hr. The acetic anhydride was removed *in vacuo*, and the residue was dissolved in 30 m*l* of ethanol. Cooling provided pale yellow plates melting at 152—153°C in a 58—60% yield.

Found: C, 43.44; H, 2.58; N, 21.27%.

This product was identified as X by an admixture-test and by a comparison of the infrared spectrum with that of an authentic sample.

BULLETIN OF THE CHEMICAL SOCIETY OF JAPAN, VOL. 44, 784—786 (1971)

Biogenesis of the Essential Oils in Camphor Trees. XXVIII.[1] On the Components of the Essential Oil of *Cinnamomum japonicum* Sieb.[2]

Yasuji FUJITA, Shin-ichi FUJITA, and Hisashi YOSHIKAWA
Government Industrial Research Institute, Osaka, Midorigaoka, Ikeda-shi, Osaka

(Received July 30, 1970)

Cinnamomum japonicum Sieb. is sometimes divided into several varieties on the basis of morphological differences in the leaves. The essential oils of samples of this plant from various parts in Japan were examined from the viewpoint of chemotaxonomy. The results obtained from the materials gathered at Mt. Satsuki, Ikeda-shi, Osaka Prefecture, will be reported here first. The characteristics of the oil of the leaves and branchlets are the abundant presence of 1,8-cineole and *p*-cymene. The rich existence of linalool in the branchlet oil may also be a characteristic of this plant.

Cinnamomum japonicum Sieb. (=*C. pedunculatum* Nees) (Japanese name, "Yabunikkei") of the Lauraceae grows widely in Japan–on Honshu, Shikoku, Kyushu, and the Ogasawara Islands; Fukushima Prefecture is the northern-most limit of its distribution. The Ryukyu Islands, Formulsa, the southern part of Korea, and Southern China are also in the area of geographical distribution of this plant. Sometimes this plant is divided into several varieties on the basis of morphological differences in the leaves.[3]

Many years ago, the essential oil of this plant was examined by Keimatsu *et al.*[4] They obtained the oil in a yield of about 1% by the steam distillation of bark from Hachijyo Island, Japan. The oil contained α-phellandrene (33%) as the main component, plus eugenol and methyleugenol. Shinozaki[5] examined the essential oil obtained in a yield of about 1% from the fresh leaves of plants of the Ogasawara Islands, and showed the presence of safrole (60%), eugenol (9%), and other compounds in the oil. Nakahara[6] also reported that plants obtained from Tane Island in Kagoshima Prefecture afforded the essential oil in a 0.3% yield, and that the oil contained camphor (25%) and cineole (16%), together with *p*-cymene and methyleugenol.

Since 1954, a careful comparison of the essential oils obtained from materials gathered from various localities in Japan has been performed in our laboratory

1) Part XXVII: Y. Fujita, S. Fujita, and S. Nishida, *Nippon Kagaku Zasshi*, **91**, 737 (1970).

2) Presented in part at the 21st Annual Meeting of the Chemical Society of Japan, Osaka, April, 1968.

3) T. Makino and K. Nemoto, "Flora of Japan," Nippon Shokubutsu Soran Pub. Assoc., Tokyo (1925), p. 924; S. Hatusima and T. Amano, "Flora of Okinawa," The Ryukyu Univ. Press, (1958), p. 34; G. Masamune, "A List of Vascular Plants of Taiwan." Hokuriku no Shokubutsu no Kai Press, (1954), p. 49; H. Liou, "Laur. Chin. Indochin.," Hermann Co., Paris (1934), p. 22; Y. Fujita, *Report of Govern. Ind. Res. Insti., Osaka*, **306**, 22 (1955); *Bot. Mag. Tokyo*, **80**, 262 (1967).

4) S. Keimatsu and Y. Asahina, *Yakugaku Zasshi*, **26**, 1095 (1906).

5) E. Shinozaki, *Kogyo Kagaku Zasshi*, **18**, 913 (1915).

6) K. Nakahara, Report of 18th Congress of Camphor Industry Engineers, (1953), p. 41.

from the view-points of chemical systematics and chemical taxonomy.

In this paper, the results of our examination of the components of the essential oils obtained from materials gathered at Mt. Satsuki in Ikeda-shi, Osaka Prefecture, will be reported.

Experimental

Isolation of the Essential Oils. *Sample I*: On May 24, 1954, the material (average weight of a twig: 65 g, consisting of 68% leaves and 32% branchlets) was gathered from a tree (diameter of the trunk at a height of one meter; 9 cmϕ) at Mt. Satsuki, in Ikeda-shi, Osaka Prefecture (320 m above sea level). On May, 25, this material (19.9 kg) was subjected to steam distillation. The distilled oil was extracted with ether, and then dried over anhydrous sodium sulfate. The oil (67.1 g), obtained in a 0.34% yield, had the following properties: d_4^{30} 0.8939, n_D^{30} 1.4800, α_D^{28} −11.00°, A.V. 0.5, E.V. 1.0.

Samples of II: On April 22, 1954, the material (average weight of a twig: 120 g, consisting of 59% leaves and 41% branchlets) was gathered from another tree (diameter: 15 cmϕ) in the same locality. The material was divided into leaves and branchlets.

II-A: On April 23, the leaves (20.0 kg) were subjected to steam distillation; the oil (168.0 g), obtained in a 0.84% yield, had the following properties: d_4^{30} 0.8792, n_D^{30} 1.4781, α_D^{28} −19.75°, A.V. 0.2, E.V. 5.0.

II-B: On April 26, the branchlets (5.5 kg) were distilled with steam; the oil (8.3 g), obtained in a 0.15% yield, had the following properties: d_4^{30} 0.9522, n_D^{30} 1.4869, α_D^{28} −9.00°, A.V. 1.0, E.V. 12.8.

Gas-liquid Chromatographic Analysis. The gas-liquid chromatography (glc) was carried out with a Shimadzu GC-1B Model apparatus, equipped with a 150×0.5 cm stainless steel column containing 30% PEG 6000 or 30% Silicone DC-550 on Celite 545 (100 mesh). Hydrogen was used as the carrier gas.

The percentages of the constituents of the oil were calculated from the areas of the peaks of the gas chromatogram.

Separation and Identification of the Individual Components. The neutral part of the sample II-A (143 g) was fractionated, by distillation under reduced pressure in a current of nitrogen with a Widmer column, into eleven fractions, as is shown in Table 1. Each fraction was then further separated into hydrocarbons and oxygenated compounds by alumina-column chromatography. The main components were isolated by preparative glc using a PEG 6000 column, and were identified by a comparison of the IR spectra and retention times (*Rt*) of glc with those of authentic samples. Some minor components were identified by a comparison of the *Rt's* with those of authentic samples obtained by the above two kinds of columns.

Table 1. Results of fractional distillation of the neutral oil (sample II-A)

Fract.	Bp (°C/mmHg)	Dist. (ml)	Bp (°C/764 mmHg)	d_4^{30}	n_D^{30}	α_D^{22}(°)
I	—83/50	25	178	0.8548	1.4719	−24.45
II	83—87/50	30	179	0.8593	1.4750	−21.80
III	87—90/50	25	179	0.8642	1.4769	−12.55
IV	90—96/50	5	180	0.8662	1.4779	−4.60
V	96—118/50	5	189	0.8747	1.4811	−7.35
VI	118—120/50	5	207	0.8929	1.4810	−12.00
VII	—104/30	5	223	0.9271	1.4819	−22.45
VIII	—115/20	5	225	0.9313	1.4819	−23.25
IX	115—122/20	5	231	0.9385	1.4902	−15.30
X	122—125/20	7	269	0.9522	1.4975	−11.45
XI	Residual	—	—	—	—	—

Table 2. The compositions of the essential oils of *C. japonicum* collected at Mt. Satsuki, Ikeda-shi, Osaka Pref.

Peak No.	Compound	Sample I (Twigs) (%)	Sample II-A (Leaves) (%)	Sample II-B (Branchlets) (%)
1	α-Pinene	2.7	3.7	0.3
2	Camphene	0.1	0.5	0.1
3	β-Pinene	2.4	3.0	0.2
4	β-Myrcene	4.7	4.7	0.9
5	*l*-α-Phellandrene	2.8	7.7	0.2
6	Limonene	2.0	3.0	0.2
7	1,8-Cineole	**23.7**	**16.5**	**12.0**
8	*p*-Cymene	**45.2**	**40.0**	**24.1**
9	3-Hexen-l-ol	0.4	0.3	0.2
10	unidentified ketone	trace	trace	trace
11	*trans*-Linalool oxide	0.1	0.1	1.3
12	*cis*-Linalool oxide	0.1	0.2	1.2
13	*l*-Linalool	3.3	2.8	**23.5**
14	*l*-Copaene	0.3	0.9	1.4
15	Camphor	0.2	0.4	0.6
16	unidentified alcohol	0.2	0.3	0.5
17	SHC	trace	0.2	0.2
18	Terpinen-4-ol	1.6	2.4	4.1
19	β-Elemene	0.1	0.2	0.4
20	*l*-Caryophyllene	1.2	0.6	0.1
21	unidentified alcohol	—	—	0.6
22	SHC	0.3	0.1	—
23	*l*-α-Terpineol	3.7	1.6	3.2
24	α-Terpinyl acetate	0.4	2.0	7.0
25	*l*-Carvotanacetone	0.1	0.5	0.2
26	α-Humulene	0.2	0.5	0.3
27	SHC (ε-Cadinene ?)	trace	trace	0.1
28	Citronellol	trace	trace	1.5
29	SHC	0.1	0.5	0.5
30	*d*-δ-Cadinene	0.4	1.0	1.1
31	Nerol	0.2	trace	trace
32	SHC	trace	0.2	trace
33	*l*-*trans*-Yabunikkeol[9]	0.5	0.5	2.5
34	Geraniol	trace	trace	1.3
35	unidentified alcohol	trace	trace	trace
36	Calamenene	0.3	0.1	0.4
37	Safrole	trace	trace	trace
38	*d*-*cis*-Yabunikkeol[9]	0.4	0.6	1.3
39	α-Calacorene	trace	0.1	0.1
40	β-Calacorene	trace	trace	0.1
41	unidentified alcohol	trace	trace	trace
42	Methyleugenol	0.2	0.1	0.5
43	Elemol	0.7	1.3	2.6
44	unidentified ketone	trace	trace	0.1
45	unidentified alcohol	trace	trace	trace
46	Eugenol	0.7	1.5	1.4
47	α-Cadinol	0.5	1.2	2.2
48	unidentified	trace	trace	1.0
49	*l*-Kaurene	trace	trace	0.5

SHC: unidentified sesquiterpene hydrocarbon

The main components may be identified as follows:

l-α-Phellandrene: Peak 5 ($[\alpha]_D^{20}$ −158.0°, c=2.2, in $CHCl_3$) was isolated from fractions I—III; it was identified as α-phellandrene by a comparison of the IR spectra.[7]

l-Linalool, Terpinen-4-ol, and l-α-Terpineol: Peak 13 ($[\alpha]_D^{20}$ −15.4°, c=4.2, in EtOH), peak 18, and peak 23 ($[\alpha]_D^{20}$ −49.6° c=4.4, in EtOH) were isolated from fraction VI and were identified as linalool, terpinen-4-ol, and α-terpineol respectively by a study of the IR spectra and *Rt's* in glc.

l-Carvotanacetone: Peak 25 ($[\alpha]_D^{20}$ −38.6°, c=4.8, in EtOH) was identified as carvotanacetone by a comparison of the IR spectrum[8] and *Rt* with those of a synthetic sample prepared from carvone.

Citronellol, Nerol, and Geraniol: A mixed sample of fractions V and VI was heated with phthalic anhydride at 80°C in a pyridine solution for one hour; the esterified part was then extracted with a sodium hydrogencarbonate solution, the sodium salt of the phthalic acid esters was saponified by potassium hydroxide, and the regenerated alcohols were distilled with steam.

These primary and secondary alcohols (peak 28, 31, and 34) were separated by preparative glc and were identified as citronellol, nerol, and geraniol respectively by a study of the IR spectra and *Rt's*.

l-trans-*Yabunikkeol and* d-cis-*Yabunikkeol*: These new monoterpene alcohols[9] (peaks 33 and 39) were also obtained from the above regenerated oil.

l-Copaene, β-Elemene, l-Caryophyllene, and β-Humulene: These sesquiterpene hydrocarbons (peaks 14, 19, 20, and 26) were isolated from fractions V—VIII and were identified as copaene ($[\alpha]_D^{20}$ −16.0°, c=4.1, in $CHCl_3$), β-elemene, caryophyllene ($[\alpha]_D^{20}$ −8.8°, c=1.7, in $CHCl_3$), and β-humulene respectively by a comparison of the IR spectra.[10]

d-*δ-Cadinene, Calamenene, α-Calacorene, and β-Calacorene*: These sesquiterpene hydrocarbons (peak 30, 36, 39, and 40) were also identified as δ-cadinene ($[\alpha]_D^{20}$ +45.6°, c=4.1, in $CHCl_3$), calamenene, α-, and β-calacorene by a comparison of the IR spectra with those of authentic samples.[10]

l-Kaurene: Peak 49 (mp 47°C, $[\alpha]_D^{20}$ −56.6°, c=4.6, in $CHCl_3$) was isolated from the residual oil of fractional distillation by column chromatography and was identified as kaurene by a study of the IR spectrum.[11]

Results and Discussion

The yields of the essential oils of this *C. japonicum* are 0.34% from the fresh twigs (sample I), 0.84% from the leaves (sample II-A), and 0.15% from the branchlets (sample II-B). Table 2 shows the compositions of these oils.

From these results, we can see it is characteristic of the oil that 1,8-cineole and *p*-cymene exist abundantly, while there are only small amounts of camphor and phenol ethers. The abundance of *l*-linalool in the branchlet oil may also be a characteristic of this plant, though the components of these oils are almost the same.

Among the other substances, we could isolate two new monoterpene alcohols, named *trans*-yabunikkeol and *cis*-yabunikkeol (*trans*- and *cis*-*p*-mentha-1(7),5-dien-2-ol), for the first time;[9] we also isolated *l*-kaurene, probably for the first time, in the Angiospermae.

7) B. M. Mitzner, E. T. Theimer, and S. K. Freeman, *Appl. Spectrosc.*, **19**, 169 (1965).

8) V. E. Veijola and A. D. Ilvespää, *Acta Chem. Scand.*, **13**, 301 (1959).

9) Y. Fujita, S. Fujita, and H. Yoshikawa, This Bulletin, **43**, 1599 (1970).

10) J. A. Wenninger, R. L. Yates, and M. Dolinsky, *J. Ass. Offic. Anal. Chem.*, **50**, 1313 (1967); J. Plíva, M. Horák, V. Herout, and F. Šorm, "Die Terpene," I, Akademie-Verlag, Berlin (1960).

11) The Infrared Data Committee of Japan, "IRDC card," No. 3306.

BULLETIN OF THE CHEMICAL SOCIETY OF JAPAN, VOL. 44, 786—791 (1971)

Infrared Spectroscopic Study of Enol and Enol Derivatives Coordinated to Platinum(II) and Palladium(II)

Yasuo WAKATSUKI,* Shun-ichi NOZAKURA, and Shunsuke MURAHASHI

Faculty of Science, Osaka University, Toyonaka, Osaka

(Received August 3, 1970)

The infrared spectra of $[Cl_2M\ Olefin]_2$ (olefin = vinyl alcohol, vinyl ethers, and their derivatives, M = Pt and Pd) have been studied in the 4000—100 cm^{-1} frequency region. A normal coordinate analysis of the coordinated vinyl alcohol indicated that the lone-pair electrons of oxygen conjugated with π-electrons of the double bond to some extent, even in the coordinated state. The coordination strengths of vinyl alcohol, vinyl ethers, and their derivatives have been examined by comparing the metal-olefin streching vibrations.

The synthesis of the vinyl alcohol complex, $[Cl_2Pt\text{-}(CH_2{=}CHOH)]_2$, has been previously reported.[1] It does not contain organic moieties other than vinyl alcohol, so the analysis of its infrared spectrum is relatively easy.

The double bond of coordinated olefin, in general, approaches a single bond to some extent, as is confirmed by the shift of the C=C stretching to the lower frequency. Nakamoto and Grogan analyzed the normal coordinate of the ethylene coordinated to platinum(II) and concluded that the force constant of the stretching of the

* Present address: The Institute of Physical and Chemical Research, Wako-shi, Saitama.

1) Y. Wakatsuki, S. Nozakura, and S. Murahashi, This Bulletin, **42**, 273 (1969).

double bond is 6.00 mdyn/Å, a value which is 19% smaller than that of free ethylene.[2] It may be thought that vinyl alcohol, like vinyl ethers, includes such a resonance structure as: CH_2=CH–OH$\longleftrightarrow$$\bar{C}H_2$–CH=$\overset{+}{O}$H. However, the contribution of such a resonance form may be decreased upon coordination to a metal, since the double-bond character of coordinated olefin is smaller than that of free olefin. In order to obtain the force constants of the C=C and C–O stretchings of the π-coordinated vinyl alcohol, the approximate in-plane normal coordinate analysis of the coordinated vinyl alcohol was carried out. It seemed that it might thereby be possible to determine whether or not the above-mentioned resonance structures really exist and the coordination of the oxygen atom to the metal.

Nakamoto and Grogan analyzed the far-infrared spectra of Zeise's dimer, $[Cl_2Pt\ C_2H_4]_2$, and its palladium analog; they assigned the metal-ethylene stretching vibration to the absorption at 408 cm^{-1} of the Pt complex and to that at 427 cm^{-1} of the Pd complex.[3] In order to ascertain the coordination power of vinyl ethers to Pt(II) and Pd(II), we measured the far-infrared spectra of vinyl ether complexes of the Zeise dimer type in the range of 700—100 cm^{-1}, and compared the frequencies of the absorptions which are assignable to the metal-olefin stretching vibrations with each other. It has often been said that the magnitude of the shift upon coordination in the C=C stretching mode reflects the strength of the metal-olefin bond. Free vinyl ethers have, however, been found to complicate two or more absorptions in the C=C stretching region;[4] moreover, the C=C stretching vibration of the coordinated olefin may strongly couple with other vibrations, as in the case of the coordinated ethylene.[2] Thus, the shift of the C=C stretching vibration upon coordination cannot be taken as a measure of the coordination power. Accordingly, the direct measurement of the metal-olefin stretching vibration, described above, is desirable.

Experimental

The Preparation of Complexes. The preparation of Pt(II) and Pd(II) complexes with vinyl ethers and their derivativs has been described in a preceding paper.[5] Vinyl alcohol and propenyl alcohol complexes with Pt(II) were synthesized as has been described in another previous paper.[1] The platinum complex of CH_2=CH–OD was obtained in a method similar to that used for the vinyl alcohol complex, that is, the hydrolysis of the silyl ether bond of the CH_2=CH–$OSiMe_3$ complex with a small amoun of heavy water.

Spectral Measurements. The spectra were obtained mainly by means of the Nujol mull technique using a Hitachi EPI-2 (4000—700 cm^{-1}), a JASCO DS-402 (700—500 cm^{-1}), and a Hitachi FIS-1 (500—100 cm^{-1}) spectrometer.

Procedure of Calculatin. It is assumed that the vinyl alcohol molecule is planar and that this plane is retained even in its coordinated state. Vinyl alcohol has 15 ($3\times7-6$) fundamental vibrations; of these, 11 are in-plane vibrations and 4 are out-of-plan vibrations. In this study, only the in-plane vibrations are examined.

It is expected that the vibrations of the vinyl alcohol molecule coordinated to a metal couple extremely weakly with other vibrations such as those due to the Pt–Cl bond. Thus, an examination of only the vibration of the vinyl alcohol coordinated to a metal is permissible.

Nakamoto *et al.* estimated that the C=C and C–H distances of the coordinated ethylene are 1.364 and 1.089 Å respectively.[2] In the case of the coordinated vinyl alcohol, these values are employed. With respect to the C–O an O–H distances, the values of 1.42 and 0.956 Å respectively are used. It is estimated that all the angles around the carbons are 120°, and that the COH angle is 110°. The conformation around the C–O bond is unclear; in this case, a trans planar conformation is assumed. Figure 1 illustrates the 13 internal coordinates employed for the calculation.

Table 1. Symmetry coordinates for the in-plane vibrations of the coordinated vinyl alcohol

Symmetry coordinate	Vibrational mode[a]
$S_1=\Delta r_1$	ν(CH)
$S_2=1/\sqrt{2}\,(\Delta r_2-\Delta r_3)$	$\nu_a(CH_2)$
$S_3=1/\sqrt{2}\,(\Delta r_2+\Delta r_3)$	$\nu_s(CH_2)$
$S_4=\Delta r_4$	ν(CO)
$S_5=\Delta r_5$	ν(OH)
$S_6=\Delta R$	ν(C=C)
$S_7=1/\sqrt{6}\,(2\Delta\beta_2-\Delta\alpha_1-\Delta\beta_1)$	δ(CCO)
$S_8=1/\sqrt{2}\,(\Delta\beta_1-\Delta\alpha_1)$	δ(CH)
$S_9=1/\sqrt{6}\,(2\Delta\alpha_2-\Delta\beta_3-\Delta\beta_4)$	$\delta(CH_2)$
$S_{10}=1/\sqrt{2}\,(\Delta\beta_3-\Delta\beta_4)$	$r(CH_2)$
$S_{11}=\Delta\sigma$	δ(OH)
$S_{12}=1/\sqrt{3}\,(\Delta\alpha_1+\Delta\beta_1+\Delta\beta_2)$	Redundant
$S_{13}=1/\sqrt{3}\,(\Delta\alpha_2+\Delta\beta_3+\Delta\beta_4)$	Redundant

a) ν_s and ν_a symmetric and asymmetric stretching; δ, bending; r, rocking.

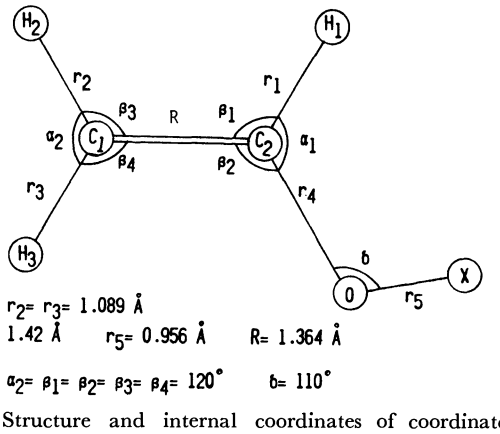

Fig. 1. Structure and internal coordinates of coordinated vinyl alcohol.

Table 1 lists the symmetry coordinates used in the present work.

The F matrix elements for the in-plane vibrations were expressed in terms of the Urey-Bradley force field.[6] A matrix secular equation of the $|GF-E\lambda|=0$[7] form was constrtcued and solved by using a NEAC 2203 computer.

2) M. J. Grogan and K. Nakamoto, *J. Amer. Chem. Soc.*, **88**, 5454 (1966).
3) M. J. Grogan and K. Nakamoto, *ibid.*, **90**, 918 (1968).
4) Y. Mikawa, This Bulletin, **29**, 110 (1956).
5) Y. Wakatsuki, S. Nozakura, and S. Murahashi, *ibid.*, to be submitted.
6) T. Shimanouchi, *J. Chem. Phys.*, **17**, 245 (1949).
7) E. B. Wilson, *ibid.*, **7**, 1047 (1939); **9**, 76 (1941).

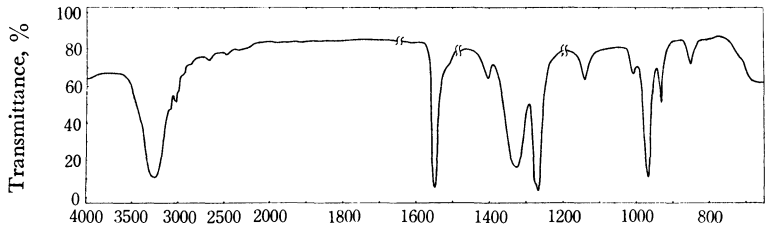

Fig. 2. IR spectrum of $[Cl_2Pt(CH_2=CH-OH)]_2$.
4000—1700 and 1500—1200 cm^{-1}; Hexachlorobutadiene mull.
1700—1500 and 1200—700 cm^{-1}; Nujol mull.

Results and Discussion

A. Normal Coordinate Analysis of Coordinated Vinyl Alcohol. The infrared spectrum of the coordinated vinyl alcohol is shown in Fig. 2, while the best sets of force constants for the coordinated vinyl alcohol are listed in Table 2.

TABLE 2. FORCE CONSTANTS FOR VINYL ALCOHOL COORDINATED TO Pt(II) (mdyn/Å)

Stretching	K(C—H)	4.63
	K(C=C)	5.85
	K(C—O)	5.00
	K(O—H)	6.00
Bending	H(HCH)	0.37
	H(HCC)	0.15
	H(CCO)	0.32
	H(HCO)	0.22
	H(COX)	0.47
Repulsive	F(H···H)	0.00
	F(H···C)	0.30
	F(C···O)	0.70
	F(H···O)	1.00
	F(C···X)	0.50

TABLE 3. VIBRATIONS OF COORDINATED VINYL ALCOHOL; $CH_2=CHOH$

Frequency, Obsd[a]	cm^{-1} Calcd	Assignment[b] (PED %)
3260 s	3345	ν(OH)(100)
3080 vw	3140	ν(CH)(99)
3020 vw	3019	$\nu_a(CH_2)$(100)
	2916	$\nu_s(CH_2)$(99)
1550 s	1567	ν(C=C)(45), δ(CH)(26), $\delta(CH_2)$(12)
1405 w	1411	$\delta(CH_2)$(65), δ(CH)(20), δ(OH)(11)
1330 s	1340	δ(OH)(48), ν(CO)(34),
1270 vs	1264	δ(CH)(43), ν(CO)(21), δ(OH)(13)
1145 w	1099	ν(C=C)(33), ν(CO)(27)
850 w	834	$r(CH_2)$(78)
497 s	495	δ(CCO)(82)
Frequencies not calculated		
1013 vw, 968 vs, 934 m		Out-of-plane bending

a) vs, very strong; s, strong; m, medium; w, weak; vw, very weak.
b) ν, stretching; δ, bending; r, rocking; s, symmetric; and a, asymmetric.
PED, Potential Energy Distribution.

TABLE 4. VIBRATIONS OF COORDINATED VINYL ALCOHOL; $CH_2=CHOD$

Frequency, Obsd[a]	cm^{-1} Calcd	Assignment[b] (PED %)
3078 w	3141	ν(CH)(99)
3015 w	3019	$\nu_a(CH_2)$(100)
	2916	$\nu_s(CH_2)$(99)
2420 m	2436	ν(OD)(100)
1527 vs	1551	ν(C=C)(47), δ(CH)(26), $\delta(CH_2)$(15)
1405 w	1401	$\delta(CH_2)$(63), δ(CH)(33)
1270 vs	1284	ν(CO)(60), δ(CH)(14)
1220 s	1169	ν(C=C)(24), δ(CH)(23), ν(CO)(18)
940 m	919	δ(OD)(76)
850 w	831	$\nu(CH_2)$(73)
490 s	490	δ(CCO)(82)
Frequencies not calculated		
1013 w, 985 s, 973 sh, 800 vw		Out-of-plane bending

a) vs, very strong; s, strong; m, medium; w, weak; vw, very weak; sh, shoulder.
b) ν, stretching; δ, bending; r, rocking; s, symmetric; and a, asymmetric.
PED, Potential Energy Distribution.

In Tables 3 and 4 the observed frequencies are compared with those for coordinated vinyl alcohol and its deuterio analog calculated by using those sets of force constants.

The product rule for isotopic frequencies[8] works extremely well in this case; thus, it supports the validity of the assignments made.

Table 2 shows that the force constant of the C=C stretching is slightly smaller than that of the coordinated ethylene (6.00 mdyn/Å),[2] and that the force constant of its C–O stretching is relatively larger than those of methanol (2.43 mdyn/Å)[9] or diethyl ether (4.38 mdyn/Å).[10] These values reasonably imply that such a resonance structure as $\bar{C}H_2$–$\overset{+}{C}H$=OH exists to some extent even in the coordinated state. The larger value of the force constant of the C–O stretching also indicates that the lone-pair electrons of the oxygen atom do not interact with platinum.

B. Metal-olefin Stretching Vibrations. Figure 3 shows the far-infrared spectra of the complexes of the

8) E. B. Wilson, J. C. Decius, and P. C. Cross, "Molecular Vibrations," McGraw-Hill, N. Y., (1955), p. 182.
9) S. Mizushima and T. Shimanouchi, "Infrared and Raman Effect," Kyoritsu, Tokyo (1958), p. 229.
10) M. Hayashi, *Nippon Kagaku Zasshi*, **78**, 222 (1957).

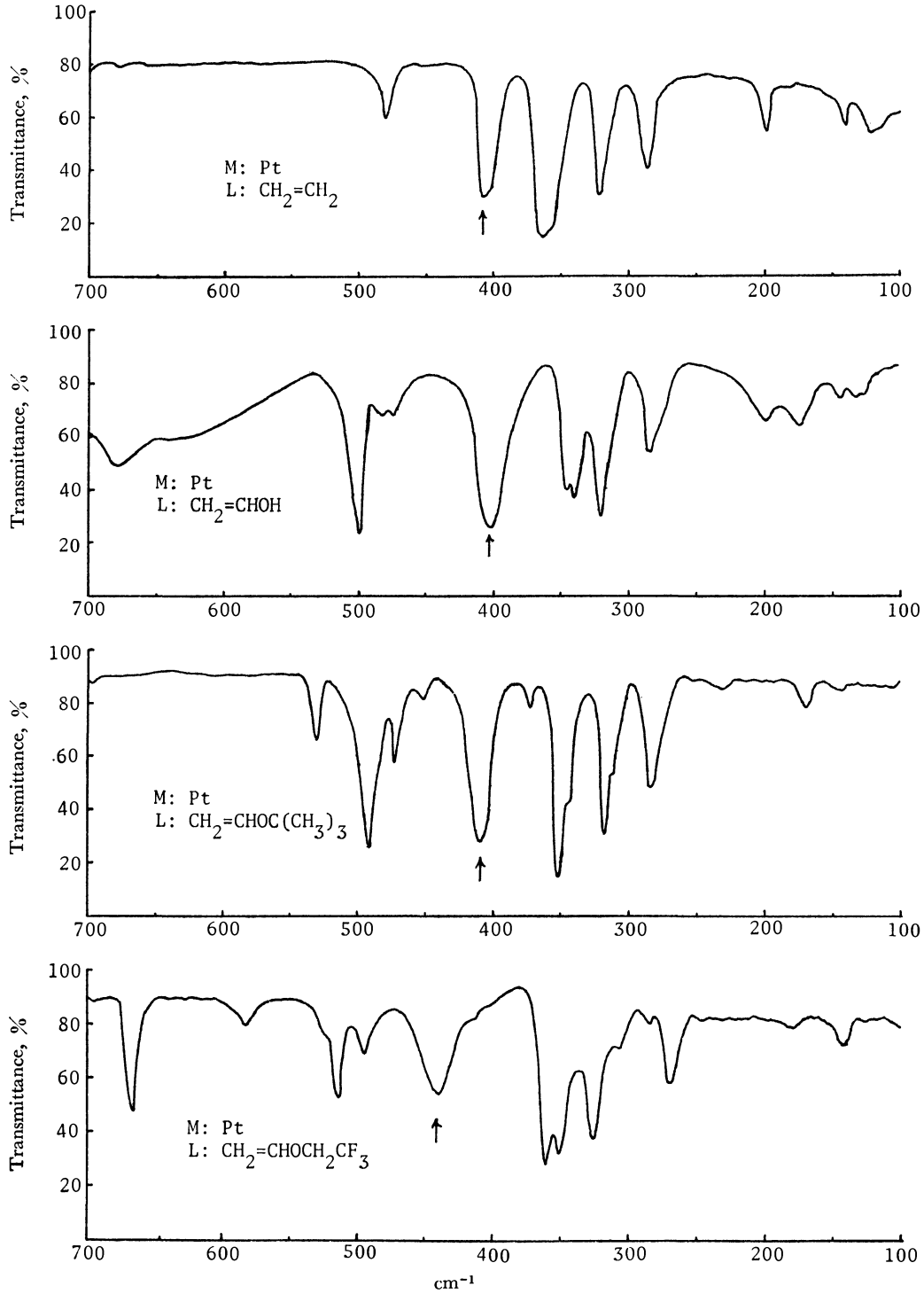

Fig. 3. Infrared spectra of $[Cl_2ML]_2$.

$[Cl_2M\ Olefin]_2$ type, in which M represents platinum or palladium.

With respect to the ethylene complexes with platinum and palladium, Nakamoto has reported that the frequency of a metal-ethylene stretching vibration is a better measure of the coordination strength than the shift width of the C=C stretching upon coordination.[3,11]

The infrared spectra of many platinum and palladium complexes of vinyl ethers, as is shown in the figure, satisfactorily correspond to the ethylene complex in the low-frequency region, and the absorption with an arrow sign can be assigned to the stretching frequency between metal and olefin. Although this absorption is not so isolated as in the case of ethylene, and hence has the possibility of coupling strongly with other vibrations, it may be regarded as a semi-quantitative measure of the coordination strength of vinyl ethers. Table 5 lists

11) M. Tsutsui, "Characterization of Organometallic Compounds," Part I, John Wiley & Sons, N. Y. (1969), p. 110.

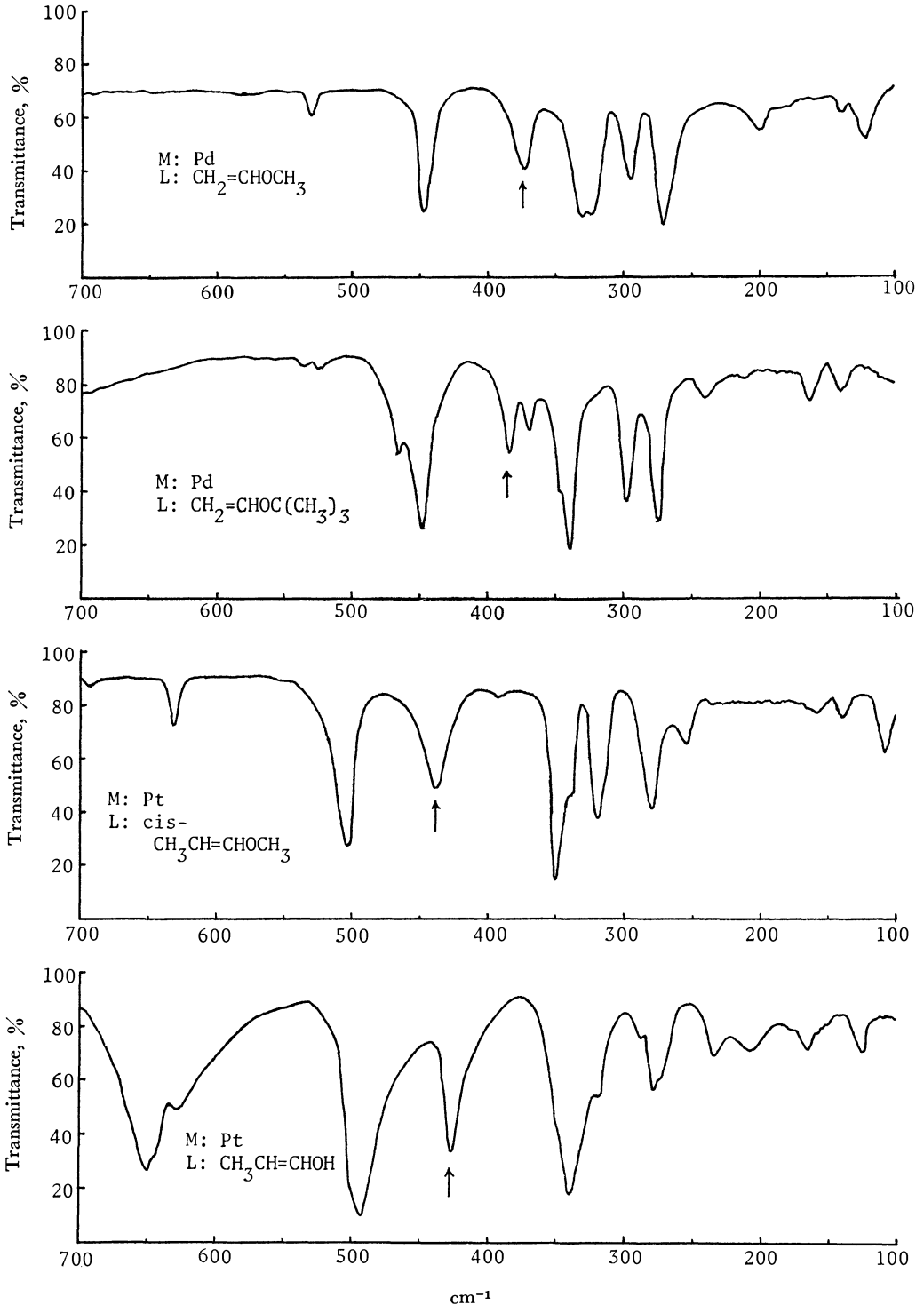

Fig. 3. Infrared spectra of $[ClM_2L]_2$.

the stretching vibrations of the metal-olefin bond thus obtained. This table suggests the following facts with respect to the coordination strength of vinyl ethers and their derivatives:

a) The coordination strength of vinyl ethers with palladium is far weaker than that with platinum. If they were comparable in magnitude, the absorption of the palladium complex should be at a frequency higher by about 20 cm^{-1} than that of the corresponding platinum complex as a result of the mass effect.

b) The coordination strength of vinyl alcohol and that of vinyl alkyl ether are almost equal to that of ethylene in the platinum complex.

c) Propenyl ethers are considerably stronger than the corresponding vinyl ethers in their coordination strength in spite of the fact that β-methyl group of the propenyl ethers may sterically interfere with the coordination, as is the case with 2-pentene.[12]

12) J. R. Joy and M. Orchin, *J. Amer. Chem. Soc.*, **81**, 310 (1959).

Table 5. Metal-olefin stretching frequencies of $[Cl_2M\ Olefin]_2$ (M=Pt, Pd)

Olefin	Metal	
	Pt	Pd
$CH_2=CH_2$	408	427 cm^{-1}
$CH_2=CHOCH_3$	(410?)	376
$CH_2=CHOC(CH_3)_3$	408	384
$CH_2=CHOCH_2CF_3$	440	—
$CH_2=CHOH$	402	—
cis-$CH_3CH=CHOCH$	438	404
cis-$CH_3CH=CHOSiMe_3$	430	—
$CH_3CH=CHOH$	427	—

d) 2,2,2-Trifluoroethyl vinyl ether is much stronger than alkyl vinyl ethers in its coordination strength.

As for the metal-olefin bonding, Chart and Duncanson's theory[13] has generally been accepted, in which the bonding is explained by a combination of the electron donation from the olefin to the metal and the electron back-donation from the metal to the olefin. The electron donation from the olefin to the metal is supposed to play an important role when the olefin has a strong electron-releasing substituent, as in the case of vinyl ethers or propenyl ethers. However, steric interactions between other ligands and a substituent on the olefin may also affect the coordination strength of the olefin; thus, the problem is complicated. At present, it seems to be difficult to interpret the relative coordination strengths of ethylene, vinyl alcohol, vinyl ethers, and their derivatives by means of a simple description.

The authors wish to express their thanks to Dr. Masamichi Kobayashi for his valuable suggestions on the analysis of the infrared spectra.

13) J. Chatt and L. A. Duncanson, *J. Chem. Soc.*, **1953**, 2939.

BULLETIN OF THE CHEMICAL SOCIETY OF JAPAN, VOL. 44, 791—793 (1971)

The Kinetics of the Reaction of Thiol Acids with Anilines

Yoshio HIRABAYASHI, Masateru MIZUTA, Masana KOJIMA,
Yukio HORIO, and Hideharu ISHIHARA
Department of Industrial Chemistry, Faculty of Engineering, Gifu University, Kakamigahara, Gifu

(Received August 6, 1970)

Studies have been made of the kinetics of the reactions of thiol acids (thiostearic acid and thioacetic acid) with anilines, such as aniline and *p*-methoxy-, *p*-ethoxy-, *p*-methyl-, *m*-methyl-, *p*-chloro, *m*-chloro-, and *m*-nitro-substituted anilines, in a chlorobenzene solution. The rate is given by $k(\text{RCO–SH})(\text{X-C}_6\text{H}_4\text{-NH}_2)$. The activation energy for the reaction of thiostearic acid with aniline is 5.3 kcal/mol. The Hammett plots give a straight line, with a value of $\rho = -2.40$ for the reactions of thiostearic acid or thioacetic acid with the anilines; the mechanism of the reaction of thiol acids with anilines is discussed.

Various observations in the literature[1] indicate that the thiol acids, RCO–SH, react with primary and secondary amines much more rapidly than the corresponding carboxylic acids, RCO–OH, and thiol acids have been frequently used as acylating agents. Some observations of Alliger *et al.*,[2] of Sheehan and Johnson,[3] and of Tarbell[1] suggest that the acylation of amines by thiol acids proceeds by a free-radical chain process. On the other hand, the kinetic study by Hawkins *et al.*[4] of the reaction of thiobenzoic acid with aniline to yield benzanilide indicates that the reaction rate in a chlorobenzene solution is given by $k(\text{C}_6\text{H}_5\text{CO–SH})(\text{C}_6\text{H}_5\text{NH}_2)$, where the constant, k, varies with the presence of small amounts of benzoic acid as an impurity, and that the rate depends on the solvent.

The present authors have undertaken kinetic studies of the reactions of thiol acids (*i. e.*, thiostearic acid and thioacetic acid) with anilines in a chlorobenzene solution to yield acyl anilides (Eq. (1)) in order to determine the mechanism of the reaction of the thiol acids with the anilines.

$$\text{RCO–SH} + \text{X–C}_6\text{H}_4\text{–NH}_2 \longrightarrow \text{RCONHC}_6\text{H}_4\text{–X} + \text{H}_2\text{S} \qquad (1)$$

R : heptadecyl or methyl group
X : H or substituent

Results and Discussion

The rate of the reaction of thiostearic acid or thioacetic acid with the anilines in a chlorobenzene solution was followed by the acid-base titration of the unreacted thiostearic acid or thioacetic acid after the hydrogen sulfide formed had been completely removed. The results gave good second-order rate constants for all the runs (Fig. 1.):

$$\text{rate} = k(\text{RCO–SH})(\text{X–C}_6\text{H}_4\text{–NH}_2) \qquad (2)$$

The observation of Hawkins *et al.*[4] of the reaction of thiobenzoic acid with aniline indicated that the

1) D. S. Tarbell and D. P. Harrish, *Chem. Rev.*, **49**, 46 (1951).
2) G. Alliger, G. E. P. Smith, Jr., E. L. Carr, and M. P. Stevens, *J. Org. Chem.*, **14**, 962 (1949).
3) J. C. Sheehan and D. A. Johnson, *J. Amer. Chem. Soc.*, **74**, 4926 (1952).
4) P. J. Hawkins, D. S. Tarbell, and P. Noble, Jr., *ibid.*, **75**, 4462 (1953).

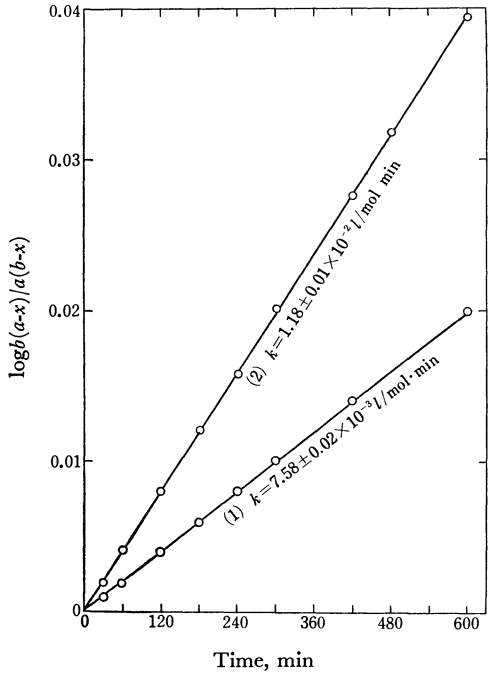

Fig. 1. The second-order plots for the reaction of thiol acid with aniline.
a and *b* are the initial concentrations of the thiol acid and aniline, respectively; *x* is the decrease of concentration of the thiol acids at time *t*.
(1) thiostearic acid: *a*, 0.1298 mol/*l*; *b*, 0.1198 mol/*l*; at 50.0°C; reaction 2.3—34.6%.
(2) thioacetic acid: *a*, 0.2435 mol/*l*; *b*, 0.2303 mol/*l*; at 40.0°C; reaction 7.7—63.0%.

reproducibility of the rate constants was not satisfactory, even though the purity of the thiol acid was better than 99%, and that this fluctuation in different samples might be due to the catalytic activity of benzoic acid present as an impurity. Accordingly, the thiostearic acid and thioacetic acid used in the present investigation were carefully purified. Thiosteric acid, with a purity of 99.3%, gave a reproducible rate constant, $(7.58\pm0.02)\times10^{-3}$ *l*/mol·min, for the reaction with aniline at 50.0°C. In thioacetic acid, the rate constants of the reactions with aniline at 40.0°C varied from one sample of thioacetic acid to another, the extreme variations being $(1.85—0.849)\times10^{-2}$ *l*/mol·min, even though the thiol acid was more than 99% pure. The sample of the thioacetic acid (purity, 99.3%), preserved in small ampoules under nitrogen and kept in an ice-box until use, gave the reproducible rate constant of $(1.18\pm0.01)\times10^{-2}$ *l*/mol·min for the reaction with aniline at 40.0°C.

Table 1 shows the rate constants of the reactions of thiostearic acid with aniline in chlorobenzene solutions at different temperatures. From the runs, the temperature coefficient of the rate constants was found to be small, and the Arrhenius plot of log *k* *vs.* $1/T$ for the data tabulated gave a straight line; the Arrhenius activation energy was found to be 5.3 kcal/mol. This value is smaller than that of the reaction of thiobenzoic acid with aniline, 7.4 kcal/mol.[4]

Table 1. The rate constants of the reaction of thiostearic acid with aniline in chlorobenzene at different temperatures

Temp. °C	$k^{a)}\times10^3$ *l*/mol·min	Temp. °C	$k^{a)}\times10^3$ *l*/mol·min
30.0	4.51	50.0	7.58
42.3	6.31	70.0	15.4

a) This is the bimolecular rate constant, determined from the plot of log $b(a-x)/a(b-x)$ *vs.* time.

Table 2. The rate constants of the reaction of thiostearic acid with the substituted anilines ($X-C_6H_4-NH_2$) in chlorobenzene at 50.0°C

Substituents X	Rate constant $k^{a)}\times10^4$ *l*/mol·min	Substituents X	Rate constant $k^{a)}\times10^4$ *l*/mol·min
p-OCH_3	356 ±4	H	75.8 ±0.2
p-OC_2H_5	407 ±5	*p*-Cl	25.0 ±0.2
p-CH_3	223 ±3	*m*-Cl	8.82±0.05
m-CH_3	97.1±0.5	*m*-NO_2	2.22±0.05

a) The bimolecular rate constant; see note a) to Table 1. Each rate constant is the average value of three runs.

Table 3. The rate constants of the reaction of thioacetic acid with the substituted anilines ($X-C_6H_4-NH_2$) in chlorobenzene at 40.0°C

Substituents X	Rate constant $k'^{a)}\times10^4$ *l*/mol·min	Substituents X	Rate constant $k'^{a)}\times10^4$ *l*/mol·min
p-OCH_3	593±7	H	118 ±1
p-OC_2H_5	672±7	*p*-Cl	36.0 ±0.4
p-CH_3	329±4	*m*-Cl	16.2 ±0.2
m-CH_3	148±2	*m*-NO_2	2.31±0.04

a) The bimolecular rate constant; see note a) to Table 1. Each rate constant is the average value of three runs.

Tables 2 and 3 show the bimolecular rate constants, *k* and *k'*, of the reactions of thiostearic acid and thioacetic acid respectively with anilines in chlorobenzene. Figure 2 shows the plots of log (k/k_0) and log (k'/k_0') *vs.* the Hammett σ-values for the substituents (k_0 and k_0'

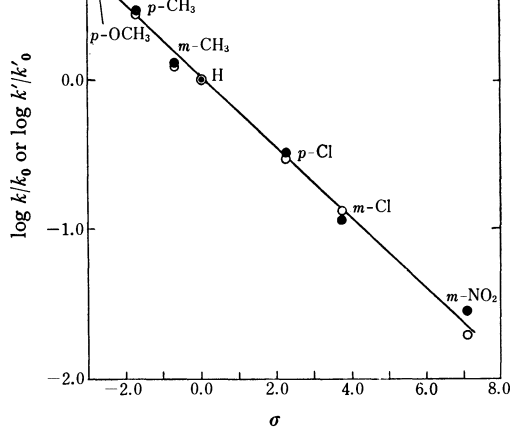

Fig. 2. Hammett's plots for the reactions of thiol acids with anilines in chlorobenzene.
● : thiostearic acid(log k/k_0); at 50.0°C
○ : thioacetic acid (log k'/k'_0); at 40.0°C.

are the rate constants of the reactions of thiostearic acid with aniline and of thioacetic acid with aniline respectively). Both plots gave straight lines, satisfying the Hammett equation; the ρ values in the Hammett equation were found to be -2.40 ± 0.09 for thiostearic acid and -2.40 ± 0.06 for thioacetic acid.

These facts indicate that the reactions between thiol acids and anilines proceed by the following pathway (Eq. 3):

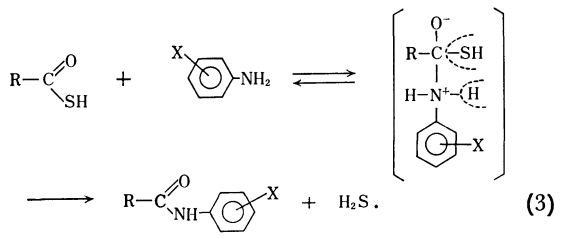

(3)

The reaction is initiated by the nucleophilic attack of the aniline on the carbonyl carbon of the thiol acid; this step probably is rate-determining and is followed by the step yielding acyl anilide and hydrogen sulfide. Consequently, the reaction is facilitated by the introduction of electron-releasing substituents into the phenyl group, but is retarded by that of electron-attracting substituents.

Experimental

Materials. *Thiostearic acid,*[5] prepared from stearoyl chloride and sodium hydrogen sulfide, was purified by repeated recrystallizations from *n*-hexane (mp 39.8—40.3°C). Its purity, as determined by the iodine method, was 99.3%. (Found: S, 10.60%. Calcd for $C_{18}H_{36}OS$: S, 10.67%).

Thioacetic acid,[6] prepared from acetic anhydride and hydrogen sulfide in the presence of sodium hydroxide, was purified by repeated fractional distillations in nitrogen (bp 87.0—87.5°C). Its purity, as determined by the iodine method, was 99.3%. (Found: S, 41.84%. Calcd for C_2H_4OS: S, 42.13%).

Chlorobenzene, obtained commercially, was washed with concd. sulfuric acid with a dilute sodium bicarbonate solution, and then with water, dried over anhydrous calcium chloride, and distilled. The fraction with a bp of 131—132°C was used.

Aniline and Substituted Anilines: All were reagent-grade chemicals obtained from the Tokyo Kasei Kogyo Co. and were purified by recrystallization or by distillation under reduced pressure in nitrogen; the materials having the following mps or bps were used: aniline, bp 82.5—83.0°C/20 mmHg; *p*-anisidine, mp 57.2—58.0°C; *p*-phenetidine, bp 127.0—128.0°C/8 mmHg; *p*-toluidine, mp 44.8—45.1°C; *m*-toluidine, bp 203.0—204.0°C; *p*-chloroaniline, mp 70.1—70.5°C; *m*-chloroaniline, bp 117.0—118.0°C/20 mmHg; *m*-nitroaniline, mp 112.9—113.1°C.

Kinetic Procedure. A standard solution of a thiol acid in chlorobenzene, prepared before each run, was pipetted into a 100-cc volumetric flask containing some chlorobenzene and a weighed sample of aniline or a substituted aniline. The volume of the solution was made up to 100 cc (thiostearic acid 0.12—0.13; thioacetic acid 0.16—0.25 mol/*l*); 10-m*l* aliquots were then removed and placed in 100-cc glass-stoppered round-bottomed flasks, which had previously been flushed with dry, oxygen-free nitrogen, in an thermostat at a prescribed temperature (accuracy ±0.1°C). The first 10-m*l* aliquot was pipetted directly into an excess of the standard base (the thioacetic acid runs: 25 cc of 0.2N potassium hydroxide; the thiostearic acid runs: 40 cc of 0.1N ethanolic potassium hydroxide and 20 cc of neutralized ethanol), and the excess base was back-titrated immediately with 0.1N hydrochloric acid by the use of thymolphthalein as the indicator. The samples were removed at regular time intervals, and the flask was immediately chilled in an ice bath; in the thioacetic acid runs, a steady stream of dry, oxygen-free nitrogen was passed through the contents of the flask for 10 min, while in the thiostearic acid runs, the flask was aspirated by a water-pump for 5 min. These procedures had been determined by preliminary experiments aimed at the complete removal of hydrogen sulfide. An excess of the standard base, mentioned above, was added to the contents of the flask, and the residual thiol acid was determined by back-titration, as has been mentioned above. In the thioacetic acid runs, it had been found, from preliminary experiments carried out under the same conditions as those used for chlorobenzene solutions of different thioacetic acid-hydrogen sulfide concentrations, that a small amount of thioacetic acid had been lost, together with the hydrogen sulfide removed; accordingly, the residual amount of thioacetic acid at each reaction time was corrected by the amounts determined for different concentrations of thioacetic acid. On the other hand, the following blank test was carried out in order to determine whether or not the thiol acid itself was changed in chlorobenzene during the reaction with aniline. Another part of the standard solution of thiol acid in chlorobenzene was diluted with chlorobenzene, and the concentration of thiol acid in the solution was made equal to that of the above thiol acid-aniline chlorobenzene solution; the subsequent treatment of the solution was just the same as has been described above. These blank samples were also removed at regular time intervals, together with the above samples, and the amount of residual thiol acid was determined; the amount of the residual thiol acid of the blank sample, determined after the removal of hydrogen sulfide, was always practically identical with that of the initial blank sample at each reaction time during the run, though the above correction value had to be taken into consideration in the thioacetic acid runs.

5) Y. Hirabayashi, M. Mizuta, and T. Mazume, This Bulletin, **37**, 1002 (1964).

6) E.K. Ellingboe, "Organic Syntheses," Vol. 31, p. 105 (1951).

Derivatives of Ditriazinylamine

Yoshiaki FUKUSHIMA, Noboru NOHARA, Yōji HASHIDA,
Shizen SEKIGUCHI, and Kohji MATSUI

Department of Synthetic Chemistry, Faculty of Engineering, Gunma University, Tenjincho, Kiryu, Gunma

(Received August 10, 1970)

Various substituted ditriazinylamines were synthesized by the reaction of *N,N*-bis(4,6-dichloro-*s*-triazin-2-yl)-amine, *N,N*-bis(4-chloro-6-phenyl-*s*-triazin-2-yl)amine, or 2-chloro-4-phenyl-*s*-triazin-2-yl-2′,4′-dichloro-*s*-triazin-2′-ylamine with nucleophilic reagents. The reaction of *N,N,N*-tris(4,6-dichloro-*s*-triazin-2-yl)amine with sodium methoxide was also examined. In this case, various products were obtained, depending upon the amount of sodium methoxide used. A Hammett plot of the substituent constants($\sum \sigma_m$) *vs.* the pK_a' or the imino proton shifts of the above-mentioned ditriazinylamines gives a linear relationship.

In a previous paper[1] we reported that ammonia or amines react with cyanuric chloride to give *N,N*-bis(4,6-dichloro-*s*-triazin-2-yl)amines (II) or *N,N,N*-tris(4,6-dichloro-*s*-triazin-2-yl)amine (III).

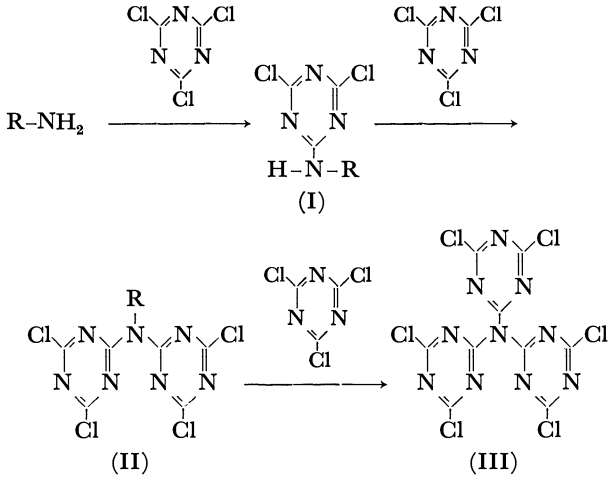

(I)

(II) (III)

R=H, Alkyl, Aryl

The active chlorine atoms of these polytriazinylamines were replaced by nucleophilic reagents much more readily than those of amino-chloro-*s*-triazines, such as I.

In addition, it was found that the *N,N*-bis(*s*-triazinyl)-amines which have been derived from I (R=H) with the replacement of the chlorine atoms behave as an acid in the presence of two triazinyl groups and that their acidities depend upon the natures of the substituents in the triazine rings.

The substituent effects in nitrogen heteroaromatic compounds have been extensively studied. For example, the Hammett equation is found to be applicable to the derivatives of the pyridine or pyrimidine series by using the substituent constants of benzene series.[2,3] However, the substituent constants applicable to triazine derivatives have not been studied systematically. Thus, with the derivatives of the *s*-triazine series substituent effects have been studied only qualitatively. Recently, the Hammett equation was observed to be applicable to the basicities of ring-nitrogen atoms of 6-substituted-2,4-diamino-*s*-triazines.[4,5] However, there have been no studies of the application of the Hammett equation to the reactions of side chains of triazine rings.

This paper will report on the nucleophilic substitution reactions of II or III, and the substituent effect on the pK_a or chemical shift of the imino protons of *N,N*-bis(*s*-triazinyl)amines.

Results and Discussion

I. Reaction of N,N-*Bis(4,6-dichloro*-s-*triazin-2-yl)amines (II) or* N,N,N-*Tris(4,6-dichloro*-s-*triazin-2-yl)amine (III) with Nucleophilic Reagents.* The reactivities of active chlorine atoms of polytriazinylamines towards nucleophilic reagents were found to be higher than those of amino-chloro-*s*-triazines (I). This is apparently a result of the larger positive charge of the carbon of *s*-triazine rings caused by two or three *s*-triazinyl groups on the same nitrogen atom. Thus, with excess amines, alcohols, mercaptans or thiophenols, II or III reacted to give replaced products, which were derived with the replacement of all the active chlorine atoms in II or III, even at room temperature, while amino-dichloro-*s*-triazines (I) reacted to give only partially-replaced products. The reaction of *N,N*-bis(4,6-dichloro-*s*-triazin-2-yl)aniline (II, R=phenyl) with primary or secondary amines gave only replaced products, but in the reaction of II (R=phenyl) or III with sodium methoxide, various products were obtained, depending upon the amount of sodium methoxide used. With excess sodium methoxide not only were the active chlorine atoms replaced, but also the cleavage of the triazinyl group was observed, even at room temperature, however, the reaction of II (R=H) with excess sodium methoxide gave only the replaced product IV.

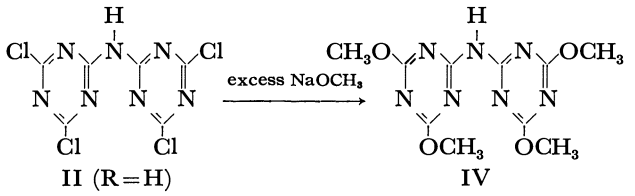

II (R=H) IV

This is probably due to the fact that IV reacts with sodium methoxide to give an anion in which the elec-

1) N. Nohara, S. Sekiguchi, and K. Matsui, *J. Heterocycl. Chem.*, **7**, 519 (1970).

2) For example, Y. Ohtsuji and E. Imoto, *Nippon Kagaku Zasshi*, **80**, 1293 (1959); H. H. Jaffé, *J. Org. Chem.*, **23**, 1790 (1958); R. Joeckle, E. D. Schmidt, and R. Meck, *Z. Naturforsch.*, **21**, 1906 (1966).

3) For example, S. Mizukami and E. Hirai, *J. Org. Chem.*, **31**, 1199 (1966).

4) G. Morimoto, *Nippon Kagaku Zasshi*, **87**, 790 (1966).

5) T. Tashiro and M. Yasuda, *Kobunshi Kagaku*, **26**, 853 (1969).

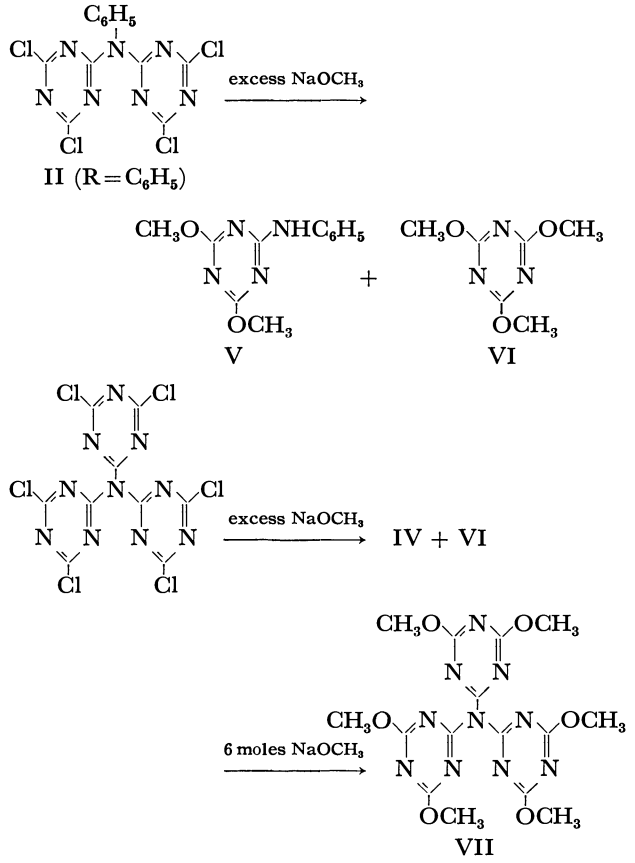

tron densities of the 2,2'-carbons of triazinyl groups are too high for them to be attacked by a methoxide anion.

II. Substituent Effects on the pK_a' Values of Ditriazinylamines. Most of the ditriazinylamines with the general formula shown in Table 1 were synthesized from I by the nucleophilic substitution described in the preceding paragraph. The ditriazinylamine (VIII) was obtained by the condensation between 2,4-dichloro-6-phenyl-*s*-triazine and 2-amino-4,6-dichloro-*s*-triazine, the compound IX, by the nucleophilic substitution of the active chlorine atoms of VIII, and the compound XVI by the condensation between 2,4-dichloro-6-phenyl-*s*-triazine and 2-amino-4-chloro-6-phenyl-*s*-triazine.

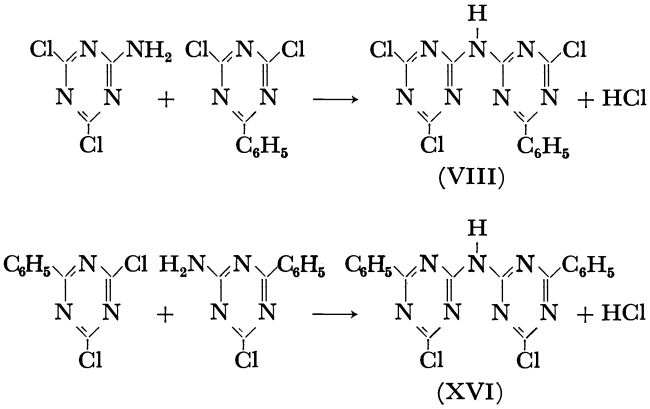

Most of these triazinyl derivatives were found to dissolve in a sodium hydroxide solution, with the simultaneous formation of the corresponding anions which have absorption bands in the region with wavelength longer than those of the original compounds. Thus, the pK_a' values of these compounds can be measured spectrophotometrically. As the measurement is carried out in a mixed solvent of water and methyl cellosolve, we will describe pK_a' instead of pK_a.[6]

However, in the cases of derivatives (VIII, XI, and XVI), the spectrophotometrical measurement of the pK_a' values was found to be impossible because of their non-solubilities in a sodium hydroxide solution or because of the ready hydrolyses of their active chlorine atoms in an aqueous solution. Table 2 lists the pK_a' values measured in a mixed solvent of methyl cellosolve and water (70/30) at 25°C. As the pK_a' values thus obtained resulted from the summation of the four substituent effects ($\sum\sigma_m$), and as the positions of the substituents correspond to the meta position of benzene derivatives, Table 2 also lists the summation of σ_m.

From these results, it is apparent that the more electron-attractive the substituent becomes, the more the acidity increases. A Hammett plot of pK_a' against $\sum\sigma_m$ is shown in Fig. 1. The ρ value calculated by the method of least squares is −4.12, with a correlation coefficient of 0.956.

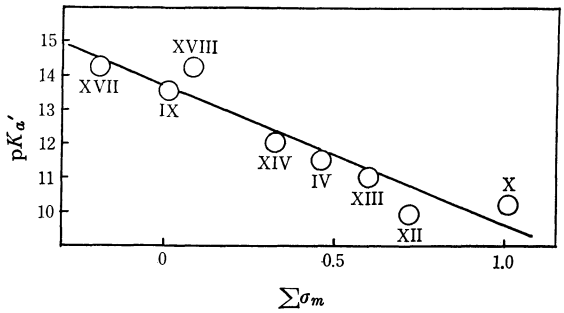

Fig. 1. Relation between pK_a' of substituted ditriazinylamines and $\sum\sigma_m$ (ρ, −4.09; r, 0.956).
The figures near the circles are the same as ones in Table 2.

From this result, it is obvious that, as a whole, the Hammett σ_m values of the benzene series are applicable to the derivatives of the triazine series.

III. Substituent Effect on Imino-proton Shifts of Ditriazinylamines. As has been mentioned in the preceding paragraph, a regular correlation was observed between pK_a' and σ_m for the dissociation of the derivatives of ditriazinylamine.

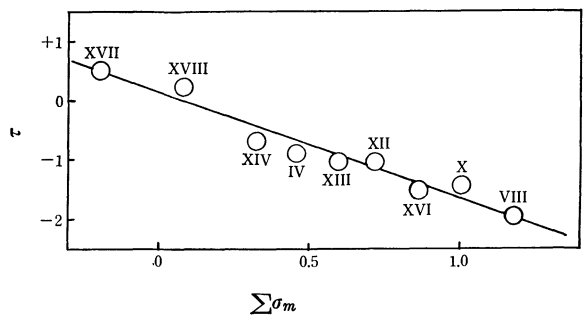

Fig. 2. Relation between imino-proton shifts of substituted ditriazinylamines and $\sum\sigma_m$ (ρ,−1.76; r, 0.977).
The figures near the circles are the same as ones in Table 3.

6) M. Syz and H. Zollinger, *Helv. Chim. Acta*, **48**, 383 (1965).
7) R. J. Ouellette, *Can. J. Chem.*, **43**, 707 (1965).

Table 1. Structures of various ditriazinylamines

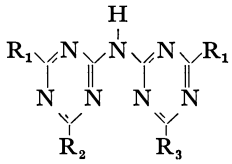

Compound No.	R_1	R_2	R_3	Yield %	Mp (°C)	Solvent for recrystallization	Anal. Found C	H	Cl
IV	CH_3O	CH_3O	CH_3O	60	185.5—186.5	Benzene	40.69	4.60	—
VIII	Cl	Cl	C_6H_5	17	204.5—206	(Sublimation)	40.63	1.83	—
IX	$(CH_3)_2N$	Cl	C_6H_5	95	202.5—204.5	Benzene-Ligroin	52.15	4.89	9.5
X	C_6H_5O	C_6H_5O	C_6H_5O	51	163—164	Methanol	66.16	3.86	—
XI	C_6H_5NH	C_6H_5NH	C_6H_5NH	57	338.5—340.5	Pyridine	66.81	4.58	—
XII	C_6H_5S	C_6H_5S	C_6H_5S	38	129.5—132	Methanol	59.52	3.38	—
XIII	CH_3S	CH_3S	CH_3S	70	183—184	Benzene	32.83	3.89	—
XIV	$(CH_3)_2N$	Cl	Cl	82	247—248.5	(Sublimation)	36.51	4.07	—
XV	$(C_2H_5)_2N$	Cl	Cl	61	112—113	Petroleum ether	43.15	5.48	—
XVI	C_6H_5	Cl	Cl	43	219.5—221	Benzene	54.95	2.99	—
XVII	$(CH_3)_2N$	CH_3O	CH_3O	81	191.5—192.5	Methanol	45.30	6.20	—
XVIII	$(CH_3)_2N$	C_6H_5O	C_6H_5O	75	190—190.5	Methanol	59.36	5.26	—

a) Measured in methanol

Table 2. pK_a' Values of derivatives of ditriazinylamines

Compound No.	$\sum\sigma_m$	pK_a'
IV	0.460[a)]	11.51
IX	0.011[a,b)]	13.59
X	1.008[a)]	10.22
XII	0.72[c)]	9.95
XIII	0.60[a)]	11.01
XIV	0.324[a,b)]	12.06
XV	—	12.43
XVII	−0.192[a,b)]	14.25
XVIII	0.082[a,b)]	14.26

a) D.H. McDaniel and H.C. Brown, *J. Org. Chem.*, **23**, 420 (1958).
b) H.H. Jaffé, *Chem. Rev.*, **53**, 191 (1953).
c) S. Oae, "Yuki Ioukagobutsu no Kagaku," Vol. 1, Tokyo Kagaku Dojin Co., Tokyo (1960), p. 117.

Table 3. Chemical shift of iminoprotons of substituted ditriazinylamines

Compound No.	$\sum\sigma_m$	τ
IV	0.460[a)]	−0.89
VIII	1.179[a)]	−1.93
X	1.008[a)]	−1.45
XI	—	+0.40
XII	0.72[c)]	−1.06
XIII	0.60[a)]	−1.04
XIV	0.324[a,b)]	−0.68
XVI	0.866[a)]	−1.54
XVII	−0.192[a,b)]	+0.49
XVIII	0.082[a,b)]	+0.23

The references a, b, and c are the same as ones in the footnote of Table 2.

In recent papers,[7,8] correlations have been noted between Hammett's σ constants and the chemical shifts of hydroxyl protons in *m*- and *p*-substituted phenols and amino protons in *m*- and *p*-substituted anilines. Consequently, a similar relation might also be expected between the chemical shifts of the imino protons of ditriazinylamines and the σ constants of substituents in the triazine rings.

Table 3 lists the imino-proton shifts of substituted ditriazinylamines, using DMSO-d_6 as a solvent at 25°C. In this solvent the positions of these signals do not shift with any variation in the concentration. A Hammett plot of imino proton shifts against $\sum\sigma_m$ is shown in Fig. 2. The ρ value was found to be 1.76, with a correlation coefficient of 0.977. From these results, it is apparent that, in the triazine derivatives, the electronic effects of the substituents are transmitted to the reaction site effectively and that, as a whole, Hammett's σ_m is also applicable to these polytriazinylamines.

Experimental

The infrared spectra were measured in potassium bromide discs on a Jasco D-301 spectrophotometer. The ultraviolet spectra were recorded on a Hitachi-124 UV-VIS spectrophotometer. The NMR spectra were recorded on a Varian A-60D spectrometer. The elemental analyses were performed in the Micro-analytical Center of the University of Gunma. All the K_a' values were determined spectrophotometrically in a mixed solvent of methyl cellosolve and water (70/30), (volume ratio), according to the method of Albert and serjeant.[9]

N,N-*Bis(4,6-dichloro-s-triazin-2-yl)amine (II, R=H).* The compound II (R=H) was prepared by the method

8) T. Yamamoto, W. F. Reynolds, and H. M. Hutton, *Can. J. Chem.*, **43**, 2668 (1965).
9) A. Albert and E. P. Serjeant, "Ionization Constants of Acids and Bases," Methuen and Co., Ltd., New York (1962).

(%) Calcd C	H	Cl	Infrared spectra (cm^{-1}) NH	triazine	UV spectra[a] λ_{max} (mμ)
40.69	4.44	—	3340	810	253
40.65	1.71	—	3240	853	—
51.68	4.88	9.5	3300	820	—
66.29	3.90	—	—	817	257
66.78	4.67	—	3400	815	—
59.28	3.48	—	3330	840	—
33.41	3.64	—	3315	850	263
36.38	4.00	—	3400	830	256
43.62	5.49	—	3260	800	—
54.56	2.80	—	3200	830	—
44.86	5.96	—	3420	810	244
59.32	5.20	—	3400	790	—

described in a previous paper.[1]

N,N-*Bis(4,6-dimethoxy-*s*-triazin-2-yl)amine (IV).* A solution of 2.3 g (0.1 mol) of sodium in 50 m*l* of methanol was added, at room temperature, to a soltion of 6.3 g (0.02 mol) of II (R=H) in 250 m*l* of methanol. After refluxing for 6 hr, the mixture was poured into 500 m*l* of ice-water neutralized with hydrochloric acid, filtered, and dried.

N,N,N-*Tris(4,6-dimethoxy-*s*-triazin-2-yl)amine (VII).* To a stirred solution of 1.0 g (0.0022 mol) of III, which is the condensation product between II (R=H) and cyanuric chloride,[1] in 30 m*l* of methanol, we added drop by drop and at room temperature, a solution of 0.3 g (0.013 mol) of sodium in 20 m*l* of methanol. After an additional 4 hr's stirring at 35—40°C, the methanol was distilled off under reduced pressure. The recrystallization of the residue from benzene yielded 0.70 g (74%) of VII; mp 206—206.5°C.

Found: C, 41.49; H, 4.14%. Calcd for $C_{15}H_{18}N_{10}O_6$; C, 41.48; H, 4.18%.

*4-Chloro-6-phenyl-*s*-triazin-2-yl-4',6'-dichloro-*s*-triazin-2'-ylamine (VIII).* To a stirred solution of 1.7 g (0.01 mol) of 2-amino-4,6-dichloro-*s*-triazine and 2.3 g (0.01 mol) of 2,4-dichloro-6-phenyl-*s*-triazine in 150 m*l* of acetone, we added, drop by drop and below 5°C, a solution of 0.4 g (0.01 mol) of sodium hydroxide in 4 m*l* of water. After an additional one hr's stirring, the mixture was poured into 500 m*l* of ice water and filtered. The filtrate was acidified with hydrochloric acid. The precipitate thus formed was filtered and dried.

*4-Dimethylamino-6-phenyl-*s*-triazin-2-yl-4'-chloro-6'-dimethylamino-*s*-triazin-2'-ylamine (IX).* Into a solution of 3.6 g (0.01 mol) of VIII in 150 m*l* of acetone, we stirred drop by drop and below 10°C, 4.6 m*l* (0.04 mol) of a 40% aqueous dimethylamine solution. After an additional 3 hr's stirring, the mixture was poured into 500 m*l* of ice water, the precipitate thus formed was filtered and dried.

In the reaction of VIII with dimethylamine, it is expected from a comparison of the σ_m values for the phenyl, chlorine, and dimethylamino substituents that, first, one of the chlorine atoms of the dichloro-*s*-triazinyl group of VIII and then chlorine atom of the chlorophenyl-*s*-triazinyl group, may be replaced by dimethylamino groups. Therefore, the main product of the above-mentioned reaction was assumed to be 4-dimethylamino-6-phenyl-*s*-triazin-2-yl-4'-chloro-6'-dimethylamino-*s*-triazin-2'-ylamine (IX).

N,N-*Bis(4,6-diphenoxy-*s*-triazin-2-yl)amine (X).* A solution of 4.0 g (0.1 mol) of sodium hydroxide in 40 m*l* of water was added, at room temperature, to a solution of 6.3 g (0.02 mol) of II (R=H) and 9.4 g (0.1 mol) of phenol in 200 m*l* of benzene. After 3 hr's stirring, the mixture was refluxed for 3 hr. The benzene layer was separated and dried over calcium chloride. Then, the benzene was distilled off under reduced pressure, and the residue was collected.

The compound XI, XII and XIII were prepared in a similar manner by the reaction of II (R=H) with aniline thiophenol, and methyl mercaptan respectively.

N,N-*Bis(4-chloro-6-dimethylamino-*s*-triazin-2-yl)amine (XIV).* Into 200 m*l* of acetone containing 3.2 g (0.01 mol) of II (R=H), we stirred, drop by drop and below 5°C, 4.5 g (0.04 mol) of a 40% dimethylamine solution. After an additional 3 hr's stirring, the mixture was poured into 300 m*l* of ice-water, filtered, and dried. The compound XV was prepared in a similar manner by the reaction of II (R=H) with diethylamine.

N,N-*Bis(4-chloro-6-phenyl-*s*-triazin-2-yl)amine (XVI).* To a stirred solution of 150 m*l* of acetone containing 2.3 g (0.01 mol) of 2,4-dichloro-6-phenyl-*s*-triazine and 2.5 g (0.012 mol) of 2-amino-4-chloro-6-phenyl-*s*-triazine, we added drop by drop and below 5°C, a solution of 0.4 g (0.01 mol) of sodium hydroxide in 4 m*l* of water. After an additional 5 hr's stirring, the mixture was poured into 1 *l* of ice-water, made alkaline with sodium hydroxide, and filtered. The filtrate was acidified with hydrochloric acid. The precipitate thus obtained was filtered and dried.

N,N-*Bis(4-dimethylamino-6-methoxy-*s*-triazin-2-yl)amine (XVII).* To a solution of 3.8 g (0.01 mol) of XIV in 150 m*l* of methanol, we added, at room temperature, a solution of 0.7 g (0.03 mol) of sodium in 30 m*l* of methanol. After the mixture had been refluxed for 3 hr, the methanol was distilled off under reduced pressure and the resulting residue was collected.

N,N-*Bis(4-dimethylamino-6-phenoxy-*s*-triazin-2-yl)amine (XVIII).* Into a solution of 3.3 g (0.01 mol) of XIV and 1.9 g (0.02 mol) of phenol in 100 m*l* of dioxane, we stirred, at room temperature, 10 m*l* of an alkaline solution containing 1.0 g (0.025 mol) of sodium hydroxide. After heating at 70—80°C for 3 hr, the mixture was poured into 300 m*l* of ice-water, filtered, and dried.

Reaction of N,N-*Bis(4,6-dichloro-*s*-triazin-2-yl)aniline (II, R=Ph) with Excess Sodium Methoxide.* A solution of 1.8 g (0.08 mol) of sodium in 50 m*l* of methanol was added, at room temperature, to a solution of 3.8 g 0.01 mol) of II (R=Ph) in 50 m*l* of methanol. The mixture was stirred at 35°C for 6 hr. Then the mixture was poured into 1 *l* of ice-water, and neutralized with hydrochloric acid. The precipitate thus formed was separated by filtration and dried. Recrystallization from ligroin yielded 1.7 g (57%), mp 133—134°C, which was found to be identical with that of an authentic sample of V by a mixed-melting-point test. After the filtrate had been extracted with benzene, the benzene layer was dried over calcium chloride. The residue obtained after distilling off the benzene was recrystallized from ligroin to give 0.9 g (66 %) of a pure material; mp 133—134°C, which was found to be identical with that of an authentic sample of trimethyl cyanurate by a mixed-melting-point test.

Reaction of N,N,N-*Tris(4,6-dichloro-*s*-triazin-2-yl)amine (III) with Excess Sodium Methoxide.* A solution of 1.0 g (0.002 mol) of III and 0.35 g (0.015 mol) of sodium in 50 m*l* of

methanol was stirred at 35—40°C for 4 hr. Then the mixture was poured into 200 m*l* of ice water. After this aqueous solution had been extracted with benzene and drying over calcium chloride, the benzene was distilled off. The residue was recrystallized from benzene. Yield, 0.4 g (68%); mp 185—186°C. By a mixed-melting-point test, this compound was proved to be IV. After the benzene had been distilled off from the filtrate, the residue was recrystallized from ligroin. Yield, 0.2 g (69%); mp 132—134°C. By a mixed-melting-point test, this compound was proved to be VI.

BULLETIN OF THE CHEMICAL SOCIETY OF JAPAN, VOL. 44, 798—802 (1971)

Studies on Cobaloxime Compounds. III. Effects of Various Cobaloximes as Vitamin B_{12} Models and of Substrate Analogs on Diol Dehydratase System

Yorikatsu HOHOKABE and Noboru YAMAZAKI

Department of Polymer Science, Faculty of Engineering, Tokyo Institute of Technology, Ookayama, Meguro-ku, Tokyo

(Received August 14, 1970)

Various types of cobaloximes with the general formula $[CoX(DH)_2B]$ or $[RCo(DH)_2B]$ (X: Cl, CN. R: alkyl groups such as methyl, ethyl, *n*-propyl, or *i*-propyl. DH: dimethylglyoximato monoanion. B: bases such as water, pyridine, nicotinamide, *γ*-picoline, *p*-toluidine, or imidazole) and some amide compounds were examined for the inhibitory effect or coenzyme activity in propanediol dehydratase of *Aerobacter aerogenes*. None of them act as coenzyme nor inhibitor, except for cyanoaquocobaloxime, which shows only a weak inhibitory effect that has been proved to be non-competitive. Water-soluble polymeric cobaloximes with the general formula [Co(OH) $(DH)_2$(Copoly–AM-VPy)] (Copoly–AM-VPy: a low molecular weight copolymer of acrylamide and 4-vinylpyridine) were also prepared and examined in the enzymatic system whose inhibitory effects were very small. Other cobaloximes with the general formula $[RCo(DH)_2(py)]$ (R: *β*-hydroxy-*n*-propyl, *β*-hydroxy-*i*-propyl, or *β*,*γ*-dihydroxy-*n*-propyl. py: pyridine) which were three of the possible intermediate models in propanediol dehydratase system, also showed little effect on the enzymatic reaction. Substrate anologs such as 2-bromo-1-propanol, 1-bromo-2-propanol, and glycerol *α*-monochlorohydrin, which are considered to interact with a nucleophilic Co(I) species, presumably a component of the active site in the holoenzyme, were found to serve as substrate.

Although many works have been done on vitamin B_{12} compounds, there are not many on the active sites in holoenzyme in which coenzyme B_{12} and substrate are assumed to be bound to apoenzyme. In the case of L-methylmalonyl-CoA mutase from sheep liver, it was assumed that holoenzyme formation involves at least a two-point attachment between the coenzyme and apoenzyme and that sulfhydryl groups are one binding site of the protein.[1] In ribonucleotide reductase from *L. leichmannii*, 5′-deoxyadenosylcobalamin with a slight alteration of *e*-propionamide group to *e*-propionic acid on the corrin ring showed neither activity nor inhibitory effect.[2] In propanediol dehydratase system, the analogs with two or three propionic acid side-chains on the corrin ring did not serve as the coenzyme, while all the three isomers of one propionic acid side-chain (at *b*, *d*, or *e* position on the corrin ring) were effective.[3]

We considered that for the appearance of the coenzyme activity in enzymatic reactions, there might be some amide groups in the neighborhood of the Co atom, since these groups in cobalamin might take part in the reactions *in vivo*, probably as binding sites to apoenzyme.[4] We have therefore studied the effect of cobaloximes having a ligand with amide groups. The resemblance of cobaloxime compounds to cobalamin compounds in chemical behavior has also been described elsewhere.[5–8]

There are a few examples dealing with the cobaloximes as the vitamin B_{12} model in biological systems. Some cobaloximes were examined in blockade of vitamin B_{12}-binding sites in gastric juice, serum, and saliva,[9] and some methylcobaloximes were demonstrated to be able to make methane in enzymatic reaction containing the extracts from *Methanobacillus omelianskii*.[10]

We have also studied the effect of various cobaloximes on propanediol dehydratase system. Among them, hydroxypropyl derivatives might be considered as model compounds for the possible intermediates in the enzymatic reaction. At present the following hypothesis seems to be acceptable: It is necessary for the appearance of coenzyme activity that Co–5′-deoxyadenosyl

1) J. J. B. Cannata, A. Focesi, Jr., R. Mazumder, R. C. Warner, and S. Ochoa, *J. Biol. Chem.*, **240**, 3249 (1965).
2) C. G. D. Morley, R. L. Blakley, and H. P. C. Hogenkamp, *Biochemistry*, **7**, 1231 (1968).
3) Y. Tamao, Y. Morikawa, S. Shimizu, and S. Fukui, *Vitamins* (Japan), **41**, 45 (1970).
4) N. Yamazaki and Y. Hohokabe, *Chem. Commun.*, **1968**, 829.
5) G. N. Schrauzer and J. Kohnle, *Chem. Ber.*, **97**, 3056 (1964).
6) G. N. Schrauzer, *Accounts Chem. Res.*, **1**, 97 (1968).
7) G. N. Schrauzer, E. Deutsch, and R. J. Windgassen, *J. Amer. Chem. Soc.*, **90**, 2441 (1968).
8) L-P. Lee and G. N. Schrauzer, *ibid.*, **90**, 5274 (1968).
9) C. W. Gottlieb, F. P. Retief, and V. Herbert, *Biochim. Biophys. Acta*, **141**, 560 (1967).
10) B. C. McBride, J. M. Wood, J. W. Sibert, and G. N. Schrauzer, *J. Amer. Chem. Soc.*, **90**, 5276 (1968).

bond in DBCC bound to apoenzyme is heterolytically cleaved, producing enzyme-bound Co(I) species. Thus, the electrophilic substrate analogs such as propylene bromohydrin are considered to have the ability to interact with the Co(I) species and serve as substrate. The results are given in the following.

Experimental

Materials. Preparative methods of various cobaloximes were reported.[11]

Imidazole-4,5-dicarboxyamide was prepared according to the method described by Baxter and Spring.[12]

Found: C, 38.47; H, 3.98; N, 36.44%. Calcd for $C_5H_6N_4O_2$: C, 38.96; H, 3.92; N, 36.35%.

2-Bromo-1-propanol was synthesized as follows: $LiAlH_4$ 5.32 g was refluxed for 3 hr in 300 m*l* of dry ether. α-Bromopropionyl bromide 43.2 g was added slowly to the mixture at 0°C for an hour followed by stirring for 2 hr. After adding 15 m*l* of H_2O and 130 m*l* of 3N H_2SO_4 to the mixture, the upper ether layer was separated. The remaining water layer was extracted with isopropyl ether, and the extract was combined with the ether layer. After drying the ether solution with Na_2SO_4, the product was fractionally distilled under a reduced pressure (bp 71°C/33 mmHg). The yield was 17.6 g (64%). The structure was confirmed by NMR and IR spectra.

Found: C, 26.85; H, 5.23; Br, 57.77%. Calcd for C_3H_7OBr: C, 25.93; H, 5.08; Br, 57.49%.

Propylene bromohydrin (commercial E. P. reagent) was a mixture of 1-bromo-2-propanol (79%) and 2-bromo-1-propanol (21%). Its composition was determined by NMR and gas chromatography, and used without further purification, because it was impossible to fractionate it by the usual fractional distillation.

5,6-Dimethylbenzimidazolylcobamide coenzyme (DBCC) was supplied by Prof. S. Fukui and Eisai Co., and propanediol dehydratase (EC. 4.2.1.28) was generously given by Prof. S. Fukui.

All other reagents were of commercial G. R. grade.

Methods. *General Method for the Enzymatic Reaction*: The enzymatic reaction was carried out in the dark. DBCC and cobaloxime or amide were mixed prior to the addition of the apoenzyme solution. A typical method is as follows: 0.1 m*l* of 0.5M KCl, and 0.2 m*l* of cobaloxime or amide solution were pipetted into an assay tube. 0.1 m*l* of DBCC solution was then added in the dark and after being cooled in an ice bath, 0.5 m*l* of cold apoenzyme solution in potassium phosphate buffer (pH 8.0) was added. The reaction was conducted for 5, and 10 min at 37°C in the dark. The mixture was then rapidly cooled in an ice bath and 0.5 m*l* of 10% trichloroacetic acid was immediately added to the mixure to stop the reaction.

In the Case of Hydroxypropylcobaloximes: The reaction was carried out for 10 min at 25°C, aerobically or anaerobically after the following treatment. A 100 W tungsten lamp was used as the light source at a distance of 4 cm.

(1) (Dark-Aerobic): A mixture of DBCC, cobaloxime, and apoenzyme was preincubated for 7 min at 25° in the dark prior to the addition of the substrate. The treatment was done in the presence of air.

(2) (Dark-Anaerobic): The same treatment as (1) but under a nitrogen atmosphere.

(3) (Light-Aerobic): A mixture of DBCC, cobaloxime, and apoenzyme was preincubated for 2 min at 25°, followed by irradiation for 5 min at 25°C prior to the addition of the substrate. The treatment was done in the presence of air.

(4) (Light-Anaerobic): The same treatment as (3) but under a nitrogen atmosphere.

In the Case of Substrate Analogs: The reaction was carried out for 2, 3.5, 7.5 (or 8), and 10 min at 25°C in the dark.

Determination of Propionaldehyde: One milliliter of 5 mM 2,4-dinitrophenylhydrazine in methanol containing a small amount of concd. HCl was added to each reaction mixture which was put to stand for 10 min at 37°C. Three milliliters of 80% aqueous pyridine were then added. The amount of hydrazone formed from propionaldehyde was colorimetrically determined at 540 mμ, 20 min or 40 min after the addition of 0.5 m*l* of alcoholic KOH (0.1 g/m*l* of 80% aqueous methanol), with a Hitachi photoelectric spectrophotometer. The absorbance was corrected by using the control solution as a reference, which is the mixture stopped immediately after the addition of apoenzyme solution. Unity of absorbance at 540 mμ, 20 min or 40 min after the addition of KOH corresponds to 0.92 and 1.09 μmol of propionaldehyde in 1 m*l* of the original reaction mixture, respectively.

The velocity was determined with the slope of the straight line passing through the time-conversion plots. The relative activity was determined as follows.

$$\text{Relative activity} = \frac{\text{Amount of aldehyde formed in the presence of additive (inhibitor)}}{\text{Amount of aldehyde formed in the absence of additive (inhibitor)}} \times 100\,(\%).$$

Results and Discussion

Polymeric Cobaloximes, Co(OH)(DH)$_2$(Copoly-AM-VPy). The enzymatic reaction was carried out in the presence of various amounts of polymeric cobaloximes in which

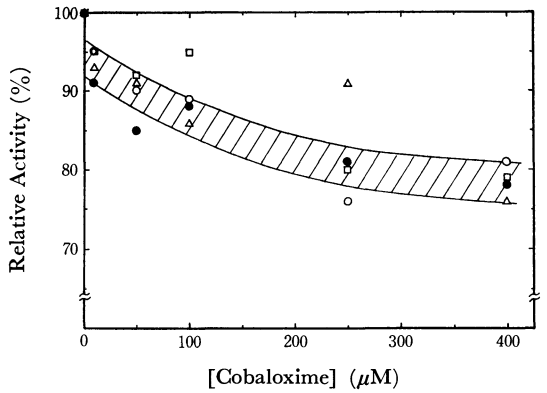

Fig. 1. Relative activity *vs.* concentration of polymeric cobaloxime plots.
The reaction mixture contained 1,2-propanediol 10 μmol, potassium chloride 50 μmol, DBCC 1.5 mμmol, apoenzyme 0.08 unit, potassium phosphate buffer (pH 8.0) 25 μmol, and polymeric cobaloxime (○ HC 025; □ HC 027; ● HC 029; △ HC 030) 0, 10, 50, 100, 250, or 400 mμmol; total volume 1.0 m*l*. The reaction was carried out for 10 min at 37°C in the dark. The average molecular weights of polymeric ligands and AM(acrylamide)/VPy(4-vinylpyridine) ratios are 3000 and 11.9 for HC 025, 2400 and 12.8 for HC 029, 1400 and 13.7 for HC027, 830 and 17.5 for HC030, respectively.

11) N. Yamazaki and Y. Hohokabe, This Bulletin, **44**, 63 (1971).

12) R. A. Baxter and F. S. Spring, *J. Chem. Soc.*, **1945**, 232.

Copoly–AM-VPy[13] coordinates with the Co atom through a pyridine residue and the amide groups are close to the cobaloxime moiety. The results are shown in Fig. 1. Although the relative activities with respect to polymeric cobaloximes decreased with the increase of the amount of cobaloximes, they decreased to *ca.* 80% even at the higher concentration of cobaloximes, and no difference in decrease with respect to the molecular weights of polymers was observed. This suggests that the polymeric cobaloximes employed in this experiment were not sufficiently small to interact with the active site in the enzyme, though their molecular weights are nearly the same as that of coenzyme B_{12} or larger only by a factor less than 2.5. This type of cobaloximes does not seem to interact with the active site in the holoenzyme.

TABLE 1. RELATIVE ACTIVITIES IN THE PRESENCE OF SOME AMIDES.

The reaction mixture contained 1,2-propanediol 10 μmol, potassium chloride 50 μmol, DBCC 1.5 mμmol, apoenzyme 0.10 unit, potassium phosphate buffer (pH 8.0) 25 μmol, and amide 250 mμmol; total volume 1.0 m*l*. The reaction was carried out for 10 min at 37°C in the dark.

Material	Relative activity (%)
None	100
Nicotinamide	90
Acetamide	92
Isobutylamide	93
Benzamide	95
Propionamide	103
Imidazole-4,5-dicarboxyamide[a)]	101

a) nearly insoluble.

Amides. From the viewpoint in the introductory, *i. e.*, some amide groups in cobalamin may take part in the reactions *in vivo*, perhaps as the binding sites to the apoenzyme, the presence of amides is expected to affect the enzymatic reaction. The results of some amides are shown in Table 1. The activity was affected slightly or not at all by the presence of amide. From the results, we see that monoamide is not bound tightly to the site because of weakeness of the hydrogen bonding. The multiple-point attachment of the amide groups in a molecule may favor the single-point attachment by the increase in total entropy and decrease in total energy by each hydrogen bonding. One of the diamide, imidazole-4,5-dicarboxyamide, however, failed to affect the active site, probably because of insolubility. It seems that some amide groups situated at an appropriate distance from each other and the cobaloxime moiety might interact with the active site.

The enzymatic reaction was also carried out in the presence of various monomeric cobaloximes.

Chloro- and Simple Alkyl-cobaloximes. All the chloro- or simple alkyl-cobaloximes were found to exert little effect on the enzymatic reaction: They include $CoCl(DH)_2B$ in which B is water, nicotinamide, pyridine, imidazole, γ-picoline, or *p*-toluidine, $CH_3Co(DH)_2B$ in which B is water, nicotinamide, pyridine, or imidazole, and $RCo(DH)_2B$ in which R is methyl, ethyl, *n*-propyl, or *i*-propyl, and B water or pyridine.

13) Copoly–AM-VPy is a low molecular weight copolymer of acrylamide (AM) and 4-vinylpyridine (VPy).

TABLE 2. RELATIVE ACTIVITIES IN THE PRESENCE OF CYANOCOBALOXIMES.

The reaction mixture contained 1,2-propanediol 10 μmol, potassium chloride 50 μmol, DBCC 1.5 mμmol, cobaloxime 250 mμmol, apoenzyme 0.083 unit (0.69 unit/mg-protein), potassium phosphate buffer (pH 8.0) 25 μmol; total volume 1.0 m*l*. The reaction was carried out for 5, or 10 min at 37°C in the dark.

Material[a)]	Relative activity (%)
None	100
NaCN(250 mμmol)	88
Co (CN)$(DH)_2(H_2O)$	57
Co(CN)$(DH)_2$(py)	90
Co(CN)$(DH)_2$(pico)	98
Co(CN)$(DH)_2$(tolu)	105

a) py: pyridine, pico: γ-picoline, tolu: *p*-toluidine.

Cyanocobaloximes. It is well known that cyanocobalamin is a strong competitive inhibitor in diol dehydratase system and other B_{12}-dependent enzymatic reactions. The effect of cyano cobaloximes was examined in comparison with cyanocobalamin. The results are shown in Table 2. They exerted no inhibition or much less inhibitory effect than cyanocobalamin; only cyanoaquocobaloxime showed a weak inhibition. From an extensive study on cyanoaquocobaloxime, it proved to be non-competitive as shown in Fig. 2. The

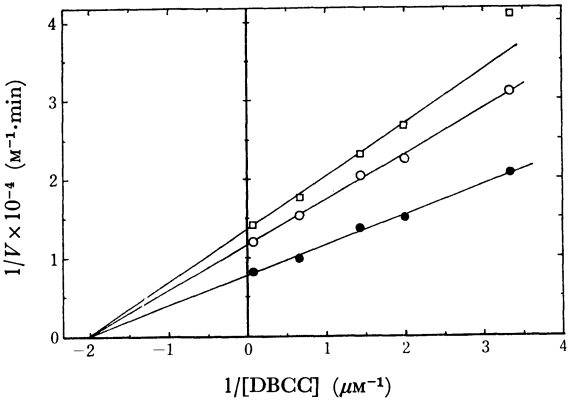

Fig. 2. Non-competitive inhibitory effect of cyanoaquocobaloxime on propanediol dehydratase system.
The reaction conditions are the same as those in Table 2, except that DBCC 0.30, 0.50, 0.70 1.50, or 15.0 mμmol, cyanoaquocobaloxime 0 (●), 200 (○), or 250 (□) mμmol, and apoenzyme 0.14 unit (0.73 unit/mg-protein) were employed.

inhibitor constant K_i was determined to be 3.3 ($\pm$0.1) $\times$ 10^{-4}M. Since the same amount of sodium cyanide exerted much less inhibition, the weak effect of cyanoaquocobaloxime is not considered to be due to free cyanide ion which might be derived from the cobaloxime. It seems that a slight conformational change of the enzyme protein occurs in the presence of the cobaloxime. A most plausible explanation of the effect is as follows. First, CN linked to cobaloxime interacts with

a given site in the protein, second, another axial ligand of the cobaloxime, *i. e.*, H_2O is displaced by a basic group of the enzyme, resulting in a slight conformational change of the tertiary structure of the enzyme.

Hydroxypropylcobaloximes. The preparation and properties of a series of hydroxyalkylcobaloximes have been reported by Schrauzer and Windgassen.[14] The Co–C bonds are readily cleaved; in mildly acidic media olefins are formed. However, in alkaline solution the products are aldehydes, ketones, or the respective aldols arising from the secondary condensation of the aldehydes. They proposed a mechanism for the action of the corrin coenzyme in diol dehydratase of *Aerobacter aerogenes*, in which they supposed that β-hydroxy-*i*-propyl derivative is the most likely organocobamide as the intermediate in glycol dehydratase system. The corresponding cobaloxime was prepared and found to produce propionaldehyde on decomposition in alkaline medium. Its effect on enzymatic reaction seems to be interesting. β,γ-Dihydroxypropylcobalamin exhibited no coenzyme activity, and exerted an inhibitory effect.[15]

Table 3. Relative activities in the presence of hydroxypropylcobaloximes under various conditions.
The reaction mixture contained 1,2-propanediol 10 μmol, potassium chloride 50 μmol, DBCC 15.0 mμmol, cobaloxime 200 mμmol, apoenzyme 0.068 unit (0.20 unit/mg-protein) for the first series of runs, and 0.086 unit (0.49 unit/mg-protein) for the second, potassium phosphate buffer (pH 8.0) 25 μmol; total volume 1.0 m*l*. Other conditions are indicated in the experimental section.
The series of runs were carried out twice and the mean values are indicated in the following table.

Material[a]	Dark		Light	
	Aerobic (1) %	Anaerobic (2) %	Aerobic (3) %	Anaerobic (4) %
None	100	133	56	89
$HOCH_2CH(OH)$-$CH_2Co(DH)_2$(py)	100	94	20	87
$HOCH_2CH(CH_3)$-$Co(DH)_2$(py)	98	119	41	101
$CH_3CH(OH)CH_2$-$Co(DH)_2$(py)	99	121	33	136

a) py: pyridine

Three of the possible intermediate models, *i. e.*, β-hydroxy-*i*-opropyl-, β-hydroxy-*n*-propyl-, and β,γ-dihydroxy-*n*-propyl-(pyridine)cobaloxime, were also synthesized and examined in propanediol dehydratase system. As the alkyl moiety of these cobaloximes are very similar to propanediol in structure, some effect could be expected; cobaloxime may block the substrate-binding site, and/or hydroxypropyl radicals arisen from the light irradiation of the cobaloximes may interact with the active coenzyme. As shown in Table 3, however, they also exerted little effect on the reaction.[16] This suggests that the cobaloximes do not contact with the active site of the holoenzyme.

All the cobaloximes described were unable to interact with the active site. Synthesis of 5′-deoxyadenosylcobaloxime failed in isolation by the usual way as carried out in the partial DBCC preparation, presumably because of its alkali and acid lability, as reported by Schrauzer.[17]

Substrate Analogs. Since it is well established that Co(I) species of cobalamin is a powerful nucleophilic agent,[18] the Co(I) nucleophile seems to play an important role in enzymatic conversion of diol to the corresponding aldehyde. Since propanediol and glycol were found not to react with Co(I) species, propanediol is considered to be activated in some form which is able to react with Co(I). Hence, three analogs, *i. e.*, $CH_3CH(OH)CH_2Br$, $CH_3CHBrCH_2OH$, and $HOCH_2CH(OH)CH_2Cl$, which are structurally similar to $CH_3CH(OH)CH_2OH$, are considered to be able to serve as a substrate or an accelerator.

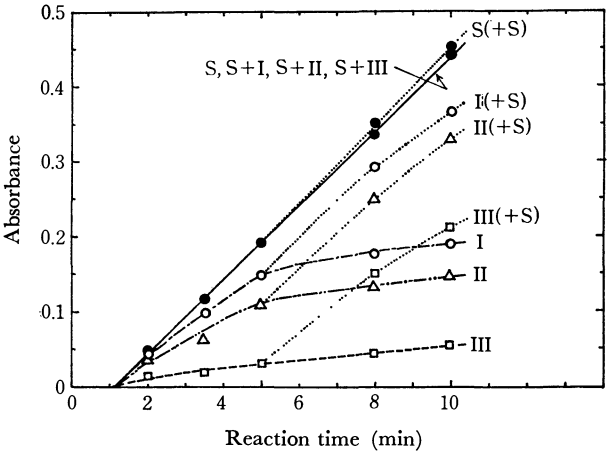

Fig. 3. Effect of substrate anologs on propanediol dehydratase system.
The reaction mixture contained I, II, III, and/or S 10 μmol, potassium chloride 50 μmol, DBCC 15.0 mμmol, apoenzyme 0.10 unit (0.61 unit/mg-protein), potassium phosphate buffer (pH 8.0) 25 μmol; total volume 1.0 or 1.1 m*l*. The reaction was carried out for 2, 3.5, 5, 8, or 10 min at 25°C in the dark. S (—●—), I (-·-○-·-), II (-···-△-···-), or III (—□—) represents the reaction in the presence of S, I, II, or III, respectively. S+I (—●—), S+II (—●—), or S+III (—●—) represents the reaction in the co-existence of S and I, S and II, or S and III, respectively. Since the reaction with S+I, S+II, or S+III proceeded in the same way as that with S, they are shown in the same line. S (+S) (···●···), I (+S) (···○···), II (+S) (···△···), or III (+S) (···□···) represents the reaction with the additional 10 μmol 1 of S during the reaction in the presence of S, I, II, or III, respectively. Unity of absorbance corresponds to 1.09 μmol of propionaldehyde. Notations on S, I, II, and III are described in the text.

14) G. N. Schrauzer and R. J. Windgassen, *J. Amer. Chem. Soc.*, **89**, 143 (1967).
15) T. Yamane, S. Shimizu, and S. Fukui, *J. Vitaminol.*, **12**, 10 (1966).
16) The enzymatic reaction was carried out at 25°C, lower than the usual 37°C, in order to minimize the inactivation of holoenzyme by incubation prior to the addition of the substrate. The holoenzyme is known to be inactivated by oxygen in the absence of the substrate.
17) G. N. Schrauzer and J. W. Sibert, *J. Amer. Chem. Soc.*, **92**, 1022 (1970).
18) G. N. Schrauzer and E. Deutsch, *ibid.*, **91**, 3341 (1969).

The following abbreviations will be used for the sake of convenience. S; 1,2-propanediol, I; propylene bromohydrin [a mixture of 1-bromo-2-propanol (79%) and 2-bromo-1-propanol (21%)], II; 2-bromo-1-propanol, III; glycerol α-monochlorohydrin.

When 10 μmol of I, II, or III was added to 10 μmol of S which was considered appropriate to give a maximum velocity V_{max}, the enzymatic reaction proceeded just the same as that in the absence of I, II, or III. I, II, or III did not inhibit the enzymatic reaction. However, they seemed to serve as substrates shown in Fig. 3; even in the absence of S, the velocity of the reaction with I or II was comparable to that with S in the initial stage of the reaction, while that with III was observed to be measurable but much less. I, II, or III is considered to interact with the same site as a normal substrate; the initial velocity of S+I, S+II or S+III would be larger than that of S which gives the V_{max}, if I, II, or III reacted with another site of the enzyme other than the normal substrate-binding site. At low concentration of S not enough to give V_{max}, addition of I or II increased the reaction velocity (Fig. 4), which supports the idea that I and/or II serve as a substrate. However, the active site in the presence of I, II, or III without S was soon inactivated as shown in Fig. 3. When such reactions were carried out anaerobically, the time-course was observed to be the same as that in aerobic conditions. It appears that inactivation is not caused by oxygen, whereas the holoenzyme is known to be inactivated by oxygen in the absence of the substrate.

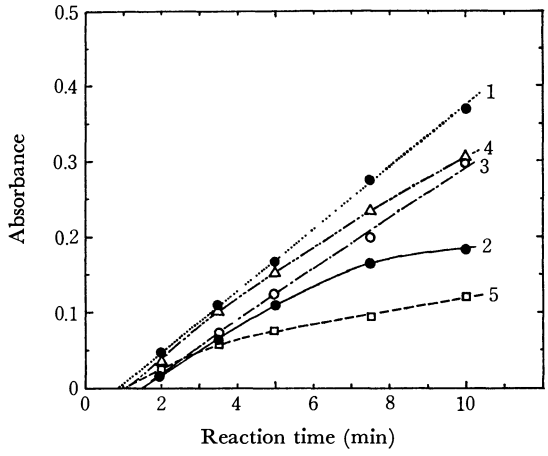

Fig. 4. Effect of substrate analogs on the propanediol dehydratase reaction in the presence of low concentration of the substrate.

The reaction mixture contained S 10 μmol (1; ···●···), S 0.15 μmol (2; —●—), S 0.15 μmol + I 10 μmol (3; -·-○-·-), S 0.15 μmol + II 10 μmol (4; -···△···-), or S 0.15 μmol+III 10 μmol (5;--□--), potassium chloride 50 μmol, DBCC 15.0 mμmol, apoenzyme 0.080 unit (0.70 unit/mg-protein), potassium phosphate buffer (pH 8.0) 25 μmol; total volume 1.0 ml. The reaction was carried out for 2, 3.5, 5, 7.5, or 10 min 25°C in the dark. Unity of absorbance corresponds to 1.09 μmol of propionaldehyde.

When 10 μmol of S was added during the course of the reaction (5 min after the initiation of the reaction) to the reaction mixture with I, II, or III in the absence of S, the expected inactivation was not observed, but the reaction proceeded with almost the same velocity as that with S which gives V_{max} (Fig. 3). This clearly indicates that the active site is temporarily blocked by some materials, and not completely inactivated in the absence of the substrate. Taking into consideration the fact that the holoenzyme initially gave the product(s) from I, II, or III but was gradually inactivated during the course of the reaction, we could consider that the temporary inactivation was caused by the formation of complex(es) between holoenzyme and the product(s) from I, II, or III. This is plausible, if we assume that the affinity to the holoenzyme decreases in the order S>product(s) from I, II, or III>I, II, or III. In the case of I holoenzyme-I complex is formed in the absence of S, which forms the product. As the amount of the product increases, holoenzyme-product complex is gradually formed, which does not interact with I and gives no more product. When S is added, the holoenzyme-product complex turns into holoenzyme-S complex, again producing the normal product. Since the affinity of S to the holoenzyme is assumed to be greater than that of analogs or product(s), the enzymatic reaction both with S and with I, II, or III proceeds the same as that in the absence of I, II, or III.

The enzymatic reaction is expected to be inhibited by the initial addition of some products estimated to be formed from I, II, or III. When 0.5 μmol of propionaldehyde and/or acetone, which appeared to be enough to block the active site as judged by the amount of the product formed from I, II, or III, were added to the system with I, II, or III, the reaction patterns did not differ from those without the addition of aldehyde and/or acetone. Although the reactions were not inhibited by propionaldehyde or acetone, the hypothesis on blocking the active site by some materials described above might still be reasonable, since other products such as aldols are expected to be produced from I, II, or III. It was recently reported that substrate analogs such as styrene glycol or 1,2-butanediol, protected the holoenzyme against inactivation by oxygen, and by displacement of the analog with the substrate the normal reaction was initiated.[19] Detailed features of the effect of the substrate analogs are not known at present.

We wish to thank Prof. S. Fukui and his coworkers of Kyoto University for kindly supplying the enzyme and giving suggestions.

19) T. Toraya and S. Fukui, *Biochem. Biophys. Res. Commun.*, **36**, 469 (1969).

Studies on Heteroaromaticity. LII.[1] Syntheses and Reactions of α-Acetylenic Ketones Containing Nitrofuran Ring

Tadashi SASAKI and Toshiyuki YOSHIOKA

Institute of Applied Organic Chemistry, Faculty of Engineering, Nagoya University, Chikusa-ku, Nagoya

(Received August 14, 1970)

2-(5-Nitro-2-furyl)-1-phenyl- (IVa), -*p*-methylphenyl- (IVb) and -(2-furyl)-acetylene (IVc) were prepared by condensation of nitrofurfural with the corresponding aryl methyl ketones, followed by bromination and dehydrobromination. Addition of aniline and cyclohexylamine to IVa afforded simple adducts Va and VIa respectively. Treatment of IVa,b with hydroxylamine, hydrazine hydrate, semicarbazide and benzamidine gave isoxazoles (VIIIa,b), pyrazoles (VIIIa,b), 1-carbamidopyrazoles (IXa,b) and pyrimidines (Xa,b) respectively. When treated with benzonitrile oxide at room temperature, IVa afforded isoxazole XIa together with furoxan, but the thermal 1,3-dipolar reactions of IVa,b with 5-nitro-2-furocarbonitrile oxide afforded exclusively isoxazoles XIIa,b. For comparison, 5-nitro-2-furfurylidenebenzophenone (IIa) was treated with benzonitrile oxide at room temperature to afford an isomeric mixture of the isoxazolines XIIIa and XIVa together with furoxan. Similar treatment of 5-nitro-2-furfurylideneacetone afforded similar results affording a mixture of XV and XVI together with furoxan. When treated with phenacylpyridinium ylide, IVa,b afforded pyrrocolines XVIIa,b. The structural elucidation of the products was carried out on the basis of the spectral data.

Saikawa *et al.*,[2] Yoshina *et al.*[3] and Sasaki and Shoji[4] reported independently on the preparation of 3-amino-6-[2-(5-nitro-2-furyl)ethynyl]-1,2,4-triazines (A), 2-(5-nitro-2-furyl)ethynylbenzothiazole (B) and 5-nitro-2-furylacetylene (C) and -propiolate (D). Saikachi and Sugimoto presented the synthesis of 3-(5-nitro-2-furoyl)prop-2-yne (E)[5] and Saikachi *et al.* that of 1-phenyl-4-(5-nitro-2-furyl)but-3-ene-1-yne (F),[6] but detailed experimental data have not been published yet. This paper deals with the syntheses of 2-(5-nitro-2-furyl)-1-aroylacetylenes (IV), another type of α-acetylenic nitrofuran, from 5-nitro-2-furfural (I) according to a sequence of the following reactions:

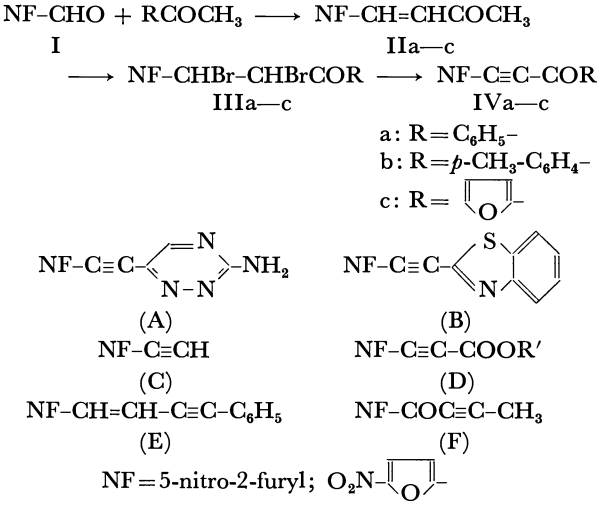

Since these α-acetylenic ketones belong to activated acetylenes,[7] several nucleophilic additions involving the 1,3-dipolar cycloaddition to amines were carried out.

Results and Discussion

Preparation of α-Acetylenic Ketones (IVa—c). In a previous paper,[8] we reported the synthesis and some reactions of the dibromide IIIa, in which we postulated the intermediacy of 2-(5-nitro-2-furyl)-1-benzoylacetylene (IVa) in the preparation of 3-(5-nitro-2-furyl)-5-phenyl-1*H*,2-pyrazole from IIIa and hydrazine hydrate. To verify this assumption, IIIa was treated in benzene with triethylamine at room temperature to afford IVa as expected. Similar treatments were applied to other dibromides IIIb,c and all afforded the corresponding acetylenic ketones IVb,c in good yields. The yields, spectral data and analyses are summarized in Table 1. The presence of a triple bond in IV is demonstrated by the appearance of $\nu_{C\equiv O}$ at 2260—2280 cm^{-1} in the IR spectra and by the hypsochromic shifts of the UV spectra from the corresponding double bonded compounds as observed by a comparison of IVb with IIb (see Experimental). Another IR spectral feature is observed in comparison of $\nu_{C=O}$; $\nu_{C=O}$ in IVb at 1620 cm^{-1} is 45—35 cm^{-1} lower in wave number than the α,β-unsaturated ketones (1675 cm^{-1}) and IIb (1655 cm^{-1}).

Simple Amine Addition. Amines are known to add most easily to the polarized triple bond in α-acetylenic ketones and secondary amines add exclusively *cis* to the acetylenes to give *trans* products in aprotic solvents,[9]

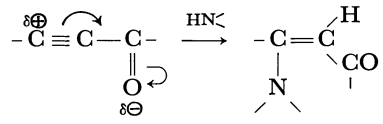

1) Part LI of this series: T. Sasaki, K. Kanematsu, and A. Kakehi, submitted to *J. Org. Chem.*

2) I. Saikawa, S. Takano, and T. Maeda, *Yakugaku Zasshi*, **87**, 1514 (1967).

3) S. Yoshina, I. Maeba, and K. Asai, *ibid.*, **88**, 984 (1968).

4) T. Sasaki and K. Shoji, *Yuki Gosei Kagaku Kyokai Shi*, **26**, 264 (1968).

5) H. Saikachi and H. Sugimoto, The Annual Meeting of the Pharmaceutical Association of Japan, D-155, Abstract, p. 103 (1966).

6) H. Saikachi, H. Ogawa, N. Shimojo, and K. Uehara, The Annual Meeting of the Pharmaceutical Association of Japan, 6p10-2, Abstract, p. 240 (1969).

7) E. Winterfeldt, *Angew. Chem. Intern. Ed.*, **6**, 423 (1967); T. F. Rutledge, "Acetylenes and Allenes," Rheinhold, New York (1969), pp. 232—271.

8) T. Sasaki and T. Yoshioka, *Yuki Gosei Kagaku Kyokai Shi*, **28**, 647 (1970).

9) C. H. Mullen and C. J. M. Stirling, *J. Chem. Soc., B*, **1966**, 1217.

Table 1. 2-(5-Nitro-2-furyl)-1-arylacetylenes (IVa—c)

Compound	Mp °C	Yield %	IR (KBr) cm^{-1} $\nu_{C\equiv C}$	IR (KBr) cm^{-1} ν_{CO}	UV λ_{max}^{EtOH} mμ	UV λ_{max}^{EtOH} (ε)	Found (Calcd) C%	H%	N%
IVa	142—144	80	2280	1625	278	(11500)	64.68	3.09	5.70
					326	(20400)	(64.73	2.93	5.81 for $C_{13}H_7O_4N$)
IVb	146—148	98	2260	1620	280	(15300)	65.63	3.66	5.47
					328	(23800)	(65.88	3.55	5.49 for $C_{14}H_9O_4N$)
IVc	226—227	70	2260	1615	230	(7400)	57.28	2.43	5.87
					300	(14800)	(57.15	2.18	6.06 for $C_{11}H_5O_5N$)
					334	(19500)			

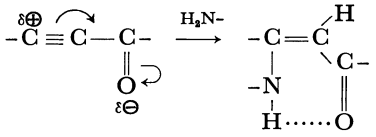

while primary amines do *trans*.[10]

Addition of aniline to IVa was carried out in benzene at room temperature to afford Va; the similarity of its IR and NMR spectral patterns to those of β-benzylamino-5-nitro-2-furfurylidenebenzophenone (G)[8] indicates that both compounds take *cis*-configuration by the *trans*-addition, forming intramolecular hydrogen bonding structure.[10] Since 1-cyclohexyl-2-(*p*-nitrophenyl)-3-benzoylaziridine (H)[11] is prepared from 2,3-dibromo-3-phenyl-*p*-nitropropiophenone and cyclohexylamine, IIIa was treated with cyclohexylamine. However, the product was shown to be not aziridine but β-cyclohexylamino-5-nitro-2-furfurylidenebenzophenone (VIa) by spectral inspection, as in the reaction with aniline.[8] Compound VIa was prepared also by addition of cyclohexylamine to IVa.

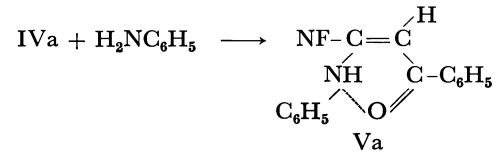

Va

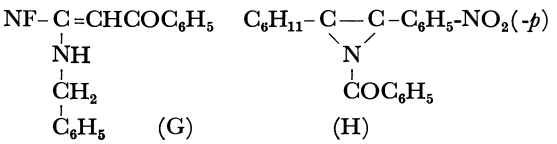

(G) (H)

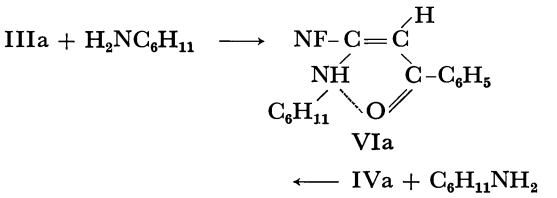

VIa

IVa + $C_6H_{11}NH_2$

Heterocyclic Preparation. Acetylenic ketones are good starting materials for synthesizing heterocycles such as isoxazoles and pyrazoles, which have been prepared from hydroxylamine[12] and hydrazine hydrate,[13] respectively. IVa,b were treated with hydroxylamine and hydrazine hydrate to give the expected corresponding isoxazoles (VIIa,b) and pyrazoles (VIIIa, b), respectively. Furthermore, when treated with semicarbazide, IVa,b afforded 1-carbamidopyrazoles (IXa, b) and with benzamidine, IVa,b yielded 2,4,6-trisubstituted pyrimidines (Xa,b), which provide a new method for the preparation of pyrimidines.

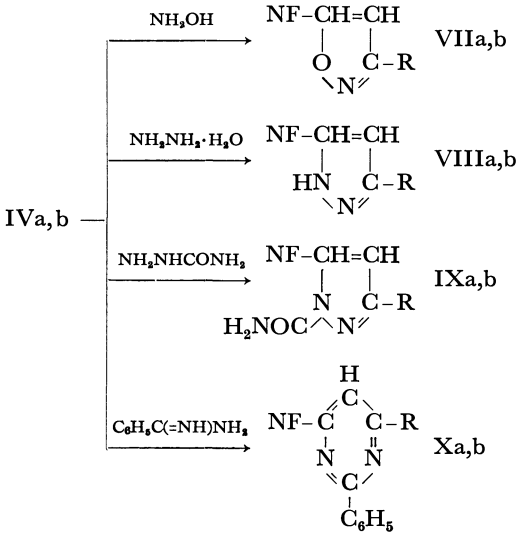

The mechanism for the formation of these heterocycles is explained by the initial Michael addition to the triple bond of IV, followed by condensation-cyclization.

1,3-Dipolar Cycloaddition as Dipolarophiles. In spite of abundant information on the cycloaddition of dimethyl acetylenedicarboxylate to several dipoles, there are few reports in literature describing similar reactions of α-acetylenic ketones; they involve the formation of benzo[*b*]furan from 1-phenyl-2-benzoylacetylene and 3,4,5,6-tetrachlorobenzene-2-diazo-1-oxide,[14] of pyrrole from 1-phenyl-2-acylacetylene and *N*-phenyl-*C*-methylsydnone,[15] and of spiroheterocycles from acylacetylene and formamidinium carbodithioates.[16] An example of the Diels-Alder reaction of 1-phenyl-2-acetylacetylene with butadiene has been reported.[17]

10) R. Huisgen, K. Herbig, and H. Huber, *Chem. Ber.*, **99**, 2526 (1966).
11) J. W. Lown, G. Dallas, and T. W. Malony, *Can. J. Chem.*, **47**, 3557 (1969).
12) C. Moureu and M. Brachin, *Bull. Soc. Chim. Fr.*, **31**, 343 (1904).
13) K. Boden and E. R. H. Jones, *J. Chem. Soc.*, **1946**, 953.
14) R. Huisgen, G. Binsch, and H. Koenig, *Chem. Ber.*, **97**, 2884 (1964).
15) R. Huisgen, *Angew. Chem.*, **74**, 29 (1962).
16) H. Behringer and J. Falkenberg, *Tetrahedron Lett.*, **1967**, 1895.
17) D. Nightingale and F. Wadsworth, *J. Amer. Chem. Soc.*, **67**, 416 (1945).

Huisgen[18] and Quilico and Speroni[19] reported isoxazole formation by the 1,3-dipolar cycloaddition of the nitrile oxides with simple acetylenes, but not with α-acetylenic ketones. IVa was therefore treated in benzene at room temperature with benzonitrile oxide prepared '*in situ*' from benzhydroxamoyl chloride and triethylamine. Column chromatography afforded 50% yield of isoxazole (XIa) together with 30% yield of side-produced furoxan. The structure of XIa was tentatively assigned as 3-phenyl-4-benzoyl-5-(5-nitro-2-furyl)-isoxazole in view of the general tendency for the direction of addition occurring at a sterically less hindered position[20] and from consideration of the electron density in IVa.[21] When 5-nitro-2-furocarbonitrile oxide was used instead of benzonitrile oxide under similar conditions, most of IVa was recovered with a small amount of furoxan, but the thermal 1,3-dipolar cycloaddition of IVa,b to the dipole afforded isoxazoles (XIIa,b) with some recovery of IVa,b. For comparison with IVa, the 1,3-dipolar cycloaddition of IIa,b with benzonitrile oxide was carried out, since Quilico[22] reported the synthesis of isoxazoline-4-ketone from α-ethylenic ketones and nitrile oxides:

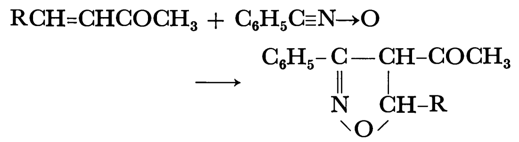

IIa was treated with benzonitrile oxide in benzene at room temperature. Chromatography afforded two crystalline products, XIIIa and XIVa, together with furoxan and some recovery of IIa. For the sake of comparison, 5-nitro-2-furfurylideneacetone was treated similarly to give also two crystalline products, XV and XVI, together with furoxan and some recovery of the starting material. From our analyses and Quilicos' results,[22] we tentatively assigned 3-phenyl-4-acetyl-5-(5-nitro-2-furyl)isoxazole for the major product XV and 3-phenyl-4-(5-nitro-2-furyl)-4-acetylisoxazole for the minor product XVI, and similarly, 3-phenyl-4-benzoyl-5-(5-nitro-2-furyl)isoxazole for the major product XIIIa and 3-phenyl-4-(5-nitro-2-furyl)-5-benzoylisoxazole for the minor product XIVa. The IR spectra of XIIIa and XIVa resembled each other as did those of XV and XVI.

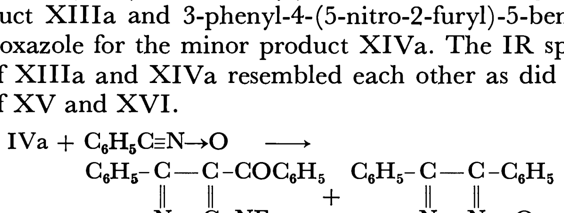

XIa

18) R. Huisgen, *Angew. Chem.*, **75**, 604 (1963).

19) A. Quilico and G. Speroni, "Five-and Six-membered Compounds," in "The Chemistry of Heterocyclic Compounds," A. Weissberger ed., Vol. 17, Wiley-Interscience, New York (1962), p. 18.

20) R. Huisgen, *J. Org. Chem.*, **33**, 2291 (1968).

21) It is reasonably assumed that the same carbon position is initially attacked by the oxygen of the nitrile oxide, where addition of amines takes place:

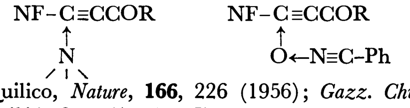

22) A. Quilico, *Nature*, **166**, 226 (1956); *Gazz. Chim. Ital.*, **80**, 831 (1950); *ibid.*, **85**, 1271 (1955).

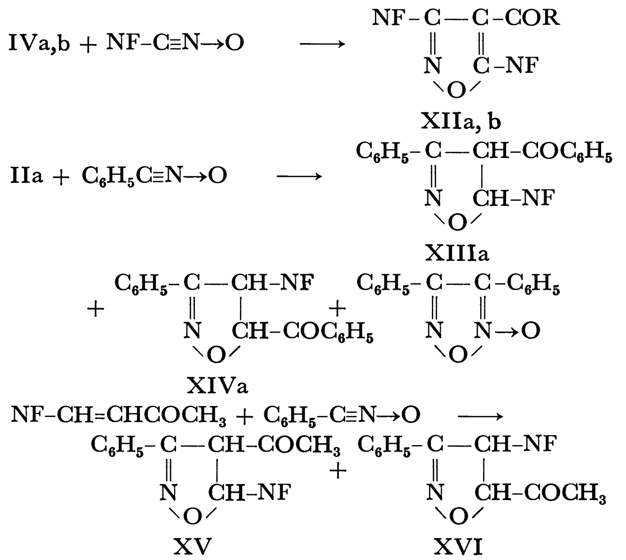

XIIa, b; XIIIa; XIVa; XV; XVI

For investigating the Diels-Alder reactivity, IVb was treated with butadiene and cyclopentadiene; heating both components in a sealed tube fused with nitrogen at 120°C for 15 hr afforded both intractable tars and with 70% recovery of the starting material in the former reaction.

Another type of 1,3-dipolar cycloaddition reaction has been reported on heterocyclic zwitterions with diethyl acetylenedicarboxylate and ethyl propiolate,[23] and cyanoacetylenes with heterocyclic *N*-ylides and *N*-imines.[24]

Treatment of IVa,b with phenacylpyridinium ylide at room temperature in benzene afforded 73 and 67% yields of XVIIa and XVIIb, respectively. The structural elucidation of XVIIa was carried out in comparison with our previous report.[24] As shown in Fig. 1, quartets centered at 0.40 τ and 1.90 τ are assignable to pyridine ring protons at C_5 and C_8, the lower field shifts being accounted for the anisotropy effect of neighboring carbonyl groups.[24] The higher field shifts of furan ring protons at 3.41 τ and 3.85 τ compared with those of the general nitrofuran derivatives[25] could be explained by the anisotropy effect of the neighboring carbonyls. Thus, the structure of XVIIa was determined as 1-benzoyl-2-(5-nitro-2-furyl)-3-benzoylpyrrocoline.

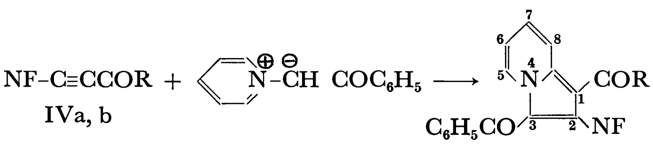

IVa, b

XVIIa,b

Experimental

Melting points were measured with a Yanagimoto micro-melting point apparatus and are uncorrected. Microanalyses

23) For a recent review, see V. Boekelheide and N. A. Fedoruk' *J. Org. Chem.*, **33**, 2062 (1969) and refs. therein.

24) T. Sasaki, K. Kanematsu, and Y. Yukimoto, *J. Chem. Soc., C*, **1970**, 481.

25) T. Sasaki, S. Eguchi, and A. Kojima, This Bulletin, **41**, 1568 (1968); *J. Heterocyclic Chem.*, **5**, 243 (1968); T. Sasaki and T. Yoshioka, This Bulletin, **41**, 2212 (1968); *ibid.*, **42**, 258 (1969).

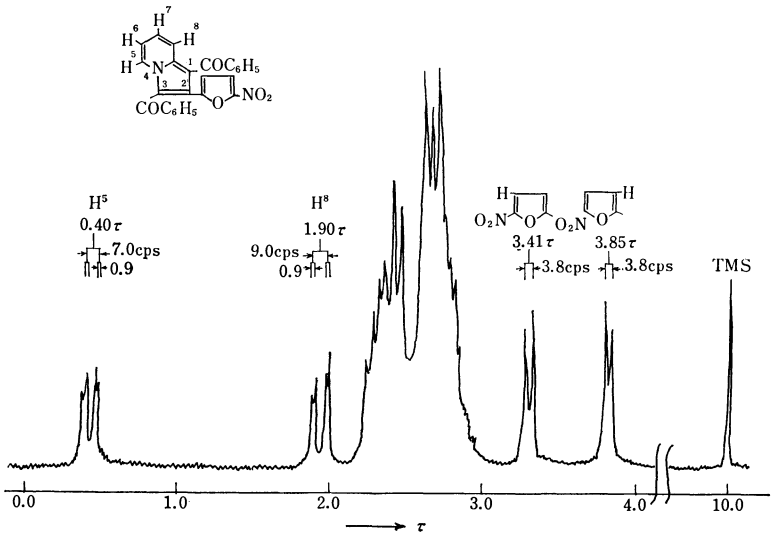

Fig. 1. NMR Spectra of XVIIa.

were performed on a Perkin Elmer 120 elemental analyzer. The NMR spectra were taken with a Jeolco Model JNM-MH-60 NMR spectrometer and with a Varian A-60 recording spectrometer with tetramethylsilane as an internal standard. The chemical shifts are expressed in τ-values. The IR spectra were taken with a JASCO Model IR-S spectrometer and the UV spectra with a JASCO rotary dispersion recorder, Model ORD/UV-5.

Condensation of Nitrofurfural with Aromatic Ketones. Differing from our previous work,[8] concentrated sulfuric acid was used as a condensation reagent as follows: To a solution of 1.4 g (10 mmol) of nitrofurfural and 1.4 g (10 mmol) of *p*-methylacetophenone in 20 m*l* of glacial acetic acid was added 2 m*l* of concentrated sulfuric acid with stirring and the mixture was stirred at 40°C for 1 day. The precipitated crystals were filtered and recrystallized from ethanol to give 1.3 g (45%) of IIb, mp 166—168°C, as pale yellow needles. IR (KBr) cm^{-1}: 1655 (CO) and 1610 (C=C). UV λ_{max}^{EtOH} mμ (ε): 296 (13100) and 348 (23100).

Found: C, 65.14; H, 4.38; N, 5.34%. Calcd for $C_{14}H_{11}O_4N$: C, 65.36; H, 4.31; N, 5.45%.

IIa was prepared similarly in a 50% yield, mp 144°C (lit,[8] 144°C). IIc was prepared by the method of Saikachi and Matsuno.[26]

Preparation of IIIa—c. IIIb,c were prepared similarly to IIIa.[8] IIIb: Yield, 98%, mp 172—174°C. IR (KBr) cm^{-1}: 1680 (CO). UV λ_{max}^{EtOH} mμ (ε): 266 (16100) and 298 (14000).

Found: C, 40.31; H, 2.69; N, 3.18%. Calcd for $C_{14}H_{11}O_4NBr_2$: C, 40.31; H, 2.66; N, 3.36%.

IIIc: Yield, 85%, mp 165—168°C. IR (KBr) cm^{-1}: 1680 (CO). UV λ_{max}^{EtOH} mμ (ε): 242 (13700) an 288 (17800).

Found: C, 33.57; H, 1.81; N, 3.33%. Calcd for $C_{11}H_7O_5NBr_2$: C, 33.70; H, 1.54; N, 3.57%.

Acetylenic Ketones (IVa—c). IVa was prepared as follows: To a stirred solution of 3.0 g (7.5 mmol) of IIIa in 100 m*l* of dry benzene was added a solution of 3 g (30 mmol) of triethylamine in 20 m*l* of dry benzene at room temperature. The mixture was stirred at room temperature for 1 day. After removing 2.5 g of triethylamine hydrobromide, the filtrate was concentrated. The residue was recrystallized from ethanol to give IVa. The yield, spectral data and analyses are given in Table 1. Similarly, IVb and IVc were prepared from IIIb and IIIc after 2 days' strring at room temperature. The results are summarized in Table 1.

Adition of Aniline to IVa. To a stirred solution of 0.4 g (1.65 mmol) of IVa in 50 m*l* of dry benzene was added a solution of 0.2 g (2.2 mmol) of aniline in 20 m*l* of dry benzene at room temperature. After 2 days' stirring at room temperature, the solvent was removed and the residue was recrystallized from ethanol to give 0.5 g (90%) of Va as yellow crystals, mp 141—143°C. IR (KBr) cm^{-1}: 1620 (CO). UV λ_{max}^{EtOH} mμ (ε): 314 (21000) and 390 (15200). NMR ($CDCl_3$)τ: −1.2 (NH), 2.0—3.0 (m, 12H, phenyl and nitrofuran ring protons), and 3.65 (s, 1H, =CH–).

Found: C, 67.85; H, 4.26; N, 8.15%. Calcd for $C_{19}H_{14}O_4N_2$: C, 68.25 H, 4.22; N, 8.38%.

β-Cyclohexylamino-5-nitro-2-furfurylidenebenzophenone (VIa). To a stirred and ice-cooled solution of 1 g (2.5 mmol) of IIIa in 50 m*l* of dry benzene was added a solution of 1.5 g (15 mmol) of cyclohexylamine in 20 m*l* of dry benzene. The solution was stirred at room temperature overnight. The solvent was removed and the residue was chromatographed on a silica-gel column using chloroform as an eluent. The first fraction afforded 0.4 g (47%) of VIa, mp 96—97°C, as red crystals (ethanol-petroleum ether). IR (KBr) cm^{-1}: 1610 (CO). UV λ_{max}^{EtOH} mμ (ε): 306 (14000) and 400 (12600). NMR ($CDCl_3$)τ: −1.3 (NH), 2.0—3.0 (m, 7H, phenyl and nitrofuran ring protons), 3.88 (s, 1H, =CH–), and 7.9—8.8 (m, 11H, cyclohexane ring protons).

Found: C, 67.39; H, 5.98; N, 8.06%. Calcd for $C_{19}H_{20}O_4N_2$: C, 67.04; H, 5.92; N, 8.23%.

The same compound was prepared quantitatively from IVa and cyclohexylamine by the same procedure as in the addition of aniline to IVa.

3-Phenyl-5-(5-nitro-2-furyl)isoxazole (VIIa). A mixture of 0.25 g (1 mmol) of IVa, 0.2 g (3 mmol) of hydroxylamine hydrochloride and 20 m*l* of ethanol was refluxed for 12 hr. After cooling, the resulting precipitates were filtered and recrystallized from ethanol to give 0.1 g (40%) of VIIa, mp 198—200°C, which showed mixed melting point depression with 3-(5-nitro-2-furyl)-5-phenylisoxazole.[27] IR (KBr) cm^{-1}: 1620 (C=N). UV λ_{max}^{EtOH} mμ (ε): 230 (18600) and 330 (14200). NMR ($CDCl_3$) τ: 2.0—2.8 (m, 7H, phenyl and nitrofuran ring protons) and 2.86 (s, 1H, isoxazole C_4-H).

Found: C, 61.18; H, 3.33; N, 11.02%. Calcd for $C_{13}H_8O_4N_2$: C, 60.94; H, 3.15; N, 10.93%.

26) H. Saikachi and J. Matsuno, *Yakugaku Zasshi*, **89**, 1622 (1969),

27) T. Sasaki and T. Yoshioka, This Bulletin, **40**, 2604 (1967).

3-(p-Methylphenyl)-5-(5-nitro-2-furyl)isoxazole (VIIb). Under similar treatment, IVb afforded 35% yield of VIIb, mp 205—207°C (ethanol). IR (KBr) cm^{-1}: 1615 (C=N). UV λ_{max}^{EtOH} mμ (ε): 232 (19000) and 332 (15000). NMR ($CDCl_3$) τ: 2.1—2.8 (m, 6H, phenyl and nitrofuran ring protons), 2.90 (s, 1H, isoxazole C_4-H), and 7.57 (s, CH_3).

Found: C, 61.76; H, 3.74; 10.14%. Calcd for $C_{14}H_{10}O_4N_2$: C, 62.22; H, 3.73; N, 10.37%.

5-(5-Nitro-2-furyl)-3-phenyl-1H,2-pyrazole (VIIIa). To a stirred solution of 0.3 g (1.25 mmol) of IVa in a mixture of 20 m*l* of benzene and 20 m*l* of ethanol was added a solution of 0.15 g (4 mmol) of 80% hydrazine hydrate in 10 m*l* of ethanol under ice-cooling. The mixture was stirred at room temperature for 2 days. The solvents were removed and the residue was treated with 20 m*l* of water. The insoluble part was filtered and recrystallized from benzene-ethanol to give 95% yield of VIIIa, mp 227°C (lit,[8] mp 225—228°C).

5-(5-Nitro-2-furyl)-3-p-methylphenyl-1H,2-pyrazole (VIIIb). Similar treatment afforded 97% yield of VIIIb, mp 241—243°C (ethanol-benzene). IR (KBr) cm^{-1}: 3180 (NH). NMR (DMSO-d_6) τ: −2.8 (NH), 2.70 (s, 1H, pyrazole C_4-H), and 7.65 (s, CH_3).

Found: C, 62.41; H, 4.28; N, 15.53%. Calcd for $C_{14}H_{11}O_3N_2$: C, 62.45; H, 4.12; N, 15.61%.

1-Carbamido-3-phenyl-5-(5-nitro-2-furyl)pyrazole (IXa). A mixture of 0.4 g (1.65 mmol) of IVa, 0.3 g (2.7 mmol) of semicarbazide hydrochloride and 25 m*l* of ethanol was refluxed for 11 hr. The solvent was removed and the residue was treated with 30 m*l* of water. The insoluble part was filtered and recrystallized from ethanol-benzene to give 0.3 g (54%) of IXa, mp 215—216°C, as pale yellow needles. IR (KBr) cm^{-1}: 3380, 3250 (NH) and 1660 (CO). NMR (DMSO-d_6) τ: 0.20 (broad s, 1H, HCl), 2.1—2.7 m, 7H, phenyl and nitrofuran ring protons, 2.66 (s, 1H, pyrazole C_4-H), and 3.4 (broad, 2H, NH_2, disappeared on deuteration).

Found: C, 50.07; H, 3.35; N, 17.02%. Calcd for $C_{14}H_9O_4N_4HCl$: C, 50.39; H, 3.02; N, 16.79%.

1-Carbamido-3-p-methylphenyl-5-(5-nitro-2-furyl)pyrazole (IXb). Similar treatment afforded 60% yield of IXb, mp 224—228C°. IR (KBr) cm^{-1}: 3400, 3250 (NH), and 1660 (CO).

Found: C, 52.00; H, 3.86; N, 16.53%. Calcd for $C_{15}H_{12}O_4N_4HCl$: C, 51.66; H, 3.76; N, 16.07%.

2-Phenyl-4-phenyl-6-(5-nitro-2-furyl)pyrimidine (Xa). A mixture of 0.4 g (1.6 mmol) of IVa, 0.3 g (2 mmol) of benzamidine hydrochloride and 20 m*l* of ethanol was refluxed for 12 hr. After cooling, the resulting precipitates were filtered and recrystallized from ethanol-benzene to give 0.13 g (25%) of Xa, mp 213—215°C, as colorless needles. UV λ_{max}^{EtOH} mμ (ε): 260 (32000) and 328 (17000). NMR ($CDCl_3$) τ: 1.2—1.7 (m, 4H, phenyl protons), 1.97 (s, 1H, pyrimidine C_5-H), and 2.3—2.6 (m, 8H, phenyl and nitrofuran ring protons).

Found: C, 69.91; H, 3.94; N, 12.28%. Calcd for $C_{20}H_{13}O_3N_3$: C, 69.96; H, 3.82; N, 12.24%.

From the filtrate, 0.16 g (40%) of IVa was recovered by column chromatography on a silica-gel using chloroform as an eluent.

2-Phenyl-4-p-methylphenyl-6-(5-nitro-2-furyl)pyrimidine (Xb). Similar treatment of IVb and amidine afforded 20% yield of Xb, mp 220—223°C (ethanol-benzene). UV λ_{max}^{EtOH} mμ (ε): 264 (37000) and 330 (18400). NMR ($CDCl_3$) τ: 1.3—1.9 (m, 4H, phenyl protons), 2.08 (s, 1H, pyrimidine C_5-H), 2.4—2.7 (m, 7H, phenyl and nitrofuran protons), and 7.55 (s, CH_3).

Found: C, 70.56; H, 4.36; N, 11.71%. Calcd for $C_{21}H_{15}O_3N_3$: C, 70.58; H, 4.23; N, 11.76%.

3-Phenyl-4-benzoyl-5-(5-nitro-2-furyl)isoxazole (XIa). To a stirred solution of 0.6 g (2.5 mmol) of IVa and 0.4 g (2.6 mmol) of benzhydroxamoyl chloride in 50 m*l* of dry benzene was added a solution of 0.9 g (9 mmol) of triethylamine in 20 m*l* of dry benzene under ice-cooling. After stirring for 1 day at room temperature, the reaction mixture was filtered and the solvent was removed from the filtrate. The residue was chromatographed on a silica-gel column using benzene as an eluent. The first fraction afforded 0.1 g (30%) of furoxan, mp 115—116°C.[27] From the second fraction a small amount of oil was obtained, which was discarded without further investigation. The third fraction afforded the main product, 0.45 g (50%) of XIa, mp 135—138°C (ethanol). IR (KBr) cm^{-1}: 1655 (CO). UV λ_{max}^{EtOH} mμ (ε): 228 (20100), 250 (16200), and 328 (14000).

Found: C, 66.48; H, 3.48; N, 7.59%. Calcd for $C_{20}H_{12}O_5N_2$: C, 66.66; H, 3.36; N, 7.78%.

Thermal 1,3-Dipolar Cycloaddition of IVa,b to 5-Nitro-2-furocarbonitrile Oxide. A solution of 0.4 g (1.65 mmol) of IVa and 0.3 g (1.6 mmol) of 5-nitro-2-furohydroxamoyl chloride in 20 m*l* of toluene was refluxed for 20 hr until the hydrogen chloride gas evolution had completely ceased. After removing the solvent, the reside was chromatographed on a silica-gel column using chloroform as an eluent. The first fraction afforded 0.1 g (25%) of recovered IVa and the second fraction yielded 0.23 g (30%) of 3,5-di(5-nitro-2-furyl)-4-benzoylisoxazole (XIIa), mp 193—195°, (ethanol-benzene). IR (KBr)cm^{-1}: 1660 (CO). UV λ_{max}^{EtOH} mμ (ε): 250 (14000) and 322 (19000).

Found: C, 55.28; H, 2.44; N, 11.13%. Calcd for $C_{18}H_9O_7N_3$: C, 55.53; H, 2.39; N, 11.08%.

Similar treatment of IVb afforded 30% recovery of IVb and 20% yield of 3,5-di(5-nitro-2-furyl)-4-methylbenzoylisoxazole (XIIb), mp 191—193°C (ethanol-benzene). IR (KBr) cm^{-1}: 1655 (CO). UV λ_{max}^{EtOH} mμ (ε): 256 (16000) and 324 (19800).

Found: C, 55.90; H, 2.86; N, 10.15%. Calcd for $C_{19}H_{11}O_8N_3$: C, 55.75; H, 2.71; N, 10.27%.

1,3-Dipolar Cycloaddition of IIa to Benzonitrile Oxide. To a stirred solution of 0.55 g (2.3 mmol) of IIa and 0.4 g (2.6 mmol) of benzhydroxamoyl chloride in 40 m*l* of dry benzene was added a solution of 0.5 g (5 mmol) of triethylamine in 20 m*l* of dry benzene under ice-cooling. The mixture was stirred at room temperature for 1 day. After removing insoluble triethylamine hydrochloride by filtration, the solvent was removed from the filtrate. The residue was chromatographed on a silica-gel column using benzene as an eluent. The first fraction afforded 0.03 g (10%) of furoxan, mp 115°C.[27] From the following fractions, 0.03 g (4%) of XIVa, mp 118—120°C, 0.2 g (40%) of recovered IIa and 0.4 g (40%) of XIIIa, mp 196—197°C (ethanol-benzene) were obtained successively. The IR spectrum of XIVa was similar to that of XIIIa.

XIIIa: IR (KBr) cm^{-1}: 1675 (CO). UV λ_{max}^{EtOH} mμ (ε): 244 (21400) and 298 (10000). NMR ($CDCl_3$) τ: 1.8—2.7 (m, 11H, phenyl and nitrofuran ring[28] protons), 3.20 (d, 1H, J=4 Hz, 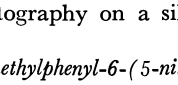) 4.10 (d, 1H, J=6 Hz, isoxazole C_5-H), and 4.28 (d, 1H, J=6 Hz, isoxazole C_4-H).

Found: C, 66.47; H, 4.03; N, 7.57%. Calcd for $C_{20}H_{14}O_5N_3$: C, 66.29 H, 3.89; N, 7.73%.

XIVa:

Found: C, 66.35; H, 3.99; N, 7.65%. Calcd for $C_{20}H_{14}O_5N_2$: C, 66.29; H, 3.89; N, 7.73%.

1,3-Dipolar Cycloaddition of 5-Nitro-2-furfurylideneacetone to Benzonitrile Oxide. From a similar treatment of 5-nitro-

28) One of two: 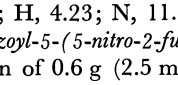

2-furfurylideneacetone[8] and benzonitrile oxide, 10% of furoxan, 10% of XVI, mp 60—62°C, and 40% of XV, mp 108—109°C (ethanol) were successively obtained. The IR spectrum of XV was similar to that of XVI.

XV: IR (KBr) cm^{-1}: 1705 (CO). UV λ_{max}^{EtOH} mμ (ε): 255 (15500) and 300 (15500). NMR (DMSO-d_6) τ: 2.2—2.6 (m, 6H, phenyl and nitrofuran[28] ring protons), 2.90 (d, 1H, J=4 Hz, 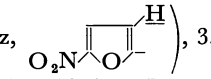), 3.76 (d, 1H, J=5 Hz, isoxazoline C_5-H), 4.51 (d, 1H, J=5 Hz, isoxazoline C_4-H), and 7.66 (s, CH_3).

Found: C, 59.85; H, 4.05; N, 9.29%. Calcd for $C_{15}H_{12}O_5N_2$: C, 60.00; H, 4.03; N, 9.33%.

XVI:

Found: C, 60.15; H, 3.95; N, 9.45%. Calcd for $C_{15}H_{12}O_5N_2$: C, 6.00; H, 4.05; N, 9.33%.

1-Benzoyl-2-(5-nitro-2-furyl)-3-benzoylpyrrocoline (XVIIa). To a stirred solution of 0.3 g (1.25 mmol) of IVa and 1 g (3.6 mmol) of phenacyl pyridinium bromide[29] in a mixture of 30 m*l* of benzene, 10 m*l* of water and 10 m*l* of ethanol was added 0.5 g (3.6 mmol) of powdered potassium carbonate under ice-cooling. The mixture was stirred at room temperature for 2 days. Water (20 m*l*) was added to the mixture and the mixture was extracted with benzene (3×50 m*l*). The benzene extracts were dried over sodium sulfate and benzene was removed from the extracts. The residue was chromatographed on a silica-gel column using chloroform as an eluent to give 0.4 g (73%) of XVIIa as yellow needles, mp 212—214°C (ethanol-benzene). IR (KBr) cm^{-1}: 1640 (CO). UV λ_{max}^{EtOH} mμ (ε): 230 (24000) and 340 (18000). NMR ($CDCl_3$) τ: 0.40 (dd, 1H, J=0.9, 7.0 Hz, C_5-H), 1.9 (dd, 1H, J=0.9, 9.0 Hz, C_8-H), 2.3—3.0 (m, 12H, phenyl (10H) and pyridine (2H) ring protons), 3.35 (d, 1H, J=4 Hz, 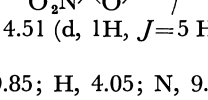) and 3.85 (d, 1H, J=4 Hz,).

Found: C, 71.74; H, 3.85; N, 6.24%. Calcd for $C_{26}H_{16}O_5N_2$: C, 71.56; H, 3.85; N, 6.42%.

1-p-Methylbenzoyl-2-(5-nitro-2-furyl)-3-benzoylpyrrocoline (XVIIb). Similar treatment afforded 70% yield of XVIIb as yellow needles, mp 195—197°C (ethanol-benzene). IR (KBr) cm^{-1}: 1640 (CO). UV λ_{max}^{EtOH} mμ (ε): 235 (23800) and 338 (20000). NMR ($CDCl_3$) τ: 0.42 (dd, 1H, J=0.9, 7.0 Hz, C_5-H), 2.02 (dd, 1H, J=0.9, 9 Hz, C_8-H), 2.4—3.1 (m, 11H, phenyl (9H) and pyridine (2H) protons), 3.35 (d, 1H, J=3.8 Hz, 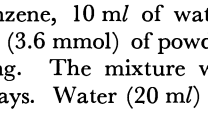), 3.80 (d, 1H, J=3.8 Hz,), and 7.73 (s, CH_3).

Found: C, 72.25; H, 4.13; N, 6.13%. Calcd for $C_{27}H_{18}O_5N_2$: C, 71.99; H, 4.03; N, 6.22%.

29) F. Kröhnke, *Chem. Ber.*, **68**, 1177 (1935).

BULLETIN OF THE CHEMICAL SOCIETY OF JAPAN, VOL. 44, 808—812 (1971)

Reactions of Haloferrocenes. IV.[1] The Condensation of Haloferrocenes with Various Carboxylic Acids in the Presence of Copper(I) Oxide

Masaru SATO, Yau Ping LAM, Izumi MOTOYAMA, and Kazuo HATA

Department of Chemistry, Faculty of Science, Tokyo Metropolitan University, Setagaya-ku, Tokyo

(Received August 21, 1970)

The condensation reaction of haloferrocenes with various carboxylic acids in the presence of copper(I) oxide was studied extensively. The reaction generally afforded the corresponding ferrocenyl carboxylates, along with a comparable amount of ferrocene. The change in the distribution of the reaction products was examined under various conditions in the reaction of bromoferrence with benzoic acid. From the discussion of the reaction mechanism, it was concluded that the ferrocenyl ester and ferrocene are produced through different active species. The reaction under proper conditions was found to be useful for the preparation of ferrocenyl esters.

The copper-catalyzed condensation reaction of halides with phenols or amines is well-known as a synthetic method of aryl ethers or arylamines.[2] However, a similar reaction of aryl halides with carboxylic acids to give aryl carboxylate has been little studied.[3] In a previous paper,[1] we reported that the reaction o haloferrocenes with copper(I) acetate in boiling pyridine gave ferrocenyl acetate; this result was different from that of aryl halides with copper(I) acetate. In this paper, the condensation reaction of haloferrocenes with various carboxylic acids in the presence of copper(I) oxide will be reported as an extension of the preceding study.

Results and Discussion

When iodoferrocene or bromoferrocene was refluxed with various carboxylic acids in the presence of copper(I) oxide in pyridine, the corresponding ferrocenyl carboxylates were obtained, together with a comparable amount of ferrocene. For example, when iodoferrocene was refluxed for half an hour with two equivalents of benzoic acid and one equivalent of copper(I) oxide in pyridine, ferrocenyl benzoate and ferrocene

1) Part III: M. Sato, I. Motoyama, and K. Hata, This Bulletin, **43**, 2213 (1970).

2) F. Ullmann, *Ber.*, **36**, 2383 (1903); F. Ullmann and P. Sponagel, *Ann.*, **350**, 83 (1906); F. Ullmann, *ibid.*, **355**, 312 (1907); F. Ullmann and C. Wagner, *ibid.*, **355**, 359 (1907).

3) J. Forrest, *J. Chem. Soc.*, **1960**, 581.

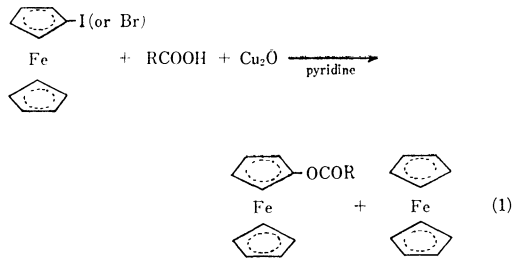

(1)

were obtained in 54% and 36% yields respectively. All the results of the reaction of iodoferrocene with the various carboxylic acids examined are summarized in Table 1. Biferrocenyl, which was obtained as a coupling product in the reaction of iodoferrocene with copper(I) acetate and benzoate, together with ferrocenyl carboxylate and ferrocene, was hardly detected at all. Especially, it was never found in the similar reaction of bromoferrocene.

Table 1. The condensation of iodoferrocene with various carboxylic acids in the presence of copper(I) oxide in pyridine

Molar ratio: iodoferrocene : carboxylic acid : copper(I) oxide = 1 : 2 : 1.
Reaction temp.: 116°C, Reaction time: 0.5 hr

Carboxylic acid	Iodoferrocene recovered (%)	Ferrocenyl ester (%)	Ferrocene (%)	Chloroferrocene (%)
p-$CH_3C_6H_4COOH$	5	47.2	35.9	
p-$CH_3OC_6H_4COOH$	29.6	30.9	34.2	
C_6H_5COOH	8.2	53.6	35.6	
p-ClC_6H_4COOH	8.5	51	27.5	
o-ClC_6H_4COOH	41.7	13.4	2.2	32.6
p-$CH_3COC_6H_4COOH$	28.8	38.1	35	
p-$NO_2C_6H_4COOH$	9.3	52.4	31.7	
o-$NO_2C_6H_4COOH$	14.9	52.0	25.1	
CH_3COOH	Trace	58.6	36.8	
CH_3CH_2COOH	1.3	54.8	34.8	
$ClCH_2COOH$	27.6	2.2[a]	31.1	38
Cl_3CCOOH	32.9	—	Trace	55.8
$C_6H_5CH=CHCOOH$	13.0	23.3	33.6	
$CH_3CH=CHCOOH$	—	41.6	44.6	

a) Ferrocenyl acetate was obtained instead of the expected chloroacetate.

As is shown in Table 1, ferrocenyl ester is a main product in most of the cases under the conditions employed. On the other hand, the corresponding reaction of 1-bromonaphthalene with acetic acid in boiling pyridine for 3 hr was reported to afford exclusively the dehalogenated product, *i.e.*, naphthalene, in a moderate yield.[4] Similarly, when *o*-nitrohalobenzene was boiled with benzoic acid in the presence of metallic copper, it was dehalogenated to give nitrobenzene.[5] The only example of the copper-catalyzed condensation, which afforded aryl carboxylate as a product, was reported as a side-reaction in the Ullmann coupling of substituted iodobenzene, using benzoic acid as the diluent.[3] The maximum yield of the aryl benzoate was reported to be 27%. The present results, shown in Table 1, are very different from those reported in the benzene series. This tendency is consistent with the fact that haloferrocene reacts easily with copper(I) acetate to give ferrocenyl acetate in a good yield,[1] while aryl halides react with the copper(I) salt to give only dehalogenated products.[4,6]

Variation in the carboxylic acid component seems to have no significant effect on the reaction and on the product distribution. The effect of the *para*-substituent of benzoic acid on the reaction is also not clear, and there is no appreciable difference in the reactivities between aromatic and aliphatic acids. These facts indicate that the reaction is not influenced by the dissociation constant of carboxylic acid. A double bond conjugated to the carboxyl group also appears to have no effect on this reaction. Although *o*-nitrobenzoic acid has been reported to be decarboxylated in the presence of copper(I) oxide at a high temperature,[7] no such decarboxylation product was found in the present reaction.

It was found, however, that the reaction was affected significantly by an α-halogen substituent of aliphatic acid or by an *ortho*-halogen substituent of benzoic acid. For instance, when iodoferrocene was refluxed with chloroacetic acid or trichloroacetic acid in the presence of copper(I) oxide in pyridine, the main product was not a corresponding ferrocenyl ester, but chloroferrocene. Similarly, the reaction of iodoferrocene with *o*-chlorobenzoic acid gave chloroferrocene as the main product, while the reaction with the *p*-isomer gave ferrocenyl *p*-chlorobenzoate and no chloroferrocene. A similar effect of the halogen substituent adjacent to the carboxyl group has been reported by Bacon and Hill[4] in the reaction of aryl halides with *o*-chlorobenzoic anhydride or chloroacetic anhydride.

It is quite interesting that the reaction of haloferrocene with any of carboxylic acids in the presence of copper(I) oxide produced a condensation product (ferrocenyl ester) together with a comparative amount of a dehalogenation product (ferrocene), whereas only dehalogenated products were obtained in the reaction of aryl halides under similar conditions. These facts inspired us to consider the mechanism of this condensation reaction. The reaction of haloferrocene with carboxylic acid in the presence of copper(I) oxide was considered to be suitable for examining the reaction mechanism, because it proceeds easily and gives good yields of the products. In the first place, the reaction between bromoferrocene and benzoic acid was investigated under various conditions. Whereas bromoferrocene reacted with benzoic acid when they were refluxed in the presence of copper(I) oxide in pyridine, no reaction occurred when bromoferrocene was treated either with copper(I) oxide or with benzoic acid alone in boiling pyridine. Therefore, it is reasonable to assume that benzoic acid initially reacts with copper(I) oxide to form a certain active species, which subse-

4) R. G. R. Bacon and H. A. O. Hill, *ibid.*, **1964**, 1112.
5) W. T. Smith, Jr., *J. Amer. Chem. Soc.*, **71**, 2855 (1949); W T. Smith, Jr., and L. Campanaro, *ibid.*, **75**, 3602 (1953).
6) W. G. H. Edwards and R. G. Stewart, *Chem. Ind.* (London), **1952**. 472.
7) M. Nilsson, *Acta Chem. Scand.*, **20**, 423 (1966).

Table 2. The influence of the molar ratio of the reaction components

Reaction temp.: 116°C, Reaction time: 0.5 hr
Bromoferrocene: 0.005 mol, Pyridine: 20 ml

Molar ratio of components			Distribution of products (%)		
FcBr	C_6H_5COOH	Cu_2O	FcBr	C_6H_5COOFc	FcH
1	1	0.5	54.9	23.5	20.4
1	2	1	23.0	34.6	40.9
1	3	1.5	3.0	36.6	56.0
1	4	2	—	35.3	62.4
1	1	0.5[a)]	44.4	32.7	21.5
1	2	0.5[a)]	46.6	27.4	24.7
1	4	0.5[a)]	56.3	13.7	18.3

a) Reaction time: 1.0 hr

quently reacts with bromoferrocene to give both the dehalogenation and the condensation products. This assumption is strongly supported by the results of the experiments listed in Table 2, in which the effect of the change in the molar ratio of the reaction components on the distribution of the products is summarized. The following facts are clearly shown in this table: (i) When the molar ratio of benzoic acid to copper(I) oxide is kept constant ($C_6H_5COOH/Cu_2O=2$) and when the molar ratio of the mixture to bromoferrocene is increased, the yields of both ferrocenyl benzoate and ferrocene increase; there is a particularly striking increase in the formation of ferrocene. (ii) When only the ratio of benzoic acid to the other components is increased, the yields of both products rather decrease. The latter fact seems to strongly support the assumption presented above.

Table 3. The reaction of various haloferrocenes with benzoic acid in the presence of copper(I) oxide in pyridine

Haloferrocene: 0.005 mol, Benzoic acid: 0.01 mol
Copper(I) oxide: 0.005 mol, Pyridine: 20 ml
Reaction temp.: 116°C, Reaction time: 0.5 hr

Haloferrocene	Haloferrocene recovered (%)	Ferrocenyl benzoate (%)	Ferrocene (%)
Iodoferrocene	8.2	53.6	35.6
Bromoferrocene	23.0	34.6	40.9
Chloroferrocene	92.5	2.6	2.4

The influence of the kind of halogen in haloferrocenes on the reaction was also studied; the results are shown in Table 3. It is clear from Table 3 that the reactivity of haloferrocene is in the order: FcI> FcBr>FcCl, an order which is similar to that in the reaction of haloferrocene with various copper(I) salts,[1,8)] and that the product distribution is also influenced by the kind of the halogen. Iodoferrocene produced predominantly ferrocenyl benzoate over ferrocene. The reaction of bromoferrocene seems to be somewhat favorable to the formation of ferrocene. As for chloroferrocene, comparable yields of both products were obtained, but the comparison of the yields seems to be of little significance because of the low reactivity of chloroferrocene.

8) M. Sato, T. Ito, I. Motoyama, K. Watanabe, and K. Hata, This Bulletin, **42**, 1976 (1969).

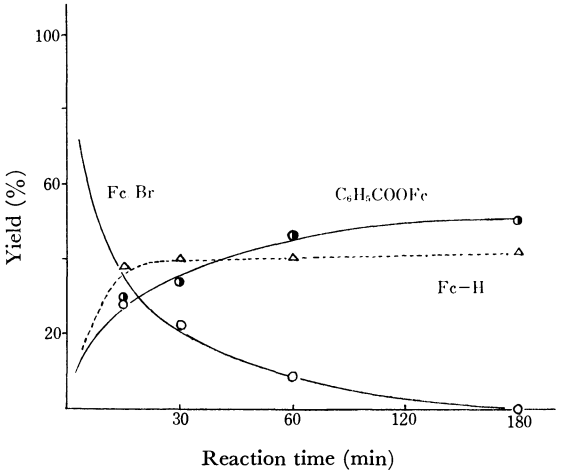

Fig. 1. The plot of the product distribution against reaction time.

It will be useful, in examining the reaction mechanism, to follow the change in the product distribution of this reaction with the lapse of the reaction time. Thus, the product distribution in the reaction of bromoferrocene with benzoic acid in the presence of copper(I) oxide in boiling pyridine was plotted against the reaction time (Fig. 1). As is shown in Fig. 1, (i) ferrocene and ferrocenyl benzoate are formed competitively in the initial stage; (ii) the formation of ferrocene is faster than that of ferrocenyl benzoate in the beginning of the reaction, but it ceases after about 30 min; (iii) the formation of the benzoate gradually increases as the reaction proceeds. The facts described above suggest unequivocally that ferrocene and ferrocenyl benzoate are produced independently through the reaction of bromoferrocene with different active species, not through an step-by-step mechanism in which one of the products is formed initially and then reacts with an active species to give the other. The more likely mechanism that the formation of ferrocene precedes that of ferrocenyl benzoate is also excluded by the fact that ferrocenyl benzoate was never obtained when ferrocene refluxed with benzoic acid and copper(I) oxide in pyridine. It is plausible, from an examination of Table 2, to conclude that the active species which affords ferrocenyl benzoate is probably copper(I) benzoate-pyridine complex, because copper(I) benzoate can be formed through the reaction of benzoic acid with copper(I) oxide in the reaction mixture.

$$2C_6H_5COOH + Cu_2O \longrightarrow 2C_6H_5COOCu + H_2O \quad (2)$$

$$C_6H_5COOCu \xrightarrow[\text{pyridine}]{} C_6H_5COOCu\text{-}Py_n$$

Since the formation of a coupling product (biferrocenyl) was never observed in this reaction, the formation of ferrocenyl benzoate seems unlikely to be through a radical mechanism. Furthermore, the radical mechanism may be excluded by the fact that, as is shown in Table 2, the formation of ferrocene does not increase even when the molar ratio of ben-

Table 4. Effect of the additional material
Bromoferrocene: 0.005 mol, Copper(I) benzoate: 0.01 mol, Annex: 0.01 mol, Pyridine: 20 ml
Reaction temp.: 116°C, Reaction time: 0.5 hr

Reaction	Annex	Product (%)		
		FcBr	C_6H_5COOFc	FcH
FcBr+C_6H_5COOH+Cu_2O[a]		23.0	34.6	40.9
FcBr+C_6H_5COOCu		11.3	62.8	2.5
FcBr+C_6H_5COOCu	H_2O	7.5	49.7	39.8
FcBr+C_6H_5COOCu	CH_3OH	—	49.7	34.4

a) Benzoic acid: 0.01 mol, Cu_2O: 0.005 mol

zoic acid as a hydrogen donor increase. Therefore, the formation of ferrocenyl benzoate is probably due to a mechanism similar to that of the reaction of haloferrocene with copper(I) benzoate in pyridine, which was reported in the preceding paper.[1]

On the other hand, the explanation of the formation of ferrocene is not yet clear, although the following considerations are possible on the basis of the results of the experiments shown in Table 4. Benzoic acid must be responsible for the formation of ferrocene, because the latter could be scarcely found at all in the reaction product when copper(I) benzoate was used instead of benzoic acid and copper(I) oxide. However, it was found that, when water or methanol was added as a hydrogen donor to the reaction of bromoferrocene with copper(I) benzoate in pyridine, the formation of ferrocene was comparable to that in the reaction using benzoic acid and copper(I) oxide. These observations support the assumption that the source of hydrogen for the formation of ferrocene in this reaction is the acidic hydrogen of benzoic acid. The acid probably reacts with copper(I) oxide to produce water through Eq. (2), and the water would react with haloferrocene through some participation in the formation of an active species such as a copper(I) complex.

Table 5. Solvent effect
Bromoferrocene: 0.005 mol, Benzoic acid: 0.01 mol
Copper(I) oxide: 0.005 mol, Solvent: 20 ml
Reaction time: 1.0 hr

Solvent	Reaction temp. (°C)	FcBr recovered (%)	Product	
			C_6H_5COOFc	FcH
Pyridine	116	9.0	47.0	40.9
Acetonitrile	82	—	89.4	8.2
Nitromethane	101	9.1	86.0	3.2
Toluene	110	28.8	42.0	26.9

Pyridine was supposed to act not only as a solvent but also as a ligand coordinating to the copper(I) salt which is formed by the reaction of benzoic acid with copper(I) oxide. Accordingly, in order to examine the role of pyridine in this reaction, the reaction was studied in other solvents; the results are summarized in Table 5. As is shown in Table 5, when the reaction was carried out in acetonitrile or nitromethane the condensation product (ferrocenyl ester) was formed in an extraordinarily high yield in place of a low yield of the dehalogenation product (ferrocene). This trend is more striking in the latter solvent. Thus, the condensation reaction in these solvents is suitable for the preparation of ferrocenyl esters. The participation of pyridine in the formation of ferrocene is obvious in Table 5. The special behavior of pyridine in this reaction is probably due to the basicity and the coordination ability of pyridine. The formation of ferrocene may be effected by the reaction of haloferrocene with a certain active species formed by the addition of water (or methanol) to the copper(I) benzoate-pyridine complex, which is expected to exist in the reaction mixture.

On the other hand, ferrocene is also obtained in a considerable amount by the reaction using toluene as a solvent. However, it seems reasonable to consider that the reaction in toluene may proceed through a different mechanism, since the product distribution is considerably different from that by the reaction using pyridine; in the previously-reported reaction between bromoferrocene and copper(I) benzoate,[1] the product distribution by the reaction using toluene as a solvent was also quite different from that by the reaction using pyridine.

Experimental

The Procedure for the Preparation of Ferrocenyl Carboxylates. Ferrocenyl Benzoate: Iodoferrocene (1.56 g, 0.005 mol), benzoic acid (1.22 g, 0.01 mol) copper(I) oxide (0.72 g, 0.005 mol), and 20 ml of pyridine were placed in a 100-ml, three-necked, round-bottomed flask fitted with a mechanical stirrer, a reflux condenser, and a gas-inlet tube. The mixture in the flask was refluxed on an oil bath maintained at 120—125°C for 0.5 hr under an atmosphere of nitrogen. After the reaction had been completed, 80 ml of ether was added to the cooled reaction mixture. The dark blue precipitate was separated by filtration and washed with a small portion of ether. The combined ether solution was washed successively with water, dilute hydrochloric acid, and water, and then dried over anhydrous magnesium sulfate. After the removal of the solvent under reduced pressure, the orange residue was chromatographed on silica gel, using *n*-hexane - benzene (1 : 1) as the eluent. The first fraction gave orange crystals (0.46 g), which were found to be a mixture of ferrocene (0.33 g, 35.6%) and iodoferrocene (0.13 g, 8.2%) by a gas-chromatographic analysis.[9] From the second fraction of the chromatography, ferrocenyl benzoate (0.82 g, 53.6%) was obtained; it was recrystallized from *n*-hexane - benzene (1 : 1), mp 108.5—109.5°C (lit,[11] 108.5—109.5°C).

The other ferrocenyl esters, listed in Table 1, were similarly prepared by the reaction of iodoferrocene with various carboxylic acids in the presence of copper(I) oxide in boiling pyridine. The analytical data of the ferrocenyl esters thus obtained are as follows:

Ferrocenyl *p*-methoxybenzoate, mp 107.2—107.8°C. Found: C, 64.47; H, 4.91%. Calcd for $C_{18}H_{16}O_3Fe$: C, 64.30; H, 4.81%.

Ferrocenyl *p*-methylbenzoate, mp 94.5—95.5°C. Found:

9) The analytical conditions for the gas-chromatographic analysis were the same as those reported in a previous paper.[10]

10) M. Sato, I. Motoyama, and K. Hata, *ibid.*, **43**, 1860 (1970).

11) A. N. Nesmeyanov, V. A. Sazonova, and V. N. Drozd, *Chem. Ber.*, **93**, 2717 (1960).

C, 67.97; H, 5.02%. Calcd for $C_{18}H_{16}O_2Fe$: C, 67.51; H, 5.05%.

Ferrocenyl *p*-chlorobenzoate, mp 109—110.5°C. Found: C, 60.09; H, 3.95%. Calcd for $C_{17}H_{13}O_2ClFe$: C, 59.94; H, 3.85%.

Ferrocenyl *o*-chlorobenzoate, orange liquid. Found: C, 61.49; H, 3.99%. Calcd for $C_{17}H_{13}O_2ClFe$: C, 59.94; H, 3.85%.

Ferrocenyl *p*-acetylbenzoate, mp 141—142°C. Found: C, 65.73; H, 4.60%. Calcd for $C_{19}H_{16}O_3Fe$: C, 65.53; H, 4.64%.

Ferrocenyl *p*-nitrobenzoate, mp 184—185°C. Found: C, 58.09; H, 3.89; N, 3.99%. Calcd for $C_{17}H_{13}O_4NFe$: C, 58.14; H, 3.74; N, 3.99%.

Ferrocenyl *o*-nitrobenzoate, mp 115—116°C. Found: C, 58.42; H, 3.89; N, 4.24%. Calcd for $C_{17}H_{13}O_4NFe$: C, 58.14; H, 3.74; N, 3.99%.

Ferrocenyl propionate, bp 108—110°C/0.05—0.06 mmHg. Found: C, 60.48; H, 5.71%. Calcd for $C_{13}H_{14}O_2Fe$: C, 60.48; H, 5.48%.

Ferrocenyl crotonate, mp 60—61.5°C. Found: C, 62.39; H, 5.21%. Calcd for $C_{14}H_{14}O_2Fe$: C, 62.24; H, 5.23%.

Ferrocenyl cinnamate, mp 88.5—90°C. Found: C, 68.81; H, 4.76%. Calcd for $C_{19}H_{16}O_2Fe$: C, 68.69; H, 4.86%.

The Reaction between Bromoferrocene and Benzoic Acid in the Presence of Copper(I) Oxide in Pyridine (Tables 2 and 3). A typical procedure was as follows. Bromoferrocene (1.33 g, 0.005 mol), benzoic acid (1.22 g, 0.01 mol), and copper(I) oxide (0.72 g, 0.005 mol) were mixed with 20 m*l* of pyridine, and then the mixture was refluxed on an oil bath for 0.5 hr under an atmosphere of nitrogen. After the reaction had been completed, the reaction mixture was treated in a manner similar to that described for the preparation of ferrocenyl benzoate. Finally, chromatographic separation afforded ferrocene, bromoferrocene, and ferrocenyl benzoate in 40.9% (0.38 g), 23.0% (0.31 g), and 34.6% (0.53 g) yields respectively.

The Reaction of Bromoferrocene with Copper(I) Benzoate in Pyridine in the Presence of Water (Table 4). Water (0.09 m*l*, 0.005 mol) was added to a mixture of bromoferrocene (1.33 g, 0.005 mol) and copper(I) benzoate (1.85 g, 0.01 mol) in 15 m*l* of pyridine; then the mixture was refluxed for 0.5 hr under an atmosphere of nitrogen. After the reaction had been completed, the reaction mixture was treated much as has been described for the preparation of ferrocenyl benzoate. The chromatography of the product gave ferrocene, bromoferrocene, and ferrocenyl benzoate in 39.8% (0.37 g), 7.5% (0.10 g), and 49.7% (0.76 g) yields respectively.

The Reaction between Bromoferrocene and Benzoic Acid in the Presence of Copper(I) Oxide in Nitromethane (Table 5). Bromoferrocene (0.67 g, 0.0025 mol), benzoic acid (0.61 g, 0.005 mol), and copper(I) oxide (0.36 g, 0.0025 mol) in 10 m*l* of nitromethane were refluxed for 1.0 hr under an atmosphere of nitrogen. After the reaction had been completed, the reaction mixture was cooled and filtered. The precipitate collected on the filter was washed with ether. The filtrate and the washings were combined, and then the combined solution was washed thoroughly with water and dried over anhydrous magnesium sulfate. After the removal of the solvent under reduced pressure, the orange residue was treated much as has been described for the preparation of ferrocenyl benzoate. Finally, ferrocene (0.015 g, 3.2% yield), bromoferrocene (0.061 g, 9.1% yield), and ferrocenyl benzoate (0.658 g, 86% yield) were obtained.

The reaction using acetonitrile or toluene as the solvent was carried out in the same manner.

BULLETIN OF THE CHEMICAL SOCIETY OF JAPAN, VOL. 44, 812—815 (1971)

Reactions of Haloferrocenes. V.[1] The Formation of Ferrocenyltriphenylphosphonium Perchlorate

Masaru SATO,[2] Izumi MOTOYAMA, and Kazuo HATA

Department of Chemistry, Faculty of Science, Tokyo Metropolitan University, Setagaya-ku, Tokyo

(Received September 5, 1970)

The reaction of haloferrocene with tetrakis(acetonitrilo)copper(I) perchlorate in nitromethane gave a 35% yield of biferrocenyl. The addition of triphenylphosphine to the reaction system causes a remarkable change in the reaction and gives ferrocenyltriphenylphosphonium perchlorate in a good yield. The scope of the formation of the quaternary salt was investigated in comparison with the corresponding reactions in the benzene series. It was found that the ligands coordinated in the intermediate copper(I) complex strongly affect the reaction. The mechanism of the formation of ferrocenyltriphenylphosphonium salt is also discussed.

Haloferrocenes are more reactive in the reactions involving metallic copper or copper(I) salt than is halobenzene. For example, the Ullmann coupling reaction of iodoferrocene takes place at 60°C,[3] and ferrocenecarbonitrile is obtained upon heating bromo- or chloroferrocene with copper(I) cyanide at 140°C.[4] It was also found that haloferrocenes reacted easily with various copper(I) salts in boiling pyridine to give substituted ferrocenes,[5-7] and that the condensation reactions of haloferrocenes with various kinds of car-

1) Part IV: M. Sato, I. Motoyama, and K. Hata, This Bulletin, **44**, 808 (1971).

2) Present address: Department of Chemistry, Saitama University, Urawa, Saitama.

3) M. D. Rausch, *J. Org. Chem.*, **26**, 1802 (1961).

4) A. N. Nesmeyanov, V. A. Sazonova, and V. N. Drozd, *Chem. Ber.*, **93**, 2717 (1960).

5) M. Sato, T. Ito, I. Motoyama, K. Watanabe, and K. Hata, This Bulletin, **42**, 1976 (1969).

6) M. Sato, I. Motoyama, and K. Hata, *ibid.*, **43**, 1860 (1970).

7) M. Sato, I. Motoyama, and K. Hata, *ibid.*, **43**, 2213 (1970).

boxylic acids easily took place in the presence of copper(I) oxide in boiling pyridine to give the corresponding ferrocenyl ester.[1] On the other hand, it is well known that similar reactions of the corresponding benzene derivatives occur only under more severe conditions.

In previous papers[5,6] it was suggested that the substitution reactions of haloferrocenes in the presence of copper(I) salts proceed through a ligand-exchange reaction within an intermediate copper(I) complex. From this point of view, it was supposed that if a copper(I) complex of a different type, in which a linkage between the metal and the ligand has no covalent character, is employed instead of the copper(I) salts used in the previous experiments, the exchange reaction will be prohibited and that the coupling reaction of haloferrocene will occur instead, even at a lower temperature. On the other hand, since such a copper(I) complex probably dissolves in a polar solvent to give a homogeneous solution, the reaction using it is expected to be advantageous for studying the reaction mechanism.

Results

In the present study, tetrakis(acetonitrilo)copper(I) perchlorate[8] (**1**) was used for the reaction. It has been reported[8,9] that the nature of the bonding between copper and perchlorate in this complex is entirely ionic in a polar solvent. When bromoferrocene was heated at 45°C for 72 hr with an equimolar amount of the complex **1** in nitromethane, biferrocenyl was obtained in a 35% yield, and 45.3% of bromoferrocene was recovered after the reaction. These results show that the copper(I) complex effects a Ullmann-type aryl-coupling reaction. However, the yield of the coupling product was too low as compared with that of a normal Ullmann reaction, in which iodoferrocene is coupled at 60°C to afford biferrocenyl quantitatively.[3] Thereupon, with a view to modifying the character of the complex in order to produce an increased yield of biferrocenyl, triphenylphosphine was added to the reaction mixture. Unexpectedly, however, when iodoferrocene was heated with triphenylphosphine in the presence of tetrakis(acetonitrilo)copper(I) perchlorate (**1**) in nitromethane, ferrocenyltriphenylphosphonium perchlorate (**2**) was obtained in a good yield. Furthermore, this reaction

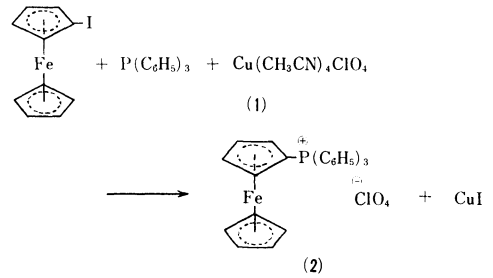

took place at a surprisingly low temperature (45°C), although never at room temperature. Bromoferrocene also reacted in a similar way, but the product was obtained only in a lower yield. These results are summarized in Table 1.

Table 1. The formation of ferrocenyltriphenylphosphonium perchlorate

Haloferrocene	Reaction temp. (°C)	Reaction time (hr)	Recovery of haloferrocene (%)	Yield (%)
FcI	44.5	15.5	35.8	61.4
FcI	101	6	14.4	80.8
FcBr	44.5	15	58.2	36.1

A reaction of this type is known also in the benzene series and is utilized as a synthetic method of aryltriphenylphosphonium salts. The reaction is generally catalyzed by anhydrous metal halide, such as aluminum chloride,[10] cobalt(II) or nickel(II) halide,[11,12] and copper(I) chloride.[13] For instance, when a substituted bromobenzene is treated with triphenylphosphine in the presence of cobalt(II) chloride or nickel(II) bromide, the corresponding aryltriphenylphosphonium bromide is obtained in a high yield, but the reaction does not occur at temperatures below 160°C.[11]

In these reactions giving quaternary phosphonium salts, haloferrocene is much more reactive than halobenzene, much as in other copper(I) salt-participating reactions. It is noticeable that the halogen atom in haloferrocene transfers to the copper(I) complex, finally giving copper(I) halide, whereas that in halobenzene moves into the phosphonium salt without coordinating to the coexisting metal halide.

As had been reported in a previous paper,[6] when the reaction of bromoferrocene with copper(I) chloride in the presence of pyridine was carried out in nitromethane, chloroferrocene was obtained. A similar reaction was attempted in the presence of triphenylphosphine instead of pyridine, but it was found that neither ferrocenylphosphonium salt nor chloroferrocene was produced. The corresponding reaction of 4-bromobiphenyl with triphenylphosphine in the presence of copper(I) chloride has been known to give 4-biphenylyltriphenylphosphonium bromide.[13]

Thus, the formation of ferrocenylphosphonium salt from iodoferrocene and triphenylphosphine was found to necessitate the presence of tetrakis(acetonitrilo)-

Table 2. The influence of the variation in molar ratio

Exp. No.	Molar ratio FcI	$P(C_6H_5)_3$	$Cu(CH_3CN)_4ClO_4$	Recovery of FcI (%)	Yield of phosphonium salt (%)
1	1	1	1	35.8	61.4
2	1	2	1	64.6	6.5
3	1	4	1	86.5	—
4	1	1	0.2	96.3	—

8) P. Hemmerich and C. Sigwart, *Experientia*, **19**, 488 (1963).
9) B. J. Hathaway, D. G. Holah, and J. D. Postlethwaite, *J. Chem. Soc.*, **1961**, 321.
10) J. Chatt and F. G. Mann, *ibid.*, **1940**, 1192.
11) L. Horner, G. Mummenthey, H. Moser, and P. Beck, *Chem. Ber.*, **99**, 2782 (1966).
12) Y. Hirusawa, M. Oku, and K. Yamamoto, This Bulletin, **30**, 667 (1957).
13) G. V. Medoks and V. F. Andronova, *J. Gen. Chem. USSR*, **22**, 2113 (1952).

copper(I) perchlorate. Moreover, the solvent effect in this reaction was found to be astonishing. When acetonitrile or pyridine instead of nitromethane was used as the solvent in this reaction, no ferrocenyltriphenylphosphonium salt was obtained, but iodoferrocene was recovered almost quantitatively.

In order to get more information, the reaction was examined under various molar ratios of the three components, using nitromethane as the solvent. The results are summarized in Table 2.

As may be seen in the table, the yield of the phosphonium salt decreases drastically as the molar ratio of triphenylphosphine increases (Exp. 1—3). This fact, together with the solvent effect described above, suggests that the reaction is strongly affected by the ligands coordinated in the copper(I) complex which serves as the intermediate in the reaction. On the other hand, when 0.2 mol of tetrakis(acetonitrilo)copper(I) perchlorate was used against 1 mol each of iodoferrocene and triphenylphosphine, no reaction was observed and the starting material was recovered almost quantitatively (Exp. 4). This observation clearly indicates that the copper(I) complex does not act as a catalyst in this reaction, unlike as in a similar reaction in the benzene series.[10-13]

Discussion

When triphenylphosphine and tetrakis(acetonitrilo)-copper(I) perchlorate was dissolved in nitromethane, a homogeneous greenish-yellow solution was obtained. As the amount of triphenylphosphine in the solution increased, the color of the solution gradually changed from greenish-yellow to almost colorless. The change in color is probably due to the change in the ligands in the copper(I) complex. It is considered probable that, when tetrakis(acetonitrilo)copper(I) salt is dissolved in nitromethane, the acetonitrile molecule coordinated in the complex is replaced by the solvent molecule. An analogous complex, in which nitromethane coordinates to the copper(I) ion instead of acetonitrile, was reported recently.[14] When iodoferrocene was added to the nitromethane solution of tetrakis(acetonitrilo)copper(I) perchlorate containing triphenylphosphine, a homogeneous reddish-orange solution was obtained, and the reaction of iodoferrocene with triphenylphosphine took place when the solution was heated. A white precipitate, which is supposed to be copper(I) iodide, was separated out as the reaction proceeded, but no change in the color of the solution was observed during the reaction. If iodoferrocene is reduced by a copper(I) complex to produce the ferrocenyl radical and the copper(II) complex, the latter may react with iodoferrocene to give a ferricenium cation, and the color of the reaction mixture ought to change during the reaction. Accordingly, the above observation suggests that this reaction does not proceed through such a radical mechanism. It seems reasonable to assume that the first step in the formation of ferrocenyltriphenylphosphonium salt is the coordination of the iodine atom in iodoferrocene to the copper(I) ion of the complex **3**, coordinated with triphenylphosphine in advance. The unstable intermediate (**4**) thus formed would provide the final product (**2**) *via* a four-centered transition state (**5**), which might have a structure similar to that proposed for the halogen-exchange reaction of haloferrocene with copper(I) chloride.[5] This assumption is

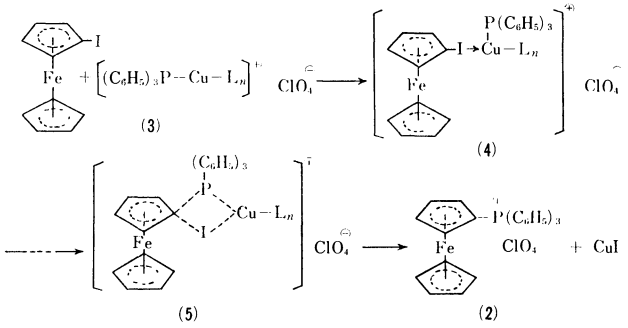

L=CH_3CN and/or CH_3NO_2

consistent with the results listed in Table 2. The coordination of iodoferrocene to the copper(I) ion is supposed to be weak, if it exists at all. Accordingly, if the amount of triphenylphosphine, which has a much stronger coordinating ability than iodoferrocene, increases, the copper(I) ion will be strongly coordinated by the triphenylphosphine; thus, the coordination by iodoferrocene will be obstructed, resulting in the reduction of the formation of ferrocenyltriphenylphosphonium salt. The solvent effect on this reaction also accords with the reaction mechanism proposed above; when acetonitrile or pyridine, which has a particular affinity to the copper(I) ion,[15] is used as a solvent, a similar obstruction of the coordination of iodoferrocene will retard the reaction.

Experimental

Materials. Iodoferrocene was prepared from chloromercuriferrocene by a slightly modified procedure of the previously-reported method.[16] Bromoferrocene was prepared from iodoferrocene according to the procedure described in a previous paper.[5] Tetrakis(acetonitrilo)copper(I) perchlorate was prepared according to the literature.[8] The solvents used in this study were purified by distillation.

Ullmann-type Coupling Reaction of Bromoferrocene Catalyzed by Tetrakis(acetonitrilo)copper(I) Perchlorate. To a pale yellow solution of tetrakis(acetonitrilo)copper(I) perchlorate (0.50 g, 0.0018 mol) in nitromethane[17] (20 ml), bromoferrocene (0.53 g, 0.0018 mol) was added at 44.5°C under a nitrogen atmosphere. The solution rapidly changed in color, from orange to black. After being heated at that temperature for 72 hr, the reaction mixture was poured into water containing tin(II) chloride. The mixture was extracted with benzene. The benzene solution was washed with water and dried over anhydrous magnesium sulfate. After the evaporation of the solvent under reduced pressure, the residue was chromatographed on alumina, using benzene - *n*-hexane (1 : 2) as the

14) W. L. Driessen and W. L. Groeneveld, *Rec. Trav. Chim. Pays-Bas*, **88**, 491 (1969).

15) I. M. Kolthoff and J. F. Coetzee, *J. Amer. Chem. Soc.*, **79**, 1852 (1957).

16) H. Shechter and J. F. Helling, *J. Org. Chem.*, **26**, 1034 (1961).

17) Nitromethane was bubbled with nitrogen before use in order to replace the dissolved oxygen with nitrogen.

solvent. From the first fraction of chromatographic separation, bromoferrocene (0.240 g, 45.3% recovery) was obtained, while from the second fraction, biferrocenyl (0.065 g, 35% yield) was isolated. The latter was recrystallized from benzene, mp 238°C (decomp.) (lit,[3] 239—240°C, decomp.), and identified by means of its NMR and IR spectra. Ferrocene could not be detected, even by gas-chromatographic analysis.

A similar reaction was attempted in acetonitrile instead of nitromethane, but it was unsuccessful.

The Reaction of Iodoferrocene with Triphenylphosphine in the Presence of Tetrakis(acetonitrilo)copper(I) Perchlorate in Nitromethane. Iodoferrocene (0.56 g, 0.0018 mol) was added, at 44.5°C in a nitrogen atmosphere, to a pale greenish-yellow solution of triphenylphosphine (0.47 g, 0.0018 mol) and tetrakis(acetonitrilo)copper(I) perchlorate (0.50 g, 0.0018 mol) in deoxygenated nitromethane[16] (20 m*l*). The color of the solution turned orange, but no further change in the color occurred during the reaction. After being heated at 101°C for 6 hr, the solution was filtered in order to remove the white precipitate separated during the reaction and the precipitate was washed with dichloromethane. The filtrate and the washing solution were then combined, and the combined solution was washed several times with water and then dried over anhydrous magnesium sulfate. The removal of the solvent under reduced pressure gave orange crystals. The crystals were dissolved again in dichloromethane, and then benzene was added to the solution. When dichloromethane was removed from the solution under reduced pressure, orange crystals of ferrocenyltriphenylphosphonium perchlorate (0.795 g, 80.8% yield) were separated out. The crystals were purified further by repeating the procedure described above; mp 175°C (decomp.). IR spectrum (KBr): 3100, 1414, 1008, 815 cm^{-1} (ferrocene nucleus); 1589, 1483, 749, 695 cm^{-1} (benzene ring); 1440, 994 cm^{-1} (P–C); and 1058—1113 cm^{-1} (perchlorate anion). NMR spectrum ($CDCl_3$): δ 4.15 (5H, singlet), 4.55 (2H, triplet), 4.90 (2H, triplet), 7.2—8.0 ppm (15H, multiplet).

Found: C, 60.83; H, 4.90%. Calcd for $C_{28}H_{24}O_4ClPFe$: C, 61.50; H, 4.43%.

Similar reactions were attempted in acetonitrile or pyridine instead of nitromethane, but they were in vain.

BULLETIN OF THE CHEMICAL SOCIETY OF JAPAN, VOL. 44, 815—818 (1971)

Formation and Properties of Phenylthiomethyl Radical. Anodic Oxidation of Sodium Phenylthioacetate and Thermal Decomposition of *t*-Butyl Phenylthioperacetate[1]

Kenji UNEYAMA, Sigeru TORII, and Shigeru OAE*

Department of Industrial Chemistry, School of Engineering, Okayama University, Okayama

* *Department of Applied Chemistry, Faculty of Engineering, Osaka City University, Osaka*

(Received September 7, 1970)

Phenylthiomethyl radical **1** was generated both from anodic oxidation of sodium phenylthioacetate **4** in sodium methoxide-methanol solution and from thermal decomposition of *t*-butyl phenylthioperacetate **5** in benzene. Both reactions afforded a similar trend of product ratios, phenyl disulfide **7** in 31—32% yield as a major product and 1,2-diphenylthioethane **6**, the dimer of radical **1** in 1—2% yield. A chemical and electrochemical reaction process of **1** along with a plausible mechanism for α-elimination of **1** is discussed.

Investigation of stability and property of thiomethyl radicals is of interest. Kinetic studies of the formation of thiomethyl radicals reveal that the radical intermediates are stabilized by divalent sulfide group.[2-6] Chemical properties of these transient reactive intermediates have attracted attention recently. Thermal decomposition of azobis-(2-phenylthio-2-propane) afforded phenyl disulfide and propylene.[7] Homolytic α-elimination of trisphenylthiomethyl radical **3** gave principally phenyl disulfide and tetrakisphenylthioethylene.[8] These results suggest that phenylthiomethyl radicals eliminate a thiophenoxy group to afford carbene intermediates. However, more data on the chemical properties of phenylthiomethyl radicals are required for a detailed discussion on the carbene mechanism. Studies on the electrochemical behavior of benzyl[9] and related radical intermediates[10] indicate that

1) Electrochemistry of organic sulfur compounds. I.

2) C. C. Price and J. Zomlefer, *J. Amer. Chem. Soc.*, **72**, 14 (1950); C. C. Price and T. C. Schman, *J. Polym. Sci.*, **16**, 577 (1955); C. E. Scott and C. C. Price, *J. Amer. Chem. Soc.*, **81**, 2670, 2672 (1959); K. Tsuda, S. Kobayashi, and T. Otsu, *J. Polym. Sci.*, **6**, 41 (1968); W. Tagaki, T. Tada, R. Nomura, and S. Oae, This Bulletin, **41**, 1696 (1968).

3) H. J. Alkema and J. F. Arens, *Rec. Trav. Chim. Pays-Bas*, **79**, 1257 (1960) and literatures cited therein.

4) K. Uneyama, H. Namba, and S. Oae, This Bulletin, **41**, 1928 (1968).

5) R. F. Bridger and G. A. Russell, *J. Amer. Chem. Soc.*, **85**, 3754 (1963).

6) C. Ruchardt, H. Bock, and I. Ruthardt, *Angew. Chem.*, **78**, 268 (1966).

7) A. Ohno and Y. Onishi, *Tetrahedron Lett.*, **1969**, 4405.

8) K. Uneyama, T. Sadakage, and S. Oae, *ibid.*, **1969**, 5193.

9) a) L. Eberson and K. Nyberg, *J. Amer. Chem. Soc.*, **88**, 1686 (1966); L. Eberson and K. Nyberg, *Tetrahedron Lett.*, **1966**, 2389. b) S. D. Ross, M. Finkelstein, and R. C. Peterson, *J. Amer. Chem. Soc.*, **89**, 4088 (1967). c) V. D. Parker and B. E. Emgert, *Tetrahedron Lett.*, **1968**, 2411, 2415. d) N. L. Weinberg and H. R. Weinberg, *Chem. Rev.*, **68**, 449 (1968).

10) a) E. J. Corey, N. L. Bould, R. T. Lalonde, J. Casanova, and E. T. Kaiser, *J. Amer. Chem. Soc.*, **82**, 2645 (1950). b) P. H. Reichenbacher, M. D. Morris, and P. S. Skell, *ibid.*, **90**, 3432 (1968); P. S. Skell and P. H. Reichenbacher, *ibid.*, **90**, 3436 (1968). c) J. G. Traynham and J. S. Dehn, *ibid.*, **89**, 2139 (1967).

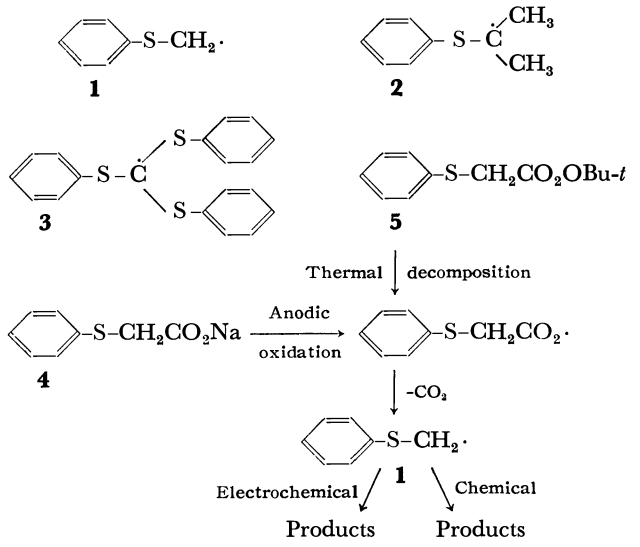

benzylic radical is oxidized to the corresponding benzylic cation. Wladislow[11] showed an example of anodic oxidation of thiomethyl radical such as α,α-diphenyl-α-phenylthiomethyl radical. However, it is impossible to work out a theory on anodic oxidation process of thiomethyl radicals from the limited result. In order to get detailed information on the chemical and electrochemical behaviors of phenylthiomethyl radical **1** as a basic model for phenylthiomethyl radicals, we have examined anodic oxidation of sodium phenylthioacetate **4** and thermal decompostion of *t*-butyl phenylthioperacetate **5**.

Results and Discussion

Phenylthioacetic acid was electrolyzed at 15—20°C in methanol-sodium methoxide at current density 30 mA/cm² and terminal voltage 25—30 volt with platinum plates. The reaction mixture in the anode compartment was handled in the usual way[12] and the product was fractionated by elution chromatography on silica gel. Current yield to the consumption of **4** was about 50%.

Phenyl disulfide **7** and phenyl methoxymethyl sulfide **9** were obtained as major products (Table 1). Phenylthioformal **8**, methyl phenylthioacetate **10** and 1,2-diphenylthioethane **6** were obtained as minor products. A trace of thioanisole **11** was also detected by vpc.

Table 1. Products formed from the electrolysis of α-phenylthioacetic acid in MeOH-MeONa

	Product	Yield (%)[a]
6	Ph-S-CH_2-CH_2-S-Ph	1.5[b]
7	Ph-S-S-Ph	32[b]
8	Ph-S-CH_2-S-Ph	4.5
9	Ph-S-CH_2-OMe	34
10	Ph-S-CH_2-CO_2Me	3.2
11	Ph-S-CH_3	trace

a) Yield based on reacted carboxylic acid
b) 2× (Yield obtained from vpc)

Table 2. Products and their yields in the thermal decompostition of *t*-butyl phenylthioperacetate in benzene at 70°C

	Product	Yield (%)[a]
6	Ph-S-CH_2-CH_2-S-Ph	2.3[b]
7	Ph-S-S-Ph	31[b]
8	Ph-S-CH_2-S-Ph	6.5[b]
12	Ph-S-CH_2-O-Bu-*t*	19
10	Ph-S-$CH_2CO_2CH_3$	0
11	Ph-S-CH_3	14
13	Ph-S-CH_2-Ph	2.5
14	CO_2	90

a) Yield based on *t*-butyl phenylthioperacetate
b) 2× (yield obtained from vpc)

In the thermolysis of *t*-butyl phenylthioperacetate **5** in benzene solution, dimer **6** was produced in only 2.3%, while disulfide **7** was obtained as a major product (Table 2). Formation of phenyl benzyl sulfide **13** indicates that phenylthiomethyl radical **1** which is undoubtedly formed as a transient intermediate attacks the solvent.

We see from the Tables that the ratios of Kolbe dimer **6** to the other principal products (**7**, **8**, **9**, and **12**) in both experiments are similar, which suggests that radical **1** would exist as an intermediate during the course of electrolysis. However, the yield of Kolbe dimer **6** was unexpectedly small as compared with the results obtained from the anodic oxidation of phenylacetic and phenoxyacetic acid.[13] One reason for this may be explained as follows, together with the mechanism of the formation of phenyl disulfide **7**. Radical **1** undergoes further electron oxidation to give phenylthiomethyl cation,[14] which undergoes solvolysis with methanol to provide the methyl ether **9** (Path A).[17] If the methanolysis of **9** took place successively in the electrolytic solution to provide thiophenol, it would readily be oxidized to thiophenoxy radical[11] whose recombination may give phenyl disulfide **7** and diphenylthioformal **8**. However, the equilibrium process of **9** in

11) B. Wladislow, *Chem. Ind.* (London), **1962**, 1868.
12) A. Takeda, S. Wada, S. Torii, and Y. Matsui, This Bulletin, **42**, 1047 (1969).
13) F. Fichter and H. Stenzl, *Helv. Chim. Acta*, **22**, 970 (1939).
14) Benzyl radical is easily oxidized to benzyl cation.[15] The oxidation potential of phenylthiomethyl radical would be lower than that of benzyl radical since solvolysis of halomethyl sulfide proceeds much faster than benzyl halide.[16] (Ref. 8)
15) V. P. Parker and B. E. Emgert, *Tetrahedron Lett.*, **1968**, 2411, 2415.
16) C. C. Price and S. Oae, "Sulfur Bonding," Ronald Press, New York (1962); H. Böhme, H. Fischer, and R. Frank, *Ann. Chem.*, **563**, 54 (1949).
17) A recombination[18] of **1** with methoxy radical can not be necessarily excluded, but the carbonium ion process (Path A) would be more favorable than (Path B) on the basis of the analogy of easy oxidation of benzyl radical and easy formation of phenylthiomethyl cation is solvolytic reaction of phenyl chloromethyl sulfide.
18) T. Inoue, K. Koyama, and S. Tsutsumi, This Bulletin, **37**, 1597 (1964); K. Sasaki, H. Urata, K. Uneyama, and S. Nagaura, *Electrochim. Acta*, **12**, 137 (1967).

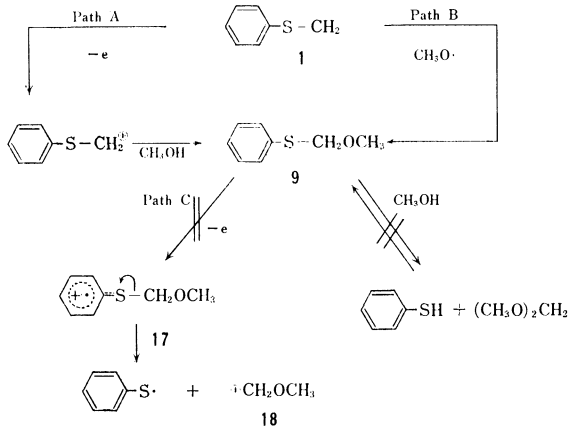

Scheme 1

alkaline methanol medium requires further investigation. Methyl ether **9** obtained by treatment of phenyl chloromethyl sulfide with sodium methoxide in methanol was subjected to solvolysis in electrolytic condition, but neither disulfide **7** nor thiophenol was detected. The fact that anodic oxidation of **16** in methanol afforded disulfide **7** and benzophenone dimethylketal[11] suggests that an intermediate **15** is more reactive than **9** in alkaline methanol medium, due to *gem*-phenyl groups.

15 **16**

Another plausible mechanism on the thiophenoxy formation from **9** is one electron oxidation of **9** to cation radical **17** followed by the elimination of thiophenoxy group to form methoxymethyl cation **18** as shown in Path C of Scheme 1. In order to examine the hypothesis, ether **9** was subjected to electrolysis in methanol-sodium methoxide solution as in the case of **4**, but no indication of the formation of **7** was observed. Thus, ether **9** is not a precursor for the thiophenoxy radical formation.

The second process is a homolytic 1,2-elimination of dimer **6** *via* intermediate **19** to produce thiophenoxy radical. Thus, 0.005 M methanol solution of **6** was electrolyzed under the condition for phenylthioacetic acid, but neither disulfide **7** nor phenyl vinyl sulfide **20** was detected by vpc. Thus, the homolytic 1,2-elimination is not plausible in our electrolysis of **4**[19,20] (Scheme 2).

The third process involves a homolytic α-elimination of the radical **1** into thiophenoxy radical and methylene carbene. In the case of phenylthioisopropyl **2** and trisphenylthiomethyl radical **3**, α-elimination has been reported.[7,8] In connection with a plausible carbene mechanism, decomposition of *t*-butyl phenylthioperacetate **5** in benzene containing 0.06—0.013 M of styrene was studied. Vpc analysis revealed the formation of phenyl cyclopropane in 0.2—0.4% yield indicating that the α-elimination occurs during thermolysis (Scheme 3). In the electrolysis, however, attempts to trap methylene group have not been achieved even when **4** was electrolyzed in methanol-sodium methoxide containing *p*-chlorothiophenol. The major products were di-*p*-chlorophenyl, *p*-chlorophenyl phenyl and diphenyl disulfides. *p*-Chlorothioanisole which might arise from the insertion of methylene group into the thiol was not confirmed by vpc. Radical **1** would split out methylene near the electrode surface which then would polymerize to afford hydrocarbons. Column chromatography of the product provided hydrocarbons. The fact that there is a similar trend of product ratios between the electrolysis and the thermolysis and the observation of hydrocarbon formation, suggests the carbene process of radical **1** in electrolysis.

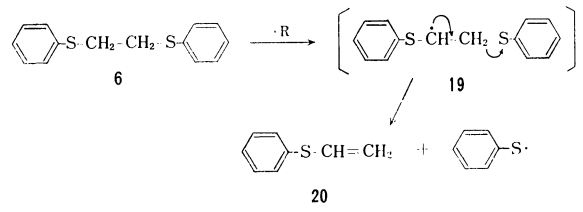

Scheme 2

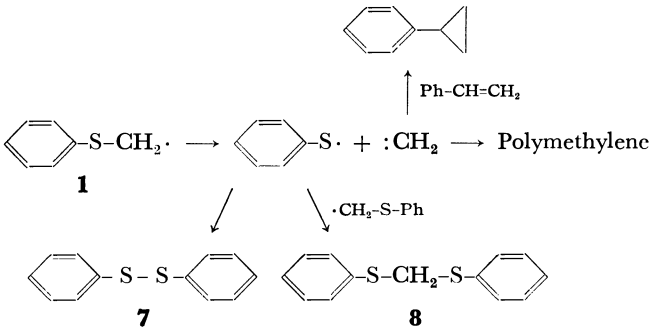

Scheme 3

In the present stage, we believe that radical **1** would undergo three chemical and electrochemical processes; (i) recombination with other radical, (ii) further one electron oxidation to phenylthiomethyl cation and (iii) α-elimination to thiophenoxy radical. The low yield of **6** in the electrolysis would be derived from the predominance of process (ii) and (iii) because of the low oxidation potential to phenylthiomethyl cation and the stable thiophenoxy radical formation from radical **1**. Extensive studies on the electrochemical fate of thiomethyl radicals having α-substituents other than hydrogen would provide more reliable information on the electrode process.

Experimental

Electrolysis of Sodium Phenylthioacetate **4**. A typical run of the electrolyses is as follows. Phenylthioacetic acid (0.46 g) dissolved in 40 m*l* of carefully distilled methanol containing 200 mg of metallic sodium was electrolyzed at 30 mA/cm² for 1 hr at terminal voltage 25—30 V in a cell (Fig. 1). The temperature was kept at 10—15°C. After electrolysis, 70 mg

19) The second process would be practical in an intrinsic radical reaction as in the peroxide decomposition of sulfides.[20] Disulfide **7** and the vinyl sulfide **20** were confirmed by vpc on decomposing di-*t*-butylperoxide in 1 M benzene solution of the sulfide **6**.

20) A. B. Terentev, R. P. Geer, A. J. Meskin, and R. M. D'Silva, *J. Amer. Chem. Soc.*, **88**, 1257 (1966); E. S. Huyser and R. M. Kellog, *J. Org. Chem.*, **31**, 3366 (1966).

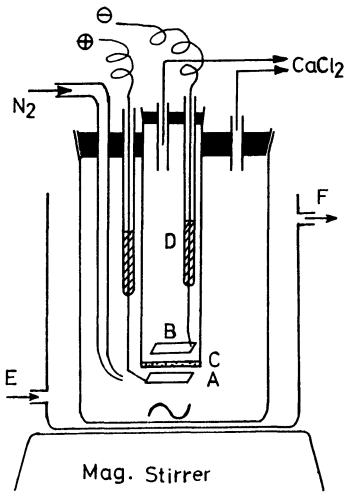

Fig. 1. Electrolysis cell.
A) Anode Pt plate (3 cm²)
B) Cathode Pt plate (3 cm²)
C) Glass filter
D) Hg pool
E) Cooling Water inlet
F) Cooling water outlet

of phenyl benzyl sulfide was added to the reaction mixture as an internal standard for vpc. After evaporation of the solvent and the usual work-up, 340 mg and 100 mg of neutral and acidic portions were obtained, respectively. The neutral portion was fractionated by elution chromatography on silica gel using *n*-hexane - benzene and each fraction was identified in comparing with authentic samples by IR, NMR, mp, vpc and tlc. Yields of the products were obtained by calculation of relative peak area of vpc (10% coated SE-30, 1 m, 150°C) using phenyl benzyl sulfide as an internal standard.

Thermal Decomposition of t-*Butyl Phenylthioperacetate* **5** *in Benzene.* Perester **5** was dissolved in dry benzene to prepare 0.01M solution. The reaction mixture was kept at 70°C for 3 hr under N_2 atmosphere. Carbon dioxide was absorbed in alkaline solution and the excess alkali was back-titrated.[21] After evaporation of benzene, residual oil was worked up as usual and the products were analyzed in a similar way to those in electrolysis. Yields of the products (Table 2) were obtained by the value of relative peak area of vpc (SE-30, 1 m, 150 and 190°C) using phenyl sulfide as an internal standard.

Thermal Decomposition of **5** *in Benzene - Styrene Solution.* Perester **5** (0.39 g) and styrene (0.31 g for run 1, 0.16 g for run 2, and 0.07 g for run 3) were dissolved in 50 m*l* of dry benzene. The reaction mixture was subjected to thermolysis at 70°C for 3 hr under N_2 atmosphere. After evaporation of the solvent, residual oil was analyzed by vpc (SE-30, 2 m, 110°C). The results are listed in Table 3.

Table 3. Yield of phenylcyclopropane in the thermolysis of the perester **5**

Run	1	2	3	4
Styrene (g)	0.31	0.16	0.07	0
Phenylcyclopropane(%)[a]	0.4	0.2	0.2	0

a) Yield based on the perester **5**

Preparation of Starting Materials and Authentic Samples. t-*Butyl Phenylthioperacetate* **5**: Into an ethereal solution of 6.3 g of *t* butyl hydroperoxide and 8 g of pyridine, 10.0 g of phenylthioacetyl chloride dissolved in 50 m*l* of dry ether was added dropwise for 20 min under cooling below −15°C. The reaction mixture was kept at −15°C for 7 hr with stirring. The mixture was then washed with 5% aqueous hydrogen chloride, then with ice water, with 5% aqueous sodium carbonate and finally with water. The ether layer was dried over anhydrous sodium sulfate for 30 min at 0°C and then ether was removed *in vacuo*. The residue was passed through an activated alumina column cooled by ice water to remove a trace of *t*-butyl hydroperoxide and acidic impurities using ether as an elute. The collected ether layer (100 m*l*) was washed with ice water and dried over sodium sulfate. After removing the solvent *in vacuo*, 6.0 g of slightly yellow colored oil was obtained. IR 1745 (C=O), 1574 (PhS–), 845 cm^{-1} (–O–O–R); NMR (CCl_4, TMS), ppm, 1.18 (s, 9H), 3.52 (s, 2H),and 7.3 (m, 5H).

Found: C, 60.13; H, 6.79%. Calcd for $C_{12}H_{16}O_3S$: C, 60.00; H, 6.71%.

*Phenyl Methoxymethyl Sulfide (***9***)*: To a solution of 9 g of thioanisole dissolved in 30 m*l* *n*-hexane, 12 g of sulfuryl chloride was added dropwise, then the mixture was refluxed for 1 hr. After evaporation of the solvent, residual oil was subjected to distillation under reduced pressure to afford 8 g of colorless oil (bp 118—120°C/20 mmHg). The chloride (6.3 g) was refluxed in 30 m*l* of methanol containing 2 g of sodium metal for 1 hr. Into the residue obtained by evaporation of methanol by a suction pump, 50 m*l* of ice water was added and organic layer was extracted with ether. Usual work-up and fractional distillation gave 5.5 g of colorless oil, bp 108—110°C/20 mmHg; IR, 2790, 1090 (OCH_3), 1591 cm^{-1} (PhS); NMR, (CCl_4, TMS), ppm, 3.38 (s, 3H), 4.90 (s, 2H), and 7.3 (m, 5H).

Found: C, 62.45; H, 6.55%. Calcd for $C_8H_{10}OS$: C, 62.33; H, 6.54%.

Phenyl t-*Butoxymethyl Sulfide (***12***)*: This was synthesized similarly by treatment of phenyl chloromethyl sulfide with potassium *t*-butoxide in *t*-butanol. Sulfide **12** is colorless oil, bp 107—109°C/6 mmHg; IR, 2960, 2920 (CH_3), 1594 (PhS), 1057 cm^{-1} (*t*-Bu–O); NMR, ($CDCl_3$, TMS), ppm, 1.26 (s, 9H), 5.01 (s, 2H) and 7.5 (m, 5H).

Found: C, 66.53; H, 8.14%. Calcd for $C_{11}H_{16}OS$: C, 67.03; H, 8.22%.

Other authentic samples and starting materials such as phenylthioacetic acid **6**, diphenylthioformal **8**,[21] 1,2-diphenylthioethane **6**,[22] phenyl disulfide **7**,[23] methylphenylthioacetate (**10**), benzyl phenyl sulfide (**13**),[24] phenyl sulfide,[25] phenyl vinyl sulfide **20**,[26] *p*-chlorothioanisole,[4] phenylcyclopropane,[27] and thioanisole were prepared as described in literatures.

21) K. Uneyama, W. Tagaki, I. Minamida, and S. Oae, *Tetrahedron*, **24**, 5271 (1968).
22) T. Fromm, *Ann. Chem.*, **253**, 161 (1922).
23) P. Hubner and G. Alsberg, *ibid.*, **156**, 330 (1912).
24) R. L. Shriner, H. C. Struck, and W. J. Jorison, *J. Amer. Chem. Soc.*, **52**, 2066 (1930).
25) W. W. Hartman, L. A. Smith, and J. B. Dickey, "Organic Syntheses," Coll. Vol. II, p. 242 (1943).
26) K. Tsuda, S. Kobayashi, and T. Otsu, *J. Macromol. Sci.*, **A1** (6), 1025 (1969).
27) The authors thank Professor M. Ikeda, Wakayama University, for kindly supplying the authentic phenylcyclopropane.

The Catalytic Reaction of Alcohols with Reduced Copper[1]

Kazuaki KAWAMOTO and Yoshiharu NISHIMURA*

Institute of Commodities, Faculty of Economics, Kagawa University, Takamatsu

(Received September 9, 1970)

The catalytic properties of a reduced copper catalyst in reaction to ethyl alcohol, *n*-propyl alcohol, *n*-butyl alcohol, 2-phenylethanol, 1-phenylethanol, 3-phenyl-1-propanol, cinnamyl alcohol, propionaldehyde, *n*-propyl propionate, and a mixture of ethyl alcohol and propionaldehyde were studied. The present investigation has been undertaken in order to find out whether or not the activity and the selectivity of reduced copper are affected by the method of the preparation of catalysts and the structure of alcohols used as the reactants, and to clarify the mechanism of the formation of the esters and ketones obtained from aliphatic alcohols. It has been found that, over reduced copper, saturated aliphatic alcohol gives considerable amounts of the corresponding aldehyde and ester. The formation of the ester may be explained by a hemiacetal mechanism. The hydroxyl group of aliphatic alcohol is very resistant to hydrogenolysis. However, with the phenyl-substituted alcohols the carbon-to-oxygen bond is easily broken.

Studies concerning the catalytic reaction of primary alcohol with various catalysts have been reported by many investigators.[2] Especially, Adkins *et al.*[2b] and Dunbar[2c] reported that, when *n*-butyl alcohol was passed over copper-chromium oxide catalysts, there were at least four important types of reactions: (1) dehydrogenation, (2) dehydration, (3) aldol condensation, and (4) ester formation by the Tischenko reaction. Dolgow *et al.*[2p] found that, on a pure copper catalyst, ethyl alcohol at 220°—300°C gave almost pure acetaldehyde and that, in the presence of a promoter, ethyl acetate was also formed, in amounts increasing with the concentration of the promoter. Further, Eto[2o] reported that the copper catalyst strongly accelerated ester formation by the Tischenko reaction.

It has been well known that the aromatic nuclear catalytic hydrogenation of benzyl-type oxygen compounds is accompanied by the hydrogenolysis of carbon-oxygen linkage.[3] The catalytic hydrogenation and hydrogenolysis of allyl alcohol, benzyl alcohol, and cinnamyl alcohol over Raney nickel, palladium on charcoal, palladium(H), Adams' platinum, ruthenium, rhodium on alumina, nickel on kieselguhr, copper-chromium oxide, palladium boride, and reduced copper as the catalysts have been investigated by many wokers.[4]

The preparation of copper catalysts and the production of acetone and oily products (isobutyl methyl ketone and diisobutyl ketone) from isopropyl alcohol have been reported in detail in previous papers.[5] It has been found that two distinct types of copper catalysts are obtained, according to the precipitants, and that the activity and the selectivity of the catalyst are affected by the reducing agent used in the preparation of the copper catalyst.

The present investigation includes an extension of this method to aliphatic primary alcohols and aromatic alcohols. Certain tendencies regarding the structure of alcohol, the ease of dehydrogenation, the ester forma-

* Present address: Department of Chemistry, Faculty of Education, Kagawa University, Takamatsu.

1) Presented at the 21st Annual Meeting of the Chemical Society of Japan, Osaka, April, 1968.

2) a) P. Sabatier, "Die Katalyse in der Organischen Chemie," Akademische Verlagsgesellschaft m. b. H., Leipzig (1927), pp. 193—202. b) H. Adkins and W. A. Lazier, *J. Amer. Chem. Soc.*, **46**, 2291 (1924); W. A. Lazier and H. Adkins, *ibid.*, **47**, 1719 (1925); H. Adkins, M. E. Kinsey, and K. Folkers, *Ind. Eng. Chem.*, **22**, 1046 (1930); H. Adkins, C. E. Kommes, E. F. Struss, and W. Dasler, *J. Amer. Chem. Soc.*, **55**, 2992 (1933). c) R. E. Dunbar, *J. Org. Chem.*, **3**, 242 (1938); R. E. Dunbar and M. R. Arnold, *ibid.*, **10**, 501 (1945). d) W. G. Palmer, *Proc. Roy. Soc.* (London), **98A**, 13 (1920); W. G. Palmer, *ibid.*, **99A**, 412 (1921); W. G. Palmer, *ibid.*, **101A**, 175 (1922); W. G. Palmer and F. H. Constable, *ibid.*, **106A**, 250 (1924); F. H. Constable, *J. Chem. Soc.*, **1927**, 2995. e) V. I. Komarewsky and J. R. Coley, *J. Amer. Chem. Soc.*, **63**, 700, 3269 (1941); V. I. Komarewsky and T. H. Kritchevsky, *ibid.*, **65**, 547 (1943); V. I. Komarewsky and L. G. Smith, *ibid.*, **66**, 1116 (1944); J. R. Coley and V. I. Komarewsky, *ibid.*, **74**, 4448 (1952). f) E. J. Badin and E. Pacsu, *ibid.*, **66**, 1963 (1944). g) M. Takayasu, *Nippon Kagaku Zasshi*, **64**, 457, 462 (1943). h) P. Y. Ivannikov, *J. Appl. Chem.* (U. S. S. R.), **13**, 118 (1940). i) S. L. Lel'chuk, A. A. Balandin, D. N. Vaskevich, and I. I. Groer, *ibid.*, **17**, 60 (1944). j) A. C. Neish, *Can. J. Res.*, **23B**, 49 (1945). k) T. Takahashi and F. Hikawa, *Kogyo Kagaku Zasshi*, **49**, 114 (1946). l) J. M. Church and H. K. Joshi, *Ind. Eng. Chem.*, **43**, 1804 (1951). m) K. Hoshiai, *Kogyo Kagaku Zasshi*, **54**, 238 (1951); K. Hoshiai, *ibid.*, **57**, 76 (1954). n) S. Kudo, *ibid.*, **58**, 719 (1955). o) K. Eto, *Yuki Gosei Kagaku Kyokai Shi*, **21**, 61 (1963). p) B. N. Dolgow, "Die Katalyse in der Organischen Chemie," VEB Deutscher Verlag der Wissenschaften, Berlin (1963), pp. 268—281; B. N. Dolgow, T. V. Nizovkina, and I. M. Stroiman, *Sbornik Statei Obshch. Khim.*, **2**, 1288 (1953); B. N. Dolgow and T. V. Nizovkina, *Zh. Obshch. Khim.*, **19**, 1125 (1949).

3) W. H. Hartung and R. Simonoff, "Organic Reactions," Vol. 7, 263 (1953).

4) a) S. Mitsui and H. Saito, *Nippon Kagaku Zasshi*, **82**, 390 (1961); S. Mitsui, S. Imaizumi, and Y. Esashi, This Bulletin, **43**, 2143 (1970); N. Oshima and S. Mitsui, *Nippon Kagaku Zasshi*, **83**, 149 (1962); N. Oshima, K. Sato, and S. Mitsui, *ibid.*, **84**, 177 (1963). b) S. Nishimura, This Bulletin, **32**, 1155 (1959); S. Nishimura and M. Hama, *ibid.*, **39**, 2467 (1966); Y. Takagi, T. Naito, and S. Nishimura, *ibid.*, **37**, 585 (1964). c) Y. Ichinohe and H. Ito, *ibid.*, **37**, 887 (1964). d) H. Adkins and L. W. Covert, *J. Phys. Chem.*, **35**, 1684 (1931); L. W. Covert, R. Connor, and H. Adkins, *J. Amer. Chem. Soc.*, **54**, 1651 (1932); R. Connor and H. Adkins, *ibid.*, **54**, 4678 (1932); E. Bowden and H. Adkins, *ibid.*, **56**, 689 (1934); H. Adkins, "Reactions of Hydrogen with Organic Compounds over Copper-Chromium Oxide and Nickel Catalysts," The University of Wisconsin Press, Madison, (1937). e) R. Baltzly and J. S. Buck, *J. Amer. Chem. Soc.*, **65**, 1984 (1943). f) J. H. Stocker, *J. Org. Chem.*, **27**, 2288 (1962); I. A. Kaye and R. S. Matthews, *ibid.*, **28**, 325 (1963); H. A. Smith and B. L. Stump, *J. Amer. Chem. Soc.*, **83**, 2739 (1961). g) M. Kawai, T. Imanaka, and S. Teranishi, *Nippon Kagaku Zasshi*, **90**, 42 (1969). h) Y. Nishimura, T. Hiraki, and K. Kawamoto, *Memoirs of the Faculty of Education, Kagawa University, Part II*, No. 179, 1 (1969).

5) K. Kawamoto, This Bulletin, **34**, 161, 795 (1961); K. Kawamoto, Y. Nishimura, and T. Hiraki, *ibid.*, **41**, 932 (1968).

tion, and the hydrogenolysis over reduced copper catalyst have been discussed. Further, this research has been undertaken in order to clarify the mechanism of the formation of the ester and the ketone.

Experimental

Reactants. The aliphatic alcohols, such as ethyl alcohol, *n*-propyl alcohol, and *n*-butyl alcohol, were purified, after being dried with calcium oxide, by distillation through a fractionating column. Propionaldehyde, *n*-propyl propionate, 2-phenylethanol, 1-phenylethanol, 3-phenyl-1-propanol, and cinnamyl alcohol were purified by being dried with anhydrous sodium sulfate, followed by fractional distillation under ordinary pressure or reduced pressure. The reactants used in this experiment showed no impurity in gas-chromatographic analysis. (Columns of PEG-6000, tricresyl phosphate, and silicone DC-550 were used.)

Preparation of Catalysts. The precipitates used in this research were identical with the Cu VII and Cu IX which were described in a preceding paper.[5] The Cu VII was prepared as follows: A solution of 30 g of cupric nitrate hexahydrate in 900 m*l* of distilled water was kept at 22°C. A sodium hydroxide solution prepared from 15 g of sodium hydroxide and 300 m*l* of distilled water was brought to the same temperature and added rapidly to the stirred copper nitrate solution. After the mixture had been stirred at this temperature for 30 min, the precipitate was washed well with distilled water by decantation, collected on a glass filter, dried in an electric oven at 105°C for 20 hr, powdered in an agate mortar, and finally stored in a stoppered bottle. The Cu IX was prepared by the same method except for the precipitant (K_2CO_3: 25 g) and the volume of distilled water (500 m*l*) used to dissolve it. These precipitates were reduced in the following ways. When hydrogen was used as the reducing agent, the hydrogen was passed at the rate 750—900 m*l* per hr. The reduction temperature was always below 185°C. In the case of the reduction of the precipitate with carbon monoxide, the flow rate of carbon monoxide was 800—900 m*l* per hr, and the reduction temperature was always below 140°C.

Apparatus and Procedure. The apparatus employed was exactly the same as that previously described.[5] The precipitate (10 g) to be reduced was placed in a Pyrex reaction tube. The furnace was heated to the reduction temperature and kept at this temperature for the period of reduction. The reducing agent was passed through the tube at a regular velocity, and the resulting catalyst was then heated to the reaction temperature. Experiments were performed at 220, 250, and 300°C under ordinary pressure, and the reactants were passed through the tube at a constant flow rate. The reaction products coming from the reaction tube were condensed by passing them through a condenser cooled with ice and were collected by two traps cooled with ice. The volume of gas evolved during the period of the reaction was measured at intervals of 30 min. All the values given in the present research are averages of two or three measurements under constant reaction conditions.

Identification and Analysis of the Reaction Products. The liquid products were identified by comparing them with authentic samples by gas chromatography. (Columns of tricresyl phosphate, PEG-6000, silicone DC-550, diethylene glycol succinate, and Hyprose SP-80 were used. For the determination of water, a 3-m column packed with Shimalite F impregnated with PEG-1000 was used.) In addition, the reaction products were dried over anhydrous sodium sulfate and then fractionally distilled, and the constituents of the fraction were identified by observing the formation of the derivatives[6] and the infrared absorption. The gaseous products were analyzed by gas chromatography. (Columns of activated charcoal, molecular sieve-13X, hexamethyl phosphoramide, tricresyl phosphate, acetonylacetone, and dimethyl sulfolane were used.) The gaseous products could not be determined quantitatively. The quantitative analysis of the liquid products in this experiment was performed by gas chromatography.

Results and Discussion

The influences of the reaction temperatures, the precipitants, and the reducing agents on the activity and the selectivity of the copper catalyst are summarized in Tables 1, 2, 4, 5, 6, 7, and 8. Experiment Nos. 11—14 of Table 2 and Experiment Nos. 15 and 16 of Table 3 were carried out in order to explain the formation mechanism of the ester and the ketone obtained by this experiment. The fluctuation in the yields of the reaction products obtained by the repeated experiments was less than 1 per cent. Since the reactants were not changed in the absence of the catalysts over a range of temperatures from 220°C to 300°C, the changes shown in Tables 1—8 do not involve the simple pyrolysis of the reactants. Further, since the evolution of the gas is constant during the reaction period, it may be concluded that the sustained activity of catalyst holds over the period of the operation.

Influences of the Precipitants and the Reducing Agents on the Catalytic Action of Reduced Copper toward Aliphatic Primary Alcohols. As may be seen from the amounts of unreacted alcohol shown in Tables 1, 2, and 4, the conversion of primary alcohol to the reaction product (aldehyde, ester, ketone, *etc.*) in the presence of the copper catalyst depends upon the temperature at which the reaction is carried out; it has been found that the yield of the reaction product increases rapidly with a rise in the reaction temperature. Dehydrogenation and the formation of the ester are the chief reactions when the catalytic reaction of aliphatic primary alcohol is carried out at 220—300°C. Even at atmospheric pressure, a considerable amounts of ester may be formed, especially at a higher temperature (300°C). From the amounts of alkenes and water present in the reaction products, it was shown that dehydration has never been a troublesome factor in studies with the aliphatic alcohol at temperatures below 300°C. As may be seen from Experiment Nos. 2 and 5 of Table 1 and Experiment Nos. 7 and 10 of Table 2, the yield of the reaction product is also affected by the sort of precipitant; it has been found that when the copper catalyst prepared with sodium hydroxide is used, the yield of the reaction product increases. As may be seen from Experiment Nos. 2 and 4 of Table 1 and Experiment Nos. 7 and 9 of Table 2, the copper catalysts prepared by treatment with hydrogen and carbon monoxide as the reducing agents are nearly equal in the yields of the reaction product, but there are the distinct differences in the amounts of aldehyde and

6) R. L. Shriner, R. C. Fuson, and D. Y. Curtin, "The Systematic Identification of Organic Compounds," 4th ed., John Wiley & Sons, New York (1956).

Table 1. Influences of the precipitants, the reducing agents and the reaction temperatures on the catalytic action of reduced copper toward ethyl alcohol

Experiment No.	1	2	3	4	5
Precipitate	CuVII				CuIX
Reducing agent	H_2	H_2	H_2	CO	H_2
Reaction temp. (°C)	220	250	300	250	250
Ethyl alcohol (g)	17.37	17.21	16.79	18.83	17.77
Velocity (g/hr)	7.6	7.1	7.1	8.7	6.9
Liquid product (g)	16.63	16.43	15.94	16.15	16.92
Composition of liquid product (%)					
Acetaldehyde	11.4	19.3	24.0	14.7	19.3
Ethyl acetate	15.5	18.7	23.5	22.6	11.5
Acetone	0.4	1.2	3.8	0.8	0.5
Acetic acid	T	T	0.7	T	T
Aldol	0.1	0.3	0.5	T	0.1
Crotonaldehyde	0.1	0.2	0.3	T	0.1
Butyraldehyde	0.1	0.2	0.4	T	0.1
2-Buten-1-ol	0.1	0.2	0.3	0.4	0.1
n-Butyl alcohol	0.2	0.4	1.0	0.3	0.2
Methyl alcohol	T	T	T	T	T
Water	T	T	T	T	T
Unidentified product	0.2	0.2	0.5	0.4	0.2
Unreacted alcohol	71.9	59.3	45.0	60.8	67.9
Gas collected[a] (*l*)	2.25	3.28	4.31	3.26	2.94

T: Trace

a) The gaseous products evolved were found to consist of hydrogen, methane, ethylene, ethane, and carbon dioxide with the exception that carbon monoxide was observed in the case of the reduction of precipitate with carbon monoxide.

Table 2. The catalytic properties of reduced copper toward *n*-propyl alcohol, propionaldehyde and *n*-propyl propionate

Experiment No.	6	7	8	9	10	11	12	13	14
Precipitate	CuVII				CuIX	CuVII			
Reducing agent	H_2	H_2	H_2	CO	H_2	H_2	H_2	CO	H_2
Reaction temp. (°C)	220	250	300	250	250	250	300	250	250
Reactant	*n*-Propyl alcohol					Propionaldehyde			*n*-Propyl propionate
Reactant charged (g)	18.93	18.73	19.16	19.00	17.16	16.19	17.72	18.96	18.08
Velocity (g/hr)	7.7	6.9	7.2	8.4	6.5	7.1	6.9	7.5	7.0
Liquid product (g)	17.97	17.72	17.99	17.93	16.20	15.15	16.59	17.38	17.02
Composition of liquid product (%)									
Propionaldehyde	11.3	15.8	22.9	11.7	17.1	—	—	—	0.3
n-Propyl propionate	9.2	14.4	19.5	20.2	11.8	0	0	0	—
Diethyl ketone	5.0	7.1	8.6	4.2	1.4	0	0	0	0.3
Propionic acid	T	0.3	0.5	T	T	2.4	4.3	2.3	0.4
n-Propyl alcohol	—	—	—	—	—	2.6	4.6	2.9	0.3
Ethyl alcohol	0.2	0.5	0.9	0.2	0.2	0	0	0	0
Methyl alcohol	0.1	0.2	0.3	0.1	0.1	0	0	0	0
Water	T	T	T	T	T	T	T	T	T
Unidentified product	0.3	1.1	1.1	1.2	0.2	T	T	0.7	0.2
Unreacted reactant	73.9	60.6	46.2	62.4	69.2	95.0	91.1	94.1	98.5
Gas collected[a] (*l*)	1.92	2.21	5.00	2.30	2.06	0.19	0.31	0.17	0.13

T: Trace

a) Gaseous products

n-Propyl alcohol: hydrogen, propylene, carbon dioxide, methane, ethane, and carbon monoxide

Propionaldehyde: carbon dioxide, hydrogen, carbon monoxide, and ethane

n-Propyl propionate: propylene and carbon dioxide

TABLE 3. THE REACTION BETWEEN ETHYL ALCOHOL AND PROPIONALDEHYDE IN THE PRESENCE OF REDUCED COPPER[a)]

Experiment No.	15	16
Reducing agent	H_2	CO
Reaction temp.(°C)	250	250
Reactant charged		
Ethyl alcohol (g)	15.35	15.20
Propionaldehyde (g)	19.28	19.32
Velocity (g/hr)	8.0	10.5
Liquid product (g)	33.20	32.88
Composition of liquid product (%)		
Acetaldehyde	3.9	4.1
Ethyl acetate	T	0.8
Ethyl propionate	15.4	7.8
Methyl ethyl ketone	0.6	0.2
n-propyl alcohol	4.8	4.1
Ethyl alcohol	30.4	34.5
Propionaldehyde	44.7	48.4
Unidentified product	0.2	0.1
Gas collected[b)] (*l*)	0.69	0.57

T: Trace
a) The precipitate (CuIX) prepared with potassium carbonate was used.
b) The gaseous products evolved contain hydrogen, carbon dioxide, ethylene, carbon monoxide, and ethane.

TABLE 4. THE CATALYTIC PROPERTIES OF REDUCED COPPER[a)] TOWARD *n*-BUTYL ALCOHOL

Experiment No.	17	18	19
Reaction temp. (°C)	220	250	300
n-Butyl alcohol (g)	18.63	19.13	19.32
Velocity (g/hr)	6.2	6.5	5.9
Liquid product (g)	17.78	18.23	18.37
Composition of liquid product (%)			
Butyraldehyde	16.2	20.1	24.2
n-Butyl-*n*-butyrate	5.7	15.0	20.9
Di-*n*-propyl ketone	0.2	0.6	5.3
Butyric acid	T	T	0.1
n-Propyl alcohol	T	0.2	0.5
Ethyl alcohol	T	0.2	0.3
Methyl alcohol	T	0.1	0.2
Water	T	T	T
Unidentified product	0.3	0.1	0.8
Unreacted alcohol	77.6	63.7	47.7
Gas collected[b)] (*l*)	1.42	2.06	3.57

T: Trace
a) The copper catalyst, prepared by treatment with sodium hydroxide followed by reduction with hydrogen, was used.
b) The gaseous products evolved contain hydrogen, carbon dioxide, 1-butene, methane, ethane, propane, and carbon monoxide.

TABLE 5. THE CATALYTIC PROPERTIES OF REDUCED COPPER TOWARD 2-PHENYLETHANOL

Experiment No.	20	21	22
Precipitate[a)]	CuVII		CuIX
Reaction temp. (°C)	250	300	250
2-Phenylethanol (g)	21.54	22.00	23.46
Velocity (g/hr)	12.6	12.1	12.5
Liquid product (g)	20.12	20.64	21.80
Composition of liquid product (%)			
Phenylacetaldehyde	17.7	9.8	8.2
Ethylbenzene	26.7	44.6	14.1
Toluene	10.8	33.3	6.9
Styrene	0.7	0.2	2.7
Methanol	0.1	T	0.2
Water	4.9	7.8	2.9
Unidentified product	0.1	0.1	6.6
Unreacted alcohol	39.0	4.2	58.4
Gas collected[b)] (*l*)	0.93	2.29	1.14

T: Trace
a) These precipitates were prepared by reduction with hydrogen.
b) The gaseous products contain hydrogen and carbon monoxide.

Table 6. The catalytic properties of reduced copper toward 1-phenylethanol

Experiment No.	23	24	25
Precipitate[a]	CuVII		CuIX
Reaction temp. (°C)	250	300	250
1-Phenylethanol (g)	20.28	20.50	21.76
Velocity (g/hr)	11.7	11.7	12.8
Liquid product (g)	18.99	19.09	20.23
Composition of liquid product (%)			
Phenyl methyl ketone	49.4	49.6	53.1
Ethylbenzene	43.1	42.8	39.4
Styrene	T	T	T
Water	7.2	7.4	6.7
Unidentified product	0	0	0
Unreacted alcohol	0.3	0.2	0.8
Gas collected[b] (*l*)	0.25	0.21	0.88

T: Trace
a) These precipitates reduced with hydrogen were used.
b) The gaseous products consist of hydrogen.

Table 7. The catalytic properties of reduced copper toward 3-phenyl-1-propanol

Experiment No.	26	27	28
Precipitate[a]	CuVII		CuIX
Reaction temp. (°C)	250	300	250
3-Phenyl-1-propanol (g)	19.77	20.00	21.07
Velocity (g/hr)	13.2	11.9	12.0
Liquid product (g)	18.31	18.50	19.49
Composition of liquid product (%)			
Phenylpropanal	13.9	33.3	12.5
n-Propylbenzene	11.4	28.4	4.8
β-Methylstyrene	2.4	9.8	1.6
Allylbenzene	0.7	1.6	0.2
Ethylbenzene	T	0.4	T
Methanol	T	T	T
Toluene	T	T	T
Ethanol	T	T	T
Water	2.1	6.3	1.2
Unidentified product	0.4	0.1	8.7
Unreacted alcohol	69.1	20.1	71.0
Gas collected[b] (*l*)	0.63	1.02	0.70

T: Trace
a) These precipitates reduced with hydrogen were used.
b) The gaseous products consist of hydrogen and the trace of carbon monoxide.

the ester in the reaction products; it has been found that the formation of the ester from alcohol is more increased by the use of the carbon monoxide-reduced copper catalyst than by the use of the hydrogen-reduced one. Judging from the values listed in Tables 1, 2, and 4, the yield of the reaction product under comparable conditions decreases with an increase in the molecular weight of alcohol. As is shown in Table 1, the copper catalyst is a good catalyst for the dehydrogenation of alcohol and for the ester formation, but it has a poor catalytic activity for aldol condensation. In the catalytic reaction of aliphatic primary alcohol, there are at least three important types of reactions which occur when primary alcohols are passed over reduced copper: (1) dehydrogenation, (2) ester formation, and (3) ketone formation.

The Mechanism of the Formation of the Main Products Obtained by the Catalytic Reaction of Aliphatic Alcohols. Many investigators[1] have found that aliphatic alcohols of n carbon atoms can be readily converted to the esters of $2n$ carbon atoms and to symmetrical ketones of $2n-1$ carbon atoms by vapor-phase contact with various catalysts. Especially, Komarewsky *et al.*[2e] reported that, in the presence of a chromium oxide catalyst, primary alcohols ranging from *n*-propyl to *n*-octadecyl alcohol can be converted to ketones by the following mechanism: (1) the dehydrogenation of alcohol to aldehyde, (2) the aldol condensation of aldehyde, (3) the removal of the carbon monoxide from the CHO group of the aldol, leaving a secondary

Table 8. The catalytic properties of reduced copper[a] toward cinnamyl alcohol

Experiment No.	29	30	31
Reaction temp. (°C)	260	280	300
Cinnamyl alcohol (g)	49.62	50.24	51.18
Velocity (g/hr)	14.9	15.8	15.9
Liquid product (g)	45.49	46.59	47.56
Composition of liquid product (%)			
Cinnamaldehyde	24.9	26.1	28.4
3-Phenylpropionaldehyde	43.5	41.1	33.3
β-Methylstyrene	19.1	20.6	22.3
Allylbenzene	2.1	2.3	2.9
3-Phenyl-l-propanol	0.8	1.0	1.2
Propylbenzene	1.1	1.4	2.3
Styrene	T	T	T
Ethylbenzene	T	0.2	0.4
Phenylacetylene	2.5	2.8	3.6
Methanol	T	T	T
Water	3.5	3.5	3.9
Unidentified product	0.6	1.0	1.7
Unreacted alcohol	1.9	0	0
Gas collected[b] (*l*)	0.06	0.05	0.02

T: Trace
a) The copper catalyst, prepared by treatment with sodium hydroxide followed by reduction with hydrogen, was used.
b) The gaseous products evolved consist of hydrogen.

alcohol, and (4) the dehydrogenation of this alcohol to ketone. On the other hand, the mechanism[7] of the conversion of ethyl alcohol into acetone was examined by Kagan and his co-workers,[8] who considered that ethyl acetate was an important intermediate in the chain of reactions involved. Dolgow and Golodnikow[9] showed that, upon passing alcohol over an activated copper catalyst or mixed catalysts (copper, nickel, zinc oxide, zirconium oxide, *etc.*) at atmospheric pressure and at 250°—300°C, a mixture of the ester and the ketone was obtained, and that the reaction was proceeded by an ester mechanism. The ester was obtained by the processes[10] to be shown below.

In the present research, propionaldehyde, *n*-propyl propionate, and a mixture of ethyl alcohol and propionaldehyde were selected for the study of the reaction mechanism. As is shown in Experiment Nos. 11—13 of Table 2, when propionaldehyde was passed over a copper catalyst, the aldehyde did not condense to give the ester, and small amounts of propionic acid and *n*-propyl alcohol were obtained. Further, as is shown in Table 3, when a mixture of ethyl alcohol and propionaldehyde was passed over reduced copper, the amount of ethyl propionate found in the reaction product was considerably higher than that of ethyl acetate. From these results, the presence of significant quantities of ester in the reaction product may be explained by a hemiacetal mechanism, as in the following schemes:

$$CH_3CH_2CH_2OH \longrightarrow CH_3CH_2CHO + H_2$$

$$CH_3CH_2CHO + CH_3CH_2CH_2OH \longrightarrow CH_3CH_2-\underset{\displaystyle H}{\overset{\displaystyle OH}{\overset{|}{\underset{|}{C}}}}-OCH_2CH_2CH_3$$

$$CH_3CH_2-\underset{\displaystyle H}{\overset{\displaystyle OH}{\overset{|}{\underset{|}{C}}}}-OCH_2CH_2CH_3 \longrightarrow CH_3CH_2-\overset{\displaystyle O}{\overset{\|}{C}}-OCH_2CH_2CH_3 + H_2$$

In the absence of the alcohol, propionaldehyde reacts to give only small amounts of acid and alcohol. These products seem to be obtained by a catalytic reaction between aldehyde and water. As is shown in Experiment No. 14 of Table 2, when *n*-propyl propionate was passed over a copper catalyst, the diethyl ketone, propionic acid, *n*-propyl alcohol, and propionaldehyde in the liquid product and the propylene and carbon dioxide in the gaseous product were obtained. Judging from these results, the formation of ketones from primary alcohols with reduced copper is probably accounted for by the Kagan process:[8]

$$2C_2H_5COOC_3H_7 \longrightarrow C_2H_5COC_2H_5 + C_3H_7OH + C_3H_6 + CO_2$$

Adkins[3d] found that when a mixture of primary alcohol and hydrogen was passed over Raney nickel at 250°C, hydrocarbon was obtained by the steps

7) $4\,C_2H_5OH \longrightarrow 4\,CH_3CHO + 2\,H_2$
$4\,CH_3CHO \longrightarrow 2\,CH_3COOC_2H_5 \xrightarrow{2H_2O} 2\,CH_3COOH + 2\,C_2H_5OH$
$2\,CH_3COOH \longrightarrow CH_3COCH_3 + CO_2 + H_2O$

8) M. J. Kagan, I. A. Sobolew, and G. D. Lubarsky, *Ber.*, **68**, 1140 (1935).

9) B. N. Dolgow and G. V. Golodnikow, *Zh. Obshch. Khim.*, **24**, 987, 1167, 1364 (1954).

10) Dolgow *et al.* proved that ethyl acetate is not primarily formed from $2C_2H_5OH \rightarrow CH_3COOC_2H_5 + 2H_2$, but, rather, by the condensation: $2CH_3CHO \rightarrow CH_3COOC_2H_5$, and that acetaldehyde, formed by the direct dehydrogenation of ethyl alcohol, is the intermediate product.

shown below.[11] Judging from the above results and from the gaseous products (alkane) obtained by this experiment, lower alcohols, such as ethyl alcohol and methyl alcohol, that were little produced by the catalytic reaction of *n*-propyl alcohol seem to be obtained by hydrogenolysis. In the case of ethyl alcohol, aldol condensation may also occur in the presence of reduced copper.

The Catalytic Properties of Reduced Copper toward Aromatic Alcohols. As may be seen from the amounts of unreacted alcohol shown in Tables 5—8, the conversion of aromatic alcohol to a reaction product varies considerably with the sort of alcohol. The percentage conversion of 2-phenylethanol is lower than that for 1-phenylethanol; this illustrates the effect of the primary or secondary nature of the alcohol on the ease of the catalytic reactions. Further, over reduced copper, 3-phenyl-1-propanol is less reactive than cinnamyl alcohol. As may be seen from Table 5, when 2-phenylethanol was passed over two types of reduced copper, heated at 250 and 300°C respectively, it was transformed into phenylacetaldehyde, ethylbenzene, toluene, styrene, methanol, and water as the liquid products. At high temperatures, the yields of toluene and carbon monoxide increased, while the yield of phenylacetaldehyde decreased. As may be seen from Table 8, cinnamyl alcohol, when passed over reduced copper heated at 260, 280, and 300°C, was converted into cinnamaldehyde, 3-phenylpropionaldehyde, β-methylstyrene, allylbenzene, 3-phenyl-1-propanol, propylbenzene, styrene, ethylbenzene, phenylacetylene, methanol, and water. Judging from the chromatograms (Columns: PEG-6000 and tricresyl phosphate) of the liquid products, the unidentified products listed in Experiment No. 22 of Table 5 and in Experiment No. 28 of Table 7 consist of a single compound. Accordingly, when the copper catalyst prepared with potassium carbonate as the precipitant was used, a different reaction seems to have occurred.

The Mechamism of the Formation of the Main Products Obtained by the Catalytic Reaction of Aromatic Alcohols. Adkins *et al.*[4d] reported that 3-phenyl-1-propanol was considerably more resistant to hydrogenolysis than 2-phenylethanol, and that, as a phenyl group became more distant from hydroxyl group, the hydrogenolysis of the carbon-oxygen linkage became more difficult. In the present research, when 3-phenyl-1-propanol was passed over the reduced copper, a large amount of *n*-propylbenzene was obtained.

The competitive hydrogenation of C=C and C=O in cinnamaldehyde over a palladium boride catalyst was studied by Kawai *et al.*[4g]; they reported that the reaction proceeded by the steps shown below.[12] Judging from the reaction products obtained by this experiment, it seems reasonable that the main products obtained by the catalytic reactions of 2-phenylethanol and cinnamyl alcohol with reduced copper were formed through the following schemes:

$$C_6H_5\text{-}CH_2\text{-}CH_2OH \longrightarrow C_6H_5\text{-}CH_2CHO + H_2$$
$$\xrightarrow{+H_2} C_6H_5\text{-}CH_2CH_3 + H_2O$$
$$C_6H_5\text{-}CH_2CHO \longrightarrow C_6H_5\text{-}CH_3 + CO$$
$$C_6H_5\text{-}CH{=}CHCH_2OH \begin{cases} \nearrow C_6H_5\text{-}CH{=}CHCHO \longrightarrow C_6H_5\text{-}CH_2CH_2CHO \\ \searrow C_6H_5\text{-}CH{=}CHCH_3 \longrightarrow C_6H_5\text{-}CH_2CH_2CH_3 \end{cases}$$

The hydrogenolysis apparently does not occur to any great extent on the catalytic reaction of the aliphatic primary alcohol with the reduced copper. However, with such aromatic alcohols as 2-phenylethanol, 1-phenylethanol, 3-phenyl-1-propanol, and cinnamyl alcohol, this is an important side-reaction. The extent of the hydrogenolysis will, therefore, depend upon the structure of the starting alcohol.

11) $RCH_2OH + H_2 \longrightarrow RH + CH_3OH$ $\qquad CH_3OH + H_2 \longrightarrow CH_4 + H_2O$

12) $C_6H_5\text{-}CH{=}CHCHO \begin{cases} \nearrow C_6H_5\text{-}CH_2CH_2CHO \\ \searrow C_6H_5\text{-}CH{=}CHCH_2OH \begin{cases} \nearrow C_6H_5\text{-}CH_2CH_2CH_2OH \\ \searrow C_6H_5\text{-}CH{=}CHCH_3 \longrightarrow C_6H_5\text{-}CH_2CH_2CH_3 \end{cases} \end{cases}$

Syntheses of 1,2,3-Trisubstituted 4-Aminoimidazolium Salts[1]

Akiko CHINONE, Sigeru SATO,* and Masaki OHTA

Department of Chemistry, Faculty of Science, Tokyo Institute of Technology, Ookayama, Meguro-ku, Tokyo

(Received September 14, 1970)

The salts of new mesoionic compounds of imidazole ring system having imino group at 4 position were synthesized by the reaction of amidines with haloacetonitriles. The resulting 4-amino-1,2,3-triphenylimidazolium salt was treated with sodium hydroxide to give an intermediate, *N*-cyanomethyl-*N*,*N'*-diphenylbenzamidine, which gave the salt of mesoionic imidazole with dry hydrogen bromide. 1,2,3-Trisubstituted 4-aminoimidazolium salts were treated with acetic anhydride or with picric acid or with silver perchlorate to give acetylated derivative, picrates and perchlorates, respectively.

Of the mesoionic imidazoles with an exo-imino group, only fused ring compounds have been reported.[2] We wish to report here the preparation of salts of 4-iminoimidazole.

As a possible route towards a synthesis of mesoionic 3,4-dihydro-4-iminoimidazole (anhydro-4-aminoimidazolium hydroxide), we tried the reaction of *N*-methyl-*N'*-phenylbenzamidine (Ia) with bromoacetonitrile (IIa) anticipating the formation of an intermediate V. When the reaction was carried out in toluene, V was not isolated, but 4-amino-3-methyl-1,2-diphenylimidazolium bromide (IVa) was obtained. Attempts to isolate the intermediate, *N*-cyanomethyl-*N*-phenyl-*N'*-methylbenzamidine, were unsuccessful even in the presence of triethylamine or sodium acetate. The structure of the salt of mesoionic compound is most likely to be IVa instead of IVa', since the alkylation of amidine occurs preferentially at the doubly-linked nitrogen atom. It is known that *N*-methyl-*N'*-phenylbenzamidine reacts preferably in form A rather than in form B.[3,4] When the diphenylbenzamidine (Ib) was treated with IIa in xylene, corresponding triphenyl substituted derivative (IVb) was obtained. By the same method, *N*-phenyl-*N'*-*p*-tolylbenzamidine (Ic) was reacted with IIa to give IVc. Considering the influence of the groups R_1 and R_3 in Ic on the basicity of the nitrogen atom, IVc seems to be preferable to IVc'.[3] In the reaction of *N*-*p*-nitrophenyl-*N'*-phenylbenzamidine (Id) with IIa, it was found that the influence of the nitro group in Id was such that no reaction occurred with IIa under the same conditions. Although the isolation of the salt III was not successful, these ring formations seem to proceed through salts III, followed by interaction of two groups, with a mechanism similar to that of sydnone imine salts formation.[5] The structure of these products was established by elementary analyses and infrared spectra, which showed bands at 3380—3100 cm^{-1} corresponding to N–H stretching vibration, and at 1650—1645 cm^{-1} due to imidazole ring.

The reaction of amidines (Ia—Ic) with chloroacetonitrile (IIb) did not take place. However, amidines (Ia—Ic) reacted with IIb and equimolar amount of potassium iodide to give corresponding imidazolium iodides (IVd—IVf) in an ethanol solution. The mechanism of formation of the imidazolium iodides seems to proceed *via* halogen exchange followed by nucleophilic attack as mentioned above. Treatment of IVa with sodium bicarbonate or triethylamine did not give free base, but resulted in recovery of starting material. This indicates that the free base of IVa is stronger than the bases. No reaction was observed also in the treatment of IVb with sodium bicarbonate or triethylamine. Treatment of IVb with sodium hydroxide did not give the free base but afforded the intermediate Va, IR spectrum of which did not show C≡N stretching vibration as in the case of *O*-cyanomethyl-*N*-phenylbenzimidate.[6] On treating Va with dry hydrogen bromide, IVb was obtained. Treatment of IVa or IVc with sodium hydroxide gave oily substance which could not be purified. Treatment of IVa with acetic anhydride gave the *N*-acetyl derivative VI. The infrared spectrum was consistent with that expected for VI, showing a weak band at 3190 cm^{-1} resulting from N–H stretching vibration, and a strong band at 1697 cm^{-1} resulting from carbonyl group. On the other hand, treatment of IVb with acetic anhydride gave hygroscopic product which could not be identified. On treating IVa or IVb with picric acid, the picrates VIIa and VIIb were obtained respectively. On treating the iodides IVd—IVf with silver perchlorate, stable perchlorates VIIIa—VIIIc were obtained in good yield. Treatment of the perchlorate with acetic anhydride resulted in the recovery of starting material instead of acetylated product.

Diaryl substituted imidazolium salts (IVa, IVd, and VIIIa) show absorption maxima at about 290 mμ and triaryl substituted imidazolium salts (IVb, IVc, IVe, IVf, VIIIb, and VIIIc) show absorption maxima at about 300 mμ irrespective of the anion, which are suggestive of their heteroaromatic system. The NMR spectrum of IVd in $CDCl_3$–CD_3CN exhibits two singlets at τ 6.40 (3H, methyl protons at 3-position) and at τ 3.03 (1H, a proton at 5-position) and multiplet at τ 2.4—2.8 (10H, protons of phenyl groups). Methyl protons of IVd are shielded to a greater extent as compared with those attached to sydnone and sydnone imine ring.[7,8] The proton at 5-position is deshielded

1) Studies of mesoionic compounds. XXXIV. Part XXXIII: A. Shaikh, A. Chinone, and M. Ohta, This Bulletin, 453 **43**, (1970).

* Present address: Mitsubishi Chemical Industries Ltd., Central Research Laboratory, 290 Isamoto, Kamoicho, Kawasaki.

2) N. W. Bristow, P. T. Charlton, D. A. Peak, and W. F. Short, *J. Chem. Soc.*, **1954**, 616.

3) F. L. Pyman, *ibid.*, **1923**, 3359.

4) C. G. Raison, *ibid.*, **1949**, 3319.

5) P. Brookes and J. Walker, *ibid.*, **1957**, 4409.

6) A. Chinone, S. Sato, T. Mase, and M. Ohta, This Bulletin, **42**, 2310 (1969).

7) K. D. Lawson, W. S. Brey, Jr., and L. B. Kier, *J. Amer. Chem. Soc.*, **86**, 463 (1964).

8) H. U. Daeniker and J. Druey, *Helv. Chim. Acta*, **45**, 2441 (1962).

as compared with imidazole. The NMR spectrum of IVe exhibits a multiplet at τ 2.40—2.95, and IVf exhibits a singlet at τ 7.65 (3H, methyl protons of *p*-tolyl group) and a multiplet at τ 2.4—3.0.

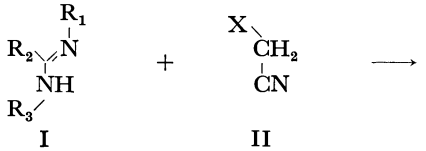

I II

Ia: $R_1=R_2=C_6H_5$, $R_3=CH_3$ IIa: X=Br IIb: X=Cl
Ib: $R_1=R_2=R_3=C_6H_5$
Ic: $R_1=R_2=C_6H_5$, $R_3=p$-$CH_3C_6H_4$
Id: $R_1=R_2=C_6H_5$, $R_3=p$-$NO_2C_6H_4$

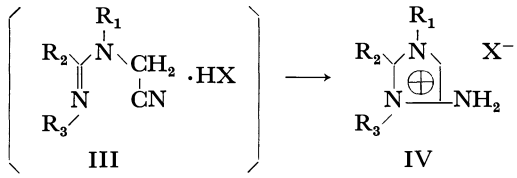

III IV

IVa: $R_1=R_2=C_6H_5$, $R_3=CH_3$, X=Br
(IVa′: $R_1=CH_3$, $R_2=R_3=C_6H_5$, X=Br)
IVb: $R_1=R_2=R_3=C_6H_5$, X=Br
IVc: $R_1=R_2=C_6H_5$, $R_3=p$-$CH_3C_6H_4$, X=Br
(IVc′: $R_1=p$-$CH_3C_6H_4$, $R_2=R_3=C_6H_5$, X=Br)
IVd: $R_1=R_2=C_6H_5$, $R_3=CH_3$, X=I
IVe: $R_1=R_2=R_3=C_6H_5$, X=I
IVf: $R_1=R_2=C_6H_5$, $R_3=p$-$CH_3C_6H_4$, X=I

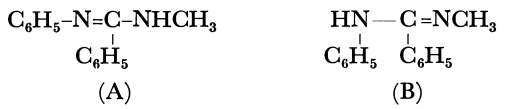

(A) (B)

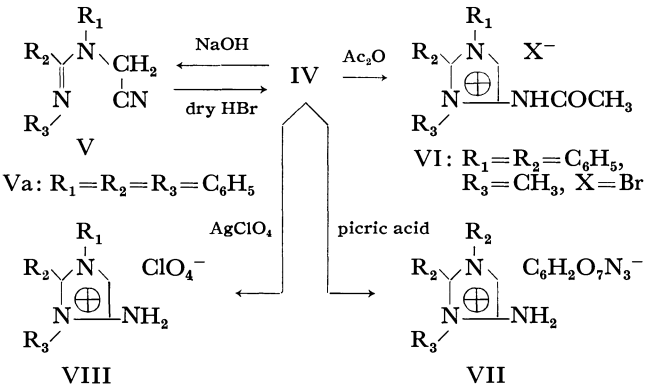

V VI

Va: $R_1=R_2=R_3=C_6H_5$
VI: $R_1=R_2=C_6H_5$, $R_3=CH_3$, X=Br

VIII VII

VIIIa: $R_1=R_2=C_6H_5$, $R_3=CH_3$
VIIIb: $R_1=R_2=R_3=C_6H_5$
VIIIc: $R_1=R_2=C_6H_5$, $R_3=p$-$CH_3C_6H_4$

VIIa: $R_1=R_2=C_6H_5$, $R_3=CH_3$
VIIb: $R_1=R_2=R_3=C_6H_5$

Experimental

All melting points were determined on a micro hot stage and are not corrected. Infrared spectra were taken on KBr tablet.

4-Amino-3-methyl-1,2-diphenylimidazolium Bromide (IVa). A solution of 2.1 g of *N*-methyl-*N*′-phenylbenzamidine and 1.2 g of bromoacetonitrile (IIa) in 30 m*l* of toluene was refluxed for 3 hr. After cooling, the precipitates were collected and washed with benzene, and recrystallized from acetonitrile to give colorless prisms with a mp of 280—285°C.

Found: C, 58.24; H, 4.71; N, 12.50%. Calcd for $C_{16}H_{16}N_3Br$: C, 58.12; H, 4.85; N, 12.73%. IR: 3440, 3275, 3140, 1660, 1647 cm^{-1}. λ_{max}^{EtOH} 290 mμ (ε 7500).

4-Amino-1,2,3-triphenylimidazolium Bromide (IVb). (i) A solution of 2.7 g of diphenylbenzamidine and 1.2 g of IIa in 30 m*l* of xylene was refluxed for 4 hr. After cooling, the precipitates which separated out were collected and recrystallized from ethanol to give colorless prisms with a mp of 282—284°C (yield 60%).

Found: C, 64.05; H, 4.88; N, 10.60%. Calcd for $C_{21}H_{18}N_3Br$: C, 64.29; H, 4.59; N, 10.71%. IR: 3380, 3110, 1646 cm^{-1}. λ_{max}^{EtOH} 302 mμ (ε 7000).

(ii) To a solution of 0.1 g of *N*-cyanomethyl-*N*,*N*′-diphenylbenzamidine in 10 m*l* of benzene, 20 m*l* of benzene containing 0.05 g of gaseous hydrogen bromide was added dropwise. Precipitates which separated out were collected and recrystallized from ethanol. No depression of the melting point was observed on admixture with the product obtained by method (i).

*4-Amino-1,2-diphenyl-3-*p*-tolylimidazolium Bromide (IVc).* A solution of 2.86 g of *N*-phenyl-*N*′-*p*-tolylbenzamidine an 1.2 g of IIa in 30 m*l* of xylene for 40 min. After cooling, the precipitates were collected and reprecipitated from and ethanol solution with ether to give colorless prisms with a mp of 267—268°C (yield 58%).

Found: C, 64.88; H, 5.12; N, 10.52%. Calcd for $C_{22}H_{20}N_3Br$: C, 65.04; H, 4.93; N, 10.35%. IR: 3400, 3100, 1650 cm^{-1}. λ_{max}^{EtOH} 298 mμ (ε 6700).

4-Amino-3-methyl-1,2-diphenylimidazolium Iodide (IVd). A suspension of 2.1 g of *N*-methyl-*N*′-phenylbenzamidine and 0.8 g of chloroacetonitrile (IIb) and 1.7 g of potassium iodide in 50 m*l* of ethanol was refluxed for 5 hr, and after cooling the precipitates were filtered off. The filtrate was treated with activated charcoal and concentrated in a vacuum to give crude product, which was reprecipitated from an ethanol solution with ether to give colorless prisms with a mp of 205—206°C (yield 24%).

Found: C, 51.02; H, 4.48; N, 11.02%. Calcd for $C_{16}H_{16}N_3I$: C, 50.94; H, 4.25: N, 11.14%. IR: 3255, 3130, 1645 cm^{-1}. λ_{max}^{EtOH} 292 mμ (ε 7100).

4-Amino-1,2,3-triphenylimidazolium Iodide (IVe). A suspension of 1.36 g of diphenylbenzamidine and 0.38 g of IIb and 0.83 g of potassium iodide in 20 m*l* of ethanol was refluxed for 7 hr. After cooling, precipitates were collected and recrystallized from ethanol to give colorless needles with a mp of 280—283°C (yield 44%).

Found: C, 57.12; H, 4.33; N, 9.73%. Calcd for $C_{21}H_{18}N_3I$: C, 57.42; H, 4.10; N, 9.57%. IR: 3400, 3140, 1645 cm^{-1}. λ_{max}^{EtOH} 300 mμ (ε 6300).

*4-Amino-1,2-diphenyl-3-*p*-tolylimidazolium Iodide (IVf).* This compound was prepared by a method analogous to that of IVd. Reprecipitation from an ethanol solution with ether gave colorless needles with a mp of 272—274°C (yield 36%).

Found: C, 58.04; H, 4.66; N, 9.34%. Calcd for $C_{22}H_{20}N_3I$: C, 58.29; H, 4.42; N, 9.27%. IR: 3400, 3150, 1650 cm^{-1}. λ_{max}^{EtOH} 300 mμ (ε 6600).

N-Cyanomethyl-N,N′-diphenylbenzamidine (Va). To a solution of 1 g of IVb in 20 m*l* of ethanol, 2 m*l* of 8% aqueous sodium hydroxide solution was added. Precipitates were collected and recrystallized from ethanol to give colorless prisms with a mp of 128—130°C (yield 60%).

Found: C, 80.96; H, 5.56; N, 13.40%. Calcd for $C_{21}H_{17}N_3$: C, 81.00; H, 5.50; N, 13.50%. IR: 1615 cm^{-1}. NMR:

τ_{Me_4Si} ($CDCl_3$) 5.2 (2H, singlet), 2.7—3.4 (15H, multiplet).

N-Acetyl-4-amino-3-methyl-1,2-diphenylimidazolium Bromide (VI). A solution of 1 g of IVa in acetic anhydride was heated at 100°C for 5 min. After cooling, ether was added to the solution, and the precipitates were collected and recrystallized from acetonitrile to give colorless prisms with a mp of 270—273°C (yield 62%).

Found: C, 57.94; H, 4.72; N, 11.18%. Calcd for $C_{18}H_{18}N_3OBr$: C, 58.07; H, 4.83; N, 11.29%. IR: 3190, 3100, 1697, 1618 cm^{-1}.

Reaction of IVa or IVb with Picric Acid. To a solution of IVa in ethanol, a solution of picric acid in ethanol was added and refluxed for 2 min. After cooling the precipitates were collected and recrystallized from ethanol-ethyl acetate to give VIIa with a mp of 193—194°C.

Found: C, 54.96; H, 3.54; N, 17.71%. Calcd for $C_{22}H_{18}N_6O_7$: C, 55.23; H, 3.79; N, 17.57%.

By the same method as mentioned above, VIIb was obtained from IVb as yellow needles with a mp of 180—182°C.

Found: C, 59.46; H, 3.95; N, 15.27%. Calcd for $C_{27}H_{20}N_6O_7$: C, 60.00; H, 3.73; N, 15.55%.

1,2,3-Trisubstituted 4-Aminoimidazolium Perchlorates (VIIIa—VIIIc). To a solution of IVd (0.33 g) in acetonitrile-chloroform, a solution of 0.21 g of silver perchlorate in chloroform-ethanol was added dropwise. The precipitates were filtered off and filtrate was concentrated in a vacuum to give crude product, which was reprecipitated from a chloroform solution with ether to give VIIIa as colorless needles with a mp of 145—146°C (yield 69%).

Found: C, 54.73; H, 4.39; N, 12.06%. Calcd for $C_{16}H_{16}N_3O_4Cl$: C, 54.94; H, 4.61; N, 12.01%. IR: 3400, 3330, 1655 cm^{-1}. λ_{max}^{EtOH} 292 mμ (ε 6500).

By the same method as mentioned above, VIIIb was obtained from IVe as colorless needles with a mp of 254—256°C (yield 75%).

Found: C, 60.94; H, 4.60; N, 10.18%. Calcd for $C_{21}H_{18}N_3O_4Cl$: C, 61.22; H, 4.40; N, 10.21%. IR: 3425, 3330, 1650 cm^{-1}. λ_{max}^{EtOH} 302 mμ (ε 6600).

By the same method as mentioned above, VIIIc was obtained from IVf as colorless needles with a mp of 204—205°C (yield 59%).

Found: C, 62.14; H, 4.97; N, 9.89%. Calcd for $C_{22}H_{20}N_3O_4Cl$: C, 62.03; H, 4.73; N, 9.87%. IR: 3410, 3325, 1650 cm^{-1}. λ_{max}^{EtOH} 300 mμ (ε 6400).

BULLETIN OF THE CHEMICAL SOCIETY OF JAPAN, VOL. 44, 828—832 (1971)

The Reaction of α-Carbonyl Sulfides with Bases. I. The Reaction between α-Carbonyl Sulfides with Thiolates

Michinori Ōki, Wataru Funakoshi, and Atsuko Nakamura
Department of Chemistry, Faculty of Science, The University of Tokyo, Hongo, Tokyo
(Received September 29, 1970)

It is found that carbonyl compounds, such as ketones and esters, bearing an alkyl(or aryl)thio group at the α-position, are smoothly reduced to the parent carbonyl compounds by the action of the thiolate anion. α-Halo or α,α-dihalo ketones are similarly reduced with the thiolate, probably *via* the corresponding sulfides. The mechanism of the reaction is discussed.

Since oxygen and sulfur belong to the same group in the periodic table, many similar reactions occur with the oxygen-sulfur analogs. However, there are also some dissimilarities, mainly because of the ability of the sulfur atom to expand its valence shell. The formations of the quadrivalent and sexivalent sulfur compounds are typical examples. As another dissimilarity of the two elements, the behavior toward bases may be cited; elemental sulfur itself and other polysulfides are known to undergo electrophilic cleavage,[1] whereas the dialkyl peroxides have seldom been reported to be cleaved by the bases.[2]

During the course of another study, we have encountered a rather curious reaction: the treatment of α-chlorodeoxybenzoin (**1**) with sodium methanethiolate (**2**) in ethanol gave rise to the formation of deoxybenzoin (**3**) instead of the expected α-(methylthio)deoxybenzoin (**4**). This finding of an unexpected reaction allured us to investigate the scope and the mechanism of the reaction. The purpose of this paper is to present the results of these studies and our conclusion that this unexpected reaction probably occurs *via* a nucleophilic attack of the thiolate ion on sulfur:

$$\underset{\text{(1)}}{C_6H_5\text{-}\underset{Cl}{CH}\text{-}\overset{O}{C}\text{-}C_6H_5} \xrightarrow[\text{(2)}]{CH_3SNa} \underset{\text{(3)}}{C_6H_5\text{-}CH_2\text{-}\overset{O}{C}\text{-}C_6H_5}$$

Results and Discussion

The cautious treatment of **1** with one equivalent of **2** in ethanol at 0°C resulted in the formation of **4** in a good yield, whereas the heating of an equimolar mixture of **1** and **2** in ethanol afforded a mixture of **3** and **4**. Thus, it is possible that the formation of **4** is the intervening process in the reduction of **1** to **3**.

$$\mathbf{1} \xrightarrow{CH_3SNa} \underset{\text{(4)}}{C_6H_5\text{-}\underset{CH_3S}{CH}\text{-}\overset{O}{C}\text{-}C_6H_5} \xrightarrow{CH_3SNa} \mathbf{3}$$

1) A. J. Parker and N. Kharasch, *Chem. Rev.*, **59**, 583 (1959).
2) Oxidation of olefins and amines with peroxy acid and Baeyer-Villiger oxidation may be considered to involve the nucleophilic cleavage of the O–O bonds. For cleavage of hydrogen peroxide with various bases, see J. O. Edwards and R. G. Pearson, *J. Amer. Chem. Soc.*, **84**, 16 (1962).

Table 1. Reduction of α-alkylthio carbonyl compounds with thiolates

Run No.	Substrate	Thiol	Molar ratio[a)]	Reaction period (hr)	Yield (%)	Products
1	$C_6H_5COCHC_6H_5$ (SC$_2$H$_5$)	C_2H_5SH	1.0	0.5	quant.	$C_6H_5COCH_2C_6H_5$
2	$C_6H_5COCH_2SC_2H_5$	C_2H_5SH	1.1	2	85	$C_6H_5COCH_3$
3	$C_6H_5COCH_2SCH_3$	C_2H_5SH	1.3	2	quant.	$C_6H_5COCH_3$
4	$C_6H_5COCH_2SCH_3$	C_6H_5SH	1.6	4	—	$C_6H_5COCH_3$ and $C_6H_5COCH_2SCH_3$ (4:1)
5	α-(Ethylthio)cyclohexanone	C_2H_5SH	1.3	10	10	Cyclohexanone
6	2-Ethylthio-1-tetralone	C_2H_5SH	1.3	2.5	62	1-tetralone
7	$CH_3SCH_2CO_2C(CH_3)_3$	CH_3SH	3.0	1.5	quant.	$CH_3CO_2C(CH_3)_3$

a) Molar ratio is expressed by dividing number of moles of the thiolates by that of the substrates.

Table 2. Reduction of α-halo carbonyl compounds with thiolates

Run No.	Substrate	Thiol	Molar ratio[a)]	Reaction period (hr)	Yield (%)	Products
8	$C_6H_5COCHClC_6H_5$	C_2H_5SH	1.0	0.4	—	$C_6H_5COCH_2C_6H_5$, $C_6H_5COCHClC_6H_5$, and $C_6H_5COCH(SC_2H_5)C_6H_5$ (3:1:4)
9	$C_6H_5COCHClC_6H_5$	C_2H_5SH	5.0	0.25	quant.	$C_6H_5COCH_2C_6H_5$
10	$C_6H_5COCH_2Cl$	C_2H_5SH	2.0	1.5	94	$C_6H_5COCH_3$
11	$C_6H_5COCH_2Cl$	CH_3SH	2.1	1.5	84	$C_6H_5COCH_3$
12	$(CH_3)_3CCOCH_2Cl$ + $(CH_3)_3CCOCHCl_2$	C_2H_5SH	—	1.5	—	$(CH_3)_3CCOCH_3$
13	2-Chlorocyclohexanone	C_2H_5SH	2.2	10	29	Cyclohexanone
14	3-Bromocamphor	C_2H_5SH	2.5	1.5	62	Camphor
15	$C_6H_5CHClCO_2C_2H_5$	C_2H_5SH	2.0	1.5	90	$C_6H_5CH_2CO_2H$ (after hydrolysis)
16	$C_6H_5CHClCO_2C_2H_5$	C_2H_5SH	2.1	0.5	—	$C_6H_5CH_2CO_2C_2H_5$ and $C_6H_5CH(SC_2H_5)CO_2C_2H_5$ (2:1)
17	$ClCH_2CO_2C(CH_3)_3$	C_2H_5SH	2.0	3.5	—	$CH_3CO_2C(CH_3)_3$ and $C_2H_5SCH_2CO_2C(CH_3)_3$

a) Molar ratio is expressed by dividing number of moles of the thiolates by that of the substrates.

Indeed, treating **4** with **2** also afforded **3** in a good yield; in order to reduce **1** to **3** in a good yield, it was necessary to use two molar portions of **2** for each mole of **1**.

In order to test the generality of the reaction, various α-halo or α-alkylthio carbonyl compounds were treated with various thiolates: the results are shown in Tables 1 and 2. It may now be said that the reduction with thiolate is a fairly general reaction. A few of the interesting points to be pointed out are as follows: 1) even α,α-dihalo ketone can be reduced to the parent ketone with thiolate (run 12); 2) α-alkylthio and α-halo esters are also reduced with thiolate (runs 7 and 17); 3) benzenethiolate is a weaker reducing agent than the alkanethiolates (run 4). It seems that the solvent must be fairly polar in order to effect the reaction, since treating α-(methylthio)acetophenone with ethanethiolate in benzene gave only a trace of the reduced material.

It is now necessary, for studying the mechanism of the reaction further, to know the fate of the sulfur compounds: it was found that dimethyl disulfide was formed when **1** was treated with **2**. Although the treatment of **4** with sodium ethanethiolate afforded dimethyl disulfide and diethyl disulfide in addition to ethyl methyl disulfide, the formations of the symmetric disulfides could be attributed to the scrambling of the ethyl methyl disulfide because of the presence of ethanethiolate anion:[1,3)]

$$RSSR' + RS^- \longrightarrow RSSR + R'S^-$$

$$RSSR' + R'S^- \longrightarrow R'SSR' + RS^-$$

Other combinations of thioethers and thiolates which could give asymmetric disulfides also afforded symmetric sulfides.

The formation of disulfides might be interpreted as indicating that the reaction proceeded *via* a radical intermediate. However, the idea is rather inconsistent with the solvent effects and the fact that the conditions

3) S. Oae and H. Tanaka, *Yukigosei Kagaku Kyokaishi*, **27**, 793 (1969).

are strongly ionic. Another fact may be added as a proof against the radical intermediate; the reduction with benzenethiolate is slow compared with that with ethanethiolate. Trapping the intermediate was thus attempted in order to ascertain the nature of this reaction.

1 was treated with sodium methanethiolate in dimethyl sulfoxide to form a deep red-orange solution. The solution was quenched with water to give **3**, whereas quenching with methyl iodide gave α-methyldeoxybenzoin (**6**). Thus, the reaction clearly proceeds *via* an ionic intermediate; otherwise it is difficult to explain the products. It is most probable to assume the intermediacy of the deprotonated anion of deoxybenzoin (**5**). Then, in ethanol and other protic solvents, **5** picks up a proton to form **3**, whereas it survives in dimethyl sulfoxide until quenched.

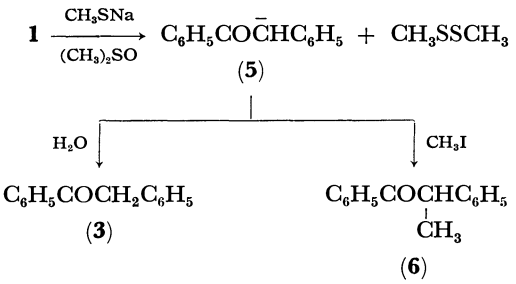

In view of the above discussion, thiolate must attack the sulfur atom of the thioethers as a nucleophile. That is, this reaction involves a nucleophilic attack at the sulfur atom of the thioether. If this mechanism is assumed, it is easy to explain the slow reaction with benzenethiolate, since benzenethiolate is a more stable anion than ethanethiolate[4] and may thus be a poorer nucleophile.

Two possibilities may be considered as the reaction mechanism: S_N1- and S_N2-type reactions at the sulfur atom of the thioether. These mechanisms may be expressed by Eqs. (1) and (2) respectively:

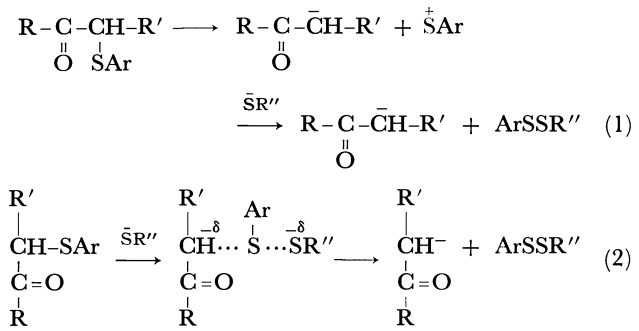

(1)

(2)

However, the possibility of the S_N1-type reaction can be ruled out for the following reason: if it were an S_N1-type reaction, there would be no reason for the alkoxide ion to fail to cause a similar reaction, but it actually is the case as will be demonstrated in the following paper.[5]

4) p*Ka* values of benzenethiol and ethanethiol are 12.0 and 8.3, respectively. M. Ōki, "San to Enki (Acids and Bases)," Baifūkan, Tokyo (1967), p. 66.

5) M. Ōki and W. Funakoshi, This Bulletin, **44**, 832 (1971).

Information about the transition state of the reaction can be obtained by measuring the substituent effects on the rates of the reaction. The pseudo-first-order rates of the reaction of α-(phenylthio)acetophenone and α-(*p*-bromophenylthio)acetophenone with sodium benzenethiolate were thus obtained using an excess of thiophenol and a reasonable amount of sodium in order to keep the concentration of the thiolate constant, while the second-order rates were calculated by using the concentration of the thiolate ion. The results are listed in Table 3. The rates are slightly diminished when the substituent is electron-withdrawing. Thus, the results may be taken as favoring the S_N2-type transition state rather than the S_N1-type, since, if it were an S_N1-type reaction, the decrease in ratio would be much larger.

Table 3. Rates of reaction of α-(arylthio)-acetophenone ($ArSCH_2COC_6H_5$) with sodium benzenethiolate in ethanol (65°C)

Ar	$k_1 \times 10^2$ hr^{-1}	$k_2 \times 10^5$ *l*·mol^{-1}·hr^{-1}
C_6H_5	2.65	1.15
p-BrC_6H_4	1.4	0.7

Another alternative may be postulated as a rate-determining step: the electron pair is donated by the anion to the sulfur *d*-orbital to form **7**:

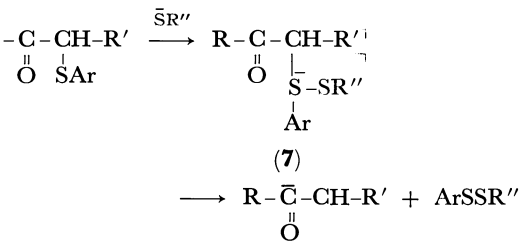

This possibility can, however, be ruled out also: if it were the case, the electron-withdrawing substituent would enhance the reaction rate.

It may be argued that reduction may not be directly caused by the thiolate anion, but by the hydride shift from either alkoxide or the thiolate anion, as many reductions are known to occur by the action of alkoxide through the hydride shift. However, this possibility can be discarded for two reasons. First, as will be discussed in the following paper,[5] ethoxide is not capable of reducing the α-alkylthio ketone. The second reason is that benzenethiolate can reduce α-alkyl(or aryl)-thio ketone in ethanol. In the latter reaction, the reducing agent must be the benzenethiolate ion, which has no α-hydrogen, since ethoxide, which may exist because of an equilibrium and also as a reaction product, has no power to reduce the alkylthio ketone.

Having established the nucleophilic nature of the reaction, the next problem is to clarify the role of the carbonyl group. The role of the carbonyl group may be considered to be two-fold. First, it acts as an anion-stabilizing substituent because of its intrinsic mesomeric and inductive nature **8**. Second, the attacking base may add to the carbonyl group first, and then within the adduct **9** a nucleophilic reaction may take place, as is indicated by the arrows:

Table 4. Reactions of some α-substituted ketones with thiolates in ethanol

Substrate	Thiol	Molar ratio[a)]	Reaction period (hr)	Yield of parent ketone (%)
$C_6H_5CH(SCN)C_6H_5$	C_2H_5SH	6.0	2	quantitative
$C_6H_5COCH_2SCN$	C_2H_5SH	2.5	7	45
$C_6H_5COCH_2Cl$	H_2S	20	5	10
$C_6H_5COCH_2SCOCH_3$	C_2H_5SH	8.0	1	84

a) Molar ratio was calculated on the basis of sodium used for making thiolates. Thiols were used always in excess relative to sodium.

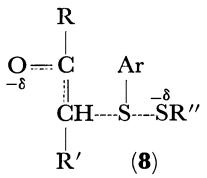

(8)

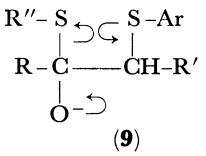

(9)

The data are rather contradictory and confusing. Triphenylmethyl chloride, ethyl triphenylmethyl thioether, phenyl trichloromethyl thioether, and *p*-benzoylbenzyl ethyl thioether gave no sign of reduction when treated with thiolate either in ethanol or in dimethyl sulfoxide-ethanol, although triphenylmethyl, trichloromethyl, and *p*-benzoylbenzyl groups are supposed to stabilize the anion to a considerable extent. These results suggest that the presence of the anion-stabilizing substituent is not good enough to cause the reaction, thus favoring the intermediate **9**. Failure of methyl *p*-tolyl sulfone to be formed from phenylthiomethyl *p*-tolyl sulfone may be added as another proof for the intermediacy of **9**, since bromomethyl *p*-tolyl sulfone is reported to be reduced by a thiolate to methyl *p*-tolyl sulfone.[6)] However, it may be argued that this is not direct proof of the importance of the carbonyl group in the reduction with thiolate, because deprotonation may compete with the nucleophilic attack at the sulfur atom.

$$p\text{-}CH_3C_6H_4SO_2CH_2Br \xrightarrow{\bar{S}C_6H_5} p\text{-}CH_3C_6H_4SO_2CH_3$$

On the other hand, there is a fact which cannot be explained by the intermediate **9**: α-(ethylthio)deoxybenzoin is smoothly reduced with triphenylphosphine. The details of the reaction will be discussed in the next paper.[5)] If the adduct **10**, which itself will be of high energy because of the charge separation and the steric effect, is formed, it has to be assumed that the positively-charged phosphorus behaves as a nucleophile: this is, though, highly unlikely.

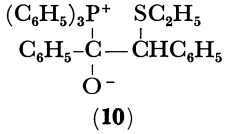

(10)

The mechanism of the reaction could be different according to the structure of the substrate and the attacking base. This point must be explored further.

6) F. G. Bordwell and B. B. Jarvis, *J. Org. Chem.*, **33**, 1182 (1968).

Finally, we wish to point out that the reaction of α-carbonyl sulfide with thiolate is not limited to α-carbonyl thioethers; some other sulfur compounds are also cleaved at the C–S bond to produce the parent carbonyl compounds. Some of the results are shown in Table 4. It will be seen that thiocyano and acetylthio ketones are smoothly reduced to the parent ketones.[7)] The isolation of acetophenone in a low yield on the treatment of α-chloroacetophenone with sodium hydrogen sulfide may be attributed to the presence of an equilibrium of ionization such as is expressed by the following equation (negative charge on the sulfur atom should certainly reduce the possibility of the nucleophilic attack):

$$C_6H_5COCH_2SH + HS^- \rightleftharpoons C_6H_5COCH_2S^- + H_2S$$

It has been well established that disulfides are cleaved at the S–S bond by various bases, and excellent reviews have been published.[1,3)] However, thioethers are known to be fairly inert toward bases, and under forcing conditions a proton alpha to the sulfur atom is removed because of the stabilization due to the sulfur atom.[8)] The reaction discovered here occurs under rather mild conditions and is a unique one in a sense mentioned above.

Experimental

Materials. The following new thioethers were identified.

α-(Methylthio)deoxybenzoin. α-Chlorodeoxybenzoin (26.5 g or 0.115 mol) was allowed to react with sodium methanethiolate in ethanol prepared from 27 g (0.56 mol) of methanethiol at −15°C. The reaction mixture was poured into water after 30 min at 0°C and extracted with ether to afford α-(methylthio)deoxybenzoin, mp 73—73.5°C, in almost quantitative yield. Found: C, 74.36; H, 5.70%. Calcd for $C_{15}H_{14}OS$: C, 74.36; H, 5.80%.

Similarly the following compounds were prepared.

α-(Ethylthio)deoxybenzoin: mp 74.1—75.5°C. Found: C, 75.29; H, 6.30%. Calcd for $C_{16}H_{16}OS$: C, 74.98; H, 6.29%.

α-(Ethylthio)cyclohexanone: bp 119—121°C/30 mmHg. Found: C, 60.70; H, 8.66%. Calcd for $C_8H_{14}OS$: C, 60.74; H, 8.92%.

7) Incidentally, this makes a very interesting contrast with the reaction between some nucleophiles and methyl α-thiocyanoacetate in that the latter yields $^-SCH_2CO_2CH_3$ anion. See R. G. Hiskey, W. H. Bower, and D. N. Harpp, *J. Amer. Chem. Soc.*, **86**, 2010 (1964); R. G. Hiskey and D. N. Harpp, *ibid.*, **86**, 2014 (1964).

8) Hydrogen atoms of the methylene group which is placed between two sulfur atoms are easily exchanged by deuterium under the influence of the basic catalyst. See for example: S. Oae, W. Takagi, and A. Ohno, *Tetrahedron*, **20**, 427 (1964).

α,α-Bis(methylthio)acetophenone: mp 65.5—66.5°C. Found: C, 56.80; H, 5.58%. Calcd for $C_{10}H_{12}OS_2$: C, 56.60; H. 5.70%.

The Reaction of Thiolates with Sulfides and Halogen Compounds. As an example of the general procedure, the reduction of α-chlorodeoxybenzoin with methanethiolate will be described. The reduction of the sulfides proceeded smoothly with equimolar thiolate, whereas the halides needed at least 2 molar portions of thiolate to produce the parent ketone in a good yield. Sometimes an excess of thiol was used to cover the loss by vaporization.

To a solution prepared from 0.3 mol of sodium and 150 m*l* of ethanol, was added 0.4 mol of methanethiol and then 0.126 mol of α-chlorodeoxybenzoin. The solution was heated under reflux and poured into water after 30 min. The subsequent extraction of the mixture gave deoxybenzoin, mp 56—57°C, in an almost quantitative yield.

The other products were analyzed by vapor-phase chromatography.

Reaction of α-(Methylthio)deoxybenzoin with Methanethiolate in Dimethyl Sulfoxide. A solution prepared from 0.958 g (0.04 mol) of sodium and 60 m*l* of ethanol was treated with an excess of methanethiol and then evaporated. The residue was taken up in 60 m*l* of dimethyl sulfoxide and mixed with a solution of 4.808 g (0.02 mol) of α-(methylthio)deoxybenzoin in 20 m*l* of dimethyl sulfoxide. The mixed solution was heated for 45 min at 85°C to produce a deep red-orange color, Quenching the solution with water gave deoxybenzoin, whereas treating the solution with methyl iodide yielded α-methyldeoxybenzoin (NMR, δ from TMS in CCl_4 4.51 (q) and 1.50 (d)).

Determination of the Reaction Rates. A solution was prepared containing *ca* 7×10^{-2} mol of α-(arylthio)acetophenone, *ca* 5 mol of thiophenol, and *ca* 2×10^{-2} mol of sodium in 200 m*l* of ethanol. Di-*p*-methoxyphenyl ketone was added to the solution for use as an internal standard of analysis. Ten-mililiter portions of the solution were sealed in separate tubes, and the decrease in the quantity of the α-keto sulfides was determined by means of NMR.

The cost of this study has been defrayed in part by the Grant-in-Aid for Fundamental Research from the Ministry of Education, to which the author's thanks are due.

BULLETIN OF THE CHEMICAL SOCIETY OF JAPAN, VOL. 44, 832—835 (1971)

The Reaction of α-Carbonyl Sulfides with Bases. II. The Effect of Variation in the Nucleophiles

Michinori Ōki and Wataru Funakoshi

Department of Chemistry, Faculty of Science, The University of Tokyo, Hongo, Tokyo

(Received September 29, 1970)

The reactions of α-alkylthio ketones with various nucleophiles were examined. It was found that such "strong bases" as ethoxide did not cause any cleavage of the C–S bond, whereas such "weak bases" as thiourea could cause the cleavage. The phenomena may be explained by the concept of soft-and-hard acids and bases. Discussions are given of some reactions of the nucleophilic attack on sulfur, which have previously been reported, in the light of this new reaction.

Since α-carbonyl sulfides were found to produce the parent keones and esters on treatment with the thiolate anion, it seemed that it would be interesting to study how widely this reaction is applicable. In the preceding paper[1] we have reported that this kind of reactions occurs not only with the α-carbonyl thioethers but also with α-thiocyano ketones and α-mercapto or α-acetylthio ketones. The purpose of this paper is to report on the effect of the kind of nucleophiles on the reaction of α-carbonyl sulfides. As examples of the latter compounds, α-alkylthio ketones were chosen because of their high reactivity.

Results and Discussion

Since thiolate was able to reduce α-alkylthio ketones, it is natural to examine the reaction of the oxygen analogs. Thus sodium ethoxide was allowed to react with α-(ethylthio)acetophenone in boiling ethanol for 1.5 hr. This treatment ended in the recovery of the starting material. One of the reasons for the recovery of this compound could be the enolization of the ketone, which might compete favorably with the nucleophilic attack on the sulfur atom. α-Methyl-α-(methylthio)-deoxybenzoin (**1**) was chosen as an example to be treated with ethoxide, because this compound has no α-hydrogen and the anion expected to be produced should be stable. The formation of the anion should thus be favored.

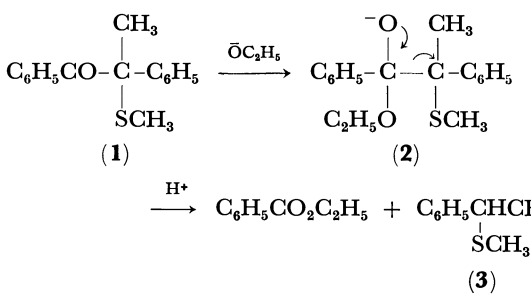

(**1**) (**2**)

$$\xrightarrow{H^+} C_6H_5CO_2C_2H_5 + C_6H_5\underset{\displaystyle SCH_3}{\underset{|}{C}}HCH_3$$

(**3**)

However, the products were not the expected α-methyl-

1) M. Ōki, W. Funakoshi, and A. Nakamura, This Bulletin, **44**, 828 (1971).

TABLE 1. THE REACTION OF α-METHYLTHIODEOXYBENZOIN WITH VARIOUS NUCLEOPHILES IN ETHANOL

Nucleophile	Heating Period (hr)	Products and Yields	Atmosphere
CN^-	15	$C_6H_5COCH_2C_6H_5$ (78%)	air
SCN^-	25	$C_6H_5COCOC_6H_5$ (trace) $C_6H_5COCH_2C_6H_5$ (trace)	N_2
$(NH_2)_2CS$	35	$C_6H_5COCH_2C_6H_5$ (13%) 85% Recovery	air
Br^-	27	92% Revovery No Product Found	N_2
Br^-	24	92% Revovery $C_6H_5COCOC_6H_5$ (trace) $C_6H_5COCH_2C_6H_5$ (trace)	air
I^-	24	$C_6H_5COCOC_6H_5$ (98%)	air
I^-	48	90% Recovery No Product Found	N_2
I^- [a]	48	No Reaction	air
$C_2H_5O^-$ [a]	25	$C_6H_5CH(CH_3)SCH_3$ and $C_6H_5CO_2C_2H_5$ only (vpc)	air
$(C_6H_5)_3P$ [b]	20	$C_6H_5COCH_2C_6H_5$ (almost quantitative)	air

a) The substrate is α-methyl-α-(methylthio)deoxybenzoin.
b) The substrate is α-(ethylthio)deoxybenzoin.

deoxybenzoin and other sulfur compounds; rather, ethyl benzoate and methyl 1-phenylethyl sulfide (**3**) were detected by means of vapor-phase chromatography. Indeed, benzoic acid was isolated after hydrolysis. It is clear that the attack by the ethoxide ion on sulfur is very slow and that the usual ketone cleavage by the base takes place *via* the adduct **2**.

Similarly, α-(methylthio)acetophenone did not give acetophenone on treament with sodium amide, although the amide anion is known to be a stronger base than ethoxide. Thus, it seemed that the capability of causing the C–S scission is not dependent on the base strength expressed by the pK_a values of the conjugate acids. This was experienced in many reactions of carbonium ions[2] and sulfur compounds;[3] the term "thiophilicity" has been proposed to express the nucleophilicity of bases when the site to be attacked is the sulfur atom. Thus, α-(methylthio)deoxybenzoin and its homologs were treated with various bases; the results are given in Table 1.

It can be pointed out that phosphine, cyanide ion, and thiourea are favorable for cleaving the C–S bond to produce deoxybenzoin. Some bases yielded benzil, which must be a product of the simultaneous desulfurization and oxidation; this tendency is clear with the iodide ion. However, in the absence of oxygen, the formation of benzil is not observed, indicating that the reaction is very probably of a radical nature. Support for this idea is given by the reaction of α-methyl-α-(methylthio)deoxybenzoin (**1**), which is not affected under similar conditions. Thus α-hydrogen is necessary to induce the change.

It seems that the higher polarity of the solvents is also a necessary condition for inducing this kind of reaction, for α-(ethylthio)acetophenone failed to give acetophenone when treated with triphenylphosphine in tetrahydrofuran.

The successful cleavage of the C–S bond of α-(alkylthio)deoxybenzoin with the cyanide ion, thiourea, and triphenylphosphine may be taken as support for the direct attack of the nucleophile on the sulfur atom, since, if the adducts **4**, **5**, and **6** are formed, neutral carbon, neutral sulfur which is next to the positive site, or positively-charged phosphorus must be the attacking base. The possibility is, however, very unlikely.

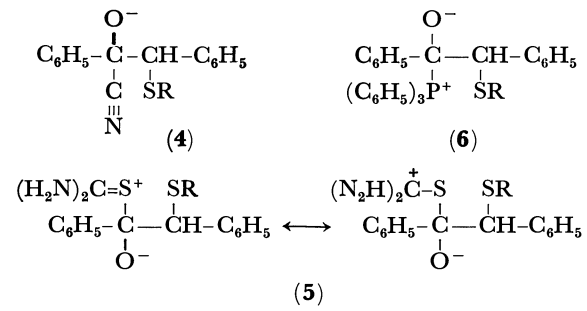

(**4**) (**6**)

(**5**)

The rough order of the reactivities of the bases is thus obtained as follows:

$$RS^- > C_6H_5S^- \sim (C_6H_5)_3P > CN^- > (H_2N)_2C{=}S > SCN^- \sim I^- \sim Br^-$$

Many papers[4,5] have been published dealing with the nucleophilicities of the bases in reactions with polysulfides and disulfides. The main difference between the nucleophilicity of the bases in relation to the polysulfides and that in relation to α-carbonyl sulfides is that hydroxide and ethoxide ions act as effective agents to cleave the S–S bond on the polysulfides, whereas,

2) C. G. Swain and C. B. Scott, *J. Amer. Chem. Soc.*, **75**, 141 (1953).
3) J. O. Edwards and R. G. Pearson, *ibid.*, **84**, 16 (1962).
4) A. J. Parker and N. Kharasch, *Chem. Rev.*, **59**, 583 (1959).
5) S. Oae and H. Tanaka, *Yukigosei Kagaku Kyokaishi*, **27**, 793 (1969).

they are ineffective in the cleavage of the C–S bond. There have been many attempts to explain the nucleophilicity of the base. Some representative theories will be discussed in an attempt to explain the above results.

Parker and Kharasch obtained the order of nucleophilicity in relation to the bivalent sulfur atom by determining the equilibrium point of the following equation:[4,6]

$$RSSR + Y^- \rightleftharpoons RS^- + RSY$$

The result was:

$$(C_2H_5O)_3P > -\overset{|}{C}^- \sim RS^- > ArS^- > (C_6H_5)_3P \sim CN^- >$$
$$SO_3^{2-} > OH^- > S_2O_3^{2-} > (H_2N)_2C{=}S > SCN^- > Br^- > Cl^-$$

An insufficient agreement of this order with the data presented here is, of course, to be expected, since those results were based on the equilibrium point and ours, on the product distribution, which is in turn determined by the one-way reaction rate.

On the other hand, Swain and Scott obtained the following order of nucleophilic constants as a fundamental characteristic of the bases:[2]

$$S_2O_3^{2-} > SO_3^{2-} \sim SH^- \sim CN^- > I^- >$$
$$SCN^- > OH^- > (H_2N)_2C{=}S$$

It may be pointed out that the placement of thiourea does not explain our results at all.

Pearson *et al.* presented the idea of the softness and hardness of the acids and bases and explained some S_N2-type organic reactions by assuming that a soft acid reacts more effectively with the soft bases. The softness is generally understood to express the higher polarizability of the acids and bases and has been obtained from the rates of the reactions of methyl iodide and *trans*-$[Pt(py)_2Cl_2]$ with various bases.[7] The order of softness thus obtained with the platinum complex is as follows:

$$(C_2H_5O)_3P > (C_6H_5)_3P \gg S_2O_3^{2-} > C_6H_5S^- \sim (H_2N)_2C{=}S >$$
$$(CH_3O)_3P > CN^- \gg SCN^- > I^- > Br^- > CH_3O^-$$

In this view of soft-and-hard acids and bases, sulfur of thioether must be one of the softest acids. Therefore, the cleavage of the C–S bond in α-carbonyl thioethers must be fast with the soft bases. The results presented here may be said to be generally in agreement with Pearson's theory, but the theory cannot explain some of the detailed results; for example, triphenylphosphine is much less reactive than predicted, and the reactivity of thiourea is less than that expected.

It may be necessary to modify the presently-proposed theories or to invent another theory to explain the results obtained with the α-carbonyl sulfides. This is also a rather expected results, since the orders of the rates of reactions of the bases with methyl iodide and the platinum complex do not agree with each other in some details.[7]

In view of the above-mentioned results, some of the points in the literature are worthy of comment. It was found that the treatment of α-(carboxymethylthio)-deoxybenzoin (**7**) with the hydroxide ion gave deoxybenzoin and glyoxylic acid in addition to hydrogen sulfide.

$$C_6H_5{-}\underset{\underset{O}{\|}}{C}{-}\underset{\underset{SCH_2CO_2H}{|}}{CH}{-}C_6H_5 \xrightarrow{OH^-}$$

(**7**)

$$C_6H_5COCH_2C_6H_5 + CHOCO_2H + H_2S$$

In order to explain these results, Iskander *et al.*[8] have assumed an attack by the hydroxide ion on sulfur, followed by cleavage to carbanion and sulfenic acid; finally, there was decomposition to glycolic acid and hydrogen sulfide.

$$-\underset{\underset{O}{\|}}{C}-\underset{|}{C}-S-\underset{|}{C}-CO_2Na \xrightarrow{OH^-} -\underset{\underset{O}{\|}}{C}-\underset{|}{C}-\underset{\underset{OH}{|}}{\bar{S}}-\underset{|}{C}-CO_2Na$$

$$\longrightarrow -\underset{\underset{O}{\|}}{C}-\underset{|}{\bar{C}}^- + \underset{\underset{OH}{|}}{S}-CH_2CO_2Na \longrightarrow$$

$$-\underset{\underset{O}{\|}}{C}-\underset{|}{CH} + CHOCO_2Na + S^{2-}$$

However, these mechanisms involve some points which are still to be clarified; especially, it is very hard to explain why carboxymethanesulfenic acid changes to glyoxylic acid and hydrogen sulfide. Since, in our experiments, proton abstraction occurs with the ethoxide, and, since the hydroxide ion is known to be a typical hard base, we favor the route of the formation of carbanion which has been proposed by Teich and Curtin:[9]

$$-\underset{\underset{O}{\|}}{C}-\underset{|}{C}-S-\underset{|}{\underset{H}{C}}-CO_2Na \xrightarrow{OH^-} -\underset{\underset{O}{\|}}{C}-\underset{|}{C}-S-\underset{|}{\bar{C}}-CO_2Na$$

$$\longrightarrow -\underset{\underset{O}{\|}}{C}-\underset{|}{\bar{C}}^- + S{=}\underset{|}{C}-CO_2Na \xrightarrow{H_2O}$$

$$-\underset{\underset{O}{\|}}{C}-\underset{|}{C}-H + O{=}\underset{|}{C}-CO_2Na + H_2S$$

We believe the similar reaction of *p*-nitrobenzylthioacetic acid in an alkaline solution reported by Schönberg and Iskander[10] can be similarly explained instead of considering the hydroxide attack on sulfur:

$$NO_2-C_6H_4-CH_2SCH_2CO_2Na \xrightarrow{OH^-}$$

$$HC(=O)-C_6H_4-N{=}N-C_6H_4-CH(=O) + CHOCO_2Na + H_2S$$

Experimental

The general procedure for the reaction was essentially the same as that reported in the preceding paper.[1] The pertinent

6) A. J. Parker and N. Kharasch, *J. Amer. Chem. Soc.*, **82**, 3071 (1960).

7) J. O. Edwards and R. G. Pearson, *ibid.*, **90**, 319 (1968), and earlier papers.

8) Y. Iskander, Y. Riad, and R. Tewfik, *J. Chem. Soc.*, **1961**, 2402, and earlier papers.

9) S. Teich and D. Y. Curtin, *J. Amer. Chem. Soc.*, **72**, 2481 (1950).

10) A. Schönberg and Y. Iskander, *J. Chem. Soc.*, **1942**, 90.

data are given in Table 1.

α-Methyl-α-(methylthio)deoxybenzoin. To a solution of 12 g (0.05 mol) of α-(methylthio)deoxybenzoin in 200 m*l* of tetrahydrofuran, 25 g (0.5 mol) of 50% sodium hydride suspension in petroleum was added, with 50 m*l* of tetrahydrofuran, over a period of 30 min. After having been stirred for 30 min at room temperature, the mixture was treated with 8 g (0.06 mol) of methyl iodide in 50 m*l* of tetrahydrofuran with ice-salt cooling. After the completion of the reaction (2 hr), the mixture was quenched with ethanol, poured into water, and extracted with ether. The extract, after evaporation and recrystallization from ethanol, afforded the desired product, mp 83—84°C. Found: C, 75.17; H, 6.06%. Calcd for $C_{16}H_{16}SO$: C, 74.96; H, 6.29%.

BULLETIN OF THE CHEMICAL SOCIETY OF JAPAN, VOL. 44, 835—841 (1971)

p-Toluenesulfonylation of 1,2-*O*-Cyclohexylidene-*myo*-inositol[1]

Tetsuo SUAMI, Seiichiro OGAWA, Takatoshi TANAKA, and Toshiki OTAKE*

Department of Applied Chemistry, Faculty of Engineering, Keio University, Koganei-shi, Tokyo

* *Nippon Electric Varian Co., Ltd., Azabu Iigura-cho, Minato-ku, Tokyo*

(Received October 15, 1970)

p-Toluenesulfonylation of 1,2-*O*-cyclohexylidene-*myo*-inositol (**1a**) afforded one mono (1), three di (1,4, 1,5, and 1,6), three tri (1,4,5, 1,4,6, and 1,5,6), and one tetra (1,4,5,6)-*O*-*p*-toluenesulfonyl derivatives of *myo*-inositol, and all the structures have been established by way of their proton magnetic resonance (PMR) spectra and the reaction sequences.

The sulfonate esters of carbohydrates are useful precursors for a wide variety of their derivatives.[2a,b] Therefore, selective sulfonylation at hydroxyl groups of sugars has been extensively studied.[2b] On the other hand, little information is, so far, known about the reactivities of the hydroxyl groups of cyclitols toward sulfonylation. Thus it seemed of interest to investigate a sulfonylation of inositols. In the present paper, we wish to report the *p*-toluenesulfonylation of 1,2-*O*-cyclohexylidene-*myo*-inositol (**1a**).[3]

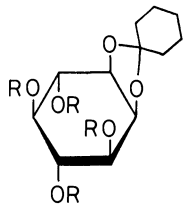

1

a: R=H
b: R=Ac

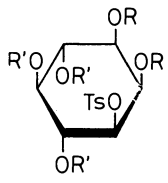

2

a: R=cyclohexylidene, R′=H
b: R=cyclohexylidene, R′=Ac
c: R=R′=H
d: R=R′=Ac

When **1a** was treated with 2 equivalents of *p*-toluenesulfonyl chloride in dry pyridine at 0—5°C for 24 hr and then at room temperature for 6 days, almost exclusively one isomer of the mono sulfonyl derivative (**2a**) was obtained in 41% yield. Acetylation of **2a** with acetic anhydride and pyridine gave tri-*O*-acetyl derivative (**2b**). Removal of cyclohexylidene group by refluxing of **2a** in 80% aqueous acetic acid afforded 1-*O*-*p*-toluenenesulfonyl-*myo*-inositol (**2c**),[4] and further acetylation of **2c** gave 1,2,4,5,6-penta-*O*-acetyl-3-*O*-*p*-toluenesulfonyl-*myo*-inositol (**2d**), which was identified with anauthentic sample.[5] Consequently, **2a** was assigned to1, 2-*O*-cyclohexylidene-3-*O*-*p*-toluenesulfonyl-*myo*-inositol. Although the same reaction was carried out with 1.5 or 3 equivalents of *p*-toluenesulfonyl chloride, **2a** was obtained in 39 or 36% yield, respectively. These results indicated that the hydroxyl group on C-3 was the most reactive one among four hydroxyl groups in **1a**, and were in accordance with the observed facilitation of acylation or sulfonylation by neighboring oxygen atoms in a cis position.[3] Other instance of this effect is the preferential *p*-toluenesulfonylation of 1,2:3,4-di-*O*-isopropylidene-*epi*-inositol in the 5-position.[6]

Then an isolation of the di-*O*-*p*-toluenesulfonyl esters was attempted. Compound **1a** was treated with

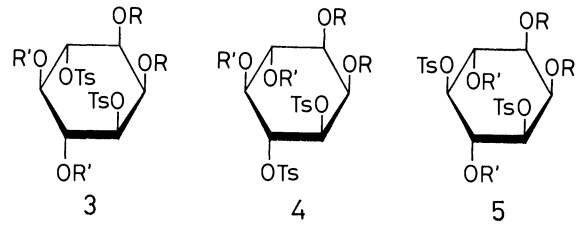

3 4 5

	R	R′
a:	cyclohexylidene	H
b:	cyclohexylidene	Ac
c:	H	H
d:	Ac	Ac

1) A part of this work was presented at the 23rd Annual Meeting of the Chemical Society of Japan, Tokyo, April, 1970 (See Abstracts of Papers of the Meeting, Vol. III, p. 1903).

2) a) R. S. Tipson, *Advan. Carbohyd. Chem.*, **8**, 107 (1953); b) D. H. Ball and F. W. Parrish, *ibid.*, **23**, 233 (1968); **24**, 139 (1969).

3) S. J. Angyal, M. E. Tate, and S. D. Gero, *J. Chem. Soc.*, **1961**, 4116.

4) S. J. Angyal, V. Bender, and J. H. Curtin, *J. Chem. Soc. (C)*, **1966**, 798.

5) S. J. Angyal, P. T. Gilham, and G. J. H. Melrose, *J. Chem. Soc.*, **1965**, 5252.

6) S. J. Angyal and P. T. Gilham, *ibid.*, **1957**, 3691.

2 equivalents of *p*-toluenesulfonyl chloride similarly a described before. After **2a** was obtained in 33% yield, its mother liquor was, then, subjected to a fractional crystallization to give a crystalline mixture of three di-esters in 41% yield. Further fractionations by a column chromatography using silica gel and recrystallization afforded chromatographically homogeneous three isomers of the di-esters (**3a**, **4a**, and **5a**). In another run, after isolating **2a** in 22% yield, the mixture was fractionated to give practically pure **3a**, **4a**, and **5a** in 20, 16 and 2.6% yield, respectively. Acetylation of **3a**, **4a**, and **5a** with acetic anhydride and pyridine gave the di-*O*-acetyl derivatives (**3b**), (**4b**), and (**5b**). Three isomers, (**3c**), (**4c**), and (**5c**), of di-*O*-*p*-toluenesulfonyl-*myo*-inositol were obtained by removal of cyclohexylidene group from **3b**, **4b**, and **5b**. On acetylation, **3c**, **4c**, and **5c** afforded tetra-*O*-acetyl derivatives (**3d**), (**4d**), and (**5d**), respectively.

In order to establish a configuration of the di-*O*-*p*-toluenesulfonyl derivatives, **2a** was further sulfonylated. When a course of the reaction with 1.5 equivalent of *p*-toluenesulfonyl chloride upon **2a**, as well as 2 equivalent upon **1a**, were monitored by a thin layer chromatography (TLC), both chromatograms were shown to be almost identical, except some traces of minor components. These results indicated that the three di-esters obtained must be derived from **2a**, and, accordingly, they should be either the 3,4-, 3,5- or 3,6-disulfonyl derivative. Also periodate oxidation was applied to an elucidation of the position of the sulfonyloxy groups in the di-esters. Compound **4a** was observed to react with periodate solution, however, neither **3a** nor **5a** would consume the reagent. So it might have been considered that the conformational rigidity of 1,2-*O*-cyclohexylidene-3,4 (or 3,6)-di-*O*-*p*-toluenesulfonyl-*myo*-inositol prevented a formation of the five membered periodate ester.[7]

Partial PMR spectrum of 3,4,5,6-tetra-*O*-acetyl-1,2-*O*-cyclohexylidene-*myo*-inositol (**1b**), as a reference compound, was shown in Fig. 1. The signals for the protons on C-1 and C-2, to which the cyclohexylidene group attached, are well upshifted and are separated

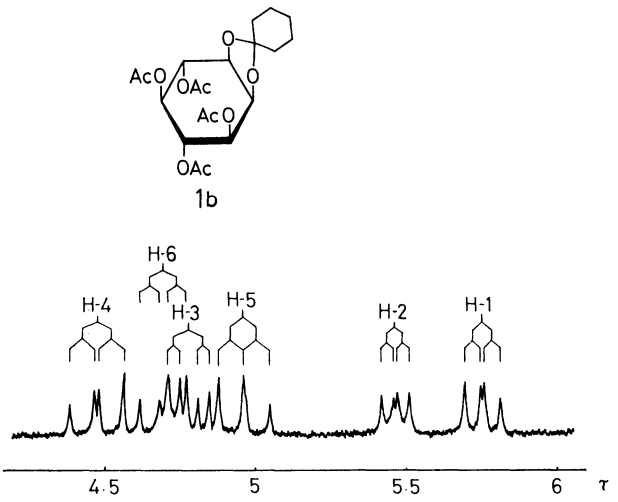

Fig. 1. Partial PMR spectrum of 3,4,5,6-tetra-*O*-acetyl-1,2-*O*-cyclohexylidene-*myo*-inositol (**1b**) (100 MHz, $CDCl_3$).

7) J. Corse and R. E. Lundin, *J. Org. Chem.*, **35**, 1904 (1970).

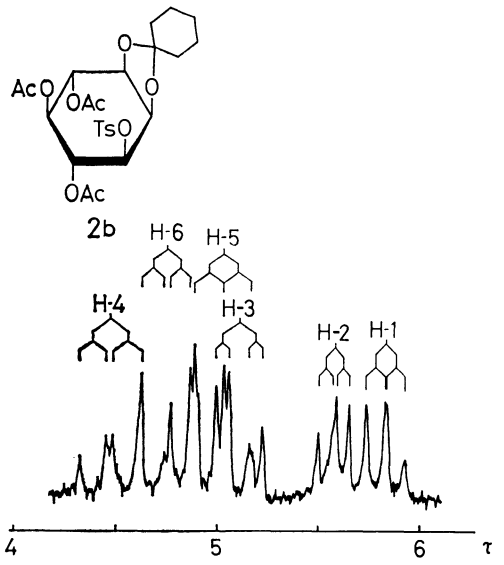

Fig. 2. Partial PMR spectrum of 4,5,6-tri- *O*-acetyl-1,2-*O*-cyclohexylidene-3-*O*-*p*-toluenesulfonyl-*myo*-inositol (**2b**) (60 MHz, $CDCl_3$).

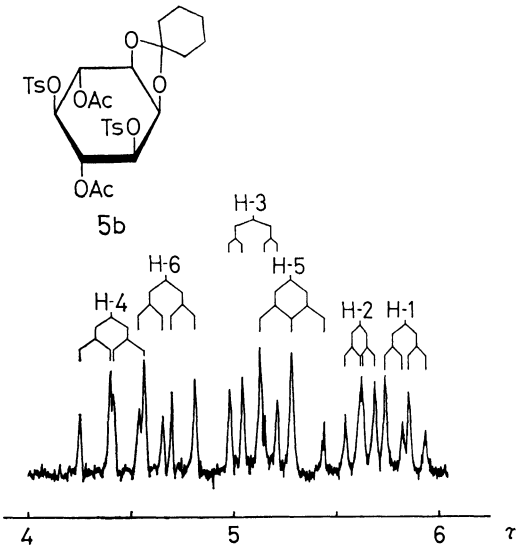

Fig. 3. Partial PMR spectrum of 4,6-di-*O*-acetyl-1,2-*O*-cyclohexylidene-3,5-di-*O*-p-toluenesulfonyl-*myo*-inositol (**5b**) (60 MHz, $CDCl_3$).

from those of the protons on the remaining carbon atoms. This simplified the assignment of signals. If it is assumed that the signal for H-1 (pseudoaxial) appears higher than that for H-2 (pseudoequatorial), all remaining signals could be adequately resolved by first-order method and assigned unambiguously to each proton, as listed in Tables 1 and 2. This assignment was further supported by the PMR spectrum of **2b** (Fig. 2). The spectral pattern is similar to that of **1b**, except that the signal for the H-3 proton is upshifted by 0.32 ppm. This can be easily understood by the fact that, in the case of **1b**, the acetoxy group on C-3 is substituted by a *p*-toluensulfonyloxy group. In the well resolved PMR spectrum of **5b** (Fig. 3), both signals for the H-3 and H-5 protons are upshifted by 0.32 ppm, comparing with those in the spectrum of **1b**. By analogy, these results might suggest that two

p-toluenesulfonyloxy groups are located at C-3 and C-5. While, in the PMR spectrum of **3b**, the quartet for the H-4 proton appears at τ 4.50, and this means that the *p*-toluenesulfonyloxy group is not located at C-4. Therefore, according to the observations of periodate oxidation and PMR spectra, **3a**, **4a**, and **5a** could be assigned to 1,2-*O*-cyclohexylidene-3,6-, 3,4- and 3,5-di-*O*-*p*-toluenesulfonyl-*myo*-inositol, respectively.

Table 1. Chemical shifts of methine protons[a)]

Compound	Chemical shifts (τ)					
	H-1	H-2	H-3	H-4	H-5	H-6
1b[b)]	5.75 q	5.46 q	4.78 q	4.47 q	4.96 t	4.69 q
2b	5.80 t	5.55 q	5.10 q	4.47 q	5.00 t	4.73 q
3b	5.84 t	5.59 q	5.14 q	4.50 q		
5b	5.83 q	5.61 t	5.10 q	4.41 t	5.28 t	4.67 q
5d	4.98 q	4.42 t	5.21 q	4.45 t	5.13 t	4.41 t
7b	5.81 t	5.59 q	5.21 q	4.54 q		

a) Measured at 60 MHz in $CDCl_3$, unless otherwise stated.
b) Measured at 100 MHz in $CDCl_3$. This compound should be named 1,4,5,6-tetra-*O*-acetyl-2,3-*O*-cyclohexylidene-*myo*-inositol, but it is not convenient for discussing the PMR spectrum.

Table 2. First-order coupling constants of methine protons

Compound	coupling constants (Hz)					
	$J_{1,2}$	$J_{2,3}$	$J_{3,4}$	$J_{4,5}$	$J_{5,6}$	$J_{6,1}$
1b	5.5	3.8	9.9	8.3	8.9	6.6
2b	5.5	4.0	10.0	8.0	8.0	6.5
3b	5.5	3.5	9.5	8.0		6.5
5b	5.0	3.5	10.0	9.0	9.0	7.0
5d	2.7	3.0	10.5	9.5	9.5	10.5
7b	6.0	3.2	10.0	6.0		5.0

It is interesting to note that the coupling constants between H-1 and H-2 are of the order of 5.0—5.5 Hz, indicating the angle between the bridgehead hydrogen atoms of a cyclohexylidene ring of approximately 35—40° on the basis of Karplus equation.[8)] Judging from the other coupling constants observed, the six-membered ring was only slightly flattened from the chair conformation by the introduction of 1,2-*O*-cyclohexylidene group into *myo*-inositol derivatives.

When a reaction mixture of **1a** and 7 equivalents of *p*-toluenesulfonyl chloride in dry pyridine was kept at room temperature until its TLC indicated an absence of the di-esters, two tri-esters (**6a** and **7a**) were obtained in a pure state by fractional crystallizations in 28 and 6% yield, respectively. The TLC of its mother liquor showed a presence of considerable amount of the tetra-ester. On acetylation, **6a** and **7a** gave di-*O*-acetyl derivatives (**6b**) and (**7b**). On acid hydrolysis with aqueous acetic acid, **6a** and **7a** gave two isomers, (**6c**) and (**7c**), of tri-*O*-*p*-toluenesulfonyl-*myo*-inositol, which, on acetylation, afforded tri-*O*-acetyl derivatives (**6d**) and (**7d**), respectively. In another run, after **6a** was crystallized out in 24% yield, the mother liquor was evaporated and the residue was subjected to an acid hydrolysis with aqueous acetic acid. From the hydrolyzate, 1,4,5,6-tetra-*O*-*p*-toluenesulfonyl-*myo*-inositol (**9a**) was recovered in 21% yield, which was converted into di-*O*-acetyl derivative (**9b**). Then the mother liquor was evaporated and the residual oil was treated with a mixture of acetic anhydride and pyridine to afford, in addition to **7d** (5%), hitherto unknown tri-*O*-acetyl-tri-*O*-*p*-toluenesulfonyl-*myo*-inositol (**8**) in 11% yield.

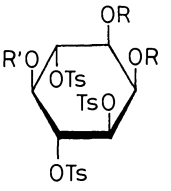

6

	R
a :	cyclohexylidene
b :	cyclohexylidene
c :	H
d :	Ac

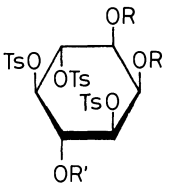

7

	R'
a :	H
b :	Ac
c :	H
d :	Ac

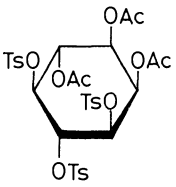

8

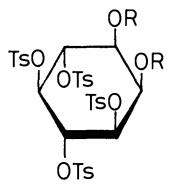

9

a : R=H
b : R=Ac

Now, sulfonylation of the three isomers of di-*O*-*p*-toluenesulfonyl derivative, **3a**, **4a**, and **5a**, were attempted for the purpose of obtaining informations on a position of sulfonyloxy groups in the tri-esters. By the TLC studies of sulfonylation products of the di-esters, it is apparent that both **6a** and **7a** were derived from **3a**, while, **6a** and **7a** were formed from **4a** and **5a**, respectively. In addition to each major component, an unidentified minor component was found in the reaction mixtures of **4a** and **5a**. Accordingly, **6a** and **7a** should be 1,2-*O*-cyclohexylidene-3,4,6- and -3,5,6-tri-*O*-*p*-toluenesulfonyl-*myo*-inositol, respectively, while, the unidentified compound might be considered to be the 3,4,5-tri-ester. These structural assignments were also confirmed by PMR spectra, and the nucleophilic displacement reaction with an azide ion, which will be described later.

The PMR spectrum of **7b** reveals a quartet at τ 4.54, which is assigned to the signal for H-4 proton. Therefore the acetoxy group is located at C-4 in **7b** and **7b** must be the 3,5,6-tri-ester. On the other hand, the absence of a quartet in a lower field in the PMR spectrum of **6b** indicated that the sulfonyloxy group is in C-4 position, and ascertained the structural assignment of **6b**.

Theoretically, four tri-esters can be derived from **1a**: the 3,4,5-, 3,4,6-, 3,5,6-, and 4,5,6-esters. So that the unidentified tri-ester (**8**) must be either the 3,4,5-

8) L. D. Hall, *Advan. Carbohyd. Chem.*, **19**, 51 (1964).

TABLE 3. CHEMICAL SHIFTS OF ACETYL METHYL PROTONS[a]

Compound	Chemical Shifts (τ)			
1b	7.99	7.98	7.92	7.88
2b	8.10	8.01	7.93	
2d	8.07	8.01	7.99[b]	7.86
3b	8.14	8.01		
3d	8.16	8.13	8.10	7.86
4b	8.05	7.99		
4d	8.06	8.01	7.98	7.86
5b	8.22	8.04		
5d	8.17	8.05	8.03	7.90
6b	8.07			
6d	8.17	8.06	7.83	
7b	8.26			
7d	8.27	8.20	7.90	
8	8.08	8.02	7.92	
9b	8.22	7.98		

a) Measured at 60 MHz in $CDCl_3$.
b) Signal of two acetyl methyl protons.

or 4,5,6-tri-ester. Had **8** been the 4,5,6-tri-ester, two acetoxy groups on C-1 and C-3 should be spectroscopically equivalent and their signals should appear as one singlet. However, **8** shows three peaks at τ 8 region: τ 7.92, 8.02 and 8.08 (Table 3). Therefore, **8** should be 1,2,6-tri-*O*-acetyl-3,4,5-*O*-*p*-toluenesulfonyl-*myo*-inositol.

The remarkable facilitation of sulfonylation have not been observed among the hydroxyl groups of **1a** other than that on C-3. Some differences in the relative proportions of the isomeric sulfonyl esters obtained are seemed to be explained by a steric and an electronic effects on a hydroxyl group toward sulfonylation.

Experimental

Melting points were determined on a Mitamura Riken micro hot stage and are uncorrected. Infrared (IR) spectra were taken in KBr disks. PMR spectra were measured on a Varian Associate A-60D (60 MHz) or HA-100D (100 MHz) spectrometer at a concentration of *ca.* 10% deuteriochloroform with tetramethylsilane as an internal standard. Chemical shifts are expressed in τ-values and signals are described as s (singlet), t (triplet), q (quartet), or m (complex multiplet). Values given for coupling constants are first-order. Thin layer chromatography (TLC) was done with silica gel (Wakogel B-10, Wako pure chemical industries Ltd.) using toluene-methyl ethyl ketone (4 : 1 or 3 : 1 volume) as the solvent system. The compounds were detected by exposing the plates to iodine vapor; the relative proportions of the compounds were estimated visually. All solutions were concentrated by a rotary evaporator at 40—50°C under reduced pressure. Whenever pyridine was employed in a reaction, the residual pyridine was removed by repeated codistillation with dry toluene.

1,2-O-*Cyclohexylidene*-myo-*inositol* (***1a***). This compound was prepared from *myo*-inositol following the method of Angyal and his coworkers[3] and purified by recrystallization two times from ethanol, mp 178—179°C (lit,[3] 179°C).

3,4,5,6-Tetra-O-*acetyl-1,2*-O-*cyclohexylidene*-myo-*inositol* (***1b***). This compound was prepared from **1a** following the method of Angyal and his coworkers,[3] mp 117—118°C (lit,[3] 118°C).

1,2-O-*Cyclohexylidene-3*-O-p-*toluenesulfonyl*-myo-*inositol* (***2a***). A solution of **1a** (5.2 g) in dry pyridine (80 m*l*) was externally cooled to 0—5°C. *p*-Toluenesulfonyl chloride (7.6 g, 2.0 equiv.) was added in one portion and dissolved under stirring, and the temperature was maintained below 5°C for 24 hr. Then the reaction mixture was stored at room temperature (15—20°C) for 6 days. The mixture was, then, poured onto ice and water (500 m*l*), and, after 24 hr at room temperature, the resulting gum was collected by decantation. The crude product was dissolved in chloroform (150 m*l*) and washed with N hydrochloric acid, 10% aqueous sodium carbonate and water successively. After drying over anhydrous sodium sulfate, the solution was evaporated to yield a semisolid, which was recrystallized from ethanol to give colorless needles (3.4 g, 41%) of **2a**, mp 225—227°C (dec.). Two recrystallization from methanol afforded an analytical sample, mp 229—230.5°C (dec.).

Found: C, 54.80; H, 6.39; S, 7.41%. Calcd for $C_{19}H_{26}O_8S$: C, 55.06; H, 6.32; S, 7.74%.

Although TLC showed the presence of considerable amounts of di- and tri-esters in the mother liquor of **2a**, further isolation was not attempted in this experiment.

In another run, the sulfonylation was carried out with 1.5 equiv. of *p*-toluenesulfonyl chloride, and the reaction mixture was kept at 0—5°C for 3 days, followed by 2 days at room temperature. The yield of **2a** was 39%. When 3.0 equiv. of *p*-toluenesulfonyl chloride was used, the yield of **2a** was 36%.

4,5,6-Tri-O-*acetyl-1,2*-O-*cyclohexylidene-3*-O-p-*toluenesulfonyl*-myo-*inositol* (***2b***). Compound **2a** (0.20 g) was treated with a mixture of acetic anhydride (2 m*l*) and pyridine (2 m*l*) at room temperature overnight. Then the reaction mixture was poured onto ice and water (20 m*l*) and the resulting crystals were collected by filtration; yield 0.23 g (88%), mp 158—160.5°C. Two recrystallization from ethanol gave fine needles (0.20 g) of **2b**, which showed the same melting point. PMR: τ 7.54 (3, s, OTs C–CH_3).

Found: C, 55.78; H, 6.05; S, 5.74%. Calcd for $C_{25}H_{32}O_{11}S$: C, 55.54; H, 5.97; S, 5.93%.

1-O-p-*Toluenesulfonyl*-myo-*inositol* (***2c***). A mixture of **2a** (1.2 g) and 80% aqueous acetic acid (20 m*l*) was refluxed for 2 hr. After cooling, the resulting precipitates were collected by filtration, washed with ethanol and dried; yield 0.74 g (77%), mp 222.5—225°C (dec.). Recrystallization from acetic acid and water gave colorless needles of **2c**, which was identified with an authentic sample (lit,[4] mp 224°C) by a mixed melting point and comparing with IR spectra.

1,2,4,5,6-Penta-O-*acetyl-3*-O-p-*toluenesulfonyl*-myo-*inositol* (***2d***). Compound **2c** (0.10 g) was treated with a mixture of acetic anhydride (2 m*l*) and pyridine (2 m*l*) at room temperature overnight. Then the reaction mixture poured onto ice and water to give colorless crystals (0.15 g, 92%) of **2d**, mp 149.5—151°C. It was identified with an authentic sample (lit,[4] mp 151°C) by a mixed melting point and comparing with IR spectra.

1,2-O-*Cyclohexylidene-3,6-di*-O-p-*toluenesulfonyl*-myo-*inositol* (***3a***), *1,2*-O-*Cyclohexylidene-3,4-di*-O-p-*toluenesulfonyl*-myo-*inositol* (***4a***) *and 1,2*-O-*Cyclohexylidene-3,5-di*-O-p-*toluenesulfonyl*-myo-*inositol* (***5a***). (a) A solution of **1a** (26.0 g) in dry pyridine (340 m*l*) was cooled to 0—5°C. *p*-Toluenesulfonyl chloride (38.0 g, 2.0 equiv.) was added in one portion and the solution was kept for 24 hr at 0—5°C, followed by 9 days at room temperature (15—20°C). Then the reaction mixture was poured onto ice and water (500 m*l*), and, after 2 days at room temperature, the water layer was separated from the resulting gum with decantation and extracted with chloroform

(2×200 ml). The extracts were washed with N hydrochloric acid, 10% aqueous sodium carbonate and water successively, and allowed to stand at room temperature overnight. The resulting crystals were collected and washed with ethanol; yield 13.9 g (33.4%), mp 225°C (dec.). Recrystallization from ethanol gave colorless needles (10.3 g, 24.7%) of **2a**, mp 229—230.5°C (dec.).

Then the gum (*ca.* 26 g) was dissolved in hot ethanol (150 ml) and kept at room temperature to give colorless crystals (10.4 g, 18.3%), which were shown to be a mixture of **3a** and **4a** by TLC. The mother liquor was evaporated and the residue was again dissolved in ethyl acetate (30 ml). Addition of benzene (60 ml) afforded the second crystals (8.45 g, 14.9%), which were composed of mainly **3a**. After 2 weeks, the third crystals (1.72 g, 3.0%) were obtained from the mother liquor and shown to be a mixture of **4a** and **5a** by TLC. Then the oily product which was obtained by evaporation of the filtrate was applied to the top of a column of silica gel (50 g, Wakogel C-200, Wako pure chemical industries Ltd.) packed in toluene-methyl ethyl ketone (5 : 1 volume). The column was eluted with the same solvent system, and the fractions were collected and combined according to the results of TLC. Evaporation of the eluates gave chromatographically pure crystals of **3a** (0.31 g), **4a** (0.53 g) and **5a** (0.78 g).

Further fractional crystallization of the first, second, and third crystals from methyl ethyl ketone and toluene gave **3a** (2.3 g), **4a** (3.6 g), and **5a** (0.9 g).

An analytical sample of **3a** was obtained by recrystallization from methyl ethyl ketone and toluene, and dried over phosphorus pentoxide *in vacuo* at 120°C; colorless granular crystals, mp 175—177.5°C.

Found: C, 55.05; H, 5.73; S, 11.41%. Calcd for $C_{26}H_{32}O_{10}S_2$: C, 54.91; H, 5.68; S, 11.28%.

Two recrystallization from methyl ethyl ketone and toluene afforded an analytical sample of **4a** as colorless cubic crystals, mp 173—175°C.

Found: C, 54.66; H, 5.63; S, 10.73%.

Recrystallization from methyl ethyl ketone and toluene gave an analytical sample of **5a** as colorless tiny needles, mp 182.5—184°C.

Found: C, 54.71; H, 5.65; S, 11.06%.

(b) Compound **1a** (26.0 g) was treated with *p*-toluenesulfonyl chloride (38.0 g) in dry pyridine (260 ml) similarly as described in (a). From the water layer, **2a** (9.3 g, 23%) was isolated. The gum was fractionally crystallized from ethyl acetate (45 ml) and benzene (100 ml) to give crystals (11.2 g, 19.6%) of **3a**, which were shown to be sufficiently pure for use in further synthetic experiment by TLC. The mother liquor was evaporated to give an oil which was crystallized from ethyl acetate and benzene to yield practically pure crystals (9.1 g, 16%) of **4a**, and, after long storage at room temperature, a crystalline mixture (8.5 g, 15%) of **3a**, **4a** and **5a** was obtained. Then the filtrate was evaporated and the resulting oil was subjected to a column chromatography similarly as described in (a). Four main components were obtained: a mixture of the tri-esters (0.59 g), **3a** (0.57 g), a mixture of **3a** and **4a** (2.92 g), and **5a** (0.43 g).

*Periodate Oxidation of **3a**, **4a**, and **5a**.* To a solution of 30 mg of 1,2-*O*-cyclohexylidene-di-*O*-*p*-toluenesulfonyl-*myo*-inositol (**3a**, **4a**, and **5a**) in 2 ml of methanol, a 1 ml portion of 50% aqueous methanolic solution of sodium metaperiodate (50 mg/ml) was added and the solution was kept for 2 days at room temperature in a dark place. The reaction mixture was analyzed directly by TLC. Judging from the results of TLC, both **3a** and **5a** did not react with periodate, and only **4a** was shown to react with periodate giving rise to another compound.

p-*Toluenesulfonylation of **2a**.* To a solution of **2a** (0.10 g) in dry pyridine (2 ml) was added *p*-toluenesulfonyl chloride (0.09 g, 1.5 equiv.) and the mixture was allowed to stand at room temperature for 4 days. The reaction mixture was analyzed directly by TLC. Monitoring by TLC, the chromatograms were found to be almost identical, except some traces of minor components, with that of the reaction mixture of **1a** and 2 equiv. of *p*-toluenesulfonyl chloride in pyridine prepared under the same condition. Even when an additional amount of *p*-toluenesulfonyl chloride was added to the mixture, both the chromatograms were identical, except some traces of minor components somewhat increased.

*4,5-Di-O-acetyl-1,2-O-cyclohexylidene-3,6-di-*O-p-*toluenesulfonyl-*myo-*inositol (**3b**).* Compound **3a** (0.20 g) was treated with a mixture of acetic anhydride (2 ml) and pyridine (3 ml) at 80°C for 1 hr. Then the reaction mixture was poured onto ice and water (10 ml) and the resulting precipitates were collected by filtration; yield 0.24 g (100%), mp 157—159°C. Two recrystallization from ethanol gave colorless needles (0.18 g, 78%) of **3b**, mp 158—160.5°C. PMR: τ 7.55 (6, s, OTs C–CH_3).

Found: C, 55.33; H, 5.39; S, 9.58%. Calcd for $C_{30}H_{36}O_{12}S_2$: C, 55.21; H, 5.56; S, 9.83%.

*5,6-Di-*O-*acetyl-1,2-*O-*cyclohexylidene-3,4-di-*O-p-*toluenesulfonyl-*myo-*inositol (**4b**).* Compound **4a** (0.45 g) was acetylated similarly as described under the preparation of **3b** to give crude crystals (0.45 g, 87%) of **4b**, mp 169—171.5°C. Two recrystallization from ethanol afforded colorless granular crystals (0.34 g, 66%), mp 170—170.5°C. PMR: τ 7.58 (6, s, OTs C–CH_3), 5.91 (1, t, H-1, J=5.5 Hz), 5.64 (1, q, H-2, J=3.5 and 5.5 Hz).

Found: C, 55.36; H, 5.66; S, 9.88%. Calcd for $C_{30}H_{36}O_{12}S_2$: C, 55.21; H, 5.56; S, 9.83%.

*4,6-Di-*O-*acetyl-1,2-*O-*cyclohexylidene-3,5-di-*O-p-*toluenesulfonyl-*myo-*inositol (**5b**).* Compound **5a** (0.13 g) was acetylated similarly as described under the preparation of **3b** to give crude crystals (0.15 g, 99%) of **5b**, mp 178.5—180°C. Two recrystallization from ethanol gave colorless needles (0.10 g, 67%), mp 166.5—168°C. Compound **5b** crystallized from ethanol in two allotropic forms: needles, mp 166.5—168°C, and rectangular plates, mp 179—180.5°C. PMR: τ 7.55 (6, s, OTs C–CH_3).

Found: C, 55.03; H, 5.61; S, 9.52%. Calcd for $C_{30}H_{36}O_{12}S_2$: C, 55.21; H, 5.56; S, 9.83%.

*1,4-Di-*O-p-*toluenesulfonyl-*myo-*inositol (**3c**).* A mixture of **3a** (0.20 g) and 80% aqueous acetic acid (10 ml) was refluxed for 2 hr. The reaction mixture was evaporated to give a crystalline residue, which was triturated with water and collected by filtration; yield 0.16 g (93%), mp 196—199°C. Recrystallization from acetic acid and water afforded colorless needles of **3c**, mp 198—200°C.

Found: C, 48.92; H, 5.02; S, 12.61%. Calcd for $C_{20}H_{24}O_{10}S_2$: C, 49.18; H, 4.95; S, 13.13%.

*1,6-Di-*O-p-*toluenesulfonyl-*myo-*inositol (**4c**).* A mixture of **4a** (0.25 g) and 80% aqueous acetic acid (10 ml) was refluxed for 2 hr. The reaction mixture was evaporated and the residue was dried by repeated codistillation with dry ethanol. Several attempts to crystallize amorphous glassy product of **4c** failed. Then it was dried over phosphorus pentoxide *in vacuo* at 110°C and analyzed; yield 0.22 g (76%), mp 155—160°C.

Found: C, 49.47; H, 5.41%. Calcd for $C_{20}H_{24}O_{10}S_2$: C, 49.18; H, 4.95%.

*1,5-Di-*O-p-*toluenesulfonyl-*myo-*inositol (**5c**).* Compound **5a** (0.29 g) was refluxed with 80% aqueous acetic acid (30 ml) for 2 hr. The reaction mixture was evaporated to dryness

and the residue was crystallized from ethanol to give colorless tiny needles (0.18 g, 71%) of **5c**, mp 211—212.5°C (dec.). Recrystallization from acetic acid and water afforded an analytical sample, mp 212—214°C (dec.).

Found: C, 48.99; H, 4.97; S, 12.85%. Calcd for $C_{20}H_{24}O_{10}S_2$: C, 49.18; H, 4.95; S, 13.13%.

1,2,4,5-Tetra-O-*acetyl-3,6-di*-O-p-*toluenesulfonyl*-myo-*inositol (**3d**).* Compound **3c** (0.24 g) was treated with a mixture of acetic anhydride (3 m*l*) and pyridine (4 m*l*) at 80°C for 1 hr. The the mixture was poured onto ice and water (20 m*l*) and the resulting precipitates were collected by filtration; yield 0.32 g (99%), mp 214—217°C. Recrystallization from chloroform and ethanol gave plates and needles (0.27 g, 84%) of **3d**, mp 216.5—217.5°C. PMR: τ 7.56 (6, s, OTs C–CH_3), 5.20 (1, q, H-3, J=3 and 10 Hz), 4.40 (1, t, H-2, J=*ca.* 3 Hz).

Found: C, 50.85; H, 5.13; S, 10.16%. Calcd for $C_{28}H_{32}O_{14}S_2$: C, 51.20; H, 4.91; S, 9.77%.

1,2,5,6-Tetra-O-*acetyl-3,4-di*-O-p-*toluenesulfonyl*-myo-*inositol (**4d**).* Crude **4c**, which was obtained from **4a** (1.01 g), was treated with a mixture of acetic anhydride (8 m*l*) and pyridine (10 m*l*) at room temperature overnight. Then the mixture was poured onto ice and water (20 m*l*) and the crystals were collected by filtration; yield 1.02 g (87%), mp 190—193°C. Recrystallization from ethyl acetate and ethanol gave colorless granular crystals of **4d**, mp 196—197.5°C. PMR: τ 7.54 (6, s, OTs C–CH_3), 5.40 (1, m, H-3), 5.07 (1, q, H-1, J=2.8 and 10 Hz).

Found: C, 51.07; H, 4.89; S, 9.64%. Calcd for $C_{28}H_{32}O_{14}S_2$: C, 51.20; H, 4.91; S, 9.77%.

1,2,4,6-Tetra-O-*acetyl-3,5-di*-O-p-*toluenesulfonyl*-myo-*inositol (**5d**).* Compound **5c** (47 mg) was treated with a mixture of acetic anhydride (0.5 m*l*) and pyridine (0.5 m*l*) at room temperature overnight. The mixture was poured onto ice and water and the resulting gum was crystallized from ethanol and water; yield 60 mg (95%), mp 160.5—162°C. Recrystallization from ethanol and water gave an analytical sample of **5d** as colorless needles, which showed the same melting point. PMR: τ 7.54 (6, s, OTs C–CH_3).

Found: C, 50.93; H, 4.88; S, 9.60%. Calcd for $C_{28}H_{32}O_{14}S_2$: C, 51.20; H, 4.91; S, 9.77%.

1,2-O-Cyclohexylidene-3,4,6-tri-O-p-*toluenesulfonyl*-myo-*inositol (**6a**) and 1,2-O-Cyclohexylidene-3,5,6-tri*-O-p-*toluenesulfonyl*-myo-*inositol (**7a**).* To a cooled solution of **1a** (26.0 g) in dry pyridine (380 m*l*), *p*-toluenesulfonyl chloride (133.5 g, 7.0 equiv.) was added in one portion, and the reaction mixture was stored at room temperature (10—15°C) for 10 days. Then any pyridine hydrochloride was removed by decantation and the solution was poured onto ice and water (1 *l*). After 2 days, the resulting gum was collected by filtration and dissolved in chloroform (300 m*l*). The chloroform solution was washed with N hydrochloric acid, 10% aqueous sodium carbonate, and water successively, and then, dried over anhydrous sodium sulfate. Then the solution was evaporated to yield a partly crystalline residue, which was triturated with chloroform and ethanol, and collected by filtration; yield 19.9 g (27.6%), mp 170—175°C. Recrystallization from chloroform and ethanol gave practically pure crystals (18.0 g) of **6a**, mp 173—177°C. An analytical sample was obtained by two recrystallizations from ethanol and dried over phosphorus pentoxide *in vacuo* at 120°C, mp 175—177.5°C.

Found: C, 54.93; H, 5.54; S, 12.70%. Calcd for $C_{33}H_{38}O_{12}S_3$: C, 54.83; H, 5.30; S, 13.30%.

From the mother liquor of **6a**, colorless plates were obtained after 1 week; yield 3.95 g (5.5%), mp 176—181°C. Two recrystallizations from chloroform and ethanol afforded an analytical sample of **7a** as colorless tiny plates, mp 183—184.5°C.

Found: C, 54.60; H, 5.27; S, 12.83%.

In another run, starting from **1a** (26.0 g), **6a** (18.2 g, (25.2%), and **7a** (2.67 g, 3.7%) were obtained from the reaction product. Then the mother liquor was evaporated and the residual oil was crystallized from methyl ethyl ketone and toluene to give a crystalline mixture (19.5 g) of mono- and di-esters. According to the result of TLC, considerable amount of tri- and tetra-esters were shown to be present in the mother liquor, but, further isolation of the isomer was not attempted.

p-*Toluenesulfonylation of **3a**, **4a**, and **5a**.* To a solution of 50 mg of 1,2-*O*-cyclohexylidene-di-*O*-*p*-toluenesulfonyl-*myo*-inositol (**3a**, **4a**, and **5a**) in 1 m*l* of dry pyridine was added 70 mg (4.0 equiv.) of *p*-toluenesulfonyl chloride and the mixture was allowed to stand at room temperature for 4 days. Then the reaction mixture was analyzed directly by TLC using toluene-methyl ethyl ketone (3:1) and benzene-ethyl acetate (9 : 4) as the solvent systems. Judging from the results of TLC, **3a** gave rise to **6a** and **7a**, while, **6a** and **7a** were formed from **4a** and **5a**, respectively. In addition to the major component, an unidentified product was found in the reaction mixture of **4a** and **5a**, which might be considered to be *1,2-O*-cyclohexylidene-*3,4,5*-tri-*O-p*-toluenesulfonyl-*myo*-inositol.

5-O-Acetyl-1,2-O-cyclohexylidene-3,4,6-tri-O-p-*toluenesulfonyl*-myo-*inositol (**6b**).* Compound **6a** (1.0 g) was treated with a mixture of acetic anhydride (5 m*l*) and pyridine (5 m*l*) at room temperature overnight. Then the reaction mixture was poured onto ice and water (30 m*l*) and the precipitates were collected by filtration; yield 1.0 g (95%), mp 177.5—179°C. Recrystallization from chloroform and ethanol afforded colorless cubic crystals (0.91 g) of **6b**, mp 179—180.5°C. PMR: τ 7.58 (9, s, OTs C–CH_3), 5.91 (1, t, H-1, J=5.5 Hz), 5.63 (1, q, H-2, J=3.5 and 5.5 Hz).

Found: C, 55.14; H, 5.47; S, 12.85%. Calcd for $C_{35}H_{36}O_{15}S_3$: C, 54.84; H, 5.27; S, 12.58%.

4-O-Acetyl-1,2-O-cyclohexylidene-3,5,6-tri-O-p-*toluenesulfonyl*-myo-*inositol (**7b**).* Compound **7a** (0.10 g) was acetylated similarly as described under the preparation of **6b** to give crystals (0.10 g, 95%) of **7b**, mp 194—195°C. Recrystallization from ethanol afforded colorless cubic crystals (0.09 g), mp 195.5—196°C. PMR: τ 7.59 (9, s, OTs C–CH_3).

Found: C, 55.05; H, 5.22; S, 12.79%. Calcd for $C_{35}H_{36}O_{15}S_3$: C, 54.84; H, 5.27; S, 12.58%.

1,4,6-Tri-O-p-*toluenesulfonyl*-myo-*inositol (**6c**).* A mixture of **6a** (2.0 g) and 80% aqueous acetic acid (40 m*l*) was refluxed for 2 hr. After cooling, the reaction mixture was poured into water (200 m*l*) and the resulting crystals were collected by filtration; yield 1.5 g (84%), mp 217—220°C. Recrystallization from ethanol gave two allotropic forms of crystals; needles and plates, mp 223—225.5°C. The melting point of the former is slightly lower than that of the latter. When the crystals were dissolved in 2-methoxyethanol and a crystallization was induced by addition of ethanol, colorless plates of **6c** were obtained homogeneously, mp 225.5—226.5°C.

Found: C, 50.68; H, 4.95; S, 14.92%. Calcd for $C_{27}H_{30}O_{12}S_3$: C, 50.47; H, 4.71; S, 14.97%.

1,4,5-Tri-O-p-*toluenesulfonyl*-myo-*inositol (**7c**).* A mixture of **7a** (0.51 g) and 80% aqueous acetic acid (10 m*l*) was refluxed for 2 hr. The reaction mixture was evaporated to dryness and the residue was digested with ethanol to give crystals (0.36 g, 81%) of **7c**, mp 205—211°C. Recrystallization from ethanol afforded colorless granular crystals, mp 208.5—210°C.

Found: C, 50.68; H, 4.87; S, 14.70%. Calcd for $C_{27}H_{30}O_{12}S_3$: C, 50.47; H, 4.71; S, 14.97%.

1,2,5-Tri-O-*acetyl-3,4,6-tri*-O-p-*toluenesulfonyl*-myo-*inositol*

(6d). Compound **6c** (0.10 g) was acetylated similarly as described under the preparation of **4d** to give crystal (0.12 g, 97%) of **6d**, mp 218.5—221°C. Recrystallization from chloroform and ethanol afforded colorless cubic crystals, which showed the same melting point. PMR: τ 7.56 (9, s, OTs C-CH_3), 5.49 (1, m, H-3), 4.48 (1, t, H-2, J=2.5 Hz).

Found: C, 51.40; H, 4.89; S, 12.69%. Calcd for $C_{33}H_{36}O_{15}S_3$: C, 51.56; H, 4.72; S, 12.49%.

1,2,4-Tri-O-*acetyl-3,5,6-tri*-O-p-*toluenesulfonyl*-myo-*inositol* ***(7d)***. Compound **7c** (0.10 g) was acetylated similarly as described under the preparation of **4d** to give crystals (0.11 g, 92%) of **7d**, mp 207—209°C (after melting and resolidifying at 180—185°C). Recrystallization from chloroform and ethanol afforded small needles, mp 210.5—212.5°C (after partly melting and showing a transition at 194—196°C). PMR: τ 7.56 (9, s, OTs C-CH_3), 5.27 (1, q, H-3, J=3 and 10 Hz).

Found: C, 51.57; H, 4.75; S, 12.30%. Calcd for $C_{33}H_{36}O_{15}S_3$: C, 51.56; H, 4.72; S, 12.49%.

1,2,6-Tri-O-*acetyl-3,4,6-tri*-O-p-*toluenesulfonyl*-myo-*inositol* ***(8)*** *and 1,4,5,6-Tetra*-O-p-*toluenesulfonyl*-myo-*inositol* ***(9a)***. A compound **1a** (5.0 g) was treated with *p*-toluenesulfonyl chloride (25.6 g, 7.0 equiv.) in dry pyridine (60 m*l*) and the reaction mixture was worked up similarly as described under the preparation of **6a** and **7a**. After **6a** (3.3 g, 24%) had been isolated by crystallization from chloroform and ethanol, the mother liquor was evaporated to dryness and the oily residue was refluxed with 80% aqueous acetic acid (50 m*l*) for 2 hr. The reaction mixture was kept for 2 days at room temperature and the resulting precipitates were collected by filtration. Then the mother liquor was again refluxed for additional 3 hr and the second crystals were obtained. The first and second crystals were combined and recrystallized two times from methyl ethyl ketone and ethanol to give colorless plates (3.3 g, 21%) of **9a**, mp 142—152°C (after sintering at 138°C). An analytical sample was obtained by recrystallization from methyl ethyl ketone and ethanol, mp 145—153°C.

Found: C, 51.59; H, 5.16; S, 15.54%. Calcd for $C_{34}H_{36}O_{14}S_4 \cdot C_2H_5OH$: C, 51.30; H, 5.03; S, 15.22%.

Then the mother liquor of **9a** was evaporated to dryness and the residue was treated with a mixture of acetic anhydride (10 m*l*) and pyridine (15 m*l*) overnight at room temperature. The reaction mixture was poured onto ice and water (100 m*l*) and, after 2 days, the resulting gum was filtered by suction. The gum was digested with chloroform and ethanol to give colorless needles (1.97 g), mp 173—177°C. Recrystallization from chloroform and ethanol afforded needles (1.6 g, 11%) of **8**, mp 194—194.5°C. PMR: τ 7.56 (9, s, OTs C-CH_3), 5.40 (1, q, H-3, J=3 and 9 Hz).

Found: C, 51.45; H, 4.53; S, 12.13%. Calcd for $C_{33}H_{36}O_{15}S_3$: C, 51.56; H, 4.72; S, 12.49%.

On addition of ethanol, the mother liquor gave plates (0.78 g, 5.3%) of **7d**, mp 202.5—206°C.

1,2-Di-O-*acetyl-3,4,5,6-tetra*-O-p-*toluenesulfonyl*-myo-*inositol* ***(9b)***. Compound **9a** (0.20 g) was acetylated as similarly as described under the preparation of **3d** to give crystals (0.23 g) of **9b**, mp 188.5—190.5°C. Recrystallization from ethanol afforded colorless needles (0.20 g, 91%), mp 189.5—190.5°C. PMR: τ 7.54 (12, s, OTs C-CH_3), 5.34 (1, q, H-3, J=3 and 8 Hz), 4.67 (1, t, H-2, J=*ca.* 3 Hz).

Found: C, 52.02; H, 4.77; S, 14.94%. Calcd for $C_{38}H_{40}O_{16}S_4$: C, 51.82; H, 4.58; S, 14.57%.

The authors are grateful to Professor Sumio Umezawa for his kind advice, to Mr. Saburo Nakada for his elementary analyses, and to Mr. Shigeyuki Itabashi and Mr. Shuichi Oki for their assistance in the preparative experiments. The financial support from the Ministry of Education for this work is gratefully acknowledged.

BULLETIN OF THE CHEMICAL SOCIETY OF JAPAN, VOL. 44, 841—844 (1971)

Iminodithiocarbonates. IV. Pyrolyses of *N*-Acyl Immonium Salts of Iminodithiocarbonates

Yoshio Ueno, Takeshi Nakai, and Makoto Okawara

Research Laboratory of Resources Utilization, Tokyo Institute of Technology, Ookayama, Meguro, Tokyo

(Received October 20, 1970)

The pyrolyses of *N*-acyl immonium salts of *S,S'*-dimethyl *N*-methyl- (II) and *N*-phenyl-iminodithiocarbonates (III) were studied. *N*-Methyl-immonium salt II gave *S*-methyl *N*-acyl-*N*-methyl-dithiocarbamate (V) at 100°C, but *N*-phenyl derivatives (III) gave phenyl isothiocyanate and *S*-methyl thiolbenzoate (VI) at 140°C. On the other hand, cyclic immonium salt, 2-(*N*-benzoyl-*N*-methyl)-1,3-dithiolanylium chloride (IV) gave 2-benzoylimino-1,3-dithiolane(VII) with elimination of *N*-methyl group at 200°C. It was found that *N*-acyldithiocarbamate V isolated was further decomposed to methyl isothiocyanate and thiolbenzoate at 200°C. Independent syntheses of *N*-acyldithiocarbamates V were performed on the reaction of *N*-monosubstituted dithiocarbamates and acyl chloride.

During the course of our study[1] on the reactivity of *N*-substitued iminodithiocarbonates, we found that the unusually stable *N*-acyl immonium salts were formed on the reaction of iminodithiocarbonates with various acid chlorides at room temperature. In the present paper, studies on the pyrolyses of these *N*-acyl immonium salts (II,III and IV) and the resulting formation of *N*-acyldithiocarbamates (V), isothiocyanates, thiolbenzoate (VI) and 2-benzoylimino-1,3-dithiolane (VII) are reported.

1) Y. Ueno, T. Nakai, and M. Okawara, Submitted, This Bulletin.

Results and Discussion

Pyrolysis of N-*Benzoyl Immonium Chloride of* S,S-*Di-*

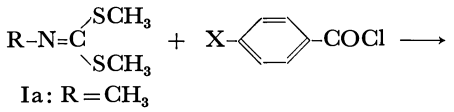

Ia: R=CH_3
Ib: R=C_6H_5

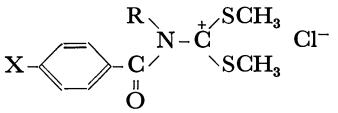

IIa: R=CH_3, X=H
IIb: R=CH_3, X=Cl
IIIa: R=C_6H_5, X=OCH_3
IIIb: R=C_6H_5, X=H

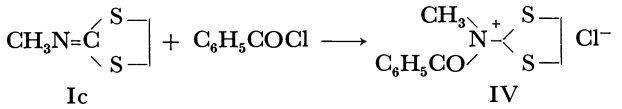

Ic IV

methyl N-*Methyl-Iminodithiocarbonate,II.* Pyrolysis of IIa at 100°C for 9 hr gave methyl *N*-benzoyl-*N*-methyl-dithiocarbamate (Va) in 90% yield. Similarly, the pyrolysis of *N-p*-chlorobenzoyl immonium chloride (IIb) gave methyl *N-p*-chlorobenzoyl-*N*-methyl-dithiocarbamate (Vb) in 79% yield.

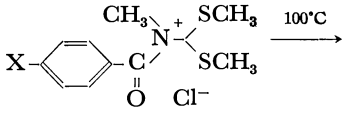

IIa: R=H
IIb: R=Cl

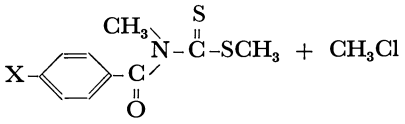

Va: R=H
Vb: R=Cl

The structure of V was established by IR, UV and NMR spectra and elemental analysis. The IR spectra showed a band at 1655—1665 cm^{-1} due to the amide-carbonyl group. The UV spectra showed two maximum absorption bands at around 240—260 mμ and 270 mμ which characterized the S–C(=S)– and N–C(=S)– resonance, respectively, in the dithiocarbamate structure. The NMR spectrum of Va fully confirmed the structure (Fig. 1). Thus signals due to S-methyl and *N*-methyl groups appeared as singlets at δ 2.58 and δ 3.66, respectively, and those due to aromatic groups as a multiplet centered at δ 7.50.

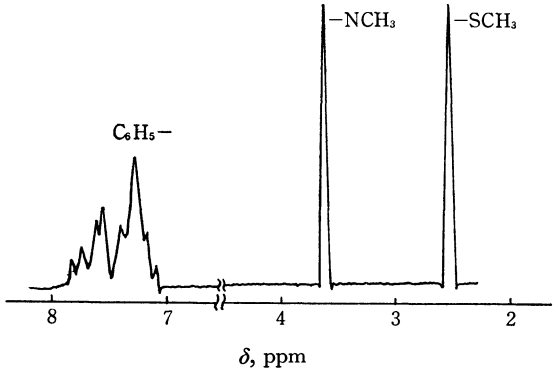

Fig. 1. The NMR spectrum of Methyl *N*-benzoyl-*N*-methyl-dithiocarbamate (Va) in $CDCl_3$.

Pyrolysis of N-*Benzoyl Immonium Chlorides of* S,S'-*Dimethyl* N-*Phenyl-Iminodithiocarbonates, III.* Pyrolysis of IIIa at 140—150°C for 7 hr gave phenyl isothiocyanate and methyl *p*-methoxythiolbenzoate (VIa) in 75 and 65% yield, respectively. Similarly, pyrolysis of the *N*-benzoyl immonium chloride (IIIb) gave phenyl isothiocyanate and methyl thiolbenzoate (VIb). In both cases, at lower temperature such as 100°C decomposition of III did not take place and the *N*-benzoyl dithiocarbamates corresponding to V were not obtained. The structures of phenylis othiocyanate and thiolbenzoate were confirmed by the spectral data and the results of elemental analysis.

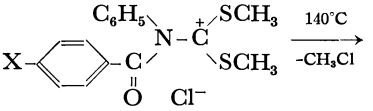

IIIa: X=OCH_3
IIIb: X=H

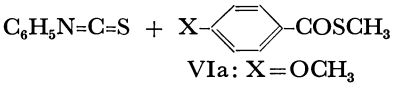

VIa: X=OCH_3
VIb: X=H

Pyrolysis of N-*Benzoyl Immonium Chloride of 2-Methyl-imino-1,3-dithiolane, IV.* Immonium chloride IV was prepared by mixing 2-methylimino-1,3-dithiolane and benzoyl chloride at room temperarture. On being heated, IV melted at about 140°C and then started to decompose at about 190°C. The reaction vessel was kept at 190—200°C for 5.5 hr. The product, 2-benzoylimino-1,3-dithiolane (VII) was obtained in 50% yield. The structure of VII was established by elemental analysis and by comparison of its IR and melting point with the data in literature.[2] The IR spectrum of VII showed a band at 1640 cm^{-1} due to the carbonyl group.

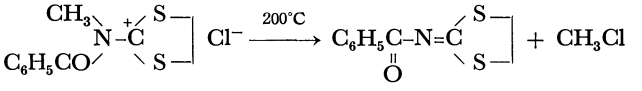

IV VII

Pyrolysis of Methyl N-*Benzoyl*-N-*Methyl-Dithiocarbamate (Va).* Although different types of products were obtained in the pyrolyses of II and III, dithiocarbamate V isolated from II seems to be an intermediate for the formation of isothiocyanate and thiolbenzoate from III. Thus the pyrolysis of *N*-benzoyl dithiocarbamate (Va) was examined. The dithiocarbamate Va was pyrolyzed at 200—220°C for 0.5 hr and resulted in the formation of methyl isothiocyanate in over 54% yield.

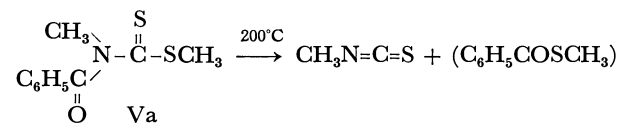

Va

Independent Synthesis of Methyl N-*Benzoyl*-N-*Phenyl-Dithiocarbamate (Vc).* Methyl *N*-benzoyl-*N*-phenyl-dithiocarbamate (Vc) was synthesized by the reaction of methyl *N*-phenyl dithiocarbamate with benzoyl chloride.

2) J. Burkhardt, R. Feinauer, E. Gulbins, and K. Hamann, *Chem. Ber.*, **99**, 1912 (1966).

Methyl *N*-phenyl dithiocarbamate was converted into the sodium salt by treating with sodium methoxide in methanol followed by treating with benzoyl chloride in benzene.

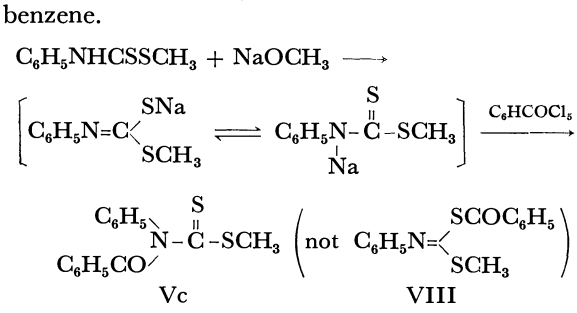

The product was assigned as *N*-benzoyl derivative Vc and the isomeric structure of *S*-benzoyl derivative VIII was eliminated by the following facts. (1). The IR spectrum showed a characteristic band of amide-carbonyl group at 1680 cm^{-1} and no band due to the ester carbonyl or imino group. (2). The UV spectrum showed two characteristic absorption at 240 mμ and 270—280 mμ due to S–C(=S)– and –N–C(=S)– resonance, respectively. (3). Formation of no picrate by the addition of picric acid indicates the absence of imino basic group. (4). The product on the reaction of methyl *N*-methyldithiocarbamate with benzoyl chloride was identical in all respects with the methyl *N*-benzoyl-*N*-methyldithiocarbamate (Va).

The structure of phenyl isothiocyanate obtained by pyrolysis of *N*-benzoyldithiocarbamate Vc at 140—150°C was confirmed by its IR spectrum. A new band at 2150 cm^{-1} due to the –N=C=S group in phenyl isothiocyanate appeared.

Pyrolytic Scheme of N-*Acyl Immonium Chloride of Iminodithiocarbonates.* From the result obtained above, the formation of isothiocyanate from *N*-phenylimmonium chloride III can be interpreted by the following scheme involving the intermediacy of the *N*-acyl dithiocarbamate V.

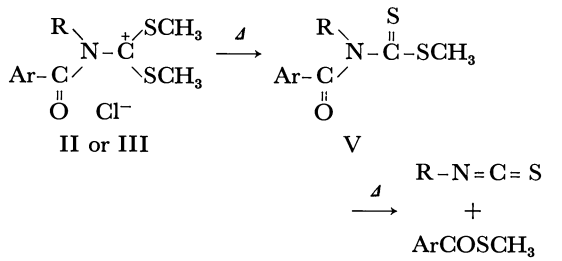

Immonium chloride II or III are pyrolyzed initially to give the dithiocarbamate V with elimination of methyl chloride. Dithiocarbamate V is further decomposed to isothiocyanate and thiolbenzoate. When R is alkyl group, the intermediate dithiocarbamate V was isolated. However, phenyl-substituted dithiocarbamate (Vc) was not isolated and spontaneously decomposed to phenyl isothiocyanate and thiolbenzoate. This indicates the less thermal stability of *N*-phenyl derivative than *N*-alkyl in compound V. While several reactions, RNX–C(=S)Y→RN=C=S+XY, are known for the formation of isothiocyanate with elimination of simple molecule, this is the first example for the formation of isothiocyanate with elimination of thiolbenzoate moiety. In contrast with the open-chain immonium salts (II or III), cyclic immonium salt IV resists the breaking at S–C bond and elimination of *N*-methyl group predominates to produce the 2-benzoylimino-1,3-dithiolane (VII).

Experimental

All melting and boiling points were uncorrected. Infrared and ultraviolet spectra were recorded on a Hitachi infrared EPI-S2 and EPS-2 spectrophotometer, respectively. The NMR spectrum was obtained with a Japan Electron Optics JNL-100 spectrophotometer in a deuteriochloroform solution using tetramethylsilane as an internal standard.

Materials. The immonium chlorides II, III, and IV were prepared by mixing the corresponding iminodithiocarbonates with benzoyl chloride derivatives at room temperature.[1] The acyl immonium chlorides thus obtained were subjected to pyrolyses without isolation.

Pyrolysis of N-*Benzoyl Immonium Chloride of* S,S-*Dimethyl*-N-*Methyl-Iminodithiocarbonate (IIa).* Immonium chloride IIa prepared from Ia (2.7 g, 0.02 mol) and benzoyl chloride (2.8 g, 0.02 mol) were heated at 100°C for 9 hr. By cooling the reaction mixture in a dry ice - acetone bath after the reaction, methyl *N*-benzoyl-*N*-methyl-dithiocarbamate (Va) was obtained (4.0 g, 90%). mp 71.5—72.0°C (recrystallized from *n*-hexane); UV: $\lambda_{max}^{cyclohexane}$ 243.5, 275 mμ, IR: (KBr): $\nu_{C=O}$ 1665 cm^{-1}.

Found: C, 53.73; H, 5.05; N, 6.26%. Calcd for $C_{10}H_{11}NOS_2$: C, 53.33; H, 4.92; N, 6.32%.

Similarly, methyl *N*-*p*-chlorobenzoyl-*N*-methyl-dithiocarbamate Vb was obtained in 79% yield: mp 64.5—65.5°C (recrystallized from *n*-hexane); UV λ_{max}^{EtOH} 260, 276 mμ, IR: $\nu_{C=O}$ 1655 cm^{-1}.

Found: C, 47.05; H, 3.74; N, 4.97%. Calcd for $C_{10}H_{10}NOS_2Cl$: C, 46.25; H, 3.88; N, 5.39%.

Pyrolysis of N-p-*Methoxybenzoyl Immonium Chloride of* S,S'-*Dimethyl*-N-*Phenyl-Iminodithiocarbonate (IIIa).* Immonium chloride IIIa prepared from *N*-phenyl iminodithiocarbonate Ib (4.0 g, 0.02 mol) and *p*-methoxybenzoyl chloride (2.9 g, 0.0017 mol) were heated at 140—150°C for 7 hr. Gas evolution was observed at about 150°C. After decomposition the reaction mixture was subjected to distillation in a vacuum, giving two fractions with a boiling point of 58—69°C/1 mmHg, (1.7 g) and 107—117°C/1 mmHg, (2.0 g). The lower-boiling fraction (74%) was identical in its infrared spectrum (2110 cm^{-1}, N=C=S) and boiling point with those of authentic phenyl isothiocyanate. The higher boiling fraction crystallized after distillation. It was recrystallized from *n*-hexane to give methyl *p*-methoxythiolbenzoate (VIa) with a melting point 41.5—42.0°C (65%); IR (KBr); $\nu_{C=O}$ 1642 cm^{-1}.

Found: C, 59.22; H, 5.30; N, 0.00%. Calcd for $C_9H_{10}O_2S$: C, 59.33; H, 5.53; N, 0.00%.

Similarly, the pyrolysis of *N*-benzoyl immonium chloride IIIb at 140—160°C for 6.5 hr gave a mixture of phenyl isothiocyanate and methyl thiolbenzoate with a boiling point of 56—75°C/4 mmHg. The IR spectrum showed a band at 2110 cm^{-1} (N=C=S) and at 1665 cm^{-1} (C=O). The close boiling point of the two products makes it difficult to separate each component by distillation. The small amount of residue on distillation was recrystallized, and was tentatively assigned as benzanilide by its IR spectrum and melting point (164.5°C). Pyrolysis of IIIb did not take place noticeably at 100°C after 8 hr.

Pyrolysis of N-*Benzoyl Immonium Chloride of 2-Methylimino-1,3-dithiolane, (IV).* 2-Methylimino-1,3-dithiolane (Ic)

(1.33 g, 0.01 mol) was mixed with benzoyl chloride (1.4 g, 0.01 mol) at room temperature. Immonium chloride IV was formed with a slight heat evolution, and which was kept at 190—200°C for 5.5 hr. Cooling the reaction mixture in a dry ice-acetone bath gave 2-benzoylimino-1,3-dithiolane (VII) (1.2 g, 50%): mp 76—77°C (recrystallized from the mixture of ether and petroleum ether) (lit,[2] 79°C): IR (KBr): $\nu_{C=O}$ 1640 cm^{-1} (lit,[2] 1640 cm^{-1}).

Found: C, 53.62; H, 3.78; N, 6.33%. Calcd for $C_{10}H_9NOS_2$: C, 53.78; H, 4.06; N, 6.28%.

Pyrolysis of Methyl N-*Benzoyl*-N-*Methyl-Dithiocarbamate (Va).* Va was heated at 200—220°C for 0.5 hr. Distillation of the reaction mixture gave two fractions with boiling points 70—80°C (0.3 g) and 120°C (0.9 g). Lower boiling fraction was identical in its IR spectrum with an authentic sample of methyl isothiocyanate. Identification of methyl isothiocyanate by transformation into thiourea derivative was carried out using *p*-methoxyaniline in ethanol solution. Recrystallization of the resulting thiourea derivative several times from ethanol gave needles of *N*-methyl-*N*-*p*-methoxyphenyl thiourea: mp 171.0—172.0°C; Found: C, 54.75; H, 5.74; C, 13.99%. Calcd for $C_9H_{12}N_2OS$: C, 55.09; H, 5.17; N, 14.28%.

Higher boiling fraction was assumed to be a mixture of methyl isothiocyanate and methyl thiolbenzoate based on its IR spectrum, at 1670 cm^{-1} (C=O) and 2130, 2240 cm^{-1} (N=C=S), but was not further investigated.

Independent Synthesis of Methyl N-*Benzoyl*-N-*Phenyl-Dithiocarbamate, (Vc).* To a solution of methyl *N*-phenyl-dithiocarbamate (3.7 g, 0.02 mol) in 20 m*l* of methanol, was added sodium methoxide (1.2 g, 0.02 mol). After stirring for 1 hr at room temperature, evaporation of methanol under reduced pressure gave white sodium dithiocarbamate. To a suspension of the sodium dithiocarbamate in 20 m*l* of dry benzene was added benzoyl chloride (2.8 g, 0.02 mol). After refluxing the mixture for 0.5 hr, filtration and evaporation of the solvent gave a yellow solid of methyl *N*-benzoyl-*N*-phenyl-dithiocarbamate (Vc) (2.5 g, 44%): mp 99—100°C (recrystallized twice from *n*-hexane); IR (KBr): $\nu_{C=O}$ 1680 cm^{-1}; UV λ_{max}^{EtOH} 244, 278 mμ.

Found: C, 62.80; H, 4.36; N, 4.90%. Calcd for $C_{15}H_{13}NOS_2$: C, 62.71; H, 4.56; N, 4.88%.

Similarly, methyl *N*-benzoyl-*N*-methyl-dithiocarbamate (Va) was synthesized on the reaction of methyl *N*-methyl-dithiocarbamate and benzoyl chloride. Thus, to a mixture of methyl *N*-methyl-dithiocarbamate (3.0 g, 0.025 mol) and sodium hydroxide (1 g, 0.025 mol) in 12 m*l* of water, was added dropwise benzoyl chloride (3.5 g, 0.025 mol) with stirring and external cooling at 7—10°C. The yellow oil separated was extracted with ether. After drying the etheral solution with anhydrous sodium sulfate, cooling the solution gave crude Va (3.3 g, 59%); mp 68—70°C. The product completely agreed with the pyrolyzed product Va in all respects in the IR and UV spectra.

NOTES

BULLETIN OF THE CHEMICAL SOCIETY OF JAPAN, VOL. 44, 845—846 (1971)

Long Spacings of ω-Cyclohexyl Alkanoic Acids

Akio Ishizawa

Department of Chemistry, Faculty of Science, Kyoto University, Sakyo-ku, Kyoto

(Received June 15, 1970)

In almost all the long chain compounds studied the chain ends are either both methyl or one of the ends is substituted with a group different in nature but similar in size with the chain constituent.[1] Studies of the long chain compounds substituted with a bulky group at the chain end in comparison with the results from such compounds as long chain *n*-paraffins or *n*-alkanoic acids will clarify the influence of the end groups on the properties of these long chain crystals. Reported here are some results from the examination of solid ω-cyclohexyl alkanoic acids $\langle\overline{\text{H}}\rangle$-$(CH_2)_n$COOH ($n$=13 to 33)[2] by X-ray powder method.

The specimens crystallized from solution (acetic acid) and those from melt gave essentially the same diffraction patterns except that in some of those obtained from solution two or more crystalline forms were observed concomitantly. The odd (n=even) and even (n=odd) members of the acids crystallized from melt, like many long chain compounds studied, differed not only in the general appearance of the diffraction patterns but also in the relation between the long spacing and the chain length.[3] Examination of the specimens crystallized from melt at temperatures just below their melting points gave the long spacings identical with those obtained at room temperature within experimental error.[4] In the thermal analysis of the specimens, the time-temperature curves increased monotonously with temperature until the temperature reached about 1°C below their melting points, where the slope of the curves became gradual. Thus, the crystalline forms obtained from melt seems stable in the range from room temperature to near their melting points.

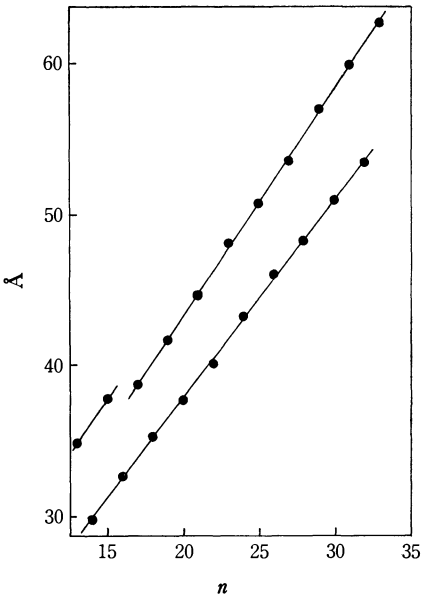

Fig. 1. Dependence of the long spacings on the chain length in $\langle\overline{\text{H}}\rangle$-$(CH_2)_n$COOH.

The effect of a bulky end group is evidently demonstrated in the long spacings. The values obtained are considerably smaller than the calculated length of the hydrogen-bonded dimeric molecule in which the chain is stretched in a straight zig-zag form. The tilt angle which refers to the angle between the chain axis and the basal plane is estimated to be about 30°

Table 1. The long spacings of cyclohexyl alkanoic acids $\langle\overline{\text{H}}\rangle$-$(CH_2)_n$COOH

n	(Å)	n	(Å)
13	34.79	14	29.74
15	37.75	16	32.53
17	38.56	18	35.17
19	41.72	20	37.46
21	44.61	22	40.01
23	48.03	24	43.16
25	50.72	26	46.00
27	53.50	28	48.21
29	56.85	30	50.92
31	59.85	32	53.31
33	62.67		

1) A. Müller, *Proc. Roy. Soc.*, **A 114**, 542 (1927); **A 120**, 437 (1928); **A 127**, 417 (1930); A. A. Schaerer, C. J. Busso, A. E. Smith, and L. B. Skinner, *J. Amer. Chem. Soc.*, **77**, 2017 (1955); F. Francis, F. J. E. Collins, and S. H. Piper, *Proc. Roy. Soc.*, **A 158**, 691 (1937); E. von Sydow, *Ark. Kemi*, **9**, 231 (1957); T. Malkin, *J. Amer. Chem. Soc.*, **52**, 3739 (1930); A. Watanabe, This Bulletin **34**, 1728 (1961); **36**, 336 (1963); A. Watanabe, A. Ishizawa, M. Kosaka, and R. Goto, *ibid.*, **42**, 1360 (1969).

2) R. Goto, A. Ishizawa, and M. Yamamura, *Nippon Kagaku Zasshi*, **88**, 678 (1967); A. Ishizawa, M. Yamamura, M. Ichii, Y. Sakashita, and R. Goto, *ibid.*, **89**, 516 (1968); A. Ishizawa, M. Yamamura, and R. Goto, *ibid.*, **89**, 815 (1968).

3) The samples were examined using Ni filtered Cu$K\alpha$ radiation (45 kV, 40—50 mA, camera distance=100 mm or 110 mm).

4) All the measurements at high temperatures were carried out within 1°C below the melting points.

from the increment of the value of the long spacing with the two additional chain units divided by twice the theoretical increase in the chain length, 2×2.515 Å. Almost all the long chain compounds studied are known to pack themselves in crystals with the chain axis inclined about 60° at most to the basal plane.[1] The marked inclination of the hydrocarbon chain of these acids seems to show the intrinsic importance of the packing of the large end groups on the arrangement of the chain molecules in crystals.

BULLETIN OF THE CHEMICAL SOCIETY OF JAPAN, VOL. 44, 846—847 (1971)

Long Spacings of ω-Cyclohexyl Alkanols

Akio ISHIZAWA

Department of Chemistry, Faculty of Science, Kyoto University, Sakyo-ku, Kyoto

(Received June 15, 1970)

It has been found that substitution of a bulky cyclohexyl group at the end of long chain alkanoic acids caused a marked change in the arrangement of the hydrocarbon chain in crystals.[1] Reported here is another similar observation on the effect of a bulky group which is introduced at the end of normal alkanols.

ω-Cyclohexyl alkanols $\langle\overline{\text{H}}\rangle$-$(CH_2)_n$OH($n$=14 to 34)

were synthesized by the reduction of ethyl (or methyl) ω-cyclohexyl alkanoates with excess lithium aluminum hydride in refluxing ether. After treatment with boiling ethanolic potassium hydroxide solution, the resulting mixture was evaporated to dryness under reduced pressure, extracted with anhydrous benzene, and the products were repeatedly recrystallized from benzene or toluene solution.

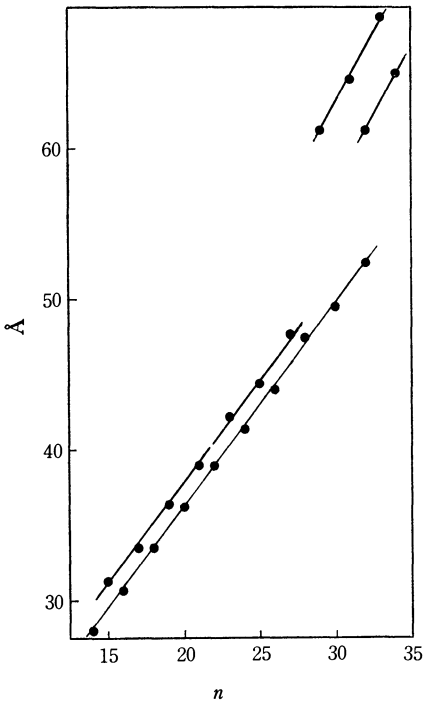

Fig. 1. Dependence of the long spacings on the chain length in $\langle\overline{\text{H}}\rangle$-$(CH_2)_n$OH.

1) A. Ishizawa, This Bulletin, **44**, 845 (1971).

As in the case of ω-cyclohexyl alkanoic acids[1] and many other long chain crystals,[2] the odd (n=odd) and even (n=even) alkanols crystallized from melt differed not only in the general appearance of the powder patterns but also in the variation of the long spacings with the chain length. As is evident from the values of long spacings, the crystalline forms of the alkanols changed at n=29 in the odd series and at n=

Table 1. Long spacings, melting points and elemental analyses of cyclohexyl alkanols

$\langle\overline{\text{H}}\rangle$-$(CH_2)_n$OH

n	Long spacing (Å)	mp (°C)	Elemental analysis (%) Calcd C	Calcd H	Found C	Found H
14	27.99	53.4—53.7	81.00	13.60	81.17	13.79
15	31.24	46.4—46.6	81.21	13.63	81.13	13.61
16	30.65	61.1—61.3	81.41	13.66	81.25	13.75
17	33.71	54.9—55.3	81.58	13.69	81.73	13.89
18	33.47	67.1—67.3	81.74	13.72	81.75	13.57
19	36.28	62.1—62.2	81.89	13.75	81.78	14.01
20	36.20	71.8—72.1	82.03	13.77	82.02	13.79
21	38.90	68.0—68.4	82.16	13.79	82.02	13.67
22	38.96	76.7—77.1	82.27	13.81	82.39	13.68
23	42.19	72.7—73.0	82.39	13.83	82.44	14.06
24	41.36	79.6—80.0	82.49	13.85	82.43	13.64
25	44.28	77.1—77.5	82.59	13.86	82.35	14.08
26	43.90	82.8—83.2	82.68	13.88	82.53	13.86
27	47.65	80.4—80.7	82.77	13.89	82.71	13.95
28	47.38	85.4—85.6	82.85	13.91	83.02	14.16
29	61.13	83.6—83.8	82.92	13.92	82.97	14.07
30	49.64	88.3—88.7	83.00	13.93	83.00	13.67
31	64.46	86.5—86.9	83.07	13.94	83.04	14.08
32	52.30 61.17	90.4—90.5	83.13	13.95	83.17	13.98
33	68.65	89.6—89.9	83.19	13.96	83.40	13.71
34	64.85	92.5—92.9	83.25	13.97	83.51	13.91

2) A. Müller, *Proc. Roy. Soc.*, **A 120**, 437 (1928); **A 127**, 417 (1930); F. Francis, F. J. E. Collins, and S. H. Piper, *ibid.*, **A 158**, 691 (1937); E. von Sydow, *Ark. Kemi*, **9**, 231 (1957); A. Watanabe, This Bulletin, **34**, 1728 (1961), **36**, 336 (1963).

32 in the even. Formation of a crystalline form with $n=32$ was found to be sensitive to the method of preparation. Rapid cooling, in general, gave the form with larger long spacing. In the other members no such behavior was observed. When the specimens were examined at temperatures immediately below their melting points,[3] those with $n\leqq 28$ gave essentially the same diffraction patterns and long spacings as were obtained at room temperature, but with the higher members ($n\geqq 29$), though the reflections at higher angles were similar to those obtained at lower temperatures, the intensity of the reflections corresponding to the long spacings became too weak to be measured. In thermal analysis, the time-temperature curves of these specimens increased linearly with temperature until the temperature reached about 1°C below their melting points, where the slope of the curves became gradual. Thus, the crystalline forms of the alkanols seemed stable in the range from room temperature to just below their melting points.

The effect of a bulky cyclohexyl end group on the chain arrangement was clearly seen in the values of the long spacings of the alkanols. The long spacings are considerably shorter than the theoretical length of the hydrogen-bonded dimeric molecule in which the chain is stretched in a zig-zag form and the tilt angle of the chain axis to the basal plane is estimated to be about 30°. The effect is similar to that observed in ω-cyclohexyl alkanoic acids and the packing of the bulky end group seems to be responsible for the change in the arrangement of the hydrocarbon chains in crystals.

3) All the measurements at high temperature were carried out within 1°C below the melting points.

BULLETIN OF THE CHEMICAL SOCIETY OF JAPAN, VOL. 44, 847—848 (1971)

Long Spacings of α,ω-Dicyclohexyl Alkanes and α, ω-Diphenyl Alkanes

Akio ISHIZAWA, Chihito FUNAYAMA, and Masao KOSAKA

Department of Chemistry, Faculty of Science, Kyoto University, Sakyo-ku, Kyoto

(Received June 15, 1970)

A bulky cyclohexyl group substituted at the chain terminal of *n*-alkanols or *n*-alkanoic acids has been found to cause a marked change in the arrangement of the hydrocarbon chains in crystals.[1] Here we report studies on α,ω-diphenyl alkanes 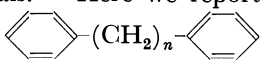 (I_n) and α,ω-dicyclohexyl alkanes 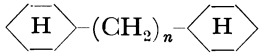 (II_n) (n=15 to 24) which are substituted with bulky groups at either ends of the chain.[2]

Like many other long chain compounds.[3] the odd (n=odd) and even (n=even) series of both I_n and II_n, crystallized from melt, gave different diffraction patterns. The long spacings also varied in different ways with chain length in the odd and even members.

At temperatures just below melting points the I_n specimens crystallized from melt gave essentially the same diffraction patterns and long spacings as those at room temperature, so that the crystalline forms seemed stable in the temperature range studied.

In II_{even} members a change in the crystalline form took place at II_{20} where the change displayed itself in the diffraction patterns as well as in the value of the long spacing. The II_{20} specimen, obtained by a similar method of preparation as for the lower members, gave two sets of long spacings. The feature of the diffraction patterns of this specimen showed no change up to a few degrees below its melting point, but at just below melting point, the crystalline form with the larger long spacing disappeared. On the other hand, the specimen obtained from melt by very rapid cooling consisted essentially of the form with the larger long spacing, the same as that was obtained for II_{22} and for II_{24}. No such behavior like that of II_{20} was ob-

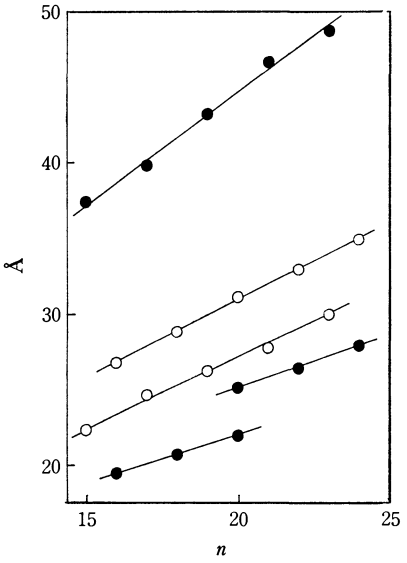

Fig. 1. Dependence of the long spacings on the chain length in 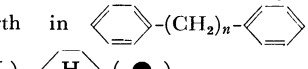 (-○-) and 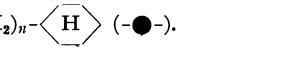 (-●-).

1) A. Ishizawa, This Bulletin, **44**, 846 (1971).

2) A. Ishizawa, M. Yamamura, and R. Goto, *Nippon Kagaku Zasshi*, **90**, 806 (1969).

3) A. Müller, *Proc. Roy. Soc.*, **A 120**, 437 (1928); **A 127**, 417 (1930); F. Francis, F. J. E. Collins, and S. H. Piper, *ibid.*, **A 158**, 691 (1937); E. von Sydow, *Ark. Kemi*, **9**, 231 (1957); A. Watanabe, This Bulletin, **34**, 1728, (1961); **36**, 336 (1963).

Table 1. The long spacings of I_n and II_n (Å)

n	I_n		II_n	
	at room temp.	at mp	at room temp.	at mp
15	22.29	22.28	37.46	37.58
16	26.72	26.86	19.46	19.34
17	24.55	24.33	39.78	40.61
18	28.75	28.71	20.62	20.89
19	26.12	25.86	43.23	43.62
20	31.03	30.87	21.89	21.95
			25.00	
21	27.37	27.54	46.52	46.45
22	32.84	33.21	26.35	26.36
23	29.92	29.67	48.72	49.57
24	34.91	34.85	27.76	27.90

served for any other II members and the crystalline forms once formed seemed stable even at temperature just below melting point.

As is evident from the long spacings of I_n and II_n, the values obtained are considerably shorter than the calculated length of the molecules in which the hydrocarbon chains are stretched in a straight zig-zag form. In crystals, II_n compounds may be considered an analogue to ω-cyclohexyl alkanoic acids and ω-cyclohexyl alkanols which exist in dimeric form by hydrogen bonding between the polar groups. The tilt angle of the hydrocarbon chain in II crystals is found unaffected by the absence of any polar groups and is calculated to be about 30° which is similar to the value obtained for ω-cyclohexyl alaknoic acids and ω-cyclohexyl alkanols.[1] The decrease of the tilt angle of I_n is less marked than that of II_n but is somewhat smaller than those which are not substituted with bulky groups.[3] These observations appear to indicate the importance of the shape and the packing of the end groups on the arrangement of the chain molecules in crystals.

BULLETIN OF THE CHEMICAL SOCIETY OF JAPAN, VOL. 44, 848—850 (1971)

Kinetic Studies of Lead Acetate Complex Formation in Aqueous Solutions

Tatsuya YASUNAGA and Shoji HARADA

Department of Chemistry, Faculty of Science, Hiroshima University, Higashi-sendamachi, Hiroshima

(Received June 26, 1970)

It is well known[1] that the rate constant of complex formation depends on the nature of the metal ion, *e.g.*, on the charge, the electric configuration, the ionic radius, and the coordination number. The Pb^{2+} ion has a noble gas electronic configuration and a large ionic radius; therefore, the rate of water substitution, which is the rate-determining step of the complex formation reaction, is expected to be very fast. The purpose of the present work is to perform kinetic studies of lead acetate complex formation with the help of the ultrasonic relaxation method.

Experimental

Reagent-grade lead acetate, lead nitrate, sodium acetate, and perchloric acid were used. Ultrasonic absorption measurements were carried out at 25°C by the pulse method over the frequency range from 15 to 95 MHz. Details of the apparatus have been described elsewhere.[2]

Theoretical

The metal ion and the ligand are hydrated in an aqueous solution. In the case of complex formation, therefore, two or three-step mechanisms, the rate-determining step of which is the release of a water molecule from the metal ion, have been proposed.[3,4] If the substitution rate of the water molecule is fast, however, the distinction of the steps is obscured. The complex formation reaction can, then, be approximately expressed by:

$$M_{aq}^{m+} + L_{aq}^{n-} \underset{k_f}{\overset{k_b}{\rightleftarrows}} ML_{aq}^{m-n} \qquad (1)$$

where M is the metal ion, L is the ligand, and ML is the complex, and where the subscript means that the ions are hydrated. The rate constants are related to the relaxation frequency, f_r, by the following form:

$$2\pi f_r = k_f + k_b(C_M + C_L) \qquad (2)$$

where C_M and C_L are the concentrations of M and L respectively. The relaxation frequency is expressed by the single relaxation equation:

$$\alpha/f^2 = A\{1 + (f/f_r)^2\}^{-1} + B \qquad (3)$$

where α is the absorption coefficient, f is the frequency, and A and B are constants.

Results and Discussion

The concentrations of the species, which were calculated by the use of the formation constants of lead acetate[5,6] and acetic acid,[7] are summarized in Table

1) M. Eigen, *Pure Appl. Chem.*, **6**, 97 (1963).
2) N. Tatsumoto, *J. Chem. Phys.*, **47**, 4561 (1967).
3) M. Eigen and K. Tamm, *Z. Elektrochem., Ber. Bunsenges. Phys. Chem.*, **66**, 93, 107 (1962).
4) M. Eigen, *ibid.*, **67**, 753 (1963).
5) N. Tanaka and K. Kato, This Bulletin, **33**, 417, 1412 (1960).
6) E. A. Burns and D. N. Hume, *J. Amer. Chem. Soc.*, **78**, 3958 (1956).
7) M. Yasuda, K. Yamasaki, and H. Ohtaki, This Bulletin, **33**, 1067 (1960).

Table 1. Experimental conditions and the relaxation frequency of the solution

Sample Number	$\sum$Pb (10^{-3} M)	$\sum$Ac (10^{-3} M)	pH	Concentration of the species (10^{-3} M)					f_r (MHz)
				Ac^-	Pb^{2+}	$PbAc^+$	$Pb(Ac)_2$	$Pb(Ac)_3^-$	
1	5	10	5.00	6	3	2	—[a]	—	25
2	15	30	4.82	12	6	9	1	—	37
3	15	50	4.72	20	4	10	1	—	35
4	25	50	4.97	20	6	17	2	1	48
5	50	30	4.58	5	30	19	1	—	50
6	50	50	5.00	12	19	29	2	—	47
7	50	100	5.02	35	8	34	7	1	61
8	50	150	5.01	63	4	32	12	2	63
9	75	50	4.55	20	6	17	2	—	53
10	75	150	5.03	47	8	50	14	2	77
11	100	50	4.58	5	61	38	1	—	82
12	100	200	4.91	54	9	66	21	4	85

a) 0.1×10^{-3} M

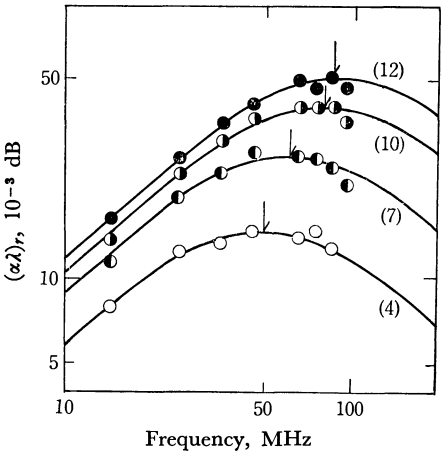

Fig. 1. Ultrasonic absorption in lead acetate solutions. $(\alpha\lambda)_r$ means the excess absorption per wavelength and the arrows indicate the relaxation frequencies. Numeral shows the sample number.

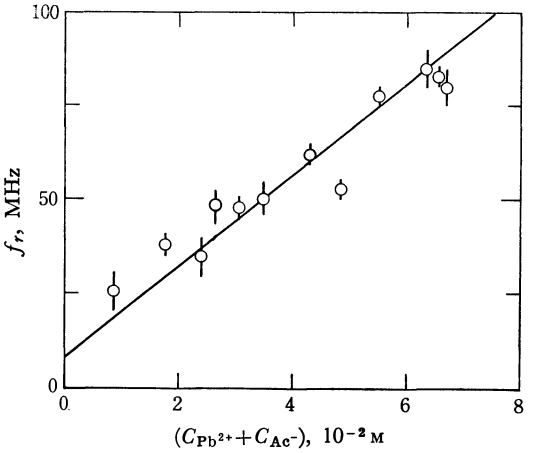

Fig. 2. Plot of relaxation frequency (f_r) *vs.* $(C_{Pb^{2+}}+C_{Ac^-})$.

1. The ionic strengths of the solutions were 0.1—0.3, but the formation constant of lead acetate at $\mu=0.2$ was used, for the change in ionic strength by an addition of $NaClO_4$ did not have a serious effect on the absorption curves. Therefore, no special care was taken with regard to the ionic strength. Representative absorption curves are shown in Fig. 1. The relaxation frequencies obtained are also listed in Table 1.

The principal equilibria between lead and acetate ions at low concentrations are:

$$Pb^{2+} + Ac^- \underset{k_{f1}}{\overset{k_{b1}}{\rightleftarrows}} PbAc^+ \qquad (4)$$

$$PbAc^+ + Ac^- \underset{k_{f2}}{\overset{k_{b2}}{\rightleftarrows}} Pb(Ac)_2 \qquad (5)$$

$Pb(Ac)_3^-$ and higher-order complexes may exist, but the concentrations are very low. Therefore, the present absorption can be attributed to one of the above two equilibria. Both of the equations have been investigated in trying to correlate the experimental data.

Equation (2) can, then, be rewritten for Eq. (4):

$$2\pi f_r = k_{f1} + k_{b1}(C_{Pb^{2+}} + C_{Ac^-}) \qquad (6)$$

With the data in Table 1, f_r is plotted against $(C_{Pb^{2+}}+C_{Ac^-})$ in Fig. 2. From the slope and the intercept of the line in Fig. 2, k_{b1} and k_{f1} were obtained; $k_{b1}=7.5\times10^9$ M^{-1} sec^{-1}, and $k_{f1}=5.7\times10^7$ sec^{-1}. The equilibrium constant of Eq. (4) is also given by $K=k_{b1}/k_{f1}=133$ M^{-1}. The equilibrium constant obtained is in good agreement with the literature value,[5,6] which had been previously used in the calculation of the ionic concentrations. On the other hand, the same plots for Eq. (5) show a linear relation, but yield a different equilibrium constant from that used before. Along with the fact that the excess ultrasonic absorption was observed in the solution where the concentration of $PbAc_2$ was very low, these results suggest that Eq. (4) is responsible for the present absorption.

The formation rate constant of Eq. (4), k_{b1}, is interesting in relation to the nature of the metal ion. Eigen and Eyring[8] obtained the rate constant of complex formation, $k_b=7\times10^9$ M^{-1} sec^{-1}, for the reaction:

$$HgCl^+ + Cl^- \underset{k_f}{\overset{k_b}{\rightleftarrows}} HgCl_2 \qquad (7)$$

They said that the value is close to the rate constants of water substitution of Pb^{2+} and Ba^{2+} ions. In this

8) M. Eigen and E. M. Eyring, *Inorg. Chem.*, **2**, 636 (1963).

work, we obtained 7.5×10^9 M^{-1} sec^{-1} for the rate constant of the complex formation of lead acetate. Considering that the Pb^{2+} ion has a large ionic radius[9] (1.32 Å) and the filled outer orbitals and, moreover, considering that the coordination number of the water molecule is larger than those of ordinary ions,[10] the above value seems to be reasonable.

9) F. Basolo and R. G. Pearson, "Mechanism of Inorganic Reactions," J. Wiley & Sons, Inc., New York (1958). p. 66.

10) T. J. Swift and W. G. Sayre, *J. Chem. Phys.*, **44**, 3567 (1966).

BULLETIN OF THE CHEMICAL SOCIETY OF JAPAN, VOL. 44, 850—851 (1971)

Acylation of Aluminum Trisacetylacetonate with *n*-Butyryl Chloride in the Presence of Aluminum Chloride[1]

Tetsuro NOJIRI,* Masatoshi MOTOI, and Iwao HASHIMOTO**

Department of Industrial Chemistry, Faculty of Technology, Kanazawa University, Kodatsuno, Kanazawa

(Received September 5, 1970)

It was reported[2] that acetylacetone reacts with *n*-butyryl chloride to give *n*-butyrylacetone (I) and di-*n*-butyrylmethane (II) in the presence of more than 2 equivalents of aluminum chloride in nitrobenzene at 45°C. These products can be rationalized by assuming initial formation of dichloroaluminum enolate of the β-diketones, acetylacetone and I, followed by butyrylation leading to the respective deacetylated products, I and II. Murdoch *et al.* and Barry reported that the metal chelates (excluding aluminum chelate) of β-diketones react with acyl chlorides in refluxing toluene or cyclohexane,[3,4] or in chloroform at room temperature[5] to afford initially triacylated methanes. Doolan and Gore[6] pointed out that aluminum trisacetylacetonate (III) or acetylacetone (regarded as converting into III during the reaction) reacts as in aromatic acylation with acetyl chloride to give diacetylated III in the presence of the excess of aluminum chloride in boiling carbon disulfide. This paper deals with the problem of deciding how the reaction of III with *n*-butyryl chloride proceeds under conditions similar to those of the above butyrylation of acetylacetone.[2]

The conditions of the present reactions and the product yields based on acetylacetone to be formed from III are given in Table 1. All the experimental procedures are similar to those for acetylacetone.[2]

The non-catalyzed reaction of III with 3 equivalents of *n*-butyryl chloride afforded I as a single product in a low yield only when the temperature was raised to 65°C. This shows that there is some difficulty at 45°C in acylating through coordination of *n*-butyryl chloride with the central metal atom of the chelate as with the mechanism proposed by Murdoch *et al.*[3,4] Even at low temperature, however, the addition of 1.5 equivalent of aluminum chloride gave II as well as I. The formation of II suggests that III can be acylated through its ring-opening during the reaction.

In the presence of 3 equivalents of aluminum chloride (1 equivalent for each acetylacetone component in III) the yields of both I and II obtained using 6 equivalents of *n*-butyryl chloride (2 equivalents for each acetylacetone component in III) increased to

TABLE 1. REACTION OF ALUMINUM TRISACETYLACETONATE WITH *n*-BUTYRYL CHLORIDE

$AlCl_3$ mole ratio	Reaction time (hr)	Product[a] and yield (%)			
		$PrCOCH_2COCH_3$	$PrCOCH_2COPr$	Total	Recovery as $(CH_3CO)_2CH_2$
0*	1	0	0	0	39
0*	1**	8	0	8	28
1.5*	1	27	6	33	17
1.5	1	34	16	50	13
3	1	37	17	54	15
3	0.5	36	18	54	14
3	24	30	21	51	11

Substrate: $Al[(CH_3CO)_2CH]_3$ 1.62 g (0.005 mol), Reactant: C_3H_7COCl 3.2 g (0.03 mol), * 1.6 g (0.015 mol)
Reaction temp.: 45°C, ** 65°C, Solvent: $C_6H_5NO_2$ 10 ml

a) Very small amounts of methyl ethyl ketone and neutral oily substance were obtained.

1) Presented at the 23rd Annual Meeting of the Chemical Society of Japan, Tokyo, April, 1970.

* Present address: FUJI CHEMICAL INDUSTRY Co., Kamiichi, Toyama.

** Present address: Wakayama Technical College, Gobo, Wakayama.

2) T. Nojiri, I. Hashimoto, M. Motoi, and K. Matsui, This Bulletin, **42**, 3359 (1969).

3) H. D. Murdoch and D. C. Nonhebel, *J. Chem. Soc.*, **1962**, 2153; *ibid.*, *C*, **1968**, 2298.

4) D. C. Nonhebel and J. Smith, *ibid.*, *C*, **1967**, 1919; D. C. Nonhebel, *ibid.*, **1962**, 4628.

5) W. J. Barry, *ibid.*, **1960**, 670.

6) P. C. Doolan and P. H. Gore, *ibid.*, *C*, **1967**, 211.

near maximum and were almost unaffected even when the reaction time was extended from 0.5 to 1 hr, but the extension of time to 24 hr allowed II to increase at the expense of I. Although the total yields increased somewhat, these findings are similar to those observed in the butyrylation reactions of acetylacetone under analogous conditions.

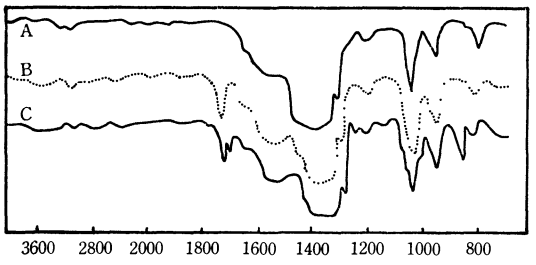

Fig. 1. Infrared spectrum of aluminum trisacetylacetonate in nitrobenzene (A); with 0.5 (B); and with 1.5 equivalent of $AlCl_3$ (C).

The infrared spectra of III in nitrobenzene solutions containing 0.5 and 1.5 equivalent of aluminum chloride show medium absorption peaks at 1688, and 1715 and 1688 cm^{-1} due to carbonyl group, respectively, which cannot be observed with the spectrum of III in nitrobenzene, as shown in Fig. 1. It can be seen that, concurrent with the ring-opening of III, a carbonyl group appears and leaves a site capable of coordinating with *n*-butyryl chloride on the central aluminum so that the butyrylation reaction proceeds easily as follows:

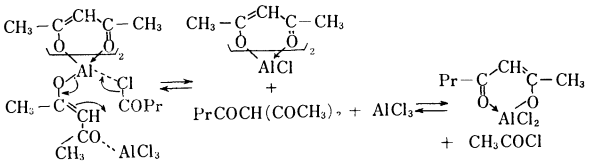

The chloroaluminum bisacetylacetonate and dichloroaluminum *n*-butyrylacetonate which were formed must be further butyrylated and then deacetylated in the same way as illustrated in the above equation. Although not produced from acetylacetone by using 0.5 equivalent of aluminum chloride,[2] II was provided from III in a nearly maximum yield of 16% even under the corresponding conditions. This high yield seems to be ascribable to the easier enolate formation of III by its ring-opening as compared with that of acetylacetone.

The authors wish to express their hearty thanks to Professor Kiyotaka Matsui for his kind guidance and encouragement.

BULLETIN OF THE CHEMICAL SOCIETY OF JAPAN, VOL. 44, 851—852 (1971)

On the Ratio of A_N to $A_{H(NH)}$ for Some Phenyl Nitric Oxide Radicals

Toshio NISHIKAWA and Kazuo SOMENO

Government Chemical Industrial Research Institute, Tokyo, Shibuya-ku, Tokyo

(Received September 14, 1970)

In an ESR study on monophenyl nitric oxide radicals (phenyl NOR) in solution, it has been suggested by Chapelet-Letourneux *et al.*[1] that the ratio of hf splitting of nitrogen to that of hydrogen attached to it, $A_N/A_{H(NH)}$, has an almost constant value of about 0.77.

TABLE 1. $A_N/A_{H(NH)}$ OF PHENYL NOR PREPARED FROM VARIOUS STARTING MATERIALS

Starting materials	$A_N/A_{H(NH)}$	Ref.
Ph-NH_2+PBA-NO_2	0.762	1
Ph-N(H)OH	0.764	1
Ph-NO_2+$LiAlH_4$	0.752	2
Ph-N(H)OH+PbO_2	0.759	3
Ph-NO+Ph-N(H)OH	0.753	4
Ph-NH_2+PBA	0.756	Present work

In the present note, some experimental results are reported in order to ascertain this constancy of the ratio, and it is also shown that phenyl NOR having intramolecular hydrogen bond (IH-bond) has another constant value of the ratio.

Well resolved ESR spectra were obtained from the radicals produced in oxidation of aniline derivatives with perbenzoic acid (PBA) at room temperature. The molecular structures of radicals were determined

TABLE 2. SOLVENT EFFECT ON $A_N/A_{H(NH)}$ OF PHENYL NOR[5]

Solvent	$A_N/A_{H(NH)}$
Ether	0.752
Tetrahydrofuran	0.752
Benzene	0.759
Toluene	0.757
Dioxane	0.756
Chloroform	0.762
Ethanol	0.759
Methanol	0.760

1) G. Chapelet-Letourneux, H. Lemaire, A. Rassat, and J. P. Ravet, *Bull. Soc. Chim. Fr.*, **1965**, 1975.

2) H. Lemaire, A. Rassat, and J. P. Ravet, *Tetrahedron Lett.*, **47**, 3507 (1964).

3) A. L. Buchachenko, *Izv. Akad. Nauk SSSR Otdel. Khim. Nauk*, **1963**, 1120; *Bull. Acad. Sci. URSS Div. Chem. Sci.*, **1963**, 1020.

4) Th. A. J. W. Wajer, A. Mackor, Th. J. deBoer, and J. D. W. vanVoorst, *Tetrahedron Lett.*, **1967**, 1941.

5) O. Kikuchi and K. Someno, This Bulletin, **40**, 2549 (1967).

Table 3. Substituent effect on $A_N/A_{H(NH)}$ of R–Ph–N(H)O

R	$A_N/A_{H(NH)}$	R	$A_N/A_{H(NH)}$
H	0.756 (0.753) [b]	*m*-Cl	0.752
p-Cl	0.754 (0.748)	-Br	0.749
-Br	0.746 (0.746)	$-CH_3$	0.758
-I	0.752	-COOH	0.752
-F	0.756 (0.760)	2,6-di-CH_3	0.756
$-CH_3$	0.746 (0.732)	*o*-Cl	0.740
$-OCH_3$	((0.760))	-Br	0.746
$-C(CH_3)_3$	(0.758)	-I	0.746 (0.741)
-COOH	0.750	-F	0.733 (0.739)
$-COOCH_3$	0.751 [a]	$-CH_3$	0.752
$-COOC_2H_5$	0.748	$-OCH_3$	0.762
$-COCH_3$	0.705	$-C(CH_3)_3$	(0.761)
		$-C_6H_5$	(0.750)

a) Methanol was used as a solvent.
b) The values in parentheses were calculated from the data presented by Wajer *et al.*[4] and double parentheses by Chapelet-Letourneux *et al.*[6]

from analysis of the spectra. The phenyl NOR was very stable in many organic solvents at room temperature. All the spectra were obtained in dioxane at room temperature unless otherwise noted. The IH-bond is formed between amino proton and carboxyl group in *o*-aminobenzoic acid and its esters. Thus phenyl NOR produced from these compounds may also have the IH-bond because of the remaining one of amino proton.

Table 4. $A_N/A_{H(NH)}$ of R–Ph–N(H)O having IH-bond

R	$A_N/A_{H(NH)}$
o-COOH	0.705
$-COOCH_3$	0.713
$-COOC_2H_5$	0.688
$-COOC_4H_9$	0.687
$-COCH_3$	0.679
-CHO [a]	0.687

a) Toluene was used as a solvent.

The ratios were obtained for some phenyl NOR under various conditions as shown in Tables 1 to 4. It may be concluded from these data (Tables 1 to 3) that the values of the ratios are in the range of 0.74—0.76 and all the effects of solvent species, substituents and steric hindrance give only less than 1% change on the ratio. This is because about 70—80% of spin density is on the nitrogen and the oxygen atoms. On other hand, as shown in Table 4, the ratio decreases to 0.71—0.68 when the radicals have the IH-bond. The only exception was in the case of *p*-acetylphenyl NOR, where the ratio decreases below the range 0.74—0.76. The ambiguity of hf splitting determination due to the complexity of the spectrum might make the ratio questionable. The effect of IH-bond seems to make a predominant contribution to the ratio. The decrement of the ratio may be used to check the IH-bond formation of phenyl NOR.

6) G. Chapelet-Letourneux, H. Lemaire, and A. Rassat, *Bull. Soc. Chim. Fr.*, **1964**, 3283.

BULLETIN OF THE CHEMICAL SOCIETY OF JAPAN, VOL. 44, 852—854 (1971)

The Carbon Dioxide-Catalyzed Ester Exchange Reaction

Yoshio Otsuji, Noboru Matsumura, and Eiji Imoto

Department of Applied Chemistry, College of Engineering, University of Osaka Prefecture, Sakai-shi, Osaka

(Received September 18, 1970)

Carbon dioxide has long been recognized as an inert gas for most neutral organic compounds. However, we have reported in a previous communication[1] that, contrary to the above view, CO_2 catalyzes the transacylation reaction from acid amides to amines. We now wish to report that CO_2 can also catalyze the ester-exchange reaction between carboxylic esters and alcohols.

Results and Discussion

A solution of butyl formate in an excess of ethanol was agitated by a stream of dry CO_2 at room temperature for 5 hr. The vpc analysis of the reaction mixture revealed that this simple treatment gave rise to an ester-exchange reaction affording ethyl formate in a 30% yield. A similar exchange reaction was also observed between other carboxylic esters and alcohols. The results are summarized in Table 1.

$$RCO_2R' + R''OH \xrightarrow{CO_2} RCO_2R'' + R'OH$$

In the controlled experiments, mixtures of butyl formate and *n*-octyl alcohol and of ethyl butyrate and butyl alcohol were allowed to stand, or were agitated by a stream of N_2, for 5 hr at room temperature. No exchange reaction was observed in any of these treatments, confirming that CO_2 must be a catalyst for the reaction.

The ester-exchange reaction was also conducted in an autoclave under the pressure of CO_2. The results are summarized in Table 2. The controlled experiments, which were carried out under the pressure of N_2, confirmed that the exchange reaction is always CO_2-catalyzed reaction, except for the reaction of butyl formate at elevated temperatures (see runs 14 and 18). The reason for this exception was clarified

1) Y. Otsuji, N. Matsumura, and E. Imoto, This Bulletin, **41**, 1485 (1968).

Table 1. The ester exchange reaction in a stream of CO_2[a)]

	Ester	Alcohol	Temp., °C[b)]	Product Compd.	Product Yield, %
1	$HCO_2C_4H_9$	C_2H_5OH	rt	$HCO_2C_2H_5$	30
2	$HCO_2C_4H_9$	$C_6H_{11}OH$	rt	$HCO_2C_6H_{11}$	10
3	$HCO_2C_4H_9$	$(CH_3)_3COH$	rt	no reaction	0
4	$HCO_2C_4H_9$	n-$C_8H_{17}OH$	0	$HCO_2C_8H_{17}$	35
5	$HCO_2C_4H_9$	n-$C_8H_{17}OH$	rt	$HCO_2C_8H_{17}$	27
6	$HCO_2C_4H_9$	n-$C_8H_{17}OH$	50—60	$HCO_2C_8H_{17}$	10
7	n-$C_3H_7CO_2C_2H_5$	n-C_4H_9OH	0	$C_3H_7CO_2C_4H_9$	27
8	n-$C_3H_7CO_2C_2H_5$	n-C_4H_9OH	rt	$C_3H_7CO_2C_4H_9$	20
9	n-$C_3H_7CO_2C_2H_5$	n-C_4H_9OH	50—60	$C_3H_7CO_2C_4H_9$	4
10	$C_6H_5CO_2C_2H_5$	n-C_4H_9OH	rt	no reaction	0

a) The reaction time was 5 hr.
b) The "rt" indicates the room temperature, which was ~20°C.

Table 2. The ester exchange reaction under the pressure of CO_2

	Ester	Alcohol	Reaction conditions Temp., °C[a)]	Reaction conditions Time, hr	Reaction conditions Press, kg/cm	Product Compd.	Product Yield, %
11	$HCO_2C_4H_9$	n-$C_8H_{17}OH$	rt	5	50	$HCO_2C_8H_{17}$	5
12	$HCO_2C_4H_9$	n-$C_8H_{17}OH$	rt	12	50	$HCO_2C_8H_{17}$	13
13	$HCO_2C_4H_9$	n-$C_8H_{17}OH$	rt	30	50	$HCO_2C_8H_{17}$	29
14	$HCO_2C_4H_9$	n-$C_8H_{17}OH$	100—110	5	150	$HCO_2C_8H_{17}$	27
15	n-$C_3H_7CO_2C_2H_5$	n-C_4H_9OH	100—110	5	150	$C_3H_7CO_2C_4H_9$	Trace
16	$C_6H_5CO_2C_2H_5$	n-C_4H_9OH	100—110	5	150	no reaction	0
			Controlled experiments[b)]				
17	$HCO_2C_4H_9$	n-$C_8H_{17}OH$	rt	5	50	no reaction	0
18	$HCO_2C_4H_9$	n-$C_8H_{17}OH$	100—110	5	50	$HCO_2C_8H_{17}$	52
19	n-$C_3H_7CO_2C_2H_5$	n-C_4H_9OH	100—110	5	50	$C_3H_7CO_2C_4H_9$	Trace

a) The "rt" indicates the room temperature, which was ~20°C.
b) The controlled experiments were conducted under the pressure of N_2.

when the reaction products were carefully analyzed. The vpc analysis of the reaction mixture obtained after the treatment of butyl formate with octyl alcohol under the pressure of N_2 at 100—110°C showed that the mixture contained formic acid and butene-1. Both products could be formed by the thermal decomposition of butyl formate. The formic acid thus produced would react with octyl alcohol to give octyl formate. The formation of the ester from formic acid under the experimental conditions was in fact verified by a separate experiment.

$$HCO_2C_4H_9 \xrightarrow{\Delta} HCO_2H + CH_3CH_2CH{=}CH_2$$

$$HCO_2H + n\text{-}C_8H_{17}OH \rightarrow HCO_2C_8H_{17}$$

Thus, the striking features of this study can be summarized by the following four items; (i) the reactivities of esters decrease in the order of; butyl formate > ethyl butyrate > ethyl benzoate (runs 5, 8, and 10), implying that the increase in the positive charge on the carbonyl carbon of the esters makes the progress of the reaction profitable; (ii) the reactivities of the alcohols decrease in the order of; primary > secondary tertiary > (runs 1, 2, 3, and 5); (iii) the yield of the exchanged esters increases with the decrease in the reaction temperature (runs 4, 5; and 6, 7, 8, and 9); and (iv) the increase in the reaction time increases the yield of the exchanged esters (runs 11, 12, and 13).

On the basis of these observations, together with those described in the previous paper,[1)] we tentatively propose the mechanism shown in Scheme 1 for the ester-exchange reaction:

$$R''OH + CO_2 \rightleftharpoons R''OCO_2H \quad (1)$$

I

$I + RCO_2R' \rightarrow$ (2)

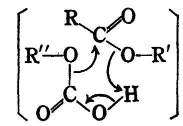

II

$$II \rightarrow RCO_2R'' + R'OH + CO_2 \quad (3)$$

Scheme 1

The reversible reaction (1) has been postulated by Hempel and Seidel,[2)] mainly on the basis of the freez-

2) W. Hempel and J. Seidel, *Ber.*, **31**, 2997 (1898).

ing-point elevation of an alcohol containing CO_2 and the molecular composition of the isolated product. However, the equilibrium constant for this reaction has not yet been determined. Nevertheless, it is reasonable to assume that the equilibrium constant for the reaction (1) in various alcohols is proportional to the solubility of CO_2 in the alcohols. The solubility data[3] of CO_2 in alcohols suggest that the equilibrium constants would decrease in the order of; primary> secondary>tertiary alcohols, an order which is in accordance with the reactivity order of the alcohols for the ester-exchange reaction. This fact and the effect of the temperature on the yield of the exchanged esters are consistent with the assumptions that reaction (1) is involved in the initial stage of the reaction and that the monoalkyl carbonate (I) is a reactive species; the concentration of I would increase with a lowering of the temperature by means of the increase in the solubility of CO_2; and accordingly, the yield of the exchanged esters would increase with a lowering of the temperature.

The monoalkyl carbonate I would then react with an ester to form a six-membered transition state (II), which would spontaneously collapse to give the exchanged ester, accompanied by the elimination of the alcohol (R'OH) and CO_2. At this stage, the nucleophilic reactivity of the alcohol may be enhanced to some extent, since the temporary formation of an alkoxide ion ($R''O^-$) would be expected at the moment of the elimination of CO_2.

3) H. Stephen and T. Stephen, "Solubilities of Inorganic and Organic Compounds," Vol. 1, Pergamon Press, Oxford, London (1963), pp. 1058—1076.

Experimental

The vpc analyses were preformed with a Yanagimoto GCG-5DH gas chromatograph, employing a stainless steel column (1.5 m × 3 mm o.d.) packed with 30% PEG-20 M on Chromosorb (80 mesh) and using helium as the carrier gas. For quantitative analyses, the respective authentic samples were used as the internal standards.

All the compounds used were purchased or prepared by the standard methods, and they were purified by distillation before use. CO_2 was generated from dry ice and was dried by passing it through concentrated H_2SO_4 and then a column packed with $CaCl_2$.

Ester-exchange Reaction in a Stream of CO_2. A solution of an ester (~0.05 mol) in an alcohol (0.1—0.2 mol) was placed in a flask equipped with a gas inlet and outlet tubes, to which a tube packed with $CaCl_2$ was connected. Dry CO_2 was then passed into the solution. The passing rate was so adjusted as to maintain the rate as constant as possible throughout the whole series of experimental runs. After an appropriate period of time, an aliquot taken up from the reaction mixture was subjected to vpc analysis.

Control experiments were carried out under conditions similar to those employed above except that the passing gas was changed from CO_2 to N_2. In these experiments, the exchanged esters were not obtained in a detectable yield, but the starting materials were recovered.

Ester-exchange Reaction under the Pressure of CO_2. To a solution of an ester (~0.03 mol) in an alcohol (0.1—0.2 mol) placed in a 300-m*l* autoclave, we added small pieces of dry ice. The autoclave was then closed and warmed to the reaction temperature. After checking the pressure, the autoclave was shaken for an appropriate period of time. An aliquot was pipetted out from the reaction mixture and then subjected to vpc analysis.

Control experiments were carried out under conditions similar to those employed above except that N_2 was used in place of CO_2.

BULLETIN OF THE CHEMICAL SOCIETY OF JAPAN, VOL. 44, 854—856 (1971)

A Spectroscopic Study on Hydrogen Bonding and Proton Transfer in Photo-Excited *p*-Hydroxybenzophenone

Akio MATSUYAMA* and Hiroaki BABA

Division of Chemistry, Research Institute of Applied Electricity, Hokkaido University, Sapporo

(Received October 6, 1970)

In a previous paper,[1] one of us (H.B.) showed that, in contrast to the case of the usual phenolic compounds,[2-4] proton transfer does not occur from *p*-hydroxybenzaldehyde to triethylamine, a strong proton acceptor, in the excited state in spite of its occurrence in the ground state. This was attributed to the fact that the lowest excited singlet of the *p*-hydroxybenzaldehyde molecule is an (n, π^*) state, where the proton-donating power of the molecule is relatively weak. In their discussion on the photochemical behavior of *p*-hydroxybenzophenone, an analogue of *p*-hydroxybenzaldehyde, Godfrey, Porter, and Suppan[5] assumed that the proton transfer would take place in the excited singlet state. In this study, the emission properties of *p*-hydroxybenzophenone coupled with proton-accepting substances have been examined to get an insight into the validity of these contradictory views.

Figure 1 shows the absorption and phosphorescence spectra of *p*-hydroxybenzophenone at 77°K in the presence of proton acceptors. The absorption spectrum of *p*-hydroxybenzophenone at 77°K in a mixture of hydrocarbons containing ether is obviously

* Present address: Biophysics Division, National Cancer Center Research Institute, Tsukiji, Chuo-ku, Tokyo.

1) H. Baba, *J. Chem. Phys.*, **49**, 1763 (1968).

2) N. Mataga and Y. Kaifu, *ibid.*, **36**, 2804 (1962).

3) H. Beens, K. H. Grellmann, M. Gurr, and A. H. Weller, *Discuss. Faraday Soc.*, **39**, 183 (1965).

4) S. Suzuki and H. Baba, This Bulletin, **40**, 2199 (1967).

5) T. S. Godfrey, G. Porter, and P. Suppan, *Discuss. Faraday Soc.*, **39**, 194 (1965).

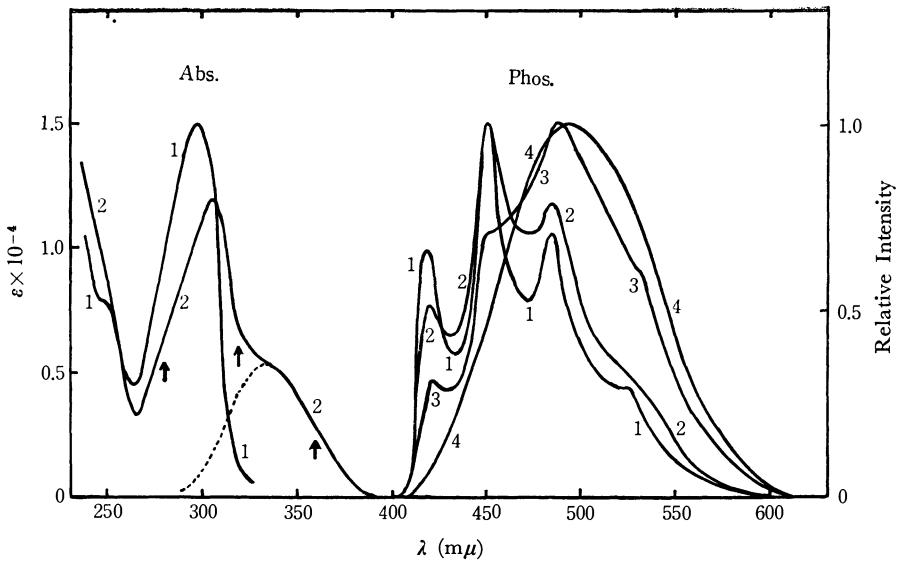

Fig. 1. Absorption (Abs.) and phosphorescence (Phos.) spectra of *p*-hydroxybenzophenone (3.03×10^{-5} mol/*l*) at 77°K.
Absorption: 1, in methylcyclohexane and isopentane (volume ratio, 1:1) containing ethyl ether (0.4 mol/*l*) as a proton acceptor; 2, in methylcyclohexane, isopentane and ethyl ether (4 : 4 : 1) containing triethylamine (4.0×10^{-3} mol/*l*).
Phosphorescence: 1, in methylcyclohexane and isopentane (1 : 1) containing ethyl ether (0.4 mol/*l*), excitation at 290 mμ; 2, 3 and 4, in methylcyclohexane, isopentane and ethyl ether (4 : 4 : 1) containing triethylamine (4.0×10^{-3} mol/*l*), excitation at 280, 320 and 360 mμ, respectively, as indicated by arrows.

ascribable to the simple hydrogen-bonded complex between *p*-hydroxybenzophenone and ether. This complex has at about 350 mμ another absorption band, which is weak and is assigned to an $n\rightarrow\pi^*$ transition. When triethylamine is added as a proton acceptor besides ether, an additional absorption band appears at 77°K in the longer wavelength region. It can be shown that in the latter case the solute molecules are associated with triethylamine owing to the much stronger basicity of the amine compared with ether. Thus, hydrogen bonding occurs between the solute and amine molecules to give a simple hydrogen-bonded complex, followed by proton transfer from the solute to the amine to yield a hydrogen-bonded ion pair. The additional absorption band can be attributed to the proton-transferred complex, *i.e.*, the hydrogen-bonded ion pair, as in the case of previous studies.[1,6,7] In the ground state of the solute molecule, an equilibrium is to be established at 77°K between the simple hydrogen-bonded complex and the ion pair.

It should be noted that in the absence of ether the *p*-hydroxybenzophenone-triethylamine system in the hydrocarbon mixture gives almost exclusively the simple hydrogen-bonded complex. This shows that the degree of proton transfer is sensitive to the polarity of the solvent.

The hydrogen-bonded complex between *p*-hydroxybenzophenone and ether gives an emission spectrum with a vibrational structure (Fig. 1). The emission has a lifetime of the order of millisecond and is assigned to the phosphorescence from the lowest triplet state of an (n, π^*) type.[8,9]

The system containing triethylamine as a proton acceptor exhibits different phosphorescence spectra, depending on the wavelengths of exciting light. Thus, excitation at 280 mμ is largely related to the hydrogen-bonded complex, the observed spectrum being essentially the same as that found in the *p*-hydroxybenzophenone molecule hydrogen-bonded with ether, whereas excitation at 360 mμ leads to a broad, long-lived ($\approx$1 sec) and red-shifted phosphorescence spectrum which is entirely different from the spectrum of the simple hydrogen-bonded complex. The broad spectrum resulting from the 360 mμ excitation may be assigned to the $\pi\leftarrow\pi^*$ phosphorescence originating in the proton-transferred complex. In this way, excitation at shorter and longer wavelengths induces phosphorescence from the simple hydrogen-bonded complex and from the proton-transferred complex, respectively. The emission obtained by excitation at intermediate wavelengths (*e.g.*, 320 mμ) is found to be a superposition of phosphorescence emissions from both complexes.

These absorption and emission characteristics of *p*-hydroxybenzophenone in relation to hydrogen bonding and proton transfer are very similar to those of *p*-hydroxybenzaldehyde,[1] except that in the former the lowest triplet is of (n, π^*) type and the proton-transferred complex gives no fluorescence. In the

6) H. Baba, A. Matsuyama, and H. Kokubun, *J. Chem. Phys.*, **41**; 895 (1964).
7) H. Baba, A. Matsuyama, and H. Kokubun, *Spectrochim. Acta*, **25A**, 1709 (1969).
8) G. Porter and P. Suppan, *Trans. Faraday Soc.*, **61**, 1664 (1965).
9) D. R. Kearns and W. A. Case, *J. Amer. Chem. Soc.*, **88**, 5087 (1966).

simple hydrogen-bonded complexes (*i.e.*, the protonated forms) of the two compounds, the lowest excited singlet (S_1) is an (n, π^*) state and the next lowest singlet (S_2) is a (π, π^*) state of charge-transfer nature. On exciting the *p*-hydroxybenzophenone-triethylamine system at shorter wavelengths (*e.g.*, 280 mμ), the protonated form is raised to its S_2 level. By the same reasoning as in the case of *p*-hydroxybenzaldehyde,[1] it is concluded that the state S_2 of the protonated form of *p*-hydroxybenzophenone is deactivated by rapid radiationless processes to the lower singlet and triplet states, phosphorescence being emitted from the protonated form itself, and that no proton transfer takes place throughout the deactivation processes.

Godfrey *et al.*[5] found that the photo-excited *p*-hydroxybenzophenone shows an anomalously low reactivity toward abstraction of a hydrogen atom from solvents. In order to interpret this phenomenon, they assumed that the proton transfer would occur in the excited singlet state of the protonated form, in marked contrast to our conclusion. It would be desirable to re-examine the anomalous photochemical behavior of *p*-hydroxybenzophenone in the light of the results of the present spectroscopic investigation.

Experimental

p-Hydroxybenzophenone was recrystallized from a mixture of water and ethanol. Methylcyclohexane of spectroscopic quality was used without further purification. Isopentane was passed through a silica-gel column. Ethyl ether was distilled over metallic sodium. Triethylamine was fractionally distilled over phosphorus pentoxide. Absorption spectra were obtained with a Hitachi EPS-3 spectrophotometer at 77°K. Emission spectra were measured at 77°K with an apparatus which was constructed using a Hitachi G-3 grating monochromator and a Hitachi EPU-2A prism monochromator.

BULLETIN OF THE CHEMICAL SOCIETY OF JAPAN, VOL. 44, 856—857 (1971)

The Spatial Distribution of Secondary Electrons Produced in the γ-Radiolysis of Cyclohexane

Shin SATO and Takefumi OKA

Department of Applied Physics, Tokyo Institute of Technology, Ookayama, Meguro-ku, Tokyo

(Received October 13, 1970)

In order to analyze the reactions of charged species produced in liquid-phase radiolysis, it is important to know the spatial distribution of secondary electrons, even if it is qualitative. Recently, Warman, Asmus, and Schuler proposed an empirical equation for the charge scavenging[1] from which they derived a distribution function for the lifetime of the charged species produced in the radiolysis of hydrocarbon solutions.[2] On the other hand, we ourselves have previously discussed the kinetics of the electron scavenging of nitrous oxide in the radiolysis of several hydrocarbons by assuming a Gauss function as the spatial distribution of secondary electrons.[3] By combining these two procedures, we have realized that it is possible to derive a spatial distribution of secondary electrons in the γ-radiolysis of cyclohexane. The present note will report the procedure of deriving the distribution function and will discuss the implications of this function.

Procedure[4]

The G-value of the electrons scavenged by an electron scavenger is expressed by the following equation, based on an appropriate assumption:[3]

$$G_s = G_{fi} + G_{gi}\left\{1-\int_0^\infty \phi(r)\ (1-N_s)^{nz}\ 4\pi r^2\ \mathrm{d}r\right\}. \qquad (1)$$

Here, G_{fi} and G_{gi} are the G-values of free and geminate electrons respectively. $\phi(r)$ is the distribution function of the distance between a thermalized electron and its parent positive ion. N_s is the mole fraction of the electron scavenger, n is the number of jumps which an electron makes before neutralization, and z is the number of new neighboring molecules when an electron makes a jump. As has been established by Williams,[5] the following relation exists between n and r: $n=r^3/3\sigma^2 r_c$. Here, r_c is the Onsager length and σ is the mean distance of a jump made by the electron.

When the concentration of the electron scavenger is not large, $(1-N_s)^{nz}$ may be replaced by $\exp(-nzN_s)$. Then, by changing a variable from r to x ($x=r^3$), we can obtain the following equation:

$$G_s = G_{fi} + G_{gi}\left\{1-\frac{4\pi}{3}\int_0^\infty \phi(x^{1/3})\ \exp(-kSx)\mathrm{d}x\right\}. \qquad (2)$$

Here, S is the concentration of the scavenger in mol l^{-1}, k is a constant $(2z/\sigma^2 r_c)(M/10^3\rho)$, M is the molecular weight of cyclohexane, and ρ is the density.

So far, two empirical equations have been proposed for expressing the relation between the G-value of scavenged electrons and the concentration of the electron scavenger. One of them has been proposed by

1) J. M. Warman, K.-D. Asmus, and R. H. Schuler, *Adv. Chem. Ser.*, **82**, 25 (1968).

2) S. J. Rzad, P. P. Infelta, J. M. Warman, and R. H. Schuler, *J. Chem. Phys.*, **52**, 3971 (1970).

3) S. Sato, T. Terao, M. Kono, and S. Shida, This Bulletin, **40**, 1818 (1967); S. Sato, *ibid.*, **41**, 304 (1968).

4) A similar treatment was proposed by M. Tatsuya at the 13th Conference of Radiation Chemistry at Tokyo, Oct., 1970, though there are small differences in details.

5) F. Williams, *J. Amer. Chem. Soc.*, **86**, 3954 (1964).

Warman, Asmus, and Schuler:[1]

$$G_s = G_{fi} + G_{gi}\frac{\sqrt{\alpha S}}{1+\sqrt{\alpha S}}. \quad (3)$$

The other has been proposed by Hummel:[6]

$$G_s = G_{fi} + G_{gi}\{1-\exp(-\sqrt{\alpha S})\}. \quad (4)$$

Here, α is a parameter which can be determined experimentally. According to Warman *et al.*, the value of α is 16 $l\,mol^{-1}$ for most of the effective electron scavengers. Now, utilizing the table of the Laplace transformation, we can derive the following two spatial distribution functions by combining Eqs. (2) and (3), and Eqs. (2) and (4):

$$\phi(r) = \frac{3k}{4\pi\alpha}\left\{\left(\frac{\alpha}{\pi kr^3}\right)^{1/2} - e^{kr^3/\alpha}\,\mathrm{erfc}\left(\frac{kr^3}{\alpha}\right)^{1/2}\right\} \quad (5)[7]$$

and

$$\phi(r) = \frac{3}{8\pi}\left(\frac{\alpha}{\pi k}\right)^{1/2} r^{-9/2}\exp\left(-\frac{\alpha}{4kr^3}\right). \quad (6)$$

Numerical calculations can easily be made by substituting the following values: r_c=280 Å (Onsager length in cyclohexane at 25°C), σ=5.4 Å (diameter of a cyclohexane molecule), and z=6. The results are shown in Fig. 1. A Gauss function used for our calculations in previous papers is also plotted.

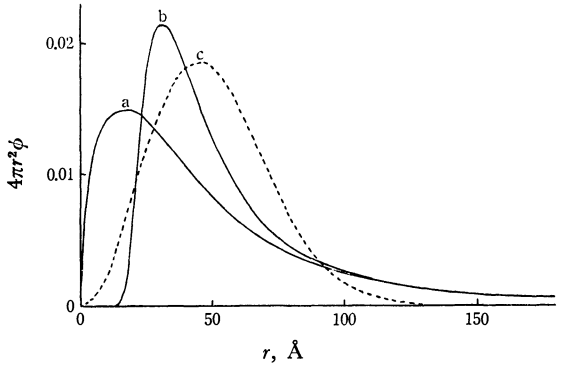

Fig. 1. Spatial distributions of secondary electron. a, Eq. (5); b, Eq. (6); c, the Gauss function (r_{av}=50 Å).

Discussion

A few years ago, Freeman and Fayadh estimated the spatial distribution of the secondary electrons produced in the γ-radiolysis of liquids[8] by using the tables proposed by Lea for the range of high-energy electron.[9] The distribution function, which is expressed by a step function, is quite similar in its form to curve b in Fig. 1. Judging from the many successful calculations made by Freeman and his collaborators,[10] the function (6) may be useful for the approximate calculation of the kinetics of the reactions of the charged species produced in the liquid-phase radiolysis because of its rather simple form.

According to Warman *et al.*, Eq. (3) is better than (4) for expressing the concentration dependence of G_s observed in the radiolysis of cyclohexane. They plotted $1/(G_s-G_{fi})$ as a function of $1/\sqrt{\alpha S}$ and estimated the value of G_{gi} by extrapolating the linear relationship to $S\to\infty$.[1] However, judging from the form of the distribution function (5), this procedure is questionable. As is shown in Fig. 1, the curve a has a large contribution at smaller values of r. Such a state, for example, at r=3 Å, would not be an ionized state, but a highly excited state, because of the strong interaction with the parent positive ion. Therefore, their procedure may include such a contribution of the reaction as the following:

$$\text{cyclo-}C_6H_{12}^* + S \rightarrow C_6H_{12}^+ + S^-$$

In other words, the value of G_{gi} estimated by their procedure may be a little larger than that of the so-called geminate ions.

6) A. Hummel, *J. Chem. Phys.*, **49**, 4840 (1968).

7) $\mathrm{erfc}(y) = 1 - \frac{2}{\sqrt{\pi}}\int_0^y e^{-t^2}dt$

8) G. R. Freeman and J. M. Fayadh, *ibid.*, **43**, 86 (1965).

9) D. E. Lea, "Actions of Radiations on Living Cells," Cambridge University Press, New York (1955), 2nd, ed., p. 29.

10) G. R. Freeman, *Radiat. Res. Rev.*, **1**, 1 (1968).

BULLETIN OF THE CHEMICAL SOCIETY OF JAPAN, VOL. 44, 858—859 (1971)

Syntheses of Fused Heterocycles *via* Cycloaddition of Hetaryne. Studies on Heteroaromaticity. Part XLVII[1]

Tadashi SASAKI, Ken KANEMATSU, and Masayuki UCHIDE

Institute of Applied Organic Chemistry, Faculty of Engineering, Nagoya University, Furo-cho, Chikusa-ku, Nagoya

(Received October 14, 1970)

In comparison with abundant examples for the cycloaddition reactions of dehydrobenzene (benzyne), only occasional reports have been made concerning the same reactions of dehydroaromatic heterocycles (hetarynes).[2] Recently, the electronic structures of hetarynes have been discussed using the extended Hückel theory,[3] by which the larger relative stability is predicted for 3-pyridyne compared with other pyridyne isomers.

These facts prompted us to report one-step syntheses of the fused bicyclic heteroaromatic ring system by the cycloaddition reactions of this hetaryne.

Expecting that the intermediate 3-pyridyne (II) might be trapped with dipolarophiles or dienophiles, the lead tetraacetate oxidation of 1-aminotriazolo-[4,5-*c*]pyridine (I)[4] was carried out in the presence of dienophilic five-membered heterocycles or some dipolarophiles.

These results are described in this note.

Results and Discussion

Only one example of 1,2-cycloaddition of dehydroheterocycle is recorded;[5] cyclopentadiene adds to 3-pyridyne in a 1,2-fashion rather than in a 1,4-fashion of Diels-Alder reaction. On the other hand, attempts to add 3-pyridyne to anthracene remain unsuccessful.[6]

In contrast, lead tetraacetate oxidation of compound I was carried out in the presence of dimethylfulvene, norbornadiene, and furan at room temperature for 1 hr. Only the *endo*-oxide III (picrate, mp 178°C) was obtained from furan in a 74% yield, which was identified by the IR and NMR spectral comparison with those of an authentic sample prepared by heating 3-pyridinediazonium-4-carboxylate in furan.[7] A recent report described the lead tetraacetate oxidation of I in the presence of tetracyclone which affords 5,6,-7,8-tetraphenylisoquinoline.[4] Neither 1,2-cycloadducts nor 1,4-Diels-Alder adducts could be isolated from the reaction of 3-pyridyne with dimethylfulvene or norbornadiene.

Similarly, 1,3-dipolar cycloaddition reactions of 3-pyridyne with dipolarophiles were also attempted.

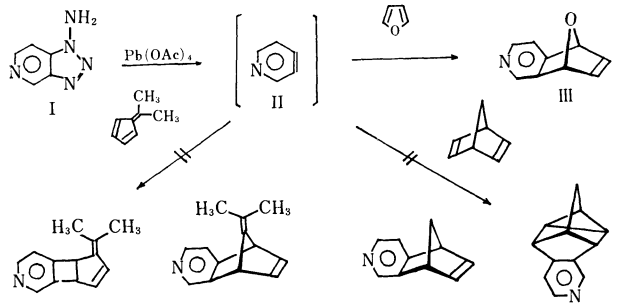

Chart 1.

There is only one example[2] known for a 1,3-addition of azide to a dehydroheterocyclic intermediate as shown by the following scheme.

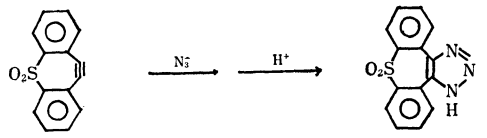

Chart 2.

Treatment of a mixture of I and *N*-phenylsydnone in 1 : 1.3 mol ratio with lead tetraacetate in tetrahydrofuran at room temperature led to the formation of 1,3-dipolar cycloadduct IV, mp 132—133°C, in a 30% yield. The NMR spectrum of IV shows signals of the ring protons at τ 0.60 (1*H*, s), 1.52 (1*H*, s), 1.77 (1*H*, d, J=7.0 Hz), and overlapping signals at τ 1.96—2.51 (1*H*-ring proton and 5*H*-phenyl protons, m). Similar oxidation of a mixture of compound I and benzaldehyde phenylhydrazone[8,9] in 1 : 1.1 mol ratio with an excess of lead tetraacetate afforded the expected cycloadduct V as pale yellow oil (picrate, mp 234—237°C) in a 15% yield. However, attempted cycloaddition of diphenyldiazomethane or benzonitrile oxide with 3-pyridyne was unsuccessful.

The orientation in the addition reaction of 1,3-dipolar *N*-phenylsydnone or diphenylnitrilimine with 3-pyridyne is not clear at present. However, the nucleophilic attack of the dipolar on 3-pyridyne might occur preferentially at the C-4 position as a consequence of its lower total electron density (3.97 against 4.35 electrons)[3] as shown by the following chart.

The structures of the 1,3-dipolar cycloadducts IV and V were tentatively assigned as 2-phenyl-2*H*-pyrazolo[4,3-*c*]pyridine and 1,3-diphenyl-1*H*-pyrazolo-

1) Part of series, XLVI., T. Sasaki and T. Yoshioka, This Bulletin, **43**, 2989 (1970).

2) R. W. Hoffmann, "Dehydrobenzene and Cycloalkynes," Academic Press, New York, N. Y. (1967), p. 199, 303, 306.

3) W. Adams, A. Grimison, and R. Hoffmann, *J. Amer. Chem. Soc.*, **91**, 2570 (1969).

4) G. W. J. Fleet and I. Fleming, *J. Chem. Soc., C*, **1969**, 1758.

5) T. Kauffmann, J. Hansen, K. Udeloft, and R. Winthwein, *Angew. Chem.*, **76**, 590 (1964).

6) T. Kauffmann, *ibid.*, **77**, 557 (1965).

7) T. Kauffmann and F. P. Boettcher, *Chem. Ber.*, **95**, 949 (1962).

8) The nitrilimines have been trapped during the oxidation of aldehyde hydrazones; W. A. F. Gladstone, J. B. Aylward, and R. O. C. Norman, *J. Chem. Soc., C*, **1969**, 2587.

9) T. Sasaki and T. Yoshioka, This Bulletin, **43**, 1254 (1970).

[4,3-*c*]pyridine, respectively. Such a fused ring system as pyrazolo[4,3-*c*]pyridine is the first in the fused heterocyclic series.

Attempted 1,3-dipolar cycloaddition reactions of 3-pyridinediazonium-4-carboxylate with dipolarophilic nitrilimines were unsuccessful.

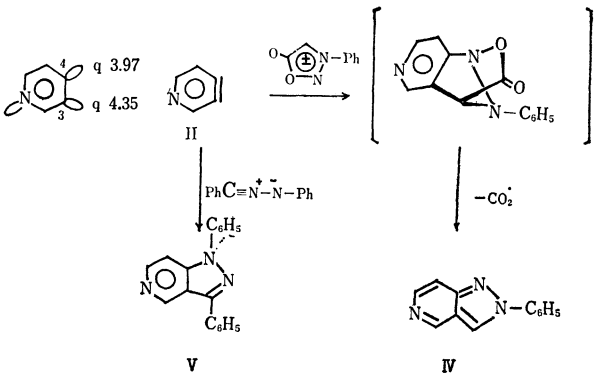

Chart 3.

Thus, it can be concluded that the cycloaddition reactivity of 3-pyridyne is generally much lower than that of benzyne, since the stereospecific 2+4 cycloaddition, the 2+2 nonconcerted cycloaddition, and the 1,3-cycloaddition for benzyne have been reported to give the corresponding cycloadducts in excellent yields.[2,10]

Experimental[11]

Lead Tetraacetate Oxidation of 1-Aminotriazolo[4,5-c]pyridine in the Presence of Furan. Compound I (390 mg) was dissolved in furan (5.1 g) and this solution was dropwise added to a stirred suspension of lead tetraacetate (1.4 g) in dichloromethane (20 m*l*) at 20°C. The reaction was always instantaneous and exothermic with evolution of nitrogen. Work-up involved filtration, evaporation of the solution, and chromatography (silicic acid, 100 mesh, Mallinckrodt) of the residue using benzene as an eluent.

Colorless oil of an *endo*-oxide III (317 mg, 75%) was obtained from the eluent; picrate, mp 178°C (lit,[7] mp 178°C).

Found: C, 48.28; H, 2.69; N, 14.97%. Calcd for $C_{15}H_{10}O_8N_4$ (picrate): C, 48.13; H, 2.69; N, 14.97%.

Reaction of 3-Pyridyne with N-Phenylsydnone. A solution of compound I (400 mg) and *N*-phenylsydnone (670 mg) in tetrahydrofuran (40 m*l*) was added dropwise to a stirred suspension of lead tetraacetate (1.2 g) in tetrahydrofuran (20 m*l*) at 20—25°C. After 1 hr, work-up as described above afforded an adduct IV (168 mg, 30%) as colorless prisms, mp 132—133°C.

Found: C, 73.56; H, 4.71; N, 21.74%. Calcd for $C_{12}H_9N_3$: C, 73.83; H, 4.65; N, 21.53%.

Reaction of 3-Pyridyne with 1,3-Diphenylnitrilimine. A solution of benzaldehyde phenylhydrazone (226 mg) and I (135 mg) in dichloromethane (20 m*l*) was added during 50 min to a stirred suspension of lead tetraacetate (1.5 g) in dichloromethane (50 m*l*) at below 10°C. The resulting thick suspension was further stirred at room temperature for 1 hr. Work-up as above afforded an adduct V (80 mg) as pale yellow oil; picrate, mp 234—237°C.

Found: C, 57.86; H, 3.29; N, 16.51%. Calcd for $C_{24}H_{16}N_6O_7$ (picrate): C, 57.60; H, 3.22; N, 16.80%.

10) For leading reference, see M. Jones, Jr., and R. H. Levin, *J. Amer. Chem. Soc.*, **91**, 6411 (1969).

11) The melting points were measured with a Yanagimoto micromelting point apparatus and are uncorrected. Microanalyses were performed on a Yanagimoto C.H.N.-Corder, Model MT-1. The NMR spectra were taken with a JEOLCO., Model JNM-MH-60 NMR spectrometer and with a Varian A-60 spectrometer with tetramethylsilane as an internal standard. The chemical shifts are expressed in τ values. The IR spectra were taken with a JASCO Model IR-S spectrometer.

BULLETIN OF THE CHEMICAL SOCIETY OF JAPAN, VOL. 44, 859—861 (1970)

Conformations of Low-molecular-weight Poly-γ-Benzyl-L-Glutamate Films

Takayoshi Iio

Department of Physics, Faculty of Science. Nagoya University, Chikusa-ku, Nagoya

(Received October 20, 1970)

We wish to report here our infrared (IR) studies of the conformations of low-molecular-weight poly-γ-benzyl-L-glutamate (PBLG) films cast from various helix-forming solvents, such as *N,N'*-dimethylformamide (DMF), *m*-cresol, dioxane, 1,2-dichloroethane (DCE), benzene, and chloroform.[1] We adopted five kinds of low-molecular-weight PBLG samples with different degrees of polymerization (DP), the DP values being 8, 13, 21, 28, and 49, and one high-molecular-weight PBLG (DP=250). The characters of the samples are shown in Table 1.

Table 1. The characters of the polymers

Sample	Initiator	A/I[a]	DP
PBLG-5	*n*-hexylamine	5	8[b]
PBLG-10	*n*-hexylamine	10	13[b]
PBLG-20	*n*-hexylamine	20	21[b]
PBLG-30	*n*-hexylamine	30	28[b]
PBLG-50	*n*-hexylamine	50	49[b]
PBLG-100	triethylamine	100	250[c]

a) Molar ratio of the anhydride to the initiator.
b) Determined by the method (1).
c) Determined by the method (2).

The IR spectra of the PBLG films are shown in Fig. 1. The high-molecular-weight PBLG exhibits the amide I band at about 1650 cm^{-1} and the amide II band at about 1548 cm^{-1}, these bands are due to the α-helix.[2]

1) S. J. Singer, *Advances in Protein Chemistry*, **14**, 1 (1959).

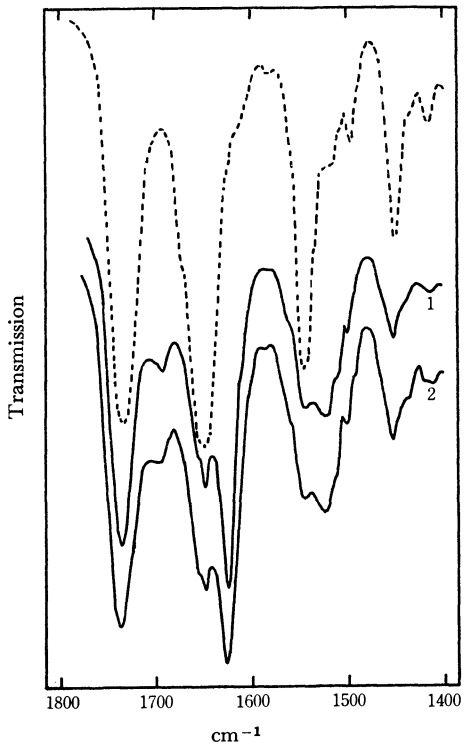

Fig. 1(a). IR spectra of PBLG-5 films cast from DMF (1) and chloroform (2) solutions. Dashed curve is that of PBLG-100 film cast from chloroform solution.

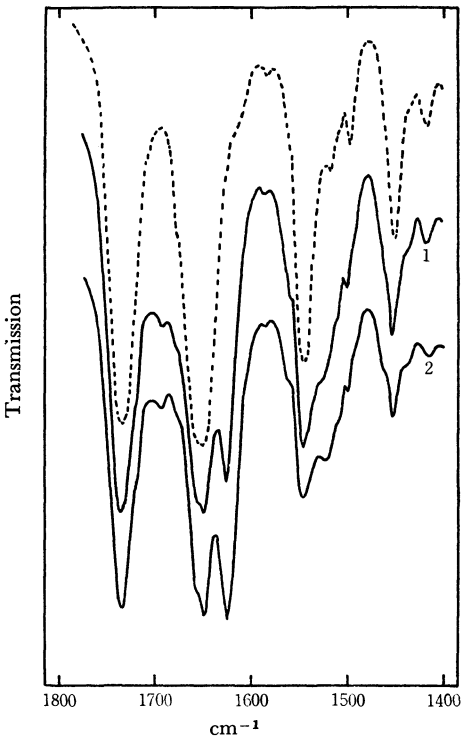

Fig. 1(b). IR spectra of PBLG-10 films.

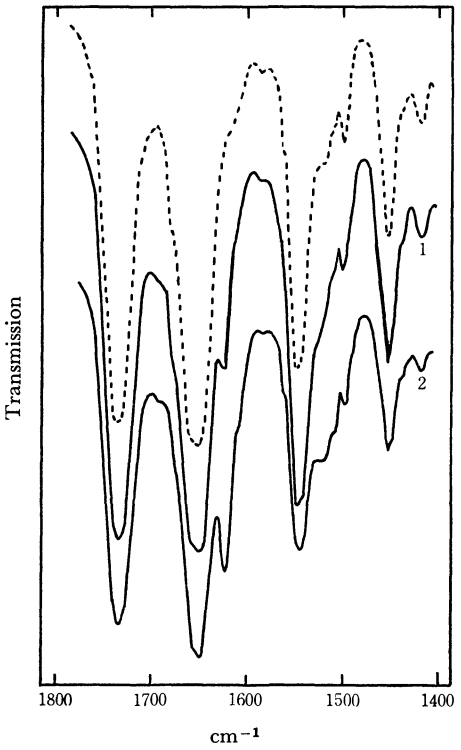

Fig. 1(c). IR spectra of PBLG-20 films.

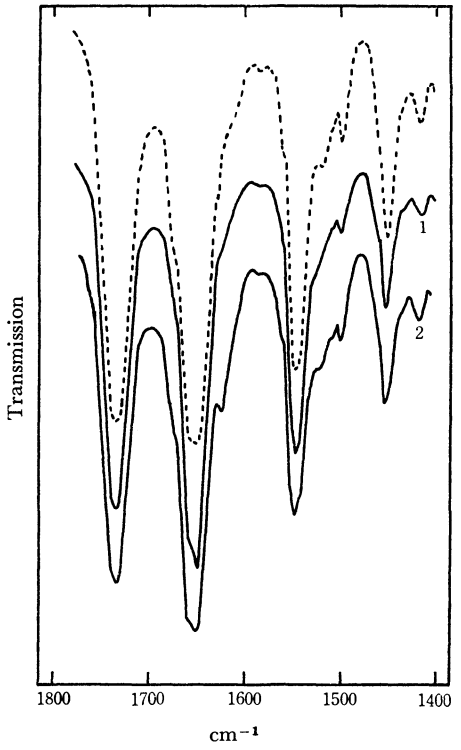

Fig. 1(d). IR spectra of PBLG-30 films.

On the other hand, the low-molecular-weight PBLG samples exhibit the amide I bands at about 1690 and 1625 cm^{-1}, positions which are attributable to the anti-parallel pleated sheet or the β-form, and at about 1650 cm^{-1}, a position which is due to the α-helix.[2] It is remarkable that the intensity of the 1625-cm^{-1} component depends not only on the value of DP, but also on the solvents from which the PBLG film was cast. This solvent effect on the degree of the β-formation is a new finding in this experiment.

2) T. Miyazawa and E. R. Blout, *J. Amer. Chem. Soc.*, **83**, 712 (1961).

The extinction coefficient of the 1625-cm^{-1} component of the amide I in the β-form is believed to be similar to that of the 1650-cm^{-1} component of the α-helix,[3] therefore, the apparent value of the β-form content, f_β, of the PBLG film may be obtained from the IR spectrum by using this equation:

$$f_\beta = \frac{OD_{1625}}{OD_{1625} + OD_{1650}}$$

where OD is the optical density of each component, calculated from the value of the transmission by the usual method.[4] The content of the α-helix equals $(1\text{-}f_\beta)$.

The f_β values are plotted in Fig. 2 as a function of the DP value. As may be seen in Fig. 2, the content of the β-form decreases as the DP value increases up to 49. The PBLG films cast from DMF and *m*-cresol solutions have smaller f_β values than have those cast from chloroform, DCE, and benzene solutions; the films from the dioxane solution have values of f_β intermediate between these two classes. Thus, it is found in this experiment that the helix-forming solvents make the low-molecular-weight PBLG films take not only the α-helix but also the β-form, and that the content of the β-form of the film depends on the solvent as follows: chloroform-benzene-DCE > dioxane > *m*-cresol-DMF.

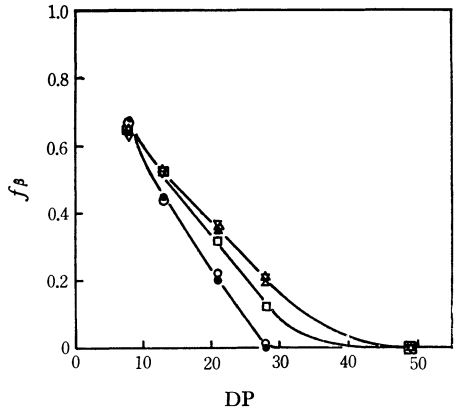

Fig. 2. Variation of the β-form content, f_β, of the PBLG films cast from the chloroform (▽), benzene (▲), DCE (△), dioxane (□), DMF (●), and *m*-cresol (○) solutions.

Experimental

Preparation of the Polymer. The low-molecular-weight PBLG samples, with different values of DP were obtained by polymerizing γ-benzyl-L-glutamate-*N*-carboxyanhydride in dioxane, using *n*-hexylamine as the initiator; the molar ratios of the anhydride to the initiator were 5, 10, 20, 30, and 50. The high-molecular-weight PBLG was obtained by using triethylamine as the initiator. The polymer was precipitated with ether from the dioxane solution, and dried under a vacuum. The DP value was determined by one of the following two methods: (1) we measured the nuclear magnetic resonance (NMR) spectra of the polymer in a chloroform and trifluoroacetic acid mixture,[5] and determined the number average DP value by calculating the ratio of the areas of the $C_\beta H_2$–$C_\gamma H_2$ proton resonances of the PBLG side-chain and the $(CH_2)_4$ proton resonances of the *n*-hexylamine bound to the C-terminal of the PBLG[6]; (2) we measured the intrinsic viscosity of the polymer in dichloroacetic acid at 25.0°C, and then applied the intrinsic viscosity *vs.* DP value relationship of Bradbury and Fenn to determine the DP value.[7] The results are summarized in Table 1.

IR Study. The dried polymer was dissolved into each helix-forming solvent, the solution was spread on a NaCl plate, and then the solvent was evaporated under a vacuum at room temperature. The IR spectrum of each unoriented film on the NaCl plate was measured with an infrared spectrophotometer, IR-G, made by the Japan Spectroscopic Co., Ltd.

The author wishes to thank Dr. Akira Minakata for his helpful advice and discussions, and Dr. Akira Warashina for his help in determining the DP values of the polymers by the NMR method.

3) a) C. H. Bamford, A. Elliott, and W. E. Hanby, "Synthetic Polypeptides," Academic Press, New York (1956), p. 143. b) S. M. Bloom, G. D. Fasman, C. deLoze, and E. R. Blout, *J. Amer. Chem. Soc.*, **84**, 458 (1962).

4) A. Elliott, "Infrared Spectra and Structure of Organic Long-Chain Polymers," Edward Arnold, London (1969), p. 30.

5) The NMR spectra were obtained on a Japan Electron Optics Laboratory Model JNM-4H-100 NMR spectrometer at a frequency of 100 MHz.

6) J. A. Ferretti and B. W. Ninham, *Macromolecules*, **3**, 30 (1970).

7) J. H. Bradbury and M. D. Fenn, *J. Mol. Biol.*, **36**, 231 (1968).

BULLETIN OF THE CHEMICAL SOCIETY OF JAPAN, VOL. 44, 862—863 (1971)

Syntheses of Alkyl *p*-Toluenesulfinates by Use of *N,N'*-Dicyclohexylcarbodiimide[1]

Yoshiko Miyaji, Hiroshi Minato, and Michio Kobayashi
Department of Chemistry, Tokyo Metropolitan University, Fukazawa, Setagaya, Tokyo
(Received October 23, 1970)

In contrast with the case of carboxylic acids, sulfinic acids cannot be converted to their esters by the reaction with alcohols in the presence of acid catalysts, since they readily undergo disproportionation to yield thiosulfonates and sulfonic acids under acid conditions. Ordinary procedures for synthesizing sulfinates utilize reactions between sulfinyl chlorides and anhydrous alcohols[2,3] or reactions between sodium sulfinates and chlorocarbonates in alcohols.[4] Investigations in our laboratories revealed that when an equimolar amount of dicyclohexylcarbodiimide (DCC) was present a sulfinic acid and an anhydrous alcohol were converted to a sulfinate in good yields. Results will be described in this paper.

Results and Discussion

The results are shown in Table 1. The procedure is very simple, and yet the yields are very good; 64—75% for ordinary sulfinates and 30% for unstable *t*-alkyl sulfinates. This method does not require sulfinyl chlorides which are thermally unstable and sensitive to moisture. This one-step synthesis of sulfinates at lower temperatures will be very effective for preparation of rather unstable sulfinates or isotope-labeled sulfinates.

When ^{18}O-labeled *p*-toluenesulfinic acid and ethanol were let to react, the ethyl ester formed contained a half of the oxygen-18 present in the acid as shown in Table 2. When this ethyl ester was made to react with phenylmagnesium bromide, the ^{18}O % of phenyl *p*-tolyl sulfoxide was the same as that of the original acid. Therefore, only one of the oxygen-18 of the sulfinic acid is contained in the sulfinate as the sulfinyl oxygen.

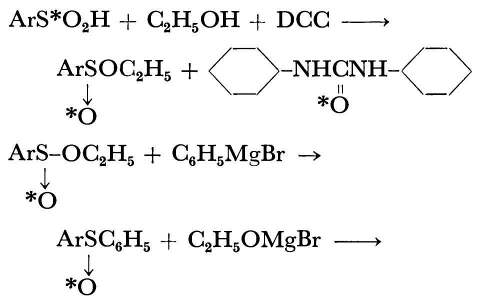

These findings suggest that the following mechanism is plausible for this reaction. Further investigation is necessary in order to determine whether the intermediate is I or II.

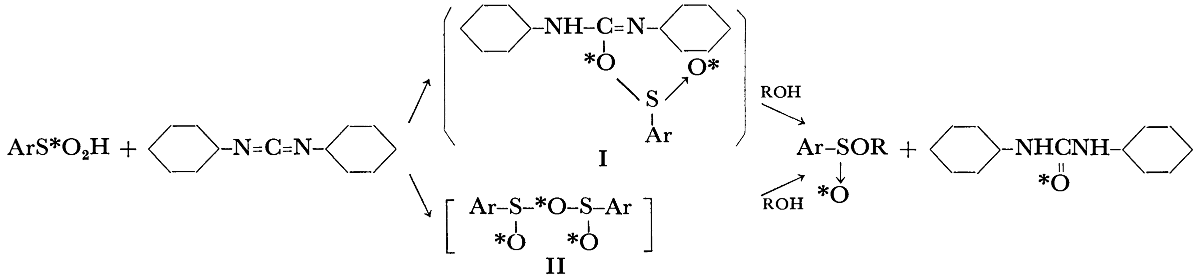

Table 1. Yields of alkyl *p*-toluenesulfinates by use of DCC

R	Method	Reagents used			Yields of products	
		$C_7H_7SO_2H$ g(mol)	ROH m*l*	DCC g(mol)	$C_7H_7SO_2R$ g(mol%)	C_6H_{11}-NHCONH-C_6H_{11} g(mol%)
Allyl	A	8.5 (0.054)	50	11.4 (0.055)	5.4 (64.5)	8.5 (73.3)
Et	A	7.5 (0.048)	50	8.8 (0.043)	5.7 (76.0)	9 (93.8)
Et	no DCC	3.6 (0.028)	18	—	0.6 (14.1)	—
i-Pr	A	2.6 (0.017)	25	3.1 (0.015)	1.9 (63.5)	2.7 (80.0)
t-Bu	B	4.0 (0.025)	3.8 (0.050)	4.61 (0.023)	1.3 (30.0)	2.6 (50.0)
l-Menthyl	B	20.5 (0.132)	21.8 (0.145)	25.3 (0.124)	10.5 (28.6)[a]	30.3 (114)

a) Crystalline *l*-menthyl *p*-toluenesulfinate obtained from a mixture of diastereomers.

1) Organic Sulfur Compounds. XXIII.
2) H. Phillips, *J. Chem. Soc.*, **1925**, 2552.
3) J. W. Wilt, R. G. Stein, and W. J. Wagner, *J. Org. Chem.*, **32**, 2097 (1967).
4) A. Yamamoto and M. Kobayashi, This Bulletin, **39**, 1292 (1966).

Table 2. Oxygen-18 distribution

Sample	Excess atom% ^{18}O	
	Found	Calcd
$CH_3C_6H_4SO_2H$[a)]	0.895	—
$CH_3C_6H_4S(=O)OEt$	0.462	0.448
$CH_3C_6H_4S(=O)C_6H_5$	0.901	0.896

a) as $CH_3C_6H_4S(=*O)-CH_2C_6H_5$ ($*O$)

Experimental

Alkyl p-*toluenesulfinates. Method A*: *p*-Toluenesulfinic acid was dissolved in large excess of an anhydrous alcohol, and 0.9—0.95 mol of DCC per mol of the sulfinic acid was slowly stirred into the solution cooled with ice. The solution immediately became turbid, and in some cases some heat was evolved. Stirring was continued for several hours or overnight. White precipitates formed were filtered off, water was added to the filtrate, and oil-soluble products were extracted with *n*-hexane. The hexane extracts were washed with a sodium carbonate solution and water, dried and then distilled. A pure alkyl sulfinate was obtained by distillation under reduced pressure or recrystallization.

Method B: To a dichloromethane solution of *p*-toluenesulfinic acid an equimolar or a little excess amount of an alcohol was added. A dichloromethane solution of DCC was slowly stirred into the sulfinic acid solution cooled with ice, and the stirring was continued for several hours or overnight. White precipitates formed were filtered off, the solvent was removed by evaporation, and the residue was dissolved in hexane. When white precipitates were formed they were removed by filtration. The rest of the procedure was the same as described in method A.

The reason why the amount of DCC used as less than equimolar is that the unreacted DCC cannot be easily separated from sulfinates by distillation. The DCC reacted can be easily removed as dicyclohexylurea. Method B is suitable for these alcohols which are solid or do not dissolve sulfinic acids readily. In this case DCC or dicyclohexylurea dissolves in dichloromethane to some extent, and these compounds must be removed by reprecipitation by addition of *n*-hexane to the residue of distillation.

Oxygen-18 Labeled Compounds. p-*Toluenesulfinic Acid-*^{18}O: Eleven grams of *p*-toluenesulfinic acid was dissolved in a mixture of 20 m*l* of $D_2{}^{18}O$ (^{18}O: 1.5 atom%) and 8.5 m*l* of dioxane. The solution was kept at 84°C for 1 hr, during which the exchange of ^{18}O is expected to be complete. After neutralization with a sodium carbonate solution and evaporation of solvent, the residue was dissolved in water. Acidification of the solution by addition of sulfuric acid yielded 8.7 g of *p*-toluenesulfinic acid-^{18}O.

Benzyl p-*Tolyl Sulfone-*^{18}O: The *p*-toluenesulfinic acid-^{18}O prepared as described above was neutralized by an aqueous sodium carbonate solution, and evaporation of the solvent yielded sodium *p*-toluenesulfinate-^{18}O. A mixture of 1 g of this sulfinate and 2 m*l* of benzyl bromide was heated at 118°C for 5 hr in a sealed tube. Benzyl *p*-tolyl sulfone produced was extracted with ether, washed with a sodium carbonate solution and water, and then dried. The ether was evaporated, and the residue was recrystallized from *n*-hexane.

The ^{18}O analyses were carried out according to the method of Rittenberg and Ponticorvo.[5)]

5) D. Rittenberg and L. Ponticorvo, *Int. J. Appl. Rad. Isotopes*, **1**, 208 (1956).

BULLETIN OF THE CHEMICAL SOCIETY OF JAPAN, VOL. 44, 863—865 (1971)

Unperturbed Dimensions of Poly-*o*-chlorostyrene

Kimiyoshi MATSUMURA, Keisuke MIZUNO, Masamichi FUKAYA, Takahiro KAMIYA, and Yasunobu SATO

Department of Chemistry, Aichi Kyoiku University, Kariya, Aichi

(Received October 30, 1970)

In a previous paper,[1] one of the present authors reported that the K_θ value of the butanone solution of poly-*o*-chlorostyrene (the theta solution at 25°C) is fairly small compared with that found from the viscosity plot for the toluene solutions; the solvent effect is considered to be the cause of the difference between these K_θ values.

In this paper, in order to examine the effect of the solvent on the K_θ value and to find the temperature dependence of the K_θ values, the viscosity measurements of poly-*o*-chlorostyrene in critical consolute solvents, which were mixtures of benzene (solvent)-cyclohexane (nonsolvent) at three ratios of mixing, were made.

Experimental

Material. The preparation and fractionation of poly-*o*-chlorostyrene were done according to the method described in a previous paper.[1] The molecular weights of the polymer fractions were determined by viscosity measurements of the toluene solutions at 25°C, with an intrinsic viscosity-molecular weight relationship of $[\eta]=1.15\times10^{-4}\cdot M^{0.66}$.[1] The molecular weights of the fractions used for the determination of the theta temperature were 141.7×10^4, 89.0×10^4, 52.5×10^4, and 23.3×10^4, while those of the fractions used for the viscosity measurements were 72.0×10^4, 59.9×10^4, 47.6×10^4, 35.8×10^4, 25.9×10^4, and 14.3×10^4.

The benzene and cyclohexane used as the solvents were purified by the methods described in a previous paper.[2] The critical consolute solvent mixtures were prepared by mixing benzene and cyclohexane by volume at 25°C; the ratios of benzene *vs.* cyclohexane were (A) 1/2.2, (B) 1/2.4,

1) K. Matsumura, *Polymer J.*, **1**, 322 (1970).

2) K. Matsumura, M. Fukaya, and K. Mizuno, This Bulletin, **43**, 1881 (1970).

and (C) 1/2.6.

Measurements. The methods used for the determination of the temperature and for the measurements of the viscosities of the solutions were the same as those in a previous paper.[2]

Results and Discussion

The Determination of the Theta Temperatures. An example of the measurements of the precipitation temperatures, T_p, and the determination of the theta temperature for poly-*o*-chlorostyrene in one critical consolute solvent mixture (A) is shown in Fig. 1. After the same procedures as that shown in Fig. 1, the theta temperatures were determined to be as follows: 31±2°C in solvent (A), 38±2°C in (B), and 45±3°C in (C).

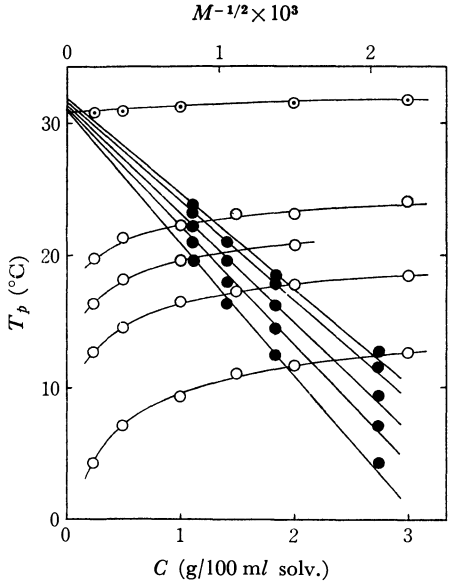

Fig. 1. The determination of the theta temperature for poly-*o*-chlorostyrene in solvent (A): ○, T_p-C for each fraction; ⊙, T_p-C for $M=\infty$; ●, T_p-$M^{-1/2}$ for several concentrations corresponding to those of ⊙.

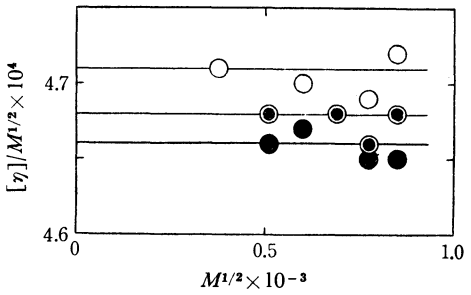

Fig. 2. Viscosity plots for poly-*o*-chlorostyrene in the critical consolute solvents: ○ (31°C), ⊙ (38°C), ● (45°C).

Viscosity. The intrinsic viscosity, $[\eta]$, and the Huggins constant, k', of poly-*o*-chlorostyrene in the critical consolute solvents are summarized in Table 1.

Discussion. As is shown in Fig. 2, the values of $[\eta]/M^{1/2}$, $(=K_\theta)$, were independent of $M^{1/2}$, as is known to be generally true for a theta solution. The K_θ values of the critical consolute solution found from Fig. 2 are shown in Table 2, together with the values of $\{\langle L^2\rangle_0/M\}^{1/2}$, $(=\{K_\theta/\Phi_0\}^{1/3})$, and σ, $(=\{\langle L^2\rangle_0/\langle L^2\rangle_{0f}\}^{1/2})$, calculated from the K_θ values, in which the value of Φ_0, the Flory parameter, was assumed to be 2.55×10^{21}, the same as that found in a previous paper.[1]

The K_θ values are in fair agreement with that of the butanone solution at 25°C (the theta solution), 4.60×10^{-4};[1] they are smaller the higher the temperature, much as with the temperature dependencies of K_θ for polystyrene and for poly-*p*-chlorostyrene.[2,3]

It was previously reported that the K_θ value of poly-*o*-chlorostyrene in butanone at 25°C is fairly small compared with that found from the viscosity plot of the toluene solution, and that this difference in K_θ values proves that the solvent effect may depend on the fact that the butanone solution gives a lower consolute temperature.

However, the results in this paper show no difference between the K_θ value of poly-*o*-chlorostyrene in a theta

Table 1. The experimental results of the viscosity measurements for poly-*o*-chlorostyrene in the critical consolute solvent mixtures

Fraction	$M\times10^{-4}$	$[\eta]$ (dl/g), solvent			k', solvent		
		(A) 31°C	(B) 38°C	(C) 45°C	(A) 31°C	(B) 38°C	(C) 45°C
2	72.0	0.401	0.397	0.395	0.45	0.46	0.42
3	59.9	0.363	0.361	0.360	0.45	0.45	0.42
4	47.6	—	0.323	—	—	0.46	—
5	35.8	0.281	—	0.279	0.53	—	0.51
6	25.9	—	0.238	0.237	—	0.47	0.50
7	14.3	0.178	—	—	0.56	—	—

Table 2. The K_θ values and the σ values of poly-*o*-chlorostyrene

Solvent	Temp. (°C)	$K_\theta\times10^4$	$\{\langle L^2\rangle_0/M\}^{1/2}$ (Å)	σ
(A)	31	4.71	0.569	2.17
(B)	38	4.68	0.568	2.17
(C)	45	4.66	0.567	2.16

3) K. Kubo, K. Ogino, and T. Nakagawa, *Nippon Kagaku Zasshi*, **88**, 1254 (1967).

solvent, which gives a lower consolute temperature, and that in a solvent, which gives a higher one. This suggests that the large value of K_θ in the toluene solution may not be caused by the solvent effect but, rather, by the downwards curvature of the viscosity plot, as was shown in a previous paper.[1] Therefore, there is difficulty in finding the value of K_θ from the viscosity plot of poly-*o*-chlorostyrene in toluene (a good solvent).

BULLETIN OF THE CHEMICAL SOCIETY OF JAPAN, VOL. 44, 865—866 (1971)

Some Benzylidene and Cyclohexylidene Derivatives of 3-Deoxy-3-nitro-α-D-glucopyranose[1]

Tohru SAKAKIBARA, Tetsuyoshi TAKAMOTO, and Toshio NAKAGAWA*

Department of Chemistry, Tokyo Institute of Technology, Ō-okayama, Meguro-ku, Tokyo

(Received October 30, 1970)

In a previous paper[2] we reported that methyl 2-*O*-acetyl-4,6-*O*-benzylidene-3-deoxy-3-nitro-β-D-glucopyranoside reacts smoothly with theophylline and 2,6-dichloropurine in the presence of sodium hydrogen carbonate to give, *via* 3-nitro-2-enoside, the corresponding 2-purinyl-glucosides in excellent yields. This finding urged us to attempt the similar reaction with 2-nitro sugars. To our knowledge, the only example belonging to this class of compounds, except 2-nitro-alditols, has been described by Lemieux *et al.*[3], *i.e.* per-*O*-acetyl-2-nitro-D-glucal, -galactal and -xylal, derived from the corresponding acetylated glycals with dinitrogen tetraoxide. But all attempts to obtain 2'-nitro nucleosides from the reaction mixtures of these compounds with some purine homologues have been hitherto unsuccessful in our laboratory.

On the other hand, we have studied on the oxidative C^1-C^2 fission of 3-deoxy-3-nitro-D-glucose (**2**) with periodate or lead tetraacetate with the aim of preparing and characterizing 2-nitro sugars, but the desired product (**7**) is likely too unstable to isolate, giving only the degradated product (**8**). In this paper, we wish to present thereof and some acetal derivatives of **2** obtained throughout this work.

Phenyl 3-deoxy-3-nitro-β-D-glycopyranoside (**1**), almost selectively prepared by successive oxidation and nitromethane condensation of phenyl β-D-glucopyranoside,[4] was hydrolyzed (4 N HCl, 100°C, 2 hr) to give the reducing 3-deoxy-3-nitro-D-glucose (**2**).[5] Treatment of **2** with benzaldehyde and zinc chloride yielded the 4,6-*O*-benzylidene derivative (**3**). Compounds **2** and **3** were isolated in high yields as an α-form (downward-mutarotating). Acetylation of **3** with acetic anhydride in pyridine gave the 1,2-di-*O*-acetate (**4**), which was deduced to be an α-anomer on the basis of its NMR spectra: (1) a relatively small value of $J_{1,2}$ (3.8 Hz)[6]; (2) an axial *O*-acetyl signal resonating at 7.84 τ($CDCl_3$).[6,7]

On an acetal exchange reaction[8] with 1,1-diethoxycyclohexane in the presence of *p*-toluenesulfonic acid (50°C/~20 mmHg), **2** gave the 1,2;4,6-di-*O*-cyclohexylidene derivative (**5**). The *α-pyranose* structure of **5** was proved by comparison of the chemical shifts and coupling constants of its ring protons[9] with those of 4,6-*O*-benzylidene-1,2-*O*-cyclohexylidene derivative (**6**), prepared by the analogous treatment of **3** (*cf.*

TABLE 1. 100 MHz NMR SPECTRA IN $CDCl_3$ (TMS as an internal standard)

Comp.	Chemical shifts in τ								Coupling constants in Hz						
	H^1	H^2	H^3	H^4	H^5	H^{6e}	H^{6a}	PhCH	$J_{1,2}$	$J_{2,3}$	$J_{3,4}$	$J_{4,5}$	$J_{5,6e}$	$J_{5,6a}$	$J_{6e,6a}$
4	3.61	4.49	4.97	5.90	5.8 ~6.2	5.65	6.13	4.45	3.5	10.5	10	9	3.5	~10	10
5	4.41	5.52	5.34	5.92	6.09	5.93	6.12	—	4.5	7	10	10	2.5	~11	11
6	4.38	5.46	5.18	6.00	5.92	5.59	6.27	4.48	4.5	6.5	10.5	11	3	~10	11
8	O-CHO (2.02); H^3 (5.09); H^{4e} (5.58); H^{4a} (6.32)							4.47	$J_{2,3}$(10); $J_{3,4e}$(5); $J_{3,4a}$(10); $J_{4a,4e}$(11)						

1) From the Master Dissertation, T. Sakakibara, Tokyo Institute of Technology, February 1970.

* Present address: Department of Chemistry, Yokohama City University.

2) T. Nakagawa, T. Sakakibara, and S. Kumazawa, *Tetrahedron Lett.*, **1970**, 1645.

3) R. U. Lemieux, T. L. Nagabhushan, and I. K. O'Neill, *Can. J. Chem.*, **46**, 413 (1968).

4) T. Nakagawa, Y. Sato, T. Takamoto, F. W. Lichtenthaler, and N. Majer, This Bulletin, **43**, 3866 (1970).

5) This compound was just described by Baer *et al.*, who prepared it by acid hydrolysis (6 N HCl, 100°C, 1 hr) of methyl 3-deoxy-3-nitro-β-D-glucopyranoside [H. H. Baer, W. Rank, and F. Kienzle, *Can. J. Chem.*, **48**, 1302 (1970)].

6) L. D. Hall, *Advan. Carbohyd. Chem.*, **19**, 51 (1964).

7) F. W. Lichtenthaler and P. Emig, *Carbohyd. Res.*, **7**, 121 (1968).

8) F. H. Bissett, M. E. Evans, and F. W. Parrish, *ibid.*, **5**, 184 (1967).

9) Moreover, if compound **5** had a *furanose* structure, $J_{2,3}$ should be ≥0.5 Hz. *Cf.* R. J. Abraham, L. D. Hall, L. Hough, and K. A. McLauchlan, *Chem. Ind.* (London), **1962**, 213; *J. Chem, Soc.*, **1962**. 3699.

Table 1).

Oxidation of **3** with periodate or lead tetraacetate gave no 2-nitro sugar **7** but a successive de-*C*-formylation occurred to form 2,4-*O*-benzylidene-1-deoxy-3-*O*-formyl-1-nitro-D-erythritol (**8**), whose structure was confirmed by its NMR spectra (Table 1).

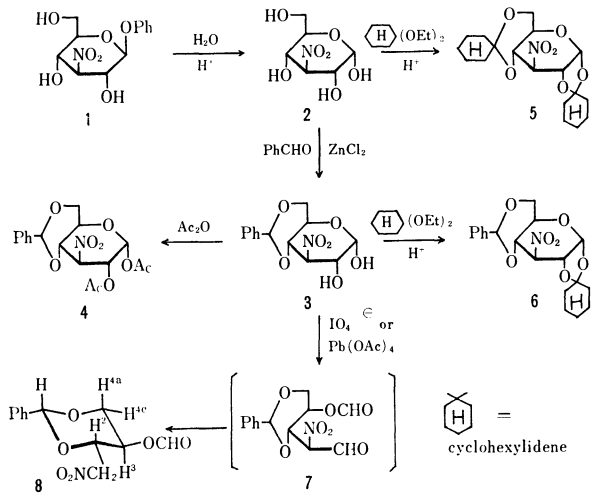

Experimental

Melting points were determined in capillaries and are uncorrected. IR spectra were obtained with a Hitachi EPI-S2 instrument. NMR spectra were taken with a JEOLCO JNM-4H-100 spectrometer, using an internal TMS standard. Optical rotations were measured with a Carl Zeiss photoelectric polarimeter.

3-Deoxy-3-nitro-α-D-glucose (2). A mixture of phenyl 3-deoxy-3-nitro-β-D-glucopyranoside[4] (10.0 g) and 4 N hydrochloric acid was refluxed for 2 hr and the resulting solution was evaporated. The residue was dissolved in hot water (*ca.* 50 m*l*), treated with active charcoal and filtered. The filtrate was evaporated, and the residue was coevaporated several times with water and then crystallized from ethanol. After washing with ethyl acetate, the crystals (colorless, 5.5 g, 75%) may be used for a synthetic purpose without further purification. A sample for analysis was recrystallized from methanol/ethyl acetate: mp 174—174.5°C (decomp.) [*lit*,[5] 176—177°C (decomp.)]; $[\alpha]_D^{20}$ +114° (*t*=0 min) → +108.5° (5 min) → +93.2° (30 min) → +79.5° (22 hr; const.) (*c* 1, H_2O)[*lit*,[5] $[\alpha]_D$ +99.6° (6 min) → +73.9° (130 min, const.) (*c* 1, H_2O)].

Found: C, 34.44; H, 5.10; N, 6.72%. Calcd for $C_6H_{11}O_7N$: C, 34.45; H, 5.30; N, 6.70%.

4,6-O-Benzylidene-3-deoxy-3-nitro-α-D-glucopyranose (3). A mixture of **2** (2.7 g), zinc chloride (4 g), and benzaldehyde (13 m*l*) was stirred for 2 days and then poured into a mixture of ice water and petroleum ether with vigorous stirring. The precipitates were collected by filtration, washed well with water and petroleum ether, and recrystallized from ethanol/water: Yield 2.9 g (76%); mp 149.5—150.5°C; $[\alpha]_D^{20}$ +34.3° (*t*=0 min) → +31.0° (2 hr 15 min) → +22.6° (24 hr) → +15.8° (3 days) → +12.2° (7 days) → +8.9° (15 days, const.)(*c* 1, dioxane). IR(KBr): 3400 cm^{-1} (OH); 1565 cm^{-1} (NO_2).

Found: C, 52.47; H, 4.81; N, 4.72%. Calcd for $C_{13}H_{15}O_7N$: C, 52.52; H, 5.09; N, 4.71%.

1,2-Di-O-acetyl-4,6-O-benzylidene-3-deoxy-3-nitro-α-D-glucopyranose (4). To a solution of **3** (0.89 g) in pyridine (9 m*l*) was added acetic anhydride (6 m*l*) under ice cooling. The reaction mixture was allowed to stand for 2 hr at room temperature and then poured into ice water. The precipitates were collected by filtration, washed well with water, and recrystallized from acetone/ethanol: Yield 1.13 g (99.2%); mp 220°C (decomp.); $[\alpha]_D^{20}$ +65.9° (*c* 1, $CHCl_3$). IR (KBr): 1755 cm^{-1} (C=O); 1565 cm^{-1} (NO_2). NMR ($CDCl_3$): 7.84 τ (3H-*s*, *ax. O*-Ac on *C*[1]); 7.99 τ (3H-*s*, *eq. O*-Ac on *C*[2]).[6,7]

Found: C, 53.39; H, 4.93; N, 3.71%. Calcd for $C_{17}H_{19}O_9N$: C, 53.54; H, 5.02; N, 3.67%.

1,2;4,6-Di-O-cyclohexylidene-3-deoxy-3-nitro-α-D-glucopyranose (5). A solution of **2** (0.63 g), 1,1-diethoxycyclohexane[10] (2 m*l*), and *p*-toluenesulfonic acid (0.01 g) in DMF (6 m*l*) was boiled at 50°C/~20 mmHg, with use of a fine stream of dry air to promote steady ebullition.[8] After 1.5 hr, the reaction mixture was neutralized with sodium hydrogencarbonate, the undissolved material was filtered off, the filtrate was evaporated *in vacuo*, and the residue was recrystallized from ethanol/petroleum ether: Yield 0.5 g (45%); mp 121—123.5°C; $[\alpha]_D^{20}$ +122° (*c* 1, $CHCl_3$). IR (KBr): 1560 cm^{-1} (NO_2).

Found: C, 58.36; H, 7.09; N, 3.78%. Calcd for $C_{18}H_{27}O_7N$: C, 58.52; H, 7.37; N, 3.79%.

4,6-O-Benzylidene-1,2-O-cyclohexylidene-3-deoxy-3-nitro-α-D-glucopyranose (6). A solution of **3** (0.89 g), 1,1-diethoxycyclohexane[10] (12 m*l*), and *p*-toluenesulfonic acid (0.01 g) in dioxane (20 m*l*) was treated for 5 hr similarly as described above. The product was recrystallized from acetone/ethanol: 0.69 g (61%); mp 155.5—156.5°C; $[\alpha]_D^{20}$ +95.5° (*c* 1, $CHCl_3$). IR (KBr): 1550 cm^{-1} (NO_2).

Found: C, 60.18; H, 5.87; N, 3.82%. Calcd for $C_{19}H_{23}O_7N$: C, 60.47; H, 6.14; N, 3.71%.

2,4-O-Benzylidene-1-deoxy-3-O-formyl-1-nitro-D-erythritol (8). a) Periodate Oxidation: Into a solution of sodium metaperiodate (0.70 g) in water (50 m*l*) was added **3** (0.89 g) and stirred at room temperature. After 6 hr, sodium hydrogencarbonate (0.25 g) was added to it and them ixture was stirred for 3 days. The precipitates were collected by filtration, washed with water, and recrystallized from ethanol/petroleum ether: colorless needles (0.404 g, 50.5%); mp 113°C; $[\alpha]_D^{20}$ −47.2° (*c* 1, EtOAc). IR (KBr): 1725 cm^{-1} (C=O); 1560 cm^{-1} (NO_2); no absorption of OH.

Found: C, 53.93; H, 4.76; N, 5.23%. Calcd for $C_{12}H_{13}O_6N$: C, 53.93; H, 4.90; N, 5.24%.

b) Lead Tetraacetate Oxidation: In a solution of lead tetraacetate (1.46 g) in dry benzene (30 m*l*) was stirred **3** (0.89 g) at room temperature for 2 hr, the precipitates were filtered off, the filtrate was evaporated, and the residue was recrystallized from ethanol/petroleum ether to give over 70% yield of colorless needles, mp and mixed mp 113°C. IR and NMR spectra were identical with those of the product obtained under (*a*).

10) J. Böeseken and F. Tellegen, *Rec. Trav. Chim. Pays-Bas*, **57**, 136 (1938).

BULLETIN OF THE CHEMICAL SOCIETY OF JAPAN, VOL. 44, 867—869 (1971)

Chemical Studies of Minerals Containing Rarer Elements from the Far East District. LXIV.[1] Abukumalite from Fusamata, Kawamata-machi, Fukushima Prefecture, Japan

Kozo Nagashima, Kazuso Nakao, Hisanobu Wakita, and Akira Kato*

* *Department of Chemistry, Tokyo Kyoiku University, Tokyo*

* *Department of Geology, National Science Museum, Ueno Park, Tokyo*

(Received November 2, 1970)

Abukumalite was first described by Hata(1938)[2] from a granite pegmatite at Suishoyama, Kawamata-machi (formerly called Iisaka Village), Fukushima Prefecture, Japan. In 1939, Machatschki[3] pointed out the isostructural relation between abukumalite and apatite due to the isomorphous coupled substitution of CaP by YSi, this being later confirmed by Omori and Hasegawa.[4] Recently, Ito(1968)[5] synthesized the intermediate members between $Ca_{10}P_6O_{24}(OH)_2$ and $Ca_6Y_4Si_6O_{24}(OH)_2$ to suggest the presence of continuous solid solution series between them, though not fully substantiated by natural materials, but partially by such a yttrian apatite as that from Naegi, Gifu Prefecture, Japan, containing 10.65% Y_2O_3 (Omori and Konno, 1962)[6] and abukumalites. Also a rare-earth ($\Sigma Ce > \Sigma Y$) silicatian apatite is reported from the Adirondack Mountains, New York.[7]

The localities of abukumalite reported thereafter include Shinden, Gifu Prefecture, Japan,[8] Hiradani, Shiga Prefecture, Japan,[9] northwestern U.S.S.R.,[10] and Pyörönmaa, Finland.[11] An aluminian variety has been reported from Siberia[12] and a cerian variety, an intermediate of abukumalite and britholite has been reported from Kola Peninsula.[13] Those from the last three foreign localities are in thermally recoverable metamict state.

The pegmatite at Fusamata, Kawamata-machi, Fukushima Prefecture, is located about 2 kilometers north of Suishoyama pegmatite, the original locality of abukumalite. In the former are known such rare earth minerals as gadolinite,[14] allanite, yttrialite, iimorite,[15] thorogummite, fergusonite, xenotime, and rare-earth-bearing zircon. The studied abukumalite was found in the dump as dark reddish brown masses up to 1 cm across and superficially coated by thorogummite.

The present report deals with the chemical analysis to specify the abukumalite from Fusamata as a fluorine dominant variety of abukumalite, and also with the determination of distribution patterns of lanthanoids in this abukumalite and that from the original locality to designate them as the members of thalenite-type (Goldschmidt and Thomassen, 1924).[16]

Chemical Composition

Chemical analysis was carried out on hand-picked material of about 3 g adopting the usual procedure for the rare earth-bearing silicates. The average atomic weight of the rare earths was determined by titrating the weighed mixed oxides with EDTA after dissolving them in hydrochloric acid. Fluorine was determined by the method proposed by Ellestad (1964).[17]

The result of chemical analysis is given in Table 1 in which that of the original abukumalite (Hata, 1938)[2] is also tabulated for comparison. The calculation of the analysis based on O+OH+F=13 gives $(\Sigma Y_{2.905}Ca_{1.388}Mn_{0.424}Fe^{3+}_{0.115}Fe^{2+}_{0.100}Al_{0.040}Na_{0.023}K_{0.015})_{5.010}(Si_{2.694}P_{0.204}Al_{0.102})_{3.000}O_{12.000}(F_{0.581}(OH)_{0.279}O_{0.140})_{1.000}$, well accounting for the ideal formula $Ca_2Y_3(SiO_4)_3(F, OH)_2$ with minor substitution of Ca by Mn, Fe, *etc.*, and the relation F>OH, differing from the original abukumalite in which OH>F.

X-Ray Studies

The precession photographs show it to be hexagonal with $a_0=9.44_1$ Å and $c_0=6.79_0$ Å, respectively, with the systematic extinction rule as: no condition for *hkil* and $l=2$ n for $000l$. Thus the possible space group is C_6^2, C_{6h}^2, or D_6^2. Though the preference should be due to its structural study, it is very probable that

1) Part LXIII: K. Sakurai, H. Wakita, A. Kato, and K. Nagashima, This Bulletin, **42**, 2725 (1969).

2) S. Hata, *Sci. Pap. Inst. Phys. Chem. Res., Tokyo*, **34**, 1018 (1938).

3) F. Machatschki, *Zentralbl. Mineral.*, **1939A**, 161 (1939).

4) K. Omori and S. Hasegawa, *J. Jap. Ass. Mineral Pertology Econ. Geol.*, **37**, 21 (1953).

5) J. Ito, *Amer. Mineral.*, **53**, 890 (1968).

6) K. Omori and H. Konno, *ibid.*, **47**, 1191 (1962).

7) M. L. Lindberg and B. Ingram, *U. S. Geol. Survey Prof. Paper*, 501-B, p. B64—B65, (1964).

8) K. Sakurai and A. Kato, *J. Mineral. Soc. Jap.*, **5**, 328 (1962).

9) K. Sakurai, A. Kato, and M. Tamura, *ibid.*, **5**, 331 (1962).

10) A. Luncs, *Latvijas PSR Zinatnu Akad. Vestis*, **1962**, No. 4, 67—76. (*Chem. Abstr.*, **57**, 8223 g (1962)).

11) A. Vorma, P. Ojanperä, V. Hoffrén, J. Siivola, and A. Löfgren, *Comptes Rendus de la Societe Geologique de Finlande*, N : o XXXVIII, 241 (1966).

12) M. A. Kudrina, V. S. Kudrin, and G. A. Sidorenko; *Geol. Mestorozhdenii Redkikh Elementov*, No. 9, 108 (1961). (*Amer. Mineral.*, **46**, 1514 (1961)).

13) N. I. Plethneva, N. A. Elina, A. P. Denisov, and A. P. Gavrilov, *Materialy po Mineralog. Kol'sk. Poluostrova, Akad. Nauk SSSR, Kol'sk. Filial*, **2**, 123 (1962). (*Chem. Abstr.*, **59**, 9678h (1963).)

14) T. Kawai, *Nippon Kagaku Zasshi*, **81**, 1054 (1960).

15) K. Nagashima and A. Kato, Preprints for 11th Annual Meeting of the Chemical Society of Japan (April, 1958).

16) V. M. Goldschmidt and L. Thomassen, Videnskab. Skrifter 1. Mat.-naturv. Klasse, **1924**, No. 5.

17) L. M. Kolthoff and E. B. Sandell, "Textbook of Quantitative Inorganic Analysis," Maruzen Asian ed., (1964), p. 721.

TABLE 1. CHEMICAL ANALYSES OF ABUKUMALITES

	1	2				
	wt%	wt%	Molecular quotient	Metal number	Oxygen number	Metal number as O+OH+F=13
SiO_2	20.84	22.59	0.3760	0.3760	0.7519	2.694
P_2O_5	5.84	2.02	0.0142	0.0285	0.0712	0.204
Al_2O_3	1.05	1.01	0.0099	0.0198	0.0297	0.142
Fe_2O_3	2.10	1.28	0.0080	0.0160	0.0240	0.115
FeO		1.00	0.0139	0.0139	0.0139	0.100
MnO	1.13	4.20	0.0592	0.0592	0.0592	0.424
CaO	13.53	10.86	0.1937	0.1937	0.1937	1.388
$\sum Ce_2O_3$	6.45	56.37	0.2028	0.4055	0.6083	2.905
$\sum Y_2O_3$	45.98					
ThO_2	0.90					
Na_2O		0.11	0.0016	0.0032	0.0016	0.023
K_2O		0.10	0.0011	0.0021	0.0011	0.015
F	0.45	1.54	0.0811			0.581
$H_2O(+)$	0.58	0.35	0.0194	0.0389	0.0194	0.279
$H_2O(-)$	0.16	0.29				
CO_2	0.05					
$-O=F_2$	−0.19	−0.65				
Total	99.09[a]	101.07				

1. Abukumalite. Suishoyama, Kawamata-machi, Fukushima Prefecture, Japan. After Hata(1938). Mean atomic weight of rare earths=112.
   a) includes MgO 0.22.
2. Abukumalite. Fusamata, Kawamata-machi, Fukushima Prefecture, Japan. The present study. Mean atomic weight of rare earths=115.

TABLE 2. X-RAY POWDER DATA FOR ABUKUMALITES AND SYNTHETIC $Ca_4Y_6Si_6O_{24}(OH)_2$

1		2		3				*hkil*
d(Å)	*I*	*d*(Å)	*I*	*d*(Å)	*I*	*Q*obs	*Q*cal	
		4.71	5					$11\bar{2}0$
4.07	20	4.07	55	4.09	20	0.060	0.060	$20\bar{2}0$
		3.88	25	3.88	15	0.066	0.067	$11\bar{2}1$
3.50	20			3.50	5	0.082	0.082	$20\bar{2}1$
3.40	40	3.411	40	3.401	10	0.0865	0.0868	0002
3.14	40	3.144	35	3.134	30	0.1019	0.1018	$10\bar{1}2$
3.08	30	3.074	40	3.089	35	0.1048	0.1047	$21\bar{3}0$
2.81	100	2.805	100	2.815	100	0.1262	0.1262	$21\bar{3}1$
2.76	60	2.769	90	2.756	65	0.1317	0.1317	$11\bar{2}2$
2.72	40	2.710	85	2.727	40	0.1345	0.1346	$30\bar{3}0$
2.62	20			2.612	10	0.1466	0.1466	$20\bar{2}2$
2.27	10	2.256	15	2.267	10	0.1945	0.1944	$31\bar{4}0$
		2.120	3	2.126	5	0.2212	0.2214	$30\bar{3}2$
2.04	10	2.046	10	2.042	10	0.2398	0.2393	$40\bar{4}0$
							0.2401	$11\bar{2}3$
1.940	30	1.932	35	1.939	15	0.2661	0.2650	$20\bar{2}3$
							0.2663	$22\bar{4}2$
1.893	10	1.883	20	1.885	10	0.2815	0.2812	$31\bar{4}2$
1.883	10	1.867	10					$32\bar{5}0$
1.829	30	1.826	35	1.826	20	0.2999	0.2999	$21\bar{3}3$
1.806	10	1.798	20	1.808	10	0.3058	0.3059	$32\bar{5}1$
1.786	20	1.776	15	1.783	10	0.3147	0.3141	$41\bar{5}0$
1.751	20	1.746	25	1.751	20	0.3262	0.3261	$40\bar{4}2$
1.705	20	1.705	15	1.696	10	0.3476	0.3470	0004
a_0=9.43 Å		a_0=9.40 Å		a_0=9.441 Å				
c_0=6.81 Å		c_0=6.81 Å		c_0=6.790 Å				

1. Abukumalite. Suishoyama, Kawamata-machi, Fukushima Prefecture, Japan. Cu/Ni radiation. Diffractometer method. After Sakurai and Kato (1962).
2. Synthetic $Ca_4Y_6Si_6O_{24}(OH)_2$. After Ito (1968).
3. Abukumalite. Fusamata, Kawamata-machi, Fukushima Prefecture, Japan. Cu/Ni radiation. Diffractometer method. The present study.

abukumalite has the same space group as ordinary apatite, C_{6h}^2.

X-ray powder data are obtained by diffractometer method employing Cu/Ni radiation. They are well coincident with those of abukumalite from the original locality, Suishoyama neighbouring to Fusamata and synthetic $Ca_{10}(PO_4)_6(OH)_2$ (Ito, 1968)[5] as shown in Table 2.

Optical Propertites

Though nearly colorless in thin section, the studied abukumalite is light brown in thick spinters with very weak dichroism: O=colorless to light brown, E= light brown; O<E.

It is uniaxial positive and the refractive indices measured by immersion method are: $\omega=1.773$, $\varepsilon=1.777$, $\varepsilon-\omega=0.004$. These values are within the variation range of those of abukumalites[8]: $\omega=$ 1.750—1.780, $\varepsilon=1.752$—1.783.

The Distribution Pattern of Lanthanoids

The distribution of lanthanoids in two abukumalites from Fusamata and Suishoyama was studied adopting about 0.5 g extracted rare earth oxides by x-ray fluorescent method, and Y, La, Ce, Pr, Nd, Sm, Gd, Tb, Dy, Ho, Er, Tm, and Yb were detected. The result of the quantitative analysis of the elements including relative error of less than 10% are plotted *versus* atomic numbers (Fig. 1). The patterns obtained show a close resemblance between Fusamata and Suishoyama abukumalites, both belonging to thalenite-type as defined by Goldschmidt and Thomassen (1924).[16] The same tendency is also found in abukumalites from Shinden,[8] Hiradani,[9] and Pyörönmaa.[11]

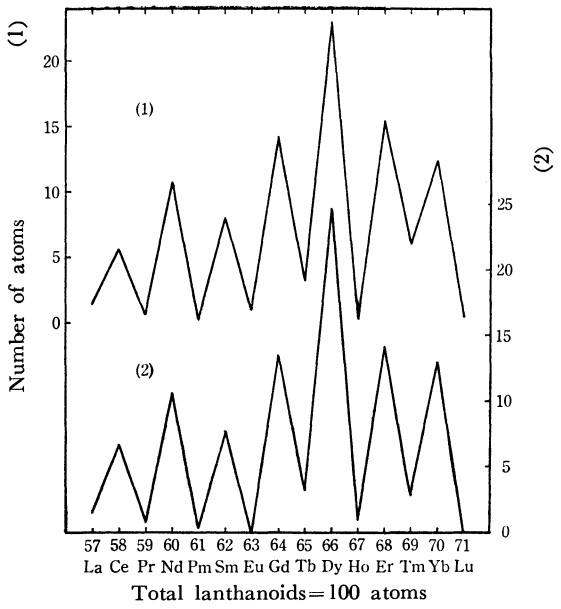

Fig. 1. Distribution patterns of lanthanoids.
(1) Abukumalite from Suishoyama, Fukushima Pref., Japan.
(2) Abukumalite from Fusamata, Fukushima Pref., Japan.

The authors express their thanks to Dr. Kin-ichi Sakurai and late Mr. Otokichi Nagashima for their kind offering of the abukumalite specimens to the authors.

SHORT COMMUNICATIONS

Ring-opening Polymerization of 2-Methyl-1,3,4-oxadiazolin-5-one

Takeshi ENDO, Takeshi INOUE, and Makoto OKAWARA
Research Laboratory of Resources Utilization, Tokyo Institute of Technology, Ookayama, Meguro-ku, Tokyo

(Received December 8, 1970)

2-Methyl-1,3,4-oxadiazolin-5-ones (I—III) were obtained easily by the reaction of corresponding hydrazides with phosgene in good yield.[1] They were confirmed by elementary analysis and IR spectrum.

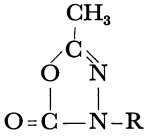

I, R=H (mp 112°C)
II, R=CH_3 (bp 70—72°C/10mmHg)
III, R=C_6H_5 (mp 92—93°C)

It is known that these derivatives are important as antibacterial compounds. The reactions of these compounds with primary amines[2] or water[3] have been reported. We found that a new type polymer IV could be synthesized by the ring-opening polymerization of 2-methyl-1,3,4-oxadiazolin-5-one (I), using tertiary amines or Lewis acids as catalysts. However, 2,4-dimethyl-1,3,4-oxadiazolin-5-one (II) and 2-methyl-4-phenyl-1,3,4-oxadiazolin-5-one (III) did not polymerize.

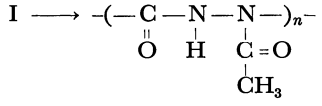

(IV)

Polymerization was carried out in sealed tubes in the absence of oxygen. The conditions for polymerization are given in Table 1. The polymer was purified by means of reprecipitation with *N,N*-dimethylformamide (DMF) and ether. The results are given in Table 1. The yield increases with the increase of the basicity of amines, although the molecular weight of the resulting polymer is low. It was found that a higher concentration of the catalyst is necessary for obtaining high yield. Compound I could also be polymerized by use of Lewis acids such as BF_3OEt_2 and $TiCl_4$, but the molecular weight and yield of the polymer obtained were low. The polymer obtained in the form of white powder is soluble in DMF, dimethyl sulfoxide (DMSO) and water, but insoluble in common organic solvents such as alcohol, acetone, and benzene. The structure of the polymer was confirmed by IR and NMR. The IR spectrum (in DMSO) indicated the three characteristic absorption bands at 3100 (N–H), 1720 (–C(=O)–CH_3) and 1690 cm^{-1} (–C(=O)–N). The absorptions attributable to carbonyl group (1770 cm^{-1}) and double bond (C=N) (1630 cm^{-1}) in the monomer disappeared. NMR spectrum of the polymer shows the two peaks at $\tau=7.35$ (singlet) and −1.15 ppm (singlet) assigned to methyl proton and N–H proton, respectively (NMR spectrum of monomer; methyl proton 7.80 ppm, N–H proton −0.55 ppm).

Table 1. Polymerization of 2-methyl-1,3,4-oxadiazolin-5-one (I)[a]

No.	Catalyst[b]	Time (hr)	Temp. (°C)	Conversion (%)	$[\eta]$[c]
1	Triethylene-diamine	30	120	48.0	0.06
2	Triethylamine	30	120	65.5	0.03
3	*N,N*-Dimethyl-benzylamine	30	120	48.0	0.07
4	Pyridine	30	120	25.5	0.05
5	$AlCl_3$	6	120	1	0.03
6	$FeCl_3$	6	120	1	0.03
7	$TiCl_4$	6	120	13	0.04
8	BF_3OEt_2	6	120	10	0.07
9	*N,N*-Dimethyl-benzylamine	20	120	93.3	0.07[d]
10	BF_3OEt_2	10	150	20	0.05

a) The polymerization of carried out in bulk.
b) Nos. 1—8, 1 mol% for monomer; Nos. 9—10, 10 mol% for monomer.
c) Measured at 30°C in water.
d) Melting point of this polymer was 224—226°C.

1) W. R. Sherman, *J. Org. Chem.*, **26**, 88 (1961).
2) A. J. Zelauskas and J. A. Aeschlimann, *ibid.*, **20**, 412 (1962).
3) W. R. Sherman and Anne von Esch, *ibid.*, **27**, 3472 (1962).

Liquid Adducts Consisting of Ammonia and Aliphatic Acid

Shizuo NAKAMURA
Sagami Chemical Research Center, Sagamihara, Kanagawa
(Received October 24, 1970)

A curious phenomenon is described herewith which takes place when a certain solid compound is added to liquid ammonia in a sealed glass tube. The compound turns liquid and remains at the bottom without being mixed with the liquid ammonia. The phenomenon does not seem to have been reported.

The following four compounds show the phenomenon: imino diacetic acid (IDA), glutaric acid (GLA), glutamic acid (GMA) and aspartic acid (ASP).

The liquid is viscous and sticky like the solution of a high molecular compound. It is not a compound in the usual sense. The ammonia content of the liquid varies with temperature. In the case of IDA the molar ratio of NH_3/IDA is 8 at dry ice temperature, and 6.5 at room temperature. The liquid becomes stiffer with the fall of temperature. At −78°C the liquid turns transparent, colorless caramel which does not flow; at −196°C it turns glassy, while liquid ammonia solidifies into a white mass. With the rise of temperature the liquid becomes turbid, but becomes transparent when left to stand for some time. The turbid liquid turns clear at once if temperature falls. This takes place at temperatures −30°C—+100°C. The phenomenon above 100°C was not studied.

The liquid is stable at room temperature under the pressure of saturated ammonia. In the case of IDA, the decomposition pressure is 2.1—2.4 atm at 22°C.

TABLE 1. TUBE SIZE AND EXPERIMENTAL CONDITIONS

Tube size			Maximum temp. °C	Maximum pressure atm.
Inner dia. mm	Outer dia. mm	Length cm		
12	17.5	28	37	14
3[a)]	8[a)]	17	100	62
2.5	9	17		
20	26	13	37	14
2.3	5	15	35	13

a) The tube burst after being kept at 100°C for one hour.

When the pressure is reduced, ammonia gas bubbles out from the viscous liquid giving rise to the formation of a white foamed mass (in the case of GLA, the mass is less sticky than in other cases, the foam being smaller). The mass is sticky at first, but turns brittle after complete separation of ammonia. It is an ammonium salt of the acid which is also dissolved forming a liquid phase like its free acid.

The liquid obtained from the four dibasic acids differ in their ammonium contents. Rough estimate at room temperature gives the results: IDA-6.5NH_3, GLA-7NH_3, GMA-6NH_3 and ASP-5NH_3.

NMR spectra of IDA-NH_3 and GLA-NH_3 at 35°C show that there is no ammonia molecule of ordinary liquid ammonia, *viz.*, NMR signal of the ammonia proton shifts from $\delta=9.88$ (ordinary liquid ammonia) to $\delta=4.74$ in the case of IDA, and to $\delta=4.26$ in the case of GLA.

The facts that the liquid does not mix with liquid ammonia, it is viscous and sticky, it exists between −196°C and +100°C, and its NMR signal of ammonia proton shifts largely from that of liquid ammonia, suggest that ammonia molecules are surrounded by atoms of acid molecules forming clathrate-like liquid structure.

Experimental. Thick glass tubes were used in order to prevent explosion. Tube size and experimental conditions are shown in Table 1.

Decomposition pressure was estimated by reading the temperature of liquid ammonia, whose vapor pressure balanced with that of the viscous liquid. The temperature range was −15°C (2.33 atm) to −17°C (2.14 atm).

In order to measure the ammonia content in the liquid, the liquid ammonia (upper phase) was made to volatilize gradually at room temperature. With the disappearance of upper phase, the tube was sealed off immediately, and weighed. The pressure was then reduced for the formation of foamed mass, and the vessel was evacuated and weighed. The results are given in Table 2. The accuracy of weighing is ±0.01 g.

TABLE 2. MASS BALANCE OF THE VISCOUS LIQUID

	Acid used g	Viscous liquid g	Ammonia content g	Molar NH_3/acid ratio	Remaining solid	
					g	Formula
IDA-NH_3	0.50	0.91	0.41	6.4	0.57	NH_4-$C_4H_6O_4N$
IDA-NH_3[a)] (−78°C)	0.50	1.02	0.52	8.1	0.58	NH_4-$C_4H_6O_4N$
GLA-NH_3	0.50	0.96	0.46	7.1	0.65	$(NH_4)_2$-$C_5H_6O_4$
GLA-NH_3	0.70	1.32	0.62	6.9	0.88	$(NH_4)_2$-$C_5H_6O_4$
GMA-NH_3	0.50	0.83	0.33	5.7	0.58	NH_4-$C_5H_8O_4N$
ASP-NH_3	0.50	0.83	0.33	5.2	0.55[b)]	NH_4-$C_4H_6O_4N$?

a) Separation of the two phases was carried out by decantation.
b) Hygroscopic.

On the Structure of Ethyl Mercaptan

Michiro HAYASHI, Hisae IMAISHI, Keiichi OHNO, and Hiromu MURATA
Department of Chemistry, Faculty of Science, Hiroshima University, Higashisenda-machi, Hiroshima
(Received November 16, 1970)

Recently, Kadzhar, Abbasov, and Imanov[1] have published a paper on the microwave spectra of trans ethyl mercaptan and its ^{34}S isotopically-substituted species. We have also independently worked on the same molecule and five isotopically-substituted species, in both the trans and gauche molecular forms.

For the trans isomer, since we have not yet finished the measurements of two ^{13}C isotopic species, the r_s structure of the molecule can not be obtained at present. A preliminary survey has shown us, however, that too many weak spectra crowd around the expected regions for the ^{13}C species, and careful measurements will be necessary for the assignment of the spectra due to two ^{13}C species in natural abundance. Therefore, we have obtained only a tentative structure which reasonably reproduces the observed rotational constants.

For the gauche isomer, we could assign the spectra only to "a"-type transitions. For "b"- and "c"-type spectra, the splittings due to the internal rotation of the SH group seem to be too large for us to get the reasonable assignments without information from theoretical treatments of the splittings, on which we are now working.

The "a" type spectra of the $J_{0J}\rightarrow(J+1)_{0J+1}$ type show no splitting, while the spectra of the $J_{1J}\rightarrow(J+1)_{1J+1}$ and $J_{1J-1}\rightarrow(J+1)_{1J}$ types are split into doublets, with separations of several mega-Hertz.

The "B" and "C" rotational constants shown in the table can be obtained by taking the average frequencies of the components of the doublets for the latter types of the spectra.

As for the "A" rotational constants, we cannot obtain them from the "a"-type spectra alone since the molecule is so close to the symmetric top. The observed rotational constants of the gauche isomer are not reproduced by simply changing the dihedral angle CCSH, while keeping the other structural parameters the same as those of the trans form; the discrepancies amount to about 5% for all isotopic species. However, reasonable agreements are obtained if we change the dihedral angle CCSH after exchanging the values of the CCS and one of the CCH angles in the CH_2 group. The CCH angle to be exchanged is the one situated at the trans position against the SH bond in the gauche isomer.

This is understandable if we have a tilted CH_2 group toward the SH bond; it is similar to the CH_3 group found, for example, in methyl mercaptan.[2]

trans isomer (MHz)	A	B	C
CH_3CH_2SH	28416.74 (9.02)[a]	5485.90 (4.08)	4882.00 (−6.32)
CH_3CH_2SD	27155.69 (30.39)	5304.20 (2.51)	4702.47 (−7.51)
$CH_3CH_2{}^{34}SH$	28330.09 (9.39)	5367.24 (3.40)	4785.07 (−6.20)
CH_3CD_2SH	22275.10 (−5.12)	5342.46 (−2.03)	4691.21 (−16.42)
CH_2DCH_2SH sym	28386.99 (24.49)	5095.23 (1.94)	4570.14 (−7.15)
asym	25913.56 (0.32)	5293.75 (3.07)	4714.34 (−7.06)

gauche isomer (MHz)	B	C
CH_3CH_2SH	5294.25 (267.27)[b] (10.34)[c]	4846.99 (155.02) (−5.97)
CH_3CH_2SD	5190.01 (262.18) (12.78)	4768.69 (153.55) (−6.72)
$CH_3CH_2{}^{34}SH$	5174.52 (259.99) (9.54)	4745.63 (152.60) (−5.90)
CH_3CD_2SH	5165.02 (237.27) (1.25)	4665.73 (120.59) (−16.17)
CH_2DCH_2SH sym	4925.07 (237.16) (7.49)	4534.85 (141.77) (−6.09)
asym-1	5107.18 (255.20) (0.35)	4680.53 (154.02) (−7.21)
asym-2	5112.46 (270.34) (14.79)	4666.62 (157.61) (−3.63)

CH_3	r(CH) 1.091 Å	∠HCH 108°00′	∠CCH 110°56′			
CH_2	r(CH) 1.091 Å	∠HCH 107°00′	∠CCH 108°12′	∠HCS 113°05′		
skeleton	r(CC) 1.535 Å	r(CS) 1.819 Å	r(SH) 1.328 Å			
	∠CCS 108°32′	∠CSH 96°35′				

a) calcd−obsd
b) calcd−obsd assuming the same structural parameters for the *trans* isomer except the dihedral angle CCSH which was taken as 60°.
c) calcd−obsd assuming the exchange of the CCS and one of the CCH angles and the change of the dihedral angle CCSH from 180° to 60° keeping the other structural parameters unchanged.

1) Ch. O. Kadzhar, A. A. Abbasov, and L. M. Imanov, *Optics and Spectry.*, **24**, 334 (1968).

2) The summary of the references is shown in L. Pierce and M. Hayashi, *J. Chem. Phys.*, **35**, 479 (1961).

Water Formation in the Gas Phase Radiolysis of Nitrous Oxide-Hydrocarbon Mixtures

Satoshi TAKAO, Yoshihiko HATANO, and Shoji SHIDA
Laboratory of Physical Chemistry, Tokyo Institute of Technology, Meguro-ku, Tokyo

(Received December 14, 1970)

The determination of water formation in the radiolysis of nitrous oxide - hydrocarbon systems is important for the elucidation of radiolytic mechanism of pure nitrous oxide, as well as the electron-scavenging process of nitrous oxide in hydrocarbons.[1] However, information is scanty and inaccurate. In previous papers,[2] an ionic mechanism in the gas-phase radiolysis of nitrous oxide was proposed and the importance of processes other than the ionic process was suggested. In the present study, the effect of hydrocarbons on the gas-phase radiolysis of nitrous oxide has been examined.

A sample containing about 90 cmHg of N_2O with small amounts of the hydrocarbons, C_2H_6, C_3H_8, C_2H_4, or C_3H_6, was irradiated by ^{60}Co-γ rays at room temperature to a total dose of 2.1×10^{20} eV/g. The products were analyzed by gaschromatography using a molecular sieve-5A column at 60°C for N_2 and CO and a polyethyleneglycol-200 column at 70°C for other oxygen-containing products. Special care was taken in the analysis of the main product H_2O.

The addition of small amounts of hydrocarbons to N_2O caused a sudden decrease in the nitrogen yield and a large increase in the yield of oxygen-containing products, giving respective plateau values. In all cases, H_2O is the major product with small amounts of alcohols or CO. A typical result for C_2H_6 is given in Fig. 1. Decrease of the observed nitrogen yield was 2.5 in G unit for C_2H_6 and C_3H_8, 2.6 for C_2H_4, and 2.7 for C_3H_6. The total yields of oxygen-containing products were 6.8 for C_2H_6, 6.9 for C_3H_8, 6.8 for C_2H_4 and 6.4 for C_3H_6. They are roughly three times, as much as the decrements of the nitrogen yield. In the presence of the hydrocarbons, NO and O_2 were not detected.

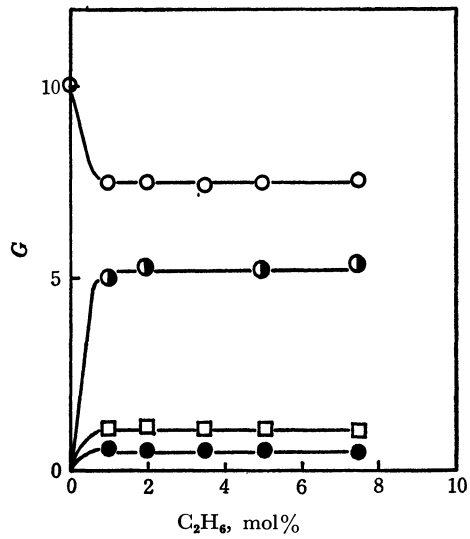

Fig. 1. The effect of C_2H_6 addition to N_2O.
○ N_2, ◑ H_2O, □ i-C_4H_9OH, ● C_2H_5OH.

From the results, the contribution from ionic processes is considered, for which the following schemes are assumed;[3]

$$N_2O \rightsquigarrow N_2O^+ + e^-,\quad N_2O^+ + RH \rightarrow N_2O + RH^+,$$

$$N_2O + e^- \rightarrow N_2O^-,$$

$$N_2O^- + RH \text{ (or } RH^+) \rightarrow N_2 + OH^- \text{ (or OH)} + R,$$

$$OH^- + RH^+ \rightarrow H_2O + R, \text{ or}$$

$$OH^- + N_2O^+ \rightarrow N_2O + OH,\quad OH + RH \rightarrow H_2O + R.$$

According to these schemes, however, nitrogen should be produced as much as H_2O and the nitrogen yield should not decrease by the addition of a hydrocarbon. The observed decrease of the nitrogen yield, then, must be ascribed to some other processes. The total yield of the oxygen-containing products is much larger than the decrease of the nitrogen yield. It seems reasonable to assume the following non-ionic processes involving two kinds of oxygen atoms; one can contribute to the decomposition of N_2O but not the other,[4] both reacting with hydrocarbons to form oxygen-containing products. On the basis of the observed decrements of the nitrogen yields in the presence of hydrocarbons, combined with the total G(NO) value and that contributed from ionic processes obtained in the radiolysis of pure N_2O,[2] it can be concluded that O* plays a major role in the non-ionic decomposition of N_2O. From the consideration of photochemical studies[5] on the reactivities of oxygen atoms, it may be inferred that O and O* are the ground $O(^3P)$ and the excited $O(^1D)$ or $O(^1S)$ atoms, respectively.

$$N_2O \rightsquigarrow \begin{cases} N_2 + O, & O + N_2O \not\rightarrow \\ N_2 + O^*, & O^* + N_2O \rightarrow N_2 + O_2,\ 2NO. \end{cases}$$

1) R. O. Koch, J. P. W. Houtman, and W. A. Cramer, *J. Amer. Chem. Soc.*, **90**, 3326 (1968); A. Menger and T. Gäumann, *Helv. Chim. Acta*, **52**, 2477 (1969).

2) S. Takao, S. Shida, Y. Hatano, and H. Yamazaki, This Bulletin, **41**, 2221 (1968); S. Takao and S. Shida, *ibid.*, **43**, 2766 (1970).

3) N. H. Sagert and A. S. Blair, *Can. J. Chem.*, **45**, 1351 (1967).

4) M. G. Robinson and G. R. Freeman, *J. Phys. Chem.*, **72**, 1394 (1968).

5) R. J. Cvetanović, "Advances in Photochemistry," Vol. 1, Interscience Publishers, New York (1963), p. 115; G. Paraskevopoulos and R. J. Cvetanović, *J. Chem. Phys.*, **50**, 590 (1969); R. A. Young, G. Black, and T. G. Slanger, *ibid.*, **49**, 4769 (1968).

On the Structure of Poly-L-lysine-metal Complexes in Aqueous Solution

Michio NAKAI, Michio YONEYAMA, and Masahiro HATANO

The Chemical Research Institute of Non-aqueous Solutions, Tohoku University, Katahira-cho, Sendai

(Received November 16, 1970)

Poly-L-lysine-copper(II) complex has been prepared as a model compound of a metalloenzyme and found to oxidize D-3,4-dihydroxyphenylalanine faster than L-enantiomorph at pH 10.5, where the polymer chain has helical structure to some extent.[1] It has been estimated that the cupric ion in the helical poly-L-lysine-copper(II) complex is coordinated by four amino nitrogens in the side chains of poly-L-lysine and, in addition, by a deprotonated nitrogen in the peptide bond of the polymer.[2]

We report herewith on the structures of the complexes prepared from poly-L-lysine and several metal salts, *i.e.*, nickel(II) nitrate, cobalt(II) nitrate, zinc(II) nitrate and potassium tetrachloropalladate(II). The pH titration and the measurements of circular dichroism (CD) and infrared absorption spectra were carried out for the polymer complexes formed in aqueous media.

The order of the stability constants of the complexes were estimated as $-Pd(II) > -Cu(II) > -Zn(II) \approx -Ni(II) \approx -Co(II)$ from modified Bjerrum plots[3] of the pH titration data obtained for the solution, with a ratio 0.15 of molar concentration of the metal ion to residual molar concentration of poly-L-lysine C_M/C_R. The Bjerrum formation functions, $\bar{n}$'s, were found to approach *ca.* 4 for all the complexes examined, which shows that each metal ion is coordinated by four amino nitrogens.

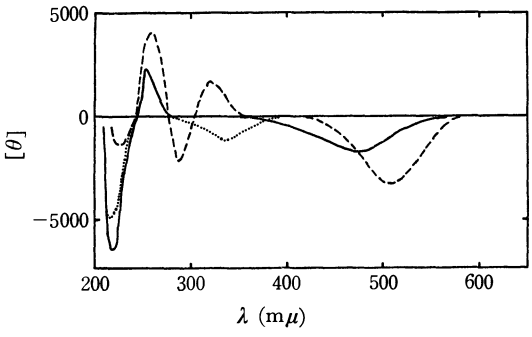

Fig. 1. CD spectra of poly-L-lysine-metal complexes (C_R= 0.005 M, C_M/C_R=0.15, pH 10.5); ---- Cu, —— Ni, ... Pd.

CD measurements were carried out at room temperature with a JASCO Model ORD/UV-5 optical rotatory dispersion recorder. The residual concentration of poly-L-lysine C_R and the ratio C_M/C_R were 0.005 mol/*l* and 0.15, respectively. All the polymer complexes showed n–π^* transition band due to helical structure at 222 mμ at pH 10.5. As in the case of poly-L-lysine-copper complex, only the poly-L-lysine-nickel and the poly-L-lysine-palladium complexes were found to show *d*–*d* transition and charge-transfer bands in addition to the band at 222 mμ (Fig. 1). The *d*–*d* transition bands are considered to be due to the vicinal effect of the asymmetric carbon of the poly-L-lysine through the coordination of the peptide group to the metal ion.

In order to ascertain the coordination of the peptide group in the cases of the nickel and the palladium complexes as done with the copper complex, the infrared absorption spectra in D_2O solutions at pD *ca.* 11 were recorded on a Hitachi Model EPI-G2 grating infrared spectrophotometer with small bags made of polyethylene film held between NaCl plates.[4] C_R and C_M/C_R were *ca.* 0.5 mol/*l* and 0.15, respectively. The amide I band of poly-L-lysine at pD *ca.* 11 shifts from 1640 cm^{-1} to 1610 cm^{-1} on the coordination of the peptide nitrogen to copper ion.[2] The band shifted to 1635 cm^{-1} and 1625 cm^{-1} for the nickel and the palladium complexes, respectively. No shift occurred in the case of the cobalt complex. The amide I band of glycylglycinate at 1632 cm^{-1} is known to shift to 1610 cm^{-1} and 1620 cm^{-1} when its deprotonated peptide nitrogen is coordinated to copper ion and nickel ion, respectively.[5] Thus the results seem to support the coordination of the peptide nitrogen to nickel and palladium ions as in the case of copper ion. They agree with those by CD measurement. In either of the nickel and the palladium complexes the metal ion seems to be coordinated by four amino nitrogens in the side chains of the helical poly-L-lysine and by a peptide nitrogen in the main chain of the polymer, which is similar to the case of poly-L-lysine-copper complex.

1) M. Hatano, T. Nozawa, and M. Yoneyama, This Bulletin, **43**, 295 (1970).
2) T. Nozawa and M. Hatano, *Makromol. Chem.*, **141**, 11 (1971).
3) T. Nozawa, M. Hatano, and S. Kambara, *Kogyo Kagaku Zasshi*, **72**, 369 (1969).
4) M. Hatano and M. Yoneyama, *J. Amer. Chem. Soc.*, **92**, 1392 (1970).
5) M. K. Kim and A. E. Martell, *ibid.*, **88**, 914 (1966); **89**, 5138 (1967).

The Synthesis and Absolute Configurations of Lilac Alcohols

Seiji WAKAYAMA, Satoshi NAMBA, Kazuo HOSOI,* and Masaji OHNO*

Chemical Laboratory, Hokkaido University of Education, Sapporo

** Basic Research Laboratories, Toray Industries, Inc., Kamakura*

(Received January 11, 1971)

Lilac alcohols have recently been isolated and assigned to the diastereomers of β,5-dimethyl-5-vinyl-2-tetrahydrofuranethanol.[1,2] We now wish to describe a total synthesis of lilac alcohols with sufficient samples for the assignment of absolute and stereochemical configurations.

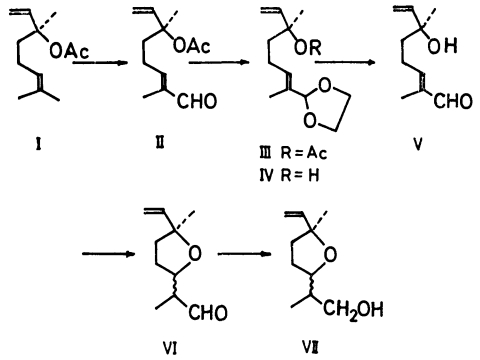

d-Linalyl acetate (I)[3] $[\alpha]_D^{25}$ +2.9 was treated with SeO_2 to afford α,β-unsaturated aldehyde II in 38% yield. Treatment of II with ethyleneglycol in the presence of *p*-toluenesulfonic acid in benzene gave ethyleneacetal III, which was hydrolysed with 5 N NaOH to afford IV. Column chromatography of IV on silica gel gave V (77% overall-yield from II to V).[4,5] The intramolecular Michael addition of alcohol to the α,β-unsaturated aldehyde was effected with NEt_3 to give VI in 43% yield. Reduction of VI with $LiAlH_4$ afforded a diastereomeric mixture (VII) of *d*-lilac alcohols in 75% yield. The mixture was separated completely by vpc to afford four diastereomers with R_t 7.1 $[\alpha]_D^{25}$ −1.4, 7.3 $[\alpha]_D^{25}$ +1.4, 8.8 $[\alpha]_D^{25}$ +6.7, and 10.1 $[\alpha]_D^{25}$ −0.5, which were shown to correspond to lilac alcohol-b, -d, -a, and -c, respectively, based on NMR, IR and optical rotations. *l*-Lilac alcohol-a $[\alpha]_D^{25}$ −11.6, -b $[\alpha]_D^{25}$ +3.0, -c $[\alpha]_D^{25}$ +2.5, and -d $[\alpha]_D^{25}$ −2.9 were synthesized from *l*-linalyl acetate[3] $[\alpha]_D^{25}$ −5.0 in a similar way, showing a contrary $[\alpha]_D$ to natural lilac alcohols. By combining the absolute configuration of *d*-linalool,[6] chemical relation to *trans*-linalool oxide,[1] and a detailed IR and NMR study of the intramolecular hydrogen bonding between the primary alcohol and ether linkage,[7] the absolute configurational assignments of lilac alcohol-a, -b, -c, and -d have been shown to be (βS, 2S, 5S), (βR, 2S, 5S), (βR, 2R, 5S), and (βS, 2R, 5S), respectively.

1) S. Wakayama, S. Namba, and M. Ohno, This Bulletin, **43**, 3319 (1970).

2) S. Namba, S. Wakayama, and M. Ohno, The 14th Symposium of Perfume, Terpene, and Essential Oil, abstracts p. 60, Kitami, Japan (1970).

3) This material was supplied by Takasago Perfumery Company. It was not perfectly pure optically, but proved to be pure enough to determine the absolute configuration.

4) During the course of our synthetic work on lilac alcohols from linalool, Naegeli and Weber published the use of aldehyde (VI) as an intermediate to davanone synthesis. P. Naegeli and G. Weber, *Tetrahedron Lett.*, **1970**, 959.

5) The direct hydrolysis of II gave V or VI in poor yield.

6) R. H. Cornforth, J. W. Cornforth, and V. Prelog, *Ann. Chem.*, **634**, 197 (1960).

7) The measurement of the intramolecular hydrogen bonding was carried out by IR and NMR.

Chronology of the Addition of 1-Cyano-1-methylethyl Radicals to 9-Bromoanthracene Studied by CIDNP

Hiizu IWAMURA, Michiko IWAMURA,* Shiro SATO,** and Katsuhiko KUSHIDA**

Department of Chemistry, Faculty of Science, The University of Tokyo, Bunkyo-ku, Tokyo

* *Department of Chemistry, Faculty of Science, Toho University, Narashino-shi, Chiba*

** *Nippon Electric Varian, Ltd., Azabu, Tokyo*

(Received January 21, 1971)

In previous papers we suggested a possible application of chemically induced dynamic nuclear polarization (CIDNP) for the determination of chronology of free radical addition reactions.[1] A typical example has now been found in the addition reaction of 1-cyano-1-methylethyl radicals to the *meso* positions of 9-substituted anthracenes.

The NMR spectrum of adduct I of 9-bromoanthracene, for example, has a doublet for the C-methyl protons at 0.86 and 0.78 ppm from the internal hexamethyldisiloxane. When 0.4 m*l* aliquot of a solution of 85 mg of 9-bromoanthracene and 112 mg of α,α'-azobisisobutyronitrile in 1.3 m*l* of tetrachloroethane was heated at 120°C in an NMR probe of a Varian HA-100 D spectrometer, it was the signal at the lower applied magnetic field (0.86 ppm) which showed an emission pattern. On the contrary, the intensity of the absorption peak at 0.78 ppm increased smoothly as expected for a normal growth of I as the reaction proceeded (see Fig. 1). Based on the empirical rule that the electronegative β-bromo substitution shifts the methyl proton resonance to the lower field by *ca.* 0.1 ppm,[2] it can be assumed that the emission signal corresponds to the methyl protons of $C_{(9)}$-CMe_2CN in I. Since the nuclear spin relaxation time T_1 of the intermediate radicals is usually short compared to their life-time, it is more probable that the nuclear spin polarization which was developed in the last step of the radical addition was detected in I. Thus the observation provides direct evidence for path a in Scheme 1 as the sequence of the addition reaction. The chronology is compatible with the knowledge that the addition proceeds through formation of a more stable intermediate radical in free radical chemistry. In the present case, II is considered to be more stable than III by additional resonance contribution of the bromine atom.

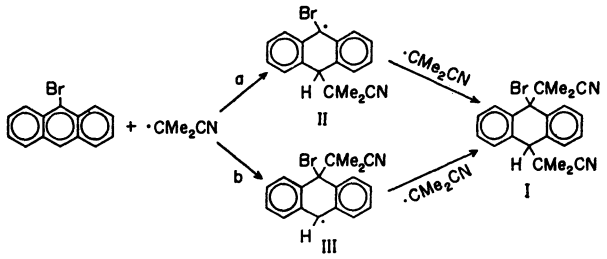

Scheme 1

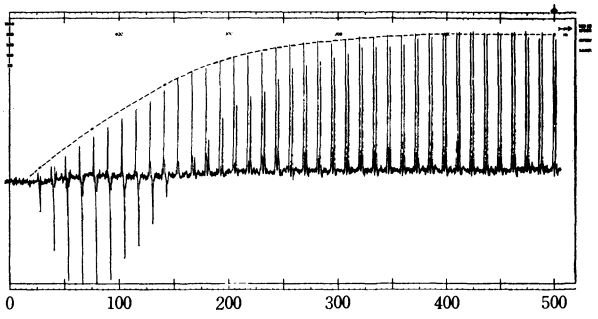

Fig. 1. Time dependence of the amplitude of the two C-methyl signals at 0.86 ppm (the upper envelope) and 0.78 ppm (the lower envelope) of I during the reaction. The dotted curve represents a theoretical increase in the concentration of I.[3]

A closer examination of the time dependence curve of the amplitude of the two C-methyl signals (Fig. 1) revealed, however, that the upper envelope representing the absorption peak at δ 0.78 ppm is not simply convex as expected for normal increase in the concentration of I as the reaction proceeds, but deviates slightly from the theoretical curve[3] in the 0—150 sec interval. The phenomenon seems to indicate that the curve could be an overlap between the normal exponential curve and a sigmoidal curve characteristic of the emission signals. The anomaly can be interpreted as a manifestation of the dual pathway of the addition reaction in which path b also contributes slightly.[4] The conclusion is consistent with that derived from the kinetic study of the reaction by Kooyman;[3] the partial rate factors at $C_{(10)}$ and $C_{(9)}$ of 9-bromoanthracene at 70°C are given as 1.37 and 0.07, respectively.[5]

1) H. Iwamura and M. Iwamura, *Tetrahedron Lett.*, **1970**, 3723; H. Iwamura, M. Iwamura, M. Tamura, and K. Shiomi, This Bulletin, **43**, 3638 (1970).

2) L. M. Jackman and S. Sternhell, "Application of Nuclear Magnetic Resonance Spectroscopy in Organic Chemistry," 2nd ed. Pergamon Press, Oxford (1969), p. 164; Ph. D. Thesis of Thomas Curphey, Harvard University.

3) Given by Equation I in E. Farenhorst and E. C. Kooyman, *Rec. Trav. Chim. Pays-Bas*, **81**, 816 (1962).

4) This effect is less conspicuous for the lower envelope representing the emission signals at 0.86 ppm in Fig. 1.

5) Reactivity at $C_{(9)}$ is calculated to be *ca.* 10% at 120°C of the present experimental conditions.

The NMR Spectra of Molten Polyethylene

Kojitsu Goto and Atsuo Nishioka*

Japan Electron Optics Lab. Co., Ltd., Akishima, Tokyo

** Tokyo Institute of Technology, Ookayama, Meguro, Tokyo*

(Received January 16, 1970)

Quantitative analyses of methyl groups and olefinic double bonds (vinyl, vinylidene, and vinylene) are usually performed by the infrared (IR) absorption method, but it can also be done by the high-resolution nuclear-magnetic-resonance (NMR) method.[1,2] The latter method has the advantage of providing an absolute measurement method if the saturation effect can be neglected. However, the analysis of the double-bond content is more difficult than that of the methyl group because of their small quantity of the order 10^{-4}/carbon atoms. To improve the signal-to-noise ratio, a molten sample was used with the NMR accumulation method at 60 MHz by Ferguson,[2] but the details were not presented.

We have obtained better results on molten polyethylene without any accumulation at 180°C by using a 100 MHz NMR spectrometer (JEOL 4H-100) with higher sensitivity than in the early studies.[1,2] The careful preparation of the sample tube is necessary to avoid the formation of voids, which disturb the homogeneity of the magnetic field. At the early stage of our experiment, polyethylene, in either pellet or powdered form, was put into the sample tube and melted on the flame of a Bunsen burner for a relatively short time (about three minutes). Figure 1 shows the NMR spectra of these samples; they consist of very sharp lines similar to those of low-molecular-weight model compounds. The double-bond signals in polyethylene were assigned by comparing them with those of the model compounds: (a) octadecene-1 ($CH_3(CH_2)_{15}CH{=}CH_2$, δ=4.72—4.98 and 5.48—5.92) for the vinyl group, (b) 2-ethyl-butene-1 ($(CH_3CH_2)_2C{=}CH_2$, δ=4.56—4.63) for vinylidene, (c) elaidic acid $(CH_3(CH_2)_7C{=}C(CH_2)_7COOH$ (H), δ=5.22—5.37) for *trans*-vinylene, and (d) oleic acid $(CH_3(CH_2)_7C{=}C(CH_2)_7COOH$ (H H), δ=5.15—5.36) for *cis*-vinylene.

However, the IR measurement of these samples showed some increase in the double-bond content compared with that of the original pellets; attributable to the dissociation by overheating during the above operation.

We then tried to prepare the sample tube under milder conditions with an oil bath maintained at 180—200°C. Figure 2 shows the spectra of these samples, which give the same kinds of signals as are shown in Fig. 1, but with some broadening and weaker intensities. It was found that the half-height widths of the methylene proton signals of both normal and dissociated samples are not very different from each other, but that the tailing part of the signal is very broad in the normal sample, corresponding to the broad molecular-weight distribution in the original sample.

Thus, the NMR spectra of molten polyethylene is very useful in determining the contents of various types of olefinic double bonds in a relatively short time without any accumulation, that is, in a single scan; moreover, this method provides a broad line width which gives us new information about the molecular motion and the molecular-weight distribution of polyethylene chains.

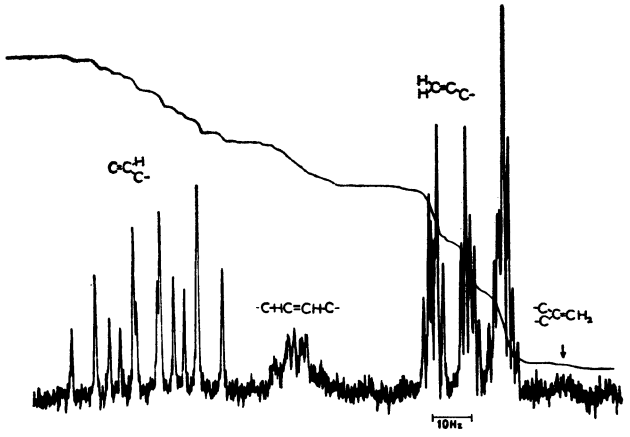

Fig. 1. Expanded spectrum of olefinic double bonds in molten high density polyethylene at 180°C.

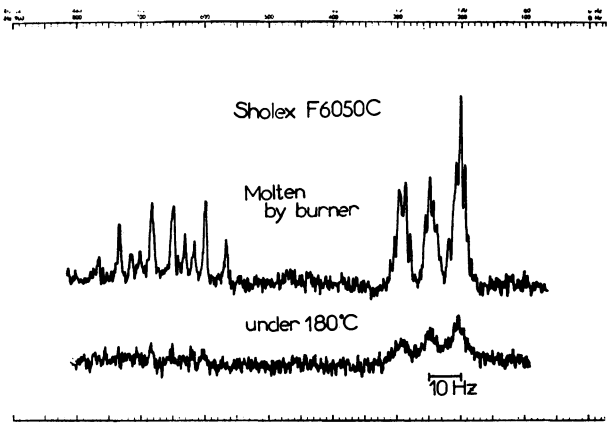

Fig. 2. Double bond spectra of molten high density polyethylene prepared by gas burner (upper) and oil bath (lower).

1) Y. Kato and A. Nishioka, This Bulletin, **39**, 1426 (1966).
2) R. C. Ferguson, *Kautschuk Gummi.*, **18**, 723 (1965).

Thermochromism in 5-Arylazo-8-quinolinols Diluted with Sodium Chloride

Yoshio MATSUNAGA
Department of Chemistry, Faculty of Science, Hokkaido University, Sapporo
(Received January 25, 1971)

Our earlier work on the diffuse reflection spectra of 1-arylazo-2-naphthols diluted with sodium chloride disclosed that the compounds in this solid two-component system exist as mixtures of the azo and hydrazone tautomers.[1] The movement of the equilibrium upon an elevation of the temperature was well demonstrated by the change in the spectrum. However, no appreciable thermochromism was noted, because the absorption bands of the two tautomers are rather coalescent. Here, we wish to report that 5-arylazo-8-quinolinols;

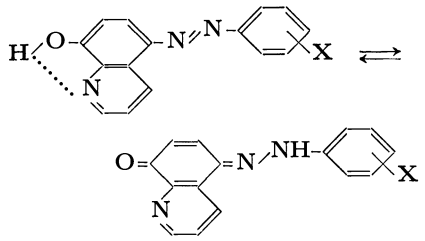

the synthesis of which was described as early as 1888 by Matheus,[2] are distinctly thermochromic when diluted with sodium chloride.

The compounds were prepared by the usual diazo-coupling reactions with 8-quinolinol. The derivatives carrying one of the following substituents in the *o*-, *m*-, or *p*-position on the phenyl ring were synthesized: methyl, chloro, methoxy, and nitro. They were easily purified by vacuum sublimation. The method of measuring the reflection spectra was the same as that described in our previous paper.[1]

For example, pure 5-(*m*-anisylazo)-8-quinolinol is orange. It turns yellowish orange upon dilution with sodium chloride. As is shown in Fig. 1, the spectrum consists of three bands, located at about 360—70 mμ, 430—40 mμ, and 540 mμ; among those, the band at 440 mμ dominates at room temperature. Upon the elevation of the temperature, the relative intensity of this band is markedly diminished at a concentration of 0.01%. The mixture is red-colored at 100°C. The direction of the spectral change upon heating in 5-phenylazo-8-quinolinol and all the *m*- and *p*-substituted compounds examined is the same as has been mentioned above. Nevertheless, various spectral features are observed because of the large difference in the relative intensities of the bands. Among the *o*-substituted compounds, only 5-(*o*-anisylazo)-8-quinolinol shows an appreciable spectral change upon the elevation of the temperature. Here, the direction of the change is the opposite of that observed in the others.

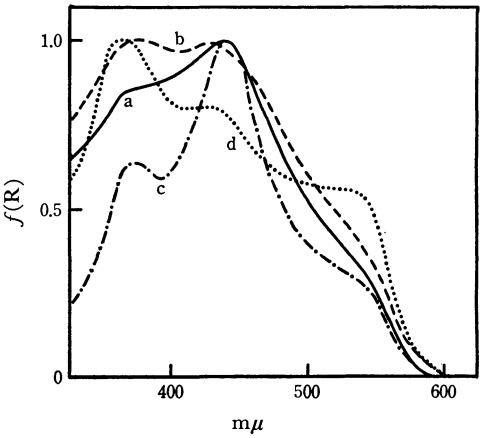

Fig. 1. Spectra of 5-(*m*-anisylazo)-8-quinolinol diluted with sodium chloride; (a) 1% at room temperature, (b) 1% at 100°C, (c) 0.01% at room temperature, and (d) 0.01% at 100°C. The maximum is arbitrarily taken as 1.00 in each spectrum.

It is likely that the azo tautomer is favored by the intramolecular hydrogen bond in the quinolinol part, the presence of which is suggested by the ease of vacuum sublimation. Therefore, the band outstanding in most of the room-temperature spectra may be ascribed to the azo tautomer. Further work is being planned to attempt a more conclusive assignment of the absorption bands to the possible tautomers.

1) C. Dehari, Y. Matsunaga, and K. Tani, This Bulletin, **43**, 3404 (1970).
2) J. Matheus, *Ber.*, **21**, 1644 (1888).

Calorimetric Study of Polystyrenes of Low Molecular Weight

Satoshi MORIMOTO

Research Institute for Polymers and Textiles, Sawatari, Kanagawa-ku, Yokohama

(Received February 5, 1970)

Heats of mixing ΔH^M at infinite dilution and integral heats of dilution ΔH_d were directly measured for the systems of atactic polystyrenes (PSt: MW$\leqq 10^4$, prepared by Pressure Chemical Co.) with benzene, toluene, and chloroform. The results are summarized as follows: (1) ΔH^M and ΔH_d decrease remarkably with the molecular weight of PSt in all solvents used. (2) The glass energies of the samples treated under the same thermal conditions were investigated and the large difference of heat capacities between liquid and glassy state of PSt was observed in the low molecular weight region. (3) Schulz's theory of osmotic second virial coefficient of athermal polymer solutions was found to agree, to a good approximation, with the differential heat $\overline{\Delta H}_1$ of dilution in toluene in the molecular weight region between 10^3 and 10^4. (4) The NMR and the X-ray diffraction analyses were performed for the PSt oligomer liquid (MW 600). All alkyl end group of molecules and an order formation in the liquid were observed. They are discussed in terms of calorimetric data.

The present study is concerned with the heats of solution and dilution in low molecular weight polystyrene-solvent systems. The heat of solution of a polymeric glass-solvent system arises partly from the glass energy of the polymer solid.[1] For atactic polystyrene (PSt), calorimetric studies[2,3] have confirmed the glass energy content, glass enthalpy which varies with the packing conditions of the polymer molecules under the glassy state. However, when polymeric glass samples of various molecular weights are treated under the same conditions, the heats of solution in the liquid polymer-solvent systems and the glass energy contents of the polymer glasses should change with their molecular weights. The heats of dilution of PSt solutions have been directly measured by several workers. In particular, studies on the low molecular weight PSt or the oligomer solutions have revealed remarkable changes of the solution properties with molecular weights in the oligomer region.[4,5]

In this work, the heats of mixing (ΔH^M) of PSt samples (prepared by Pressure Chemical Co., average molecular weight $\bar{M}\leqq 10^4$), treated under the same thermal conditions in benzene, toluene and chloroform at infinite dilution, and the heats of dilution of the solutions have been measured. Dependence of the values on molecular weight was examined and information on the polymer and the solution was obtained from the results.

Experimental

Materials. PSt polymers of narrow molecular weight distribution, $\overline{M_w}/\overline{M_n}\leqq 1.10$, products of the Pressure Chemical Co., were used. For the measurement of the ΔH^M, the polymers were subjected to the same thermal treatment with the exception of the polymer of $\bar{M}=600$, a viscous liquid. After removing air in a vacuum 10^{-5} mmHg, PSt samples were heat-treated at 130°C for 10 min in N_2 gas current and were annealed at room temperature. The liquid solute ethylbenzene and the solvents benzene, toluene, and chloroform were commercial products of the highest quality. All but chloroform were dried with sodium wire and fractionally distilled over phosphorus pentoxide before use. Chloroform was washed repeatedly with distilled water, dried over calcium sulfate and fractionally distilled before use.

Calorimetry. For the measurement of ΔH^M, a rotational twin conduction calorimeter[6] in which a mixing cell similar to that described by Malcolm and Rowlinson[7] was used. The principle of the detection of heat is similar to that reported previously.[8] Almost all ΔH^M values at infinite dilution were obtained from the measurements for final concentration of 0.7—1.3% using 20—30 mg of the solute and about 3 m*l* of the solvent. Measurements were performed within ±4% of standard deviation. For the determination of the integral heat of dilution (ΔH_d), a revised type of calorimeter[9] with multiple modules[10] was used. The ΔH_d values were obtained by diluting 1—7 m*l* of 5—10% solution to about 2×10^{-3} % concentration, *i.e.*, almost infinite dilution. The values were obtained with a maximum error of ±20%.

Density Measurements. Measurement of the change in density Δd between pure solvent and PSt dilute solution was carried out by means of Cahn electromagnetic balance RG using a density cell at 25°C. The measurement is entirely similar to that reported by Elgret *et al.*[11] The apparent specific valumes v_2^* of PSt oligomers in dilute solution were found from the equation[12]

$$v_2^* = d^{-1}(1+\Delta d/c) \qquad (1)$$

where d is the density of pure solvent and c is polymer concentration. The PSt concentrations were about 2% in benzene and in toluene, and about 1% in chloroform. Reproducibility of the values of v_2^* derived from the value of Δd was within ±0.1% on an average. The densities measured were 0.87405 for benzene, 0.86273 for toluene,

1) G. V. Schulz, K. V. Guenner, and H. Gerrens, *Z. Phys. Chem. (N. F.)*, **4**, 192 (1955).
2) A. A. Tager, M. V. Tsilipotkina, A. I. Podlensnjak, and E. V. Makovskaya, International Symposium on Macromolecular Chemistry, Tokyo-Kyoto, 1966, preprints VII, p. 89.
3) U. Bianchi, C. Cuniberti, E. Pedemonte, and C. Rossi, *J. Polym. Sci., Part A-2*, **5**, 743 (1967).
4) G. V. Schulz and A. Horbach, *Z. Phys. Chem. (N. F.)*, **22**, 377 (1959).
5) H. Sotobayashi and K. Ueberreiter, *J. Polym. Sci.*, **A, 2**, 1257 (1964).
6) K. Amaya, S. Takagi, and S. Hagiwara, 2nd Calorimetry Conference, Japan (1966), p. 16.
7) G. N. Malcolm and J. S. Rowlinson, *Trans. Faraday Soc.*, **53**, 921 (1967).
8) S. Morimoto, *J. Polym. Sci., Part A-1*, **6**, 1547 (1968).
9) K. Amaya and S. Hagiwara, 2nd Calorimetry Conference, Japan (1966) p. 18.
10) S. Morimoto, 4th Calorimetry Conference, Japan (1968), p. 103.
11) K. F. Elgert and K. Camman, *Z. Anal. Chem.*, **226**, 193 (1967).
12) B. Rosen, *J. Polym. Sci.*, **17**, 559 (1955).

0.4753 for chloroform, and 0.86281 g/ml for ethylbenzene.

Other Measurements. NMR spectra were taken with a Nihon Denshi C-60 HL spectrometer using about 5% solution of the sample in $CDCl_3$. X-ray diffraction diagrams and photographs were obtained with a Rigaku Denki X-ray diffraction apparatus.

Results and Discussion

Heats of Solution. The results are given in Figs. 1 and 2. In Fig. 1, the values of ΔH^M of the low molecular weight PSt samples, subjected to the same thermal treatment in three solvents at 18 and 45°C are plotted against the molecular weights. The values of ΔH^M of ethylbenzene which can be regarded as the monomeric substance of PSt were endothermic for benzene, athermal for toluene and exothermic for chloroform. The larger exothermic change in ΔH^M suggests the larger exothermic contribution from the glass enthalpies which increase with the molecular weight of PSt. This tendency is made clear by the study of Schulz *et al.*[1] and also by the relation between the heat capacity C_p and the temperature of the

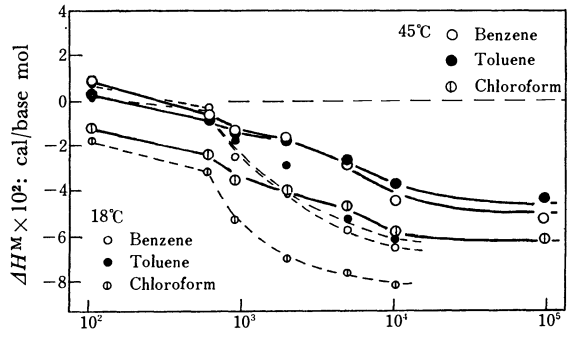

Fig. 1. Heats of mixing ΔH^M at infinite dilution of PSt samples plotted against their avg. molecular weights.

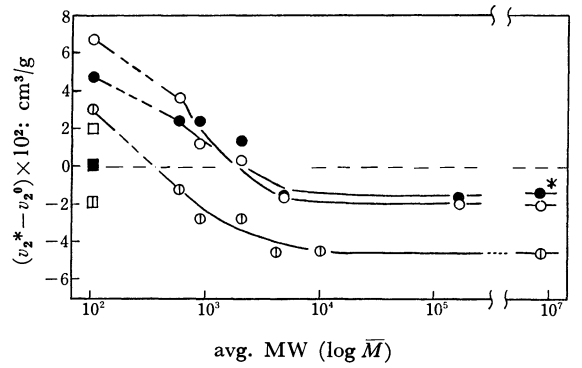

Fig. 2. Excess volume *vs.* avg. molecular weight of PSt. The values v_2^0 are those reported by Fox-Loshaek.[15] Square and asterisked marks are the calculated values from measured v_2^0 and from the reported v_2^* values,[11] respectively.

○ Benzene ● Toluene ⓘ Chloroform

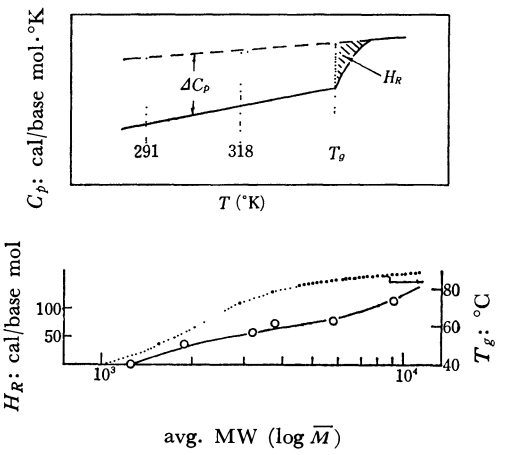

Fig. 3. Correlation of heat capacity with temperature, and the values of H_R[13] and T_g[13] *vs.* the molecular weight of PSt.

glass transition of PSt as shown in Fig. 3. The relation between the glass enthalpy and the heat of mixing ΔH_l^M of liquid polymer at infinite dilution is given by

$$\Delta H^M = \Delta H_l^M - \Delta H_g^M \tag{2}$$

$$\Delta H_g^M = \int_T^{T_g} \Delta C_p \, dT + H_R \,, \tag{3}$$

where $-\Delta H_g^M$ is the contribution due to glass enthalpy, T temperature, T_g glass temperature, ΔC_p the difference in C_p between glass polymer and liquid polymer to be assumed at the same temperature as shown in Fig. 3, H_R the rest enthalpy arising from the transition which takes place slowly from the glassy state to liquid phase, and shown as the shaded portion in Fig. 3. This relation can be used to estimate the contributions either of ΔH_l^M or ΔH_g^M to the ΔH^M values. Another approach to the estimation of the value of ΔH^M is from the apparent specific volume of the PSt in dilute solution. Horth *et al.*[14] found that the difference between v_2^* and the specific volume v_2^0 of the pure liquid polymer is approximately proportional to the ΔH_l^M, *viz.*,

$$v_2^* - v_2^0 = \beta \boldsymbol{R} T \kappa_1 v_2^0 \varphi_1 / V_1 (1+\alpha T)$$
$$= [\beta/(1+\alpha T)] \Delta H_l^M / M_0 \,, \tag{4}$$

where α and β are the coefficients of thermal expansion and the compressibility of the solution, φ_1 and V_1 the volume fraction and the molar volume of the solvent, $\boldsymbol{R}$ gas constant, κ_1 Flory's enthalpy parameter, and M_0 the molecular weight of the repeating unit of the polymer. Using the empirical v-T-M equation,[15] we obtained a relative relation between v_2^*-v_2^0 and $\overline{M}$ for the oligomers as shown in Fig. 2. Although not presented here, a similar figure is obtained using the other v-T-M relation.[16] The specific volume v_2^0 of ethylbenzene measured was 1.15900 which was used for the calculation. In the high molecular weight

13) E. Jenckel and K. Ueberreiter, *Z. Phys. Chem., Abt.* **A182**, 36 (1938).

14) A. Horth, D. Patterson, and M. Rinfret, *J. Polym. Sci.*, **39**, 189 (1959).

15) T. G. Fox and S. Loshaek, *ibid.*, **15**, 371 (1955).

16) T. G. Fox and P. J. Flory, *J. Appl. Phys.*, **21**, 581 (1950).

region, the partial specific volume of PSt is almost constant and has been reported[11] to be 0.911 in benzene and 0.917 in toluene solution. These values agree fairly well with our results, 0.911 and 0.914, respectively, obtained as the apparent specific volumes v_2*. Calculated values $(1+\alpha T)/\beta$ were 316 for benzene, 330 for toluene, and 363 cal/cm^3 for chloroform system by using the values[17] of pure solvents instead of the solutions for α and β. These values are almost the same for the three solvent systems. It is understood that the behavior shown in Fig. 2 is consistent with the one obtained from direct calorimetric measurements.

In Figs. 1 and 2, the values ΔH_l^M for all solvent systems show a similar tendency for the change of molecular weight. However, the tendency slightly differed with the characteristics of the solvents. In the case of monomeric solute-ethylbenzene, ΔH^M of toluene system showed lower values than those of other systems. However, this relation was reversed when the molecular weight increased. This reversal was observed in the molecular weight region between 10^3 and 10^4, which shifted lower when the temperature was lowered.

The value of ΔH_l^M in PSt ($\overline{M}$: 3,980)-toluene system at 25°C has been obtained as 60 cal/base mol from the ΔH_l^M and C_p measurements by Schulz.[1] According to this scheme, the ΔH_l^M at the higher molecular weight region in benzene and chloroform systems should be constant, *i.e.*, about −100 and −300 cal/base mol for benzene and chloroform systems respectively. This exothermic effect in benzene or chloroform system is attributable to the interactions between the solvent molecules and the phenyl components in PSt molecules, although the slightly exothermic factor can not be ignored when the solute chain length increases.[5,18] The interaction between the solvent and the constituent of polymer molecule is introduced to interpreted ΔH_l^M qualitatively.[5,18,19] The values of ΔH^M of benzene and *n*-heptane both with chloroform were directly measured and the values −398 and 719 cal/mol were obtained, respectively. A considerably large exothermic value of ΔH^M in the chloroform system, as compared with PSt-benzene system, reflects the interactions between the chloroform and the phenyl group in PSt molecule.

A characteristic feature throughout this experiment is that the difference of the glass energies at different temperatures can be estimated from the measurements. In Fig. 4, the difference of the measured ΔH^M values at 18°C and 45°C are plotted against the molecular weight of PSt, although the temperature dependence of ΔH_l^M values are not completely negligible. The differences in the ΔH^M values thus obtained in this molecular weight region were somewhat scattered, but the large difference of glass energies is evident in the range $\overline{M}=10^3$—10^4. The magnitude of the difference in glass energy, when compared for a constant difference in temperature, corresponds to the mean values of ΔC_p between the measured temperatures

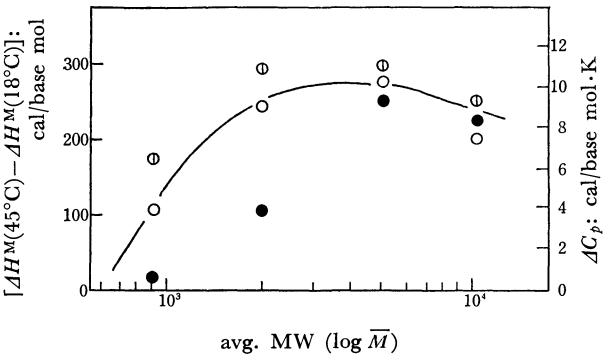

Fig. 4. The difference of glass energies between two measured temperatures and concluded ΔC_p value plotted against the avg. molecular weight of PSt.
○ Benzene ● Toluene ⓘ Chloroform

as shown in Fig. 4. The ΔC_p, or more exactly the ΔC_v at constant volume (generally at T_g), is the contribution of the conformational change of the polymer chains between the rubber and glassy states to the value of C_p, and is called conformational heat capacity.[20] Conversion of ΔC_p to ΔC_v might clarify this behavior, but the constants in the low molecular weight region have not been obtained. In connection with the movement of molecular chains,[21] the larger ΔC_p values may be explained as caused by the increase of the molecular cohesion in the glass of this molecular weight region or by the larger mobility of shorter chains in the liquid state, even though the cohesion might be independent of molecular weight. The sudden increase and the partially higher ΔC_p values were observed in the PSt oligomer region. The ΔC_p value of the higher molecular weight PSt agreed well with the reported value 0.09 cal/g. K[1,3] in this region.

Heats of Dilution. Measurement of the heats of dilution in the three solvent systems was performed at 25°C by diluting about 5 m*l* solution of the concentration 5—10% to infinite dilution for the toluene and the benzene systems and by diluting about 1 m*l* solution of the concentration 10% to infinite for the chloroform system. In order to obtain the differential heat $\Delta\overline{H}_1$ of dilution per mol solvent and the enthalpy term $B_H(=\boldsymbol{R}TA_{2,H})$ of the second virial coefficient $B(=\boldsymbol{R}TA_2)$ from the heats of dilution ΔH_d measured, the following equations were used.[4,22]

$$B_H = (\Delta H_d/w_2)/(c_e-c_a) \quad (5)$$

$$B_H = \boldsymbol{R}TA_{2,H} = -\Delta\overline{H}_1/\overline{V}_1c^2 \quad (6)$$

where A_2 and $A_{2,H}$ are the second virial coefficient and the enthalpy term of A_2, w_2 the weight of the solute to be diluted, c_a and c_e the initial and the final concentration of the solution. The value of B_H was found to depend on the concentration[4,23] and molecular weight,[24] but the dependence was neglected here for the sake of simplicity. The results are given in Fig. 5.

17) "International Critical Tables," McGraw-Hill, New York (1933), **3**, pp. 27, 35.
18) H. Sotobayashi, *Makromol. Chem.*, **123**, 157 (1969).
19) W. Bruns, F. Mehdorn, K. Mirus, and K. Ueberreiter, *Kolloid-Z. Z. Polym.*, **224**, 17 (1968).
20) B. Wunderlich, *J. Chem. Phys.*, **37**, 2429 (1962).
21) A. J. Kovacs, *Fortschr. Hochpolym. Forsh.*, **3**, 394 (1964).
22) G. V. Schulz and H. Doll, *Z. Electrochem.*, **56**, 248 (1952).
23) A. Kagemoto, S. Murakami, and R. Fujishiro, This Bulletin, **39**, 15 (1966).
24) A. Kagemoto, S. Murakami, and R. Fujishiro, *ibid.*, **40**, 11 (1967).

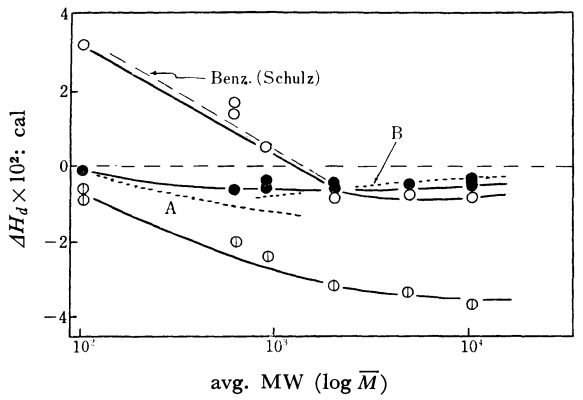

Fig. 5. Heat of dilution *vs.* molecular weight of PSt. Dotted lines A and B are shown for the values from Eqs. (7) and (8), respectively.
○ Benzene ● Toluene ⓘ Chloroform.

The values of ΔH_d were calculated from the B values according to the above equations, assuming that the c_a and $(c_a - c_e)$ are both 7.0×10^{-2} g/cm^3. The ΔH_d value corresponds to the heat arising from the dilution of 5 m*l* solution from 7% to infinite dilution. In Fig. 5, the molecular weight dependence is similar to that of ΔH_l^M at infinite dilution obtained from the heat of solution.

A characteristic feature of this experiment is the behavior of the toluene system which can be considered as an athermal solution. Theories of the second virial coefficient A_2^{ath} for athermal solutions have been given by several authors. From the equation derived by Schulz for A_2^{ath}[25] and by Schulz, Inagaki, and Kirste[26] for the relation between A_2 and $A_{2,H}$, the following equations are derived approximately for the value of B_H^{ath}.

$$B_H^{ath} = \boldsymbol{R}T^2\alpha\bar{v}_2(\pi^3 a^3 \boldsymbol{N}_A)^{1/2}/M_0(4^3 M_0\bar{v}_2)^{1/2} \quad (7)$$

$$B_H^{ath} = \boldsymbol{R}T^2\alpha\bar{v}_2(\pi^3 a^3 \boldsymbol{N}_A)^{1/2}/M_0(4^3 M_0\bar{v}_2)^{1/2}h(z)\,, \quad (8)$$

where α is the thermal expansion coefficient of the solution, $\bar{v}_2$ the partial specific volume of PSt, a the length of monomer unit, $\boldsymbol{N}_A$ the Avogadro number. With regard to the flexibility of polymer molecules, Schulz, Baumann, and Darskus[27] tried to combine the effect of coiling of long chain molecules. Miltiplying $A_{2,H}^{ath}$ by function $h(z)$ derived by Casassa,[28] they obtained good agreement with the experimental A_2 of athermal high polymer solutions. Equation (8) was thus derived and its applicability was examined. As seen in Fig. 5, our results show good agreement with the calculated values and the theory expresses the molecular weight dependence of the heat of dilution fairly well. Definite changes in the solution properties of the oligomers ($\overline{M}$: 10^3—10^4) have been observed by the measurements of the second virial coefficient,[5] the intrinsic viscosity,[29] and the partial specific compressibility.[30] The behavior can be explained as due to the flexibility of molecular chains in the solution (*i.e.*, rigid nature of the short chain molecule). This effect was observed in the direct measurement at the molecular weights between 10^3 and 10^4.

The enthalpy parameters χ_H and the $z\Delta w/\boldsymbol{k}T$ values[31] both involved in the Van Laar equation were calculated as a function of the molecular weight as shown in Fig. 6.

$$\chi_H = \overline{\Delta H}_1/\boldsymbol{R}T\varphi_2^2 \quad (9)$$

$$\chi_H = (\bar{V}_1/\bar{V}_2)z\Delta w/\boldsymbol{k}T\,, \quad (10)$$

Where φ_2 is the volume fraction of the solute PSt, z the coordination number, Δw the interchange energy, $\boldsymbol{k}$ the Bolzmann constant, $\bar{V}_2$ the partial molar volume of PSt. The $z\Delta w/\boldsymbol{k}T$ values of the benzene system for the higher molecular weight PSt ($\overline{M} \geqq 3000$) coincide with those for the toluene system. The comparatively higher χ_H values were observed in the low oligomer region as shown in Figs. 5 and 6. The con-

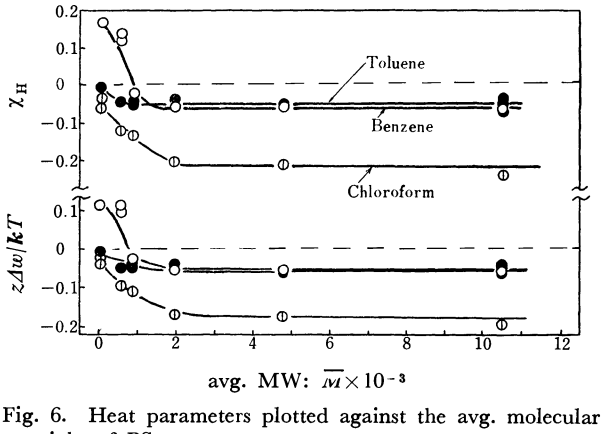

Fig. 6. Heat parameters plotted against the avg. molecular weight of PSt.

centration dependence of the enthalpy parameter was calculated on the basis of the quasi-chemical approximation for polymer solutions,[32,33]

$$\chi_H \equiv -T\left(\frac{\partial\chi_1}{\partial T}\right)$$
$$= [4\theta^2\Delta w(1-\theta)/\beta\varphi_2^2\boldsymbol{k}T(\beta+1-2\theta)(\beta+1)]$$
$$\times \exp(2\Delta w/z\boldsymbol{k}T) \quad (11)$$
$$\theta = \varphi_2(z-2)/(z-2\varphi_2)$$
$$\beta^2 = 1 + 4\theta(1-\theta)[\exp(2\Delta w/z\boldsymbol{k}T) - 1]\,.$$

The concentration dependence of the enthalpy parameter in the three solvent systems is shown in Fig. 7. The parameters χ_H were calculated on the basis of the $z\Delta w/\boldsymbol{k}T$ values, Eq. (11), and the ΔH_l^M values were obtained from Eq. (9) at $\varphi_2 = 1$ and the following

25) G. V. Schulz, *Z. Naturforsch.*, *A*, **2**, 27 (1947).
26) G. V. Schulz, H. Inagaki, and R. Kirste, *Z. Phys. Chem. (N. F.)*, **24**, 390 (1960).
27) G. V. Schulz, H. Baumann, and R. Darskus, *ibid.*, **70**, 3647 (1966).
28) E. F. Casassa, *J. Chem. Phys.*, **31**, 800 (1959).
29) U. Bianchi and A. Peterlin, *J. Polym. Sci., Part A-2*, 1759 (1968).
30) Y. Nomura and Y. Miyahara, *Nippon Kagaku Zasshi*, **89**, 142 (1968).
31) H. Tompa, "Polymer Solutions," Butterworths, London (1956), Chapt. III.
32) W. J. C. Orr, *Trans. Faraday Soc.*, **40**, 320 (1944).
33) C. Booth, G. Gee, G. Holden, and G. R. Williamson, *Polymer*, **5**, 343 (1964).

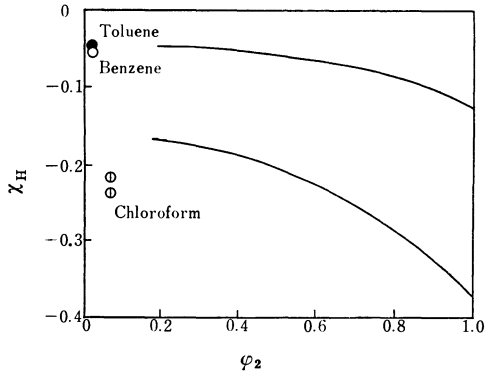

Fig. 7. Concentration dependences of the values of χ_H calculated on the basis of the quasi-chemical approximation. The avg. MW of PSt in toluene and in benzene are both 10500 and those in chloroform are 4800 and 10500.

equation which is expressed by the Van Laar equation.[31]

$$\Delta H_l^M \simeq (\bar{V}_2/\bar{V}_1)RT\chi_H \quad (12)$$

The ΔH_l^M values were −60, −80, and −300 cal/base mol for toluene, benzene, and chloroform solvent systems, respectively, and agreed well with the ΔH_l^M obtained from the direct measurements of the ΔH^M in the glassy PSt-solvent systems. From the results, the glass enthalpies of the higher molecular weight PSt can be calculated to be about 300 cal at 45°C and about 600 cal/base mol at 18°C.

An Order formation in the Oligomer Liquid. In examining the molecular weight dependence of ΔH^M and $\overline{\Delta H_1}$, we came across some problems concerning the behavior of low oligomers, in particular, the oligomer liquid ($\bar{M}$: 600, T_g: −18——20°C). First, the integral heat of dilution ΔH_d of the benzene solution at 25°C has a larger positive value than that reported.[4] Secondly, the heat of mixing ΔH^M at infinite dilution in the system, on the contrary, is exothermic, *i.e.*, of negative value. This suggested some questions on the chemical composition and ordering structures of the PSt oligomer sample.

The NMR spectrum of the oligomer showed the existence of long alkyl group, possibly *n*-butyl group, to the end as expected from the method of polymerization.[34] The NMR spectra of PSt and the oligomer are shown in Fig. 8. From the integral curves given by the dotted lines, the ratios of the number of protons from the phenyl groups of PSt molecule at the lower magnetic field to that from the methylene and methyne group at the higher field were compared. The ratio of 5 to 3 which is equal to the theoretical value was obtained for the high molecular weight PSt sample of the $\bar{M}$: 10500. For the oligomer sample, the ratio was 1 to 1. This shows that the oligomer molecule has an additional alkyl group, *i.e.* the *n*-butyl end group. Taking this fact into account, we can explain the larger heat of dilution by the endothermic interactions with solvent benzene.

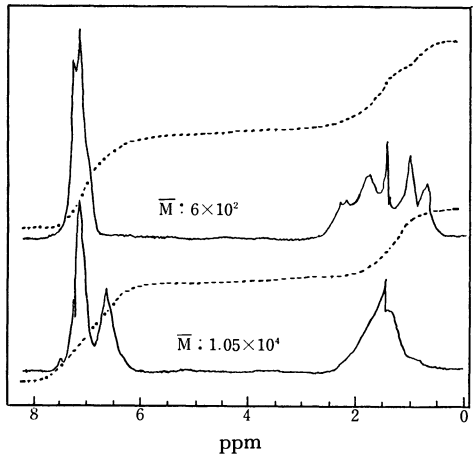

Fig. 8. NMR spectra of PSt and it's oligomer: dotted lines are the integral curves.

In order to check the possible existence of some ordered structure in the oligomer liquid, X-ray diffraction analysis was carried out at room temperature. The results are shown in Figs. 9 and 10. The diffracted amorphous halo of which 2θ is about 5° was found from both the X-ray diffraction intensity curve and photograph. On the other hand, the amorphous haloes ($2\theta \approx 10°$ and 20°) have been observed for the atactic PSt glass. The period calculated according to the Bragg equation was 17 Å, almost equal to the extended molecular chain length.

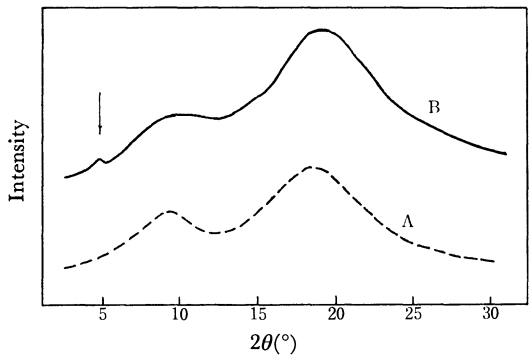

Fig. 9. X-Ray (CuKα_1) diffraction diagrams of PSt glass (A) and its oligomer ($\bar{M}$: 600) liquid (B).

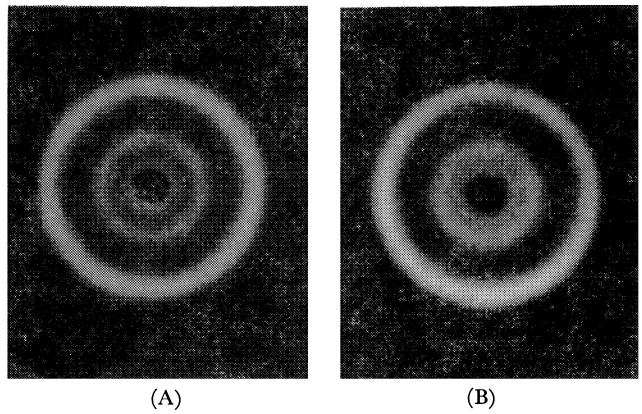

(A) (B)

Fig. 10. X-Ray (CuKα_1) diffraction photographs of PSt glass (A) and its oligomer ($\bar{M}$: 600) liquid (B).

34) T. Altares, Jr., D. P. Wyman, and V. R. Allen, *J. Polymer Sci., Ser. A*, **2**, 4533 (1964).

Such extended chain molecules which have a lower intramolecular energy than the coiled one, should bring an endothermic contribution to ΔH^M. This contribution is contrary to our result. Thus some exothermic contributions corresponding to the state of higher energy such as glass should be considered even in liquid state. If not, some strong rotational restriction of the side phenyl group in the ordered molecules is attributable to the endothermic effect. It has not been made clear, however, how such arrangements of chain molecules in general contribute thermally to the ΔH^M when dissolved. However, results suggest the existence of a smectic phase of short and rigid PSt oligomer molecules which are arranged parallel to each other in the liquid state. An exothermic contribution to ΔH^M was found in this oligomer liquid.

The author is indebted to Professor Ryoichi Fujishiro of Osaka City University, Dr. Kazuo Amaya of Government Chemical and Industrial Research Institute of Tokyo, and Dr. Hisashi Uedaira of this Institute for their valuable advice and encouragement.

BULLETIN OF THE CHEMICAL SOCIETY OF JAPAN, VOL. 44, 884—887 (1971)

An Interpretation of Mass Spectra of Disubstituted Benzenes by Simple LCAO MO Calculation. I

Susumu TAJIMA, Nobuhide WASADA, and Toshikazu TSUCHIYA

Government Chemical Industrial Research Institute, Tokyo, Honmachi, Shibuya-ku, Tokyo

(Received April 13, 1970)

A part of the mass spectra for derivatives of aniline and anisole was interpreted using the results of MO calculation. Compounds studied were: aniline derivatives: *o*-, *m*-, and *p*-compounds of anisidine, aminophenol, chloroaniline, nitroaniline, aminobenzoic acid, and aminoacetophenone; and anisole derivatives: *o*-, *m*-, and *p*-compounds of anisidine, methoxyphenol, chloroanisole, nitroanisole, methoxybenzoic acid, and methoxybenzaldehyde. The intensities of certain fragment ions in the mass spectra of these compounds were compared with the results of simple LCAO MO calculation for these compounds. A simple relation was found between the intensity and the partial bond order for a frontier electron of the bond ruptured.

Other than the well known quasi-equilibrium theory[1] (Q.E.T.), a method for theoretical interpretation of mass spectra of larger organic compounds has been reported by Hirota *et al.*[2,3] In this method, it is assumed that the scission probability of each of the skeletal bonds of the parent ion is proportional to the positive charge density of the highest occupied molecular orbital localized at the bond. Though the method has been applied successfully to paraffins[2] including cycloparaffins,[3] the basis for the interpretation has not yet been scrutinized as thoroughly as has been done for Q.E.T. The fundamental idea of Q.E.T. is generally accepted now, and the mass spectra of various aliphatic compounds[4-7] have been interpreted by the theory. The calculations involved, however, are rather tedious even for such a simple compound as propane. Nounou[8] has applied Q.E.T. to large aromatic compounds and successfully interpreted the mass spectra of substituted phenanthrenes. Recently, Dougherty[9] reported an interpretation of the decomposition of parent ions caused by electron impact with the perturbation MO method. Difference of mass spectra between aromatic isomers has been elucidated by Tatematsu *et al.*[10] on the basis of the difference of radical electron density, calculated by simple LCAO MO method, on the atoms in the isomers.

The purpose of the present paper is to find an approach to interpret the mass spectra of some aromatic compounds and to clarify the fragmentation mechanism by the results of simple LCAO MO calculation. In the procedure, various factors such as electron density, bond order *etc.* have been calculated by the method on a series of disubstituted benzenes and were compared with the intensity of certain fragment ions in their mass spectra.

Experimental

Mass spectra were obtained with a CEC 21—103C mass spectrometer. Conditions of measurement were: magnetic field, 4100 gauss; ion accelerating voltage, 3500—500 V; electron accelerating voltage, 70 eV; trap current, 10 μA; temperature of ion source, 250°C; temperature of sample manifold, 125—130°C.

The following derivatives of aniline and anisole were investigated: Aniline derivatives—*o*-, *m*-, and *p*-compounds

1) H. M. Rosenstock, M. B. Wallenstein, A. L. Wahrhaftig, and H. Eyring, *Proc. Natl. Acad. Sci. U.S.*, **38**. 667 (1952).
2) K. Fueki and K. Hirota, *Nippon Kagaku Zasshi*, **81**, 212 (1960).
3) K. Hirota and Y. Niwa, *Tetrahedron Lett.*, **1966**, 5757.
4) H. M. Rosenstock, Doctorial Dissertation, *Univ. of Utah. Salt Lake City*, 1952.
5) L. Friedman, F. A. Long, and M. Wolfsberg, *J. Chem. Phys.*, **27**, 613 (1957).
6) A. B. King and F. A. Long, *ibid.*, **29**, 374 (1958).
7) F. W. Lampe and F. H. Field, *J. Amer. Chem. Soc.*, **81**, 3238 (1959).
8) P. Nounou, *Advan. Mass Spectrometry*, No. 4, 551 (1967).
9) R. C. Dougherty, *J. Amer. Chem. Soc.*, **90**, 5780 (1968).
10) H. Nakata and A. Tatematsu, *Tetrahedron Lett.*, **1969**, 4303.

of anisidine, aminophenol, chloroaniline, nitroaniline, aminobenzoic acid, and aminoacetophenone; Anisole derivatives—*o*-, *m*-, and *p*-compounds of anisidine, methoxyphenol, chloroanisole, nitroanisole, methoxybenzoic acid, and methoxybenzaldehyde. The compounds were guaranteed reagents. obtained from Tokyo Kasei Co., Ltd., and were used without further purification.

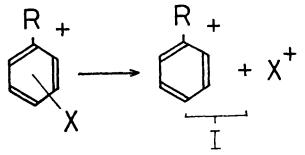

Fig. 1. Fragment ions investigated.

In Fig. 1, R denotes the common substituent, NH_2 or OCH_3, in the derivatives of aniline or anisole, respectively, and X denotes the other substituent, such as Cl, NO_2 *etc.* The summation of the intensity of ions shown in the right side of Fig. 1, *i.e.*, the ions inferred to be produced directly by a rupture of the bond between the aromatic moiety and the substituent X, was investigated. *I* desotes the summation of intensity of the ions mentioned above, normalized by the total ion intensity of the compound, *i.e.*, for aniline derivatives, *I* desotes the normalized ion intensity of $C_6H_4NH_2^+$ (*m/e* 92) plus X^+, and for anisole derivatives, *I* denotes that of $C_6H_4OCH_3^+$ (*m/e* 107) plus X^+. As shall be described, a simple correlation was found to be valid between log *I* and the partial bond order P^h for the frontier electron of the bond mentioned above.

Table 1. Partial bond order (P^h) of frontier electron

Aniline derivatives X	P^h *o*-	P^h *m*-	P^h *p*-
OCH_3	−0.136	−0.017	−0.134
OH	−0.126	−0.012	−0.126
Cl	−0.043	−0.002	−0.046
COOH	0.020	0.001	0.023
NO_2	0.024	0.001	0.028
$COCH_3$	0.037	0.001	0.046
Anisole derivatives X	P^h *o*-	P^h *m*-	P^h *p*-
NH_2	−0.154	−0.107	−0.151
OH	−0.146	−0.049	−0.143
Cl	−0.049	−0.002	−0.054
COOH	0.017	0.001	0.020
NO_2	0.021	0.001	0.026
CHO	0.035	0.002	0.045

A FACOM 270—30 computer was used for calculation. The parameters used in the calculation were quoted from the accepted values in the literature[11,12]. The results are shown in Table 1, where P^h is the partial bond order for a frontier electron of the bond between the substituent X and the aromatic moiety containing amino or methoxy group.

11) L. E. Orgel, T. L. Cottrel, W. Dick, and L. E. Sutton, *Trans. Faraday Soc.*, **47**, 113 (1951).
12) H. H. Jaffé, *J. Chem. Phys.*, **20**, 279 (1952).

Results and Discussion

Correlation between the ion intensity *I*, described above, and various calculated quantities, such as electron density, free valence, and bond order for the molecules, were scrutinized. As a consequence of the investigation, a simple relation was found to be valid between the partial bond order P^h (shown in Table 1) for a frontier electron of the bond ruptured and log *I*. In Figs. 2, 3, and 4, log *I versus* P^h relation for each of *o*-, *m*-, and *p*-aniline derivatives, respectively, is plotted. The same plot for anisole derivatives is shown

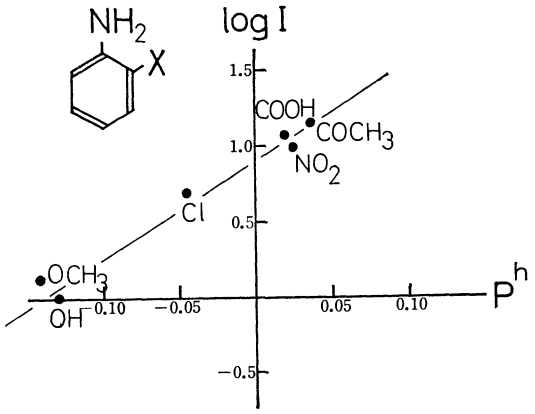

Fig. 2. log *I versus* partial bond order of the frontier electron for *o*-aniline derivatives.

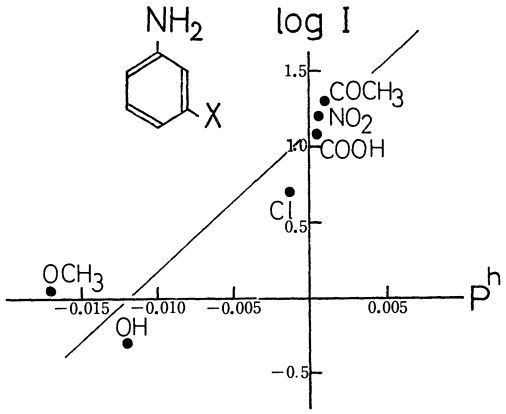

Fig. 3. log *I versus* partial bond order of the frontier electron for *m*-aniline derivatives.

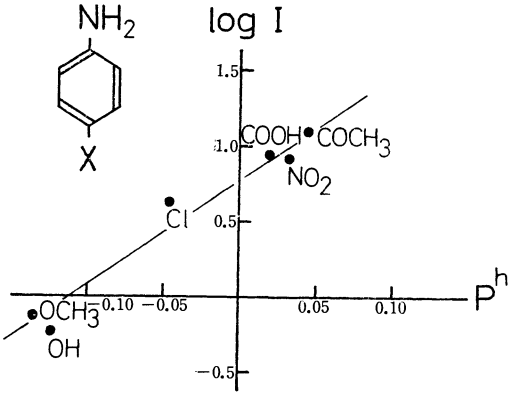

Fig. 4. log *I versus* partial bond order of the frontier electron for *p*-aniline derivatives.

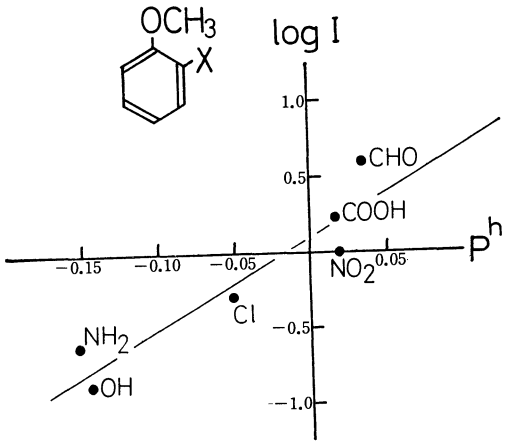

Fig. 5. log I *versus* partial bond order of the frontier electron for *o*-anisole derivatives.

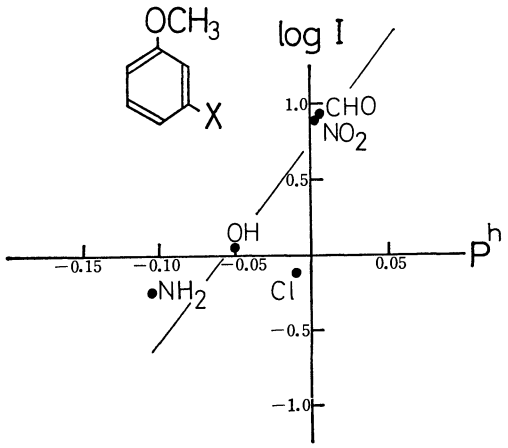

Fig. 6. log I *versus* partial bond order of the frontier electron for *m*-anisole derivatives.

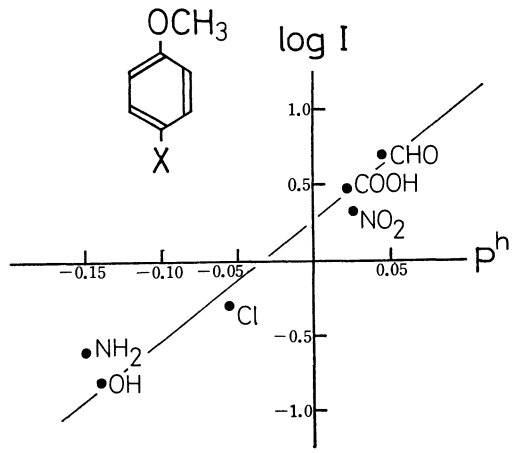

Fig. 7. log I *versus* partial bond order of the frontier electron for *p*-anisole derivatives.

in Figs. 5, 6, and 7.

Almost every compound studied exhibited a metastable peak corresponding to decomposition of M^+ into the aromatic moiety of interest, *i.e.*, into $C_6H_4NH_2^+$ for aniline derivatives, and $C_6H_4OCH_3^+$ for anisole derivatives, suggesting that at least a part of the process proceeds according to Q.E.T. mechanism. The implication is that the half life of parent ions is about 10^{-5} sec. The life time of an ion in its excited states is considered to be nearly 10^{-8} sec[13,14]. A molecular ion in its excited states does not decompose immediately after it is produced by electron impact, but rather undergoes many vibrations. During these vibrations there is a high probability of radiationless transitions among the many potential surfaces for the molecular ion, and the ion falls into its ground state or its low lying electronic states before it eventually decomposes.[1]

A linear relation was found between the vertical ionization potential measured by electron impact and H.M.O. coefficient of π-electron obtained by simple LCAO MO calculation for anisidines and chloroanilines. From the results it has been inferred that the first three ionizations of these compounds correspond to removal of a π-electron.[15] Similar conclusion has been obtained for other compounds under consideration in the present study.[16] Thus it is legitimately assumed that the low lying electronic states for the molecular ions in the present investigation are those produced by loss of a π-electron.

In view of the results so far achieved, the experimental results of the present study can be explained by Q.E.T. mechanism as follows. According to the theory, the excited molecular ion produced by electron impact does not decompose immediately into the various fragment ions, but the excited molecular ion falls into its ground or low lying electronic states by radiationless transition in less than 10^{-8} sec. Then the molecular ion decomposes by unimolecular decomposition into fragment ions mentioned above, *i.e.*, $C_6H_4NH_2^+$ and X^+ in the case of aniline derivatives or $C_6H_4OCH_3^+$ and X^+ in the case of anisole derivatives. If these fragment ions are produced from the molecular ion in its electronic ground state, as is assumed in Q.E.T., close correlation would be expected between some of the characteristic quantities of the molecular ion in its electronic ground state and the ion intensity of fragment ions inferred to be produced from the ion. A molecular ion in its electronic ground state is produced when a frontier electron is lost by the molecule. Figures 2—7 illustrate simple relations between the partial bond order for the frontier electron and the summation of the intensity of the fragment ions concerning the bond, normalized by the total ion intensity, and show considerable parts of the fragment ions referred are produced by this mechanism.

In simple LCAO MO calculation, the following expression is derived for the energy E_i of the ith molecular orbital,[17]

$$E_i = \alpha + 2\sum P_j^i \beta$$

where P_j^i is the partial bond order of an electron in the

13) H. Sponer, *Radiat. Res., Suppl.* **1**, 558 (1959).
14) M. A. Linotengarten, *Bull. Acad. Sci. USSR, Phys. Ser.*, **24**, 1050 (1960).
15) S. Tajima, N. Wasada, and T. Tsuchiya, *Tetrahedron Lett.*, **1970**, 139.
16) S. Tajima, N. Wasada, and T. Tsuchiya, to be published elsewhere.
17) C. A. Coulson and H. C. Longuet-Higgins, *Proc. Roy. Soc.*, **A191**, 39 (1947).

ith MO for the jth bond, α is the Coulomb integral and β is the resonance integral, respectively. One can see that the larger the value of P_j^i for an electron is, the more the electron contributes to the stabilization of the bond. When a molecular ion M^+ in its ground state decomposes into the fragment ions mentioned above by unimolecular decomposition, the larger the partial bond order between the aromatic moiety and the substituent X of the frontier electron removed from the molecule is, the more the strength of the bond decreases by the removal of the electron and the more easily the bond ruptures. The results shown in Figs. 2—7 can be explained qualitatively by the rationalization.

We have not considered on ortho effect in our calculation. If there are appreciable ortho effects, the points in Figs. 2 and 5 will not lie close to a straight line, because the ortho effects may be different as the substituents differ.

For m-compounds for aniline derivatives, the partial bond order for the frontier electron in the bond under consideration is very small (Table 1), and the influence of the loss of a frontier electron on the bond strength is considered to be very small, though a trend similar to Figs. 2 and 4 manifests itself as is seen in Fig. 3. For m-compounds, when log I is compared with the partial bond order for the second highest occupied molecular orbital P' instead of that for the highest occupied molecular orbital, a relation similar to Fig. 2 and Fig. 4 is obtained as is shown in Fig. 8, except for chloroaniline. From the result, the molecular ions in the state which corresponds to the loss of an electron in the second highest occupied orbital appear to be mainly responsible for the rupture of the bond under consideration in this case. For o-, p-compounds for

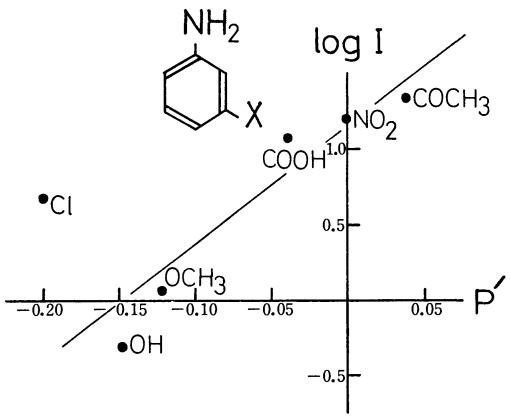

Fig. 8. log I *versus* partial bond order of an electron in the second highest occupied molecular orbital for m-aniline derivatives.

aniline derivatives, the partial bond order of the bond for the second highest occupied orbital is very small. For meta anisole derivatives, however, the loss of a frontier electron from the bond under consideration seems to decrease the stability of the bond more effectively than for meta aniline derivatives, since the partial bond order of the frontier electron in the m-compounds are larger for anisole derivatives than for aniline derivatives, as is seen in Table 1.

Studies on more numerous compounds are desirable, and a quantitative rationalization of the current phenomena and explanation for the abnormal behavior of m-chloroaniline, *etc.* deserve further investigation.

The authors wish to thank Dr. Akira Kuboyama of this Institute for his valuable discussions.

Purity Determination of Organic Compounds by a Newly Designed DTA Apparatus[1)]

Yo-ichiro MASHIKO, Takako SHINODA, and Hisae ENOKIDO*

Government Chemical Industrial Research Institute, Tokyo, Shibuya-ku, Tokyo

(Received May 21, 1970)

An apparatus of differential thermal analysis has been designed and constructed for the purpose of determining the purity of organic compounds with as small an amount of sample as possible, within a short time and yet with an accuracy of better than ±0.001 mol%. Degussa platinum thermometers were used. They were calibrated with a precision of better than ±0.004° against a standard platinum resistance thermometer. Methods for determining the impurities in samples on the basis of irreversible thermodynamics have been developed. The results were compared with those obtained by using an adiabatic calorimeter of our laboratory and by the National Bureau of Standards. The apparatus proved to be useful in determining the purity of about 1 m*l* of samples, whose melting points lie in the temperature range −200°C—+200°C within an accuracy of ±0.004 mol% in about 1.5 hr.

Differential thermal analysis (DTA) is widely used as a dynamic method of thermal analysis in various fields. However, in order to apply it to purity determination, the apparatus and procedure should be designed taking the following facts into consideration.

The accuracy of evaluation of impurities in the sample is dependent upon the precision of the thermometer. Thermocouples are used for DTA measurements, but it is difficult to calibrate them with a precision better than ±0.01°. In the DTA apparatus reported here, platinum thermometers calibrated against a standard platinum thermometer were employed. The temperature of the sample and the temperature difference between the sample and reference substance were recorded simultaneously as functions of time.

The DTA method is a dynamic one and the observed temperature is not measured at equilibrium. It is necessary therefore to analyze the resulting curves on the basis of irreversible thermodynamics instead of reversible thermodynamics.

Before testing the DTA apparatus with the NBS Standard Sample 217b 2,2,4-trimethylpentane, a comparison of the purity obtained by the NBS and that by our adiabatic calorimeter[2)] was made.

An extrapolation method as well as comparative methods for purity determination by the DTA measurements were developed.

Experimental

Apparatus. An apparatus was constructed to obtain DTA and total thermal analysis (TTA) curves simultaneously at temperatures from −200°C to 200°C. The cryostat of the apparatus was so designed that the amount of the sample can be as small as possible. The general assembly is illustrated in Fig. 1. A copper block A with two holes drilled symmetrically with respect to the center, is hung inside jacket E by means of three constantan cords. A heating wire is wound around A. In operation, the cryostat is sealed at the top plate F with Wood's metal or solder and mounted in a glass Dewar vessel containing coolant. All electric lead wires (#38 copper) come from the top of the cryostat through a stainless steel pipe at the center and are connected at the terminal D. They are then wound around A so as to secure good thermal contact. The inside of E is evacuated, and the cooling and heating rates are controlled by adjusting the amount of helium gas in it.

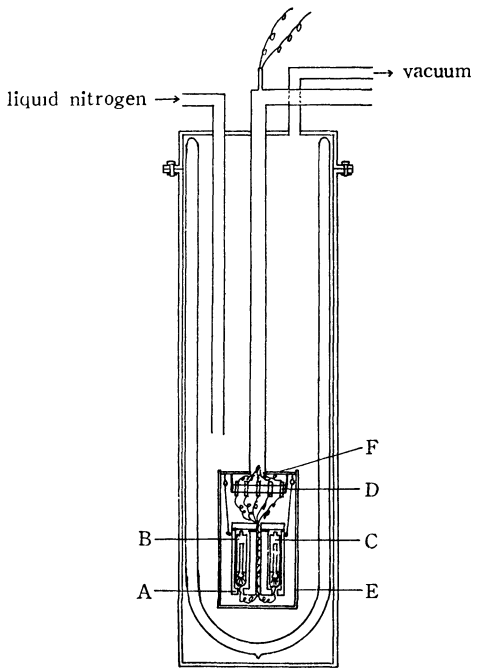

Fig. 1. Cross-section of the cryostat.
(A) copper block; (B) sample cell; (C) reference cell; (D) terminal of lead wires; (E) jacket; (F) top plate of the container

The details of sample or reference cell are shown in Fig. 2. Cell a is made of silver-plated copper (0.2 mm thick) with internal volume about 1 m*l*. Four vanes are soldered to the inside wall of the cell. The cap of the cell has a copper capillary tube c through which the inside can be evacuated. The platinum thermometer b is cast into a re-entrant well of the cell with indium alloy. Sample and reference cells, to which are attached silver-plated copper sheaths d, are set in the holes of A.

Since the cells are too small to fit standard platinum thermo-

1) Presented before the 5th Japanese Calorimetry Conference, Osaka, November, 1969.

* Present address: Tokyo Kasei Kogyo Co., Ltd., 6-Chome, Toshima, Kita-ku, Tokyo, Japan.

2) T. Shinoda, H. Enokido, Y. Maeda, and Y. Mashiko, *unpublished.*

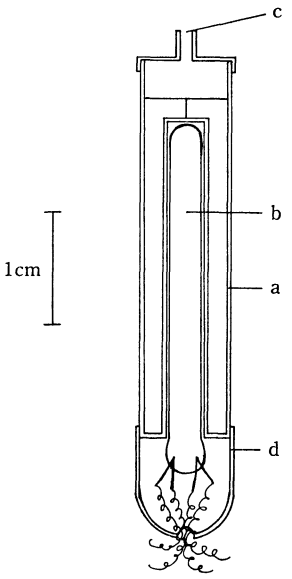

Fig. 2. Cross-section diagram of sample or reference cell.
(a) vessel of sample or reference substance
(b) Degussa platium thermometer
(c) copper capillary tube
(d) sheath

meters, small platinum-in-glass thermometers (Degussa-Hanau Model P4) are employed. The Degussa thermometer was originally supplied with two nickel lead wires. It was modified by fixing four platinum lead wires instead of two nickel wires. The thermometers were then calibrated against a Leeds & Northrup platinum thermometer certified by the National Bureau of Standards. For the intercomparison of resistance values, two kinds of thermometers were cast with indium alloy into three re-entrant wells drilled in a copper block. The copper block was placed within an adiabatic shield of the adiabatic calorimeter assembly.[2] Some 50 comparisons of each Degussa thermometer with the standard thermometer were made in the temperature range from −180°C to 70°C under practically adiabatic conditions. Attempts were made to find coefficients which would fit the following formula separately in the temperature regions above and below 0°C to the observed resistance-temperature data for each Degussa thermometer.

$$R_t/R_0 = 1+\alpha t[1+\delta(1-t\cdot 10^{-2})10^{-2} + \beta t^2(1-t\gamma 10^{-2})10^{-6}] \quad (1)$$

Here t is the temperature in degrees Celsius, and R_t and R_0 are the resistances of the Degussa thermometer at t°C and 0°C, respectively. Coefficients determined are given in Table 1. Deviations of the observed resistances from the calculated resistances, obtained by means of Eq. (1) are within ±0.004° as shown in Fig. 3.

The temperature of a given sample and the difference in temperature between the sample and reference substance are simultaneously recorded on a Shimadzu Precision Recording Thermometer Type CT3 whose precision is 0.01° or 0.001° according to its two ranges.

Material. 2,2,4-trimethylpentane used in this experiment was the Standard Sample 217b which was purified and certified as 99.993±0.003 mol% by the National Bureau of Standards. Commercial 2,2,4-trimethylpentane and *n*-pentadecane of Extra Pure Grade were also obtained from Tokyo Kasei Kogyo Co., Ltd. α-Al_2O_3 which was supplied by Shimadzu Co. was used as a reference substance.

Table 1. Coefficients determined by fitting the calibration data to Eq. (1) for Degussa platinum-resistors

	Resistor 1	Resistor 2
	t above 0°C	
R_0 (ohms)	99.7245	99.7541
δ	1.38640	1.47009
α	0.00385854	0.00391828
β	0.0	0.0
	t below 0°C	
R_0 (ohms)	99.7225	99.7515
δ	1.59087	1.70733
α	0.00385205	0.00390511
β	0.0741392	−0.0364007
γ	1.54525	−4.05087

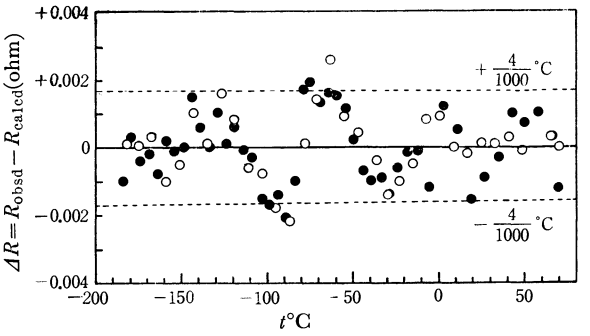

Fig. 3. Deviation of observed resistance of two Degussa thermometers from the calculated resistance by using Eq. (1).
○ thermometer 1 ● thermometer 2

Results and Discussion

Principle of Purity Determination from the Freezing or Melting Point Measurement. For impurities that are completely soluble in the liquid phase but insoluble in the solid phase, a thermodynamic relation between the amount of impurities N in mole fraction and the equilibrium temperature T, for an ideal or sufficiently dilute solution, is given by

$$-\ln(1-N)/r = (T^*_{m0}-T)\Delta H_m/\boldsymbol{R}(T^*_{m0})^2 \quad (2)$$

where T_{m0} is the melting point of pure compound, r the fraction melted or crystallized, ΔH_m the heat of fusion at T_{m0} of the pure compound, and $\boldsymbol{R}$ the gas constant. When the temperature T given by a time-temperature curve is not measured at equilibrium, the equation for the amount of impurities should be derived from irreversible thermodynamics as follows[3]:

$$-\ln(1-N)/r = (\Delta H_m/\boldsymbol{R})(1/T-1/T_{m0}^*) + (\Delta C_p/\boldsymbol{R})[\ln(T_{m0}^*/T) + 1 - (T_{m0}^*/T)] + A(T,r)/\boldsymbol{RT}. \quad (3)[4]$$

Here ΔC_p denotes the difference of the heat capacity between liquid and solid state of a pure compound,

3) I. Prigogin and R. Defay, "Chemical Thermodynamics," Longmans, Green and Co., Ltd, (1954) p. 373.

4) For samples of purity above 99 mol% the approximate equation $-\ln(1-N)\simeq N$ may be used in Eqs. (2) and (3).

and $A(T, r)$ the affinity. The value of A changes as a function of given temperature or time. If A can be neglected, Eq. (3) is reduced to Eq. (2).

When $A=0$ for a specific sample, the values of temperature obtained and the fraction melted or crystallized can be used for the determination of purity by means of Eq. (2). Usually, it is however not possible to find the point at which $A=0$ in the time-temperature curve of DTA measurements. Attempts were made, therefore, to develop methods of evaluating the purity by means of Eq. (3) from the DTA and TTA curves. The methods are divided into two procedures as follows.

(a) Melting Point Depression Method Using Extrapolation: When the melting point (or freezing point[5]) of a pure compound T^*_{m0} and that of a given sample T^*_m at $r=1$ are known, it is possible to give the amount of impurities in the sample from the melting point depression $T^*_{m0}-T^*_m$. In the first place, the purity of NBS Standard Sample 217b 2,2,4-trimethylpentane was reexamined using the precision adiabatic calorimeter.[2] The result, $99.991_2\pm0.0014$ mol%, is in excellent agreement with the given purity, 99.993 ± 0.003 mol% by the NBS within probable error. The melting point T^*_{m0} of pure compound was found to be 165.821_5°K as shown in Fig. 4. Two measurements of

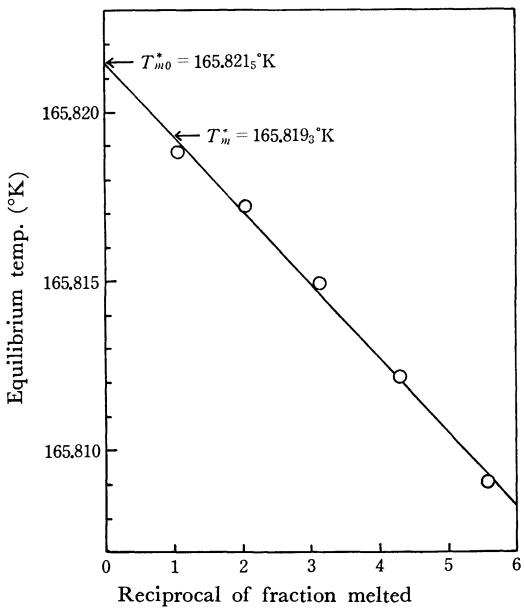

Fig. 4. Relationship between equilibrium temperatures and reciprocal of fraction melted for NBS Standard Sample 2,2,4-trimethylpentane.

TABLE 2. HEAT OF FUSION OF 2,2,4-TRIMETHYLPENTANE
mol wt 114.223; 0.208706 mol

Temperature Interval(°K)	Heat Input (cal/mol)	$\int C_p dT$ (cal/mol)	ΔH_m (cal/mol)
165.027–166.219	2285.8	86.4	2199.4
165.080–166.453	2296.8	98.6	2198.2
		average	2198.8±0.6

5) The melting point is exactly equal to the freezing point under an equilibrium condition.

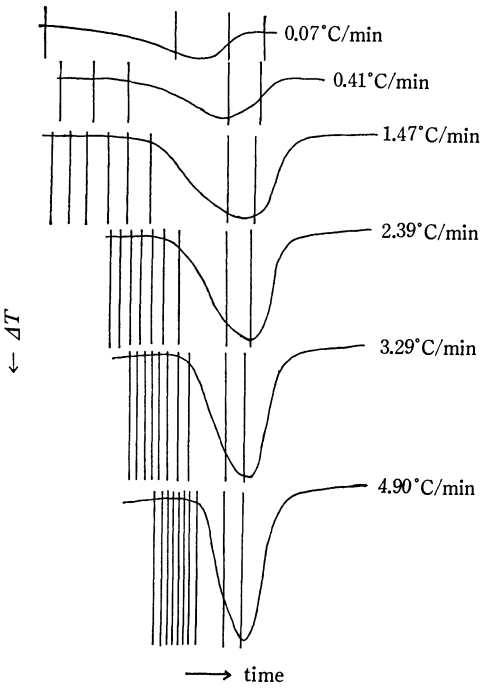

Fig. 5. DTA curves observed at various heating rates of commercial sample of 2,2,4-trimethylpentane.

the heat of fusion ΔH_m were also made, and the result is in good agreement with the literature value,[6] 2198 cal/mol, as summarized in Table 2.

DTA measurements at several heating rates were made using the NBS and commercial 2,2,4-trimethylpentane. Fig. 5 shows some examples of the DTA curves obtained.

As a matter of principle, the temperature at a peak maximum in a DTA curve obtained by this apparatus can be assumed to be equal to a quasi-melting point and depends upon the heating rate. The plots of temperatures at peak maxima (T_{max}) of DTA curve *versus* heating rates (a) for two samples of 2,2,4-trimethylpentane are shown in Fig. 6. Extrapolation of the curves obtained for two samples to $a=0$ gives the values of T_{max} $(a=0)$. We may assume that at T_{max} $(a=0)$ melting is complete under equilibrium condition, *viz.*, T_{max} $(a=0)$ agrees with the true melting point T^*_m of a given sample. We can then estimate the purity of sample by means of Eq. (2), where $r=1$ (complete melting) for T_{max} $(a=0)$. The values of T_{max} $(a=0)$ for the NBS and commercial samples were found to be 165.819°K and 165.334°K, and the purities 99.990 ± 0.004 mol% and 98.054 ± 0.004 mol%, respectively.

(b) Comparative Method: (i) If the affinity A in Eq. (3) at $T=T_{max}$ is denoted by A_{max}, it may be assumed that the value of A_{max} for the same material is dependent only upon heating rate a as shown in Fig. 6 for a highly purified sample. Since highly accurate result has been given for the purity of the NBS standard sample by adiabatic calorimetry, the value of A_{max} for 2,2,4-trimethylpentane can be calculated as a function of the heating rate by means of Eq. (3). The plotted result shows a smooth curve as in Fig. 7. The

6) American Petroleum Institute Research Project 6.

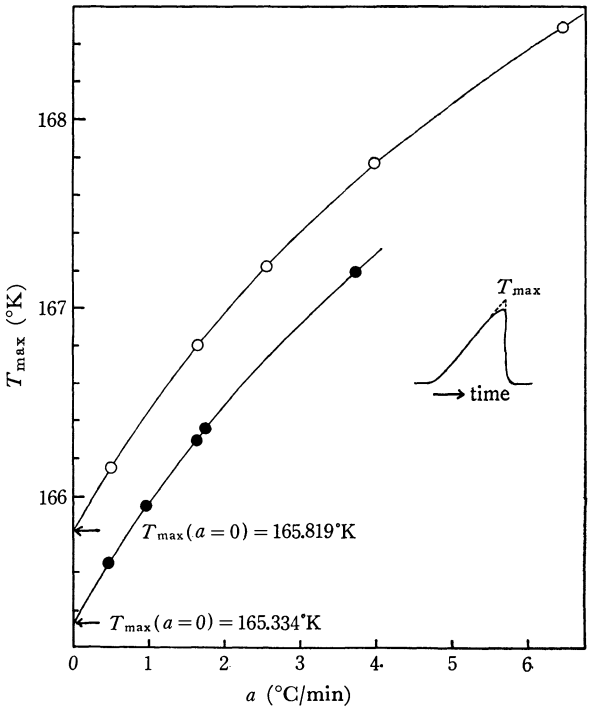

Fig. 6. Relationships between T_{max} and heating rate a for two samples of 2,2,4-trimethylpentane of different purity.
○ NBS sample ● commercial sample

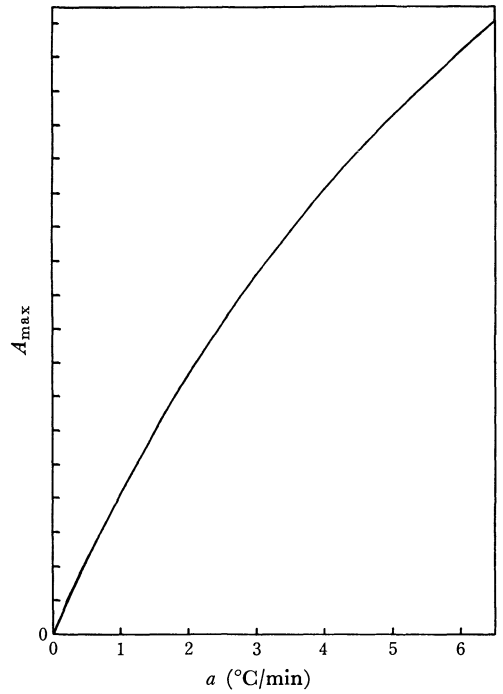

Fig. 7. Relationship between A_{max} and heating rate a for 2,2,4-trimethylpentane.

figure obtained on the NBS sample can be assumed to be applicable to the commercial sample, since the purity difference between the samples is small. Thus, from the values of T_{max} for the commercial sample observed at five different heating rates and the values of A_{max} obtained from the graph of A_{max} *versus* a of Fig. 7, the purity of the commercial sample was calculated by means of Eq. (3). The results are summarized in Table 3, and are in good agreement with that obtained by the melting point depression method (Fig. 6).

TABLE 3. RESULTS OF PURITY DETERMINATION BY COMPARATIVE METHOD (i) FROM THE DATA OBTAINED AT FIVE DIFFERENT HEATING RATES FOR COMMERCIAL SAMPLE OF 2,2,4-TRIMETHYLPENTANE

a (°C/min)	T_{max} (°K)	A_{max}/R	N (mol%)
0.47_2	165.644	2.068	98.05_4
0.96_8	165.949	4.111	98.05_4
1.61_1	166.295	6.443	98.04_8
1.73_7	166.354	6.830	98.05_0
3.72_1	167.193	12.459	98.05_6
		average	$98.05_2 \pm 0.004$

(ii) Indices 1 and 2 will be used in the following to denote two samples of different purity for DTA measurement. We will compare the purities at $T_1 = T_2 = T_{2,max}$ ($r_2 = 1$) with a fixed heating rate (a=const.). Then from Eq. (3) we obtain the relation

$$-\ln(1-N_1)/r_1 + \ln(1-N_2)/r_2 = (1/T_{2,max})(1/R)(A_1 - A_2), \quad (4)$$

where r_1 is the fraction melted at $T_1 = T_{2,max}$ for sample 1. In principle, a peak area of a DTA curve is proportional to the heat of fusion of the compound.[7] We can thus estimate the value of r by making use of the ratio of the peak area against time, *i.e.*, the value of $r(t')$ at time $t=t'$ is given by

$$r(t') = \left[\int_{t_i}^{t'} (y-y_s)dt + \int_{t''}^{t_f} (y-y_s)dt\right] \Big/ \left[\int_{t_i}^{t_f} (y-y_s)dt\right] \quad (5)$$

Here t_i and t_f are the times at which melting begins and finishes, t'' the time when $y=y(t')$ after the peak maximum, and y_s a steady state value of the differential temperature. Thus, if the amount of impurities N_1 for sample 1 is known, and the values of r_1, A_1, and A_2 ($=A_{max}$) in Eq. (4) are obtained from the $1/r_1$—$1/T$ relation, Eq. (3) and Fig. 7, respectively, then the amount of impurities N_2 for sample 2 can be calculated by means of Eq. (4). Here, sample 1 must be a substance with higher purity than the sample 2 ($N_1 < N_2$).

We employed the NBS and commercial 2,2,4-trimethylpentane as samples 1 and 2. Comparison of DTA data was made at the heating rate of 1.64_5°C/min for the NBS sample and 1.61_1°C/min for the commercial sample. The purity of the commercial sample was 98.04_8 mol% which is in good agreement with those obtained previously. Though the heating rates were adjusted to be as close as possible, it was difficult to obtain exactly the same heating rate for both samples. Method (ii) is therefore inferior to method (i) in accuracy.

Conventional Melting Point Method. In a melting curve the temperature which is given by the intersection of an extrapolated solid warming line with the extended backward liquid warming line, as shown in

7) M. J. Vold, *Anal. Chem.*, **21**, 683 (1949).

Fig. 8, has been regarded as an equilibrium point ($A=0$) of the melting curve.[8] The behavior of affinity A during the melting was investigated on two samples of 2,2,4-trimethylpentane to check whether $A=0$ is actually established at this point. Fig. 9 shows plots of A *versus* $1/r$ obtained from the peak area for the NBS and commercial samples. It is seen in Fig. 9 that an equilibrium point ($A=0$) not always realized in the melting curve, and the plots of the two samples differ largely in the $1/r<2$ region but are in agreement in the $1/r<2$ region. Although it is thought that the point of half melting ($1/r=2$) is mostly at equilibrium during the melting, the closest points to equilibrium for the NBS and commercial samples give the values of 2.13 and 1.65 for $1/r$, respectively, as shown in Fig. 9. It is therefore concluded that the well-known method of thermal analysis shown in Fig. 8 can not give a highly accurate result. It is desirable to make use of the comparative methods described previously in the region of the melting curve where $1/r<2$.

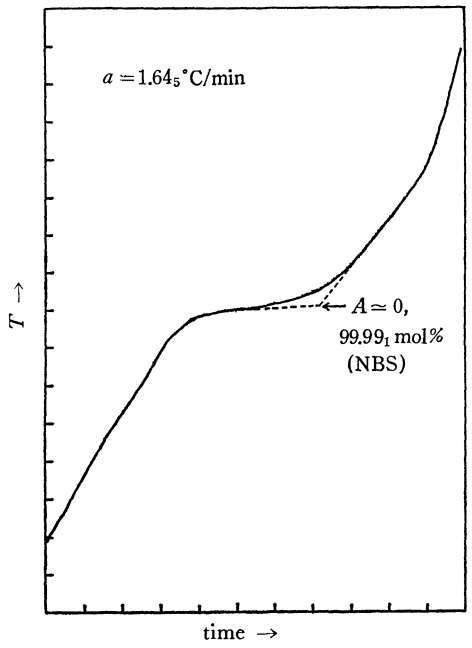

Fig. 8. Time-temperature melting curve for NBS sample of 2,2,4-trimethylpentane.

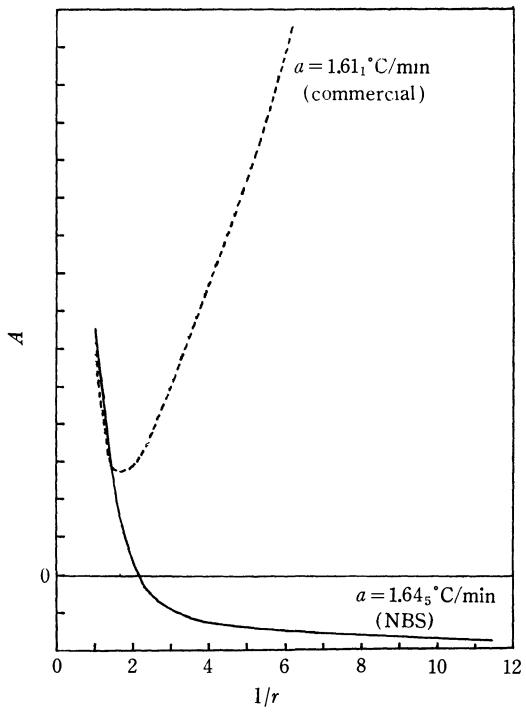

Fig. 9. Relationships between affinity A and reciprocal of fraction melted $1/r$ for NBS and commercial samples of 2,2,4-trimethylpentane.

The purity of two samples of 2,2,4-trimethylpentane determined by the methods described above are summarized in Table 4.

Table 4. Results of purity determination by various methods for 2,2,4-trimethylpentane samples of different purity

Method	Standard sample (NBS) (mol%)	Commercial sample (mol%)
Freezing point (NBS)	99.993 ±0.003	—
Calorimetric	99.991_2±0.0014	—
DTA		
(a) Melting point depression using extrapolation ($T_{max}(a=0)$)	99.99_0 ±0.004	98.05_4
(b) Comparative (i)	—	98.05_2±0.004
Comparative (ii)	—	98.04_8
(c) Melting point ($T(A=0)$, Fig. 8)	99.99_1	—

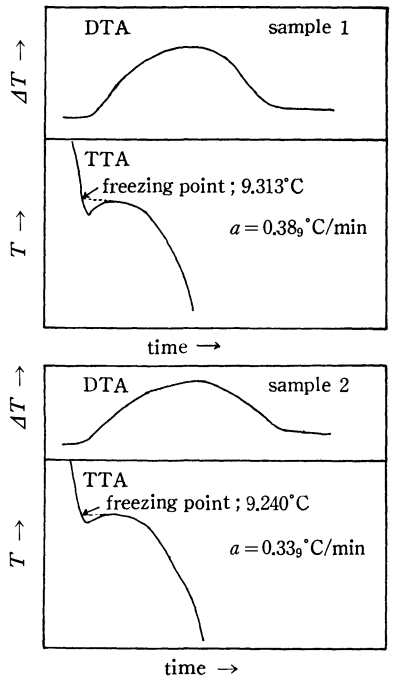

Fig. 10. DTA and TTA freezing curves for two samples of different purity of *n*-pentadecane.

8) W. J. Taylor and F. D. Rossini, *J. Res. NBS*, **32**, 197 (1944); A. R. Glasgow, Jr., A. J. Streinffand, and F. D. Rossini, *ibid.*, **35**, 355 (1945).

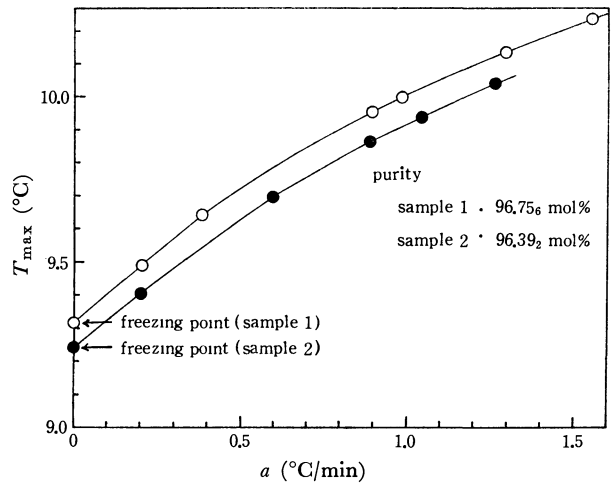

Fig. 11. Relationships between T_{max} and heating rate a for two samples of *n*-pentadecane of different purity.

Freezing DTA Measurement. The DTA data for two commercial *n*-pentadecane samples of different purity are given in Fig. 10. The freezing points of the samples were obtained by the well-known method[7] from the time-temperature cooling curves. The T_{max} ($a=0$) of the samples was obtained by the melting point depression method using extrapolation, as shown in Fig. 11. T_{max} ($a=0$) values are in excellent agreement with freezing points obtained from the freezing curves, and give the purity of each sample in terms of Eq. (2), as given in Fig. 11.

It can therefore be pointed out that when the sample is successfully supercooled, the freezing point obtained from the cooling curve is nearly at a temperature under equilibrium condition.

The authors wish to thank Dr. W. Wayne Meinke of the National Bureau of Standards for the supply of the Standard Sample 217b 2,2,4-trimethylpentane.

BULLETIN OF THE CHEMICAL SOCIETY OF JAPAN, VOL. 44, 893—895 (1971)

Brönsted and Lewis Acidity of Solid Nickel Sulfate

Hideshi HATTORI, Shun-itsu MIYASHITA, and Kozo TANABE
Department of Chemistry, Faculty of Science, Hokkaido University, Sapporo

(Received June 2, 1970)

The distribution of Brönsted and Lewis acidities of nickel sulfates heat-treated at various temperatures in air or in a vacuum has been determined by observing the infrared spectra of pyridine adsorbed on the sulfates in the range 1300—1600 cm^{-1}. It has been found that the Brönsted acidity increases with the rise of temperature of heat treatment in air, attains a maximum value at 250°C and then decreases, while the maximum of the Lewis acidity appears at a higher temperature (about 400°C), the sum of both acidities giving the total acidity measured by *n*-butylamine titration method. An experiment in a vacuum showed that Lewis acid is converted into Brönsted acid by the addition of water. The structural nature and the catalytic activity of the Brönsted and Lewis acid sites on nickel sulfate are discussed.

Solid nickel sulfate shows remarkable acidic property on being subjected to heat treatment[1] and is used as a new type of effective catalysts in a number of acid-catalyzed reactions.[2] It was found that the total acidity[3] (Brönsted plus Lewis acidity) of the sulfate heat-treated at various temperatures measured by *n*-butylamine titration method correlates well with the catalytic activity of the depolymerization of paraldehyde,[1] polymerization of propylene[4] and aldehydes,[5] hydration of propylene,[6] exchange reaction of chlorine between benzyl chloride and hydrogen chloride,[7] *etc.* However, no good correlation was found for the isomerization of α-pinene[8] and the hydrolysis of methylene chloride.[9] This was tentatively interpreted as due to the fact that isomerization depends on Brönsted acidity and hydrolysis on Lewis acidity,[2] on the basis of the structural study of acid sites.[10] However, since we have no experimental evidence for each type of acid site, we have attempted to measure Brönsted and Lewis acidities separately, by employing the infrared spectroscopic method[11] of pyridine adsorbed on the solid acid catalyst. The results are discussed in connection with the nature and the activity of acid sites of nickel sulfate catalyst.

Experimental

Infrared spectra of adsorbed pyridine were measured for nickel sulfate heat-treated in air or in a vacuum *in situ* cell. Heptahydrate of nickel sulfate was heat-treated in a glass

1) K. Tanabe and R. Ohnishi, *J. Res. Inst. Catalysis, Hokkaido Univ.*, **10**, 229 (1962).
2) K. Tanabe and T. Takeshita, *Adv. in Catalysis*, **17**, 315 (1967).
3) Acidity is defined as an acid amount in the present paper.
4) Y. Watanabe and K. Tanabe, *J. Res. Inst. Catalysis, Hokkaido Univ.*, **12**, 56 (1964).
5) H. Takida and K. Noro, *Kobunshi Kagaku*, **21**, 23 and 109 (1964).
6) Y. Ogino, *J. Catalysis*, **8**, 64 (1967).
7) M. Ogasawara, K. Tanabe, and T. Takeshita, *J. Res. Inst. Catalysis, Hokkaido Univ.*, **17**, 28 (1969).
8) R. Ohnishi, T. Takeshita, and K. Tanabe, *Shokubai* (Tokyo), **7**, 306 (1965).
9) T. Yamaguchi and K. Tanabe, Fourth International Congress on Catalysis, Moscow, 1968, Preprint of the Paper, No. 80.
10) T. Takeshita, R. Ohnishi., T. Matsui, and K. Tanabe, *J. Phys. Chem.*, **69**, 4077 (1965).
11) E. P. Parry, *J. Catalysis*, **2**, 371 (1963).

tube at various temperatures in the range 200—500°C for 3 hr in air and the glass tube was sealed off. Immediately after the tube was opened, it was connected to vacuum apparatus and evacuated to 10^{-6} mmHg for 30 min at room temperature and then pyridine (about 2 mmHg) was introduced and adsorbed for 10 min. After removing excess pyridine by evacuating for 30 min at room temperature, 5 mg of the sample was mixed with 200 mg of KBr powder and pressed into a tablet 12 mm in diameter by means of a pressure approximately 3000 kg/cm^2. The spectrum range in the 1300—1700 cm^{-1} was observed with an infrared spectrophotometer (Hitachi EPI-2).

In an *in situ* cell experiment, nickel sulfate mounted on silica gel (35 wt% as anhydride) was used. The sample discs were placed in the cell and heat-treated at various temperatures in a vacuum for 3 hr. After cooling to room temperature, pyridine (about 2 mmHg) was introduced and adsorbed for 15 min. After evacuation for 30 min at 50°C and further evacuation for 30 min at 100°C, the spectra were recorded on a Hitachi EPI-G2 double beam grating spectrophotometer. In some experiments, the effect of water on the spectrum of chemisorbed pyridine was examined to see whether Lewis acid can be converted into a Brönsted one. Weight loss of heptahydrate of nickel sulfate by dehydration in air or in a vacuum with the rise of temperature of heat treatment was also measured by weighing the samples treated for 3 hr at various temperatures.

Pyridine was purified by dehydration over molecular sieve 4A and by distillation in a vacuum. Heptahydrate of nickel sulfate was a guaranteed reagent of Kanto Chemical Co. Tokyo. Silica gel used was prepared by the hydrolysis of ethylorthosilicate, which had little acidity on the surface.

Results and Discussion

The spectra of pyridine adsorbed on nickel sulfate heat-treated at various temperatures in air are shown in Fig. 1, where two main absorption bands (1520 and 1425 cm^{-1}) are observed. Since the band of higher frequency disappears when the sample was heat-treated at 350°C, while the band of lower frequency still remains even by heat treatment at 450°C, both the bands seem to be those of different species of adsorbed pyridine. It is known that the band of coordinately bonded pyridine appears at 1445—1460 cm^{-1} on the surface of η-alumina,[11] silica-alumina,[11,12] and cation exchanged zeolites,[13–15] while the band of pyridinium ion or salts at 1530—1540 cm^{-1} on silica-alumina,[11,12] cation exchanged zeolites[13–15] or in various pyridine complexes.[16] Therefore, the band near 1520 cm^{-1} in Fig. 1 has been assigned to the band due to pyridinium ion and that at 1425 cm^{-1} due to coordinately bonded pyridine. Since the acid strength of the sulfate is lower than those of the solid acids mentioned above,[2] and it is known that the band of pyridine adsorbed on weaker acid site appears at lower frequency,[15] it seems likely that the species responsible for the bands at 1520 and 1425 cm^{-1} were adsorbed on much weaker Brönsted and Lewis acids respectively. Thus, the bands at 1520 and 1425 cm^{-1} in Fig. 1 can be respectively taken as those corresponding to Brönsted and Lewis acid. Figure 2 shows the changes in intensities of these two bands with change of temperature of heat treatment. It is seen that Brönsted acidity shows its maximum when the sample was heat-treated at 250°C, whereas Lewis acidity attains its maximum at about 400°C.

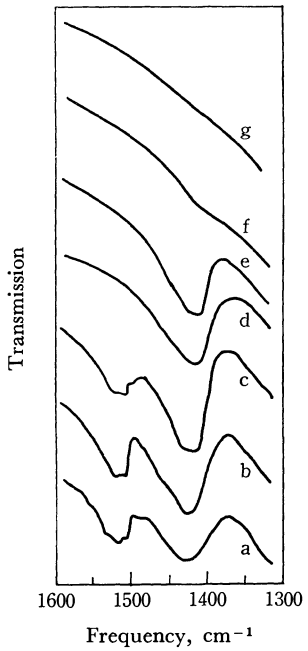

Fig. 1. Infrared spectra of pyridine on nickel sulfates heat-treated at various temperatures in air.
a : 200°C, b : 250°C, c : 300°C, d : 350°C, e : 400°C, f : 450°C, g : 500°C

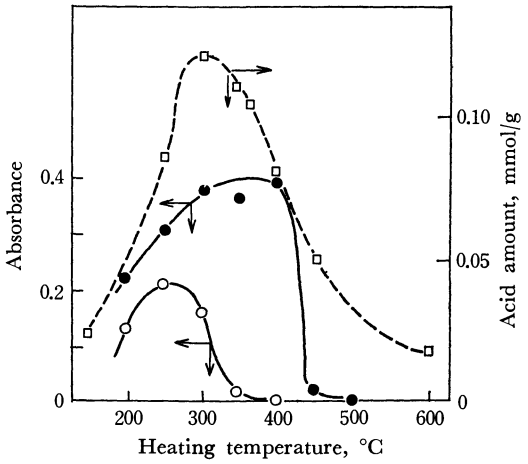

Fig. 2. Variation of absorbances at 1425 cm^{-1} (●) and at 1520 cm^{-1} (○) with heating temperature. Dotted line shows acid amount at acid strength $H_0 \leqq 3.3$ measured by *n*-butylamine titration[1].

The spectra of pyridine adsorbed on nickel sulfate heat-treated in a vacuum are shown in Fig. 3. The shape of the bands differs somewhat from that ob-

12) M. R. Basila, T. R. Kantner, and K. H. Rhee. *J. Phys. Chem.*, **68**, 3197 (1964).
13) J. W. Ward, *J. Catalysis*, **9**, 225 (1967).
14) B. V. Liengme and W. K. Hall, *Trans. Faraday Soc.*, **62**, 3229 (1966).
15) H. Hattori and T. Shiba, *J. Catalysis*, **12**, 111 (1968).
16) N. S. Gill, R. H. Nuttall, D. E. Scaife, and D. W. A. Sharp, *J. Inorg. Nucl. Chem.*, **18**, 79 (1961).

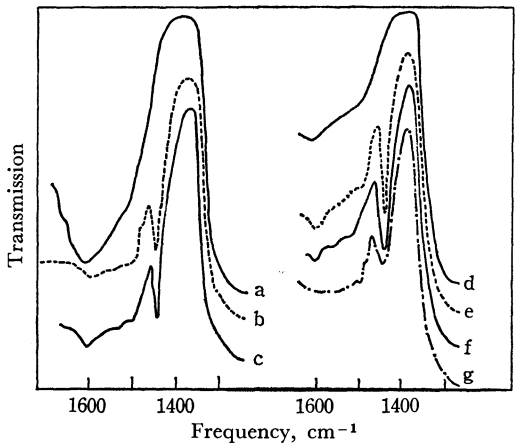

Fig. 3. Infrared spectra of pyridine on silica supported nickel sulfates heat-treated in a vacuum.
a ; background spectrum of silica supported nickel sulfate heat-treated at 150°C for 3 hr
b ; a+pyridine and evacuated at 50°C for 30 min
c ; further evacuation of b at 100°C for 30 min
d ; background spectrum of silica supported nickel sulfate heat-treated at 200°C for 3 hr
e ; d+pyridine and evacuated at 50°C for 30 min
f ; further evacuation of e at 100°C for 30 min
g ; f+water vapor of about 2 mmHg and evacuated at room temperature for 30 min

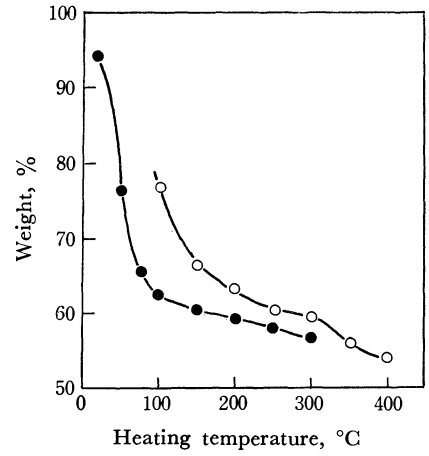

Fig. 4. Weight loss of nickel sulfate as a result of dehydration by heating in a vacuum (●) and in air (○). Weight % of anhydrous sulfate is calculated to be 55.1%, by taking weight % of the heptahydrate as 100%.

served for the samples heat-treated in air, though both spectra are essentially the same. The difference is considered due to the fact that the absorption bands of pyridine[11] adsorbed on silica which was used as a carrier in a vacuum experiment are superposed near 1600 cm^{-1} and 1440 cm^{-1}. Thus, the bands at 1490—1550 cm^{-1} become broader and those at 1440 cm^{-1} become sharper in the case of vacuum experiment (Fig. 3). The bands at 1490—1550 cm^{-1} for the samples heat-treated at 150°C seem to be large compared with those at 200°C (compare b and c with e and f in Fig. 3; the relative strength of the absorption at 1490—1540 cm^{-1} to that at 1440 cm^{-1} is larger for the samples heat-treated at 150°C than for those at 200°C). This indicates that Brönsted acidity decreases with the rise of temperature of heat treatment from 150 to 200°C in a vacuum. Dehydration curves in air and in a vacuum shown in Fig. 4 reveal that the temperature of heat treatment required for a definite extent of dehydration is about 100°C lower in a vacuum than in air. Thus, Brönsted acidity is expected to show its maximum value when heat-treated at about 150°C in a vacuum. The addition of water resulted in a decrease in the intensities of the 1440 cm^{-1} band and in a slight increase in the intensities of the 1490—1550 cm^{-1} band (Fig. 3, curves f and g). This indicates that Lewis acid is converted into Brönsted acid to some extent by the addition of water.

We shall now give some explanation on the Brönsted and Lewis acidity curves in Fig. 2, by taking into account the structural nature of acid sites of nickel sulfate. According to our studies with infrared, X-ray, electron spin resonance, *etc.*,[10] the acid center of nickel sulfate is considered to be an empty orbital on the nickel ion which appears in an incompletely dehydrated, metastable transition structure. Intermediate configuration is formed between the monohydrate and anhydrous form. The vacant orbital, and the resulting affinity for an electron pair, explains the Lewis acid nature of nickel sulfate. The Brönsted acidity arises from two sources. One is the water coordinated directly with a nickel ion. The nickel ion tends to attract the oxygen atom, thus setting a hydrogen ion free. The other is the surface water acidified by the inductive effect of neighboring cationic Lewis acid centers. Thus, Brönsted acid appears when the vacant orbital of nickel ion is formed by dehydration and its acidity increases with the rise of dehydration temperature. However, since the amount of hydrated water decreases as the temperature of heat treatment is increased, the Brönsted acidity begins to decrease at 250°C (Fig. 2). The Lewis acidity also increases with the rise of dehydration temperature, but does not decrease until the metastable structure having the vacant orbital collapses and changes to a stable structure at 450°C. Therefore, the maximum of Brönsted acidity appears at a lower temperature (250°C) and that of Lewis acidity at a higher temperature (400°C). The sum of both acidity curves gives the total acidity which was measured by *n*-butylamine titration method[1] (Fig. 2).

We reported that the rate maxima of the isomerization of α-pinene to camphene[8] and the formation of formaldehyde by the hydrolysis of methylene chloride[9] with nickel sulfates heat-treated in air at various temperatures were observed respectively at 250°C and 400°C, which do not coincide with the maximum of total acidity measured by *n*-butylamine titration method. The rate maxima coincide respectively with the maxima of Brönsted and Lewis acidity observed in the present experiment, and the activity curves for isomerization and hydrolysis plotted against the temperature of heat treatment of nickel sulfate correlate well with Brönsted and Lewis acidity curves shown in Fig. 2. This confirms our conclusions[2,9] that the isomerization of α-pinene is catalyzed by Brönsted acid, and the hydrolysis of methylene chloride by Lewis acid.

Group Interactions in Polyelectrolytes. V. The Kinetics of the Amination of Chloromethylated Polystyrene with 2-Aminobutanol

Hiroshi KAWABE and Masaya YANAGITA

The Institute of Physical and Chemical Research, Wako-shi, Saitama

(Received August 7, 1970)

The amination of chloromethylated polystyrene with 2-aminobutanol in dioxane was studied. The apparent rate constatns, k_{app}, as computed by the simple second-order equation, were found to increase linearly with the degree of amination; this was in contrast with the amination with *n*-butylamine, in which the k_{app} decreased as the amination proceeded. By assuming that the reactivity of the chloromethyl group is enhanced when it is situated next to the already-aminated group as a result of the "hydrophilic effect" of the hydroxyl group, rate equations which give the elementary rate constants were derived. In the presence of a large excess of amine, the over-all kinetics can be expressed by:

$$dx/dt = [ab/(3k_1-k_2)][3k_1(k_1-k_2)e^{-3k_1at} + 2k_1k_2e^{-k_2at}]$$

where x is the concentration of chloride ions at time t; where a is the initial concentration of amine, and b, that of the chloromethyl group, and where k_1 and k_2 are the rate constants of the elementary reactions which are independent of the neighboring group and under the influence of it respectively. The values of k_{app} calculated on the basis of k_1 and k_2 were also found to agree with the observed values.

Amination kinetics of chloromethylated polystyrene with *n*-butylamine or di-*n*-butylamine in dioxane was reported previously.[1] The apparent rate constant, as calculated by the simple second-order rate equation, k_{app}, decreased as the amination proceeded. The results were interpreted in terms of the two-step amination resulting from the steric effect of already-aminated neighboring groups, and the over-all kinetics in the presence of a large excess of amine could be expressed by an equation containing two rate constants.

In the present study, the amination of chloromethylated polystyrene with 2-aminobutanol has been carried out in dioxane, and k_{app} has been found to increase linearly with the degree of amination. The difference between the kinetic behavior in the amination of chloromethylated polystyrene with *n*-butylamine and with 2-aminobutanol is considered to arise from the different position of the amino group in the amines and the presence of the hydroxyl group in 2-aminobutanol. Analysis of the experimental data reveals that the amination proceeds in two steps. Rate equations for this reaction are derived on the basis of the kinetic data.

Experimental

Materials. Polystyrene and chloromethylated polystyrene were prepared by the procedure described in the previous paper;[1] their molecular weights were determined, by means of osmometry in toluene, to be 5.44×10^4 and 7.33×10^4 respectively. These results indicate that neither cross-linking nor degradation of the polymer occurred in the chloromethylation process. The chlorine content of the chloromethylated polystyrene, which was purified by reprecipitation with dioxane and methanol, was 22.87%, corresponding to the degree of chloromethylation of 97.8%. (−)-2-aminobutanol was prepared from its tartaric acid salt by the use of an ion-exchange resin column (Dowex-50, X-8, 20—50 mesh) according to the procedure reported by Tsuboyama *et al.*[2] It had a bp of 86—87°C/15 mmHg; n^{20} 1.4532; $[\alpha]_D^{20}$ −10.23. All the other chemicals were of a reagent grade, and de-ionized, de-carbonized water was used throughout the experiments.

Kinetic Measurement of the Amination. Fifty milliliters of a dioxane solution containing one gram of chloromethylated polystyrene, benzyl chloride, or ethylene bromide was throughly mixed with 100 m*l* of a dioxane solution containing a large excess of 2-aminobutanol (about twenty times as many moles as the chloromethyl group). The solution thus obtained was stirred during the reaction, and its temperature was maintained within ±0.1°C by means of a thermostat. Throughout the reaction, the system was kept homogeneous. At appropriate intervals, aliquots were taken out; each of them was poured into dilute nitric acid and titrated potentiometrically with 0.1 N silver nitrate. The experimental conditions are listed in Table 1.

Table 1. Experimental conditions of amination

Run	Temp. °C	Halide	b[b] mol/*l*	a[b] mol/*l*	a/b
A	40	Benzyl Chloride	0.0541	1.0561	19.5
B	50.5	Benzyl Chloride	0.0525	1.0538	20.1
C	60	Benzyl Chloride	0.0528	1.0550	20.0
D	70	Benzyl Chloride	0.0528	1.0542	20.0
E	70	Ethylene Bromide	0.0725	1.4212	19.6
F	40	CMPS[a]	0.0430	0.8549	19.9
G	50	CMPS[a]	0.0431	0.8590	19.9
H	60	CMPS[a]	0.0441	0.8589	19.5
I	70	CMPS[a]	0.0439	0.8641	19.7

a) Chloromethylated polystyrene (Cl: 22.87%)
b) a: initial concentration of 2-aminobutanol
b: initial concentration of halide expressed by mol of halogen per *l*

Results

Benzyl chloride was quantitatively aminated with 2-aminobutanol in dioxane, and its rate constant was

1) H. Kawabe and M. Yanagita, This Bulletin, **41**, 1518 (1968).

2) K. Tsuboyama, S. Tsuboyama, and M. Yanagita, *Reports I.P.C.R.* (in Japanese), **41**, 194 (1965).

given by the second-order equation:

$$k = \frac{1}{(a-b)t} \ln \frac{b(a-x)}{a(b-x)} \quad (1)$$

where a is the initial concentration of the amine and b, that of benzyl chloride, while x is the concentration of chloride ions at time t. Although chloromethylated polystyrene was also quantitatively aminated with 2-aminobutanol in dioxane without any separation of the polymer, the rate constant computed by Eq. (1) increased as the reaction proceeded. The experimental results are summarized in Figs. 1 and 2, where t is the time and $\overline{kt}$ is the term defined as follows:

$$\overline{kt} \equiv \frac{1}{a-b} \ln \frac{b(a-x)}{a(b-x)} \quad (2)$$

In the case of benzyl chloride (Fig. 1), the plot of $\overline{kt}$ against t is represented by a single line, while in the case of chloromethylated polystyrene (Fig. 2), the plot is divided into two lines which intersect at one-third of the amination. These results may be explained by assuming that the chloromethyl group of the polymer

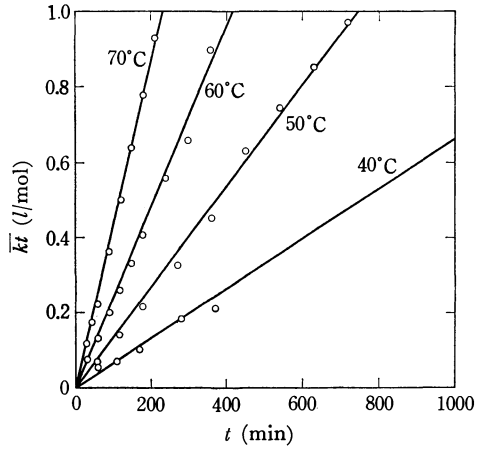

Fig. 1. Amination of benzyl chloride.

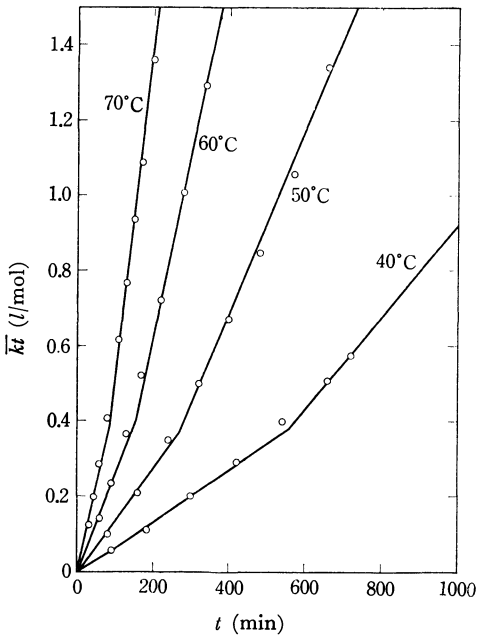

Fig. 2. Amination of chloromethylated polystyrene.

is aminated at a normal rate unless its neighboring group is changed, while the amination is accelerated when one of the nearest-neighbors is aminated. This assumption is partly supported by the amination of ethylene bromide shown in Fig. 3, where $\beta(=x/b)$

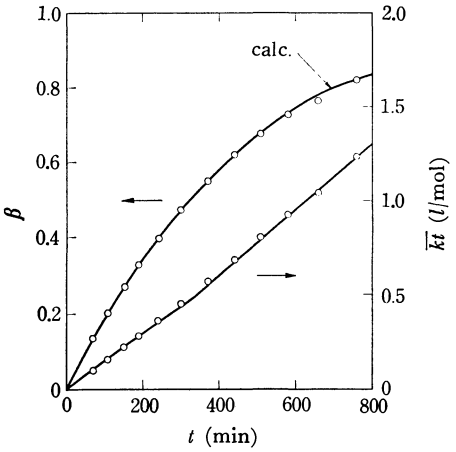

Fig. 3. Amination of ethylene bromide.

denotes the degree of amination. Acceleration, as expected, is observed in this reaction, though it is not very remarkable and the $\overline{kt}$ *vs.* t plot intersects nearly at half-amination. These results are in contrast with those of the amination of ethylene bromide with *n*-butylamine and di-*n*-butylamine, which is controlled by a single rate constant.[1)]

Sakurada[3)] reported that the rate of the alkaline hydrolysis of polyvinyl acetate in an aqueous acetone solution increased as indicated in the following relation:

$$dx/dt = k_0(1 + m\beta)(a - x)(b - x) \quad (3)$$

where k_0 and m are constants and where $\beta=x/b$. On the other hand, we may express the rate of bimolecular polymer reaction by:

$$dx/dt = k_{app}(a - x)(b - x) \quad (4)$$

where k_{app} is the apparent rate constant. On the basis of Eqs. (3) and (4), we obtain the relation:

$$k_{app} = k_0(1 + m\beta) \quad (5)$$

which means that k_{app} is a linear function of β.

The above relation has also been found in the present study to be applicable to the amination of chloromethylated polystyrene, as is shown in Fig. 4. The values of k_0 and m thus determined are listed in Table 2. Although k_0 increases with an increase in the tem-

Table 2. k_0 and m in the amination of chloromethylated polystyrene

Run	Temp. °C	$k_0 \times 10^3$ l/mol min	m
F	40	0.56	1.14
G	50	1.12	1.20
H	60	2.10	1.24
I	70	3.78	1.16

3) I. Sakurada, *Kobunshi*, **17**, 21 (1968). I. Sakurada and Y. Sakaguchi, *Kobunshi Kagaku*, **13**, 441 (1956).

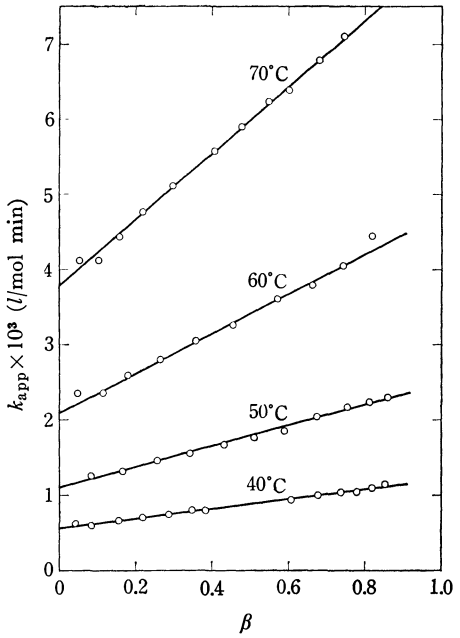

Fig. 4. Dependence of apparent rate constant on fractional conversion in the amination of chloromethylated polystyrene.

perature, m has an almost constant value irrespective of the temperature. It is interesting that these different kinds of reaction can be expressed by such a simple linear relation. It should be noted that k_{app} in the amination with n-butylamine or di-n-butylamine is not a linear function of β, but decreases markedly beyond half-amination.

Sakurada[3] ascribed the acceleration of the alkaline hydrolysis of polyvinyl acetate to the adsorption of alkali by the hydroxyl group formed in the polymer. He suggested the designation of "hydrophilic effect" for this phenomenon. It also seems possible that aminated groups in chloromethylated polystyrene adsorb 2-aminobutanol in dioxane because of the hydroxyl groups.

Rate Equations

The amination of chloromethylated polystyrene, as described in the preceding section, is a two-step reaction composed of two elementary reactions, one of which is independent of the neighbors and the other of which is accelerated by the neighboring aminated group. The rate equations for this reaction are derived on the model of low-molecular compounds to be described below.

Bifunctional Compound Model (Model I). The rate equation for a bifunctional compound, whose reactivity alters when one of the groups is changed, has previously been described.[1] It is given by:

$$dx/dt = (a-x)[k_1 b - 2(k_2 - k_1)x_1 - k_2 x] \quad (6)$$

$$k_1 = \frac{1}{[(2 - k_2/k_1)a - b]t} \ln \frac{1-\alpha}{1-(2-k_2/k_1)\beta} \quad (7)$$

$$k_2 = \frac{1}{(a-b)(t-\tau)}\left(\ln \frac{1-\alpha}{1-\beta} - \ln \frac{1-\chi/a}{1-\chi/b}\right) \quad (8)$$

where x_1 is the concentration of the first changed group; τ and χ are the values of t and x when $x_1 \simeq b/2$; $\alpha = x/a$ and $\beta = x/b$. When a large excess of a reagent is used ($a \gg b$), the over-all kinetics is expressed by this equation:

$$\beta = 1 - \frac{k_1 - k_2}{2k_1 - k_2} e^{-2k_1 at} - \frac{k_1}{2k_1 - k_2} e^{-k_2 at} \quad (9)$$

The amination of ethylene bromide can properly be expressed by this equation. These rate equations were found to be useful in describing the amination kinetics of chloromethylated polystyrene with n-butylamine or di-n-butylamine, in which the amination of a chloromethyl group placed between two already-aminated neighbors is sterically hindered and the $\overline{kt}$ *vs.* t plot is divided into two lines intersecting nearly at $\beta = 0.5$.[1]

Trifunctional Cyclic Compound Model (Model II). In the reaction of chloromethylated polystyrene with 2-aminobutanol, in which the intersection lies nearly at $\beta = 1/3$, the amination of a chloromethyl group is assumed to be accelerated when one of its neighbors is aminated. Accordingly, the chloromethyl groups may be classified into three groups depending upon their environment; one is situated between unchanged neighbors, another is situated next to an aminated neighbor, while a third is situated between two aminated neighbors. In this case, the trifunctional cyclic compound model, shown below, is considered to be more suitable than Model I:

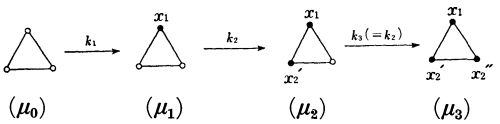

In the above figure illustrating the reaction of a trifunctional compound and a reagent, the white circles represent unchanged groups, and the black circles, changed groups. The relationships among the concentrations are:

$$\mu_0 = M - x_1 = (b/3) - x_1 \quad (10)$$

$$\mu_1 = x_1 - x_2, \ \mu_2 = x'_2 - x_2'' \quad (11)$$

$$x = x_1 + x_2, \ x_2 = x_2' + x_2'' \quad (12)$$

where M is the initial concentration of the compound and b, that of the reactive group of the compound; $\mu_n (n=0, 1, 2, \text{and } 3)$ is the concentration of the compound, n groups of which are changed at time t; x_1, x_2', and x_2'' are the concentrations of the first, secondary and last changed group respectively at time t. Since only two steps are observed in the amination of chloromethylated polystyrene with 2-aminobutanol, k_3 is simply assumed to be equal to k_2 in this case.

The over-all rate of the above reaction with the two rate constants of k_1 and k_2 is given by:

$$dx/dt = (a-x)[3k_1\mu_0 + k_2(2\mu_1 + \mu_2)]$$
$$= (a-x)[k_1 b - 3(k_1 - k_2)x_1 - k_2 x] \quad (13)$$

where a is the initial concentration of a reagent. On the assumption that $x \simeq x_1$ in the initial stage of reaction ($\beta < 1/3$) and that $x_1 \simeq b/3$ in the final stage ($\beta > 1/3$), the integration of Eq. (13) yields:

$$k_1 = \frac{1}{[(3 - 2k_2/k_1)a - b]t} \ln \frac{1-\alpha}{1-(3-2k_2/k_1)\beta} \quad (14)$$

$$k_2 = \frac{1}{(a-b)(t-\tau')}\left[\ln\frac{1-\alpha}{1-\beta} - \ln\frac{1-\chi'/a}{1-\chi'/b}\right] \quad (15)$$

where τ' is a time when $x_1 \simeq b/3$ and χ' is a value of x at this time. When a large excess of reagent is used ($a \gg b$), the term ($a-x$) in Eq. (13) can be replaced by a, and x_1 is given by:

$$x_1 = b(1 - e^{-3k_1 at})/3 \quad (16)$$

Hence, by integrating Eq. (13), we obtain;

$$x = b\left[1 - \frac{k_1 - k_2}{3k_1 - k_2}e^{-3k_1 at} - \frac{2k_1}{3k_1 - k_2}e^{-k_2 at}\right] \quad (17)$$

and the over-all rate is given by:

$$dx/dt = \frac{ab}{2k_1 - k_2}[2k_1(k_1 - k_2)e^{-2k_1 at} + k_1 k_2 e^{-k_2 at}] \quad (18)$$

Equations (14) and (15) can also be derived by considering the polymer reaction itself. The relative position of changed groups on a polymer molecule may be illustrated as follows:

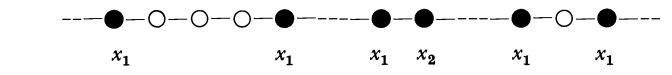

Two groups may be situated independently (I), side by side (II), or with an unchanged group between them (III). In the initial stage of the reaction, the situation [III] can be neglected; the rate is then given by:

$$dx/dt = dx_1/dt + dx_2/dt$$
$$= (a-x)[k_1\{(b-x) - 2x_1\} + 2k_2 x_1] \quad (19)$$

On the assumption that $x \simeq x_1$ in the initial stage, we obtain;

$$dx/dt = (a-x)[k_1 b - (3k_1 - 2k_2)x] \quad (20)$$

In the final stage of the reaction, only reactive groups next to the changed group are left and the rate is given by:

$$dx/dt = k_2(a-x)(b-x) \quad (21)$$

By integrating Eqs. (20) and (21), we obtain Eqs. (14) and (15) respectively.

Discussion

The rate constants of the amination of ethylene bromide at 70°C were calculated on the basis of Eqs. (7) and (8) for Model I (bifunctional compound model) to give $k_1 = 1.39 \times 10^{-3}$ ($k_1' = 1.45 \times 10^{-3}$) and $k_2 = 1.91 \times 10^{-3}$ l/mol min respectively; k_1' is an approximate value of k_1 which is obtained from the slope of the $\overline{kt}$ *vs.* t plot according to:

$$k_1' = \Delta\overline{kt}/\Delta t \quad (22)$$

The values of β calculated on the basis of Eq. (9) by using the above values of k_1 and k_2 are plotted against t in Fig. 3, in which a solid line show this calculated plot. The experimental values, which are represented by white circles, fall excellently on this plot.

In the case of chloromethylated polystyrene, the rate constants were calculated on the basis of Eqs. (7) and (8), on the one side, and on the basis of Eqs. (14) and (15) for Model II (the trifunctional compound model), on the other side. The results are summarized in Table 3, where the rate constants of benzyl chloride are also listed. The over-all kinetics expressed by Eq. (9) for Model I and by Eq. (17) for Model II were evaluated by using the respective values of k_1 and k_2. In Fig. 5, the broken and solid lines are the calculated plots for Model I and II respectively, and the white circles represent observed values. The agreement of the calculated and observed values are not so excellent as in the case of ethylene bromide, though Model II expresses the experimental results more closely than does Model I.

Table 3. Rate constants of the amination with 2-aminobutanol

Temp. °C	Rate constants $\times 10^3$, l/mol min: Chloromethylated polystyrene k_1' Eq. (22)	k_1 Model I Eq. (7)	k_1 Model II Eq. (14)	k_2 Eq. (8) or (15)	Benzyl chlorride k Eq. (1)
40	0.709	0.596	0.529	1.32	0.678
50	1.41	1.19	1.05	2.77	1.35
60	2.78	2.25	2.07	4.81	2.46
70	4.49	4.04	3.51	9.30	4.48

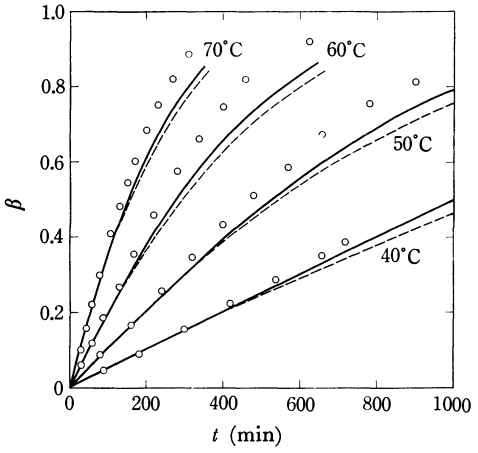

Fig. 5. Amination of chloromethylated polystyrene.
---- calculated for Model I
—— calculated for Model II
○ observed values

Equation (6) for Model I can be expressed in the form of Eq. (3) as follows:

$$dx/dt = k_1\left[1 + (k_2/k_1 - 1)\left(\frac{2\beta_1/\beta - 1}{1-\beta}\right)\beta\right](a-x)(b-x)) \quad (23)$$

where β_1 is given by the following equation when $a \gg b$:

$$\beta_1 = x_1/b = (1 - e^{-2k_1 at})/2 \quad (24)$$

By comparing Eqs. (23) with (4), we obtain:

$$k_{app}/k_1 = 1 + (k_2/k_1 - 1)(2\beta_1 - \beta)/(1-\beta) \quad (25)$$

Equation (13) for Model II can also be transformed to:

$$dx/dt = k_1\left[1 + (k_2/k_1 - 1)\left(\frac{3\beta_1/\beta - 1}{1-\beta}\right)\beta\right] \quad (26)$$

and:

$$k_{app}/k_1 = 1 + (k_2/k_1 - 1)(3\beta_1 - \beta)/(1 - \beta) \quad (27)$$

where β_1 is given by Eq. (16) when $a \gg b$.

The value of k_{app} at a given time can be calculated as a function of k_1, k_2, and t on the basis of Eqs. (25) and (27) respectively; the calculated values are compared with the observed values in Fig. 6. The agreement of the two sets of values is better in Model II than in Model I.

On the other hand, k_{app}/k_1 in Eqs. (25) and (27) has the same meaning as k_{app}/k_0 in Eq. (5), since the values of k_0 and k_1 are almost the same, as is shown in Tables 2 and 3. The plots of k_{app}/k_0 against β for Model I, Model II, and the original data are shown in Fig. 7. The plot for Model II is closer to the observed one than is that for Model I.

It may be concluded, on the basis of the facts to be summarized below, that Model II is better for such a self-accelerated reaction as that shown in the present study: (i) the intersection in the $\overline{kt}$ *vs.* t plot lies near $\beta=1/3$; (ii) the amination of ethylene bromide is also self-accelerated; (iii) the rate equations for Model II which give k_1 and k_2 can be derived in terms of the polymer reaction; (iv) the calculated plot of β *vs.* t for Model II is closer to the observed one than is that for Model I, and (v) the k_{app} values calculated for Model II are almost the same as the observed values.

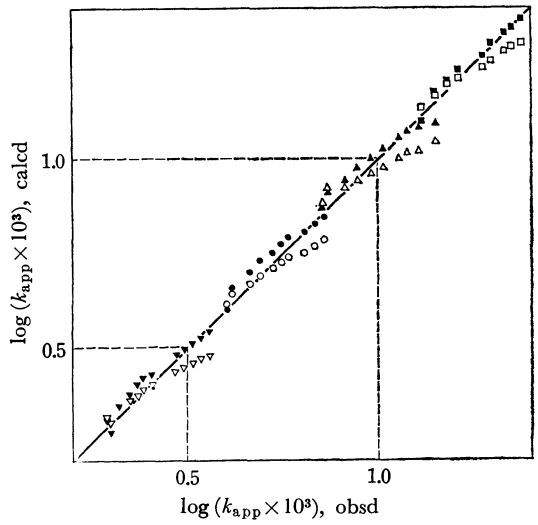

Fig. 6. Comparison between calculated and observed values of apparent rate constant in the amination of chloromethylated polystyrene.
Model I ▽ : 40°C, ○ : 50°C, △ : 60°C, □ : 70°C
Model II ▼ : 40°C, ● : 50°C, ▲ : 60°C, ■ : 70°C

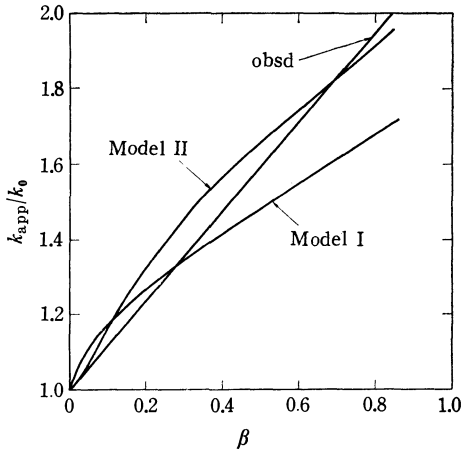

Fig. 7. Plots of k_{app}/k_0 *vs.* β in the amination of chloromethylated polystyrene.

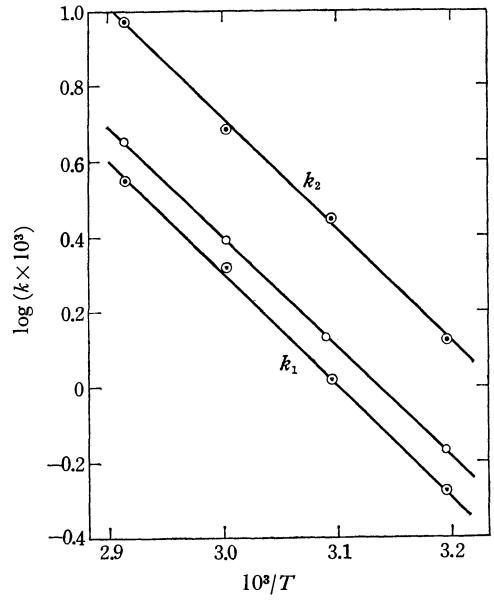

Fig. 8. Dependence of rate constants on temperature in the amination with 2-aminobutanol.
○ : Benzyl chloride
⊙ : Chloromethylated polystyrene

The Arrhenius plots of the rate constants listed in Table 3 are shown in Fig. 8, where the plot for k_1 is the one calculated on the basis of Model II. The values of E_a, the activation energy, which were calculated by the least-squares method, are listed in Table 4, where the mean values of A, the frequency factor, have been computed by means of:

$$k = A\exp(-E_a/\boldsymbol{R}T)\ l/\text{mol min}$$

In the table are also listed the mean value of $\Delta S_0^{\neq}$, the entropy of activation, which was calculated by:

$$A/60 = e(\boldsymbol{k}T/\boldsymbol{h})\exp(\Delta S_0^{\neq}/\boldsymbol{R})$$

TABLE 4. ACTIVATION ENERGIES, FREQUENCY FACTORS, AND ACTIVATION ENTROPIES OF AMINATION

Halide	Amine		E_a kcal/mol	A l/mol min	$\Delta S_0^{\neq}$ cal/deg mol
Chloromethylated polystyrene	2-Aminobutanol	k_1	13.6±0.2	1.57×10^6	−40.5
		k_2	13.6±0.1	4.50×10^6	−38.4
Benzyl chloride	2-Aminobutanol		13.4±0.1	1.60×10^6	−40.5
Benzyl chloride	*n*-Butylamine		12.5±0.2	7.88×10^5	−41.8

where $e=2.713$, k is the Boltzmann constant, and h, the Planck constant; the standard state refers to a unit concentration of one mole per liter.

The same value of E_a is obtained for k_1 and k_2; this value is comparable to that of the monomeric one, benzyl chloride. The value of A or $\Delta S_0^{\neq}$ for k_2 is slightly higher than that for k_1, whereas the latter is consistent with the values for benzyl chloride. This suggests that the amination of chloromethylated polystyrene proceeds normally in the initial stage.

The above-described facts also support the assumption that the self-acceleration in the amination is due to the adsorption of 2-aminobutanol by the hydroxyl group in the nearest-neighbor. In addition, the stronger self-acceleration has been observed in the amination with diethanolamine in dioxane.[4] On the other hand, such a steric hindrance of the neighboring groups as is observed in the amination with *n*-butylamine has not been found in the amination with 2-aminobutane in dioxane.[4] The "hydrophilic effect" of the hydroxyl group can, therefore, be considered to be the predominant factor in the amination of chloromethylated polystyrene with 2-aminobutanol in dioxane.

The authors wish to express their thanks to Mr. M. Takahashi for his technical assistance in preparing the polymer and in carrying out the measurement.

4) The present authors' unpublished data.

BULLETIN OF THE CHEMICAL SOCEITY OF JAPAN, VOL. 44, 901—907 (1971)

Excitation of Sodium Atoms by Collisions with Vibrationally Excited Molecules behind Shock Waves

Soji TSUCHIYA and Isao H. SUZUKI

Department of Pure and Applied Sciences, College of General Education, The University of Tokyo, Meguro-ku, Tokyo

(Received August 20, 1970)

Simultaneous measurements of Na D and CO fundamental emissions have been made behind a shock wave in CO–Ar or CO–N_2–Ar mixture containing a trace of Na vapor. The relaxation of a population in each vibrational level is calculated by use of Montroll-Shuler equation. The Na D emission intensity behind the shock wave in the 1.5% CO+Ar mixture nearly follows the relaxation of CO molecules excited to a vibrational level $v=3$ or 4, which is energetically lower than the 3^2P state of Na. This means that most Na atoms are excited by collisions with CO molecules in a level higher than $v=3$, and that the Na D reversal temperature exceeds the vibrational temperature of CO molecules behind the shock wave. In contrast to this, excitation of Na behind the shock wave in the 1.7% CO+49.3% N_2+49.0% Ar mixture is due to collisions with N_2 molecules in a level higher than $v=6$, and a nearly resonant vibrational-to-electronic energy transfer is realized. The relative values of the exciting rate k_v^e by collisions with CO or N_2 in a level v are determined to be $k_1^e : k_2^e : k_3^e : k_4^e : k_5^e = <0.01 : 0.04 : 1 : 1.6 : <2$ for Na–CO and $k_4^e : k_5^e : k_6^e : k_7^e : k_8^e = <0.03 : 0.21 : 1 : 1.4 : <2$ for Na–N_2 collisions at about 2600°K.

It is well known that the collision cross-section of an inert monoatomic gas for quenching the Na D fluorescence is very small or zero, while those of molecular gases are of the same order of magnitude as the gas kinetic ones. This is one of the evidences of the efficient energy transfer from the electronic to vibrational modes of molecules and the very poor coupling between the electronic and translational motions. Gaydon and Hurle[1,2] proposed that the Na D reversal temperature behind a shock wave in N_2 or other molecular gases was the same as the vibrational temperature of molecules, and they determined the vibrational relaxation times of some diatomic gases from the profiles of Na D reversal temperature behind shock waves. This means that Na atoms are excited by collisions with molecules in a vibrational level nearly resonant to the 3^2P state of Na. Other results in line with the above idea have been reported on the electronic excitation of Na atoms by collisions with vibrationally excited N_2 molecules in an electrical discharge[3] and in thermal beams.[4] However, these experiments could not give direct information on a vibrational state of N_2 whose energy was transferred to the electronic state of Na. To clarify this point, two experiments concerning the quenching process of excited atoms were carried out. Polanyi and coworkers observed the infrared emission induced in CO[5] and NO[6] through the quenching of Hg(6^3P), and concluded that less than half of the electronic energy was transferred to vibrations of CO and NO. Burrow and Davidovits[7] examined the vibrational state of N_2 which quenched Rb(5^2P) by the superelastic electron impact method, and found the vibrational state of a certain quantity of N_2 to be $v=5$ which was

1) A. G. Gaydon and I. R. Hurle, Eighth Symposium (International) on Combustion, Williams & Wilkins (1962), p. 309.

2) I. R. Hurle, *J. Chem. Phys.*, **41**, 3911 (1964).

3) W. L. Starr, *ibid.*, **43**, 73 (1965).

4) J. E. Mentall, H. F. Krause, and W. L. Fite, *Discuss. Faraday Soc.*, **44**, 157 (1967).

5) G. Karl, P. Kruus, and J. C. Polanyi, *J. Chem. Phys.*, **46**, 224 (1967).

6) G. Karl, P. Kruus, J. C. Polanyi, and I. W. M. Smith, *ibid.*, **46**, 244 (1967).

7) P. D. Burrow and P. Davidovits, *Phys. Rev. Lett.*, **21**, 1789 (1968).

nearly resonant to the 5^2P state.

In this work, we have measured the emissions of CO fundamental and Na D line at the same position behind shock waves in CO–Ar and CO–N_2–Ar mixtures containing a trace of Na vapor, and found a correlation between vibrational relaxation and electronic relaxation. The purpose of this experiment is to examine whether the electronic excitation temperature of Na is the same as the vibrational temperature or not, and to determine vibrational levels of diatomic molecules that can excite Na atoms most efficiently.

Experimental

The shock tube used is a stainless steel pipe of 10 cm i.d. with the test section of 460 cm and the driver section of 100 cm in length. The test section was evacuated to less than 10^{-4} Torr, and the leak rate was about 10^{-2} Torr/hr. Mylar film was used as a diaphragm which was ruptured spontaneously by the accumulating pressure of H_2 gas. Three windows are placed 400 cm away from the diaphragm; two quartz windows for measurement of the Na D doublet lines and calibration of a glass prism monochromator by passing a light beam across the tube from an appropriate light source, and the other CaF_2 window perpendicular to the light path of Na D line for the infrared emission. An infrared filter (Optical Coating Lab., LO-04260) and an Au-doped Ge detector (Philco, GPC-201A) were used to isolate and detect the CO fundamental emission. The time constant of the detector and an amplifier system was about 2 μsec. The Na D doublet was measured by a monochromator with a photomultiplier 1P21. The shock velocity was determined by two Pt film gauges placed 30 cm in front of and behind the observation windows.

The sample gases Ar, N_2, and CO were commercially available ones, and their nominal purities were 99.99% for Ar, 99.98% for N_2, and 99.5% for CO. The CO gas was purified by successive distillation using molecular sieve 5A at liquid nitrogen temperatare, and other gases were introduced into a mixing tank through a trap cooled by liquid nitrogen. A trace of Na vapor was added to the sample gas as fine dust by feeding the gas into the shock tube through a trap filled with Na vapor at 10^{-2}—10^{-3} Torr. By this method, a roughly controlled quantity of Na vapor could be mixed in the shock-heated gas, and the time required for colloidal Na to vaporize was very short. This was ascertained by measurement of the absorption of Na D line. No Na D emission was observed in a shock-heated gas without introduction of Na vapor by the above procedure.

Results

Figure 1(a) shows an example of emission profiles of CO fundamental and Na D line behind a shock wave in the 1.5% CO+Ar mixture. The intensity of CO fundamental increases exponentially with a time lapse after the shock arrival, and that of Na D line rises gradually toward its equilibrium value. The latter phenomenon is explained by the fact that Na atoms are excited by collisions with vibrationally excited CO molecules. Previously,[8] we ascertained that the collision cross-section of Ar atom for quenching Na(3^2P) was less than 10^{-3}Å^2. A similar conclusion for a Cs(6^2P)–He collision was reported by Dodd, Enemark, and Gallagher.[9] Thus, Ar atoms have no role in the excitation of Na atoms in a shock-heated CO–Ar mixture.

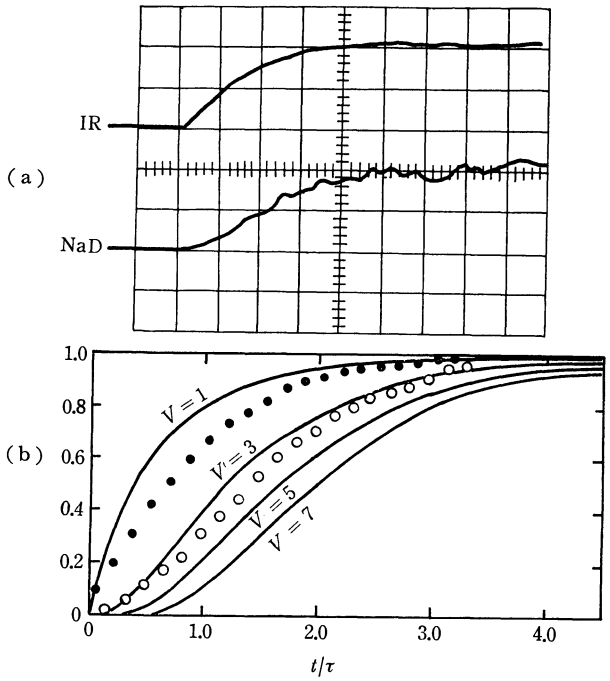

Fig. 1. (a) Emission profiles of CO fundamental and Na D line behind a shock wave in the 1.5% CO+Ar mixture.
(b) Vibrational relaxation of CO molecules in level v calculated from the above result and the excitation relaxation of Na atoms. Shock condition: $U_s=1.63$ mm/μsec, $p_2=518$ Torr, $T_2=2620$°K, $p_2\tau=74.0$ atm. μsec, and sweep velocity=20 μsec/division. #332.
– $\frac{x_v(t)}{x_v(\infty)}$, ● $\frac{I_{CO}(t)}{I_{CO}(\infty)}$, ○ $\frac{I_{Na}(t)}{I_{Na}(\infty)}$

The vibrational relaxation of CO in the CO–Ar mixture can be followed by the CO fundamental emission. Here, we make three assumptions: (1) the vibration of CO is harmonic, (2) only single quantum transitions are possible, and (3) the transition probability from $v=i$ to $v=i-1$ and that from $v=i$ to $v=i+1$ obey the relations, $P(i;-1)=iP(1;-1)$ and $P(i;+1)=(i+1)P(1;+1)$. For this case, Montroll and Shuler[10] showed that the vibrational distribution in each level was of the Boltzmann type, and the vibrational temperature T_v could be defined throughout the relaxation process. Thus, the concentration of CO in the v-th vibrational level should be given by

$$x_v = M(1 - e^{-\Theta})e^{-v\Theta}, \quad (1)$$

where $\Theta=\boldsymbol{hc}\omega/\boldsymbol{k}T_v$ (ω=vibrational frequency in cm^{-1}) and M is the total concentration of CO, *i.e.*, $M=\sum_v x_v$. The relaxation of the vibrational energy $E(T_v)$ is formulated to be

8) S. Tsuchiya and K. Kuratani, *Combustion and Flame*, **8**, 299 (1964).

9) J. N. Dodd, E. Enemark, and A. Gallagher, *J. Chem. Phys.*, **50**, 4838 (1969).

10) E. W. Montroll and K. E. Shuler, *ibid.*, **26**, 454 (1957).

$$1 - E(T_v)/E(T) = e^{-t/\tau}, \quad (2)$$

where $E(T)$ is the vibrational energy in equilibrium with the translational temperature T and τ the vibrational relaxation time. Since the vibrational energy is proportional to the intensity of the fundamental vibration, the relaxation time is determined experimentally by use of Eq. (2), and the vibrational temperature during the course of the relaxation can be expressed as a function of t/τ considering the relation $E(T_v) = Mhc\omega e^{-\theta}/(1-e^{-\theta})$. The concentration in each vibrational level during the relaxation can then be calculated as shown in Fig. 1(b). Applicability of the Montroll-Shuler equation to the present problem will be discussed later.

The Na D emission intensity can be assumed as a thermal emission under optically thick conditions, since the concentration of Na atoms is about 10^{11}—10^{12} atoms/cc, which is estimated from absorption measurement. Hence, the imprisonment of the Na D resonance line is effective for the present system, and the intensity is given by

$$I_{Na} = E_D B^\circ(\omega_D, T_{exc})\overline{\Delta\omega}\cdot\Delta\Omega\cdot\Delta s, \quad (3)$$

where B° is a steradiancy from the black body at a temperature T_{exc}, ω_D the wavenumber of Na D line, $\overline{\Delta\omega}$ a spectral slit width of the monochromator, $\Delta\Omega$ a solid angle of a light flux incident on the monochromator, Δs an area of the slit, and E_D an effective emissivity defined by

$$E_D = \int g(\omega', \omega_D)\{1 - \exp[-k(\omega')L]\}d\omega' \Big/ \int g(\omega', \omega_D)d\omega', \quad (4)$$

where $g(\omega',\omega_D)$ is a slit function of the monochromator set at the wavenumber of ω_D, $k(\omega)$ absorption coefficient, and L the optical depth of gaseous emitter. The emissivity depends only on the concentration of Na atoms, and is assumed to be constant in the flowing gas behind a shock wave. Therefore, the ratio of the intensity at time t to that at an equilibrium region far from a shock front is

$$\begin{aligned} I_{Na}(t)/I_{Na}(\infty) &= B^\circ(\omega_D, T_{exc})/B^\circ(\omega_D, T_2) \\ &= \exp[-(hc\omega_D/k)(1/T_{exc} - 1/T_2)] \\ &= [Na^*]_t/[Na^*]_\infty, \end{aligned} \quad (5)$$

where T_2 is the translational temperature behind a shock wave, and Na* denotes Na(3^2P) atom. Thus, the relative concentration of Na(3^2P) or the excitation temperature T_{exc} can be obtained from the Na D emission measurement.

The energy exchange process between the electronic and vibrational states of Na and CO is represented by

$$Na + CO(v) \rightleftarrows Na^* + CO(v - \Delta), \quad (6)$$

where the vibrational quanta Δ of CO is transferred to or from the electronic state of Na, and the exciting and quencing rates are denoted by $k^e_{v,\Delta}$ and $k^q_{v-\Delta,\Delta}$. The quenching process occurs efficiently in every gas kinetic collision, and the exciting probability is very large in a collision with a CO molecule in a particular vibrational level. Thus, the quasi-equilibrium between the electronic and vibrational states of Na and CO can be assumed, *viz.*, the relation,

$$[Na^*]/[Na] = (\sum_v k_v^e x_v)/[(\sum_v k_v^q x_v) + k_r], \quad (7)$$

holds during the relaxation process behind a shock wave. In this equation

$$k_v^e = \sum_{0\le\Delta\le v} k^e_{v,\Delta} \text{ and } k_v^q = \sum_{0\le\Delta\le v^*} k^q_{v,\Delta},$$

where v^* is the nearly resonant level to the 3^2P state of Na; $v=8$ for CO and $v=7$ or 8 for N_2, and k_r is a rate of radiative loss. In the present experimental condition, the radiative loss of Na(3^2P) can be neglected as shown previously,[8] and the denominator on the right-hand side of Eq. (7) is close to $k_0^q x_0 + k_1^q x_1$, which is nearly constant throughout the relaxation process. Reasons for this are: (1) a very poor population in a vibrational level higher than $v=2$ in the temperature range of the present experiment, and (2) it is reasonable to assume that the quenching rate of molecules in the vibrationally ground state does not differ from that of first excited molecules (Ref. 17 and Discussion). The emission intensity relative to that at the equilibrium region far after the shock arrival is then represented by

$$\begin{aligned} I_{Na}(t)/I_{Na}(\infty) &= \sum_v k_v^e x_v(t)/\sum_v k_v^e x_v(\infty) \\ &= \text{const.} \sum_v k_v^e[e^{-v\theta}(1 - e^{-\theta})], \end{aligned} \quad (8)$$

and the relative values of k_v^e's can be estimated by comparing the profile of I_{Na} with the calculated ones of x_v's.

It is seen from Fig. 1(b) that the experimental plots of $I_{Na}(t)/I_{Na}(\infty)$ nearly agree with those of $x_v(t)/x_v(\infty)$ when $v=3$ or 4. This seems that Na atoms are excited mainly by collisions with CO molecules in the vibrational level $v=3$ or 4, *i.e.*, the contribution of terms with $v=3$ or 4 to the right-hand side of Eq. (8) is very large as compared with that of a term with another v. Hence, the relative values of k_v^e's may be calculated by the least square method using the equation

$$\begin{aligned} y(\equiv I_{Na}(t)/I_{Na}(\infty)(1 - \chi)^{-1}) &= \sum_v k_v'\chi^v \\ &\approx k_2'\chi^2 + k_3'\chi^3 + k_4'\chi^4, \end{aligned}$$

where $\chi = e^{-\theta}$ and $k_v' = \text{const. } k_v^e$. The calculation was made by using observed values of y and χ at an interval of 0.1 of t/τ in the range that $t/\tau = 0.3$—3.0. The maximum value of k_1' was estimated by the assumption that $y = k_1'\chi$ when $t/\tau = 0$—0.3, and that of k_5' by the equation

$$\sum[y - (k_2'\chi^2 + k_3'\chi^3 + k_4'\chi^4) = k_5'\sum\chi^5,$$

where the notation $\sum$ means to sum up the experimental values at an interval of 0.1 of t/τ. In order to ascertain the reliability of the result obtained by the above method, the same procedure was applied to a case of contribution from other vibrational states, *e.g.*, $v=1$, 2, and 3 or $v=4$, 5, and 6. However, the result was physically untenable, since the conditions $k_v^e \ge 0$ and $k_v^e \ge k_{v-1}^e$ were not satisfied. The relative values of k_v^e's thus calculated are summarized in Table 1, from which we can conclude that most Na atoms are excited by collilions with CO molecules in a level higher than $v=3$. The experimental accuracy of Na D emission intensity is not enough to determine the

Table 1. Relative value of the exciting rate k_v^e of Na atoms in Na–CO collisions behind shock waves in the 1.5% CO + Ar mixture

Exp. no.	U_s mm/μsec	p_2 Torr	T_2 °K	$p_2\tau$ atm. μsec	k_1^e	k_2^e	k_3^e	k_4^e	k_5^e	k_6^e
332	1.63	518	2620	74.0	<0.01	0.09	1	1.9	<2.4	—
348	1.66	522	2710	59.7	<0.01	0.05	1	1.3	<1.8	—
368	1.67	502	2730	58.9	—	<0.02	1	3.3	4.3	< 6
381	1.815	469	3190	41.7	<0.09	0.3	1	1.4	<1.7	—
387	1.48	667	2220	194	<0.09	0.5	1	3.0	<4.5	—
363	1.54	570	2370	133	<0.07	0.3	1	3.7	<7.3	—
				mean[a]	<0.01	0.04	1	1.6	<2.0	—

a) Mean values of k_v^e's are calculated by the least square method using the former three data, nos. 332, 348, and 368, with the assumption $T_2=2690$°K.

Table 2. Relative value of the exciting rate k_v^e of Na atoms in Na–N_2 collisions behind shock waves in the 1.7% CO+49.3% N_2+49.0% Ar mixture

Exp. no.	U_s mm/μsec	p_2 Torr	T_2 °K	$p_2\tau$ atm. μsec	k_3^e	k_4^e	k_5^e	k_6^e	k_7^e	k_8^e
240	1.945	427	2540	138	<0.01	0.03	0.3	1	<3.0	—
242	1.96	418	2580	133	<0.03	0.09	0.2	1	<2.5	—
244	1.96	415	2570	126	—	<0.04	0.08	1	3.7	< 5
				mean[a]	—	<0.03	0.2	1	1.4	< 2

a) Mean values of k_v^e's are calculated by the least square method using all the data with the assumption $T_2=2560$°K.

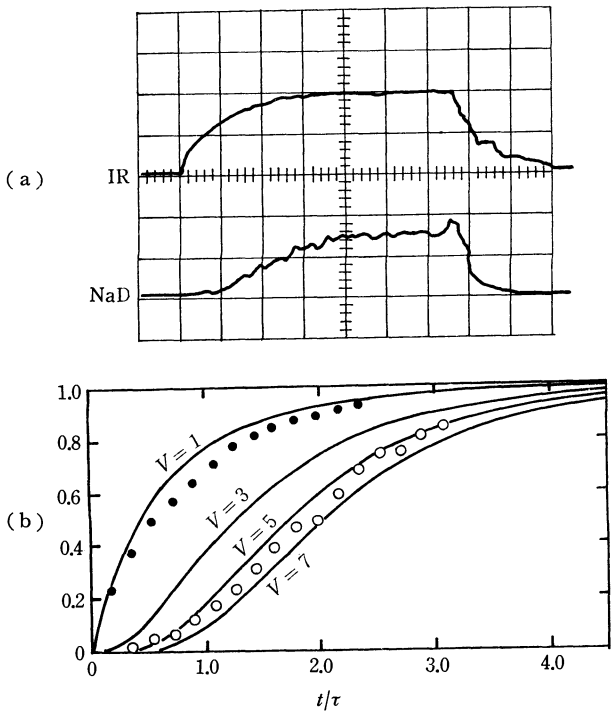

Fig. 2. (a) Emission profiles of CO fundamental and Na D line behind a shock wave in the 1.7% CO+49.3% N_2+49.0% Ar mixture.
(b) Vibrational relaxation of N_2 molecules in level v calculated from the above result and the excitation relaxation of Na atoms. Shock condition: $U_s=1.945$ mm/μsec, $p_2=427$ Torr, $T_2=2540$°K, $p_2\tau=138$ atm. μsec, and sweep velocity=50 μsec/division. #240.
— $\frac{x_v(t)}{x_v(\infty)}$, ● $\frac{I_{CO}(t)}{I_{CO}(\infty)}$, ○ $\frac{I_{Na}(t)}{I_{Na}(\infty)}$,

relative values of k_v^e's more than three, and the error is large for k_v^e at high vibrational levels owing to poor population.

The observed emission profiles of Na D and CO fundamental behind a shock wave in the 1.7% CO+49.3% N_2+49.0% Ar mixture are shown in Fig. 2(a). In a previous paper,[11] we proposed the vibrational relaxation equation for a diatomic gas mixture, and obtained the collision probability of the vibration-vibration energy exchange between CO and N_2. According to the result, the vibrational relaxation of CO should closely follow that of N_2. Since the concentration of CO is much smaller than that of N_2, and the collision cross-sections of CO and N_2 for quenching Na(3^2P) are of a similar magnitude,[12] the exciting or quenching collisions of CO molecules with Na atoms scarcely contribute to the whole intensity of Na D line. Analysis for the determination of relative values of k_v^e's is the same as that for the case of CO. As seen from Fig. 2(b), the excitation of Na atoms is made mainly by collisions with N_2 molecules in vibrational levels $v=5$—7. The calculated results are shown in Table 2. A nearly resonant vibrational-to-electronic energy transfer between N_2 and Na can be concluded. This is in line with Gaydon and Hurle's postulate.[1]

Discussion

The relaxation of the population in each vibrational level has been calculated by use of the Montroll-Shuler equation, based on the foregoing three assumptions.

11) Y. Sato, S. Tsuchiya, and K. Kuratani, *J. Chem. Phys.*, **50**, 1911 (1969).
12) D. R. Jenkins, *Proc. Roy. Soc.* (London), **A303**, 453 (1968).

Appropriateness of this procedure should be discussed. The vibrational excitation of CO in a CO–Ar mixture proceeds by two processes (this is the same for a N_2–Ar mixture). One is a gain or loss of vibrational quanta Δ by collision with Ar or CO through the translation-vibration (T-V) energy transfer

$$\text{(i)}\quad \mathrm{CO}(i) + \mathrm{M} \rightleftarrows \mathrm{CO}(i+\Delta) + \mathrm{M}.$$

The other is a resonant or near-resonant vibration-vibration (V-V) energy transfer process

$$\text{(ii)}\quad \mathrm{CO}(i) + \mathrm{CO}(j) \rightleftarrows \mathrm{CO}(i+\Delta) + \mathrm{CO}(j-\Delta).$$

According to this mechanism, the relaxation of population x_i in the i-th vibrational level is given by

$$\begin{aligned} dx_i/dt = {} & Z\sum_{\Delta\geq 1}\{[P(i-\Delta;\ \Delta)x_{i-\Delta} + P(i+\Delta;-\Delta)x_{i+\Delta}] \\ & - [P(i;\ -\Delta) + P(i;\ \Delta)]x_i\}N \\ & + Z\sum_{j}\sum_{\Delta\geq 1}\{[Q(i-\Delta, j;\ \Delta)x_{i-\Delta}x_j + Q(i+\Delta, j;\ -\Delta)x_{i+\Delta}x_j] \\ & - [Q(i, j;\ -\Delta) + Q(i, j;\ \Delta)]x_i x_j\}, \end{aligned} \tag{9}$$

where Z is the collision frequency, N the concentration of whole particles CO and Ar, and the probabilities for the forward processes of (i) and (ii) are represented respectively by $P(i;\ \Delta)=\phi_{\mathrm{A}}P_{\mathrm{A}}(i;\ \Delta)+\phi_{\mathrm{CO}}P_{\mathrm{CO}}(i;\ \Delta)$ and $Q(i,j;\ \Delta)$, in which ϕ_{A} and ϕ_{CO} are mole fractions of Ar and CO, and P_{A} and P_{CO} are the corresponding T-V probabilities by collisions with Ar and CO, respectively. Since $Q \gg P$, a quasi-equilibrium in the distribution of population in each vibrational level can be assumed during the relaxation process as proposed by Treanor, Rich, and Rhem.[13] That is, the vibrational relaxation proceeds keeping the second term in Eq. (9) equal to zero.

If we can assume that a CO molecule is a harmonic oscillator, the quasi-equilibrium condition results in the Boltzmann distribution, and the vibrational temperature can be defined. Then, Eq. (9) is reduced to

$$\begin{aligned} dx_i/dt = {} & ZN\sum_{\Delta\geq 1}[P(i;\ -\Delta)(\rho^{\Delta}x_{i-\Delta} - x_i) \\ & - P(i+\Delta;\ -\Delta)(\rho^{\Delta}x_i - x_{i+\Delta})], \end{aligned} \tag{10}$$

where $\rho=\exp(-\boldsymbol{hc}\omega/\boldsymbol{k}T)$ and $P(i-\Delta;\ \Delta)=\rho^{\Delta}P(i;\ -\Delta)$ from the detailed balancing. Here, we will take a first momentum $V=\sum_i ix_i$ from Eq. (10). The result is

$$dV/dt = ZN\sum_{\Delta\geq 1}\Delta\sum_{i}P(i+\Delta;\ -\Delta)(\rho^{\Delta}x_i - x_{i+\Delta}). \tag{11}$$

By assuming the Landau-Teller rule of transitions,

$$\begin{aligned} P(i+\Delta;\ -\Delta) = {} & (1/\Delta!)(i+1)(i+2) \\ & \cdots\cdots(i+\Delta)P(\Delta;\ -\Delta), \end{aligned} \tag{12}$$

Eq. (11) can be written as

$$\begin{aligned} dV/dt = {} & ZNM\sum_{\Delta\geq 1}\Delta P(\Delta;\ -\Delta)\{\rho^{\Delta}[1 + (V/M)]^{\Delta} \\ & - (V/M)^{\Delta}\}, \end{aligned} \tag{13}$$

where $M=\sum_i x_i$. If the quantity, $X=1-E/E(T)$ is defined to represent the departure of vibrational energy E from $E(T)$ in equilibrium with translational temperature T, the relaxation of vibrational energy can be written as

$$\begin{aligned} -dX/dt = {} & ZN\sum_{\Delta\geq 1}\Delta(\rho/1-\rho)^{\Delta-1}P(\Delta;\ -\Delta)[(1-\rho X)^{\Delta} \\ & - (1-X)^{\Delta}], \end{aligned} \tag{14}$$

where the relations $M=E(T)(1-\rho)/\rho\boldsymbol{hc}\omega$ and $V=E(T_v)/\boldsymbol{hc}\omega$ are used to derive the above equation from Eq. (13). This shows that the multiple quanta transitions cause non-linearity in the relaxation equation, and that the relaxation cannot be described as a simple exponential approach toward the equilibrium state. If all the terms higher than X in Eq. (14) are neglected, the equation should be similar to that of Landau-Teller, and an apparent relaxation time τ can be defined as

$$1/\tau = ZN\sum_{\Delta\geq 1}\Delta^2\rho^{\Delta-1}/(1-\rho)^{\Delta-2}P(\Delta;\ -\Delta). \tag{15}$$

In Fig. 3, the exact calculation for the system, where both the single and double quanta transitions contribute to relaxation, is compared with the above approximate solution, and the diference between the relaxing vibrational energies in both models is only 10% even if $P(2;\ -2)/P(1;\ -1)=0.1$. Therefore, to apply the Landau-Teller relaxation equation to the experimental analysis means to automatically take into account to a certain extent the contribution from multiple quanta transitions.

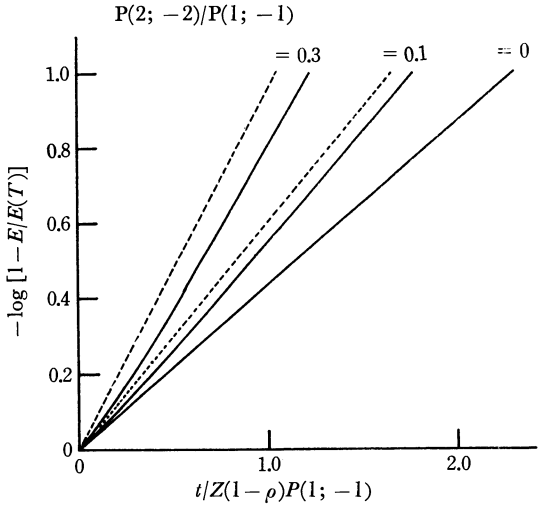

Fig. 3. Relaxation profile of CO behind a shock wave of 2000°K with single and double quanta transitions.
Solid line: exact solution, dotted line: approximate solution neglecting X^2 term.

It is probable that the real vibrational relaxation deviates from that of the Landau-Teller-Montroll-Shuler equation due to anharmonicity, especially for molecules in a high vibrational level. The quasi-equilibrium condition for a system of anharmonic oscillators results in a non-Boltzmann distribution.[13] In the shock-tube experiment, the translational temperature is higher than the vibrational one, though the latter cannot be uniquely defined. For this case, an effective vibrational temperature θ_v^* for a vibrational level v is lower than θ_1^* for the level $v=1$. Calculation of θ_v^*/θ_1^* as a function of θ_1^*/T shows that θ_v^*/θ_1^* is 0.97 for CO in a level $v=8$ when $\theta_1^*/T=0.3$. This value of θ_v^*/θ_1^* is for the initial stage of the relaxation where the population of highly excited molecules which contribute to the excitation of Na is very small.

13) C. E. Treanor, C. W. Rich, and R. G. Rhem, *J. Chem. Phys.*, **48**, 1798 (1968).

Table 3. Relative values of the exciting and quenching rates k_{Δ}^{e} and k_{Δ}^{q} of Na atom in Na–CO and Na–N_2 collisions at about 2600°K

vib. quanta transferred, Δ		1	2	3	4	5	6	7	8
Na–CO	k_{Δ}^{e}	<0.01	0.04	1	0.6	<0.4	—	—	—
	k_{Δ}^{q}	<0.1	0.1	1	0.2	<0.04	—	—	—
	k_{Δ}^{q} (calcd)[a]	0	0.72	1	1.3	0.94	0.34	0.16	0.03
Na–N_2	k_{Δ}^{e}	—	—	—	<0.04	0.3	1	0.5	<0.8
	k_{Δ}^{q}	—	—	—	<0.5	1.0	1	0.1	<0.06
	k_{Δ}^{q} (calcd)[a]	0	0.35	0.62	0.97	1.30	1	0.32	0

a) Relative values of k_{Δ}^{q} (calcd) at 0.1 and 0.2 eV of initial kinetic energies for Na–N_2 and Na–CO collisions, repectively, are those calculated by Bauer *et al.*[17]

Thus, a large deviation from the Boltzmann distribution cannot be expected in the present experimental condition. The remaining effects of the anharmonicity are the enhancement of the multiple quanta transitions and the difference in values of $\exp(-E_v/\boldsymbol{k}T_v)$ (E_v is a real energy level) and $\exp(-v\boldsymbol{hc}\omega/\boldsymbol{k}T_v)$. The former can be rejected from the preceding discussion, and the latter effect causes little change in curves of $x_v(t)/x_v(\infty)$ in Figs. 1 and 2. The absolute values of x_v must be corrected by a factor $\exp[(v\boldsymbol{hc}\omega-E_v)/\boldsymbol{k}T_v]$, which does not produce a serious effect on the present conclusion.

The uncertainty in the population distribution can be eliminated by a direct measurement of the vibrational relaxation of highly excited molecules, especially in a level energetically near the 3^2P state. Lack of this experiment is the weakest point in this kind of work. However, we can say at least that the excitation temperature of Na atoms does not agree strictly with the the vibrational temperature of CO, while it nearly agrees with that of N_2 if the molecules are assumed to undergo relaxation of the Landau-Teller type.

The detailed balancing equation for process (6) is

$$k^{e}_{v,\Delta}/k^{q}_{v-\Delta,\Delta} = (g^*/g)\exp[-(E^* - \Delta\boldsymbol{hc}\omega)/\boldsymbol{k}T], \quad (16)$$

where g is the degeneracy of Na(3^2S), g^* the combined degeneracies of the two 3^2P states, E^* the electronic energy of Na(3^2P), and T a translational or rotational temperature. If it is possible to suppose that the exciting or quenching rate is only dependent on the vibrational quanta Δ transferred to or from the electronic state of Na and independent of vibrational states of colliding molecules, the exciting rate k_{Δ}^{e} and consequently the quenching rate k_{Δ}^{q} can be estimated as shown in Table 3. This means that the energy transfers of vibrational quanta $\Delta=3$—4 in Na–CO collisions and $\Delta=5$—6 in Na–N_2 collisions are most effective. Thus, about half of the electronic energy must be supplied from the translational or rotational motion to excite Na(3^2S) by collision with CO.

The relation between the excitation temperature of Na and the vibrational temperature of molecules may be discussed by Eqs. (7) and (16). Equation (7) can be simplified by the aforementioned assumption that $k^{e}_{v,\Delta}=k_{\Delta}^{e}$ and $k^{q}_{v,\Delta}=k_{\Delta}^{q}$ for all v, and is written as

$$[Na^*]/[Na] = \sum_{0\le\Delta\le v^*} k_{\Delta}^{e}\exp(-\Delta\boldsymbol{hc}\omega/\boldsymbol{k}T_v)/\sum_{0\le\Delta\le v^*} k_{\Delta}^{q},$$

where the radiative process is neglected. Combining the above equation with the equation of detailed balancing Eq. (16), the following relation can be derived.

$$\exp(-E^*/\boldsymbol{k}T_{exc}) = \sum_{0\le\Delta\le v^*} k_{\Delta}^{q}\exp[-(E^*/\boldsymbol{k}T) + (\Delta\boldsymbol{hc}\omega/\boldsymbol{k})(1/T - 1/T_v)]/\sum_{0\le\Delta\le v^*} k_{\Delta}^{q}. \quad (17)$$

In a thermal equilibrium system in which $T=T_v$, Eq. (17) shows that $T_{exc}=T$, while $T_{exc}\neq T$ in the system of $T\neq T_v$. For the latter, the relation of T_{exc} to T_v can be clarified by assuming that only the vibrational energy of $\Delta^*\boldsymbol{hc}\omega$ is exchanged with the electronic state of Na, where Δ^* means the most effective vibrational quanta transferred in the vibrational-to-electronic energy transfer, that is, $k_{\Delta q}=0$ when $\Delta\neq\Delta^*$. Then, we have

$$1/T_{exc} = (\Delta^*\boldsymbol{hc}\omega/E^*)/T_v + [1 - (\Delta^*\boldsymbol{hc}\omega/E^*)]/T. \quad (18)$$

In the case of resonant vibrational-to-electronic energy transfer, we get

$$\Delta^* = v^*,\ T_{exc} = T_v.$$

On the other hand, in a non-resonant case, $\Delta^*<v^*$, we obtain

$$T < T_{exc} < T_v \quad \text{or} \quad T > T_{exc} > T_v.$$

The vibrational relaxation time obtained by measuring the Na D emission behind a shock wave in CO should be shorter than that determined from the CO fundamental emission, since $T_{exc}>T_v$. Figure 4(a) represents the relaxation of the vibrational energy calculated from the emission profiles of CO fundamental and Na D emissions, for which the assumption $T_v=T_{exc}$ is made. The vibrational energy defined by the Na excitation is nearer to its equilibrium value than the real energy observed by the infrared emission. This may be referred to the fact that the main contribution to the excitation of Na is caused from CO molecules in a level $v=3$ or 4. However, an apparent relaxation time which is determined from a slope of linear plots, $\log(1-E/E(T))$ *vs.* t, does not differ so much from the true one. The difference between the two slopes is less than 10%, which is of a magnitude comparable to an experimental error of the Na D emission measurement. Thus, vibrational relaxation times in CO or CO–Ar mixture observed by separate measurements of the Na D and CO fundamental emissions appear to agree with each other as Russo has found.[14] The same analysis for a CO–N_2–Ar mixture is shown in Fig. 4(b), and the vibrational relaxations measured

by both methods agree quite well. This indicates the resonant mechanism in the vibrational-to-electronic energy transfer, and is in line with Hurle's experiment.[2]

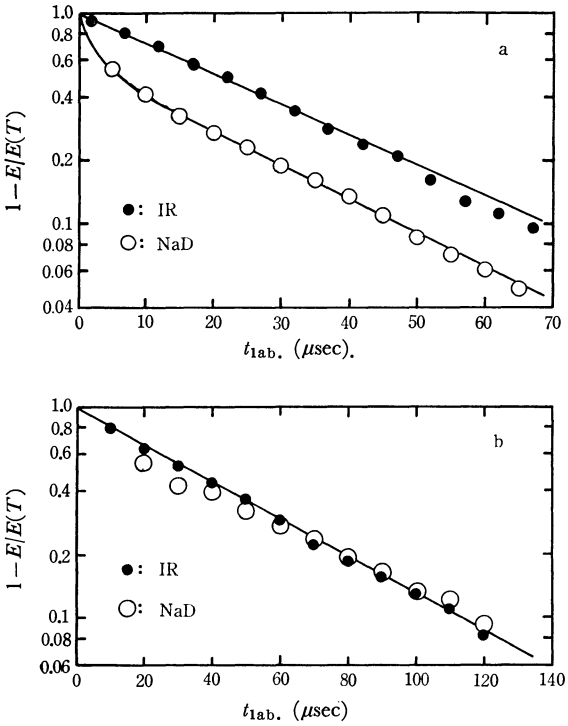

Fig. 4. (a) Relaxation of the vibrational energy of CO behind a shock wave in the 1.5% CO+Ar mixture.
(b) Relaxation of the vibrational energy of N_2 behind a shock wave in the 1.7% CO+49.3% N_2 +49.0% Ar mixture. Two values of $E/E(T)$ are determined from infrared emission measurement, $I_{CO}(t)/I_{CO}(\infty)$, and from the NaD emission by assuming that $T_v=T_{exc}$.

Russo[14] also observed the vibrational relaxation in the expanding flow of the 5%CO+Ar mixture by measuring the Na D reversal and CO vibrational temperatures, and found that the ratio of the relaxation time τ_e to that of the shock-wave experiment τ_s is 10^{-2}—10^{-3} for the infrared method, and 10^{-1}—10^{-2} for the Na D method. Since $T_v>T$ in the expanding flow and $\Delta^*=3$—4, T_{exc} must be lower than T_v if a non-Boltzmann distribution is not taken into account. This suggests a smaller value of τ_e/τ_s for the Na D method than that for the infrared method, while a non-Boltzmann distribution caused by the V-V coupling of anharmonic oscillators has a reverse effect. However, it seems impossible to explain the difference in values of τ_e/τ_s observed by two methods in terms of the latter effect. A later experiment by Rosenberg, Taylor, and Teare[15] shows that H atoms as an impurity reduce considerably the relaxation time of CO in the expanding flow. Hence, the Na excitation temperature observed by Russo might be abnormally high by the chemi-excitation mechanism $H+H+Na\rightarrow H_2+Na^*$.

Theoretical calculation for the quenching process, $Na(3^2P)+N_2(0)\rightarrow Na(3^2S)+N_2(v)$, was made by Bjerre and Nikitin[16] and by Bauer, Fisher, and Gilmore.[17] They proposed that the adiabatic potentials of $Na(3^2P)+N_2(^1\Sigma_g^+)$ and $Na(3^2S)+N_2(^1\Sigma_g^+)$ were crossed by the surface $Na^++N_2^-$, and that the non-adiabatic transitions occurred at these crossing points. This model explains well the large quenching cross-section of N_2, though the collision process without crossing or approaching of initial and final potential surfaces results in a very small cross-section.[18] Bjerre and Nikitin calculated the classical trajectories on the potential surfaces by applying the Landau-Zener formula to the transitions at crossing points, and obtained the final classical vibrational energies of N_2 and quenching probabilities. Their result shows the vibrational states of N_2 molecules, to which the energy of $Na(3^2P)$ is transferred, to be mostly in $v=1$—4. This is incompatible with our results. Bauer *et al.* treated the process in terms of a diffusion of the probability flux through a two-dimensional network of potential curves characterized by the electronic and the vibrational states of N_2 and N_2^-. The transition probability at each crossing point is given by the Landau-Zener formula, in which the transition matrix element is the product of an electronic interaction function and a Franck-Condon factor between the vibrational states of N_2 and N_2^-. In Table 3, their results are compared with ours in order to show qualitative agreement.

Conclusion

The excitation of Na atoms to the 3^2P state behind the shock wave in a CO–Ar mixture follows the vibrational excitation of CO molecules to levels $v=3$—4 rather than to a level $v=8$ which is energetically resonant to the 3^2P state of Na. The result is derived with the assumption that the vibrational relaxation of CO proceeds under the condition of Landau-Teller. Analysis of this result shows that most Na atoms are excited by collisions with CO molecules in a vibrational level higher than $v=3$, and the remaining energy to excite Na atoms is supplied from the translational or rotational motion of the colliding atom and molecule. In contrast to this, the excitation of Na atoms is made by collisions with vibrationally excited N_2 molecules in levels $v=5$—7, and the process is a nearly resonant vibrational-to-electronic energy transfer. Thus, the Na excitation temperature behind the shock wave in a N_2–Ar mixture is nearly in agreement with the vibrational temperature of N_2. The results are compatible with the theoretical calculation based on the mechanism that a Na atom is excited *via* an ionic state $Na^+\cdots CO^-$ or $Na^+\cdots N_2^-$ in the process of molecular collision.

The authors thank Mr. Yukinori Sato for his valuable discussion on the analysis of vibrational relaxation.

14) A. L. Russo, *J. Chem. Phys.*, **47**, 5201 (1967).
15) C. W. von Rosenberg, R. L. Taylor, and J. D. Teare, *ibid.*, **48**, 5731 (1968).
16) A. Bjerre and E. E. Nikitin, *Chem. Phys. Lett.*, **1**, 179 (1967).
17) E. Bauer, E. R. Fisher, and F. R. Gilmore, *J. Chem. Phys.*, **51**, 4173 (1969).
18) P. G. Dickens, J. W. Linnett, and O. Sovers, *Discuss. Faraday Soc.*, **33**, 52 (1962).

Studies on Salt Solution Aerosols. V.[1] The Effect of Surface Active Substance upon the Droplet Size of an Aqueous NaCl Solution Aerosol

Yasuo Ueno and Isamu Sano

Department of Chemistry, Faculty of Science, Nagoya University, Chikusa-ku, Nagoya

(Received August 25, 1970)

An aqueous NaCl solution (10%) containing a surface active substance was dispersed to a mist with a Dautrebande type atomizer. The influence of the surface active substance on the droplet size and mass concentration of the mist during aging was studied. We examined ethyl alcohol, acetic acid, ethyl acetate, acetone, glycerine, and a commercial nonionic surfactant. From the results it was found that at an early stage of aging, the droplet number present in mist was inversely proportional to the fourth power of droplet size.

In a previous study,[2] we carried out an experiment on the production of aqueous NaCl solution aerosols by atomizing an aqueous NaCl solution containing or not containing a surfactant with an atomizer. We found that the droplet size decreases with the increase of the concentration of the surfactant or with the decrease of the surface tension of the dispersing solution. Surfactants used were commercial products of polyoxyethylene nonylphenyl ether, $C_9H_{19}C_6H_4O(CH_2CH_2O)_nH$ with $n=6$, 9, and 21.

In the present study we worked with a Dautrebande's baffle type atomizer, which is superior to the intercepting glove type used earlier as it produces droplets finer than 1.2 μ diameter.

Unlike the above-mentioned polymeric surfactants with the c.m.c. ranging from 10^{-1} to 10^{-2}% by weight, almost all the surface active substances examined in the present work are of much higher solubility so that they enabled us to conduct the experiment over a wider range of concentration to gain knowledge of the role of surface active substance in the production of mist and, moreover, of the correlation between the size and number of the droplets present in mist immediately after its formation.

Various methods[3] of measuring the size of droplets of a mist have been presented, but they are laborious and troublesome on account of the volatility of the droplets causing alteration in their size. For example, in the chemical spot method,[3] it involves preparation of a series of calibration curves. The method adopted in the present study takes advantage of the volatility and is of significance as being applicable and available to much the same extent as the other methods.

Experimental

Materials. Ethyl alcohol, acetic acid, ethyl acetate, acetone, and glycerine used were of the extra pure grade. Commercial surfactant, EA-80 (polyoxyethylene nonylphenyl ether, $n=9$), was used as obtained from a chemical supply house.

Apparatus and Procedure. The over-all experimental

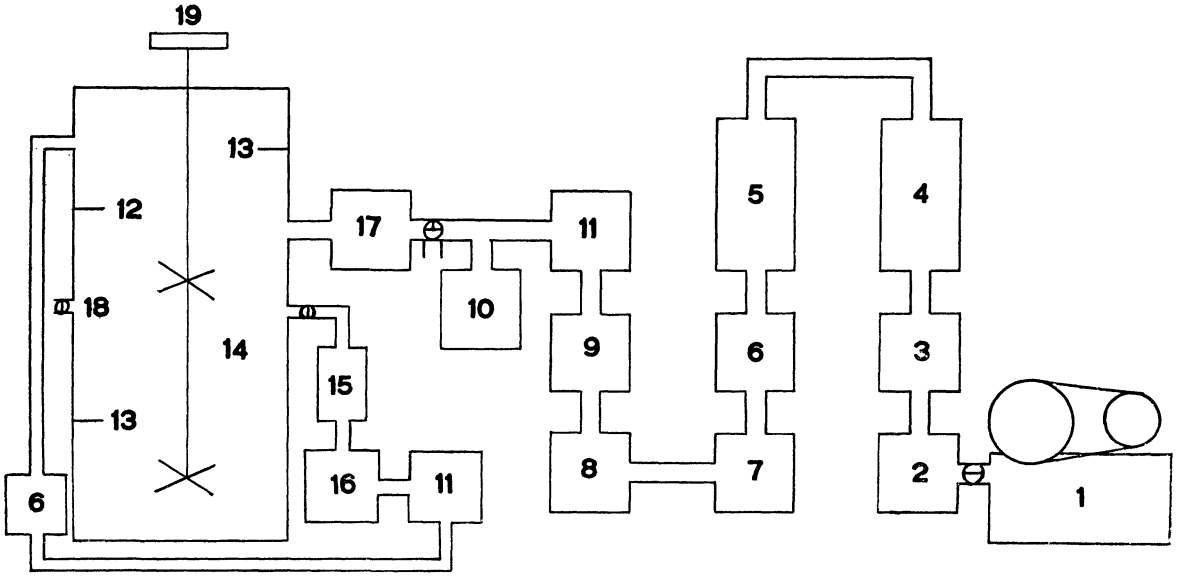

Fig. 1. Over-all experimental arrangement.
1) compressure 2) air cleaner 3) pressure regulator 4) tubes of glass fibers 5) tubes of absorbent cotton 6) bubbling bottles for humidification 7) large bottles for air buffering 8), 9) pressure regulators 10) manometer 11) flowmeter 12) hygrometer 13) glass thermometer 14) chamber 15) electrical precipitator 16) air pump 17) atomizer 18) sampling hole 19) stirrer.

1) Part IV: This Bulletin, **44**, 637 (1971).
2) I. Sano, S. Hikita, and Y. Ueno, *Nippon Kagaku Zasshi*, **90**, 876 (1969).
3) Y. Ueno and I. Sano, This Bulletin, **44**, 637 (1971).

arrangement is illustrated in Fig. 1. The compressed air at 5 kg/cm² (1) was driven through an air cleaner (2) and its pressure was reduced to 3 kg/cm² by a pressure regulator (3). The air was passed through filter tubes of glass fibers (4) and of absorbent cotton (5) for elimination of air-borne dust and then, it was humidified by bubbling through the same solution (6) as that to be dispersed and released from gustiness of flow with the aid of two large bottles (7). Finally, the pressure was adjusted and maintained constant at 2 kg/cm² by regulators (8) and (9). The mist thus generated with an atomizer (17) was introduced for 10 min into a mist chamber which had previously been saturated with water vapor of the dispersing solution. The humidity and temperature in the chamber were measured by means of an electrical resistance type hygrometer (12) and a glass thermometer (13) before and after the run. The temperature was kept at 20.0°±0.5°C throughout all the runs of experiment. The mist was subjected to aging with a constant rate stirrer (50 rev/min) (19) for an hour. The recorded time was reckoned from the moment of stopping the introduction of mist. At frequent intervals, portions of the mist were drawn for determination of mass concentration and particle size. The total amount of the portions of mist drawn from the chamber, so that it would scarcely affected the accuracy of the determination.

The solution to be dispersed was an aqueous NaCl solution (10%) or that containing a surface active substance in such an amount that the diminution of NaCl was within 0.05%.

Mist Generator. The mist generator employed is a modification of the Dautrebande type[4] and is illustrated in Fig. 2. The amount of the dispersing solution present in the generator is maintained constant by feeding fresh solution from the bottom of a cylindrical reservior (7) of 7 cm diameter, and the excess leaves the generator to a sink through a level tube (not shown in Fig. 2) whose height is adjustable as one wishes. The solution is drawn up by virture of the Venturi effect through the annular channel between the nozzle (3) and the filtering column (4). The atomized droplets impinge against the upper part of the filtering cap (5); the coarser ones are unstable to precipitate and run down into the dispersing solution (10), while those surviving are driven to pass through about fifty, small holes of 1.0 mm diameter (8) in the filtering column (4) and some of them encounter one another and coalesce. The stabilized and finer mist is thus generated through a mouthpiece (6).

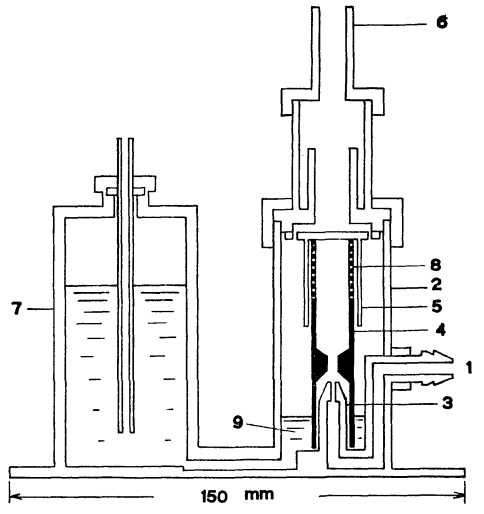

Fig. 2. Aerosol generator equipped with a constant feeding reservior.
1) compressed air tubing 2) plastic cylinder 3) air nozzle 4) filtering column topped by filtering holes 5) filtering cap 6) mouthpiece 7) reservior 8) small holes of 1.0 mm diameter in filtering column 9) dispersing solution

It is well known that this device can favourably be utilized for generation of submicronic droplets on account of its merit that size selection is effectively made through a liquid filtration mechanism, whereby coarser droplets are obligatory removed from the mist in the inner column.

Mass Concentration Analysis. Portions of the mist were periodically drawn with a constant rate air pump and passed through an electrical precipitator under a voltage of 7200 V/cm. The deposit in it was dissolved in 20 cc of distilled water and the weight was determined by electrical conductivity measurement with an error of less than 5%. With the volume of the mist drawn, which was recorded on the flowmeter, the concentration was calculated as milligrams of NaCl per cubic centimeter.

Particle Size Analysis. Portions of the mist were drawn into a silica gel holding syringe and dried, and they were passed to a precipitator at a rate of 15 cc/min. The precipitator used was that of Shibata Scientific Instrument Co. Estimates of the particle size were made on the thermal precipitator samples with a Hitachi HU-11DS electron microscope at a magnification of 3000 X. Electron microscope collodion mesh grids were mounted on a circular cover glass which was fitted close to a heated wire of the thermal precipitator. The sodium chloride particles were cubic crystals, and the number averaged width of their one crystal face was regarded as the representative size. From the average width (L) thus found, we calculated the radius (R) of the sphere corresponding to a 10% solution droplet.

Results and Discussion

Time Variation of Mass Concentration. Figure 3 shows that the mass concentration decreases with the

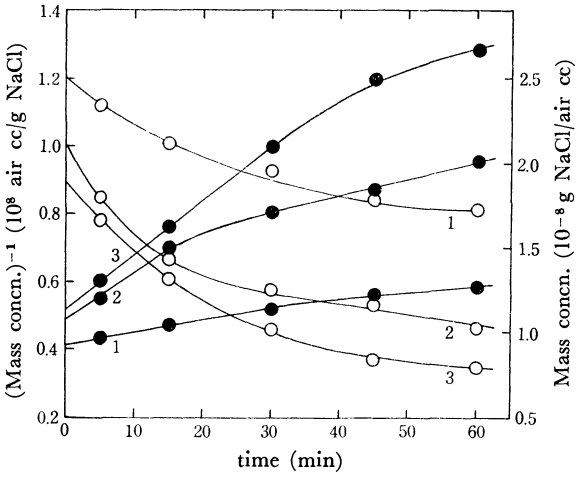

Fig. 3. Time variation of mass concentration.
(1) with no surface active substance
(2) acetone, 0.25 mol/*l*
(3) acetone, 0.50 mol/*l* solid circles refer to the left-hand axis and open circles the right one.

4) L. Dautrebande, H. Beckmann, and W. Walkenhorst, *Arch. intern. Pharmacodynamide*, **66**, 170 (1958); L. Dautrebande, "Microaerosols," Acad. Press, London and New York (1962); W. Walkenhorst and L. Dautrebande, *Staub.*, **24**, 505 (1964); M. J. Matteson and M. Stober, *J. Colloid & Interface Sci.*, **23**, 203 (1967); M. Suzuki, S. Watanabe, S. Hongo, and T. Ohata, *Zairyo*, **17**, 564 (1968).

elapse of time and markedly with the addition of a surface active substance to the dispersing solution. It will be seen that if the reciprocal of the mass concentration is plotted against the time, a linear relation holds in the early stages of nearly all the runs, revealing that the rate of the decrease in mass concentration follows the rate law of a second order reaction.

Time Variation of Particle Size Distribution and Number Concentration. The variation in particle size distribution with time is given in Fig. 4. It is evident in the figure that the size of a sodium chloride particle as represented by the width of one crystal face increases with time and, with the particles obtained from the solution droplets containing ethyl acetate, the size gets smaller as the surface active substance is more concentrated. The similar results were found for another surface active substances such as ethyl alcohol, acetic acid, acetane, glycerine, and polyoxyethylene nonylphenyl ether.

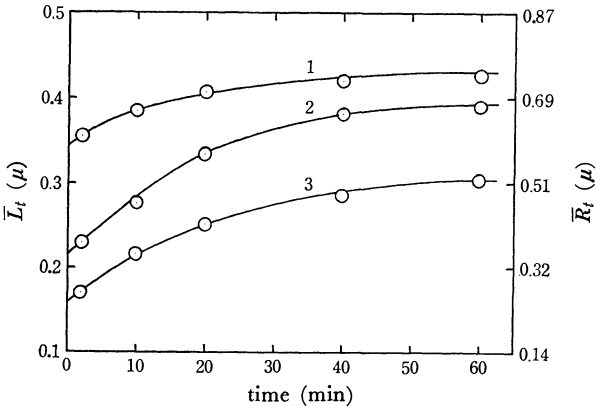

Fig. 4. Time variation of particle size distribution.
(1) with no surface active substance (2) ethyl acetate, 0.20 mol/l (3) ethyl acetate, 0.45 mol/l

We calculate the average droplet radius ($\bar{R}_t$) from the average crystal size ($\bar{L}_t$) by use of the relation

$$4/3\cdot\pi\bar{R}_t^3\cdot\rho_1\cdot W/100 = \rho_2\bar{L}_t^3 \qquad (1)$$

where W is the NaCl concentration of dispersing solution, ρ_1 and ρ_2 are the densities of the solution and NaCl crystal, respectively, and the subscript t is the time elapsed, while the bar over a letter signifies the average. On the right axis in Fig. 4 is shown the radius (R_t).

Size Distribution and Number Concentration Immediately after Atomization. Let us express the average of crystal size, droplet radius, mass concentration, and number concentration at zero time by L_0, R_0, C_0, and N_0, respectively. The value of L_0 or R_0 is found by extrapolation of the plot of L_t or R_t *vs.* t to the intercept in Fig. 4 and similarly the value of C_0 in Fig. 3. The number concentration N_0 can be estimated by

$$N_0 = C_0/(L_0^3\rho_2) = C_0/(4/3\cdot\pi R_0^3\rho_1\cdot W/100) \qquad (2)$$

Figure 5 indicates the relationship between the droplet radius (R_0) or number concentration (N_0) and the surface tension of dispersing solution. From the figure, it will be noted that as the surface tension is decreased, the smaller radius and the higher concentration are attained except the case of glycerine which exhibits that the plotted points deviate largely from the curves for the radius as well as the concentration probably because of comparatively high viscosity of the solution. Figure 6 shows the relationship of R_0 or N_0 and the viscosity, with the exception of the solutions of EA-80 and ethyl acetate which are of low viscosity. Remark should be made, here, of the fact that the relation of R_0 to the viscosity is in the reverse to that in the previous paper;[5] the reason may be possibly be that the working mechanism of the present atomizer is different from that of the atomizer employed previously. We will later report the effect of viscosity in more detail with particular reference to the experiments using glycerine, ethylene glycol and so on as a surface active substance.

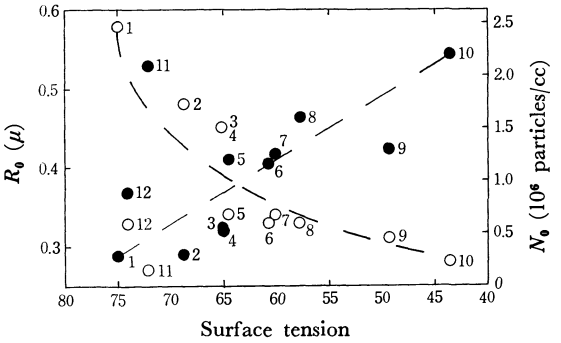

Fig. 5. Relation between R_0 or N_0 and the surface tension of dispersing solution.
(1) with no surface active substance (2) acetic acid, 0.25 mol/l (3) ethyl alcohol, 0.25 mol/l (4) acetone, 0.25 mol/l (5) acetic acid, 0.50 mol/l (6) ethyl alcohol, 0.50 mol/l (7) acetone, 0.50 mol/l (8) EA-80, 10^{-2}% (9) ethyl acetate, 0.20 mol/l (10) ethyl acetate, 0.45 mol/l (11) glycerine, 1.00 mol/l (12) glycerine, 0.50 mol/l (○ : R_0, ● : N_0)

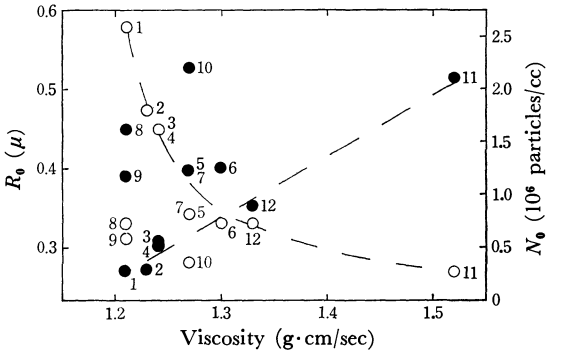

Fig. 6. Relation between R_0 or N_0 and the viscosity of dispersing solution.
With regard to the legends, confer Fig. 5. (○ : R_0, ● : N_0)

If it is assumed that a mechanical W is required for a large number of droplets, whose surface area taken together runs up to A_2, to be formed from a bulk solution of surface area A_1, then

$$W = \gamma\Delta A = \gamma(A_2 - A_1) \qquad (3)$$

where γ is the surface tension. Neglecting A_1 in comparison with A_2 and denoting the surface active substance containing NaCl solution by a prime,

$$\gamma A_2 = \gamma' A_2' \qquad (4)$$

5) I. Sano and Y. Ueno, *Nippon Kagaku Zasshi*, **90**, 47 (1969).

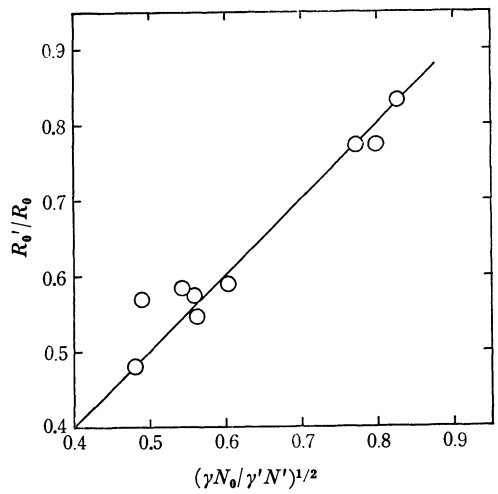

Fig. 7. Plot of R_0'/R_0 against $(\gamma N_0/\gamma' N_0')^{1/2}$.

and

$$\gamma'/\gamma = A_2/A_2' = N_0 S_0/N_0' S_0' \tag{5}$$

where N_0 and S_0 represent the number concentration of the droplets present in the mist chamber and the average area per droplet, respectively. Since S_0 is equal to $4\pi R_0^2$, it follows from Eq. (5) that

$$R_0'/R_0 = (\gamma N_0/\gamma' N_0')^{1/2} \tag{6}$$

The validity of Eq. (6) is as given in Fig. 7.

According to the results previously reported,[2]

$$R_0'/R_0 = (a\gamma'^{1/2} - b)(a\gamma^{1/2} - b) \tag{7}$$

where a and b are empirical constants. From Eqs. (6) and (7), we get

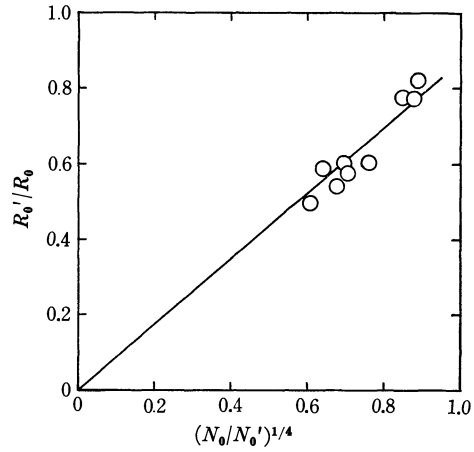

Fig. 8. Plot of R_0'/R_0 against $(N_0/N_0')^{1/4}$.

$$R_0'/R_0 = (N_0/N'_0)^{1/4}[(1 - b/a \cdot \gamma'^{-1/2})/(1 - b/a \cdot \gamma^{-1/2})]^{1/2} \tag{8}$$

The magnitude of the 1/2-power term of the right side is clearly less than unity as γ' is smaller than γ, and would be supposed to remain nearly constant for the range studied. Experimental verification of Eq. (8) is presented in Fig. 8; there is a straight line of a slope slightly lower than 45° which is in conformity with expectation. This reveals that the Eq. (8) might be approximated to

$$R_0'/R_0 = (N_0/N_0')^{1/4} \tag{9}$$

It will be a useful relation for the estimation of the droplet size or the number concentration in aerosol at zero time without knowledge of the surface tension of the solution to be dispersed.

The Catalytic Oxidation of Hydrogen on Titanium Dioxide; Anatase and Rutile

Yoshito ONISHI

Department of Chemistry, Faculty of Industrial Arts, Kyoto Technical University, Matsugasaki, Sakyo-ku, Kyoto

(Received August 26, 1970)

To clarify the reaction mechanism of catalytic oxidation of hydrogen on titanium dioxide, the rate of catalytic oxidation of hydrogen by oxygen and the reduction rate of titanium dioxide by hydrogen have been measured by a static method in temperature range of 400—650°C at 10^{-2} mmHg. The results were compared with those of carbon monoxide which were reported in the previous papers. The oxidation reactions of hydrogen on anatase and rutile were first order with respect to hydrogen and independent of the oxygen pressure. The oxidation rate was almost the same as the reduction rate of titanium dioxide by hydrogen. The activation energy was 29.2 kcal/mol for anatase and 17.8 kcal/mol for rutile, and the difference between these values for two crystal forms was nearly equal to that of the oxidation of carbon monoxide. Therefore, it may be considered that the mechanism of oxidation of hydrogen is analogous to that of carbon monoxide. The electric conductivity of the catalyst during the oxidation of hydrogen was larger than that in oxygen at the same temperature, and was still larger than that during the oxidation of carbon monoxide except for a few cases on anatase. There were close correlations between the electric conductivity and the amount of active oxygen of the catalyst and the reduction rate constant of titanium dioxide by both hydrogen and carbon monoxide.

As a series of investigations of the catalytic action of titanium dioxide, the catalytic oxidation of carbon monoxide[1,2] and the catalytic decomposition of nitrous oxide[3] have been carried out. It was confirmed from the results that the difference between anatase and rutile in the catalytic action is owing to the difference in the desorption rates of the active oxygen from the catalysts. Furthermore, in order to examine whether the reaction mechanism of carbon monoxide is applied to other reactions, the catalytic oxidation of hydrogen was examined because hydrogen is a reducing gas analogous to carbon monoxide.

There have been published several papers concerning the oxidation of hydrogen on the metallic oxide catalysts,[4-12] and some of them [4-7,10] compared the reaction mechanisms of the oxidation of hydrogen with those of carbon monoxide. But except for a few papers on the adsorption of hydrogen on titanium dioxide,[13] there is none which treated systematically the catalytic oxidation of hydrogen on titanium dioxide.

Experimental

The catalysts[1] used in the present investigation were anatase (A) and rutile (R) which was obtained from the sample A by heating it at 1150°C for 3 hr. The specific surface areas of anatase and rutile estimated by B.E.T. method using nitrogen as the adsorbate were 10.3 m^2/g and 1.0 m^2/g, respectively. Polymorphic forms of two samples were confirmed by X-ray diffraction. Hydrogen, oxygen, and carbon monoxide from the commercial cylinders were purified by passing through a liquid nitrogen cooled trap. The apparatus had a trap, a Pirani gauge, a McLeod gauge, and a sample tube of fused quartz. Pressure of gas was usually measured by the Pirani gauge but sometimes by the McLeod gauge. The trap in the apparatus was cooled by liquid nitrogen in order to protect the sample from grease and mercury vapors and also to catch the oxidation product of hydrogen, H_2O.

The catalyst heated to 600°C for 3 hr in oxygen under a pressure of about 70 mmHg was called to be in its starting state.[2] After this treatment, the catalytic oxidation of hydrogen was measured at a definite temperature and under pressure of about 10^{-2} mmHg by using a mixed gas with a composition of $H_2/O_2=2/1$. The reaction product H_2O is condensed in the liquid nitrogen trap, and the oxidation rate of hydrogen can be determined by measuring the rate of decrease of the pressure. The distance between the trap and the sample tube was so small and the pressure in the reaction system was so low that the reaction product was caught rapidly in the trap. Therefore, even without a circulating pump, there was no trouble for the measurement. For the purpose of estimating the order of reaction, the reaction rate was also determined by using a mixed gas with a composition of $H_2/O_2=3/1$. The electric conductivity of the catalyst was measured by using the apparatus for the experiment under gas pressures of 10 mmHg and above, which was described in the previous paper.[1]

Results and Discussion

Dependence of Catalytic Activity on Specific Surface Area and Crystal Form. The rates of the catalytic oxidation of hydrogen on two crystal forms were determined in temperature range of 400—650°C and under pressure of about 10^{-2} mmHg. The reaction was first order with respect to the total pressure of the reac-

1) Y. Onishi and T. Hamamura, This Bulletin, **43**, 996 (1970).
2) Y. Onishi, *ibid.*, in press.
3) Y. Onishi, *ibid.*, to be published.
4) L. Glukhovskaya and B. Bruns, *J. Phys. Chem. (U.S.S.R.)*, **19**, 262 (1945); *Chem. Abstr.*, **40**, 514[4] (1946).
5) G. Rienäcker, M. Birckenstaedt, and R. Burmann, *Z. Anorg. Chem.*, **262**, 81 (1950); *Chem. Abstr.*, **44**, 10473h (1950).
6) M. I. Silich and B. P. Bruns, *Zhur. Fiz. Khim.*, **24**, 1179 (1950); *Chem. Abstr.*, **49**, 2166b (1955).
7) M. E. Dry and F. S. Stone, *Discuss. Faraday Soc.*, **28**, 192 (1959).
8) N. A. Krohn, *U. S. At. Energy Comm.* **ORNL-2878**, 73, (1960); *Chem. Abstr.*, **54**, 12757i (1960).
9) V. V. Popovskii and G. K. Boreskov, *Problemy Kinetiki i Kataliza Akad. Nauk S.S.S.R.*, **1960**, **No. 10**, 67; *Chem. Abstr.*, **55**, 11040f (1961).
10) T. T. Bakumenko, *Kinet. Katal.*, **6**, 74 (1965); *Chem. Abstr.*, **62**, 13900c (1965).
11) J. P. Beaufils, *Compt. Rend., Ser.* **C 263**, 7 (1966); *Chem. Abstr.*, **65**, 12894e (1966).
12) J. A. Maymo and J. M. Smith, *Amer. Inst. Chem. Engrs. J.*, **12**, 845 (1966); *Chem. Abstr.*, **65**, 16539c (1966).
13) L. G. Maidanovskaya and B. V. Spitsyn, *Uchenye Zapiski Tomsk. Gosudarst. Univ. im. V.V. Kuibysheva* **1959**, **No. 29**, 42; *Chem. Abstr.*, **55**, 10018e (1961).

tant gas P, and its rate can be expressed as follows:

$$d(H_2O)dt = 2/3k \cdot P \quad (1)$$

where k is a constant. The Arrhenius plots on two crystal forms are shown in Fig. 1 by △. As shown in this figure the experimental points of k are linear for both anatase and rutile, and activation energies were calculated to be 29.2 kcal/mol and 17.8 kcal/mol, respectively.

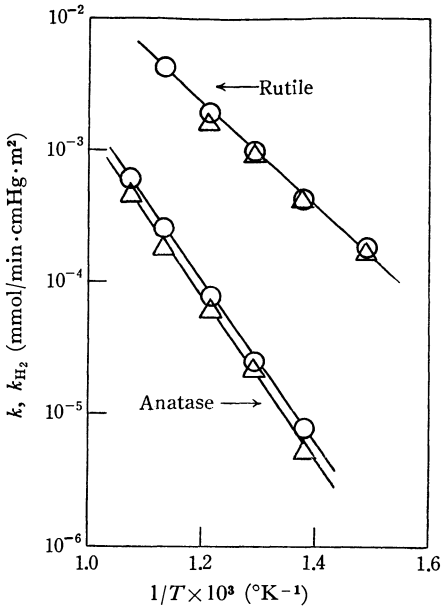

Fig. 1. Effect of temperature on the rate constant of oxidation of hydrogen.
△: k ○: k_{H_2}

Dependence of Reaction Rate and Partial Pressures of Hydrogen and Oxygen. To examine the effect of the partial pressures of hydrogen and oxygen on the reaction rate, the oxidation rate of hydrogen was measured in temperature range of 400—650°C and under pressure of about 10^{-2} mmHg keeping the initial partial pressure of oxygen constant and changing the partial pressure of hydrogen, or *vice versa*. The results are shown in Figs. 2 and 3. It is found from the figures that the oxidation rate of hydrogen is first order with

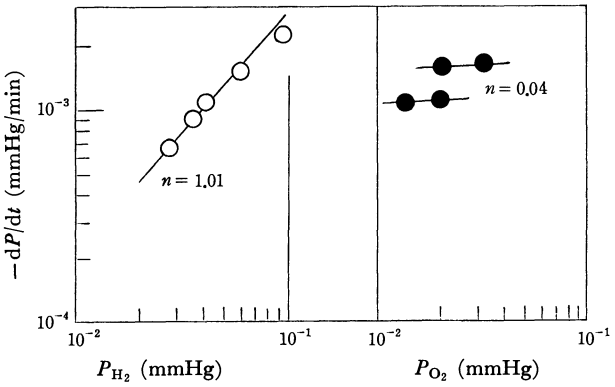

Fig. 2. Kinetics of the oxidation of hydrogen for anatase at 600°C. Open circles refer to constant O_2 partial pressure and changing H_2 pressures. Filled circles refer to constant H_2 partial pressure and changing O_2 pressures. n is the order of reaction.

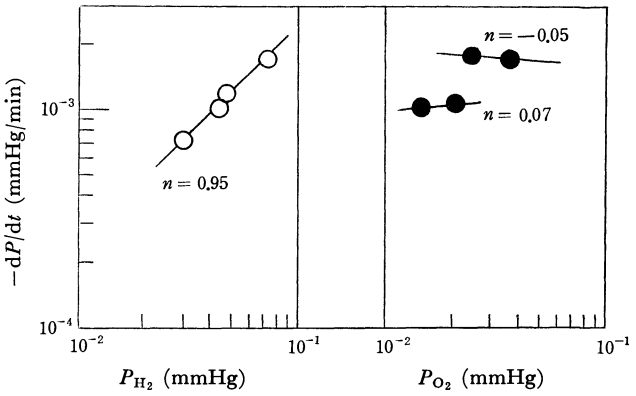

Fig. 3. Kinetics of the oxidation of hydrogen for rutile at 450°C. Open circles refer to constant O_2 partial pressure and changing H_2 pressures. Filled circles refer to constant H_2 partial pressure and changing O_2 pressures. n is the order of reaction.

respect to the hydrogen pressure P_{H_2} and independent of the oxygen pressure P_{O_2}, therefore, the following equation is obtained:

$$d(H_2O)/dt = k \cdot P_{H_2} \quad (2)$$

Reaction of Active Oxygen of Catalyst with Hydrogen. When the catalyst in the starting state was exposed to hydrogen under pressure of about 10^{-2} mmHg at a definite temperature, hydrogen reacted slowly with the active oxygen of the catalyst and water vapor thus formed was condensed in the trap and the pressure of hydrogen decreased. It was found from the results that the formation rate of water depends upon P_{H_2} and is expressed as follows:

$$d(H_2O)/dt = k_{H_2} \cdot P_{H_2} \quad (3)$$

where k_{H_2} is a rate constant of reduction of titanium dioxide by hydrogen. The Arrhenius plots on two crystal forms are shown in Fig. 1 by ○, and the value k_{H_2} is almost the same as the rate constant of the catalytic oxidation of hydrogen k above mentioned.

Electric Conductivity of the Catalyst. The temperature-dependence of electric conductivities for the catalysts of two crystal forms measured in various conditions are shown in Figs. 4 and 5. It is seen that the values in $H_2/O_2=2/1$ are larger than those in oxygen in the measured temperature range and are still larger than those in $CO/O_2=2/1$ except for the values at the temperatures lower than 450°C on anatase. From the results, it is considered that the catalyst during the oxidation of hydrogen would be in more reduced state than in the case of the oxidation of carbon monoxide except for the case at the lower temperatures mentioned above for anatase. As is listed in Table 1, the trend in conductivity coincides well with the trend in the rate constants k_{H_2} and k_{CO}.

As the slopes of the temperature-dependence of electric conductivity in oxygen and in vacuum are parallel to each other for two crystal forms, as shown in Figs. 4 and 5, it is probable that the surface state of titanium dioxide preheated at 600°C in oxygen is stable under the experimental temperatures. In the previous papers,[1,2] it is mentioned that the electric conductivity of the catalyst during the oxidation of carbon monoxide is larger than that in oxygen be-

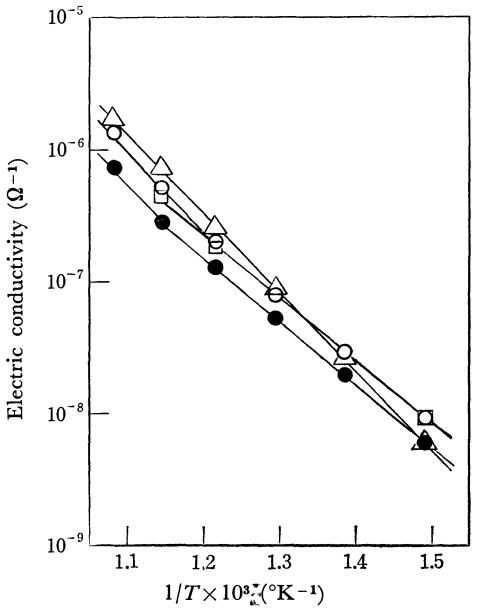

Fig. 4. Effect of temperature on electric conductivity of anatase.
△: in $H_2/O_2=2/1$ (10^{-2} mmHg)
○: in $CO/O_2=2/1$ (70 mmHg)
●: in O_2 (70 mmHg)
□: in vacuum (10^{-6} mmHg)

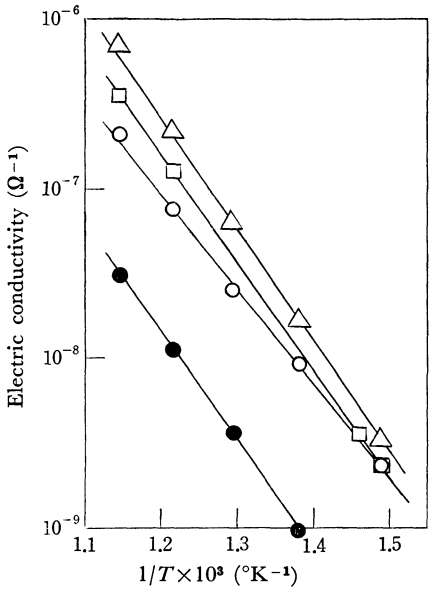

Fig. 5. Effect of temperature on electric conductivity of rutile.
△: in $H_2/O_2=2/1$ (10^{-2} mmHg)
○: in $CO/O_2=2/1$ (70 mmHg)
●: in O_2 (70 mmHg)
□: in vacuum (10^{-6} mmHg)

cause a part of active oxygen on the catalyst is removed by the reaction with the carbon monoxide in the mixed gas. Therefore, from the same reason, the electric conductivity of the catalyst during the oxidation of hydrogen is larger than that in oxygen and, in narrow conductivity range, the amount of increase of conductivity will depend upon the number of the active oxygen defect. By utilizing this relation, the deficiency of active oxygen during the oxidation of hydrogen

TABLE 1. RATE CONSTANTS OF REDUCTION OF CATALYSTS BY HYDROGEN AND CARBON MONOXIDE

Temp. (°C)	650	600	550	500	450	400
$k_{H_2}\times10^4$ (H_2O mmol/min·cmHg·m²)						
Anatase	5.8	2.5	0.88	0.27	0.074	—
Rutile	—	41.0	21.5	10.8	4.6	1.9
$k_{CO}\times10^4$ (CO_2 mmol/min·cmHg·m²)						
Anatase	—	0.75	0.396	0.176	0.0896	—
Rutile	—	3.01	2.24	1.83	1.36	—

can be estimated from the electric conductivities in oxygen and in $CO/O_2=2/1$.

On the other hand, it was mentioned in the previous paper[2] that when titanium dioxide in the starting state is exposed to carbon monoxide under pressure of 10—150 mmHg at a definite temperature, after a certain period, all the surface oxygen which reacts easily with carbon monoxide is used up and the decrease of CO pressure stops. The reactive surface oxygen is called active oxygen on the oxidation of carbon monoxide. Similarly an amount of active oxygen for the oxidation of hydrogen can be determined. When the catalyst in the starting state was exposed to a circulating hydrogen under pressure of about 50 mmHg, hydrogen reacted with the surface oxygen of the catalyst to form water which was condensed in the trap, and H_2 pressure decreased. But the decrease stopped after a definite period as is the case of carbon monoxide. Thus the amount of active oxygen for the oxidation of hydrogen was estimated from the total decrease of the H_2 pressure. The amounts for two catalysts at various temperatures agreed within the experimental error with those of carbon monoxide. Therefore, the amount of active oxygen for the oxidation of hydrogen seems to be approximately equal to that for carbon monoxide at the same temperature. Therefore, the values of active oxygen listed in the previous paper[2] are also applicable to the oxidation of hydrogen. In Table 2, the deficiency of active oxygen on the oxidati on o hydrogen $(1-\theta)$, the rate constant of oxidation of the reduced titanium dioxide by oxygen k_{O_2} listed in the previous paper,[2] and the values of $k_{O_2}\cdot(1-\theta)^2$ are shown, where θ is the fraction of coverage of active oxygen. θ is equal to 1 at the starting state. The value $k_{O_2}\cdot(1-\theta)^2$ agrees almost with k_{H_2} which is listed in

TABLE 2. CALCULATED VALUES OF $(1-\theta)$, k_{O_2}, AND $k_{O_2}\cdot(1-\theta)^2$

k_{O_2} and $k_{O_2}\cdot(1-\theta)^2$ ($-O_2$ mmol/min·cmHg·m²)				
Temp. (°C)	600	550	500	450
Anatase				
$(1-\theta)\times10^2$	3.27	2.80	2.14	1.54
$k_{O_2}\times10$	2.35	1.20	0.55	0.25
$k_{O_2}\cdot(1-\theta)^2\times10^4$	2.5	0.93	0.25	0.059
Rutile				
$(1-\theta)\times10^2$	4.90	5.83	5.43	5.70
$k_{O_2}\times10$	18.0	7.50	3.40	1.33
$k_{O_2}\cdot(1-\theta)^2\times10^4$	43	26	10	4.2

Table 1, and from these values, the following equation may be satisfied approximately because the value θ is nearly equal to 1 during the oxidation of hydrogen:

$$P_{H_2} \cdot k_{H_2} \cdot \theta = 2P_{O_2} \cdot k_{O_2} \cdot (1-\theta)^2 \quad (4)$$

The above equation is entirely similar with that for the oxidation of carbon monoxide. Therefore, the catalytic oxidation of hydrogen seems to proceed with the same mechanism as that of the oxidation of carbon monoxide, as will be mentioned below.

Reaction Mechanism of Oxidation of Hydrogen. It has been described in the previous paper[1] that the electric conductivities of the catalysts of two crystal forms in oxygen at a definite temperature are constant independently of oxygen pressure. This shows that the surface of the catalyst is saturated with oxygen under pressure above 10^{-2} mmHg. It seems from this fact that the oxidation rate of the reduced catalyst by oxygen is extremely fast. In fact, these values are 920—4400 times as large as the reduction rates of the catalyst by hydrogen in temperature range of 450—600°C. Therefore, from Eqs. (1), (2), and (3), and from the results shown in Fig. 1, the reaction of the oxidation of hydrogen may consist of two steps; 1) the active oxygen of the catalyst reacts with hydrogen which is physisorbed or has just collided with the surface from the gas phase, and water thus formed is desorbed leaving an oxygen defect on the surface, and 2) the oxygen defect is quickly refilled with oxygen from the gas phase. The reaction steps are expressed by the following equations:

$$H_2(g) + O(s) \not\rightarrow H_2O(g) + (s) \quad (5)$$

$$(s) + 1/2\, O_2(g) \rightarrow O(s) \quad (6)$$

where O(s) refers to the active oxygen of the catalyst and (s) the oxygen defect on the surface. The rate of step (6) is extremely faster than that of step (5), therefore, the rate of water formation depends upon only P_{H_2}.

For the oxide catalysts other than titanium dioxide, there are several papers[4-8] which state that the rate of catalytic oxidation of hydrogen depends upon only P_{H_2}, and some papers[4-7,10] compared the reaction mechanism with that of carbon monoxide and found the similar mechanism for both gases. For titanium dioxide, the mechanism of oxidation of hydrogen is entirely similar to that of carbon monoxide, and the electric conductivities of the catalysts during the oxidation of both gases are larger than those in oxygen at the same temperatures. Moreover, the effect of crystal form for the oxidation of hydrogen and carbon monoxide is similar, *i.e.*, the activation energy of the oxidation of hydrogen on anatase is larger about 10 kcal/mol than that on rutile, as is the case for carbon monoxide. The reason of this agreement is explained by the fact that the rate-determining steps of two oxidation reactions are considered to be the reaction between the active oxygen of the catalyst and hydrogen or carbon monoxide. Therefore, the difference of 10 kcal/mol comes from the difference in the readiness of reaction between the gases and the active oxygen of the two forms, *i.e.*, the readiness of desorption of the active oxygen from the catalysts, and has almost no correlation with the kinds of the reactant gases. The activation energy of the thermal desorption of the active oxygen atoms of anatase is about 10 kcal/mol larger than that of rutile[1] and this difference can be compared with the difference in activation energies of the oxidation of hydrogen by two crystal forms.

The author wishes to express their deep thanks to Professor Takuya Hamamura of Kyoto Technical University and Professor Kumasaburo Kodera of Kyoto University for their kind advices and discussions.

Electron Donor-acceptor Complexes between Group IV Tetrahalides and Methylbenzenes

Masahiro HATANO and Osamu ITO

The Chemical Research Institute of Non-Aqueous Solutions, Tohoku University, Sendai

(Received August 27, 1970)

The charge-transfer bands of the loose complexes between Group IV tetrahalides (chlorides and bromides) and methylbenzenes were observed, and the electron affinities of these tetrahalides were systematically evaluated from these observed charge-transfer bands. The semi-empirical molecular orbital calculations (the extended Hückel method) for these tetrahalides revealed that the tetrahalides interact with the benzene ring using the vacant molecular orbital involving the empty *d* atomic orbital of the halogen atom in the tetrahalides. Moreover, the meanings of the electron affinities estimated in this study were discussed in terms of the molecular orbitals, by comparing them with the values of the electron affinities evaluated by other methods.

Extensive studies have been made of the complexes between Group IV tetrahalides and *n*-donors by means of the thermodynamic[1] and the spectroscopic measurements, such as IR[2] and NMR.[3] Since Mulliken developed the theory of the donor-acceptor complex,[4] it has been reported that these tetrahalides form not only stable complexes with *n*-donors, but also loose complexes with aromatic π-donors.

As for the carbon tetrachloride and carbon tetrabromide, many workers have studied the formation of loose complexes with π-donors.[5-8] The formation of loose complexes between tin tetrachloride and aromatic hydrocarbons has been studied by Tsubomura[9] and by Myher and Russell.[10] By the spectroscopic measurements, Krauss and his co-workers have found that the titanium tetrachloride and vanadium tetrachloride form loose complexes with π-donors.[11]

Although there have been many investigations of the tetrahalide complexes, many essential problems have not yet been solved. Some of them are as follows:

i) What are the structures of these complexes?

ii) What is the order of the electron affinities of the tetrahalides, which are evaluated from the charge-transfer bands, and what are the meanings of these electron affinities?

iii) What are the molecular orbitals of the tetrahalides which are used to accept the aromatic π-electrons of the donors?

The aim of the present study is to settle some of these problems as definitely as possible. In order to accomplish this purpose, we undertook to measure the UV and visible spectra and to carry out some molecular orbital calculations on these tetrahalides.

Experimental

Materials. Cyclohexane of a spectral-use grade was refluxed over calcium hydride and was distilled and stored under nitrogen gas. The hexamethylbenzene (HMB) and pentamethylbenzene (PMB) were recrystallized and sublimated twice, whereas durene purified by zone-refining was used without further purification. The Mesitylene was refluxed, distilled, and stored in a sealed vessel under nitrogen gas. All the tetrachlorides and tetrabromides, of an extra pure grade, were distilled *in vacuo* and then were immediately used.

Procedure. After the glass apparatus had been dried in a high vaccum and baked to a high temperature, the donor and acceptor solutions were made separately, with air excluded, in glass apparatus, and then degassed in a high vaccum to follow the mixing of both solutions. The concentrations of the solutions were varied over a wide range to obtain the new absorption bands clearly. The absorption spectra were measured by a Cary model 14M recording spectrophotometer, and fused quartz cells with a light-path length of 0.1—10 mm were used.

Experimental Results and Discussion

Electron Donor-acceptor Complexes between Tin Tetrachloride and Methylbenzenes. The mixed solutions of tin tetrachloride and methylbenzenes, *i.e.*, mesitylene, durene, PMB, and HMB, in cyclohexane showed significant absorption bands in the UV and visible regions, where solutions of the individual components show negligible absorption; only in the appropriate concentrations of the donor (0.050—0.075 mol/*l*) and those of the acceptor (0.025—0.050 mol/*l*) solutions were new absorption maxima clearly separated, as is shown in Fig. 1.

The plotting of the transition energies of the new absorption bands ($h\nu_{CT}$) against the ionization potentials(I_P)[12] of the corresponding donors exhibits a linear relationship, as is shown in Fig. 2-I. A similar linear relationship has been established in the iodine molecular

1) D. P. N. Satchell and R. S. Satchell, *Chem. Rev.*, **69**, 251 (1969).
2) D. G. Brown, R. S. Drago, and T. F. Bolles, *J. Amer. Chem. Soc.*, **90**, 5706 (1968).
3) J. F. Deters, P. A. McCusker, and R. C. Pilger, *ibid.*, **90**, 4583 (1968).
4) R. S. Mulliken, *ibid.*, **74**, 811 (1952).
5) F. J. Striter and D. H. Templeton, *J. Chem. Phys.*, **37**, 161 (1962).
6) F. Dorr and G. Buttgereit, *Ber. Bunsenges. Physik. Chem.*, **67**, 867 (1963).
7) R. F. Weimer and J. M. Fransnitz, *J. Chem. Phys.*, **42**, 3643 (1965).
8) K. M. C. Davis and M. F. Farmer, *J. Chem. Soc., B*, **1967**, 28.
9) H. Tsubomura, This Bulletin, **27**, 1 (1954).
10) J. J. Myher and K. E. Russell, *Can. J. Chem.*, **42**, 1555 (1964).
11) a) H. L. Krauss and H. Hüttmann, *Z. Naturforsch.*, **18b**, 976 (1963); b) H. L. Krauss and J. Nickl, *ibid.*, **20b**, 630 (1965). c) H. L. Krauss and H. Hüttmann, *ibid.*, **21b**, 490 (1966).
12) K. Watanabe, *J. Chem. Phys.*, **26**, 542 (1957).

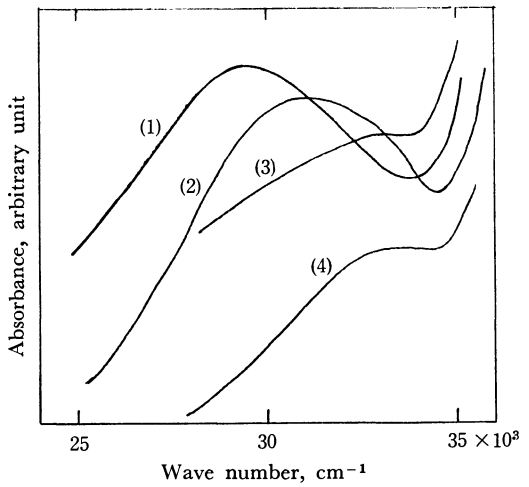

Fig. 1. Absorption spectra of various donors with $SnCl_4$ in cyclohexane (at 24.5°C).
(1) HMB, (2) PMB, (3) durene, (4) mesitylene.

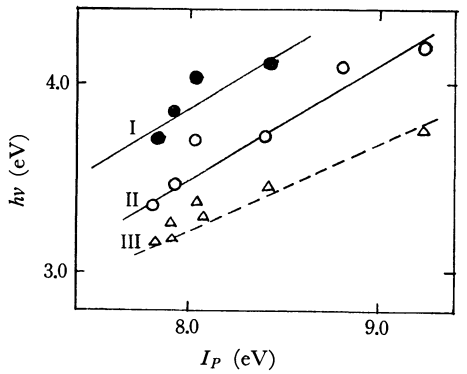

Fig. 2. Relationships between transition energies and I_P of aromatics.
I: $SnCl_4$-aromatics
II: I_2-aromatics
III: σ-complexes or protonated carbonium ions of aromatics

complexes with methylbenzenes (Fig. 2-II).[13] The transition energies of the absorption bands for the σ-complexes or protonated carbonium ions of methylbenzenes are also plotted in Fig. 2-III against I_P.[14-16] From a comparision of I with II and III in Fig. 2, it could be confirmed that the new absorption bands are due not to the σ-complexes or protonated carbonium ions, but to the electron donor-acceptor complexes.[17] Moreover, the similarity of the slopes of I and II in Fig. 2 suggests that the properties of these tin tetrachloride complexes resemble those of the iodine molecular complexes.

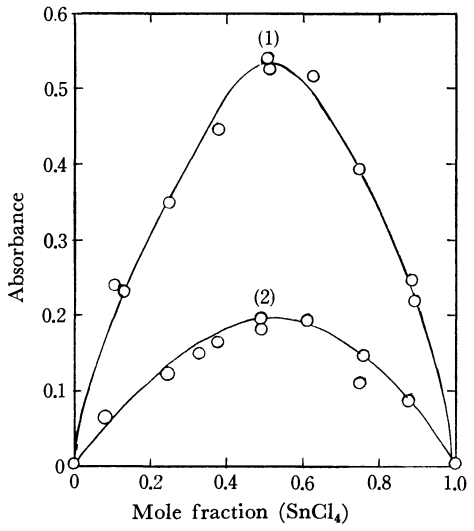

Fig. 3. Continuous variation plots for the absorbance of $SnCl_4$-HMB solution in cyclohexane.
$SnCl_4$+HMB=0.2 mol/l, (1) at 33.3 kK (absorption maximum), (2) at 31.3 kK.

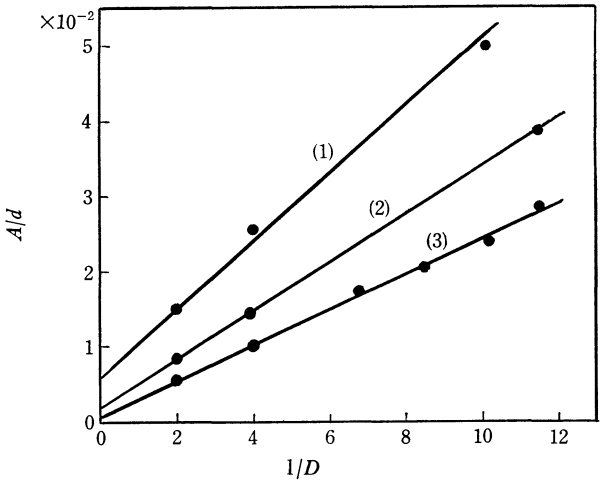

Fig. 4. Plots of Benesi-Hildebrand for $SnCl_4$-mesitylene at high concentration of mesitylene in cyclohexane (24.5°C).

$$\frac{A}{d}=\frac{1}{\varepsilon K}\cdot\frac{1}{D}+\frac{1}{\varepsilon}$$

A,D: concentrations of acceptor and donor, respectively, d: absorbance, ε: molar extinction coefficient, K: formation constant, (1) 340 nm, (2) 320 nm, (3) 300 nm

Continuous variation plots for the absorbance of the solutions of tin tetrachloride and HMB in cyclohexane are given in Fig. 3. At both 300 nm (a maximum of the charge-transfer absorption) and 320 nm, these plottings indicate that a 1 : 1 complex is formed in this system; this finding is consistent with that of Myher and Russell.[10] Since the formation of a 1 : 1 complex was confirmed, the Benesi-Hildebrand plots for this system were attempted, as is shown in Fig. 4, which shows straight lines. The formation constant and molar extinction coefficient of this complex were estimated to be as shown in Table 1, in which the formation constants varied greatly with the wavelength. It has been reported that the dependence of the formation constants on the wavelength occur, when a contact charge-transfer complex or another com-

13) G. Briegleb, "Electron-Donor-Acceptor-Komplexe," Springer, Berlin (1961).
14) H. H. Perdampus and T. H. Kranz, *Z. Physik. Chem. Neue Folge*, **38**, 295 (1963).
15) C. Dallinger, E. L. Macker, and A. A. Verrijn Stuart, *Mol. Phys.*, **1**, 123 (1958).
16) In Fig. 2-III, it seems as if the plots for σ-complexes fit a linear relationship, but it has been established that, for aromatic hydrocarbons with lower I_P values, such as polyacenes, the plots deviate from this linearity.[13]
17) M. Hatano and O. Ito, This Bulletin, **42**, 1780 (1969).

TABLE 1. FORMATION CONSTANT (K) AND MOLAR EXTINCTION COEFFICIENT (ε) FOR $SnCl_4$-MESITYLENE AT 24.5°C

Wavelength(nm)	K(mol^{-1} l)	ε
300[a)]	0.43	1000
320	0.95	357
340	1.30	167

a) Absorption maximum.

TABLE 2. FORMATION CONSTANTS (mol^{-1} l) FOR $SnCl_4$ AND CCl_4 COMPLEXES WITH METHYLBENZENES OR BENZENE

	HMB	Mesitylene	Benzene
$SnCl_4$[a)]	1.68	0.43	—
CCl_4[b)]	0.64	0.113	0.0009

a) Values estimated at the maxima of charge-transfer bands in cyclohexane at 24.5°C.
b) Ref. 7, values estimated near the maxima of charge-transfer bands in n-hexane at 25°C.

position is included in the system,[18,19] but we could not determine which case is more likely in this system. However, when the formation constant of one system is compared with that of another system, only the values obtained at or near the maxima of the charge-transfer absorptions may be suitable. The estimated values of the formation constants at the absorption maxima are shown in Table 2, together with the literature values for the carbon tetrachloride complexes, which were measured near the maxima of the charge-transfer bands.[7] Moreover, from the temperature changes of the formation constants, the formation enthalpy for this system was estimated to be −2.8 kcal/mol; this value was comparable with the previously reported values.[9,10]

The Charge-transfer Bands of the Other Tetrahalide Complexes with HMB. As for the other tetrachloride complexes and tetrabromide complexes with HMB, all the spectra except the carbon tetrahalide complex were measured (Fig. 5—10); the absorption maxima of the newly-appearing absorption bands are summarized in Table 3, together with the reported charge-transfer bands. The shapes and positions of these absorption spectra are characteristic of the charge-transfer bands. In the case of silicon tetrahalides, the approximate values are shown in Table 3, since the new absorptions seemed to overlap with those of the donor.

In the systems of titanium tetrahalides and methylbenzenes (Figs. 8 and 9), two absorption peaks appeared, as had been reported by Dijkgraaf[20] and by Ott and his co-workers.[21] Since a peak at a shorter wavelength changed its position with a variation in the concentrations of the donor and the acceptor, this

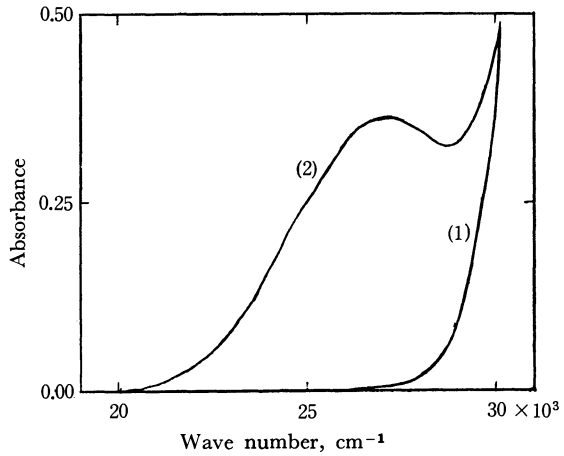

Fig. 5. Absorption spectra of $SnBr_4$-HMB in cyclohexane.
(1) $SnCl_4$(2.5×10^{-2} mol/l) in cyclohexane
(2) $SnCl_4$(2.5×10^{-2} mol/l)+HMB(7.5×10^{-2} mol/l)
10 mm cell

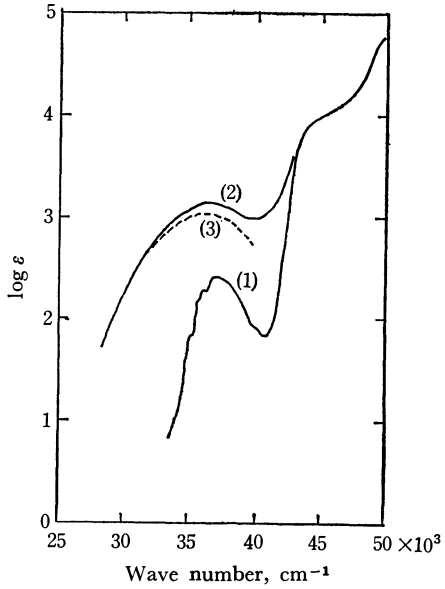

Fig. 6. Absorption spectra of $GeCl_4$-HMB in cyclohexane.
(1) HMB in cyclohexane
(2) HMB in mixed system ($GeCl_4$: cyclohexane=1:1)
(3) (2)—(1)

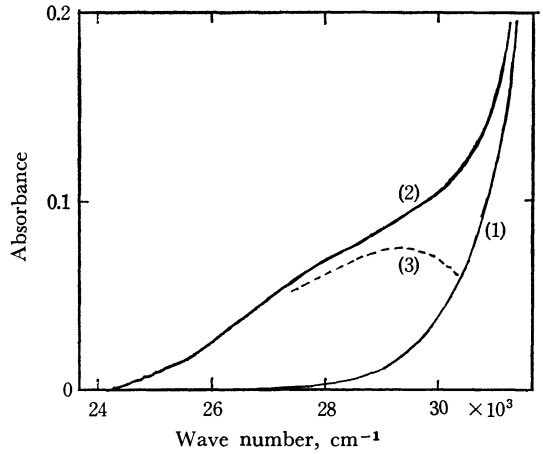

Fig. 7. Absorption spectra of $GeBr_4$-HMB in cyclohexane.
(1) mixed system ($GeBr_4$: cyclohexane=1:1)
(2) HMB (5.0×10^{-2} mol/l) in mixed system of (1)
(3) (2)—(1), 0.1 mm cell

18) G. Dana Johnson and Ronald E. Bowen, *J. Amer. Chem. Soc.*, **87**, 1655 (1965).
19) M. J. S. Dewar and C. C. Thompson, Jr., *Tetrahedron, Suppl.*, **no. 7**, 97 (1966).
20) C. Dijkgraaf, *J., Phys. Chem.*, **69**, 660 (1965).
21) J. B. Ott, J. R. Goates, R. J. Jensen, and N. F. Mangelson, *J. Inorg. Nucl. Chem.*, **27**, 2005 (1965).

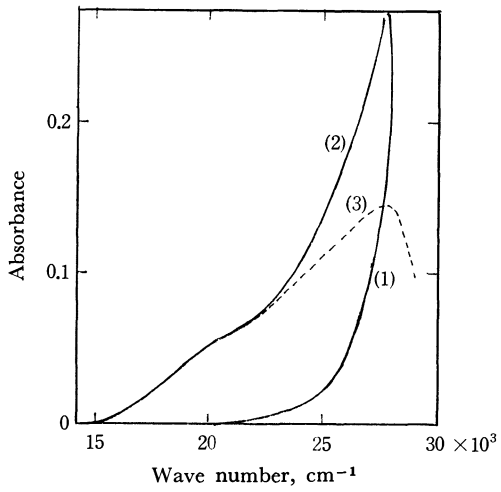

Fig. 8. Absorption spectra of $TiCl_4$-HMB in cyclohexane.
(1) $TiCl_4$ (2.7×10^{-3} mol/l)
(2) $TiCl_4$ (2.7×10^{-3} mol/l)+HMB(5.0×10^{-2} mol/l)
(3) (2)—(1), 2 mm cell

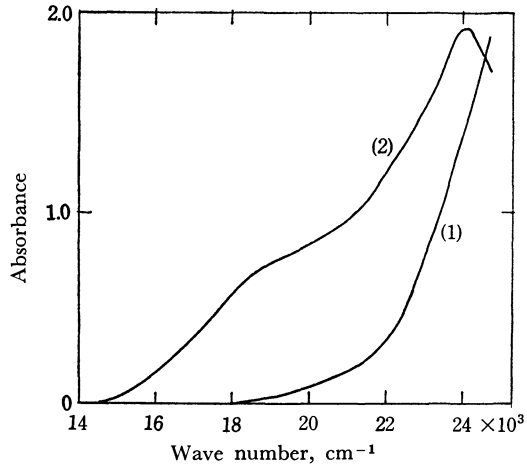

Fig. 9. Absorption spectra of $TiBr_4$-HMB in cyclohexane.
(1) $TiBr_4$ (2.5×10^{-2} mol/l)
(2) $TiBr_4$ (2.5×10^{-2} mol/l)+HMB (7.5×10^{-2} mol/l)
ref. $TiBr_4$ (1), 10 mm cell

peak was deduced to be an apparent absorption peak which emerged from the difference between the absorption of titanium tetrahalide in the complex system and that of titanium tetrahalide itself in cyclohexane. Therefore, only the absorptions at longer wavelengths were deduced to be the charge-transfer bands which correspond to the values reported by Krauss and his co-workers.[11]

On the basis of these measurements, it may be pointed out that the charge-transfer bands of the tetrabromides appear in a longer-wavelength region than those of the corresponding tetrachlorides and the charge-transfer bands of tetrahalides including the transition elements appear in a longer-wavelength region than those of tetrahalides including non-transition elements.

Evaluation of Electron Affinities of the Tetrahalides from the Charge-transfer Bands. The electron affinities

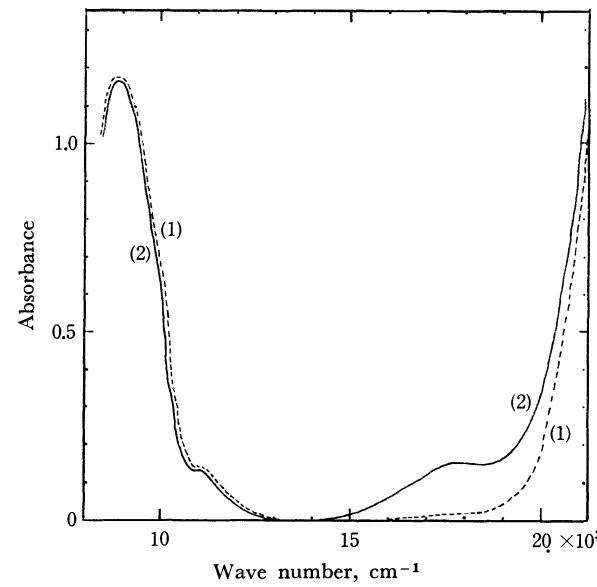

Fig. 10. Absorption spectra of VCl_4-HMB in cyclohexane.
(1) VCl_4 (2.5×10^{-2} mol/l)
(2) VCl_4 (2.5×10^{-2} mol/l)+HMB (5.0×10^{-2} mol/l), 1 mm cell

Table 3. Systematic data for the electron donor-acceptor complexes between tetrahalides and aromatic hydrocarbons

	$h\nu_{CT}$(HMB) in nm	E_A^{CT} in eV	ΔH(HMB) in kcal/mol	R(M-X)[c] in Å
CCl_4	242[a]	0.15	−0.54[a]	1.767
$SiCl_4$	230	−0.3	—	2.019
$GeCl_4$	280	0.87	—	2.113
$SnCl_4$	339	1.57	−2.8	2.31
$TiCl_4$	510	2.87	−1.8[b]	2.169
VCl_4	550	3.27	—	2.137
CBr_4	303[a]	1.17	—	1.942
$SiBr_4$	250	0.13	—	2.15
$GeBr_4$	342	1.60	—	2.266
$SnBr_4$	370	1.92	—	2.44
$TiBr_4$	540	2.97	—	2.31

a) Ref. 8.
b) Toward phenanthlene in CCl_4, Ref. 11.
c) R(M-X) means M-X distance (Ref. 30).

of electron acceptors have been evaluated on the basis of the charge-transfer bands by many investigators.[22,23] Using the same donor, neglecting the differences in the coulombic interaction energies between the components in the complexes, and neglecting the contributions of the local excitations to the charge-transfer transition, the following approximate equation can be derived:

$$(E_A)_i - (E_A)_0 = (h\nu_{CT})_0 - (h\nu_{CT})_i \quad (1)$$

Here, the suffixes o and i indicate the standard and any given acceptor respectively. Since the "vertical" ionization potential and electron affinity should be involved in the charge-transfer transition according to Mulliken's theory,[4] the values used here and evaluated on the basis of Eq. (1) are not "adiabatic"

22) M. Batley and L. E. Lyons, *Nature*, **196**, 573 (1962).
23) G. Briegleb, *Angew. Chem.*, **76**, 326 (1964).

but "vertical." Here, choosing the iodine molecule and HMB as the standard system, and assuming the electron affinity of the iodine molecule to be 1.8_0 eV[22] and the charge-transfer transition energy of this system to be 3.4_7 eV,[13] the electron affinities of all the tetrachlorides and tetrabromides could be evaluated systematically, as is shown in Table 3.

The electron affinities of titanium tetrachloride and vanadium tetrachloride evaluated by Krauss and his co-workers[11] are smaller by 1 eV than the values evaluated in this study, because they evaluated them assuming the electron affinity of iodine molecule to be 0.8 eV[23] and used that value as the standard in Eq. (1). Therefore, these electron affinities are meaningful only as relative values. As was expected from the transition energies of the charge-transfer bands, the electron affinities of transition-element tetrahalides are larger than those of non-transition element tetrahalides, and the electron affinities of bromides are larger than those of chlorides.

TABLE 4. ELECTRON AFFINITY OF CARBON TETRACHLORIDE AND *p*-BENZOQUINONE ESTIMATED FROM DIFFERENT METHODS

	E_A^{CT} (eV)[a]	E_A^{mag} (eV)[b]	ΔH(HMB) in kcal/mol
CCl_4	0.15	2.1[d]	−0.54[e]
p-Benzoquinone	2.02[c]	1.4[d]	−1.8[f]

a) Electron affinity estimated from charge-transfer band.
b) Electron affinity estimated by magnetron method.
c) Ref. 21, d) Refs. 24 and 25, e) Ref. 8, f) Ref. 13.

Moreover, it was pointed out by Davis and Farmer[8] that the electron affinity of carbon tetrachloride as evaluated from the charge-transfer band was smaller than the corresponding values of *p*-benzoquinone; on the other hand, this order was reversed when the electron affinity was evaluated by the magnetron method (Table 4).[24,25] In the following section we will attempt to explain this anomaly in terms of the molecular orbital.

Structure of the Loose Complexes between Tetrahalides and Methylbenzenes. In general, tetrahalides form 1 : 2 stable complexes with *n*-donors, the structures being as shown in Fig. 11-A,[26] while, with aromatic π-donors, tetrahalides form loose complexes, whose structures have not yet been made clear except a carbon tetrabromide complex with *p*-xylene (Fig. 11-B).[5] If tetrahalides form A-type complexes, some spectral changes might occur accompanying a conformational change from the T_d to the D_{4h} of tetrahalides. These changes in the electronic spectra were indicated by Bridgland and McGregor in their study of vanadium tetrachloride complexes with *N*-oxides;[27] that is, in a ligand field with a D_{4h} symmetry of vanadium tetrachloride in the

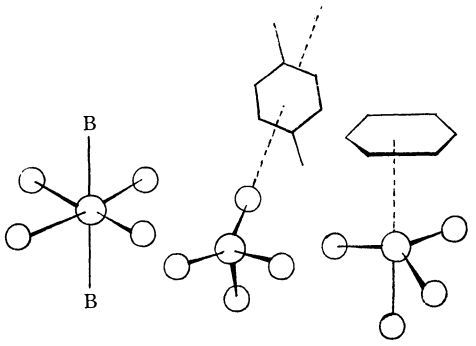

Fig. 11. Structures of tetrahalide complexes.
[A] a stable complex toward *n*-donors
[B] a loose complex between CBr_4 and *p*-xylene proposed by Striter and Templeton[5]
[C] a possible structure between $SnCl_4$ and methylbenzene

A-type complex, the $2T_{2g}-2E_g$ intramolecular charge transition of the T_d symmetry split into two transitions. However, in the case of the vanadium tetrachloride-HMB complex, the spectral change was not observed, as is shown in Fig. 10; this indicates that vanadium tetrachloride retains the T_d symmetry even in the complex with methylbenzenes. As for the tetrachlorides, since the order of the atomic distance between the central atom and the halogen atom of tetrachlorides is $CCl_4<SiCl_4<GeCl_4<TiCl_4<VCl_4<SnCl_4$ (Table 3), it may be presumed that tetrachlorides, whose distance are smaller than vanadium tetrachloride, will tend to form a structure similar to that of the vanadium tetrachloride complex with methylbenzenes, that is, a B-type structure (Fig. 11).

The only remaining problem here is, then, the analysis for the tin tetrachloride complex, for which Tsubomura[9] assumed that the tin atom may be coordinated directly to either one or two benzene rings. On the other hand, it has been reported that, although the stable complexes show a 1 : 2 composition, the loose complexes show a 1 : 1 composition. Even in the case of the tin tetrachloride complexes with methylbenzenes, the formation of 1 : 1 complexes was confirmed (Fig. 3); this suggests that the tetrachlorides composed of a relatively large-sized central atom such as tin tetrachloride also form B-type complexes. This suggestion was supported by the order of the formation constants, which increase in the same order as those of the carbon tetrachloride complexes (Table 2), whose structures were presumed to be B-type.[5]

Since the unstability accompanying the conformational change from the T_d to the D_{4h} or from the T_d to the "Pyramidal" of tetrachloride is too large to form a complex between the central atom and the benzene ring, the A- and C-type structures may be excluded. The same discussions may be extended to the tetrabromide complexes.

Theoretical Considerations and Discussions

It has been presumed by some workers that the carbon tetrahalides accept the π-electron of the benzene ring using the empty *d* atomic orbitals of halogen

24) A. F. Gaines, J. Kay, and F. M. Page, *Trans. Faraday Soc.*, **62**, 874 (1966).
25) A. L. Farragher and F. M. Page, *ibid.*, **62**, 3072 (1966).
26) S. Ichiba, M. Mishima, and H. Negita, This Bulletin, **42**, 1486 (1969).
27) B. E. Bridgland and W. R. McGregor, *J. Inorg. Nucl. Chem.*, **31**, 43 (1969).

Table 5. Valence state ionization potentials of group IV elements and halogen atoms in eV

	C	Si	Ge	Sn	Ti	V	Cl	Br
s	20.78[a]	17.31[a]	17.90[b]	17.75[b]	9.86[c]	9.99[c]	25.27[d]	23.81[d]
p	11.31[a]	9.19[a]	7.40[b]	8.19[b]	5.62[c]	6.89[c]	13.69[d]	11.85[d]
d	—	—	—	—	—	—	1.61[e]	1.74[e]

a) J. Hinze and H. H. Jaffé, *J. Amer. Chem. Soc.*, **84**, 540 (1962).
b) C. E. Moore, "Atomic Energy Levels," *N. B. S. Circular*, (1948).
c) H. Basch, A. Viste, and H. B. Gray, *J. Chem. Phys.*, **44**, 10 (1966).
d) H. O. Pritchard and H. A. Skinner, *Chem. Rev.*, **55**, 745 (1955).
e) W. Kauzman, "Quantum Chemistry," Academic Press Inc., New York (1957), p. 326.

atoms (3*d* for chlorides and 4*d* for bromides).[28] To ascertain the truth of this assumption for all tetrahalide complexes, molecular orbital calculations were carried out by an extended Hückel method for tetrachlorides and tetrabromides.[29] In these calculations, in addition to *s* and *p* atomic orbitals, empty *d* atomic orbitals of halogen atoms were considered. All the valence state ionization potentials used in this study are summarized in Table 5, together with the literatures.

The distances between the central atoms and the halogen atoms are shown in Table 3.[30] The overlap integrals were calculated using the Slater-type atomic orbitals by means of the method of Roothaan,[31] whose program was reported by Offenhartz.[32,33]

Table 6. Some results of extended Hückel calculations of some T_d symmetry tetrachlorides

	$E_{H.O.}$ (eV)[a]	I_p (obsd)[b]	$E_{L.V.}$ (eV)[c]	E_A^{CT} (eV)	S_{AD}[d]
CCl_4	−13.29	11.47	−10.7	0.15	0.017
$SiCl_4$	−11.51	11.6	−8.8	−0.3	0.022
$GeCl_4$	−13.58	11.0	−6.7	0.87	0.011
$SnCl_4$	−13.64	10.5	−7.7	1.57	0.011
$TiCl_4$	−13.16	11.7	−8.2	2.67	0.030

a) Energy level of the highest occupied orbital.
b) From Ref. 34.
c) Energy level of the lowest vacant orbital.
d) Overlap integral in complex.

Some of the results of the calculations are shown in Table 6. The calculated ionization potentials of tetrachlorides may be compared with the measured values;[34] the agreement is as good as is generally achieved for this quantity. On the other hand, the electron affinity calculated by the extended Hückel method could not be compared directly with the measured values, but it may be possible to compare them relatively. However, no correlation, not even a relative one, could be found between the lowest vacant orbital energies and the electron affinities evaluated from the charge-transfer bands. As for the non-transition element tetrahalides, when the vacant molecular orbitals (E_V) involving the *d* atomic orbital of the halogen atom, which appeared at a higher energy level than those of the lowest vacant orbital, are plotted against

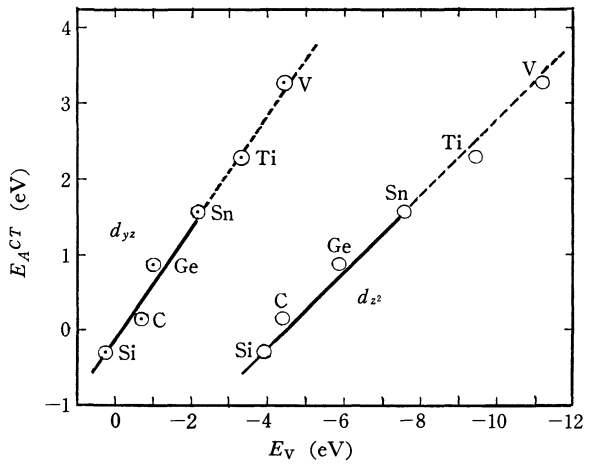

Fig. 12. Plots of E_A^{CT} against energies of vacant molecular orbitals of tetrachlorides, (E_V), which are used to accept aromatic π-electrons.
d_{z^2}: molecular orbitals involving $3d_{z^2}$ of chlorine atom
d_{yz}: molecular orbitals involving $3d_{yz}$ of chlorine atom

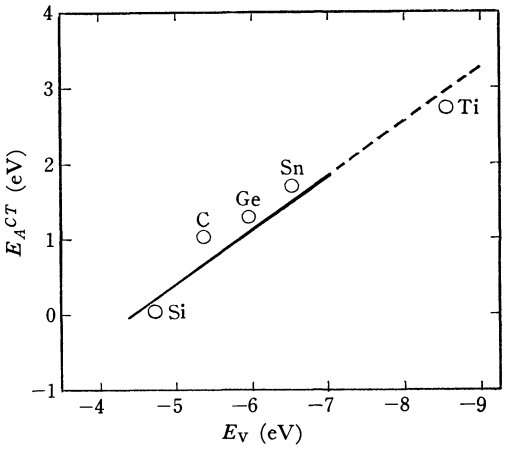

Fig. 13. Plots of E_A^{CT} against energies of vacant molecular orbitals of tetrabromides(E_V), which are used to accept aromatic π-electrons.
d_{z^2}: molecular orbitals involving $4d_{z^2}$ of bromine atom

28) a) J. R. Goates, R. J. Sullivan, and J. B. Ott, *J. Phys. Chem.*, **63**, 589 (1954). b) R. Anderson and J. M. Prausnitz, *J. Chem. Phys.*, **39**, 1225 (1963).
29) R. Hoffmann, *J. Chem. Phys.*, **40**, 2474 (1964).
30) Ed. Nihon-kagaku-kai, "Kagaku-binran," Maruzen, Tokyo (1966), p. 1203.
31) C. C. J. Roothaan, *J. Chem. Phys.*, **19**, 1445 (1951).
32) P. O. Offenhartz, *J. Chem. Educ.*, **44**, 604 (1967).
33) This program was presented by the Quantum Chemistry Program Exchange (Indiana University), and all the calculations were executed on the Tohoku University NEAC-2200 Model 500 computer.
34) S. P. Ionov and J. V. Ionova, *Zh. Neorgan. Khim.*, **13**, 1, (1968).

TABLE 7. MOLECULAR ORBITALS, INVOLVING $3d_{z^2}$ OF Cl, WHICH FIT A LINEAR RELATIONSHIP AGAINST E_A^{CT} IN FIG. 13

	M[a]	X_1[a]	S_{AD}[b]
CCl_4	$-0.28\,s+\cdots+$	$0.09\,s-0.02\,p_z+0.46\,d_{z^2}+\cdots$	0.06
$SiCl_4$	$-0.20\,s+\cdots+$	$0.08\,s-0.20\,p_z+0.41\,d_{z^2}+\cdots$	0.05
$GeCl_4$	$-0.54\,s+\cdots+$	$0.13\,s-0.28\,p_z+0.30\,d_{z^2}+\cdots$	0.04
$SnCl_4$	$-0.71\,s+\cdots+$	$0.20\,s-0.38\,p_z+0.17\,d_{z^2}+\cdots$	0.04
$TiCl_4$	$-0.86\,s+\cdots+$	$0.20\,s-0.10\,p_z+\cdots\cdots\quad\cdots$	0.03
VCl_4	$-0.49\,s+0.86\,d_{z^2}$	$\cdots\cdots+0.10\,p_z+\cdots\cdots\quad\cdots$	0.03

a) M and X mean the central atom and halogen atom, respectively.
b) Overlap integral in complexes (*AD*).

TABLE 8. MOLECULAR ORBITALS, $3d_{yz}$ OF Cl, WHICH FIT A LINEAR RELATIONSHIP AGAINST E_A^{CT} IN FIG. 13

	M	X_1-X_2
CCl_4	$0.22(p_x+p_y)+\cdots$	$+(0.74(d_{yz}(X_1)-d_{yz}(X_2)+\cdots)$
$SiCl_4$	$0.36(p_x+p_y)+\cdots$	$+(0.78(d_{yz}(X_1)-d_{yz}(X_2)+\cdots)$
$GeCl_4$	$0.25(p_x+p_y)+\cdots$	$+(0.73(d_{yz}(X_1)-d_{yz}(X_2)+\cdots)$
$SnCl_4$	$0.13(p_x+p_y)+\cdots$	$+(0.99(d_{yz}(X_1)-d_{yz}(X_2)+\cdots)$
$TiCl_4$	$0.58\,p_x+\cdots\cdots$	$+(0.22(d_{yz}(X_1)-d_{yz}(X_2)+\cdots)$
VCl_4	$0.61\,p_x+\cdots\cdots$	$+(0.20(d_{yz}(X_1)-d_{yz}(X_2)+\cdots)$

TABLE 9. MOLECULAR ORBITALS, INVOLVING $4d_{z^2}$ OF Br, WHICH FIT A LINEAR RELATIONSHIP AGAINST E_A^{CT} IN FIG. 14

	M	Br_1	$+\cdots$
CBr_4	$-0.17\,s+\cdots\cdots$	$(-0.26\,p_z+0.36\,d_{z^2}+\cdots)$	$+\cdots$
$SiBr_4$	$-0.14\,s+\cdots\cdots$	$(-0.19\,p_z+0.39\,d_{z^2}+\cdots)$	$+\cdots$
$GeBr_4$	$-0.56\,p_x+\cdots\cdots$	$(-0.05\,p_z+0.16\,d_{z^2}+\cdots)$	$+\cdots$
$SnBr_4$	$-0.58\,p_x+\cdots\cdots$	$(-0.06\,p_z+0.11\,d_{z^2}+\cdots)$	$+\cdots$
$TiBr_4$	$-0.82\,d_{xy}+\cdots\cdots$	$(-0.15\,s+0.16\,p_z+\cdots)$	$+\cdots$

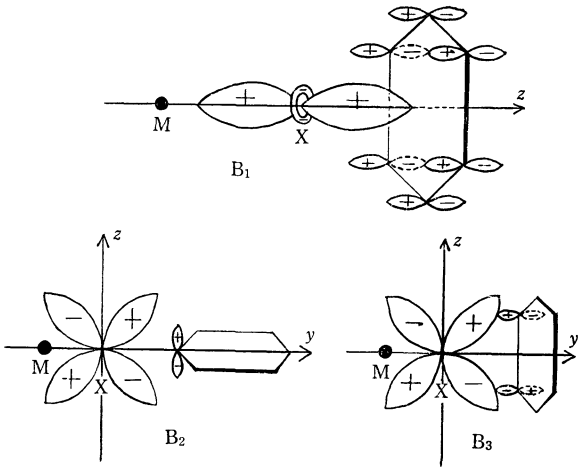

Fig. 14. Assumed structures of loose complexes between tetrahalides and methylbenzenes.
[B_1]: d_{z^2} orbital on halogen atom,
[B_2] and [B_3]: d_{yz} orbital on halogen atom.

the electron affinities evaluated from the charge-transfer bands, the molecular orbitals involving the $3d_{z^2}$ and $3d_{yz}$ of chlorides or the $4d_{z^2}$ of bromides all satisfy a linear relationship, as is shown in Figs. 12 and 13 respectively. The corresponding vacant molecular orbitals of the transition-element tetrahalides, which could be found by extrapolating the plots for the non-transition-element halides, do not always involve empty *d* atomic orbitals on the halogen atoms. These molecular orbitals are summarized in Tables 7 and 8 for the chlorides and in Table 9 for the bromides. From the geometry of the empty *d* atomic orbitals, some structures of the complexes with benzene rings could be presumed, as is illustrated in Fig. 14.

Since it has been accepted that the charge-transfer force is determined mainly by the electron affinity and the overlap integral (S_{AD}) between the donor and the acceptor orbital, these overlap integrals were evaluated approximately, assuming an a_{2u} molecular orbital of benzene as the donor orbital and using the coordination system shown in Fig. 14-B_1. These results are shown in Tables 6 and 7. Since the overlap integrals for the lowest vacant orbitals are very small compared with that of the iodine-benzene complex, which was evaluated by Aono to be 0.11,[35] it is not considered that these molecular orbitals of tetrachlorides accept the π-electrons of the donor. However, the overlap integrals of the molecular orbitals in Table 7 are suitable values for explaining the formations of the weak complexes. Since the electron affinities of titanium tetrachloride and vanadium tetrachloride are larger than these of tin tetrachloride and carbon tetrachloride, and since the order of the overlap integrals are reversed, the compensation between the electron affinity and the overlap integral might induce the lack of variation in the formation enthalpies in the complexes.

On the basis of these results, we could explain the anomaly in the meaning of the electron affinity shown in Table 4. That is, although carbon tetrachloride accepts the free electron by using the lowest vacant orbital, and although the result of this process might correspond to the value measured by the magnetron method, the π-electrons of the benzene ring are accepted by the molecular orbital involving the empty *d* orbital of the chlorine atom in carbon tetrachloride; this process corresponds to the charge-transfer transition. On the other hand, an organic π-acceptor such as *p*-benzoquinone accepts both the free electron and the π-electrons of the donor by using the lowest vacant orbital, for this orbital expands outside of the acceptor molecule.

As has been discussed above, the results on the struc-

35) S. Aono, *Progress Theor. Phys.*, **22**, 313 (1959).

tures of the complexes and on the molecular orbitals of tetrahalides permit the explanation of many phenomena, such as the order of the electron affinities and formation enthalpies; therefore, it may safely be concluded that the tetrahalides interact with the benzene ring using the vacant molecular orbitals involving empty *d* atomic orbitals on halogen atoms of tetrahalides. Moreover, this conclusion suggests that the weak other charge-transfer bands from the donor orbital to the lowest vacant orbital of tetrahalide may appear in a wavelength region longer than those observed in this study. However, more detailed studies of the shapes of the charge-transfer bands, especially of their tails, are needed.

The authors wish to thank to Professor T. Nakajima and Dr. A. Tajiri of Tohoku University and Dr. M. Okuda of the University of California for their useful discussions and for making extended Hückel programs. Acknowledgement is also due to the Ministry of Education for the financial support granted for this research.

BULLETIN OF THE CHEMICAL SOCIETY OF JAPAN, VOL. 44, 923—928 (1971)

An Infrared Spectroscopic Study of Hydrogen Bonds. The Liquid-Liquid Interaction of Solvents with Trimethylsilanol

Tsutomu KAGIYA, Yūzō SUMIDA, Takeshi WATANABE, and Toshihiro TACHI

Faculty of Engineering, Kyoto University, Sakyo-ku, Kyoto

(Received September 7, 1970)

An infrared spectroscopic study of the hydrogen-bonding interaction of binary solvents (S_1–S_2) with trimethylsilanol has been made, where CCl_4 is used as S_1 and the aromatic hydrocarbons and the O- and N-containing solvents, as S_2. On the basis of the findings on the O–H frequency shifts ($\Delta\nu_{OH}$) of trimethylsilanol, the equilibrium constants (K) and the preferential coordination constants (α_{1-2}) of hydrogen-bond formation, the difference in the O–H···π and the O–H···n hydrogen-bonding interactions has been discussed. The free-energy changes ($-\Delta G$) were found to be better related to the apparent half-widths ($\Delta\nu_{1/2}$) of the O–H bands than the $\Delta\nu_{OH}$. The $\Delta\nu_{OH}$ of trimethylsilanol caused by the interaction with the solvent was in good correlation with the donor number defined as the heat of mixing of the solvent with antimony(V) chloride. From the linear relationship between the $\Delta\nu_{OH}$ of trimethylsilanol and the $\Delta\nu^{S}_{OH}$ of the surface silanol caused by the gas-phase adsorption on silica gel, it was also found that the proton-donating power of the surface silanol was considerably larger than that of trimethylsilanol and was nearly equal to that of *p*-nitrophenol. There existed a linear relationship through the point of origin between the α_{1-2} and the separation factors (α^{S}_{1-2}) in the liquid-phase adsorption on the silica gel surface.

Many interesting studies of the intramolecular and the intermolecular hydrogen bonds have been made by using such analytical instruments as IR, NMR, and Raman spectrometers.[1] Especially, the O–H···π hydrogen-bonding interactions between the proton donors and the solvents containing π-electrons have been systematically studied with the IR technique.[2-4] On the other hand, the spectroscopic studies of the O–H···n interactions of the proton donors with the solvents containing hetero atoms have been mainly focussed on the O–H frequency shifts, the equilibrium constants, and the enthalpy changes of hydrogen-bond formations.[5-10] Many investigations of the hydrogen bond have, in any case, been made in very dilute solutions of such inert solvents as CCl_4. Little attention has been paid to the quantitative difference or to the correlation between the O–H···π and the O–H···n interactions.[1] Moreover, few systematic studies of hydrogen-bonding interactions in correlation with the gas-phase and/or the liquid-phase adsorption phenomena on a solid surface have been reported, except for the gas-phase adsorption on silica gel.[11,12] On the other hand, despite the vastness of the literature on intermolecular interactions in solution, the correlation between the nucleophilic coordinations of solvents to the Brönsted acids and the Lewis acids has never been discussed because of the different types of interactions

1) The studies of the hydrogen bonds were summarized in G. C. Pimentel and A. L. McClellan, "The Hydrogen Bond," W. H. Freeman & Co., San Francisco, Calif., (1960).

2) a) R. West, *J. Amer. Chem. Soc.*, **81**, 1614 (1959); b) D. L. Powell and R. West, *Spectrochim. Acta*, **20**, 984 (1964).

3) B. Ghosh and S. Basu, *Trans. Faraday Soc.*, **61**, 2097 (1965).

4) a) Z. Yoshida, E. Osawa, and R. Oda, *J. Phys. Chem.*, **68**, 2895 (1964); b) Z. Yoshida and E. Osawa, *J. Amer. Chem. Soc.*, **87**, 1467 (1965); c) Z. Yoshida and E. Osawa, *ibid.*, **88**, 4019 (1966).

5) W. Gordy and S. C. Stanford, *J. Chem. Phys.*, **9**, 204 (1941).

6) M. St. C. Flett, *J. Soc. Dyers Colourists*, **68**, 59 (1952).

7) T. Tsubomura, *J. Chem. Phys.*, **23**, 2130 (1955).

8) a) T. D. Epley and R. S. Drago, *J. Amer. Chem. Soc.*, **89**, 5770 (1967); b) K. F. Purcell and R. S. Drago, *ibid.*, **89**, 2874 (1967); c) R. S. Drago and T. D. Epley, *ibid.*, **91**, 2883 (1969); d) R. S. Drago, N. O'Bryan, and G. C. Vogel, *ibid.*, **92**, 3924 (1970).

9) J. H. Nelson, L. C. Nathan, and R. O. Ragsdale, *ibid.*, **90**, 5754 (1968).

10) T. Kagiya, Y. Sumida, and T. Inoue, This Bulletin, **41**, a) 767, b) 773, c) 779 (1968); d) T. Kagiya, Y. Sumida, and T. Tachi, *ibid.*, **43**, 3716 (1970).

11) T. Kagiya, Y. Sumida, and T. Tachi, *ibid.*, in press. (1971).

12) a) V. Ya. Davydov, A. V. Kiselev, and V. I. Lygin, *Dokl. Akad. Nauk, SSSR*, **147**, 131 (1962); b) G. A. Galkin, A. V. Kiselev and V. I. Lygin, *Trans. Faraday Soc.*, **60**, 431 (1964); c) L. H. Little, "Infrared Spectra of Adsorbed Species," Academic Press, London-New York (1966), p. 274.

involved.[13]

In this paper, the hydrogen-bonding interaction has been studied by means of the IR technique between various proton-acceptor solvents (S_2) in carbon tetrachloride (S_1) solutions and trimethylsilanol, which has a partial structure (SiO–H bond) analogous to the silanol group on the silica gel surface.[14] The objectives of the present work are; (1) to discuss the different types of hydrogen bonds, *i.e.*, the O–H···π and the O–H···n interactions; (2) to compare the hydrogen-bonding interaction with trimethylsilanol with the nucleophilic coordination to antimony(V) chloride as a Lewis acid, and (3) to ascertain the relationship between the liquid-liquid interaction with trimethylsilanol and the gas-phase adsorption (solid-gas interaction) or the liquid-phase adsorption (solid-liquid interaction) on silica gel.

Experimental

Materials. All the solvents were obtained commercially and were purified by the usual methods. The trimethylsilanol was synthesized by the method of Sommer.[15]

Spectra Measurements. The composition of the binary mixture of carbon tetrachloride (S_1) and the second solvent (S_2) was cautiously determined by weighing and was varied over quite a wide concentration range. A small quantity of trimethylsilanol was added to a weighing bottle containing the binary mixture to make a solution of 0.004—0.015 mol/*l*. The KBr cell, with an optical thickness of 0.20 cm and filled with the solution, was placed in the irradiation path of infrared light, controlled at 28±3°C, and then allowed to equilibrate before scanning. All the spectral measurements were made by using a Japan Spectroscopic Co., Ltd., Model DS-403G infrared spectrophotometer. The spectral slit width was 1.7 cm^{-1} in the O–H fundamental regions (3400—3700 cm^{-1}).

Analysis of Spectra. The O–H frequency shifts ($\Delta\nu_{OH}$) of trimethylsilanol caused by the S_2 were expressed as the difference from the free O–H absorption frequency in CCl_4 ($\nu_{OH}(CCl_4)=3702$ cm^{-1});

$$\Delta\nu_{OH} = \nu_{OH}(CCl_4) - \nu_{OH}(S_2) \quad (1)$$

In the following equilibrium reaction;

$$SiOH\cdots S_1 + S_2 \rightleftarrows SiO\text{–}H\cdots S_2 + S_1 \quad (2)$$

the concentration ([SiOH···S_1] or [SiO–H···S_2]) of trimethylsilanol solvated by S_1 or S_2 in the binary mixture was estimated from the calibration curve of the trimethylsilanol concentration in each solvent against the absorbance, which had been drawn in advance. However, the O–H absorption band of trimethylsilanol in the polar solvent differed considerably in frequency, in intensity, and in shape from that caused by the solvent in the binary mixture. The concentration [SiO–H···S_2] of trimethylsilanol solvated by such solvents as ethyl acetate (EA), acetonitrile (AN), dioxane (DOX), and tetrahydrofuran (THF) was replaced by [SiOH]$_0$−[SiOH···S_1], where [SiOH]$_0$ was the initial concentration. Moreover, in order to evaluate the apparent molar absorption coefficients (κ_2) of hydrogen-bonded complexes with the hetero atoms, the check for the Lambert-Beer rule was made in such dilute solutions of CCl_4 that the free O–H band disappeared, that is, in solutions with volume ratios of CCl_4 : EA=1 : 1, CCl_4 : AN=1 : 1, CC_4 : DOX=2 : 1, and CCl_4 : THF=2 : 1. The concentration [SiO–H···S_2] estimated by using the apparent molar absorption coefficients agreed, within the limits of experimental error (3—5%), with [SiOH]$_0$−[SiOH···S_1]. The equilibrium constant (α_{1-2}) in Eq. (2), which we called the preferential coordination constant, was calculated by the use of Eq. (3);

$$\alpha_{1-2} = \frac{[SiO\text{–}H\cdots S_2]([S_1]_0 - [SiOH\cdots S_1])}{[SiOH\cdots S_1]([S_2] - [SiO\text{–}H\cdots S_2])} \quad (3)$$

The equilibrium constant (K) of hydrogen-bond formation in very dilute solutions of CCl_4 was estimated from the α_{1-2}.

Results and Discussion

Figures 1 and 2 show typical examples of O–H···π and O–H···n spectra observed in CCl_4-benzene and CCl_4-tetrahydrofuran solutions respectively. The

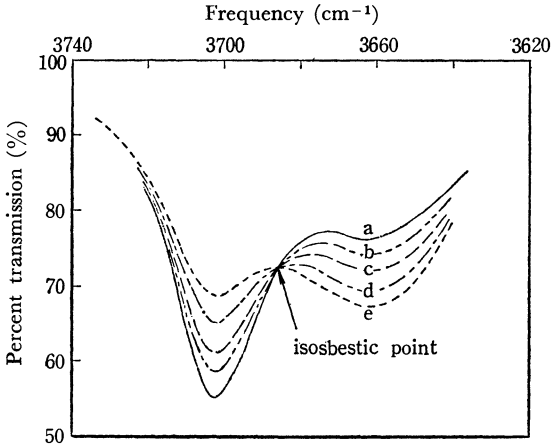

Fig. 1. The O–H stretching absorption spectra of 0.012 mol/*l* of trimethylsilanol in the CCl_4-benzene solutions.
Volume ratios of CCl_4 : Benzene: a, 12 : 3; b, 11.5 : 3.5; c, 11:4; d, 10:5; e, 9 : 6.

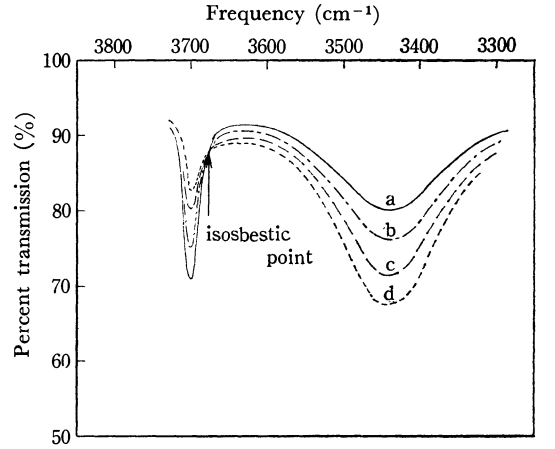

Fig. 2. The O–H stretching absorption spectra of 0.0063 mol/*l* of trimethylsilanol in the CCl_4-tetrahydrofuran solutions.
Volume ratios of CCl_4 : tetrahydrofuran: a, 14.9 : 0.1; b, 14.75 : 0.25; c, 14.5 : 0.5; d, 14 : 1.

13) a) V. Gutmann, A. Steininger, and E. Wychera, *Mh. Chem.*, **97**, 460 (1966); b) V. Gutmann and E. Wychera, *Inorg. Nucl. Chem. Lett.*, **2**, 257 (1966); c) V. Gutmann, "Coordination Chemistry in Non-Aqueous Solution," Springer-Verlag, Wien-New York (1968).

14) R. West and R. H. Baney, *J. Amer. Chem. Soc.*, **81**, 6146 (1959).

15) L. H. Sommer, E. Pietrusza, and F. C. Whitmore, *ibid.*, **68**, 2282 (1946).

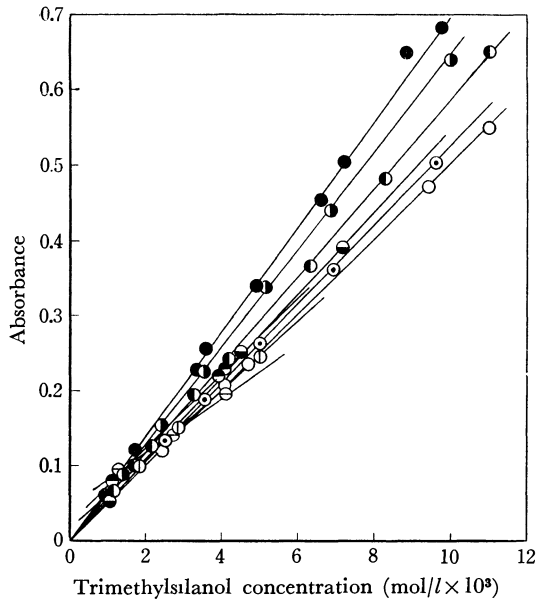

Fig. 3. The Lambert-Beer rule between the concentrations of trimethylsilanol solvated by solvents and the absorbances at the maximum points of O-H stretching absorption bands.
●, Carbon tetrachloride; ○, Benzene; ⊙, Chlorobenzene; ◐, Toluene; ◑, *p*-Xylene; ◓, Ethyl acetate (in 50 volume % CCl_4 solution); ◒, Acetonitrile (in 50% CCl_4); ⓓ, Dioxane (in 67% CCl_4); ⓕ, Tetrahydrofuran (in 67% CCl_4).

Lambert-Beer rule held fairly well over a wide concentration range of trimethylsilanol in CCl_4 and in the aromatic hydrocarbons, but not in solvents containing oxygen and nitrogen atoms diluted by CCl_4, as has been described in the experimental section (Fig. 3). This may be due to the large polarity of the hydrogen-bonded complex with the hetero atom. As is shown in Figs. 1 and 2, the isosbestic points were observed in every binary solution studied in the present work except the CCl_4-acetonitrile solution.[16] This fact leads to the conclusion that all hydrogen-bonded complexes have compositions of 1 : 1.[4c] Moreover, the fact that the preferential coordination constants, calculated on the basis of the 1 : 1 complex, are reasonably constant over the wide concentration range of the S_2 provides indirect support for the 1 : 1 assumption.

In Table 1, the apparent molar absorption coefficients (κ_2) and the apparent half-widths ($\Delta\nu_{1/2}$) of the O–H bands bonded by the solvents, the equilibrium constants (K) of the hydrogen-bond formation in very dilute CCl_4 solutions, and the preferential coordination constants (α_{1-2}) of the binary mixtures are summarized, together with the O–H frequency shifts ($\Delta\nu_{OH}$) of trimethylsilanol caused by the S_2. The error limits in Table 1 are believed to be within about 5%.[4c]

Difference in the O–H···π and O–H···n Hydrogen Bonds. It should be noted in Table 1 that the apparent molar absorption coefficients which are characteristic of the hydrogen-bonded complexes are nearly equal within 230—300 l/mol·cm, even though the O–H···π and O–H···n hydrogen bonds are of different types.[17] On the other hand, the half-widths, expressing the relaxation phenomenon of the complexes, changed markedly with different forms of hydrogen-bonding interaction, *i.e.*, ~50 cm^{-1} for O–H···π and 120—160 cm^{-1} for O–H···n complexes.[18] Moreover, the $\Delta\nu_{OH}$, α_{1-2}, and K values of solvents containing the oxygen and nitrogen atoms are large in comparison with those of the aromatic hydrocarbons. These results suggest the stronger nucleophilic coordination of the lone-pair-electrons of the hetero atom to trimethylsilanol than that of the π-electrons of the benzene nuclei. A major difference in the two types of hydrogen-bonding interactions is considered to appear more conspicuously in the entropy effect than in the enthalpy effect.

In order to confirm this theory, the free-energy changes ($-\Delta G$) of hydrogen-bond formation were plotted against the $\Delta\nu_{OH}$ values, which were propor-

Table 1. Spectral properties, equilibrium constants and preferential coordination constants of hydrogen bond between trimethylsilanol and proton acceptor solvents (S_2) in CCl_4 solutions

Solvent (S_2)	Mole fraction of S_2 in CCl_4-S_2	κ_2[a] (l/mol·cm)	$\Delta\nu_{1/2}$[a] (cm^{-1})	$\Delta\nu_{OH}$ (cm^{-1})	α_{1-2}	K (l/mol)	$-\Delta G$ (kcal/mol)
Chlorobenzene	0.24—0.45	264	43±1	29±1	1.97±0.21	0.19±0.02	−0.98±0.07
Benzene	0.21—0.45	252	52±3	40±1	2.25±0.07	0.22±0.01	−0.90±0.03
Toluene	0.18—0.78	293	50±2	59±1	2.36±0.21	0.23±0.02	−0.87±0.07
p-Xylene	0.15—0.75	326	35±1	63±1	2.59±0.18	0.25±0.02	−0.82±0.05
Ethyl acetate	0.03—0.50	258	131±6	146±3	15.5 ±0.3	1.50±0.03	0.24±0.02
Acetonitrile	0.02—0.65	275	128±8	140—175[b]	18.1 ±3.8	1.76±0.37	0.34±0.14
Dioxane	0.01—0.23	229	145±9	220±6	30.6 ±7.6	2.97±0.74	0.65±0.17
Tetrahydrofuran	0.01—0.08	—	150±9	265±3	35.6 ±4.1	3.46±0.39	0.74±0.07

a) As for the free O–H absorption band in CCl_4, κ_1=356 l/mol·cm and $\Delta\nu_{1/2}$=18±1 cm^{-1}.
b) The $\Delta\nu_{OH}$ increases with the increase in the acetonitrile concentration in the binary mixture.[16]

16) A. Allerhand and P. von Schleyer, *ibid.*, **85**, 371 (1963).
17) The κ_2 and $\Delta\nu_{1/2}$ values of the O–H absorption band in *p*-xylene were 326±5 l/mol·cm and 35±1 cm^{-1} respectively. This may be caused by the asymmetric O–H band in *p*-xylene, which differs from the symmetric bands in other aromatic hydrocarbons.
18) The $\Delta\nu_{1/2}$ values of O–H···n complexes decreased slightly with an increase in the concentration of trimethylsilanol.

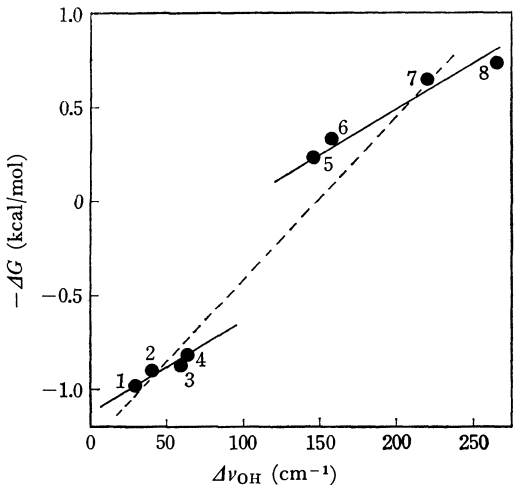

Fig. 4. Relationship between the free energy changes ($-\Delta G$) of hydrogen bond formation and the O-H frequency shifts ($\Delta\nu_{OH}$).
1, Chlorobenzene; 2, Benzene; 3, Toluene; 4, *p*-Xylene; 5, Ethyl acetate; 6, Acetonitrile; 7, Dioxane; 8, Tetrahydrofuran.

tional to the enthalpy changes of hydrogen-bond formation, as had been pointed out in the earlier papers.[1,8] As is shown in Fig. 4, a linear relationship is apparently obtained between them. However, further observation indicates different straight lines for the aromatic hydrocarbons and the solvents containing the hetero atoms, whose slopes are nearly equal to each other. This can be explained as resulting from the remarkable difference in the entropy effects of π- and n-hydrogen bonds. A similar result had been reported for the phenol adducts with π-electron and lone-electron donors.[4b,c]

On the other hand, the $\Delta\nu_{1/2}$ value should be an overall value expressing the molecular movement of the O–H group in solutions, including the enthalpy and the entropy changes. Therefore, the ΔG value may be expected to have a better correlation with the $\Delta\nu_{1/2}$ value than with the $\Delta\nu_{OH}$. As is confirmed in Fig. 5, the ΔG *vs.* $\Delta\nu_{1/2}$ relationship is satisfied in various binary solutions, regardless of the form of the hydrogen bond.

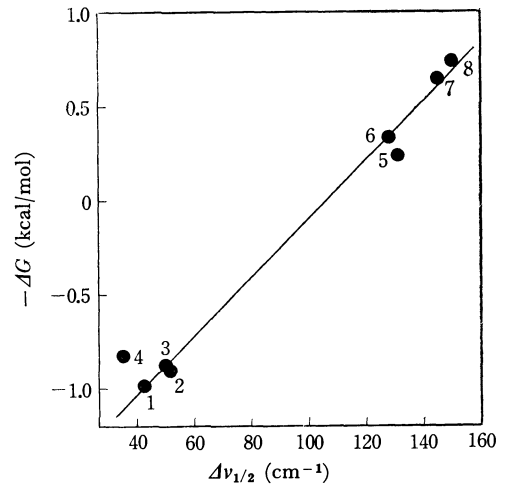

Fig. 5. Relationship between the free energy changes ($-\Delta G$) of hydrogen bond formation and the apparent half-widths ($\Delta\nu_{1/2}$) of O-H bands.
1, Chlorobenzene; 2, Benzene; 3, Toluene; 4, *p*-Xylene; 5, Ethyl acetate; 6, Acetonitrile; 7, Dioxane; 8, Tetrahydrofuran.

Interaction Forces of Solvents toward the Brönsted and Lewis Acids. As has been mentioned in the previous papers,[10a,d] the $\Delta\nu_{OH}$ can be regarded as a measure of the proton-accepting (the electron-donating) properties of S_2 toward the Brönsted acid. On the other hand, Gutmann *et al.* have made quantitative calorimetric measurements of the interactions of a number of solvents containing the hetero atoms with antimony(V) chloride and have proposed a donor number for each of the solvents toward the Lewis acid.[13] A comparison of the electron-donating properties of the solvents toward the different kinds of acids, *e.g.*, the Brönsted and Lewis acids, is shown in Fig. 6, where the $\Delta\nu_{OH}$ values of pyridine, dimethyl sulfoxide, dimethylformamide, and *N*,*N*-dimethylacetamide have been approximated from the data for deuteromethanol as a proton donor.[10a] The $\Delta\nu_{OH}$ increased linearly with the increase in the donor numbers. It seems that it can be concluded from this fact that there exists a certain physicochemical rule between the intermolecular interactions toward the Brönsted acid and the Lewis acid, despite the different types of interactions.

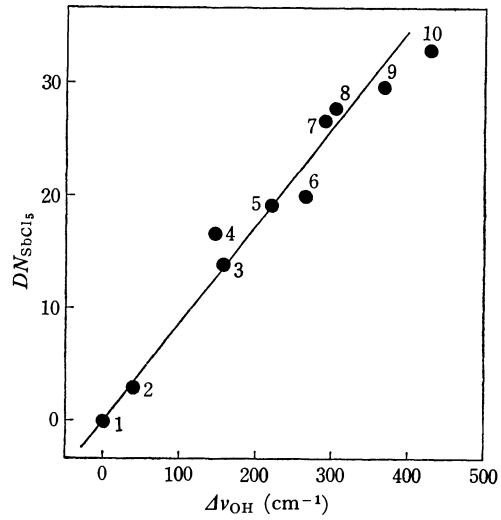

Fig. 6. Relationship between the donor numbers (DN_{SbCl_5}) and the O-H frequency shifts ($\Delta\nu_{OH}$).
1, Carbon tetrachloride; 2, Benzene; 3, Acetonitrile; 4, Ethyl acetate; 5, Dioxane; 6, Tetrahydrofuran; 7, Dimethylformamide; 8, *N*,*N*-Dimethylacetamide; 9, Dimethyl sulfoxide; 10, Pyridine.
The $\Delta\nu_{OH}$ values of solvents (7—10) were estimated from the data for deuteromethanol.
The DN_{SbCl_5} of CCl_4 was approximated by that of 1,2-dichloroethane.

Liquid-liquid Interaction with Trimethylsilanol and Solid-gas and Solid-liquid Interaction with the Silica Gel Surface. It is well known that the silanol group on the silica gel surface plays an effective role in the catalytic reactions. In order to make clear the intermolecular interactions on the silica gel surface, the liquid-liquid interaction with trimethylsilanol was compared with the gas-phase adsorption (solid-gas interaction) and

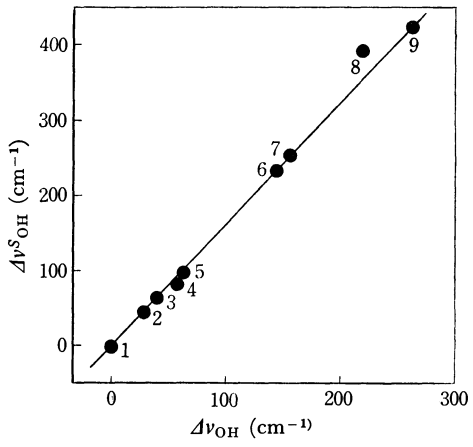

Fig. 7. Relationship between the O-H frequency shifts ($\Delta\nu^S_{OH}$) of silica gel surface silanol by gas-phase adsorption and the O-H frequency shifts ($\Delta\nu_{OH}$) of trimethylsilanol.
1, Carbon tetrachloride; 2, Chlorobenzene; 3, Benzene; 4, Toluene; 5, *p*-Xylene; 6, Ethyl acetate; 7, Acetonitrile; 8, Dioxane; 9, Tetrahydrofuran.

the liquid-phase adsorption (solid-liquid interaction) on silica gel.

The $\Delta\nu_{OH}$ values of trimethylsilanol were plotted against the $\Delta\nu^S_{OH}$ values, which were the O–H frequency shifts of the surface silanol caused by the monolayer adsorption of gases on silica gel,[12,19] where the O–H absorption frequency by CCl_4 vapor was taken to be 3704 cm^{-1}. As is shown in Fig. 7, a good linear relationship, with a slope of 1.60 was obtained between them. The value of this slope indicates that the O–H group of the surface silanol is more acidic than that of trimethylsilanol; that is, the ionic dissociation energy

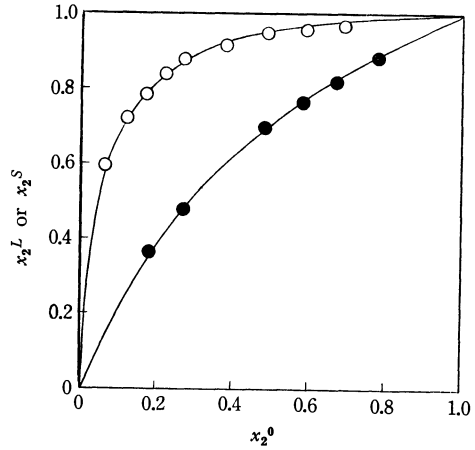

Fig. 8. Plots of the mole fractions (x_2^L) of trimethylsilanol bonded by S_2 or the mole fractions (x_2^S) of S_2 adsorbed on silica gel against the mole fractions (x_2^0) of non-bonded S_2.
●; Carbon tetrachloride-Toluene (Trimethylsilanol), $\alpha_{1-2}=2.36$
○; Cyclohexane-Toluene (Silica gel), $\alpha^S_{1-2}=18.6$.

19) The silanol O–H frequency shifts on the silica gel surface depend slightly on the surface coverage; they grow considerably with the surface coverage up to a monolayer, while on further adsorption they change very slowly.
20) For such a homologous series of adsorbates as the aromatic hydrocarbons, the $\Delta\nu_{OH}$ increases as the differential heat of adsorption becomes larger.

of the surface O–H bond is smaller than that of the trimethylsilanol O–H bond.[10d] This may correspond to the fact that the O–H fundamental frequency of silica gel is 3749 cm^{-1} in the gas-phase,[12] considerably larger than that (*ca.* 3710 cm^{-1}) of trimethylsilanol.[10d] In a previous paper,[10d] we defined the proton-donating power (Φ_D) of the donor, independent of the kind of proton acceptor, as the ratio of the O–H frequency shift of the proton donor in a certain acceptor to that of methanol as a standard proton donor;

$$\Phi_D = \frac{\Delta\nu_{RO-H}(\text{proton acceptor})}{\Delta\nu_{MeO-H}(\text{proton acceptor})} \quad (4)$$

This definition rests on the fact that there exists a linear relationship, through the point of origin, between $\Delta\nu_{RO-H}$ and $\Delta\nu_{MeO-H}$ in the same proton acceptor.[8d,10d] According to our definition, the Φ_D of the trimethylsilanol and the silica gel surface silanol were determined to be 1.65 and 2.65 respectively. The value of

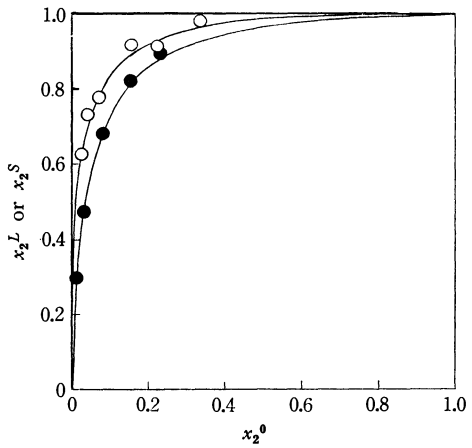

Fig. 9. Plots of the mole fractions (x_2^L) of trimethylsilanol bonded by S_2 or the mole fractions (x_2^S) of S_2 adsorbed on silica gel against the mole fractions (x_2^0) of non-bonded S_2.
●; Carbon tetrachloride-Dioxane (Trimethylsilanol), $\alpha_{1-2}=30.6$
○; Cyclohexane-dioxane (silica gel), $\alpha^S_{1-2}=63.3$.

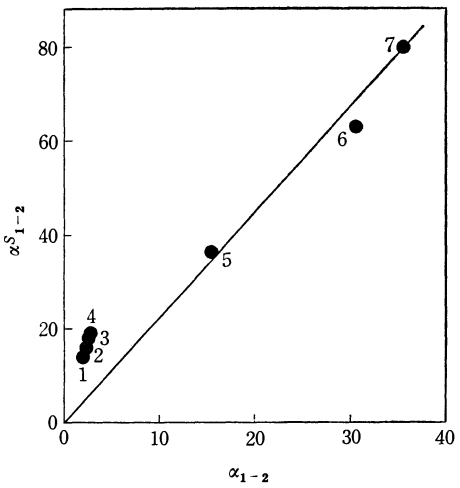

Fig. 10. Relationship between the preferential coordination constants (α_{1-2}) of trimethylsilanol and the separation factors (α^S_{1-2}) of silica gel.
1, Chlorobenzene; 2, Benzene; 3, Toluene; 4, *p*-Xylene; 5, Ethyl acetate; 6, Dioxane; 7, Tetrahydrodrofuran.

surface silanol is nearly equal to that (2.92) of *p*-nitrophenol. On the other hand, the $\Delta\nu_{OH}$ is not related to the differential heat of adsorption, expressing the total energy of the complicated interaction with the surface at a given coverage.[20] However, from a comparison of the homogeneous and heterogeneous hydrogen-bonding interactions, it can be concluded that there is a difference in the Φ_D, namely, the sensitivity to proton acceptors, but no essential difference in the nucleophilic coordination phenomena.

In order to compare the liquid-liquid interaction with trimethylsilanol with the solid-liquid interaction with the silica gel surface, we examined the relationship between the preferential coordination constants (α_{1-2}) to trimethylsilanol and those ($\alpha^S{}_{1-2}$) on silica gel, that is, the separation factors. The latter was obtained from the data on the preferential adsorption from the binary solution of cyclohexane(S_1)-second solvent(S_2) on silica gel.[11] In Fig. 8 and 9, the mole fractions ($x_2{}^L$) of trimethylsilanol bonded by the S_2 or those ($x_2{}^S$) of the S_2 adsorbed on the silica gel are plotted against the mole fractions ($x_2{}^0$) of the non-bonded S_2 in the equilibrium solution. It should be noted in Figs. 8 and 9 that the binary mixtures are better separated on the silica gel surface than in trimethylsilanol. The separation power of silica gel or trimethylsilanol is characterized by the $\alpha^S{}_{1-2}$ or the α_{1-2}. A quantitative relationship between the α_{1-2} and the $\alpha^S{}_{1-2}$ is illustrated in Fig. 10. A straight line, though not good, is drawn with a slope of 2.2 through the point of origin. This may correspond to the fact that the Φ_D of surface silanol is larger than that (1.65) of trimethylsilanol.[10d] It can be said from the above considerations that the separation powers of proton donors in the same binary mixture become larger as the Φ_D values of the donors increase.

BULLETIN OF THE CHEMICAL SOCIETY OF JAPAN, VOL. 44, 928—933 (1971)

The Molecular and Crystal Structure of 3,4-Furandicarboxylic Acid Dimethylester

Yasuyoshi OKADA,* Kazumi NAKATSU,** and Akira SHIMADA

Department of Chemistry, Faculty of Science, Osaka City University, Sugimotocho, Osaka

(Received September 9, 1970)

The crystals of 3,4-furandicarboxylic acid dimethylester are monoclinic of the space group $P2_1/a$, with unit cell dimensions $a=12.64$, $b=8.16$, $c=7.97$ Å, and $\beta=100.0°$. An approximate structure was determined by application of the symbolic addition phase determining procedure. After several cycles of least-squares refinement, the discrepancy index for the 901 observed reflections was reduced to 14%. In the molecule the furan ring is planar, and one carbomethoxy group is almost on the same plane as the furan ring, while the other makes an angle of 10.5° with the ring. The bond lengths and angles do not differ appreciably from the values found in the other compounds, except for those of C(3)–C(4)=1.41 Å, C(4)–C(3)–C(6)=131° and C(3)–C(4)–C(7)=132°, the latter two being larger than normal values probably because of interaction between the carbonyl-oxygens. The mode of packing of the molecules and a scheme of twinning found in this crystal is discussed.

3,4-Furandicarboxylic acid dimethylester (I) (MW 184, mp 47°C) was studied by means of X-ray crystal analysis to elucidate its molecular structure and the mode of packing in the crystal. Several structures similar to that of the present molecule were studied. They include 3,4-furandicarboxylic acid,[1] furan-α,α'-dicarboxylic acid[2] (or 2,5-furandicarboxylic acid), and 3,4-thiophendicarboxylic acid dimethylester.[3] It would be of interest to compare the present structure with the others, especially about the configurations of the two substituents with respect to the furan ring and the bond distances and angles inside it.

(I)

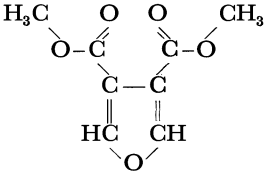

Experimental

Specimens of suitable size for X-ray work were crystallized from the aqueous solution in the form of a transparent, colorless column elongated along the c axis.[4] The crystals have a cleavage plane normal to the a^* axis.

The compound crystallizes always in a twinned form; the twinning is found to be such that the twins have common a^* and b^* but different c^* direction. Twinning made the accurate intensity determinations difficult, for partial or heavy overlappings of the reflections from the twins occurred in some zones.

Since the crystals sublime readily in the air at room temperature, the specimen was enclosed in a capillary tube during exposure to X-rays. Multiple Weissenberg intensity data were collected with Ni-filtered Cu $K\alpha$ radiation along axis c from zeroth to fifth layer and along axes a and b for zeroth layer only. The intensities were estimated visually with the use of a calibrated scale. Altogether 1239 independent reflections were observed, and 338 of them were too weak to be

* Present address: NIKKI Chemical Co., Ltd., 4-51 Kitahama, Osaka.

** Present address: Faculty of Science, Kwansei Gakuin University, 1-2 Uegahara, Nishinomiya.

1) D. E. Williams and R. E. Rundle, *J. Amer. Chem. Soc.*, **86**, 660 (1964).

2) E. Martuscelli and C. Pedone, *Acta Crystallogr.*, **B24**, 175 (1968).

3) H. Yoshioka, K. Nakatsu, and A. Shimada, to be published.

4) The crystals were kindly prepared by Professor S. Oae, Faculty of Technology of Osaka City University.

measured. No correction was made for absorption and extinction. After the Lorentz and the polarization corrections were made, intensities were placed on a same relative scale.

The crystal data are as follows:

Monoclinic,

$a=12.64\pm0.04$ Å

$b=8.16\pm0.02$

$c=7.97\pm0.02$

$\beta=100.0\pm0.1°$

Systematic Absences, $h0l$ with h odd and $0k0$ with k odd

Space Group, $P2_1/a$

Density, $D_m=1.50$ g cm^{-3}, $D_x=1.51$ g cm^{-3}

Z 4

Absorption Coefficient, $\mu=12.7$ cm^{-1} (for Cu $K\alpha$).

Structure Determination

Since attempts to solve the Patterson map were not successful, the direct phase determining method, or so-called symbolic addition method[5] by Karle *et al.*, was applied. Professor Y. Okaya of State University of New York kindly supplied us with a copy of his program.[6]

In this procedure normalized structure factors may be used, being defined as

$$E_h^2 = F_h^2/\varepsilon \sum_{j=1}^{N} f^2{}_j h^2, \qquad (1)$$

where F_h is the observed structure factor for the reflection $\boldsymbol{h}$, and N is the number of atoms in the unit cell. ε is a factor that depends on the space group extinctions, and $\varepsilon=1$ in the space group $P2_1/a$ except for the $h0l$ and $0k0$ reflections, where $\varepsilon=2$. The distribution and the statistical averages of the normalized structure factor are given in Table 1. The experimental values imply that the crystal is centrosymmetric.

To initiate the symbolic addition procedure, three linearly independent reflections were chosen to specify the origin. The signs of two other reflections were specified symbolically by letters. These five reflections forming the basic starting set are as follows:

Table 1. Statistical averages and distribution of the normalized structure factors

	Experimental	Theoretical	
		Centric	Acentric
$\langle\|E^2\|\rangle$	1.000[a]	1.000	1.000
$\langle\|E^2-1\|\rangle$	1.059	0.968	0.736
$\langle\|E\|\rangle$	0.726	0.798	0.886
$\|E\|>3$	0.26%	0.3%	0.01%
$\|E\|>2$	5.1	5.0	1.8
$\|E\|>1$	31.0	32.0	36.8

a) Normalized to the unity.

$h\ k\ l$	$\|E\|$	sign	$h\ k\ l$	$\|E\|$	sign
1 1 2	3.63	+	3 5 0	3.53	A
5 3 1	2.76	+	8 2 0	2.72	B
3 4 1	2.67	+			

These reflections were chosen on the basis of the large number of interactions obtained from application of the Σ_2 formula and on their relatively high $|E|$ values. The Σ_2 formula is

$$sE_h \approx s\sum_{k} E_k \cdot E_{h-k}, \qquad (2)$$

where s means "sign of". The probability $P_s(E_h)$ that a symbolic phase s determined by the Σ_2 formula is valid is given by[6]

$$P_s(E_h) = 1/2 + 1/2 \tanh\left(\frac{\sigma_3}{\sigma_2^{3/2}}|E_h|\cdot R_s\right), \qquad (3)$$

where $\sigma_n=\sum_{j=1}^{N} Z_j{}^n$, Z_j is the atomic number of the jth atom and R_s is the difference between the sum of the products $E_k \cdot E_{h-k}$ associated with the dominant symbol(s) and the sum of the products of all other symbols.

Table 2. A typical sigma-2 list

Reflection $\boldsymbol{h}=(3\ 6\ 3)$ $|E|=1.69$

$\boldsymbol{k}$			$\|E_k\|$	$\boldsymbol{h-k}$			$\|E_{h-k}\|$	T[a]	s_k[b]	s_{h-k}	s_h
9	4	3	3.41	−6	2	0	2.13	12.27	−A B		
9	5	1	2.61	−6	1	2	1.82	8.03	B	−A B	−A
1	8	1	3.11	2	−2	2	1.95	10.25	A	− B	−A B
10	3	5	2.49	−7	3	−2	2.41	10.14	−A B		
10	3	1	2.48	−7	3	2	2.90	12.15		B	
0	8	2	2.35	3	−2	1	2.17	8.62		B	
0	9	3	2.16	3	−3	0	1.72	6.28	+	−A	−A
2	7	1	1.85	1	−1	2	3.63	11.35	−A B	+	−A B
8	1	2	1.82	−5	5	1	1.66	5.11	−		
8	−1	2	1.82	−5	7	1	1.61	4.95	+		
6	1	−2	1.82	−3	5	5	2.49	7.66	A B	−	−A B
4	0	3	1.82	−1	6	0	1.70	5.20	B	−A	−A B

$R_s=11.91$ $P_s(E_h)=0.9965$ Phase $=-$AB

a) $T=|E_h \cdot E_k \cdot E_{h-k}|$

b) s's mean sign or phase of $\boldsymbol{h}$, $\boldsymbol{k}$, or $(\boldsymbol{h-k})$.

5) J. Karle and I. L. Karle, *Acta Crystallogr.*, **21**, 849 (1966).

6) Y. Okaya and A. Bednowitz, *ibid.*, **22**, 111 (1967).

Only 220 reflections with $|E|$ greater than 1.5 were considered. As many terms in Σ_2 as possible were used to determine each phase. An example of Σ_2 list is given in Table 2, which contains all the interaction pairs giving the index triplet for which a phase should be assigned. Some of these terms seem to indicate a relationship between the unknown symbols. After four cycles of iterations, the phases for 138 reflections were expressed by the combinations of A and B. Inspection of all the Σ_2 interaction lists showed that there was only one possible assignment for the unknown A and B, that is, A=+ and B=+. Any other assignment would have resulted in discrepancies in a number of contributors to Σ_2. This relation was taken into account and 29 additional phases of the reflections were determined. Thus 167 phases were settled.

E maps (Fourier map with E rather than F values for coefficients) were computed with both the 138 and 167 reflections. All the thirteen non-hydrogen atoms in the asymmetric unit were resolved. Sections from these maps are illustrated in Figs. 1(a) and (b). On the E map shown in Fig. 1(b), the peak values for all the atoms exceeded 220 (on an arbitrary scale), while the maximum value of the rapidly varying background was 193.

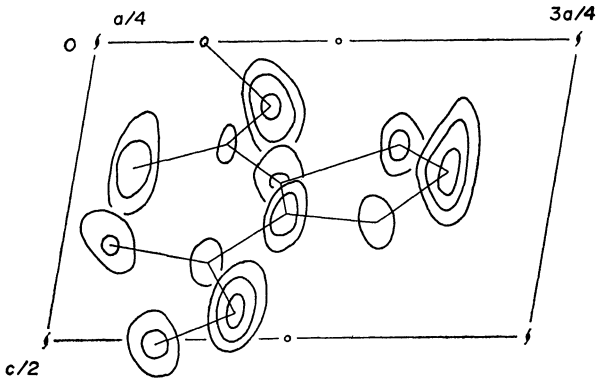

(a)

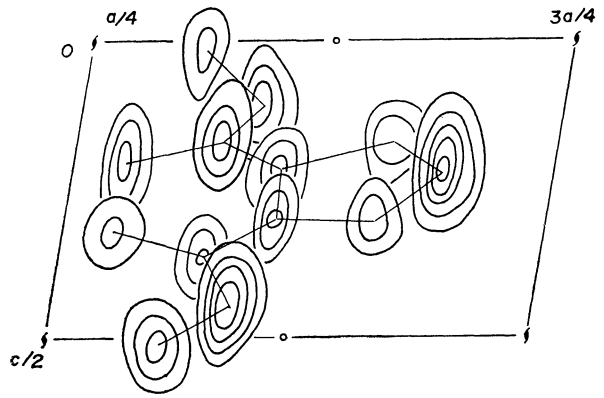

(b)

Fig. 1. E maps computed with 138 terms (a) and 167 terms (b).

Coordinates for the thirteen non-hydrogen atoms as read from the E map were subjected to a least-squares refinement, using all the reflection data. After three cycles of diagonal least-squares calculations, the discrepancy index $R=\Sigma||F_o|-|F_c||/\Sigma|F_o|$ was reduced to 0.21 for the non-zero reflections only. Successive two cycles of block-diagonal calculations lowered R only by 2%.

Electron density and difference Fourier syntheses were calculated at this stage of refinement. Sections of the three-dimensional electron density map projected on (010) are given in Fig. 2. Since remarkable anisotropic thermal vibration of the atoms were implied from the difference Fourier map, further refinement was carried out with the anisotropic temperature factors applied to the thirteen non-hydrogen atoms. Two more cycles of block-diagonal least-squares calculations improved R to 0.135. The peaks of hydrogen atoms did not appear in the difference map even at this stage.

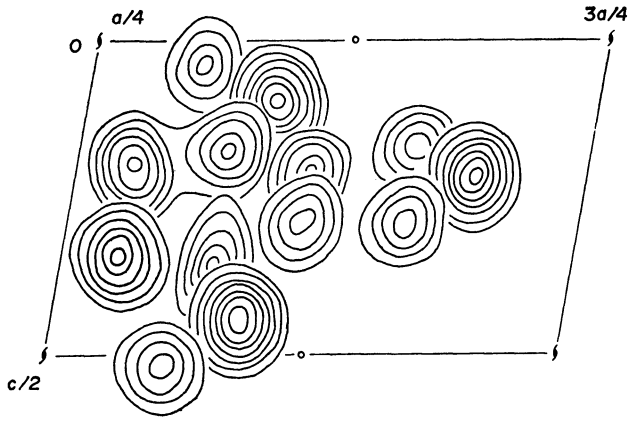

Fig. 2. Sections of electron density distribution projected onto (010) plane. Contours are drawn at intervals of 1 e·Å^{-3}, starting at 2 e·Å^{-3}.

Results and Discussion

The final coordinates and temperature factors of the atoms are listed in Table 3(a) and (b), respectively, and the intramolecular distances and angles are given in Table 4 and Fig. 3. In Table 5 the bond distances and angles inside the furan ring found in the several similar molecules are compared with the mean values in the present one, where the furan ring has approximately a mirror symmetry through O(1) and the midpoint of C(3)–C(4) bond.

The ring C–O lengths of 1.36 and 1.35 Å are very close to the values found in various compounds. The double bond lengths of 1.37 and 1.38 Å in the ring are nearly equal to the value of 1.361 Å found in furan, but greater than the values 1.351 and 1.35$_4$ Å found in 3,4-acid and α,α'-acid, respectively. The single bond distance 1.41 Å in the ring appears to be significantly shorter than the value 1.462 Å found in 3,4-acid. The single bonds between the ring and the carbonyl group are 1.45 and 1.47 Å long, the former

Table 3. Atomic parameters

(a) Fractional Coordinates and Their Standard Deviations

Atom	x	$10^4\sigma(x)$	y	$10^4\sigma(y)$	z	$10^4\sigma(z)$
O (1)	0.6383	6	0.0405	9	0.2204	10
C (2)	0.5794	8	−0.0929	14	0.1699	15
C (3)	0.4782	8	−0.0739	12	0.2128	13
C (4)	0.4783	8	0.0802	12	0.2934	14
C (5)	0.5785	9	0.1448	13	0.2973	16
C (6)	0.3949	9	−0.1991	13	0.1734	15
C (7)	0.3958	8	0.1673	12	0.3676	14
O (8)	0.4320	6	−0.3240	9	0.0954	10
O (9)	0.3059	6	−0.1923	11	0.2059	12
O (10)	0.3032	6	0.1293	11	0.3453	12
O (11)	0.4350	6	0.2979	9	0.4465	10
C (12)	0.3567	10	−0.4578	16	0.0345	18
C (13)	0.3621	9	0.4007	14	0.5227	16

(b) Thermal Parameters and Their Standard Deviations ($\times 10^4$)

Temperature factor $=\exp[-(\beta_{11}h^2+\beta_{22}k^2+\beta_{33}l^2+\beta_{12}hk+\beta_{13}hl+\beta_{23}kl)]$

Atom	β_{11}	σ	β_{22}	σ	β_{33}	σ	β_{12}	σ	β_{13}	σ	β_{23}	σ
O (1)	53	5	172	13	211	18	−18	14	96	15	−76	25
C (2)	52	8	151	18	187	25	−11	20	62	21	−35	36
C (3)	43	7	127	15	146	22	−6	17	57	18	−12	31
C (4)	46	7	108	15	167	23	4	17	62	19	−10	31
C (5)	53	8	142	18	240	27	10	20	83	23	−49	36
C (6)	56	8	125	16	193	26	−2	16	45	21	−20	34
C (7)	53	7	126	16	153	23	−3	18	62	20	1	32
O (8)	57	6	161	13	232	19	−14	15	89	16	−142	26
O (9)	59	6	193	16	355	23	−50	17	144	19	−143	31
O (10)	55	6	204	16	336	23	−2	17	102	19	−147	31
O (11)	56	5	160	13	194	17	2	14	73	15	−81	25
C (12)	71	10	185	22	272	32	−63	25	72	27	−151	44
C (13)	72	9	166	19	195	27	40	22	80	24	−188	39

Table 4. Interatomic distances and bond angles in a molecule (standard deviations in parenthesis)

Interatomic distances (Å)		Bond angles (°)	
O(1)–C(2)	1.364 (0.014)	C(2)–O(1)–C(5)	108.9 (0.9)
C(2)–C(3)	1.383 (0.016)	O(1)–C(2)–C(3)	108.9 (1.0)
C(3)–C(4)	1.412 (0.015)	C(2)–C(3)–C(4)	106.7 (1.0)
C(4)–C(5)	1.374 (0.017)	C(3)–C(4)–C(5)	106.7 (1.0)
C(5)–O(1)	1.362 (0.015)	C(4)–C(5)–O(1)	108.8 (1.0)
C(3)–C(6)	1.454 (0.016)	C(2)–C(3)–C(6)	121.9 (1.0)
C(4)–C(7)	1.468 (0.016)	C(4)–C(3)–C(6)	131.4 (1.0)
C(6)–O(8)	1.323 (0.015)	C(5)–C(4)–C(7)	121.1 (1.0)
C(6)–O(9)	1.210 (0.015)	C(3)–C(4)–C(7)	132.2 (1.0)
C(7)–O(10)	1.197 (0.015)	C(3)–C(6)–O(8)	110.0 (1.0)
C(7)–O(11)	1.294 (0.014)	C(3)–C(6)–O(9)	126.5 (1.1)
O(8)–C(12)	1.477 (0.016)	O(8)–C(6)–O(9)	123.5 (1.1)
O(11)–C(13)	1.459 (0.015)	C(4)–C(7)–O(10)	123.9 (1.1)
		C(4)–C(7)–O(11)	110.9 (0.9)
C(2)–O(8)	2.639 (0.014)	O(10)–C(7)–O(11)	124.8 (1.1)
C(5)–O(11)	2.642 (0.015)	C(6)–O(8)–C(12)	117.9 (1.0)
O(9)–C(12)	2.700 (0.017)	C(7)–O(11)–C(13)	117.6 (0.9)
O(9)–O(10)	2.849 (0.013)		
O(10)–C(13)	2.672 (0.016)		

Table 5. Comparison of bond lengths and angles in furan ring with similar substances

	3,4-ester[a]	2,5-acid[b]	3,4-acid[c]	furan[d]
O(1)–C(2)[e]	1.36_3 Å	1.36_8 Å	1.361 Å	1.3621 Å
C(2)–C(3)	1.37_9	1.35_4	1.351	1.3609
C(3)–C(4)	1.41_2	1.44_2	1.462	1.4309
$\sigma \times 10^3$(Å)	14—17	6—8	3—5	1—2
C(2)–O(1)–C(5)	108.9°	104.4°	107.2°	106.55°
O(1)–C(2)–C(3)	108.9	112.3	110.3	110.68
C(2)–C(3)–C(4)	106.7	105.4	105.7	106.05
σ(°)	0.9—1.1	0.5	0.2—0.3	0.067

a) Present work. The mean values are shown. b) 2,5-furandicarboxylic acid (furan-α,α'-dicarboxylic acid)[2]. c) 3,4-furandicarboxylic acid[1]. d) Results from microwave spectroscopy[7]. e) Key;

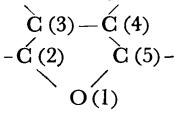

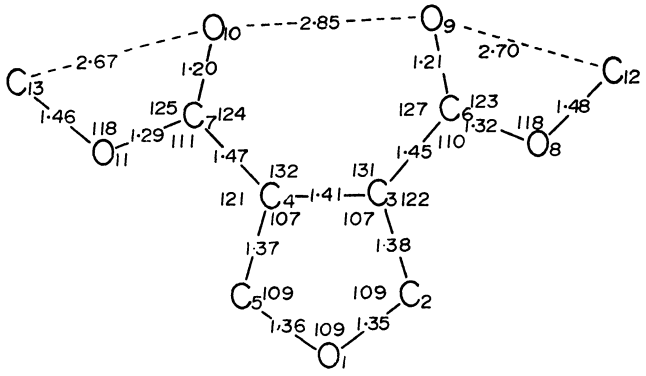

Fig. 3. The molecular structure projected on the plane of furan rin . Standard deviations are about 0.016Å and 1.0°.

is slightly shorter than the usual value.

The furan ring is accurately planar, and the equation of the mean plane and the deviations of the atoms from this plane are given in Table 6, in which the planes of carbonyl groups are also described. The oxygen atoms in one of the carboxyl group, O(10) and O(11), are markedly out of the plane of furan ring; the twist angle of the carboxyl group with respect to the ring plane is 10.5°. The other carboxyl oxygen atoms, O(8) and O(9), on the other hand, are almost completely on the same plane as the ring.

The distance between the two carboxyl oxygen atoms is 2.85 Å, which is just the twice of the van der Waals radius of oxygen atom and should be compared to the value of 2.91 Å found in 3,4-thiophendicarboxylic acid dimethylester.[3] The angles C(4)–C(3)–C(6)= 131° and C(3)–C(4)–C(7)=132° deviate considerably from the ideal value 126°. This would be due to the steric hindrance between the two substituents. The interaction would also cause the distortion of the bond angles around C(6) and C(7), *viz.*, C(3)–C(6)–O(9) and C(4)–C(7)–O(10) are increased, while C(3)–C(6)–O(8) and C(4)–C(7)–O(11) are reduced by several degrees each.

The mode of packing of the molecules in the crystal can be seen in Figs. 4 and 5. The furan rings incline

Table 6. Mean plane parameters and deviations of the atoms from the plane

Plane 1. Furan ring defined by O(1), C(2), C(3), C(4), and C(5).

$-0.1718X+0.4360Y-0.8834Z+2.7242=0$

Atom	Deviation	Atom	Deviation
O(1)	+0.0060 Å	O(8)	−0.0064 Å
C(2)	−0.0022	O(9)	−0.0036
C(3)	−0.0024	O(10)	+0.2138
C(4)	+0.0060	O(11)	−0.1501
C(5)	−0·0074	C(12)	+0.0881
C(6)	−0.0034	C(13)	−0.1360
C(7)	−0.0013		

Plane 2. Carboxyl group defined by C(3), C(6), O(8), and O(9).

$-0.1716X+0.4346Y-0.8841Z+2.7251=0$

Atom	Deviation	Atom	Deviation
C(3)	−0.0002 Å	O(9)	−0.0002 Å
C(6)	+0.0005	C(12)	+0.0964
C(8)	−0.0002		

Plane 3. Carboxyl group defined by C(4), C(7), O(10), and O(11).

Atom	Deviation	Atom	Deviation
C(4)	+0.0081 Å	O(11)	+0.0086 Å
C(7)	−0.0294	C(13)	+0.0209
O(10)	+0.0132		

Dihedral angles between the planes.

Plane 1—Plane 2 0.1°

Plane 1—Plane 3 10.5°

by 64° to the (010) plane, and contact each other alternatively with the interplanar separation of 3.28 Å across the center of symmetry at (1/2, 0, 1/2) and 2.83 Å across that at (1/2, 0, 0). Hence, the molecules are thought to be stacked along the *c* direction with their planes parallel to each other but in opposite orientation. There are gaps between the molecular layers parallel to the *bc* plane. This explains for the crystals showing a cleavage parallel to this plane. The intermolecular distances less than 3.7 Å are listed in Table

7) B. Bak, D. Christensen, W. B. Dixon, L. Hansen-Nygaad, J. R. Andersen, and M. Schottlander, *J. Mol. Spectrosc.*, **9**, 124 (1962).

Table 7. Intermolecular distances less than 3.7 Å

From	To	At	Distance	From	To	At	Distance
O(1)	C(3)	IV	3.52 Å	C(2)	C(13)	VII	3.50 Å
	C(6)	IV	3.35	C(3)	C(7)	VII	3.53
	C(8)	IV	3.42		O(11)	VII	3.30
	O(9)	III	3.56	C(4)	C(4)	VII	3.50
	O(10)	VII	3.68	C(5)	C(7)	VII	3.66
	C(12)	III	3.42		O(8)	IV	3.44
	O(10)	IX	3.45		O(10)	IX	3.35
	C(13)	IX	3.42	C(6)	O(11)	VII	3.49
C(2)	C(2)	IV	3.42	O(8)	C(12)	V	3.51
	C(3)	IV	3.30		C(13)	VII	3.70
	C(4)	IV	3.63	O(9)	C(13)	VIII	3.37
	C(6)	IV	3.68		C(12)	II	3.19
	C(7)	VII	3.70	O(10)	C(13)	VIII	3.12
	O(9)	III	3.33		C(12)	II	3.41
	O(11)	VII	3.52	O(11)	C(13)	VI	3.53

I	x	y	z	VI	$1-x$	$1-y$	$1-z$
II	$1/2-x$	$1/2+y$	$-z$	VII	$1-x$	$-y$	$1-z$
III	x	$-1+y$	z	VIII	$1/2-x$	$-1/2+y$	$1-z$
IV	$1-x$	$-y$	$-z$	IX	$1/2+x$	$1/2-y$	z
V	$1-x$	$-1-y$	$-z$				

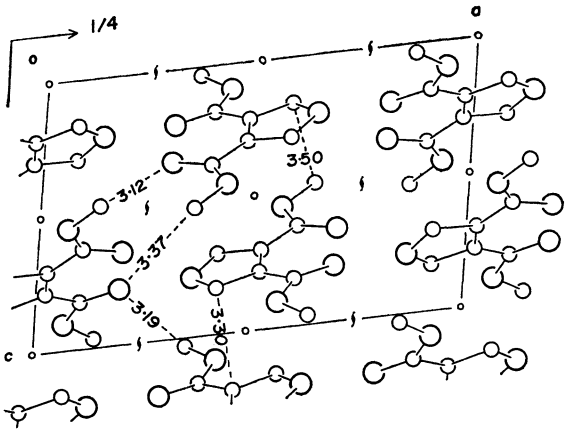

Fig. 4. The crystal structure viewed along the b axis.

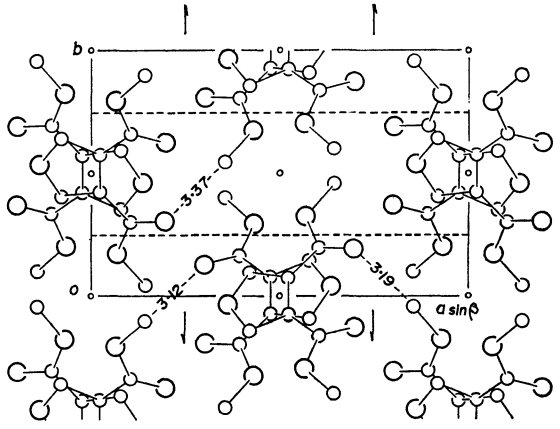

Fig. 5. The crystal structure viewed along the c axis.

7, in which several close approaches are found between the carbonyl oxygen atom and the methyl group, and between the furan ring carbon atoms.

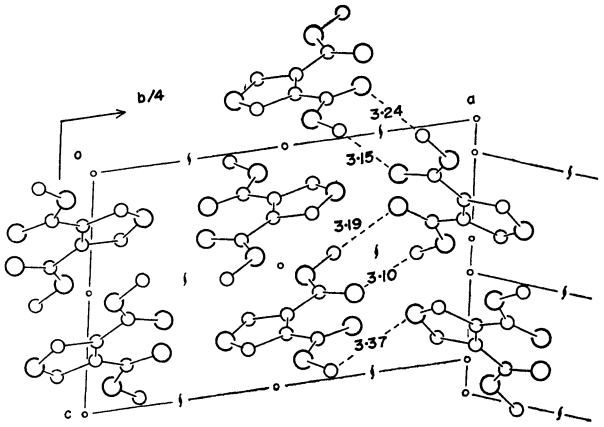

Fig. 6. Proposed scheme of twinning.

A submicroscopic scheme of twinning is proposed, as shown in Fig. 6. The boundary surface of the twin components is assumed on the crevice that lies between the molecular layers parallel to the bc plane, and the layer on $x=a$ is inverted and translated along axes b and c so that the twins have common a^* and b^* directions but different c^* direction. Thus, the resultant intermolecular distances across the crevice on $x=a/2$ and $x=a$ take reasonable values as shown in the figure.

The authors wish to express their sincere thanks to Professor Yoshiharu Okaya of State University of New York and Professor Tamaichi Ashida of Osaka University who kindly gave us computing facilities.

Tables of the observed and calculated structure factors are kept as Document No. 7104 at the office of the Bulletin of the Chemical Society of Japan. A copy may be secured by citing the document number and by remitting, in advance, ¥ 600 for photoprints. Pay by check or money order payable to: Chemical Society of Japan.

Effect of Phase on Excitation Transfer in the Radiolysis of Isobutane

Tetsuo MIYAZAKI, Takahisa YAMADA, Terunobu WAKAYAMA, Kenji FUEKI, and Zen-ichiro KURI

Department of Synthetic Chemistry, Faculty of Engineering, Nagoya University, Chikusa-ku, Nagoya

(Received September 10, 1970)

The effects of CCl_4 on the formation of H_2 and C_4H_9 radicals in the radiolysis of i-C_4H_{10} have been studied in glass at 77°K and the liquid at 195°K. The yield of H_2, which is not affected by the addition of N_2O or SF_6, decreases sharply upon the addition of CCl_4 in the glass, as in the crystal (This Bulletin, **42**, 1164 (1969); **43**, 1017 (1970).), while it does not so sharply decrease in the liquid as in the solid. The effects of CCl_4 on the yields of H_2 correspond fairly well to those on the yields of the C_4H_9 radicals. The effects of CCl_4 in the glass are explained by the excitation transfer from the excited butane molecule to CCl_4, as in the radiolysis of i-C_4H_{10} in the crystal. A kinetic treatment suggests that its mechanism may be the exciton transfer. Some remarks on the primary process of ionization in the radiolysis of solid hydrocarbons are given from the viewpoint of exciton transfer.

We have studied the radiolysis of isobutane in the crystalline state at 77°K by ESR spectroscopy and product analysis. Though the yields of C_4H_9 radicals and hydrogen do not decrease in the presence of conventional electron scavengers, they decrease remarkably upon the addition of CCl_4.[1] The characteristic effects of CCl_4 have been ascribed to exciton transfer from a kinetic consideration. Recently it has been found that the radiolysis of solid isobutane is affected appreciably by its state, by whether it is glass or polycrystal.[2] Although the isobutyl radical is formed in the crystalline state by γ-irradiation, the t-C_4H_9 radical is formed in the glassy state. The yields of CH_4 and C_3H_6 in the radiolysis of solid isobutane are much higher in the polycrystalline state than in the glassy state. It has been suggested that a plausible explanation of the phase effect is in terms of the difference between the efficiency of energy transfer in the glass and that in the polycrystal.

Here we have studied the effects of the phase on the excitation transfer to CCl_4 in the radiolysis of isobutane.

Experimental

The isobutane, methylcyclohexane (MCH), nitrous oxide, and carbon tetrachloride were all the same as those which had been used before.[1,2] The sulfur hexafluoride (Matheson Co.) was of a high purity. The samples were irradiated with Co-60 γ-rays at a dose rate of 4.2×10^5 rad/hr. The ESR measurements were made on a JES-3BX ESR spectrometer. The gaseous products not condensable at the temperature of liquid nitrogen were analyzed by a gas burette connected to a Toepler pump and a copper oxide furnace kept at 240°C.

Pure isobutane forms a polycrystalline solid at 77°K. When a sample of isobutane containing a small amount of MCH is plunged into liquid nitrogen, it forms a clear glass. The concentration of MCH in the radiolysis of glass for the product analysis is different from that for the ESR measurement. This is because the state of the glass depends upon the concentration of MCH. The glass at a high concentration of MCH is unfavourable for the detection of radicals by ESR, because the matrix is so soft that the radicals are not trapped. Therefore, the concentration of MCH chosen for the measurement of the C_4H_9 radical is 4 mol/100 mol of i-C_4H_{10}. The glass at a low concentration of MCH is, however, so unstable that it becomes crystalline during a long γ-irradiation time. Therefore, when the yield of H_2 is measured in the radiolysis in the glassy state, the chosen concentration of MCH is 10 mol/100 mol of i-C_4H_{10}.

Results

Formation of Hydrogen. In the radiolysis of i-C_4H_{10}-MCH(10 mol/100 mol of i-C_4H_{10}) system, N_2O and SF_6 are added in the glassy state in order to suppress the formation of hydrogen by a neutralization reaction (reactions (1) and (2)), if any should occur:

$$C_4H_{10} \rightsquigarrow C_4H_{10}^+ + e^- \quad (1)$$

$$C_4H_{10}^+ + e^- \rightarrow H,\ H_2,\ P \quad (2)$$

where P represents some radicals or molecules. As is shown in Table 1, the yield of hydrogen does not decrease at all upon the addition of electron scavengers, such as N_2O and SF_6. Since $G(N_2)$ amounts to 1.4—1.6 in the radiolysis of i-C_4H_{10}-MCH(10 mol/100 mol of the i-C_4H_{10})-N_2O(3 mol/100 mol of i-C_4H_{10}) system, N_2O captures electrons efficiently to produce N_2, as

Table 1. Radiolysis of i-C_4H_{10}—MCH(10[a]) system in the glassy state at 77°K
Total dose: 4.3×10^6 rad

	$G(H_2)$	$G(CH_4)$	$G(N_2)$
i-C_4H_{10}—MCH(10[a])	3.94	0.87	—
	3.94	0.94	—
i-C_4H_{10}—MCH(10[a])—SF_6(3[a])	4.11	0.81	—
	4.06	0.74	—
i-C_4H_{10}—MCH(10[a])—N_2O(3[a])	4.00	0.78[b]	1.62[b]
	4.20	0.78[b]	1.43[b]

a) Unit, mol/100 mol of i-C_4H_{10}

b) It is assumed that the efficiency of N_2O(3 mol/100 mol of i-C_4H_{10}) is approximately the same as that of SF_6 (3 mol/100 mol of i-C_4H_{10}).
$G(CH_4)$ from non-ionic process in the radiolysis of i-C_4H_{10}—MCH(10[a])—N_2O(3[a]) system, therefore, is assumed to be the same as that in the radiolysis of i-C_4H_{10}—MCH(10[a])—SF_6(3[a]) system.
$G(N_2)$ is obtained by the relation:
$G(N_2)=G(N_2+CH_4)_{i\text{-}C_4H_{10}\text{—MCH(10}^{a)}\text{)—}N_2O(3^{a)})\ \text{system}} - G(CH_4)_{i\text{-}C_4H_{10}\text{—MCH(10}^{a)}\text{)—}SF_6(3^{a)})\ \text{system}}$

1) a) T. Wakayama, T. Miyazaki, K. Fueki, and Z. Kuri, This Bulletin, **42**, 1164 (1969). b) T. Wakayama, T. Kimura, T. Miyazaki, K. Fueki, and Z. Kuri, *ibid.*, **43**, 1017 (1970).

2) a) T. Miyazaki, T. Wakayama, K. Fueki, and Z. Kuri, *ibid.*, **42**, 2086 (1969). b) T. Wakayama, T. Miyazaki, K. Fueki, and Z. Kuri, *J. Phys. Chem.*, **74**, 3584 (1970). c) Y. Saitake, T. Wakayama, T. Kimura, T. Miyazaki, K. Fueki, and Z. Kuri, This Bulletin, **44**, 301 (1971).

in the radiolysis of liquid cyclohexane.[3] Therefore, it can be concluded that hydrogen is not formed by the neutralization reaction in the radiolysis of isobutane in the glassy state as it is in the crystalline state.[1]

The effect of CCl_4 on the yield of hydrogen in the radiolysis of isobutane in the liquid, glass, and polycrystal are shown in Fig. 1. Since a part of the hydrogen formation in the radiolysis of liquid isobutane[4] is due to the neutralization reaction of cation and an electron, SF_6 was added in order to suppress the formation of hydrogen by the ionic process. Since the hydrogen is not formed in the radiolysis of the glassy and polycrystalline states by the neutralization reaction, the effect of CCl_4 is not influenced by the presence of an electron scavenger such as N_2O.

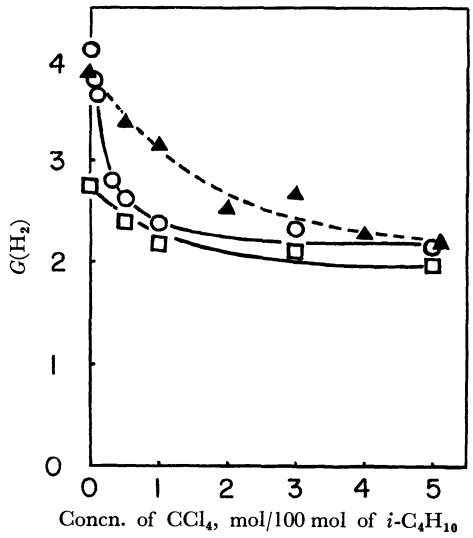

Fig. 1. Effect of CCl_4 on the hydrogen formation in the radiolysis of isobutane. Total dose: 4.3×10^6 rad.
○—○: i-C_4H_{10}—MCH(10[a])—N_2O(3[a])) system in the glass at 77°K
□—□: i-C_4H_{10}—SF_6(3[a])) system in the liquid at 195°K
▲—▲: i-C_4H_{10} in the polycrystal at 77°K[1]
a) Unit, mol/100 mol of i-C_4H_{10}

Formation of C_4H_9 Radical. The effects of CCl_4 on the yields of t-C_4H_9 radicals in the radiolysis of the i-C_4H_{10}-MCH (4 mol/100 mol of i-C_4H_{10}) system in the glass are shown in Fig. 2. The correlation between the yields of H_2 and those of the C_4H_9 radicals, as plotted against the concentration of CCl_4, is also shown in Fig. 2. Since the effect of CCl_4 on the yields of H_2 is completed at 5 mol of CCl_4/100 mol of i-C_4H_{10}, the yield of hydrogen $G'(H_2)$, which is affected by the addition of CCl_4, can be estimated by the following equation: $G'(H_2)=G(H_2)-G(H_2)_c$. $G(H_2)_c$ is $G(H_2)$ at 5 mol of CCl_4/100 mol of i-C_4H_{10}, and $G'(H_2)$ and $G(C_4H_9)$ are, in the absence of CCl_4, both normalized to unity. The fact that the yields of the C_4H_9 radicals coincide fairly well with $G'(H_2)$ indicates that the formation of the C_4H_9 radical is closely related to the formation of H_2.

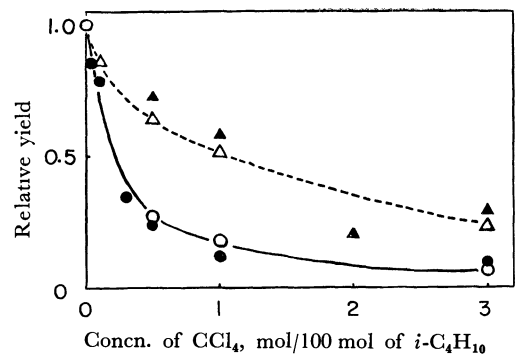

Fig. 2. Effect of CCl_4 on the C_4H_9 radical formation in the radiolysis of solid isobutane at 77°K. $G'(H_2)$ is plotted for comparison. Total dose: 1.7×10^5 rad.
○—○: Yields of C_4H_9 radicals in the γ-irradiated i-C_4H_{10}—MCH(4[a])) glass
● : $G'(H_2)$ in the γ-irradiated i-C_4H_{10}—MCH(10[a])—N_2O(3[a])) glass
△—△: Yields of C_4H_9 radicals in the γ-irradiated i-C_4H_{10} polycrystal[1]
▲ : $G'(H_2)$ in the γ-irradiated i-C_4H_{10} polycrystal[1]
a) Unit, mol/100 mol of i-C_4H_{10}

Discussion

Excitation Transfer. It can be considered that the C_4H_9 radical and H_2 are formed mainly by the decomposition of excited molecules produced directly by the γ-irradiation of solid isobutane. This conclusion is based on the following observations, made both here and in a previous study:[1]

1) The yields of the C_4H_9 radical in the radiolysis of polycrystalline isobutane are not changed by the presence of conventional electron scavengers, such as phenyl iodide, ethyl iodide, nitrous oxide, and sulfur hexafluoride.[1]

2) The yields of the C_4H_9 radical do not increase upon the photobleaching of toluene anions in the γ-irradiated isobutane-toluene(5 mol/100 mol of i-C_4H_{10}) system in the polycrystalline state.[1]

3) The yields of the C_4H_9 radical do not increase upon the photobleaching of electrons trapped in the γ-irradiated isobutane-MCH(4 mol/100 mol of i-C_4H_{10}) system in the glassy state or the photobleaching of benzene anions in the γ-irradiated isobutane-MCH (4 mol/100 mol of i-C_4H_{10})-benzene(5 mol/100 mol of i-C_4H_{10}) system in the glassy state.

4) The yields of H_2 in the radiolysis of glassy isobutane are not changed at all by the presence of conventional electron scavengers, such as nitrous oxide and sulfur hexafluoride.

The yields of the C_4H_9 radical and H_2 decrease sharply, however, upon the addition of CCl_4 in the radiolysis of solid isobutane (Figs. 1 and 2). Let us ascribe this effect to excitation transfer from the excited isobutane molecule to CCl_4 and the suppression of the decomposition of the excited isobutane:

$$C_4H_{10} \xrightarrow{I} C_4H_{10}^* \quad (3)$$

$$C_4H_{10}^* \xrightarrow{k_d} C_4H_9 + H \quad (4)$$

$$H + H \longrightarrow H_2 \quad (5)$$

$$H + C_4H_{10} \longrightarrow C_4H_9 + H_2 \quad (6)$$

3) S. Sato, R. Yugeta, K. Shinsaka, and T. Terao, *ibid.*, **39**, 156 (1966).
4) K. Tanno, S. Shida, and T. Miyazaki, *J. Phys. Chem.*, **72**, 3496 (1968).

$$C_4H_{10}^* + CCl_4 \xrightarrow{k_q} C_4H_{10} + CCl_4^* \quad (7)$$

where I is the rate of reaction (3) and where k is the rate constant. The yield of the thermal hydrogen atom captured by ethylene is measured by ESR and found to be rather small in the radiolysis of i-C_4H_{10} containing C_2H_4.[1] Therefore, it is likely that some of the H atoms in reaction (4) are hot atoms.

As is shown in Fig. 1, the efficiency of excitation transfer depends upon the phases; its order in this system is as follows:

glass > crystal > liquid

The reason why the excitation transfer is more efficient in the glass than in the crystal is not clear at present. It is noted that the yields of hydrogen do not decrease upon the addition of CCl_4 in the liquid phase (Fig. 1).

The C–H bond rupture of the excited butane molecule in reaction (4) may occur in the period of one vibration ($\sim 10^{-13}$ sec). Since the excitation transfer in reaction (7) competes with reaction (4), the rate of excitation transfer is probably extremely high. Therefore, the mechanism of the excitation transfer may be exciton transfer.

Now let us consider the excitation transfer in the glass by the kinetic treatment on hydrogen formation. The formation of hydrogen may be expressed as in reactions (3)—(7). The rate of excitation transfer (reaction (7)) cannot be expressed a priori, as that of the bimolecular reaction. Therefore, the following expression is adopted:[5]

$$R_q = k_q[C_4H_{10}^*][CCl_4]^{n/3} \quad (I)$$

where R_q is the rate of reaction (7). Since the rate of excitation transfer is usually expressed as some integral power function of the distance between two interacting molecules, it is assumed here that $R_q \propto [CCl_4]^{n/3}$, where n is an integer. $[CCl_4]^{1/3}$ is proportional to the reciprocal of the average distance between the molecules of carbon tetrachloride and excited butane. The rate of excitation transfer for various theoretical models is expressed as follows:[6]

a) Exciton transfer:

$$R_q \propto \frac{1}{r^3}$$

b) Vibrational-relaxation resonance transfer:

$$R_q \propto \frac{1}{r^6}$$

where r is the distance between interacting molecules. The steady-state treatment leads to:

$$\frac{1}{G'(H_2)} = \frac{1}{I} + \frac{k_q}{Ik_d}[CCl_4]^{n/3} \quad (II)$$

where n is taken to be 3 or 6, depending upon the models. Kinetic plots of our data for (a) and (b) are shown in Fig. 3. The experimental points fall reasonably well

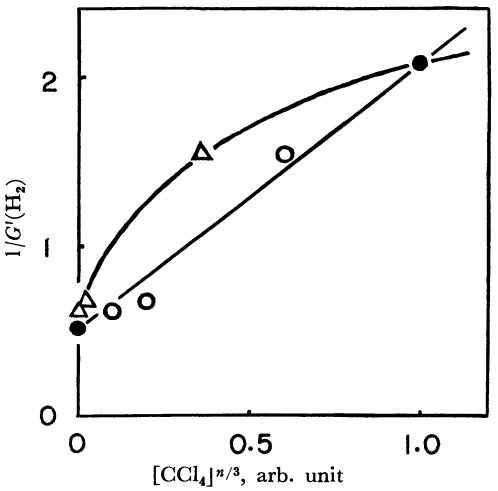

Fig. 3. Relations between $1/G'(H_2)$ and $[CCl_4]^{n/3}$ in the radiolysis of i-C_4H_{10}—MCH(10[a])—N_2O(3[a]) system at 77°K. When $[CCl_4]=0.5$[a], $[CCl_4]^{n/3}$ is nomalized to be 1.
○—○: $n=3$
△—△: $n=6$
a) Unit, mol/100 mol of i-C_4H_{10}

on a straight line for $n=3$; thus,

$$R_q \propto [CCl_4] \propto \frac{1}{r^3}$$

The kinetic treatment suggests that the mechanism of excitation transfer in the glass is exciton transfer. The same conclusion was previously obtained for the butyl-radical formation in the crystalline state.[1]

Primary Process of Ionization in the Radiolysis of Solid Hydrocarbons. There are some peculiar phenomena in the solid-state radiolysis, as compared with the radiolysis in the liquid phase.

First, the fragmentation of an excited isobutane ion is negligible in the radiolysis of isobutane in the polycrystal and glass,[1,2b] while it plays an important role in the radiolysis of liquid isobutane.[4] The excited isobutane ion has an electronic excitation energy of more than 1.8 eV and decomposes instantaneously in one vibration to form the $C_3H_7^+$ ion and the CH_3 radical.[7] When the excited isobutane ion is produced by the charge-transfer reaction from Kr^+ in the γ-irradiated Kr-i-C_4H_{10} system at 77°K, it has an excitation energy of more than 1.8 eV and decomposes even in the solid matrix of Kr.[8] Since it seems that the matrix of the i-C_4H_{19}-MCH (10 mol/100 mol of i-C_4H_{10}) system is softer than that of solid Kr at 77°K, we cannot ascribe the depression of the fragmentation of excited ion in the γ-irradiated glassy isobutane to the cage effect by the matrix. Therefore, it is conceivable that the yields of the excited ion are lower in the solid state than in the liquid state.

Second, the yields of hydrogen, which are not affected by the addition of N_2O and which correspond to those from nonionic processes, are much higher in the γ-irradiated glassy isobutane than in the liquid state. Therefore, it is conceivable that the yields of

5) U. A. Kolanovsky and L. S. Polak, *Dokl. Akad. Nauk SSSR*, **135**, 361 (1960).

6) a) M. Kasha, *Radiat. Res.*, **20**, 55 (1963). b) Th. Förster, "Comparative Effects of Radiation" (M. Burton, J. S. Kirby-Smith, and J. L. Magee, Eds.), John Wiley & Sons, New York, (1960), p. 300.

7) a) T. Miyazaki, K. Tanno, and S. Shida, This Bulletin, **42**, 362 (1969). b) T. Miyazaki, T. Kohama, K. Fueki, and Z. Kuri, *ibid.*, **42**, 894 (1969).

8) T. Wakayama, A. Miwa, T. Miyazaki, K. Fueki, and Z. Kuri, unpublished results.

the nonionic species are higher in the solid state than in the liquid state.

Third, it has been reported by several investigators that the yields of the electrons which can be captured by electron scavengers are 1.5—2.0 G-units in the radiolysis of hydrocarbon glasses at 77°K. They used biphenyl,[9] alkyl disulfide,[10] benzene,[11] iodobenzene,[12] and nitrous oxide[12] as electron scavengers. The yields of the electrons captured by these scavengers were determined by measurements of the optical[9,10] or ESR absorption[11] of the anions, or by product analysis.[12] It is very interesting that G(e) values obtained by different scavengers and measurements are 1.5—2.0 in the γ-irradiated hydrocarbon glasses, while the G(e) values amount to 3—4 in γ-irradiated liquid hydrocarbon. Therefore, it is conceivable that the yields of ionization may be smaller in the solid state than in the liquid state.

One possible explanation of these characteristic phenomena of solid radiolysis will be given here from the viewpoint of the formation of the exciton. It may be said, from the above considerations, that the exciton plays an important role in the γ-irradiated solid, though it plays only a minor role in the liquid phase. When the exciton is formed by γ-irradiation in the solid hydrocarbon, the electronic absorption spectrum of the solid can be expected to differ from that of the liquid; that is to say, Davydov splitting can be expected to occur.[13] If a fraction of the ionization occurs from superexcited states, as proposed by Platzman,[14] and if the state of the exciton corresponds to the superexcited state, the following schemes may represent the ionization of i-C_4H_{10}: In the liquid state:[4]

$$i\text{-}C_4H_{10} \rightsquigarrow C_4H_{10}^{**} \quad (8)$$

$$C_4H_{10}^{**} \longrightarrow C_4H_{10}^{+*} + e^- \quad (9)$$
$$\longrightarrow C_4H_{10}^{+} + e^- \quad (10)$$

$$C_4H_{10}^{+*} \longrightarrow C_3H_7^{+} + CH_3 \quad (11)$$

where $C_4H_{10}^{**}$ represents isobutane in the superexcited states and where $C_4H_{10}^{+*}$ represents the excited isobutane ion. In the solid state:

$$i\text{-}C_4H_{10} \rightsquigarrow C_4H_{10}^{*} \quad (3)$$

$$C_4H_{10}^{*} \longrightarrow C_4H_9 + H \quad (4)$$
$$\longrightarrow C_4H_{10}^{+} + e^- \quad (12)$$

where $C_4H_{10}^{*}$ represents the exciton which produces mainly a butyl radical, a hydrogen atom, a butane ion, and an electron. A mechanism by which the exciton may be related to the ionization was also suggested in the solid radiolyses of polyethylene[15] and succinic acid.[16]

It can be understood from the above reaction scheme that the fragmentation of the excited ion occurs only in the radiolysis of liquid isobutane. The yields of hydrogen from nonionic processes may be larger in the radiolysis of solid isobutane than in that of the liquid phase, because reaction (4) is involved. Since the exciton produces mainly neutral fragments in the radiolysis of glass (reaction (4)), the yields of electrons may be rather low in γ-irradiated glass as compared with those in the liquid phase.

The authors wish to thank Dr. Kanji Katsuura of the Kurashiki Rayon Company for his helpful discussions.

9) J. P. Guarino and W. H. Hamill, *J. Amer. Chem. Soc.*, **86**, 777 (1964).
10) T. Shida, *J. Phys. Chem.*, **74**, 3055 (1970).
11) T. Wakayama, T. Miyazaki, K. Fueki, and Z. Kuri, This Bulletin, **43**, 3761 (1970).
12) T. Kimura, T. Miyazaki, K. Fueki, and Z. Kuri, *ibid.*, **41**, 2861 (1968).
13) A. S. Davydov, "Theory of Molecular Excitons," (translated by M. Kasha and M. Oppenheiner, Jr.) McGraw-Hill Book Company, New York, 1962.
14) R. Platzman, *Radiat. Res.*, **17**, 419 (1962).
15) a) R. H. Partridge, *J. Chem. Phys.*, **52**, 2485 (1970). b) R. H. Partridge, *ibid.*, **52**, 2491 (1970).
16) a) T. Miyazaki, S. Okada, T. Wakayama, K. Fueki, and Z. Kuri, This Bulletin, **43**, 1907 (1970). b) T. Miyazaki, Y. Fujitani, T. Wakayama, K. Fueki, and Z. Kuri, *ibid.*, **43**, 984 (1971).

Electronic Absorption Spectra of Crystals of Thymine, Uracil, and Their Derivatives

Masashi TANAKA and Jiro TANAKA

Department of Chemistry, Faculty of Science, Nagoya University, Chikusa, Nagoya

(Received September 21, 1970)

The electronic structures and spectra of thymine, uracil, and their derivatives have been studied by measuring the electronic absorption spectra of the single crystals. In the polarized absorption spectra of the crystal, an unusual absorption band appears at about 285 mμ in the tail of the usual $\pi\rightarrow\pi^*$ transition when the crystal has the C=O···H–N-type hydrogen bond. The direction of the transition moment of this band is found to be along the direction of the hydrogen bond between a pair of C=O···H–N-groups, the nature of which is discussed from several viewpoints. The direction of the transition moment of the first and second $\pi\rightarrow\pi^*$ bands is determined to be inclined at about $+38°$ and $+86°$ from the $C_4\cdots N_1$ line toward the C_5 atom. The result for the first band is not in perfect agreement with the finding of Stewart and Davidson regarding 1-methylthymine, who regarded this angle as either $-14°$ or $+19°$.

Thymine and uracil are important base components of DNA and RNA molecules. The electronic structures and spectra of these molecules are significant in studying the conformation and optical properties of poly-nucleotide, since the hypochromic and circular dichroic effects are governed mainly by the nature of the electronic transitions and the interaction of excited states of these base pairs. Although many investigations have appeared on the spectra of DNA bases and these derivatives in solution,[1-5] little work has been done with the polarization of the transition moments. Stewart and Davidson[6] reported on the absorption spectra of single crystals of 9-methyladenine and 1-methylthymine. Chen and Clark[7] measured the polarized reflection spectra of the purine crystal. The present research was undertaken in order to find the polarization of each band by measurements of the absorptions on the single crystals of several of these base components. The polarized crystal absorption spectra of several kinds of crystals of thymine, uracil, and these derivatives were measured; these bases all have the same π-electron framework and, to a first approximation, may have the same polarization property if we disregard the effect of substituent methyl groups. The exciton-type interaction between different excited states (second-order exciton effects) will be disregarded because the transition moments are not very large. The dichroic ratios are used with the oriented gas model to find the directions of two $\pi\rightarrow\pi^*$ transitions in the 220 and 280 mμ regions.

In the crystalline spectra, we have noticed a particular kind of absorption band which is accompanied by a C=O···H–N-type hydrogen bond: The polarization character of this band is rather specific, and its nature will be discussed from several points of view.

Experimental

Materials. The 5-ethyl-6-methyluracil was kindly supplied by Dr. Marsh of the California Institute of Technology, while the 1,3-dimethyl thymine and 1,3-dimethyluracil were synthesized by Dr. Sakabe of our laboratory. All the other compounds were obtained from the Sigma Chemical Company, the California Corporation for Biochemical Research, or the Nakarai Chemical Company. All these compounds were recrystallized from water or ethanol before measurement.

Apparatus. The crystal spectra were recorded at room temperature on a specially-designed microspectrophotometer consisting of: (i) an Olympus polarizing microscope with Zeiss Ultrafluar objectives and a quartz Rochon polarizer, (ii) a Zeiss PMQII monochromater with tungsten and hydrogen sources, and (iii) a 1P28 photomultiplier tube with a standard Zeiss detection system.

Results

1,3-Dimethylthymine. The absorption spectrum of the single crystal of 1,3-dimethylthymine is shown in Fig. 1. The crystal absorption spectrum is similar to that of the solution spectrum, and the $\pi\rightarrow\pi^*$ band is observed at about 270 mμ. The direction of the transition moment can not be discussed with this crystal since the crystal structure has not yet been analyzed.

Calcium Thymidylate. The absorption spectrum of the single crystal of calcium thymidylate has been measured and is shown in Fig. 2-a. The crystal structure analysis has been carried out by Trueblood, Horn, and Luzzati,[8] who showed that the crystal belongs to the space group of C_{2h}-$P2_1$ and that two molecules are included in a unit-cell. The unit-cell dimensions are $a=14.40$, $b=6.87$, $c=9.81$ Å, and $\beta=90°58'$. On the basis of this finding, the projection of molecules onto the developed plane (100) is pictured in Fig. 2-b. A thymine ring is found nearly perpendicular to the bc plane; it is related to another ring with a two-fold screw axis parallel to the *b* axis. The distance between the two thymine rings is 3.43 Å, and no hydrogen bonding of the C=O···H–N-type is involved between the base rings. The crystalline absorption spectrum

1) S. F. Mason, *J. Chem. Soc.*, **1960**, 219; **1954**, 20.
2) D. Voet, W. B. Gratzer, R. A. Cox, and P. Doty, *Biopolymers*, **1**, 193 (1963).
3) K. Nakanishi, N. Suzuki, and F. Yamazaki, *ibid.*, **34**, 53 (1961).
4) L. B. Clark and I. Tinoco, Jr., *J. Amer. Chem. Soc.*, **87**, 11 (1965).
5) M. Tanaka and S. Nagakura, *Theor. Chim. Acta*, **6**, 320 (1966).
6) R. F. Stewart and N. Davidson, *J. Chem. Phys.*, **39**, 255 (1963).
7) H. H. Chen and L. D. Clark, *ibid.*, **51**, 1862 (1969).
8) K. N. Trueblood, P. Horn, and V. Luzzati, *Acta Crystallogr.*, **14**, 965 (1961).

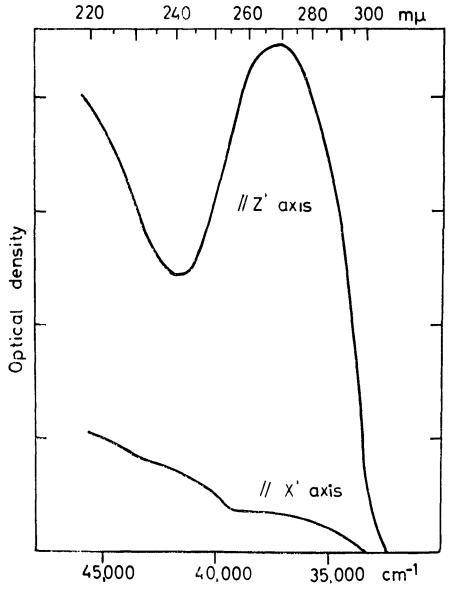

Fig. 1. The polarized absorption spectrum of the single crystal of 1,3-dimethylthymine.

is measured on the bc plane. In the *c* axis spectrum, two peaks are observed at 275 and 220 mμ but the *b*-axis spectrum has only a peak at 280 mμ in the region between 330 and 220 mμ. Each peak shifts to a longer wavelength as compared with the solution spectrum, but no extra band is observed. The dichroic ratio for the first $\pi\rightarrow\pi^*$ band in the vicinity of 280 mμ is determined from the areas under two perpendicularly-polarized absorption curves and it gives $I_c : I_b = 10 : 1$. If θ is the angle which the transition moment projected onto the bc plane makes with the *c* axis, then the polarization ratio ($I_c : I_b$) is equal to $\cot^2\theta$. From the crystal structure data, we may be able to find the relation of the molecular frame to the *b* axis and, finally,

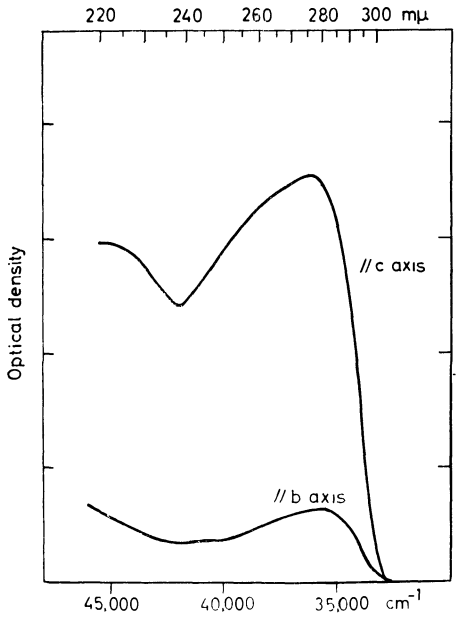

Fig. 2-a. The polarized absorption spectrum in the (100) plane of the single crystal of calcium thymidylate.

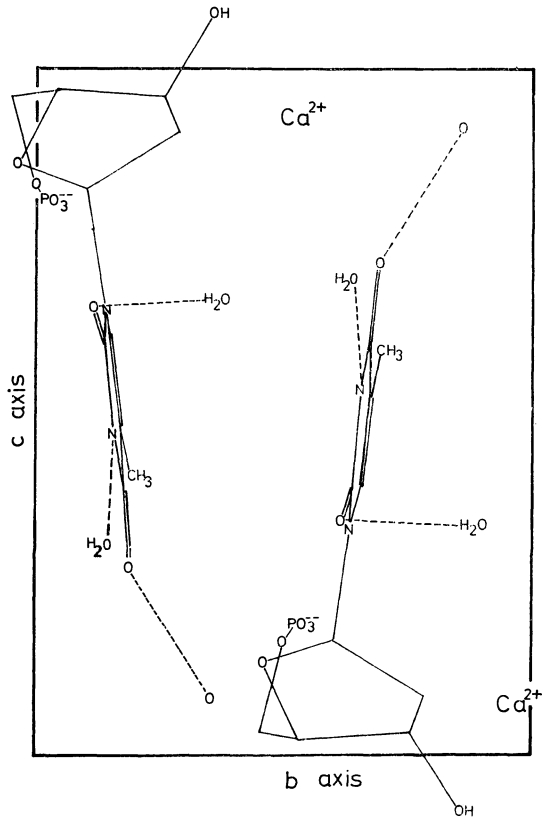

Fig. 2-b. Projection of calcium thymidylate molecules onto the (100) plane.

to determine the direction of the transition moment in the molecular plane. By this method, the transition moment of this band is determined to lie at either +79° or +97° inclined to the reference axis, which is settled along the line joining the C_4 atom and its para partner (N_1) as is shown in Fig. 3. Here, the positive sign of the angle indicates clockwise rotation around the center of the ring. The dichroic ratio of the second $\pi\rightarrow\pi^*$ band is about 6 : 1 ($I_c : I_b$) as measured from the observed band intensities. From these results, the transition moment to the reference axis is estimated as being inclined to +82° or +94°. These angles are found to be more or less likely for the first and second bands, but this result is not reasonable from a theoretical point of view. The accuracy of the measurement is poor, because the molecular plane is sharply tilted to the developed crystalline plane. In such a configuration an accurate determination will be rather difficult, but it will provide some auxiliary information.

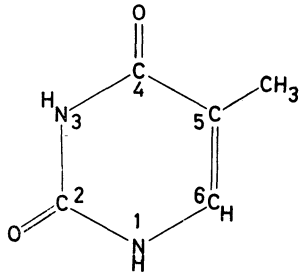

Fig. 3. Numbering of the atoms of thymine molecule.

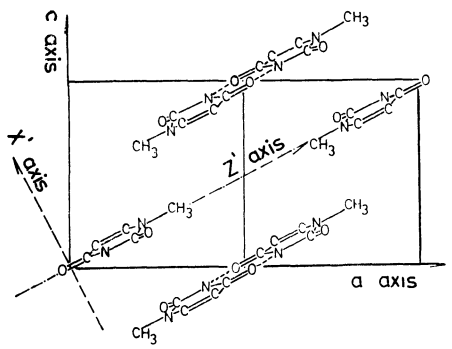

Fig. 4-a. Projection of 1-methylthymine molecules onto the (010) plane.

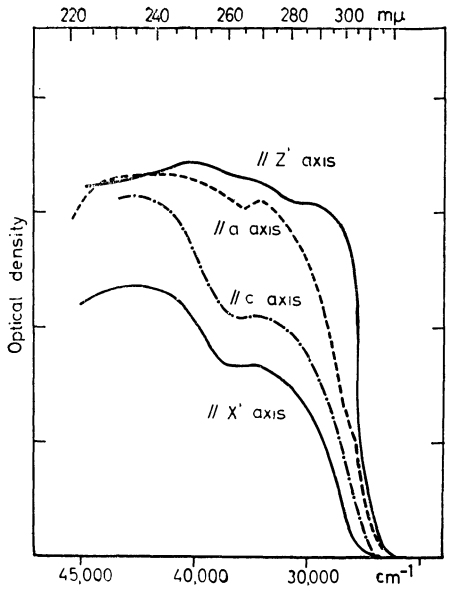

Fig. 4-b. The polarized absorption spectrum in the (010) plane of the single crystal of 1-methylthymine.

1-Methylthymine. Hoogsteen[9] analyzed the crystal structure of 1-methylthymine and showed that the crystal belongs to the space group of C_{2h}-$P2_1/c$, including four molecules in a unit-cell. The unit-cell dimensions are $a=7.53$, $b=12.09$, $c=7.60$ Å, and $\beta=89°58'$. The projection of molecules onto the developed cleavage plane (010) is pictured in Fig. 4-a. The molecules are arranged in layers closely parallel to the (102) plane and nearly perpendicular to the ac plane. The molecules are joined together in pairs by two C=O···H–N-type hydrogen bonds around a center of symmetry. The absorption spectra have been measured along the a and c crystal axes as well as along the Z' and X' optical axes, as is shown in Fig. 4-b. Here, the optical axis Z' is placed within the (102) plane and the X' axis is normal to its plane. Stewart and Davidson[6] measured the polarized absorption spectrum with the (102) plane, in which they used a crystal cut by a diamond knife of ultramicrotome. Our spectra are different from their spectrum in that an extra peak appears in the vicinity of 310 mμ. This band is nearly perfectly polarized along the Z' axis. Therefore, the direction of the transition moment must be along the direction of the hydrogen bond. Accordingly, the origin of this band might be intimately connected with the existence of the hydrogen bond of a C=O···H–N-type. This absorption characteristic is also found with other types of crystals containing the C=O···H–N-hydrogen bond between the base rings; we will discuss its nature in a later section. The next peak is found in the 270 mμ region; this peak may be assigned to the first $\pi\rightarrow\pi^*$ band. In the determination of the dichroic ratio of these bands, two methods are employed. One is to subtract the extra band from the observed spectral curve, regarding it as of different electronic origin. The other method is to include it into a single $\pi\rightarrow\pi^*$-type transition. By the first method the observed dichroic ratio is about 6 : 1 ($I_{z'}$: $I_{x'}$) and the direction of the transition moment

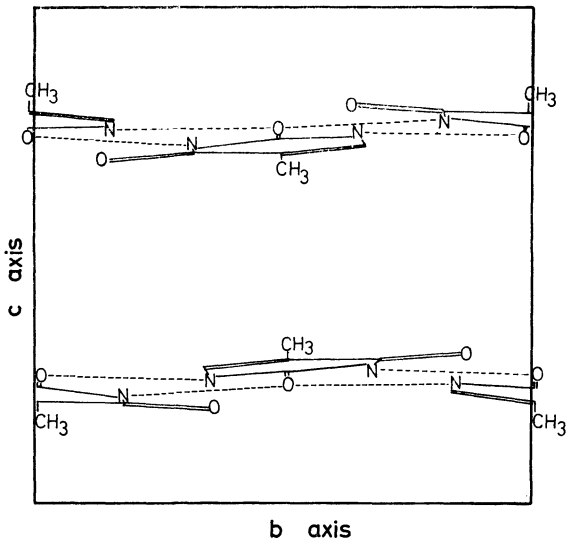

Fig. 5-a. Projection of thymine molecules onto the (100) plane.

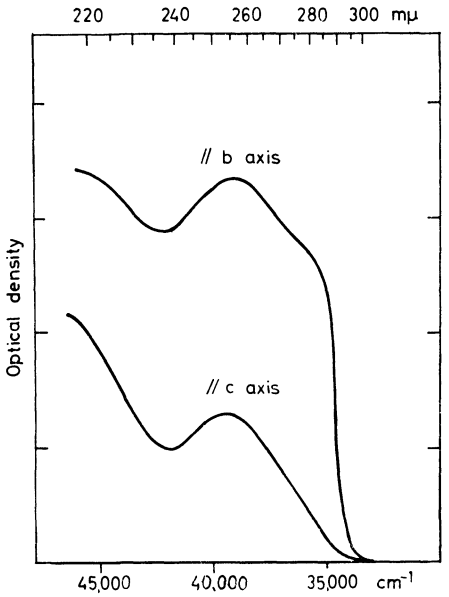

Fig. 5-b. The polarized absorption spectrum in the (100) plane of the single crystal of thymine.

9) K. Hoogsteen, *Acta Crystallogr.*, **16**, 28 (1963).

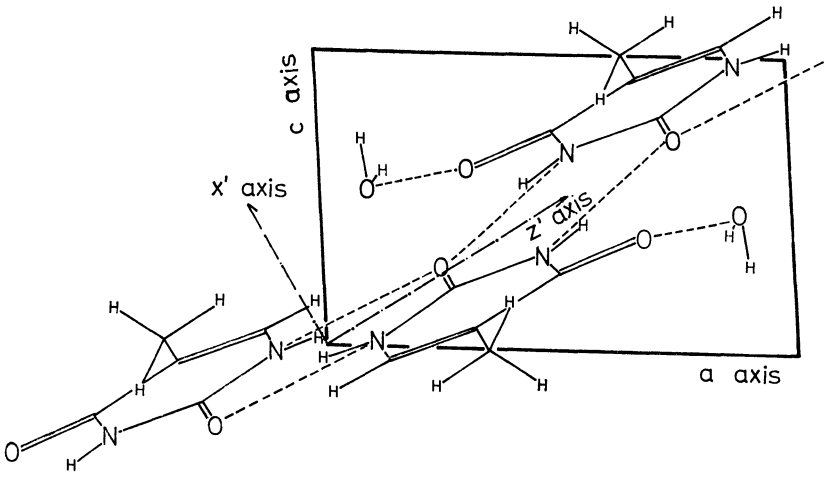

Fig. 6-a. Projection of thymine monohydrate molecules onto the (010) plane.

is deduced to be either +84° or +103° to the C_4-N_1 reference axis. By the latter method, the angle is found to be +80° or +110°. The second $\pi\rightarrow\pi^*$ band exists in the region of 235 mμ, with the dichroic ratio of 1.5 : 1 ($I_{z'} : I_{x'}$). From this value, the transition moment is determined to lie at +87° or +96° inclined to the reference axis. In this case also, the first and the second bands show similar polarizations; this must be due to the conditions of the developed plane being unfavourable for the measurement of the first band.

Thymine. The crystal structure of thymine anhydrate has been analyzed by Ozeki, Sakabe, and Tanaka[10] in our laboratory. The crystal belongs to the space group of C_{2h}–$P2_1/c$ and includes four molecules in a unit-cell. The unit-cell dimensions have been found to be as follows; a=12.87, b=6.83, c=6.70 Å, and β=105°. The projection of molecules onto the cleavage plane (100) is pictured in Fig. 5-a. The plane of the molecule is nearly parallel to the (001) plane and is included at 3.3° and 4.1° to the a and b axes respectively. The molecules are connected by two hydrogen bonds of the C=O···H–N-type. The crystalline absorption spectrum has been measured on the (100) plane; it is shown in Fig. 5-b. In the spectrum parallel to the b axis, an extra hump is observed at about 285 mμ and no component is detected along the c axis. Accordingly, this band may be related to the hydrogen bond of the C=O···H–N-type; it will be discussed in a later section, The peak of the first $\pi\rightarrow\pi^*$ band exists at 255 mμ in both the b- and c-axes spectra, and the observed dichroic ratio is about 3.6 : 1 ($I_b : I_c$). The direction of the transition moment is determined to be either +50° or +68° (or, alternatively, +52° or +66°) to the C_4–N_1 axis. In the second $\pi\rightarrow\pi^*$ band, a maximum is observed at 220 mμ in the b axis spectrum, but no peak is found in the c-axis spectrum down to 220 mμ. The dichroic ratio is determined to be 2 : 1 ($I_b : I_c$), and the transition moment is estimated to be either +55° or +63° for the reference axis.

Thymine Monohydrate. The crystal structure of thymine monohydrate was analyzed by Gerdil.[11] The crystal belongs to the space group of C_{2h}–$P2_1/c$ and includes four molecules in a unit-cell. The unit-cell dimensions are a=6.08, b=27.76, c=3.82 Å, and β=94°19′. The projection of molecules onto the developed plane (010) is pictured in Fig. 6-a. The hydrogen bonds of the C=O···H–N-type extend along the direction of the Z' optical axis. The polarized absorption spectrum was measured in the (010) plane; it is shown in Fig. 6-b. The spectrum has an extra band at about 285 mμ in addition to two $\pi\rightarrow\pi^*$ bands at 265 and 220 mμ. The extra band is polarized along the direction of the Z' axis, which is the direction of the maximum refractive index. The observed dichroic ratios for two $\pi\rightarrow\pi^*$ bands at 265 and 220 mμ are about 3.4 : 1 and 1.4 : 1 ($I_{z'} : I_{x'}$) respectively. The angles between the transition moment and reference axes are determined to be +24° or +81° (or,

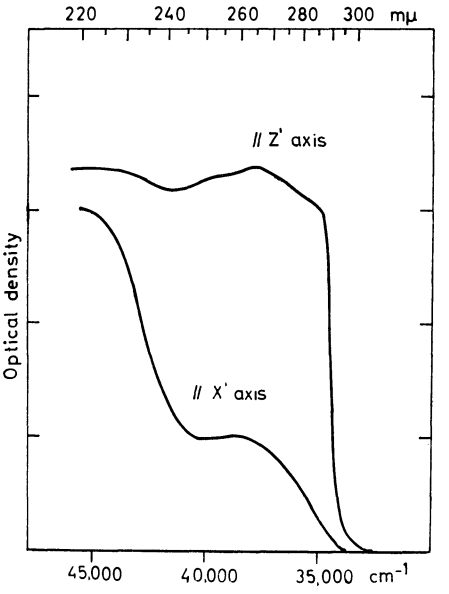

Fig. 6-b. The polarized absorption spectrum in the (010) plane of the single crystal of thymine monohydrate.

10) K. Ozeki, N. Sakabe, and J. Tanaka, *Acta Crystallogr.*, **B25**, 1038 (1969).

11) R. Gerdil, *ibid.*, **14**, 333 (1961).

alternatively, +35° or +78°) for the first band and +43° or +76° for the second band.

1,3-Dimethyluracil. The absorption spectrum of the single crystal of 1,3-dimethylthymine is shown in Fig. 7. The crystal absorption spectrum is similar to the solution spectrum, and the first $\pi\rightarrow\pi^*$ band is observed at about 265 mμ. The peak of the second $\pi\rightarrow\pi^*$ band exists below 220 mμ. The direction of the transition moments of these two bands can not be discussed on the basis of the crystal spectra, since the crystal structures have not yet been analyzed.

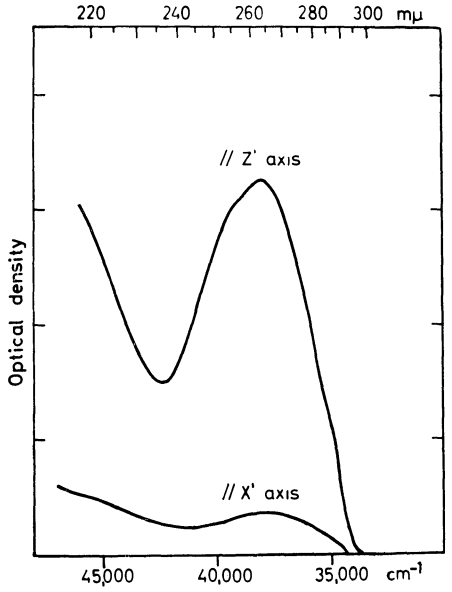

Fig. 7. The polarized absorption spectrum of the single crystal of 1,3-dimethyl uracil.

Sodium Uridine-5'-phosphate. The absorption spectrum of the single crystal of sodium uridine-5'-phosphate has been measured; it is shown in Fig. 8. The crystal structure is not known, but there seems to be

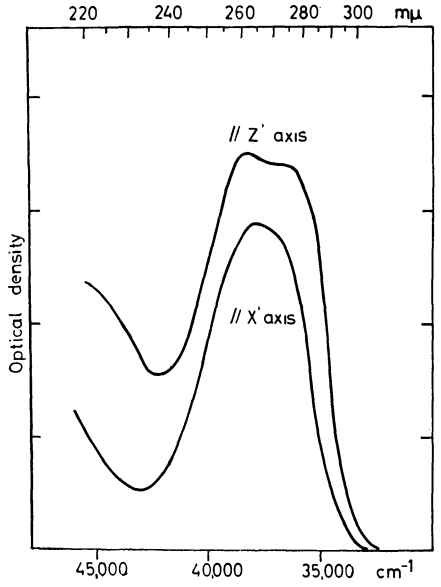

Fig. 8. The polarized absorption spectrum of the single crystal of sodium uridine-5'-phosphate.

no hydrogen bond of the C=O···H–N-type between the bases. The absorption spectrum is similar to that in solution, as expected, and no anomalous extra band is observed.

Uracil. The optical property of this crystal was studied by Gilpin and McCrone,[12] while the crystal structure was analyzed by Parry.[13] The crystal belongs to the space group of C_{2h}–$P2_1/a$ and includes four molecules in a unit-cell. The cell dimensions are $a=11.82$, $b=12.35$, $c=3.62$ Å, and $\beta=120°$. The projection of molecules onto the ac plane is pictured in Fig. 9-a. The molecules are arranged in a hydrogen-bonded layer parallel to the (001) plane. In this crystal, one oxygen atom (O_8) forms two hydrogen bonds with nitrogen atoms in the neighbouring molecules. The crystalline absorption spectrum was measured on the ac plane by means of a polarized light; the results are shown in Fig. 9-b. For the spectrum on the ac plane, an extra peak is observed along the direction of the Z' optical axis, which is related to the hydrogen bond of the C=O···H–N-type. The peak of the first $\pi\rightarrow\pi^*$ band exists at 255 mμ, and the dichroic ratio is about 1.4 : 1 ($I_{z'} : I_{x'}$). Accordingly, the angle between the transition moment and the reference axis is estimated to be +19° or +23° for this plane. For the second $\pi\rightarrow\pi^*$ band, a peak

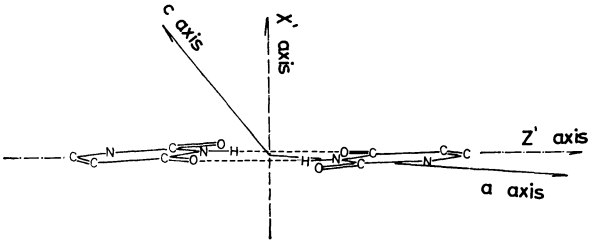

Fig. 9-a. Projection of uracil molecules onto the (010) plane.

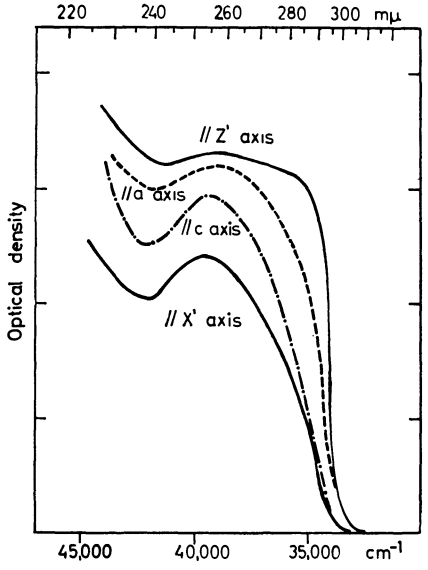

Fig. 9-b. The polarized absorption spectrum in the (010) plane of the single crystal of uracil.

12) V. Gilpin and W. C. McCrone, *Anal. Chem.*, **22**, 368 (1950).
13) G. S. Parry, *Acta Crystallogr.*, **7**, 313 (1954).

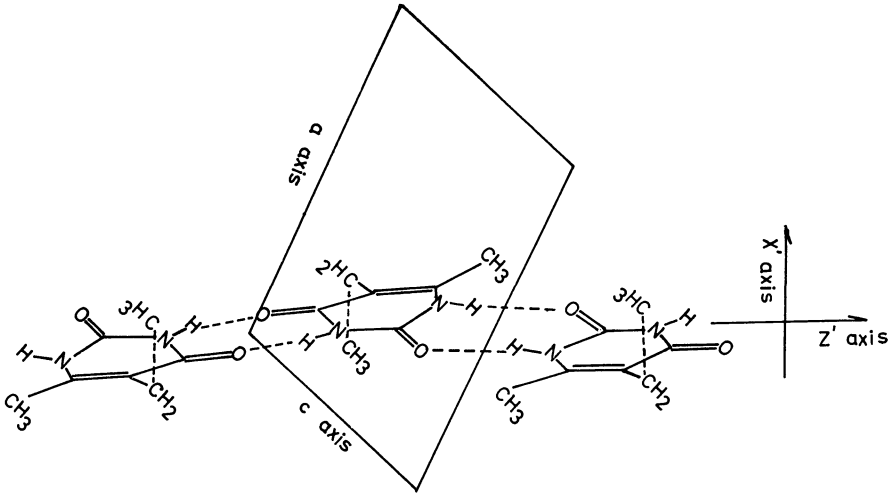

Fig. 10-a. Projection of 2-ethyl-5-methyluracil onto the (010) plane.

was not observed and so it would be difficult to obtain the dichroic ratio and to determine the direction of the transition moment.

2-Ethyl-5-methyluracil. Reeke and Marsh[14] had analyzed the crystal structure of 5-ethyl-6-methyluracil and had shown that the crystal belongs to the space group of $P\bar{1}$ and includes two molecules in a unit-cell. The projection of molecules onto the developed cleavage plane (010) is pictured in Fig. 10-a. Molecules are held together by C=O···H–N-type hydrogen bonds to form chains along the [102] direction. The absorption spectrum has been measured on the ac plane; it is shown in Fig. 10-b. In the polarized absorption spectra parallel to the Z' optical axis, an extra peak has been observed at about 290 mμ, and it has no component along the X' axis. Therefore, this band may be connected with the hydrogen bond

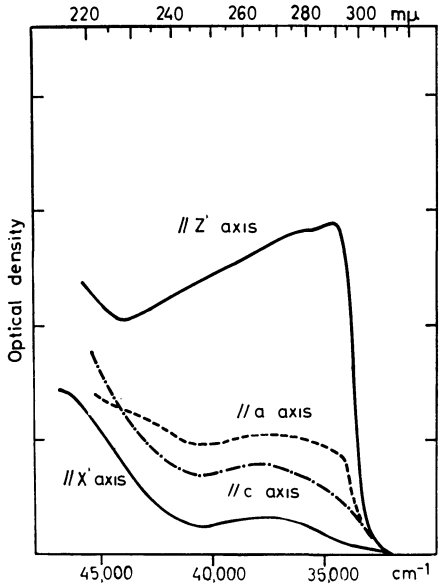

Fig. 10-b. The polarized absorption spectrum in the (010) plane of the single crystal of 2-ethyl-5-methyluracil.

14) G. N. Reeke, Jr., and R. E. Marsh, *Acta Crystallogr.*, **20**, 703 (1966).

of the C=O···H–N-type. The peak of the first $\pi\rightarrow\pi^*$ band is supposed to lie at 265 mμ; the observed dichroic ratio is about 9 : 1 ($I_{z'} : I_{x'}$), and it gives the direction of the transition moment to be either $+45°$ or $-60°$ to the reference axis. In the second $\pi\rightarrow\pi^*$ band, no peak is observed down to 220 mμ, but the dichroic ratio may be determined to be 3 : 1 ($I_{z'} : I_{x'}$) from the intensities in the measured region. Therefore. the transition moment is estimated to be either $+35°$ or $+100°$ for the C_4–N_1 axis.

Discussion

The directions of the transition moments obtained from these measurements are tabulated in Table 1. The values for the first and the second $\pi\rightarrow\pi^*$ bands are rather scattered, and a careful consideration is needed to determine the average angle. First of all, the accuracy of the dichroic measurement with each crystalline plane is not sufficient enough to decide the angle within an error of $\pm10°$, because several bands overlap in this region. Secondly, the estimation of the angle is particularly difficult when the molecular plane is sharply tilted to the developed crystalline plane and the transition moment projected on the crystalline plane is placed nearly parallel to the line at which the molecular plane intersects the crystalline plane. For this reason, the results on calcium thymidylate and 1-methyl thymine are disregarded for the determination of the direction of the transition moment of the first $\pi\rightarrow\pi^*$ band; the results with four other crystals yielded the average value of $+38°$, with a probable error of $\pm14°$. This value is not in exact agreement with the value obtained by Stewart and Davidson,[6] who regarded this angle as $-14°$ or $+19°$ on 1-methylthymine. The second $\pi\rightarrow\pi^*$ band will be perpendicular to the first $\pi\rightarrow\pi^*$ band because of the orthogonal relation, and the transition moment of the second band is placed perpendicularly to the intersecting line in the cases of calcium thymidylate and 1-methylthymine. Therefore, the results with five crystals are estimated to be $+86°$. The above-mentioned results are shown in Fig. 11. The deviations

TABLE 1. DIRECTION OF THE TRANSITION MOMENTS DETERMINED FROM THE OBSERVED DICHROIC RATIOS

Compound	First $\pi\rightarrow\pi^*$ band (I)[a]		First $\pi\rightarrow\pi^*$ band (II)[b]		Second $\pi\rightarrow\pi^*$ band	
		angle[c]		angle[c]		angle[c]
Calcium thymidylate	$I_c : I_b$ 10 : 1	+79° or + 97°			6 : 1	+82° or + 92°
1-Methyl thymine	$I_{z'} : I_{x'}$ 6 : 1	+84° or +103°	7 : 1	+80° or +110°	1.5 : 1	+87° or + 96°
Thymine	$I_b : I_c$ 3 : 1	+52° or + 66°	3.6 : 1	+50° or + 68°	2 : 1	+55° or + 63°
Thymine monohydrate	$I_{z'} : I_{x'}$ 3.4 : 1	+35° or + 78°	4.4 : 1	+24° or + 81°	1.4 : 1	+43° or + 76°
Uracil	$I_{z'} : I_{x'}$ 1.5 : 1	+19° or + 23°	1.9 : 1	+16° or + 26°		
2-Ethyl-5-methyl uracil	$I_{z'} : I_{x'}$ 9 : 1	+45° or − 60°	14 : 1	+48° or − 55°	3 : 1	+35° or +100°

a) The hump in the vicinity of 285 mμ is thought as another extra band which is assumed to have a line shape of gaussian type.
b) The hump in the vicinity of 285 mμ is thought as part of the same band.
c) The angle which the transition moment makes with the line joining the nitogen (N_1) and its para partner (C_4) (clockwise rotation denoted as positive in Fig. 3)

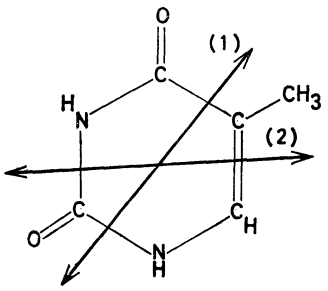

Fig. 11. Directions of the transition moments of the two $\pi\rightarrow\pi^*$ bands in the vicinity of 260 mμ (1) and 220 mμ (2).

between the observed values and average values may be interpreted by the mixing effect of the crystal field. It is now necessary to develop the experimental and theoretical studies of this effect.

Finally, let us discuss the nature of the additional band. Two prominent characteristics are noticed with this extra band; one is its polarization parallel to the direction of the hydrogen bonding, and the second is that it is observed as a hump on the tail of the first π—π^* band. We can imagine several explanations for this band; a charge-transfer point of view associated with a strong hydrogen bonding is stressed in a previous short communication.[15] Another explanation, which seems much more reasonable, is based on the consideration of the potential curve for the excited and the ground states. It is well known that the potential function of the hydrogen bonding has two minima along the direction of the hydrogen-stretching coordinate. It is very probable that the excited state has a displaced potential minimum relative to that of the ground state, as is shown in Fig. 12, because the N–H bond of the excited molecule may have a stronger acidity or hydrogen-donating power than the normal molecule, or the carbonyl group may

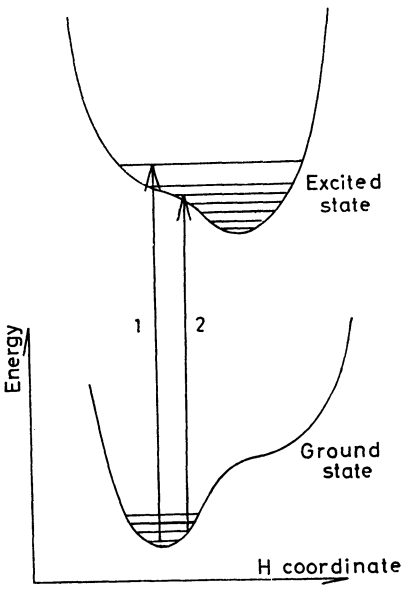

Fig. 12. The potential curve along the hydrogen bond.

have a stronger accepting power. For this particular potential problem, the vibrational structure of the electronic transition must be greatly modified. Specifically, the lower energy transitions are accompanied by a large displacement of the hydrogen coordinate and a large vibrational Frank-Condon factor, which causes the polarization to be along the direction of the hydrogen bonding. An alternative idea to explain this pattern is that the energy of the first $\pi\rightarrow\pi^*$ excited configuration is modified by the perturbation of the charge-transfer excited configuration; this may be regarded as a kind of vibronic perturbation in the excited state. These considerations are really suggestive of the shape and the electronic structures of the excited hydrogen bonding system in connection with the photochemical changes and mutations induced by ultraviolet light and radiation in DNA bases.

15) J. Tanaka and M. Tanaka, *Nature*, **213**, 68 (1967).

The Hydrogenation of Butadiene Catalyzed by Pentacyanocobaltate(II) in Aqueous and Non-aqueous Solvents

Takuzo FUNABIKI and Kimio TARAMA
Faculty of Engineering, Kyoto University, Sakyo-ku, Kyoto
(Received September 21, 1970)

The hydrogenation of butadiene catalyzed by pentacyanocobaltate(II) was studied in water and in glycerol-methanol-water and ethylene glycol-methanol solutions. The amount of hydrogen absorbed, and the rate of hydrogen absorption, in the water solvent were much greater than in the other solvents. The composition of the butenes produced by the hydrogenation in the water solution was *trans*-2-≫1->*cis*-2-butene at CN/Co<5.1, and 1-≫*trans*-2->*cis*-2-butene at CN/Co>5.1; this composition was affected by the concentration of the complex. The composition of the butenes produced in the glycerol-methanol solution was *trans*-2-≫1->*cis*-2-butene at CN/Co<5.4 and 1->*cis*-2-≫*trans*-2-butene at CN/Co>5.4; a concentration effect similar to that in the water solution was observed. The composition of butenes in the glycerol-methanol-water solution at CN/Co=6.0 was remarkably affected by the composition of the solvent. In the ethylene glycol-methanol solution, *cis*-2-butene was much more producible than in the glycerol-methanol solution. The mechanism of the hydrogenation of butadiene by pentacyanocobaltate(II) was discussed on the basis of these solvent effects on the composition of products, and on the basis of the kinetical behavior of this hydrogenation reaction.

Pentacyanocobaltate(II) is a typical and interesting complex in the areas of both coordination chemistry and catalysis,[1] and its typical nature has been made clear in recent years as part of development of the chemistry of homogeneous catalysis, but our understanding of this complex can still be said to be inadequate. Recently, the present authors investigated this complex with two objects; one was to find organic solvents to increase the reactivity of this complex, and the other was to make sure of the radical mechanism proposed for the reaction of this complex. We found that pentacyanocobaltate(II) easily initiates the halomethylation of olefin in the glycerol-methanol solvent.[2] In a study related to this interesting solvent effect, we have found that the hydrogenation of butadiene catalyzed by pentacyanocobaltate(II) in the glycerol-methanol solvent gives very different results from those in water, as has already reported briefly.[3] It has been also found that butadiene is hydrogenated in the absence of hydrogen in these solvents,[3] but the results are somewhat different from those in the presence of hydrogen. In this paper, we will report more detailed results of the hydrogenation of butadiene in these solvents in the presence of hydrogen.

Experimental

Reagents. The glycerol and ethylene glycol (Nakarai Chemicals, LTD., Guaranteed Pure Grade) were distilled *in vacuo*. The methanol (Nakarai Chemicals, LTD., Guaranteed Pure Grade) was dried by the use of magnesium methoxide. The KCN (Nakarai Chemicals, LTD., Guaranteed Pure Grade) was dried in a vacuum desicator containing P_2O_5. Anhydrous $CoCl_2$ (Nakarai Chemical, Extra Pure Grade), butadiene (Takachiho Chemicals, containing 0.5—0.7% 1-butene), and hydrogen and nitrogen gases (Teikoku-Sanso) in commercial cylinders were all used without further purification.

Apparatus. The reaction vessel was 100-m*l*, three-necked flask equipped with a 50-m*l* dropping funnel; it was connected to two gas burets for hydrogen and butadiene, a mercury manometer, a gas-flow meter, and a stroke pump (Rigo-sha), which was used to circulate the gases in the reaction vessel through the solution at a flow rate of about 500 m*l* per minute. The solution was stirred magnetically and maintained at 20°C by means of a thermostat.

Procedure. The procedure consisted of two steps: the first step was hydrogen absorption by pentacyanocobaltate(II), and the second step was butadiene hydrogenation by the solution obtained in the first step.

(a) Hydrogen Absorption: In a hydrogen atmosphere, 10 m*l* of the $CoCl_2$ solution in the dropping funnel was added to 40 m*l* of the KCN solution in the reaction vessel while the solution was stirred vigorously and the gas was circulated, the volume of hydrogen absorbed at a constant atmospheric pressure was recorded as a function of the time for 1 hr in the case of the water solution and for 2 hr in the case of the glycerol-methanol solution. (When a mixture of 35 m*l* of glycerol and 15 m*l* of methanol was used as the solvent, the $CoCl_2$ was dissolved in 10 m*l* of methanol.) 10 mmol of $CoCl_2$ was used, except in examining the effect of the concentration of the complex.

(b) Hydrogenation of Butadiene: After the hydrogen-absorption procedure (a), about 130 m*l* of butadiene was introduced into the reaction vessel in such a way as replacing the hydrogen in the gas phase by butadiene as completely as possible. Stirring and circulation were started again after the above procedure. (This is the start of the hydrogenation.) While butadiene was supplied to maintain a constant atmospheric pressure, 2-m*l* gas samples were picked out by an injection-syringe at 10- or 20-min intervals for 4 hr; these samples were analyzed by means of a gas chromatograph (Shimadzu, Type GC-2B), using a 3.5-m column of DMS at room temperature. The moles of each butene produced were calculated, assuming that the sums of the relative amounts of butene and butadiene on the gas chromatograph correspond to the total moles of butadiene introduced into the reaction vessel until the sampling time.

Results

Hydrogen Absorption. Figure 1 shows typical examples of the hydrogen absorption by pentacyano-

1) See the recent review by J. Kwiatek, "Catalysis Reviews" Vol. 1, ed. by H. Heinemann, Marcel Dekker, New York (1968), p. 37.

2) K. Tarama and T. Funabiki, *Nippon Kagaku Zasshi*, **89**, 88 (1968).

3) K. Tarama and T. Funabiki, This Bulletin, **41**, 1744 (1968).

cobaltate(II) in water and the glycerol-methanol solution respectively. In the water, an initial rapid absorption of hydrogen was observed and the amount of hydrogen absorbed was nearly equal to the expected value (from the concentration of the complex), but in the glycerol-methanol solution, the rate of absorption was much slower and the amount of it was much less. (In the latter case, an initial increase in the gas volume was observed during the addition of the $CoCl_2$ solution to the KCN solution.) The amount of hydrogen absorbed tended to decrease with an increase in the CN/Co ratio; this tendency was more remarkable in the glycerol-methanol solution than in the water.

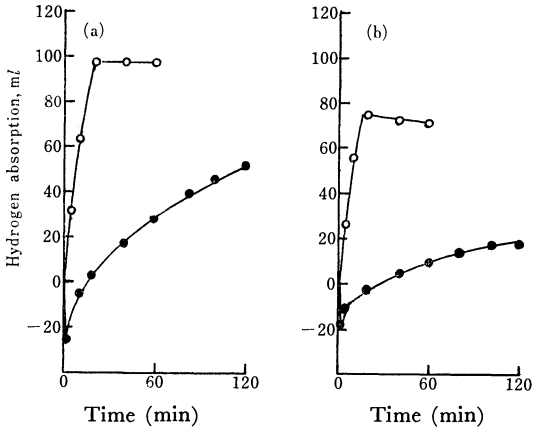

Fig. 1. Hydrogen absorption by pentacyanocobaltate(II).
(a) CN/Co=5.0 (b) 6.0
○ in water (50 ml)
● in glycerol (35 ml)+methanol(15 ml)
$CoCl_2$=10 mmol, 20°C

Hydrogenation of Butadiene in Water Solution. The Effect of the CN/Co Ratio: As is shown in Fig. 2,[4] a result similar to those obtained by other authors[5,6] was obtained: *trans*-2-butene is selectively produced in the low CN/Co region, and 1-butene in the high CN/Co region, while *cis*-2-butene is always negligible. The variation in the total yield of butenes was not remarkable. Figure 3 shows the time courses of the formation of each butene at several CN/Co ratios; it is known that the hydrogenation almost stops within 1 hr.

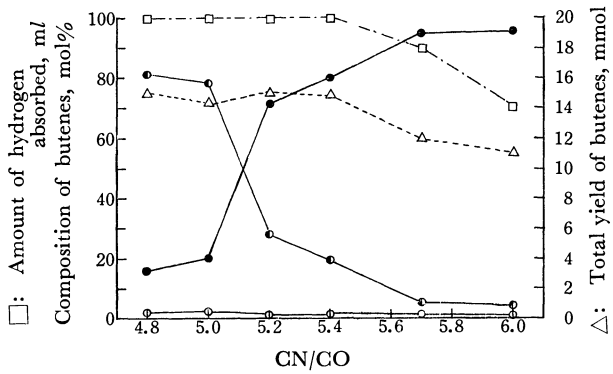

Fig. 2. Effect of CN/Co ratio in water.
● 1-butene, ◐ *trans*-2-butene, ○ *cis*-2-butene
Solvent: water 50 ml, $CoCl_2$=10 mmol, 20°C

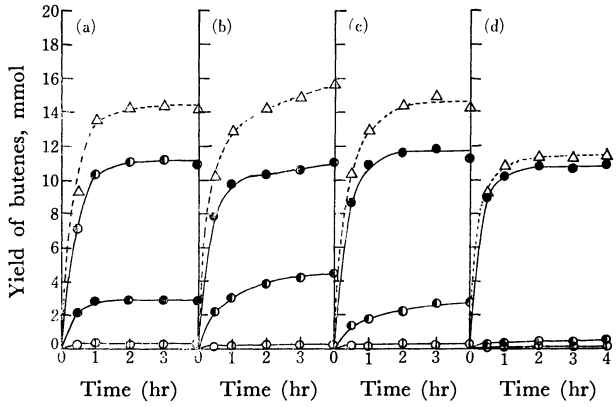

Fig. 3. Butene formation at different CN/Co ratio in water.
(a) CN/Co=5.0 (b) 5.2 (c) 5.4 (d) 6.0
● 1-butene, ◐ *trans*-2-butene, ○ *cis*-2-butene,
△ Total yield of butenes
Solvent: water 50 ml, $CoCl_2$=10 mmol, 20°C

Effect of the Concentration of the Complex: Figure 4 shows the results of the experiments in which the concentration of the complex was varied between 0.05 M and 0.25 M at CN/Co=5.0 (Fig. 4-a), and between 0.10 M and 0.20 M at CN/Co=6.0 (Fig. 4-b). At CN/Co=5.0, the mole fraction of *trans*-2-butene in the product decreased, while those of 1- and *cis*-2-butene increased with a decrease in the cobalt concentration[7]: at CN/Co=6.0, that of 1-butene decreased with the cobalt concentration. The total yield of butenes decreased linearly with the cobalt concentration.

Hydrogenation of Butadiene in the Glycerol-Methanol Solution. The Effect of the CN/Co Ratio: The

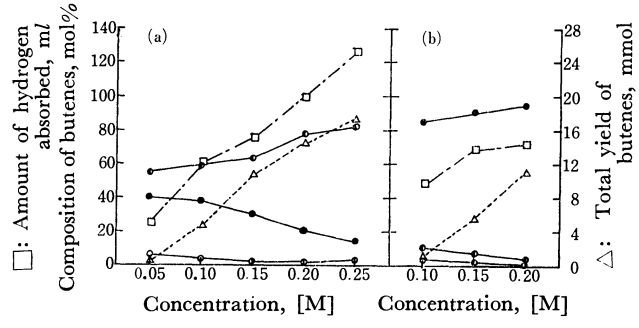

Fig. 4. Effect of concentration of the complex in water.
(a) CN/Co=5.0 (b) 6.0
● 1-butene, ◐ *trans*-2-butene, ○ *cis*-2-butene,
Solvent: water 50 ml, 20°C

4) The data for the composition and yield of each butene in Figures 2, 4, 5, 7, 8, and 10 are those obtained 3 hr after the start of the hydrogenation of butadiene. The data for the amount of hydrogen absorbed are those obtained by the procedure (a).

5) M. S. Spencer and D. A. Dowden (Imperial Chemical Industries Ltd.), U. S. 3009969 (1061).

6) J. Kwiatek, I. L. Mador, and J. K. Seyler, *Advan. Chem. Ser.*, **37**, 201 (1963).

7) This result at CN/Co=5.0 is not consistent with that obtained by Piringer *et al.*, in which the main product was 1-butene at a high cobalt concentration. *cf.* A. Farcus, U. Luca, and O. Piringer, "Progress in Coordination Chemistry" (Proceedings of the 11th International Conference on Coordination Chemistry Haifa and Jersulem, September, 1968), ed. by M. Cais, Elsevier Publishing Company, Amsterdam (1968), p. 29.

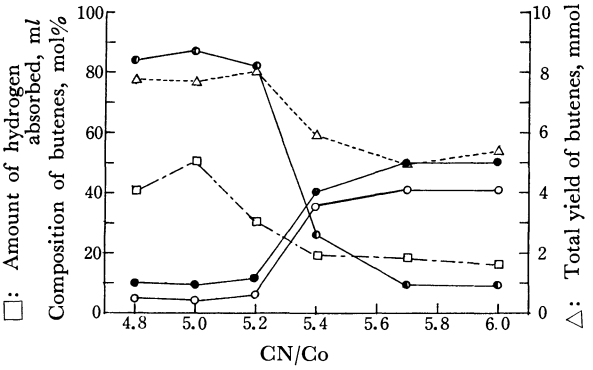

Fig. 5. Effect of CN/Co ratio in glycerol-methanol.
● 1-butene, ◐ *trans*-2-butene, ○ *cis*-2-butene,
Solvent: glycerol (35 m*l*)+methanol (15 m*l*),
$CoCl_2$=10 mmol, 20°C

results of the hydrogenation in the glycerol (35 m*l*)-methanol (15 m*l*) solution were remarkably different from those in the water, as is shown in Fig. 5 (*cf.* Fig. 2). *trans*-2-Butene was exclusively produced in the low CN/Co region, as in the water, while *cis*-2-butene was produced as much as 1-butene in the high CN/Co region. That is to say, the composition of the products was *trans*-2-≫1->*cis*-2-butene at CN/Co<5.4, and 1->*cis*-2-≫*trans*-2-butene at CN/Co>5.4. The total yield of butenes and the amount of hydrogen absorbed decreased with an increase in the CN/Co ratio. The results in water and in glycerol-methanol are compared in Table 1.

Table 1. Effect of CN/Co ratio in the butadiene hyerogenation in water and in glycerol-methanol[a)]

CN/Co	Composition of butenes (mol%)[b)]					
	in water			in glycerol-methanol		
	1-	*trans*-2-	*cis*-2-	1-	*trans*-2-	*cis*-2-
4.8	16	81	2	10	84	5
5.0	20	78	2	9	87	4
5.2	71	28	1	12	82	6
5.4	80	19	1	40	26	35
5.7	94	5	1	50	9	41
6.0	95	4	1	50	9	41

a) Water (50 m*l*), Glycerol (35 m*l*)+Methanol(15 m*l*), $CoCl_2$=10 mmol, 20°C
b) Composition after 3 hr from the start of the hydrogenation

Figure 6 shows the time courses of the formation of butenes at several CN/Co ratios in the glycerol-methanol solvent. Although almost all the *trans*-2-butene was formed within the initial hour at a rapid rate, *cis*-2-butene and 1-butene were formed gradually at rather slow rates. In comparison with the formation of *cis*-2-butene, an initial rapid formation was observed in the case of 1-butene.

Effect of the Concentration of the Complex. Figure 7 shows the results when the concentration of the complex was varied between 0.05 M and 0.20 M at CN/Co=5.0 and 6.0 in the glycerol (35 m*l*)-methanol (15 m*l*) solution. At CN/Co=5.0, the mole fraction of *trans*-

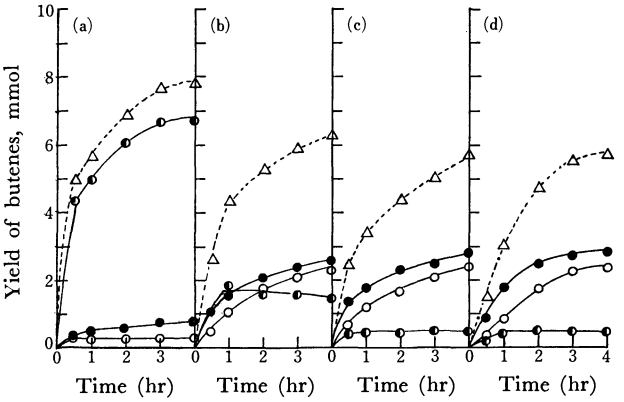

Fig. 6. Butene formation at different CN/Co ratio in glycerol-methanol.
(a) CN/Co=5.0 (b) 5.4 (c) 5.7 (d) 6.0
● 1-butene, ◐ *trans*-2-butene, ○ *cis*-2-butene,
△ Total yield of butenes
Solvent: glycerol (35 m*l*)+methanol (15 m*l*), $CoCl_2$=10 mmol 20°C

2-butene in the products decreased, and those of 1- and *cis*-2-butene increased, with a decrease in the cobalt concentration (Fig. 7-a). At CN/Co=6.0, the mole fraction of 1-butene decreased and that of *cis*-2-butene increased with a decrease in the cobalt concentration (Fig. 7-b). The total yield of butenes decreased linearly with the cobalt concentration, but this tendency was greater at CN/Co=5.0 than at CN/Co=6.0.

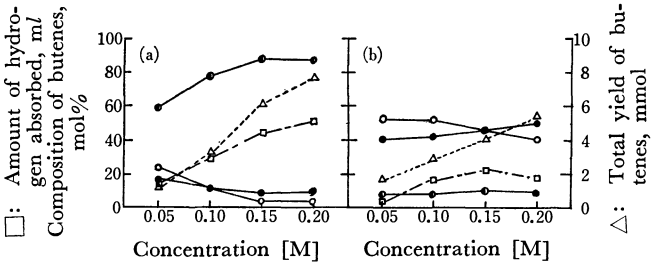

Fig. 7. Effect of concentration of the complex in glycerol-methanol.
(a) CN/Co=5.0 (b) 6.0
● 1-butene, ◐ *trans*-2-butene, ○ *cis*-2-butene,
Solvent: glycerol(35 m*l*)+methanol(15 m*l*), 20°C

Effect of Solvent Composition in the Glycerol-Methanol-water Solutions: Figure 8 shows the results at CN/Co=6.0 in the solvents with a total volume of 50 m*l*, containing glycerol (35 m*l*), methanol (15→0 m*l*), and water (0→15 m*l*). The increase in the water content (which involves, at the same time, the decrease in the methanol content) resulted in a great increase in the mole fraction of 1-butene and a decrease in that of *cis*-2-butene. The amount of hydrogen absorbed and the total yield of the butenes showed little change. Figure 9 shows the time courses of the formation of butenes in these solvents; it indicates that, although the initial rate of the formation of 1-butene changes little, that of *cis*-2-butene greatly decreases as the content of water increases.

Figure 10 shows the results at CN/Co=6.0 in the solvents containing glycerol (35 m*l*), methanol (15 m*l*),

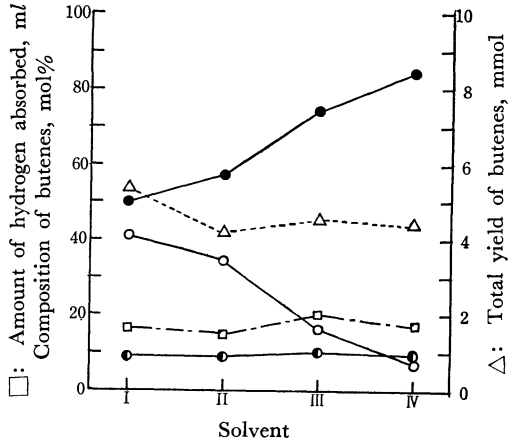

Fig. 8. Effect of composition of solvent in glycerol-methanol-water at CN/Co=6.0 (1).
● 1-butene, ◐ *trans*-2-butene, ○ *cis*-2-butene

	Glycerol	MeOH	H_2O
I	35 m*l*	15 m*l*	0 m*l*
II	35 m*l*	10 m*l*	5 m*l*
III	35 m*l*	5 m*l*	10 m*l*
IV	35 m*l*	0 m*l*	15 m*l*

$CoCl_2$=10 mmol, 20°C

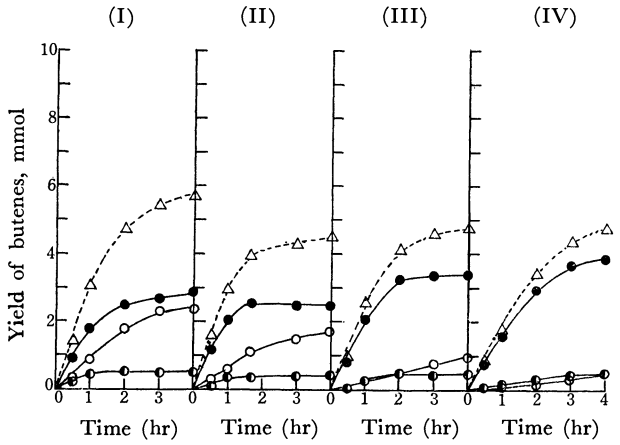

Fig. 9. Effect of composition of solvent in glycerol-methanol-water at CN/Co=6.0 (1).
● 1-butene, ◐ *trans*-2-butene, ○ *cis*-2-butene
△ Total yield of butenes
Solvents in I-IV corresponds to those in Fig. 8

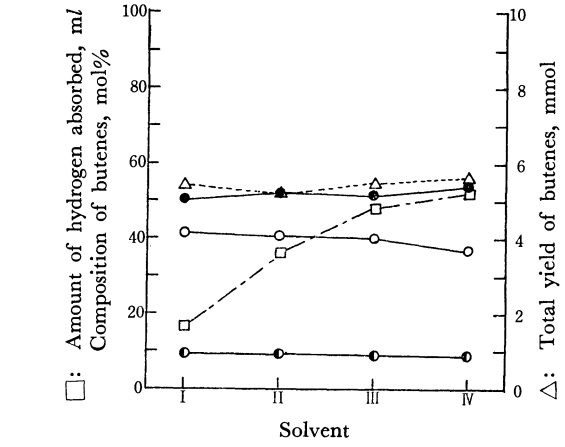

Fig. 10. Effect of composition of solvent in glycerol-methanol-water at CN/Co=6.0 (2).
● 1-butene, ◐ *trans*-2-butene, ○ *cis*-2-butene

	Glycerol	MeOH	H_2O
I	35 m*l*	15 m*l*	0 m*l*
II	35 m*l*	15 m*l*	5 m*l*
III	35 m*l*	15 m*l*	10 m*l*
IV	35 m*l*	15 m*l*	15 m*l*

$CoCl_2$=10 mmol, 20°C

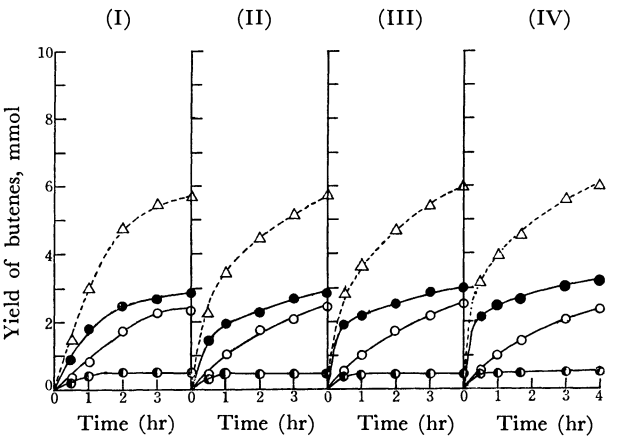

Fig. 11. Effect of composition of solvent in glycerol-methanol-water at CN/Co=6.0 (2).
● 1-butene, ◐ *trans*-2-butene, ○ *cis*-2-butene
△ Total yield of butenes
Solvents in I-IV corresponds to those in Fig. 10.

and water (0→15 m*l*). Remarkably different from the results shown in Fig. 8, the composition and the total yield of butenes did not vary in spite of the increase in the water content, although the amount of hydrogen absorbed increased with the water content. Figure 11 shows the time courses of the formation of butenes in these solvents; it indicates that, although the initial rate of the formation of 1-butene increases with the water content, that of *cis*-2-butene is little affected.

Color of the Solution: The aqueous solution of pentacyanocobaltate(II) was dark green and clear just after its preparation so long as CN/Co>4.8 ([Co]=0.2 M). After the hydrogen absorption, the color of the solution changed from dark green to a greenish yellow. Upon the introduction of butadiene to the solution, the solution became dark green within about 5 min, but it turned yellow green or yellow as the reaction proceeded. During the hydrogen absorption and the hydrogenation processes, a precipitate was formed at CN/Co<5.0. In the case of the glycerol (35 m*l*)-methanol (15 m*l*) solvent ([Co]=0.2 M), the solution was always clear, even in the low CN/Co region. At CN/Co<5.2, the dark green which was found just after the preparation of the complex soon turned dark brown and changed to red brown in the process of the hydrogen absorption. When butadiene was introduced, the red brown rapidly changed to dark brown, but it became red brown again during the process of the hydrogenation. At CN/Co>5.7, a color change similar to that in the water solution was observed, except that the yellow color was generally deeper in this solvent. In the region of CN/Co=5.2—5.7, a color change intermediate between the above two typical cases was observed.

Hydrogenation of Butadiene in the Ethylene Glycol-Methanol Solution. The preliminary experiment of the

hydrogenation of butadiene in the ethylene glycol (35 m*l*)-methanol (15 m*l*) solution showed rather different features from that in the glycerol-methanol solution. At CN/Co=6.0, the solution of the complex, just after having been prepared in a hydrogen atmosphere, was dark green and contained a precipitate, although the KCN and $CoCl_2$ solutions were both clear before mixing. After the hydrogen absorption (47 m*l* of hydrogen was absorbed), the solution remained dark green and contained a precipitate. When butadiene was introduced, a rapid absorption of butadiene was observed for the initial 10 min; the solution immediately became clear and yellow in its color within 5 min. The composition of butenes was *cis*-2->1-≫*trans*-2-butene even in the initial stage; after 3 hr, it was *cis*-2-(50%)>1-(45%)≫*trans*-2-butene (5%).

At CN/Co=5.0, the solution after the hydrogen absorption (41 m*l* of hydrogen was absorbed) was also dark green and contained many precipitates. When hydrogenation was started, a rapid absorption of butadiene was observed, but the change in color (to orange) and disappearance of the precipitate was slow. The composition of butenes was *trans*-2->*cis*-2->1-butene in the initial stage, but it became *cis*-2-(44%)>1-(36%)>*trans*-2-butene(20%) after 3 hr. The time courses of the formation of butenes at CN/Co=5.0 and 6.0 are shown in Fig. 12.

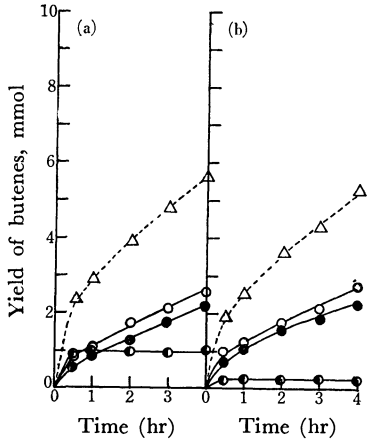

Fig. 12. Butene formation in ethylene glycol-methanol.
(a) CN/Co=5.0, (b) 6.0
● 1-butene, ◐ *trans*-2-butene, ○ *cis*-2-butene
△ total yield of butenes
Solvents: ethylene glycol (35 m*l*)+methanol (15 m*l*)
$CoCl_2$=10 mmol, 20°C

Discussion

The hydrogenation of butadiene by pentacyanocobaltate(II) was first reported by Spencer and Dowden,[5] who described that 1-butene was produced at a high CN/Co ratio and *trans*-2-butene, at a low ratio. Kwiatek *et al.*[6] studied this reaction in detail, varying the CN/Co ratio, changing the order of the introduction of hydrogen and butadiene into the complex solution, and using deuterium instead of hydrogen; they reported that the composition of butenes varies at CN/Co=5.5—6.0,[8] that the active species of the reaction is the hydrido-complex $HCo(CN)_5^{3-}$, and that the reaction intermediates are fairly stable organocyanocobaltates(III). They have proposed the following mechanism (Eqs. (1)—(3)), in which the rate-determining step is (3):

$$2\,Co(CN)_5^{3-} + H_2 \rightleftarrows 2\,Co(CN)_5H^{3-} \quad (1)$$

$$Co(CN)_5H^{3-} + C_4H_6 \rightleftarrows Co(CN)_5(C_4H_7)^{3-} \quad (2)$$

$$Co(CN)_5H^{3-} + Co(CN)_5(C_4H_7)^{3-} \rightarrow 2\,Co(CN)_5^{3-} + C_4H_8 \quad (3)$$

As the structure of the intermediate complex, $Co(CN)_5(C_4H_7)^{3-}$, the following three types have been proposed:[9,10] two σ-type complexes (σ_1 and σ_2) and one π-allyl-type complex (π), and it has been considered that the composition of butenes depends on the concentration of each intermediate. Kwiatek and Seyler considered that, in the high CN/Co region, (σ_1) is the most stable and 1-butene is produced exclusively from it, while in the low CN/Co region, (π) is the most stable and 2-butene (*trans*≫*cis*) is produced exclusively from it. On the other hand, Burnett *et al.*,[11] who studied this butadiene hydrogenation kinetically, proposed a mechanism in which 1-butene is produced from (σ_2); *trans*- and *cis*-2-butene, from (σ_1), and *trans*-2- and 1-butene, from (π). The basic difference between the two mechanisms is in the way of the

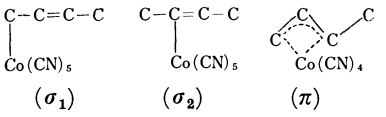

attack of the hydrido-complex $HCo(CN)_5^{3-}$ on butadiene and on the intermediate complexes; in the former mechanism, it is a 1,4-addition and γ-attack, while in the latter, it is a 1,2-addition and α-attack. Although Jackman *et al.*[12] reported that the reaction of conjugated olefin with hydridopentacyanocobaltate occurs in the *cis*-1,2-addition, the present authors consider that the hydrogenation of a conjugated diene such as butadiene must be a special case.

In discussing the mechanism of the hydrogenation of butadiene by pentacyanocobaltate(II), it should be noticed that the results which have been obtained by other authors were obtained in water and so the proportion of *cis*-2-butene to *trans*-2- and 1-butene was always negligible. The most characteristic result which was obtained in the glycerol-methanol solution was that *cis*-2-butene is produced in the high CN/Co region, and the time course of its formation is very different from that of *trans*-2-butene; in the case of *trans*-2-butene, a rapid initial formation, followed by

8) Suzuki reported later that the composition varies very sharply at CN/Co=5.1—5.2 (*cf.* T. Suzuki and T. Kwan, *Nippon Kagaku Zasshi*, **86**, 713 (1965)).

9) J. Kwiatek and J. K. Seyler, Proceedings of the 8th International Conference on Coordination Chemistry, Vienna, 1964 (V. Gutmann, ed.), Springer, Vienna (1964), p. 308.

10) J. Kwiatek and J. K. Seyler, *J. Organometal. Chem.*, **3**, 421 (1965).

11) M. G. Burnett, P. J. Connoly, and C. Kemball, *J. Chem. Soc., A*, **1968**, 991.

12) L. M. Jackman, J. A. Hamilton, and J. M. Lawlor, *J. Amer. Chem. Soc.*, **90**, 1914 (1968).

a slow formation or none at all, is observed, while *cis*-2-butene is produced gradually and successively. Therefore it is reasonable to assume that the structure of the intermediate for the *cis*-2-butene formation resembles that for 1-butene rather than that for *trans*-2-butene. If it is supposed that such organocyano-complexes as (σ_1), (σ_2), and (π) are the intermediates for the butadiene hydrogenation by pentacyanocobaltate(II),[13] and that σ complex is stable in the high CN/Co region, it is natural to consider that the (σ_1) of the *cis* configuration (*cis*-σ_1) is probably an intermediate for the *cis*-2-butene formation, because with other σ complexes such as the (σ_1) with a *trans* configuration and the (σ_2), there is the great probability of the formation of *trans*-2-butene besides *cis*-2-butene.

As an intermediate for 1-butene formation, two complexes (σ_1 and σ_2), should be considered, because either complex may produce 1-butene, by the γ- or the α-attack of the hydrido-complex. Although it is difficult to decide which is the proper intermediate, at this stage we prefer *cis*-σ_1, because it seems to be more appropriate to consider a common intermediate for the two butenes (1- and *cis*-2-butene) rather than different intermediates. Hence, in the mechanism here proposed, butadiene and the hydro-complex react in the 1,4-addition to form a *cis*-butenyl complex at first.

The present authors observed a difference in the time courses of the formation of 1- and *cis*-2-butene in the glycerol-methanol and the glycerol-methanol-water solutions. The rate of the formation of 1-butene in the initial stage is greater than that of *cis*-2-butene; this difference becomes more obvious with an increase in the water content in the solvent. This result may be explained in terms of the difference in the reactivity of the two active reducing species, provided that there exists another reactive reducing species besides the hydrido-complex: The reaction of the hydrido-complex with *cis*-σ_1 is rapid and produces exclusively 1-butene in the initial stage (the quantity of 1-butene produced by this reaction may be rather small, because the amount of hydrogen absorbed in this solvent is generally small), but another reactive reducing species, which may be a solvent molecule or a cyanocobalt-complex coordinated by the solvent, reacts to produce nearly equal amounts of 1- and *cis*-2-butene at a relatively slower rate than the hydrido-complex. This may be written schematically as in Scheme 1, where CoH, CoROH and ROH denote the hydrido-com-

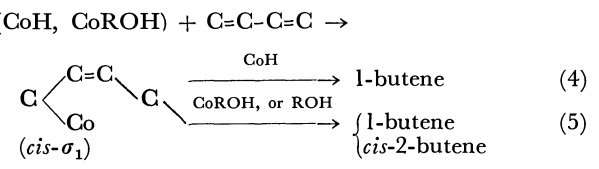

Scheme 1

plex, the cyanocobalt complex coordinated by an alcoholic solvent, and the alcoholic solvent respectively. If there is enough CoH for the second step in Scheme 1, an initial rapid formation of 1-butene will be observed, and *vice versa*. This proposal may well be supported by the following facts: 1) In the water solution, 1-butene is selectively formed in the high CN/Co region; this can be ascribed to the selective performance of reaction (4). 2) In the glycerol-methanol solution in the high CN/Co region in the absence of hydrogen, the composition of butenes is *cis*-2->1-$\gg$*trans*-2-butene;[3] this can be ascribed to the absence of the hydrido-complex. 3) In the ethylene glycol-methanol solution at CN/Co=6.0, the composition of butenes is also *cis*-2->1-$\gg$*trans*-2-butene, even in the initial stage; this can be ascribed to the rapid reaction of butadiene with hydrido-complex to produce the intermediate complex (*cis*-σ_1) without saving the hydrido-complex for the second step. (This may be connected with the rate of the dissolution of butadiene into the solvent or with the precipitate formation.)

The probable intermediate for the *trans*-2-butene formation may well be a π-methallyl-complex (π), as was proposed by Kwiatek,[9] but it seems to be rather difficult to explain the initial rapid formation of *trans*-2-butene from the (π) complex, for the rate of isomerization between σ-allyl and π-allyl complexes presumed from the NMR spectra with an allyl-pentacyanocobaltate(III)[10] is not very great. We wish here to propose another route for the formation of *trans*-2-butene, in which *trans*-2-butene is produced in one step via a butadiene-bridged transition state which is produced by one molecule of butadiene and a dimeric-type hydrido-complex, such as proposed by Piringer and Farcas;[14] the mechanism may be shematically written as in Scheme 2:

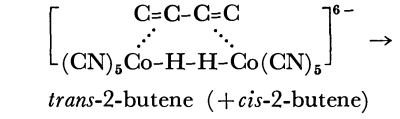

trans-2-butene (+*cis*-2-butene)

Scheme 2

In these mechanisms, the selectivity of the hydrogenation of butadiene by pentacyanocobaltate(II) largely depends on the type of hydrido-complexes which are in equilibrium in the solution and whose equilibrium constant is affected by the CN/Co ratio and the concentration of the complex. It is supposed that the monomeric form exists selectively in the high CN/Co region, and that the monomeric form increases with the a decrease in the concentration in the low CN/Co region (*cf.* Figs. 4 and 7).

The color change of the solution suggests a variation of the structure of the complexes in solution, but we should be careful in discussing these data. At this stage, it cannot be decided whether or not the brown color observed in the glycerol-methanol solution in the low CN/Co region is connected with the structure of the complex which produces *trans*-2-butene.

13) Although the present authors have proposed another possible mechanism of the formation of 1- and *cis*-2-butene in the high CN/Co region, supposing that the *cis*-2-buteneyl radical is the intermediate, this radical mechanism will not be discussed further in this paper (*cf.* K. Tarama, T. Funabiki, and M. Mohri, *Shokubai*, **11**, 35 (1969)).

14) O. Piringer and A. Farcas, *Z. Phys. Chem. N.F.*, **46**, 190 (1965).

The solvent effect on the hydrogenation by pentacyanocobaltate(II) is rather complicated. The presence of water is surely important in 1-butene formation (Fig. 8), but it is not decisive (Fig. 9). The presence of methanol seems to be important for the *cis*-2-butene formation, but the role of methanol cannot be discussed in detail before the effect of glycerol becomes clear. At this stage, the results in the solvent containing glycerol-methanol-water (Figs. 8—11) may be explained as follows, on the basis of the proposed mechanism: the constancy of the initial rate of the formation of 1-butene in the solvents of Figs. 8 and 9 may be ascribed to the constancy of the concentration of the hydridocomplex (the amount of hydrogen absorbed in each solvent was nearly constant), and the great decrease in the rate of formation of *cis*-2-butene may be ascribed to the decrease in the methanol content. The increase in the initial rate of formation of 1-butene with the increase in the water content in the solvents of Figs. 10 and 11 may be ascribed to the increase in the concentration of the hydrido-complex (the amount of hydrogen absorbed increases with an increase in the water content), and the constancy of the rate of the formation of *cis*-2-butene may be ascribed to the nearly constant content of methanol. The present authors consider that the difference in the reactivity of pentacyanocobaltate(II) between that in water and that in these alcoholic solvents is due partly to the difference in the structures of the reactive species, to for example, the difference between the free ion in water and the ion-pair in alcoholic solvents, and partly to the difference of the solvating ability of the solvents.

BULLETIN OF THE CHEMICAL SOCIETY OF JAPAN, VOL. 44, 951—957 (1971)

Optical Activity of Nucleic Acid-Thionine Complexes[1)]

Yasumasa J. I'HAYA and Tomoyasu NAKAMURA

Department of Materials Science, The University of Electro-Communications, Chofu-shi, Tokyo

(Received October 1, 1970)

The absorption spectra, optical rotatory dispersion, and circular dichroism (CD) of the DNA- and RNA-thionine complexes were measured at the nucleic acid phosphate to dye ratios (P/D) 0.01—50 and at the temperature range 20—85°C. The Cotton effects of P/D >3 complexes were observed in the wavelength region 520—680 nm, being resolved at least into four partial Cotton effects. From their transient profiles with changing P/D values and the observed temperature effect, they were interpreted to be induced from the dye monomers bound near the asymmetric environment of nucleic acids. The Cotton effects of P/D <2 complexes in the wavelength region 450—580 nm are new and have not been reported for other DNA-dye systems. The trough of these Cotton effects completely disappeared at 50°C and the decreasing profile of its relative rotation with increasing temperature was roughly parallel to that of the dimer fraction. The newly developed Cotton effects are inferred to result from an interaction between the dye dimers aggregated in a helical fashion along the nucleic acid helices. The negative sign CD maximum observed in the wavelength region 300—330 nm is probably due to DNA-dye interactions, but its origin is not clear.

It is well known that some basic dyes show photodynamic and mutagenic actions for microorganisms.[2,3)] Binding of such dyes to biological macromolecules, such as nucleic acids and polysaccarides, induces the bathochromic and hypochromic effects in the visible electronic absorption region of the dyes.[4-7)] Concerning the nucleic acid-aminoacridine dye complexes, the binding mechanism and conformations have been studied extensively by many investigators using the optical rotatory dispersion (ORD) and circular dichroism (CD) methods.[8-11)] Acridine orange (AO) and/or proflavine is an optically inactive molecule. When either dye binds to a biological helical polymer, anomalous optical rotation (Cotton effect) is observed in the spectral region of the dye. Blake and Peacocke[9)] observed this "extrinsic Cotton effect" by means of ORD measurement, and Gardner and Mason[11)] by CD measurement under various experimental conditions, *viz.*, by changing the nucleic acid phosphate to dye ratio (P/D), pH, and ionic strength. In order to explain the induced anomalous optical rotations for nucleic acid-dye complexes, particularly for the DNA-AO complexes, the following models have been proposed: for their conformations, helical arrangement of the dye along the macromolecule or helical tangential extension of the dye hanging on the anionic residue of the macromolecule, and for their

1) Presented in part at the 23rd Annual Meeting of the Chemical Society of Japan, Tokyo, 1970.

2) N. Yamamoto, *Virus*, **6**, 510, 522, 531 (1956).

3) F. H. Crick, L. Barnett, S. Brenner, and R. J. Watts Robin, *Nature*, **192**, 1227 (1961).

4) F. W. Morthland, P. P. H. de Bruyn, and N. H. Smith, *Exp. Cell Res.*, **7**, 201 (1954).

5) M. Semmel and M. Daune, *Biochim. Biophys. Acta*, **145**, 561 (1967).

6) H. Ito and Y. J. I'Haya, *Intern. J. Quantum Chem.*, **2**, 5 (1968).

7) Teh Fu Yen, M. Davar, and A. Rembaum, *Biochim. Biophys. Acta*, **184**, 646 (1969).

8) A. R. Peacocke and J. N. H. Skerett, *Trans. Faraday Soc.*, **52**, 261 (1956).

9) A. Blake and A. R. Peacocke, *Biopolymers*, **4**, 1091 (1966).

10) K. Yamaoka and R. A. Resnik, *J. Phys. Chem.*, **70**, 4051 (1966).

11) B. J. Gardner and S. F. Mason, *Biopolymers*, **5**, 79 (1967).

interaction mechanism, dipole-dipole interaction between the stacked and/or intercalated dyes or asymmetric environment of the binding sites.

Much has been said for and against these models. In the DNA-AO complexes, there appear two or three negative CD maxima in the visible absorption region of the dye, in addition to the positive CD maximum in the longer wavelength region. However, the primary source of the Cotton effects, *i.e.*, whether they are induced from monomerically bound AO or from dimerically bound AO, has not been established.

Thionine forms molecular complexes with nucleic acids. In this paper we report results of the measurement of the induced Cotton effects and absorption spectra resulting from the interaction of thionine with native DNA and RNA. We show how Cotton effects change their profiles with P/D and temperature. Comparing the results with those obtained for the DNA-AO complexes, we will discuss the origin of the induced Cotton effects, in particular the contribution of the thionine dimer. Certain inferences will be made as to the binding conformations of the nucleic acid-thionine complexes.

Experimental

Commercial calf-thymus DNA (Sigma Type 1) was used without further purification. Unfractioned RNA was prepared from rat-liver according to Kirby's method.[12] Stock solutions of nucleic acids (30 mg/25 m*l*) were stored in the cold and diluted just prior to use. Thionine (3,7-diaminophenothiazonium chloride; Lauth's violet) (Tokyo Kasei) was purified by recrystallization twice from aqueous solution. In this purified dye, no detectable impurity was found through Sephadex LH-20 column chromatography. Stock solutions of the dye were stored in the dark in order to avoid photosensitized reactions.

Stock aqueous solutions of the dye and nucleic acids were dissolved in 0.01 M phosphate buffer (pH 6.84). The concentration of nucleic acids, expressed in terms of phosphate residues, was determined as usual by the measurement of the absorbance at 260 nm and using the known molar extinction coefficients $\varepsilon_P^{260}=6{,}650$ and $\varepsilon_P^{260}=8{,}190$ for DNA and RNA, respectively. Within the concentration range of $(1—3)\times10^{-5}$ M, $\varepsilon^{598}=54{,}200$ was obtained for thionine in the phosphate buffer. This value is nearly in accord with that given by Rabinowitch and Epstein.[13]

Total concentration of the dye in the complexes was selected to be from 1.0×10^{-5} M to 3.3×10^{-5} M, since the observed extrinsic Cotton effects of the complexes strongly depended upon the concentration of the dye. Using a Jasco ORD/UV-5 recording spectrophotometer, absorption, ORD, and CD spectra were measured at various temperatures (20—85°C). Temperature studies were carried out with a specially designed variable temperature cell. Sample temperatures were measured with a copper-constantan thermocouple while spectra were being taken.

Results

Morthland *et al.*[4] reported that the absorption spectrum of thionine shifts to the red, losing its intensity, upon formation of the complex with nucleic acids. Although our experimental conditions differ somewhat from theirs, analogous bathochromism and hypochromism are observed except for extremely low P/D complexes (Fig. 1). When P/D exceeds 10, a new absorption maximum appears at about 610 nm, while the absorption maximum at 598 nm is diminished in intensity and remains as a shoulder in this region. In contrast to such high P/D complexes, the extremely low P/D ones show slight broadening of the shorter wavelength limb together with slight depression of the absorption maximum at 598 nm. The absorption spectrum of the dye alone, when the concentration

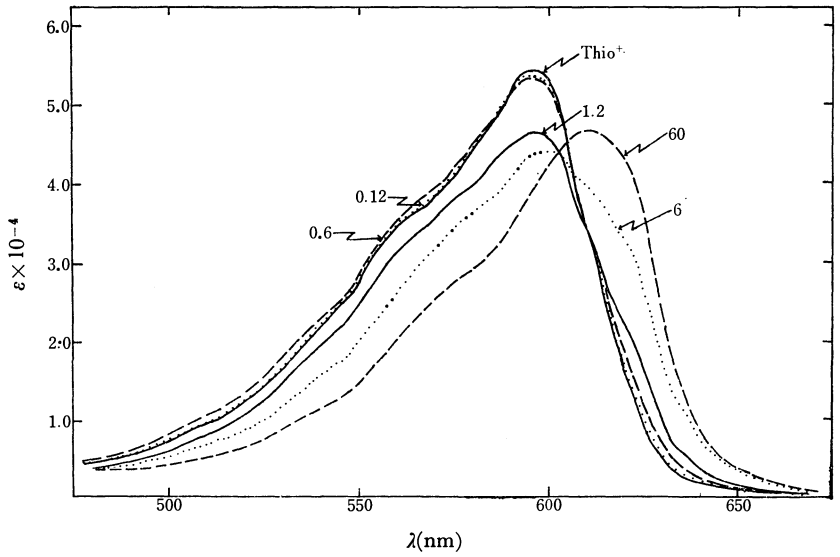

Fig. 1. Absorption spectra of Calf-thymus DNA-thionine complexes in 10^{-2} M phoshate buffer (pH=6.84). Total concentration of thionine, 2×10^{-5} M. Each figure shows P/D value of the complexes.

12) K. S. Kirby, *Biochem. J.*, **64**, 405 (1956).

13) E. Rabinowitch and L. F. Epstein, *J. Amer. Chem. Soc.*, **63**, 69 (1941).

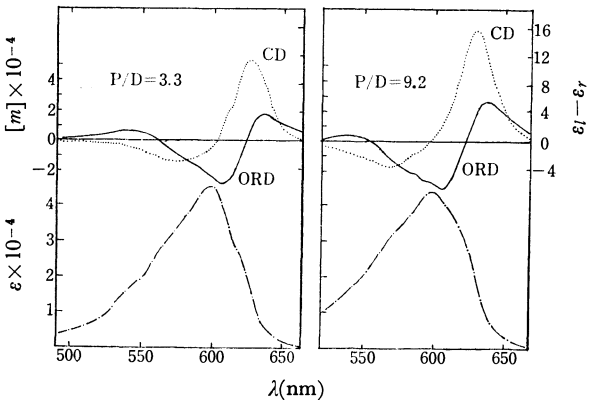

Fig. 2. ORD, CD (upper), and absorption (lower) spectra of DNA-thionine (left) and RNA-thionine (right) complexes at high P/D values. Total concentration of thionine, 1×10^{-5} M.

of the dye is sufficiently high (about 10^{-3} M), shows another maximum at 560 nm. This has been assigned to a dimer band of thionine.[13] The 610 nm (monomer) band of the high P/D and the 560 nm (dimer) band of the low P/D DNA-thionine complexes seem to correspond to the α-(or complex II) and β-(or complex I) bands of the DNA-AO complexes, respectively. At further increased P/D values, two isosbestic points are obtained at 608 nm and 602 nm. The former can be observed even when the concentration of DNA is not very high. The latter, however, can be observed only in the complexes of P/D values greater than 20. Metachromatic properties of the RNA-thionine complex are almost the same as those of the DNA-thionine complex described above.

Figures 2 and 3 show the representative ORD and CD spectra of the DNA- and RNA-thionine complexes. These data together with those for the absorption spectra are summarized in Table 1. At relatively high P/D values, the general shapes of these ORD and CD spectra resemble those of the DNA-AO complex.[9-11] It is apparent that there are one positive (*ca.* 626 nm) and one negative (*ca.* 576 nm) Cotton effect in the visible absorption spectral region of these complexes, as seen in Fig. 2 and Table 1. When P/D decreases to less than 2, new Cotton effects are observed in the region of 450—580 nm (Fig. 3). These types of Cotton effects have not been observed in other DNA-dye complexes. It should be noted that even in the DNA-thionine system the following conditions are required for observation: low P/D value (less than 2), high total concentration of the dye (at least, more than 2×10^{-5} M), and moderate temperature (below 50°C).

The decrease in P/D gives rise to the decrease in molar rotation of the peak at 636 nm and the trough at 606 nm and the increase in that of the trough at 525 nm. After passing intermediate P/D values where all these peaks and troughs are detected, only the trough

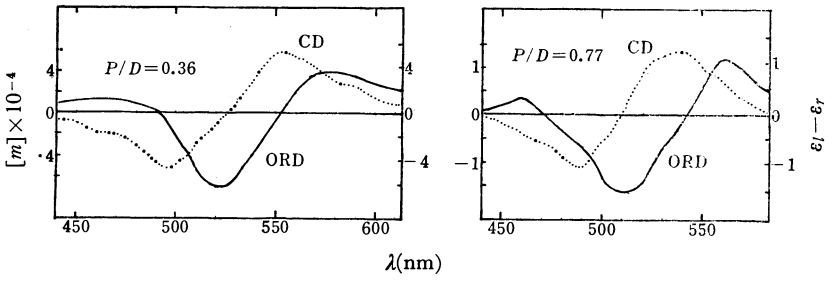

Fig. 3. ORD and CD spectra of DNA-thionine (left) and RNA-thionine (right) complexes at low P/D values. Total concentration of thionine, 3.3×10^{-5} M.

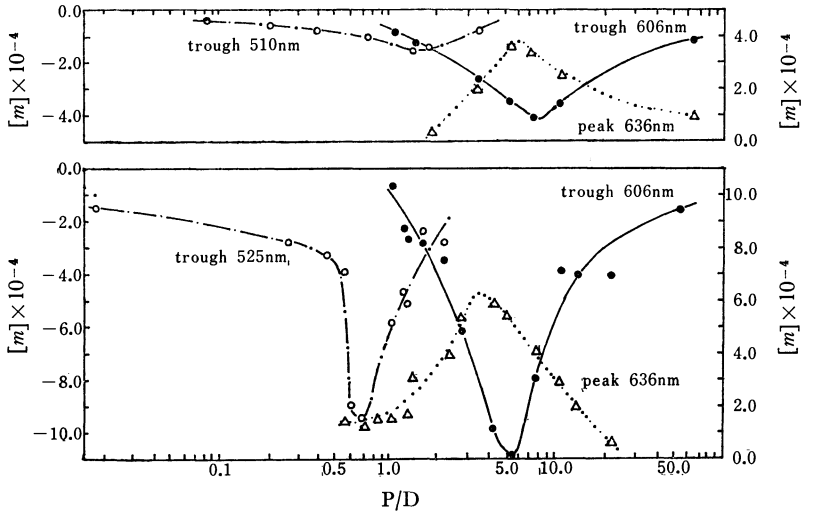

Fig. 4. Plot of molar rotation against P/D value for RNA-thionine (upper, thionine conc., 2×10^{-5} M) and DNA-thionine (lower, thionine conc., 3×10^{-5} M) complexes. Left hand scale applies to each trough and right hand scale to each peak.

Table 1. Absorption, ORD, and CD spectral data for DNA- and RNA-thionine complexes (nm)

Thionine-DNA					
Total conc. of thionine (M)	1.00×10^{-5}	2.95×10^{-5}	2.95×10^{-5}	2.95×10^{-5}	3.33×10^{-5}
P/D	3.3	0.27	1.36	5.43	0.36
Absorption					
peaks	602	596	596	602	596
shoulders	~570, ~615	~565	~540, ~565	~565, ~615	~565
ORD[a]					
peaks	635 (1.69)		635 (3.39)	637 (5.42)	
					~580 (2.36)
troughs	607 (−2.83)		604 (−2.71)	609 (−11.19)	
		527 (−2.71)	525 (−5.08)		522 (−6.31)
shoulder				590 (−6.11)	
inflextion points	623	560	622		490, 556
CD[b]					
(+) maxima	626 (11.88)				555 (4.80)
(−) maxima	576 (−3.20)				494 (−4.50)

Thionine-RNA					
Total conc. of thionine	1.00×10^{-5}	2.30×10^{-5}	2.30×10^{-5}	2.30×10^{-5}	3.33×10^{-5}
P/D	9.2	0.37	1.85	11.13	0.77
Absorption					
peaks	599	596	596	601	592
shoulders	~560, ~620	~565	~510, ~565	~575, ~620	~565
ORD[a]					
peaks	636 (2.50)		640 (0.43)	640 (2.60)	
		555 (0.65)	550 (0.65)		562 (1.05)
troughs	607 (−3.13)			606 (3.47)	
		510 (−0.65)	506 (−1.30)		512 (−1.65)
shoulder					
inflextion points	622	535	622, 565, 520	624	541
CD[b]					
(+) maxima	627 (16.26)				540 (1.20)
(−) maxima	570 (−3.96)				490 (−1.05)

a) Values in braces show molar rotations [m] in units of degrees mol^{-1} $decimeter^{-1}$ $ml\times10^{-4}$.
b) Values in braces show circular dichroic absorptions $\varepsilon_l-\varepsilon_r$ in units of l cm^{-1} mol^{-1}.

at 525 nm can be observed clearly even at extremely low P/D values. These variations in the ORD profile are illustrated in Fig. 4, together with those of the RNA-thionine complexes.

Figure 5 shows the effect of temperature on the ORD curves. The relative amplitudes (or relative molar rotations) at various temperatures are plotted in Fig. 6 where the value of the amplitude (or molar rotation) at 20°C is taken to be unity. The relative amplitude of the P/D=2.6 complex begins to decrease at about 40°C, reaches a value 0.5 at 60°C, but is still observable even at 85°C, beyond which the measurements become impossible to be carried out (Fig. 6a). This trend is quite similar to that of the DNA-AO complex.[14] For the P/D=0.36 complex, the effect of temperature is more drastic. At about 35°C the re-

14) M. Zama and S. Ichimura, *Biopolymers*, **9**, 53 (1970).

lative molar rotation of this complex reaches a value 0.5 and vanishes completely at temperatures higher than 50°C (Fig. 6b).

Thionine shows absorption also in the ultraviolet absorption region of nucleic acids. A negative CD band, which seems to correspond to the absorption shoulder of the dye at 310 nm, appears in the DNA-thionine complex. Figure 7 shows the Cotton effects of the complex and DNA alone developing in this spectral region, together with the absorption spectra of the complex and thionine alone. These CD spectra

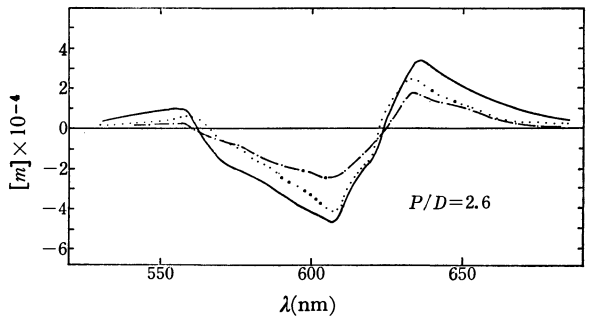

Fig. 5a. Effect of temperature on the ORD curves of the DNA-thionine P/D=2.6 complex. ——: 25°C, ·····: 50°C, —·—·: 70°C.

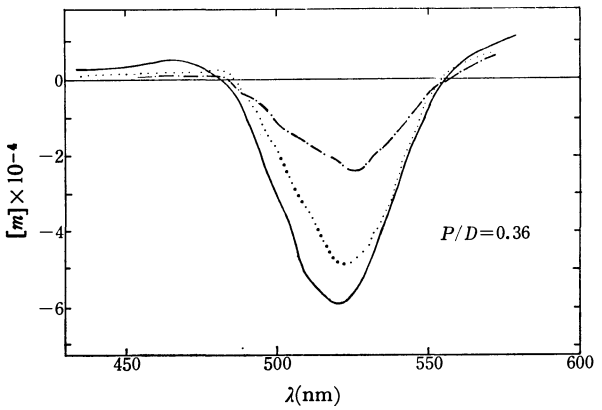

Fig. 5b. Effect of temperature on the ORD curves of the DNA-thionine P/D=0.36 complex. ——: 25°C, ·····: 32°C, —·—·: 40°C.

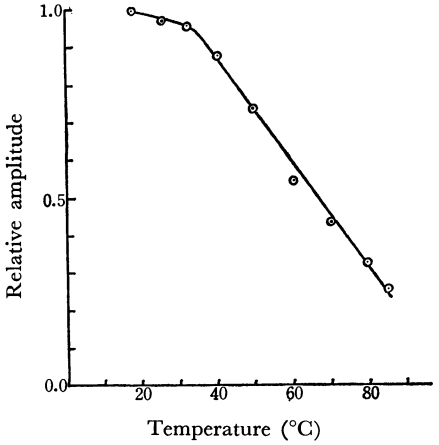

Fig. 6a. Temperature dependence of the relative amplitude of the DNA-thionine P/D=2.6 complex. Values are normalized against that at 20°C.

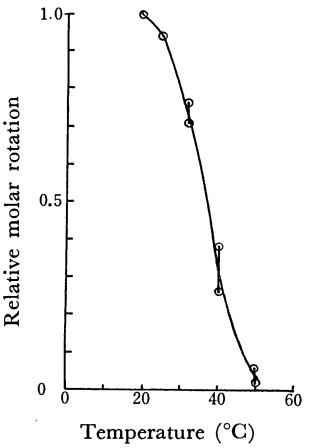

Fig. 6b. Temperature dependence of the relative molar rotation at 250 nm of the DNA-thionine P/D=0.36 complex. Vertical lines show experimental errors.

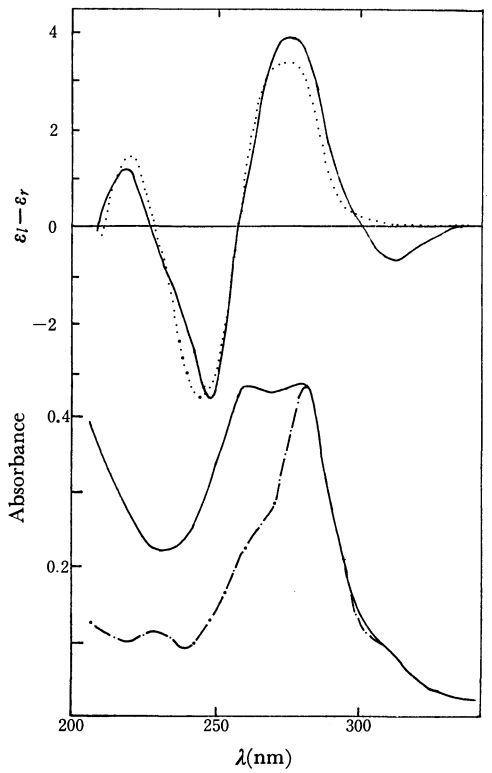

Fig. 7. CD spectra of DNA (upper, ——) and of the DNA-thionine P/D=3.2 complex (upper, ·····) and absorption spectra of thionine (lower, —·—) and of the DNA-thionine complex (lower, ——).

are corrected in magnitude in order that the negative CD maximum of the complex around at 250 nm coincides with the corresponding maximum of DNA. Similar effects are observed in the RNA-thionine complex. No quantitative measurements with respect to these Cotton effects developing in the ultraviolet absorption region of the complexes have been carried out.

Discussion

Interactions between nucleic acids and dyes have been a subject of both experimental and theoretical

studies concerning the effect on the electronic spectra, the change in the thermodynamic parameters, hydrodynamic characters and other physical and chemical properties of complexes.[15] A problem of current interest in chemistry of macromolecule-dye complexes is the study of the induced optical activity of these systems. Many workers have studied the Cotton effects of complexes such as DNA-aminoacridine dyes,[8-11] DNA-actinomycine,[16] and polysaccaride-various dyes complexes by means of ORD and CD measurements.[17]

Yamaoka and Resnik[10] and Gardner and Mason[11] independently suggested the existence of the four partial Cotton effects observable in the visible absorption spectral region of the DNA-AO complex. Their concepts, however, are not in accord with each other with respect to the signs of Cotton effects. Yamaoka and Resnik resolved the resultant CD curves, derived from the experimental ORD spectrum by the Kroning-Kramers transform, into four components (partial CD bands) *viz.*, a positive CD band located at the longest wavelength and three successive negative CD bands. Gardner and Mason, on the contrary, directly measured the CD spectrum and concluded that there are one positive and two negative Cotton effects, of which the longer wavelength positive CD band possesses two positive components. Yamaoka and Resnik ascribed the interaction mechanism to the asymmetric environment due to the asymmetric carbon atoms of the macromolecule, in accordance with model I proposed and rejected by Stryer and Blout.[18] According to their interpretation these four CD bands correspond to four monomer transitions. The positive CD maximum is assigned to the ^1L_a forbidden transition of the free AO molecule and the other three negatives to the 0–0, 0–1, and 0–2 vibrational transitions of the ^1L_b allowed band.

The ORD and CD spectra of the DNA-thionine P/D=3.3 complex (Fig. 2) resemble very closely those of the DNA-AO complex (for example the P/D=5 complex given in Fig. 4 of Ref. 9). The binding conformation of the DNA-thionine complex is supposed to be quite similar to that of the DNA-AO complex, being supported by the flow dichroism experiment of Nagata *et al.*[19] on the complexes of DNA-phenothiazine dyes, such as methylene blue and toluidine blue, and of DNA-acridine dyes. From these similarities, the observed Cotton effects of the DNA-thionine P/D>3 complexes are inferred to be resolved into at least four components, all of them being due to monomer dye-asymmetric site and/or monomer dye-monomer dye interactions (vide post).

The Cotton effects newly developed at low P/D values (Fig. 3) seem to be caused by an interaction between the dimerically bound or more aggregated dyes in view of the following results experimental findings. (1) The Cotton effects are found near the dimer band. (2) Occurrence of this phenomenon strongly depends upon the total concentration of the dye. (3) At low P/D values, the visible absorption spectrum of the complex shows a slight blue shift (Fig. 1). (4) The Cotton effects of low P/D complexes undergo more rapid and more drastic temperature effect than those of high P/D complexes.

A question arises with respect to items (1) and (2). Is the existence of two CD maxima, a positive one at 555 nm and a negative one at 494 nm, consistent with the assumption that the Cotton effects of the low P/D complexes are due to the 560 nm dimer band of the dye? This can be answered by the concept of exciton splitting. The dimer transition may split into two transitions through interaction between the dimerically bound dyes. In the present case, an absorption spectrum corresponding to the negative CD maximum is uncertain, but it should be observed under some optimum experimental conditions, for example at lower temperature.

At extremely low P/D values, it appears that the amount of the dye dimers greatly increases since the dye monomers will closely bind to almost all possible binding sites of nucleic acids. This is confirmed by the fact that the longer wavelength Cotton effects, assigned to the monomerically bound dye molecules, disappear at extremely low P/D values (Fig. 4). From item (3), the bound dye dimer may form a face-to-face arrangement, the so-called stacking model, along the helix of nucleic acid.

The Cotton effects developing in the spectral region of 450—580 nm at low P/D values are ascribable to the dimer or higher aggregates of thionine. This is supported more strongly by the transient profiles of these Cotton effects accompanied with increasing temperature (item (4)). The decrease in the relative amplitude with increasing temperature, for the Cotton effects of the DNA-thionine P/D=2.6 complexes (Fig. 6a), appears to be due to the detachment of the bound dye from DNA and/or to a relatively mild structural change not so drastic as to induce the denaturation of DNA. Since the melting temperature of calf-thymus DNA is 85.2°C (in 0.15 M NaCl+0.05 M Na citrate solution),[20] we may infer that the decomposition of the DNA helices in the complex occurs at temperatures higher than 85°C, although the accurate melting temperature of the complex is not known. The fact that the relative amplitude is still non-zero even at this limiting temperature suggests that the Cotton effects of the P/D=2.6 complexes may be induced not from an interaction between the dye molecules aggregated in a helical fashion but to the dye bound near the asymmetric carbon atoms of nucleic acids. The bound dye is supposed to be primarily of the monomeric form, since there may exist quite a small amount of dye dimers at such high temperatures. This conclusion is also supported by Yamaoka and Resnik's experiment on the sodium poly-α, L-glutamate-AO complexes which shows optical activity

15) G. Löber, *Z. Chem.*, **9**, 252 (1969).
16) Y. Courtois, W. Guschlbauer, and P. Fromageet, *Eur. J. Biochem.*, **6**, 106 (1968).
17) A. L. Stone, *Biopolymers*, **3**, 617 (1965).
18) L. Stryer and E. R. Blout, *J. Amer. Chem. Soc.*, **83**, 1411 (1961).
19) C. Nagata, M. Kodama, Y. Tagashira, and A. Imamura, *Biopolymers*, **4**, 409 (1966).
20) S. Yabuki and A. Wada, *Seibutsu Butsuri*, **6**, 31 (1966).

even at very high P/D values (P/D $\sim 10^4$).

In the case of the P/D=0.36 complex, the trough of the newly developed Cotton effects at 520—525 nm completely disappears at about 50°C (Fig. 6b). This critical temperature becomes lower with the decrease of the total concentration of dye. Using the data for the dimerization constants of thionine in aqueous solution,[13] the dimer fraction for the 3.3×10^{-5} M solution is calculated and plotted in Fig. 8 against temperature. The dimer fraction of the dye undergoes rapid reduction with increasing temperature. The trend resembles quite well the decrease in relative molar rotations. Since the dimerization constants used are of pure thionine in aqueous solution, there remains the question whether it is correct to use these values to estimate the dimer fraction of the dye in the DNA-thionine complex. We may suppose that the amount of the dimeric dyes bound to DNA in the complex is roughly proportional to the amount of the dye dimers in aqueous solution of the dye alone.

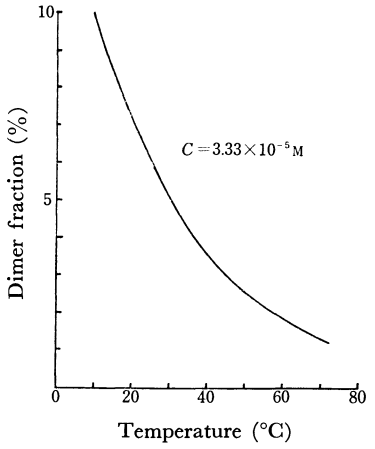

Fig. 8. Plot of dimer fraction of thionine in aqueous solution against temperature.

It appears reasonable therefore, to conclude that these newly developed Cotton effects for the low P/D complexes are ascribable to the dye dimer and that the disappearance of optical activity at about 50°C is due to the absence of dye dimer bound to DNA. Since DNA may still possess their helical structures at 50°C, there is possibly a model in which the dye dimers are bound in a repetitive fashion along the DNA helix to interact with each other. This model is supported by the general shapes of the ORD and CD curves of the low P/D complexes. We tentatively conclude, therefore, that the primary source of the optical activity newly found at 450—580 nm may be an electrostatic interaction between the dye dimers bound to DNA probably in a repetitive fashion to form a dye dimer super-helix. Vicinal disymmetry might play a sufficient role to induce optical activity, just as the case of the 520—650 nm Cotton effects.

A negative CD maximum appearing at 300—330 nm for the P/D=3.2 complex may be assigned to the absorption shoulder of thionine (Fig. 7). This has not been observed in the DNA-AO system. It was reported that DNA has a negative CD maximum in the same spectral region,[21] but we did not observe this. However, if it could be observed, it should be as small as one-tenth of the CD maximum of the complex. Therefore, the latter is undoubtedly due to an interaction between DNA and thionine. Our data are insufficient to estimate its origin, however.

It should be added that all of the foregoing discussion on the DNA-thionine complexes equally applies to the RNA-thionine complexes.

Conclusion

The results on the optical activity of the DNA- and RNA-thionine complexes are summarized as follows:

(a) The Cotton effects of the high P/D complexes are observed in the wavelength region 520—680 nm (Optical Activity I), both of them being resolved at least into four components.

(b) The Cotton effects of the low P/D complexes are observed in the wavelength region 450—580 nm (Optical Activity II). These are new types of Cotton effects which have not been observed in other DNA (or RNA)-dye systems.

(c) Optical Activity I which is predominant at the P/D values 4—5 diminishes rapidly with decreasing P/D values and Optical Activity II develops at about P/D=2.

(d) The effect of temperature on Optical Activity I differs from that on Optical Activity II. The former is observed even at 85°C, the latter completely disappears at 50°C.

(e) Unlike the DNA-AO complex, a negative CD maximum appears in the wavelength region 300—330 nm.

Interpretation of the results is summarized as follows:

(1) Optical Activity I is induced from the dye monomers bound near the asymmetric carbon atoms of nucleic acids.

(2) Optical Activity II results from an interaction between the dye dimers aggregated probably in a helical fashion along the nucleic acid helices.

(3) A negative CD maximum developing at 300—330 nm is probably due to DNA-dye interactions, but its origin is uncertain.

This work was supported in part by a grant-in-aid from the Ministry of Education.

21) Jen Tsi Yang and T. Samejima, *Biochem. Biophys. Res. Commun.*, **33**, 793 (1968).

Electronic Spectra and Electrical Resistivities of the Molecular Complexes of Benzidine and Its Derivatives

Yoshio MATSUNAGA and Gunzi SAITO

Department of Chemistry, Faculty of Science, Hokkaido University, Sapporo

(Received October 6, 1970)

The electronic structures of about sixty polycrystalline molecular complexes of benzidine and its derivatives have been examined on the basis of the vibrational and electronic spectra. The complexes show a strong tendency to be non-ionic, in spite of the low ionization potentials of the electron donors. Several non-ionic complexes exhibiting resistivities of the order of 10^3—10^5 ohm cm have been found. The optical and electrical properties of the complexes consisting of donor molecules with amino groups and of acceptor molecules with carbonyl groups are distinctly different from those of the others. The first charge-transfer absorption band of the solid complex in the former group appears at an energy considerably lower than that of the corresponding complex in chloroform. Moreover, the activation energy for semiconduction seems to be appreciably reduced by the formation of a hydrogen bond.

On the basis of the electronic and vibrational spectra, it has been established that the crystal charge-transfer complexes can be rather sharply divided into two groups, namely, those having essentially non-bonding ground states (hereafter to be called "non-ionic complexes") and those having dative ground states("ionic complexes").[1-3] In general, an ionic complex may be formed when a donor molecule with a low ionization potential is combined with an acceptor molecule with a high electron affinity. However, one of the present authors has demonstrated that the electrostatic energy of the charged lattice is as important as the energy needed to charge the constituent molecules in governing the formation of an ionic crystal complex.[4] Among the donor compounds examined in our previous paper, tetramethylbenzidine was found to show a very strong tendency to form non-ionic complexes in spite of its low ionization potential, which has been estimated to be as low as 6.8 eV.[5] In connection with this observation, it is noteworthy that most of the noticeably semiconducting quinone complexes are ionic.[6] Furthermore, non-ionic complexes display relatively low resistivities only when the charge-transfer absorptions are located in an exceptionally low-energy region. The tetramethylbenzidine-*p*-chloranil complex, which has a resistivity of 10^7 ohm cm, is known to be such an example. Therefore, one may hope to have a good chance of examining the physical properties of a large number of non-ionic complexes exhibiting charge-transfer absorptions at unusually low energies by studying the crystal complexes of benzidine and its derivatives.

Experimental

Materials. The following five compounds, the ionization potentials of which are supposed to increase in the order of numbering, were used as donors: *N,N,N',N'*-tetramethylbenzidine (I), *o*-tolidine (II), benzidine (III), *o,o'*-dibromo-*o*-tolidine (IV), and *o,o'*-dichloro-*o*-tolidine (V). The first three compounds were commercially obtained. They were purified by recrystallization and then by sublimation in a vacuum. The last two were prepared by the halogenation of compound II, as has been reported by Schlenk.[7] The fifteen acceptors used in this work were as follows: 2,3-dichloro-5,6-dicyano-*p*-benzoquinone (DDQ) (a), tetracyano-*p*-benzoquinodimethane (TCNQ) (b),[8] tetracyanoethylene (TCNE) (c), 2,3-dicyano-*p*-benzoquinone (d),[9] 2,3-dicyano-α-naphthoquinone (e),[10] 9-dicyanomethylene-2,4,7-trinitrofluorene (f), *p*-chloranil (g), 2,5-dichloro-3,6-dibromo-*p*-benzoquinone (h),[11] *p*-bromanil (i),[12] *p*-fluoranil (j), 2,5-dichloro-*p*-benzoquinone (k), 2,3-dichloro-*p*-benzoquinone (l),[13] 2,6-dichloro-*p*-benzoquinone (m), dichloro-*p*-xyloquinone (n),[14] and *s*-trinitrobenzene (TNB) (o). Their electron affinities decrease in approximately the above order. These compounds were obtained from commercial sources unless references are cited.

The molecular complexes were prepared by mixing the component compounds, previously separately dissolved in a hot solvent, usually benzene, chloroform, or dichloroethane. They were crystallized upon cooling or were precipitated immediately. Some ion-radical salts, the vibrational and electronic spectra of which were to be compared with those of the molecular complexes, were also prepared. The oxidation of the donor compounds was carried out with bromine according to the procedure of Hughes and Hush.[15] The acceptor compounds, a, b, d, and f, were reduced with the iodide ion following the methods reported by various workers.[2,16,17]

Measurements. The vibrational spectra of the crystal complexes were determined as Nujol mineral oil mulls with a Jasco IR-G infrared spectrophotometer, and the electronic spectra, with a Beckman DK-2A spectrophotometer with the

1) R. Foster and T. J. Thomson, *Trans. Faraday Soc.*, **59**, 296 (1963).
2) Y. Matsunaga, *J. Chem. Phys.*, **41**, 1609 (1964).
3) K. M. C. Davis and M. C. R. Symons, *J. Chem. Soc.*, **1965**, 2079.
4) Y. Matsunaga, This Bulletin, **42**, 2490 (1969).
5) T. Amano, H. Kuroda, and H. Akamatu, *ibid.*, **42**, 671 (1969).
6) Y. Matsunaga, *Nature*, **205**, 72 (1965).
7) W. Schlenk, *Ann.*, **363**, 277 (1908).
8) D. S. Acker and W. R. Hertler, *J. Amer. Chem. Soc.*, **84**, 3370 (1962).
9) J. Thiele and F. Gunther, *Ann.*, **349**, 45 (1906).
10) G. A. Reynolds and J. A. VanAllan, *J. Org. Chem.*, **29**, 3591 (1964).
11) A. R. Ling, *J. Chem. Soc.*, **61**, 558 (1892).
12) H. A. Torrey and W. H. Hunter, *J. Amer. Chem. Soc.*, **34**, 702 (1912).
13) J. B. Conant and L. F. Fieser, *ibid.*, **45**, 2194 (1923).
14) E. Carstanjen, *J. Prakt. Chem.*, (2), **23**, 421 (1881).
15) G. K. Hughes and N. S. Hush, *J. Proc. Roy. Soc. N. S. W.*, **81**, 48 (1947).
16) L. R. Melby, R. J. Harder, W. R. Hertler, W. Mahler, R. E. Benson, and W. E. Mochel, *J. Amer. Chem. Soc.*, **84**, 3374 (1962).
17) T. K. Mukherjee and L. A. Levasseur, *J. Org. Chem.*, **30**, 644 (1965).

aid of a reflectance attachment. The procedure in the latter measurements was similar to that described in our previous paper.[18] The charge-transfer absorption spectra were also examined in solution. The solvent used throughout was chloroform, Wako Special Reagent. As the present donor compounds dissolved in chloroform are easily oxidized with air, sample solutions were prepared immediately before measurements by dissolving appropriate amounts of the component compounds.

The resistivities up to 10^8 ohm cm were examined by a voltage-current method employing a cell similar to that designed by LaFlamme.[19] The temperature was adjusted in the range from 20 to 60°C using a heating tape wrapped around the cell and connected to a variable transformer.

Results and Discussion

Characterization of Complexes. The complexes were classified into two groups, namely, non-ionic and ionic complexes, on the basis of the vibrational spectra. This method was described in detail in a previous paper.[2] In short, when the vibrational spectrum of a complex is well approximated by a superposition of the spectra of the component compounds, the complex is considered to be non-ionic. If the spectrum consists of the spectra of the ionized components, namely, D^+ and A^- free-radical ions, the complex is characterized as ionic. The vibrational spectrum of the A^- ion is usually readily distinguishable from that of the A molecule; therefore, it is not difficult to characterize the complexes by this technique. The results of the characterization are presented in Fig. 1. In this diagram the complexes have been arranged by placing the ionization potentials of the donors on the abscissa and the electron affinities of the acceptors on the ordinate. As had been proposed earlier,[4] the energy of the charge-transfer absorption in the TNB

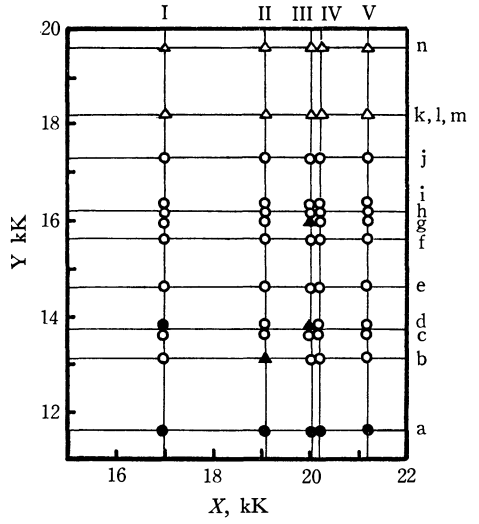

Fig. 1. Electronic structures of molecular complexes as revealed by the vibrational spectra. Non-ionic complexes are indicated by open circles and ionic ones by shaded circles. As to notations I—V, a—o and X and Y, see text.

complex, X, as determined in a chloroform solution, was taken as a measure of the former quantity, and that in the pyrene complex, Y, as a measure of the latter (see Eq. (1) in next section). The complexes which were found to be non-ionic are indicated by open circles, and those found to be ionic, by shaded circles. The following three, shown by shaded triangles, are of a complicated nature or are unstable: IIb, IIIc, and IIIg; therefore, they could not be well characterized. The complex IIb has a composition different from that calculated for 1 : 1, and it gives a vibrational spectrum which is too complicated to be considered as simply either non-ionic or ionic. A similar phenomenon has been disclosed by Ohmasa *et al.* in a closely related complex, benzidine-TCNQ, IIIb, when solvent molecules are occluded.[20] It has been known for a long time that benzidine forms a very unstable complex with *p*-chloranil.[21] Furthermore, this complex, IIIg, has been reported to be non-stoichiometric.[22]

For the combinations expressed by open triangles, no solid complex could be isolated. As may be seen in Fig. 1, most of the complexes examined in this work are non-ionic. The only exceptions are the DDQ complexes of I—V and the complex Id. These observations are in good accordance with our earlier view that the remarkably strong tendency to be non-ionic found in the tetramethylbenzidine complexes arises from the size and shape of this donor molecule, factors which are unfavorable to strong electrostatic interaction with acceptors.

Electronic Spectra. The energy of the charge-transfer absorption, $h\nu_{CT}$, in a non-ionic, 1 : 1 single complex may be written, as a good approximation:[23]

$$h\nu_{CT} = I_D - A_A - C' , \qquad (1)$$

where I_D is the ionization potential of the donor molecule and where A_A is the electron affinity of the acceptor molecule. The term C', the magnitude of which is known to be relatively insensitive to the kinds of donor and acceptor, arises largely from the electrostatic energy in the dative-bond structure. The complexes on the $Y=-X+$ constant line in Fig. 1 should all exhibit charge-transfer absorptions at nearly the same energy. The values of $h\nu_{CT}$, as estimated by the use of Fig. 1, are equal to:

$$\begin{aligned} &h\nu_{CT}(\mathrm{D\cdot TNB}) + h\nu_{CT}(\mathrm{pyrene\cdot A}) - h\nu_{CT}(\mathrm{pyrene\cdot TNB}) \\ &\quad = I_D - A_A - C'(\mathrm{D\cdot TNB}) - C'(\mathrm{pyrene\cdot A}) \\ &\quad + C'(\mathrm{pyrene\cdot TNB}) . \end{aligned} \qquad (2)$$

In Fig. 2, the $h\nu_{CT}$ values observed in chloroform solutions are plotted against the $h\nu_{CT}$ values estimated by the use of Eq. (2). The agreement is generally excellent; this confirms the assumption that the observed low-energy absorption is due to the charge-transfer from the donor molecule to the acceptor molecule. Double charge-transfer absorptions were recorded in

18) K. Abe, Y. Matsunaga, and G. Saito, This Bulletin, **41**, 2852 (1968).
19) P. M. LaFlamme, *Rev. Sci. Instrum.*, **35**, 1193 (1964).
20) M. Ohmasa, M. Kinoshita, and H. Akamatu, This Bulletin, **42**, 2402 (1969).
21) H. Fecht, *Ber.*, **41**, 2983 (1909).
22) H. Kusakawa and S. Nishizaki, This Bulletin, **38**, 2201 (1965).
23) H. M. McConnell, J. S. Ham, and J. R. Platt, *J. Chem. Phys.*, **21**, 66 (1953).

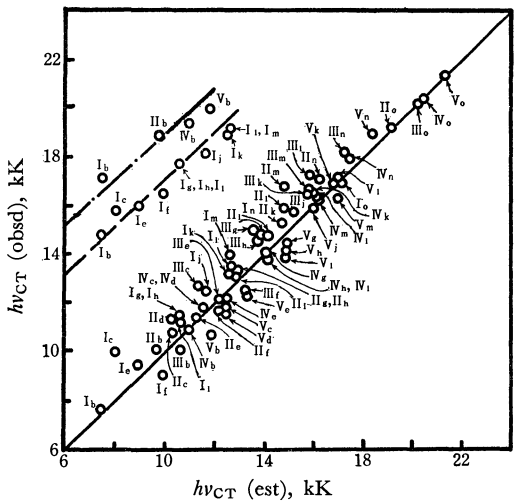

Fig. 2. Comparison between the observed energies of charge-transfer bands measured in solutions and the energies estimated by Fig. 1.

some combinations. The plot of the energy of the second absorption against the above-mentioned estimated $h\nu_{CT}$ values indicates that the second absorptions may be classified into two different classes. As one of them is characteristic of the complexes of tetramethylbenzidine, the absorption is apparently to be assigned to the charge-transfer from the second highest occupied orbital of the donor to the lowest vacant orbital of the acceptor. The absorption bands characteristic of the complexes of TCNQ form the other class. In this instance, the appearance of the second absorption is due to the charge-transfer from the highest occupied orbital of the donor to the second lowest vacant orbital of TCNQ. The average difference of 9.3 kK between the first and second bands in the TCNQ complexes is in agreement with the difference between the first and second transition energies in the TCNQ molecule as calculated by means of the molecular orbital method.[24] The existence of two classes in the second absorptions leads to the appearance of triple charge-transfer bands in the TCNQ complex of tetramethylbenzidine, as is shown in Fig. 3. The first band in the crystal complex is shifted to the low-energy side, and the second and third bands, to the high-energy side, compared to the corresponding bands observed in chloroform. An examination of Fig. 2 indicates that the third band is associated with the second lowest vacant orbital of TCNQ.

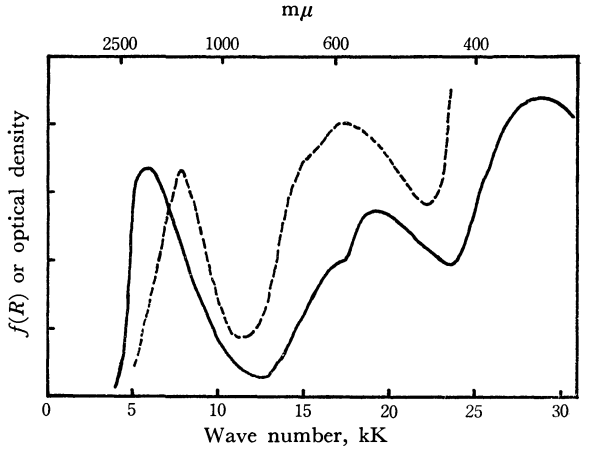

Fig. 3. Electronic spectra of tetramethylbenzidine-TCNQ in the solid state (——) and in a chloroform solution (----).

In Table 1 the energies of the charge-transfer absorptions of the solid complexes are summarized, along with the amounts of the shifts compared to the energies observed for the complexes in chloroform. As was noted in Fig. 1, the complexes with the acceptors, k, l, m, and n, could not be crystallized from the solution. For some of them, the charge-transfer absorptions in the solid phase could be measured with samples made by grinding together mixtures of the solid components. The energies obtained in this way are also presented in Table 1. Amano *et al.* have examined the polarized absorption spectra using single crystals of several complexes of benzidine and its tetramethyl derivative.[5,25] Their compounds include the following seven: Ib, Ig, Io, IIIb, IIIg, IIIk, and IIIo. The results given by Amano, which are cited for the sake of comparison in the footnote in Table 1, are in essential agreement with ours.

The first charge-transfer bands in all the solid complexes but Ij are shifted to the low-energy side if compared with those of the complexes in chloroform. A closer consideration of the amounts of the shifts shows that these non-ionic complexes must be further classified into two subgroups. With the donor I, the shifts are no more than 3.0 kK. Secondly, when the acceptor is not a quinone, the largest shift observed is 2.9 kK in the complexes Ic and IIb. Thus, the red-shifts found in this subgroup are usually small, and they may be explained in terms of a change in the surrounding molecules acting as a dielectric medium or by a change in the relative arrangement of the donor and acceptor molecules.[26,27] The second subgroup comprises complexes of quinones combined with the donors II—V, which bear unsubstituted amino groups. The red-shifts are quite substantial, ranging from 2.7 kK in the complex Vd to 6.0 kK in the complex Vn. In this respect, the complexes with *p*-fluoranil are quite exceptional; even a blue-shift was found in the complex Ij. The presence of amino groups in the donor molecules and carbonyl groups in the acceptor molecules induces the formation of hydrogen bonds in the crystal complexes. As it is a common feature that the donor and acceptor molecules are alternatively stacked, face-to-face, on each other along one of the crystal axes, the donor molecules linked to the acceptor molecules by hydrogen bonds should belong to different stacks. Thus, the effects of the hydrogen-bond formation, if any, must be observable only in the crystal complexes. A large red-shift of the charge-transfer absorption in quinhydrone as a result of the crystal-

24) D. A. Lowitz, *ibid.*, **46**, 4698 (1967).

25) T. Amano, H. Kuroda, and H. Akamatu, Preprint of the Symposium on Molecular Structures, 3B2 (1967).

26) H. Kuroda, K. Yoshihara, and H. Akamatu, This Bulletin, **35**, 1604 (1962).

27) T. Matsuo and H. Aiga, *ibid.*, **41**, 271 (1968).

TABLE 1. THE ENERGIES OF CHARGE-TRANSFER ABSORPTIONS IN THE SOLID COMPLEXES OF BENZIDINE AND ITS DERIVATIVES AND THE AMOUNTS OF SHIFTS COMPARED TO THOSE OF THE COMPLEXES IN CHLOROFORM (IN kK)

A	D									
	I		II		III		IV		V	
b	5.9[a]	(−1.8)	7.2	(−2.9)	8.0[b]	(−2.1)	8.9	(−2.0)	9.1	(−1.6)
	16.9	(+2.1)	17.4		20.0		19.6	(+0.2)	20.0	(0.0)
	19.0	(+1.8)								
c	7.0	(−2.9)	9.8	(−1.1)	11.0	(−1.8)	9.9	(−1.9)	10.0	(−1.9)
	16.0	(+0.6)			24.6		20.5		21.0	
d							9.0	(−2.8)	9.1	(−2.7)
							18.2		18.5	
e	7.7	(−1.8)	8.0	(−3.4)	9.1	(−3.0)	6.7	(−5.5)	8.4	(−3.9)
	16.3	(+0.3)			20.2		18.7		19.0	
f	8.7	(−0.4)	10.3	(−1.5)	11.5	(−1.0)	12.0		12.5	
	17.3	(+0.8)			17.0					
g	9.5[c]	(−1.9)	9.2	(−4.0)	[d]		9.1	(−5.0)	9.5	(−5.0)
	17.9	(−0.1)	19.7				20.5		20.8	
h	8.4	(−3.0)	9.4	(−3.8)	9.8	(−4.8)	9.3	(−4.6)	9.6	(−4.7)
	17.7	(−0.1)	19.7		20.4		20.3		20.7	
i	8.4	(−2.9)	9.1	(−4.0)			9.2	(−4.7)	9.9	(−4.3)
	17.5	(−0.3)	19.7				20.5		20.5	
j	13.2	(+0.7)	13.9	(−0.9)	9.5[e]		14.5	(−1.2)	14.7	(−1.2)
	20.5	(+2.3)	23.2		20.4		24.1		26.0	
k			12.3	(−3.1)	12.0[e]	(−4.5)				
			25		25.3					
l	12.0	(−1.3)	12.1	(−3.8)						
	20.2		23							
m	13.3	(−0.2)					11.7	(−4.7)	11.8	(−4.5)
	22.5						22.9			
n	13.3	(−1.5)					13.7	(−4.3)	13.1	(−6.0)
o	16.2[f]	(−0.8)	17.6	(−1.6)	19.0[g]	(−1.2)	18.2	(−2.2)	19	(−2.3)
	24.0									

a) 7.5 and 16.5, b) 8 and 18, c) 8—9 and 18.3, d) 10 and 22.2, e) 12.5, f) 16.7 and 23.9, g) 18.3 and 26 were reported by Amano, Kuroda, and Akamatu, see Refs. 5 and 25.

lization has also been ascribed to the intermolecular hydrogen bond.[28]

The location of the second charge-transfer bands in the complexes of tetramethylbenzidine is only slightly affected by a change in the state. The nature of these absorptions has been speculated upon by Amano *et al.* on the basis of their measurements of the polarized absorption spectra.[5]

A striking resemblance between the spectra of the ionic DDQ complexes and the solid cation-radical salts derived from the donors should be mentioned. For example, the spectrum of the complex IVa is compared with that of solid *o,o'*-dichloro-*o*-tolidine bromide in Fig. 4. The latter is very similar to those of the solid bromides of benzidine, *o*-tolidine, and tetramethylbenzidine described in our earlier papers.[29,30]

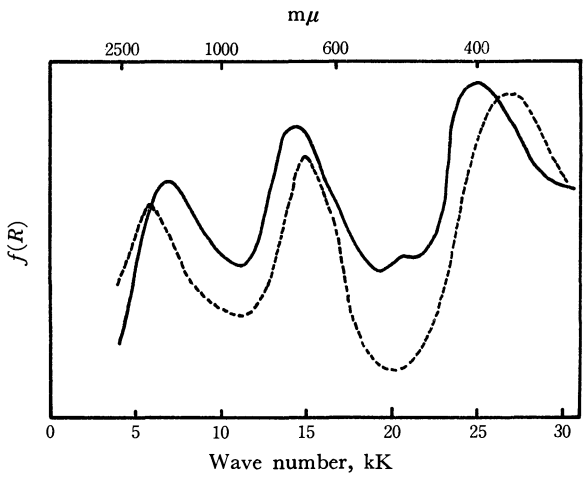

Fig. 4. Diffuse reflection spectra of dichloro-*o*-tolidine-DDQ (——) and dichloro-*o*-tolidine bromide (----).

The electronic spectra of ion-radical salts have been known to depend considerably upon the mode of intermolecular interaction. The spectrum shown in Fig.

28) T. Amano, H. Kuroda, and H. Akamatu, Preprint of the 21th Annual Meeting of the Chemical Society of Japan, 19222 (1968).
29) Y. Iida and Y. Matsunaga, This Bulletin, **41**, 2615 (1968).
30) A. Hakusui, Y. Matsunaga, and K. Umehara, *ibid.*, **43**, 709 (1970).

Table 2. Electrical resistivities (in ohm cm) at room temperature and activation energies for semiconduction (in eV) of the solid complexes of benzidine and its derivatives

A	D									
	I		II		III		IV		V	
a	6×10^{3}		1×10^{3} [a]		6×10^{3}		2×10^{3}		7×10^{3}	
b	2×10^{6}	0.36	2×10^{4}		5×10^{6}	0.38	3×10^{6}	0.27	2×10^{7}	0.42
c	2×10^{8}		8×10^{8}	0.51	2×10^{8}	0.53	6×10^{8}	0.43	5×10^{7}	0.38
			(10^{16}) [b]		(10^{14}	0.71) [b]				
d			2×10^{3}				5×10^{4}	0.27	8×10^{4}	0.30
e			2×10^{5}	0.13	7×10^{5}	0.31	4×10^{7}	0.31	1×10^{7}	0.36
g	9×10^{7}	0.49	4×10^{6}	0.20			1×10^{8}	0.21	6×10^{7}	0.27
	(10^{7}) [c]		(4×10^{9}	0.53) [b]						
h	3×10^{7}	0.56	5×10^{7}	0.39			4×10^{7}	0.40	7×10^{7}	0.38
i	1×10^{6}	0.50	3×10^{8}				2×10^{7}	0.30	2×10^{7}	0.31
	(10^{8}) [d]									
j	(10^{12}) [c]									
o	(1×10^{17}	0.81) [e]								

a) The initial value in the measurement because of the slow but steady increase on standing.
b) By Kusakawa and Nishizaki, Ref. 22.
c) By Schwarz, Davies and Dobriansky, Ref. 32.
d) By Matsunaga, Ref. 6.
e) By Kuroda, Yoshihara and Akamatu, Ref. 26.
f) By van der Hoek, Lupinski and Oosterhoff, Ref. 31.

4, which bears no resemblance to either the monomer or dimer spectrum and which is extended into a lower-energy region, is assigned to the cation-radicals in a strong more-than-by-pairs interaction. Consequently, we may conclude that the ionized donor molecules in these DDQ complexes strongly interact with each other. Such an interaction is possible, even if the donor and acceptor molecules are alternately stacked, because of the rather large difference in the size and shape of the component molecules.

Electrical Properties. The electrical resistivities, ρ, at room temperature and the activation energies for semiconduction, E_a, as defined by

$$\rho = \rho_0 \exp(E_a/kT) \tag{3}$$

are presented in Table 2, along with the values appearing in the literature.[6,22,26,31,32] The ionic DDQ complexes exhibiting resistivities of the order of 10^3 ohm cm are the most conductive ones in the present series of complexes. Nevertheless, it must be noted that the non-ionic complexes can be as conductive as the ionic ones if the component molecules are properly chosen. Their resistivities are continuously distributed from 10^3 ohm cm on upward; one in the order of 10^3, IId, three in the order of 10^4, IIb, IVd, and Vd, and two in the order of 10^5, IIe and IIIe. Thus, the resistivity of a complex seems to be very much determined by the acceptor. The complexes of the acceptors d and e tend to exhibit low resistivities. On the other hand, the TCNE complexes have resistivities of the order of 10^7 or 10^8 ohm cm, and the complexes of the acceptors f and j—o have resistivities higher than our upper limit, 10^8 ohm cm.

The electronic spectra and electrical resistivities in the series of the TCNE complexes and also the TNB complexes have been examined by Kuroda *et al.*[26,33] They have pointed out that $2E_a$, the energy gap if the conduction is intrinsic, is approximately equal to the energy of the charge-transfer absorption in the crystal complex. The empirical relation between these two quantities may be expressed, in general, by this equation:

$$2E_a = h\nu_{CT}(\text{solid}) - \Delta\,, \tag{4}$$

where Δ is nearly constant in a series of molecular complexes with a given acceptor if the donor molecules are of the same type. The magnitude of Δ varies within a rather narrow range, *e.g.*, 0.2 eV for the TNB complexes of aromatic amines. In Fig. 5, we plotted twice the activation energy for semiconduction against the energy of the first charge-transfer absorption given in Table 1. The complexes in the first subgroup are indicated by open circles, and those in the second, by shaded circles.

Another result which seems to be the consequence of the hydrogen bonding is clearly demonstrated here; that is, considerable deviations from Eq. (4) are observed with the complexes in the latter subgroup. The direction of the deviation is in accordance with the conclusion by Gravatt and Gross that an extended intermolecular overlap resulting from the hydrogen bonding produces a decrease in the activation energy for semiconduction.[34] However, their resistivities are close to those of the corresponding complexes of

31) J. A. van der Hoek, J. H. Lupinski, and L. J. Oosterhoff, *Mol. Phys.*, **3**, 299 (1960).
32) M. Schwarz, H. W. Davies, and B. J. Dobriansky, *J. Chem. Phys.*, **40**, 3257 (1964).
33) H. Kuroda, M. Kobayashi, M. Kinoshita, and S. Takemoto, *ibid.*, **36**, 457 (1962).
34) C. C. Gravatt and P. M. Gross, *ibid.*, **46**, 413 (1967).

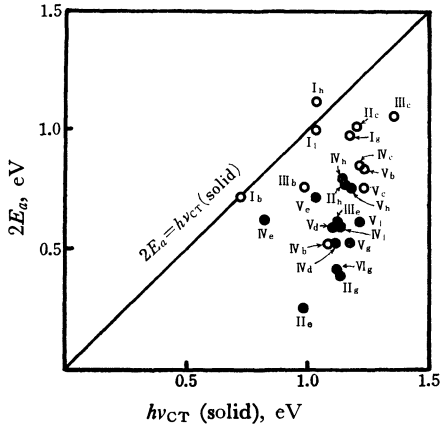

Fig. 5. Plot of twice the activation energy for semiconduction against the energy of the first charge-transfer band in solid complex. As to the meaning of open and shaded circles, see text.

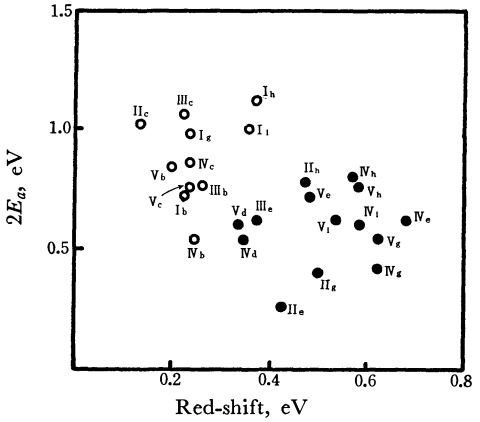

Fig. 6. Classification of molecular complexes on the basis of twice the activation energy for semiconduction and the amount of red-shift in the first charge-transfer band caused by crystallization.

tetramethylbenzidine. The decrease in the activation energy is apparently compensated for by an increase in the preexponential factor in Eq. (4), ρ_0. As the hydrogen bonding causes; (i) a large red-shift in the first charge-transfer band by crystallization and (ii) a substantial decrease in the activation energy for semiconduction, the molecular complexes can be quite distinctly divided into the two subgroups in a diagram such as that shown in Fig. 6. However, the mechanisms involved in these electronic processes are yet unknown.

BULLETIN OF THE CHEMICAL SOCIETY OF JAPAN, VOL. 44, 963—967 (1971)

The Preparation and Nonstoichiometry of Samarium Hexaboride

Koichi NIIHARA
The Research Institute for Iron, Steel and Other Metals, Tohoku University, Sendai

(Received October 7, 1970)

Samarium hexaboride was prepared by the borothermal reaction; $2\,Sm_2O_3+(6+4x)B=4\,SmB_x+3\,B_2O_2$. The residual oxygen content amounted to less than 0.03 w/o under optimum reaction conditions heating at 1650°C for 2 hr under a high vacuum. It was found by X-ray intensity and density measurements that the samarium hexaboride stayed stable over a large nonstoichiometric region from $Sm_{0.68}B_6$ to SmB_6. These extensive nonstoichiometric properties of samarium hexaboride can be explained in terms of the required electron numbers of the SmB_6 network in hexaboride.

In recent years the rare earth elements and their high-temperature compounds have been intensively investigated since their applications range over an extensive area of new technology, including radio engineering, electronics, metallurgy, machine construction, and electrical engineering. In particular, the hexaborides of the rare earth elements have become a subject of increasing importance and interest because of their high melting points, low electric resistivities, low values of the electron work function, high emission-current densities, and thermal stabilities.

All the rare earth metals, as well as scandium, strontium, barium, and plutonium, form isostructural hexaborides. The crystal structure of hexaborides was first determined by Stackelberg and Neuman.[1] According to them, the crystal structure is cubic and of the cesium chloride type, in which the metal atom is held in the center of a cage of boron atoms (just as the cesium atom is held in the CsCl crystal); six boron atoms in the octahedral form are located at the corners of the cell, in the same position as the chloride ion in cesium chloride.

The theoretical treatments by Longuet-Higgins and Roberts,[2] Eberhardt[3] and Yamazaki[4] have led to the conclusion that each boron octahedron requires 20 electrons, of which 18 come from the boron atoms and 2 from the metal atom. Out of the total of 20 electrons, 14 supposedly form bonds within the octahedron, and 6 enter into the external two-electron covalent bonds connected with neighboring octahedra. Therefore, it is possible that the rare earth hexaborides have a

1) Stackelberg, M. Von, and F. Neumann, *Z. Phys. Chem.*, **B19**, 314 (1932).

2) H. C. Longuet-Higgins and M. Dev. Roberts, *Proc. Roy. Soc. (London)*, **A223**, 336 (1954).

3) W. H. Eberhardt, B. L. Crawford, and W. N. Lipscob, *J. Chem. Phys.*, **22**, 989 (1954).

4) M. Yamazaki, *J. Phys. Soc. Japan*, **12**, 1 (1957).

relatively wide range of homogeneity, for the rare earth metals have three valence electrons.

The present study has been carried out so as to investigate the nonstoichiometric properties of pure samarium hexaboride. The results show that the study of nonstoichiometric propeties of the hexaboride will also provide useful information on the electronic configuration.

Experimental

Materials. Samarium sesquioxide, Sm_2O_3,[5] was separated from a crude rare earth mixture at this laboratory by replacement chlomatography, using the EDTA solution as the solvent. The Sm_2O_3 obtained by this method was over 99.9% pure, and other rare earth elements were found to be negligible in quantity by mass spectrography and radioactivation analysis.

The crystal boron, 99.9% pure and containing 0.11% oxygen. was obtained from Wako Pure Chemical Industries, Ltd, Tokyo.

Preparation of Samples. The hexaboride was prepared by the borothermal reduction[6-10] of samarium oxide, Sm_2O_3, according to the following equation:

$$2Sm_2O_3 + (6 + 4x)B = 4SmB_x + 3B_2O_2 \quad (1)$$

The lower volatile suboxide of the boron, B_2O_2, was removed upon reduction under a vacuum.

The samarium sesquioxide and boron were mixed in the desired mole proportions and ground carefully in a sardonyx mortar for complete homogenization. Samples weighing 4—5 g were heated at 1650°C in a tantalum crucible placed in an electric-resistance heater in a vacuum of 10^{-4}—10^{-6} mmHg at several temperatures for different times. The temperature was read with a W-WRe thermocupple and an optical pyrometer, corrected for window and prism absorptions.

X-Ray Diffraction. X-ray photographs of the products were taken using CuK_α and FeK_α radiations and a Debye-Scherrer X-ray powder camera (114.8 mm diameter). The precise lattice constants for the cubic hexaboride samples were calculated by extrapolating a plot of lattice constants *vs.* $\cos^2\theta$ to $\theta=90°$. The X-ray intensity ratio between the particular diffraction planes for the hexaboride was measured using an X-ray diffractometer equipped with a monochrometer.

Chemical Analysis. The boride samples were dissolved in Na_2CO_3 aq., and then their pH values were adjusted to 5.2 with $(CH_2)_6N_4$. After adding the XO indicator, analyses of the samarium were performed by titration with a 1/100 mol EDTA standard aquasolution. Boron analyses were performed by titration with a 1/10 N NaOH aquasolution after dissolving the samples in Na_2CO_3, adjusting their pH to 6.9, and adding Mannitol. Oxygen analyses were performed by the inert-gas-fusion coulonic titration method.

Density Measurements. The powdered specimens of 325—400 mesh were prepared by grinding them carefully in the sardonyx mortar. The density was determined at 20.5°C by a flotation technique using CCl_4.

Resistivity Measurements. For the resistivity measurements, a current of about 0.04 to 0.5 A was passed through the specimens and a standard resistance connected in series. A simple two-point apparatus and a standard potentiometric method were used. The resistivity measurements were carried out from the temperature of liquid nitrogen to 1000°K. The specimens used were $3\times5\times16$ mm blocks which were cut from annealed pellets using a diamond cutter.

Results and Discussion

Determination of Reaction Conditions. The samarium sesquioxide-boron compacts mixed at a 1 : 15 mol ratio were heated in a vacuum at 900—1900°C for 30 min. A loss weight results from the vaporization of the lower volatile oxide of boron, B_2O_2. The loss weight percentage after the heating reaction is plotted against the reaction temperature in Fig. 1. The dotted line indicates the theoretical loss weight percentage when the reaction is performed according to Equation (1).

Figure 1 shows that the borothermal reaction begins at about 1350°C and exceeds the theoretical weight loss at 1600°C. Figure 2 shows the oxygen content *vs.* the reaction time when the samarium sesquioxide-boron compact was reacted in a vacuum at 1650°C for different times. From Fig. 2 it is clear that the products contain only 300 ppm oxygen when reacted at 1650°C for 2 hr in a high vacuum.

From the results shown in Fig. 1 and Fig. 2, it can

TABLE 1. THE ANALYSES OF THE PRODUCTS

Nominal composition B/Sm_2O_3	B/Sm			Phases
	Theo.[a]	Theo.[b]	Analyses	
9	3.0	3.5	5.54	SmB_6+SmB_4
9.5	3.3	3.8	5.65	SmB_6+SmB_4
10	3.5	4.0	5.71	SmB_6+SmB_4
11	4.0	4.5	5.88	SmB_6+SmB_4
12	4.5	5.0	5.93	SmB_6+SmB_4
13	5.0	5.5	5.96	SmB_6
14	5.5	6.0	6.02	SmB_6
15	6.0	6.5	6.13	SmB_6
16	6.5	7.0	6.51	SmB_6
17	7.0	7.5	7.01	SmB_6
18	7.5	8.0	7.49	SmB_6
18.5	7.75	8.25	7.82	SmB_6
19	8.0	8.5	8.13	SmB_6
20	8.5	9.0	8.52	SmB_6
21	9.0	9.5	8.86	SmB_6
22	9.5	10.0	9.27	SmB_6+B (trace)
23	10.0	10.5	9.62	BmB_6+B
24	10.5	11.0	10.41	SmB_6+B
25	11.0	11.5	11.02	SmB_6+B
26	11.5	12.0	12.28	SmB_6+B

a) Calculated values on the assumption of formation of B_2O_2 during reaction.
b) Calculated values on the assumption of formation of B_2O_3 during reaction.

5) S. Yajima, K. Sasaki, and M. Noro, *Kogyo Kagaku Zasshi*, **72**, 1213 (1969).
6) E. Felten, J. Binder, and B. Post, *J. Amer. Chem. Soc.*, **80**, 3479 (1958).
7) G. L. Galloway and H. A. Eick., *J. Inorg. Nucl. Chem.*, **27**, 293 (1965).
8) H. A. Eick and P. W. Gilles, *J. Amer. Chem. Soc.*, **81**, 5030 (1959).
9) B. Post, S. Moskowitz, and F. W. Glaser, *ibid.*, **78**, 1800 (1956).
10) G. Blznakov and P. Peskev., *J. Less-com. Met.*, **7**, 441 (1964).

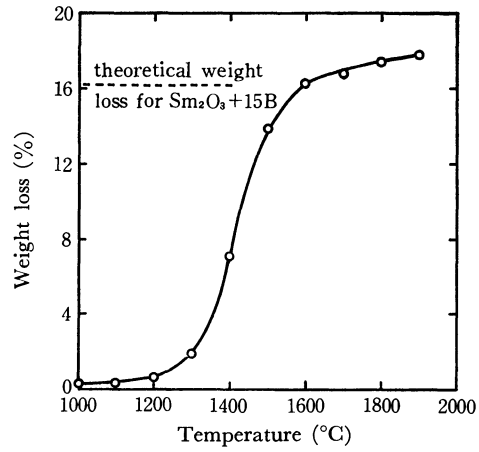

Fig. 1. The effect of temperature on the weight loss of Sm_2O_3+15B mixtures after 30 min.

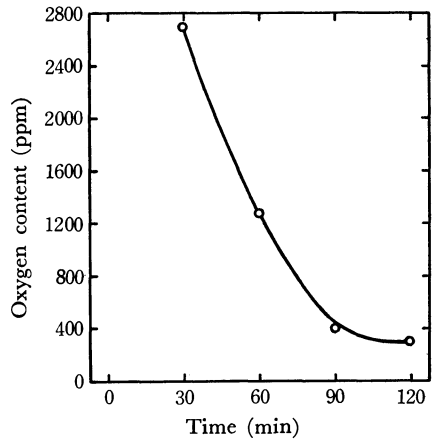

Fig. 2. The effect of time on the oxygen content after heating Sm_2O_3+15B mixtures at 1650°C in 10^{-4}—10^{-6} mmHg.

be seen that the borothermal reaction is almost completed by heating at 1650°C for 2 hr in a vacuum.

Preparation of Samarium Hexaboride. The samarium sesquioxide-boron compacts mixed at various ratios were heated under a vacuum of 10^{-4}—10^{-6} mmHg at 1650°C for 2 hr. The results of chemical and X-ray analyses are summarized in Table 1. In the regions of 13—21 and 9—12 in the nominal composition ratio, B/Sm_2O_3, only samarium hexaboride, SmB_6, and both samarium tetraboride, SmB_4, and samarium hexaboride, SmB_6, were observed, respectively. In the region of 22—26 in the nominal composition, SmB_6 and a trace of boron were observed. In this region, samarium dodecaboride, SmB_{12}, was not detected at all. If the borothermal reaction takes place according to Eq. (1), the boron-samarium atomic ratio, B/Sm, must agree with the theoretical values shown in the second column in Table 1. Felten *et al.*[6] have reported that boric anhydride, B_2O_3, vaporizes during the reaction. If the boric anhydride, B_2O_3, vaporizes during the reaction, the B/Sm ratio in the region of 14—26 in the nominal composition is in good agreement with the theoretical values shown in the third column. However, the observed values coincide well with the theoretical values in the second column. From this fact, it may be concluded that, during the reaction, not boric anhydride, B_2O_3, but a volatile suboxide of the B_2O_2 boron is formed in the region of 15—26 in the nominal composition. In the region of 9—14, the analytical values of B/Sm are considerably different from the theoretical values. It is reasonable to think the borothermal reaction takes place in this region following these equations.

$$Sm_2O_3 + (15 - 2x)B = (2 - x)SmB_6 + xSmB_4 + (3/2)B_2O_2(g) \quad (2)$$

$$SmB_4 = SmB_6 + Sm(g) \quad (3)$$

Samsonov[11,12] has reported that an approximate thermodynamic calculation of either the suboxide of the B_2O_2 boron or boric anhydride, B_2O_3, but that SmB_4 is decomposed into SmB_6 and Sm(g) according to Eq. (3).

Nonstoichiometric Properties. As can be seen from Table 1, the samarium hexaboride is stable in the nonstoichiometric composition of 5.96—9.27 at the boron-samarium atomic ratio. The variation in the lattice parameter of the cubic hexaboride *vs.* B/Sm is shown in Fig. 3. The lattice parameter decreases with an increase in the B/Sm ratio in the region of the monophase hexaboride.

If the nonstoichiometric properties of samarium hexaboride are related to the position of samarium metal, the X-ray diffraction intensity will vary considerably because the magnitude of the atomic scattering factor of samarium is much larger than that of boron. The diffraction of the 100 and 110 planes is sensible for the position of samarium metal. The variation in the X-ray intensity ratio of the 100 diffraction plane *vs.* the 110 plane is plotted against the B/Sm ratio in Fig. 4. The dotted line shows the value of the calculated X-ray intensity ratio. These calculated values are obtained according to Eq. (4), supposing that is the formation of $Sm_{1-x}B_6$, the excess boron does not enter into interstitial sites in unit cells, but vacancies form at random in the sites of the samarium metal:

$$I \propto |F|^2 p \frac{1 + \cos^2 2\theta}{\sin^2 \theta \cos \theta}$$

$$\frac{I_{100}}{I_{110}} \propto \frac{|F_2|^2 p_2 \dfrac{1 + \cos^2 2\theta_2}{\sin^2 \theta_2 \cos \theta_2}}{|F_1|^2 p_1 \dfrac{1 + \cos^2 2\theta_1}{\sin^2 \theta_1 \cos \theta_1}} \quad (4)$$

where p is the permutation factor.

The variation in the density against B/Sm=1+y in SmB_{1+y} or 1−x in $Sm_{1-x}B_6$ is plotted in Fig. 5. The solid line (a) shows the experimental values, both the closed circles (b) and the open circles (c) being the theoretical values. The values of the closed circles and open circles are calculated on the assumption that the nonstoichiometric composition can be indicated by the $Sm_{1-x}B_6$ formula or the SmB_{6+y} formula respectively. The experimental results are in good

11) G. V. Samsonov, *Uspekki Khim.*, **28**, 189 (1959).

12) G. V. Samsonov, Boride of the rare earth metals. "High temperature compounds of the rare earth metals with nonmetals," Edited by G. V. Samsonov, Consultants Bureau, New York (1965), p. 56.

agreement with the values of the closed circles. From the variations in the lattice parameter, the X-ray intensity ratio, and the density, it seems probable that the samarium hexaboride phase is stable from SmB_6 to $Sm_{0.68}B_6$. Johnson and Daane[13] have found that the lantanum hexaboride phase is stable from LaB_6 to $LaB_{7.8}$. It is probably more exact to refer to the latter as $La_{0.76}B_6$.

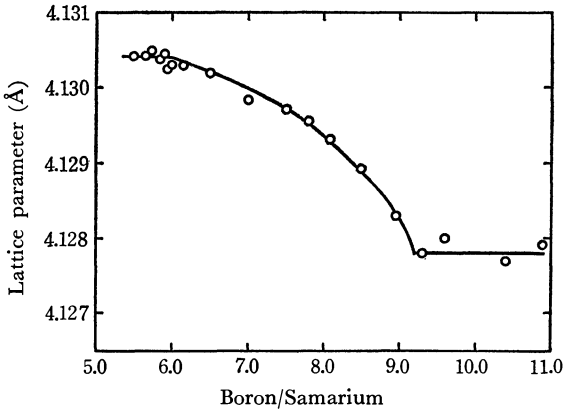

Fig. 3. The variation in the lattice parameter of samarium hexaboride.

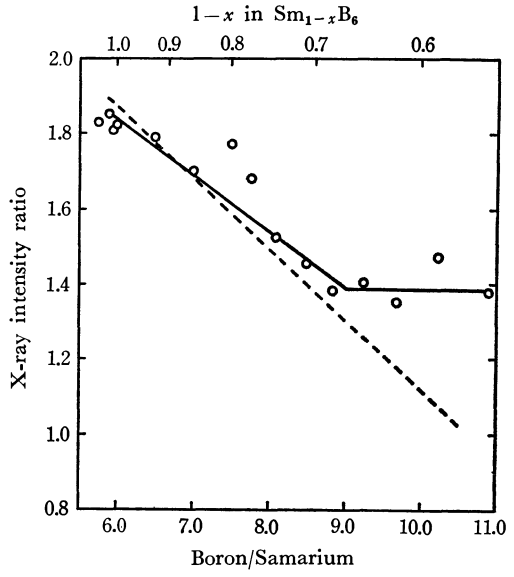

Fig. 4. The variation in the X-ray intensity ratio, $I(100)/I(110)$, against nonstoichiometric composition of samarium hexaboride.
-○-: experimental values, ----: calculated values.

Relationship between a Wide Homogeneity Range and Bonding. The wide range of homogeneity in samarium hexaboride can be explained in terms of the required electron numbers of the boron network and the availability of such electrons in the valence band of the metal atom. Calculations by Longuet-Higgins and Roberts[2] and Lipscomb and Britton[3] indicate that two electrons must be transferred to each boron octahedron in the hexaboride structure to ensure its

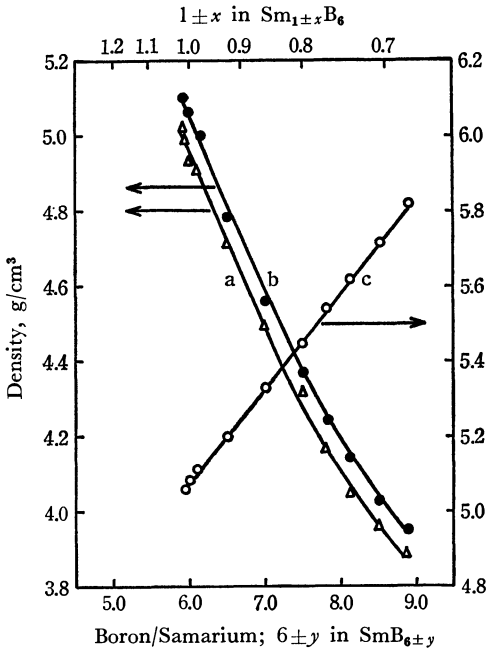

Fig. 5. The variation of density against nonstoichiometric composition of samarium hexaboride.
a(-Δ-): experimental values, b(-●-) and c(-○-) are X-Ray density calculated on the assumption that $Sm_{1-x}B_6$ or SmB_{6+y} respectively.

stability. In stoichiometric SmB_6 there is, therefore, one excess valence electron for each samarium atom because the rare earth metals generally have three valence electrons. This excess metal valence electron is responsible for the metallic properties. The lower limit of $Sm_{0.67}B_6$ is theoretically possible, with each samarium atom contributing all three valence electrons to the boron net; at that composition, the phase is presumably an electrical insulator.

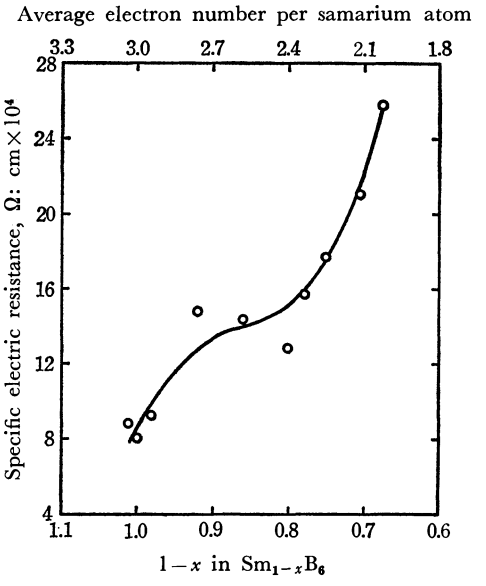

Fig. 6. The plot of specific electric resistivity *vs.* $1-x$ in $Sm_{1-x}B_6$ or average electron number per samarium metal atom.

Generally the temperature dependence of the electric resistance of a number of hexaborides of the rare

13) R. W. Johnson and A. H. Danne, *J. Phys. Chem.*, **65**, 909 (1961).

earth metals[12,14,15] showed a positive value of the temperature coefficient of the resistance, just as we should have expected for a substance with metallic conductivity. An exception is the hexaboride of samarium, which possesses a negative value of the thermal coefficient of the resistance. This fact can be explained by the change in the ratio of divalent and trivalent samarium with the temperature.[16-18] In the present work, $Sm_{1-x}B_6$ possessed a negative value of the temperature coefficient of resistance, very small in absolute magnitude at temperatures above 500°C. The variation in the electrical resistivity at 25°C against the electron number to be transfered to each boron octahedron is shown in Fig. 6. The electrical resistivity varies from 8×10^{-4} to 26×10^{-4} $\Omega\cdot$cm with an increase in the number of samarium-metal atom vacancies. At the lower limit of the homogeneity range, $Sm_{0.68}B_6$ (electron number, 2.04), the electrical conductivity is relatively large, probably due to: (a) impurities, (b) the effect of the d band of samarium metal, and (c) more few electrons being required to form the B_6 net.

Referring to (c) among these three factors, $Ba_{0.57}Na_{0.43}B_6$ and $Th_{0.23}Na_{0.77}B_6$ are stable in the $(NaMe)B_6$ system[19,20] and correspond to 1.60 electrons per metal atom. If the formation of the bond of boron in the SmB_6 phase requires 1.60 electrons, a somewhat smaller electron number per metal atom than two, the remaining electrons ($2.04-1.60=0.44$) per samarium atom in $Sm_{0.68}B_6$ can enter into the conduction band and its electrons can be responsible for the comparatively high electroconductivity at the lower limit of the nonstoichiometric composition.

From this standpoint, the limit of the homogeneity range existing between SmB_6 and $Sm_{0.53}B_6$ can be explained theoretically. The lower limit observed in this study was $Sm_{0.68}B_6$. It seems that the lower limit may be determined by the onset of mechanical instability in the boron lattice due to the large number of metal-atom vacancies. This point is still open to question, though, and further work is called for.

The author would like to thank Professor Seishi Yajima for his guidance and encouragement, and Mr. Masahiko Sase for his chemical analyses.

14) G. V. Samsonov and A. E. Grodshtein, *Zh. Fiz. Khim.*, **30**, 379 (1956).
15) Paderno, Yu. B., *Dokl. Akad. Nauk SSSR*, **11**, 1215 (1959); *ibid.*, **137**, 646 (1961).
16) A. Menth, E. Buehler, and T. H. Geballe, *Phys. Rev. Lett.*, **22**, 295 (1969).
17) E. E. Vainshtein, S. M. Vlokhim, and Yu. B. Paderno, *Sov. Phys.-Solid State*, **6**, 2318 (1965).
18) L. M. Falicov and J. C. Kimball, *Phys. Rev. Lett.*, **22**, 997 (1969).
19) F. Bertant and P. Blum, *Compt. Rend.*, **234**, 265 (1952).
20) P. Blum and F. Bertant, *Acta. Cryst.*, **7**, 81 (1954).

BULLETIN OF THE CHEMICAL SOCIETY OF JAPAN, VOL. 44, 967—970 (1971)

The Effect of Pressure on the Association of Dye Molecules in an Aqueous Solution[1)]

Keizo SUZUKI and Masao TSUCHIYA[2)]

Department of Chemistry, Faculty of Science and Engineering, Ritsumeikan University, Kita-ku, Kyoto

(Received October 12, 1970)

The effect of pressure on the association of rhodamine B (RB) and methylene blue (MB) in water has been investigated on the basis of their absorption spectra under hydrostatic pressures up to 4500 atm at room temperatures. Pressure increases the association of these dyes. The volume changes accompanying the 2 monomer$\rightleftarrows$ dimer process are calculated. The values are -10.4 cc/mol and -10.6 cc/mol in RB and MB respectively. These negative values are inconsistent with the suggestions by Rohatgi and Singhal and by Mukerjee and Ghosh that hydrophobic bonds are responsible for the associations of RB and MB. It is more plausible to assume that the hydrogen bond is the main binding force in the dye associations. London's dispersion force and the increase in the dielectric constant of water with the increase in the pressure may also assist the dye associations.

Dye association in an aqueous solution has, in general, been deduced from nonconformity with Beer's law. Various mechanisms have been advanced for the association of dyes. However, no definite mechanism has been put forward to explain the forces holding the dye molecules together. Mukerjee and Ghosh[3)] have recently suggested the contribution of the hydrophobic bond in the formation of the dimer from the fact that urea decreases the association of methylene blue. Rohatgi and Singhal[4)] also considered the hydrophobic bond as responsible for the association of rhodamine B because of the positive entropy change (+5.3 eu). If the hydrophobic bond is responsible for dye association, as they suggested, it could be expected that the equilibrium would shift to the monomer side under a high pressure, because the formation of the hydrophobic bond accompanies a positive volume

1) Presented at the 20th Annual Meeting of the Chemical Society of Japan, Tokyo, 1967, and the 21st Annual Meeting of the same society, Osaka, 1968.

2) Present address: Laboratory of Biology and Chemistry, College of Naval Architecture of Nagasaki, Nagasaki.

3) P. Mukerjee and A. K. Ghosh, *J. Phys. Chem.*, **67**. 193 (1963).

4) K. K. Rohatgi and G. S. Singhal, *ibid.*, **70**, 1695 (1966).

change.[5,6]

In this communication we will attempt to interpret the nature of bonding in the association of two dyes, rhodamine B and methylene blue, by measuring the absorption spectra of these aqueous dye solutions under high pressure. No study of the effects of applied pressure on the dye association has yet been reported. The molecular formulas of these dyes may be represented as follows:

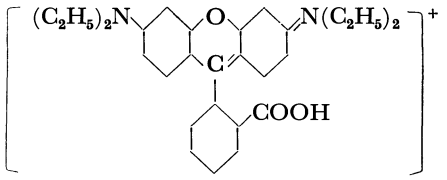

Rhodamine B (RB)

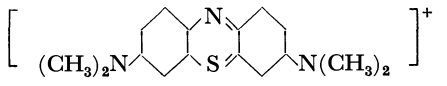

Methylene blue (MB)

Experimental

Methods. High-pressure optical equipment of the Drickamer type[7] was used, along with a Hitachi-Perkin Elmer 139 type spectrophotometer. The absorption cell used is shown in Fig. 1, and the dye solution was sealed with mercury. Silicone oil was used as a pressure medium. The concentration of the dye solution under pressure was corrected by using the compressibility data of water.[8] The concentration of the solutions was limited to below *ca.* 10^{-3} mol/*l* in such a manner so as to form an isosbestic point, indicating that primarily there are present only two absorbing species (monomer and dimer) at 1 atm.

Materials. The rhodamine B (RB, Sumitomo Chemical Co.) and the methylene blue (MB, Nakarai Chemical Co.) were recrystallized twice, from acetone and ethanol respectively, and then dried at 110°C. The purity of the samples was judged from the values of their peak wavelengths at the monomer band. These values are tabulated in Table 1, along with the values for reference.

Table 1. Peak wavelength at each M-band of RB and MB

Dye	Wavelength (*mμ*)	
	This work	Ref.
RB	554 (30°C)	554 (30°C)[a]
		555 (—)[b]
MB	665 (18°C)	656 (27°C)[c]
		664 (25°C)[d]
		660 (20°C)[e]
		665 (30°C)[f]

a) Rohatgi and Singhal (1966)[4]
b) Glowacki (1964)[9]
c) Rabinowitch and Epstein (1941)[16]
d) Bergmann and O'Konski (1963)[22]
e) Mukerjee and Ghosh (1963)[3]
f) Braswell (1968)[21]

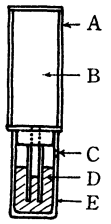

Fig. 1. Optical cell.
A: Glass cell, B: Sample solution, C: Entrance and exit of pressure medium, D: Mercury, E: Holder of mercury made of poly vinylchloride tubing.

Results and Discussion

Figure 2 shows the spectra of aqueous RB solutions at concentrations from 10^{-3} to 10^{-5} mol/*l* at 1 atm. The absorption bands at 554 and 524 m*μ* correspond to those of the monomer (M) and the dimer (D) respectively, and an isosbestic point appears at 533 *mμ*. These spectra coincide well with those in the literature.[9]

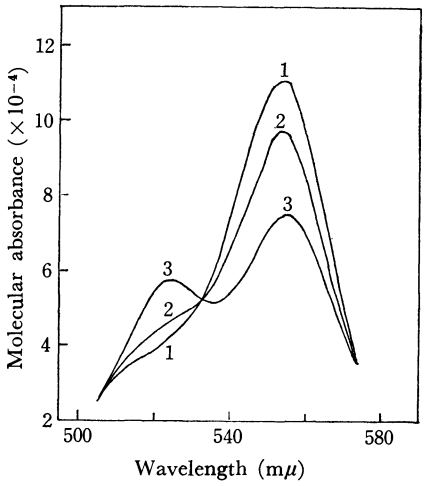

Fig. 2. Effect of concentration on absorption spectra of RB in aqueous solution at 1 atm and 30°C.
Concn. of RB (mol/*l*)
1 1×10^{-5}
2 1×10^{-4}
3 1×10^{-3}

Figure 3 shows the absorption spectra of RB (5.00×10^{-5} mol/*l*) under pressures of up to 4500 atm. It can be found from this figure that both the absorption bands shift to the red and that the absorption of the M-band decreases, while the absorption of the D-band increases, with an increase in the pressure. That is, the influence of the pressure is similar to the increase in the concentration, as is shown in Fig. 2, with the exception of the band shift. Such a band shift is a general phenomena observed in the absorption spec-

5) W. Kauzmann, *Advan. Protein Chem.*, **14**, 1 (1959).
6) G. Némethy and H. A. Scheraga, *J. Phys. Chem.*, **66**, 1773 (1962); *J. Chem. Phys.*, **36**, 3401 (1962).
7) K. Suzuki, Y. Miyosawa, and C. Suzuki, *Arch. Biochem. Biophys.*, **101**, 225 (1963).
8) P. W. Bridgman, *Proc. Amer. Acad. Arts and Sci.*, **48**, 309 (1912).
9) J. Glowacki, *Acta Phys. Polonica*, **26**, 905 (1964).

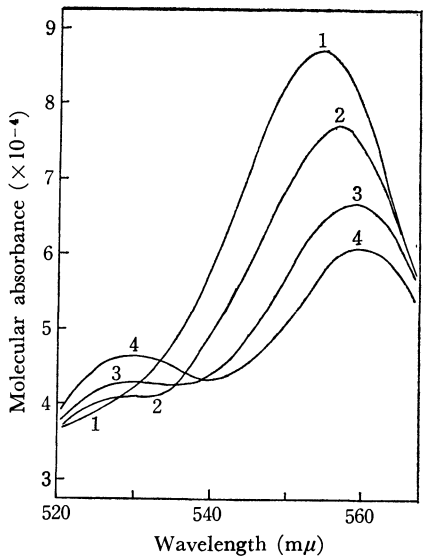

Fig. 3. Effect of pressure on the absorption spectra of RB in aqueous solution (5×10^{-5} mol/l) at 30°C.

	Pressure (atm)
1	1
2	1800
3	3600
4	4500

trum under high pressure; it may be attributed to a solvent effect deduced from the increase in the dielectric constant of the solvent.[10,11] If the shift at each pressure is restored to 1 atm, an isosbestic point can be demonstrated at 533 mμ, as in Fig. 2. We can, then, assume that only the dimer is formed in the experimental ranges of pressure and concentration.

The equilibrium constant, K, of 2 monomer $\rightleftarrows$ dimer was calculated according to the method of Rohatgi and Singhal.[4] The values of K from 1 to 4500 atm are tabulated in Table 2. The volume change accompanying the dimerization, ΔV, is calculated from the following relation;

$$\Delta V = -RT\left(\frac{\partial \ln K}{\partial P}\right)_T$$

Table 2. Effect of pressure on the equilibrium constant K of 2 monomer $\rightleftarrows$ dimer of RB (30°C) and MB (20°)

Pressure (atm)	Equilibrium constant K (l/mol)[a]	
	RB ($\times10^3$)	MB($\times10^4$)
1	6.01	5.56
900	7.48	8.52
1800	10.1	10.7
2700	14.8	15.1
3600	23.2	27.7
4500	39.8	42.2

a) The volume change accompanying association calculated from the above data is −10.4 cc/mol in RB and −10.6 cc/mol in MB.

10) F. G. Wick, *Proc. Amer. Acad. Arts and Sci.*, **58**, 555 (1923).
11) W. W. Robertson, S. E. Babb, and F. A. Matson, *J. Chem. Phys.*, **26**, 367 (1957).

The value of ΔV thus calculated is −10.4 cc/mol.

If the dimer is formed by a hydrophobic bond, as has been suggested by Rohatgi and Singhal,[4] the volume change accompanying the dimerization should be positive, because the formation of the hydrophobic bond is accompanying by a positive volume change, as has been reported by Kauzmann[5] and Scheraga *et al.*[6] Even if the participation of hydrophobic interaction in the dimerization process can not be neglected, another interaction, such as a hydrogen bond, should be predominant. The structure of the RB molecule fully admits the possibility of hydrogen-bond formation by the carboxyl group. It is plausible to assume that the hydrogen bond is concerned in the dimerization process of RB, because the formation of the hydrogen bond is accompanied by a negative volume change.[12-15]

Figure 4 represents the pressure effect on the absorption spectrum of MB in an aqueous solution. Absorption peaks appear at about 665 and 610 mμ; they correspond to the M-band and the D-band respectively, as has been reported by Rabinowitch and Epstein[16] and by others.[3,17-23] Both the absorption

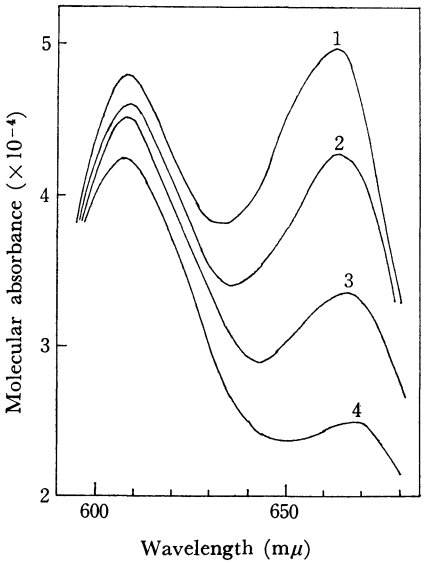

Fig. 4. Effect of pressure on the absorption spectra of MB in aqueous solution (1×10^{-4} mol/l) at 18°C.

	Pressure (atm)
1	1
2	900
3	2700
4	4500

12) S. D. Hamann, "Physico-chemical Effects of Pressure," Butterworths Sci. Publications, London (1957), p. 147.
13) E. Fishman and H. D. Drickamer, *J. Chem. Phys.*, **24**, 548 (1956).
14) J. Osugi and Y. Kitamura, *Rev. Phys. Chem. Jap.*, **35**, 25 (1965).
15) K. Suzuki, Y. Miyosawa, M. Tsuchiya, and Y. Taniguchi, *ibid.*, **38**, 63 (1968).
16) E. Rabinowitch and L. F. Epstein, *J. Amer. Chem. Soc.*, **63**, 69 (1941).
17) G. Holst, *Z. Physik. Chem.*, **A182**, 321 (1938).
18) L. Michaelis and S. Granick, *J. Amer. Chem. Soc.*, **67**, 1212 (1945).

bands decrease with an increase in the pressure, and no isosbestic point appears. It has been known that the absorption decreases under high pressure in other cases.[11] It should be mentioned, however, that the ratio of the optical density at the D-band (D_d) to that of the M-band (D_m), D_d/D_m, increases with the pressure. Moreover, no other absorption band besides the M-band and the D-band can be found at the shorter wavelengths 600 mμ to 400 mμ. The equilibrium constant, K, can be calculated according to the method of Rohatgi and Singhal,[4] as in RB. The values are tabulated in Table 2. The volume change accompanying the dimerization, ΔV, is calculated to be -10.6 cc/mol from Eq. (1).

The MB results also show that the dye association is promoted by compression, as in the case of RB. It has been found that the presence of urea and alcohol decreases the self-association of MB.[3] Therefore, the effect of the pressure on the association of MB is the opposite of the effects of urea and alcohol. From the viewpoint of the value of ΔV (negative sign), the association of MB can not be interpreted in terms of a hydrophobic bond, as has been suggested by Mukerjee and Ghosh.[3]

If the value of ΔV is taken into account, hydrogen bonding may be concerned in the self-association of MB. The structure of MB, however, does not admit the possibility of direct hydrogen bonding. A hydrogen bond through sandwiched water molecules may be involved in this phenomenon, as has been suggested by previous investigators.[23,24]

London's dispersion force could also cause a stacking of dye molecules so as to decrease the volume when the monomer units are in a sandwich with the principal molecular axes parallel, as has been suggested by Förster[25] and by Bergmann and O'Konski.[22] The increase in the dielectric constant with an increase in the pressure[26] may assist the association of dye ions, for an increase in the dielectric constant reduces the coulombic repulsive forces between the ionic parts of the dye ion.[27]

The authors wish to express their thanks to Professor W. Kauzmann of Princeton University for his valuable suggestions. The financial support given by the Ministry of Education is also gratefully acknowledged.

19) T. Vickerstaff and D. R. Lemin, *Nature*, **157**, 373 (1946); D. R. Lemin and T. Vickerstaff, *Trans. Faraday Soc.*, **43**, 491 (1947).
20) M. Schubert and A. Levine, *J. Amer. Chem. Soc.*, **77**, 4197 (1955).
21) E. Braswell, *J. Phys. Chem.*, **72**, 2477 (1968).
22) K. Bergmann and C. T. O'Konski, *ibid.*, **67**, 2169 (1963).
23) J. A. Bergeron and M. Singer, *J. Biophys. Biochem. Cytol.*, **4**, 433 (1958).
24) S. E. Sheppard and A. L. Geddes, *J. Amer. Chem. Soc.*, **66**, 2003 (1944).
25) T. Förster, *Naturwissenschaften*, **33**, 166 (1946).
26) B. K. P. Scaife, *Proc. Phys. Soc.* (London), **B68**, 790 (1955).
27) R. F. Tuddenham and A. E. Alexander, *J. Phys. Chem.*, **66**, 1839 (1962).

An MO-theoretical Interpretation of the Origin of the Orienting Effect in Aliphatic Systems

Hiroshi FUJIMOTO, Shinichi YAMABE, and Kenichi FUKUI
Faculty of Engineering, Kyoto University, Sakyo-ku, Kyoto

(Received October 14, 1970)

The importance of the charge-transfer interaction from the highest occupied (HO) molecular orbital (MO) of a donor to the lowest unoccupied (LU) MO of an acceptor molecule has been stressed on the basis of the numerical results of the calculation on a model of the S_N2 reaction of methyl chloride. The effect of a counter ion on the frontier orbitals has been discussed. For the E2 reaction of ethyl chloride, it has been discussed how the orienting effect of the leaving nucleophile is transmitted to the *trans*-β-hydrogen by means of the frontier electron density. The influence of the rotation about the C_α–C_β bond upon the reactivity of β-hydrogen has also been discussed.

In one of our previous papers, we have discussed the interaction energy between two reactant systems, *A* and *B*, partitioning it into four terms: the Coulomb, exchange, delocalization, and polarization interaction terms.[1] A succinct expression for each of these four terms has also been derived. On the basis of the three principles which govern the orientation and the spatial direction of chemical reactions, it has also been pointed out that the cooperation of the change in the molecular shape in the neighborhood of the reaction center with the charge-transfer interaction can be a driving force in a majority of chemical reactions.[2]

In this paper, we will present a further discussion of the physical meaning of the charge-transfer interaction and the orienting effect in the chemical reactions of aliphatic systems. To save space, the same notations as the previous paper[1] will be used, and no explanation will be repeated here.

The Delocalization Interaction

First of all, let us briefly mention the delocalization interaction terms in order to clarify the later discussion of the numerical computations. The delocalization interaction energy, *D*, is generally given by:

$$D = \sum_{i}^{occ}\sum_{l}^{uno} \frac{|H_{0,i\to l} - S_{0,i\to l}H_{0,0}|^2}{H_{i\to l,i\to l} - H_{0,0}} + \sum_{k}^{occ}\sum_{j}^{uno} \frac{|H_{0,k\to j} - S_{0,k\to j}H_{0,0}|^2}{H_{k\to j,k\to j} - H_{0,0}} \quad (1)$$

The denominator, $H_{i\to l,i\to l} - H_{0,0}$, can be expressed in terms of the ionization potential and the electron affinity:

$$H_{i\to l,i\to l} - H_{0,0} = I_{Ai}^{(B)} - E_{Bl}^{(A-i)} = I_{Ai}^{(B+l)} - E_{Bl}^{(A)} \quad (2)$$

in which:

I_{Ai}: the vertical ionization potential of the electron in the *i*th MO of the reactant *A*, and

E_{Bl}: the vertical electron affinity of the reactant *B* with respect to the *l*th MO.

$I_{Ai}^{(B+l)}$ is the value of I_{Ai} in the case of the approach of the system *B* with an additional electron occupying the *l*th originally unoccupied MO, and where $E_{Bl}^{(A-i)}$ is the value of E_{Bl} in the case of the approach of the system *A*, in which one electron occupying the *i*th MO is subtracted. The relations given in Eq. (2) can be easily visualized by means of a schematic diagram of the electron configurations without any formalism, as has been shown in one of our previous papers.[1]

The Delocalization Interaction and the Frontier Orbitals

Let us first consider the case in which two electronically neutral molecules interact with each other. The denominator of Eq. (1) is not simply expressed as $I_{Ai}-E_{Bl}$. The quantity $I_{Ai}^{(B)}$ represents the ionization potential of the *i*th MO of the reactant *A* under the influence of the reactant *B*. Since *B* is electronically neutral, $I_{Ai}^{(B)}$ may not differ very much from I_{Ai}. On the other hand, $E_{Bl}^{(A-i)}$ is the electron affinity of the *l*th MO of the reactant *B* in the cationic field of the reactant *A*, in which an electron in the *i*th MO is subtracted. Therefore, $E_{Bl}^{(A-i)}$ may be much greater than E_{Bl}. This implies that the denominator of Eq. (1) can be small enough in comparison with $I_{Ai}-E_{Bl}$.

Secondly, let us consider the case in which the reactant *A* is an anion and the reagent *B* is a neutral molecule. In this case, $E_{Bl}^{(A-i)}$ may be close to E_{Bl}, since the system *A* in which an electron in the *i*th MO is subtracted, is electronically neutral, while $I_{Ai}^{(B)}$ may be much smaller than those in neutral systems.

Lastly, let us consider the case where *A* is neutral and *B* is cationic. In this case, the $E_{Bl}^{(A)}$ may be greater than those in neutral systems, although $I_{Ai}^{(B+l)}$ may rather be close to I_{Ai}. Thus, we may come to the conclusion that the denominator of Eq. (1) is small enough when *i* denotes the HO MO of the donor, and *l*, the LU MO of the acceptor, among the various terms in *D*, in comparison with those simply expected from the $I_{Ai}-E_{Bl}$ of neutral molecules. In the interaction between an anion, *A*, and a cation, *B*, there may be cases in which $I_{Ai}^{(B)}-E_{Bl}^{(A-i)}$ is zero.

Even in not exactly degenerate case, the one-term approximation of *D*, such as Eqs. (4) and (5) in Ref. 2, may be valid for a majority of chemical interactions between the two reactant systems.

To exemplify these circumstances, we have carried out a numerical calculation on a model of the S_N2 reaction shown in Fig. 1. The MO's of the isolated species were obtained by means of an all-valence-shell ASMO SCF method which was similar to the one developed by Yonezawa *et al.*[3] The Coulomb electron repulsion integrals were estimated by point-charge approximation for intermolecular AO pairs. The

1) K. Fukui and H. Fujimoto, This Bulletin, **41**, 1989 (1968).
2) K. Fukui and H. Fujimoto, *ibid.*, **42**, 3393 (1969).

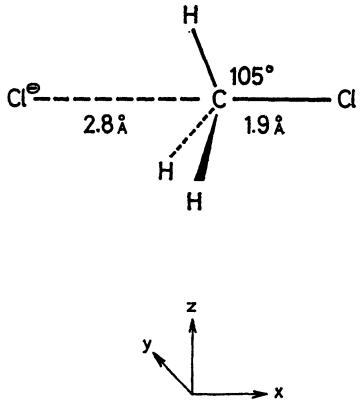

Fig. 1. The model of S_N2 reaction employed in this calculation.

integral, $\int t(1)(Z_\alpha e^2/r_{\alpha 1})t(1)dv(1)$, was taken to be equal to $Z_\alpha e^2/R_{\alpha\gamma}$ if the AO t belongs to the γ ($\gamma \neq \alpha$) nucleus, while, when t belongs to α, it was estimated using the Slater AO's. The other multi-center integrals were all calculated by the use of the Mulliken approximation.[4] The results of the calculation on various $(H_{i\to l,i\to l}-H_{0,0})$ are given in Table 1. We can see that the terms corresponding to the charge-transfer configurations from the p_x, p_y, and p_z of the attacking chloride ion to the LU MO of methyl chloride are relatively small in comparison with the other terms. Three p orbitals in the attacking chloride ion are degenerate in the isolated state, while this degeneracy is removed in the event of interaction with methyl chloride.

Table 1. The values of $H_{i\to l,i\to l}-H_{0,0}$ (in eV) for the various charge-transfer configurations of $CH_3Cl\cdots Cl\ominus$ system

i	l			
	LU	LU+1	LU+2	LU+3
s	15.4819	27.9199	27.9199	33.2388
x	3.2279	16.3913	16.3913	22.7129
y	6.3149	17.5828	17.9707	24.9383
z	6.3149	17.9706	17.5828	24.9383

Orienting Effect

The numerator of Eq. (1) may be supposed to be proportional to the overlap integral between the wave function of a charge-transfer configuration and that of the zero configuration. Moreover, we have a relation:

$$S_{0,i\to l} \cong \sqrt{2}\, s_{il} \tag{3}$$

This implies that the ease of the mixing of the charge-transfer configuration from the ith occupied MO of the system A to the lth unoccupied MO of the system B is proportional to the overlapping of these specific MO's. Table 2 shows the values of s_{il} calculated with respect to the nuclear configuration shown in Fig. 1.

3) T. Yonezawa, K. Yamaguchi, and H. Kato, This Bulletin, **40**, 535 (1967).

4) R. S. Mulliken, *J. Chim. Phys.*, **46**, 497 (1949).

Table 2. The values of $|s_{il}|$ for the various charge-transfer configurations of $CH_3Cl\cdots Cl\ominus$ system

i	l			
	LU	LU+1	LU+2	LU+3
s	0.0434	0	0	0.0740
x	0.0608	0	0	0.0504
y	0	0.0346	0.0008	0
z	0	0.0008	0.0346	0

We can see that the p_y and p_z orbitals are orthogonal to the LU MO of methyl chloride, while p_x has the largest overlap with the LU MO. This is due to the symmetry of the LU MO of methyl chloride, which has its maximum extension in the direction of the x-axis. Here it should be noted that the attack of the chloride ion and the departure of the chlorine of methyl chloride take place in the direction parallel with the x-axis. As we have previously discussed,[2] the LU MO of methyl chloride has the largest partial electron population at the carbon atom and antibonding character in the region of the carbon-chlorine bond, supplying a cause of inversion in the event of a S_N2 reaction. Although the values of $(H_{i\to l,i\to l}-H_{0,0})$ for the $i=s$ of the chloride ion and the $l=$LU+3 of the methyl chloride are large, the overlap integral, s_{il}, corresponding to this charge-transfer configuration is quite large, also. However, according to the second principle in our previous paper,[2] the contribution of this configuration becomes less and less important as the nuclear configuration change takes place along with the chemical reaction. Moreover, the importance of the charge-transfer term from the HO MO of the donor to the LU MO of the acceptor is accentuated by the aid of the cationic species which are present in the environment of the electron-acceptor molecule and by the aid of the anionic species which exist in the neighbor of the electron-donor molecule. We have made a calculation of the system composed of methyl chloride and the lithium cation, as is shown in Fig. 2. The

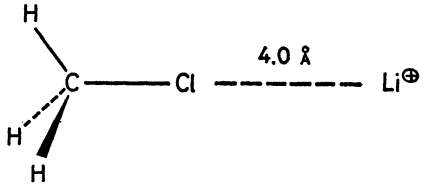

Fig. 2. The model employed for the calculation of the effect of a counter ion.

energy of the LU MO of methyl chloride is calculated to be 2.9570 eV, while that of the system shown in Fig. 2 is −4.5212 eV. In this case, the LU MO of the system comes to be almost degenerate with the HO MO of the chloride ion, which is calculated to be −3.4667 eV in our calculation. In real chemical MD of the chloride ion, which is calculated to be reactions, a reactant may hardly be exposed to the positive field of a bare nucleus. However, the one-term approximation of D, represented by Eqs. (4) and (5) in Ref. 2, might be valid in a majority of electron donor-acceptor interactions. Such an effect on MO's as to change their energy levels is an important role

of counter ions, catalysts, solvents, and so on. This point will be discussed elsewhere.

Thus, we can conclude, as has already been discussed in our previous papers,[1,2] that the chemical reaction takes place at the position and in the direction where the overlapping of the HO MO of the electron-donor and the LU MO of the electron-acceptor is at its maximum; the present results support the conclusion fully.

Next, let us consider how the orienting effect of a nucleophile is transmitted to the *trans*-β-hydrogen, taking the case of the E2 reaction of ethyl chloride as an example. The partial valence-inactive population (C_r^2) and the partial valence-active population (v_r)[5] of β-hydrogen in the LU MO are given in Table 3.

Table 3. The partial valence-inactive and partial valence-active populations of hydrogens in LU of ethyl chloride

		Model I	Model II $F_{rs}\}=0$ s_{rs} $r=\mathrm{Cl}_{s,x,y,z}$ $s=\mathrm{H}_3,\mathrm{H}_4,\mathrm{H}_5$	Model III $F_{rs}\}=0$ s_{rs} $r=\mathrm{Cl}_{s,x,y,z}$ $\mathrm{H}_1,\mathrm{H}_2$ $s=\mathrm{H}_3,\mathrm{H}_4,\mathrm{H}_5$
$(C_r^{LU})^2$	3	0.0058	0.0058	0.0115
	5	0.0447	0.0453	0.0529
$v_r^{(LU)}$	3	−0.0027	−0.0030	−0.0065
	5	−0.0282	−0.0256	−0.0305

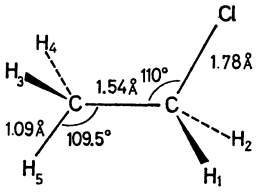

Model I is ethyl chloride, with the valence-angles and bond-lengths shown in the table, while Model II corresponds to the one in which the integrals between the chlorine and the 3, 4, and 5 hydrogens are put equal to zero in the secular equations and Model III is obtained by removing further the integrals between the 1 and 2 α-hydrogens and the 3, 4, and 5 β-hydrogens from Model II. We can see that the β-hydrogen *trans* to the chlorine has the largest frontier electron density ($(C_r^{(LU)})^2$) and anti-bonding character ($(v_r^{(LU)})^2$) among the three β-hydrogens in all of the three models presented in Table 3. This implies that the orienting effect of the nucleophile is transmitted to the *trans*-β-hydrogen mainly through the bonds having their maximum extension in the plane defined by chlorine, α,β-carbons, and *trans*-β-hydrogen.

Next, let us examine the change in the partial valence-inactive population and the partial valence-active population of hydrogens in the LU MO in the case of the rotation about the carbon α and carbon β bond axis. The results of the calculations on *n*-propyl chloride are shown in Table 4. It can be seen that the partial valence-inactive population of hydrogen in the LU MO is at its minimum when the plane involving the hydrogen and the α, β-carbons is perpendicular

5) K. Ruedenberg, *Rev. Mod. Phys.*, **34**, 326 (1962).

Table 4. The partial valence-inactive and partial valence-active populations of hydrogens in LU of *n*-propyl chloride

$\theta°$	$(C_{H_1}^{LU})^2$	$v_{H_1}^{(LU)}$
0	0.0400	−0.0205
30	0.0261	−0.0132
60	0.0063	−0.0030
90	0.0003	−0.0003
120	0.0120	−0.0074
150	0.0330	−0.0200
180	0.0461	−0.0283

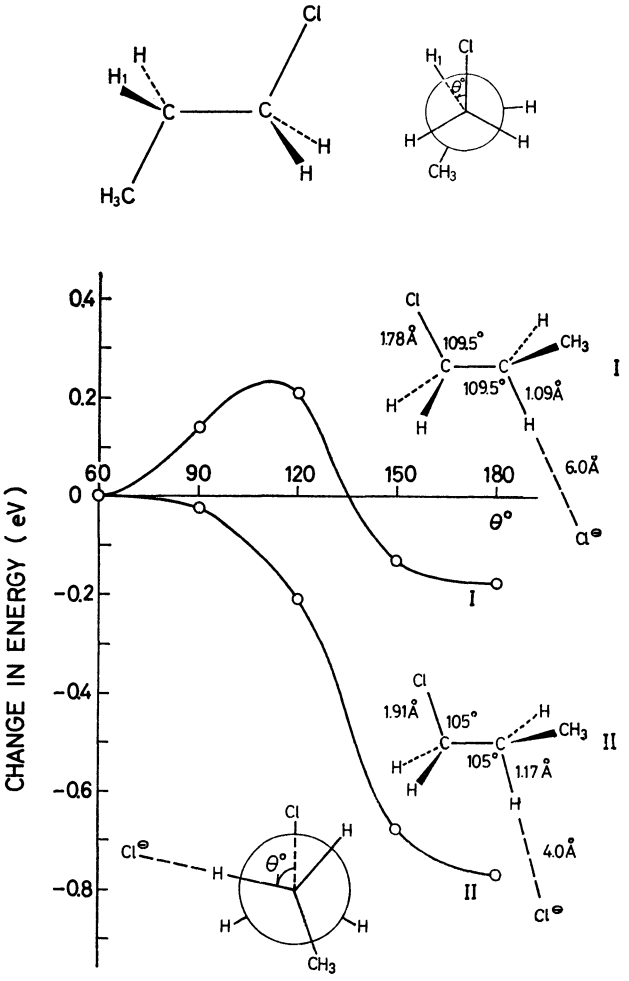

Fig. 3. The change in the energy of $CH_3CH_2CH_2Cl$----$Cl^{\ominus}$ system with the rotation about C_α—C_β axis.

to the one determined by the chlorine and the α, β-carbons, while it is at its maximum when the former is identified as the latter. When the methyl group is located *trans* to chlorine, the partial valence-inactive population of hydrogen in the LU MO is 0.0063. If the hydrogen comes to the *trans* position with respect to chlorine, the partial valence-inactive population increases to 0.0461. We have calculated the total energy of the system composed of *n*-propyl chloride and chloride ion in Fig. 3. The results shown in Fig. 3 have been obtained with reference to the approximation employed by Del Re and Parr in estimating

the nuclear repulsion energy.[6] We can see that the *gauche* form ($\theta=180°$) with respect to methyl and chlorine has a lower total energy than the *trans* form ($\theta=60°$) separated by a relatively low rotation barrier. A distinct parallelism has been shown to exist between the experimentally-observed rate constant of the E2 reaction and $(C_r^{(LU)})^2$, an approximate form of D, for a variety of alkyl halides.[7] *n*-Propyl bromide is found to be more reactive than ethyl bromide.[8] This also seems to indicate that hydrogen in *n*-propyl chloride is liable to be abstracted at the *trans* position to chlorine. This is conceivable, since the partial valence-inactive population of *trans*-β-hydrogen of ethyl chloride in the *staggered* form is 0.0447. Similar considerations may hold for other alkyl chlorides.

The results in Table 4 show that the β-hydrogen at the *cis* position to chlorine in an *eclipsed* *n*-propyl chloride ($\theta=0°$) has a larger reactivity toward a nucleophile than the other β-hydrogen ($\theta=120°$). This implies that if a molecule is rigidly fixed to the *eclipsed* form, selective *cis* elimination may take place. This may be a principal reason for the preferential *cis-exo* elimination of hydrogen bromide in *exo*-2-bromonorbornane.[9] Such an orienting effect of the leaving nucleophile should always be kept in mind in discussing the chemical reactivity of hydrogens in cyclic systems.

We have discussed the important role of the charge-transfer between the frontier orbitals and the origin of the orienting effect in terms of the frontier electron density for several chemical reactions of aliphatic systems, demonstrating how the so-called "anti-coplanar" selectivity in E2 reactions could arise.

The authors wish to express their appreciation to the Data Processing Center of Kyoto University for its generous permission to use the FACOM 230.60 computer.

6) G. Del Re and R. G. Parr, *Rev. Mod. Phys.*, **35**, 604 (1963).
7) K. Fukui, H. Hao, and H. Fujimoto, This Bulletin, **42**, 348 (1969).
8) C. K. Ingold, "Structure and Mechanism in Organic Chemistry," Cornell University Press, Ithaca (1969), p. 651.
9) E. C. Kooyman and G. C. Vegter, *Tetrahedron*, **4**, 382 (1958).

BULLETIN OF THE CHEMICAL SOCIETY OF JAPAN, VOL. 44, 974—977 (1971)

Semiconductivity and Photoconductivity of TCNQ Crystal

Shoji HIROMA,* Haruo KURODA, and Hideo AKAMATU**

Department of Chemistry, Faculty of Science, The University of Tokyo, Hongo, Tokyo

(Received October 24, 1970)

The results of a preliminary investigation on the semiconductive and photoconductive behaviors of the TCNQ crystal are described. The single crystal of TCNQ shows a resistivity of the order $10^{11}\ \Omega\cdot$cm at room temperature with an activation energy of about 0.6 eV. The photoconductive sensitivity of a TCNQ crystal is comparatively high. There are two types of crystal with respect to sensitivity to visible light. In both cases, the low-energy tail is extended up to about 1.5 eV. It is shown that both the activation energy of photoconduction and the light-intensity dependence of photocurrent differ appreciably in visible and ultraviolet regions.

Although extensive investigations have been carried out on the electrical properties of anion radical salts of 7,7,8,8-tetracyano-*p*-quinodimethane (TCNQ),[1] a good organic semiconductor, little is known on the properties of a TCNQ crystal itself. We could expect some interesting aspects on the electrical conduction in a TCNQ crystal. First, a low energy for the conduction state could be expected as will be discussed later. If this is the case, a TCNQ crystal will show a relatively good conductivity as well as some characteristic photoconductive behaviors. Secondly, we could easily inject electrons into a TCNQ crystal because of its high electron affinity.

In a previous paper,[2] we reported the polarized absorption spectra of the single crystal of TCNQ. We will report the results of a preliminary experiment on the semiconductivity and photoconductivity of a TCNQ crystal.

Experimental

TCNQ was synthesized by the method described by Acker and Hartler,[3] and purified first by recrystallization and then by repeated sublimation *in vacuo*. Because of the high electron affinity of TCNQ, it is apt to take donor-type impurities to form TCNQ ion radical. The purified specimen was checked with ESR, and confirmed to show no detectable signal. This means that the concentration of TCNQ ions, if present at all, might be less than $8\times10^{-16}\ g^{-1}$.

Single crystals were prepared by slow sublimation *in vacuo*, or by crystallization from ethylacetate solution. Most crystals thus obtained were a parallelepiped bounded with (001), (110). The developed face was usually (001). The size of a typical crystal used for the measurement was 0.5 cm × 0.5 cm × 0.05 cm.

For electrical measurements, electrodes were put on the

* Present address: Hitachi Research Laboratory, Hitachi Ltd., Hitachi, Ibaraki.

** Present address: Yokohama National University, Yokohama.

1) W. J. Siemons, P. E. Bierstedt, and R. G. Kepler, *J. Chem. Phys.*, **39**, 3523 (1963); L. R. Melby, *Can. J. Chem.*, **43**, 1448 (1965); J. P. Farges, A. Brau, D. Vasilescu, P. Dupuis, and J. Neel, *Phys. stat. sol.*, **37**, 745 (1970).

2) S. Hiroma, H. Kuroda, and H. Akamatu, This Bulletin, **43**, 3626 (1970).

3) D. S. Acker and W. R. Hartler, *J. Amer. Chem. Soc.*, **84**, 3370 (1962).

developed face of the crystal to form a sandwich-type arrangement. Although several different electrode materials were tested, most photoconductivity experiments were carried out by using a vacuum-deposited gold film as an illuminating electrode and carbon-paint electrode as another one.

DC currents were measured with a Toa Dempa Microvolt-ammeter Model PM-18. For illumination with a monochromatic light, a quartz-prism monochrometer was used with a Ushio 500 W Xe-lamp, or a tungsten lamp as the light source. The light intensity was measured with a calibrated germanium phototransistor, or a photomultiplier tube. Most measurements were carried out by placing the crystal in a vacuum of 10^{-4}—10^{-5} mmHg.

Results and Discussion

Dark Conduction. A TCNQ crystal shows a relatively high dark conduction. The single crystal showed a resistivity of 5×10^{11} Ω·cm at room temperature. The resistivity measured with a powder sample under compression of 116 kg/cm^2 was 1×10^{11} Ω·cm. These values are considerably low in comparison with the resistivity reported for polycyclic aromatic hydrocarbons of comparative molecular size, such as pyrene[4] and perylene.[5]

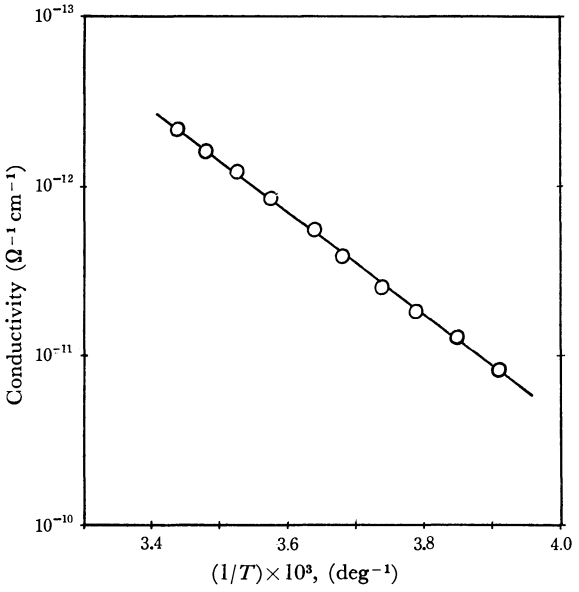

Fig. 1. Temperature dependence of conductivity of TCNQ crystal.

The temperature dependence of dark conduction was measured in the temperature range 200—290°K. An example is shown in Fig. 1. The results can be well described with the exponential equation

$$i = i_0 \exp(-\Delta E/kT) \quad (1)$$

The values of activation energy, ΔE, were found to differ a little with different crystals, but all of them fall in the range 0.45—0.6 eV. The highest value obtained in the present experiment was 0.6 eV.

Thus, if we assume that the carriers are formed by the intrinsic mechanism, not from impurity, the energy gap can be taken to be about 1.2 eV. The energy gap ε can be related to the ionization potential I and the electron affinity A of the component molecule by the relation

$$\varepsilon = I - A - 2P \quad (2)$$

where P is the polarization energy. From the magnetron experiment, Farragher and Page[7] have determined the electron affinity of TCNQ to be 2.88 eV. No experimental value is known for the ionization potential. From a molecular orbital calculation,[8] we predicted that $I=7.83$ eV and $A=2.35$ eV. Thus, the difference $I-A$ will be 5.48 eV if we take our theoretical values, and 4.95 eV if we take Page's value for A.[9] Although we have not estimated the polarization energy in a TCNQ crystal, it does not seem unreasonable to assume it to be about 2 eV according to the known data for various organic crystals.[7] Thus, we can predict that the energy gap in a TCNQ crystal might be in the range 1—1.5 eV. Hence the energy gap determined from the temperature dependence of dark conduction is not inconsistent with this estimation. Naturally, we can not exclude the possibility that the observed dark current is due to the impurity effect or the injection from electrode. The observed variation of the activation energy from crystal to crystal suggests that such extrinsic effects are not negligible. We only wish to point out that our highest experimental value, 1.2 eV, is not unreasonable for the true energy gap.

Spectral Response of Photoconduction. A TCNQ crystal exhibits a rather high photoconductive sensitivity as compared with usual polycyclic aromatic hydrocarbons. The photocurrent was found to be proportional to the applied field up to 10^3 V/cm.

The photocurrent *vs.* wavelength curve directly obtained with our experimental set-up is shown in Fig. 2(a). On examining a number of crystals, we found that TCNQ crystals can be classified into at least two types with respect to their spectral response of photoconduction, one which shows a lower sensitivity (*curve A*), and the other a higher sensitivity (*curve B*) in the visible region. We shall denote these two types by A and B, respectively.[11]

If we normalize the observed photocurrent to a constant light intensity, we obtain the curves shown in

4) H. Inokuchi, This Bulletin, **29**, 131 (1956).
5) M. Sano and H. Akamatu, *ibid.*, **34**, 1569 (1961).
6) In the case of powder sample, ΔE was measured to be 0.45 eV.
7) A. L. Farragher and F. M. Page, *Trans. Faraday. Soc.*, **63**, 2369 (1967).
8) c. f. T. L. Kunii and H. Kuroda, *Theor. Chim. Acta* (Berl), **11**, 97 (1968).
9) From the contact potential measurement, Kotani has determined the Fermi level of TCNQ crystal as 5.1 eV (M. Kotani, PhD Thesis, 1970). The values of I and A mentioned above give the prediction of Fermi level at 5.1—5.3 eV, in agreement with this experimental value.
10) L. E. Lyons, *J. Chem. Soc.*, **1957**, 5001; F. Gutman and L. E. Lyons, "Organic Semiconductors," John-Wiley, New York (1967); M. Batley and L. E. Lyons, *Molec. Cryst. Liqu. Cryst.*, **6**, 299 (1970).
11) At present, we do not know the reason for their appearance. Both types were found among crystals prepared by the same procedure. They can not be distinguished either from appearance or from the crystallographic character of the prominent face of the crystal.

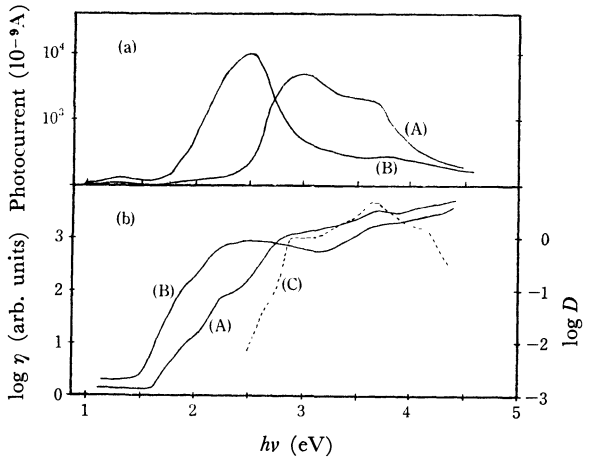

Fig. 2. Spectral response of photoconduction of crystal of A (*Curve A*), and crystal of B (*Curve B*). In Fig. 2(a), the photocurrent directly obtained without any correction for light intensity is plotted against the photon energy ($h\nu$). In Fig. 2(b), the logarithm of the apparent photoconductive sensitivity (η) is plotted against $h\nu$, together with the logarithm of the optical density (D) of the absorption spectrum of the crystal (*Curve C*).

Fig. 2(b), where the logarithm of η(Photocurrent/light intensity) is plotted against photon energy. The absorption spectrum of a TCNQ crystal is also shown. It can be seen that the spectral response curve of the A-type crystal corresponds to the absorption spectrum as regards the locations of the maxima, whereas there is an extra band in the 20—25 kK region in the case of the B-type crystal. It should be noted also that, in both cases, the tail of spectral response curve is extended into the lower energy region well outside the absorption edge. Such a tail seems to have a threshold at about 1.5 eV, which nearly coincides with the energy gap experimentally estimated from the temperature dependence of dark current.

We have examined the presence of electrode effect by using evaporated-film electrodes of different kinds of metal, *i.e.*, Au, Al, Pb, and Mg and a conducting glass electrode. But no specific effect of electrode material was found as far as the spectral response curve is concerned.

At present we do not know the reason for the difference in spectral response between A and B. It could be associated with the defect concentration of crystal. Another possibility might be the effect of impurity, or that of TCNQ ions which are produced either by impurity or the injection from electrodes. However, we have found that no marked change is produced in the spectral response curve, even if a large amount of TCNQ ions are introduced into the crystal by the doping of Li or ammonia.

Effects of Temperature and Light Intensity on Photocurrent. Photocurrent increases exponentially with temperature. An example of the experimental results obtained for crystal of A is shown in Fig. 3. From the results, the activation energy for photoconduction is estimated to be 0.15 and 0.03 eV for the wavelength of light 400 mμ and 500 mμ, respectively. The same results were obtained also for crystal of B.

The logarithm of the observed photocurrent against

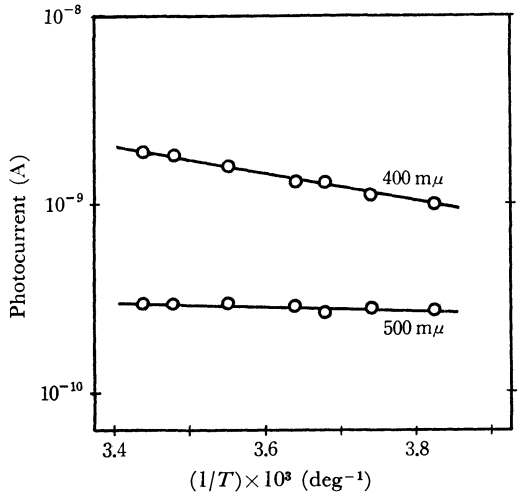

Fig. 3. Temperature dependence of photocurrent. (Crystal of A of TCNQ)

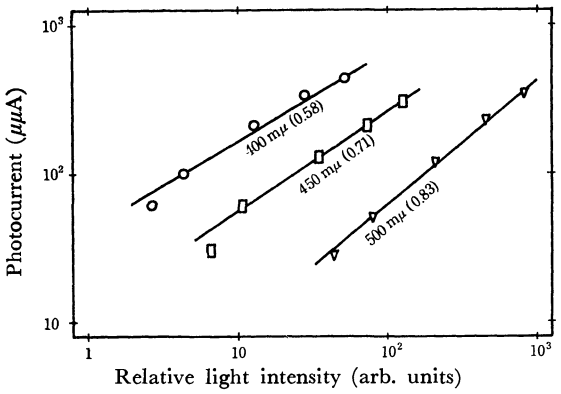

Fig. 4. Dependence of photocurrent (i_p) on the light intensity (L). (Crystal of A of TCNQ); the wavelength of the light is indicated in the figure, the number in the parentheses is the value of n obtained by assuming that $i_p \propto L^n$.

that of relative light intensity is plotted in Fig. 4. The data shown here were measured on crystal of A, but essentially the same results were obtained also for B type crystals. We can thus conclude that in both A and B types, the photocurrent is nearly proportional to the light intensity in the visible region, whereas it is almost proportional to the square root of the light intensity in the ultraviolet region. It is well known that photocurrent becomes proportional to the square root of light intensity when the concentration of charge carrier is controlled by the recombination of photogenerated carriers.[12] Such an effect is usually observed at very high light intensity. In the present experiments, the intensity of monochromatized light is not high, and is considerably lower in the ultraviolet region than in the visible region. It should be noted, however, that the absorption coefficient of a TCNQ crystal is quite high in the ultraviolet region, so that the incident light is strongly absorbed in a very thin region near the illuminated surface of the crystal, while the light in the visible region can penetrate deep into

12) N. Almeleh and S. E. Harrison, *J. Phys. Chem. Solids*, **26**, 1571 (1965).

the bulk of the crystal. Thus, it is most likely that an ultraviolet light produces a considerably high carrier concentration near the illuminated surface, where recombination could play an important role.

If this is actually the case, the temperature dependence of the steady-state photocurrent with an ultraviolet light will be dependent, not only on the carrier trapping in the bulk, but also on the recombination process. This could be the reason for the difference in activation energy between the visible and ultraviolet regions.

Effect of Electron Donor. We prepared a Li-doped polycrystalline film from a melt of TCNQ containing 1—2 weight percent of Li(TCNQ). The pale-green film thus obtained showed a considerably higher dark current, and the ratio of photocurrent to dark current was markedly reduced. However, no specific change was found in the shape of the spectral response curve of photoconduction. Similarly, a TCNQ crystal showed a pale green color when it was kept for a long period in ammonia vapor. The dark current in TCNQ crystal gradually increased with time on exposure to ammonia vapor. In the case of crystal of A, the photocurrent was lowered to about half of the original value throughout the spectral region after exposure to 15 mmHg ammonia vapor for 22 hr. Again, no specific change was found in the spectral response curve.

These results suggest that the doping of an electron donor, or the introduction of TCNQ ion into the crystal, markedly affects the dark conduction, but does not give rise to additional mechanism of charge carrier formation in photoconduction.

BULLETIN OF THE CHEMICAL SOCIETY OF JAPAN, VOL. 44, 977—984 (1971)

Observation and Interpretation of Triplet-Triplet Absorption Spectra of Substituted Naphthalenes[1)]

Takeshi TAKEMURA, Kiyoaki HARA, and Hiroaki BABA

Division of Chemistry, Research Institute of Applied Electricity, Hokkaido University, Sapporo

(Received October 30, 1970)

Triplet-triplet (T-T) absorption spectra of naphthalene, α- and β-naphthol, and α- and β-methoxynaphthalene have been observed in rigid-glass solutions at 77°K by the rapid-scan spectrophotometric method and in fluid solutions at room temperature by the flash spectroscopic method. Hydrogenbonding effects on the T-T absorption spectra were examined for α- and β-naphthol. α-Naphthol was found to give different absorption spectra, depending upon the solvents employed. In a certain case the spectrum is attributed to a photoproduct rather than to the triplet state of α-naphthol. Analysis of the spectral data leads to the conclusion that the T-T absorption spectra in α-derivatives involve two different electronic transitions, and those in β-derivatives are due to a single electronic transition which is analogous to the transition in naphthalene. In agreement with these observations, calculations performed by the Pariser-Parr-Pople method predict that in the low-energy region, α-naphthol should have two allowed and detectable transitions, ${}^3\Psi_1 \rightarrow {}^3\Psi_7$ and ${}^3\Psi_1 \rightarrow {}^3\Psi_8$, and naphthalene and β-naphthol have only one such transition, ${}^3\Psi_1 \rightarrow {}^3\Psi_9$. The wave functions of triplet states are subjected to configuration analysis, with the result that ${}^3\Psi_7$ and ${}^3\Psi_8$ of α-naphthol are related predominantly to ${}^3\Psi_8$ and ${}^3\Psi_9$ of naphthalene, respectively.

Triplet-triplet (T–T) absorption spectra give useful information concerning the electronic structure of higher triplet states as well as of the lowest triplet of molecules. Until now a number of studies have been made both experimentally and theoretically on the T–T transitions in aromatic hydrocarbons such as naphthalene.[2,3)] It is to be expected that we get a deeper insight into the nature of triplet states by investigating the effect of substitution on the T–T transitions. There have been, however, relatively few systematic studies of T–T absorption for substituted aromatic hydrocarbons.

The present paper deals with T–T absorption spectra of some substituted naphthalenes. The parent hydrocarbon, naphthalene, is one of the molecules whose T–T transitions have attracted much attention.[2,3)] The naphthalene molecule shows at about 400 mμ a T–T absorption consisting of three sharp peaks. Recent studies including polarization measurements[4–6)] and molecular orbital calculations[7,8)] have demonstrated that this T–T absorption is due to a single electronic transition which has three peaks as vibrational components. In their theoretical study on T–T absorption spectra of substituted naphthalenes, Kla-

1) Presented at the Symposium on Molecular Structure, held by the Chemical Society of Japan, at Towa University, Kyushu, Oct. 1969.

2) S. K. Lower and M. A. El-Sayed, *Chem. Revs.*, **66**, 199 (1966).

3) S. P. McGlynn, T. Azumi, and M. Kinoshita, "Molecular Spectroscopy of the Triplet State," Prentice-Hall, Englewood Cliffs, New Jersey (1969).

4) M. A. El-Sayed and T. Pavlopoulos, *J. Chem. Phys.*, **39**, 834 (1963).

5) D. P. Craig and G. Fischer, *Trans. Faraday Soc.*, **63**, 530 (1967).

6) D. Lavalette, *Chem. Phys. Lett.*, **3**, 67 (1969).

7) R. L. de Groot and G. J. Hoytink, *J. Chem. Phys.*, **46**, 4523 (1967).

8) M. K. Orloff, *ibid.*, **47**, 235 (1967).

sinc and Sommer[9] paid attention to the experimental fact that the β-derivatives of naphthalene give an absorption spectrum similar to the spectrum of the parent molecule, but the α-derivatives show one or more new absorption bands.[10]

In this study, α- and β-naphthol and α- and β-methoxynaphthalene were treated as substituted naphthalenes. Our particular attention was directed to the distinction between the absorption arising from the triplet state and that possibly from a photoproduct, as well as to the distinction between individual transitions when different electronic transitions were involved in a T–T absorption. For naphthols, hydrogen-bonding effects were investigated on the T–T absorption spectra to obtain information on the origin of the spectra and also on the electronic properties of the triplet states concerned. In addition to these experimental investigations, calculations have been made for the triplet states of naphthols by the Pariser-Parr-Pople method,[11,12] and the resulting wavefunctions have been subjected to the configuration analysis proposed by Baba, Suzuki, and Takemura[13] with a view to revealing the electronic structure of the triplet states and making a reasonable assignment of the observed spectra.

Experimental

Materials. Naphthalene was purified by vacuum sublimation. α-Naphthol was recrystallized from ligroin, and β-naphthol from water and ligroin; both were further purified by vacuum sublimation. α-Methoxynaphthalene was purified by high-vacuum distillation over metallic sodium, and was then passed through an activated alumina column with a mixture of petroleum ether and ethyl ether as the solvent. After eliminating the solvent by distillation in an atmosphere of nitrogen, the α-methoxynaphthalene was again subjected to high-vacuum distillation. β-Methoxynaphthalene was recrystallized from ethanol and from *n*-heptane and was sublimed *in vacuo*.

Isopentane was distilled over phosphorus pentoxide. Methylcyclohexane and *n*-hexane of spectroscopic quality were used without further purification. Ethyl ether was treated with 10% sodium bisulfite solution, dried with calcium chloride and finally distilled over metallic sodium. Triethylamine was refluxed with phosphorus pentoxide and then fractionally distilled.

Apparatus and Procedure. Triplet-triplet absorption spectra were measured by two different methods. In the first method, the spectra were obtained with a rapid-scan spectrophotometer (Hitachi Model RSP-2[14]) in rigid-glass solutions at 77°K, as shown in Fig. 1. The spectrophotometer is a double-beam instrument, and scans from 220 to 700 mμ in 150 msec at a rate of 3 scans/sec. It is suitable for use in the present experiment since all the compounds studied have triplet lifetimes of about 2 sec.

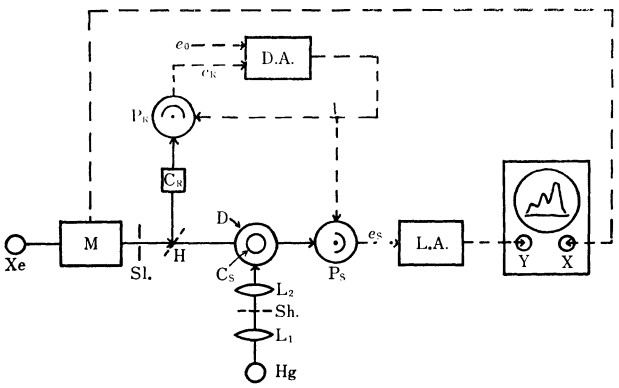

Fig. 1. A schematic diagram of the rapid-scan spectrophotometer as used for measuring T–T absorption spectra at 77°K. Xe, xenon light source; M, monochromator; Sl., slit; H, half-mirror; D, quartz Dewar; Hg, high-pressure mercury lamp for excitation; L_1 and L_2, lenses; Sh., shutter; D.A., differential amplifier; L.A., logarithmic amplifier; see text for other symbols.

Light from a 150-W xenon lamp, the source, is dispersed by a grating monochromator, and the resulting monochromatic light is divided into two beams which pass through the reference cell C_R and sample cell C_S, and then fall on the reference photomultiplier P_R and sample photomultiplier P_S, respectively. The difference between the output voltage e_R of P_R and a standard voltage e_0 is amplified, and the resulting voltage V is fed back to the cathode of P_R. By making the degree of amplification sufficiently great, e_R is held at a constant level (e_0) even if the wavelength of the monochromatic light is changed according to scanning. The voltage V is also applied to the photomultiplier P_S, so that the output voltage e_S of P_S becomes proportional to the transmittance of the sample. The output e_S is fed into a logarithmic amplifier to produce a voltage proportional to the absorbance of the sample. Absorption spectra corresponding to desired scans can be obtained on a storage oscilloscope for a desired wavelength range, with a linear wavelength scale which is calibrated with reference to the absorption spectrum of holmium.

In the T–T absorption measurements, the sample solution in a quartz cell of test-tube type was placed in a quartz Dewar and was cooled down to 77°K. An Osram HBO 100-W high-pressure mercury lamp was used for excitation. Several T–T absorption spectra were obtained in each measure-

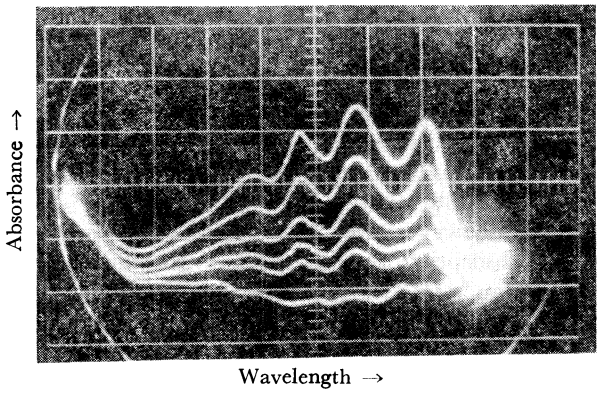

Fig. 2. T–T absorption spectra of α-naphthol in PME containing triethylamine at 77°K, measured by the rapid-scan spectrophotometer. The region of scanning is from 335 mμ to 535 mμ; the scan time is about 60 msec for this region.

9) L. Klasinc and U. Sommer, *Chem. Phys. Lett.*, **3**, 107 (1969).
10) G. Heinrich, H. Blume, and D. Schulte-Frehlinde, unpublished work cited in Ref. 9.
11) R. Pariser and R. G. Parr, *J. Chem. Phys.*, **21**, 466, 767 (1953).
12) J. A. Pople, *Trans. Faraday Soc.*, **49**, 1375 (1953).
13) H. Baba, S. Suzuki, and T. Takemura, *J. Chem. Phys.*, **50**, 2078 (1969).
14) H. Baba and Y. Shindo, *Bunseki Kagaku*, **16**, 653 (1967).

ment. They included the spectrum corresponding to the scan immediately after shutting off the exciting light and also the spectrum (or base line) after completion of the triplet decay; allowance was made for the base line in determination of the true absorption. An example of the measurement by the rapid-scan method is shown in Fig. 2.

In the second method, T–T absorption spectra were obtained by means of flash spectroscopy. The technique and procedure were similar to those described by Porter and Windsor.[15,16] Two xenon flash tubes for excitation were mounted parallel to a sample quartz cell, 10 mm in diameter and 10 cm in length. The cell, was connected to a reservoir where the sample solution was degassed by repeated freeze-thaw cycles. The energy of the excitation flash was about 100 J. Another xenon flash tube was used to take the T–T absorption spectrum on the X-ray film set on a Shimadzu plane-grating spectrograph, Model GE-100. The density of the film was measured by a microphotometer.

Theoretical

Calculations on the Triplet States. Molecular orbital (MO) calculations have been made for the π-electronic triplet states of naphthalene and α- and β-naphthol by the semiempirical LCAO-SCF MO method including configuration interaction (CI), the Pariser-Parr-Pople method, to obtain the excitation energies and oscillator strengths of their T–T absorption transitions.

It is assumed that all the C–C distances are 1.40 Å, all the bond angles 120°, and the C–O distance is 1.37 Å. The valence-state ionization potentials I, valence-state electron affinities A, and resonance integrals β are taken to be as follows:

$$I_C = 11.16\,\text{eV}, \qquad I_O = 32.9\,\text{eV}$$
$$A_C = 0.03\,\text{eV}, \qquad A_O = 11.7\,\text{eV}$$
$$\beta_{CC} = -2.48\,\text{eV}, \qquad \beta_{CO} = -2.30\,\text{eV}$$

The Coulomb repulsion integrals γ_{pq} are calculated in units of eV by the formula

$$\gamma_{pq} = 14.40/[a \exp(-0.3\,r^2) + r] \qquad (1)$$

where r is the distance in units of Å between a pair of atoms p and q, and

$$a = 14.40/\{(1/2)[(I_p - A_p) + (I_q - A_q)]\}$$

with I and A expressed in units of eV. Atoms p and q may include both carbon and oxygen atoms, and Eq. (1) is used for $p=q$ as well as for $p \neq q$.

The values of I_C and A_C are taken from the data presented by Hinze and Jaffé.[17] In the derivation of Eq. (1), we first assumed a general formula

$$\gamma_{pq} = 14.40/[a \exp(-br^n) + r]$$

where b and n are adjustable parameters. (The formula proposed by Nishimoto and Mataga[18] is obtained by taking b as zero, while the formula by Knowlton and Carper[19] corresponds to $n=1$.) The values of b and n adopted here, together with the integral β_{CC}, are so chosen that the calculated excitation energies for the $^1B_{2u}$, $^1B_{1u}$, $^1E_{1u}$, and $^3B_{1u}$ states of benzene are in best agreement with the observed ones as measured at the maximum of the whole absorption band corresponding to each of the electronic transitions from the ground state to these singlet and triplet states. The values of I_O, A_O, and β_{CO} are determined so that the results of calculation and experiment may agree well as to the energy shifts of the lower singlet and triplet levels which are produced on going from benzene to phenol.

Twelve singly excited triplet configurations of lower energy are included in the CI calculations. If the SCF MO's of naphthalene and naphthols are numbered from 1 to 10 and from 1 to 11, respectively, in order of increasing orbital energy, the twelve configurations concerned are represented by the following one-electron transitions: for naphthalene 5→6, 7, 8, 9; 4→6, 7, 8, 9; 3→6, 7; 2→6, 7; and for naphthols 6→7, 8, 9, 10; 5→7, 8, 9, 10; 4→7, 8; 3→7, 8.

Configuration Analysis. The general procedure for configuration analysis has been described in a previous paper.[13] The wavefunctions $^3\Psi_1$, $^3\Psi_2$, ⋯ for the triplet states of α- or β-naphthol are collected in a row vector $^3\boldsymbol{\Psi}$. Each of these wavefunctions is expressed in terms of the reference state wavefunctions $^3\Psi_1{}^0$, $^3\Psi_2{}^0$, ⋯ that are built up from the MO's localized either on the naphthalene or on the substituent. The reference state wavefunctions collected in a row vector $^3\boldsymbol{\Psi}^0$ involve locally excited states and charge-transfer states. By introducing a matrix $^3\mathbf{M}$, $^3\boldsymbol{\Psi}$ is written as

$$^3\boldsymbol{\Psi} = {}^3\boldsymbol{\Psi}^0({}^3\mathbf{M}) \qquad (2)$$

The matrix $^3\mathbf{M}$ can be determined by the method developed previously.[13]

Results and Discussion

Figure 3 shows transient absorption spectra obtained by the rapid-scan method for naphthalene, α- and β-naphthol in a mixture of isopentane, methylcyclohexane and ether (PME; volume ratio, 6 : 1 :

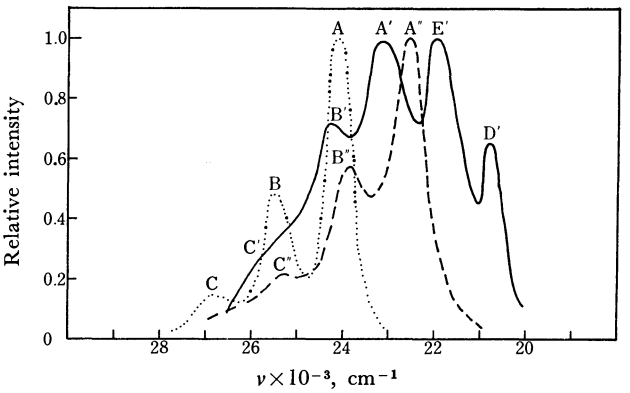

Fig. 3. Transient absorption spectra of naphthalene (·····), α-naphthol (——), and β-naphthol (- - -) in PME at 77°K. Concentrations of solutes: naphthalene, 8.3×10^{-4} mol/l; α-naphthol, 1.8×10^{-4} mol/l; β-naphtol, 1.7×10^{-4} mol/l.

15) G. Porter, *Proc. Roy. Soc. London*, **A200**, 284 (1950).
16) G. Porter and M. W. Windsor, *Discuss. Faraday Soc.*, **17**, 178 (1954).
17) J. Hinze and H. H. Jaffé, *J. Amer. Chem. Soc.*, **84**, 540 (1962).
18) K. Nishimoto and N. Mataga, *Z. physik. Chem. N.F.*, **12**, 335 (1957).
19) P. Knowlton and W. R. Carper, *Mol. Phys.*, **11**, 213 (1966).

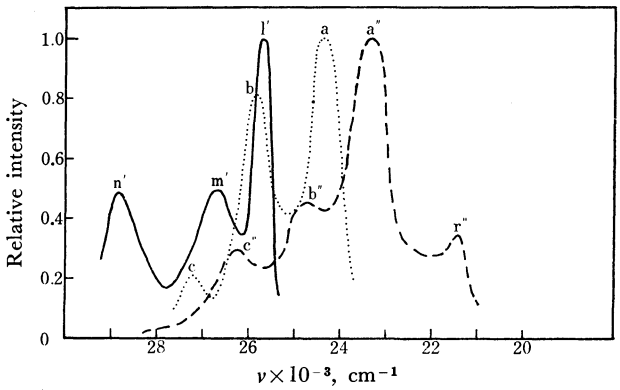

Fig. 4. Transient absorption spectra of naphthalene (·····), α-naphthol (——), and β-naphthol (- - -) in *n*-hexane at room temperature. Concentrations of solutes: naphthalene, 8.5×10^{-4} mol/*l*; α-naphthol, 3.07×10^{-4} mol/*l*; β-naphthol, 3.3×10^{-4} mol/*l*.

TABLE 1. BAND MAXIMA OF ABSORPTION SPECTRA

	Rapid-scan method in PME at 77°K			Flash method in *n*-hexane at room temperature		
	Band	λ(mμ)	ν(cm^{-1})	Band	λ(mμ)	ν(cm^{-1})
Naphthalene	A	414.5	24130	a	410.5	24360
	B	392.0	25510	b	387.5	25810
	C	372.5	26850	c	368.0	27170
α-Naphthol	D'	481.0	20790	l'	389.0	25710
	E'	455.0	21980	m'	374.5	26700
	A'	431.5	23180	n'	347.5	28780
	B'	412.0	24270			
	C'	—	—			
β-Naphthol				r''	467.0	21410
	A''	443.0	22570	a''	429.0	23310
	B''	419.0	23870	b''	404.0	24750
	C''	395.5	25280	c''	381.0	26250

0.7)[20] at 77°K, and Fig. 4 those obtained by the flash method in *n*-hexane at room temperature. In this paper all the spectra are given in such a way that the intensity of the maximum of the whole absorption spectrum is normalized to unity, since we are not concerned with the absolute absorption intensities. The numerical data on band maxima are presented in Table 1.

As has been mentioned, the absorption spectrum of naphthalene consists of three vibrational bands which belong to a single T–T electronic transition. In Figs. 3, 4 and Table 1, the absorption bands for naphthalene and its derivatives are denoted in the following way. The bands observed in the PME rigid glass are written in capital letters, while those observed in *n*-hexane by the flash method are written in small letters; the prime and double prime refer to α- and β-naphthol, respectively. As will be seen, bands of the same type are represented by letters of the same kind.

20) Ether was added to eliminate the possibility of association of the naphthol molecules.

Confirmation of T–T Absorption. The lifetimes of the transient absorption spectra in PME at 77°K shown in Fig. 3 were measured and found to be equal to the respective phosphorescence lifetimes of naphthalene, α- and β-naphthol observed under the same conditions. All the absorption spectra in Fig. 3 are therefore regarded as due to T–T transitions.

The T–T absorption spectra of naphthalene in Figs. 3 and 4 agree in their features, though a slight frequency shift is found. The corresponding spectra of β-naphthol also agree with each other and with the naphthalene spectra except for an additional band appearing in the spectrum of Fig. 4. Thus, on changing the solvent from the PME rigid glass to the fluid *n*-hexane, bands A'', B'', and C'' show a shift to higher frequencies, resulting in a'', b'', and c'', respectively. On the other hand, a new band referred to as r'' appears in the β-naphthol spectrum obtained by the flash method (Fig. 4). This band cannot be due to β-naphthol itself, but should be assigned to a certain molecular species produced by flash photolysis. In fact, r'' is identical with the absorption band at 21500 cm^{-1} which was found by Jackson and Porter[21] in flash photolysis of β-naphthol in viscous paraffin and assigned to the β-naphthoxyl radical.

The absorption spectrum of α-naphthol shown in Fig. 4 is similar to the spectrum attributed to a T–T transition in α-naphthol by Porter and Windsor.[22] However, the spectrum of α-naphthol in Fig. 4 differs entirely from the spectrum in Fig. 3, so that the former should not be identified with the T–T absorption. This is also supported by the following.

A rapid-scan measurement of the transient absorption spectrum was made for α-naphthol at 77°K in a hydrocarbon solvent of isopentane-methylcyclohexane (PM) mixture. In contrast to the case of Fig. 3, this did not contain ether. The spectrum thus obtained was very different from the T–T spectrum of α-naphthol in Fig. 3, and was analogous to the spectrum in Fig. 4. It was found that the absorption spectrum obtained in this way did not vanish so long as the sample was kept at low temperature, and disappeared on warming. This clearly shows that the spectrum in question, and hence the spectrum of α-naphthol in Fig. 4, cannot be due to a T–T transition, and should be attributed to a free radical produced by flash photolysis. The spectral behavior of α-naphthol thus changes with the constituent of the solvent employed, and it does not depend on the temperature or rigidity of the solvent.

In PME, the naphthol must form a hydrogen bond with ether. We assume that formation of a hydrogen bond between α-naphthol and a proton-accepting substance like ether gives rise to stabilization of the triplet state of the α-naphthol molecule and leads to the normal T–T absorption spectrum. It might be noted that a solution of α-naphthol in PME containing triethylamine as a proton acceptor also gives the T–T absorption at 77°K (*vide infra*).

21) G. Jackson and G. Porter, *Proc. Roy. Soc. London*, **A260**, 13 (1961).

22) G. Porter and M. W. Windsor, *Proc. Roy. Soc. London*, **A245**, 238 (1958).

Analysis of T–T Absorption Spectra. The three absorption bands of naphthalene (Fig. 3) belong to one and the same electronic transition and constitute a vibrational progression. Thus all these bands are known to be polarized along the long axis of the molecule,[4–6] and the spacings A···B and B···C are equally $\sim$1400 cm^{-1}, which can be assigned to a totally symmetric vibration of naphthalene. Similarly, the three absorption bands of β-naphthol are considered to constitute an analogous vibrational progression. The T–T absorption spectrum of α-naphthol (Fig. 3) involves five bands, which are not likely to belong to a single electronic transition. In connection with this problem, we will refer to additional experimental results.

The T–T absorption spectra at 77°K of α-naphthol in PME containing triethylamine as a proton acceptor and of α-methoxynaphthalene in PME are shown in Fig. 5, and the corresponding spectra of the β-derivatives in Fig. 6. In these figures the spectra of the naphthols in PME at 77°K are also given for comparison.

As regards the hydrogen bonding effects on electronic transitions, a thorough investigation has been carried out on the usual singlet transitions of hydroxylic compounds including α- and β-naphthol.[23] It was concluded that frequency shifts accompanying the formation of hydrogen bond differ in magnitude among different electronic transitions in a given molecule, and all the vibrational components for a given transition show a uniform shift. Intensity changes accompanying the formation of hydrogen bond also differ. These conclusions may be applied to the case of T–T transitions.

It is expected that triethylamine produces far greater hydrogen bonding effects on the T–T transitions of naphthols than does ether, since the former is known to have a much stronger proton-accepting power.[24,25]

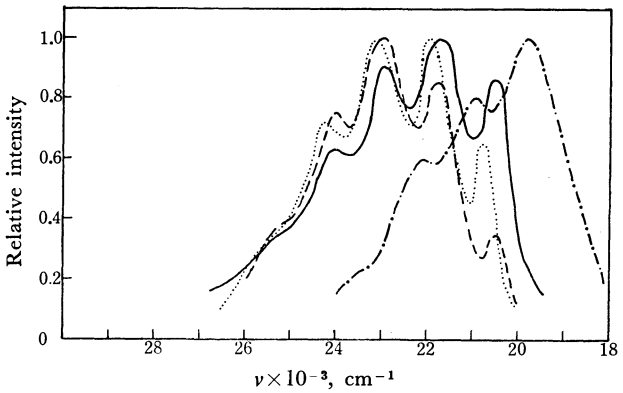

Fig. 5. T–T absorption spectra of α-substituted naphthalenes at 77°K: ·····, α-naphthol in PME; ——, α-naphthol in PME containing triethylamine (0.2 mol/*l*); —·—·, α-naphthol in an ethanol-methanol mixture containing potassium hydroxide (0.11 mol/*l*); – – –, α-methoxynaphthalene in PME. Concentrations of solutes: α-naphthol, 1.8×10^{-4} mol/*l* in all cases; α-methoxynaphthalene, 1.7×10^{-4} mol/*l*.

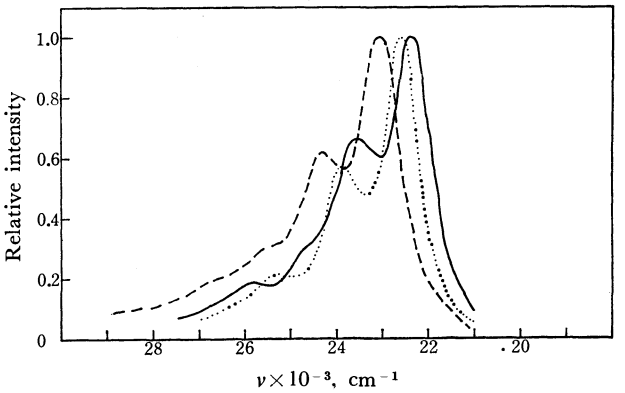

Fig. 6. T–T absorption spectra of β-substituted naphthalenes at 77°K: ·····, β-naphthol in PME; ——, β-naphthol in PME containing triethylamine (0.2 mol/*l*); – – –, β-methoxynaphthalene in PME. Concentrations of solutes: β-naphthol, 1.7×10^{-4} mol/*l* in all cases; β-methoxynaphthalene, 1.6×10^{-4} mol/*l*.

For β-naphthol (Fig. 6), the three bands show a uniform red shift on changing the proton acceptor from ether to triethylamine. Furthermore, the absorption spectrum of β-methoxynaphthalene resembles the spectrum of β-naphthol. These observations confirm the view that the absorption bands of β-naphthol or of β-methoxynaphthalene are to be associated with a single T–T transition.

In the case of α-naphthol (Fig. 5), when the proton acceptor is changed from ether to triethylamine, the two bands at lower frequencies, D′ and E′ (*cf.* Fig. 3), are red-shifted and intensified to a greater extent than the remaining three bands, A′, B′, and C′, suggesting that D′ and E′ belong to a different T–T transition from that to which A′, B′, and C′ belong. α-Methoxynaphthalene gives a spectrum which is, as a whole, similar to the α-naphthol spectrum. It is seen, however, that the bands corresponding to D′ and E′ are of lower intensity in α-methoxynaphthalene than in α-naphthol. In Fig. 5 is also shown the T–T absorption spectrum at 77°K of α-naphthol in an alkaline ethanol-methanol mixture (volume ratio, 5 : 1), where the naphthol molecule is converted to the naphtholate ion. Owing to the highly electron-donating character of the $-O^-$ group, the absorption spectrum of the α-naphtholate ion is markedly displaced to the red with a considerable change in appearance as compared with the spectrum of α-naphthol. It can be assumed here that in the naphtholate ion the bands D′ and E′ coalesce into one broad band with the maximum at 19800 cm^{-1}, and that the three bands at the higher frequencies correspond to A′, B′, and C′, with the band at 21000 cm^{-1} assigned as A′.

Thus, all the observations for the α-derivatives of naphthalene indicate that the absorption spectrum of α-naphthol or of α-methoxynaphthalene originates in two different T–T transitions, one leading to the bands A′, B′, and C′ and the other to D′ and E′. It is to be noted that the relative intensity of the T–T transition with which D′ and E′ are associated increases

23) H. Baba and S. Suzuki, *J. Chem. Phys.*, **35**, 1118 (1961).
24) S. Nagakura and M. Gouterman, *J. Chem. Phys.*, **26**, 881 (1957).
25) For this reason, in PME containing triethylamine, naphthols are considered to form a hydrogen bond with triethylamine.

TABLE 2. CALCULATED STATE ENERGIES RELATIVE TO THE GROUND STATE AND f VALUES FOR THE T–T TRANSITIONS

Wave-function	Naphthalene						α-Naphthol		β-Naphthol	
	This work			Pariser						
	Symmetry	Energy (cm^{-1})	f	Symmetry	Energy (cm^{-1})	f	Energy (cm^{-1})	f	Energy (cm^{-1})	f
$^3\Psi_1$	B_{2u}^+	23360	Ref.	B_{2u}^+	17590	Ref.	21830	Ref.	22680	Ref.
$^3\Psi_2$	B_{1g}^+	30600	0	B_{1g}^+	27620	0	29940	0.002	29880	0.001
$^3\Psi_3$	B_{3u}^+	33080	0	B_{3u}^+	29360	0	31240	0.001	31960	0
$^3\Psi_4$	B_{3u}^-	36060	0	B_{3u}^-	32420	0	35440	0.002	34150	0.005
$^3\Psi_5$	A_{1g}^+	37850	0	B_{2u}^+	34040	0	38360	0.002	36930	0.004
$^3\Psi_6$	B_{2u}^+	38740	0	A_{1g}^+	35770	0	39160	0	39220	0.004
$^3\Psi_7$	B_{1g}^+	48390	0	B_{1g}^+	44580	0	47250	0.254	46440	0.081
$^3\Psi_8$	A_{1g}^-	48460	0.134	A_{1g}^-	46100	0.084	48120	0.645	48530	0.065
$^3\Psi_9$	B_{1g}^-	50560	0.990	B_{1g}^-	48280	0.451	49770	0.076	49950	0.990
$^3\Psi_{10}$	A_{1g}^+	56760	0	A_{1g}^+	48560	0	55180	0.025	56260	0.072
$^3\Psi_{11}$	A_{1g}^-	62630	0.523	B_{3u}^+	51070	0	61040	0.823	60830	0.457
$^3\Psi_{12}$	B_{1g}^-	70630	0.013	B_{2u}^+	54090	0	69250	0.008	68380	0.010

in the order: α-methoxynaphthalene<α-naphthol hydrogen-bonded with ether<α-naphthol hydrogen-bonded with triethylamine<α-naphtholate ion.

In general the frequency shift of an electronic transition produced by hydrogen bonding is due to the difference between the energies of hydrogen bond for the electronic states which are concerned in that transition.[23] All the T–T absorption transitions in α- and β-naphthol treated in this study are found to be shifted to the red upon formation of the hydrogen bond. This means that in all cases the proton-donating power of the naphthols is stronger in the higher triplet state than in the lowest triplet. It should be noted that the frequency shifts for the T–T transitions of α- and β-naphthol are comparable in magnitude to those for the transitions from the ground state to excited singlet states of the naphthols.[23,24]

Theoretical Interpretation of T–T Transitions. The calculated energies for triplet states, relative to the ground state, and the oscillator strengths (f) for transitions from the lowest triplet state to higher triplet states are summarized in Table 2. In all cases, the triplet state wavefunctions are numbered from 1 to 12 in order of increasing energy. For naphthalene, the results of calculation by Pariser[26] are also given in the same table. It should be noted that Pariser included all singly excited configurations in his CI calculation. Of the resulting twenty-five state wavefunctions twelve are given in Table 2. The symmetry types are shown for the wavefunctions of the naphthalene molecule (symmetry group, D_{2h}). The long and short molecular axes are chosen as x and y coordinate axes, respectively, and the plus and minus signs have the same meaning as those used by Pariser.[26]

In Fig. 7 the results of calculations are compared with the spectral data obtained at 77°K in rigid-glass solution. The magnitudes of the calculated oscillator strengths f are represented by the lengths of solid lines in such a way that the largest f value for each of the molecules is normalized to unity. However, for the triplet states with f values less than one-tenth of the largest f, only their energy levels are shown in the figure by dotted lines. In each of the molecules, the experimental energy level for $^3\Psi_1$ represents the position of the 0–0 band of the phosphorescence spectrum measured in PME at 77°K; the spacing between the experimental level for $^3\Psi_1$ and the absorption curve given in the figure corresponds to the observed T–T transition energy.

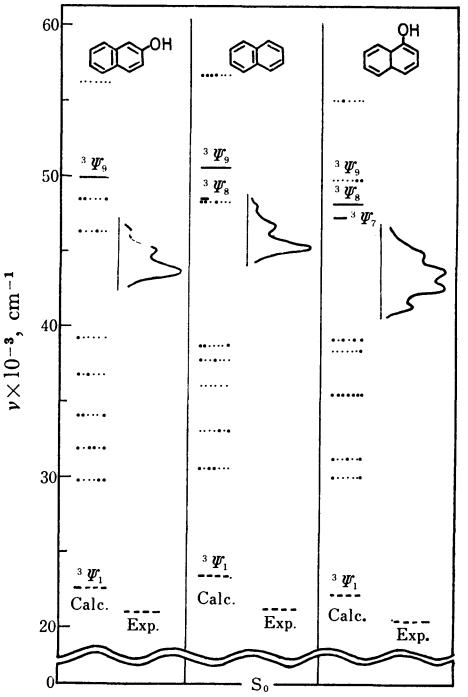

Fig. 7. Calculated and experimental energies of triplet states in naphthalene, α- and β-naphthol. Energies are expressed in wavenumbers relative to the ground state (S_0). The intensities of T–T transitions from the lowest triplet to higher triplet states are represented by solid lines of different lengths or by dotted lines according to the magnitudes of the calculated oscillator strengths; see text for the details.

Since the lowest triplet of naphthalene is a $^3B_{2u}^+$

26) R. Pariser, *J. Chem. Phys.*, **24**, 250 (1956).

state, only the transitions to the triplet states characterized by g and minus are to be allowed. From a comparison of the f values, it follows that the T–T absorption in β-naphthol as well as in naphthalene is due to $^3\Psi_1 \rightarrow {}^3\Psi_9$ transition, the adjacent transition $^3\Psi_1 \rightarrow {}^3\Psi_8$ being assumed to be too weak to be observed. In the case of α-naphthol, there is no large difference between the f values for $^3\Psi_1 \rightarrow {}^3\Psi_7$ and $^3\Psi_1 \rightarrow {}^3\Psi_8$, so that these transitions are expected to appear in the T–T absorption spectrum. Thus, of the two transitions observed for α-naphthol, the one of lower energy is assigned to $^3\Psi_1 \rightarrow {}^3\Psi_7$ and the other to $^3\Psi_1 \rightarrow {}^3\Psi_8$.

The triplet-state energies obtained from our calculations should in principle be related to the Franck-Condon maxima of absorption transitions which might be supposed to occur from the ground state to the triplet states concerned. If allowance is made for this fact, it might be said that the calculated energies are in general agreement with the experimental ones, at least with respect to the relative positions of the triplet levels

Table 3. Configuration analysis for α-naphthol

	$^3\Psi_1$	$^3\Psi_2$	$^3\Psi_3$	$^3\Psi_4$	$^3\Psi_5$	$^3\Psi_6$	$^3\Psi_7$	$^3\Psi_8$	$^3\Psi_9$	$^3\Psi_{10}$
$^3\Psi^0_1$	**78.3**	6.2		0.7		0.3	1.0	0.3		
$^3\Psi^0_2$	2.9	**70.2**	3.4		0.4	0.9	0.3			0.2
$^3\Psi^0_3$		2.4	**54.3**	27.9	0.1	0.3	2.7		0.1	
$^3\Psi^0_4$			17.6	**38.6**	9.6	20.1	0.6	0.5	0.4	0.4
$^3\Psi^0_5$	0.2	0.5	3.6	18.2	22.7	29.0	0.1	2.1	0.3	0.2
$^3\Psi^0_6$				0.1	**53.0**	**34.7**	0.2	0.3	0.2	0.1
$^3\Psi^0_7$					0.2		15.4	9.4	**51.4**	
$^3\Psi^0_8$			0.9		0.6		**39.0**	5.3	32.1	1.7
$^3\Psi^0_9$				0.3		0.2	11.6	**60.8**	2.3	0.6
$^3\Psi^0_{10}$							0.3		0.2	**75.1**
$^3\Psi^0_{11}$					0.2				0.1	1.8
$^3\Psi^0_{12}$										
$^3\Psi^0_{CTO\rightarrow6}$	11.4	5.7		1.8	0.6	2.5	7.0	2.3	0.3	1.2
$^3\Psi^0_{CTO\rightarrow7}$		0.9	9.5	1.6		0.3	10.0	2.8	1.7	3.4
$^3\Psi^0_{CTO\rightarrow8}$	0.2	4.8	0.2	0.1		0.2	1.2	5.5		
$^3\Psi^0_{CTO\rightarrow9}$			0.3	0.8	1.6	1.3	0.5		0.4	4.2
$^3\Psi^0_{3\rightarrow8}$		0.3					0.2	1.4		
$^3\Psi^0_{3\rightarrow9}$					0.2	0.1				0.7
$^3\Psi^0_{2\rightarrow8}$										
Total weight (%)	93.0	91.0	89.8	90.1	89.2	89.9	90.1	90.7	89.5	89.6

Table 4. Configuration analysis for β-naphthol

	$^3\Psi_1$	$^3\Psi_2$	$^3\Psi_3$	$^3\Psi_4$	$^3\Psi_5$	$^3\Psi_6$	$^3\Psi_7$	$^3\Psi_8$	$^3\Psi_9$	$^3\Psi_{10}$
$^3\Psi^0_1$	**83.9**	2.7	0.7	0.6		0.3		2.8	0.1	
$^3\Psi^0_2$	0.5	**63.6**	21.1	0.6	0.4		0.2	1.6		
$^3\Psi^0_3$	0.5	1.2	**54.2**	5.5	16.3	0.2			0.2	0.4
$^3\Psi^0_4$	1.2	3.1	2.8	**46.0**	5.1	22.5	8.1		0.1	
$^3\Psi^0_5$	0.4	0.9	2.4	0.2	**40.9**	14.7		0.8		1.1
$^3\Psi^0_6$				16.3	13.0	**42.2**	15.1	2.5		
$^3\Psi^0_7$				1.2	0.2		**22.0**	18.1		
$^3\Psi^0_8$	0.3	0.4	0.2			0.6	17.4	**50.9**		
$^3\Psi^0_9$					0.4	0.1	0.1	0.5	**80.1**	8.4
$^3\Psi^0_{10}$					0.4	0.1	0.2	0.5	1.8	**56.5**
$^3\Psi^0_{11}$					0.3	0.2		0.7	0.3	3.1
$^3\Psi^0_{12}$							0.4	0.3	0.6	0.9
$^3\Psi^0_{CTO\rightarrow6}$	5.8	7.4	4.7	1.4	5.4	1.0	0.5	2.0	3.6	8.8
$^3\Psi^0_{CTO\rightarrow7}$	0.1	0.4	0.5	9.9	1.8	1.4	4.8	1.1	0.1	2.1
$^3\Psi^0_{CTO\rightarrow8}$	0.2	2.7			2.6	1.4	1.9	2.2	3.0	4.0
$^3\Psi^0_{CTO\rightarrow9}$				0.2	0.5		2.7	0.5		0.7
$^3\Psi^0_{3\rightarrow8}$					0.1		0.2	0.4		0.3
$^3\Psi^0_{3\rightarrow9}$							0.1	0.2		
$^3\Psi^0_{2\rightarrow8}$		0.2			0.3	0.1	0.3	0.2	0.2	0.5
Total weight (%)	92.9	82.6	86.6	81.9	87.7	84.8	74.0	85.3	90.1	86.8

for naphthalene and its two derivatives.

In the T–T absorption spectrum of α-naphthol in PME at 77°K, the two transitions have almost the same intensities, whereas theory predicts that the intensity of the first transition should be about two-fifths of that of the second (Table 2). In PME, however, naphthol is linked to ether through a hydrogen bond, which will result in an increase in the relative intensity of the first transition. In fact, α-methoxynaphthalene, which is expected to have a π-electronic structure similar to that of α-naphthol and has no possibility of forming a hydrogen bond with ether, gives in PME a T–T absorption spectrum in which the first transition is weak compared with the second (see Fig. 5).

Recently Klasinc and Sommer[9] have made calculations on the T–T transitions of naphthalene and naphthols by the Pariser-Parr-Pople method. Their results differ in detail from the results of the present calculations, but they also reached the conclusion that one new transition should appear in the T–T absorption spectrum of α-naphthol.

Tables 3 and 4 give the results of configuration analysis. The triplet-state wavefunctions ${}^3\Psi_1$, ${}^3\Psi_2$, ⋯, ${}^3\Psi_{10}$ for the naphthols are analyzed into the wavefunctions for reference triplet states, *viz.*, the locally excited states related to naphthalene ${}^3\Psi_1{}^0$, ${}^3\Psi_2{}^0$, ⋯, ${}^3\Psi_{12}{}^0$, charge-transfer (CT) configurations ${}^3\Psi^0{}_{\mathrm{CTO}\to k}$, formed by transferring an electron from the orbital localized on the oxygen atom to the kth MO of naphthalene, and some other singly locally excited configurations ${}^3\Psi^0{}_{i\to k}$. The numbering of the MO's localized on naphthalene is the same as described previously. In the columns of Tables 3 and 4, the weights in percent of the ${}^3\Psi^0$'s obtained as the squares of the elements of the matrix ${}^3\mathbf{M}$ in Eq. (2), are shown for each of the ${}^3\Psi$'s, the weights less than 0.1% being omitted.[27]

It is seen from the tables that in β-naphthol the wavefunction ${}^3\Psi_9$ consists mainly of ${}^3\Psi_9{}^0$, while in α-naphthol ${}^3\Psi_7$ and ${}^3\Psi_8$ consist predominantly of ${}^3\Psi_8{}^0$ and ${}^3\Psi_9{}^0$, respectively. The lowest triplet state ${}^3\Psi_1$ is largely due to ${}^3\Psi_1{}^0$ in both α- and β-naphthol. Thus, ${}^3\Psi_1\to{}^3\Psi_7$ and ${}^3\Psi_1\to{}^3\Psi_8$ transitions in α-naphthol are to be related, respectively, to local transitions ${}^3\Psi_1{}^0(B_{2u}{}^+)\to{}^3\Psi_8{}^0(A_{1g}{}^-)$ and ${}^3\Psi_1{}^0(B_{2u}{}^+)\to{}^3\Psi_9{}^0(B_{1g}{}^-)$, and ${}^3\Psi_1\to{}^3\Psi_9$ in β-naphthol to ${}^3\Psi_1{}^0(B_{2u}{}^+)\to{}^3\Psi_9{}^0(B_{1g}{}^-)$. It will be found, on closer inspection of Table 3, that the appearance of a new transition in the α-derivative of naphthalene is due to the fact that ${}^3\Psi_7$ involves the characters ${}^3\Psi_9{}^0(B_{1g}{}^-)$ and CT configurations to an appreciable extent. The total weight of CT configurations amounts to as much as 18.7%.

We wish to express our thanks to Dr. Satoshi Suzuki for his co-operation and discussion in carrying out the calculations, and to Mr. Yoshio Shindo and Mr. Masahisa Fujita for their help in constructing the apparatus for flash spectroscopy.

27) Numbers written in boldface represent the largest weights.

BULLETIN OF THE CHEMICAL SOCIETY OF JAPAN, VOL. 44, 984—988 (1971)

The Role of Reaction Sites in the Radiolysis of Solid Succinic Acid

Tetsuo MIYAZAKI, Yoshiteru FUJITANI, Terunobu WAKAYAMA, Kenji FUEKI, and Zen-ichiro KURI

Department of Synthetic Chemistry, Faculty of Engineering, Nagoya University, Chikusa-ku, Nagoya

(Received November 2, 1970)

The main gaseous products in the radiolysis of solid succinic acid are CO_2, CO, and H_2. It was found that the $G(CO+H_2)$ from the powder is much higher than that from the single crystal, while there is no difference in $G(CO_2)$ between the powder and the single crystal, indicating that CO_2 is produced homogeneously in the solid. The clear difference in the $G(CO+H_2)$ between the powder and the single crystal cannot be attributed to the analytical procedure, the secondary reaction of CO, or the presence of H_2O as an impurity. It may be due to the difference in the primary process of the radiolysis. It is conceivable that the mobile active entity formed by the γ-irradiation of the crystal migrates to the special reaction sites and produces CO and H_2. The difference in $G(CO+H_2)$ may also be due to the different numbers of the sites between the powder and the single crystal. It is discussed whether the mobile entity is a cation, an electron, or an exciton.

We have previously studied the radiolysis in the solid state in order to elucidate the primary process of radiolysis in the solid state and in order to obtain information about reaction kinetics in the solid state. In the previous studies, some peculiar phenomena in solid-state radiolysis have been reported.[1,2] The formation of the exciton may play an important role in the radiolysis of solid isobutane, while it plays only a minor role in the liquid phase.[1] When solid isobutane is γ-irradiated, an isobutyl radical is formed in the crystalline state, while a tertiary butyl radical is formed in the glassy state.[2] This result cannot be

1) a) T. Wakayama, T. Miyazaki, K. Fueki, and Z. Kuri, This Bulletin, **42**, 1164 (1969). b) T. Wakayama, T. Kimura, T. Miyazaki, K. Fueki, and Z. Kuri, *ibid.*, **43**, 1017 (1970). c) T. Miyazaki, T. Yamada, T. Wakayama, K. Fueki, and Z. Kuri, *ibid.*, **44**, 934 (1971).

2) a) T. Miyazaki, T. Wakayama, K. Fueki, and Z. Kuri, This Bulletin, **42**, 2086 (1969). b) T. Wakayama, T. Miyazaki, K. Fueki, and Z. Kuri, *J. Phys. Chem.*, **74**, 3584 (1970).

explained by the ordinary theory of a unimolecular reaction in the gas phase.

In a previous communication, the preliminary findings on the effect of crystal size on the radiolysis of succinic acid have been reported. In this work we will study this effect in more detail in order to get a better understudying of solid-state radiolysis.

Experimental

The succinic acid was supplied by the Katayama Chemical Co. and was more than 99.8% pure. The acid was in the form of a single crystal 0.5—1.0 cm long, and its melting point was 185°C. The single crystal was ground into powder with an agate mortar. The diameter of the powder was measured with a microscope and found to be about 2×10^5 Å.

After the samples of the single crystal or the powder had been degassing for more than 3 hours on a vacuum line, they were irradiated with γ-rays from Co-60 at a dose rate of 4.4×10^{19} eV/g hr. After irradiation, the sample was melted at 185°C, and then the gaseous products were analyzed as follows: the gaseous products (mixtures of CO and H_2) not condensable at the temperature of liquid nitrogen were analyzed by a gas burette connected to a Toepler pump and a cupric oxide furnace kept at 240°C, while another gaseous product (CO_2) not condensable at the temperature of dry ice was measured by means of the gas burette alone.

Results and Discussion

Gaseous Products in the Radiolysis of Solid Succinic Acid. The main gaseous products in the radiolysis of solid succinic acid are shown in Table 1. When succinic acid is γ-irradiated at −196°C in the powdered form or in the single crystal, the $G(CO+H_2)$ values are about 0.3 and 0.04 respectively at a dose of 6.6×10^{20} eV/g. The fact that the $G(CO+H_2)$ value is different from the previously-reported value[3] may be due to the difference in dose between the two cases. On the contrary, there is no clear difference in the yield of CO_2 between the powder and the single crystal. The yield of CO is about four times that of H_2. It should be noted that the $G(CO+H_2)$ value from the powder is much higher than that from the single crystal.

Table 1. Radiolysis of solid succinic acid

State	Irrad. Temp.	Method of Analysis	$G(CO+H_2)$	$G(CO_2)$
Powder	−196°C	Melting	0.20[a]+0.11[b]	2.01
Powder	−196°C	Melting	0.20[a]+0.10[b]	1.90
Single Crystal	−196°C	Melting	0.06	1.89
Single Crystal	−196°C	Melting	0.02	1.60
Powder	−196°C	Dissolved in ethanol	0.24	
Single Crystal	−196°C	Dissolved in ethanol	0	
Powder	30°C	Melting	0.92	4.92
Single Crystal	30°C	Melting	0.24	4.60

a) Yield before melting the sample
b) Yield after melting the sample
Dose: 6.6×10^{20} eV/g

3) T. Miyazaki, S. Okada, T. Wakayama, K. Fueki, and Z. Kuri, This Bulletin, **43**, 1907 (1970).

The possibility that the difference in $G(CO+H_2)$ value may be attributed to thermal decomposition during the analysis can be excluded for the following two reasons. First, two-thirds of the total yields of $CO+H_2$ could be measured at room temperature without melting the irradiated powder at 185°C, and the yields are much higher than the total yields from the single crystal. Second, when the CO and H_2 were measured after the γ-irradiated sample had been dissolved in ethanol at room temperature, the clear difference in $G(CO+H_2)$ value between the powder and the single crystal was also observed.

Does the CO produced in the single crystal react with the trapped radicals to result in the low yield of CO, while CO in the powder diffuses to the surface without the reaction? The yields of $CO+H_2$ trapped in the powder at the irradiation temperature of −196°C and 30°C are 0.1 and 0.5 respectively. These values are higher than the total yields from the single crystal at each temperature. The difference in $G(CO+H_2)$ value between the powder and the single crystal cannot be ascribed to this cause.

Therefore, the difference in $G(CO+H_2)$ may represent the difference in the yields of products in the radiolysis of succinic acid.

Effect of H_2O on the Radiolysis of Succinic Acid. Solid succinic acid contains a small amount of water in its crystal. When a solid succinic acid is melted at 185—190°C, the water is vaporized from the acid; then the vapor pressure of water can be measured after the sample has been rapidly cooled to room temperature. In order to examine whether or not water was produced by the thermal decomposition of succinic acid at 185—190°C, the samples were held at this temperature for different times and then the amounts of water were measured. As is shown in Table 2, the amounts of water do not depend upon the time the substances are kept at 185—190°C; therefore, they represent the amounts of water present in the crystal as an impurity.

Table 2. Amounts of H_2O as an impurity in the succinic acid

State	Time held at 185—190°C	H_2O (mol%)
Single Crystal	0.3 hr	10
Single Crystal	1.5 hr	8
Single Crystal	3.0 hr	13
Powder	0.3 hr	13

Since the water usually acts as an effective cation scavenger in the radiolysis, there is a possibility that the amount of water in the powder is smaller than that in the crystal and that the difference in $G(CO+H_2)$ value between the powder and the single crystal is due to this effect. Table 2 shows, however, that the amount of water in the powder is approximately equal to that in the single crystal. When the polycrystalline sample from which water has been completely removed

TABLE 3. EFFECT OF H_2O ON THE RADIOLYSIS OF SUCCINIC ACID AT $-196°C$

State	$G(CO+H_2)$	$G(CO_2)$
Sample A	0.22	2.01
Sample B	0.19	1.83
Powder	0.31	1.96

Sample A: Polycrystal, from which H_2O is removed completely by melting the powder.
Sample B: Polycrystal, from which H_2O is removed completely by melting the single crystal.
Dose: 6.6×10^{20} eV/g

by melting and degassing, is γ-irradiated, the yield of $CO+H_2$ is rather smaller than that from the powder (Table 3). Therefore, the difference in $G(CO+H_2)$ value between the powder and the single crystal cannot be ascribed to the effect of water, but must be ascribed to a difference in the physical state, such as the surface area or the defects in the crystal.

Effect of Total Dose. The dependence of gaseous products on the total dose is shown in Figs. 1 and 2. The rate of the production of $CO+H_2$ decreases gradually with an increase in the dose, while the yield of CO_2 increases linearly with an increase in the dose. These results suggest that the mechanism of the formation of CO and H_2 differs from that of CO_2. If it is supposed that CO and H_2 are produced at special active sites of the crystal, the sites may be gradually consumed with an increase in the dose, resulting in a decrease in the rate of the formation of $CO+H_2$. The yields of $CO+H_2$ in the radiolysis of the single crystal at $-196°C$ seem to be negligibly small at a low dose. This is because the analysis of a small amount of $CO+H_2$ with Toepler pump is very difficult. On the contrary, CO_2 may be produced homogeneously in the crystal.

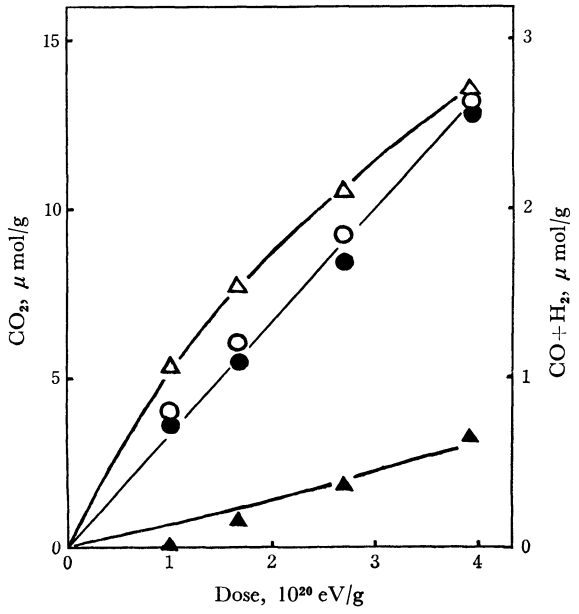

Fig. 1. Yield of gaseous products in the radiolysis of solid succinic acid at $-196°C$ against the total dose.
△: Yields of $CO+H_2$ from succinic acid in the powder.
▲: Yields of $CO+H_2$ from succinic acid in the single crystal.
○: Yields of CO_2 from succinic acid in the powder.
●: Yields of CO_2 from succinic acid in the single crystal.

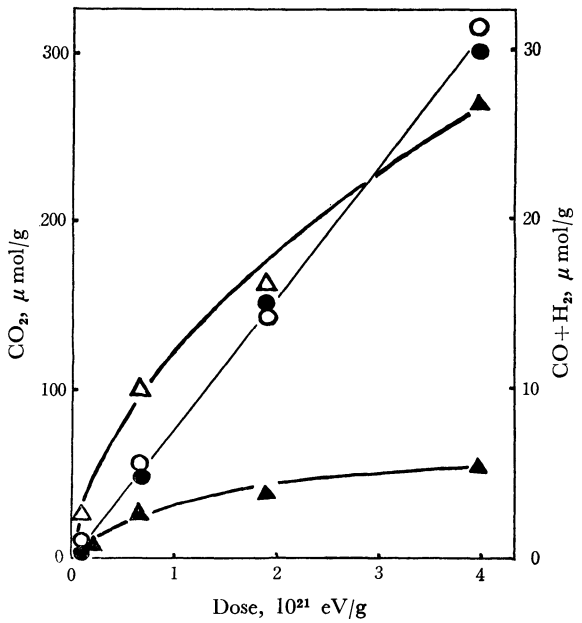

Fig. 2. Yields of gaseous products in the radiolysis of solid succinic acid at room temperature against the total dose.
△: Yields of $CO+H_2$ from succinic acid in the powder.
▲: Yields of $CO+H_2$ from succinic acid in the single crystal.
○: Yields of CO_2 from succinic acid in the powder.
●: Yields of CO_2 from succinic acid in the single crystal.

Yield Measured at Room Temperature without Melting. A fraction of the gaseous products can be measured at room temperature without melting the irradiated sample; the measurable yields depend upon the storage time at room temperature (Fig. 3). When the powdered succinic acid is irradiated at $-196°C$, the

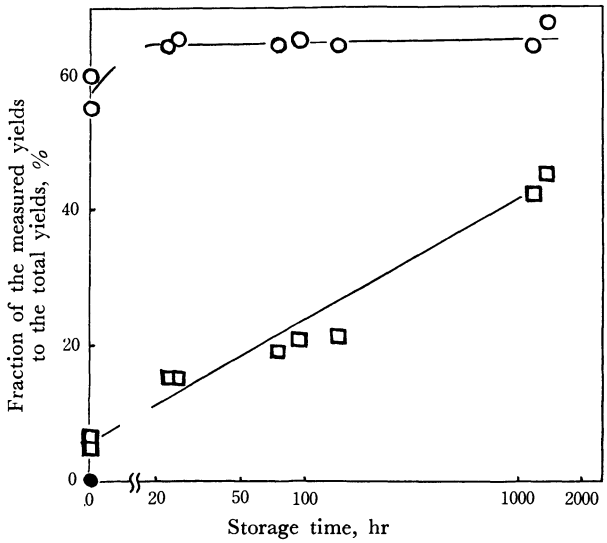

Fig. 3. Effect of storage time on the yields measured at room temperature before melting the irradiated sample.
○: Yields of $CO+H_2$ measured at room temperature before melting the irradiated sample.
□: Yields of CO_2 measured at room temperature before melting the irradiated sample.

$CO+H_2$ cannot be measured at $-196°C$, but two-thirds of the total yield can be measured immediately after warming up to room temperature. The measurable amount of $CO+H_2$ does not increase even if the sample is stored for longer than 1000 hr at room temperature. On the contrary, the amount of CO_2 measurable at room temperature gradually increases with the passage of the storage time. As will be discussed in the next section, the gaseous products may be formed mainly by warming the irradiated sample to room temperature. Two-thirds of CO and H_2 may be formed at some sites such as the surface and may come out easily from the crystal. The residue may be formed at another type of site, such as defects of the crystal, and be tightly trapped in the crystal. The results indicate that CO_2 may be formed uniformly in the crystal and may gradually diffuse to the surface during storage at room temperature.

Mechanism of Reaction. Since the effect of reaction sites on the radiolysis has not been reported previously, and since our information about the solid-state kinetics of molecular compounds is very scanty at present, it is not possible to explain this effect in a satisfactory way. We will discuss here a possible mechanism for this effect. Several investigators have proposed the following mechanism for explaining the ESR results on succinic acid:[4]

$$HOOCCH_2CH_2COOH \rightsquigarrow HOOCCH_2CH_2COOH^+ + e^- \quad (1$$

$$HOOCCH_2CH_2COOH^+ + HOOCCH_2CH_2COOH \rightarrow HOOCCH_2CH_2COO\cdot + HOOCCH_2CH_2COOH_2^+ \quad (2)$$

$$HOOCCH_2CH_2COO\cdot \rightarrow HOOCCH_2CH_3\cdot + CO_2 \quad (3)$$

$$e^- + HOOCCH_2CH_2COOH \rightarrow HOOCCH_2CH_2COOH^- \quad (4)$$

$$HOOCCH_2CH_2COOH^- \rightarrow HOOCCH_2CH_2 + CO_2^- \quad (5)$$

$$HOOCCH_2CH_2\cdot + HOOCCH_2CH_2COOH \rightarrow HOOCCH_2CH_3 + HOOCCH_2\dot{C}HCOOH \quad (6)$$

$$HOOCCH_2CH_2\cdot \rightarrow HOO\dot{C}CHCH_3 \quad (7)$$

Reactions (1), (2), and (4) take place at $-196°C$ by γ-irradiation. Reactions (3), (5), (6), and (7) represent the reactions which occur when the irradiated sample is warmed from $-196°C$ to room temperature. The facts that CO_2 is the main gaseous product in the radiolysis of succinic acid and that it is formed homogeneously in the crystal can be explained by the above reaction mechanism.

On the other hand, it is conceivable that CO and H_2 may be produced when the mobile active entity formed by γ-irradiation migrates to the reaction sites, such as the surface and defects in the crystal. We will now discuss whether the mobile entity is a cation, an electron, or an exciton.

(a) Cation: A crystal of succinic acid is a monoclinic plate; its structure was determined by Broadley *et al.* (Fig. 4).[5] Two nearest neighbor molecules of succinic acid are tightly combined by two hydrogen bonds between their carboxyl groups. Once a succinic acid cation is formed in reaction (1), its proton may be transferred easily to the second molecule by a quantum-tunneling process in a hydrogen bond (reaction (2)).[6] It is, however, difficult for the proton transfer to the third molecule to occur by this process, since there is no hydrogen bond between the protonated second molecule and the third molecule which is not depicted in Fig. 4.

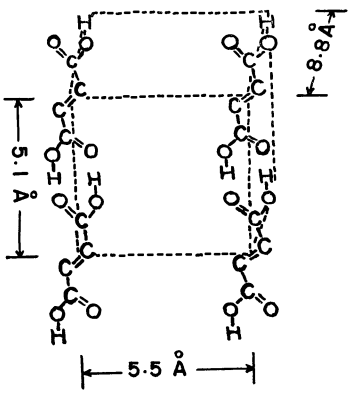

Fig. 4. Structure of the crystal of succinic acid in the unit cell.

The interaction between the protonated second molecule and the third molecule can roughly expressed by a charge-induced dipole interaction:

$$E = -\frac{e^2\alpha}{2r^4} \quad (I)$$

where E is the energy of interaction, and r, the distance between a charge and an induced dipole. α is the effective polarizability and is taken as 2×19^{-24} cc for a carbonyl group. Assuming that the charge of the protonated second molecule is localized on the oxygen atom, the distance (r) between the charge and a carbonyl group of the third molecule is 3.14 Å. From Eq. (I), we get $E\sim-1$ Kcal, which is rather less than the energy of the hydrogen bond, suggesting that the ion-molecule reaction would not occur easily.

Since water is an effective proton scavenger in the radiolysis, the fact that water does not affect the yields of CO and H_2 suggests that the proton does not move in the crystal.

(b) Electron: When 2-methyltetrahydrofuran (MTHF) glass containing a small amount of succinic acid is γ-irradiated at $-196°C$, the electrons are completely captured by the acid.[7] Since the efficiency of electron capture by maleic acid (HOOCCHCHCOOH) is 5—10 times as great as that of biphenyl in MTHF glass at $-196°C$,[8] succinic acid also may cap-

4) R. N. Schwartz, M. W. Hanna, and B. K. Bales *J. Chem. Phys.*, **51**, 4336 (1969). The related papers on ESR studies are cited therein.

5) J. S. Broadley, D. W. J. Cruickshank, J. D. Morrison, J. M. Robertson, and H. M. M. Shearer, *Proc. Roy. Soc.* (London), **A251**, 441 (1959).

6) I. Miyagawa, N. Tamura, and J. W. Cook, *J. Chem. Phys.*, **51**, 3520 (1969).

7) T. Suzuki, T. Miyazaki, A. Torikai, K. Fueki, and Z. Kuri, unpublished results.

8) A. Torikai, T. Suzuki, T. Miyazaki, K. Fueki, and Z. Kuri, *J. Phys. Chem.*, (1971) **75**, 482 (1971).

ture electrons efficiently in the solid state.

Since the absorption spectrum of the succinic-acid anion is not observed in the visible region, it is expected that the acid may possess a high electron affinity and that the anion, once it is formed, does not release an electron easily. Therefore, it seems that an electron does not move a long distance in the crystal of succinic acid.

(c) Exciton: In the previous studies of the radiolysis of solid isobutane,[1] it has been suggested that an exciton may play an important role in the solid-state radiolysis and that it will migrate to a distance of 20—30 Å. Since all the molecules of succinic acid in the crystal are combined by hydrogen bonds in one direction, an exciton, if it is formed, can migrate to a farther distance in the succinic acid than in saturated hydrocarbons. If it is supposed that the exciton migrates to the surface of succinic acid and is ionized there (reaction (9)), CO and H_2 may be formed by the neutralization of the succinic-acid ion by warming the sample up to room temperature (reaction (10)). This opinion is based on the findings that CO and H_2 are not observed at −196°C, and that CO is not adsorbed on the surface of succinic acid at −196°C. The reaction scheme may be represented as follows:

$$HOOCCH_2CH_2COOH \rightsquigarrow (HOOCCH_2CH_2COOH)_n^* \quad (8)$$

(in the crystal)

$$(HOOCCH_2CH_2COOH)_n^* \rightarrow HOOCCH_2CH_2COOH^+ + HOOCCH_2CH_2COOH^- \quad (9)$$

(at the surface)

$$HOOCCH_2CH_2COOH^+ + HOOCCH_2CH_2COOH \rightarrow HOOCCH_2CH_2COO\cdot + HOOCCH_2CH_2COOH_2^+ \quad (2)$$

$$HOOCCH_2CH_2COOH_2^+ + HOOCCH_2CH_2COOH^- \rightarrow CO,\ H_2,\ \text{other products} \quad (10)$$

(warming up to room temperature)

where $(HOOCCH_2CH_2COOH)_n^*$ is an exciton. The possibility that the exciton state in the solid may correspond to the superexcited state and be related to the ionization of the solid has also been suggested for the radiolysis of solid isobutane.[1c]

The authors wish to express their appreciation to Dr. Machio Iwasaki of the Government Industrial Research Institute of Nagoya for many fruitful discussions, and to Dr. Nobuo Tagusagawa of Nagoya University for his measurement of the crystal size of the powder.

BULLETIN OF THE CHEMICAL SOCIETY OF JAPAN, VOL. 44, 988—992 (1971)

Dielectric Relaxation and Molecular Structure. V. Application of the Single Frequency Method to Systems with two Debye Dispersions

Keniti HIGASI, Yoshinori KOGA, and Masahiko NAKAMURA
School of Science and Engineering, Waseda University, Shinjuku, Tokyo

(Received November 28, 1970)

There are four Debye equations for dilute solutions which can be used to determine the relaxation time of a polar solute molecule. This paper offers a critical examination of these equations, especially two representative formulas which are mutually independent. If the solute molecule has a non-rigid configuration and has two relaxation times, τ_1 and τ_2, for overall and internal rotations, respectively, average relaxation times will be obtained from these equations based on measurements at a single frequency. However, the analysis of this paper shows that under a certain condition (if a proper frequency for the measurement and a suitable equation for the calculation are employed) one may make a crude estimate regarding one of the two relaxation times. Further, the ratio of two relaxation times seems to afford a clue for investigating the mechanism of internal rotation. In addition, Cole-Cole dispersion and atomic polarization problems are also discussed.

The dielectric constant ε' and loss ε'' of the dilute solution are represented by the following equations

$$\left.\begin{aligned} \varepsilon' &= \varepsilon_1' + a'w_2 \\ \varepsilon_0 &= \varepsilon_{10} + a_0 w_2, \quad \varepsilon_\infty = \varepsilon_{1\infty} + a_\infty w_2 \\ \varepsilon'' &= \varepsilon_1'' + a''w_2 \end{aligned}\right\} \tag{1}$$

in which subscript 1 refers to the pure solvent and 2 refers to the solute, while subscript 0 refers to the zero frequency measurement in the static field and ∞ to the infinite frequency measurement (at a very high frequency). The concentration w_2 in the present work is the weight fraction but any concentration units (*e.g.*, mole fraction) can be used instead.

The Debye equations for dilute solutions are[1)]

$$\frac{a' - a_\infty}{a_0 - a_\infty} = \frac{1}{1 + \omega^2\tau^2} \tag{2}$$

and

$$\frac{a''}{a_0 - a_\infty} = \frac{\omega\tau}{1 + \omega^2\tau^2} \tag{3}$$

where a', a_0, a_∞, and a'' are the so-called "slopes" defined by Eq. (1), ω is the angular frequency and τ the relaxation time. The relaxation time τ is obtained from Eq. (2)

$$\tau = \frac{1}{\omega}\sqrt{\frac{a_0 - a'}{a' - a_\infty}} \tag{4}$$

1) K. Higasi, This Bulletin, **39**, 2157 (1966).

And from Eq. (3)

$$\tau = \frac{1}{\omega}[A \pm \sqrt{A^2 - 1}] \tag{5}$$

where

$$A = \frac{a_0 - a_\infty}{2a''}$$

Combination of Eqs. (2) and (3) gives two independent equations

$$\tau = \frac{1}{\omega}\frac{a''}{a' - a_\infty} \tag{6}$$

and

$$\tau = \frac{1}{\omega}\frac{a_0 - a'}{a''} \tag{7}$$

If the solute molecule is provided not with one relaxation time but with two relaxation times, τ_1 and τ_2, Eqs. (2) and (3) will lead to the following expressions:

$$\frac{a' - a_\infty}{a_0 - a_\infty} = \frac{1 - C_2}{1 + \omega^2\tau_1^2} + \frac{C_2}{1 + \omega^2\tau_2^2} \tag{8}$$

$$\frac{a''}{a_0 - a_\infty} = \frac{(1 - C_2)\omega\tau_1}{1 + \omega^2\tau_1^2} + \frac{C_2\omega\tau_2}{1 + \omega^2\tau_2^2} \tag{9}$$

The coefficients, $C_1 \equiv 1 - C_2$ and C_2 are the weight factors of the two Debye processes defined by τ_1 and τ_2 respectively. The purpose of this paper is to make a critical examination of the average τ values obtained from a_0, a', a'', and a_∞ by the use of Eqs. (6) and (7) when the dielectric system actually does follow Eqs. (8) and (9).

Results

(I) $\tau(1)$ from Eq. (6). By dividing Eq. (9) by Eq. (8) we get

$$\frac{a''}{a_0' - a_\infty} = \frac{\dfrac{(1 - C_2)\omega\tau_1}{1 + \omega^2\tau_1^2} + \dfrac{C_2\omega\tau_2}{1 + \omega^2\tau_2^2}}{\dfrac{1 - C_2}{1 + \omega^2\tau_1^2} + \dfrac{C_2}{1 + \omega^2\tau_2^2}}$$

Consequently, the relaxation time τ defined by Eq. (6) will become

$$\tau(1) = \frac{1}{\omega}\frac{a''}{a' - a_\infty}$$

$$= \frac{(1 - C_2)\tau_1 + C_2\tau_2 + \omega^2\tau_1\tau_2[(1 - C_2)\tau_2 + C_2\tau_1]}{1 + [(1 - C_2)\tau_2^2 + C_2\tau_1^2]\omega^2} \tag{10}$$

Put $$\tau_1 = m\tau_2: \quad \omega\tau_2 = x \tag{11}$$

and we get

$$\tau(1) = A\tau_2 \tag{12}$$

where

$$A = \frac{[m - (m - 1)C_2] + mx^2[1 + (m - 1)C_2]}{1 + [1 + (m^2 - 1)C_2]x^2} \tag{13}$$

Eq. (13) contains a term m which was defined in Eq. (11) as the ratio of τ_1 to τ_2. The molecular relaxation time, τ_1, for overall rotation has been well investigated over the past twenty years. The relation between τ_1 and the molecular size and shape has been fairly well established so that one may be able to make a good guess for any polar molecule under given conditions,[2] although opinions may differ as to the accuracy of such an estimation.[3]

More recently extensive investigation have been made concerning the second relaxation time, τ_2, which arises from internal rotation of a polar group in the molecule.[2] The magnitude of τ_2 for a given polar group varies according to the investigator. For instance, German workers[4] find τ_2 in the range of 0.5—3 psec, mostly 1—2 psec, while American[2] and British[5] scientists give somewhat higher τ_2 values for the same group often in the range of 2—4 psec. Accuracy for the determination of τ_2 from the measurement is considered to be lower than that for τ_1. The value of τ_1,[2,3] the relaxation time for overall rotation is much larger and depends on the viscosity of the solvent. Perhaps τ_1 for a benzene derivative in benzene solution would be around 8—15 psec and those for molecules with two benzene rings in the same solvent would be 16—30 psec. According to the above estimates of τ_1 and τ_2 one may consider

$$1 < m \simeq 2 - 30$$

At the frequency of 100 GHz ($\omega = 0.6282 \times 10^{12}$), the condition $\omega\tau = 1$ gives $\tau = 1.59$ psec which corresponds to an average value of $\tau_2 \simeq 1$—2 psec estimated by Knobloch[4] and other German workers: $x = 1 (\omega\tau_2 = 1)$. And $x = 2 (\omega\tau_2 = 2)$ at 100 GHz will be in accordance with other estimate for τ_2.[2,5]

From Eq. (13) it follows:

Overall rotation only:

$$C_2 = 0: \quad A = \frac{m + mx^2}{1 + x^2} = m \quad \tau(1) \to \tau_1$$

Internal rotation only:

$$C_2 = 1: \quad A = \frac{1 + mx^2}{1 + mx^2} = 1 \quad \tau(1) \to \tau_2$$

Further $$m \to \infty \quad A \to \frac{C_2x^2}{C_2x^2} = 1 \qquad \tau(1) \to \tau_2$$

In Fig. 1 the relation of A *versus* C_2 is plotted for four cases, viz., $m = 10$ $x = 1$, $x = 0.3$; $m = 5$ $x = 1$, $x = 0.3$. It will be seen that with increase in m and x the curve becomes flat, A approaching to unity in the region of large C_2 values. For example, $1 < A \leq 1.2$ if $C_2 \geq 0.5$, $m \geq 10$ and $x \geq 1$. This will imply that the average relaxation time, $\tau(1)$, obtained at 100 GHz by use of the Eq. (6) would be larger by only 20% than the smaller relaxation time τ_2, if the absorption intensity due to the internal rotation is significant and two absorption peaks are fairly separated. However, at lower frequencies such as $x \to 0$, Eq. (13) gives $A \to (1/2)(m+1)$ at $C_2 = 1/2$, i.e.,

$$\tau(1) \to (1/2)(\tau_1 + \tau_2) \quad \text{at } C_2 = 0.5.$$

(II) $\tau(2)$ from Eq. (7). We may denote the relaxation time defined by Eq. (7) as $\tau(2)$ and will obtain

2) C. P. Smyth, *Ann. Rev. Phys. Chem.*, **17**, 433 (1966).
3) K. Chitoku and K. Higasi, This Bulletin, **36**, 1064 (1963); O. Kiyohara and K. Higasi, *Bull. Res. Inst. Appl. Elec.*, **18**, 123, 138 (1966).
4) For instance, P. Knobloch, *Z. Naturforsch.*, **20a**, 580 (1965).
5) S. W. Tucker and S. Walker, *Can. J. Chem.*, **47**, 681 (1969).

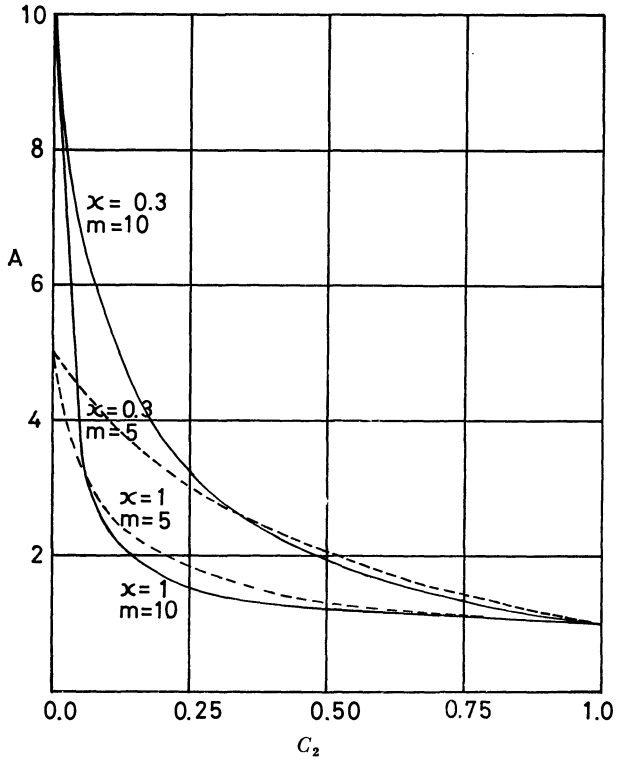

Fig. 1. Graphs relating ratio $\tau(1)/\tau_2 \equiv \boldsymbol{A}$ to the weight factor for internal rotation C_2, when $\tau_1/\tau_2 \equiv m = 5$, 10 and $\omega\tau_2 \equiv x = 0.3$, 1. The plots are based on Eq. (13).

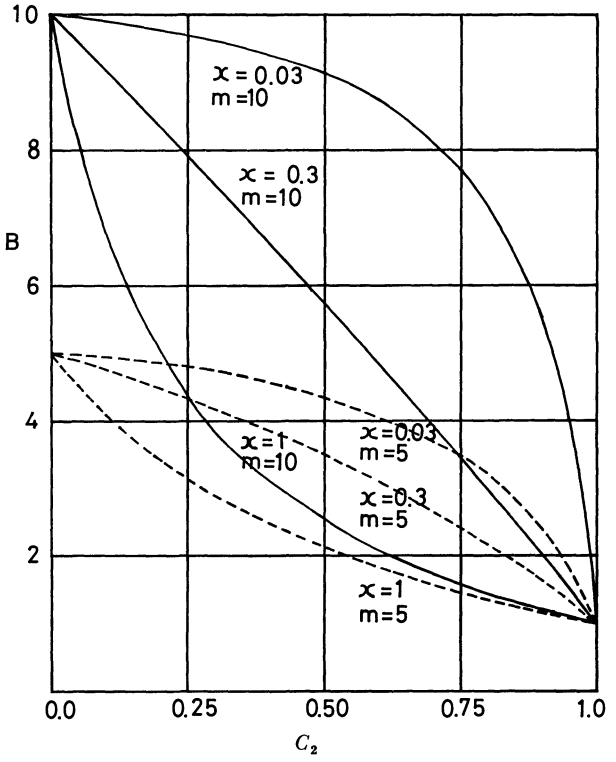

Fig. 2. Graphs relating ratio $\tau(2)/\tau_2 \equiv \boldsymbol{B}$ to the weight factor for internal rotation C_2, when $\tau_1/\tau_2 \equiv m = 5$, 10 and $x = \omega\tau_2 = 0.03$, 0.3, 1. Plots are based on Eq. (15).

$$\tau(2) = \frac{1}{\omega}\frac{a_0 - a'}{a''} = \boldsymbol{B}\tau_2 \tag{14}$$

where

$$\boldsymbol{B} = \frac{m^2 - (m^2 - 1)C_2 + m^2x^2}{m - (m - 1)C_2 + mx^2[1 + (m - 1)C_2]} \tag{15}$$

Overall rotation only:

$$C_2 = 0: \quad \boldsymbol{B} = \frac{m^2 + m^2x^2}{m + mx^2} = m, \quad \tau(2) \to \tau_1$$

Internal rotation only:

$$C_2 = 1: \quad \boldsymbol{B} = \frac{1 + m^2x^2}{1 + m^2x^2} = 1, \quad \tau(2) \to \tau_2$$

Further at lower frequencies ($x \to 0$)

$$\boldsymbol{B} \to m, \quad \tau(2) \to \tau_1$$

In Fig. 2 the relation of $\boldsymbol{B}$ to C_2 is plotted for six cases, $m = 10$, 5 and $x = 1$, 0.3, 0.03. It will be seen $\tau(2)$ gives a larger relaxation time than $\tau(1)$ for the dielectric system consisting in two Debye dispersions.

Gopala Krishna's equation[6] is based essentially on the same principle[1] with Eq. (7); recently, Vij and Srivastava[7] made a critical analysis of these equations. The relaxation times of non-rigid molecules[7,8] calculated by Gopala Krishna's procedure as well as by Eq. (7) would correspond to $\tau(2)$ for a given frequency.

(III) $\boldsymbol{B}/\boldsymbol{A}$ and C_2. We have $\tau(1) = \boldsymbol{A}\tau_2$ and $\tau(2) = \boldsymbol{B}\tau_2$. The ratio $\boldsymbol{B}/\boldsymbol{A}$ is unity at $C_2 = 0$ and $C_2 = 1$ and varies with m, x and C_2. In Fig. 3 are shown curves of $\boldsymbol{B}/\boldsymbol{A}$ *vs.* C_2 for $m = 5$ and 10 and $x = 1$ and 3. The maximum of $\boldsymbol{B}/\boldsymbol{A}$ becomes larger with increase in m.

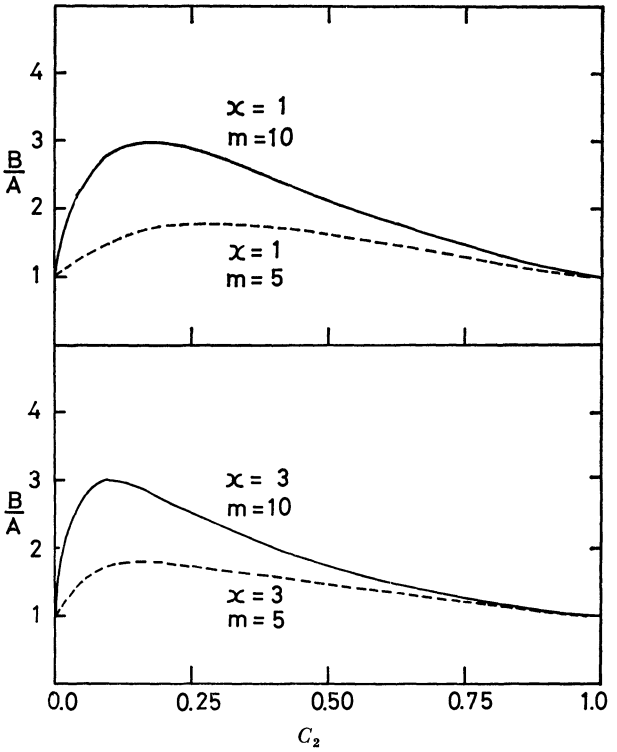

Fig. 3. Graphs relating ratio $\tau(2)/\tau(1) \equiv \boldsymbol{B}/\boldsymbol{A}$ to the weight factor C_2, when $\tau_1/\tau_2 \equiv m = 5$, 10, $\omega\tau_2 \equiv x = 3$, 1.

6) K. V. Gopala Krishna, *Trans. Faraday Soc.*, **53**, 767 (1957).
7) J. K. Vij and K. K. Srivastava, *ibid.*, **66**, 1087 (1970).
8) K. K. Srivastava and J. K. Vij, This Bulletin, **43**, 2307, 2313 (1970).

The literature[2,4] gives values of τ_2 to be 1—4 psec and almost independent of solvent. This would imply $x \rightarrow 1$—3 for $\omega \simeq 0.6 \times 10^{12}$ (100 GHz). Regarding τ_1 for overall rotation we might make a good guess[2,9] for a molecule with known molecular size and shape if the solvent and temperature are known. For given m and x the weight factor C_2 will be found to be associated with $\boldsymbol{B}/\boldsymbol{A}$.

(IV) $\tau(3)$ and $\tau(4)$ from Eqs. (4) and (5). We may call the relaxation time from Eq. (4) as $\tau(3)$.

$$\tau(3) = \frac{1}{\omega}\sqrt{\frac{a_0 - a'}{a' - a_\infty}} = \frac{1}{\omega}\sqrt{\frac{a''}{a' - a_\infty} \cdot \frac{a_0 - a'}{a''}}$$

from Eqs. (6) and (7)

$$\tau(3) = \sqrt{\tau(1) \cdot \tau(2)} \tag{16}$$

Thus, $\tau(3)$ is a geometric mean of $\tau(1)$ and $\tau(2)$.

$\tau(4)$ is the relaxation time which follows from Eq. (5) and is not independent of $\tau(1)$ and $\tau(2)$. Since Debye introduced a variation of Eq. (3) first in estimating the relaxation time of a polar molecule by the dilute solution method, Eq. (3) as well as its variations have been employed by many workers.[10,11] Figure 4 provides $\tau(4)$ *vs.* C_2 curves for systems with two Debye dispersions.

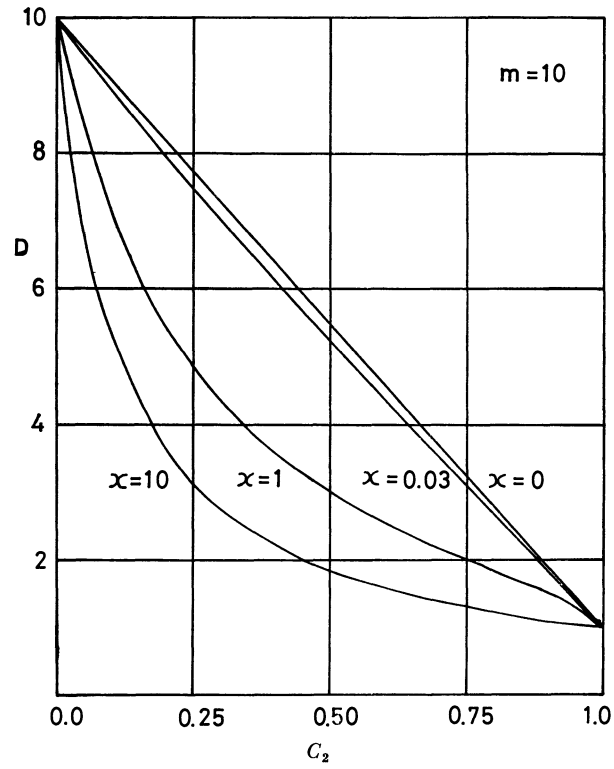

Fig. 4. Graphs relating ratio $\tau(4)/\tau_2 \equiv \boldsymbol{D}$ to the weight factor C_2 when $\tau_1/\tau_2 \equiv m = 10$ and $\omega\tau_2 \equiv x = 0$, 0.03, 1 and 10.

One will find from the upper curve in Fig. 4 that if $x = \omega\tau_2 \rightarrow 0$

$$\tau(4) = \tau_2[m - (m-1)C_2] = (1 - C_2)\tau_1 + C_2\tau_2 \tag{17}$$

This is an equation for internal rotation often utilized in the measurements at lower frequencies.[12]

$$\tau_{\text{eff}} = \left(\frac{\mu_1}{\mu}\right)^2 \tau_1 + \left(\frac{\mu_2}{\mu}\right)^2 \tau_2 \tag{18}$$

in which μ_1 and μ_2 are the two components of the molecular dipole μ.

(V) Problem of a_∞ and α. Equations for evaluating the relaxation time, Eqs. (4), (5), and (6) have a common weakness; they have uncertainty as to the choice of a_∞. Studies on chlorobenzene and other polar molecules by Smyth and his co-workers[13] seems to suggest $a_\infty \simeq a_D$—certainly this approximation, if true, would be very convenient. In most cases, however, $a_\infty \geq a_D$ would be more likely. The values $\tau(1)$ estimated based on $a_\infty \simeq a_D$ will be too small if actually a_∞ is larger than a_D.

If the dielectric system of dilute solution of a polar substance in non-polar solvent happens to obey the Cole-Cole empirical rule,[14] the following expression[1] will become valid.

$$\frac{a' - ja'' - a_\infty}{a_0 - a_\infty} = \frac{1}{1 + (j\omega\tau_0)^{1-\alpha}} \tag{19}$$

τ_0 is the most probable relaxation time, and α is the distribution parameter. From Eq. (19) $\tau(1)$ and $\tau(2)$ become

$$\tau(1) = \frac{1}{\omega} \frac{(\omega\tau_0)^{1-\alpha} \cos(\pi\alpha/2)}{1 + (\omega\tau_0)^{1-\alpha} \sin(\pi\alpha/2)} \tag{20}$$

$$\tau(2) = \frac{1}{\omega} \frac{(\omega\tau_0)^{1-\alpha} + \sin(\pi\alpha/2)}{\cos(\pi\alpha/2)} \tag{21}$$

Both $\tau(1)$ and $\tau(2)$ have smaller values than τ_0 for $\alpha \neq 0$. For example, at 100 GHz $\tau(1) = 4.3$ psec, $\tau(2) = 7.9$ psec for $\alpha = 0.1$ and $\tau_0 = 9$ psec; $\tau(1) = 3.1$ psec, $\tau(2) = 7.4$ psec for $\alpha = 0.17$ and $\tau_0 = 9$ psec.

Concluding Remarks

1. For the study of dielectric behavior of polar molecules it would be most desirable to obtain the complete spectrum of dielectric constants and losses in the whole frequency range where the dispersion takes place. However, this is an almost impossible task, unless the dispersion occurs only in the lower frequencies, say, below 7 GHz. Unfortunately the dipole dispersions due to group rotation in non-rigid molecules appear in much higher frequency range than this. In fact the single frequency method has been employed[6,7] in spite of all its theoretical defects for studies in the microwave frequencies.

2. If one uses Gopala Krishna's method[6] for determining the relaxation time of a non-rigid molecule, it should be noted that this equation provides a *mean* values. Its value, *i.e.* $\tau(2)$ is given by Eqs. (14) and (15) if the system is a superposition of two Debye dispersions.

9) K. Higasi, *Kagaku*, **37**, 261 (1967); *Kagaku-no-Ryoiki*, (Supplement) **82**, 3 (1968).

10) N. E. Hill, W. E. Vaughan, A. H. Price, and M. Davies, "Dielectric Properties and Molecular Behaviour," Van Nostrand, Reinhnld, London (1969); p. 289, Eq. (5.5).

11) C. P. Smyth, "Dielectric Behavior and Structure," McGraw-Hill, New York (1955) p. 64,

12) E. Fischer, *Z. Naturforsch.*, **4a**, 707 (1949); *Z. Phys.*, **127**, 49 (1949); A. Aihara and M. Davies, *J. Colloid Sci.*, **11**, 671 (1956).

13) S. K. Garg, H. Kilp, and C. P. Smyth, *J. Chem. Phys.*, **43**, 2341 (1965).

14) K. S. Cole and R. H. Cole, *ibid.*, **9**, 341 (1941).

3. The analysis of $\tau(1)$ shows that the relaxation time for internal rotation τ_2 may be estimated from high frequency measurements if we could have a true a_∞ value. In fact, τ_2 is closely associated with a_∞. Both quantities are of extreme importance in molecular science. They might be estimated with some accuracy but at present we do not have any absolutely reliable method to determine them.

We thank Professor H. Takahashi for helpful discussion. We are also grateful to the Toray Science Foundation for the financial aid.

BULLETIN OF THE CHEMICAL SOCIETY OF JAPAN, VOL. 44, 992—997 (1971)

Dielectric Relaxation and Molecular Structure. VI. Dielectric Measurements at the Frequency of 100 GHz

Kazuo CHITOKU* and Keniti HIGASI**

Research Institute of Applied Electricity, Hokkaido University, Sapporo

Masahiko NAKAMURA, Yoshinori KOGA, and Hiroaki TAKAHASHI

School of Science and Engineering, Waseda University, Shinjuku, Tokyo

(Received November 28, 1970)

This paper gives details of the equipment and the method of the measurement at 100 GHz. Dielectric constants and losses are measured at this frequency for ten organic molecules in benzene and four (aniline, phenol, and its derivatives) both in benzene and in dioxane. A majority of the molecules studied are of non-rigid configuration. Discussion is given of the relaxation times and the mechanism of internal rotation involved. Hydrogen bonding effects in aniline, phenol, and its derivatives are also discussed.

For many years a number of dielectric measurements have been carried out using a variety of frequency ranges. However, there are few dielectric data obtained in the range of very high frequency above 60 GHz, *i.e.*, below five millimeters in the wavelength. And this range of frequencies is a field which is still unexplored and need careful investigations.[1] For example, non-polar liquids such as benzene or carbon tetrachloride are found to show dielectric absorption in this frequency range[1] in a sharp contrast to the old belief that all the non-polar liquids should show no appreciable absorption in any range of frequencies.

According to Poley[2] polar liquids consisting of rigid molecules such as chlorobenzene and nitrobenzene are provided with an additional absorption at the high frequency end of millimeter band. This novel absorption became an object of intensive research.[3,4]

For a non-rigid molecule having a rotatable polar group or groups one finds two or more absorption peaks. The absorption due to internal rotation takes place in the millimeter range. For these reasons the dielectric measurements at a frequency of the wavelength less than 5 millimeters are of considerable interest.

In the present paper the writers wish to report on the millimeter wave apparatus for 100 GHz (3 mm), the method of measurements, the experimental results, and the dielectric relaxation times of the organic molecules obtained in dilute solution. Most of the substances chosen for the solute are of non-rigid configuration; and benzene was employed as solvent and for some solutes with hydrogen bonding capacity, *p*-dioxane was also used for comparison.

Apparatus

The experimental technique is based on the free space method.[5] For measuring dielectric constants and losses at 100 GHz the usual transmission line (wave guide) method is not much use since its upper limit is estimated to be about 75 GHz.[5] The apparatus is the microwave equivalent of Michelson interferometer and is of the same type with that of Garg, Kilp, and

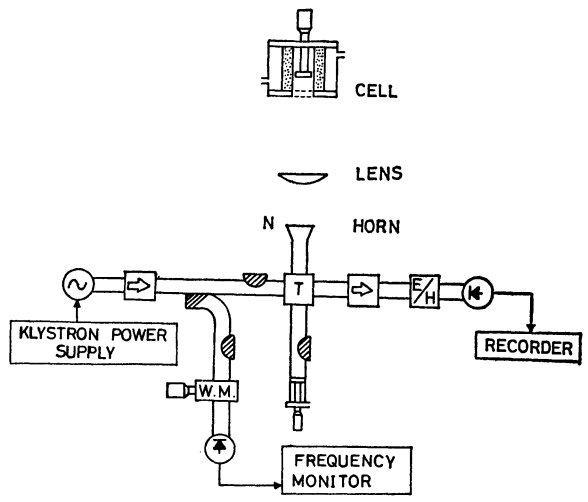

Fig. 1. Schematic of 100 GHz apparatus, microwave analog of the Michelson interferometer.

* Present address: Naka Works, Hitachi, Ltd., Katsuta, Ibaraki.

** Now at School of Science and Engineering, Waseda University, Shinjuku, Tokyo.

1) N. E. Hill, W. E. Vaughan, A. H. Price, and M. Davies, "Dielectric Properties and Molecular Behaviour," Van Nostrand Reinhold, London (1969), pp. 298—311.

2) J. Ph. Poley, *J. Appl. Sci.*, **B4**, 337 (1955).

3) G. W. Chantry and H. A. Gebbie, *Nature*, **208**, 378 (1965).

4) M. Davies, G. W. F. Pardoe, J. Chamberlain, and H. A. Gebbie, *Trans. Faraday Soc.*, **66**, 273 (1970).

5) N. E. Hill *et al.*, Ref. 1. See Chapter 2.

Smyth.[6,7] The schematic diagram of the apparatus is shown in Fig. 1.

The klystron (Oki 100 V 10 A) generates millimeter waves of about 3 mm in wavelength and its frequency is monitored by a cavity resonator (W 2203). The microwave energy is divided by a hybrid ring T (W 3701) in equal parts. Half passes through the transmitting horn N out into free space. A dielectric lens (TRGW 986) is used to produce a well-collimated beam, which traversed the liquid in the cell, reflected by the plunger, retraverses the liquid and finally is focussed by the lens back into the horn. In the reference arm the other half of the microwave energy from the hybrid is reflected by an adjustable plunger. The interference of the two beams takes place in the wave guide leading to the detective device and finally to the recorder (QPD 53).

Calculation of n and k

The complex index of refraction (n^*) of the material is defined as

$$n^* = n - jk \tag{1}$$

and the dielectric constant (ε') and the loss (ε'') of the same material are related to the above quantities according to

$$\left.\begin{aligned} \varepsilon' &= n^2 - k^2 \\ \varepsilon'' &= 2nk \end{aligned}\right\} \tag{2}$$

The evaluation of n and k values are essentially the same as employed by Garg, Kilp, and Smyth.[6] The final equation for obtaining k is

$$\begin{aligned} \frac{I_{max}(1)-I_{min}(1)}{I_{max}(2)-I_{min}(2)} &= \exp\left(-2\beta_0 k[h_1-h_2]\right) \\ &\times\left[\frac{(1+n)-(1-n)\exp\left(-4\beta_0 kh_1\right)}{(1+n)-(1-n)\exp\left(-4\beta_0 kh_2\right)}\right] \\ &\times\left[\frac{(1+n)^2-(1-n)^2\exp\left(-4\beta_0 kh_2\right)}{(1+n)^2-(1-n)^2\exp\left(-4\beta_0 kh_1\right)}\right]^2 \end{aligned} \tag{3}$$

The final electric intensity (I) at the detector has maxima and minima with the change of liquid thickness (h). The relative maximum (I_{max}) and the adjacent relative minimum (I_{min}) corresponding to a given liquid thickness h are observed; they are denoted by $I_{max}(1)$, $I_{min}(1)$ for h_1 and $I_{max}(2)$ and $I_{min}(2)$ for h_2, *etc.*. The phase constant β_0 is given by $\beta_0=2\pi/\lambda_0$ where λ_0 is the wavelength in air.

Smyth *et al.*[6] used an electronic computer to find n and k to fit the experimental curve. In the present work this formidable task of fitting was successfully replaced by a simple procedure which is based on a least-square method. (See Appendix.)

Purification of Materials

The organic compounds studied were all commercially available. Purchased materials of best grade were fractionally distilled before use. Solvents, benzene and *p*-dioxane, were carefully purified in the usual way.

Results

Measurements of ε' and ε'' for three to four dilute solutions for each solute were made and the so-called "slopes" a', a'', *etc.* were obtained on the assumption that the linear relationship of ε' and ε'' with the concentration (weight fraction) w_2 exists.

$$\left.\begin{aligned} \varepsilon' &= \varepsilon_1' + a'w_2 \\ \varepsilon'' &= \varepsilon_1'' + a''w_2\ ;\ \varepsilon_1'' \simeq 0 \\ \varepsilon_0 &= \varepsilon_{10} + a_0 w_2 \\ n_D^2 &= n_{1D}^2 + a_D w_2 \end{aligned}\right\} \tag{4}$$

in which subscript 1 refers to the pure solvent and 2 to the solute and the symbols have the usual meaning.

The relaxation time of a polar solute is obtained by the use of two equations.[8] We shall denote them by $\tau(1)$ and $\tau(2)$ in the following manner.

$$\left.\begin{aligned} \tau(1) &= \frac{1}{\omega}\cdot\frac{a''}{a'-a_\infty} \\ \tau(2) &= \frac{1}{\omega}\cdot\frac{a_0-a'}{a''} \end{aligned}\right\} \tag{5}$$

There is no reliable method to evaluate a_∞. The most common approximation is to assume a_∞ to be equal to a_D. This may be equivalent to say that both atomic polarization term and correction due to Poley's absorption[2] can be neglected.

Grant[9] suggests the use of the following equation in evaluating ε_∞ (*viz.*, a_∞ in this case)

$$a_\infty(\equiv a_G) = a' - \frac{(a'')^2}{a_0-a'} \tag{6}$$

We shall write the value given by Eq. (6) as a_G. The two values for relaxation times, $\tau(1)$ and $\tau(2)$, become identical with the use of this a_G value—the condition of $a_\infty=a_G$ may be a criterion for the pure Debye system with a single relaxation time. Contrary to this, $\tau(1)$ and $\tau(2)$ should have different vafues for a system with two Debye dispersions. They differ also for a system which obeys Cole-Cole's empirical rule.[8] Experimental values of a' and a'' obtained at about 100 GHz, *viz.*, 96.027 GHz are collected in Table 1. (See Eqs. (4) for the definition of a' and a''.) In the same table a_0 and a_D defined by Eqs. (4) are given together with a_G which is obtained from a', a'', and a_0 (see Eq. (6)).

Magee and Walker[10] proposed a new method for evaluating ε_∞ (hence a_∞) from the Cole-Cole arc for systems which really have two Debye dispersions. Their method was employed when sufficient data were available for the plot. When there are no reliable data, a tentative choice was made with the condition in mind that $a_D \leq a_\infty \leq a_G$.

In Table 2 a collection is given of experimental re-

6) S. K. Garg, H. Kilp, and C. P. Smyth, *J. Chem. Phys.*, **43**, 2341 (1965).

7) The writers are grateful to Professor C. P. Smyth, Princeton University, for providing them with an absorption material (Teflon impregnated with carbon) which was used in the cell cylinder.

8) K. Higasi, Y. Koga, and M. Nakamura, This Bulletin, **44**, 988 (1971).

9) One of the writers is grateful to Dr. E. H. Grant, London University, for discussions on the use of Eq. (6). See also N. E. Hill, *Trans. Faraday Soc.*, **59**, 344 (1963).

10) M. D. Magee and S. Walker, *J. Chem. Phys.*, **50**, 2580 (1969).

Table 1. Slopes a', a'' obtained at 100 GHz in benzene (20°) and a_0, a_D, and a_G

Substance	a_0	a'	a''	a_D	a_G
Diphenyl ether	1.085	0.383	0.321	0.217	0.236
Dibenzyl ether	1.155	0.343	0.166	0.185	0.309
Benzophenone	5.982	0.608	0.550	0.282	0.551
Dibenzyl ketone	3.947	0.547	0.463	0.193	0.484
Chlorobenzene	2.477	0.263	0.497	0.052	0.151
Benzyl chloride	3.228	0.565	0.618	0.094	0.421
p-Xylene chloride	3.517	0.848	0.858	0.137	0.573
p-Dimethoxy benzene	2.551	0.564	0.481	0.060	0.447
p-Diethoxy benzene	2.130	0.474	0.399	0.018	0.378
Anisole	1.717	0.370	0.326	0.043	0.291
Aniline	2.806	1.141	0.678	0.219	0.865
(in dioxane)	4.407	1.239	0.521	0.514	1.153
Phenol	3.344	0.621	0.413	0.144	0.558
(in dioxane)	4.784	0.738	0.340	0.395	0.709
2,6-Dimethyl phenol	1.930	0.461	0.370	0.081	0.368
(in dioxane)	3.518	0.609	0.311	0.353	0.576
2,6-Di-*t*-butyl phenol	1.394	0.271	0.326	0.0	0.177
(in dioxane)	1.947	0.526	0.356	0.280	0.437

Table 2. Relaxation times $\tau(1)$ and $\tau(2)$ [This Experiment] and τ_0, τ_1, and τ_2 [Literature] in psec

Substance	$\tau(1)$	$\tau(2)$	Literature values
Diphenyl ether	3.2	3.6	τ_0 3.4[11] 4.0[12] 4.1[13]
Dibenzyl ether	1.7	8.1	τ_0 18[12]; τ_1 33[14] L; τ_2 3.9[14]L
Benzophenone	2.8	16.2	τ_0 16.4[15] 18.3[16] 20.4[17] 22[18]; τ_1 27[19] C; τ_2 3.5[19] C
Dibenzyl ketone	2.2	12.2	
Chlorobenzene	3.9	7.4	τ_0 8.3[6] 9.6[13] 8.6[17] 8.3[18] 10.8[20] L
Benzyl chloride	2.2	7.1	τ_0 9.9[15]; τ_1 14.0[22] 18.7[23] 20[21] 23.7[23]; τ_2 1.4[22] 2.3[23] 2.9[23] 4[21]
p-Xylene chloride	2.0	5.2	τ_0 3.0[24] 5.0[15]; τ_2 3.0[24]
p-Dimethoxy benzene	1.6	6.8	τ_0 6.2[25] 6.9[26] 9.7[27]; τ_1 8.5[22] 14.7[28] L; τ_2 0.75[22] 5.6[29]
p-Diethoxy benzene	1.4	6.9	
Anisole	1.6	6.9	τ_0 6.6[25] 7.6[15]; τ_1 9.0[22] 20[25]; τ_2 0.9[22] 3.2[29] 6.5[25]
Aniline	1.2	4.1	τ_0 9.78[30] L; τ_1 7.15[22] 22.2[28] L; τ_2 0.9[28] L 0.5[22]
Aniline (in dioxane)	1.2	10.1	τ_0 19.4[31]
Phenol	1.4	10.9	τ_0 9.3[32] C; τ_1 11.4[22]; τ_2 1.1[22]
Phenol (in dioxane)	1.6	19.7	
2,6-Dimethyl phenol	1.6	6.6	τ_0 5.3[33]; τ_1 13.7[33]; τ_2 3.4[33] 3.5[34]
2,6-Dimethyl phenol (in dioxane)	2.0	15.5	
2,6-Di-*t*-butylphenol	2.0	5.7	
2,6-Di-*t*-butylphenol (in dioxane)	2.4	6.6	

L liquid C cyclohexane T carbon tetrachloride

11) J. T. Vij and K. K. Srivastava, This Bulletin, **43**, 2313 (1970).
12) J. E. Anderson and C. P. Smyth, *J. Chem. Phys.*, **42**, 473 (1965).
13) J. Schneider, *ibid.*, **32**, 665 (1960).
14) K. Bergmann, D. M. Roberti, and C. P. Smyth, *J. Phys. Chem.*, **64**, 665 (1960).
15) E. Fischer, *Z. Naturforsch.*, **4a**, 707 (1949).
16) W. Jackson and J. G. Powles, *Trans. Faraday Soc.*, **42A**, 101 (1946).
17) K. Chitoku and K. Higasi, This Bulletin, **36**, 1064 (1963).
18) D. H. Whiffen and H. W. Thompson, *Trans. Faraday Soc.*, **42A**, 149 (1949); D. H. Whiffen, *ibid.*, **46**, 130 (1950).
19) D. Farmer and S. Walker, *Tetrahedron*, **22**, 111 (1966).
20) S. K. Garg and C. P. Smyth, *J. Chem. Phys.*, **42**, 1397 (1965).
21) E. M. Turner, W. W. Ehrhardt, G. Leone, and W. E. Vaughan, *J. Phys. Chem.*, **74**, 3543 (1970).
22) G. Klages and P. Knobloch, *Z. Naturforsch.*, **20a**, 580 (1965); P. Knobloch, *ibid.*, **20a**, 851 (1965).
23) W. P. Purcell, K. Fish, and C. P. Smyth, *J. Amer. Chem. Soc.*, **82**, 6299 (1960).
24) S. Dasgupta and C. P. Smyth, *ibid.*, **90**, 6318 (1968).
25) E. Forest and C. P. Smyth, *ibid.*, **86**, 3474 (1964).
26) E. Fischer, *Z. Naturforsch.*, **9a**, 909 (1954).
27) D. M. Roberti and C. P. Smyth, *J. Amer. Chem. Soc.*, **82**, 2106 (1960).
28) S. K. Garg and C. P. Smyth, *J. Chem. Phys.*, **46**, 373 (1967).
29) C. P. Smyth, "Molecular Relaxation Processes," Chem. Soc. Special Publ. No. 20, Chemical Society, London (1966), p. 6.
30) E. Fischer, *Z. Physik*, **127**, 49 (1949).
31) K. Chitoku and K. Higasi, This Bulletin, **39**, 2160 (1966).
32) E. Fischer and R. Fessler, *Z. Naturforsch.*, **8a**, 177 (1953).
33) F. K. Fong and C. P. Smyth, *J. Amer. Chem. Soc.*, **85**, 1565 (1963).
34) A. Aihara and M. Davies, *J. Colloid Sci.*, **11**, 671 (1965).

laxation times in the units of psec (10^{-12} sec). Solvent is benzene if not stated; and temperature is 20°C for the present work and 15°—25° for the literature values. $\tau(1)$ and $\tau(2)$ are calculated by the use of a', a'', a_0, and a_D values recorded in Table 1. Since a_D is used instead of a_∞ throughout, $\tau(1)$ calculated from Eq. (5) is too low in general. Regarding the literature values τ_0 denotes the average relaxation time, τ_1 the relaxation time for overall rotation and τ_2 the relaxation time for internal rotation.

Discussion

Table 2 shows that diphenyl ether has two close values for the relaxation time $\tau(1)=3.2$ psec and $\tau(2)=3.6$ psec and according to Table 1 a_G is found to be near a_D. In contrast to this benzophenone has $\tau(1)=2.8$ psec and $\tau(2)=16.2$ psec and a_G is much larger than a_D. If an intermediate value 0.51 between a_D and a_G is taken for a_∞, $\tau(1)$ will become larger, *viz.*, 9.5 psec. Assuming that diphenyl ether and benzophenone have the same relaxation mechanism associated with $\tau_1=19.9$ psec and $\tau_2=3.31$ psec one will find the weight factor for internal rotation to be very big, *viz.*, $C_2=0.92$, in diphenyl ether, while the same factor is very small in benzophenone, *viz.*, $C_2=0.06$ for $\tau(1)=9.5$ psec and $\tau(2)=16.2$ psec.—The method of the analysis is given in the preceding paper.[8] These findings are in good agreement with the experimental results in the liquid state[35] and with the internal rotation mechanism based on the mesomeric effects.[36]

Two opposite views are available in connection with the dielectric anomaly of diphenyl ether.[37] One is based on the belief that the molecular moment of diphenyl ether lies in the direction of the line dividing the C–O–C angle of the molecule in two equal parts. This makes overall rotation, rotation of the whole molecules, to be the only cause of dielectric absorption. This is because rotation of two rings will not produce any change in the direction of the molecular moment. The other view[36] is based on the assumption that there might be a dipole component perpendicular to the line dividing the C–O–C angle equally and if so, this component (due to mesomerism) would be appreciable in diphenyl ether and very small in benzophenone. The advantage of the second view is that rotation of two rings alone can produce a change in the orientation of the molecular moment.

According to the former view one has to assume a special kind of overall rotation coupled with rotation of two rings[38] which would not occur so frequently. The weakness of the second mechanism is the lack of direct evidence for it[39]—although there is no reliable evidence against it[12,40,41] either.

Introduction of two CH_2 groups between O or C=O and two aromatic rings in the molecule of diphenyl ether or benzophenone will reduce the mesomeric effect and at the same time it will give a greater flexibility to the molecule.[42] It is interesting to find in this connection that $\tau(2)$ in Table 2 increases with the order: diphenyl ether, dibenzyl ether, dibenzyl ketone, and benzophenone.

Relaxation times for chlorobenzene (Table 2) are $\tau(1)=3.9$ psec and $\tau(2)=7.4$ psec, these being obtained on the assumption $a_\infty=a_D=0.05$. Contrary to this, or better a_∞ is estimated from the Cole-Cole plot, —we shall call it a_{CC}; Garg, Kilp, and Smyth[6] provided $a_{CC}=0.15$ which happens to be equal to a_G (Table 1). If this a_{CC} is used as a_∞, $\tau(1)=\tau(2)=7.4$ psec and Poley's absorption[2] will not exist or will be too weak to be detected at 100 GHz.

If a little smaller value $a_\infty=0.11$ is tentatively chosen, one would reach a conclusion that such an absorption does exist at the shorter end of millimeter band. For example, a weak absorption with $\tau_2=0.5$ psec, $C_2=0.1$ with the molecular rotation $\tau_1=8.5$ psec will be expected[8] on the assumption of two Debye processes. One of us (Takahashi)[43] confirmed Poley's absorption at about 2000 GHz (60 cm^{-1}) by a far infra-red spectrometer (FIS-3).

Dielectric relaxation of benzyl chloride has been analysed by Knobloch[22] and Purcell *et al.*[23]; the former gives $\tau_1=14.0$ psec, $\tau_2=1.4$ psec, $C_2=0.30$ while the latter gives two sets of $\tau_1=18.7$, $\tau_2=2.9$, and $\tau_1=23.7$, $\tau_2=2.3$ (all in psec). The present data lead to $\tau_1=12.4$ psec, $\tau_2=2.48$ psec and $C_2=0.24$[8] with the use of $a_{CC}=0.31$.[23] It appears fairly certain that there exist two dispersion regions in this molecule.

It is not clear, however, whether *p*-xylene chloride has such two relaxation processes or not. If $a_\infty=a_G=0.573$ is true, $\tau(2)=5.2$ psec will be the intramolecular relaxation time. On the other hand if the group rotation has a shorter relaxation time 1—2 psec,[22] we shall have to assume some contribution from overall rotation. An analysis[8] of the present data gives $\tau_1=11.6$ psec, $\tau_2=1.65$ psec, $C_2=0.25$ with $a_\infty=0.25$; or $\tau_1=11.6$ psec, $\tau_2=3.31$ psec, $C_2=0.55$ with $a_\infty=0.48$.

It is possible that both *p*-dimethoxy benzene and *p*-diethoxy benzene have two distinct relaxation processes, *viz.*, due to overall rotation as well as to internal rotation.[44] This is because if two methoxy or two ethoxy groups have freedom of rotation around the C–O axes, the components of the two mesomeric moments along the direction of the molecular axis would not cancel each other.

Now, consider the mesomeric moment arising from the upper OCH_3 group (see Fig. 2). The mesomeric moment depends upon the angle of rotation, φ_1, measured from the plane of the benzene ring.[45]

35) W. E. Vaughan and C. P. Smyth, *J. Phys. Chem.*, **45**, 98 (1961); W. E. Vaughan, W. S. Lovell, and C. P. Smyth, *J. Chem. Phys.*, **36**, 535 (1962).
36) K. Higasi, This Bulletin, **35**, 632 (1962); K. Higasi and C. P. Smyth, *J. Amer. Chem. Soc.*, **82**, 4759 (1960).
37) K. Higasi, "Dipole, Molecule and Chemistry," Hokkaido Univ., Sapporo (1965). Chapter II, pp. 19—36.
38) F. K. Fong, *J. Chem. Phys.*, **40**, 132 (1964).
39) K. Chitoku and K. Higasi, *Bull. Res. Inst. Appl. Elec.* (Hokkaido Univ.), **19**, 32 (1967).
40) K. Higasi, *Kagaku to Kogyo*, **15**, 118 (1962).
41) D. B. Farmer and S. Walker, *Trans. Faraday Soc.*, **63**, 966 (1967).
42) A. Aihara, Private Communication.
43) H. Takahashi, to be published.
44) K. Higasi, "Dielectric Relaxation and Molecular Structure," Hokkaido Univ., Sapporo (1961), p. 34.
45) K. Higasi, H. Baba, and A. Rembaum, "Quantum Organic Chemistry," Interscience, New York (1965), p. 157.

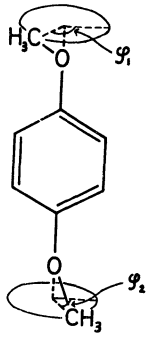

Fig. 2. Internal rotation in *p*-dimethoxybenzene and two angles of rotation, φ_1 and φ_2.

$$\mu_m(\text{upper}) = \mu_{max} \cos^2 \varphi_1$$

Similarly for the lower OCH_3 group

$$\mu_m(\text{lower}) = \mu_{max} \cos^2 \varphi_2$$

where φ_2 is the angle of rotation of the lower group. The component along the molecular axis is

$$\mu_m(\text{upper}) - \mu_m(\text{lower}) = \mu_{max}(\cos^2 \varphi_1 - \cos^2 \varphi_2)$$

The average $<\cos^2 \varphi_1 - \cos^2 \varphi_2>$ is 1/4 for free rotation and is not equal to zero in general. Contributions from overall rotation would be appreciable unless the maximum mesomeric moment μ_{max} of a methoxy group attached to a benzene ring is very small.[44]

The present data of $\tau(1)$ and $\tau(2)$ seem to support the above view, since the weight factor for molecular rotation $1-C_2$ is found to be quite large in several analyses[8] of the data. For example, for *p*-dimethoxy benzene $\tau_1=11.55$ psec, $\tau_2=1.65$ psec, $C_2=0.20$ with $a_\infty=0.30$ and for *p*-diethoxybenzene $\tau_1=11.55$ psec, $\tau_2=1.65$ psec, $C_2=0.20$ with $a_\infty=0.25$. These data can well be compared with the result of Klages and Knobloch's[22] analysis on *p*-dimethoxybenzene, or with Klages and Zenteks[46] $C_2=0.17$, $\tau_1=8.8$ psec, $\tau_2=(0.4)$ psec. More recently Vaughan *et al.*[47] give $C_2=0.13$ with $\tau_1=6.2$ psec and $\tau_2=0.9$ psec for liquid. However, there is uncertainty regarding the choice of a_∞. Anisole is in accord with $\tau_1=9.90$ psec, $\tau_2=1.65$ psec, $C_2=0.16$ with $a_\infty=0.21$. Again, it would be most desirable to have a reliable a_∞ value in order to find how important is the contribution of overall rotation.

Last group of four molecules are studied by the use of two solvents, benzene and dioxane, with a view to examining the hydrogen bonding effects of the solute with the solvent. According to the previous method of analysis[8] of two mean relaxation times $\tau(1)$ and $\tau(2)$ obtained at this high frequency one can make a very crude estimate of τ_1 and τ_2. The relaxation time τ_1 for overall rotation is closer $\tau(2)$ than to $\tau(1)$ and the relaxation time for internal rotation τ_2 is near to the observed $\tau(1)$ value. Recorded $\tau(1)$ values of these molecules are about 1—3 psec which is in good agreement with τ_2 for the OH and also for the NH_2 groups given by Knobloch.[48] In contrast to $\tau(1)$, $\tau(2)$ varies greatly with solutes and solvents and has values 4—20 psec. The ratio of $\tau(2)$ obtained in dioxane to that in benzene, τ_D/τ_B, is 2.48 (aniline), 1.81 (phenol), 2.36 (2,6-dimethyl phenol) and 1.16 (2,6-di-*t*-butyl phenol). The ratio of viscosities of two solvents is 1.2836 : 0.6466=1.99 : 1, while τ_D/τ_B for chlorobenzene and nitrobenzene are 1.57 and 1.51 respectively. The observed high increase of τ values from benzene to dioxane in aniline, phenol, and 2,6-dimethyl phenol is an indication that an oxygen atom of dioxane forms a hydrogen bond with amino-hydrogen atoms in aniline or with the hydrogen atom in phenol or of its derivative.[31] However, on account of the steric hindrance of the bulky substituents the OH group in 2,6-di-*t*-butyl phenol is not able to form a hydrogen bond with the solvent molecule. It is impressive to find small $\tau(2)$ values for this molecule both in benzene and dioxane. The group rotation seems to predominate in this molecule, as is the case of 2,4,6-tri-*t*-butyl phenol in decalin.[49] Further, the solute molecules tend to associate through hydrogen bonds. This association seems to take place in case of phenol in benzene.[50] Without such an effect the ratio τ_D/τ_B of phenol would possibly be much larger than the observed.

Appendix

1. *Calculation of n.* The real part of the refractive index n is expressed as

$$n = \sqrt{\frac{\left(\frac{\lambda_0}{\lambda_d}\right)^2+\left(\frac{\lambda_0}{\lambda_c}\right)^2}{1+\left(\frac{\lambda_0}{\lambda_c}\right)^2}} \qquad \text{(A-1)}$$

where λ_0, λ_d, and λ_c are the wavelength in air, the wavelength in the sample and the cut-off wavelength, respectively.

2. *Calculation of k.* The imaginary part of the refractive index k is calculated according to Eq. (3) by a least square method. Eq. (3) can be replaced in the following integrated form (A-2) using the relation:

$$h_m = \frac{1}{2} m\lambda_d$$

and

$$\beta_0 = 2\pi/\lambda_0$$

where $m=1, 2, \cdots, t$.

$$Y_m = -A_m k - B_m(k) + C \qquad \text{(A-2)}$$

where

$$Y_m = \ln[I_{max}(m) - I_{min}(m)]$$

$$A_m = \frac{2\pi\lambda_d}{\lambda_0} m$$

$$B_m(k) = \ln \frac{\left[(1+n)^2-(1-n)^2\exp\left(-\frac{4\pi\lambda_d km}{\lambda_0}\right)\right]^2}{\left[(1+n)-(1-n)\exp\left(-\frac{4\pi\lambda_d km}{\lambda_0}\right)\right]}$$

C is an integration constant.

46) G. Klages and A. Zentek, *Z. Naturforsch.*, **16a**, 1016 (1961).
47) W. E. Vaughan, S. B. W. Roeder, and T. Provder, *J. Chem. Phys.*, **39**, 701 (1963).
48) P. Knobloch, *Ber. Bunsenges. Phys. Chem.*, **69**, 296 (1965).
49) M. Davies and R. J. Meakins, *J. Chem. Phys.*, **26**, 1584 (1957).
50) K. Higasi, This Bulletin, **25**, 159 (1952).

The observed values of Y_m are expressed in a matrix form.

$$\tilde{\mathbf{Y}}^\circ = (Y_1^\circ, Y_2^\circ, \cdots, Y_t^\circ)$$

The unknown parameters in Eq. (A-2) are k and C. Therefore it is desired to obtain the values of k and C which give the calculated values of $\tilde{\mathbf{Y}}=(Y_1, Y_2, \cdots, Y_t)$ closest to $\tilde{\mathbf{Y}}^\circ$.

This may be done by the following procedure. Let k^{I} and C^{I} be the first guessed values of k and C and $\tilde{\mathbf{Y}}^{\mathrm{I}}=(Y_1^{\mathrm{I}}, Y_2^{\mathrm{I}}, \cdots, Y_t^{\mathrm{I}})$ be the calculated values of $\tilde{\mathbf{Y}}$ using k^{I} and C^{I}. To get the corrections Δk^{I} and ΔC^{I} from the difference $\Delta\mathbf{Y}=\mathbf{Y}^\circ-\mathbf{Y}^{\mathrm{I}}$, let us assume the corrected values to be k^{II} and C^{II} and the calculated values to be $\tilde{\mathbf{Y}}^{\mathrm{II}}=(Y_1^{\mathrm{II}}, Y_2^{\mathrm{II}}, \cdots, Y_t^{\mathrm{II}})$. The purpose of the least square method is to minimize the value of S which is expressed as:

$$S = (\tilde{\mathbf{Y}}^\circ-\tilde{\mathbf{Y}}^{\mathrm{II}})\mathbf{W}(\mathbf{Y}^\circ-\mathbf{Y}^{\mathrm{II}})$$

where $\mathbf{W}$ is a diagonal matrix whose element w_i is the weight factor of Y_i°.

An assumption is made that the variation of $\mathbf{Y}$ is linearly proportional to Δk and ΔC when they are very small. That is:

$$\mathbf{Y}^{\mathrm{II}} - \mathbf{Y}^{\mathrm{I}} = \mathbf{J}^{\mathrm{I}}\Delta\mathbf{K}^{\mathrm{I}}$$

where $\mathbf{J}^{\mathrm{I}}$ is a Jacobian matrix expressed as:

$$\mathbf{J}^{\mathrm{I}} = \begin{pmatrix} \frac{\partial Y_1^{\mathrm{I}}}{\partial k^{\mathrm{I}}} & \frac{\partial Y_1^{\mathrm{I}}}{\partial C^{\mathrm{I}}} \\ \frac{\partial Y_2^{\mathrm{I}}}{\partial k^{\mathrm{I}}} & \frac{\partial Y_2^{\mathrm{I}}}{\partial C^{\mathrm{I}}} \\ \vdots & \vdots \\ \frac{\partial Y_t^{\mathrm{I}}}{\partial k^{\mathrm{I}}} & \frac{\partial Y_t^{\mathrm{I}}}{\partial C^{\mathrm{I}}} \end{pmatrix}$$

and

$$\Delta\mathbf{K}^{\mathrm{I}} = \begin{pmatrix} \Delta k^{\mathrm{I}} \\ \Delta C^{\mathrm{I}} \end{pmatrix}$$

then

$$S = (\Delta\tilde{\mathbf{Y}}^{\mathrm{I}}-\Delta\tilde{\mathbf{K}}^{\mathrm{I}}\tilde{\mathbf{J}}^{\mathrm{I}})\mathbf{W}(\Delta\mathbf{Y}^{\mathrm{I}}-\mathbf{J}^{\mathrm{I}}\Delta\mathbf{K}^{\mathrm{I}}) \tag{A-3}$$

In order to mimimize S, the differenciation of S by $\Delta\mathbf{K}^{\mathrm{I}}$ must be zero. One obtains the following simultaneous linear equation

$$\tilde{\mathbf{J}}^{\mathrm{I}}\mathbf{W}\mathbf{J}^{\mathrm{I}}\Delta\mathbf{K}^{\mathrm{I}} = \tilde{\mathbf{J}}^{\mathrm{I}}\mathbf{W}\Delta\mathbf{Y}^{\mathrm{I}} \tag{A-4}$$

This equation may be solved if $|\tilde{\mathbf{J}}^{\mathrm{I}}\mathbf{W}\mathbf{J}^{\mathrm{I}}|\neq 0$ which is usually satisfied. Using the above calculated values of $\Delta\tilde{\mathbf{K}}^{\mathrm{I}}=(\Delta k^{\mathrm{I}}. \Delta C^{\mathrm{I}})$ the most appropriate second guessed values k^{II} and C^{II} are obtained.

$$k^{\mathrm{II}} = k^{\mathrm{I}} + \Delta k^{\mathrm{I}}$$
$$C^{\mathrm{II}} = C^{\mathrm{I}} + \Delta C^{\mathrm{I}}$$

The final values of k and C which give the best fit between observed and calculated values of $\mathbf{Y}$ can be obtained by repeating this process until S cannot be reduced any further.

We are grateful to Professor S. Nagakura, the University of Tokyo, and Prof. H. Baba, Hokkaido University, for their invaluable help in the present work. Thanks are due to the Ministry of Education and the Toray Science Foundation for the financial aid.

BULLETIN OF THE CHEMICAL SOCIETY OF JAPAN, VOL. 44, 997—1000 (1971)

Osmotic Pressures of Polystyrene, Poly-*p*-chlorostyrene and Poly-*o*-chlorostyrene Solutions

Kenji KUBO and Kazuyoshi OGINO

Department of Pure and Applied Sciences, College of General Education, The University of Tokyo, Tokyo

(Received November 30, 1970)

Second virial coefficients for polystyrene (PS), poly-*p*-chlorostyrene (PPCS), and poly-*o*-chlorostyrene (POCS) were determined in various solvents by osmotic-pressure measurements. Free-energy parameters, χ, were estimated from the values of the second virial coefficients. It was shown that the values of χ in each solvent at 30°C became larger in the following order: PS, POCS, PPCS in toluene; PS, PPCS, POCS in chlorobenzene; PPCS, PS, POCS in *n*-butyl acetate. It was indicated that, in addition to the effect of intermolecular forces, another parameter related to the stiffness of the polymer chains should be considered in order to discuss the thermodynamic properties of polymer solutions. It was shown that the values of χ for two polychlorostyrenes in *n*-butyl acetate increased with an increase in the temperatures, unlike the behavior of PS in the same solvent.

In a preceding paper,[1] it was shown that the thermodynamic properties of solutions of poly-*p*-chlorostyrene (PPCS) were markedly different from those of polystyrene (PS) because of the effect of the polar substituent at the para position.

In this paper, the variation in the thermodynamic properties due to the various positions of substituent was examined by osmotic-pressure measurements for PS, PPCS, and poly-*o*-chlorostyrene (POCS) in different solvents.

Experimental

Materials. *o*-Chlorostyrene, a monomer, was prepared from commercial *o*-chlorobenzaldehyde by the following process: *o*-chlorophenylmethylcarbinol was synthesized by a Grignard reaction and was then dehydrated by potassium bisulfate.[2] The monomer was polymerized in bulk at 60°C, in the presence of azo-bis-isobutyronitrile as an

1) K. Kubo, K. Ogino, and T. Nakagawa, *Nippon Kagaku Zasshi*, **88**, 1254 (1967).

2) L. A. Brooks, *J. Amer. Chem. Soc.*, **66**, 1295 (1944).

initiator, under nitrogen gas. The polymer was fractionated from a dilute benzene solution by a successive precipitation procedure using methanol. One separate from nine fractions was used for the osmotic-pressure measurements.

Each fraction of PPCS was the same as has been described in the previous paper.[1] The monodispersed polystyrene used in this experiment was from the Pressure Chemical Company; we assumed that this will not be of the isotactic type, for it was soluble in 2-butanone.

The solvents were dried, toluene and chlorobenzene with calcium chloride, and *n*-butyl acetate with magnesium sulfate, and were freshly distilled before each measurement.

Measurements. The osmotic pressures were determined using a Hewlett-Packard High Speed Membrane Osmometer (Model 503) and Schleicher & Schuell membranes (Type 08) at various temperatures; in toluene and chlorobenzene at 30°C and in *n*-butyl acetate at 5, 30, and 55°C. Pycnometer was used in determining the partial specific volumes in benzene at 30°C; these volumes were found to be 0.797 for PPCS and 0.792 (cc/g) for POCS.

Results

The second virial coefficient, A_2, was obtained from the osmotic pressure by the use of the following equation;

$$\pi/c = \boldsymbol{R}T(1/M_n + A_2c) \tag{1}$$

or;

$$(\pi/c)^{1/2} = (\boldsymbol{R}T/M_n)^{1/2}(1 + M_nA_2c/2) \tag{2}$$

where π is the osmotic pressure; c, the concentration; M_n, the number-average molecular weight; $\boldsymbol{R}$, the gas constant, and T, the absolute temperature. The data observed in toluene and chlorobenzene fit Eq. (2), and those in *n*-butyl acetate fit Eq. (1); several examples are shown in Figs. 1 and 2. The results for M_n and A_2 are summarized in Table 1.

According to the lattice theory of polymer solutions by Flory and Huggins, the free-energy parameter, χ, is related to A_2 by the following relation;

$$A_2 = (1/2 - \chi)\bar{v}_2^2/V_1 \tag{3}$$

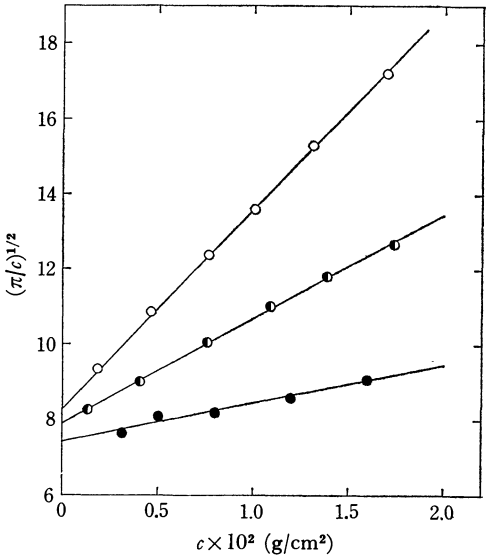

Fig. 1. Plots of $(\pi/c)^{1/2}$ against c in toluene at 30°C.
○ for PS, ◐ for POCS, and ● for PPCS-f6

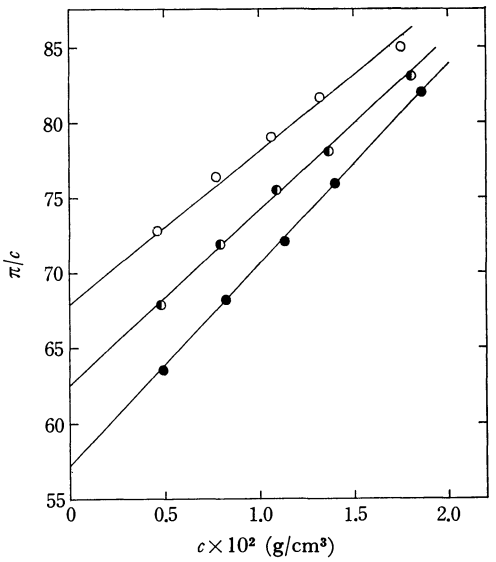

Fig. 2. Plots of π/c against c for POCS in *n*-butyl acetate.
● at 5°C, ◐ at 30°C, and ○ at 55°C

where $\bar{v}_2$ is the partial specific volume of the polymer and where V_1 is the molar volume of the solvent. Since a strong molecular-weight dependence of A_2 in dilute solutions has been observed, especially in good solvents, it is not reasonable, in a strict sense, to discuss the thermodynamic properties of polymer solutions in terms of χ values estimated from Eq. (3). In dilute polymer solutions, A_2 is generally given by the relation using Flory's notation:

$$A_2 = (1/2-\chi)(\bar{v}_2^2/V_1)h(z/\alpha_s^3) \tag{4}$$

with:

$$z = 2(3/2\pi)^{3/2}(\bar{v}_2^2/N_AV_1)(\overline{r^2}_0/M)^{-3/2}M^{1/2}(1/2-\chi). \tag{5}$$

Here, N_A is Avogadro's number, $\overline{r^2}_0$ is the unperturbed mean-square end-to-end distance of the polymer, and the latter is proportional to the molecular weight, M. The α_s quantity is the expansion factor related to the statistical radius. Several forms of $\alpha_s(z)$ consistent with $h(z/\alpha_s^3)$ have been reported. Recently, it has been shown by Fujita *et al.* that their experimental results can be explained well[3] by a combination of $\alpha_s(z)$ and $h(z/\alpha_s^3)$, which Yamakawa and his coworkers presented.[4,5] Therefore, employing their results we estimated χ as:

$$\alpha_s^2 = 0.541 + 0.459(1+6.04z)^{0.46} \tag{6}$$

and:

$$h(z/\alpha_s^3) = \{1-(1+4.454z/\alpha_s^3)^{-0.2867}\}/1.277(z/\alpha_s^3). \tag{7}$$

The value of χ is obtained as follows: by combining Eqs. (4)—(7), $A_2M^{1/2}(\overline{r^2}_0/M)^{-3/2}$ can be represented, and plotted, as a function of z only. The value of z, which corresponds to the A_2 and M_n values obtained from the osmotic-pressure measurements, can be found on the graph when we know the value of $(r_0^2/M)^{1/2}$.

3) T. Norisuye, K. Kawahara, A. Teramoto, and H. Fujita, *ibid.*, **49**, 4330 (1968).
4) H. Yamakawa and G. Tanaka, *J. Chem. Phys.*, **47**, 3991 (1967).
5) H. Yamakawa, *ibid.*, **48**, 2103 (1968).

Table 1. Experimental results of osmotic pressure measurements and values of free energy parameters for polystyrene, poly-*p*-chlorostyrene and poly-*o*-chlorostyrene in various solvents

Polymer -Fract.	Solvent	Temp. °C	$M_n \times 10^{-4}$	$A_2 \times 10^4$ $\left(\frac{cm^3 \cdot mol}{g^2}\right)$	$\chi^{a)}$	$\chi^{b)}$
PS	Toluene	30	37.3	3.45	0.456	0.383
	Chlorobenzene	30	38.8	3.77	0.454	0.370
	n-Butyl acetate	5	41.1	1.88		
		30	40.4	2.08	0.466	0.423
		55	40.2	2.00		
PPCS-f6	Toluene	30	46.3	0.625	0.489	0.483
-f7	Chlorobenzene	30	31.6	2.17	0.465	0.411
-f8	*n*-Butyl acetate	5	18.0	2.96		
-f8		30	17.6	2.39	0.448	0.380
-f8		55	16.5	1.90		
POCS	Toluene	30	40.7	1.73	0.470	0.435
	Chlorobenzene	30	40.6	1.72	0.472	0.439
	n-Butyl acetate	5	41.5	0.570		
		30	40.3	0.449	0.490	0.488
		55	40.1	0.337		

a) Estimated from Eq. (3).
b) Estimated from Eqs. (4)—(7).

Then, the value of χ corresponding to the z can be readily obtained from Eq. (5). The values of χ, summarized in Table 1, are estimated, using the values of $\bar{v}_2$ in cc/g and $(\overline{r^2}_0/M)^{1/2}$ in cm·mol$^{1/2}$/g$^{1/2}$, to be as follows:

	$\bar{v}_2$	$(\overline{r^2}_0/M)^{1/2} \times 10^{11}$
PS	0.920[6]	670[7]
PPCS	0.797	584[1]
POCS	0.792	633[8]

The values of χ obtained from Eq. (3) are also summarized in Table 1.

Discussion

A free-energy parameter, χ, is resolved into an enthalpy term, χ_h, and an entropy term, χ_s. The enthalpy term is represented by Hildebrand's expression:[9]

$$\chi = V_1(\delta_s - \delta_p)^2/RT. \quad (8)$$

Here, the solubility parameter, δ, is given by $(\Delta E/V)^{1/2}$, where ΔE is the molar energy of vaporization, and the suffix s or p represents the solvent or the polymer respectively. It was shown by Huggins that χ_s is expressed as $1/z$ (z: coordination number); thus, χ should increase in accordance with $|\delta_s - \delta_p|$. From the results in toluene, taking account of δ_s (toluene)$=$ 8.9 and δ_p (PS)$=$9.3,[10] it seems to be reasonable to assume that δ_p increases in the order of PS, POCS, and PPCS. The assumption that the δ_p of POCS is smaller than that of PPCS suggests that the effect of the *o*-chlorine atom on an intermolecular force is not so large as that of the *p*-chlorine atom because of the screening effect by a main chain for the *o*-chlorine atom.

If the order of δ_p shown above can be used, and in view of δ_s (chlorobenzene)$=$9.50, the increase in χ does not correspond to the order of $|\delta_s - \delta_p|$ in chlorobenzene. Therefore, in addition to the effect of intermolecular forces, another parameter may be introduced so as to represent the difference in the thermodynamic properties of polymer solutions. Thus, it is reasonable to take into account a theory of the average-potential method proposed by Prigogine and his co-workers.[11] In this theory, external degrees of freedom of r-mer are defined as the remainder left by internal degrees associated with intramolecular valence forces from a total of $3r$ degrees of freedom; they are taken to be $3c$ in number. With a sufficiently large r, c/r tends to 0 for a "perfect rigid r-mer" and to 2/3 for a "perfect flexible r-mer." The parameter c has a value which decreases with an increase in the "stiffness' of the polymer chain. The intermolecular potential energy between elements of i and j is taken to be a Lennard-Jones 6-12 potential-energy type with characteristic parameters for the pair, ε^*_{ij} and r^*_{ij}, where r^*_{ij} is the distance between the centers of the elements, at a minimum potential energy of ε^*_{ij}. The element of the monomer is the monomer itself, and the submolecule of the polymer is treated as an element. If the "sizes" of the elements of A (monomer) and B

6) M. Griffel, R. S. Jessup, J. A. Cogliano, and R. P. Park, *J. Research NBS*, **52**, 217 (1954).
7) M. Kurata and W. H. Stockmayer, *Fortscr. Hochpolym.-Forsch.*, **3**, 196 (1963).
8) K. Matsumura, *Makromol. Chem.*, **124**, 204 (1969).
9) J. H. Hildebrand and R. L. Scott, "The Solubility of Nonelectrolytes," Dover Publications Inc., New York, N.Y. (1964), p. 131.
10) T. G. Fox, *Polymer*, **3**, 111 (1962).
11) I. Prigogine (with the collaboration of A. Bellemans and V. Mathot), "The Molecular Theory of Solutions," North-Holland Publishing Co., Amsterdam (1957), Chapters 16 and 17.

(r-mer) are equal,

$$r^*_{AA} = r^*_{BB} = r^*_{AB}. \quad (9)$$

If the minima of potential energies are also equal,

$$\varepsilon^*_{AA} = \varepsilon^*_{BB} = \varepsilon^*_{AB}. \quad (10)$$

The free-energy parameter in the (r-mer)-monomer system can, then, be approximately represented by this theory by the relation:

$$\chi = 1/z + (C_{P,A}/2R)(1 - c_B/q_B)^2 \quad (11)$$

where $C_{P,A}$ is the molar configurational heat capacity of the monomer and where q_B is given by $(rz-2r+2)/z$. Using the parameters assumed by Eqs. (9) and (10) along with Eq. (11), it can readily be understood that χ is larger in positive value the stiffer the polymer. The systems of polychlorostyrenes-chlorobenzene are treated as such cases in a crude sense. On the basis of this crude assumption, the χ values for these systems are not worth discussing quantitatively, but the finding that the value of χ for POCS in chlorobenzene is larger than the corresponding value for PPCS may be qualitatively attributed to the enlarged chain stiffness of POCS, which in turn may be due to the steric hindrance of the rotation of the main chain by the chlorine atom at the ortho position.

The second virial coefficients for PPCS and POCS in n-butyl acetate decrease with an increase in the temperature. This behavior is different from that of PS in the same solvent, and it is equivalent to a decrease in the intrinsic viscosity with an increase in the temperature, as has been reported previously for PPCS in n-butyl acetate.[1] In view of an inappreciable temperature coefficient of $\bar{r}_0^2$ for PPCS in the same solvent,[12] it seems reasonable to conclude that the values of χ for PPCS, and perhaps for POCS in n-butyl acetate, increase with an increase in the temperatures. This fact may suggest the existence of a strong interaction between the chlorine atom in the polymer and the solvent molecule. The solubility of POCS in n-butyl acetate in poorer than that of PPCS. This fact may be attributed to the difference in stiffness between the two polychlorostyrenes.

From the relations for A_2 and M_n reported in the literature, the values of A_2 can be estimated for polymers with the same molecular weights as those of the polymer fractions employed in this work. The values of A_2 thus obtained are 3.67[13] and 3.54×10^{-4} [14] for atactic PS in toluene; a value of 3.45×10^{-4} ($cm^3\cdot mol/g^2$) is obtained by us, which is slightly smaller than the former and is nearly equal to the latter. The values of A_2 for PPCS in toluene, 0.80[15] and 1.00×10^{-4},[16] are slightly larger than our corresponding value, 0.625×10^{-4} ($cm^3\cdot mol/g^2$). These discrepancies may be partly attributed to the difference in the molecular-weight distributions of the polymers; the deduced conclusion seems not to be affected by these discrepancies. The results for A_2 obtained from light scattering for poly-m-chlorostyrene in toluene[17] were not taken into account of our present discussion, because a value of A_2 obtained from such a measurement is not essentially equivalent to that obtained from osmotic pressure for a polymer fraction with a molecular-weight distribution.

The difference in solubility between PS and various polychlorostyrenes in toluene has been represented by Matsumura[8] on the basis of the data of the polymer-coil dimensions as measured by light scattering. The order of the solubilities of PS and PPCS among these polymers is the reverse of that estimated from our osmotic-pressure measurements. From the fact that our results on osmotic pressure for PS and PPCS in toluene are essentially identical with the corresponding data in the literature cited here, we have some question about the results of light scattering which have been referred to by Matsumura.[18,19]

We intend to proceed with our studies in concentrated polymer solutions by means of vapor-pressure measurements, by which a free-energy parameter is directly estimated; it seems that it will be interesting to discuss quantitatively the effect of the stiffness of a polymer chain on the thermodynamic properties, basing our discussion on the average-potential method or on Flory's method, presented lately.[20]

12) K. Kubo and K. Ogino, *Rep. Prog. Poly. Phys. Japan*, **10**, 111 (1967).
13) W. R. Krigbaum and P. J. Flory, *J. Amer. Chem. Soc.*, **75**, 1775 (1953).
14) F. Danusso and G. Moragrio, *J. Polymer. Sci.*, **24**, 161 (1957).
15) N. Kuwahara, K. Ogino, A. Kasai, S. Ueno, and M. Kaneko, *ibid.*, **A3**, 985 (1965).
16) K. Takamizawa, This Bulletin, **39**, 1186 (1965).
17) K. Matsumura, *ibid.*, **42**, 1874 (1969).
18) T. Oyama and K. Kawahara, *Nippon Kagaku Zasshi*, **78**, 484 (1957).
19) T. Saito, This Bulletin, **35**, 1580 (1962).
20) P. J. Flory, *J. Amer. Chem. Soc.*, **87**, 1833 (1965).

Non-Equilibrium Thermodynamics: Steady State Thermodynamic Relations in the Non-Linear Current-Affinity Region

R. J. Tykodi

Department of Chemistry, Southeastern Massachusetts University, North Dartmouth, Massachusetts, 02747, U. S. A.

(Received June 6, 1969)

A simple heat conduction example is used to show that the choice of boundary conditions for describing a steady process, although of no consequence in the linear current-affinity region, governs the applicability (or the lack thereof) of various thermodynamic assertions to the non-linear current-affinity region. The need for a whole family of classificatory principles to aid us in organizing our knowledge about steady processes is pointed out.

Steady state non-equilibrium situations can be described in thermodynamic terms;[1] the rate of entropy production $\theta \equiv \dot{S}(\text{system}) + \dot{S}(\text{surroundings})$ normally plays a central role in such descriptions. By combined use of the First and Second Laws of thermodynamics it is always possible to resolve the rate of entropy production in a steady state into a set of *currents* Y_i and *affinities* Ω_i, with the currents being time derivatives of extensive thermodynamic variables:

$$\theta = \sum_i Y_i \Omega_i \geqq 0. \tag{1}$$

In a neighborhood of a thermodynamic equilibrium state σ, we can express each current Y_i as a Taylor's series in the affinities Ω_j:

$$Y_i = Y_i(\Omega_j, \sigma) = \sum_j L_{ij}(\sigma)\Omega_j + 1/2\sum_{j,k} L_{ijk}(\sigma)\Omega_j\Omega_k + \cdots ; \tag{2}$$

the coefficients are functions of the parameters describing the thermodynamic equilibrium state σ. If we stop with the linear terms in the expansion in Eq. (2), we define a *linear* current-affinity *neighborhood* of the thermodynamic reference state σ. In such a linear neighborhood of a reference state σ, many interesting theorems hold for situations not involving magnetic or centrifugal fields:[1-3]

a) The matrix of the coefficients L_{ij} is symmetric: $L_{ij}=L_{ji}$.

b) The determinant of the coefficients L_{ij} and all principal minors of that determinant are positive: $L_{ii}>0$, $L_{ii}L_{jj}-L_{ij}L_{ji}>0$ $(i \neq j), \cdots$.

c) For a given reference state σ and a set of affinities Ω_j and currents Y_j $(j \neq i)$, the following relations hold:

$$(\partial Y_i/\partial \Omega_i)_{\Omega_j,\sigma} \geqq (\partial Y_i/\partial \Omega_i)_{Y_j,\sigma} > 0.$$

d) For a given reference state σ and a constant set of affinities Ω_j $(j \neq i)$, the rate of entropy production has a minimum at the point $Y_i=0$;

$$0 = (\partial\theta/\partial Y_i)_{\Omega_j,\sigma}|_{Y_i=0}, \quad 0 < (\partial^2\theta/\partial Y_i^2)_{\Omega_j,\sigma}|_{Y_i=0}.$$

e) For any given expression involving only the rate of entropy production, the currents Y_i, and the affinities Ω_i (in any combination), consider whether the expression equals zero or does not equal zero—*i.e.*, consider the *mystic properties* (the vanishing or non-vanishing) of the expression. Generate from the given expression a *dual* expression by everywhere exchanging the roles of currents and affinities, and examine the mystic properties of the dual expression. In the linear neighborhood of a reference state σ, a given expression of the appropriate type and its dual expression have the same mystic properties.

Let

$$B_{ij}(\sigma) \equiv (\partial Y_i/\partial \Omega_j)_{\Omega',\sigma}, \quad D_{ij} \equiv (\partial Y_i/\partial \Omega_j)_{Y',\sigma},$$

$$(\delta/\tilde{\delta}Y_j)_{\Omega',\sigma} \equiv (\partial/\partial Y_j)_{\Omega',\sigma}|_{Y_j=0},$$

$$(\delta/\tilde{\delta}\Omega_j)_{Y',\sigma} \equiv (\partial/\partial \Omega_j)_{Y',\sigma}|_{\Omega_j=0},$$

where the subscript $\Omega'(Y')$ means constant $\Omega_k(Y_k)$ for each $k \neq j$. Then in the linear current-affinity neighborhood of σ, the relations a)—e) take the forms

$$B_{ij}(\sigma) = B_{ji}(\sigma), \tag{3}$$

$$B_{ii}(\sigma) > 0, \quad B_{ii}(\sigma)B_{jj}(\sigma) - B_{ij}(\sigma)B_{ji}(\sigma) > 0 \quad (i \neq j), \cdots, \tag{4}$$

$$B_{ii}(\sigma) \geqq D_{ii}(\sigma) > 0, \tag{5}$$

$$(\delta\theta/\tilde{\delta}Y_i)_{\Omega',\sigma}, \quad (\delta^2\theta/\tilde{\delta}Y_i^2)_{\Omega',\sigma} > 0, \tag{6a, b}$$

$$0 = (\delta\theta/\tilde{\delta}Y_i)_{\Omega',\sigma=0} \leftrightarrow (\delta\theta/\tilde{\delta}\Omega_i)_{Y',\sigma=0}, \text{ etc.} \tag{7}$$

The question of interest is; Are there any general relations of the form (3)—(7) that hold *outside* the linear current-affinity neighborhood of reference state σ?

I shall now describe a simple heat conduction example that yields non-linear current-affinity relations and which is particularly rich in counter-examples for relations of the type (3)—(7).

Heat Conduction Example

Stretch a homogeneous metallic wire between two heat reservoirs (thermostats) α, β; cut the wire at its mid point and let the two thereby exposed faces of the wire communicate with a thermostat (heat reservoir) x; insulate the wire so that there are no lateral heat losses. Consider the case of a wire of constant thermal conductivity κ, and choose the dimensions of the wire so that $2\mathcal{B}\kappa/\mathcal{A}=1$, where $\mathcal{A}$ is the length and $\mathcal{B}$ is the cross sectional area of the wire. Let $\dot{Q}_\alpha{}^{(r)}$, $\dot{Q}_\beta{}^{(r)}$, $\dot{Q}_x{}^{(r)}$ represent the rate of influx of heat into the appropriate reservoir (of temperature T_α, T_β, or T_x). In the steady state we have the following relations:

$$\dot{Q}_\alpha{}^{(r)} + \dot{Q}_\beta{}^{(r)} + \dot{Q}_x{}^{(r)} = 0, \tag{8}$$

1) R. J. Tykodi, "Thermodynamics of Steady States," The Macmillan Company, New York (1967).

2) S. de Groot, "Thermodynamics of Irreversible Processes," North-Holland Publishing Company, Amsterdam (1951).

3) I. Prigogine, "Introduction to the Thermodynamics of Irreversible Processes," John Wiley & Sons, New York (1968).

$$\dot{Q}_\alpha^{(r)} = T_x - T_\alpha, \quad \dot{Q}_\beta^{(r)} = T_x - T_\beta,$$
$$\dot{Q}_x^{(r)} = T_\alpha + T_\beta - 2T_x, \tag{9}$$
$$\theta = \dot{Q}_\alpha^{(r)}\left(\frac{1}{T_\alpha} - \frac{1}{T_x}\right) + \dot{Q}_\beta^{(r)}\left(\frac{1}{T_\beta} - \frac{1}{T_x}\right)$$
$$\equiv Y_1\Omega_1 + Y_2\Omega_2, \tag{10}$$
$$= \dot{Q}_\alpha^{(r)}\left(\frac{1}{T_\alpha} - \frac{1}{T_\beta}\right) + \dot{Q}_X^{(r)}\left(\frac{1}{T_X} - \frac{1}{T_\beta}\right)$$
$$\equiv y_1\omega_1 + y_2\omega_2. \tag{11}$$

For a given thermodynamic state σ the linear current-affinity neighborhood is infinitesimal; it is thus easy to investigate relations such as (3)—(7) in the non-linear current-affinity region. By way of example, note that at constant T_β (let the state at β play the role of a reference state σ, *i.e.*, $\sigma=\beta$)

$$\dot{Q}_\alpha^{(r)} = Y_1 = Y_1(\Omega_1, \Omega_2, \sigma) = T_x - T_\alpha$$
$$= T_\beta(1 - T_\beta\Omega_2)^{-1} - T_\beta(1 + T_\beta\Omega_1 - T_\beta\Omega_2)^{-1}$$
$$= T_\beta\{T_\beta\Omega_1 - (T_\beta\Omega_1)^2 + 2T_\beta^2\Omega_1\Omega_2$$
$$+ (T_\beta\Omega_1)^3 + \cdots\}. \tag{12}$$

Let us now check the validity of relations (3)—(7) in the non-linear current-affinity region for various choices of reference state σ: $\sigma=\alpha, \beta, x$; a subscript σ in an equation means that the thermodynamic state at σ is being held constant, *i.e.*, subscript σ means constant T_σ.

Relations (3). The validity of relations (3) varies with the choice of reference state σ; thus (*e.g.*)

$$B_{12}(x) = B_{21}(x) = 0, \quad b_{12}(x) = b_{21}(x) = -T_\alpha^2, \tag{13}$$

but

$$B_{12}(\beta) \neq B_{21}(\beta), \quad b_{12}(\beta) \neq b_{21}(\beta), \tag{14}$$

except in the limit $T_\alpha \to T_\beta$, $T_x \to T_\beta$. (The upper and lower case convention introduced in Eqs. (10) and (11) applies throughout the paper.)

Relations (4). Relations (4) remain valid for either choice of currents and affinities—Eq. (10) or (11)—and for all choices of reference state.

Relations (5). The validity of relations (5) varies with the choice of reference state; thus (*e.g.*)

$$B_{ii}(\sigma) = D_{ii}(\sigma) > 0, \quad \sigma = \alpha, \beta, x, \quad i = 1, 2 \tag{15}$$

and

$$b_{11}(\beta) > d_{11}(\beta) > 0, \tag{16}$$

but

$$b_{11}(\alpha) = T_x^2, \quad d_{11}(\alpha) = T_\beta^2/2. \tag{17}$$

There is, consequently, no necessary ordering relation between $b_{11}(\alpha)$ and $d_{11}(\alpha)$, except in the limit $T_x \to T_\alpha$, $T_\beta \to T_\alpha$.

Relations (6). The relations

$$(\partial^2\theta/\partial Y_i^2)_{\Omega',\sigma} > 0, \quad (\partial^2\theta/\partial y_i^2)_{\omega',\sigma} > 0,$$
$$\sigma = \alpha, \beta, x, \quad i = 1, 2, \tag{18}$$

hold for all choices of reference state, but the validity of the relations

$$(\delta\theta/\tilde{\delta}Y_i)_{\Omega',\sigma} = 0, \quad (\delta\theta/\tilde{\delta}y_i)_{\omega',\sigma} = 0$$

varies with the choice of reference state; thus (*e.g.*)

$$(\delta\theta/\tilde{\delta}Y_1)_{\Omega_2,\beta} = 0, \quad (\delta\theta/\tilde{\delta}y_1)_{\omega_2,\beta} = 0, \tag{19}$$

but

$$(\delta\theta/\tilde{\delta}Y_1)_{\Omega_2,\alpha} \neq 0, \quad (\delta\theta/\tilde{\delta}y_1)_{\omega_2,\alpha} \neq 0, \tag{20}$$

and

$$(\delta\theta/\tilde{\delta}y_2)_{\omega_1,\sigma} \neq 0 \quad \sigma = \alpha, \beta, x, \tag{21}$$

except in the appropriate limit.

Relations (7). A given expression and its dual expression need not have the same mystic properties outside the linear current-affinity region; thus (*e.g.*)

$$(\delta\theta/\tilde{\delta}y_1)_{\omega_2,x} = 0 \text{ and } (\delta\theta/\tilde{\delta}\omega_1)_{y_2,x} = 0, \tag{22}$$

$$(\delta\theta/\tilde{\delta}y_2)_{\omega_1,\beta} \neq 0 \text{ and } (\delta\theta/\tilde{\delta}\omega_2)_{y_1,\beta} \neq 0, \tag{23}$$

but

$$(\delta\theta/\tilde{\delta}y_1)_{\omega_2,\beta} = 0 \text{ whereas } (\delta\theta/\tilde{\delta}\omega_1)_{y_2,\beta} \neq 0, \tag{24}$$

$$(\delta\theta/\tilde{\delta}y_2)_{\omega_1,\alpha} \neq 0 \text{ whereas } (\delta\theta/\tilde{\delta}\omega_2)_{y_1,\alpha} = 0, \tag{25}$$

except, of course, in the appropriate limit.

Observations

The relations (3)—(7) form an interrelated, compact set in the linear neighborhood of any arbitrary thermodynamic reference state σ. As we move outside the linear current-affinity region, we find that relations (4) and (6b) remain generally valid, but that the other relations become sensitive to the choice of reference state and cannot be counted on to remain valid for any arbitrary choice of reference state. Outside the linear current-affinity region, then, we can expect to find [with the exception of relations (4) and (6b)] only a series of special thermodynamic relations, relations that hold only for special choices of current-affinity representation and for special sets of reference states. We are thus faced with the task of categorizing steady states in such a way that we can immediately tell which of relations (3)—(7) is applicable to a given situation.

Consider, for example, the following situation: for an arbitrary reference state σ and fixed affinities Ω_j $(j\neq k)$ make a plot of θ *versus* Y_k; such a plot will always be concave upward—relation (6b)— and will always show a minimum. Now, start from an equilibrium configuration, the entire system being in state σ, and make θ *vs.* Y_k plots for various choices of the affinities Ω_j, moving (with each successive plot) farther and farther away from reference state σ. Let us examine the locus of the minima in the θ *vs.* Y_k plots as we move away from the equilibrium state; we observe one of two patterns: i) either the locus of the minima lies on the line $Y_k=0$ (Fig. 1), or ii) the locus of the minima lies off the line $Y_k=0$ (Fig. 2). We can accordingly categorize steady state situations by noting whether they follow the pattern of Fig. 1 or whether they follow that of Fig. 2—the thermoelectric effect[1] (*e.g.*), with Y_k being the electric current, follows the Fig. 1 pattern, whereas our heat conduction example, with $Y_k=\dot{Q}_x^{(r)}$ [Eq. (21)], follows the Fig. 2 pattern. What we would very much like to have is a criterion for recognizing a Fig. 1 situation *without* actually having to compute θ as a function of Y_k.

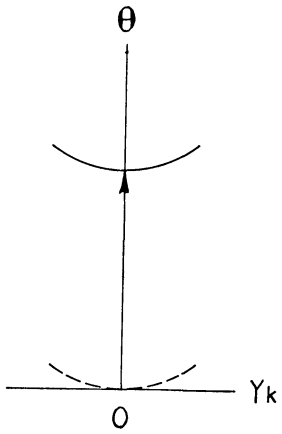

Fig. 1

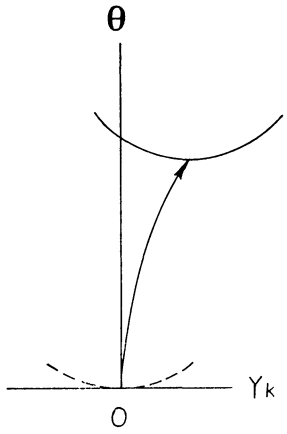

Fig. 2

A fruitful field for further effort, then, is the search for classificatory principles, *a la* Mendeleeff, for steady state situations so that we can treat such situations in groups according to their thermodynamic deserts.

Appendix

In this appendix I offer a tentative criterion for a situation of the Fig. 1 type. From the various steady-state currents Y_k, I single out a class of *conservative currents* Y_k^*: a conservative current (i) flows in a closed loop or (ii) flows from a source (χ) to a sink (ψ) without loss or branching, *i.e.* $Y_k^*(\chi)+Y_k^*(\psi)=0$, or (iii) is the rate of change of the degree of reaction variable ($\dot{\xi}$) for a chemical reaction. In considering the flow of a given current, I single out a class of *associated fundamental reference states* σ^*: an associated fundamental reference state for a current Y_k is a reference state such that the condition of constant Ω', σ implies that all the intensive variables in each Ω' are kept constant. To illustrate these ideas in terms of the heat conduction example of this paper, note that none of the currents $\dot{Q}_\alpha^{(r)}$, $\dot{Q}_\beta^{(r)}$, $\dot{Q}_x^{(r)}$ are conservative currents since they satisfy the three-term relation (8) instead of the two-term relation [(ii) above] required of a conservative current. Note also that in Eq. (10) with respect to current Y_1 reference state x is an associated fundamental reference state since constant Ω_2, x implies constant T_β, T_x; on the other hand reference state α is not an associated fundamental reference state for Y_1 since constant Ω_2, α implies only that the combination $T_\beta^{-1}-T_x^{-1}$ is to remain constant whereas the separate temperatures T_β, T_x may change.

The criterion that I tentatively propose is the following: A situation involving both a conservative current Y_k^* and an associated fundamental reference state σ^* follows the pattern of Fig. 1, *i.e.*

$$(\delta\theta/\tilde{\delta}Y_k^*)_{\Omega',\sigma^*}=0. \tag{26}$$

Of the four possible combinations of current type (Y_k^* or Y_k) and reference state type (σ^* or σ)$-(\delta\theta/\tilde{\delta}Y_k^*)_{\Omega',\sigma^*}$, $(\delta\theta/\tilde{\delta}Y_k^*)_{\Omega',\sigma}$, $(\delta\theta/\tilde{\delta}Y_k)_{\Omega',\sigma^*}$, $(\delta\theta/\tilde{\delta}Y_k)_{\Omega',\sigma}$—we know that each of the four expressions vanishes in a linear neighborhood of the appropriate thermodynamic reference state; I am now suggesting that it is only the Y_k^*,σ^* combination that unfailingly continues to vanish outside the appropriate linear neighborhood.

In considering the behavior of θ as a current Y_k vanishes, let the residual currents (the non-vanishing currents) be indicated by Y_i. If any of the Y_i are mass currents involving sensible amounts of kinetic energy, it is generally impossible to find an associated fundamental reference state σ^* for the vanishing current Y_k. This observation means that relation (26) can only be tested in the case of a vanishing current (Y_i) of mass or electricity or chemical reaction ($\dot{\xi}$) in the presence of a residual current (or currents) Y_i of heat or electricity. The various steady-state non-equilibrium effects that could conceivably meet the requirements of Eq. (26) are some of the electrokinetic effects, the thermomolecular pressure effect, thermoösmosis, thermal diffusion, thermoelectricity, and effects involving a stationary chemical reaction ($\dot{\xi}=0$) in the presence of residual flows of heat or electricity; see Ref. 1 for a full discussion of these non-equilibrium effects.

Salt and Medium Effects on H_ Indicators

N. CHATTANATHAN and C. KALIDAS

Department of Chemistry, Indian Institute of Technology, Madras, India

(Received September 29, 1970)

The activity coefficients of the molecular forms of a few nitrodiphenylamine indicators were determined by a solubility method in basic solutions of ethylene and propylene glycols. The medium effects on the ions of these indicators were also obtained by determination of the medium effects of their molecular forms separately by solubility measurements. Variation of the activity coefficients and the medium effects on the ions of the indicators are discussed.

In earlier papers on this subject,[1,2] it was shown that the validity of the acidity function concept is based on two conditions. For a pair of successive indicators B and B_1 in the overlapping range, the equality of the activity coefficient ratios

$$\frac{f_{B^{0,-}}}{f_{A^{+,0}}} = \frac{f_{B_1{}^{0,-}}}{f_{A_1{}^{+,0}}} \quad (1)$$

must be satisfied where A, B and A_1, B_1 are the indicator acid-base pairs. The superscripts $B^{0,-}$ indicate an uncharged or a negatively charged basic indicator used in H_0 or H_- measurements, respectively. The charges on the other species can be explained in a similar manner. The relative strengths of a pair of indicators must remain unchanged on changing the medium. Although the equality of the ratios of the above type has approximately been shown to hold by indirect methods for indicators of similar structure in water and some non-aqueous solvents of fairly high dielectric constant, the recent work of Boyd[3] has clearly established that there are quite large variations in the individual values of the activity coefficient for both the neutral bases and their conjugate acids. A direct determination of the activity coefficients of the indicators is, therefore, necessary not only for an evaluation of the relative contributions of the various terms in the appropriate acidity function but also to understand[4] the dependence of the acidity function on the indicator structure and in particular on the site of ionisation. Although several classes of indicators have been employed[5-7] for H_- measurements in aqueous and non-aqueous solutions of bases, no data are hitherto available on the variation of their activity coefficients with changing medium. The present work deals with the determination of the activity coefficients of the molecular forms of a few nitrodiphenylamines (which have earlier been employed for H_- measurements in glycols[2]) in sodium glycollate solutions of ethylene and propylene glycols and also their medium effects.

Experimental

Preparation of Solvents, Indicators, and Base. The purification of ethylene and propylene glycols has been described elsewhere.[2] The indicators 2,4,3′-trinitrodiphenylamine (2,4,3′-TNDA), 2,4-dinitrodiphenylamine (2,4-DNDA), and 2,4-dinitro-4′-aminodiphenylamine (2,4-DN-4′-amino-DA) were employed. They were prepared and purified according to standard methods in literature.[8] The preparation and standardization of sodium glycollate in ethylene and propylene glycols has been described.[2]

Solubility Measurements. The solubility measurements of the indicators at various concentrations of the base in the two glycol were carried out at 30±0.5°C. Their saturated solutions were obtained by shaking mixtures of the solid with the appropriate base solution for about 48 hr in a thermostat maintained at a fixed temperature. Known volume of the saturated solution was diluted suitably with the appropriate solvent (the pure solvent or a base solution of the desired concentration) to get convenient values of optical density. The optical densities were measured at the wavelength of maximum absorption of the molecular forms in a P.M.Q. II Carl Zeiss Spectrophotometer and the concentrations were calculated using the known extinction coefficients of the indicators in these solvents at this wavelength. In addition, solubility measurements of the various indicators in water at the same temperature were carried out to compute the medium effects. All solubility measurements were carried out at least in duplicate to confirm the reproducibility of results.

Results

The activity coefficients were calculated from

$$f_{HA} = \frac{S_0}{S}\left(1+\frac{K_{HA}}{h_-}\right) \quad (2)$$

where S_0 and S refer to the solubilities of the given indicator in the pure glycol and the base solution, respectively. K_{HA} is the thermodynamic dissociation constant of the indicator, the activity coefficients being referred to a value of unity at infinite dilution in the given solvent and $\log h_- = -H_-$ on the solvent standard state.

Table 1 gives the solubility and activity coefficient data for different indicators in the two solvents. The medium effects on the molecular and ionic forms of these indicators are presented in Table 2. The medium effect on the ions was calculated by adding the medium effect of the corresponding molecular acids to the overall medium effect which is given by pK^s_{HA}—pK^w_{HA} where pK^s_{HA} and pK^w_{HA} refer to the negative logarithm of thermodynamic ionisation constants of a given indicator in solvent "S" and water, respectively.

1) C. Kalidas and S. R. Palit, *J. Chem. Soc.*, **1961**, 3998.
2) N. Chattanathan and C. Kalidas, *Aust. J. Chem.*, in press.
3) R. H. Boyd, *J. Amer. Chem. Soc.*, **85**, 1555 (1963).
4) L. M. Sweeting and K. Yates, *Can. J. Chem.*, **44**, 2395 (1966).
5) K. Bowden, *Chem. Rev.*, **66**, 119 (1966).
6) C. H. Rochester, *Quart. Rev.*, **21**, 494 (1967).
7) G. Yagil, *J. Phys. Chem.*, **71**, 1034 (1967).
8) R. Stewart and J. P. ODonnell, *Can. J. Chem.*, **42**, 1681 (1964).

TABLE 1. ACTIVITY COEFFICIENT DATA OF THE MOLECULAR FORM OF THE VARIOUS INDICATORS

Solvent: Ethylene glycol
Indicator: 2,4,3'-TNDA

Base concn. (mol/l)	Solubility $\times 10^4$ (mol/l)	log f_{HA}
0.00	4.27	—
5.00×10^{-4}	3.50	+0.088
1.00×10^{-3}	4.25	+0.008
1.00×10^{-2}	5.28	−0.037
1.10×10^{-1}	7.68	+0.041

Solvent: Propylene glycol
Indicator: 2,4,3'-TNDA

Base concn. (mol/l)	Solubility $\times 10^4$ (mol/l)	log f_{HA}
0.00	4.79	—
2.50×10^{-4}	5.05	−0.017
5.00×10^{-4}	5.99	−0.096
1.00×10^{-3}	6.48	−0.109
5.00×10^{-3}	6.69	−0.049

Indicator: 2,4-DNDA

Base concn. (mol/l)	Solubility $\times 10^3$ (mol/l)	log f_{HA}
0.00	2.21	—
5.00×10^{-4}	1.93	+0.060
1.00×10^{-3}	2.24	−0.005
5.00×10^{-3}	2.30	−0.015
1.00×10^{-2}	1.93	+0.061
1.00	1.97	+0.160

Indicator: 2,4-DNDA

Base concn. (mol/l)	Solubility $\times 10^3$ (mol/l)	log f_{HA}
0.00	3.98	—
2.50×10^{-4}	3.53	+0.053
5.00×10^{-4}	4.57	−0.060
1.00×10^{-3}	4.80	−0.081
5.00×10^{-3}	4.81	−0.080
5.00×10^{-2}	3.88	+0.032

Indicator: 2,4-DN-4'-amino-DA[a)]

0.00	3.97	—
5.00×10^{-4}	3.83	+0.016
1.00×10^{-3}	3.66	+0.035
5.00×10^{-3}	3.39	+0.069
5.00×10^{-1}	3.33	+0.081
1.25	4.03	+0.033

a) The tabular columns have the same headings as for the above indicator.

TABLE 2.

Indicator	ΔpK in E.G.	ΔpK in P.G.	log f^o_{HA} in E.G.	log f^o_{HA} in P.G.	log $(f^o_{H^+}\cdot f_{A^-})$ in E.G.	log $(f^o_{H^+}\cdot f_{A^-})$ in P.G.
2,4,6-TNDA[a)]	2.01	2.53	−2.27	−2.11	−0.26	+0.42
2,4,2',4'-TNDA[b)]	1.90	2.27	−2.13	−1.78	−0.23	+0.49
2,4,3'-TNDA	1.91	2.53	−1.83	−1.88	+0.08	+0.65
2,4-DNDA	2.25	3.02	−2.54	−2.79	−0.29	+0.23
2,4-DN-4'-amino-DA	2.07	—	−2.47	—	−0.40	—

E.G. = Ethylene glycol; P.G. = Propylene glycol.
a) 2,4,6-trinitrodiphenylamine
b) 2,4,2',4'-tetranitrodiphenylamine

The medium effect of the molecular acid was calculated from

$$\log f^o_{HA} = \log \frac{S_w}{S_g} \qquad (3)$$

where S_w and S_g are the solubilities of the indicator in water and the glycol, respectively. The results of Table 1 are plotted in Fig. 1.

Discussion of the Activity Coefficients. We see from Table 1 as well as from Fig. 1 that the activity coefficients of all the indicators vary considerably in the range of base concentrations employed contrary to general assumption. Generally, the indicator molecules are 'salted in' in the presence of the base except in the case of 2,4-DN-4'-amino-DA. There is, however, a tendency for the activity coefficients to increase *i.e.* show a 'salting out effect' at low base concentrations as well as at higher base concentrations.

A similar variation of the activity coefficients of some nitroanilines and amides was noted by others[3,4,9)] in acid solutions although no attempt was made to explain the variation. Qualitatively this can be explained in terms of three types of hydrogen bonded interactions when base concentration is increased. At low concentrations, the base, being a strong hydrogen bond acceptor, removes the solvent molecules bonded to the indicator thus decreasing its solubility. At intermediate concentrations, the increased indicator ionization coupled with the solvation of the indicator ion increases its solubility. At higher concentrations, this is opposed by hydrogen bonding between the base molecules, the effect being less on the sol-

9) M. I. Vinnik and N. Librovich, *Tetrahedron*, **22**, 2945 (1966).

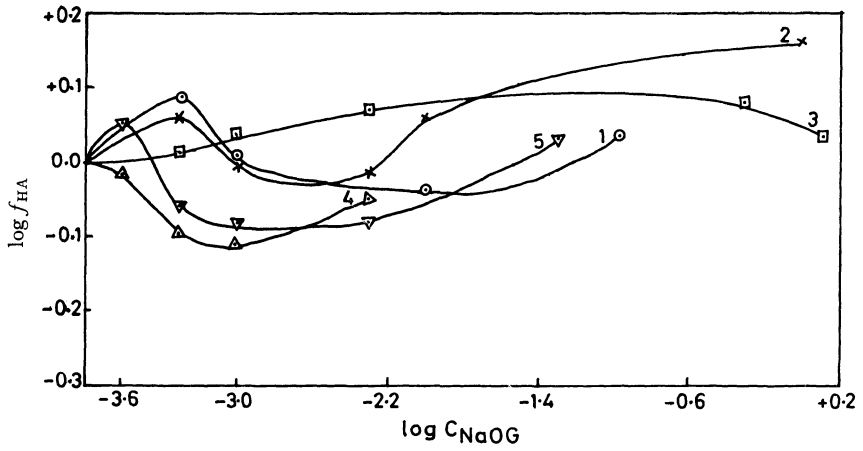

Fig. 1. Plot of $\log f_{HA}$ against $\log C_{NaOG}$ for various indicators in ethylene and propylene glycols.
Curves 1,2,3 are in ethylene glycol and 4,5 are in propylene glycol.
⊙,△ refer to 2,4,3′-TNDA. ×,▽ refer to 2,4-DNDA. ▣ refers to 2,4-DN-4′-amino-DA.

vation of the indicator ion thus decreasing its solubility. In the case of 2,4-DN-4′-amino-DA the ionization of the indicator being much less, predominantly salting out effect is observed.

Our results show that the ratio of the activity coefficients of two successive indicators in the overlap region decreases from unity at higher base concentrations in ethylene glycol while it increases in propylene glycol. Since it was shown[2] that Eq. (1) is applicable for nitrodiphenylamines in basic solutions of ethylene and propylene glycols, a similar variation should be expected in the case of the activity coefficient ratio of the anionic forms of the indicators. An increase in the number of nitro groups leads to a greater "salting in" effect presumably due to the strong hydrogen bond interactions between these groups and the solvent, the effect being much more pronounced in propylene glycol than in ethylene glycol.

Discussion of Medium Effects. The medium effects for the ions of the various indicators in ethylene glycol are smaller than those in propylene glycol, and the free energy change for the transfer of the ions from water to ethylene glycol is negative while it is positive for propylene glycol.

Application of the Born equation reveals that the free energy change associated with the transfer of the indicator ions (the proton and the indicator anion) from a solvent of high to a low dielectric constant should be positive. Although the results in propylene glycol are in qualitative agreement with that predicted by the Born equation, the results in ethylene glycol are contradictory. This is not surprising since the Born equation takes into account only the electrostatic contribution to the free energy change of transfer while other factors, such as ion-solvent interactions, which depend on solvent basicity and contribute to the non-electrostatic part of the free energy change are ignored. The opposite signs of the medium effects of the indicator ions in the two solvents are undoubtedly due to the differences[2,10] in their solvent basicities. The differences in the medium effects of the ions of the various indicators in a given solvent most possibly arise from the changes in the delocalization of charge caused by the introduction of nitro or amino groups in various positions in the benzene ring. Such differences in charge delocalization affect the ion-solvent interactions considerably.

Grateful thanks are due to Professor M.V.C. Sastri, Head of the Department, for his constant encouragement throughout the work.

10) R. G. Bates, "Determination of pH. Theory and Practice," John Wiley & Sons Inc., New York (1964), p. 194.

Corrosion Reaction of Iron in Phosphatizing Solution

Ryokai SHIRAKAWA,* Shiro TAKEDA,** Takao UMEGAKI,*** and Taijiro OKABE

Department of Applied Chemistry, Faculty of Engineering, Tohoku University, Sendai

(Received June 3, 1970)

An electrochemical investigation was made on the corrosion reaction of iron in phosphatizing solution to clarify the mechanism of the formation of phosphate coating. Polarization characteristic curves revealed the corrosion of iron to be under cathodic control implying that the formation of phosphate coating occurs thus under cathodic control. The corrosion rate increased considerably by the addition of KNO_3 or KNO_2 which is used as an accelerator in phosphatization. The formation of phosphate coating was much accelerated by cathodic polarization of iron, but repressed by anodic polarization and rotation of the iron electrode.

The rate of phosphate coating formation is believed to be controlled by the corrosion rate of metal surface phosphatized. The corrosion reaction is divided into two electrochemical reactions, anodic and cathodic.

It was suggested by Machu[1-3] that the rate of phosphate coating formation is controlled by the anodic reaction at the anodic area, occupying more than 99% of metal surface and shows first order dependency on the anodic area. However, the relation between this rate and the anodic area fails by the addition of an accelerator to the phosphatizing solution because of its depolarization effect.

We found that the phosphate coating formation is basically under cathodic control which seems quite reasonable since the corrosion reaction of metal is usually under cathodic control.

Measurement of polarization characteristic and the rate of dissolution of iron in phosphatizing solutions of various compositions were made to decide the rate-determining step and the rate of corrosion reaction. The influence of the cathodic polarization of iron in the phosphate coating formation was examined.

Experimental

Polarization Characteristic. Solutions having the compositions shown in Table 1 were prepared by dissolving guaranteed pure chemical reagents in redistilled water (electroconductivity 2.2×10^{-6} mho·cm). Because of complications that may arise due to the formation of zinc phosphate coating on iron electrode, no zinc was added to the solution.

Iron electrode, 5 mm in diameter, was cut out from a commercial mild steel whose composition is given in Table 2. The bottom was polished with 0/5 emery paper, degreased with benzene just before the measurement and the other end was inserted into a glass tube support to be rotated in the solution. The rest of the electrode surface was covered with epoxy resin for the sake of insulation from solution. The rotation speed of the iron electrode was changed from 200 to 800 rpm.

TABLE 1. COMPOSITION OF SOLUTION FOR POLARIZATION CHARACTERISTIC

H_3PO_4	KNO_3	KNO_2	pH	Atmosphere
0.23 M	0 M	0 mM	2.6	nitrogen
0.23	0	0	2.6	air
0.23	0.10	0	2.6	nitrogen
0.23	0.10	5	2.6	nitrogen

TABLE 2. COMPOSITION OF MILD STEEL USED (wt%)

C	Si	Mn	P	S	Cu	Cr	Ni
0.12	0.29	0.35	0.002	0.030	0.35	0.06	0.09

The apparatus is shown in Fig. 1. The current was recorded 30—60 sec after the application of a constant potential to the iron electrode by a potentiostat. First anodic and then cathodic polarization characteristics were measured. All the experiments were carried out at 25°C.

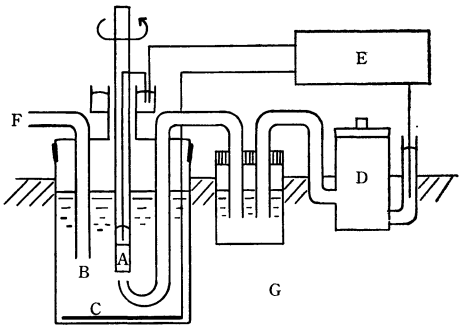

Fig. 1. Apparatus for polarization characteristic.
A: iron electrode, B: phosphatizing solution, C: Pt-electrode, D: SCE, E: potentiostat, F: N_2 or air inlet, G: thermostat

Corrosion Rate. Solutions having compositions given in Table 3 were prepared from reagent grade chemicals and distilled water. The iron electrode and cell used in the measurement of polarization characteristic were used. A polished iron electrode was dipped into the solution, rotated for a certain time and the amount of dissolved iron was determined.

TABLE 3. COMPOSITION OF SOLUTION FOR CORROSION RATE

H_3PO_4	KNO_3	KNO_2	pH	Atmosphere
0.23 M	0 M	0 mM	2.6	nitrogen
0.05—0.50	0	0	2.6	air
0.23	0.05—0.50	0	2.6	air
0.23	0	5—20	2.6	air

* Present address: The Furukawa Electric Co. Ltd., Nikko.
** Present adress: The Fujitsu Co. Ltd., Kawasaki.
*** Present address: The Tokyo Metropolitan Univ., Tokyo.

1) W. Machu, *Chem. Fabrik*, **13**, 461 (1940).
2) W. Machu, *Korrosion u. Metallschutz*, **17**, 157 (1941); **18**, 89 (1942), **20**, 1 (1944).
3) W. Machu, *Arch. Metallkde*, **1**, 1 (1948); **3**, 203 (1949).

Influence of Polarization on Phosphate Coating Formation. The composition of the solution is given in Table 4. The solution was prepared by dissolving ZnO in H_3PO_4 and HNO_3 and diluting with distilled water. The pH of the solution was controlled by addition of K_2CO_3.

TABLE 4. COMPOSITION OF PHOSPHATIZING SOLUTION

H_3PO_4	ZnO	HNO_3	pH
0.20 M	0.10 M	0.07 M	2.6

The same iron electrode and apparatus as those used in the experiment for polarization characteristic were used, except for the replacement of the potentiostat with a galvanostat.

A constant current was applied on the iron electrode in the phosphatizing solution and the change of iron electrode potential with time against SCE was recorded. The phosphate coating formed on the electrode was observed with a microscope.

Results and Discussion

Typical polarization characteristic curves of iron in solutions of various compositions at 600 rpm are shown in Fig. 2.

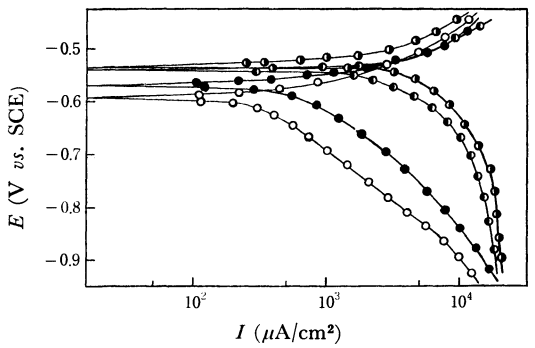

Fig. 2. Polarization characteristic of iron.
○: 0.23 M H_3PO_4 in N_2, ●: 0.23 M H_3PO_4 in air,
◐: 0.23 M H_3PO_4 + 0.10 M KNO_3 in N_2,
◑: 0.23 M H_3PO_4 + 0.10 M KNO_3 + 5 mM KNO_2 in N_2

The anodic polarization curves are smooth in all cases indicating the anodic reactions to be under diffusion control.

On the other hand, the cathodic polarization curves change appreciably with the composition of solution.

In pure H_3PO_4 under nitrogen atmosphere, a straight line called "Tafel slope" is observed on the cathodic polarization curve between the apparent current density of 500 and 5000 $\mu A/cm^2$ indicating the reaction to be under activation control. The intersection of extrapolated line of the Tafel slope and the corrosion potential gives an approximately 300 $\mu A/cm^2$ estimation of the corrosion current.

The polarization curves and the corrosion currents in this condition are not affected by the increase of rotation speed of iron electrode from 200 to 800 rpm except when current density is greater than 5000 $\mu A/cm^2$ where the cathodic polarization becomes slightly smaller with the increase of rotation speed. This could also be explained by the activation control of the corrosion reaction of iron.

In the air, the cathodic polarization curves are smooth for all rotation speeds throughout the range of current density. This indicates the cathodic reaction to be under diffusion control. In this case the corrosion potential becomes more noble than that under nitrogen atmosphere, as the rotation speed increases.

By addition of accelerators such as KNO_3 or KNO_2, the cathodic polarization curves show limiting currents and reactions proceed under diffusion control. The influence of dissolved oxygen is negligible in the presence of the accelerator.

It should be noted that in all cases, the polarization characteristic indicates that the corrosion reaction of iron in the phosphatizing solution namely the phosphate coating formation, is under cathodic control.

Figure 3 shows the corrosion current of iron in pure H_3PO_4 calculated from the amount of dissolved iron, assuming that the reaction is $Fe \rightarrow Fe^{2+} + 2e$, and applying the Faraday rule.

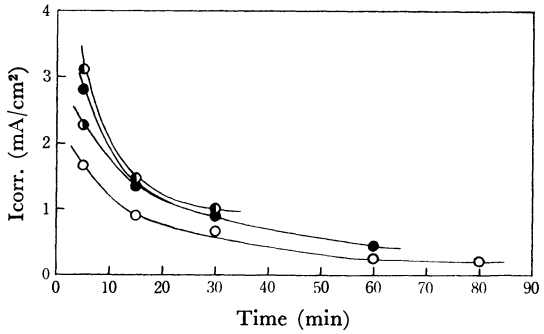

Fig. 3. Corrosion current of iron in H_3PO_4.
H_3PO_4 concn. ◐: 0.10 M Atmosphere ○: N_2
●○: 0.23 ●◐◑: air
◑: 0.50

The corrosion current diminishes exponentially with time and approaches a constant value under nitrogen or air atmosphere because of inactivation of iron surface. In the air, the corrosion rate is always greater than that under nitrogen atmosphere, while the difference of concentration of H_3PO_4 shows no influence on corrosion current. This shows that the reaction is mainly due to the oxygen dissolved in solution.

The corrosion current 300 $\mu A/cm^2$ obtained from the polarization characteristic corresponds to the value shown at 60—80 min in this case.

Figure 4 shows the corrosion rate of iron expressed by the dissolution rate of iron in H_3PO_4 containing various amounts of KNO_3 and KNO_2. Each plot is an average of three values obtained at 5, 15, and 30 min except those in pure H_3PO_4 which was taken only at 15 min. This is because when either KNO_3 or KNO_2 is present in the solution, the dissolved iron increases linearly with time showing constant corrosion rate within a deviation ±10%, while the corrosion rate changes considerably in the case of pure H_3PO_4. The corrosion rate increases with the increase of the concentration of added KNO_3. An increase of KNO_3 concentration from 0.05 to 0.50 M accelerates the corrosion rate by a factor of 4. KNO_2 has 30—70 times greater accelerating effect on the corrosion rate than

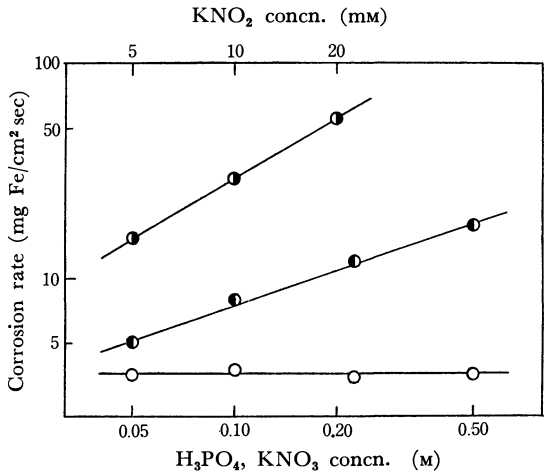

Fig. 4. Corrosion rate of iron in H_3PO_4 with KNO_3 or KNO_2.
○: pure H_3PO_4, ◐: 0.23 M H_3PO_4 + KNO_3,
◑: 0.23 M H_3PO_4+KNO_2

KNO_3.

It has also been found that the corrosion rate is not affected at all by the change of pH of the solution from 1.5 to 4.5 in pure H_3PO_4 but decreases to almost 1/6 by the same pH elevation when KNO_3 or KNO_2 is present in the solution. The increase of rotation speed of iron electrode from 100 to 600 rpm increases the corrosion rate by a factor of 2 in H_3PO_4 containing 0.1 M of KNO_3. This indicates that the corrosion rate is approximately proportional to the square root of the rotation speed of iron electrode.

When a cathodic current is applied to the iron electrode, active area on the iron surface decreases with the formation of phosphate coating, the iron electrode potential falling gradually, suddenly drops to the potential of electrodeposition of zinc. The time lap between the application of cathodic current and the sudden change of potential was measured as a phosphatizing time τ of iron electrode. Reproducibility of τ was examined and the deviation was found to be within ±20%.

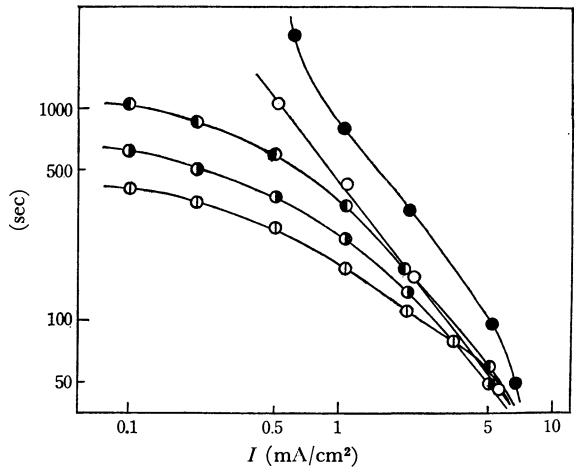

Fig. 5. Influence of cathodic polarization.
KNO_2 concn. ○●: 0 mM Rotation speed ○: 0 rpm
◐: 2.5 ●◐◑◌: 600
◑: 5
◌: 10

It is obvious from Fig. 5 that the cathodic polarization accelerates the coating formation considerably, but the rotation of electrode at 600 rpm represses it. This is due to the excessively large corrosion rate of iron surface caused by the rotation of the electrode. Coating formation is accelerated to a greater extent with the concentration of added KNO_2. The influence of cathodic polarization of iron electrode on

Fig. 6. Phosphate coating on buff-polished iron. (5 min, ×160)
Cathodic current 3 mA/cm², without rotation.

Fig. 7. Phosphate coating on buff-polished iron. (5 min, ×160)
Without cathodic current and rotation.

Fig. 8. Phosphate coating on buff polished iron.
(5 min, ×160)
Without cathodic current, rotation at 600 rpm.

the coating formation is clearly seen in Figs. 6 and 7. This shows the phosphate coating formed on the buff-polished iron electrode.

The cathodic polarization increases the number and growth rate of phosphate crystals (Fig. 6) in comparison with that which is not polarized (Fig. 7). The rotation represses the phosphate coating and increases the corrosion of iron surface as seen in Fig. 8.

On the other hand, the anodic polarization of iron electrode shows no comparable effect on the coating formation as observed with the cathodic polarization when polarization is small. As the polarization is increased, the coating formation is repressed and the dissolution of iron electrode increases.

Conclusions

The corrosion reaction of iron which is the first step of phosphate coating formation was investigated from an electrochemical viewpoint and the following conclusions were obtained.

1) The corrosion reaction of iron in the phosphatizing solution is under cathodic control. Thus, the phosphate coating formation is also under cathodic control. The influence of diffusion rate can not be neglected.

2) The corrosion rate of iron is increased by KNO_3 and KNO_2, the latter being more effective.

3) The cathodic polarization of iron accelerates the phosphate coating formation considerably, while anodic polarization and rotation of the iron electrode represses it.

BULLETIN OF THE CHEMICAL SOCIETY OF JAPAN, VOL. 44, 1010—1013 (1971)

The Spectroscopic Observation of the Selective Volatilization of Metal Solid Samples in a Nitrogen Plasma Flame[1)]

Masaoki Oku and Kichinosuke Hirokawa

The Research Institute for Iron, Steel and Other Metals, Tohoku University, Sendai

(Received June 5, 1970)

Some metal solid samples were burned in a nitrogen plasma flame, and the spectrum intensity-time curves were spectrographically observed. The curves indicated that the fractional distillation of alloying elements was caused by the reactions of the solid-alloy sample and nitrogen gas. The fractional distillation was explained in terms of the difference in the stabilities of the metal nitrides. The distribution of the emission species and the temperature of the flame suggested that there were few chemical reactions in the flame or that the chemical reactions in the flame had little effect on the spectrum intensities. In an appendix, the method of line-pair selections for obtaining the correct temperature is considered.

Many molecular species, such as MO, OH, and CN, are produced by the introduction of solution samples into a plasma flame; they cause the high background spectra. The use of a metal solid sample instead of the solution may eliminate some of them, but the difficulties of the use of a solid sample are present in the complications of sample charging, high-temperature physicochemical reactions in an electrode, and the evaporation process of electrode materials. Several excellent discussions of fractional distillation or selective vaporization have already been reported.[2-4)] However, few papers have discussed the fractional distillation resulting from the reactions of elements in a metal electrode with gases which produce plasmas. In a previous report,[5)] a burner which produced a current-free nitrogen plasma jet flame was used for the spectrographic analysis of metal solid samples. With it, satisfactory calibration curves were obtained

1) This paper was read at the 23 rd Annual Meeting of the Chemical Society of Japan, Tokyo, April, 1970.

2) L. H. Ahrens and S. R. Taylor, "Spectrochemical Analysis," Addison-Wesley Publ. Co., Reading, Mass. (1961).

3) O. Leuchs, *Spectrochim. Acta*, **4**, 237 (1950).

4) E. Schroll, *Z. Anal. Chem.*, **198**, 40 (1963).

5) K. Hirokawa and H. Goto, This Bulletin, **42**, 693 (1969).

for the determination of some alloying elements in iron alloys, but for the alloying elements in aluminum alloy the precision was not satisfactory because of the sputtering of aluminum as aluminum nitride. In this report, the evaporation process of aluminum alloy and iron alloy, the emission profiles for metallic species in the nitrogen plasma flame, and the flame temperature will be investigated.

Experimental

The apparatus was the same as that described in the previous report.[5] The spectra were photographed under the following conditions: sample, 15 mm in length and 5 mm in diameter; polarity, anode; condenser voltage, 230—250 V; arc current, 13—15 A; tangentially-introduced gas-flow rate, 1.4 *l*/min; atomizer gas-flow rate, 4.2 *l*/min; slit width of spectrograph, 30 μ. Fuji spectrographic plates were developed with F.D. 131 at 20°C for 5 min. In order to measure the distribution of spectrum intensities along the vertical axis of the nitrogen plasma flame, the flames were imaged on the spectrographic slit with a 10-sec exposure after a predischarge of 120 sec. The intensity-time curves were obtained by a focused image of the flames on a condenser lens and by repeating a 10-sec exposure and a 20-sec interval after a predischarge of 5 sec. A Shimadzu ARL electron X-ray microprobe analyser was used for microanalysis; it had an accelerating voltage of 20 kV.

Results and Discussion

The vertical emission profiles for metallic species in the nitrogen plasma flames produced by an aluminum alloy (Si, 0.75; Cu, 0.90; Mg, 2.32; Zn, 3.06; Fe, 0.09; Mn, 0.274; Pb, 0.40; Bi, 0.58; Cr, 0.177; Ti, 0.266%) and by an iron alloy (V, 1.72%) are shown in Figs. 1 and 2 respectively. The spectrum intensities are normalized to the intensity of the part, 0.3 to 0.9 mm above the top of the burner. There were no proper two lines for measuring the temperature for the aluminum alloy flame. Therefore, the temperature was measured only for the iron alloy flame with the line-pair of FeI 3214.40 and FeI 3219.59. The method of selecting line-pairs for obtaining the correct temperature will be considered in an appendix. The temperature distribution curve along the vertical axis of the plasma flame is shown in Fig. 3. The higher a position in the flame, the lower the temperature. This suggests that the flame is cooled by the surrounding air and has no exothermic reactions at least. Moreover, the monotonous and nearly uniform decrease in the spectrum intensities with the height of the flame indicates that there are few reactions in the flame or that the chemical reactions have little effect on the

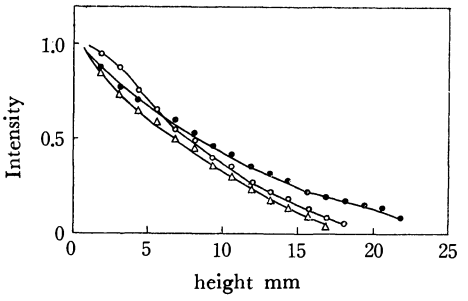

Fig. 1. The vertical emission profile for metallic species in the nitrogen plasma flame produced by Al-alloy.
○, TiI 3642.68; ●, CrI 3020.67; △, MgI 3096.90

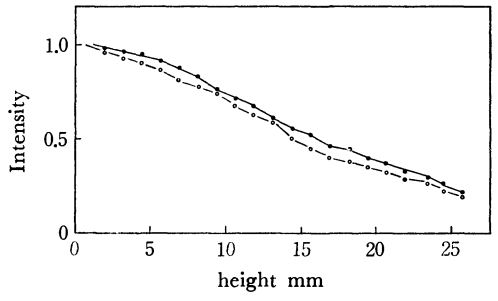

Fig. 2. The vertical emission profile for metallic species in the nitrogen plasma flame produced by Fe-alloy.
●, VI 3185.40; ○, FeI 3184.90

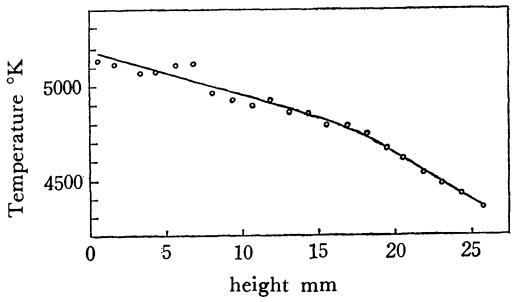

Fig. 3. The temperature curve along the vertical axis of iron-nitrogen plasma flame.

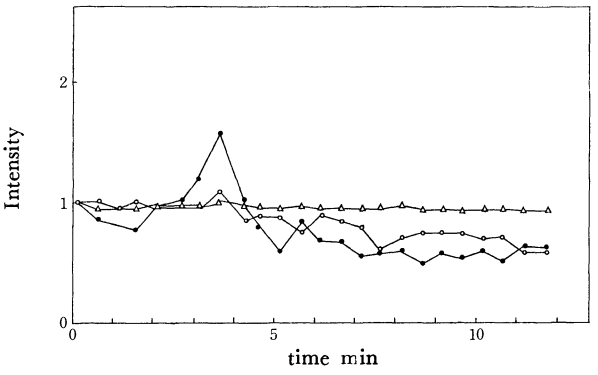

Fig. 4. Intensity-time curve for Cr, Si, Al in Al-alloy.
△, CrI 3593.49; ●, SiI 2881.58; ○, AlI 2567.99

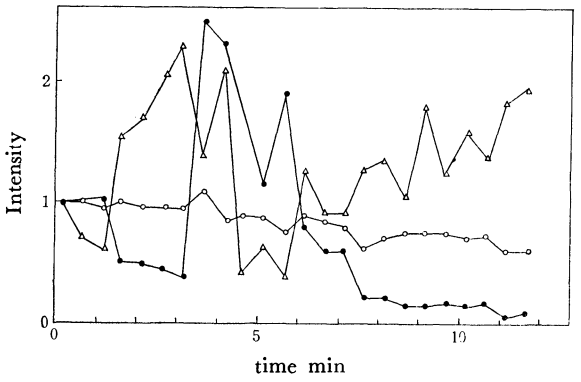

Fig. 5. Intensity-time curve for Mn, Ti, Al in Al-alloy.
△, MnII 12605.69; ●, TiI 3642.68; ○, AlI 2567.99.

spectrum intensities.

For some elements in aluminum alloy, the intensity-time curves are shown in Figs. 4 and 5. Aluminum, magnesium, silicon, chromium, nickel, zinc, and lead make one group. Their intensities decreased with the time, though the rates of decrease were small. However, the intensity of manganese had risen in the early stage, and then, after a diminution, increased gradually again. The spectral intensity of titanium had decreased at first and then after an increase, decreased again. The intensity-time curve of a solid sample was not, of course, the same in each discharge, but the patterns of the curves appeared similar.

For some elements in iron alloys, the intensity-time curves are shown in Figs. 6 and 7. Nearly constant spectral line-intensity ratios with time were obtained for manganese, molybdenum, and vanadium in iron. On the other hand, the spectrum intensity ratios aluminum and titanium to iron decreased with the time. These patterns were also similarly maintained in each discharge.

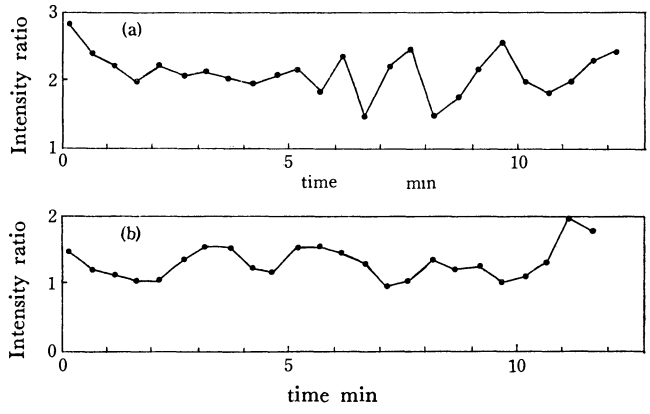

Fig. 6. Intensity-time curve for Mn in Al-Mn-Steel, MnI 2801.06/FeI 2840.42 (a); and Mo in Mo-Steel, MoI 3864.11/FeI 3805.34 (b).

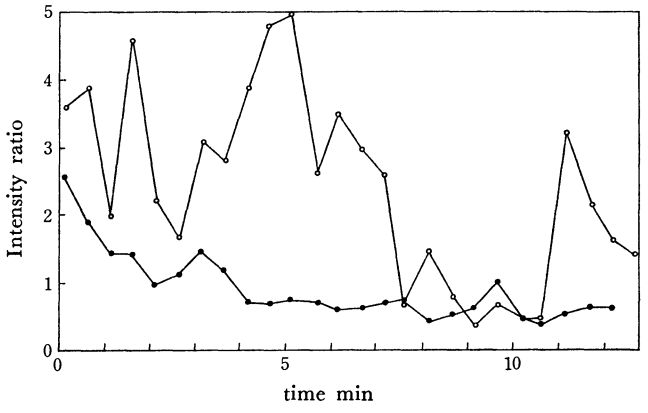

Fig. 7. Intensity-time curve for Ti, in Ti-Steel, and Al in Al-Mn-Steel.
○, TiI 3653.50/FeI 3451.92; ●, AlI 3092.71/FeI 3142.45

The flame temperature of titanium-iron alloy was around 4600—4900°K during the burning period. The flame used was current-free, so that violent change in the excitation conditions of the plasma during the burning period is not considered. Since the emission-spectral-line intensities from the flame under constant conditions are proportional to the concentration of the elements in the flame, the intensity-time curves are considered to be equivalent to the evaporation rate-time curves. The evaporation rates may depend to a considerable degree upon the chemical reactions on the electrode. Figures 4 to 7 may, consequently, indicate that there is a relationship between the intensity-time curves and the reactions on the electrode. The equilibrium between metals and the corresponding nitrides have been represented graphically by Darken and Garry.[6] The equilibrium is represented:

$$x\mathrm{M}_{(\mathrm{solid})} + \mathrm{N}_{2(\mathrm{gas})} = \mathrm{M}_x\mathrm{N}_{2(\mathrm{solid})}$$

Iron nitride decomposes at a low temperature, and titanium nitride is more stable at a high temperature. The partial pressure of the nitrogen of other metal system comes between the partial pressure of the iron system and that of the titanium system at the same temperature, as in Darken and Garry's graph. In the case of the aluminum matrix, the evaporation-rate ratio of aluminum to metal, which forms not so stably as aluminum, is nearly constant. Titanium is concentrated on the electrode surface of the electrode, titanium may intermittently evaporate in large quantities; then a second decrease is observed. In the case of the iron matrix, aluminum and titanium behave similarly. In electron-microprobe analysis, the intensity of Ti$K\alpha$ on the discharged surface of the sample was higher than that of other parts, and N$K\alpha$ was observed in the same places. These findings indicated that titanium was concentrated as titanium nitride there. Titanium nitride was observed even in the heated area of the bulk sample. However, the behavior of manganese could not be explained.

Conclusion

The reactions of solid-sample metal with nitrogen gas, which produces an arc plasma, cause a fractional distillation of the elements in samples. It indicates that a nitrogen plasma flame may not be adequate for the determination of titanium and zirconium in some alloys because of the higher stabilities of their nitrides. The differences in the stabilities of metal nitrides cause a fluctuation in the emission spectral intensity ratios.

Appendix

The fundamental equation for temperature measurement according to the two-line procedure is:

$$I_a/I_b = (gA)_a/(gA)_b \cdot \nu_a/\nu_b \cdot \exp(-(V_a - V_b)/kT).$$

if the lines are labelled a and b (I, relative intensity; g, statistical weight; A, relative transition probability; ν, frequency; V, excitation potential). Boumans[7] discussed the effect of $V_a - V_b$ and the $(gA)_a/(gA)_b$ ratio upon the relative error ($\Delta T/T$) of the temperature. The error, however, depends not only on them but also on the value of the I_a/I_b ratio.

6) L. S. Darken and R. W. Gurry, "Physical Chemistry of Metals," McGraw-Hill Book Co., Inc., New York, Tront, London (1954).

7) P. W. J. M. Boumans, "Theory of Spectrochemical Excitation," Plenum Press, New York (1966).

EXPERIMENTALLY MEASURABLE TEMPERATURE RANGES BY TWO-LINE PROCEDURE[a)]

TABLE 1. $2.00\,\text{eV} < V_a - V_b < 2.50\,\text{eV}$

$V_a - V_b$	(eV)	2.32	2.28	2.27	2.14
$(gA)_a/(gA)_b$		28.1	100	268	635
λ_a	(Å)	3265.62	3760.05	3956.46	4282.41
λ_b	(Å)	3440.99	3683.06	3940.88	4216.41
A	(°K)	4800—12000	3900—11000	3400—8000	2900—5900
B	(°K)		3900— 5100	3400—5200	2900—5000

TABLE 2. $2.50\text{eV} < V_a - V_b < 3.00\,\text{eV}$

$V_a - V_b$	(eV)	2.70	2.73	2.67	2.72
$(gA)_a/(gA)_b$		34.2	200	382	745
λ_a	(Å)	2887.81	3638.30	3684.11	3677.63
λ_b	(Å)	2969.36	3707.82	3683.06	3683.06
A	(°K)	5400—15000	4200—10000	3800—8500	3600—7300
B	(°K)		4200— 6200	3800—6200	3600—6100

TABLE 3. $3.00\,\text{eV} < V_a - V_b < 3.50\,\text{eV}$

$V_a - V_b$	(eV)	3.35	3.37	3.30	3.27
$(gA)_a/(gA)_b$		94.1	250	473	945
λ_a	(Å)	3553.74	3805.34	3738.31	3586.11
λ_b	(Å)	3443.88	3922.91	3906.48	3683.06
A	(°K)	5800—17000	5000—12000	4500—9800	4200—8200
B	(°K)		5000— 8100	4500—7600	4200—7000

TABLE 4. $3.50\,\text{eV} < V_a - V_b$

$V_a - V_b$	(eV)	3.93	3.75	3.84	3.75
$(gA)_a/(gA)_b$		62.7	308	763	2160
λ_a	(Å)	5292.52+	3282.33++	3353.03+++	3345.02++
λ_b	(Å)	5105.54	3075.90	3351.97	3075.90
A	(°K)	7200—23000	5500—13000	5000—10000	4400—8200
B	(°K)		5500—8500	5000— 8500	4400—8200

a) In lines A and B the ratio $\Delta I/I$ ($I=I_a/I_b$) is larger than 4% and 10% respectively when the ratio $\Delta T/T$ is 2%. The combinations were made by atomic spectra line-pairs of iron expect Table 4. +, CuI; ++, ZnI; +++, CrI.

In experiments, especially with photographic plates, the range of the intensity ratio, $I(I_a/I_b)$, may be restricted to that between 0.1 and 10.0. The usual relative standard deviation of the spectrum intensity is larger than 2 per cent. Thus, if the $\Delta I/I$ is smaller than 4 per cent when I varies from I to $I+\Delta I$, the calculated temperature is not reliable. Since the small standard deviation in the temperature by the plotting method is 110°K at 5100°K,[8)] temperature ranges where where determination errors are within 2 per cent are presented in the tables. Tables 1—4 show the combination of $V_a - V_b$, $(gA)_a/(gA)_b$, the corresponding temperature ranges. The values of gA are based on the measurement of Corliss and Bozman.[9)] In the A and B lines, the $\Delta I/I$ ratios are larger than 4 per cent and 10 per cent respectively when the $\Delta T/T$ ratios are 2 per cent.

8) C. H. Corliss, *J. Research NBS*, **66A** (Phys. and Chem.), 5 (1966).

9) C. H. Corliss and W. R. Bozman, "Experimental Transition Probabilities for Spectral Lines of Seventy Elemests," NBS Monograph 53, Washington, D.C. (1962).

Thermal Annealing Behavior of the Recoil ^{57}Co Formed by the Decay of ^{57}Ni-Labeled Hexamminenickel(II) Complexes

Takashi Omori, Shaw-Chii Wu, and Takanobu Shiokawa
Department of Chemistry, Faculty of Science, Tohoku University, Katahira, Sendai
(Received August 26, 1970)

Thermal annealing reactions of ^{57}Co formed by the EC and β^+-decay of the ^{57}Ni-labeled hexamminenickel(II) halide complexes were investigated in detail by means of ion-exchange techniques. When the annealing is carried out at high temperatures, the chemical behavior of ^{57}Co is remarkably affected by the thermal decomposition of the parent and daughter complexes. In the intrinsic annealing, however, the annealing curves have characteristic shapes and the plateau yields of $^{57}Co(NH_3)_6^{3+}$ ion are independent of the temperature, depending on the nature of the outer-sphere anion. The unusual oxidation reaction of the recoil ^{57}Co(II) species is explained by the action of the crystal defects in the near-neighborhood of the recoil site.

Since Collins and Harbottle[1] found that the annealing reaction can take place in the hexabromoethane even if the γ-dose is negligibly small, there have appeared several studies of the intrinsic annealing of the recoil atom in the decay-atom system. For instance, Andersen *et al.*[2,3] have reported that, in the β^--decay process of $K_2{}^{125}SnCl_6$, the distribution of ^{125}Sb is strongly affected by the inherent crystal defects in the crystal, while in the IT process of $^{127m}Te(OH)_6$, the influence of crystal defects introduced prior to the decay event on the initial distribution of ^{127}Te and on the thermal annealing reaction can be ignored. In the IT process of $K^{80m}BrO_3$, it has also been found that the thermal annealing might be promoted by the inherent crystal defects.[4]

Studies of the intrinsic annealing process, therefore, would seem to provide very important information on the recombination mechanism in the solid phase. In a previous paper,[5] the chemical behavior of the ^{57}Co produced by the EC and β^+-decay of the ^{57}Ni-labeled hexamminenickel(II) complex was reported. The results showed that a fairly large amount of the ^{57}Co(III) species is produced, depending on the nature of the outer-sphere anion. Moreover, the heating of the sample at 60°C generally increases the yield of the cobalt(III) species. The present study has been carried out in order to clarify the thermal-annealing behavior of ^{57}Co in the hexamminenickel(II) halide complexes.

Experimental

All the reagents used were of a guaranteed-reagent grade.

Nickel-57 was produced by a (γ, n) reaction using an electron linear accelerator of Tohoku University. Nickel oxide which had been irradiated by bremsstrahlung with a maximum energy of 40 MeV was dissolved in concentrated hydrochloric acid, and then the solution was passed through an anion-exchange resin in order to separate the ^{57}Co produced by the EC and β^+-decay of ^{57}Ni and that produced by the (γ, p) reaction.[6] The ^{57}Ni-labeled hexamminenickel(II) halides were synthesized by ordinary methods[7] and were then stored in the dark at the temperature of dry ice. After the complete decay of the ^{57}Ni, the ^{57}Co-labeled species were separated by means of a cation-exchange resin method, with reference to the procedure previously reported by Ikeda *et al.*[8]

The thermal-annealing procedure was carried out in a constant boiling bath or in an electric oven. Crystals were placed in brown glass tubes in air unless otherwise stated. The macroscopic thermal decomposition of the hexamminenickel(II) complexes was studied under the same conditions as was the thermal annealing.

The radioactivity of ^{57}Co was measured with a 100-channel pulse-height analyzer equipped with an NaI(Tl) well crystal.

Results and Discussion

In the present investigation, the following ^{57}Co recoil species were separated by means of a cation-exchange resin method: $^{57}Co^{2+}$, $^{57}CoX(NH_3)_5^{2+}$, and $^{57}Co(NH_3)_6^{3+}$, where X denotes Cl, Br, or I. The experimental results for the initial distribution of ^{57}Co-labeled species in the hexamminenickel(II) complexes are summarized in Table 1. The yields shown are average values of at least five determinations.

Table 1. Initial yield of ^{57}Co-labeled species in hexamminenickel(II) halides

Compound	Yield of ^{57}Co-labeled species (%)		
	Co^{2+}	$CoX(NH_3)_5^{2+}$	$Co(NH_3)_6^{3+}$
$[^{57}Ni(NH_3)_6]Cl_2$	72.6±1.5	2.3±0.5	24.7±0.8
$[^{57}Ni(NH_3)_6]Br_2$	72.8±1.7	1.6±0.4	25.7±1.6
$[^{57}Ni(NH_3)_6]I_2$	70.3±2.0	2.7±0.6	26.9±1.5

Although the initial yields of the radioactive ^{57}Co species in the hexamminenickel(II) halides are nearly all equal, there appears a remarkable difference among the isothermal annealing curves, as is shown in Figs.

1) K. E. Collins and G. Harbottle, *Radiochim. Acta*, **3**, 21 (1964).
2) T. Andersen, F. Christensen, and K. Olesen, *Trans. Faraday Soc.*, **62**, 248 (1966).
3) T. Andersen, L. Johansen, and K. Olesen, *ibid.*, **63**, 1730 (1967).
4) T. Shiokawa, T. Sasaki, and S. Takahashi, *Radiochem. Radioanal. Lett.*, **1**, 31 (1969); T. Shiokawa and T. Sasaki, This Bulletin, **43**, 2835 (1970).
5) T. Omori, S. C. Wu, and T. Shiokawa, *Radiochem. Radioanal. Lett.*, **3**, 405 (1970).
6) G. E. Moore and K. A. Kraus, *J. Amer. Chem. Soc.*, **74**, 843 (1952).
7) H. Ito, "Jikken Kagaku Koza," Vol. 11, Maruzen, Tokyo (1956), p. 74.
8) N. Ikeda, K. Yoshihara, and S. Yamagishi, *Radiochim. Acta*, **3**, 13 (1964).

1—3. In all cases, an increase in the $^{57}Co(NH_3)_6^{3+}$ yields corresponds substantially to a decrease in the $^{57}Co^{2+}$ yield, and the yield of the ^{57}Co-labeled halopentamminecobalt(III) fraction is almost independent of the heating time and the temperature. Thus changes in the $^{57}CoX(NH_3)_5^{2+}$ yield are not plotted in the figures.

Figure 1 shows the annealing curves for the chloride complex. For temperatures below 80°C, the annealing isotherms exhibit normal kinetic patterns. At 119°C, the yield of the $^{57}Co(NH_3)_6^{3+}$ fraction increases at first, then reaches a maximum after 2 hrs' heating and subsequently decreases. This kind of annealing pattern is presumably due to the thermal decomposition of the reformed complex.

In the bromide complex, the annealing isotherms at various temperatures are shown in Fig. 2. Up to 100°C, the annealing curves possess characteristic shapes; that is, they show the inflection near the point

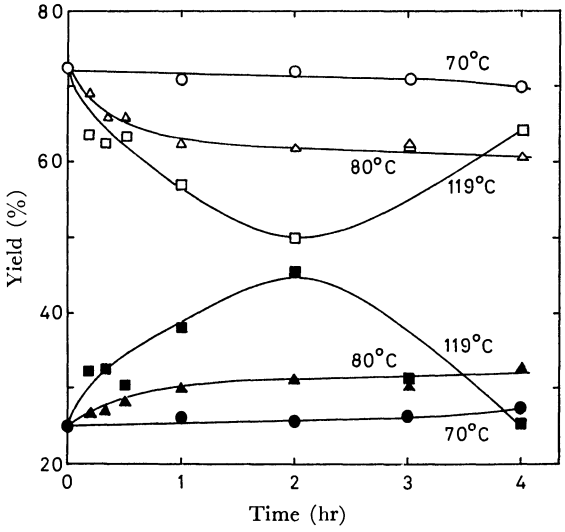

Fig. 1. Isothermal annealing curves of ^{57}Co in $[^{57}Ni(NH_3)_6]Cl_2$.
○, △, □: $^{57}Co^{2+}$; ●, ▲, ■: $^{57}Co(NH_3)_6^{3+}$

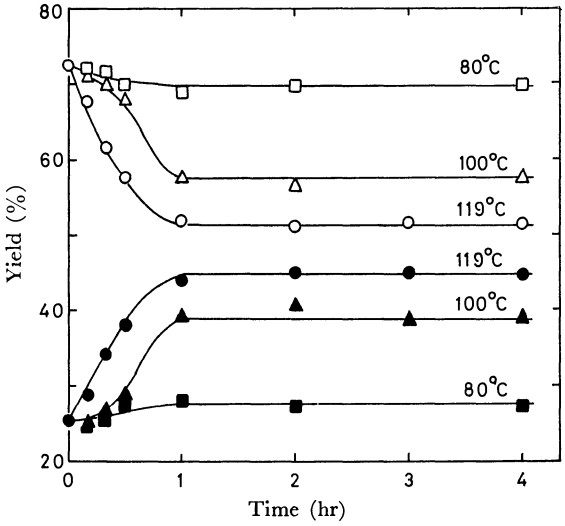

Fig. 2. Isothermal annealing curves of ^{57}Co in $[^{57}Ni(NH_3)_6]Br_2$.
○, △, □: $^{57}Co^{2+}$; ●, ▲, ■: $^{57}Co(NH_3)_6^{3+}$

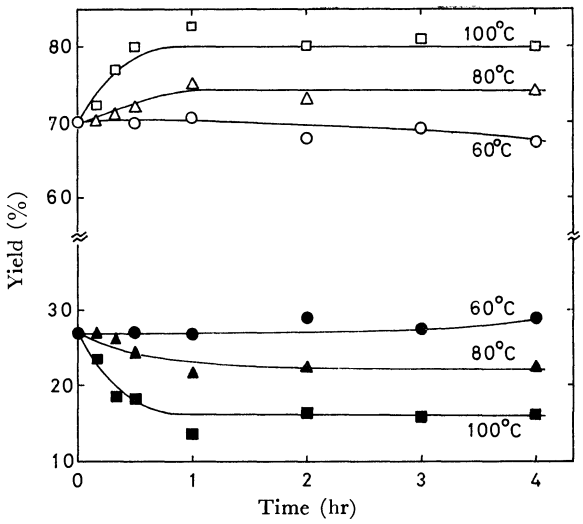

Fig. 3. Isothermal annealing curves of ^{57}Co in $[^{57}Ni(NH_3)_6]I_2$.
○, △, □: $^{57}Co^{2+}$; ●, ▲, ■: $^{57}Co(NH_3)_6^{3+}$

of origin. However, the curve at 119°C shows a normal kinetic pattern.

In the iodide complex, the annealing isotherms differ appreciably from those of the chloride and bromide complexes, as is shown in Fig. 3. The $^{57}Co(NH_3)_6^{3+}$ yield decreases gradually at 80°C, though it increases slightly at 60°C after 4 hrs' heating.

These experimental results suggest that the chemical behavior of the recoil ^{57}Co atoms in the nickel(II) complexes is influenced by the thermal decomposition of the daughter cobalt complexes. It is necessary to study also the effect of the thermal decomposition of the parent complexes, because the hexamminenickel(II) chloride decomposes at a lower temperature than does the hexamminecobalt(III) chloride.[9]

The macroscopic thermal decomposition of the hexamminenickel(II) chloride was noticeable after heating for 4 hr at 80°C, where it amounted to 6.2 per cent, while at 70°C no appreciable decomposition was observed after 20 hrs' heating. In the bromide and iodide complexes, no macroscopic decomposition of the crystal took place after 4 hrs' heating at 80°C, but the decomposition began at 100°C.

On the basis of the data for the thermal decomposition of the parent nickel(II) complexes, the chemical behavior of the recoil ^{57}Co atoms can be explained as follows: when the parent complex is thermally stable, the annealing reaction does not proceed essentially after 4 hrs' heating. On the contrary, when the parent complex, $[Ni(NH_3)_6]Cl_2$, begins to decompose, the $^{57}Co(NH_3)_6^{3+}$ yield increases remarkably. This suggests that freely-available ammonia molecules will participate in the formation reaction of the hexamminecobalt(III) complex. In the iodide, however, the decrease in the $^{57}Co(NH_3)_6^{3+}$ yield at 80°C is possibly to be ascribed to low thermal stability of hexamminecobalt(III) iodide, since the thermal

9) W. W. Wendlandt and J. P. Smith, "Thermal Properties of Transition-Metal Ammine Complexes," Elsevier, Amsterdam (1967).

decomposition of the hexamminenickel(II) iodide can be ignored.

In the (n, γ) process of the hexamminecobalt(III) complexes, Yasukawa and Saito[10,11] have also found that the thermal annealing reaction of ^{60}Co to reform the parent is promoted by the atmosphere of ammonia gas. This effect was interpreted in terms of the diffusion of ammonia, penetrating into the interior of the crystal and reacting with fragments to reform the parent.

Extensive kinetic studies of the thermal decomposition of the hexamminecobalt(III) complexes have been carried out by Tanaka and Nagase.[12] They proposed that the decomposition of $[Co(NH_3)_6]Cl_3$ *in vacuo* proceeds as follows:

$$[Co(NH_3)_6]Cl_3 \rightarrow [Co(NH_3)_6]Cl_2 + Cl \rightarrow CoCl_2 + 6NH_3 + (1/2)Cl_2 \quad (1)$$

The first step, which is rate-determining, is the electron-transfer process from the outer-sphere chloride ion to the central cobalt(III) ion. The reaction of the second step is very fast, because hexamminecobalt(II) chloride is thermally unstable. On the other hand, when the samples were treated in a sealed system or in air, the reaction was complicated:

$$[Co(NH_3)_6]Cl_3 \overset{A}{\rightleftharpoons} [Co(NH_3)_6]Cl_2 + (1/2)Cl_2 \rightleftharpoons R$$
$$\overset{B}{\longrightarrow} [CoCl(NH_3)_5]Cl_2 + NH_3 \overset{A'}{\rightleftharpoons}$$
$$[Co(NH_3)_5]Cl_2 + (1/2)Cl_2 + NH_3 \rightleftharpoons R \quad (2)$$

where R represents the mixture of the decomposition products. The B process takes place when the electron-transfer reaction is strongly interfered with. It should be noticed that the A process of Eq. (2) is a reversible electron-transfer reaction, in which oxygen in the air can oxidize the cobalt(II) to cobalt(III) complexes instead of halogen molecules. In both systems, the order of the increase in the rate of the electron-transfer reaction is expressed as follows: $[Co(NH_3)_6]Cl_3 < [Co(NH_3)_6]Br_3 < [Co(NH_3)_6]I_3$.

In the present system, the apparent annealing reaction is the oxidation of the cobalt(II) ion to the cobalt(III) ion. Since the yield of the halopentammine-cobalt(III) ion does not vary during the annealing reaction, the oxidation reaction seems to proceed as the reverse of the reaction expressed in the A process of Eq. (2). Furthermore, the fact that, when the ammonia molecules produced by the thermal decomposition of the parent complex are available, the formation of the hexamminecobalt(III) ion proceeds rapidly and extensively, suggests that the reformation of $^{57}Co(NH_3)_6^{2+}$ is also a rate-determining step in the thermal annealing.

In order to study further the effect of the ammonia molecules, a thermal annealing reaction in air was compared with that in a vacuum-sealed tube. After heating for 12 hr at 80°C, the $^{57}Co(NH_3)_6^{3+}$ yield increases to 24.9 per cent in the sealed system, but only to 15.1 per cent in air. In the sealed system, the ammonia molecules formed by the decomposition of the hexamminenickel(II) ion cannot escape from the system and participate in the reformation reaction.

In Mössbauer studies, the formation of $^{57}Fe(III)$ species is often observed in the EC process of the ^{57}Co-(II) compound.[13] In the hot-atom chemistry of the solid state, however, few examples have been reported of the oxidative reaction in the recoil process.[14] In other words, the recoil species other than the parent are, as a general rule, found, partly or entirely, in an oxidation state lower than their original condition. On annealing, the parent compound is reformed, even if the recoil species is found in a higher oxidation state than is the parent. These trends suggest that the chemical behavior of the recoil species is influenced mostly by the crystal matrix of the parent compound and secondarily by the chemical nature of the recoil species.

The present results contrast strongly with the general trends and indicate that the chemical property of the daughter species plays an important role in determining the chemical fate of the recoil atom in the foreign matrix. As an extension of this discussion, further study of the chemical behavior of the recoil ^{57}Co was designed in the temperature region where the effect of the thermal decomposition could be ignored. The experimental results are summarized in Fig. 4.

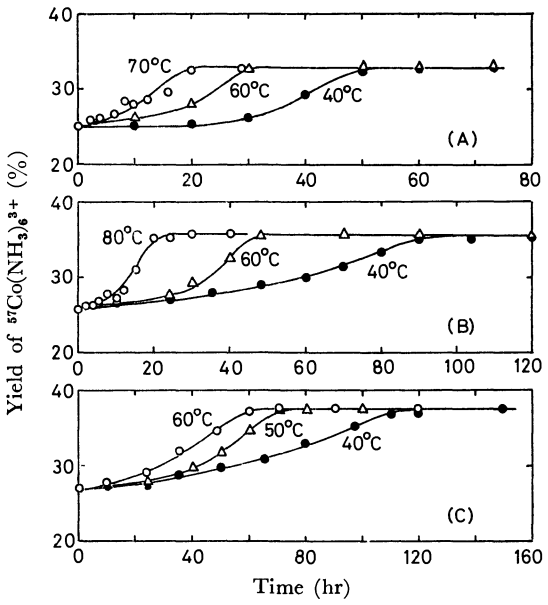

Fig. 4. Increase of $^{57}Co(NH_3)_6^{3+}$-yield by thermal annealing at relatively low temperatures.
(A): $[^{57}Ni(NH_3)_6]Cl_2$; (B): $[^{57}Ni(NH_3)_6]Br_2$;
(C): $[^{57}Ni(NH_3)_6]I_2$

10) T. Yasukawa and N. Saito, *J. Inorg. Nucl. Chem.*, **27**, 1433 (1965).
11) T. Yasukawa, *ibid.*, **28**, 17 (1966).
12) N. Tanaka and K. Nagase, This Bulletin, **40**, 546 (1967).
13) For example, R. Ingalls and G. Depasquali, *Phys. Lett.*, **6**, 169 (1966); A. Nath, M. P. Klein, W. Kundig, and D. Lichtenstein, *Radiation Effects*, **2**, 211 (1969); J. M. Friedt, A. Creset, L. Asch, and J. P. Adloff, *Radiochem. Radioanal. Lett.*, **3**, 81 (1970).
14) J. S. Butterworth and G. Harbottle, *Radiochim. Acta*, **6**, 169 (1966); A. H. W. Aten, Jr., and J. C. Kapteyn, *ibid.*, **9**, 223, 224 (1968).

Table 2. Thermal annealing of ^{57}Co-doped hexamminenickel(II) complexes

Compound	Thermal treatment	Yield of ^{57}Co-labeled species (%)		
		Co^{2+}	$CoX(NH_3)_5^{2+}$	$Co(NH_3)_6^{3+}$
$[Ni(NH_3)_6]Cl_2$	None	51.8	0.1	48.2
	100°C, 4 hr	50.6	0.5	48.9
$[Ni(NH_3)_6]Br_2$	None	57.5	0.1	42.4
	100°C, 4 hr	57.3	0.2	42.5

The shape of these annealing curves is similar to that in the bromide complex at 100°C. However, some interesting features can be found: the characteristic plateau values are dependent on the nature of the outer-sphere anions, but independent of the temperature, and the order of the increase in the rate of the annealing reaction is expressed as follows: chloride> bromide>iodide.

Mathematical analyses showed that a composite annealing curve for the present data is incompatible with a single first- or second-order rate process, nor does it fit error-function kinetics. However, some qualitative explanation would be possible on the supposition that, in this temperature region, the annealing reaction could be considered to be stoichiometrically the same as that taking place at higher temperatures.

About 53 per cent of the decay events of ^{57}Ni is the EC process, and the remainder is the β^+-decay.[15] The recoil energy (max. 34 eV) is too low for the ^{57}Co atoms to allow displacement into the interstitial site.[16] However, the electronic excitation following the decay will affect the chemical behavior of the daughter species.

The emission of a positron from the nucleus of a constituent atom should produce a negatively-charged species. Accordingly, the immediate effect of the decay of the $^{57}Ni(II)$ complex would be the formation of the univalent cobalt complex, and this cobalt complex would be found in the cobalt(II) species upon dissolution. On the other hand, the decrease in nuclear charge by electron capture is balanced by the decrease in the number of electrons. However, the vacancy created in the K shell is followed by the Auger cascade, which results in a multiply charged daughter species.[17] The neutralization of the charged ion causes the decomposition of the compound and creates the crystal defects surrounding the recoil atom. In this case, the recoil species will be found in the oxidation states of Co(II) and Co(III).[13]

The electron-transfer reaction is also affected by the oxidative power of the outer-sphere anion.[5] In the halide complexes, the driving force for the oxidation seems to be electron trapping by positive holes produced during the neutralization of multiply-charged recoil species. In fact, the annealing rates increase with an increase in the electron affinity of the halogen atom. A thermal ionization mechanism for the thermal annealing of ^{60}Co in the hexamminecobalt(III) bromide has been proposed by Yoshihara and Harbottle.[18] This explanation was further confirmed by the ^{57}Co-doping experiment. The ^{57}Co-doped hexamminenickel(II) complexes which were synthesized from a solution of the nickel(II) ion containing carrier-free ^{57}Co were subjected to thermal treatment. In this case, all the ^{57}Co may exist in the form of the hexammine complex. The experimental results are listed in Table 2. The fairl large $^{57}Co(NH_3)_6^{3+}$ yield is due to the air-oxidation of the cobalt(II) ion during synthesis. No appreciable change in the $^{57}Co(NH_3)_6^{3+}$ yield is observed at 100°C, where the annealing behavior of the recoil ^{57}Co is noticeable, as may be seen in Fig. 1. This fact indicates that, when the crystal defects are absent in the near-neighborhood of the ^{57}Co atom, the oxidation reaction of the cobalt(II) species does not take place.

The temperature-independent plateau value of the $^{57}Co(NH_3)_6^{3+}$ yield suggests that the intrinsic annealing takes place in a small region affected by the recoil. If the damage to the crystal lattice is extensive, synthetic reaction such as the formation of the pentamminecobalt(III) complex will occur simultaneously, as has been pointed out by Yoshihara.[19]

We wish to express our thanks to Dr. M. Yagi and the operating group of LINAC for their kind arrangements for the irradiation and to Dr. K. Yoshihara for his valuable discussion. We are also very grateful to the Ministry of Education for a grant to T. O., and to the Atomic Energy Council, Republic of China, for a grant to S. C. W.

15) C. M. Lederer, J. M. Hollander, and I. Perlman, "Table of Isotopes" (Sixth edition), John Wiley & Sons, New York (1967).
16) K. Yoshihara, M. H. Yang, and T. Shiokawa, *Radiochem. Radioanal. Lett.*, **4**, 143 (1970); K. Yoshihara and H. Kudo, *J. Chem. Phys.*, **52**, 2950 (1970).
17) S. Wexler, "Actions Chemiques et Biologiques des Radiations" (ed. M. Haissinsky), Masson, Paris (1965), Vol. 8, pp. 180—193.
18) K. Yoshihara and G. Harbottle, *Radiochim. Acta*, **1**, 68 (1963).
19) K. Yoshihara, *Nature*, **204**, 1296 (1964).

Kinetic Studies of the Electron Transfer Reaction in Iron(II) and Iron(III) Systems. III. Complex Formation and Catalytic Action with Thiocyanate Ion in Dimethyl Sulfoxide[1]

Goro WADA, Noriko YOSHIZAWA, and Yoko SAKAMOTO

Department of Chemistry, Nara Women's University, Nara

(Received August 28, 1970)

The formation constants K_1 and K_2 of the complexes $Fe(NCS)^{2+}$ and $Fe(NCS)_2^+$ in dimethyl sulfoxide (DMSO) and the rate constants and the activation parameters of the electron transfer reaction between Fe(II) and Fe(III) in DMSO catalyzed by thiocyanate ion were measured. K_1 and K_2 are $(8.4\pm0.9)\times10^2$ M^{-1} and $(0.97\pm0.10)\times10^2$ M^{-1} at $\mu=0.1$ M and 25°C, respectively. The apparent rate constant k_{app} is nearly independent of acid concentrations and increases markedly with total thiocyanate ion concentration. The rate constants k_1 and k_2 of Fe^{2+}-$Fe(NCS)^{2+}$ and Fe^{2+}-$Fe(NCS)_2^+$ systems are $(2.24\pm0.35)\times10^2$ M^{-1}sec^{-1} and $(2.96\pm0.64)\times10^3$ M^{-1}sec^{-1} at $\mu=0.2$ M and 25°C, respectively. $\Delta H_1^{\neq}=8.9\pm1.0$ kcal/mol and $\Delta S_1^{\neq}=-17\pm3$ cal/deg·mol are obtained from the temperature dependence of k_{app}. From a comparison with the data of cases catalyzed by Cl^- and SCN^- ions in water and DMSO, the present electron transfer reaction is deduced to proceed probably *via* the inner-sphere mechanism with the SCN^- ion as a bridging ligand, similar to the Cl^- ion-catalyzed reaction in DMSO.

In the electron transfer reaction between iron(II) and iron(III) species in aqueous solutions, the hydrogen atom transfer mechanism seemed to prevail because the hydrogen atoms of water molecules played an important role.[2] This was proved directly and indirectly by further evidence that the reaction still proceeded at a considerable rate even in the solid state[3] or in the very concentrated perchloric acid media[4] and that the reaction rate decreased with the addition of certain substances, such as nitromethane,[5] 2-propanol,[6] and some other alcohols,[7] because no or less exchangeable hydrogen atoms attached to the molecules of these substances. However, dimethyl sulfoxide (DMSO) was found to be not a substance making the reaction proceed slower but rather to be a medium better than water for the reaction, although DMSO seems to have no such exchangeable hydrogen atoms through which long chains of molecules are formed by hydrogen bondings, as water molecules easily do.[8] Moreover, the rate constants of the electron transfer reaction catalyzed by the chloride ion in this solvent are much larger than those in water.[9] Thus, there must be a reaction path other than the path *via* the hydrogen atom transfer mechanism.

According to recent more precise investigations, the electron transfer reactions of both the Fe^{2+}-$FeCl^{2+}$ [10] and Fe^{2+}-$FeNCS^{2+}$ [11] systems proceed predominantly even in aqueous solutions, *via* the inner-sphere mechanism and not *via* hydrogen atom transfer mechanism.

The present work was undertaken to see what effect thiocyanate ion has on the rate of the electron transfer reaction in DMSO, as compared with the case in which chloride ion was used in the same solvent.[9] In order to obtain the individual rate constants of the elementary reactions, the formation constants for the complexes between the existing species in DMSO had to be determined first. This was performed by the methods used in our previous investigation in the iron(III)-chloride ion-DMSO system.[12]

Experimental

Materials. Commercial DMSO of guaranteed reagent grade was distilled under a reduced nitrogen atmosphere of 3—4 mmHg, dried by shaking with activated alumina, and redistilled under the same condition. Iron(II) perchlorate crystal was prepared by dissolving pure iron wire in dilute perchloric acid and recrystallizing under an atmosphere of nitrogen. Iron(III) perchlorate was, then, easily prepared by oxidation of the iron(II) salt by hydrogen peroxide and the following recrystallization. Both crystals were not anhydrous but contained some lattice water. This did not matter at all, since the crystals were used only at very dilute concentrations and it was confirmed that a small amount of water does not seriously influence the results. Anhydrous sodium perchlorate was obtained by drying monohydrous salt recrystallized from water at 300°C. Anhydrous ammonium thiocyanate was obtained by storing wet crystal in a desiccator at room temperature, after recrystallization twice. The perchloric acid in DMSO was prepared by means of cation exchange resin. Dowex 50 w×8 resin of 50—100 mesh was treated with 6 N hydrochloric acid to transform it into H-type, washed with water to eliminate chloride ion completely, dried in an electric oven at a temperature not over 100°C, allowed to swell in DMSO, filled in a column, and then made to pass through a DMSO solution of 0.7 M ammonium perchlorate, until ammonium ion became detectable by the Nessler reagent in the eluent. The ammonium-free perchloric acid in DMSO obtained

1) Previous paper: G. Wada and R. Yoshihara, *Kogyo Kagaku Zasshi*, **73**, 2309 (1970).
2) W. L. Reynolds and R. W. Lumry, *J. Chem. Phys.*, **23**, 2460 (1955).
3) R. A. Horne, *J. Inorg. Nucl. Chem.*, **25**, 1139 (1963).
4) D. L. Baulch, F. S. Dainton, D. A. Ledward, and H. Sugier, *Trans. Faraday Soc.*, **62**, 2200 (1966).
5) A. G. Maddock, *ibid.*, **55**, 1268 (1959).
6) N. Sutin, *J. Phys. Chem.*, **64**, 1766 (1960).
7) R. A. Horne, "Exchange Reactions," I.A.E.A., Vienna, (1965), p. 67.
8) J. Menashi, W. L. Reynolds, and G. van Auken, *Inorg. Chem.*, **4**, 299 (1965).
9) G. Wada and W. L. Reynolds, *ibid.*, **5**, 1354 (1966).
10) R. J. Campion, T. J. Conocchioli, and N. Sutin, *J. Amer. Chem. Soc.*, **86**, 4591 (1964).
11) T. J. Conocchioli and N. Sutin, *ibid.*, **89**, 282 (1967).
12) G. Wada, This Bulletin, **41**, 882 (1968).

was titrated with sodium hydroxide.

The stock solution of the radioactive tracer of ^{59}Fe was manufactured as follows: The radioactive $*FeCl_3$ in hydrochloric aqueous solution was heated in an evaporating dish, and a few drops of perchloric acid were added just before dryness. After repeating the procedure several times, the final perchloric salt was dissolved in DMSO and stored in the cold.

Photometry. For determination of optical densities of sample solutions, a Hitachi-Perkin-Elmer UV-VIS spectrophotometer Model 139 was used with a thermostated cell compartment and 1-cm silica cells.

Rate Measurements of Electron Transfer Reactions. The reaction was started by mixing two solutions, A and B, in a reaction vessel in a thermostat. Contents of solution A were $Fe(ClO_4)_3$ (labeled with ^{59}Fe), NH_4SCN, $HClO_4$, and $NaClO_4$. Those of solution B were the same as solution A except for $Fe(ClO_4)_2$ in place of $Fe(ClO_4)_3$. Nitrogen gas saturated with DMSO vapor was continuously bubbled through the reaction solution before and after the initiation of the reaction. Nitrogen bubbling was carried out not only for stirring but also for preventing oxidation. At certain intervals, an aliquot of the reaction solution was quickly taken out by a syringe or a thermostated pipet, into a quenching solution containing 2,2′-bipyridyl which immediately stopped the reaction because of quick formation of $Fe(bipy)_3^{2+}$. The quenching solution also contained aluminum nitrate. By addition of ammonia, aluminum ion was coprecipitated with iron(III) ion as hydroxide. The precipitate was filtered from the solution and the radioactivity of a definite portion of the filtrate was measured with a well-type scintillation counter. The rest of the filtrate was used for optical determination of the concentration of iron(II) in the form of $Fe(bipy)_3^{2+}$ at 522 nm. The sample of the reaction solution at infinite time was taken at least ten half lives of the reaction after the initiation. In order to determine the total concentration of iron species in the system, the iron(III) was reduced to iron(II) by hydroxylamine. A more detailed procedure of the rate measurement was described previously.[8,9]

Results and Discussion

Absorption Spectra and Formation Constants of Fe^{3+}-SCN^- *Complexes in DMSO.* The absorption spectra of $Fe(ClO_4)_3$ and of $Fe(ClO_4)_3$–NH_4SCN in DMSO at $HClO_4$ concentration of 0.02 M are shown in Fig. 1. Curves A and B show respectively the spectrum of the simply solvated Fe^{3+}, and that of a mixture of Fe^{3+} and SCN^-, which partly form monothiocyanato complex. By combining both curves and the value of K_1 which will be obtained later, curve C can be calculated as the true spectrum of $FeNCS^{2+}$ complex, which exhibits a peak at 450 nm. The spectra A and C coincide well with those of Wada *et al.*[9,12] and Csiszar *et al.*,[13] respectively. The spectra were not influenced by the change in acid concentration.

The formation constant of $FeNCS^{2+}$, $K_1=[FeNCS^{2+}]/[Fe^{3+}][SCN^-]$, was determined by means of Job's continuous variation method.[12] Job's curves at $C_a=1.00\times10^{-3}$ and $C_b=0.70\times10^{-3}$ M are depicted in Fig. 2, C_a and C_b being the sum of the total concentrations of iron(III) and thiocyanate ion, $[Fe^{3+}]_0$ and $[SCN^-]_0$. The maximum points appear just at the center of the symmetrical curves indicating that the complex formed at these concentrations is of the composition $Fe^{3+}:SCN^-=1:1$. The observations were carried out at 440, 450, and 460 nm. K_1 and the

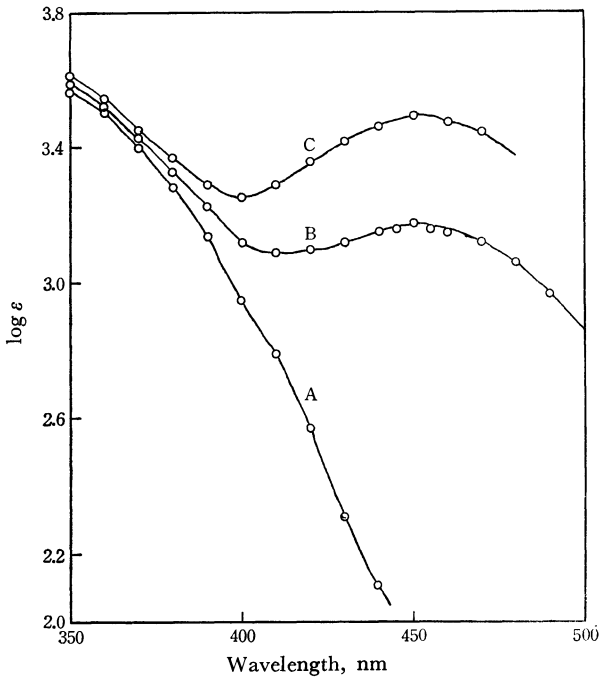

Fig. 1. Absorption spectra of Fe^{3+}, $FeNCS^{2+}$ in DMSO, at $[HClO_4]=0.02$ M, $\mu=0.10$ M and 25°C.
Curve A. $[Fe^{3+}]_0=5.40\times10^{-5}$ M
Curve B. $[Fe^{3+}]_0=5.40\times10^{-5}$ M, $[SCN^-]_0=9.78\times10^{-4}$ M
Curve C. Calculated for $FeNCS^{2+}$

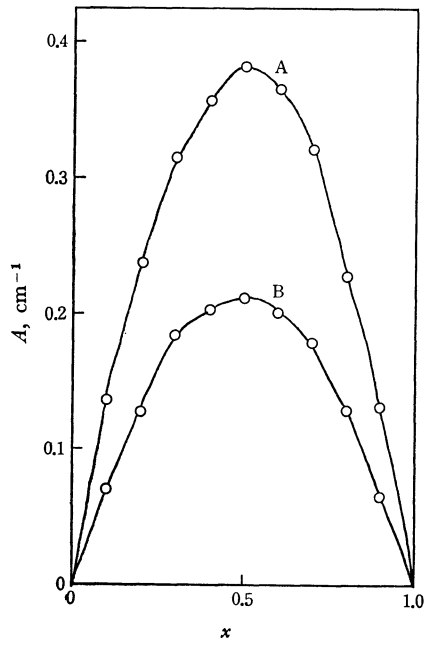

Fig. 2. Job's curves for Fe^{3+}-SCN^- system in DMSO at $[HClO_4]=0.02$ M, $\mu=0.10$ M, 25°C and 450 nm.
Curve A. $C_a=1.00\times10^{-3}$ M
Curve B. $C_b=0.700\times10^{-3}$ M

13) B. Csiszar, V. Gutmann, and E. Wychera, *Monatsh. Chem.*, **98**, 12 (1967).

molar extinction coefficient ε_1 of $FeNCS^{2+}$ are calculated by the following equation.[12]

$$A = \varepsilon_0[Fe^{3+}] + \varepsilon_1[FeNCS^{2+}] - \varepsilon_0[Fe^{3+}]_0$$
$$= (\varepsilon_1-\varepsilon_0)[FeNCS^{2+}] \quad (1)$$

$$[FeNCS^{2+}] = \frac{x_a(1-x_a)C_a^2-x_b(1-x_b)C_b^2}{C_a-C_b} \quad (2)$$

$$[Fe^{3+}] = x_aC_a - [FeNCS^{2+}] \quad (3)$$

$$[SCN^-] = (1-x_a)C_a - [FeNCS^{2+}] \quad (4)$$

$$\varepsilon_1 = \frac{A}{[FeNCS^{2+}]} + \varepsilon_0 \quad (5)$$

The values of $\varepsilon_0[Fe^{3+}]+\varepsilon_1[FeNCS^{2+}]$ in Eq. (1) correspond to the observed absorbances of the sample at individual wavelengths. By means of Eqs. (2), (3), and (4), the following value was obtained.

$$K_1 = (8.4\pm0.9) \times 10^2\ M^{-1} \text{ at } 25°C \quad (6)$$

Another K_1 value obtained by means of stopped flow method by other authors is $1.18\times10^3\ M^{-1}$ at $\mu=0.024$ M and 25°C, which is a little larger than ours.[14,15]

At higher concentrations, dithiocyanato complex seems to be formed gradually, because the linearity between $\bar{\varepsilon}$ and $(\bar{\varepsilon}-\varepsilon_0)/[SCN^-]$ is no longer established.[12,16] However, the linear relationship between $\bar{\varepsilon}$ and $\Delta\bar{\varepsilon}(1+K_1[SCN^-])/K_1[SCN^-]^2$ becomes noticeable, according to the equation

$$\bar{\varepsilon} = \varepsilon_2 - \frac{1}{K_2}\frac{\Delta\bar{\varepsilon}(1+K_1[SCN^-])}{K_1[SCN^-]^2} \quad (7)$$

where $\bar{\varepsilon}$ is the apparent molar extinction coefficient of iron(III), $\Delta\bar{\varepsilon}$ the deviation of the observed $\bar{\varepsilon}$ from hypothetical $\bar{\varepsilon}$ which would have been obtained if no $Fe(NCS)_2^+$ formation occurred, and K_2 is defined to be the stepwise formation constant $K_2=[Fe(NCS)_2^+]/[FeNCS^{2+}][SCN^-]$. Figure 3 shows the straight line according to Eq. (7), from whose intercept and slope ε_2 and K_2 are obtained at 25°C as follows:

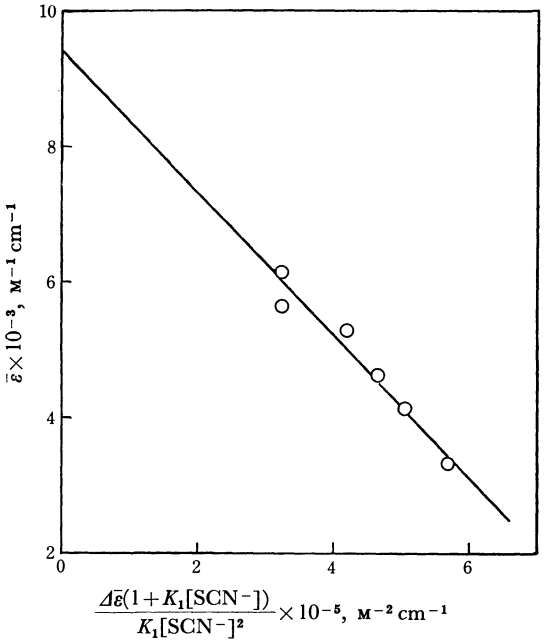

Fig. 3. Linear relation of $\bar{\varepsilon}$ against $\Delta\bar{\varepsilon}(1+K_1[SCN^-])/K_1[SCN^-]^2$ at $[HClO_4]=0.02$ M, $\mu=0.10$ M, 25°C and 450 nm.
$[Fe^{3+}]_0=1.89\times10^{-4}$ M
$[SCN^-]_0=(3.14-11.73)\times10^{-3}$ M

$$\varepsilon_2 = (9.4\pm0.5) \times 10^3\ M^{-1}\,cm^{-1} \text{ at } 450\ nm \quad (8)$$

$$K_2 = (0.97\pm0.10) \times 10^2\ M^{-1} \text{ at } 25°C \quad (9)$$

The dependence of K_1 and K_2 upon the dielectric constant of the solvents is listed in Table 1, in which the solvents are arranged in the sequence of their dielectric constants. It is seen that the lower the dielectric constant, the larger the stability of the complex, as expected theoretically. The linear relationship of $\log K_1$ *vs.* the reciprocal of the dielectric constant is roughly established.

By similar trials to determine the formation constant

Table 1. Dependence of K_1 and K_2 upon the dielectric constant of solvents

Solvent	Temperature °C	Dielectric constant	$\log K_1$	$\log K_2$	Ref.
H_2O 0.5 M $NaClO_4$	25	80	2.14	1.31	17)
H_2O 0.128 M $HClO_4$	—	80	2.37	—	18)
20% acetone 0.1 H^+	20	71	2.43	—	19)
40% acetone 0.1 H^+	20	58	2.57	—	19)
DMSO $\mu=0.1$	25	46.7	2.92	1.99	Present work
DMSO $\mu=0.024$	25	46.7	3.07	—	14)
80% acetone 0.1 H^+	20	32	3.2	—	19)
90% ether	—	29.8	4.70	—	20)

14) C. H. Langford and F. M. Chung, *J. Amer. Chem. Soc.*, **90**, 4485 (1968).

15) According to Keiko Ohnishi in our laboratory, the value of K_1 determined by conductivity method is $6\times10^4\ M^{-1}$, which is much larger than that by spectrophotometry. The discrepancy indicates that iron(III) ion has a widely spread ionic atmosphere around itself with its high electric charges in low dielectric medium. The value determined by the spectrophotometry only measures the complex which coordinates with thiocyanate ion in the first coordination sphere of the central ion.

16) T. W. Newton and G. M. Arcand, *ibid.*, **75**, 2449 (1953).

17) G. S. Laurence, *Trans. Faraday Soc.*, **52**, 236 (1956).

18) H. S. Frank and R. L. Oswalt, *J. Amer. Chem. Soc.*, **69**, 1321 (1947).

19) A. K. Babko and L. V. Markova, *Ukr. Khin. Zh.*, **25**, 363 (1959).

20) A. K. Babko and V. S. Kodenskaya, *Zh. Obshch. Khim.*, **17**, 1080 (1947).

of the Fe^{2+}-SCN^--DMSO system, no formation of complex species was recognized, in spite of the fact that the formation of $FeNCS^+$ has been found with the equilibrium constant $7.0\pm0.5\ M^{-1}$ by a flow technique in water.[11]

Rate Constants of Electron Transfer Reaction. According to McKay, isotopic exchange reactions including such types as the present electron transfer generally obey the rate equation[21-23]

$$\ln\left(1-\frac{x}{x_\infty}\right) = -\frac{a+b}{ab}Rt \qquad (10)$$

in which x and x_∞ represent radioactivity at time t and infinite time t_∞, respectively, and a and b the analytical total concentrations of iron(II) and iron(III), respectively, employed in the reaction system. R is the reaction rate. A typical linear relation of $\log(x_\infty-x)$ *vs.* time is drawn in Fig. 4. If the half life of the reaction is denoted by $t_{1/2}$, and if the reaction is regarded as that of first order with respect to both iron(II) and iron(III) concentrations, the apparent second order rate constant k_{app} is given by

$$k_{app} = \frac{0.693}{(a+b)t_{1/2}} \qquad (11)$$

If the reaction is of first order with respect to the individual concentrations of both iron(II) and iron(III), a rate equation $R=k_{app}ab$ is doubtlessly established, since the arbitrary variation in both concentrations gave a good constant k_{app} as long as other conditions of the reaction were kept unchanged, although it was practically impossible to assure the separate concentration dependence of both iron(II) and iron(III) because of experimental difficulty.

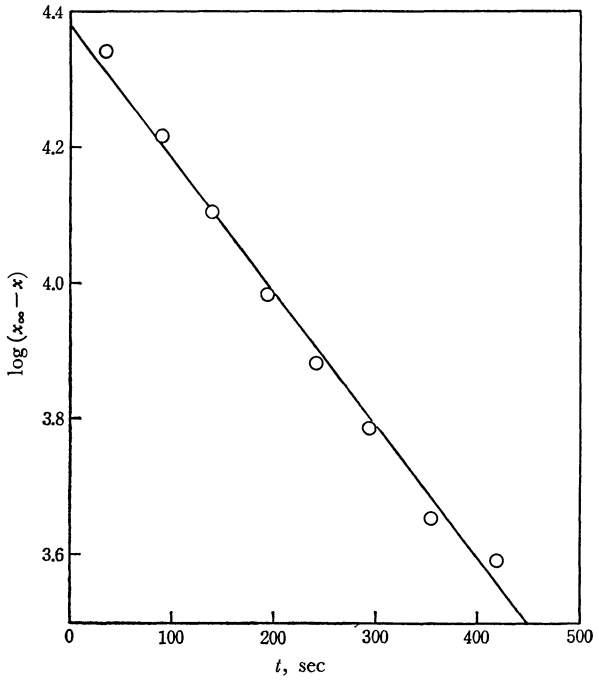

Fig. 4. Typical rate measurement of the reaction at 25°C.
$[Fe(II)]_0=3.69\times10^{-5}$ M
$[Fe(III)]_0=2.61\times10^{-5}$ M
$[SCN^-]_0=2.32\times10^{-4}$ M
$[HClO_4]=1\times10^{-2}$ M
$\mu=0.2$ M

Calculation of the values of k_{app} was performed by the method of least squares. The probable error was usually less than 5%.

Dependence of k_{app} on Acid Concentrations. Table 2 shows the dependence of k_{app} on the variation of acid concentrations in the range 6.9×10^{-5}—1.01×10^{-1}M. This indicates a slight but regular decrease of k_{app} with the increase of acid concentration. Acid concentration dependence of k_{app} appears to be much less than in the case of chloride ion-catalyzed electron transfer reaction in DMSO.[24] It might be said that k_{app} is nearly independent of the acid concentration except at very high acid concentration.

Table 2. Dependence of k_{app} upon acid concentration
$[SCN^-]_0=3.07\times10^{-4}$ M, $\mu=0.2$ M, 25°C

$[HClO_4]$ M	$[Fe(II)]_0\times10^5$ M	$[Fe(III)]_0\times10^5$ M	k_{app} $M^{-1}sec^{-1}$
6.9×10^{-5}	5.27	2.77	84.9
1.4×10^{-4}	9.67	3.36	79.6
3.4×10^{-4}	6.63	3.85	79.5
1.03×10^{-3}	7.28	2.06	79.2
5.15×10^{-3}	10.32	1.68	78.8
1.00×10^{-2}	3.86	1.46	77.3
1.01×10^{-1}	7.77	1.14	58.5

Dependence of k_{app} on SCN^- Ion Concentration. The reaction is markedly catalyzed by thiocyanate ion; its effects on k_{app} are summarized in Table 3. k_{app} is accelerated by the presence of SCN^- ion, similar as to the case of Cl^- ion.[9] Thus, the following three reaction paths can be considered to represent the principal mechanisms.

$$Fe^{2+} + {}^*Fe^{3+} \rightarrow Fe^{3+} + {}^*Fe^{2+} \qquad k_0 \quad (12)$$

$$Fe^{2+} + {}^*FeNCS^{2+} \rightarrow FeNCS^{2+} + {}^*Fe^{2+} \qquad k_1 \quad (13)$$

$$Fe^{2+} + {}^*Fe(NCS)_2{}^+ \rightarrow Fe(NCS)_2{}^+ + {}^*Fe^{2+} \qquad k_2 \quad (14)$$

The symbols Fe^{2+}, Fe^{3+}, $FeNCS^{2+}$, and $Fe(NCS)_2{}^+$ in the equations stand for the individual solvated species $Fe(DMSO)_6{}^{2+}$, $Fe(DMSO)_6{}^{3+}$, $Fe(DMSO)_5(NCS)^{2+}$, and $Fe(DMSO)_4(NCS)_2{}^+$, respectively, and the rate constants for the reactions (12), (13), and (14) are represented by k_0, k_1, and k_2, respectively. The first five values of k_{app} in Table 3 indicate that $k_0=34.4\ M^{-1}sec^{-1}$ as the mean value.

Since the observed rate is the sum of the values through the three paths, and the concentrations of the complexes involved in the reaction are decided by their formation constants, k_{app} is written as follows:

$$k_{app} = \frac{k_0+k_1K_1[SCN^-]+k_2K_1K_2[SCN^-]^2}{1+K_1[SCN^-]+K_1K_2[SCN^-]^2} \qquad (15)$$

When the denominator in Eq. (15) is substituted into D for simplicity, Eq. (15) can be rearranged to

21) H. A. C. Mckay, *Nature*, **42**, 997 (1938).
22) J. Silverman and R. W. Dodson, *J. Phys. Chem.*, **56**, 846 (1952).
23) T. Takaishi, This Bulletin, **42**, 1266 (1969).
24) G. Wada and W. L. Reynolds, "Exchange Reactions," I.A.E.A., Vienna (1965), p. 59.

TABLE 3. DEPENDENCE OF k_{app} UPON THIOCYANATE ION CONCENTRATION
$[HClO_4]=0.01$ M, $\mu=0.2$ M, 25°C

$[SCN^-]_0\times10^4$ M	$[SCN^-]\times10^4$ M	$[Fe(II)]_0\times10^5$ M	$[Fe(III)]_0\times10^5$ M	k_{app} $M^{-1}sec^{-1}$
—	—	11.4	4.35	33.7
—	—	6.68	2.71	37.7
—	—	11.6	3.66	35.3
—	—	12.0	3.91	33.5
—	—	8.15	6.25	32.0
0.77	0.765	5.76	1.30	44.9
1.08	1.06	3.15	2.28	62.7
1.55	1.54	3.75	0.87	51.9
1.55	1.53	2.66	1.84	61.9
2.32	2.28	3.69	2.61	73.4
2.32	2.295	5.32	1.47	71.8
3.07	3.04	3.86	1.46	77.3
3.09	3.06	4.07	1.26	87.1
3.30	3.26	7.01	1.14	94.1
3.87	3.83	3.69	1.63	120.5
3.87	3.83	6.25	1.47	136.3
3.87	3.83	2.01	1.74	99.1
4.64	4.585	4.35	1.95	123.6
5.41	5.36	3.59	1.73	141.2
6.19	6.14	2.44	1.47	178.3
6.96	6.90	7.17	1.74	177.3
7.73	7.565	6.02	4.28	166.2
7.73	7.675	4.40	1.41	176.2
7.73	7.66	2.01	1.79	177.4
9.29	9.19	5.11	2.11	248.2
10.83	10.76	6.08	1.52	256.7

express a linear relationship between Y and $[SCN^-]$:

$$Y=\frac{k_{app}D-k_0}{[SCN^-]}=k_1K_1+k_2K_1K_2[SCN^-] \quad (16)$$

The plot of Y against $[SCN^-]$ is shown in Fig. 5. The intercept and the slope of the straight line give k_1 and k_2 respectively, by the least squares calculation, using the given values of K_1 and K_2:

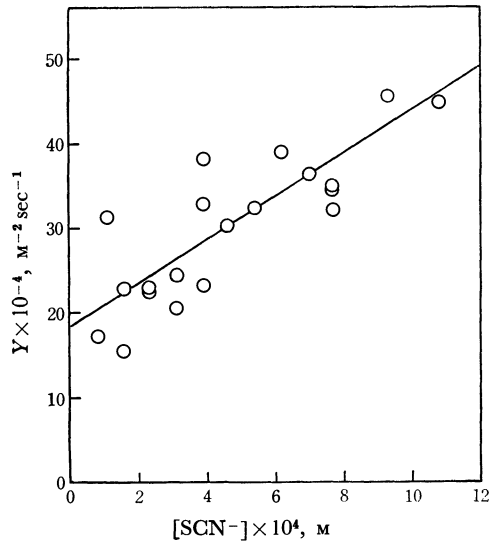

Fig. 5. Linear relation of Y against $[SCN^-]$ at $[HClO_4]=0.01$ M, $\mu=0.2$ M, 25°C.

$$k_1=(2.24\pm0.35)\times10^3\ M^{-1}sec^{-1} \quad (17)$$

$$k_2=(2.96\pm0.64)\times10^3\ M^{-1}sec^{-1} \quad (18)$$

Temperature Dependence of k_{app} and Activation Parameters. At constant acid and thiocyanate ion concentrations, the reaction rate was measured at different temperatures; 20, 25, 30, and 35°C. The results are given in Table 4. The plots of $\log k_0$ and $\log k_1$ against $1/T$ correspond to the activation parameters in the following:

$$\Delta H_0^{\neq}=9.7\pm0.7\ kcal/mol \quad (19)$$

$$\Delta H_1^{\neq}=8.9\pm1.0\ kcal/mol \quad (20)$$

$$\Delta S_0^{\neq}=-19\pm2\ cal/deg\cdot mol \quad (21)$$

$$\Delta S_1^{\neq}=-17\pm3\ cal/deg\cdot mol \quad (22)$$

The values of $\Delta H_0^{\neq}$ and $\Delta S_0^{\neq}$ agree with those by Menashi *et al.*[8]; $\Delta H_0^{\neq}=9.6$ kcal/mol and $\Delta S_0^{\neq}=$

TABLE 4. TEMPERATURE DEPENDENCE OF k_0 AND k_1
$[HClO_4]=0.01$ M, $\mu=0.2$ M

Temperature °C	$[SCN^-]_0=0$ k_0 $M^{-1}sec^{-1}$	$[SCN^-]_0=3.30\times10^{-4}$ M k_1 $M^{-1}sec^{-1}$
20	26.5	216
25	34.4	310
30	44.1	380
35	60.4	461

−20 cal/deg·mol.

General Discussion. The various elementary rate constants at room temperature and the activation enthalpies and entropies of the electron transfer reactions between iron(II) and iron(III) uncatalyzed and catalyzed by Cl^- and SCN^- ions in water and DMSO are collected and listed in Table 5. Generally speaking, k_0, k_1, and k_2 in DMSO are much larger than the corresponding ones in water, k_1 catalyzed by SCN^- ion is about twice as large as k_1 catalyzed by Cl^- ion in both solvents. So is also k_2 catalyzed by SCN^- ion compared to k_2 catalyzed by Cl^- ion in DMSO, while k_2 catalyzed by SCN^- ion is much smaller than k_2 catalyzed by Cl^- ion in water.

The exchange rates of DMSO molecules between the molecules coordinated to Co(II) or Ni(II) and the ones in the bulk in DMSO[25] and in mixed solvents of DMSO and nitromethane[26] are known by the NMR method. If the exchange rates in the case of iron ions do not differ very much from those of Co(II) and Ni(II), since the solvated species of these metal ions are considered to be high spin complexes, the exchange rate constant of DMSO may be greater than the rate constants of the electron transfer reaction k_0 and k_1 in DMSO listed in Table 5. Langford and Chung[14] determined the rate constant of the anation reaction $FeS_6^{3+}+SCN^-\rightarrow FeS_5(NCS)^{2+}+S$ in which S stands for DMSO by the stopped-flow method to be 670 ± 10 $M^{-1}sec^{-1}$, which is also greater than k_0 and k_1 in DMSO in Table 5. Considering this with the fact that DMSO has no hydrogen atoms which would play an important role in the hydrogen atom transfer mechanism, it is very probable that the inner-sphere mechanism is the path actually occurring in the electron transfer reaction in DMSO. Thus, the effects of the bridging ligands appear clearly in DMSO, although it is not the case in water, where the role of the anions is indirect and latent when the reaction proceeds through the hydrogen atom transfer mechanism. Recently, however, Cl^- and SCN^- ions were found to act as bridging anions in the inner-sphere mechanism even in water,[11] as stated before. As a bridging ligand, SCN^- ion appears to be better than Cl^- ion in both water and DMSO. A detailed discussion on the observed values of the activation parameters is not possible as yet.

Appendix: Incomplete Separation of Radioactive Precipitate. In the rate measurements, we frequently experienced a small fraction of the radioactive iron(III) to penetrate through filter paper into the filtrate liquid containing iron(II), when iron(III) was coprecipitated with aluminum hydroxide by ammonia. Thus, the extent of the electron transfer reaction at time t looked apparently larger than the true rate, because the radioactivity of the filtrate was larger than that purely due to the iron(II) species only. According to preliminary tests, however, the penetration factor of iron(III) through the precipitate layer leaking into the filtrate, α, was independent of the concentrations of iron(II) and iron(III) under the present experimental conditions, as long as the concentrations of aluminum ion and ammonia were kept constant. Consequently, the α can be easily fixed to be constant throughout at least one kinetic run.

When radioactivity at time t of iron(II), iron(III), and total iron is represented by x, y, and c respectively, then $x+y$ is equal to c, where c is time-independent. Since the radioactivity of iron(III) which has leaked into iron(II) is $(c-x)\alpha$, the apparent radioactivity of iron(II) at time t, x', is given by

$$x' = x + (c-x)\alpha \tag{23}$$

In the same way, the apparent radioactivity of iron(II) at time t_∞, x'_∞, is given by

$$x'_\infty = x_\infty + (c-x_\infty)\alpha \tag{24}$$

In the actual plotting of Eq. (10), $1-(x'/x'_\infty)$ is used instead of $1-(x/x_\infty)$. Then, the following ratio β is defined by use of Eqs. (23) and (24).

$$\beta = \frac{1-(x'/x'_\infty)}{1-(x/x_\infty)} = \frac{(1-\alpha)x_\infty}{(1-\alpha)x_\infty+c\alpha} \tag{25}$$

The value of β at any different time is shown to be constant for a kinetic run, because β is independent of x, x', and x'_∞, being smaller than unity ($\beta=1$ only when $\alpha=0$). Thus, the linearity of $\log(x'_\infty-x')$ and $\log(x_\infty-x)$ *vs.* time is given by

Table 5. Summarized data of the Fe(II)-Fe(III) electron transfer reaction catalyzed by Cl^- and SCN^- ions in H_2O and DMSO at 25°C

Solvent	Catalyst	k_0 $M^{-1}sec^{-1}$	k_1 $M^{-1}sec^{-1}$	$\Delta H_0^\ddagger$ or $\Delta H_1^\ddagger$ kcal/mol	$\Delta S_0^\ddagger$ or $\Delta S_1^\ddagger$ cal/deg·mol	k_2 $M^{-1}sec^{-1}$	Ref.
H_2O	—	4.0	—	10.5	−20.6	—	a)
	Cl^-	—	22.8[e]	11.0	−15	53[e]	b)
	SCN^-	—	41.5	7.9	−26	7	c)
DMSO	—	34.4	—	9.7	−19	—	—
	Cl^-	—	130[e]	5.2	−27	1.02×10^{3} [e]	d)
	SCN^-	—	224	8.9	−17	2.96×10^{3}	—

a) S. Fukushima and W. L. Reynolds, *Talanta*, **11**, 283 (1964).
b) N. Sutin, J. K. Rowley, and R. W. Dodson, *J. Phys. Chem.*, **65**, 1248 (1961); Ref. 22.
c) G. S. Laurence, *Trans. Faraday Soc.*, **53**, 1326 (1957).
d) Ref. 9.
e) Observed at 20°C.

25) S. Thomas and W. L. Reynolds, *J. Chem. Phys.*, **46**, 4164 (1967).
26) L. S. Frankel, *Chem. Commun.*, **1969**, 1254.

$$\log (x'_\infty - x') = \log x'_\infty + \log \beta - \frac{(a+b)R}{2.303\,ab}t \quad (26)$$

$$\log (x_\infty - x) = \log x_\infty - \frac{(a+b)R}{2.303\,ab}t \quad (27)$$

The slope of the straight line does not change even if x' and x'_∞ are used instead of x and x_∞ respectively, whereas the intercept of the straight line is lowered by $(\log x'_\infty + \log \beta) - \log x_\infty$, since $x'_\infty \beta / x_\infty$ is equal to $1-\alpha$. As a result of the lowering of the straight line, the reaction seemingly proceeds somewhat faster than the true reaction. Theoretically, x should be zero at time zero, but it frequently happens that x shows an appreciable value when time is extrapolated to zero. This does not affect the rate constant, as long as the leaking of iron(III) occurs by a definite factor α.

BULLETIN OF THE CHEMICAL SOCIETY OF JAPAN, VOL. 44, 1024—1027 (1971)

Infrared Spectra of Pentacyanonitrosylmanganese (^{14}NO and ^{15}NO) Complexes

Eiichi Miki, Soto-o Kubo,* Kunihiko Mizumachi, Tatsujiro Ishimori, and Hisateru Okuno

Department of Chemistry, College of Science, Rikkyo University, Nishi-Ikebukuro, Toshima-ku, Tokyo

(Received September 14, 1970)

The ^{15}NO-complexes for $K_3[Mn(CN)_5(NO)]\cdot 2H_2O$, $K_3[Mn(CN)_5(NO)]$ and $Ag_2[Mn(CN)_5(NO)]$ were prepared. By measuring and calculating the effect of the nitrogen isotope ^{15}N on the infrared spectra, the Mn–N–O arrangement was found in all the complexes, and the absorption bands due to the skeletal vibrations between the manganese and the NO group were clearly assigned.

X-Ray crystal structures have been determined for a number of transition-metal nitrosyl compounds. However, the X-ray method does not seem to be useful for distinguishing nitrogen from oxygen in the NO group.

Recently, for the nitrosylruthenium(III), nitrosylchromium(II) and nitrosylcobalt(II) complexes, the effect of the nitrogen isotope ^{15}N on the infrared spectra was measured, and the isotopic shifts were compared with those calculated by the simple three-body model of the metal and the NO group.[1,2] This method was found to be useful for determining the coordinating atom of the NO group to the metal atom, and for assigning the skeletal vibrations between the metal and the NO group.

In this paper are described infrared studies on $K_3[Mn(CN)_5(NO)]\cdot 2H_2O$, $K_3[Mn(CN)_5(NO)]$, $Ag_2[Mn(CN)_5(NO)]$ and their ^{15}NO-complexes.

Experimental

$K_3[Mn(CN)_5(NO)]\cdot 2H_2O$ with normal nitrogen isotopes was prepared by the method of Blanchard and Magnusson[3] who used NO gas, and was purified by the method of Cotton *et al.*[4] $K_3[Mn(CN)_5(NO)]$ and $Ag_2[Mn(CN)_5(NO)]$ were also prepared according to the same method. $K_3[Mn(CN)_5(NO)]\cdot 2D_2O$ was prepared by treating the unhydrated salt with D_2O in a vacuum line.

The ^{15}NO-complexes were prepared on about 1/10 the ordinary scale. $K_3[Mn(CN)_5(^{15}NO)]$ was prepared in a vacuum line; with the aid of liquid nitrogen, 3 mmol of ^{15}NO gas derived from $K^{15}NO_3$ (^{15}N atom% = 99) was trapped in a reaction vessel containing an outgassed pale-greenish slurry which was prepared by mixing 2 mmol of $Mn(C_2H_3O_2)_2\cdot 4H_2O$/(2.5 m*l* H_2O), 3 mmol of KOH/(2.5 m*l* H_2O), and 10 mmol of KCN/(2.5 m*l* H_2O) in succession. The reaction vessel was shaken under running water until the frozen solution was molten. The pale-greenish slurry was shaken for 5—6 hr at room temperature to give a clear violet solution containing $[Mn(CN)_5(^{15}NO)]^{3-}$. The yield of the purified $K_3[Mn(CN)_5(MO)]\cdot 2H_2O$ was about 50% based on $Mn(C_2H_3O_2)_2\cdot 4H_2O$. Preparation of the ^{15}NO-complexes on such a semi-micro scale was thought to give the correct products because the ^{14}NO-complexes prepared on the semi-micro scale gave the same infrared spectra as those prepared on an ordinary scale, and their elementary analyses showed the correct values.

Found: K, 31.9; Mn, 15.1; C, 16.5; N, 23.3; H_2O, 9.79%. Calcd for $K_3[Mn(CN)_5(NO)]\cdot 2H_2O$: K, 31.84; Mn, 14.9; C, 16.30; N, 22.82; H_2O, 9.78%. Found: C, 18.5; N, 25.2%. Calcd for $K_3[Mn(CN)_5(NO)]$: C, 18.07; N, 25.29%. Found: Ag, 49.4; Mn, 12.4; C, 14.1; N, 18.7%. Calcd for $Ag_2[Mn(CN)_5(NO)]$: Ag, 50.07; Mn, 12.75; C, 13.94; N, 19.51%.

Infrared spectra were measured over 200—4000 cm^{-1} in Nujol mull, hexachlorobutadiene mull, and a potassium bromide disk. The spectra were recorded on JASCO DS-402G (700—4000 cm^{-1}), JASCO model IR-F, and Hitachi EPI-L type (200—700 cm^{-1}) infrared spectrophotometers. The wave numbers of the observed absorption bands were calibrated with 1,2,4-trichlorobenzene, polystyrene film and water vapour. Reproducibility was about ± 1 cm^{-1} in the region 200—3000 cm^{-1}, and ± 10 cm^{-1} in the region 3000—4000 cm^{-1}.

Results

Assignments of Infrared Spectra. Assignments of the N–O stretching and the skeletal vibrations between the manganese and the NO group were made on the

* Present address: Central Laboratory, Kurita Water Industry Co. Ltd., 1723, Bukkoh-choh, Hodogaya-ku, Yokohama.

1) E. Miki, T. Ishimori, H. Yamatera, and H. Okuno, *Nippon Kagaku Zasshi*, **87**, 703 (1966).

2) E. Miki, This Bulletin, **41**, 1835 (1968).

3) A. A. Blanchard and R. R. Magnusson, *J. Amer. Chem. Soc.*, **63**, 2236 (1941).

4) F. A. Cotton, R. R. Monchamp, R. J. M. Henry, and R. C. Young, *J. Inorg. Nucl. Chem.*, **10**, 28 (1959).

Table 1. Wave numbers and assignment of infrared absorption bands in $K_3[Mn(CN)_5(NO)]\cdot 2H_2O$, $K_3[Mn(CN)_5(NO)]\cdot 2D_2O$, $K_3[Mn(CN)_5(NO)]$, and $Ag_2[Mn(CN)_5(NO)]$

$K_3[Mn(CN)_5(NO)]\cdot 2H_2O$ and $K_3[Mn(CN)_5(NO)]\cdot 2D_2O$

^{14}NO-complex		^{15}NO-complex	Assignment
3600 m	(2653 m)[a]	3610 m	O-H str.
3410 m, b	(2496 m, b)	3420 m, b	
3250 w	(2405 w)	3250 w	
2129 w	(2128 w)	2129 w	C-N str.
2095 vs	(2095 vs)	2095 vs	
2054 sh	(2054 sh)	2054 sh	
1741 vs	(1736 vs)	1704 vs	N-O str.
1733 vs	(1728 vs)	1694 vs	
1657 w	(1220 sh)	1658 w	O-H bend.
1638 m	(1208 m)	1639 m	
663 m	(663 m)		Mn-^{14}N str. + Mn-^{14}N-O bend.
		660 w	Mn-^{15}N str.
653 w	(653 w)		Mn-^{14}N-O bend.
		651 w	Mn-^{15}N-O bend.
		646 m	Mn-^{15}N-O bend.
494 m	(490 m, b)	493 m	Mn-C str. + Mn-C-N bend.
470 sh		470 sh	
451 vs[b]	(455 vs)	451 s	
435 sh		435 sh	
423 m	(421 sh)	423 m	
405 s	(405 s)	404 s	
365 s	(365 s, b)	364 s	
	(330 m, b)[c]		
318 m	(315 m, b)	317 m	

$K_3[Mn(CN)_5(NO)]$

^{14}NO-complex	^{15}NO-complex	Assignment
3610 vw, b	3620 vw, b	
3420 vw, b	3300 vw, b	
2129 w	2125 w	C-N str.
2103 vs	2103 vs	
2065 sh	2064 sh	
1711 vs	1675 vs	N-O str.
1695 vs	1663 vs	
659 s		Mn-^{14}N str. + Mn-^{14}N-O bend.
	661 w	Mn-^{15}N str.
	648 s	Mn-^{15}N-O bend.
490 w	487 w	Mn-C str. + Mn-C-N bend.
455 m	454 m	
447 m	446 m	
405 s	404 s	
368 s, b	368 s, b	
315 w	314 w	

$Ag_2[Mn(CN)_5(NO)]$

^{14}NO-complex	^{15}NO-complex	Assignment
2166 m	2166 m	C-N str.
1888 vs	1850 vs	N-O str.
628 m, b	620 m, b	Mn-N str. + Mn-N-O bend.
468 vs, b	482 vs, b	Mn-C str. + Mn-C-N bend.
417 vs	417 vs	
346 s	345 s	
310 m	310 m	

a) The wave numbers of the bands in parentheses are for the deuterated complex.
b) The 450 cm^{-1} band includes H_2O libration mode.
c) The 330 cm^{-1} band includes D_2O libration mode.
Abbreviations: str.=stretching; bend.=bending; vs=very strong; s=strong; m=medium; w=weak; vw=very weak; sh=shoulder; b=broad.

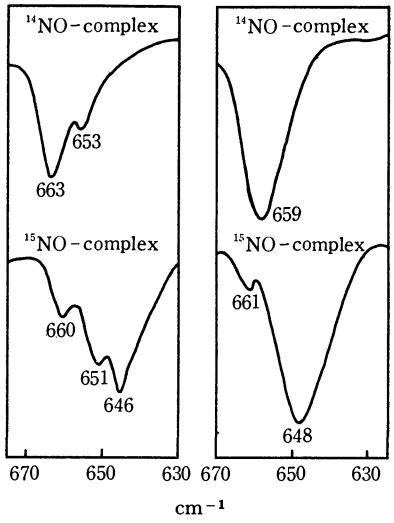

Fig. 1. Infrared spectra of $K_3[Mn(CN)_5(NO)]\cdot 2H_2O$ and $K_3[Mn(CN)_5(NO)]$ in the region 630—670 cm^{-1}.

basis of the ^{15}N-isotopic shifts. The observed frequencies and their assignments for $K_3[Mn(CN)_5(NO)]\cdot 2H_2O$, $K_3[Mn(CN)_5(NO)]$ and $Ag_2[Mn(CN)_5(NO)]$ are shown in Table 1. The two very strong absorption bands in the region 1700—1740 cm^{-1} of $K_3[Mn(CN)_5(^{14}NO)]\cdot 2H_2O$ and its unhydrate correspond to the N–O stretching vibrations since these bands shift upon ^{15}N-substitution. The wave number of the stronger peak was used to calculate the isotopic shifts. For the hydrate, the absorption bands at 663 and 653 cm^{-1} shifted and split to 660, 651 and 646 cm^{-1} upon ^{15}N-substitution as shown in Fig. 1. These bands can be assigned to the skeletal vibrations between the manganese and the NO group because the wave numbers for the deuterate hydrate were the same as those for the normal hydrate. For $K_3[Mn(CN)_5(NO)]$, on the other hand, the single absorption band at 659 cm^{-1} split into two peaks at 661 and 648 cm^{-1} upon ^{15}NO-substitution as shown in Fig. 1. For $Ag_2[Mn(CN)_5(NO)]$, a strong band of the ^{14}NO-complex at 1888 cm^{-1} was assigned to the N–O strethcing vibration; this band shifted to 1850 cm^{-1} upon ^{15}NO-substitution. A broad absorption at 628 cm^{-1} shifted to 620 cm^{-1} upon ^{15}NO-substitution, but did not split. This band seems to be due to the skeletal vibrations between the manganese and the NO group.

A number of absorption bands observed in a region lower than 620 cm^{-1} could be assigned to the skeletal vibrations between the manganese and the CN group.[5] For $K_3[Mn(CN)_5(NO)]\cdot 2H_2O$, such bands were observed on the background of a very broad absorption band centered at about 450 cm^{-1}. This broad band seems to be due to the libration of the crystal water because the absorption shifted to about 330 cm^{-1} upon deuterium substitution.

Calculation of Isotopic Shifts. An X-ray study of $K_3[Mn(CN)_5(NO)]\cdot 2H_2O$ has shown an approximately linear arrangement of the manganese and the

5) D. M. Adams, "Metal-Ligand and Related Vibrations," Edward Arnold Publishers Ltd., London (1967), p. 169—173.

Table 2. Observed and calculated isotopic shifts ($\Delta\nu_{obsd}$ and $\Delta\nu_{calcd}$ in cm^{-1}) of $K_3[Mn(CN)_5(NO)]$ and $Ag_2[Mn(CN)_5(NO)]$

$K_3[Mn(CN)_5(NO)]$

^{15}NO-compex wave number (cm^{-1})	$\Delta\nu_{obsd}$	$\Delta\nu_{calcd}$			
		Assignment 1		Assignment 2	
		model MnNO	MnON	MnNO	MnON
1663	32	38	22	38	23
661	(−2)*	4	10	17	6
648	11	17	6	4	10

$Ag_2[Mn(CN)_5(NO)]$

^{15}NO-complex wave number (cm^{-1})	Assignment	$\Delta\nu_{obsd}$	$\Delta\nu_{calcd}$	
			model MnNO	MnON
1850	a	38	40	28
620	b	(8)**	5	8
620	c	(8)**	16	6

$\Delta\nu_{obsd} = \nu_{^{14}NO\text{-complex(obsd)}} - \nu_{^{15}NO\text{-complex(obsd)}}$

$\Delta\nu_{calcd} = \nu_{^{14}NO\text{-complex(calcd)}} - \nu_{^{15}NO\text{-complex(obsd)}}$

Assignment 1: Of the two wave numbers in the region 630—670 cm^{-1}, the higher wave number is assigned to the stretching vibration between the manganese and the NO group and the lower one to the bending vibration.

Assignment 2: The reverse of Assignment 1.

a: The N–O stretching vibration.

b: The stretching vibration between the manganese and the NO group.

c: The bending vibration between the manganese and the NO group.

*: This observed isotopic shift($\Delta\nu_{obsd}$) is explained by Ref. 8.

**: These observed isotopic shifts are very rough values since the two skeletal vibrations appear to be adjacent to each other.

NO group.[6] The isotopic shifts were calculated for $K_3[Mn(CN)_5(NO)]\cdot 2H_2O$, its unhydrate[7] and $Ag_2[Mn(CN)_5(NO)]$[7] by the use of the two linear three-body models, Mn–N–O and Mn–O–N as described previously.[1,2] A probable assignment of the skeletal vibrations and determination of the arrangement were based on a comparison of the calculated isotopic shifts with the observed ones. Table 2 shows the observed and the calculated isotopic shifts for $K_3[Mn(CN)_5(NO)]$ and $Ag_2[Mn(CN)_5(NO)]$.

Arrangement and Assignment. The calculated isotopic shifts in the case of the Mn–N–O arrangement with Assignment 1 for the unhydrate (see Table 2) are in agreement with the observed ones. The Mn–N stretching and the Mn–N–O bending vibrations seem to overlap accidentally at 659 cm^{-1}. They shifted and split into the 661 cm^{-1} (the Mn–N stretching vibration) and 648 cm^{-1} (the Mn–N–O bending vibration) bands upon ^{15}NO-substitution.[8] Both the hydrate and $Ag_2[Mn(CN)_5(NO)]$ were found to show the Mn–N–O arrangement from the observed isotopic shifts for the N–O stretching vibrations upon ^{15}NO-substitution.

For $K_3[Mn(CN)_5(NO)]\cdot 2H_2O$, three absorption bands were observed in the region 640—670 cm^{-1} on the ^{15}NO-complex, and two on the ^{14}NO-complex. They are caused by the skeletal vibrations of the Mn–NO group. The doubly degenerate Mn–N–O bending vibrations of the free complex ion can be assumed to split into two absorption bands in the crystalline state. For the isotopic shifts of the absorption bands, the following assignments may be most probable. Two absorption bands due to the Mn–N stretching and one of the Mn–N–O bending vibrations overlap at 663 cm^{-1} for the ^{14}NO-complex. They shift and split into two bands at 660 cm^{-1} (the Mn–^{15}N stretching vibration) and 651 cm^{-1} (the Mn–^{15}N–O bending vibration), while another Mn–^{14}N–O bending vibration (653 cm^{-1}) shifts to 646 cm^{-1} upon ^{15}NO-substitution (Fig. 1).

Discussion

The Mn–N–O arrangement was found in the pentacyanonitrosylmanganese complexes as conventionally described for metal nitrosyl complexes. In $K_2[RuX_5(NO)]$ (X=Cl and Br), the overtone band of the Ru–N–O linear bending vibration is observed in the frequency region near twice the value of the fundamental frequency of the Ru–N–O bending vibration.[9] $K_3[Mn(CN)_5(NO)]\cdot 2H_2O$ and its unhydrate show bands at 1325 and 1313 cm^{-1}; these frequencies are nearly

6) A. Tullberg and N. Vannerberg, *Acta Chem. Scand.*, **21**, 1462 (1967).

7) For $K_3[Mn(CN)_5(NO)]$ and $Ag_2[Mn(CN)_5(NO)]$, the linear three-body model was assumed although a crystal X-ray study was not carried out.

8) The absorption intensity of the Mn–N stretching vibration would be very weak as compared with that of the Mn–N–O bending vibration. If the two absorptions are adjacent to each other, the wave number of the overlapping bands will be approximately equal to that of the Mn–N–O bending vibration and roughly to that of the stretching vibration. The Mn–^{14}N stretching vibration can be estimated to appear at about 665 cm^{-1} by calculation of the isotopic shift as shown in Table 2.

9) J. Hiraishi, Ph. D. Thesis, The University of Tokyo (1956).

the same as twice the 663 and 659 cm^{-1} bands ($663\times 2=1326$ and $659\times 2=1318$). From this observation, the 663 and 659 cm^{-1} bands can be assigned to the Mn–N–O linear bending vibrations. This is in agreement with the assignment by the comparison of the observed isotopic shifts with the calculated ones. For $Ag_2[Mn(CN)_5(NO)]$, the overtone band of the Mn–N–O bending vibration was not observed.

One Mn–N stretching and two Mn–N–O bending vibrations were observed in $K_3[Mn(CN)_5(NO)]\cdot 2H_2O$. This can be explained as follows. The $[Mn(CN)_5(NO)]^{3-}$ ion belongs to the point-group symmetry C_{4v} and the reduced representation can be shown as $8A_1+A_2+4B_1+2B_2+9E$. The A_1 and the E species are infrared active, and the N–O and the Mn–N stretching vibrations belong to the A_1 species and the Mn–N–O bending vibration to the E species. $K_3[Mn(CN)_5(NO)]\cdot 2H_2O$ crystallizes in the space group No. 9 Cc,[6] where E species is expected to split into infrared active A' and A'' species, but not A_1 species. Thus, one Mn–N stretching and two Mn–N–O bending vibrations are expected to be observed in crystalline state.

The wave numbers of the N–O stretching vibrations increase in the order of $K_3[Mn(CN)_5(NO)]$, $K_3[Mn(CN)_5(NO)]\cdot 2D_2O$ and $K_3[Mn(CN)_5(NO)]\cdot 2H_2O$ (see Table 1). The changes suggest that hydrogen bonds are formed between the NO group and the crystal waters as revealed by X-ray study of $K_3[Mn(CN)_5(NO)]\cdot 2H_2O$.[6] The changes were observed in the N–O stretching vibrations but hardly at all in C–N stretching vibrations.

The wave numbers of the N–O and the C–N stretching vibrations for $Ag_2[Mn(CN)_5(NO)]$ are higher than those for $K_3[Mn(CN)_5(NO)]\cdot 2H_2O$ and its unhydrate, while the reverse is observed for the skeletal vibrations between the manganese and the NO group. This can be explained from the difference of oxidation states of the manganese atom; the oxidation state of the manganese atom for the K-salts and the Ag-salt are II and III, respectively.

The assignment of the skeletal vibrations between the manganese and the NO group for the examined complexes is tentative, and no distinction between the skeletal vibrations was made.[10] However, a probable assignment of the skeletal vibrations for $K_3[Mn(CN)_5(NO)]\cdot 2H_2O$ and its unhydrate is thought to have been established.

The present work has been supported in part by a Grant for Scientific Research from the Ministry of Education.

10) P. Gans, A. Sabatini, and L. Sacconi, *Inorg. Chem.*, **5**, 1877 (1966).

BULLETIN OF THE CHEMICAL SOCIETY OF JAPAN, VOL. 44, 1027—1030 (1971)

Formation of Hypophosphate in the Radiolysis of Phosphite Solution

Niro MATSUURA, Masahito YOSHIMURA, Masao TAKIZAWA,* and Yukio SAKAKI*

Department of Pure and Applied Sciences, The University of Tokyo, College of General Education, Komaba, Meguro-ku Tokyo

**Tokyo Institute of Photographic Technology, Atsugi, Kanagawa*

(Received September 14, 1970)

The formation of hypophosphate and phosphate in the radiolysis of a phosphite solution was established by the anion-exchange chromatographic technique. The quantitative determination of their yields was made by colorimetry of the phosphate and hypophosphate with the Mo(V)+Mo(VI) reagent, which develops molybdenum-blue colors in two steps at different temperatures. The G values in an aerated condition are 0.01 molecules/100 eV in acid and 0.1 molecule/100 eV in neutral pH with respect to the hypophosphate formation, independent of the phosphite concentration. In a deaerated system much higher values are obtained, amounting to around 0.5 molecules/100 eV at a phosphite concentration of 10^{-3} M. The G values of hypophosphate plus phosphate are around 3.0; this is in agreement with the half-value of the primary radical yields, $1/2\cdot(g_{red}+g_{OH})$, reported in the data derived from the radiation-chemical studies in the aqueous system. The hypothesis that the hypophosphate (IV) ion radical is a transient species in the oxidation of phosphite to phosphate is supported by the results obtained in this work.

The neutron activation of phosphate in an aqueous solution produces ^{32}P-labelled hypophosphate simultaneously with other oxyphosphorus compounds of different oxidation numbers.[1] However, we failed in an attempt to prepare hypophosphate from phosphite by oxidation in an aqueous medium, despite its high stability and inertness.[2] The synthesis of labelled hypophosphate could not be ascribed absolutely to the recoil process of ^{32}P hot atoms, because the transformation of a primary product of labelled phosphite into hypophosphate under ambient radiations in nuclear reactor might be involved. Cottin and Haissinsky[3] proposed a reaction mechanism for the radiolysis of phosphite to phosphate in the aqueous phase by assuming that the hypophosphate-ion radical is a transient intermediate. Hypophosphate-ion radicals have been detected by ESR study in a gamma-irradiated orthophosphate in the form of $\cdot H_2PO_3$.[4] The

1) N. Matsuura and Tsing-Ko Lin, *J. Inorg. Nucl. Chem.*, **32**, 353 (1970).

2) A. D. Mitchell, *J. Chem. Soc.*, **125**, 1013 (1924); Van Wazer, "Phosphorus and Its Compounds," Vol. I, Interscience Pub., New York (1958), pp. 406—411.

3) M. Cottin and M. Haissinsky, *J. Chim. Phys.*, **53**, 917 (1951).

4) A. Treinin, "Radical Ions," Interscience Pub., New York (1968), p. 525.

defect formed by gamma-irradiation in glassy P_2O_5 or glassy alkaline phosphate has been ascribed to this radical,[5] but with no chemical evidence. Haissinsky's report stated that the hypophosphate-ion radicals produced during the radiolysis of phosphite were oxidized further by certain additives, such as O_2, H_2O_2, and N_2O, and that there was little chance to form hypophosphate by a recombination of $\cdot H_2PO_3$.[6] A new technique of the colorimetry of hypophosphate developed by Ohashi *et al.*[7] is now available for determining the yields of hypophosphate in the radiolysis of phosphite by the application of the Mo(V)+Mo(VI) reagent.[8]

Experimental

Materials and Reagents. Sodium phosphite salt, $Na_2HPO_3 \cdot 5H_2O$, was purchased from Wako Pure Chemicals Co., Ltd., and was used without purification. Sodium hypophosphate salt was prepared from elemental phosphorus by hypochlorite oxidation according to the procedure described in the literature.[9] Triply-distilled water was used for preparing the samples to be irradiated.

Irradiation. The sample solutions, in Pyrex tubes, were irradiated with ^{60}Co gamma-ray source (3.8×10^{18} eV/g·hr at 10 cm from the center); the experiments were done in the Institute for Solid State Physics, The University of Tokyo. Irradiations were performed at room temperature, and the absorbed gamma-dose was calibrated by means of a Fricke dosimeter under the same conditions as were used for the irradiation of the samples by assuming $G(+Fe^{3+})=15.5$.

Chemical Analysis. For the detection of hypophosphate the development of the molybdenum-blue color by Mo(V)+Mo(VI) reagent[8] was effected in three different stages. First, a sample solution kept for 30 min at 25°C after the addition of the reagent develops a full color as a result of the hypophosphate. Second, heating on a boiling water bath for some ten minutes results in an increase in the blue color by an amount corresponding to the orthophosphate concentration. Finally, the color due to phosphite is developed on a separate sample solution by the use of the same reagent, with acid sulfite added. The last treatment provides the total content of the oxyphosphorus acid present in the irradiated solution. A batch test tried on synthetic samples showed a slight deviation in the observed values from the expected values as a result of background absorption by the successive treatment of the color development. On the basis of the batch-test data, a correction was made on the measured absorbancies, but it amounts to less than 10%, depending on the amounts of phosphate and hypophosphate present. A phosphite solution, when heated at near the boiling point of water, degrades into phosphate and hydrogen or phosphine.[10] If phosphite is concentrated too much in a sample solution, the "autoredox" decomposition of phosphite also affects the results of the absorbancy by augmenting the phosphate content during the heat treatment for the color development in the second stage. However, the background absorbancy caused by the thermal degradation of phosphite can be disregarded if the phosphite concentration is less than 10^{-3} M. According to our observations, the rate of phosphate formation was proportional to the square of the phosphite concentration, but independent of the concentration of dissolved oxygen. A sharp increase in phosphate was observed at a phosphite concentration higher than about 10^{-3} M. For this reason, the measurements of the radiation-induced yields of phosphate from phosphite were carried out at the concentrations lower than 10^{-3} M.

The ion-exchange chromatographic separation of hypophosphate from phosphate and phosphite was effected by the gradient elution technique, running 0.1 to 0.3 M KCl solutions through a 20-cm Dowex 1×8 anion-exchange resin column. Each 5-ml fraction was subjected to colorimetry by the molybdenum-blue method.

Results and Discussion

Evidence for the formation of hypophosphate in an irradiated solution of phosphite was given by the chromatographic technique combined with the colorimetry of phosphorus by the molybdenum-blue method. Gradient elution with 0.1 M to 0.3 M potassium chloride solutions, buffered with borate at pH 8 develops the phosphoxy-acids of different oxidation states in the order of: hypophosphite, phosphate, phosphite, and hypophosphate. The elution peak at 190 ml in the chromatographic pattern shown in Fig. 1 can be assigned to the peak due to hypophosphate.[11] The yield of hypophosphate in the radiolysis of the phosphite solution was computed from the area of the chromoatogram peak, whose value was in good agreement with the value found by the differential colorimetry of hypophosphate.

A systematic survey of the yields of hypophosphate in the radiolysis of phosphite was made by the differential-colorimetric method both in 0.5 N sulfuric acid and in a neutral solvent under aerated or deaerated conditions. The yields are plotted against the absorbed gamma-dose for a given concentration

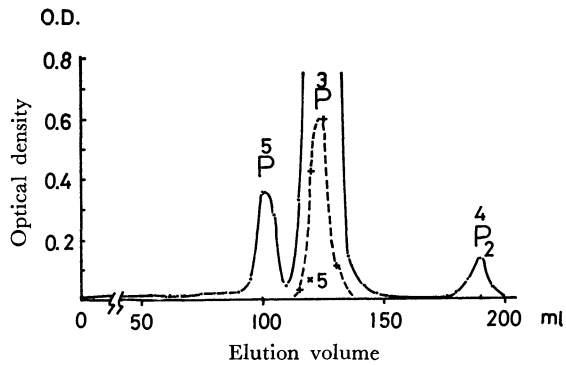

Fig. 1. Chromatographic analysis of gamma-irradiated phosphite solution.
2 ml of 5×10^{-3} M phosphite solution was adsorbed on the anion-exchange resin Dowex 1-8, subjected to gradient elution with 0.1 to 0.3 M KCl and each 5 ml fraction was under examination for phosphorus content by Mo(V)+Mo(VI) reagent

5) T. Feldmann and N. Treinin, *J. Chem. Phys.*, **47**, 2754 (1967); *J. Phys. Chem.*, **72**, 3768 (1968).
6) M. Haissinsky, *J. Chim. Phys.*, **62**, 1141, 1149 (1965).
7) N. Yoza and S. Ohashi, This Bulletin, **37**, 33, 37 (1964).
8) F. Lucena-Conde and L. Prat, *Anal. Chim. Acta*, **16**, 473 (1957).
9) E. Leininger and T. Chulski, "Inorganic Synthesis," Vol. IV, ed. by J. C. Bailar, McGraw Hill, New York (1953), p. 68.
10) Van Wazer, *loc. cit.*, p. 380.
11) N. Matsuura, M. Kobayashi, and Tsing-Ko Lin, This Bulletin, **43**, 2850 (1970).

of phosphite in Fig. 2. These plots provide a straight line falling on the abscissa at a point corresponding to the gamma-dose of around 2×10^{17} eV/m*l* for the radiolysis in both acid and neutral media, irrespective of the presence of oxygen. In an acid medium under aerated conditions, there is practically no formation of hypophosphate, as may be seen in Fig. 2.

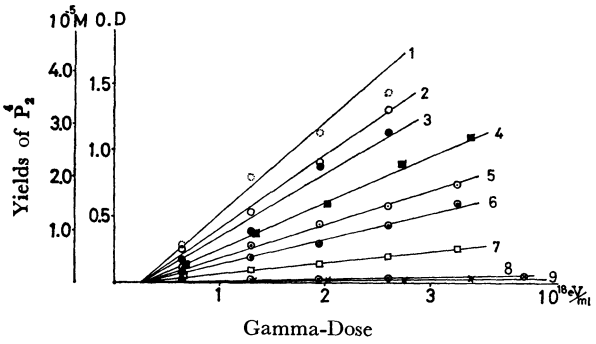

Fig. 2. Yields of hypophosphate (P_2^4)-gamma dose relationship.
1. (○) phosphite concentration of 10^{-3} M
2. (○) 5×10^{-4} M
3. (●) 10^{-4} M in neutral pH
4. (■) 10^{-3} M
5. (⊙) 5×10^{-4} M
6. (◎) 10^{-4} M in acid under deaerated condition
7. (□) 5×10^{-4} M in neutral pH
8. (⊗) 5×10^{-4} M
9. (×) 10^{-4} M in acid under aerated condition

The radiation-chemical yields in *G* value were determined at a gamma-dose of 6.4×10^{17} eV/m*l* as a function of the phosphite concentration. The results are represented in Fig. 3. The *G* value of hypophosphate formation in an aerated neutral solution attains a value of 0.1 ions per 100 eV, independent of phosphite concentration. In a deaerated solution, on the other hand, the *G* values increase with an increase in the concentration of phosphite. The hypophosphate detected in the radiation-induced oxidation of phosphite to phosphate is strong evidence that the hypophosphate-ion radicals are in the monomer form, produced as transient intermediates and acting as precursors of hypophosphate. The fact that the yields of hypophosphate are greatly influenced by the concentration of phosphite is connected with the properties of the hypophosphate-ion radicals, which are relatively inert to the radical species of water radiolysis as compared with the reactivity of the phosphite. The reaction between the phosphite and hydrogen peroxide occurs only very slowly, while it proceeds at an appreciable rate under the influence of ultra-violet rays, which generate the OH radicals by the decomposition of hydrogen peroxide. The hypophosphate is described in the literature as being resistant to the attack of the common redox reagents. In our experiments, too, the yields of phosphate from hypophosphate in the radiolysis were observed to be relatively small and to be entirely suppressed in the presence of phosphite.

From these facts and observations, we assumed that the radiolysis of phosphite was initiated through process (1) by the abstraction of the hydrogen atom from

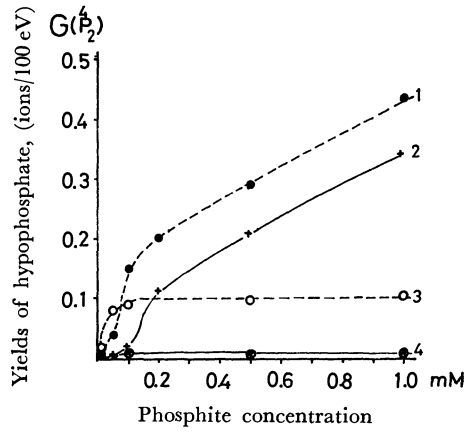

Fig. 3. *G* values of hypophosphate formation as fnuction of phosphite concentration.
1. in deaerated neutral solution, 2. deaerated acid solution, 3. aerated neutral solution, and 4. aerated acid solution

the P–H bond of phosphite ions:

$$H\text{-}\underset{\underset{OH}{|}}{\overset{\overset{O}{\|}}{P}}\text{-}OH + H \text{ (or OH)} = \cdot\underset{\underset{OH}{|}}{\overset{\overset{O}{\|}}{P}}\text{-}OH + H_2 \text{ (or } H_2O) \quad (1)$$

The hypophosphate radicals thus formed are oxidized further into phosphate by the OH radicals, but the rate of oxidation may be slowed down so long as phosphite is predominant as a powerful radical scavenger. When the hypophosphate-ion radicals are accumulated to a certain extent by the absorption of the critical gamma-dose, the recombination reaction through (2) competes with the oxidation by the OH radicals through (3):

$$2\cdot H_2PO_3 = H_4P_2O_6 \quad (2)$$

$$\cdot H_2PO_3 + OH = H_2PO_4^- + H^+ \quad (3)$$

Since, $G(H_2)=g_{H_2}+g_H$ has been known in the acid radiolysis of phosphite,[3] the reduction of the hypophosphate radical to phosphite by the reducing radicals to provide $G(H_2)=g_{H_2}+g_H/2$ is improbable. However, in the presence of oxygen, the H atoms acting as reducing agents are converted into the HO_2 radicals through (4) as the oxidizing agent, and the reducing radicals in turn take part in the oxidation of the hypophosphate radicals through (5):

$$H + O_2 = HO_2 \quad (4)$$

$$\cdot H_2PO_3 + HO_2 + H_2O = H_3PO_4 + H_2O_2 \quad (5)$$

Consequently, the low yields of hypophosphate in the radiolysis under aerated conditions can be explained by the contribution of the HO_2 radical to phosphate formation by reactions (4) and (5) in stead of to hypophosphate formation in the dimer form by (2).

The yields of phosphate in the radiolysis of phosphite were determined by differential colorimetry, along with the yields of hypophosphate. The *G* values of phosphate formation plus hypophosphate formation, thus determined, are shown in Fig. 4 as a function of the phosphate concentration. The results show that the *G* values tend to attain a certain limiting value at a concentration of phosphite higher than 10^{-4} M beyond this concentration all the radical products of water

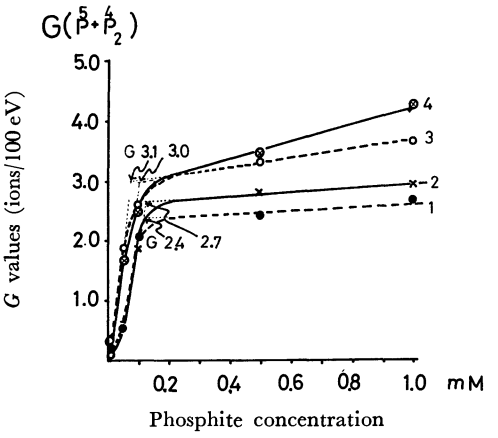

Fig. 4. G values of phosphate plus hypophosphate as function of phosphite concentration in
1. deaerated neutral solution, 2. deaerated acid solution, 3. aerated neutral solution, 4. aerated acid solution.

radiolysis that escape from recombination in the spur space are swept away by the phosphite. The steep rises in the curves, followed by plateaus, make it possible to find the lowest concentration of phosphite necessary for fulfilling the above-cited conditions by the extension of the ascending and plateau parts of the curve, as is shown in Fig. 4. At these particular points, the G values are from 2.4 to 2.7 for the radiolysis in the deaerated system and from 3.0 to 3.1 for the radiolysis in the aerated system.

Since the conversion of phosphite to phosphate is a two-equivalent oxidation, these G values must be a half of the sum of the primary radical yields with respect to the OH and the reducing species. Accordingly, the G values of phosphate plus hypophosphate shown in Fig. 4 can be interpreted in terms of the primary radical yields, denoted by g_{OH} and g_H as below by (6). According to (6), the observed value of G agrees well with the theoretically-derived value,[12] 3.35 at pH 0.2 or 3.5 at pH 6.0:

$$G(\overset{5}{P} + \overset{4}{P_2}) = 1/2 \cdot (g_H + g_{OH}) \qquad (6)$$

In (6) g_H implies the primary yields of the reducing radicals, the H atoms as well as the solvated electrons.

In our experiment, the G values steadily increase beyond 10^{-4} M of phosphite, and at 10^{-3} M the observed G value is 4.3 in the aerated-acid medium. However, an extraordinary G value by the chain mechanism has not yet been observed. The slow increase, followed by a rapid rise in $G(\overset{4}{P_2}+\overset{5}{P})$, can be ascribed to the fact that radical products remaining alive in the spurs come to be partially scavenged by phosphite. The contribution of hydrogen peroxide from the molecular product of radiolysis to the increasing $G(\overset{4}{P_2}+\overset{5}{P})$ can not be excluded, particularly in the aerated system, even though the rate of the reaction of hydrogen peroxide with phosphite is very slow where there is no influence of radiation. Since there is no formation of hypophosphate below a critical gamma-dose of about 2×10^{17} eV/ml, denoted by D_{crit}, the hypophosphate ion radicals must attain a stationary concentration amounting to $2G\cdot(\overset{4}{P_2}+\overset{5}{P})\cdot D_{crit}$. The stationary concentration of the hypophosphate ion radicals under consideration is around 2×10^{-5} M, if the $G(\overset{4}{P_2}+\overset{5}{P})$ value is taken to be 3.0 on the average. The latter concentration is about ten times smaller than the phosphite concentration, giving plateau G values, 1×10^{-4} M. By comparing the phosphite concentration of 10^{-4} M for reaction (1) with the hypophosphate ion radical concentration of 2×10^{-5} M for reaction (2), a majority of the radical OH can be said to react with phosphite through (1) unless the second-order rate constant of (1) is much smaller than that of (3). Our results show that the phosphate formation (3), which is at least ten times larger than that of reaction (1).

In connection with the protective action of phosphite, the effect of hypophosphite was studied in order better to understand the critical dose, D_{crit}, in this system. If hypophosphite solution is irradiated with gamma-rays, no phosphate is formed and the increase of phosphite continues until a greater part of the hypophosphite is consumed. Thus, the oxidation of phosphite to phosphate is entirely protected against the attack of the radical products of water radiolysis, as may be seen in Fig. 5. The critical gamma-dose for

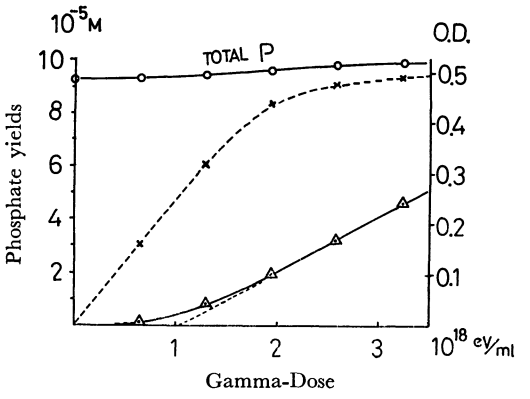

Fig. 5. Yields of phosphate ($\overset{5}{P}$) in the radiolysis of 10^{-4} M hypophosphite (full line curve with △).
Total phosphorus content, including hypophosphite, phosphite, hypophosphate, and phosphate, for checking the amount lost by thermal degradation during the heat treatment of color development (upper full line with ○).
For the sake of comparison the yields of phosphate in the radiolysis of the same concentration of phosphite solution are plotted by the break line with ×.

the complete protection of phosphate formation was 1.0×10^{18} eV/ml. At this critical value, the hypophosphite concentration is lowered significantly to such an extent that the rate of oxidation of phosphite to phosphate becomes compatible with the rate of the conversion of hypophosphite to phosphite.

12) E. Hayon, "Radiation Chemistry of Aqueous Systems," ed. by G. Stein, Interscience Pub., Jerusalem (1968).

Photon-Activation Analysis for Zirconium with Molybdenum Used as the Internal-Reference Element[1)]

Tong-Chuin PUNG,* Toyoaki KATO, and Yoshinaga OKA**
Department of Chemistry, Faculty of Science, Tohoku University, Katahira-cho, Sendai
(Received September 16, 1970)

A method for the determination of zirconium has been studied by activation analysis with bremsstrahlung photons, with molybdenum used as the internal-reference element. This method is based on the γ-ray spectrometric measurement of the ^{89}Zr activity produced by the ^{90}Zr(γ,n) reaction and on the comparison of this activity with the ^{88}Zr activity formed by the (γ,α) reaction on molybdenum. The reaction products and their rates of production in zirconium and in molybdenum have also been examined as functions of bremsstrahlung maximum energies up to 60 MeV, and the best conditions for the determination of zirconium are proposed. When the maximum energy was set at 20 MeV, no interfering reactions occurred; under the present experimental conditions, a zirconium content down to about 18 μg can be determined accurately. The reliability and the versatility of this method are demonstrated.

A minute amount of zirconium can be determined by photon-activation analysis using ^{89}Zr activity induced in an irradiated sample. This technique has been applied to the determination of zirconium in hafnium samples, using the non-destructive internal-reference method.[2,3)]

In a previous report,[4)] a method for the determination of niobium by photon-activation analysis has been proposed, with molybdenum used as the internal-reference element. The activity of the ^{92m}Nb produced by the (γ,n) reaction was utilized for the determination, while ^{95m}Nb or ^{96}Nb activities coming from molybdenum by the (γ,p) processes were used as references. On the basis of similar principles, methods for the determination of arsenic,[5)] rubidium,[6)] and cesium[7)] have also been established. Besides the (γ,n) and the (γ,p) reactions, the (γ,α) reactions can be induced by activation with photons in the giant resonance-energy region; the yields of (γ,α) reactions in several medium-weight nuclei for 20 MeV bremsstrahlung were given previously.[8)]

Thus, an element can be determined by comparing the activity of its (γ,n) reaction product with the activity induced by the (γ,α) reaction on the reference element having an atomic number higher by two.

The present work concerns a method for the determination of zirconium using molybdenum as the internal-reference element. In order to determine the best conditions for this purpose, some work has also been carried out on the yields of photonuclear reactions over the energy range of bremsstrahlung photons up to 60 MeV. When a maximum energy was set at 20 MeV, no interfering reactions occurred, and traces of zirconium down to about 18 μg could be determined accurately.

Experimental

Materials and Irradiation. The zirconium oxide was of an analytical-reagent grade and was from the Johnson Mathey Corp. The molybdenum was a metallic powder of 99.9% purity, from Wako Pure Chemical Industries, Ltd. Synthetic mixtures of these two samples, with known zirconium-to-molybdenum weight ratios ranging from 2.46×10^{-3} to 2.49×10^{-5}, were prepared in order to examine the sensitivity and the accuracy of the method. Each sample, weighing from 0.1 to 2 g, was placed either in a silica or Pyrex tube with an internal diameter of 8 mm. The tube was then placed in a water-cooled target holder immediately behind the bremsstrahlung generator, a 3-mm-thick platinum plate, and was irradiated. The irradiation periods varied between 1 and 3 hr.

Two kinds of linear-electron accelerators of Tohoku University were the bremsstrahlung sources. One of them provided a 20 MeV-electron beam. The other machine, which was capable of accelerating electrons with much higher energies, was used as the 30-to-60 MeV bremsstrahlung source. The experimental method, involving bremsstrahlung-flux monitoring, and the details of the irradiation were essentially the same as have been described in detail in a previous report.[9)]

Separation of Zirconium. The separation of zirconium activities from an irradiated sample was performed, after the addition of a zirconium carrier (10 mg), by means of the anion-exchange method, with a mixture of hydrofluoric and hydrochloric acid as the eluent.

The method was essentially the same as has been described in a previous report.[4)] The zirconium activities were eluted from a Dowex 1×8 column[10)] with 80 m*l* of a 0.01 N hydrofluoric acid - 9 N hydrochloric acid mixture. To this fraction, 5 m*l* of a saturated aqueous solution of boric acid were added. The zirconium hydroxide was precipitated from this solution by the addition of aqueous ammonia, filtered, washed, and then ignited to give zirconium oxide. This was wrapped with a thin sheet of aluminum for γ-ray counting. The chemical yield was determined, if needed.

1) Study of Activation Analysis Using the Internal-Reference Method. XVII; Part XVI: H-T. Tsai, *Nippon Kagaku Zasshi*, **92**, 93 (1971).

* Present address: The Research Institute for Iron, Steel, and Other Metals, Tohoku University, Katahira-cho, Sendai.

** Present address: Department of General Education, Kitasato University, Sagamihara, Kanagawa.

2) Y. Oka, T. Kato, and M. Sasaki, *Nippon Kagaku Zasshi*, **84**, 588 (1963).

3) Y. Oka and T. Kato, *ibid.*, **86**, 835 (1965).

4) Y. Oka, T-C. Pung, and T. Saito, This Bulletin, **43**, 1083 (1970).

5) Y. Oka, T. Kato, and Y. Konami, *Bunseki Kagaku*, **18**, 971 (1969).

6) H-T. Tsai, T. Kato, and Y. Oka, This Bulletin, **43**, 2823 (1970).

7) H-T. Tsai, *Nippon Kagaku Zasshi*, **92**, 60 (1971).

8) Y. Oka, T. Kato, K. Nomura, T. Saito, and H-T. Tsai, This Bulletin, **41**, 2660 (1968).

9) Y. Oka, T. Kato, and N. Sato, This Bulletin, **42**, 387 (1969).

10) 1 cm $\phi\times40$ cm, 100—200 mesh.

TABLE 1. NUCLEAR DATA FOR ZIRCONIUM NUCLIDES

Target nuclide (abundance, %)	Reaction type	Product nuclide	Mass threshold ($-Q$, MeV)	Coulomb barrier (MeV)	Half-life of product	Decay mode	Principal γ-rays
^{90}Zr (5.46)	(γ, n)	^{89}Zr	12.00	—	78.4 hr	EC, β^+	0.910, 1.710
	$(\gamma, 2n)$	^{88}Zr	21.14	—	85 d	EC	0.394
	$(\gamma, 3n)$	^{87}Zr	33.81	—	1.6 hr	EC, β^+	1.220
	(γ, pn)	^{88}Y	20.20	6.44	108.1 d	EC, β^+	0.898, 1.836
	(γ, d)	^{88}Y	17.63	6.15	108.1 d	EC, β^+	0.898, 1.836
	$(\gamma, \alpha n)$	^{85}Sr	18.22	11.43	64.0 d	EC	0.514
^{91}Zr (11.23)	$(\gamma, 2n)$	^{89}Zr	19.19	—	78.4 hr	EC, β^+	0.910, 1.710
	$(\gamma, 3n)$	^{88}Zr	30.18	—	85 d	EC	0.394
	(γ, p)	^{90m}Y	6.86	6.40	3.1 hr	IT, β^-	0.202, 0.482
^{92}Zr (17.11)	(γ, p)	^{91m}Y	9.40	6.38	50 min	IT	0.551
	(γ, pn)	^{90m}Y	17.33	6.40	3.1 hr	IT, β^-	0.202, 0.482
	(γ, d)	^{90m}Y	15.10	6.11	3.1 hr	IT, β^-	0.202, 0.482
^{94}Zr (17.40)	(γ, p)	^{93}Y	10.33	6.35	10.3 hr	β^-	0.267, 0.940
^{96}Zr (2.80)	(γ, n)	^{95}Zr	7.84	—	65.5 d	β^-	0.724, 0.756
^{92}Mo (15.86)	(γ, α)	^{88}Zr	5.46	13.65	85 d	EC	0.394
	$(\gamma, \alpha n)$	^{87}Zr	17.65	13.69	1.6 hr	EC, β^+	1.220
^{94}Mo (9.12)	$(\gamma, \alpha n)$	^{89}Zr	14.06	13.62	78.4 hr	EC, β^+	0.910, 1.710
^{100}Mo (9.62)	$(\gamma, \alpha n)$	^{95}Zr	11.02	13.40	65.5 d	β^-	0·724, 0.756

Measurement of Radioactivity. The γ-ray measurements were made with a Ge(Li) detector, with a sensitive volume of 36 cm^3, coupled to a TMC 1024-channel pulse-height analyzer. The counting system had a resolution of 4 keV for the 661.6 keV γ-line of ^{137}Cs. The sample was measured at a fixed position, 1 cm from the sensitive surface of the detector.

A 3″ dia. × 3″ NaI(Tl) crystal was also used as the detector. This was coupled to an 800-channel pulse-height analyzer made by the Tokyo Shibaura Electric Co., Ltd. The sample was located at a distance of 1 cm from the crystal surface.

For the study of various photonuclear reaction products, in which a much greater resolving power was required, the Ge(Li) detector was used exclusively. For analytical purposes, the NaI(Tl) detector was used.

Results and Discussion

Photonuclear Reaction. The nuclear data of present importance are given in Table 1. For a zirconium sample irradiated with 20 MeV bremsstrahlung, ^{89}Zr and ^{95}Zr produced by the (γ,n) reactions and ^{91m}Y produced by the (γ,p) reaction were measured at a cooling time of 45 min. At 30 MeV, ^{88}Zr was produced by the $(\gamma,2n)$ reaction and ^{90m}Y and ^{93}Y were produced by the (γ,p) reactions, beside the above products. With this energy, ^{88}Y formed by the (γ,pn) and (γ,d) reactions on ^{90}Zr was also recognized after the relatively short-lived products had decayed away. In addition, the ^{90}Zr$(\gamma, 3n)^{87}$Zr reaction occurred for an energy beyond 45 MeV. These zirconium and yttrium activities are summarized in terms of their γ-ray photopeak intensities, and are plotted against bremsstrahlung maximum energy, in Fig. 1. All the activity data are expressed in counts per minute per milligram of zirconium at the end of an 1-hr irradiation by bremsstrahlung with the given maximum energies, after being normalized to a standard dose rate required to produce 1.0 μCi ^{196}Au by the 1-hr irradiation of 1 mg of gold. It is clear that the

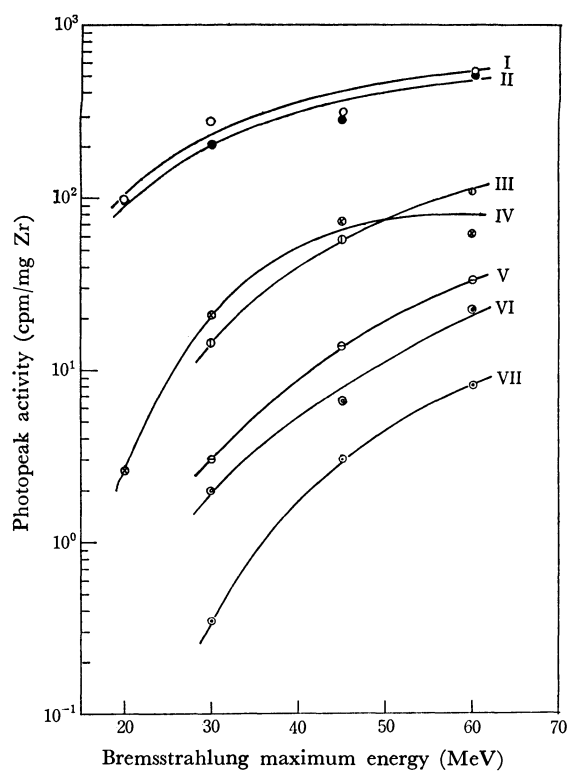

Fig. 1. Photopeak activities of zirconium and yttrium nuclides formed in zirconium as a function of bremsstrahlung maximum energy with a 36 cm^3 Ge(Li) detector.
I: ^{89}Zr 0.910 MeV γ-ray V: ^{90m}Y 0.482 MeV γ-ray
II: ^{89}Zr 0.511 MeV γ-ray VI: ^{93}Y 0.267 MeV γ-ray
III: ^{90m}Y 0.202 MeV γ-ray VII: ^{88}Zr 0.394 MeV γ-ray
IV: ^{91m}Y 0.551 MeV γ-ray

TABLE 2. R_W *versus* R_{A_0} FOR ZIRCONIUM-MOLYBDENUM MIXTURES

R_W (Zr/Mo)	R_{A_0}		R_W/R_{A_0}	
	^{89}Zr(0.511 MeV)	^{89}Zr(0.910 MeV)	^{89}Zr(0.511 MeV)	^{89}Zr(0.910 MeV)
2.460×10^{-3}	9.55×10^{1}	1.33×10^{2}	2.58×10^{-5}	1.85×10^{-5}
2.220×10^{-3}	8.33×10^{1}	1.15×10^{2}	2.64×10^{-5}	1.91×10^{-5}
6.272×10^{-4}	2.27×10^{1}	3.27×10^{1}	2.76×10^{-5}	1.92×10^{-5}
1.902×10^{-4}	7.04×10^{0}	1.02×10^{1}	2.70×10^{-5}	1.86×10^{-5}
1.390×10^{-4}	5.39×10^{0}	6.74×10^{0}	2.58×10^{-5}	2.06×10^{-5}
2.490×10^{-5}	8.99×10^{-1}	1.22×10^{0}	2.77×10^{-5}	2.04×10^{-5}
		Mean :	2.67×10^{-5}	1.94×10^{-5}
		Std. dev. :	$\pm0.08\times10^{-5}$	$\pm0.08\times10^{-5}$

0.910 MeV γ-ray of ^{89}Zr gives the highest photopeak activity for all the bremsstrahlung maximum energies. The annihilation radiation (0.511 MeV) can also be used for the sensitive determination of zirconium.

When molybdenum was irradiated with 20 MeV bremsstrahlung and the zirconium activity was separated, only the 0.394 MeV γ-ray was observed; it was attributed to ^{88}Zr produced by the ^{92}Mo(γ,α)^{88}Zr reaction. With 30 MeV bremsstrahlung, γ-rays due to the ^{89}Zr produced by the ^{94}Mo(γ,αn) reaction have also been measured. In addition, ^{87}Zr and ^{95}Zr were produced by the (γ,αn) reactions on molybdenum at energies beyond 45 MeV. Since the ^{89}Zr activity was used in the determination of zirconium, the irradiation conditions leading to the production of ^{89}Zr from molybdenum had to be avoided. Below 20 MeV, only the ^{94}Mo(γ,αn)^{89}Zr reaction ($-Q=14.06$ MeV) can produce ^{89}Zr. The experimental results showed that no appreciable amount of ^{89}Zr was produced from molybdenum with 20 MeV bremsstrahlung.

The Determination of Zirconium. The annihilation radiation or the 0.910 MeV γ-ray photopeak can be utilized for the determination of zirconium, while the ^{88}Zr activity arising from molybdenum can be used as a reference. The accuracy of the method was assessed by processing synthetic zirconium-molybdenum mixtures. They were irradiated with 20 MeV bremsstrahlung for 3 hr at a dose rate of 8×10^{4} R/min.[11] After the irradiation, the zirconium activities were separated chemically as has been described above. Figure 2 shows a typical γ-ray spectrum of the zirconium fraction. The photopeak area of the 0.511 MeV or 0.910 MeV peak of ^{89}Zr was measured and compared with that of the 0.394 MeV peak of ^{88}Zr. The results are given in Table 2. In each case, a good proportionality was obtained between R_W and R_{A_0}, where R_W is the weight ratio of zirconium to molybdenum and where R_{A_0} is the ratio of the photopeak activities corrected at the end of a 3-hr irradiation. The zirconium content can be determined down to 45 μg by this relationship, with a relative error of within 4% under the present experimental conditions.

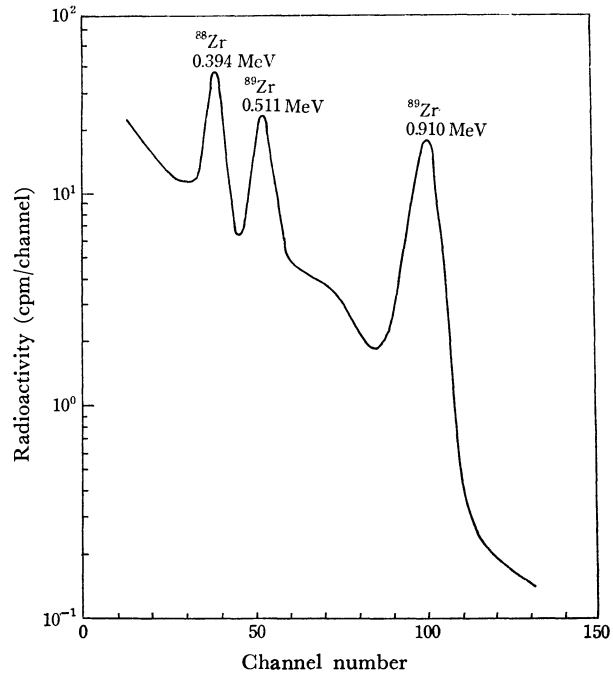

Fig. 2. γ-Ray spectrum of radiozirconium separated from a mixed sample (Zr 45.2 μg + Mo 1.815 g), 23.3 hr after irradiation with 20 MeV bremsstrahlung for 3 hr with a NaI(Tl) detector.

When a photopeak activity of 10 cpm is selected as the limit of determination, about 18 μg of zirconium in 2 g of molybdenum can be determined. With an accelerator giving a higher bremsstrahlung dose rate, the sensitivity is improved. In the energy region of 20 MeV bremsstrahlung, no interfering photonuclear reactions can occur from the coexisting elements. In the present case, the neutron reactions which arise from photoneutrons cause no serious problems.

This method can be used generally for the determination of zirconium when we add a proper amount of molybdenum, 2 g in most cases, to the sample as the reference element. When this method is combined with that reported previously for the determination of niobium,[4] zirconium and niobium may be determined simultaneously with molybdenum used as the reference.

In conclusion, the present authors believe that the method presented here is promising for the accurate

11) The dose-rate determination has been done by means of a method reported earlier.[12]

12) Y. Oka, T. Kato, and I. Nagai, *J. Nucl. Sci. Tech.*, **4**, 300 (1967).

determination of zirconium in samples of various origins, provided that those samples do not contain a large amount of molybdenum.

The authors express their appreciation to members of the linac staff at the Institute of Nuclear Science, Tohoku University, for their very fine services.

BULLETIN OF THE CHEMICAL SOCIETY OF JAPAN, VOL. 44, 1034—1039 (1971)

Studies of Ethylenediamine-*N,N'*-diacetatocobalt(III) Complexes. I. The Preparation and Some Properties of Ethylenediamine-*N,N'*-diacetatocobalt(III) Complexes, with Chloride, Water, Ammonia, Ethylenediamine, 1,10-Phenanthroline, and 2,2'-Dipyridyl as the Additional Ligands

Kashiro KURODA and Kiyokatsu WATANABE

Department of Chemistry, Faculty of Science, Ehime University, Matsuyama, Ehime

(Received September 29, 1970)

A series of cobalt(III) complexes containing the tetradentate ethylenediamine-*N,N'*-diacetate anion (EDDA) and chloride, water, ammonia, ethylenediamine, 1,10-phenanthroline, and 2,2'-dipyridyl as the ligands occupying the residual coordination positions have been prepared, and some of their physical and chemical properties have been examined. Two isomers have been isolated in the cases of the phenanthroline and dipyridyl complexes; they have been inferred to be the *α-cis*(pink) and the *β-cis*(red) isomers* on the basis of their electronic absorption spectra. A new convenient route for the preparation of the series has been presented, a route which passes through the dichloro, chloroaquo, and diaquo complexes.

Although a number of cobalt(III) complexes which contain the tetradentate ethylenediamine-*N,N'*-diacetate anion (EDDA) have been reported in the literature,[1-6] the number is still small in comparison with those of such other series as the triethylenetetraminecobalt(III) and nitrilotriacetatocobalt(III) series. The main reason for the rather few instances of isolation is undoubtedly the large solubilities or the difficulty in the crystallization of the members of the series. The addition of an organic solvent such as ethanol to a concentrated reaction mixture, a method which is often used in the complex preparations, almost always gives oily materials or highly hygroscopic precipitates in this series. For example, the carbonato-(ethylenediamine-*N,N'*-diacetato)cobalt(III) ion reacts with various anions in the acidic solution, but the addition of ethanol to the reaction mixture gives no satisfactory materials. In order to obtain good crystals, we attempted the crystallization or precipitation of a complex from an aqueous solution, keeping the other components in the solution as few in number as possible. Thus, several new complexes as well as the known species have been isolated in the nonhygroscopic state. A new convenient route of preparation will be reported in this communication.

Theoretically, a di(monodentate)-EDDA-Co(III) complex may exist in three different stereoisomers, and a bidentate-EDDA-Co(III) complex in two, as is shown in Fig. 1. Legg and Cooke isolated *α-cis*-[Co(EDDA)(en)]NO_3 and *β-cis*-[Co(EDDA)(en)]-ClO_4.[2] From the very low yield of the *β-cis* isomer and the failure to isolate *β-cis*-[Co(EDDA)$(NH_3)_2$]X, it has been considered that EDDA very much prefers the *α-cis* coordination mode.[2-5] Recently, Coleman, Legg, and Steele obtained the *α-cis* and *β-cis* isomers of oxalato-EDDA-Co(III) and malonato-EDDA-Co-

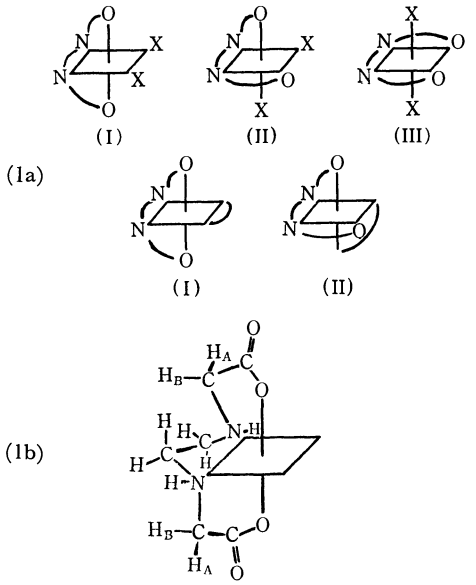

Fig. 1. Coordination modes of EDDA-Co(III) complexes.
(1a) (I) *α-cis*-configuration
(II) *β-cis*-configuration
(III) *trans*-configuration
(1b) conformation of EDDA in the *α-cis*-isomer

* In this article, the nomenclature proposed by A. M. Sargeson and G. H. Searle (*Inorg. Chem.*, **4**, 45 (1965)) has been adopted in order to distinguish the isomers. The *trans* and *cis* isomer named in several articles are *α-cis* and *β-cis* isomer here, respectively.

1) M. Mori, M. Shibata, E. Kyuno, and F. Maruyama, This Bulletin, **35**, 75 (1962).
2) J. I. Legg and D. W. Cooke, *Inorg. Chem.*, **4**, 1576 (1965).
3) J. I. Legg, D. W. Cooke, and B. E. Douglas, *ibid.*, **6**, 700 (1967).
4) C. W. Van Saun and B. E. Douglas, *ibid.*, **8**, 115 (1969).
5) P. J. Garnett, D. W. Watts, and J. I. Legg, *ibid.*, **8**, 2537 (1969).
6) P. F. Coleman, J. I. Legg, and J. Steele, *ibid.*, **9**, 937 (1970).

(III) complexes.[6] In these cases, the yields of the two isomers were comparable. It has not yet been clearly established what factors determine the coordination mode of EDDA around the central cobalt ion. In our new preparative procedure, in which the chloroaquo or the diaquo complex was used as the starting material, both *α-cis* and *β-cis* isomers were obtained in the cases of the 1,10-phenanthroline and the 2,2'-dipyridyl complexes. It was possible to control the yield of the isomers by adjusting the reaction temperature.

Experimental

Materials. The ethylenediamine-*N,N'*-diacetic acid (Dotite Reagents), 1,10-phenanthroline, and 2,2'-dipyridyl (Nakarai Chemicals) and all the other reagent-grade chemicals were used without further purification.

Analysis. The cobalt was analysed by a direct EDTA titration, using murexide as an indicator, after the decomposition of a complex with hot concentrated sulfuric and nitric acid. The other elements were analysed at the Institute for Chemical Research in Kyoto University.

Apparatus and Measurements. The visible and ultraviolet absorption spectra were measured with a Hitachi ESP-3 Recording Spectrophotometer. The infrared spectra were recorded with a Hitachi EPI-G Spectrophotometer. The proton nuclear magnetic resonance spectra were recorded with a Japan Electron Optics JNM-4H-100 Spectrometer (100 MHz), using deuterium oxide as the solvent. The temperature of the probe was maintained at 22±1°C. The chemical shifts, referred to TMS as zero, were calculated from the observed shifts of a complex from the resonance of HDO (4.69 ppm downfield from the TMS resonance). The solubility measurements and the reactions with various anionic reagents were carried out by a procedure described elsewhere.[7]

*Preparations. (1) Hydrogen Dichloro(ethylenediamine-*N,N'*-diacetato)cobaltate(III), H[Co(EDDA)(Cl)$_2$]*: In 40 m*l* of water, ethylenediamine-*N,N'*-diacetic acid (1.76 g), sodium hydroxide (0.8 g), and cobalt(II) chloride hexahydrate (2.3 g) were added in this order. We then started to bubble air into the mixture, and 10 m*l* of hydrogen peroxide (30%) were added, drop by drop, through the air inlet. Air bubbling was continued for 5 hr, during which time the color of the solution changed from brown to dark red-violet and finally deep red-violet. Eighty milliliters of concentrated hydrochloric acid were added to the oxidation product, and then the mixture was concentrated on a steam bath, with continuous stirring, to about 60 m*l*. The color changed to a dark bluish green; at the same time a dark green precipitate appeared. After cooling, the precipitate was collected on a filter, and washed with concentrated hydrochloric acid, methanol, and ether. Yield, 2 g.

Found: Co, 19.35; C, 23.43; H, 3.65; N, 9.02%. Calcd for H[Co(EDDA)(Cl)$_2$]=$CoC_6H_{11}O_4N_2Cl_2$ (305.00): Co, 19.32; C, 23.63; H, 3.64; N, 9.18%.

An additional product was obtained by the further evaporation of the filtrate, but the deposit contained colorless crystals (NaCl). This product was useful for the preparation of the following chloroaquo complex.

*(2) Chloroaquo(ethylenediamine-*N,N'*-diacetato)cobalt(III) Monohydrate, [Co(EDDA)(Cl)(H$_2$O)]·H$_2$O*: One gram of hydrogen dichloro(ethylenediamine-*N,N'*-diacetato)cobaltate(III) was dissolved in a minimal amount of water (~30 m*l*); then the solution was kept at room temperature for one day. The blue-violet crystals which deposited were washed with cold water, ethanol, and ether. Yield, 0.5 g. The mother liquid was useful for the preparation of the following diaquo complex.

Found: Co, 19.27; C, 23.71; H, 4.59; N, 8.85%. Calcd for [Co(EDDA)(Cl)(H$_2$O)]·H$_2$O=$CoC_6H_{14}O_6N_2Cl$ (304.58): Co, 19.35; C, 23.66; H, 4.63; N, 9.20%.

*(3) α-cis-Diaquo(ethylenediamine-*N,N'*-diacetato)cobalt(III) Perchlorate, α-cis-[Co(EDDA)(H$_2$O)$_2$]ClO$_4$*: In 30 m*l* of water, 1 g of the above chloroaquo complex was suspended, and the mixture was heated at 60°C. After the starting complex had dissolved and the color of the solution had changed from blue-violet to red-violet, the solution was concentrated to 5 m*l*, and then 2 m*l* of 6 N $HClO_4$ was added. The mixture was placed in a refrigerator for 1—2 days. The red crystals which formed was washed with methanol and ether. Yield, 1 g. In order to deposit the complex more quickly or to recover the material from the filtrate in this procedure and from the filtrate in the chloroaquo complex preparation, the solution was evaporated in a large, flat dish with an aid of an air stream and gentle heating. When the solution contained a relatively large amount of chloride ions (in the case of the recovery), repeated evaporation was necessary to let chloride ions leave as hydrogen chloride; otherwise, the evaporation residue consisted mainly of the chloroaquo complex.

Found: Co, 15.73; C, 19.70; H, 3.82; N, 7.42%. Calcd for [Co(EDDA)(H$_2$O)$_2$]ClO$_4$=$CoC_6H_{14}O_{10}N_2Cl$ (368.57): Co, 15.99; C, 19.55; H, 3.83; N, 7.60%.

*(4) α-cis-Ethylenediamine-*N,N'*-diacetato(diammine)cobalt(III) Perchlorate Monohydrate, α-cis-[Co(EDDA)(NH$_3$)$_2$]ClO$_4$·H$_2$O*: Though the nitrate of this complex had previously been prepared by Legg and Cooke,[2] the following procedure was found to be simpler. The mixture of cobalt(II) chloride hexahydrate (2.3 g), ethylenediamine-*N,N'*-diacetic acid (1.8 g), active charcoal (0.5 g), and 10 m*l* of 6 N ammonia in 80 m*l* of water was oxidized by vigorous air bubbling for 4 hr. After the removal of the charcoal by filtration, 10 m*l* of 6 N $HClO_4$ were added to the red-purple filtrate. A large amount of crystals appeared after a while. The precipitate was recrystallized from 150 m*l* of warm (~50°C) water with the addition of a few milliliters of 6 N $HClO_4$ for complete precipitation. It was washed with ethanol and ether. Yield, 2.0 g.

Found: Co, 15.35; C, 18.50; H, 4.55; N, 14.42%. Calcd for [Co(EDDA)(NH$_3$)$_2$]ClO$_4$·H$_2$O=$CoC_6H_{18}O_9N_4Cl$ (384.62): Co, 15.32; C, 18.74; H, 4.72; N, 14.57%.

The same product was obtained from [Co(EDDA)(Cl)(H$_2$O)]·H$_2$O. A suspension which contained 0.5 g of the chloroaquo complex in 40 m*l* of water was heated until the complex dissolved completely. The complex aquated during the dissolution, and the color of the solution was red-violet. By the addition of 5 m*l* of 6 N ammonia, the color changed immediately to a more reddish tone. After the solution had been heated till the odor of ammonia vanished, 3 m*l* of 6 N $HClO_4$ were added. The precipitate thus obtained showed properties identical with those of the product prepared by the preceding procedure.

*(5) α-cis-Ethylenediamine-*N,N'*-diacetato(ethylenediamine)-cobalt(III) Perchlorate, α-cis-[Co(EDDA)(en)]ClO$_4$*: Although a procedure for the preparation for the nitrate of this complex had previously been described by Legg and Cooke,[2] the following more simple procedure was found to give a satisfactory yield. A mixture of cobalt(II) chloride hexahydrate (2.3 g), ethylenediamine-*N,N'*-diacetic acid (1.8 g),

7) K. Kuroda and P. S. Gentile, This Bulletin, **38**, 1362 (1965).

ethylenediamine (0.8 g), and active charcoal (0.5 g) in 80 ml of water was oxidized by vigorous air bubbling for 4 hr. After the removal of the charcoal by filtration, the red solution was concentrated to about 30 ml and then cooled. A large amount of a fibrous material thus appeared. (This material, which is probably the chloride of the desired complex, has a curious character; it gets entangled like fine threads in a liquid.) The material was recrystallized from warm water. When it was then mixed with concentrated perchloric acid, the crystalline form changed to powder. The perchlorate thus obtained was washed with ethanol and ether. Yield, 2.2 g.

Found: Co, 14.93; C, 24.52; H, 4.56; N, 14.24%. Calcd for $[Co(EDDA)(en)]ClO_4 = CoC_8H_{18}O_8N_4Cl$ (392.64): Co, 15.01; C, 24.47; H, 4.62; N, 14.27%.

The same product was obtained from the chloroaquo complex (2). In 40 ml of water, 0.5 g of the chloroaquo complex was aquated by gentle heating. An aqueous solution, which contained the equivalent amount of ethylenediamine (0.11 g), was then added. The color of the solution changed immediately from red-violet to reddish orange. After evaporation to about 10 ml, 3 ml of concentrated perchloric acid were added. The precipitate thus formed showed properties identical with those of the product prepared by the preceding procedure.

(6) α - cis - Ethylenediamine - N,N' - *diacetato (1,10 - phenanthroline) cobalt(III) Perchlorate, α-cis-[Co(EDDA)(phen)]ClO₄*: A mixture of the diaquo complex (0.3 g), 1,10-phenanthroline monohydrate (0.165 g), and active charcoal (0.1 g) in 50 ml of a methanol (70%)-water mixture was heated at 40°C for 1 hr with continuous stirring. After the removal of the charcoal by filtration, 2 ml of 6 N $HClO_4$ was added to the filtrate. The precipitate thus formed was collected on a filter and then extracted by warm water. The first 10 ml extract was disregarded. A few drops of 6 N $HClO_4$ were added to the last main extract (~80 ml). The pink precipitate thus formed was washed with ethanol and ether. Yield, 0.3 g.

Found: C, 42.38; H, 3.58; N, 10.85%. Calcd for $[Co(EDDA)(phen)]ClO_4 = CoC_{18}H_{18}O_8N_4Cl$ (512.75): C, 42.16; H, 3.54; N, 10.93%.

(7) β - cis - Ethylenediamine - N,N' - *diacetato (1,10 - phenanthroline) cobalt(III) Perchlorate, β-cis-[Co(EDDA)(phen)]ClO₄*: A suspension of 0.3 g of the chloroaquo complex in 20 ml of water was gently heated until the complex dissolved completely. The resulting solution was mixed with 0.1 g of active charcoal and a solution which contained 0.217 g of 1,10-phenanthroline in 30 ml of methanol, and then the mixture was concentrated to ~10 ml with continuous stirring on a steam bath. The reaction temperature was about 90°C. After the removal of the charcoal by filtration, 2 ml of 6 N $HClO_4$ were added to the filtrate. The viscous phase which was thus formed became solid after a day. This solid, after crushing, was collected on a filter and then extracted by warm water. The first extract (10 ml) was disregarded. To the main extract (~70 ml), a few milliliters of 6 N $HClO_4$ were added. The red precipitate thus formed was recrystallized once again in the same way. It was washed with methanol and ether. Yield, 0.15 g.

Found: C, 41.71; H, 3.70; N, 10.55%. Calcd for $[Co(EDDA)(phen)]ClO_4 = CoC_{18}H_{18}O_8N_4Cl$ (512.75): C, 42.16; H, 3.54; N, 10.93%.

(8) α - cis - Ethylenediamine - N,N' - *diacetato (2,2' - dipyridyl) cobalt(III) Perchlorate Monohydrate, α-cis-[Co(EDDA)(dipy)]ClO₄·H₂O*:

(9) β - cis - Ethylenediamine - N,N' - *diacetato (2,2' - dipyridyl) cobalt(III) Perchlorate Monohydrate, β-cis-[Co(EDDA)(dipy)]ClO₄·H₂O*:

These two isomers were separated from one reaction product. It is also possible to prepare each isomer separately by procedures similar to those for the phenanthroline complexes described above.

A mixture of 0.3 g of the diaquo complex (3), 0.127 g of 2,2'-dipyridyl, and 0.1 g of active charcoal in 50 ml of methanol (70%)-water mixture was heated at 55°C for 1 hr with continuous stirring. After the removal of the charcoal, the filtrate was condensed to 20 ml. A pink precipitate began to appear by cooling; it grew to a considerable amount by the addition of a few drops of 6 N $HClO_4$. This precipitate was recrystallized twice from warm water. The filtrate which was separated from the above precipitate was concentrated to 10 ml, and then 1 ml of 6 N $HClO_4$ was added. The red precipitate thus formed was recrystallized twice from warm water. Both products were washed with ethanol and ether. Yield: the pink *α-cis* isomer, 0.15 g; the red *β-cis* isomer, 0.13 g.

Found: C, 37.77; H, 3.45; N, 11.05% for the pink isomer; C, 37.47; H, 3.82; N, 10.99% for the red isomer. Calcd for $[Co(EDDA)(dipy)]ClO_4 \cdot H_2O = CoC_{16}H_{20}O_9N_4Cl$ (506.74): C, 37.92; H, 3.98; N, 11.06%.

Results and Discussion

Preparation Procedures. The preparative procedures used in this study are shown schematically

TABLE 1. PREPARATION SCHEME OF EDDA-Co(III) COMPLEXES
(The water of crystallization is omitted.)

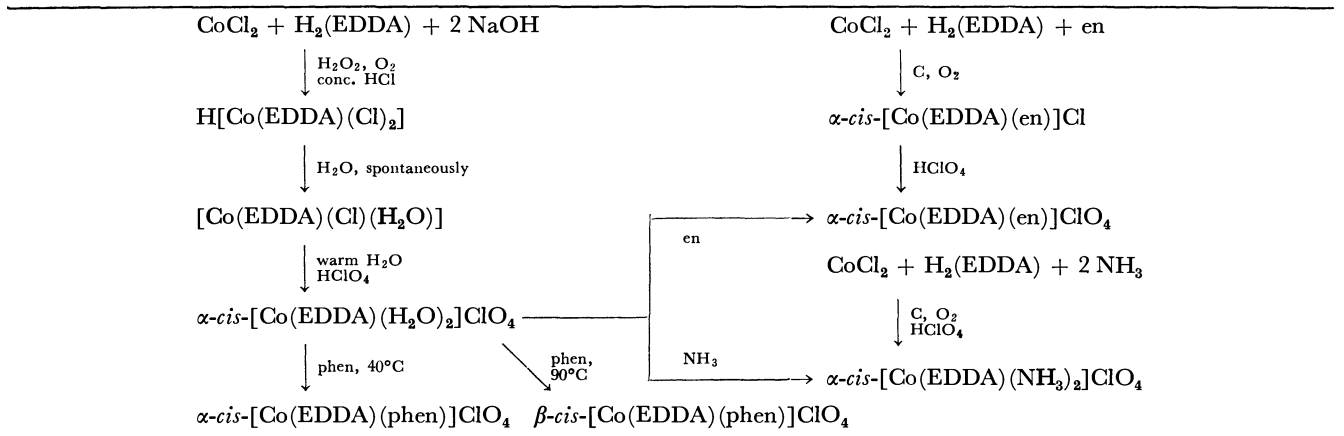

Table 2. Reactions of cationic EDDA-Co(III) complexes with various anionic reagents

	NaBr NaI	Na_2CO_3 $Na_2C_2O_4$	CH_3CO_2Na CCl_3CO_2Na	$NaNO_2$ Na_2SO_3	NaCN NaSCN	Na_2HPO_4	Solubility (m*l*-H_2O/g)
α-cis-[Co(EDDA)$(NH_3)_2$]ClO_4 (red-violet)	—	—	—	—	—	—	240
	ppt	—	ppt	—	—		
α-cis-[Co(EDDA)(en)]ClO_4 (red)	ppt	—	—	—	—	—	90
	—	—	ppt	—	—		
cold	—	violet	—	—	red-brown	violet	
	red	—	—	—	—		
α-cis-[Co(EDDA)$(H_2O)_2$]ClO_4 (pink-violet)	—	brown-violet	violet deeper	orange-red	brown-yellow	violet	very soluble
warm	brown-yellow	red-violet	violet deeper	red-brown	red-brown		

—: no observable reaction
ppt: a precipitate occurred
The name of color means the original color changed to the listed color.
No observable reaction occurred by 2 N NH_4Cl, 2 N $NaNO_3$, 2 N $(NH_4)_2SO_4$ with any of the complexes.

Table 3. Absorption maxima of the electronic spectra of Co(III)-EDDA complexes

	Ia		Ib		II	
	$\bar{\nu}$(kK)	(ε)	$\bar{\nu}$(kK)	(ε)	$\bar{\nu}$(kK)	(ε)
α-cis-[Co(EDDA)$(NH_3)_2$]ClO_4	18.59	(92.0)	~22	sh	27.55	(118.2)
α-cis-[Co(EDDA)(en)]ClO_4	18.84	(89.0)	~22	sh	27.70	(113.8)
H[Co(EDDA)$(Cl)_2$]	16.61	(176)	*		23.75	(133)
[Co(EDDA)(Cl)(H_2O)]	17.36	(144.5)			24.69	(97.3)
α-cis-[Co(EDDA)$(H_2O)_2$]ClO_4	18.21	(136.0)			25.71	(76.2)
α-[Co(EDDA)(phen)]ClO_4	18.52	(121.6)	*		~26	sh
β-[Co(EDDA)(phen)]ClO_4	*		20.00	(166.8)	~27	sh
α-[Co(EDDA)(dipy)]ClO_4	18.57	(129.4)	*		~26	sh
β-[Co(EDDA)(dipy)]ClO_4	*		20.04	(182.5)	~27	sh

* A deformation is observable in the region of the first band.

in Table 1. In this new preparative route for the series, the dichloro complex was synthesized first. All of the other species were derived from this complex, although the ethylenediamine and the diammine complexes were synthesized from cobalt(II) chloride and the ligands, too. The preparative procedure for the dichloro complex followed those of *trans*-[Co$(Cl)_2(en)_2$]Cl and the analogous dichloro complexes. It is satisfactorily simple and gives a good yield.

The solubility of [Co(EDDA)(Cl)(H_2O)], the first aquation product of the dichloro complex, is exceptionally small among the various Co(III)-EDDA complexes. It spontaneously comes out from the concentrated solution of the dichloro complex. It aquates in warm water, resulting in the diaquo complex without any decomposition. The diaquo complex reacts with various anions and neutral ligands almost instantaneously. Therefore, the chloroaquo complex is the most suitable starting substance for the syntheses of the series. This has been illustrated in the present study and will be discussed further in subsequent communications.

In the preparation of the phenanthroline and the dipyridyl complexes, the reaction temperature strongly affected the yield of the *α-cis* and the *β-cis* isomers. The *α-cis* isomer occurred at relatively low temperatures (~40°C), whereas the *β-cis* isomer was formed at higher temperatures (>55°C). Because the starting diaquo complex is the *α-cis* isomer and the *α-cis* configuration is probably more stable than the *β-cis* configuration, it is reasonable to consider that the occurrence of the *β-cis* isomer needs the heat of the rearrangement of the ligands and, hence, a higher temperature.

Reactions with Anionic Reagents. The solubility and the reactions with various anionic reagents were examined on several of the cationic complexes prepared. The results are summarized in Table 2. The color change in the diaquo complex with CN^-, NO_2^-, NCS^-, *etc.* are undoubtedly due to the substitution of the coordinated water by the anions. The isolation of these acido-complexes will be reported in subsequent communications.

It has been reported that trichloroacetic acid makes precipitates with *trans*-[CoN_4O_2]-type complexes, but not with their *cis*-isomers in general.[8] The diammine and the ethylenediamine complexes in this study, which have the *α-cis* configuration (the *trans* configuration with respect to O), as will be discussed below, make precipitates with trichloroacetate, as is indicated in Table 2; that is to say, the two complexes also have the common property observed previously in the other *trans*-[CoN_4O_2]-type complexes.

Electronic Absorption Spectra. Table 3 and Figs. 2—4 show the visible and ultraviolet absorption spectra

8) K. Kuroda and P. S. Gentile, *ibid.*, **38**, 1368 (1965).

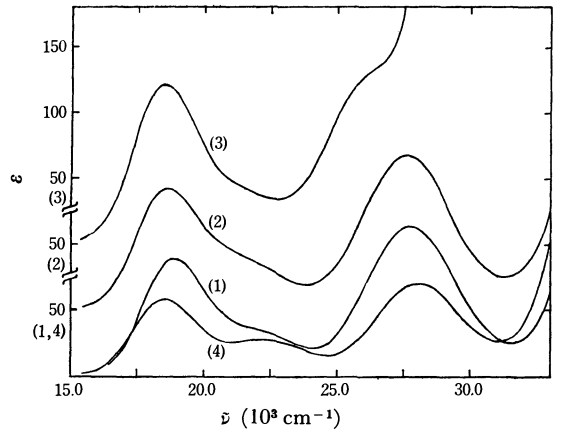

Fig. 2. Absorption spectra of some EDDA-Co(III) complexes, I.
(1) α-*cis*-[Co(EDDA)(en)]ClO_4
(2) α-*cis*-[Co(EDDA)$(NH_3)_2$]ClO_4
(3) α-*cis*-[Co(EDDA)(phen)]ClO_4
(4) *trans*-[Co$(CH_3CO_2)_2(en)_2$]ClO_4

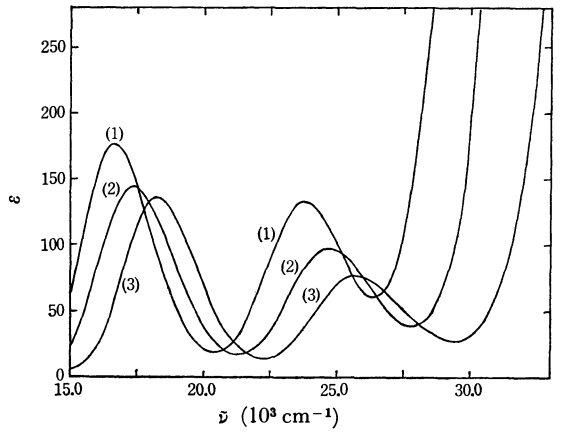

Fig. 3. Absorption spectra of some EDDA-Co(III) complexes, II.
(1) H[Co(EDDA)$(Cl)_2$]
(2) [Co(EDDA)(Cl)(H_2O)]
(3) [Co(EDDA)$(H_2O)_2$]ClO_4

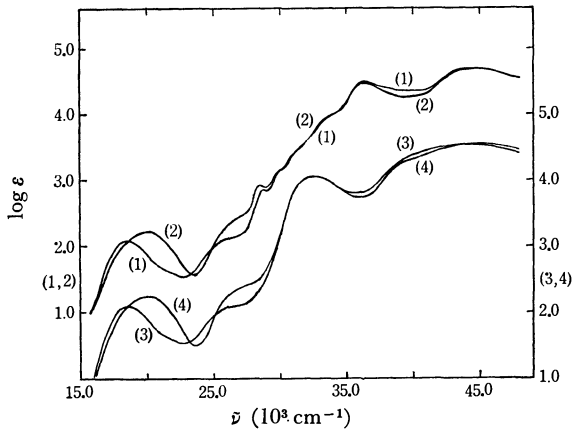

Fig. 4. Absorption spectra of some EDDA-Co(III) complexes, III.
(1) α-*cis*-[Co(EDDA)(phen)]ClO_4
(2) β-*cis*-[Co(EDDA)(phen)]ClO_4
(3) α-*cis*-[Co(EDDA)(dipy)]ClO_4
(4) β-*cis*-[Co(EDDA)(dipy)]ClO_4

of the complexes studied. Two samples of the diammine complex as well as of the ethylenediamine complex, which were obtained by the two different procedures, showed completely identical spectra; those spectra also agreed with those obtained by Legg and Cooke[2] within the limits of experimental error. The absorption curves have the characteristic feature of *trans*-isomers, namely, a large split in the first band, and are similar to those of *trans*-[Co$(CH_3CO_2)_2(NH_3)_4]^+$ and *trans*-[Co$(CH_3CO_2)_2(en)_2]^+$ previously studied.[8] The spectra show clearly that the complexes have the α-*cis* configuration.

The absorption maxima and their intensities of the dichloro, chloroaquo, and diaquo complexes are on the ordinary line of the spectrochemical and hyperchromic series:

$$\bar{\nu}_{Cl_2} < \bar{\nu}_{ClH_2O} < \bar{\nu}_{(H_2O)_2}$$

$$\varepsilon_{Cl_2} > \varepsilon_{ClH_2O} > \varepsilon_{(H_2O)_2}$$

The spectrum of the dichloro complex is worth examining in relation to its structure. Although the shape of the first band is nearly symmetrical, a small deformation (expansion) in the higher-wave-number region ($\sim 19\times10^3$ cm^{-1}) of the band is observable, as may be seen in Fig. 3. If the complex be the *trans*-isomer (III in Fig. 1), a large split in the first band would be expected as the spectrum of *trans*-[Co$(Cl)_2(en)_2]^+$, because of the *trans*-coordination of the two chlorine atoms. Therefore, the possibility of the III mode may be eliminated. If the complex be the β-*cis* isomer (II), two atoms of the same kinds (Cl–Cl, N–N, O–O) are at the *cis*-positions. In this configuration, a very intense absorption would be expected, since the ligand field around the central atom is highly unsymmetrical. The α-*cis* configuration (I), though the evidence from the spectrum alone is not conclusive, is the most reasonable assignment for the dichloro complex, and the small deformation mentioned above may be attributed to the *trans(O)*-component of the coordination mode.

Since ethylenediamine, 1,10-phenanthroline, and 2,2′-dipyridyl are near to each other in the spectrochemical series, the spectra of the α-*cis* isomer of the phenanthroline and the dipyridyl complexes are expected to resemble that of α-*cis*-[Co(EDDA)(en)]$^+$, at least in the *d-d* transition region. As may be seen in Figs. 2 and 4, one of the two isomers of the phenanthroline and dipyridyl complexes shows an analogous absorption curve between 15×10^3 and 25×10^3 cm^{-1} to that of the ethylenediamine complex, although the Ib absorption is less pronounced. Therefore, the pink isomers have undoubtedly the α-*cis* configuration. It has been observed that the first band of a *cis*-[CoN_4O_2]-type complex has a slight deformation in the lower-wave-number region of the band and has a higher absorption intensity than the corresponding *trans*-isomer.[9] The red isomers of both the phenanthroline and the dipyridyl complexes showed these characteristics. The facts indicate that the red isomers have the β-*cis* configuration. In the ultraviolet region of

9) K. Kuroda and P. S. Gentile, *J. Inorg. Nucl. Chem.*, **27**, 155 (1965).

the spectra of these complexes, there are several maxima and shoulders, as may be seen in Fig. 4. These absorptions are sure to be originated from the conjugate π-bond systems of the bidentate ligands. The complete similarity of the curves between the two geometrical isomers means that the ligand specific bands are little influenced by the structure as a whole and that, furthermore, the two substances are certainly a pair of different configurational isomers.

Infrared Spectra. The infrared spectra were supplementally used in this study for the estimation of the structure of the complexes prepared. The anhydrous dichloro complex showed only one strong absorption (3165 cm^{-1}) in the NH, OH stretching region, whereas three peaks (3625, 3495, 3170 cm^{-1}) were observed in the chloroaquo complex (monohydrate) and two peaks (3470, 3300 cm^{-1}) in the diaquo complex (anhydrous). Two absorptions, that at 3170 cm^{-1} of the chloroaquo and that at 3300 cm^{-1} of the diaquo complex, may be assigned to the NH-stretching mode. It may be considered that the other two peaks of the former come from the lattice and the coordinated water, and that one peak of the latter originates from the equivalent H_2O ligands of the *α-cis* configuration.

In the complexes which contain ligands with a carboxyl group, another noteworthy region in the infrared spectra is around 1650 cm^{-1}, the CO-stretching region. Each of the complexes studied showed a broad strong absorption in this region, which is considered to be due to the CO-stretching overlapped by the NH_2 and OH_2 deformation modes. The lack of absorption between 1700--1800 cm^{-1} indicates that the two carboxyl groups of EDDA certainly coordinate to the central cobalt and are not present as the free-acid type.[10]

Proton Nuclear Magnetic Resonance Spectra. Van Saun and Douglas measured the PMR spectra of the M[Co(EDDA)(AA)] they had prepared, where AA= ox, mal; they observed only one AB quartet pattern due to the glycinate ring protons of EDDA.[4] Because CO_3, of the equivalency of the two glycinate rings in the *α-cis* configuration, they concluded that their complexes were *α-cis* isomers. Recently, Coleman, Legg, and Steele prepared the *β-cis* isomers of $[Co(EDDA)(ox)]^-$ and $[Co(EDDA)(mal)]^-$ and analysed the PMR spectra of the isomers as well as the *α-cis* isomers.[6] As expected from the configuration of the *β-cis* isomers, the spectra were much more complicated than those of the *α-cis* isomers.

The PMR spectrum of $[Co(EDDA)(H_2O)_2]ClO_4$ is shown in Fig. 5. It can be seen that one AB quartet pattern due to the glycinate protons and a symmetrical

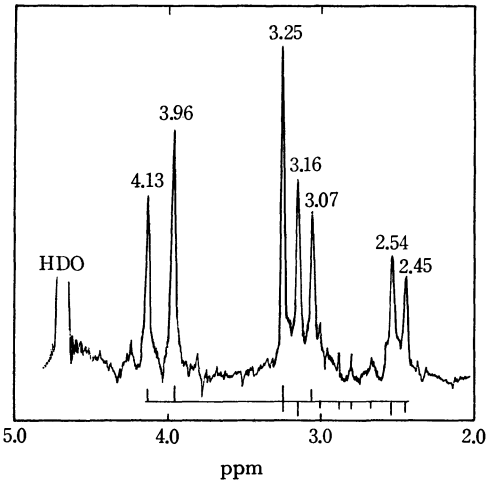

Fig. 5. PMR spectrum of D_2O solution of $[Co(EDDA)(H_2O)_2]ClO_4$.

A_2B_2 pattern due to the ethylene backbone protons are present, although not all the resonances of the latter protons theoretically expected (12 resonances) can be clearly observed. The chemical shifts of the glycinate protons (H_A and H_B in Fig. 1b) are 4.04 and 3.17 respectively, and the coupling constant, J_{AB}, is 18 Hz. These values are in agreement with those which have been obtained previously with the analogous complexes.[2-6] These results indicate that the diaquo complex is the *α-cis* isomer.

The spectra of the other complexes are a little more difficult to measure or to analyse because of the low solubility (chloroaquo complex), the rapid aquation (dichloro complex), or the presence of many kinds of protons in a complex ion (phenanthroline and dipyridyl complexes). The research is still in progress.

Conclusion

Seven new complexes, $H[Co(EDDA)(Cl)_2]$, $[Co(EDDA)(Cl)(H_2O)]\cdot H_2O$, *α-cis*-$[Co(EDDA)(H_2O)_2]ClO_4$, *α-cis*- and *β-cis*-$[Co(EDDA)(phen)]ClO_4$, *α-cis*- and *β-cis*-$[Co(EDDA)(dipy)]ClO_4\cdot H_2O$, as well as two known complexes, *α-cis*-$[Co(EDDA)(NH_3)_2]ClO_4\cdot H_2O$ and *α-cis*-$[Co(EDDA)(en)]ClO_4$, have been prepared by new, simple preparation procedures. The *α-cis* and *β-cis* isomers of the phenanthroline and the dipyridyl complexes have been identified by means of their electronic absorption spectra. The *α-cis* configuration of the diaquo complex has been confirmed by a study of the PMR spectrum. The dichloro and the chloroaquo complexes are supposed to be *α-cis* isomers from the electronic absorption spectra, although this is not completely certain.

10) D. H. Busch and J. C. Bailar, *J. Amer. Chem. Soc.*, **75**, 4574 (1953).

The Indirect Determination of Microamounts of Mercury(II) by Means of Dithizone Extraction and AC Polarography

Tomihito KAMBARA and Minoru HARA

Department of Chemistry, Faculty of Science, Hokkaido University, Sapporo

(Received October 12, 1970)

It was found that dithizone in an aqueous alkaline solution shows sharp AC polarographic peaks; the indirect determination of mercury by means of these peaks was investigated. After the extraction of mercury(II) dithizonate into benzene, the excess dithizone was eliminated. Then the mercuric ion was stripped into the aqueous phase containing the iodide ion. The isolated dithizone in the benzene layer was back-extracted into the alkaline supporting electrolyte solution and the polarogram was recorded. By the present method, up to 30 μg of mercury can be determined.

Dithizone(H_2Dz) is a very sensitive reagent which has been used for the colorimetric determination of many metals. Separation by means of solvent extraction is very easy, useful, and selective. In polarographic determinations of copper, zinc,[1] lead,[2] and cadmium,[3] the metals are extracted as dithizonates into an organic layer, the solvent is evaporated, and the residue is redissolved in water, or the dithizonates are back-extracted from the organic phase into a suitable aqueous solution. Recently Yamashita[4] has reported the interesting polarographic behavior of dithizone and metal dithizonates in a ternary solvent mixture consisting of chloroform, water, and methylcellosolve.

The present authors have now found that dithizone in an aqueous alkaline solution gives sharp peaks in AC polarography, and have investigated the application of these dithizone peaks to the microdetermination of mercury. In the present method, the microamount of mercury is extracted into benzene, and then the excess dithizone in organic layer is back-extracted into an aqueous ammonia solution. Then, dithizone is stripped from the mercury dithizonate by shaking it with an aqueous potassium iodide solution. The dithizone remains in benzene, but the mercury goes into the aqueous phase as an iodo-complex. The electrolysis solution was prepared by shaking the supporting electrolyte solution, consisting of sodium sulfate and sodium hydroxide, with the remaining organic layer, containing the isolated dithizone. The mercury is determined indirectly from the height of the dithizone peak. The fundamental conditions for this method are discussed below.

Experimental

Reagents. 30 mg of dithizone (Wako Chemicals Co., guaranteed reagent) were dissolved in benzene and purified as usual; then the volume was made up to 200 m*l* with benzene. This stock solution was diluted, and the concentration of the dithizone was estimated by the absorbance and the molar absorptivity at 620 mμ.[5]

The standard stock solution of mercury(II) was prepared by dissolving 0.1354 g of mercuric chloride in 100 m*l* of 1 N sulfuric acid and was then diluted when used.

The stripping solution was prepared by dissolving 10 g of potassium hydrogen phthalate and 25 g of potassium iodide in 500 m*l* of distilled water, a few crystals of sodium thiosulfate being added to reduce any trace of the iodine liberated. The solution was then further purified by shaking it with a dithizone-benzene solution in order to remove any heavy metal.

The supporting electrolyte solution was prepared by mixing 250 m*l* of 0.4 M sodium sulfate and an appropriate volume of 1 N sodium hydroxide, and by then making the volume up to 500 m*l* with distilled water.

The other chemicals used were all guaranteed reagents.

Apparatus. AC polarographic measurements were performed by using a Yanagimoto polarograph, type PA-102. The dropping mercury electrode with the following characteristics was used: $m=0.526$ mg/sec, $t=5.57$ sec at $h=65.0$ cm, at an open circuit in the deaerated supporting electrolyte solution.

The absorbances and absorption spectra were measured with a Shimadzu spectrophotometer, type QV-5, by the aid of a 1-cm glass cell. The pH of the solutions was measured with a Hitachi-Horiba glass electrode pH meter, type F-5.

Established Procedure. Take the sample solution up to 50 m*l* containing mercury up to 30 μg that is made about 0.5 N in sulfuric acid. If necessary, add masking reagents. Add 10 m*l* of 1×10^{-4} M dithizone-benzene solution and shake for 1 min. Transfer the organic layer to another separating funnel. Add 10 m*l* of 0.15 N ammonium hydroxide, shake for 15 sec, and discard the aqueous solution. Repeat this operation once again. The excess dithizone is thus removed. Add 10 m*l* of the above-cited stripping solution into a separating funnel, in which the benzene layer containing only mercury dithizonate should remain, and shake for 1 min. Then mercury(II) is transfered into the aqueous solution. Allow the mixture to stand for a while, transfer 5 m*l* of the benzene layer containing the isolated dithizone to another separating funnel containing 5 m*l* of the supporting electrolyte solution (pH=12.5), and shake for 10 sec. Transfer the aqueous solution into a polarographic cell. Record an AC polarogram at 25±0.1°C, after deaeration by passing nitrogen gas through for 5 min.

Results and Discussion

AC Polarogram of Dithizone. Figure 1 shows the AC polarogram of dithizone in a 0.2 M sodium sulfate alkaline solution. Two prominent peaks are observed in the AC polarogram, but the corresponding DC

1) G. B. Jones, *Anal. Chim. Acta*, **7**, 578 (1952).
2) J. Cholak and K. Bambach, *Ind. Eng. Chem., Anal. Ed.*, **13**, 583 (1941).
3) J. Cholak and D. M. Hubbard, *ibid.*, **16**, 333 (1944).
4) K. Yamashita, *Rev. Polarog.* (Japan), **15**, 65 (1968).
5) G. Iwantscheff, "Das Dithizon und seine Anwendung in der Mikro- und Spurenanalyse," Verlag Chemie, Weinheim (1958), p. 17.

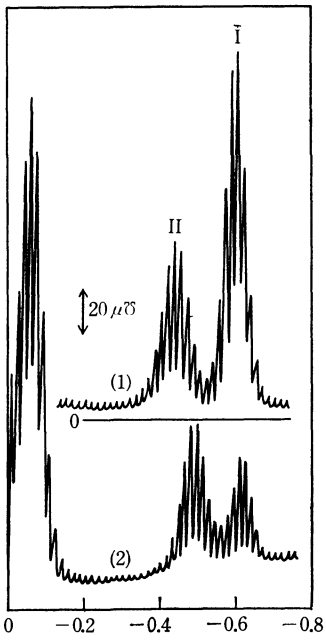

Fig. 1. (1) AC polarogram of 2.0×10^{-5} M dithizonate ion(HDz^-) in a deaerated solution of 0.2 M Na_2SO_4, *ca.* 0.01 M NaOH (pH=12.56) at 25°C.
(2) AC polarogram of 2.0×10^{-5} M dithizonate ion in an air-saturated supporting electrolyte solution.

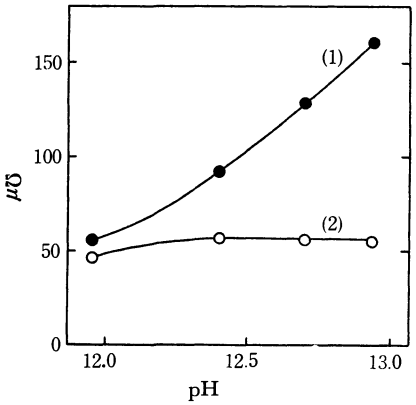

Fig. 2. Effect of pH of the electrolysis solution on the AC peak heights of dithizonate ion.
HDz^-: 1.65×10^{-5} M, 0.2 M Na_2SO_4 (NaOH added), 25°C.
(1) peak I. (2) peak II.

steps are very ill-defined. Without deaeration, the heights of the two peaks tend to decrease; peak I, appearing at the more negative potential, decreases especially rapidly.

The effect of the pH of the supporting electrolyte solution on the heights of the two peaks is shown in Fig. 2. The height of the peak I increases linearly with the increasing pH, but that of peak II remains constant in the pH region between 12.4 and 12.9.

Figure 3 shows the temperature dependance of the AC peaks. Although the height of peak I increases with the temperature, that of peak II shows an almost constant value. Under the above conditions, the peak I is always higher than peak II. This indicates that the determination of dithizonate using peak I is more sensitive; however, the height of peak I is remarkably

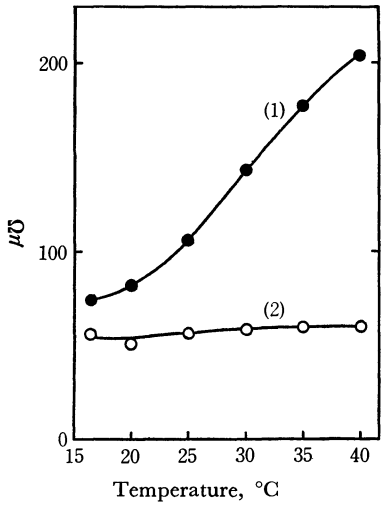

Fig. 3. Effect of temperature on the AC peak heights of dithizonate ion.
HDz^-: 2.22×10^{-5} M, 0.2 M Na_2SO_4 (NaOH added).
pH=12.47 at 19°C.
(1) peak I. (2) peak II.

influenced not only by the pH but also by the temperature. Hence, a little deviation in pH and temperature would cause a significant analytical error. In order to avoid these errors, the present authors employed peak II for the determination of dithizone. The temperature was fixed at 25±0.1°C, and the pH was adjusted to about 12.5. Under the above conditions, the AC peak height shows a linear relationship up to a dithizone concentration of 3×10^{-5} M. In the concentration range higher than the above value, the polarogram becomes ill-defined.

Extraction of Mercury and Elimination of Excess Dithizone. It was first confirmed that 20 μg of mercury(II) in 10 m*l* of 0.5 N in sulfuric acid can be extracted quantitatively by shaking it for only 30 sec with a 4.4×10^{-5} M dithizone-benzene solution.

Now, the method of eliminating the excess dithizone from organic solution will be investigated. When the organic solution is shaken with 10 m*l* of 0.15 N ammonium hydroxide, the free dithizone in the organic solution is back-extracted. In order to eliminate the free dithizone completely, this operation is done once again. 10 m*l* of a 1×10^{-4} M dithizone-benzene solution was found to show no absorbance at 620 mμ after these operations. Milton and Hoskins[6] investigated the mono-color determination method of mercury(II) dithizonate, in which the excess dithizone is removed by shaking with dilute ammonia. According to them, shaking with 0.75 N ammonium hydroxide converts the primary dithizonate, $Hg(HDz)_2$, into the secondary dithizonate, HgDz. When 0.75 N ammonium hydroxide is used in the present study, the longer the shaking time, the greater the decrease in the absorbance at the wavelength of the maximum absorption of mercury (II) dithizonate, $Hg(HDz)_2$. However, the evidence for the formation of the secondary complex has not been found, the shape of the absorption spectrum showing no change. When 0.15 N ammonium hydro-

6) R. F. Milton and J. L. Hoskins, *Analyst*, **72**, 6 (1947).

xide is used, neither a change in the absorption spectrum nor a decrease in the absorbance was recognized. It was found that 10 m*l* of a 1×10^{-4} M dithizone-benzene solution can extract 20 μg of mercury quantitatively from 60 m*l* of an aqueous solution.

Stripping of Mercury. In order to isolate the dithizone from the mercury dithizonate, the reversion method proposed by Irving *et al.*[7] was used. That is, the mercuric ion was back-extracted into the acidified iodide solution, presumably as triiodo-mercurate(II).

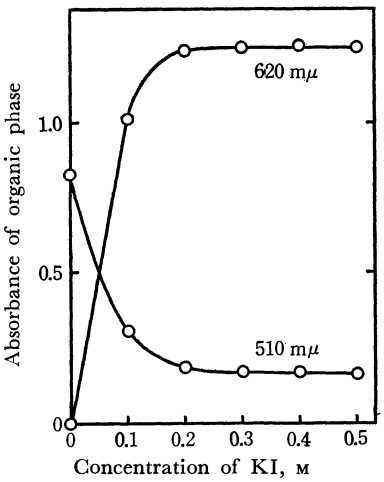

Fig. 4. Effect of the concentration of potassium iodide on the back-extraction of mercury.
$Hg(HDz)_2$ in org. soln.: 1.61×10^{-5} M
pH=3.67 (0.1 M phthalate buffer)
Shaking time: 2 min
$V_{org.} = V_{aq.} = 10$ m*l*

Figure 4 shows the effect of the iodide concentration on the stripping of mercury. 10 m*l* of the organic layer is shaken for 2 min with an equal volume of an iodide solution. The maximum absorbance of dithizone in benzene at 620 mμ shows a constant value when the concentration of potassium iodide is higher than 0.3 M. Also, at 510 mμ, at which dithizone has its minimum absorptivity but mercuric dithizonate shows a high extinction, shaking with a potassium iodide solution higher than 0.3 M results in a constant absorbance. The absorption spectra of these organic layers being the same as that of dithizone in a benzene solution, the existence of the mercury dithizonate in the organic layer may be disregarded.

Thus, it is confirmed that the 0.3 M potassium iodide solution can back-extract mercury quantitatively from an equal volume of a benzene solution of mercury dithizonate. The shaking time of 30 sec is found to be sufficient for the back-extraction under the above conditions. Further, it is found that the ratio of the concentration of the isolated dithizone to that of the mercury taken is two. Hence, the extraction and back-extraction of mercury can be carried out quantitatively. Furthermore, the mercury dithizonate, $Hg(HDz)_2$, is not converted into the secondary complex, HgDz.

Aqueous Solution of Dithizone. The step in which the isolated dithizone is transferred into the supporting electrolyte solution is investigated. A 0.2 M sodium sulfate solution, the pH of which is adjusted with a sodium hydroxide solution, is used as the supporting electrolyte solution. When the pH of the supporting electrolyte solution is higher than 11.5, the dithizone in the benzene layer is back-extracted into the aqueous solution as the dithizonate ion. Irving *et al.*[8] reported the decomposition of dithizone in an aqueous alkaline solution. They stated that dithizone in 1.5 N ammonium hydroxide decomposes at a rate of 20—30%/hr, but in 0.15 N ammonium hydroxide the velocity becomes very slow.

In the present experiment, the dithizonate ion is stable for one hour, at least in 0.2 M sodium sulfate solution, the pH of which is adjusted to 12.52 with sodium hydroxide.

Thus, in this procedure the decomposition of the dithizonate ion can be neglected. It should be further mentioned that the electrolysis solution should be completely free from the iodide ion. Because the iodide ion shows a broad peak as the result of an anodic process, the peak of dithizone is very much disturbed. When a 5-m*l* portion of the isolated dithizone solution is pippeted out to another separating funnel, contamination by the iodide ion is avoided.

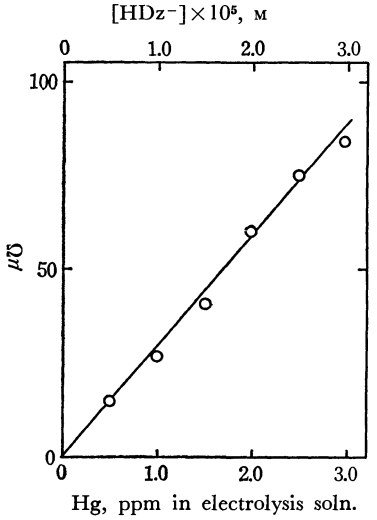

Fig. 5. Calibration curve.

Calibration Curve. The calibration curve obtained according to the above procedure is shown in Fig. 5. Up to 30 μg of mercury the peak height is proportional to the amount of mercury taken. When the determination of 20 μg of mercury was repeated seven times, the relative standard deviation was 4.2%.

For comparison, the same amount of mercury was determined by dithizone spectrophotometric methods. The relative standard deviation of six measurements was 4.6% in the mixed color method and 3.1% in the mono-color method. In the method of the measuring the absorbance of the free dithizone in benzene which is liberated from the mercury(II) dithizonate by stripping mercury(II) with the iodide ion, the relative standard deviation was 2.1%.

7) H. Irving, G. Andrew, and E. J. Risdon, *J. Chem. Soc.*, **1949**, 541.

8) H. Irving, S. J. H. Cooke, S. C. Woodger, and R. J. P. Williams, *ibid.*, **1949**, 1847.

Table 1. Effect of diverse ions
Mercury(II) taken: 20 μg in 20 m*l*

Interfering ion added	Method of masking	Peak height $\mu\mho$	Peak height, $\mu\mho$, in 95% confidence limits	F_0	t_0
None		58, 62 61, 58 60, 65 63	61.0±2.3		
Ag(I) 2.2 mg	(1)	66 60 67	64.3±9.1	2.22	1.63
Cu(II) 1.3 mg	(2)	63 62 62	62.3±1.3	18.03	0.833

$F(2, 6, 0.025)=7.26 > F_0=2.22$
$F(6, 2, 0.025)=39.3 > F_0=18.03$
$t(8, 0.025)=2.306 > t_0$
(1) Add 200 mg of NaCl, discard the aqueous layer, shake with 10 m*l* of 1% NaCl in 0.5 N H_2SO_4.
(2) Add 200 mg of EDTA-2Na salt.

Effect of Diverse Ions. The mercury(II) sample solution is 0.5 N in sulfuric acid, so it is supposed that gold(III), palladium(II), platinum(II), silver(I), and copper(II) are extracted together and that they interfere with the determination of mercury. It is known, however, that these ions are masked with the chloride ion and EDTA.[9] In this work the interferences by silver and copper have been investigated.

The extraction of 20 μg of mercury was investigated; the results are shown in Table 1. When 2.2 mg of silver(I) coexists in 20 m*l* of the sample solution, it is not masked completely by adding 200 mg of sodium chloride. However, as may be seen in Table 1, the silver(I) ion does not interfere if the benzene extract is shaken once again with 10 m*l* of a 1% sodium chloride solution in 0.5 N sulfuric acid; further, 1.3 mg of copper(II) is masked completely with EDTA. According to the familiar *t*-test, no significant difference is found between the means of the peak heights at the 95% significant level.

9) E. B. Sandell, "Colorimetric Determination of Traces of Metals," Interscience Publishers, New York (1959), p. 627.

BULLETIN OF THE CHEMICAL SOCIETY OF JAPAN, VOL. 44, 1043—1047 (1971)

The Effect of Solvents on the Adduct Formation of Uranyl Thenoyltrifluoroacetonate with Tributyl Phosphate

Kenichi Akiba and Nobuo Suzuki*

Research Institute of Mineral Dressing and Metallurgy, Tohoku University, Sendai

(Received October 28, 1970)

Addition compound formation between uranyl bis-thenoyltrifluoroacetonate (UO_2A_2) and tributyl phosphate(S) was studied by a partition method, using uranium-237 as the tracer. The formula of the adduct complex was shown to be $UO_2A_2 \cdot S$. The solvent effect on the adduct formation constant was taken into account in connection with the activity; the activity coefficients of each species in various solutions were calculated from the molar volume and the solubility parameter. The formation constants based on the molar fraction, K_x, in a number of solvents were pre-estimated, employing $\log K_x = 7.08$ in carbon tetrachloride as a reference. They are in agreement with the observed values. The formation constant in terms of activity was found to be constant $\log K_S^\circ = 5.77 \pm 0.30$. A correlation between the formation constants of the two adducts, $UO_2A_2 \cdot S$ and $ZnA_2 \cdot S$, was demonstrated.

An addition of one or more basic molecules to a formally neutral chelate with unsaturated coordination sites has been found in many organic solutions. Most of the synergistic effects in extraction are ascribed to the formation of addition compounds, though various explanations of these effects have been postulated.[1] The adduct formations of uranyl complexes with neutral ligands have received much attention; several authors have investigated the effects of β-diketones (*e.g.*, TTA) and/or organophosphorous esters (*e.g.*, TBP).[2-4] However, there have been only a few systematic studies of the solvent properties governing the equilibrium constants in synergistic extraction processes.

In previous papers, the solvent effect on distribution coefficients was elucidated in typical extraction systems.[5-7] Further, the adduct formation constants of the zinc-TTA chelate with TBP in a variety of organic solvents were correlated with the activity coefficients of the substances involved in the reaction.[7]

* Present address: Department of Chemistry, Faculty of Science, Tohoku University, Sendai.

1) Y. Marcus and A. S. Kertes, "Ion Exchange and Solvent Extraction of Metal Complexes," Wiley-Interscience, London (1969), p. 815.

2) K. Batzar, D. E. Goldberg, and L. Newman, *J. Inorg. Nucl. Chem.*, **29**, 1511 (1967).

3) T. V. Healy, *ibid.*, **19**, 314 (1961).

4) H. Irving and D. N. Edgington, *ibid.*, **15**, 158 (1960).

5) K. Akiba, N. Suzuki, H. Asano, and T. Kanno, *Radioanal. Chem.*, in press, "Regularities of Extraction of Uranyl Thenoyltrifluoroacetonate into a Number of Solvents."

6) N. Suzuki and K. Akiba, *J. Inorg. Nucl. Chem.*, in press, "Distribution Regularity of the Divalent Metal Chelate into Various Organic Solvents-Distribution of Beryllium Thenoyltrifluoroacetonate."

7) K. Akiba, N. Suzuki, and T. Kanno, This Bulletin, **42**, 2537 (1969).

The present study has been undertaken in order to clarify the regularities in the formation of an adduct complex between a coordinatively unsatulated chelate, uranyl bis-thenoyltrifluoroacetonate, and tributyl phosphate. The formation constants are pre-estimated from the calculated activity coefficients and are compared with those observed. The relation between the formation constants of uranyl -and zinc-TTA adducts with TBP is also investigated.

Experimental

Materials. A radioisotope of uranium-237 was produced by irradiating natural uranium with a 60 MeV bremsstrahlung from a linear electron accelerator in the Laboratory of Nuclear Sciences, Tohoku University. The irradiated sample was then treated as before.[5]

Thenoyltrifluoroacetone (TTA) was purified by sublimation under reduced pressure, while tributyl phosphate (TBP) was purified as before.[7]

The organic solvents used were purified in the usual manner.

Procedure. An aqueous $(H,Na)ClO_4$ solution (ionic strength=0.10) including ^{237}U was shaken for 20 hr with an equal volume of a desired organic solution containing TTA and TBP. The phases were separated by centrifugation, and aliquots of both phases were taken for the measurement of the γ-radioactivity. All the experiments were performed in a room thermostated at 25±1°C.

Results and Discussion

The adduct formation of the neutral chelate in the organic solution is expressed by:

$$UO_2A_2 + m\,S \rightleftarrows UO_2A_2 \cdot m\,S \qquad (1)$$

$$K_S = \frac{[UO_2A_2 \cdot m\,S]}{[UO_2A_2][S]^m} \qquad (2)$$

where UO_2A_2 represents the uranyl-TTA chelate; S, tributyl phosphate, and K_S, the molar formation constant of the adduct.

In the extraction of the uranyl complex with a TTA solution containing TBP from an aqueous medium, the distribution ratio of uranium ($D_{M,S}$) is given by:

$$D_{M,S} = \frac{P_M\beta_2[A^-]_{aq}^2\{1+\sum K_S[S]^m\}}{1+\sum\beta_n[A^-]_{aq}^n} \qquad (3)$$

where $P_M=[UO_2A_2]_{org}/[UO_2A_2]_{aq}$ and $\beta_n=[UO_2A_n^{(2-n)+}]/[UO^{2+}][A^-]_{aq}^n$. At a fixed aqueous concentration of the TTA anion, the next equation is given:

$$\frac{D_{M,S}}{D_M} = 1 + \sum K_S[S]^m \qquad (4)$$

where D_M is the distribution ratio in the absence of TBP. When only one adduct is predominant, Eq. (4) may be simplified to:

$$K_S = \frac{D_{M,S}}{D_M}\frac{1}{[S]^m} \qquad (5)$$

The formation constant can be obtained by a curve fitting method[8] according to Eq. (4) or by Eq. (5).

Distribution of Uranyl Complexes. The distribution ratios in the presence of TBP are independent of the uranyl concentration in the experimental range of 10^{-7} to 10^{-4} M, as Fig. 1 shows, even for paraffinic solvents such as *n*-hexane where the influence of the uranyl concentration has been found in the absence of TBP, as has been described previously.[5] It seems likely that the addition of organophilic TBP very greatly increases the solubility of the uranyl complex in these solvents and eliminates the change in the activity coefficients with an increase in the concentration.

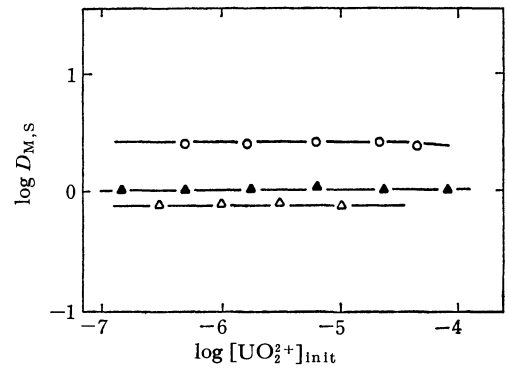

Fig. 1. Distribution ratios of uranyl complexes as a function of uranyl concentration.
[HA]=10^{-2} M; [S]=3.66×10^{-3} M; ○, *n*-hexane (pH=1.76); ▲, carbon tetrachloride (pH=1.76); △, benzene pH=1.80)

The uranyl concentration was kept at 10^{-5} M in subsequent experiments.

The plots of log $D_{M,S}$ against pA at a fixed concentration of TBP gave a series of straight lines, with a slope of −2, which run parallel with the broken line for benzene at no TBP, as Fig. 2 shows; the addition

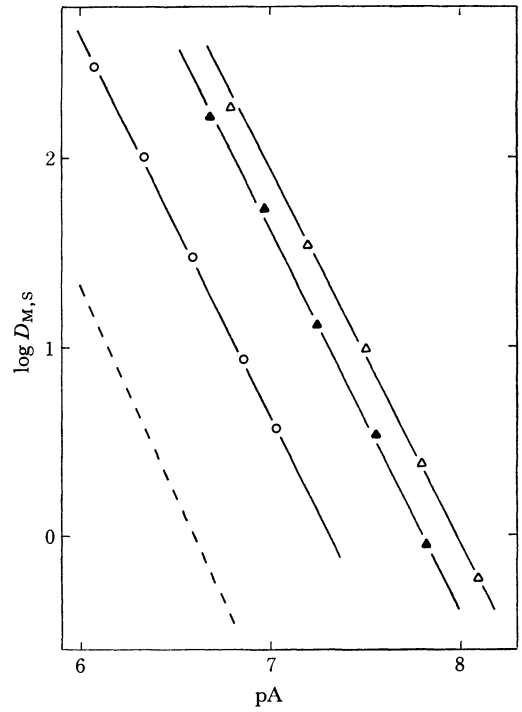

Fig. 2. Distribution ratios of uranyl complexes in the presence of TBP.
[HA]=10^{-2} M; [S]=3.66×10^{-3} M; ○, *n*-hexane ▲, carbon tetrachloride; △, benzene; broken line: benzene at no TBP.

8) T. Sekine and M. Ono, This Bulletin, **38**, 2087 (1965).

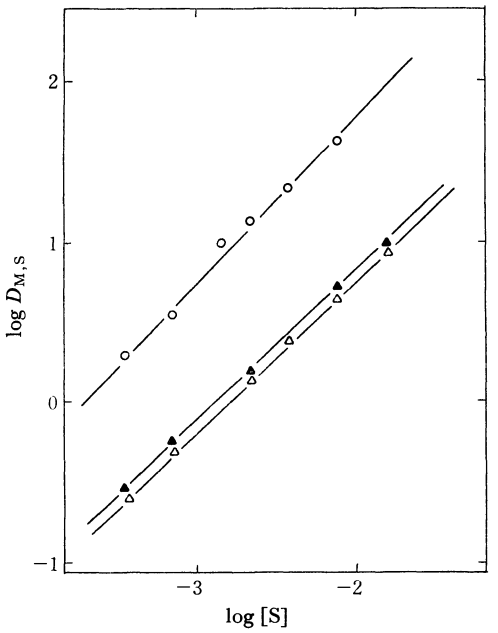

Fig. 3. Distribution ratios of uranyl complexes as a function of TBP concentration.
[HA]=10^{-2} M; ○, *n*-hexane (pH=2.24); ▲, carbon tetrachloride (pH=1.96); △, benzene (pH=2.03)

of TBP much enhances the distribution ratios, but the uranyl complexes still retain the two molecules of TTA which are bonded with each uranyl ion. It seems that the formally neutral chelate transfers to the organic phase from the aqueous phase and associates with TBP to form a coordinatively saturated adduct, or that, preferably, the water molecules in the complex are replaced by hydrophobic-donor molecules of TBP.

The variation in $\log D_{M,S}$ with $\log [S]$ were represented by a family of straight lines with a slope of 1, as Fig. 3 shows; this indicates that only one molecule of TBP is associated with the chelate and that there is no higher adduct, $UO_2A_2 \cdot mS$ ($m>1$), under the experimental conditions here adopted. The extraction of the uranyl complex with TBP alone, free from any chelating agent, is negligibly small at these low concentrations of TBP and acid. Accordingly, only one adduct, $UO_2A_2 \cdot S$, is taken up in this study.

Estimation of Adduct Formation Constants. An equilibrium constant will be strongly influenced by the nature of the medium, though the stoichiometry of the adduct remains unaltered. For a comparison of reactions in different media, the formation constant should be considered in connection with the activity, because the activity coefficient of the solute is very sensitive to the properties of the medium and the concentration is not always directly proportional to the activity. In a previous paper, an approach to the problem of the role of solvents in the adduct formation of the zinc-TTA chelate with TBP was made from this point of view; the regularity of equilibrium constants in various organic solutions was fairly well established.[7] Such a treatment seems to be valid for the uranyl adduct in this work.

The formation constant expressed in activities is:

$$K_S^\circ = \frac{a_{M \cdot S}}{a_M \cdot a_S} \tag{6}$$

where a is the activity, and where the two subscripts, M and M·S, denote the molecules of the chelate and its adduct respectively. When the activity of a pure supercooled-liquid is chosen as the standard state, K_S° can be considered to be constant, regardless of the solvents; the effect of the solvent may be connected with the change in the activity coefficient with the solvent properties. In using the expression based on the molar fraction for thermodynamic convenience, K_S° is represented by:

$$K_S^\circ = \frac{x_{M \cdot S}}{x_M \cdot x_S} \cdot \frac{\gamma_{M \cdot S}}{\gamma_M \cdot \gamma_S} \tag{7}$$

where x is the molar fraction, and γ, the activity coefficient. Eq. (7) is then rewritten as follows:

$$\log K_x = \log K_S^\circ - \log F_\gamma \tag{8}$$

where $K_x = x_{M \cdot S}/x_M \cdot x_S$ and $F_\gamma = \gamma_{M \cdot S}/\gamma_M \cdot \gamma_S$. Therefore, when the quantity related to the activity coefficients is given in the desired solvents, the constant, K_S°, can be derived from the K_x value obtained experimentally in a certain solvent; the K_x values in others can be pre-estimated from the values of K_S° and F_γ.

The activities of TBP have been measured in many solutions,[9,10] but those of the uranyl chelate and the adduct have never been given. It is not always easy to measure the activity, but the activity may be practically evaluated by the aid of the following equation for a regular solution consisting of two components, A and B:[11]

$$RT \ln a_A = RT\left[\ln \varphi_A + \varphi_B\left(1 - \frac{V_A}{V_B}\right)\right] + V_A \varphi_B^2 (\delta_A - \delta_B)^2 \tag{9}$$

where φ is the volume fraction; V, the molar volume, and δ, the solubility parameter. Taking into account the dilute solution of the solute A in the solvent B, the activity coefficient based on molar fraction can be written as:

$$RT \ln \gamma_A = RT\left[\ln \frac{V_A}{V_B} + \left(1 - \frac{V_A}{V_B}\right)\right] + V_A (\delta_A - \delta_B)^2 \tag{10}$$

Accordingly, the activity coefficient can be calculated from the physicochemical properties of a pure liquid, *i.e.*, the molar volumes and the solubility parameters of the solute and of the solvent.

As to the chelate, it is reasonable to postulate that $\delta_M \fallingdotseq \delta_{HA} = 9.9$ (HA denotes the TTA molecule) and $V_M \fallingdotseq 2V_{HA} = 320$ m*l* as has been described previously.[5] We have no sufficient data to evaluate the V and δ of the uranyl adduct. The solubility parameter of $UO_2A_2 \cdot S$ is probably close to that of $ZnA_2 \cdot S$, because the molecular forms of the adducts appear to be similar to each other. The $\gamma_{M \cdot S}$ values were calculated on the assumption that $\delta_{UO_2A_2 \cdot S} \fallingdotseq \delta_{ZnA_2 \cdot S} = 9.4$ and that $V_{M \cdot S} = V_M + V_S = 593$ m*l*.[7] The γ_S values were ob-

9) K. Alcock, S. S. Grimley, T. V. Healy, J. Kennedy, and H. A. C. McKay, *Trans. Faraday Soc.*, **52**, 39 (1956).
10) S. Siekierski, *J. Inorg. Nucl. Chem.*, **24**, 205 (1962).
11) J. H. Hildebrand R. L. Scott, "Solubility of Nonelectrolytes," 3rd Ed., Dover, New York (1964), p. 119.

Table 1. Adduct formation constants of uranyl bis-thenoyltrifluoroacetonate with tributyl phosphate at 25°C

No.	Solvent	δ	V	$\log F_\gamma$	$\log K_x$ Calcd from Eq. (8)	$\log K_x$ Calcd from Eq. (12)	$\log K_x$ Obsd	$\log K_S$ Obsd
1	*n*-Hexane	7.3	130	−1.25	7.10	7.69	7.56	6.67
2	*n*-Heptane	7.4	140	−1.38	7.23	7.74	7.32	6.47
3	Cyclohexane	8.2	108	−1.81	7.66	7.61	7.78	6.81
4	Methylene chloride	9.7	64			5.85	5.61	4.42
5	Chloroform	9.3	81	−0.19	6.04	5.50	5.55	4.46
6	Carbon tetrachloride	8.6	96	−1.23	7.08[a]	7.08[a]	7.08	6.06
7	Bromoform	10.5	87	−0.15	6.00	5.53	5.92	4.86
8	Benzene	9.2	89	−1.29	7.14	6.69	6.59	5.54
9	Toluene	8.9	107	−1.13	6.98	6.63	6.67	5.70
10	Isopropylbenzene	8.5	140			6.57	6.24	5.39
11	Chlorobenzene	9.5	102	−0.79	6.64	6.35	6.42	5.43
12	*o*-Dichlorobenzene	10.0	113	−0.52	6.37	6.48	6.57	5.62

a) Observed value employed as reference.

tained from the data on TBP.[9,10]

The constant, $\log K_S^\circ = 5.85$, was given from the calculated F_γ value and $\log K_x = 7.08$ in carbon tetrachloride, which was used as a reference solvent. The adduct formation constants pre-estimated according to Eq. (8) are listed in the sixth column of Table 1. No estimate in methylene chloride or isopropylbenzene is given because of the lack of data on TBP.

The relation between the formation constants for uranyl and zinc adducts with TBP is considered, as the formation constants of $ZnA_2 \cdot S$ have been obtained in various organic solutions.[7] The formation constant for $ZnA_2 \cdot S$ is also expressed as:

$$K^\circ_{S(Zn)} = \frac{x_{ZnA_2 \cdot S}}{x_{ZnA_2} \cdot x_S} \cdot \frac{\gamma_{ZnA_2 \cdot S}}{\gamma_{ZnA_2} \cdot \gamma_S} = K_{x(Zn)} \cdot F_{\gamma(Zn)} \qquad (11)$$

The activity coefficients of different solutes having the same values of the solubility parameter and of the molar volume should be equal to one another in a given solvent, according to Eq. (10), so long as the specific interaction between the solute and solvent molecules is small enough to be neglected. As the above assumptions for the δ and V of uranyl chelate seem to hold also for the zinc chelate, the activity coefficients of these chelate are taken as equal to each other. Similarly, the γ values for uranyl and zinc adducts may be identical in the same media. These findings lead to the conclusion that $F_{\gamma(U)} \fallingdotseq F_{\gamma(Zn)}$ in a given solvent. Each K_S° value for uranyl and zinc adducts is constant; therefore, the following relation can be given by eliminating the terms of the activity coefficients:

$$\frac{K_{x(U)}}{K_{x(Zn)}} = \frac{K^\circ_{S(U)}}{K^\circ_{S(Zn)}} = h \qquad (12)$$

or $\log K_{x(U)} = \log K_{x(Zn)} + \log h$

The formation constants of the uranyl adduct can also be estimated from those of the zinc adduct. The constant, $\log h = 1.63$, was obtained from the observed values for two adducts in carbon tetrachloride. The estimates from Eq. (12) are shown in the seventh column of Table 1.

Regularities in Adduct Formation. The observed adduct formation constants are summarized in Table 1. The molar formation constants ($K_S/K_x = V_B/1000$) are also tabulated. The observed values are in rough accord with the estimates; they are especially consistent with the pre-estimations from Eq. (12). The K_S values in two solvents have been reported. The present datum in cyclohexane agrees with $\log K_S = 6.77$,[12] but that in benzene is larger than the $\log K_S = 5.28$ and 4.74 in the literature.[1]

Figure 4 shows the relation between the adduct

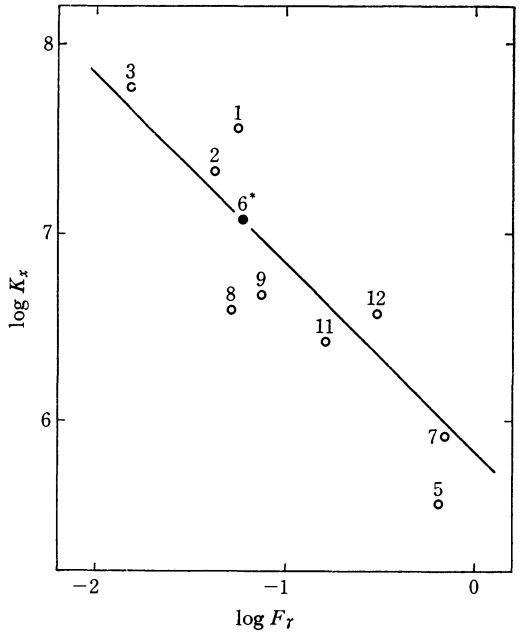

Fig. 4. Relation between the adduct formation constants and the activity coefficients.
The numbers in Figs. 4 and 5 correspond to those in Table 1.
* Employed as reference

12) H. Irving and D. N. Edgington, *J. Inorg. Nucl. Chem.*, **20**, 314 (1961).

formation constants and the activity coefficients. The straight line with a slope of −1 passing through a experimental point in carbon tetrachloride is the estimate. The points observed are close to the line, although negative deviations are found in benzene and chloroform and a positive one in *n*-hexane. This tendency is similar to the case of the zinc adduct.[7] The negative deviation in chloroform appears to be due to the formation of a hydrogen bond between TBP and solvent molecules.[13] The values of log K_S° were found to be 5.77±0.30 by the method of least-squares. Thus, the solvent effect on the equilibrium constant was explained in connection with the activity coefficients evaluated from the properties of pure substances.

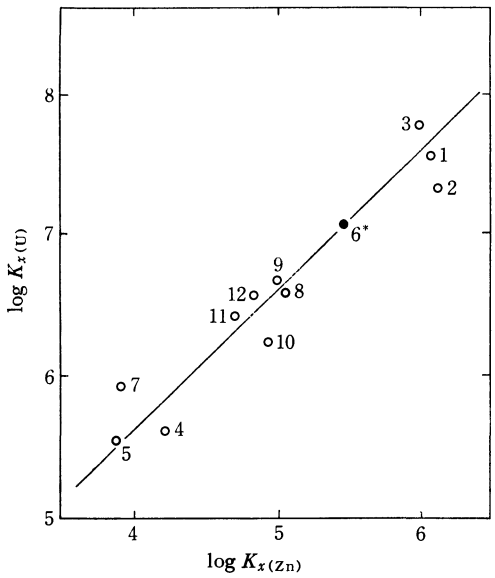

Fig. 5. Relation between the formation constants of $UO_2A_2 \cdot S$ and $ZnA_2 \cdot S$.
The $K_{x(Zn)}$ values were given from Ref. 7.
* Reference

13) M. F. Pushlenkov, E. V. Komarov, and O. N. Shuvalov, *Radiokhim.*, **2**, 537 (1960).

The formation constants of the uranyl adduct are plotted against those of the zinc adduct in Fig. 5. The values thus established are in accord with the estimated line, with a slope of 1, passing through the point in carbon tetrachloride. There are small deviations even in the solvents such as chloroform where some deviations are found in evaluating from the activity coefficients. This shows that the influence of the solvent on the formation of the uranyl adduct is essentially the same as that in the case of the zinc adduct, as was expected. In the estimation by Eq. (12), since there is no need to calculate the γ values, the estimates seems to be free from errors due to the evaluation of such fundamental values as V or δ. This method may be practically useful for the reactions involving components with unknown V or δ values, when we have evidence that these values of the desired substance are equal to those of the reference. For example, the formation constants for the same type of adducts may be estimated in a similar manner. However, it should be remembered that this simple method is based on the similarity of complexes and is not always valid for different types of adducts. In general, the change in the activity coefficients should be taken into account for each species in solution.

The authors are grateful to Professor T. Kanno for his interest in this study, and to the members of the Laboratory of Nuclear Sciences, Tohoku University, for the irradiation of uranium. Thanks are also due to Miss H. Asano for her assistance in the experimental work.

Synthesis and Properties of Two α-Phenylazostilbenes. A New Method for the Elimination of Water and *p*-Toluensulphonate Ion from Substituted Phenylhydrazones[1]

Luciano CAGLIOTI and Angelo G. GIUMANINI*

Istituto di Chimica Organica e Industriale, Universita' di Bologna, 40136 *Bologna, Italy*

(Received October 2, 1970)

The synthesis of a linear azoalkene, α-phenylazostilbene (**1**), not conjugated to strong electron withdrawing groups is reported. α-(*p*-Methoxyphenylazo)stilbene (**3**) was prepared by a direct method. The mass spectra of **1** and **3** showed a rearrangement yielding positive ions of benzonitrile and benzaldehyde anils (**7**).

We wish to report a facile one step preparation of α-phenylazostilbene (**1**) which appears to be the first[2] azoalkene isolated in which the carbon-carbon double bond is not part of a ring[3] or conjugated to a strongly electron withdrawing group.[4] When benzoin phenylhydrazone (α- or β-form, **2**) was stirred with an equimolecular amount of *p*-tosyl chloride in pyridine at 40°C during 10—20 hr, a 45—73% yield of **1** could be obtained as a red stable crystalline solid, mp 90.5—91°C, IR (KBr) bands at 6.94, 10.96, 13.09, 13.22, 13.29, 14.25, and 14.66 μ, PMR ($CDCl_3$) peaks at 7.16 and 7.34 (m, 14 H) and 7.78 ppm (m, 2 H, δ values). The mass spectrometrically determined MW was 284 (calcd 284) with structurally important ions at *m/e* values of 207 (−Ph), 193 (−PhN), 180 (−H, $-C_6H_5CN$), 179 (base peak, $-PhN_2$), 105 ($-Ph_2C_2H$), 103 ($PhCN^+$), 93 (PhN^+), and 77 (Ph^+). The structure of **1** was proved chemically by transforming it into benzoin osazone (mp 234—235°C, no depression with authentic sample) upon reflux with phenylhydrazine in glacial acetic acid. The UV spectrum of **1** resembles very closely that of *trans*-azobenzene[5] with maxima (in *n*-C_6H_{14})[6] at 233.0 ($\varepsilon=1.38\times10^4$), 325.0 ($3.54\times10^4$), 344.5 ($3.68\times10^4$), and 444.0 nm ($6.20\times10^2$). **1** dissolved in 97% sulphuric acid to give a colourless solution (UV max at 247.0 ($\varepsilon=1.135\times10^4$), 275.0 ($1.042\times10^4$) and 348.0 nm ($1.201\times10^4$)) which turned violet in *ca.* 10 min (*vis* max at 538.0 nm ($\varepsilon=6.97\times10^2$)). The stable colouration can be ascribed to the formation of a carbonium ion.[7] **1** could be exactly titrated with *n*-butyllithium, one equivalent of this reagent being used up for the disappearance of the red colour from an hexane solution of **1**.

The mechanism of formation of **1** appears to involve the *O*-tosyl derivative of **2** for which pyridine performs a 1,4 ionic elimination of *p*-toluensulphonic acid. Pure pyridine (14 hr at 45°C) produced no **1**.

It is of interest that a derivative of **1**, namely α-(*p*-methoxyphenylazo)stilbene (**3**), was obtained by simply bringing *p*-methoxy-phenylhydrazine in contact with benzoin at 105°C during 14 hr without solvent. The new compound, obtained in 30% yield, was an orange, stable crystalline solid, mp 106—107°C (109—111°C for an analytical sample), whose analysis, MW (M^+ at 314), infrared, PMR and mass spectra are in agreement with the proposed formula.

The present synthesis affords an easy access to these new compounds which cannot be prepared by the diazo coupling method,[8,9] and represent new examples

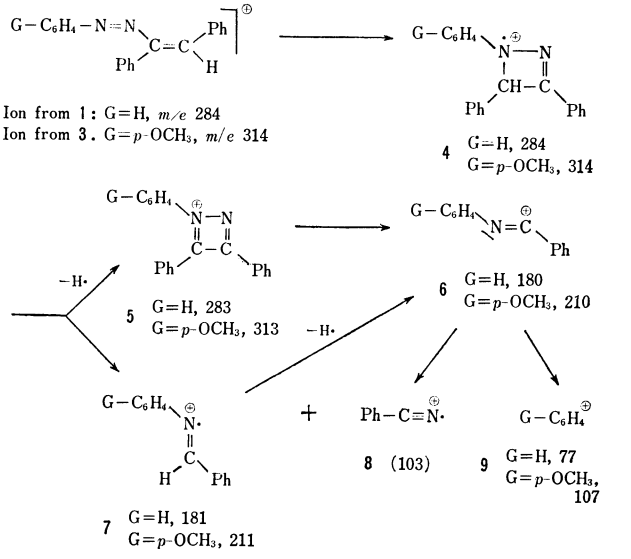

Scheme 1

1) This work was supported by CNR grant n. 69.00367.115.621. One of us (AGG) gratefully acknowledges a CNR research fellowship (1967—8) during which this work was carried out.

* Present address: Center for Mass Spectrometry, Via S. Giacomo, 5-40126 Bologna, Italy.

2) During the writing of this manuscript, a paper describing the preparation of **1** from α-chlorodesoxybenzoin and phenylhydrazine appeared: S. Brodka and H. Simon, *Chem. Ber.*, **102**, 3647 (1969).

3) L. Caglioti, P. Grasselli, and G. Rosini, *Tetrahedron Lett.*, **1965**, 4545 and unpublished results from L. Caglioti and G. Rosini; G. J. F. Chittendem and R. D. Guthrie, *J. Chem. Soc., C*, **1967**, 1703 and J. Buckingham and R. D. Guthrie, *ibid.*, **1967**, 1700. See also Ref. 2.

4) J. Van Alphen, *Rec. Trav. Chim. Pays-Bas*, **64**, 109, 305 (1945).

5) H. H. Jaffe, S.-J. Yeh, and R. W. Gardner, *J. Mol. Spectrosc.*, **2**, 120 (1958).

6) The whole spectrum undergoes a red shift of small entity in methanol except for the longest wavelength band. The individual shifts amount to 2.9, 2.9, and 1.4 kcal/mol in the order of increasing wavelength. This can be interpreted in terms of small alteration of charge distribution in the corresponding excited states. Even the longest wavelength maximum, a n-π^* transition is completely unaffected by solvent change, thus indicating that a large charge reorganization should take place. A similar phenomenon was observed for azobenzene: H. H. Jaffe and M. Orchin, "Theory and Application of Ultraviolet Spectroscopy," John Wiley and Sons, New York (1965), p. 286.

7) R. Wizinger and B. Cyriax, *Helv. Chim. Acta*, **28**, 1018 (1945).

8) A. P. Terentiev and L. L. Gomberg, *J. Gen. Chem. U.S.S.R.*, **8**, 662 (1938).

9) S. M. Parmenter, Ch. 1 in "Organic Reactions," ed. by R. Adams, J. Wiley and Sons, New York (1959).

of 1,4 sulphonic acid and water[10] elimination in the azoalkene preparation from hydrazonic substrates.

If our interpretation of the low resolution mass spectra of **1** and **3** concerning ions at 180 and 211, respectively, is correct, an interesting rearrangement with intermediate four member ring charged species **4** and **6** took place, as evidenced by the detection of the corresponding fragments **5**, **6**, and **7** (Scheme 1). Structure **5** is very likely to be correct. However, formula **6** most probably only reflects the composition of the actual ion.

Experimental

UV spectra were recorded with a Unicam sp. 800, IR spectra with a Beckman IR 5 (KBr pellet technique), PMR spectra[11] with a Varian DP60 and low resolution mass spectra[11] with a Perkin Elmer 270. Values of *m/e* for the 10 highest peaks are reported with relative abundance in brackets. "Half" masses (hm) due to double charged ions and metastable ions (mi) are reported when considered of interest.

α-Benzoin Phenylhydrazone. This compound was prepared according to Smith and Ranson.[12] The solvent was evaporated in a vacuum and the thick residue washed thoroughly with hot hexane. A fractional crystallization from benzene gave the lower melting isomer (*β*-form, mp 95—96°C): hexane was added to the mother liquor, from which the α-isomer was obtained, mp 159—161°C. Yield: 45% (α and *β*). One recrystallization from hexane - ether gave slightly yellow compound, mp 161°C (lit,[12] 158—159°C). PMR (d_6-acetone): 5.88 (1H, s, CH), 6.31 (1H, s, OH), 6.83 (1H, s, NH), 7.1, 7.2, 7.8 ($3H_{ar}$, $10H_{ar}$, $2H_{ar}$, m). UV (hexane) max:[13] 214.0 ($\varepsilon = 1.71 \times 10^4$), 235.0 ($1.53 \times 10^4$), 297.5 ($0.79 \times 10^4$), and 342 nm ($1.97 \times 10^4$).

β-Benzoin Phenylhydrazone. This compound was prepared in 57% yield by bringing equimolecular amounts of benzoin and phenylhydrazine[14] in contact at 120°C for 30 min, extracting the resulting thick oil many times with hexane and recrystallizing from hot ethanol, mp 101—102°C (lit[12,14] 106°C). PMR (d_6-acetone): 4.98 (1H, d, $J = 4.5$ Hz, CH), 5.59 (1H, d, $J = 4.5$ Hz, OH), 7.25 (15H, m, arom. protons), and 8.15 (1H, s, NH). UV (hexane) max:[13] 216.0 ($\varepsilon = 1.71 \times 10^4$), 253.0 ($1.39 \times 10^4$), 258.0 ($1.54 \times 10^4$), 264.5 ($1.50 \times 10^4$), 272.3 ($1.48 \times 10^4$), and 305.3 nm ($1.11 \times 10^4$).

The actual structure of the two benzoin phenylhydrazones was discussed by a number of workers.[13,15,16]

α-Phenylazostilbene (**1**). 1) A solution of 15.09 g *p*-tosyl chloride and 23.94 g of a mixture of α- and *β*-isomers of benzoin phenylhydrazone in 150 m*l* dry pyridine was refluxed for 7 hr. An intensely red colouration appeared immediately and a white precipitate formed. The cool mixture was washed with brine, dried over sodium sulphate and the solvent evaporated to give a red oil. Since direct crystallization from common solvents failed to yield a solid product, absorption chromatography (silica gel, hexane - benzene 1 : 1 vol) was employed to give 3 well separated fractions: the first eluted was a trace of a rose oil not further analyzed, the second was a red oil (55% yield), which was recrystallized to the desired compound (mp 89—90°C) from methanol, the third unreacted α-benzoin phenylhydrazone (mp 155—158°C).

2) *From Benzoin Phenylhydrazone*: A solution of the α-benzoin phenylhydrazone (3.83 g) and tosyl chloride (3.38 g) in 23 m*l* pyridine was stirred at 40°C for 33 hr. The red colour appeared very soon after mixing the reactants. The reaction mixture was heated with 50 m*l* water and extracted with hexane. The organic layer, dried over sodium sulphate, was freed from solvent, to yield a viscous red oil. Chromatography on a 4×30 cm silica gel column, using benzene as an eluent, gave, after a 200 m*l* forerun, compound **1** (3.60 g, 72.5%, 250 m*l*) as a thick red oil, homogeneous by tlc analysis (R_f 0.75, on silica gel with cyclohexane - ethylacetate 85/15 vol).[17] Two recrystallizations from alcohol gave red-orange crystals, mp 90.5—91°C (lit,[1] 90°C).

3) *From β-Benzoin Phenylhydrazone*: Using the same procedure as described above for the reaction of the α-form, we obtained the same product **1** 45%, mp 90°C (lit,[1] 90°C), mixed mp with that obtained from the α-form showed no depression.

Found: C, 84.21; H, 5.55; N, 10.04%. Calcd for $C_{20}H_{16}N_2$: C, 84.47; H, 5.67; N, 9.85%. PMR ($CDCl_3$):[18] 7.16 and 7.34 (14H, partially overlapped multiplets), 7.78 (2H, m). IR (KBr):[19] 6.26 w, 6.81 w, 6.94 m, 7.02 s, 7.03 m, 7.10 m, 7.41 w, 7.43 w, 7.80 w, 8.66 w, 9.31 w, 9.45 m, 9.49 m, 9.85 m, 9.93 w, 10.95, and 10.98 (doublet, m), 11.32 w, 11.45 m, 12.93 w, 13.09 vs, 13.22 s, 13.29 s, 13.34 vs, 13.59 w, 14.17 vs, 14.25 vs, 14.50 vs, 14.66 vs, 14.69 vs, 16.04 s, 16.47 m, 17.15 s, 19.32 w, 19.38 w, 20.06 s, and 20.19*μ* s. UV maxima are indicated in the descriptive part. Mass spectrum:[20] 179 (100, $-PhN_2$), 284 (82, parent peak), 178 (73, $PhCCPh^+$), 283 (31, −H), 77 (30, Ph^+), 180 (26, −H, −PhCN), 285 (18, +H), 177 (12), 181 (10, −PhCN), 105 (10, PhN_2^+), 193 (10, −PhN) and 207 (10, −Ph); hm: 142.5 ($M+1^{2+}$), 142 (M^{2+}) and 141.5 ($M-1^{2+}$).

Reactions of **1**. *A) Reaction with* n-*Butyllithium*: The red colour of a hexane solution of **1** changed to pale yellow and a white precipitate appeared upon dropwise addition of one equivalent of *n*-butyllithium (hexane solution). The reactions were instantaneous. No attempt was made to separate and identify the product(s).

B) Reaction with Phenylhydrazine: A mixture of **1** (251 mg) and phenylhydrazine (381 mg) in glacial acetic acid (4 m*l*) was refluxed for 7 hr, the solvent was then evaporated under reduced pressure, the solid yellow residue taken up with chloroform and washed with aqueous bicarbonate, the organic solution was dried over sodium sulphate and evaporated to yield the crude benzoin osazone, mp 325—328°C.

10) H. Simon and W. Moldendauer found that 2-cyclohexanolone phenylhydrazone exchanged the OH substituent with a MeO group in methanol in *acidic* conditions. They *proposed* the intermediary of 1-phenylazocyclohexene, *Chem. Ber.*, **101**, 2124 (1968).

11) We are indebted to Mrs. A. B. Giumanini for recording the spectra.

12) A. Smith and J. H. Ramson, *J. Amer. Chem. Soc.*, **16**, 108 (1894).

13) C. C. Baly, W. B. Tuck, E. G. Marsden, and M. Gazdar, *J. Chem. Soc.*, **91**, 1573 (1907) reported the higher wavelength part of the electronic spectrum of this compound.

14) G. J. Bloink and K. H. Pausaker, *ibid.*, **1952**, 661.

15) S. B. Hendricks, O. R. Wulf, G. E. Hilbert, and U. Liddel, *J. Amer. Chem. Soc.*, **58**, 1991 (1936).

16) E. M. Tanner, *Spectrochim. Acta*, **16**, 20 (1959).

17) Work in progress in our laboratory by G. Rosini has shown that two stereoisomers of **1** could be obtained from α-acetoxydesoxybenzoin and phenylhydrazine.

18) The physical properties here recorded are identical for **1** from any of the **3** preparations described.

19) This spectrum was recorded with a Perkin Elmer Grating Spectrometer model 225.

20) The sample was vapourized in a chamber of ion source at 85°C; the chamber was kept at 150°C and the electron energy at 80 eV.

Crystallization from chloroform - ethanol gave a product (43.5%) melting at 234—235°C, showing no depression with an authentic sample of the β-osazone prepared from benzoin and phenylhydrazine in refluxing acetic acid.[21] Mass spectrum:[22] 386 (−4H!), 298 (−PhNH), 215, 194, 192, 104, 103, 93, 92, 91, 77, and 65.

p-*Methoxyphenylazostilbene (**3**).* *p*-Anisylhydrazine (5.0 g), prepared according to Padoa's method[23] and benzoin (7.32 g) were heated without solvent at 105°C under reduced pressure (10 Torr) for 1 hr. The reaction of water elimination was very prompt as was the appearance of a red colouration of the melt. The obtained oil was chromatographed in small lots (*ca.* 4 g) on a silica gel 5×40 cm column using benzene as eluent. A 30% yield of a red oil, crystallizing in beautiful red needles from ethanol, mp 110—111.5°C, one spot on tlc, was obtained. Found: C, 80.62; H, 5.57; 8.78%. Calcd for $C_{21}H_{18}N_2O$: C, 80.23; H, 5.72; N, 8.91%. PMR ($CDCl_3$): 15 protons in the "aromatic" region, accounting for all *ar*-H and the olefinic H, with prominent peaks at 6.84, 7.00, 7.17, 7.35, 7.70, 7.85, and a singlet (3H, CH_3) at 3.81. Mass spectrum:[20] 314 (100, parent peak), 107 (81, An^+), 179 (64, $-AnN_2$), 178 (63, $PhCCPh^+$), 135 (42, AnN_2^+), 77 (34, Ph^+), 211 (20, −PhCN), 315 (19, +H), 313 (17, −H), and 196 (16); hm: 157.5 ($M+1^{2+}$), 157 (M^{2+}) and 149.5 (299^{2+}, $-CH_3$); mi.: *ca.* 312 and 85. IR (KBr): 6.25 s, 6.32 m, 6.68 m, 6.95 m, 7.60 w, 7.98 s, 8.47 w, 8.55 w, 8.77 s, 9.73 s, 10.87 w, 11.38 w, 11.92 s, 12.46 w, 13.06 w, 13.16 w, 13.60 m, 14.17 s, 14.51 s, and 15.73μ w.

21) A. Purgotti, *Gazz. Chim. Ital.*, **22**, II, 611 (1892).

22) The sample was vaporized at *ca.* 160°C, the ion source temperature was kept at 180°C and the electron energy at 70 eV.

23) M. Padoa, *Gazz. Chim. Ital.*, **44**, II, 535 (1914).

BULLETIN OF THE CHEMICAL SOCIETY OF JAPAN, VOL. 44, 1050—1054 (1971)

The Solvent Effect on the Reaction of 1,1,4,4-Tetraphenyl-2-halobuta-2,3-dien-1-ol with Mercuric Halide

Fumio Toda, Nobuhiro Ooi, and Katsuhiko Akagi

Department of Industrial Chemistry, Faculty of Engineering, Ehime University, Matsuyama

(Received August 3, 1970)

The reaction of the title compound (I) with mercuric halide in an aprotic and in a protic solvent afforded the fulvene derivative (VII) and the dihydrofuran derivative (VIII or IX) respectively. Both the cross-reactions (bromo-analog of I (Ia)+$HgCl_2$, chloro-analog of I (Ib)+$HgBr_2$) in an aprotic solvent afforded the chloro-fulvene derivative (VIIb). However, when the above reactions were carried out in a protic solvent, the product was the dihydrofuran derivative (IX), in which the halogen combining with carbon is chlorine and that combining with mercury is bromine. On the basis of the results of those cross-reactions, the reaction mechanism will be discussed. Acetonitrile showed distinctive behavior. In acetonitrile, the bromine of Ia was easily exchanged with the chlorine of sodium chloride at room temperature, and Ib was obtained quantitatively.

In a previous paper,[1] we have reported the reaction of the bromo-analog of the title compound (Ia) with mercuric acetate to afford various reaction products, depending on the nucleophilicity of the solvent used. When the reaction was carried out in acetic acid, the acetoxymercuration product II was obtained as the sole product. The reaction in alcohol, however, afforded the corresponding alkoxy acetylene alcohol (III), derived by the retropropargyl rearrangement,[2] and the mercurated dihydrofuran derivative (IV), derived by mercuration, followed by intramolecular cyclization, in various ratios depending on the bulkiness of the alkyl of the alcohol used. In the solvent with which it is not necessary to take account of its nucleophilicity, such as acetone, the reaction of Ia with mercuric acetate afforded the naphthalenone derivatives (V and VI), probably *via* an allenic epoxide intermediate.

In order to clarify the role of a protic solvent on the reaction of I with mercuric salt, we have studied the halomercuration of I in various protic and aprotic solvents. We have found that the variation in the

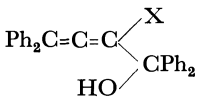

(I) a: X=Br; b: X=Cl

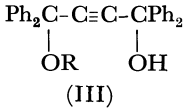

(III)

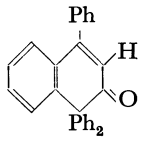

(V)

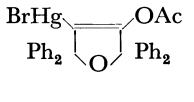

(II)

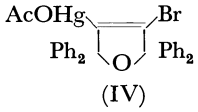

(IV)

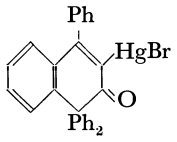

(VI)

main reaction product depends on whether the solvent used is protic or aprotic.

Results. The treatment of an acetone solution of I with an equimolar amount of mercuric halide (HgX_2) for 1 hr at room temperature afforded mainly the fulvene derivative (VII) in the yields shown in Scheme 1 in addition to a small amount of the dihydrofuran derivative (VIII or IX). The structures of the main products were determined by a comparison of their mp's and infrared spectral data with those of

1) F. Toda and K. Akagi, *Tetrahedron*, **25**, 3795 (1969).
2) F. Toda, M. Higashi, and K. Akagi, This Bulletin, **42**, 829 (1969).

the corresponding authentic samples, VIIa[3] and VIIb.[4] Since both the cross reactions, Ia+$HgCl_2$ and Ib+$HgBr_2$ yielded the same product, VIIb, and since the VII product did not exchange the halogen upon treatment with HgX_2 under the same conditions as those employed for the halomercuration reaction, the reaction must proceed through a process in which halogen-exchange is possible. The above observation is important in order to clarify the reaction mechanism. It will be discussed in the following section.

The same treatment of I with HgX_2 in *t*-butanol as that employed for the reaction in acetone afforded VIII or IX in the yields shown in Scheme 2. The reaction of Ia+$HgBr_2$ and Ib+$HgCl_2$ afforded di-dibromo (VIIIa) and dichloro-derivatives (VIIIb) respectively. The two cross reactions, Ia+$HgCl_2$ and Ib+$HgBr_2$, however, yielded the same product, bromochloro derivative (IX), in which the halogen combining with carbon is chlorine and that combining with mercury is bromine. The results show again that the reaction proceeds *via* an intermediate in which halogen-exchange occurs. The reaction mechanism will be described in detail in the Discussion section.

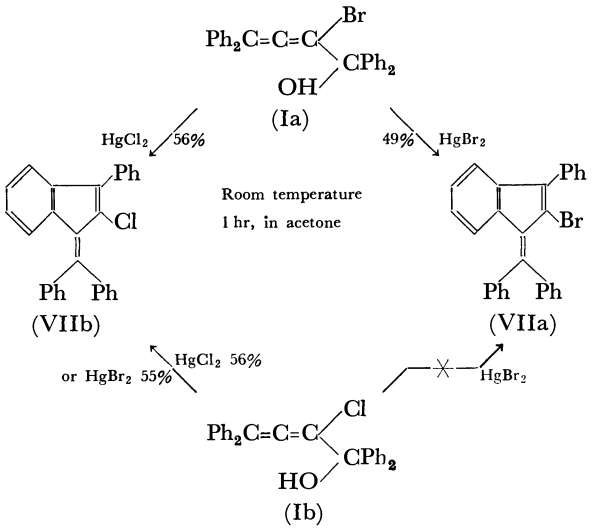

Scheme 1

The structures of VIII and IX were determined by the methods shown in Scheme 3. The infrared spectral data of VIIIa thus obtained were identical with those of an authentic sample[1] prepared by shaking an acetone solution of IV with aqueous potassium bromide. The treatment of VIIIa with sodium borohydride in alcohol at room temperature afforded a demercurated product,

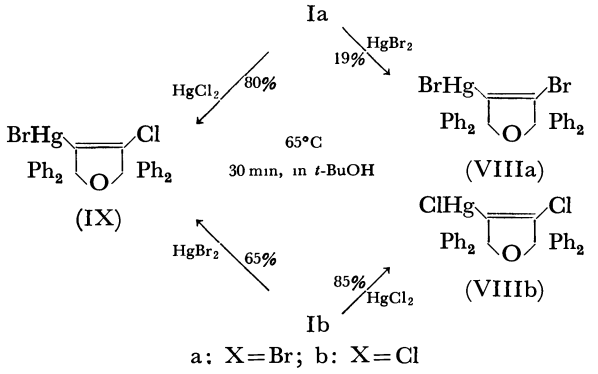

a: X=Br; b: X=Cl

Scheme 2

Xa, quantitatively. The spectral data of Xa were identical with those of an authentic sample prepared according to a previously-reported method[3], the acid-catalyzed cyclization of Ia. The sodium borohydride reduction of VIIIb and IX gave the same product, Xb, and its spectral data were identical with those of an authentic sample prepared by the acid-catalyzed cyclization of Ib.

As was described above, the type of the main product of the reaction of I with HgX_2 depends on the solvent used. In order to test the generality of the solvent effect on the reaction, several aprotic and protic solvents were employed for the reaction. The yields of the products of the reaction of Ia and $HgCl_2$ are summarized in Table 1, together with the reaction conditions. Because of the difference in the solubility of the reactants and in the reaction rate, the reaction condition differs slightly from each other. However, the product ratio was slightly affected by the reaction temperature and the time.

In all the aprotic solvents, the major product was VIIb. In some cases, however, IX was isolated as a minor product in addition to VIIb. Reversely, the major product of the reaction in a protic solvent, such as *t*-amyl, *t*-butyl and cyclohexyl alcohol, was IX. The anomalous behavior of acetic acid, phenol, and acetonitrile was also observed.

Discussion. On the basis of the finding that the reaction of Ia with $HgCl_2$ in aprotic and protic solvests afforded mainly the fulvene derivative (VIIb) and dihydrofuran derivative (IX) respectively (Table 1), and of the results of the cross reactions (Schema 1,2), the reaction mechanism which is shown in Scheme 4 was postulated. In Scheme 4, ketone is representative of the aprotic solvent.

For the intermediate (XI) initially produced by

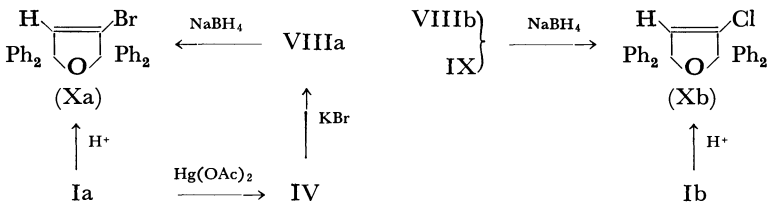

Scheme 3

3) F. Toda, T. Komoda, and K. Akagi, *ibid.*, **41**, 1493 (1968).

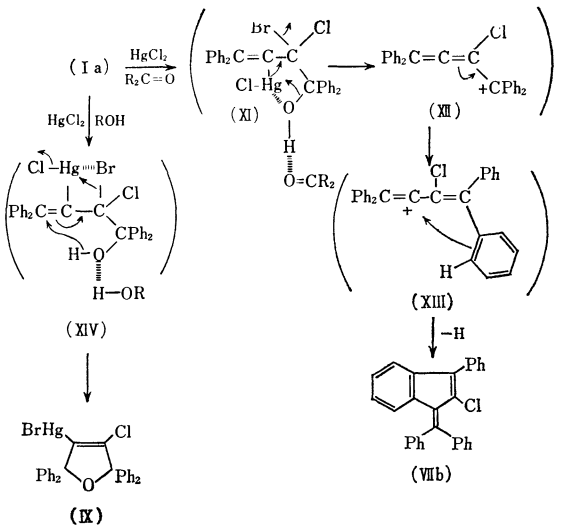

Scheme 4

Table 1. Yield of the products of the reaction of Ia and $HgCl_2$

Reaction condition			Product (%)	
Temp.	Time (hr)	Solvent	VIIb	IX
r. t.[a]	1	Me_2CO	56	12
65°C	0.5	$(t\text{-Bu})_2CO$	95	—
65°C	0.5	cyclohexanone	82	—
refl.[b]	0.5	THF	71	6
refl.	0.5	Et_2O	82	9
r. t.	1	CS_2	56	6
r. t.	0.5	MeCN	77	(VIIIb, 6)
refl.	0.5	MeCN	97	—
r. t.	0.5	$MeCO_2H$	66	—
65°C	0.5	PhOH	61 (XV, 11)	—
65°C	0.5	*t*-AmOH	—	84
65°C	0.5	*t*-BuOH	15	80
65°C	0.5	cyclohexanone	15	42

a) Room temperature, b) Reflux.

the chloromercuration on Ia, an aprotic solvent serves as an electron-donor species and coordinates with the hydrogen of the hydroxyl group. The hydrogen bonding increases the electron density around the oxygen of the hydroxyl, and facilitates the coordination between mercury and the hydroxyl oxygen. Dechloromercuration, followed by the dehydroxylation of XI, affords the cation (XII). It is reasonable to consider that Br^- is more facile at leaving a moiety than Cl^- and that XI affords the chlorine-substituted cation (XII). The intramolecular cyclization of the cation (XIII) derived by the migration of the double bond of allene in XII affords VIIb.

In a protic solvent, however, the mercury-oxygen coordination in the chloromercurated intermediate (XIV) is inhibited because of the decreased electron density around the hydroxyl oxygen resulting from hydrogen bonding between the protic solvent and the hydroxyl oxygen. Therefore, the coordination between mercury and bromine is preferable. Intramolecular coordination between mercury and bromine has been postulated.[1,5] Of two halogens on the carbon of XIV, the elimination of Br^- occurs predominantly. Therefore, the reaction can be interpreted by a combination of the following two main processes: the Br^- attacks the mercury, and then the Cl^- leaves the mercury. The migration of the double bond and the intramolecular cyclization yields IX.

Of the five protic solvents cited in Table1, acetic acid and phenol differed widely from the others in the mode of reaction. In those solvents, the main reaction product was VIIb, not IX. A strong acid, such as acetic acid or phenol, would promote the dehydroxylation of the intermediate XI and finally afford VIIb *via* XII. The observation that the heating of Ia in acetic acid for 1 hr at 75°C afforded VIIa in a 68% yield, supports the above assumption. The conversion of I into VII by treatment with sulfuric acid has been reported.[2] Nevertheless, since the reaction of Ia with $HgCl_2$ in acetic acid afforded the halogen-exchanged product VIIb, but not VIIa, the process must also contain a halomercurated intermediate such as XI. The same interpretation is applicable to the reaction in phenol, which affords mainly a halogen-exchanged product VIIb and a small amount of halogen-free fulvene (XV). The process giving XV must proceed by a direct reaction of Ia and phenol, since the treatment of Ia with phenol at 65°C for 30 min afforded XV in an 90% yield (Scheme 5), even though its mechanism is not clear.

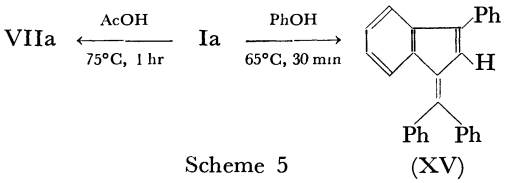

Scheme 5 (XV)

It is reasonable to assume that the halogen-exchange process on the reaction of I and HgX_2 is a part of the reaction, as has been discussed above, since neither of the reaction products, VII and VIII, exchanged its halogens with those of HgX_2 under the same conditions as were employed for the halomercuration. Nevertheless, the possibility that the exchange occurs before the reaction starts cannot be ruled out. If the halomercuration process of I to afford XI or XIV is reversible, halogen-exchange will occur before the reaction starts. This possibility can, however, be disregarded on the basis of the following observation. The reaction of Ia with five molar amounts of $HgCl_2$ in *t*-butyl alcohol afforded IX, but not any detectable VIIIb. If the halogen-exchange process precedes the reaction to afford the dihydrofuran derivative, the reaction product might be VIIIb or, at least, might be contaminated with VIIIb.

The reaction of Ia and $HgCl_2$ in acetonitrile is distin-

4) E. D. Bergmann, E. Fischer, and J. H. Jaffe, *J. Amer. Chem. Soc.*, **75**, 3230 (1953).

5) E. F. Kiefer and W. Gericke, *ibid.*, **90**, 5131 (1968).

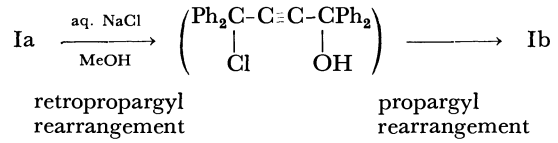

Scheme 6

guishable from those in other aprotic solvents. The reaction at room temperature in acetonitrile afforded VIIIb (6%) instead of IX, in addition to VIIb (77%). Since shaking an acetonitrile solution of IX with $HgCl_2$ did not yield VIIIb, and since IX was recovered quantitatively, the complete halogen-exchange leading to VIIIb should occur before the completion of reaction. It can reasonably be assumed that the chloro-analog of Ia (Ib) initially formed by a halogen exchange between Ia and $HgCl_2$ reacts with $HgCl_2$ to afford VIIIb. This assumption was certified by shaking an acetonitrile solution of Ia with sodium chloride at room temperature for 30 min; this afforded Ib quantitatively. The halogen-exchange probably proceeds by the sequence of retropropargyl-propargyl rearrangements shown in Scheme 6. The exchange, however, was not observed in other aprotic solvents tested, such as acteone and tetrahydrofuran. The treatment of Ib with aqueous potassium bromide in acetonitrile, however, did not afford Ia.

Experimental

All the melting points were uncorrected. The infrared spectra were recorded in Nujol mull on a spectrophotometer, IR-E, of the Japan Spectroscopic Co. The molecular weights were determined by means of a molecular-weight apparatus of Hitachi-Perkin Elmer, model 115, in benzene.

1,1,4,4-Tetraphenyl-2-halobuta-2,3-dien-1-ol (I). The bromo-analog (Ia) was prepared according to a previously-reported method.[3] The chloro-analog (Ib) was prepared by a modified version of that method used for the preparation of Ia. Into an ice-cooled solution of 1,1,4,4-tetra-phenyl-but-2-yne-1,4-diol (5 g, 13 mmol) in acetic acid (30 m*l*) - benzene (12 m*l*), concentrated hydrochloric acid (5 m*l*) dissolved in acetic acid (20 m*l*) was stirred drop by drop, over a period of 10 min. After the stirring had then been continued for a further 30 min, ice water (100 m*l*) was added to the reaction mixture. The crude product which separated was extracted with ether. The ether solution was washed with water, aqueous sodium bicarbonate, and water successively, and dried over sodium sulfate. The crude crystals obtained by the evaporation of the solvent were recrystallized from benzene - petroleum ether to afford Ib as colorless prisms (2.7 g) (51%); mp 100—101°C. IR 3400 (OH) and 1945 cm^{-1} (C=C=C).

Found: C, 82.16; H, 5.38%. Calcd for $C_{28}H_{21}OCl$: C, 82.25; H, 5.14%.

Acid-catalyzed Intramolecular Cyclization of Ib. A solution of Ib (0.1 g) in acetone (3 m*l*) containing two drops of concentrated hydrochloric acid was heated under reflux for 10 min. The crude crystals obtained by the evaporation of the solvent were washed with water and recrystallized from methyl alcohol to give Xb as colorless needles (0.03 g) (30%); mp 169—169.5°C. IR 1630 (C=C) and 1020 cm^{-1} (C–O).

Found: C, 81.98; H, 5.07%. Calcd for $C_{28}H_{21}OCl$: C, 82.25; H, 5.14%.

General Procedure of the Reaction of I and HgX_2. A mixture of I (1 mmol), HgX_2 (1 mmol), and solvent (5 m*l*) was treated under the reaction conditions summarized in Table 1 and in Scheme 1 and 2. When the reaction was carried out in a solvent with a boiling point lower than 100°C, such as all the aprotic solvent used except di-*t*-butyl ketone and cyclohexanone, the reaction product was isolated by the evaporation of the solvent. On the other hand, when the reaction was carried out in a solvent which boils at temperature higher than 100°C, the reaction product was isolated by adding petroleum ether to the reaction mixture.

The crude product thus obtained was purified by recrystallization or was fractionated into components by fractional recrystallization.

Some examples of each case are shown in the following columns.

Reaction of Ia and $HgCl_2$ in Acetone. A solution of Ia (0.46 g, 1 mmol) and $HgCl_2$ (0.28 g, 1 mmol) in dry acetone stirred at room temperature for 1 hr. The crude product obtained by the evaporation of the acetone was extracted with petroleum ether (20 m*l*). The evaporation of the solvent afforded VIIb as red prisms (0.22 g) (56%); mp 158°C (lit,[4] mp 159—160°C). The spectral data of VIIb were identical with those reported in the literature.[4] The residue remaining after the extraction with petroleum ether was extracted with cyclohexane (20 m*l*). The removal of the solvent of the cyclohexane solution afforded IX as colorless plates (0.08 g) (12%); mp 194—195°C. IR 1610 (C=C) and 1015 cm^{-1} (C–O).

Found: C, 48.67; H, 2.92%; mol wt (benzene), 696. Calcd for $C_{28}H_{20}OHgBrCl$: C, 48.84; H, 2.91%; mol wt 688.

The reaction of IX by sodium borohydride in ethyl alcohol yielded Xb in an almost quantitative yield.

By the same procedure, Ib was treated with $HgBr_2$ in acetone to afford VIIb (55%) and IX (9%).

Under the same conditions, Ia reacted with $HgBr_2$ to give VIIa (49%) as red prisms; mp 160°C (lit,[3] mp 160—161°C).

Under the same conditions, Ib reacted with $HgCl_2$ and yielded VIIb (56%) and VIIIb (4%) as colorless plates; mp 253—260°C. IR 1615 (C=C) and 1020 cm^{-1} (C–O).

Found: C, 52.85; H, 3.23%; mol wt (benzene), 669. Calcd for $C_{28}H_{20}OHgCl_2$: C, 52.26; H, 3.11%; mol wt, 644.

The sodium borohydride reduction of VIIIb afforded Xb quantitatively.

Reaction of Ia and $HgCl_2$ in t-Butyl Alcohol. A mixture of Ia (0.46 g, 1 mmol), $HgCl_2$ (0.28 g, 1 mmol), and *t*-butyl alcohol (5 m*l*) was stirred at 65°C for 30 min. The crystals which separated out upon the addition of petroleum ether (20 m*l*) to the reaction mixture were collected by filtration and were recrystallized from cyclohexane to afford IX (0.48 g) (70%). The petroleum ether solution remaining after the removal of IX was concentrated to dryness. The fractional recrystallization of the residue from petroleum ether afforded VIIb (0.06 g) (15%) and some additional IX (0.07 g) (10%).

By the same procedure as was employed for the above reaction, Ia was treated with $HgBr_2$ in *t*-butyl alcohol to afford VIIIa (19%) and (2%). The structure of VIIIa was determined by a comparison of its infrared spectrum (1620 (C=C) and 1015 cm^{-1} (C–O)) with that of an authentic sample prepared according to the previously-reported method,[1] as is shown in Scheme 3. The sodium borohydride reduction of VIIIa gave Xa quantitatively.

The reactions of Ib+$HgCl_2$ and Ib+$HgBr_2$ in *t*-butyl alcohol afforded VIIIb (85%), and VIIIb (65%) and VIIb (15%), respectively.

Reaction of Ia and $HgCl_2$ in Phenol. A mixture of Ia (0.46 g, 1 mmol), $HgCl_2$ (0.28 g, 1 mmol), and phenol (5 m*l*) was stirred at 65°C for 30 min. After cooling, water was added to the reaction mixture, the product which was crystallized out was fractionated by fractional recrystallization from *n*-hexane to afford VIIb (0.24 g, 61%) and XV (0.05 g, 11%) as yellow prisms; mp 204°C (lit,[3,6] mp 204—205°C). The infrared spectral data of XV were identical with those of an authentic sample prepared according to the literature.[3]

Reaction of Ia and Phenol. A solution of Ia (0.23 g, 0.5 mmol) in phenol (2.5 m*l*) was heated at 65°C for 30 min. After cooling, the reaction mixture was diluted with water to give XV (0.16 g) (90%).

Reaction of Ia with Acetic Acid. A solution of Ia (0.23 g, 0.5 mmol) in acetic acid (2.5 m*l*) was heated at 75°C for 1 hr. The evaporation of the solvent gave VIIa, after recrystallization from acetone (0.15 g) (68%).

Reaction of Ia with Five Molar Amounts of $HgCl_2$ in t-Butyl Alcohol. A mixture of Ia (0.46 g, 1 mmol), $HgCl_2$ (1.35 g, 5 mmol) and *t*-butyl alcohol (5 m*l*) was heated at 65°C under stirring for 30 min. The residue remaining after evaporation of the solvent under reduced pressure was extracted with cyclohexane (20 m*l*). The evaporation of the solvent of the cyclohexane solution afforded IX (0.688 g) (100%). The bromochloro compound (IX) thus obtained was proven, by a careful infrared spectral study, not to be contaminated with any detectable amount of dichloro-analog (VIIIb).

Reaction of Ia with Aqueous Sodium Chloride in Acetonitrile. A solution of Ia (0.23 g, 0.5 mmol) in acetonitrile (2.5 m*l*) was shaken with saturated aqueous sodium chloride (2.5 m*l*) at room temperature for 30 min. An acetonitrile layer was then separated and concentrated to dryness to afford Ib (0.19 g) (97%).

Reaction of Ia with Aqueous Sodium Chloride in Acetone (or Tetrahydrofuran). The same treatment of Ia as above with aqueous sodium chloride in acetone (or tetrahydrofuran) gave the recovered Ia in a quantitative yield in both cases.

The authors wish to express their thanks to Mr. Shoichi Kato for the elemental analyses, and to Miss Toshiko Matsumoto for her measurement of the molecular weights.

6) J. Salkind and A. Kruglo, *Ber.*, 61, 2306 (1928).

BULLETIN OF THE CHEMICAL SOCIETY OF JAPAN, VOL. 44, 1054—1062 (1971)

Electronic Spectra of Phenanthrene Derivatives. Effect of Substitution

Shuzo AKIYAMA, Masazumi NAKAGAWA, and Kichisuke NISHIMOTO*

Department of Chemistry, Faculty of Science, Osaka University, Toyonaka, Osaka

**Department of Chemistry, Faculty of Science, Osaka City University, Sumiyoshi-ku, Osaka*

(Received August 5, 1970)

During the course of studies on the spectral regularities of linear conjugated systems bearing aromatic terminal groups (*cf. Tetrahedron Lett.*, **1964**, 719; *ibid.*, **1968**, 1121; This Bulletin, **39**, 2320 (1966); *ibid.*, **40**, 340 (1967)), we found that the free electron model (FEM) cannot explain the effect of substitution on the electronic spectrum of phenanthrene. In order to get further information the electronic spectra of forty-eight phenanthrene derivatives each bearing a substituent at 2-, 3-, or 9-positions have been examined, and it was found that the electronic spectra of these derivatives also cannot be explained on the basis of FEM. SCF-MO-CI calculation has been carried out on phenanthrylpoly-ynes and hydroxyphenanthrenes revealing that the discrepancy between the observation and the expectation from FEM in the behavior of L_a and L_b of phenanthrene derivative is attributable to a complex configuration interaction.

It is well-known that the free electron model (FEM) proposed by Platt[1] gave a satisfactory explanation for the electronic spectra of polycyclic aromatic compounds. In the case of linear polyacenes, it was concluded on the basis of FEM treatment that the polarizations along the short axis (y-axis) were responsible for the B_a and L_a bands, and the transitions associated with L_b and B_b bands were considered to be polarized in the direction of the long axis (x-axis) (Fig. 1).

Empirical assignment of polarization on the basis of the substituent effect,[2] the result of the measurement of polarized spectrum of crystal[3] and the conclusion of MO calculation were found to be consistent with the FEM assignment.

For the electronic spectrum of phenanthrene, the first member of phene series, Platt assigned[1] long

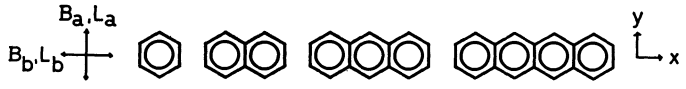

Fig. 1. Polarization diagram of linear-polyacenes on the basis of FEM.

1) H. B. Klevens and J. R. Platt, *J. Chem. Phys.*, **17**, 470 (1949); J. R. Platt, *ibid.*, **17**, 489 (1949).

2) *E.g.*, for anthracene derivatives, see, R. N. Jones, *Chem. Rev.*, **32**, 1 (1943).

3) D. P. Craig and P. C. Hobbins, *J. Chem. Soc.*, **1955**, 539.

axis polarized transitions to L_a and B_b species, and short axis polarized transitions to L_b and C_b species. However, the strong transition, called B_b by Platt[1] was relabeled B_a by Ham and Ruedenberg.[4]

Since SCFMO calculation[5] was consistent with that of Ham and Ruedenberg, the state assignment indicated in Fig. 2 was employed in this paper. Little experimental verification of the assignment has been done, probably owing to the lack of spectral data on phenanthrene derivatives.

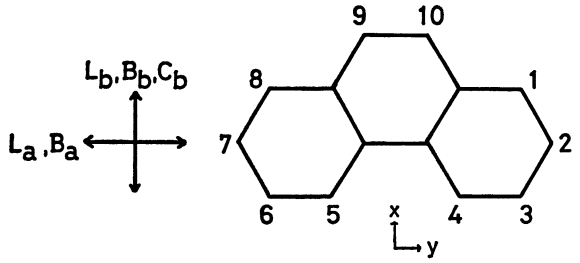

Fig. 2. Polarization diagram of phenanthrene.

During the course of studies on the regularities of the electronic spectra of diarylpoly-ynes,[6] we noticed that the behavior of L_a and L_b bands in the spectra of substituted phenanthrenes could not be explained simply on the basis of FEM. It was desirable to get further spectral data on monosubstituted phenanthrene derivatives to solve the interesting problem. Several monosubstituted derivatives bearing a substituent at 2-, 3-, or 9-positions have been prepared.[7] It was anticipated that the substituent may exert a distinctly different effect on the electronic spectrum at these three positions. The electronic spectra of the 37 phenanthrene derivatives we prepared, together with those of the reported ones (11 compounds), were examined with respect to the nature and position of the substituent, and were compared with the expected effect from FEM consideration. The 48 compounds are given in Fig. 11.

Electronic Spectra[8]

The absorption bands of phenanthrene have been assigned to be L_b, L_a, B_a, and C_b in the sequence of diminishing wavelength.[4,5] From the standpoint of FEM, it was anticipated that a substitution at 2-position of phenanthrene may exert a more marked effect on the B_a and L_a bands than does a substitution at the 3- or 9-position, and C_b and L_b bands should be affected more strongly by a substitution at 3- or 9-position than that at 2-position.

A brief summary of the substituent effect observed in some of the substituted phenanthrenes is given in the following.

Methyl and Hydroxymethylphenanthrenes [R-CH_3 *and* R-CH_2OH] *(R=phenanthryl).* An essestial difference between the electronic spectra of phenanthrene and of methylphenanthrenes could not be observed.[9] As illustrated in Fig. 3, similar spectra have been obtained in hydroxymethylphenanthrenes. The difference of position of substitution gave no appreciable change in the electronic spectra, indicating the lack of electronic interaction between these substituents and the nucleus.

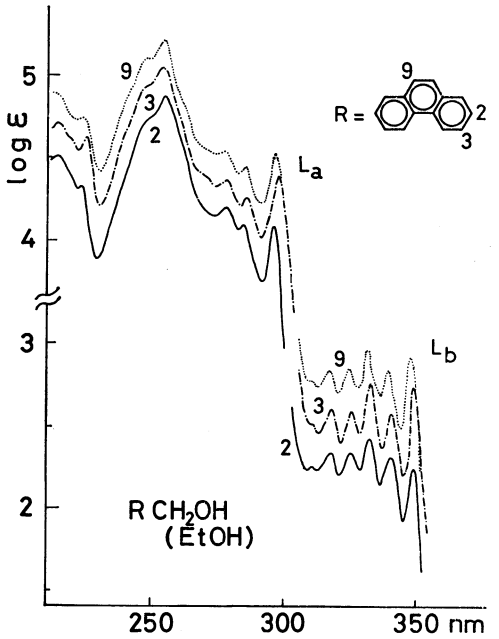

Fig. 3. The absorption curves of hydroxymethylphenanthrenes. The curves, with the exception of 2-substituted compound at the bottom, have been displaced upward on the ordinate axis by 0.1 log ε unit increments from the curve immediately below.

Acetylphenanthrenes [$RCOCH_3$] *and Formylphenanthrenes* [RCHO]. The absorption curves of the methylketones and the aldehydes are given in Figs. 4 and 5. The spectra of 2-isomers show close resemblance to that of phenanthrene itself, while the 3- and 9-isomers exhibit similar absorption curves which differ from that of the 2-isomer. The large red-shift of B_a band of 2-isomers as compared with 3- and 9-isomers is in line with the expectation from FEM. In the case of 3- and 9-isomers, the C_b bands seem to submerge under the B_a bands resulting in broad absorption bands around 250 nm. The large red shift of C_b band of 3- or 9-isomer is also in line with FEM anticipation. On the other hand, contrary to expectation from FEM consideration, the largest blue-shift of L_a band of the

4) N. S. Ham and K. Ruedenberg, *J. Chem. Phys.*, **25**, 13 (1956).

5) K. Nishimoto and L. S. Forster, *Theor. Chim. Acta*, **3**, 407 (1965).

6) S. Akiyama and M. Nakagawa, *Tetrahedron Lett.*, **1964**, 719; K. Nishimoto, R. Fujishiro, S. Akiyama, and M. Nakagawa, This Bulletin, **39**, 2320 (1966); S. Akiyama and M. Nakagawa, *ibid.*, **40**, 340 (1967); S. Akiyama, K. Nakasuji, K. Akashi, and M. Nakagawa, *Tetrahedron Lett.*, **1968**, 1121.

7) The synthesis of these substituted phenanthrenes will be reported in the near future as Part V of "Linear Conjugated Systems bearing Aromatic Terminal Groups."

8) The electronic spectra were obtained on a Hitachi EPS-3T spectrophotometer at room temperature using a well-matched pair of 1 cm quartz cell.

9) Reliable spectra of 3- and 9-methyl derivatives were reported in "UV Atlas of Organic Compounds," Vol. III, Butterworths, London and Verlag Chemie, Weinheim (1967). The 2-isomer has been prepared by us.

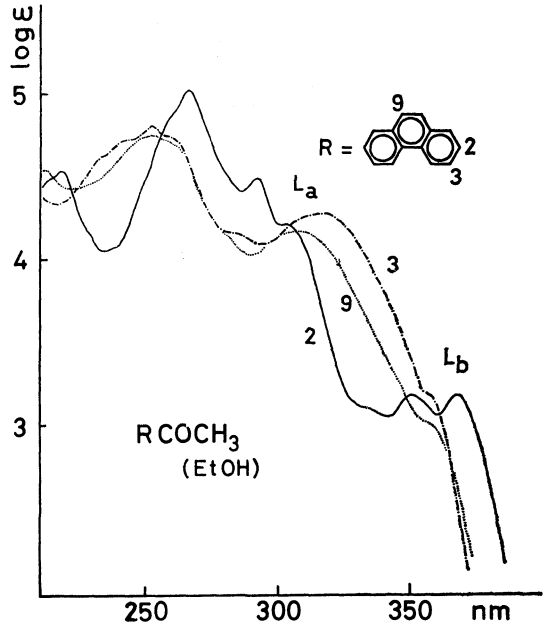

Fig. 4. The absorption curves of acetylphenanthrenes.

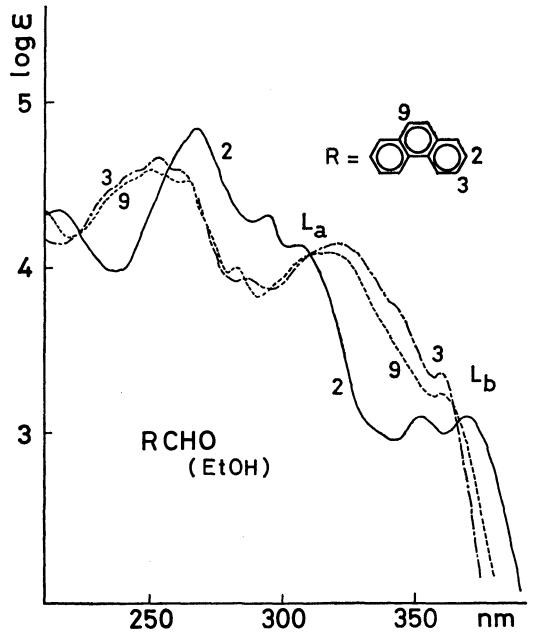

Fig. 5. The absorption curves of formylphenanthrenes.

2-isomer was observed, and the L_b band showed the largest red-shift in the case of 2-isomer.

Ethynylphenanthrenes [R–C≡CH]. The electronic spectrum of 2-ethynylphenanthrenes was found to be closely related with that of phenanthrene (Fig. 6). 3- and 9-Isomers exhibited C_b bands (230—240 nm) at longer wavelength than 2-isomer (200 nm), and the B_a band of 2-isomer showed a bathochromic shift accompanied with appreciable hyperchromism as compared with B_a bands of 3- and 9-isomers. The spectral change caused by the change of position of substitution is consistent with FEM anticipation. However, though the L_a bands of 3- and 9-isomers showed an appreciable red-shift as compared with that of phenanthrens, no shift of the L_a band was observed in 2-isomer. With regard to the L_b band, the 2-isomer

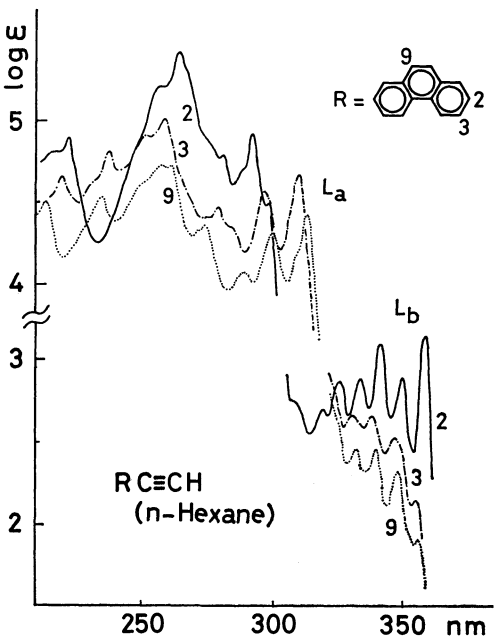

Fig. 6. The absorption curves of ethynylphenanthrenes. The curves, with the exception of 9-substituted compound at the bottom, have been displaced upward on the ordinate axis by 0.2 log ε unit increments from the curve immediately below.

absorbed at the longest wavelength. Thus behavior of L_a and L_b bands are inconsistent with FEM argument.

Diphenanthrylpoly-ynes [R(C≡C)$_n$R]. As illustrated in Fig. 7, 2,2′-diphenanthrylacetylene (n=1) exhibited a characteristic absorption curve owing to the marked red-shift of the B_a band. The broad band observed at around 250 nm in the spectra of the 3- and 9-isomers seem to be the composite of B_a and submerged C_b bands. The increasing red-shift of L_a band in the sequence of 2-, 3-, and 9-isomers is in contrast with the expectation from FEM. The trend observed in the spectra of diphenanthrylacetylenes was also observed in the spectra of di- (n=2), tri- (n=3) and pentaacetylenes (n=5) (Figs. 8, 9, and 10). The regular bathochromic shift of L_a band in line with the increasing number of n is impressive (*cf.*, Fig. 11).

From the results, it is evident that the behavior of C_b and B_a bands is in line with FEM anticipation. However, the spectral shifts of L_a and L_b bands were found to be inconsistent. The effect of substitution

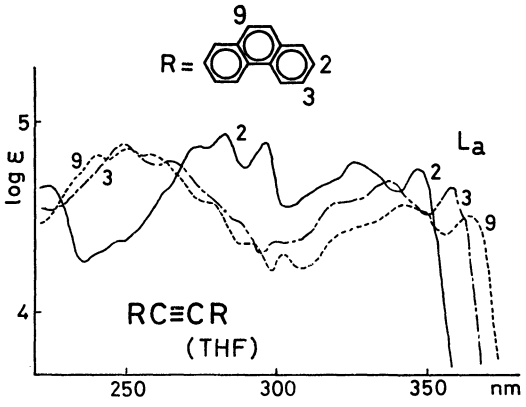

Fig. 7. The absorption curves of diphenanthrylacetylenes.

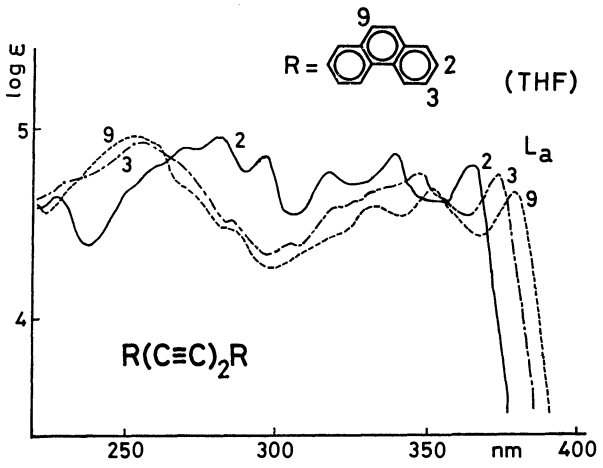

Fig. 8. The absorption curves of diphenanthryldiynes.

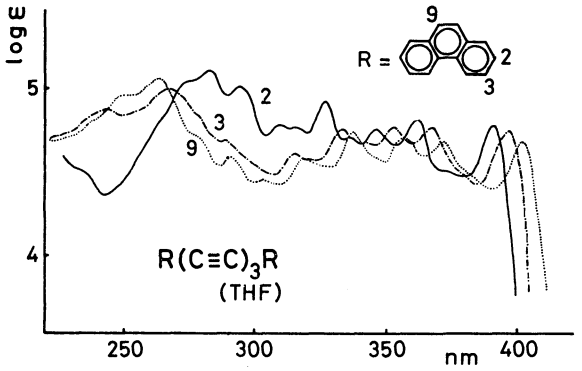

Fig. 9. The absorption curves of diphenanthryltriynes.

on the shifts of L_a and L_b bands is summarized in Fig. 11. When a bulky group such as $NHCOCH_3$, $COCH_3$, or CHO is introduced to the 9-position of phenanthrene nucleus, it should interfere sterically with the hydrogen atom at the 8-position. This seems to be responsible for the observed small red-shift and the hypochromism of the L_a band of phenanthrene bearing a large group at 9-position. The increasing red-shift of L_a band in phenanthryl mono-, di-, and tri-acetylenes [$\mathbf{R(C{\equiv}C)_nH}$, $n=1,2$, and 3] in the sequence of 2-<3-<9-isomers seems to support the above argument, as the linear substituents should suffer minor steric interference from the hydrogen at 8-position.

The Results of Semi-Empirical SCF-MO-Cl Calculation

The apparent contradiction between the observed spectral behavior of substituted phenanthrenes and the expected spectral change from the FEM of substituted phenanthrenes prompted us to elucidate this problem theoretically. In previous papers,[10] it was concluded theoretically that a linear polyacene having a substituent at α-position, such as α-naphthol, should exhibit an electronic spectrum having practically the same band characteristics as those of the parent hydrocarbon. On the other hand, in the electronic spectrum of a β-substituted linear polyacene, such as β-naphthol, a considerable mixing of the L_a and L_b species should occur modifying the band characteristics of the parent hydrocarbon. In the case of β-naphthol, the longest-wavelength absorption band should be the L_b band containing about 30% of L_a component.

Phenanthrene can be regarded as benznaphthalene. Consequently, the 9-position in phenanthrene is either an α- or a β-position of the naphthalene nucleus. Thus a more complicated spectral change by introduction of a substituent in the nucleus of phene-series is expected as compared with that of acene-series.

We have calculated the electronic structures of phenanthrene, 2-, 3-, and 9-phenanthrylpoly-ynes, and 2-, 3-, and 9-hydroxyphenanthrenes by a semi-empirical SCF-MO-CI method based on π-electron approximation and variable β approximation.[3] Two-centre electron repulsion integrals were calculated by the method proposed previously by one of us (K. N.).[11] As shown by Hinze and Jaffé,[12] the valence state ionization potential (I) and the electron affinity (A) associated with carbon atom are almost independent of hybridization. The same values of I and A were used for all carbon atoms in this paper. The parameters are summarized in Table 1. In the vari-

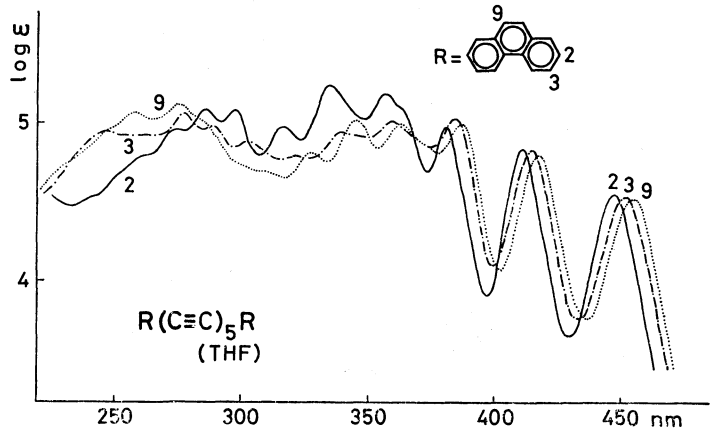

Fig. 10. The absorption curves of diphenanthrylpentaynes.

10) K. Nishimoto, *J. Phys. Chem.*, **67**, 1443 (1963); K. Nishimoto and R. Fujishiro, This Bulletin, **37**, 1660 (1964).

11) K. Nishimoto, *Theor. Chim. Acta*, **5**, 74 (1966).

12) J. Hinze and H. H. Jaffé, *J. Amer. Chem. Soc.*, **84**, 540 (1962).

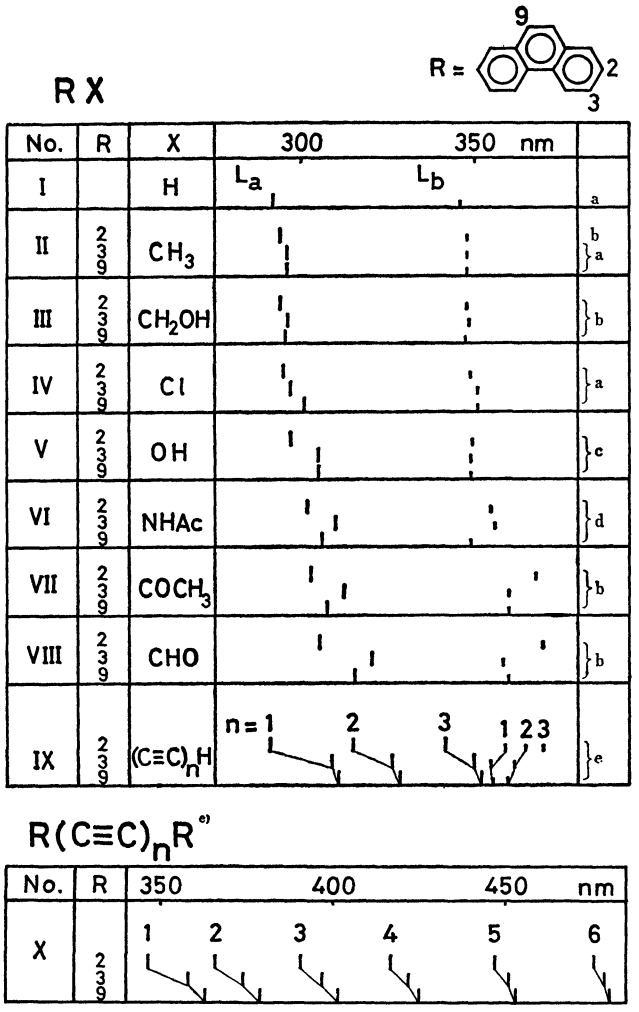

Fig. 11. Solvent: I and IX: hexane; II, III, V, VI, VII, and VIII: ethanol; IV: light petroleum (bp 100—120°C); X: tetrahydrofuran.
a) "UV Atlas of Organic Compounds," Vol. III, Butterworths, London and Verlag Chemie, Weinheim (1967). b) measured by the present authors. c) Table 2, Ref. d. d) "Absorption Spectra in the Ultraviolet and Visible Region," Vol. I, ed. by L. Lang, Publishing House of the Hungarian Academy of Sciences, Budapest (1961), pp. 213, 217, and 221. e) synthesized and measured by the present authors.

Table 1. Parameters

	I (eV)	A (eV)
C^+	6.60	0.00
C^{2+}	30.88	10.85

$\beta_{C-C}=\beta_{C=C}=\beta_{C\equiv C}=-0.51p-1.84$ eV
$\beta_{C-O}=-0.56p-2.20$ eV

able β approximation, a conventional geometry is assumed in which all the bond lengths are set at 1.40 Å.[13] The transition energies have been computed after including approximately the same amount of configuration interaction as involved for phenanthrene.[13] Singly excited configurations up to 3.0 eV from the lowest excited configuration are included in the calculation. The calculated transition energies and intensities are summarized together with experimental data in Table 2. A satisfactory agreement between the calculated results and experimental data was obtained affording theoretical basis to the observed bathochromic shift of L_a band in the 2-, 3-, and 9-substituted phenanthrenes (2-<3-<9-) and that of L_b band (9-<3-<2-).

It is interesting to note that the B_a and B_b species of phenanthrene are approximately degenerated (*i.e.*, $\Delta E(B_a)=4.91$ eV, $\Delta E(B_b)=5.00$ eV). However, B_a should be very intense ($f(B_a)=1.260$; $f(B_b)=0.425$). According to the present calculation, the absorption band at around 250 nm region of phenanthrene is associated with the long-axis (y-axis) polarized transition. The result is in line with the assignment by Ham and Ruedenberg.[4]

For phenanthrene, there are as usual two non-mixing pairs of states. As the calculation indicates, the b states arising from the paired excitation $\psi_7\rightarrow\psi_9$ and $\psi_6\rightarrow\psi_8$ are associated with the short-axis polarized transitions, and the a states which arise from $\psi_7\rightarrow\psi_8$ and $\psi_6\rightarrow\psi_9$ are related with the long-axis polarized transitions. In the case of phenanthrene derivatives, because of the complete loss of molecular symmetry, all the singly excited configurations usually interact with each other. However, by means of the criteria we obtained,[10] we can assign the state levels as shown in Table 3.

Table 2. Transition energies (eV) and intensities of phenanthrene and its derivatives

Molecule	Transition energy: Singlet Calcd	Singlet Obsd	Triplet Calcd	Triplet Obsd	Oscillator strength Calcd	Oscillator strength Obsd	Polarization[a] Calcd	Polarization[a] Obsd
Phenanthrene	3.58	3.75[b]	2.57	2.68[c]	0	0.003[b]	x	x[b]
	4.27	4.23[b]			0.459	0.18[b]	y	y[b]
	4.91	4.91[b]			1.260	1.09[b]	y	y[b]
	5.00				0.425		x	
	5.32				0.435			
2-Ethynylphenanthrene	3.53	3.45	2.63		0			
	4.24	4.26			0.514		1°	
	4.36	4.70			1.700		175°	
	4.89				0.650		72°	
	5.24				0.225		94°	

13) K. Nishimoto, *Theor. Chim. Acta*, **7**, 207 (1967).

TABLE 2 continued

Molecule	Transition energy				Oscillator strength		Polarization[a]	
	Singlet		Triplet					
	Calcd	Obsd	Calcd	Obsd	Calcd	Obsd	Calcd	Obsd
3-Ethynylphenanthrene	3.57	3.49	2.53		0			
	4.04	4.01			0.856		161°	
	4.75	4.80			0.822		154°	
	4.97				0.544		106°	
	5.07				1.106		52°	
9-Ethynylphenanthrene	3.67	3.49	2.37		0			
	3.99	3.98			0.688		153°	
	4.75	4.77			1.030		78°	
	4.82				0.778		177°	
	4.99				0.348		4°	
2-Butadiynylphenanthrene	3.65	3.40	2.72		0			
	4.03	3.94			2.125		176°	
	4.30				0.097		8°	
	4.82				0.653		81°	
	5.24				0.148		17°	
3-Butadiynylphenanthrene	3.73	3.42	2.43		0			
	3.86	3.80			1.283		147°	
	4.48				0.496		110°	
	4.96				1.041		55°	
	5.12				0.618		9°	
9-Butadiynylphenanthrene	3.67	3.44	2.45		0			
	3.75	3.77			1.148		137°	
	4.47				0.732		85°	
	4.76				0.884		18°	
	5.02				0.417		163°	
2-Hexatriynylphenanthrene	3.64		2.49		0			
	3.73	3.62			2.253		177°	
	4.33				0.204		7°	
	4.75				0.586		91°	
	5.01				0.239		19°	
3-Hexatriynylphenanthrene	3.55	3.54	2.29		1.970		136°	
	3.73				0			
	4.32				0.354		82°	
	4.88				0.881		50°	
	5.09				0.589		172°	
9-Hexatriynylphenanthrene	3.54	3.52	2.41		1.624		132°	
	3.68				0			
	4.34				0.534		75°	
	4.74				0.816		23°	
	5.01				0.601		160°	
2-Hydroxyphenanthrene	3.51	3.37[d]	2.58		0.015		101°	
	4.26	4.25[d]			0.296		1°	
	4.71	4.86[d]			1.445		176°	
	4.95				0.507		68°	
	5.28				0.316		101°	
3-Hydroxyphenanthrene	3.52	3.41[d]	2.54		0.018		21°	
	4.13	4.06[d]			0.536		174°	
	4.91	5.00[d]			1.120		3°	
	4.96				0.330		115°	
	5.20				0.629		84°	
9-Hydroxyphenanthrene	3.56	3.39[d]	2.75		0.026		32°	
	4.09	4.06[d]			0.456		169°	
	4.84	5.00[d]			0.851		23°	
	4.89				0.462		157°	
	5.10				0.389		116°	

a) The numerical value gives the angle between the transition moment vector and y-axis of the molecule.
b) H. B. Klevens and J. R. Platt, *J. Chem. Phys.*, **17**, 470 (1949).
c) D. S. McClure, *ibid.*, **17**, 905 (1949).
d) C. Djerassi, H. Bendes, and P. Sengupta, *J. Org. Chem.*, **20**, 1046 (1955).

Table 3. The coefficients of lowest singly excited configurations in the lowest excited states of phenanthrene and its derivatives

State	Coefficients of						Classification
	$\chi_{m\to m+1}$	$\chi_{m-1\to m+2}$	$\chi_{m\to m+2}$	$\chi_{m-1\to m+1}$	$\chi_{m\to m+3}$	$\chi_{m-2\to m+1}$	
				Phenanthrene			
1	0	0	0.6755	0.6755	−0.0768	0.0768	L_b
2	0.9482	−0.2710	0	0	0	0	L_a
3	0.2442	0.9532	0	0	0	0	B_a
4	0	0	−0.6036	0.6036	−0.3151	−0.3151	B_b
5	0	0	−0.3472	0.3472	0.5303	0.5303	C
				2-Hydroxyphenanthrene			
1	0.5303	0.4405	−0.3858	0.5335	−0.1156	−0.0287	L_a+L_b
2	0.6484	0.2483	0.2582	−0.6437	0.0959	0.0325	
3	−0.2038	0.5361	0.6873	0.2777	0.0016	0.1366	B_a+B_b
4	−0.4133	0.6157	−0.2994	−0.3441	0.0491	−0.2661	
5	−0.1835	0.1645	−0.2651	−0.2289	−0.4220	0.5286	C
				3-Hydroxyphenanthrene			
1	0.1757	0.0797	0.7194	−0.6038	0.0512	0.0434	L_b
2	0.9437	0.2138	−0.1368	0.1377	−0.0202	0.0106	L_a
3	−0.1925	0.9197	−0.1215	−0.0879	0.1001	−0.1023	B_a
4	−0.0696	0.2417	0.4796	0.5579	−0.3772	0.3376	B_b
5	0.0108	−0.0251	0.3963	0.4489	0.4295	−0.5394	C
				9-Hydroxyphenanthrene			
1	0.2527	0.1128	0.7051	−0.5876	−0.0949	0.0524	L_b
2	0.9213	0.2123	−0.2397	0.1437	0.0431	−0.0302	L_a
3	−0.1831	0.6469	−0.4172	−0.3725	−0.1712	−0.0854	B_a+B_b
4	−0.1224	0.6358	0.3188	0.4075	0.4696	0.0346	
5	−0.0051	−0.2499	−0.2487	−0.3488	0.7610	−0.111	C
				2-Ethynylphenanthrene			
1	0	0	−0.6679	0.6679	−0.0475	−0.0475	L_b
2	0.9196	0.2402	−0.1209	−0.1209	−0.0620	0.0620	L_a
3	−0.1234	0.8835	0.2692	0.2692	−0.0153	0.0153	B_a
4	0.2494	−0.3357	0.5783	0.5783	0.1568	−0.1568	B_b
5	−0.0808	0.0857	−0.2417	−0.2417	0.3617	−0.3617	—
				3-Ethynylphenanthrene			
1	0	0	−0.6835	0.6835	−0.0446	−0.0446	L_b
2	0.9737	0.1339	0.0062	0.0062	−0.0185	0.0185	L_a
3	−0.0697	0.7975	−0.0113	−0.0113	0.3889	−0.3889	B_a
4	−0.0420	0.2902	0.5583	0.5583	−0.2856	0.2856	B_b
5	0.0575	−0.4224	0.4057	0.4057	0.4329	−0.4329	—
				9-Ethynylphenanthene			
1	0	0	0.6850	0.6850	0.0907	0.0907	L_b
2	0.9710	−0.1813	−0.0237	0.0237	−0.0431	0.0431	L_a
3	0.0160	−0.1779	0.6257	−0.6257	0.1959	−0.1959	B_b
4	0.1180	0.8035	0.2395	−0.2395	−0.2933	0.2933	B_a
5	0.1160	0.4753	−0.1007	0.1007	0.5669	−0.5669	C

The following conclusions can be deduced from Table 3.

1) The nature of the excited states of phenanthrene derivatives is considerably dependent on the type of substituent.

2) The effect of substituent on the mixing of configurations at the lower excited states is found to be the largest at 2-position and rather small at 3- and 9-positions.

3) The L_a species of phenanthrene is considerably shifted by the substitution at 3- and 9-positions. Since it was indicated that a rather large interaction between L_a and L_b species should be produced by the substitution at 2-position, very much shifts of the L_a species in 2-substituted derivatives are expected. In fact as indicated in Fig. 11, a small change of L_a band of

phenanthrene by substitution at the 2-position was observed [*e.g.*, phenanthrene: 292 nm (in *n*-hexane); 2-ethynylphenanthrene: 291 nm (in *n*-hexane); 2-hydroxyphenanthrene: 292 nm (in ethyl alcohol)].

This suggests that 3- and 9-positions should resemble the α-position in linear polyacenes, while the 2-position would be similar to the β-position in polyacenes.

The intensities of L_b species of phenanthrylpoly-ynes are calculated to be zero. However, if we use different valence state ionization potentials for different hybridization, we will have non-zero, but very small intensities.

The calculation reveals that the discrepancy between the observation and the expectation from FEM

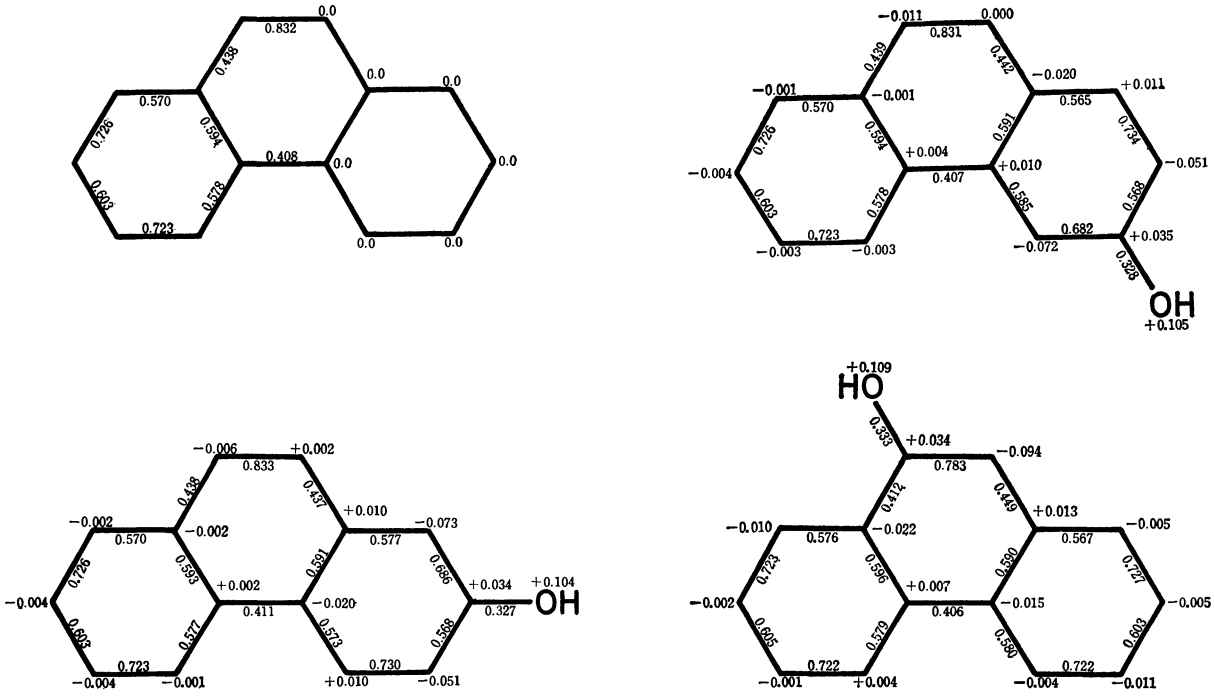

Fig. 12. Molecular diagrams of phenanthrene and its hydroxy derivatives in the ground states.

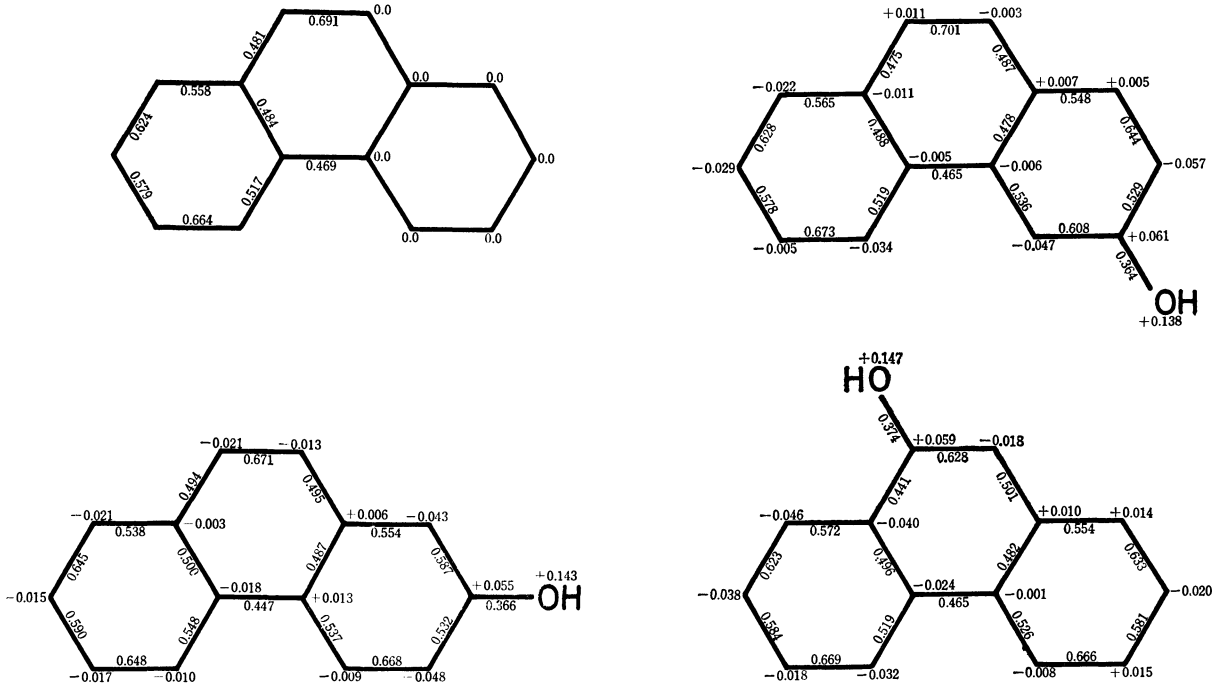

Fig. 13. Molecular diagrams of phenanthrene and its hydroxy derivatives in the lowest exited singlet states.

on the behavior of L_a and L_b species of phenanthrene derivatives should be attributed to a complex configuration interaction. It should be noted that the FEM treatment should be carefully applied to phene-series, especially in the case of qualitative argument of substituent effect on the electronic spectra of phene-series.

Appendix

Appendix 1. Changes of the molecular properties of hydroxyphenanthrenes by excitation.

The molecular diagrams of phenanthrene and its hydroxy derivatives are given in Figs. 12 and 13. The molecular properties, expected by the present SCF-MO calculation are summarized as follows:

Molecular Geometry: As indicated by the molecular diagram (Fig. 12), the molecule will expand and take a round shape in the excited state. The marked change of the bond order at 9—10 position is noteworthy.

Reactivity: In the ground state, the nucleus bearing hydroxy group will be most reactive. However, in the excited state, the 1-, 3-, 8-, and 9-positions in 2-hydroxy derivative, the 2-, 4-, 5- and 7-positions in 3-hydroxy isomer and 5-, 7-, and 8-positions in 9-hydroxy derivative are expected to be reactive.

pK_a: The molecular diagrams indicate that the acidity (pK_a) of the hydroxy derivatives will be as follows:

Ground state: $2 \approx 3 > 9$

Excited state: $3 > 2 > 9$

The change of charge density in hydroxy derivatives on excitation is found to be fairly large. On the other hand, no change of charge density is found in the phenanthryl-poly-ynes on excitation.

Appendix 2. Calculated ionization potentials and electron affinity of phenanthrene and its derivatives (eV).

Molecule	I	A
Phenanthrene	8.14	1.46
2-Hydroxyphenanthrene	8.01	1.35
3-Hydroxyphenanthrene	7.78	1.28
9-Hydroxyphenanthrene	7.71	1.21
2-Ethynylphenanthrene	8.14	1.46
3-Ethynylphenanthrene	7.98	1.63
9-Ethynylphenanthrene	7.91	1.69
2-Butadiynylphenanthrene	7.99	1.61
3-Butadiynylphenanthrene	7.83	1.77
9-Butadiynylphenanthrene	7.74	1.86
2-Hexatriynylphenanthrene	7.80	1.80
3-Hexatriynylphenanthrene	7.70	1.90
9-Hexatriynylphenanthrene	7.62	1.98

BULLETIN OF THE CHEMICAL SOCIETY OF JAPAN, VOL. 44, 1062—1067 (1971)

Sterically Controlled Syntheses of Optically Active Organic Compounds. XIII. Catalytic Hydrogenation of Symmetric Substrates in the Presence of Asymmetric Molecules[1]

Takao YOSHIDA and Kaoru HARADA

Institute of Molecular Evolution and Department of Chemistry, University of Miami, Coral Gables, Florida 33134, U.S.A.

(Received August 10, 1971)

Several organic acids which contain C=O, C=N, and C=C double bonds are catalytically hydrogenated in the presence of various optically active organic bases by the use of several solvent systems. Effects of bases and solvents on the optical activities of the products are examined.

Many asymmetric hydrogenation reactions have been reported;[2-7] however, only few reports on the asymmetric hydrogenation using symmetric substrate and catalyst in the presence of asymmetric molecules have appeared in the literature. Lipkin and Stewart[8] reported the catalytic hydrogenation of β-methylcinnamate and β-(α-naphthyl)-cinnamate with hydrocinchonine, in which a small degree of asymmetric hydrogenation was demonstrated. Nakamura[9] reported asymmetric hydrogenation of acetophenone oxime in the presence of *l*-menthoxyacetic acid.

In this paper, catalytic hydrogenations of various symmetric organic acids which contain C=O, C=N, and C=C double bonds were carried out by using several solvent systems in the presence of asymmetric organic bases. The substrates used were: benzoylformic acid, α-acetamidoacrylic acid, α-acetamidocinnamic acid, β-phenylpyruvic acid, and α-oximino-propionic acid. Optically active organic bases used were: *l*-sparteine, *l*-ephedrine, (S)-(−)- and (R)-(+)-α-methylbenzylamine, (R)-(+)-α-ethylbenzylamine, and (S)-(−)- and (R)-(+)-α-(1-naphthyl)ethylamine. The

1) Contribution no. 163 of the Institute of Molecular Evolution, Universitv of Miami. Part XII, K. Harada and T. Yoshida, *Chem. Commun.*, **1970**, 1071.

2) S. Akabori, T. Ikenaka, and K. Matsumoto, *Nippon Kagaku Zasshi*, **73**, 112 (1952).

3) Y. Izumi, M. Imaida, H. Fukawa, and S. Akabori, This Bulletin, **36**, 21 (1963).

4) J. C. Sheehan and R. E. Chandler, *J. Amer. Chem. Soc.*, **83**, 4795 (1961).

5) R. G. Hiskey and R. C. Northrop, *ibid.*, **83**, 4798 (1961).

6) K. Harada, *Nature*, **212**, 1571 (1967); *J. Org. Chem.*, **32**, 1790 (1967).

7) J. Mathieu and J. Weill-Raynal, *Bull. Soc. Chim. Fr.*, **1968**, 1211.

8) D. Lipkin and T. D. Stewart, *J. Amer. Chem. Soc.*, **61**, 3295 (1939).

9) Y. Nakamura, *Nippon Kagaku Zasshi*, **61**, 1051 (1940).

solvents used were: water, methanol, ethanol, isopropanol, *t*-butanol, and dioxane. Results are summarized in Tables 1, 2, and 3 and in Figs. 1, 2, and 3.

In Fig. 1, optical purities of mandelic acid (reaction A), alanine (reaction B), phenylalanine (reaction C), and β-phenyllactic acid (reaction D) prepared in the presence of *l*-sparteine by the use of various solvents are presented. The discontinuity of optical purity curves in reactions A, B, and C by the use of various solvents is observed between methanol and ethanol, and in reaction D, discontinuity is found between ethanol and isopropanol.

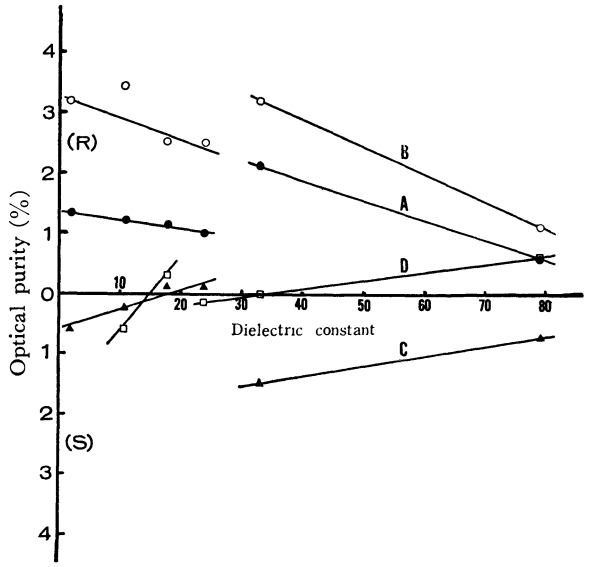

Fig. 1. Catalytic hydrogenation in the presence of *l*-sparteine.
A Benzoylformic acid+*l*-sparteine
B α-Acetamidoacrylic acid+*l*-sparteine
C α-Acetamidocinnamic acid+*l*-sparteine
D Phenylpyruvic acid+*l*-sparteine

In Fig. 2, the optical purity of mandelic acid (reaction E), alanine from α-acetamidoacrylic acid (reaction F), alanine from α-oximino-propionic acid (reaction G), and β-phenyllactic acid (reaction H) are shown. In reaction G, optical purity of alanine from α-oximino propionic acid is rather high and the value reaches 10% by the use of isopropanol. Optical activity of β-phenyllactic acid reaches 7.5% by the use of methanol. The discontinuity of optical purity curves of the products is found in all reactions E, F, G, and H. Inversion of configuration of the products is observed in reactions E, F, and G.

In Fig. 3, alanine formation from α-acetamidoacrylic acid by the use of various optically active bases is presented. In reactions I and J, S-(−)-α-methylbenzylamine and (R)-(+)-α-methylbenzylamine are used respectively for the synthesis of alanine. The optical purity curve of reactions I and J are similar in magnitude but are opposite in sign. The antipodal results are also obtained in the formation of alanine by the use of (R)-(+)-α-(l-naphthyl)ethylamine (reaction L) and (S)-(−)-α-(l-naphthyl)ethylamine (reaction M). The magnitude of optical activity and also sign of configuration of the resulting alanine change, depending on the solvent used. The discontinuity

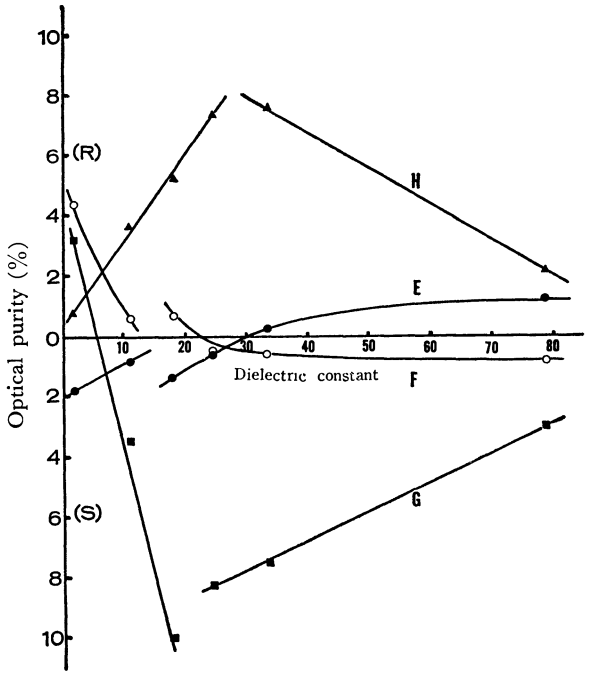

Fig. 2. Catalytic hydrogenation in the presence of *l*-ephedrine.
E Benzoylformic acid+*l*-ephedrine
F α-Acetamidoacrylic acid+*l*-ephedrine
G Oximino propionic acid+*l*-ephedrine
H Phenylpyruvic acid+*l*-ephedrine

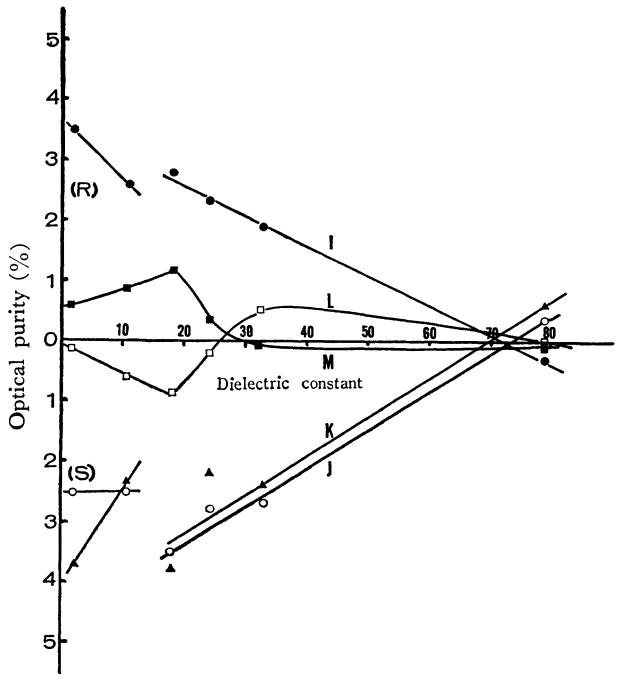

Fig. 3. Catalytic hydrogenation of α-acetamidoacrylic acid in the presence of various optically active amines.
I α-Acetamidoacrylic acid+(S)-(−)-α-methylbenzylamine
J α-Acetamidoacrylic acid+(R)-(+)-α-methylbenzylamine
K α-Acetamidoacrylic acid+(R)-(+)-α-ethylbenzylamine
L α-Acetamidoacrylic acid+(R)-(+)-α-(l-naphthyl)ethylamine
M α-Acetamidoacrylic acid+(S)-(−)-α-(l-naphthyl)ethylamine

Table 1. Catalytic hydrogenation in the presence of *l*-sparteine

No.	Substrate	Amine	Solvent	Yield (%)	$[\alpha]_D^{25}$ a)	Config.	P(%) b)
A-1	$C_6H_5COCOOH$ (450 mg)	*l*-Sparteine (700 mg)	H_2O	400 mg (88)	−1.0 (c=2.21)	R	0.6
2			MeOH	400 (88)	−3.3 (c=1.68)	R	2.1
3			EtOH	430 (94)	−1.6 (c=2.46)	R	1.0
4			*i*-PrOH	420 (92)	−1.8 (c=2.23)	R	1.1
5			*t*-BuOH	430 (94)	−2.0 (c=2.85)	R	1.2
6			Dioxane	420 (92)	−2.1 (c=2.64)	R	1.3
B-1	CH_2=C(NHAc)-COOH (390 mg)	*l*-Sparteine (700 mg)	H_2O	200 mg (75)	−1.6 (c=0.34)	R	1.1
2			MeOH	250 (94)	−4.6 (c=0.34)	R	3.2
3			EtOH	240 (90)	−3.6 (c=0.15)	R	2.5
4			*i*-PrOH	230 (86)	−3.6 (c=0.28)	R	2.5
5			*t*-BuOH	240 (90)	−4.9 (c=0.20)	R	3.4
6			Dioxane	240 (90)	−4.6 (c=0.25)	R	3.2
C-1	C_6H_5CH=C(NHAc)-COOH (615 mg)	*l*-Sparteine (700 mg)	H_2O	420 mg (85)	−0.6 (c=2.45)	S	0.7
2			MeOH	380 (77)	−1.4 (c=1.21)	S	1.5
3			EtOH	400 (81)	+0.1 (c=2.13)	R	0.1
4			*i*-PrOH	400 (81)	+0.1 (c=2.23)	R	0.1
5			*t*-BuOH	400 (81)	−0.2 (c=2.72)	S	0.2
6			Dioxane	360 (73)	−0.6 (c=2.68)	S	0.6
D-1	$C_6H_5CH_2COCOOH$ (820 mg)	*l*-Sparteine (1.170 g)	H_2O	640 mg (78)	+0.13 (c=3.63)	R	0.6
2			MeOH	650 (79)	0 (c=3.71)		0.0
3			EtOH	600 (73)	−0.02 (c=3.62)	S	0.1
4			*i*-PrOH	620 (75)	+0.06 (c=2.88)	R	0.3
5			*t*-BuOH	630 (76)	−0.14 (c=2.84)	S	0.6

a) (S)-(+)-Mandelic acid: $[\alpha]_D$=+156.2° (H_2O)
DNP-(S)-(+)-Alanine: $[\alpha]_D$=+143.9° (1 N NaOH)
(R)-(+)-β-Phenyllactic acid: $[\alpha]_D$=+22.2° (H_2O)
DNP-(S)-(−)-Phenylalanine: $[\alpha]_D$=−93.7° (1 N NaOH).
b) Optical purity is defined as ($[\alpha]_D$ obs/$[\alpha]_D$ lit)×100.

of optical purity curves is observed in reactions I, J, and K.

An explanation of these results would be very difficult because of the complexity of the reaction system. A substrate (acid) and a base would interact with each other, and these two kinds of molecules would also be absorbed on the catalyst surface. The solvent molecule in the reaction system would also interact with the substrate, the base, and the catalyst.

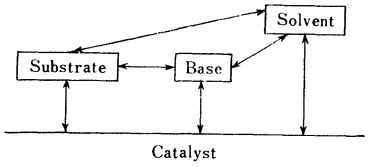

In reaction (A), optical purity of mandelic acid prepared from benzoylformic acid tends to increase to the R-configuration depending on the decrease of dielectric constant of the solvent used. On the other hand, in reaction (D), optical purity of β-phenyllactic acid from phenylpyruvic acid tends to increase to the S-configuration, depending on the decrease of polarity of the solvent used. In reaction (B), the configuration of alanine from α-acetamidoacrylic acid is R and the optical purity increases to the R-configuration depending on the use of less polar solvents. However, in reaction (C), configuration of phenylalanine from α-acetamidocinnamic acid which is a similar homologue of α-acetamidoacrylic acid, is S and the direction of increase of optical purity curve is antipodal to the reaction (B). These results suggest that the phenyl residue of acetamidocinnamic acid could be an important factor to determine the conformation of the substrate on the catalyst surface.

In reaction (A) and (B), by the use of *l*-sparteine, configurations of mandelic acid and alanine are both found to be R and optical activity curves change similarly to the R-configuration, depending on the decrease of polarity of the solvent. However, in reactions (E) and (F) by the use of *l*-ephedrine, configurations of mandelic acid and alanine from the same substrate are antipodal to each other. These results suggest that the replacement of optically active base could

Table 2. Catalytic hydrogenation in the presence of *l*-ephedrine

No.	Substrate	Amine	Solvent	Yield (%)	$[\alpha]_D^{25}$ a)	Config.	P(%)b)
E-1	$C_6H_5COCOOH$ (750 mg)	*l*-Ephedrine (830 mg)	H_2O	630 mg (83)	−1.9 (c=2.04)	R	1.2
2			MeOH	680 (90)	−0.4 (c=2.15)	R	0.2
3			EtOH	650 (86)	+0.1 (c=2.03)	S	0.6
4			*i*-PrOH	640 (84)	+2.0 (c=2.06)	S	1.3
5			*t*-BuOH	630 (83)	+1.4 (c=1.91)	S	0.9
6			Dioxane	640 (84)	+2.8 (c=2.76)	S	1.8
F-1	CH_2=C(NHAc)-COOH (390 mg)	*l*-Ephedrine (500 mg)	H_2O	250 mg (94)	+1.2 (c=0.32)	S	0.8
2			MeOH	240 (90)	+0.9 (c=0.52)	S	0.6
3			EtOH	260 (97)	+0.7 (c=0.49)	S	0.5
4			*i*-PrOH	250 (94)	−1.0 (c=0.51)	R	0.7
5			*t*-BuOH	250 (94)	−0.8 (c=0.57)	R	0.6
6			Dioxane	250 (94)	−6.3 (c=0.26)	R	4.4
G-1	CH_3-C(NOH)-COOH (310 mg)	*l*-Ephedrine (500 mg)	H_2O	150 mg (56)	+4.4 (c=0.33)	S	3.0
2			MeOH	150 (56)	+10.8 (c=0.26)	S	7.5
3			EtOH	50 (19)	+11.8 (c=0.39)	S	8.2
4			*i*-PrOH	— (16)c)	+14.4 (c=0.41)	S	10.0
5			*t*-BuOH	— (20)c)	+5.0 (c=0.44)	S	3.5
6			Dioxane	— (8)c)	−4.4 (c=0.48)	R	3.1
H-1	$C_6H_5CH_2COCOOH$ (820 mg)	*l*-Ephedrine (825 mg)	H_2O	700 mg (85)	+0.5 (c=2.07)	R	2.2
2			MeOH	640 (78)	+1.7 (c=1.13)	R	7.6
3			EtOH	680 (82)	+1.6 (c=2.39)	R	7.3
4			*i*-PrOH	670 (81)	+1.2 (c=1.89)	R	5.2
5			*t*-BuOH	640 (78)	+0.8 (c=1.71)	R	3.6
6			Dioxane	550 (67)	+0.2 (c=2.34)	R	0.9

a) (S)-(+)-Mandelic acid: $[\alpha]_D$=+156.2° (H_2O)
DNP-(S)-(+)-Alanine: $[\alpha]_D$=+143.9° (1 N NaOH)
(R)-(+)-β-Phenyllactic acid: $[\alpha]_D$ +22.2° (H_2O).
b) Optical purity is defined as ($[\alpha]_D$ obs/$[\alpha]_D$ lit)×100.
c) Yields are calculated from DNP-alanine.

result in the change of the conformation of the substrate molecule on the catalyst surface. The discrepancies between reactions (A) and (B) and reactions (E) and (F) might be accounted for by the fact that *l*-sparteine has a rigid structure and *l*-ephedrine has a relatively flexible structure. The optical purity of mandelic acid (reaction E) is rather low, however, while the optical purity of β-phenyllactic acid (reaction H), which is a similar homologue of mandelic acid, is rather high (~8%).

In reactions (J) and (K), alanine was prepared by the use of (R)-(+)-α-methylbenzylamine and (R)-(+)-α-ethylbenzylamine. The optical purity curves of (J) and (K) are almost the same as shown in Fig. 3. This implies that the difference between methyl and ethyl residue in the optically active amines does not affect the optical purity of the resulting alanine.

In order to avoid fractionation of the partially optically active amino acids during the isolation and purification procedures, a part of the amino acids were converted to DNP-derivatives. The DNP-amino acids were purified by using Celite column chromatography[10] without fractionation of the optical isomers.[11] Optical activities of mandelic acid and β-phenyllactic acid were measured before recrystallization to avoid fractionation of these optical isomers.

Experimental

All hydrogenations were carried out by the use of Parr 3910 shaker type hydrogenation apparatus at room temperature (23—25°C) with initial pressure of 40 psi.

All optical rotation measurements were carried out by the use of JASCO-ORD-UV-5 spectropolarimeter. The length of the cell used for the measurement of optical activity were 1 cm and 10 cm. All solutions for the measurement of optical activity were filtered through 0.2 μ Millipore filter or whatman No. 50 hardened filter paper. Optical rotatory

10) J. C. Perrone, *Nature*, **167**, 513 (1951); A. Court, *Biochem. J.*, **58**, 70 (1954).
11) K. Harada and K. Matsumoto, *J. Org. Chem.*, **32**, 1794 (1967); K. Harada and T. Yoshida, This Bulletin, **43**, 921 (1970).

Table 3. Catalytic hydrogenation of α-acetamidoacrylic acid in the presence of various optically active amines

No.	Substrate	Amine	Solvent	Yield (%)	$[\alpha]^{25}$ a)	Config.	P(%) b)
I-1	$CH_2=C(NHAc)-COOH$ (260 mg)	(S)-$C_6H_5CH(NH_2)CH_3$ (240 mg)	H_2O	160 mg (90)	+0.4 (c=0.69)	S	0.3
2			MeOH	150 (84)	−2.8 (c=0.53)	R	1.9
3			EtOH	150 (84)	−3.3 (c=0.61)	R	2.3
4			*i*-PrOH	150 (84)	−4.0 (c=0.75)	R	2.8
5			*t*-BuOH	170 (96)	−3.7 (c=0.68)	R	2.6
6			Dioxane	160 (90)	−5.1 (c=0.67)	R	3.5
J-1	$CH_2=C(NHAc)-COOH$ (260 mg)	(R)-$C_6H_5CH(NH_2)CH_3$ (240 mg)	H_2O	150 mg (84)	−0.5 (c=4.29)	R	0.3
2			MeOH	150 (84)	+3.8 (c=2.84)	S	2.7
3			EtOH	130 (73)	+4.1 (c=3.74)	S	2.8
4			*i*-PrOH	150 (84)	+5.0 (c=2.83)	S	3.5
5			*t*-BuOH	150 (84)	+3.6 (c=2.35)	S	2.5
6			Dioxane	160 (90)	+3.6 (c=2.97)	S	2.5
K-1	$CH_2=C(NHAc)-COOH$ (260 mg)	(R)-$C_6H_5CH(NH_2)C_2H_5$ (340 mg)	H_2O	150 mg (84)	−0.9 (c=2.68)	R	0.6
2			MeOH	150 (84)	+3.5 (c=2.81)	S	2.4
3			EtOH	160 (90)	+3.2 (c=2.87)	S	2.2
4			*i*-PrOH	160 (90)	+5.4 (c=2.48)	S	3.8
5			*t*-BuOH	160 (90)	+3.3 (c=2.74)	S	2.3
6			Dioxane	150 (84)	+5.4 (c=2.52)	S	3.7
L-1	$CH_2=C(NHAc)-COOH$ (260 mg)	(R)-$C_{10}H_7CH(NH_2)CH_3$ (340 mg)	H_2O	160 mg (90)	0 (c=2.56)		0
2			MeOH	160 (90)	−0.8 (c=1.85)	R	0.5
3			EtOH	160 (90)	+0.3 (c=2.33)	S	0.2
4			*i*-PrOH	160 (90)	+1.2 (c=2.45)	S	0.8
5			*t*-BuOH	160 (90)	+0.9 (c=2.49)	S	0.6
6			Dioxane	160 (90)	+0.2 (c=2.59)	S	0.1
M-1	$CH_2=C(NHAc)-COOH$ (260 mg)	(S)-$C_{10}H_7CH(NH_2)CH_3$ (318 mg)	H_2O	150 mg (84)	+0.3 (c=3.81)	S	0.2
2			MeOH	160 (90)	+0.1 (c=4.06)	S	0.1
3			EtOH	160 (90)	−1.0 (c=2.74)	R	0.7
4			*i*-PrOH	150 (84)	−1.9 (c=3.05)	R	1.3
5			*t*-BuOH	150 (84)	−1.1 (c=4.02)	R	0.8
6			Dioxane	160 (90)	−0.8 (c=5.23)	R	0.6

a) DNP-S(+)-Alanine: $[\alpha]_D$ = +143.9° (1 N NaOH).
b) Optical purity is defined as ($[\alpha]_D$ obs/$[\alpha]_D$ lit)×100.

dispersion curves of some of the samples were recorded in order to determine that the rotatory power of the samples was due to the optically active specific compounds which formed by the asymmetric hydrogenation.

Elemental analyses were carried out by Micro-Tech Laboratories, Inc., Skokie, Illinois. Melting points were measured by the use of Mel-Temp apparatus. Melting points measured were uncorrected.

Dielectric constants of the solvents used were as follows:

H_2O	78.5
MeOH	32.6
EtOH	24.3
i-PrOH	18.3
t-BuOH	10.9
Dioxane	2.2

Optically active amines used were: *l*-(−)-sparteine, $[\alpha]_D^{25}$ −4.59° (benzene); *l*-(−)-ephedrine, $[\alpha]_D^{25}$ −5.13° (ethanol); S-(−)-α-methylbenzylamine, $[\alpha]_D^{25}$ −42.4° (benzene); R-(+)-α-methylbenzylamine, $[\alpha]_D^{25}$ +40.0° (benzene); R-(+)-α-ethylbenzylamine, $[\alpha]_D^{25}$ +21.7° (benzene); R-(+)-α-(1-naphthyl)ethylamine, $[\alpha]_D^{25}$ +77.8° (benzene); S-(−)-α-(1-naphthyl)ethylamine, $[\alpha]_D^{25}$ −80.0° (benzene).

Hydrogenation of Benzoylformic Acid with l-*Sparteine.* A mixture of benzoylformic acid (450 mg, 0.003 mol) and *l*-sparteine (700 mg, 0.003 mol) in 15 m*l* of water was subjected to hydrogenation at room temperature with 500 mg of 5% palladium on charcoal. After the hydrogenation was over, the catalyst was removed by filtration and the filtrate was concentrated under reduced pressure. The residual oil was dissolved in 6 N hydrochloric acid and the mixture was extracted with ether several times. The combined ethereal extract was washed once with water and dried with anhydrous sodium sulfate. After evaporation of ether, mandelic acid was crystallized. Yield, 400 mg (88%), mp 116.5—117°C, $[\alpha]_D^{32}$ −0.96° (*c* 2.21, H_2O), optical purity 0.6%. A part of this sample was recrystallized from benzene, mp 120—121°C.

Found: C, 62.92; H, 5.25%. Calcd for $C_8H_8O_3$: C, 63.15; H, 5.30%.

Similar experiments by using other solvents are listed in Table 1 (A).

Hydrogenation of Benzoylformic Acid with l-*Ephedrine.* The hydrogenation procedures are the same as described above. The results are summarized in Table 2 (E).

Hydrogenation of α-Acetamidoacrylic Acid with l-*Sparteine.* A mixture of α-acetamidoacrylic acid (390 mg, 0.003 mol) and *l*-sparteine (700 mg, 0.003 mol) in 30 m*l* of water was hydrogenated with 5% palladium on charcoal (500 mg). After hydrogenation was over, the catalyst was removed by filtration. The filtrate was concentrated *in vacuo*. The residual oil was hydrolyzed with 6 N hydrochloric acid (20 m*l*) under reflux for 5 hr. The hydrolyzate was evaporated to dryness under reduced pressure. The residue was dissolved in 10% aqueous sodium carbonate solution and the solution was extracted with ether repeatedly to remove sparteine. The aqueous solution was acidified and was evaporated to dryness *in vacuo*. The residual amino acid hydrochloride was extracted with absolute ethanol. The ethanol solution was evaporated under reduced pressure. Free alanine was obtained by using a Dowex-50 ion exchange column. Yield, 200 mg (75%), DNP-alanine, $[\alpha]^{25}$ −1.56° (*c* 0.34, 1 N NaOH), optical purity, 1.1%, mp 178—179°C.

Found: C, 42.50; H, 3.53; N, 16.9%. Calcd for $C_9H_9O_6N_3$: C, 42.36; H, 3.55; N, 16.47%.

Similar experiments by the use of other solvents are summarized in Table 1 (B).

Hydrogenation of α-Acetamidoacrylic Acid with l-*Ephedrine.* The hydrogenation procedures are similar to those described above. The results are summarized in Table 2 (F).

Hydrogenation of α-Acetamidoacrylic Acid with S-(−)-α-Methylbenzylamine. The procedures are similar to those described above. The results are summarized in Table 3 (I, J, K, L, M).

Hydrogenation of α-Acetamidocinnamic Acid with l-*Sparteine.* The procedures are similar to those described above. From α-acetamidocinnamic acid (615 mg, 0.003 mole) and *l*-sparteine (700 mg, 0.003 mole), 420 mg of phenylalanine was obtained (85%), DNP-phenylalanine, $[\alpha]^{25}$ −0.61° (*c* 2.45, 1 N NaOH), optical purity 0.65%, mp 216.5—217.5°C.

Found: C, 54.11; H, 3.84; N, 12.57%. Calcd for $C_{15}H_{13}O_6N_3$: C, 54.38; H, 3.96; N, 12.68%.

Other results obtained by the use of other solvents are listed in Table 1 (C).

Hydrogenation of Phenylpyruvic Acid with l-*Epherine.* Phenylpyruvic acid (820 mg, 0.005 mole) and *l*-ephedrine (825 mg, 0.005 mole) were dissolved in 30 m*l* of water. The mixture was hydrogenated and β-phenyllactic acid was isolated as above. Yield, 700 mg (85%), mp 94—95°C, $[\alpha]_D^{25}$ +0.48° (*c* 2.07, H_2O), optical purity 2.2%. A part of the sample was recrystallized from benzene, mp 96—97°C.

Found: C, 62.92; H, 5.25%. Calcd for $C_9H_{10}O_3$: C, 63.15; H, 5.30%.

Other results obtained by using other solvents are summarized in Table 2 (H).

This work was supported by Grant No. NSG 10-007-052 of the National Aeronautics and Space Administration.

Sterically Controlled Syntheses of Optically Active Organic Compounds. XIV. Syntheses of Dipeptides from *N*-(α-Ketoacyl)-α-amino Acid Esters[1]

Kaoru HARADA and Kazuo MATSUMOTO

Institute of Molecular Evolution and Department of Chemistry, University of Miami, Coral Gables, Florida 33134, U.S.A.

(Received August 10, 1970)

Optically active α-amino acids were synthesized from azomethines of *N*-α-ketoacyl-amino acid esters by catalytic hydrogenation. When optically active (S)-alanine was used, (R)-amino acyl-(S)-alanine ester was obtained. When alkyl groups of optically active (S)-amino acids in the *N*-α-ketoacyl-amino acid esters were larger than ethyl group, the configurations of newly formed amino acids were found to be (S). From these results possible steric courses of the asymmetric syntheses are discussed.

Several nonenzymatic asymmetric syntheses of α-amino acids from α-keto acids have been reported.[2–14] Hiskey and Northrop[4] published a description of a stereospecific synthesis of dipeptide from benzylamine Schiff bases of *N*-pyruvoyl-(S)-alanine. They discussed the question of whether (S)-alanyl-(S)-analine would result (Scheme I), if the catalytic hydrogenation of the Schiff base were to follow the "Prelog Rule".[15] However, the ratio of resulting dipeptide, (R)-ala-(S)-ala: (S)-ala-(S)-ala, was found to be 2: 1. The results indicate that the catalytic hydrogenation does not follow the Prelog rule.

In order to clarify the stereochemical course of the sterically controlled synthesis, several reactions were carried out.[8] Oximes of (S)- and (R)-*N*-phenylglyoxyl-oyl-α-methylbenzylamine and *N*-(S)- and (R)-ethyl-

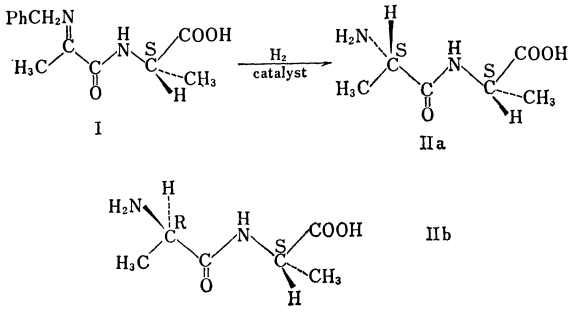

Scheme 1

benzoylformamide were hydrogenated and the hydrogenated products were hydrolyzed. When optically active (S)- or (R)-α-methylbenzylamine was used, the configuration of the resulting phenylglycine was (R) and (S), respectively,[8] which agreed with the results obtained by Hiskey and Northrop.[4] However, when (S)- or (R)-α-ethylbenzylamine was used, the resulting phenylglycine was (S) or (R) respectively, which agreed with the configurations expected by the formal application of the Prelog rule. The clear inversion of the configuration of the products depending on the α-methyl- and α-ethylbenzylamines could not be explained by an electronic effect. These results suggest that the reaction would be controlled by steric factors. In order to solve the problem, it has been proposed that the substrate might form a five-membered chelate ring structure with the catalyst (Scheme 2).[8] When (S)-α-methylbenzylamine was used as an optically active moiety of benzoylformamide, the conformation was proposed as structure III (conformation A). However, when (S)-α-ethylbenzylamine was used, the conformation of the substrate could be structure IV (conformation B). Since the ethyl group is bulkier than the methyl group, the ethyl group could reach the catalyst surface if the substrate were to take on con-

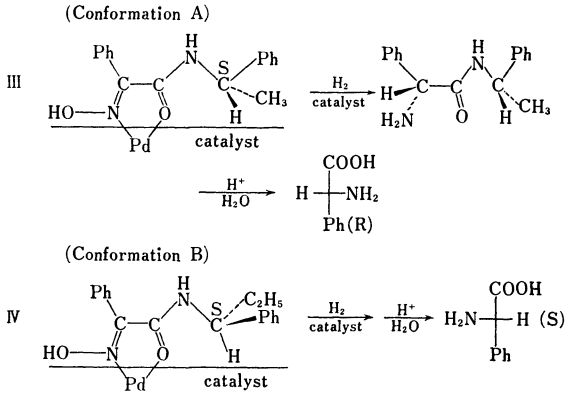

Scheme 2

1) For part XIII, T. Yoshida and K. Harada, This Bulletin, **44**, 1062 (1971). Presented in part at the Peptide Symposium at Yale University, August (1968). Contribution no. 121 of the Institute of Molecular Evolution, University of Miami.

2) S. Akabori and S. Sakurai, *Nippon Kagaku Zasshi*, **78**, 1629 (1957).

3) R. G. Hiskey and R. C. Northrop, *J. Amer. Chem. Soc.*, **83**, 4798 (1961).

4) R. G. Hiskey and R. C. Northrop, *ibid.*, **87**, 1753 (1965).

5) A. N. Kost, R. S. Sagitullin, and M. A. Yurouskaja, *Chem. Ind.* (London), **1966**, 1494.

6) A. Kanai and S. Mitsui, *Nippon Kagaku Zasshi*, **87**, 183 (1966).

7) K. Matsumoto and K. Harada, *J. Org. Chem.*, **31**, 1956 (1966).

8) K. Harada and K. Matsumoto, *ibid.*, **32**, 1794 (1967).

9) K. Harada, *Nature*, **212**, 1571 (1966); *J. Org. Chem.*, **32**, 1790 (1967).

10) K. Harada and K. Matsumoto, *J. Org. Chem.*, **33**, 4467 (1968).

11) K. Matsumoto and K. Harada, *ibid.*, **33**, 4526 (1968).

12) K. Harada and T. Yoshida, This Bulletin, **43**, 921 (1970).

13) K. Harada and J. Oh-hashi, *ibid.*, **43**, 960 (1970).

14) K. Harada and T. Yoshida, *Chem. Commun.*, **1970**, 1071.

15) V. Prelog, *Helv. Chim. Acta*, **36**, 308 (1953). The Prelog rule was originally proposed for homogeneous reactions. Therefore, the Prelog rule might not be applicable for catalytic hydrogenation of the Schiff base of α-keto acid amides. It is important to consider that the configurational agreement of the final product does not always mean that the conformation of the substrate follows the Prelog rule, because several possible conformations of the substrate would result in the specific configuration predicted by the Prelog rule.

Table 1. Sterically controlled syntheses of alanyl dipeptides

$$CH_3\text{-}\underset{\underset{\underset{CH_2Ph}{|}}{N}}{\overset{\overset{}{\|}}{C}}\text{-}CONH\text{-}\overset{*}{C}H(R)\text{-}COOiBu \xrightarrow[\text{catalyst}]{H_2} \text{Alanyl dipeptides}$$

R	Asymmetric moiety	Yield of alanine % a)	Ratio of diastereomeric dipeptides	Newly formed alanine: Config'n	Newly formed alanine: $[\alpha]_D$ of DNP-Alanine (1 N NaOH, c=0.3—0.6)	Newly formed alanine: Optical purity % d)	Conform'n of substrate
CH_3	(S)-ala-*i*-Bu	15	R-S:S-S=82:18	R	b)	64	A
	(S)-ala-Me	25	76:24	R	b)	52	A
Et	(S)-α-NH_2-*n*-Bu-*i*-Bu	16	29:71	S	c)	41	B
i-Pr	(S)-val-*i*-Bu	11	34:66	S	+45.5	32	B
	(R)-val-*i*-Bu	12	34:66	R	−45.3	32	B
	(S)-val-Me	12	42:58	S	+24.6	17	B
i-Bu	(S)-leu-*i*-Bu	19	32:68	S	+56.7	39	B
	(S)-leu-Me	18	41:59	S	+25.2	18	B
Benzyl	(S)-ph-ala-*i*-Bu	26	37:63	S	+36.4	25	B
$-CH_2COOiBu$	(S)-asp-di-*i*-Bu	11	37:63	S	+36.0	25	B
ϕ	(R)-ph-gly-*i*-Bu	27	50:50	±	0	0	B

a) Yields are calculated from pyruvic acid.
b) The ratio of diastereomeric dipeptides was measured by amino acid analyzer after saponification. From these results optical purities were calculated.
c) The optical activity of alanine was calculated from the results of $[\alpha]_D$ of free amino acid mixture and the composition of amino acids.
d) Optical purity defined as ($[\alpha]_D$ observed/$[\alpha]_D$ literature)×100, DNP-(S)-alanine, $[\alpha]_D$=+143.9° (1 N NaOH).

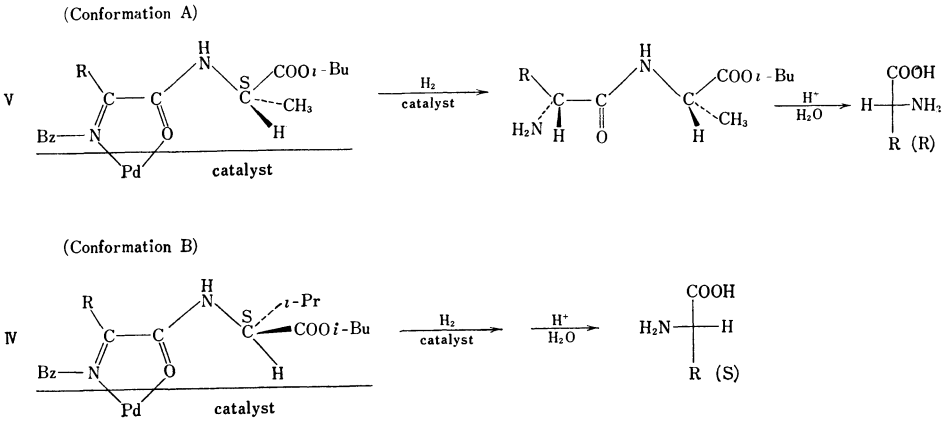

Scheme 3

formation A. Therefore, the most probable conformation is structure IV (conformation B) when the R-group of the amine is larger than the ethyl group. Then the cyclic intermediate complex could be adsorbed on the less bulky side of the molecule and the hydrogenation reaction would take place (Scheme II)[8] (two step mechanism).

In order to confirm further the proposed steric course of the asymmetric synthesis, a series of dipeptide syntheses were carried out in the study reported here. When benzylamine Schiff base of *N*-pyruvoyl-(S)-alanine isobutyl ester was used as a starting material, the configuration of the newly formed alanine was (R), (R)-ala-(S)-ala : (S)-ala-(S)-ala=82 : 18. When isobutyl (S)-α-aminobutyrate was used as an asymmetric center, (S)-alanine was obtained, (R)-ala-(S)-NH_2-Bu : (S)-ala-(S)-NH_2-Bu=29 : 71. In this series of reactions, also the inversion of configuration of the resulting amino acid was observed when asymmetric moieties containing methyl or ethyl residues were used. Results are summarized in Table 1. These results agreed with those obtained in the phenylcine synthesis.[8] The possible steric course of the reactions is shown in Scheme 3.

When the alkyl group of the asymmetric moiety is methyl (alanine isobutyl ester), structure A could be the preferred conformation. When the alkyl group is larger than the ethyl group (isobutyl α-aminobutyrate), structure B could be the major conformation in the sterically controlled syntheses of dipeptides. Intermediates A and B were then absorbed on the catalyst at the less bulky side and the hydrogenation reaction could take place. Optical purities of the newly formed alanine using valine and leucine isobutyl ester

TABLE 2. STERICALLY CONTROLLED SYNTHESES OF α-AMINOBUTYRYL PEPTIDES

$$C_2H_5\text{-}C(=N\text{-}CH_2Ph)\text{-}CONH\text{-}CH(R)\text{-}COO\text{-}i\text{-}Bu \xrightarrow[\text{catalyst}]{H_2} \xrightarrow[H_2O]{H^+} \alpha\text{-Aminobutyric Acid}$$

Asymmetric moiety	Yield a) %	Newly formed α-amino-*n*-butyric acid: Config'n	Newly formed α-amino-*n*-butyric acid: [α] of DNP-Derivative (1N NaOH, c=0.3—0.6)	Newly formed α-amino-*n*-butyric acid: Optical purity b)	Conform'n of substrate
(R)-φ-gly-*i*-Bu (oxime)	67	—	0	0	B
(S)-φ-ala-*i*-Bu (oxime)	56	S	+12.1	12	B
(S)-φ-ala-*i*-Bu	65	S	+8.8	9	B
(S)-asp-di-*i*-Bu	53	S	+25.7	26	B

a) Yields are calculated from α-ketobutyric acid.
b) Optical purity defined as ($[\alpha]_D$ observed/$[\alpha]_D$ literature)×100. DNP(S)-α-amino-*n*-butyric acid, $[\alpha]$=+98.8° (1 N NaOH)

are larger than those of alanine obtained by the use of valine or leucine methyl ester. This finding may also support the fact that structure B could be the major conformation in these reactions.

If structure B is the preferred conformation when the R group is larger than the ethyl group, one could state an order of effective bulkiness of the R group in this reaction by the use of the optical purity of newly formed alanine. When R is phenyl, the optical purity of newly formed alanine is zero, so that the effective bulkiness of the phenyl group and of the –COO–*i*-Bu group are the same. In the same way, the bulkiness of the benzyl group and of the $-CH_2COO$–*i*-Bu group are almost the same. However, these are smaller than those of the phenyl or –COO–*i*-Bu groups. The order of effective bulkiness of the R group could be arranged as shown below.

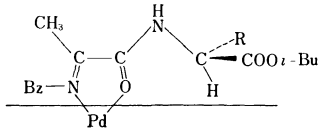

(Conformation B)

$$-COO\text{-}i\text{-}Bu \sim Ph > -CH_2Ph \sim -CH_2COO\text{-}i\text{-}Bu > i\text{-}Pr > i\text{-}Bu > Et$$

The order of bulkiness does not agree with the order of residue weight. In the order of effective bulkiness, the phenyl group is larger than the benzyl group and also the isopropyl group is larger than the isobutyl group. This relationship can be explained on the basis that the phenyl group and isopropyl group are rigid and branched and that these groups also cannot be bent. On the other hand, benzyl and isobutyl groups are flexible; these are not branched at the α-carbon to which these groups are attached. Therefore, the effective bulkiness of rigid and branched phenyl and isopropyl groups does not follow the order of residual weight.

Table II describes α-aminobutyryl peptides. The reaction products have all S–S and R–R structures. The R groups used were phenyl, benzyl, and $-CH_2$–COO–*i*-Bu. Therefore, structure B could be the major conformation in these reactions.

In summary, (a) a chelation hypothesis in the sterically controlled synthesis of dipeptide is proposed; (b) an order of effective bulkiness of side chains is assigned by the use of optical purity of the newly formed amino acids; (c) the dimension of the space between substrate and catalyst surface is inferred by the use of chemical data; (d) the possibility is advanced that one can determine the configurations of structurally unknown primary amines by the use of these results, when the proposed stereochemical course is further established.

Experimental

Amino Acid Esters. Amino acid methyl ester hydrochlorides were prepared by the thionyl chloride method.[16] Amino acid isobutyl ester *p*-toluenesulfonates (amino acid ester PTS) were prepared by the use of the azeotropic method in benzene with a Dean and Stark separation tube.[17] Yields were between 70 to 80%, (Table 3).

N-α-*Ketoacyl-α-amino Acid Esters.* Experimental procedures in the syntheses of dipeptide esters are similar to those described earlier.[8] α-Keto acid (0.03 mol) and α-amino acid ester (hydrochloride or *p*-toluenesulfonate), (0.03 mol) were dissolved in anhydrous tetrahydrofurane (150 m*l*) or freshly purified chloroform (100 m*l*). The solution was cooled to about −15°C. To this, 2.75 m*l* (0.03 mol) of phosphorus oxychloride was added dropwise in a period of 10 min. The mixture was kept at −10°C for 1 hr and at 0°C for 30 min. Then the mixture was again cooled to −15°C. To this solution 7.5 m*l* (0.09 mol) of pyridine was added dropwise in a period of 30 min at −15——10°C. After the addition, the solution was kept at −10——5°C for 1 hr, then the solution was brought to room temperature. Solvent was removed under reduced pressure. The residual syrup was dissolved in ethyl acetate and the solution was washed with 1 N hydrochloric acid, 5% sodium hydrogen carbonate, and then with water. The solution was dried with anhydrous sodium sulfate. Ethyl acetate was evaporated under reduced pressure. The attempt to crystallyze the residual yellow syrup was unsuccessful. The syrup was

16) W. J. Humphlett and C. V. Wilson, *J. Org. Chem.*, **26**, 2507 (1961).
17) L. Zervas, M. Winitz, and J. P. Greenstein, *ibid.*, **22**, 1515 (1957); M. Winitz, L. Block-Frankenthal, N. Izumiya, S. M. Birnbaum, C. G. Baker, and J. P. Greenstein, *J. Amer. Chem. Soc.*, **78**, 2424 (1956).

Table 3. Elemental analyses of amino acid esters

	Mp °C	$[\alpha]_D^{25}$ (EtOH)		C%	H%	N%
(S)-Ala *i*-Bu PTS	120—121	−1.1	Found	53.04	7.36	4.42
			Calcd	52.98	7.30	4.41
(S)-NH_2-Bu *i*-Bu HCl	124—125	+6.5	Found	49.29	9.36	7.11
			Calcd	49.05	9.27	7.15
(R)-Val *i*-Bu PTS	146—147	−9.1	Found	55.82	8.00	4.08
			Calcd	55.62	7.87	4.05
(S)-Leu *i*-Bu PTS	137—138	+10.3	Found	57.07	8.33	4.03
			Calcd	56.79	8.13	3.89
(S)-Phe *i*-Bu PTS	165—166	+24.9	Found	60.89	6.99	3.56
			Calcd	61.04	6.91	3.55
(R)-Phgly *i*-Bu PTS	185—186	−61.8	Found	60.16	6.74	3.74
			Calcd	60.13	6.64	3.69
(S)-Asp di-*i*-Bu PTS	128—129	+11.5	Found	54.64	7.61	3.40
			Calcd	54.65	7.48	3.35

used for further experiment.

Alanyl and α-Aminobutyryldipeptide Isobutyl Esters. *N*-α-Ketoacyl-α-amino acid ester and an equimolar amount of benzylamine were dissolved in benzene. The solution was gently refluxed for 20 minutes with a Dean-Stark separator. The benzene was removed under reduced pressure. The residual syrup was dissolved in absolute methanol. Hydrogenation and hydrogenolysis were carried out with 10% palladium on charcoal at room temperature, by the use of a Parr 3910 shaker type hydrogenation apparatus. After the reaction was over, the catalyst was removed and the methanol was evaporated under reduced pressure. The residue was dissolved in ethyl acetate and the solution was extracted with 1 N hydrochloric acid. To the aqueous solution, sodium hydrogencarbonate was added to bring the pH to 8. The solution was extracted with ethyl acetate. The solution was dried with anhydrous sodium sulfate and the solvent was evaporated under reduced pressure. The residual product (dipeptide ester) was used for further experiments (for saponification or for hydrolysis).

Optical Purity of Newly Formed Amino Acid Residues. Dipeptide esters were refluxed with 6 N hydrochloric acid for 8 hr. The hydrolyzate was evaported to dryness *in vacuo*. The residue was dissolved in a small amount of water and the solution was applied to a Dowex 50×2 column (hydrogen form, 100—200 mesh, 20×1.8 cm). After washing with water, amino acid mixture was eluted with 1 N aqueous ammonia. After evaporation of water and ammonia under reduced pressure, a mixture of free amino acids was obtained. The amino acid mixture was treated with 2,4-dinitrofluorobenzene in a conventional manner.[18] The resulting DNP-amino acids were separated by the use of a Celite column treated with pH 7.0 citrate buffer[19] without fractionation of optical isomer.[8,12]

In the synthesis of alanylphenylalanine in Table 1, DNP-(S)-alanine was isolated and analyzed.

Found: C, 42.42; H, 3.66; N, 16.64%. Calcd for $C_9H_9O_6N_3$; C, 42.36; H, 3.55: N, 16.47%.

In the synthesis of alanylaspartic acid in Table 1, free (S)-alanine was isolated by the use of Dowex 50×2 column.

Found: C, 40.68; H, 8.01; N, 15.58%. Calcd for $C_3H_7O_2N$: C, 40.44; H, 7.92; N, 15.72%.

Optical activities of separated DNP-amino acids were measured in 1 N sodium hydroxide by the used of a Rudolph model 80 polarimeter with PEC-101 photometer. In the case of alanyl-α-aminobutyric acid synthesis, the optical purity of alanine was determined by the measurement of specific rotation and composition of free amino acid mixture which was obtained by acid hydrolysis. The amino acid compositions were determined by the used of a Phoenix model K-5000 automatic amino acid analyzer.

This work was supported by Grant NGR 10-007-052 from the U.S. National Aeronautics and Space Administration.

18) F. Sanger, *Biochem. J.*, **39**, 507 (1945); K. R. Rao and H. A. Sober, *J. Amer. Chem. Soc.*, **76**, 1328 (1954).

19) J. C. Perrone, *Nature*, **167**, 513 (1951); A. Court, *Biochem. J.*, **58**, 70 (1954).

The Catalytic Dehydrogenation of Alcohols with Reduced Copper under Ultraviolet Light[1]

Shigeaki NAKAMURA and Kazuaki KAWAMOTO[2]
Department of Chemistry, Takamatsu Technical College, Takamatsu
(Received August 15, 1970)

In order to investigate whether or not the dehydrogenation activity of the reduced copper is affected by ultraviolet light, the reaction of such alcohols as ethanol, 1-propanol, 2-propanol, and 1-butanol was carried out with reduced copper and ultraviolet light at 250°C. It was found that the conversion of alcohols and the yield of aldehydes were larger with the reduced copper under ultraviolet light than without the light, and that aldol condensation for the ethanol reaction was recognizable when the reduced copper catalyst was used without ultraviolet light.

Many papers have reported on the decomposition of alcohols with copper catalysts.[3-6] The main products of the formation of a complex[4,7] between the alcohols and the copper catalysts were found to be aldehydes, ketones, and esters. On the other hand, the photochemical reaction of alcohols has been carried out recently.[8,9]

It has been reported that the radical formation of alcohol under ultraviolet light produced mainly RR'-$\dot{C}$OH,[9] from which aldehyde, pinacol, and so on were obtained. Although the photo-oxidation of such reactants as alcohol, water, and carbon monoxide has been studied with ZnO[10] sensitized by ultraviolet light, the reaction of gaseous alcohol in the presence of a reduced copper catalyst and ultraviolet light has not been carried out. Accordingly, the present work was carried out in order to study the difference between the catalytic reaction of alcohols with the reduced copper alone and that with the reduced copper under ultraviolet light. It was found that the yield of aldehydes and the conversions of ethanol, 1-propanol, and 1-butanol increased considerably with the catalytic reaction under ultraviolet light, with the exception of 2-propanol, and that 1-butanol might be formed from ethanol through an aldol condensation mechanism with the catalyst without ultraviolet light.

Experimental

Preparation of Catalyst. Copper nitrate, the starting material, was prepared from electrolytic copper and nitric acid.

A mixture of 20 g of electrolytic copper in an aqueous solution of nitric acid (90 g of 60% HNO_3 and 90 m*l* of distilled water) was heated gradually on a sand bath.

After the electrolytic copper has been completely dissolved, the solution was diluted with the same amount of distilled water and filtered through a glass filter. The diluted solution was evaporated below 60°C to give crystals of cupric nitrate hexahydrate. The blue crystals were dried under reduced pressure for several hours. A solution of 30 g of cupric nitrate hexahydrate, prepared by the method described above in 900 m*l* of distilled water, was kept at 22°C. A sodium hydroxide solution prepared from 15 g of sodium hydroxide and 300 m*l* of distilled water was brought to the same temperature and added rapidly to a stirred copper nitrate solution.

After the mixture had been stirred at this temperature for 30 min, the precipitate was washed well with distilled water by decantation, collected on a glass filter, dried in an electric oven at 105°C for 20 hr, powdered in an agate mortar, and finally stored in a stoppered bottle. The precipitates were reduced in the following ways. When hydrogen (or carbon monoxide) was passed through at the rate of 750—900 m*l* per hour over 10 g of the precipitate, the reduction temperature was always below 180°C in the case of hydrogen and below 140°C in the case of carbon monoxide, and the reduction time was 4—5 hr.

Apparatus and Procedure. The apparatus employed was similar to that used in the previous investigation,[6] with the exception that a low-pressure mercury lamp (UL1—8 DQ 80 W made by Ushio Electric Co., Ltd.) was inserted into the center of the reaction tube (Fig. 1). A definite amount (10 g) of the precipitate was spread in a Pyrex reaction tube (reaction part: 35 mm in inside diameter and 550 mm long), which was then set in an electrically-heated furnace of the horizontal type.

The furnace was heated to the reduction temperature and kept at this temperature for the period of the reduction.

The resulting catalyst was then heated to the reaction temperature (250°C) under ordinary pressure. The alcohols (ethanol, 1-propanol, 2-propanol, and 1-butanol) purified by the ordinary method were passed through the tube at a constant flow rate of 7.2 to 9.3 g per hour (carrier gas, nitrogen).

1) The major part of this research was presented at the 22nd Annual Meeting of the Chemical Society of Japan, Tokyo, March 31, 1969.

2) Present address: Institute of Commodities, Faculty of Economics, Kagawa University, Takamatsu.

3) E. F. Armstrong and T. P. Hilditch, *Proc. Roy. Soc.* (London), **97A**, 259 (1920); W. G. Palmer, *ibid.*, **101A**, 175 (1922); K. Kawamoto, This Bulletin, **41**, 932 (1968).

4) W. G. Palmer and F. H. Constable, *Proc. Roy. Soc.* (London), **106A**, 250 (1924).

5) P. Sabatier, "Die Katalyse in der Organischen Chemie," Akademische Verlag Gesellschaft m. b. H., Leipzig (1927).

6) K. Kawamoto, This Bulletin, **34**, 161, 795, 799 (1961).

7) A. A. Balandin, *Z. Physik. Chem.* (Leipzig), **B2**, 289 (1929); W. G. Palmer and F. H. Constable, *Proc. Roy. Soc.* (London), **107A**, 255, 270 (1925).

8) G. Leuschner and K. Pfordte, *Ann. Chem.*, **619**, 1 (1958); Y. Odaira, A. Morimoto, H. Yamamoto, and S. Tsutsumi, *Kogyo Kagaku Zasshi*, **64**, 457 (1961); K. Shima and S. Tsutsumi, *ibid.*, **64**, 460 (1961); K. Hatano, M. Yanagida, Y. Fujita, and T. Kwan, *ibid.*, **72**, 123 (1969).

9) G. Gibson, *Trans. Faraday Soc.*, **53**, 914 (1957); D. Ingram, *ibid.*, **54**, 1304 (1958).

10) I. Komuro, Y. Fujita, and T. Kwan, This Bulletin, **32**, 884 (1959); J. Kuriacose and M. C. Markham, *J. Catal.*, **1**, 498 (1962); E. Bauer and C. Neuweiler, *Helv. Chim. Acta*, **10**, 901 (1921); A. Berna, *J. Phys. Chem.*, **68**, 2047 (1964); W. Doerffler and K. Hauffe, *J. Catal.*, **3**, 156 (1964).

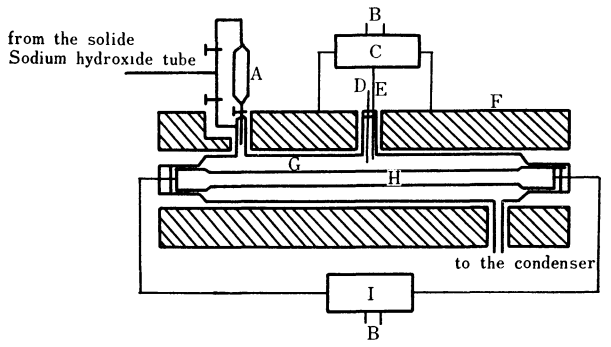

Fig. 1. Apparatus.
A: Funnel, B: Electric source, C: Temp. regulator, D: Thermometer, E: Thermocouple, F: Electric furnace, G: Reaction tube, H: Mercury lamp, I: Voltage stabilizer.

The reaction products coming out of the reaction tube were removed by being passed through a condenser filled with ice water, supplemented by two traps which were cooled with dry ice and acetone. The volume of gas evolved was determined by allowing it to displace the water from a graduated 2-*l* cylinder.

All the values given in the present research are averages of two to three measurements under constant reaction conditions, as Tables 1—4 show.

Analysis of the Products. The reaction products were identified by comparing them with authentic samples obtained by gas chromatography. In addition, the liquid products were dried over anhydrous sodium sulfate and then fractionally distilled, and the constituents of the cut were identified by their boiling points, densities, refractive indices, and the formation of the corresponding derivatives. All the derivatives for the identification of the reaction products were made by the Shriner, Fuson, and Curtin method.[11]

The reaction products were analyzed quantitatively by gas chromatography, using a Shimadzu Type GC-2C apparatus. A 5-m column of the filler (polyethylene glycol-6000, tricresyl phosphate, silicone DC-550 and diethylene glycol succinate in the case of the liquid products, and activated charcoal, molecular sieve-13X, hexamethylphosphoramide, tricresyl phosphate, acetonylacetone and dimethylsulfolane in the case of the gaseous products) was used at an operating temperature of 100°C and a flow rate of 22.0 ml/min of helium. For the determination of the water, a 3-m column packed with Shimalite F impregnated with polyethylene glycol-1000 was used at 100°C, with a hydrogen carrier and at 11.5 ml/min.

Results and Discussion

Tables 1—5 show the results of the present experiments.

Table 1. Catalytic dehydrogenation of ethanol with reduced copper under ultraviolet light
(Reaction temp.: 250°C)

Experiment No.	1	2	3	4	5	6
Catalyst	Abs.	Pres.	Pres.	Pres.	Pres.	Pres.
Reducing agent	—	H_2	CO	H_2	CO	Non
Ultraviolet light	Irra.	Non	Non	Irra.	Irra.	Irra.
Ethanol used (g)	20.82	20.10	20.02	19.86	20.05	19.99
Liquid products (g)	19.86	19.02	19.02	18.53	18.19	18.65 17.89[b]
Conversion[a] (%)	2.01	38.28	37.91	66.59	65.92	65.62[c]
Composition of Liquid Products (%)						
Ethanal	1.2	18.1	13.8	29.7	21.8	49.9
Ethyl acetate	—	16.8	21.2	25.4	33.9	12.6
Propanone	0.4	1.6	1.4	10.2	8.9	1.9
Aldol	—	0.3	T	0	0	0
2-Butenal	—	0.2	0.2	0	0	0
Butanal	—	0.2	0.2	0	0	0
2-Buten-1-ol	—	0.2	0.2	0	0	0
1-Butanol	—	0.4	0.4	T	T	T
2,3-Butanediol	T	—	—	T	T	T
2-Propanol	0.2	—	—	0.4	0.4	0.4
1-Propanol	T	—	—	T	T	T
Methanol	0.1	0.1	0.1	0.3	0.3	0.3
2-Butanol	0.1	—	—	0.2	0.1	0.1
Water	T	T	T	T	T	(0.76 g)
Unidentified product	T	0.4	0.4	0.4	0.5	0.4
Unreacted alcohol	98.0	61.7	62.1	33.4	34.1	34.4

Abs.: absent. Pres.: present. Irra.: irradiated. T: trace.
a) The conversion was given by 100·(grams of liquid product - grams of unreacted alcohol) divided by grams of liquid product.
b), c) The values were obtained by means of excluding water from the liquid products. The value in parentheses shows the weight of water formed.

11) R. L. Shriner, R. C. Fuson, and D. Y. Curtin, "The Systematic Identification of Organic Compounds," John Wiley & Sons, New York (1956).

TABLE 2. CATALYTIC DEHYDROGENATION OF 1-PROPANOL WITH REDUCED COPPER UNDER ULTRAVIOLET LIGHT
(Reaction temp.: 250°C)

Experiment No.	1	2	3	4	5	6
Catalyst	Abs.	Pres.	Pres.	Pres.	Pres.	Pres.
Reducing agent	—	H_2	CO	H_2	CO	Non
Ultraviolet light	Irra.	Non	Non	Irra.	Irra.	Irra.
1-Propanol used (g)	19.98	19.96	19.99	20.07	19.95	19.68
Liquid products (g)	19.35	19.00	18.84	19.26	18.50	19.10 18.46[b]
Conversion[a] (%)	1.81	37.32	36.78	62.62	62.38	62.19[c]
Composition of Liquid Products (%)						
Propanal	1.1	15.4	10.3	30.3	20.4	48.2
Propyl propionate	—	13.7	19.2	20.8	31.2	9.6
3-Pentanone	—	6.4	5.6	8.6	7.9	1.5
Ethanol	0.2	0.5	0.4	0.6	0.6	0.6
Methanol	T	0.2	0.2	0.2	0.2	0.3
3,4-Hexanediol	T	—	—	T	T	T
2-Butanol	0.2	—	—	0.4	0.4	0.4
2-Methyl-1-propanol	—	—	—	0.3	0.2	0.2
Hexane	T	—	—	T	T	T
Ethanal	0.2	—	—	T	T	T
Propanone	0.1	—	—	T	T	T
Water	T	T	T	T	T	(0.64 g)
Unidentified product	T	1.1	1.1	1.4	1.5	1.4
Unreacted alcohol	98.2	62.7	63.2	37.4	37.6	37.8

Abs.: absent. Pres.: present. Irra.: irradiated. T: trace.
a) The conversion was given by 100·(grams of liquid product - grams of unreacted alcohol) divided by grams of liquid product.
b), c) The values were obtained by means of excluding water from the liquid products. The value in parentheses shows the weight of water formed.

TABLE 3. CATALYTIC DEHYDROGENATION OF 1-BUTANOL WITH REDUCED COPPER UNDER ULTRAVIOLET LIGHT
(Reaction temp.: 250°C)

Experiment No.	1	2	3	4	5	6
Catalyst	Abs.	Pres.	Pres.	Pres.	Pres.	Pres.
Reducing agent	—	H_2	CO	H_2	CO	Non
Ultraviolet light	Irra.	Non	Non	Irra.	Irra.	Irra.
1-Butanol used (g)	20.07	19.98	19.91	19.96	19.98	19.92
Liquid products (g)	18.44	18.84	18.61	18.05	17.96	19.11 18.52[b]
Conversion[a] (%)	1.08	35.77	35.20	60.50	60.30	58.42[c]
Composition of Liquid Products (%)						
Butanal	0.7	18.9	13.7	30.2	22.8	48.4
Butyl butyrate	—	15.7	20.2	26.7	33.9	6.7
4-Heptanone	—	0.5	0.3	0.5	0.4	0.5
1-Propanol	0.2	0.2	0.2	0.3	0.4	0.4
Ethanol	T	0.2	0.2	0.2	0.2	0.2
Methanol	T	0.1	0.1	0.1	0.1	0.1
2-Pentanol	0.2	—	—	0.5	0.5	0.4
2-Methyl-1-butanol	0.1	—	—	0.2	0.3	0.2
3-Methyl-1-butanol	T	—	—	0.1	0.1	0.1
Ethanal	T	—	—	T	T	T
Propanone	T	—	—	T	T	T
Water	T	T	T	T	T	(0.59 g)
Unidentified product	0.2	0.4	0.5	1.7	1.6	1.4
Unreacted alcohol	98.6	64.0	64.8	39.5	39.7	41.6

Abs.: absent. Pres.: present. Irra.: irradiated. T: trace.
a) The conversion was given by 100·(grams of liquid product - grams of unreacted alcohol) divided by grams of liquid product.
b), c) The values were obtained by means of excluding water from the liquid products. The value in parentheses shows the weight of water formed.

Table 4. Catalytic dehydrogenation of 2-propanol with reduced copper under ultraviolet light
(Reaction temp.: 250°C)

Experiment No.	1	2	3	4	5	6
Catalyst	Abs.	Pres.	Pres.	Pres.	Pres.	Pres.
Reducing agent	—	H_2	CO	H_2	CO	Non
Ultraviolet light	Irra.	Non	Non	Irra.	Irra.	Irra.
2-Propanol used (g)	19.86	20.05	20.04	19.96	19.86	19.93
Liquid products (g)	18.28	17.84	18.43	18.62	18.44	20.39 19.42[b]
Conversion[a] (%)	1.81	90.19	90.61	92.37	92.68	91.19[c]
Composition of Liquid Products (%)						
Propanone	1.4	53.3	52.1	75.9	90.1	90.1
4-Methyl-2-pentanone	—	16.6	17.2	9.8	1.6	0.1
2,6-Dimethyl-4-heptanone	—	11.9	12.4	2.3	T	0
4-Methyl-2-pentanol	—	1.7	1.9	0.6	T	0
2,3-Dimethyl-2,3-butanediol	T	—	—	T	T	T
Water	T	5.6	6.0	2.8	T	(0.97 g)
2,3-Dimethylbutane	T	—	—	0.3	0.3	0.3
2-Butanol	0.2	—	—	0.4	0.4	0.4
Ethanal	0.2	—	—	0.3	0.3	0.3
Ethanol	T	—	—	T	T	T
Unidentified product	T	1.1	1.0	T	T	T
Unreacted alcohol	98.2	9.8	9.4	7.6	7.3	8.8

Abs.: absent. Pres.: Present. Irra.: irradiated. T: trace.
a) The conversion was given by 100·(grams of liquid product - grams of unreacted alcohol) divided by grams of liquid product.
b), c) The values were obtained by means of excluding water from the liquid products. The value in parentheses shows the weight of water formed.

Table 5. Catalytic reaction of alcohols with copper catalyst under ultraviolet light
Gaseous Products

Reactant	Catalyst	Light	Product
Ethanol	Pres.	Abs.	H_2, C_2H_4, CO, CO_2
	Pres.	Pres.	H_2, CH_4, C_2H_6, C_2H_4, n-C_4H_{10}, CO, CO_2
1-Propanol	Pres.	Abs.	H_2, C_3H_6, CO, CO_2
	Pres.	Pres.	H_2, CH_4, C_2H_6, C_2H_4, C_3H_8, C_3H_6, CO, CO_2
1-Butanol	Pres.	Abs.	H_2, 1-C_4H_8, CO, CO_2
	Pres.	Pres.	H_2, CH_4, C_2H_6, C_2H_4, C_3H_8, C_3H_6, n-C_4H_{10}, 1-C_4H_8, CO, CO_2
2-Propanol	Pres.	Abs.	H_2, CO
	Pres.	Pres.	H_2, CH_4, C_2H_6, C_3H_8, C_3H_6, CO

Pres.: present. Abs.: absent.

Comparison of the Copper Catalyst under Ultraviolet Light with the Non-irradiated Copper Catalyst. In the case of the gaseous reaction of ethanol, as is shown in Table 1, the conversion in the presence of the copper catalyst under ultraviolet light was much larger than that without the light.

The conversion of ethanol under only ultraviolet light was smaller than all those obtained in the presence of the copper catalyst.

As is shown in Tables 1—3, the conversion of 1-propanol and 1-butanol had an inclination similar to that of ethanol, but it was found that the conversions of the primary alcohols decreased slightly in proportion to the molecular weights of the primary alcohols. As is shown in Table 4, the conversion of 2-propanol in the presence of the catalyst and the light was almost the same as that obtained with the catalyst without the light. In the case of the catalytic reaction of 2-propanol, it is considered that the 2-propanol reaction differs from those of other primary alcohols by having the reactive α-hydrogen atom.

The total amounts of the main products of the alcohols, such as the aldehydes, the esters and the ketones, accounted for over 95% of the conversions of the present alcohols for both the catalytic reaction under ultraviolet light and the reaction without the light. The aldol condensation was observed with the catalytic reaction of ethanol in the absence of the light, but it did not occur quite as in the cases of the other alcohols.

The formation of diols by the use of ultraviolet light

was observed in the cases of ethanol, 1-propanol, and 2-propanol, but not in the case of 1-butanol. The gaseous products are shown in Table 5. When the reaction of alcohol in the presence of the catalyst and ultraviolet light was compared with that in the presence of the non-irradiated catalyst, more gaseous products were found to be formed under the former reaction conditions.

Comparison between the Reduced Copper Catalysts. As is shown in Table 1, the formation of ethanal from ethanol by dehydrogenation was more increased by the use of the hydrogen-reduced copper catalyst than by the use of the carbon monoxide-reduced copper catalyst and was further promoted by ultraviolet light. The same tendency was observed in the formation of propanal and butanal from 1-propanol and 1-butanol respectively, as is shown in Tables 2 and 3. As is shown in Table 4, the formation of propanone from 2-propanol by dehydrogenation was remarkably accelerated by ultraviolet light. The conversion of 2-propanol into propanone with the carbon monoxide-reduced catalyst under ultraviolet light was above 90% in all the products (included the unreacted alcohol). The aldehydes and the ketone mentioned above were obtained in any small amounts under ultraviolet light without the catalyst. Esters were obtained in larger quantities by the use of a reduced copper catalyst treated with carbon monoxide than with one reduced with hydrogen, and the production was further promoted by ultraviolet light. From the results mentioned above, it was found that the formation of the esters occurred preferentially with the carbon monoxide-reduced catalyst, and that the copper catalyst treated with hydrogen as the reducing agent was suitable for the formation of the aldehyde. The above facts suggest that the different structures of the catalyst surface are formed by the different reducing agents used. As Table 1 shows, the yield of propanone, which seems to have been formed by the secondary reaction process of ethanol, was nearly proportional to that of ethanal from ethanol. A similar tendency was also observed in the formation of 3-pentanone from 1-propanol, but little 4-heptanone was formed from 1-butanol.

Non-reduced Copper Catalyst. As is shown by Experiment No. 6 in Tables 1—3, the yield of aldehydes, such as ethanal from ethanol, propanal from 1-propanol, and butanal from 1-butanol, was the largest, and much more water was formed than under other experimental conditions. The hydrogen formed by dehydrogenation and the non-reduced copper catalyst might react to form water on the surface of the catalyst.

Formation Mechanism of the Main Products from Ethanol in the Presence of the Catalyst. From the facts mentioned above, the reaction mechanism of ethanol is considered to be as follows.

The main products, such as ethanal and ethyl acetate, appear to be formed by the following schemes:[5,12,13]

$$C_2H_5OH \rightarrow CH_3CHO + H_2$$

$$C_2H_5OH + CH_3CHO \rightarrow$$

$$CH_3CH(OH)OC_2H_5 \xrightarrow{-H_2} CH_3COOC_2H_5$$

The formation of propanone from ethanol with a catalyst can probably be presented by Kagan's process,[14] with the result that ethylene and carbon dioxide are formed:

$$2CH_3COOC_2H_5 \rightarrow$$

$$CH_3COCH_3 + C_2H_5OH + C_2H_4 + CO_2$$

Judging from such gaseous products as methane and hydrogen, methanol, which was little produced in a catalytic reaction, seems to be formed by hydrogenolysis:[13]

$$C_2H_5OH \xrightarrow{H_2} CH_3OH + CH_4$$

The ethylene in gas products is considered to be provided by dehydration,[13] also. Morgan and Kagan proposed the following mechanism for the formation of alcohol by aldol condensation and hydrogenation as follows:[15]

$$2CH_3CHO \rightarrow CH_3CH(OH)CH_2CHO \xrightarrow[H_2]{-H_2O}$$

$$CH_3CH_2CH_2CHO \xrightarrow{H_2} CH_3CH_2CH_2CH_2OH$$

Accordingly, 1-butanol seems to be formed by the aldol condensation of ethanal, which is itself the product of the primary catalytic reaction process of ethanol. Aldol condensation was not observed under ultraviolet light. On the other hand, one of the present authors has previously reported that the main reaction mechanism of 2-propanol with the copper catalyst is represented by the steps shown below.[6]

$$(CH_3)_2CHOH \rightarrow (CH_3)_2CO + H_2$$

$$(CH_3)_2CHOH + (CH_3)_2CO \rightarrow$$

$$(CH_3)_2CHCH_2COCH_3 + H_2O$$

$$(CH_3)_2CHOH + CH_3COCH_2CH(CH_3)_2 \rightarrow$$

$$(CH_3)_2CHCH_2COCH_2CH(CH_3)_2 + H_2O$$

2-Methyl-2-pentanol may be formed from 4-methyl-2-pentanone by hydrogenation.

Photochemical Reaction Mechanism of Ethanol. As is shown in Table 6, the photochemical reaction of ethanol seems to proceed without a catalyst, judging from the products obtained in the present work and from the results previously reported.[8,9]

12) W. G. Palmer, *Proc. Roy. Soc.* (London), **98A**, 13 (1920); H. Adkins, K. Folkers, and M. Kinsey, *J. Amer. Chem. Soc.*, **53**, 2714 (1931); M. Ya. Kagan, and O. M. Podurovskaya, *J. Appl. Chem. (U. S. S. R.)*, **5**, 378 (1932); B. N. Dolgov and T. V. Nizovkina, *Zh. Obshch. Khim.*, **19**, 1125 (1949); B. N. Dolgov, T. V. Nizovkina, and I. M. Strouman, *Sbornik Statei Obshch. Khim.*, **2**, 1288, 1293 (1953).

13) B. N. Dolgow, "Die Katalyse in der Organischen Chemie," Veb Deutscher Verlag Der Wissenschaften, Berlin (1963).

14) M. Ya. Kagan, I. A. Sobolev, and G. D. Lyubarskii, *Ber.*, **68B**, 1140 (1935).

15) G. T. Morgan, *Proc. Roy. Soc.* (London), **127A**, 240 (1930); G. T. Morgan and D. V. N. Hardy, *Chem. Ind.* (London), **1933**, 518; M. Ya. Kagan, G. D. Lyubarskii, and S. F. Fedorov, *J. Appl. Chem. (U. S. S. R.)*, **7**, 135 (1934).

TABLE 6. PHOTOCHEMICAL REACTION SCHEME
(Reactant: Ethanol)

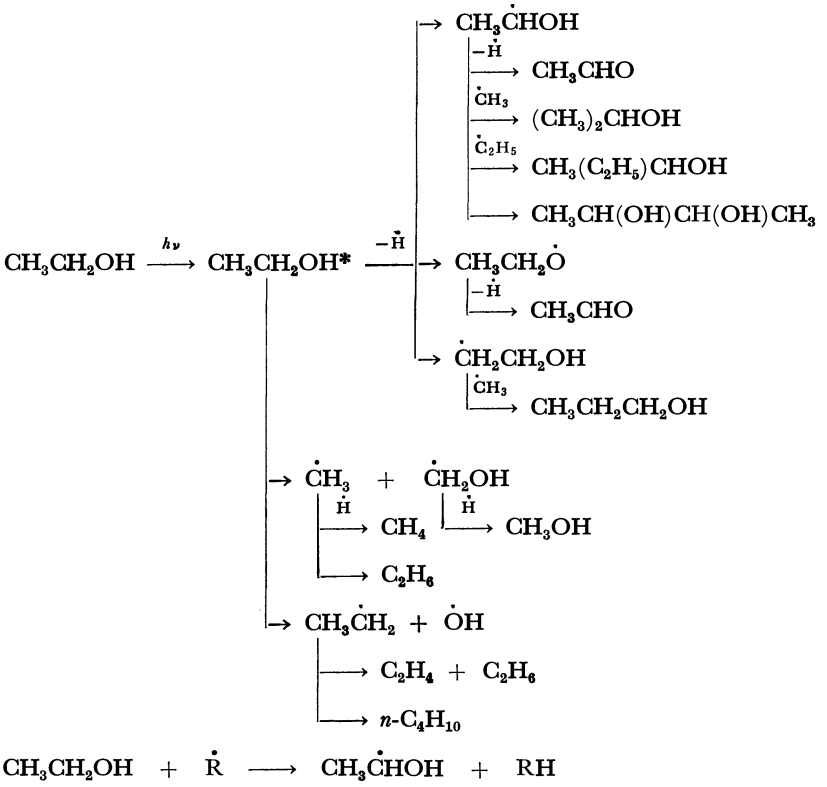

Reaction Process of Alcohol with the Catalyst under Ultraviolet Light. The reaction of the alcohols with the catalyst under ultraviolet light promoted the formation of aldehydes and esters, and their conversions, except in the case of 2-propanol, were much accelerated by ultraviolet light. By the use of the non-reduced copper catalyst under the light, the formation of aldehyde from alcohol was especially remarkable.

However, the conversion of alcohol under ultraviolet light without the copper catalyst was small. Accordingly, it is considered that the scarcely no decomposition of alcohol occurs under ultraviolet light without the catalyst, and that the main products were almost all formed by the catalytic reaction of alcohol. The facts mentioned above may be represented by the two following reaction processes.

The first is:

$$S \xrightarrow{h\nu} S^*$$

$$R + S^* \rightarrow R\cdots\cdots S^* \rightarrow \text{Products} + S$$

where:

S, catalyst; R, alcohol; h, Plank's constant, and ν, the frequency of ultraviolet light.

As is shown in Table 1, no aldol condensation was observed under ultraviolet light, but it occurred slightly with the non-irradiated catalyst. The above facts suggest that the surface of the catalyst was altered slightly by the irradiation of ultraviolet light. One of the present authors has previously reported that the formation of higher ketones from 2-propanol with the reduced copper catalyst seems to be attributable to the effect either of a trace of water or of a lower oxide of copper in the catalyst.[6] Also, from the fact that the copper catalyst reduced in the present work was reddish purple, it seems to include such oxides of copper as Cu_2O,[16] which shows photoconductivity, though no strong and sharp absorption of copper and copper compounds has been observed in the range of ultraviolet light.[17] Accordingly, we consider that the copper catalyst gives rise to electrons and positive holes which may enhance the activity of the catalyst when irradiated under ultraviolet light. The above process has been reported for the ZnO - O_2 system by Kwan.[18]

16) T. S. Moss, "Photoconductivity in the Elements," Academic Press, New York (1953); R. H. Bube, "Photoconductivity of Solids," John Wiley, New York (1960).

17) Miner (1903), Tool (1910), Mecke and Ley (1924), and French and Lowry (1924). In "International Critical Tables of Numerical Data, Physics, Chemistry and Technology," Vol. V, ed. by J. W. Clarence, McGraw Hill Book Co., New York and London (1933), pp. 249, 330.

18) T. Kwan, "Photochemistry and Its Application," ed. by M. Koizumi *et al.*, Kagaku Dojin Tokyo, Tokyo (1965), pp. 101—119.

The reaction schemes described in the above report are as follows:

$$M \xrightarrow{h\nu} M^* \xrightarrow{O_2} MO_2^*(MO_2) \xrightarrow{B} M + BO_2 \quad (1)$$

$$M \xrightarrow{h\nu} M^* \xrightarrow{B} MB^*(MB) \xrightarrow{O_2} M + BO_2 \quad (2)$$

where M is a photocatalyst and B is the reactant oxidized. In the present work, oxygen was not present in the reaction system.

Accordingly, it is considered that the photo-response may occur in the adsorption of alcohol on the surface of the present catalyst, as is shown in Scheme (2).

The second is:

$$R + S \rightarrow R\cdots\cdots S \xrightarrow{h\nu} (R\cdots\cdots S)^* \rightarrow \text{Products} + S$$

Although alcohols like ethanol show the absorption in the extreme range of ultraviolet light,[19] the wavelength of its absorption seems to be shifted[20] when it is adsorbed on the surface of the catalyst. Accordingly, an intermediate state like an activated complex seems to be excited by ultraviolet light, and its decomposition seems to be promoted. When the reaction with the copper catalyst under ultraviolet light was compared with that in the presence of the non-irradiated copper catalyst, the species of the main products, such as ethanal, ethyl acetate, and propanone, were, in the case of ethanol, almost the same in both the experiments, and the yields of the main products increased in all the main products upon irradiation of ultraviolet light. Moreover, the total amounts of the main products accounted for over 95% of the conversions of the primary alcohol for both the catalytic reaction under the light and the reaction without the light. From the above facts, it can be considered that the direction of the catalytic reaction with the catalyst and the light may be almost the same as that of the catalytic reaction without the light, and that the reaction velocity may be accelerated by the irradiation. In the case of the first process, the species of the main products with the catalyst under ultraviolet light may differ somewhat from those obtained with the catalyst alone, so the state of the non-irradiated catalyst might be altered considerably by ultraviolet light. Accordingly, the second reaction process may occur rather than the first process. The tendency of the catalytic reactions of 1-propanol and 1-butanol was similar to that of ethanol. In the case of 2-propanol, the dehydrogenation may be more rapid than that of the primary alcohols,[7] so 2-propanol may have a reactive α-hydrogen atom, though the second process is considered to be valid for the catalytic reaction under the light. Accordingly, the yield of propanone by the catalytic dehydrogenation may be especially large and may be further promoted by ultraviolet light.

The authors wish to thank Dr. Yoshio Masuyama, President of Takamatsu Technical College, for his encouragement throughout this work.

19) A. J. Harrison, B. J. Cederbolm, and M. A. Terwillinger, *J. Chem. Phys.*, **30**, 355 (1959).
20) K. Kimura and S. Nagakura, *Spectrochim. Acta*, **17**, 166 (1961).

Anodic Reaction of 5-Alkyl-2-furoic Acids in Protic Solvents

Sigeru Torii, Hideo Tanaka, Hitosi Ogo, and Siro Yamasita
Department of Industrial Chemistry, Okayama University, Okayama
(Received August 26, 1970)

Anodic oxidation of 5-alkyl-2-furoic acids (**4** and **10**) in protic solvents has been studied. The major products were 1-butenolides (**12**, **13**, **16**, and **17**) and γ-keto esters (**11** and **15**) and their acids (**14** and **18**). Methyl 5-*n*-hexyl-2,5-dimethoxy-2,5-dihydro-2-furoate **19** was converted into γ-keto ester **11** and its acid **14** by hydrolysis with alkali and into 1-butenolide **12** by electrolysis of the alkaline solution. A possible mechanism of the anodic oxidation of 5-alkyl-2-furoic acids has been discussed.

Anodic oxidation of a number of furan derivatives in protic media in the presence of appropriate electrolytes gives mainly 2,5-disubstituted 2,5-dihydrofurans.[1] However, similar experiments on 2-furoic acids have not been described, except for one by Hellström.[2] We are especially interested in 2-furoic acids both for their synthetic utility[3,4] and for anodic oxidation that is expected on both the furan ring and carboxyl group. We report that the anodic oxidation of 5-*n*-hexyl and 5-

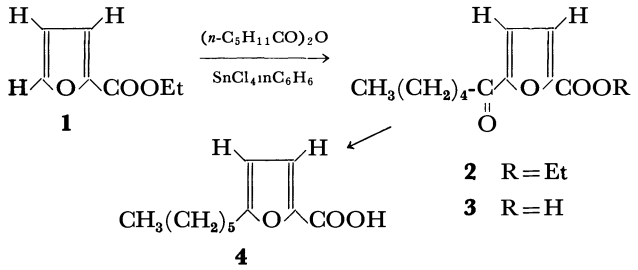

1 4

(1,1-dimethylbutyl)-2-furoic acids (**4** and **10**) in protic media can lead to γ-hexyl-γ-keto acid derivatives and also to γ-alkyl-1-butenolides, which can be rationalized as arising from 2,5-substituted intermediates (b).

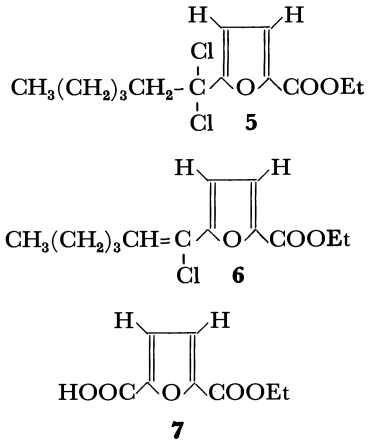

5-Alkyl-2-furoic acids have been synthesized by Gilman and Calloway[5] from the condensation of alkyl 2-furoates with alkyl halides using aluminum chloride. *n*-Alkyl chains are found to be isomerized to give secondary and tertiary derivatives.[5] An attempt to prepare 5-*n*-alkyl-2-furoic acids by the reaction of 2-furoates with acid anhydrides has been reported.[6]

The reaction of ethyl 2-furoate **1** with *n*-hexanoic anhydride in the presence of stannic chloride was reinvestigated and found to give a 4—10% yield of oily materials which seem to be a mixture containing **5** and **6**, in addition to the expected crystalline ester (**2**, 15—20%). A constituent of the crude oil was isolated by preparative vpc after treatment with pyridine, and assigned to be **6** on the basis of spectral data and elemental analysis.

In the initial stage of this reaction, a large amount of *gem*-dichloride **5** is believed to be produced, but the high reactivity and instability of the dichloride function has precluded its isolation and characterization. As a matter of fact, halide **6** was converted into 5-carbethoxy-2-furoic acid[7] liberating hydrogen chloride while the oil stood at room temperature for several hours. Preferential formation of the mixture of chlorides (**5** and **6**) over **2** occurred when the reaction of **1** with *n*-hexanoyl chloride in carbon tetrachloride was carried out using ferric chloride as a catalyst.[8] Conversion of **2** into **4** *via* **3** was realized by the Huang-Minlon reduction.[9]

We studied in detail the structure of the products in the alkylation of **1** with *n*-hexyl bromide. By fractional distillation, two components of bp 140—142.5°C/20 mmHg could be isolated in the ratio 3:1 and the analytical specimens (**8** and **9**) were obtained by preparative vpc. The structure of **8**, a fraction boiling at 142°C/20 mmHg, was assigned from spectral data and elemental analysis. By comparing the NMR spectrum of **8** with that of **9**, a conspicuous difference was found at τ 8.00—9.50. In this region the NMR spectrum of **9** exhibited a triplet at 9.26 (6H), a singlet at 8.78 (3H), a triplet at

1) a) N. L. Weinberg and H. R. Weinberg, *Chem. Revs.*, **68**, 499 (1968); b) S. D. Ross, M. Finkelstein, and J. J. Uebel, *J. Org. Chem.*, **34**, 1018 (1969); c) S. Arita, Y. Takahashi, and K. Takeshita, *Kogyo Kagaku Zasshi*, **72**, 2289 (1969); d) K. Yoshida and T. Fueno, This Bulletin, **42**, 2411 (1969).

2) N. Hellström, *Svensk Kem. Tid.*, **60**, 214 (1948); *Chem. Abstr.*, **43**, 1271 (1949).

3) A. Takeda, H. Hosisima, and S. Torii, This Bulletin, **39**, 1354 (1966).

4) A. Takeda, K. Takahashi, S. Torii, and T. Moriwake, *J. Org. Chem.*, **31**, 616 (1966).

5) Isolation of the corresponding side chain isomers was not attempted: H. Gilman and N. O. Calloway, *J. Amer. Chem. Soc.*, **55**, 4197 (1933).

6) Without isolating intermediates, impure oily 5-alkyl-2-furoic acids were used for the synthesis of antitubercular active compounds: K. Kawabe, T. Suzui, and M. Iguchi, *Yakugaku Zasshi*, **80**, 58 (1960).

7) R. Andrisano and A. Tundo, *Gazz. Chim. Ital.*, **81**, 414 (1951); *Chem. Abstr.*, **46**, 55736 (1952); Beilstein Org. Chem., H. **18**, 329.

8) G. G. Galustyan and I. P. Tsukervanik, *Zh. Obshch. Khim.*, **34**, 1478 (1964).

9) Huang-Minlon. *J. Amer. Chem. Soc.*, **68**, 2487 (1964).

Table 1. Reaction procedures and yields of products

Experiment	1	2	3	4	5	6
Substrate	4	4	4	11	11	11
(g)	1.5	1.0	0.9	2.7	1.8	0.8
Solvent						
AcOH* (m*l*)	20+60*a)	35+10*b)	—	50+100*c)	20+40*d)	—
MeOH (m*l*)	15	—	20	10.2	15	20
H_2O (m*l*)	10	—	10	15.5	10	10
Electrolyte	KOH	AcONa	KOH	KOH	KOH	KOH
(g)	0.65	0.6	0.3	1.15	0.65	0.3
Reaction Time (hr)	26	8	2	24	27	2.5
Terminal Voltage (V)	16—17	50	15	15	15	12
Current (A)	0.8—1.2	0.2—0.3	1.0	1.3—1.8	0.7—1.2	1.0
Temp (°C)	29—34	28—35	25—26	25—35	25—30	19—20
End point (pH)	4	—	8	4	4	8
Procucts						
Neutral (g)	1.2	0.8	0.7	2.0	1.3	0.7
Acidic (g)	0.3	—	0.15	0.5	0.1	0.15

* After electrolysis was continued for 2—3 hr, additional acetic acid was added as follows: a) 10 m*l* every 4 hr, b) 5 m*l* every 2.5 hr, c) 10 m*l* every 2 hr, d) 10 m*l* every 5 hr.

Table 2. Composition of the products (peak area % on vpc)

Experiment	1	2	3	4	5	6
Constituents						
R	n-C_6H_{13}-			$CH_3(CH_2)_2C(CH_3)_2$-		
Neutral portion						
R-CO-CH_2-CH_2-COOMe	28	—	42	5	26	83
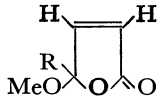	46	—	21	18	32	(11)[a]
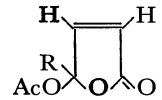	—	71	—	30	—	—
Unknown	—	—	37	—	—	—
Others (several peaks)	26	29	—	47	42	6
Acidic portion						
R-CO-CH_2-CH_2-COOEt	60	—	93	61	60	97

a) Identification was carried out by comparison of retention time on vpc.

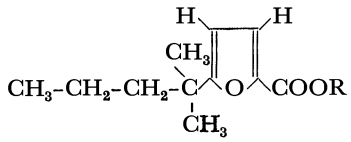

8 R=Et
10 R=H

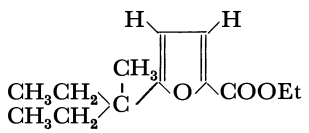

9

8.65 (3H), and a multiplet at 8.34 (4H). Except for the region 1250—1150 cm^{-1} the infrared spectra of **8** and **9** are similar with respect to all major peaks. Hydrolysis of **8** in the usual manner gave **10** in good yield.[5]

Electrolysis of furoic acids (**4** and **10**) was carried out in various protic media, using two platinum foil electrodes. Details of the experimental conditions along with the results are shown in Tables 1 and 2. In runs 1 and 5, mixtures of γ-keto esters (**11** and **15**), 1-butenolides (**12** and **16**) and γ-keto acids (**14** and **18**) were obtained. In experiments 2 and 4, an increase in the proportion of acetic acid in the electrolyte solution facilitated the formation of γ-acetoxy-1-butenolides (**13** and **17**). In procedures 3 and 6, formation of both γ-keto acids (**14** and **18**) and their methyl esters (**11** and **15**) increased considerably. Analytical samples of these compounds were obtained by preparative vpc.

The structures of **11** and **14** were confirmed by comparison of their NMR and infrared spectra with those of authentic specimens.[4,10] The proposed structure for **15** was supported by its infrared spectrum, showing γ-keto ester carbonyls at 1745 and 1709 cm^{-1}, and

10) Authentic methyl 4-oxo-decanoate was prepared from the corresponding acid by methylation with diazomethane.

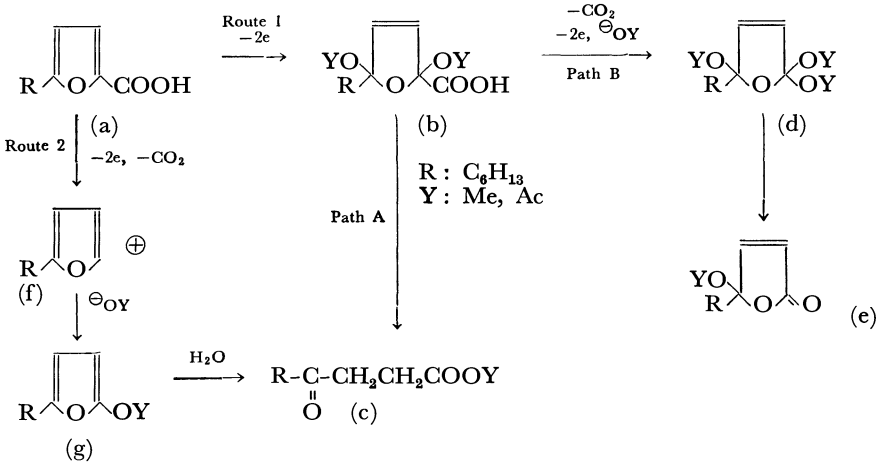

Scheme 1

R-C(=O)-CH_2CH_2COOR'

11 R=*n*-C_6H_{13}- R'=CH_3
14 R=*n*-C_6H_{13}- R'=H
15 R=$CH_3(CH_2)_2C(CH_3)_2$- R'=CH_3
18 R=$CH_3(CH_2)_2C(CH_3)_2$- R'=H

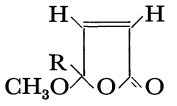

12 R=*n*-C_6H_{13}-
16 R=$CH_3(CH_2)_2C(CH_3)_2$-

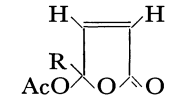

13 R=*n*-C_6H_{13}-
17 R=$CH_3(CH_2)_2C(CH_3)_2$-

by its NMR spectrum which shows geminal methyls at τ 8.86 as a singlet, and also by its elemental analysis. The γ-keto acid **18** was converted into **15** by the action of diazomethane. The structures of γ-methoxybutenolides (**12** and **16**) were deduced from their spectral properties and elemental analyses. The infrared spectra of both **12** and **16** had equal absorption bands at 3100, 1830, 1778, and 1613 cm^{-1}. NMR spectra of **12** and **16** exhibited a three-proton signal at τ 6.88 and 6.83, respectively, in place of the peak at τ 7.92 due to methyl protons of the acetoxy group of **13** and **17**. The NMR spectrum of **17** showed two doublets at τ 2.56 and 3.71 (J=6Hz) ascribable to olefinic protons. The NMR spectrum of **13** closely resembled that of **17**. Further evidence confirming the structural similarity of **13** and **17** was found in the absorption bands at 1786 and 1760 cm^{-1} due to lactone and acetoxy carbonyls, respectively.

The electrochemical behavior of 5-alkyl-2-furoic acids (a) is of particular interest in clarifying competitive anodic oxidation between the furan ring and carboxyl group. A tentative mechanism for the formation of γ-keto derivatives (c) and 1-butenolides (e) is shown in Scheme 1. As seen in route 1, anodic oxidation of furoic acids (a) would occur *via* two electron oxidation of the furan ring similar to the mechanism previously proposed, which involves cation radical or dication intermediates.[1] On the other hand, plausible intermediates (g) that may be derived from two electron oxidation of the carboxyl group of (a) *via* cation precursor (f) as shown in route 2 might be subjected to hydrolysis to give (c). Some evidence is required of the presence of the obtainable intermediates (g) in the initial products from the anodic oxidation of (a), but no appreciable amount of (g) was detected on vpc. Thus, it seems that an initial oxidation mechanism of the furan ring (route 1) for the anodic oxidation of (a) accounts for the results.

In order to obtain evidence for the proposed mechanism, anodic oxidation of (b) under our conditions was attempted. Anodic oxidation of methyl 5-*n*-hexyl-2-furoate in methanol in the presence of a catalytic amount of sulfuric acid afforded *trans* and *cis* isomers of 2,5-dimethoxy derivatives (**19**a and **19**b). Isolation of both **19**a and **19**b could be carried out by preparative vpc.

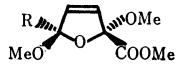

19a, *trans*

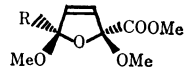

19b, *cis*

Hydrolysis of **19** in aqueous methanol-potassium hydroxide gave an alkaline solution from which only γ-keto ester **11** and γ-keto acid **14** were obtained after acidification with dilute sulfuric acid. Evolution of carbon dioxide took place when the pH of the alkaline solution fell below 7. This suggests that 2, 5-dimethoxy derivative (b) is a precursor of **11** and **14** (path A). On the other

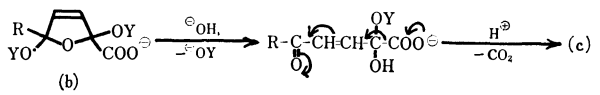

Y=H, Me Path A

hand, electrolysis of the alkaline solution gave 10—15% yield of 1-butenolide **12** together with **11** and **14**. The result reveals the probability of 2,5-dimethoxy derivative (b) as an intermediate which can lead to **12** (path B). Further two electron oxidation of the carboxyl group of (b) might give an unstable compound (d) *via* cation intermediates (h and/or i) as shown in Scheme 2.

Alkaline hydrolysis, followed by treatment with mineral acid, of 2,5-dimethoxy-2-*n*-hexyl-2,5-dihydrofuran (m) resulting from anodic dimethoxylation of 2-*n*-hexylfuran (l), which may be derived from one electron oxidation of (a) and (b) as shown in path C and D in

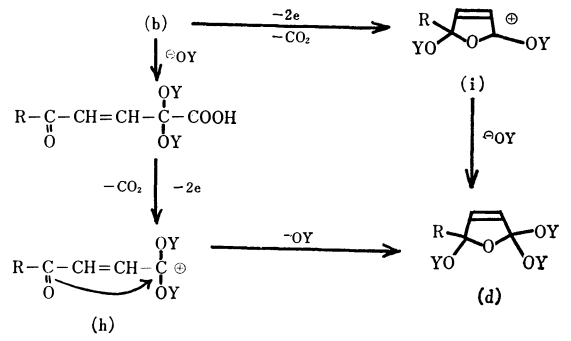

Scheme 2

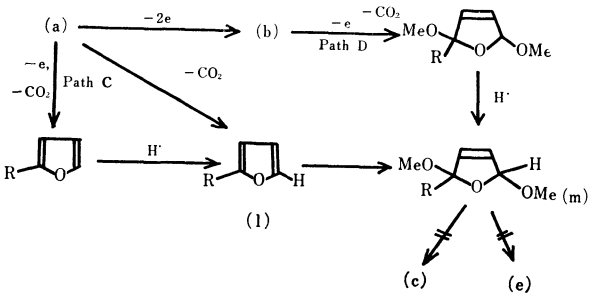

Scheme 3

Scheme III, provided no evidence for the presence of (c) and (e).

Experimental[11]

Reaction of Ethyl 2-Furoate (1) with n-*Hexanoic Anhydride.* Condensation of **1** (14.0 g) with *n*-hexanoic anhydride (21.4 g) in benzene (50 ml) in the presence of stannic chloride (52 g) was carried out. A mixed oil was obtained (7.1 g) according to the procedure reported by Kawabe *et al.*[6] Upon standing for several hours, white crystals **2** were precipitated and purified by preparative vpc to give analytical sample of **2**, mp 57—58°C: IR (neat) 3150 (=C–H), 3100 (=C–H), 1730 (ester C=O), 1675 (C=O), 1570 (C=C), 1503, 1295, 1260, 1220, 1165, 1015, 960, 770 cm^{-1}; NMR ($CDCl_3$) τ 2.80 (s, 2H, =C–H), 5.60 (q, 2H, J=5.6 Hz, O–CH_2–C), 7.10 (t, 2H, –CH_2CO), 8.25 (m, 8H, –$(CH_2)_4$–), 8.60 (t, 3H, J=5.6 Hz, O–C–CH_3), 9.10 (t, 3H, C–CH_3).

Found: C, 65.78; H, 7.82%. Calcd for $C_{13}H_{18}O_4$: C, 65.53; H, 7.61%.

Ketonic component **2** was separated from the oily filtrate by extraction with Girard reagent P.[12] A total 4.5 g of **2** was obtained. The residual yellow oil, after being treated with a few drops of pyridine, was purified by distillation to give 2.2 g of **6**, bp 125—128°C/2 mmHg. The analytical specimen was obtained by preparative vpc; IR (neat) 3150 (=C–H), 3100 (=C–H), 1725 (ester C=O), 1640 (C=C), 1580 (C=C), 1510, 1300, 1258, 1211, 1140, 1014, 800, 755 cm^{-1}; NMR ($CDCl_3$) τ 2.86 (d, 1H, J=2.7 Hz, =C–H), 3.36 (t, 1H, J=5.6 Hz, CCl=C–H), 3.40 (d, 1H, J=2.7 Hz, =C–H), 5.60 (q, 2H, J=5.6 Hz, O–CH_2–C), 7.58 (m, 2H, =C–CH_2), 8.00—8.70 (m, 4H, –$(CH_2)_2$–), 8.60 (t, 3H, J=5.6 Hz, O–C–CH_3), 9.07 (t, 3H, C–CH_3).

Found: C, 60.44; H, 6.74%. Calcd for $C_{13}H_{17}ClO_3$: C, 60.82; H, 6.68%.

The chlorovinyl derivative **6** was decomposed on standing for several days to give crystals **7**, mp 147.5—148°C (lit,[7] mp 149°C); IR (Nujol mull) 3700—2100 (COOH), 1733 and 1685 (ester and carboxyl C=O) cm^{-1}.

The solid **7** was esterified with diazoethane[13] to give diethyl 2,5-difuroate whose infrared spectrum was superimposable in every detail with that of the authentic specimen.[14]

Preparation of Ethyl 5-Hexyl-2-furoates (8 and 9). Condensation of ethyl 2-furoate (23 g) with *n*-hexyl bromide (28 g) in carbon disulfide (100 m*l*) in the presence of aluminum chloride (43 g) was carried out at room temperature according to the procedure by Gilman and Calloway.[5] After being treated in the usual manner, distillation of the product gave a fraction (20 g) boiling at 110—130°C/10 mmHg. Upon fractional redistillation of the fraction using a spinning band-type distillation apparatus, two major fractions were obtained in the ratio 3:1, one was assigned to **8** (rich fraction) boiling at 142°C/20 mmHg and the other (**9**) boiling at 143°C/20 mmHg.[15] Analytical specimens (**8** and **9**) were provided by preparative vpc (Rt: 18.0 and 19.2 min, respectively). Ethyl 5-(1,1-dimethylbutyl)-2-furoate **8**, IR (neat) 3100 (=C–H), 1725 (conjugated ester C=O), 1590 (C=O), 1520 (C=C), 1300, 1135, 1016, 800, 760 cm^{-1}; NMR ($CDCl_3$) τ 2.95 (d, 1H, J=2.7 Hz, =C–H), 3.89 (d, 1H, J=2.7 Hz, =C–H), 5.67 (q, 2H, J=5.6 Hz, O–CH_2–C), 8.16—8.60 (m, 4H, –$(CH_2)_2$–), 8.64 (t, 3H, J=5.6 Hz, O–C–CH_3), 8.70 (s, 6H, *gem*-CH_3), 9.14 (t, 3H, C–CH_3).

Found: C, 69.88; H, 8.69%. Calcd for $C_{13}H_{20}O_3$: C, 69.61; H, 8.99%.

Ethyl 5-(1-methyl-1-ethylpropyl)-2-furoate **9**, IR (neat) 3100, 1725, 1590, 1520, 1300, 1135, 1018, 760 cm^{-1}; NMR ($CDCl_3$) τ 2.93 (d, 1H, J=2.7 Hz, =C–H), 3.87 (d, 1H, J=2.7 Hz, =C–H), 5.67 (q, 2H, J=5.6 Hz, O–CH_2–C), 8.32 (m, 4H, *gem*-CH_2–C), 8.65 (t, 3H, J=5.6 Hz, O–C–CH_3), 8.78 (s, 3H, C–CH_3), 9.26 (t, 6H, J=6.2 *gem*-C–CH_3).

Found: C, 69.59; H, 9.31%. Calcd for $C_{13}H_{20}O_3$: C, 69.61; H, 8.99%.

Hydrolysis of Ethyl 5-(1,1-Dimethylbutyl)-2-furoate (8). A mixture of **8** (5 g), potassium hydroxide (1.8 g), and ethanol (7 m*l*) with a few drops of water was heated at 80°C for 30 min with stirring, then poured into 100 m*l* of ice water and acidified with dilute sulfuric acid to give **10** (3.1 g), mp 60.5°C (crude); IR (Nujol mull) 1689 (carboxylic acid C=O), 1600 (C=C), 1528, 1310, 1160, 1019 cm^{-1}. By treating **10** with diazomethane, methyl 5-(1,1-dimethylbutyl)-2-furoate was obtained, bp 91—92°C/4 mmHg. Purification of the methyl ester of **10** was performed by preparative vpc: IR (neat) 3150, 1735, 1593, 1520, 1308, 1142, 1022, 990, 926, 795, 760 cm^{-1}.

Found: C, 68.43; H, 8.72%. Calcd for $C_{12}H_{18}O_3$: C, 68.55; H, 8.63%.

Electrolysis Apparatus. The electrolysis cell was a

11) All melting and boiling points are uncorrected. Preparative gas chromatography was operated by a partially modified Yanagimoto GCG-550T type apparatus fitted with 10% coated SE-30 packed column, 3 m long, carrier gas H_2 20 m*l*/min at 130—175°C. Infrared spectra were determined with a Hitachi EPI-S2 spectrophotometer. NMR spectra were obtained on a Japan Electron Optics Laboratory spectrometer (JNM-C-60) in deuteriochloroform with TMS as an internal reference. Microanalyses were carried out by Miss M. Harada of our laboratory.

12) A. Girard and G. Sandulesco, *Helv. Chim. Acta*, **19**, 1095 (1936).

13) B. Eistert and L. Klein, *Chem. Ber.*, **101**, 900 (1968).

14) R. Andrisano, *Ann. Chim.* (Rome), **40**, 30 (1950); *Chem. Abstr.*, **45**, 7563 (1951).

15) The constitution of both fractions was estimated as follows: the former fraction contained 97% of **8** and the latter 50% of **9**, elucidated by vpc using poly-neopentyl glycol succinate 10% coated Diasolid L. M. column.

water-jacketed beaker, 3.2 cm long in diameter and 10 cm high, fitted with a gas lead pipe, a thermometer, and a magnetic stirrer. The electrodes were two platinum foils (1.5×2.0 cm^2) about 1 mm apart from each other. Current was controlled by manually adjusting the applied voltage as required. The direction of current was changed every 30 sec by means of a commutator.

*Electrolysis of 5-n-Hexyl-2-furoic Acid (**4**) in Acetic Acid-Methanol-Water.* A solution of **4** (1.5 g), potassium hydroxide (0.65 g) in acetic acid (20 ml)-methanol (15 m*l*)-water (10 m*l*) was electrolyzed at 29—34°C for 26 hr under a current of 0.8—1.2 A at 16—17 V (Experiment 1, Table 1). 10 m*l* of acetic acid was added every 4 hr. The reaction mixture was poured into 200 m*l* of ice water and extracted with ether. The ethereal solution was washed with aqueous sodium bicarbonate followed by aqueous sodium chloride and dried over Na_2SO_4. Evaporation of the solvent gave 1.2 g of neutral product, whose vpc analysis showed presence of two main constituents (Rt min, peak area%): **11** (14.2, 28) and **12** (15.4, 46), along with minor constituents (total peak area 26%) as shown in Table 2. Analytical specimens (**11** and **12**) were obtained by preparative vpc. IR spectrum and retention time of **11** on vpc were identical with those of authentic sample.[4] The physical data of **12** together with microanalytical results are as follows: IR (neat) 3100 (=C–H), 1830 (shoulder), 1779 (lactone C=O), 1613, 1463, 1171, 912, 822 cm^{-1}; NMR ($CDCl_3$) 2.90 (d, 1H, J=5.6 Hz, =C–H), 3.79 (d, 1H, J=5.6 Hz, =C–H), 6.88 (s, 3H, O–CH_3), 7.90—8.30 (m, 2H, C–CH_2–C–C=C–C=O), 8.73 (broad, 8H, –$(CH_2)_4$–) and 9.14 (t, 3H, C–CH_3).

Found: C, 66.52; H, 9.32%. Calcd for $C_{11}H_{18}O_3$: C, 66.64; H, 9.15%.

The alkaline solution was acidified with dilute sulfuric acid and extracted with ether. The ethereal solution was washed with aqueous sodium chloride, dried over Na_2SO_4 and concentrated *in vacuo*. The remaining oil was treated with diazomethane to give 0.3 g of methyl ester whose vpc showed a sharp peak at Rt 14 min (peak area 60%) along with many minor peaks. The major constituent after purified by preparative vpc was identical with that of authentic sample **11**.

In a similar manner, electrolysis of 5-(1,1-dimethylbutyl)-2-furoic acid **10** in acetic acid-methanol-water media, as seen in Experiment 4, gave 2.0 g of neutral and 0.5 g of acidic portions. Vpc analysis of the neutral portion showed presence of three main compounds (Rt min, peak area%): **15** (11.7, 5), **16** (13.6, 18) and **17** (28.6, 30) along with many minor constituents. From the acidic portion, 0.5 g of methyl ester was obtained after being treated with diazomethane. Vpc analylysis showed a sharp peak (Rt 11.7 min, peak area 61%) and minor peaks (total 10 peaks). IR spectrum of the main component, after being purified by preparative vpc, was identical with that of **15**. Compound **15**: IR (neat) 1745 (ester C=O), 1709 (ketone C=O), 1471, 1440, 1369, 1213, 1170, 1090, 840 cm^{-1}; NMR ($CDCl_3$) τ 6.32 (s, 3H, O–CH_3), 7.30 (m, 4H, CO–$(CH_2)_2$–CO), 8.11—8.90 (broad, 4H, –$(CH_2)_2$–), 8.86 (s, 6H, *gem*-CH_3), 9.10 (t, 3H, C–CH_3).

Found: C, 66.01; H, 10.04%. Calcd for $C_{11}H_{20}O_3$: C, 65.97; H, 10.07%.

Compound **16**: IR (neat) 3100 (=C–H), 1830 (shoulder), 1778 (lactone C=O), 1613, 1134, 1108, 914, 826 cm^{-1}; NMR ($CDCl_3$) τ 2.80 (d, J=6.0 Hz, 1H, =C–H), 3.70 (d, J=6.0 Hz, 1H, =C–H), 6.83 (s, 3H, O–CH_3), 8.65 (m, 4H, –CH_2–), 9.03 (s, 9H, $3CH_3$).

Found: C, 66.70; H, 9.46%. Calcd for $C_{11}H_{18}O_3$: C, 66.64; H, 9.15%.

Compound **17**: IR (neat) 3100 (=C–H), 1786, 1760 (acetoxy, lactone C=O), 1619, 1394, 1372, 1333, 1223, 1124, 1097, 1055, 1015, 992, 913, 840, 820, 736 cm^{-1}; NMR ($CDCl_3$) τ 2.56 (d, 1H, J=6.0 Hz, =C–H), 3.71 (d, 1H, J=6.0 Hz, =C–H), 7.92 (s, 3H, O–CO–CH_3), 8.65 (m, 4H, –$(CH_2)_2$–), 8.98—9.03 (s, 9H, $3CH_3$).

Found: C, 63.50; H, 8.47%. Calcd for $C_{12}H_{18}O_4$: C, 63.70; H, 8.02%.

*Electrolysis of 5-n-Hexyl-2-furoic acid (**4**) in Acetic Acid.* A solution of **4** (1.0 g) and potassium acetate (0.6 g) in acetic acid (35 m*l*) was electrolyzed at 28—35°C for 8 hr under a current of 0.2—0.3 A at 50 V (Experiment 2, Table 1). After the usual working-up, 0.8 g of neutral oily material was obtained. Vpc analysis showed presence of a major constituent **13** (Rt: 29.0 min, peak area 71%) along with minor constituents (total 12 peaks). Analytical specimen **13** provided by preparative vpc has following physical constants: IR (neat) 3100 (=C–H), 1781, 1750 (acetate and lactone C=O), 1383, 1220, 816 cm^{-1}; NMR ($CDCl_3$) τ 2.42 (d, 1H, J=5.6 Hz, =C–H), 3.79 (d, 1H, J=5.6 Hz, =C–H), 7.91 (s, 3H, O–CO–CH_3), 8.68 (broad, 10H, 5–CH_2–), 9.11 (t, 3H, C–CH_3).

Found: C, 63.86; H, 8.17%. Calcd for $C_{12}H_{18}O_4$: C, 63.70; H, 8.02%.

*Electrolysis of 5-n-Hexyl-2-furoic Acid (**4**) in Aqueous Methanol.* A solution of **4** (0.9 g) and potassium hydroxide (0.3 g) in 66% aqueous methanol (30 m*l*) was electrolyzed at 25—26°C for 2 hr under a current of 1 A at 15 V (Experiment 3, Table 1). After the usual working-up, 0.7 g of neutral and 0.5 g of crystalline acidic portions were obtained. Analytical data of the neutral portion are shown in Table 2. An acid, mp 64—65°C (*n*-hexane) (lit,[4] mp 60—60.5°C), treated with diazomethane, gave the corresponding methyl ester whose IR spectrum and retention time on vpc coincided with those of authentic sample **11**. Similarly, electrolysis of 5-(1,1-dimethylbutyl)-2-furoic acid **10** in acetic acid-methanol-water media and in aqueous methanol were carried out (Experiments 5 and 6). These results are also shown in Table 2.

*Methyl 5-n-Hexyl-2,5-dimethoxy-2,5-dihydro-2-furoates (**19**a and **19**b).* A solution of methyl 5-*n*-hexyl-2-furoate (1.1 g) in 25 m*l* of methanol containing two drops of concentrated sulfuric acid was electrolyzed with platinum electrodes at 20°C for 6 hr under a current density of 0.06 A/cm^2 at 15.5—16 V. The reaction mixture was concentrated *in vacuo* and extracted with ether. The ethereal solution was washed with aqueous sodium chloride and then concentrated *in vacuo*. Distillation of the residue gave 1.3 g of oil, bp 115—120°C/2.5 mmHg, consisting of two products (Rt 11.5 and 12.8 min in a ratio of 1:0.7). Isolation of two stereoisomers of methyl 5-*n*-hexyl-2,5-dimethoxy-2,5-dihydro-2-furoates was carried out by preparative vpc; **19**b (*cis* isomer) Rt: 11.5 min, **19**a (*trans* isomer) Rt: 12.8 min. *trans* Isomer **19**a, IR (neat) 3100 (=C–H), 1755 (ester C=O), 1635 (C=C), 1465, 1442, 1260, 1064, 1035, 857, 794 cm^{-1}; NMR ($CDCl_3$) τ 3.91 (s, 2H, =C–H), 6.17 (s, 3H, –CO–O–CH_3), 6.61 (s, 3H, O–CH_3), 6.80 (s, 3H, O–CH_3), 8.20 (m, 2H, C–CH_2–C–C=C–C=O), 8.68 (m, 8H, 4–CH_2–), 9.10 (t, 3H, C–CH_3).

Found: C, 61.65; H, 9.00%. Calcd for $C_{14}H_{24}O_5$: C, 61.75; H, 8.88%.

cis-Isomer **19**b: IR (neat) 3100 (=C–H), 1755 (ester C=O), 1635 (C=C), 1465, 1442, 1340, 1270, 1160—1000, 940, 859, 794 cm^{-1}; NMR ($CDCl_3$) τ 3.91 (s, 2H, =C–H), 6.17 (s, 3H, CO–O–CH_3), 6.55 (s, 3H, O–CH_3), 6.70 (s, 3H, O–CH_3), 8.15 (m, 2H, C–CH_2–C–C=C–C=O), 8.68 (broad, 8H,

4-CH_2-), 9.10 (t, 3H, C-CH_3).

Found: C, 61.65; H, 8.96%. Calcd for $C_{14}H_{24}O_5$: C, 61.75; H, 8.88%.

Hydrolysis of Methyl 5-n-Hexyl-2,5-dimethoxy-2,5-dihydro-2-furoate. A solution of 0.5 g of **19**, potassium hydroxide (0.1 g) and two drops of water in methanol (2.2 m*l*) was stirred at room temperature for 24 hr. The mixture was poured into 25 m*l* of ice water, neutralized with acetic acid to pH 7.0—7.5 and extracted with ether. The extracts, after being concentrated in *vacuo*, gave a trace of oil whose vpc chart showed no peak corresponding to **19**. The aqueous solution was acidified to pH 4—5 with dilute sulfuric acid. Carbon dioxide was evolved. The organic layer was taken up in ether, washed with aqueous sodium bicarbonate and aqueous sodium chloride and concentrated in *vacuo*. The residue (0.25 g) contained a constituent corresponding to the γ-keto ester **11** (peak area 85% on vpc). IR spectrum of the analytical specimen coincided well with that of authentic sample mentioned in the preceeding paragraph. The alkaline solution was acidified with dilute sulfuric acid, taken up in ether, washed with aqueous sodium chloride and concentrated in *vacuo*, giving 1.5 g of oily material. On treatment with diazomethane the corresponding methyl ester **11** was obtained.

Electrolysis of the alkaline solution obtained by hydrolysis of **19** was carried out as follows: to a methanol solution prepared from 0.5 g of **19**, 1.0 g of potassium hydroxide and 2.2 m*l* of methanol with a few drop of water, 12.8 m*l* of methanol and 5 m*l* of water were added (in total methanol 15 m*l*, water 5 m*l*). The solution was electrolyzed at 23—27°C for 0.5 hr under a current of 0.33 A at 14.4—15 V. The reaction solution was concentrated in *vacuo*, poured into 25 m*l* of ice water, neutralized with acetic acid to pH 7.0—7.5 and extracted with ether. Evaporation of the solvent gave 0.28 g of neutral portion whose vpc data are very similar to those of Experiment 3 in Table 2. The aqueous solution was acidified with dilute sulfuric acid and extracted with ether. After the usual working-up, the ethereal solution gave a crystal (0.05 g): mp 64.5—65°C from *n*-hexane (lit,[4] mp 60—60.5°C). The crystal was treated with diazomethane to give **13** whose retention time on vpc and IR spectrum are identical with those of the specimen mentioned in the paragraph above.

BULLETIN OF THE CHEMICAL SOCIETY OF JAPAN, VOL. 44, 1084—1089 (1971)

Syntheses and Reactions of Functional Polymers. LIV. Syntheses and Polymerizations of *O*-Substituted-*N*-hydroxymaleimides

Mitsuaki NARITA, Takero TERAMOTO, and Makoto OKAWARA

Research Laboratory of Resources Utilization, Tokyo Institute of Technology, Ookayama, Meguro-ku, Tokyo

(Received September 11, 1970)

The reverse Diels-Alder reaction of *N*-substituted maleimide adducts of furan is a useful method for the preparation of *N*-substituted maleimides which can not be obtained by the direct dehydration of maleamic acids owing to the formation of the corresponding isomaleimides. *O*-Benzyl, *O*-acetyl, *O*-benzoyl, *O*-benzenesulfonyl, and *O*-methyl-*N*-hydroxymaleimide adducts of furan decompose at 140—190°C to produce the corresponding maleimides. The homo- and co-polymerization with styrene of these maleimides were carried out and monomer reactivity ratios and *Q-e* values for these maleimides were determined. The copolymer obtained were converted to the copolymer of *N*-hydroxymaleimide and styrene.

We reported the preparation of polymers having the *N*-hydroxyimide structure in the chain and activation of carboxylic acid group by use of those polymers.[1,2] Syntheses of several *N*-substituted maleimides were investigated for the preparation of such polymers.[3] However, the dehydrocyclizations of *N*-substituted maleamic acids afforded only isomaleimides instead of maleimides. Several attepmpts to convert isomaleimides to maleimides were unsuccessful except for a special case.

In this paper, we report a new method to obtain *N*-substituted maleimides effectively *via* the Diels-Alder adducts. The homo- and co-polymerization with styrene of these maleimides were carried out and the polymers obtained were hydrolyzed to give the corresponding *N*-hydroxyimide structure.

Results and Discussion

Preparation of O-*Substituted*-N-*hydroxymaleimide Adducts of Furan.* Dehydration of *N*-substituted maleamic acids produces the corresponding maleimides or isoimides depending on the nature of the maleamic acids and the conditions for dehydration.[4,5] On the other hand, it is well known that dehydration of *N*-substituted saturated amic acids produce only the corresponding imides except for *N*-substituted camphoramic acids.[5] The reverse Diels-Alder reaction is known to be a useful method for the preparation of maleimides. Maleic anhydride adducts of anthracene and cyclopolyenes give imides by treatment with amines since the dehydration of the *N*-substituted saturated amic acids produce only the corresponding imides. When these imides are pyrolized at 200—500°C, maleimides are

1) M. Akiyama, M. Narita, and M. Okawara, *J. Polymer Sci., Part A-1*, **7**, 1299 (1969).

2) M. Akiyama, Y. Yanagisawa, and M. Okawara, *ibid., A-5*, **7**, 1905 (1969).

3) M. Narita, M. Akiyama, and M. Okawara, This Bulletin, **44**, 437 (1971).

4) E. Hedaya, R. L. Hinman, and S. Theodoropulos, *J. Org. Chem.*, **31**, 1311, 1317 (1967).

5) W. R. Roderick and P. L. Bhatia, *ibid.*, **28**, 2018 (1963).

obtained.[6] Thus, the reverse Diels-Alder reaction is thought to be a very useful method for the preparation of *N*-substituted maleimides which can not be obtained by direct dehydration of maleamic acids owing to the formation of the corresponding isomaleimides.

The maleic anhydride adduct of furan, which is obtained easily in quantitative yield by the reaction of furan with maleic anhydride at room temperature, decomposes at lower temperature (*ca.* 125°C) than maleic anhydride adducts of anthracene and cyclopolyenes. We therefore prepared *N*-substituted maleimide adducts of furan by the reaction of the maleic anhydride adduct of furan with amines and decomposed them to synthesize *N*-substituted maleimides.

The maleic anhydride adduct of furan (3,6-endoxo-1,2,3,6-tetrahydrophthalic anhydride) reacted with *N*-benzyloxyamine produce *O*-benzyl-*N*-hydroxymaleimide adduct of furan (*O*-benzyl-*N*-hydroxy-3,6-endoxo-1,2,3,6-tetrahydrophthalimide) (I) in quantitative yield in benzene by heating. Similarly the *N*-hydroxymaleimide adduct of furan (II) was obtained by treatment of maleic anhydride adduct of furan with hydroxylamine in 64% yield in methanol as shown below.

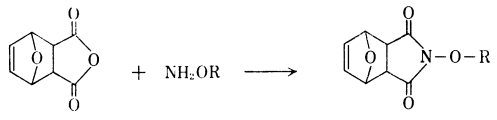

R=$CH_2C_6H_5$, H

I: R=$CH_2C_6H_5$
II: R=H

Scheme 1

The *N*-hydroxymaleimide adduct of furan (II) reacted with acetic anhydride, benzoyl chloride, benzenesulfonyl chloride and methyl iodide to produce the corresponding *O*-substituted-*N*-hydroxymaleimide adducts of furan (*O*-acetyl, *O*-benzoyl, *O*-benzenesulfonyl, and *O*-methyl-*N*-hydroxy-3,6-endoxo-1,2,3,6-tetrahydrophthalimide) as shown below.

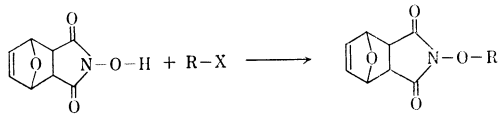

III-VI

III: R=CH_3CO (X=$OCOCH_3$)
IV: R=C_6H_5CO (X=Cl)
V: R=$C_6H_5SO_2$ (X=Cl)
VI: R=CH_3 (X=I)

Scheme 2

The structures were confirmed by elemental analyses and infrared spectra. The results are summarized in Table 1 and Table 2. A characteristic feature of five membered ring imides is the presence of bands at *ca.* 1780 cm^{-1} (medium) and 1730 cm^{-1} (strong) in the infrared spectra. Infrared spectra of isoimides generally exhibit a strong absorption due to carbonyl group at 1780 cm^{-1} and a medium absorption due to imine linkage at 1670 cm^{-1}. All the compounds in Table 2 exhibit characteristic absorptions of imides.

We did not investigate the stereochemistry of the compounds. However it is well known that furan forms *exo* adducts exclusively with maleic anhydride[7] and maleimide.[8] From the results and the reaction condition, we presume that compounds (I—VI) are *exo* adducts.

Syntheses of O-*Substituted*-N-*hydroxymaleimides by Pyrolyses of Those Adducts of Furan.* We carried out the reverse Diels-Alder reaction of the *O*-substituted-*N*-hydroxymaleimide adducts of furan (preceding section). The compounds decompose at 140—190°C producing

Table 1. *N*-Substituted maleimide adducts of furan

Compd. Formula	Yield (%)	Mp (°C) (dec. temp.)	Anal. (Calcd) (%) C	H	N
I	95	115—116	66.88	4.58	5.16
$C_{15}H_{13}NO_4$		(~150)	(66.41)	(4.83)	(5.16)
II	64	187—188	53.39	3.75	7.96
$C_8H_7NO_4$		(~150)	(53.04)	(3.90)	(7.73)
III	97	137—138	54.20	4.02	6.34
$C_{10}H_9NO_5$		(~150)	(53.81)	(4.06)	(6.28)
IV	84	134.5—136	63.59	3.68	5.00
$C_{15}H_{11}NO_5$		(~150)	(63.16)	(3.89)	(4.91)
V	73	168—171	52.39	3.35	4.36
$C_{14}H_{11}NO_6S$[a]		(~150)	(52.33)	(3.45)	(4.36)
VI	40	139—140.5	55.85	4.63	7.22
$C_9H_9NO_4$		(~150)	(55.38)	(4.65)	(7.18)

a) S%, Found (Calcd): 9.94 (9.98).

Table 2. Infrared data of *N*-substituted maleimide adducts of furan

Compd.	Characteristic absorption (cm^{-1}) imide	R[assignment]
I	1784(m)[a] 1728(s)[a]	3025(w)[a] [-C_6H_5]; several absorptions below 900 [-$CH_2C_6H_5$]
II	1785(m) 1725(s)	3470(m) (sh)[b], 3300(m) [-OH]
III	1782(s) 1745(s)	1805(m) [-CO-CH_3]; 1376(m) [CH_3-CO-]
IV	1775(s) 1742(s)	1800(m) [-CO-C_6H_5]; 1600(w), 1450(w) [-C_6H_5]
V	1791(m) 1747(s)	1580(w), 1450(m) [-C_6H_5]; 1392 (s) [ν_{as} SO_2]; 1182(s) [ν_s SO_2]
IV	1778(m) 1725(s)	2950(w); 1372(m) [-CH_3]

a) Absorption intensity: s=strong, m=medium, w=weak.
b) sh=shoulder.

6) E. J. Prill, U. S. 2524136; *Chem. Abstr.*, **45**, 1162 (1951).

7) H. Stockmann, *J. Org. Chem.*, **26**, 2025 (1961).

8) H. Kwart and I. Burchuk, *J. Amer. Chem. Soc.*, **74**, 3094 (1952).

the corresponding maleimides and furan except for the *N*-hydroxyimide (II) as shown below.

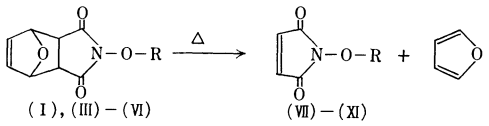

(I), (III)–(VI) (VII)–(XI)

VII; R=$C_6H_5CH_2$, VIII; R=CH_3CO,
IX; R=C_6H_5CO, X; R=$C_6H_5SO_2$,
XI; R=CH_3

Scheme 3

The *N*-hydroxyimide (II) was decomposed at 190°C, but no *N*-hydroxymaleimide was obtained since it is probably unstable thermally. Confirmation of the structures of compounds (VII—XI) was achieved from elemental analyses, infrared and NMR spectra. Results are summarized in Tables 3, 4, and 5. The NMR spectra of compounds (VII—XI) were measured in deuteriochloroform solutions using tetramethylsilane as an internal reference. We stated that the NMR spectra of isomaleimides show two doublets due to unsymmetrical nature of olefinic hydrogen and maleimides have only one singlet due to the symmetrical nature of olefinic hydrogen[3]. The NMR data in Table 4 show only one singlet due to the symmetrical nature of olefinic hydrogen in every case and indicate the compounds to be maleimides. We described further that isomaleimides generally have two sharp bands in the infrared at *ca.* 1780 cm^{-1} (strong) and 1670 cm^{-1} (medium) which are associated with the anhydride-like carbonyl and imine bonds present in the isomaleimide ring and that maleimides have a characteristically broad carbonyl band in the infrared with maxima near 1720 cm^{-1}.[3] The infrared data in Table 5 show two bands at *ca.* 1780 cm^{-1} (medium) and 1740 cm^{-1} (strong) which are characteristic of five membered ring imides and indicate the compounds to be maleimides.

TABLE 3. *O*-SUBSTITUTED-*N*-HYDROXYMALEIMIDES

Compd. Formula	Yield (%)	Mp (°C) (bp)	Anal. (Calcd) (%) C	H	N
VII	93	89.5—91	65.08	4.09	6.85
$C_{11}H_9NO_3$			(65.02)	(4.46)	(6.89)
VIII	95	70.5—71.5	46.37	3.09	9.13
$C_6H_5NO_4$		(~140°C/ 25 mmHg)	(46.46)	(3.25)	(9.03)
IX	94	87—89	61.33	3.00	6.48
$C_{11}H_7NO_4$			(60.83)	(3.25)	(6.45)
X	90	108—109.5	47.35	2.71	5.46
$C_{10}H_7NO_5S$[a]			(47.43)	(2.79)	(5.53)
XI	80	109—111	47.50	3.75	11.23
$C_5H_5NO_3$		(~128°C/ 27 mmHg)	(47.25)	(3.97)	(11.02)

a) S%, Found (Calcd): 12.57 (12.66).

TABLE 4. DETAILS OF THE NMR SPECTRA

Compd.	Chemical shift (δ)	Multiplicity[a]	Number of protons	Assignment
VII[1]	5.06	S	2	methylenic H
	6.53	S	2	olefinic H
	7.25—7.55	M	5	aromatic H
VIII	2.32	S	3	CH_3CO–
	6.75	S	2	olefinic H
IX	6.82	S	2	olefinic H
	7.40—8.25	M	5	aromatic H
X	6.86	S	2	olefinic H
	7.60—8.25	M	5	aromatic H
XI	3.93	S	3	CH_3-O-
	6.62	S	2	olefinic H

a) S=singlet, M=multiplet.

TABLE 5. INFRARED DATA OF *O*-SUBSTITUTED-*N*-HYDROXYMALEIMIDES

Compd.	Characteristic absorption (cm^{-1}) imide	R[assignment]
VII	1780(w)[a](sh)[b]	1500(w), 1455(w) [-C_6H_5];
	1725(s)[a]	1480(w) [-CH_2-]; several
	1710(s) (sh)	absorptions below 900
		[-CH_2-C_6H_5]
VIII	1780(m)[a]	1814(s) [-CO-CH_3];
	1741(s)	1380(m) [CH_3-CO-]
IX	1770(s)	1600(w), 1580(w), [-C_6H_5]
	1742(s)	
X	1780(m) (sh)	1580(w), 1450(m) [-C_6H_5];
	1742(s)	1390(s) [ν_{as} SO_2];
		1196(s) [ν_s SO_2]
XI	1775(m) (sh)	2970(w) [CH_3-];
	1740(s)	1386(m) [CH_3-]
	1720(s) (sh)	

a) Absorption intensity: s=strong, m=medium, w=weak.
b) sh=shoulder.

Polymerization of O-*Substituted*-N-*hydroxymaleimides.* It is known that the radical homopolymerization of 1,2-disubstituted ethylenes proceeds only with great difficulty. The polymerization of maleic anhydride and maleimide was reported recently.[9]

Homopolymerization of the maleimides obtained above was carried out in dioxane with azobisisobutyronitrile (AIBN) at 70°C. The results are summarized in Table 6. The inherent viscosities observed were low, but the infrared absorption band at 810—830 cm^{-1} which can be associated with out-of-plane deformations of hydrogen of the -CH=CH- link disappeared completely in the products. The copolymerization of those maleimides (M_2) with styrene (M_1) were conducted in dioxane by use of AIBN as an initiator at low temperature (35°C) to suppress the rapid polymerization. Typical results (VIII-styrene) are shown in Table 7.

9) R. M. Joshi, *Makromol. Chem.*, **53**, 33 (1962); P. O. Tawney, R. H. Snyder, R. P. Conger, K. A. Leibbrand, and C. H. Stiteler *J. Org. Chem.*, **26**, 15 (1961).

Table 6. Homopolymerization of maleimides[a)]

Compd. (g) Formula	Yield (g)	Mp (°C)	$\eta_{acetone}^{30°C}$ (0.5 g/dl)	Anal. (Calcd) (%) C	H	N
VII (2.03) $C_{11}H_9NO_3$	1.82	190—205	0.055	63.83 (65.02)	4.26 (4.46)	6.75 (6.89)
VIII (1.98) $C_6H_5NO_4$	1.25	229—241	0.015	45.73 (46.46)	3.48 (3.25)	8.18 (9.03)
IX (1.09) $C_{11}H_7NO_4$	0.89	231—239	0.020	59.68 (60.83)	3.13 (3.25)	6.14 (6.45)
X (1.27) $C_{10}H_7NO_5S$	0.74	189—193	0.029	(47.43)	(2.79)	(5.53)
XI (1.27) $C_5H_5NO_3$	0.65	253—266	0.023	45.38 (47.25)	4.35 (3.97)	9.91 (11.02)

a) Polymerization conditions; 70°C, 10 hr in 5 ml of dioxane, 0.082 g of AIBN as initiator, in sealed tube.

Table 7. Copolymerization of *N*-acetoxymaleimide (M_2) with styrene (M_1)[a)]

Initial mixture M_1 mol%	Initial mixture M_2 mol%	Polymerization time(min)	Conversion %	Analysis N, %	Polymer composition M_1 mol%	Polymer composition M_2 mol%
95	5	135	5.5	4.40	61.1	38.9
90	10	105	5.9	4.67	58.2	41.8
80	20	120	9.9	4.84	56.3	43.7
70	30	30	9.2	5.01	54.5	45.5
50	50	30	9.3	5.26	51.7	48.3
30	70	30	10.3	5.16	52.8	47.2
20	80	30	14.3	5.27	51.5	48.5
10	90	30	10.1	5.40	50.1	49.9
5	95	50	8.9	5.46	49.4	50.6

a) Polymerization conditions; 35°C in dioxane, monomer mixture 1.0 mol/*l*, AIBN initiator 0.025 mol/*l*.

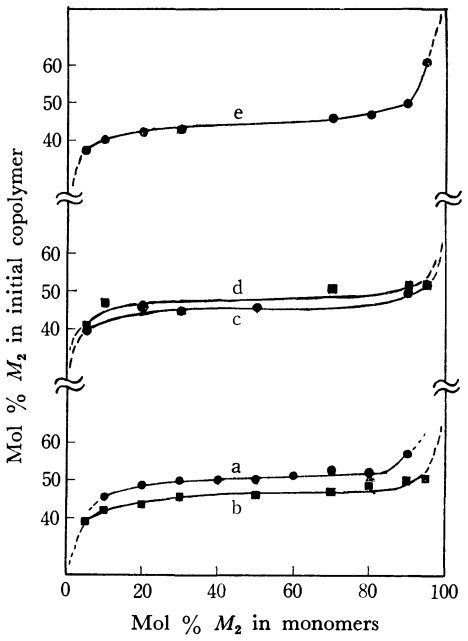

Fig. 1. Copolymerization diagram for *N*-substituted maleimides (M_2) and styrene (M_1).
a: VII, b: VIII, c: IX, d: X, e: XI

The polymerization curves were determined by inserting successive values of r_1 and r_2 in the following equation, until the best fit of the resulting curve with the experimental points was obtained.

$$\frac{m_1}{m_2} = \frac{M_1}{M_2} \cdot \frac{r_1 M_1 + M_2}{r_2 M_2 + M_1}$$

A marked tendency for alternation can be observed as shown in copolymerization diagram for *N*-substituted maleimides and styrene (Fig. I). The Q and e values for these maleimides were calculated by means of the equation of Alfrey-Price with the values of r_1 and r_2, and the results are shown in Table 8. The high Q value as well as a strong alternation tendency would be explained by the fomation of molecular complexes in the transition

Table 8. Monomer reactivity ratios and Q-e values of maleimides (M_2) [(M_1)=styrene]

M_2	r_1	r_2	Q_2	e_2
VII	0.02	0.03	5.65	1.93
VIII	0.02	0.01	4.85	2.12
IX	0.03	0.01	3.42	2.05
X	0.02	0.03	5.65	1.93
XI	0.02	0.02	5.32	2.00

state between styrene and maleimides as in the case of styrene and maleic anhydride. The formation of charge transfer complex was examined by measurement of UV spectrum in the N-actoexymaleimide-styrene system. However, neither the change of λ_{max} (290 mμ) of *N*-acetoxymaleimide nor an appearance of new absorption band due to the C-T complex formation was observed by the addition of styrene.

Conversion of Copolymers into N-*Hydroxymaleimide-Styrene Copolymer.* Treatment of the *N*-benzyloxyimide polymer (VII′) with hydrogen bromide in acetic acid,[3] gave debenzylated *N*-hydroxymaleimide type copolymer (XIII). The structure of polymer was confirmed by the agreement of infrared absorption peaks with those of the polymer obtained previously.[2] The *N*-acetoxyimide polymer (VIII′) was hydrolyzed into the hydroxymaleimide type copolymer (XIII) when the polymer in dioxane containing 6N hydrochloric acid was refluxed for ten hours. Treatment of the copolymer (VIII′), (IX′), and (X′) with water - triethylamine in dioxane gave also hydrolyzed polymer (XIII). However, the polymers obtained were combined with triethylamine tightly. Polymer (XIII) showed imide carbonyl absorption band at 1710 cm^{-1} in the infrared spectrum, while in the case of the polymer (XIII′) it shifted to 1710 and 1680 cm^{-1}. In order to confirm the interaction of triethylamine with the *N*-hydroxyimide group, the model reaction was carried out. Thus *N*-hydroxysuccinimide and triethylamine gave a 2:1 molecular compound, whose infrared specturm also showed two peaks at 1710 and 1680 cm^{-1}.

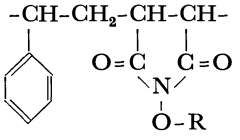

VII′: R=CH_2-C_6H_5
VIII′: R=$COCH_3$
IX′: R=COC_6H_5
X′: R=SO_2-C_6H_5
XIII: R=H

$$\text{VII}' \xrightarrow[CH_3COOH]{HBr} \text{XIII} \xleftarrow[\text{dioxane}]{6N\ HCl} \text{VIII}'$$

$$\text{VIII}', \text{IX}', \text{and X}' \xrightarrow[\text{dioxane}]{Et_3N\text{-}H_2O} \text{XIII}\cdot Et_3N\ (\text{XIII}')$$

Experimental

All melting and boiling points are uncorrected. Infrared spectra of the products were obtained as potassium bromide disks using a Hitachi Infrared Photometer Model EPI-S2. NMR spectra were obtained with a Japan Electron Optics C-100 spectrometer in deuteriochloroform solution with tetramethylsilane as an internal standard. Solvents used for reactions were purified by the usual method.

Preparation of N-*Benzyloxymaleimide Adduct of Furan (I).* Maleic anhydride adduct of furan (4.15 g) was dissolved in 100 m*l* of benzene and 3.08 g of *N*-benzyloxyamine was added. The mixture was refluxed for 3 hr and then concentrated to *ca.* 15 m*l* and cooled. The white crystals (6.33 g) were filtered off and washed with ethanol, yield 95%. They are recrystallized from ethanol, mp 115—116°C (dec. 150°C).

Preparation of N-*Hydroxymaleimide Adduct of Furan (II).* Maleic anhydride (300 g) was added to a solution of 210 g of furan in 400 m*l* of benzene and the mixture was kept overnight at room temperature with stirring. The mixture became a lump. The lump was added little by little by cooling with ice-cold water and stirring to a solution of 102 g of hydroxylamine in 1.5 *l* of methanol prepared by Lashua's procedure.[10] When heat evolution from the reaction mixture ceased, the mixture was kept for 7 hr at room temperature. Benzene and methanol were then distilled off and 700 m*l* of ethanol was added to the residue. The mixture was refluxed for 3 hr and cooled by ice-cold water. The white crystals were filtered off and washed with ethanol, yield 270 g, mp 187—188°C (dec.). After concentration of the mother liquor, an additional 78 g of the product was obtained to give a total yield of 64%.

Preparation of N-*Acetoxymaleimide Adduct of Furan (III).* *N*-Hydroxymaleimide adduct of furan (II) (7.0 g) was suspended in 20 m*l* of acetic anhydride and kept at 80—90°C for 3 hr when all the compounds dissolved in the solution gradually. After the reaction was over, it was cooled with ice-cold water and the product was filtered under suction and washed thoroughly with benzene, yield 5.0 g, mp 135—136°C (dec.). After concentration of the mother liquor, an additional 2.4 g of the product was obtained to give a total yield of 97%. It was recrystallized from benzene, mp 137—138°C (dec.).

Preparation of N-*Benzoyloxymaleimide Adduct of Furan (IV).* *N*-Hydroxymaleimide adduct of furan (II) (54.6 g) and 48 g of benzoyl chloride were dissolved in 200 m*l* of *N,N*-dimethylformamide. Pyridine (27 g) was added dropwise to this solution with stirring and by cooling with ice-cold water. The mixture was stirred for 7 hr at 0—20°C and then poured into 1 *l* of water. The precipitate was filtered off and washed with water. Recrystallization from benzene gave 68 g of the product, mp 134.5—136°C. After concentration of the mother liquor, an additional 4 g of the product was obtained to give a total yield of 84%.

Preparation of N-*Benzenesulfonyloxymaleimide Adduct of Furan (V).* *N*-Hydroxymaleimide adduct of furan (II) (36.4 g), 40 g of benzenesulfonyl chloride, and 18 g of pyridine were dissolved in 400 m*l* of benzene. The mixture was refluxed for 3 hr and then cooled. The crystals were filtered off and washed thoroughly with water. Recrystallization from acetone gave 29 g of the product, mp 171—173°C (dec.). After concentration of the mother liquor, an additional 17.5 g of the product was obtained to give a total yield of 73%.

Preparation of N-*Methoxymaleimide Adduct of Furan (VI).* *N*-Hydroxymaleimide adduct of furan (II) (18.2 g) and 56 g of methyl iodide were dissolved in 100 m*l* of *N,N*-dimethylformamide (free from water). Granulated barium oxide (45 g) was added to this solution and allowed to stand for 15 hr at room temperature. The precipitates of barium oxide and barium iodide were filtered off and the filtrate was concentrated under reduced pressure. The viscous residue was poured into 300 m*l* of water. The precipitate was filtered off and washed with water, yield 7.8 g, mp 138—140°C (dec.). It was recrystallized from ethanol, mp 139—140.5°C (dec.).

Synthesis of N-*Benzyloxymaleimide (VII).* The *N*-benzyloxyimide (I) (2.0 g) was heated in an oil bath at 170—180°C under a gentle stream of air. The solid slowly melted with vigorous furan evolution. After 1 hr, the yellowish liquid was cooled. Recrystallization from *n*-hexane gave 1.4 g (95% yield) of the product, mp 88—90°C. A second recrystallization from *n*-hexane gave light yellow crystals, mp 89.5—91°C (lit,[3] 89.5—91).

Synthesis of N-*Acetoxymaleimide (VIII).* The *N*-acetoxyimide (III) (36g) was pyrolized in an oil bath at 180—190°C under reduced pressure (25 mmHg). The solid slowly melted

10) S. C. Lashua, U. S. 3202689 (1965); *Chem. Abstr.*, **64**, 599d (1966).

with vigorus furan evolution and *N*-acetoxymaleimide was distilled at ~140°C (25 mmHg), yield 23.8 g (95 %), mp 68—71°C. Recrystallization of crude product from carbon tetrachloride furnished white crystals, mp 70.5—71.5°C.

Synthesis of N-*Benzoyloxymaleimide (IX).* The *N*-benzoyloxyimide (IV) (20 g) was dissolved in 70 m*l* of nitrobenzene and heated in an oil bath at 170—175°C for 1 hr under a gentle stream of air. Nitrobenzene was then distilled off under reduced pressure. The residue was recrystallized from carbon tetrachloride to give 14.3 g of the product, yield 95%, mp 85—88°C. A second recrystallization from *n*-hexane - carbon tetrachloride using charcoal gave white crystals, mp 87—89°C.

Synthesis of N-*Benzenesulfonyloxymaleimide (X).* The *N*-benzenesulfonyloxyimide (V) (13 g) was heated in an oil bath at 190—195°C under a gentle stream of air. The solid solwly melted with vigorous furan evolution. After 20—30 min, the liquid was cooled and combined with 50 m*l* of acetone and allowed to stand in a refrigerator overnight. Crystals (V) were filtered off and the filtrate was concentrated and the residue was recrystallized from carbon tetrachloride-chloroform to give 9 g of the product, yield 90%, mp 107—109°C. Further recrystallization from carbon tetrachloride-chloroform gave white crystals, mp 108—109.5°C.

Synthesis of N-*Methoxymaleimide (XI).* The *N*-methoxyimide (VI) (18 g) was pyrolyzed in an oil bath at 180—185°C under reduced pressure (27 mmHg). The solid slowly melted with vigorous furan evolution and *N*-methoxymaleimide was distilled at 128°C/27 mmHg, yield 80%, mp 102—108°C. Recrystallization from carbon tetrachloride - *n*-hexane using charcoal gave light yellow crystals, mp 108—110°C.

Homopolymerization of O-*Substituted*-N-*hydroxymaleimides.* Homopolymerization of maleimides (VII, VIII, IX, X, and XI) was performed in 5 m*l* of dioxane with 0.082 g of AIBN as an initiator at 70°C. The amounts of monomers used are described in Table 6. The polymerization tubes were sealed off in a vacuum. After 10 hr, the polymer solution was poured into ether and the polymer obtained was purified by dissolving twice in dioxane and precipitating in ether.

Copolymerization of O-*Substituted*-N-*hydroxymaleimides.* Copolymerization of maleimides (VII, VIII, IX, X, and XI) with styrene was perfomred in dioxane with AIBN as an initiator. The total amount of monomers was 1.0 mol/*l* and the amount of initiator was 0.025 mol/*l*. The polymerization tubes were sealed off in a vacuum and heated in a thermostated bath at 35°C, till a yield of approximately 10% of polymer was obtained. The polymer solution was then poured into ether, and the polymer was purified by reprecipitation from dioxane to ether. The polymer composition was determined by nitrogen analysis. The measurement of UV spectrum of *N*-acetoxymaleimide (VIII) was carried out for the ethylene chloride solution (2.5—10^{-3} mol/*l*) in the absence or presence of a large excess of styrene with a Hitachi Spectrophotometer EPS-3T.

Conversion of Copolymers into N-*Hydroxymaleimide-Styrene Copolymer.* Treatment of the *N*-benzyloxymaleimide type copolymer (VII′) with hydrogen bromide in acetic acid was performed as mentioned previously.[3] The *N*-acetoxyimide polymer (VIII′) (15.0 g) was dissolved in 250 m*l* of dioxane containing 50 m*l* of 6N hydrochloric acid and refluxed for 10 hr. The polymer solution was poured into 1 *l* of water and the polymer obtained (XIII) was purified by dissolving twice in dioxane and precipitating in ether. Yield 11.7 g.

The *N*-acetoxymaleimide polymer (VIII′) (0.3 g) was hydrolyzed in 10 m*l* of dimethylformamide containing 1 m*l* portions of water and triethylamine at room temperature for 7 hr. The polymer solution was poured into ether and 0.2 g of polymer (XIII′) was obtained. Hydrolysis of polymer IX′ and X′ was carried out in the same procedure.

Molecular Compound of N-*Hydroxysuccinimide with Triethylamine.* To a solution of *N*-hydroxysuccinimide (1.16 g) in 10 m*l* of tetrahydrofuran, was added 2.02 g of triethylamine. The precipitate appeared instantly, and the reaction mixture was kept at room temperature for 30 min. The precipitate was filtered and washed with tetrahydrofuran, yield 1.97 g, mp 112—113°C. From elemental analyses, the product was found to consist of 2 moles hydroxysuccinimide and 1 mole triethylamine.

Found: C, 50.99; H, 7.62; N, 12.70%. Calcd for $2C_4H_5NO_3C_6H_{15}N(C_{14}H_{25}N_2O_3)$: C, 50.74; H, 7.61; N, 12.68%.

The Stereochemistry of Nucleophilic Addition. I. The Reformatsky Reaction of 2-Methyl- and 2-Ethylcyclohexanones[1]

Takashi MATSUMOTO and Kenji FUKUI

Department of Chemistry, Faculty of Science, Hiroshima University, Higashi-sendamachi, Hiroshima

(Received September 24, 1970)

The Reformatsky reaction of 2-methyl- or 2-ethylcyclohexanone with ethyl bromoacetate gave a mixture of epimeric alcohols, which were then separated by column chromatography in an 80 : 20 ratio. The configurations of these major and minor products were identified as ethyl *trans*- and ethyl *cis*-2-methyl (or ethyl)-1-hydroxycyclohexylacetate respectively on the basis of their IR analyses, their chromatographic behavior, and correlation with the products of the Grignard reaction, the stereochemistry of which is well known. The NMR spectra of these epimeric alcohols are also discussed, and it is suggested that the chemical shifts of the methylene protons alpha to the ethoxycarbonyl group and of the proton of the hydroxyl group gives useful data for their stereochemical assignments. From these results, it is evident that the Reformatsky and the Grignard reactions proceed in a similar fashion; that is, the entering group predominantly approaches to the carbonyl group from the equatorial side. The stereoselectivity of the Reformatsky reaction is slightly less than that of the Grignard reaction.

The Reformatsky reaction[2] has been utilized for over eighty years as a convenient method for preparing β-hydroxy-carboxylic esters, which in turn can be converted to the corresponding unsaturated esters and acids. However, the stereochemistry of this reaction with cyclic ketones containing a substituent in the position alpha to the carbonyl group has been little studied.

Recently Epstein and Sonntag[3] reported that the condensation of 2-chlorocyclohexanone with methyl bromoacetate gives only one diastereomer, methyl *trans*-2-chloro-1-hydroxycyclohexylacetate. More recently, the Reformatsky reactions of monocyclic terpenes ((−)-menthone, (+)-isomenthone, and (−)-carvomenthone) with ethyl bromoacetate have also been reported by Perry and Maroni-Barnaud;[4] the stereochemistry of the major products in these reactions assigned the *trans*-configuration of the ester group to the alpha-substituted alkyl group.

During the course of other synthetic experiments in this laboratory, we also studied the stereochemistry of the Reformatsky reaction with 2-methyl- and 2-ethylcyclohexanones; the present paper will describe our results.

The condensation of 2-methylcyclohexanone (I) with ethyl bromoacetate is known to yield ethyl 2-methyl-1-hydroxycyclohexylacetate (II),[5] but the composition of the mixture of the isomers formed was not examined. In the present study, this reaction was reinvestigated in more detail; the results are summarized in Table 1, which lists the average values obtained from two or more determinations. It can be seen from Table 1 that a good yield (84%) of the β-hydroxy ester was obtained by the use of an excess of the bromoester and zinc in a benzene solution, while when tetrahydrofuran was used as the solvent in place of benzene, the yield was somewhat low (63%). The distilled product was successfully separated by means of column chromatography on sillica gel to give two epimeric oily esters (IIa and IIb) in an approximately 80: 20 ratio. Each of these esters(IIa and IIb) was converted to the corresponding crystalline acid (IIIa, mp 78—79°C and IIIb, mp 80—81°C) by alkaline hydrolysis. The reported melting point for 2-methyl-1-hydroxycyclohexylacetic acid is 67—68°C;[5] this substance is apparently a mixture of the epimers (IIIa and IIIb), thus accounting for the lower melting point. The acids (IIIa and IIIb) were further characterized as their *p*-bromophenacyl esters (IVa, mp 86—88°C and IVb, mp 91.5—92.5°C, respectively). The configurations of IIa and IIb are assigned on the basis of the following evidence. The reduction of IIa and IIb with $LiAlH_4$ in ether afforded, respectively, the corresponding diols (Va, mp 67—68°C and Vb, liquid). Subsequently, Va and Vb were subjected to tosylation with *p*-toluenesulfonyl chloride in pyridine, followed by the reduction of the resulting tosylates (VIa and VIb) with $LiAlH_4$ in tetrahydrofuran; this gave the epimeric 2-methyl-1-ethylcyclohexanols, VIIa and VIIb, respectively.

Since it is well known[6-8] that the Grignard reaction of 2-alkylcyclohexanones with simple alkylmagnesium halides yields *cis*-2-alkylcyclohexanol derivatives possessing an axial hydroxyl group as the major product, the preparation of the epimeric 2-methyl-1-ethylcyclohexanols by the Grignard reaction was attempted in order to make possible direct comparisons with the above alcohols (VIIa and VIIb). Although the Grignard reaction of I with ethylmagnesium iodide has already been reported by Cook and Laurence[9] the composition of the epimeric alcohols was not examined. Therefore, the separation of the epimers was carried out by means

1) Although the formulas depicted represent only one enantiomer, they are taken to indicate a racemate.

2) S. Reformatstky, *Ber.*, **20**, 1210 (1887). For a review of this, see R. L. Shriner, "Organic Reactions", Vol. 1, Wiley, New York (1942), p. 1.

3) W. W. Epstein and A. C. Sonntag, *Tetrahedron Lett.*, **1966**, 791.

4) M. Perry and Y. Maroni-Barnaud, *Bull. Soc. Chim. Fr.*, **1969**, 3574.

5) O. Wallach and E. Beschke, *Ann. Chem.*, **347**, 337 (1906); K. Auwers and Ph. Ellinger, *ibid.*, **387**, 230 (1912).

6) A. V. Kamernitzky and A. A. Akhren, *Tetrahedron*, **18**, 705 (1962), and the references cited therein.

7) H. O. House and W. L. Respess, *J. Org. Chem.*, **30**, 301 (1965).

8) F. Rocquet, J. P. Battioni, M. L. Capman, and W. Chodkiewicz, *C. R. Acad. Sci.*, **268**, 1449 (1969); *Chem. Abstr.*, **71**, 29919h (1969).

9) J. W. Cook and C. A. Laurence, *J. Chem. Soc.*, **1938**, 58.

Table 1. The data of the Reformatsky reaction

	Starting substance (mol)			Solvent[a]	Product		Ratio of epimers[b]	
	Ketone	$BrCH_2CO_2Et$	Zn		Bp (°C/mmHg)	Yield[b] (%)	*trans*	*cis*
I	0.050	0.050	0.050	B	119—122/10	68	80	20
I	0.050	0.075	0.075	B	119—122/10	84	81	19
I	0.050	0.075	0.075	THF	127—129/15	63	75	25
VIII	0.040	0.060	0.060	B	137—141/14	83	80	20

a) Solvent abbreviations: B=Benzene, THF=tetrahydrofuran.
b) The individual values obtained differ from these average values by not more than ±1%.

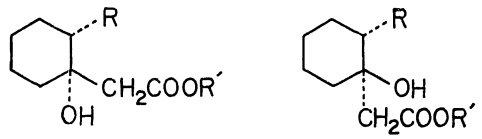

IIa R=Me, R'=Et IIb
IIIa R=Me, R'=H IIIb
IVa R=Me, R'=p-Br-phenacyl IVb
IXa R=R'=Et IXb

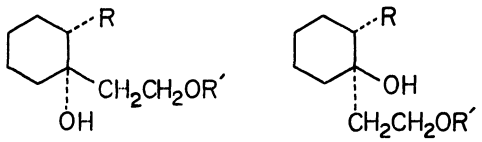

Va R=Me, R'=H Vb
VIa R=Me, R'=Ts VIb
Xa R=Et, R'=H Xb
XIa R=Et, R'=Ts XIb

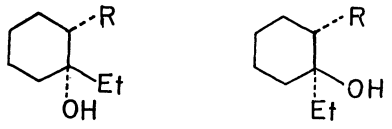

VIIa R=Me VIIb
XIIa R=Et XIIb

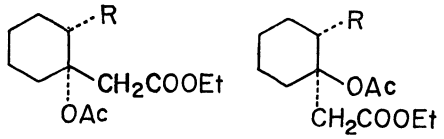

XIIIa R=Me XIIIb
XIVa R=Et XIVb

of column chromatography; two epimeric alcohols were thus successfully separated in a 90: 10 ratio. The major and minor alcohols of this reaction were shown to be identical with VIIa and VIIb respectively by comparisons of their IR and NMR spectra.

Similarly, 2-ethylcyclohexanone (VIII) was also condensed with ethyl bromoacetate to give an 83% yield of epimeric β-hydroxy-carboxylic esters, which were then separated into IXa (liquid) and IXb (mp 50.5—51.5°C) in an 80:20 ratio. The reduction of the major (IXa) and minor (IXb) esters with $LiAlH_4$ gave the corresponding diols (Xa, mp 93.5—94.5°C and Xb, mp 73—73.5°C), which were then further converted to the corresponding 1,2-diethylcyclohexanols (XIIa and XIIb) *via* tosylates (XIa and XIb). The Grignard reaction[10] of VIII with ethylmagnesium bromide gave epimeric alcohols in a 93:7 ratio; these major and minor alcohols were also shown to be identical with XIIa and XIIb respectively.

The IR spectra of IIa, IIb, IXa, and IXb are summarized in Table 2, in which the hydroxyl absorption bands have been assigned by comparing their spectra with those of the corresponding acetates (XIIIa, XIIIb, XIVa, and XIVb). The IR spectra of IIa and IXa showed bands at 988 cm^{-1} and at 986 cm^{-1} respectively; they suggest the presence of the axial hydroxyl groups, while in the cases of IIb and IXb their spectra (IIb: 1050 cm^{-1} and IXb: 1056 cm^{-1}) suggest the presence of the equatorial hydroxyl groups. These stereochemical assignments of the hydroxyl groups were further supported by the chromatographic behavior of mixtures of isomeric alcohols. Winstein and Holness[11] have stated that isomers with equatorial hydroxyl groups can be expected to be adsorbed more strongly on chromatography and, therefore, to be more difficult to elute than the isomers with the more hindered axial hydroxyls. In the present study, the isomers (IIa, VIIa, IXa and XIIa) assigned to the axial hydroxyl group were eluted first in each instance.

Table 2. The IR spectra of IIa, IIb, IXa and IXb in $CHCl_3$ (cm^{-1})

	IIa	IXa	IIb	IXb
OH	3512	3512	3512	3520
OH	988	986	1050	1056
C=O	1710	1710	1708	1708

The NMR spectra are shown in Tables 3–7. It is of interest to note the difference in the signals due to methylene protons alpha to the ethoxycarbonyl group. As is shown in Tables 3 and 4, the methylene protons of

10) J. R. Dice, L. E. Loveless, Jr., and H. L. Cates, Jr., *J. Amer. Chem. Soc.*, **71**, 3546 (1949).
11) S. Winstein and N. Holness, *ibid.*, **77**, 5562 (1955).

TABLE 3. THE NMR SPECTRA OF ETHYL 1-HYDROXY-2-METHYLCYCLOHEXYLACETATES

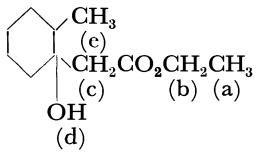

		a	b	c	d	e
IIa (major)	$CDCl_3$	1.27 (t, J=7.0)	4.15 (q, J=7.0)	2.29 (d, J=15) 2.68 (d, J=15)	3.07 (bs)	0.92
	Py-d_5	1.14 (t, J=7.0)	4.12 (q, J=7.0)	2.71 (s)	—	1.10 (d, J=5.0)
	$\Delta^{12)}$	+0.13	+0.03	−0.22	—	−0.18
IIb (minor)	$CDCl_3$	1.28 (t, J=7.0)	4.17 (q, J=7.0)	2.48 (s)	3.64 (bs)	0.92 (d, J=6.0)
	Py-d_5	1.13 (t, J=7.0)	4.13 (q, J=7.0)	2.58 (s)	—	1.03 (d, J=6.5)
	$\Delta^{12)}$	+0.15	+0.04	−0.10	—	−0.11

TABLE 4. THE NMR SPECTRA OF ETHYL 1-HYDROXY-2-ETHYLCYCLOHEXYLACETATES

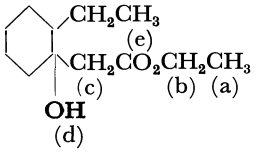

		a	b	c	d	e
IXa (major)	$CDCl_3$	1.28 (t, J=7.0)	4.18 (q, J=7.0)	2.33 (d, J=15) 2.76 (d, J=15)	*ca* 2.9 (bs)	0.87 (t, J=6.0)
	Py-d_5	1.16 (t, J=7.0)	4.15 (q, J=7.0)	2.78 (s)	—	0.90 (t, J=7.0)
	$\Delta^{12)}$	+0.12	+0.03	−0.24	—	−0.03
IXb (minor)	$CDCl_3$	1.29 (t, J=7.0)	4.20 (q, J=7.0)	2.47 (d, J=16) 2.56 (d, J=16)	3.65 (bs)	0.95 (t, J=4.0)
	Py-d_5	1.14 (t, J=7.0)	4.14 (q, J=7.0)	2.61 (s)	—	0.94 (t, J=4.5)
	$\Delta^{12)}$	+0.15	+0.06	−0.10	—	+0.01

TABLE 5. THE NMR SPECTRA OF THE ACETATE (XIIIa AND XIIIb) IN $CDCl_3$

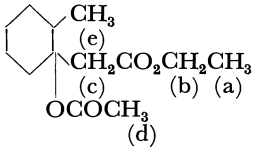

	a	b	c	d	e
XIIIa	1.23 (t, J=7.0)	4.07 (q, J=7.0)	2.79 (d, J=14) 3.27 (d, J=14)	1.99 (s)	0.96 (d, J=7.0)
XIIIb	1.23 (t, J=7.0)	4.09 (q, J=7.0)	2.75 (d, J=14) 3.01 (d, J=14)	2.00 (s)	1.00 (d, J=7.0)

TABLE 6. THE NMR SPECTRA OF THE ACETATES (XIVa AND XIVb) IN $CDCl_3$

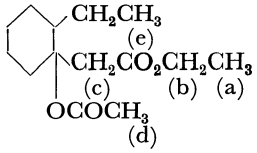

	a	b	c	d	e
XIVa	1.25 (t, J=7.0)	4.10 (q, J=7.0)	2.86 (d, J=14) 3.32 (d, J=14)	1.99 (s)	0.90 (m)
XIVb	1.24 (t, J=7.0)	4.08 (q, J=7.0)	2.75 (d, J=14) 2.99 (d, J=14)	2.01 (s)	0.89 (t, J=5.0)

the major products (IIa and IXa) are observed as well-defined AB-type quartets in $CDCl_3$, while completely-collapsed singlets result in pyridine-d_5. On the other hand, the methylene protons of the minor products (IIb and IXb) in $CDCl_3$ are observed as a singlet and as a slightly separated quartet, respectively, which is also collapsed to a singlet in pyridine-d_5. All of the acetates show well-defined quartets arising from methylene protons alpha to the ethoxycarbonyl group in $CDCl_3$. Tables 3 and 4 report the Δ values[12] for the methyl and methylene protons present in the ethyl cyclohexylacetate derivatives obtained in this study. It is evident from the data presented in these tables that definite relationships exist between the chemical-shift values induced in pyridine (Δ values) and the location and orientation of solute protons. The methyl protons of the ester group experience shielding effects of 0.12—0.15 ppm in pyridine relative to chloroform, while those of methylene protons of the ester group are small, 0.03—0.06 ppm. Since the differences in these values due to the ester group of epimeric alcohols are very small, these shifts induced in pyridine have no value for conformational analysis. However, in IIa and IXa the Δ values observed for methylene protons alpha to the ethoxycarbonyl group are large (Δ= −0.22 and −0.24 ppm respectively), while relatively small values are observed in IIb (Δ= −0.10 ppm) and IXb (Δ= −0.10 ppm). Therefore, these pyridine-induced shifts of the methylene protons of $-CH_2CO_2R$ group seem to be useful for the conformational analysis. Furthermore, the $\delta_A-\delta_B$ values[13] which are summarized in Table 7 are also useful for this purpose, for the compounds (IIa, IXa, XIIIa, and XIVa) possessing an equatorial $-CH_2CO_2R$ group have larger values than the compounds (IIb, IXb, XIIIb, and XIVb) possessing an axial $-CH_2CO_2R$ group. The chemical shift of the hydroxyl proton also depends on its conformation. As may be seen in the IIa (3.07 ppm) and IXa (*ca.* 2.9 ppm) compounds, the axial hydroxyl protons show signals in a higher magnetic field than do those of equatorial hydroxyl protons (IIb: 3.64 ppm and IXb: 3.65 ppm).

TABLE 7. THE $\delta_A-\delta_B$ VALUES OF METHYLENE PROTONS OF CH_2CO_2R GROUP IN $CDCl_3$

$-CH_2CO_2R$ (Hz)			
equatorial		axial	
IIa	23	IIb	0
IXa	26	IXb	6
XIIIa	29	XIIIb	16
XIVa	28	XIVb	14

From the above correlation between the Reformatsky and the Grignard reaction products, the results of the spectral analysis, and the chromatographic behavior, the configurations of the entering ester group relative to the alkyl group at the 2 position of the major products (IIa and IXa) in the Reformatsky reaction may be identified as *trans* configurations, while those of the minor products (IIb and IXb) are *cis*. Therefore, it is evident that the Reformatsky and the Grignard reaction with 2-alkylcyclohexanones proceed in a similar fashion; that is, the entering group predominantly approaches to the carbonyl group from the equatorial side, which derives to the axial hydroxyl compound.

The stereoselectivity of the Reformatsky reaction observed is slightly less than that of the Grignard reaction.

Experimental

All the melting and boiling points are uncorrected. The NMR spectra were taken on a Hitachi Model R-20 NMR spectrometer (60 MHz), using tetramethylsilane as the internal standard. Their chemical shifts are presented in terms of δ values; s: singlet; bs: broad singlet; d: doublet; t: triplet; q: quartet. The column chromatography was performed on Merck silica gel (0.08 mm).

Ethyl 2-Methyl-1-hydroxycyclohexylacetate (II). A solution of ethyl bromoacetate (12.5 g: 0.075 mol) in dry benzene (12.0 m*l*) was added, drop by drop at 80°C and over a period of 25 min, to a thoroughly stirred mixture of 2-methylcyclohexanone (5.6 g: 0.050 mol), purified zinc powder[14] (4.9 g: 0.075 mol), and dry benzene (6.0 m*l*). When the exothermic reaction started, the heating bath was removed, if neccessary; the temperature was kept at 80—87°C during the addition. After the addition was complete, the mixture was refluxed for 30 min, cooled, decomposed with dilute hydrochloric

12) Δ ppm=δ in $CDCl_3$−δ in pyridine-d_5.

13) Calculated from the chemical shifts (AB-type quartets) of the methylene protons alpha to the ethoxycarbonyl group.

14) R. L. Shriner, "Organic Reactions," Vol. 1, Wiley, New York (1942), p. 16.

acid (5%: 60 ml), and then extracted with ether. The ether extract was successively washed with water, a sodium hydrogencarbonate solution, and water, and then dried over sodium sulfate. The solvent was evaporated and the residue was distilled to give II as an oil; bp 119—122°C/10 mmHg; yield 8.4 g (84%). The other runs of this condensation are summarized in Table 1.

Separation of II into IIa and IIb. A 4.2×30 cm column was prepared from silica gel (200 g) suspended in purified benzene. To this was added the above sample (II: 2.520 g), after which elution with benzene containing 3% ether was carried out. Fractions 1—8 (800 ml) were discarded. Fractions 9—19 (550 ml) were evaporated to give IIa (2.035 g) as an oil.

Found: C, 65.87; H, 10.11%. Calcd for $C_{11}H_{20}O_3$: C, 65.97; H, 10.07%.

Fraction 20 (50 ml) gave nothing. Fractions 21—36 (800 ml) were evaporated to give IIb (0.458 g) as an oil.

Found: C, 66.21; H, 9.82%. Calcd for $C_{11}H_{20}O_3$: C, 65.97; H, 10.07%.

Hydrolysis of IIa and IIb. *a*) A mixture of IIa (1.00 g), aqueous sodium hydroxide (10%: 4.0 ml), and methanol (10 ml) was refluxed for 1.5 hr. After a usual work-up, the crude product was recrystallized from petroleum benzin containing a small amount of ether to give *trans*-2-methyl-1-hydroxycyclohexylacetic acid (IIIa) as colorless crystals; mp 78—79°C; yield 780 mg. A mixed-melting-point determination with IIIb (mp 80—81°C) showed 68—71°C. NMR in $CDCl_3$: 0.94 (3H, bs, $-C\underline{H}_3$), 2.36 and 2.77 (2H, each d and J=15 Hz, $-C\underline{H}_2CO_2H$), 6.80 (2H, bs, $-O\underline{H}$ and $-CO_2\underline{H}$). NMR in pyridine-d_5: 1.14 (3H, d, J=5.0 Hz, $-C\underline{H}_3$), 2.78 and 2.91 (2H, each d and J=14 Hz, $-C\underline{H}_2CO_2H$).

Found: C, 62.73; H, 9.55%. Calcd for $C_9\underline{H}_{16}O_3$: C, 62.76; H, 9.36%.

The *p*-bromophenacyl ester (IVa) was prepared from IIIa by a usual method. The crude product was recrystallized from aqueous methanol to give colorless crystals, mp 86—88°C, which gave a positive Beilstein halogen test.

Found: C, 55.12; H, 5.79%. Calcd for $C_{17}H_{21}O_4Br$: C, 55.29; H, 5.73%.

b) A mixture of aqueous sodium hydroxide (10%: 2.0 ml) and IIb (500 mg) in methanol (5.0 ml) was treated as has been described for IIIa; *cis*-2-methyl-1-hydroxycyclohexylacetic acid (IIIb) was thus obtained as colorless crystals; mp 80—81°C; yield 300 mg. NMR in $CDCl_3$: 0.94 (3H, d, J=7.0 Hz, $-C\underline{H}_3$), 2.53 (2H, s, $-C\underline{H}_2CO_2H$), 7.08 (2H, bs, $-O\underline{H}$ and $-CO_2\underline{H}$). NMR in pyridine-d_5: 1.05 (3H, d, J=6.5 Hz, $-C\underline{H}_3$), 2.72 (2H, s, $-C\underline{H}_2CO_2H$).

Found: C, 62.68; H, 9.51%. Calcd for $C_9H_{16}O_3$: C, 62.76; H, 9.36%.

The *p*-bromophenacyl ester (IVb), colorless crystals, mp 91.5—92.5°C, was prepared from IIIb by a usual method.

Found: C, 54.97; H, 5.84%. Calcd for $C_{17}H_{21}O_4Br$: C, 55.29; H, 5.73%.

Reduction of IIa and IIb with $LiAlH_4$. *a*) A solution of IIa (1.760 g) in dry ether (15 ml) was added, drop by drop and over a period of 50 min, to a suspension of $LiAlH_4$ (650 mg) in dry ether (15 ml) at room temperature, and then the mixture was gently refluxed for 2 hr. After a usual work-up, the crude product was recrystallized from petroleum benzin to give Va as colorless crystals; mp 67—68°C; yield 1.140 g (82%).

Found: C, 68.46; H, 11.63%. Calcd for $C_9H_{18}O_2$: C, 68.31; H, 11.47%.

b) The IIb ester (2.770 g) was reduced with $LiAlH_4$ (1.060 g) by a method similar to that used for Va. The diol, Vb, was thus obtained as an oil (2.060 g) which showed no carbonyl absorption band in its IR spectrum and which could be used for the next step without purification. For analysis it was purified by means of column chromatography on silica gel.

Found: C, 68.10; H, 11.68%. Calcd for $C_9H_{18}O_2$: C, 68.31; H, 11.47%.

cis- *and* trans-*2-Methyl-1-ethylcyclohexanols (VIIa and VIIb).* *a*) *From Va and Vb*: A mixture of Va (1.100 g) and *p*-toluenesulfonyl chloride (1.330 g) in dry pyridine (10 ml) was allowed to stand at room temperature for 30 hr and then poured into a mixture of ice and dilute hydrochloric acid (10%: 50 ml). The mixture was extracted with ether, and the extract was washed with water, dried over sodium sulfate, and then evaporated under a vacuum to give crude VIa as a yellow oil (1.284 g).

A solution of the above crude tosylate (VIa) in dry tetrahydrofuran (10 ml) was added, drop by drop and over a period of 10 min at room temperature, to a suspension of $LiAlH_4$ (500 mg) in dry tetrahydrofuran (10 ml); there after then the mixture was refluxed for 3 hr. After a usual work-up, the crude product was purified by means of chromatography on silica gel (70 g), after which elution with benzene containing 3% ether was carried out. Fractions 1—7 (350 ml) were discarded. Fractions 8—14 (175 ml) were evaporated to give VIIa (293 mg) as a colorless oil.

Found: C, 75.74; H, 12.71%. Calcd for $C_9H_{18}O$: C, 75.99; H, 12.76%.

When elution was continued with benzene containing 50% ether, the starting Va was recovered as colorless crystals (219 mg: mp 67—68°C).

By a method similar to that used for VIIa, the Vb diol (2.060 g) was tosylated with *p*-toluenesulfonyl chloride and then reduced with $LiAlH_4$ to give crude VIIb (1.359 g). When this was purified by means of chromatography on silica gel (150 g), pure VIIb (306 mg) was obtained as a colorless oil.

Found: C, 75.80; H, 12.68%. Calcd for $C_9H_{18}O$: C, 75.99; H, 12.76%.

The starting Vb (451 mg) was also recovered.

b) *From the Grignard Reaction*: 2-Methyl-1-ethylcyclohexanol (VII: bp 70—74°C/11 mmHg) was prepared in a 75% yield from I and ethylmagnesium iodide by the method of Cook and Laurence.[9] The product (2.078 g) was chromatographed on silica gel (200 g), after which elution with benzene containing 3% ether was carried out. The first (1.220 g) and second (0.115 g) fractions thus obtained were shown to be identical with the above VIIa and VIIb respectively by a spectral comparison.

Ethyl trans- *and* cis-*2-Ethyl-1-hydroxycyclohexylacetates (IXa and IXb).* A mixture of 2-ethylcyclohexanone (VIII: 5.00 g), purified zinc powder (3.90 g), and dry benzene (5.0 ml) was treated with a solution of ethyl bromoacetate (10.0 g) in dry benzene (10 ml) by a method similar to that used for II. The crude product was distilled under a vacuum to give a colorless oil (7.10 g: bp 137—141°C/14 mmHg) in an 83% yield.

The above ester (2.190 g) was chromatographed on silica gel (200 g), after which elution with benzene containing 3% ether was carried out. Fractions 1—18 (900 ml) were discarded. Fractions 19—25 (350 ml) were evaporated to give *trans*-2-ethyl-1-hydroxycyclohexylacetate (IXa: 1.687 g) as a colorless oil.

Found: C, 67.06; H, 10.43%. Calcd for $C_{12}H_{22}O_3$: C, 67.25; H, 10.35%.

Fraction 26 (50 ml) was evaporated to give a colorless oil (0.105 g) which was shown to be a mixture (*ca.* 1:1) of IXa and IXb by IR and NMR analyses. Fractions 27—36 (500 ml) were evaporated to give *cis*-2-ethyl-1-hydroxycy-

clohexylacetate (IXb: 0.386 g) as colorless crystals; mp 50.5—51.5°C.

Found: C, 67.05; H, 10.42%. Calcd for $C_{12}H_{22}O_3$: C, 67.25; H, 10.35%.

Reduction of IXa and IXb with $LiAlH_4$. *a*) The IXa ester (1.280 g) was reduced with $LiAlH_4$ (0.450 g) by a method similar to that used for Va. The product was recrystallized from petroleum benzin containing a small amount of ether to give Xa as colorless crystals; mp 93.5—94.5°C; yield, 0.850 g.

Found: C, 69.68; H, 11.83%. Calcd for $C_{10}H_{20}O_2$: C, 69.72; H, 11.70%.

b) The IXb ester (0.720 g) was also reduced with $LiAlH_4$ to give Xb as colorless crystals; mp 73—73.5°C; yield, 0.400 g.

Found: C, 69.66; H, 11.83%. Calcd for $C_{10}H_{20}O_2$: C, 69.72; H, 11.70%.

cis- *and* trans-*1,2-Diethylcyclohexanols (XIIa and XIIb).* *a*) *From Xa and Xb*: By a method similar to that used for VIIa, the Xa diol (350 mg) was tosylated and then reduced to give crude XIIa (280 mg), which was subsequently chromatographed on silica gel (30 g) to give pure XIIa (161 mg) as a colorless oil.

Found: C, 76.69; H, 12.93%. Calcd for $C_{10}H_{20}O$: C, 76.86; H, 12.90%.

XIIb was also obtained from Xb by a method similar to that used for XIIa.

Found: C, 76.82; H, 12.88%. Calcd for $C_{10}H_{20}O$: C, 76.86; H, 12.90%.

b) *From the Grignard Reaction*: 1,2-Diethylcyclohexanol was prepared by the method of Dice *et al.*[10] This (2.300 g) was chromatographed on silica gel (200 g), after which elution with benzene containing 3% ether was carried out. The first (1.753 g) and second (0.123 g) fractions obtained were shown to be identical with XIIa and XIIb respectively by a spectral comparison.

The Acetates (XIIIa, XIIIb, XIVa and XIVb). *a*) A mixture of IIa (930 mg), *p*-toluenesulfonic acid monohydrate (50 mg), isopropenyl acetate (2.0 m*l*), and dry toluene (10 m*l*) was refluxed for 3 hr; then the solvent was slowly distilled off over a period of 60 min to *ca.* 5 m*l*. To the cold solution solid sodium hydrogencarbonate (200 mg) was added, and, after stirring for 10 min, the mixture was filtered. The filtrate was evaporated under a vacuum, and the residue was purified by chromatography to give XIIIa as a colorless oil; yield, 1.105 g.

Found: C, 64.58; H, 9.26%. Calcd for $C_{13}H_{22}O_4$: C, 64.44; H, 9.15%.

b) The other acetates (XIIIb, XIVa, and XIVb) were also prepared in an almost quantitative yield by a method similar to that used for XIIIa.

XIIIb, Found: C, 64.27; H, 9.21%. Calcd for $C_{13}H_{22}O_4$: C, 64.44; H, 9.15%.

XIVa, Found: C, 65.61; H, 9.56%. Calcd for $C_{14}H_{24}O_4$: C, 65.59; H, 9.44%.

XIVb, Found: C, 65.53; H, 9.51%. Calcd for $C_{14}H_{24}O_4$: C, 65.59; H, 9.44%.

BULLETIN OF THE CHEMICAL SOCIETY OF JAPAN, VOL. 44, 1095—1101 (1971)

The Catalytic Dehydrogenation, Dehydroxylation, and Dehydroxymethylation of Benzyl Alcohol. II. The Effects of Sodium Compounds as Additives

Masayoshi ISHIGE,* Koji SAKAI, Masatoshi KAWAI, and Kazuo HATA

Department of Chemistry, Faculty of Science, Tokyo Metropolitan University, Setagaya-ku, Tokyo

(Received September 29, 1970)

The reaction of benzyl alcohol has been examined over stabilized nickel (S-Ni) catalysts which have been modified by treating the catalyst surface with solutions of sodium compounds; this has been done in order to obtain some information about the relation between the behavior of the molecule adsorbed on the metal catalyst and the chemical nature of the catalyst surface. On the basis of the f_H, f_{CH_3}, and f_{CHO} values, which were defined as representing the catalytic activity for the formation of benzene, toluene, and benzaldehyde respectively, the variation in the activity for each modified S-Ni was evaluated. The general aspects may be summarized as follows: (1) The reaction is generally retarded with an increase in the amount of a sodium compound which is adsorbed on the catalyst during the modification process. (2) When the modification is of a lower grade, the effect of additives on the catalytic activity represented by f values is in the following order: $NaNO_3 < NaOH < Na_2S_2O_3 < NaI < NaBr < NaCl$. (3) A proper amount of NaCl on the catalyst promotes the reaction. The increase in S_H and S_{CH_3} values, which were defined as representing the selectivity factors for the formation of benzene and toluene toward that of benzaldehyde, is roughly associated with the increase in the corresponding f values.

As was reported in the previous paper,[1] the concurrent dehydrogenation, dehydroxylation, and dehydroxymethylation of benzyl alcohol was observed when it was heated at 150—170°C in the presence of various kinds of metal catalysts. The proportions of benzaldehyde, toluene, and benzene in the reaction product were found to be greatly affected by the chemical nature of the catalysts used, and it was assumed that the reaction proceeded through a metal benzyl complex, which was considered to be an adsorbed transition complex on the catalysts.

In order to obtain more detailed information regard-

* Present address: Chemical Laboratory, Ochanomizu University, Otsuka, Bunkyo-ku, Tokyo.

1) Part I: M. Ishige, K. Sakai, M. Kawai, and K. Hata, This Bulletin, **43**, 2186 (1970).

TABLE 1. THE CATALYTIC ACTIVITIES OF S-Ni MODIFIED BY TREATING WITH HYDROXIDE SOLUTIONS OF VARYING CONCENTRATIONS

Concn. of aq. NaOH (N)	Amount of NaOH adsorbed (meq/g)	Rate constant of the decomposition of H_2O_2 $k \times 10^2$ (min^{-1})	Yield of PhCHO (%)
0.0000	—	1.094	46.7
0.02352	>0.0000	0.4885	42.7
0.04824	0.0031	0.4903	21.9
0.09929	0.0844	1.088	10.7
0.1966	0.1860	2.321	10.7
0.2487	0.2620	1.047	10.7

ing the relationship between the behavior of the adsorbed molecule and the chemical nature of the catalysts, an extensive study of the catalytic reaction of benzyl alcohol was carried out in the presence of various kinds of modified nickel catalysts; these catalysts had been prepared by treating their surfaces with various inorganic sodium compounds.

Several observations have been reported on the variation in the catalytic activity and selectivity of the catalysts modified by a variety of additives on the surface of the catalyst: for example, there is the promoting or poisoning effect of a small amount of platinic chloride or amines in hydrogenation on Raney nickel,[2] and that of the pyridine and thiophene which were added to Raney nickel in the reductive dehydroxymethylation of alcohols.[3] There is also the interesting instance of an optically-active alcohol synthesized from methyl acetoacetate by hydrogenation in the presence of modified Raney nickel catalysts; the surfaces of these catalysts had been treated with optically-active carboxylic acids or amino acids.[4] These results suggest that a small amount of an additive on the catalyst surface interacts both with the catalyst metal and with the reactant, thereby bringing about not only a change in the conditions of the catalyst surface, but also a change in the behavior of the reactant molecule on the catalyst. Pines and his collaborators proposed that nickel[3,5] and alumina[6] catalysts possess inherent acid properties, and that the poisoning of active contact sites of the catalysts by sulfur-containing compounds causes an accentuation of the acid properties of the catalysts. However, it is necessary to examine other operative factors of the catalysis in addition to the dual-function mechanism of the reforming catalyst,[7] because the stereospecific property or the reaction selectivity in the catalysis has not yet been sufficiently elucidated.

Results

The Modification of a Stabilized Nickel Catalyst. It has been found that nickel catalysts, such as Raney nickel, Urushibara nickel A, and Stabilized nickel, are useful for the dehydrogenation of benzyl alcohol.[1] Stabilized nickel (abbreviated as S-Ni)[8] was employed in all the following experiments, because it is the most stable in the air and the most convenient of the three catalysts cited. Various kinds of modified S-Ni were prepared by treating S-Ni with sodium hydroxide or various sodium salts. S-Ni was kept soaking for 24 hr in an aqueous solution of the respective sodium compound. Then, the catalyst was separated from the solution and dried at below 80°C. Since the degree of the modification of the catalyst is dependent on the initial concentration of the solution,[9] modified nickels of the

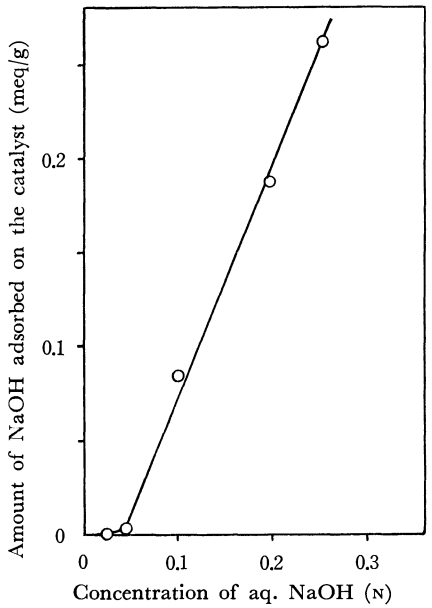

Fig. 1. Relation of the amount of adsorbate *vs.* concentration of aq. NaOH.

2) D. R. Levering, F. L. Morritz, and E. Lieber, *J. Amer. Chem. Soc.*, **72**, 1190 (1950).

3) H. Pines, M. Shamaiengar, and W. S. Postl, *ibid.*, **77**, 5099 (1955).

4) S. Tatsumi, M. Imaida, Y. Fukuda, Y. Izumi, and S. Akabori, This Bulletin, **37**, 846 (1964); **38**, 1206 (1965).

5) V. N. Ipatieff, F. J. Pavlike, and H. Pines, *J. Amer. Chem. Soc.*, **75**, 3179 (1953); H. Pines, A. Rudin, G. M. Bô, and V. N. Ipatieff, *ibid.*, **76**, 2740 (1954).

6) H. Pines and C. T. Chen, *ibid.*, **82**, 3562 (1960); H. Pines and S. M. Csicsery, *ibid.*, **84**, 292 (1962); K. Watanabe, C. N. Pillai, and H. Pines, *ibid.*, **84**, 3949 (1962).

7) *Cf.* G. C. Bond, "Catalysis by Metals," Academic Press, London and New York (1962), p. 443.

8) S-Ni(S 10) is a nickel catalyst made from reduced nickel by treating it with inert gas, such as CO_2. The adsorbed CO_2 can be expelled completely when the catalyst is allowed to coexist with water; T. Yamanaka, *Kagaku Gijitsu*, **2**, 57 (1958); T. Yamanaka and Y. Takagi, *J. Sci. Res. Inst.*, **51**, 168 (1957); T. Yamanaka, K. Taya, and Y. Takagi, *ibid.*, **52**, 143 (1958); *Sci. Pap. Inst. Phys. Chem. Res.* (Tokyo), **52**, 224 (1958).

9) K. Mukaida, A. Akiyoshi, and T. Shirasaki, *Shokubai*, **8**, 236 (1966).

same kind but of a different degree of modification were expected to be obtained when solutions of various concentrations were used in treating the catalyst.

The Nature of Stabilized Nickel Modified by Sodium Hydroxide. (*a*) *The Measurement of the Amount of NaOH Adsorbed on S-Ni*: The amount of sodium hydroxide on the catalyst surface adsorbed from solutions of various concentrations was measured by the following method. A definite amount of S-Ni was separately soaked in aqueous NaOH solutions of various concentrations and then allowed to stand at room temperature for 24 hr. Then, the diminution in the concentration of each solution was measured by titration with a standard solution of hydrochloric acid. The relation of the amounts of NaOH adsorbed per gram of nickel to the initial concentration of the NaOH solution is shown in Table 1 and Fig. 1. Figure 1 shows an approximately linear relationship between these quantities.

(*b*) *The Measurement of the Activity of the Modified S-Ni to Decompose H_2O_2*: Hydrogen peroxide is readily decomposed in first order in the presence of S-Ni.[10] Thus, it is expected that the degree of modification of the modified S-Ni may be represented in terms of the rate constant of the decomposition of H_2O_2. The rate constant of this reaction in the presence of each modified S-Ni cited in the preceding section is evaluated by means of the volumetric measurement of the oxygen generated at 20.03°C. The experimental results are shown in Table 1 and Fig. 2. By referring to the preceding experiment, it was found that the rate constant does not always increase with an increase in the amount of OH^- adsorbed on the surface of the catalyst. However, the intercept of a straight line through the three points in the middle range of the graph provides a value zero for the rate constant at the zero concentration. The slope of this line may represent the relation between the catalytic activity for the decomposition of H_2O_2 and the amount of OH^- on the surface of the catalyst. The deviation of the plots at both ends of the graph clearly suggests the complicated catalytic behavior of each modified catalyst.

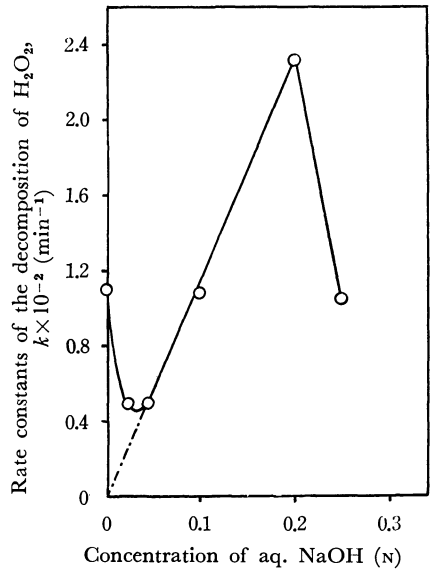

Fig. 2. Relation of the rate constant of the decomposition of H_2O_2 *vs.* concentration of aq. NaOH.

(*c*) *The Relative Catalytic Activities of Modified S-Ni for the Dehydrogenation of Benzyl Alcohol*: Benzyl alcohol was dehydrogenated to benzaldehyde by refluxing at 151—156°C for 24 hr in the presence of each catalyst. After 24 hrs' refluxing, the yield of benzaldehyde was estimated by gas chromatography. The yields of benzaldehyde are shown in Table 1 and Fig. 3. In the region of relatively little modification, the reaction was found to be retarded by an increase in the amount of OH^- on the catalyst. However, the yield of benzaldehyde remained almost constant in the presence of the highly-modified catalysts.

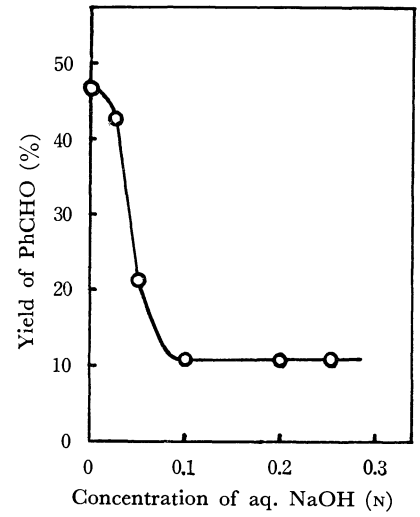

Fig. 3. Relation of relative ratio of the dehydrogenation of benzyl alcohol *vs.* concentration of aq. NaOH.

The Effects of Various Additives on the Catalytic Reaction of Benzyl Alcohol. Different modified nickel catalysts were prepared from S-Ni by treating it with various sodium salts, such as NaCl, NaBr, NaI, $Na_2S_2O_3$, and $NaNO_3$. The same procedure as was used in the preparation of the NaOH-modified S-Ni was employed; variation in the degree of modification was also attained by the use of different concentrations of the salt solution.

The catalytic reaction of benzyl alcohol in the presence of these modified S-Ni catalysts was examined from the point of view of the variation in the catalytic activity and the selectivity of these catalysts. In each of the following experiments, benzyl alcohol was heated in a sealed tube at 154.5—155.0°C in the presence of a modified S-Ni. After the mixture was kept on heat for 24 hr, the sealed tube was cooled to 0°C; the composition of the reaction mixture was then evaluated by gas chromatography. The results are summarized in Table 2. Since it was assumed that the reaction proceeds competitively through an adsorbed transition complex on the

10) It is well-known that the catalytic decomposition of H_2O_2 is often utilized to estimate the excess oxygen on the metal oxide surface, which is an important factor of the activity of the oxide catalysts: *Cf.*, S. E. Voltzi and S. E. Weller, *J. Amer. Chem. Soc.*, **76**, 1586 (1954); Y. Matsunaga, This Bulletin, **30**, 984 (1957); I. Mazin and T. Braun, *J. Phys. Chem.*, **24**, 532 (1963).

Table 2. Catalytic reactions of benzyl alcohol in sealed tubes in the presence of various modified S-Ni

Additive		Benzyl alcohol reacted (%)	Composition of product (mol %)			Rate constants[a] $k\times10^3$ (hr^{-1})	Activity			Selectivity	
Compound	Concn. of solution(N)		PhH	$PhCH_3$	PhCHO		f_H	f_{CH_3}	f_{CHO}	S_H	S_{CH_3}
None		21.2	28.8	46.7	24.5	9.89	28.5	46.2	24.2	7.19	28.3
NaOH	0.02	2.2	3.7	16.1	80.2	0.925	0.313	1.49	7.42	−134	−69.6
	0.05	3.0	8.8	22.2	69.0	1.27	1.12	2.82	8.76	−89.5	−49.2
	0.10	6.3	19.8	31.6	48.6	2.72	5.39	8.60	13.2	−38.9	−18.7
	0.15	6.9	24.7	36.0	39.3	2.98	7.36	10.7	11.7	−20.2	−3.80
	0.20	0.4	0.0	7.5	92.5	0.167	0.00	0.125	1.54	—	−209
	0.25	1.1	15.4	18.2	66.4	0.461	0.710	0.839	3.06	−63.4	−56.2
NaCl	0.02	27.5	26.9	46.6	26.6	13.4	36.1	62.4	35.7	0.40	24.3
	0.04	20.0	31.6	42.6	25.8	9.32	29.4	39.7	25.0	8.80	21.8
	0.08	15.0	30.3	39.2	30.5	6.79	20.6	26.6	20.7	−0.20	10.9
	0.16	11.9	34.6	29.8	35.6	5.28	18.3	15.7	18.8	−1.20	−7.70
NaBr	0.02	17.9	25.0	46.0	29.0	8.25	20.6	37.9	23.9	−6.40	20.1
	0.04	17.0	28.3	44.6	27.1	7.78	22.0	34.7	21.1	1.70	21.8
	0.08	13.0	29.2	41.4	29.4	5.80	16.9	24.0	17.0	−0.26	14.9
	0.16	9.9	35.3	33.6	31.1	4.32	15.2	14.5	13.4	5.40	3.40
NaI	0.02	17.5	28.1	41.9	30.0	8.04	22.6	33.7	24.1	−2.80	14.5
	0.04	13.6	36.0	35.2	28.8	6.08	21.9	21.4	17.5	9.70	8.6
	0.08	8.3	23.1	35.0	41.9	3.60	8.31	12.6	15.1	−25.8	−7.8
	0.16	6.0	28.4	26.0	45.6	2.56	7.27	6.65	11.7	−20.6	−24.4
$Na_2S_2O_3$	0.02	14.0	13.9	45.0	31.1	6.19	8.75	28.3	19.6	−35.0	16.2
	0.04	14.2	27.1	43.3	29.6	6.40	17.3	27.7	18.9	−3.80	16.4
	0.08	11.6	32.2	41.0	26.8	5.14	16.5	21.0	13.8	17.9	18.4
	0.16	11.1	33.9	40.7	25.4	4.93	16.7	20.1	12.3	12.6	20.4
$NaNO_3$	0.02	4.1	8.0	48.9	43.1	0.592	0.474	2.90	2.55	−73.2	5.40
	0.04	4.0	7.1	42.2	50.7	0.575	0.408	2.60	2.92	−85.4	−7.80
	0.08	0.0	0.0	0.0	0.0	0.00	—	—	—	—	—
	0.16	0.0	0.0	0.0	0.0	0.00	—	—	—	—	—

a) Rate constant of the conversion of benzyl alcohol.

catalyst,[1] the activity of each catalyst for the formation of benzene, toluene, and benzaldehyde was expressed in terms of the f_H, f_{CH_3}, and f_{CHO} factors respectively; these factors are proportional to the approximate values of the rate constants for the formation of each product in the early period of the reaction (within the period in which 30% of the alcohol reacted).[11] The f_H, f_{CH_3}, and f_{CHO} were defined as follows:

$$\left.\begin{aligned} f_H &= 100\ k_{alc}\ (\text{mol\% of PhH}) \\ f_{CH_3} &= 100\ k_{alc}\ (\text{mol\% of PhCH}_3) \\ f_{CHO} &= 100\ k_{alc}\ (\text{mol\% of PhCHO}) \end{aligned}\right\} \quad (1)$$

where k_{alc} is the first-order rate constant in the disappearance of the alcohol.

The selectivity factors for the formation of benzene and toluene toward that of benzaldehyde were represented by S_H and S_{CH_3}, which were defined as follows:

$$\left.\begin{aligned} S_H &= 100 \log (f_H/f_{CHO}) \\ &= 100 \log (\text{mol\% of PhH/mol\% of PhCHO}) \\ S_{CH_3} &= 100 \log (f_{CH_3}/f_{CHO}) \\ &= 100 \log (\text{mol\% of PhCH}_3\text{/mol\% of PhCHO}) \end{aligned}\right\} \quad (2)$$

The values of the f and S factors are shown in Table 2.[12] Figures 4 and 5 illustrate the relations of these values *vs.* the approximate degrees of the modification of the catalyst, which were represented by the initial concentrations of the solution used for modifying the catalyst, on the assumption that the degree of modification and the concentration of the sulution are proportional in the region of low concentration.

The results shown in Table 2 indicate that the catalytic activity and selectivity of the catalyst are affected by the nature of the adsorbate on the catalyst surface. The general aspect may be summarized as follows: (1) an increase in the amount of the adsorbate generally brings about a retardation of the reaction; (2) a proper amount of NaCl on the catalyst surface promotes the reaction; (3) variations in the kind and amount of the adsorbate have particular effects on the production of toluene, whereas they have a lesser effect on the formation of benzene; (4) the effect of additives on the catalyst activity, which is expressed by the values f_H, f_{CH_3}, and f_{CHO}, is generally in this order for the S-Ni

11) With the further progress of the reaction, the aspect of the reaction becomes complicated and the simple expression adopted here is no more valid.

12) A positive value of S_H and S_{CH_3} indicates that the formation of benzene or toluene is superior to that of benzaldehyde, whereas a negative value means the less formation of benzene or toluene than that of benzaldehyde.

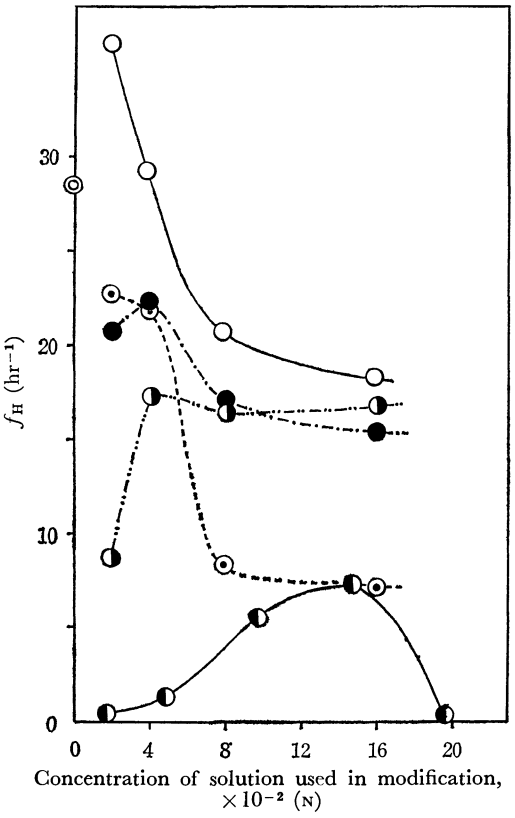

(a)

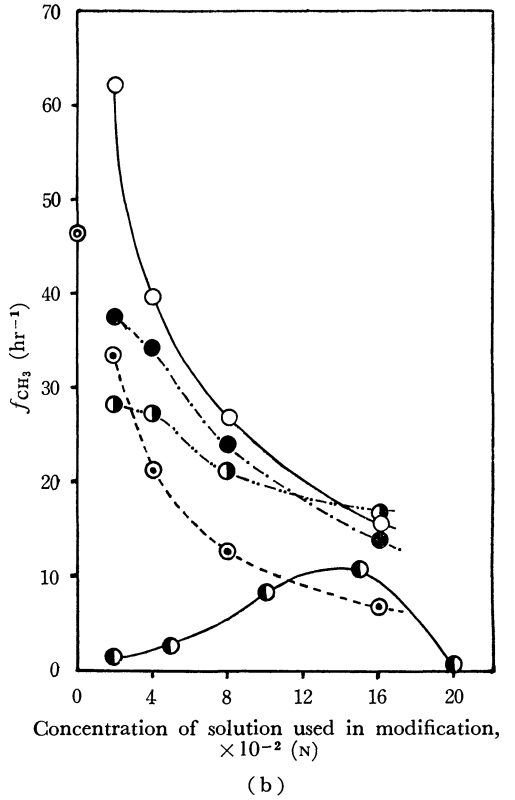

(b)

modified to a lesser degree: $NaNO_3$ <NaOH< $Na_2S_2O_3$ <NaI<NaBr<NaCl; (5) the increase in f values is roughly associated with the increase in S values; (6) with regard to the selectivity change for the formation of

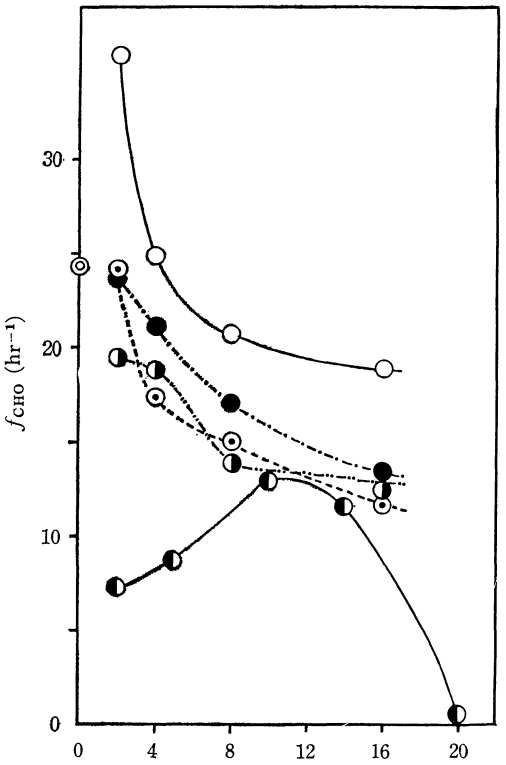

(c)

Fig. 4. The activities of modified catalysts for the formation of benzene, toluene, and benzaldehyde.
○, NaCl; ●, NaBr; ⊙, NaI; ◑, $Na_2S_2O_3$; ◐, NaOH; ◎, control (unmodified S-Ni catalyst)

toluene when the amount of the adsorbate is increased, the sodium compounds as additives may be classified into two groups: one with decreasing S_{CH_3} values, and the other with increasing S_{CH_3} values. The compounds with larger f_{CH_3} values generally belong to the former group, whereas those with smaller f_{CH_3} values belong to the latter. On the other hand, the effects of various additives on the selectivity for the formation of benzene can not be estimated so clearly as for the formation of toluene. However, an appreciable change in the S_H value is observed with an increase in the amount of the adsorbate in the cases of additives with smaller f_H values.

Discussion

The increasing coverage of the catalyst surface by additive substances might necessarily lead to a decrease in the catalytic activity due to the hindrance of the approach of the benzyl alcohol molecule to the catalyst surface. The data in Table 2 are generally consistent with this consideration, but some of them deviate. Especially, the change in selectivity caused by the additives on the catalyst cannot be simply understood by the coverage, though selectivity does not undergo so great a change as activity as a result of the presence of the additives on the catalyst. It is, however, noteworthy that the observed S values are somewhat influenced by the kinds and the amounts of the additives, and that the

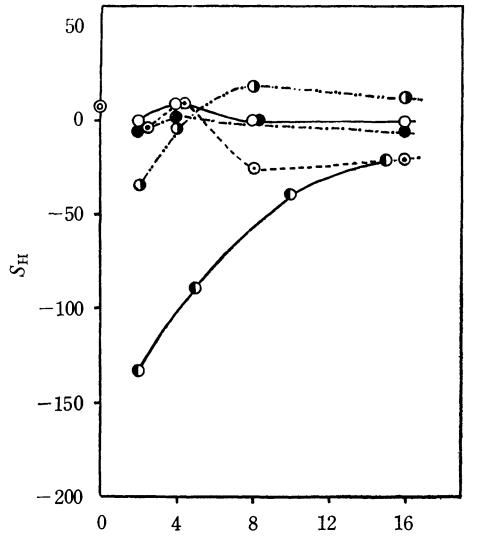

(a)

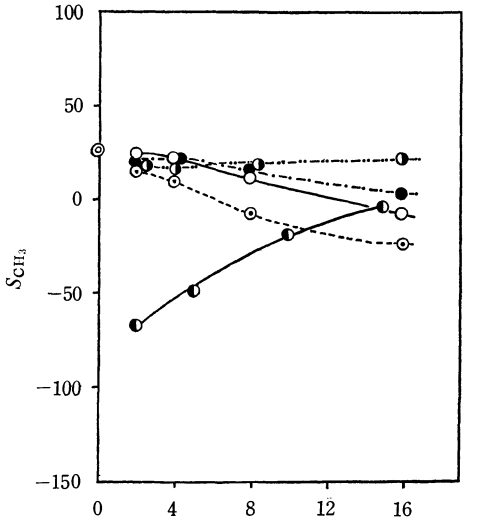

(b)

Fig. 5. The selectivities of modified catalysts for the formation of benzene and toluene toward benzaldehyde. (The notations are the same as Fig. 4.)

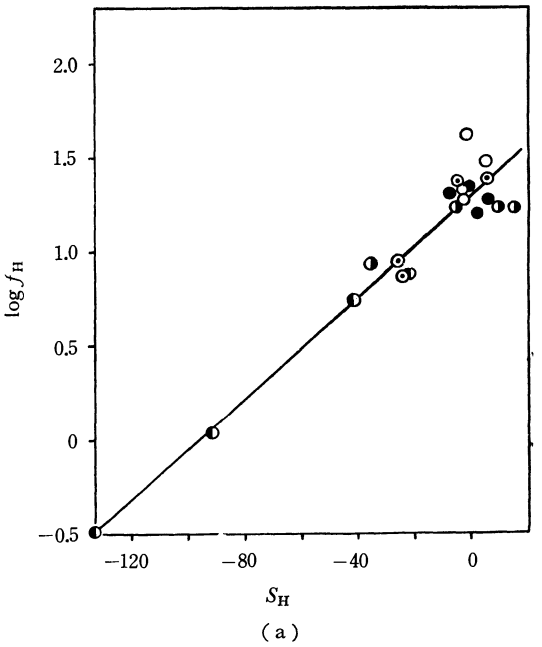

(a)

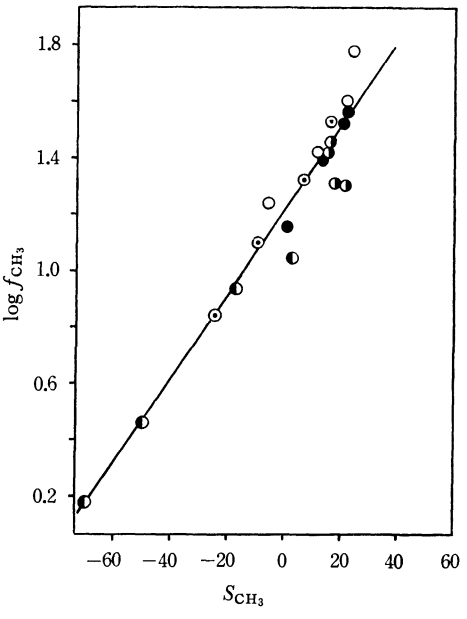

(b)

Fig. 6. The plots of $\log f$ *vs.* S for benzene and toluene. (The notations are the some as in Fig. 4.)

influence is related to the f value under the given conditions. This fact suggests the possibility that the change in the catalytic activity for the formation of each product might bring about a change in selectivity for the corresponding product. Therefore, the correlation between f and S values was examined. As is shown in Fig. 6, the plots of $\log f$ *versus* S in each graph were distributed near a straight line, which can be represented by the following equation:

for the formation of benzene,

$$\log f_H = 0.0137 S_H + 1.31$$

for the formation of toluene,

$$\log f_{CH_3} = 0.0147 S_{CH_3} + 1.23 \qquad (3)$$

However, no such a linerar relation was observed when the reaction proceeded either too fast or too slow.

It is assumed that the first step in the reaction is the dehydrogenation of benzyl alcohol to benzaldehyde through an adsorbed transition complex on the catalyst, and that the succeeding dehydroxylation and dehydroxymethylation utilize the hydrogen generated by the dehydrogenation. If each product of the reaction is competitively produced from the same transition intermediate at an early stage of the reaction, it is understandable that the selectivity is correlative with the activity of the catalyst. The deviation from the linear relation between $\log f$ and S by the faster reaction can be explained as follows: the faster approach to the pseudo-equilibrium between benzyl alcohol and benzaldehyde brings about a feedback of benzaldehyde to

benzyl alcohol, resulting in an increase in the apparent S_H and S_{CH_3} values.

A small amount of sodium chloride was found to promote the reaction. The increase in the activity of the catalyst as a result of the presence of halide ions is found to be in an order consistent with the basicity or inductive effect of halogens.[13] This fact suggests that halide anions on the catalyst surface induce electron transfer around them, thus accentuating the acid property of the catalyst surface.[3,5,14] However, the possibility cannot be excluded that, as has been observed in the catalysts modified by some potassium halides,[15] different amounts of the anion adsorbed from solutions of different halides of the same concentration affect the catalytic activity.[16] Nevertheless, the unique promotion by a proper amount of NaCl as additive indicates that the chloride ion might play an important role in the catalytic reaction.[17] It implies that the change in catalytic activity is mainly dependent on the intrinsic property of the halide ion, rather than being a mere coverage-change.

In the preceding paper, we proposed the intervention of a metal benzyl complex in the reaction. If this is the case, the anions on the catalyst surface might participate as ligands in the complex, thus exerting a certain influence on the activity of the catalyst.

Experimental

Material. Benzyl Alcohol: Benzyl alcohol was purified according to the procedure described previously.[1] The purity was found to be over 99% by gas chromatography.

Catalyst: A commercial stabilized nickel (S 10) (supplied by Nikko Shokai Co., Ltd.), containing 50% of kieselguhr, was used as the catalyst.

Preparation of Modified S-Ni. (i) Sodium hydroxide (10.3 g) was dissolved in distilled water, and then diluted to 1 *l* to make a 0.2487N NaOH solution. The concentration of the solution was determined by titration with a standard solution of oxalic acid. Several portions of the NaOH solution were taken out and separately diluted to prepare 0.1966, 0.09929, 0.04824, and 0.02352N solutions. Every 3.00-g portion of the S-Ni catalyst was soaked in a 30.0-m*l* portion of the NaOH solution, and then left to stand for 24 hr at room temperature. After the adsorption equilibrium had been attained, a 10.0-m*l* portion of the solution was taken out from the upper layer and titrated with 0.1084N hydrochloric acid. The amount of NaOH adsorbed was calculated from the difference in the concentrations.

(ii) Aqueous solutions of NaCl, NaBr, NaI, $Na_2S_2O_3 \cdot 5H_2O$, and $NaNO_3$ were prepared, the concentrations of the solution being regulated to 0.02, 0.04, 0.08, and 0.16N respectively. In an Erlenmeyer flask we then placed a 30-m*l* portion of a solution and a 3-g portion of S-Ni; the mixture was left to stand under a cork-stopper for 24 hr at room temperature. Then, the aqueous layer was removed by decantation, and the catalyst was dried for 12 hr at below 80°C. The catalysts modified by NaOH and $Na_2S_2O_3$ were dried in a desiccator for more than 24 hr at room temperature.

Decomposition of H_2O_2 by Modified S-Ni. Commercial H_2O_2 (30%) was diluted with water to about fifty times the initial volume. In a 30-m*l* flask joined to a gas burette we then placed 20 m*l* of the H_2O_2 solution; the temperature was regulated to maintain 20.03°C. Then, a 0.1210-g portion of modified S-Ni was quickly added; the oxygen generated was measured volumetrically after a proper interval.

Reaction of Benzyl Alcohol in the Presence of Modified S-Ni under Ordinary Pressure. Benzyl alcohol (6 m*l*) and modified S-Ni (1 g) were placed in a 30-m*l*, round-bottomed flask equipped with a reflux-condenser. The content was refluxed for 24 hr in an oil bath, which had been heated at 151—156°C in advance. After the reaction was over, the reaction mixture was analyzed by gas chromatography in order to estimate the amount of benzaldehyde produced.

Reaction of Benzyl Alcohol in the Presence of Modified S-Ni in a Sealed Tube. Benzyl alcohol (2.00 g) and a modified S-Ni catalyst (0.333 g) were heated at 155°C for 24 hr in a sealed tube. After the reaction was over, the tube was cooled with ice, and the composition of the reaction mixture was analyzed by gas chromatography.

The authors wish to express their hearty thanks to Dr. Ken-ichi Watanabe for his helpful encouragement.

13) E. Naruko, *Kogyo Kagaku Zasshi*, **67**, 2023 (1964).

14) I. D. Chapman and M. L. Hair, *J. Catal.*, **2** 145 (1963); C. J. Plank, D. J. Sibbert, and R. B. Smith, *Ind. Eng. Chem.*, **49**, 742 (1957).

15) L. Michaelis and H. Lachs, *Kolloid Z.*, **9**, 279 (1911).

16) In the case of reactive adsorbates, such as NaOH and $Na_2S_2O_3$, it might also be considered that a change in quality occurs to some extent as a result of the contact with the air during the preparation of modified catalyst or of the thermal decomposition during the catalytic reaction in the presence of them.

17) A few studies have been reported on the accelerating effect of NaCl on the reaction: *Cf.*, T. Nakabayashi, *J. Amer. Chem. Soc.*, **82**, 3900 (1960); K. Sakai, M. Ishige, K. Watanabe, and K. Hata, This Bulletin, **43**, 1172 (1970).

Photochemical Reduction of Nitrobenzene and Its Reduction Intermediates. IX. The Photochemical Reduction of 4-Nitropyridine in a Hydrochloric Acid-Isopropyl Alcohol Solution[1]

Shizunobu HASHIMOTO, Koji KANO, and Kazuo UEDA
Department of Applied Chemistry, Doshisha University, Kamikyo-ku, Kyoto

(Received October 3, 1970)

The photochemical reduction of 4-nitropyridine has been investigated in hydrochloric acid-isopropyl alcohol solutions. 4-Nitropyridine was not photoreduced in isopropyl alcohol, whereas when the photolysis was carried out in hydrochloric acid-isopropyl alcohol solutions, the photoreduction of 4-nitropyridine proceeded from its n,π^* triplet state to give 4-hydroxylaminopyridine in a quantitative yield. The quantum yields for the disappearance of 4-nitropyridine in hydrochloric acid-isopropyl alcohol solutions increased with the concentration of hydrochloric acid up to 3.6×10^{-2} mol l^{-1} ($\Phi=0.27$—0.94). These results suggest that the hydrogen abstraction of photoexcited 4-nitropyridine proceeds electrophilically because of the decrease in the electron density of the nitro group, in decrease resulting from the protonation of heterocyclic nitrogen and the n,π^* excitation of the nitro group.

It is well-known that aromatic nitro compounds are photoreduced in hydrogen-donative solvents to give the corresponding amino or hydroxylamino compounds.[2] Few investigation of the relationships between the electronic structures of photoexcited nitro compounds and their reactivities of hydrogen abstraction have, however, been done to date. Hurley and Testa[3] have reported that the reactivity of the hydrogen abstraction of the protonated nitrobenzene triplet is greater than that of the unprotonated nitrobenzene triplet. Janzen and Gerlock[4] reported the substituent effects on the photochemistry and nitroxide-radical formation of nitro aromatic compounds, as studied by electron-spin-resonance spin-trapping techniques. Meanwhile, we ourselves have reported that, when the photoreduction of *para*-substituted nitrobenzenes is done in isopropyl alcohol (IPA), there is a linear correlation between the log-values of the relative quantum yields of nitrobenzenes and the nitrobenzene and the Hammett constants (ρ: +); therefore, the hydrogen abstraction of photoexcited nitrobenzenes may proceed electrophilically.[1] On the other hand, 4-nitropyridine is not reduced photochemically in IPA, and it is photoreduced in hydrochloric acid (HCl) - IPA solutions to give 4-hydroxylaminopyridine in a quantitative yield.[5] These facts are very interesting and may prove useful in investigating the correlation between the reactivity of the photochemical reduction and the electronic structure of nitro aromatic compounds in the photoexcited states.

In this paper, we wish to report in detail our findings on the photoreduction of 4-nitropyridine and to discuss the photoreduction mechanism. Both the reporting and discussing were begun in a communication (Ref. 5).

Results

Photochemical Reduction of 4-Nitropyridine. Identification of the Reduction Products. Figure 1 shows the progressive spectral change during the course of the photolysis of a 2×10^{-3} mol l^{-1} solution of 4-nitropyridine in IPA on irradiation with an immersion-type 130-W high-pressure mercury lamp under a nitrogen atmosphere at room temperature. As Fig. 1 shows, no isosbestic points were observed on the spectra, and the reaction product (Product A) had an absorption at 250 mμ. "Product A" (mp>300°C, brown plate from ethanol) has not yet been identified; however, it is clearly not a reduction product of 4-nitropyridine, such as 4-hydroxylamino-, 4,4'-azoxy-, 4,4'-azo-, and/or 4-aminopyridine, as has been shown by a comparison of the UV spectra with those of authentic samples.

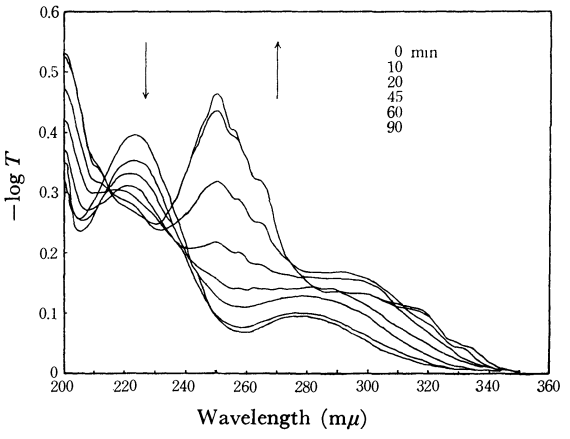

Fig. 1. The progressive spectral change of the photoreaction of 4-nitropyridine in IPA.

Meanwhile, the progressive spectral change during the reaction of a 2×10^{-3} mol l^{-1} solution of 4-nitropyridine in a 4 vol% concentrated HCl - IPA solution on irradiation with an immersion-type 130-W high pressure mercury lamp under a nitrogen atmosphere at room temperature is shown in Fig. 2. Two isosbestic points were observed at 214 and 244 mμ respectively. The absorption at 273 mμ (Product B) gradually in-

1) Part VIII: S. Hashimoto and K. Kano, *Tetrahedron Lett.* **1970**, 3509.
2) Y. Ogata, *Kogyo Kagaku Zasshi*, **72**, 23 (1969); "The Chemistry of the Nitro and Nitroso Groups," ed. by H. Feuer, Interscience, New York (1969), p. 181.
3) R. Hurley and A. C. Testa, *J. Amer. Chem. Soc.*, **89**, 6917 (1967).
4) E. G. Janzen and J. L. Gerlock, *ibid.*, **91**, 3108 (1969).
5) S. Hashimoto, K. Kano, and K. Ueda, *Tetrahedron Lett.*, **1969**, 2733.

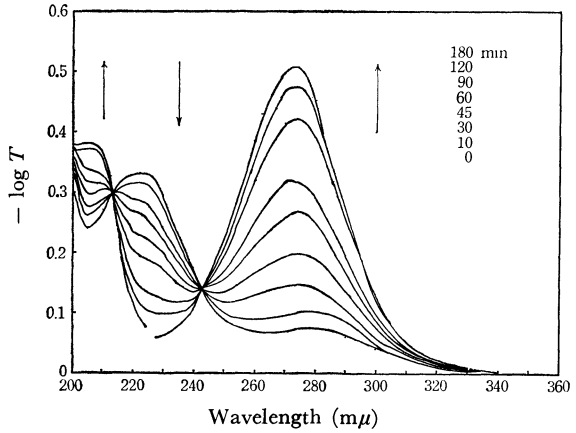

Fig. 2. The progressive spectral change of the photoreduction of 4-nitropyridine in HCl-IPA solution.

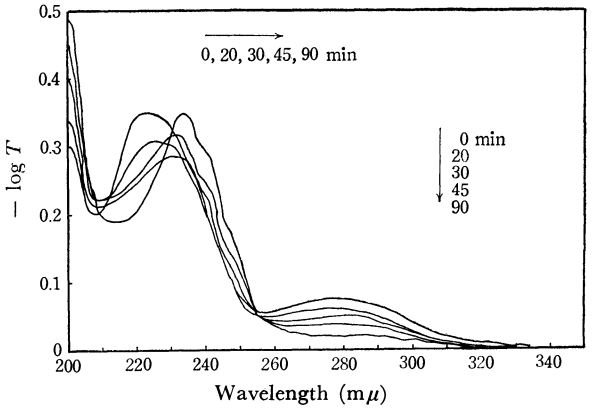

Fig. 3. The progressive spectral change of the photoreaction of 4-nitropyridine in HCl-IPA solution under an oxygen atmosphere.

creased in intensity with the progress of the photolysis. "Product B" was converted by alkali to afford 4,4'-azopyridine (yield 32%), and then converted to 4,4'-azoxypyridine (yield 24%) on treatment in a neutral solution. It has been established that 4-hydroxylaminopyridine 1-oxide converts to 4,4'-azopyridine 1,1'-dioxide on treatment in an alkaline solution, and converts to 4,4'-azoxypyridine 1,1'-dioxide on treatment in a neutral solution,[6] while phenylhydroxylamine converts to azoxybenzene.[7] These facts suggest that "Product B", which is a precursor of 4,4'-azopyridine and 4,4'-azoxypyridine, is 4-hydroxylaminopyridine.

Effect of Triplet Quenchers. The quenching effects for the photoreduction of 4-nitropyridine in HCl-IPA solutions were investigated by using 1,3-pentadiene and/or oxygen as triplet quenchers.

A 2×10^{-3} mol l^{-1} solution of 4-nitropyridine in a 4 vol% concentrated HCl-IPA solution containing 1,3-pentadiene (2.5×10^{-2} mol l^{-1}) was irradiated with an immersion-type 130-W high-pressure mercury lamp under a nitrogen atmosphere at room temperature. In the photoreduction of 4-nitropyridine in the absence of 1, 3-pentadiene, about 3.0 hr is required to complete the photolysis, but in the presence of 1,3-pentadiene, which is 1.5 times as large in quantity as 4-nitropyridine, about 4.5 hr is required. The photoreduction of 4-nitropyridine proceeded under irradiation by a near 316 mμ light, and we do not need consider the inner-filter effect by 1,3-pentadiene ($\lambda_{max}^{IPA}=223$ mμ) in this reaction. These facts suggest that the photoreduction of 4-nitropyridine is quenched by 1,3-pentadiene.

The quenching effect by oxygen was also studied. A 2×10^{-3} mol l^{-1} solution of 4-nitropyridine in a 4 vol% concentrated HCl - IPA solution was irradiated with an immersion-type 130-W high-pressure mercury lamp under an oxygen atmosphere at room temperature. The progressive spectral change during the photolysis is shown in Fig. 3. As Fig. 3 shows, the photochemical reaction of 4-nitropyridine under an oxygen atmosphere proceeded in a complicated way; finally, a product which had an absorption at 235 mμ was generated. The generation of 4-hydroxylaminopyridine was not observed on the UV spectrum. A reaction other than photoreduction might occur, and so it could not clarified whether or not the photoreduction of 4-nitropyridine was quenched by oxygen. Kaneko *et al.*[8] have reported that 4-nitropyridine 1-oxide is not reduced photochemically in ethanol under an oxygen atmosphere, and that 4-hydroxypyridine 1-oxide is thus prepared. The photolysis of 4-nitropyridine in oxygen-saturated solutions is now under investigation.

The Role of HCl. The Quantum Yield for the Disappearance of 4-Nitropyridine. HCl plays an important role in the photochemical reduction of 4-nitropyridine. The quantum yields for the disappearance of 4-nitropyridine (Φ) were measured in order to clarify the role of HCl.

Several 1×10^{-3} mol l^{-1} solutions of 4-nitropyridine in 80% IPA-water solutions containing varying amounts of HCl were irradiated by a 316-mμ light under a nitrogen atmosphere at room temperature. Here, 4-hydroxylaminopyridine was the only product. The correlation between the quantum yields and the concentration of HCl is shown in Fig. 4. The quantum yields of the 4-nitropyridine disappearance increased

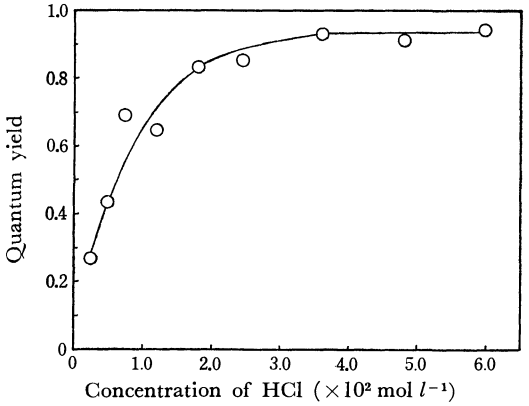

Fig. 4. The correlation of the quantum yields for the disappearance of 4-nitropyridine and the concentration of HCl.

6) F. Parisi, P. Bovina, and A. Quilico, *Gazz. Chim. Ital.*, **90**, 903 (1960).

7) Y. Ogata, M. Tsuchida, and Y. Takagi, *J. Amer. Chem. Soc.*, **79**, 3397 (1957); Y. Ogata, Y. Sawaki, J. Mibae, and T. Morimoto, *ibid.*, **86**, 3854 (1964).

8) C. Kaneko, I. Yokoe, and S. Yamada, *Tetrahedron Lett.*, **1967**, 775.

with the concentration of HCl up to 3.6×10^{-2} mol l^{-1}, and while they were constant above this concentration ($\Phi_{av.}=0.93$). The quantum yields of the 4-nitropyridine disappearance ($\Phi=0.27-0.94$) were greater than that of nitrobenzene in IPA ($\Phi=0.0114$)[9] and/or IPA - HCl solutions ($\Phi=0.04-0.14$).[3]

Discussion

It has been studied by several workers how aromatic nitro compounds, such as nitrobenzene,[9-11] *para*-substituted nitrobenzenes,[1,12] 1-nitronaphthalene,[13,14] and 4-nitropyridine 1-oxide,[15,16] are photoreduced in hydrogen-donative solvents to give the corresponding amino or hydroxylamino compounds. On the other hand, 4-nitropyridine was not photoreduced in IPA, but was reduced photochemically in HCl-IPA solutions under a nitrogen atmosphere to afford 4-hydroxylaminopyridine in a quantitative yield.

The photoreduction of 4-nitropyridine was quenched by 1,3-pentadiene; this suggested that the hydrogen abstraction proceeded from the excited triplet state of 4-nitropyridine. However, it seems that the quenching effect by 1,3-pentadiene is not significant in the photoreduction of 4-nitropyridine. This finding is similar to the oxygen quenching of the nitrobenzene triplet.[9] The photochemical behavior of nitro compounds in hydrogen-donative solvents may be written as in the following sequence:

$$N + h\nu \xrightarrow{k_1} N^{*(1)} \quad (1)$$

$$N^{*(1)} \xrightarrow{k_2} N \quad (2)$$

$$N^{*(1)} \xrightarrow{k_3} N^{*(3)} \quad (3)$$

$$N^{*(3)} \xrightarrow{k_4} N \quad (4)$$

$$N^{*(3)} + Q \xrightarrow{k_5} N + Q \quad (5)$$

$$N^{*(3)} + AH \xrightarrow{k_6} NH + A \quad (6)$$

A steady-state approximation for solutions containing quenchers such as 1,3-pentadiene and/or oxygen leads to this expression for the disappearance of nitro compounds:

$$\Phi = \frac{\Phi_T}{\left[1+\frac{k_4+k_5(Q)}{k_6(AH)}\right]}$$

where Φ is the quantum yield for the disappearance of nitro compounds, Φ_T is the yield of the triplet, (AH) is the concentration of the hydrogen-donative solvents, and (Q) is the concentration of the quenchers. It can be explained, in accounting for the ineffective oxygen quenching of the nitrobenzene triplet, that k_4 is greater than $k_5(Q)$.[9] In the photoreduction of 4-nitropyridine, however, k_4 may be small, since the quantum yield for the disappearance of 4-nitropyridine was about 0.9 in the absence of 1,3-pentadiene when an IPA solution of 4-nitropyridine containing 4 vol% concentrated HCl was irradiated with the 316 mμ light.[17] Therefore, it is reasonable to expect that $k_6(AH)$ will be greater than $k_5(Q)$.

Meanwhile, 4-nitropyridine in IPA absorbed broadly near the 340—420 mμ light. Since this weak band overlapped with the intense π,π^* band, it was impossible to distinguish the n,π^* band. It has been established that the hydrogen abstraction of photoexcited benzophenones proceeds from their n,π^* triplet states and that the reactivity of hydrogen abstraction falls off in their π,π^* triplet states.[18] By the way, the quantum yields for the diappearance of 4-nitropyridine in HCl-IPA solutions were strikingly large ($\Phi=0.27$—0.94). These facts suggest that the photoreduction of 4-nitropyridine proceeds from its n,π^* triplet state.

In the photoreduction of 4-nitropyridine to 4-hydroxylaminopyridine, HCl had to exist in the reaction system. The UV spectra of 4-nitropyridine in acidic IPA solutions, suggest that the protonation of heterocyclic nitrogen proceeded, while the protonation of the nitro group in the ground state does not occur, in the range of the HCl concentration used in our experiments, since the absorption of the conjugated acid of 4-nitropyridine at 280 mμ in IPA increased in its intensity with an increase in the acidity and the isosbestic point was observed at 248 mμ. These results suggest that 4-nitropyridine hydrochloride is reduced photochemically. It seemed that, since 4-nitropyridine partly forms its hydrochloride in the range of the HCl concentration from 0.24×10^{-2} to 3.6×10^{-2} mol l^{-1}, the quantum yield for the disappearance of 4-nitropyridine increased with the concentration of HCl; above this concentration, the formation of hydrochloride was perfect, and so the quantum yields became constant.

The electron density on the nitro group of 4-nitropyridine may be lower than that of nitrobenzene because of the electron-withdrawing effect of heterocyclic nitrogen. When the lone pair of heterocyclic nitrogen is protonated, the electron-withdrawing effect will be enhanced; therefore, the electron density on the nitro group of protonated 4-nitropyridine may be lower than that of unprotonated 4-nitropyridine.

Meanwhile, the n-π^* transition of the nitro group may be pictured as follows:[19]

9) R. Hurley and A. C. Testa, *J. Amer. Chem. Soc.*, **88**, 4330 (1966).
10) S. Hashimoto, J. Sunamoto, H. Fujii, and K. Kano, This Bulletin, **41**, 1249 (1968).
11) J. A. Barltrop and N. J. Bunce, *J. Chem. Soc.*, **1968**, 1467.
12) R. A. Finnegan and D. Knutson, *J. Amer. Chem. Soc.*, **90**, 1670 (1968).
13) S. Hashimoto and K. Kano, *Kogyo Kagaku Zasshi*, **72**, 188 (1969).
14) W. Trotter and A. C. Testa, *J. Phys. Chem.*, **74**, 845 (1970).
15) C. Kaneko, S. Yamada, I. Yokoe, N. Hata, and Y. Ubukata, *Tetrahedron Lett.*, **1966**, 4729.
16) N. Hata, E. Okutsu, and I. Tanaka, This Bulletin, **41**, 1769 (1968).
17) Although the quantum yield in the presence of 1,3-pentadiene could not determine exactly because of the difficulty of the determination of 4-nitropyridine, it was estimated to be about 0.6 when a solution of 4-nitropyridine (1×10^{-3} mol l^{-1}) in 4 vol% concentrated HCl-IPA solution containing 1,3-pentadiene (2.5×10^{-2} mol l^{-1}) was irradiated with the 316 mμ light.
18) T. Tezuka, *Yuki Gosei Kagaku Kyokai Shi*, **27**, 309 (1969).
19) "The Chemistry of the Nitro and Nitroso Groups," ed. by H. Feuer, Interscience, New York (1969), p. 169.

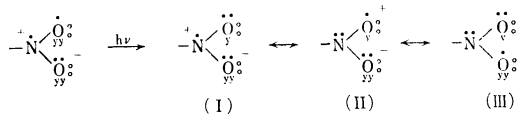

(I) (II) (III)

Ground state n,π^* Excited state

·: π electron; ∘: sp electron; y: p_y electron

The structure (I) and (III) imply that a nitro n,π^* excited state exhibits biradical properties. On the other hand, as is shown in the structure (II), n,π^* excitation removes an electron from the oxygen atom and promotes it to same π^* orbital, which is then shared by both atoms, formally leaving a 1/2 positive charge on oxygen. For these reasons, the n,π^* excited states of nitro compounds are similar to those of carbonyl compounds; therefore, it is reasonable to assume that the reactivity of the hydrogen abstraction of the n,π^* photoexcited nitro compounds is also similar to that of carbonyl compounds. Porter and Suppan[20] have reported that the reactivity of the hydrogen abstraction of benzophenones may be classified, in decreasing order, as n,π^*, π,π^*, and charge-transfer (CT) states; these properties can be interpreted in term of the electron distribution in the lowest triplet level.

As has been mentioned above, the formal positive charge at oxygen atoms on the nitro group of 4-nitropyridine, may increase in this order: the unprotonated 4-nitropyridine, protonated 4-nitropyridine, and the n,π^* excited state of protonated 4-nitropyridine. In view of the above facts, it seems reasonable to assume that the hydrogen abstraction of photoexcited 4-nitropyridine may be dominated by the electron density on the oxygen of the nitro group, and that it proceeds electrophilically similarly to that of photoexcited benzophenones. This deduction may be supported by the fact that there is a linear correlation between the log-values of the quantum yields for the disappearence of *para*-substituted nitrobenzenes and the Hammett constants (ρ: +) when the photoreduction of *para*-substituted nitrobenzenes is done in IPA.[1]

Experimental

Materials. The 4-nitropyridine was prepared according to the procedures described in the literature.[21] Reagent-grade IPA was distilled prior to use. 1,3-Pentadiene commercially obtained was further purified by distillation (bp 42—45°C).

Determination of Quantum Yields. The 316-mμ light was isolated from a high-pressure 130-W mercury lamp with a combination filter of Toshiba UV-D25, an aqueous nickel sulfate solution, and carbon tetrachloride. The light intensities were determined with a potassium ferrioxalate actinometer described by Hatchard and Parker.[22]

Analytical Procedures. The disappearance of 4-nitropyridine was determined by measuring the optical densities of photolyzed solutions. Polarographic analysis for following the 4-nitropyridine disappearance was also undertaken (pH=6.0, $E_{1/2}=-0.3$ V), but satisfying data could not obtained by this method. A Hitachi 124 spectrophotometer was used for the quantitative absorbance measurements and for following the progressive spectral change in the 4-nitropyridine photochemistry.

Preparation of 4,4'-Azoxypyridine and 4,4'-Azopyridine by the Photolysis of 4-Nitropyridine. A mixture of 0.62 g (5×10^{-3} mol) of 4-nitropyridine and 2.5 m*l* of concentrated HCl was exactly diluted to 1 *l* with IPA, and then irradiated with an immersion-type 130-W high-pressure mercury lamp for 10 hr under a nitrogen atmosphere at room temperature. After the irradiation, the photolyzed solution was evaporated to half of its volume *in vacuo*; the "reaction mixture" was thus obtained. The "reaction mixture" was neutralized with an aqueous sodium carbonate solution, and then evaporated to 100 m*l* of its volume. The brown residue thus obtained was heated to *ca.* 95°C for 2.5 hr and then extracted with chloroform. After the evaporation of the chloroform, the residue was recrystallized from water. The plate crystal thus obtained was identified as 4,4'-azoxypyridine; yield, 0.12 g (24%); mp 125—126.5°C. In mass spectroscopy, a molecular radical ion M^+ (*m/e* 200), was found corresponding to the molecular formula of $C_{10}H_8N_4O$.

Found: C, 60.10; H, 4.05; N, 28.12; O, 7.73%. Calcd for $C_{10}H_8N_4O$: C, 59.99; H, 4.03; N, 27.99; O, 7.99%.

The UV and IR spectra of 4,4'-azoxypyridine are shown in Figs. 5 and 6.

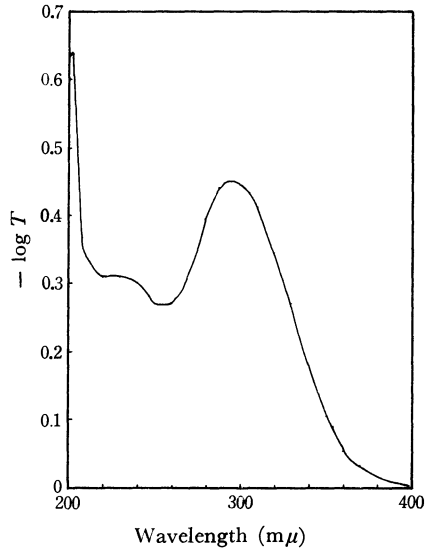

Fig. 5. UV-spectrum of 4,4'-azoxypyridine (4×10^{-5} mol l^{-1}).

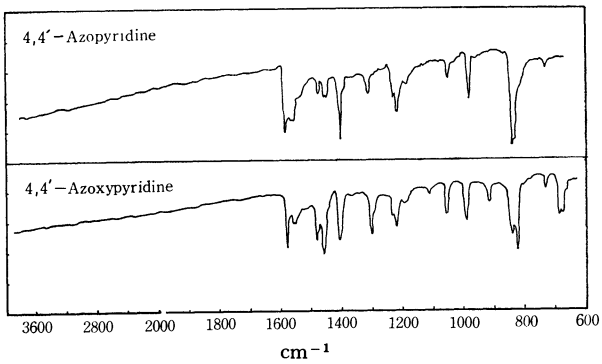

Fig. 6. IR-spectra of 4,4'-azoxypyridine and 4,4'-azopyridine (KBr).

20) G. Porter and P. Suppan, *Trans. Faraday Soc.*, **61**, 1664 (1965).
21) E. Ochiai, *J. Org. Chem.*, **18**, 534 (1953).
22) C. G. Hatchard and C. A. Parker, *Proc. Roy. Soc.* (London), **A235**, 518 (1956).

The "reaction mixture" was basified with 300 m*l* of a 33% aqueous sodium hydroxide solution, and then evaporated as far as possible. The redish-orange residue was dissolved in water and extracted with chloroform. After the evaporation of the chloroform, the residue was recrystallized from water. The redish-orange needles thus obtained were identified as 4,4′-azopyridine; yield, 0.15 g (32%); mp 109—110.5°C (lit,[6] mp 108—109°C). In mass spectroscopy, a molecular radical ion, M^+ (*m/e* 184), was found corresponding to the molecular formula of $C_{10}H_8N_4$.

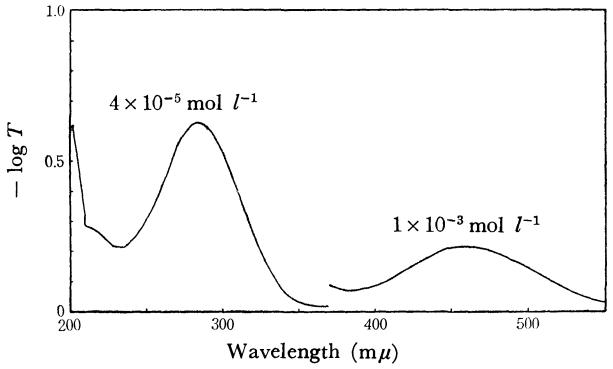

Fig. 7. UV-spectrum of 4,4′-azopyridine in IPA.

Found: C, 65.39; H, 4.22; N, 30.16%. Calcd for $C_{10}H_8N_4$: C, 65.20; H, 4.38; N, 30.42%.

The UV and IR spectra of 4,4′-azopyridine are shown in Figs. 7 and 6.

The authors wish to thank Mr. Ikuo Takada and Miss Tomi Inoue for their assistance in the experiments.

BULLETIN OF THE CHEMICAL SOCIETY OF JAPAN, VOL. 44, 1106—1107 (1971)

Alkoxysilanes. VII. The Preparation of Alkylalkoxysiloxanes

Ichiro KIJIMA, Keisuke OKUDA, and Yoshimoto ABE*

Department of Industrial Chemistry, Faculty of Engineering, Science University of Tokyo, Kagurazaka, Shinjuku-ku, Tokyo

(Received October 6, 1970)

Trimethylsiloxytri-*t*-butoxysilane (I), bis(trimethylsiloxy)di-*t*-butoxysilane (II), and bis(trimethylsiloxy)bis-(tri-*t*-butoxysiloxy)silane (III) were prepared by the reaction of trimethylchlorosilane with tri-*t*-butoxysilanol, di-*t*-butoxysilanediol, and bis(tri-*t*-butoxysiloxy)silanediol respectively. Bis(tri-*t*-butoxysiloxy)dimethylsilane (IV) was also obtained by the reaction of dimethyldichlorosilane with tri-*t*-butoxysilanol. The reaction of dimethyldichlorosilane with di-*t*-butoxysilanediol or bis(tri-*t*-butoxysiloxy)silanediol gave tetramethyltetra-*t*-butoxy (V) or tetramethyltetra(tri-*t*-butoxysiloxy)cyclooctasiloxane (VI). These compounds were identified by means of elemental analysis, molecular-weight determination, and a study of the IR and NMR spectra.

Alkylalkoxysiloxanes have been obtained by the hydrolysis of alkylalkoxychlorosilanes and alkylalkoxysilanes,[1,2] but the preparation of the alkylalkoxysiloxanes[3] by the reaction of alkoxysilanols with alkylchlorosilanes has not been described. In this paper, we wish to report an investigation of the preparation of alkylalkoxysiloxanes bearing methyl and *t*-butoxy groups as organic radicals.

Since we had already prepared several alkoxysilanols, tri-*t*-butoxysilanol,[4] di-*t*-butoxysilanediol,[5] and bis-(tri-*t*-butoxysiloxy)silanediol, we expected that the reaction of these silanols with alkylchlorosilanes would lead to the formation of mixed siloxanes. Furthermore, polyalkylalkoxysiloxanes may be obtained by the reactions of the silanediols with dichlorosilanes. It was found that the following reactions, (A) and (B), easily afforded the products (I), (II), (III), and (IV):

$$Me_3SiCl + (RO)_{4-n}Si(OH)_n + nC_5H_5N \rightarrow (RO)_{4-n}Si(OSiMe_3)_n + nC_5H_5NHCl \quad (A)$$

where R=Bu^t and n=1: (I), n=2: (II)
R=(Bu^{t}O)$_3$Si and n=2: (III)

$$Me_2SiCl_2 + 2(RO)_3SiOH + 2C_5H_5N \rightarrow [(RO)_3SiO]_2SiMe_2 + 2C_5H_5NHCl \quad (B)$$

where R=Bu^t (IV)

These products could be distilled as a colorless viscous liquid (IV) which solidified as soon as distilled. As Table 1 shows, the results of the elemental analysis and molecular-weight determination agreed with the calculated values for the compounds. The IR spectra of these comopunds are essentially identical and show absorption peaks at 1388 and 1360 (branching of the alkyl group), 1240 and 1255 (Si–Me$_3$, methyl group), 1052 (Si–O–Si), 841 (Si–Me$_3$), and 799 (Si–Me$_2$)cm^{-1}.[6] The NMR spectra of the compound (I) also show the proton signals at 8.73 (Bu^t) and 9.90 (Me) τ. The formation of these compounds indicates that the hydroxy groups in the silanols are easily replaced by the trimethylsiloxy group, although they are sterically hindered. It is generally known that it is difficult to replace the X group in the alkoxysilanes $(RO)_{4-n}SiX_n$

* Present address: Faculty of Science and Technology, Science University of Tokyo, Noda City (278).

1) K. A. Andrianov and M. Kamenskaya, *J. Gen. Chem.*, (U. S.S.R.), **8**, 969 (1938); K. A. Andrianov and O. Gribanova, *ibid.*, **8**, 552 (1938).

2) K. A. Andrianov and B. A. Izmaylov, *J. Organometal. Chem.*, **8**, 443 (1967).

3) J. R. Wright, R. O. Bolt, A. G. Goldschmidt, and A. D. Abbott, *J. Amer. Chem. Soc.*, **80**. 1733 (1958).

4) Y. Abe and I. Kijima, This Bulletin, **42**, 1118 (1969).

5) Y. Abe and I. Kijima, *ibid.*, **43**, 466 (1970).

6) R. E. Richards and H. E. Thompson, *J. Chem. Soc.*, **1949**, 125.

Table 1. Alkylalkoxysiloxanes

Reactants (g) A	B	N	Products	Yield (%)	Bp °C/mmHg	n_D^{20}	Mol wt Found (Calcd)	Found Anal % (Calcd) Si
14.1	34.2	10.2	(I)	57	102/16[a]	1.3974	336 (337)	15.89 (16.69)
5.1	4.8	3.3	(II)	21	110—111/23[a]	1.3946	364 (353)	22.33 (23.89)
3.2	8.8	2.4	(III)	20	167—169/1	1.4141	600 (687)	16.23 (16.35)
8.9	36.3	10.9	(IV)	28	150—153/1 38.5—40 (Mp)	—	535 (585)	14.44 (14.40)

A: Chlorosilane, B: Silanol, a) Fractionally distilled

Table 2. Cyclic Alkylalkoxysiloxanes

Reactants (g) A	B	N	Products	Yield (%)	Mp °C	Mol wt Found (Calcd)	Found Anal % (Calcd) C	H	Si
21.0	34.0	25.4	(V)	66	109—110[a]	527 (529)	45.31 (45.51)	9.56 (9.15)	21.31 (21.24)
1.5	6.6	1.8	(VI)	35	132—133[b]	1294 (1290)	47.71 (48.41)	8.82 (9.32)	17.62 (17.42)

A: Dichlorosilane, B: Silanediol, a) Recrystallized from *n*-hexane, b) Recrystallized from ethanol

(n=halogen, amino group; R=t-alkyl group; n=1 or 2) by a bulky alkoxy group.[7-9] In the present case, however, the replacement is very easy. This difference seems to result from the difference in the bond length between the Si–O–C and Si–O–Si bonds.

Since it was found that the reaction of (A) and (B) easily afforded the alkylalkoxysiloxanes, we can expect that the reaction of dialkyldichlorosilanes with silanediols will produce polyalkylalkoxysiloxanes. With this view, the following reaction was carried out:

$$Me_2SiCl_2 + (RO)_2Si(OH)_2 + 2C_5H_5N \rightarrow \text{(cyclic tetrasiloxane)} + 2C_5H_5NHCl \quad \text{(C)}$$

where R=Bu^t: (V), R=(Bu^{t}O)$_3$Si: (VI)

The products obtained (V and VI) could be distilled or recrystallized. As is shown in Table 2, (V) solidified as soon as distilled (mp 109—110°C); (VI) could not be distilled because of the decomposition (240°C/1mmHg), but it was recrystallized from ethanol (mp 132—133°C). These products were soluble in common organic solvents. The analytical data and the results of the molecular-weight determination agreed with the calculated values for the cyclooctasiloxanes shown by Equation (C).

The formation of these compounds was also confirmed by the spectroscopic data; the IR spectra of these compounds show the absorption peaks at 1388 and 1360 (Bu^t), 1252 and 1240 (Si–Me), 1060 (Si–O–Si), and 799 (Si–Me$_2$) cm^{-1}. The NMR spectra of (V) show proton signals at 8.72 (Bu^t) and 9.87 (Me) τ. In this reaction, the formation of the cyclic alkylalkoxysiloxanes may be ascribed to the steric effect of the t-butoxy and tri-t-butoxy-siloxy groups.

Experimental

All the experiments were carried out under a dry atmosphere. The melting and boiling points are uncorrected.

Materials. Commercially-available trimethylchlorosilane and dimethyldichlorosilane were redistilled before use.[10] The aldoxysilanols used were prepared by a method already described.[4,5]

Preparation of Alkylaldoxysiloxanes. To a solution of silanol or silanediol and pyridine in toluene, dimethyldichlorosilane in the same solvent was added, drop by drop, about 0°C. After the mixture had been refluxed for 2 hr, pyridine hydrochloride was filtered off; then the solvent was removed, and the residue was recrystallized or distilled *in vacuo*, giving crystals or a liquid.

Instruments. The molecular weight was determined by the cryoscopic method in benzene. The IR spectra were measured in a liquid film or KBr disk by means of a Hitachi EPI-S2 spectrometer. The NMR spectra were measured with a Varian A-60 spectrometer in a carbon tetrachloride solution, with tetramethylsilane as the internal standard.

7) H. J. Backer and H. A. Klasens, *Rec. Trav. Chim.*, **61**, 500 (1942).
8) H. Breederveld and H. I. Waterman, *ibid.*, **72**, 166 (1953).
9) C. S. Miner, L. A. Bryan, R. P. Holyz, and G. W. Pedlow, *Ind. Eng. Chem.*, **39**, 1368 (1947).

10) The authors wish to thank the Matsumoto Pharmaceutical Co. for the supply of methylchlorosilanes.

Peptide Synthesis by Oxidation-Reduction Condensation. I. Use of NPS-Peptides as Amino Component

Masaaki Ueki, Hiroshi Maruyama, and Teruaki Mukaiyama

Laboratory of Organic Chemistry, Tokyo Institute of Technology, Ookayama, Meguro-ku, Tokyo

(Received October 12, 1970)

Sulfenamides were found to react readily with soft nucleophiles in the presence of active hydrogen compounds. A new method for the synthesis of carboxamide from metal carboxylate, sulfenamide and tertiary phosphine was developed. The effects of metal component were examined. Copper(II) salts gave the best result. In a similar way, peptides were synthesized by the reaction of copper(II) salts of acylamino acid, or free acylamino acid in the presence of cupric chloride and triethylamine, with NPS-amino acid derivatives and triphenylphosphine. When organo-mercuric compounds such as dianisylmercury were used in place of cupric chloride and triethylamine in the above reaction, almost complete retention of configuration was observed by the Young test.

In a previous communication,[1] a new amide (peptide) forming reaction by use of sulfenamide as an amino component was reported. The reaction is described more in detail in this paper.

Most sulfenic acid derivatives such as sulfenyl halide, sulfenate ester, disulfide, thiocyanate react very easily with phosphite triester. However, sulfenamide does not react with the ester because of the least polarizability of sulfur-nitrogen bond. On the other hand, sulfenamide is easily attacked by phosphite diester, which has a similar nucleophilicity as triester, to yield thiophosphate and amine.[2] The difference in reactivity between phosphite di- and tri-esters could be attributed to the presence or absence of active hydrogen. Mercaptan, which possesses a soft nucleophilic center and a proton in the molecule, also readily reacts with sulfenamide to give disulfide and amine. This reaction has been used for the removal of *o*-nitrophenylsulfenyl (NPS) protecting group introduced to α-amino function in peptide synthesis.[3] This shows that sulfenamides are activated by the protonation to yield active species, which are in turn easily attacked by soft nucleophile.

The reaction of sulfenamide and tertiary phosphine, a representative soft nucleophile, in the presence of active hydrogen compounds such as water and alcohol was tried first. When *p*-chlorobenzenesulfenanilide was allowed to react with triphenylphosphine in ether saturated with water, quantitative cleavage of sulfur-nitrogen bond was observed. On the other hand, no reaction occurred when the same reaction was tried in anhydrous methanol. However, quantitative cleavage of sulfur-nitrogen bond was observed by the addition of boron trifluoride etherate to the reaction system.

The same reaction of sulfenamide, phosphine and active hydrogen compound was tried by using carboxylic acid. After a short reaction period, acetomorpholide was obtained in a 63% yield from *o*-nitrobenzenesulfenic morpholide, triphenylphosphine and acetic acid. Formation of carboxamide is well explained by considering a subsequent acylation of the liberated amine with acyloxyphosphorane.

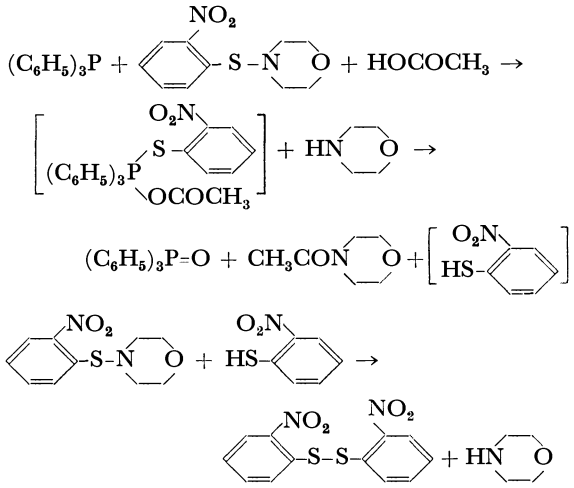

This reaction is not sufficient for the preparation of carboxamide because of the undesirable consumption of the starting sulfenamide by the subsequent reaction with mercaptan produced. This side reaction can be minimized by employing a mercaptan scavenger, which turns mercaptan into an inactive form. For example, when copper(II) hexanoate was allowed to react with *N*-*n*-butylbenzenesulfenamide and triphenylphosphine, a 95% yield of *N*-*n*-butylhexanamide was obtained, as shown in the following equation.

$$(R^1CO_2)_2Cu + 2R^2SNR^3R^4 + 2(C_6H_5)_3P \rightarrow 2R^1CONR^3R^4 + [(R^2S)_2Cu] + 2(C_6H_5)_3P{=}O$$

Since the copper(II) mercaptide produced does not react at all with sulfenamide in this reaction, yields of carboxamides are good as shown in Table 1. It is to be noted that mercury(II) and lead (II) salts of hexanoic acid also gave good results.

It is known that sulfenyl groups such as tritylsulfenyl and *o*-nitrophenylsulfenyl (NPS) can be used selectively as removable protecting groups in peptide synthesis. It can be expected that new peptide bond formation could be completed without removing the protecting group by the application of the above method to NPS-amino acid derivatives. *N*-Benzyl-*o*-nitrobenzenesulfenamide was chosen as a model compound and allowed to react with triphenylphosphine and benzoic acid. Contrary to expectation, the sulfenamide strongly resisted the

1) T. Mukaiyama, M. Ueki, H. Maruyama, and R. Matsueda, *J. Amer. Chem. Soc.*, **90**, 4490 (1968).

2) K. A. Petrov, N. K. Blinznyuk, and V. A. Savostenok, *Zh. Obshch. Khim.*, **31**, 1361 (1961); *Chem. Abstr.*, **55**, 23317e (1961).

3) L. Zervas, D. Borovas, and E. Gazis, *J. Amer. Chem. Soc.*, **85**, 3660 (1963).

Table 1. Reactions of metal carboxylates, sulfenamides, and triphenylphosphine

Metal Carboxylate	Sulfenamide	Products: Carboxamide Structure	Products: Carboxamide Yield (%)	Products: $(C_6H_5)_3P=O$ Yield (%)
$(CH_3CO_2)_2Cu$	$C_6H_5S-N(C_2H_5)_2$	$CH_3CO-N(C_2H_5)_2$	60	quantitative
$(CH_3CO_2)_2Cu$	$C_6H_5S-NH(n-C_4H_9)$	$CH_3CO-NH(n-C_4H_9)$	quantitative	quantitative
$(CH_3CO_2)_2Cu\cdot H_2O$	$C_6H_5S-NH(n-C_4H_9)$	$CH_3CO-NH(n-C_4H_9)$	57	quantitative
$(n-C_5H_{11}CO_2)_2Cu$	$C_6H_5S-NH(n-C_4H_9)$	$n-C_5H_{11}CO-NH(n-C_4H_9)$	95	93
$(C_6H_5CO_2)_2Cu$	$C_6H_5S-NH(n-C_4H_9)$	$C_6H_5CONH(n-C_4H_9)$	62	quantitative
$(p-CH_3C_6H_4CO_2)_2Cu$	$C_6H_5S-NH(n-C_4H_9)$	$p-CH_3C_6H_4CONH(n-C_4H_9)$	80	90
$(n-C_5H_{11}CO_2)_2Hg$	$p-ClC_6H_4S-NH(n-C_4H_9)$	$n-C_5H_{11}CO-NH(n-C_4H_9)$	74	89
$(n-C_5H_{11}CO_2)_2Pb$	$p-ClC_6H_4S-NH(n-C_4H_9)$	$n-C_5H_{11}CO-NH(n-C_4H_9)$	68	84

reaction. This might be due to the lower electron density on nitrogen atom of this sulfenamide by conjugation with nitro group through sulfur *d* orbital and aromatic ring. However, it was found that addition of equimolar excess of triphenylphosphine gave rise to reaction. After the reaction period of 3 hr, *N*-benzylbenzamide was obtained in 90% yield by separating by column chromatography on silica gel. During the reaction about 1.5 equivalents of triphenylphosphine were oxidized even when reaction was carried out under nitrogen atmosphere, and copper mercaptide was obtained as a complex with triphenylphosphine. The detailed mechanism of the oxidation of the excess phosphine is not made clear as yet.

The above mentioned reaction of the preparation of carboxamide was modified to start from free carboxylic acid and sulfenamide. When *N*-*n*-butylbenzenesulfenamide was treated with hexanoic acid and triphenylphosphine in the presence of mercury(II) chloride and triethylamine. *N*-*n*-butylhexanamide was obtained in 79% yield. Various inorganic metallic compounds were examined through the reactions by using *N*-benzyl-*o*-nitrobenzenesulfenamide (see Table 2). The effcts of the metallic compounds in these reactions are explained by means of the following mechanism.

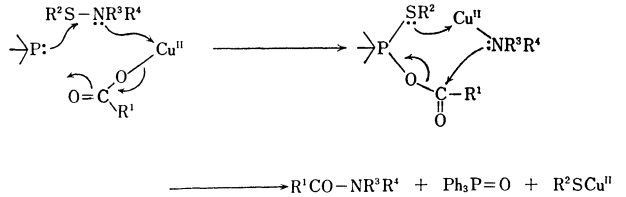

In the first stage of the reaction, metallic compound activates sulfur-nitrogen bond by accommodating the lone pair electrons on nitrogen atom. Thus a hard metal such as zinc is more effective in this stage. In the second stage, a metal component is used for mercaptide forming reaction. Thus a soft metal such as mercury(II) is more effective. The presence of both zinc chloride and mercuric chloride in the reaction gave good results as expected.

The new method was applied to the peptide synthesis by using NPS-amino acid derivatives as amino component. First, synthesis of benzyloxycarbonyl (Z)-L-phenylalanylglycine ethyl ester, which is free from the problem of racemization, was tried. Copper(II) Z-L-phenylalaninate was prepared by treating sodium salt with aqueous copper(II) sulfate solution. To a stirred mixture of the copper salt in methylene chloride, NPS-Gly-OEt and 1 molar excess of triphenylphosphine were added. The copper salt dissolved soon and a clear reddish brown solution resulted. Z-L-Phe-Gly-OEt was obtained by ordinary treatment in 96% yield. Further, it was found that the reaction of free Z-L-Phe-OH with NPS-Gly-OEt and excess triphenylphosphine in the presence of copper(II) chloride and triethylamine also gave dipeptide in 90% yield.

Table 2. Reaction of benzoic acid, *N*-benzyl-*o*-nitrobenzenesulfenamide, and triphenylphosphine in the presence of metal chloride and triethylamine

Metal chloride	Conditions	Products: $C_6H_5CONHCH_2C_6H_5$ Yield (%)	Products: $(C_6H_5)_3P=O$ Yield (%)
$CuCl_2$	RT 1 day	88	150
$HgCl_2$	RT 1 day	no reaction	—
$ZnCl_2$	RT 3 hr	71	100
$CuCl_2+ZnCl_2$	RT 1 day	75	100
$HgCl_2+ZnCl_2$	RT 1 day	80	92

2 equiv of triphenylphosphine was used.

The test for racemization in these two types of reactions was carried out by employing the Young method.[4] When copper(II) benzoyl(Bz)-L-leucinate, NPS-Gly-OEt and triphenylphosphine were allowed to react in methylene chloride at room temperature, Bz-Leu-Gly-OEt was obtaind in 77% yield. Its specific rotation was −19.0° (*c* 3.1, EtOH), which indicated that the L-isomer content was 57%. When Bz-L-Leu-OH, NPS-Gly-OEt and triphenylphosphine were allowed to react in the presence of copper(II) chloride and triethylamine in methylene chloride at room temperature for 15 hr, completely racemized Bz-Leu-Gly-OEt was obtained in 72% yield. No improvement was observed even when they were allowed to react at −70°C for 5 hr.

It is most probable that the racemization occurs

4) M. W. Williams and G. T. Young, *J. Chem. Soc.*, **1963**, 881.

through as oxazolone derived from the postulated acyloxyphosphorane intermediate. Thus, it is expected that basic species such as triethylamine and copper amide involved in the reaction would accelerate the formation of oxazolone from the intermediate.

It is known that the addition of acidic substances is very effective for the prevention of racemization in DCC[5] and mixed anhydride methods.[6] The effects of the acidic additives in this method were examined (Table 3). As expected, it was found that racemization was considerably suppressed by acidic additives according to their acidity except for *N*-hydroxysuccinimide. From its pK_a value, *N*-hydroxysuccinimide was more effective than expected. Pivalic acid, which showed no effect in the DCC method,[6] also showed some prevention. It was found that the reaction could be carried out without use of excess triphenylphosphine. Thus it is clear that acidic substances are useful not only for the prevention of racemization, but also for the activation of sulfenamides.

Table 3. Reaction of copper(II) Bz-L-leucinate, NPS-Gly-OEt, and triphenylphosphine in the presence of acidic additives

Additive	pK_a	Bz-L-Leu-Gly-OEt	
		Yield (%)	L-Isomer content (%)
none	—	77	57
C_6H_5OH	9.89	75	0
	9.40	64	84
p-$O_2NC_6H_4OH$	7.15	90	11
$(CH_3)_3CCO_2H$	5.01	57	39
2,4-$(O_2N)_2C_6H_3OH$	3.96	81	77
2,4,6-$(O_2N)_3C_6H_2OH$	0.38	48	80

From these findings basic substances such as triethylamine can be expected to be purged by employing the metallic salts derived from the above mentioned acidic compounds,mercaptan scavenger, in place of copper(II) chloride and triethylamine. This makes the reaction medium acidic and racemization would consequently be prevented. Mercury was found to be the best metal, since in such conditions metallic compounds are necessary only for complete trapping of mercaptan produced and not for the activation of sulfenamides. Mercury(II) bis-2,4-dinitrophenolate was prepared and the reaction of Bz-L-Leu-OH, NPS-Gly-OEt and triphenylphosphine was tried in the presence of the mercuric salt. As expected, Bz-L-Leu-Gly-OEt was obtained in 88% yield and its L-isomer content was 74%. When aryl mercuric compounds such as dianisyl mercury and anisyl mercuric bromide were used as a mercaptan scavenger, almost complete retention of configuration was observed as shown in Table 4.

Table 4. Reactions of Bz-L-Leu-OH, NPS-Gly-OEt, triphenylphosphine, and organomercuric compounds

Organomercuric compounds	Bz-L-Leu-Gly-OEt		$(C_6H_5)_3P=O$ Yield (%)
	Yield (%)	L-Isomer (%)	
$[2,4\text{-}(O_2N)_2C_6H_3O]_2Hg$	88	74	87
$(p\text{-}CH_3OC_6H_4)_2Hg$	93	87	99
p-$CH_3OC_6H_4HgBr$	92	93	97

In conclution, highly optically pure peptides can be prepared by the new method starting from the NPS-peptides as amino component by a one step procedure. Mild reaction condition starting with free carboxyl component is a merit of this new method as compared with the other method using NPS-peptides as an amino component.[7]

Experimental

Reagents. Sulfenamides were prepared from the corresponding chloride and amines. NPS-Gly-OEt was prepared by the method in literature.[3] Bz-L-Leu-OH, commercial product of Takara Kosan Co., was used without further purification.

Copper(II) salts of acylamino acids were prepared by treating the sodium salts of acylamino acids with copper (II) sulfate in aqueous solution. The copper salts precipitated were extracted with ethyl acetate, and the extracts were dried and evaporated *in vacuo*. The crude copper salts were purified by reprecipitation from chloroform-petroleum ether (bp 30—50°C).

(Z-L-Phe-O)$_2$Cu Found: C, 61.13; H, 5.04; N, 4.33%. Calcd for $C_{34}H_{32}N_2O_8Cu$; C, 61.86; H, 4.89; N, 4.24%.

(Bz-L-Leu-O)$_2$Cu Found: C, 57.87; H, 6.27; N, 4.97%. Calcd for $C_{26}H_{32}N_2O_6Cu$; C, 58.65; H, 6.02; N, 5.27%.

Mercury (II) bis-2,4-dinitrophenolate was prepared by the following procedure. A solution of 2,4-dinitrophenol and mercuric acetate in 1/1(v/v) aqueous ethanol was refluxed. Precipitates were collected by filtration and washed with water and acetone and dried.

Found: C, 30.51; H, 1.76; N, 5.61%. Calcd for $C_{12}H_8N_2O_6Hg$; C, 30.25; H, 1.68; N, 5.88%. *p*-Anisylmercuric bromide[8] and bis-*p*-anisylmercury[9] were prepared according to literature.

Reactions of Metal Carboxylates, Sulfenamides, and Triphenylphosphine(I). (General Procedure) Sulfenamide (10 mmol) in anhydrous methylene chloride (10 m*l*) was added drop by drop to a vigorously stirred mixture of metal carboxylate (5 mmol) and I (10 mmol) in methylene chloride (20 m*l*). The mixture was stirred for several hours and kept standing overnight. The precipitated copper mercaptide was removed by filtration, and carboxamide was obtained from the filtrate by distillation or chromatography on silica gel. Physical properties are as follows: $CH_3CON(C_2H_5)_2$, bp 93—100°C/40 mmHg; $CH_3CONH(n\text{-}C_4H_9)$, bp 110—112°C/22 mmHg; $n\text{-}C_5H_{11}CONH(n\text{-}C_4H_9)$, bp 95—98°C/0.05 mmHg; $C_6H_5CONH(n\text{-}C_4H_9)$, mp 68—70°C; $p\text{-}CH_3C_6H_4CONH(n\text{-}C_4H_9)$, mp 55—57°C: [Found: C, 75.60; H, 8.83; N, 7.30%. Calcd for $C_{12}H_{17}NO$; C, 75.75; H, 8.96; N, 7.32%.

5) E. Wünsch and F. Drees, *Chem. Ber.*, **99**, 110 (1966); J. E. Zimmerman and G. W. Anderson, *J. Amer. Chem. Soc.*, **89**, 7151 (1967).

6) G. W. Anderson, F. M. Callahan, and J. E. Zimmerman, *ibid.*, **89**, 178 (1967).

7) J. Savrda and D. H. Veyrat, *Tetrahedron Lett.*, **1968**, 6253; H. Faulstich, *Chimia*, **23**, 150 (1969).

8) F. Challenger and S. A. Miller, *J. Chem. Soc.*, **1938**, 894.

9) F. R. Preuss and I. Janshen, *Arch. Pharm.*, **293**, 933 (1960).

Reaction of Copper(II) Benzoate, N-*Benzyl-o-nitrobenzenesulfenamide, and I.* Reaction was carried out under the same conditions as described above except that I was used in one molar excess. The resulting solution was evaporated and reddish brown copper complex was precipitated from the residue by trituration with methanol. After filtration of the precipitate, the filtrate was condensed and chromatographed on silica gel. Copper complex and a small amount of disulfide were eluted by benzene. Elution with 1:1 mixture of benzene-methylene chloride gave *N*-benzylbenzamide (90%), mp 104—105°C. Further elution with 9:1 mixture of methylene chloride - methanol gave triphenylphosphine oxide (159%).

Reaction of Hexanoic, Acid, N-n-*Butylbenzenesulfenamide, and I in the Presence of Mercury(II) Chloride and Triethylamine(TEA).* Ten mmol of the sulfenamide in methylene chloride (10 m*l*) was added to a vigorously stirred mixture of hexanoic acid (10 mmol), I (10 mmol), mercuric chloride (5 mmol) and TEA (10 mmol) in methylene chloride (15 m*l*). After stirring for 3 hr at room temperature, mercury mercaptide precipitated was filtered off. The organic layer was dried and evaporated. From the residue, insoluble materials in petroleum ether (30—50°C) were removed by filtration. The filtrate was condensed and distilled to give *N-n*-butylhexanamide, (77%), bp 105—108°C/0.20 mmHg, which was purified by passing short column of silica gel.

Reactions of Benzoic Acid, N-*Benzyl-o-nitrobenzenesulfenamide, and I in the Presence of Metal Chlorides and TEA.* Reaction was carried out under similar conditions as mentioned above except that I was used in one molar excess when copper(II) chloride was employed. Isolation was carried out by chromatography on silica gel. The results are listed in Table 2.

Reaction of Copper(II) Z-L-phenylalaninate, NPS-Gly-OEt, and I. The copper salt (5 mmol), NPS-Gly-OEt (10 mmol), and I (20 mmol) were mixed in methylene chloride at room temperature. The resulting solution was stirred for 3 hr and kept standing overnight. After evaporation of the solvent, copper mercaptide-phosphine complex was precipitated by the addition of methanol and filtered off. The filtrate was condensed to about 5 m*l*, and 15 m*l* of ether and 25 m*l* of petroleum ether (30—50°C) were added to give Z-L-phe-Gly-OEt, 2.60 g (68%), mp 96—100°C. Additional 1.10 g (29%) of the peptide, mp 96—112°C, was obtained by chromatography on silica gel. The sample for analysis was recrystallized from ethyl acetate - petroleum ether, mp 109—111°C, $[\alpha]_D^{20}$ −17.0° (*c* 2, EtOH), lit,[10] mp 110—113°C, $[\alpha]_D^{20}$ −16.6° (*c* 2, EtOH).

Found: C, 65.59; H, 6.34; N, 7.02%. Calcd for $C_{21}H_{24}N_2O_5$; C, 65.61; H, 6.29; N, 7.29%.

10) R. W. Young, K. H. Wood, R. T. Joyce, and G. W. Anderson, *J. Amer. Chem. Soc.*, **78**. 2126 (1956).

Reaction of Z-L-Phe-OH, NPS-Gly-OEt, and I in the Presence of Copper(II) Chloride and TEA. NPS-Gly-OEt (10 mmol) in methylene chloride was added at room temperature to the stirred mixture of Z-L-Phe-OH (10 mmol), I (20 mmol), copper(II) chloride (5 mmol) and TEA (10mmol) in methylene chloride. The mixture was stirred for 1 day, washed with water and dried. The products were separated by chromatography on silica gel to give copper mercaptide-phosphine complex 3.12 g; Z-L-Phe-Gly-OEt 3.58 g, mp 109—112°C, $[\alpha]_D^{20}$ −17.3° (*c* 2, EtOH) and triphenylphosphine oxide, 4.28 g (154%).

Test for Racemization in This Type of Reaction by the Young Method.[4] *A) Reaction of Copper(II) Bz-L-leucinate, NPS-Gly-OEt, and I:* The reaction was carried out in the same manner as in the synthesis of Z-L-Phe-Gly-OEt. Hydrogen sulfide gas was introduced for 1 hr to the resulting solution. Cupric sulfide precipitated was filtered off and the filtrate was washed with 1N HCl, 5% $NaHCO_3$ solution and water, and dried. The products were then separated by preparative thin layer chromatography to give Bz-Leu-Gly-OEt 2.47 g (77%), mp 148—149°C. The crude material was subjected to measurement of optical purity without any purification to avoid fractionation, $[\alpha]_D^{20}$ −19.0° (*c* 3.1, EtOH), L-isomer content 56%.

B) Reaction of Bz-L-Leu-OH, NPS-Gly-OEt, and I in the Presence of Copper(II) Chloride and TEA: The reaction was carried out in the same manner as in the synthesis of Z-L-Phe-Gly-OEt starting from free carboxyl component. Hydrogen sulfide gas was introduced for 1 hr to the resulting solution. On filtering off the precipitated copper mercaptide, the filtrate was condensed and chromatographed on silica gel to give bis-*o*-nitrophenyl disulfide (quantitative), Bz-Leu-Gly-OEt 2.30 g (72%), mp 143—145°C, $[\alpha]_D^{20}$ 0°(*c* 3.1, EtOH) and triphenylphosphine oxide 3.34 g (120%).

Reaction of Copper(II) Bz-L-Leucinate, NPS-Gly-OEt, and I in the Presence of Acidic Additives. Copper(II) Bz-L-leucinate (5 mmol), NPS-Gly-OEt (10 mmol), I (10 mmol), and acidic substances listed in Table 3 (10 mmol) were mixed in methylene chloride at room temperature. The mixture was stirred for several hours and kept standing overnight. On filtering off copper mercaptide the filtrate was washed with 1N HCl, 5% $NaHCO_3$ solution and water and dried. On evaporation of the solvent, chromatographic separation gave crude Bz-Leu-Gly-OEt, which was subjected to the measurement of optical purity. The results are listed in Table 3.

Reactions of Bz-L-Leu-OH, NPS-Gly-OEt, I, and Organomercuric Compounds. The reaction was carried out by mixing equimolar amounts of Bz-L-Leu-OH, NPS-Gly-OEt, I, and bis(*p*-anisyl)mercury, mercury bis(2,4-dinitrophenolate) or *p*-anisylmercuric bromide in methylene chloride at room temperature. Work-up was done as above and results are listed in Table 4.

Decomposition of *cis*- and *trans*-α-Phenylcinnamoyl Peroxide and *t*-Butyl *cis*- and *trans*-α-Phenylperoxycinnamate. Stereochemistry of 1,2-Diphenylvinyl Radical[1]

Naoto WADA, Katsumi TOKUMARU, and Osamu SIMAMURA

Department of Chemistry, Faculty of Science, The University of Tokyo, Hongo, Tokyo

(Received October 23, 1970)

Decomposition of *trans*- and *cis*-α-phenylcinnamoyl peroxide and *t*-butyl *trans*- and *cis*-α-phenylperoxycinnamate were carried out in solution and the products were determined. *t*-Butyl *trans*- and *cis*-α-phenylperoxycinnamate, on decomposition in carbon tetrachloride, gave mixtures of *cis*- and *trans*-α-chlorostilbene in the same *cis* to *trans* ratio at 110°C, but in different ratios at 80°C, the higher ratio being obtained from *t*-butyl *trans*-α-phenylperoxycinnamate. In the decomposition of *trans*- and *cis*-α-phenylcinnamoyl peroxide in various solvents at 60°C, the α-halostilbenes formed in carbon tetrachloride and bromotrichloromethane and the stilbenes produced in cumene, chloroform and triethylsilane were shown to be richer in the isomer of the same configuration as the peroxide decomposed. The stereochemical course of the reaction of the 1,2-diphenylvinyl radical generated from these peroxy-esters and peroxides is discussed.

The stereochemistry of vinyl radicals has recently been investigated by several groups of workers.[2-8] Unsubstituted vinyl[2,3] and 1-methylvinyl radicals[2] have been shown by electron spin resonance measurements to exist not in an *sp*-hybridized linear form but in two sp^2-hybridized bent forms which are interconvertible. However, from the viewpoint of organic reaction mechanisms, the stereochemical behaviour of various vinyl radicals can not be regarded as completely clarified.[4-8]

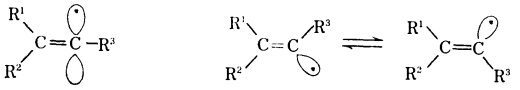

Linear form Bent forms

In a previous paper,[6] we showed that styryl radicals exist in two bent forms from the finding that *trans*- or *cis*-cinnamoyl peroxide, on decomposition in carbon tetrachloride at 77°C, gave mixtures of *trans*- and *cis*-β-chlorostyrene in the same ratio, whereas in bromotrichloromethane at 77°C, *trans*- and *cis*-β-bromostyrene were produced in different ratios. Singer and Kong have also presented evidence that 1-bromo-2-phenylvinyl radicals have *cis*- and *trans*-forms.[4d] Sargent and Browne have shown that *cis*- or *trans*-3-chloro-3-hexene, on treatment with sodium naphthalenide in tetrahydrofuran or dimethoxyethane, gave mixtures of *trans*- and *cis*-3-hexene in different *cis* to *trans* ratios which suggest that the 1-ethyl-1-butenyl radicals intermediately formed are in two bent forms.[7]

It seemed of interest to investigate the stereochemistry of the 1,2-diphenylvinyl radical. It is possible that it might exist in linear form, since this form could be stabilized by a possible conjugation between the unpaired electron in a *p*-orbital on the *sp*-hybridized α-carbon atom and the π-electron system on the adjacent α-phenyl group. Singer and Kong considered these radicals, which they generated by decomposition of *t*-butyl *trans*- and *cis*-α-phenylperoxycinnamate in solution at 110°C, to exist in two bent forms in equilibrium[4b] by analogy with the structure of simpler vinylic radicals.[2,3] Kopchik and Kampmeier have recently concluded that the 1,2-diphenylvinyl radical is *sp*-hybridized at the radical centre, from the analysis of experimental data and of molecular orbital calculations with the 1-vinylvinyl radical as a model.[5d]

In the present investigation, *trans*- and *cis*-α-phenylcinnamoyl peroxide (I) and *t*-butyl *trans*- and *cis*-α-phenylperoxycinnamate (II) were allowed to decompose in solution in order to generate 1,2-diphenylvinyl radicals and the products were examined.

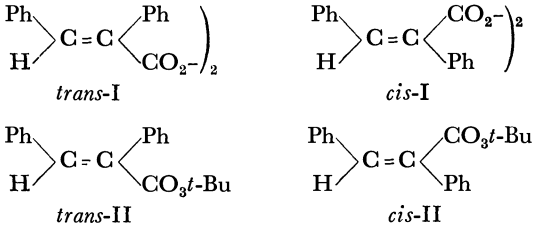

trans-I *cis*-I

trans-II *cis*-II

Results and Discussion

Preparation and Properties of α-Phenylcinnamoyl Peroxides. *trans*-α-phenylcinnamoyl peroxide was prepared by treatment of *trans*-α-phenylcinnamoyl chloride with sodium peroxide. It showed characteristic absorption

1) Most of the contents of this article was presented at the 20th (April, 1967, Tokyo) and the 21st (April, 1968, Osaka) Annual Meetings of the Chemical Society of Japan.

2) R. W. Fessenden and R. H. Schuler, *J. Chem. Phys.*, **39**, 2147 (1963).

3) E. L. Cochran, F. J. Adrian, and V. A. Bowers, *ibid.*, **40**, 213 (1964).

4) a) L. A. Singer and N. P. Kong, *Tetrahedron Lett.*, **1966**, 2089. b) L. A. Singer and N. P. Kong, *J. Amer. Chem. Soc.*, **88**, 5213 (1966). c) L. A. Singer and N. P. Kong, *ibid.*, **89**, 5251 (1967). d) L.A. Singer and N.P. Kong, *Tetrahedron Lett.*, **1967**, 643.

5) a) J. A. Kampmeier and R. M. Fantazier, *J. Amer. Chem. Soc.*, **88**, 1959 (1966). b) R.M. Fantazier and J.A. Kampmeier, *ibid.*, **88**, 5219 (1966). c) J. A. Kampmeier and G. Chen, *ibid.*, **87**, 2608 (1965). d) R. M. Kopchik and J. A. Kampmeier, *ibid.*, **90**, 6733 (1968).

6) O. Simamura, K. Tokumaru, and H. Yui, *Tetrahedron Lett.*, **1966**, 5141.

7) G. D. Sargent and M. W. Browne, *J. Amer. Chem. Soc.*, **89**, 2788 (1967).

8) R. C. Neuman, Jr., and G. D. Holmes, *J. Org. Chem.*, **33**, 4317 (1968).

bands of diacyl peroxides at 1750 and 1772 cm^{-1} (Nujol). The isomeric *cis*-peroxide was prepared according to Greene and Kazan's procedure[9] from *cis*-α-phenylcinnamic acid and hydrogen peroxide with *N*, *N'*-dicyclohexylcarbodiimide as a condensing agent. Preparation both from *cis*-α-phenylcinnamoyl chloride and sodium peroxide by the conventional procedure[10] and from *cis*-α-phenylcinnamoylimidazole and hydrogen peroxide[11] was unsuccessful. The *cis*-α-phenylcinnamoyl peroxide obtained was a pale yellowish oil at room temperature, and displayed characteristic bands of diacyl peroxides at 1779 and 1795 cm^{-1} (Nujol).

Both peroxides, particularly the *cis*-peroxide, were found unstable in neat state or in solution even at room temperature. The instability of α-phenylcinnamoyl peroxides is attributable to facile conversion into their carboxy-inversion products from the following observations. When the *trans*-peroxide was allowed to stand as Nujol mull at room temperature, its infrared absorption bands due to a diacyl peroxide group at 1750 and 1772 cm^{-1} gradually decreased in intensity and finally disappeared, while new absorption bands at 1810 and 1740 cm^{-1} characteristic of alkyl alkanoyl carbonates[12] appeared and increased in intensity (see Fig. 1); in fact the product from this change was shown to be 1,2-diphenylvinyl *cis*-1,2-diphenylethylenecarbonyl carbonate.[13]

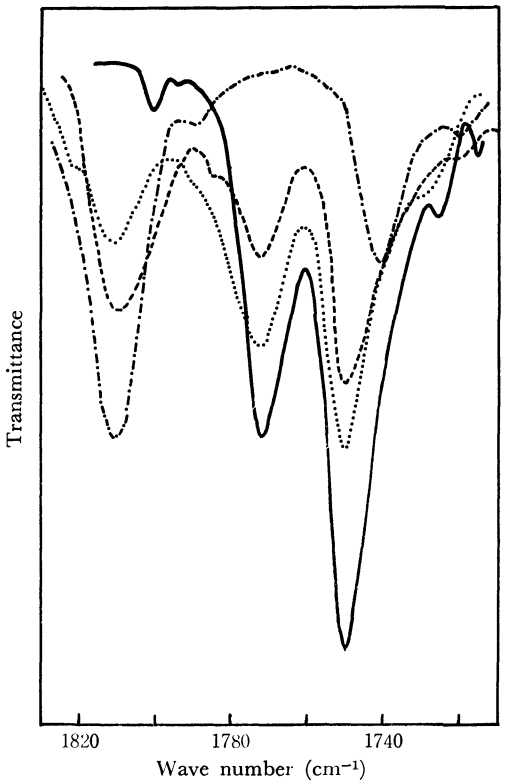

Fig. 1. IR spectra at various times of *trans*-α-phenylcinnamoyl peroxide (Nujol mull) at 24.5°C.
—— immediately after the preparation of the mull; ····· after 55 hr; ---- after 79 hr; —·—· after 258 hr.

The unsuccessful attempt to prepare *cis*-α-phenylcinnamoyl peroxide by treatment of *cis*-α-phenylcinnamoyl chloride with sodium peroxide gave an oily material, which solidified at −78°C, contained no peroxidic oxygen and displayed infrared absorption bands at 1740 and 1803 cm^{-1} characteristic of an alkyl alkanoyl carbonate.[12] On being dissolved in dichloromethane at room temperature, it decomposed spontaneously giving *cis*-α-phenylcinnamic anhydride, while with alkali it afforded *cis*-α-phenylcinnamic acid and diphenylacetylene. This suggests that the reaction of *cis*-α-phenylcinnamoyl chloride with sodium peroxide once gave *cis*-α-phenylcinnamoyl peroxide, which, under the experimental conditions, readily rearranged into the carboxy-inversion product, 1,2-diphenylvinyl *trans*-1, 2-diphenylethylenecarbonyl carbonate, and that this carbonate subsequently decomposed, as is generally known to be the case with acyl alkyl carbonates,[12b] to give *cis*-α-phenylcinnamic anhydride and 1,2-diphenylvinyl carbonate, the latter probably giving rise to diphenylacetylene.

Products from Thermal Decomposition. *trans*- and *cis*-α-Phenylcinnamoyl peroxide were allowed to decompose in carbon tetrachloride at 60, 80, and 110°C, and in bromotrichloromethane, chloroform, cumene, and triethylsilane at 60°C, and *t*-butyl *trans*- and *cis*-α-phenylperoxycinnamate were also subjected to decomposition in carbon tetrachloride at 80 and 110°C. The products from these decompositions are listed in Tables 1, 2, and 3.

Operation of a homolytic mechanism in the decomposition of the peroxides and the peroxy-esters is demonstrated by the formation of bicumyl in cumene and of hexachloroethane in carbon tetrachloride, bromotrichloromethane, and chloroform, both arising from dimerization of the radical derived from solvents, and also by the production of α-halostilbenes in carbon tetrachloride and bromotrichloromethane resulting from abstraction of a halogen atom by the 1,2-diphenylvinyl radical; this is further supported by the finding that the presence of 2,2-diphenyl-1-picrylhydrazyl completely suppressed the formation of α-chlorostilbene in the decomposition of the *trans*-peroxide in carbon tetrachloride. The sole production of the α-phenylcinnamic acid of the same geometrical configuration as the starting peroxide or the peroxy-ester shows that neigher the starting materials nor the intermediate α-phenylcinnamoyloxy radicals isomerize to their isomeric forms under the reaction conditions employed. Separate experiments also confirmed that no isomerization of stilbenes or α-halostil-

9) F. D. Greene and J. Kazan, *J. Org. Chem.*, **28**, 2168 (1963).
10) L. F. Fieser and A. E. Oxford, *J. Amer. Chem. Soc.*, **64**, 2060 (1942).
11) H. A. Staab, W. Rohr, and F. Graf, *Chem. Ber.*, **98**, 1122, 1128 (1965); H. A. Staab, *Angew. Chem. Intern. Ed.*, **1**, 351 (1962).
12) a) D. S. Tarbell and N. A. Leister, *J. Org. Chem.*, **23**, 1149 (1958). b) D. S. Tarbell and E. J. Longosz, *ibid.*, **24**, 774 (1959).
13) Formation of such a carboxy-inversion product is frequently observed with diacyl peroxides such as 4-*t*-butylcyclohexanecarbonyl peroxide,[14] cyclohexanecarbonyl peroxide,[15] α-methylbutyryl peroxide,[16] isobutyryl peroxide[16] and β-phenylisobutyryl peroxide.[17]
14) F. D. Greene, H. P. Stein, Chin-Chiun Chu, and F. M. Vane, *J. Amer. Chem. Soc.*, **86**, 2080 (1964).
15) R. C. Lamb, J. G. Pacifici, and P. W. Ayers, *ibid.*, **87**, 3928 (1965).
16) J. K. Kochi, *ibid.*, **85**, 1958 (1963).
17) S. Oae, T. Kashiwagi, and S. Kozuka, *Chem. Ind.* (London), **1965**, 1694.

TABLE 1. PRODUCTS FROM DECOMPOSITION OF *trans*- AND *cis*-α-PHENYLCINNAMOYL PEROXIDE IN CARBON TETRACHLORIDE AND YIELDS IN MOL% OF PEROXIDE[a]

Run No.	1	2	3[b]	4	5[c]	6[d]
Temp. °C	80	80	60	60	110	60
Peroxide	*trans*	*cis*	*trans*	*cis*	*trans*	*trans*
Initial concn. (M)	0.0226	0.0090	0.0109	0.0086	0.0083	0.0146
trans-PhCH=CPhCO$_2$H	21.8	0	43.2	0	+	8.8
cis-PhCH=CPhCO$_2$H	0	35.6	0	35.0	0	0
cis-PhCH=CPhCl	78.0	0.3	27.6	2.0	54.0	0
trans-PhCH=CPhCl	1.2	0.1	0.7	2.6	6.8	0
cis-PhCH=CHPh	1.4	0	1.0	1.0	2.4	0
trans-PhCH=CHPh	2.8	1.5	8.8	10.4	1.2	0
PhC≡CPh	7.6	0.6	31.4	3.2	48.4	53.8
PhCH$_2$COPh	4.0	0	19.2	13.2	25.6	
(PhCOCHPh)$_2$	0	24.4	0	10.0	0	0
C_2Cl_6	+	+	+	+	+	+
(*cis*-PhCH=CPhCl)/(*trans*-PhCH=CPhCl)	99 : 1	75 : 25	97 : 3	43 : 57	89 : 11	

a) A + sign denotes that the product was detected but not determined.
b) Yield of carbon dioxide was determined to be 130 mol% of the peroxide.
c) Carried out in a sealed tube.
d) In the presence of DPPH (six moles per mole of the peroxide).

TABLE 2. PRODUCTS FROM DECOMPOSITION OF *trans*- AND *cis*-α-PHENYLCINNAMOYL PEROXIDE IN CUMENE, CHLOROFORM, BROMOTRICHLOROMETHANE, AND TRIETHYLSILANE AND YIELDS IN MOL% OF PEROXIDE[a]

Run No.	7	8	9	10	11	12	13[b]
Solvent	cumene	cumene	$CHCl_3$	$CHCl_3$	$BrCCl_3$	$BrCCl_3$	Et_3SiH
Temp. °C	60	60	60	60	60	60	60
Peroxide	*trans*	*cis*	*trans*	*cis*	*trans*	*cis*	*trans*
Initial concn. (M)	0.0214	0.0085	0.0201	0.0090	0.0194	0.0157	0.0505
trans-PhCH=CPhCO$_2$H	52.0	0	15.4	0	50.0	0	+
cis-PhCH=CPhCO$_2$H	0	24.0	0	28.4	0	38.6	0
cis-PhCH=CPhX			0	1.2[c]	8.8[d]	1.0[d]	
trans-PhCH=CPhX			0	5.4[c]	1.0[d]	1.0[d]	
cis-PhCH=CHPh	34.0	0.8	36.0	1.4	0.1	0.1	16.5
trans-PhCH=CHPh	4.0	3.2	4.8	16.0	0	4.1	5.3
PhC≡CPh	44.0	0.8	15.4	1.4	1.4	0.6	57.4
PhCH$_2$COPh	32.0	+	3.2	0	~50	0	~40
(PhCOCHPh)$_2$	0.8	10.0	0	5.0	0	+	0
C_2Cl_6			+	+	+	+	
PhCMe$_2$CMe$_2$Ph	+	+					
(*cis*-PhCH=CPhX)/(*trans*-PhCH=CPhX)	89 : 11[e]	20 : 80[e]	88 : 12[e]	6 : 94[e]	89 : 11[f]	48 : 52[f]	76 : 24[e]

a) A + sign denotes that the product was detected but not determined.
b) Hexaethyldisilane was detected by vpc.
c) α-Chlorostilbene.
d) α-Bromostilbene.
e) The isomer ratio of *cis*- to *trans*-stilbene.
f) The isomer ratio of *cis*- to *trans*-α-bromostilbene.

TABLE 3. ISOMER RATIO OF α-CHLOROSTILBENE FROM DECOMPOSITION OF *t*-BUTYL *trans*- AND *cis*-α-PHENYLPEROXYCINNAMATE IN CARBON TETRACHLORIDE[a]

Temp. °C	100	110	80	80
Peroxy-ester	*trans*-II	*cis*-II	*trans*-II	*cis*-II
(*cis*-PhCH=CPhCl)/(*trans*-PhCH=CPhCl)	73 : 27[b]	76 : 24[b]	84 : 16[c]	77 : 23[c]

a) Initial concentrations of peroxy-ester were between 0.06 and 0.1 M. Decompositions were carried out in sealed tubes. The yields of α-chlorostilbenes were between 30 and 40%.
b) Mean of triplicate runs.
c) Mean of duplicate runs.

benes took place under the reaction conditions used or in the work-up process. These observations enable us to discuss the stereochemical behaviour of intermediate 1,2-diphenylvinyl radicals by examining the isomer ratio of α-halostilbenes formed in carbon tetrachloride or bromotrichloromethane.

The *trans*- and *cis*-peroxide were found to give more complex mixtures of products than the peroxy-esters. Moreover, the *cis*-peroxide, compared with the *trans*-peroxide, afforded much lower yields of those products which could arise from the reaction of 1,2-diphenylvinyl radicals with solvents. *cis*- and *trans*-Stilbene were produced from the peroxides, not only in solvents carrying a transferable hydrogen atom such as chloroform, cumene, and triethylsilane, but also, though in smaller yields, in solvents containing no hydrogen atom such as carbon tetrachloride and bromotrichloromethane, indicating that the stilbene was not exclusively formed by abstraction of a hydrogen atom by 1,2-diphenylvinyl radicals from solvents. Diphenylacetylene and deoxybenzoin were also shown to arise from both *cis*- and *trans*-peroxides in various solvents. *dl*-1,2-Dibenzoyl-1,2-diphenylethane resulted from the *cis*-peroxide. Some of these compounds might have been formed as cage reaction products or the products from the decomposition of 1,2-diphenylvinyl 1,2-diphenylethylenecarbonyl carbonate.

Decomposition of *cis*- and *trans*-peroxy-ester in carbon tetrachloride, on the other hand, gave neither stilbene nor 1,2-dibenzoyl-1,2-diphenylethane, although diphenylacetylene was formed in lower yield than in the case with the peroxides, showing that the peroxy-esters decompose with less complexity than the peroxides.

Isomer Ratios of Olefins Resulting from Decomposition. Decomposition of *t*-butyl *cis*- or *trans*-α-phenylperoxycinnamate in carbon tetrachloride at 110°C gave α-chlorostilbenes in an approximately equal ratio of the *cis*- to *trans*-isomer, *viz.*, 73:27 from the *trans*- and 76:24 from the cis-peroxy-ester. Decreasing the reaction temperature to 80°C, however, resulted in different *cis* to *trans* ratios of the chloro-olefins: 84:16 from the *trans*- and 77:23 from the *cis*-peroxy-ester. These findings clearly exclude the possibility that the 1,2-diphenylvinyl radical is directly produced in linear form by homolysis of the peroxy-esters, because the linear radical would lead to the same *cis* to *trans* ratio of α-chlorostilbenes, irrespective of the configuration of the peroxy-ester decomposed. Thus, the results are readily explained by assuming that the 1,2-diphenylvinyl radical exists in two bent forms corresponding to *cis* and *trans* configurations in line with the prevalent view on the structure of various vinylic radicals,[2-8,18] and the reaction steps are formulated in the following scheme (RX=CCl_4).

Both forms of the 1,2-diphenylvinyl radical, at 110°C, rapidly isomerize to each other to attain equilibrium before abstraction of a chlorine atom from carbon tetrachloride, so that the same *cis* to *trans* ratio of the the products is obtained irrespective of the configuration of the starting material. Singer and Kong concluded

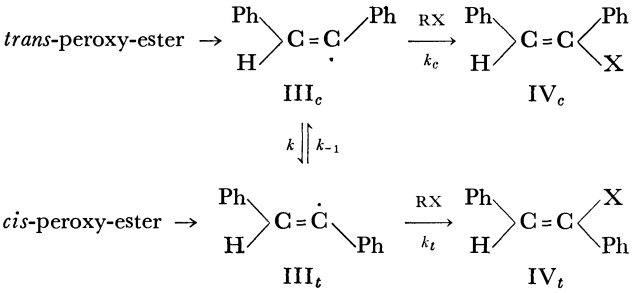

Scheme 1.

such a rapid equilibration for this radical on the basis of the finding that the ratio of *cis*- to *trans*-stilbene resulting from decomposition of both *t*-butyl *cis*- and *trans*-α-phenylperoxycinnamate in cumene, cyclohexane or toluene at 110°C were not dependent on the configuration of the peroxy-esters.[4b] However, it is evident that at 80°C, the equilibration of these radicals is sufficiently slow in rate for the abstraction from carbon tetrachloride to compete with it; the *trans* peroxy-ester, therefore, gave a higher *cis* to *trans* ratio of α-chlorostilbenes (84:16) than the *cis* peroxy-ester (77:23), the configuration of the starting peroxy-ester being partly reflected in the isomer ratio.

Decomposition of *cis*-α-phenylcinnamoyl peroxide in carbon tetrachloride gave mixtures of *cis*- and *trans*-α-chlorostilbene in *cis* to *trans* ratios of 43:57 at 60°C and of 75:25 at 80°C, while the *trans*-peroxide gave *cis* to *trans* ratios of 97:3 at 60°C, 99:1 at 80°C, and 89:11 at 110°C; it is apparent that with decreasing temperature these peroxides tend to yield α-chlorostilbene predominantly of the same configuration as the starting peroxide. The same tendency was also observed in the decomposition at 60°C in some other solvents (Table 2), indicating that, at 60°C, the interconversion between *cis*- and *trans*-1,2-diphenylvinyl radicals is not so rapid as to complete the equilibration before abstraction.

In a previous paper,[6] decomposition of *trans*- or *cis*-cinnamoyl peroxide at 77°C was shown to afford mixtures of *trans*- and *cis*-β-chlorostyrene in the same *cis* to *trans* ratio in carbon tetrachloride, but mixtures of *trans*- and *cis*-β-bromostyrene in different *cis* to *trans* ratios in bromotrichloromethane, the *cis*-peroxide giving a higher *cis* to *trans* ratio. These findings led to the conclusion that the isomerization between *cis*- and *trans*-styryl radicals takes place rapidly enough to be complete before the abstraction of a chlorine atom from carbon tetrachloride, but its rate is comparable with that of the abstraction of a bromine atom from bromotrichloromethane. However, in contrast with this, the isomerization between isomeric 1,2-diphenylvinyl radicals at 60°C or 80°C is not so rapid as to complete equilibration before reaction with various solvents. This difference between the styryl and 1,2-diphenylvinyl radical is attributed to the presence, in the latter, of an α-phenyl group, which is heavier than the α-hydrogen in the former, the phenyl group moving less rapidly than the hydrogen in the isomerization step. This result is in line with the observation by Singer and Kong that 1-bromo-2-phenylvinyl radicals do not equilibrate at 110°C, owing to the presence of a heavier α-bromine atom,[4d] and with the fact that, according to the electron spin

18) O. Simamura, "Topics in Stereochemistry," Vol. 4, ed. by N. L. Allinger and E. L. Eliel, Wiley-Interscience, New York (1969), p. 21.

resonance spectroscopy, at −172°C, 1-methylvinyl radicals do not isomerize,[2] whereas unsubstituted vinyl radicals isomerize.[2,3]

Notwithstanding the above arguments, the possibility is not ruled out that a linear form of 1,2-diphenylvinyl radical corresponding to a state of energy minimum exists between those two bent forms in which the radicals are initially produced and which also correspond to energy minima. If the linear form exists as well, the *cis* to *trans* product ratio should be the same irrespective of the configuration of the starting material or reflect its difference according to whether the equilibration among the three forms of the radical is rapid or slow.

The Difference in Reactivity between cis- *and* trans-*1,2-Diphenylvinyl Radicals; the Steric Effect.* By reference to Scheme 1 ($RX=CCl_4$) the product isomer ratio and the four reaction rate constants are correlated, so that a quantitative measure of the difference in reactivity between *cis*- and *trans*-1,2-diphenylvinyl radicals may be obtained on the assumption that a linear form of this radical is not involved. The ratio of *cis*- to *trans*-α-chlorostilbene formed from *trans*-peroxy-ester, $(IV_c/IV_t)_{yield}$, which may be denoted by C, is expressed by the use of the steady state approximation as follows:

$$C = (IV_c/IV_t)_{yield} = k_c/k_t \cdot \{k_{-1} + k_t[CCl_4]\}/k \quad (1)$$

Similarly, the ratio of *trans*- to *cis*-olefin, arising from *cis*-peroxy-ester, $(IV_t/IV_c)_{yield}$, which may be denoted by T, isgiven as follows:

$$T = (IV_t/IV_c)_{yield} = k_t/k_c \cdot \{k + k_c[CCl_4]\}/k_{-1} \quad (2)$$

Elimination of the concentration of carbon tetrachloride $[CCl_4]$ from Eqs. (1) and (2) leads to

$$(T + 1)/(C + 1) = k_t/k_c \cdot k/k_{-1} \quad (3)$$

When the isomeric vinyl radicals III_c and III_t equilibrate, we have $k/k_{-1}=[III_t]/[III_c]=K_{eq}$ where K_{eq} denotes the equilibrium constant of interconversion between these radicals. In the absence of any evidence available for assessment of the equilibrium constant K_{eq}, this value may be assumed to be approximated by the equilibrium constant of isomerisation between *trans*- and *cis*-stilbene, since it does not seem unreasonable that the steric effect caused by an odd electron is not significantly different from that caused by a hydrogen atom. The value for K_{eq} or k/k_{-1} is therefore estimated at 100 and 180 at 110°C and 80°C, respectively, on the basis of the data reported for stilbenes.[19]

Substitution of the observed values of C and T and of the estimated values of k/k_{-1} in equation 3 gives $k_t/k_c = 1.2\times10^{-3}$ at 80°C and 3.5×10^{-3} at 110°C. Thus, the *cis* radical III_c abstracts a chlorine atom from carbon tetrachloride several hundred times faster than the *trans* radical III_t; evidently, this difference is attributable to a crowded situation around the radical centre of the *trans* radical, which places steric hindrance to an incoming molecule of carbon tetrachloride.

The above ratios of the rate constants at 80°C and 110°C correspond to the difference in activation free energy of 4.7 and 5.1 kcal/mol, respectively, since $\Delta G_t^{\ddagger} - \Delta G_c^{\ddagger} = -2.3RT\cdot\log(k_t/k_c)$. These values are larger than what one would expect on the ground of the presence of a phenyl group at the β-position, since the *cis*-styryl radical reacts with carbon tetrachloride at 77°C with an activation free energy higher by 1.0 kcal/mol than the *trans*-styryl radical, the cause of this being evidently steric retardation exerted by the *cis*-phenyl group.[8,16] The higher value of $\Delta G_t^{\ddagger} - \Delta G_c^{\ddagger}$ for the 1,2-diphenylvinyl radical is explained by the fact that the disposition of the α-phenyl group is different between III_c and III_t. In III_t the α-phenyl lies in the plane of the double bond, so that its ortho-hydrogen exerts steric hindrance toward an approaching carbon tetrachloride molecule in addition to that exerted by the β-phenyl group, whereas, in III_c, the α-phenyl is twisted away from the plane of the C=C double bond because of the β-phenyl group on the same side of it,[20] so that the hindrance due to the ortho-hydrogen is absent.

Experimental

Preparation of trans-α-*Phenylcinnamoyl Peroxide. trans*-α-Phenylcinnamic acid, prepared by the usual procedure,[21] was treated with six molar equivalents of thionyl chloride in dry benzene at room temperature for 52 hr and the resulting *trans*-α-phenylcinnamoyl chloride was recrystallized from petroleum ether (boiling below 40°C), mp 42.5—44°C (lit,[22] mp 47—48°C). This chloride (3.2 g, 0.0132 mol) was added with stirring to a mixture of sodium peroxide (2.4 g, 0.031 mol), ice (15 g), water (15 m*l*), and petroleum ether (40 m*l*) cooled in an ice bath. Stirring was continued for 5 hr, and the precipitate was filtered off by suction, washed repeatedly with cold water, and dried between sheets of filter paper in a vacuum for 2 hr at 8°C to afford 2.0 g (68%) of the required peroxide (purity, 94.0% as determined by iodometric titration). It decomposed at 52—55°C with gas evolution. IR($\nu_{C=O}$): 1750 and 1772 cm^{-1} (Nujol). NMR: τ 2.1 (singlet, 1H) and 2.8 (multiplet, 10H); *trans*-α-phenylcinnamic acid shows peaks at τ 2.1 (singlet, 1H) and 2.7 (multiplet, 10H).

Preparation of cis-α-*Phenylcinnamoyl Peroxide.* This peroxide was prepared according to Greene and Kazan's procedure.[9] To a cold stirred solution of *N,N'*-dicyclohexylcarbodiimide (2.0 g, 0.01 mol) and anhydrous solution (10 m*l*) of hydrogen peroxide in ether (5M) was added dropwise a solution of *cis*-α-phenylcinnamic acid[23] (2.2 g, 0.01 mol) in dichloromethane (25 m*l*). The mixture was stirred at 0°C for 3 hr and then filtered by suction through a sintered glass funnel, and the *N,N'*-dicyclohexylurea collected in the funnel was slurried three times with 20 m*l* portions of cold dichloromethane and the washings were added to the main filtrate. This filtrate was added with 60 m*l* of cold ether and was

19) The equilibrium ratio of *trans*- to *cis*-stilbene of 96 : 4 at 200°C (T. W. J. Taylor and A. R. Murray, *J. Chem. Soc.*, **1938**, 2078). corresponds to the difference in free energy of $\Delta G=3.03$ kcal/mol. This value and the difference in heat of hydrogenation between *cis*- and *trans*-stilbene, 5.7 kcal/mol (R. B. Williams, *J. Amer. Chem. Soc.*, **64**, 1395 (1942).), which corresponds to ΔH, give the difference in entropy of 5.7 e.u. These values enable ΔG, and, accordingly, equilibrium constants at given temperatures to be estimated.

20) H. Suzuki, This Bulletin, **33**, 379 (1960).

21) R. E. Buckles and K. Bremer, "Organic Syntheses," Coll. Vol. IV, p. 777 (1963).

22) R. Riemschneider and H. Kampfer, *Monatsh. Chem.*, **90**, 518 (1959).

23) L. F. Fieser, "Experiments in Organic Chemistry," Maruzen, Tokyo (1958), p. 182.

washed in succession with three 25 m*l* portions of cold saturated ammonium sulphate solution, two 25 m*l* portions of cold 10% sodium carbonate solution, and two 25 m*l* portions of cold aqueous saturated sodium chloride solution. The organic layer was dried over anhydrous sodium sulphate and the solvent was completely removed under reduced pressure at 0°C in a rotary film evaporator. The remaining *cis*-α-phenylcinnamoyl peroxide (0.35 g, yield 17%) was pale yellowish oil at room temperature and solidified at −35°C (purity, about 30% as determined by iodometry). It was extremely unstable at room temperature and decomposed with gas evolution, and attempted recrystallization from several solvents was unsuccessful. IR($\nu_{C=O}$): 1779 and 1795 cm^{-1} (Nujol).

Preparation of t-*Butyl* trans-α-*phenylperoxycinnamate.* This compound was prepared according to the procedure of Milas and Surgenor.[24] To a cold stirred mixture of *t*-butyl hydroperoxide (4.5 g, 0.05 mol) and potassium hydroxide (2.8 g, 0.05 mol) in 60 m*l* of water was added dropwise a solution of *trans*-α-phenylcinnamoyl chloride (8.0 g, 0.034 mol) in 60 m*l* of ether in 10 min, and the mixture was stirred for a further 22 hr at room temperature. The reaction mixture was then washed with three 150 m*l* portions of 5% aqueous sodium carbonate and dried over anhydrous sodium sulphate. After removing ether, the remaining white material was recrystallized from ether–petroleum ether to give 5.0 g (50% yield) of the required peroxy-ester, mp 107—108°C (purity, 99% as determined by iodometric titration. Found: C, 76.89; H, 6.80%; Calcd for $C_{19}H_{20}O_3$: C, 77.03; H, 6.76%). Its spectroscopic data (IR and NMR) were in accord with those reported by Singer and Kong.[4b]

Preparation of t-*Butyl* cis-α-*phenylperoxycinnamate.* *cis*-α-phenylcinnamic acid (5.0 g, 0.022 mol) was treated with thionyl chloride (20.0 g, 0.17 mol) in dry benzene at room temperature for 49 hr in the dark. Volatile matter was removed from the resulting mixture in a rotary film evaporator, and the remaining yellowish matter was repeatedly recrystallized from petroleum ether to give *cis*-α-phenylcinnamoyl chloride, mp 66.0—68.0°C (Found: C, 73.74; H, 4.62%; Calcd for $C_{15}H_{11}OCl$: C, 74.08; H, 4.53%). IR($\nu_{C=O}$): 1740 cm^{-1} (Nujol). NMR: τ 2.60 (multiplet, 10H) and 3.16 (singlet, 1H). The required peroxy-ester was prepared from this chloride in a similar way to the preparation of the *trans* isomeride. The *cis*-peroxy-ester, mp 78—80°C (purity, 99%), obtained in 60% yield, showed satisfactory spectroscopic data[4b] (IR and NMR) and elementary analysis (Found: C, 77.05; H, 6.95%; Calcd for $C_{19}H_{20}O_3$: C, 77.03; H, 6.76%).

Authentic Materials and Solvents. The authentic samples, used for comparison with reaction products, of *cis*- and *trans*-α-chlorostilbene, *cis*- and *trans*-α-bromostilbene, *cis*- and *trans*-stilbene, deoxybenzoin, diphenylacetylene, and bicumyl *etc.* were prepared in the usual way. Carbon tetrachloride (Wako, special grade) was used without further purification. Commercial chloroform was shaken with concentrated sulphuric acid, washed with 5% aqueous sodium carbonate and water, dried over calcium chloride and distilled. Cumene was shaken with concentrated sulphuric acid, washed with water and 5% aqueous sodium carbonate, dried over calcium chloride, and distilled over sodium wire. Bromotrichloromethane (Eastman Kodak) was distilled in the dark immediately before use. Triethylsilane was prepared from trichlorosilane and ethylmagnesium bromide.[25]

Decomposition of trans-α-*Phenylcinnamoyl Peroxide at Room Temperature.* The infrared spectrum of this peroxide was examined in five times amount of Nujol at 24.5°C at intervals with a Hitachi EPI-G2 infrared spectrophotometer. The spectrum in the carbonyl region changed during 258 hr as shown in Fig. 1. Another specimen of the same peroxide was set aside at 24.5°C for 258 hr without apparent change, but it displayed the same infrared spectrum as the above sample in Nujol after 258 hr, and was further shown, by iodometric titration, to contain only 2.8% of the active oxygen initially present in the peroxide. This material (0.87 g) was dissolved in 20 m*l* of ether and extracted with three 200 m*l* portions of 5% aqueous sodium carbonate to afford 0.224 g of *trans*-α-phenylcinnamic acid on acidification of the extract. Removal of ether from the organic layer gave 0.665 g of a yellowish solid, and it was recrystallized twice from chloroform–petroleum ether to give 1,2-diphenylvinyl *cis*-1,2-diphenylethylenecarbonyl carbonate, mp 127—135°C (Found: C, 80.88; H, 4.71%; Calcd for $C_{30}H_{22}O_4$: C, 80.72; H, 4.93%); IR($\nu_{C=O}$): 1810 and 1740 cm^{-1} (Nujol).

Decomposition of cis-α-*phenylcinnamoyl Peroxide at Room Temperature.* To a cold solution of *cis*-α-phenylcinnamoyl chloride (2.0 g, 8.2 mmol) in 30 m*l* of tetrahydrofuran were added dropwise 1.0 g (8.7 mmol) of 30% aqueous hydrogen peroxide and 2 m*l* of aqueous sodium hydroxide (0.33 g, 8.3 mmol), and the mixture was stirred at 0°C for 26 hr. Cold dichloromethane (50 m*l*) was added. It was then washed with three 100 m*l* portions of cold water and three 100 m*l* portions of 5% sodium hydrogen carbonate, and dried over anhydrous sodium sulphate. The solvent was removed at 0°C in a rotary film evaporator, the remaining yellowish oil was dissolved in a small amount of dichloromethane, methanol was added to the solution at 10°C and this was cooled to −78°C to deposit a white solid. The mixture was centrifuged at −78°C and the supernatant liquid removed with a pipette; the remaining solid was washed with cold methanol and dried *in vacuo* at −78°C to give 1.5 g of a white solid. This was found to contain only a trace of active oxygen by iodometric titration, and showed absorption bands at 1803 and 1740 cm^{-1} (in carbon tetrachloride) characteristic of the alkyl alkanecarbonyl carbonate. When a portion of this substance was added to dichloromethane at room temperature in an attempt at recrystallization, gas evolved vigorously indicating its decomposition; work-up of the mixture gave *cis*-α-phenylcinnamic anhydride, characterized by mp and mixed mp 149.5—150°C, and comparison of its spectrum with an authentic specimen. Hydrolysis of the above substance by heating with potassium hydroxide (5 g) for an hour in a mixture of 40 m*l* of ethanol and 20 m*l* of water afforded *cis*-α-phenylcinnamic acid and trace of diphenylacetylene.

General Procedure for Thermal Decomposition. In a round-bottomed three-necked flask fitted with a gas inlet, a stopper, and a reflux condenser, to which were connected a trap cooled with dry ice–ethanol, a magnesium perchlorate tube and an Ascarite tube, in the order mentioned, was placed a measured amount of a solvent (60—100 molar excess of the peroxide to be added). This was heated under reflux in a slow stream of nitrogen for an hour and cooled down to room temperature; then a weighed amount of the peroxide was added. The resulting solution was allowed to stand under nitrogen in a thermostat kept at a specified temperature until the peroxide had been completely decomposed (6—10 hr). In the decomposition of *cis*-α-phenylcinnamoyl peroxide which is unstable, reaction solutions were prepared by dissolving in a measured amount of a solvent the *cis*-peroxide immediately after it was obtained by removal of the solvent from the reaction mixture for

24) N. A. Milas and D. M. Surgenor, *J. Amer. Chem. Soc.*, **68**, 642 (1946).

25) H. Ishii, "Yukikagobutsu Goseiho," Vol. IV, Gihodo, Tokyo (1966), p. 107.

the preparation of this peroxide, and the concentration of the peroxide in the solution was determined by iodometry.

In decompositions conducted at higher temperatures, a solution of the peroxide or peroxy-ester (0.3—0.5 g) in 20 m*l* of a solvent was placed in a small pyrex ampoule which was connected to a vacuum line, degassed by three cycles of the usual procedure consisting of solidification by chilling, evacuation and thawing, and sealed at 3×10^{-3} mmHg. The ampoule was kept in a thermostat until the peroxide had been completely decomposed.

Product Analysis. A reaction mixture, transferred to a separating funnel with ether, was shaken with three 100 m*l* portions of 5% aqueous sodium carbonate to isolate and determine α-phenylcinnamic acid. The organic layer was dried over anhydrous sodium sulphate and ether was distilled off. The residue was subjected to vpc (Perkin-Elmer 154-D with a column of silicone oil) for determination of products; products in some runs were isolated by either column or gas chromatography and identified by comparison with authentic specimens.

BULLETIN OF THE CHEMICAL SOCIETY OF JAPAN, VOL. 44, 1118—1121 (1971)

Oligomerization of Isoprene by Vanadium Catalysts

Yasuzo UCHIDA, Ken-ichi FURUHATA, and Hisayasu ISHIWATARI

Department of Industrial Chemistry, Faculty of Engineering, The University of Tokyo, Hongo, Tokyo

(Received November 5, 1970)

Oligomerization of isoprene by the catalyst system consisting of $VO(OEt)_3$ and organoaluminum compounds was studied. Isoprene was oligomerized to a mixture of dimers, trimers and higher oligomers by $VO(OEt)_3$–Et_2AlCl catalyst system. 2,6-Dimethyl-1,*trans*-3,6-octatriene was the main dimer of isoprene in this reaction. The addition of tetrahydrofuran, dioxane, triphenylphosphine, bis-diphenylphosphinoethane, triethylamine or tetramethylethylenediamine to this catalyst system raised the reaction rate and the selectivity for the dimer at lower donor/$VO(OEt)_3$ molar ratios but suppressed the reaction at higher molar ratios. By $VO(OEt)_3$–Et_3Al catalyst system, isoprene was converted to a liquid polymer and by $VO(OEt)_3$–$EtAlCl_2$ catalyst system, it was cyclopolymerized to an insoluble polymer. Structures of two new oligomers of isoprene were also reported.

The oligomerization of isoprene to linear oligomers of head-to-tail structures is of great interest for the synthesis of raw materials of terpenic compounds. A linear dimer of isoprene, 2,6-dimethyl-1,3,6-octatriene which is formed by the head-to-tail addition of isoprene, was formed by titanium,[1] chromium,[2] or nickel[3] based catalysts but by these catalysts cyclic dimers were also formed. Palladium based catalyst[4] gave selectively 2,7-dimethyl-1,3,7-octatriene from isoprene but this compound has a tail-to-tail structure.

We reported previously the oligomerization of isoprene by zirconium[5] and hafnium[6] based catalysts. By these catalysts, 2,6-dimethyl-1,*trans*-3,6-octatriene was formed without six- or eight-membered cyclic dimers, and in the case of zirconium based catalysts, the addition of electron donors such as triphenylphosphine to the catalyst system raised the selectivity for this dimer to over than 90%.

In this paper we report the oligomerization of isoprene by the catalyst system consisting of ethyl orthovanadate and organoaluminum compounds.

Experimental

Reagents. Isoprene, benzene, tetrahydrofuran, 1,4-dioxane, triethylamine, *N,N,N′,N′*-tetramethylethylenediamine and tetrahydrothiophene were dried and distilled under a nitrogen stream.

Organoaluminum compounds were purified by distillation and were diluted in benzene.

Ethyl orthovanadate synthesized by the reported method[7] was diluted in benzene and stored in a refrigerator.

1,2-Bisdiphenylphosphinoethane was synthesized by the reported method.[8]

Commercial triphenylphosphine was used without further purification.

Reaction Procedure. In a typical reaction, to a 20 m*l* glass ampule filled with nitrogen, 3.75 g of benzene, 50 mmol of isoprene, 0.5 mmol of ethyl orthovanadate (14.3 wt% benzene solution) and 6.0 mmol of diethylaluminum chloride (14.8 wt% benzene solution) were charged in this order with syringes under a nitrogen stream. The total amount of benzene was controlled to be 8.3—8.5 g. The ampule was then sealed and kept at 70°C for 1 hr.

Analysis. The gas chromatography was used for calculating the conversion percent of isoprene and quantitative analysis of products. A 2 m stainless steel column,

1) a) L. I. Zakharkin, *Dokl. Akad. Nauk S.S.S.R*, **131**, 1069 (1960). b) H. Takahashi and M. Yamaguchi, *Osaka Kogyo Gijutsu Shikensho Kiho*, **15**, 271 (1964). c) L. I. Zakharkin and V. M. Akhmedev, *Azerb. Khim. Zh.*, **1969**, 58.

2) G. Wilke, *J. Polym. Sci.*, **38**, 45 (1959).

3) S. Watanabe, K. Suga, and H. Kikuchi, *Aust. J. Chem.*, **23**, 385 (1970).

4) N. Takahashi, T. Sibano, and N. Hagihara, *Shokubai (Catalyst)*, **11**, 4 (1969).

5) A. Misono, Y. Uchida, K. Furuhata, and S. Yoshida, This Bulletin, **42**, 2303 (1969).

6) A. Misono, Y. Uchida, K. Furuhata, and S. Yoshida, *ibid.*, **42**, 1383 (1969).

7) W. Prandtl and L. Hess, *Z. Anorg. Chem.*, **82**, 103 (1913).

8) W. Hewertson and H. R. Watson, *J. Chem. Soc.*, **1962**, 1490.

4 mm in diameter, packed with polydiethylene glycol succinate on Shimalite was used. Operation conditions: column temperature, 120°C and 180°C for dimers and trimers, respectively; flash evaporator, 300°C; carrier gas(helium) speed, 30 ml/min. Benzene was used as an internal standard.

Infrared spectra were taken using a Hitachi infrared spectrophotometer EPI-S2.

Nuclear magnetic resonance spectra were taken using a JMN-4H-100(Japan Electron Optics Laboratory Co.).

Results and Discussion

Oligomerization of Isoprene by $VO(OEt)_3$—Et_2AlCl Catalyst System. Isoprene was oligomerized to a mixture of dimers, trimers and higher oligomers by this catalyst system. Two dimers were found on gas chromatography and the structure of the main dimer was determined to be 2,6-dimethyl-1,*trans*-3,6-octatriene by comparing the infrared spectrum with that of the pure sample obtained by the zirconium catalyst.[5] The yield of another dimer was less than 14% of that of 2,6-dimethyl-1,*trans*-3,6-octatriene. As shown from the gas chromatographic data, the mixture of trimers was consisted of more than six isomers in which four were predominantly formed.

The Effect of the Al/V Molar Ratio: The effect of the molar ratio of diethylaluminum chloride to ethyl orthovanadate is shown in Fig. 1. Reactions were carried

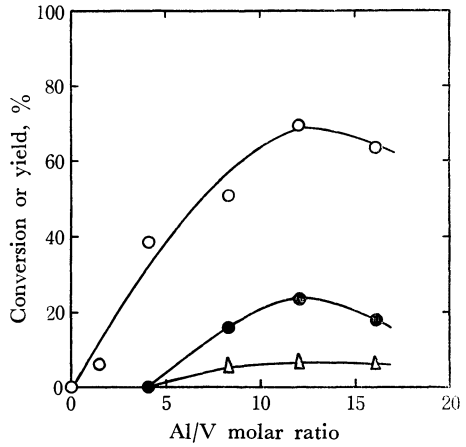

Fig. 1. Effect of the molar ratio of Et_2AlCl to $VO(OEt)_3$.
-○-: Conversion of isoprene, %
-●-: Yield of 2,6-dimethyl-1, *trans*-3,6-octatriene, %
-△-: Yield of trimers, %
Reaction temp.: 70°C; reaction time: 1 hr;
Isoprene/$VO(OEt)_3$: 100

out at 70°C for 1hr. At the molar ratio 4, the reaction solution was very viscous and no low oligomers were formed. A yellow, wax-like polymer of isoprene obtained at this ratio contained 67% of *cis*-1,4-, 25% of *trans*-1,4-, 6% of 3,4- and 2% of 1,2-structures.[9]

The maximum yield of 2,6-dimethyl-1,*trans*-3,6-octatriene was accomplished when the molar ratio of diethylaluminum chloride to ethyl orthovanadate was 12. The yield and the selectivity for this dimer at this ratio were 23.3% and 33.4%, respectively. The infrared spectrum of the mixture of higher oligomers obtained at this ratio showed absorptions due to methyl and methylene groups (2960, 2920, 2850, 1450, and 1380 cm^{-1}), a three-substituted double bond (1670 and 840 cm^{-1}), a terminal methylene group (1650 and 890 cm^{-1}) and a *trans* two-substituted double bond (980 cm^{-1}, weak). At higher molar ratios, the conversion of isoprene and the yield of dimers slightly decreased.

The Effect of Electron Donors: The effect of electron donors on the oligomerization by this catalyst system was studied using monodentate and potentially bidentate compounds (Figs. 2—5). The reactions were carried out at 70°C for 1 hr keeping the molar ratio of diethylaluminum chloride to ethyl orthovanadate constant at 12.0. The addition of tetrahydrofuran, 1,4-dioxane, triethylamine, *N,N,N',N'*-tetramethylethylenediamine,

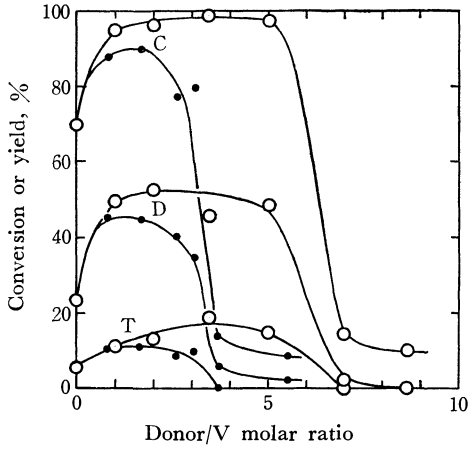

Fig. 2. Effect of tetrahydrofuran and dioxane.
-○-: Tetrahydrofuran
-●-: Dioxane
C: Conversion of isoprene, %
D: Yield of 2,6-dimethyl-1, *trans*-3, 6-octatriene, %
T: Yield of trimers, %
Reaction conditions: 70°C, 1 hr,
Isoprene/$VO(OEt)_3$: 100, $Et_2AlCl/VO(OEt)_3$: 12

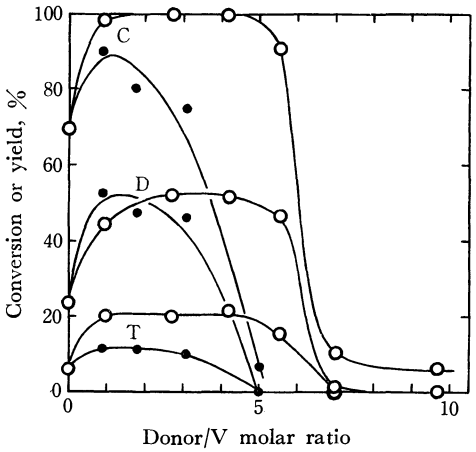

Fig. 3. Fffect of triethylamine and tetramethylethylenediamine.
-○-: Triethylamine
-●-: Tetramethylethylenediamine
C: Conversion of isoprene, %
D: Yield of 2,6-dimethyl-1, *trans*-3,6-octatriene, %
T: Yield of trimers, %
Reaction conditions: 70°C, 1 hr,
Isoprene/$VO(OEt)_3$: 100, $Et_2AlCl/VO(OEt)_3$: 12

9) W. S. Richardson and A. Sacher, *J. Polym. Sci.*, **10**, 353 (1953).

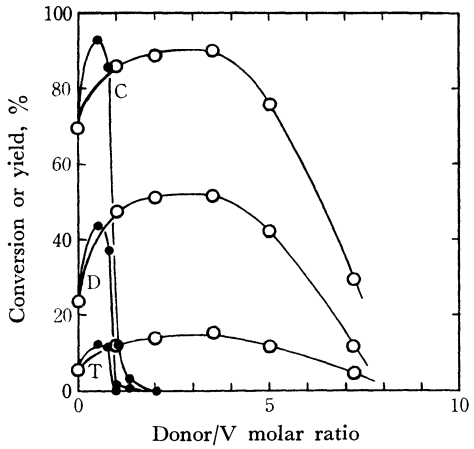

Fig. 4. Effect of triphenylphosphine and bis-diphenylphosphinoethane.
-○-: Triphenylphosphine
-●-: Bis-diphenylphosphinoethane
C: Conversion of isoprene, %
D: Yield of 2,6-dimethyl-1, *trans*-3,6-octatriene, %
T: Yield of trimers, %
Reaction conditions: 70°C, 1 hr,
Isoprene/$VO(OEt)_3$: 100, $Et_2AlCl/VO(OEt)_3$: 12

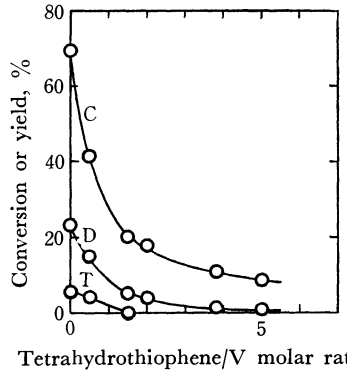

Fig. 5. Effect of tetrahydrothiophene.
C: Conversion of isoprene, %
D: Yield of 2,6-dimethyl-1, *trans*-3,6, octatriene, %
T: Yield of trimers, %
Reaction conditions: 70°C, 1 hr,
Isoprene/$VO(OEt)_3$: 100, $Et_2AlCl/VO(OEt)_3$: 12

triphenylphosphine or 1,2-bis-diphenylphosphinoethane raised the reaction rate at lower donor/$VO(OEt)_3$ molar ratios. The selectivity for 2,6-dimethyl-1,*trans*-3,6-octatriene was also raised to 50—60%. The reactions were suppressed at higher molar ratios. Tetrahydrothiophene suppressed the reaction at every molar ratio.

Reaction of Isoprene by $VO(OEt)_3$—Et_3Al or $VO(OEt)_3$—$EtAlCl_2$ Catalyst System. By the catalyst system consisting of ethyl orthovanadate and triethylaluminum, isoprene was consumed nearly completely and was converted into a liquid polymer in the reaction at 40—100°C for 1 hr. Only small amount of the dimer (less than 1.3%) was formed at 40—70°C. The infrared spectrum of the brown liquid polymer obtained in the reaction at 70°C for 1 hr and at the molar ratio of triethylaluminum to ethyl orthovanadate 5—10 showed absorptions due to methyl and methylene groups (2950, 2925, 2850, 1455, and 1380 cm^{-1}), a terminal methylene group (1790, 1650, and 890 cm^{-1}), three-substituted and *trans* double bonds (1670, 970, 840, and 810 cm^{-1}) and a vinyl group (910 cm^{-1}, sh). It contained about 55% of 1,4-, 40% of 3,4- and 5% of 1,2-structures.[9]

The catalyst system consisting of ethyl orthovanadate and ethylaluminum dichloride caused the vigorous polymerization of isoprene at room temperature. The infrared spectrum of the insoluble polymer obtained showed only methyl and methylene absorption (2925, 2850, 1455, and 1380 cm^{-1}) and did not show any absorption due to carbon-carbon double bonds. This spectrum was idential with that of the polymer formed by the cationic cyclopolymerization of isoprene by ethylaluminum dichloride.[10]

Structures of New Oligomers of Isoprene. The minor dimer formed by the catalyst consisting of ethyl orthovanadate and diethylaluminum chloride had the same gas chromatographic retention times as the dimer obtained in a small amount by zirconium[5] and hafnium[6] based catalysts. The mixture of dimers obtained by the zirconium catalyst was fractionated by distillation and the sample of the minor dimer (92% purity, containing 8% of 2,6-dimethyl-1,*trans*-3,6-octatriene) was analyzed with the use of infrared and nuclear magnetic resonance spectra. The infrared spectrum showed absorptions due to methyl and methylene groups (2965, 2925, 2850, 1440, and 1380 cm^{-1}), a conjugated double bond (1610 cm^{-1}), a vinyl group (1795, 1645, 990, and 895 cm^{-1}), a three-substituted double bond (1670 and 810 cm^{-1}) and a weak absorption at 960 cm^{-1} due to 2,6-dimethyl-1,*trans*-3,6-octatriene. The nuclear magnetic resonance spectrum showed the presence of three methyl groups (τ=8.41, doublet; 8.38, singlet; 8.24, singlet), one methylene group between two double bonds (τ=7.17, doublet), one vinyl group (τ=5.17—4.87, three absorptions; 3.68, double doublet) and two olefinic protons (τ=4.90—4.55, complex absorptions). Thus the structure of this compound is considered to be 3,6-dimethyl-1,3,6-octatriene.

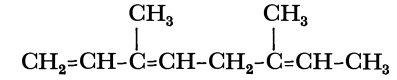

Relative retention times (retention time of benzene =1) of four main trimers obtained by the catalyst system consisting of ethyl orthovanadate and diethylaluminum chloride were 4.1, 4.6, 6.8, and 9.9 (operation conditions of gas chromatography, see experimental part). Two isomers (relative retention time, 6.8 and 9.9) were gas chromatographically identical with those obtained by the zirconium based catalyst and one isomer (relative retention time, 9.9) was assumed to be 3,6,10-trimethyl-2,5,*trans*-7,10-dodecatetraene.[5]

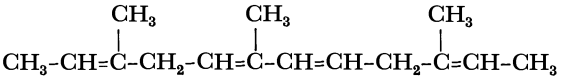

trans

The mixture of trimers obtained by the zirconium catalyst was fractionally distilled and the isomer with the relative retention time 6.8 was obtained in a pure

10) I. Koessler, M. Stolka, and K. Mach, *J. Polym. Sci. Pt C*, **No. 4**, 977 (1963).

state. The infrared spectrum of this isomer showed absorption due to methyl and methylene groups (2970, 2925, 2850, 1455, 1445, and 1380 cm^{-1}), a conjugated double bond (1610 cm^{-1}), a *trans* double bond (1670 and 970 cm^{-1}), a terminal methylene group (1780, 1650, and 885 cm^{-1}) and three-substituted double bonds (1670, 840, and 810cm^{-1}). Its nuclear magnetic resonance spectrum showed the presence of four methyl groups(τ= 8.45, doublet; 8.34, singlet, two methyl groups; 8.20, singlet), two adjacent methylene groups between doubl bonds (τ=7.98—7.90), one methylene group between double bonds (τ=7.20, doublet), one terminal methyl group (τ=5.16, singlet), two olefinic protons (τ=4.92 —4.70, complex absorptions) and one *trans* two-substituted double bond (τ=4.48, double triplet; 3.88, doublet). Thus the structure of this isomer is considered to be 2,6,10-trimethyl-1,*trans*-3,6,10-dodecatetraene or 2,7,10-trimethyl-1,*trans*-3,7,10-dodecatetraene.

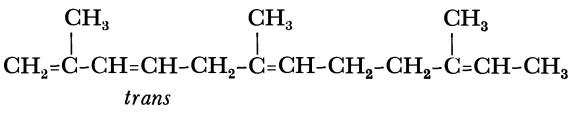

or

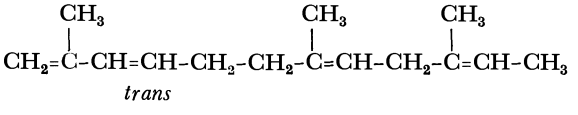

BULLETIN OF THE CHEMICAL SOCIETY OF JAPAN, VOL. 44, 1121—1125 (1971)

The Thermal Rearrangement and Degradation of 2,3-Bis(alkylimino)oxetane

Takeo SAEGUSA, Naotake TAKA-ISHI, and Yoshihiko ITO
Department of Synthetic Chemistry, Faculty of Engineering, Kyoto University, Sakyo-ku, Kyoto

(Received November 20, 1970)

The thermal rearrangement of 2,3-bis(alkylimino)oxetane (**1**) was investigated. At 200°C, 2,3-bis(secondary alkylimino)oxetane was converted into 3-imidazolin-5-one (**8**). 2,3-Bis(tertiary alkylimino)oxetane was stable at 200°C, but it was rearranged at 300°C to a cyclobutanone derivative (**18**). A mechanism involving the β-lactam intermediate (**12**) (**17**) formed by the Chapman rearrangement of **1** was proposed.

This paper will describe the thermal rearrangement and the accompanying decomposition of 2,3-bis(alkylimino)oxetane (**1**).

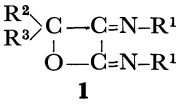

1

The rearrangement of **1** constitutes a significant extension of the molecular rearrangement of methylenecyclopropane derivatives with hetero atoms in their framework (Eq. (1)), which has recently attracted considerable attention.[1,2]

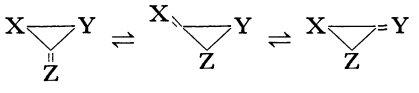

(1)

Among several examples, the tautomeric interconversion of three-membered α-lactam (**2**) and imino-oxirane (**3**) reported by Sheehan and Lengyel[2] (Eq. (2)) is taken to be especially closely related to the present study.

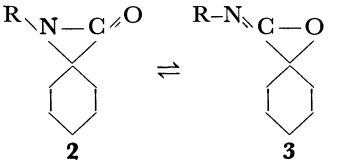

2 **3** (2)

Further, the imino-oxirane–lactam rearrangement has been assumed in the following scheme of the $BF_3 \cdot OEt_2$-catalyzed reactions of isocyanides[3] with carbonyl compounds[4] to produce 2,3-diimino-oxetane (**1**).[3-7] The formation of a by-product, **7**, in the acid-catalyzed reaction of isocyanide with carbonyl compounds has been explained by a process involving the molecular rearrangement of **4** to **5** (Scheme 1).

The course of the thermal rearrangement of **1** is dependent upon the nature of alkyl groups (R^1) attached to the imino nitrogen atoms. When R^1 is a secondary alkyl, the rearrangement occurs at 200°C and takes the course of Eq. (3), in which the migration of the secondary hydrogen atom of one alkyl group is involved:

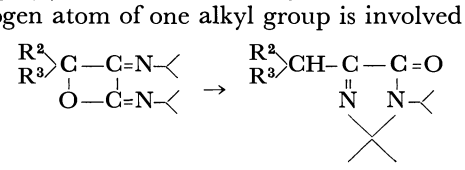

(3)

When R^1 is a tertiary alkyl in **1**, rearrangement requires a higher temperature of 300°C and involves the migration of the hydrogen of the alkyl group of R^2 or R^3 (Eq. (4)):

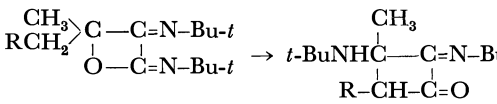

(4)

1) J. A. Deyrup and R. B. Greenwald, *Tetrahedron Lett.*, **1966**, 5091; J. A. Deyrup, M. M. Vestling, W. V. Hagan, and H. Y. Yun, *Tetrahedron*, **25**, 1467 (1969).

2) J. C. Sheehan and I. Lengyel, *J. Amer. Chem. Soc.*, **86**, 746 (1964); J. C. Sheehan and I. Lengyel, *ibid.*, **86**, 1356 (1964); J. C. Sheehan and I. Lengyel, *Angew. Chem. Internat. Ed.*, **7**, 25 (1968).

3) T. Saegusa, N. Taka-ishi, and H. Fujii, *Polymer Lett.*, **5**, 779 (1967).

4) T. Saegusa, N. Taka-ishi, and H Fujii, *Tetrahedron*, **24**, 3795 (1968)

5) H. J. Kabbe, *Angew. Chem.*, **80**, 406 (1968).

6) H. J. Kabbe, *Chem. Ber.*, **102**, 1404 (1969).

7) B. Zeeh, *Tetrahedron Lett.*, **1969**, 113.

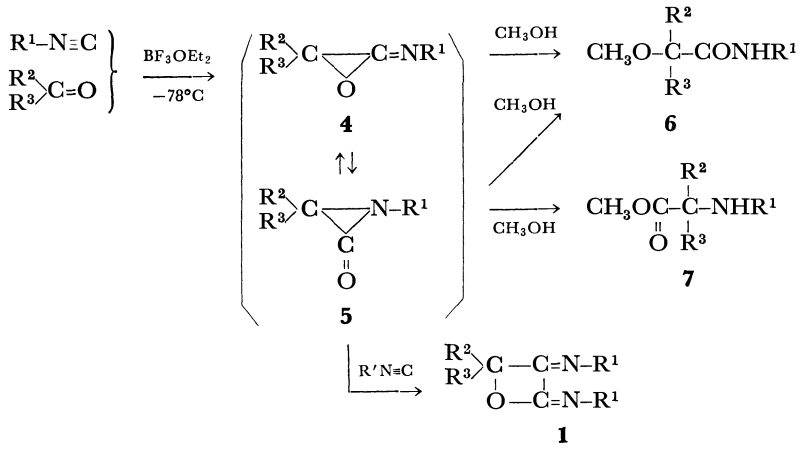

Scheme 1

Results and Discussion

When **1a** (R^1=  , R^2=R^3=Me) was heated at 200°C, the rearranged compond **8a** was obtained in a yield of 43%, along with small amounts of 2-hydroxy-2-methyl-*N*-cyclohexylpropionamide (**9a**) and *N*-cyclohexylformamide (**10a**) (Scheme 2). The structure of **8a** was established on the basis of spectral analyses in addition to elemental analysis. The presence of the isopropyl group in **8a** was clearly demonstrated by the NMR spectrum. The absence of NH and OH groups was indicated by the IR spectrum. Other observations of the IR and NMR spectra as well as the results of the elemental analysis fit the structure **8a** (see Experimental Section).

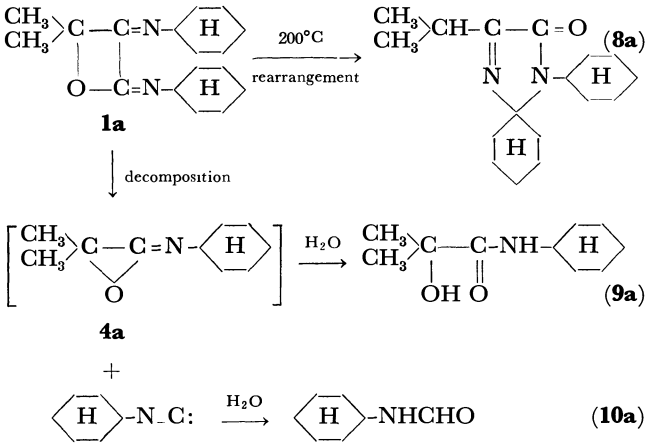

Scheme 2

Additional support for the structure **8a** was given by acid hydrolysis, which produced an α-keto acid amide (**11**) and cyclohexanone:

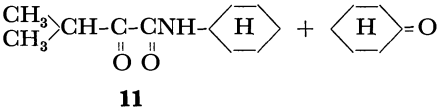

11

Some other homologues, **1b** (R^1=  , R^2=Me, R^3=Et) and **1c** (R^1=*i*-Pr, R^2=Me, R^3=Et), were also converted to the corresponding 3-imidazolin-5-one. The results are shown in Table 1. The employment of a solvent such as benzyl benzoate and diphenylmethane did not increase the yield of the rearranged product.

TABLE 1. REARRANGEMENT OF 2,3-BIS(SECONDARY ALKYLIMINO)OXETANE

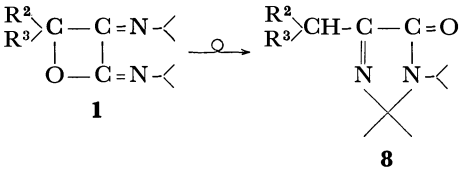

Compound	-<	R^2	R^3	Solvent	Yield of **8** (%)
1a	- 	CH_3	CH_3	—	43
1b	- 	CH_3	C_2H_5	—	62
1c	$-CH(CH_3)_2$	CH_3	C_2H_5	—	49
1c	$-CH(CH_3)_2$	CH_3	C_2H_5	$C_6H_5CH_2OCOC_6H_5$	38
1c	$-CH(CH_3)_2$	CH_3	C_2H_5	$(C_6H_5)_2CH_2$	37

As to the reaction mechanism, the normal Chapman reaction may be thought of an as antecedent process which may produce a precursor intermediate (**12**).

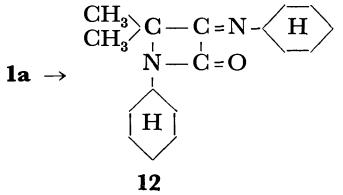

12

However, several attempts to isolate **12** were all unsuccessful. The structure of the product shows unequivocally the cleavage of the O–4C bond. The position of the bond-cleavage of the thermal rearrangement is the same as that of the cationic reaction of 2,3-bis-iminooxetane. The cationic ring-opening of **1** by acid, producing **13**, has been previously reported by Kabbe[8] and by us.[4] When the R^1 or R^2 of **1** is an aromatic ring, the BF_3-catalyzed bond-cleavage takes place at the O–4C bond

8) H. J. Kabbe, *Chem. Ber.*, **102**, 1410 (1969).

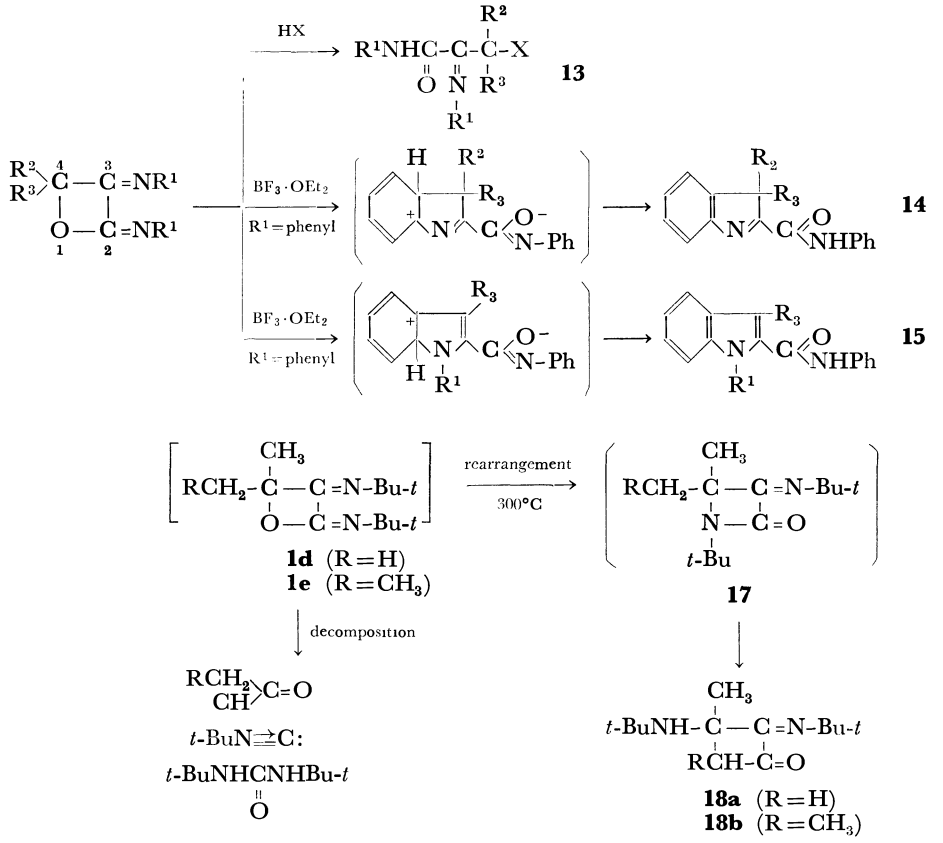

to produce indol derivatives, **14** and **15**.[9,10]

The formation of by-products of **9a** and **10a** may be explained by assuming the decomposition of **1a** into cyclohexyl isocyanide and an unstable imino-oxirane **4a**. The hydrolytic cleavage of **4a** affords **9a**, and the hydrolysis of cyclohexyl isocyanide gives rise to **10a**. The decomposition of **1a** depicted in Scheme 2 resembles the decomposition of imino-oxirane (**16**) to isocyanide and a carbonyl compound, as has been reported by Kagen and Lillien.[11] (Eq. (4)):

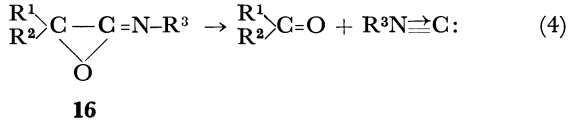

(4)

16

The bis(tert-alkylimino)homologue of **1** has no hydrogen at the α-carbon atom of nitrogen, and its thermal rearrangement takes a different route. At 200°C, **1d** (R^1=*t*-Bu, R^2=R^3=Me) is stable and does not rearrange. The rearrangement of **1d**, however, occurs at 300°C to produce **18a**. The concurrent decomposition of **1d** takes place to give *t*-butyl isocyanide, acetone, and di-*t*-butylurea.

The structure **18a** was established by a study of the spectral data and by elemental analysis. The presence of a secondary amino group was indicated in both the IR and the NMR spectra. In the NMR spectrum, the appearance of two new peaks at τ 6.50 (NH) and τ 6.28 (-CH_2)-was taken to support the structure **18a**. Similarly, **1e** (R^1=*t*-Bu, R^2=Me, R^3=Et) was converted into **18b**. The acetylation of **18b** with acetyl chloride gave the *N*-acetyl derivative. This result also supports the structure of **18b**.

As to the mechanism of the rearrangement of **1d** and **1e**, the structure of the product **18** may be taken to suggest a scheme *via* an intermediate of β-lactam (**17**) which is formed by the Chapman rearrangement of **1**. The cleavage of the bond between the amide nitrogen and the carbonyl carbon atom in **17** leads to the formation of **18**. The rearrangement **1d** and **1e** may be compared with the thermal reactions of the related compounds. Sheehan has reported[12,13] the rearrangement of triphenyl-substituted α-lactam (**19**) which proceeded the analogous bond cleavage. Singer and Barlett[14] have shown the photo- and thermal-decomposition of an iminooxetan (**20**) into the corresponding isocyanate (**21**) and olefin (**22**).

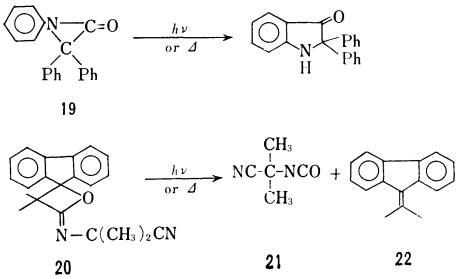

9) B. Zeeh, *Tetrahedron Lett.*, **1967**, 3881; B. Zeeh, *Chem. Ber.*, **102**, 678 (1969).
10) B. Zeeh, *Angew. Chem.*, **79**, 415 (1967); B. Zeeh, *Chem. Ber.*, **101**, 1753 (1968).
11) H. Kagen and I. Lillien, *J. Org. Chem.*, **31**, 3728 (1966).
12) J. C. Sheehan and J. W. Frankenfeld, *J. Amer. Chem. Soc.*, **83**, 4792 (1961).
13) J. C. Sheehan and I. Lengyel, *J. Org. Chem.*, **28**, 3252 (1963).
14) L. A. Singer and P. D. Barlett, *Tetrahedron Lett.*, **1964**, 1887.

Table 2. Characterizations of 2,3-bis(alkylimino)oxetanes

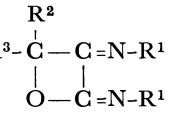

Compd	R_1	R_2	R_3	Bp C°/mmHg	Formula	Anal Calcd % C	H	N	Found % C	H	N	NMR absorption, τ
1b	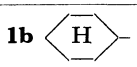	CH_3	Et	129—130/[a]								m 5.9 (1H), m 6.45 (1H) s 8.52 (3H), t 9.00 (3H)
1c	*i*-Pr	CH_3	Et	78—80/12	$C_{12}H_{22}N_2O$	68.53	10.54	13.32	68.42	10.69	13.21	m 5.55 (1H), m 6.16 (1H) q 8.22 (2H), s 8.52 (3H) d 8.85 (6H), d 8.88 (6H) t 9.00 (3H)
1d	*t*-Bu	CH_3	CH_3	94—96/32[b]	$C_{13}H_{24}N_2O$	69.60	10.78	12.49	69.44	10.95	12.37	s 8.50 (6H), s 8.58 (9H) s 8.68 (9H)
1e	*t*-Bu	CH_3	Et	74—76/7	$C_{14}H_{26}N_2O$	70.54	10.99	11.75	70.79	11.03	11.66	q 8.25 (2H), s 8.57 (3H) s 8.64 (9H), s 8.70 (9H) t 9.05 (3H)
1f	*t*-Bu	CH_3		110/18	$C_{15}H_{26}N_2O$	71.95	10.47	11.19	71.66	10.23	11.27	s 8.45 (3H), s 8.60 (9H) s 8.70 (9H), m 8.8—9.6 (5H)

a) Distilled with partial degradation. b) Lit, bp 76°C/10 mmHg.[6]

A bis(alkylimino)oxetane with a cyclopropane ring at 4-C (**1f**, R^1=*t*-Bu, R^2=Me, R^3=cyclopropyl) rearranged *via* different way, one involving the cleavage of the cyclopropane ring. The product was a picolinamide (**25**).

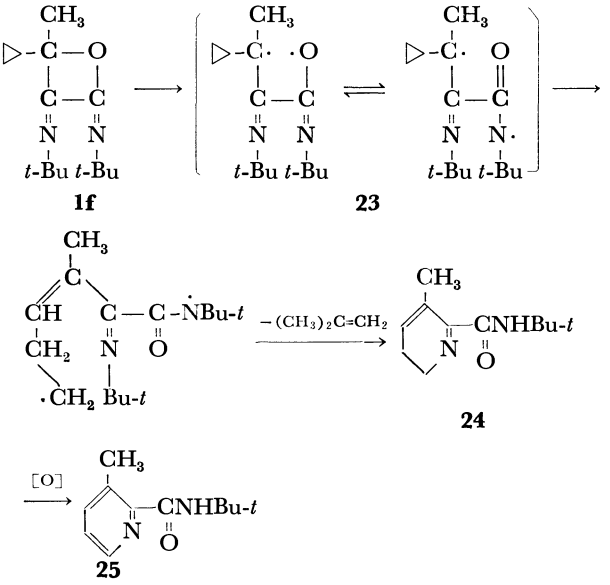

In the above scheme, the first step is the cleavage of the carbon oxygen bond at the same position as that of Scheme 2. The ring-opening of the cyclopropane ring of **23** followed by the cyclization of the resulting radical, with the elimination of isobutene, will produce a dihydropicolinamide derivative (**24**), whose dehydrogenation then gives rise to **25**.

Experimental

Materials. 2,3-Bis(cyclohexylimino)-4,4-dimethyloxetane[4] (**1a**) and 2,3-bis(*t*-butylimino)-4,4-dimethyloxetane[6] (**1d**) have been previously reported. The other iminooxetanes were prepared by a procedure described previously.[4] The properties of the iminooxetanes are shown in Table 2.

Thermal Rearrangement of 2,3-Bis(cyclohexylinino)-4,4-dimethyloxetane (**1a**). At 200°C, 1.1 g (4 mmol) of **1a** was heated for 7 hr and then subjected to distillation. From the distillate, bp 150—153°C/8 mmHg, 1-cyclohexyl-4-isopropyl-2,2-pentamethylene-3-imidazolin-5-one(**8a**) was obtained in a yield of 43%.

Found: C, 73.07; H, 10.51; N, 9.76%. Calcd for $C_{17}H_{28}N_2O$: C, 73.87; H, 10.21; N, 10.13%. IR spectrum (neat): 1680 ($\nu_{C=O}$) and 1625 ($\nu_{C=N}$) cm^{-1}; NMR spectrum ($CDCl_3$): τ 8.78 (doublet, 6H, $(\underline{CH_3})_2CH$–), 7.8—9.0 (complex, 20H, $-CH_2-$ of cyclohexyl ring), 7.2—7.8 (broad multiplet, 1H, –CH– of the cyclohexyl ring), 7.05 (multiplet, 1H, $(CH_3)_2\underline{CH}$–). The by-products, *N*-cyclohexylformamide (**10a**) and 2-hydroxy-2-methyl-*N*-cyclohexylpropionamide (**9a**), were isolated by preparative glpc in yields of 4% and 8% respectively. **9a** was identified by a comparison of the glpc retention time and IR spectrum with those of an authentic sample prepared according to the method of Hagedorn.[15]

Hydrolysis of 1-Cyclohexyl-4-isopropyl-2,2-pentamethylene-3-imidazolin-5-one (8a). A solution of 1.4 g (5 mmol) of **8a** in 20 ml of ethanol saturated with hydrochloric acid was refluxed for 1 day. After the ethanol has then been evaported, the reaction mixture was treated with aqueous sodium hydrogencarbonate and extracted with methylene chloride. The methylene chloride extract was washed with water and then subjected to glpc analysis. Cyclohexanone and *N*-cyclohexyl-3-methyl-2-oxobutyramide (**11**) were obtained in yields of 70% and 78% respectively.

Found: C, 66.30; H, 9.76; N, 6.82%. Calcd for $C_{11}H_{19}NO_2$: C, 66.97; H, 9.71; N, 7.10%. IR spectrum (neat): 1725 ($\nu_{C=O}$) and 1665 ($\nu_{N-C=O}$) cm^{-1}, NMR spectrum ($CDCl_3$):

15) I. Hagedorn and U. Eholzer, *Chem. Ber.*, **98**, 936 (1965).

τ 8.85 (doublet, 6H, $(\underline{CH_3})_2CH$), 7.8—9.0 (complex, 11H, cyclohexane ring protons) 6.4 (multiplet, 1H, $(CH_3)_2C\underline{H}$), 3.2 (broad multiplet, 1H, N$\underline{H}$).

*1-Cyclohexyl-4-*sec*-butyl-2,2-pentamethylene-3-imidazolin-5-one (8b).* **8b** was obtained in a yield of 62% by the thermal rearrangement of 2,3-bis(cyclohexylimino)-4-ethyl-4-methyloxetane (**1b**), bp 155—160°C/3 mmHg. IR spectrum (neat): 1685 ($\nu_{C=O}$) and 1630 ($\nu_{C=N}$) cm^{-1}; NMR spectrum ($CDCl_3$); τ 9.10 (triplet, 3H, $\underline{CH_3}CH_2$–), 8.78 (doublet, 3H, $\underline{CH_3}CH$), 7.5—9.0 (complex, 21H, cyclohexane ring protons), 7.25 (multiplet, 1H, $CH_3\underline{CH}$); Mass spectrum: *m/e* 290 (M^+).

*4-*sec*-Butyl-1-isopropyl-2,2-dimethyl-3-imidazolin-5-one (8c).* **8c** was obtained in a yield of 49% by the thermal rearrangement of 2,3-bis(isopropylimino)-4-ethyl-4-methyloxetane (**1c**), bp 89—90°C/18 mmHg.

Found: C, 68.25; H, 10.82; N, 13.07%. Calcd for $C_{12}H_{22}N_2O$: C, 68.53; H, 10.54; N, 13.32%. IR spectrum (neat): 1680 ($\nu_{C=O}$) and 1625 ($\nu_{C=N}$) cm^{-1}; NMR spectrum ($CDCl_3$): τ 9.08 (triplet, 3H, $\underline{CH_3}CH_2$), 8.77 (doublet, 3H, $\underline{CH_3}CHCH_2CH_3$), 8.55 (singlet, 6H, N–C$(CH_3)_2$–N), 8.53 (doublet, 6H, $(\underline{CH_3})_2CH$), 8.35 (multiplet, 2H, $CH_3\underline{CH_2}$–CH), 7.22 (multiplet, 1H, $CH_3\underline{CH}CH_2CH_3$), 6.25 (multiplet, 1H, $(CH_3)_2\underline{CH}$).

*Thermal Rearrangement of 2,3-Bis(*t*-butylimino)-4,4-dimethyloxetane (1d).* At 300—350°C, 2 g (9 mmol) of **1d** was heated for 1 hr and then distilled. The volatile material trapped by a dry ice-methanol bath, was shown to be a mixture of acetone and *t*-butyl isocyanide by a study of the glpc and NMR spectra. From the distillation condensate, bp 118°C/12 mmHg, 3-*t*-butylamino-2-*t*-butylimino-3-methylcyclobutanone (**18a**) was obtained by means of preparative glpc in a yield of 30%.

Found: C, 68.94; H, 10.55; N, 12.66%. Calcd for $C_{13}H_{24}N_2O$: C, 69.60; H, 10.78; N, 12.49%. IR spectrum (neat): 3350 (ν_{NH}) and 1665 ($\nu_{C=O}$ and $\nu_{C=N}$) cm^{-1}; NMR spectrum ($CDCl_3$): τ 8.77 (singlet, 9H, *t*-Bu), 8.55 (singlet, 9H, *t*-Bu), 8.00 (singlet, 3H, CH_3), 6.50 (singlet, 1H, NH), 6.28 (singlet, 2H, CH_2), Mass spectrum: *m/e* 224 (M^+). From the residue, 1,3-di-*t*-butylurea was obtained in a yield of 11%; it was identified by a comparison of IR and NMR spectra with those of the authentic sample.

3-t-Butylamino-2-t-butylimino-3,4-dimethylcyclobutanone (18b). **18b** was obtained in a yield of 64% by the thermal rearrangement of 2,3-bis(*t*-butylimino)-4-ethyl-4-methyloxetane (**1e**), bp 135°C/12 mmHg.

Found: C, 69.97; H, 11.39; N, 11.60%. Calcd for $C_{14}H_{26}N_2O$: C, 70.54; H, 10.99; N, 11.75%. IR spectrum (neat): 3350 (ν_{NH}) and 1665 ($\nu_{C=O}$ and $\nu_{C=N}$) cm^{-1}. NMR spectrum ($CDCl_3$): τ 8.78 (singlet, 9H, *t*-Bu), 8.65 (doublet, 3H, $\underline{CH_3}CH$), 8.50 (singlet, 9H, *t*-Bu), 8.05 (singlet, 3H, CH_3), 6.85 (singlet, 1H, NH), 6.10 (quartet, 1H, $CH_3\underline{CH}$). Mass spectrum: *m/e* 238 (M^+).

Acetylation of 3-t-Butylamino-2-t-butylimino-3,4-dimethylcyclobutanone (18b). Into a solution of 0.5 g of **18b** (2 mmol) and 0.5 m*l* of triethylamine in 10 m*l* of ether, we stirred, drop by drop, 1 m*l* of acetyl chloride at room temperature. After standing for 20 hr, the reaction mixture was treated with aqueous sodium hydrogencarbonate. The ether layer was then subjected to glpc analysis to yield the *N*-acetylated compound quantitatively.

Found: C, 68.30; H, 10.00; N, 9.71%. Calcd for $C_{16}H_{28}N_2O_2$: C, 68.53; H, 10.07; N, 9.99%. IR spectrum (neat): 1660 cm^{-1}; NMR stectrum ($CDCl_3$): τ 8.58 (doublet, 3H, $\underline{CH_3}CH$), 8.57 (singlet, 9H, *t*-Bu), 8.49 (singlet, 9H, *t*-Bu), 8.21 (singlet, 3H, CH_3), 8.08 (singlet, 3H, CH_3), 5.95 (multiplet, 1H, $CH_3\underline{CH}$). Mass spectrum: *m/e* 280 (M^+).

N-t-*Butyl-3-methylpicolinic Amide (25).* At 200°C, 1 g (4 mmol) of 2,3-bis(*t*-butylimino)-4-cyclopropyl-4-methyloxetane (**1f**) was heated for 1 hr and then subjected to glpc analysis. **25** was thus obtained in a yield of 23%.

Found: C, 68.92; H, 8.64; N, 14.69%. Calcd for $C_{11}H_{16}N_2O$: C,68.72; H, 8.39; N, 14.57%. IR spectrum (neat): 3350 (ν_{NH}), 1670 ($\nu_{C=O}$), and 1510 (ν_{NH}) cm^{-1}. NMR spectrum (CCl_4): τ 8.52 (singlet, 9H, *t*-Bu), 7.30 (singlet, 3H, CH_3), 2.80 (multiplet, 1H, $\underline{H}C{=}C{-}CH_3$), 2.50 (multiplet, 1H, $\underline{H}C{=}CH{-}N$), 2.50 (broad singlet, 1H, NH), 1.70 (multiplet, 1H, CH=N). Mass spectrum: *m/e* 192 (M^+).

BULLETIN OF THE CHEMICAL SOCIETY OF JAPAN, VOL. 44, 1125—1127 (1971)

Radical Cations of Halogenated Tetrahydroxybenzene Diethylene Ethers

Teruzo ASAHARA, Manabu SENŌ, and Takuma TESHIROGI

Institute of Industrial Science, The University of Tokyo, Roppongi, Minato-ku, Tokyo

(Received November 30, 1970)

It was observed that two newly-prepared substances, 3,6-dichloro- and 3,6-dibromo-1,2,4,5-tetrahydroxybenzene diethylene ether, underwent one-electron oxidation to afford the corresponding radical cations in concentrated sulfuric acid. Their electronic spectra and ESR spectra were recorded in a sulfuric acid and nitromethane - $AlCl_3$ medium. The chloro - compound gives an ESR spectrum with a hyperfine structure, while the bromo-compound shows a spectrum without hyperfine splitting. Some different behavior was observed in several model compounds with similar structures.

Some aspect of the behavior of methoxybenzenes in concentrated sulfuric acid have been investigated, and the formation of the corresponding radical cations has been confirmed by means of a study of the ESR[1] and electronic absorption spectra.[2] We reported in a preceding paper[3] the syntheses of 3,6-dichloro- and 3,6-dibromo-1,2,4,5-tetrahydroxybenzene diethylene ether

1) A. Zweig, W. G. Hodgson, and W. H. Jura, *J. Amer. Chem. Soc.*, **86**, 4124 (1964).

2) K. Kimura and H. Yamada, This Bulletin, **42**, 3032 (1969).

3) T. Asahara, M. Senō, S. Shiraishi, and T. Teshirogi, *Kogyo Kagaku Zasshi*, **74**, 231 (1971).

(I and II) through the reaction of 2,5-dichloro- and 2,5-dibromo-3,6-dihydroxy-*p*-benzoquinone respectively with ethylene glycol. During the course of investigation of these properties, we observed the red coloration and ESR spectra of the compounds I and II in a sulfuric acid medium.

For comparison, some model compounds–2,5-dichloro- and 2,5-dibromohydroquinone dimethyl ether (III and IV), tetrachloro- and tetrabromohydroquinone dimethyl ether (V and VI), and 3,6-dichloro- and 3,6-dibromo-1,2,4,5-tetramethoxybenzene (VII and VIII)– were synthesized, and their ESR and electronic spectra were examined in sulfuric acid. The results will be presented in this paper.

Experimental

Syntheses. Compounds I and II synthesized according to the description in a previous paper.[3] Compound III was prepared from hydroquinone dimethyl ether and chlorine gas according to the method of Habermann,[4] mp 125°C (lit, 126°C), while V was prepared by treating III with chlorine gas, mp 165°C (lit, 164°C). Compound IV was prepared from the reaction of hydroquinone dimethyl ether with bromine, mp 141°C (lit, 142°C), and VI was prepared by the reaction of tetrabromohydroquinone with a potassium hydroxide solution of dimethyl sulfate, mp 193°C (lit, 194°C). Although the syntheses of compounds VII and VIII were described by Marini-Bettolo's report,[5] where chloranil or bromanil was methoxylated reductively in a zinc-methanol system, another procedure was adopted here; that is, 2,5-dichloro- or 2,5-dibromo-3,6-dimethoxy-*p*-benzoquinone was reduced with sodium dithionite and then reacted with dimethyl sulfate in an aqueous potassium solution. The products were recrystallized from ethanol-water; mp 114°C (VII) and 107°C (VIII). The electronic spectra were recorded on a Hitachi EPS-3T spectrophotometer, while the ESR spectra were measured by means of a JEX-3X ESR spectrometer. The sulfuric acid used for the solvent was of a special grade (98%) and nitromethane - aulminium chloride was prepared according to the description in the literature.[6]

Results and Discussion

The electronic spectra of I and II in concentrated sulfuric acid are shown in Fig. 1. The absorptions in the visible region (500 and 540 mμ) may be supposed to result from the radical cations which are formed through the one-electron oxidation of the original compounds. These absorptions correspond to the peaks at 440 and 460 mμ respectively of hydroquinone dimethyl ether, which was analysed by Kimura.[2]

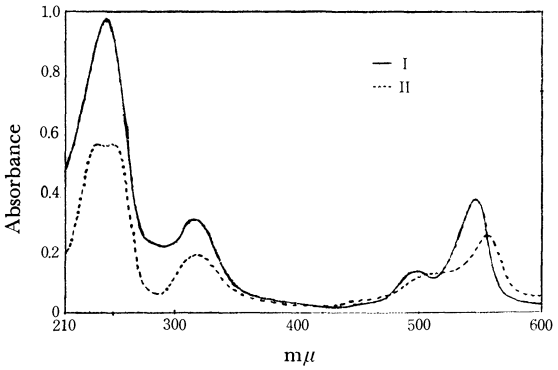

Fig. 1. Electronic spectra of I and II in sulfuric acid. (concn. 4×10^{-5} mol/*l*)

The ESR spectra of I and II in sulfuric acid are shown in Figs. 2 and 3. The spectrum of I has an hfs with nine

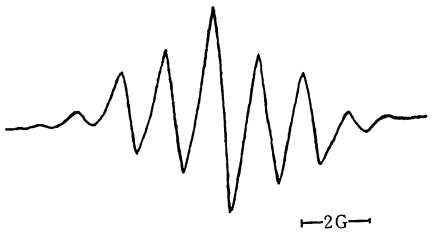

Fig. 2. ESR spectrum of I in concentrated sulfuric acid. (concn. 2×10^{-4} mol/*l*).

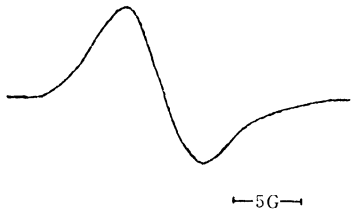

Fig. 3. ESR spectrum of II in concentrated sulfuric acid. (concn. 2×10^{-4} mol/*l*)

peaks. This is ascribed to the splitting by eight equivalent hydrogen atoms of I and has the expected intensity ratio of 1 : 8 : 28 : 56 : 70 : 56 : 28 : 8 : 1. The coupling constant, a^H is 1.33 gauss; this may be compared with the value, 2.21 gauss, for 1,2,4,5-tetramethoxybenzene.[1] The spectrum of II shows no hfs. Shine *et al.*[7] observed that 2,7-dichlothianthrene shows a three-line spectrum, but 2,7-dibromothianthrene shows a single broad-line spectrum.

Similar ESR spectra were observed in the nitromethane - aluminium chloride medium.[6] The hfs splitting of the spectrum of I is poorer under similar conditions in this medium than in sulfuric acid. The spectrum of II is a single broad line in this medium. The lack of any splitting into hfs in the spectra of II is probably the result of the spin-orbit coupling, as has been suggested by Shine *et al.*[7] An anisotropy is observed in these spectra; it is probably the result of the high viscosity of the medium and the spin-orbit interaction. The electronic spectra of I and II in this medium are nearly the same as those in sulfuric acid, (I, λ_{max} 498, 538 mμ; II λ_{max} 508, 546 mμ).

As has been stated above, the spectra of the radical cations of the chloro derivative are different from those of the bromo derivative. In order to obtain further information on this question, the spectra of several model compounds were examined. The model compounds synthesized for this purpose were as follows:

4) J. Habermann, *Chem. Ber.*, **11**, 1034 (1878).
5) C. B. Marini-Bettolo and F. S. Trucco, *Gazz. Chim. Ital.*, **73**, 300 (1943).
6) W. F. Forbes and P. D. Sullivan, *J. Amer. Chem. Soc.*, **88**, 2862 (1966).
7) H. J. Shine, C. F. Dais, and R. J. Small, *J. Chem. Phys.*, **38**, 569 (1963).

Table 1. Electronic spectra in sulfuric acid

Compound	I		II		III		IV		VII		VIII	
λ_{max} (mμ)	502	542	512	552	457	490	485	518	454	481	438	464
log ε	3.62	3.99	3.57	3.83	3.48	3.68	3.45	3.63	2.04	2.18	1.90	2.32

Table 2. ESR spectra

Compound	No. of lines (in concentrated sulfuric	Hyperfine splitting	Over-all splitting acid)	g-Values	No. of lines (in nitromethane - aluminium	Hyperfine splitting	Over-all splitting chloride)
I	9	1.33	12.0	2.0025	5[a]	—	18.5
II	1	—	16.5	2.0036	1	—	20.0
VII	5	1.74	12.0	2.0023	9	1.97	19.0
VIII	11[a]	—	20.5	2.0034	11	2.25	19.5

a) Poorly resolved.

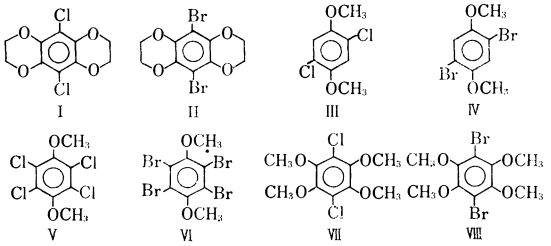

The tetrahalogeno compounds (V and VI) are insoluble in sulfuric acid, probably because of the electron-withdrawing property of halogens. The other compounds are soluble in sulfuric acid to form red solutions. The absorption peaks in the visible region, which are supposed to be due to radical cations, are characterized as is shown in Table 1. While the red solutions of VII and VIII show ESR spectra, no signals of ESR were observed for the red solutions of III and IV. The chloro compound VII has an ESR spectrum with only five peaks. The bromo compound VIII also shows an hfs; this hfs is very complicated, probably because of the restricted rotation of the four methoxy groups. When nitromethane - aluminium chloride was used instead of sulfuric acid as an oxidation medium, the hfs was also observed for the compounds VII and VIII. The results of the ESR spectra are summarized in Table 2. It should be noted that nitromethane - aluminium chloride is a stronger oxidation medium than sulfuric acid and that the radical cations of the bromo compounds have a more labile unpaired electron than the radical cations of chloro compounds. Moreover, a comparison of the signal intensities revealed that the chloro compounds have a higher radical concentration than the corresponding bromo compounds. The g-values are smaller for the chloro compounds than for the bromo compounds, as is to be expected from the values of the spin-orbit coupling constant.

The authors wish to thank Dr. Kōzi Ōhigashi, Basic Research Laboratories, Toray Co., for many useful suggestions regarding the ESR spectra.

BULLETIN OF THE CHEMICAL SOCIETY OF JAPAN, VOL. 44, 1127—1130 (1971)

Stereoselectivity of Phenylcarbenoid of Zinc in Cycloaddition with Olefin

Jun NISHIMURA, Junji FURUKAWA,* Nariyoshi KAWABATA,** and Hiroaki KOYAMA
Department of Synthetic Chemistry, Kyoto University, Sakyo-ku, Kyoto

(Received December 2, 1970)

The stereoselectivity of phenylcarbenoid of zinc generated from diethylzinc and benzal iodide was investigated in the cycloaddition reaction with olefin. The carbenoid showed larger *syn*-selectivity than phenylcarbenoid of lithium. Electron-donating substituent attached to the phenyl group of the phenylcarbenoid enhanced the *syn*-selectivity of the carbenoid. The *syn*-selectivity of the phenylcarbenoid was larger in ether than in *n*-pentane, contrary to the case of phenylcarbenoid of lithium.

The authors have reported briefly the formation of phenylcyclopropane by the reaction of diethylzinc and benzal iodide in the presence of olefin.[1] The generation of an phenylcarbenoid of zinc was assumed in the reaction.

* To whom inquiries should be directed.
** Present address: Department of Chemistry, Kyoto Institute of Technology, Matsugasaki, Kyoto.

1) J. Furukawa, N. Kawabata, and J. Nishimura, *Tetrahedron Lett.*, **1968**, 3495.

The present paper describes details of the stereochemistry of this reaction.

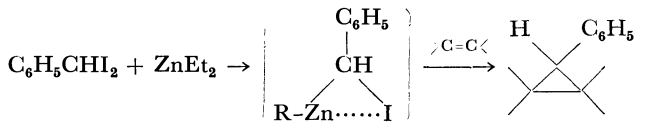

(1)

The reaction of diethylzinc and the substituted benzal iodide with 2-methylbut-2-ene and cyclohexene in moderate reaction conditions gave arylcyclopropanes in 18—69% yield. Results are given in Table 1.

TABLE 1. FORMATION OF ARYLCYCLOPROPANES

X- 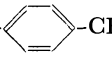 -CHI_2	2-Methylbut-2-ene[a]		Cyclohexene[c]	
	syn/*anti*	Yield (%)[b]	*syn*/*anti*	Yield (%)[b]
p-CH_3	5.3	30	—	—
H	4.2	42	17.1	69[d]
p-Cl	2.0	18	—	—

a) Reactions were carried out at room temperature.
b) Based on the iodide.
c) Ref. 1.
d) Determined by vapor phase chromatography.

As was mentioned before,[1] this phenylcarbenoid of zinc shows the *syn*-selectivity.

In the reaction of diethylzinc and ethylidene iodide with olefin, methylcyclopropanes were formed with the result that *syn* isomer generally predominated over *anti* isomer.[2]

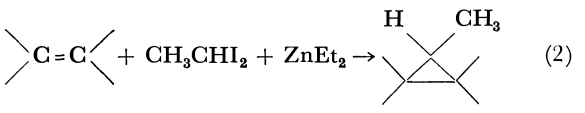

(2)

The electrostatic interaction between methyl group of the methylcarbenoid and substituents of olefin was proposed to explain the *syn*-selectivity of reaction (2).[2]

In the reactions with cyclohexene, the phenylcarbenoid in reaction (1) showed higher *syn*-selective behavior (*syn*/*anti*=17.1)[1] than the methylcarbenoid in reaction (2) (*syn*/*anti*=1.5).[2] As can be seen in Table 1, the electron-donating substituent attached to the phenyl group of benzal iodide enhanced the *syn*-selectivity of reaction (1). The electrostatic interactions between substituents in carbenoid and olefin may be significant factors which determine the isomer ratio in reaction (1).

The stereoselectivity of phenylcarbenoid in reaction (1) is compared with those of other phenylcarbene and carbenoids (Table 2).

The *syn*-selectivity of phenylcarbenoid in reaction (1) is higher than that of phenylcarbenoid of lithium,[3] but is much the same order of magnitude as that of other phenylcarbenoid of zinc.[4]

2) J. Nishimura, N. Kawabata, and J. Furukawa, *Tetrahedron*, **25**, 2647 (1969), and the literatures cited therein.
3) G. L. Closs and R. A. Moss, *J. Amer. Chem. Soc.*, **86**, 4042 (1964).
4) S. H. Goh, L. E. Closs, and G. L. Closs, *J. Org. Chem.*, **34**, 25 (1969).

TABLE 2. STEREOSELECTIVITY OF VARIOUS ARYLCARBENE AND CARBENOIDS

Reaction	Olefin	*syn*/*anti*	Yield %	Reference
$C_6H_5CHN_2$ + *hv*		1.1	—	3
$C_6H_5CHBr_2$ + MeLi		1.3	23	3
$C_6H_5CHI_2$ + Et_2Zn		4.2	42	This work
p-$CH_3C_6H_4CH_2$ + ZnI_2		2.6	—	4
$C_6H_5CHN_2$ + $ZnBr_2$		4.7	70	4

The *syn*/*anti* isomer ratio of 7-phenylnorcarane produced by reaction (1) depends largely upon the nature of solvents.

TABLE 3. SOLVENT EFFECT UPON *syn*/*anti* ISOMER RATIO IN REACTION (1) WITH CYCLOHEXENE[a]

Solvent	Isomer ratio (*syn*/*anti*)	Yield[b] (%)
n-Pentane	6.6	68
Benzene	6.2	67
Cyclohexanone	9.3	low
Acetonitrile	9.5	low
Diethyl ether	17.1	69
Di-*n*-butyl ether	16.0	68
t-Butyl methyl ether	14.0	67
Di-*iso*-propyl ether	12.0	71
Diethylene glycol dimethyl ether	9.6	low
Tetrahydrofuran	9.6	low

a) Reactions were carried out at 25°C.
b) Determined by vapor phase chromatography and based on the iodide.

The phenylcarbenoid shows much higher *syn*-selective behavior in ethers than in hydrocarbons. The *syn*/*anti*

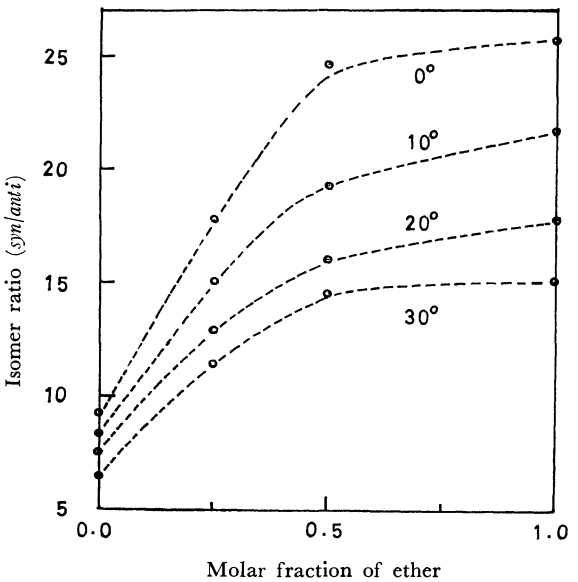

Fig. 1. Dependence of *syn*/*anti* isomer ratio on ether content in reaction (1) with cyclohexene in ether-pentane mixture.

Table 4. Temperature dependence of *syn*/*anti* isomer ratio in reaction (1) with cyclohexene in ether-pentane mixture

No.	Molar fraction of ether	Isomer ratio (*syn*/*anti*) 0°C	10°C	20°C	30°C	$\Delta H_s^{\ddagger} - \Delta H_a^{\ddagger}$ (kcal/mol)	$\Delta S_s^{\ddagger} - \Delta S_a^{\ddagger}$ (e. u.)
1	1.00	25.6	21.7	17.9	15.1	−2.91	−4.18
2	0.50	24.6	19.3	16.1	14.6	−2.88	−4.23
3	0.25	17.7	15.0	12.9	11.4	−2.41	−3.14
4	0.00	9.2	8.3	7.5	7.3	−1.31	−0.42

isomer ratio in reaction (1) with cyclohexene was examined in the mixed solvent of ether and *n*-pentane. The *syn*/*anti* isomer ratio increased with the molar fraction of ether in the mixed solvent as is shown in Fig. 1. These facts show the special solvent effect of aliphatic ethers upon the stereoselectivity of reaction (1), which might include the coordination of ether to zinc atom of the carbenoid. In the case of the reaction of *n*-butyllithium and *p*-methylbenzal bromide with *cis*-but-2-ene in the mixed solvent of ether and *n*-pentane,[3] the *syn*/*anti* isomer ratio of 1-*p*-tolyl-*cis*-2,3-dimethylcyclopropane decreased with the increasing molar fraction of ether contrary to the case of reaction (1). Metal atom of carbenoid may play an important role in this solvent effect.

Temperature dependence of the *syn*/*anti* isomer ratio in reaction (1) with cyclohexene in the ether - pentane mixture is given in Table 4.

According to the theory of absolute reaction rate,[5] $\ln(k_s/k_a)$ is given by Eq. (3) if transmission coefficients κ_s is equal to κ_a:

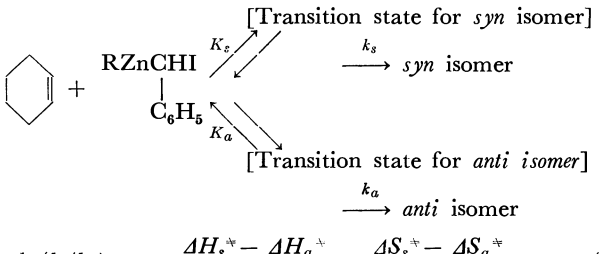

$$\ln(k_s/k_a) \cong -\frac{\Delta H_s^{\ddagger} - \Delta H_a^{\ddagger}}{RT} + \frac{\Delta S_s^{\ddagger} - \Delta S_a^{\ddagger}}{R} \qquad (3)$$

where k_s and k_a are the rate constants for the formation of *syn* and *anti* isomer, respectively. If the reaction is kinetically controlled, k_s/k_a can be calculated from the *syn*/*anti* isomer ratio with Eq. (4).

$$[syn \text{ isomer}]/[anti \text{ isomer}] = k_s/k_a \qquad (4)$$

The isomerization between *syn*- and *anti*-7-phenylnorcaranes is not very significant under the conditions of reaction (1) and subsequent experimental procedures,[6] and consequently this reaction can be assumed to be kinetically controlled. The differences in activation enthalpy and entropy between *syn* and *anti* isomer formation in reaction (1) were calculated and given in Table 4.

The activation enthalpy and the activation entropy for the *syn* isomer formation are smaller than those for the *anti* isomer formation. This result means that the transition state for *syn* isomer formation is energetically more stable than that for *anti* isomer formation, but entropically the situation is reverse.

The difference in activation energy between *syn* and *anti* isomer formation is larger in ether than in *n*-pentane. The phenomenon might be attributed to the specific solvation of ether to zinc atom of the carbenoid. Further experiments are required to discuss this point.

Experimental

Elemental analyses were performed at the Elemental Analyses Center of Kyoto University. NMR spectra were obtained with a Varian associates A-60 NMR Spectrometer or a Japan Electron Optics Lab. Model C60H Spectrometer in carbon tetrachloride using tetramethylsilane as the internal standard. Vapor phase chromatographic analyses were made on a Shimadzu GC-2C gas chromatograph. Melting points were corrected, but boiling points were not.

Materials. *t*-Butyl methyl ether was prepared according to the procedure of Norris and Rigby.[7] Tosylhydrazones of arylaldehydes[3] and ring substituted benzal iodides[8] were prepared by conventional methods: $C_6H_5CHI_2$, mp 44—46°C; p-$CH_3C_6H_4CHI_2$, mp 36—38°C (lit,[8] 35—37°C); p-$ClC_6H_4CHI_2$, mp 55—57°C.

Solvents were purified by the usual methods.[9] Other reagents were purified as described in the previous paper.[10]

Aryl-2,2,3-trimethylcyclopropanes. The reaction procedure was the same as have been described in a previous paper.[2] The reaction was carried out at room temperature. Stereochemical structures of products were determined by NMR chemical shift of methyl protons as shown in Table 5.[3] Physical properties and analytical data of the compounds were given in Table 6.

Temperature and Solvent Dependence of endo/exo *Isomer Ratio in Reaction (1) with Cyclohexene.* Cyclohexene (0.10 mol, 10.2 m*l*), benzal iodide (0.01 mol, 3.44 g) and solvent (20 m*l*) were placed in a 50 m*l* three necked flask equipped with a magnetic stirrer, a reflux condenser, a dropping funnel, and a gas-inlet with three-way cock under an atmosphere of nitrogen. The mixture was heated or chilled to prescribed temperature, and diethylzinc (0.02 mol, 2 m*l*) was added slowly from dropping funnel. After stirred for 5 hr, tetralin (0.005 mol) was added as internal standard for vapor phase chromatographic analysis. The reaction mixture was treated with aqueous ammonium chloride and analysed by vapor phase chromatography.

5) S. Glasstone, K. J. Laidler, and H. Eyring, "The Theory of Rate Processes," McGraw-Hill, New York & London (1941).
6) See experimental section.
7) J. F. Norris and G. W. Rigby, *J. Amer. Chem. Soc.*, **54**, 2088 (1932).
8) R. A. Moss, *J. Org. Chem.*, **30**, 3261 (1965).
9) A. Weisserberger, E. P. Proskauer, J. A. Riddick, and E. E. Toops, Jr., "Organic Solvents," Interscience, New York (1957).
10) J. Furukawa, N. Kawabata, and J. Nishimura, *Tetrahedron*, **24**, 53 (1968).

TABLE 5. CHEMICAL SHIFT (τ) OF METHYL PROTONS OF ARYL-2,2,3-TRIMETHYLCYCLOPROPANE

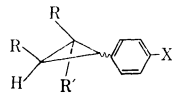

($R=R'=CH_3$)

X	Obsd (Reported)[a]			
	syn Isomer		*anti* Isomer	
	R	R'	R	R'
p-CH_3	9.10 (9.12)	8.79 (8.82)	—	—
H	9.14 (9.10)	8.82 (8.78)	8.81 (8.83)	9.24 (9.23)
p-Cl	9.12 (9.12)	8.79 (8.78)	8.80 (8.82)	9.21 (9.22)

a) Ref. 3.

TABLE 6. ARYL-2,2,3-TRIMETHYLCYCLOPROPANES PREPARED BY REACTION (1) WITH 2-METHYLBUT-2-ENE

$XC_6H_4CH—CHCH_3$ $\diagdown\ \diagup$ $C(CH_3)_2$	Bp (lit)[a] (°C/mmHg)	Elemental analysis Calcd (Found)		
		C	H	Cl
p-CH_3	81—88/9 (43/0.8)	89.59 (89.62)	10.41 (10.29)	
H	91—92/19 (61/3.5)	89.94 (90.15)	10.06 (10.01)	
p-Cl	55—57/5 (70/0.2)	74.03 (74.22)	7.77 (7.97)	18.21 (18.43)

a) Ref. 3.

The reaction of diethylzinc, methylene iodide, and cyclohexene was carried out under a similar reaction condition for 5 hr at room temperature in the presence of an isomer mixture (*syn*/*anti*=19.4) of 7-phenylnorcarane. The reaction mixture was treated in a similar manner as mentioned above. Vapor phase chromatographic analysis of the reaction mixture indicated that the *syn*/*anti* isomer ratio of the recovered 7-phenylnorcarane was 18.4. Thus, the isomerization between *syn*- and *anti*-7-phenylnorcarane during reaction (1) and subsequent experimental procedures is not so significant.

BULLETIN OF THE CHEMICAL SOCIETY OF JAPAN, VOL. 44, 1130—1133 (1971)

The Pyrolysis of Halocyclopropanes at High Temperatures

Teruzo ASAHARA, Katsumichi ONO,* and Kazuki TANAKA

Institute of Industrial Science, The University of Tokyo, Roppongi, Minato-ku, Tokyo

(Received December 14, 1970)

The pyrolysis reactions of dihalocyclopropanes and monohalocyclopropanes were carried out at 200—400°C. Bromo-substituted cyclopropanes were readily decomposed in this temperature range. In all cases, the pyrolysis products were ring-opened olefinic hydrocarbons. As for the monohalocyclopropanes, the reactions proceed in a stereospecific manner. The possible mechanism was discussed in terms of the requirements of the electrocyclic ring opening.

The slow solvolysis rates of cyclopropyl compounds have attracted much attention from organic chemists. The low reactivity of these compounds toward nucleophilic substitution has been attributed to the steric strain of the ring, which makes the intermediate cyclopropyl cation unstable.[1] Generally, the solvolysis, products are exclusively ring-opened allyl derivatives.

Examples of this type of transformation, the so-called cyclopropyl-allyl transformation, have been reported by many authors; the reaction presented in our next report, in which ring-opened products were obtained by the Friedel-Crafts reaction of halocyclopropanes, may also be included in this category.

The transformation requires the rotation of substituted groups on the cyclopropane ring. As a result, several steric courses may be considered with regard to the direction of rotation. According to the proposal of Woodward and Hoffmann,[2] the steric course of this process is determined by the symmetry of the highest occupied orbital of the ground state. They predicted

* Present address: Chemical Research Institute of Non-aqueous Solutions, Tohoku University, Sendai.

1) H. C. Brown, R. S. Fletcher, and R. B. Johannesen, *J. Amer. Chem. Soc.*, **73**, 212 (1951).

2) R. B. Woodward and R. Hoffmann, *ibid.*, **87**, 395 (1965).

Table 1. Pyrolysis of dihalocyclopropanes

Cyclopropane	Pyrolysis temperature (°C)	Total[a] pyrolysate (%)	Pyrolysis product	Yield (%)	Recovered[b] cyclopropane (%)
I-Cl	392	63	$CH_2=\overset{Cl}{\overset{|}{C}}-\overset{CH_3}{\overset{|}{C}}=CH_2$	24	31
I-Br	350	34	$CH_2=\overset{Br}{\overset{|}{C}}-\overset{CH_3}{\overset{|}{C}}=CH_2$	70	1
II	390—400	68		0	48
III	320—325	26		54	3
VI	390	43			12

a) The weight % of condensed hydrocarbons to the starting material.
b) The weight % of pyrolysis product to total pyrolysate.

that the direction of the ring opening of the cyclopropyl cation must be disrotatory. Some experimental evidence has been given by the solvolysis reactions of substituted cyclopropyl tosylates.[3,4]

In the present investigation, the pyrolysis reaction of halocyclopropanes was studied. Some differences with regard to the stereospecificity may be expected between the pyrolysis and cationic ring-opening reactions of cyclopropanes. Since the pyrolysis rates of halocylopropanes are quite fast at 200—400°C, this reaction is suitable for the investigation of the reactivity of chemically-inactive halocyclopropanes. The steric course of the pyrolysis reaction will be discussed on the basis of analyses of the pyrolysis products.

Results and Discussion

It is expected that dihalocyclopropanes are less reactive than the corresponding monohalocyclopropanes as a result of the introduction of electron-withdrawing halogen atoms. However, the thermal decompositions of some dichlorocyclopropanes have been reported recently,[5,6] and it has been recognized that, at temperatures higher than 400°C, even these chemically stable cyclopropanes can be decomposed.

In this work, the pyrolysis reactions of *gem*-dibromocyclopropanes were mainly investigated. The results for *gem*-dihalocyclopropanes are summarized in Table 1. The pyrolysis products which could not be isolated were identified by the use of a mass spectrometer directly connected to a gas chromatograph.

1,1-Dichloro-2,2-dimethylcyclopropane (I-Cl) was pyrolyzed at 390°C to give 2-chloro-3-methylbutadiene. This reaction has already been reported by Robinson.[5] Similarly, 1,1-dibromo-2,2-dimethylcyclopropane (I-Br) gave 2-bromo-3-methylbutadiene as a sole product at lower temperatures.

The formation of the butadiene derivative may be attributed to the above-described cyclopropyl-allyl

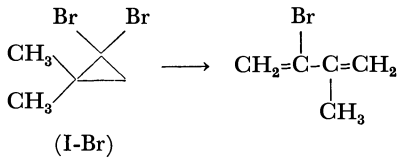

(I-Br) (1)

transformation, followed by the migration of the bromine atom, just as in the case of dichlorocyclopropanes. It must be noted that the ring opening is accompanied by the elimination of hydrogen bromide. As is well known, halogenated hydrocarbons easily decompose to olefins in the above temperature range, with the elimination of hydrogen halide. Therefore, dehydrohalogenation would seem to occur simultaneously with ring opening under the conditions studied in this work. This consideration is supported by the absence of ring-opened dibromides in the pyrolysis products.

The pyrolysis of 7,7-dibromonorcarane (III) gave cycloheptatriene as has been reported[6] for the high-temperature pyrolysis of 7,7-dichloronorcarane (II). However, the yield was relatively poor because of the carbonization of the starting material.

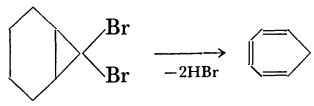

(III) (2)

II did not decompose in the temperature range studied in this work. 1,1-Dibromo-2-phenylcyclopropane (IV) gave complex products at 350°C which could not be identified.

The pyrolysis of monohalocyclopropanes was carried out under the same conditions as were used for dihalocyclopropanes. As it was very difficult to separate completely *cis*- and *trans*-isomers of monohalocyclopropanes by distillation, mixtures of the two isomers were pyrolyzed.

Bromocyclopropane (V) was prepared by the bromination of cyclopropane carboxylic acid.[7] The other monohalocyclopropanes were prepared by the reduction of the corresponding dihalocyclopropanes with tri-*n*-butyltin hydride. The ratio of the *cis* isomer to the *trans*

3) C. H. DePuy, L. G. Schnack, J. W. Hausser, and W. Wiedemann, *ibid.*, **87**, 4006 (1965).
4) P. von R. Schleyer, G. W. VanDine, U. Schöllkopf, and J. Paust, *ibid.*, **88**, 2868 (1966).
5) G. C. Robinson, *J. Org. Chem.*, **33**, 607 (1968).
6) G. C. Robinson, *ibid.*, **29**, 3433 (1964).
7) J. S. Meek and D. T. Osuga, "Organic Syntheses," Vol. 43, p. 9 (1963).

Table 2. Pyrolysis of monohalocyclopropanes

Cyclopropane	Pyrolysis temperature (°C)	Total pyrolysate (%)	Pyrolysis product	Yield (%)	Recovered cyclopropane (%)
V	303	61	$CH_2=CH-CH_2Br$	72	1
VI	300	34	$CH_2=C(CH_3)-CH=CH_2$	98	0
	210	49		90	0
VII	355	43		61	6
	300	53		56	5
	253	41		40	8
VIII	300	37	$CH(C_2H_5)=CH-CH=CH_2$	75	0
	250	34		66	0

one was determined by using a gas chromatograph and NMR as has been described by Seyferth.[8]

The pyrolysis of V gave allyl bromide as the main product. This bromide was identified by a comparison of its gas chromatograph with that of an authentic sample. The elimination of hydrogen bromide did not occur in this case.

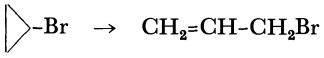

(3)

1-Bromo-2,2-dimethylcyclopropane (VI) was pyrolyzed almost completely at 300°C. None of the stereoisomers exist for this cyclopropane. Carbonization was not observed, and the single product was identified as isoprene. Isoprene is probably formed by the dehydrohalogenation after the rearrangement of VI to 2-bromo-2-methylbutene-1. However, the rearranged bromide was not found in the pyrolysis product.

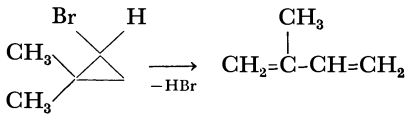

(4)

(VI)

A mixture of *exo*- and *endo*-7-bromonorcarane (VII) gave a hydrocarbon with a parent mass of 94. However, a considerable amount of the starting material was recovered. The hydrocarbon in the pyrolysate was separated by distillation and was identified as 1,3-cycloheptadiene by NMR and elemental analysis. On the other hand, the recovered starting material was

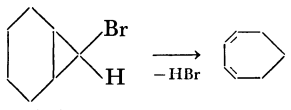

(5)

(VII)

found by gas-chromatographic analysis to be an almost pure *exo* isomer of VII. It is evident that the *endo* isomer was completely decomposed to 1,3-cycloheptadiene, while the *exo*-isomer was quite stable in the temperature range studied in this work.

A mixture of *cis*- and *trans*-1-bromo-2-propylcyclopropane (VIII) was pyrolyzed to give two major products with a parent mass of 82. The product formed in the higher yield may be *trans*-1,3-hexadiene, as the results of the NMR analysis indicate. The other product is probably *cis*-1,3-hexadiene, but no unambiguous assignment for the two isomers formed in this reactions was possible because of the presence of other components.

Monohalocyclopropanes with a phenyl group, *i.e.*, 1-bromo-2-phenylcyclopropane and 1-bromo-2-methyl-2-phenylcyclopropane, were also investigated. However, the products were complex and could not be identified.

The pyrolysis conditions for monohalocyclopropanes are summarized in Table 2.

In view of the pyrolysis product of V, it is rather surprising that the only product of the pyrolysis of VI was isoprene, which may be formed by the dehydrobromination of 3-bromo-3-methylbutene-1. Another possible bromide, 1-bromo-3-methylbutene-2, probably rearranges to 3-bromo-3-methylbutene-1 to form the same product.

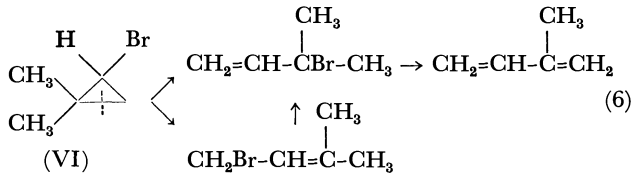

(6)

The lack of the reactivity of *exo*-norcaranyl compounds toward solvolysis reaction was attributed to its incapability of forming an intermediate allylic carbonium ion by the outward rotation of groups trans to the leaving group, as is shown in Fig. 1.[3]

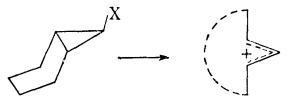

Fig. 1

Analogous considerations can possibly explain the great difference in the pyrolysis rates of *exo*- and *endo*-7-bromonorcarane. As is shown in Fig. 2, if the electrons of the C_2–C_3 bond move to the back face of the C_1–Br bond, as has been described by DePuy[3], the bromine atom would migrate to the C_2 or C_3 position along the lower side of the plane formed by the three-membered ring. On the other hand, if the electrons of the C_2–C_3 bond move to the same side of the bromine atom with respect to the cyclopropane ring, the bromine atom must go across the plane of cyclopropane to migrate to the C_2 or C_3 position.

8) D. Seyferth, H. Yamazaki, and D. L. Alleston, *J. Org. Chem.*, **28**, 703 (1963).

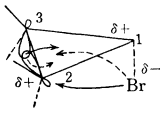

Fig. 2

In conclusion, in the pyrolytic rearrangement of halocyclopropanes, the direction of the rotation of the groups on the cyclopropane ring also obeys the rule proposed by DePuy,[3] *i.e.*, the groups *trans* to the halogen atom rotate outward, while the groups *cis* to the halogen atom rotate inward. As for the *exo* isomer VII, the groups *trans* to the bromine atom are ristricted by the cyclohexane ring. Therefore, the outward rotation of these groups is impossible.

Experimental

gem-Dihalocyclopropanes. Dihalocarbenes generated from haloform and potassium *t*-butoxide were added to the corresponding olefins, and finally purified by distillation.[9] The dihalocyclopropanes investigated in this work were 1,1-dichloro-2,2-dimethylcyclopropane (I-Cl) (bp 120—121°C), 1,1-dibromo-2,2-dimethylcyclopropane (I-Br) (bp 62—64°C/21 mmHg), 7,7-dichloronorcarane (II) (bp 78—79°C/15 mmHg), 7,7-dibromonorcarane (III) (bp 104°C/3 mmHg), and 1,1-dibromo-2-phenylcyclopropane (VI) (bp 110—112°C/4 mmHg).

Monohalocyclopropanes. These cyclopropanes were prepared by the reduction of the corresponding *gem*-dihalocyclopropanes with tri-*n*-butyltin hydride.[8] The monohalocyclopropanes thus obtained were mixture of *cis* and *trans* isomers. The clear separation of these isomers by distillation could not be achieved. The ratios of the *cis* isomer to the *trans* one were determined by gas chromatography with the aid of the NMR spectra, as has been reporyed bt Seyferth.[8]

1-Bromo-2,2-dimethylcyclopropane (VI)
bp 50—52°C/130 mmHg, lit,[8] 107—108°C.

7-Bromonorcarane (VII)
bp 86—96°C/28 mmHg, lit,[8] 94—109°C/24—27 mmHg.
cis/*trans* : 2.8.

1-Bromo-2-propylcyclopropane (VIII)
bp 52—54°C/33 mmHg, *cis*/*trans* : 2.0.

1-Bromo-2-phenylcyclopropane
bp 93—102°C/3 mmHg, lit,[8] 48—50°C/0.15 mmHg.

1-Bromo-2-methyl-2-phenylcyclopropane
bp 80—83°C/4 mmHg.

The accurate determination of the *cis*-to-*trans* ratios for the last two cyclopropanes were not possible because of their decompositions in the column of the gas chromatograph.

Bromocyclopropane (V) was prepared by the bromination of cyclopropane carboxylic acid[7] (bp 67—68.5°C, lit, 69°C).

Pyrolysis Apparatus. The pyrolysis reactions were carried out in a vertical electric furnace equipped with a calcium oxide column. From the top of the furnace, halocyclopropanes were introduced, drop by drop, with nitrogen as the carrier gas. The hydrogen halide evolved in the couse of the reaction was absorbed by calcium oxide. The gaseous pyrolysis products were condensed in a dry ice - methanol bath. The trapped pyrolysates were dried and distilled or were directly analyzed by gas chromatography. The pyrolysis temperature was 200—400°C.

Identification of Pyrolysis Products. 2-Chloro-3-methylbutadiene had a bp of 89—95°C (lit,[5] 91—101°C).

Found: C, 58.37; H, 7.05; Cl, 34.57%. Calcd for C_5H_7Cl: C, 58.55; H, 6.88; Cl, 34.73%.

2-Bromo-3-methylbutadiene had a bp of 36—37°C/35 mmHg, (lit,[10] 35°C/40 mmHg).

Found: C, 40.23; H, 4.79; Br, 54.88%. Calcd for C_5H_7Br: C, 40.85; H, 4.80; Br, 54.35%.

Cycloheptatriene had a bp of 53.5—55°C/97 mmHg, (lit,[6] 61°C/125 mmHg).

Found: C, 90.91; H, 8.37%. Calcd for C_7H_8: C, 91.25; H, 8.75%.

NMR signals (in carbon tetrachloride): $\tau=3.5$, 3.7, 4.7 (olefinic protons), $\tau=7.83$ (methylene protons, triplet).

The allyl bromide was identified by comparing the retention time of its gas chromatograph with that of an authentic sample.

Found: C, 30.04; H, 4.07; Br, 65.79%. Calcd for C_3H_5Br: C, 29.78; H, 4.17; Br, 66.05%.

The isoprene was also identified by gas chromatography using an authentic sample.

Found: C, 88.35; H, 11.85%. Calcd for C_5H_8: C, 88.16; H, 11.84%; mol wt (parent mass), 68.

1,3-Cycloheptadiene had a bp of 119—121°C (lit,[11] 121.5°C).

Found: C, 89.24; H, 10.90%. Calcd for C_7H_{10}: C, 89.29; H, 10.71%; mol wt (parent mass), 94.

NMR signals (in carbon tetrachloride): $\tau=4.33$ (olefinic protons), $\tau=7.69$, 8.10 (methylene protons).

The pyrolysis product of VIII was distilled to give a fraction of 67.5—73°C. The gas chromatograph of this fraction showed two major components, both of which have a parent mass of 82. The NMR signals indicate that the product formed in a higher yield may be *trans*-1,3-hexadiene.

Found: C, 86.79; 13.06%. Calcd for C_6H_{10}: C, 87.73; H, 12.27%.

NMR signals: $\tau=8.7$ (methylene protons), $\tau=9.0$ (methyl protons, triplet). The signals for the olefinic protons were complex and could not be assigned.

9) W. von E. Doering and A. K. Hoffmann, *J. Amer. Chem. Soc.*, **76**, 6162 (1954).

10) A. A. Petrov, *Zh. Obshch. Khim.*, **13**, 748 (1948).

11) J. B. Conn, G. B. Kistiakowsky, and E. A. Smith, *J. Amer. Chem. Soc.*, **61**, 1868 (1939).

The Anchoring Effect of the Fine, Powdery Copolymer of Glycidyl Methacrylate-Divinyl Benzene for Antioxidants in Polypropylene

Yukio MIZUTANI, Koshi KUSUMOTO, and Shigeo HISANO
Tokuyama Soda Co., Ltd., Tokuyama, Yamaguchi
(Received September 14, 1970)

The anchoring effect of the fine, powdery copolymer of glycidyl methacrylate-divinylbenzene, blended in polypropylene, for phenolic antioxidants was studied by the oxygen absorption method and by studying the infrared spectrum. As a result, the anchoring effect was recognized, and it was confirmed that the effect came from the reaction between the phenolic hydroxyl groups of antioxidants and the epoxy groups of the fine, powdery copolymer and that, furthermore, the anchoring effect was related to the molecular structure of the antioxidants. It is interesting to note that these results suggests that polymeric antioxidants practically overcome the defect of the migration or the volatility observed on low-molecular-weight antioxidants.

In a previous paper,[1] we reported that the fine, powdery copolymer of glycidyl methacrylate-divinylbenzene was useful as a mordant for the dyeing of polypropylene fiber, and showed the anchoring phenomena of the dye with the amino group in the substrate, a phenomena resulting from the reaction between the epoxy group of the fine, powdery copolymer and the amino group of the dye.

The reaction between the phenolic hydroxyl group and the epoxy group is well known.[2] These facts suggest that the fine, powdery copolymer might be effective in anchoring the phenolic antioxidant in polypropylene. This effect was studied by the oxygen-absorption method and by infrared spectroscopy.

Experimental

Materials. The polypropylene (PP) powder used contains no antioxidant. The properties were as follows: melt index (at 230°C, load; 2.16 kg/cm^2): 0.25 g/10 min, specific gravity (at 23°C): 0.912 g/cm^3, and grain size: under 30 mesh.

Fine, powdery copolymers (PFPC) of glycidyl methacrylate (GMA)-divinylbenzene (DVB) [PFPC-GD] and styrene (St)-DVB [PFPC-St] were prepared by the procedure described in the previous paper.[3] The synthetic conditions of PFPC and the epoxy values are shown in Table 1. The epoxy value was determined by the HCl-dioxane method.[4]

TABLE 1. SYNTHETIC CONDITIONS AND EPOXY GROUP CONTENT OF PFPC

PFPC	Condition		Epoxy group content
PEPC-GD	GMA	: 180 g	6.21 mmol/g-powder
	DVB	: 20 g	
	BPO	: 10 g	
	n-Heptane	: 2.8 *l*	
	at 70°C	5 hr	
PFPC-St	St	: 225 g	—
	DVB	: 25 g	
	BPO	: 10 g	
	iso-PrOH	: 2.5 *l*	
	at 70°C	4 hr	

1) Y. Mizutani, This Bulletin, **39**, 1088 (1966).
2) P. E. Parker, *Chem. Rev.*, **59**, 737 (1959).
3) Y. Mizutani, K. Yamamoto, and S. Matsuoka, This Bulletin, **39**, 1792 (1966).
4) G. King, *Nature*, **164**, 1106 (1949).

TABLE 2. STRUCTURAL FORMULAS OF ANTIOXIDANTS

	Structural formula
DVMP	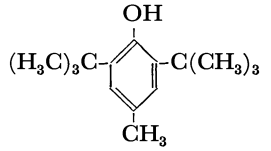
MTVP	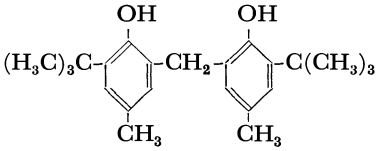
VHMP	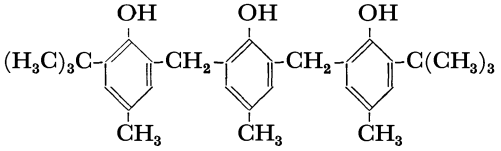
MDTP	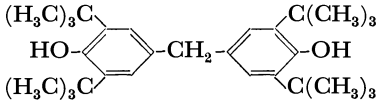
TTBP	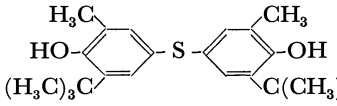
DLTDP	$S(CH_2CH_2COOC_{12}H_{25})_2$

The antioxidants used are shown in Table 2.

Preparation of Samples. PP powder and PFPC were mixed in a sufficient amount of methanol with a mixer. The polymer mixture thus obtained was filtered and dried in a vacuum at room temperature. Then, the polymer mixture was dipped into an acetone solution of the antioxidant, after which the acetone was evaporated at room temperature under reduced pressure. The mixture was extruded at 200—230°C with an extruder (Type MK-1, from the Modern Machinery Co., Ltd.) and then pelletized.

In order to obtain the specific surface area of the sample over the safe limit of the specific surface area for an oxygen-absorption reaction[5] and in order to eliminate the unreacted antioxidant, the pellets were dissolved in hot *p*-xylene under a nitrogen atomosphere, poured into methanol, filtered out, extracted with acetone for about 16 hr, and then dried in a vacuum at room temperature.

5) Y. Mizutani, H. Ihara, K. Yamamoto, and S. Matsuoka, *Kobunshi Kagaku*, **21**, 437 (1964).

The Measurement of Oxygen Absorption. The measurements were carried out with an apparatus previously described.[5] The reaction temperature was maintained by means of a vapor bath. As a vapor bath, monochlorobenzene, *p*-xylene, and a mixture of them with a trace of ethanol were used. The amount of oxygen absorbed was transformed into the value at 25°C and 760 mmHg.

The amount of oxygen absorbed gradually increased in the initial stage, and then it increased steadily. The oxygen absorption rate at the steady state (Kc, ml/min·g) was determined by the slope of the linear part of the oxygen absorption curve, and the induction period (P, min), by the extrapolation of the slope.[5]

The Measurement of the Infrared Spectrum. The spectrum was measured on a filmy sample with a Hitachi model EPI-G_2 spectrometer. For the accuracy of the experiment, an equimolar antioxidant (MTVP) to the epoxy-group of PFPC-GD was added, and the absorption intensity of the hydroxyl group of MTVP ($(\log I_0/I)/d$; where $\log I_0/I$ was the absorbance and d was the thickness of the film) was calculated. This value was used as a measure of the concentration of the antioxidant.

Results and Discussion

Anchoring Effect of PFPC-GD in the Practical Recipe. The compositions of the samples used are summarized in Table 3. DLTDP was used as a co-inhibitor.[6] P-1

Table 3. Compositions of samples in practical recipe

Sample	Added material,	wt %
P-1	MTVP	0.056
	DLTDP	0.110
P-2	PFPC-St	4.55
	MTVP	0.056
	DLTDP	0.110
P-3	PFPC-GD	4.55
	MTVP	0.056
	DLTDP	0.110

contains no polymeric, fine powder, and P-2 contains PFPC-St, which has no reactive group. These two samples were used as the reference samples. P-3 contains PFPC-GD, which has an epoxy group. Examples of the oxygen absorption curves of these three samples are shown in Fig. 1. It was observed that the induction period of the oxygen absorption curve of P-3 was longer than that of either reference sample, P-1 or P-2. The co-inhibitor (DLTDP) was not detected in these samples by studying the infrared spectrum. Therefore, the difference in the induction period shows that the antioxidant (MTVP) was anchored in PP resin and was not extracted with acetone. In P-2, the anchoring effect was not observed, because PFPC-St had no reactive group. These results suggest that the anchoring effect comes from the reaction between the epoxy groups of PFPC-GD and the phenolic hydroxyl groups of the antioxidant (MTVP).

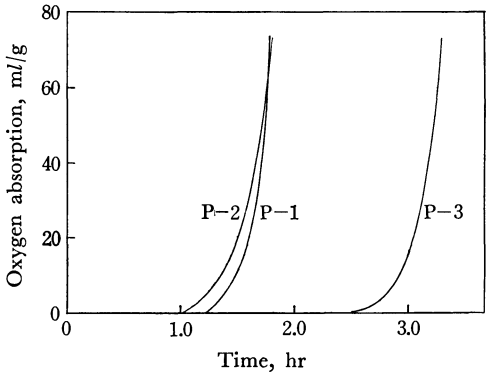

Fig. 1. Oxygen absorption curves in practical recipe at 133°C.

The reciprocal of the induction period ($1/P$) and oxygen absorption rate at the steady state (K_c) were obtained from the oxygen absorption curves at various

Table 4. The values of $1/P$ and Kc at various temperature in the practical recipe

Sample		Reaction temp., °C			
		133	128.6	125	121
P-1	$(1/P)\times10^2$, min^{-1}	1.11	0.781	0.602	0.417
	K_c, ml/min·g	4.3	3.5	2.2	1.0
P-2	$(1/P)\times10^2$, min^{-1}	1.36	0.877	—	0.426
	K_c, ml/min·g	4.3	2.8	—	0.9
P-3	$(1/P)\times10^2$, min^{-1}	0.549	0.444	0.355	0.448
	K_c, ml/min·g	4.6	2.6	2.1	0.68

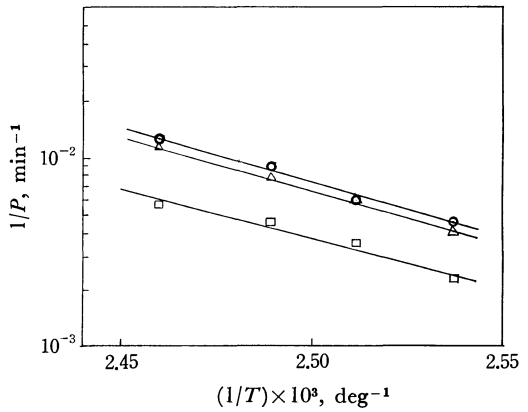

Fig. 2. Arrhenius plot of $1/P$ in practical recipe.
△: P-1, ○: P-2, □: P-3

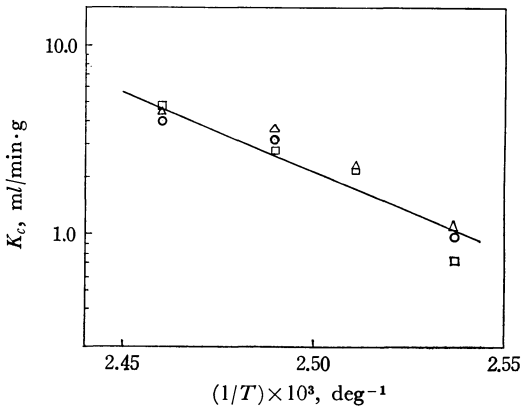

Fig. 3. Arrhenius plot of K_c in practical recipe.
△: P-1, ○: P-2, □: P-3

6) N. P. Neureiter and D. E. Bown, *Ind. Eng. Chem., Prod. Res. Develop.*, **1**, 236 (1962).

temperatures, as is shown in Table 4. The activation energy of the reaction in the induction region (E_t) and that in the steady state (E_s) were calculated from the Arrhenius plots shown in Fig. 2 and Fig. 3. The values of the activation energies were as follows: E_t=25—28 kcal/mol and E_s=40 kcal/mol. These values almost correspond with those reported in a previous paper[5] (E_i=22 kcal/mol, E_s=43 kal/mol).

Confirmation of the Reaction between PFPC-GD and MTVP by Studying the Infrared Spectrum in a Model Recipe. The polypropylene powder in a model recipe contains 4.6 wt% ofPFPC-GD and 3.2 wt% of MTVP.

The infrared spectra of the samples investigated are shown in Fig. 4. P-4-1 consisted of pellets obtained by

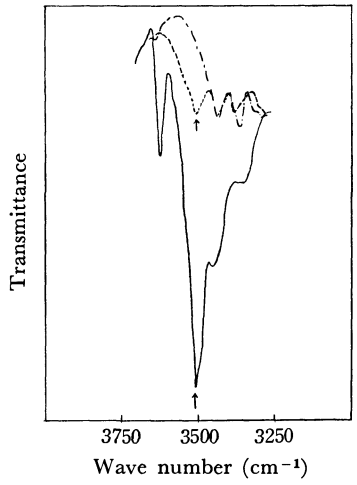

Fig. 4. Infrared spectra in model recipe.
——— Reference, —— P-4-1, ---- P-4-2, P-4-3, P-4-4

extruding the PP powder of the model recipe, P-4-2 consisted of the powder obtained by treating the pellets with hot *p*-xylene, and P-4-3, and P-4-4 consisted of the powder extracted with acetone. As the reference sample, pellets without any added MTVP were used. The infrared spectra of P-4-2, P-4-3, and P-4-4 were identical. The absorption band at 3510 cm^{-1} was assigned to the characteristic band of the phenolic hydroxyl groups of MTVP, and the absorption intensities of the band were calculated. The results are shown in Table 5. The constancy of the value under treatment

TABLE 5. THE CHANGE OF ABSORPTION INTENSITY IN THE MODEL RECIPE

Sample[a]	Time of aceton-extraction (hr)	$(\log I_0/I)/d$[d]
P-4-1[b]	—	20.3
P-4-2[c]	—	2.7
P-4-3	6	2.8
P-4-4	16	2.8

a) PFPC-GD: 4.6 wt%, MTVP: 3.2 wt%.
b) Pellets after extruding.
c) Powder obtained by treating with hot *p*-xylene.
d) Based upon the value of reference sample, PP+PFPC-GD.

with hot *p*-xylene (P-4-2) and the extraction time with acetone shows that the antioxidant (MTVP) reacted with PFPC-GD and was anchored in PP resin.
The decrease in the absorption intensity upon treatment with hot *p*-xylene or upon extraction with acetone shows that the degree of the reaction of MTVP with PFPC-GD was low. For reference, the induction period of the oxygen-absorption reaction of P-4-3 at 128°C was over 10 hr.

Influence of the Molecular Structure of Antioxidants on the Anchoring Effect. If the reactivities of the phenolic hydroxyl groups are equal, it seems that quantity of antioxidants to be anchored will be greater as the numbers of the hydroxyl groups in a molecule increases. Also when the numbers of the hydroxyl groups are equal, it seems that the quantity will be mainly due to the reactivity of the hydroxyl group. In order to confirm the above suppositions, oxygen absorption curves on various antioxidants are compared in Fig. 5. The anti-

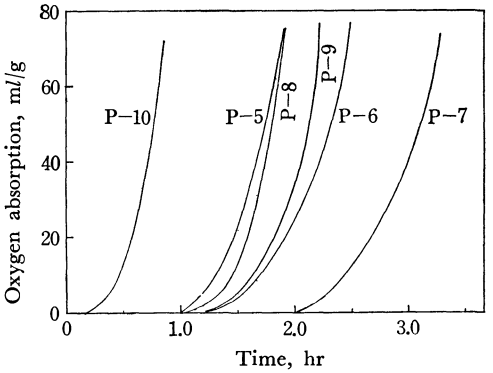

Fig. 5. Influence of the molecular structure of antioxidants on anchoring effect. (at 129°C)

oxidants used and the quantities added, which were so fixed that the quantities of the phenolic hydroxyl groups were equal, are shown in Table 6. Figure 5 shows that

TABLE 6. NUMBERS OF PHENOLIC HYDROXYL GROUPS AND QUANTITIES OF ANTIOXIDANTS ADDED

Sample[a]	Antioxidant	Number of -OH in a molecule	Antioxidant added mmol/g
P-5	DVMP	1	4.0×10^{-3}
P-6	MTVP	2	2.0×10^{-3}
P-7	VHMP	3	1.3×10^{-3}
P-8	MDTP	2	2.0×10^{-3}
P-9	TTBP	2	2.0×10^{-3}
P-10	—	—	—

a) PFPC-GD content: 4.6 wt%.

the induction period increases as the number of hydroxyl group increases. Also, the induction period increased in such an order as: P-8 (MDTP) <P-9 (TTBP) <P-6 (MTVP); this order may be mainly due to the decrease in the steric hindrance to the hydroxyl groups of antioxidants, as can be guesssed from the molecular structure. However, it has not yet been explained why the induction period of P-5 (DVMP)(shown in Fig. 5), the one phenolic hydroxyl group of which may be consumed in the reaction with the epoxy groups of PFPC-GD was longer than that of P-10.

The authors wish to thank Professor Y. Takegami of the Faculty of Engineering, Kyoto University, for his valuable advice.

NOTES

BULLETIN OF THE CHEMICAL SOCIETY OF JAPAN, VOL. 44, 1137—1139(1971)

Intramolecular Hydrogen Bonds. XVI.[1] Preferable Conformation of 1-Tetralols

Nobuo Mori, Mitsuo Yoshifuji, Yoshihiro Asabe, and Yojiro Tsuzuki
Department of Chemistry, Science University of Tokyo, Kagurazaka, Shinjuku-ku, Tokyo
(Received July 10, 1970)

It has recently been suggested[2,3] that, for the OH–π interaction in 1-tetralols, the *quasi-equatorial* conformation of the hydroxyl group is preferable to the *quasi-axial* one. This seems contradictory if the hydrogen-accepting site is the π-electrons on the 9-position as in benzyl alcohols,[4] because examination of the model shows that the *quasi-axial* conformation is sterically preferable for the interaction. In order to solve this problem, the steric and electronic effects of substituents on the infrared OH spectra of 1-tetralols have been investigated in their dilute carbon tetrachloride solutions.

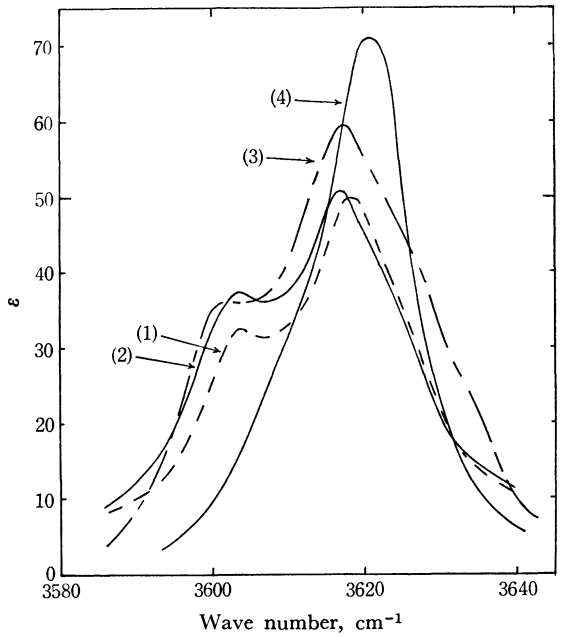

Fig. 1. OH Spectra of 1-tetralols: unsubst. (1), 7-methoxy (2), 7-nitro (3), and 5,8-dimethyl (4).

The OH spectra of 1-tetralols and 1-methyl-1-tetralols, which consist of two split bands, are in contrast with each other (Figs. 1 and 2). In the former the higher-frequency band is stronger, while in the latter the lower-frequency band is stronger, and the weaker bands of both spectra almost disappear by the 8-methyl substitution. The following can be considered as reasons for band splitting: (1) interaction between the OH group and the π-electrons,[4,5] (2) rotational isomerism of the OH group about the C–O bond,[4,5] and (3) conformational isomerism of the OH group to be caused by the ring conversion of the saturated-ring portion. The observed spectra should be contributed by different OH species. However, the pronounced spectral change by the 8-methyl substituent can be explained mainly by (3), *viz.*, by the conformational interconversion of the saturated-ring portion resulting from the steric interaction between the *quasi-equatorial* 1- and the 8-substituents, because the 8-substituent is not expected to have a similarly significant influence on (1) and (2). It thus appears that the steric repulsion between the *quasi-equatorial* 1- and the 8-substituents is sufficiently high to overcome the steric interaction between the *quasi-axial* 1-substituent and the *axial* 3-hydrogen atom.[6] Therefore, the hydroxyl groups in 1-tetralols are preferably in a *quasi-axial* conformation, while in 1-methyl-1-tetralols they are in a *quasi-equatorial* conformation, as can be expected from the oridnary order of steric size: H<OH<CH_3.

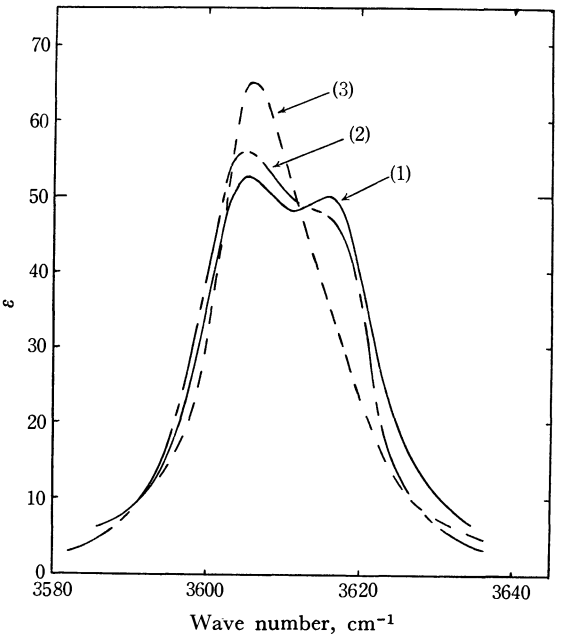

Fig. 2. OH Spectra of 1-tetralols: 1-methyl (1), 1-methyl-7-methoxy (2), and 1,5,8-trimethyl (3).

The higher- and the lower-frequency bands can thus be assigned to the *quasi-axial* and *-equatorial* OH groups,

1) Part XV; N. Mori, Y. Asabe, J. Tatsumi, and Y. Tsuzuki, This Bulletin, **43**, 3227 (1970).
2) K. Hanaya, *Nippon Kagaku Zasshi*, **90**, 314 (1969).
3) K. Hanaya, *ibid.*, **91**, 82 (1970).
4) M. Ōki and H. Iwamura, This Bulletin, **32**, 955 (1959); **35**, 1552 (1962).
5) M. Ōki and H. Iwamura, This Bulletin, **32**, 950 (1959).
6) A similar effect of steric interaction is recognized in several 1-substituted cyclohex-2-enes.[3,7]
7) E. W. Garblish, Jr., *J. Org. Chem.*, **27**, 4249 (1962).

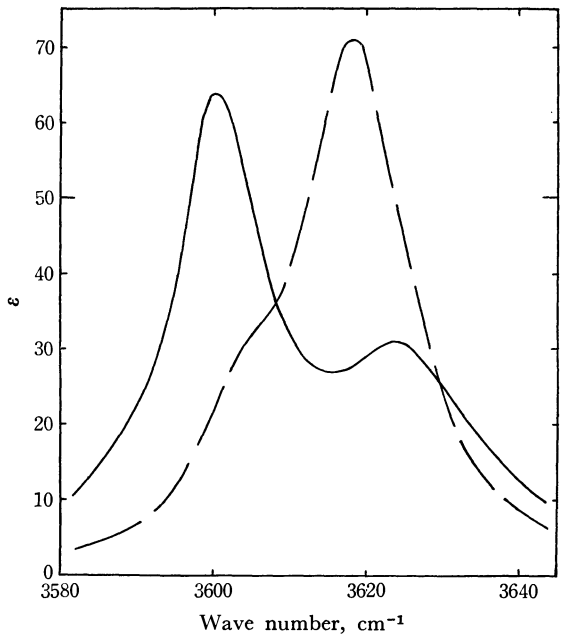

Fig. 3. OH Spectra of *cis*- and *trans*-3-phenyl-1-tetralols: *cis* (——), *trans* (— —).

respectively. They probably contain further absorption bands due to the other OH species, such as their conformational and/or rotational isomers, to some extent.

In the interaction with the π-electrons, the observed effect of a 7-substituent on the intensity ratio indicates that one or both of the *quasi-axial* and *-equatorial* OH groups participate. The *quasi-equatorial* one evidently interacts, since the frequency is lower than both of the free ν_{OH} values (3627 and 3620 cm^{-1}) and the interacted ν_{OH} values (3616 and 3607 cm^{-1}) of α-phenylethanol and -isopropanol.[4] Substantially all the OH species in the *quasi-equatorial* conformation seem to interact, since 1,5,8-trimethyl-1-tetralol shows, apart from a very intense band of the *quasi-equatorial* interacted OH group, only a very low unsymmetry due to other OH species on the higher-frequency side.

Whether the *quasi-axial* OH group interacts is not clear on account of the fact that the OH frequencies of 1-tetralols are very close to the interacted OH frequency of α-phenylethanol, while those of 1-methyl-1-tetralols are close to the free OH frequency of α-phenylisopropanol. However, there are several suggestions for the *quasi-axial* OH group to be free; if it is assumed that *trans*-3-phenyl-1-tetralol is fixed in such a conformation that the hydroxyl and the phenyl group are *quasi-axial* and *equatorial*, respectively, the strong band observed at 3618 cm^{-1} should be assigned to the free OH species, with the unsymmetry of the band being attributable to the rotational isomerism about the C–O axis or the interacted OH species. The same assignment should be given for the unsymmetric band of 5,8-dimethyl-1-tetralol whose OH group should preferably be *quasi-axial*. If interaction take place, the *quasi-axial* OH group would be prone to an electronic effect of substituents. However, even the 7-nitro substitution results in no appearance of a significant band on the higher-frequency side, suggesting that the *quasi-axial* OH group is practically free, and the observed intensity ratio of the two bands (*quasi-axial* to *quasi-equatorial*) increases with the 7-substituents in the order: $CH_3O<H<NO_2$, suggesting that the electronic effect is operative on the *quasi-equatorial* OH group and the interaction between this group and the π-electrons becomes weaker in that order, thereby some of the interacted OH species becoming free and then *quasi-axial*. For the electronic effect of substituents, a further study of 5- and 6-substituted 1-tetralols would be desirable.

In the case of isomeric 3-phenyl-1-tetralols[8] (Fig. 3), the *trans* isomer may exist predominantly in a conformation with the *quasi-axial* OH group, as mentioned above. The *cis* isomer exists in two conformations; one con-

Table 1. Physical constants and apparent spectral data of 1-tetralols

Substituents in 1-tetralols	Mp (Bp) °C	ν_{OH}, cm^{-1}		
		*q.-ax.*OH (ε_a)	*q.-eq.*OH (ε_e)	$\varepsilon_a/\varepsilon_e$
Unsubstituted[9]	(126/12)	3618 (50)	3603 (32)	1.56
7-Methoxy[10]	38.2— 38.7	3616 (51)	3603 (37)	1.39
7-Nitro[11]	108 —108.5	3614 (60)	3601 (36)	1.67
5,8-Dimethyl[12]	92.0	3621 (65)		
		3610[a]		
1-Methyl[13]	88.5— 89.0	3616 (50)	3605 (53)	0.94
1-Methyl-7-methoxy	68 — 69	3616 (47)	3605 (56)	0.84
1,5,8-Trimethyl[14]	136	3615[a]	3606 (71)	
3-Phenyl (*cis*)[b]	99.5—100.5	3624 (31)	3600 (64)	0.46
(*trans*)[b]	98.5— 99.5	3618 (71)		
		3603[a]		

a) ν_{OH} at the shoulder part (the assignment is uncertain).

b) Configuration was determined by NMR spectroscopy.[15]

8) In the presence of a shoulder, the spectrum of the *trans* isomer differs somewhat from that reported by Hanaya,[2] probably because of the different temperatures of measurement (25°C in Hanaya's work, 20°C in our work).

9) F. Strauss and L. Lemmel, *Ber.*, **54**, 25 (1921).

10) D. G. Thomas and A. H. Nathan, *J. Amer. Chem. Soc.*, **70**, 331 (1948).

11) Y. Asahina and T. Momose, *Yakugaku Zasshi*, **64**, 154 (1944).

12) W. Cocker, B. E. Cross, J. T. Edward, D. S. Jenkinson, and J. McCormick, *J. Chem. Soc.*, **1953**, 2355.

13) T. Kusama and D. Koike, *Nippon Kagaku Zasshi*, **72**, 683 (1951).

14) E. D. Barnett and F. G. Sanders, *J. Chem. Soc.*, **1933**, 434.

tains the OH group in the *quasi-axial* conformation and the other, in the *quasi-equatorial* one. Preference of the latter indicates that the steric interaction between the *quasi-axial* 1-hydroxyl and the *axial* 3-phenyl group is higher than that between the *quasi-equatorial* 1-hydroxyl group and the 8-hydrogen atom. Accordingly, our spectral data support the configurations proposed by Mitsui *et al.* on the basis of NMR spectroscopy.[15]

Experimental

Samples. All the tetralols, except for 1-methyl-7-methoxy-1-tetralol, were prepared and purified by the methods described in the literature. Isomeric 3-phenyl-1-tetralols were further purified through chromatography on silica gel using a mixture of hexane and benzene. Their melting and/or boiling points were equal, or very close, to those reported. The above 7-methoxy-compound was prepared in the usual manner[13] from 7-methoxy-1-tetralone. (Found: C, 75.16; H, 8.50%. Calcd for $C_{12}H_{16}O_2$: C, 74.97; H, 8.39%).

Infrared Measurement. This was carried out at *ca.* 20°C in the same manner as described previously.[1] The concentration used was 0.003 mol/*l* in carbon tetrachloride and the cells used had a path-length of 5.0 cm.

The spectral data are summarized in Table 1 together with the physical constants.

15) S. Mitsui, A. Kasahara, and K. Hanaya, This Bulletin, **41**, 2526 (1968).

BULLETIN OF THE CHEMICAL SOCIETY OF JAPAN, VOL. 44, 1139—1141 (1971)

The Syntheses and Hydrolyses of *p*-Substituted Phenyl Phosphosulfates[1]

Waichiro TAGAKI, Toshio EIKI, and Itsuya TANAKA

Department of Chemistry, Faculty of Technology, Gunma University, Kiryu, Gunma

(Received August 5, 1970)

Very recently, Benkovic and Hevey have reported a study on the mechanism of nonenzymatic hydrolysis of phenyl phosphosulfate.[2] Independently, we have also been investigating the mechanism of the hydrolysis of the same compound. Since little is known about the chemistry of phosphosulfate linkage and in view of its importance for biochemistry,[3] it seems to be significant to report our own results. In this paper, we will describe the syntheses and hydrolyses of *p*-substituted phenyl phosphosulfates (PPS, I).

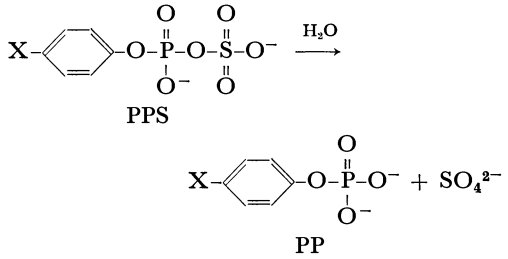

PPS

PP

I. X=CH_3O, CH_3, H, Cl (diammonium salts)

Results and Discussion

Syntheses of PPS (I). Pyridine-SO_3 complex has been used for the preparation of PPS.[2] However much better yield of PPS (usually 60—70%) was obtained when the reaction was conducted using the diammonium salts of PP and dimethylformamide (DMF)-SO_3 complex in DMF.

Hydrolyses of PPS. The products were found to be exclusively phenyl phosphate (PP) and inorganic sulfate under both alkaline and acidic conditions.

1. The rate of alkaline hydrolysis was first order with respect to the hydroxide ion concentration in a range of [NaOH]=0.01—1.0 M. The substituent effect was larger than that for the acidic hydrolysis (Fig. 1). The value of entropy of activation (Table 1) was in the range expected for a bimolecular reaction.[4]

In an alkaline solution, the major ionic form of PPS is undoubtedly the dianion. This dianion would undergo a nucleophilic attack by hydroxide ion on either sulfur or phosphorus to give PP and inorganic sulfate in the rate determining step. An alternative mechanism is a rate determining unimolecular fission of S-O bond of

Table 1. Kinetics of hydrolyses of unsubstituted phenyl phosphosulfate

	Reagent	Temp., °C	$k_{obs}\times 10^4 sec^{-1}$	
1.	Alkaline hydrolysis			
	0.5N NaOH	70	1.31	
	0.5N NaOH	85	3.43	E_a=15.9 kcal/mol
	0.5N NaOH	98	7.65	$\Delta S^{\neq}$=−32.5 e.u. (98°C)
2.	Acidic hydrolysis			
	0.5N HCl	17.8	8.55	
	0.5N HCl	30	33.8	E_a=20.3 kcal/mol
	0.5N HCl	39.5	99.5	$\Delta S^{\neq}$=−4.9 e.u. (30°C)
	0.5N DCl[a]	30	98.5	k^{D_2O}/k^{H_2O}=2.91 (30°C

a) In D_2O

1) A part of this study has been reported at the 23rd Annual Meeting of the Chemical Society of Japan, April 4, 1970, Tokyo.

2) S. J. Benkovic and R. C. Hevey, *J. Amer. Chem. Soc.*, **92**, 4971 (1970).

3) a) P. W. Robbins and F. Lipmann, *ibid.*, **78**, 2652, 6409 (1956); b) P. W. Robbins and F. Lipmann. *J. Biol. Chem.*, **229**, 837 (1957); c) P. W. Robbins and F. Lipmann, *ibid.*, **233**, 686 (1958); d) F. Lipmann, *Science*, **128** 575 (1958).

4) F. A. Long, J. G. Pritchard, and F. E. Stafford, *ibid.*, **79**, 2363 (1957).

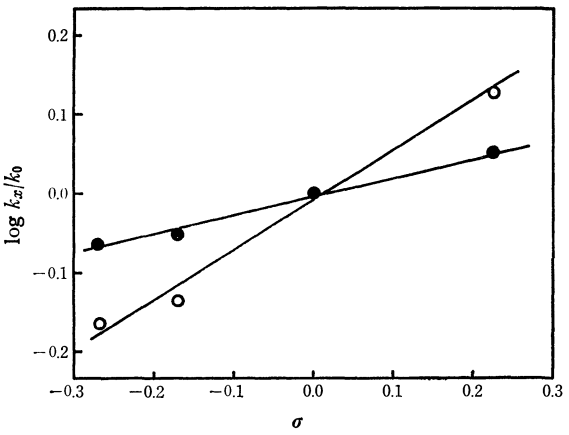

Fig. 1. Hammett substituent effect for the hydrolyses of *p*-substituted phenyl phosphosulfates.
●: 0.8N HCl, 30°C, $\rho=0.22$
○: 0.01N NaOH, 98°C, $\rho=0.67$

PPS to give PP and sulfur trioxide. The above results seem to support the first bimolecular mechanism.

2. The rate of acidic hydrolysis was first order with respect to the hydronium ion concentration in a range of $-\log[H^+]=0-2$. The ρ value for the substitution effect was small (Fig. 1). Such small ρ values have also been observed in the hydrolyses of sulfates[5] and phosphates[6] of substituted phenols, and the values have been interpreted as to support A-1 type mechanisms. The value of entropy of activation (Table 1) was appreciably larger than that for the alkaline hydrolysis and is consistent with that expected for an A-1 type solvolysis. The solvent isotope effect (Table 1) was also in the range expected for an A-1 type mechanism.[7]

Experimental

DMF-SO_3 solution was prepared by distilling SO_3 into anhydrous DMF, and the concentration of SO_3 was estimated by an alkaline titration and by the yield of *p*-nitrophenyl sulfate (obtained by the reaction wih sodium *p*-nitrophenoxide). *DCl-D_2O solution* (5N) for the determination of the isotope effect was prepared by dissolving dry DCl gas in D_2O (99.8%, Showa Denko).

p-*Substituted Phenyl Phosphorodichloridates* were prepared by the reaction of phenols and $POCl_3$ at 110°C and the desired fractions were collected by distilling the reaction mixture under reduced pressure.[8]

p-*Substituted Phenyl Phosphates (PP)* were prepared by the hydrolyses of the above dichloridates in water at room temperature:[8] *p*-substituent, mp (°C); CH_3O, 90—100; CH_3, 113—114; H, 99—100; Cl, 123—124.

Diammonium salts of p-*Substituted Phenyl Phosphosulfates (PPS, 1).* The diammonium salt of unsubstituted PP (2.0g, 9.6 mmol) was dissolved in DMF solution (16*ml*) of DMF-SO_3 complex (14.4 mmol), and this reaction mixture was left at room temperature for one hour. The reaction mixture was then cooled down to about −50°C and neutralized with a saturated ethanol solution of ammonia to give somewhat pasty mass. This mixture was allowed to warm up to room temperature and ether was added to effect further precipitation. The solid was collected by filtration, and then dissolved in ethanol and filtered again to remove some insoluble solid. The filtrate was concentrated to give colorless needles. This was recrystallized twice from ethanol ether mixture to give pure diammonium salt of PPS, yield 1.7 g. A small amount of the starting PP was recovered from the mother liquor.

The other substituted PPS were prepared similarly. The R_f values of paper chromatography and elementary analyses of thus obtained diammonium salts of PPS are shown in Tables 2 and 3.

Table 2. The R_f values in paper chromatography[a]

Substituent	Phenyl phosphosulfate[b]	Phenyl phosphate
CH_3O	0.67	0.50
CH_3	0.72	0.54
H	0.65	0.48
Cl	0.77	0.60
	SO_4^{2-}[b]	HPO_4^{2-}[b]
	0.33	0.0

a) Conditions: paper, Toyo Filter Paper No. 50; solvent, *n*-PrOH: NH_3: H_2O=6: 3: 1 v/v
b) Diammonium salts

Table 3. The elementary analyses of the diammonium salts of *p*-substituted phenyl phosphosulfates (PPS)

Substituent	Found (Calcd)			
	C%	H%	N%	P%[a]
CH_3O	26.75	4.89	7.65	9.78
	(26.42	4.75	8.81	9.74)
CH_3	27.50	5.03	8.25	10.09
	(27.82	5.00	9.25	10.25)
H	24.64	4.43	9.88	10.98
	(25.02	4.51	9.72	10.77)
Cl	23.33	4.45	9.02	
	(22.33	3.74	8.68)	

a) Determined by the method of Fleury and Leclere (P. Fleury and M. Leclere, *Bull. Soc. Chim. Biol.*, **25**, 201 (1943)).

The following UV absorption maxima were observed for the substituted PPS and PP in alkaline solutions. a) For PPS, *p*-substituent and λ_{max} in mμ (ε_{max}) were: CH_3O, 276 (1420); CH_3, 267 (720); H, 260 (440); Cl, 269 (530). b) For PP: CH_3O, 280(1830); CH_3, 274(1100); H, 267(740); Cl, 274(840).

Kinetics. a) Alkaline hydrolysis. An alkaline solution of PPS (1.0×10^{-3}M) was sealed in 10 ampoules and kept in a constant temperature bath. At suitable time intervals, an ampoule was withdrawn and chilled in an ice-water bath, and the optical density of the content was recorded at the absorption maximum of PP which increased smoothly as the reaction proceeded. From this optical density change, good first order rate costants (deviation, within ±3%) were calculated by using an equation, $k_{obs}=1/t \ln (OD_\infty-OD_0)/(OD_\infty-OD_t)$.

At high temperature (98°C) and with a high hydroxide ion concentration (>0.5 N NaOH), further hydrolysis was observed giving an absorption at 290 mμ due to the formation of phenoxide ion. However, the amount of phenol produced at the end

5) E. J. Fendler and J. H. Fendler, *J. Org. Chem.*, **33**, 3852 (1968).
6) G. Disabato and W. P. Jencks, *J. Amer. Chem. Soc.*, **83**, 4400 (1961).
7) C. A. Bunton and V. J. Shiner, *ibid.*, **83**, 3207 (1961).
8) H. F. Freeman and C. W. Colver, *ibid.*, **60**, 750 (1938).

of reaction was estimated to be less than 1%, and therefore the correction of optical density for the phenol formation was neglected. Plots of log k_{obs} against log[OH^-] gave a straight line with a slope=1.0. Other data are shown in Table 1 and Fig. 1.

b) Acidic hydrolysis. Aqueous solutions of PPS and HCl were temperature equilibrated and mixed to make a reaction mixture containing PPS, 1.0×10^{-2}M, and the acid of desired concentration. A part of this reaction mixture was quenched at suitable time intervals by diluting with an alkaline solution (to 1.0×10^{-3}M of PPS) and the optical density change was recorded as described above. The formation of phenol was not detected. Plots of log k_{obs} against log[H^+] gave a straight line with a slope=1 as observed by Benkovic and Hevey.[2] Other data are shown in Table 1 and Fig. 1.

This research has been initiated at the laboratory directed by Professor Shigeru Oae at Osaka City University. The authors wish to thank Professor Oae and the members of his research group.

BULLETIN OF THE CHEMICAL SOCIETY OF JAPAN, VOL. 44, 1141—1143(1971)

The Photodecomposition of *N*-Bromosulfonamides

Takehisa OHASHI, Mitsuo OKAHARA, and Saburo KOMORI

Department of Applied Chemistry, Faculty of Engineering, Osaka University, Yamadakami, Suita, Osaka

(Received August 18, 1970)

In a previous paper,[1] the present authors reported a competitive hydrogen abstraction by the chlorine atom and the sulfonamide radical, and the predominant intramolecular hydrogen abstraction by the sulfonamide radical in an aqueous solution in the photodecomposition of *N*-alkyl-*N*-chloroalkanesulfonamides. It has also been reported[1,2] that *N*-*t*-butyl-*γ*-bromo-*n*-butanesulfonamide was formed in the photodecomposition of *N*-bromo-*N*-*t*-butyl-*n*-butanesulfonamide, unlike the result[1] obtained in the photodecomposition of *N*-*t*-butyl-*N*-chloro-*n*-butanesulfonamide. In this experiment, the photodecomposition of *N*-alkyl-*N*-bromo-*n*-alkanesulfonamides was investigated in order to study hydrogen abstraction by the sulfonamide radical.

N-Alkyl-*N*-bromo-*n*-alkanesulfonamides were prepared by the treatment of *N*-alkyl-*n*-alkanesulfonamides with freshly-prepared NaOBr in a buffer solution (Table 1). The results of the photodecomposition of *N*-bromosulfonamides are listed in Table 2. In the reaction of *N*-bromo-*N*-*t*-butyl-*n*-hexanesulfonamide in benzene, glpc and NMR analyses showed the formation of *N*-*t*-butyl-*γ*-bromo- (I) and *N*-*t*-butyl-*δ*-bromohexanesulfonamide (II), while the *ε*-bromo isomer was not formed. This suggests that the *γ*-and *δ*-bromo isomers were formed *via* intramolecular 1,5 and 1,6 hydrogen transfer by the sulfonamide radical, and that no intermolecular hydrogen abstraction by the sulfonamide radical or the bromine atom occurs; this is distinct from the result[1] observed in the reaction of *N*-*t*-butyl-*N*-chloro-*n*-hexanesulfonamide, in which the participation of the chlorine atom was observed. This must be due to the difference in reactivity between bromine and chlorine.

The isomer ratio (I/II=1.96—1.98) in this reaction was similar to that (*N*-*t*-butyl-*γ*-chlorohexanesulfonamide/*N*-*t*-butyl-*δ*-chlorohexanesulfonamide=1.93—1.94) observed in the reaction of *N*-*t*-butyl-*N*-chloro-*n*-hexanesulfonamide in an aqueous solution (AcOH/H_2O=2.1)[1]; a similar value (I/II=2.04) was obtained in the reaction of *N*-bromo-*N*-*t*-butyl-*n*-hexanesulfonamide in the AcOH–H_2O system. These facts support the hypothesis described in the previous paper[1] that the reactivity of the chlorine atom is retarded by solvation, that the predominant intramolecular hydrogen abstraction by the sulfonamide radical occurs in an aqueous solution, and that the reactivity in the hydrogen abstraction of the sulfonamide radical in the aqueous solution does not differ from that of the sulfonamide radical in benzene. The same result was obtained in the reaction of *N*-bromo-*N*-*t*-butyl-*n*-pentanesulfon-

TABLE 1. PROPERTIES AND ANALYSES OF *N*-BROMOSULFONAMIDES

RSO_2NBrR'	n_D	IR, cm^{-1}	UV[a] λ_{max}, nm(ε)	Br, %[b]
R=*n*-C_3H_7 R'=*t*-C_4H_9	1.4910[c]	2960, 1350, 1150, 890	315 (148)	30.7 (30.95)
R=*n*-C_4H_9 R'=*t*-C_4H_9	1.4955[d]	2960, 1340, 1145, 890	317 (149)	29.2 (29.36)
R=*n*-C_4H_9 R'=Me	1.5047[d]	2960, 1340, 1150, 790	310 (136)	34.5 (34.72)
R=*n*-C_5H_{11} R'=*t*-C_4H_9	1.4950[c]	2960, 1340, 1145, 890	318 (131)	27.6 (27.91)
R=*n*-C_6H_{13} R'=*t*-C_4H_9	1.5030[c]	2960, 1340, 1150, 890	320 (115)	26.5 (26.61)

a) In cyclohexane.
b) Values in parentheses are calculated values.
c) n_D^{32} d) n_D^{20}

1) T. Ohashi, S. Takeda, M. Okahara, and S. Komori, This Bulletin, **44**, 771 (1971).

2) R. S. Neale and N. L. Marcus, *J. Org. Chem.*, **34**, 1808 (1969).

Table 2. Photodecomposition of *N*-bromosulfonamides[a)]

RSO_2NBrR'		Concn. mol/*l*	React. time, min	Recovery rate,[c)] %	Composition[b)] of reaction product			
					I %	II %	III %	Isomer ratio, II/III
R=*n*-C_6H_{13}	R'=*t*-C_4H_9	0.2 in benzene	35	95	16.4	55.3	28.2	1.96
R=*n*-C_6H_{13}	R'=*t*-C_4H_9	0.4 in benzene	30	92	22.8	50.5	25.5	1.98
R=*n*-C_5H_{11}	R'=*t*-C_4H_9	0.2 in benzene	30	96	7.0	50.0	42.1	1.19
R=*n*-C_4H_9	R'=*t*-C_4H_9	0.2 in benzene	25	94	20.0	79.3	—	—
R=*n*-C_4H_9	R'=*t*-C_4H_9	0.2 in CCl_4	40	94	17.3	82.1	—	—
R=*n*-C_4H_9	R'=*t*-C_4H_9	0.2 in *t*-BuOH-H_2O[d)]	120	82	35.7	64.0	—	—
R=*n*-C_3H_7	R'=*t*-C_4H_9	0.2 in benzene	20	92	28.0	72.5	—	—
R=*n*-C_6H_{13}	R'=*t*-C_4H_9	0.2 in AcOH-H_2O[e)]	180	71	57.1	28.4	13.9	2.04
R=*n*-C_4H_9	R'=Me	0.2 in benzene	40	78	58.3	28.1[f)]	—	—

a) N_2 flow rate is 150m*l*/min.
b) Determined by glpc (wt %).
c) (The weight of the product obtained/the weight of *N*-bromosulfonamide) × 100
d) *t*-BuOH/H_2O=1.7 (volume ratio)
e) AcOH/H_2O=2.1 (volume ratio)
f) In addition to the compounds listed, the high molecular weight of product was observed (*m/e*=320).
I=RSO_2NHR', II=*N*-Alkyl-*γ*-bromo-*n*-alkanesulfonamide, III=*N*-Alkyl-*δ*-bromo-*n*-alkanesulfonamide

amide. The isomer ratio of the two rearranged products (*γ*-bromo isomer/*δ*-bromo isomer=1.19) was similar to that (*N*-*t*-butyl-*γ*-chloropentanesulfonamide/*N*-*t*-butyl-*δ*-chloropentanesulfonamide=1.14)[1)] obtained in the reaction of *N*-*t*-butyl-*N*-chloro-*n*-pentanesulfonamide in an aqueous solution. In the decomposition of *N*-bromosulfonamides in the aqueous solution, the low yield of conversion to the rearranged products is due to the unstability of *N*-bromosulfonamides in the aqueous solution and to the reduction to the original sulfonamides. Several sultam derivatives were obtained by the treatment of rearranged products with ethanolic NaOH (see Experimental Section).

Experimental

Apparatus. The glpc analyses were conducted by a Shimadzu GC-3A using Apieson L grease 10% or Silicone oil 550 10% on Diasolid L, 60—80 mesh, 1 m column. The Hg lamp was an Eikosha 150 W high-pressure Hg lamp.

Materials. The benzene, AcOH, and CCl_4 were purified by an ordinary method.

General Procedure of N-*Bromination.* *N*-Alkyl-*n*-alkanesulfonamide (0.05 mol) was suspended in a buffer solution (100m*l*, pH=6.6), and to the solution, a 50-m*l* portion of aqueous NaOBr (freshly prepared from Br_2 (24 g) and Na_2CO_3 (16 g)) was added; the solution was then stirred for 4 hr at room temperature. The insoluble oil separated as a lower layer was collected and dissolved in CCl_4 and dried over Na_2SO_4, and the solvent was evaporated. Yield, 75—80%.

Photodecomposition of N-*Bromosulfonamides.* *N*-Bromosulfonamides were irradiated at 28—30°C under N_2 until the active bromine was negligible.

Isolation and Analyses of Reaction Products. Analyses of the products in the reaction of *N*-bromo-*N*-*t*-butylbutanesulfonamide, the alkali treatment, and analyses of sultams were carried out as has been described in our previous papers.[1,3)]

N-t-*Butyl-γ-bromo*-n-*propanesulfonamide.* This substance was obtained by adding hexane to an ether solution of reaction products and was recrystallized from cold ether. Mp 76°C. IR: 3285, 2960, 1315, and 1135 cm^{-1}, NMR (in $CDCl_3$): τ; 5.45 (lH), 6.45(triplet, 2H), 6.80(triplet, 2H), 7.65(multiplet, 2H), 8.62(singlet, 9H).

Found: C, 32.80; H, 6.20; N, 5.25; Br, 30.8%. Calcd for $C_7H_{16}BrNO_2S$: C, 32.57; H, 6.25; N, 5.43; Br, 30.95%.

N-t-*Butylpropanesultam.* This was obtained by the ethanolic treatment of *N*-*t*-butyl-*γ*-bromopropanesulfonamide with ethanolic NaOH. Yield, 96%. Mp 56°C. IR: 2960, 1310, 1210, 1130, 1000, and 730 cm^{-1}. NMR (in $CDCl_3$): τ; 6.55—6.98 (multiplet, 4H), 7.55—7.90(multiplet, 2H), 8.63(singlet, 9H).

Found: C, 47.46; H, 8.51; N, 7.72%. Calcd for $C_7H_{15}NO_2S$: C, 47.43; H, 8.53; N, 7.90%.

N-t-*Butyl-δ-bromo*-n-*pentanesulfonamide.* This was obtained by cooling the hexane solution of the reaction mixture and was recrystallized from cold ether. Mp 55°C. IR: 3280, 2960, 1310, and 1130 cm^{-1}. NMR(in $CDCl_3$):τ; 5.60(1H), 5.95(multiplet, IH), 6.95(triplet, 2H), 8.05(multiplet, 4H), 8.25(doublet, 3H), 8.62(singlet, 9H).

Found: C, 37.44; H, 7.24; N, 4.85; Br, 27.7%. Calcd for $C_9H_{20}BrNO_2S$: C, 37.77; H, 7.04; N, 4.89; Br, 27.91%.

The alkali treatment of this product gave *N*-*t*-butylpent-3-enesulfonamide.[1)] Yield, 91%.

N-t-*Butyl-γ-bromo*-n-*pentanesulfonamide.* The presence of this isomer was confirmed by the formation of *N*-*t*-butyl-3-ethylpropanesultam[3)] by the alkali treatment of the reaction mixture obtained after the removal of the *δ*-bromo isomer.

N-t-*Butyl-δ-bromo*-n-*hexanesulfonamide (II).* On cooling the hexane solution of the products to −50°C, a white precipitate was obtained; this was shown to be a mixture of two isomers by glpc and elementary analyses. On the cooling of an ether solution of this mixture, II was isolated and recrystallized from ether and hexane. Mp 63°C. IR: 3280, 2960, 1320, and 1140 cm^{-1}. NMR(in CCl_4): τ; 4.85(1H), 6.05(multiplet, 1H), 7.00 (multiplet, 2H), 7.80—8.30 (multiplet, 6H), 8.62 (singlet, 9H), 8.93(triplet, 3H).

Found: C, 40.16; H, 7.43; N, 4.59; Br, 26.5%. Calcd for $C_{10}H_{22}BrNO_2S$: C, 40.00; H, 7.39; N, 4.67; Br, 26.61%.

4-Ethylbutanesultam[1)] was obtained by the alkali treatment of the *δ*-bromohexanesulfonamide produced by the treatment of II with HCl in a similar manner to that described in a previous paper.[1)] Yield, 87%.

N-t-*Butyl-γ-bromo*-n-*hexanesulfonamide (I).* When the hexane solution of the filtrate was cooled to −70°C after the

3) M. Okahara, T. Ohashi, and S. Komori, *J. Org. Chem.*, **33**, 3066 (1968).

the removal of the δ-bromo isomer, I was isolated as a white precipitate which melted at room temperature. n_D^{20} 1.4838. IR: 3280, 2960, 1320, and 1140 cm^{-1}. NMR (in CCl_4): τ; 4.75(1H), 5.95 (multiplet, 1H), 6.90(triplet, 2H), 7.60—8.35 (multiplet, 6H), 8.63 (singlet, 9H), 9.00 (triplet, 3H).

Found: C, 40.30; H, 7.54; N,4.26; Br, 26.4%. Calcd for $C_{10}H_{22}BrNO_2S$; C, 40.00; H, 7.39; N, 4.67; Br, 26.61%.

3-Propylpropanesultam[1] was obtained from I in the same manner as has been described above. Yield, 80%.

N-*Methyl-γ-bromo*-n-*butanesulfonamide.* The presence of this compound was confirmed by a study of the NMR of the reaction mixture. NMR (in $CDCl_3$): τ; 5.85(multiplet, CHBr), 8.25(doublet, CH_3CHBr).

Furthermore, the formation of *N*-methyl-3-mehtylpropanesultam was observed by glpc and NMR of the products obtained by the alkali treatment of the reaction mixture described above.

N-*Methyl-3-methylpropanesultam.* An authentic sample of this sultam was obtained by the alkali treatment of *N-methyl-γ*-chloro-*n*-butanesulfonamide.[1] Bp 78—80°C/0.2mmHg, n_D^{32} 1.4660. IR: 2960, 1310, 1140, 1050, 930, 845, and 755cm^{-1}. NMR(in $CDCl_3$): τ; 6.65—7.05(mutiplet, 3H), 7.40(singlet, 3H), 7.50-8.10(multiplet, 2H), 8.72(doublet, 3H).

Found: C, 39.96; H, 7.12; N, 9.40%. Calcd for $C_5H_{11}NO_2S$: C, 40.26; H, 7.43; N, 9.39%.

BULLETIN OF THE CHEMICAL SOCIETY OF JAPAN, VOL. 44, 1143—1144(1971)

Synthetic Studies of the Flavone Derivatives. XX.[1] The Synthesis of Sorbifolin

Mitsuru NAKAYAMA, Kenji FUKUI, Tokunaru HORIE,*
Masao TSUKAYAMA,* and Mitsuo MASUMURA*

Department of Chemistry, Faculty of Science, Hiroshima University, Higashisenda-machi, Hiroshima
** Department of Applied Chemistry, Faculty of Engineering, University of Tokushima, Tokushima*

(Received August 19, 1970)

Recently, sorbifolin[2] was isolated, along with sorbarin (scutellarein-7-monorhamnoside), from the fresh leaves of *Sorbaria stellipila* SCHNEID. Its structure was identified as 7-methoxy-5,6,4′-trihydroxyflavone (I) on the basis of chemical and spectral evidence.[2]

The present paper will describe the synthesis of I from 3,6-dihydroxy-2,4-dimethoxyacetophenone (II).[3] The monobenzyl ether (III)[4] of II was esterified with *p*-benzyloxybenzoyl chloride in the presence of anhydrous pyridine, and then the resulting ester was converted into 3-benzyloxy-2,4-dimethoxy-6-hydroxy-ω-(4-benzyloxybenzoyl)acetophenone (IV) by Baker-Venkataraman transformation. The cyclodehydration of IV with anhydrous sodium acetate in acetic acid afforded 6,4′-dibenzyloxy-5,7-dimethoxyflavone (V). The debenzylation of V by hydrogenolysis gave the 6,4′-dihydroxyflavone derivative (VI). Then, the partial demethylation of VI with anhydrous aluminum chloride in acetonitrile gave the desired flavone I, which was easily converted into the acetate (VII).

I and VII were shown to be identical with the natural pigment and its acetate respectively by a mixed-melting-point determination and by NMR, IR, and UV spectral comparisons.

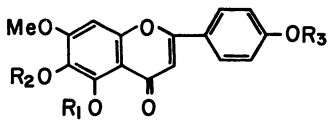

I $R_1 = R_2 = R_3 = H$

V $R_1 = Me,\ R_2 = R_3 = C_6H_5CH_2$

VI $R_1 = Me,\ R_2 = R_3 = H$

VII $R_1 = R_2 = R_3 = Ac$

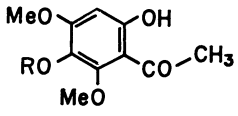

II $R = H$

III $R = C_6H_5CH_2$

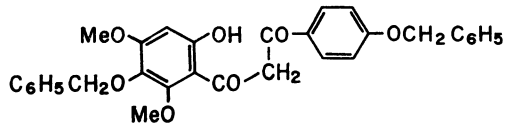

IV

1) XIX of this series: M. Nakayama, K. Fukui, T. Horie, and M. Masumura, *Nippon Kagaku Zasshi*, **91**, 739 (1970).
2) M. Arisawa, T. Takakuwa, and T. Nakaoki, *Chem. Parm. Bull.* (Tokyo), **18**, 916 (1970).
3) V. D. Nageswara Sastri and T. R. Seshadri, *Proc. Indian Acad, Sci. Sect. A*, **23**, 262 (1946).
4) K. Fukui, M. Nakayama, M. Matsui, M. Masumura, and T. Horie, *Nippon Kagaku Zasshi*, **90**, 1270 (1969).

Experimental[5]

3-Benzyloxy-2,4-dimethoxy-6-hydroxy-ω-(4-benzyloxybenzoyl)-acetophenone (IV). A mixture of the crude III[4] (2 g) and *p*-benzyloxybenzoyl chloride (2.5 g) in anhydrous pyridine (10 ml) was heated at 120°C for 2 hr. The cooled reaction mixture was poured into dilute hydrochloric acid and then extracted with ether. The removal of the solvent gave a semi-solid (a crude ester).

A mixture of the above ester, freshly-powdered potassium hydroxide (2.0 g), and pyridine (15ml) was heated at 60°C for 4 hr with stirring. The reaction mixture was acidified with dilute hydrochloric acid, and then extracted with ether. The ether layer was washed with a sodium carbonate solution and water, and then evaporated. The resulting residue was treated with methanol-ether (1:1). The separated crystals were recrystallized from methanol-ethyl acetate to give IV as yellow prisms; mp 111—112.5°C; yield, 1.0 g (30% from III).

Found: C, 72.58; H, 5.52%. Calcd for $C_{31}H_{28}O_7$: C, 72.64; H, 5.51%.

6,4'-Dibenzyloxy-5,7-dimethoxyflavone (V). A mixture of IV (720 mg) and anhydrous sodium acetate (1.6 g) in acetic acid (8 ml) was heated at 140°C for 1 hr. The reaction mixture was then diluted with water and ether. The separated crystals were recrystallized from ethyl acetate to give V as colorless prisms; mp 154.5—155.5°C; yield, 600 mg (86%). UV: λ_{max}^{EtOH} mμ(log ε); 271(4.26), 330(4.50). NMR: ($CDCl_3$) 6.53(s, H-3), 6.72(s, H-8), 7.02(d, J=9.0 Hz, H-3', -5'), 7.80(d, J=9.0 Hz, H-2', -6').

Found: C, 75.07; H, 5.24%. Calcd for $C_{31}H_{26}O_6$: C, 75.29; H, 5.30%.

6,4'-Dihydroxy-5,7-dimethoxyflavone (VI). A mixture of V (890 mg) and Pd-C (10%; 90 mg) in ethyl acetate-methanol (2:1:150 ml) was shaken in an atmosphere of hydrogen for 5 hr. After the catalyst had been filtered off, the filtrate was evaporated. The residue was recrystallized from ethanol to give VI as colorless needles; mp 286—288°C; yield, 500 mg (88%). UV: λ_{max} mμ (log ε); (EtOH) 280(4.30), 334(4.50); (EtOH-AcONa) 285_{sh}(4.21),[6] 332 (4.32), 380(4.15). NMR: (DMSO) 6.56(s, H-3), 6.89(d, J=8.3 Hz, H-3', -5'), 7.08(s, H-8), 7.88(d, J=8.3 Hz, H-2', -6').

Found: C, 64.87; H, 4.24%. Calcd for $C_{17}H_{14}O_6$: C, 64.96; H, 4.49%.

Diacetate: mp 213—214°C (colorless prisms from ethyl acetate). UV: λ_{max}^{EtOH} mμ (log ε); 264(4.35), 312(4.41). NMR: ($CDCl_3$) 6.58(s, H-3), 6.80(s, H-8), 7.21(d, J=9.0 Hz, H-3', -5'), 7.88(d, J=9.0 Hz, H-2', -6').

Found: C, 63.03; H, 4.63%. Calcd for $C_{21}H_{18}O_8$: C, 63.31; H, 4.55%.

Sorbifolin (7-Methoxy-5,6,4'-trihydroxyflavone) (I). A mixture of VI (300 mg) and anhydrous aluminum chloride (2.0 g) in anhydrous acetonitrile (20 g) was heated at 65°C for 12 hr. The reaction mixture was then diluted with 1% hydrochloric acid (100 ml). After the solvent had been removed as much as possible under a vacuum, the separated solid was recrystallized from methanol to give I as yellow needles; mp 290—292°C; yield, 140 mg (49%). UV: λ_{max} mμ (log ε); (EtOH) 290(4.31), 343(4.41); (EtOH-$AlCl_3$) 306 (4.38), 366(4.47); (EtOH-AcONa) 380(4.25) (natural pigment:[7] (EtOH) 290(4.29), 343(4.39); (EtOH-$AlCl_3$) 306 (4.36), 366(4.44); (EtOH-AcONa) 380(4.17)). NMR: (DMSO) 3.89(s, OCH_3), 6.75(s, C-3 or -8), 6.80(s, H-8 or -3), 6.90(d, J=8.3 Hz, H-3', -5'), 7.93(d, J=8.3 Hz, H-2', -6'), 8.63(bs, OH-6), 10.3(bs, OH-4'), 12.65(s, OH-5).

Found: C, 64.06; H, 3.93%. Calcd for $C_{16}H_{12}O_6$: C, 64.00; H, 4.03%.

Triacetate (VII): mp 228—229°C (colorless needles from methanol). UV: λ_{max}^{EtOH} mμ (log ε); 261.5(4.28), 310(4.43).

Found: C, 61.70; H, 4.22%. Calcd for $C_{22}H_{18}O_9$: C, 61.97; H, 4.26%.

The authors are grateful to Dr. Munehisa Arisawa, Kokando Co., Ltd., for his gifts of the natural pigment and its acetate.

5) All the melting points are uncorrected. The NMR spectra were measured with a Hitachi R-20 spectrometer (60 MHz), using tetramethylsilane as the internal standard (δ, ppm); s, singlet; bs, broad singlet; d, doublet.

6) sh=shoulder

7) The natural pigment was measured in this laboratory.

BULLETIN OF THE CHEMICAL SOCIETY OF JAPAN, VOL. 44, 1145—1146(1971)

Inverse Gas Chromatographic Investigation of Fractionated Polycarbonates

Yoshiyuki YAMAMOTO, Shin TSUGE, and Tsugio TAKEUCHI

Department of Synthetic Chemistry, Faculty of Engineering, Nagoya University, Chikusa-ku, Nagoya

(Received August 24, 1970)

Inverse gas liquid chromatography (glc) has recently been used to measure the interactions between stationary test compounds and solute vapors. Davis, *et al.*[1] characterized asphalts by means of inverse glc. Lavoie and Guillet,[2] and Smidsrød and Guillet[3] also investigated second order transitions (*e.g.* glass transition, *Tg*) and polymer-solute interactions for polymeric materials using this method.

Poly[2,2-propanebis(4-phenyl carbonate)] (PC) is a most thermostable polymer and has the following repeating unit.

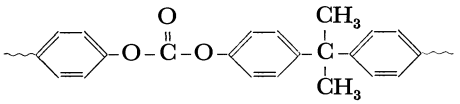

However, PC synthesized by the solvent method (SM-PC), in which *p-t*-butylphenol is used as terminater, provides the next end group.

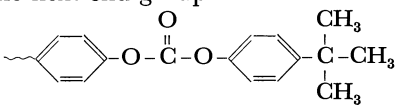

On the other hand, PC synthesized by the melt method (MM-PC) is known to yield either end groups.[4]

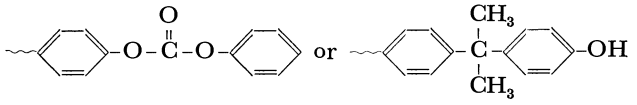

In this work, fractionated PC with various molecular weight was investigated by means of inverse glc. Effect of the end groups, molecular weights, and *Tg* of PC on the retention behaviors are also discussed.

Results and Discussion

Molecular Weight of PC and Retention Behaviors. When polymers are used as a stationary phase in glc, it is expected that the smaller the molecular weights of the polymers, the stronger the interactions between their end groups and test solute. The interactions can also be affected by the nature of the end groups.

Figure 1 gives schematic chromatograms of benzene and diphenylmethane obtained by use of MM-PC with various molecular weights as the stationary phase in glc at 220°C. The retention time of diphenylmethane changes markedly as a function of the molecular weight of PC, while that of benzene is almost constant regardless of its molecular weight. The same tendency was observed for SM-PC.

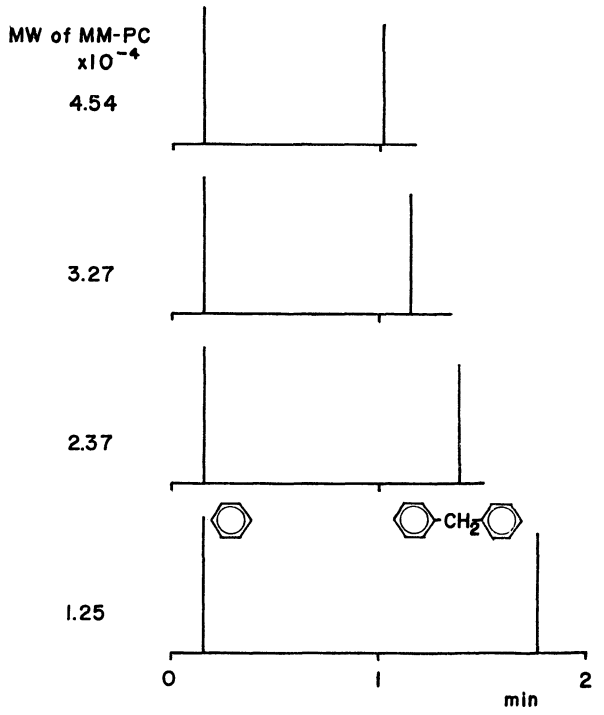

Fig. 1. Schematic chromatograms of benzene and diphenylmethane obtained by use of MM-PC with various molecular weights as the stationary phase in glc at 220°C.

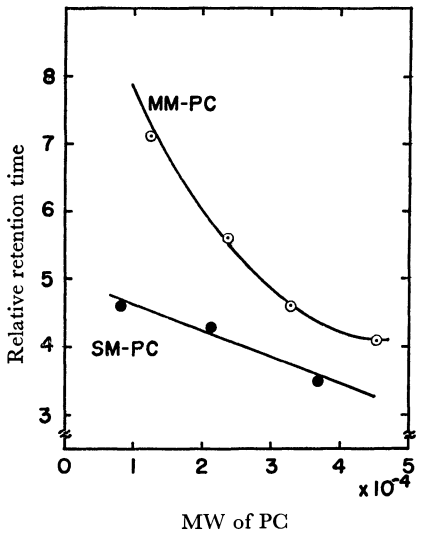

Fig. 2. The relationship between the relative retention time of diphenylmethane to benzene and the molecular weight of PC.

The results are shown in Fig. 2, where the relative retention time of diphenylmethane to benzene is plotted against the molecular weight of PC.

The relative retention time was adopted for compensa-

1) T. C. Davis, J. C. Peterson, and W. E. Haines, *Anal. Chem.*, **38**, 241 (1966).
2) A. Lavoie and J. E. Guillet, *Macromol.*, **2**, 445 (1969).
3) O. Smidsrød and J. E. Guillet, *ibid.*, **2**, 272 (1969).
4) S. Tsuge, T. Okumoto, Y. Sugimura, and T. Takeuchi, *J. Chromatogr. Sci.*, **7**, 253 (1969).

tion of small changes in the experimental conditions such as flow rate of carrier gas and column temperature.

We see from Fig. 2 that the polarity of MM-PC column decreases nearly hyperbolically with the increase of molecular weight. This is mainly due to the end hydroxy groups of MM-PC. On the other hand, the retention data of SM-PC shows relatively small changes because of the terminal *t*-butyl groups, whose polarity is smaller than that of the hydroxy group.

These data suggest that rough estimation of the molecular weight of PC is possible by this method, provided that the synthetic method is known.

Retention Behavior near T_g. The chain mobility of polymer varies considerably before and after T_g, which is expected to cause remarkable change of its interaction with the solute.

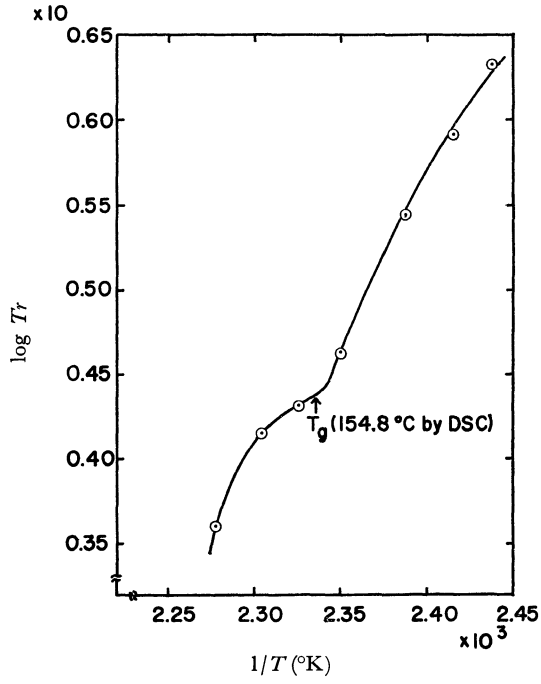

Fig. 3. The relationship between the reciprocal of the absolute column temperature and logarithms of the relative retention time (*Tr*) of *N,N*-dimethylformamide to cyclohexane near *Tg* for MM-PC.

Figure 3 shows the relationship between the reciprocal of the absolute column temperature and logarithms of the relative retention time of *N,N*-dimethylformamide to cyclohexane near T_g (154.8°C by DSC) for MM-PC. The relative retention time decreases with the rise of column temperature. However, a point of inflection exists near T_g. The same inclination was obtained for SM-PC. However, no appreciable differences were observed with variation of the molecular of PC.

Experimental

Materials. Fractionated PC-samples having molecular weights 10000—50000 were used. Raw PC was fractionated as reported previously[4] by successive precipitation method in methylene chloride-*n*-pentane system and the molecular weight of each fraction was measured by the viscosimetric method.

Preparation of Column Packing. PC weighting aboug 0.25 g was dissolved in 50 m*l* of methylene chloride. Then 0.75g of Celite 545 (80-100 mesh) was added to the solution. After the solvent was evaporated at 50°C in a vaccum with constant stirring, the coated support was packed in a column tube.

Gas Chromatographic Conditions. a) *For Measurement of Molecular Weight Effect*;
Gas chromatograph: Yanagimoto GCG Model 220 with TCD
Column: 2 mm, i. d. × 50 cm copper tube
Column temperature: 150 and 220°C
Carrier gas: H_2, 12 m*l*/min
Sample: mixture of benzene and diphenylmethane
Sample size: 10 μl

b) Measurement of Retention Behavior near T_g;
Gas chromatograph: Yanagimoto GCG 550 F with FID
Column: 2mn, i. d. × 100cm copper tube
Column temperature: 137—166°C
Carrier gas: N_2, 10m*l*/min
Sample: mixture of cyclohexane and *N,N*-dimethylformamide
Sample size: 0.1μl

c) Determination of Tg;
DSC: Rigaku Denki Model DT-10 Differential Scanning Calorimeter
Sample size: 25mg
Heating rate: 10°C/min

BULLETIN OF THE CHEMICAL SOCIETY OF JAPAN, VOL. 44, 1147—1148(1971)

The Chemical Modification of Biopolymers. IV. The Introduction of Succinyl Groups into Bacterial α-Amylase

Shuichi SUZUKI, Yutaka HACHIMORI, Ryuichi MATOBA, and Kinya TAKASAKI
Research Laboratory of Resources Utilization, Tokyo Institute of Technology, Meguro-ku, Tokyo
(Received October 1, 1970)

The introduction of functional groups into enzymes has been studied for its effect on enzymic properties. As has been shown previously, the mercaptosuccinylation of Taka-amylase A[1] (EC. 3.2.1.1) caused an increase in the enzymic activity, but the enzymic activity was not elevated, but was lowered, by succinylation.

However, the introduction of succinyl groups into bacterial α-amylase (*Bacillus subtilis*, EC. 3.2.1.1) raised the activity.

The preparation of succinyl α-amylase and their properties has been studied.

Experimental

Activity Measurements. The hydrolytic activity of the native and modified α-amylase was measured by studying the decrease in absorbance at 700 mμ due to iodine-amylose complex formation (the blue-value method),[2] and by studying the increase in the reducing groups (the Somogyi-Nelson method).[3,4] The digestion was conducted at 37°C for 30 min in a 0.07 M acetate buffer.

The protein concentration was estimated by spectrophotometry with the extinction coefficient, $E^{1\%}_{1cm}$ of 25.3 at 280mμ,[5] or by the method of Lowry.[6]

Preparation of Succinyl α-Amylase. Succinyl α-amylase was prepared as follows: One milliliter of a succinic anhydride solution in dioxane (2.2×10^{-6} mol to 2.2×10^{-4} mol) was added to 20 ml of the buffered protein solution (4.4×10^{-7} mol in a 0.2 M phosphate buffer, pH 8.0) at 2—4°C. After 30 min, 6 ml of a 0.4M hydroxylamine solution in a 0.2M phosphate buffer (pH 7.5) were added in order to stop the reaction. The reaction mixture was then dialyzed against distilled water for 24 hr at 5°C. The extent of succinylation was estimated by studying the decrease in the amino groups by the method of Matsushima *et al.*[7]

Results and Discussion

Determining the Extent of Succinylation of α-Amylase. Figure 1 shows the effect of the concentration of succinic anhydride on succinylation at 2°C. The extent of the succinylation of lysyl residues increased in accordance with the increase in the concentration of succinic anhydride. Fifteen succinyl groups per mole of enzyme was obtained when a 500-fold mole excess was used.

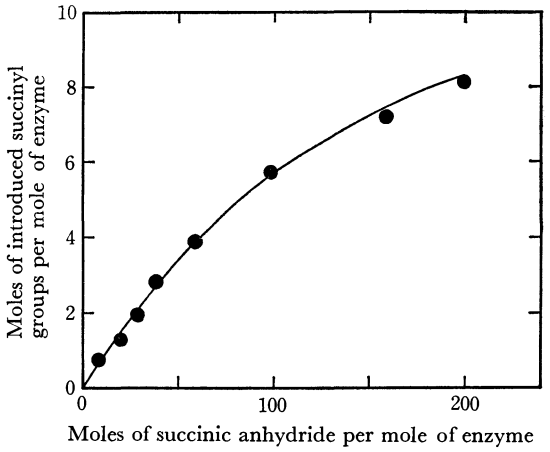

Fig. 1. The effect of concentration of succinic anhydride on degrees of succinylation of α-amylase.

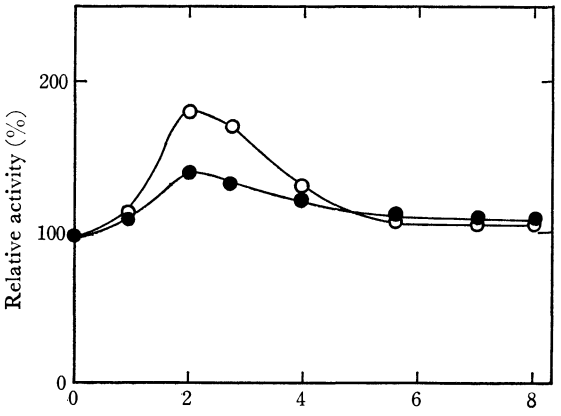

Fig. 2. The activities of the native and modified α-amylase on amylose measured at these pH optima in a 0.07 M acetate buffer and a 4.1×10^{-3}M amylose solution by the blue-value method (Curve A, open circle) and by the Somogyi-Nelson method (Curve B, closed circle).

Enzymic Activities of Succinyl α-Amylase. The enzymic activities of the modified enzymes are shown as curve A (the blue-value method) and curve B (the Somogyi-Nelson method) in Fig. 2. The enzymic activities were measured in a 4.1×10^{-3}M amylose solution and are expressed in percentages of the native enzymic activity. The enzymic reactions were carried out at the optimal pH values, which were shifted by the succinylation as is shown below. When two moles of succinyl groups were introduced per mole of enzyme, the activity on amylose, as measured by the blue-value method, increased to 180%, while that as measured by the Somogyi-Nelson method increased to 140%, of that of the native enzymic activity.

1) S. Suzuki, Y, Hachimori, and R. Matoba, This Bulletin, **43**, 3849 (1970).
2) H. Fuwa, *J. Biochem.* (Tokyo), **41**, 583 (1954).
3) M. Somogyi, *J. Biol. Chem.*, **195**, 19 (1952).
4) N. Nelson, *J. Biol. Chem.*, **153**, 375 (1944).
5) J. Hsiu, E. H. Fischer, and E. A. Stein, *Biochemistry*, **3**, 61 (1964).
6) O. H. Lowry, N. J. Rosebrough, A. L. Farr, and R. J. Randall, *J. Biol. Chem.*, **193**, 265 (1951).
7) A. Matsushima, Y. Hachimori, Y. Inada, and K. Shibata, *J. Biochem.* (Tokyo), **63**, 328 (1967).

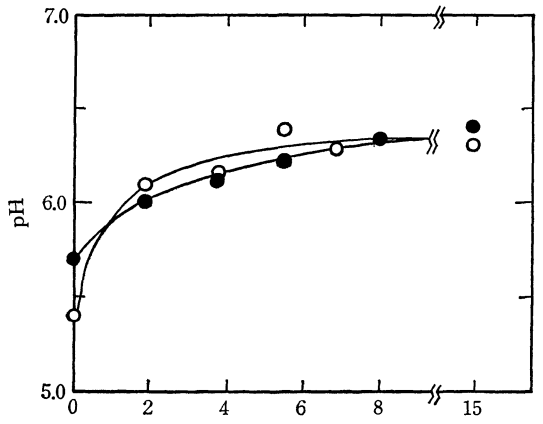

Fig. 3. The effect of the extent of succinylation of α-amylase on pH optima in a 0.07M acetate buffer and a 4.1×10^{-3}M amylose solution by the blue-value method (Curve A, open circle) and by the Somogyi-Nelson method (Curve B, closed circle).

pH Optima of Succinyl α-Amylase. The pH optima of the native and modified α-amylase are plotted against the numbers of the introduced succinyl groups by curve A (the blue-value method) and curve B (the Somogyi-Nelson method) in Fig. 3.

The pH optima were shifted higher with the progress of succinylation. The pH optima of the native enzymes were 5.4 and 5.7, as measured in a 4.1×10^{-3}M amylose solution by the blue-value method and by the Somogyi-Nelson method respectively, while the pH optima of the modified enzyme into which 15 succinyl groups per mole of enzyme has been introduced were 6.3 (the blue-value method) and 6.4 (the Somogyi-Nelson method).

Properties and Characteristics of Succinyl α-Amylase. The kinetic properties of the native and modified amylase with two succinyl groups per mole of enzyme were determined by the Lineweaver-Burk method.

The V_{max} values for the native and modified enzymes were 1.3×10^4 and 1.4×10^4 mol per min per mole of enzyme respectively.

However, succinylation decreased the K_m for amylose from 4.4×10^{-3}M^{-1} to 2.6×10^{-3}M^{-1}.

These results suggest that the increase in enzymic activity is due to the increase in affinity for amylose.

The reaction with succinic anhydride replaces the positively charged ammonium groups, NH_3^+, at a neutral pH with a $NHCOCH_2CH_2COO^-$ function. The changes that had been produced in the viscosity and sedimentation behavior of succinylated proteins would suggest a considerable expansion or unfolding of the molecular structure.

The $S^0_{20,w}$ values for the native and modified enzymes were found to be 4.4 and 5.0 respectively by ultracentrifugal analysis. That this is not primarily due to aggregation of the molecules is likely to be indicated by the fact that the change in the sedimentation constant is small and the ultracentrifugal patterns of the modified amylase showed a single well-defined peak. The native and the succinyl α-amylase show intrinsic viscosities of 0.024 *dl*/g and 0.021 *dl*/g respectively.

From these experiments, we have concluded that the effective volume occupied by the succinyl amylase molecule increased compared to that of untreated α-amylase, and that the increase in the affinity for amylose is likely to be due to the expansion of the molecular structure. As has been reported previously,[1] the succinylation of Taka-amylase A caused a decrease in the enzymic activity. The difference in the effects of succinylation on the two enzymic activities seem to be due to the extent of conformational change taking place by succinylation.

BULLETIN OF THE CHEMICAL SOCIETY OF JAPAN, VOL. 44, 1148—1150(1971)

Electrochemical Evidence for the Mechanism of the Primary Stage of Photosynthesis[1)]

Akira FUJISHIMA and Kenichi HONDA

Institute of Industrial Science, The University of Tokyo, Roppongi, Minato-ku, Tokyo

(Received October 13, 1970)

A phenomenon analogous to photosynthesis was observed by using an electrochemical system involving semiconductor electrodes, such as *n*-type titanium dioxide (rutile) single crystals. The results help greatly to establish the nature of the initial stage of photosynthesis, especially the oxygen evolution reaction, from the electrochemical point of view. One of the most important processes in the photosynthesis is a hole injection into a water molecule, though it is not clear whether the hole exists before injection in a localized level or in an excess hole band of chlorophylls. Since van Niel[2)] proposed that the photolysis of water was the basic reaction for converting light into chemical energy, Arnon and others[3)] have developed this idea, especially the relation between the excitation of chlorophylls and oxygen evolution. According to the results of Arnon's primary photochemical reaction, an absorbed light quantum excites a chlorophyll molecule and expels an

1) Studies on Photosensitive Electrode Reactions. III.

2) C. B. van Niel, "Photosynthesis in Plants," Iowa State College Press (1949), p. 437.

3) D. I. Arnon, *Nature*, **184**, 10 (1959).

electron. This electron naturally has a higher potential energy at the expense of the energy of the absorbed light quantum. The chlorophyll molecule, as it expels an electron, becomes ready to accept another from water with oxygen evolution and, in this way, returns to a normal state. However, the mechanism of the oxygen evolution reaction has not yet been sufficiently explained.

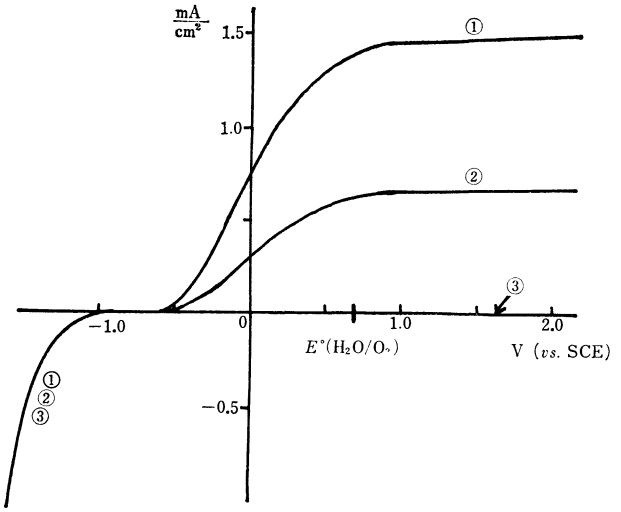

Fig. 1. Current-voltage curves of TiO_2 electrode with and without irradiation of light in the buffered solution of pH 4.7.
Curve ①: under irradiation (relative intensity of light, 100%).
Curve ②: under irradiation (relative intensity of light, 50%).
Curve ③: without irradiation.

Photosensitized Electrolytic Oxidation. The present authors[4] have previously studied the electrochemical behavior of semiconductor electrodes under the irradiation with light. In the present experiment, *n*-type titanium dioxide (TiO_2) single crystals were used after reduction treatment in order to increase the electric conductivity. The current voltage data were obtained potentiostatically. Figure 1 shows typical current-voltage curves with and without irradiation. Without irradiation, hydrogen evolution occurred in the cathodic polarization region, but the anodic current was extremely small. Under irradiation, the cathodic branch of the current-voltage curve was not influenced, but a large anodic current flowed at a potential more positive than −0.5 V (*vs.* SCE) in a neutral electrolyte solution. The magnitude of the anodic current was proportional to the light intensity and depended on the wavelength of the light. A large anodic current flowed when the semiconductor electrode was irradiated with light with an energy higher than the band gap of TiO_2, 3.0 eV.

This anodic reaction may be related to the holes, the minority carriers, which are produced in the valence band of TiO_2 by light. When an anodic current flowed, gas evolution was observed at the TiO_2 electrode surface. It was observed by gas chromatography that the gas was oxygen. As TiO_2 is very stable, it seems unlikely that the TiO_2 electrode was decomposed under irradiation. Even after the anodic current had flowed for a long time with a strong light, the TiO_2 electrode surface was not at all changed and no titanium ions could be detected in the electrolyte solution. In a 0.1 N Na_2SO_4 electrolyte solution, the relation between the change in the pH and the amount of current at 0.0 V in the case of the TiO_2 electrode was the same as that when the Pt electrode was used at 1.0 V. Therefore, the anodic reaction may be attributed to the electrolytic oxidation of water to oxygen gas.

Though the reversible oxidation potential of water to oxygen is 0.7 V (*vs.* SCE) at pH 4.7, the anodic current flowed, in fact, at potentials more positive than −0.5 V under irradiation. This fact indicates that the oxidation potential of water shifts by about 1.2 V towards the more negative region at pH 4.7. From the results described above, a mechanistic model of the electrochemical reaction at the *n*-type TiO_2 electrode is proposed; it is illustrated in Fig. 2. We call the above-mentioned phenomenon "photosensitized electrolytic oxidation." The origin of the photosensitized electrolytic oxidation is, of course, the absorption of the energy of light by the semiconductor electrode.

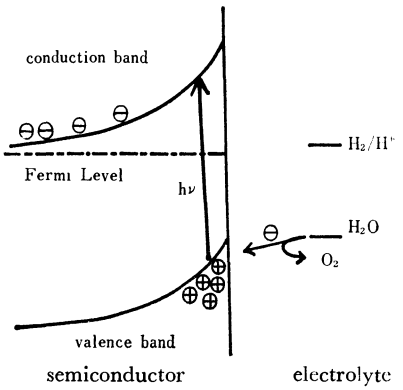

Fig. 2. A mechanistic model of photosensitized electrolytic oxidation.

If the electrolyte solution involved halogen ions, such as iodide or bromide ions, they are also oxidized in competition with the oxygen evolution reaction in relation to the concentration of halogen ions. Recently, we have investigated the photo-electrochemical reactions of *n*-type semiconductor electrodes of the zinc oxide single crystal and the cadmium sulfide single crystal;[5] under anodic polarization these crystals are dissolved because of the positive holes formed in the valence band by the irradiation with light. In the electrolyte solution involving halogen ions, the electrochemical oxidation of these anions occurs instead of the dissolution reaction on both ZnO and CdS electrodes. The oxidation potentials of halogen ions on TiO_2, ZnO, and CdS electrodes are more negative than the standard oxidation potential. Therefore, the photosensitized electrolytic oxidation of halogen ions seems to occur even with ZnO and CdS electrodes.

Photo-electrochemical Cell and Its Relation to the Primary

4) A. Fujishima, K. Honda, and S. Kikuchi, *Kogyo Kagaku Zasshi*, **72**, 108 (1969).

5) A. Fujishima, M, Matsukura, K.Honda, and S.Kikuchi, Preprint of the Annual Meeting of the Electrochemical Society of Japan, 1969, P.c-45, A.Fujishima, E.Sugiyama and K.Honda, This Bulletin, **44**, 304 (1971).

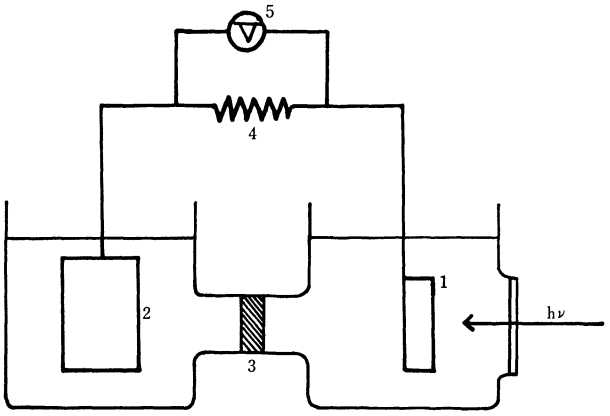

Fig. 3. An electrochemical cell with TiO_2 electrode under irradiation.
1: TiO_2 electrode, 2: Pt electrode, 3: sinter-glass diaphragm, 4: an outer load, 5: a voltmeter

Stage of Photosynthesis. The function of the TiO_2 semiconductor electrode in relation to the primary stage of photosynthesis can be better understood by constructing an electrochemical cell with a semiconductor electrode under irradiation, as is shown in Fig. 3. When the surface of the TiO_2 electrode was irradiated, the current which passed through the load was proportional to the light intensity. It was seen from the direction of the current that an oxidation reaction occurred at the TiO_2 electrode and a reduction, at the Pt electrode. The oxidation reaction was oxygen evolution resulting from water electrolysis. This fact indicates that the TiO_2 electrode absorbed the energy of light and caused the electrolysis of water to oxygen gas without any applied electric power and that, at the same time, a reduction occurred at the Pt counter electrode and electric energy was supplied to the outer load.

There has previously been presented a model[6] which regarded aggregated chlorophylls as a kind of semiconductor. This opinion has been supported in part by experimental results with regard to the photoconductivity[7] and the delayed light emission[8] of chloroplasts and other phenomenon. It may be considered that the reaction at the TiO_2 electrode and the Pt counter electrode, and the work done by electric energy to the outer load, approximately correspond to those which occur in chlorophylls, carbon assimilation, and photophosphorylation respectively. In a model of photosynthesis[9,10] where oxidation-reduction potentials were introduced with a view of placing great emphasis on the electron transfer in plants, the stages of the photoexcitation of chlorophylls and oxygen evolution are similar to the mechanism of photosensitized electrolysis at the TiO_2 electrode. This kind of work with an electrochemical system containing a semiconductor or insulator electrode will be of great help in studying the primary processes involved in photosynthesis.

The authors wish to thank Dr. M. Sukigara for his useful discussions.

6) E. Katz, "Photosynthesis in Plants," Iowa State College Press, (1949), p. 291.
7) R. C. Nelson, *J. Chem. Phys.*, **27**, 864 (1957).
8) B. L. Strehler and W. Arnold, *J. Gen. Physiol.*, **34**, 809 (1951).
9) J. A. Bassham, *Advan. Enz.*, **25**, 39 (1963).
10) M. Calvan and G. M. Androes, Proc. Photosynthesis Conf., Paris (1962).

BULLETIN OF THE CHEMICAL SOCIETY OF JAPAN, VOL. 44, 1150—1152(1971)

Asymmetric Reduction of Some Dehydrophenylalanyl Peptides[1]

Mikizo NAKAYAMA, Gun'ichi MAEDA, Takeo KANEKO,* and Hakuji KATSURA*

Faculty of Education, Mie University, Tsu, Mie

**Department of Chemistry, Faculty of Science, Osaka University, Toyonaka, Osaka*

(Received October 14, 1970)

Recently, Sheehan *et al.*[2] reported the stereoselective reduction of *N*-acetyldehydrovaline *S*-α-phenylethylamide by means of Raney-nickel catalyst. To clear stereochemical factors of this type of asymmetric reduction, authors carried out stereospecific reduction of a dehydropeptide, *N*-acetyldehydrophenylalanyl-D-valine and its esters. After saponification, D-phenylalanine was afforded, having specific rotation between +6.29°—+15.88° (optical purity 18—45%).

N-Acetyldehydrophenylalanyl-D-valine, prepared by the condensation reaction[3] of 4-benzal-2-methyl-5-oxazolone[4] and D-valine, was esterified in alcohols by treatment with a small amount of hydrochloric acid. The dehydropeptide and its esters were hydrogenated with palladium on charcoal, then hydrolyzed by refluxing with hydrochloric acid. From the reaction mixtures, D-valine and D-phenylalanine were separated in chemically pure states according to the method of Partridge.[5] Following table shows these results.

1) This paper is dedicated to Emeritus Professor Munio Kotake in Commemoration of his 75th birthday, November 30, 1969.

2) J. C. Sheehan and R. E. Chandler, *J. Amer. Chem. Soc.*, **83**, 4795 (1961).

3) O. K. Behrens, D. G. Doherty, and M. Bergmann, *J. Biol. Chem.*, **136**, 61 (1940).

4) R. M. Herbst and D. Shemin, "Organic Syntheses," Coll. Vol. II, p. 1 (1948).

5) S. M. Partridge, *Biochem. J.*, **44**, 521 (1949).

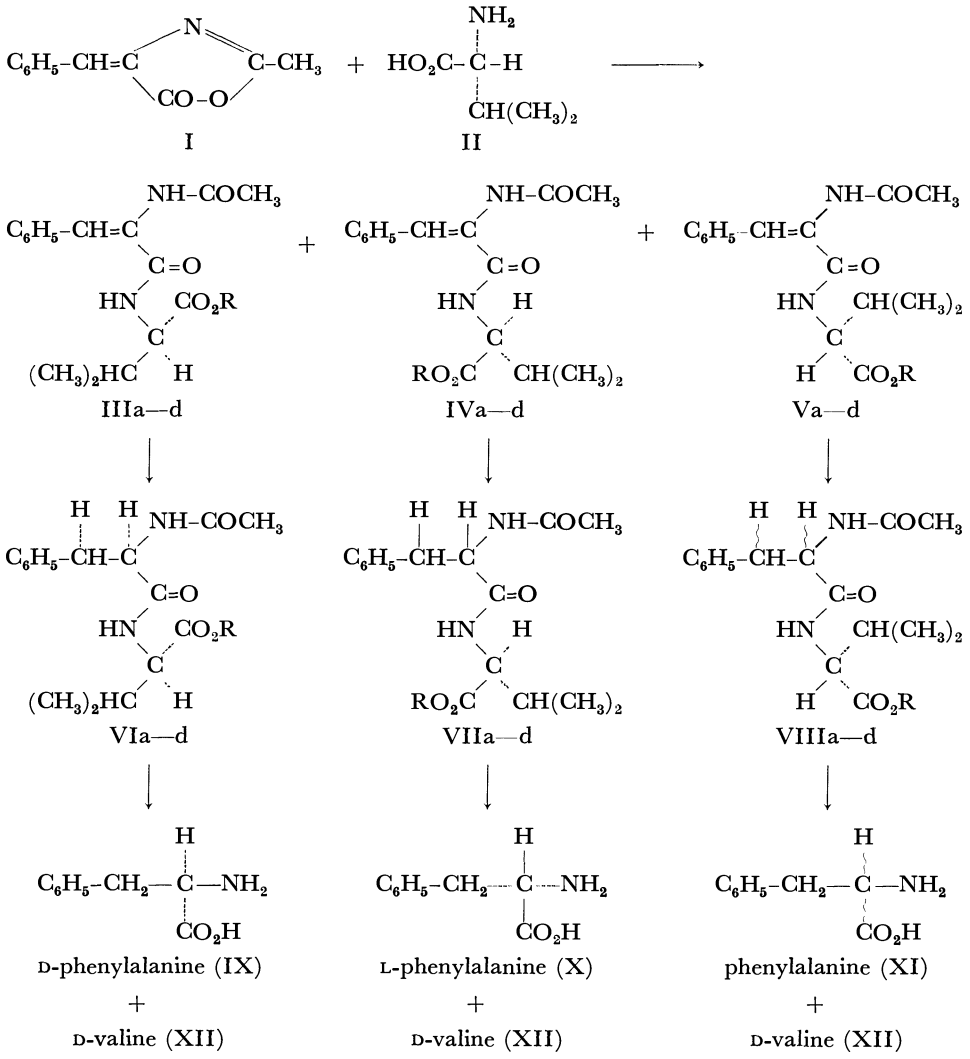

a, R=H; b, R=CH_3; c, R=C_2H_5; d, R=n-C_3H_7

Table 1. Asymmetric reduction of dehydrophenylalanyl peptides

	R	$[\alpha]_D$ (Py)	IX $[\alpha]_D$ (H_2O)	Optical[a] yield %	XII $[\alpha]_D$ (6N HCl)
IIIa	H	−35.96	+14.23	40.7	—
IIIa	H	−35.94	+12.12	34.6	−22.90
IIIb	CH_3	−24.14	+15.88	45.3	−21.80
IIIb	CH_3	−22.92	+13.83	39.5	−21.43
IIIc	C_2H_5	−34.44	+8.84	25.2	−21.40
IIIc	C_2H_5	−32.49	+10.42	29.8	−21.44
IIId	C_3H_7	−38.93	+6.29	18.0	−21.05
IIId	C_3H_7	−38.12	+8.87	25.3	−20.83

a) Specific rotations of optically pure L-phenylalanine and L-valine are −35.0° (H_2O) and +23.0° (6N HCl), respectively.

Experimental

N-Acetyldehydrophenylalanyl-D-valine (IIIa). To a solution of 11.7g (0.1mol) of D-valine ($[\alpha]_D$ −23.0°) in 200m*l* of 0.5N sodium hydroxide solution, was added 18.8 g (0.1mol) of 4-benzal-2-methyl-4-oxazolone[4] followed by about 190 m*l* of acetone until the mixture became clear. After standing overnight, the reaction mixture was acidified by adding 100m*l* of 1N hydrochloric acid. Crude crystals separated were recrystallized from 99% ethanol; pure crystals (yield, 19.5g (64%)) mp 218°C, $[\alpha]_D^{27}$ −24.0° (*c* 2.32, 99% ethanol), $[\alpha]_D^{25.5}$ −35.94° (*c* 2.96, pyridine). Found: C, 63.14; H, 6.62; N, 9.21%. Calcd for $C_{16}H_{20}O_4N_2$: C, 62.95; H, 6.69; N, 9.22%.

N-Acetyldehydrophenylalanyl-D-valine Esters (IIIb, c, and d). To a solution of 5.0g of above peptide (IIIa) in 100 m*l* of methanol was added 2m*l* of concentrated hydrochloric acid at 0°C. After standing for 2 days at room temperature, separated crystals were filtered off, and pure crystals were obtained by recrystallization from a mixture of water and methanol.

Methyl Ester (IIIb): mp 195°C (yield, 76%), $[\alpha]_D^{25}$ −24.13° (*c* 3.22, pyridine).
Found: C,64.16; H,7.01; N,8.63%. Calcd for $C_{17}H_{22}O_4N_2$: C, 64.13; H, 6.97; N, 8.80%.

Ethyl ester (IIIc) and *n*-propyl ester (IIId) were afforded by the analogous methods described above.

Ethyl Ester (IIIc): mp 154°C (yield, 82%), $[\alpha]_D^{25}$ −34.44° (*c* 3.20, pyridine).
Found: C, 65.19; H, 7.20; N, 8.43%. Calcd for $C_{18}H_{24}O_4N_2$: C, 65.04; H, 7.28; N, 8.43%.

n-Propyl Ester (IIId): mp 151°C (yield, 76%). $[\alpha]_D^{25}$ −38.73° (*c* 4.83, pyridine).
Found: C,65.34; H,7.52; N,8.27%. Calcd for $C_{19}H_{26}O_4N_2$:

C, 65.87; H, 7.57; N, 8.09%.

Asymmetric reduction and hydrolysis. A solution of 1.5g of the peptide or its esters in 100m*l* of ethanol was hydrogenated with 0.1g of 5% palladium on charcoal under atmospheric pressure at room temperature. After absorption of hydrogen was ended (about 45 min), catalyst was filtered off and the filtrate was evaporated to dryness under reduced pressure. The residue was hydrolyzed by refluxing with 15m*l* of concentrated hydrochloric acid for 50 min, and the hydrolysate was evaporated at below 40°C to dryness under reduced pressure. To the residue water was added and evaporated again as described above. These procedures were repeated until free hydrochloric acid was removed completely from the residue. The hydrolysate was treated with the activated charcoal prepared according to the method of Partridge.[5] From the aqueous layer D-valine was obtained, and from the charcoal D-phenylalaine was eluted. These amino acid fractions were neutralized by means of Amberite IR-4B resin. The optical rotation of D-valine was measured in solution of 6N hydrochloric acid.

As the solubility of optically active phenylalanine in water is larger than that of racemic isomer, to avoid fractional crystallization a part of a solution of phenylalanine obtained above was completely evaporated to dryness and weighed, then the residue was dissolved in a definite volume of water and optical rotation of this solution was measured. In each instance the identity and purity of the amino acids were confirmed by paper chromatography developed by 80% phenol. The phenylalanine (R_f=0.87) and valine (R_f=0.79) obtained above, showed single ninhydrin-positive spots which had the same R_f values as those of authentic samples, respectively.

Discussion

As dehydrophenylalanyl peptides may be regarded as derivatives of cinnamic acid, phenyl and carboxyl groups of the peptides should be oriented "trans" position to each other with regard to double bond, since the longest conjugated system is the most stable configuration. The peptides in this paper, would have three staggered conformations as shown by III, IV, and V. According to the assumptions by Prelog[6] and Sheehan,[2] hydrogen will be absorbed on the surface of catalyst and the substrate will approach the catalyst surface from the least sterically hindered side. From III, VI will be deduced, and from IV, VII will be expected. Stereostructure of VIII, the reduction product from V, is yet obscure, because of no significant difference between the bulkiness of "isopropyl" and "carboxylate" groups. After saponification, the products obtained from VI will be D-(R)-phenylalanine and D-(R)-valine, on the other hand L-(S)-phenylalanine and D-(R)-valine will be given from VII, but from VIII, D-valine and racemic or faintly optically active phenylalanine will be obtained. Because D-phenylalanine produced predominantly in these experiments, it is supposed that the conformer III is the most preferable one among the three probable conformers (III, IV, and V) of dehydrophenylalanyl peptides.

6) V. Prelog, *Helv. Chim. Acta*, **36**, 308 (1953).

BULLETIN OF THE CHEMICAL SOCIETY OF JAPAN, VOL. 44, 1152—1153(1971)

The Mass Spectra of 2-Oxo-3-aryl-1,2,3-oxathiazolidines

Fukiko YAMADA, Tomihiro NISHIYAMA, Yasuyoshi FUJIMOTO, and Motokazu KINUGASA

Department of Applied Chemistry, Faculty of Engineering, Kansai University, Senriyama, Suita, Osaka

(Received October 24, 1970)

Various oxathiazolidines are easily prepared by the reactions of *N*-sulfinylanilines with alkene oxides.[1,2] We have prepared 2-oxo-3-phenyl-1,2,3-oxathiazolidine (I) and 2-oxo-3-*p*-tolyl-1,2,3-oxathiazolidine (II) by a reported method[2] and have examined their mass spectra. In this report, we wish to describe the fragmentation schemes of the compounds I and II; the correlation between the fragmentation pathways and the related organic reaction mechanisms will also be discussed.

The mass spectral data of I and II are shown in Table 1. The compounds gave distinct molecular ions, as would be predicted from the presence of the aromatic nucleus; the fragment ions were formed by loss of SO_2 from the molecular ions. The base peaks occur from the loss of the SO_2 group, followed by the loss of the methyl radical. The most prominent fragment ions of the masses at 104 and 118 lose HCN to give hydrocarbon ions with masses of 77 II and 91 respectively. There are three steps of cleavage in the oxathiazolidine ring, the eliminations of SO_2 (1), the methyl radical (2), and HCN (3). The path of the fragmentation of the ring in the compounds I and II is indicated

TABLE 1. MASS SPECTRAL DATA OF COMPOUNDS I AND II[a] (75 eV)

No.	I			II		
	m/e	Ion composition[b]	Rel. Int. (%)	*m/e*	Ion composition	Rel. Int. (%)
1	183	$C_8H_9NO_2S$	55	197	$C_9H_{11}NO_2S$	84
2	119	C_8H_9N	16	133	$C_9H_{11}N$	22
3	118	C_8H_8N	18	132	$C_9H_{10}N$	24
4	105	C_7H_7N	30	119	C_8H_9N	38
5	104	C_7H_6N	100	118	C_8H_8N	100
6	91	C_6H_5N	24	105	C_7H_7N	43
7	77	C_6H_5	78	91	C_7H_7	80

a) The NMR and IR spectra of the compounds were consistent with the assigned structures.[2]

b) The high-resolution mass spectra of these compounds gave the correct composition of all the ions mentioned in the table within an error of ±5 millimass units.

1) V. S. Etlis, A. P. Sineokov. and M. E. Sergeeva, *khim. Geterotsikl. Soedin.*, 682 (1966).

2) F. Yamada, T. Nishiyama, M. Kinugasa, and M. Nakatani, This Bulletin,**43**, 3611 (1970).

by the dotted lines in the diagram below.

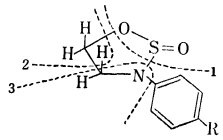

I, R=H II, R=CH_3

These phenomena can be explained in part by the observation that the bond connecting the SO group and the nitrogen atom in the oxathiazolidine ring of I and II has a high probability of fission.

It is interesting to compare this spectrum with the spectra of the other oxathiazolidines reported by Deyrup and Moyer.[3,4] In contrast to the present behavior, the major peak in the fragmentation of 2-oxo-3-*t*-butyl-1,2,3-oxathiazolidine occurs from the loss of the methyl radical, followed by the loss of SO_2, as follows:

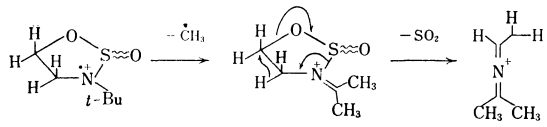

2-Oxo-3-aryl-1,2,3-oxathiazolidines, I and II, can be converted to the corresponding *N,N'*-diarylpiperazines by thermal decomposition and can easily be hydrolyzed to the *N*-(2-hydroxyethyl)anilines by water.[2] In the case of the above reactions, we suggest that, after the loss of the SO_2 group, the remaining atoms in the oxathiazolidine ring are rearranged to become an intermediate which has the same composition as the ion 2, as is shown in Table 1. Thus, the intermediate reacts with another one to give *N,N'*-diarylpiperazines or with water to give *N*-(2-hydroxyethyl)anilines. The ions, although few in number, are detected in both the spectra. This is best explained by the formation of the piperazine molecule and of *N*-(2-hydroxyethyl)-aniline.

Moyer[4] attempted the pyrolysis of some 2-oxo-3-*t*-butyl-1,2,3-oxathiazolidines; however, the reaction products have not been determined. Attempts to hydrolyze the above oxathiazolidines under homogeneous basic aqueous conditions failed. These compounds can only be hydrolyzed to the corresponding amino alcohols by dilute acid.

These differences can be explained by the mass spectral data that, in the first step of the fission, the two compounds, I and II, both produce ions corresponding to the loss of the SO_2 group from the molecules, whereas no corresponding ions from the 2-oxo-3-*t*-butyl-1,2,3-oxathiazolidines are observed.

Experimental

The mass spectra were obtained with a Japan Electron Optics Co., Ltd., JMS-O1SG Mattauch-Herzog double-focusing mass spectrometer. In the photographic-plate measurements, about 50μg of a sample was introduced with a marker (PFK), under normal operating conditions (accelerating voltage, 6.4kV). Accurate masses were determined by using a JMC-1A comparator, while the elemental compositions were evaluated by using Lederberg's Table.[5]

3) J. A. Deyrup and C. L. Moyer, *J. Org. Chem.*, **34**, 175 (1969).

4) C. L. Moyer, Dissertation on 2-Oxo-1,2,3-oxathiazolidines, Harvard University, (1968).

5) J. Lederberg, "Computation of Molecular Formulas for Mass Spectrometry," Holden-Day, San Francisco, (1964), p. 12.

BULLETIN OF THE CHEMICAL SOCIETY OF JAPAN, VOL. 44, 1153—1154(1971)

The Mercury Content of Several Acid Hot Springs in Japan

Naoichi OHTA and Minoru TERAI

Department of Chemistry, Faculty of Science, Tokyo Metropolitan University, Setagaya-ku, Tokyo

(Received October 24, 1970)

The geochemical data of mercury are still insufficiently especially for materials related to volcanic activity.[1] As to hot spring waters, two investigations have been reported hitherto. Stock and Cucuel[2] found 0.0001—0.0005g/ton mercury in spring water. Iwasaki *et al.*[3] reported on the chemical composition of Tamagawa Hot Spring, Akita Prefecture, in which the amount of mercury was estimated to be 0.01ppm. In this paper, the present authors will report the results of a quantitative estimation of mercury in several acid hot springs in Japan.

Sampling and Analytical Method

The samples shown in Table 1 were collected from 10 hot springs distributed around the Shirane volcano, Gunma Prefecture, on July 17th, 1970. The pH values and the temperatures were measured at the orifice of the springs. The determination of mercury was carried out in the laboratory according to the method of a previous work.[4] Mercuric sulfide should be

1) K. Rankama and Th. G. Sahama, "Geochemistry," The University of Chicago Press, Chicago (1950), p. 715.

2) A. Stock and F. Cucuel, *Naturwissenschaften,* **22,** 390 (1934).

3) I. Iwasaki, T. Katsura, T. Tarutani, T. Ozawa, M. Yoshida, B. Iwasaki, M. Hirayama, and M. Kamada, "Geochemistry of the Tamagawa Hot Springs," Dedicated to Prof. E. Minami by his friends and students on his sixtieth birthday, Published in Tokyo (1963), p.23; Y. Uzumasa, "Chemical Investigation of Hot Springs in Japan," Tsukiji Shokan Co., Ltd. (1965), p. 83.

4) N. Ohta, M. Terai, and M. Isokawa, *Nippon Kagaku Zasshi,* **91,** 351 (1970).

Table 1. Mercury content of acid hot springs

Sample	Temperature (°C)	pH	Hg ($\mu g/l$)
Yubatake, Kusatu	64.8	1.7	7.2
Gunma Univ. Hospital, Kusatu	56.5	1.7	19
Sainokawara No. 4, Kusatu	54.4	1.8	19
Sainokawara No. 6, Kusatu	45.8	1.8	30
Ubayu, Manza	81.0	2.3	<0.1
Ōnigayu, Manza	71.0	2.0	<0.1
Suzunoyu, Manza	96.5	2.0	<0.1
Karabuki, Manza	94.0	1.3	<0.1
Syakunage, Manza	90.0	1.8	<0.1
Yukama, Mt. Shirane	16.4	0.8	17

precipitated as quickly as possible after the sample has been collected in order to prevent any loss of mercury. Cadmium nitrate solution containing 2.5 mg of cadmium was added to 500 m*l* of sample water as a carrier. The acidity of the solution was adjusted to 0.1N. After the solution had then been saturated with hydrogen sulfide, 0.5 m*l* of 5% aluminum nitrate solution was added and the mixture was mixed well. After not less than 24 hr, the sulfide precipitate was filtered and treated with 3 m*l* of aqua regia. The solution was aerated for several minutes, and then 2 m*l* of 20% hydroxylamine hydrochloride solution were added. The pH of the solution was adjusted to 4.5 with ammonium hydroxide; the final volume should be approximately 50 m*l*. The cupric ion was eliminated from this solution by adding 5 m*l* of 0.1 mol/*l* trifluoroacetylacetone-chloroform solution and shaking it for 10 minutes. The aqueous solution was separated and adjusted to 0.25N in sulfuric acid. Five milliliters of 0.001% dithizone-chloroform solution were added to the solution, and the mixture was shaken for one minute. The chloroform phase was separated, and the absorbance was measured at 490 mμ with a Shimadzu-Bausch & Lomb Spectronic 20 spectrophotometer.

Results and Discussion

The mercury contents of the acid hot springs are shown in Table 1, together with the pH values and the temperatures. The average mercury contents of hot springs of the Kusatu and Manza districts are shown in Table 2, along with the previously-reported values of various natural waters.

The mercury content of spring water seems to differ much according to the locality and the type of each hot spring. The values of Kusatu and Yukama are high and close to the data reported by Iwasaki *et al.*[3] On the other hand, the values of Manza are low and resemble the data of Stock and Cucuel.[2]

Table 2. Mercury content of natural waters

Sample	Location	Hg ($\mu g/l$)	Reference
Hot spring	Kusatu	19(av. of 4 samples)	This work
	Manza	<0.1(av. of 5 samples)	This work
	Tamagawa	10	Iwasaki *et al.*[3]
		0.1 —0.5	Stock and Cucuel[2]
Mineral water		15	Krainov[5]
Sea water	Ramapo Deep, Japan Trench	0.08—0.15	Hamaguchi *et al.*[6]
	Minamata Bay	1.6 —3.6	Hosohara *et al.*[7]
	Sagami Bay	2.7	Ohta *et al.*[4]
River water	Tokyo-to	2.8	Ohta *et al.*[4]

Kusatu and Manza hot springs are located at the east and the west foot of the Shirane volcano, respectively. It was suggested by Noguchi *et al.*[8] that the Kusatu and Manza hot springs belong to different types of springs. Both Kusatu and Manza are of the strong-acid type, but the contents of many chemical constituents, such as alkali metals, magnesium, calcium, iron, arsenic, vanadium, chloride and sulfate, differ considerably; for example, chloride is more abundant in Kusatu (231—622 mg/*l*) than in Manza (139—197 mg/*l*).[8,9] However, the difference in mercury contents between Kusatu and Manza is excessively large compared to that of other constituents. This fact is of great interest and suggests a relationship between the mercury content and the mechanism by which the spring water wells out.

The authors wish to thank Mr. T. Araki, Tokyo Metropolitan University, for his useful comments.

5) S. R. Krainov, *Byul. Nauchn. Tekhn. Inform. Min. Geol. i Okhrany Nedr. SSSR.* (1961), No. 2, 19; *Chem. Abstr.*, **57**, 7029h (1962).
6) H. Hamaguchi, R. Kuroda, and K. Hosohara, *Nippon Kagaku Zasshi*, **82**, 347 (1961).
7) K. Hosohara, H. Kozuma, K. Kawasaki, and T. Turuta, *ibid.*, **82**, 1479 (1961).
8) K. Noguchi, M. Ichikuni, T. Araki, T. Nishiido, A. Noguchi, and Y. Nakagawa, *Onsen Kagaku*, **17**, 9 (1966).
9) T. Araki, *ibid.*, **19**, 69 (1968).

BULLETIN OF THE CHEMICAL SOCIETY OF JAPAN, VOL. 44, 1155—1156 (1971)

Addition Reactions of Heterocumulenes to the Sb-N Bond

Jugo KOKETSU, Masaki OKAMURA, and Yoshio ISHII

Department of Synthetic Chemistry, Faculty of Engineering, Nagoya University, Furo-cho, Chikusa-ku, Nagoya

(Received October 15, 1970)

Even though much information on the reactions of Group Va metal amides with various unsaturated compounds is available, it has largely been limited to those of phosphorus and arsenic amide.[1-3] In this communication, some of our results on the reactions of organoantimony(III) amide with alkyl or aryl isocyanate or isothiocyanate are presented.

The reactions of *N,N*-dimethylaminodimethylstibine with equimolar alkyl or aryl isocyanate or isothiocyanate in ethyl ether took place exothermally at room temperature to give the simple insertion products as shown below.

$$Me_2SbNMe_2 + RNCX \longrightarrow Me_2Sb(R)NC(X)NMe_2$$

R=Me, Et, Bu^t, Ph; X=O or S

These addition products are very hygroscopic liquids and decomposed into white solids when exposed to air. The yield, physical properties, and the relevant spectral data are shown in experimental section and Tables 1 and 2.

The spectral data suggest that the 1:1 addition products are formed across the Sb–N bond.

Hydrolysis of all the addition products was performed with dilute hydrochloric acid, and the hydrolysis product were identified as trisubstituted urea and thiourea derivatives by their spectral data and by their failure to depress the melting points on admixture with authentic samples.

Experimental

Preparation of N,N-*Dimethylaminodimethylstibine.* To a solution of lithium amide, prepared from dimethylamine and *n*-buthyllithium in petroleum ether, an equimolar amount of dimethylchlorostibine, prepared according to the method of Davies,[4] was added slowly with ice cooling. The reaction mixture was heated for 1hr under reflux. Separation of lithium chloride by decantation and removal of the solvent gave crude *N,N*-dimethylaminodimethylstibine, which was purified by column distillation. Bp 62—65°C/75mmHg, yield 46%.

TABLE 1. PHYSICAL PROPERTIES AND ELEMENTAL ANALYSES OF $Me_2Sb(R)NC(X)NMe_2$

	Compound	Reaction	Bp (°C/mmHg) [Mp °C]	Yeild (%)	Found (%)			Calcd (%)		
					C	H	N	C	H	N
I	R=Et, X=O	Exothermic	72.5— 73.5/0.25	78	32.07	6.37	10.80	31.49	6.42	10.49
II	R=Bu^t, X=O	Exothermic	28.5— 29.0/0.15	72	36.91	7.35	9.23	36.64	7.17	9.49
III	R=Ph, X=O	Exothermic	98 — 99/0.07 [59.0— 60.0]	62	42.94	5.32	8.15	41.94	5.44	8.89
IV	R=Me, X=S	Exothermic	76 — 77/0.31	59	26.20	5.69		26.79	5.62	
V	R=Ph, X=S	Exothermic	117 —118/0.02	73	39.69	5.02	8.95	39.91	5.18	8.46

TABLE 2. RELEVANT IR FREQUENCIES AND NMR ABSORPTIONS OF $Me_2Sb(R)NC(X)NMe_2$

Compound	(IR cm^{-1})[a]				NMR (τ, ppm)[c]
	ν(N=C=X)[b]		ν(SbC_2)		
	asym.	sym.	asym.	sym.	
I	1638 (s)	1523 (s)	532 (w)	518 (w)	6.70 (q, 2H, NCH_2-), 8.92 (t, 3H, -CH_3) 7.15 (s, 6H, NMe_2), 9.05 (s, 6H, $SbMe_2$)
II	1640 (s)	1513 (s)	533 (w)	518 (w)	7.05 (s, 6H, NMe_2), 8.71 (s, 9H, NBu^t) 9.08 (s, 6H, $SbMe_2$)
III	1680 (w)	1560 (s)	519 (w)	509 (w)	3.20 (m, 5H, NPh), 7.43 (s, 6H, NMe_2) 9.45 (s, 6H, $SbMe_2$)
IV	1540 (s)	1345 (s)	522 (w)	518 (w)	6.65 (s, 3H, NMe), 7.00 (s, 6H, NMe_2) 9.06 (s, 6H, $SbMe_2$)[d]
V	1580 (s)	1360 (s)	515 (w)	510 (w)	3.29 (m, 5H, NPh), 7.00 (s, 6H, NMe_2) 9.22 (s, 6H, $SbMe_2$)

a) In $CHCl_3$, b) X=O or S, c) 10% solution in $CHCl_3$, d) 10% solution in C_6H_6

1) G. Oertel, H. Mals, and H. Haltschmidt, *Chem. Ber.*, **97**, 891 (1964).
2) H. J. Vetter and H. Nöth, *Angew. Chem.*, **75**, 417 (1963).
3) H. J. Vetter and H. Nöth, *Z. Naturforsch.* **19b**, 167 (1964).
4) G. T. Morgan and G. R. Davies, *Proc. Roy. Soc.*, **110**, 523 (1926).

Reaction of N,N-*Dimethylaminodimethylstibine with Isocyanates.* Typical experiment is described. Further details are shown in Tables 1 and 2. Methyl isocyanate (0.38 g, 6.67 mmol) in ethyl ether was added dropwise with constant stirring to *N,N*-dimethylaminodimethylstibine (1.30 g, 6.64 mmol) in the same solvent (5 m*l*). The reaction was exothermic. The white crystals formed. The crystals, *N,N,N'*-trimethylureidodimethylstibine (1.05g, 63%), were collected by filtration and washed several times with ethyl ether. Mp 75°C; ν(N=C=O), 1640(s), 1530(s); $\nu(SbC_2)$, 530, 518cm^{-1}; τ, 7.10 (s, 3H, NMe), 7.12 (s, 6H, NMe_2), 9.05 (s, 6H, $SbMe_2$).

Found: C, 27.91; H, 6.57; N, 11.38%. Calcd for $C_6H_{15}N_2OSb$: C, 28.49; H, 5.98; N, 11.08%.

A portion (0.1g) of this product was treated with dilute hydrochloric acid to give white crystals which were proved to be *N,N,N'*-trimethylurea (0.37g, 98%) by comparison of its mp and spectral data with those of an authentic sample.

BULLETIN OF THE CHEMICAL SOCIETY OF JAPAN, VOL. 44, 1156—1158(1971)

Proton NMR Spectrum of *N*-Phenethyl-*o*-anisidine[1)]

Teruzo Asahara, Manabu Senō, Sadayoshi Tanaka, and Masatoshi Akiyama
Institute of Industrial Science, The University of Tokyo, Roppongi, Minato-ku, Tokyo

(Received November 2, 1970)

It was reported that anionic telomerizations where anisidines and phenetidines were allowed to react as a telogen with styrene as a taxogen in the presence of alkali metals gave phenethylamines.[1)] Each of the telomers showed two methylene triplets in the NMR spectrum, the assignment of which was not elucidated.

This paper reports on the preparation of mixed telomers composed of *N*-phenethyl-*o*-anisidine and *N*-phenethyl-*β*-*d*-*o*-anisidine and the assignment of NMR spectrum of *N*-phenethyl-*o*-anisidine done by analyzing the NMR spectra of the mixed telomers.

Results and Discussion

Exchange Reaction between O-*Anisidine and Deuterium Oxide*

The exchange reaction between *o*-anisidine and deuterium oxide in the presence of a small amount of potassium deuteroxide gave mixed amines, *i.e. o*-

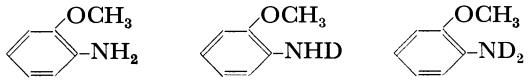

1 **2** **3**

anisidine **1**, *o*-anisidine-*N*-*d* **2**, and *o*-anisidine-*N*-d_2 **3**. Since the above is an equilibrium reaction, the partly deuterated *o*-anisidine may be composed of **1**, **2**, and **3**. The extent of deuteration of the amino group calculated from the integral curve of NMR spectrum was 55%. On treating *o*-anisidine with deuterium oxide, the intensity of –NH– stretching vibration of the amine at 3350—3450 cm^{-1} decreased and –ND– stretching vibration appeared at 2400—2600 cm^{-1}. This is consistent with the fact that the amino group of *o*-anisidine was partly deuterated.

Anionic Telomerization of Mixed o-*Anisidine with Styrene.*

In the first place the mixed *o*-anisidine was allowed to react with an alloy of sodium and potassium to form organometallic compounds **5** and **6**, which acted as an initiator (I). In the next place telomerization was carried out by dropping styrene into the amine-alloy system (II,III). Finally, the reaction product was washed with water and dried, and thereafter purified by vacuum distillation (IV) : bp 156°C/2mmHg, n_D^{25} 1.5747, mol wt by VPO 229. Found: C, 79.02 ; H, 7.73; N, 6.40 %. Calcd for $[C_{15}H_{16}NO]_{0.48}$ $[C_{15}H_{15}DNO]_{0.52}$: C, 79.08; H and D, 7.79; N, 6.15 %.

These reactions are summarized as follows.

Thus, a mixture of *N*-phenethyl-*o*-anisidine **13** and *N*-phenethyl-*β*-*d*-*o*-anisidine **14** was prepared by the telomerization of styrene with the mixed amines.

Proton NMR Spectrum of Mixed Telomers **13** *and* **14**.

Figures 1 and 2 show the proton NMR spectrum of *N*-phenethyl-*o*-anisidine and that of the mixed telomers derived from the partly deuterated *o*-anisidine, respectively. In Fig. 1 two triplets with equal intensities appear at 2.79 ppm and 3.27 ppm, while in Fig. 2 the area of the triplet at 2.79 ppm decreases and the shape of the signal at 3.27 ppm is modified.

It may be derived from the reaction scheme and the consideration on the spectra that a triplet signal at 2.79 ppm should originate from the methylene group neighboring to the phenyl group and the other triplet at 3.27 ppm should be assigned to the methylene group attached to the nitrogen atom. The extent of deuteration of the obtained telomers, calculated from the integral curve in Fig. 2, reached 52 % of the mixed telomers.

The proton NMR spectra of *N*-phenethyl-*m*-anisidine, *N*-phenethyl-*p*-anisidine, *N*-phenethyl-*o*-phenetidine, *N*-phenethyl-*m*-phenetidine, and *N*-phenethyl-*p*-phenetidine previously reported[1)] can be interpreted in the same manner.

1) Anionic Telomerizaions. VI. Part V of this series: T. Asahara, M. Senō, S. Tanaka, and M. Akiyama, *Bull. Jap. Petrol. Inst.*, to be published.

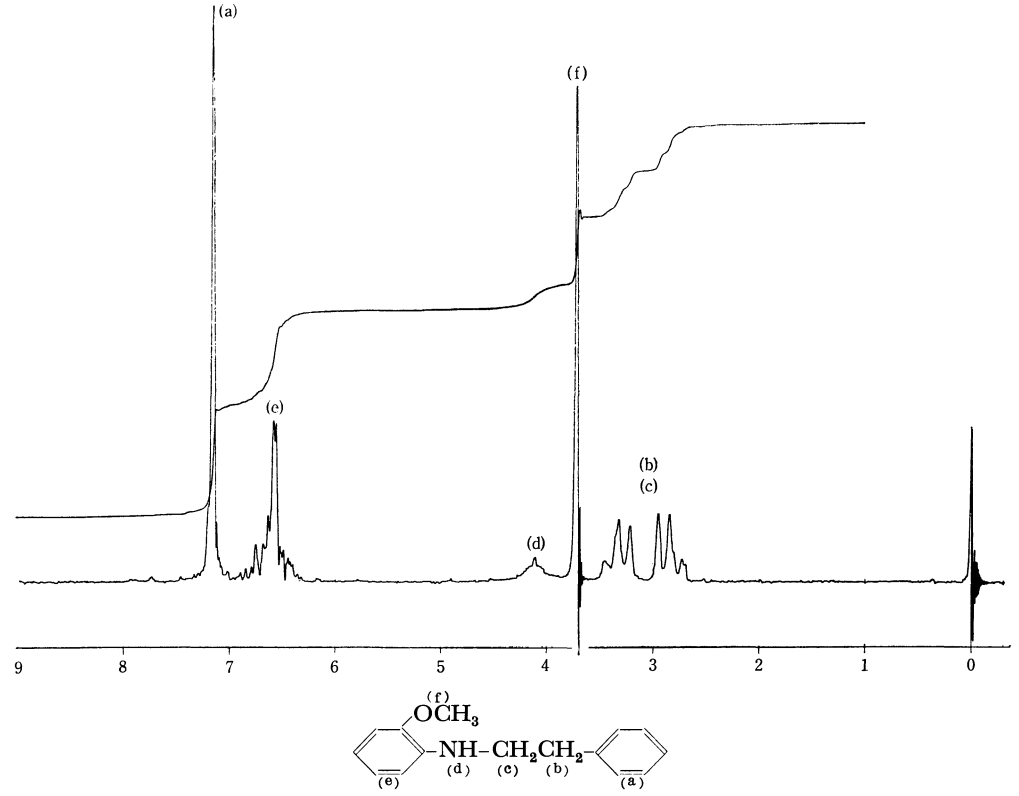

Fig. 1. Proton NMR spectrum of *N*-phenethyl-*o*-anisidine.

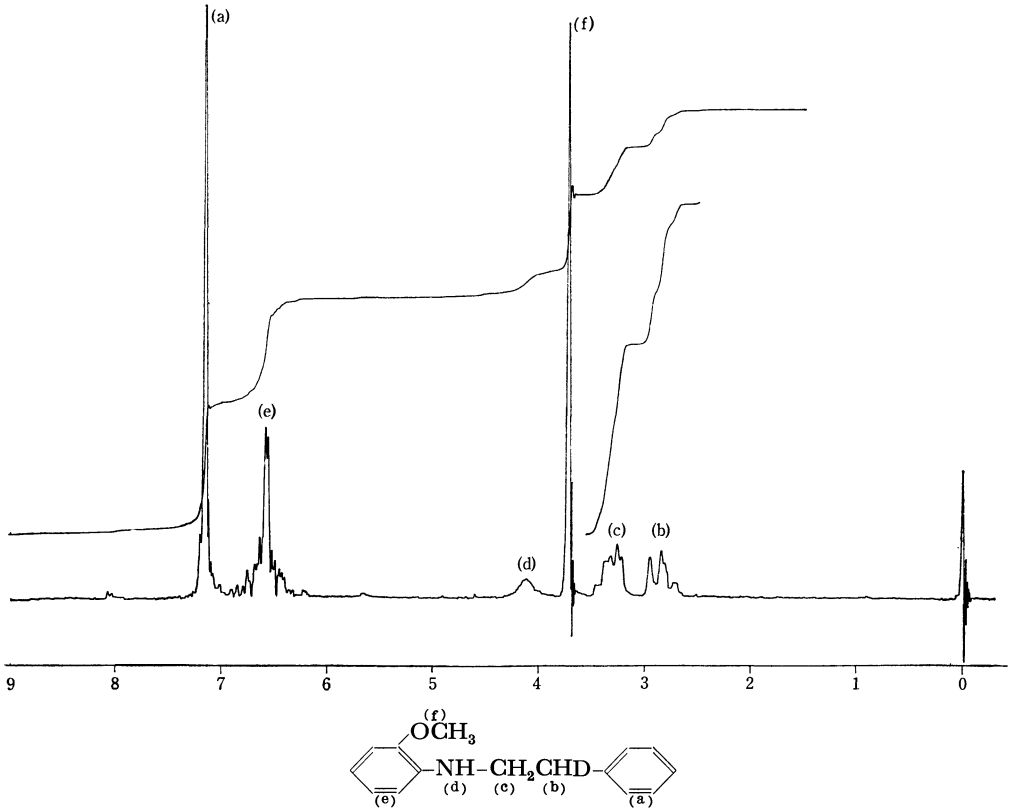

Fig. 2. Proton NMR spectrum of the mixed telomers composed of *N*-phenethyl-*o*-anisidine and *N*-phenethyl-*β*-*d*-*o*-anisidine.

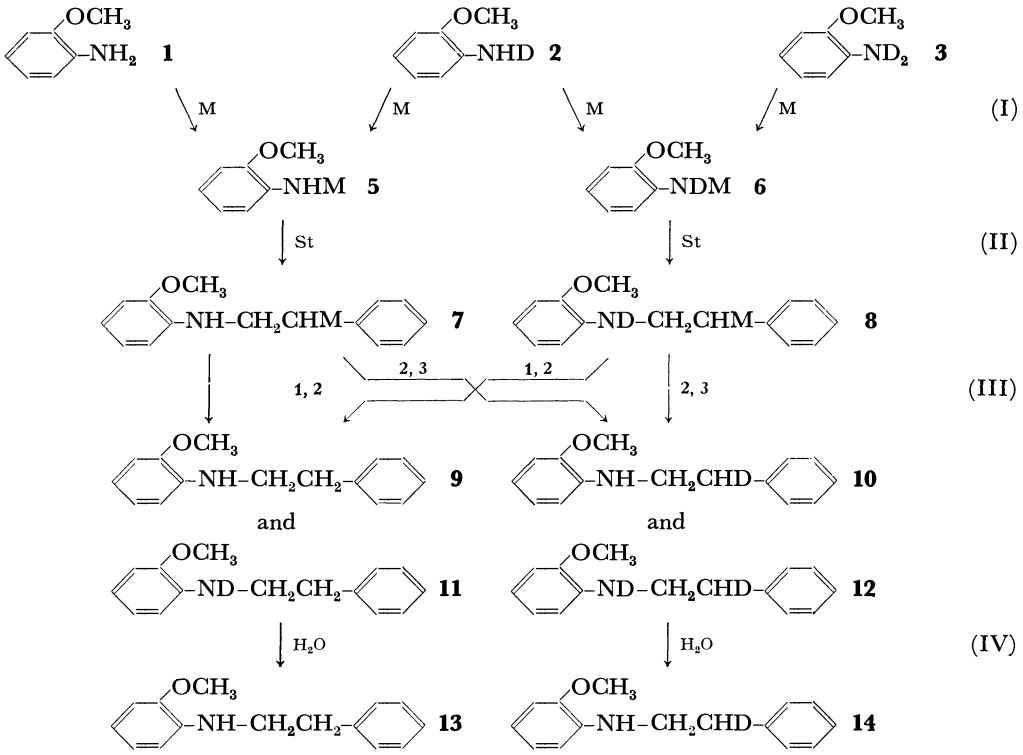
OCH3
-NH2 1
OCH3
-NHD 2
OCH3
-ND2 3
M
M
M
M
(I)
OCH3
-NHM 5
OCH3
-NDM 6
St
St
(II)
OCH3
-NH-CH2CHM- 7
OCH3
-ND-CH2CHM- 8
1, 2
2, 3
1, 2
2, 3
(III)
OCH3
-NH-CH2CH2- 9
and
OCH3
-NH-CH2CHD- 10
and
OCH3
-ND-CH2CH2- 11
OCH3
-ND-CH2CHD- 12
H2O
H2O
(IV)
OCH3
-NH-CH2CH2- 13
OCH3
-NH-CH2CHD- 14

M: Na or K

BULLETIN OF THE CHEMICAL SOCIETY OF JAPAN, VOL. 44, 1158—1160(1971)

On the Mechanism of Bromination of Olefins with Cupric Bromide

Takashi KOYANO

Central Research Laboratory, Toa Nenryo Kogyo Co., Oi-machi, Iruma-gun, Saitama

(Received November 2, 1970)

Although it is generally accepted that cupric chloride does not liberate chlorine molecule in chlorination of organic substances,[1] the active species has not been established in bromination of organic compounds with cupric bromide. The bromination of acetone to bromoacetone in methanol at 0°C has been explained as the reaction of cupric bromide molecule,[2] while in the nuclear bromination of alkylbenzenes at 110—120°C a possibility of participation of bromine molecule has been suggested.[3] Rate of the bromination of allyl alcohol to form 2,3-dibromopropanol in refluxing methanol has been reported to be second order in cupric bromide and independent of olefin.[4] This rate equation was

$$\text{rate} = k[CuBr_2]^2 \qquad (1)$$

explained by assuming the dissociation of cupric bromide to molecular bromine, which was claimed to be the actual brominating agent in the reaction. Consumption of bromine[4] or removal of cuprous bromide by complex formation with olefin[5] has been believed to be a driving force for the dissociation of cupric bromide.

$$2CuBr_2 \underset{k_b}{\overset{k_a}{\rightleftharpoons}} 2CuBr + Br_2 \qquad (2)$$

In order to obtain further experimental results to discuss the reaction mechanism, the bromination of 1-hexene has been kinetically investigated in methanol.

The products were the dibromide (I) and the methoxybromide (II) with a small amount of by-products ($<1\%$). To avoid complication by the effect of resulting cuprous bromide, the rates are expressed by initial rates and shown in Table 1.

Plots of log[$CuBr_2$] and log[hexene] *vs.* log v showed straight lines, and rate orders were calculated from these lines. The rates were expressed by following equations, where v_1 and v_2 are the rates of formations of I and II, respectively.

$$v_1 = k_1[\text{hexene}][CuBr_2]^{1.8-2.0} \qquad (3)$$

$$v_2 = k_2[\text{hexene}][CuBr_2] \qquad (4)$$

Since the rate order in [$CuBr_2$] is smaller for II, I can not be a precursor of II, that is, II was not formed by methanolysis of I.

1) T. Koyano, This Bulletin, **43**, 1439 (1970), and references cited therein.

2) S. Kawaguchi and Y. Kojima, *Shokubai*, **8**, 239 (1966).

3) P. Kovacic and K. E. Davis, *J. Amer. Chem. Soc.*, **86**, 427 (1964).

4) C. E. Castro, E. J. Gaughan, and D. C. Owsley, *J. Org. Chem.*, **30**, 587 (1965).

5) W. C. Baird, Jr., and J. H. Surridge, *ibid.*, **35**, 2090 (1970).

Table 1. Rate of reaction

Method	Temp. (°C)	hexene (mol/l)	$CuBr_2$ (mol/l)	$v_1 \times 10^6$ (mol/l·sec)	$v_2 \times 10^6$ (mol/l·sec)	n_1	n_2	m_1	m_2
A	40	0.184	0.197	3.96	2.99	2.0	1.1		
		0.182	0.288	8.56	4.73				
		0.192	0.374	14.3	5.82				
B	50	0.088	0.291	4.23	3.47	1.8	1.0	1.1	1.0
		0.175	0.290	9.38	6.75				
		0.350	0.287	18.3	12.5				
		0.350	0.453	41.3	19.3				

$v_1 = k_1[\text{hexene}]^{m1}[CuBr_2]^{n1}$ $v_2 = k_2[\text{hexene}]^{m2}[CuBr_2]^{n2}$

If the equilibrium of Eq. 2 had been attained rapidly, Eq. (5) must have been realized.

$$k_a[CuBr_2]^2 = k_b[CuBr]^2[Br_2] = 4k_b[Br_2]^3 \quad (5)$$

Then, concentration of bromine should be approximately proportional to the 2/3 power of cupric bromide added. The present data are hardly interpreted as the bromination with bromine.

If the reaction proceeds by bromination with bromine, an allylic bromination may be expected.[6] However, the bromination of cyclohexene with cupric bromide in refluxing carbon tetrachloride afforded 1,2-dibromocyclohexane but no 3-bromocyclohexene.

A possible explanation is that the olefin initially forms a complex with cupric bromide, followed by competitive attack of this complex by solvent methanol and another cupric bromide molecule or bromide ion. The latter step should be rate-determining.

We have also studied the bromination of isomeric 2-butenes in refluxing methanol. The resulted dibromides were composed exclusively of those expected from "*trans*" addition of bromine, in contrast to the case with cupric chloride, where a mixture of diastereomeric dichlorides was obtained.[7] Similarly, the products from cyclohexene have been reported to be only *trans*-dibromide and *trans*-methoxybromide,[5] while cupric chloride yielded the corresponding *cis*-compounds at the same time.[7] Therefore, the intermediate complex must resemble a bridged bromonium ion type species.

In summary, the reaction may be represented by the following scheme.

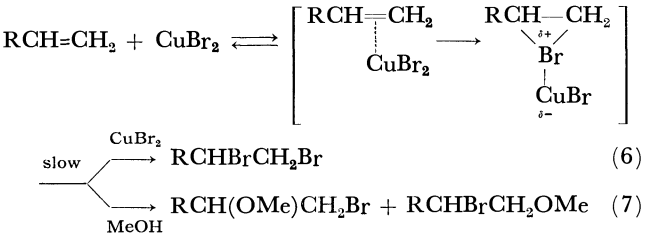

$$\xrightarrow[\text{slow}]{CuBr_2} RCHBrCH_2Br \quad (6)$$

$$\xrightarrow[MeOH]{} RCH(OMe)CH_2Br + RCHBrCH_2OMe \quad (7)$$

Experimental

Materials. All the reagents were the commercially available purest reagents, purified appropriately when necessary. I and II, 1,2-dibromocyclohexane, and diastereomeric 2,3-dibromobutanes were synthesized by addition of bromine to 1-hexene in methanol,[8] cyclohexene in CCl_4,[9] and *trans*- and *cis*-2-butenes in CH_2Cl_2,[10] respectively. 3-Bromocyclohexene was prepared by allylic bromination of cyclohexene with NBS in CCl_4 in the presence of benzoyl peroxide[11] (bp 65—66.5°C/20 mmHg).

Analysis. Cupric ion was determined by iodometry.[12] Cuprous ion was titrated with the standard ceric solution using ferroin as the indicator.[13] Glpc was performed on a Shimadzu GC-4AF gas chromatograph (dioctyl sebacate on Chromosorb W, 135°C, H_2 flame detector).

Kinetic Measurements. *Method A*: A solution of cupric bromide in methanol was placed in a Schlenk tube under N_2 and prewarmed in a constant temperature bath (±0.05°C). A measured amount of 1-hexene was added in the solution and the reaction was started. From time to time 10m*l* of the reaction solution was removed and was poured into 20ml of 0.05 M ferric ammonium sulfate solution (in 3N H_2SO_4) immediately after taking a small amount of sample for glpc, and the cuprous ion was titrated.

Method B: A sealed tube technique was employed; in each 15m*l* glass sealed tube 10m*l* of the reaction mixture was placed under N_2. At intervals the tube was taken out from the bath (± 0.05°C), cooled in ice-water, and kept in a freezer (−20°C). After the last tube was removed, the reaction solutions were analyzed as quickly as possible.

The amount of consumed cupric bromide was divided between the dibromide and the methoxybromide in the ratio of the glpc analysis. Then, amounts of the products were calculated on assumption that one mole of either product was formed by consumption of two moles of the cupric salt. The methoxy-bromide was composed of approximately 18% of 1-methoxy-2-bromohexane and 82% of 1-bromo-2-methoxyhexane (by Hitachi 063 gas chromatograph with Apiezon L capillary column at 90°C).

Reaction of Cyclohexene. A mixture of cyclohexene (3.3g, 0.04 mol) and cupric bromide (8.9g, 0.04mol) in CCl_4 (40 m*l*) was refluxed for 1hr under N_2. The resulted grey powder was dissolved in aqueous methanol after drying under reduced pressure, and cupric ion was titrated. The conversion was *ca.* 98%. The main reaction product was 1,2-dibromocyclohexane with some by-products (*ca.* 5%), and 3-bromocyclohexene was

6) B. P. McGrath and J. M. Tedder, *Proc. Chem. Soc.*, **1961**, 80.
7) T. Koyano, This Bulletin, **43**, 3501 (1970).
8) W. H. Puterbaugh and M. S. Newman, *J. Amer. Chem. Soc.*, **79**, 3469 (1957).
9) H. R. Snyder and L. A. Brooks, "Organic Syntheses", Coll. Vol. II. p.173 (1943).
10) J. H. Rolston and K. Yates, *J. Amer. Chem. Soc.*, **91**, 1469 (1969).
11) L. F. Hatch and G. Bachmann, *Chem. Ber.*, **97**, 132 (1964).
12) W. T. Elwell and D. Price, "Comprehensive Analytical Chemistry", Vol. Ic. ed. by C. L. Wilson and D. W. Wilson, Elsevier Publishing Co., Amsterdam (1962), p.371.
13) I. M. Kolthoff and R. Belcher, "Volumetric Analysis", Vol. III, Interscience, New York (1957), p. 121.

not detected by glpc.

Reaction of 2-Butenes. A solution of cupric bromide in methanol (0.50 mol/*l*) was refluxed for 4 hr under 2-butene atmosphere (1 atm). The results were (the starting 2-butene, conversion, and ratio of the dibromide (III) to the methoxybromide (IV)): *trans*, 14.1%, 0.87; *cis*, 25.3%, 1.07. The dibromides formed were exclusively the "*trans*" addition products, *i.e.*, *meso* from *trans* and *dl* from *cis*.

The dibromides were sufficiently stable under the reaction conditions. When III (4 mmol) was heated in refluxing methanol (30 m*l*) with cupric bromide (15 mmol) for 4 hr under N_2, 1.1% of *erythro*-IV was formed from the *meso*-III and 0.2% of *threo*-IV from the *dl*-III.

BULLETIN OF THE CHEMICAL SOCIETY OF JAPAN, VOL. 44, 1160(1971)

The Synthesis of 2,8-Diphenyl-4*H*,10*H*-benzodipyran-4,10-dione

Yoshimori OMOTE, Yasuomi TAKIZAWA, and Noboru SUGIYAMA
Department of Chemistry, Tokyo Kyoiku University, Otsuka, Bunkyo-ku, Tokyo
(Received November 6, 1970)

Recently one of the present authors has reported a new flavone, "arthraxin" (I), with a 4*H*,10*H*-benzodipyran-4,10-dione skeleton.[1] Now the unequivocal synthesis of 2,8-diphenyl-4*H*,10*H*-benzodipyran-4,10-dione (II) has been performed in a way which will be described below.

The acetylation of 5,7-dihydroxyflavone (III) with acetic acid in the presence of boron trifluoride affords 8-acetyl-5,7-dihydroxyflavone (IV). The alternative structure V is rejected by means of a study of the NMR spectrum, as is shown in Table 1. From the calculation, based on the analysis in terms of the additive substituent shielding values,[2-4] each proton at H-6 or H-8 can be predicted to have the same value. The difference between the real value of the protons at H-6 and H-8 can be explained as being caused by the ring current of the structure IX. Heating an *o*-hydroxyacetophenone, IV, with benzoic anhydride and sodium benzoate gives the title compound, II. All the spectral data as well as the result of the elemental analysis support this structure.

TABLE 1. (δ)

Compound	H-8	H-6	H-3
III	6.55	6.25	6.85
IV		6.35	6.70
VI	6.57	6.36	6.65
VII	6.56	6.38	6.63
VIII	6.86	6.56	6.73

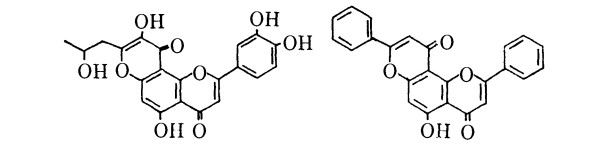

I

II

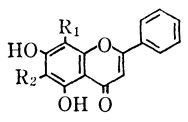

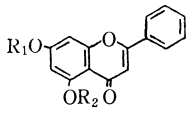

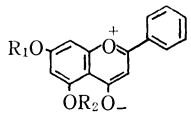

III: $R_1=R_2=H$ VI: $R_1=R_2=CH_3$
IV: $R_1=COCH_3$, $R_2=H$ VII: $R_1=CH_3$, $R=H$
V: $R_1=H$, $R_2=COCH_3$ VIII: R_1COCH_3, $R_2=H$

Experimental

8-Acetyl-5,7-dihydroxyflavone (IV). Through a solution of 5,7-dihydroxyflavone (III) (0.4g) in acetic acid saturated with boron trifluoride, boron trifluoride gas was passed for 5 hr with stirring. The color of the reaction mixture turned from yellow to brown, and then yellow precipitates appeared. The precipitates were filtered and treated by heating under reflux in 200m*l* of water for 20 min to produce IV as yellow precipitates. This was purified by sillica-gel-column chromatography, using a benzene-ethyl acetate (2:1) mixture, to give pale yellow needles; mp 208 —209°C; UV, 235 (15700), 248 (15200), and 276 (16700) nm (ε); IR (KBr), 3450, 1655, 1605, and 1590 cm^{-1}; NMR ($CDCl_3$), δ 2.85 (s, 3H, $PhCOCH_3$), 6.35 (s, 1H, H-6), 6.70 (s, 1H, H-3), 7.5—8.0 (m, 5H, H-2', 3', 4', 5', 6'), 13.8 (s, IH), 14.3 (s, 1H).

Found: C, 69.04; H, 4.22%. Calcd for $C_{17}H_{12}O_5$: C,68.91; H, 4.08%.

2,8-Diphenyl-4H,10H-benzodipyran-4,10-dione (II). A mixture of 8-acetyl-5,7-dihydroxyflavone (0.5 g), benzoic anhydride (10 g), and sodium benzoate (1 g) was blended in a mortar and then heated in an oil bath at 180°C for 6 hr. The reaction mixture was dissolved in 30 m*l* of ethanol, and to this solution a solution of potassium hydroxide (3.2 g) in water (2 m*l*) was added; the mixture was then heated under reflux for 30 min to decompose a benzene of II. After the ethanol had been evaporated from the mixture, water was added and a stream of carbon dioxide was passed through to give yellow precipitates. The precipitates were filtered, washed with acetone, and then reprecipitated from a benzene-ethyl acetate (1:1) mixture to afford pale yellow powders; mp 275°C (decomp.); UV, 256 (41900) and 287 (40700) nm(ε); IR, 3450, 1655, 1640, and 1585 cm^{-1}; NMR δ 6.85 (s, 1H), 6.95 (s, 1H), 7.30—7.65 (m, 7H), 7.8—8.1 (m, 4H), 12.25 (s, 1H).

Found: C, 75.02; H, 3.79%. Calcd for $C_{24}H_{14}O_5$:C, 75.39; H, 3.69%.

1) M.Kaneta and N.Sugiyama, This Bulletin, **42**, 2984 (1969).
2) H. Spiesecke and W. G. Schneider, *J. Chem. Phys.*, **35**, 731 (1961).
3) P. Diehl, *Helv. Chim. Acta*, **44**, 829 (1961).
4) J. A. Ballantine and C. T. Pillinger, *Tetrahedron*, **23**, 1691 (1967).

BULLETIN OF THE CHEMICAL SOCIETY OF JAPAN, VOL. 44, 1161—1162(1971)

Spontaneous Electron Transfer from Amines to Simple Quinones in an Aqueous Medium

Kazuhiro MARUYAMA, Shigetoshi SUZUE, and Jiro OSUGI

Department of Chemistry, College of Liberal Arts and Science, and Department of Chemistry, Faculty of Science, Kyoto University, Kyoto

(Received November 6, 1970)

The formation of radical anions arising from thermal electron transfer between tetrahalogenated *p*-benzoquinone and *N*-tetramethyl-*p*-phenylenediamine has already been established.[1] Photochemically-activated electron transfer from amines to carbonyl compounds to result in the corresponding radical anions has also been recently reported by Davidson and Wilson.[2] The use of tetrahalogenated *p*- or *o*-benzoquinones as mild dehydrogenating reagents provides us with a useful method for preparing less stable quinones from the corresponding hydroquinones; the subject has been well documented by several authors.[3]

Recently we found that spontaneous electron transfer from amines to simple quinones without any electron-attracting substituents can occur in a deaerated aqueous medium. Stable radical anions of quinones, such as phenanthraquinone, acenaphthenequinone, and potassium phenanthraquinone-2-sulfonate, can be detected by ESR spectroscopy. The radical anions thus obtained are identified by comparison with that produced by the reduction of the corresponding quinone with alkali metal in tetrahydrofuran. Although phenanthraquinone and acenaphthenequinone are only slightly soluble in water, one can observe a strong ESR signal if the aqueous quinone solution saturated with a suitable amine is deaerated thoroughly. The ESR spectra of typical radical anions observed are shown in Fig. 1, together with that of the radical anion produced by the reduction of phenanthraquinone with calcium metal. The amines examined in these expreiments are ethylamine, diethylamine, and triethylamine. The mode of electron transfer may be formulated as follows:

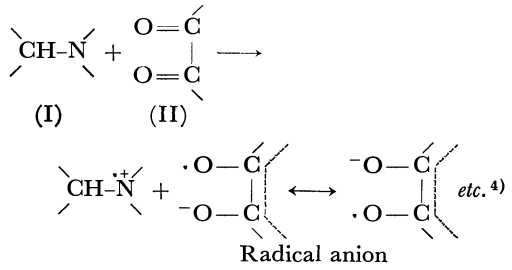

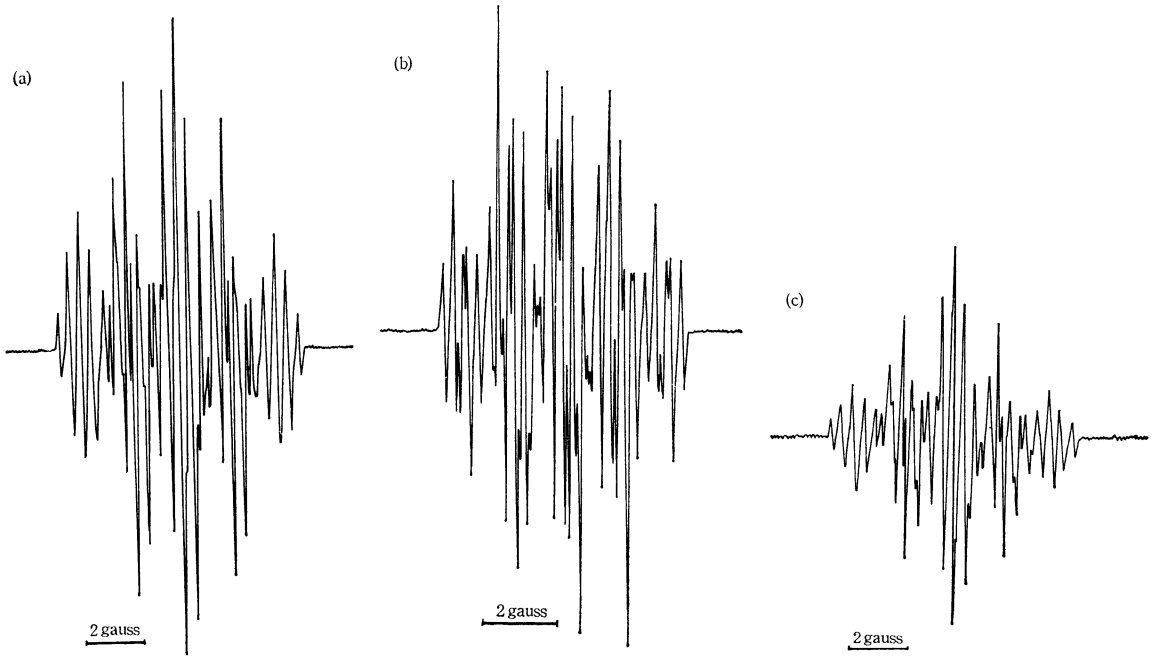

Fig. 1. (a) ESR spectrum of phenanthraquinone radical anion observed in the system phenanthraquinone-diethylamine-water (2H:1.73 gauss, 2H:1.69 gauss, 2H:0.41 gauss).
(b) ESR spectrum of potassium phenanthraquinone-2-sulfonate radical anion observed in the system potassium phenanthraquinone-2-sulfonate-diethylamine-water.
(c) ESR spectrum of radical anion produced by reduction of phenanthraquinone with metallic calcium-Hg in THF.

1) E.M.Kosower "An Introduction to Physical Organic Chemistry", John Wiley & Sons, New York, (1968), p. 189.
2) R.S.Davidson and R.Wilson, *J. Chem. Soc., B*, **1970**, 71.
3) D. Walker and J. D. Hiebert, *Chem. Rev.*, **67**, 153 (1967); W. M. Horspool, *Quart. Rev.* (London), **23**, 204 (1969); Hans-Dieter Becker, *J. Org. Chem.*, **34**, 1198, 1203, 1211 (1969).
4) A detailed chemical analysis of the products derived from amines is now being performed.

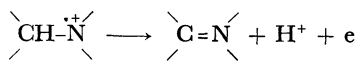

(III)

The *g*-values of the radical anions are summarized in Table 1.

TABLE 1. *g*-VALUES OF RADICAL ANIONS

Quinone	Reducing Reagent	*g*-Value
phenanthraquinone	diethylamine	2.0049[a]
phenanthraquinone	Na	2.0050[b]
phenanthraquinone	K	2.0051[b]
acenaphthenequinone	triethylamine	2.0049[a]
potassium phenanthraquinone-2-sulfonate	diethylamine	2.0050[a]
potassium phenanthraquinone-2-sulfonate	triethylamine	2.0050[a]

a) in water b) in tetrahydrofuran

For a comparison of the effect of the presence or absence of a counter cation around a radical anion molecule, the *g*-values of phenanthraquinone potassium and sodium ketyls have been determined; they are also tabulated in Table 1. However, although the distribution of the unpaired electron in radical anions is much affected by the presence or absence of a counter cation,[5] no meaningful difference in *g*-value between a free radical anion and an ion-paired one is observed.

Procedure. Quinone, dissolved in pure water, and amine were each deaerated, mixed by means of the technique of a breakable seal in the dark, and left overnight. The characteristic color of the radical anion gradually appeared; thereupon the sample was submitted to ESR spectroscopy. An X-band ESR spectrophotometer with 100 Kc modulation manufactured by JEOL was used in this research.

5) K.Maruyama and R.Goto, *Rev. Phys. Chem. Jap.*, **34**, 30(1964); K.Maruyama, M.Yoshida, and J.Osugi, *ibid.*, **39**, 117 (1969).

BULLETIN OF THE CHEMICAL SOCIETY OF JAPAN, VOL. 44, 1162—1164(1971)

Fluorescence and Phosphorescence Spectra of α-Naphthol in Relation to Hydrogen Bonding and Proton Transfer

Akio MATSUYAMA* and Hiroaki BABA

Division of Chemistry, Research Institute of Applied Electricity, Hokkaido University, Sapporo

(Received November 9, 1970)

Formation of a hydrogen bond between α-naphthol and a suitable proton-accepting substance may result in a change of the fluorescent state (or the lowest excited singlet state S_1) of α-naphthol from ^1L_b to ^1L_a state. It is possible that the proton may be transferred from the naphthol to the proton acceptor in the fluorescent state.[1] These problems were discussed in a previous paper by Suzuki and Baba using ether and triethylamine as proton acceptors.[2] The present note reports the results of further investigations on the same problems and also on the possibility of proton transfer in the phosphorescent state (or the lowest triplet state T_1). In this study we have employed dimethylformamide as a proton acceptor in addition to ether and triethylamine.

Figure 1 shows fluorescence and phosphorescence spectra of α-naphthol at 77°K in a mixture of isopentane and methylcyclohexane containing ether, dimethylformamide, or triethylamine.

From the behavior of the excitation-polarization spectra related to fluorescence, it has been demonstrated that the naphthol-ether system forms a simple hydrogen-bonded complex in S_1 state of ^1L_b type, while in the naphthol-triethylamine system the proton transfer takes place to yield an ion pair within the lifetime of the excited singlet state, and the fluorescence originates in the ion pair from its S_1 state which can be assigned to ^1L_a state[2].

It is seen from Fig. 1 that on changing the proton acceptor from ether to dimethylformamide the fluorescence spectrum is displaced to the red, as expected from the greater proton-accepting power of the amide as compared to ether.[3,4] In the case of dimethylformamide as acceptor, however, the fluorescence spectrum is located at a considerable distance from the spectrum of the ion pair of naphthol-triethylamine system. Thus the former is regarded as due to the α-naphthol molecule which forms a simple hydrogen bond with the amide. On the other hand, the spectrum of the naphthol-amide system is structureless, suggesting the S_1 state to be ^1L_a. The excitation-polarization spectrum related to the fluorescence of this system was measured and found to be very similar to the corresponding polarization spectrum obtained for the ion pair of naphthol-amine system.[2] We thus conclude that the fluorescent state of the hydrogen-bonded complex between the naphthol

*Present address: Biophysics Division, National Cancer Center Research Institute, Tsukiji, Chuo-ku, Tokyo.

1) N. Mataga and Y. Kaifu, *J. Chem. Phys.*, **36**, 2804 (1962); H. Baba, *ibid.*, **49**, 1763 (1968) and papers cited therein.

2) S. Suzuki and H. Baba, This Bulletin, **40**, 2199 (1967).

3) G. C. Pimentel and A. L. McClellan, "The Hydrogen Bond," W. H. Freeman and Company, San Francisco, Calif. (1960), Appendices.

4) When dimethylformamide was used as proton acceptor, a small amount of ether (0.2 mol/*l*) was added to get a better rigid glass. However, owing to the greater proton-accepting power of the amide, α-naphthol is considered to form the hydrogen bond only with the amide molecule.

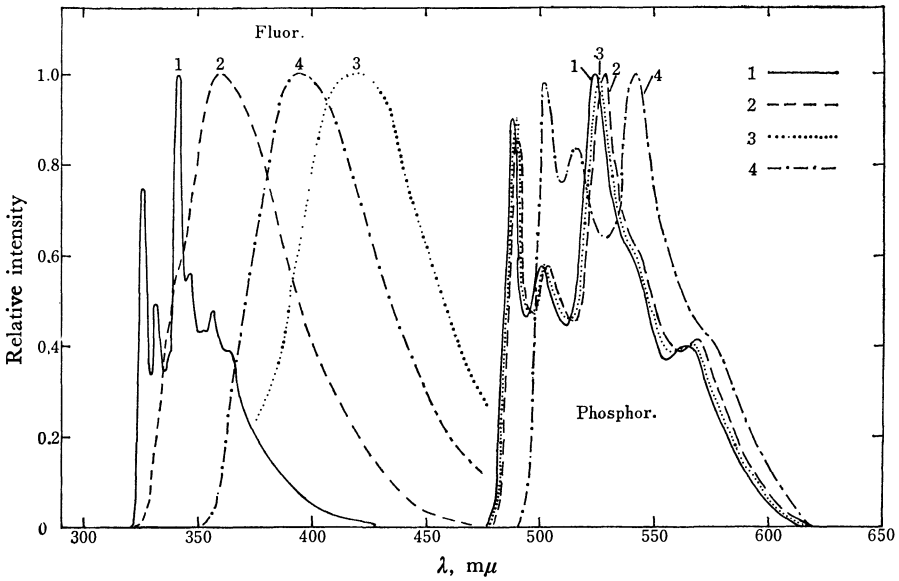

Fig. 1. Fluorescence and phosphorescence spectra of α-naphthol at 77°K: 1, 2, and 3, in isopentane-methylcyclohexane (volume ratio, 1:1) containing ether (1.0 mol/*l*), dimethylformamide (0.015 mol/*l*), and triethylamine (0.2 mol/*l*), respectively; 4, in ethanol-methanol (5:1) containing potassium hydroxide (5×10^{-3} mol/*l*).

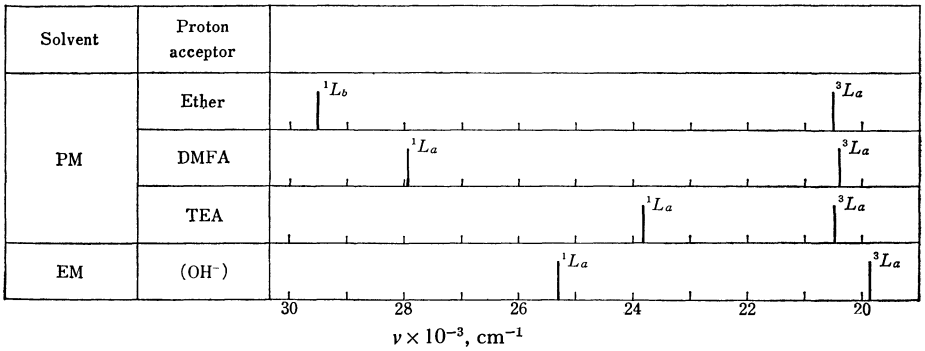

Fig. 2. Location of fluorescence maxima and phosphorescence 0–0 bands at 77°K for α-naphthol hydrogen-bonded with proton acceptors of different strengths and for α-naphtholate ion. PM, isopentane-methylcyclohexane (1 : 1); EM, ethanol-methanol (5 : 1); DMFA, dimethylformamide; TEA, triethylamine.

and dimethylformamide is of ^1L_a type.

In Fig. 1 are also shown the fluorescence and phosphorescence spectra of α-naphthol in an alkaline ethanol - methanol mixture in which the naphthol is converted to the naphtholate ion. Figure 2 shows the positions of the fluorescence and phosphorescence spectra of α-naphthol coupled with different proton acceptors, together with the positions of spectra of naphtholate ion. The emitting states are given in the Platt notation; the phosphorescent states are assigned to ^3L_a, as is generally accepted.[5] It should be noted that S_1 and T_1 states have the same electron configuration L_a in all cases except for the case of ether as proton acceptor.

The phosphorescence spectrum of α-naphthol - triethylamine system closely resembles the corresponding spectra of the naphthol - ether and naphthol - dimethylformamide systems both in position and in shape. The phosphorescence spectra of the naphthol associated with any of the proton-accepting substances are quite different from the spectrum of the α-naphtholate ion. Consequently, it is reasonable to attribute the former spectra to the respective hydrogen - bonded complexes in which no proton transfer occurs. Thus, phosphorescence is emitted solely from the simple hydrogen - bonded species even when triethylamine is used as the proton acceptor. Since in the naphthol - triethylamine system the ion pair is responsible for the fluorescence, proton transfer must occur in the reverse direction within the lifetime of T_1 state.

The results of the present investigations on the fluorescence and phosphorescence spectra of α-naphthol in relation to hydrogen bonding and proton transfer are consistent with the view that the acidity of a phenolic compound is in general much weaker in the triplet state than in the excited singlet state.[6]

5) S. P. McGlynn, T. Azumi, and M. Kinoshita, "Molecular Spectroscopy of the Triplet State," Prentice-Hall, Englewood Cliffs, N. J. (1969).

6) G. Jackson and G. Porter, *Proc. Roy. Soc. Ser.*, *A*, **260**, 13 (1961).

Experimetal

α-Naphthol was recrystallized from ligroin and was sublimed *in vacuo*. Methylcyclohexane of spectroscopic quality was used without further purification. Isopentane was passed through a silica-gel column. Ethyl ether was distilled over metallic sodium. Dimethylformamide was shaken with potassium hydroxide and calcium oxide and was then distilled. Triethylamine was fractionally distilled over phosphorus pentoxide. Absorption and emission spectra and excitation-polarization spectra were measured at 77°K in the same way as described previously.[7]

7) T. Takemura and H. Baba, This Bulletin, **42**, 2756 (1969).

BULLETIN OF THE CHEMICAL SOCIETY OF JAPAN, VOL. 44, 1164—1165 (1971)

Elementary Reactions of Metal Alkyl in Anionic Polymerization. VI. The Synthesis and Reactivity of Calciumzinc Tetra-*n*-butyl

Yusuke KAWAKAMI, Yoshiro YASUDA, and Teiji TSURUTA
Faculty of Engineering, The University of Tokyo, Bunkyo-ku, Tokyo

(Received November 14, 1970)

According to the standard method proposed by Gilman,[1] calciumzinc tetraethyl ($CaZnEt_4$) is prepared in benzene by an interchange reaction between diethylzinc and metallic calcium. Diethyl ether cannot be used for the solvent, because it is too reactive, the calcium ate complex formed being decomposed by the ether.[2] Diethyl ether, on the other hand, has been found to be an appropriate solvent for the preparation of calciumzinc tetra-*n*-butyl ($CaZn(n\text{-}Bu)_4$).

Experimental

*Preparation and Analysis of Calciumzinc Tetra-*n*-butyl.* A mixture of 4.0g (0.10 atom) of calcium metal, 27 m*l* (0.155 mol) of $n\text{-}Bu_2Zn$, and 27 m*l* of diethyl ether was heated, under stirring, to 50—60°C (bath temperature), the temperature was maintained at that value for about 24hr. During the reaction a reddish suspension was produced. After 24hr, heating and stirring were stopped and the reaction mixture was allowed to stand at least one night. The supernatant layer was then taken out with a syringe and put into a 100-m*l* flask. Then the ether and the unreacted $n\text{-}Bu_2Zn$ were removed under reduced pressure. The yellow residue was washed with *n*-heptane several times and then freeze-dried from benzene. The residue was dissolved again into diethyl ether, and the calciumzinc tetra-*n*-butyl in the supernatant solution was analyzed by EDTA chelate titration, NMR, and vapor-phase chromatography(vpc). The tetrabutyl compound, unlike $CaZnEt_4$, cannot be prepared in benzene. The use of tetrahydrofuran as a solvent resulted in producing the ate compound in a lower yield. Dimethoxyethane and 1,4-dioxane could not be used as solvents because of their high reactivities toward the calcium compound.

*Analysis of Calciumzinc Tetra-*n*-butyl.* In EDTA chelate titration, the amount of zinc was determined by using xylenol orange (XO) as an indicator at pH 5.0—5.5 (CH_3COOH-CH_3COONa buffer solution).[3] The total amount of calcium plus zinc was determined by using Eriochrome Black T (EBT) as an indicator at pH 10.0 (NH_3-NH_4Cl buffer solution).[3] The results of the analyses are shown in Table 1. As is shown in Table 1, the ratio of calcium to zinc(1.05±0.02), as well as that of *n*-butyl to metal (4.1±0.1), is in accordance with the $CaZn(n\text{-}Bu)_4$ composition. A new triplet, observed in the vicinity of 9.8 τ in the NMR spectrum of Fig. 1, is assigned to the methylene signal of metal-CH_2- in the ate complex.

TABLE 1 EDTA AND VPC ANALYSES OF $CaZn(n\text{-}Bu)_4$

No	Ca/Zn	*n*-Butyl/Ca	*n*-Butyl/Zn
1	1.03	4.0	4.1
2	1.07	4.1	4.2

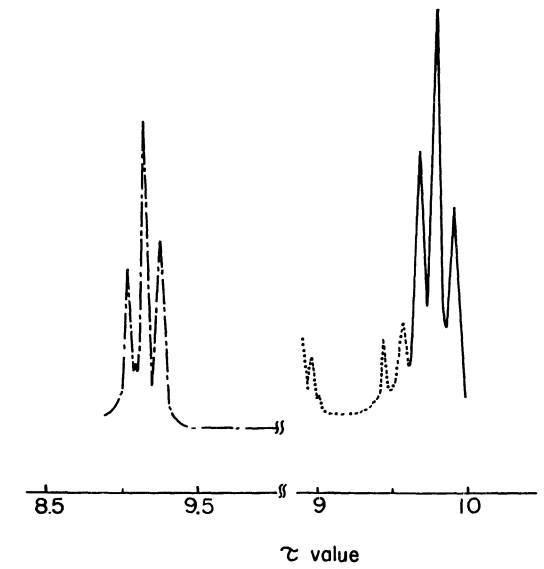

Fig. 1. NMR spectra of M-CH_2 in $Zn(n\text{-}Bu)_2$ and $CaZn(n\text{-}Bu)_4$. 60 MHz, room temperature.
Sample, 10 mol% of diethyl ether solution was used.
——$CaZn(n\text{-}Bu)_4$, ——$Zn(n\text{-}Bu)_2$, -----ether

1) H. Gilman and L. A. Woods, *J. Amer. Chem. Soc.*, **67**, 520 (1945).

2) A. Isobe, H. Aoi, M. Ishimori, and T. Tsuruta, unpublished data.

3) K. Ueno, "Chelate Titration," (in Japanese), Nankodo, Tokyo, (1960), p. 230, 241.

TABLE 2. REACTION OF $CaZn(n\text{-}Bu)_4$ WITH CCl_4

Initial $CaZn(n\text{-}Bu)_4$	Recovered *n*-butane from supernatant (A)		Titrated metal in supernatant (A)		*n*-Butyl/Zn
	before drying-up	after drying-up	Zn	Ca	
0.390 mmol	0.787 mmol	0.784 mmol	0.389 mmol	0.0	2.0

Reaction with Carbon Tetrachloride. Di-*n*-butylzinc scarcely reacts with carbon tetrachloride. On the other hand, as is shown in Table 2, calciumzinc tetra-*n*-butyl, when reacted with exess CCl_4 to form white precipitates in diethyl ether, leaves di-*n*-butylzinc in the supernatant diethyl ether solution, (A), no calcium being detected by the EDTA chelate titration of the supernatant. Since *n*-butane corresponding to a half of the *n*-butyl groups of the $CaZn(n\text{-}Bu)_4$ used was recovered after the hydrolysis of the supernatant (A), the zinc alkyl component in $CaZn(n\text{-}Bu)_4$ was considered to survive in the supernatant without any reactions with carbon tetrachloride. This consideration was further supported by the following results: (i) The amount of the *n*-butane recovered by hydrolyzing the supernatant (A) after the "drying-up" procedure[4] was just the same as that of the *n*-butane recovered from (A) before the "drying-up" procedure.

(ii) The supernatant (A) polymerized methyl vinyl ketone (MVK) to give a stereoregular polymer. The behavior of (A) was in harmony with that of a zinc alkyl solution.[6]

(iii) Copolymerization between MVK and styrene initiated with (A) was shown to possess an anionic character in a way similar to the copolymerization initiated with zinc alkyl.

(iv) α,β-Unsaturated esters, *e.g.*, methyl methacrylate (MMA), were not polymerized by the supernatant (A). If the supernatant had contained a trace of calcium species, the unsaturated esters would have been polymerized anionically.

Judging from the data described above, $CaZn(n\text{-}Bu)_4$ seems to have an ate complex structure consisting of $Ca(n\text{-}Bu)_2$ and $Zn(n\text{-}Bu)_2$. Recently, a detailed report about the nature of the $MZnEt_4$, (in which M=Ca, Ba, and Sr) was published.[7] Another report concerning the structure of the ate complexes of the alkaline earth metals will be published elsewhere.[2]

Reaction with α,β-Unsaturated Ketones. The only elementary reaction of calciumzinc tetra-*n*-butyl with the saturated ketone or aldehyde is the hydrogen abstraction reaction. The calcium ate compound can virtually cause no carbonyl addition reaction, even with such a reactive carbonyl group as those of C_2H_5CHO, $C_2H_5COC_2H_5$, and CH_3COCH_3, as is shown in Table 3. The addition reaction would result in a decrease in the *n*-butane recovered before the "drying-up" procedure. When an α,β-unsaturated ketone was treated with $CaZn(n\text{-}Bu)_4$, no carbonyl addition products were detected, the elementary reactions between $CaZn(n\text{-}Bu)_4$ and α,β-unsaturated ketones presumably being conjugate addition and hydrogen abstraction reactions in the same way as is the case with $n\text{-}Bu_2Zn$.[5] When a diethyl ether solution of $CaZn(n\text{-}Bu)_4$ was added to MVK in diethyl ether (molar ratio 1 : 100), a rapid polymerization of MVK was observed, thus forming polymer precipitates. The supernatant (B) was found to contain neither MVK monomer nor any calcium compounds, the only species detected in (B) by EDTA chelate titration being zinc compound. When MVK was newly added to the supernatant (B), the polymerization of MVK was observed to take place, giving a stereoregular polymer.[6] MMA was not polymerized by the supernatant(B). The chemical behavior of the supernatant layer, (B), toward the α,β-unsaturated ketone and ester seems to coincide with the known chemical behavior of zinc alkyl. These observations showed that the calcium-alkyl part of $CaZn(n\text{-}Bu)_4$ reacted with MVK very rapidly, forming polymer precipitates, and that $n\text{-}Bu_2Zn$ was liberated in the supernatant layer, (B). The liberated $n\text{-}Bu_2Zn$ was reacted with MVK competitively with the calcium-alkyl part, though the reactivity of the former was much lower than that of the latter.

TABLE 3. REACTION OF $CaZn(n\text{-}Bu)_4$ WITH CARBONYL COMPOUNDS[a]

Compound	Recovered *n*-butane from supernatant (B)	
	before drying-up[b] (%)	after drying-up[c] (%)
C_2H_5CHO	96	14
$C_2H_5COC_2H_5$	98	30
CH_3COCH_3	98	19
$CH_2=CHCOCH_3$	51	42
$CH_2=C(CH_3)COCH_3$	50	41[3]
$CH_3CH=CHCOCH_3$	75	5
$(CH_3)_2C=CHCOCH_3$	100	0

a) 30°C in Et_2O; $[CaZn(n\text{-}Bu)_4]$ 0.004 mol/*l*; [carbonyl compound] 0.40 mol/*l*; reaction time, 24 hr.
b) represents 100(1—fraction of *n*-butyl group consumed in the addition reactions) %.
c) represents % of unreacted metal-*n*-butyl linkage.

4) By means of the "*drying-up*" procedure,[5] *n*-butane liberated from butylmetal is removed, while the unreacted butylmetal is left in the residue.

6) T. Tsuruta, R. Fujio, and J. Furukawa, *Makromol. Chem.*, **80**, 172 (1964).

7) F. Kaufmann, A. Geraudelle, B. Kaempf, F. Schue, A. Deluzarche, and A. Maillard, *J. Organometal. Chem.*, **24**, 13 (1970).

5) Y.Kawakami, Y. Yasuda, and T. Tsuruta, *J. Macromol. Sci.-Chem.*, *A***3(2)**, 205 (1969).

SHORT COMMUNICATIONS

On Electro-optic Effect in Lyotropic Liquid Crystals

Taro TACHIBANA and Mitsuko TANAKA
Department of Chemistry, Ochanomizu University, Bunkyo-ku, Tokyo
(Received November 13, 1970)

Some semitransparent lyotropic liquid crystals become turbid at once on application of an electrical potential and recover rapidly on removal of the potential. This phenomenon, found at first by Winsor[1] with the aqueous solutions of ionic surfactants of alkyl sulfate type, was attributed to the alignment of a randomly oriented liquid crystal by the electrical field. We have found a similar electro-optic effect in some lyotropic liquid crystals of ternary systems composed of ionic surfactant-amphiphile-water[2].

The systems examined were I, Na caprylate-caprylic acid (or decanol)-water, II, K caprylate-decanol-water, and III, cetyltrimethylammonium bromide-hexanol-water. The samples contained in a narrow-bore glass tube like a salt bridge between two electrodes were visually observed. A DC potential of about 100 V/cm was applied between two electrodes as a pulse of the order of 10 msec. Though a current of several milliamperes passed through the samples, the short time was sufficient for observing the turbidity preventing the sample from undue heating. The electro-optic effect was examined for all regions of the phase diagram.

According to Mandell and Ekwall,[3] there are structurally different liquid crystalline phases designated B, C, D, E, and F in the ternary systems I, II, and III. We found that the regions exhibiting the electro-optic effect were confined to phase B (*e.g.* 9.0% KC_8, 9.0% C_8-acid, and 82% H_2O) for system I, phases B (*e.g.* 8.6% KC_8, 9.3% decanol, and 82.1% H_2O) and C (*e.g.* 20.6% KC_8, 24.4% decanol, and 55.0% H_2O) for system II, and a part[4] of water-rich region of phase D (*e.g.* 7.6% CTAB, 5.0% hexanol, and 87.4% H_2O) for system III. Turbidity was produced only in phase B also when the alcohol in the systems was replaced by heptanol or octanol. This shows that the effect is specific for such types of liquid crystal. Phase B is smectic and has a lamellar structure comprising parallel layers of amphiphilic ions and molecules with interlayer water. Fontel *et al.*[5] considered from X-ray and other data that, in phase B, the stability of the double layers is possibly so low that they are easily divided into smaller fractions of varying size. Such a labile structure also might be associated with electro-optic effect.

Thin films of the samples in these phases were examined under a microscope between crossed Nichols. They showed weak birefringence with a woven texture. On application of a continuous potential (about 1.5 sec) of 50 V/cm to opposite edges of the film, it became turbid and the microscopic texture changed rapidly from woven to granular. At the same time the field of view as a whole darkened, showing a decrease of birefringence. This could be accounted for by assuming that the structure of liquid crystal is disrupted in part, probably by the shear induced in the liquid crystal by ionic migration, and that the fractions of liquid crystal thus produced disperse as large micelles in the medium and act as light-scattering centers.

Electro-optical turbidity effect has been also found in thin layers of some thermotropic liquid crystals of nematic class. Heilmeier *et al.*[6] attributed this effect to the orientation fluctuation produced by disruptive effects of ions in transit through the aligned nematic medium. In contrast to this case, the turbidity effect in lyotropic liquid crystals might be due to density fluctuation.

1) P. A. Winsor, *J. Colloid Sci.*, **10**, 101 (1955).
2) Winsor stated in his recent review that the Na caprylate-decanol-water system showed the electro-optic effect in a composition in region B (*Chem. Rev.*, **68**, 1 (1968)).
3) L. Mandell and P. Ekwall, Proc. Intern. Congr. Surface Active Substances 4th Brussels, Vol. 2, 659 (1964).
4) This region also may be phase B, since the microscopic texture is similar to that observed for phase B in system I or II.
5) K. Fontel, L. Mandell, H. Lehtinen, and P. Ekwall, *Acta Polytech. Scand. ch.*, **74**, 111 (1968).
6) G. H. Heilmeier, L. A. Zanoni, and L. A. Barton, *Proc. IEEE.*, **56**, 1162 (1968).

A New Oxygen-Insertion Reaction into Silicon-Silicon Bonds with Tertiary Amine Oxides

Hideki SAKURAI, Mitsuo KIRA, and Makoto KUMADA*

Department of Chemistry, Faculty of Science, Tohoku University, Sendai

**Department of Synthetic Chemistry, Faculty of Engineering, Kyoto University, Kyoto*

(Received December 1, 1970)

We reported an oxidation reaction of organodisilanes with perbenzoic acid.[1] Spialter and Austin subsequently described oxidative cleavage of the silicon-silicon bonds with oxides of nitrogen[2] and ozone.[3] These reagents are regarded as electrophilic and kinetic investigations led to the suggestion of a mechanism similar to that of epoxidation.[1,3] We now wish to describe a new and mechanistically interesting insertion reaction of oxygen from tertiary amine oxides into silicon-silicon bonds. The reaction also constitutes a new reduction of amine oxides.[4]

Trimethylamine *N*-oxide reacts exothermally with phenoxypentamethyldisilane in dimethyformamide (DMF), yielding phenoxypentamethyldisiloxane in a moderate yield.[5] Oxidation of hexamethyldisilane to hexamethyldisiloxane with trimethylamine *N*-oxide required somewhat drastic conditions, the yield being 71% after heating at 90—100°C for 6 hr in DMF. Vinylpentamethyldisilane afforded vinylpentamethyldisiloxane in contrast to the reaction with perbenzoic acid.[1]

$$CH_2{=}CHSiMe_2SiMe_3 \xrightarrow{Me_3NO} CH_2{=}CHSiMe_2OSiMe_3$$

$$CH_2{=}CHSiMe_2SiMe_3 \xrightarrow{PhCO_3H} CH_2{-}CHSiMe_2OSiMe_3 \quad (\backslash O /)$$

Pyridine *N*-oxide reacts more slowly than does trimethylamine *N*-oxide. Treatment of phenoxypentamethyldisilane with pyridine *N*-oxide in DMF, dioxane or toluene afforded phenoxypentamethyldisiloxane in over 85% yield. Although hexamethyl disilane did not react with pyridine *N*-oxide, other organodisilanes such as phenyl, 1,2-diphenyl-, and 1,1-diphenyl-substituted permethylated disilanes gave the corresponding disiloxanes as single products together with pyridine in dioxane.

$$X\text{-}SiMe_2SiMe_3 + C_5H_5NO \longrightarrow X\text{-}SiMe_2OSiMe_3 + C_5H_5N$$

These results suggest a nucleophilic attack of *N*-oxides on the silicon-silicon bond as a primary step, which was supported by kinetic studies.

Table 1. Second Order rate constants for oxidation reaction of phenoxypentamethyldisilanes with pyridine *N*-oxide in toluene at 135.0°C[a]

Substituent	$10^5\ k$,[b] $l\ mol^{-1}\ sec^{-1}$
p-CH_3O	6.43±0.27
m-CH_3	6.32±0.16
H	9.74±0.50
p-Cl	21.9 ±0.7
m-CF_3	38.7 ±2.4
p-CH_3CO	37.5 ±0.8

a) Initial concentrations of silanes and pyrdine *N*-oxide were 0.02—0.21 mol l^{-1} and 0.03—0.3 mol l^{-1}, respectively.

b) Average of two to four runs.

The extent of reaction of substituted phenoxypentamethyldisilane with pyridine *N*-oxide in toluene at 135.0°C was followed by the disappearance of disilanes (glpc), the second-order rate law being found to hold accurately. The results are listed in the Table.

A tolerably good Hammett plot was obtained between log (k/k_H) and σ (r=0.971). A positive reaction constant ρ = +1.18 indicates nucleophilic attack of *N*-oxides at silicon to be involved in the rate-determining step.

The mechanism and rate parameters of the reaction appeared interesting in connection with the peracid oxidation of disilanes.[1]

1) H. Sakurai, T. Imoto, N. Hayashi, and M. Kumada, *J. Amer. Chem. Soc.*, **87**, 4001 (1965).

2) L. Spialter and J. D. Austin, *ibid.*, **88**, 1828 (1966).

3) L. Spialter and J. D. Austin, *Inorg. Chem.*, **5**, 1975 (1966).

4) K. Naumann, G. Zon and K. Mislow, *J. Amer. Chem. Soc.*, **91**, 2788, 7012 (1969), reported the use of hexachlorodisilane as a reducing agent for phosphine oxides, amine oxides, and sulfoxides. They suggested the intermediacy of hexachlorodisiloxane formed by a mechanism involving a free trichlorosilyl anion. In the present study, however, it has been disclosed that organodisilanes are generally capable of reducing amine oxides.

5) Yields of disiloxane depend on the degree of dehydration of $Me_3NO{\cdot}2H_2O$. Main by-products were phenol and $(Me_3SiMe_2Si)_2O$ through hydrolysis.

Elektronenübertragungsfähigkeit des durch die Elektroreduktion entstandenen Dimeres der 1,3-disubstituierten Pyridine

Shozo KATO, Jun'ichi NAKAYA,* und Eiji IMOTO

Department of Applied Chemistry, College of Engineering, University of Osaka Prefecture, Sakai, Osaka

**Department of Chemistry, Faculty of Liberal Arts and Sciences, University of Osaka Prefecture, Sakai, Osaka*

(Eingegangen am 7. Januar, 1971)

Es scheint selbstverständlich, daß der Dihydropyridinring im allgemeinen als eine Art Elektronendonator geeignet ist, weil das 1,4,4-Trimethyl-1,4-dihydropyridin mit dem Maleinsäureanhydrid einen *CT*-Komplexe bilden kann.[1] Andererseits erwähnt Wallenfels,[2] daß das Tetracyanoäthylenradikal auf die Reaktion zwischen Dihydropyridin und TCNE momentan zurückgeführt werden kann. Auch berichteten er und Gellrich,[3] daß bei der metallischen Reduktion von *N*-alkylierten Nicotinamiden das Dimere hergestellt wird und daß es beim Vergleich der UV-Spektren[3] order NMR-Spektren[4] in 6-Stellung des Pyridinrings verknüpft ist.

Bisher haben wir einige einelektronische Reduktionsprodukte von aza-heteroaromatischen Verbindungen einheitlich beobachtet; bei der im allgemeinen als Energie für die Reduktion das beschränkte Potential auf Grund der polarographischen ersten Welle verwendet wurde. Wenn durch eine derartige Elektroreduktion das Dimere der 1,3-disubstituierten Pyridine entsteht, für das wir uns als Modellverbindung der NADH interessieren, wird man auch die Möglichkeit einer Elektronenübertragungsfähigkeit statt einer Dihydroverbindung erwarten können. Bei der elektrolytischen Reduktion kennzeichnet es sich durch den radikalischen Angriff, infolgedessen ist die Struktur des einelektronischen Reduktionsproduktes nicht das Dimere des 1,4-Dihydrotyps, wie es bei der Reduktion mit Natriumdithionit der Fall ist, sondern 1,6-Dihydrotyp.[5]

Hier wollten wir die Elektronenübertragungsfähigkeit des von *N*-Benzyl-3-carbamoylpyridinium Chlorid (Ia) hergestellten Dimeres (Ib)[5] mit *N*-Benzyl-3-carbamoyl-1,4-dihydropyridin (Ic) vergleichen. In der Pufferlösung (pH 10) zeigt Ib seine polarographische Oxydationswelle an −0,30 V (*vs.* SCE), aber nach dem Verlauf ergibt sich eine andere Reduktionswelle an −0,97 V, die der Reduktion von Ia zukommt.[5] Es ist bemerkenswert, daß Ic keine Oxydationswelle im Gebiet von anliegender Spannung zeigen kann. Unter Hinweis darauf, ist das Verhalten des von *N*-Benzyl-3-carboxylpyridinium Chlorid (IIa) hergestellten Dimeres (IIb), das die allernegativste Oxydationswelle (−0,59 V) innerhalb des Dimeres von derartigem *N*-Alkyl-3-substituierten Pyridin ergeben konnte,[5] in Kürze zugefügt worden; über die ordnungsgemäß berichtet werden soll.

In der elektrolytischen Zelle, in der man gleichzeitig das UV-Spektrum messen kann,[6] werden 2, 13 mg ($5\cdot10^{-6}$ mol) Ib mit 1,72 g Tetrabutylammonium Perchlorat in 50 m*l* DMF aufgelöst. Sobald man 2,46 mg ($1\cdot10^{-5}$ mol) Chloranil Zufügt, färbt sich die Lösung tiefgelb. Nachdem ungefähr 10 min unter der stickstoff'schen Atmosphäre gerührt wurde, mißt man Polarogramme und Spektren. Auf dem Polarogramm erscheint die neue Oxydationswelle (0,0V) des Chloranilanionradikals statt Ib quantitativ. Die Erscheinung des Radikals wird auch nach der Entstehung eines stark absorbierten ESR-Spektrums festgestellt. Durch den Vergleich der Extinktion der langwelligen Bande (450 mμ) des UV-Spektrums, die dem Chloranilanionradikal zukommt, kann man erkennen, daß im Fall von Ic diese nur 27%-ige Elektronenübertragungsfähigkeit gegen Ib besitzt. Ib reagiert außerdem mit TCNQ in DMF quantitativ und ergibt das grün gefärbte Tetracyanochinodimethananionradikal, das auf Grund der Absorption des ESR-Spektrums ermittelt wurde. Und das von *N,N'*-Diphenyl-*p*-phenylendiamin elektrolytisch entstandene Kationradikal,[7] das sich blau in Acetonitril gefärbt hat, entfärbt sich sofort durch Zusatz von Ib.

Wenn man *p*-Phenanthrolin-di-methiodid in der Lösung von IIb (pH 10) zufügt, entsteht sogleich das einelektronische Reduktionsprodukt, ein tiefrotes Radikal, das wegen seiner kationischen Abstoßung sehr stabil ist. Dieses Radikal selbst ist durch das polarographische Verhalten[6] bestätigt worden.

Die ganze Übersicht ist wie folgt schematisiert:

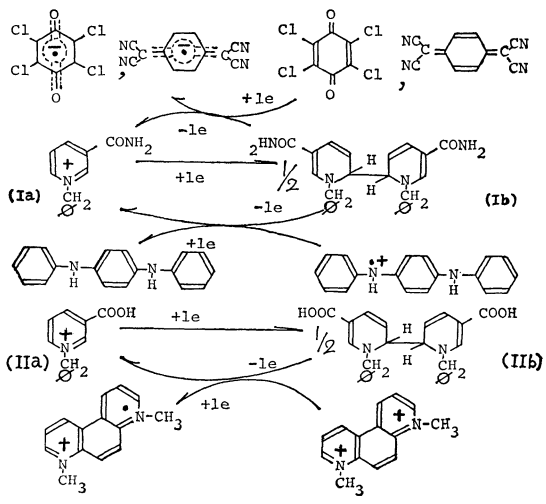

1) E. M. Kosower und T. S. Sörensen, *J. Org. Chem.*, **27**, 3764 (1962).

2) H. Sund, H. Diekmann, und K. Wallenfels, "Advance in Enzymology," Bd. 26, herausgegeben von F. F. Nord, John Wiley und Sons, Inc., New York, London (1964), S. 144.

3) K. Wallenfels und M. Gellrich, *Chem. Ber.*, **92**, 1406 (1959).

4) H. Diekmann, G. Englert, und K. Wallenfels, *Tetrahedron*, **20**, 281 (1964).

5) J. Nakaya, S. Kato, und E. Imoto, "Heterocyclische Verbindung Toron-kai Koen-yoshi-shu," Bd. 3, Japan (1970), S. 79.

6) Der Apparat ist im Bericht beschrieben, der z.Z. in "Review of Polarography" (Japan) eingesandt ist.

7) S. Musha, S. Munemori, und H. Aoki, "Poarograph Toronkai Koen-yoshi-shu," Bd. 15, Japan (1969), S. 32.

Photoaddition Reactions of Pyromellitic Acid Tetramethylester to Olefins

Yutaka KATSUHARA, Yasuo SHIGEMITSU, and Yoshinobu ODAIRA

Department of Petroleum Chemistry, Faculty of Engineering, Osaka University, Suita, Osaka

(Received January 28, 1971)

In our previous paper, we reported the photoadditions of some aromatic carboxylate esters with one or two electron-withdrawing groups to 1,1-diphenylethylene (I).[1] As part of our series of studies of the photochemistry of aromatic carboxylate esters, we will now report on the photoreactions of pyromellitic acid tetramethylester (II) with olefins.

A mixture of 0.03 mol of II and 0.09 mol of I in acetonitrile was irradiated through a Pyrex filter with a 500-W high-pressure mercury lamp for 120 hr under a nitrogen atmosphere to give pale yellow needles (mp 108—109°C) in a 95% yield based on the reacted ester. This photoproduct was identified as the olefin (III) by a study of its IR, NMR, and mass spectra and by elemental analysis. Obviously, III would be derived from an intermediary oxetane (A) by deformylation due to the steric hindrance of the adjacent *o*-methoxycarbonyl group.

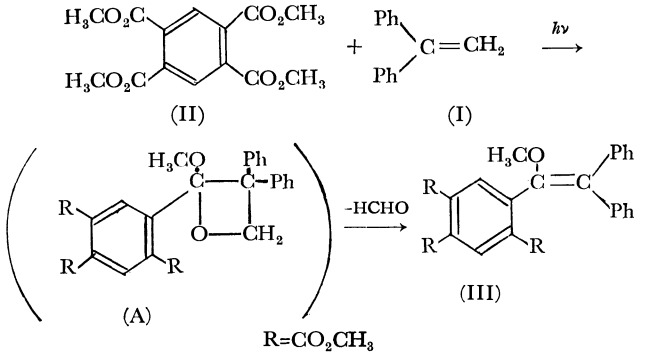

(II) (I) (A) (III)

R=CO_2CH_3

Recently Koltzenburg *et al.* reported that benzene reacted photochemically with butadienes at the 1,4-position of the aromatic ring to give cycloadducts.[2] On the other hand, we have observed a photocycloaddition of the aromatic ring of trimesic acid triesters to cyclooctene (IV).[3] In order to examine the possibility of photocycloaddition at the aromatic ring of II, the following photoreactions of II with some olefins were done.

First, a solution of 0.02 mol of II and 0.10 mol of 2,3-dimethylbutadiene (V) was irradiated for 20 hr under the conditions described above. The diene product (VI), consisting of S-*cis*- and S-*trans*-forms, was obtained in a 13% yield, together with large amounts of butadiene polymers, but no photocycloaddition reaction at the aromatic ring took place at all. It was also reasonable to consider that VI was formed *via* an unstable oxetane (B).

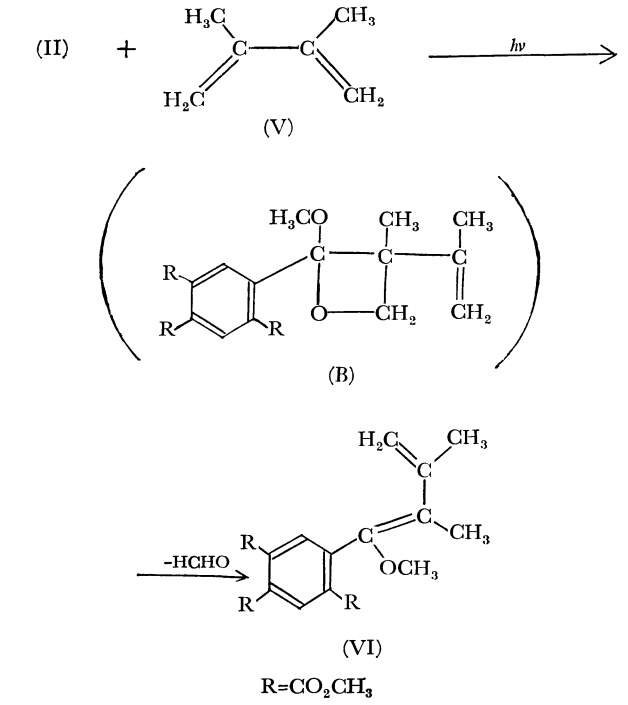

(II) (V) (B) (VI)

R=CO_2CH_3

Second, a solution of 0.03 mol of II and 0.09 mol of IV was irradiated in a similar manner, an unstable oxetane (VII) was thus obtained in a 16% yield as the sole detectable product.

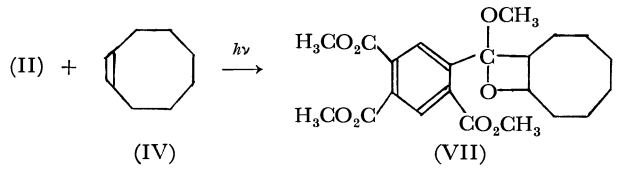

(IV) (VII)

From the facts that only one isomeric oxetane was formed in each photocycloaddition of II to olefins, and that acetone was produced by the photoreduction of II in 2-propanol, the reactive species of these reactions were assumed to be n-π^* in nature. Studies of the reactive species of polysubstituted aromatic carboxylate esters are currently in progress.

1) Y. Shigemitsu, H. Nakai, and Y. Odaira, *Tetrahedron*, **25**, 3039 (1969).

2) K. Kraft and G. Koltzenburg, *Tetrahedron Lett.*, **1967**, 4357, 4723.

3) Unpublished.

A New Tetrahedral Nickel(II) Complex—Bis(*N*-4-methoxyphenyl-3-methoxysalicylideneiminato)nickel(II)

Akira TAKEUCHI and Shoichiro YAMADA

Institute of Chemistry, College of General Education, Osaka University, Toyonaka, Osaka

(Received February 6, 1971)

It was concluded[1,2] that bis(*N*-aryl-substituted salicylideneiminato)nickel(II) complexes (abbreviated as Ni(X-SAL·R)$_2$, Formula I) in non-donor solvents existed as an equilibrium mixture composed of various species such as planar, tetrahedral and associated forms, the equilibrium depending upon the nature of X and R as well as upon concentration and temperature. Both a planar and an associated species could be isolated as crystals, but no tetrahedral species has so far been obtained for these complexes. The present communication describes the first isolation of a tetrahedral species, which has been achieved with bis(*N*-4-methoxyphenyl-3-methoxysalicylideneiminato)nickel-(II).

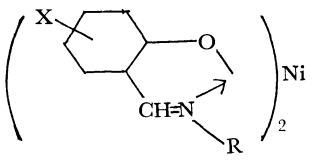

Formula I

The crude product of Ni(3-CH_3OSAL·4-CH_3O–Ph)$_2$ was obtained, Ph being phenyl group, by a reaction of bis(3-methoxysalicylaldehydato)-nickel(II) (0.01 mol) with 4-methoxyphenyl amine (0.02 mol) in ethanol or chloroform. A solution of the crude product in chloroform or benzene was slowly evaporated at about 50°C, until red-brown crystals separated out. The red-brown crystals were filtered off, while the solution was kept warm. Mp 239—240°C. Found: C, 62.66; H, 4.92; N, 4.78%. Calcd for Ni($C_{15}H_{14}NO_3$)$_2$: C, 63.07; H, 4.94; N, 4.90%.

Planar coordination is ruled out for this compound, since it is paramagnetic with a magnetic moment of 3.30 B.M. at room temperature. The solid spectrum of this complex displays main features typical of the tetrahedral nickel(II) complex,[3] having *d-d* bands at about 5.7, 8.0, and 14.0 kK. It is concluded that the red-brown form of Ni(3-CH_3O–SAL·4-CH_3O–Ph)$_2$ has a tetrahedral configuration. Inspection of electronic spectra also reveals that Ni(3-CH_3O–SAL·4-CH_3O–Ph)$_2$ in chloroform exists predominantly as a tetrahedral species.

It is presumed that the steric hindrance arising from the methoxy-group at the 3-position does not absolutely exclude the planar configuration for Ni(3-CH_3O–SAL·4-CH_3O–Ph)$_2$, since Ni(3-CH_3O–SAL·2,6-$(CH_3)_2$Ph)$_2$, in which steric hindrance is much higher, was concluded to have a planar configuration in solid state and in non-donor solvent.[4] For occurrence of the tetrahedral species in crystalline state, the steric condition is not considered to be the only responsible factor. Another important factor might be the suitable field strength produced by the ligand 3-CH_3O–SAL·4-CH_3O–Ph, which seems to be low enough to disfavour the planar configuration for the complex.

Besides the red-brown crystals, olive-green crystals with composition of Ni(3-CH_3O–SAL·4-CH_3O–Ph)$_2$·H_2O have also been isolated by recrystallization of the crude product from 95% ethanol.

1) L. Sacconi, *Coord. Chem. Rev.*, **1**, 126, 192 (1966); L. Sacconi and M. Ciampolini, *J. Chem. Soc.*, **1964**, 276.

2) R. H. Holm and K. Swaminathan, *Inorg. Chem.*, **2**, 181 (1963).

3) S. Yamada and H. Nishikawa, This Bulletin, **36**, 755 (1963); L. Sacconi, P. Paoletti, and M. Ciampolini, *J. Amer. Chem. Soc.*, **85**, 411 (1963).

4) S. Yamada, A. Takeuchi, K. Yamanouchi, and K. Iwasaki, This Bulletin, **42**, 131 (1969).

Phase Transition in Hexammine Nickel Halides

Takasuke MATSUO, Hiroshi SUGA, and Syûzô SEKI
Department of Chemistry, Faculty of Science, Osaka University, Toyonaka, Osaka
(Received February 15, 1971)

Palma-Vittorelli *et al.*[1] found a sudden broadening of the ESR absorption line of Ni^{2+} in $[Ni(NH_3)_6]X_2$ crystals (X; halogens) at low temperature. It was pointed out that this anomalous behavior is not of magnetic origin but is concerned with the motional state of ammonia. Aiello *et al.*[2] showed that over a narrow range temperature a sharp line was superposed on a broader one in the ESR spectrum of the chloride, indicating coexistence of the two phases. These works and an entropy anomaly in the analogous iodide briefly mentioned by van Kempen *et al.*[3] stimulated us to investigate the thermodynamic property of the substances. We report here a preliminary result of a heat capacity measurement on $[Ni(NH_3)_6]Cl_2$ and $[Ni(NH_3)_6]Br_2$. The specimens were crystals 0.5—1 mm in size prepared by the standard method and dried in a desiccator over calcium oxide for a year. The heat capacity measurement was performed between 12 and 300 K with an adiabatic calorimeter of nearly the same construction as that of the previous one.[4,5] the accuracy of the measurement was estimated to be better than 1% at 30 K and 0.3% at 200 K. In total 132 heat capacity data were collected for the chloride and 125 data for the bromide, some of which are shown in Fig. 1. The anomalous increase of heat capacity was found to occur with peaks at 83.17 K and 34.99 K for the chloride and the bromide, respectively. These temperatures are to be compared with 82.5 K and 35 K at which the line width transitions were observed in the ESR spectra.[1] Time required for attaining thermal equilibrium in the calorimeter was usually 5—10 min, but in the transition region of the chloride more than 45 min was required, while for the bromide roughly 20 min was sufficient even at the peak of the anomaly. In contrast to the sharp peak of the bromide the peak of the chloride is rather broad. A preliminary estimate of the entropy of transition was made by interpolating the normal heat capacity smoothly to the transition region. It was found to be 35.1 $JK^{-1}mol^{-1}$ for the chloride and 17.4 $JK^{-1}mol^{-1}$ for the bromide, with a somewhat larger ambiguity for the latter due to larger arbitrariness in the interpolation.

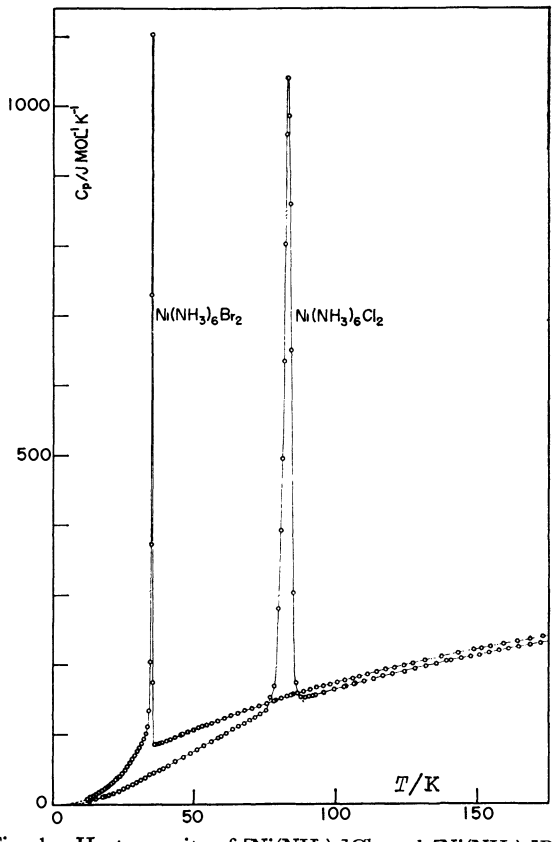

Fig. 1. Heat capacity of $[Ni(NH_3)_6]Cl_2$ and $[Ni(NH_3)_6]Br_2$.

Recently, Klaaijsen *et al.*[6] found heat capacity anomalies in several hexammine metal iodides. They inferred from the estimated entropy change that the transitions in the series of the iodides might have the same physical background. As Bates and Stevens[7] pointed out on an electrostatic model, it is possible that there are eight equivalent configurations which the single complex cation can take in the isolated state. If one of them is favorable at low temperature, the transition entropy would amount to Rln8, which is close to the estimated value for the bromide.

1) M. B. Palma-Vittorelli, M. U. Palma, and F. Persico, *J. Phys. Soc. Jap.*, **17**, Suppl. B1, 475 (1962).
2) G. Aiello, M. U. Palma, and F. Persico, *Phys. Lett.*, **11**, 117 (1964).
3) H. van Kempen, T. Garofano, A. R. Miedema, and W. J. Huiskamp, *Physica*, **31**, 1096 (1965).
4) H. Suga and S. Seki, This Bulletin, **38**, 1000 (1965).
5) T. Matsuo, H. Suga, and S. Seki, *J. Phys. Soc. Jap.*, **30**, 785 (1971).
6) F. W. Klaaijsen, H. Suga, and Z. Dokoupil, to be published in *Physica*.
7) A. R. Bates and K. W. H. Stevens, *J. Phys.*, **C, 2**, 1573 (1969).

Binuclear Copper(II) Complexes Derived From 3-Formyl-5-methylsalicylaldehyde and Glycine

Hisashi Okawa and Sigeo Kida

Department of Chemistry, Faculty of Science, Kyushu University, Hakozaki, Fukuoka

(Received February 17, 1971)

Although many binuclear copper(II) complexes have been synthesized, there are few in which two copper (II) ions are bridged with two different groups.[1,2] We report here the syntheses of three new binuclear copper (II) complexes formed by the reaction of copper(II) ion with 3-formyl-5-methylsalicylaldehyde and glycine. These complexes possess the same surrounding organic moiety except for the second bridging group, which is chloride, bromide, or hydroxide anion (Fig. 1), and seem useful in investigating the role of the bridging group in exchange interaction.

The Cl-bridged complex (green needles) was prepared as follows. To a hot ethanolic solution of copper(II) chloride dihydrate and aldehyde was added an aqueous solution of a stoichiometric amount of glycine. The resulting clear solution was heated on a water-bath for ten min to give green needles. The same procedure was employed in the synthesis of the corresponding Br-bridged complex (green needles) by using anhydrous copper(II) bromide instead of copper(II) chloride dihydrate. The OH-bridged complex was obtained as blue prisms, when copper(II) acetate monohydrate or copper(II) sulfate pentahydrate was used as a metal source. Analytical data of the complexes given in Table 1 agree with the formulas shown in Fig. 1.

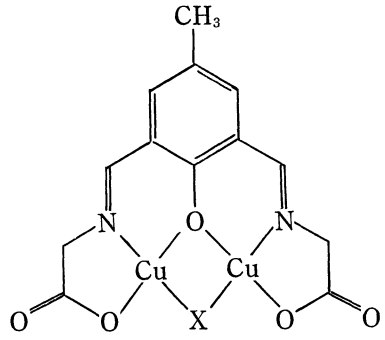

X=Cl, Br, OH

Fig. 1.

Table 1. Analytical data of complexes

Complex	Found(%)			Calcd(%)		
	C	H	N	C	H	N
X=Cl	35.42	2.67	6.11	35.67	2.53	6.40
Br	32.65	2.41	5.51	32.38	2.30	5.81
OH	35.88	3.25	6.33	35.70	3.23	6.41[a]

a) Calculated for monohydrate.

Infrared spectra of the complexes exhibit no $\nu_{C=O}$ mode of a formyl group and show a strong broad band due to the C=O (carboxylate), C=N, and C=C vibration in the region 1645—1600 cm^{-1}. The reflectance spectra of the Cl-, Br-, and OH-bridged complexes show one broad *d–d* band at 695, 695, and 650 mμ respectively. The Cl- and Br-bridged complexes seem to take a binuclear structure in water as well as in pyridine, judging from the close resemblance of the spectra in solutions to those in solid states. Magnetic moments of the Cl- and Br-bridged complexes measured at room temperature were 1.72 and 1.76 B.M. respectively, which are close to the value 1.73 B.M. calculated from the spin-only formula. The magnetic moment of the OH-bridged complex was 1.09 B.M., suggesting a fairly strong antiferromagnetic interaction between the copper (II) ions.

1) H. Okawa, This Bulletin, **43**, 3019 (1970).
2) R. Robson, *Inorg. Nucl. Chem. Lett.*, **6**, 125 (1970); *Aust. J. Chem.*, **23**, 2217 (1970).

The Photo-doping of Metals into Solids for New-type Imaging Systems

Isamu SHIMIZU, Hiraku SAKUMA, Hiroshi KOKADO, and Eiichi INOUE

Imaging Science and Engineering Laboratory, Tokyo Institute of Technology, Ookayama, Meguro-ku, Tokyo

(Received February 23, 1971)

New imaging systems are presented by using photosensitive thin films of chalcogenides-metal or metal halogenides-metal systems. Photosensitive thin films of PbI_2-Ag have been used for recording the hologram by Tubbs,[1] and the photoreaction was described as follows:

$$PbI_2 \xrightarrow{h\nu} (PbI_2)^*$$
$$(PbI_2)^* + 2Ag \longrightarrow Pb + 2AgI \quad (1)$$

Kostyshin *et al.*[2] mentioned, without giving any details, that Ag could be reacted with As_2S_3 by light.

The photosensitive double layers were prepared by the successive vacuum (10^{-5} Torr) evaporation of viterous chalcogenides (ex., As_2S_3, $As_2Se_3As_2Te_3$, *etc.*) and metal (Ag, Cu, Cd, *etc.*) on glass supports. When the (As_2S_3-Ag) sample was irradiated with light at room temperature, a metal (Ag) was diffused into the chalcogenide layer (As_2S_3). The photoinduced reaction may be presented as follows:

$$As_2S_3 + Ag \xrightarrow{h\nu} As_2S_3(Ag) \quad (2)$$

The name "photo-doping" is given to the reaction. The light absorption in the visible region due to the Ag layer was diminished by the irradiation. On the other hand, the absorption edge of the Ag-doped As_2S_3 layer (As_2S_3 (Ag)) was shifted to a longer wavelength. The absorption spectra of As_2S_3 and As_2S_3 (Ag) are shown in Fig. 1. The reaction (2) occurred upon irradiation with light from a He–Ne laser (6328Å). As the light absorption was not admitted at 6328Å on the As_2S_3 layer, the photoreaction seemed to be induced by the excitation of Ag with light as follows:

$$Ag \xrightarrow{h\nu} Ag^*$$
$$Ag^* + As_2S_3 \longrightarrow As_2S_3(Ag) \quad (3)$$

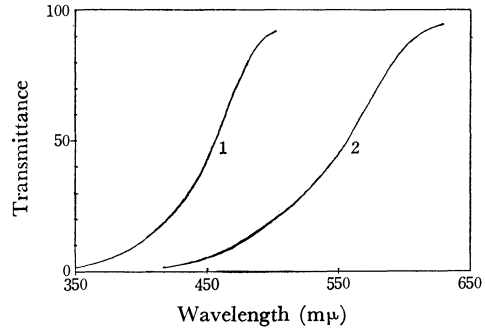

Fig. 1. Absorption spectra of As_2S_3 and As_2S_3(Ag).
1. As_2S_3
2. As_2S_3(Ag)
} thickness 1250 Å

After the image-wise exposure, the fixed image was obtained by dissolving out the unchanged Ag layer by using a mixture of sulfuric acid and potassium dichromate. As As_2S_3 was easily soluble in an alkali solution, while As_2S_3 (Ag) was not, an As_2S_3 (Ag) image which well resists etching with acids, including that of a HF solution, was obtained by dissolving the As_2S_3 part.

The photo-doping efficiency greatly depended on the host materials. A layer of Ag more than 0.1 μ thick was doped in the $As_2Se_3As_2Te_3$ layer (1 μ thick) within a few seconds by irradiation with a 250W-Hg lamp. The "photo-doping" process has a number of advantages, such as a high resolution, a wide range of sensitivity in the visible region, and a higher sensitivity than photopolymers; it is thus of considerable interest in the recording of images and photomicrofabrication.

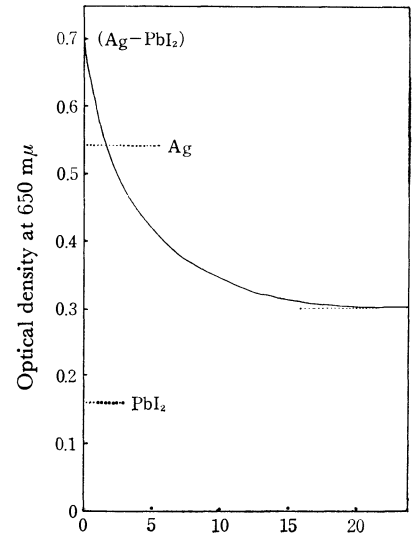

Fig. 2. Density change of PbI_2-Ag system under illumination of a Hg lamp.
thickness of PbI_2: 0.2 μ
light intensity (high pressure Hg lamp): 3.5×10^{-2} W/cm^2

Concerning the PbI_2-Ag system, the Ag layer was diffused into the PbI_2 layer by irradiation with light, and it educed Pb upon continuous irradiation. The relation between the irradiation time and the density change in the PbI_2-Ag system is shown in Fig. 2. The photoinduced reaction of PbI_2-Ag may be represented as follows:

$$(PbI_2)^* + 2Ag \longrightarrow PbI_2(2Ag)$$
$$PbI_2(2Ag) \longrightarrow Pb + 2AgI \quad (4)$$

The first step of this reaction is similar to the photo-doping of the As_2S_3-Ag system. The difference in electrical resistivity between PbI_2 and PbI_2 (Ag) was enough to make electrophotographic images. The electrical properties were also drastically changed by the photo-doping of metals in viterous semiconductive chalcogenides; this is of interest for the making of electronic devices.

1) M. R. Tubbs, *J. Photogr. Sci.*, **17**, 162 (1969).
2) M. T. Kostyshin, E. V. Mikhailovskaya, and P. F. Romanenko, *Soviet Phys. Solid State*, **8**, 451 (1966).

The Vibrational Structure of the Charge-Transfer Band in Solution

Jun-ichi AIHARA
Department of Chemistry, Faculty of Science, Hokkaido University, Sapporo
(Received March 3, 1971)

Several authors have reported the existence of a vibrational structure in the absorption spectra of charge-transfer (CT) complexes in the solid state, while the solution spectra of the complexes are generally likely to be continuous.[1,2] No one has yet observed the fine structure in the solution spectra, though we have no definite evidence for its absence.[3]

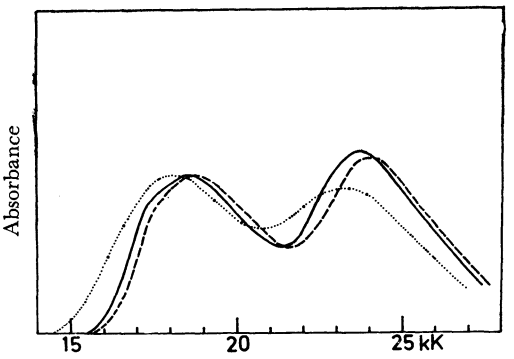

Fig. 1. Absorption spectra of the naphthalene-TCNE complex in cyclohexane (——), in *n*-hexane (------), and in methylene chloride (·····).

Recently, we undertook a further investigation of the solution spectra of the CT complexes; partial success has been achieved in detecting some structure in the solution spectra of the naphthalene-tetracyanoethylene (TCNE) complex. Figure 1 shows typical CT absorption spectra of the naphthalene-TCNE complex in solution. This complex is known to have two CT absorption bands which correspond to the transitions from the highest and the second-highest filled orbital of naphthalene to the lowest vacant orbital of TCNE.[4]

We first found some anomaly on the low-energy side of the first CT band in *n*-hexane. The absorption maximum is preceded by a distinct shoulder; the locations are at 18800 and 17500 cm^{-1} respectively. The separation between them is approximately 1300 cm^{-1}, the uncertainty of this figure being ± 100 cm^{-1}. The spectrum of the cyclohexane solution has a close resembrance to that of the *n*-hexane solution. A similar situation is also found among other saturated hydrocarbon solutions of this complex. The spacings are approximately equal in these solvents. These are listed in Table 1.

Table 1. Absorption maxima and shoulders of the first CT band of the naphthalene-TCNE complex in various solvents (cm^{-1})

Solvent	Maximum	Shoulder	Difference
n-Hexane	18800	17500	1300
n-Heptane	18800	17400	1400
Cyclohexane	18500	17200	1300
Methylcyclohexane	18600	17300	1300

On the other hand, the majority of the solvents do not cause such a distinct structure in the CT spectra. As is exemplified in Fig. 1, the spectrum in methylene chloride appears very continuous and structureless, as usual. Various solvents, classified as benzenes, haloalkanes, ethers, and alcohols, do not induce such a structure. Hence, the appearance of the shoulder is confined to the saturated hydrocarbon solutions.

What is the origin of such a structure? The possibility of a third CT band in this region can be precluded as was recently proved by photoelectron spectroscopy and by theoretical calculations.[4,5] It seems that this structure is not due to another rotational isomer, either, in view of the fact that the second CT band is not accompanied by such a shoulder before the peak. The structure is characteristic of only the first CT band. Accordingly, we concluded that the fine structure originates from the vibronic interaction of the charge-transfer transition with the vibrational mode belonging to either the donor or the acceptor molecule. This presumption seems acceptable, though doubts may be voiced. It is not necessary to take the vibration of the donor against the acceptor into consideration, since the frequency of this mode is expected to be 100—200 cm^{-1}.[3]

Another support for this came from the fact that there exists a similar vibrational structure in the photoelectron spectrum of the molecular naphthalene.[5] When naphthalene is photo-ionized by the 584-Å radiation, a distinct 1410 cm^{-1} progression appears in the spectrum of the photoelectrons from the uppermost filled orbital. It is missing in that from the second highest filled orbital. This parallelism is quite consistent, since the ionization process of naphthalene is also involved in the charge-transfer transition of the naphthalene-TCNE complex.

As has been mentioned above, we could detect the fine structure of the CT bands in solution very rarely. However, its finding at all effectively aids the analysis of the electronic structure of the CT complex in solution. We will go on to examine the absorption spectra of other CT complexes in solution.

1) S. K. Lower, R. M. Hochstrasser, and C. Reid, *Mol. Phys.*, **4**, 161 (1961).
2) H. Kuroda, I. Ikemoto, and H. Akamatsu, *J. Mol. Spectrosc.*, **22**, 60 (1967).
3) R. S. Mulliken and W. B. Person, "Molecular Complexes. A Lecture and Reprint Volume." Chapter 8, Wiley, New York (1969).
4) T. Ohta, H. Kuroda, and T. L. Kunii, *Theor. Chim. Acta*, **19**, 167 (1970).
5) D. W. Turner, *Chem. Brit.*, **4**, 435 (1968).

The Effect of Pressure on the Rate of the Acid-catalyzed Hydration of Propylene

Haruo TAKAYA, Naoyuki TODO, Tadasuke HOSOYA, and Toshio MINEGISHI
The Government Chemical Industrial Research Institute, Tokyo, Mita, Meguro-ku, Tokyo
(Received March 14, 1970)

In order to confirm whether a water molecule (or molecules) is held in a protonated activated complex by electrostatic interaction or by a partial valence bond, the pressure dependency of the activation volume, ΔV^{*}, for the hydration of propylene was measured at 180°C. The pressure effect on the rate of the hydration of propylene was studied in such dilute sulfuric acid solutions of a 0.0000108 mole fraction (0.00060N under S.T.P.) that the dielectric constant, D, and the density of pure water could be replaced for those of the reacting solution. The absolute value of the ΔV^{*} decreases steeply from 19 ml/mol at 300 kg/cm² to 4 ml/mol at 5000 kg/cm². The activation energies and entropies, obtained from the temperature dependency of the reaction rate, are 22.7 kcal/mol and −16.6 e.u./mol respectively at 1000 kg/cm² and 21.9 kcal/mol and −17.0 e.u./mol respectively at 3000 kg/cm². The ΔV^{*} is approximately proportional to the $-\partial D/D^{2}\partial p$ value, (D: dielectric constant of medium; p: pressure), which follows from the Krichevski equation; hence, it was concluded that the contraction of water around an activated complex by electrostatic interaction contributes to the ΔV^{*} and that a water molecule (or molecules) is held in the activated complex by electrostatic interaction. The case of a water molecule being held by a partial valence bond was discussed in terms of the molar volumes of the reactants.

Investigations of the transition state of the acid-catalyzed hydration of olefins have been made by several workers.[1-3] It has been reported that the rate-determining step, for simple olefins, is either the formation of a carbonium ion, which is rapidly captured by water,[1] or a proton transfer from a hydrated proton to an olefin.[4] In any case, the transition state contains perhaps one or more molecules of water. In order to determine the rate-determining step, it is valuable to investigate the behavior of water molecules in the transition state.

Baliga and Whalley[5] studied the pressure effects on the rates of the hydration of ethylene, propylene, and isobutene; they obtained activation volumes of −15.5 ml/mol at 180°C, −9.6 ml/mol at 100°C, and −11.5 ml/mol at 35°C. They concluded that, at the transition states for these reactions, the partial covalent bond is formed between a protonated olefin and a water molecule. The proposed state, however, is based on the assumption that there is only a small difference between the contraction of water around an activated complex and the electrostriction of the proton in the formation of the transition state.

On the other hand, Taft[1] found that the logarithm of the rate of the hydration of isobutene is proportional to the acidity function, $-H_0$, and concluded that the transition state is a "free" carbonium ion. By "free" carbonium ion he meant an ion hydrated only by ion-dipole interaction, without any strong covalent interactions between the ion and a water molecule. This mechanism was, however, proposed on the basis of the Zucker-Hammett hypothesis, and this hypothesis has been shown not always to be applicable to the reactions thus far examined.[6-9] Moreover, this mechanism presents another contradiction: the ratio of the rate constant in D_2O to that in H_2O was actually close to unity, although the values of the ratio for most A-1 reactions are between two and three.

In order to confirm whether a water molecule (or water molecules) is held in the protonated activated complex by electrostatic interaction or by a partial valence bond, the present investigation into the pressure dependency of the activation volume, ΔV^{*}, for the hydration of propylene was undertaken at 180°C. At 180°C the dielectric constant of water, which affects the electrostatic interaction, increases considerably with the pressure, but the decrease in the molar volume of water is small,—*i.e.*, the decrease in the radius of a water molecule is small. If the electrostatic bonds between the protonated activated complex and water result in a larger contraction of water around an activated complex than that around the hydrated proton,—if, *i.e.*, the principal term contributing to ΔV^{*} is a change in the contraction of water between an activated complex and a hydrated proton, —the absolute value of ΔV^{*} will decrease considerable with the pressure as a result of the increase in the dielectric constant with the pressure. On the other hand, if the formation of a partial valence bond between a protonated propylene and a water molecule contributes to the activation volume, ΔV^{*}, the decrease in the absolute value of ΔV^{*} with the pressure will be small since the decrease in the molar volume of water with pressure is small.

Experimental

Materials. The water used in this experiment was purified by passing it through two kinds of ion exhange-resin; it was subsequently distilled twice to remove fine particles of the exchange-resins, which have a superior catalytic activity

1) R. W. Taft, Jr., *J. Amer. Chem. Soc.*, **74**, 5372 (1952).
2) C. A. Bunton and V. J. Shiner, Jr., *ibid.*, **83**, 42 (1961). *ibid.*, **83**, 3215 (1961).
3) E. L. Puelee and R. W. Taft, Jr., *ibid.*, **78**, 5807 (1956).
4) F. A. Long and M. A. Paul, *Chem. Revs.*, **57**, 935 (1957).
5) B. T. Baliga and E. Whalley, *Can. J. Chem.*, **42**, 1019 (1964); *ibid.*, **43**, 2453 (1965).
6) J. F. Bunnett, *J. Amer. Chem. Soc.*, **83**, 4956 (1961).
7) R. W. Taft, Jr., N. C. Deno, and P. S. Skell, *Ann. Rev. Phys. Chem.*, **9**, 306 (1958).
8) R. P. Bell, "The Proton in Chemistry," Cornell University Press, Ithaca, New York (1959).
9) H. Takaya, N. Todo, and T. Hosoya, This Bulletin, **42**, 2748 (1969).

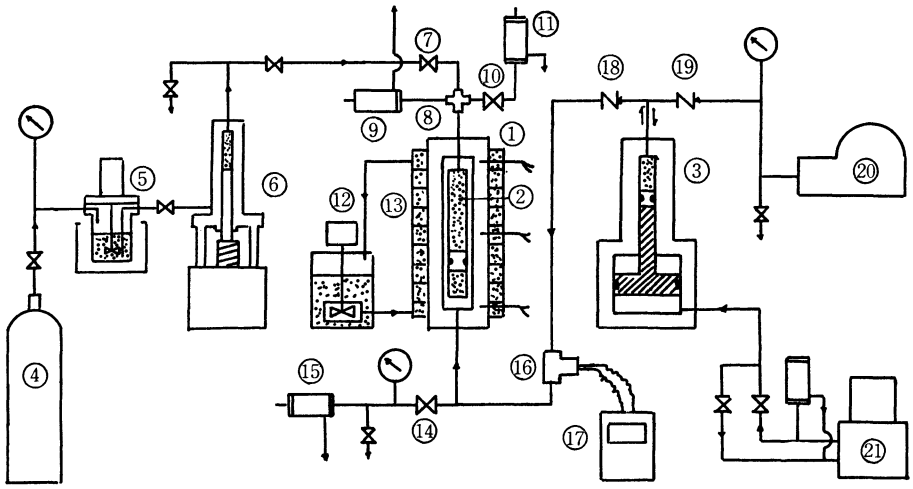

Fig. 1. Equipment used under pressure.

1: Reaction vessel	2: Reactor	3: Pressure intensifier
4: Cylinder of propylene	5: Propylene absorber	6: Injector of reacting solutions
7: Valve	8: Cross fitting	9: Safety valve
10: Valve	11: Relief valve	12: Circulater of heated oil
13: Jacket of reactor for heating	14: Valve	15: Relief valve
16: Manganin pressure cell	17: Pressure recorder	18, 19: Check valve
20: Pump for charging silicone oile	21: Pump for driving intensifier	

for the hydration of olefin. The propylene (extra-pure grade), obtained commercially, and the sulfuric acid (guaranteed reagent) were used without further purification.

Apparatus and Procedure. The equipment used is shown in Fig. 1, while the details of the pressure technique were described in an earlier paper.[10] The reacting solution in the reactor (2), which is contained in a high-pressure vessel (1), can be repeatedly replaced at chosen reaction temperatures under a pressure of 300 kg/cm². The reacting solutions were prepared by dissolving propylene into aqueous acid in a pressure vessel (5) at 0°C under high pressures (up to 8 atm); they were then injected into the reactor (2), kept at chosen reaction temperatures under the pressure of 300 kg/cm² by using a high-pressure injector (6). The reactor (2) was constructed so as to keep the solution in contact only with Teflon. The mole fraction of the propylene dissolved as the reactant was varied from 0.006 to 0.0010

Analysis. The progress of the hydration of propylene was followed by analyzing the product extracted at fixed intervals. The gaseous propylene in the products was measured by a gas burette, while the amount of propylene dissolved in the products was determined by gas chromatography. The column used for this measurement was 2 m in length, and 4 mm in dia., and it was packed with 25% P.E.G. 1500 on celite 545 (60-80 mesh).

Results

The reaction was the first order in propylene,[5] and the rate constant, k_1, was calculated by the usual equation (1):

$$\ln x = -k_1 t + \text{constant} \quad (1)$$

where x is the ratio of the mole fraction of the unreacted propylene at the reaction time, t, to the initial mole fraction. For the reactions in the dilute sulfuric acid solution of a mole fraction 0.0000108 (0.00060N under

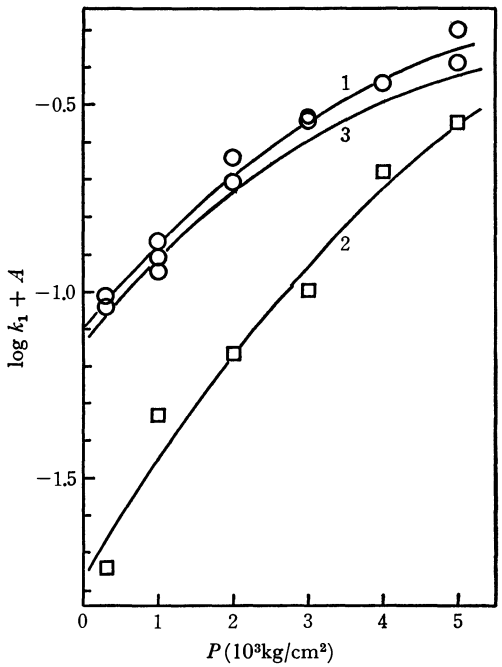

Fig. 2. Effect of pressure on the rate of hydration of propylene at 180°C. The curves 1, 2, and 3 correspond to Eqs. (2), (3), and (4) resperctively.
Curve 1: in aqueous sulfuric acid, $A=0$.
Curve 2: in aqueous solution without acid catalysis, $A=0.6$.
Curve 3: log K_{1c}, A=0.

S.T.P.) at 180°C, the correlation of log k_1 with the pressure, p, was as is shown in Fig. 2, where the log k_1 increases from −1.0 at 300 kg/cm² to −0.3 at 5000 kg/cm² and is represented by Eq. (2):

$$\log k_1 = -1.109 + 0.245 \times 10^{-3}p - 0.0182 \times 10^{-6}p^2 \quad (2)$$

In the present work, considerably diluted acid was used as the catalyst since the dielectric constant and the density of a diluted acid solution could be replaced with

10) T. Hosoya, T. Minegishi, H. Takaya, N. Todo, and M. Yoneoka, *Tokyo Kogyo Shikensho Hokoku*, **64**, 499 (1969).

those of pure water. Therefore, it was necessary to measure the rate for the solution consisting of pure water and propylene. As is shown in Fig 2, it was observed that the reaction without any acid catalysts proceeds, though the rate, k_{1w}, was much lower than that for the solution with an acid catalyst. The log k_{1w} was represented by Eq. (3):

$$\log k_{1w} = -2.371 + 0.347 \times 10^{-3}p - 0.0203 \times 10^{-6}p^2 \quad (3)$$

Accordingly, the correct rate constant, k_{1c}, with an acid catalyst was calculated by subtracting those of k_{1w} from k_1. In Fig. 2 the log k_{1c} is also plotted against p, its dependence on p can be represented by Eq. (4):

$$\log k_{1c} = -1.144 + 0.247 \times 10^{-3}p - 0.0203 \times 10^{-6}p^2 \quad (4)$$

In Fig. 3 the relation between the activation volume, ΔV^*, as defined by Eq. (5), and the reacting pressure is shown.

$$\Delta V^* = -2.303RT\frac{\partial \log k_1}{\partial p} \quad (5)$$

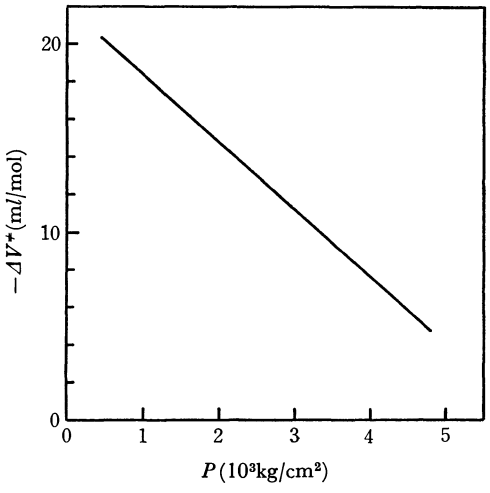

Fig. 3. Effect of pressure on volume of activation for the acid-catalyzed hydration of propylene in water at 180°C.
$-\Delta V^* = 21.9 - 3.6 \times 10^{-3}p$ (ml/mol)

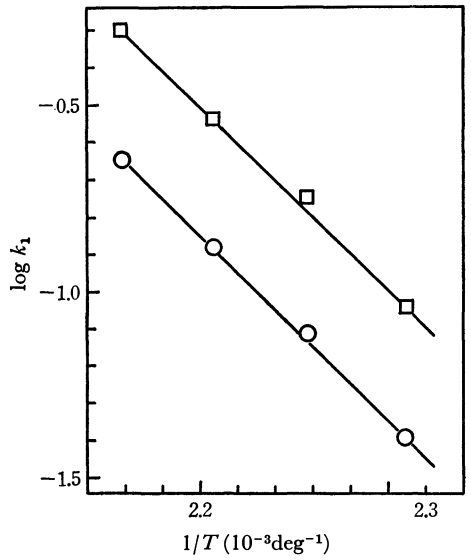

Fig. 4. Effect of temperature on the rate of the acid-catalyzed hydration of propylene. ○: at 1000 kg/cm^2. □: at 3000 kg/cm^2.

This figure indicates that the absolute values of the activation volume, the pressure dependency of which is represented by Eq. (6), decrease steeply with the pressure as the same manner as in the case of the hydration of ethylene observed by Baliga at 180°C.[5] However, the absolute value obtained at 180°C under 300 kg/cm^2, 19 ml/mol, is twice as large as the value, 9.6 ml/mol, obtained by Baliga[5] for propylene at 100°C under about 1 kg/cm^2.

$$-\Delta V^* = 21.9 - 3.6 \times 10^{-3}p \text{ (ml/mol)} \quad (6)$$

The temperature dependency of the reaction is shown by Arrhenius plots in Fig. 4. The activation energies and entropies are 22.7 kcal/mol and −16.6 e.u./mol respectively at 1000 kg/cm^2 and are 21.9 kcal/mol and −17.0 e.u./mol respectively at 3000 kg/cm^2, where the entropies are calculated in the same manner as in Baliga's report.[5]

Discussion

As was shown in the preceding paper[9] the mechanism of the acid-catalyzed hydration of propylene can be represented by Eq. (7) and Eq. (8):

$$C_3H_6 + H^+ \cdot h_2H_2O + (h_1 - h_2)H_2O \overset{K_1}{\rightleftharpoons} [C_3H_6 \cdot H^+ \cdot h_1H_2O]^* \quad (7)$$

$$[C_3H_6 \cdot H^+ \cdot h_1H_2O]^* \rightarrow C_3H_7OH + H^+ \cdot h_2H_2O + (h_1 - h_2 - 1)H_2O \quad (8)$$

where h_1 and h_2 are the hydration numbers of the activated complex and the proton respectively; the hydration number of propylene has been considered to be zero. The activation volume for the reaction represented by Eq. (7) can be defined by Eq. (9)[11]:

$$\Delta V^* = \bar{V}_{act.} - \bar{V}_{prop.} - \bar{V}_{h.p.} - (h_1 - h_2)\bar{V}_w \quad (9)$$

$$= \Delta V_{act.} - \Delta V_{H^+} \quad (10)$$

where $\bar{V}_{act}$, $\bar{V}_{prop.}$, $\bar{V}_{h.p.}$, and $\bar{V}_w$ are the partial molar volumes of the activated complex, propylene, the hydrated proton, and water respectively, and where $\Delta V_{act.}$ and ΔV_{H^+} are defined by Eq. (11) and Eq. (12) respectively:

$$\Delta V_{act.} = \bar{V}_{act.} - \bar{V}_{prop.} - h_1\bar{V}_w \quad (11)$$

$$\Delta V_{H^+} = \bar{V}_{h.p.} - h_2\bar{V}_w \quad (12)$$

Here, the volume change, ΔV_{H^+}, is the electrostriction of the proton. In connection with $\Delta V_{act.}$, it is convenient to split it into two terms: $\Delta_1 V_{act.}$, which is the change in the volume of the reacting molecules when they form the transition state, and $\Delta_2 V_{act.}$, which is the accompanying change in the volume of the surrounding liquid water, arising principally from the change in the contraction of water around an ion by means of electrostatic interaction. Equation (10) can, then, be rewritten as Eq. (13):

$$\Delta V^* = \Delta_1 V_{act.} + \Delta_2 V_{act.} - \Delta V_{H^+} \quad (13)$$

According to Baliga and Whalley, the principal term contributing to the ΔV^* is $\Delta_1 V_{act.}$, and the contribution

11) S. D. Hamann, "High Pressure Physics and Chemistry," Vol. 2, ed. by R. S. Bradley, Academic Press, London and New York (1963), p. 165.

of the ($\Delta_2V_{act.}$ $-\Delta V_{H^+}$) term to the ΔV^* may be very small. Their consideration, however, is based on the assumption that the size of the activated complex is larger than that of H_3O^+, though it is known that the formula of the hydrated proton is not H_3O^+, but $H^+ \cdot h_2H_2O$, where h_2 is, *e.g.*, about 4 at 25°C. It seems, therefore, more likely that the size of the ionic activated complex is smaller than that of the hydrated proton. It is probable, then, that $\Delta_2V_{act.}$ is smaller than ΔV_{H^+} and that $\Delta_1V_{act.}$ is negligibly small; the principal term contributing to the ΔV^* is ($\Delta_2V_{act.}$ $-\Delta V_{H^+}$).

Let us now discuss which of the two cases is related to the observed large decrease in the absolute value of the activation volume with the pressure: the case 1, where the term contributing to ΔV^* is ($\Delta_2V_{act.}$ $-\Delta V_{H^+}$); and the case 2, where the term contributing to ΔV^* is $\Delta_1V_{act.}$

Case 1. In order to discuss the contraction of water around an ion, the method of the calculation of the contraction must first be considered. The contraction is expressed by Krichevski equation, which follows from Born's model:

$$\Delta V_{el.} = -\frac{z^2e^2\partial D}{2rD^2\partial p} \qquad (14)^{11}$$

where $\Delta V_{el.}$ denotes the contraction of a medium of the dielectric constant, D, around a sphere of the radius, r, carrying a charge of ze, e being the electronic charge, and z, an intergal number, and where p is the pressure. Hamann[11] derived the equation of the contraction by considering the pressure dependency of r. In order to calculate the correct value of the contraction, the arrangements of the water molecules at the nearest neighbor of an ion must be taken into account.[12] The arrangement effect is especially important in the case of a small ion.[12] However, there have been reported none of the experimental data necessary to evaluate the arrangements of the water molecules and the pressure dependency of r at high temperatures and pressures. Therefore, in this paper it is assumed, neglecting these effects, that $\Delta V_{el.}$ is proportional to the $-\partial D/D^2\partial p$ value. This assumption is partly supported by the fact that the radius of a protonated activated complex is large and by the following facts. The variation of the radius of *n*-heptane, even at 300°C, is only about 10 per cent with the increase in pressure from 1000 kg/cm² to 5000 kg/cm², since their molar volumes under pressures of 1000 kg/cm² and 5000 kg/cm² are 164 m*l* and 129 m*l* respectively.[13] Those molar volumes are not greatly different from that under S.T.P. (145 m*l*). Therefore, it may be deduced that the variation in the radius of propylene is also small, since the molar volume of propylene, 79 m*l*, at 180°C under a pressure of 1000 kg/cm² is not greatly different from that in the liquid state, 60 m*l*.

If the principal terms contributing to ΔV^* are the ($\Delta_2V_{act.}$ $-\Delta V_{H^+}$) terms, ΔV^* should be proportional to the $-\partial D/D^2\partial p$ value, because $\Delta_2V_{act.}$ and ΔV_{H^+} are both proportional to the $-\partial D/D^2\partial p$ value. Figure 5 shows that the observed activation volumes, in which the values observed by Baliga at 100°C have been included, are approximately proportional to the $-\partial D/D^2\partial p$ value. Here, the values, $-\partial D/D^2\partial p$, for pure water were calculated by the Quist equation,[14] and the density of water, which is necessary to evaluate the dielectric constant, was obtained from Sharp's report.[15] From this figure it may be reasonable to conclude that the main contribution to the ΔV^* consists of the ($\Delta_2V_{act.}$ $-\Delta V_{H^+}$) terms; that is, water molecules (or a water molecule) are held in an activated complex by electrostatic interaction.

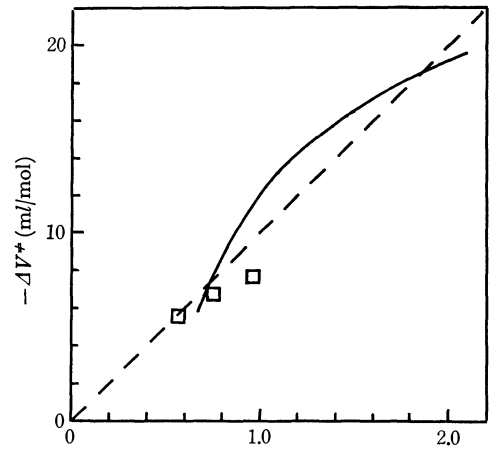

Fig. 5. $-\Delta V^*$ *versus* $-\partial D/D^2\,\partial p$.
—: present results.
□: Baliga, at 100°C. Ref. 5.

Case 2. By the following procedure it can be shown that the Case 2 is unlikely. If the principal term contributing to ΔV^* is $\Delta_1V_{act.}$, the observed ΔV^* should be caused by contraction, δl, from the length of a van der Waals bond between a propylene and a water molecule into that of a partial valence bond between a protonated propylene and a water molecule. Therefore, the activation volume, ΔV^*, can be approximately represented by Eq. (15):

$$\Delta V^* = -S\delta l \qquad (15)$$

where S is a cross-sectional area for a water molecule. The observed $-\Delta V^*$ value, 18 m*l*/mol, at a pressure of 1000 kg/cm² is nearly equal to a molar volume of water under the same conditions, 19.1 m*l*/mol.[15] This means, from Eq. (15), that a water molecule is completely embraced in a protonated propylene upon the formation of the activated complex. From the above conception of the activation process, the $-\Delta V^*$ value at a pressure of 5000 kg/cm² should be a molar volume of water, 17 m*l*/mol.[15] However, the observed $-\Delta V^*$ value at a pressure of 5000 kg/cm² is only 4 m*l*/mol. The large discrepancy shows that the case 2 is unlikely.

12) B. E. Conway, J. E. Desnoyers, and A. C. Smith, *Phil. Trans. Roy. Soc. London*, **256**, 389 (1964).
13) A. D. Doolittle, *Chem. Eng. Progr. Symp. Ser.*, **59**, 1 (1963).
14) A. S. Quist and W. L. Marshall, *J. Phys. Chem.*, **69**, 3165 (1965).
15) W. E. Sharp, *University of California Radiation Laboratory Report* UCRL-7118 (1962).

The Nature of a Bond between a Water Molecule and a Protonated Propylene in the Activated Complex for the Acid-catalyzed Hydration of Propylene

Haruo TAKAYA, Naoyuki TODO, Tadasuke HOSOYA, and Toshio MINEGISHI
The Government Chemical Industrial Research Institute, Tokyo, Mita, Meguro-ku, Tokyo
(Received March 14, 1970)

The nature of a bond between a water molecule and a protonated propylene in the activated complex for the acid-catalyzed hydration of propylene was discussed. The number of water molecules contained in the activated complex, 1.3, was obtained by applying the acidity function, T_0, to the dependency of the log k_1 on the acid concentration for the hydration of various olefins. The general relationship between the electrostriction and the hydration number of various uni-valent cations was also discussed, and these ions were divided into two separate groups. In the first group, the hydration was caused by electrostatic interaction, while in the second group, the hydration was caused mainly by covalent bond formation. Since the representative point of the hydration of propylene was located near the first group, it was concluded that a molecule of water is held in the activated complex by electrostatic interaction. On the basis of these considerations, the present authors propose a hypothesis which is useful in characterizing the nature of a bond between a water molecule and a protonated substrate in an activated state: (a) If the log k_1 for a reaction increases linearly with $-H_0$, a water molecule (or molecules) is held in an activated complex by electrostatic interaction. (b) If the log k_1 for a reaction increases linearly with the log m_a, a water molecule is held in an activated complex by the formation of a covalent bond. k_1: the first order rate constant; H_0: Hammett's acidity function; m_a: acid concentration.

In an earlier paper[1], the following mechanisms of acid-catalyzed reactions in moderately concentrated acid solutions have been proposed:

$$S\cdot h_5H_2O + H^+\cdot h_2H_2O + (h_1-h_2-h_5)H_2O \overset{K_1}{\rightleftharpoons} [SH^+\cdot h_1H_2O]^* \quad (1)$$

$$[SH^+\cdot h_1H_2O]^* \rightarrow \text{Product} \quad (2)$$

where S is a substrate and where h_1, h_2, and h_5 are the hydration numbers of the activated complex, the proton, and the substrate respectively. The number of water molecules contained in an activated complex, h_1, can be calculated from the dependency of the log k_1 on the acid concentrations:

$$\log k_1 = C - T_0 \quad (3)$$

where k_1 and C are a rate constant and a constant respectively, and where T_0 is a new acidity function which varies with the hydration number, h_1, and with the acid concentrations. The respective acidity functions T_0, for various acid solutions are given by Eqs. (4)–(6): in hydrochloric acid solutions:

$$T_0 = 2.4(3.9-h_1+h_5)\log a_w - \log m_a \quad (4)$$

in nitric acid solutions:

$$T_0 = 2.3(3.9-h_1+h_5)\log a_w - \log m_a \quad (5)$$

in perchloric acid solutions:

$$T_0 = 2.3(3.9-h_1+h_5)\log a_w - \log m_a \quad (6)$$

where a_w is the activity of water and where m_a is the molality of acid. Usually, the hydration number of a substrate, h_5, is zero because, as was shown in the derivation process of T_0, the hydration number even of a water molecule, which has a larger affinity for water than hydrocarbons, is zero. These equations are derived in much the same manner as in the Glueckauf's calculation of the hydration numbers of ions in aqueous solutions,[2] therefore, the hydration number of an activated complex, h_1, as calculated by these equations, can be treated equally as the hydration numbers of various kinds of alkali metal ions as calculated by his method.

The present authors previously studied the pressure effect on the rate of the acid-catalyzed hydration of propylene and reported that the absolute values of the observed activation volume are approximately proportional to the value, $-\partial D/D^2\partial P$, derived from the Drude and Nernst equation; here D is a dielectric constant of water and p is a pressure.[3] From this result, it was concluded that the activation volume is caused by the contraction of water around a protonated propylene by electrostatic interaction; that is water molecules (or a water molecule) may be held in the activated complex by electrostatic interaction.

In this paper the above conclusion will be discussed in terms of the relationship between the hydration number and the electrostriction of various uni-valent cations.

Calculation and Discussion

Hydration Number of a Hammett Base. In order to examine the process of calculating the hydration number of an activated complex, h_1, first, the hydration numbers of a protonated Hammett base in various acid solutions were calculated.

The acidity function, T_0, for the protonation of a Hammett base is equal to the acidity function, H_0,[4] as defined by Eq. (7), because the value of m_{AH^+}/m_A in Eq.(7) is equivalent to the first-order rate constant, k_1, in Eq.(3) and both the H_0 and T_0 functions are defined as being equal to $-\log m_a$ in a dilute acid solution[1]:

1) H. Takaya, N. Todo, and T. Hosoya, This Bulletin, **42**, 2748 (1969).

2) E. Glueckauf, *Trans. Faraday Soc.*, **51**, 1235 (1955).

3) H. Takaya, N. Todo, T. Hosoya, and T. Minegishi, This Bulletin, **44**, 1175 (1971).

4) M. A. Paul and F. A. Long, *Chem. Rev.*, **57**, 1 (1957).

$$\log \frac{m_{AH^+}}{m_A} = C - H_0 \quad (7)$$

where A is a Hammett base and where AH^+ is a protonated Hammett base. By the substitution of the values in Table 1 into Eq.(5) and Eq.(6), the hydration number of a protonated Hammett base, h_1, can be calculated. The results obtained are 0.8 and 0.4 in nitric acid and in perchloric acid respectively, as is shown in the last column of Table 1. As for the value in hydrochloric acid, it was shown in an earlier paper that h_1 is 0.7.[1] It seems to be possible to decide that the hydration numbers do not vary with the kind of acid. The small disagreement among these values, which is caused probably by omitting a part of the salting-out effects in the course of the calculation of the T_0, may be interpreted on the assumption that the salting-out effects for a protonated Hammett base are almost completely canceled by those for the Hammett base. The fact that there was not so large a disagreement among the hydration numbers of a Hammett base in various acids suggests that the same procedure can be used in calculating the hydration numbers for other protonated activated complexes.

TABLE 1. HYDRATION NUMBER OF A HAMMETT BASE IN VARIOUS ACID SOLUTIONS

	Molality	$\log m_a$	H_0 or T_0	$\log a_w$	h_1
in HNO_3	3.0	0.477	−0.94	−0.065	0.8
in $HClO_4$	3.0	0.477	−1.07	−0.074	0.4

Numbers of Water Molecules Contained in the Activated Complexes for Hydration of Olefins. The dependency of $\log k_1$ on the acid concentrations for the hydration of propylene has not been observed. Therefore, the hydration numbers were calculated by using the results observed by Taft for the hydration of various olefins,[5] and the average value of these was used as the number of water molecules contained in the activated complex for the hydration of propylene. The $\log k_1$, which was represented by $\log k_c$ in Taft's paper, is represented by:

$$\log k_1 = -\rho' H_0 + C \quad (8)$$

where ρ' is a parameter to be determined by experiments. By comparing Eq.(8) with Eq.(3), it can be seen that $\rho' H_0$ must be T_0. In Table 2 the observed values of $-\rho' H_0$ (or $-T_0$) and also the hydration numbers of the various protonated olefins calculated by Eq.(5) are tabulated. From Table 2 it can be seen that the average hydration number is 1.3.

TABLE 2. THE OBSERVED $-\rho' H_0$ (or $-T_0$) AND THE HYDRATION NUMBERS CALCULATED BY Eq. (5)

Substrate	HNO_3 Molarity	$-\rho' H_0$ or $-T_0$	Hydration number
Trimethylethylene	2.995[a]	0.88	1.7
Methylenecyclobutane	2.995[a]	1.00	1.0
Triptene	2.995[a]	0.89	1.6
Isobutene	2.525[b]	0.81	1.0

a) $\log m_a = 0.52$ and $\log a_w = -0.071$.
b) $\log m_a = 0.44$ and $\log a_w = -0.056$.

5) R. W. Taft, Jr., E. L. Purlee, P. Riesz, and C. A. DeFazio, *J. Amer. Chem. Soc.*, **77**, 1584 (1955).

Relationship between the Conventional Electrostriction, $\Delta_c V_{el.}$, and the Hydration Number, h_1, of Uni-valent Cations. The relationship between the conventional electrostriction, $\Delta_c V_{el.}$, of various uni-valent alkali metal cations[6] and hydration number is shown in Fig. 1, where the value of $\Delta_c V_{el.}$ is represented by setting the $\Delta_c V_{el.}$ of H^+ as zero. The conventional electrostriction of a cation, $\Delta_c V_{el.}$, is correlated with its electrostriction, $\Delta V_{el.}$, as is shown by Eq. (9)[7]:

$$\Delta_c V_{el.} = \Delta V_{el.} - \Delta V_{el.H^+} \quad (9)$$

where $\Delta V_{el.H^+}$ is the electrostriction of the proton. From this figure, it can clearly be seen that the alkali metal ions are divided into the following separate two groups. In the first group, which consists of Rb^+, K^+ and Na^+, the values of $\Delta V_{el.}$ can be represented by the value, $-Bz^2/r_s$,[8] derived from the Drude and Nernst equation. Here, r_s is the radius of an ion, which has a charge of z, and B is a constant. Since the Drude and Nernst equation was derived by using the theory of the electrostriction of a homogeneous dielectric around a charged sphere, it seems to suggest that the hydration of the ions in the first group is caused by electrostatic interaction. On the other hand, the $\Delta V_{el.}$ of the second group, which consists of H^+ and Li^+, can not be given by the $-Bz^2/r_s$ value; moreover, the electrostriction of H^+ is small because of the large radius of the hydrated proton, the formula of which is accepted as $H^+ \cdot (H_2O)_4$.[2,8]

It may be generalized from the discussion above described that if the representative point for a reaction is located near the first group, the water molecules are held in an activated complex by electrostatic interaction and the number of water molecules may be 0, 1, or 2. On the other hand, if the representative point for a reaction is located near the second group, that is, if its hydration number is 3 and the activation volume is nearly zero, the structure of the activated complex may be similar to that of a hydrated proton, $H^+ (H_2O)_4$.

Consideration of an Activation Volume, ΔV^*. It can be shown by the following treatment that the change in volume for the reaction of Eq. (1), ΔV^*, as defined by Eq. (11), is equivalent to the electrostriction in Fig. 1, $\Delta_c V_{el.}$:

$$\Delta V^* = \bar{V}_{act.} - \bar{V}_S - \bar{V}_{h.p.} - (h_1 - h_2)\bar{V}_w \quad (11)$$

where $\bar{V}_{act.}$, $\bar{V}_S$, $\bar{V}_{h.p.}$, and $\bar{V}_w$ are partial molar volumes of the activated complex, the substrate, the hydrated proton, and water respectively. Equation (11) can be re-written as Eq. (12) and Eq. (13):

$$\Delta V^* = (\bar{V}_{act.} - \bar{V}_S - h_1\bar{V}_w) - (\bar{V}_{h.p.} - h_2\bar{V}_w) \quad (12)$$

$$= \Delta V_{act.} - \Delta V_{H^+} \quad (13)$$

where $\Delta V_{act.}$ and ΔV_{H^+} are defined by Eq. (14) and Eq. (15) respectively:

$$\Delta V_{act.} = \bar{V}_{act.} - \bar{V}_S - h_1\bar{V}_w \quad (14)$$

6) R. M. Noyes, *ibid.*, **86**, 971 (1964).

7) The electrostriction of an ion is defined by Eq. (10) where the partial molar volume, $\bar{V}_0$, can be determined by experiments, however, the intrinsic ionic volume, V, can not be done by experiments but only deduced theoretically.

$$\Delta V_{el} = \bar{V}_0 - V, \quad (10)$$

8) P. Mukerjee, *J. Phys. Chem.*, **65**, 740 (1961).

$$\Delta V_{H^+} = \bar{V}_{h.p.} - h_2\bar{V}_w \quad (15)$$

Generally, the electrostriction of a proton, $\Delta V_{el.H^+}$, is determined on the basis of the assumption that the intrinsic molar volume of H^+, V in Eq. (10),[7] is zero. However, if a proton is hydrated in water, the above assumption means that the intrinsic molar volume of $H^+ \cdot h_2H_2O$ is equal to the volume of h_2H_2O, *i.e.*, h_2V_w. Therefore,

$$\Delta V_{H^+} = \Delta V_{el.H^+} \quad (16)$$

On the other hand, the electrostriction of an activated state, $\Delta V_{el.act.}$, is given by Eq. (17):

$$\Delta V_{el.act.} = \bar{V}_{act.} - V_{SH\cdot h_1H_2O} \quad (17)$$

where $V_{SH.h_1H_2O}$ is the intrinsic molar volume of an activated complex, and where $SH \cdot h_1H_2O$ is a imaginary and non-cationic activated complex, one which is formed by the imaginary subtraction of an univalent charge from an activated complex, $[SH^+ \cdot h_1H_2O]^*$. On the basis of the same assumption as was used in the case of H^+, the value of $V_{SH.h_1H_2O}$ can be determined by Eq. (18):

$$V_{SH\cdot h_1H_2O} = \bar{V}_S + h_1\bar{V}_w \quad (18)$$

In this case, the substrate, S, corresponds to a water molecule in a hydrated proton, $H^+(H_2O)_4$. Therefore, from Eqs. (14), (17), and (18), we can obtain Eq. (19):

$$\Delta V_{act.} = \Delta V_{el.act.} \quad (19)$$

From Eqs. (13), (16), and (19), we can obtain Eq. (20):

$$\Delta V^* = \Delta V_{el.act.} - \Delta V_{el.H^+} \quad (20)$$

It is evident from a comparison of Eq. (20) and Eq. (9) that the ΔV^* is equivalent to $\Delta_c V_{el.}$.

Application of the Relationship to Reactions. First, the relationship shown in Fig. 1 was applied to the classification of protonation of ammonia and enolization of acetone.

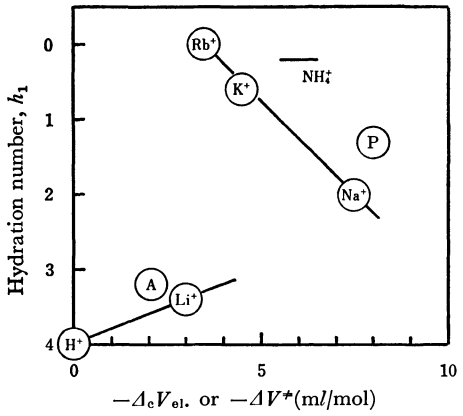

Fig. 1. Hydration number*1 *versus* conventional electrostriction, $\Delta_c V_{el}$, or activation volume, ΔV^*, of uni-valent cations at 25°C.
Ⓟ: hydration of propylene ($\Delta V = -8$ml/mol Ref. 3, $h_1 = 1.3$)
Ⓐ: enolization of acetone ($\Delta V^* = -2.1$ ml/mol Ref. 11, $h_1 = 3.2$ Ref. 12)
*1 The hydration number is obtained by calculating the entropy change; thus, the water molecules in hydration should be tightly bond with the ion.

The former reaction is represented by Eq. (21):[9]

$$H_3^+O + NH_3 \rightleftharpoons H_2O + NH_4^+ \quad (21)$$

For this reaction, $-\Delta V_{el.}$ is 5.5—6.5 ml/mol[9] and the hydration number, h_1, is 0.2.[2] Since its position is located near the first group, the hydration may be caused by electrostatic interaction. The nature of the electrostriction of the ammonium ion is the same as those of alkali metal cations, since the hydration number of the ammonium ion can be correlated with Pauling's ionic radius in the same manner as in the case of the alkali metal cation.[2] In Fig. 1 the absolute value of the electrostriction of the ammonium ion deviates from that of the first group by 2 ml/mol. This may arise partly from the values of the electrostrictions of alkali metal cations used, since the $\Delta V_{el.}$ is not a completely experimental value.[7]

For the latter reaction there is general agreement that the slow step is the removal of a proton from the α-carbon of the protonated ketone by water acting as a base.[10] For this reaction, the ΔV^* is −2.1 ml/mol,[11] and the h_1 is 3.2,[12] and the representative point is located near the second group; the probable structure of the activated complex is, then, similar to that of a hydrated proton, as is shown in Fig. 2. In this model the bond between the proton and the oxygen in the water molecule must be strong and covalent, since two hydrogen atoms of the water molecule must be cationic enough to attract two more water molecules.

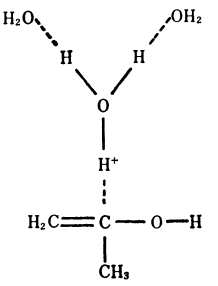

Fig. 2. Probable structure of the activated complex for enolization of acetone.

Consideration of the Activated Complex for the Hydration of Propylene. Since ΔV^* is −8 ml/mol[13] and h_1 is 1.3, the representative point of the hydration of propylene is located near the first group, as is shown in Fig. 1. As a consequence, it is a reasonable interpretation that the hydration of the activated complex is caused by electrostatic interaction and that the structure of the activated complex can not be similar to that of a hydrated proton.

Bunton[14] proposed two models for the activated state

9) E. Whalley, *Trans. Faraday Soc.*, **55**, 798 (1959).
10) R. P. Bell, "Advances in Catalysis," Vol. IV, Academic Press Inc., New York (1952), pp.165—182.
11) E. Whalley, *Can. J. Chem.*, **42**, 1835 (1964).
12) The values of w^* from Bunnett's report for the reaction are 1.42 and 1.66 in hydrochloric acid. Hence 3.2 is obtained as h_1 by using Eq. (4). J. F. Bunnett, *J. Amer. Chem. Soc.*, **83**, 4956 (1961).
13) At 25°C the ΔV^* is about −8 ml/mol from the Fig. 5 in an earlier paper,[3] since the value $-\partial D/D^2\partial p$ under S. T. P. is 0.8×10^{-6} cm²/kg.
14) C. A. Bunton and V. J. Shiner, Jr., *J. Amer. Chem. Soc.*, **83**, 3207 (1961).

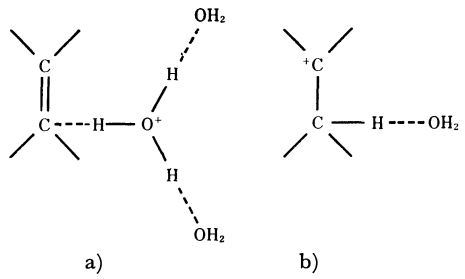

Fig. 3. Two models for the activated state of hydration of olefin proposed by Bunton (Ref. 14).
a) The activated state is similar to initial state. In his paper a hydrated proton is represented by H_3O^+, however, in this paper it is done by $H(H_2O)_4^+$.
b) The activated state is akin to the carbonium ion.

of the hydration of various olefins; by the use of these models the observed isotope effect can be rationally explained: a) the activated state is similar to the initial state, and b) the activated state is akin to the carbonium ion, *i.e.*, the proton is bound to the reaction center (Fig. 3). In view of the hydration number, it is necessary to exclude the a) structure, since its hydration number, 3, is different from the value, 1.3, obtained in the present investigation. On the other hand, the b) model is in good agreement with the results of this study.

According to our results, the "free" carbonium ion model proposed by Taft[15] is plausible for the activated complex, and one molecule of water may be bound to the "free" carbonium ion by electrostatic interaction.

If the observed value of the activation volume[3], -8 m*l*/mol, is caused by the partially covalent bond formation between a protonated olefin and a water molecule, as was proposed by Baliga,[16] its bond must be strong and nearly equal to the covalent bond, since the value of 8 m*l*/mol corresponds to nearly half of the molar volume of water. The covalent bond may be formed by the transfer of an electron from the oxygen in a water molecule to the protonated olefin. Hence, the two hydrogen atoms of the water molecule become cationic and attract two more water molecules. This means that the number of the water molecules contained in the activated complex must be 3; this is inconsistent with the observed hydration number of 1.3.

New Hypothesis as to the Nature of a Bond between a Water Molecule and a Protonated Substrate in an Activated Complex. Zucker and Hammett have proposed a hypothesis which seemed useful in distinguishing the A-1 mechanism from the A-2 mechanism according to whether log k_1 increases linearly with log c_{H^+} or with $-H_0$, where c_{H^+} is the concentration of the acid.[17] This hypothesis has, however, been sharply criticized by several authors[12,18] and has not been generally accepted.

The present authors hereby propose a hypothesis which is useful in characterizing the nature of a bond between a water molecule and a protonated substrate in an activated state: (a) If the log k_1 for a reaction increases linearly with $-H_0$, a water molecule (or water molecules) is held in an activated complex by electrostatic interaction.

(b) If the log k_1 for a reaction increases linearly with log m_a, a water molecule is held in an activated complex by a covalent bond.

Strictly speaking, the water molecule held in an activated complex by a weakly and partially covalent bond can not be distinguished from that contained by electrostatic interaction. However, this does not seem significant, because, in the present state, a discussion of such a fine difference between the two cases seems meaningless.

15) R. W. Taft, Jr., *J. Amer. Chem. Soc.*, **74**, 5372 (1952).
16) B. T. Baliga and E. Whalley, *Can. J. Chem.*, **42**, 1019 (1964); *ibid.*, **43**, 2453 (1965).
17) L. Zucker and L. P. Hammett, *J. Amer. Chem. Soc.*, **61**, 2791 (1939); F. A. Long and M. A. Paul, *Chem. Rev.*, **57**, 935 (1957).
18) R. W. Taft, Jr., N. C. Deno, and P. S. Skell, *Ann. Rev. Phys. Chem.*, **9**, 306 (1958); R. P. Bell, "The Proton in Chemistry," Cornell University Press, Ithaca, N. Y. (1959).

A Theoretical Study of the Possible Interaction between Sulfonium Salts and Molecular Oxygen

Katsutoshi OHKUBO* and Tokio YAMABE

Faculty of Engineering, Kyoto University, Sakyo-ku, Kyoto

(Received August 17, 1970)

The interaction between sulfonium salts and molecular oxygen was studied by the ASMO SCF method. Firstly, the results of the ASMO SCF calculation of trimethylsulfonium chloride suggested that the bond between the sulfonium cation and the anion was constituted mainly of the bonding $(d\text{-}p)\pi$-type overlaps (made by $3d_{yz}$- (or $3d_{xz}$-) of S and $3p_y$ (or $3p_x$) of Cl) and of the antibonding $(d\text{-}p)\sigma$-type overlaps (made by $3d_{z^2}$ (or $3p_z$) of S and $3p_z$ (or $3d_{z^2}$) of Cl). Secondly, the sulfonium salt interacts with molecular oxygen mainly through a $(d\text{-}p)$ σ-type overlap between the $3d_{yz}$-(or $3d_{xz}$-)orbital of the former and the $(1\pi_g)_z$-orbital of the latter. Thirdly, a maximum overlap formed between $3d$-sulfur orbitals and $1\pi_g$-orbitals of O_2 is established at the O_2-rotation angle of $\pi/4$ to the direction of the d-orbital expansion. Finally, the change in the energy state of O_2 caused by the sulfonium-salt interaction was discussed.

Some theoretical investigations into the interaction of oxygen with various organic or inorganic compounds have been made: a donor-acceptor interaction with organic solvents by Hoijtink[1] and by others[2,3] (experimentally by Evans,[4-8] Tsubomura *et al.*,[2,9] and many other authors[10-15]) with pottasium chloride by Känzig,[16] and with iodides;[17] moreover, Khan and Kearns[18] calculated the energy of the interaction of molecular oxygen with organic molecules. These studies are characterized by discussions based on the donor-acceptor interaction.

From our own previous work[19] on the catalytic nature of sulfonium salt based on the interaction with molecular oxygen, it was suggested that the "partially-occupied" d-orbitals on the central sulfur of the sulfonium ion might interact with $1\pi_g$-orbitals of the oxygen molecule and that the interaction might be possible through the orbital symmetries between the d_{yz} (or d_{xz})-sulfur orbitals and the $(1\pi_g)_z$-orbital of the oxygen molecule (a strong $(d\text{-}p)\sigma$ type) and between d_{xy} and $(1\pi_g)_x$ (a weak $(d\text{-}p)\pi$ type). Moreover, from the ultraviolet spectroscopic study[20] of the interaction between the sulfonium salts and molecular oxygen, it was found that the characteristic band near 200 mμ should not be assigned to the charge-transfer bands, but to the transition from the nonbonding $3p_z$ lone pair-orbital on the central sulfur to the $3d$-sulfur orbitals. Moreover, it was found that the molecular oxygen interacting with the sulfonium salt shifted the band to the longer wavelength in the energy region of *ca.* 0.05—0.25 eV.

It is of interest to investigate further the interaction of sulfonium salts with molecular oxygen from a theoretical point of view. The present theoretical study intends to clarify the following: a) the nature of the bond[19] between the sulfonium cation and the counter anion; b) the configuration of the mode of interaction between the sulfonium and molecular oxygen, and c) the chemical property of the oxygen molecule "activated" through the interaction with the sulfonium salts. A zero-differerential-overlap approximated ASMO SCF method including the d-orbitals of sulfur was employed for the investigations of these three features.

Method of Calculation

For the sake of mathematical convenience, a zero-differential-overlap approximated ASMO SCF method was used for the calculations of trimethylsulfonium chloride, by itself and also in interaction with oxygen.

For the calculations, the values of the orbital exponents of H, C, O, S, and Cl were supplied from the data of Clementi;[21] the ionization potentials and electron affinities of the above atoms were chosen from the values calculated by Jaffé,[22] while the values of the effective nuclear charge and the ionization potential of $3d$-sulfur orbitals were taken from Levison and Perkins.[23] These values are listed in Table 1. For one-center exchange repulsion integrals, the values of the Frank-

* Present address: Faculty of Engineering, Kumamoto University, Kurokami-machi, Kumamoto.

1) G. J. Hoijtink, *Mol. Phys.*, **3**, 67 (1960).
2) H. Tsubomura and R. S. Mulliken, *J. Amer. Chem. Soc.*, **82**, 5966 (1960).
3) J. N. Murrel, *ibid.*, **3**, 319 (1960).
4) D. F. Evans, *J. Chem. Soc.*, **1953**, 345.
5) D. F. Evans, *ibid.*, **1957**, 1351, 3885.
6) D. F. Evans, *ibid.*, **1959**, 2753.
7) D. F. Evans, *ibid.*, **1960**, 1737.
8) D. F. Evans, *ibid.*, **1961**, 1987.
9) H. Ishida, H. Takahashi, H. Sato, and H. Tsubomura, *J. Amer. Chem. Soc.*, **92**, 275 (1970).
10) J. Jorthner and U. Sokolov, *J. Phys. Chem.*, **65**, 1633 (1961).
11) L. Paoloni and M. Cignitti, *Sci. Rept. Inst. Super. Sanita*, **2**, 45 (1962).
12) E. C. Lim and V. L. Kowalski, *J. Chem. Phys.*, **36**, 1729 (1962).
13) H. Bradley and A. D. King, *ibid.*, **47**, 1189 (1967).
14) A. U. Munck and J. F. Scott, *Nature*, **177**, 587 (1956).
15) L. J. Heidt and L. E. Ekstrom, *J. Amer. Chem. Soc.*, **79**, 1260 (1967).
16) W. Känzig, *J. Phys. Chem. Solids*, **23**, 479 (1962).
17) H. Leavanon and G. Navon, *J. Phys. Chem.*, **73**, 1861 (1969).
18) A. U. Khan and D. R. Kearns, *J. Amer. Chem. Soc.*, **48**, 3272 (1968).
19) K. Fukui, K. Ohkubo, and Yamabe, This Bulletin, **42**, 312 (1969).
20) K. Ohkubo, K. Nakai, and T. Yamabe, to be published.
21) E. Clementi and D. Raimondi, *J. Chem. Phys.*, **38**, 2686 (1963).
22) J. Hinze and H. H. Jaffé, *J. Amer. Chem. Soc.*, **84**, 540 (1962).
23) K. A. Revison and P. G. Perkins, *Theor. Chim. Acta* (Berl.), **14**, 206 (1969).

Condon parameters calculated by Hinze and Jaffé[24] were used, while for one-center coulomb repulsion integrals, the Pariser approximation[25] was used, as usual. For two-center coulomb repulsion integrals, the Ohno approximation[26] was employed.

TABLE 1. PARAMETERS USED FOR THE CALCULATION

Atom	Orbital	Orbital exponent	Ionization potential (eV)	Electron affinity (eV)
S	3*s*	2.1223	20.08	11.54
	3*p*	1.8273	13.32	3.50
	3*d*	1.00	3.06	1.63
C	2*s*	1.6083	21.01	8.91
	2*p*	1.5679	11.27	0.34
H	1*s*	1.00	13.60	0.75
Cl	3*s*	2.3561	24.02	14.45
	3*p*	2.0387	13.39	3.73
O	2*s*	2.2458	36.07	18.44
	2*p*	2.2266	18.53	3.40

For the assumed configuration of the sulfonium salt, a D_3 propeller-like configuration is most plausible, as was discussed in our previous report.[19] The bond distances and angles were set up as follows: S–C=1.82 Å, C–H=1.10 Å, S–Cl=2.5—4.5 Å and ∠HCH=109°28′, ∠CSC=120°, ∠CSCl=90°. The geometry used for the ASMO SCF calculation is illustrated in Fig. 1.

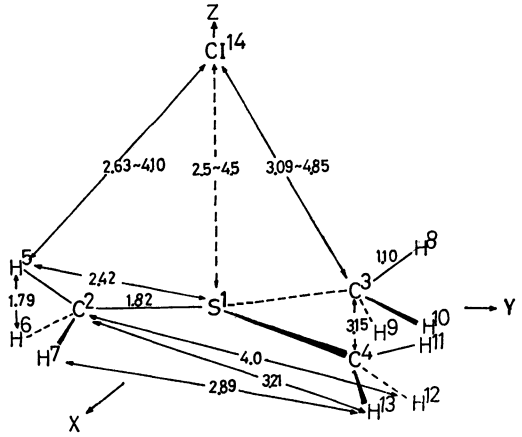

Fig. 1. Geometry used for the calculation.

Results and Discussion

Contributions of d-*Sulfur Orbitals to the Electronic State of Sulfonium Salt. Atom Population and Bond Population, Total Energy and Dipole Moment.* In order to estimate the contribution of *d*-sulfur orbitals to the S–Cl bond, an ASMO SCF calculation of trimethylsulfonium chloride was carried out both with and without inclusion of the *d*-sulfur orbitals with respect to the S–Cl distance of 2.5—4.5Å. The atom population, total energy, and dipole moment are shown in Fig. 2. As is shown in Fig. 2, in the case including *d*-sulfur orbitals, the contribution of *d*-orbitals may be reflected by the results of the smaller atom population of Cl and the significant amounts of the charge density at the *d*-orbitals of sulfur. Moreover, the charge of the C-atoms of methyl substituents becomes larger through *d*-π conjugation.[27] The *d*-π conjugation between the sulfonium cation and the counter chloride anion is directly related to the covalent nature of the S–Cl bond, as has been discussed previously.[19] On the other hand, the minimum total energy at the S–Cl distance of 3.5Å in the assumed configurations of the sulfonium chloride suggests the ionic molecular structure of the salt, considering the van der Waals radii of S (1.85 Å) and Cl (1.80Å).

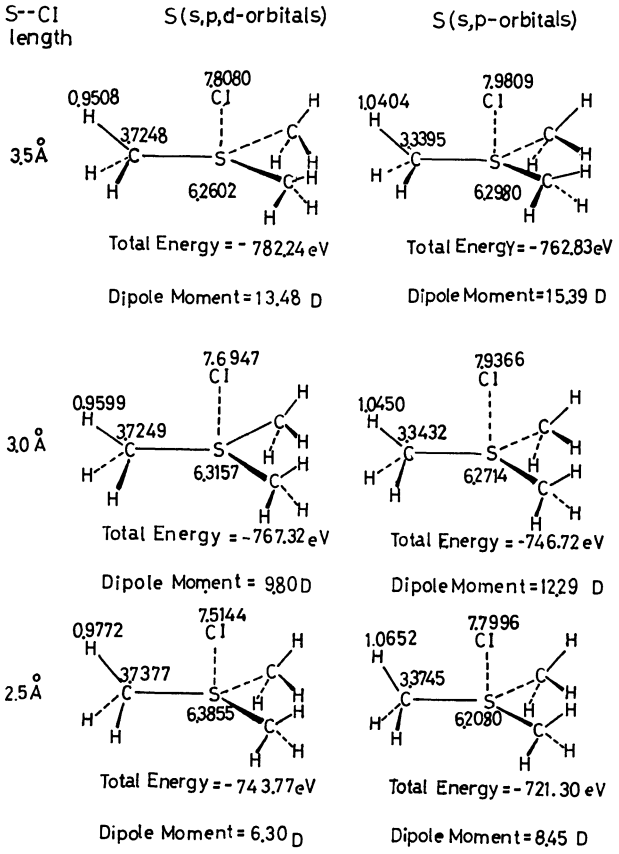

Fig. 2. The atomic population of $(CH_3)_3SCl$.

The Property of the Bond between the Sulfonium Cation and the Anion. It is well known that the orbital overlapping between atoms gives some idea of the aspects of the bond nature.

The bond property of S–Cl was, then, investigated from the viewpoint of the orbital overlappings in the coulomb and van der Waals distances of S–Cl (2.0 and 3.65 Å respectively). In this case, the contribution of the *s*-orbitals of both atoms to the bond formation can be neglected. The modes of the orbital overlappings of various orbitals are shown in Fig. 3. The overlap

24) J. Hinze and H. H. Jaffé, *J. Chem. Phys.*, **38**, 1834 (1963).
25) R. Pariser and R. G. Parr, *ibid.*, **21**, 466, 767 (1953).
26) K. Ohno, *Theor. Chim. Acta*, **2**, 219 (1964).

27) In the case of triphenylsulfonium tetrafluoroborate, the *d*-π conjugation between the *d*-sulfur orbitals of the central sulfur atom and the π-orbitals of phenyl substituents was reflected by the red shift of the ^1L_b transition of the sulfonium in the order of 0.27 eV, as compared with the ^1L_b transition of triphenylcarbonium tetrafluoroborate, as established ultraviolet spectroscopic study (K. Ohkubo and T. Yamabe, *Bull. Japan Petr. Inst.*, **12**, 130 (1970)).

between the *d*-orbitals of sulfur and those of chlorine does not participate dominantly in the bond formation, even though a suitable maximum overlap appears in the 2.5—4.5 Å region of S-Cl, because of the vacancy of the *d*-orbitals on both atoms. The bond formation can, then, be considered to be mainly dependent on the $(d\text{-}p)\sigma$ and $(d\text{-}p)\pi$ overlaps, because the contribution of the $p\sigma$ and $p\pi$ overlaps is not so dominant in the separation beyond the distance of 3 Å. Therefore, the atomic orbital populations of both atoms and the bond orders between the atoms exhibit the bond natures characteristic of the $(d\text{-}p)\pi$ bonding orbital between the d_{xz} (or d_{yz}) of sulfur and the p_x (or p_y) of chloride and the $(d\text{-}p)\sigma$ antibonding orbital between d_{z^2} (or p_z) of S and p_z (or d_{z^2}) of Cl (see Table 2).

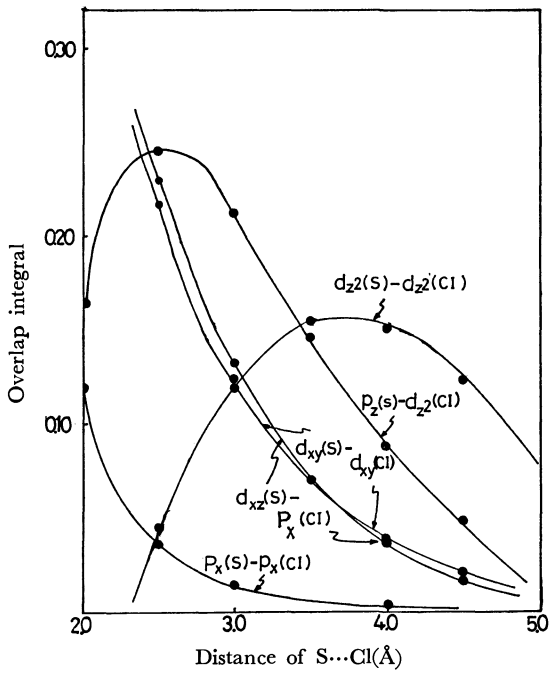

Fig. 3. Orbital overlaps between the orbitals of the central sulfur and those of the chloride.

From Table 2, the decrease in the distance of S-Cl promotes the charge transfer, as is shown in the following schemes:

Electron migration through the π-bonding orbital:

$$p_x^{(Cl)}\,(\text{or } p_y^{(Cl)}) \xrightarrow{\text{through } d_{xz}^{(S)}-p_x^{(Cl)} \text{ or } d_{yz}^{(S)}-p_y^{(Cl)}} d_{xz}^{(S)}\,(\text{or } d_{yz}^{(S)})$$

The electrons of $p_x^{(Cl)}$ which migrate to d_{xz} (or d_{yz}) push out the electrons of $p_x^{(S)}$ (or $p_y^{(S)}$) to $p_x^{(Cl)}$ (or $p_y^{(Cl)}$):

$$p_x^{(S)}\,(\text{or } p_y^{(S)}) \xrightarrow{\text{through } p_x^{(S)}-p_x^{(Cl)}} p_x^{(Cl)}\,(\text{or } p_y^{(Cl)})$$

Electron migration through the σ-antibonding orbital:

$$p_z^{(Cl)} \xrightarrow{\text{through } d_{z^2}^{(S)}-p_z^{(Cl)}} d_{z^2}^{(S)}$$

The electron of $p_z^{(Cl)}$ which has migrated to $d_{z^2}^{(S)}$ repulses the electrons of $p_z^{(S)}$, thus promoting the migration of the electrons of $p_z^{(S)}$ to $p_z^{(Cl)}$ or $d_{z^2}^{(S)}$.

$$p_z^{(S)} \xrightarrow{\text{through } p_z^{(S)}-p_z^{(Cl)}} \begin{cases} p_z^{(Cl)} \\ d_{z^2}^{(S)} \end{cases}$$

Table 2. The bond nature of S-Cl of trimethylsulfonium chloride

Distance of S-Cl	AO population of S				AO population of Cl	
	$p_x=p_y$	p_z	$d_{xz}=d_{yz}$	d_{z^2}	$p_x=p_y$	p_z
4.5	1.2201	1.9290	0.0425	0.0673	1.9956	1.9447
3.5	1.1997	1.9249	0.0621	0.1413	1.9736	1.8818
3.0	1.1840	1.9173	0.0906	0.1830	1.9416	1.8601
2.5	1.1649	1.8840	0.0812	0.2347	1.9042	1.8371

AO Bond order of S-Cl

Distance of S-Cl	$p_x^{(S)}-p_x^{(Cl)}=p_y^{(S)}-p_y^{(Cl)}$	$p_z^{(S)}-p_z^{(Cl)}$	$d_{xz}^{(S)}-p_x^{(Cl)}=d_{yz}^{(S)}-p_y^{(Cl)}$	$d_{z^2}^{(S)}-p_z^{(Cl)}$
4.5	0.0022	0.0002	0.0839	−0.2841
3.5	0.0116	−0.0093	0.2122	−0.4264
3.0	0.0279	−0.0310	0.3162	−0.4469
2.5	0.0639	−0.0843	0.4340	−0.4116

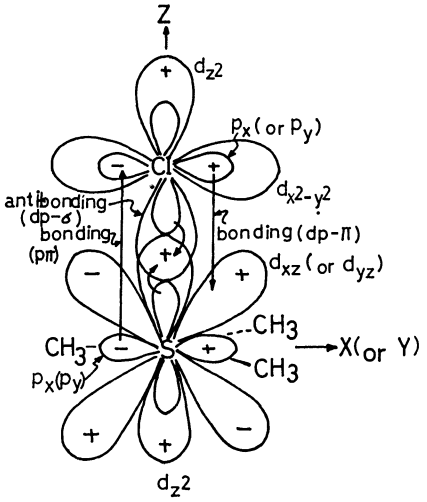

Fig. 4. The directions of electron migrations between sulfonium cation and chloride anion in the case of the decrease of S···Cl bond length.

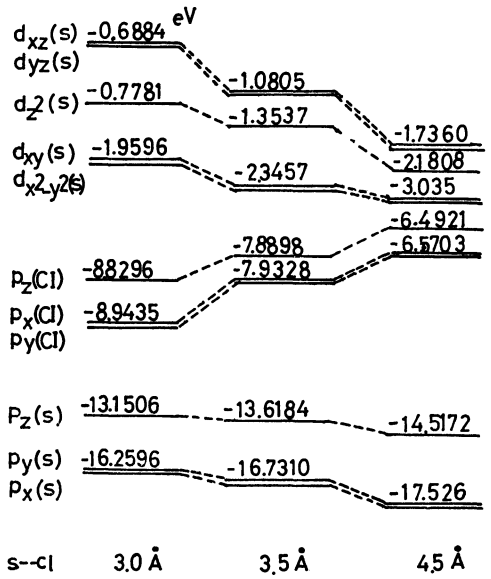

Fig. 5. An energy diagram of $(CH_3)_3SCl$.

These circumstances are illustrated in Fig. 4.
In this case, the changes in the net charges of carbon and hydrogen were very small as compared with those of sulfur and chlorine. The change in the energy levels of the *p*- and *d*-orbitals of the central sulfur and the chlorine atom with the variation in the S-Cl bond length is shown in Fig. 5.
From Fig. 5, it may be seen that, at the larger separation between S and Cl (4.5 Å), the $p_z^{(Cl)}$ is the highest occupied orbital and the $d_{x^2-y^2}^{(S)}$ is the lowest unoccupied one, while at the smaller separation (3.0 Å), the former is lowered remarkably because of the outdrawing of the charge and, as a result, the latter comes to have a partially-occupied nature, with an elevation of the energy level.

Interaction between the Sulfonium Salt and Molecular Oxygen. For the interaction between the sulfonium salt and molecular oxygen, two probable configurations can be considered as the model for the mode of interaction: One is the parallel form, and the other is the triangular one, as is shown in Fig. 6. Among the orbital overlaps between the *d*-orbitals of the central sulfur atom and the $1\pi_g$-orbitals of the oxygen molecule, a $(d\text{-}p)\pi$-type overlap or d_{yz}-$(1\pi_g)_x$ and a $(d\text{-}\pi)$ π-type overlap of d_{xy}-$(1\pi_g)_y$ for the parallel form, and $(d\text{-}p)\sigma$-type overlaps of d_{xy}-$(1\pi_g)_x$ and d_{yz}-$(1\pi_g)_y$ for the triangular form, are possible.

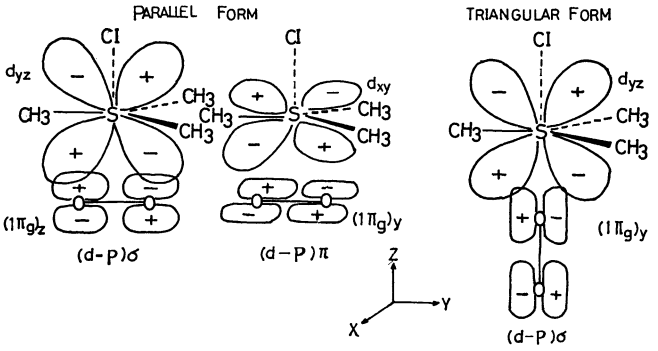

Fig. 6. Interactions between *d*-orbitals of trimenthylsulfonium chloride and $1\pi_g$-orbitals of molecular oxygen.

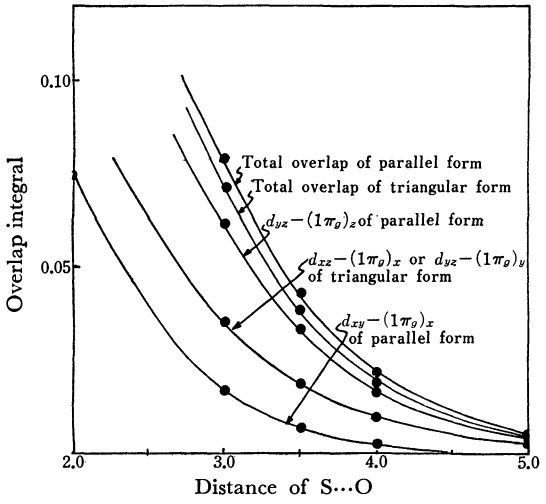

Fig. 7. Orbital overlap between *d*-orbitals of central sulfur of sulfonium and $1\pi_g$-orbitals of molecular oxygen.

The individual values of their overlap integrals were calculated. The geometry used for the mode of interaction between trimethylsulfonium chloride and the oxygen molecule is indicated in Fig. 6. As is indicated in Fig. 7, the total overlap of the parallel form is larger than that of the triangular one, and the $(d\text{-}p)\sigma$-type overlap is apparently larger than the $(d\text{-}p)\sigma$-type one; this is in agreement with the previous discussion.[19]

The Dependence of Orbital Overlaps on the Rotation around the Bond Axis between Two Oxygen Atoms.
The ASMO SCF calulation was further adopted for the parallel form, in which the oxygen molecule rotates in a way parallel to the sp^2-hybrid ligand plane, as is shown briefly in Fig. 8.

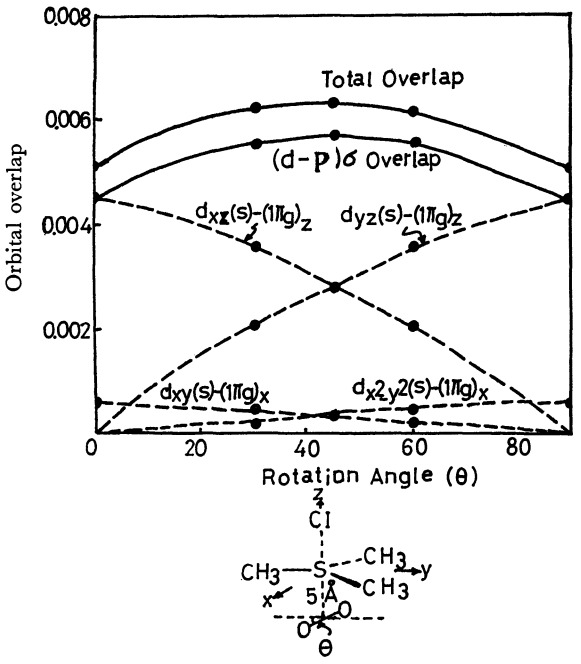

Fig. 8. Orbital overlap in case of O_2 rotation.

The dependence of the orbital overlap integrals on the rotation of the molecular axis of the oxygen molecule is indicated in Fig. 8.
Fig. 8 shows that the most preferable overlap is brought about at the rotation angle of 45° to the direction of *d*-orbital expantion. In this situation, the orbital symmetry is favorable for the formation of a methane-like bonding overlap. These circumstances are illustrated in Fig. 9. Here, it is necessary to consider the chemical nature of the oxygen molecule activated through the interaction with the sulfonium salt. When the *d*-orbitals of the central atom interact with the $1\pi_g$-orbitals of the oxygen molecule, the partially-occupied *d*-sulfur orbitals[19] (d_{yz} or d_{xz}) to which the electron flows from the counter anion may transfer the charge to the $(1\pi_g)_z$-orbital of O_2, and the $(1\pi_u)_z$-orbital electron may back-donate to the d_{z^2}-sulfur orbital. Such electron migrations promote the increase in the bond length of the oxygen molecule by the electron repulsion, and the odd-electron-charge density may localize in each oxygen atom so as to increase the radical nature of O_2. In this situation, the half-occupied, doubly-degenerated $1\pi_g$-orbitals come to be free from the de-

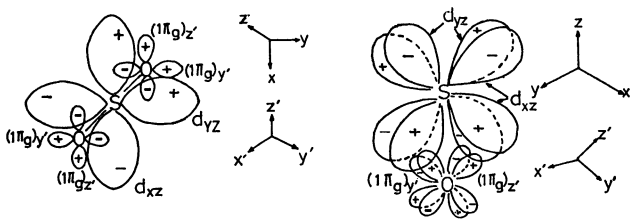

Fig. 9. An optimized interaction between sulfur *d*-orbitals and 1π-orbitals of oxygen molecule.

generated state, considering the Jahn-Teller effect.[28,29] It should be stressed here that the electron affinity and the ionization potential of the oxygen molecule are 0.15 eV[30,31] and 12.075 eV[32,33] respectively. Considering that the energy levels of the $3d$-sulfur orbitals, in particular those of d_{xz} and d_{yz}, are -0.688, -1.736 eV at the S-Cl distances between 3.0 and 3.4 Å (see Fig. 5), the energy level of -0.15 eV of the oxygen molecule might play an important role in the interaction with the $3d$-sulfur orbitals because of possibility of perturbation between them. Further work about the electronic state of the oxygen molecule calculated by means of non-empirical calculation may clarify this point.

28) H. A. Jahn and E. Teller, *Proc. Roy, Soc.*, **A 161**, 220 (1937).
29) H. A. Jahn, *ibid.*, **A 164**, 117 (1938).
30) D. S. Burch, S. J. Smith, and L. M. Branscomb, *Phys. Rev.*, **112**, 171 (1958).
31) R. S. Mulliken, *ibid.*, **115**, 1225 (1959).
32) K. Watanabe, *J. Chem. Phys.*, **26**, 542 (1957).
33) Other data are 12.2 ± 0.3 eV (G. L. Weissler, J. A. R. Samson, M. Ogawa, and G. R. Cook, *J. Opt. Soc. Amer.*, **49**, 338 (1959)) and 12.21 ± 0.04 eV (D. C. Frost and C. A. McDowell, in "Advance in Mass Spectrometry," edited by J. D. Waldron, Pergamon Press, London (1959), p. 413).

The most suggestive results obtained from this study may be summarized as follows:

a) The bond between the sulfonium cation and the anion of the sulfonium salts is constituted mainly by the bonding $(d\text{-}\pi)\pi$-type overlaps made by the $3d_{yz}$- (or $3d_{xz}$-) sulfur orbital and the $3p_y$- (or $3p_x$-) chloride orbital and by the antibonding $(d\text{-}\pi)\sigma$-type overlaps made by the $3d_{z_2}$- (or $3p_z$-) sulfur orbital and the $3p_z$- (or $3d_{z_2}$-) chloride orbital.

b) As to the interaction between the *d*-orbitals of sulfonium salt and the $1\pi_g$-orbitals of the oxygen molecule, orbital symmetries allow two modes of interaction (the parallel form and the triangular one). The former is stronger than the latter. In the parallel form of the interaction, a $(d\text{-}p)\sigma$-type overlap is predominant over a $(d\text{-}p)\pi$-type overlap, as has been suggested previously.[19]

c) The maximum overlap of the $(d\text{-}p)\sigma$ type formed between the sulfonium salt and molecular oxygen is possible when the oxygen molecule rotates at the angle of $\pi/4$ around its bond axis parallel to the sp^2-hybrid ligand plane of the sulfonium cation.

d) The electron inflowing from the $3d$-orbitals of the sulfonium to the $1\pi_g$-orbitals of O_2 localizes the electron charge of the orbitals, which may be connected with the increase in the radical nature of O_2.

The calculations have been carried out on the FACOM 230.60 computer at the Computer Center of Kyoto University.

The authors wish to express their cordial thanks to Professor Kenichi Fukui, who made a number of valuable suggestions and commented on major portions of this study.

A Theoretical Study of the Catalytic Activity of Group I Metal Salts in the Homogeneous Liquid-Phase Oxidation

Katsutoshi OHKUBO, Hidetoshi SHIMADA, Yasuhiro SHIOTANI, and Masahide OKADA
Faculty of Engineering, Kumamoto University, Kurokami-machi, Kumamoto
(Received October 1, 1970)

A theoretical consideration of the catalytic activity of group I metal salts, especially of lithium ones, for the homogeneous liquid-phase oxidation of hydrocarbons was developed by extended Hückel molecular orbital calculations, with particular reference to the interaction between the salts and molecular oxygen. We made several findings. First, a marked activity of lithium salt-catalysts was reflected by a remarkable "electron-partial occupation" of the lithium cation in their salts. Second, a strong interaction of the lithium catalyst with O_2 occurred at the angle of 15° to the direction of the $1\pi_g$-orbital expansions of O_2. Third, the lithium catalyst participated strongly in the activation of O_2 at the distance of 2 Å—3 Å, increasing the electron-population of one oxygen atom located farther from the lithium cation. Finally, the contribution of the "activated" oxygen molecule to the initiation of the oxidation of hydrocarbons was discussed.

In the field of liquid-phase catalytic oxidations, it is usually accepted that oxidation catalysts such as transition metal compounds[1] exhibit catalytic effects on the acceleration of the reaction rate through the so-called "*Haber-Weiss*"mechanism.[2] On the other hand, the different proposals of some other authors[3-5] have been based on the concept that oxidation catalysts might interact with molecular oxygen to form "*activated*" oxygen. This concept is surely plausible considering that the main product (hydroperoxide) accumulated is little decomposed by the catalyst in low-temperature oxidation in spite of the appreciable amounts of oxygen consumed to hydrocarbons. However, the above concept has not been confirmed precisely on the basis of experimental work.

It is hard to deny that hydroperoxides formed in such small amounts (below 2%[6] of the total conversion, as determined from the amount of O_2 absorbed) during the induction period initiate the oxidation reaction as radical initiators through their thermal or catalytic decompositions. In this case, radicals produced secondarily from such a hydroperoxide take part in the decomposition of the hydroperoxide formed successively.

From our previous works concerning the catalytic behavior of such salt-type catalysts as onium compounds[7-9] and metal salts[10] in the homogeneous liquid-phase oxidation, the phenomena of the increasing rates at the initial stage of the reaction could be well explained by the assumption of an interaction between the catalysts and molecular oxygen; furthermore, this assumption was supported more precisely by a spectroscopic study[11] of the above interaction. Recently, the donor-acceptor interaction[12-14] between organic compounds (donor) and molecular oxygen (acceptor) has been studied in detail in connection with the "*contact charge-transfer complex*";[15-17] a theoretical calculation of this complex can be found in Ref. 18. Moreover, a possible interaction of KCl with O_2 has been confirmed by Känzig and Cohen[19] by a study of the ESR spectra, which indicated the presence of the O_2^- anion. It was found in our recent study[10] that alkali metal salts, in particular lithium salts, promote the oxidation reaction remarkably without an incubation period: this suggests the interaction of the salts with molecular oxygen at the initial, short stage of the reaction.

The aim of this study is to clarify the following points: a) the electronic states of metal salts, especially of lithium salts, and their correlations to the catalytic activity of the salt-type catalysts, b) the mode of the intraction of the catalysts with molecular oxygen, and c) the chemical property of the oxygen molecule "*activated*" through the interaction with the above salt-type catalysts. The extended Hückel method proposed by Hoffman[20] was employed to investigate these items.

Methods of Calculation

The calculations by the extended Hückel method were performed at first on group I metal chlorides and

1) For instance, W. F. Brill, *Ind. Eng. Chem.*, **52**, 837 (1960); A. Robertson and W. A. Walters, *J. Chem. Soc.*, **1947**, 492; E. R. Muller, *Ind. Eng. Chem.*, **46**, 562 (1954); N. Ohta and S. Marumo, *Kogyo Kagaku Zassi*, **58**, 798 (1955), and the references cited therein.
2) F. Harber and P. Weiss, *Proc. Roy. Soc.* (London), **A 147**, 233 (1939).
3) N. Uri, *Nature*, **177**, 1177 (1956).
4) H. Kropf, *Ann.*, **637**, 73 (1960).
5) H. Kropf and Hd. Hoffman, *Tetrahedron Lett.*, **1967**, 659.
6) It is generally considered that the hydroperoxide formed (mol) corresponds at most to 98% of the total conversion on the basis of the amount of O_2 absorbed (mol).
7) K. Fukui, K. Ohkubo, and T. Yamabe, This Bulletin, **42**, 312 (1969).
8) K. Ohkubo, T. Yamabe, and K. Fukui, *ibid.*, **42**, 1800 2220 (1969).
9) K. Ohkubo and T. Yamabe, *Bull. Japan Petrol. Inst.*, **12**, 130 (1970).
10) K. Ohkubo and T. Yamabe, *ibid.*, **12**, 123 (1970).
11) K. Ohkubo, K. Nakai, and T. Yamabe, to be published.
12) D. F. Evans, *J. Chem. Soc.*, **1953**, 345; **1957**, 1351, 3883; **1959**, 2753; *Proc. Roy. Soc.* (London), **A 255**, 55 (1960).
13) A. U. Munk and J. F. Scott, *Nature*, **177**, 587 (1956).
14) H. Tsubomura and R. S. Mulliken, *J. Amer. Chem. Soc.*, **82**, 5966 (1960).
15) R. S. Mulliken, *Rec. Trav. Chim.*, **75**, 845 (1956); L. E. Orgel and R. S. Mulliken, *J. Amer. Chem. Soc.*, **79**, 4839 (1957).
16) D. F. Evans and R. S. Mulliken, *J. Chem. Phys.*, **23**, 1424, 1426 (1955).
17) J. N. Murrell, *J. Amer. Chem. Soc.*, **81**, 5073 (1959).
18) A. U. Khan and D. R. Kearns, *J. Chem. Phys.*, **48**, 3272 (1968).
19) W. Känzig and M. H. Cohen, *Rev. Lett.*, **3**, 509 (1959).
20) R. Hoffmann, *J. Chem. Phys.*, **39**, 1397 (1963); **40**, 2474 (1964).

several lithium salts: LiCl, NaCl, KCl, RbCl, LiBr, LiI, LiF, Li_2SO_4, Li_2CO_3, LiO_2CH, $LiO_2CC_2H_5$, $LiNO_3$, $(LiO_2C)_2$, Li_3PO_4, and so on. Secondly, the calculations were carried out for the interaction between LiCl and O_2 with the variation in the bond angles of OOLi at 0°, 10°, 15°, 30°, 60°, and 90° at a fixed distance (O_2–LiCl=3.0 Å). Thirdly, the calculations were performed on the interactions between LiCl and O_2 at the distances (O_2–LiCl) of 1.0—5.0 Å at a fixed angle ($\angle$OOLi=15°). For the calculations, the values of the orbital exponents for H, Li, Na, Rb, Be, C, N, O, P, S, and Cl were taken from the data of Clementi[21], while the valence-state ionization potentials used for the diagonal *H*-matrix elements (H_{ii}) were supplied by Hinze[22,23] and Pople[24]. These parameters are listed in Table 1. For the off-diagonal matrix elements (H_{ij}), the Wolfsberg-Helmholtz approximation[25] was employed:

$$H_{ij} = K(H_{ii}+H_{jj})S_{ij}/2$$

where the value of K is taken to be 1.75[26] and where S_{ij} is the overlap integral between AO's.

In regard to the bond lengths and angles of the metal salts, they are indicated in the proper tables and figures in this paper. For the H_{ij} of the O atom, there exist three different sets of values for cheking the charge of the atom: H_{ii}(eV)=−36.02 (O 2*s*) and −18.53 (O 2*p*) (Method I), −32.38 (O 2*s*) and −15.85 (O 2*p*) (Method II), and −35.30 (O 2*s*) and −13.61 (O 2*p*) (Method III). Finally, the contour maps of the interaction between the partially-occupied *s*-Li^+ orbital and $1\pi_g$-orbitals of O_2 were portrayed using the effective nuclear charges of the two atoms as derived from Slater's rule.[27]

Table 1. Parameters used for the calculations

Atom	Orbital exponent	Ionization potential (eV)	
		s	*p*
H	1.0	13.60	
Li	0.6396	5.39	3.54
Na	0.8358	5.14	3.04
K	0.8738	4.34	2.73
Rb	0.9969	4.18	2.60
Be	0.9560	9.92	5.96
C	1.5679	21.01	11.27
N	1.9170	26.92	14.42
O	2.2266	36.07[a]	18.53[a]
		32.38[b]	15.85[b]
		35.30[c]	13.61[c]
P	1.6288	20.20	12.49
S	1.8273	20.08	13.32
Cl	2.0387	24.02	13.39

a) Method I, b) Method II, c) Method III

21) K. Clementi and D. Raimondi, *J. Chem. Phys.*, **38**, 2686 (1963).
22) J. Hinze and H. H. Jaffé, *J. Amer. Chem. Soc.*, **84**, 540 (1962).
23) J. Hinze and H. H. Jaffé, *J. Phys. Chem.*, **67**, 1501 (1963).
24) J. A. Pople, D. P. Santry, and G. A. Segal, *J. Chem. Phys.*, **43**, S129 (1965).
25) M. Wolfsberg and L. Helmholtz, *ibid.*, **20**, 837 (1952).
26) R. Hoffmann, *ibid.*, **39**, 1397 (1963); **40**, 2474, 2480, 2745 (1964).
27) J. C. Slater, *Phys. Rev.*, **36**, 57 (1930).

Results and Discussion

The Correlation between the Catalytic Activity of the Metal Salt and the Atom Population of its Metal Ion. Before discussing the correlation between the catalytic activity of metal salt and the atomic population of its metal cation ($M(M^+)$), it is necessary to emphasize that the catalytic activity of metal salt is not directly dependent upon the counter anion of the salt, but upon its metal cation, and that it is affected mediately by the difference in the structures of the anions. Moreover, the counter anion of the effective salt-type catalyst is not required to have a radical as metal halide.[28] Among the group I metal salts tested, lithium salts exhibited a striking catalytic activity for the acceleration of the reaction rate, without the decomposition of the hydroperoxide formed at the initial stage of the oxidation. It was considered that such a remarkable activity of lithium salts was related to the small 2*s*-lithium orbital "partially occupied" by an electron-inflowing from the counter anion. The lowest vacant *s*-orbital (speaking strictly, a partially occupied one) of Li^+ would thus play an important role in the catalytic activity. This consideration may be true in the case of the $M(M^+)$ of Li^+. The relation between $M(M^+)$ and the catalytic activity (defined by the maximum rate of reaction (R_{max})) is shown in Table 2. Table 2 indicates the marked partial electron-occupation on the vacant orbital of Li^+ in a large separation[29] at a van der Waals distance of Li–Cl (3.31 Å), even though all the $M(M^+)$ values except $M(Li^+)$ is almost zero. This feature of the partial electron-occupation on the vacant orbital of the cation may be related to the weak covalent nature of lithium salts, in view of the appreciable value of the overlap population (indicated by M(M–Cl)) as compared with the negligible populations of other group I metal salts. Such a weak covalency of lithium salts can be understood in terms of the very appreciable solubilities of lithium salts to organic solvents, such as alcohol and ether.

The Bond Nature of Lithium Salts. In order to investigate the nature of the bond of lithium salts, the extended Hückel molecular orbital calculation for Li_3PO_4 was carried out with the bond lengths of Li–O varying from an ionic distance (2.91 Å) to the covalent one (2.30 Å). The changes in the atomic population and the total energy with those of the distance are illustrated in Fig. 1, where the geometry used for the calculation is also portrayed. As is shown in Fig.1, the total energy of Li_3PO_4 indicates, interestingly, that the ionic structure of this phosphate is very stable. In this case, however, the total energy excludes the energies of core repulsions and electron-electron interactions. Considering the circumstances of the hydrocarbons around the metal salt-catalysts in the reaction system, it seems preferable to use the ionic structures of the catalysts. The present calculations will hereafter

28) In fact, phosphate, formate, *etc.* of lithium salts are more effective than halides in tetralin oxidation.[10]
29) The bond distance of Li–Cl has been reported to be *ca.* 2.2029 Å (L. Pauling, "The Nature of the Chemical Bond," Cornell Univ. Press, Ithaca, N. Y. (1960), p. 532).

TABLE 2. THE RELATION BETWEEN THE CATALYTIC ACTIVITY OF GROUP I METAL CHLORIDES AND THE ELECTRONIC STATES OF THEM

Compound (MCl) M	Distance of M–Cl (Å)	L.V. orbital of M^+	$R_{max} \times 10^{4a)}$ (mol/l·sec)	M (M^+)[b]	N(M–Cl)[c]	L. V. level of s-orbital of M (eV)
Li	3.31	2s	1.20	0.0200	0.016	−5.090
Na	3.65	3s	0.07	0.0055	0.004	−5.018
K	4.05	4s, 3d	0.10	0.0012	0.001	−4.268
Rb	4.25	5s, 4d	0.12	0.0003	0.0003	−4.164
NH_4[d]		3s	0.08			
($BeCl_2$)[d]	2.02	2p (or 2s)[e]	0.13	0.7037	0.2575	−4.338[f]
None			0.05			

a) This maximum rate was determined by the moles of O_2 absorbed corresponding to those of hydroperoxide formed in the oxidation of cumene saturated with the metal chlorides at 70°C.
b) Atomic population of the metal cation.
c) Overlap bond population between the metal cation and the anion.
d) They were taken for the purpose of comparison.
e) The L.V. orbital of $BeCl_2$ is 2p-one in the case of sp-hybrid-valence state, while that of Be^{2+} is a vacant 2s-orbital. The former may be preferable because of the feeble ionic character of $BeCl_2$.
f) This level corresponds to the vacant p-Be orbital.

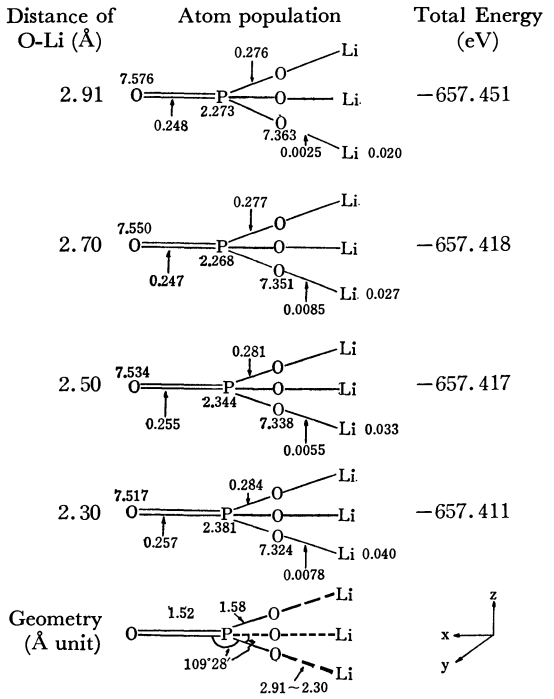

Fig. 1. Electronic states of Li_3PO_4 in some possible structures.

be performed on the ionic structures of the salts.

The Correlation between the Catalytic Activity of Several Lithium Salts and the Atomic Population of the Lithium Cation (M(Li$^+$)) in Them. The counter anions of salt-type catalysts appreciably affect the catalytic activity, as has been discussed previously.[7-10] It is of interest to investigate the relation between the activity (defined by R_{max}[30]) and M(Li$^+$). In this case, M(Li$^+$) would be related directly to the covalency of the bond between the lithium cation and the counter anion, as is indicated by the total overlap population of Li^+–X^-, (M(Li^+–X^-)). R_{max}, M(Li$^+$), and M(Li^+–X^-) are listed in Table 3. An interesting correlation between R_{max} and M(Li$^+$) could be found with some irregularities caused by a gap between the structures calculated and those in the reaction system. This correlation suggests that electrons on the "partially occupied" orbitals of lithium cation participate directly in the activity and that the counter anion contributes not a little toward the changing of the electron-occupation on the cation by an electron-inflow through the somewhat "covalent" bond.

Interaction between the Lithium-salt Catalysts and Molecular Oxygen. The catalytic activity of lithium salts as effective catalysts for the oxidation may be attributed to the contribution of the partially-occupied 2s-lithium orbital, in view of the above discussion. It is plausible here to discuss the interaction between the orbital mentioned above and the half occupied,doubly-degenerated 1π_g-orbitals of $^3\Sigma^-$ molecular oxygen, because the catalysts are unlikely to promote the reaction by the decomposition of the hydroperoxide formed, especially during the initial stage of the reaction.[10] There exist three different representative configurations of the interaction (angular-, linear-, and triangular one), as Fig. 2 indicates. Our previous report[10] demonstrated that the "angular interaction" is plausible in view of the orbital symmetry. From Fig. 2 in which the total orbital overlaps between the orbitals of Li^+ and 1π_g-orbitals of O_2 are recorded, the demonstration mentioned above may be seen to be in good agreement with the present results of calculations, because the overlaps of the angular interaction is larger than those of the others. However, the strength of the interaction should vary with the direction of the orbitals of the Li^+ to 1π_g-orbitals of O_2; it is also affected by the total orbital overlaps between the lithium cation and the 1π_g-orbitals (S(Li^+–O_2(1π_g))). The variation in S(Li^+–O_2(1π_g)) with the angles of the interaction is shown in Table 4. Moreover, the participation of the catalyst in the electronic state of molecular oxygen accompanies the energy splitting of the 1π_g-orbitals from the degenerated state, reflecting the Jahn-Teller

30) This was determined by means of the quantity of O_2 consumed to tetralin at 120°C during the formation of equimolar quantities of its hydroperoxide to those of O_2.

Table 3. Correlation between the catalytic activity of lithium salts and the atomic population of lithium cation

Catalyst	M (Li^+)[a]		M (Li^+-X^-)[b]		R_{max}[c] (mol/l·sec $\times 10^4$)
	Method I	Method II	Method I	Method II	
LiF	−0.003		−0.008		1.98
LiCl	0.020		0.032		2.68
LiBr	0.020		0.034		2.96
LiI	0.032		0.054		0.28
$LiNO_3$	−0.012	—	−0.002	—	1.76
Li_2CO_3	0.001	0.006	0.002	0.010	1.13
Li_2SO_4	0.013	0.024	0.004	0.008	1.41
Li_2PO_4	0.008	0.020	0.0	0.006	2.05
LiOH	—	−0.001	—	−0.018	1.27
LiO_2CH	—	0.002	—	0.012	3.88
$LiO_2C_2H_5$	−0.002	—	0.0016	—	1.27
$(LiO_2C)_2$	0.0004	—	0.0008	—	1.69

a) Atomic population of Li^+.
b) Overlap bond population between Li^+ cation and X^- anion.
c) These values were obtained from the data of the tetralin-oxidation catalyzed by lithium salts (2.4×10^{-2} mol/l) at 120 °C for 3.0 hr, where the moles of tetralin hydroperoxide formed corresponded to those of O_2 absorbed.

Table 4. The variation in the electronic state of O_2 with the angular interaction between LiCl and O_2

Angle of OOLi	$S(Li^+-O_2\cdot(1\pi_g))$[a]	M (O–O)[b]		P (O–O)[c]		ΔE ($1\pi_g$)[d] (eV)	
		Method I	Method II	Method I	Method II	Method I	Method II
0°	0.007	0.476	0.460	−0.607	−0.619	0.0009	0.0010
10°	0.036	0.474	0.453	−0.607	−0.619	0.0010	0.0011
15°	0.048	—	0.730[e]	—	−0.666[e]	—	0.0014[e]
30°	0.043	0.468	0.454	−0.607	−0.619	0.0011	0.0014
60°	0.007	0.466	0.450	−0.606	−0.618	0.0006	0.0007
90°	0.036	0.464	—	−0.606	—	0.0	—
O_2 only		0.830		−0.596		0.0	

a) Total orbital overlap between the orbitals of Li^+ and $1\pi_g$-ones of O_2.
b) Atomic bond population between two oxygen atoms.
c) Bond order density of the $sp\sigma$-type bond of O_2.
d) The energy difference of the 1π-orbitals removing from the degenerated state.
e) These values were obtained from the calculations by Method III.

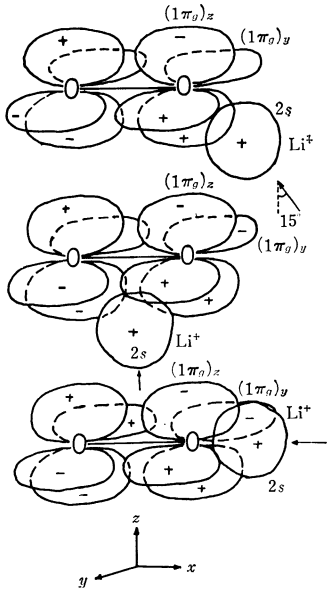

Fig. 2. Configurations of interaction between the partially occupied 2s-orbital of Li^+ and the half-occupied, doubly degenerated 1π-orbitals of O_2.

effect.[31,32] This situation may be understood in terms of the energy difference between the removed $1\pi_g$-orbitals (indicated by the notation of "$\Delta E(1\pi_g)$" in Table 4). The value of $\Delta E(1\pi_g)$ suggests that the larger it becomes, the more O_2 comes to have an active radical nature.

From the data of the extended Hückel calculations by both methods (Methods I and II), shown in Table 4, $S(Li^+-O_2(1\pi_g))$ and $\Delta E(1\pi_g)$ shown clearly that the strongest interaction occurrs at the angle of 15° to the direction of $1\pi_g$-orbital expansion. This fact may be closely related to the bond angles of ROOH ($\angle$ROO $=105°$[33]), H_2O ($\angle$HOH$=104°27'$[34,35]), CH_3OH ($\angle$COH$=104°40'$[36]), *etc.* The change in the angles of the interaction, however, has little influence upon the

31) H. A. Jahn and E. Teller, *Proc. Roy. Soc.*, **A 161**, 220 (1937).
32) H. A. Jahn, *ibid.*, **A 164**, 117 (1938).
33) L. E. Sutton, editor, "Interatomic Distances," The Chemical Society, London (1958).
34) D. M. Dennison, *Rev. Mod. Phys.*, **12**, 175 (1940).
35) G. Herzberg, "Infrared and Raman Spectra," D. Van Nostrand Co., New York (1945).
36) K. J. Tauer and W. N. Lipscomb, *Acta Crystallogr.*, **5**, 606 (1952); D. Dreyfus-Alain and R. Viallard, *Compt. Rend.*, **234**, 536 (1952).

TABLE 5. THE VARIATION IN THE ELECTRONIC STATE OF O_2 WITH THE ANGULAR INTERACTION BETWEEN LiCl AND O_2

Distance of Li–O (Å)	$S(Li^+O_2\cdot(1\pi_g))$[a]	M (O–O)[b] Method		M (Li^+)[c] Method		P (O–O)[d] Method		ΔE ($1\pi_g$)[e] (eV) Method		M (O_f) M (O_n)[f] Method	
		II	III	II	III	II	III	II	III	II	III
5	0.008	0.444	0.716	0.036	0.038	−0.628	−0.679	0.0001	0.0001	0.0005	0.0008
4	0.021	0.446	—	0.037	—	−0.626	—	0.0003	—	0.0030	—
3	0.048	0.458	0.730	0.040	0.053	−0.619	−0.666	0.0012	0.0014	0.0154	0.025
2	0.082	0.504	0.782	0.022	0.042	−0.605	−0.647	0.0017	0.0017	0.0456	0.066
1	0.059	—	0.864	—	−0.03	—	−0.654	—	0.0099	—	0.072
O_2 only		0.830				−0.596					

a), b), c), d), and e) are found in Table 2 or Table 3.
f) Difference between the atomic population of the farther oxygen atom (M (O_f)) and that of the neighboring atom (M (O_n)) for the catalyst. The former was larger than the latter.

state of the antibonding $sp\sigma$-type orbitals of the O–O bond, as is shown by the bond-order density (P(O–O)) in Table 4.

The investigation of the interaction of the lithium catalyst with molecular oxygen was, then, developed further by calculating the angular interaction with the variation in the distances of O_2-LiCl from 5 Å to 1 Å at a fixed angle of 15°. The data obtained from the calculations are summarized in Table 5. As is shown in Table 5, a monotonous increase in the total overlap, S (Li^+–O_2 ($1\pi_g$)), with a shortening of the distance between the catalyst and O_2 brings about a larger separation in the orbital energies ($\Delta E(1\pi_g)$). However, in the case of the distance of 1 Å, hardly no interaction might occur because of the core repulsions of the two molecules; this is reflected by the relatively small value of $S(Li^+–O_2(1\pi_g))$. On the other hand, when the lithium catalyst interacts with O_2 at 4 Å—5 Å, the catalyst has little effect upon the activation of O_2, as is suggested by the fact that the values of $S(Li^+–O_2(1\pi_g))$ are so much smaller than those at 3 Å and 4 Å. The contour map for the interaction (at 5 Å) between the $1\pi_g$-orbitals of O_2 and the partially-occupied s-lithium orbital of the catalyst indicates little influence of the catalyst upon the orbitals of O_2, as is shown in Fig. 3. In this situation of the

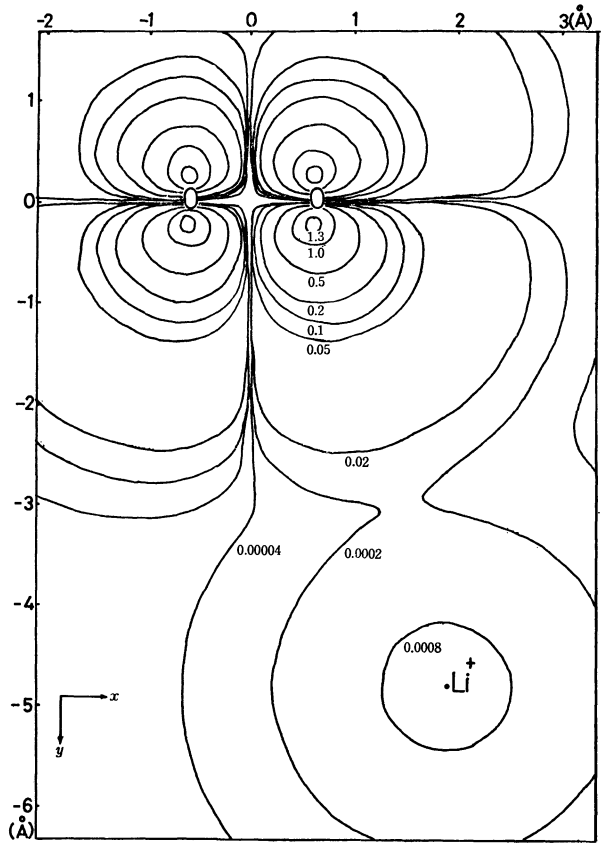

Fig. 3. Contour map for the angular interaction between the 1π-O_2 orbitals and the partially occupied s-Li orbital at 5Å. The values of the contour in this map and the following ones are those of the wave functions.

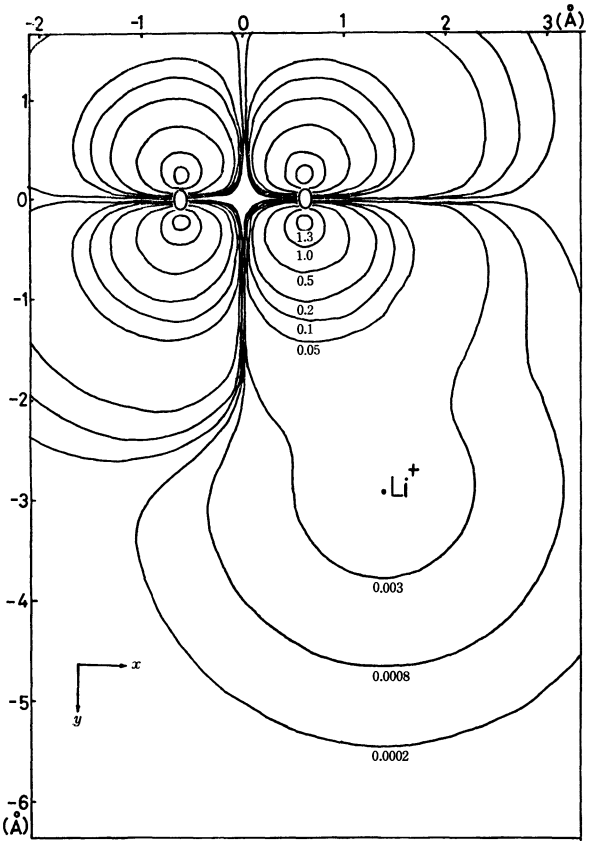

Fig. 4. Contour map for the angular interaction between the $1\pi_g$-O_2 orbitals and the s-Li orbitals at 3Å.

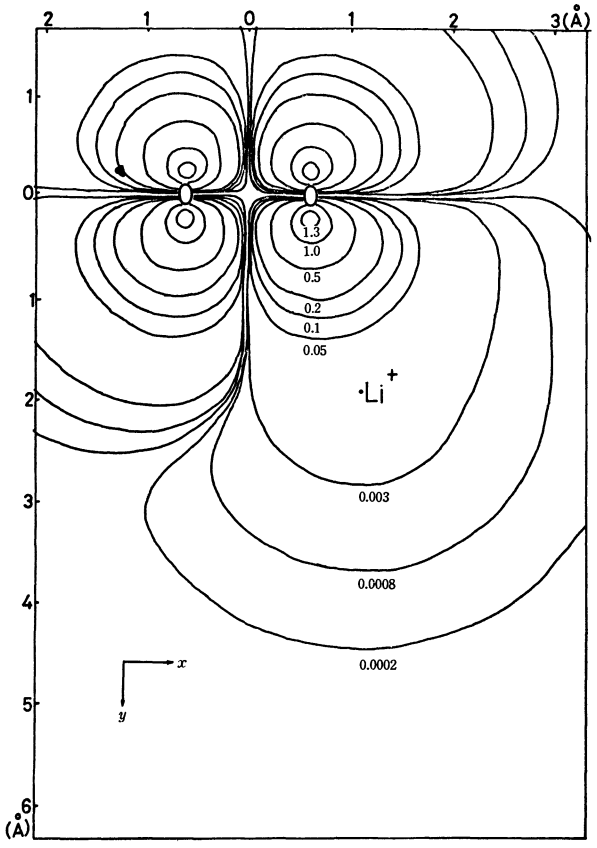

Fig. 5. Contour map for the angular interaction between the $1\pi_g$-O_2 orbitals and the s-Li orbital at 2Å.

small $S(Li^+–O_2(1\,\pi_g))$ value, electrons may be transferred mainly from the $1\,\pi_u$-orbitals of O_2 to the lithium cation to some extent, considering the increase in the atomic population of Li^+ ($M(Li^+)$) with the decrease in the distance between O_2 and the catalyst, while the total population of Cl^- stays constant. Then a favorable interaction would occur at distances from 2 Å to 3 Å, considering the $2p$-orbital expansions of O_2 and the small $2s$-orbital of Li^+. These circumstances are comprehensible in terms of the maps in Figs. 4 and 5. In this case, it is expected that electrons migrate from the partially-occupied $2s$-Li^+ orbital to the $1\,\pi_g$-orbitals of O_2, with a back-donation from the the $1\,\pi_u$-orbitals of the latter to the former. This is suggested by the decreasing $M(Li^+)$.[37]

Speaking about the population of the two oxygen atoms in O_2, the one atom remote from the catalyst, O_f, accepts more electrons than the other (O_n). Further, the $sp\sigma$-type O–O bond may lengthen its interatomic distance, since its bond-order density, P(O–O), is not only negative but also appreciably smaller than that of normal $^3\sum_g^-$ O_2 (see Table 5). Under the circumstances of hydrocarbons (RH), the position of O_f will be the more active side in O_2 for the reaction with RH: the electrons of O_f may transfer to the lowest laying, antibonding σ^*-orbital of RH through the $1\,\pi_g$-orbitals, thus increasing the antibonding character of the bond and causing the scission of the bond. When a hydrogen is abstracted from RH by O_2 through the cleavage of the R-H linkage, electrons migrating from O_2 to RH will be back-donated to the catalyst through the same $1\,\pi_g$-orbitals. Further work on the precise calculation including RH will clarify this assumption.

Finally, the results obtained from the present study may be summarized as follows:

a) Among group I metal salts, as calculated by the extened Hükel method, lithium salts were found to bear a remarkable electron-occupancy in their $2s$-orbitals; in this connection, lithium salts have a somewhat covalent bond.

b) The catalytic activity of group I metal salts can be well explained on the basis of their close relation to the atomic population of the metal cation, and the high activity of the lithium catalyst is reflected by the remarkable population of Li^+.

c) The lithium catalyst interacts most strongly with molecular oxygen at the angle of 15° to the direction of the $1\,\pi_g$-orbital expansions of O_2: this was understood on the basis of the suitable orbital overlap between the "partially-occupied" orbitals of Li^+ and the $1\pi_g$-orbitals of O_2.

d) Such an effect of the lithium-salt catalyst was exhibited best at the distance of 3 Å—2 Å from O_2. The electrons of Li^+ may inflow to the $1\,\pi_g$ of O_2 with the back-donation of $1\,\pi_u$ of the latter and an increase in the electron population of the farther oxygen atom (O_f) for the catalyst. This phenomenon furthered the orbital-removement of $1\,\pi_g$ from the degenerated state.

e) As for the hydrogen abstraction of "activated" O_2 from hydrocarbons, the orbitals of O_f take part in the abstraction more effectively than those of O_n.

The calculations were carried out on the FACOM 230.60 computer at the computation center of University of Kyushu.

37) The atomic population of Cl also stayed constant.

Analysis of Skeletal Deformation Vibration Spectra in Relation to the Molecular Structure

Tsunetake FUJIYAMA

Department of Chemistry, Faculty of Science, The University of Tokyo, Hongo, Bunkyo-ku, Tokyo

(Received August 19, 1970)

Deformation vibrations associated with displacements of skeletal heavy atoms are mainly discussed. It is shown that skeletal deformation vibrations are sensitive to the change of an azimuthal angle θ and that the frequencies of the vibrations are specific for the structure of rotational isomers. The θ-dependency of skeletal deformation vibrations corresponds exactly to that of elements of a kinetic energy matrix $\bar{G}$. The results emphasize the simplicity and the usefulness of the approximate normal coordinate treatment in which only skeletal heavy atoms are taken into account.

The concept of group frequencies has played an important role in the interpretation of vibration spectra, and it has contributed greatly to the progress of vibration spectroscopy. On analysing the spectra of large molecules, however, it is difficult to find those appropriate frequencies in the so-called finger print region because of the complexity of the coupling between the group frequencies and the overlapping of vibration bands. Sometimes the normal coordinate treatment affords a useful solution of the problem. However, many of the molecules which arouse great interest of chemists are composed of many atoms and the normal coordinate treatment for such molecules is often time consuming. Moreover, it is not always easy to obtain a reasonable set of force constants that can explain very complicated spectra.

A series of studies on molecular structures for various aliphatic compound showed that it is very hard to make a complete analysis of the vibration spectra of the molecules which have internal rotation axes because of their complexity. In order to overcome the difficulties we tried to find the absorption bands which are sensitive to the change of geometry of rotational isomers and are easily found in the spectra free from the overlapping of other absorption bands. The skeletal deformation vibrations are just the absorption bands satisfying the above requirements and will become still more useful with the remarkable progress in far-infrared spectrometers and laser-Raman instruments. Details of the spectral data used in the present report will be found in the references.[1-3]

Basic Concept

Intrinsic Frequency. The vibrations discussed herewith are deformation vibrations associated with displacements of skeletal heavy atoms of a given molecule. The basic concept of the vibrations will be drawn from the vibration frequencies of the CH_3CH_2X type molecules, because a molecule of this type has only one skeletal deformation vibration.

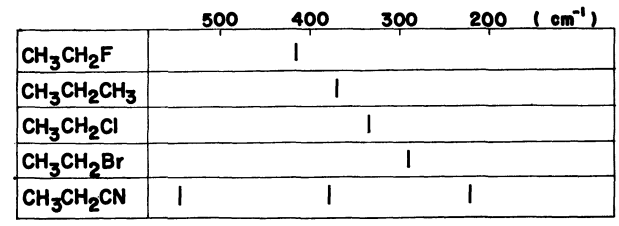

Fig. 1. Observed frequencies for CH_3CH_2X type molecules.

Figure 1 shows the observed frequencies of CH_3CH_2X type molecules. It is clear that the frequency of the deformation vibration decreases with the increase of the mass of atom X. This implies that deformation vibration frequency is determined mainly by the diagonal element of a kinetic energy matrix $\bar{G}$ corresponding to a coordinate $\Delta\alpha_{CCX}$, where $\Delta\alpha_{CCX}$ represents the change of the angle C–C–X. The calculated diagonal elements of $\bar{G}$ matrices for the CH_3CH_2X type molecules are compared with the observed deformation vibration frequencies in Table 1, where g_{CCX} denotes the diagonal element of $\bar{G}$ matrix corresponding to the coordinate $\Delta\alpha_{CCX}$ in $amu^{-1}\cdot A^{-2}$, ν the deformation vibration frequency in cm^{-1}, and A or f_{CCX} is defined by the relations

Table 1. Relation between frequencies and diagonal elements of $\bar{G}$ and $\bar{F}$ matrices of CH_3CH_2X type molecules

Molecule	ν (cm^{-1})	A (amu^{-1} A^{-1} md)	g_{CCX} ($amu^{-1}A^{-2}$)	f_{CCX} (md A)
CH_3CH_2F	415	0.103	0.168	0.61
$CH_3CH_2CH_3$	371	0.082	0.163	0.50
CH_3CH_2Cl	336	0.066	0.126	0.52
CH_3CH_2Br	290	0.053	0.115	0.46

$$A = \frac{4\pi^2 c^2}{N}\nu^2, \tag{1}$$

and

$$f_{CCX} = A/g_{CCX}. \tag{2}$$

In these equations f_{CCX} is expressed in md·A, A is in $amu^{-1}\cdot A^{-1}\cdot md$, while N and c represent the Avogadro number and the velocity of light, respectively. We see that a close relationship exists between g_{CCX} and A as expected. The observed frequencies of Fig. 1 are not assigned exactly to the CCX deformation modes, but they might be considered, to the first approximation,

1) T. Fujiyama, MA thesis submitted to the University of Tokyo (1963).

2) T. Fujiyama, Ph. D. thesis submitted to the University of Tokyo (1966).

3) Tables of Molecular Vibrational Frequencies, Part 1, U. S. Department of Commerce, N. B. S. (1967), and the references cited therein,

to be the *intrinsic frequencies* of the deformation vibrations expressed by the coordinate $\Delta\alpha_{CCX}$. The f_{CCX}'s are values calculated by Eq. (2), and not the real values of $\bar{F}$ matrices. However, the values can be used for the estimation of the intrinsic frequencies.

The frequencies of CH_3CH_2CN exhibit quite exceptional behaviour in the group, because the molecule has two extra vibrations occurring from the linear part of a cyanide group. The intrinsic frequency of a CCN bending vibration is expected to be near 370 cm^{-1}, because the degenerate CCN bending vibration of CH_3CN occurs at 370 cm^{-1}. The CCC deformation vibration and the parallel component of the CCN bending vibration have strong mutual interaction because of the closeness of their unperturbed frequencies, and separate into 544 cm^{-1} and 226 cm^{-1}, leaving the unperturbed perpendicular component of the CCN bending vibration at 378 cm^{-1}. We designate these three vibrations occurring at 544, 226, and 378 cm^{-1} as A, C, and B type vibrations of a cyanide group,

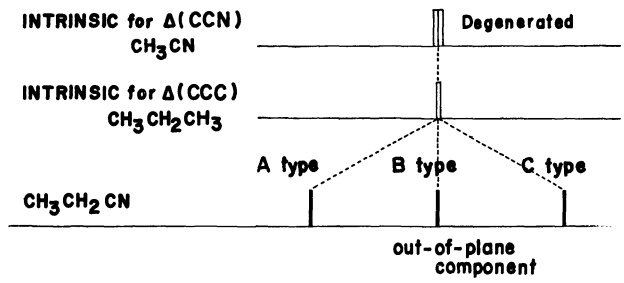

Fig. 2. Frequency diagram for CH_3CH_2CN.

respectively. Figure 2 shows the frequency diagram for CH_3CH_2CN. It seems better to classify CH_3CN into a CH_3CH_2X group rather than CH_3CH_2CN as far as skeletal deformation vibrations are concerned. Then the intrinsic frequency for a cyanide group may be chosen near 370 cm^{-1} referring to the spectra of CH_3CN. However, much clearer pictures would be obtained if one chooses the frequencies of CH_3CH_2CN as the intrinsic frequencies of cyanide compounds. The choice of an intrinsic frequency may be changed inaccordance with the characteristics of a given molecule so as to make the results of spectral analysis clearer and simpler.

Coupling between Intrinsic Frequencies. As intrinsic frequencies can be obtained from the observed frequencies of CH_3CH_2X type molecules, the next step is to estimate the feature and the degree of interaction between them.

$CH_3CH_2CH_2X$ Type Molecules: This type of molecule is expected to have two skeletal deformation vibrations corresponding to the coordinates, $\Delta\alpha_{CCC}$ and $\Delta\alpha_{CCX}$ whose intrinsic frequencies are known from the observed frequencies for $CH_3CH_2CH_3$ and CH_3CH_2X, respectively. The $\bar{G}$ and $\bar{F}$ matrices of this type of molecules are

$$G = \begin{array}{c} \begin{matrix} \text{other} \\ \text{coordinates} \end{matrix} \quad \begin{matrix} \Delta\alpha_{CCC} & \Delta\alpha_{CCX} \end{matrix} \\ \begin{pmatrix} & \\ \hline & \begin{matrix} g_1 & c \\ c & g_2 \end{matrix} \end{pmatrix} \end{array}, \tag{3}$$

$$F = \begin{array}{c} \begin{matrix} \text{other} \\ \text{coordinates} \end{matrix} \quad \begin{matrix} \Delta\alpha_{CCC} & \Delta\alpha_{CCX} \end{matrix} \\ \begin{pmatrix} & \\ \hline & \begin{matrix} f_1 & \\ & f_2 \end{matrix} \end{pmatrix} \end{array}, \tag{4}$$

where the matrix elements g_1 and f_1 are associated with the coordinate $\Delta\alpha_{CCC}$, g_2 and f_2 are associated with the coordinate $\Delta\alpha_{CCX}$, and c is the cross term of the coordinates $\Delta\alpha_{CCC}$ and $\Delta\alpha_{CCX}$. Of these five elements, only c depends on the angle θ through the relation:

$$c = \text{Constant} \times \cos\theta, \tag{5}$$

where θ is the azimuthal angle of the skeleton C–C–X.

Consider, to a first approximation, the two dimensional parts of the matrices $\bar{G}$ and $\bar{F}$, which are indicated in Eqs. (3) and (4). The frequencies of the two deformation vibrations are then expressed as

$$\nu_{\pm} = [(g_1f_1+g_2f_2) \pm \sqrt{(g_1f_1-g_2f_2)^2+4c^2f_1f_2}]/2. \tag{6}$$

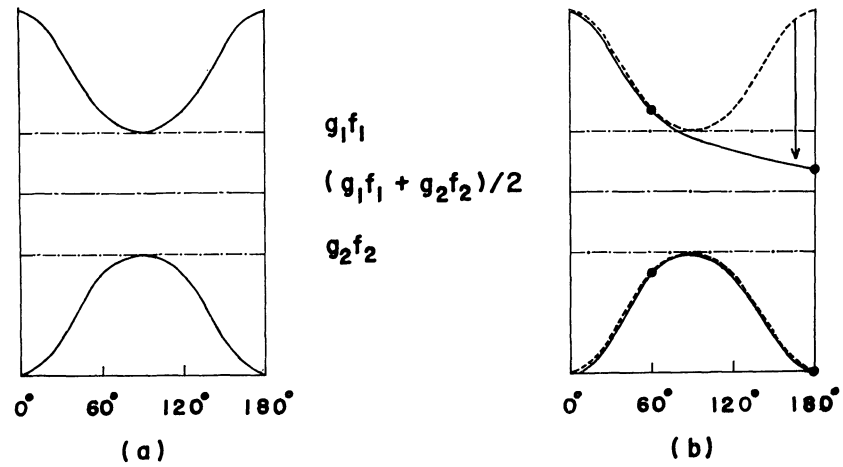

Fig. 3. θ-dependency of skeletal deformation vibration.
(a) Effect of deformation-deformation interaction.
(b) Effect of stretching-deformation interaction.

Equation (5) shows that the element c is zero when θ is 90° and has the largest value when θ is 0° or 180°. Thus, we can understand from Eq. (6) that frequency separation of these two vibrations, $\nu_+ - \nu_-$, is the largest for $\theta=0°$ or for $\theta=180°$ and the smallest for $\theta=90°$. Figure 3(a) shows the θ-dependency for the skeletal deformation frequencies. If c is zero, ν is either g_1f_1 of g_2f_2, which is the intrincis frequency associated, respectively, with $\Delta\alpha_{CCC}$ or $\Delta\alpha_{CCX}$.

The effects of the other vibrations such as a stretching vibration of C-X bond are considerable in this case. In addition to deformation-deformation interaction, we have to consider the effect of stretching-deformation interaction. It is known that the effect of the latter interaction if remarkable when azimuthal angle θ takes a value larger than 90°.[5] Usually the frequency of C–X stretching vibration is higher than those of deformation vibrations. Therefore the effect is remarkable only for ν^+ of Eq. (6). Thus, the θ-dependency of the skeletal deformation frequencies of $CH_3CH_2CH_2X$ type molecules leads to that shown in Fig. 3 (b).

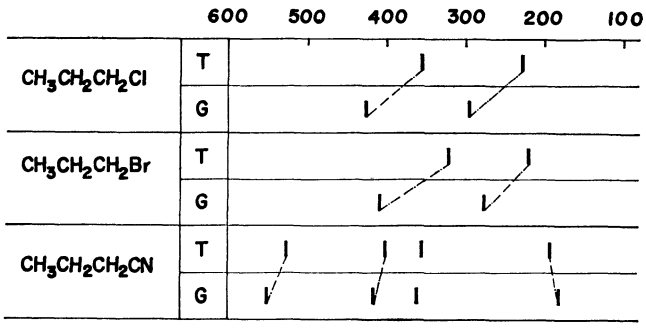

Fig. 4. Observed frequencies for $CH_3CH_2CH_2X$ type molecules.

The observed skeletal deformation frequencies of the $CH_3CH_2CH_2X$ type molecules are summarized in Fig.4. Recall that *trans* (hereafter T) and *gauche* (hereafter G) forms of these molecules correspond to the values of azimuthal angles of 180° and 60°, respectively. Then the correspondence of Fig. 3(b) and Fig. 4 is most striking.

For $CH_3CH_2CH_2CN$, it is convenient to consider the coupling between the intrinsic frequencies taken from CH_3CH_2CN and the additional intrinsic frequency taken from $CH_3CH_2CH_3$. In this case, it is sufficient to consider the interaction between the A and the C type vibrations of cyanide group and the intrinsic vibration for $\Delta\alpha_{CCC}$; the type B vibration of cyanide group is perpendicular to the plane of the skeleton. The interaction of the A and the C type vibrations with the additional $\Delta\alpha_{CCC}$ vibration is also very small, because these frequencies are well separated from each other. One remarkable change thus expected is a slight lowering of the frequency of the type A deformation for the T form due to the stretching-deformation interaction. Figure 5 shows the frequency diagram for $CH_3CH_2CH_2CN$.

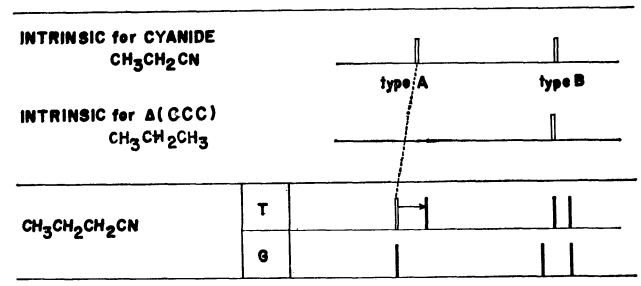

Fig. 5. Frequency diagram for $CH_3CH_2CH_2CN$.

It is interesting to note that the stretching-deformation interaction pushes the C–X stretching vibration of T form up to higher frequency side. This situation explains the well-known empirical rule which correlates molecular conformation and the C–Cl stretching frequencies.[4]

XCH_2CH_2X Type Molecules: The deformation vibrations of these molecules are analyzed satisfactorily by taking into account the two vibrations corresponding to the coordinates $\Delta\alpha_{CCX}$'s. Therefore, a similar approach used in the last section may be applied for this case. The only difference comes from the fact that the two intrinsic frequencies are identical, *i.e.*, $g_1f_1=g_2f_2$. Thus, the extent of coupling becomes most sensitive for

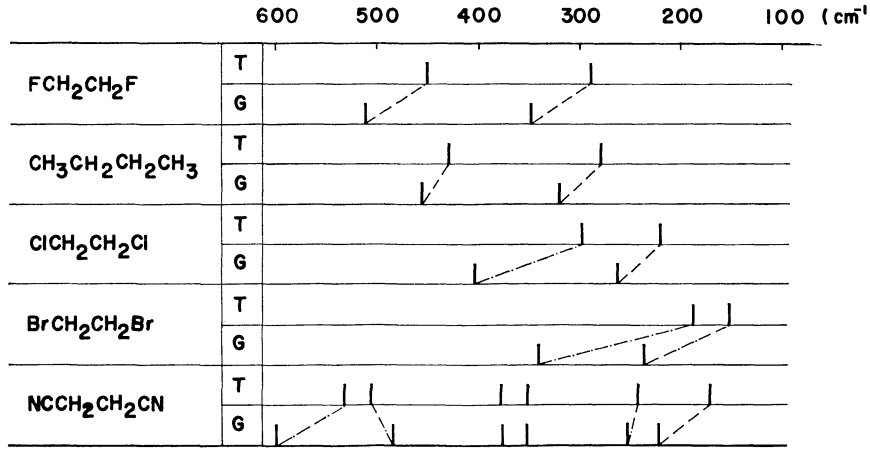

Fig. 6. Observed frequencies for XCH_2CH_2X type molecules.

4) T. Shimanouchi, S. Tsuchiya, and S. Mizushima, *J. Chem, Phys.*, **30**, 1365 (1959).

5) Here, the term stretching is used symbolically. The frequency of the stretching vibration under consideration is the lowest of all the other vibrations which interact with skeletal deformation vibrations indirectly. For a complete description of the deformation-stretching interaction, see I. Nakagawa, *Nippon Kagaku Zasshi*, **76**, 813 (1955), and the related reports cited therein.

the change of the element c of Eq. (6). Figure 6 shows the observed frequencies for XCH_2CH_2X type molecules and the close similarity of Fig. 4 and Fig. 6 is quite obvious.

For succinonitrile, the vibration frequencies of type A and type C exhibit similar patterns, respectively, in the 600—500 cm^{-1} and the 250—150 cm^{-1} regions. The B type vibrations locate in the region of 350—380 cm^{-1} and change their frequencies little for all θ.

Application to More Complicated Molecules

$XCH_2CH_2CH_2X$ Type molecules. This type of molecule has three skeletal deformation vibrations associated with the coordinates $\Delta\alpha^1_{CCX}$, $\Delta\alpha_{CCC}$, and $\Delta\alpha^2_{CCX}$. The submatrix of $\bar{G}$ corresponding to the three deformation coordinates is given as:

$$\bar{G} = \begin{array}{c} \begin{matrix} \Delta\alpha_{CCC} & \Delta\alpha^1_{CCX} & \Delta\alpha^2_{CCX} \end{matrix} \\ \begin{pmatrix} A & & \\ C_1 & B & \\ C_2 & D & B \end{pmatrix} \end{array}, \qquad (7)$$

where A and B are independent of θ, C_1, C_2, and D are related with θ by the relations:

$$C_1 = \text{Constant} \times \cos\theta_1, \qquad (8)$$

$$C_2 = \text{Constant} \times \cos\theta_2, \qquad (9)$$

and $$D = \text{Constant}\,(\sin\theta_1 \sin\theta_2 - (1/3)\cos\theta_1 \cos\theta_2). \qquad (10)$$

In these equations, θ_1 and θ_2 are two azimuthal angles made by the skeleton of $XCH_2CH_2CH_2X$ and the coefficients are calculated by assuming all the valence angles are tetrahedral. For this case we may well consider the coupling of the skeletal deformation vibrations in two steps, of which the first is the interaction between $\Delta\alpha^1_{CCX}$ and $\Delta\alpha^2_{CCX}$. The second is that between $\Delta\alpha_{CCC}$ and the two resultant vibrations from the first step. The matrix element D plays a dominant role in the first stage, while C_1 and C_2 do in the second process. If we use the matrix expression, the first process corresponds to stransforming the three deformation coordinates by an unitary matrix $\bar{U}$, where

$$\bar{U} = \begin{pmatrix} 1 & 0 & 0 \\ 0 & 1/\sqrt{2} & 1/\sqrt{2} \\ 0 & 1/\sqrt{2} & -1/\sqrt{2} \end{pmatrix} \qquad (11)$$

After the trasformation, the matrix **G** of Eq. (7) becomes

$$\bar{G}_s = \bar{U}\bar{G}\tilde{\bar{U}} = \begin{array}{c} \begin{matrix} S_1 & S_2 & S_3 \end{matrix} \\ \begin{pmatrix} A & & \\ (C_1+C_2)/\sqrt{2} & B+D & \\ (C_1-C_2)/\sqrt{2} & 2 & B-D \end{pmatrix} \end{array} \qquad (12)$$

and the relation between the two sets of coordinates is

$$\begin{pmatrix} S_1 \\ S_2 \\ S_3 \end{pmatrix} = \bar{U} \times \begin{pmatrix} \Delta\alpha_{CCC} \\ \Delta\alpha^1_{CCX} \\ \Delta\alpha^2_{CCX} \end{pmatrix} \qquad (13)$$

Consider the three rotational isomers, TT, TG, and GG of the $XCH_2CH_2CH_2X$ type molecules, then the magnitude of D is calculated for these three rotational isomers from Eq. (10) as:

$$D(\text{TT}) : D(\text{TG}) : D(\text{GG}) = 2 : 1 : 4.$$

Thus the frequency separation due to the first step coupling is expected to be that of Fig. 7.

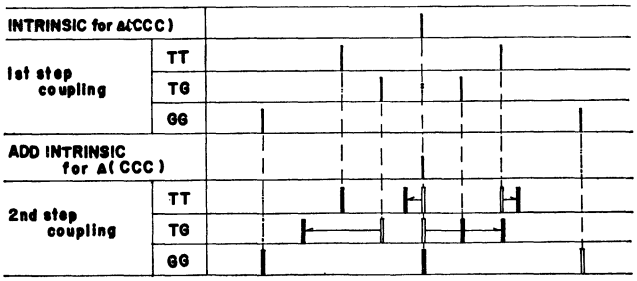

Fig. 7. Frequency diagram for $XCH_2CH_2CH_2X$ type molecules.

The second step is explained by the magnitude and the θ-dependency of C_1 or C_2. The magnitudes of (C_1+C_2) and (C_1-C_2) give the measures of coupling between S_1 and S_2, or between S_1 and S_2, respectively. Referring to the calculated C_1 and C_2 values and to the intrinsic frequency of S_1 obtained from $CH_3CH_2CH_3$, we can expect the frequencies of $CH_3CH_2CH_2CH_2CH_3$, the results of which are shown in Fig. 7. In fact, the observed frequencies given in Fig. 8 for pentane follow the expected pattern reasonably.

As for $NCCH_2CH_2CH_2CN$, the first step coupling is essential, because the intrinsic frequencies for cyanide groups are far apart from that of the intrinsic frequency for $\Delta\alpha_{CCC}$. Both the A type and the C type frequencies of cyanide groups exhibit the patterns quite close to that expected from the first step interaction. They are found, respectively, in the region of 600—400 cm^{-1} and of 200—100 cm^{-1}. The frequencies observed in the region of 400—300 cm^{-1} correspond to the $\Delta\alpha_{CCC}$ and type B vibrations of cyanide groups.

From the analogy of the cyanide compounds, it is convenient to designate the frequencies separated into the higher and the lower frequency regions by the first step coupling as A type and C type deformation vibrations, respectively, and to designate the additional

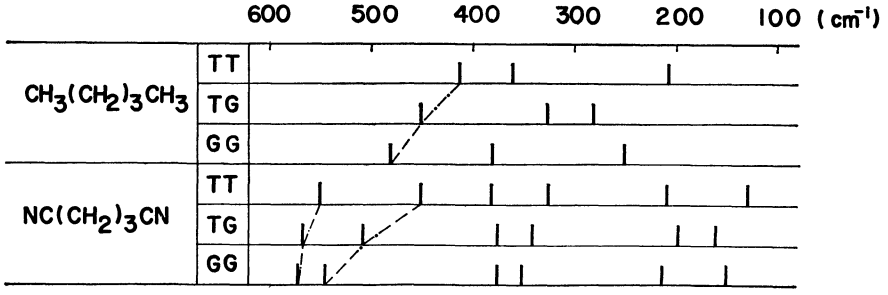

Fig. 8. Observed frequencies for $XCH_2CH_2CH_2X$ type molecules.

intrinsic frequencies for the second step coupling as B type deformation vibration. Generally, the deformation vibrations of type A occur in the region around 600—400 cm^{-1} and are appropriate vibration to study molecular conformation. The frequencies of the A type vibrations are moderately sensitive to the change of azimuthal angles and their relative locations originated from different rotational isomers are fairly analogous with different molecules. On the other hand, the B and the C type vibrations are not always useful for the purpose. Although the C type vibrations are also sensitive to the molecular geometry, the coupling effects with torsional vibrations spoil the structural specificity of the spectral pattern. The frequencies of B type vibrations are almost the same as those of intrinsic freuqencies and, therefore, insensitive to molecular structures. The spectral analysis of CH_3-$CH_2CH_2CH_2Cl$ is the most striking example demonstrating this conclusion.

$CH_3CH_2CH_2CH_2Cl$: This molecule has five possible rotational isomers, TT, GT, TG, GG, and GG'. A similar approach used in the last section is applicable to this case.

The matrix element D of Eq. (7) changes its magnitude in accordance with the conformation of the molecule. The magnitude of D is calculated for the five possible rotational isomers from Eq. (10) as:

$$D(\mathrm{TT}):D(\mathrm{GT}):D(\mathrm{TG}):D(\mathrm{GG}):D(\mathrm{GG}') = 2:1:1:4:5$$

Thus, the general pattern of the frequency separations due to the first step coupling is expected to be that of

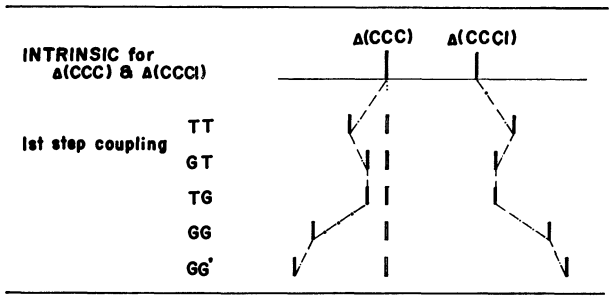

Fig. 9. Frequency diagram for $CH_3CH_2CH_2CH_2Cl$.

Fig. 9. If we neglect the second step interaction, it is clear that the A type vibrations occur in the region around 500—400 cm^{-1}. With reference to the A type vibrations of $CH_3CH_2CH_2CH_2CH_3$ of Fig. 8, the highest and the lowest frequencies of the A type vibrations of $CH_3CH_2CH_2Cl$ are expected, respectively, to be 500 cm^{-1} and 370 cm^{-1}, since the intrisic frequency for $\Delta\alpha_{CCCl}$ is lower than that of $\Delta\alpha_{CCC}$. The frequency diagram of Fig. 7 indicates that the A type vibrations of GT and TG forms are shifted to the higher frequency side by the second step coupling effect. Thus, the A type vibrations of this molecule are expected to occur in the frequency order:

$$\nu(\mathrm{GG}') > \nu(\mathrm{GG}) > \nu(\mathrm{TG}) \gtrsim \nu(\mathrm{GT}) > \nu(\mathrm{TT}).$$

Figure 10 shows the observed infrared spectra of liquid $CH_3CH_2CH_2CH_2Cl$ in the region of 700—200 cm^{-1}. Actually, four bands are seen in the A region of the spectra, namely 472, 456, 435, and 380 cm^{-1}. This

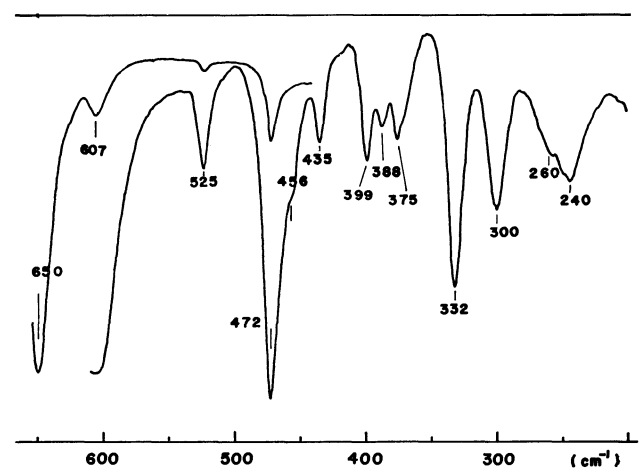

Fig. 10. Infrared spectra of liquid $CH_3CH_2CH_2CH_2Cl$ in the region of 700—200 cm^{-1}.

indicates the existence of at least four rotational isomers in liquid $CH_3CH_2CH_2CH_2Cl$. A more detailed analysis of the spectra including the B and the C type vibrations will be reported elsewhere.

Molecules Having Side Chains. We have discussed so far the normal chain molecules. The skeletal deformation vibrations of molecules having side chains are also interesting. The intrinsic frequencies of these molecules are reasonably obtained from the vibration spectra of $(CH_3)_2CHX$ type molecules.

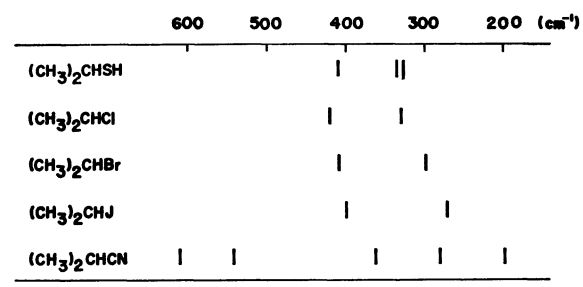

Fig. 11. Observed frequencies for $(CH_3)_2CHX$ type molecules.

$(CH_3)_2$ CHX type molecules: The observed frequencies for the molecules of this type are summarized in Fig. 11. These molecules have three skeletal deformation vibrations, of which two are of the species A' and the other is of the species A''. The A'' vibration which is called an out-of-plane bending vibration is expected to show strong frequency dependency on the mass of X atom. The A' vibrations are assigned either to CH_3–C–CH_3 bending or to inplane C–X bending vibration. It is seen from Fig. 11 that the former exhibit almost the same frequency regardless of the X atom. The slight difference in frequency may be attributed to the effect of the intraction with the C–X stretching vibration.

For $(CH_3)_2CHCN$ also, the intrinsic frequencies can be found as is the case for CH_3CH_2CN. Define the internal coordinates, $\Delta\alpha_1$, $\Delta\alpha_2$, $\Delta\alpha_3$, $\Delta\beta_s$, and $\Delta\beta_p$, which are associated with the skeletal displacements of $(CH_3)_2CHCN$ molecule, then the symmetry coordinates which define the approximate vibrational modes of the molecule are:

$$S_1 = (2\Delta\alpha_1 - \Delta\alpha_2 - \Delta\alpha_3)/\sqrt{6}$$
$$\sqrt{2}S_2 = (\Delta\alpha_1 + \Delta\alpha_2 + \Delta\alpha_3)/\sqrt{3} - \Delta\beta_p,$$
$$\sqrt{2}S_3 = (\Delta\alpha_1 + \Delta\alpha_2 + \Delta\alpha_3)/\sqrt{3} + \Delta\beta_p, \quad (14)$$
$$\sqrt{2}S_4 = (\Delta\alpha_2 - \Delta\alpha_3)/\sqrt{2} - \Delta\beta_s,$$
and $$\sqrt{2}S_5 = (\Delta\alpha_2 - \Delta\alpha_3)/\sqrt{2} + \Delta\beta_s,$$

where $\Delta\alpha_1$ corresponds to the change of an angle CH_3–C–CH_3, $\Delta\alpha_2$ and $\Delta\alpha_3$ to those of CH_3–C–CN, and $\Delta\beta_s$ and $\Delta\beta_p$ to the parallel and the perpendicular bending of C–C≡N part, respectively. The coordinates, S_1, S_2, and S_3, belong to A' species, while S_4 and S_5 to A'' species. The S_2 and the S_4 vibrations are called A type intrinsic vibrations of a cyanide group and occur in the region of 600—550 cm^{-1}. The S_3 and the S_5 vibrations are called C type vibrations of a cyanide group and occur in the region of 300—100 cm^{-1}. The CH_3–C–CH_3 deformation vibration occurring at 360 cm^{-1} corresponds to the coordinate S_1 and is called B type vibration. The frequency of the B type vibration is close to the intrinsic frequency of $\Delta\alpha_{CCC}$ for normal chain molecules. These five frequencies of $(CH_3)_2$-CHCN molecule can be chosen as the intrinsic frequencies of the cyanide group attached to a secondary carbon atom, the details of which are seen in the lower part of Fig. 13.

$CH_3CH(CN)CH_2CH_3$: 2-cyanobutane is chosen as an appropriate example of application to secondary substituted molecules with an internal rotation axis. In addition to the five intrinsic frequencies obtained from $(CH_3)_2CHCN$, it is enough to consider one skeletal deformation vibration corresponding to the coordinate $\Delta\alpha_{CCC}$, whose intrinsic frequency is supposed to be near 370 cm^{-1}. The first step coupling takes place between the two vibrations, $\Delta\alpha_{CCC}$ at 370 cm^{-1} and the B type vibration of $(CH_3)_2CHCN$ at 360 cm^{-1}. As already discussed, this type of coupling has the most serious effect on frequencies when the molecule takes T form. The second step coupling corresponds to the interaction of the A type vibrations of cyanide part with the resultant vibrations from the first step interaction. The effect of the interaction is strong when the molecule takes G form both for the out-of-plane and the in-plane vibrations of the type A. When the molecule takes T conformation, the frequency shift due to the coupling is expected to be very small, so that the vibration of the A type would not be affected much. Thus, we can expect the frequency diagram of this molecule as shown in Fig. 12.

Figure 13 shows the observed inrfared spectra of liquid 2-cyanobutane in the region of 700—100 cm^{-1} together with the skeletal deformation frequencies of $(CH_3)_2CHCN$ at the bottom. From the spectra the existence of at least two rotational isomers is concluded because there appear thirteen bands in the region of 600—100 cm^{-1} when only six skeletal deformation vibrations are expected for each rotational isomer. It is seen in the figure that there exist four bands with strong intensities in the 600—500 cm^{-1} region where the A type vibrations of cyanide group are expected to occur. The bands at 577 cm^{-1} and 528 cm^{-1} increase their relative intensities in the low temperature spectra, while those at 602 cm^{-1} and at 555 cm^{-1} follow the reverse tendency. This implies that those frequencies correspond, in pairs, to the stable rotational isomers T and G. From the frequency diagram of Fig. 12, we may conclude that the pair at 577 and 528 cm^{-1} is assigned to that of T form, while the pair at 602 and 555 cm^{-1} is assigned to that of G form. It is also understood that the T form is a more stable rotational isomer. It should be noticed that two bands are found at 666 and 492 cm^{-1} in the spectra of Fig. 13. These may also be of the A type and may be assigned to the rotational isomer G which is assumed to be most unstable form. In fact, the bands disappear in the low temperature spectra.

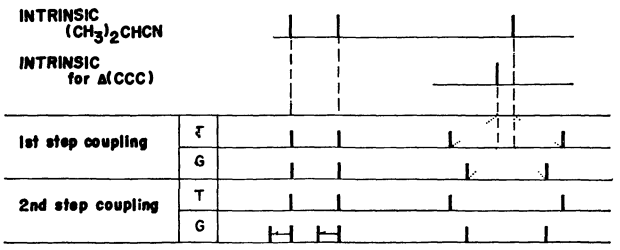

Fig. 12. Frequency diagram for $CH_3CH(CN)CH_3CH_2$.

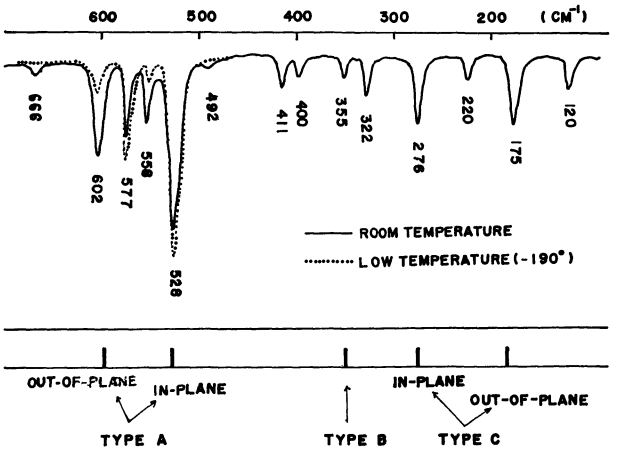

Fig. 13. Infrared spectra of liquid $CH_3CH(CN)CH_2CH_3$. Solid line: room temperature, Dotted line: low temperature (−190°C, glass) Bottom: observed frequencies for $(CH_3)_2$-CHCN.

Discussion

It was shown in the former sections that the molecular conformations of same complicated molecules could be determined by the analyses of skeletal deformation vibrations. The process of the analysis may be summarized as follows.

(a) Find the intrinsic frequencies from the simpler molecules which have the similar chemical structures or substituents as those of molecules in question. The molecules suitable for this purpose are of the type CH_3CH_2X, $(CH_3)_2CHX$, and $(CH_3)_3CX$. The choice of the intrinsic frequencies should be made so as to make the analyses simpler.

(b) Consider the coupling between the intrinsic frequencies. The frequency shift due to the coupling can be estimated from the off-diagonal elements of

$\bar{G}$ matrix associated with the two coordinates of the intrinsic frequencies in question.

(c) We may consider the couplings in several steps. The resultant frequencies from one interaction step will play a role as the intrinsic frequencies in the next process.

(d) When the matrix elements of $\bar{G}$ depend on the azimuthal angle θ, the frequencies involved are naturally θ-dependent. When the diagonal elements of the deformation coordinates involved have θ-dependency, it is not very hard to determine the structure of the molecule by comparing the observed frequencies with the expected values for skeletal deformation frequencies. Therefore, when off-diagonal elements of $\bar{G}$ matrix are θ-dependent, it is desirable to make transformation which brings the θ-dependency into the diagonal parts.

(e) Sometimes it is necessary to take into account the effect of the stretching vibrations, the frequencies of which are located close to those of the skeletal deformation vibrations. The effect is important when the substituents X are composed heavy atoms, because the stretching vibration frequencies come close to those of the skeletal deformations. The effects are often θ-dependent.

(f) Throughout the analyses, a $\bar{F}$ matrix is tacitly assumed to be diagonal. The validity of the assumption can hardly be guaranteed theoretically, but the good correspondence between the expected and the observed spectral patterns indicates the practical usefulness of the method.

The above discussions lead to the very important conclusion about the normal coordinate treatment of complicated molecules. It is good enough to take into account the skeleton of a given molecule in the calculation, if the determination of the molecular structures of rotational isomers is the main object of the calculation. In that case the force constants used for the calculations are purely empirical parameters appropriate to explain the vibration frequencies produced by the displacements of heavy atoms. Mostly it is possible to choose the suitable set of force constants to explain spectra of skeletal deformation region. The simplicity and usefulness of such treatment may easily be understood by considering the size of the secular determinant to be solved. In the case of *n*-butylchloride, for example, the determinant is 36 in its order if all the atoms were considered, while mine order matrix is necessary if we neglect the light atoms.

It must be emphasized here, however, that the estimated frequencies from the above processes are of course not exact. It is always necessary to compare the expected frequencies with the observed as a group or as a pattern. Vital to this type of work is the isolation of the bands originating from one rotational isomer from those of the others. This can be done by examining the effects of temperature and of solvents on the spectra as well as by observing the spectra in various phases.

This work was performed under the guidance of Professor Takehiko Shimanouchi in the University of Tokyo. The author is grateful to Professor T. Shimanouchi for helpful discussion. He also wishes to acknowledge helpful correspondence with Professor Ichiro Nakagawa and Dr. Isao Suzuki of the University.

Electronic Structures of the Oxocarbon Anions. III. Application of the Extended Hückel and Variable Electronegativity Extended Hückel Methods[1]

Kazuyoshi SAKAMOTO[2] and Yasumasa J. I'HAYA

Department of Materials Science, The University of Electro-Communications, Chofu-shi, Tokyo

(Received August 20, 1970)

The extended Hückel (EH) method with different basis functions and the variable electronegativity extended Hückel (VEEH) method are applied first to the calculation of the electronic structure of CO and then to that of three oxocarbon anions, $(C_4O_4)^{2-}$, $(C_5O_5)^{2-}$, and $(C_6O_6)^{2-}$. MO energies of CO calculated by both methods are closer to those computed by a non-empirical SCF method and also to observed values, compared with those obtained by the CNDO/1 method. It is also found for CO and the three anions that in the EH method the charge distributions are not dependent on the basis functions chosen and are much more localized on the oxygen atoms than in the VEEH method. The latter method yields a π-electron distribution which is close to that predicted by the variable electronegativity π-electron SCF method. The EH and VEEH methods predict reasonable values for the lower excitation energies of these oxocarbon anions; specifically the calculated $\sigma \rightarrow \pi^*$ excitation energy of $(C_4O_4)^{2-}$ agrees well with an observed value.

In previous papers,[3,4] the lower π-electronic states of three oxocarbon anions, $(C_4O_4)^{2-}$, $(C_5O_5)^{2-}$, and $(C_6O_6)^{2-}$, have been investigated by a Pariser-Parr-Pople type self-consistent field (PPP-SCF) method with configuration interaction including up to doubly excited configurations. The calculated lowest $\pi \rightarrow \pi^*$ transition energies for these anions were shown to be in good agreement with observed values. However, we have so far not referred to their σ-electronic structures, in other words we have assumed the sp^2 hybridized σ-skeletons for all anions. Recently, we observed a new absorption band of $(C_4O_4)^{2-}$ at 325 mμ with $\varepsilon =$ 174[5] and confirmed that this band is most probably due to an $n \rightarrow \pi^*$ transition.[6] Partly for explaining this theoretically and partly for elucidating the σ-structures of the anions, we feel the need of an all valence electron treatment not only for $(C_4O_4)^{2-}$ but for the series of oxocarbon anions.

For this purpose, we first take up the extended Hückel (EH) method.[7,8] As is well known, the method has many advantages but has some drawbacks also. Some disadvantages are: (1) in heteroatom-containing molecules, the resultant charge distribution becomes unrealistic, *i.e.* excess amounts of charge tend to concentrate on more electronegative centers; (2) the results for molecule ions are not good. To improve this, we first try to choose an appropriate basis set which is different from Slater orbitals ordinarily used. In so far as we know, such sort of attempts has not been made elsewhere.

Alternatively, several authors[9-12] have tried iterative methods in which matrix elements H_{pp} are assumed to be linear functions of a net atomic charge q_N or of both q_N and a total gross population in each AO (AO population).

Such iterative methods, however, do not always lead to satisfactory conclusions. For example, Carroll *et al.*[10] compared the usual EH calculation with the iterative one for small inorganic molecules and gave no definite answer to a question of which procedure was preferred. Duke[12] indicated, in the calculation of relatively small molecules, that a similar iterative method does not always lead to improvements in the wave functions but some better tendency is found for molecule ions.

In this paper, a somewhat different procedure is proposed for solving an iterative EH equation with the intention of improving the above-mentioned weak points of the usual EH treatment. In the method, tentatively called a variable electronegativity extended Hückel (VEEH) method, the valence state ionization potentials (VSIP) are taken to be quadratic functions of the effective nuclear charge Z_p, just like the case of the π-electron SCF treatment (VESCF for example). We first apply the method to a pilot molecule, CO, in order to see whether the calculated charge distribution is reasonable, then to the series of oxocarbon anions. Overall comparison of the EH method with different basis sets and the VEEH method will be made in regard to the electronic structures of the oxocarbon anion series together with that of carbon monoxide.

1) Part of this paper was read before the 23rd Annual Meeting of the Chemical Society of Japan, Tokyo, April, 1970.

2) Japan Society for the Promotion of Science Postdoctral Fellow.

3) K. Sakamoto and Y. J. I'Haya, *Theor. Chim. Acta*, **13**, 220 (1969), called Part I of this series.

4) K. Sakamoto and Y. J. I'Haya, *J. Amer. Chem. Soc.*, **92**, 2636 (1970), called Part II of this series.

5) K. Sakamoto, K. Ikegami, and Y. J. I'Haya, *Reports of the University of Electro-Communications*, **28**, 95 (1970).

6) Although Skujins and Webb observed a new absorption band at 3.99 eV with $\varepsilon = 87$, they did not refer to its assignment; S. Skujins and G. A. Webb, *Spectrochim. Acta*, **25A**, 917 (1969).

7) M. Wolfsberg and L. Helmholtz, *J. Chem. Phys.*, **20**, 837 (1952).

8) R. Hoffmann, *ibid.*, **39**, 1397 (1963); **40**, 2047, 2474, 2480, 2745 (1964).

9) L. C. Cusachs, *ibid.*, **43**, S157 (1965); L. C. Cusachs and J. W. Reynolds, *ibid.*, **43**, S160 (1965).

10) D. G. Carroll, A. T. Armstrong, and S. P. McGlynn, *ibid.*, **44**, 1865 (1966); D. G. Carroll and S. P. McGlynn, *ibid.*, **45**, 3827 (1966).

11) J. E. Baldwin and W. D. Foglesong, *J. Amer. Chem. Soc.*, **90**, 4311 (1968).

12) B. J. Duke, *Theor. Chim. Acta*, **9**, 260 (1968).

Method of Calculation

In the EH calculations, the following three basis sets are used for the sake of comparison: (a) Slater-type orbitals (STO) in which the orbital exponent ζ is determined by Slater's rule, (b) the free-atom-ζ single-ζ STO's,[13,14] (c) the free-atom-ζ double-ζ STO's.[13,15] Within the framework of the EH method, the diagonal matrix elements H_{pp} are chosen to be the negative of the VSIP, *i.e.* $H_{pp}=-I_p$. The values of I_p's are taken from Pritchard's paper[16] and are assumed to be constant throughout the whole calculation. The off diagonal matrix elements H_{pq} are assumed to take the form

$$H_{pq} = (K/2)(H_{pp}+H_{qq})S_{pq}, \quad K = 1.75 \qquad (1)$$

The reason for this is as follows. The alternative formula assumes $K=2-|S_{pq}|$, *i.e.*

$$H_{pq} = [(2-|S_{pq}|)/2](H_{pp}+H_{qq})S_{pq} \qquad (2)$$

and both Eqs. (1) and (2) have been used successfully.[8,9] To check which formula is more favorable, both equations are applied to preliminary calculations of the oxocarbon anions. In Tables 1 and 2 are illustrated the results for $(C_4O_4)^{2-}$ obtained when the free-atom-ζ single-ζ basis set is used. As these tables show, the electronic distributions and excitation energies are not very much dependent on the assumption of which formula is used. Similar results are obtained for other oxocarbon anions. Therefore, Eq. (1) is chosen hereafter in this paper only for its simpler form.

In the VEEH method, the values of the matrix elements are modified by new Z_p's at each stage of the iteration process. The values of Z_p for $2s$ and $2p$ valence orbitals of carbon and oxygen are determined by

$$Z_p = N_x - 1.35 - 0.35M_x \qquad (3)$$

where N_x stands for the atomic number of atom x contributing pth orbital, and M_x is the atomic population of atom x determined by Mulliken's population analysis.[17] A new M_x is estimated from the previous one, M_x*, by the following equation[18]

$$M_{x\,\text{input}} = M^*_{x\,\text{input}} - \lambda(M^*_{x\,\text{input}} - M^*_{x\,\text{output}}) \qquad (4)$$

with a constant λ, the steepest decent parameter, which value is taken to be 0.1 in this paper. Being assumed the quadratic dependence on Z_p, the VSIP's for $2s$ and $2p$ orbitals of carbon and oxygen are obtained as shown in Table 3. These quadratic formulae are determined from atomic spectroscopic data[16,19-23] for the corresponding iso-electronic series by least squares method, as usual. The whole iteration process is continued until the total gross atomic population (atomic population) remains constant within the limits of 0.01. Such convergence was obtained by fifteen iterations, on the average. The computations used a double precision (18 places) routine.[24]

TABLE 1. AO POPULATION OF $(C_4O_4)^{2-}$ BY DIFFERENT PARAMETER K IN EH METHOD WITH BASIS SET (b)[a]

Atom	AO	$K=1.75$	$K=2-\|S_{pq}\|$
C	$2s$	1.01	0.99
	$2p_x$	0.74	0.75
	$2p_y$	0.74	0.75
	$2p_z$	0.61	0.62
O	$2s$	1.78	1.83
	$2p_x$	1.87	1.84
	$2p_y$	1.87	1.84
	$2p_z$	1.89	1.88

a) See the text.

TABLE 2. LOWEST EXCITATION ENERGIES OF $(C_4O_4)^{2-}$ BY DIFFERENT PARAMETER K IN EH METHOD CALCULATED WITH BASIS SET (b)[a]

Transition	$K=1.75$	$K=2-\|S_{pq}\|$
$\pi\rightarrow\pi^*$	4.16	4.38
$\sigma\rightarrow\pi^*$	3.53	3.63
$\sigma\rightarrow\sigma^*$	20.52	19.08

a) See the text.

TABLE 3. Z_p DEPENDENCE OF IONIZATION POTENTIAL I_p[a]

Iso-electronic Series and Atomic Valence State	AO	a_0	a_1	a_2
C: $(B^-,C,N^+,O^{+2},F^{+3})$	$2s$	3.5563	−5.8864	2.6669
$(2s)$ $(2p)$ $(2p)$ $(2p)$	$2p$	3.3668	−7.6466	0.5758
O: $(N^-,O,F^+,Ne^{+2},Na^{+3})$[b]	$2s$	3.4060	−6.9846	−4.2390
$(2s)$ $(2p)^2$ $(2p)^2$ $\underline{(2p)}$	$2p$	0.1055	15.2424	−53.8253

a) $I_p=a_0Z_p^2+a_1Z_p+a_2$.
b) I_p of the underlined $2p$ orbital.

Both EH and VEEH methods are first applied to a pilot molecule, CO, to examine which procedure is more preferable in regard to the prediction of the electronic states of heteroconjugated molecules. Afterwards we apply the methods to the three oxocarbon anions whose bond lengths are given in the previous paper.[4]

Results and Discussion

The calculated MO energies of CO are listed in Table 4. For comparison, the results obtained by the

13) The terminology is shown in Mulliken's paper; *Rev. Mod. Phys.*, **32**, 232 (1960).
14) E. Clementi and D. L. Raimondi, *J. Chem. Phys.*, **38**, 2686 (1963).
15) E. Clementi, *ibid.*, **40**, 1944 (1964).
16) H. O. Pritchard and H. A. Skinner, *Chem. Rev.*, **55**, 745 (1955).
17) R. S. Mulliken, *J. Chem. Phys.*, **23**, 1833, 1841 (1955).
18) D. R. Hartree, "The Calculation of Atomic Structure," Wiley, New York (1957), p. 88.
19) C. E. Moore, "Atomic Energy Levels" (National Bureau of Standards), Circular No. 467 (1949).
20) H. A. Skinner and H. O. Pritchard, *Trans. Faraday Soc.*, **49**, 1254 (1953).
21) J. M. Parks and R. G. Parr, *J. Chem. Phys.*, **32**, 1657 (1960).
22) G. Pilcher and H. A. Skinner, *J. Inorg. Nucl. Chem.*, **24**, 937 (1962).
23) J. Hinze and H. H. Jaffé, *J. Amer. Chem. Soc.*, **84**, 540 (1962); *J. Phys. Chem.*, **67**, 1501 (1963).
24) The calculations were carried out using a HITAC 5020E computer at the computer center of the University of Tokyo.

Table 4. Orbital energies of CO calculated by various methods (eV)[a]

MO's and their symmetry	EH basis (a)	EH basis (b)	EH basis (c)[b]	VEEH	Non-empirical[c]	CNDO/1[d]	observed[e]
6σ (a_1)	44.11	49.64	46.21	43.83	23.47	13.64	
2π (e_1)	−9.37	−9.13	−7.94	−10.27	6.12	5.38	
5σ (a_1)[f]	−14.68	−14.52	−13.19	−14.82	−13.74	−17.35	−14.01
1π (e_1)	−18.27	−18.32	−18.52	−17.10	−16.61	−20.87	−16.51
4σ (a_1)	−20.66	−20.72	−21.23	−20.44	−20.66	−24.67	−19.72
3σ (a_1)	−37.21	−37.26	−37.29	−34.93	−41.76	−45.44	

a) The observed bond length (1.128 Å) is used (D. B .Neumann and J. W. Moskowitz, *J. Chem. Phys.*, **50**, 2216 (1969)).
b) See the text.
c) Ref. 26.
d) Ref. 25.
e) Ref. 27.
f) The highest occupied MO.

Table 5. AO and atomic populations of CO calculated by various methods

			EH basis (a)	EH basis (b)	EH basis (c)[a]	VEEH	Non-empirical[b]	CNDO/1[c]
AO-population	C	$2s$	1.44	1.43	1.37	1.47	1.66	1.70
		$2p_\sigma$	1.09	1.10	1.17	1.20	0.93	1.09
		$2p_\pi$	0.24	0.26	0.33	0.51	0.62	0.62
	O	$2s$	1.71	1.70	1.69	1.63	1.86	1.70
		$2p_\sigma$	1.77	1.77	1.77	1.69	1.54	1.51
		$2p_\pi$	1.76	1.74	1.67	1.49	1.38	1.38
Atomic population	C		3.00	3.04	3.19	3.69	3.83	4.03
	O		7.00	6.96	6.81	6.31	6.17	5.97

a) See the text.
b), c) See footnotes c and d of Table 4.

CNDO/1[25] and a non-empirical LCAO-SCF[26] are included. The occupied MO energies calculated by the EH and the VEEH methods are rather close to those computed by the non-empirical SCF method, and also to observed values,[27] compared with those of the CNDO/1 calculation.

The AO population and the atomic population of CO calculated by various methods are compared in Table 5. The charge tends to delocalize in going from basis (a) to basis (c) in the EH method. When the VEEH approximation is applied the charge distribution gets closer to that calculated by the non-empirical SCF method. The dipole moments of CO, including the atomic polarization term,[25] are calculated to be 2.86, 2.58, and 1.59 Debyes, respectively, for three basis sets (a), (b), and (c) in the EH method, all in the sense of C^+O^- polarity. On the other hand, the VEEH method yields a dipole moment 0.22 Debye, the polarity being C^-O^+. This explains well the observed sign and magnitude of the dipole moment of CO.[28] From the above, the following points are noteworthy. (1) The MO energies and charge distributions produced by the VEEH approach are pretty close to those obtained by a non-empirical SCF calculation, and the calculated dipole moment is in accord with the observed value. (2) In the EH method, the charge distributions and orbital energies are hardly influenced by suitable choices of basis functions.

In Table 6 are shown the calculated orbital energies and their symmetries of three oxocarbon anions, $(C_4O_4)^{2-}$, $(C_5O_5)^{2-}$, and $(C_6O_6)^{2-}$. Only the results obtained by the EH method with basis (a) are listed, since the data for those calculated with bases (b) and (c) and also by the VEEH method are not very much different from the entries in Table 6. In particular, in the EH calculation the energies of the occupied MO's

Table 6. Orbital energies calculated from EH method with STO basis set (eV)[a]

$(C_4O_4)^{2-}$ Energy	Symmetry	$(C_5O_5)^{2-}$ Energy	Symmetry	$(C_6O_6)^{2-}$ Energy	Symmetry
15.04	e_u	9.74	a_2'	7.80	e_{1u}
5.30	a_{2g}	9.08	e_1'	−4.14*	b_{2g}
−4.67*	b_{1u}	−5.60*	e_2''	−7.38*	e_{2u}
−9.45*	e_g	−10.79*	e_1''	−11.55*	e_{1g}
−12.86†	b_{1g}	−13.15†	e_2'	−12.78†	a_{2g}
−13.26*	a_{2u}	−13.23*	a_2''	−13.17*	a_{2u}
−14.94	e_u	−16.24	e_1'	−14.00	e_{2g}
−17.88	a_{1g}	−17.77	a_2'	−16.88	e_{1u}

a) Asterisk denotes π-MO's and others correspond to σ-MO's. Dagger denotes the highest occupied MO's.

25) J. A. Pople, D. P. Santry, and G. A. Segal, *J. Chem. Phys.*, **43**, S129 (1965); J. A. Pople and G. A. Segel, *ibid.*, **43**, S136 (1965).
26) H. Brion and C. Moser, *ibid.*, **32**, 1194 (1960).
27) M. I. Al-Joboury and D. W. Turner, *J. Chem. Soc.*, **1964**, 4434.
28) B. Rosenblum and A. H. Nethercot, Jr., *J. Chem. Phys.*, **27**, 828 (1957).

are not affected so much by the starting basis functions, just as in the case of CO. In both EH and VEEH calculations, it is found that each highest occupied MO of the anions is made up of a linear combination of $2p_x$ and $2p_y$ AO's centered on all the carbon and oxygen atoms and does not contain a $2s$ character.[29] Therefore these highest occupied MO's are characterized to be not a so-called lone-pair orbital but a σ-type orbital. Furthermore, it is found that the charge flows from oxygen to carbon in the EH method, while in the VEEH method the situation is reverse and the degree of delocalization increases. On the other hand, the second highest occupied and the lowest and the second lowest vacant MO's are all clearly specified to be of pure π-characters.[30]

TABLE 7. LOWER EXCITATION ENERGY FOR OXOCARBON ANIONS (eV)

Molecule	Transition	EH basis (a)	EH basis (b)	EH basis (c)[a]	VEEH	Obsd.
$(C_4O_4)^{2-}$	$\pi\rightarrow\pi^*$ E_u	3.81	4.16	5.19	2.41	4.60
	E_u	8.59	9.62	11.85	6.72	
	$\sigma\rightarrow\pi^*$ E_g	3.41	3.53	3.44	2.18	3.81[b]
	A_{1u}	8.19	8.99	10.10	6.49	
	$\sigma\rightarrow\sigma^*$ B_{2g}	18.16	20.52	21.76	16.12	
	E_u	27.90	31.60	32.05	23.80	
$(C_5O_5)^{2-}$	$\pi\rightarrow\pi^*$ E_1'	2.45	2.67	3.44	1.39	3.40
	E_2'	7.63	8.52	10.55	5.85	
	$\sigma\rightarrow\pi^*$ E_1''	2.37	2.30	1.70	1.28	
	E_1''	7.55	8.15	8.81	5.75	
	$\sigma\rightarrow\sigma^*$ E_1'	22.23	24.80	26.19	19.16	
$(C_6O_6)^{2-}$	$\pi\rightarrow\pi^*$ E_{1u}	1.62	1.76	2.35	0.82	2.56
	E_{2g}	5.79	6.40	8.02	4.11	
	$\sigma\rightarrow\pi^*$ E_{1g}	1.24	1.07	0.27	0.69	
	E_{2u}	5.40	5.71	1.53	3.97	
	$\sigma\rightarrow\sigma^*$ E_{1u}	20.58	22.85	24.53	18.35	

a) See the text.
b) Ref. 5.

The lower excitation energies for the anions, being assumed to be orbital energy differences, are given in Table 7. The $\sigma\rightarrow\pi^*$ excitation energy of $(C_4O_4)^{2-}$, 3.41 eV, which corresponds to an electron excitation from the highest occupied (σ-type) to the lowest vacant (π-type) orbital, is in good accord with our observed value, 3.81 eV.[5] The overall agreement with the experimental $\pi\rightarrow\pi^*$ excitation energies is fairly good in the EH treatment; specifically the method with the use of basis (c) is the best.

As for the VEEH treatment, the calculated $\pi\rightarrow\pi^*$ and $\sigma\rightarrow\pi^*$ excitation energies of $(C_4O_4)^{2-}$ are qualitatively consistent with the experimental conclusion that the $\pi\rightarrow\pi^*$ excitation energy is larger than the $\sigma\rightarrow\pi^*$ one. However, the $\pi\rightarrow\pi^*$ excitation energies predicted by the VEEH method for other anions are too low to be compared with the corresponding observed values. This can not be understood at present, but will be improved by the inclusion of electronic repulsion.[31]

TABLE 8. AO POPULATION FOR OXOCARBON ANIONS

Molecule	Atom	AO	EH basis (a)	EH basis (b)	EH basis (c)[a]	VEEH	PPP–VESCF[b]
$(C_4O_4)^{2-}$	C	$2s$	1.02	1.01	0.98	1.11	
		$2p_\sigma$	1.47	1.48	1.52	1.67	
		$2p_\pi$	0.62	0.61	0.65	0.92	0.94
	O	$2s$	1.79	1.78	1.77	1.67	
		$2p_\sigma$	3.72	3.73	3.73	3.54	
		$2p_\pi$	1.90	1.89	1.85	1.58	1.56
$(C_5O_5)^{2-}$	C	$2s$	1.03	1.03	0.99	1.12	
		$2p_\sigma$	1.44	1.45	1.50	1.65	
		$2p_\pi$	0.51	0.52	0.57	0.91	0.93[c]
	O	$2s$	1.79	1.78	1.77	1.67	
		$2p_\sigma$	3.73	3.74	3.74	3.56	
		$2p_\pi$	1.89	1.88	1.83	1.49	1.47[c]
$(C_6O_6)^{2-}$	C	$2s$	1.03	1.03	1.00	1.11	
		$2p_\sigma$	1.43	1.44	1.48	1.64	
		$2p_\pi$	0.46	0.47	0.51	0.91	0.92
	O	$2s$	1.79	1.78	1.77	1.68	
		$2p_\sigma$	3.74	3.75	3.75	3.57	
		$2p_\pi$	1.88	1.87	1.82	1.43	1.41

a) See the text.
b) Under the approximation of Pariser-Parr equation for two-center electronic repulsion integral and of including all the terms for resonance integral.
c) Ref. 3.

The results of the AO population analysis are given in Table 8. The overall charge distribution obtained by the EH method is not very much dependent on starting basis functions as before. Comparing the VEEH method with the EH method, the former yields more delocalized picture for electrons than the latter does. Furthermore, the former computes the π-type AO populations (indicated as $2p_\pi$ in Table 8) very close to the π-electron densities calculated by a Pariser-Parr type π-electron approximation (see the last column

TABLE 9. ATOMIC BOND POPULATION FOR OXOCARBON ANIONS AND CARBON MONOXIDE

Molecule	Bond	EH basis (a)	EH basis (b)	EH basis (c)[a]	VEEH
$(C_4O_4)^{2-}$	C–C	0.93	0.95	0.96	0.87
	C–O	0.64	0.65	0.65	0.94
$(C_5O_5)^{2-}$	C–C	0.94	0.96	0.98	0.90
	C–O	0.65	0.67	0.68	0.95
$(C_6O_6)^{2-}$	C–C	0.91	0.93	0.94	0.90
	C–O	0.66	0.68	0.70	0.96
CO	C–O	1.11	1.15	1.24	1.44

a) See the text.

29) The highest occupied MO of $(C_5O_5)^{2-}$ contains a small amount of $2s$ component.

30) That is, σ-MO's levels are embedded between π-MO's levels. Indeed, such a behavior is noted for many aromatic substances, for example benzene.[8]

31) A study on the electronic structures of the same anion series by means of a semi-empirical VESCF method including all valence electrons has just been completed and will be submitted for publication in the future.

of Table 8). The effective σ-type AO populations, that is, ratios of the $2s$ and $2p_\sigma$ AO populations, do not change from anion to anion and from method to method, and are approximately $2s^{1.0}\ 2p_\sigma^{1.5}$ for the carbon atom and $2s^{1.0}\ 2p_\sigma^{2.0}$ for the oxygen atom.

In Table 9 are presented the results of the atomic bond population analysis for the three anions and CO. It is found that the atomic bond population for CO is always larger than those for the C–O bonds of the anions, irrespective of the method of calculation. This is consistent with the observed fact that the bond length in CO (1.128 Å) is shorter than any C–O bond length in the three anions (1.259—1.262 Å).

The values of VSIP's produced at the final stage of iteration in the VEEH method are considerably different from the constant values used in the EH method. For example, with regard to the carbon atom of $(C_4O_4)^{2-}$, the quantity obtained from the VEEH method is greater than that used in the EH method, by 1.7 eV for $2s$ AO's and by 1.5 eV for $2p$ AO's. As for the oxygen atom, the former is less than the latter, the differences being 6.5 and 4.0 eV for $2s$ and $2p$ AO's, respectively. A similar conclusion is also obtained in other two anions.

BULLETIN OF THE CHEMICAL SOCIETY OF JAPAN, VOL. 44, 1205—1212(1971)

The Emission Spectra of Pyrazine and Deuterated Pyrazines in the Vapor and in Rigid Matrices at 90°K

Hajime Ishii, Motohiko Koyanagi, and Yoshiya Kanda
Department of Chemistry, Faculty of Science, Kyushu University, Fukuoka
(Received August 31, 1970)

Emission spectra of pyrazine and its deuterated derivatives have been observed in the vapor and the vibronic structure has been analyzed in detail. The vibronic structures of the phosphorescence spectra of these compounds have been explained all in terms of totally symmetrical vibrations, while the first main bands of the fluorescence spectra were anomalous as well as their progression bands in respect to the band position and intensity distribution. For comparison, the fluorescence spectra have also been studied in rigid matrices at 90°K.

The fluorescence and phosphorescence spectra of pyrazine-d_0 and -d_4 in the vapor were first observed by Logan and Ross.[1] The 0—0 bands of the phosphorescence spectra of these compounds coincided with those of the lowest T←S absorption spectra, and the shorter-wavelength region emissions were identified with the fluorescence spectra. The observation of the fluorescence spectrum of pyrazine gave a great sensation together with a similar report on 1,2- and 1,3- diazines[2] since it had been generally accepted that the fluorescence should be, if any, too weak to be observed for such a compound with a $^1(n,\pi^*)$ level as the lowest excited singlet state. The fluorescence spectrum has also been studies in rigid solution,[1] in fluid solutions,[3] and in the crystal at 77°K.[4] However, no vibrational analyses of those spectra have yet been made in detail. On the other hand, photoisomerization efficiency from pyrazine to pyrimidine has been discussed in the vapor[5] and in solutions.[6]

The fluorescence and phosphorescence spectra of pyrazine and deuterated pyrazines have been studied here in the vapor. For comparison the fluorescence spectra of pyrazines were also observed in rigid solutions at 90°K. The vibronic structures will be discussed. It is interesting that the phosphorescence spectra from photochemically produced pyrimidines have been observed when the pyrazines in solutions have been excited with the 2537 Å line of the Hg-lamp in agreement with the result by Lahmani *et al.*[6] in which the photochemical products were detected by gas chromatography.

Experimental

A quartz cell for study of emissions in the vapor is essentially the same as that reported by Base and Sponer.[7] A super high pressure Hg-lamp was used as a light source. Two filter systems were employed. One was a combination consisting of a path of 5 cm saturated *aq.* solution of $NiSO_4$ with a little amount of $CoSO_4$ added and that of 1 cm *aq.* solution of mono sodium phthalate of sufficient concentration to cut off the exciting light shorter in wavelength than 3000 Å for observation of the emissions in the vapor and the other consisted of the former of the above filter combination and a path of 1 cm D_3P[8] *aq.* solution for the emissions in solutions. The former combination is suitable for taking out mainly 3130 Å of the Hg-lamp and so is the latter for 2537 Å. The vapor pressure was estimated from the temperature near the outside of the bottom of a side tube where a sample was placed,

1) L. M. Logan and I. G. Ross, *J. Chem. Phys.*, **43**, 2903 (1965).
2) B. J. Cohen, H. Baba, and L. Goodman, *J. Chem. Phys.*, **43**, 2902 (1965).
3) H. Baba, L. Goodman, and P. C. Valenti, *J. Amer. Chem. Soc.*, **88**, 5410 (1966).
4) P. Loustauneau and G. Nouchi, *Compt. Rend.*, **261**, 4693 (1965).
5) F. Lahmani and N, Ivanoff. *Tetrahedron Lett.*, **40**, 3913 (1967).
6) F. Lahmani, N. Ivanoff, and M. Magat, *Compt. Rend.*, **263**, 1005 (1966).
7) A. M. Bass and H. Sponer, *J. Opt. Soc. Amer.*, **40**, 389 (1950).
8) L. C. Braga and M. D. Lumb, *J. Sci. Instrum.*, **43**, 341 (1966).

according to the equations cited in Ref. 1. The temperature of the sample vapor was assumed equal to the inside temperature of the main oven in which the main part of the fluorescence cell was mounted. With an increase in temperature of the vapor the phosphorescence decreased considerably in intensity while the fluorescence remained unchanged in intensity. Pyrazine obtained from Tokyo Kasei Co., Ltd. was first converted into its salt form with sulfuric acid, recrystallized from alcohol, delivered from the salt form, and sublimed several times in vacuum. Pyrazine-d_4 and -2,3-d_2 were synthesized in the same way as that previously given,[9,10] and sublimed several times in vacuum. Spectra were photographed with a Shimadzu quartz spectrograph type QM-60. Slitwidths employed were 50 μ and 100 μ for measurement of the emissions in the vapor and solutions, respectively. The spectral position was determined within an accuracy of 3 cm^{-1} for the phosphorescence in the vapor, and 5 cm^{-1} and 20 cm^{-1} for the fluorescence in the vapor and in solution, respectively.

Results and Discussion

The Phosphorescence Spectra in the Vapor State. The phosphorescence spectra of pyrazine-d_0, -2, 3-d_2 and -d_4 were observed in the vapor. The microphotometer tracings and the spectral data are given in Figs. 1—3 and Tables 1—3, respectively. As has been pointed out by Logan and Ross,[1] the origin bands of the phosphorescence spectra of pyrazine-d_0 and -d_4 coincided exactly within experimental errors with those of the previously reported T←S absorption spectra.[11] The 0—0 band of pyrazine-2,3-d_2 was located at 26895cm^{-1} and the promotion energy in substitution of an H with a D was found to be 37 cm^{-1} in the vapor, very close to a value of 35 cm^{-1} in the crystal.[9] The overall spectral pattern is rather simple in all three cases as can be seen in Figs. 1—3. Active vibrations observed in the phosphorescence

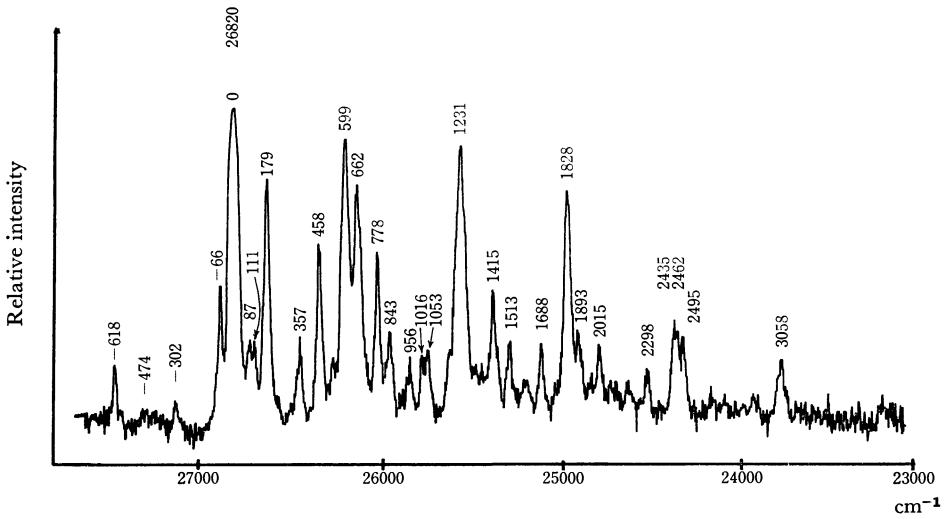

Fig. 1. Phosphorescence spectrum of pyrazine-d_0 in the vapor.

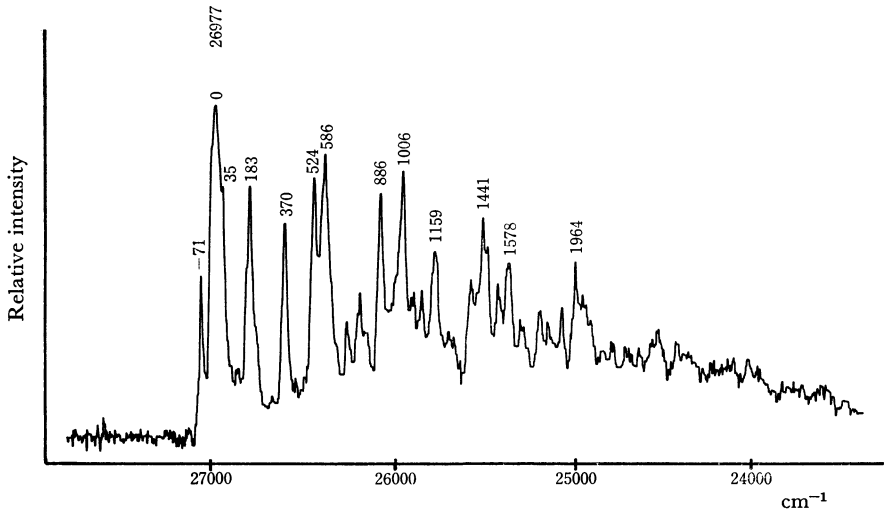

Fig. 2. Phosphorescence spectrum of pyrazine-d_4 in the vapor.

9) M. Koyanagi, T. Shigeoka, and Y. Kanda, "Molecular Luminescence," E. C. Lim, ed., Benjamin, Inc., New York, (1969), p. 765.

10) S. Califano, G. Adembri, and G. Sbrana, *J. Mol. Spectrosc.*, **20**, 385 (1964).

11) K. K. Innes, J. P. Burne, and I. G. Ross, *ibid.*, **22**, 125 (1967), (Review).

Table 1. Vibrational analysis of the phosphorescence spectrum of pyrazine-d_0 in the vapor

ν (cm^{1-})	Rel.[a] Int.	$\Delta\nu$ (cm^{-1})	Assignment[b]	ν (cm^{1-})	Rel.[a] Int.	$\Delta\nu$ (cm^{-1})	Assignment[b]
27438	m	−618	$0+\nu_{6a}'$	25307	m	1513	$0-\nu_{10a}\times 2$
27294	mw	−474	$0+\nu_{16b}'\times 2$	25228	w	1592	$25405+(\nu_{16b}'-\nu_{16b})$
27237	w	−417		25207	w	1613	$0-\nu_{6a}-\nu_1$
27122	m	−302		25132	m	1688	$(2)-\nu_{9a}$
26886	m	− 66	$=(5)$	25049	w	1771	
26841	w	− 21	$0+\nu_{6a}'-\nu_{6a}$	24992	s	1828	$0-\nu_{6a}-\nu_{9a}$
26820	ss	0	$=0$: 0—0 band	24978	w	1842	$0-\nu_5\times 2$
26733	m	87	$=(6): 0+\nu_{9a}'-\nu_{9a}$	24927	m	1893	$(3)-\nu_{9a}$
26709	m	111		25854	w	1966	
26641	s	179	$=(1): 0+\nu_{16b}'-\nu_{16b}$	24805	m	2015	$25405-\nu_{6a}$
26483	m	337	sh.	24739	w	2081	$25405-\nu_{16a}\times 2$
26463	m	357	$0+(\nu_{16b}'-\nu_{16b})\times 2$	24628	m	2192	$25405+(\nu_{16b}'-\nu_{16b})-\nu_{6a}$
26362	s	458	$=(2): \nu_5'-\nu_5$	24572	w	2248	$0-\nu_1-\nu_{9a}$
26292	w	528	$(5)-\nu_{6a}$	24522	m	2298	
26221	s	599	$0-\nu_{6a}$	24385	ms	2435	$25405-\nu_1$
26158	s	662	$=(3): 0-\nu_{16a}\times 2$	24358	ms	2462	$0-\nu_{9a}\times 2$
26135	m	685	$(6)-\nu_{6a}$	24325	ms	2495	$(3)-\nu_{6a}-\nu_{9a}$
26042	s	778	$(1)-\nu_{6a}$	24212	mw	2608	$25405+(\nu_{16b}'-\nu_{16b})-\nu_1$
25977	s	843	$(3)+(\nu_{16b}'-\nu_{16b})$	24175	mw	2645	$25405-\nu_{9a}$
25881	w	939	sh.	24145	mw	2675	$((3)+(1))-\nu_{6a}-\nu_{9a}$
25864	m	956	$0+(\nu_{16b}'-\nu_{16b})\times 2-\nu_{6a}$	24082	mw	2738	$0-\nu_{10a}\times 2-\nu_{9a}$
25804	m	1016	$0-\nu_1$	23996	w	2824	$25405+(\nu_{16b}'-\nu_{16b})-\nu_{9a}$
25767	m	1053	$(2)-\nu_{6a}$	23972	w	2848	$0-\nu_{6a}-\nu_1-\nu_{9a}$
25657	m	1163	$(5)-\nu_{9a}$	23762	ms	3058	$0-\nu_{6a}-\nu_{9a}\times 2$
25589	s	1231	$0-\nu_{9a}$	23748	w	3072	$0-\nu_5\times 2-\nu_{9a}$
25566	w	1254	$(3)-\nu_{6a}$	23622	mw	3198	
25504	w	1316	$(6)-\nu_{9a}$	23574	mw	3246	$25405-\nu_{6a}-\nu_{9a}$
25475	w	1345		23477	mw	3343	
25405	ms	1415	$(1)-\nu_{9a}$ or $0-\nu_4\times 2$	23294	mw	3526	

a) Estimated intensity: ss> s > ms > m > mw > w. b) Bands (1)···(6), see also Fig. 4.

Table 2. Vibrational analysis of the phosphorescence spectrum of pyrazine-d_4 in the vapor

ν (cm^{-1})	Rel. Int.	$\Delta\nu$ (cm^{-1})	Assignment[a]	ν (cm^{-1})	Rel. Int.	$\Delta\nu$ (cm^{-1})	Assignment[a]
27546	mw	−569	$0+\nu_{6a}'$	25783	mw	1194	$(1)-\nu_{9a}$
27401	w	−424	$0+\nu_{16b}'\times 2$	25724	mw	1253	$(2)-\nu_1$
27193	w	−216		25690	mw	1287	
27101	w	−124		25602	m	1375	$(2)-\nu_{9a}$
27048	m	− 71	$=(5)$	25570	mw	1407	$(3)-\nu_1$
26996	w	− 19	sh.	25536	ms	1441	$0-\nu_5\times 2$
26977	ss	0	$=0$: 0—0 band	25507	ms	1470	$0-\nu_{6a}-\nu_1$
26938	m	39	pyrazine-d_3 0—0	25447	m	1530	$(3)-\nu_{9a}$
26857	mw	120		25399	m	1578	
26794	s	183	$=(1): 0+(\nu_{16b}'-\nu_{16b})$	25386	m	1591	$0-\nu_{6a}-\nu_{9a}$
26607	s	370	$=(2): 0+(\nu_5'-\nu_5)$	25323	mw	1654	$(1)-\nu_{6a}-\nu_1$
26453	s	524	$=(3): 0-\nu_{16a}\times 2$	25306	mw	1671	
26391	s	586	$0-\nu_{6a}$	25213	m	1764	$0-\nu_1\times 2$
26281	m	696		25169	mw	1808	
26219	w	758		25092	m	1885	$0-\nu_1-\nu_{9a}$
26207	m	770	$(1)-\nu_{6a}$	25013	ms	1964	$(2)-\nu_1-\nu_{9a}$ or $(3)-\nu_5\times 2$
26162	m	815	$(5)-\nu_1$	24972	mw	2005	$0-\nu_{9a}\times 2$
26091	s	886	$0-\nu_1$	24951	mw	2026	$0-\nu_{6a}-\nu_5\times 2$
26019	m	956	$(2)-\nu_{6a}$	24929	mw	2048	$0-\nu_{6a}\times 2-\nu_1$
25971	s	1006	$0-\nu_{9a}$	24870	w	2107	$(3)-\nu_{6a}-\nu_{9a}$
25912	m	1065	$(1)-\nu_1$	24854	w	2123	
25871	m	1106	$(3)-\nu_{6a}$	24798	mw	2179	$0-\nu_{6a}\times 2-\nu_{9a}$
25818	ms	1159	$0-\nu_{10a}\times 2$	24776	w	2201	
25802	m	1175	$0-\nu_{6a}\times 2$				

a) Bands (1)···(6), see also Fig. 4.

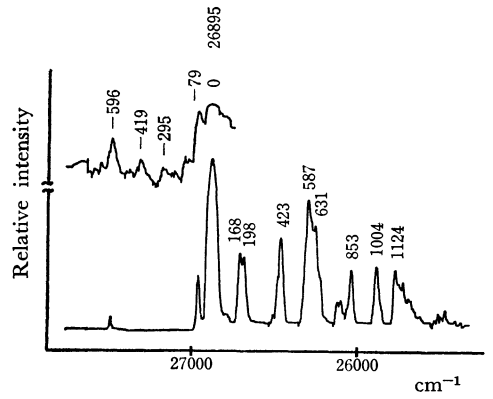

Fig. 3. Phosphorescence spectrum of pyrazine-2,4-d_2 in the vapor.

Table 3. Vibrational analysis of the phosphorescence spectrum of pyrazine-2,3-d_2 in the vapor

ν (cm^{-1})	Rel. Int.	$\Delta\nu$ (cm^{-1})	Assignment[a]
27491	m	−596	$0+\nu_{6a}'$
27314	w	−419	$0+\nu_{16b}'\times 2$
27190	w	−295	$0+\nu_{16a}'\times 2$
26974	m	− 79	=(5)
26895	ss	0	=0: 0—0 band
26803	w	92	=(6)
26782	w	113	
26727	ms	168	$=(4): 0+(\nu_{16a}'-\nu_{16a})$
26697	ms	198	$=(1): 0+(\nu_{16b}'-\nu_{16b})$
26472	s	423	$=(2): 0+(\nu_5'-\nu_5)$
26386	w	509	$(5)-\nu_{6a}$
26344	w	551	
26308	s	587	$0-\nu_{6a}$
26264	ms	631	$=(3): 0-\nu_{16a}\times 2$
26235	m	660	sh.
26140	m	755	$(4)-\nu_{6a}$
26116	m	779	$(1)-\nu_{6a}$
26042	ms	853	$=(7): 0-\nu_{15}$
25891	s	1004	$0-\nu_1$
25771	s	1124	$0-\nu_{9a}$

a) Bands (1)···(7), see also Fig. 4.

spectra are the modes of ν_{6a}, ν_{9a}, and ν_1 and their combinations.[12] However, there are many bands that lie with considerable intensity between 27100 and 25900 cm^{-1} and it is impossible to analyze them in terms of the normal mode frequencies in the ground state only. They are schematically reproduced in Fig. 4, and referred hereafter to the band (1), (2),···(7). The assignments are wholly based on the band positions since no other information is available. For instance a study of temperature dependence of the vapor spectra proved of no help, since it was practically impossible to compare the band intensities under different temperatures. With an increase in temperature, the continuous emission from the vapor overlapping on the phosphorescence spectrum increased in intensity, while the

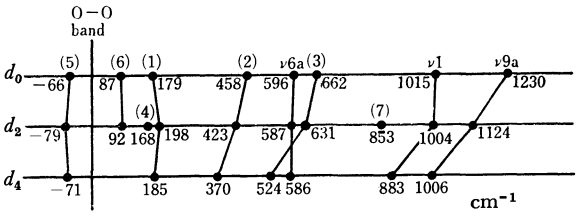

Fig. 4. Schematic representation of first main bands of the phosphorescence spectra of pyrazines in the vapor.

phosphorescence spectrum decreased in intensity. This made a precise measurement of the band intensity impossible.

The band (1) may be ascribed to the 1–1 transition of the ν_{16b}, since hot bands −474 (d_0), −419 (d_2), and −424 cm^{-1} (d_4) could be assigned to the overtones of this vibrational mode in the excited state, and fundamental frequencies of this mode are 416, 409, and 399 cm^{-1} in the ground state, respectively. This situation is analogous to the first S←S (π^*–n) absorption spectrum of pyrazine-d_0.[13] Similarly, the band (2) may arise from the 1–1 transition due to the mode ν_5 if we take 461, 442, and 351 cm^{-1} as ν_5 frequencies in the triplet state which are smaller in frequency by about 50% than those in the ground state, but still greater as compared with the value in the lowest singlet (n,π^*) state.[14] Here, the ν_5 mode frequency of pyrazine-2,3-d_2 in the ground state has been taken to be 865 cm^{-1}. Whether this is valid will be discussed later in connection with the band (7). On the basis of the numerical relationships found in the pyrazine-2,3-d_2 spectrum, the band (3) was assigned to an overtone frequency of a non-totally symmetrical mode in the ground state. These are; 631↔316×2 (ground state), −295↔−148 ×2 (excited state), 168 (band (4))↔316−148 (1–1 transition). Thus the frequencies 331 (d_0), 316 (d_2), and 262 cm^{-1} (d_4) were obtained as fundamentals of a non-totally symmetrical mode in the ground state of the respective compounds in the parentheses, which could be assigned to the ν_{16a} vibrational mode. The experimental value of the frequency has not yet been established but a value of 340 cm^{-1} (d_0) has tentatively been given, which has been taken from the Raman data in the liquid phase[15] and has been supported by the normal mode calculation based on the valency force constants transferred from benzene.[16] The band (5) has its counterpart in the T←S absorption spectrum, but has not been assigned.[17] The band (6) is the 1–1 transition of the ν_{9a} according to a list of designation in Ref. 11. The band (7) has a frequency difference of 853 cm^{-1} from the 0–0 band and this is too large to be interpreted as 1–1 transition. This band is also too strong in intensity to be accounted for as 2–2 transition, *e.g.*, overtone of the 423 cm^{-1} band. From its magnitude

12) The mode numbers employed here are the same as those used in, J. D. Simmons, K. K. Innes, and G. M. Begun, *J. Mol. Spectrosc.*, **14**, 190 (1964).

13) M. Ito, R. Shimada, T. Kuraishi, and W. Mizushima, *J. Chem. Phys.*, **26**, 1508 (1957).

14) K. K. Innes, J. D. Simmons, and S. G. Tilford, *J. Mol. Spectrosc.*, **11**, 257 (1963).

15) R. C. Lord, A. L. Marston, and F. A. Miller, *Spectrochim. Acta*, **9**, 113 (1957).

16) D. B. Scully, *ibid.*, **17**, 233 (1961).

17) K. K. Innes and L. E. Giddings, Jr., *Discuss. Faraday Soc.*, **35**, 192 (1963).

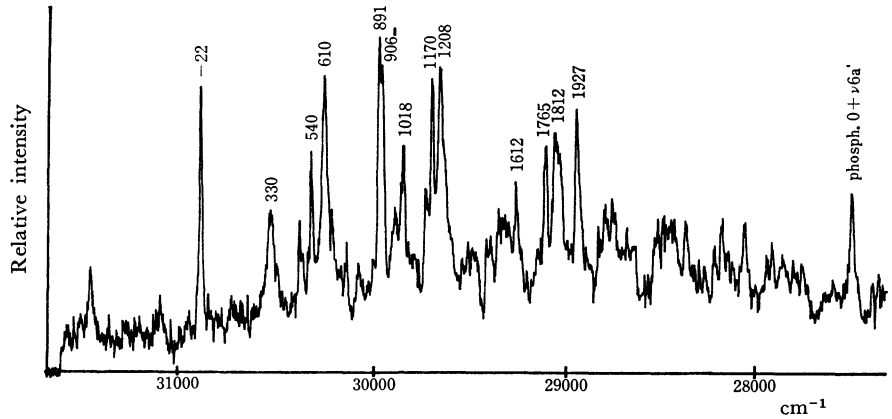

Fig. 5. Fluorescence spectrum of pyrazine-d_0 in the vapor.

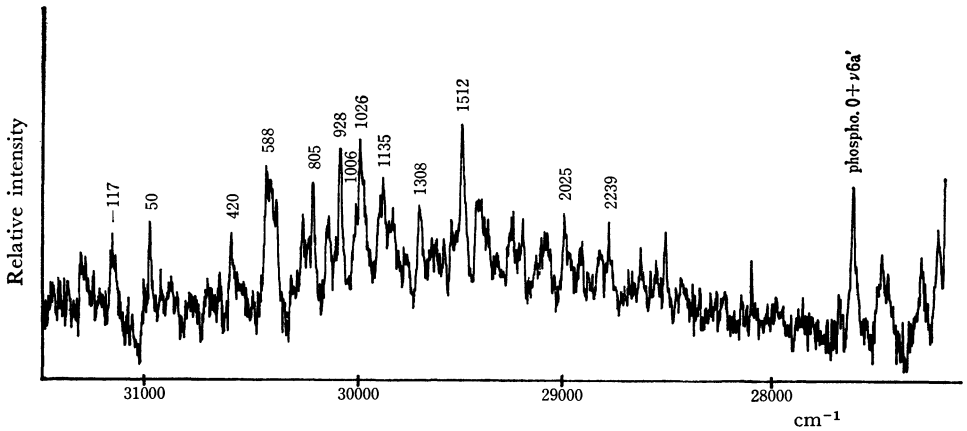

Fig. 6. Fluorescence spectrum of pyrazine-d_4 in the vapor.

TABLE 4. VIBRATIONAL ANALYSIS OF THE FLUORESCENCE SPECTRUM OF PYRAZINE-d_0 IN THE VAPOR

ν (cm^{-1})	Rel. Int.	$\Delta\nu$[a] (cm^{-1})	Band relation[b]	ν (cm^{-1})	Rel. Int.	$\Delta\nu$[a] (cm^{-1})	Band relation[b]
31315	w	−440	=(1): (ν_{6a})	29804	m	1071	(3)−ν_5
31292	w	−417		29740	m	1135	(2′)−ν_{6a}
31207	w	−332		29705	s	1170	(2)−$\nu_{6a}\times 2$
31130	w	−255		29667	s	1208	(2)−ν_{9a} or (3′)−ν_{6a}
31099	w	−224		29605	w	1270	
30897	s	− 22	=(2): (ν_1)	29427	m	1448	(2′)−ν_5
30829	w	46		29312?	mw	1563	(1′)−ν_{9a}
30811	w	64		29263	ms	1612	(4′)−ν_{6a}
30746	w	129		29110	ms	1765	(2′)−ν_{9a} or (2)−$\nu_{6a}\times 3$
30726	w	149	=(3): ($\nu_{6a}\times 2$)	29063	ms	1812	(2)−$\nu_5\times 2$
30687	mw	188	=(4): (ν_{9a})	28948	ms	1927	(4′)−ν_5
30633	w	242		28830	mw	2045	(2′)−$\nu_{6a}-\nu_5$
30570	mw	305		28797	m	2078	(2)−$\nu_{6a}\times 2-\nu_5$
30545	m	330	=(1′): [c]	28757	m	2118	(2)−$\nu_5-\nu_{9a}$
30400	m	475	(1)−ν_5	28669	w	2206	(4′)−$\nu_{6a}\times 2$
30335	ms	540	=(2′): ($\nu_5'-\nu_5$)	28630	mw	2245	(4′)−ν_{9a}
30265	s	610	=(3′): (ν_{6a})	28502	m	2373	(2′)−$\nu_5\times 2$
30191	m	684		28479	m	2396	(2)−$\nu_{6a}\times 2-\nu_{9a}$
30152	m	723		28356	m	2519	(4′)−$\nu_{6a}-\nu_5$
30090	mw	785	(1)−ν_{9a}	28196	m	2679	(2′)−$\nu_5-\nu_{9a}$ or (2)−$\nu_{6a}\times 3-\nu_5$
29984	s	891	(2)−ν_5	28156	m	2719	(2)−$\nu_{6a}-\nu_5-\nu_{9a}$
29969	ms	906		28027	m	2848	(4′)−$\nu_5\times 2$ or (4′)−$\nu_{6a}-\nu_{9a}$
29857	ms	1018	=(4′): (ν_1)	27872	m	3003	(2)−$\nu_{6a}\times 3-\nu_{9a}$

a) $\Delta\nu=\nu_{abs}^{0-0}-\nu$ ($\nu_{abs}^{0-0}=30875$ cm^{-1}).

b) Bands (1′)···(4′) could be assigned as are shown in parentheses, but agreement between the observed vibrational frequencies and the data in Ref. 12 in the case for pyrazine-d_0 are rather worse than that of pyrazine-d_4 emission (see also Table 5). Bands (1)···(4) are assigned as are shown in parentheses on the assumption that a false origin lies at 31913 cm^{-1}.

c) The frequency difference is in agreement with that of a hot band observed in Ref. 13 in the ultraviolet absorption spectrum in the vapor, but its assignment remains unknown.

Table 5. Vibrational analysis of the fluorescence spectrum of pyrazine-d_4 in the vapor

ν (cm^{-1})	Rel. Int.	$\Delta\nu$[a] (cm^{-1})	Band relation[b]	ν (cm^{-1})	Rel. Int.	$\Delta\nu$[a] (cm^{-1})	Band relation[b]
31281	m	−251		29919	m	1111	
31157	ms	−117	=(1*)	29898	ms	1135	
31130	m	−100		29860	w	1170	(2′)−ν_{6a}
31005	m	25		29852	ms	1178	
30980	ms	50	=(1): (ν_{9a})	29808	w	1222	(1)−$\nu_{6a}\times 2$
30885	m	150	=(2*)	29785	m	1245	
30788	w	242		29745	w	1285	
30772	w	258		29722	ms	1308	
30719	m	311		29660	m	1370	(1′)−ν_1
30664	m	366		29646	m	1384	(2)−ν_{6a}
30610	ms	420	=(1′): ($\nu_5'-\nu_5$)	29602	m	1428	(1′)−ν_{9a}
30593	w	437		29566	m	1464	(1*)−$\nu_{6a}-\nu_{9a}$
30570	m	460	(1*)−ν_{6a}	29552	w	1478	
30514	m	516		29539	w	1491	
30442	s	588	=(2′): (ν_{6a})	29518	s	1512	(1)−$\nu_{6a}-\nu_1$
30434	w	596		29441	ms	1589	(2′)−ν_{9a}
30396	s	634	(1)−ν_{6a}	29385	m	1645	
30382	w	648		29344	m	1686	(2)−ν_1
30319	ms	711		29278	m	1752	(2′)−$\nu_{6a}\times 2$
30295	w	735	(2*)−ν_{6a}	29268	m	1762	(1*)−$\nu_1-\nu_{9a}$
30275	ms	755	(1*)−ν_1	29219	m	1811	(2)−ν_{9a}
30225	s	805	=(2): ($\nu_1\times 2$)	29140	m	1890	(3′)−ν_{9a}
30154	ms	876	(1*)−ν_{9a}	29122	m	1908	
30144	m	886	=(3′): (ν_1)	29095	m	1935	(1)−$\nu_1-\nu_{9a}$
30102	s	928	(1)−ν_1	29065	w	1965	(2)−$\nu_{6a}\times 2$
30041	w	989		29020	w	2010	(4′)−ν_{9a}
30024	m	1006	=(4′): (ν_{9a}) or (1′)−ν_{6a}	29005	m	2025	
30004	s	1026	(2*)−ν_1	28930	mw	2100	(1)−$\nu_{6a}\times 2-\nu_1$
29990	m	1040	(1*)−$\nu_{6a}\times 2$	28892	w	2138	
29980	w	1050	(1)−ν_{9a}	28853	mw	2177	(4′)−$\nu_{6a}\times 2$
29959	m	1071		28837	w	2193	
29945	w	1085		28791	m	2239	

a) $\Delta\nu=\nu_{abs}^{0-0}-\nu$ ($\nu_{abs}^{0-0}=31030$ cm^{-1}).

b) Bands (1′)···(4′) could be assigned as are shown in parentheses, and those are possible in contrast to the pyrazine-d_0 spectrum since the numerical agreement is fair and the vibrational modes are the same as those observed in the fluorescence in solution. Bands (1) and (2) are assigned as are shown in parentheses on the assumption that a false origin lies at 31988 cm^{-1}.

in frequency two assignments may be possible; $\nu_5(a_2$ in $C_{2v})$ and $\nu_{15}(a_1$ in $C_{2v})$. In order to clarify this point, the hot bands of the lowest S←S absorption spectrum of pyrazine-2,3-d_2 in the vapor was investigated and two bands were found at 854 and 865 cm^{-1} from the 0—0 band located at 30952 cm^{-1}, the latter being much stronger in intensity. The fact that ν_5 appears strongly in the absorption spectra of pyrazine-d_0 and -d_4 in the vapor[14] suggests that 865 cm^{-1} may be of the mode ν_5 and 853 cm^{-1} the mode ν_{15}, in good agreement with Ref. 18.[19] Therefore, it has been concluded that all the progressions observed in the phosphorescence spectra of pyrazines in the vapor with sufficient intensity are of totally symmetrical, *i.e.*, a_g (or a_1) mode, overtone vibration, or arise from v–v transitions.

The Fluorescence Spectra in the Vapor State. The fluorescence spectra of pyrazine-d_0 and -d_4 have been studied in the vapor. The microphotometer tracings and the spectral data are given in Figs. 5 and 6 and Tables 4 and 5, respectively, although no unambiguous interpretation of these spectra has yet completely been made. It seems strange to say that the emission spectrum of pyrazine between 31500 and 28000 cm^{-1} is not explainable. But this is not a result conflicting with Ref. 1, in which the identification of the fluorescence spectra was based on the rough coincidence in the Franck-Condon contour between the emissions and the hot bands of the lowest S←S absorption spectra in the vapor. The details will be discussed in the following: At first, let us consider a difference between the tracing curves given by Logan and Ross and those of the present work (Figs. 5 and 6). The most remarkable one lies on a band denoted as −22 cm^{-1} in pyrazine-d_0 spectrum in Fig 5 (−22 cm^{-1} means its distance from the origin band of the first S←S (π^*-n) absorption spectrum). This is one of the strongest bands in our fluorescence spectrum but missing from that by Logan

18) E. F. Zalewski, Ph. D. Thesis, University of Chicago, 1968.

19) However, ν_5 mode has been observed with moderately strong intensity in the phosphorescence spectra of pyrazine-d_0, -d_2, and -d_4 at the isotopically mixed crystal experiments. M. Koyanagi, T. Shigeoka, and Y. Kanda, This Bulletin, to be submitted.

and Ross. The observation was repeatedly made at various temperatures and pressures with and without foreign gas (air). A careful comparison of the curve by Logan and Ross with our various tracing curves showed that the $-22\ cm^{-1}$ band was possibly reabsorbed by the origin band and the hot bands lying close to it in the curve by Logan and Ross since the curve in a region between -500 to $+1000\ cm^{-1}$ coincided well with one of the tracing curves with a strong continuous background of the exciting light source and an intense absorption or reabsorption appearing on it.

No bands that correspond to the hot bands in the absorption were observed in the fluorescence spectrum of gaseous pyrazine-d_0, but several bands in that of gaseous pyrazine-d_4. These phenomena shoud not be attributed to reabsorption or difference in absorbance due to low population of "hot molecules" in the ground state. On the other hand, there are many bands that can be analyzed in terms of four normal mode frequencies of pyrazines, such as the modes of ν_1, ν_5, ν_{6a}, and ν_{9a}, if several origins are tentatively assumed as given in Tables 4 and 5. One of the most probable interpretations of the fluorescence spectra in the vapor may be based on the so-called resonance spectra. An attempt along this line shows that several strong bands become explainable with pseudo-origins. Another may be to assume many abnormally populated emitting levels higher than the zero vibrational level in the excited state. This is probable but too speculative.

Fluorescence in Solution at Low Temperature. The fluorescence spectra of pyrazine-d_0 and -d_4 in methyl cyclohexane and pyrazine-d_0 in benzene have been measured at 90°K. The fluorescence spectrum of pyrazine in methyl cyclohexane consists of somewhat broad bands but becomes rich in structure in benzene solution. The 0—0 band diminishes its intensity with an increase of the concentration. N_{6a} and ν_5 are active vibrations in pyrazine-d_0 in methyl cyclohexane, but whether its 600 cm^{-1} long progressions are overtones of ν_{6a} or combinations of ν_{6a} and ν_{9a} was not certain bacause of its broad linewidth. In a benzene solution they are clearly of the latter type. The spectrum in a benzene solution was rather complicated because there are several sub-systems besides its main progressions.

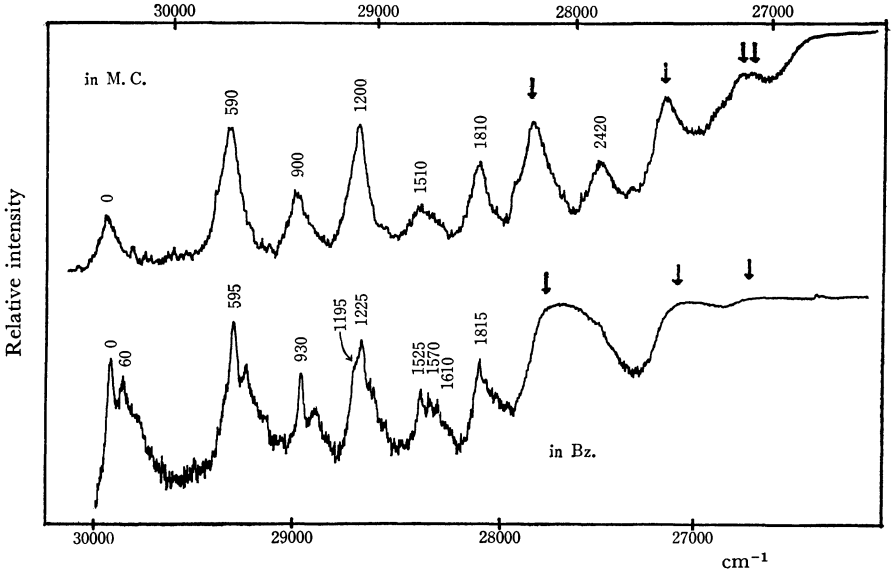

Fig. 7. Fluorescence spectra of pyrazine-d_0 in solutions at 90°K. Downward arrows denote the phosphorescence from pyrimidine-d_0.

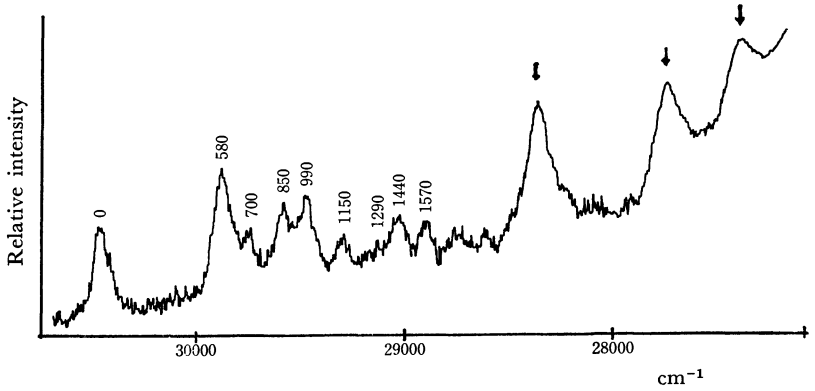

Fig. 8. Fluorescence spectrum of pyrazine-d_4 in methyl cyclohexane at 90°K. Downward arrows denote the phosphorescence from pyrimidine-d_4.

Table 6. Vibrational analysis of the fluorescence spectra of pyrazine-d_0 in solution at 90°K

in M.C. ν (cm^{-1})	Rel.[a] Int.	$\Delta\nu$[b] (cm^{-1})	in benzene ν (cm^{-1})	Rel.[a] Int.	$\Delta\nu$[b] (cm^{-1})	Assignment
30310	3	0	29895	7	0	=0: 0-0 band
			29835	6	60	0−(60)
29720	8	590	29300	9	595	$0-\nu_{6a}$
			29245	7	650	$0-\nu_{6a}-(55)$
			29150	sh	745	$0-\nu_{10a}$
29410	4	900	28965	7	930	$0-\nu_5$
			28900	6	995	$0-\nu_5-(65)$
29100	7	1200	28700	sh	1195	$0-\nu_{6a}\times 2$
			28670	8	1225	$0-\nu_{9a}$
			28615	6	1280	$0-\nu_{9a}-(55)$
28800	2	1510	28370	6	1525	$0-\nu_{6a}-\nu_5$
			28325	6	1570	$0-\nu_{8a}$
			28285	6	1610	$0-\nu_{11}\times 2$
28500	5	1810	—	—	—	$0-\nu_{6a}\times 2$
			28080	7	1815	$0-\nu_{6a}-\nu_{9a}$
			28045	6	1850	$0-\nu_{6a}\times 2$
28220	(s)	(0)	27750	(s)	(0)	pyrimidine-d_0 phospho. 0—0
27890	3	2420	—	—	—	$0-\nu_{6a}\times 4, 0-\nu_{9a}\times 2$
27540	(s)	(680)	27100	(s)	(650)	pyri.-d_0 phospho.
27150	(s)	(1070)	—	—	—	pyri.-d_0 phospho.
27100	(s)	(1120)	—	—	—	pyri.-d_0 phospho.

a) sh: shoulder, s: strong.
b) ( ): phosphorescence bands of pyrimidine-d_0.

Table 7. Vibrational analysis of the fluorescence spectrum of pyrazine-d_4 in methyl cyclohexane at 90°K

ν (cm^{-1})	Rel.[a] Int.	$\Delta\nu$[b] (cm^{-1})	Assignment
30460	4	0	=0: 0—0 band
29880	6	580	$0-\nu_{6a}$
29760	2	700	$0-\nu_5$
29610	4	850	$0-\nu_1$
29470	4	990	$0-\nu_{9a}$
29310	2	1150	$0-\nu_{6a}\times 2$
29170	1	1290	$0-\nu_{6a}-\nu_5$
29020	3	1440	$0-\nu_{6a}-\nu_1$
28890	3	1570	$0-\nu_{6a}-\nu_{9a}$
28730	0	1730	$0-\nu_{6a}\times 3$
28590	0	1870	$0-\nu_{6a}\times 2-\nu_5$
28330	(s)	(0)	pyrimidine-d_4 phospho. 0—0
27680	(s)	(650)	pyri.-d_4 phospho.
27280	(s)	(1050)	pyri.-d_4 phospho.

a) s: strong.
b) ( ): phosphorescence bands of pyrimidine-d_4.

A separation of about 60 cm^{-1} associated with this spectrum may be due to a lattice vibration.[20] In pyrazine-d_4, ν_{6a}, ν_5, ν_{9a}, and ν_1 are active. This last mode was not found in pyrazine-d_0. The observation of the $0-\nu_5$ band in the fluorescence spectra at low temperature in both -d_0 and -d_4 favors the interpretation given by Innes *et al.* that all strong vibronic bands of the 3200 Å absorption system of pyrazine must be assigned to a single electronic transition of mixed character in polarization.[14] An alternative assignment had been given to this band by Ito *et al.* as belonging to an electronically forbidden transition into an another $^1(n, \pi^*)$ state.[13] However, in the case of ordering of energy levels, the fluorescence will occur solely from the lower one at low temperature, especially if the higher transition is of forbidden character and the lower one is of allowed one. Thus it has been concluded that the fluorescence spectrum in solution is explainable by one electronic transition and is a normal one.

The phosphorescence spectra from photochemically produced pyrimidines were also observed, whose 0—0 bands were located at 28220 (d_0) and 28330 cm^{-1} (d_4) and separated by about 1500 cm^{-1} to the shorter wavelengths from that of the pyrazine phosphorescence. This additional emission did not appear when the 3130 Å system of the Hg-lamp was used as an exciting light in agreement with the results by Lahmani *et al.*[5] The mechanism of the photoisomerization of pyrazine has been discussed by several investigators,[6,5,21] and a diazavenzvalene has been proposed as a reaction intermediate. A thermally promoted rearrangement has also been reported.[21] It may be of another interest to examine whether the reversed photoreaction, *i.e.*, pyrimidine into pyrazine, may occur or not.

From the analyses of the vibronic structure of the emission spectra of pyrazine and its deuterated compounds in the vapor, it has been found that the phosphorescence spectrum is straightforward but the fluorescence spectrum is anomalous, and several fundamentals of the vibrations including ν_{16a} mode have been found. They are summarized in Table 8. It has also been found that the fluorescence spectrum of pyrazine in solution at liquid air temperature is of single electronic transition and the photochemical reaction of pyrazine occurs even at such temperature.

Table 8. Fundamental frequencies of pyrazines observed in the phosphorescence spectra in the vapor

vib. mode	elec.[a] state	fundamental frequencies (cm^{-1}) -d^0	-2,3-d^2	-d^4
ν_{16b}	T	237	210	214
ν_{16a}	G	331	316	262
	T		148	
ν_5	T	461	442	351
	G		(865)	
ν_{15}	G		853	

a) T: triplet, G: ground state.

The authors wish to thank Dr. R. Shimada for his helpful advice on instruments for the vapor spectra measurement, and Dr. T. Edamura for his information to us about his unpublished results on the absorption and fluorescence spectra of crystalline pyrazine.

20) A similar interpretation has been given by T. Shigeoka, Master Thesis, Kyushu Univ., 1967.

21) W. D. Crow and C. Wentrup, *Tetrahedron Lett.*, **27**, 3115 (1968).

Spectroscopic Determination of Quenching Cross-Sections of Excited Mercury Atoms (6^3P_1, 6^3P_0) in Molecular Collisions

Hiroyuki HORIGUCHI and Soji TSUCHIYA

Department of Pure and Applied Sciences, College of General Education, The University of Tokyo, Meguro-ku, Tokyo

(Received September 4, 1970)

The concentrations of $Hg(6^3P_1)$ and (6^3P_0) atoms, $[Hg_1^*]$ and $[Hg_0^*]$, were determined from the absorptions of 4358 and 4047 Å lines in the Ar-diluted mercury vapor in the presence of several quenching molecules, under the radiation of 2537 Å emission. An apparent absorption intensity was not proportional to $[Hg_1^*]$ or $[Hg_0^*]$, and was sensitive to the ratio of the spectral half-width of the light source to that of the absorption line. Therefore, a method to correct an absorption intensity was proposed. The relation of $[Hg_1^*]$ to [Q], a concentration of quenching molecules, is explained well by the Stern-Volmer equation. The value of $[Hg_0^*]$ increases with [Q] until it reaches a maximum at a certain value of [Q], and a further increase of [Q] results in a decrease of $[Hg_0^*]$. These findings are explained well by the following mechanism: (1) $Hg+h\nu \rightarrow Hg_1^*$, (2) $Hg_1^* \rightarrow Hg+h\nu$, (3) $Hg_1^*+Q \rightarrow Hg+Q$, (4) $Hg_1^*+Q \rightarrow Hg_0^*+Q$, (5) $Hg_0^*+Q \rightarrow Hg+Q$, (6) $Hg_0^* \rightarrow Hg$ (by collisions with a wall). The respective values of cross-sections (σ^2) of N_2, CO, and NO for process (3) are ≤ 0.03, 0.60, and 20 Å^2, and those for process (4) are 0.36, 2.1 and 5 Å^2, and those for process (5) are $\leq 3.6\times10^{-4}$, 0.15 and 8.0 Å^2.

The collisional cross-section for quenching an excited mercury atom $Hg(6^3P_1)$ has been obtained by the intensity measurement of the fluorescence from $Hg(6^3P_1)$[1,2] or by observing directly a lifetime of 6^3P_1 state[3]. However, the cross-section thus determined is the sum for the two quenching processes, *i.e.*, from 6^3P_1 to the ground state 6^1S_0 and to the metastable state 6^3P_0. Scheer and Fine[4] found that collisional cross-sections of CO and N_2 for quenching 6^3P_1 to 6^3P_0 were nearly the same, and concluded that CO was a more efficient quencher than N_2 for the process 6^3P_1 to 6^1S_0. Later, Callear and Williams[5] observed the time history of the absorption due to the existence of $Hg(6^3P_0)$ after the flash excitation of mercury atoms, and concluded that all of the cross-sections of various molecules for the process 6^3P_0 to 6^1S_0 were very small compared with the 6^3P_1 quenching cross-sections. Furthermore, they could not find any systematic relation between a cross-section for quenching 6^3P_1 to 6^3P_0 and an energy discrepancy which could not be converted to the vibration of a quenching molecule. Kimbell and Le Roy[6] previously determined the stationary concentration of $Hg(6^3P_0)$ in the system of N_2 gas with mercury vapor illuminated by the mercury resonance line assuming the Lambert-Beer rule. However, their assumption should be uncertain.

In this paper, we propose an accurate method to determine the concentrations of $Hg(6^3P_1)$ and (6^3P_0) from the absorptions of 4358 Å (7^3S_1—6^3P_1) and 4047 Å (7^3S_1—6^3P_0) spectral lines. Based on this method, the cross-sections of N_2, CO, and NO for the quenching processes, $^3P_1 \rightarrow {}^1S_0$, $^3P_1 \rightarrow {}^3P_0$, and $^3P_0 \rightarrow {}^1S_0$ are determined.

Experimental

An outline of the apparatus in this experiment was similar to that used by Karl, Kruus, and Polanyi.[7] The reaction cell was a Vycol glass tube, 4 cm in diameter and 100 cm long, and was surrounded by four low pressure mercury lamps (Toshiba Electric Co., germicidal lamp) that were made from quartz tubes, 2.5 cm in diameter and 89.3 cm long. Each of these exciting lamps was operated by the direct current and had a power of 7.5 watt at 2537 Å radiation, and the emission intensities of other spectral lines were less than 1/30 of that of 2537 Å line. The intensity of 2537 Å radiation from the exciting lamps was monitored by a photoelectric tube (Toshiba Electric Co., PV-43), that was sensitive only to the 2537 Å line. Another low pressure mercury lamp (Ushio Co., ULO-6DQ), d.c. operated, was used as a light source for the measurement of absorption. Apparent concentrations of $Hg(6^3P_1)$ or (6^3P_0) atoms were determined in terms of the optical density, $\log I_0/I$, at 4358 Å for 6^3P_1 atoms and 4047 Å for 6^3P_0 atoms. The light beam, 5 mm in diameter, from the ULO-6DQ lamp was modulated at 25 Hz by a chopper before entering the cell and was passed longitudinally through the cell. The intensity of the beam was measured by a grating monochrometer (Japan Spectroscopic Co., CT-1), and the out-put from the photomultiplier was filtered by a 25 Hz tuned amplifier. The spectral slit-width of the monochromator was usually about 2 cm^{-1}, so that the observed intensity was an integrated one of 4358 or 4047 Å spectral line profile.

Sample gases used were all commercial ones, and their nominal purities were 99.99% for Ar. 99.999% for N_2, 99.5% for CO, and 98.5% for NO. Argon and nitric oxide were purified by successive distillation at liquid nitrogen temperature, and other gases passed through a U-shaped glass tube packed with active charcoal. In order to minimize the pressure dependence of the absorption intensity, quenching gases were diluted in argon, and the total pressure in the reaction cell was kept constant, where argon could be assumed to be a very poor quencher. A quenching gas diluted in argon, from which mercury vapor was removed by passing through a spiral tube cooled to an appropriate temperature, −194.5°C or −119°C, was fed into the reaction cell *via* a mercury saturator at a constant temperature.

1) A. C. G. Mitchell and M. W. Zemansky, "Resonance Radiation and Excited Atoms," Cambridge University Press, Cambridge, (1934), Chap. IV.

2) R. J. Cvetanović, "Progress in Reaction Kinetics," Vol. 2, Pergamon Press, London, (1964), p. 39.

3) C. G. Matland, *Phys. Rev.*, **92**, 637 (1953).

4) M. D. Scheer and J. Fine, *J. Chem. Phys.*, **36**, 1264 (1962).

5) A. B. Callear and G. J. Williams, *Trans. Faraday Soc.*, **60**, 2158 (1964).

6) G. H. Kimbell and D. J. Le Roy, *Can. J. Chem.*, **38**, 1714 (1960).

7) G. Karl, P. Kruus, and J. C. Polanyi, *J. Chem. Phys.*, **46**, 224 (1967).

Results and Analyses

Absorption Intensity and Concentration of Excited Mercury Atom. The absorptions of 4047 and 4358 Å lines were seen, when a gaseous mixture of Ar, N_2, and Hg was irradiated by the exciting lamp. In this case, the Lambert-Beer rule cannot be applied, since it is well known in atomic absorption spectroscopy that the properties of the spectral line itself, *i.e.* (1) the hyperfine structure of the lines, (2) the ratio of the absorption and emission line widths, (3) the resonance line broadening, must be considered. To investigate this point in experiment, it was examined how the absorption intensity of 4047 Å line was dependent on the intensity of 2537 Å radiation from the exciting lamp. Two examples of the results are shown by curves A and B in Fig. 1. The optical density is not in a linear relation to the intensity of exciting radiation, though the concentration of $Hg(6^3P_0)$ in the cell should be proportional to the intensity of 2537 Å line.

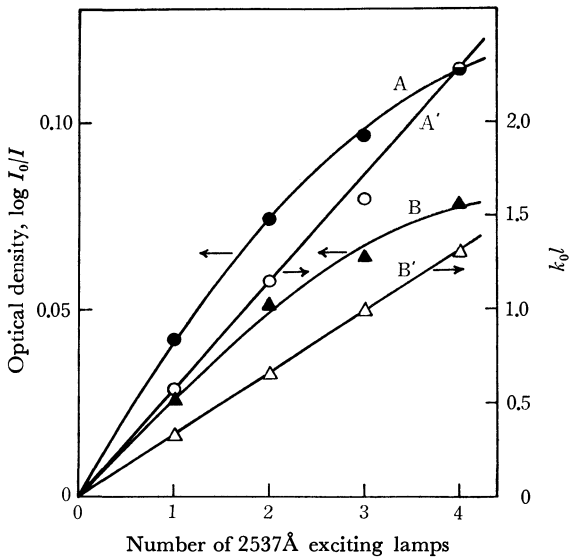

Fig. 1. Relative intensity of 2537Å radiation *vs.* the optical density at 4047Å, and relative intensity *vs.* calculated values of $[Hg_0^*]$ in k_0l unit.
A(●), A'(○): $p(N_2)=0.03$ Torr, $p(Ar)=4.97$ Torr; B(▲), B'(△): $p(N_2)=0.03$ Torr, $p(Ar)=0.97$ Torr.

To analyze this result, the profiles of the 4047 Å line from the light source and the absorption line of $Hg(6^3P_0)$ are assumed to be of Doppler broadened type. This assumption is only approximately applicable, because the spectral line profile from the discharge lamp must be dependent on many factors, *e.g.*, Doppler, collision, Stark effects, *hfs*, *etc.*, and the absorption line has a combined form of Doppler and collision broadened profiles with *hfs*. However, the purpose of the present experiment is not to clarify the spectral line profile, but to find the physical quantity proportional to the concentration of the excited mercury atoms from the optical density. Therefore, we tried to correct the curves of the absorption intensities in Fig. 1 to be linear to the intensity of 2537 Å line under the above assumption. The spectral intensity, E_ν, at a wave number ν from the light source is represented by[1]

$$E_\nu = \text{const} \times \exp[-(\omega/\alpha)^2], \quad (1)$$

where

$$\omega = 2(\nu-\nu_0)(\ln 2)^{1/2}/\Delta\nu_D,$$

$\Delta\nu_D$, the Doppler breadth of the absorption line, and ν_0 is the wave number at the line center or peak of the profile, and α is the ratio of the emission line breadth to absorption line breadth. Equating the absorption coefficient, k_ν, to $k_0\exp(-\omega^2)$ in Doppler broadening, the absorbancy A is

$$A = \int_{-\infty}^{+\infty}[\exp-(\omega/\alpha)^2]\{1-\exp[-k_0l(\exp-\omega^2)]\}d\omega \Big/ \int_{-\infty}^{+\infty}\exp-(\omega/\alpha)^2 d\omega, \quad (2)$$

where l is the length of the reaction cell, and k_0 is the absorption coefficient at the peak, that can be related to the oscillator strength f as

$$k_0 = 2(\ln 2/\pi)^{1/2}(\pi e^2 fN/mc\Delta\nu_D), \quad (3)$$

where e and m are electron's charge and mass, respectively, c, the light velocity, and N, the concentration of absorbing atoms per unit volume. Using the theoretical value of f,[8] k_0 for Hg (6^3P_1) and (6^3P_0) are 6.21×10^{-12} N and 5.90×10^{-12} N cm^{-1}, respectively. The absorbancy can be developed as[1]

$$A = \sum_n(-1)^n(k_0l)^n/n!(1+n\alpha^2)^{1/2}, \quad (4)$$

and this value is calculated by the HITAC 5010 computer with various values of α and k_0l, where l is 100 cm in this study. Some of the calculated results from Eq. (4) are shown graphically in Fig. 2, where the optical density, derived from the calculated value of $A(=(I_0-I)/I_0)$, is used. It is seen from this figure that the optical density is strongly dependent on the value

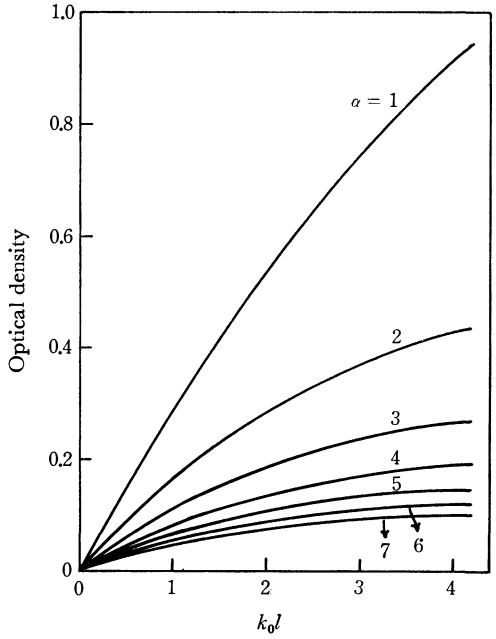

Fig. 2. Relation of the calculated optical density to k_0l with various values of α.

8) N. P. Penkin, *J. Quant. Spectrosc. Radiat. Transfer*, **4**, 74 (1964).

of α, that is, when the half-width of the spectral line from the light source is larger than that of the absorption line, the absorption intensity becomes small though the concentration of absorbing atoms is constant.

The experimental curves in Fig. 1 should be represented by one of the theoretical curves in Fig. 2. When the scale of the abscissae in Figs. 1 and 2 is converted to the logarithmic one, one can seek a theoretical curve that agrees with the experimental one in the range of 0.04—0.06 of the optical density. The values of α thus obtained are 5.2 for 1 Torr of the total pressure, and 5.0 for 5 and 10 Torr. A small dependence of α on the total pressure is due to the fact that the half-width of the collision-broadened line is about 1/10 that of the Doppler broadened one at 10 Torr if the optical collision cross-section of Ar or N_2 is 100 Å^2. By the use of the theoretical curves in Fig. 2 and the obtained value of α, a value of $k_0 l$, in other words, a concentration of $Hg(6^3P_0)$ can be determined from an absorption intensity. The curves A′ and B′ in Fig. 1 are thus obtained, and show that the concentration of $Hg(6^3P_0)$ is proportional to the intensity of 2537 Å radiation from the exciting lamp. It is also seen from Fig. 1 that the absorption intensity for 5 Torr of the total pressure is larger than that for 1 Torr even if the partial pressure of N_2 is the same. This is due to the fact that the deactivation of $Hg(6^3P_0)$ is governed by the collision with the wall of the reaction vessel. The collisional frequency with the wall is much dependent on the total pressure (see later).

In conclusion, the simple application of the Lambert-Beer rule is inappropriate in the present experimental condition, and the total pressure must be kept constant to avoid the collision broadening effect and the influence of wall collisions. In the following experiment, it is assumed that argon and quenching molecules have the same optical collision cross-section, and that the 4358 Å line profile from the light source has the same line-width as the 4047 Å line. The latter assumption may be open to question, but an apparent optical density is nearly proportional to the concentration of $Hg(6^3P_1)$, which is very small compared with that of $Hg(6^3P_0)$.

Quenching Mechanism and Rates. The following processes are considered as a quenching mechanism in the present system,

$$\text{(i)}\quad Hg(6^1S_0) + h\nu \xrightarrow{k_1} Hg(6^3P_1),$$

$$\text{(ii)}\quad Hg(6^3P_1) \xrightarrow{k_2} Hg(6^1S_0) + h\nu,$$

$$\text{(iii)}\quad Hg(6^3P_1) + Q \xrightarrow{k_3} Hg(6^1S_0) + Q,$$

$$\text{(iv)}\quad Hg(6^3P_1) + Q \xrightarrow{k_4} Hg(6^3P_0) + Q,$$

$$\text{(v)}\quad Hg(6^3P_0) + Q \xrightarrow{k_5} Hg(6^1S_0) + Q,$$

$$\text{(vi)}\quad Hg(6^3P_0) \xrightarrow{k_6} Hg(6^1S_0),$$

where Q represents a quenching molecule, and the concentration of $Hg(6^3P_1)$ will be denoted by $[Hg_1^*]$, and that of $Hg(6^3P_0)$ by $[Hg_0^*]$, and that of $Hg(6^1S_0)$ by [Hg]. McAlduff and Le Roy[9] have proposed further processes including the collision between an excited mercury atom and a ground state atom;

$$\text{(vii)}\quad Hg(6^3P_1) + Hg(6^1S_0) \longrightarrow Hg_2^*,$$

$$\text{(viii)}\quad Hg_2^* \longrightarrow Hg(6^3P_0) + Hg(6^1S_0),$$

$$\text{(ix)}\quad Hg_2^* + Q \longrightarrow Hg_2 + Q.$$

If these processes take place besides the reactions (i)—(vi), the concentration of $Hg(6^3P_0)$ produced in the system of Ar, N_2, and Hg mixture, must not have a simple linear relation to the pressure of mercury vapor. This is not the case in the present experiment, since $[Hg_0^*]$ has been found proportional to a pressure of mercury vapor in the range of 2×10^{-5}—1.9×10^{-4} Torr. Here, the pressure of mercury vapor was ordinarily 1.9×10^{-4} Torr, that is the saturated one at 0°C, and the effective collision frequency of an excited mercury atom with ground state atoms is very small compared with that of quenching by N_2 molecules, even if the collision cross-section of an excited mercury atom with a ground state atom is supposed about 100 Å^2.

From the reactions (i)—(vi), the stationary concentration of $Hg(6^3P_1)$ is expressed by

$$[Hg_1^*] = k_1 I[Hg]/\{k_2+(k_3+k_4)[Q]\}, \qquad (5)$$

where I is an intensity of 2537 Å radiation. If $[Hg_1^*]$ without quenching molecules is denoted by $[Hg_1^*]_0$, Eq. (5) reduces to the Stern-Volmer relation,

$$[Hg_1^*]_0/[Hg_1^*] = 1 + [(k_3+k_4)/k_2][Q]. \qquad (5')$$

The concentration of $Hg(6^3P_0)$ can be formulated as

$$[Hg_0^*] = k_2k_4[Hg_1^*]_0[Q]/\{(k_3+k_4)k_5[Q]^2 + [k_2k_5+(k_3+k_4)k_6][Q]+k_2k_6\}. \qquad (6)$$

The value of $[Hg_0^*]$ increases with increasing [Q] untill [Q] reaches $[Q]_{max}$,

$$[Q]_{max} = [k_2k_6/(k_3+k_4)k_5]^{1/2}. \qquad (7)$$

With this value of [Q], $[Hg_0^*]$ has a maximum value. Further increase of [Q] results in a decrease of $[Hg_0^*]$, and finally $[Hg_0^*]$ reduces to zero with very large amount of quenching molecules. Eq. (6) can be rewritten as

$$[Hg_0^*] = (k_4/k_6)[Hg_1^*]_0[Q]/\{([Q]/[Q]_{max})^2 + [(k_5/k_6)+(k_3+k_4)/k_2][Q]+1\}. \qquad (6')$$

The observed relation of $[Hg_1^*]$ or $[Hg_0^*]$ against [Q] is explained well by the above equations, and $(k_3+k_4)/k_2$, k_4/k_6, and k_5/k_6 can be determined.

The experimental values of $[Hg_1^*]_0/[Hg_1^*]$ are plotted in Fig. 3 against the partial pressure of N_2, CO, or NO as a quencher. The linear slope of the curve in Fig. 3 gives a value of $(k_3+k_4)/k_2$. As is mentioned, the line broadening effect by the existence of argon atoms causes an increase of $[Hg_1^*]$, because the absorption of 2537 Å radiation becomes more effective. Here, $[Hg_1^*]_0$ is 4.8×10^7 atoms cc^{-1} with 5 Torr of argon pressure, and 3.5×10^7 with 1 Torr.

Figure 4(a) shows that $[Hg_0^*]/[Hg_1^*]_0$ increases monotonously with increasing pressure of N_2, and that $[Hg_0^*]/[Hg_1^*]_0$ at 5 Torr of the total pressure is larger than that at 1 Torr. The former fact means that the value of $[Q]_{max}$ is far from the present experimental

9) J. E. McAlduff and D. J. Le Roy, *Can. J. Chem.*, **43**, 2279 (1965).

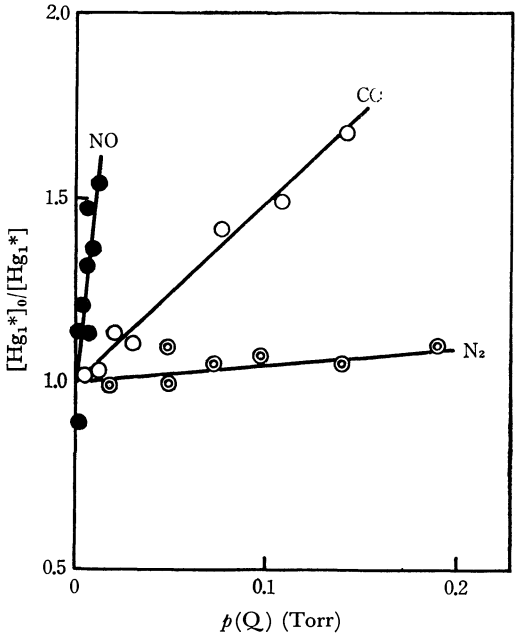

Fig. 3. Plots of $[Hg_1^*]_0/[Hg_1^*]$ *vs.* partial pressure of quencher. Total pressure in the cell is 5 Torr, and a partial pressure of Hg vapor is 1.9×10^{-4} Torr. N_2: ◎, CO: ○, NO: ●

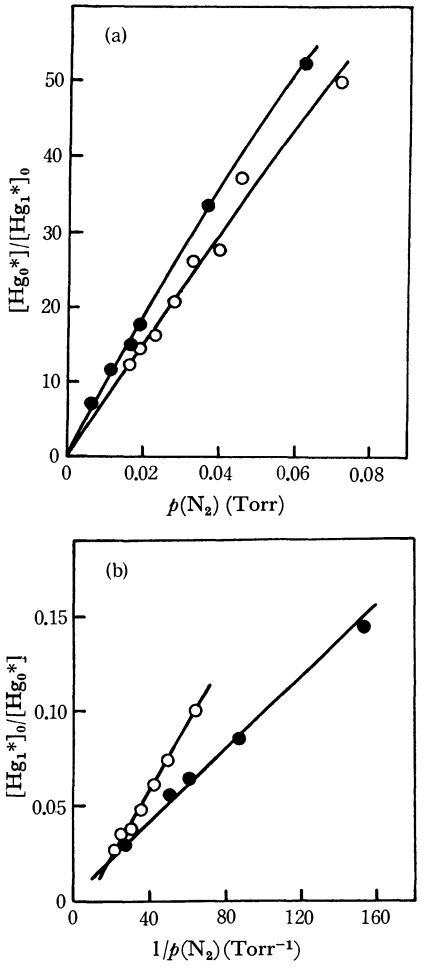

Fig. 4. (a) Plots of $[Hg_0^*]/[Hg_1^*]_0$ *vs.* partial pressure of N_2. Total pressure in the cell is 5 Torr (●) and 1 Torr (○), and a partial pressure of Hg vapor is 1.9×10^{-4} Torr.
(b) Plots of $[Hg_1^*]_0/[Hg_0^*]$ *vs.* $1/p(N_2)$.

range, *i.e.*, k_5 is very small. The later experimental finding is to be explained by the fact that a value of k_6 becomes larger as a total pressure decreases. This shows that the deactivation of $Hg(6^3P_0)$ is not due to a radiative process, but to collisions with the wall of the cell. Very long radiative lifetime of $Hg(6^3P_0)$, *i.e.*, 5.6 sec,[10] supports this explanation. Under the condition, $[Q]\ll[Q]_{max}$, Eq. (6′) can be approximated to,

$$[Hg_1^*]_0/[Hg_0^*] = (k_6/k_4)(1/[Q]) + (k_5/k_4) + [(k_3+k_4)k_6/k_2k_4]. \quad (8)$$

The values of $[Hg_1^*]_0/[Hg_0^*]$ are plotted *vs.* $1/[Q]$ in Fig. 4(b), using the data in Fig. 4(a), and a value of k_6/k_4 is obtained from a slope of a straight line in Fig. 4(b).

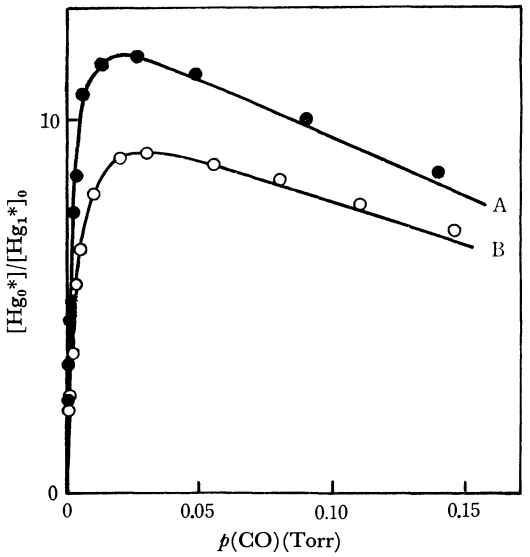

Fig. 5. Plots of $[Hg_0^*]/[Hg_1^*]_0$ *vs.* partial pressure of CO. Total pressure in the cell is 5 Torr (●) and 1 Torr (○), and a partial pressure of Hg vapor is 1.9×10^{-4}Torr. The curves, A and B, show the calculated values of $[Hg_0^*]/[Hg_1^*]_0$ from Eq. (6′) with the following values, $(k_3+k_4)/k_2=1.50\times10^{-16}$ cc·molecules^{-1}, $k_4/k_6=2.25\times10^{-13}$ (the curve A), $=8.47\times10^{-14}$ (the curve B) cc·molecules^{-1} and $k_5/k_6=1.61\times10^{-14}$ (A), $=7.14\times10^{-15}$ (B) cc·molecules^{-1}.

The experimental relation between $[Hg_0^*]/[Hg_1^*]_0$ and [CO] is shown in Fig. 5, and is explained well by Eq. (6). The larger value of $[Hg_0^*]/[Hg_1^*]_0$ at 5 Torr of the total pressure than that at 1 Torr arises from the longer lifetime of Hg (6^3P_0) at 5 Torr than at 1 Torr, and this also causes an decrease in a value of $[Q]_{max}$ at higher pressure. In the pressure range of CO that is very small compared with $[Q]_{max}$, the same procedure as the case of N_2 can be applied for the determination of k_4/k_6. By the use of this value of k_4/k_6, $[Q]_{max}$ can be found by fitting the experimental values of $[Hg_0^*]/[Hg_1^*]_0$ with the curve calculated by Eq. (6′). Then, a value of k_5/k_6 can be obtained by substituting the value of $k_2/(k_3+k_4)$ into Eq. (7). In the case of quenching by NO, the experimental curve of $[Hg_0^*]/[Hg_1^*]_0$ *vs.* partial pressure of NO could not be observed accurately owing to a very small

10) R. H. Garstang, *J. Opt. Soc. Amer.*, **52**, 845 (1962).

concentration of $Hg(6^3P_0)$, that is caused by an efficient quenching of the 6^3P_1 state to 6^1S_0 or 6^3P_0 to 6^1S_0. This also explains the fact that Callear and Williams[5] have not been able to detect the $Hg(6^3P_0)$ atoms by the flash excitation of Hg in NO or other polyatomic gases. The observed value of $[Hg_0^*]/[Hg_1^*]_0$ was 0.11 when a partial pressure of NO was 3.65×10^{-4} Torr at 10 Torr of the total pressure. By the direct measurement (see next) of the lifetime of $Hg(6\,^3P_0)$ in the same experimental condition, k_5 and k_6 were found to be 1.24×10^{-10} cc molecules^{-1} sec^{-1} and 1.0×10^2 sec^{-1}, respectively. Substituting these rate constants into Eqs. (7) and (6'), 3.7×10^{-4} Torr of $[Q]_{max}$ and 5.3 Å^2 of k_4 are obtained.

Table 1. Observed values of quenching rates (cc·molecules^{-1}) of Hg (6^3P_1) and Hg (6^3P_0)

Quencher	$(k_3+k_4)/k_2$	k_4/k_6	k_5/k_6
N_2	2.2×10^{-17}	3.2×10^{-14}	$\leq1\times10^{-17}$
CO	1.5×10^{-16}	2.2×10^{-13}	1.6×10^{-14}
NO	1.4×10^{-15}	5.5×10^{-13}	8.3×10^{-13}

These data are obtained at a total pressure of 5 Torr and a partial pressure of Hg of 1.9×10^{-4} Torr.

The observed values of $(k_3+k_4)/k_2$, k_4/k_6, and k_5/k_6 are summarized in Table 1. The lifetimes of $Hg(6^3P_1)$ and $Hg(6^3P_0)$, *i.e.*, k_2 and k_6, cannot be determined in the present experiment. The value of k_2 should be $1/\tau$, where τ is a radiative lifetime of $Hg(6^3P_1)$, 1.0×10^{-7} sec. However, the peak absorption coefficient, k_0 for 2537 Å line is 4.0 cm^{-1} in the present experimental condition, and the imprisonment effect of the radiation must be considered. Here, the effective radiative lifetime τ' given by Milne[11] is adopted. In his calculation, τ' for the case of infinite slab is,

$$\tau'/\tau = 1 + (k_0 l/\lambda)^2, \qquad (10)$$

where $\lambda\tan\lambda = k_0 l$. Kibble, Copley, and Krause[12] ascertained that the observed radiative lifetime of Na (3^2P) was in good agreement with the value calculated by Eq. (10). In our case, τ' is 3.52×10^{-6} sec, from which we can calculate the total quenching cross-section of $Hg(6^3P_1)$ as shown in Table 2.

To determine the rate of deactivation of $Hg(6^3P_0)$, the time history of the absorption of 4047 Å after the excitation radiation was suddenly turned off, was observed in the system of $Ar+N_2+Hg$ mixture, where N_2 molecules could be assumed as very inefficient quenchers of $Hg(6^3P_0)$ atoms. The result shows that a lifetime of $Hg(6^3P_0)$ is 2.8 msec at 1 Torr of the total pressure, 6.7 msec at 5 Torr, and 10 msec at 10 Torr, and is independent of a pressure of Hg atoms. This shows that the deactivation of $Hg(6^3P_0)$ is mainly caused by collisions with the wall of the reaction vessel as already pointed out. The details of this experiment will be reported in near future. Thus, the cross-sections for the processes, $6^3P_1\rightarrow6^3P_0$ and $6^3P_0\rightarrow6\,^1S_0$, can be calculated, and are shown in Table 2. The uncertainty in a value of k_2 produces a somewhat unaccuracy in an absolute value of the total quenching cross-section for $6^3P_1\rightarrow6^3P_0$, 6^1S_0. Hence, the calculated cross-section for the process $6^3P_1\rightarrow6^1S_0$ as the difference of $\sigma^2(6^3P_1\rightarrow6^1S_0, 6^3P_0)$ and $\sigma^2(6^3P_1\rightarrow6^3P_0)$ is most unreliable in the present results. However the present finding that the cross-section of N_2 for $6^3P_1\rightarrow6^1S_0$, 6^3P_0 is very close to that for $6^3P_1\rightarrow6^3P_0$, is consistent with the experimental result of Samson.[13] This is also supported by the later experiment of Matland,[3] who has found that the temperature dependence of the quenching cross-section of $Hg(6^3P_1)$ is nearly explained by $\exp(-\Delta E/kT)$, where ΔE is 0.07 eV. This value of the ΔE is necessary for a N_2 molecule as a kinetic energy if the energy difference between the 6^3P_1 and 6^3P_0 states is transferred to the vibration of N_2 molecule. Therefore, the result of Matland shows that the quenching of $Hg(6^3P_1)$ is mainly to the 6^3P_0 state and scarcely to the 6^1S_0 state. Thus, the estimated value of k_2 is not very different from the true one, and the cross-sections for the process 6^3P_1—6^1S_0 in Table 2 are reliable at least in an order of magnitude except that of N_2, whose cross-section for this process might be hidden in errors of the observed ones for the processes $6^3P_1\rightarrow6^3P_0$ and $6^3P_1\rightarrow6^1S_0$, 6^3P_0.

Table 2. Cross-sections (σ^2 in Å^2) for quenching $Hg(6^3P_1)$ and $Hg(6^3P_0)$

Quencher	$^3P_1\rightarrow{}^1S_0$	$^3P_1\rightarrow{}^3P_0$	$^3P_0\rightarrow{}^1S_0$	$^3P_1\rightarrow{}^3P_0$, $^1S_0$
N_2 this work	≤0.03	0.36	$\leq3.6\times10^{-4}$	0.39
others	0.02[a]	0.31[a]	$\leq2\times10^{-6}$[a], 9.0×10^{-6}[b]	0.33[a], 0.13[c], 0.27[d]
CO this work	0.60	2.1	0.15	2.7
others	—	—	0.028[b], 0.08—0.5[e]	5.8[d]
NO this work	20	5	8.0[h]	25
others	—	—	0.34[b], >0.38[f]	35.3[d], 24.7[g]

a) E.W. Samson,[13]
b) A.B. Callear and G.J. Williams,[5]
c) C.G. Matland,[3]
d) A.C.G. Mitchell and M.W. Zemansky,[1]
e) G. Karl, P. Kruus and J. C. Polanyi,[7]
f) G. Karl, P. Kruus, J. C. Polanyi, and I.W.M. Smith,[16]
g) J.R. Bates,[17]
h) This value is obtained by the measurement of the lifetime of $Hg(6^3P_0)$ in the mixture of $Ar+N_2+NO+Hg$.

11) E. A. Milne, *J. London Math. Soc.*, **1**, 40 (1926).
12) B. P. Kibble, G. Copley, and L. Krause, *Phys. Rev.*, **153**, 9 (1967).
13) E. W. Samson, *ibid.*, **40**, 940 (1932).

Discussion

The quenching cross-section of 6^3P_0 to 6^1S_0 obtained by us show a marked difference from those by Callear and Williams.[5] In their flash experiment, the half-width of flash duration reaches 51 μsec, and the production of $Hg(6^3P_0)$ from $Hg(6^3P_1)$ may not be neglected about 100—150 μsec after a flash excitation. Hence, there might be a possibility to underestimate a value of k_5. For the quenching process $6^3P_1 \rightarrow 6^3P_0$, Scheer and Fine[4] obtained $k_4(\text{for CO})/k_4(\text{for } N_2)$ to be about 1, while its value was 5.8 in our result. However, absorption of 2537 Å radiation might become smaller as the total pressure in the cell decreased, owing to the pressure dependency of α, as we already discussed. In their experimental condition, the pressure of CO in the cell was lower than that of N_2 by one order of magnitude, and this might cause that the absorption of 2537 Å line for the case of CO in the cell is smaller than that for the case of N_2, and that the apparent value of $k_4(\text{for CO})/k_4(\text{for } N_2)$ become large compared with the true value.

Callear and Oldman[14] assumed that collisional transitions between spin-orbit splitting levels of various atoms are due to the electronic-to-vibrational energy transfer, and found the systematic relations of cross-sections to energy discrepancies between spin-orbit splittings and vibrational quanta of colliding molecules. In the present case, the ratio of cross-sections for $6^3P_1 \rightarrow 6^3P_0$ is,

$$\sigma^2(N_2):\sigma^2(CO):\sigma^2(NO) = 1:5.8:14.$$

Dickens, Linnett, and Sovers[15] calculated this ratio, assuming that the repulsive potential of exponential type, $\exp(-\alpha \mathbf{r})$, where $\mathbf{r}$ means the distance between an atom and a molecule, made a perturbation to the nuclear motion of molecule and the electronic one in $Hg(6^3P_1)$ atom at an instance of collision. Their calculated ratio is 1: 9.8: 250 in the case of $\alpha = 5$ Å^{-1}. Therefore, the quenching process $6^3P_1 \rightarrow 6^3P_0$ of N_2 or CO may be explained by a small perturbation due to the repulsive potential between Hg atom and N_2 or CO molecule, but the mechanism for $Hg(6^3P_1)$—NO collision is far from this explanation. Since NO molecule has an unpaired electron, its collisional process with $Hg(6^3P_1)$ atom must be a strongly non-adiabatic one. This is perhaps a reason why the quenching cross-section of NO for 6^3P_1—6^1S_0 is much larger than that of N_2 or CO.

Conclusion

Conclusions derived in this work are following. (1) The concentration of $Hg(6^3P_1)$ and $Hg(6^3P_0)$ atoms can be determined from the absorption intensity of 4358 and 4047 Å lines emitted from a mercury discharge lamp. Here, the Lambert-Beer rule is not applicable since the spectral half-width of the 4358 or 4047 Å line is five times of the absorption line, *i.e.*, a Doppler half-width at 300°K. (2) The energy transfer mechanism in the system of Ar+Quencher+Hg illuminated with the 2537 Å radiation is: (i) $Hg + h\nu \rightarrow Hg_1^*$, (ii) $Hg_1^* \rightarrow Hg + h\nu$, (iii) $Hg_1^* + Q \rightarrow Hg + Q$, (iv) $Hg_1^* + Q \rightarrow Hg_0^* + Q$, (v) $Hg_0^* + Q \rightarrow Hg + Q$, (vi) $Hg_0^* \rightarrow Hg$ (by collisions with a wall). The cross-sections for the processes, $6^3P_1 \rightarrow 6^1S_0$, $6^3P_1 \rightarrow 6^3P_0$, and $6^3P_0 \rightarrow 6^1S_0$ can be determined as shown in Table 2. (3) Most of the quenching process of $Hg(6^3P_1)$ by a collision with N_2 or CO is $6^3P_1 \rightarrow 6^3P_0$, while the process is mainly $6^3P_1 \rightarrow 6^1S_0$ in a quenching collision with NO. (4) The cross-section for quenching 6^3P_1 to 6^1S_0 is larger by several-fold than that for quenching 6^3P_0 to 6^1S_0. The latter value is not very small except for N_2. (5) A systematic relation of cross-sections for $6^3P_1 \rightarrow 6^3P_0$ to vibrational frequencies can not be found.

14) A. B. Callear and R. J. Oldman, *Trans. Faraday Soc.*, **63**, 2888 (1967).

15) P. G. Dickens, J. W. Linnett, and O. Sovers, *Discuss. Faraday Soc.*, **33**, 52 (1962).

16) G. Karl, P. Kruus, J. C. Polanyi, and I. W. M. Smith, *J. Chem. Phys.*, **46**, 244 (1967).

17) J. R. Bates, *J. Amer. Chem. Soc.*, **54**, 569 (1932).

Note added in proof: It has been reported by Callear and McGurk (*Chem. Phys. Letters.*, **6**, 417 (1970)) with a new flash device that $\sigma^2(^3P_0 \rightarrow {}^1S_0)$ of NO, CO_2, and H_2 are 16.2, 0.033, and 0.95 Å^2 and that these values are much greater than previous estimates by Callear and Williams[5] with the standard flash technique.

Liquid-phase Adsorption from Binary Solutions on Silica Gel. Separation Factors and Orientation of Adsorbed Components on the Surface

Tsutomu KAGIYA, Yūzō SUMIDA, and Toshihiro TACHI
Faculty of Engineering, Kyoto University, Sakyo-ku, Kyoto
(Received September 7, 1970)

The preferential adsorption equilibria of various binary solutions of cyclohexane-aromatic compounds and cyclohexane-cyclic ethers on chromatographic silica gel have been studied at 30°C. On the basis of the assumption that the adsorption is of the Langmuir-type, the separation factors (α) and the numbers of moles in the adsorbed-phase per unit mass of silica gel (n^σ/m) have been calculated. The values of log α correlate well not only with the electron-donating properties of the preferentially-adsorbed components, but also with the powers of the gas-phase adsorption on silica gel and of the liquid-liquid interaction with liquid trimethylsilanol. Moreover, on the basis of the information on n^σ/m, the orientation angles of the adsorbed components on the surface have been evaluated. The adsorption of the aromatic hydrocarbons was nearly flat to the surface, and that of the cyclic ethers, perpendicular.

Theoretical and experimental studies of the gas-phase adsorption on the solid surface have been actively made since the latter half of the 1910's.[1] The chemical structures of the surface have also been made clearer by means of analytical instruments.[2] The liquid-phase adsorption on the solid surface has been mainly studied from the standpoint of the industrial purifications of the organic solvents, the lubricating oils, and so on.[3-6] Little attention has, however, been paid to quantitative discussions of the power of adsorption from solutions on the solid surface and of the orientation of the adsorbed components on the surface, although they have been some qualitative studies.[7-9]

In this investigation, the adsorption equilibria of various binary solutions of cyclohexane-aromatic compounds and cyclohexane-cyclic ethers on chromatographic silica gel have been studied at 30°C. The objectives of the present work are: (1) to discuss the separation factors in connection with the electronic properties of the adsorbed components, (2) to compare the liquid-phase adsorption on silica gel (solid-liquid interaction) with the gas-phase adsorption on silica gel (solid-gas hydrogen bond) and with the liquid-phase coordination to trimethylsilanol (liquid-liquid hydrogen bond), and (3) to evaluate the orientation angles of the components adsorbed on the surface.

Experimental

Materials. Spectro-grade cyclohexane, benzene, toluene, *p*-xylene, chlorobenzene, anisole, dioxolane, 1,4-dioxane, and tetrahydrofuran were used as the adsorbates. These adsorbates were dried with silica gel and were then used without further purification. The adsorbent was silica gel (100−200 mesh) for thin-layer chromatography. The silica gel (dried at 160°C) had the following characteristics; B.E.T.(N_2) area = 383 m^2/g, and pH of aqueous suspension = 7.0.

Adsorption Equilibria. Portions of about 4 g of accurately-weighed silica gel, dried at 160°C, were placed in glass ampoules and degassed for about 6 hr. The ampoules were then filled with about 10 m*l* of a binary solution of the cyclohexane-second solvent of a known composition. The sealed ampoules were placed in a constant-temperature bath controlled at 30 ± 0.2°C and then allowed to equilibrate while being stirred frequently. The analysis of the equilibrium mixture was made with a Shimadzu gas chromatograph, GC-4AIT.

Results and Discussion

In order to discuss quantitatively the adsorption equilibrium of the mixture of the cyclohexane (S_1)-second solvent (S_2) on the silica gel, we must first determine the form of the adsorption isotherm. The selective adsorbed capacity (a_2) of the preferentially-adsorbed component, which is S_2 in each binary solution, can be approximately calculated by the following equation:[8]

$$a_2 = \frac{V_{M2} \cdot n^0}{m} \frac{x_2^0 - x_2^l}{1 - x_2^l} \quad (1)$$

where V_{M2} is the molar volume of S_2 (ml/mol); m, the weight of silica gel (g); n^0, the total number of moles of the original mixture (mol), and x_2^0 and x_2^l, the mole fractions of S_2 in the original liquid and the non-adsorbed liquid at equilibrium respectively. It can be said that Eq. (1) holds over a wide concentration range ($0 < x_2^l < 1$) when the adsorption power of S_2 is so large in comparison with that of S_1 that the surface

1) S. Brunauer, "The Adsorption of Gases and Vapors," Vol. 1, Oxford Univ. Press, Oxford (1945).
2) M. L. Hair, "Infrared Spectroscopy in Surface Chemistry," Marcel Dekker, INC., New York (1967).
3) B.J. Mair and A.F. Forziati, *J. Res. Nat. Bur. Stand.*, **32**, 151, 165 (1944).
4) A. E. Hirschler and T. S. Mertes, *Ind. Eng. Chem.*, **47**, 193 (1955).
5) a) E. Funakubo, *Sekiyu Kagaku Zasshi*, **6**, 759 (1963); b) H. Takisawa, E. Funakubo, and I. Moritani, *Brennstoff-Chem.*, **43**, 7 (1962); c) E. Funakubo, I. Moritani, N. Toshima, and T. Nagai, *Kogyo Kagaku Zasshi*, **66**, 237 (1963).
6) a) T. Yagi, K. Uchimoto, K. Shimizu, and M. Hirahama, *ibid.*, **68**, 326 (1965); b) T. Yagi, K. Shimizu, and K. Uchimoto, *ibid.*, **68**, 331 (1965); c) T. Yagi, K. Shimizu, K. Uchimoto, and S. Maeda, *ibid.*, **68**, 335 (1965).
7) J. L. Olsen, U. S. Patent 2564717 (Sun Oil Co., 1951); R. K. Iler, "The Colloid Chemistry of Silica and Silicates," Cornel Univ. Press, Ithaca, New York (1955), p. 150.
8) S. Eagle and J. W. Scott, *Ind. Eng. Chem.*, **42**, 1287 (1950).
9) D. Hadzi, "Hydrogen Bonding," Pergamon Press, New York (1959), p. 449.

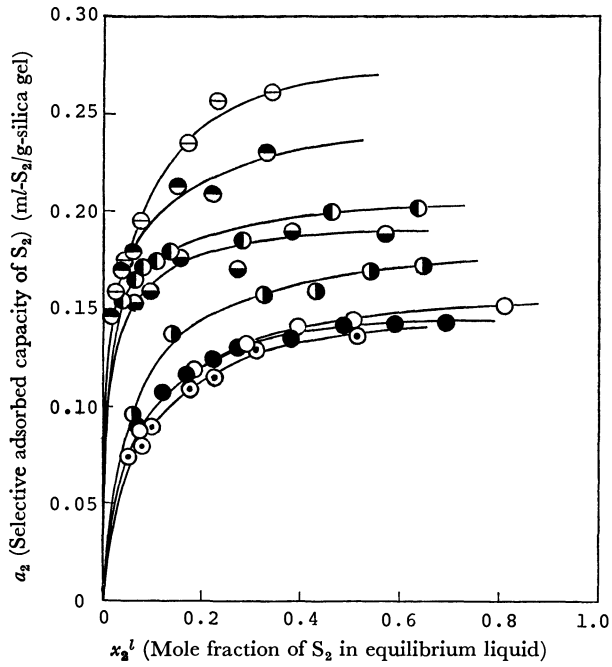

Fig. 1. Adsorption isotherms for cyclohexane (S_1)-second solvent (S_2) mixtures on silica gel.
S_2: ⊙, Chlorobenzene; ○, Benzene; ●, Toluene; ◑ *p*-Xylene; ◐, Anisole; ⊖, Dioxolane; ◓, 1,4-Dioxane; ◒, Tetrahydrofuran.

can be almost entirely covered by S_2, even in a low concentration range of S_2. The above condition was assumed to be satisfied for the present binary solutions.

The adsorption isotherms of a_2 *versus* x_2^l are shown in Fig. 1. In the high concentration range of S_2, it is so difficult to evaluate accurately the very small difference between the x_2^0 and the x_2^l that the experimental error in the a_2 becomes larger. However, there are good linear relationships between x_2^l/a_2 and x_2^l, as is shown in Fig. 2. From these results, we assumed that the adsorption from the mixtures used in this experiment was of the Langmuir-type.[10]

On the other hand, according to Everett,[11] the behavior of a perfect solution in contact with a Langmuir-type adsorbing surface can be discussed on the basis of the following equation:

$$\frac{x_1^l \cdot x_2^l}{n^0 \cdot \Delta x_2^l/m} = \frac{m}{n^\sigma}\left(x_2^l + \frac{1}{\alpha - 1}\right) \qquad (2)$$

where n^σ is the number of moles in the adsorbed-phase; Δx_2^l, the change in the mole fraction of S_2 due to the adsorption, and α, the separation factor for the equilibrium reaction:

$$(S_1)^\sigma + (S_2)^l \rightleftarrows (S_1)^l + (S_2)^\sigma \qquad (3)$$

The above equation (2) rests on the assumptions that; (i) the adsorption is of the Langmuir-type; (ii) α remains constant over the entire concentration range; (iii) the ratio of the activity coefficients ($\gamma_1^l\gamma_2^\sigma/\gamma_1^\sigma\gamma_2^l$) can be approximated to unity, and (iv) the adsorbed components have similar molecular sizes in the adsorbed-phase or the S_2 covers the surface entirely, even in the low concentration range of S_2. Regarding assumption (ii), Yagi *et al.* have reported that the values of α in the *n*-heptane-aromatic hydrocarbon systems are constant over a wide concentration range ($0.2 < x_2^l < 1.0$).[6] Assumption (iii) cannot be checked at present because of the difficulties in measuring the activity coefficients

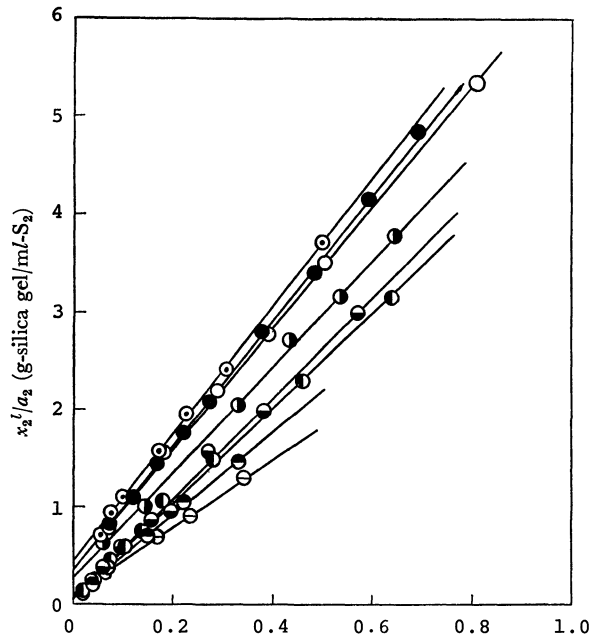

Fig. 2. Langmuir plots for cyclohexane (S_1)-second solvent (S_2) mixtures on silica gel.
S_2: ⊙, Chlorobenzene; ○, Benzene; ●, Toluene; ◑, *p*-Xylene; ◐, Anisole; ⊖, Dioxolane; ◓, 1,4-Dioxane; ◒, Tetrahydrofuran.

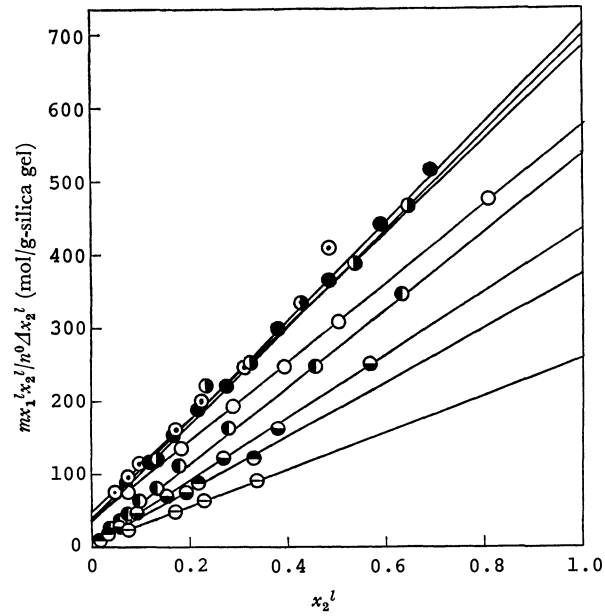

Fig. 3. Everett plots of $mx_1^l x_2^l/n^0 \Delta x_2^l$ *vs.* x_2^l for cyclohexane (S_1)-second solvent (S_2) mixtures on silica gel.
S_2: ⊙, Chlorobenzene; ○, Benzene; ●, Toluene; ◑, *p*-Xylene; ◐, Anisole; ⊖, Dioxolane; ◓, 1,4-Dioxane; ◒, Tetrahydrofuran.

10) Yagi *et al.* pointed out that the adsorption of the *n*-heptane-aromatic hydrocarbon systems on silica gel was of the Freundlich type.[6]

11) D. H. Everett, *Trans. Faraday Soc.*, **60**, 1803 (1964); D. H. Everett, *ibid.*, **61**, 2478 (1965).

Table 1. Separation factors and numbers of moles of adsorbed components in cyclohexane - preferentially adsorbed component mixtures

Preferentially adsorbed components	α	$n^{\sigma}/m \times 10^4$ (mol/g)
Chlorobenzene	14.0_6	15.3_8
Benzene	16.0_3	18.4_8
Toluene	18.5_5	14.8_0
p-Xylene	19.3_8	15.0_4
Anisole	49.2_4	18.9_9
Dioxolane	37.8_0	40.3_2
1,4-Dioxane	63.2_2	27.6_6
Tetrahydrofuran	80.0_2	23.4_5

of the components in the adsorbed-phase.[11-13]

Figure 3 shows the analytical data for various binary solutions plotted according to Eq. (2). The good linear relationships may indicate that the above assumptions are almost satisfied over the concentration range used in this experiment, in spite of the difference in the chemical structures of S_2. The separation factor (α) and the number of moles in the adsorbed-phase per unit mass of adsorbent (n^{σ}/m) are listed in Table 1.[14] It should be noted in Table 1 that the α and n^{σ}/m values of dioxolane, 1,4-dioxane, and tetrahydrofuran are sufficiently large in comparison with those of the aromatic hydrocarbons. This suggests difference in the adsorption behavior, *i.e.*, the adsorption power and the orientation of adsorption.

The Separation Factors and the Electron-donating Properties of Solvents. It may be considered that the values of log α, indicating the power of the nucleophilic adsorption of S_2 on the silica-gel surface covered with cyclohexane (S_1), are related to the electron-donating properties of S_2. The log α of the aromatic hydrocarbons and derivatives are plotted against the ionization potentials (I_p) and the Hammett's substituent constants (σ_p) in Fig. 4.[15] The log α increased linearly as the ionization potentials became smaller and as the electron-relieving properties of the substituents became larger. This suggests that the adsorption of the aromatic hydrocarbons is mainly caused by the π-electrons of the benzene nuclei.[19] The deviation of chlorobenzene from the log α-I_p line may imply that the first ionization of chlorobenzene was not caused by the benzene ring. On the other hand,

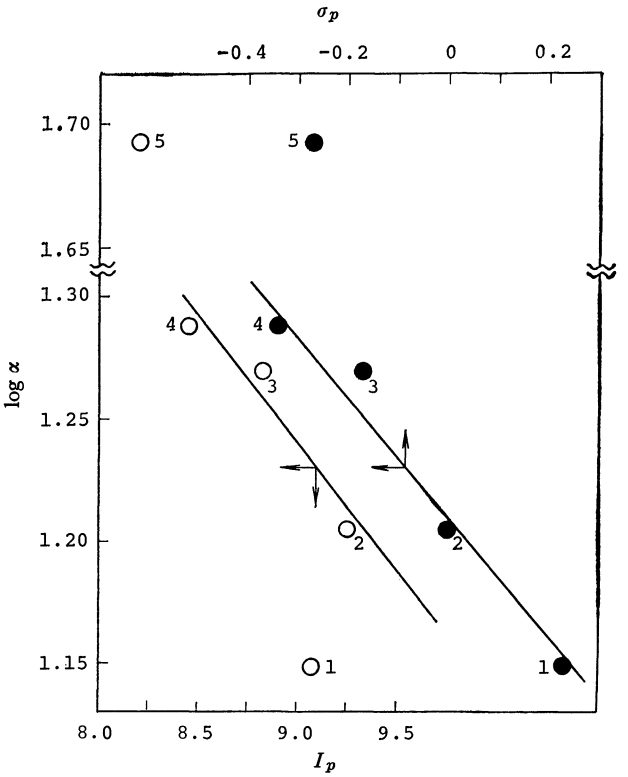

Fig. 4. Relation between log α and ionization potentials (I_p) or Hammett's substituent constants (σ_p) for substituted benzene derivatives.
1, Chlorobenzene; 2, Benzene; 3, Toluene; 4, *p*-Xylene; 5, Anisole.

the declination of anisole from both lines can be inferred to indicate the existence of strong adsorption by the oxygen atom rather than weak adsorption by the benzene nuclei.

The Separation Factors and the Hydrogen-bonding Interaction with the Surface Silanol or Liquid Trimethylsilanol. In order to make clear the liquid-phase adsorption phenomenon, we discussed the separation factors, *i.e.*, the liquid-phase adsorption powers, in connection with the strengths of the solid-gas and liquid-liquid hydrogen-bonding interactions. The strength of the solid-gas hydrogen bond can be evaluated by the IR technique as the difference ($\Delta\nu^S_{OH}$) in the adsorption frequencies of the free O-H band and the bonded O-H band caused by the monolyaer adsorption of gas on silica gel:[20,21]

$$\Delta\nu^S_{OH} = \nu^S_{OH}(\text{free}) - \nu^S_{OH}(\text{bonded})$$

That of the liquid-liquid hydrogen bond can be similarly estimated by means of the frequency shift ($\Delta\nu^L_{OH}$) of liquid trimethylsilanol caused by the solvent, which has a chemical structure (SiO-H bond) analogous to the silanol group on the silica-gel surface:[22]

12) a) S. K. Suri and V. Ramakrishna, *J. Phys. Chem.*, **72**, 1555 (1968); b) S. K. Suri and V. Ramakrishna, *Trans. Faraday Soc.*, **65**, 1690 (1969).
13) B. C.-Y. Lu and R. F. Lama, *ibid.*, **63**, 727 (1967).
14) In the cyclohexane - benzene systems, the value of n^{σ}/m was independent of the adsorption temperature.
15) This order of the adsorption powers of the benzene derivatives agrees well with the experimental results of Brown,[16] Giles *et al.*,[17] and Kiselev *et al.*[18] However, Funakubo *et al.* reached the reverse conclusion on the basis of their findings on the ultraviolet adsorption spectrum of the adsorbed-phase.[5b]
16) H. C. Brown, *J. Amer, Chem. Soc.*, **74**, 3570 (1952).
17) C. H. Giles and R. B. Mckay, *J. Chem. Soc.*, **1961**, 58.
18) G. A. Galkin, A. V. Kiselev, and V. I. Lygin, *Trans. Faraday Soc.*, **60**, 431 (1964).
19) N. Okuda, *Nippon Kagaku Zasshi*, **82**, 1118 (1961).
20) a) V. Ya. Davydov, A. V. Kiselev, and V. I. Lygin, *Dokl. Akad. Nauk, SSSR*, **147**, 131 (1962); b) L. H. Little, "Infrared Spectra of Adsorbed Species," Academic Press, London-New York (1966), p. 274.
21) The silanol O–H frequency shifts on the silica-gel surface depend slightly on the surface coverage; they grow considerably with the surface coverage up to a monolayer, while on further adsorption they change very slowly.[18]
22) a) T. Kagiya, Y. Sumida, and T. Tachi, This Bulletin, **43**, 3716 (1970); b) T. Kagiya, Y. Sumida, T. Watanabe, and T. Tachi, *ibid.*, **44**, 923 (1971).

TABLE 2. EFFECTIVE MOLECULAR OCCUPANCIES AND ORIENTATION ANGLES OF PREFERENTIALLY ADSORBED COMPONENTS ON SILICA GEL

Preferentially adsorbed components	A_2 (Å²/molecule)	d_2[a] (Å)	h_2[a] (Å)	θ (degree)	A_2[b] (Å²/molecule)	S[b] (m²/g)
Chlorobenzene	41.3_4	5.45_9	7.34_2	3	30.9_1	$286._4$
Benzene	34.4_1	5.45_9	6.30_3	0	27.9_2	$310._8$
Toluene	42.9_6	5.45_9	7.53_8	5	31.4_6	$280._5$
p-Xylene	42.2_8	5.45_9	8.74_5	11	34.7_3	$314._7$
Anisole	33.4_8	5.45_9	7.71_5	17	31.9_5	$365._5$
Dioxolane	15.7_7	5.37_8	5.11_5	77	23.8_0	$578._1$
1,4-Dioxane	22.9_9	5.38_3	6.21_6	90	27.1_5	$452._4$
Tetrahydrofuran	27.1_1	5.65_0	5.37_1	86	26.0_0	$367._2$

a) Values calculated from Eq. (6).
b) Values calculated from the assumption of the spherical molecules for the preferentially adsorbed components.

$$\Delta\nu^L_{OH} = \nu^L_{OH}(\text{bonded by benzene}) - \nu^L_{OH}(\text{bonded})$$

where benzene is conveniently employed as a reference solvent. As is shown in Fig. 5, good correlations between logα and $\Delta\nu^S_{OH}$ or $\Delta\nu^L_{OH}$ were obtained; that is, the values of logα increased linearly with the increase in the $\Delta\nu^S_{OH}$ or the $\Delta\nu^L_{OH}$. From the relationships, we may conclude that the liquid-phase adsorption on silica gel is mainly governed by the proton-accepting properties of solvents. A comparison of $\Delta\nu^S_{OH}$ and $\Delta\nu^L_{OH}$ shows a large proton-donating property of surface silanol.[22]

The Orientation Angles of the Components Adsorbed on the Surface. According to Schay and Nagy,[12b,23] if the effective molecular occupancies (A) of the two components in the adsorbed-phase are known, the total surface area per unit mass of solid (S) is given by the following equation:

$$S = N\left(\frac{n_1^\sigma}{m}A_1 + \frac{n_2^\sigma}{m}A_2\right) \quad (4)$$

where n_1^σ and n_2^σ are, respectively, the number of moles of S_1 and S_2, and where N is the Avogadro number. When the α of S_2 is so large that the surface is preferentially covered with S_2, or when $A_1=A_2$, Eq. (4) can be approximated with Eq. (5):

$$S = \frac{n^\sigma}{m}A_2N \quad (5)$$

The above conditions can be considered to be satisfied for the binary mixtures in this paper. By assuming that the specific surface area is equal to the B.E.T. (N_2) area, the effective molecular occupancies were calculated from Eq. (5); they are summarized in the second column of Table 2. The values of A in the sixth column of Table 2 are calculated from $A=(V_M/N)^{2/3}$.[12b,24] This calculation rests on the assumption that the adsorbed molecules are cube-shaped and have the same packing on the surface as the molecules of the adsorbed liquid have in the neat solution. The specific surface area, listed in the last column of Table 2, was calculated with the n^σ/m values and the A_2 values obtained with the latter method. It appears that the S values calculated by the above method yield lower values for the aromatic compounds and higher values for the cyclic ethers in comparison with the B.E.T. (N_2) area of 383 m²/g for the adsorbent.[12] This disagreement in the areas provides negative support for the assumption of the spherical molecules in the adsorbed phase and suggests the orientation of the adsorbed components on the surface.

We then tried to estimate the orientation of the adsorption by the use of the effective molecular occupancy. If the preferentially-adsorbed molecules with six- or five-membered rings are cylindrical (diameter=d(Å) and height=h(Å)), then we can approximately obtain the following equation:

$$\pi\left(\frac{d}{2}\right)^2 h\cdot N = V_M \quad (6)$$

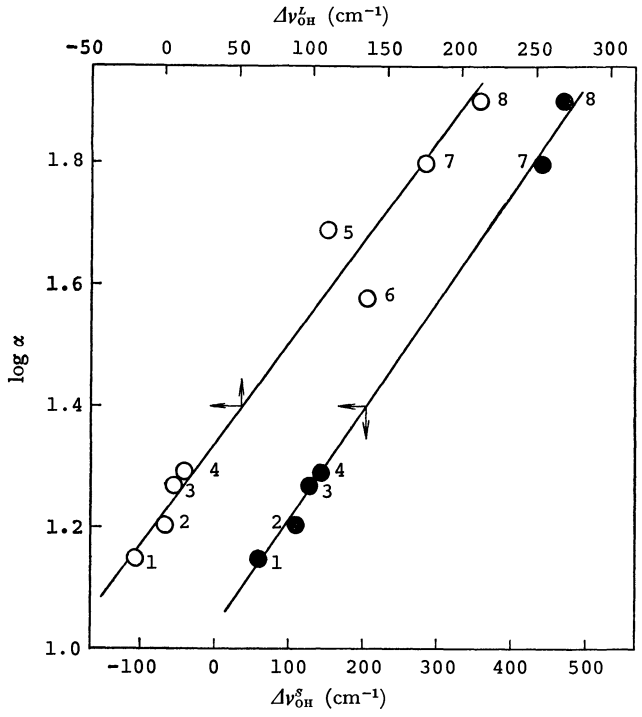

Fig. 5. Relationship between log α and O–H frequency shifts ($\Delta\nu^S_{OH}$) of silica gel surface silanol by gas-phase adsorption or O–H frequency shifts ($\Delta\nu^L_{OH}$) of trimethylsilanol by solvents.
1, Chlorobenzene; 2, Benzene; 3, Toluene; 4, *p*-Xylene; 5, Anisole; 6, Dioxolane; 7,1,4-Dioxane; 8, Tetrahydrofuran.

23) a) G. Schay, L. Gy. Nagy, and T. Szekrenyesy, *Periodica Polytechnica*, **6**, 91 (1962); b) L. Gy. Nagy, *ibid.*, **7**, 75 (1963).

24) F. Paneth and W. Vorwerk, *Z. Phys. Chem.*, **101**, 445 (1922).

Between the diameter and the height, these relations may hold; $d=h\cdot\cos 30°$ for benzene and 1,4-dioxane, and $h=d\cdot\cos 18°$ for tetrahydrofuran and dioxolane. By substituting the above relations into Eq. (6), the diameters and the heights of S_2 molecules were calculated. The diameters of the other aromatic derivatives were taken to be that of benzene.

When the preferentially-adsorbed component adsorbs with an orientation angle (θ) on the surface, it should be given by the following equation:

$$A_2 = \pi\left(\frac{d}{2}\right)^2 \sin\theta + hd\cdot\cos\theta \qquad (7)$$

The values of θ obtained are also listed in the fifth column of Table 2. It is obvious from Table 2 that the adsorptions of all the aromatic compounds except anisole are nearly flat to the surface and that those of the cyclic ethers are nearly perpendicular (Fig. 6-a,b). The orientation angle ($\theta=77°$) for dioxolane may be understood as the simultaneous adsorption by two oxygen atoms in a dioxolane molecule, although it cannot be exactly illustrated. If the adsorption of anisole is caused only by the interaction force between the oxygen atom in an anisole molecule and the surface, the orientation angle should be nearly equal to 30°. On the contrary, for the adsorption due to the benzene nuclei, it should be nearly zero. Therefore, it can be considered that the orientation angle ($\theta=17°$) obtained for anisole suggests the existence of the two kinds of

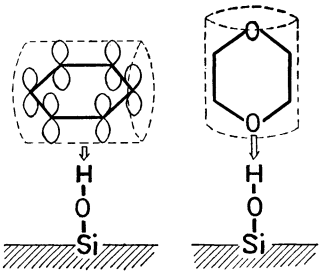

(a) Benzene (b) 1,4-Dioxane

Fig. 6. Adsorption models of benzene and 1,4-dioxane on silica gel.

interactions, that of the strong adsorption by the oxygen atom and that of the weak adsorption by the benzene nuclei.[25] This consideration also agrees with the discussion of the large deviation of anisole from both straight lines of log α *versus* I_p and σ_p. This conclusion corresponds well to the spectroscopic data that the two unassociated O-H vibrational bands of trimethylsilanol appear in the anisole solution; the one showing the large shift and intensity is assigned to the O-H band due to the hydrogen bond formed by the lone-pair-electrons of ether oxygen, and the other, showing the small shift and intensity, to that formed by the benzene nuclei.[22a]

25) M. J. D. Low and J. A. Cusumano, *Can. J. Chem.*, **47**, 3906 (1969).

Ultrasonic and Thermodynamic Study on Solute-Solvent Interaction. Binary Mixtures of *t*-Butyl Chloride, *t*-Butyl Bromide and 1,1,1-Trichloroethane with Carbon Tetrachloride, Benzene and *p*-Xylene

Osamu KIYOHARA and Kiyoshi ARAKAWA
Research Institute of Applied Electricity, Hokkaido University, Sapporo
(Received September 7, 1970)

Sound velocity and density of binary mixtures of *t*-butyl chloride (*t*BC), *t*-butyl bromide (*t*BB), and 1,1,1-trichloroethane (TCE) with carbon tetrachloride (CT), benzene (B), and *p*-xylene (*p*X) were measured at temperatures, 25 and 35°C. The excess molar volume and excess compressibility of these systems were calculated. The temperature dependency of excess volume was negative for aromatic solutions and positive for CT solutions. The temperature coefficients of excess compressibility were negative for all systems. The relation between thermodynamic properties and intermolecular interactions in these systems were discussed. Two systems, B-TCE and CT-TCE, were found to be nearly ideal. The solute-solvent interactions in CT-*t*BC and *t*BC-TCE systems were found to be more attractive than in other systems.

Adiabatic compressibility of binary mixtures has been studied by a number of investigators using ultrasonic methods.[1-8] Though considerable data are found in literature, there are not many systematic studies on the dependency of compressibility upon the interaction between unlike molecules. It has been pointed out by several workers that the excess thermodynamic functions are sensitively dependent not only on the difference in intermolecular forces, but also on the difference in size of molecules.[9,10] It is obvious that the study of excess compressibility and excess molar volume gives important information on intermolecular forces determining the properties of mixtures.

The purpose of the present study is to investigate the solute-solvent interaction from ultrasonic velocity and density data, using the statistical theory of solutions.[9]

In this study, *t*-butyl chloride, *t*-butyl bromide, and 1,1,1-trichloroethane were used as solutes which are polar and nearly spherical in molecular shape, and carbon tetrachloride, benzene and *p*-xylene as solvents. Carbon tetrachloride was chosen as a typical solvent which is spherical in molecular shape.

Measurements of sound velocity and density were carried out at 25 and 35°C for nine binary mixtures.

Experimental

Samples of carbon tetrachloride (CT),[11] benzene (B), *p*-xylene (*p*X), *t*-butyl chloride (*t*BC), *t*-butyl bromide (*t*BB), and 1,1,1-trichloroethane (TCE) are guaranteed reagents obtained from Wako Pure Chemical Industry Co. Ltd., and used after purification.[12] Boiling points agreed with the values in literature. The purity of samples was examined by the measurements of density at 25°C.

Sample	Observed values of density at 25°C	Literature values[13]
Carbon tetrachloride	1.58446	1.58434
Benzene	0.87361	0.87362
p-Xylene	0.85663	0.85669
t-Butyl chloride	0.8356_1	0.8354[a]
t-Butyl bromide	1.2131_1	1.2132_1[a]
1,1,1-Trichloroethane	1.3293_3	1.3293_5[a]

a) Interpolated values

The sound velocity was measured at 3 Mc. The interferometer used is described in a previous paper.[7] The results are accurate within 0.3 m/sec. Density measurements were made using a pycnometer of the usual type. Its accuracy is within 0.01%. *t*-Butyl bromide is fairly unstable at ordinary temperatures and should be treated carefully. Thus, the accuracy of the sound velocity and density in the systems including *t*-butyl bromide is within 0.5 m/sec and 0.03%, respectively.

Results

The density d and sound velocity v were measured over the whole concentration range at 25 and 35°C for nine systems: CT-*t*BC, CT-*t*BB, CT-TCE, B-*t*BC, B-*t*BB, B-TCE, *p*X-*t*BC, *p*X-TCE, and *t*BC-TCE.

Excess Molar Volume on Mixing. Excess molar volume V^E was calculated from the density data, and its dependency of mole fraction is shown in Figs. 1(a)-(i) for each system. The abscissa x represents the mole fraction of solutes. The accuracy of V^E is about ± 0.02 cc/mole, except for that of *t*-butyl bromide solutions, which is ± 0.05 cc/mole.

1) G. A. Holder and E. Whalley, *Trans. Faraday Soc.*, **58**, 2108 (1962).
2) H. Sackmann and A. Boczek, *Z. Phys. Chem.*, **29**, 329 (1961).
3) E. A. Moelwyn-Hughes and P. L. Thorpe, *Proc. Roy. Soc.* (London), **A268**, 574 (1964).
4) K. C. Reddy, S. V. Subrehmanyan, and J. Bhmasenachar, *J. Phys. Soc. Japan*, **19**, 559 (1964).
5) R. J. Fort and W. R. Moore, *Trans. Faraday Soc.*, **61**, 2102 (1965).
6) L. A. Staveley, W. R. Tupman, and K. R. Hart, *ibid.*, **51**, 323 (1955).
7) O. Kiyohara and K. Arakawa, This Bulletin, **43**, 3037 (1970).
8) G. H. Findenegg and F. Kohler, *Trans. Faraday Soc.*, **63**, 870 (1967); E. Wilhem, R. Schano, G. Becker, G. H. Findenegg, and F. Kohler, *ibid.*, **65**, 1443 (1969).
9) K. Arakawa and O. Kiyohara, This Bulletin **43**, 975 (1970).
10) J. S. Rowlinson, "Liquids and Liquid Mixtures," 2nd ed., Butterworth, London (1969).
11) Abbreviations are used for each substance.
12) J. A. Riddick and E. E. Toops, Jr., "Organic Solvents," Vol. II, 2nd edit., Interscience Publishers, Inc., New York (1967).
13) J. Timmermans, "Physicochemical Constants of Pure Organic Compounds," Elsevier Publishing Co., Amsterdam, The Netherlands, Vol. I (1950) and Vol. II (1965).

All the systems except CT-TCE, B-*t*BB, B-TCE, and *p*X-TCE give negative values of V^E. The V^E *vs.* mole fraction curves in B-*t*BB and B-TCE systems are of nearly inverse S type, and that for CT-TCE system positive. The temperature dependency of V^E is negative for B-*t*BC, B-TCE, *p*X-*t*BC, and *p*X-TCE, and positive for CT-*t*BC and *t*BC-TCE systems. However, the temperature coefficients are very small, and those for CT-*t*BB, CT-TCE, and B-*t*BB are zero within experimental error.

Mathot and Desmyter[14] measured the V^E of CT-*t*BC and CT-TCE systems and obtained −0.26 cc/mol and 0.25 cc/mole for equimolar mixtures at 0°C, respectively. The values we obtained are −0.36 and 0.04 cc/mol for CT-*t*BC and CT-TCE at 25°C, respectively. There is a discrepancy between these values, which is larger in CT-TCE system.

The values of V^E can be represented by

$$V^E = x(1-x)\sum_{t=0}^{2} A_t \cdot (1-2x)^t \qquad (1)$$

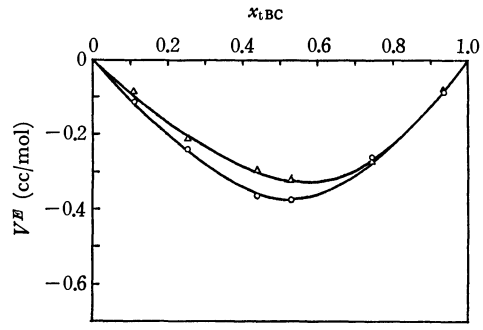

Fig. 1. 1(a). Excess molar volume of CT-*t*BC system.
○ 25°C, △ 35°C

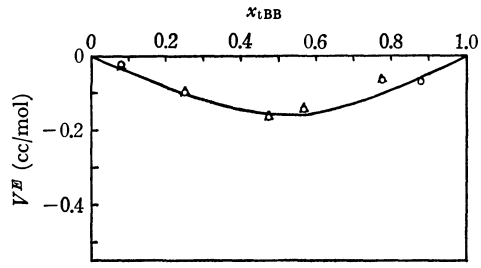

Fig. 1(b). Excess molar volume of CT-*t*BB system.
○ 25°C, △ 35°C

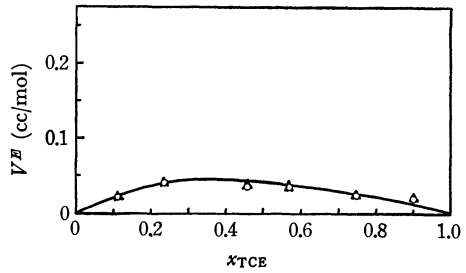

Fig. 1(c). Excess molar volume of CT-TCE system.
○ 25°C, △ 35°C

14) V. Mathot and A. Desmyter, *J. Chem. Phys.*, **21**, 782 (1953).

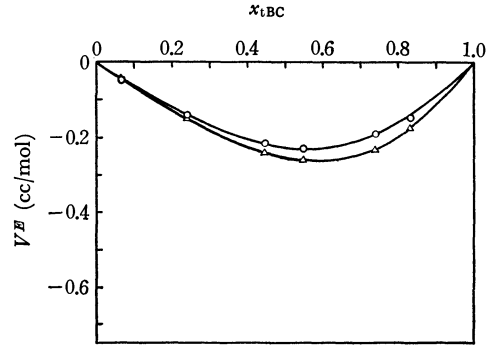

Fig. 1(d). Excess molar volume of B-*t*BC system.
○ 25°C, △ 35°C

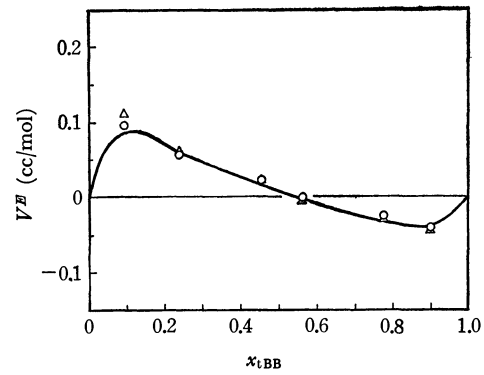

Fig. 1(e). Excess molar volume of B-*t*BB system.
○ 25°C, △ 35°C

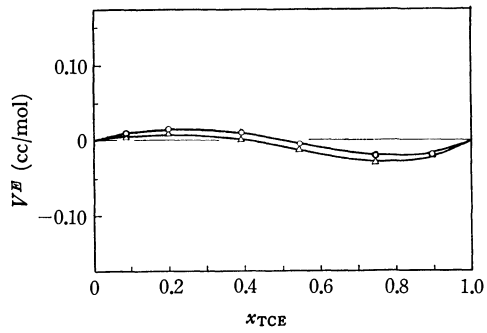

Fig. 1(f). Excess molar volume of B-TCE system.
○ 25°C, △ 35°C

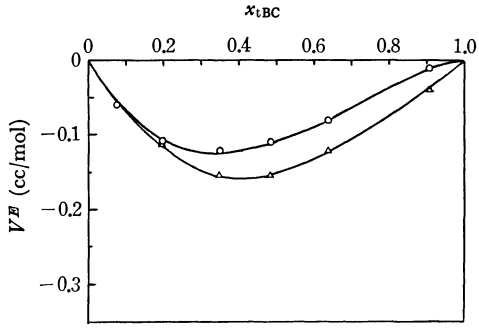

Fig. 1(g). Excess molar volume of *p*X-*t*BC system.
○ 25°C, △35°C,

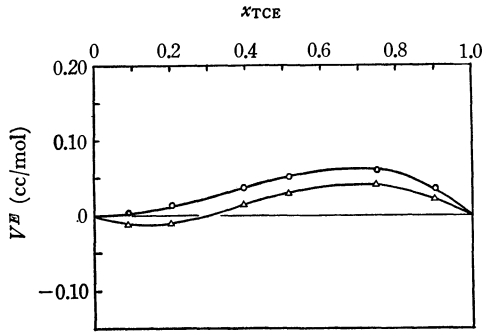

Fig. 1(h). Excess molar volume of *p*X-TCE system.
○ 25°C, △ 35°C

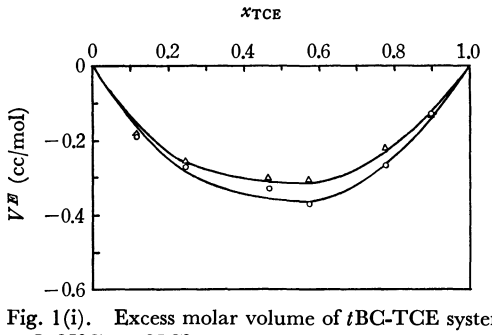

Fig. 1(i). Excess molar volume of *t*BC-TCE system.
○ 25°C, △ 35C°

where x is the mole fraction of solute. The coefficients A_i, which were determined for each system by the method of least squares, are given in Table 1(a).

TABLE 1(a). VALUES OF THE COEFFICIENTS A_i

System	T (°C)	A_0	A_1 (cc/mol)	A_2
CT-*t*BC	25	−1.449	0.067	0.453
	35	−1.278	0.275	0.317
CT-*t*BB	25	−0.567	0.105	0.204
	35	−0.379	0.262	0.138
CT-TCE	25	0.146	0.010	0.154
	35	0.163	0.019	0.139
B-*t*BC	25	−0.903	0.191	−0.069
	35	−1.022	0.370	0.051
B-*t*BB	25	0.019	0.802	0.443
	35	−0.012	0.921	0.602
B-TCE	25	0.003	0.225	−0.109
	35	−0.033	0.209	−0.110
*p*X-*t*BC	25	−0.428	−0.418	−0.069
	35	−0.587	−0.239	−0.100
*p*X-TCE	25	0.199	−0.205	0.036
	35	0.111	−0.235	−0.070
*t*BC-TCE	25	−1.436	−0.212	−0.296
	35	−1.248	−0.212	−0.507

Sound Velocity. The values of sound velocity in pure components are given in column 3 of Table 2, together with literature values in the last column. The sound velocity of all these systems deviates negatively from linear addivity in mole fraction, and the deviation decreases with the rise of temperature. The sound velocity *vs.* concentration curves for CT-TCE, B-TCE, *p*X-TCE, and *t*BC-TCE systems at 25°C are shown in Fig. 2.

Adiabatic Compressibility. The values of adiabatic compressibility calculated from the values of v and d by means of the equation

$$\kappa_s = 1/(v^2 d) \tag{2}$$

are given in column 4 of Table 2 for pure liquids.

The excess compressibility $(V\kappa_s)^E$ is defined by means of the equation

$$(V\kappa_s)^E = V\kappa_s - (V_{AA}\kappa_{s,AA}x_A + V_{BB}\kappa_{s,BB}x_B) \tag{3}$$

where V, V_{AA} and V_{BB} are the molar volume of solution and pure liquids for species A and B, respectively, and $\kappa_{s,AA}$ and $\kappa_{s,BB}$ are the adiabatic compressibility of pure liquids A and B, respectively. The values of $(V\kappa_s)^E$ are shown in Figs. 3(a)—(i) for each system. $(V\kappa_s)^E$ becomes linear in mole fraction if a system behaves like an ideal solution.[7]

TABLE 1(b). VALUES OF THE COEFFICIENTS B_i

System	T (°C)	B_0	B_1 (bar^{-1} × 10^{-6})	B_2
CT-*t*BC	25	−23.180	4.040	−0.668
	35	−25.268	2.530	1.961
CT-*t*BB	25	− 8.098	0.291	0.200
	35	—	—	—
CT-TCE	25	1.546	−1.770	1.613
	35	1.004	−0.470	−0.470
B-*t*BC	25	−28.104	1.333	−1.015
	35	−33.208	0.988	−1.384
B-*t*BB	25	− 9.176	−0.658	−0.453
	35	−11.099	−0.944	−1.020
B-TCE	25	− 0.691	−0.370	−1.182
	35	− 3.188	−1.464	−2.755
*p*X-*t*BC	25	− 9.962	1.982	−1.942
	35	−13.564	1.510	−0.602
*p*X-TCE	25	5.878	−1.089	0.061
	35	5.902	0.469	−1.044
*t*BC-TCE	25	−17.703	−1.475	1.502
	35	−20.784	−1.032	0.772

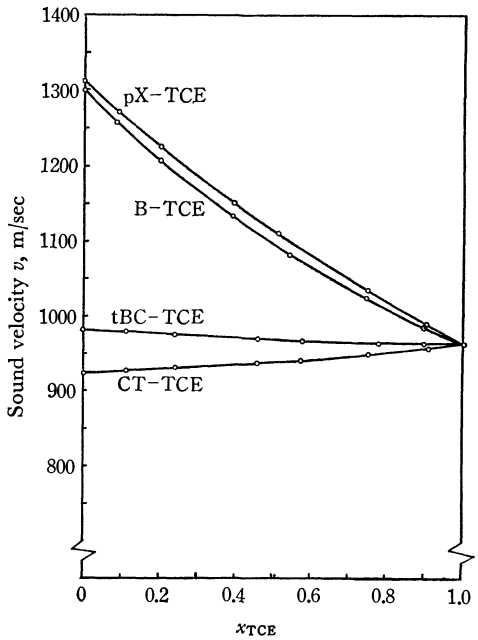

Fig. 2. Sound velocity of B-TCE, CT-TCE, *p*X-TCE and *t*BC-TCE systems.

Table 2. Sound velocity and compressibility of pure liquids

Substance	T (°C)	v (m/sec)	κ_s (bar$^{-1}\times 10^{-6}$)	Lit. values of sound velocity
Benzene	25	1299.1	67.8_3	1299,[a] 1307,[b] 1295[c]
	35	1251.3	74.0_1	1253,[a]
Carbon tetrachloride	25	921.2	74.3_7	923,[d] 927[b]
	35	890.4	80.6_0	892[d]
p-Xylene	25	1309.6	68.0_7	
	35	1268.0	73.3_5	
t-Butyl chloride	25	981.1	124.3_3	984[e]
	35	940.3	137.3_9	
t-Butyl bromide	25	903.$_3$	101.0_3	
	35	868.$_4$	110.7_5	
1,1,1-Trichloroethane	25	963.4	81.0_5	
	35	930.1	88.0_5	

a) A. Van Itterbeek and A. De Bock, *Physica*, **14**, 609 (1949).
b) Ref. 5.
c) D. D. Deshpande and L. G. Bhatgadde, *J. Phys. Chem.*, **72**, 261 (1968).
d) R. T. Legemann, D. R. McMillan, and W. E. Woolf, *J. Chem. Phys.*, **17**, 369 (1949).
e) G. W. Willard, *J. Acous. Soc. Amer.*, **19**, 235 (1947).

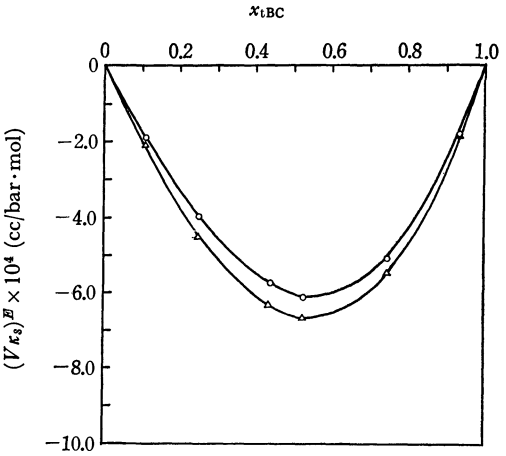

Fig. 3.(a). $(V\kappa_s)^E$ for CT-*t*BC system.
○ 25°C, △ 35°C

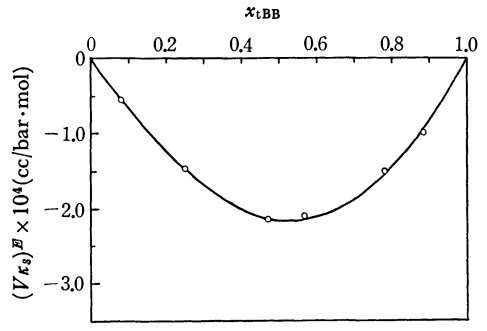

Fig. 3(b). $(V\kappa_s)^E$ for CT-*t*BB system at 25°C.

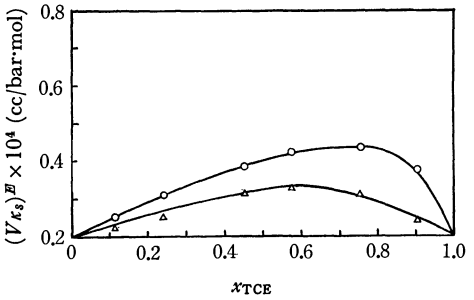

Fig. 3(c). $(V\kappa_s)^E$ for CT-TCE system.
○ 25°C, △ 35°C

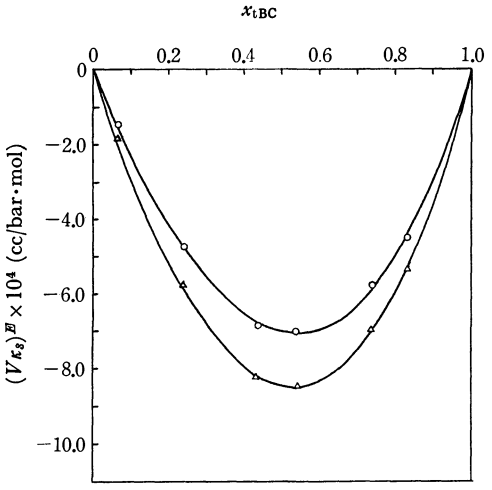

Fig. 3(d). $(V\kappa_s)^E$ for B-*t*BC system.
○ 25°C, △ 35°C

The $(V\kappa_s)^E$ values of all systems except CT-TCE have negative values and their dependency on temperature is negative for all systems except *p*X-TCE system, where it is zero within experimental error. The κ_s^E *vs.* mole fraction curves fit into the following equation.

$$\kappa_s^E = x(1-x)\sum_{i=0}^{2} B_i \cdot (1-2x)^i \qquad (4)$$

Coefficients B_i are given in Table 1(b). The accuracy of κ_s^E is within 0.05%, and that for *t*-butyl bromide solutions within 0.1%.

Discussion

The curves of excess volume with respect to mole fraction differ from those of excess compressibility.

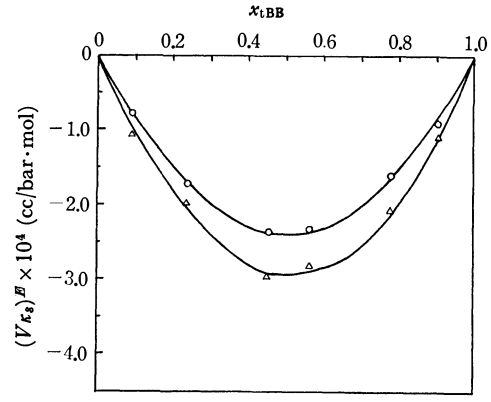

Fig. 3(e). $(V\kappa_s)^E$ for B-*t*BB system.
○ 25°C, △ 35°C

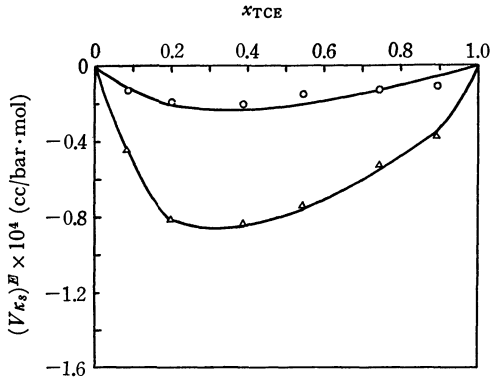

Fig. 3(f). $(V\kappa_s)^E$ for B-TCE system.
○ 25°C, △ 35°C

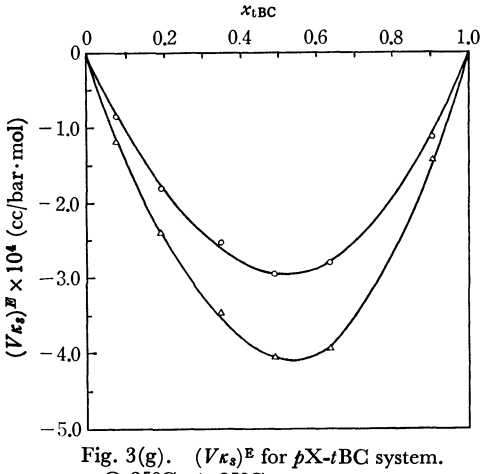

Fig. 3(g). $(V\kappa_s)^E$ for *p*X-*t*BC system.
○ 25°C, △ 35°C

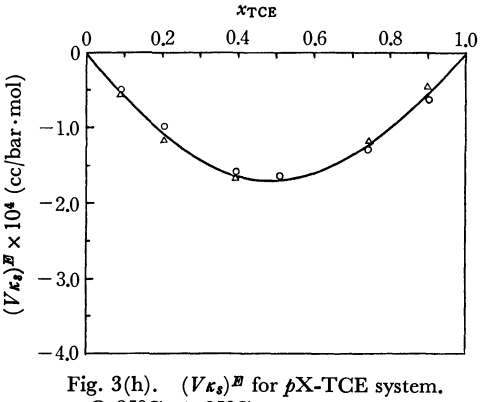

Fig. 3(h). $(V\kappa_s)^E$ for *p*X-TCE system.
○ 25°C, △ 35°C

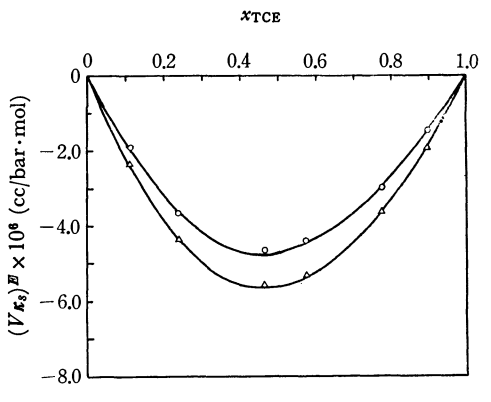

Fig. 3(i). $(V\kappa_s)^E$ for *t*BC-TCE system.
○ 25°C, △ 35°C

The latter are more symmetrical except for CT-TCE system. In particular, asymmetry of V^E is marked in aromatic systems.

It is seen that the temperature dependency of V^E has negative coefficients for aromatic solutions and positive ones for CT solutions, although the temperature coefficients are very small for all systems. The general trend in temperature dependency of κ_s^E and $(V\kappa_s)^E$ seems to be negative.

The interaction between unlike molecules in these systems seems to be ascribed to dispersion forces and dipole-induced dipole interactions, considering the chemical nature of the species in these systems. Recently, Fort, Jr., and Lindstrom[15] reported that there is no complex formation.

Molecular size V^* for pure liquids was obtained from the values of molar volume V and thermal expansion coefficient α, by the equation[9].

$$V^* = V \times \left[(1+\alpha T) \Big/ \left(1+\frac{4}{3}\alpha T\right) \right]^3. \tag{5}$$

The values of these parameters are listed in Table 3, together with dipole moments of solute.

We showed that the V^E was expressed as the sum of two terms[9]: the one V^E_{size} associated with the size difference of molecules and the other $V^E_{int.}$ associated with the interaction forces between molecules. Thus, for a mixture composed of species A and B, we have

$$V^E = V^E_{size} + V^E_{int.} \tag{6}$$

and

$$V^E_{size} = [(V^*_A - V^*_{AA})x_A + (V^*_B - V^*_{BB})x_B] \times [1-(9RT/\pi)(V^0/W_m)]^{-1} \tag{7}$$

where $W_m = N^2 \times (\gamma\varepsilon_A{}^* r_A{}^{*3} x_A + \gamma\varepsilon_B{}^* r_B{}^{*3} x_B)$, $V^* = N\beta r^{*3}$, $V^\circ = V_{AA}x_A + V_{BB}x_B$, and pure components are denoted by AA and BB. γ, β, r^*, and ε^* have the same meaning as in the previous paper.[9] r^* and ε^* are related to those of pure liquids by means of the equations

$$r^*_A = r^*_{AA}x_A + r^*_{AB}x_B, \quad r^*_B = r^*_{AB}x_A + r^*_{BB}x_B,$$
$$r^*_{AB} = (r^*_{AA} + r^*_{BB})/2 \tag{8}$$

and

$$\varepsilon^*_A = \varepsilon^*_{AA}x_A + \varepsilon^*_{AB}x_B, \quad \varepsilon^*_B = \varepsilon^*_{AB}x_A + \varepsilon^*_{BB}x_B \tag{9}$$

The relation of molar volume and interaction energy

15) R. C. Fort, Jr., and T. R. Lindstrom, *Tetrahedron*, **23**, 3227 (1967).

Table 3. Molecular parameters of pure liquids (25 °C)

Substance	V (cc/mol)	$\alpha \times 10^3$ (deg.$^{-1}$)	V^* (cc/mol)	μ (D)
Benzene	89.41	1.223[a]	69.22	
Carbon tetrachloride	97.09	1.226[b]	75.13	
p-Xylene	123.93	1.013[c]	99.11	
t-Butyl chloride	110.78	1.427[c]	83.34	2.12[d]
t-Butyl bromide	112.91	1.275[c]	86.75	2.19~2.21[e]
1,1,1-Trichloroethane	100.36	1.245[c]	77.44	1.79[d]

a) S. E. Wood and J. P. Brusi, *J. Amer. Chem. Soc.*, **65**, 189 (1943).
b) E. L. Washington and R. Battino, *J. Phys. Chem.*, **72**, 4496 (1968).
c) Estimated from the data on densities at various temperature summarized in Ref. 13.
d) Ref. 12.
e) A. L. McClellan, "Tables of Experimental Dipole Moments," W. H. Freeman Co., San Francisco and London (1963).

for a mixture is given by

$$W_m = (9RT/2\pi) \times [V^2/(V-V^*)] \quad (10)$$

where $V^* = V_A^* x_A + V_B^* x_B$ and V is molar volume of solution, and that for a pure liquid A by

$$N^2 \gamma \varepsilon_{AA}^* r_{AA}^{*3} = (3RT/2\pi) \times [V_{AA}^{4/3}(V_{AA}^{1/3} - V_{AA}^{*1/3})] \quad (11)$$

The value of θ, which is associated with intermolecular interaction energy ε_{AB}^*, is defined as follows.

$$\theta = [\varepsilon_{AB}^* - (\varepsilon_{AA}^* + \varepsilon_{BB}^*)/2]/\varepsilon_{AA}^* \quad (12)$$

The values ε_{AB}^* for equimolar mixtures are calculated from the observed values of V^E and the molecular parameters in Table 3, using Eqs. (6)—(11). The values of θ are determined from ε_{AB}^* and are given in Table 4. $\theta_{disp.}$, obtained using Bertholet's relation $\varepsilon_{AB}^* = (\varepsilon_{AA}^* \cdot \varepsilon_{BB}^*)^{1/2}$, and the values of V_{size}^E and $V_{int.}^E$ obtained for equimolar mixtures are also listed.

We see that the values of θ are negative and smaller than those of $\theta_{disp.}$, except for the systems CT-*t*BC and *t*BC-TCE which has positive values of θ. All the systems except these two have positive values of $V_{int.}^E$.

It is seen that the values of θ decrease in the order CT, B, and *p*X as solvents for a common solute and those of $V_{int.}^E$ increase in this order. The results are consistent with the idea that the attractive interaction between solute and solvent becomes stronger in the order *p*X, B, and CT as solvents.[9]

Carbon tetrachlordie, *t*-butyl chloride, trichloroethane, and *t*-butyl bromide are similar chemically. They are regarded as derivatives of CH_4: in the first three compounds H atoms of CH_4 are replaced by Cl and CH_3 groups and in the last by Br and CH_3 groups. The molecular shape of these four compounds are nearly spherical. Carbon tetrachloride is non-polar and the other three have the dipole moment about 2D as given in Table 3.

In CT-TCE system, the observed values of V^E and $(V\kappa_s)^E$ are one order smaller than those in other systems, and the magnitude of θ is negative and small. Similar situations are found in B-TCE systems. Thus, it is concluded that these two systems are nearly ideal. Turner *et al.*[16] reached the same conclusion from the measurements of dielectric relaxation times, boiling point diagram and heat of mixing of B-TCE system. From the fact that CT-B system is nearly ideal,[9] it can be said that all binary mixtures consisting of CT, B, and TCE are regarded as ideal solutions.

As seen in Table 4, the observed values of V^E and $(V\kappa_s)^E$ in the systems including *t*BC are negative and comparatively larger in their absolute magnitude, compared with those in the systems including TCE. Moreover, the values of θ in CT-*t*BC and TCE-*t*BC systems are positive, which is in sharp contrast to the situation in CT-TCE and B-TCE systems. This means that the solute-solvent interactions in CT-*t*BC and *t*BC-TCE systems are more attractive than those in other systems.

The molecules of *t*BC and TCE have structures in which methyl groups and chlorine atoms are exchanged and have nearly the same dipole moments.

Table 4. Thermodynamic quantities of equimolar mixtures (25 °C)

System	$V^E_{obs.}$	V^E_{size} (cc/mol)	$V^E_{int.}$	$(V\kappa_s)^E \times 10^4$ (cc/bar·mol)	θ (10^{-3})	$\theta_{disp.}$
CT-*t*BC	−0.36	−0.10	−0.26	-6.0_0	5.7	−0.5
CT-*t*BB	−0.14	−0.20	0.06	-2.1_2	−1.0	−0.0
CT-TCE	0.04	−0.01	0.05	0.3_8	−2.3	−0.0
B-*t*BC	−0.23	−0.31	0.08	-7.0_1	−7.7	−0.5
B-*t*BB	0.00	−0.46	0.46	-2.3_2	−16.5	−0.0
B-TCE	0.00	−0.11	0.11	-0.1_6	−4.2	−0.0
*p*X-*t*BC	−0.11	−0.31	0.20	-2.9_2	−16.1	−3.1
*p*X-TCE	0.05	−0.59	0.64	1.6_5	−21.2	−1.2
*t*BC-TCE	−0.36	−0.05	−0.31	-4.6_6	9.4	−0.4

16) E. M. Turner, D. W. Anderson, L. A. Reich, and W. E. Vaughan, *J. Phys. Chem.*, **74**, 1275 (1970).

The molecular size V^* of CT, *t*BC, and TCE do not differ much. This is shown in Table 3. It might be concluded that the nature of more attractive interactions in CT-*t*BC and TCE-*t*BC systems is due to the interactions between methyl groups and chlorine atoms. This suggests that the interaction between these molecules can not be described by means of the central force field which is a function of the separation between molecular centers.[10] This might be assumed to be an interaction through molecular surfaces.[17]

17) P. J. Flory, *J. Amer Chem. Soc.*, **87**, 1833 (1965); A. Abe and P. J. Flory, *ibid.*, **87**, 1838 (1965).

The values of dipole moments of 1,2-dichloroethane (DCE) in pure liquid (2.1 D) and in benzene solution (1.7 D) are nearly equal in the order of magnitude to those of *t*BC and TCE, respectively. However, B-DCE system has positive values of V^E, $(V\kappa_s)^E$ and θ, which are in marked contrast to the negative values in B-*t*BC and B-TCE.[7] A more refined treatment of a ternary mixture, which includes the conversion between gauche and trans forms in DCE, is desirable for B-DCE system.

In the systems including B and *p*X as solvents, the values of θ in *p*X solutions are more negative than those in B solutions. It indicates that the solutes studied are more attractive to B than to *p*X.

BULLETIN OF THE CHEMICAL SOCIETY OF JAPAN, VOL. 44, 1230—1233(1971)

ESR Study of Adsorbed Monomer and Dimer Cation Radicals of Benzene and Its Methyl Derivatives

Siro NAGAI, Shun-ichi OHNISHI, and Isamu NITTA

Osaka Laboratory for Radiation Chemistry, Japan Atomic Energy Research Institute, Neyagawa City, Osaka

(Received September 14, 1970)

Benzene, toluene, *o*-, *m*-, *p*-xylene, and mesitylene adsorbed on silica gel were γ-irradiated at -196°C. ESR spectra observed at -196°C for these systems at low contents of the methylbenzenes were assigned to the respective monomer cations. Dimer cations of benzene, toluene, and *p*-xylene were produced on γ-irradiation at -196°C of the adsorbed systems at higher contents and also by the reaction of monomer cations and neutral molecules at higher temperature than -160°C.

Edlund *et al.*[1] reported that the monomer and dimer cations of benzene were produced in γ-irradiated benzene-silica gel system and these authers[2] studied the formation of these cations, as well as neutral radicals, as functions of adsorption amount and irradiation dosage. Tanei[3] also observed these cations adsorbed on silica gel by ultraviolet irradiation. In the present paper, we describe results of our study on γ-irradiated methylbenzenes adsorbed on silica gel. From the analysis of the ESR spectra, we determined the structure of the radicals produced on the gel and followed reactions of the radicals on raising the temperature.

Experimental

Silica gel (Mallinckrodt Chemical Works, 100 mesh) was heated *in vacuo* at 500—550°C for 10 hr before use. The BET surface area determined by N_2 adsorption was 500 m^2/g. Chemicals were obtained from commercial sources; spectro-grade benzene from Merck and toluene, *o*-, *m*-, *p*-xylene, and mesitylene from Nakarai Chemical Co., Ltd. (reagent grade). These reagents were used without further purification. Adsorbed samples were prepared by adding methylbenzene gas of known volume to silica gel in a vacuum line at room temperature, and a part of them (*ca.* 300 mg) was transferred *in vacuo* to spectrosil tube for ESR measurement. Amount of adsorption was determined with a Hg manometer, and was limited in the present study to the low coverage region, from 1.0×10^{-5} mol/g to the amount of monolayer. The amount of monolayer (coverage) was estimated from the area occupied by an adsorbed methylbenzene molecule[4] and the BET surface area. The obtained value was approximately 2×10^{-3} mol/g for benzene and its methyl derivatives.

γ-Irradiation was carried out at -196°C with a 2,000 Ci Co-60 source to a dose of 5.0×10^5R. ESR spectra were recorded using a Varian V-4500 spectrometer and variable temperature accessorries at various temperatures from -196°C to room temperature. The ESR signal from the γ-irradiated silica gel did not contribute significantly to the observed spectra for the methylbenzene-silica gel system.

Results and Discussion

ESR Spectra of Irradiated Adsorbed Aromatic Compounds. ESR spectrum of the adsorbed benzene was dependent on the amount of adsorption as reported by Edlund *et al.*[2] The adsorbed methylbenzenes also showed quite similar dependence. When the adsorbed amount was about 1/100 of the monolayer coverage, the ESR spectra shown in Figs. 1 to 5 were observed. For benzene, the observed spectrum (Fig. 1a) was the same as that reported by Edlund *et al.*[2]; the seven lines with

1) O. Edlund, P.-O. Kinell, A. Lund, and A. Shimizu, *J. Chem. Phys.*, **46**, 3678 (1967).

2) O. Edlund, P.-O. Kinell, A. Lund, and A. Shimizu, "Advances in Chemistry Series," Vol. 82, ed. by R. F. Gould, American Chemical Soceity Publications, Washington, D.C. (1968), p. 311.

3) T. Tanei, This Bulletin, **41**, 833 (1968).

4) R. N. Smith, C. Pierce, and H. Cordes, *J. Amer. Chem. Soc.*, **72**, 5595 (1950).

asymmetric individual lines, the splitting value being $a_H=4.4$ gauss. Toluene gives the 5-line spectrum of $a_H=14.0$ gauss with additional splitting of 3 gauss (Fig. 2a). The spectrum of *p*-xylene consists of seven lines ($a_H=14.5$ gauss) with additional 3 gauss splitting (Fig. 3a). The splitting values for *m*-xylene, *o*-xylene, and mesitylene are 11.0 gauss, 11.0 gauss with additional splitting of 6 gauss, and 8.0 gauss, respectively.

When the amount of adsorption was increased, but still smaller than the monolayer coverage, the spectra for benzene, toluene, and *p*-xylene changed into those having splitting values a'_H equal to one half of a_H. No half-field resonances were observed for benzene. Benzene gives the 13-line spectrum with $a'_H=2.2$ gauss (Fig. 1b), in agreement with the result by Edlund *et al.*[1] The spectra for toluene and *p*-xylene have the splitting values $a'_H=7.0$ gauss, and 7.5 gauss, respectively. For *m*-xylene, *o*-xylene, and mesitylene, on the other hand, no such spectra with $a'_H=a_H/2$ were observed. Instead, the spectra became broadened, as shown in in Fig. 4 for *m*-xylene.

On increasing the adsorption amount further, close to and larger than the monolayer coverage, all the samples gave broad spectra which can be assigned to the cyclohexadienyl type radicals. These types of spectra were observed as trace background also for the lower coverage samples.

Assignment of the Spectra. ESR spectra observed

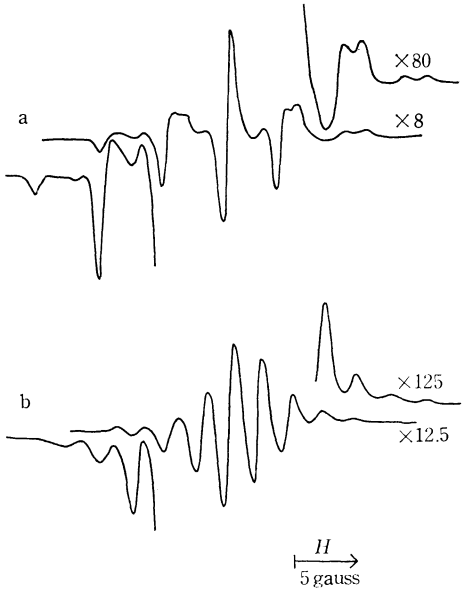

Fig. 1. ESR spectra from γ-irradiated benzene-silica gel at benzene content
(a) 2.4×10^{-5} mol/g, (b) 6.0×10^{-5} mol/g.

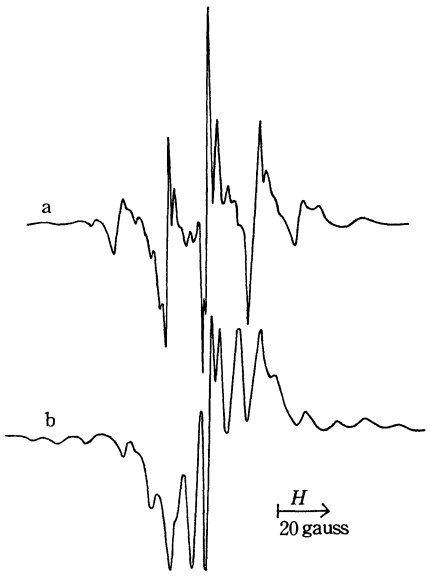

Fig. 3. Typical spectra from *p*-xylene-silica gel
(a) 2.1×10^{-5}mol/g, (b) 7.7×10^{-5} mol/g.

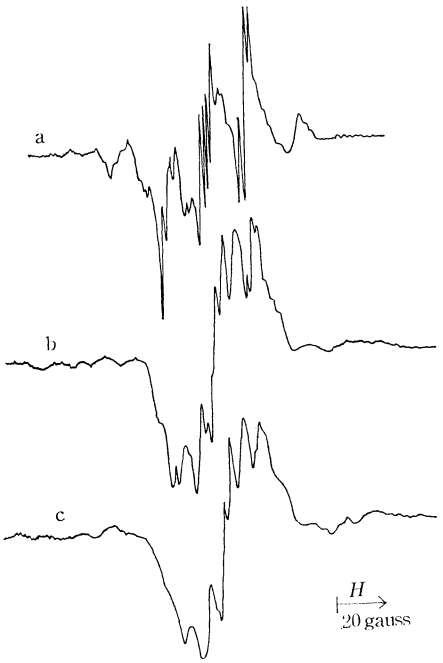

Fig. 2. ESR spectra from toluene-silica gel at toluene content
(a) 3.7×10^{-5} mol/g, (b) 7.5×10^{-5} mol/g, (c) 1.3×10^{-4} mol/g.

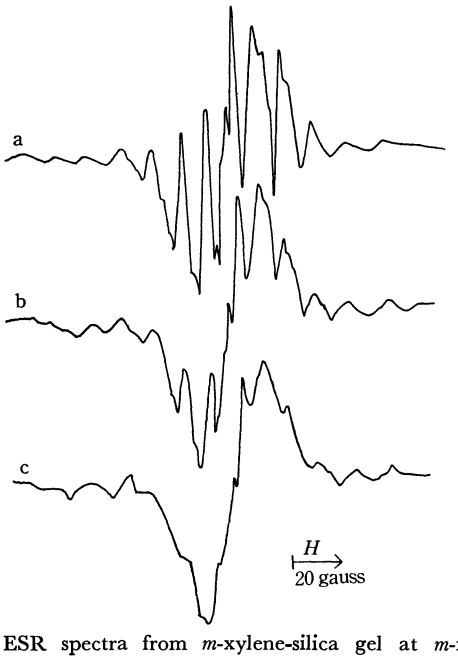

Fig. 4. ESR spectra from *m*-xylene-silica gel at *m*-xylene content
(a) 1.9×10^{-5} mol/g, (b) 4.1×10^{-5} mol/g, (c) 7.3×10^{-5} mol/g.

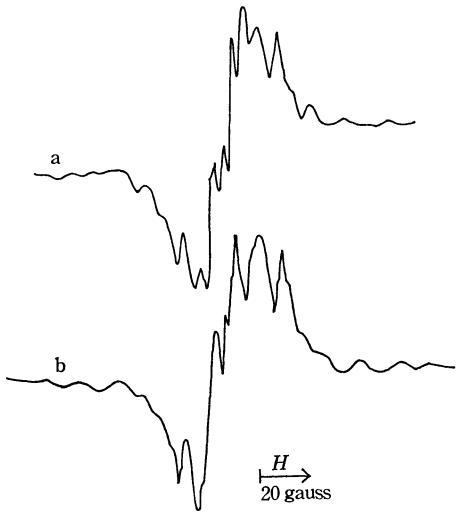

Fig. 5. ESR spectra from *o*-xylene and mesitylene-silica gel systems at low contents.
(a) *o*-xylene, (b) mesitylene

for the adsorbed compounds with the lowest coverages can be assigned to the respective monomer cations. Theoretical hyperfine splitting values are calculated by the simple Hückel MO method. The splitting values of the methyl protons, taking $Q_H^{CCH_3}=44$ gauss obtained for the cation of durene,[5] are 14.7 gauss for the cations of toluene and *p*-xylene, 11.0 gauss for *o*- and *m*-xylene, and 7.3 gauss for mesitylene. These theoretical values agree well with the observed values. The additional splittings are due to the ring protons and the observed equal splittings for toluene and *p*-xylene are reasonable, in view of the same spin density (1/12) at the 2,3,5,6-ring carbon atoms of the two methylbenzenes.

Difference in the spectra for *o*-xylene and *m*-xylene cannot be explained by the simple Hückel theory. With the perturbation calculation,[6] however, this difference could be explained; the 4,5-protons in *o*-xylene would have smaller splitting values than the 4,6-protons in *m*-xylene.

ESR spectra of toluene and *p*-xylene at the intermediate coverages can be asigned to the respective dimer cations, in view of the half splitting values a_H'.

Formation of Dimer Cations

ESR spectra of the adsorbed benzene, toluene, and *p*-xylene became those of the dimer cations, through intermediate composite spectra, as the adsorption amounts were increased.

This change of monomer to dimer was studied for benzene as a function of absorption amount and temperature. At −196°C, the formation of dimer cation began at the benzene content as low as 2×10^{-5} mol/g and the dimer increased at the expense of monomer, as the adsorption amount became larger (Fig.6).

The monomer spectrum was stable at −196°C for several weeks. At about −160°C, the seven-line

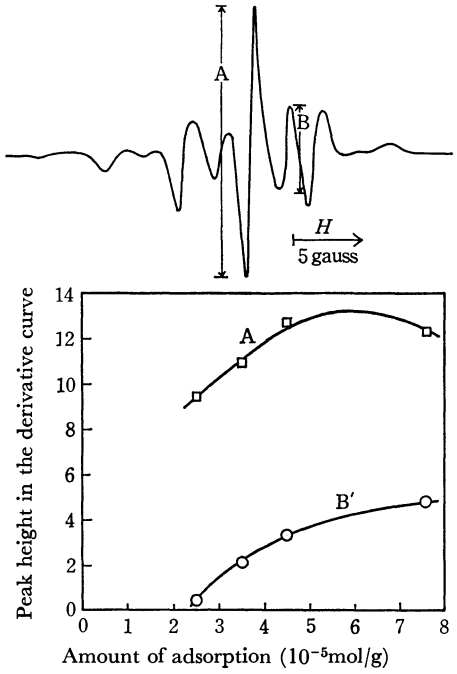

Fig. 6. Formation of the dimer cation as a function of the benzene content. The peak height B', which is the peak height B multiplied by the binomial ratio 924/792, was plotted against the content. The peak A is a superposition of the peaks of the spectra of the monomer and the dimer cations.

spectrum began to change and the 13-line spectrum appeared. The latter spectrum became predominant at −140°C and at still higher temperatures it began to decay, the individual lines of the spectrum becoming sharp. Formation of the dimer at higher temperatures was studied with benzene by following spectral change at a constant temperature −155°C (Fig. 7). The result suggests that the dimer cations are produced from the monomer cations. The temperature for this conversion depends on the heat-treatment of silica gel. On a silica gel heat-treated at 850°C, the conversion occurs even at −196°C, while it hardly occurs at about −140°C with a silica gel heated at 200°C.

At −196°C, the adsorbed benzene as well as the monomer cation radicals produced by irradiation does

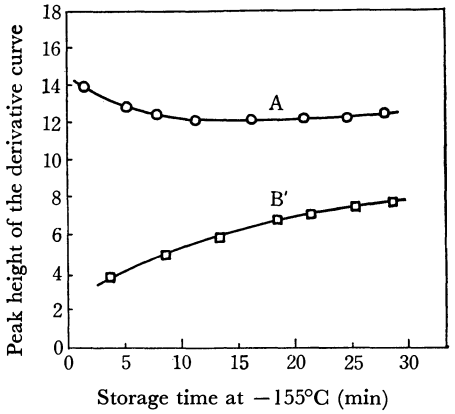

Fig. 7. Change in the concentration of the dimer cation at −155°C. The peak height B'=B×(924/792) was plotted against storage time at −155°C. See legend to Fig. 6 as for other notations.

5) R. Hulme and M. C. R. Symons, *J. Chem. Soc.*, **1965**, 1120.
6) T. H. Brown, M. Karplus, and J. C. Shug, *J. Chem. Phys.*, **38**, 1749 (1963).

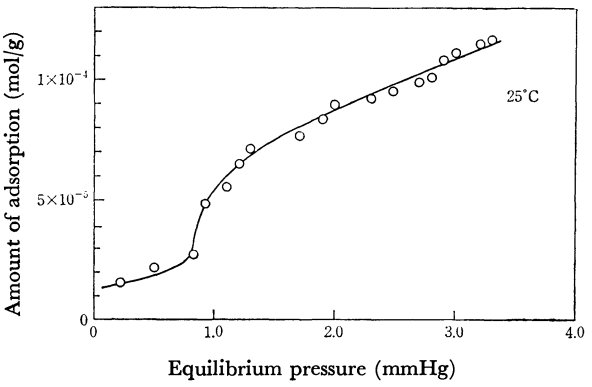

Fig. 8. Adsorption isotherm of benzene on silica gel at 25°C.

not have sufficient mobility to come close to form the dimer cation radicals. When the adsorption amount exceeds 2×10^{-5} mol/g, there seems to occur a certain change in the mode of adsorption as evidenced from the adsorption isotherm (Fig. 8). Adsorptions as benzene dimer might occur and these species would give the dimer cation on irradiation. The slower rates of motions of the monomer and dimer cations at −196°C can be noted from the asymmetry of the individual lines of the 7-line spectrum and the line-widths variation of the 13-line spectrum depending on the total nuclear quantum numbers.

At higher temperatures, the adsorbed monomer cations and molecules become mobile to come close to form the dimer cations. Such mobilization can be seen from the spectral changes and the decay. Different behavior for the monomer-to-dimer conversion with silica gels subjected to different heat-treatments suggests alterations in mobility of adsorbed benzene on silica gel heat-treated at various temperatures.

The same mechanism would also hold for the dimer formation of toluene and *p*-xylene. At higher temperatures, the spectra of dimer cations were observed.

For the cases of *o*-xylene, *m*-oxylene and mesitylene, such clear evidence for the dimer formation was not obtained from ESR spectra. At higher temperatures, however, the adsorbed molecules become also mobile in view of decay of the signals. The spectra also change to the broad spectra, which might be responsible for the dimer cation radials.

BULLETIN OF THE CHEMICAL SOCIETY OF JAPAN, VOL. 44, 1233—1238(1971)

The Crystal Structure of *cis*-Ammonium Disulfitotetrammine-cobaltate(III) Trihydrate, $NH_4[Co(SO_3)_2(NH_3)_4]\cdot 3H_2O$[1]

Teruo NOMURA and Masayoshi NAKAHARA
Department of Chemistry, Rikkyo University, Ikebukuro, Tokyo

(Received September 22, 1970)

The structure of $NH_4[Co(SO_3)_2(NH_3)_4]\cdot 3H_2O$ has been determined by the heavy-atom method and refined to $R=0.12$ by a least-squares analysis based on 874 three-dimensional visual data. The compound crystallizes in the orthorhombic space group $P2_12_12_1$, with unit cell dimensions of $a=10.995$, $b=17.563$, $c=6.834$ Å, and $Z=4$. The two sulfito groups in the complex anion are coordinated to the central cobalt atom in *cis* positions through their sulfur atoms, with Co-S distances of 2.23 Å (mean). The *cis*-configuration of brown sodium salt, with an absorption spectrum similar to that of the trihydrate of ammonium salt, has also been established.

There are two stereoisomers conceivable for the disulfitotetramminecobaltate(III) complex anion: the *cis* and *trans* forms. In fact, in the case of the ammonium salt of this complex, the two isomers have been known as the dark brown trihydrate and the reddish brown tetrahydrate respectively. The absorption spectrum of the dark brown ammonium salt in an aqueous solution has a chage-transfer band at 265 mμ and a sulfito-specific band at 297 mμ in the ultraviolet region, whereas that of the reddish brown ammonium salt has only a sulfito-specific band at 274 mμ. In the sodium salts, the spectra are nearly identical with those of the corresponding ammonium salts; that is, the brown salt corresponds to the dark brown ammonium salt, and the golden-yellow salt, to the reddish brown ammonium salt. These spectra were first measured by Shimura[2] and are followed in the present work (Fig.1).

The assignment of the configurations of these salts has not yet been established; Hofmann and Jenny,[3] who first prepared the two isomers of sodium salts, designated a brown, less soluble dihydrate as the *cis* form and another golden-yellow, more soluble tetrahydrate as the *trans* form. They also concluded that the dark brown and reddish brown ammonium isomers correspond to the brown or golden-yellow sodium salts, respectively. Schwarz and Tede[4] showed, from their studies of the photochemical decomposition of the ammonium salts, that the dark brown, more decomposable salt is the *cis*-isomer and the reddish brown, less

1) T. Nomura, M. Nakahara, and Y. Kondo, presented at the 23rd Annual Meeting of the Chemical Society of Japan, Tokyo, April, 1970.

2) Y. Shimura, *J. Amer. Chem. Soc.*, **73**, 5079 (1951); This Bulletin, **25**, 46 (1952).

3) K. A. Hofmann and A. Jenny, *Ber.*, **34**, 3855 (1901).

4) R. Schwarz and K. Tede, *ibid.*, **60**, 63 (1927).

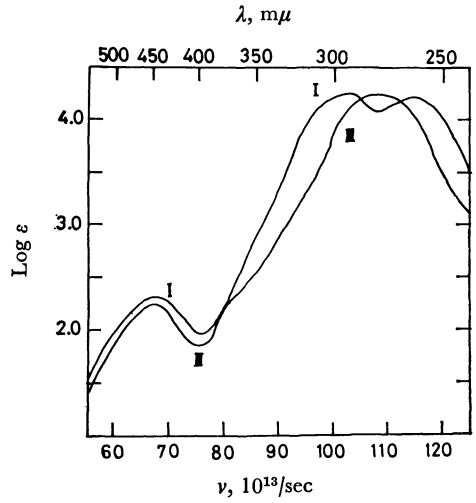

Fig. 1. Absorption spectra of the dark brown isomer (I) and of the reddish brwon isomer (II) of ammonium salt in a 3% aqueous solution of ammonia.

decomposable salt is the *trans*-isomer. Klement[5] and Bailar and Peppard[6] also concluded that the sulfito groups of the dark brown trihydrate must be located in the *cis* positions, in view of the fact that only two ammonia molecules are replaced by an ethylenediamine molecule. On the other hand, in view of the position of the charge-transfer band, Shimura[2] suggested that the dark brown salt has a *trans* configuration with respect to the sulfito groups and assumed, from the first absorption band at 465 mμ, that the sulfito groups in the complex anion were more symmetrical or more stable than a free SO_3 radical, that is, that they were bonded through the sulfur atom to the central atom.

In the present work, the dark brown trihydrate, $NH_4[Co(SO_3)_2(NH_3)_4]\cdot 3H_2O$, has been subjected to a three-dimensional X-ray analysis in order to establish the structure of the complex anion and in order to elucidate in detail the way of the coordination of the sulfito groups to the metal.

Experimental

Ammonium disulfitotetramminecobaltate(III) trihydrate was prepared by the method of Bailar and Peppard.[6] This compound crystallizes in dark brown pillars elongated along the *c* axis, the shortest crystallographic axis. The specimens used for the collection of the intensity data were reformed into cylinders with diameters of 0.024 cm and of 0.026 cm, the axes of which were parallel to the *c* and *a* axes respectively. Using Fe*K*α radiation, Weissenberg photographs with spot-integrating procedure were taken from the zero to fourth levels and from the zero to seventh levels about the *c* and *a* axes respectively. The intensities were measured visually by use of standard calibrated scales and were converted to structure amplitude values in the usual way. Corrections were also applied for absorption, the crystal being assumed to be perfectly cylindrical.[7] A total of 874 independent intensity data were collected.[8]

The crystal data are as follows: $NH_4[Co(SO_3)_2(NH_3)_4]\cdot 3H_2O$, F.W.=359.3, orthorhombic, space group $P2_12_12_1$ (D_2^4, No. 19); a=10.995(6), b=17.563(15), c=6.834(5) Å, U=1322 Å^3; D_m=1.81 g·cm^{-3}. Z=4, D_x=1.80 g·cm^{-3}; linear absorption coefficient for Fe*K*α radiation, μ=94.5 cm^{-1}.

Determination of the Structure

The location of the cobalt atom could be readily determined from Patterson projections, $P(u, v)$ and $P(v, w)$ (Fig. 2).

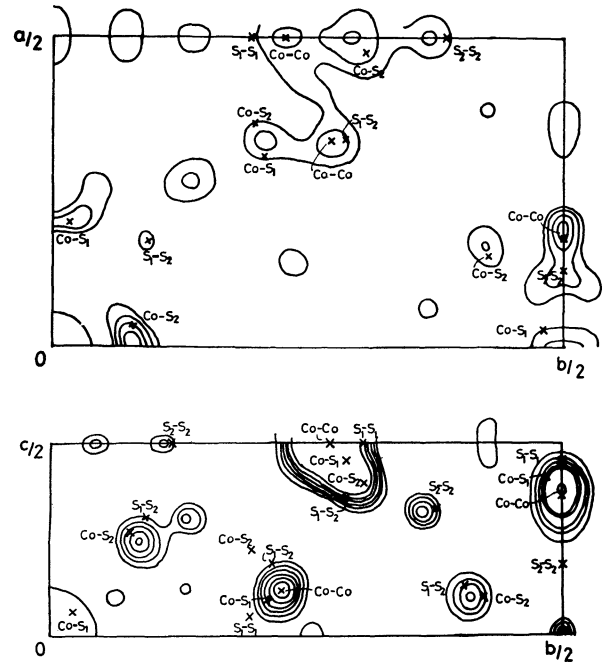

Fig. 2. Patterson projections, $P(u,v)$ and $P(v,w)$, where the vectors between heavy atoms are shown by the crosses.

However, the positions of the two sulfur atoms of the sulfito groups could not be definitely fixed from Patterson maps until a three-dimensional Fourier synthesis has been calculated by the use of phases based on the cobalt atom. The coordinates of these heavy atoms were refined by the block-diagonal, least-squares method.[9] The discrepancy factor, $R=\sum(|F_o|-|F_c|)/\sum|F_o|$, decreased to 0.30. A three-dimensional Fourier synthesis with phases determined by the heavy atoms allowed the four nitrogen atoms to be located around the cobalt atom. Successive refinements were carried out and the positions of all the remaining lighter atoms except those of the hydrogen atoms were revealed, though the nitrogen atom of the ammonium ion and the oxygen atoms of the water molecules were not sufficiently distingushed from each other. These syntheses also indicated that

5) R. Klement, *Z. Anorg. Chem.*, **150**, 117 (1926).

6) J. C. Bailar, Jr., and D. F. Peppard, *J. Amer. Chem. Soc.*, **62**, 105 (1940).

7) International Tables for X-Ray Crystallography, Vol. II, Kynoch Press, Birmingham (1959).

8) A FFLP program written by Dr. F. Iwasaki and Dr. H. Iwasaki was used for the Lorentz and polarization corrections of the intensity data.

9) The Fourier synthesis and least-squares program used was HBLS-4 (in the "Universal Crystallographic Computation Program System" edited by Dr. T. Sakurai and published by the Crystallographic Society of Japan), written by Dr. T. Ashida. The weights at the final least-squares refinement were assumed to be as follows: $w=(3.52/F_0)^2$ if $F_0\geq 3.52$, and $w=1$ if $F_0\leq 3.52$.

anisotropic temperature factors should be used for all the atoms.

After several cycles of least-squares refinement with anisotropic thermal parameters, the discrepancy fractor became 0.12. A final difference Fourier synthesis gave no significant indications of the positions of the hydrogen atoms. The atomic scattering factors were taken from International Tables for X-ray Crystallography.[10]

At a later stage of the refinement, extinction corrections were applied for some of the larger F_o values.

The final three-dimensional electron density map is shown in Fig. 3. The final parameters are given in Tables 1 and 2.

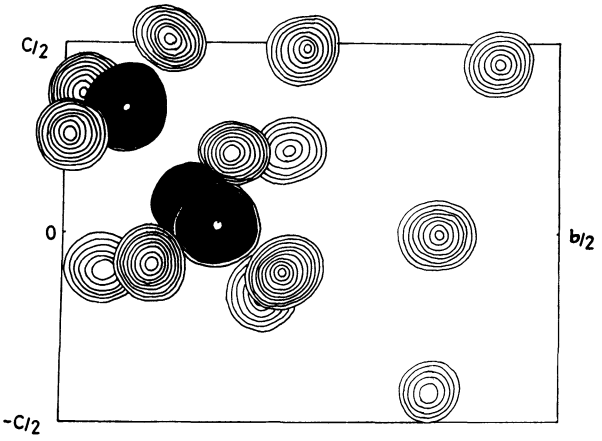

Fig. 3. The final three-dimensional electron density map composed of sections through the atomic centers parallel to (100). The contours are drawn at intervals of 1.0 e.Å^{-3} starting with 1.0 e.Å^{-3}.

The agreement between the observed and calculated structure amplitudes is reasonable.[11]

The standard deviations of the coordinates, estimated from the least-squares results, are 0.004 Å (mean) for the cobalt and sulfur atoms and 0.02 Å (mean) for the others.

Description of the Structure and Discussion

A projection of the contents of an asymmetric unit along the *a* axis is presented in Fig. 4. The bond lengths

Table 1. Final fractional coordinates and their e.s.d.'s

Atom	$x(\sigma(x))\times 10^4$	$y(\sigma(y))\times 10^4$	$z(\sigma(z))\times 10^4$
Co	0891(2)	1326(1)	0747(5)
S(1)	−1101(4)	1529(3)	0238(7)
S(2)	0538(4)	0595(3)	3327(8)
N(1)	0894(18)	2276(10)	2351(29)
N(2)	2655(16)	1194(9)	1250(26)
N(3)	0864(17)	0384(10)	−0916(25)
N(4)	1290(17)	1988(10)	−1681(35)
N(5)	0244(21)	3686(12)	−4179(33)
O(1)	−1796(17)	1673(9)	2093(23)
O(2)	−1730(15)	0845(7)	−0816(25)
O(3)	−1288(13)	2209(8)	−1064(21)
O(4)	0161(17)	1069(9)	5128(21)
O(5)	1645(14)	0157(8)	3745(25)
O(6)	−0530(16)	0035(9)	2826(22)
O(7)	3339(17)	2368(9)	4850(28)
O(8)	0655(15)	3739(10)	−0037(26)
O(9)	2305(16)	4360(10)	4598(25)

Table 2. Final thermal parameters and their e.s.d.'s

Temperature factors are of the form:

$\exp[-(h^2\beta_{11}+k^2\beta_{22}+l^2\beta_{33}+2hk\beta_{12}+2hl\beta_{13}+2kl\beta_{23})]$

Atom	$\beta_{11}\times 10^6$	$\beta_{22}\times 10^6$	$\beta_{33}\times 10^6$	$\beta_{12}\times 10^6$	$\beta_{13}\times 10^6$	$\beta_{23}\times 10^6$
Co	0532(0)	0241(0)	1672(2)	0008(0)	0031(0)	0011(0)
S(1)	0500(0)	0193(0)	1225(2)	0013(0)	−0136(1)	0132(0)
S(2)	0397(0)	0191(0)	1392(2)	−0091(0)	0046(1)	0046(0)
N(1)	0644(1)	0292(0)	2431(11)	0045(0)	0362(4)	0377(1)
N(2)	0681(1)	0267(0)	1447(9)	−0201(0)	−0177(3)	0200(1)
N(3)	0911(2)	0314(0)	1000(8)	−0089(1)	−0043(3)	0051(1)
N(4)	0438(1)	0274(0)	3225(13)	0251(0)	−0108(4)	−0035(1)
N(5)	1195(2)	0530(0)	1958(11)	−0245(1)	0397(4)	−0274(2)
O(1)	0941(1)	0359(0)	1924(9)	−0001(0)	−0139(3)	−0018(1)
O(2)	0851(1)	0155(0)	2664(10)	−0049(0)	0527(3)	−0049(1)
O(3)	0457(1)	0355(0)	1602(8)	−0172(0)	−0141(1)	0050(1)
O(4)	1424(2)	0379(0)	0556(7)	−0062(0)	0904(3)	−0007(1)
O(5)	0583(1)	0314(0)	2786(10)	0082(0)	0243(3)	0398(1)
O(6)	1002(2)	0462(0)	1675(9)	−0404(1)	−0074(3)	−0064(1)
O(7)	1104(2)	0308(0)	2918(10)	0062(0)	−0313(4)	0133(1)
O(8)	0903(1)	0453(0)	2147(9)	0266(1)	0147(3)	0333(1)
O(9)	1128(2)	0375(0)	2310(10)	−0031(1)	0193(4)	0158(1)

10) International Tables for X-Ray Crystallography Vol. III, Kynoch Press, Birmingham (1962).

11) A complete list of the observed and calculated structure factors has been submitted to, and is kept as Document No. 7105 by, the office of the Bulletin of the Chemical Society of Japan, 1—5 Kanda-Surugadai, Chiyoda-ku, Tokyo. A copy may be secured by citing the Document number and by remitting, in advance, ¥400 for photo prints. Pay by check or money order payable to: Chemical Society of Japan.

TABLE 3. THE INTERATOMIC DISTANCES AND BOND ANGLES IN THE COMPLEX ANION, $[Co(SO_3)_2(NH_3)_4]$
Their e.s.d.'s are given in parentheses

Co–S(1)	2.245(6)Å	S(1)–O(6)	3.24(2)	N(3)–N(4)	2.90(3)Å	O(4)–O(5)	2.47(2)
Co–S(2)	2.215(6)	S(2)–N(1)	3.05(2)	N(3)–O(1)	4.23(2)	O(4)–O(6)	2.50(2)
Co–N(1)	2.00(2)	S(2)–N(2)	2.92(2)	N(3)–O(2)	2.96(2)	O(5)–O(6)	2.47(2)
Co–N(2)	1.98(2)	S(2)–N(3)	2.94(2)	N(3)–O(3)	3.98(2)	S(1)–Co–S(2)	92.5(2)°
Co–N(3)	2.01(2)	S(2)–N(4)	4.29(2)	N(3)–O(4)	4.37(2)	S(1)–Co–N(1)	87.4(6)
Co–N(4)	2.07(2)	S(2)–O(1)	3.30(2)	N(3)–O(5)	3.32(2)	S(1)–Co–N(2)	177.4(5)
S(1)–O(1)	1.50(2)	S(2)–O(2)	3.80(2)	N(3)–O(6)	3.06(2)	S(1)–Co–N(3)	91.6(5)
S(1)–O(2)	1.56(1)	S(2)–O(3)	4.59(1)	N(4)–O(1)	4.30(3)	S(1)–Co–N(4)	89.6(5)
S(1)–O(3)	1.50(1)	N(1)–N(2)	2.81(3)	N(4)–O(2)	3.92(3)	S(2)–Co–N(1)	92.7(6)
S(2)–O(4)	1.54(2)	N(1)–N(3)	4.00(3)	N(4)–O(3)	2.89(2)	S(2)–Co–N(2)	88.0(5)
S(2)–O(5)	1.47(2)	N(1)–N(4)	2.83(3)	N(4)–O(4)	5.08(3)	S(2)–Co–N(3)	88.3(5)
S(2)–O(6)	1.56(2)	N(1)–O(1)	3.14(3)	N(4)–O(5)	4.92(3)	S(2)–Co–N(4)	177.6(5)
Co–O(1)	3.15(2)	N(1)–O(2)	4.39(2)	N(4)–O(6)	5.04(3)	N(1)–Co–N(2)	90.1(8)
Co–O(2)	3.19(2)	N(1)–O(3)	3.35(2)	O(1)–O(2)	2.46(2)	N(1)–Co–N(3)	178.6(8)
Co–O(3)	3.11(1)	N(1)–O(4)	2.96(2)	O(1)–O(3)	2.42(2)	N(1)–Co–N(4)	88.3(8)
Co–O(4)	3.13(2)	N(1)–O(5)	3.93(2)	O(1)–O(4)	3.17(2)	N(2)–Co–N(3)	90.9(7)
Co–O(5)	3.02(2)	N(1)–O(6)	4.25(2)	O(1)–O(5)	4.76(2)	N(2)–Co–N(4)	89.8(7)
Co–O(6)	3.11(2)	N(2)–N(3)	2.84(2)	O(1)–O(6)	3.24(2)	N(3)–Co–N(4)	90.7(8)
S(1)–S(2)	3.227(7)	N(2)–N(4)	2.86(3)	O(2)–O(3)	2.45(2)	O(1)–S(1)–O(2)	107.1(9)
S(1)–N(1)	2.93(2)	N(2)–O(1)	5.00(2)	O(2)–O(4)	4.58(2)	O(1)–S(1)–O(3)	107.2(9)
S(1)–N(2)	4.23(2)	N(2)–O(2)	5.06(2)	O(2)–O(5)	4.99(2)	O(2)–S(1)–O(3)	106.1(8)
S(1)–N(3)	3.05(2)	N(2)–O(3)	4.95(2)	O(2)–O(6)	3.17(2)	O(4)–S(2)–O(5)	110.5(10)
S(1)–N(4)	3.05(2)	N(2)–O(4)	3.82(2)	O(3)–O(4)	4.94(2)	O(4)–S(2)–O(6)	107.4(9)
S(1)–O(4)	3.71(2)	N(2)–O(5)	2.73(2)	O(3)–O(5)	5.85(2)	O(5)–S(2)–O(6)	109.4(9)
S(1)–O(5)	4.54(2)	N(2)–O(6)	4.20(2)	O(3)–O(6)	4.74(2)		

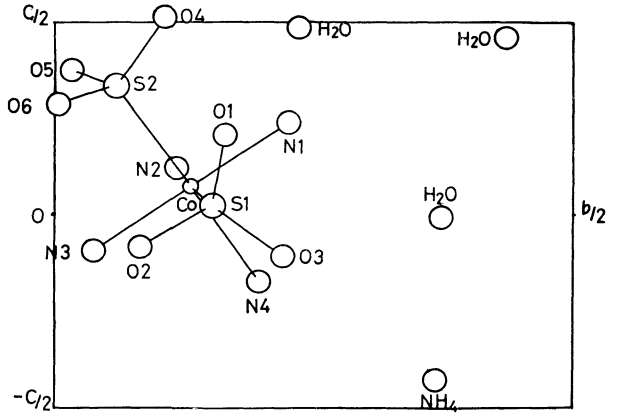

Fig. 4. The structure in an asymmetric unit, viewed along the *a* axis.

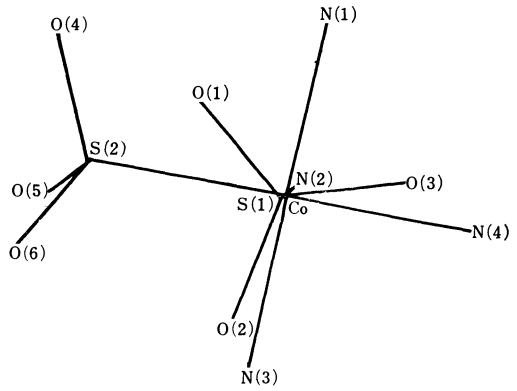

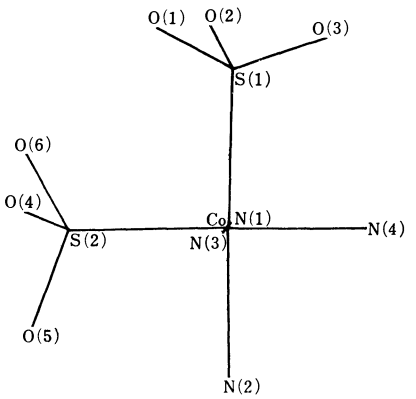

Fig. 5. Projections of the complex anion onto (a) the plane defined by the three oxygen atoms of O(1), O(2), and O(3) in a sulfito group and (b) the least-squares plane for Co, S(1), S(2), N(2), and N(4).

and angles with their e.s.d.'s are listed in Table 3, while the pertinent intermolecular contacts (*i.e.*, those less than 3.22 Å) are given in Table 5.

In the complex anion, the two sulfito groups are coordinated to the central cobalt atom in *cis* positions through their sulfur atoms, the Co-S distances of 2.22 Å and 2.25 Å. These bond lengths are somewhat shorter than the sum of the covalent radii (2.26 Å) obtained from the radius of 1.22 Å for Co(III) and that of 1.04 Å for tetrahedral sulfur, while they are a little longer than the Co-S distance of 2.20 Å found in the crystal of $[Co(SO_3)(SCN)en_2]$,[12] whose crystal structure was first determined among the Co(III) complexes containing the sulfito group as a ligand. The sulfito groups are of a somewhat distorted trigonal-pyramidal struc-

12) S. Baggio and L.N. Becka, *Acta Crystallogr.*, **B25**, 946 (1969).

ture, three oxygen atoms and a lone pair of electrons being bound tetrahedrally around the central sulfur atom; they do not possess a strict three-fold symmetry. The O–S distances range from 1.47 to 1.56 Å, the values of the S–O–O angles being 106°—111°. In the crystals of $(NH_4)_2SO_3\cdot H_2O$[13] and $NiSO_3\cdot 6H_2O$[14] containing ionic sulfito groups, the mean values of the S–O distances and the O–S–O angles are 1.53 Å and 104° respectively, whereas, in the crystals of $[Co(SO_3)(SCN)en_2]$ and $[Pd(SO_3)(NH_3)_3]$[15] involving the coordinated sulfito groups, the corresponding values are 1.49 Å and 110° respectively.

The planes formed by O(1), O(2), and O(3), and O(4), O(5), and O(6), are approximately perpendicular to the Co–S(1) and Co–S(2) bonds respectively (*cf.*, Fig. 5(a)).

The intermolecular distances, Co–N(NH_3), are 1.98—2.01 Å and are quite normal, with the exception only of 2.07 Å of Co–N(4), which is slightly longer.

The nitrogen and sulfur atoms are displaced from the regular octahedral positions around the central cobalt atom. The displacement is irregular, though the geometry is partially kept almost regular as may be seen in, for example, the dimensions of two of the triangles formed by three nitrogens. Mainly as a result of the repulsions between the non-bonded oxygen atoms belonging to different sulfito groups, the S-Co-S angle is larger than 90° (Fig. 5(b)) and two sulfito groups are located so as to keep their oxygen atoms at distances longer than 3.17 Å from those in another (Fig. 6 and Table 3). This distortion of the complex anion from the regular octahederal configuration seems to make the complex more photochemically decomposable than another isomer.[4]

The crystal is essentially ionic. The layers of the complex anions and those of the ammonium ions are alternately piled up, approximately parallel with the (120) and (1$\bar{2}$0) planes. The interstices among the complex anions form channels, which are elongated

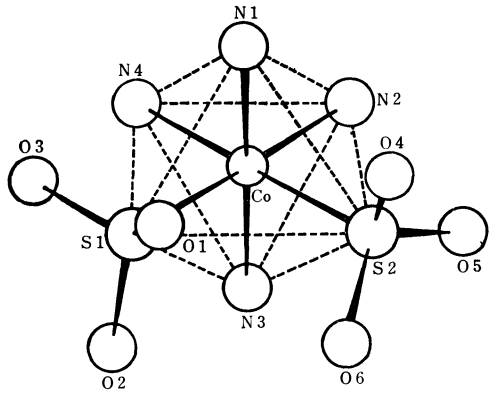

Fig. 6. A drawing of the complex anion, viewed along the direction perpendicular to the plane composed of three nitrogen atoms, N(2), N(3), and N(4). The displacement of sulfur and nitrogen atoms from their regular octahedral positions and the relative locations of oxygen atoms belonging to different SO_3 groups are also shown.

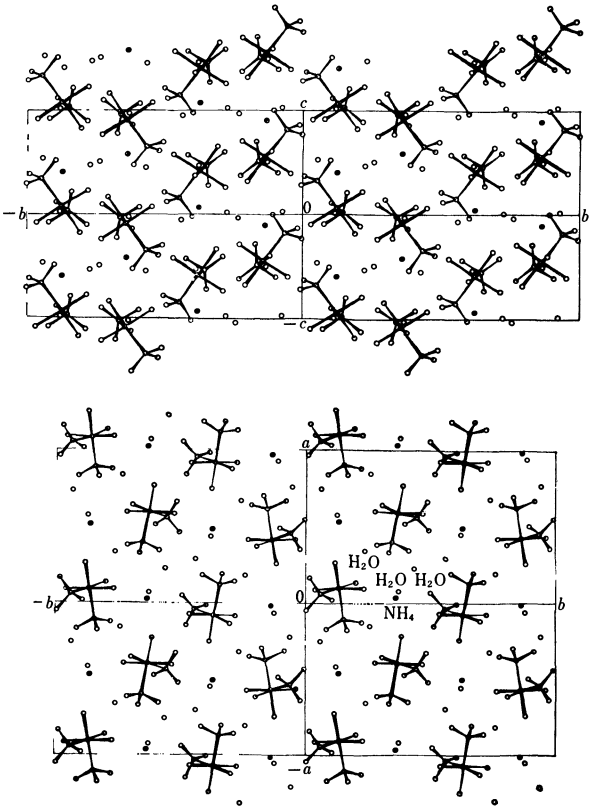

Fig. 7. Arrangement of the complex anions, ammonium ions, and water molecules in the crystal lattice.

along the *c* and *a* axes and which are packed with ammonium ions and water molecules (Fig. 7).

A complex anion is surrounded by six ammonium ions: four closest N···NH_4 and two O···NH_4 approaches can be found at distances ranging from 3.22 to 3.62 Å (Table 4).

TABLE 4. SIX CLOSER APPROACHES FROM AMMONIUM IONS TO NITROGEN AND OXYGEN ATOMS IN ANIONS

Reference atom at (x,y,z)				Distances
N(1)-N(5) at (	x,	y,	$1+z$)	3.50(3)Å
N(2)-N(5) at (	$1/2+x$,	$1/2-y$,	$-z$)	3.48(3)
N(3)-N(5) at (	$-x$,	$-1/2+y$,	$-1/2-z$)	3.22(3)
N(4)-N(5) at (	x,	y,	z)	3.62(3)
O(1)-N(5) at (	$-1/2+x$,	$1/2-y$,	$-z$)	3.61(3)
O(6)-N(5) at (	$-x$,	$-1/2+y$,	$-1/2-z$)	3.47(3)

The closest O···N contact occurs at a distance of 2.69 Å between NH_4 and H_2O (9[a]), the closest O···O distance being 2.69 Å between O(1) and H_2O (7[f]) and the closest N···N distance being 3.22 Å between N(3) and NH_4[d], while the van der Waals radii are 1.50 Å for nitrogen and 1.40 Å for oxygen. Intermolecular contacts less than 3.22 Å are presented in Table 5, while the short contacts in the structure are shown in Fig. 8. The complex anions are held together in the crystal by hydrogen bonds of the N–H···O and O–H···O types. These bonds involve each complex anion in a three-dimensional bonding network.

In the present structural study, the configuration of the dark brown ammonium trihydrate salt, NH_4-

13) L. F. Battle and K. N. Trueblood, *Acta Cryst.*, **19**, 531 (1965).
14) S. Baggio and L. N. Becka, *ibid.*, **B25**, 1150 (1969).
15) M. A. Spinnler and L. N. Becka, *J. Chem. Soc., A*, **1967**, 1195.

TABLE 5. INTERMOLECULAR CONTACTS LESS THAN 3.22 Å AND THEIR e.s.d.'s. IN PARENTHESES

Superscripts used are as follows:

No symbol	x,y,z		
a)	$x,$	$y,$	$-1+z$
b)	$1/2+x,$	$1/2-y,$	$-z$
c)	$1/2-x,$	$-y,$	$-1/2+z$
d)	$-x,$	$-1/2+y,$	$-1/2-z$
e)	$-1/2+x,$	$1/2-y,$	$-z$
f)	$-1/2+x,$	$1/2-y,$	$1-z$
g)	$-x,$	$-1/2+y,$	$1/2-z$

N(1)-O(7)	3.17(3)Å	N(5)-O(7^e)	2.83(3)Å
N(1)-O(8)	3.05(3)	O(1)-O(7^f)	2.69(2)
N(2)-O(3^b)	3.04(2)	O(1)-O(9^e)	3.06(2)
N(2)-O(5^c)	3.02(3)	O(2)-O(8^e)	3.02(2)
N(3)-O(4^a)	3.06(2)	O(2)-O(9^e)	2.82(2)
N(3)-O(5^c)	2.91(2)	O(2)-O(9^g)	2.81(2)
N(3)-N(5^d)	3.22(3)	O(3)-O(7^e)	2.72(2)
N(4)-O(4^a)	2.98(3)	O(6)-O(9^f)	3.13(2)
N(4)-O(1^b)	3.17(2)	O(6)-O(8^g)	2.72(2)
N(5)-O(9^a)	2.69(3)	O(6)-O(9^g)	2.83(2)
N(5)-O(8)	2.87(3)	O(1)-O(8^e)	3.22(2)

$[Co(SO_3)_2(NH_3)_4]\cdot 3H_2O$, has been established as the *cis* form. It may also be concluded that the brown sodium salt with an absorption spectrum similar to that of the present substance is the *cis* isomer. The results thus obtained are consistent with those of several other studies.[3-6]

Both of the sulfito groups are pyramidal and are bonded to the cobalt through the sulfur atom.This is consistent with the prediction of Shimura.[2] The large value of the molar extinction coefficient in the charge-transfer band (log ε=4.20) can be reasonably explained by the coordination of the sulfito group through the sulfur.

During the preparation of the manuscript of this report, a short communication about the structure of this complex anion has been published by other workers.[16]

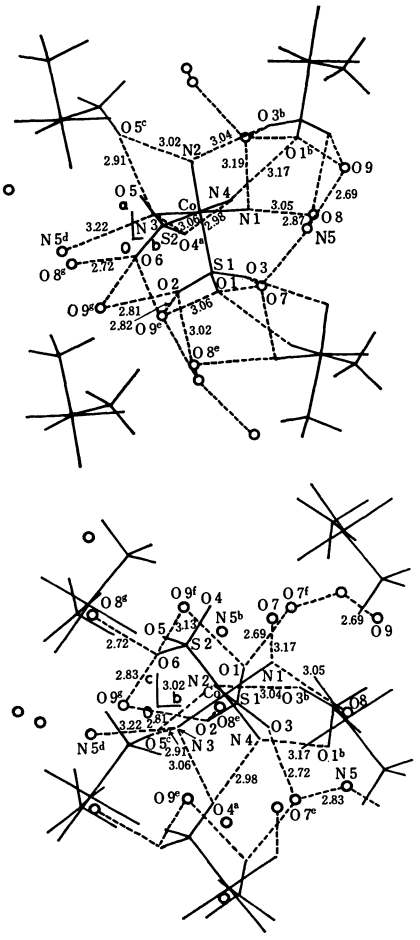

Fig. 8. Intermolecular contacts less than 3.22 Å.

The authors wish to express their thanks to Professor Y. Saito for his kind advice and encouragement, and also wish to thank Professor Y. Kondo for his kind support of their study. This research was partly defrayed by grants from Matsunaga Science Foundation, to which the authors' thanks are also due.

16) A. V. Ablov, L. I. Landa, Yu. A. Simonov, T. I. Malinovskii, and A. B. Tovis, *Dokl. Akad. Nauk. SSSR*, **1970**, 190 (3) 579—581 (Chem.).

The Codimerizations of Styrene with Vinyl Compounds Catalyzed by Olefin-palladium(II) Chloride Complexes

Keiji KAWAMOTO, Atsushi TATANI, Toshinobu IMANAKA, and Shiichiro TERANISHI

Department of Chemical Engineering, Faculty of Engineering Science, Osaka University, Machikaneyama, Toyonaka, Osaka

(Received September 26, 1970)

The codimerization of styrene with vinyl compounds catalyzed by di-μ-chloro-dichlorobis(styrene)dipalladium(II), $(Pd(C_6H_5CH{=}CH_2)Cl_2)_2$, was investigated in a homogeneous system under mild conditions. The reaction of styrene and methyl acrylate carried out at 50°C for 6 hr yielded 220% codimers, 169% dimers of methyl acrylate, and 18% dimers of styrene, on the basis of the palladium(II) used. The codimerizations of styrene with vinyl acetate and with methyl vinyl ketone gave 50% codimer and 125% codimers respectively. When nitroethylene and *n*-butyl vinyl ether were used as the vinyl compound, no codimers were formed. The codimerization of styrene-d_3 with ethylene was also carried out. The reaction mechanism involving the five-coordinate hydridopalladiumolefin intermediate was proposed and discussed in the terms of the distribution of deuterium in the codimer of styrene-d_3 and ethylene, the functional group effects of vinyl compounds, and solvent effects on the codimerization.

Many investigations have recently been reported for the cooligomerizations of conjugated dienes with mono-olefins catalyzed by transition-metal compounds. Few reports have appeared, however, concerning the codimerizations of simple olefins with vinyl compounds and the dimerizations of vinyl compounds.[1)]

As has been reported in a preliminary communication,[2)] we have found that olefin-palladium chloride complexes are an effective catalyst for the codimerization of styrene with ethylene. Afterwards, Barlow and his co-workers reported the dimerizations and the codimerizations of olefins catalyzed by a benzonitrile palladium chloride complex and suggested that the palladium hydride is an intermediate.[3)] The investigations of the substituent effects of vinyl compounds and the structure of codimers on codimerization reactions give an important suggestion as to the reaction mechanism of the oligomerizations of olefins. In this paper, the codimerization of styrene with various vinyl compounds will be investigated. A reaction mechanism involving the five-coordinate hydridopalladium-olefin intermediate will be proposed and discussed in the terms of the functional group effects of vinyl compounds and solvent effects on the codimerization.

Experimental

Codimerization of Styrene with Vinyl Compounds. A reaction vessel was charged with 10.7 mmol of a styrene-palladium complex, 0.7 mol of styrene, and 0.7 mol of a vinyl compound; then, the mixture was stirred at 50°C for 6 hr. This solution thereby turned reddish-brown. The resulting solution was diluted with petroleum ether after the unreacted reagents had been removed under reduced pressure at 50°C; then it was filtered to remove the catalyst and palladium metal. The filtrate was distilled under reduced pressure. The products were separated by distillation or preparative-glcg, and were identified by infrared spectroscopy (Jasco model IR-E), proton magnetic resonance spectroscopy (JNM-4H-100 and JNM-C60HL), mass spectrometry (Hitachi RMS-4 mass spectrometer), and elemental analysis.

Methyl *trans*-5-phenyl-4-pentenoate: IR spectrum: C=O 1735 cm^{-1}, *trans*-HC=CH-963 cm^{-1}, phenyl 747 and 695 cm^{-1}. NMR spectrum: CH_3 τ 6.39 (s), CH_2 τ 7.58 (m), -HC=CH- τ 3.61 (d) and 3.89 (m), phenyl τ 2.78 (m). Found: C, 76.12; H, 7.55%. Calcd for $C_{12}H_{14}O_2$; C, 75.76; H, 7.42%.

Methyl *trans*-2-methyl-4-phenyl-3-butenoate: IR spectrum: C=O 1735 cm^{-1}, *trans*-HC=CH- 966 cm^{-1}, phenyl 749 and 699 cm^{-1}. NMR spectrum: CH_3 τ 6.36 (s) and 8.68 (d), CH τ 7.50 (m), -HC=CH- τ 3.58 (d) and 3.83 (m), phenyl τ 2.78 (6).

Methyl *trans*-5-phenyl-3-pentenoate: IR spectrum: C=O 1735 cm^{-1}, *trans*-HC=CH- 966 cm^{-1}, phenyl 749 and 699 cm^{-1}. NMR spectrum: CH_3 τ 6.36 (s), CH_2 τ 6.70 (m) and 6.95 (m), -HC=CH- τ 4.38 (m), phenyl τ 2.78 (m).

trans-1-Phenyl-4-acetoxy-1-butene: IR spectrum: C=O 1735 cm^{-1}, *trans*-HC=CH- 967 cm^{-1}, phenyl 748 and 696 cm^{-1}. NMR spectrum: CH_3 τ 8.04 (s) CH_2 τ 5.91 (m) and 7.53 (q), -HC=CH- τ 3.57 (d) and 3.92 (m), phenyl τ 2.79 (m).

trans-1-Phenyl-4-acetyl-1-butene: IR spectrum: C=O 1712 cm^{-1}, *trans*-HC=CH- 967 cm^{-1}, phenyl 752 and 697 cm^{-1}. NMR spectrum: CH_3 τ 7.94 (s), CH_2 τ 7.54 (m), -HC=CH- τ 3.63 (d) and 3.91 (m), phenyl τ 2.81 (m).

Methyl *trans*-3-pentenoate: NMR spectrum: CH_3 τ 6.38 (s) and 8.31 (d), CH_2 τ 7.06 (m), -HC=CH- τ 4.50 (m).

Methyl *trans*-2-pentenoate: IR spectrum: C=O 1730 cm^{-1}, *trans*-HC=CH- 981 cm^{-1}. NMR spectrum: CH_3 τ 6.33 (s) and 8.91 (t), CH_2 τ 7.75 (m), -HC=CH- τ 3.04 (m) and 4.24 (d).

Codimerization of Styrene-d_3 with Ethylene. Styrene-d_3 was prepared using the method described by Kirchner.[4)] Mixtures of acetophenone (25 g), 99.75% D_2O (30 m*l*), and 40% NaOD in D_2O (0.3 m*l*) were stirred at 85°C for 10 hr. The resulting solutions gave 98% acetophenone-d_3 (23 g) when the same procedure was repeated three times. The reduction of acetophenone-d_3 with $LiAlD_4$ (4 g) gave $C_6H_5CD(OH)CD_3$ (20.5 g). The alcohol was dehydrated using

1) a) T. Alderson, E. L. Jenner, and R. V. Lindsey, Jr., *J. Amer. Chem. Soc.*, **87**, 5638 (1965). b) H. Müller, D. Wittenberg, H. Seibt, and E. Scharf, *Angew. Chem. Intern. Ed.*, **4**, 327 (1965). c) A. Misono, Y. Uchida, M. Hidai, and H. Kanai, *Chem. Commun.*, **1967**, 357. d) T. Saegusa, Y. Ito, H. Kinoshita, and S. Tomita, This Bulletin, **43**, 877 (1970).

2) K. Kawamoto, T. Imanaka, and S. Teranishi, *Kogyo Kagaku Zasshi*, **72**, 1612 (1969).

3) M. G. Barlow, M. J. Bryant, R. N. Hanszeldine, and A. G. Mackie, *J. Organometal. Chem.*, **21**, 215 (1970).

4) K. Kirchner, *Makromol. Chim.*, **96**, 179 (1966).

the method of Overberger *et al.*[5] to give styrene-d_3 (12.5 g). From the analysis of the integral curve of the NMR spectrum, assuming the phenyl protons to be 5H, the α and β protons of styrene were found to contain 0.02H and 0.04H respectively. A glass autoclave was charged with an ethylene-palladium complex (1.5 g) and styrene-d_3 (10 g). The autoclave was flushed with ethylene and pressured to 4 atm, and then the mixture was stirred at 50°C for 6 hr. From the NMR spectrum analysis of the codimer thus obtained, assuming the phenyl protons to be 5H, it was calculated that olefinic methynyl, saturated methylene, and methyl protons in *trans*-1-phenyl-1-butene contained 0.97H, 0.78H, and 0.98H respectively. The estimated error in the observed values of the protons was *ca.* 0.02H.

Results and Discussion

The codimerization reaction of styrene with ethylene reported in a preliminary communication[2] was applied to the system of ethylene and methyl acrylate with a functional group. Ethylene was bubbled into a methyl acrylate solution containing an ethylene-palladium chloride complex catalyst at 50°C for 6 hr. The following products were thus obtained:

$$CH_2{=}CH_2 + CH_2{=}CH{-}COOCH_3 \longrightarrow$$

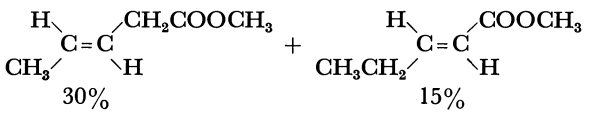

(based on palladium(II))

Methyl acrylate also could be successfully codimerized with ethylene. However, the yield is rather low because ethylene dissolves slightly in methyl acrylate under atmospheric pressure; therefore, the codimerization reactions of styrene instead of ethylene with various vinyl compounds were investigated.

The codimerization reactions of styrene with vinyl compounds catalyzed by the styrene-palladium chloride complex were carried out at 50°C for 6 hr. The results are shown in Table 1. The codimerization reaction of styrene with methyl acrylate gave not only the codimers of styrene and methyl acrylate, but also the dimers of methyl acrylate. When the other polar vinyl compound were used, no dimers of polar vinyl compounds were formed. Though the codimerization rate of styrene with vinyl acetate is slow, the complex remains as a stable catalyst for at least 6 hr. As is shown in Table 1, it was found that the codimers obtained as the main products have a linear structure in which the β carbon of styrene is bonded to the β carbon of the vinyl compound, with a shifting of the hydrogen on the β carbon of styrene. The relation between the functional groups on vinyl compounds and the yields of the codimers is shown in Table 2. When methyl acrylate bearing a carbomethoxy group is used as the vinyl compound, the best yield of codimers is obtained; the yield decreases in the following sequence: $-CO_2CH_3 > -COCH_3 > -OCOCH_3$. When nitroethylene, which has a strongly electron-withdrawing group, and *n*-butyl vinyl ether, bearing a *n*-butoxy group which is an electron-donating group are used, no codimer has been formed. When nitroethylene is used as the vinyl compound, we obtained a stable yellow-brown precipitate which shows the presence of phenyl and nitro groups in its infrared spectrum. When *n*-butyl vinyl ether is used, a viscous solution containing a higher polymer of *n*-butyl vinyl ether whose infrared spectrum shows the presence of a C–O–C bond is instantaneously formed.

Table 2. Relation between functional groups of vinyl compounds (CH_2=CH–X) and yield of codimers

X	$-NO_2$	$-\overset{\overset{O}{\|}}{C}-CH_3$	$-\overset{\overset{O}{\|}}{C}-O-CH_3$	$-O-\overset{\overset{O}{\|}}{C}-CH_3$	$-OC_4H_9$
Yield[a], %	—	125	220	50	—

a) Yields are based on the catalyst used.

The dependence of the concentration of vinyl compounds on the rates of the codimerization reactions of styrene with methyl acrylate and with vinyl acetate is shown in Fig. 1. The rate of the codimerization of styrene with methyl acrylate is proportional to the concentration of methyl acrylate in a high concentration of styrene and is independent of the concentrations of the reactants in a high concentration of methyl acrylate, because the styrene-palladium chloride complex has been used as a catalyst and the rate of the codimerization was

Table 1. Reaction of styrene and vinyl compounds

Vinyl compound	Products[a]
CH_2=CH–CO_2CH_3	*trans*-$C_6H_5CH{=}CH(CH_2)_2CO_2CH_3$, 190%; *trans*-$C_6H_5CH_2CH{=}CHCH_2CO_2CH_3$, 10%. *trans*-$C_6H_5CH{=}CHCH(CH_3)CO_2CH_3$, 20%. *trans*-$CH_3O_2CCH{=}CH(CH_2)_2CO_2CH_3$, 153%; *trans*-$CH_3O_2CCH_2CH{=}CHCH_2CO_2CH_3$, 16%. Dimers of styrene[b], 18%.
CH_2=CH–$OCOCH_3$	*trans*-$C_6H_5CH{=}CH(CH_2)_2OCOCH_3$, 50%. Dimers of styrene,[b] 32%.
CH=CH–$COCH_3$	*trans*-$C_6H_5CH{=}CH(CH_2)_2COCH_3$, 18%; isomers of codimer,[c] 107%. Dimers of styrene,[b] 14%.

Styrene-palladium complex (Pd): 10.7 mmol, styrene: 0.7 mol, vinyl compound: 0.7 mol. 50 C, 6 hr.
a) Yields are based on the catalyst used.
b) Four isomers of dimer of styrene containing *trans*-1,3-diphenyl-1-butene.
c) Three isomers of codimer of styrene with methyl vinyl ketone which were identified by infrared spectrum.

5) C. G. Overberger and J. H. Saunders, "Org. Syn.," Coll. Vol. 3, p. 204.

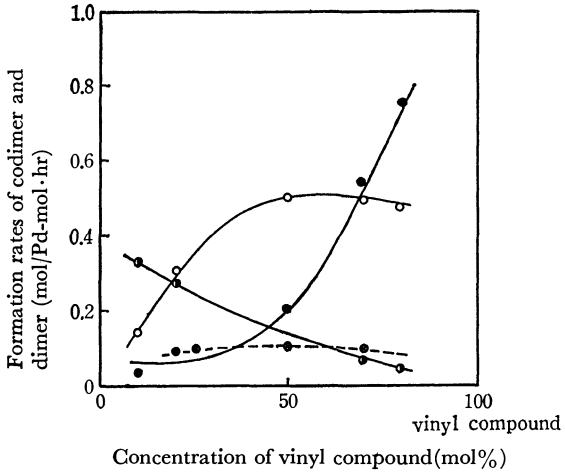

Fig. 1. The dependence of the concentration of vinyl compounds on the formation rates of codimerization and dimerization reactions.
○: Codimer of styrene with methyl acrylate, ●: dimer of methyl acrylate, ◑: dimer of styrene, ⊗: codimer of styrene with vinyl acetate. Styrene-palladium complex (Pd): 10.7 mmol, styrene+vinyl compound: 0.94 mol, nitromethane: 0.47 mol. 50°C.

measured at the point where codimers were formed in an equal amount of the catalyst used. The dimerization rates of styrene and methyl acrylate increase with increases in the styrene and methyl acrylate concentrations respectively, and the increase in the dimerization rate of methyl acrylate is larger than that in the dimerization rate of styrene. An induction period has been observed in the dimerization of methyl acrylate, but not in the dimerization of styrene; this may result from the use of the styrene-palladium complex as a catalyst. The rate of the codimerization of styrene with vinyl acetate is smaller than that of styrene with methyl acrylate and is not remarkable dependent upon the concentration of the reactants.

The solvent effect on the codimerization of styrene with methyl acrylate and on the dimerization of methyl acrylate is summarized in Table 3.[6] The formation ratio of the codimer to the dimer does not remarkably depend on the solvents except in the case of acetic acid. As was observed in the dimerization of ethylene and in the codimerization of styrene with ethylene in previous papers,[7,8] the reaction rate is enhanced in solvents containing the oxygen atom, such as phenol, nitromethane, and nitrobenzene. The reaction rate is larger in systems without a solvent than in acetic acid and benzene solvents. It appears that the reactant itself is a good solvent. Since the solvent effect was not observed in benzene on the dimerization of ethylene[7] or on the codimerization of styrene with ethylene,[8] benzene is deduced to play a role in diluting the catalytic solution. On the other hand, in contrast with the rate of the codimerization of styrene with methyl acrylate, the rate of the dimerization of methyl acrylate in acetic acid is lower than that in benzene. Since acetic acid is a good solvent in the dimerization of ethylene[7] and in the codimerization of styrene with ethylene[8], and since the dimer of styrene in acetic acid is formed in more than 3 mol equivalents of that in systems without a solvent, it may be suggested that acetic acid disturbs the coordination of methyl acrylate to the catalyst through some interactions between acetic acid and methyl acrylate.

Table 3. Solvent effects on the codimerization of styrene with methyl acrylate and on the dimerization of methyl acrylate

Solvent	Formation rate of codimer (mol/Pd-mol·hr)	Formation rate of dimer (mol/Pd-mol·hr)	Dielectric constant[6] ε(°C)
Phenol	0.530	0.311	6.15(20)
Nitromethane	0.495	0.192	22.7(10)
Nitrobenzene	0.431	—	34.8(25)
Dioxane	0.304	0.118	2.28(0)
Non solvent	0.218	0.103	—
Acetic acid	0.197	0.035	9.78(60)
Benzene	0.109	0.063	2.44(0)

Styrene-palladium complex (Pd): 10.7 mmol, styrene: 0.47 mol, methyl acrylate: 0.47mol, solvent: 0.47 mol. Reaction temperature: 50°C.

Furthermore, when the codimerization of styrene-d_3 with ethylene was carried out at 50°C for 6 hr, the results were as follows:

$$CH_2{=}CH_2 + C_6H_5CD{=}CD_2 \longrightarrow CH_{2.02}D_{0.98}{-}CH_{1.22}D_{0.78}{-}CH{=}CH{-}C_6H_5$$
$$H:D = 1.03:0.97$$

This experimental evidence on the distribution of deuterium can be interpreted according to the following scheme:[9]

$$CH_2{=}CH_2 + C_6H_5CD{=}CD_2 \longrightarrow CH_2{=}CH{-}CD_2{-}CHD{-}C_6H_5 \longrightarrow CH_2D{-}CH{=}CD{-}CHD{-}C_6H_5 \longrightarrow$$
$$CH_2D{-}CHD{-}CH{=}CD{-}C_6H_5 \text{ and } CH_2D{-}CH_2{-}CD{=}CD{-}C_6H_5$$

The codimerization reactions of styrene with vinyl compounds have the following characteristic features: (i) the use of methyl acrylate as a vinyl compound gives more codimers than that of the other vinyl compounds; (ii) the codimers produced as main products have a linear structure in which the β carbon of styrene is bonded to the β carbon of vinyl compound *via* a hydrogen shift of the β carbon of styrene; (iii) this reaction is enhanced in solvents containing the oxygen atom, particularly in weak dissociated solvents and in strongly polar solvents such as nitrobenzene, and (iv) the use of nitrobenzene or dioxane as solvent which can not be considered to be hydride sources makes it easy to give the codimer. The codimerization reaction includes the following two processes: (a) the coordina-

6) Chem. Soc. Japan, "Kagaku Binran, Kisohen I(Chem. Table, Basic I)," Maruzen, Tokyo (1966), p. 1003.

7) K. Kawamoto, T. Imanaka, and S. Teranishi, *Nippon Kagaku Zasshi*, **91**, 39 (1970).

8) K. Kawamoto, T. Imanaka, and S. Teranishi, This Bulletin, **43**, 2512 (1970).

9) Harrod and his co-workers reported that the palladium complexes isomerize the olefins by a C_3—C_1 hydrogen shift in the isomerization of 1-heptene-3-d_3.[10]

10) J. F. Harrod and A. J. Chalk, *J. Amer. Chem. Soc.*, **88**, 3491 (1966).

tion reaction includes the following two processes: (a) the coordination of the vinyl compound to the palladium ion, and (b) the hydrogen shift between the coordinated styrene and the vinyl compound. An electron-withdrawing property of the functional groups decreases in the following order on the basis of Hammett's σ value:[11]

$-NO_2 > -COCH_3 > -CO_2CH_3 > -OCOCH_3 >$ Phenyl $> n$-butoxy

If the π-bond formation between olefins and the palladium (II) ion depends predominantly on the back-donation of filled d-electrons in the palladium ion, the π-bonding ability of the vinyl compound to the palladium ion will decrease with a decrease in the σ value. On the other hand, since hydrogen is easily bonded to most transition metals as a hydride, the ease with which the hydride is formed from the coordinated vinyl compound is the opposite of the order of the σ values. It may be assumed that the best yield of the codimer when methyl acrylate is used in the codimerization of styrene with vinyl cmpounds is derived from these two opposite components.

Recently, Ketley *et al.* have suggested the following mechanism for the palladium-catalyzed dimerization of ethylene;[12]

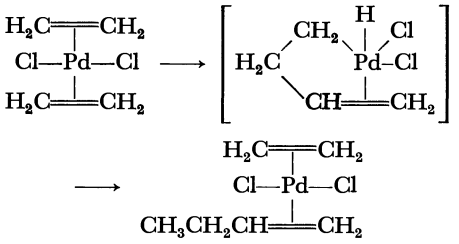

This mechanism can not, however, account for the main process of the dimerization reaction of ethylene, namely, the insertion reaction, because the carbon atom of the ethylene π-bonded to palladium has a partially positive charge, unlike free ethylene, and so the insertion reaction between π-bonded ethylenes can not be expected. It can also not account for the remarkable effect of the solvents described above.

Barlow *et al.* have reported a mechanism of the dimerization of olefins which involves the formation of the palladium hydride as a catalytic active species:[3]

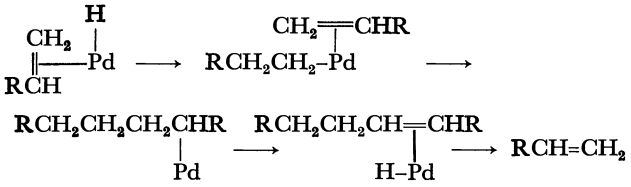

The hydrogen of the initially-formed Pd^{II}–H has been described as resulting from the solvents or the olefins as is shown in the following scheme:

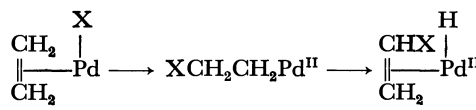

However, this mechanism, assuming the Pd^{II}–H to be a catalytic active species, can not reasonably account for the following facts: (a) styrene and vinyl compounds readily codimerize in systems without a solvent or in such solvents as nitrobenzene and dioxane, which can not be considered to be hydride sources; (b) analysis of the reaction solutions by glcg show no trace of the corresponding halogenated compound, and (c) in the experiment of the codimerization of styrene-d_3 with ethylene, if ethylene and styrene-d_3 are codimerized by Pd^{II}–H and Pd^{II}–D without any exchange reaction of Pd^{II}–H and Pd^{II}–D in the isomerization, the expected products are CH_3–CH_2–CD=CD–C_6H_5 and mixtures of CH_3–CHD–CD=CH–C_6H_5 and CH_3–CHD–CD=CD–C_6H_5 or of CH_2D–CH_2–CD=CD–C_6H_5 and CH_3–CHD–CD=CD–C_6H_5. These results are different from this experimental evidence. On the other hand, the presence of the exchange reaction of Pd^{II}–H and Pd^{II}–D in every stage of the isomerization gives mixtures of numerous products in which deuterium is distributed in various ways. Therefore, the ratio of hydrogen to deuterium in the methyl group of the codimer can be expected to be higher than 2 in the Pd^{II}–H mechanism; the observed ratio was found to be approximately 2 in this experiment. We are inclined to believe that the codimerization proceeds through a reaction path which requires no external source of hydride.

On the basis of the above facts (i)—(iv) and the results of the codimerization reaction of styrene-d_3 with ethylene, we wish to propose the reaction mechanism, with a hydride shift between coordinated styrene and vinyl compound, shown in Scheme 1.[13]

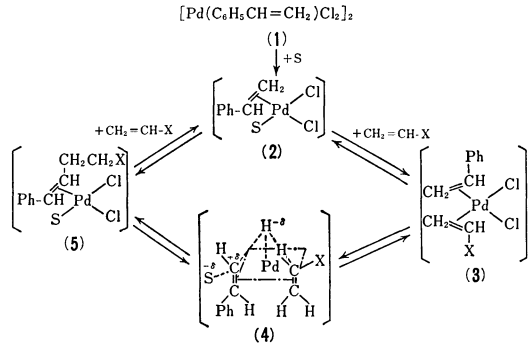

Scheme 1

The styrene-palladium complex (1) initially dissociates into a complex (2) in the presence of a solvent. The coordination of the vinyl compound with the complex (2) results in another complex (3). In the stage of the insertion reaction from the complex (3) to the complex (5) *via* an intermediate (4), the palladium ion easily abstracts the β carbon of styrene as a hydride rather than the vinyllic hydrogen of the vinyl compound, with an electron-withdrawing group, thus reforming the five-coordinate hydridopalladium-olefin intermediate (4). This hydride is added to the α carbon of the vinyl compound with the electron-withdrawing

11) J. Hine, "Physical Org. Chem.," Mcgrew-Hill, N. Y. (1956), p. 65.

12) A. D. Ketley, L. P. Fisher, A. J. Berlin, C. R. Morgan, E. H. Gorman, and T. R. Steadman, *Inorg. Chem.*, **6**, 657 (1967).

13) K. Kawamoto, T. Imanaka, and S. Teranishi, *Nippon Kagaku Zasshi*, **89**, 639 (1968).

group to the four-coordinate palladium-alkyl complex and then, this alkyl group is inserted into the partially-positive β carbon of styrene, thus reforming the complex (5) through the coordination of the solvent to a vacant coordination site. The codimerization reaction may proceed by repeating these processes. A nucleophilic approach of the solvent can facilitate the abstraction of a hydride from styrene by the palladium ion and stabilize the partially-positive β carbon of styrene. These functions of the solvent were suggested by Volger in the oxidative dimerization of β-substituted α-olefins by palladium acetate.[14] Recently, Fackler *et al.* have reported ascertaining the presence of the five-coordinate complex by nuclear magnetic-resonance spectroscopy in reactions of xanthates and dithiocarbamates of palladium (II) and platinum (II) with methyldiphenylphosphine[15] while Tayim *et al.* have proposed a reaction mechanism involving the five-coordinate complex as an intermediate in the isomerization catalyzed by the platinum complexes.[16] In addition to the function of the solvent described above, the solvent may catalytically keep the coordination site active through its coordination in the stage of changing from the complex (3) to the complex (5) and may also accelerate the coordination of the vinyl compound through its dissociation in the stage of changing from the complex (2) to the complex (3). The same argument was previously made by the present authors in attempting to explain the dimerization of ethylene[7] and the codimerization of styrene with ethylene.[8]

14) H. C. Volger, *Rec. Trav. Chim.*, **86**, 677 (1967).

15) J. P. Fackler, Jr., W. C. Seidel, and John A. Fetchin, *J. Amer. Chem. Soc.*, **90**, 2707 (1968).

16) H. A. Tayim and J. C. Bailar, Jr., *ibid.*, **89**, 3420 (1967).

BULLETIN OF THE CHEMICAL SOCIETY OF JAPAN, VOL. 44, 1243—1248(1971)

Conformation of Adsorbed Polymeric Chain. III

Kinsi MOTOMURA, Kōjū SEKITA, and Ryohei MATUURA
Department of Chemistry, Faculty of Science, Kyushu University, Fukuoka

(Received October 9, 1970)

Average properties of a copolymeric chain in which a segments of the kind A and b segments of the kind B occur alternatively are calculated for an infinite chain length. For the simplest case of $a=b=1$, *i.e.* an alternating copolymeric chain $(-A-B-)_N$, the average number of adsorbed segments of A, $\bar{\nu}_A$, that of B, $\bar{\nu}_B$, and the mean square end-to-end distance $\overline{r^2}$ are computed numerically as functions of the adsorption energies ε_A and ε_B. The values of $\bar{\nu}_A$, $\bar{\nu}_B$, and $\overline{r^2}$ are proportional to N for larger values of η_A $(=\exp(\varepsilon_A/kT))$ than the critical value $(\eta_A)_c$ at fixed η_B, as found for the case of a homogeneous polymeric chain. It is seen that the behavior of the copolymeric chain near an interface is affected distinctively by the adsorption energies of the segments A and B, and the copolymeric chain is forced to adsorb even for a fairly low adsorption energy of the segment of one kind if the adsorption energy of the segment of the other kind is sufficiently large.

Statistical-mechanical theories of the adsorption of polymeric chains at interfaces have been presented by many investigators.[1-7] For the homogeneous polymeric chain which is a long sequence of segments of the same kind, it was shown that the conformation of the isolated polymeric chain near the interface changes discontinuously at a certain value of the adsorption energy which depends on a lattice model used. In the case of the polymeric chain consisting of $n+1$ segments on a simple cubic lattice we obtained results where the average number of adsorbed segments is given by

$$\begin{aligned}
\bar{\nu} &= n\{1-\eta[2(\eta-1)]^{-1} \\
&\quad + \eta[4(\eta-1)^2+(\eta-1)]^{-1/2}\}, && \eta>\eta_c \\
\bar{\nu} &= (5/2)(\pi n/6)^{1/2}, && \eta=\eta_c \\
\bar{\nu} &= 6/(6-5\eta), && \eta<\eta_c
\end{aligned} \tag{1}$$

and the mean-square end-to-end distance by

$$\begin{aligned}
\overline{r^2} &= 2l^2n(\eta-1)[4(\eta-1)^2+(\eta-1)]^{-1/2}, && \eta>\eta_c \\
\overline{r^2} &= (8/9)l^2n, && \eta=\eta_c \\
\overline{r^2} &= l^2n, && \eta<\eta_c
\end{aligned} \tag{2}$$

where η is related to the energy gain per segment associated with the adsorption $-\varepsilon$, by the equation

$$\eta = \exp(\varepsilon/kT), \tag{3}$$

η_c equals 6/5, and l is the distance between neighboring segments.[6,7] It is interesting to estimate the effect

1) R. Simha, H. L. Frisch, and F. R. Eirich, *J. Phys. Chem.*, **57**, 584 (1953).
2) A. Silberberg, *J. Phys. Chem.*, **66**, 1872 (1962); *J. Chem. Phys.*, **46**, 1105 (1967); *ibid.*, **48**, 2835 (1968).
3) E. A. DiMarzio, *J. Chem. Phys.*, **42**, 2101 (1965); E. A. DiMarzio and F. L. McCrackin, *ibid.*, **43**, 539 (1965); C. A. J. Hoeve, E. A. DiMarzio, and P. Peyser, *ibid.*, **42**, 2558 (1965); C. A. H. Hoeve, *ibid.*, **43**, 3007 (1965).
4) R.-J. Roe, *Proc. Nat. Acad. Sci.*, **53**, 50 (1965); *J. Chem. Phys.*, **43**, 1591 (1965); *ibid.*, **44**, 4264 (1966).
5) R. J. Rubin, *J. Chem. Phys.*, **43**, 2392 (1965); *J. Res. Nat. Bur. Stand.*, **B70**, 237 (1966).
6) K. Motomura and R. Matuura, *Mem. Fac. Sci., Kyushu Univ.*, **C6**, 97 (1968).
7) K. Motomura and R. Matuura, *J. Chem. Phys.*, **50**, 1281 (1969); *ibid.*, **51**, 4681 (1969).

of foreign segments introduced into the polymeric chain upon the above equations. This is useful to understand better the strange behavior of copolymers at interfaces.

We extended the theoretical treatment given in previous papers to a copolymeric chain consisting of segments of various kinds. For convenience, we consider a copolymeric chain in which the segments of kinds A and B, the same in size, occur in alternative succession of a segments of the kind A and b segments of B.

Theoretical

1. Probability of an Adsorbed Polymeric Chain. The behavior of polymer molecules near an interface is represented by a symmetrical random walker whose way is blocked by the interface when the self-excluded volume is neglected and the concentration is extremely dilute. We are concerned with a polymeric chain $(-A_a-B_b-)_N$ consisting of $(a+b)N$ segments lying in the positive z domain of a simple cubic lattice and adsorbing at the interface which is the xy plane through $z=0$. We also assume that the polymeric chain is always adsorbed by the end segments of the chain on the interface, because the dangling chain ends make a negligible contribution to the properties in an adsorbed state $(\eta>\eta_c)$.[4,7] A given conformation of the absorbed polymeric chain, of which one chain end is located at the origin and the other end at a point $(x,y,0)$, is characterized by a sequence of random walkers which touch the interface only at two ends and have probabilities $f_{k_j}(x_j,y_j)$. The probability of the adsorbed polymeric chain is then given by

$$p_{(a+b)N}(x,y,\eta_A,\eta_B) = \sum_m \sum_k \sum_{x,y} \eta_A\eta_B f_{k_m}(x_m,y_m) \prod_{j=1}^{m-1} \eta_j f_{k_j}(x_j,y_j), \tag{4}$$

where

$$\eta_A = \exp(\varepsilon_A/\boldsymbol{k}T), \quad \eta_B = \exp(\varepsilon_B/\boldsymbol{k}T), \tag{5}$$

and η_j takes η_A or η_B according to whether the j-th random walker terminates in the segments A or in B. A set of $\boldsymbol{k}$, $\boldsymbol{x}$, and $\boldsymbol{y}$ means a microscopic state satisfying the conditions

$$\sum_{j=1}^{m} k_j = (a+b)N - 1 \tag{6}$$

which come from the fact that the polymeric chain of $(a+b)N$ segments is replaced by the random walk of $(a+b)N-1$ steps,

$$\sum_{j=1}^{m} x_j = x, \quad \text{and} \quad \sum_{j=1}^{m} y_j = y, \tag{7}$$

and the sums are taken over all possible values. On introducing generating functions

$$\sum_{x,y} p_{(a+b)N}(x,y,\eta_A,\eta_B) \exp(ix\theta+iy\phi) = P_{(a+b)N}(\theta,\phi,\eta_A,\eta_B)$$

$$\sum_{N=1}^{\infty} P_{(a+b)N}(\theta,\phi,\eta_A,\eta_B) w^{(a+b)N-1} = P(\theta,\phi,\eta_A,\eta_B;w) \tag{8}$$

and

$$\sum_{x,y} f_{(a+b)n+k}(x,y) \exp(ix\theta+iy\phi) = F_{(a+b)n+k}(\theta,\phi)$$

$$\sum_{n=0}^{\infty} F_{(a+b)n+k}(\theta,\phi) w^{(a+b)n+k} = F_k(\theta,\phi;w), \tag{9}$$

Eq. (4) becomes

$$P(\theta,\phi,\eta_A,\eta_B;w) = \eta_A \boldsymbol{a}\left(\sum_{m=1}^{\infty} \mathbf{M}^m\right)\boldsymbol{\beta}^+ = \eta_A \boldsymbol{a}\mathbf{M}(\mathbf{I}-\mathbf{M})^{-1}\boldsymbol{\beta}^+, \tag{10}$$

where

$$\mathbf{M} = \begin{pmatrix} \eta_A F_{a+b} & \eta_A F_1 & \cdots \eta_A F_{a-1} & \eta_B F_a & \cdots \eta_B F_{a+b-1} \\ \eta_A F_{a+b-1} & \eta_A F_{a+b} \cdots & \eta_A F_{a-2} & \eta_B F_{a-1} \cdots & \eta_B F_{a+b-2} \\ \cdots\cdots & \cdots\cdots & \cdots\cdots & \cdots\cdots & \cdots\cdots \\ \eta_A F_1 & \eta_A F_2 & \cdots \eta_A F_a & \eta_B F_{a+1} \cdots & \eta_B F_{a+b} \end{pmatrix}, \tag{11}$$

$$\boldsymbol{a} = (1\ 0\ \cdots\ 0), \text{ and } \boldsymbol{\beta} = (0\ \cdots\ 0\ 1).$$

Substituting Eq. (A9) in the Appendix into the above equation, we obtain

$$P(\theta,\phi,\eta_A,\eta_B;w) = \eta_A \Delta_1(1)/D(1), \tag{12}$$

where

$$D(1) = (-1)^{a+b} \begin{vmatrix} \eta_A F_{a+b}-1 & \eta_A F_1 & \cdots \eta_B F_{a+b-1} \\ \eta_A F_{a+b-1} & \eta_A F_{a+b}-1 \cdots & \eta_B F_{a+b-2} \\ \cdots\cdots & \cdots\cdots & \cdots\cdots \\ \eta_A F_1 & \eta_A F_2 & \cdots \eta_B F_{a+b}-1 \end{vmatrix} \tag{13}$$

and

$$\Delta_1(1) = \begin{vmatrix} \eta_A F_1 & \eta_A F_2 \cdots \eta_B F_{a+b-1} \\ \eta_A F_{a+b}-1 & \eta_A F_1 \cdots \eta_B F_{a+b-2} \\ \cdots\cdots & \cdots\cdots \\ \eta_A F_3 & \eta_A F_4 \cdots \eta_B F_1 \end{vmatrix} \tag{14}$$

It is now necessary to know $F_k(\theta,\phi;w)$ as a function of θ, ϕ, and w in order to have an explicit expression of $P(\theta,\phi,\eta_A,\eta_B;w)$.

2. Evaluation of $F_k(\theta,\phi;w)$. There exist relations between the probabilities $f_{(a+b)n+k}(x,y)$ and corresponding probabilities $u_{(a+b)n+k}(x,y)$ of an unrestricted random walk:

$$\begin{aligned} u_{(a+b)n+k}(x,y) &= \sum_{x',y'} f_1(x',y') u_{(a+b)n+k-1}(x-x',y-y') \\ &+ 2\sum_j \sum_{x',y'} f_{(a+b)j+1}(x',y') u_{(a+b)(n-j)+k-1}(x-x',y-y') \\ &+ \cdots\cdots \\ &+ 2\sum_j \sum_{x',y'} f_{(a+b)(j+1)}(x',y') u_{(a+b)(n-j-1)+k}(x-x',y-y'), \\ & k = 1, 2, \cdots, a+b. \end{aligned} \tag{15}$$

Defining generating functions

$$\sum_{x,y} u_{(a+b)n+k}(x,y) \exp(ix\theta+iy\phi) = U_{(a+b)n+k}(\theta,\phi)$$

$$\sum_{n=0}^{\infty} U_{(a+b)n+k}(\theta,\phi) w^{(a+b)n+k} = U_k(\theta,\phi;w)^{8)} \tag{16}$$

analogous to Eq. (9), Eq. (15) becomes

$$\begin{aligned} U_k(\theta,\phi;w) &= [2F_1(\theta,\phi;w) - wF_1(\theta,\phi)]U_{k-1}(\theta,\phi;w) \\ &+ 2F_2(\theta,\phi;w)U_{k-2}(\theta,\phi;w) + \cdots \\ &+ 2F_{a+b}(\theta,\phi;w)U_k(\theta,\phi;w), \\ & k = 1, 2, \cdots, a+b-1 \\ U_{a+b}(\theta,\phi;w) - U_0(\theta,\phi) &= [2F_1(\theta,\phi;w) \\ &- wF_1(\theta,\phi)]U_{a+b-1}(\theta,\phi;w) \\ &+ 2F_2(\theta,\phi;w)U_{a+b-2}(\theta,\phi;w) + \cdots \\ &+ 2F_{a+b}(\theta,\phi;w)U_{a+b}(\theta,\phi;w). \end{aligned} \tag{17}$$

Rearranging the above equations after introducing

8) For $k=a+b$ the equation is slightly modified by adding $U_0(\theta,\phi)$ to the left-hand side.

$$U_0(\theta, \phi) = 1 \text{ and } F_1(\theta, \phi) = c/3 \tag{18}$$

where

$$c = \cos\theta + \cos\phi, \tag{19}$$

we obtain

$$\begin{aligned}
&U_{k-1}(\theta, \phi; w)F_1(\theta, \phi; w) + U_{k-2}(\theta, \phi; w)F_2(\theta, \phi; w) + \cdots \\
&\quad + U_k(\theta, \phi; w)F_{a+b}(\theta, \phi; w) = (1/2)[U_k(\theta, \phi; w) \\
&\quad + (cw/3)U_{k-1}(\theta, \phi; w)], \quad k = 1, 2, \cdots, a+b-1 \\
&U_{a+b-1}(\theta, \phi; w)F_1(\theta, \phi; w) + U_{a+b-2}(\theta, \phi; w)F_2(\theta, \phi; w) + \cdots \\
&\quad + U_{a+b}(\theta, \phi; w)F_{a+b}(\theta, \phi; w) = (1/2)[U_{a+b}(\theta, \phi; w) \\
&\quad + (cw/3)U_{a+b-1}(\theta, \phi; w) - 1].
\end{aligned} \tag{20}$$

These equations allow us to evaluate $F_k(\theta, \phi, w)$. We have

$$\begin{aligned}
F_1(\theta, \phi; w) &= cw/6 + D_1/D \\
F_k(\theta, \phi; w) &= D_k/D, \quad k = 2, 3, \cdots, a+b-1 \\
F_{a+b}(\theta, \phi; w) &= 1/2 + D_{a+b}/D,
\end{aligned} \tag{21}$$

where

$$D = \begin{vmatrix} U_{a+b} & U_{a+b-1} \cdots U_1 \\ U_1 & U_{a+b} \cdots U_2 \\ \cdots\cdots & \cdots\cdots \\ U_{a+b-1} & U_{a+b-2} \cdots U_{a+b} \end{vmatrix} \tag{22}$$

and D_k is the determinant obtained on replacing the respective elements in the k-th column of D by

$$0, 0, \cdots, 0, -1/2.$$

$U_j(\theta, \phi; w)$ in the determinants are given by

$$\begin{aligned}
U_j(\theta, \phi; w) &= \frac{1}{2\pi}\int_{-\pi}^{\pi} d\phi \left[\frac{w}{3}(c+\cos\phi)\right]^j \Big/ \\
&\quad \left\{1 - \left[\frac{w}{3}(c+\cos\phi)\right]^{a+b}\right\} \\
&= [3/(a+b)]\sum_{l=0}^{a+b-1} \{1/\omega^{(a+b-j)l}[(3 - cw/\omega^l)^2 \\
&\quad - (w/\omega^l)^2]^{1/2}\}, \quad j = 1, 2, \cdots, a+b,
\end{aligned} \tag{23}$$

where

$$\omega = \exp[2\pi i/(a+b)]. \tag{24}$$

3. Expressions for Average Properties. We may write $P(\theta, \phi, \eta_A, \eta_B; w)$, which we will denote by $P(c, \eta_A, \eta_B; w)$ hereafter, as an explicit function of c, η_A, η_B, and w. It is now possible to calculate the average properties of the adsorbed polymeric chain. Taking into account Eqs. (4) and (8), the mean square end-to-end distance is given by

$$\overline{r^2} = l^2[c\{\partial P_{(a+b)N}(c, \eta_A, \eta_B)/\partial c\}/P_{(a+b)N}(c, \eta_A, \eta_B)]_{c=2}, \tag{25}$$

where $P_{(a+b)N}(c, \eta_A, \eta_B)$ is used instead of $P_{(a+b)N}(\theta, \phi, \eta_A, \eta_B)$. On the other hand, the average number of adsorbed segments of the kind A per polymeric chain is computed by

$$\bar{\nu}_A = \eta_A\{\partial P_{(a+b)N}(2, \eta_A, \eta_B)/\partial\eta_A\}/P_{(a+b)N}(2, \eta_A, \eta_B) \tag{26}$$

and that of B by

$$\bar{\nu}_B = \eta_B\{\partial P_{(a+b)N}(2, \eta_A, \eta_B)/\partial\eta_B\}/P_{(a+b)N}(2, \eta_A, \eta_B). \tag{27}$$

In order to carry out the calculation of Eqs. (25), (26), and (27), it is necessary to know $P_{(a+b)N}(c, \eta_A, \eta_B)$ and its derivatives with respect to c, η_A, and η_B. These functions are found by applying Cauchy's residue theorem to Eq. (8). We obtain

$$\begin{aligned}
P_{(a+b)N}(c, \eta_A, \eta_B) &= (1/2\pi i)\oint_{C_0} (1/w^{(a+b)N}) \\
&\quad \times P(c, \eta_A, \eta_B; w)dw,
\end{aligned} \tag{28}$$

$$\begin{aligned}
[\partial P_{(a+b)N}(c, \eta_A, \eta_B)/\partial c]_{c=2} &= (1/2\pi i)\oint_{C_0} (1/w^{(a+b)N}) \\
&\quad \times [\partial P(c, \eta_A, \eta_B; w)/\partial c]_{c=2}dw,
\end{aligned} \tag{29}$$

$$\begin{aligned}
\partial P_{(a+b)N}(2, \eta_A, \eta_B)/\partial\eta_A &= (1/2\pi i)\oint_{C_0} (1/w^{(a+b)N}) \\
&\quad \times \{\partial P(2, \eta_A, \eta_B; w)/\partial\eta_A\}dw,
\end{aligned} \tag{30}$$

and

$$\begin{aligned}
\partial P_{(a+b)N}(2, \eta_A, \eta_B)/\partial\eta_B &= (1/2\pi i)\oint_{C_0} (1/w^{(a+b)N}) \\
&\quad \times \{\partial P(2, \eta_A, \eta_B: w)/\partial\eta_B\}dw,
\end{aligned} \tag{31}$$

where the contour C_0 includes only the pole at $w=0$.

4. Average Properties of $(-A-B-)_N$. Taking up the simplest case $a=b=1$, *i.e.* an alternating copolymeric chain $(-A-B-)_N$, we will consider the effect of different adsorption energies of segments A and B on the conformation. Let us first derive the generating functions of unrestricted random walk $U_1(c; w)$ and $U_2(c; w)$ which are necessary for knowing $F_1(c; w)$ and $F_2(c; w)$. This is done by introducing $a=b=1$ and $\omega=-1$ resulting from Eq. (24) into Eq. (23); we have

$$\begin{aligned}
U_1(c; w) &= (3/2)\{[(3-cw)^2 - w^2]^{-1/2} - [(3+cw)^2 - w^2]^{-1/2}\} \\
U_2(c; w) &= (3/2)\{[(3-cw)^2 - w^2]^{-1/2} + [(3+cw)^2 - w^2]^{-1/2}\}.
\end{aligned} \tag{32}$$

Substituting these equations and Eq. (22) into Eq (21), we get

$$\begin{aligned}
F_1(c; w) &= cw/6 - (1/12)\{[(3-cw)^2 - w^2]^{1/2} \\
&\quad - [(3+cw)^2 - w^2]^{1/2}\} \\
F_2(c: w) &= 1/2 - (1/12)\{[(3-cw)^2 - w^2]^{1/2} \\
&\quad + [(3+cw)^2 - w^2]^{1/2}\}.
\end{aligned} \tag{33}$$

The generating function of the probability of adsorbed polymeric chain is connected with $F_1(c; w)$ and $F_2(c; w)$ with the aid of Eqs. (12), (13), and (14), and is expressed as the explicit function of c, η_A, η_B, and w:

$$P(c, \eta_A, \eta_B; w) = \eta_A\eta_B F_1(c; w)/D(c, \eta_A, \eta_B, w), \tag{34}$$

where

$$\begin{aligned}
D(c, \eta_A, \eta_B, w) &= 1 - (\eta_A + \eta_B)F_2(c; w) \\
&\quad + \eta_A\eta_B[F_2(c: w)^2 - F_1(c; w)^2] \\
&= \frac{(\eta_A+\eta_B)^2}{4\eta_A\eta_B}\left\{\left(1 - \frac{1}{6}\frac{2\eta_A\eta_B}{\eta_A+\eta_B}(3+cw\right.\right. \\
&\quad \left.\left. - [(3-cw)^2 - w^2]^{1/2}\right)\left(1 - \frac{1}{6}\frac{2\eta_A\eta_B}{\eta_A+\eta_B}\right.\right. \\
&\quad \left.\left. \times (3 - cw - [(3+cw)^2 - cw^2]^{1/2})\right) \right. \\
&\quad \left. - \left(\frac{\eta_A - \eta_B}{\eta_A + \eta_B}\right)^2\right\}.
\end{aligned} \tag{35}$$

On introducing Eq. (34) into Eq. (28), the generating function $P_{2N}(2, \eta_A, \eta_B)$ is given by

$$P_{2N}(2, \eta_A, \eta_B) = \frac{1}{2\pi i}\oint_{C_0} \frac{1}{w^{2N}} \frac{\eta_A\eta_B F_1(2; w)}{D(2, \eta_A, \eta_B, w)} dw. \tag{36}$$

It is seen from Eq. (35) that the equation $D(2, \eta_A, \eta_B, w)=0$ has two roots w_1 and w_2 which are related to each other by

$$w_1 = -w_2 \tag{37}$$

and coincide with branch-points $w=1$ and -1 respectively for a set of η_A and η_B satisfying

$$36 - 6(3-6^{1/2})(\eta_A+\eta_B) - 5(24^{1/2}-1)\eta_A\eta_B = 0. \tag{38}$$

We are interested in the behavior of the adsorbed polymeric chain only when the values of η_A and η_B are larger than the critical values given by Eq. (38), because the polymeric chain is in reality in the adsorbed state for the values of η_A and η_B. If the values of η_A and η_B are larger than the critical values and N is infinitely large, the principal contribution to the integral of Eq. (36) comes from residues of w_1 and w_2.[5,6] Thus we have

$$P_{2N}(2, \eta_A, \eta_B) = -\frac{1}{{w_1}^{2N}} \frac{\eta_A\eta_B F_1(2; w_1)}{\partial D(2, \eta_A, \eta_B, w_2)/\partial w} - \frac{1}{{w_2}^{2N}} \frac{\eta_A\eta_B F_1(2; w_2)}{\partial D(2, \eta_A, \eta_B, w_2)/\partial w}, \tag{39}$$

where $\partial D(2, \eta_A, \eta_B, w_1)/\partial w$ and $\partial D(2, \eta_A, \eta_B, w_2)/\partial w$ denote the values of $\partial D(2, \eta_A, \eta_B, w)/\partial w$ at $w=w_1$ and w_2, respectively. Combining

$$\partial D(2, \eta_A, \eta_B, w)/\partial w = -(\eta_A+\eta_B)\partial F_2(2; w)/\partial w + 2\eta_A\eta_B[F_2(2; w)\partial F_2(2; w)/\partial w - F_1(2; w)\partial F_1(2; w)/\partial w] \tag{40}$$

where

$$\partial F_1(2; w)/\partial w = 1/3 + (1/4)\{(2-w)[(3-2w)^2-w^2]^{-1/2} + (2+w)[(3+2w)^2-w^2]^{1/2}\}$$
$$\partial F_2(2; w)/\partial w = (1/4)\{(2-w)[(3-2w)^2-w^2]^{-1/2} - (2+w)[(3+2w)^2-w^2]^{-1/2}\} \tag{41}$$

with Eq. (37), we obtain

$$\partial D(2, \eta_A, \eta_B, w_1)/\partial w = -\partial D(2, \eta_A, \eta_B, w_2)/\partial w. \tag{42}$$

From this and

$$F_1(2; w_1) = -F_1(2; w_2), \tag{43}$$

Eq. (39) is reduced to

$$P_{2N}(2, \eta_A, \eta_B) = -\frac{2}{{w_1}^{2N}} \frac{\eta_A\eta_B F_1(2; w_1)}{\partial D(2, \eta_A, \eta_B, w_1)/\partial w} \tag{44}$$

On the other hand, the substitution of the derivative of $P(c, \eta_A, \eta_B; w)$ with respect to c into Eq. (29) gives

$$\left[\frac{\partial P_{2N}(c, \eta_A, \eta_B)}{\partial c}\right]_{c=2} = \frac{1}{2\pi i}\oint_{c, w^{2N}} \frac{dw}{} \left[\frac{\eta_A\eta_B\partial F_1(2; w)/\partial c}{D(2, \eta_A, \eta_B, w)} - \frac{\eta_A\eta_B F_1(2; w)\partial D(2, \eta_A, \eta_B, w)/\partial c}{D(2, \eta_A, \eta_B, w)^2}\right], \tag{45}$$

where

$$\partial D(2, \eta_A, \eta_B, w)/\partial c = -(\eta_A+\eta_B)\partial F_2(2; w)/\partial c + 2\eta_A\eta_B[F_2(2; w)\partial F_2(2; w)/\partial c - F_1(2; w)\partial F_1(2; w)/\partial c] \tag{46}$$

in which

$$\partial F_1(2; w)/\partial c = w/6 + (w/12)\{(3-2w)[(3-2w)^2-w^2]^{-1/2} + (3+2w)[(3+2w)^2-w^2]^{-1/2}\}$$
$$\partial F_2(2; w)/\partial c = (w/12)\{(3-2w)[(3-2w)^2-w^2]^{-1/2} - (3+2w)[(3+2w)^2-w^2]^{-1/2}\}. \tag{47}$$

Carrying out integration in a similar way and retaining the predominant term in the limit $N\gg1$, Eq. (45) becomes

$$\left[\frac{\partial P_{2N}(c, \eta_A, \eta_B)}{\partial c}\right]_{c=2} = -\frac{2N}{{w_1}^{2N+1}} \frac{\eta_A\eta_B F_1(2; w_1)\partial D(2, \eta_A, \eta_B, w_1)/\partial c}{[\partial D(2, \eta_A, \eta_B, w_1)/\partial w]^2}. \tag{48}$$

We may obtain expressions for $\partial P_{2N}(2, \eta_A, \eta_B)/\partial\eta_A$ and $\partial P_{2N}(2, \eta_A, \eta_B)/\partial\eta_B$ by using a method similar to that used to derive the above equation:

$$\frac{\partial P_{2N}(2, \eta_A, \eta_B)}{\partial\eta_A} = -\frac{2N}{{w_1}^{2N+1}} \frac{\eta_A\eta_B F_1(2; w_1)\partial D(2, \eta_A, \eta_B, w_1)/\partial\eta_A}{[\partial D(2, \eta_A, \eta_B, w_1)/\partial w]^2}$$
$$\frac{\partial P_{2N}(2, \eta_A, \eta_B)}{\partial\eta_B} = -\frac{2N}{{w_1}^{2N+1}} \frac{\eta_A\eta_B F_1(2; w_1)\partial D(2, \eta_A, \eta_B, w_1)/\partial\eta_B}{[\partial D(2, \eta_A, \eta_B, w_1)/\partial w]^2} \tag{49}$$

where

$$\partial D(2, \eta_A, \eta_B, w)/\partial\eta_A = -F_2(2; w) + \eta_B[F_2(2; w)^2-F_1(2; w)^2]$$
$$\partial D(2, \eta_A, \eta_B, w)/\partial\eta_B = -F_2(2; w) + \eta_A[F_2(2; w)^2-F_1(2; w)^2]. \tag{50}$$

The final equations for the average properties are derived by substituting Eqs. (44), (48), and (49) into Eqs. (25), (26), and (27):

$$\overline{r^2} = 2Nl^2\frac{2}{w_1}\frac{\partial D(2, \eta_A, \eta_B, w_1)/\partial c}{\partial D(2, \eta_A, \eta_B, w_1)/\partial w}, \tag{51}$$

$$\bar{\nu}_A = 2N\frac{\eta_A}{w_1}\frac{\partial D(2, \eta_A, \eta_B, w_1)/\partial\eta_A}{\partial D(2, \eta_A, \eta_B, w_1)/\partial w}, \tag{52}$$

and

$$\bar{\nu}_B = 2N\frac{\eta_B}{w_1}\frac{\partial D(2, \eta_A, \eta_B, w_1)/\partial\eta_B}{\partial D(2, \eta_A, \eta_B, w_1)/\partial w}. \tag{53}$$

We can now calculate the average values $\overline{r^2}$, $\bar{\nu}_A$, and $\bar{\nu}_B$ of the polymeric chain $(\text{–A–B–})_N$ at the interface as functions of η_A and η_B and compare them with previous results.

Discussion

Let us first consider how the average number of adsorbed segments of kind A in the alternating copolymeric chain $(\text{–A–B–})_N$ varies with η_A in the limit $N\gg1$ when η_B has a given value. This is determined by numerical calculation of Eq. (52) which is made by evaluating one root w_1 of the equation $D(2, \eta_A, \eta_B, w)=0$ at a given set of η_A and η_B and then substituting the root into Eq. (52) with Eqs. (40) and (50). The variation of $\bar{\nu}_A$ with η_A at few fixed values of η_B is illustrated in Fig. 1, where the ratio $\bar{\nu}_A/2N$ is plotted against ε_A measured in the unit kT. It is seen that the average number of adsorbed segments is proportional to the total number of segments of the copolymeric chain for values of η_A larger than the critical value $(\eta_A)_c$ derived from Eq. (38) at given η_B, as found for the case of a homogeneous polymeric chain consisting of identical segments. The critical value $(\eta_A)_c$ increases remarkably with the decrease in η_B. The increase of $\bar{\nu}_A$ with η_A is slower than the corresponding one of the homogeneous polymeric chain calculated by Eq. (1).

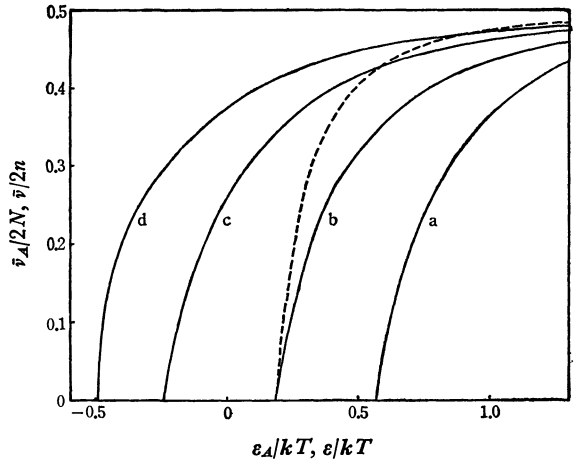

Fig. 1. The ratio $\bar{\nu}_A/2N$ of the copolymeric chain $(-A-B-)_N$ is plotted against ε_A/kT in the limit $N \gg 1$: (a) $\varepsilon_B/kT = -0.223$, (b) 0.182, (c) 0.588, (d) 0.916. The dotted line corresponds to the homogeneous polymeric chain calculated by Eq. (1).

It is probable that the adsorption of the segment A in the copolymeric chain is obstructed by the existence of the segment B having a low adsorption energy when $\eta_B > 6/5$ ($\varepsilon_B/kT < 0.182$). On the other hand, when $\eta_B > 6/5$, adsorption is preferred at the initial stage, becomes equal to that of the homogeneous polymeric chain at $\eta_A = \eta_B$, and then accepts a negative contribution at larger η_A.

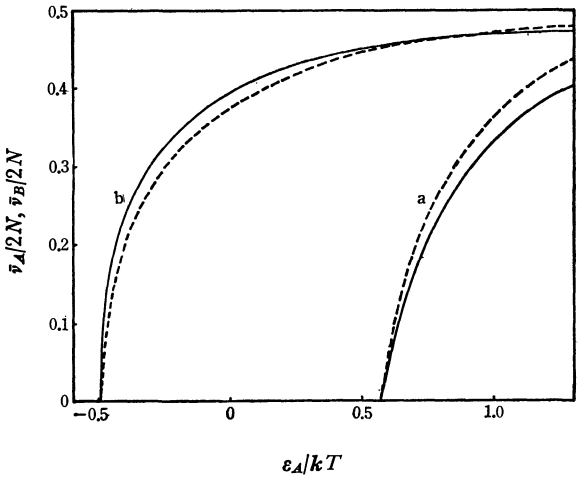

Fig. 2. Comparison of $\bar{\nu}_B/2N$ *versus* ε_A/kT (solid line) and $\bar{\nu}_A/2N$ *versus* ε_A/kT (dotted line) at (a) $\varepsilon_B/kT = -0.223$ and (b) 0.916.

It is also interesting to see the variation of the average number of adsorbed segments of kind B with η_A when η_B is given. The plot of $\bar{\nu}_B/2N$ against ε_A/kT is shown in Fig. 2 where the curves are calculated by Eq. (53) by a similar procedure. Adsorption of segment B occurs and increases gradually with η_A even when η_B has a value lower than 6/5 at which the homogeneous polymeric chain consisting of B segments does not exist in the adsorbed state. For $\eta_B > 6/5$, the value of $\bar{\nu}_B$ increases fairly steeply with η_A.

From the above results, we can know the effect of the adsorption energy of the segments on the total average number of adsorbed segments of the alternating

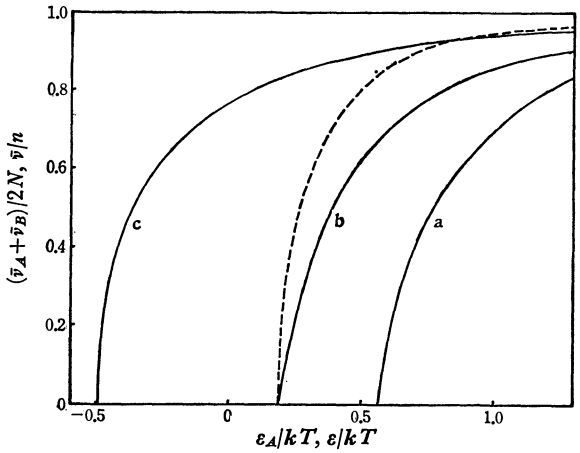

Fig. 3. The sum $(\bar{\nu}_A+\bar{\nu}_B)/2N$ is plotted against ε_A/kT: (a) $\varepsilon_B/kT = -0.223$, (b) 0.182, (c) 0.916. $\bar{\nu}/n$ of Eq. (1) is shown by the dotted line.

copolymeric chain. In Fig. 3, the sum of $\bar{\nu}_A/2N$ and $\bar{\nu}_B/2N$ given in Figs. 1 and 2 *versus* ε_A/kT curves at fixed values of η_B are illustrated together with the curve of a homogeneous polymeric chain calculated by Eq. (1). It is noticeable that the behavior of the copolymeric chain near an interface is affected distinctly by the adsorption energies of segments A and B, and the copolymeric chain is forced to adsorb even for a fairly low adsorption energy of the segment of one kind if the adsorption energy of the segment of the other kind is sufficiently large.

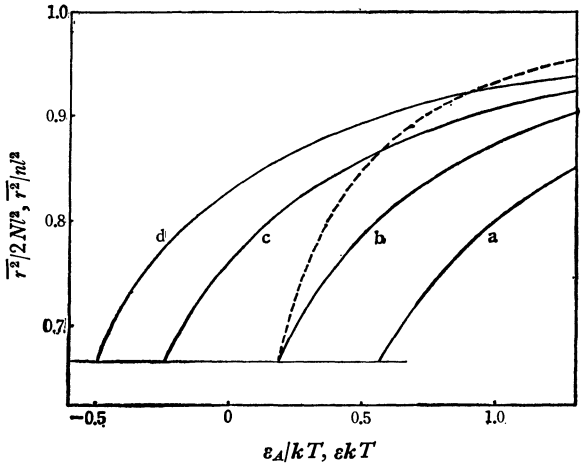

Fig. 4. The ratio $\overline{r^2}/2Nl^2$ of the copolymeric chain is plotted against ε_A/kT: (a) $\varepsilon_B/kT = -0.223$, (b) 0.182, (c) 0.588, (d) 0.916. The dotted line indicates $\overline{r^2}/nl^2$ given by Eq. (2).

Finally we evaluate the end-to-end distance of the copolymeric chain $(-A-B-)_N$ in the limit $N \gg 1$. The value of $\overline{r^2}$ calculated from Eq. (51) by a similar procedure is given as a function of ε_A/kT at the constant value of ε_B/kT in Fig. 4. The effect of adsorption energies on the end-to-end distance is remarkably large in comparison to those on the average number of adsorbed segments. This seems in part due to the fact that the symmetric random walk model which allows any step to retrace the previous one on a simple cubic lattice shortens specifically the end-to-end distance

of the alternating copolymeric chain at the small value of η_B.

Average properties of copolymeric chains of other kinds will be discussed elsewhere.

Appendix

The square matrix of order $a+b$, **M**, of Eq. (11) is related to a diagonal matrix by

$$\mathbf{M} = \mathbf{T}\Lambda\mathbf{T}^{-1}, \tag{A1}$$

where

$$\Lambda = \begin{pmatrix} \lambda_1 & 0 & \cdots & 0 \\ 0 & \lambda_2 & \cdots & 0 \\ \cdots & \cdots & \cdots & \cdots \\ 0 & 0 & \cdots & \lambda_{a+b} \end{pmatrix}, \tag{A2}$$

λ_i being the eigenvalues of **M**. The eigenvectors of **M** can be obtained by solving simultaneous equations:

$$\begin{aligned} &(\eta_A F_{a+b}-\lambda_j)t_{1,j} + \eta_A F_1 t_{2,j} + \cdots + \eta_B F_{a+b-1} t_{a+b,j} = 0 \\ &\eta_A F_{a+b-1} t_{1,j} + (\eta_A F_{a+b}-\lambda_j)t_{2,j} + \cdots + \eta_B F_{a+b-2} t_{a+b,j} = 0 \\ &\cdots\cdots\cdots\cdots\cdots\cdots\cdots\cdots\cdots\cdots\cdots\cdots\cdots\cdots\cdots\cdots \\ &\eta_A F_1 t_{1,j} + \eta_A F_2 t_{2,j} + \cdots + (\eta_B F_{a+b}-\lambda_j)t_{a+b,j} = 0, \\ &\qquad j = 1, 2, \cdots, a+b. \end{aligned} \tag{A3}$$

For notational simplicity it may be taken that

$$t_{1,j} = 1, \quad j = 1, 2, \cdots, a+b. \tag{A4}$$

The other vector elements are obtained from the $a+b-1$ equations out of Eq. (A3); we have

$$t_{i,j} = \Delta_i(\lambda_j)/\Delta_1(\lambda_j), \quad i = 2, 3, \cdots, a+b. \quad \text{and} \quad j = 1, 2, \cdots, a+b, \tag{A5}$$

where

$$\Delta_1(\lambda_j) = \begin{vmatrix} \eta_A F_1 & \eta_A F_2 \cdots \eta_B F_{a+b-1} \\ \eta_A F_{a+b}-\lambda_j & \eta_A F_1 \cdots \eta_B F_{a+b-2} \\ \cdots\cdots & \cdots\cdots\cdots\cdots \\ \eta_A F_3 & \eta_A F_4 \cdots \eta_B F_1 \end{vmatrix} \tag{A6}$$

and $\Delta_i(\lambda_j)$ is the determinant obtained on replacing the respective elements in the $(i-1)$-th column of $\Delta_1(\lambda_j)$ by

$$-(\eta_A F_{a+b}-\lambda_j), \; -\eta_A F_{a+b-1}, \; \cdots, \; -\eta_A F_2.$$

The transformation matrix **T** consists of the eigenvectors obtained above:

$$\mathbf{T} = (t_{i,j}) \tag{A7}$$

$$\mathbf{T}^{-1} = (t_{i,j}^{-1}) \tag{A8}$$

where

$$t_{i,j}^{-1} = \text{cofactor}\,(t_{j,i})/|\mathbf{T}|.$$

By use of Eq. (A1) with Eqs. (A2), (A7), and (A8), it follows that

$$\begin{aligned} \boldsymbol{\alpha}\mathbf{M}(\mathbf{I}-\mathbf{M})^{-1}\boldsymbol{\beta}^+ &= \boldsymbol{\alpha}\mathbf{T}\Lambda(\mathbf{I}-\Lambda)^{-1}\mathbf{T}^{-1}\boldsymbol{\beta}^+ \\ &= \sum_{j=1}^{a+b} t_{1,j}\lambda_j(1-\lambda_j)^{-1}t_{j,a+b}^{-1} \\ &= \Delta_1(1)/D(1), \end{aligned} \tag{A9}$$

where

$$D(1) = (-1)^{a+b}|\mathbf{M}-\mathbf{I}| \tag{A10}$$

and $\Delta_1(1)$ is Eq. (A6) where λ_j is equated to unity.

BULLETIN OF THE CHEMICAL SOCIETY OF JAPAN, VOL. 44, 1248—1252(1971)

Conformation of Adsorbed Polymeric Chain. IV

Kinsi MOTOMURA, Yoshikiyo MOROI, and Ryohei MATUURA
Department of Chemistry, Faculty of Science, Kyushu University, Fukuoka

(Received October 9, 1970)

In order to develop further the theoretical treatment of a polymeric chain adsorbed at an interface, a random walk model, in which each step has the same probability except that no step can retrace the preceding one on a simple cubic lattice, has been used. The average number of adsorbed segments $\bar{\nu}$, the average number of trains $\bar{m}$, and the mean square end-to-end distance $\overline{r^2}$ are calculated as functions of the adsorption energy of segment ε and the number of segments n when n is infinitely large. The average numbers of segments in a train and a loop, $\bar{k}'$ and $\bar{k}$, are also calculated. Through the increment in the value of critical adsorption energy ε_c, prohibition of immediate reversal for the random walk fairly influences the average properties of adsorbed polymeric chain. The decrease in $\bar{m}$ and the increase in $\bar{k}'$ with ε/kT at its large values are remarkable in comparison with those of the symmetric random walk, which may be accounted for by the diminution of the chance of making loops. It is shown that $\overline{r^2}$ is equivalent to the mean square two-dimensional end-to-end distance of a restricted random walk without immediate reversals on a simple cubic lattice at ε_c/kT and approaches that on a simple square lattice in the limit $\varepsilon/kT\rightarrow\infty$.

In the previous papers[1-3] the adsorption of polymeric chains at an interface was analyzed by making use of the symmetric random walk in which the probability of the next step at any stage is not influenced by that of the preceding one. McCrackin[4] and Bluestone and Cronan[5] have estimated numerically average

1) K. Motomura and R. Matuura, *Mem. Fac. Sci., Kyushu Univ.*, **C6**, 97 (1968).
2) K. Motomura and R. Matuura, *J. Chem. Phys.*, **50**, 1281 (1969); *ibid.*, **51**, 4681 (1969).
3) K. Motomura, K. Sekita. and R. Matuura, This Bulletin, **44**, 1243 (1971).
4) F. L. McCrackin, *J. Chem. Phys.*, **47**, 1980 (1970).
5) S. Bluestone and C. L. Cronan, *J. Phys. Chem.*, **70**, 306 (1966).

properties of the adsorbed polymeric chain having a relatively small number of segments by performing a Monte Carlo calculation to treat the effect of the self-exclusion. Rubin[6] has derived the expressions for the average number of adsorbed segments per polymeric chain and the mean distance of the end of a polymeric chain from the interface by means of a random walk model, when the number of segments of the polymeric chain is much larger than unity. In his model the direction of each step is assumed to be at right angles to the direction of the preceding step. A better knowledge about the behavior of a polymer molecule at an interface in an extreme dilution may be obtained by taking a correlation between steps of a random walker into consideration.

In this paper we wish to consider a restricted random walk in which each step has the same probability except that any step is forbidden to retrace its previous one on the simple cubic lattice and to know how the correlation between neighboring steps affects the conformation of the adsorbed polymeric chain.

Theoretical

1. Probability of an Adsorbed Polymeric Chain. As we are concerned only with the behavior of a polymeric chain in an adsorbed state, we assume that both the end segments of the polymeric chain are adsorbed on an interface; the adsorbed polymeric chain consists of an alternate sequence of trains and loops. Denoting the probabilities of loop and train by $f_{kj}(x_j, y_j)$ and $g_{k'j}(x'_j, y'_j)$, the probability of the adsorbed polymeric chain composed of $n+1$ segments is given by

$$p_n(x,y,t,\eta) = \sum_m \sum_{\mathbf{k}} \sum_{\mathbf{x},\mathbf{y}} \prod_{j=1}^{m} [t\eta^{k'_j+1} g_{k'_j}(x'_j, y'_j)] \prod_{j=1}^{m-1} f_{k_j}(x_j, y_j) \tag{1}$$

where

$$\eta = \exp(\varepsilon/kT). \tag{2}$$

Here $-\varepsilon$ is the energy gain per segment associated with the adsorption and t is the parameter to evaluate the number of trains. A set of $\mathbf{k}$, $\mathbf{x}$, and $\mathbf{y}$ means a microscopic state satisfying

$$n = \sum_j k_j + \sum_j k'_j, \quad x = \sum_j x_j + \sum_j x'_j,$$
$$\text{and} \quad y = \sum_j y_j + \sum_j y'_j$$

and the sums are taken over all possible values. On introducing generating functions

$$P_n(\theta,\phi,t,\eta) = \sum_{x,y} p_n(x,y,t,\eta) \exp(ix\theta + iy\phi)$$

$$P(\theta,\phi,t,\eta;w) = \sum_{n=1}^{\infty} P_n(\theta,\phi,t,\eta) w^n \tag{3}$$

and the corresponding ones for $f_k(x, y)$ and $g_k(x, y)$, we obtain

$$P(\theta,\phi,t,\eta;w) = t\eta G(\theta,\phi;\eta w)/[1 - t\eta G(\theta,\phi;\eta w) F(\theta,\phi;w)]. \tag{4}$$

It is now necessary to calculate $F(\theta, \phi; w)$ and $G(\theta, \phi; \eta w)$. Let us define the probability of the restricted random walk which arrives at a point $(x, y, 0)$ from the origin after n steps are $q_n(x, y)$ and that in which the direction of the final step is $-z$ as $q_n^{-z}(x, y)$. There exists a relation between $q_n(x, y)$, $q_n^{-z}(x, y)$, and $f_n(x, y)$:

$$q_n^{-z}(x,y) = \sum_{x',y'} \sum_{l=3}^{n} [q_{n-l}(x-x', y-y') - q_{n-l}^{-z}(x-x', y-y')] f_l(x', y'). \tag{5}$$

Introducing the generating functions analogous to Eq. (3), the above equation becomes

$$F(\theta,\phi;w) = [Q(\theta,\phi;w) - 1/6]/[Q(\theta,\phi;w) - Q^{-z}(\theta,\phi;w)] - 1. \tag{6}$$

With the help of the generating function of the random walk with no immediate reversals on the simple cubic lattice derived by Domb and Fisher[7]

$$Q(\theta,\phi,\psi;w) = [15 - (\cos\theta + \cos\phi + \cos\psi)w]/[15 - 6(\cos\theta + \cos\phi + \cos\psi)w + 3w^2], \tag{7}$$

$Q(\theta, \phi; w)$ is given by the expression

$$Q(\theta,\phi;w) = (1/2\pi)\int_{-\pi}^{\pi} Q(\theta,\phi,\psi;w)\,d\psi = (1/6)\{(25-w^2)[(5-2cw+w^2)^2 - 4w^2]^{-1/2} + 1\}, \tag{8}$$

where

$$c = \cos\theta + \cos\phi. \tag{9}$$

By a similar procedure, it follows that

$$Q(\theta,\phi;w) - Q^{-z}(\theta,\phi;w) = (5/12)\{5 + 2cw - w^2 + [(5-2cw+w^2)^2 - 4w^2]^{1/2}\}[(5-2cw+w^2)^2 - 4w^2]^{-1/2}. \tag{10}$$

Substituting Eqs. (8) and (10) into Eq. (6), we obtain

$$F(\theta,\phi;w) = (1/5)\{25 - 10cw + 3w^2 - 5[(5-2cw+w^2)^2 - 4w^2]^{1/2}\}/\{5 + 2cw - w^2 + [(5-2cw+w^2)^2 - 4w^2]^{1/2}\}. \tag{11}$$

On the other hand, $g_n(x, y)$ is the probability of a two-dimensional random walk in which the probability of each step is equal to 1/5 except that no step retraces the previous one on a simple square lattice and is correlated with the probability of the corresponding symmetric random walk $u_n(x, y)$:

$$u_{n+2}(x,y) = (1/9)u_n(x,y) + (1/12)\sum_{l=1}^{n} \sum_{x',y'} (5/6)^l g_l(x', y') \times u_{n-l}(x-x', y-y') + (5/6)^{n+2} g_{n+2}(x,y). \tag{12}$$

By applying the generating function

$$U(\theta,\phi;w) = \sum_{n=0}^{\infty} (6/5)^n U_n(\theta,\phi) w^n = \sum_{n=0}^{\infty} (6/5)^n w^n [\sum_{x,y} u_n(x,y) \exp(ix\theta + iy\phi)] = 5/(5-2cw) \tag{13}$$

and the generating function of $g_n(x, y)$ to Eq. (12), we can obtain an explicit expression for $G(\theta,\phi;w)$:

$$G(\theta,\phi;w) = 2(5c-2w)w/(25-10cw+3w^2). \tag{14}$$

Substituting Eqs. (11) and (14) into Eq. (4) and rearranging the resulting equation, we obtain the general solution for the adsorbed polymeric chain

6) R. J. Rubin, *J. Res. Nat. Bur. Stand.*, **B69**, 301 (1965).

7) C. Domb and M. D. Fisher, *Proc. Cambridge Phil. Soc.*, **54**, 48 (1958).

$$P(\theta, \phi, t, \eta; w) = N(c, t, \eta, w)/D(c, t, \eta, w) \quad (15)$$

where

$$N(c, t, \eta, w) = 10t\eta^2 w(5c-2\eta w)\{5+2cw-w^2 + [(5-2cw+w^2)^2-4w^2]^{1/2}\} \quad (16)$$

and

$$D(c, t, \eta, w) = 5(25-10c\eta w+3\eta^2 w^2)\{5+2cw-w^2 + [(5-2cw+w^2)^2-4w^2]^{1/2}\} - 2t\eta^2 w(5c-2\eta w) \times\{25-10cw+3w^2-5[(5-2cw+w^2)^2-4w^2]^{1/2}\}. \quad (17)$$

2. Evaluation of Average Properties. It is now possible to evaluate average properties of the adsorbed polymeric chain based on the model in which the random walk has no immediate reversals. The average number of adsorbed segments per polymeric chain $\bar{\nu}$ can be obtained by noting Eqs. (1) and (3):

$$\bar{\nu} = \eta[dP_n(2, 1, \eta)/d\eta]/P_n(2, 1, \eta) \quad (18)$$

where $P_n(c, t, \eta)$ is used instead of $P_n(\theta, \phi, t, \eta)$. In a similar manner we have for the average number of trains per polymeric chain the following equation:

$$\bar{m} = [\partial P_n(2, t, \eta)/\partial t]_{t=1}/P_n(2, 1, \eta). \quad (19)$$

It also follows that

$$\overline{r^2} = a^2[c\partial P_n(c, 1, \eta)/\partial c]_{c=2}/P_n(2, 1, \eta), \quad (20)$$

where $\overline{r^2}$ is the mean square end-to-end distance and a is the distance between neighboring segments.

Explicit expressions for $P_n(c, t, \eta)$ and its derivatives are immediately derived from Eq. (15). According to Cauchy's residue theorem, $P_n(2, 1, \eta)$ is found to be

$$P_n(2, 1, \eta) = (1/2\pi i)\oint_{C_0}(1/w^{n+1})P(2, 1, \eta; w)dw = (1/2\pi i)\oint_{C_0}(1/w^{n+1})[N(2, 1, \eta, w)/D(2, 1, \eta, w)]dw, \quad (21)$$

where C_0 includes only the pole at $w=0$. Denoting the smallest root of

$$0 = D(2, 1, \eta, w) = (5-\eta w)[5(5-3\eta w)\{5+4w-w^2+[(5-4w+w^2)^2 - 4w^2]^{1/2}\} - 4\eta^2 w\{25-20w+3w^2-5[(5-4w+w^2)^2 - 4w^2]^{1/2}\}] \quad (22)$$

by w_1, which coincides with the branch-point $w=1$ at the value $\eta=5/4$ which corresponds to the critical value of the adsorption energy, the integral of Eq. (21) may be approximated by the residue at $w=w_1$ when n is infinitely large. Thus we obtain

$$P_n(2, 1, \eta) = -\frac{1}{w_1^{n+1}}\frac{N(2, 1, \eta, w_1)}{\partial D(2, 1, \eta, w_1)/\partial w} \quad (23)$$

where

$$\partial D(2, 1, \eta, w_1)/\partial w = -(5-\eta w_1)[(5-4w_1+w_1^2)^2-4w_1^2]^{-1/2} \times\{[25(4\eta^2+3\eta-4)-10(16\eta^2-12\eta-5)w_1+9\eta(4\eta-5)w_1^2] \times[(5-4w_1+w_1^2)^2-4w_1^2]^{1/2}-5\eta(4\eta-3)[(5-4w_1+w_1^2)^2 - 4w_1^2]+10[5+\eta(4\eta-3)w_1](10-11w_1+6w_1^2-w_1^3)\}. \quad (24)$$

The derivative of $P_n(2, 1, \eta)$ with respect to η in the numerator of Eq. (18) is evaluated similarly. If terms which are not proportional to n are dropped, we have

$$\frac{dP_n(2, 1, \eta)}{d\eta} = \frac{1}{2\pi i}\oint_{C_0}\frac{1}{w^{n+1}}\frac{\partial P(2, 1, \eta; w)}{\partial \eta}dw = -\frac{n}{w_1^{n+2}}\frac{N(2, 1, \eta, w_1)dD(2, 1, \eta, w_1)/d\eta}{[\partial D(2, 1, \eta, w_1)/\partial w]^2} \quad (25)$$

where

$$dD(2, 1, \eta, w_1)/d\eta = -(5-\eta w_1)w_1\{25(8\eta+3)-20(8\eta-3)w_1 + 3(8\eta-5)w_1^2-5(8\eta-3)[(5-4w_1+w_1^2)^2-4w_1^2]^{1/2}\}. \quad (26)$$

The same procedure gives the expressions for $[\partial P_n(2, t, \eta)/\partial t]_{t=1}$ and $[\partial P_n(c, 1, \eta)/\partial c]_{c=2}$ in the limit $n \gg 1$. The results are

$$\left[\frac{\partial P_n(2, t, \eta)}{\partial t}\right]_{t=1} = -\frac{n}{w_1^{n+2}}\frac{N(2, 1, \eta, w_1)\partial D(2, 1, \eta, w_1)/\partial t}{[\partial D(2, 1, \eta, w_1)/\partial w]^2} \quad (27)$$

and

$$\left[\frac{\partial P_n(c, 1, \eta)}{\partial c}\right]_{c=2} = -\frac{n}{w_1^{n+2}}\frac{N(2, 1, \eta, w_1)\partial D(2, 1, \eta, w_1)/\partial c}{[\partial D(2, 1, \eta, w_1)/\partial w]^2} \quad (28)$$

where

$$\partial D(2, 1, \eta, w_1)/\partial t = -4\eta^2 w_1(5-\eta w_1)\{25-20w_1+3w_1^2 - 5[(5-4w_1+w_1^2)^2-4w_1^2]^{1/2}\} \quad (29)$$

and

$$\partial D(2, 1, \eta, w_1)/\partial c = -10w_1[(5-4w_1+w_1^2)^2-4w_1^2]^{-1/2} \times\{[25(\eta^2+\eta-1)-40\eta(\eta-1)w_1+\eta(4\eta^2-5)w_1^2] \times[(5-4w_1+w_1^2)^2-4w_1^2]^{1/2}-5\eta(\eta-1)[(5-4w_1+w_1^2)^2 - 4w_1^2]+[25+20\eta(\eta-1)w_1-\eta^2(4\eta-3)w_1^2] \times(5-4w_1+w_1^2)\}. \quad (30)$$

We can now calculate the average properties of the polymeric chain adsorbed on an interface in the limit $n \gg 1$. Combining Eqs. (23) and (25) with Eq. (18), the expression for the average number of adsorbed segments per polymeric chain is obtained:

$$\bar{\nu} = n\frac{\eta}{w_1}\frac{dD(2, 1, \eta, w_1)/d\eta}{\partial D(2, 1, \eta, w_1)/\partial w}. \quad (31)$$

For the average number of trains per polymeric chain and the mean square end-to-end distance, we obtain

$$\bar{m} = n\frac{1}{w_1}\frac{\partial D(2, 1, \eta, w_1)/\partial t}{\partial D(2, 1, \eta, w_1)/\partial w} \quad (32)$$

and

$$\overline{r^2} = a^2 n\frac{2}{w_1}\frac{\partial D(2, 1, \eta, w_1)/\partial c}{\partial D(2, 1, \eta, w_1)/\partial w}. \quad (33)$$

The derivatives on the right-hand side of the above formulas are already given explicitly in Eqs. (24), (26), (29), and (30).

Discussion

The average properties of the adsorbed polymeric chain based on the model in which no step of a random walk can retrace the previous one on the simple cubic lattice have been evaluated as functions of the adsorption energy and the chain length for infinite chain length. Computing w_1 satisfying Eq. (22) and substituting this value into Eq. (31) with Eqs. (24) and (26), we obtain

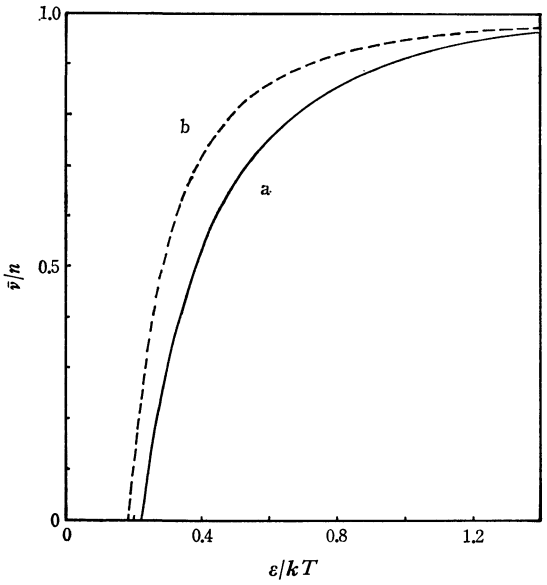

Fig. 1. The ratio of $\bar{\nu}$ to n is plotted against ε/kT in the limit $n \gg 1$: (a) restricted random walk without immediate reversal, (b) symmetric random walk.[1)]

the average number of adsorbed segments per polymeric chain. This is graphically shown in Fig. 1 where the ratio of $\bar{\nu}$ to n is plotted against the adsorption energy ε measured in unit kT. For comparison the ratio $\bar{\nu}/n$ for the symmetric random walk model discussed in Part I is also given in Fig. 1. We see that the prohibition of immediate reversals for the random walk fairly influences the amount of segments adsorbed on the interface. The resulting enhancement of critical adsorption energy and diminution of the average number of adsorbed segments can be explained by the difference between decreases in statistical weights of the two-dimensional and three-dimensional random walks, due to the restriction for the step to retrace the preceding step.

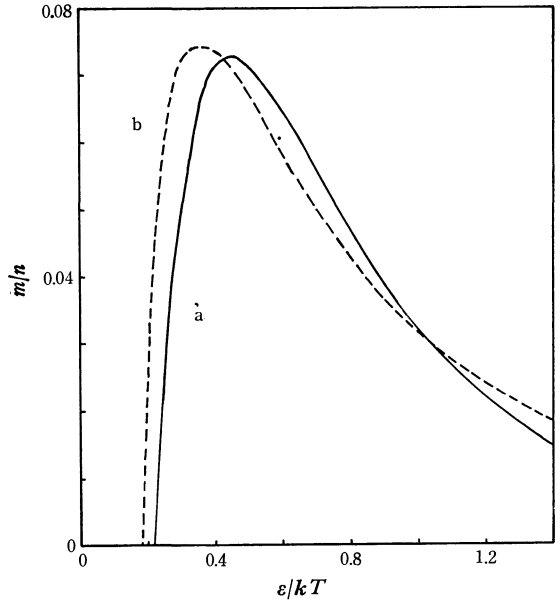

Fig. 2. The ratio $\bar{m}/n$ is plotted against ε/kT: (a) restricted random walk without immediate reversal, (b) symmetric random walk.[2)]

The average number of trains per polymeric chain $\bar{m}$ is calculated in the same way. The plot of ratio $\bar{m}/n$ against ε/kT is illustrated in Fig. 2 with the corresponding one of the symmetric random walk. Shapes of the curves, $\bar{m}/n$ *versus* ε/kT, seem to be alike as a whole, while the decrease of the value of $\bar{m}/n$ of the restricted random walk without immediate reversals at large values of η is rather steep. The smaller average number of trains (the smaller average number of loops) for large values of η may be accounted for by the diminution of the chance of making loops. The smallest number of segments in the loop for the restricted random walk without immediate reversals is $\bar{k}=2$ instead of $\bar{k}=1$ for the symmetric random walk, where $\bar{k}$ is the average number of segments in the loop and is given by

$$\bar{k} = (n-\bar{\nu})/(\bar{m}-1). \tag{34}$$

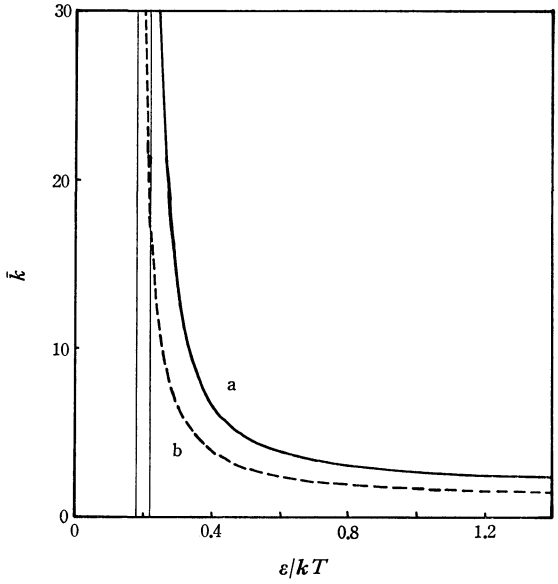

Fig. 3. $\bar{k}$ is plotted against ε/kT: (a) restricted random walk without immediate reversal (b) symmetric random walk.[2)]

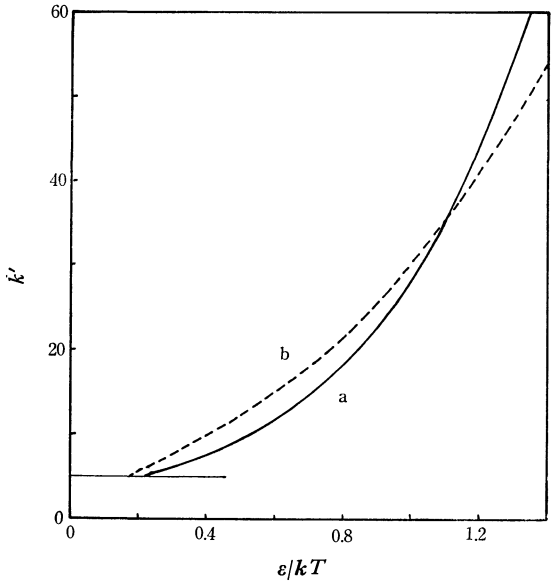

Fig. 4. $\bar{k}'$ is plotted against ε/kT: (a) restricted random walk without immediate reversal, (b) symmetric random walk.[2)]

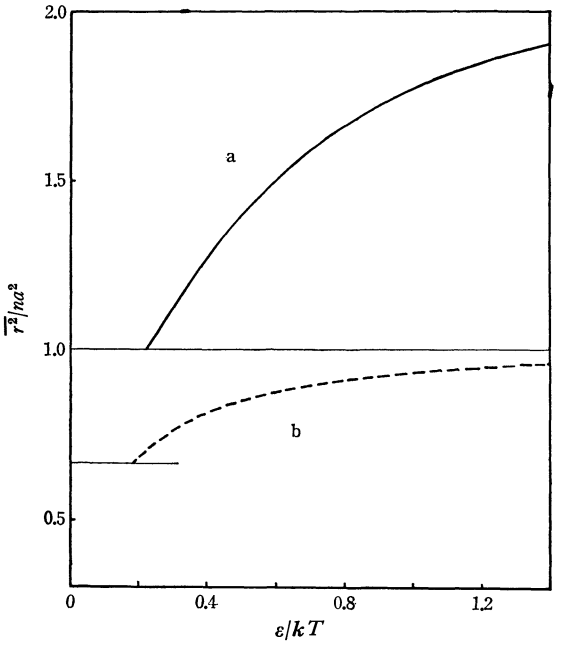

Fig. 5. The ratio $\overline{r^2}/na^2$ is plotted against ε/kT: (a) restricted random walk without immediate reversal, (b) symmetric random walk.[1]

The value of $\bar{k}$ computed is plotted against ε/kT in Fig. 3. We might expect that the average number of segments in the train $\bar{k}'$ increases rapidly with the adsorption energy. The value of $\bar{k}'$ is easily evaluated by the relation

$$\bar{k}' = \bar{\nu}/\bar{m}, \tag{35}$$

which is depicted against ε/kT in Fig. 4. Increase of $\bar{k}'$ *versus* ε/kT curve is remarkable compared with that obtained previously.[2]

Finally the mean square end-to-end distance in the limit $n \gg 1$ is calculated from Eq. (33) with Eqs. (24) and (30) by a similar procedure. The result is illustrated in Fig. 5 where the ratio $\overline{r^2}/na^2$ is plotted against ε/kT. It is clear that the polymeric chain of the restricted random walk without immediate reversals has a fairly extended conformation in comparison with that of the symmetric random walk in spite of the small value of the average number of adsorbed segments per polymeric chain. The value of $\overline{r^2}$ is na^2 at the critical adsorption energy and approaches $2na^2$ for infinite adsorption energy. According to Domb and Fisher,[7] the mean square end-to-end distance of the restricted random walk with no immediate reversals on lattices in the limit $n \gg 1$ is given by

$$(\overline{r^2})_{\mathrm{DF}} = na^2(1+\delta)/(1-\delta) \tag{36}$$

where

$$\delta = 1/(q-1), \tag{37}$$

q being the coordination number of lattice used. Equation (36) results in $(\overline{r^2})_{\mathrm{DF}} = (3/2)na^2$ for the random walk on a simple cubic lattice and $(\overline{r^2})_{\mathrm{DF}} = 2na^2$ on a simple square lattice. It is easily recognized that the mean square end-to-end distance of the adsorbed polymeric chain is equivalent to that of the restricted random walk without immediate reversals, of which both ends are located on xy plane through $z=0$ in the simple cubic lattice, at the critical adsorption energy and approaches that of the two-dimensional one on the simple square lattice for infinite adsorption energy.

BULLETIN OF THE CHEMICAL SOCIETY OF JAPAN, VOL. 44, 1252—1256(1971)

The Surface Properties of the Silica-Titania System Prepared by the Hydrolysis of Metal Alkoxides

Hiroshi HOSAKA and Kenjiro MEGURO

Department of Applied Chemistry, Faculty of Science, Science University of Tokyo, Kagurazaka, Shinjuku-Ku, Tokyo

(Received October 22, 1970)

The surface and bulk properties of silica-titania systems, prepared by the co-hydrolysis of silicon ethoxide and titanium tetrabutoxide, were investigated by measuring the heat of immersion, the adsorption of nitrogen, water, and ammonia, the X-ray diffraction, the DTA, and the TGA. It was found that the addition of silica to titania has a large suppressive effect on the crystal growth of anatase and on the transformation of anatase to rutile. The heat of immersion, the surface hydrophilicity (the surface area by water adsorption/the surface area by nitrogen adsorption) and the amount of ammonia adsorbed gave inverted sigmoid curves when the titania content was varied. Especially, the shape of the curve of the change in the heat of immersion coincides approximately with that of the surface hydrophilicity.

Recently, the methods of the preparation of metal oxides by the hydrolysis of metal alkoxides have often been reported. Such oxides synthesized by an ion-free process are suitable for the study of the surface properties of metal oxides. Meguro *et al.*[1,2] studied the surface properties of alumina-titania and silica-alumina systems prepared by the co-hydrolysis of metal alkoxides.

In this experiment, we have investigated the surface properties of the silica-titania system obtained by the co-hydrolysis of silicon ethoxide and titanium tetrabutoxide.

1) H. Murayama, K. Kobayashi, M. Koishi, and K. Meguro, *J. Colloid Interface Sci.*, **32**, 470 (1970).

2) H. Murayama and K. Meguro, This Bulletin, **43**, 2386 (1970).

Experimental

Materials. Several samples of the silica-titania system were obtained by the co-hydrolysis of silicon ethoxide and titanium tetrabutoxide mixtures with different molar ratios. The purities of the alkoxides were checked by infrared analysis. The hydrolysis reaction was carried out by dropping a water-methanol mixture (water : methanol= 4:1 in weight) into a butanol solution of alkoxide (butanol : alkoxide= 1:1 in weight), keeping the total molar ratio of the water to alkoxide at 20:1. The water used was deionized and was then distilled. The alcohols used were of a reagent grade. After the liquid had been stirred for 10 hr at the boiling point, the precipitate was separated, washed with deionized water and then methanol, and dried at 100°C *in vacuo*. The dried samples were calcined for 2 hr in an electric furnace at temperatures from 500 to 1000°C. The samples calcined at 500°C were used for the study of the surface properties. The composition of the samples, as determined by X-ray fluorescence analysis were 21, 55, and 83 in the weight-percentage ratio: (titania)/(silica+titania); they will be designated as 4ST (silica : titania≒4:1 in weight), ST, and S4T respectively.

Apparatus and Procedure. The thermogravimetric and differential thermal analyses of the samples have been made by means of an automatic recording instrument of the Shimadzu Seisakusho Co.; the rate of heating was 10°C per minute. The X-ray diffraction patterns were recorded with a Geigerflex X-ray diffractometer of the Rigaku Denki Co., using Ni-filtered Cu radiation.

The heat of immersion was measured with a semimicro-calorimeter which had been devised in our laboratory.[3,4] A thermistor was used for measuring small temperature changes. A wide-mouthed, silvered Dewar flask with a 400 m*l* capacity served as the calorimeter vessel. It was attached to a Bakelite flange with stainless steel rings equipped with a Neoprene gasket. The calorimeter assembly included a small, 10 ohm heating manganin wire for calibration, a stirrer, a sample holder, and a thermistor. The whole assembly was immersed in a constant-temperature bath at 25°C. The heat evolved at immersion was calculated by means of galvanometer readings. The adsorption isotherms of nitrogen at −195°C, of water at 25°C, and of ammonia at 260°C were determined by means of a conventional, volumetric, gas-adsorption apparatus. For the water adsorption, the apparatus was maintained at 25°±0.5°C in an air thermostat. Each sample for water adsorption was outgassed at 100°C for 1 hr at 10^{-5} Torr and then cooled to 25°C prior to the adsorption studies. The nitrogen and water-surface areas of the samples were calculated by the BET formula, using 16.2 and 10.8 Å^2 for the cross-sectional areas of the nitrogen and water molecules respectively.

The compositions of all the samples were measured with a Rigaku Denki X-ray vacuum spectrograph by means of X-ray fluorometry.[5] The analyser crystal was ethylenediamine ditartrate. The chromium target was adjusted at 45KV, 12 mA (for Si) and 30KV, 6mA (for Ti). The X-radiation was detected by a proportional counter (90% Ar+10% CH_4) and discriminated as follows: for Si: base line, 70/1000, and channel width, 100/100, and for Ti: base line, 80/1000, and channel width, 100/100.

3) K. Meguro, M. Koishi, and N. Okabe, *Kogyo Kagaku Zasshi*, **68**, 2055 (1965).

4) K. Meguro, M. Koishi, M. Aizawa, N. Uchino, K. Matsumoto, H. Kimoto, Y. Kumaki, and H. Sawai, *Kogyo Kagaku Zasshi*, **69**, 1724 (1966).

5) A. Leonard, S. Suzuki, J. Fripiat, and C. De Kimpe, *J. Phys. Chem.*, **68**, 2608 (1964).

Results and Discussion

(*i*) *Differential Thermal Analysis, Thermogravimetric Analysis, and X-Ray Investigation.* Typical results of the differential thermal analysis (DTA) and the thermogravimetric analysis (TGA) are shown in Fig. 1. The DTA of the samples are given in Fig. 1; they are characterized with an endothermic peak at 150°C and a small broad exothermic peak at 250—400°C. The endothermic peak is supposed to be due to the loss of adsorbed water, while the exothermic peak is supposed to be caused by the oxidation of a chemically-adsorbed solvent, which seems to be identified by the weight loss shown in the TGA curves at the same temperature. Therefore, in order to avoid the effect of the adsorbed solvent on the surface property, the chosen temperature of calcination was 500°C.

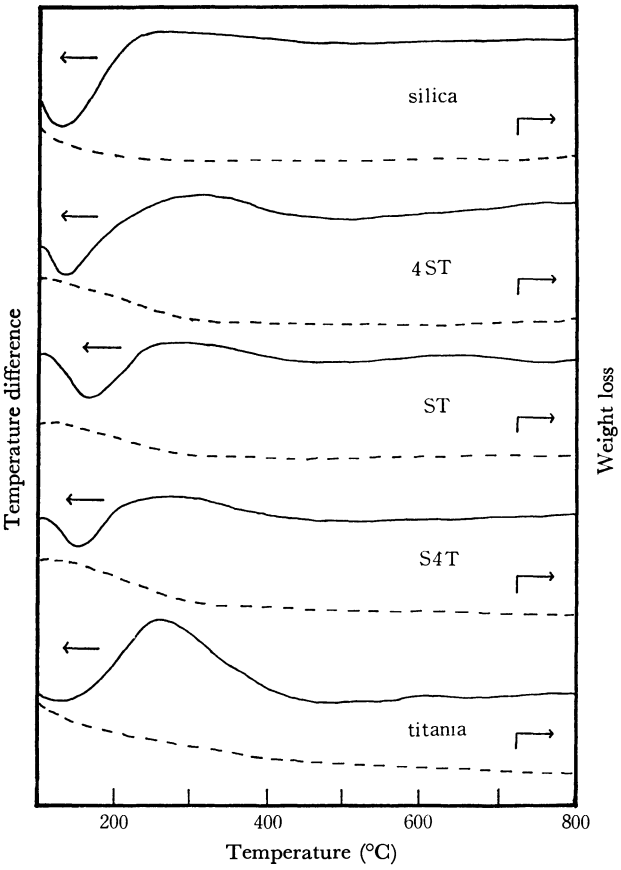

Fig. 1. DTA (solid lines) and TGA (dotted lines) curves of the silica-titania systems.

Typical X-ray diffraction patterns of the samples are shown in Fig. 2. The patterns of the silica calcined at 100—1000°C showed an almost amorphous structure. Broad lines characteristic of anatase are seen in the patterns of the titania heated at 100°C. These broad lines became sharper with a rise in the temperature of calcination. Moreover, the lines of rutile begin to appear in the patterns of the product calcined at 600—700°C. The silica-titania systems have different X-ray patterns from the parent oxides, but they show no lines which are not found in the patterns of the parent oxides. The X-ray-diffraction study showed that the addition of silica to titania has a large suppressive effect on the

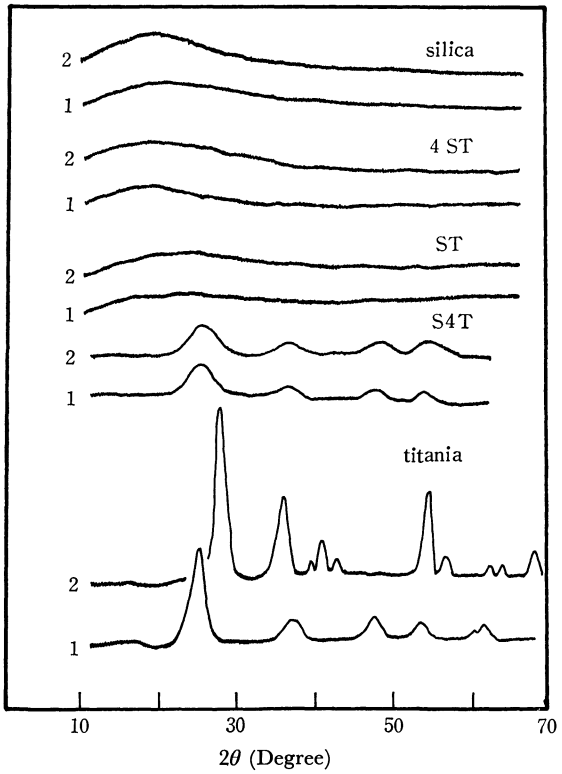

Fig. 2. X-Ray diffraction patterns at different temperatures (1:500°C 2:800°C) of the silica-titania systems.

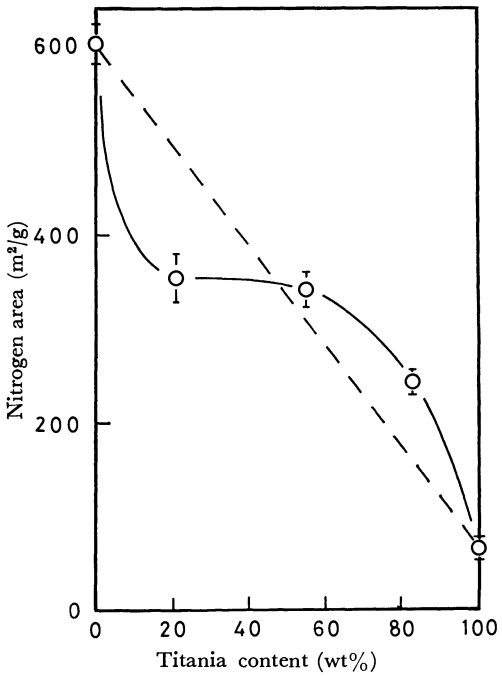

Fig. 3. The change of the nitrogen surface area of the silica-titania systems calcined at 500°C with composition. Dotted line, the dry-mixed oxides.

crystal growth of anatase and on the transformation of anatase to rutile. This effect was evidenced by the fact that the samples of 4ST and ST remained amorphous even when the calcining temperature was raised to 800°C. In the case of S4T, which has a higher titania content, only broad lines of anatase was observed in the calcination at 500°C; this anatase pattern remained the same up to 800°C. This suppressive effect increases as the silica content increases. Typical patterns are shown in Fig. 2. It is well known that the rate of the anatase-rutile transformation is affected by the presence of foreign ions, entering either substitutionally or interstitially.[6] From the suppressive effects on the crystal growth and the transformation, it may be supposed that the silica-titania systems prepared by the co-hydrolysis are different in structure from simple mechanical mixtures of dry silica and titania.

(*ii*) *Specific Surface Area.* The specific surface areas of the samples obtained by nitrogen adsorption change with the titania content, giving a sigmoid curve, as is shown in Fig. 3, in which the surface area is plotted as a function of the weight percentage of titania. This is compared with the straight dotted line in Fig. 3, which shows the theoretical surface area as calculated as the mechanical mixtures. In practice, however, the specific surface areas of the samples do not change proportionally with the composition, but give a sigmoid curve. The surface area decreases steeply between silica (600m²/g) and S4T (348m²/g), gradually decreases between 4ST and S4T (239m²/g), and then decreases steeply again between S4T and titania (63.9m²/g).

(*iii*) *Water Adsorption and Heat of Immersion.* Figure 4 represents the specific surface area derived from the water adsorption versus the composition of the silica–titania systems. The curve of the surface area versus the composition in Fig. 4 is not a straight line, as might be expected in the case of a simple mixture of dry silica and titania.

Healey and his co-workers[7] have shown that the ratio of the apparent surface area, as determined by the water adsorption, to the total area, as determined by the nitrogen adsorption, is a direct measure of the fraction of the hydrophilic surface present in a finely-

Table 1. Surface properties of the silica-titania system calcined at 500°C for2 hr

Sample composition wt % (TiO_2/SiO_2+TiO_2)	X-Ray diffraction	S_{N_2} (m^2/g)	S_{H_2O} (m^2/g)	$S_{H_2O}/S_{N_2}\times 100$	H_t (erg/cm^2)	Amounts of NH_3 adsorbed (ml/m^2)
0	amorphous	600	81.3	14	119	0.001
21	amorphous	348	155	44	303	0.0124
55	amorphous	343	203	59	346	0.0166
83	weak anatase lines	239	142	60	332	0.0380
100	weak anatase lines	63.9	55	86	506	0.105

6) R. D. Shannon, and J. A. Pask, *J. Amer. Ceram. Soc.*, **48**, 391 (1965).

7) F. H. Healey, Y. F. Yu, and J. J. Chessick, *J. Phys. Chem.*, **59**, 399 (1955).

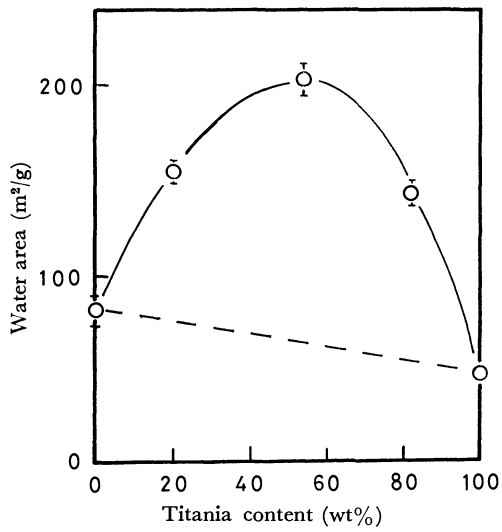

Fig. 4. The change of the water surface area of the silica-titania systems with composition. Dotted line, the dry-mixed oxides.

divided solid. The ratio may also be considered to be a measure of the hydrophobicity; the smaller the ratio the more hydrophobic the surface. Therefore, the surface hydrophilicity in percentage may be expressed as: (the surface area by water adsorption/the surface area by nitrogen adsorption) × 100. The change in the surface hydrophilicity of the samples is illustrated in Fig. 5 as a function of the titania content. The straight dotted line in Fig. 5 shows the theoretical surface hydrophilicity calculated as were the mechanical mixtures. It is noticeable that the experimental hydrophilicity deviates from the straight line. The hydrophilicity of the samples rises steeply between silica (14%) and 4ST (44%), rises gradually between 4ST (60%), and then again rises steeply beween S4T and titania (86%).

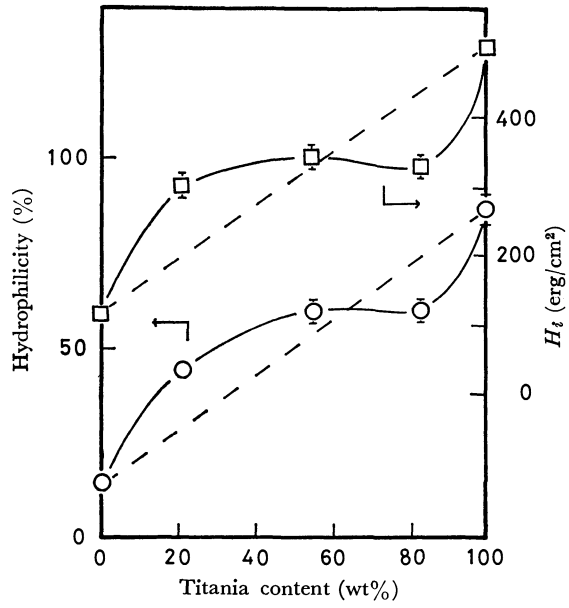

Fig. 5. The change of the heat of immersion and the surface hydrophilicity of the silica-titania systems with composition. □-Heat of immersion. ○-Surface hydrophilicity. Dotted lines, the dry-mixed oxides.

The change in the heat of immersion with the composition of the samples is represented in Fig. 5, in which the heat of immersion is plotted as a function of the titania content. The straight dotted line in Fig. 5 shows the theoretical heat of immersion calculated as were the mechanical mixtures. The heat of immersion increases steeply between silica (119erg/cm²) and 4ST (303erg/cm²), changes gradually between 4ST and S4T (332erg/cm²), and then increases greatly between S4T and titania (506erg/cm²). The crystal structures of silica, 4ST, and ST are almost amorphous, while those of S4T and titania are anatase. From these results, it may be concluded that the heat of immersion of the samples is not affected by the change in the crystal structure. The change in the surface hydrophilicity with the composition approximately coincides with that of the heat of immersion, as is shown in Fig. 5. The same results have been reported on alumina-titania[1] and silica-alumina[2] systems. The coincidence of the changes in the surface hydrophilicity of these samples with the composition and those of the heat of immersion of these samples with the composition can be explained as resulting from the fact that alumina, silica and titania surfaces are usually covered with hydroxyl groups, which act as primary adsorption sites for polar molecules. Since the surface hydrophilicity has an intimate relation with surface hydroxyl groups, the coincidence of this curve with that of the heat of immersion is reasonable.

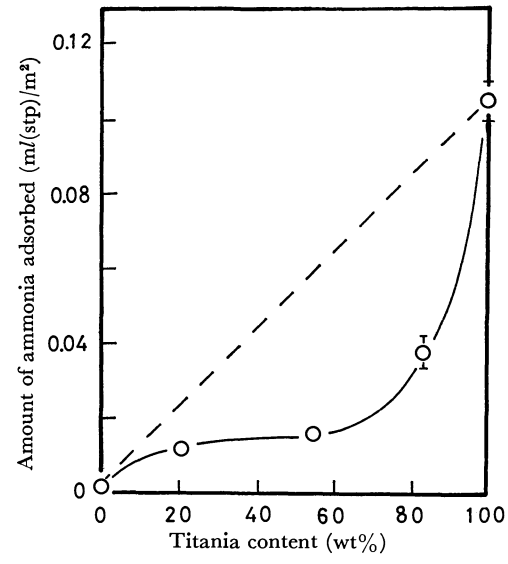

Fig. 6. The change of the amount of ammonia adsorbed on the silica-titania systems with composititon. Dotted line, the dry-mixed oxides.

(iv) Surface Acidity. Another important character of the surface of the silica-titania system is the surface acidity. The ammonia adsorption isotherm at 260°C, where the highest equilibrium pressure was about 10Torr, was determined.[8,9] The surface acidity of the samples was determined by the adsorption of ammonia at 260°C. The shape of the adsorption

8) T. Shiba and E. Echigoya, *Nippon Kagaku Zasshi*, **76**, 1046 (1955).

9) J. J. Fripiat, A. Leonard, and J. B. Uytterhoeven, *J. Phys. Chem.*, **69**, 3274 (1965).

isotherms of the samples is that of the Langmuir type. The saturated amount of the adsorption of ammonia can be calculated from the Langmuir equation; the calculated values of the saturated adsorption are listed in Table 1. Figure 6 shows the relation between the amount of ammonia and the titania content in the silica-titania system. In this case, the amount of ammonia adsorbed on the samples does not change proportionally with the titania content. The straight dotted line in Fig. 6 shows the theoretical value of ammonia adsorption, calculated as were the mechanical mixtures. The change in the surface acidity with the titania content shows an inverted sigmoid curve like those of the heat of immersion and of the hydrophilicity. This suggests that there is a relationship between the sites responsible for the ammonia adsorption and the surface hydroxyl groups. This suggestion agrees with the results of Stöber.[10]

It should be noted that the observed values of the silica-titania system, such as those of the nitrogen area, the water area, the surface hydrophilicty, the heat of immersion, and the surface acidity, are very different from those obtained on the assumption that this system is composed of a simple mechanical mixture of the two components. These deviations may originate in the method of the preparation of the systems; they suggest that the surface structures of the systems prepared by the co-hydrolysis of these metal alkoxides are different from those of simple mechanical mixture of dry silica and titania.

10) W. Stöber, *Kolloid-Z.Z.Polym.*, **145**, 17 (1956).

BULLETIN OF THE CHEMICAL SOCIETY OF JAPAN, VOL. 44, 1256—1261 (1971)

Photochemical Reaction of 9-Cl-Acridine in Aerated and Deaerated Ethanol. I

Katsumi NAKAMARU, Shigeya NIIZUMA, and Masao KOIZUMI
Department of Chemistry, Faculty of Science, Tohoku University, Katahira, Sendai

(Received October 22, 1970)

It was established that upon irradiation, the degassed ethanol solution of 9-chloroacridine is quickly converted into 9,9′-biacridyl by the reaction $2(\text{9-Cl-acridine}) \xrightarrow[(h\nu)]{+2H} \text{9,9′-biacridyl} + 2HCl$ and that 9,9′-biacridyl produced is then reduced photochemically to 9,9′-biacriden as the main product. The reaction scheme completely denies the scheme previously proposed (V. Zanker and W. Flügel, *Z. Naturforsch.*, **19(b)**, 376 (1964)) in which the primary photoproduct is a charge transfer complex between 9-Cl-acridine and its reduced form. 9,9′-biacridyl is photoreduced to an acridan-like compound even in the aerated solution perhaps *via* molecular mechanism in contrast to 9-Cl-acridine which yields acridone under similar conditions. ESR spectrum with hfs was detected in the acidic solution (degassed) containing 9,9′-biacriden produced photochemically. The mechanism of its production was discussed. Similar reactions using various solvents (aerated and deaerated) were examined and the general feature of the primary processes was described.

Photoreduction of acridine in various H-containing solvents has been studied extensively by the authors[1-3] and others.[4-7] Reactive sites on the acridine molecule are always 9C– and 10N– positions, the latter usually being hydrogenated preferentially in the primary act; the final products are acridans or biacridan according to experimental conditions.

Concerning the effect of substitution at 9-position, Zanker and Flügel studied the photoreaction of 9-halogen-acridine under various conditions[8] and reported that 9-Cl-acridine (9-Cl-A) in the aerated ethanol yields acridone while in the atmosphere of nitrogen, a photoproduct of quite a different type having an absorption peak at 430 nm (for the sake of convenience will refer to it as X-species) is produced which by prolonged irradiation is gradually transformed into another different species (Y-species) with a peak at 530 nm. Although they gave no suggestions as to the structure of Y-species, they proposed that X-species may be a charge transfer type molecular complex between the starting substance and the phtoproduct, perhaps 9-Cl-acridan. No work has been reported on these interesting reactions since then.

1) M. Koizumi, Y. Ikeda, and T. Iwaoka, *J. Chem. Phys.*, **48**, 1869 (1968); M. Koizumi, Y. Ikeda, and H. Yamashita, This Bulletin, **41**, 1056 (1968).
2) A. Kira and M. Koizumi, This Bulletin, **42**, 625 (1969).
3) Y. Miyashita, S. Niizuma, and M. Koizumi, *ibid.*, **43**, 3435 (1970).
4) V. Zanker, E. Erhardt, F. Mader, and J. Thies, *Z. Naturforsch.*, **21b**, 102 (1966); V. Zanker, E. Erhardt, and H. Mantsch, *Z. physik. Chem. N. F.*, **58**, 1 (1968); V. Zanker and E. Erhardt, *Ber. Bunsenges. phys. Chem.*, **72**, 267 (1968); V. Zanker and G. Prell, *ibid.*, **73**, 791 (1969).
5) A. Kellmann and J. T. Dubois, *J. Chem. Phys.*, **42**, 2518 (1965).
6) E. Vander Donkt and G. Porter, *ibid.*, **46**, 1173 (1967).
7) F. Wilkinson and J. T. Dubois, *ibid.*, **48**, 2651 (1968).
8) V. Zanker and W. Flügel, *Z. Naturforsch.*, **19(b)**, 376 (1964).

We found a CT type complex somewhat analogous to that stated by Zanker and Flügel in a solution containing acridine and acridan or phenazine and dihydrophenazine.[9] The latter system has also been investigated by Bailey *et al.*[10] It was also found that these systems give ESR signals under suitable conditions. We were interested in the complex formation between oxidized and reduced forms and investigated the reaction of 9-Cl-A (I), studying in particular the reaction scheme up to the formation of X-species in detail. Careful reinvestigation of the overall reaction has revealed, however, that the fomation of X-species is preceded by another quite rapid process which yields 9,9′-biacridyl (II), and that X-species is 9,9′-biacriden (III) instead of a C-T complex.

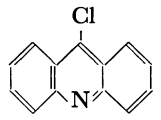

(I)

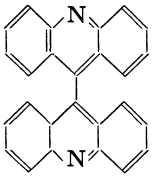

(II)

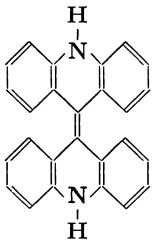

(III)

Another interesting finding is that the photoproduct at the stage of X-species fomation, gives an ESR spectrum in acidic medium. Zanker and Flügel's observation of acridone formation in the aerated solution has been reconfirmed but we strongly suggest quite a different mechanism. Solvent effect on the reactions both in aerated and deaerated solutions has been examined.

Experimental

Materials. 9-Cl-acridine was prepared and purified according to the method of Albert and Ritchie (*Organic Synthesis*, **22**, 5 (1942)). Since 9-Cl-acridine in ethanol easily undergoes thermal transformation into acridone, the solution was always prepared immediately before the experiment. The concentration was 1×10^{-4}M unless otherwise stated. Ethanol was dried according to the method of Lund and Bjerrum.[11] Methyltetrahydrofuran was dehydrated with Na-K alloy in vacuo repeating freeze-pump-thaw 7—8 times.

Apparatus and Procedures. The apparatus for reaction was a similar one to that employed in our laboratory. The light source is a 100 W high pressure mercury lamp. 365 nm monochromatic light was taken out through a filter system consisting of a glass plate and U-2 filter. Fluorescence spectrum was measured with a Hitachi MPF-2 spectrofluorometer, and ESR spectrum with a JEOL P-10 type ESR spectrometer.

Results and Discussion

Reaction in the Deaerated Ethanol Solution. Figure 1 shows the change in the absorption spectrum caused by irradiation.

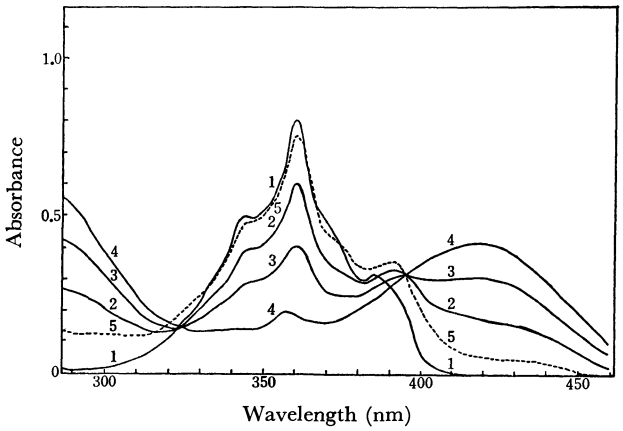

Fig. 1. Change of absorption spectra when the degassed ethanol solution of 9-Cl-A was irradiated by 365 nm (25°C).
1) 9-Cl-A
2) 1 min and 10 sec irradiation
3) 3 min and 20 sec irradiation
4) 7 min irradiation
5) air is introduced to 4),
for about 40 sec irradiation of 9-Cl-A, essentially the same spectrum as 5).

About 40 seconds after starting irradiation, the main peak shifted slightly to the shorter wavelength accompanied with a complicated change in the 385 nm region. This stage was then followed by a second extensive change *i.e.* a large decline of the main peak and a rise of a new broad maximum around 420 nm (X-species). Prolonged irradiation caused a gradual replacement of this band with a new band near 530 nm (Y-species). The two last changes are in complete agreement with Zanker and Flügel's observation but the first one escaped their notice. In Fig. 2, curve a) is the plot of $\ln(e^{acd}-1)$ (α, absorption coefficient at 365 nm; c, concentration of 9-Cl-A) against time for the reaction of 9-Cl-A. It is evident that a certain type of induction period exists corresponding to the spectral change in the earliest stage.

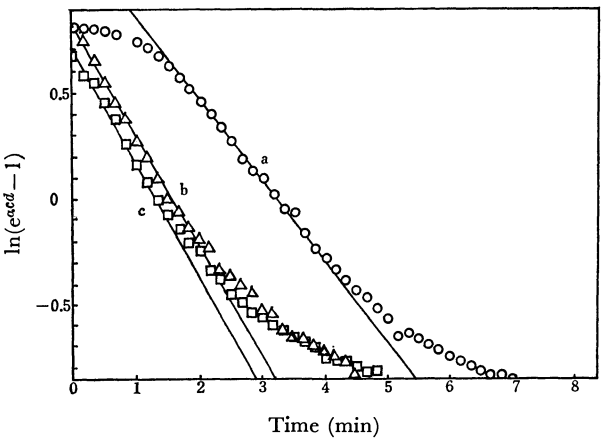

Fig. 2. Plot of $\ln(e^{acd}-1)$ *vs.* t for the degassed ethanol solution of 9-Cl-A (1×10^{-4}M) and of Z-species (see Text).
(excitation at 365 nm; temp., 25°C)
a) —○—○— first run (for 9-Cl-A)
b) -△-△- second run (for Z-species)
c) -□-□- third run (for Z-species)

9) T. Iwaoka, S. Niizuma, and M. Koizumi, This Bulletin, **43**, 2786 (1970).
10) D. N. Bailey, D. K. Roe, and D. M. Hercules, *J. Amer. Chem. Soc.*, **90**, 6291 (1968).
11) H. Lund and J. Bjerrum, *Ber.*, **64**, 210 (1931).

Concerning the behavior of X-species, Zanker and Flügel only mentioned that it is gradually reconverted into the initial substance in the dark. We have found in addition to this recovery of absorption spectrum (but not of the initial substance), that the introduction of air quickly converts X-species into a compound with a spectrum resembling that of 9-Cl-A, as shown in Fig. 1. We concluded, however, by close examination that the spectrum agrees almost completely with that of the species produced during the first 40 second irradiation. This solution when irradiated again after having been degassed, turned into X-species. We found no induction period in this case, and the spectrum changed with a clear isosbestic point at 393 nm from the beginning. Quantum yield for X formation was almost the same as the value for 9-Cl-A obtained from the run after the induction period. The chemical behavior of this compound was found to be quite different from that of 9-Cl-A. Thus the latter is transformed into acridone when the aerated ethanol solution is irradiated as observed by Zanker and Flügel and as confirmed by us, whereas the former gives acridan-like product instead of acridone. This is shown in Fig. 3.

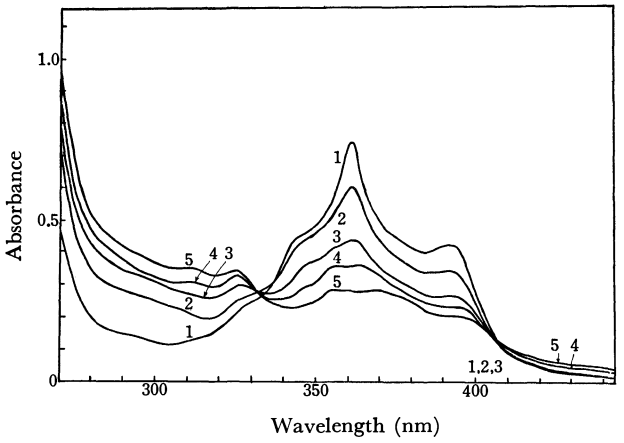

Fig. 3. Spectral change of Z-species in the aerated ethanol solution upon irradiation at 365 nm (25°C). Time of irradiation,
1) 0
2) 2 min and 30 sec
3) 9 min and 30 sec
4) 22 min
5) 127 min

These findings strongly suggest that 9-Cl-A is quickly transformed photochemically into a different substance which we denote tentatively by Z-species. The Z-species (oxidized form) is reduced to X which is reoxidized by oxygen to Z. It was confirmed that the reactions

$$Z \xrightarrow[h\nu]{\text{in ethanol}} X \qquad X \xrightarrow{O_2} Z \qquad (1)$$

can be repeated as shown by curves b) and c) in Fig. 2. Thus the identification of Z-species prior to that of X-species is required.

Identification of Z-species. It is well known that 9-Cl-A is susceptible to dechlorination and dimerization and yields 9,9′-biacridyl under reductive conditions such as with Raney nickel in methanol, with hydrogen and palladium on barium sulphate and with zinc dust in hydrochloric acid.[12] This leads to the expectation that Z-species in the present system is 9,9′-biacridyl. If a chlorine atom remains in the molecule, the molecular weight is ~214, while the molecular weight of 9,9′-biacridyl is 356. Hence a mass spectrometric determination of molecular weight was undertaken. To do this, preparation of Z-species was carried out on a large scale using a Riko-Kagaku K.K.'s irradiation apparatus. 1—1.5 *l* of the ethanol solution of 9-Cl-A $1—2 \times 10^{-4}$M, was irradiated by 365 nm in the atomsphere of argon. It was confirmed that the product gives the same spectrum as that for Z-species obtained by small-scale reaction. The crystal obtained by distilling off the solvent was subjected to thin layer chromatography and Z-species was separated by using the mixture of benzene (10) and ethylacetate (1) as a developer. It was established that the material thus separated undergoes essentially the same reactions as those for Z-species.

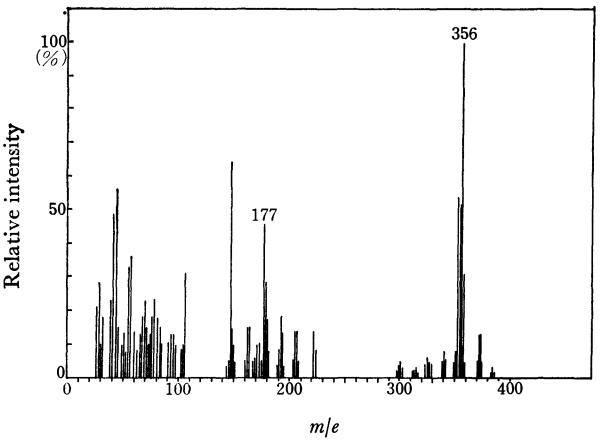

Fig. 4. Mass spectrum of Z-species prepared on a large scale and purified by thin layer chromatography. Relative intensity in reference to that for m/e=356 (100%). Temperature measured, 160°C.

Results of mass spectrometry are shown in Fig. 4. It is seen that a principal peak lies at 356 and there is no peak near 214. All the physical properties observed support the view that Z-species is 9,9′-biacridyl. Thus we have the results:

1) melting point, 379°C (literature value, 382°C[13])
2) Scarecely soluble in nearly all the solvents
3) The absorption spectrum agrees with that reported by Levshin.[14]
4) pH dependence of the absorption indicates the presence of two nitrogen atoms in a molecule as shown in Fig. 5.

It was confirmed that the solution, after 9-Cl-A has been converted into X-species, contains chlorine anion and is acidic and that the spectrum of Z-species in the solution (aerated) agrees very well with that for 10^{-4}M HCl given in Fig. 5.

12) R. M. Acheson, "Acridines," Interscience Pub., New York (1956), p. 277.
13) H. Decker and W. Petsch, *J. prak. Chem.*, **143**, 211 (1935).
14) L. V. Levshin, *Zh. Eksp. i Theor. Fiz.*, **28**, 213 (1955).

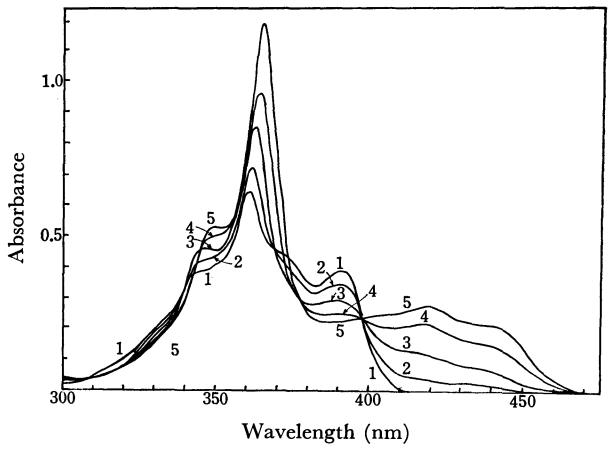

Fig. 5. Effect of the addition of HCl on the absorption spectra of the ethanol solution of Z-species (purified by thin layer chromatography).
Concentration of HCl,
1) 0
2) 1×10^{-4}M
3) 5×10^{-4}M
4) 5×10^{-3}M
5) 0.1M

We can now conclude that Z-species is 9,9′-biacridyl which is produced by reaction

$$2(9\text{-Cl-A}) \xrightarrow[(h\nu)]{2H} \text{biacridyl} + 2HCl \qquad (2)$$

X-Species and ESR Spectrum of the Photoproduct. Now that Z-species, a precursor of X-species, has been identified to be 9,9′-biacridyl, it is highly probable that X-species is a compound obtained by the photochemical reduction of 9,9′-biacridyl. 9,9′-biacriden is considered most likely to be such a compound. This compound was prepared by Decker and Petsch for the first time. According to their results, *N,N′*-dimethyl derivative is stable in the air, but not *N*-monomethyl derivative. These compounds emit green fluorescence as X-species does. Figure 6 shows the fluorescence spectrum of X-species together with those of 9-Cl-A and of Y. The absorption and fluorescence spectra of *N,N′*-dimethyl derivative reported recently by Legg and Hercules[15] essentially agree with those of X-species. Thus we can conclude that X-species is biacriden.

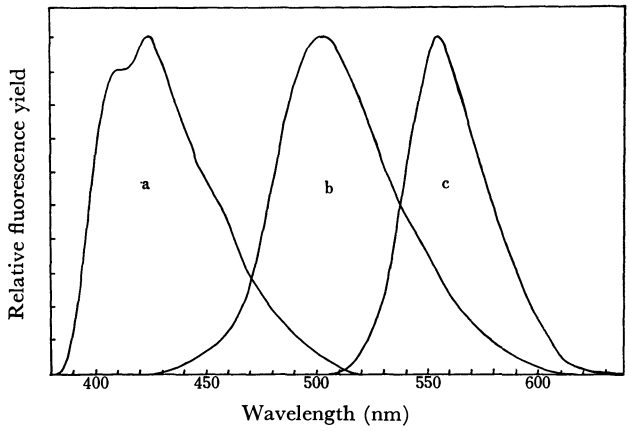

Fig. 6. Fluorescence spectra of 9-Cl-A, X, and Y in ethanol.
a : 9-Cl-A
b : X (obtained by 10 minutes irradiation of the degassed solution of 9-Cl-A)
c : Y (obtained by 33 hours irradiation of the degassed solution of 9-Cl-A)

The photoproduct involving X-species has been found to give ESR spectrum with well separated hfs, the analysis of which has not yet been completed. At present it is interesting to note that the general feature of the spectrum strongly suggests the existence of the two equivalent NH groups which supports the view that the radical is originated from biacriden. Another important fact is that the ethanol solution of 9,9′-biacridyl separated by thin layer chromatography exhibits no ESR spectrum upon irradiation, although on the basis of quite a similar spectral change the photochemical reaction is thought to proceed essentially in the same way, as shown in Fig. 7. In view of scheme (2) for the photochemical formation of biacriden from

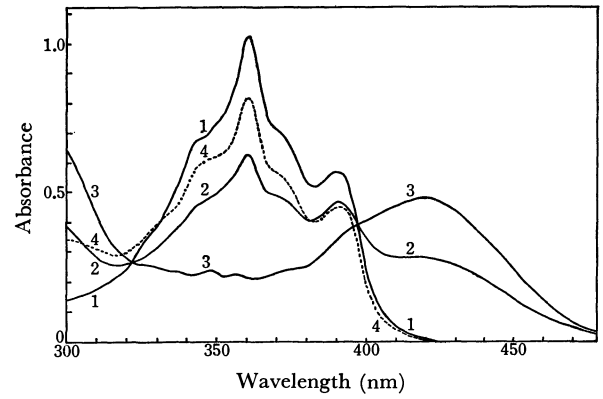

Fig. 7. Change of absorption spectra of Z (obtained on a large scale and purified by thin layer chromatography) in the degassed ethanol solution upon irradiation.
Time of irradiation,
1) 0
2) 1 min and 10 sec
3) 6 min
4) air introduced to 3)
T, 25°C; λ excitation, 365 nm

9-Cl-A, it was suspected that the acidic medium is necessary for the appearance of ESR. In fact we could confirm that the irradiated solution of the separated 9,9′-biacridyl in ethanol gives a similar ESR spectrum when a small quantity of HCl was added to the solution in a degassed condition. It should be added that 9,9′-biacridyl dissolved in acetic acid does not undergo photoreduction. This may be due to the non-reactivity of the double protonated species.

Reaction in the Aerated Ethanol Solution. Zanker and Flügel's observation that acridone is the main photoproduct in the aerated ethanol solution was reconfirmed. The solvent they used was 96% aqueous ethanol. They proposed the following mechanism for the photochemical reactions as well as for the thermal reaction.

About 100 times increase of the rate in the photochemical reaction as compared with that in the thermal one was attributed to the increased basicity of the

15) K. D. Legg and M. Hercules, *J. Amer. Chem. Soc.*, **91**, 1902 (1969).

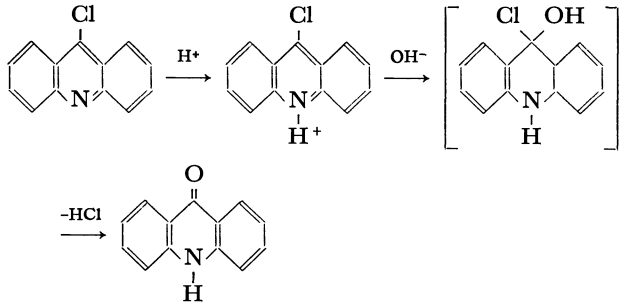

excited state.

Our results on the effect of oxygen concentration and of the addition of water are shown in Figs. 8 and 9. It is evident from Fig. 8 that the existence of oxygen above 5×10^{-4}M is necessary for the occurrence of photochemical formation of acridone. Figure 9 shows that the addition of a large quantity of water does not induce the formation of acridone in the absence of oxygen. The results indicate that oxygen instead of water plays a dominant role in the reaction. In order to confirm definitely the none-participation of water in the reaction we carried out an experiment using a carefully dehydrated ethanol (aerated). It was found that the formation of acridone proceeds at essentially the same rate. A similar experiment was repeated using carefully dehydrated methyltetrahydrofuran. Formation of acridone was confirmed, though acridan-type compound was produced at the same time. Thus,

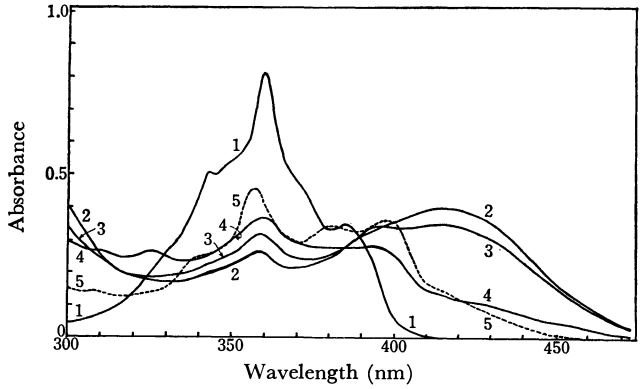

Fig. 8. Absorption spectra of irradiated ethanol solutions of 9-Cl-A dissolving various concentrations of oxygen. (Time of irradiation, 8—9 min at 365 nm, temp., 25°C)
1) 9-Cl-A
Concentration of oxygen of the irradiated solutions,
2) 1.6×10^{-6}M
3) 1.4×10^{-5}M
4) 7.4×10^{-5}M
5) 5.1×10^{-4}M

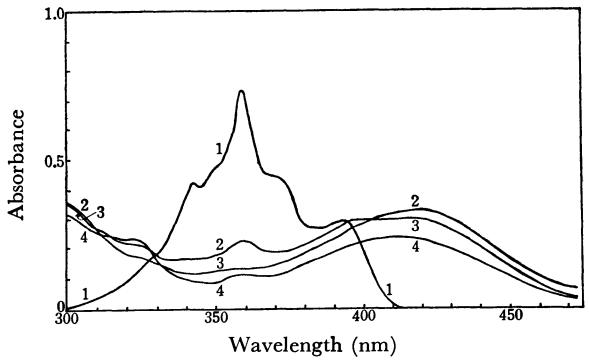

Fig. 9. Absorption spectra of irradiated solutions of 9-Cl-A in the mixed solvents of water and ethanol of various composition (time of irradiation, 9 min at 365 nm).
1) 9-Cl-A in the mixture of ethanol (3) and water (1). The ratio of ethanol to water (in vol) in the irradiated solution,
2) 3:1
3) 1:1
4) 1:2

TABLE 1. TYPES OF REACTION IN VARIOUS SOLVENTS (Φ,[c] Quantum yield)

	Solvent	Aerated	Deaerated
A)	Methanol	Acridone ($\Phi=0.016$)	Biacriden ($\Phi=0.0011$)
	Ethanol	Acridone ($\Phi=0.033$)	Biacriden ($\Phi=0.011$)
	Isopropanol	Acridone ($\Phi=0.012$)	Biacriden ($\Phi=0.012$)
	n-Butanol	Acridone	Biacriden
	n-Amyl alcohol	Acridone ($\Phi=0.0026$)	Biacriden
	s-Amyl alcohol	Acridone ($\Phi=0.0045$)	Biacriden
	t-Amyl alcohol	Acridone ($\Phi=0.0026$)	Biacriden
	Ethyleneglycol	Acridone ($\Phi=0.013$)	Biacriden
	Benzyl alcohol	Acridone + biacriden	Biacriden ($\Phi=0.033$)
	Cyclohexanol	Acridone ($\Phi=0.0062$)	Acridone
	Toluene	Acridone ($\Phi=0.0024$)[a]	Biacriden
B)	*β*-Phenetyl alcohol	Acridone ($\Phi=0.0076$)	Acridan type
	Tetrahydrofulfuryl alcohol	Acridone ($\Phi=0.026$)	Acridan type ($\Phi=0.041$)
	Tetrahydrofuran	Acridone ($\Phi=0.0041$)[a]	Acridan type ($\Phi=0.035$)
	Cyclohexane	Acridone ($\Phi=0.0076$)[a]	
	Dioxane: H_2O[b] = 1:1 in vol	Acridone ($\Phi=0.011$)	Acridan type ($\Phi=0.048$)
	Trichloroethylene	Acridone ($\Phi=8.5\times10^{-4}$)[a]	
	n-Heptane	Acridone ($\Phi=0.0056$)[a]	
C)	Benzene	no reaction	no reaction
	CCl_4[b]	no reaction	no reaction

a) acridan-type compound may be produced simultaneously.
b) agrees with Zanker's result.
c) Quantum yields are the preliminary values obtained simply from the decrease of the optical density.

there is no room to doubt that the formation of acridone proceeds in a different mechanism from Zanker and Flügel's, in which oxygen instead of water plays an essential role.

Investigations on the Solvent Effect on the Reactions in Aerated and Deaerated Conditions. Table 1 gives preliminary results on the type of reaction and their quantum yields for various solvents aerated and deaerated.

A survey of the results leads us to the following conclusion. In an aerated condition, formation of acridone proceeds in all the solvents except for benzene and carbon tetrachloride which have no easily detachable hydrogen atoms. This suggests that the primary process for the production of acridone is the formation of semiquinone of 9-Cl-acridine with H-atom attached on N-atom, (C-radical). A larger quantum yield of acridone formation in ethanol than in methanol is also in line with this view. The effect of the addition of water to the aerated ethanol on the acridone formation quantum yield, also supports this view (Table 2).

Table 2. Quantum yield (Φ) of acridone formation in the aerated ethanol-water mixture

$EtOH:H_2O$ (in vol%)	100:0	95:5	90:10	75:25	50:50	33.3:66.7
Φ	0.033	0.027	0.020	0.016	0.009_3	0.005_1

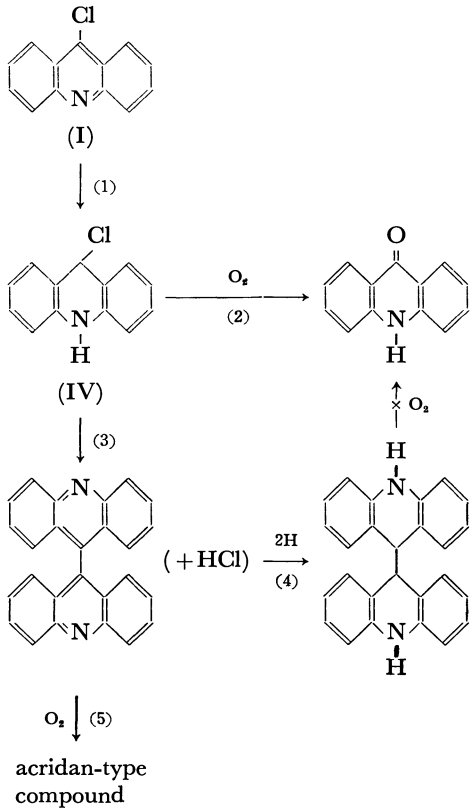

Oxygen may perhaps oxidize the semiquinone and the resulting HO_2 or H_2O_2 may lead to acridone formation. A slight increase of the rate of acridone formation by the addition of H_2O_2 seems to support this mechanism. There is scarcely any sign of the formation of acridan-type compound in the solvents of A group. In the deaerated solution, two types of reaction occur, the formation of acridan-type compound and the formation of biacriden. However, it is not known whether the formation of acridan-type compound occurs *via* biacridine or directly from 9-Cl-acridine in the solvents of B group. Whether biacridan- or 9-(9-acridanyl)-acridine-type compound is produced in the former case is also unknown. One exception is cyclohexanol in which acridone is formed even in the absence of oxygen. Benzyl alcohol is of particular interest for its high reactivity and for the result that biacriden is likely to be produced even in the presence of oxygen.

Conclusion

A general feature of the photochemical reaction of 9-Cl-acridine may be summarized as follows.

Process (1) may occur both in the presence and in the absence of oxygen. One conceivable scheme for Process (2) is the formation of HO_2 and H_2O_2 and their attack on (IV). Process (3) is suppressed when the oxygen concentration is larger than $\sim 10^{-4}$M. It is not known whether the detachment of HCl preceeds or succeeds the dimerization. It is most likely that molecular mechanism does not occur at all or is negligible for 9-Cl-acridine in alcohols. Process (5) occurs most likely *via* molecular mechanism; primary product may perhaps be 9-(9-acridanyl)-acridine compound. In the deaerated alcohols, the reaction yielding biacriden is predominant, but formation of acridan-type compound can also occur *via* molecular mechanism. The relative magnitudes of the two type reactions depend on the nature of the solvent.

The formation of radical species (most likely radical ion) might be due to some kind of reaction between two substances, for instance, electron transfer between biacriden and 9,9′-biacridyl or between biacriden and 9-(9-acridanyl)-acridine. This is likely because the concentration of radical species is very small compared with that of biacriden. That the acidic medium is necessary for the appearance of ESR[16] suggests an analogous mechanism to that for the system of phenazine (ϕ) and dihydrophenazine (ϕH_2), in which radical cation is produced by the interaction of ϕ and ϕH_2 in a strong acidic medium[10] or by acidifying the ethanol solution containing an associated complex between ϕ and ϕH_2.

16) According to Maeda and Hayashi, lucigenine (10,10′-dimethyl 9,9′-biacridinium dinitrate) exhibits ESR in the solid state while 10,10′-dimethylbiacriden does not. These observations might have some relation with the present result. K. Maeda and T. Hayashi, This Bulletin, **40**, 169 (1967).

The Crystal and Molecular Structure of 2,5-Distyrylpyrazine

Yoshio SASADA, Hirotaka SHIMANOUCHI, Hachiro NAKANISHI,* and Masaki HASEGAWA*

Laboratory of Chemistry for Natural Products, Tokyo Institute of Technology, Meguro-ku, Tokyo

**Research Institute for Polymers and Textiles, Kanagawa-ku, Yokohama*

(Received October 27, 1970)

2,5-Distyrylpyrazine($C_{20}H_{16}N_2$), which has photo-polymerizability in the crystalline state, crystallizes in the orthorhombic system with cell dimensions of $a=20.638$, $b=9.599$, and $c=7.655$ Å, including four molecules in the unit cell. The space group is *Pbca*. The structure has been determined by the direct method and refined by the block-diagonal-matrix least-squares method using three-dimensional data. The molecules is not planar; the average plane of the pyrazine ring makes a dihedral angle of 12.09° with that of the benzene ring. The molecules are spaced by the *c*-translation forming an almost parallel plane-to-plane stack. In this stack, the ethylenic double bonds approach each other at the shortest intermolecular distances of 3.939 Å, since the long axis of the molecule makes an angle of about 30° with the *c*-axis. Therefore, the polymerization may occur between these double bonds to form a cyclobutane ring.

Recently, Hasegawa and his collaborators have reported that 2,5-distyrylpyrazine (DSP) (I) is polymerized by photo-irradiation in the crystalline state to result in a linear polymer (II) containing a cyclobutane ring in the main chain.[1,2]

In the course of exploring the photo-polymerizability of various related diolefinic compounds, it has been found that 1,4-bis[β-pyridyl-(2)-vinyl]benzene (P2VB) (III) gives a polymer just like DSP.[2] Under a polarizing microscope, both polymers look like aggregates of bar-like crystals which are elongated in the direction of the *c*-axis of the monomer crystal.[3] The crystallinity of these polymers corresponds to the highest among known polymers.

In order to investigate the mechanism of polymerization, X-ray powder photographs have been taken for these two monomers and the related diolefinic compounds.[4] The powder diagrams of DSP and P2VB are nearly identical with each other.

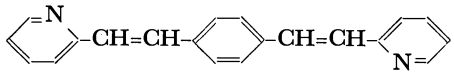

III

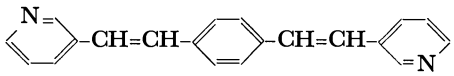

VI

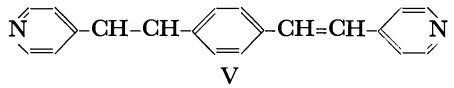

V

On the other hand, 1,4-bis[β-pyridyl-(3)-vinyl]benzene (P3VB) (IV) and 1,4-bis[β-pyridyl-(4)-vinyl]benzene (P4VB) (V), which have nearly the same molecular dimensions as P2VB, give X-ray patterns different from those of I and III, and do not polymerize under the same conditions. These observations suggest that the molecules of DSP and P2VB are favourably arranged for polymerization in the crystal, while P3VB and P4VB are not.

Moreover, the results of the analysis of kinetic behavior indicate that the polymerization of DSP is controlled by the molecular arrangement in the monomer crystal.[3]

The present paper will deal with the crystal structure of DSP as one of a series of studies aiming to clarify the relationship between the polymerization mechanism and the molecular arrangement in the crystal.

Experimental

DSP was prepared by the dehydration of 1 mol of 2,5-dimethylpyrazine and 2 mol of benzaldehyde in the presence of benzoic anhydride. By the slow evaporation of a saturated THF solution at room temperature, crystals suitable for the X-ray work were obtained. They were yellowish-green hexagonal plates with a thickness of about 1 mm.

The unit cell dimensions were determined by the least-squares treatment of the spacing of high-angle *hk*0 and *h*0*l* reflections, which were measured on Weissenberg photographs and calibrated with the powder lines of Al-wire. The density calculated by assuming 4 molecules in a unit cell, is 1.244 $g \cdot cm^{-3}$, while the density measured by floatation is 1.257

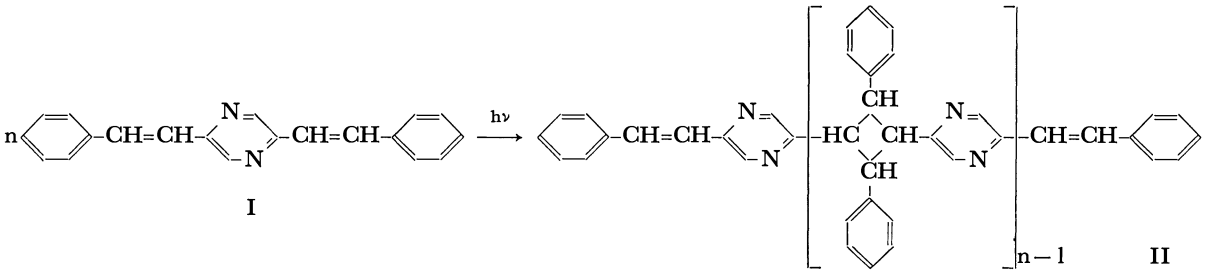

I II

1) M. Hasegawa and Y. Suzuki, *J. Polymer Sci., Part B* **5**, 813 (1967).

2) M. Hasegawa, Y. Suzuki, F. Suzuki, and H. Nakanishi, *ibid., Part A-1*, **7**, 743 (1969).

3) H. Nakanishi, Y. Suzuki, F. Suzuki, and M. Hasegawa, *ibid., Part A-1*, **7**, 753 (1969).

4) M. Iguchi, H. Nakanishi, and M. Hasegawa, *ibid., Part A-1*, **6**, 1055 (1968).

$g \cdot cm^{-3}$. From the systematic absences of reflections, the space group is determined to be *Pbca*; the absent reflections are $0kl$ when k is odd, $h0l$ when l is odd, and $hk0$ when h is odd. Since the general positions are eight-fold in this space group, the number of the molecules in the unit cell indicates that the molecule must have a centre of symmetry. The crystal data of DSP are given in Table 1.

Table 1. Crystallographic and physical data

Formula	$C_{20}H_{16}N_2$
MW	284
Mp	230°C
Crystal system	Orthorhombic
Space group	*Pbca*
a	20.638 Å
b	9.599 Å
c	7.655 Å
Z	4
Vol.	1517 Å^3
D_{calcd}	1.244 g·cm^{-3}
D_{obsd}	1.257 g·cm^{-3}
μ	6.83 cm^{-1}
$F(000)$	600

The intensity data were collected from equi-inclination multiple-film Weissenberg photographs. The layers from 0 to 5 along the c-axis and from 0 to 7 along the b-axis were recorded using Cu-Kα radiation. The crystals used had cross sections, perpendicular to the rotation axis, of 0.10×0.05 cm and of 0.05×0.05 cm for the c- and b-axis rotations respectively. The intensities were measured visually by comparison with a calibrated scale prepared with the same crystal. Of these 1246 reflections, 297 were measured as having zero intensity, while the others range from 1 to 19837 in their relative intensities. Corrections were made for the Lorentz and polarization factors and for spot size, but not for absorption. The data were put onto an absolute scale by means of Wilson's plot. The structure factors, $|F_h|$, and the normalized structure factors, $|E_h|$, were computed together.

Structure Determination

The symbolic addition procedure was applied for sign determination. As a starting set, the signs of five strong reflections were chosen; three of them specified the origin, and the other two were symbols, as is shown in Table 2. After six cycles of the phase-determining process using the Σ_2 relationship, the signs of 103 reflections out of 180 with $|E_h|>1.5$ were determined in terms of the a and b with a probability greater than 0.97. Further, by investigating the list of the Σ_2 relations, it seemed most probable that $a=+$ and $b=-$.

An E-map was computed using these 103 reflections with $a=+$ and $b=-$. All eleven non-hydrogen

Table 2. Assignment of signs of five strong reflections

h	k	l	E	Sign
1	1	7	4.31	+
3	7	6	3.95	+
4	1	1	3.24	+
12	4	4	5.04	a
3	7	2	3.12	b

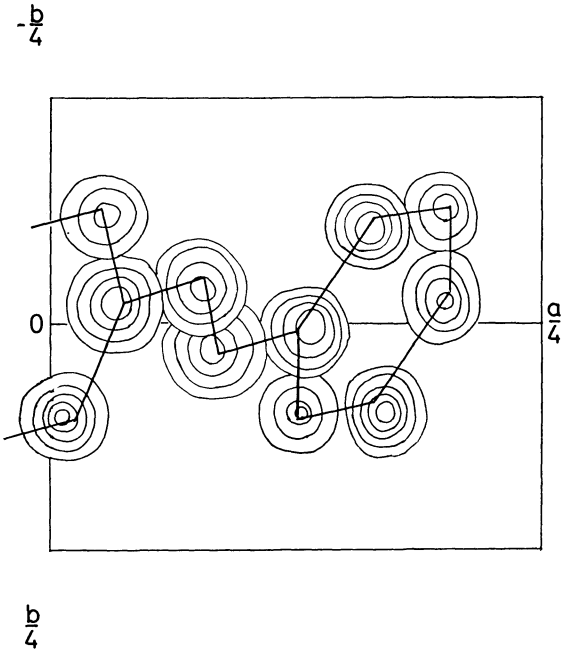

Fig. 1. Composite E-map. Contours are at equal intervals on an arbitrary scale. The final molecular shape is indicated with solid line.

atoms in the asymmetric unit were well resolved in the resulting E-map, as is shown in Fig. 1. Two additional appreciable peaks appeared, one of which is at the centre of the pyrazine ring, and the other, at the centre of the benzene ring; they were easily excluded as being insignificant. The only ambiguity was in the choice of the position of the N atom from between the alternative assignments.

Refinement

The coordinates of the eleven atoms as read on the E-map were subjected to Fourier refinement. On the first electron-density distribution map, the N atom was assigned easily from the peak height. The discrepancy factor, $R=\Sigma||F_o|-|F_c||/\Sigma|F_o|$, was 0.284 for the observed reflections. The parameters were refined by the block-diagonal-matrix least-squares method using isotropic temperature factors for all the atoms. After four cycles, the R value was reduced to 0.150. Further refinement was performed by introducing anisotropic temperature factors of the $exp\{-(B_{11}h^2+B_{22}k^2+B_{33}l^2+B_{12}hk+B_{13}hl+B_{23}kl)\}$ form. After four cycles, the R value became 0.132. A difference Fourier synthesis at this stage revealed all the hydrogen atoms. The absence of a residual peak outside the N atom proved that the assignment of nitrogen based on the peak height was correct. The subsequent refinement was, however, initiated by using the positions of hydrogens computed by assuming suitable geometries of the C–H bond (C–H=1.08 Å), and the parameters of all the atoms including isotropic hydrogens were refined. After four cycles, the R value was 0.098. In the final cycles of refinement, the strongest reflection, 020, was excluded because it seemed to suffer from extinction. After four cycles, the R value reached 0.086.

The final atomic coordinates and the temperature

factors are given in Table 3, and their standard deviations, in Table 4. The observed and calculated structure factors are listed in Table 5. The final three-dimensional electron density distribution is shown in Fig. 2.

The atomic scattering factors used in the calculation were taken from the International Tables for X-ray Crystallography (1962). The computations were done on CDC 3600 and HITAC 5020E computers with the programs written by T. Ashida.

Results and Discussion

Molecular Structure. The bond lengths and angles are listed in Table 6, along with their standard deviations; they are also shown in Fig. 3.

The mean value of the C–C bond lengths in the benzene ring is 1.397 Å, very close to that given by Sutton.[5] The C(6)–C(5)–C(7) angle, 117.7°, is somewhat smaller than the others. A decrease in the corresponding angle is observed in the benzene ring with the –CH=CHR substituent: 118.2 and 117.5° in 1,1-di-*p*-toluylethylene,[6]

TABLE 3. FINAL ATOMIC COORDINATES AND TEMPERATURE FACTORS

The anisotropic temperature factors are expressed in the form of $exp\{-(B_{11}h^2+B_{22}k^2+B_{33}l^2+B_{12}hk+B_{13}hl+B_{23}kl)\}$

Atom	x/a	y/b	z/c	B_{11} or B	B_{22}	B_{33}	B_{13}	B_{13}	B_{23}
N(1)	0.0111	0.1073	0.8780	0.00294	0.00982	0.01939	0.00071	0.00195	0.00074
C(1)	0.0254	−0.1253	0.9812	0.00291	0.00911	0.02153	0.00115	0.00139	0.00043
C(2)	0.0367	−0.0223	0.8568	0.00275	0.01040	0.01563	0.00004	0.00074	0.00093
C(3)	0.0771	−0.0504	0.7043	0.00304	0.00957	0.01857	0.00046	0.00124	−0.00197
C(4)	0.0848	0.0331	0.5676	0.00263	0.00980	0.01896	−0.00002	0.00051	−0.00129
C(5)	0.1252	0.0074	0.4135	0.00253	0.01030	0.01648	−0.00057	−0.00131	−0.00327
C(6)	0.1257	0.1050	0.2760	0.00331	0.01129	0.01886	−0.00075	−0.00060	0.00110
C(7)	0.1638	−0.1118	0.3953	0.00288	0.01178	0.01732	0.00042	0.00051	−0.00079
C(8)	0.1644	0.0848	0.1301	0.00409	0.01470	0.02104	−0.00276	0.00272	0.00287
C(9)	0.2024	−0.1323	0.2492	0.00314	0.01393	0.02249	0.00005	0.00139	−0.00750
C(10)	0.2029	−0.0338	0.1158	0.00372	0.01702	0.02048	−0.00233	0.00399	−0.00461
H(1)	0.0484	−0.2214	0.9619	6.10					
H(3)	0.1029	−0.1503	0.7026	6.14					
H(4)	0.0587	0.1307	0.5702	6.11					
H(6)	0.0950	0.1958	0.2855	5.66					
H(7)	0.1629	−0.1890	0.4978	5.72					
H(8)	0.1653	0.1624	0.0321	6.10					
H(9)	0.2337	−0.2227	0.2395	5.68					
H(10)	0.2339	−0.0463	0.0065	5.78					

TABLE 4. ESTIMATED STANDARD DEVIATIONS

($\sigma(x)$, $\sigma(y)$, and $\sigma(z)$ in Å, $\sigma(B)$ in Å^2)

Atom	$\sigma(x)$	$\sigma(y)$	$\sigma(z)$	$\sigma(B_{11}$ or $B)$	$\sigma(B_{22})$	$\sigma(B_{33})$	$\sigma(B_{12})$	$\sigma(B_{13})$	$\sigma(B_{23})$
N(1)	0.0039	0.0038	0.0040	0.00011	0.00045	0.00083	0.00038	0.00052	0.00113
C(1)	0.0048	0.0046	0.0052	0.00013	0.00052	0.00107	0.00046	0.00066	0.00134
C(2)	0.0045	0.0046	0.0046	0.00013	0.00054	0.00088	0.00045	0.00058	0.00124
C(3)	0.0049	0.0045	0.0049	0.00014	0.00052	0.00103	0.00046	0.00063	0.00133
C(4)	0.0046	0.0045	0.0049	0.00012	0.00053	0.00099	0.00044	0.00061	0.00130
C(5)	0.0044	0.0045	0.0047	0.00012	0.00054	0.00090	0.00044	0.00058	0.00126
C(6)	0.0051	0.0048	0.0052	0.00015	0.00059	0.00107	0.00052	0.00067	0.00142
C(7)	0.0048	0.0049	0.0049	0.00014	0.00059	0.00096	0.00048	0.00062	0.00139
C(8)	0.0058	0.0056	0.0056	0.00018	0.00074	0.00118	0.00063	0.00078	0.00163
C(9)	0.0052	0.0053	0.0058	0.00015	0.00066	0.00116	0.00055	0.00073	0.00164
C(10)	0.0056	0.0058	0.0056	0.00017	0.00081	0.00116	0.00064	0.00076	0.00176
H(1)	0.0508	0.0587	0.0586	1.61					
H(3)	0.0540	0.0567	0.0581	1.62					
H(4)	0.0544	0.0586	0.0577	1.60					
H(6)	0.0508	0.0526	0.0576	1.55					
H(7)	0.0512	0.0532	0.0573	1.55					
H(8)	0.0535	0.0563	0.0581	1.60					
H(9)	0.0501	0.0553	0.0569	1.50					
H(10)	0.0538	0.0550	0.0558	1.57					

5) L. E. Sutton, "Tables of Interatomic Distances and Configuration in Molecules and Ions," The Chemical Society, London (1958). S 13.

6) G. Casalone, A. Gavezotti, C. Mariani, A. Mugnoli, and M. Simonetta, *Acta Crystallogr.*, **B26**, 1 (1970).

TABLE 5. OBSERVED AND CALCULATED STRUCTURE FACTORS
Both structure factors are multiplied by 4.5.

H FO FC	H FO FC	H FO FC	H FO FC	H FO FC	H FO FC	H FO FC	H FO FC
K,L= 0 0	2* 0 7	5* 0 9	9 382 378	9 17 16	5 190-165	6 86 -90	1 113 -94	6 62 61
2 249 275	4 12 -17	6* 0 -10	10 69 -67	10 20 16	6 111 99	7 92 -95	2 20 14	7 45 -42
4 122-131	6 61 64	7 84 -81	11 147 140	11* 0 -8	7 11 -10	8 90 -89	3 18 21	8* 0 -14
6 272 287	8 57 60	8 47 43	12 66 63	12* 0 0	8 30 -28	9 75 -78	4 9 14	9 33 36
8 36 -32	10 15 -17	9 86 -83	13 35 33	13* 0 3	9 7 2	10 62 64	5 32 33	10* 0 10
10 111 113	K,L= 11 0	10 23 -29	14 56 -54	14 57 -56	10 82 75	11 60 -60	6 113 103	11 16 23
12 13 -9	4 23 -22	11 26 -26	15 44 -42	15 41 38	11 9 -12	12* 0 5	7* 0 -1	12 64 64
14 33 29	6 41 41	12 21 -20	16 51 -47	16 13 -17	12 63 59	13 24 -28	8 14 16	13 20 -24
16 33 -34	8 45 37	13 18 -19	17* 0 3	17* 0 3	13 24 22	14 36 34	9* 0 4	14 10 9
18 60 -57	K,L= 12 0	14* 0 -4	18* 0 -1	18 18 -20	14 25 24	15 11 -13	10 28 27	15 17 -20
20 63 -55	0 36 -40	15 19 -20	19 48 44	19* 0 8	15 16 14	16 11 -17	11* 0 -8	16 16 -12
22 37 -37	K,L= 1 1	16 24 -28	20 19 -17	20* 0 11	16 41 39	17 13 14	12 43 42	17 11 10
24 57 62	1 74 73	17* 0 0	21* 0 -4	21 13 -12	17* 0 9	18 45 -43	13 11 -13	18 24 23
K,L= 1 0	2 254-245	18 29 -28	22* 0 1	22 23 21	18* 0 -7	19* 0 2	14 30 27	19 10 11
2 52 57	3 308 308	19 20 25	23* 0 1	K,L= 6 2	19 29 -29	20 8 9	15* 0 1	20 11 11
4 105-108	4 620 665	20 10 -8	24 10 -11	0 67 64	20 24 -24	21 6 -9	16 37 37	K,L= 7 4
6 269 295	5 533 562	21* 0 10	K,L= 1 2	1 38 34	21 21 -18	K,L= 7 3	17* 0 2	3 16 -18
8 10 -13	6 178 178	22 24 -23	1 13 11	2* 0 8	22 9 13	3 15 -16	18* 0 6	4 12 -11
10 17 -19	7 62 63	K,L= 6 1	2 33 34	3 36 33	23* 0 -10	4* 0 3	19* 0 8	5 43 44
12 10 11	8 8 9	0 129-115	3 170 171	4 74 -65	24 7 11	5 29 30	20* 0 7	6 94 -94
14* 0 0	9 11 12	1 94 88	4 68 72	5 12 -19	K,L= 2 3	6 67 68	21* 0 8	7 50 52
16* 0 8	10 60 -63	2 59 -59	5* 0 4	6 11 -17	0 190 181	7 26 30	22 8 11	8 21 -27
18 43 -43	11 22 -25	3 15 18	6 85 -84	7* 0 4	1 62 64	8* 0 -4	K,L= 2 4	9* 0 6
20* 0 -2	12 11 17	4 57 -60	7 10 -6	8 34 35	2 131 129	9 11 4	0 218-213	10 38 -39
22* 0 -8	13 65 -64	5 14 -18	8 149 141	9 33 34	3 84 79	10 26 -27	1 18 15	11 36 -38
24 27 -23	14 123 115	6 34 -35	9 163 161	10* 0 2	4 99 -92	11* 0 7	2 4 5	12 36 -36
K,L= 2 0	15 33 -34	7* 0 0	10 81 77	11* 0 -1	5 64 52	12* 0 9	3* 0 9	13 42 -43
0 775 896	16 25 28	8 54 52	11 14 15	12* 0 -6	6 10 -2	13* 0 2	4 25 -28	14* 0 -10
2 147 160	17 31 -32	9 33 -37	12 22 20	13 23 -23	7 113 112	14 16 22	5 62 -55	15* 0 -4
4 148-158	18* 0 7	10* 0 -5	13 15 -12	14 14 11	8 73 73	15 10 -9	6 94 -79	16 24 -20
6 57 -54	19 21 23	11* 0 -13	14 17 17	15 23 -26	9 33 34	16 10 13	7 39 -35	17 13 13
8 47 -45	20 37 -36	12 22 -28	15 72 67	16 23 23	10 21 8	17* 0 0	8 15 16	18 12 13
10 45 46	21* 0 8	K,L= 7 1	16 24 -23	17 15 -12	11 20 -23	18 13 -16	9 18 19	K,L= 8 4
12 27 -28	22* 0 3	2 15 -27	17 15 9	18* 0 -3	12 79 73	K,L= 8 3	10* 0 -2	2 21 -23
14 19 21	23 30 -28	3 79 85	18 26 21	19* 0 -3	13 94 90	0 12 -17	11* 0 -4	3* 0 -3
16* 0 -4	24* 0 2	4 9 13	19* 0 -9	20 14 -17	14 27 24	1 12 -14	12 49 46	4 11 14
18 52 -48	25 14 -13	5 35 41	20* 0 1	21 17 -17	15 65 61	2 12 -13	13 31 -29	5 21 -22
20 36 -39	26 16 -15	6* 0 1	21 9 11	K,L= 7 2	16 12 17	3* 0 10	14 23 18	6* 0 0
22* 0 2	K,L= 2 1	7 13 -20	K,L= 2 2	1 51 -49	17 12 11	4* 0 -9	15 15 -16	7 11 6
24 51 44	0 29 25	8 45 51	0 35 34	2 97 -95	18 12 13	5* 0 0	16 11 12	8* 0 -11
K,L= 3 0	1 82 -84	9* 0 -5	1 100-100	3 136-131	19 23 24	6 50 -53	17 15 16	9 23 25
2 24 -23	2 123-126	10* 0 7	2 86 -81	4 79 -74	20 19 -21	7 55 -54	18 12 3	10 12 13
4 38 -35	3 76 79	11* 0 4	3 85 84	5* 0 0	21 10 9	8 51 -49	19 33 32	11 10 16
6 295 270	4 316 330	12* 0 5	4 33 -29	6 18 20	22* 0 7	9 30 -32	K,L= 3 4	12 21 -23
8 48 -46	5 258 269	13* 0 -9	5 25 -24	7 15 -17	23* 0 -2	10 11 12	1 120 -98	13* 0 6
10 48 -48	6 149 154	14 24 26	6 33 -30	8 14 -10	24 10 12	11 11 -12	2* 0 3	14 10 -6
12 11 3	7 72 -74	15 12 -15	7 23 17	9 47 -49	K,L= 3 3	12 27 31	3 24 27	K,L= 9 4
14 12 -11	8 69 -71	16 23 -27	8 48 46	10* 0 -6	1 127-107	13 10 -11	4 35 35	5 10 14
16* 0 12	9 8 5	17 19 -24	9 244 248	11* 0 -8	2 121-106	14 9 12	5 66 64	6 10 -13
18 51 -55	10 126.128	K,L= 8 1	10 50 43	12* 0 -5	3 20 -20	15* 0 2	6 61 59	7 10 16
20* 0 -7	11 129 128	1 56 62	11 84 79	13 10 8	4 86 84	16 14 -18	7 25 24	8 15 -18
22* 0 -13	12 12 20	2 66 -68	12 9 -5	14 21 -20	5 60 -59	17 14 16	8 20 20	9* 0 3
24 36 -31	13 46 -47	3 32 35	13 21 -17	15 9 -2	6 13 -16	18 14 -16	9* 0 4	10* 0 11
K,L= 4 0	14 38 41	4 46 -48	14 12 -5	16 12 -12	7* 0 5	K,L= 9 1	10* 0 -2	11 24 -22
0 212-213	15 11 -13	5* 0 4	15 65 -66	17* 0 5	8 46 45	3 22 -21	11 23 -25	12 25 5
2 17 -8	16 12 -13	6* 0 -8	16* 0 2	18 14 -15	9* 0 10	4 18 25	12 41 39	13 23 -21
4 105-106	17 27 25	7 20 29	17 14 -10	19 15 14	10 109-108	5* 0 0	13 42 -38	K,L= 10 4
6 360-323	18* 0 7	8* 0 -4	18* 0 -3	20 9 10	11 38 41	6 30 32	14 50 49	0 37 -34
8 70 -71	19 37 -39	9* 0 0	19 15 15	21 14 -18	12 33 -32	7* 0 11	15* 0 -9	1* 0 7
10 20 -24	20 47 46	10* 0 13	20* 0 4	K,L= 8 2	13 70 64	8* 0 -7	16 31 36	2 13 -14
12 69 -61	21 25 -28	11 12 6	21 20 -17	0 36 33	14 92 86	9* 0 -2	17 14 10	3* 0 -5
14 13 -9	22 11 -11	12 12 -18	K,L= 3 2	1 67 64	15 40 41	10 10 15	18 15 16	4 9 -8
16* 0 13	K,L= 3 1	13 20 25	1 16 16	2 57 58	16 46 -46	11 9 -15	19 14 16	5 8 -12
18 34 -36	1 211-185	14* 0 8	2 23 -18	3 50 50	17 32 33	12 9 13	20 9 10	6 24 -20
20* 0 -6	2 185 164	15 20 21	3 195 177	4* 0 7	18 35 -36	13 16 -17	21 10 12	K,L= 11 4
22 35 37	3 118-109	K,L= 9 1	4 70 -61	5* 0 -11	19* 0 6	14 19 2	22 13 12	2 11 -13
24 11 15	4 68 70	1 32 34	5 38 37	6* 0 -1	20 12 -17	15 6 -12	K,L= 4 4	K,L= 1 5
K,L= 5 0	5 154 144	2 64 -68	6 81 -80	7 27 26	K,L= 4 3	16 22 18	0 118 -93	1 33 -33
2 38 -39	6 91 89	3 79 80	7 21 -22	8* 0 5	0 191 154	K,L= 10 3	1* 0 -2	2* 0 -1
4 79 77	7 72 -72	4* 0 1	8 177 174	9 34 34	1 45 37	0 10 14	2* 0 8	3 21 -25
6 55 49	8 8 -15	5 25 27	9 200 192	10 10 -14	2 21 21	1* 0 -8	3 7 11	4 10 -15
8 16 -20	9 102 -96	6 37 40	10 122 116	11* 0 10	3 55 48	2* 0 -2	4 7 1	5 43 -42
10 14 13	10 52 -59	7* 0 -9	11 8 7	12 24 18	4* 0 -4	3* 0 4	5 56 -53	6* 0 -7
12 41 -37	11 25 -33	8 12 20	12 15 19	13 13 14	5 22 -19	4 10 -17	6 46 51	7 45 47
14 30 -33	12 12 -13	9 11 8	13 19 -17	14* 0 -6	6 53 -51	5* 0 7	7 87 -84	8 41 -41
16* 0 0	13 33 -31	10 16 17	14* 0 -8	15 8 9	7* 0 -1	6* 0 1	8 12 11	9* 0 -12
18 12 5	14 16 18	11 16 17	15 112 109	16 9 -9	8 21 -26	7* 0 -1	9 20 24	10 96 -95
K,L= 6 0	15 24 -25	12 21 21	16 32 -35	K,L= 9 2	9 37 -40	8* 0 -6	10 25 -25	11 33 -23
0 28 -31	16* 0 4	K,L= 10 1	17 17 14	1 32 -28	10 58 62	9* 0 4	11 13 14	12 15 -18
2* 0 1	17* 0 0	0 14 20	18 19 20	2 44 -37	11 75 -76	10* 0 3	12 170 145	13* 0 -13
4 9 -5	18 32 -30	1 25 27	19 15 -8	3 61 -57	12 21 28	11* 0 2	13 64 -61	14 58 58
6 82 -81	19 43 46	2 25 -28	20* 0 6	4* 0 1	13 43 42	12 37 31	14 27 22	15 32 -35
8 12 -11	20 16 -20	3 29 34	21 9 10	5* 0 7	14 46 44	K,L= 11 3	15 38 -36	K,L= 2 5
10 13 16	21 11 15	4* 0 0	K,L= 4 2	6* 0 4	15 26 27	0 18 0	16 14 -5	0 9 -11
12 82 -86	22 16 -19	5 21 26	0 103 89	7* 0 5	16* 0 5	1 11 -21	17 14 17	1 51 55
14 21 -20	23* 0 -7	6* 0 11	1 58 -56	8 31 32	17 12 11	2 11 -14	18 54 50	2 81 -79
16* 0 2	24 15 -15	7 11 14	2 158-144	9* 0 -2	18 23 -25	3 7 -13	19 16 18	3 13 17
18 28 -32	K,L= 4 1	8 16 -21	3 40 33	10 14 15	19 15 18	4 10 8	20 9 11	4 26 -20
K,L= 7 0	0 134-118	9* 0 6	4 164-146	11* 0 1	K,L= 5 3	K,L= 0 4	K,L= 5 4	5 54 -56
2 15 22	1 53 49	10 17 19	5 9 -13	12* 0 5	1 43 -39	0 175-169	1 19 -24	6 27 -26
4 21 22	2 24 -27	11 24 21	6 55 -53	13* 0 0	2 43 -38	1 27 27	2* 0 2	7 72 73
6 27 25	3 16 18	12 21 23	7 41 -36	14 9 9	3* 0 -6	2 35 -35	3* 0 -4	8 87 -88
8 19 17	4 87 87	13* 0 8	8 20 18	15 14 12	4* 0 4	3 9 8	4* 0 8	9 104 99
10 48 54	5 59 61	14 14 15	9 80 72	K,L= 10 2	5 11 19	4 19 -25	5 65 67	10* 0 -7
12* 0 0	6 31 35	K,L= 11 1	10 74 70	0 9 10	6 20 28	5 39 -35	6 105-102	11 17 20
14 26 -30	7 47 -50	2 25 -30	11* 0 5	1 37 33	7 13 21	6 193-179	7 70 68	12* 0 0
16 12 17	8 23 27	3* 0 2	12 63 -60	2* 0 1	8 20 28	7 30 26	8* 0 -5	13 46 48
K,L= 8 0	9 38 -38	4 15 -22	13 65 -64	3 37 34	9 13 16	8* 0 1	9* 0 5	14* 0 -8
0 126 131	10 70 64	5* 0 -9	14 36 37	4* 0 4	10 130-129	9 36 34	10 64 -62	15* 0 11
2 37 36	11 50 48	6 20 23	15 74 -74	5* 0 2	11 44 49	10 32 30	11 37 -36	16 14 -17
4 18 24	12* 0 9	7* 0 -15	16 54 53	6* 0 -7	12 40 -39	11 14 -15	12 40 -40	17* 0 -5
6 85 87	13 27 -29	8* 0 -1	17 27 -25	7* 0 -1	13 47 48	12 63 -57	13 54 -51	18* 0 -5
8 61 64	14* 0 7	9* 0 -11	18* 0 0	8 19 -18	14 79 75	13* 0 6	14 19 21	19 24 25
10* 0 8	15* 0 -1	10* 0 10	19 18 -18	9* 0 5	15 21 26	14* 0 9	15 13 -14	20 11 12
12 50 -58	16* 0 -7	11 18 18	20 16 11	10* 0 1	16 43 -43	15* 0 0	16 24 -26	21 9 10
14 17 -21	17* 0 4	K,L= 0 2	21 31 -29	11 11 10	17 23 24	16 14 19	17 15 14	K,L= 3 5
K,L= 9 0	18* 0 11	0 60 -47	K,L= 5 2	K,L= 11 2	18 44 -45	17 14 13	18 16 19	2 17 19
2 32 35	19 30 -31	1 82 -77	1 36 -33	7 16 16	19 15 18	18 38 -42	19 9 11	3 13 -10
4 19 -27	20 23 25	2 187 181	2 79 -75	8 8 13	K,L= 6 3	19 41 40	K,L= 6 4	4 53 -50
6 67 69	21 12 -16	3 160 163	3 76 -71	9 27 28	0 15 20	20* 0 -11	0 11 3	5 73 -70
8 52 48	K,L= 5 1	4 91 94	4 157-149	K,L= 1 3	1 11 -16	21* 0 8	1* 0 -2	6* 0 1
10. 27 32	1 154-136	5 28 -23	5 23 20	1 47 -50	2 30 -30	22* 0 -4	2 13 -18	7 47 49
12 20 22	2 143 130	6 116 113	6 9 12	2 69 -83	3 11 14	23 7 -8	3* 0 7	8 88 -86
K,L= 10 0	3 64 -68	7 97 101	7 33 -32	3 31 -31	4 12 17	24 15 -18	K,L= 1 4	9 59 59
0 38 38	4 55 -55	8 41 42	8* 0 -13	4 229 205	5 25 -27	K,L= 1 4	5 38 -40	10 47 -41

TABLE 5. Continued

H	FO	FC	H	FO	FC	H	FO	FC	H	FO	FC	H	FO	FC	H	FO	FC	H	FO	FC	H	FO	FC
11	13	-16	6*	0	-12	1	47	45	10	38	-42	K=L=	3	6	K=L=	6	6	9*	0	-4	K=L=	0	8	1	24	-31
12*	0	-2	7	40	44	2	34	-32	11	38	38	3	89	-82	4	14	17	10	23	-22	0	57	62	2*	0	2
13*	0	-5	8	52	-53	3	13	-15	12*	0	9	4	67	70	5*	0	13	K=L=	3	7	1*	0	-22	3*	0	-7
14*	0	2	9	52	55	4	14	17	13	34	-34	5	47	-47	6*	0	9	1	35	39	2*	0	-13	4*	0	-5
15	17	21	10*	0	0	5	13	-16	14	29	-28	6*	0	-10	7*	0	0	2*	0	8	3*	0	3	5*	0	5
16	30	34	11*	0	-11	6	13	-14	15	32	-26	7*	0	2	8*	0	-4	3*	0	-4	4	41	43	6	13	17
17	20	22	12*	0	1	7	13	16	16	27	-27	8*	0	3	9	18	-19	4*	0	11	5	62	67	7*	0	1
K=L=	4	5	13*	0	4	K=L=	8	5	K=L=	1	6	9	59	-61	K=L=	7	6	5	15	-29	6	68	75	8	12	-13
0	15	17	14*	0	-9	0	44	46	3	76	-73	10	31	37	1	12	17	6	15	-10	7*	0	27	K=L=	4	8
1*	0	-6	15	33	33	1	56	-54	4	57	59	11*	0	-15	2	21	26	7	26	-28	8*	0	1	0	48	-50
2	20	23	16	28	29	2	34	39	5	45	-42	12*	0	4	3	76	79	K=L=	4	7	9	18	-22	1*	0	18
3	37	-35	17	22	20	3	24	-32	6*	0	-13	13*	0	5	4*	0	2	4	19	-18	10*	0	0	2*	0	-9
4	12	-14	18	10	8	K=L=	9	5	7*	0	0	14*	0	4	5	12	14	5	30	31	11*	0	4	3*	0	5
5	65	-56	19	12	-12	0	17	0	8*	0	14	15	13	-17	6*	0	5	K=L=	5	7	12	15	-19	4*	0	8
6*	0	-7	K=L=	6	5	1	21	17	9	33	-36	K=L=	4	6	7*	0	2	4	13	19	13	14	13	5*	0	-2
7	28	27	0	54	53	2	20	-23	10	27	29	2	19	-25	8*	0	-6	5	13	-19	14*	0	-6	6	15	-14
8	24	-30	1	76	-77	3*	0	-24	K=L=	2	6	3	52	-53	9*	0	4	6*	0	0	15	12	16	7	10	17
9	60	56	2	79	81	4*	0	-4	0	52	-48	4	14	19	10	17	-22	7	18	-27	K=L=	1	8	K=L=	6	8
10	24	-25	3	60	-62	5*	0	-6	1*	0	4	5	14	-17	11	9	6	8	12	-16	1	14	-20	0	16	-18
11*	0	0	4*	0	6	6	10	3	2*	0	14	6	19	22	K=L=	1	7	9*	0	0	K=L=	2	8	K=L=	1	9
12	20	21	5*	0	-11	7*	0	-12	3	74	-76	7	14	14	1	131	130	10	11	15	0	12	5	5	10	18
13	14	14	6*	0	5	8	23	9	4	66	68	8	24	-28	2	81	83	11*	0	-11	1*	0	-1	6*	0	-2
14	19	-22	7	23	-27	9	15	-18	5	59	-56	9	24	-23	3*	0	-3	12*	0	7	2*	0	-10	7	9	-13
15*	0	-11	8	25	29	K=L=	0	6	6*	0	12	K=L=	5	6	4	35	-40	13	9	-14	3*	0	4	8	29	31
16	18	-20	9*	0	-2	0	103	-99	7*	0	0	1	33	33	K=L=	2	7	K=L=	6	7	4	25	26	9*	0	8
17	17	-17	10	14	-13	1*	0	15	8	24	-24	2	29	34	0	70	-73	0	28	33	5	35	35	10	27	32
18	10	-5	11	14	-15	2	72	71	9*	0	-3	3	29	39	1*	0	-19	1*	0	11	6	36	34	K=L=	2	9
19	9	12	12	13	16	3	73	-75	10	18	-24	4*	0	3	2*	0	-8	2*	0	8	7	21	22	7	11	-13
K=L=	5	5	13	13	-17	4	94	97	11	13	16	5*	0	5	3*	0	-6	3*	0	5	8*	0	-1	K=L=	3	9
1	38	35	14	12	-15	5	75	-67	12*	0	0	6*	0	5	4	39	-43	4*	0	10	9	18	-18	2	17	8
2*	0	-7	15	31	-26	6*	0	8	13	12	-15	7*	0	4	5	37	43	5*	0	5	10*	0	-8	K=L=	4	9
3*	0	2	16	18	-7	7	34	-13	14	12	-13	8	14	-18	6	36	-41	6	29	30	11*	0	-3	3	10	-13
4*	0	-8	17	23	-19	8*	0	-10	15	14	-14	9	14	-18	7*	0	16	K=L=	7	7	12	17	-17			
5	52	-52	K=L=	7	5	9*	0	10	16	20	-18	10	13	-12	8*	0	16	10	11	13	K=L=	3	8			

TABLE 6(a). BOND LENGTHS WITH THEIR e. s. d.'s

	Length (Å)	e.s.d. (Å)
N(1)–C(1)	1.328	0.007
N(1)–C(2)	1.364	0.006
C(1)–C(2)	1.395	0.007
C(2)–C(3)	1.463	0.007
C(3)–C(4)	1.330	0.007
C(4)–C(5)	1.469	0.007
C(5)–C(6)	1.412	0.007
C(5)–C(7)	1.405	0.007
C(6)–C(8)	1.389	0.008
C(7)–C(9)	1.389	0.008
C(8)–C(10)	1.394	0.008
C(9)–C(10)	1.394	0.008
C(1)–H(1)	1.050	0.059
C(3)–H(3)	1.100	0.058
C(4)–H(4)	1.083	0.059
C(6)–H(6)	1.083	0.058
C(7)–H(7)	1.082	0.058
C(8)–H(8)	1.062	0.058
C(9)–H(9)	1.087	0.057
C(10)–H(10)	1.061	0.056

TABLE 6 (b). BOND ANGLES WITH THEIR e. s. d.'s

	Angle(Å)	e.s.d.(Å)
C(2)–N(1)–C(1)	115.8	0.5
C(2)–C(1)–N(1)	124.1	0.6
N(1)–C(2)–C(1)	120.2	0.4
C(1)–C(2)–C(3)	120.8	0.4
N(1)–C(2)–C(3)	119.0	0.4
C(2)–C(3)–C(4)	126.0	0.5
C(3)–C(4)–C(5)	127.0	0.5
C(4)–C(5)–C(7)	122.7	0.4
C(4)–C(5)–C(6)	119.6	0.4
C(6)–C(5)–C(7)	117.7	0.4
C(5)–C(6)–C(8)	120.7	0.5
C(5)–C(7)–C(9)	121.5	0.5
C(6)–C(8)–C(10)	120.6	0.5
C(7)–C(9)–C(10)	120.1	0.5
C(8)–C(10)–C(9)	119.4	0.5
C(2)–C(1)–H(1)	117.0	3.2
C(2)–C(3)–H(3)	116.6	3.1
C(4)–C(3)–H(3)	117.4	3.1
C(3)–C(4)–H(4)	116.7	3.1
C(5)–C(4)–H(4)	116.4	3.1
C(5)–C(6)–H(6)	118.8	3.1
C(8)–C(6)–H(6)	120.5	3.1
C(5)–C(7)–H(7)	118.6	3.1
C(9)–C(7)–H(7)	120.0	3.1
C(6)–C(8)–H(8)	118.7	3.2
C(10)–C(8)–H(8)	120.7	3.2
C(7)–C(9)–H(9)	120.6	3.0
C(10)–C(9)–H(9)	119.3	3.0
C(8)–C(10)–H(10)	120.0	3.1
C(9)–C(10)–H(10)	120.5	3.1

118.2° in diethylstilbestrol,[7] 118.2° in 1.8-diphenyl-1,3,5,7-octatetraene,[8] 118.2° in chalcone,[9] 117° in *p*-methoxychalcone[10] and 118.4° in *p*-coumaric acid.[11] Such a decrease may be interpreted as being due to interatomic repulsion induced by the substituent.

In the pyrazine ring there are two kinds of C–N bonds. The C–N bond adjacent to the substituent (C(2)–N(1)=1.346 Å) is longer than the other (C(1)'–N(1)=1.328 Å). Similar differences are observed in the substituted pyridine ring: 1.37 and 1.35 Å for 2,2-bipyridine,[12] and 1.362 and 1.337 Å for 2-(2-pyridylmethyldithio)benzoic acid.[13] The C–C bond length of the pyrazine ring, 1.395 Å, is compared to that of the benzene ring. These bond lengths are different

7) a) C. M. Weeks, A. Cooper, and D. A. Norton, *ibid.*, **B26**, 429 (1970). b) I. E. Smiley and M. G. Rossmann, *Chem. Commun.*, **1969** 198.

8) W. Drenth and E. H. Wiebenga, *Acta Crystallogr.*, **8**, 755 (1955).

9) D. Rabinovich, *J. Chem. Soc., B*, **1970**, 11.

10) D. Rabinovich and G. M. J. Schmidt, *ibid., B*, **1970**, 6.

11) H. Utsumi, K. Fujii, H. Irie, A. Furusaki, and I. Nitta, *Nippon Kagaku Zasshi*, **91**, 439 (1970).

12) L. L. Merritt, Jr., and E. D. Schroeder, *Acta Crystallogr.*, **9**, 801 (1956).

13) J. Karl, I. L. Karl, and D. Mitchell, *ibid.*, **B25**, 866 (1969).

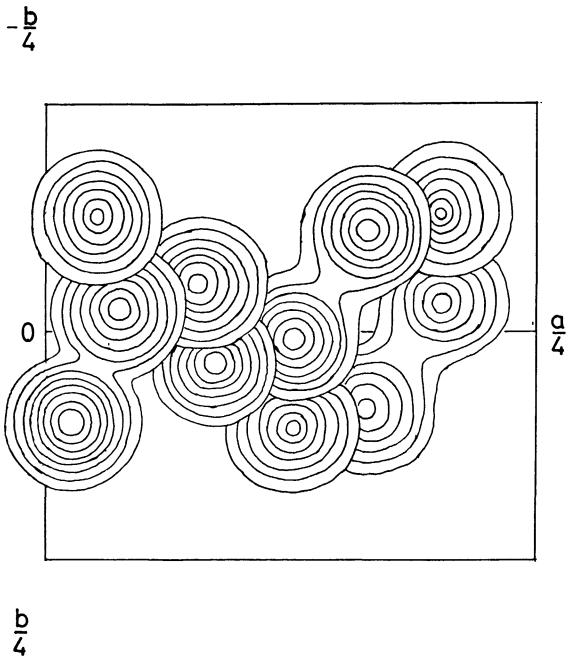

Fig. 2. Composite electron density diagram of sections parallel to (001). Contours are at intervals of 1.0 e.Å^{-3}, starting at 1.0 e.Å^{-3}.

from those of pyrazine itself;[14] C–N and C–C are 1.334 and 1.378 Å respectively. The C–N–C bond angle, 115.8°, is similar to that of pyrazine, 115.7°, and somewhat smaller than that in substituted pyridine: 116.7° in 1-phenyl-2-(2-pyridyl)ethanedione-1,2,[15] 118.5° in 2-(2-pyridylmethyldithio)benzoic acid,[13] and 120.6° in *cis*-β-bromo-β-(2-pyridyl)styrene.[16]

The bond lengths of C(2)–C(3) (1.463 Å), C(4)–C(5) (1.469 Å), and C(3)–C(4) (1.330 Å) are reasonable as those in a conjugated system; for example, in 1,8-diphenyl-1,3,5,7-octatetraene[8] the single bond length is 1.468 Å and the double bond length is 1.350 Å. The C(2)–C(3)–C(4) angle (126.0°) and the C(3)–C(4)–C(5) angle (127.0°) are considerably greater than 120°. Similar results have been reported for di-substituted ethylene: 128° for stilbene,[17] 126.8° for 1,8-diphenyl-1,3,5,7-octatetraene,[8] 127.6° for chalcone,[9] 127.2° for *p*-methoxychalcone,[10] 125.8° for *p*-coumaric acid,[11] 122.2° for diethylstilbestrol,[7] and 122.7° for 1,2-di-2-pyridylethenediol-1,2.[18]

It is noteworthy that the bond angles of nearly planar styryl groups (in the above-mentioned substances as well as the present compound) show very common features. The angles of C(3)–C(4)–C(5), C(4)–C(5)–C(7), and C(6)–C(5)–C(7) are 127°, 123°, and 118° respectively within a range of about one degree.

The equations of the average planes were evaluated by the method of least-squares. None of the hydrogen atoms were include because of the large standard deviations in their atomic coordinates. The equations are:

$$0.78278x + 0.41637y + 0.46215z - 3.53357 = 0 \quad (1)$$

for the plane of all eleven atoms;

$$0.75315x + 0.48099y + 0.44879z - 3.39271 = 0 \quad (2)$$

for the plane of the benzene ring;

$$0.81100x + 0.28777y + 0.50939z - 3.89936 = 0 \quad (3)$$

for the plane of the pyrazine ring, and

$$0.77506x + 0.43947y + 0.45404z - 3.46952 = 0 \quad (4)$$

Table 7. Displacements (Å) from the average planes

	plane (1)	plane (2)	plane (3)[a]	plane (4)
N(1)	−0.1813		−0.0059	−0.2119[b]
C(1)	0.1532		−0.0062	0.1809[b]
C(2)	−0.0010		0.0061	−0.0012
C(3)	−0.0018	0.0077[b]	0.0018[b]	0.0012
C(4)	0.0234	−0.0278[b]	0.1763[b]	0.0012
C(5)	0.0185	−0.0078		−0.0012
C(6)	0.1068	0.0071		0.0579[b]
C(7)	−0.0652	0.0034		−0.0544[b]
C(8)	0.0763	−0.0019		
C(9)	−0.0880	0.0018		
C(10)	−0.0188	−0.0026		

a) In addition to these three atoms, the centre of symmetry(0,0,1) was included in the plane evaluation.
b) These atoms were not included in the plane evaluation.

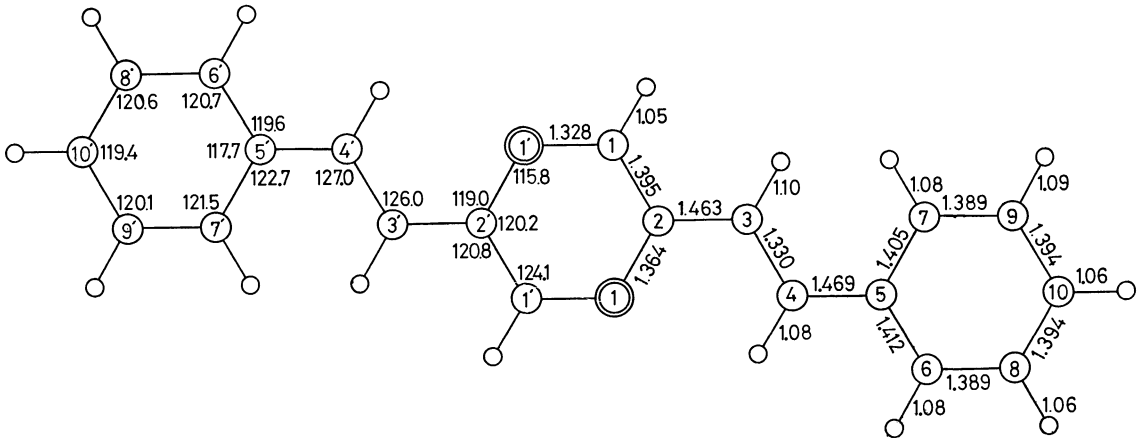

Fig. 3. Bond lengths (Å) and angles (degrees).

14) P. J. Wheatley, *ibid.*, **10**, 182 (1957).
15) T. Ashida, S. Hirokawa, and Y. Okaya, *ibid.*, **21**, 506 (1966).
16) H. Utsumi, A. Takenaka, A. Furusaki, and I. Nitta, *Nippon Kagaku Zasshi*, **91**, 443 (1970).
17) J. M. Robertson and I. Woodward, *Proc. Roy. Soc., Ser. A*, **162**, 568 (1939).
18) T. Ashida, S. Hirokawa, and Y. Okaya, *Acta Crystallogr.*, **18**, 122 (1965).

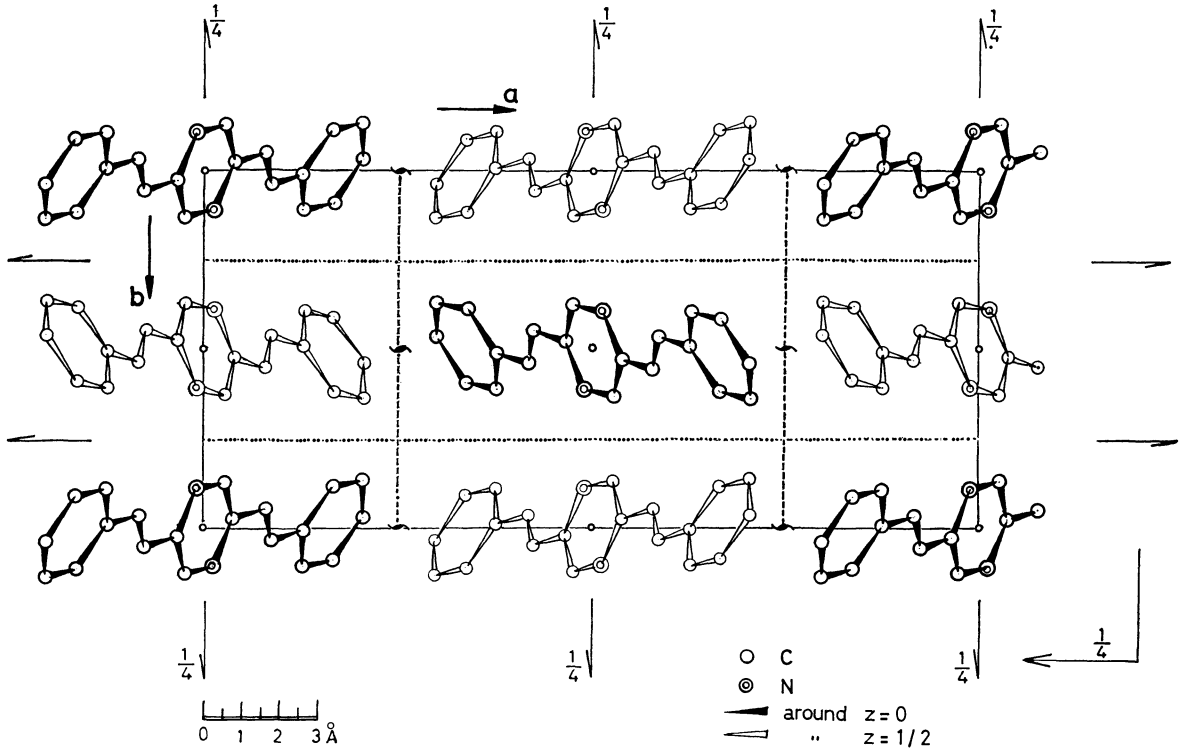

Fig. 4. The crystal structure viewed along the *c*-axis.

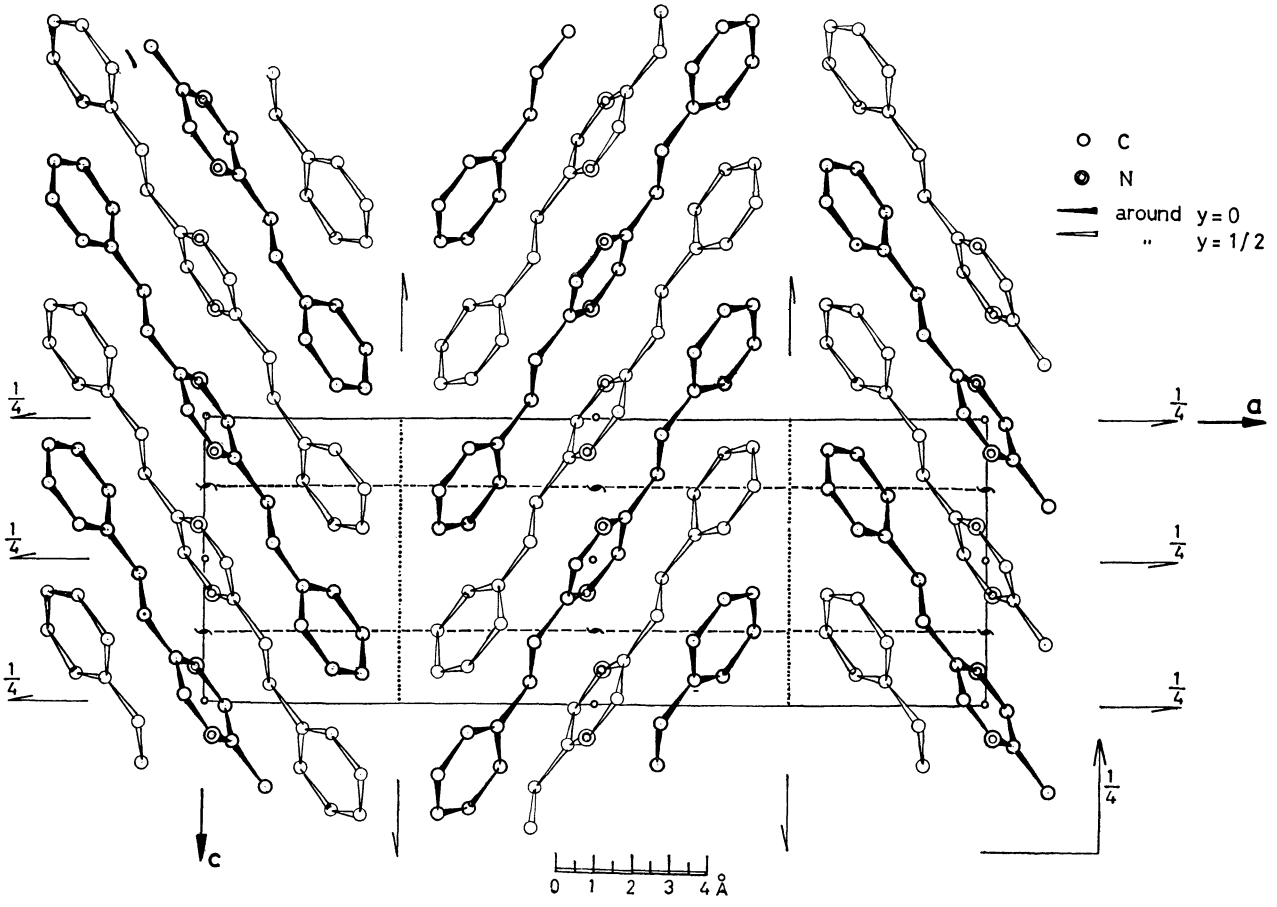

Fig. 5. The crystal structure viewed along the *b*-axis.

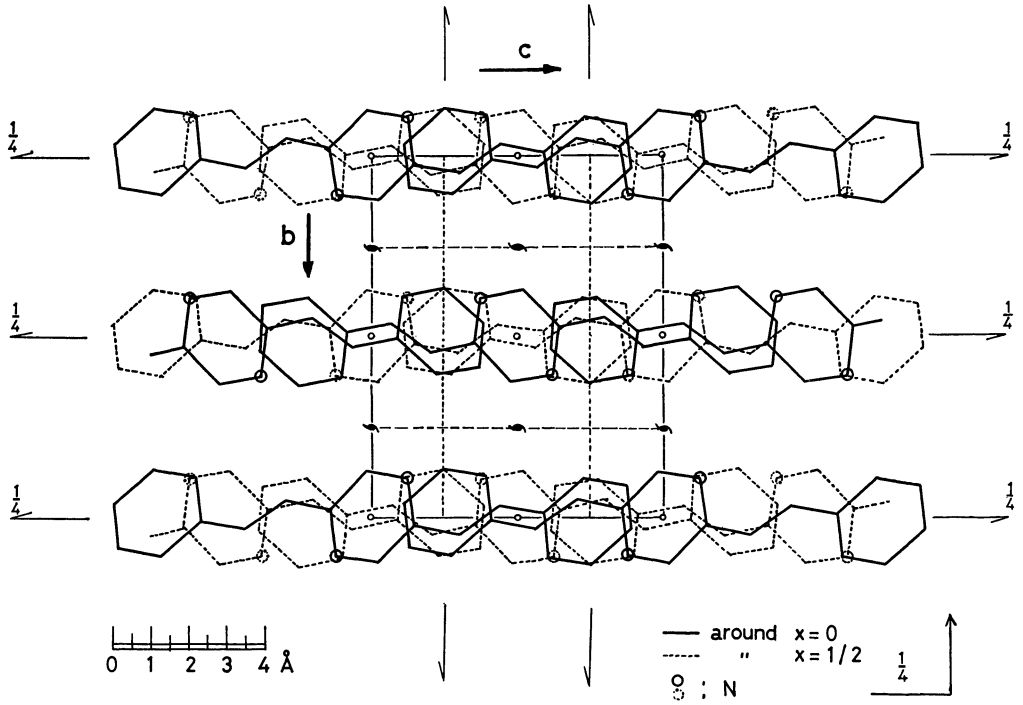

Fig. 6. The crystal structure viewed along the *a*-axis.

for the plane through the atoms C(2), C(3), C(4), and C(5), where x, y, and z are in Å.

The displacement of the atoms from each plane are shown in Table 7. The maximum deviations are 0.008 Å for the plane (2), 0.006 Å for the plane (3), and 0.001 Å for the plane (4). Therefore, these three groups of the atoms are planar.

However, the molecule as a whole is not planar, as may be seen from Table 7. The benzene ring rotates by 2.61° about the bond C(4)–C(5), and the pyrazine ring rotates by 9.42° about C(2)–C(3) in the opposite direction. Therefore, the dihedral angle between the planes (2) and (3) is 12.09°. The rotation about C(4)–C(5) may be due to a repulsion between the

Table 8. Intermolecular distances less than 4.0 Å

Atom in molecule 1	Atom	in molecule	Distance (Å)	Atom in molecule 1	Atom	in molecule	Distance (Å)
C(6)	C(1)	2	3.775	C(6)	N(1)′	2	3.675
C(6)	C(2)	2	3.893	C(5)	C(10)	3	3.880
C(6)	N(1)	2	3.856	C(7)	C(8)	3	3.980
C(8)	C(1)	2	3.688	C(7)	C(10)	3	3.515
C(8)	C(2)	2	3.520	C(9)	C(10)	3	3.773
C(8)	C(3)	2	3.945	C(3)	C(1)	4	3.706
C(8)	N(1)	2	3.715	C(7)	C(1)	4	3.869
C(10)	C(1)	2	3.905	C(7)	C(3)	4	3.981
C(10)	C(2)	2	3.963	C(9)	C(7)	4	3.740
C(1)	C(6)′	2	3.692	C(10)	C(7)	4	3.880
C(2)	C(5)′	2	3.932	C(3)	C(3)	4	5.414[a]
C(2)	C(6)′	2	3.590	C(1)	N(1)′	4	3.837
C(3)	C(4)′	2	3.939	C(3)	N(1)′	4	3.807
C(4)	C(3)′	2	3.939	C(6)	C(4)	5	3.912
C(4)	C(4)′	2	3.702	C(6)	N(1)	5	3.719
C(5)	C(2)′	2	3.932	C(4)	C(4)	5	5.652[a]
C(5)	N(1)′	2	3.755	N(1)	C(1)′	5	3.837
C(6)	C(1)′	2	3.692	N(1)	C(3)′	5	3.807
C(6)	C(2)′	2	3.590				

a) Listed for investigating the distances between double bonds.

Molecule	General coordinate
1	x, y, z
2	$x, y, -1.0+z$
3	$0.5-x, -y, 0.5+z$
4	$x, -0.5-y, -0.5+z$
5	$x, 0.5-y, -0.5+z$

hydrogen atoms attached to C(3) and C(7). The interatomic distance between these hydrogen atoms is 2.04 Å (e.s.d.=0.08 Å). Although, for the rotation about C(2)–C(3), no such repulsion is operative because of the absence of any hydrogen attached to the N atom, the rotation about C(2)–C(3) is larger than that about C(4)–C(5). This may be interpreted in terms of some intermolecular interactions.

Crystal Structure. The arrangements of molecules in the crystal viewed along the *c*-, *b*-, and *a*-axes are shown in Fig. 4, 5, and 6 respectively. Intermolecular distances less than 4.0 Å are listed in Table 8. No unusual short approaches are observed.

The molecules are oriented in such a way that their long axes are nearly perpendicular to the *b*-axis, as may be seen in Figs. 4 and 6. This arrangement can well explain the UV dichroism; the absorption parallel to the *c*-axis is ten times as strong as that parallel to the *b*-axis when measured on (100).[19]

The molecules spaced by the *c*-translation are also related by the centre of symmetry, the corresponding planar parts in these molecules being parallel to each other. As the long axis of the molecules makes an angle of about 30° to the *c*-axis, the molecules are piled up infinitely plane-to-plane, sliding in the direction of the long axis by half a molecule, as may be seen in Fig. 7.

The ethylenic double bonds, which are antiparallel to each other, approach to a distance of 3.939 Å from each other. This intermolecular distance between ethylenic double bonds is the shortest, while the second shortest contact of the same kind is 5.417 Å found between the molecules which are related by the *b*-glide plane. It is most probable that the double bonds related by the centre of symmetry react to form a a cyclobutane ring by photo-irradiation,[20] resulting in a linear ploymer. Thus, polymer chains should grow in the direction of the *c*-axis. This is confirmed by X-ray-crystallographic[21] and electron-microscopic[22] studies of the polymer thus obtained.

In order to investigate the intermolecular contacts involving the double bonds, the molecule 2 is projected on the best plane of the moecule 1 in Fig. 7. The

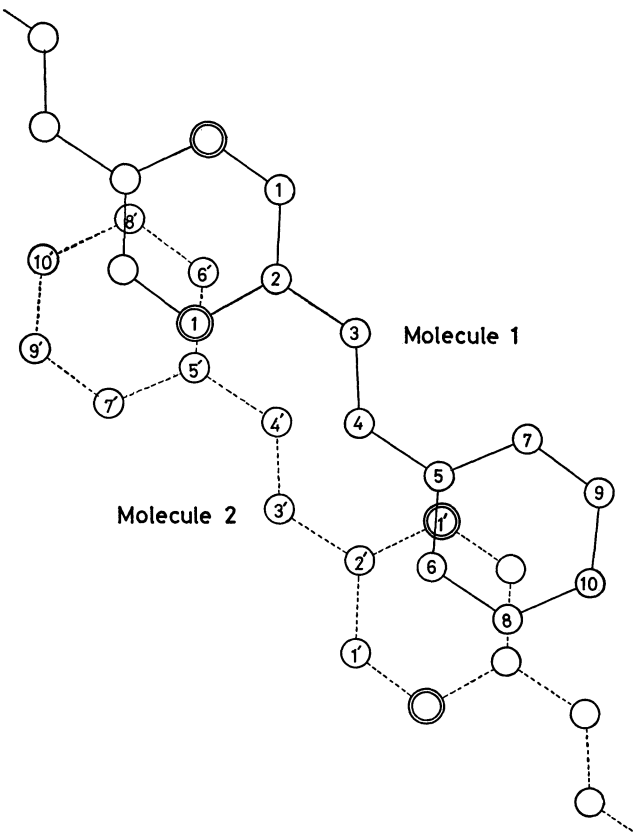

Fig. 7. The overlapping of the molecules viewed along the normal of the average plane of the reference molecule.

benzene ring in one molecule overlaps with the pyrazine ring in the other molecule. This type of parallel stacking of the aromatic rings has been observed in several other compounds. In the crystals of 1-phenyl-(2-pyridyl)ethanedione-1,2[15] and 2,2-pyridyl,[23] there are parallel pairs between the same aromatic rings and the perpendicular distances range from 3.49 to 3.80 Å. In the present crystal there are close contacts between unlike rings, with a plane-to-plane distance of 3.52 Å. Similar contacts are found in 2-(2-pyridylmethyl-dithio)benzoic acid. The UV spectrum of DSP in the crystalline state is different from that in solution, the former having a shoulder on the side of the longer wavelength[19]. The fact indicates that there is some kind of intermolecular interaction. As the short contacts are observed only between the parallel rings, it may be that the interaction of the overlapping part in Fig. 7, mainly determines the packing of the molecules in the crystal.

19) T. Tamaki, Y. Suzuki, and M. Hasegawa, Paper presented at the 19th Annual meeting of the Society of Polymer Science, Japan, Tokyo, May, 1970, p. 108.

20) G. M. J. Schmidt, *J. Chem. Soc.*, **1964**, 2014.

21) H. Nakanishi, M. Hasegawa, Y. Sasada, and H. Shimanouchi, Paper presented at the 19th Annual meeting of the Society of Polymer Science, Japan, Tokyo, May, 1970, p. 337 and to be published.

22) H. Nakanishi, M. Nakano, and M. Hasegawa, *J. Polymer Sci.*, **B8**, 755 (1970).

23) a) S. Hirokawa and T. Ashida, *Acta Crystallogr.*, **14**, 774 (1961). b) T. Ashida and S. Hirokawa, *ibid.*, **B26**, 454 (1970).

Some Information Derived from the Infrared Spectra of Ion-radical Molecules. The Spin-density Distribution for the *p*-Chloranil Anion Radical[1]

Yôichi IIDA

Department of Chemistry, Faculty of Science, Hokkaido University, Sapporo

(Received October 30, 1970)

The spin-density distribution in the *p*-chloranil anion radical was determined by means of the difference in the bond orders of the conjugated systems between *p*-chloranil and its anion radical, which was estimated on the basis of the stretching force constants. It was found that the spin-density distribution calculated by this method was in good agreement with that estimated by means of the molecular orbital calculations or by means of the hyperfine splitting constants in the ESR absorption. In view of these results, it was suggested that the present method might become a new tool for investigating the unpaired electron distributions of ion-radical molecules in general.

The infrared spectrum of an ion radical is known to be appreciably different from that of its neutral molecule.[2,3] In a previous paper,[3] we examined the infrared spectra(650—4000cm^{-1}) of *p*-chloranil and its anion radical.[4] In order to explain the appreciable frequency differences between their corresponding bands, the fundamental frequencies were assigned, and the simple Urey-Bradley force fields were determined for both the neutral and anion radical molecules. Their stretching-force constants for the bonds in the π conjugated systems were related to the bond orders by the use of the formula of Coulson and Longuet-Higgins.[5] The values of the bond orders thus obtained for *p*-chloranil ant its anion radical were in good agreement with those evaluated by the molecular orbital calculation, except for the C=O bond in the anion radical. These results are presented in Table 1. In view of these results, it seems that the difference in the infrared spectra between these two molecules is almost entirely attributable to the difference in their electronic structures caused by an extra electron on the *p*-chloranil anion radical.[3]

TABLE 1. THE VALUES OF THE BOND ORDERS OF THE C–C, C=C, AND C=O BONDS FOR *p*-CHLORANIL AND ITS ANION RADICAL

Bond	*p*-Chloranil		Its anion radical	
	IR[a]	MO[b]	IR[a]	MO[b]
C–C	0.27	0.30	0.37	0.41
C=C	0.87	0.91	0.79	0.81
C=O	0.82	0.85	0.40	0.70

a) The values obtained from the stretching force constants, which were evaluated from the fundamental frequencies observed in the infrared spectra.

b) The values calculated from the molecular orbitals for *p*-benzoquinone. See T. L. Kunii and H. Kuroda; Rep. Compt. Centre, Univ. Tokyo, **1**, 119 (1968).

The purpose of the present paper is to indicate that the difference in the bond orders between *p*-chloranil and its anion radical, which was obtained from their infrared spectra, leads to the spin-density distribution for the *p*-chloranil anion radical. In this respect, it is interesting to compare the results of our calculations with the spin-density distribution derived from the molecular orbital calculations and with that derived from the hyperfine splitting constants in the ESR absorption.

Calculations

It was assumed, to a first approximation, that the coefficients of the atomic orbitals for the molecular orbitals of the *p*-chloranil anion radical were not so different from the respective ones of *p*-chloranil, when an extra electron enters into the lowest vacant orbital of *p*-chloranil.[6] In this case, the difference in the bond orders between *p*-chloranil and its anion radical seems to be caused solely by the extra electron in the half-occupied molecular orbital of the *p*-chloranil anion radical. The effect of chlorine can be taken into account either by treating chlorine as a heteroatom or by treating the carbon atom bonded to chlorine as a heteroatom.[7] As will be explained below, it was

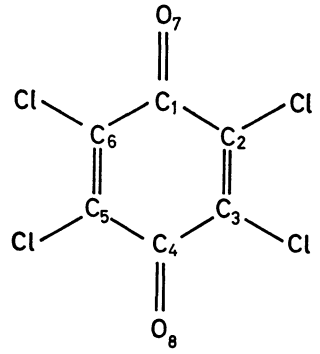

Fig. 1. The structural formula and the numbering of atoms for *p*-chloranil anion radical.

1) This work was presented at the Symposium on Molecular Structure, Tokyo, October, 1970.

2) Y. Matsunaga, *Canad. J. Chem.*, **38**, 1172 (1960); Y. Matsunaga, *Helv. Phys. Acta*, **36**, 800 (1963); Y. Matsunaga, *J. Chem. Phys.*, **41**, 1609 (1964); M. Kinoshita and H. Akamatu, *Nature*, **207**, 291 (1965); J. Stanley, D. Smith, B. Latimer, and J. P. Devlin, *J. Phys. Chem.*, **70**, 2011 (1966).

3) Y. Iida, This Bulletin, **43**, 345 (1970).

4) Actually, the infrared spectrum of the anion radical was measured as that of the crystalline salt with the potassium cation (K^+ *p*-Chloranil$^-$).

5) C. A. Coulson and H. C. Longuet-Higgins, *Proc. Roy. Soc.* (London), **A193**, 456 (1948).

6) A. Streitwieser, Jr., "Molecular Orbital Theory for Organic Chemists," John Wiley & Sons, New York and London, 139 (1961).

7) M. Broze, Z. Luz, and B. L. Silver, *J. Chem. Phys.*, **46**, 4891 (1967).

found that the result of our calculations can be well understood by the latter approach. Therefore, let c_i (i=1—8) be the coefficient of the i th atomic orbital in the half-occupied molecular orbital for the p-chloranil anion radical, the structural formula and the numbering of atoms of which are illustrated in Fig. 1. Since, as has already been remarked in a previous paper,[3] the value of the C=O bond order obtained for the anion radical involves some contribution of the self-polarizability, this value must be excluded in our treatment. We use only the values of the bond orders for the homopolar C=C and C–C bonds. Then, from Table 1, as for the C=C bond:

$$c_2c_3 = -0.08 \pm 0.005. \quad (1)$$

The point group for the p-chloranil anion radical belongs to the D_{2h} symmetry. From the symmetry properties, the absolute value of c_2 is equal to that of c_3. If we take c_2 as positive, these relations lead to:

$$c_2 = -c_3 = 0.283 \pm 0.009. \quad (2)$$

As for the C–C bond:

$$c_1c_2 = 0.10 \pm 0.005. \quad (3)$$

Putting the c_2 value into Eq. (3), we obtain:

$$c_1 = 0.354 \pm 0.029. \quad (4)$$

Similarly, since $c_1c_6=c_3c_4=c_1c_2$, and $c_5c_6=c_2c_3$:

$$c_6 = -c_5 = c_2, \quad (5)$$

$$c_4 = -c_1. \quad (6)$$

Although, as has been mentioned above, the values of c_7 and c_8 cannot be obtained directly from Table 1, the following normalization condition allows us to compute these values as:

$$|c_7|^2 = |c_8|^2 = \frac{1}{2}(1.00 - 2|c_1|^2 - 4|c_2|^2)$$

$$= 0.213 \pm 0.010. \quad (7)$$

As we can see from Table 1, the C=O bond order is obviously decreased in the anion radical: $c_1c_7=c_4c_8<0$. Therefore,

$$c_7 = -c_8 = -0.462 \pm 0.010.^{8)} \quad (8)$$

Judging from the signs of the coefficients of the atomic orbitals, the symmetry of the half-occupied molecular orbital for the p-chloranil anion radical proves to belong to the b_{3g} irreducible representation; this is in good accordance with that predicted by the electronic-spectrum measurements or the molecular-orbital calculations.[9-11]

The spin density, ρ_i(IR), at the ith atom can, then, be calculated by:[12]

$$\rho_i(\mathrm{IR}) = |c_i|^2. \quad (9)$$

The values of ρ_i(IR) thus obtained for i=1, 2, and 7 are collected in Table 2.

Table 2. The spin density distribution in p-chloranil anion radical

Position, i[a]	ρ_i(IR)[b]	ρ_i(MO)[c]
1	0.127±0.020	0.0918
2	0.080±0.005	0.1025
7	0.213±0.010	0.2031

a) Numbering as in Fig. 1.
b) The values calculated from the difference of the bond orders between p-chloranil and its anion radical, which were derived from the difference of the stretching force constants in their infrared spectra.
c) The values estimated from the molecular orbital calculation by Broze, Luz, and Silver. See Ref. 7.

Discussion

Comparison with the Results of the Molecular-orbital Calculations. In order to account for the ^{17}O hyperfine splitting constant in the ESR absorption, Broze *et al.* have calculated the Hückel molecular orbitals for the p-chloranil anion radical.[7] They assumed the carbon atom bonded to chlorine to be a heteroatom, X, and determined the best-fit value for the ^{17}O hyperfine splitting constant. The optimum parameters for the heteroatom, X, are:

$$\alpha_X = \alpha - 0.012\beta, \quad (10)$$

$$\beta_{CX} = 0.962\beta. \quad (11)$$

As for the oxygen atom:

$$\alpha_O = \alpha + 1.17\beta, \quad (12)$$

$$\beta_{CO} = 1.46\beta. \quad (13)$$

They calculated the spin density, ρ_i(MO), for the p-chloranil anion radical by means of McLachlan's approximation. The values of ρ_i(MO) for i=1,2, and 7 are also collected in Table 2.[7]

As is shown in Table 2, although ρ_1(IR) $-\rho_1$(MO) $\approx$ 0.035, ρ_2(IR) $-\rho_2$(MO) ≈ -0.023, and ρ_7(IR) $-\rho_7$(MO) $\approx$0.010, the agreement between ρ_i(IR) and ρ_i(MO), where i=1, 2, and 7, is fairly good.

Since the α_X and β_{CX} values in Eqs. (10) and (11) are close to those of the corresponding carbon atoms in the p-benzoquinone anion radical, the unpaired-electron distribution in the conjugated system for the p-chloranil anion radical appears to be similar to that for the p-benzoquinone anion radical.

Comparison with the Results on the ESR Hyperfine Splitting Constants. As the p-chloranil anion radical does not include any hydrogen atom, no experimental

8) By the use of the c_1c_7 value and the C=O bond order for p-chloranil, the C=O bond order for the anion radical is corrected to 0.66±0.02. According to the formula of Coulson and Longuet-Higgins,[5] a C=O stretching force constant, K(C=O), in the infrared spectrum is represented by:

$$K(\mathrm{C{=}O}) = \{(1-p(\mathrm{C{=}O}))K_s + p(\mathrm{C{=}O})K_d\} + \left[\left\{\frac{K_sK_d(s-d)}{K_s(1-p(\mathrm{C{=}O}))+K_dp(\mathrm{C{=}O})}\right\}^2 \frac{\pi(\mathrm{COCO})}{2}\right].$$

The notation of this equation and the values of K_s=5.0 md/Å and K_s=10.7 md/Å have already been described in a previous paper.[3] If this equation is applicable to the p-chloranil anion radical, the first term is found to be equal to 8.8 md/Å by the use of p(C=O)=0.66. In this case, since the observed K(C=O) value for the anion radical is 7.3 md/Å, the numerical difference, −1.5 md/Å, may be attributable to the second term involving the self-polarizability. See Ref. 3.

9) Y. Harada, *Mol. Phys.*, **8**, 273 (1964).
10) K. Kimura, H. Yamada, and H. Tsubomura, *J. Chem. Phys.*, **48**, 440 (1968).
11) Y. Iida, This Bulletin, **43**, 2772 (1970).
12) The notation, ρ_i(IR), was used for distinguishing it from the ρ_i(MO) or ρ_i(ESR) to be described in the next section.

result is available for the hyperfine splitting constants except for that due to the ^{17}O of the carbonyl group. Broze *et al.* examined the ESR spectra of the ^{17}O-labeled *p*-chloranil anion radical in various solvents.[7] For example, the ^{17}O hyperfine splitting constant was found to be $a_7^O(\text{obs}) = -8.89 \pm 0.02$ G in a dimethylformamide solution. On the other hand, the theoretical oxygen hyperfine splitting constant, $a_7^O(\text{calc})$, in a carbonyl group can be evaluated by the following equation:[7,13,14]

$$a_7^O(\text{calc}) = Q_{OC}^O \rho_O + Q_{CO}^O \rho_O, \qquad (14)$$

where the values of $Q_{OC}^O = -40.7 \pm 5.2$ G and $Q_{CO}^O = -9.5 \pm 6.1$ G were proposed by Broze *et al.*;[7] ρ_O and ρ_C are the spin densities in the $p\pi$ orbitals of the oxygen and the neighbouring carbon atoms respectively. If the values of $\rho_1(\text{IR})$ and $\rho_7(\text{IR})$ are put into Eq. (14), $a_7^O(\text{calc})$ is evaluated to be -10.05 ± 2.48 G; this value is in good agreement with the foregoing experimental value of -8.89 ± 0.02 G.

At present, there appear no experimental data for use in comparing the spin densities on the carbon atoms in the *p*-chloranil anion radical. However, since the unpaired-electron distribution in the conjugated system for the *p*-chloranil anion radical seems to be similar to that for the *p*-benzoquinone anion radical, the values of $\rho_i(\text{IR})$ were compared with the spin densities of the *p*-benzoquinone anion radical as determined from the hyperfine splitting constants.

Das and Fraenkel measured the proton and ^{13}C hyperfine splittings in the ESR spectrum of the *p*-benzoquinone anion radical; they found $a_2^H = -2.395 \pm 0.002$ G and $a_1^C = -2.21 \pm 0.02$ G in the dimethoxyethane solution, while the values were $a_2^H = -2.368 \pm 0.001$ G and $a_1^C = -0.40 \pm 0.04$ G in the C_2H_5OH-H_2O solution.[13] When $i=1$, 2, and 7, the spin densities, $\rho_i(\text{ESR})$, derived from these experimental results were 0.1487, 0.0896, and 0.1721 in the dimethoxyethane solution, while they were 0.1796, 0.0877, and 0.1450 in the C_2H_5OH-H_2O solution respectively.[13] Although there are appreciable differences in the spin densities for the two solvents at the carbonyl carbon and oxygen atoms, we can see that the set of $\rho_i(\text{IR})$, where $i=1$, 2, and 7, is well fitted to that of $\rho_i(\text{ESR})$ in the dimethoxyethane solution. In the case of the C_2H_5OH-H_2O solution, the agreement between $\rho_i(\text{IR})$ and $\rho_i(\text{ESR})$ is not satisfactory, except for that between $\rho_2(\text{IR})$ and $\rho_2(\text{ESR})$.

Concluding Remarks

It has been well established that hyperfine splitting constants in the ESR spectra provide one of the most important means for determining the spin-density distribution of radical molecules.[14] However, this technique involves the following difficulties:

(1) If a radical molecule does not include atoms with a nuclear magnetic moment, no experimental data are available for the hyperfine splitting constants. In practice, when the H, ^{13}C, ^{14}N, or ^{17}O atom is not contained in a radical molecule, the information is, accordingly, quite limited.

(2) If radical molecules exist in an aggregate state, such as in the solid state or in a highly concentrated solution, the hyperfine splittings should be narrowed by intermolecular spin-exchange interaction, which gives only a single exchange-narrowed line.[15] Therefore, the hyperfine splitting constants cannot be obtained in such a situation.

Instead of the use of the hyperfine splitting constants, the spin-density distribution of a radical molecule can be evaluated, in some cases, on the basis of an accurate determination of the *g*-values in the ESR absorption or from the chemical shifts in the NMR spectrum.[14] However, besides these techniques, the present use of the infrared spectra of a neutral molecule and its ion radical constitutes a new approach to this problem. In contrast to the use of hyperfine splitting constants, our method has the following advantages:

(1) A radical molecule need not necessarily include atoms with a nuclear magnetic moment, because the spin densities are derived from the differences in the bond orders.

(2) One can estimate the spin-density distribution for a radical molecule not only in an isolated state, but also in an aggregate state. The latter information seems to be valuable for investigating the intermoleculer interaction of radical molecules. In fact, the values of $\rho_i(\text{IR})$, where $i=1$, 2, and 7, of the *p*-chloranil anion radical are those in the solid state,[3] in which the charge-transfer interaction between *p*-chloranil anion radical molecules has been known to take place by means of the solid-state spectrum.[11] In this respect, one reason for the previously-mentioned small deviation of the $\rho_i(\text{IR})$ values from the $\rho_i(\text{MO})$ or $\rho_i(\text{ESR})$ values, where $i=1$, 2, and 7, may be the difference in the spin-density distributions between the solid state and the isolated state. However, we should keep in mind that, in our treatment, the $\rho_i(\text{IR})$ values include some uncertainties in the course of the derivation of the bond orders from the stretching force constants. This means that more reliable values for the spin densities will be obtained if a more precise estimation of the bond orders and the self-polarizabilities can be made from the stretching force constants.

13) M. R. Das and G. K. Fraenkel, *J. Chem. Phys.*, **42**, 1350 (1965).

14) J. R. Bolton, "Radical Ions," ed. by E. T. Kaiser and L. Kevan, Interscience Publishers, New York, London, and Sydney (1968), p. 1.

15) G. E. Pake, "Paramagnetic Resonance," W. A. Benjamin, New York, 79 (1962).

The Crystal and Molecular Structure of Pyromellitic Acid Dihydrate (Benzene-1,2,4,5-tetracarboxylic Acid Dihydrate)[1]

Fusao TAKUSAGAWA, Ken HIROTSU, and Akira SHIMADA

Department of Chemistry, Faculty of Science, Osaka City University, Sugimoto-cho, Sumiyoshi-ku, Osaka

(Received November 4, 1970)

The crystal structure of pyromellitic acid dihydrate has been determined by the method of X-ray diffraction. The crystal is triclinic in the $P\bar{1}$ space group, with $Z=1$ and cell dimensions of $a=10.05$, $b=6.45$, $c=5.45$ Å, $\alpha=74.5°$, $\beta=112.2°$, and $\gamma=77.3°$. The structure was derived from the three-dimensional Patterson function and was later refined by the least-squares method, using the anisotropic thermal parameters, to give a final R index of 7.4%. All the hydrogen atoms were located on the difference-synthesis map. The average C(ring)–C(ring) distance is 1.386 Å, while the average C(ring)–C(carboxyl) distance is 1.496 Å. One carboxyl group is twisted by 17.9°, and the other is twisted by 74.5°, out of the plane of the benzene ring. The C–O(H) and C=O distances differ significantly from each other, the average values being 1.302 and 1.211 Å respectively. Four types of hydrogen bonds, with an average O–H···O distance of 2.732 Å, form a three-dimensional network. Thus, each molecule is joined, through hydrogen bonds around the center of symmetry, to two other molecules, forming an endless chain in the [1 $\bar{1}$ 1] direction. Water molecules are arranged on the plane parallel to (1 1 0) so as to hold the chains together by hydrogen bonds.

The pyromellitic acid dihydrate, $C_6H_2(COOH)_4\cdot 2H_2O$, with two pairs of vicinal carboxyl groups, is one of 12 benzene carboxylic acids. The crystal structures of several of these acids have already been studied by means of X-ray work to give valuable information in the field of crystal chemistry: benzoic acid;[2] phthalic acid;[3,4] terephthalic acid;[5] trimesic acid[6] and mellitic acid.[7] However, no X-ray investigation has been reported on hydrates of these benzene carboxylic acids. In view of this situation, it seemed that it would be of interest to examine the crystal and molecular structure of this compound in detail, so as to elucidate the steric hindrance of adjacent carboxyl groups and the way of hydrogen bonding in this crystal. It will also be of significance to compare the results of this study with the results of studies of other carboxylic acids, such as the oxalic acid,[8–17] thoroughly investigated, with special reference to the hydrogen-bond formation in the crystal.

Experimental

The crystals were obtained in the form of colorless plates by recrystallization from an aqueous solution. The cell dimensions were measured from zero-layer Weissenberg photographs, which were calibrated with superimposed Al powder lines. They are given with other crystal data in Table 1. By the assumption of one chemical unit in a unit cell, the density is calculated to be 1.64 g/cm³, this value is in good agreement with the observed value (1.63 g/cm³) determined by the floatation method.

Table 1. Crystal data

Pyromellitic acid dihydrate,	$C_6H_2(COOH)_4\cdot 2H_2O$
Formula weight, 290.20	
Crystal system, Triclinic	Space group, $P\bar{1}$
Cell dimension	
$a=10.05(1)$Å	$\alpha=74.5(3)°$
$b=6.45(2)$	$\beta=112.2(1)$
$c=5.45(1)$	$\gamma=77.3(1)$
$D_m=1.63$ g/cm³	
$D_c=1.64$ g/cm³ (Z=1)	
$\mu_r=15.223$ cm^{-1} (CuK_α)	

The crystals were ground to cylinders with average diameters of 0.26 mm for the b-axis and 0.33 mm for the c-axis specimens. They had lengths of 0.83 and 0.74 mm along the b and c axes respectively. The intensity data were collected for the 0-3 layers around the b and c axes by the use of the multiple-film equi-inclination Weissenberg technique, using Cu$K\alpha$ radiation. The intensities of the diffraction spots were estimated visually by comparison with a calibrated intensity standard. Of the possible 1370 reflections within the Cu$K\alpha$ sphere, 1100 independent reflections were measured; 148 were too weak to be measured. The data were corrected for spot-shape, absorption, and Lorentz and polarization factors. They are then correlated and reduced to the structure factors by the procedure presented by Hamilton, Rollet and Sparks.[18] Finally, the structure factors were placed approximately on an absolute scale by the method of Wilson.[19]

1) A preliminary account has already appeared in This Bulletin, **42**, 3368 (1969). The major part of this paper was read at the 23rd Annual Meeting of the Chemical Society of Japan, Tokyo, April, 1970.
2) G. A. Sim, J. M. Robertson, and T. H. Goodin, *Acta Crystallogr.*, **8**, 157 (1955).
3) H. Jaggi, *Z. Kristallogr.*, **109**, 3 (1957).
4) W. Nowacki and H. Jaggi, *ibid.*, **109**, 272 (1957).
5) M. Bailery and C. J. Brown, *Acta Crystallogr.*, **22**, 387 (1966).
6) D. J. Duchamp and R. E. Marsh, *ibid.*, **B25**, 5 (1969).
7) S. F. Darlow, *ibid.*, **14**, 159 (1961).
8) S. B. Hendricks, *Z. Kristallogr.*, **91**, A, 48 (1935).
9) E. G. Cox, M. W. Dougill, and G. A. Jeffrey, *J. Chem. Soc.*, **1952**, 4854.
10) J. M. Robertson and I. Woodward, *ibid.*, **1936**, 1817.
11) F. R. Ahmed and D. W. J. Cruickshank, *Acta Crystallogr.*, **6**, 385 (1953).
12) R. G. Delaplane and J. A. Ibers, *ibid.*, **B25**, 2423 (1969).
13) T. M. Sabine, G. W. Cox, and B. M. Craven, *ibid.*, **B25**, 2437 (1969).
14) P. Coppens and T. M. Sabine, *ibid.*, **B25**, 2442 (1969).
15) P. Coppens, T. M. Sabine, R. G. Delaplane, and J. A. Ibers, *ibid.*, **B25**, 2451 (1969).
16) F. F. Iwasaki and Y. Saito, *ibid.*, **23**, 56 (1967).
17) F. F. Iwasaki, H. Iwasaki, and Y. Saito, *ibid.*, **23**, 64 (1967).
18) W. C. Hamilton, J. S. Rollett, and R. A. Sparks, *ibid.*, **18**, 129 (1965).
19) A. J. C. Wilson, *Nature* (London), **150**, 151 (1942).

There were no reflections systematically absent. Of the two possible space groups, $P\bar{1}$ and $P1$, the former was assigned by testing the intensity distributions.

Structure Determination

Since the crystal belongs to the $P\bar{1}$ space group with only one molecule in the unit cell, the center of a benzene ring of pyromellitic acid must lie on a center of symmetry. This is of considerable aid in structure analysis. At first, two three-dimensional unsharpened and sharpened Patterson maps were calculated to derive a rough idea of the orientation of the benzene ring. Although these two maps differed from each other in several features, they gave trial coordinates of the three carbon atoms forming the benzene ring with the knowledge of the aromatic carbon-carbon distance.

With this orientation of the benzene ring, three arrangements of the two carboxyl groups are possible. Hence, attempts were made, using conventional bond distances and angles, to fit the interatomic vectors among the carboxyl groups to the observed peaks in the Patterson maps. However, this method could not give a fruitful clue, so three sets of structure factors and three-dimensional Fourier syntheses were calculated in order to rule out the wrong arrangements. The R indices for the three sets were found to be almost the same, but one of the three electron-density maps indicated the peaks of five oxygen atoms of the two carboxyl groups and one water molecule, as well as those of two carbon atoms of the carboxyl groups.

The refinement of the positional parameters, thermal parameters, and the scale factor was carried out by means of the block-diagonal least-squares method, using a modified version of the HBLS program written by Okaya and Ashida.[20] The initial calculations were based on about 600 reflections with $\sin\theta/\lambda \leq 0.5$ and the weighting scheme of $w=1.0$ to accelerate the convergence. Five cycles of refinement with isotropic themal parameters lowered the R index to 18.0%. At this stage, anisotropic thermal parameters were introduced for all the atoms except the hydrogen atoms; four subsequent cycles of refinement dropped the R index to 10.0%. However, several reflections showed rather large $|Fo-Fc|$ discrepancies; this disagreement in structure factors seemed to be caused by the neglect of the hydrogen atoms.

Therefore, we have prepared a three-dimensional difference map, using $(Fo-Fc')$ as the coefficients; here Fc' stands for the calculated structure factor with all the atoms except the hydrogen atoms. This map showed the peaks for hydrogen atoms near the positions expected, although there remained a few spurious peaks comparable in height to those of the hydrogen atoms. Several cycles of least-squares refinement were attempted with the hope of improving the parameters belonging to the atoms beside the hydrogen atoms. In this case, we did not try to refine the parameters of the hydrogen atoms. During these cycles, the residual did not reduce significantly; the weighting scheme was altered to $w=A/Fo$ for $Fo \geq A$, $w=1.0$ for $1.5 \leq Fo \leq A$ and $w=0.5$ for $Fo \leq 1.5$ in later refinements. The A parameter was re-evaluated several times during the refinement so as to give approximately a constant average of $w(Fo-Fc)^2$ in groups of increasing $\sin\theta/\lambda$—0.000—0.291, 0.291—0.411, 0.411—0.503, 0.503—0.650; the final value was 5.0. After several least-squares cycles, the difference map was again calculated without hydrogen atoms. This new map indicated the peaks of five hydrogen atoms with several ghost peaks. With anisotropic thermal parameters for non-hydrogen atoms and isotropic thermal parameters for hydrogen atoms, the final R index was 7.4%, excluding unobserved reflections. The observed and calculated structure factors are listed in Table 2.[21]

Table 3. The final parameters and their standard deviations (in parentheses)

The coordinates of the heavy atoms have been multiplied by 10^4; those of the hydrogen atoms, by 10^3. The anisotropic temperature parameters of the heavy atoms are of the form $\exp[-(b_{11}h^2+b_{22}k^2+b_{33}l^2+2b_{12}hk+2b_{13}hl+2b_{23}kl)]$, and have been multiplied by 10^5. For the hydrogen atoms the values listed are isotropic temperature parameters B.

Atom	X	Y	Z	b_{11}	b_{22}	b_{33}	b_{12}	b_{13}	b_{23}
C(1)	889(3)	−1826(6)	−233(7)	460(37)	2213(108)	2356(158)	−214(103)	593(128)	−717(229)
C(2)	1597(3)	−941(6)	1743(7)	330(38)	2196(114)	2332(161)	−107(108)	383(130)	−620(249)
C(3)	709(3)	879(6)	1969(7)	492(33)	2362(108)	2547(151)	−263(100)	512(118)	−1042(230)
C(4)	1821(3)	−3887(6)	−372(7)	509(39)	2174(109)	2255(160)	−131(106)	547(131)	−651(232)
C(5)	3322(3)	−1756(6)	3480(7)	371(36)	2432(113)	2659(168)	−106(104)	352(129)	−901(246)
O(1)	1130(3)	−4188(6)	−2720(6)	626(33)	2943(99)	3781(148)	32(93)	431(117)	−1855(217)
O(2)	3089(3)	−5140(5)	1581(6)	584(33)	3146(102)	3200(141)	198(94)	312(112)	−1149(213)
O(3)	3844(3)	−2903(5)	6236(6)	407(30)	4307(119)	2444(147)	−143(96)	332(111)	−701(219)
O(4)	4120(3)	−1291(5)	2387(6)	377(31)	4108(120)	3399(143)	−335(90)	626(112)	−308(208)
O(5)	7187(3)	−2369(5)	2972(6)	589(32)	2805(92)	3551(123)	−298(95)	791(98)	−1295(207)
H(1)	113(4)	162(6)	329(8)	0.5(7)					
H(2)	173(7)	−550(12)	−244(14)	4.5(15)					
H(3)	473(9)	−341(14)	698(20)	7.5(16)					
H(4)	638(10)	−237(14)	330(18)	7.5(16)					
H(5)	686(4)	−104(7)	137(9)	0.7(8)					

20) Y. Okaya and T. Ashida, HBLS IV. The Universal Crystallographic Computing System (I), p. 65, Japanese Crystallographic Association (1967).

21) The complete data of the F_o-F_c table are kept as Document No. 7106 at the office of the Bulletin of the Chemical Society of Japan. A copy may be secured by citing the document number and remitting, in advance, ¥900 for photoprints. Pay by check or money order payable to: Chemical Society of Japan.

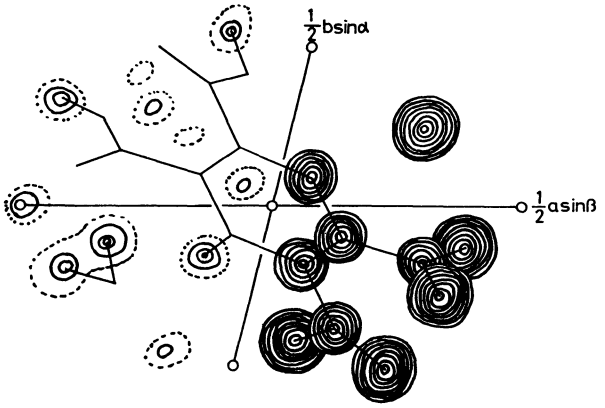

Fig. 1. The projection of the electron density along the *c* axis.

Discussion of the Structure

The final positional and thermal parameters are listed, along with their standard deviations, in Table 3. Figure 1 shows the electron-density and difference maps along the *c* axis calculated at the end of the refinement.

The right-hand side is a composite of a number of electron-density sections. The left-hand side is composite of difference sections calculated with the structure factors excluding the hydrogen atoms. The bond distances and angles are listed, along with their estimated standard deviations, in Table 4 and are also given in Fig. 2, which shows the projection of a molecule onto the plane of the benzene ring. In Table 5, the molecular dimensions obtained in the present crystal are compared with those of related benzene carboxylic acids.

Table 4. Least-squares plane of the ring

Equation of the plane defined by the six ring atoms
$-0.59635X-0.40280Y+0.69434Z=0.0$
X, *Y*, and *Z* are coordinates in Å referred to an orthogonal set of axes, where *Y* is parallel to *b* and *X* lies in the *ab* plane.
Deviations of atoms.

Atom	From the plane	Atom	From the plane
C(1)	−0.0005Å	C(4)	0.0861Å
C(2)	−0.0005	C(5)	−0.1216
C(3)	0.0005	H(1)	−0.0237
C(1′)	0.0005	C(4′)	−0.0861
C(2′)	0.0005	C(5′)	0.1216
C(3′)	−0.0005	H(1′)	0.0237

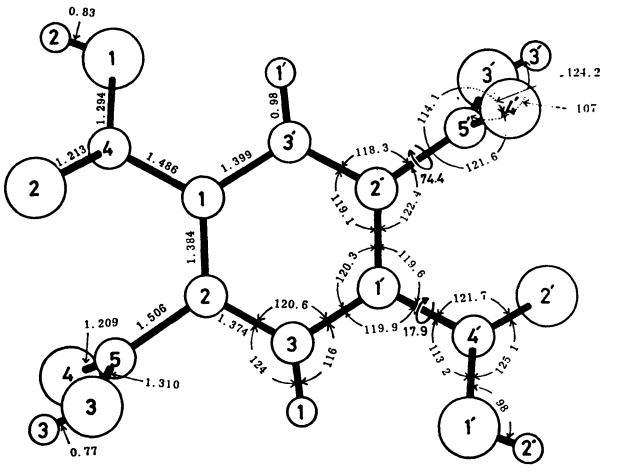

Fig. 2. Bond distances and angles in a molecule.

Table 5. Bond lengths and bond angles

C(1)–C(2)	1.384(6)Å	C(5)–O(3)	1.310(5)Å
C(1)–C(3′)	1.399(5)	C(5)–O(4)	1.209(6)
C(1)–C(4)	1.486(6)	O(1)–H(2)	0.83(7)
C(2)–C(3)	1.374(6)	O(3)–H(3)	0.77(7)
C(2)–C(5)	1.506(5)	O(5)–H(4)	0.89(9)
C(3)–H(1)	0.98(5)	O(5)–H(5)	0.93(4)
C(4)–O(1)	1.294(5)		
C(4)–O(2)	1.213(4)		
C(2)–C(1)–C(3′)	120.3(4)°	C(1)–C(4)–O(1)	113.2(3)°
C(2)–C(1)–C(4)	119.6(3)	C(1)–C(4)–O(2)	121.7(4)
C(3′)–C(1)–C(4)	119.9(4)	O(1)–C(4)–O(2)	125.1(4)
C(1)–C(2)–C(3)	119.1(3)	C(2)–C(5)–O(3)	114.1(4)
C(1)–C(2)–C(5)	122.4(4)	C(2)–C(5)–O(4)	121.6(3)
C(3)–C(2)–C(5)	118.3(4)	O(3)–C(5)–O(4)	124.2(3)
C(1′)–C(3)–C(2)	120.6(4)	C(4)–O(1)–H(2)	98(5)
C(1′)–C(3)–H(1)	116(2)	C(5)–O(3)–H(3)	110(6)
C(2)–C(3)–H(1)	124(2)	H(4)–O(5)–H(5)	107(5)

There are three structurally distinct ring C–C distances. The average value is 1.386 Å; this does not differ significantly from the accepted value. Similarly, the bond angles in the benzene ring require no special comment. The least-squares plane was calculated through the six ring atoms. The benzene ring is essentially planar. The equation of the plane is given in Table 6, together with the out-of-plane distances of various atoms in a molecule. The dimensions of the two carboxyl groups are very similar to each other, but the two C–O distances in each group are distinctly different. The bonds between the carbon and carbonyl oxygen atoms, C(4)–O(2) and C(5)–O(4), are shorter than those between the carbon and hydroxyl oxygen atoms, C(4)–O(1) and C(5)–O(3), by an average value of 0.091 Å. The hydrogen atoms of pyromellitic acid are definitely associated with the hydroxyl oxygen atoms, as no evidence was found for any disordering of the hydrogen position or the presence of the H_3O^+ ion. In both carboxyl groups, the C–C–O angles associated with the short C–O bonds are smaller than those associated with the longer C–O bonds by an average value of 9.7°; the O–C–O angles are also found to be clearly larger than 120°, as is usually observed in carboxylic acids.

One carboxyl group is twisted by 17.9° out of the plane of the benzene ring, while the other is twisted by 74.4°. Furthermore, C(4) and C(5) deviate from the least-squares plane by 0.12 and −0.08 Å respectively. These twists and deviations might be due to the repulsion of the oxygen atoms of the adjacent carboxyl groups, and also to the formation of the hydrogen-bond network, as will be discussed later. The C(1)–C(2)–C(5) angle is 122.4°, which is significantly larger than 120°; this might also be caused by the interaction of the vicinal carboxyl groups, although the corresponding angle related to another carboxyl group does not differ significantly from 120°. In general, the distances of the C–C bond external to the central ring fall in the

Table 6. Comparison of the molecular shapes in benzene carboxylic acids

Molecule	C–C[a]Å	C–C[b]Å	C=OÅ	C⁼⁼OÅ	C–O(H)Å	Dihedral angle[c]	References
Benzoic acid	1.39*	1.48	1.24	—	1.29	0.0°	d
Phthalic acid	1.38*	1.49	1.22	—	1.30	34.0	e, f
Terephthalic acid	1.392*	1.483	1.262	—	1.272	5.3	g
Trimesic acid	1.390*	1.493*	1.244*	—	1.291*	14.9*	h
		1.483*	—	1.258*	—	5.5*	
Pyromellitic acid dihydrate	1.386*	1.486	1.213	—	1.294	17.9	this study
		1.506	1.209	—	1.310	74.4	
Mellitic acid	1.391*	1.548	—	1.236	—	66.8	i
		1.520	1.260	—	1.340	80.7	
		1.521	1.199	—	1.320	25.7	
		1.508	—	1.269	—	24.6	
	1.383*	1.505	—	1.233	—	55.5	
		1.508	1.226	—	1.286	44.0	
		1.532	1.188	—	1.290	66.0	
		1.512	—	1.251	—	51.5	

a) C(ring)-C(ring)
b) C(ring)-C(carboxyl)
c) The dihedral angle between the planes of the benzene ring and the carboxyl group
d) G. A. Sim, J. M. Rodertson, and T. H. Goodin, *Acta Crystallogr.*, **8**, 157 (1955).
e) H. Jaggi, *Z. Kristallogr.*, **109**, 3 (1957).
f) W. Nowacki and H. Jaggi, *ibid.*, **109**, 272 (1957).
g) M. Bailery and C. J. Brown, *Acta Crystallogr.*, **22**, 387 (1966).
h) D. J. Duchamp and R. E. Marsh, *ibid.*, **B25**, 5 (1969).
i) S. F. Darlow, *ibid.*, **14**, 159 (1961).
* Average value

range of 1.48 and 1.54 Å, such as found in the benzoic acid[2] and the acetic acid,[22] which vary according to the differences in the contribution of the π-bond character. In the present structure, the two C(ring)-C(carboxyl) distances are 1.486 and 1.506 Å respectively. The difference between these two distances may be inside the limits of experimental error. However, it is likely that the changing of these bond lengths can be explained by the difference in the contribution of the π-bond character resulting from the twisting angles of related carboxyl groups.

The most interesting features of the structure are the intricate arrangement of hydrogen bonds and the resulting three-dimensional network. Four types of hydrogen bonds, with O-H···O distances of 2.549, 2.687, 2.807, and 2.876 Å, form a three-dimensional net work, as is shown in Figs. 3 and 4. Each molecule is joined, through a hydrogen bond around the center of symmetry, to two other molecules, forming an endless chain in the [1 $\bar{1}$ 1] direction. Water molecules are arranged on the plane parallel to (1 1 0) so as to hold the chains together by hydrogen bonds. The distance between the oxygen atoms of the carboxyl groups related by a center of symmetry is 2.687 Å; this is normal for this type of hydrogen bond. The three hydrogen bonds through the medium of a water molecule differ significantly in length and strength, the distances being 2.549 Å for the H_2O···HO bond and 2.807 and 2.876 Å for the two O···H_2O bonds. The O(1‴)–H(2‴)··· O(5″) angle of 166° indicates that the hydrogen atom lies more closely to the line joining O(1‴) and O(5″) (2.549 Å) than in the case of the weaker O(5″)–H(4″)··· O(4″) (2.876 Å) and O(5″)–H(5″)···O(4⁗) (2.807 Å) hydrogen bonds, in which the corresponding angles are 152° and 165° respectively.

In connection with the mode of hydrogen bonding in this crystal mentioned above, it is interesting to compare it with that found in the oxalic acid, which

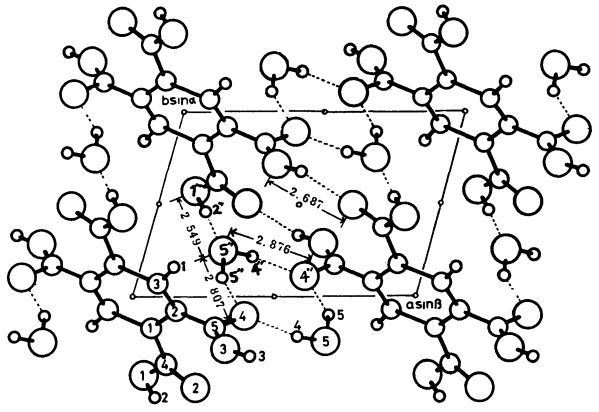

Fig. 3. The projection of the crystal structure along the *c* axis.

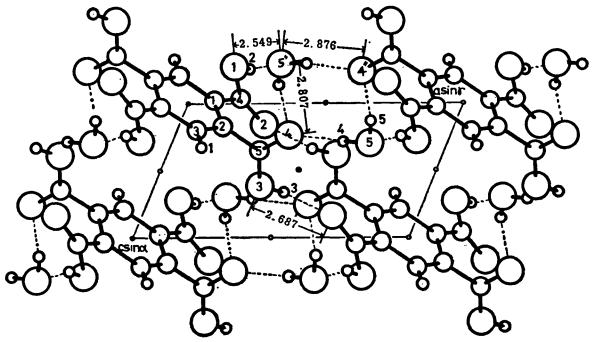

Fig. 4. The projection of the crystal structure along the *b* axis.

22) R.E. Jones and D.H. Templeton, *Acta Crystallogr.*, **11**, 484 (1958).

Table 7. Comparison of hydrogen bond distances and angles in pyromelltic acid dihydrate and oxalic acid dihydrate

	Pyromellitic acid dihydrate	α-oxalic acid dihydrate
(Distance)		
O(1‴)-O(5″)	2.549(6)Å	2.512Å
O(5″)-O(4)	2.807(8)	2.864
O(5″)-O(4″)	2.876(5)	2.883
(Angle)		
O(1‴)-O(5″)-O(4″)	130.3(2)°	136.0°
O(1‴)-O(5″)-O(4)	107.1(2)	119.8
O(4″)-O(5″)-O(4)	86.3(2)	84.4
O(5)-O(4″)-O(5″)	93.7(2)	97.9

has been studied in detail. The oxalic acid is well known to have polymorphs, occurring in two anhydrous forms[8,9] and also in two dihydrate forms,[10-17] one of which is found in the deutrated dihydrate. While there is only one independent carboxyl group in an oxalic acid molecule, there are two independent carboxyl groups in a pyromellitic acid. It will be seen that one kind of hydrogen bond is used to form the endless chain, as in the β-form of the anhydrous oxalic acid. Except for this hydrogen bond, there still remain six hydrogen atoms to be hydrogen bonded in a pyromellitic acid dihydrate as in an oxalic acid dihydrate. The hydrogen bonds formed by those remaining hydrogen atoms seem to resemble those found in the α-form of oxalic acid dihydrate. The hydrogen-bonding distances and angles are compared in Table 7. Moreover, the direction of the line joining the water oxygen atom and carboxyl hydrogen atom O(5″)···H(2‴) makes an angle of 47° with the plane of the water molecule in the present crystal. The corresponding angle in the oxalic acid dihydrate is 51°; this is one of the main features of hydrogen bonds in the α-oxalic acid dihydrate.[14,17]

This research was partly supported by the Scientific Research Grant of the Ministry of Education.

BULLETIN OF THE CHEMICAL SOCIETY OF JAPAN, VOL. 44, 1278—1281 (1971)

Photochemical Reactions of Uranyl Ions with Organic Compounds III. The Correlation between the Reaction Mode and the Pre-Equilibrium in the Photolysis of the Uranyl-lactate System

Shukichi SAKURABA and Ryoka MATSUSHIMA
Faculty of Engineering, Shizuoka University, Hamamatsu

(Received November 28, 1970)

On the basis of the assumed mechanism for the photolysis of the uranyl-lactate system, the equilibrium constant for the complex formation, K, was evaluated from the photo-kinetic data by using a monochromatic 4047 Å light; it was then compared with those obtained from the usual spectrophotomeric measurements. A comparison of the K values obtained by means of the photo-kinetic data ($1.0-1.1\times10^{-1}$) and by means of the analytical data ($1.1-1.2\times10^{-1}$) gave an excellent agreement; there was also a good agreement between the slope of the plot of the photo-kinetic data and that predicted from the assumed mechanism. The results supported the crude mechanism assumed earlier.

In a previous paper[1] it was reported that the photo-oxidation of lactic acid by uranyl ions gave acetaldehyde (with an evolution of carbon dioxide) and pyruvic acid as the oxidation products besides, the equimolar uranium-(IV) species as the reduction product. The dependence of the relative ratio of the organic products upon the various experimental conditions was attributed to the difference in the initial species of the system to be photolized; the formation of acetaldehyde involves an intra-molecular decomposition of the uranyl-lactate complex initially formed, while the formation of pyruvic acid involves encounter collisions between lactic acid and the excited uranyl ions (initially uncomplexed):

$$U + HL \rightleftharpoons UL + H^+$$

$$U + h\nu \longrightarrow U^*$$

$$UL + h\nu \longrightarrow UL^*$$

$$U^* \xrightarrow{k_1} U + h\nu' \text{ or heat}$$

$$UL^* \xrightarrow{k_2} UL + h\nu'' \text{ or heat}$$

$$U^* + HL \xrightarrow{k_3} U(V) + HL^+$$

$$UL^* \xrightarrow{k_4} UL' + CO_2$$

$$HL^+ + U \xrightarrow{\text{fast}} \text{pyruvic acid} + U(V) + 2H^+$$

$$2U(V) \xrightarrow[H^+]{\text{fast}} U(IV) + U$$

$$UL' \xrightarrow{\text{fast}} \text{acetaldehyde} + U(IV) + H^+$$

where U: uranyl ion; HL: lactic acid; HL^+: intermediate radical cation $CH_3C^+H(OH)CO_2H$, and UL′: intermediate species, such as $CH_3C^+H\!\!<\!\!\begin{matrix}O\\H\end{matrix}\!\!>UO^+_2$ (the last

1) S. Sakuraba and R. Matsushima, This Bulletin, **43**, 1950 (1970).

two intermediates would lose protons to form radicals, but the true intermediate species are still uncertain).

The present investigation was undertaken to see whether or not the equilibrium constant (for the uranyl lactate complex) which can be evaluated from the kinetic data by using the assumed equations is consistent with that determined by means of the usual analytical method.

Experimental

De-oxygenated solutions containing 0.2M lactic acid and 0.02M uranyl nitrate, of the pH-range of 0.1—2.5 and the ionic strength of 0.3—0.5, were irradiated with the light of the 4047—4078 Å region at 20°C by means of an interference filter and a 500-W high-pressure mercury arc. The concentrations of the acetaldehyde (A) and pyruvic acid (P) formed were determined spectrophotometrically as their 2,4-dinitrophenylhydrazones. The separation of the hydrazone derivative from each other was carried out with ethyl acetate[2] and an aqueous Na_2CO_3 (0.5N) solution.[1]

The quantum yield of the formation of pyruvic acid, ϕ_P, and that of acetaldehyde, ϕ_A, under various pH's were obtained from the molar ratios [A]/[P] by using a calibrated graph of the total quantum yield[3] as a function of the pH preliminarily measured repeatedly with a much more stable Hg-lamp source(100W). This method seems to make possible simplified procedures and a much higher accuracy than the direct measurements of the quantum yields, since the [A]/[P] ratio is independent of the total number of the light quanta absorbed by the system.[1] The adjustments of the pH(or [H]) of the solutions, both that to be photolyzed and that for analytical use (for the measurement of the k value), were carried out with solutions of perchloric acid and sodium hydroxide, using a pH-meter (Toa Denpa Co., Ltd.).

Results and Discussion

The Photo-Kinetic Results. For simplification, the experimental conditions were so chosen that only the 1:1 complex of the uranyl-lactate was formed;

$$U + HL \overset{K}{\rightleftarrows} UL + H^+$$

It is evident both from Fig. 1 and from the linearity of the plots in Figs. 5 and 6 that only the 1:1 complex[4] is formed when the initial concentrations, at pH≤3, of the uranyl ions and lactic acid are 0.02M and 0.2M respectively. The hydrolysis and polymerizations of uranyl ions are negligible at pH values below 2.5.[5]

The formation quantum yields, ϕ_P and ϕ_A, for the photolysis of the uranyl-lactate system in which initial formation of the 1:1 complex is involved will be given by the following equations, (1) and (2) respectively,

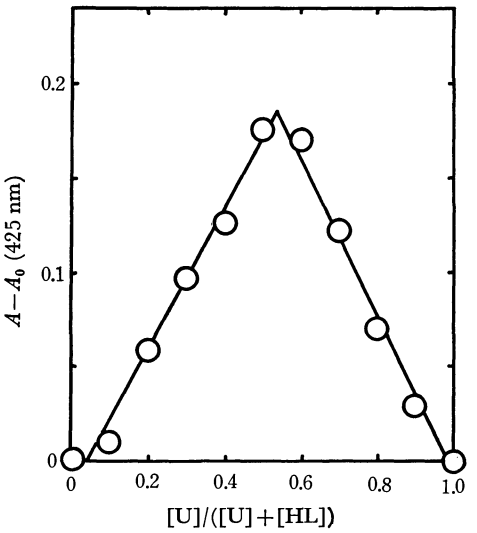

Fig. 1. Application of the continuous variation method to the uranyl-lactate system, as measured at 425 nm peak. [U]+[HL]= 0.04M, pH=3.0.

which are based on the assumed mecahnism.

$$\phi_P = \frac{k_3[HL]}{k_1 + k_3[HL]} \cdot \frac{\varepsilon_1[U]}{\varepsilon_1[U] + \varepsilon_2[UL]} \quad (1)$$

$$\phi_A = \frac{k_4}{k_2 + k_4} \cdot \frac{\varepsilon_2[UL]}{\varepsilon_1[U] + \varepsilon_2[UL]} \quad (2)$$

Equations (1) and (2) can be rewritten as Eqs. (1′) and (2′):

$$\log\left(\frac{\phi_P^0}{\phi_P} - 1\right) = \log C + \mathrm{pH} \quad (1')$$

$$\log\left(\frac{\phi_A^0}{\phi_A} - 1\right) = -\log C - \mathrm{pH} \quad (2')$$

where:

$$\phi_P^0 = k_3[HL]/(k_1 + k_3[HL]) \quad (3)$$

$$\phi_A^0 = k_4/(k_2 + k_4) \quad (4)$$

$$C = \varepsilon_2 K[HL]/\varepsilon_1 \quad (5)$$

$$K = [UL][H]/[U][HL] \quad (6)$$

ε_2 and ε_1 are the absorption coefficients of the complex and the uncomplexed uranyl ions respectively at the

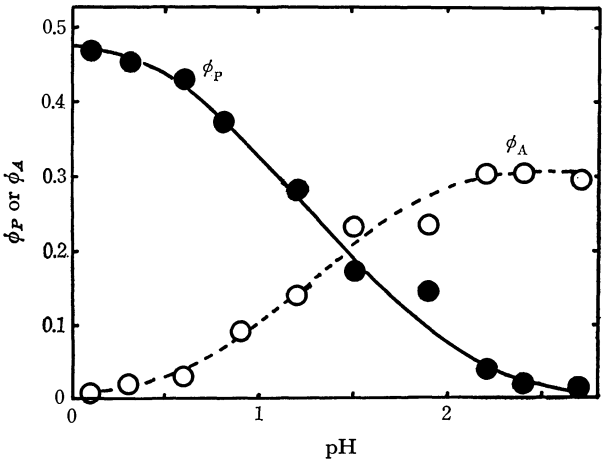

Fig. 2. Plots of the quantum yields *vs.* pH, showing $\phi_P^0 = \phi_P(\text{at } \phi_A \to 0) = 0.48$, $\phi_A^0 = \phi_A(\text{at } \phi_P \to 0) = 0.32$.
ϕ_A: The quantum yield of acetaldehyde formation.
ϕ_P: The quantum yield of pyruvic acid formation.

2) The extraction by ethyl acetate was superior to the extraction by chloroform or carbon tetrachloride because of its higher solubility and more complete separation.

3) The total quantum yield was equal to the quantum yield of the U(IV) formation.[1]

4) See also I. Feldman and J. R. Harvill, *J. Amer. Chem. Soc.*, **76**, 2114, 4726 (1954).

5) E. Rabinowitch and R. L. Belford, "Spectroscopy and Photochemistry of Uranyl Compounds," Pergamon Press, London (1964) pp. 91—110.

6) Y. Oka, "Zikken Kagaku Koza," 2nd Series, Vol. 7, Maruzen, Tokyo (1966), p. 210.

irradiated wavelength (4047 Å). ϕ_P^0 can be regarded as a limited value of ϕ_P when ϕ_A reaches zero (Eqs. (1) and (3)), and ϕ_A^0 as a limited value of ϕ_A when ϕ_P reaches zero (Eqs. (2) and (4))(*cf.* Fig. 2). When the initial concentration of lactic acid is much higher than that of the uranyl ion, the change in the lactic acid concentration due to the complex formation may be neglected: $[HL]_i \gg [U]$, $[HL]_i \gg [UL]$. Thus, Eqs. (5) and (6) may be rewritten as Eqs. (5′) and (6′):

$$C = \varepsilon_2 K[HL]_i/\varepsilon_1 \ (=\text{constant}) \qquad (5')$$

$$K = [UL][H]/[U][HL]_i \qquad (6')$$

Then, if the quantum yields, ϕ_P and ϕ_A, are measured under various pH's, with the initial concentration of lactic acid kept constant and much higher than that of the uranyl ion, the plot of log $(\phi_P^0/\phi_P - 1)$ *vs.* pH and log $(\phi_A^0/\phi_A - 1)$ *vs.* pH should be straight lines with slopes of 1 and −1 respectively. A good agreement with these predictions is shown in Fig. 3, though the A plot is somewhat scattered. Either from the intercept of the P plot or from that of the A plot, the equilibrium constant, K, can be evaluated by using Eq. (5′) if ε_1 and ε_2 are determined by an appropriate method. The absorption coefficient of the uranyl ions, ε_1, at 4047 Å was 7.0 and was constant over the pH range from 0.1 to 2.4 (Fig. 4). The absorption coefficient of the complex, ε_2, at 4047 Å can be obtained from the intercept of the corresponding plot in Figs. 5 or 6 by using Eq. (7). The 3 plot in Fig. 5 gives $\varepsilon_2 - \varepsilon_1$ (at 405 nm) = 7.0, and the 1 plot in Fig. 6 gives $\varepsilon_2 - \varepsilon_1$(at 405 nm) = 7.1. When $[HL] = 0.20$ M, $\varepsilon_1 = 7.0$, $\varepsilon_2 = 14.0$, and log $C = -1.35$ (the intercept of plot P in Fig. 3), are substituted in Eq. (5′), K becomes 1.1×10^{-1}; while the substitution of $-\log C = 1.4$ (the intercept of plot A) gives $K = 1.0 \times 10^{-1}$.

Determination of the Equilibrium Constant by the Spectrophotometric Method[6,7] In order to compare the K-value evaluated on the basis of the photo-kinetic data with those evaluated by means of the usual analytical

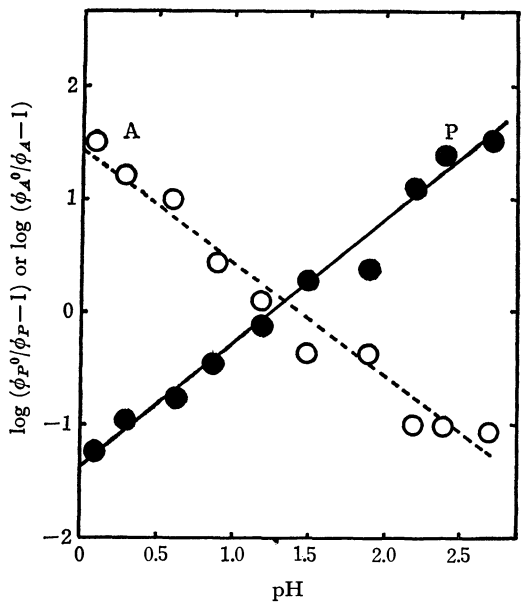

Fig. 3. Plots of log $(\phi_P^0/\phi_P - 1)$ and log $(\phi_A^0/\phi_A - 1)$ *vs.* pH.
P: Plot of log $(\phi_P^0/\phi_P - 1)$ *vs.* pH
A: Plot of log $(\phi_A^0/\phi_A - 1)$ *vs.* pH
$[U]_i = 0.02$ M, $[HL]_i = 0.2$ M, $\lambda = 4047$ Å, Temperature = 20°C.

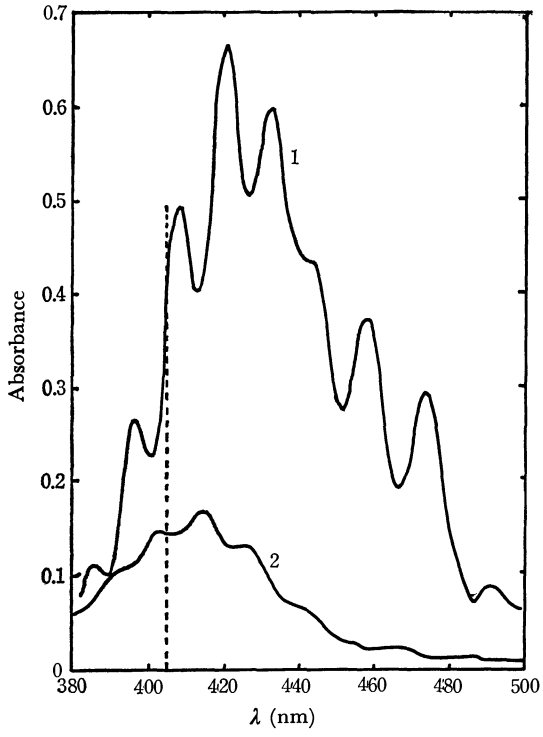

Fig. 4. Absorption spectra of the uranyl-lactate complex and the uncomplexed uranyl ions.
1: The increment in absorption due to the complex formation, $(A - A_0) \times 10$, at pH = 1.7 and $[UO_2^{2+}]_i = 0.02$M.
2: Absorption spectrum of the uncomplexed uranyl ion at pH values 0.1 to 2.4. The dotted vertical line indicates the wavelength of the 4047 Å radiation used for the photolysis.

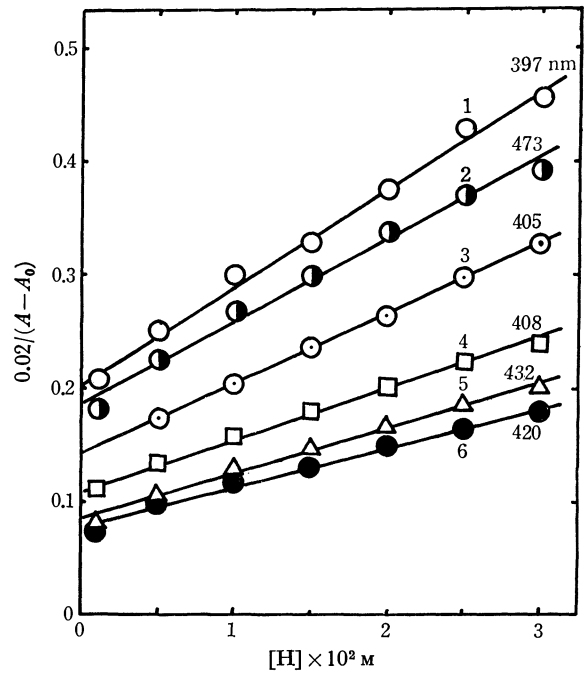

Fig. 5. Plots of $[U]_i/(A - A_0)$ *vs.* [H].
$[U]_i = 0.02$M, $[HL]_i = 0.2$M, Temperature = 20°C.
Plot 3 gives $\varepsilon_2 - \varepsilon_1$ (at 405 nm) = 7.0

7) Y. Oka, "Zikken Kagaku Koza," 2nd Series, Vol. 7, Maruzen, Tokyo (1966), p. 202.

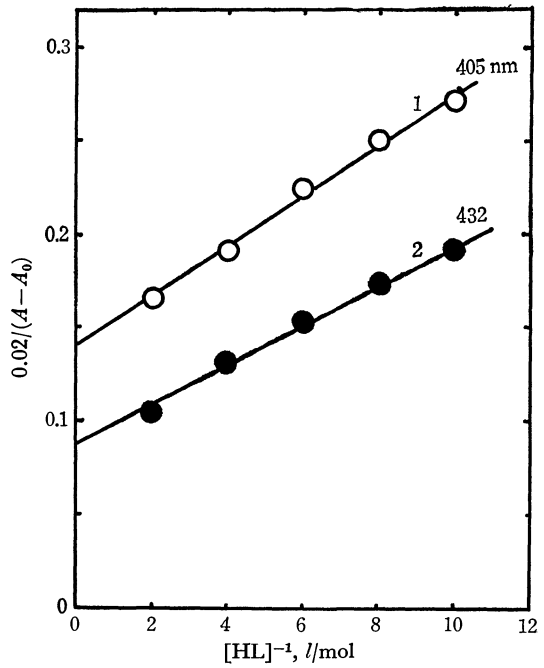

Fig. 6. Plots of $[U]_t/(A-A_0)$ *vs.* $[HL]_t^{-1}$.
$[U]_t$=0.02 M pH=2.0, Temperature=20°C.
Plot 1 gives $\varepsilon_2-\varepsilon_1$ (at 405 nm)=7.1

method, spectrophotometric measurements were made for the uranyl-lactate system prior to photolysis under the conditions mentioned above. The absorption spectra of the uranyl-lactate complex and the uncomplexed uranyl ions are shown in Fig. 4. The equilibrium constant, K, can be obtained from the plot of $[U]_t/(A-A_0)$ either as a function of [H] by keeping $[HL]_t$ constant, or as a function of $[HL]_t^{-1}$ by keeping [H] constant, using Eq. (7):

$$\frac{[U]_t}{A-A_0} = \frac{1}{\varepsilon_2-\varepsilon_1} + \frac{[H]}{(\varepsilon_2-\varepsilon_1)K[HL]_t} \qquad (7)$$

Here, A is the total absorption of the system at a wavelength in the visible region (where absorption by lactic acid is zero), A_0 is equal to $\varepsilon_1[U]_t$ at the same wavelength, and $[U]_t$ is kept constant (0.02M). The results,

Table 1. Equilibrium constant of the complex formation, measured by spectrophotometric method

Wavelength (nm)	$K^{a)} \times 10$	$K^{b)} \times 10$
363	1.19	
397	1.27	
405	1.20	1.13
408	1.20	
432	1.03	1.00
458	1.20	

a) Obtained from the plot of $[U]_t/(A-A_0)$ *vs.* [H]
b) Obtained from the plot of $[U]_t/(A-A_0)$ *vs.* $[HL]_t^{-1}$

measured at several wavelengths, are shown in Figs. 5 and 6, while the K values are listed in Table 1. A comparison of these values with those evaluated from the photo-kinetic data ($1.0—1.1\times10^{-1}$) gave excellent agreement.

The close relationship indicates that the variation in the reaction mode (or in the molar ratio of the products) is merely a direct reflection of the initial equilibria of the solutions to be photolyzed. Thus, the assumptions that the formation of acetaldehyde involves an intramolecular decomposition of the uranyl-lactate complex initially formed, and that the formation of pyruvic acid involves collisions between the excited uranyl ions initially uncomplexed, are supported. The results also suggest that the formation of an intermediate donor-acceptor complex during the lifetime of the excited state is not likely to be an important factor in governing the variations in the reaction mode in the photolysis of the uranyl-lactate system, though such an intermediate complex (exciplex) seems to play an important role in the transfer mechanisms of many other systems.[8,9] Of course, our results give no information on the redox-intermediate species (radical or radical ions), on which further clarification is needed.

8) N. Uri, *Advan. Chem. Ser.*, **36**, 102 (1962).
9) G. W. Robinson and R. P. Forsch, *J. Chem. Phys.*, **38**, 1187 (1963); R. E. Kellogg and N. C. Wyeth, *ibid.*, **45**, 3156 (1966); W. Siebrand, *ibid.*, **47**, 2411 (1967); D. P. Chock, J. Jorther, and S. A. Rice, *ibid.*, **49**, 610 (1968); E. A. Chandross and C. J. Dempster, *J. Amer. Chem. Soc.*, **92**, 3586 (1970).

The Adsorption of Water on SiO_2, Al_2O_3, and $SiO_2 \cdot Al_2O_3$. The Relation between the Amounts of Physisorbed and Chemisorbed Water

Tetsuo Morimoto, Mahiko Nagao, and Junichiro Imai

Department of Chemistry, Faculty of Science, Okayama University, Tsushima, Okayama

(Received December 14, 1970)

The specific surface area, the water content, and the water adsorption isotherm have been measured in order to investigate the interaction between the surfaces of SiO_2, Al_2O_3, and $SiO_2 \cdot Al_2O_3$ and water molecules. Al_2O_3 gives II-type adsorption isotherms and the amount of adsorbed water on it increases with a rise in the temperature of pretreatment, whereas SiO_2 gives isotherms approximate to the III-type and the amount of adsorbed water is larger when treated at lower temperatures. With $SiO_2 \cdot Al_2O_3$, it was found that the type of isotherms and the effect of the pretreatment temperature are similar to those of Al_2O_3, and that the amount of adsorption increases with an increase in the Al_2O_3 content. By analysing the adsorption data, the ratio of the amount of physisorbed water in the first layer to the amount of the underlying chemisorbed water was calculated. As a result, it was found that the H_2O:OH ratio is 1:2 on the surface of Al_2O_3, whereas it is 1:1 on the surface of SiO_2. The analysis of the isotherms on $SiO_2 \cdot Al_2O_3$ showed that the adsorption property of water on them is not additive: *e.g.*, the amount of adsorbed water on $SiO_2 \cdot Al_2O_3$ is larger than the sum of the water adsorbed on each component. Thus, it has been concluded that, on the surface of SiO_2 in contact with Al_2O_3, the surface hydroxylation proceeds more rapidly than on the surface of pure SiO_2.

Silica-alumina ($SiO_2 \cdot Al_2O_3$) is a catalyst widely used for such reactions as cracking and isomerization, and its surface properties have been studied extensively. Among these, the relation between the surface acidity and the catalytic activity[1-4] has been the most important property; it has been studied by using such basic substances as ammonia,[5-7] amine,[8] and pyridine[9,10] as adsorbates. Recently, it has become clear that the surface hydroxyl groups are present on the surfaces of most metal oxides placed in the usual atmosphere, that they affect their surface properties, and that they also play important roles in catalytic actions.[11,12] Finch and Clark[12] have reported that more than 0.45% water is necessary for the isomerization reaction of 1-butene by using $SiO_2 \cdot Al_2O_3$ as a catalyst; in this case, water acts cooperatively with a complex for polymerization.

In the preceding papers the ratio of the number of physisorbed water molecules to the amount of the underlying chemisorbed water (surface hydroxyl groups) has been investigated; it was found to be 1:2 (H_2O:OH) for TiO_2 (rutile) and α-Fe_2O_3[13] and 1:1 for ZnO[14] in the monolayer coverage of physisorbed water. On the surface of the $SiO_2 \cdot Al_2O_3$ catalyst there should be two kinds of surface hydroxyl groups, silanol and aluminol, differing in properties. It has been reported that the remaining surface hydroxyl groups of $SiO_2 \cdot Al_2O_3$ after the treatment at higher temperatures were those on SiO_2.[15] There have been many discussions of the nature of acidic sites on $SiO_2 \cdot Al_2O_3$,[16] but the water adsorption property, which should affect the surface acidity, has not yet been investigated in detail. The purpose of this work is to investigate the water adsorption property on SiO_2, Al_2O_3, and three kinds of $SiO_2 \cdot Al_2O_3$, all differing in composition in order to ascertain the relation between the amounts of physisorbed and chemisorbed water on them, and to clarify the details of the interaction between oxide surfaces and water molecules.

Experimental

Materials. Pure SiO_2 gel (S) was produced by the hydrolysis of ethyl-silicate with water at 100°C, the latter being purified by double distillation from a commercial, guaranteed reagent. Al_2O_3 gel (A) was prepared by the following process. Metallic aluminum was treated with a 5% NaOH solution to remove the surface impurity, and then washed with water, absolute ethanol, and ether. The 25 g of metallic aluminum thus treated were permitted to react with 300 m*l* of pure isopropanol in a reflux flask, in the presence of 1 g of mercuric chloride as a catalyst. The aluminum isopropoxide thus formed[17] was distilled under a reduced pressure of 2.5 Torr (108—108.5°C). An Al_2O_3 gel sample was obtained by the hydrolysis of this aluminum isopropoxide in a mixed solution of isopropanol and water (3:1). Three kinds of $SiO_2 \cdot Al_2O_3$ were obtained by mixing SiO_2 (S) and Al_2O_3 (A) samples of different compositions. SA-25, SA-50, and SA-75 contain Al_2O_3 gel of 25, 50, and 75wt.% respec-

1) O. Johnson, *J. Phys. Chem.*, **59**, 827 (1955).
2) R. L. Richardson and S. W. Benson, *ibid.*, **61**, 405 (1957).
3) M. W. Tamele, *Discuss. Faraday Soc.*, **8**, 270 (1960).
4) D. M. Brouer, *J. Catal.*, **1**, 22 (1962).
5) J. E. Mapes and R. P. Eischens, *J. Phys. Chem.*, **58**, 1059 (1954).
6) A. Clark, V. C. F. Holm, and D. M. Blackburn, *J. Catal.*, **1**, 244 (1962).
7) P. L. Hseih, *ibid.*, **2**, 211 (1963).
8) A. C. Zettlemoyer and J. J. Chessick, *J. Phys. Chem.*, **64**, 1131 (1960).
9) E. P. Parry, *J. Catal.*, **2**, 371 (1963).
10) M. R. Basila, J. R. Kantner, and K. H. Rhee, *J. Phys. Chem.*, **68**, 3197 (1964).
11) T. C. Franklin and M. Kawamata, *ibid.*, **71**, 4213 (1967).
12) J. N. Finch and A. Clark, *ibid.*, **73**, 2234 (1969).
13) T. Morimoto, M. Nagao, and F. Tokuda, *ibid.*, **73**, 243 (1969).
14) T. Morimoto and M. Nagao, This Bulletin, **43**, 3746 (1970).
15) M. R. Basila, *J. Phys. Chem.*, **66**, 2223 (1962).
16) *E.g.*, K. Tanabe and T. Takeshita, "San Enki Shokubai (Acid-Base Catalysis)," Sangyo Tosho, Tokyo (1966), p. 187.
17) A. L. Wilds, *Org. Reaction*, **2**, 198 (1944).

tively. The mixing of SiO_2 and Al_2O_3 gels was carried out in an agate-ball mill. Finally, the pure and mixed gels thus obtained were washed sufficiently with distilled water, dried at 100°C, and calcined at 500°C for 10 hr in air.

Specific Surface Area. The specific surface area of the samples pretreated at 600°C for 4 hr under the reduced pressure of 10^{-5} Torr was measured by applying the BET theory[18] to the nitrogen adsorption data at −196°C. The conditions of the pretreatment were the same as those for the water adsorption measurement. The molecular area of nitrogen was assumed to be 16.2 Å^2. The values obtained on the S, A, SA-25, SA-50, and SA-75 samples were 640, 189, 423, 427, and 317 m^2/g respectively.

Water Content. The water content of the samples was measured by the successive-ignition-loss method.[19] The samples were treated in the same apparatus as was used for the adsorption measurement for 4 hr at various temperatures, from room temperature to 1100°C; the vapor evolved was determined volumetrically at each step. From these data, the water content remaining on the surface could be obtained as a function of the pretreatment temperature. In this calculation the water content at 1100°C was assumed to be zero, as the amount of water vapor expelled at 1100°C was negligibly small.

Water-adsorption Isotherm. The sample was at first treated at 600°C for 4 hr under the reduced pressure of 10^{-5} Torr. The measurement of the water adsorption isotherm was carried out volumetrically at 20°C, by using an oil manometer to read the equilibrium pressure. After the first adsorption isotherm had been determined, the sample was again treated at 30°C for 4 hr at 10^{-5} Torr, and then the second adsorption isotherm was measured at the same temperature as before. The same adsorption measurements were repeated subsequently for one sampling after the sample had been treated at various temperatures, from 100 to 500°C.

Results

The water content of the samples is shown in Fig. 1 as a function of the pretreatment temperature. It indicates the amount of water bonded to the surface treated at the given temperatures, expressed in the number of hydroxyl groups per 100 Å^2. At lower temperatures there is a large possibility that it includes the amount of physisorbed water. It can be seen from Fig. 1 that the water content of pure Al_2O_3 is the most, and that the value of SiO_2 is the least. With $SiO_2 \cdot Al_2O_3$, the greater the portion of Al_2O_3, the more the water content. Furthermore, the water-content curve of pure SiO_2 is characteristic in that it decreases almost linearly with the rise in the temperature.

The water-adsorption isotherms of five samples are given in Figs. 2—4. In the case of Al_2O_3, the adsorption isotherms belong to the II-type of Brunauer's classification;[20] the amount of adsorbed water is the largest in the measurement after 600°C treatment, and the smallest in the measurement after 30°C treatment. When the pretreatment temperature rises from 30

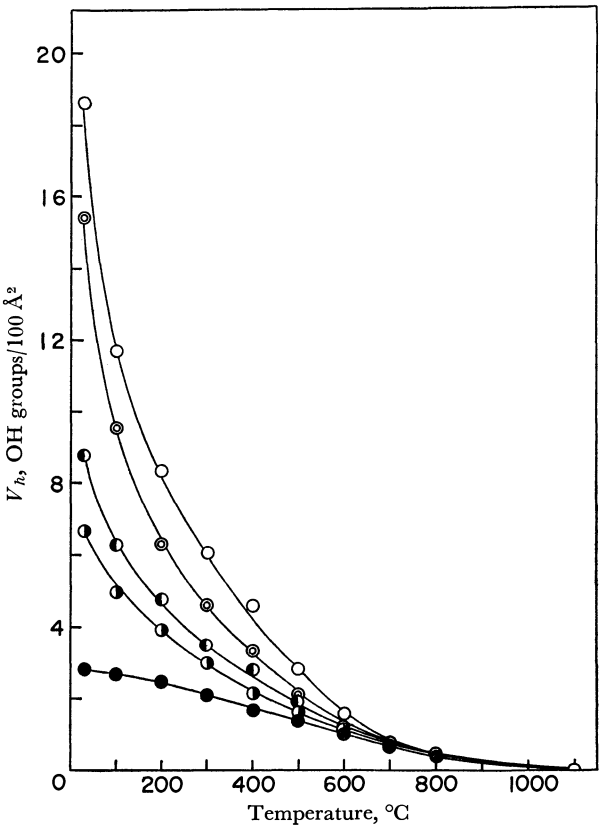

Fig. 1. Water content of SiO_2, Al_2O_3, and $SiO_2 \cdot Al_2O_3$: ●, S; ○, A; ◑, SA-25; ◐, SA-50; ◎, SA-75.

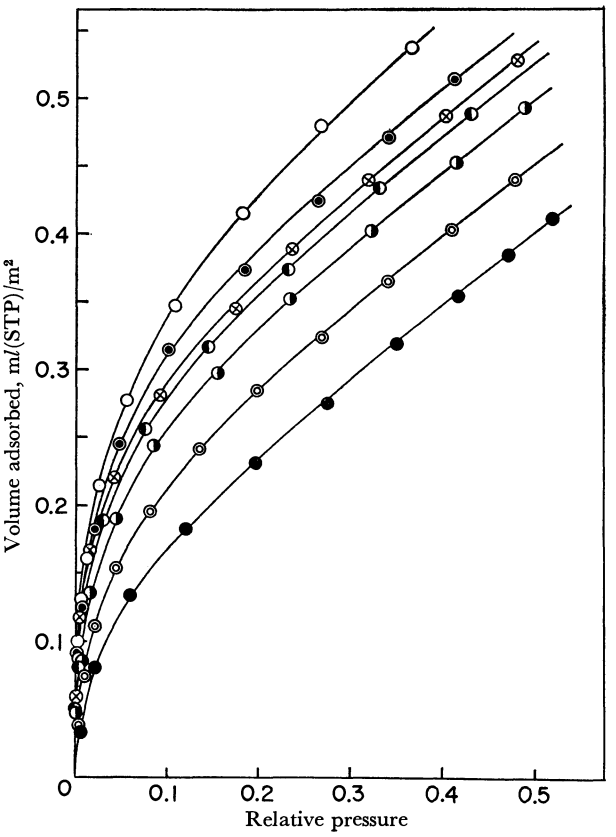

Fig. 2. Water-adsorption isotherm on Al_2O_3 at 20°C, pretreated at 600°C, ○; 30°C, ●; 100°C, ◎; 200°C, ◑; 300°C, ◐; 400°C, ⊗; 500°C, ◉.

18) S. Brunauer, P. H. Emmett, and E. Teller, *J. Amer. Chem. Soc.*, **60**, 309 (1938).

19) T. Morimoto, K. Shiomi, and H. Tanaka, This Bulletin, **37**, 392 (1964).

20) S. Brunauer, "The Adsorption of Gases and Vapors," Princeton University Press, Princeton (1945).

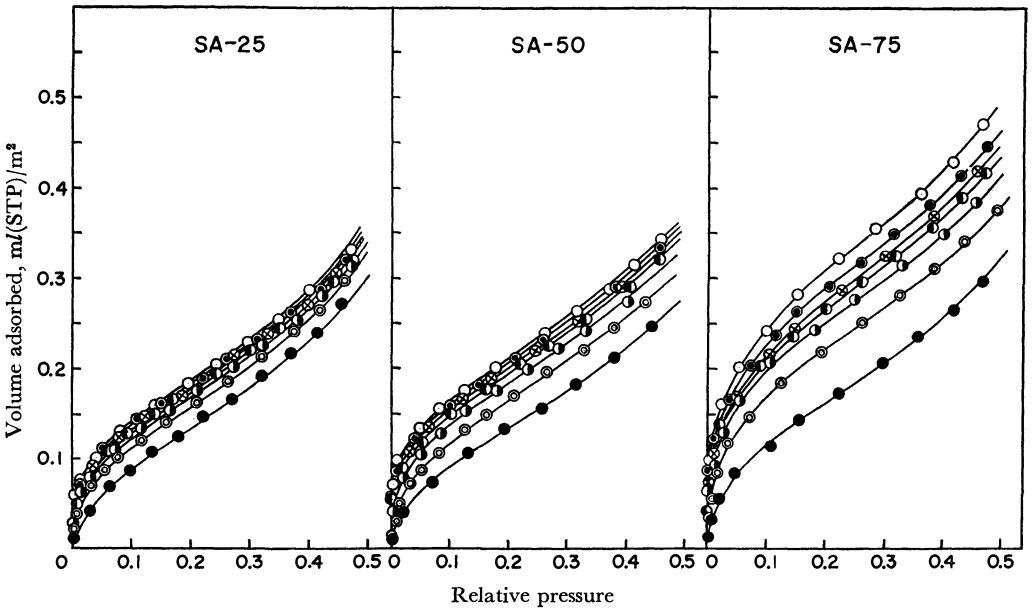

Fig. 3. Water-adsorption isotherm on $SiO_2 \cdot Al_2O_3$ at 20°C, pretreated at 600°C, ○; 30°C, ●; 100°C, ◎; 200°C, ◑; 300°C, ◐; 400°C, ⊗; 500°C, ◉.

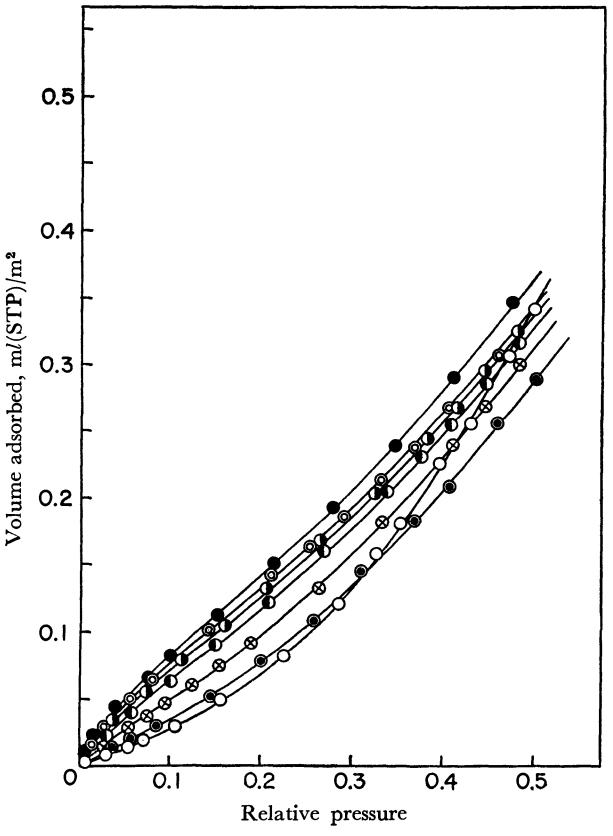

Fig. 4. Water-adsorption isotherm on SiO_2 at 20°C, pretreated at 600°C, ○; 30°C, ●; 100°C, ◎; 200°C, ◑; 300°C, ◐; 400°C, ⊗; 500°C, ◉.

to 500°C, the amount of adsorbed water increases and approaches the value of the 600°-treated sample. Moreover, Fig. 2 shows that the sample of Al_2O_3 chemisorbs water considerably. The same situation appears in the case of $SiO_2 \cdot Al_2O_3$ (Fig. 3), and the amount of adsorbed water increases with an increase in the content of Al_2O_3.

The water-adsorption isotherms on pure SiO_2 are given in Fig. 4; they are quite different from those on pure Al_2O_3 and $SiO_2 \cdot Al_2O_3$. First, the results generally show that the higher the pretreatment temperature, the less the amount of adsorbed water. Second, the shape of the isotherms on the sample pretreated at lower temperatures is of the II-type, whereas it seems to approach the III-type when the pretreatment temperature rises. Young[21] has reported that, on a flame silica, the water-adsorption isotherms were of the III-type and that the amount of adsorbed water decreased with the rise in the pretreatment temperature to 450°C. Most metal oxides chemisorb water molecules, even at the lowest equilibrium pressure, to form surface hydroxyl groups, and further physisorb water molecules on them through hydrogen bonding, resulting in II-type isotherms, as is shown in Figs. 2 and 3. On the contrary, the surface of pure SiO_2 adsorbs more water when the pretreatment temperature is lower and, accordingly, when the remaining surface hydroxyl groups are larger in number, as may be seen from Figs. 1 and 4. Moreover, the amount of adsorbed water on the 600°C-treated sample is quite small at lower pressures, but it increases more sharply at higher pressures compared to the cases of the other samples, as is shown in Fig. 4. These results suggest that the rate of the surface hydroxylation of SiO_2 is slower than in the cases of Al_2O_3 and other metal oxides and that, therefore, the physisorption only occurs during the water-adsorption measurement. Our experience has shown that, in the first adsorption-isotherm measurement on SiO_2 (after 600°C treatment), the time required for the attainment of the equilibrium pressure was within 20 min in the low-pressure range, but was prolonged in the higher-pressure range,

21) G. J. Young, *J. Colloid Sci.*, **13**, 67 (1958).

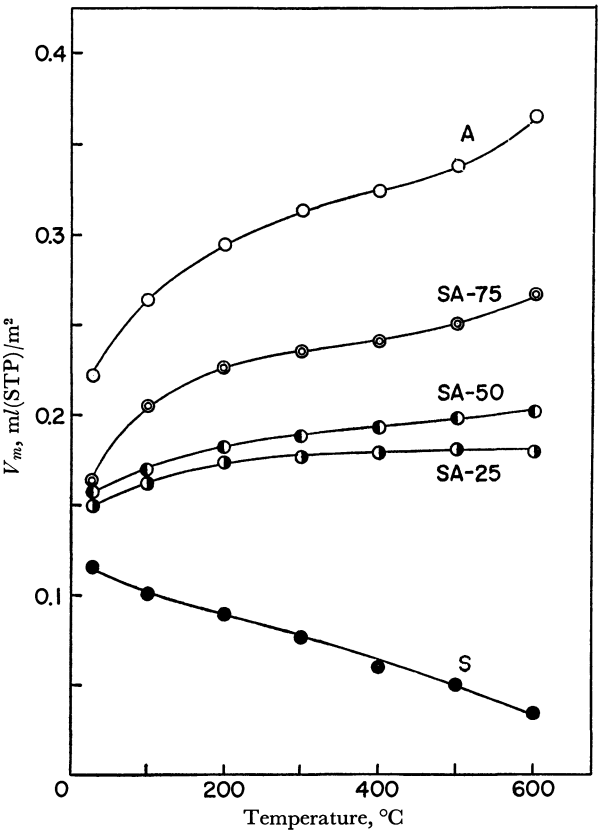

Fig. 5. Dependence of V_m value on pretreatment temperature.

taking more than a few hours. In the second adsorption measurement, however, the equilibrium was attained within 30 min over the whole range of pressure. The results of Hockey and Pethica[22] and those of Egorova *et al.*[23] agree with the present findings, supporting of the idea that, on the surface of SiO_2, the rate of surface hydroxylation is so slow that the surface can only be hydroxylated at higher relative pressures.

By applying the BET method[18] to the adsorption isotherms, the monolayer capacity, V_m, of water was calculated and plotted against the pretreatment temperature (Fig. 5). The V_m value on Al_2O_3 increases with a rise in the temperature of pretreatment. In a previous paper, the same plot was taken on ZnO, TiO_2, and α-Fe_2O_3.[24] In the cases of ZnO and TiO_2, the temperature at which the steep increase in V_m starts was distinct; this was explained in terms of the commencement of the removal of chemisorbed water by the pretreatment and the reversible rehydroxylation on exposing the surface to water vapor. Also, in the present case additional chemisorption on Al_2O_3 is considered to occur, though the temperature showing the commencement of the steep increase in V_m is not clear similarly to the case of α-Fe_2O_3. The removal of chemisorbed water may occur at least at 150°C, as is to be expected from Fig. 1. On the other hand, the V_m value of SiO_2 decreases almost linearly with the rise in the pretreatment temperature; this is parallel to the decrease in water content shown in Fig. 1. This suggests that, on the surface of SiO_2, the physisorption of water only occurs on the surface hydroxyl groups during the adsorption measurement. With $SiO_2 \cdot Al_2O_3$, the V_m value increases similarly to that of pure Al_2O_3, but the increase in V_m becomes slower when the content of SiO_2 is greater, as is shown in Fig. 5.

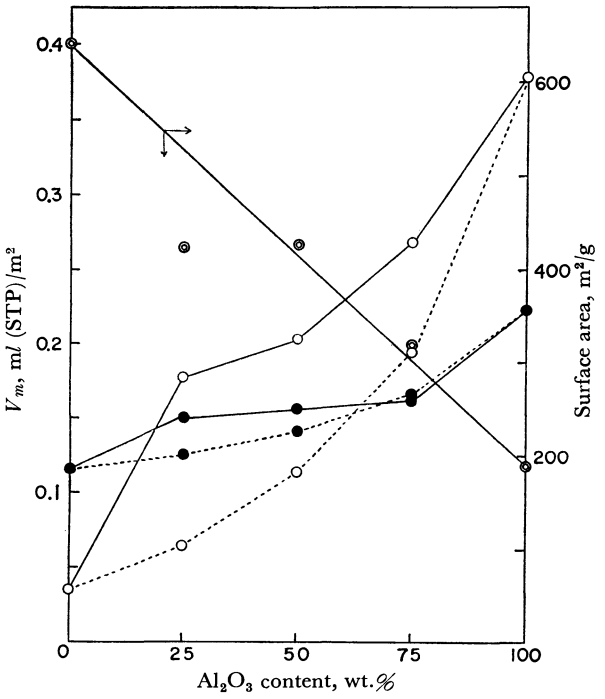

Fig. 6. Dependence of V_m value and specific surface area on Al_2O_3 content: pretreated at 600°C, ○; 30°C, ●.

In order to ascertain the dependence of V_m on the composition, V_m is replotted against the Al_2O_3 content in Fig. 6. This plot can be taken for each pretreatment temperature, but in Fig. 6 only two limiting cases are represented (600° and 30°C treatments). The other plots at the intermediate temperatures can be inserted in a regular order between them. The specific surface area of the sample is also plotted in Fig. 6. As may be seen from Fig. 6, the surface areas of $SiO_2 \cdot Al_2O_3$ are almost all on the straight line connecting the values of SiO_2 (640 m²/g) and Al_2O_3 (189 m²/g); the one exception is the SA-25 sample, which gives a fairly smaller value than would be expected from the composition. If the surface area of $SiO_2 \cdot Al_2O_3$ is composed of the sum of each component, the portion of the surface of Al_2O_3 in $SiO_2 \cdot Al_2O_3$, $S_{(A)}/S_{(SA)}$, is about 9, 23, and 47% for SA-25, SA-50, and SA-75 respectively. Furthermore, if the water adsorption occurs additively on the surfaces of $SiO_2 \cdot Al_2O_3$, the V_m value will change as shown by the dotted curves. The experimental results on $SiO_2 \cdot Al_2O_3$, especially on SA-25, deviate greatly from these synthetic curves, indicating that the water adsorption does not occur additively on the surface of $SiO_2 \cdot Al_2O_3$. It has been established that $SiO_2 \cdot Al_2O_3$ of a composition of 13—25 wt.% Al_2O_3

22) J. A. Hockey and B. A. Pethica, *Trans. Faraday Soc.*, **57**, 2247 (1961).
23) T. S. Egorova, Yu. A. Zarif'yants, V. F. Kiselev, K. G. Krasil'nikov, and V. V. Murina, *Zh. Fiz. Khim.*, **36**, 1458 (1962).
24) T. Morimoto, M. Nagao, and F. Tokuda, This Bulletin, **41**, 1533 (1968).

Table 1. Relation between the amounts of physisorbed and chemisorbed water on SiO_2, Al_2O_3, and $SiO_2 \cdot Al_2O_3$ (SA-50)

Sample	Treat. temp., °C	V_m, ml(STP)/m²	V_p, H_2O molecules/100Å²	V_c,	V_h, OH groups/100Å²	V_c+V_h,	$\frac{V_p}{V_c+V_h}$, H_2O/OH
SiO_2	30	0.116	3.12	—	2.78	—	—
	100	0.100	2.69	—	2.72	2.72	0.99
	200	0.089	2.40	—	2.50	2.50	0.96
	300	0.077	2.07	—	2.10	2.10	0.99
	400	0.060	1.62	—	1.69	1.69	0.96
	500	0.051	1.37	—	1.40	1.40	0.98
	600	0.035	0.94	—	1.03	1.03	0.91
Al_2O_3	30	0.223	6.00	—	18.66	—	—
	100	0.264	6.00	2.20	11.92	13.92	0.43
	200	0.295	6.00	3.87	8.28	12.15	0.49
	300	0.314	6.00	4.89	6.04	10.93	0.55
	400	0.324	6.00	5.43	4.58	10.01	0.60
	500	0.336	6.00	6.08	2.80	8.88	0.68
	600	0.378	6.00	8.34	1.60	9.94	0.60
SA-50	30	0.157	4.23	—	8.78	—	—
	100	0.169	4.23	0.64	6.26	6.90	0.61
	200	0.182	4.23	1.34	4.76	6.10	0.69
	300	0.188	4.23	1.66	3.50	5.16	0.82
	400	0.193	4.23	1.93	2.82	4.75	0.89
	500	0.198	4.23	2.20	1.99	4.19	1.01
	600	0.203	4.23	2.47	1.17	3.64	1.16

has a large catalytic activity.[6,25] The present results seem to show a characteristic activity of SA-25 in the adsorption of water.

Discussion

On the basis of these experimental results, the relation between the amounts of physisorbed and chemisorbed water on pure SiO_2 and Al_2O_3 was first obtained as is shown in Table 1. V_m is the monolayer capacity obtained from the water-adsorption isotherm. This may be considered to include only physisorbed water in the case of SiO_2, as has been discussed above. V_p is the amount of physisorbed water, expressed in the number of water molecules per 100 Å². For the same reason, the amount of chemisorbed water, V_c, on SiO_2 is zero in the initial stage of the adsorption process. V_h is the water content; it indicates the amount of water chemisorbed before the adsorption measurement, expressed in the number of hydroxyl groups per 100 Å². Thus, the value of V_h is equal to the total amount of chemisorbed water in the case of SiO_2. It may be seen from Table 1 that the ratio of V_p to V_h is approximate to 1 on every surface of SiO_2 treated at different temperatures. This finding indicates that the initial physisorption of water occurs only on silanol groups in the ratio of 1:1. The surface density of silanol groups is 2.78 OH groups/100 Å² at most; this is reasonable compared with the maximum value calculated by Schneider[26] on the surface of amorphous SiO_2 (5.0 OH groups/100 Å²), although it is considerably smaller than the number of surface hydroxyl groups on Al_2O_3 and the other metal oxides.[13] Several authors have also found that the number of the surface hydroxyl groups on SiO_2 is small.[21,22,27] These silanol groups are, therefore, believed to be scattered and isolated on the surface of SiO_2, on which each water molecule is bonded through hydrogen bonding in the ratio of 1:1. On the surface of ZnO a similar ratio has also been found,[14] but there the mechanism of water adsorption seems to be different from the present case.

The V_m value on Al_2O_3 treated at various temperatures is composed of both physisorbed and chemisorbed water, as has been described above, but the second adsorption isotherm obtained after the treatment at 30°C contains only physisorbed water, for the reason discussed in previous papers.[13,24] Therefore, in the case of Al_2O_3, the V_m value obtained from the second adsorption isotherm (after the 30°C treatment) was taken as the amount of physisorbed water, V_p, and the difference between V_m and V_p, as the amount of the chemisorbed water, V_c.[28] The sum of V_c and V_h is, accordingly, the total amount of the chemisorbed water after the adsorption measurement. Thus, in the case of Al_2O_3, the $V_p:(V_c+V_h)$ ratio should be the true ratio of the amounts of physisorbed and chemisorbed water in the first layer of physisorption; it is found to be approximately 1 : 2, as is shown in Table 1. This suggests that, on the surface of Al_2O_3, one water molecule is physisorbed onto two surface hydroxyl groups, as in the cases of TiO_2 (rutile) and α-Fe_2O_3.[13] In addition, when the pretreatment temperature of Al_2O_3 rises over 200°C, V_h decreases, V_c

25) A. Clark and V. C. F. Holm, *J. Catal.*, **2**, 16, 21 (1963).
26) M. Schneider, Ph. D. Thesis, University of Heidelberg, Germany (1962); H. P. Boehm, *Advan. Catal.*, **16**, 179 (1966).
27) G. J. Young and T. P. Bursh, *J. Colloid Sci.*, **15**, 361 (1960).
28) J. J. Jurinak, *ibid.*, **19**, 477 (1964).

Table 2. Relation between the amounts of physisorbed and chemisorbed water on $SiO_2 \cdot Al_2O_3$ (SA-50)

Treat. temp., °C	$V_{m(SA)}$, ml(STP) /m²	$V_{m(A)}$, ml (STP) /0.23 m²	$V_{p(A)}$, H_2O molecules/23 Å²	$V_{c(A)}$,	$V_{h(A)}$,	$V_{c(A)}+V_{h(A)}$,	$\frac{V_{p(A)}}{V_{c(A)}+V_{h(A)}}$, H_2O/OH
				OH groups/23 Å²			
30	0.157	0.068	1.83	—	6.64	—	—
100	0.169	0.092	1.83	1.30	4.17	5.47	0.33
200	0.182	0.114	1.83	2.45	2.83	5.28	0.35
300	0.188	0.129	1.83	3.27	1.88	5.15	0.36
400	0.193	0.147	1.83	4.24	1.52	5.76	0.32
500	0.198	0.159	1.83	4.89	0.91	5.80	0.32
600	0.203	0.177	1.83	5.82	0.38	6.20	0.30

increases, and the sum of V_h and V_c is almost constant; this suggests that the rehydroxylation of the dehydroxylated sites occurs reversibly on the surface of Al_2O_3 upon exposure to water vapor.

In the case of $SiO_2 \cdot Al_2O_3$, the meaning of the H_2O: OH ratio is fairly obscure, since water molecules can be adsorbed differently on the two kinds of surfaces. The SA-50 data listed in Table 1 are temporarily-calculated values, the mean value of the values on the two kinds of surfaces, which are obtained by the same method as was used in the case of pure Al_2O_3. In this calculation it is assumed that the physisorption only occurs on the 30°-treated surface of SA-50, and that V_p is constant on every surface treated at different temperatures. The H_2O:OH ratio of SA-50 thus calculated increases remarkably with the rise in the pretreatment temperature, though the values of pure SiO_2 and Al_2O_3 are almost invariable. This tendency becomes smaller in the order: SA-25 (0.72—1.53), SA-50 (0.61—1.16), SA-75 (0.36—0.63); the larger the portion of SiO_2, the greater the effect. Certainly, this effect results from the fact that, when the surface treated at higher temperatures is exposed to water vapor, the rehydroxylation occurs reversibly and rapidly on the dehydroxylated sites of both SiO_2 and Al_2O_3 in $SiO_2 \cdot Al_2O_3$, as in the case of pure Al_2O_3, in spite of the fact that the rehydroxylation is difficult on SiO_2. Since the physisorption of water initially occurs on the surface hydroxyl groups, the amount of physisorbed water on $SiO_2 \cdot Al_2O_3$ is also expected to decrease, as in the case of pure SiO_2, when the pretreatment temperature rises. Thus, in calculation of SA-50 shown in Table 1, V_p was overestimated and, accordingly, V_c+V_h was underestimated, resulting in the increase in the H_2O:OH ratio at higher pretreatment temperatures.

Another calculation was made on the SA-50 sample as an example (Table 2), assuming that the surface of SiO_2 in $SiO_2 \cdot Al_2O_3$ only physisorbs only water molecules. On this sample, the portion of the surfaces occupied by Al_2O_3 is 23%. By subtracting the amount of physisorbed water on 77 Å² of pure SiO_2 from the V_m value of SA-50, we can obtain the sum of the amounts of physisorbed and chemisorbed water, $V_{m(A)}$, on 23 Å² of Al_2O_3. By means of the same method as was used in the case of Al_2O_3, $V_{m(A)}$ can be separated into the amounts of chemisorbed ($V_{c(A)}$) and physisorbed water ($V_{p(A)}$); assuming that the $V_{m(A)}$ value obtained after the 30°C treatment is composed of only the amount of physisorbed water, as in the case of pure Al_2O_3, the $V_{p(A)}$ value of 1.83 water molecules per 23 Å² for SA-50 is obtained. On the measurements after the pretreatment at higher temperatures, the chemisorption of water also occurs; its amount can be determined by subtracting $V_{p(A)}$ from $V_{m(A)}$. On the other hand, the water content of SA-50 illustrated in Fig. 1 should be composed of those on SiO_2 and Al_2O_3. On the basis of the above assumption that the surface of SiO_2 does not chemisorb water molecules, the water content of Al_2O_3, $V_{h(A)}$, can be calculated. Thus, the ratio of the amount of physisorbed water ($V_{p(A)}$) to the total amount of chemisorbed water ($V_{c(A)}+V_{h(A)}$) can be given as 0.30—0.36 for every measurement, whatever the treatment temperature may be, as is shown in Table 2. Similar results were obtained on the SA-25 (0.21—0.31) and SA-75 (0.24—0.34) samples; they are all considerably smaller than that on pure Al_2O_3 (0.5).

Such small values seem to be quite difficult to accept if we take into account the surface hydrophilicity of pure Al_2O_3. These unlikely small values probably arise from the assumptions that the water chemisorption does not occur on the surface of SiO_2 and that, consequently, all the chemisorption of water on $SiO_2 \cdot Al_2O_3$ in the adsorption process is to be attributed to the surface of Al_2O_3 in $SiO_2 \cdot Al_2O_3$. Rather, it may be reasonable

Table 3. Amount of chemisorbed water on SiO_2 in $SiO_2 \cdot Al_2O_3$

Treat. temp., °C	SA-25			SA-50			SA-75		
	$V_{c(A)}$,	$V_{m(S)}$,	$V_{c(S)}$,	$V_{c(A)}$,	$V_{m(S)}$,	$V_{c(S)}$,	$V_{c(A)}$,	$V_{m(S)}$,	$V_{c(S)}$,
	OH groups/100 Å²			OH groups/100 Å²			OH groups/100 Å²		
100	16.44	1.41	0.47	5.65	1.03	0.34	6.02	3.40	1.13
200	29.67	2.55	0.85	10.65	2.03	0.68	9.19	4.72	1.57
300	36.78	3.15	1.05	14.22	2.79	0.93	10.98	5.40	1.80
400	48.33	4.24	1.41	18.43	3.88	1.29	12.57	6.34	2.11
500	54.00	4.74	1.58	21.26	4.53	1.51	14.15	7.15	2.38
600	60.89	5.37	1.79	25.30	5.06	1.69	17.17	7.83	2.61

Table 4. Comparison of V_h values of $SiO_2 \cdot Al_2O_3$ (OH groups/100 Å^2)

Temp., °C	S exp.	SA-25 calcd	SA-25 exp.	SA-50 calcd	SA-50 exp.	SA-75 calcd	SA-75 exp.	A exp.
30	2.78	4.21	6.67	6.43	8.78	10.24	16.46	18.66
100	2.72	3.53	4.91	4.79	6.26	6.95	9.64	11.72
200	2.50	3.02	3.94	3.83	4.76	5.22	6.32	8.28
300	2.10	2.45	3.02	3.01	3.50	3.95	4.68	6.04
400	1.69	1.95	2.16	2.35	2.82	3.05	3.34	4.58
500	1.40	1.53	1.61	1.72	1.99	2.06	2.04	2.80
600	1.03	1.08	1.03	1.16	1.17	1.30	1.06	1.60

to suppose that water molecules can be chemisorbed also on the surface of SiO_2 in $SiO_2 \cdot Al_2O_3$. In the calculation in Table 2, the number of the silanol groups thus probably formed is included in $V_{c(A)}$; this results in the overestimation of $V_{c(A)}$ and, accordingly, the underestimation of $V_{p(A)}$: $(V_{c(A)} + V_{h(A)})$. The overestimation of $V_{c(A)}$ can be understood more clearly by recalculating the data per 100 Å^2 from those per 23 Å^2, as in Table 3. The number of surface aluminum atoms of α-Al_2O_3 is estimated crystallographically to be 10.20 aluminum atoms per 100 Å^2 on the (0001) plane of α-Al_2O_3. Peri and Hannan[29] assumed the value of 12.5 OH groups/100 Å^2 as the surface density of hydroxyl groups on the fully hydroxylated surface of γ-Al_2O_3. The surface density of aluminum atoms and, accordingly, the maximum number of surface aluminol groups on the $SiO_2 \cdot Al_2O_3$ samples tested here can be expected to be almost the same as has been cited above. The V_c values on pure Al_2O_3 in Table 1 are, therefore, reasonable, but the $V_{c(A)}$ values are extraordinarily large, as is shown in Table 3; this proves that $V_{c(A)}$ has been overestimated.

Next, let us estimate the amount of chemisorbed water on SiO_2 in $SiO_2 \cdot Al_2O_3$, as has just been suggested. On the basis of the value of $V_{c(A)}$ in Table 3 and that of V_c of pure Al_2O_3 in Table 1, the excess amount of chemisorbed water per 23 Å^2 can be calculated; this water is transferred to the surface of 77 Å^2 of SiO_2. Here, the amount of water chemisorbed on Al_2O_3 in $SiO_2 \cdot Al_2O_3$ is assumed to be the same as that chemisorbed on pure Al_2O_3. The $V_{m(S)}$ value thus obtained is given in Table 3, expressed in the number of hydroxyl groups per 100 Å^2. When the chemisorption of water occurs on SiO_2 to form the silanol groups, additional physisorption will also occur on them. Accordingly, assuming that the physisorption on SiO_2 in $SiO_2 \cdot Al_2O_3$ would occur in the ratio of 1:1 (H_2O:OH), as in the case of pure SiO_2, one third of the $V_{m(S)}$ value is the amount of chemisorbed water. The $V_{c(S)}$ value thus obtained is 2.61 OH groups/100 Å^2 at most, as is shown in Table 3; this is comparable with the V_h value on SiO_2 and indicates the number of silanol groups retained before the water-adsorption measurement. $V_{c(S)}$ is the mean value on the unit surface area of SiO_2 in $SiO_2 \cdot Al_2O_3$, but the silanol groups newly formed during the adsorption process are probably concentrated in the contacting surface region of SiO_2 and Al_2O_3.

Finally, assuming that the V_h value of each oxide in $SiO_2 \cdot Al_2O_3$ is the same as that of single oxide, and taking into account the surface areas occupied by the two components, we can calculate the V_h values of $SiO_2 \cdot Al_2O_3$ and compare them with the experimental data read from Fig. 1 (Table 4). It may be seen from Table 4 that the experimental V_h value is always larger than the calculated one, but that the former approaches the latter as the sample is pretreated at higher temperatures. In other words, the water content is not additive and the partial chemisorption of water occurs on $SiO_2 \cdot Al_2O_3$ before the adsorption measurement.

From the above results and considerations, we may conclude, with a large degree of probability, that the formation of silanol groups or new kinds of hydrated sites is fairly easy on SiO_2 in $SiO_2 \cdot Al_2O_3$, but is difficult on pure SiO_2. The mechanism of this reaction can be considered to be as follows: each aluminum atom on the surface of Al_2O_3 will attract lone-pair electrons from the surface oxygen atom of SiO_2 when they come in contact with each other. Such an excited site formed on the contacting surface region of the two oxides will react easily with a water molecule according to the formula:

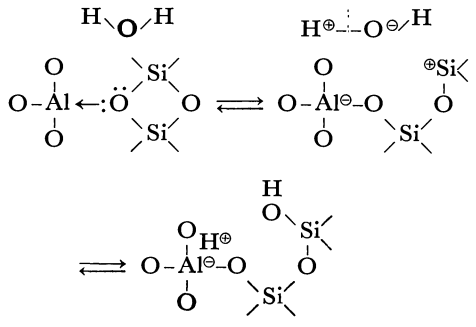

In this process, the water molecule can be adsorbed *via* dissociation; on the surface of SiO_2 a silanol group is formed, and on the surface of Al_2O_3, H^+ is adsorbed on the negative site of the aluminum atom.

29) J. B. Peri and R. B. Hannan, *J. Phys. Chem.*, **64**, 1526 (1960).

Stability Constants of Cu(II) Chelates with *o*-Phenylenediamine Derivatives

Kenyu KINA and Kyoji TÔEI

Department of Chemistry, Faculty of Science, Okayama University, Tsushima, Okayama

(Received May 11, 1970)

The stability constants of copper(II) chelates with *o*-phenylenediamine derivatives have been determined by the pH titration method. The measurements have been carried out at 25.0±0.1°C and μ=0.10(by KNO_3). *o*-Phenylenediamine derivatives, which have a substituent group (CH_3, CH_3O, COOH, or Cl, *etc.*) at the 4 positions, were used as ligands. The overall stability constants of the copper chelates are of the order: CH_3, CH_3O, H, COO^-, Cl, COOH; their values were 8.50, 8.42, 7.72, 7.06, 5.76, and 5.35 respectively. The effects of substituent groups on the stability constants have been studied. The plot of the overall stability constants against the sum of Hammett σ_m and σ_p values was found to be linear. The chelate stability and acid dissociation constants of the acido complexes of 3,4-diaminobenzoic acid were determined by the use of an augmented matrix.

Chelate-compound formation between transition metal ions and aliphatic diamines such as ethylenediamine has been extensively studied.[1] However, an aromatic diamine has not yet been widely studied. The present investigation was undertaken in order to determine the stability constants of copper(II) chelates of aromatic diamines, that is, *o*-phenylenediamine and its derivatives. The stability constants were calculated by the method of the least squares. If the acido complexes are present, the calculation will become enormously troublesome. According to Schwarzenbach, some kinds of ionic species can be neglected in a solution with a certain ratio of the ligand to the metal ion. From this point of view, the problem can be simplified; the acid dissociation and stability constants of acido complex were thus determined.

Experimental

Reagents. *m*-Phenylenediamine, *p*-phenylenediamine, 4-methyl-*o*-phenylenediamine (Wako Pure Chemical Co.), *o*-phenylenediamine (Daiichi Pure Chemical Co.), 4-chloro-*o*-phenylenediamine, 1,2,4-triaminobenzene dihydrochloride (Tokyo Chemical Industry Co.), and 3,4-diaminobenzoic acid (Aldrich Chemical Co.) were treated with active carbon and were recrystallized from conc. HCl before use.[2] 4-Methoxy-*o*-phenylenediamine was systhesized by the reduction of 2-nitro-4-methoxyaniline.[3] The dihydrochlorides of *o*-phenylenediamine derivatives, and 1,2,4-triaminobenzene trihydrochloride were obtained as white crystals. The hydrochlorides were used for the titration. A carbonate-free potassium hydroxide solution was prepared by the method of ion exchange and was standardized with potassium hydrogen phthalate titrimetrically.

Reagent Solutions. The stock solution of copper(II) ($Cu(NO_3)_2 \cdot 3H_2O$) was standarized by the usual procedures of chelatometric titration.[4] Solutions of all the ligands were made up with redistilled water just before the titration.

pH Titration Method. The hydrogen-ion concentration was measured by using an HRL-Model P pH meter (made by the Horiba Instruments Inc., Kyoto), with glass and calomel electrodes. Before and after each titration, the pH meter was calibrated with an acetate buffer.[5] The titration was carried out in a jacketed titration cell the volume of which was 100m*l*. For the determination of the dissociation constants of the protonated ligands, 2.5×10^{-3}M solutions of ligand in 0.10M potassium nitrate were used. On the other hand, solutions containing 1:1, 2:1, 3:1, 4:1, 5:1, 6:1, or 10:1 molar ratios of the ligand to the metal ion were used for the determination of the stability constants, while the ionic strength was maintained at approximately 0.10M with potassium nitrate. By circulating water from a constant-temperature bath through the water jacket, the temperature of the solution to be measured was kept at 25.0±0.1°C, and the room temperature, at 25±1°C. A carbon dioxide-free nitrogen atmosphere was maintained above the solution.

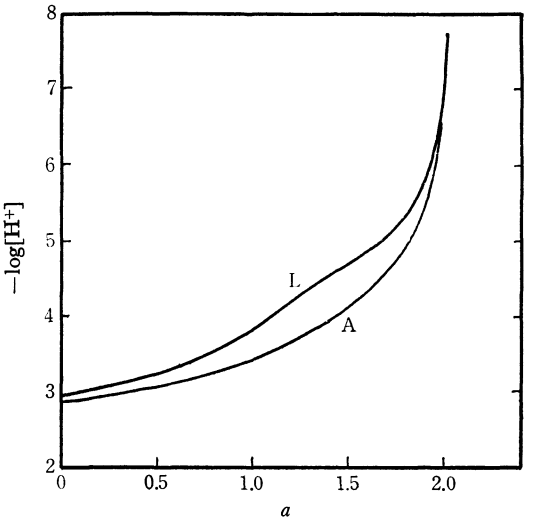

Fig. 1. Titration of *o*-phenylenediamine dihydrochloride, and 2:1 metal chelate, at 25°C, μ=0.10, L, ligand only; A, Cu(II) and ligand mixture [Ligand]=2[Metal ion]=1.052×10^{-3}M, [KOH]=1.072×10^{-3}M, *a*=moles of base added per mol of ligand.

Mathematical Treatment

a) Acid-dissociation Constants. The acid-dissociation constants of the protonated ligands were calculated

1) L. G. Sillén and A. E. Martell, "Stability Constants of Metal-Ion Complexes," Special Publication No. 17, The Chemical Society, Burlington House, London (1964), P. 390.

2) K. Tôei and K. Ito, *Talanta*, **12**, 773 (1965).

3) F. Wrede and E. Strack, *Ber.*, **62**, 2050 (1920).

4) K. Ueno, "Chelatemetric Titration" (in Japanese), Nankodo, Ltd., Tokyo (1967), P. 250.

5) S. Nakashima, H. Miyata, and K. Tôei, This Bulletin, **40**, 870 (1967).

by a method analogous to that of Murakami *et al.*[6] The equilibria and the dissociation constants involved are:

$$H_2L^{2+} \rightleftarrows H^+ + HL^+, \quad K_{a1} = [H^+][HL^+]/[H_2L^{2+}],$$
$$HL^+ \rightleftarrows H^+ + L, \quad K_{a2} = [H^+][L]/[HL^+],$$
$$1/K_{a1} = AK_{a2} + B \qquad (1)$$

where:

$$A = (2T_L - T_{OH} - [H^+] + [OH^-])/[H^+]^2(T_{OH} + [H^+] - [OH^-])$$
$$B = (T_L - T_{OH} - [H^+] + [OH^-])/[H^+](T_{OH} + [H^+] - [OH^-]),$$

and where L represents the *o*-phenylenediamine or its derivatives. T_L and T_{OH} are the total ligand concentration, and the concentration of the base added to the system, respectively. In all the calculations, the concentrations were corrected for the change in volume produced by the addition of the KOH. The acid-dissociation constants for protonated ligands were calculated by solving simultaneous equations from two points on the titration curve in the range of the buffer region. The pK_{a2} can be determined accurately by solving the simultaneous equations, because it has an order of magnitude of 3—5. If the pK_{a1} is below 2.0, an accurate value can not be obtained by this method. On the basis of Eq. (1) we assume that pK_{a1} is known and that pK_{a2} is the unknown. Then, pK_{a1} is obtained by the application of iterative approximation, by using an electronic computer (NEAC-2203: Nippon Electric Co., Ltd.).

b) Stability Constants. The ligands, 4-chloro, 4-methyl, or 4-methoxy-*o*-phenylenediamine and *o*-phenylenediamine, can have only one proton in the pH 2.8—4.5 region. Such ligands are treated as monoprotic acid in such a region. The equilibria and the stability constants are as follows:

$$M^{2+} + L \rightleftarrows ML^{2+}, \quad K_1 = [ML^{2+}]/[M^{2+}][L],$$
$$ML^{2+} + L \rightleftarrows ML_2^{2+}, \quad K_2 = [ML_2^{2+}]/[ML^{2+}][L].$$

The stability constants, K_1 and K_2, were calculated by fitting the data to the Irving and Rossotti equation:[7]

$$\bar{n}/(\bar{n}-1)[L] = [(2-\bar{n})[L]/(\bar{n}-1)]K_1K_2 - K_1, \qquad (2)$$

which is a linear form.

Here

$$\bar{n} = (T_L - [L] - [HL^+])/T_M,$$
$$[L] = K_{a2}(2T_L - T_{OH} - [H^+] + [OH^-])/[H^+],$$
$$[HL^+] = (2T_L - T_{OH} - [H^+] + [OH^-]),$$

and T_M is the total metal-ion concentration. The stability constants, K_1 and K_2, are best evaluated by the method of "least squares." The reliability of the constants was verified the theoretical formation curve with the experimental one. Eq. (2) can be rewritten as follows:

$$[L] = [(1-\bar{n}) - \{(\bar{n}-1)^2K_1^2 - 4\bar{n}(\bar{n}-2)K_1K_2\}^{1/2}/K_1]2(\bar{n}-2)K_2. \qquad (3)$$

The theoretical formation curves can be generated by the stability constants reported in Table 3 and by Eq. (3).

When the acido complex are present, the acid dissociation and chelate stability constants are obtained by a treatment based on that described by Nagano *et al.*[8] The following equation and equilibria were considered in the 3,4-diamino-benzoic acid system:

$$M^{2+} \overset{9)}{\rightleftarrows} M(OH)^+ \overset{10)}{\rightleftarrows} M(OH)_2$$
$$K_{M1} \updownarrow$$
$$MHL^{2+} \overset{k_1}{\rightleftarrows} ML^+$$
$$K_{M2} \updownarrow$$
$$M(HL)_2^{2+} \overset{k_2}{\rightleftarrows} ML(HL)^+ \overset{k_2'}{\rightleftarrows} ML_2.$$

The equilibrium constants are defined as follows:

$$K_{M1} = [MHL^{2+}]/[M^{2+}][HL],$$
$$K_{M2} = [M(HL)_2^{2+}]/[MHL^{2+}][HL],$$
$$k_1 = [H^+][ML^+]/[MHL^{2+}],$$
$$k_2 = [H^+][ML(HL)^+]/[M(HL)_2^{2+}],$$
$$k_2' = [H^+][ML_2]/[ML(HL)^+],$$
$$K_{a1} = [H^+][H_2L^+]/[H_3L^{2+}],$$
$$K_{a2} = [H^+][HL]/[H_2L^+],$$
$$K_{a3} = [H^+][L^-]/[HL].$$

The first step of the acid dissociation of protonated ligands is thus complete. As for the total ligand concentration, T_L, the total proton concentration, T_H and the total metal-ion concentration, T_M, the following relations hold:

$$T_L = \sum_{j=0}^{2}[H_jL] + [MHL^{2+}] + [ML^+] + 2[M(HL)_2^{2+}] + 2[ML(HL)^+] + 2[ML_2] \qquad (4)$$

$$T_H - [H^+] + [OH^-] = T_L \cdot g = \sum_{j=0}^{2} j[H_jL] + [MHL^{2+}] + 2[M(HL)_2^{2+}] + [ML(HL)^+] \qquad (5)$$

$$T_M = [M^{2+}] + [MHL^{2+}] + [ML^+] + [M(HL)_2^{2+}] + [ML(HL)^+] + [ML_2] \qquad (6)$$

The average number of hydrogen ions bound per total of the ligands, g, is given by the expressions:

$$g = \sum_{j=1}^{3} j[H_jL]/T_L, \quad g = 3 - a + ([OH^-] - [H^+])/T_L,$$

a=moles of base added per mole of ligand.

Here a group of brief symbols will be introduced:

$$A = T_L, \quad B = T_L \cdot g, \quad C = T_M, \quad D_1 = K_{M1}, \quad D_2 = K_{M1}k_1,$$
$$D_3 = K_{M1}K_{M2}, \quad D_4 = K_{M1}K_{M2}k_2, \quad D_5 = K_{M1}K_{M2}k_2k_2',$$
$$m = [M^{2+}], \quad h = [HL], \quad a_0 = (K_{a3}/[H^+] + 1 + [H^+]/K_{a2}),$$
$$b_0 = (1 + 2[H^+]/K_{a2}).$$

Equations (5), (6), and (7) may be rewritten as follows:

$$A = h\{a_0 + (D_1 + D_2/[H^+])m + (2D_3 + 2D_4/[H^+] + 2D_5/[H^+]^2)mh\} \qquad (7)$$

$$B = h\{b_0 + D_1m + (2D_3 + D_4/[H^+])mh\} \qquad (8)$$

6) Y. Murakami, K. Nakamura, and M. Tokunaga, This Bulletin, **36**, 669 (1963).

7) H. Irving and H. S. Rossotti, *J. Chem. Soc.*, **1953**, 3397.

8) K. Nagano, H. Kinoshita, and Z. Tamura, *Chem. Pharm. Bull.* **11**, 999 (1963).

9), 10) The hydroxo complexes were not taken into consideration, because the equilibria were investigated between pH 2.5 and 5.0.

$$C = m\{1 + (D_1+D_2/[H^+])h + (D_3+D_4/[H^+] + D_5/[H^+]^2)h^2\}. \quad (9)$$

The elemination of h and m from three independent equations, (7), (8), and (9) will lead to one equation, into which the observed values of five points on the titration curves may be substituted; if the simultaneous equations are solved, all constants can, in principle, be obtained. However, their solution is, in practice, enormously troublesome. This difficulty was overcome by selecting suitable experimental conditions and by iterative approximation using the electronic computer.

1) *Metal-ion-excess Solution.* In this case, the concentration of the free neutral ligand, h, is very small, and only 1:1 species can be present. Equations. (7), (8), and (9) then become:

$$A = h\{a_0 + (D_1+D_2/[H^+])m\} \quad (10)$$

$$B = h(b_0+D_1m) \quad (11)$$

$$C = m\{1 + (D_1+D_2/[H^+])h\}. \quad (12)$$

The elimination of the h from (10) and (11) will lead to Eq. (13), $D_1=\{(b_0-ga_0)/m(g-1)\}-\{gD_2/[H^+](g-1)\}$. Assuming that m is approximately equal to the total metal concentration, and solving simultaneous equations from two points on the titration curve, a first approximation of D_1 and D_2 can be obtained; their temporary constants and m are then substituted into Eq. (10), from which a reasonable value of h is obtained. By the use of these h, D_1, and D_2 values, a more reasonable value of m can be calculated by Eq. (12). This value of m is substituted into Eq. (13), and more reasonable values of D_1 and D_2 are obtained by solving simultaneous equations from two points on the titration curve. This procedure is repeated until the values of these constants converge.

2) *Ligand-excess Solution.* Here, D_1 and D_2 have already been determined from the above solution. In this condition, three chelates, $M(HL)_2^{2+}$, $ML(HL)^+$, and ML_2, are present. The elimination of the m from Eqs. (7), (8), and (9) will lead to Eq. (14):

$$l_3D_3 + l_4D_4 + l_5D_5 = L \quad (14)$$

where;

$$l_3 = (Cf_3-Fh)h,$$
$$l_4 = (Cf_4-F[H^+]^{-1}h)h,$$
$$l_5 = (Cf_5-F[H^+]^{-2}h)h,$$
$$L = F\{1 + (D_1+D_2/[H^+])h\} - C(f_1D_1-f_2D_2),$$

$f_1 = (g-1)$, $f_2 = g[H^+]^{-1}$, $f_3 = 2f_1$, $f_4 = (2g-1)[H^+]^{-1}$, $f_5 = 2g[H^+]^{-2}$, $b_0 - ga_0 = F$.

As l_3, l_4, l_5, and L are entirely of known or measurable quantities, D_3, D_4, and D_5 can be obtained by solving simultaneous equations. For the treatment of Eq. (14), a matrix representation is extremely useful. The augmented matrix is:

$$\begin{bmatrix} l_{31} & l_{41} & l_{51} & L_1 \\ l_{32} & l_{42} & l_{52} & L_2 \\ l_{33} & l_{43} & l_{53} & L_3 \end{bmatrix} \quad (15)$$

which is solved by the method of Gauss-Jordan.

Results and Discussion

Acid-dissociation Constants. The acid-dissociation constants of protonated *o*-phenylenediamine derivative were calculated from the titration curve; they are summarized in Table 1. An example of the titration curve is given in Fig. 1. The first step of the acid dissociation of protonated *o*-phenylenediamine derivatives is very

Table 1. Acid dissociation constants of protonated *o*-phenylenediamine derivatives

Ligand	pK_{a1}	pK_{a2}	pK_{a3}	σ_m [a)]	σ_p [a)]	$\sigma_m+\sigma_p$
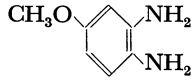	*	5.10		+0.115	−0.268	−0.153
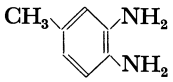	*	4.79		−0.069	−0.170	−0.239
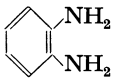	*	4.63		0.000	0.000	0.000
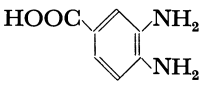	*	3.69	4.75	−0.45	−0.37	+0.82
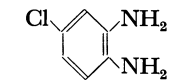	(0.6)	3.94		+0.373	+0.227	+0.600
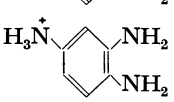	(1.2)	3.20	5.95	+0.63	+0.56	+1.19
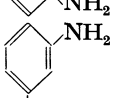	2.40	4.89				
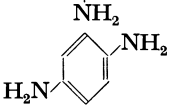	2.87	6.06				

* not measurable owing to very strong acid

a) H.H. Jaffé, *Chem. Rev.*, **53**, 191 (1953).

strong. This may be attributed to the steric hindrance. When the substituent group is a chloride or amino group, the pK_{a1} values of these derivatives can be calculated by the iterative approximation method; the pK_{a1} values are (0.6) and (1.2) respectively. The introduction of a chlorine atom to *o*-phenylenediamine decreases the value of pK_{a2}; the same effect is observed in carboxyl and amino groups. The relation between the pK_{a2} and the σ_p values shows a good linearity, but the σ_m values do not show such a good linearity. It is implied that the para-position effect, that is, the mesomeric effect, is the main factor rather than the inductive effect (the meta-position effect). The second dissociation of 3,4-diaminobenzoic acid is due to one of the diammonium protons, while the third dissociation is due to the carboxyl proton, because the pK_a (4.75) is comparable with those of 3-aminobenzoic acid (4.79) and 4-aminobenzoic acid (4.92). Table 2 shows the pK_a values for amino-substituted benzoic acids.

Table 2. Value of pK_a for amino-substituted benzoic acids in water[12]

X	*ortho*	*meta*	*para*
(H)	(4.20)	(4.20)	(4.20)
NH_2	4.98	4.79	4.92
NHMe	5.33	5.10	5.04
NMe_2	8.42	5.10	5.03
NH_3^+	2.04	—	—

The pK_a values of *o*-phenylenediamine derivatives with CH_3, H, Cl, or CH_3O as a substituent group at the 4 position, are 4—5. The second dissociation of 1,2,4-triaminobenzene trihydrochloride is depressed to an order of magnitude of 3 by the electron-withdrawing effect of the NH_3^+ group.

Stability Constants. The formation curve was obtained by titration. The values of $\bar{n}$ near the center of the formation curve ($0.9<\bar{n}<1.1$) are omitted, because they are very sensitive to slight experimental errors. Selected values of $\bar{n}$ and [L] were used to calculate the overall chelate stability constants, β_1 and β_2, by the use of the method of least squares on a linear form of the Irving and Rossotti equation. The theoretical formation curve is generated by the stability constants reported in Table 3. As can be seen from Fig. 2, the theoretical formation curve was in good agreement with the experimental one.

When 3,4-diaminobenzoic acid system is treated, the relationship between the equilibrium constants and $\log D_i$ ($i=1,2,\cdots,5$) is as follows:

$$\log K_{M1} = \log D_1,\ pk_1 = \log D_1 - \log D_2,\ \log K_{ML} = pK_{a3} + \log D_2,\ pk_2 = \log D_3 - \log D_4,\ \log K_{M2} = \log D_3 - \log D_1,$$
$$pk_2' = \log D_4 - \log D_5,\ \log K_{ML_2} = 2pK_{a3} + \log D_5.$$

The pK_{a3} value of the 3,4-diaminobenzoic acid was 4.75; however, the acid-dissociation constant (pK_{a1}) of the Cu(II) chelate was 3.84. The depression of the pK_a value is 0.91 (=4.75−3.84). The pK_a values of benzoic acid and *p*-nitro-benzoic acid are 4.18 and 3.43 respectively.[11] Therefore, the *p*-nitro group has

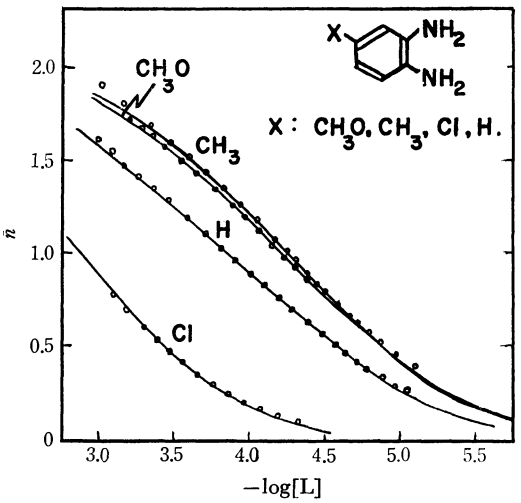

Fig. 2. Experimental and theoretical formation curve, at 25°C and $\mu=0.10$.
—, Theoretical; ○, Experimental

Table 3. Stability constants of Cu (II) complexes with *o*-phenylenediamine derivatives

Ligand	$\log K_1$	$\log K_2$	$\log K_1K_2$
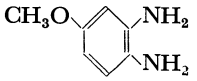	4.78	3.64	8.42
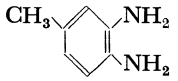	4.74	3.76	8.50
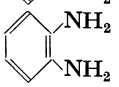	4.55	3.17	7.72
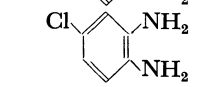	3.32	2.44	5.76

an electron-withdrawing effect of 0.75 pK_a units. The Cu(II) ion has a stronger electron-withdrawing effect than does the *p*-nitro group. The introduction of substituent groups in the 4 position of *o*-phenylenediamine leads to marked changes in the log β_2 value, changes which clearly reveal two effects (inductive and meso-

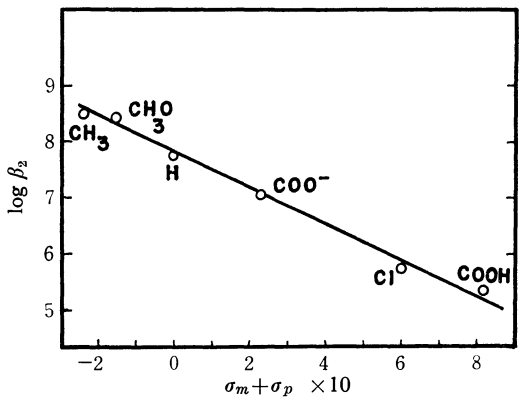

Fig. 3. Relationship between log β_2 and the sum of Hammett's sigma values.

11) A. Albert and E. P. Serjeant, "Ionization Constants of Acids and Bases," Methuen, London (Japanese Edition, Maruzen) (1962), P. 121.

12) S. Patai, "The Chemistry of the Amino Group," John Wiley and Sons, London (1968), p. 224.

meric). The plot of log β_2 against the sum of σ_m and σ_p was found to be linear. As can be seen from Fig. 3, the sums of the Hammett's σ_m and σ_p values of the COOH group and the COO^- group are 0.82 and 0.23 respectively. The difference in value between the COOH and COO^- groups is 0.59; that is, the electron-withdrawing effect is decreased after the dissociation, and as a result log β_2 is increased 0.71 units. When the ligand is 1,2,4-triaminobenzene, some converged values were obtained from the metal-ion-excess condition, but different behavior was observed in the ligand-excess condition; therefore, calculation became very difficult. In the reaction between *o*-phenylenediamine and other divalent ions (Mn, Co, Ni, Zn, *etc.*), the pH effect was very small; therefore, their stability constants may be lower.

The authers are grateful to Dr. G. Nakayama (Tokyo Chemical Industry Co.) for a gift of 1,2,4-triamino-benzene dihydrochloride.

BULLETIN OF THE CHEMICAL SOCIETY OF JAPAN, VOL. 44, 1293—1296(1971)

Electron-Transfer Reactions of Multidentate Ligand Cobalt(III) Complexes. I. The Reductions of Some Chloro(triethylenetetramine)cobalt(III) Complexes by Iron(II)

Yoshimi KURIMURA, Kousaburo OHASHI,* Toshio OHTSUKI,* and Katsumi YAMAMOTO*

College of General Education, Ibaraki University, Mito

**Department of Chemistry, Ibaraki University, Mito*

(Received May 27, 1970)

The kinetics of Fe^{2+} reductions of *cis*-α-Co(trien)Cl_2^+, *cis*-α-Co(trien)OH_2Cl^{2+} and *cis*-β_1-Co(trien)OH_2Cl^{2+} (trien=triethylenetetramine) have been studied at 25°C, $[H^+]=0.10$ M and $\sum[ClO_4^-]=1.0$ M. The second-order rate constants obtained are 4.0×10^{-4} M^{-1} sec^{-1}, 1.6×10^{-4} $M^{-1}sec^{-1}$, and 9.8×10^{-5} M^{-1} sec^{-1} for *cis*-α-Co(trien)Cl^{+2}, *cis*-α-Co(trien)OH_2Cl^{2+}, and *cis*-β_1-Co(trien)OH_2Cl^{2+} respectively. It is demonstrated, by comparing with other rate data for the Fe^{2+} reductions of *cis*-CoN_4XCl^{n+} (N=NH_3, 0.5 en and 0.25 trien, and X=H_2O and Cl^-) that the rate decreases with an increase in the number of chelate rings in the Co(III) complexes. The chelate effect of the nonbridging ligand on the electron-transfer reactions of Co(III) complexes is discussed on the basis of a model which involves the ligand-field strength of the *trans*-ligand to the bridging one, the energy needed for stretching the *trans*-group away from the Co(III) center, and the effect of the solvation.

The iron(II) reductions of $Co(en)_2XY^{n+}$ [1,2] and $Co(NH_3)_4XCl^{n+}$ [3] and electron-transfer reactions between aquochromium(II) ion and chromium(III) complexes[4-10] have been studied in order to investigate the effect of the nonbridging ligand on the rate of electron-transfer reactions. The effect of the nonbridging ligand on the electron-transfer reactions of $Co(en)_2XY^{n+}$ can be classified in the following three categories[2]: i) the effect of the geometry, ii) the effect of changing the nature of one nonbridging ligand, and iii) the effect of chelation. The investigation was also carried out on the effect of chelation by nonbridging ligands on the reductions of aquo-, sulfato- and chlorocobalt(III) complexes by chromium(II) and vanadium(II).[11,12] Fraser[12] introduced the solvation theory to explain the results obtained by these reactions. However, it has since been suggested that the results for the reactions of *cis*- and *trans*-$Co(en)_2XCl^{n+}$ complexes with iron(II) did not conform to this solvation treatment of the chelation effect.[2]

The present authors wish now to report the effects encountered in the reductions of some Co(trien)XCl^{n+} complexes by iron(II).

Experimental

Preparation of Complexes. The *trans*-[Co(trien)Cl_2]Cl, *cis*-α-[Co(trien)Cl_2]Cl, and *cis*-β-[Co(trien)Cl_2]Cl were prepared in a manner previously described.[13] The identity and purity of the complexes were confirmed analytically and spectrophotometrically.

Materials. A solution of iron(II) perchlorate was prepared by dissolving analytical-grade iron wire in an excess of perchloric acid. The concentration of the iron(II) was determined by titration with a standared potassium permanganate solution. The iron(III) concentration was calculated

1) C. Bifano and R. G. Linck, *J. Amer. Chem. Soc.*, **89**, 3945 (1967).
2) P. Benson and A. Haim, *ibid.*, **87**, 3826 (1965).
3) R. G. Linck, *Inorg. Chem.*, **7**, 2394 (1968).
4) A. Haim and N. Sutin, *J. Amer. Chem. Soc.*, **88**, 434 (1966).
5) J. H. Espenson and D. W. Carlyle, *Inorg. Chem.*, **5**, 1887 (1966).
6) D. E. Pennington and A. Haim, *ibid.*, **5**, 1887 (1966).
7) J. H. Espenson and B. G. Slocum, *ibid.*, **6**, 906 (1967).
8) A. Adin, J. Dole, and A. G. Sykes, *J. Chem. Soc., A*, **1967**, 1504.
9) J. M. DeChant and J. B. Hunt, *J. Amer. Chem. Soc.*, **89**, 5988 (1967).
10) D. E. Pennington and A. Haim. *Inorg. Chem.*, **6**, 2138 (1967).
11) R. T. M. Fraser, *Proc. Chem. Soc.*, **1963**, 262.
12) R. T. M. Fraser, *Inorg. Chem.*, **2**, 954 (1963).
13) a) A. M. Sargeson and G. H. Seale, *ibid.*, **6**, 787 (1967). b) D. A. Buckingham, P. A. Mazill, and A. M. Sargeson, *ibid.*, **6**, 1032 (1967).

from the difference in the amonts of the total iron and that of the iron(II) found. In all cases, the amounts of iron(III) were less than 5% of the total iron. The perchlorate concentration was analyzed by the titration of the hydrogen-ion concentration when an aliquot of the iron(II) solution was passed through a column of cation-exchange resin in the hydrogen form. The hydrogen-ion concentration of the iron(II) solution was calculated from the concentrations of perchlorate, ion(II), and iron(III). In most cases, the hydrogen-ion and perchlorate concentrations of the iron(II) solution were adjusted to 0.20 M and 2.0 M respectively by the addition of perchloric acid and sodium perchlorate solutions. All the other chemicals were of a reagent grade.

Kinetic Measurements. Erlenmeyer flasks containing the iron(II) solution, redistilled water, and weighed amounts of the solid complex respectively were kept in a thermostat. A 5-m*l* portions of the water was pipeted into the flask, and, after the complete dissolution of the complex had been achieved, 5-m*l* of the iron(II) solution were added by means of an injection syringe. Then, this solution was rapidly transferred into a spectrophotometer cell of a Hitachi Model 125 spectrophotometer. The reaction rate was measured at a sufficiently high concentration of iron(II) in order to minimize the complications arising from aquation.

Reductions of cis-α-*Co(trien)*Cl_2^+ *and* cis-α-*Co(trien)* OH_2Cl^{2+}. The aquation processes and the rate constants for the aquation reactions of the Co(III) complexes under investigation have been given by Sergeson and Searle.[14,15] The rate constant for the aquation of the first chloride ion in *cis*-α-RCl_2^+, where R represents $Co(trien)^{3+}$, is 9.4×10^{-3} min^{-1} at 25°C. Since *cis*-α-ROH_2Cl^{2+} is formed in a 100% retention by aquation of the *cis*-α-RCl_2^+ and since the rate of aquation of the second chloride ion in the *cis*-α-ROH_2Cl^{2+} is very slow,[2] a kinetic scheme for the iron(II) reductions of *cis*-α-RCl_2^+ and *cis*-α-ROH_2Cl^{2+} is given by:

$$\begin{array}{ccc} cis\text{-}\alpha\text{-}RCl_2^+ & \xrightarrow{k_{a_1}} & cis\text{-}\alpha\text{-}ROH_2Cl^{2+} \\ k_1 \downarrow \ Fe^{2+} & & k_2 \downarrow \ Fe^{2+} \\ Co(II) + Fe(III) & & Co(II) + Fe(III) \end{array}$$

The rate constant of k_{a1} is known, and the two rate constants to be determined are k_1 and k_2. Since the rate of the aquation of *cis*-α-RCl_2^+ is relatively large as compared with the reduction rates of *cis*-α-RCl_2^+ and *cis*-α-ROH_2Cl^{2+} even at high iron(II) concentrations, k_1 and k_2 were determined in a manner similar to that used by Benson and Haim.[2] The absorbance of the reaction mixture was measured at 525 nm, which is the isosbestic point for *cis*-α-RCl_2^+ and *cis*-α-ROH_2Cl^{2+}, as a function of the time. Then, values of $\log(A_t-A_\infty)$, where A_t is the absorbance at time t, and A_∞, the absorbance after all the Co(III) complex has been reduced to Co(II), were plotted as a function of the time. One of the plots is illustrated in Fig. 1. After a certain period of time, the plots conformed to linearity; the slope of the linear portion gives a measure of the pseudo-fist-order rate constant for the disappearance of *cis*-α-ROH_2Cl^{2+}. The linear behavior begins when the *cis*-α-RCl_2^+ has been exhausted and the only Co(III) species present in an appreciable concentration is *cis*-α-ROH_2Cl^{2+}. The linear portion of the $\log(A_t-A_\infty)$ *vs.* t plot gives a slope which is equal to $-k_2[Fe^{2+}]/2.303$. When A_c is defined as the value of A_t obtained by extrapolating the linear portion of the $\log(A_t-A_\infty)$ *vs.* t plot to zero time, the plot of $\log(A_t-A_c)$ *vs.* t gives a slope which is equal to $-\{k_{a1}+k_1[Fe^{2+}]\}/2.303$.

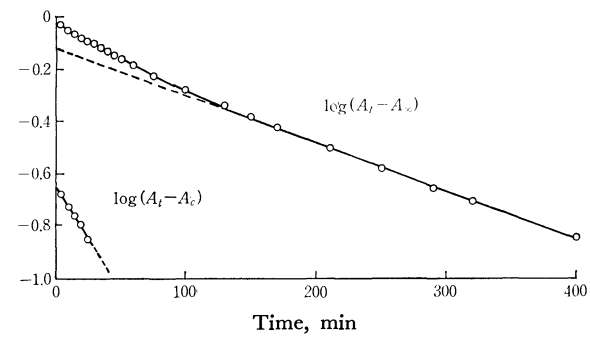

Fig. 1. Plots of log (A_t-A_∞) *vs.* time and log (A_t-A_c) *vs.* time for iron(II) reduction of *cis*-α-$Co(trien)Cl_2^+$.
8.28×10^{-3} M *cis*-α-$[Co(trien)Cl_2]Cl$, 0.415 M Fe^{2+}, $[H^+]=0.10$ M, $\sum(ClO_4^-)=1.0$ M, 525 nm, 25°C.

The values of k_1 and k_2 were calculated from the known values of k_{a1}, $[Fe^{2+}]$, and the slope.

Reduction of cis-β_1-*Co(trien)*OH_2Cl^{2+}. Our attempt to determine the rate constant for the ion(II) reduction of *cis*-β-RCl_2^+ by this method failed because of the fast aquation ($k=8.7\times10^{-2}$ min^{-1} at 25°C)[14] of this complex. Since the aquation of the *cis*-β-RCl_2^+ gives two different species of the mono-aquo complexes (94% of *cis*-β_1-ROH_2Cl^{2+} and 4% of *cis*-β_2-ROH_2Cl^{2+}),[14] the rate constants for the iron(II) reductions of these complexes could not be determined separately either by the method in which *cis*-β-RCl_2^+ was used as a starting material. A rapid first aquation of *trans*-RCl_2^+ ($k=21.1\times10^{-2}$ min^{-1} at 25°C)[14] gives only *cis*-β_1-ROH_2Cl^{2+}, and the rate of aquaion of the latter species is relatively slow ($k=1.40\times10^{-3}$ min^{-1} at 25°C).[14] The *trans*-species is almost completely converted into the *cis*-β_1-species about 30 min after the dissolution of the *trans*-species at 25°C, and the min after the dissolution of the *trans*-species at 25°C, and the aquation of the second chloride ion of the *cis*-β_1-species produced in the aquation reaction can be neglected within this period. Therefore, the determination of the rate constant for *cis*-β_1-ROH_2Cl^{2+} could be achieved by adding the iron(II) solution to that of *cis*-β_1-ROH_2Cl^{2+} which had been prepared by keeping the pure *trans*-RCl_2^+ solution in a thermostat for 30 min at 25°C. The kinetic scheme for the iron(II) reduction of *cis*-β_1-ROH_2Cl^{2+} is given as follows:

$$\begin{array}{ccccc} trans\text{-}RCl_2^+ & \xrightarrow{25°C,\ 30\ min} & cis\text{-}\beta_1\text{-}ROH_2Cl^{2+} & \xrightarrow{k_{a_2}} & cis\text{-}\beta\text{-}R(OH_2)_2^{3+} \\ & & k_3 \downarrow \ Fe^{2+} & & \\ & & Co(II) + Fe(III) & & \end{array}$$

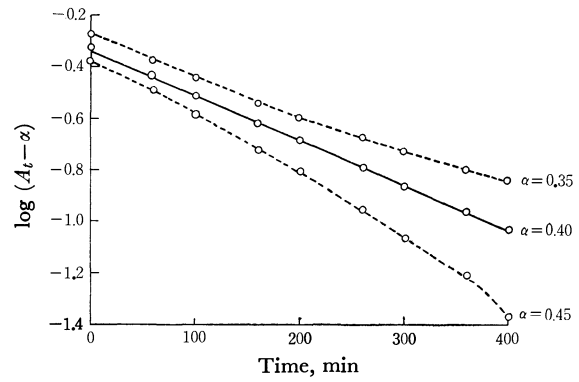

Fig. 2. Plots of log $(A_t-\alpha)$ *vs.* time for iron(II) reduction of *cis*-β_1-$Co(trien)OH_2Cl^{2+}$.
9.1×10^{-3}M *cis*-β_1-$[Co(trien)OH_2Cl]Cl_2$, 0.448M Fe^{2+}, $[H^+]=0.10$M, $\sum(ClO_4^-)=1.0$M, 488 nm, 25°C.

14) A. M. Sargeson and G. H. Searle, *Nature*, **200**, 356 (1963).
15) A. M. Sargeson and G. H. Searle, *Inorg. Chem.*, **6**, 2172 (1967).

As will be shown in the Appendix, the following equation can be derived when the width of the cell used is 1-cm:

$$A_t - \alpha = (E'_t - E')\{[ROH_2Cl]_0 - A\}e^{-Bt}$$

In this equation, the A_t is the absorbance of the reaction mixture at the isosbestic point (488 nm) for the ROH_2Cl^{2+} and $R(OH_2)_2^{3+}$, and E_t' and E' are the molar extinction coefficients of these species, and that of aquo-cobalt(II) ion at this wavelength, respectively. The A, B, and α are obtained by means of the equations shown in the Appendix. Since the value of α was unknown, the value of k_3 was determined as follows: as may be seen in Fig. 2, a straight line is obtained by adjusting the α value so that a plot of the $\log(A_t - A_\infty)$ *vs.* t becomes linear. Since the linear plot gives a slope which is equal to $-(ka_2 + k_3[Fe^{2+}])/2.303$, k_3 can be obtained from the known values of k_{a_2} and $[Fe^{2+}]$.

Results and Discussion

Since $CoCl^{2+}$ [16] and, probably, $Co(en)_2XCl^{n+}$ (X= H_2O and Cl^-)[2] react with Fe^{2+} *via* the chloride-bridged activated complex, it is reasonable to assume a similar mechanism for our reactions.

Table 1. Rate constants[a] for reductions of $RXCl^{n+}$ by Fe(II) (R=Co (trien), X=H_2O and Cl^-)

Complex	Rate constant ($M^{-1}sec^{-1}$)
cis-α-RCl_2^+	4.0×10^{-4}
cis-α-ROH_2Cl^{2+}	1.6×10^{-4}
cis-β_1-ROH_2Cl^{2+} [b]	9.8×10^{-5}

a) At 25° C, $\sum(ClO_4^-)=1.0$ M, $[H^+]=0.10$ M
b) Starting material is *trans*-RCl_2^+.

The values of the measured second-order rate constants and the specific rates of *cis*-CoN_4XCl^{n+} with Fe^{2+} are represented in Tables 1 and 2 respectively. The relatively low reduction rate of the $CoN_4OH_2Cl^{2+}$ as compared with that of the corresponding $CoN_4Cl_2^+$ may be mainly due to its dipositive charge.

In the *cis*-$CoN_4Cl_2^+$ system, the order of effectiveness is $Co(en)_2Cl_2^+ > Co(trien)Cl_2^+$, while in the *cis*-$CoN_4OH_2Cl^{2+}$ system it is $Co(NH_3)_4OH_2Cl^{2+} > Co(en)_2OH_2Cl^{2+} > \alpha$-$Co(trien)OH_2Cl^{2+} > \beta_1$-$Co(trien)OH_2Cl^{2+}$. The configurations of the *cis*-α- and *cis*-β_1-ROH_2Cl^{2+} have been determined by Sergeson *et al.*[13,14] As the rate constants for the *cis*-α- and *cis*-β_1-ROH_2Cl^{2+} are in the same order, the rate seems not to be strinkingly affected by their configurations with respect to the ligand of trien.

Table 2. Rate constants for Fe^{2+} reductions of *cis*-$CoN_4Cl_2^+$ and *cis*-$CoN_4OH_2Cl^{2+}$ (N=NH_3, 0.5 en and 0.25 trien)

Complex	Rate constant[a]	R_{NH3}[b]	R_{en}[c]
$Co(en)_2Cl_2^+$	16[e]		1
$Co(trien)Cl_2^+$	4.0		0.25
$Co(NH_3)_4OH_2Cl^{2+}$	353[d]	1	
$Co(en)_2OH_2Cl^{2+}$	4.5[e]	0.013	
α-$Co(trien)OH_2Cl^{2+}$	1.6	0.0045	
β_1-$Co(trien)\ OH_2Cl^{2+}$	0.98	0.0028	

a) At 25° C, $\sum(ClO_4^-)=1.0$ M, $[H^+]=0.10$ M, units are 10^{-4} M^{-1} sec^{-1}.
b) Ratio of rate constant to the rate constant for $Co(NH_3)_4OH_2Cl^{2+}$.
c) Ratio of rate constant to the rate constant for $Co(en)_2Cl_2^+$.
d) From Ref. 3.
e) From Ref. 2.

The results indicate that the relative effectiveness is decreased with an increase in the number of the chelate ring, so the trend in the rate can be ascribed to the chelate effect of the nonbridging ligand on the electron-transfer reactions. Orgel[17] and Taube[18] suggested that electron-transfer to the unoccupied d_{z^2} orbital on the Co(III) will take place more rapidly the lower the energy of the d_{z^2} orbital. The orbital energy would be lower by: (i) a *trans*-ligand to the bridgnig one with a weak ligand field,[2,17,18] and (ii) the removal of the *trans*-ligand in the z direction away from the Co(III) center.[2]

The rate of the Cr^{2+} reductions of $CoN_5SO_4^+$ (N_5= $(NH_3)_5$, $(en)_2NH_3$, and tetren[19]) is rather decreased with an increase in the number of the chelate ring in the Co(III) complexes, whereas the rate is hardly affected by an increase in the number of the chelate ring in the Cr^{2+} reductions of CoN_5OAc^{2+} and perhaps CoN_5Cl^{2+}.[12] Fraser explained these results on the basis of solvation. Such a solvation effect is now represented by the effect (c).

The effects of the ligand-field strength of the *trans*-ligand (represented by the effect (a)) and the energy for the bond stretching in the Co–N bond in the z direction (represented by the effect (b)) appear to be of little importance in such reaction as the Cr^{2+} reductions of *cis*- and *trans*-$Co(en)_2NH_3Z^{2+}$ (Z=Cl^- and OH^-),[19] nor as has been described above, in the Cr^{2+} reductions of CoN_5Cl^{2+}, CoN_5OAc^{2+}, and, possibly, $CoN_5SO_4^+$.[12] This may be ascribed to the fact that the relative bond-stretching energies in the Co-N bonds in such reactions as CoN_5Cl^{2+}, CoN_5OAc^{2+}, and $CoN_5SO_4^+$ with Cr^{2+}

Table 3. Analysis of chelate effect in electron-transfer reactions

Type of reaction	Example	$\Delta F_s/\Delta F^{\neq}$	Effects[c,d] a	b	c	Effects of chelation[b]
A	$Cr^{2+}-CoN_5Cl^{2+}$ [a]	small	−	−	−	−
	$Cr^{2+}-CoN_5OAc^{2+}$ [a]		−	−	−	−
	$Cr^{2+}-CoN_5SO_4^+$ [a]		−	−	+	+
B	$Fe^{2+}-CoN_4Cl_2^+$ [b]	large	+	+	+	+
	$Fe^{2+}-CoN_4OH_2Cl^{2+}$ [b]		+	+	−	+

a) $N_5=(NH_3)_5$, $(en)_2$ NH_3, and tetren.
b) N=NH_3, 0.5 en and 0.25 trien.
c) + indicates that effect is relatively large, −, effect is negligible small.
d) a, b, and c indicate that the effect of ligand field strength of the *trans*-ligand, effect of removal of the *trans*-ligand away from the Co(III) center and effect of solvation, respectively.

16) T. J. Concochioli, G. Nancollas, and N. Sutin, *J. Amer. Chem. Soc.*, **86**, 1453 (1953).
17) L. Orgel, Report of the Tenth Solvay Conference, Brussels, 289 (1956).
18) H. Taube, *Adv. Inorg. Chem. Radiochem.*, **1**, 1 (1959).
19) tetren=tetraethylenepentamine.

(type-A reactions) would be small compared with those in such reactions as the Fe^{2+} reductions of *cis*-CoN_4XCl^{n+} (type-B reactions). In fact, it was demonstrated by Green *et al.*[20] that there is little stretching of the Co-N bonds in the reactions of *cis*- and *trans*-$Co(en)_2NH_3Z^{2+}$ complexes with Cr^{2+}. The relative bond-stretching energy mentioned above is defined as: $\Delta F_s/\Delta F^*$ where ΔF_s is a free-energy change to stretch the Co-N bond in the z direction away from the Co(III) center prior to the transfer of an electron.

An analysis of the chelate effect on the electron-transfer reactions of the CoN_5X^{n+} and CoN_4XCl^{n+} complexes is shown in Table 3. In the Fe^{2+} reductions of *cis*-$CoN_4OH_2Cl^{2+}$, where the relative bond-stretching energy would be important and where the effect of solvation energy may be less important since the resulting cobalt(II) and iron(III) in the reactions have over-all charges of +2, there should be no change in the ΔF^* as the chelation is increased;[12] the results obtained can be explained mainly by the (a) and (b) effects. Since the order of the increasing ligand-field strength may be: $NH_3 <$ en $<$ trien and that of the increasing energy for the removal of the *trans*-ligand seems to be: $NH_3 <$en $<$ trien, it is expected that the relative rate will decrease with an increase in the number of the chelate ring in the Fe^{2+} reductions of CoN_4XCl^{n+}. It is considered that the energy required to stretch the metal-ligand bond along the z axis in the *cis*-CoN_4XCl^{n+} is increased as the stability of the complex increases, though the approximation is poor because of the lack of information about the force constants for the Co-N bonds discussed.

Appendix

The kinetic scheme for the Fe^{2+} reductions of *cis*-β_1-ROH_2Cl^{2+} is:[21]

$$ROH_2Cl + Fe^{2+} \xrightarrow{k_3} Co(II) + Fe(III) \quad (1)$$

$$ROH_2Cl + H_2O \xrightarrow{k_{a_1}} R(OH_2)_2 + Cl^- \quad (2)$$

The integrated rate equations for reactions (1) and 2) are:

$$[ROH_2Cl]_t = [ROH_2Cl]_0 e^{-Bt} \quad (3)$$

$$[R(OH_2)_2] = A - Ae^{-Bt} \quad (4)$$

where:

$$A = \frac{k_{a_1}[ROH_2Cl]_0}{k_{a_1} + k_3[Fe^{2+}]}$$

$$B = k_{a_1} + k_3[Fe^{2+}]$$

By stoichiometric considerations, the absorbance at the isosbestic point of ROH_2Cl and $R(OH_2)_2$ at time t is found to be:

$$A_t = E_t'[ROH_2Cl]_t + E_t'[R(OH_2)_2]_t + E'[Co(II)]_t$$

where E_t' is the molar extinction coefficient for ROH_2Cl and $R(OH_2)_2$ at the isosbestic point and where E' is the molar extinction coefficient for the Co(II) ion.

Since

$$[Co(II)]_t = [ROH_2Cl]_0 - [ROH_2Cl]_t - [R(OH_2)_2]_t$$

$$A_t = E'[ROH_2Cl]_0 + (E_t' - E')\{[ROH_2Cl]_t + [R(OH_2)_2]_t\} \quad (5)$$

from Eqs. (3), (4), and (5), we obtain:

$$A_t - \alpha = (E_t' - E')\{[ROH_2Cl]_0 - A\}e^{-Bt}$$

where:

$$\alpha = E'[ROH_2Cl]_0 + (E_t' - E')A$$

A part of this research was carried out with a Scientific Research Grant from the Ministry of Education, to which the authors thanks are due.

20) M. Green, K. Schung, and H. Taube, *Inorg. Chem.*, **4**, 1184 (1956).

21) The charges of the Co(III) complexes in the following equations are omitted for the sake of simplicity.

The Thermodynamic Properties of the Nonstoichiometric Ceric Oxide at Temperatures from 900 to 1300°C

Bunji IWASAKI* and Takashi KATSURA

Department of Chemistry, Tokyo Institute of Technology, Ookayama, Meguro-ku, Tokyo

(Received October 8 ,1970)

Oxygen partial pressure in equilibrium with nonstoichiometric ceric oxide of a definite composition were determined by equilibration with pure oxygen, air, CO_2, and CO_2-H_2 mixtures at 900, 1000, 1100, 1227, and 1300°C, using a thermobalance. The values for the activities and the relative partial enthalpies and entropies of both Ce_2O_3 and CeO_2 were calculated on the basis of the relation between the P_{O_2} and its composition.

During the last 10 years, studies of nonstoichiometric ceric oxide have been made by many investigators, especially from a view to clarifying the behavior of the solid solution in the Ce_2O_3-CeO_2 system at high temperatures. Brauer *et al.*,[1] for example, determined oxygen-dissociation pressures in the Ce_2O_3-CeO_2 system at temperatures from 600 to 1050°C by a thermogravimetric technique and calculated the enthalpy of oxidation of Ce_2O_3 to CeO_2. Furthermore, Brauer and Gingerich[2] determined the phase relations in the same system at temperatures from 20 to 1000°C using a high-temperature X-ray diffractometer and constructed a phase diagram. Kuznetsov *et al.*[3] reported on oxygen-dissociation pressures in the same system at temperatures from 694 to 1010°C; their results were based on emf measurements. Bevan and Kordis[4] reported their results on the same system at temperatures from 636 to 1169°C; these results were based on thermogravimetry.

These investigations have indeed revealed the presence of an extensive solid solution with a definite structure of CeO_2, but it is still desirable to study in more detail the relationship between the composition and the oxygen partial pressure at which the composition is equilibrated, especially at temperatures above 1100°C, in order to determine the precise thermodynamic properties. It is also necessary to measure directly the actual oxygen partial pressure in the furnace instead of using the calculated oxygen partial pressure based on the thermochemical data.

The objectives of the present study are, therefore, to determined the oxygen partial pressure in equilibrium with the ceric oxide of a definite composition by means of a solid electrolyte cell and thermogravimetry at temperatures from 900 to 1300°C, and to present some thermodynamic properties of the present solid solution.

Experimental

The ceric oxide obtained from the Nichisan Rare Element Co., was 99.9% pure. The oxide sample was heated at 1200°C in the air for 2 hr to make a suitable pellet.

The details of the procedure have been described by Katsura and Muan,[5] Katsura and Kimura,[6] and Katsura and Hasegawa.[7] A brief description will suffice for the general procedure.

A thermobalance was used to measure the isothermal weight change of a pellet as a function of the oxygen partial pressure. A quenching method was also used to check the thermogravimetric result.

As a results of the preliminary work, it was found that the weight of a pellet remained constant over a range of oxygen partial pressures from 0.2 to 1 atm at all the temperatures used. In addition, the chemical analysis of the quenched samples obtained from this range of oxygen partial pressures always had the stoichiometric composition of $CeO_{2.00}$, as may be seen in Table 1. On the basis of these facts, we chose the $CeO_{2.000}$ prepared under an oxygen partial pressure of 0.2 or 1 atm as the reference-weight standard.

The desired partial pressures of oxygen were obtained by using pure oxygen, air, carbon dioxide, and CO_2-H_2 mixtures. The actual oxygen partial pressures in the CO_2 and CO_2-H_2 mixtures at 900 to 1227°C were measured by an improved solid electrolyte cell composed of $(ZrO_2)_{0.85}(CaO)_{0.15}$.[7] It had been found previously[7,8] that the actual oxygen partial pressures produced by the CO_2-H_2 mixtures at 1300°C agreed well with the values calculated on the basis of the thermochemical data within the limits of experimental error. Thus, the oxygen partial pressures in the mixtures at 1300°C were calculated from the data summarized by Elliott and Gleiser[9] and by Coughlin.[10]

The O/Ce ratio in the weight-standard material, $CeO_{2.000}$ was determined volumetrically by using the persulfate method.[11] The O/Ce ratios in samples quenched in various atmospheres were determined thermogravimetrically by a weight-gain method as follows: the samples of the inner parts obtained by being taking the outer parts out of the the quenched samples were heated at 1000°C for 2 hr in the air until complete oxidation to $CeO_{2.000}$ had been achieved. The weight-gain corresponds to the increase in oxygen content in the quenched samples.

The phase present in the inner parts of the quenched samples were identified by an X-ray diffraction method using CuKα.

The rate of approach to the equilibrium state was studied thermogravimetrically. To ensure the equilibrium, the

* Present address: Research Institute of Underground Resources, Akita University, Akita.

1) G. Brauer, K. A. Gingerich, and U. Holtschmidt, *J. Inorg. Nucl. Chem.*, **16**, 77 (1960).
2) G. Brauer and K. A. Gingerich, *ibid.*, **16**, 87 (1960).
3) F. A. Kuznetsov, V. I. Belyi, and T. N. Rezukhina, *Dokl. Akad. Nauk SSSR*, **139**, 1405 (1961).
4) D. J. M. Bevan and J. Kordis, *J. Inorg. Nucl. Chem.*, **26**, 1509 (1964).
5) T. Katsura and A. Muan, *Trans. AIME.*, **230**, 77 (1964).
6) T. Katsura and S. Kimura, This Bulletin, **38**, 1664 (1965).
7) T. Katsura and M. Hasegawa, *ibid.*, **40**, 561 (1967).
8) M. Wakihara and T. Katsura, *Met. Trans.*, **1**, 363 (1970).
9) J. F. Elliott and M. Gleiser, "Thermochemistry for Steelmaking," Addison-Wesley Publ. Co., Reading, Mass. (1960).
10) J. P. Coughlin, *Bureau of Mines, Bull.* 542, U. S. A. (1954).
11) H. Willard and H. P. Young, *J. Amer. Chem. Soc.*, **50**, 1379 (1928).

Table 1. Comparisons of O/Ce ratios determined by various methods and of the phases present in the quenched samples

Temp., °C	$-\log P_{O_2}$	O/Ce by thermogravimetry	O/Ce by weight-gain method	phase present[a)]
1300±3	0	2.000±0.001	2.00 ±0.01[b)]	cubic
	9.03	1.901±0.001	1.926±0.002	cubic
	12.14	1.792±0.001	1.814±0.001	cubic
	15	1.697±0.001	1.722±0.002	cubic
1000±3	19.14±0.05	1.775±0.001	1.801±0.002	cubic
900±3	19.78±0.05	1.900±0.001	1.909±0.002	cubic+pseu.
	20.47±0.05	1.824±0.001	——	cubic+pseu.
	20.77±0.05	1.804±0.001	1.832±0.001	cubic+pseu.

a) Abbreviations used have the following meanings: cubic=cubic fluorite structure and pseu.=pseudo-cubic fluorite structure.
b) Obtained by volumetric analysis.

equilibrium composition was established from two courses, *i.e.*, the course from a reduced state to an oxidized, and the reverse course. It was found that, in general, the equlibrium was approached quickly, even in the slowest case, in which the time of equilibration was approximately 2 hr.

The weight-loss due to the vaporization of the nonstoichiometric ceric oxide could not be observed even in the case of the lowest oxygen partial pressure at 1300°C.

Results

Table 1 compares the O/Ce ratios determined by various methods and the phases present in the quenched samples, together with the maximum uncertainties in the measurements. As is shown in Table 1, the O/Ce ratios obtained by a weight-gain method are slightly larger than the thermogravimetric results. As an O/Ce ratio is found to become slightly larger with a falling temperature at a given ratio of CO_2 to H_2 in the atmosphere, and as the reaction rate is rapid, as has been described previously, these results obtained by a weight-gain method are considered to be due to oxidation during quenching. As may be seen in Table 1, the cubic form of the sample at 900°C could not be quenched to ice temperature without an exsolution of the pseudo-cubic form. Judging from the shape of the curve of the oxygen partial pressure against CeO_{2-x} at 900°C in Fig. 1, as will be seen later, and the phase diagram obtained by a high-temperature X-ray-diffraction method,[2)] the phase assemblages of the CeO_{2-x} obtained in the present study at all the temperatures used are considered to be a single solid solution.

Table 2 shows the experimental results obtained thermogravimetrically at various temperatures.

Table 2. Equilibrium oxygen partial pressures over the nonstoichiometric ceric oxide of a given composition at 900, 1000, 1100, 1227, and 1300°C

O/Ce	$-\log P_{O_2}$	O/Ce	$-\log P_{O_2}$	O/Ce	$-\log P_{O_2}$	O/Ce	$-\log P_{O_2}$	O/Ce	$-\log P_{O_2}$
900°C		1000°C		1100°C		1227°C		1300°C	
2.000	0.68	2.000	0.68	2.000	0	2.000	0	2.000	0
1.998	3.12	1.997	3.20	1.999	2.41	1.998	2.77	2.000	0.68
1.996	11.05	1.993	10.18	1.993	6.79	1.991	6.25	1.995	3.43
1.995	13.15	1.987	13.82	1.989	8.78	1.988	6.63	1.976	6.29
1.994	14.12	1.983	15.04	1.981	10.14	1.980	7.48	1.967	6.87
1.993	15.85	1.973	15.77	1.970	10.92	1.976	7.96	1.959	7.32
1.992	17.13	1.959	16.18	1.960	11.56	1.965	8.49	1.953	7.48
1.990	18.00	1.933	16.60	1.938	12.35	1.946	9.17	1.949	7.65
1.978	19.07	1.893	17.04	1.915	12.76	1.926	9.72	1.946	7.82
1.964	19.33	1.871	17.34	1.899	13.08	1.895	10.45	1.940	7.96
1.940	19.56	1.857	17.60	1.886	13.35	1.876	10.90	1.929	8.21
1.925	19.64	1.837	18.00	1.870	13.70	1.861	11.29	1.924	8.38
1.913	19.71	1.803	18.64	1.851	14.13	1.848	11.60	1.901	9.03
1.907	19.74	1.775	19.14	1.803	15.52	1.834	11.97	1.886	9.46
1.900	19.78			1.777	16.27	1.817	12.46	1.875	9.73
1.870	20.00					1.797	13.08	1.860	10.14
1.850	20.18					1.790	13.32	1.847	10.51
1.824	20.47					1.768	13.84	1.830	10.96
1.804	20.77					1.742	14.61	1.816	11.40
								1.792	12.14
								1.776	12.55
								1.769	12.70
								1.738	13.81
								1.727	14.13

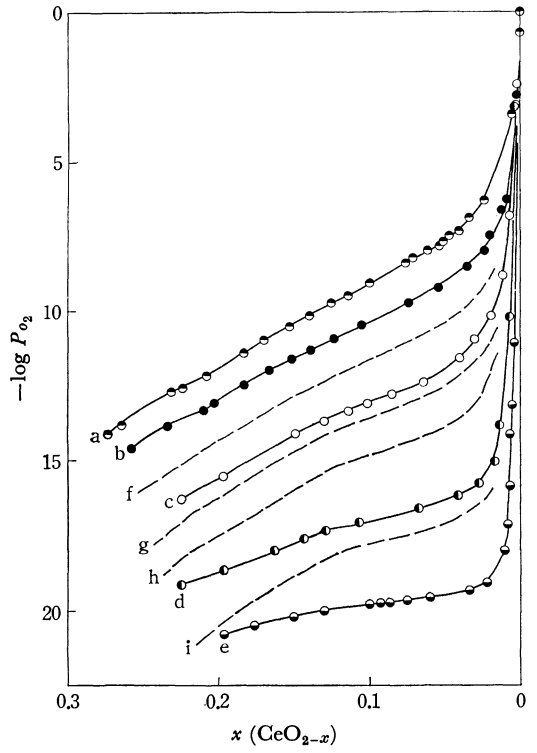

Fig. 1. $-\log P_{O_2}$ *vs.* x in CeO_{2-x} at each temperature.
—— This work; Temp.: (a) 1300°C, (b) 1227°C, (c) 1100°C, (d) 1000°C, (e) 900°C
—— Data of Bevan and Kordis: Temp.: (f) 1169°C, (g) 1080°C, (h) 1023°C, (i) 916°C

Discussion

Variation in the Composition of CeO^{2-x} with the Oxygen Partial Pressure. Figure 1 shows the variation in the composition of the nonstoichiometric ceric oxide with the oxygen partial pressures at various temperatures, together with the results of Bevan and Kordis.[4] These curves above 1100°C nearly agree with those of Bevan and Kordis[4] in shape, but the curves below 1000°C are inconsistent with each other, especially from 0.1 to about 0.2 of x. This might be largely the result of the oxygen partial pressure calculated in the study of Bevan and Kordis,[4] because, in the case of such a low temperature, the establishment of the equlibrium within the gas phase may be suspicious, even at a usual flow-rate of gases of, say, about 1 cm/sec. Therefore, the P_{O_2} must be actually measured by the solid electrolyte cell used in the present study. We will use the present results in respect to composition and P_{O_2} as the most reliable relation to calculate the thermodynamic properties of the Ce_2O_3-CeO_2 system, as will be seen later.

Activities of Ce_2O_3 and CeO_2 in Nonstoichiometric Ceric Oxide. To begin with, we assume that the nonstoichiometric ceric oxide is a mixture of two components, CeO_2 and O_2. The real composition of the CeO_2 phase is, however, CeO_{2-x}, and the reaction between these components may be written as follows;

$$CeO_2 = CeO_{2-x} + x/2O_2 \qquad (1)$$

Thus, from the Gibbs-Duhem Equation, the activity of CeO_2 in the solution may be related as follows;

$$\log a_{CeO_2} = \int_2^x (2-x)\mathrm{d}\log P_{O_2}^{1/2} \qquad (2)$$

where x is related to Eq. (1). The activity of CeO_2 is planimetrically measured by the integration of Eq. (2) from the stoichiometric composition to that under consideration.

Next, we may take the present solid solution as a homogeneous mixture of two components, CeO_2 and Ce_2O_3. Since the activity of CeO_2 has already been determined as a function of P_{O_2}, the activity of the other component, Ce_2O_3, may be determined directly. However, the α-function method[12] is more reliable

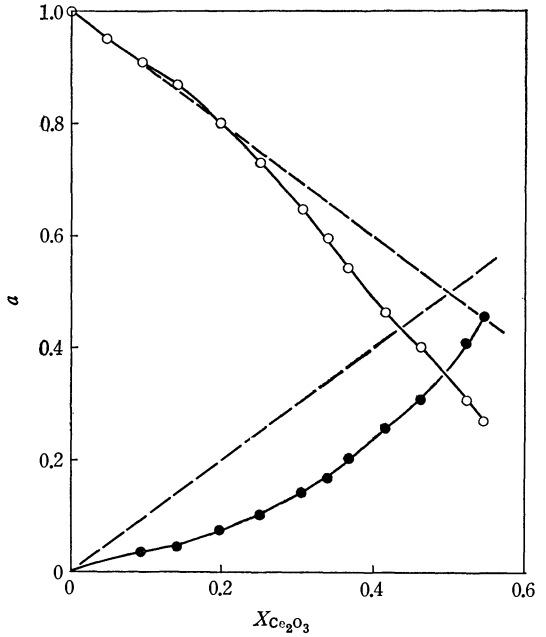

Fig. 2. Activity *vs.* mol fraction at 1300°C.
—— ● $a_{Ce_2O_3}$, ○ a_{CeO_2}, —— Raoult's law

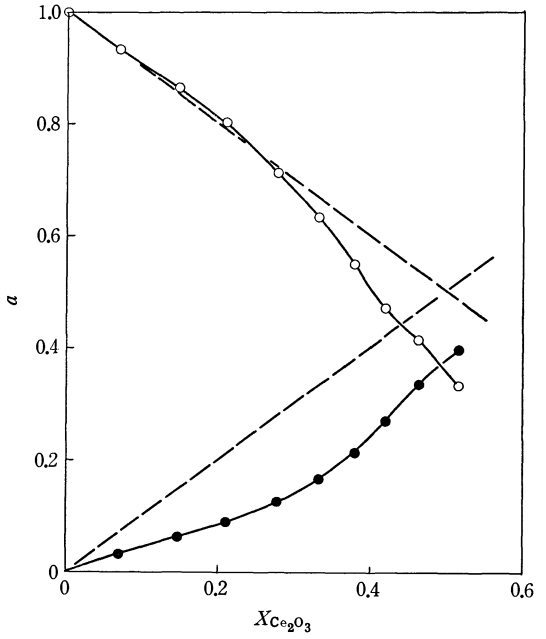

Fig. 3. Activity *vs.* mol fraction at 1227°C.
—— ● $a_{Ce_2O_3}$, ○ a_{CeO_2}, —— Raoult's law

12) L. S. Darken and R. W. Gurry, "Physical Chemistry of Metals," McGraw-Hill Book Co., New York, N. Y. (1953), p. 264.

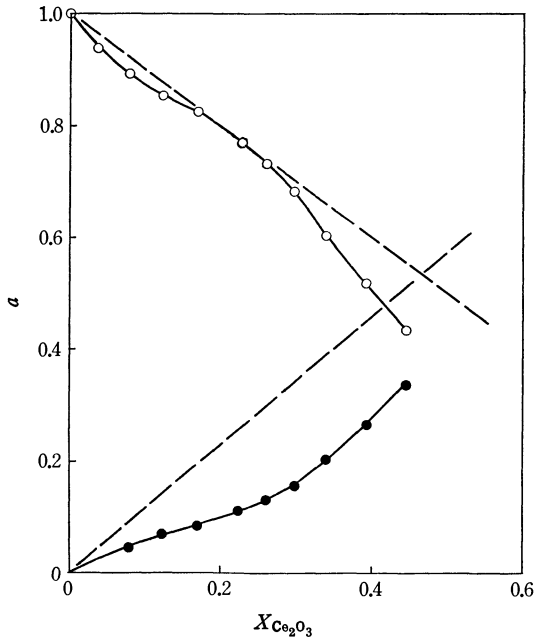

Fig. 4. Activity *vs.* mol fraction at 1100°C.
—— ● $a_{Ce_2O_3}$, ○ a_{CeO_2}, —— Raoult's law

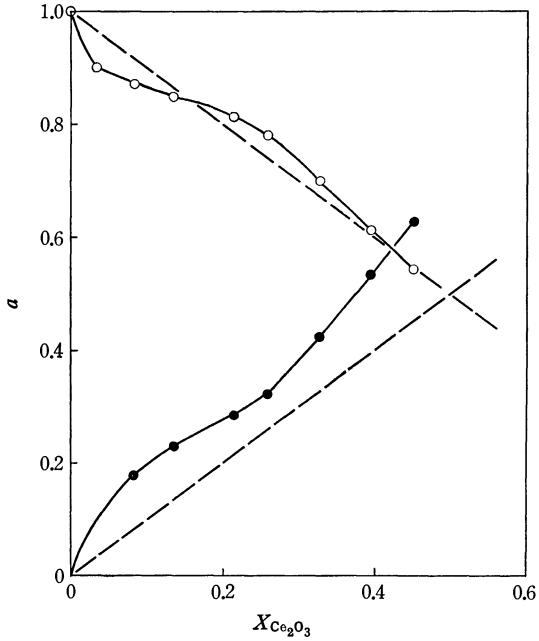

Fig. 5. Activity *vs.* mol fraction at 1000°C.
—— ● $a_{Ce_2O_3}$, ○ a_{CeO_2}, —— Raoult's law

for graphic integration, and here we may adopt the equation proposed by Wagner,[13] which may, in order to calculate the activity of Ce_2O_3, be written as follows;

$$\log a_{Ce_2O_3} = \int_0^Y \frac{\log a_{CeO_2}}{(1-Y)^2} dY - \frac{Y}{1-Y} \log a_{CeO_2} \qquad (3)$$

where Y is the mol fraction of CeO_2 in the binary system.

The first term on the right side of Eq. (3) is obtained by integration from the stoichiometric composition of Ce_2O_3 to that under consideration. The value of $(\log a_{CeO_2})/(1-Y)^2$ at the stoichiometric composition of Ce_2O_3

13) C. Wagner, "Thermodynamics of Alloys," Addison-Wesley Publ. Co., Reading, Mass. (1952), p. 16.

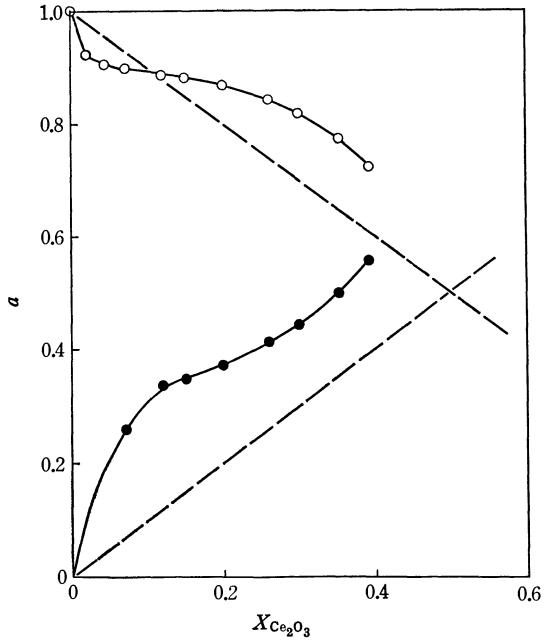

Fig. 6. Activity *vs.* mol fraction at 900°C.
—— ● $a_{Ce_2O_3}$, ○ a_{CeO_2}, —— Raoult's law

is an extrapolated value.

The activity relations thus obtained at various temperatures are illustrated in Figs. 2—6, together with the lines giving the behavior of an ideal solution. It is clear from these figures that the activity of CeO_2 obeys Raoult's law up to a 0.2 mol fraction of Ce_2O_3 at temperatures above 1200°C, but at 1000 and 900°C the activity of CeO_2 changes in a singular manner and

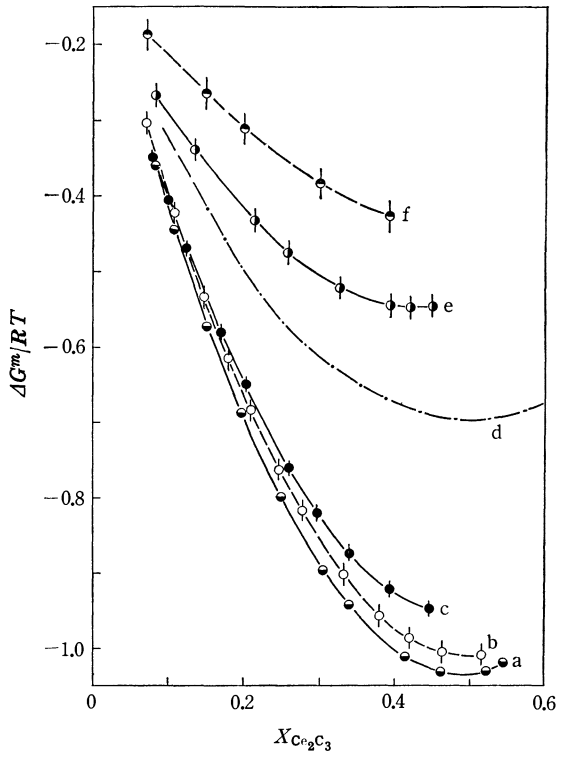

Fig. 7. $\Delta G^m/RT$ *vs.* mol fraction at each temperature.
Temp.: (a) 1300°C, (b) 1227°C, (c) 1100°C, (d) $\Delta G^m/RT$ of an ideal solution, (e) 1000°C, (f) 900°C

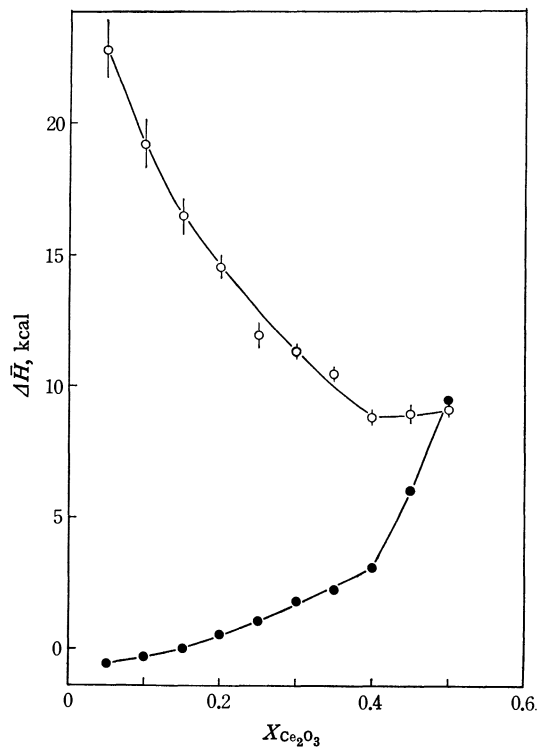

Fig. 8. Relative partial molal enthalpy *vs.* mol fraction.
● $\Delta\bar{H}_{Ce_2O_3}$, ○ $\Delta\bar{H}_{CeO_2}$

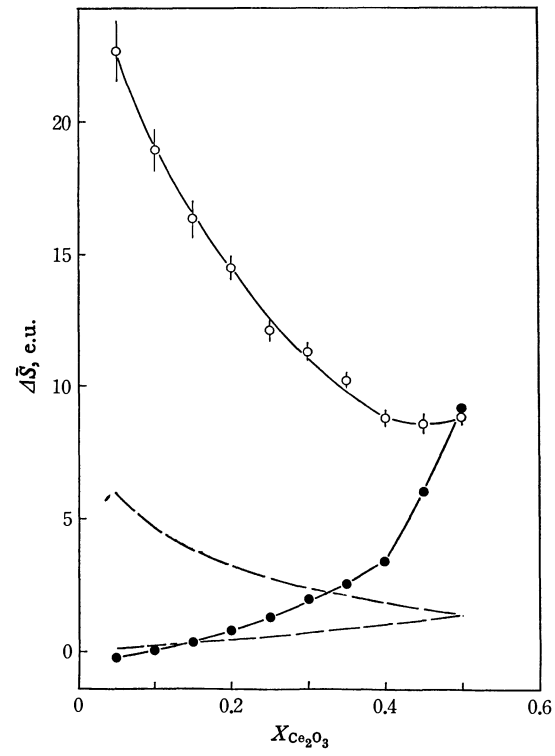

Fig. 9. Relative partial molal entropy *vs.* mol fraction.
—— ● $\Delta\bar{S}_{Ce_2O_3}$, ○ $\Delta\bar{S}_{CeO_2}$
—— Relative partial molal entropy of a regular solution

obeys Raoult's law only in a narrowly limited range of mol fractions of Ce_2O_3. The a_{CeO_2}-$X_{Ce_2O_3}$ relation at 1100°C seems to be intermediate between those obtained at higher and lower temperatures. Thus, the Ce_2O_3-CeO_2 solid solution will continuously change in its thermodynamic properties with a decrease in the temperature. However, the change in the same relation is very rapid at temperatures between 1000 and 1100°C compared with that at other intervals of temperature.

The activity of Ce_2O_3 reflects the behavior of the activity of CeO_2 at each temperature; it seems to obey Henry's law up to a 0.2 mol fraction of Ce_2O_3 above 1100°C.

Variation in the Free Energy of Mixing with the Temperature. In order to avoid a direct temperature effect, $\Delta G^m/\boldsymbol{R}T$ was selected instead of the total free energy of mixing ΔG^m, where $\boldsymbol{R}$ is gas constant and T is the absolute temperature. Figure 7 shows the variation in $\Delta G^m/\boldsymbol{R}T$ with the mol fraction of Ce_2O_3 at various temperatures, together with the curve showing the $\Delta G^m/\boldsymbol{R}T$ of an ideal solution. The widths of the lines in Fig. 7 show the experimental errors.

As is shown in Fig. 7, these curves move upward with a fall in the temperature. Considered this fact and the activity relations shown in Figs. 2—6, this tendency seems to show a tendency toward the immiscibility of the solid solution. This inference is consistent with the fact that a miscibility-gap appears about 685°C at a composition of $CeO_{1.92}$.[2)]

As is shown in Fig. 7, these curves above 1100°C deviate negatively from the curve giving the ideal behavior. According to a quasi-chemical approach,[14)] this indicates an attractive interaction of the same atom. Thus, this may be assumed to be due to a tendency toward ordering or clustering in which cerium ions in normal sites enter interstitial sites.

Relative Partial Enthalpy and Entropy of Mixing. The relative partial enthalpies and entropies of the mixing of CeO_2 and Ce_2O_3 obtained by means of the mean least-squares method from the activity relations are shown in Figs. 8 and 9 respectively. The widths of the lines how the experimental errors. Curves showing the relative partial entropy of a regular solution are also included in Fig. 9.

As is shown in Fig. 9, these observed curves are similar in shape to those of a regular solution, but deviate too much from those of a regular solution.

The minimum of the curves of CeO_2 in Figs. 8 and 9 may be assumed to be due to a tendency toward compound formation.

Dr. Iwaji Iwasaki, Professor of chemistry, Toho University, encouraged us throughout the present study.

14) R. A. Swalin, "Thermodynamics of Solids," John Wiley & Sons, New York, N. Y. (1962), p. 109.

The pH Dependence of Anion Exchange Chromatographic Separation of Tri- and Tetraphosphate Anions

Terumasa NAKAMURA, Mitsuyasu KIMURA,* Hirohiko WAKI, and Shigeru OHASHI

Department of Chemistry, Faculty of Science, Kyushu University, Hakozaki, Fukuoka

(Received October 9, 1970)

The anion-exchange distribution ratios of tri-, tetra-, and pentaphosphate were determined in a Dowex 1-X4-potassium chloride system at different pH by the batch method. The difference between the mean charges of the phosphates in resin phase and solution was explained in terms of a higher pH of resin phase than that of the solution. pH dependence of the separation factors for tri- and tetraphosphate and for tetra- and pentaphosphate was estimated from the batch equilibrium data, and the relative elution positions of these phosphates were confirmed by the practical chromatographic runs.

We employed gradient-elution chromatography with anion-exchange resins for the separation of a series of linear oligophosphates.[1,2] In the course of the experiments[1,2] we found that when ammonium acetate solutions with pH 7 or potassium chloride solutions with pH 8 are used as an eluent, a mixture of linear oligophosphates can be almost completely separated from one another, but the difference between the elution positions of tri- and tetraphosphate is remarkably smaller than that between the elution positions of other adjacent pairs. However, when the mixture is eluted with potassium chloride solutions with pH 9.3, separation of tri- and tetraphosphate does not occur. The same pH dependence of the elution positions of these two phosphates can be seen in the elution diagrams for a series of linear oligophosphates by Matsuhashi.[3]

The present investigation was undertaken to clarify the pH dependence of the anion-exchange chromatographic separation of tri- and tetraphosphate. The mean charges of these phosphates in a resin phase and in a solution at equilibrium are discussed.

Experimental

Batch Experiment. Resin: The anion-exchange resin Dowex 1-X4 (100—200 mesh) was conditioned to chloride form and dried at 60°C in a vacuum desiccator for 5 hr.

Preparation of Sample Solutions: Commercial pentasodium triphosphate hexahydrate was purified by recrystallization with ethyl alcohol, and dissolved in potassium chloride solutions of various concentrations and pH values. Chloride concentrations; 0.150, 0.200, 0.250, 0.300, and 0.350 M. pH 5.2; 0.001 M potassium hydrogen phthalate-dilute sodium hydroxide buffer. pH 7.1; 0.003 M sodium maleate-dilute acetic acid buffer. pH 9.5; 0.010 M ammonium chloride-dilute aqueous ammonia buffer. Solutions of tetra- and pentaphosphate were prepared from glassy sodium polyphosphate with an average degree of polymerization of 4.5 by means of the gradient-elution chromatographic method. Fractions of the effluent-containing tetra- or pentaphosphate were collected, and after addition of 1 g of dry Dowex 1-X4 the volume of this mixture was increased by a factor of more than 100 times with water so that the greater part of the phosphate anions was adsorbed in the resin phase. The resin was then separated from the solution and immersed in a concentrated potassium chloride solution for 1 hr. The phosphate anions adsorbed in the resin phase were thus recovered into the solution. From this solution, tetra- or pentaphosphate solutions of the different chloride concentrations and pH values were prepared.

Determination of Distribution Ratios: A weighed amount of dry Dowex 1-X4 (about 0.5 g) was put into a stoppered Erlenmeyer flask which contains 10 m*l* of a potassium chloride solution with a definite chloride concentration and pH. This was kept standing overnight, and after 5 m*l* of a linear oligophosphate solution of the corresponding chloride concentration and pH value was added, the mixture was shaken for 2 hr at 20°C.

The phosphorus content in the solution was determined colorimetrically with the molybdenum(V)-molybdenum(VI) reagent.[4] The distribution ratio D is defined by the equation

$$D = \frac{\text{millimoles of phosphorus per m}l\text{ resin bed}}{\text{millimoles of phosphorus per m}l\text{ solution}} \quad (1)$$

Gradient-Elution Chromatography. Glassy Sodium Polyphosphate: Glassy sodium polyphosphate with an average degree of polymerization of 4.5 was prepared by quenching the melt of a mixture of sodium dihydrogen orthophosphate dihydrate and disodium hydrogen orthophosphate dodecahydrate with a molar ratio of 5 to 4 after complete dehydration and condensation.

Chromatographic Run: An aliquot of a solution containing 1 mg of sodium dihydrogen orthophosphate dihydrate and 50 mg of the glassy sodium polyphosphate was loaded on a column of Dowex 1-X4 (100—200 mesh, ϕ 1.24×66.5 cm) and eluted with potassium chloride solution by means of gradient-elution technique. The initial chloride concentration of the eluent in a mixing bottle and the chloride concentration of the eluent in a reservoir were 0.209 and 0.468 M, respectively. The pH of the eluents was adjusted to 4.5 with 0.001 M potassium hydrogen phthalate and dilute sodium hydroxide solution or to 3.0 with 0.001 M potassium hydrogen phthalate and dilute hydrochloric acid. The volume of the eluent in the mixing bottle was kept to 1000 m*l*. Chromatographic runs were carried out with the flow rate of 36—45 m*l*/hr at 20°C. Effluents were collected into 9 m*l* fractions with an automatic fraction collector.

Determination of Phosphorus and Chloride Concentrations: Molybdenum(V)-molybdenum(VI) reagent was used for the determination of phosphorus contents. Determination of chloride

* Present address: Osaka Aerosol Industries Co., Yodomizu, Fushimi, Kyoto.

1) T. Nakamura, K. Ujimoto, N. Yoza, and S. Ohashi, *J. Inorg. Nucl. Chem.*, **32**, 3191 (1970).

2) S. Ohashi, N. Tsuji, Y. Ueno, M. Takeshita, and M. Muto, *J. Chromatogr.*, **50**, 349 (1970).

3) M. Matsuhashi, *J. Biochem.*, **44**, 65 (1957).

4) F. Lucena-Conde and L. Prat, *Anal. Chim. Acta*, **16**, 473 (1957).

concentrations was carried out by Mohr's method for the fractions containing no phosphate anions.

Results and Discussion

Koguchi *et al.*[5] reported that the mean charge of the phosphate species in a resin phase $\bar{i}_R$ is given by the following equation for the system of an anion-exchange resin and an ammonium acetate solution.

$$\partial \log D/\partial \log(AcO^-) = \bar{i}_R \quad (2)$$

This treatment is applicable to the system where potassium chloride is used in place of ammonium acetate as follows. The linear phosphate anion with a degree of polymerization of n, $H_{n+2-j}P_nO_{3n+1}^{j-}$, is abbreviated to $H_{a-j}P^{j-}$ or P^{j-}. The distribution ratio D and the dissociation constants in a resin phase and in a solution $\bar{K}_j$ and K_j are defined by the following equations for a given linear phosphate.

$$D = \sum[P^{j-}]/\sum(P^{j-}) = \{[P^0]+[P^-]+\cdots+[P^{j-}]+\cdots+[P^{a-}]\}/\{(P^0)+(P^-)+\cdots+(P^{j-})+\cdots+(P^{a-})\} \quad (3)$$

$$\bar{K}_j = [H^+]^j[P^{j-}]/[H_aP] \quad (4)$$

$$K_j = (H^+)^j(P^{j-})/(H_aP) \quad (5)$$

where the concentrations of ions in the resin phase and in the solution are distinguished by [ ] and ( ), respectively. Donnan's equilibrium gives the following equation for the pair of hydrogen and chloride ions.

$$[H^+]\cdot[Cl^-] = (H^+)\cdot(Cl^-)\cdot\gamma_{(H^+)}\cdot\gamma_{(Cl^-)}/\gamma_{[H^+]}\cdot\gamma_{[Cl^-]}$$

where γ's represent activity coefficients. The distribution coefficient of a non-ionized phosphate species between the resin phase and the solution are considered to be constant,

$$[P^0]/(P^0) = \gamma_{(P^0)}/\gamma_{[P^0]} = \text{constant} \quad (7)$$

From Eqs. (3), (4), and (5), we get

$$D = \{[P^0]/(P^0)\}\cdot\{1+\cdots+K_j/[H^+]^j+\cdots+K_a/[H^+]^a\}/\{1+\cdots+K_j/(H^+)^j+\cdots+K_a(H^+)^a\} \quad (8)$$

If a pH of the solution is kept constant,

$$\{[P^0]/(P^0)\}/\{1+\cdots+K_j/(H^+)^j+\cdots+K_a/(H^+)^a\} = K(\text{const.}) \quad (9)$$

From Eqs. (8) and (9), we get

$$\log D = \log K + \log(1+\cdots+\bar{K}_j/[H^+]^j+\cdots+\bar{K}_a/[H^+]^a) \quad (10)$$

In order to differentiate Eq. (8) with respect to $\log(Cl^-)$, the following relation is used.

$$\{\partial \log D/\partial \log(Cl^-)\}_{(H^+)=\text{const.}} = \left\{\frac{\partial \log D}{\partial[H^+]}\cdot\frac{\partial[H^+]}{\partial(Cl^-)}\cdot\frac{\partial(Cl^-)}{\partial \log(Cl^-)}\right\}_{(H^+)=\text{const.}} \quad (11)$$

The components of the right-hand side of Eq. (11) are expressed as follows.

$$\partial[H^+]/\partial(Cl^-) = \{(H^+)/[Cl^-]\}\cdot\gamma_{(H^+)}\gamma_{(Cl^-)}/\gamma_{[H^+]}\gamma_{[Cl^-]} \quad (12)$$

$$\partial \log D/\partial[H^+] = \{-\bar{K}_1/[H^+]^2-\cdots-j\bar{K}_j/[H^+]^{j+1}-\cdots-a\bar{K}_a/[H^+]^{a+1}\}/\{1+\bar{K}_1/[H^+]+\cdots+\bar{K}_j/[H^+]^j+\cdots+\bar{K}_a/[H^+]^a\} \quad (13)$$

$$\partial(Cl^-)/\partial \log(Cl^-) = (Cl^-) \quad (14)$$

Thus, Eq. (11) can be written as

$$\{\partial \log D/\partial \log(Cl^-)\}_{(H^+)=\text{const.}} = \{[P^-]+\cdots+j[P^{j-}]+\cdots+a[P^{a-}]\}/\{[P^0]+[P^-]+\cdots+[P^{j-}]+\cdots+[P^{a-}]\} = \sum j[P^{j-}]/\sum[P^{j-}] = \bar{i}_R \quad (15)$$

The distribution coefficient of a particular ionic species P^{j-}, f_j, is derived from Donnan's equilibrium for the pair of this ionic species and chloride ion:

$$f_j = [P^{j-}]/(P^{j-}) = \{[Cl^-]/(Cl^-)\}^j\cdot\gamma_{(P^{j-})}\gamma^j_{[Cl^-]}/\gamma_{[P^{j-}]}\gamma^j_{(Cl^-)} \quad (16)$$

Eq. (15) can then be transformed into the following equation.

$$\bar{i}_R = \{f_1(P^-)+\cdots+jf_j(P^{j-})+\cdots+af_a(P^{a-})\}/\{f_0(P^0)+f_1(P^-)+\cdots+f_j(P^{j-})+\cdots+f_a(P^{a-})\} = \sum jf_j(P^{j-})/\sum f_j(P^{j-}) \quad (17)$$

On the other hand, the mean charge of the phosphate species in the solution, $\bar{i}$, is given by

$$\bar{i} = \sum j(P^{j-})/\sum(P^{j-}) \quad (18)$$

The concentration of chloride ion in the resin phase is usually much greater than that in the solution, thus Eq. (16) gives

$$f_j \gg 1 \quad (19)$$

From Eqs. (17), (18), and (19), the following relation can be obtained.

$$\bar{i}_R \geqq \bar{i} \quad (20)$$

This relation can be understood from the fact that a weak acid such as phosphoric acids is much dissociated at a higher pH and that the hydrogen ion concentration in an anion-exchange resin phase is in general higher than that in a solution.

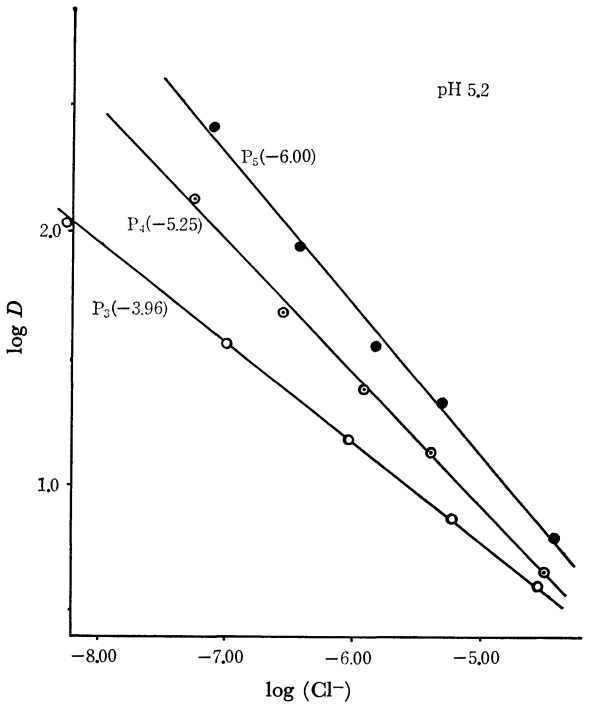

Fig. 1. $\log D$ *vs.* $\log(Cl^-)$ for tri-(P_3), tetra-(P_4) and penta-(P_5) phosphate at pH 5.2. The slope for each straight line is given in parentheses.

5) K. Koguchi, H. Waki, and S. Ohashi, *J. Chromatogr.*, **25**, 398 (1966).

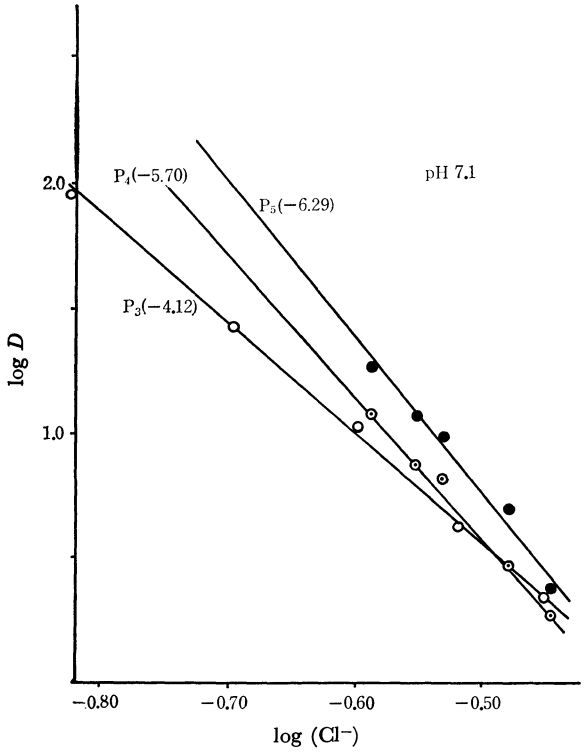

Fig. 2. log D *vs.* log(Cl⁻) for tri-, tetra-, and pentaphosphate at pH 7.1.

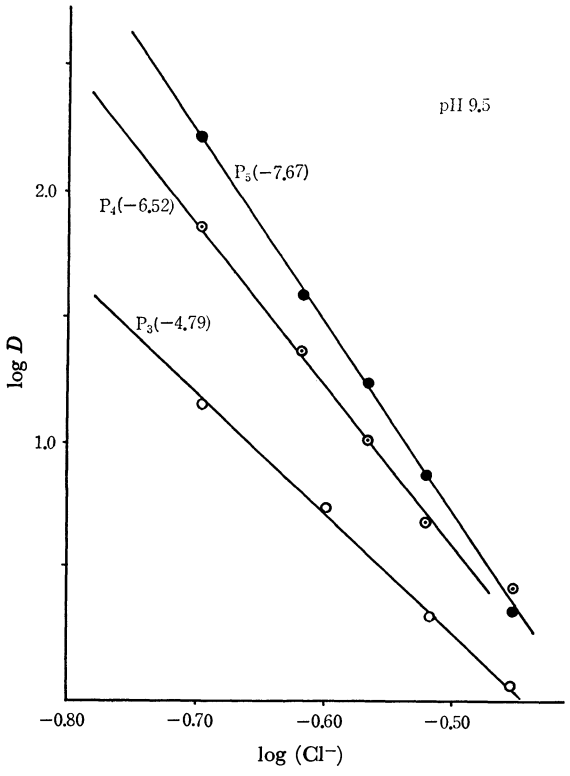

Fig. 3. log D *vs.* log (Cl⁻) for tri-, tetra-, and pentaphosphate at pH 9.5.

The relationship between the distribution ratio and the chloride ion concentration in the solution is given in Figs. 1, 2, and 3. From Eq. (15), the slope of each straight line gives the mean charge of each phosphate

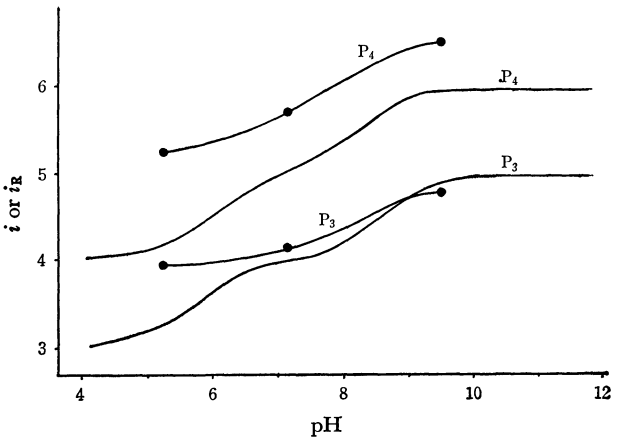

Fig. 4. Relationship between $\bar{i}$ or $\bar{i}_R$ and the pH values in solution.
——: calculated $\bar{i}$ values, ●—●: observed $\bar{i}_R$ values.

species in the resin phase at a given pH of the solution. In Fig. 4, the resulting mean charges are compared with the calculated mean charges in the solution for tri- and tetraphosphate. For these calculations the dissociation constants obtained by Irani and Callis[6] were employed. The relationship of Eq. (20) is confirmed by Fig. 4. Since in the higher pH region the fully dissociated phosphate species predominate in both phases, the decrease of the difference between $\bar{i}_R$ and $\bar{i}$ is expected from Eqs. (17) and (18). The difference still remaining will be attributed to the change of the activity coefficients.

The chromatographic separation of linear oligophosphates will be discussed in terms of a separation factor α_a^b which is defined by

$$\alpha_a^b = D_b/D_a \qquad (21)$$

where D_a and D_b represent the distribution ratios of phosphate species a and b, respectively. From the definition, α_3^4 and α_4^5 were calculated from the batch distribution ratios for the pairs of tri- and tetraphosphate

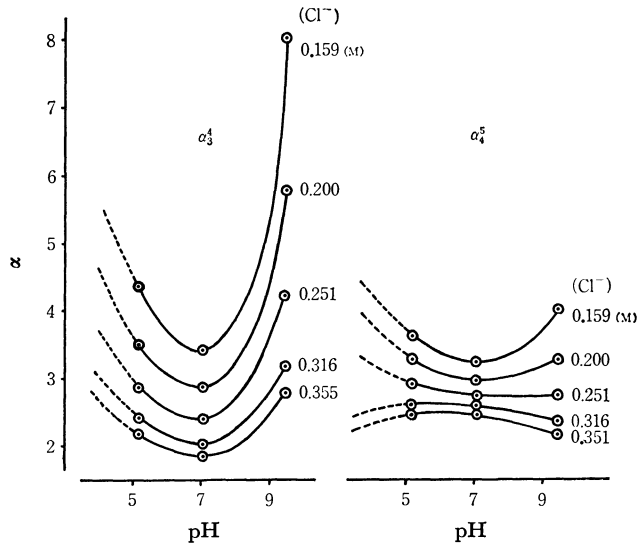

Fig. 5. The pH dependence of α_3^4 and α_4^5 at various chloride concentrations.

6) R. R. Irani and C. F. Callis, *J. Phys. Chem.*, **65**, 934 (1961).

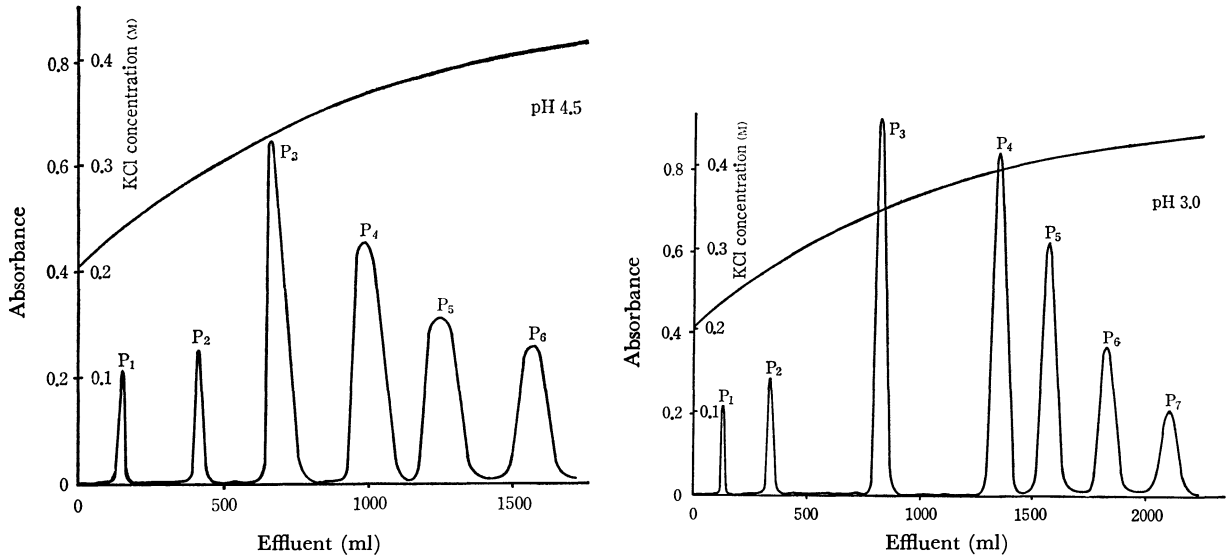

Fig. 6. Elution curves of linear oligophosphates at pH 4.5 and 3.0.

and of tetra- and pentaphosphate. The pH dependence of these separation factors is shown in Fig. 5. All the curves for α_3^4 give the minium values near pH 7 for all chloride concentrations. On the other hand, the curves for α_4^5 exhibit a tendency similar to those for α_3^4 at low chloride concentrations, but those at the high chloride concentrations seem to have maximum values. This suggests that the separation of tri- and tetraphosphate will be improved if the pH of eluent is kept apart from pH 7, but the separation of tetra- and pentaphosphate will not appreciably improved by changing the pH of eluent in the high chloride concentration region where these two phosphates are practically eluted out. This was confirmed by the chromatographic runs at different pH values of 4.5 and 3.0, which are shown in Fig. 6. The two elution diagrams indicate that the separability of tri- and tetraphosphate is improved by decreasing a pH, but not of tetra- and pentaphosphate.

BULLETIN OF THE CHEMICAL SOCIETY OF JAPAN, VOL. 44, 1305—1310(1971)

The Chemistry of Protactinium. IX. A Study of the Solvent Extraction of Protactinium(V) from a Perchloric Acid Solution Using Di(2-ethylhexyl)phosphoric Acid as the Extractant

Toshiaki MITSUGASHIRA

The Research Institute for Iron, Steel and Other Metals, Tohoku University, Katahira, Sendai

(Received November 5, 1970)

Studies of the chemical behavior of protactinium(V) in a perchloric acid solution were carried out by the HDEHP-benzene extraction method. When the protactinium concentration was lower than 10^{-7} M, the extraction reaction was considered to proceed as:

$$PaO(OH)^{2+}_{aq.} + 3(HA)_{2\ org.} = PaO_p(OH)_qA_{5-2p-q}(HA)_{2p+q+1\ org.} + 2H^+_{aq.} + (2-p-q)H_2O_{aq.}$$

where $p=1$, $q=0$ or 1, and $p=2$, $q=0$

and

$$Pa(OH)_3{}^{2+}_{aq.} + 3(HA)_{2\ org.} = PaO_p(OH)_qA_{5-2p-q}(HA)_{2p+q+1\ org.} + 2H^+_{aq.} + (3-p-q)H_2O_{aq.}$$

where $p=0$, q=0, 1, 2, or 3; p=1, $q=0$ or 1 and $p=2$, $q=0$.

It has been said that the aqueous solution of protactinium(V) is unstable because of its strong tendency to hydrolyze and to precipitate, even in a relatively strong acid solution. This tendency is especially noticeable in a perchloric acid solution, which is considered to be the most fundamental of the aqueous systems. Although many investigations have been carried out into the chemistry of protactinium(V) in a perchloric acid solution, the species present in this medium are far from having been established.

Suzuki and Inoue[1] reported that protactinium(V) in a perchloric acid solution existed in the forms of PaO-

1) S. Suzuki and Y. Inoue, This Bulletin, **39**, 1705 (1966).

$(OH)^{2+}$ or $Pa(OH)_3^{2+}$ and PaO^+_2, $PaO(OH)_2^+$ or $Pa(OH)_4^+$ when the concentration of protactinium(V) was lower than 10^{-6}M and the acidity was 0.3—2.0 M; they reached these conclutions by means of an investigation by the TTA-benzene extraction method, by the ion-exchange adsorption method, and by a filtration method using several kinds of filter paper and of membrane filter. They also observed that the distribution ratio (D) of protactinium (V) in the TTA-benzene extraction varied with the method of the preparation of the perchloric acid solution of protactinium, and pointed out that this fact was one of the reasons for the disagreement among the results obtained by various authers. This implies the necessity for a suitable choice of the experimental conditions if the thermodynamic treatment is to be made possible. Even when precautions were taken, the experimental error was too high for quantitative knowledge to be obtained.

Recently, solvent extraction studies using acidic organophosphoric esters have been successful. Among these esters di(2-ethylhexyl)phosphoric acid(HDEHP) is known to be effective for the separation of the lanthanides and of the actinides, particularly of the transplutonium elements, by means of extraction chromatography.[2-6] The acidic organophosphoric esters have greater acid dissociation constants than TTA.[7,8] HDEHP is considered to extract cations by a cation-exchange mechanism and thus is expected to have a selectivity in the solvent extraction according to the charge of the cation. Therefore, for a complete understanding of the chemical behavior of protactinium in the perchloric acid solution, it is worthwile to make a solvent-extraction study by using HDEHP as an extractant, for it has different characteristics than TTA.

Akatsu[9] pointed out, in her paper on the chemistry of neptunium, that protactinium(V) had a greater distribution ratio than neptunium(V) in a HDEHP-perchloric acid extraction system. She also emphasized the difference in the acid dependency of the distribution ratio between protactinium(V) and neptunium(V); *i.e.*, protactinium(V) showed an inversely second-power dependency, while neptunium(V) showed an inversely proportional dependency. However she did not say anything about the extraction mechanism of protactinium(V) nor the abnormal behavior of protactinium(V) in the perchloric acid solution pointed out by Suzuki and Inoue in their TTA-extraction studies. If her results indicate a special stability of the Pa(V)-HDEHP extraction system, we can except that remarkable progress in Pa(V)-solution chemistry can be attained by HDEHP-extraction study.

In this investigation, the author studied the HDEHP-extraction in order to clarify the chemical species of protactinium(V) in a perchloric acid solution.

Experimental

Reagents and Apparatus. *^{231}Pa and ^{233}Pa*: ^{231}Pa which had been obtained from The Radio-chemical Centre (Amersham, England) was purified by a method reported previously.[10] The radiochemical purity was certified by α-ray and γ-ray spectroscopy. The concentration of protactinium in the ^{231}Pa solution was determined by absolute α-ray counting and by gravimetry, using protactinium pentoxide as the weighing form. These two results agreed well within the limits of experimental error, so we can say that there was no contamination by non-radioactive impurities.

^{233}Pa was prepared by the method of Suzuki and Inoue.[10]

HDEHP and Other Reagents: Commercially-available HDEHP was purified by the method reported by Peppard *et al.*[11] In order to determine the purity of HDEHP, about a 0.1 N HDEHP-10% alcohol-benzene solution was titrated by a 0.1 N NaOH standard solution. The purity was at least 99.8%. Benzene was used as a diluent of HDEHP, which is dimeric in this solvent.[11] The benzene was purified by extracting thiophene by concentrated sulfuric acid, followed by distillation. The other reagents used in this experiment were of the highest purity.

Glass Apparatus: All of the glass apparatus, including pipettes, beakers, separatory funnels and flask, used in this experiment was preliminarily saturated with protactinium by being brought in contact with the perchloric acid solution of protactinium for a time sufficient for the saturation of the adsorption to be reached. The material balance held well under this treatment, except otherwise noted.

Procedures. *The Preparation of the Pa-perchloric Acid Solutions*: Appropriate amounts of the ^{231}Pa-stock solution and the ^{233} Pa-stock solution were placed in a platinum dish and evaporated to dryness. The residue was dissolved in concentrated perchloric acid. The solution was then diluted to 10^{-7}M with respect to protactinium with perchloric acid of a suitable concentration. In order to regulate the ionic strength (μ) of the solution, the lithium perchlorate solution, which has the same acidity as the Pa-perchloric acid solution under investigation, was added.

The Determination of the Distribution Ratio: Ten milliliters of a Pa-perchloric acid solution and 10 ml of a HDEHP-benzene solution were mixed in a separatory funnel for 15 min. After the two phases had completely separated, an aliquot of each phase was taken into a polyethylene test tube and the γ-radioactivity of ^{233}Pa was counted by means of a $1^1/_2''$ welltype NaI(Tl) scintillation counter. The distribution ratio was calculated by means of the usual relationship:

$$D = \frac{\gamma\text{-radioactivity per ml of the organic phase}}{\gamma\text{-radioactivity per ml of the aqueous phase}}$$

As a result of the preliminary experiment, it was established that the distribution ratio did not change even when the Pa-perchloric acid solution was left to stand for 1—7 days after its preparation. Thereafter, the distribution ratio gradually varied with time. This change reflects the change in the composition of the Pa-species in the perchloric acid solution. In this experiment, the solutions which were allowed to stand

2) J. W. Winchester, *J. Chromatogr.*, **10**, 502 (1963).
3) R. J. Sochacka and S. Siekierski, *ibid.*, **16**, 376 (1964).
4) S. Siekierski and R. J. Sochacka, *ibid.*, **16**, 385 (1964).
5) E. P. Hotwitz, C. A. A. Bloomquist, and D. J. Henderson, *J. Inorg. Nucl. Chem.*, **31**, 1149 (1969).
6) E. P. Horwitz, C. A. A. Bloomquist, D. J. Henderson, and D. E. Nelson, *ibid.*, **31**, 3255 (1969).
7) D. F. Peppard, D. W. Mason, and C. M. Anderjasich, *ibid.*, **27**, 697 (1965).
8) E. H. Cook and R. W. Taft, Jr., *J. Amer. Chem. Soc.*, **74**, 6103 (1952).
9) E. Akatsu, **JAERI 1099** (1965).
10) S. Suzuki and Y. Inoue, This Bulletin, **39**, 490 (1966).
11) D. F. Peppard, J. R. Ferraro, and G. W. Mason, *J. Inorg. Nucl. Chem.*, **7**, 231 (1958).

for 1—4 days were used, unless otherwise noted. Thus, the error in the distribution ratio was minimized to about 10% when the distribution ratio was nearly 1.0.

It was found that a 10 min shaking was sufficient to get a constant distribution ratio. The equilibrium in the aqueous phase which is established in a 10 min shaking, is called "rapid equilibrium" in the rest of this report.

The distribution ratio obtained from the backward extraction varied markedly with respect to the standing time of the Pa-HDEHP-benzene solution and did not show a constant value in any interval of the standing time. The distribution ratio obtained from the backward extraction was generally higher than that obtained from the forward extraction.

Thus, in this investigation one can not, contrary to expectations, make a quantitative discussion of the thermodynamic equilibrium of the protactinium in a perchloric acid solution but can merely get the extraction behavior of Pa-species which are in rapid equilibrium with the extractable species.

Results

The Relation between the Distribution Ratio and the Acidity. The influence of the acidity on the distribution ratio was investigated by means of the constant ionic strength of the aqueous phase, as is shown in Fig. 1.

One of the important results concerns the different acid dependency between the solutions with the inonic strengths of 2.5 and 1.5. In the former case, the log-log plot of D and the acidity shows a linear relation, with a slope of -2, if the acidity is higher than 0.7 M. In the latter case, however, the slope is about -1.2. When the acidity of the aqueous phase was very low, the material balance did not hold well because protactinium was adsorbed on the wall of the glass separatory funnel in every experiment, even though the vessels had first been saturated with protactinium from a perchloric acid solution of moderate acidity. This tendency was prominent at acidities lower than 0.5 M when the ionic strength was 2.5. When the ionic strength was 1.5, this tendency was even more pronounced, and, in addition, inextractable species were found. The percentage fraction of the total protactinium contributed by the inextractable species was greater than 30% when the acidity was between 0.15 M and 0.3 M. Therefore, Fomin's method was applied in order to obtain the true distribution ratio (D_t) of the extractable species.[12] The results are shown in Fig. 2. The maximum standard deviation of D_t amounted to about 50%. This large error seems to be caused by two independent factors: one is the scattering of data caused by the adsorption of protactinium on the wall of separatory funnel, and the other is the limitation in the application of the Fomin method. In spite of this difficulty, one can read from Fig. 2 that the log-log plot of D_t and the acidity shows a linear relation, with a slope of -2, similar to the case of the inoic strength of 2.5.

The Relation between the Distribution Ratio and the HDEHP Concentration. The relation between the distribution ratio and the HDEHP concentration was

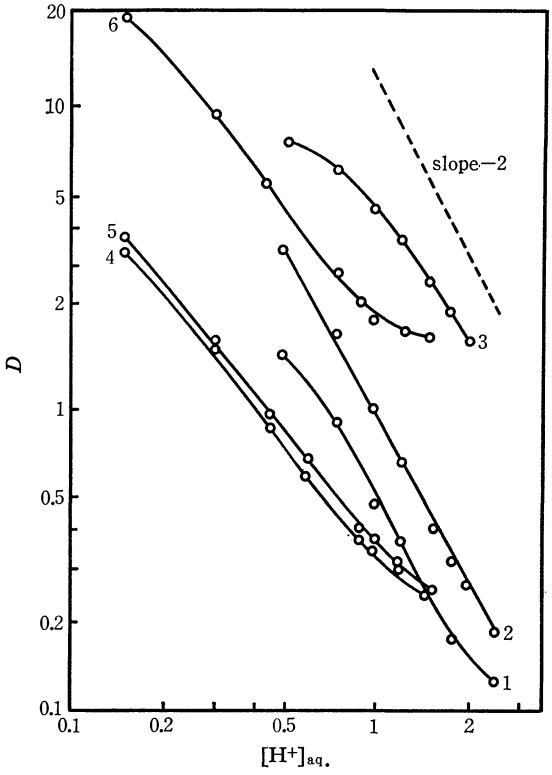

Fig. 1. The relation between the distribution ratio and the acidity.
1, $\mu=2.5$, $[(HA)_2]_{org.}=5\times10^{-2}$M, Standnig time is 10 hr
2, $\mu=2.5$, $[(HA)_2]_{org.}=5\times10^{-3}$M, Standing time is 3 days
3, $\mu=2.5$, $[(HA)_2]_{org.}=1\times10^{-2}$M, Standing time is 3 days
4, $\mu=1.5$, $[(HA)_2]_{org.}=5\times10^{-3}$M, Standing time is 1 day
5, $\mu=1.5$, $[(HA)_2]_{org.}=5\times10^{-3}$M, Standing time is 5 days
6, $\mu=1.5$, $[(HA)_2]_{org.}=1\times10^{-2}$M, Standing time is 5 days

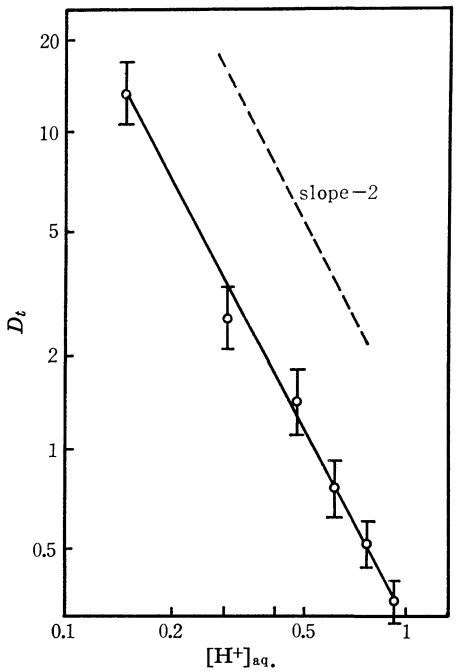

Fig. 2. The relation between the true distribution ratio obtained by the Fomin's method and the acidity.
$[(HA)_2]_{org.}=5\times10^{-3}$M, $\mu=1.5$

12) V. V. Fomin, E. P. Mairova, M. I. Krapivin, and V. G. Yudina, *Zh. Neorg. Khim.*, **3**, 2113 (1958).

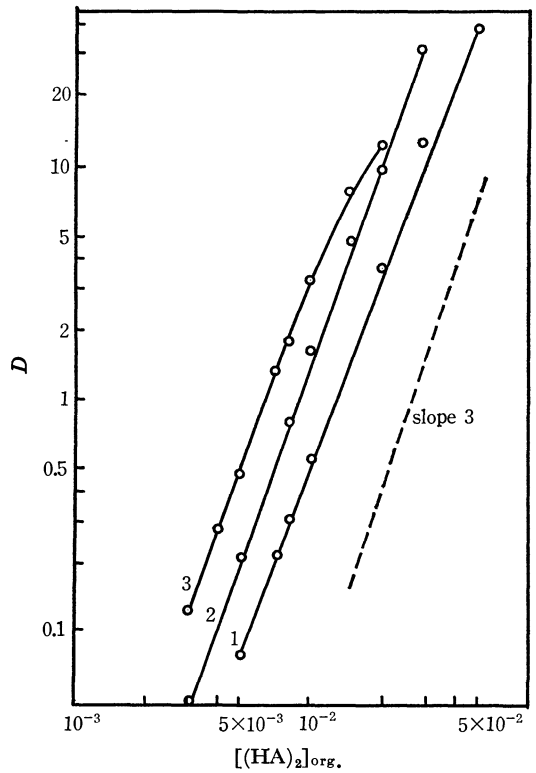

Fig. 3. The relation between the distribution ratio and the HDEHP concentration.
1, 2.32M $HClO_4$, 2, 1. 16M $HClO_4$, 3, 0. 58M $HClO_4$

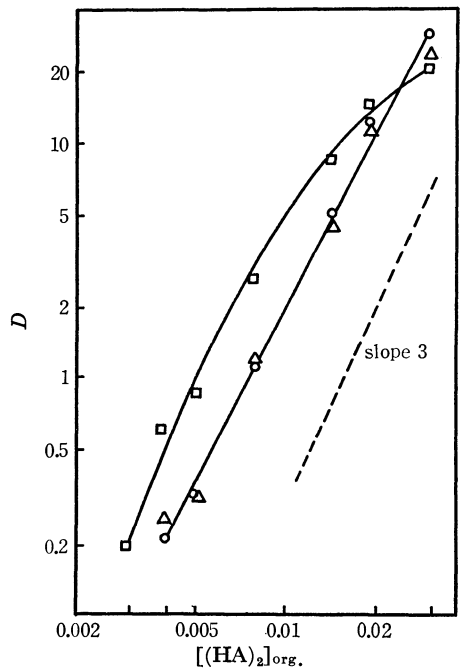

Fig. 4. The relation between the distribution ratio and the HDEHP concentration. The acidity of the aqueous phase was kept constant but the ionic strength was changed.
○ μ=1.3, *i. e.* no lithium perchlorate in the aqueous phase
△ μ=2.5, □ μ=4.8

also investigated; the results are shown in Figs. 3 and 4. Figure 3 was obtained from the solution without lithium perchlorate, and Fig. 4 was obtained from the solution of a constant acidity, but at various ionic strengths. The dotted line indicates the slope of +3. It is clear from these figures that the log-log plot of D and the concentration of the dimeric HDEHP shows a linear relation, with a slope of about 3.

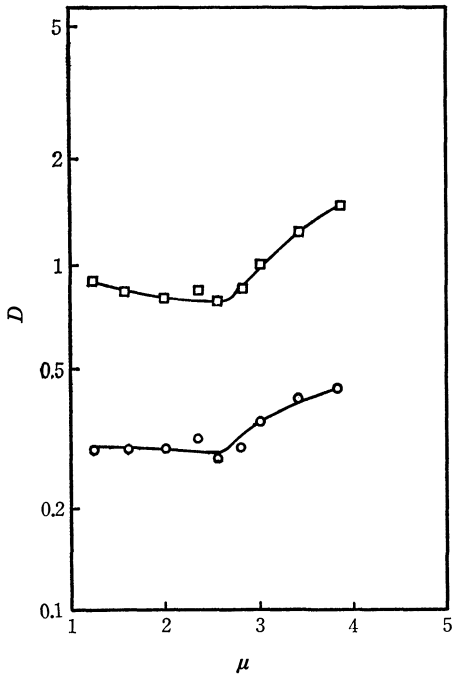

Fig. 5. The change of the distribution ratio by the change of the ionic strength of the aqueous phase.
○ org. phase, 5×10^{-3}M $(HA)_2$
□ org. phase, 7.5×10^{-3}M $(HA)_2$

The Relation between the Distribution Ratio and the Ionic Strength. The relation between the distribution ratio and the ionic strength is shown in Fig. 5. In this experiment the acidity was kept constant (1.3 M). When the ionic strength is not higher than 2.5, the distribution ratio does not vary when the ionic strength does. On the other hand, when the ionic strength is higher than 2.5, the distribution ratio increases with an increase in the ionic strength. This observation is consistent with the results shown in Fig. 4, where the values of the distribution ratio and its dependency on the HDEHP concentration are shown to be the same in the solutions having ionic strengths of both 1.5 and 2.5, but in the case of an ionic strength of 4.8 the values of the distribution ratio become larger and the linearity between the logarithm of the distribution ratio and the logarithm of the HDEHP concentration becomes poor.

Discussion

It is obvious from Figs. 1 through 4 that the distribution ratio is proportional to the cube of the HDEHP concentration and inversely proportional to the square of the acidity. If the species extractable into the organic phase are considered to have no charge, the general equation for the HDEHP extraction reaction can be written as:

$$PaO_m(OH)^{5-2m-n}_{n\,aq.} + k(HA)_{2\,org.} = PaO_p(OH)_qA_{5-2p-q}(HA)_{2k+2p+q-5\,org.} + (5-2m-n)H^+_{aq.} + (m+n-p-q)H_2O_{aq.} \quad (1)$$

where HA, $(HA)_2$, and A^- represent the HDEHP molecule, the dimeric HDEHP, and the dissociated HDEHP anion respectively. The distribution ratio is defined by the following relation (if one omits the designation of the phase for the sake of simplicity):

$$D = \frac{\sum_{p,q,k}[PaO_p(OH)_qA_{5-2p-q}(HA)_{2k+2p+q-5}]}{\sum_{m,n}[PaO_m(OH)_n{}^{5-2m-n}]} \quad (2)$$

where brackets show the activity of the enclosed species. The equilibrium constant is defined by the following relation:

$$K_{m,n,p,q,k} = \frac{[PaO_p(OH)_qA_{5-2p-q}(HA)_{2k+2p+q-5}][H^+]^{5-2m-n}[H_2O]^{m+n-p-q}}{[PaO_m(OH)_n{}^{5-2m-n}][(HA)_2]^k} \quad (3)$$

By taking the partial derivative of the logarithm of the distribution ratio with respect to the logarithm of $[(HA)_2]$ and of $[H^+]$, we obtain:

$$\frac{\partial \ln D}{\partial \ln [(HA)_2]} = \sum_{p,q,k} k f_{p,q,k} \quad (4)$$

and

$$\frac{\partial \ln D}{\partial \ln [H^+]} = -5 + \sum_{m,n} (2m+n) f_{m,n} \quad (5)$$

where $f_{p,q,k}$ is the fraction of the total activity of protactinium in the organic phase contributed by the $PaO_p(OH)_qA_{5-2p-q}(HA)_{2k+2p+q-5}$ species and where $f_{m,n}$ is that of the aquous phase contributed by the $PaO_m(OH)_n$ species.

If the activity coefficients of any species are assumed to be constant over the entire range of the conditions in a series of experiments, Eqs. (4) and (5) are valid when the activities are replaced by the concentrations. The conditions applied in this experiment can be considered to satisfy this assumption. Thus, according to the results of this experiment, $\partial \ln D/\partial \ln [(HA_2)]$ should be 3 and $\partial \ln D/\partial \ln [H^+]$, -2. Thus we obtain:

$$\sum_{p,q,k} k f_{p,q,k} = 3 \quad (6)$$

and

$$\sum_{m,n} (2m+n) f_{m,n} = 3 \quad (7)$$

If one excludes the fortuitous agreement between the slope obtained empirically and the values calculated from the left-hand sides of Eqs. (6) and (7) by considering the complex combination of many species, Eqs. (8) and (9) are obtained from Eqs. (6) and (7):

$$k = 3 \quad (8)$$

$$2m + n = 3 \quad (9)$$

Therefore, the species of protactinium in the perchloric acid solution are considered to be $PaO(OH)^{2+}$ or $Pa(OH)_3{}^{2+}$. The existence of such species as $Pa(OH)_4{}^+$, $PaO(OH)_2{}^+$ or $PaO_2{}^+$, which were observed by the TTA-extraction, is negligible.

We can make some assumptions which seem reasonable considering the nature of the strong Pa-O bond and the large acid-dissociation constant of HDEHP. The former tells us that p is equal to or larger than m, while the latter tells us that q is queal to or less than n, as long as the molecular form of HDEHP is present in the extracted species. Furthermore, the degree of hydrolysis can not proceed by the complex formation, *i.e.*, $p+q \leq m+n$.

From the above consideration, one can represent the reaction mechanism as:

$$PaO(OH)^{2+}{}_{aq.} + 3(HA)_{2\,org.} = PaO_p(OH)_qA_{5-2p-q}(HA)_{2p+q+1\,org.} + 2H^+{}_{aq.} + (2-p-q)H_2O_{aq.} \quad (10)$$

where $p=1$, $q=0$ or 1 and $p=2$, $q=0$,
and:

$$Pa(OH)_3{}^{2+}{}_{aq.} + 3(HA)_{2\,org.} = PaO_p(OH)_qA_{5-2p-q}(HA)_{2p+q+1\,org.} + 2H^+{}_{aq.} + (3-p-q)H_2O_{aq.} \quad (11)$$

where $p=0$, $q=0$, 1, 2, or 3; $p=1$, $q=0$ or 1, and $p=2$, $q=0$.

In Fig. 1, the absolute value of the slope of log-log plot of D and the acidity is lower than 2 and the presence of the charge of $+1$ and $+2$ was expected when the ionic strength was 1.5. However, this is the effect of the existence of the inextractable species, as is quite clear from the results shown in Fig. 2. This conclusion seems at first sight to be contradictory to the results reported by Suzuki and Inoue,[1] but it can at least qualitatively be explained by the following consideration. In the TTA-benzene extraction, the inextractable species were not observed [1,13] but unadsorbable species were observed in the cation exchange study.[1] Essentially, the reaction of the HDEHP-extraction reaction is considered to be a cation-exchange reaction; therefore, the existence of the inextractable species is not so surprising. Figure 2 shows the results obtained by the Fomin method, in which the contribution from the inextractable species can be omitted. This shows the prominent species, which is in rapid equilibrium with the extraction, to have a charge of $+2$. Thus, no contributions from such species as $PaO(OH_2)^+$, $Pa(OH)^+_4$, and $PaO_2{}^+$ were observed, though the existence of these species had been concluded in the TTA-extraction. Therefore, the inextractable species may be $PaO(OH)^+_2$, $Pa(OH)^+_4$, or PaO^+_2 if we do not take the presence of the polymer into account.

Thus far we have considered the monomeric species only, but it is natural also to consider the inextractable species to be some polymeric species whose charge per atom of Pa is lower than 1. Further study is necessary to make a correct choice out of two possibilities mentioned above. At any rate, the presence of the TTA anion will play an important role in the establishment of the equilibrium between the extractable and the inextractable species.

Another interesting fact is shown in Fig. 1. Although the extraction conditions of the curves 1 and 2 were identical except for the standing time, the values of the distribution ratio were not the same. This difference can be explained by the difference in the standing time; *i.e.*, the equilibrium in the aqueous phase has not yet been established in the curve 1 while it has nearly been

13) R. T. Kolarich, V. A. Ryan, and R. P. Schuman, *J. Inorg, Nucl. Chem.*, **29**, 783 (1967).

established in the curve 2. On the other hand, when the ionic strength is 1.5, the difference in the distribution ratio is not observed between the curves 4 and 5, which were obtained under identical extaction conditions except for the standing time. These observations are consistent with the results of the preliminary experiment and show that the choice of the length of the standing time; *i.e.*, 1—4 days, is proper. However, their distribution ratios in the low acidity range are not identical with the extrapolated values of the curve 1 nor of the curve 2, although the HDEHP concentration is identical; *i.e.*, 5×10^{-3} M. Then the correction by the Fomin method was made, as is shown in Fig. 2, and the corrected distribution ratio was compared with the curves 1 and 2. Even by this procedure, the difference was still pronounced. In order to investigate this difference in more detail, the dependency of the distribution ratio on the perchloric acid concentration was examined by using a 5×10^{-3} M HDEHP-benzene solution. The results were compared with the results obtained by the use of the Fomin method (Fig. 2) and with the curve 2 in Fig. 1 (*cf.* Fig. 6).

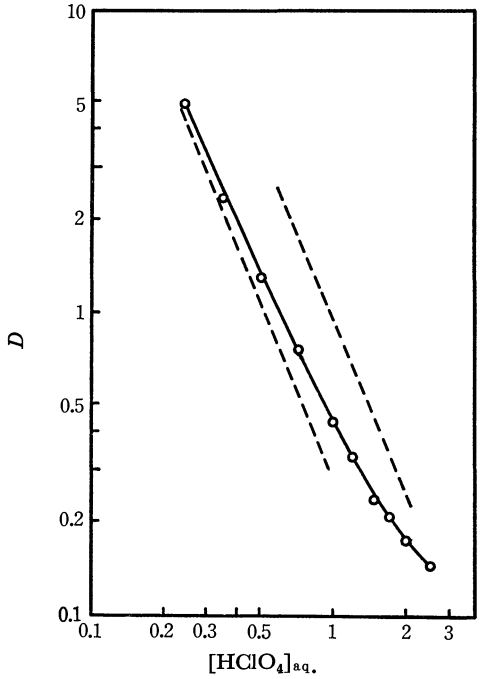

Fig. 6. The relation between the distribution ratio and the perchloric acid concentration. The upper dotted line indicates the curve 2 in Fig. 1 and the lower one, curve in Fig. 2.

In this figure the upper dotted line corresponds to the curve 2 of Fig. 1 and the lower one, to the curve shown in Fig. 2. The values of the distribution ratio obtained by extraction from the pure perchloric acid solution are distributed between the two dotted lines. The slope of the curve obtained by plotting the logarithm of the distribution ratio *vs.* the logarithm of the perchloric acid concentration asymptotically approaches −2 with a decrease in the acid concentration. This tendency is not so unusual in the adsorption on the cation-exchange resin. The most significant difference in the physical properties of the solution is the activity of water; in this case, the activity is higher when the ionic strength is 1.5. The transformation to the inextractable species and the adsorption on the glass vessel seem to occur upon the addition of lithium perchlorate to the perchloric acid solution of protactinium. However, as has been outlined above, their contribution to the distribution ratio is negligible when the acidity is 1.3 M or higher.

Therefore, the gradual approach of the slope to −2 seems to be explainable by the gradual increase in the activity of water. If there exists this equilibrium;

$$PaO(OH)^{2+} + H_2O = Pa(OH)_3^{2+} \qquad (12)$$

between the extractable species, the $Pa(OH)_3^{2+}$ must be more stable than $PaO(OH)^{2+}$ at lower acid concentrations or in media of lower ionic strengths, where the activity of water is lower. Thus, the dependency of the distribution ratio on the inoic strength can be explained by the change in $f_{1,1}$ and $f_{0,1}$ in Eq. (7). In order to confirm this assumption, it is necessary to investigate directly the dependency of the distribution ratio on the activity of water.

The author wishes to thank professor Shin Suzuki and Dr. Yasushi Inoue for their valuable advice throughout this study.

The Reaction of Acetylenecarboxylic Acid with Amines. XV.[1] Reaffirmation of the Enamine Structure Facilitated by Intramolecular Hydrogen Bonding Common to the Reaction Products

Yasuo IWANAMI
Sasaki Institute, Kanda-Surugadai, Tokyo
(Received March 3, 1970)

The reactions of dimethyl acetylenedicarboxylate (V) with *p*-chloroaniline, ethanolamine, ethylenediamine, *o*-aminophenol, and *o*-phenylenediamine gave dimethyl *N*-(*p*-chlorophenyl)aminofumarate(VI), 3-methoxycarbonylmethylene-3,4,5,6,-tetrahydro-2*H*-1,4-oxazin-2-one (VII), 3-methoxycarbonylmethylenepiperazin-2-one (VIII), 3-methoxycarbonylmethylene-3,4,-dihydro-2*H*-1,4-benzoxazine-2-one(IX), and 3-methoxycarbonylmethylene-3,4-dihydro-2(1*H*)-quinoxalinone(X), respectively. It has been shown that methoxycarbonylmethylene is a common structural element in all products, where the carbonyl is hydrogen-bonded with an amino group to form an enamine form. The spectra measured for crystals (IR) and for solutions in inert solvents (NMR) exhibited the fixation of the enamine form preferentially to the imine form, while NMR spectra for trifluoroacetic acid solutions indicated both forms in equilibrium. Tautomerization occurring in the acid is discussed.

In a preceding paper of this series,[2] we reported that the substance customarily called ethyl 2(1*H*)-quinoxalinone-3-acetate (I) should be named 3-ethoxycarbonylmethylene-2-oxo-1,2,3,4-tetrahydroquinoxaline (II) in consideration of IR spectral data, *viz.*, this compound exists in the enamine form as expressed by II which is facilitated by an intramolecular hydrogen bonding.

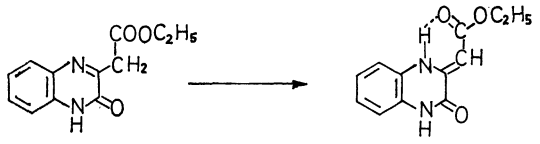

I II

The preceding report was the first to present evidence for the structural predomination common to a series of pyrazinone-type compounds (III and IV) having a *β*-carbonyl group in their side chain.[3,4] It was also reported that such a carbonylmethylene structure, facilitated by hydrogen bonding, predominates not only in these heterocycles but also commonly in *β*-iminopropionyl derivatives.[5]

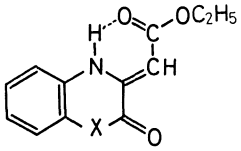

X=NH, O and S
(II: *X*=NH)
III

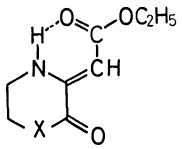

X=NH and O
IV

Chapman[6] described the same enamine structure of I (*i.e.*,II) five years after. There is a contradiction[7] between his and our results, and our reports are inadequately cited in his paper. Some other workers also described simliar enamine forms[8–10] of heterocycles closely related to I or II, and they refer the enamine structure to imine-enamine tautomerism. In our papers, however, we refrained from explaining the enamine form by tautomerism, since we could not obtain any evidence for the presence of the corresponding imine form in our experiments carried out under ordinary conditions.

This paper deals with a reconfirmation of the enamine structure of several types of compounds with emphasis on the point that the imine form can not be detected in chloroform and methanol solutions.

Results

We synthesized methyl ester homologues of the compounds,[2–5] in order to extend our study on their enamine structures by means of IR and NMR spectroscopy. The syntheses were carried out by the reactions of dimethyl acetylenedicarboxylate (V) with *p*-chloroaniline, ethanolamine, ethylenediamine, *o*-aminophenol and *o*-phenylenediamine, as follows:

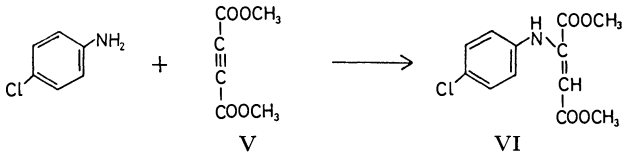

V VI

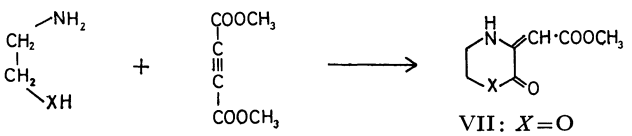

X=O and NH V VII: *X*=O
VIII: *X*=NH

1) Part XIII: This Bulletin, **37**, 1745 (1964), and Part XIV: *Nippon Kagaku Zasshi*, **85**, 704 (1964). Presented in part at the 21st Annual Meeting of the Chemical Society of Japan, Osaka, April, 1968.

2) Y. Iwanami, *Nippon Kagaku Zasshi*, **82**, 778, 780 (1961).

3) Y. Iwanami, *ibid.*, **83**, 100, 161, 316, 593, 597 (1962); H. Sasaki, H. Sakata, and Y. Iwanami, *ibid.*, **85**, 704 (1964).

4) Y. Iwanami, Y. Kenjo, K. Nishibe, M. Kajiura, and S. Isoyama, This Bulletin, **37**, 1740 (1964); Y. Iwanami, S. Isoyama, and Y. Kenjo, *ibid.*, **37**, 1745 (1964).

5) Y. Iwanami, *Nippon Kagaku Zasshi*, **82**, 632, 634 (1961); **83**, 600 (1962).

6) D. D. Chapman, *J. Chem. Soc.*, **1966**, 806.

7) If not a contradiction, it could be a serious misprint.

8) R. Mondelli and L. Merlini, *Tetrahedron*, **22**, 3253 (1966).

9) W. von Philipsborn, H. Stierlin, and W. Traber, *Helv. Chim. Acta*, **46**, 2592 (1963).

10) L. Merlini, W. von Philipsborn, and M. Viscontini, *ibid.*, **46**, 2597 (1963).

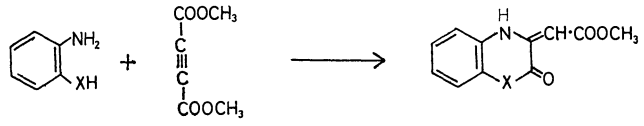

X=O and NH V IX: X=O X: X=NH

The IR spectra of these reaction products (VI—X) were measured for potassium bromide disks. All ester carbonyl bands exhibit marked lower frequency shifts compared to those of normal esters. Since absorption bands of the carbon-carbon double bond are observed in all cases, a double bond adjacent to the carbonyl (α, β-unsaturated) probably contributes to the shifts. Every carbonyl band, however, is not in the expected range[11] of 1730—1717 cm^{-1} for an α, β-unsaturated ester carbonyl, but in a less wave number region of 1696—1659 cm^{-1}. This can be explained by the intramolecular hydrogen bonding of the carbonyl with the amino group displacing its band toward much lower frequency side.[11] These results show that all the products are in enamine structure but not in imine form.

The products are thus to be named dimethyl *N*-(*p*-chlorophenyl)aminofumarate (VI), 3-methoxycarbonylmethylene-3,4,5,6-tetrahydro-2*H*-1,4-oxazin-2-one (VII), 3-methoxycarbonylmethylenepiperazin-2-one (VIII), 3-methoxycarbonylmethylene-3,4-dihydro-2*H*-1,4-benzoxazin-2-one (IX), 3-methoxycarbonylmethylene-3,4-dihydro-2(1*H*)-quinoxalinone (X).

The NMR spectra of VI, VII, VIII, and IX in deuteriochloroform commonly show singlets due to an olefinic (methine) proton instead of expected methylene if they exist in imine forms. Moreover, each spectrum shows at least one amino proton signal, the integration of which represents a single proton on nitrogen (two signals appear in the case of VIII). Its position in a lower field suggests hydrogen bonding involving the amino proton.

Main IR absorption bands and NMR signals of these compounds are shown in Fig. 1, together with the structural formulas which illustrate the actual forms of enamine type (the ring amide structures of VIII and X are also supported by both spectral data). Since IR spectra were measured for potassium bromide disks and NMR spectra for solutions, all these compounds can be satisfactorily expressed by the formulas shown in Fig. 1 both in solution and crystalline states.

If interconversion of imine and enamine (tautomerism) takes place, the hydrogen of side chain methine or methylene should be exchangeable with deuterium in the presence of deuterium oxide. One of the possible exchange mechanisms would be as follows:

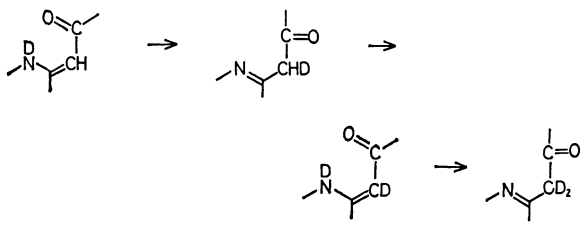

When the NMR spectra of these compounds were measured in deuteriomethanol (CD_3OD), exchange with deuterium oxide removed the amino proton signal(s) (Table 1). Nevertheless, the signal of the methine proton did not disappear. Its relative intensity remained unchanged to afford 1:3 ratio to the integration of methyl singlet in every case. Hence it appears that tautomerism never occurs in deuteriomethanol and probably in deuteriochloroform.

On the other hand, some different results were

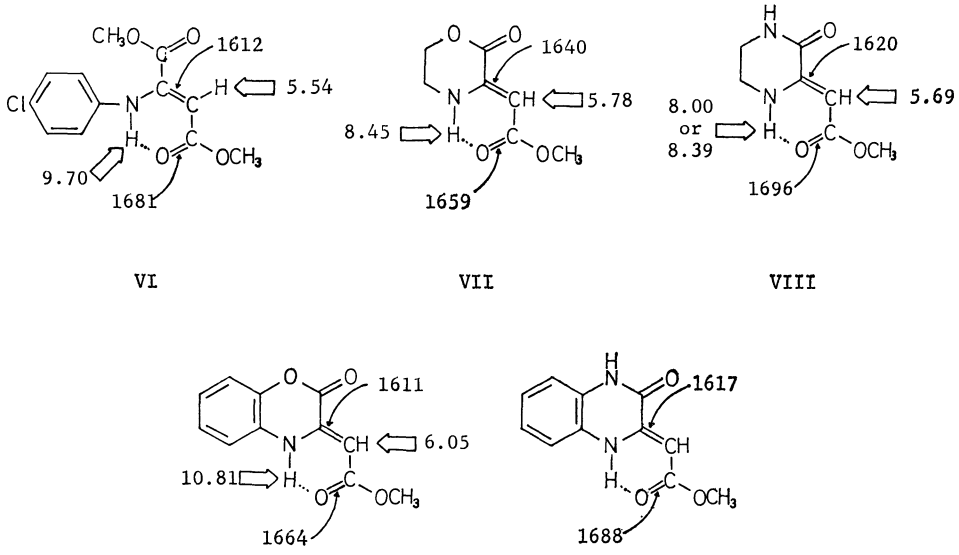

VI VII VIII

IX X

Fig. 1. Structural formulas of the products. Large arrow ⇨ shows the position of the NMR signal (δ) in deuteriochloroform, and small arrow → indicates the IR absorption (cm^{-1}) for potassium bromide disk. Compound X was insoluble in deuteriochloroform.

11) L. J. Bellamy, "The Infrared Spectra of Complex Molecules," Methuen & Co., London (1958), p. 179.

Table 1. Chemical shifts of the products

Compound	CD_3OD			CF_3COOH		
	CH_3	CH_2	=CH	CH_3	CH_2	=CH
VI	3.42	—	5.11	3.36 3.49	3.46	4.48
VII	3.39	—	5.18	3.52	3.55	5.62
VIII	3.37	—	5.14	3.42	3.54	5.52
IX	3.49	—	6.92	3.52	3.52	5.62

The values are in ppm (δ) relative to internal tetramethylsilane. The mark—: no indication of the signal (side chain) at all. Compound was sparingly soluble in CD_3OD. The signals of X in CF_3COOH were already reported.[8]

obtained from the measurement using trifluoroacetic acid. Both methine and methylene proton signals are exhibited in this acid as listed in Table 1. Methylene proton signals can be interpreted as due to the side chain methylene of each compound existing in the imine form. The enamine and imine forms are, therefore, equilibrated in the acid.

A variety of the existing ratios of enamine to imine in the acid are shown by calculation based upon the relative intensities of methine singlets, as follows: approximately 1:2, 1:0.5, 1:8, and 1:>10 for VI, VII, VIII, and IX, respectively.

In deuteriotrifluoroacetic acid, either methine or methylene proton signal disappears by replacement with deuterium. It can therefore be said that tautomerization becomes possible under certain conditions caused by trifluoroacetic acid.

Discussion

The phenomenon observed on the compounds in trifluoroacetic acid is noteworthy. However, there is an essential difference between the compounds and β-diketones such as acetylacetone or ethyl acetoacetate, which ordinarily exist as an equilibrium mixture of keto and enol tautomers, while all the compounds in the present study shut themselves much more firmly in the enamine form in crystals and chloroform or methanol solution (at least the imine form is extremely minimized). The imine formation and tautomerization therewith in trifluoroacetic acid may be caused by a concerted reaction[12] which proceeds by simultaneous attack of the acid and the base as illustrated below.

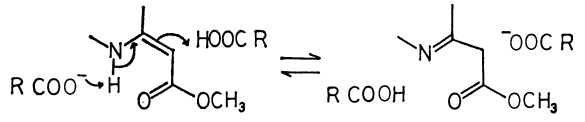

Generally, imine form is predominant[13,14] in imine-enamine tautomerism:

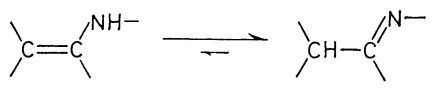

Enamines are stable only when there is no hydrogen on the nitrogen (—C=C–NRR′).[13,14] It is interesting that all our products possess a hydrogen on the nitrogen atom but the enamine forms remain stable.

This series represents a special case of proton-shift isomerization or tautemerization. However, we recently encountered a perfectly converse predominance of the imine form observed on the same side-chain derivative of a more complicated heterocycle, which will be reported in the following paper.

Experimental

IR spectra were measured for KBr disks with a Nippon Bunko DS-301 spectrophotometer, and NMR spectra were determined on a Hitachi H-60 model.

The synthetic procedures of the all compounds were essentially the same as the corresponding ethyl derivatives[2-5] except that diethyl acetylenedicarboxylate was replaced by dimethyl acetylenedicarboxylate (V) and methanol was used as the solvent instead of ethanol. Only their melting points (uncorr.), yields in percent, and data of elementary analyses are described.

Dimethyl N-(p-Chlorophenyl)aminofumarate (*VI*). This was prepared by the reported procedure.[5] Yield 83%; mp 75—76°C.

Found: C, 53.59; H, 4.82; N, 5.06%. Calcd for $C_{12}H_{12}O_4NCl$: C, 53.44; H, 4.49; N, 5.19%.

3-Methoxycarbonylmethylene-3,4,5,6-tetrahydro-2H-1,4-oxazin-2-one (*VII*). This was prepared by the reported procedure.[2] Yield 69%; mp 81—82°C.

Found: C, 49.36; H, 5.52; N, 7.97%. Calcd for $C_7H_9O_4N$: C, 49.12; H, 5.30; N, 8.18%.

3-Methoxycarbonylmethylenepiperazin-2-one (*VIII*). This was prepared by the reported procedure.[4] Yield 88%; mp 173—174°C.

Found: C, 49.55; H, 6.14; N, 16.61%. Calcd for $C_7H_{10}O_3N_2$: C, 49.40; H, 5.92; N, 16.46%.

3-Methoxycarbonylmethylene-3,4-dihydro-2H-1,4-benzoxazine-2-one (*IX*).[15] This was prepared by the reported procedure.[2] Yield 67%; mp 170°C (lit.[15,16] mp 170°C).

Found: C, 60.49; H, 4.33; N, 6.45%.

3-Methoxycarbonylmethylene-3,4-dihydro-2(1H)quinoxalinone (*X*). This was prepared by the reported procedure.[2] Yield 75%; mp 227°C (lit.[17,18] mp 225°C).

Found; C, 60.67; H, 4.43; N, 12.78%.

Grateful acknowledgement is made to Miss Masako Asahina, and Dr. Yutaka Fujise, Tohoku University, for NMR spectroscopy, to Dr. Tomohisa Takita, Institute of Microbial Chemistry, for helpful discussion on NMR data, and to Prof. Hiro-oki Sasaki of this institute for his interest and encouragement.

12) E. S. Gould, "Mechanism and Structure in Organic Chemistry," Henry Holt and Co., Inc., London (1960), p. 385.

13) J. March, "Advanced Organic Chemistry: Reactions, Mechanisms, and Structure," McGraw-Hill Book Co., New York (1968), p. 62.

14) J. D. Roberts and M. C. Caserio, "Basic Principles of Organic Chemistry," W. A. Benjamin, Inc., New York (1964), p. 486.

15) A compound probably identical with this product has been reported to be its isomer, 2-methoxycarbonylmethylene-3,4-dihydro-2*H*-1,4-benzoxazin-3-one.[16] Chemical shifts and melting point of the compound described in the paper supports its identity. The structure allocated as IX is more satisfactory for interpretation of its IR absorption bands in comparison with those of the oxazinone derivatives[2-4] including VII of the present report.

16) R. M. Acheson, M.W. Foxton, and G. R. Miller, *J. Chem. Soc.*, **1965**, 3200.

17) F. Weygand, W. Steglich, and H. Tanner, *Ann, Chem.*, **658**, 128 (1962).

18) Reported as methyl 2-hydroxyquinoxaline-3-acetate.

The Reaction of Acetylenecarboxylic Acid with Amines. XVI.[1] Formation of Alkyl Isoxanthopterinacetates Possessing Imine Structure[2]

Yasuo IWANAMI
Sasaki Institute, Kanda-Surugadai, Tokyo
(Received March 3, 1970)

Methyl and ethyl isoxanthopterin-6-acetates and their 4-amino analogues have been prepared *via* a new route from acetylenedicarboxylate and 2,5,6-triamino-4-hydroxypyrimidine or 2,4,5,6-tetraaminopyrimidine. These compounds uniquely exist in the imine form as evidenced by NMR and IR spectral data. This is the only exceptional case so far examined, since a number of related compounds exist in enamine form. When dissolved in sulfuric acid, however, tautomerization of imine to enamine is observed. It was demonstrated by NMR inspection that the methylene hydrogen on the side chain is exchangeable with deuterium. The tautomerism in sulfuric acid is discussed.

The reactions of ethyl and methyl acetylenedicarboxylates (Ia and Ib) with 2,5,6-triamino-4-hydroxypyrimidine (IIa) or 2,4,5,6-tetraaminopyrimidine (IIb) gave the corresponding alkyl isoxanthopterin-6-acetates (IIIa and IIIb) or their 4-amino analogues (IIIc and IIId). Although the preparation of the ethyl ester (IIIa and IIIc) by a different route is known,[3] this procedure provides another route.

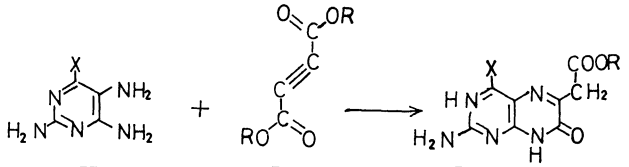

II
a : X=OH
b : X=NH_2

I
a : R=Et
b : R=Me

III
a : X=OH; R=Et
b : X=OH; R=Me
c : X=NH_2; R=Et
d : X=NH_2; R=Me

In a previous paper[4] we reported that the compound customarily called ethyl 2(1*H*)-quinoxalinone-3-acetate exists in the enamine form, *i.e.* in a structure to be named 3-ethoxycarbonylmethylene-3,4-dihydro-2(1*H*)-quinoxalinone. The enamine form is facilitated by an intramolecular hydrogen bonding. The preceding report was the first to present evidence for such a chelate structure. Since then, many examples of similar enamines possessing intramolecular hydrogen bonding have been reported from our laboratory in condensed[1,4-6] and noncondensed[1,4,6] nitrogen-containing heterocycles of five-,[5] six-,[1,4-6] and seven-membered[5] rings or even in simpler alkyl β-aminoacrylates.[1,5,7]

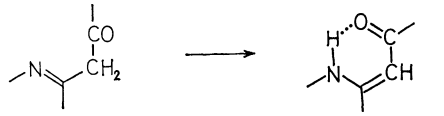

imine form enamine form

Because of their structural resemblance to the heterocycles,[1-4] compounds IIIa—d were expected to exist in the enamine form. Nevertheless, IR and NMR spectroscopic data have disclosed the predominancy of the imine form both in their solution and crystalline states.

The IR spectra of III exhibited ester carbonyl bands in the range 1747—1716 cm^{-1}, but not 1698—1644 cm^{-1}, which was expected for an intramolecularly hydrogen-bonded α,β-unsaturated ester carbonyl common to all the related compounds reported in the preceding papers. This suggests that the side chain of III exists in an alkyl acetate form rather than in chelated alkoxycarbonylmethylene form.

In order to obtain further evidences the NMR spectra of III were examined. Although solubility of III in the usual solvents was not high enough for the spectroscopy, we found that sulfuric acid was good solvent in which III was stable at ordinary temperature.

The NMR spectra of IIIa in sulfuric acid are shown in Fig. 1. A triplet at 1.78 ppm and a quartet at 4.75 ppm are observed besides two broad signals due to NH protons at 5.24 and *ca.* 8.00 ppm. The profile of the quartet appears deformed. The relative intensity of the quartet represents 4: 3 to the triplet due to methyl protons of the ethoxyl group. This can be explained by the overlapping of a quartet due to methylene protons of the ethoxyl group with a singlet due to the other methylene protons adjacent to the pteridine ring. In deuteriosulfuric acid, the coinciding singlet has disappeared together with amino proton signals, and the intensity of the remaining quartet diminishes to two-thirds that of the triplet. Namely, the triplet and quartet turn out typical bands of an ethoxyl group.

The spectrum of IIIa in deuteriodimethyl sulfoxide is essentially the same as that in sulfuric acid. Similar phenomena have been observed in the spectra of IIIb—d.

From these results except those in deuteriosulfuric acid, it is evident that this compound exists as ethyl isoxanthopterin-6-acetate (IIIa) but not as 6-ethoxy-

1) Part XV: Y. Iwanami, This Bulletin, **44**, 1311 (1971).
2) Presented in part at the IVth International Symposium on Pteridines, Toba, July, 1969, and also partially described in The Symposium Proceedings, "Chemistry and Biology of Pteridines," International Academic Printing Co., Yamabuki-cho Shinjuku-ku, Tokyo (1970), p. 129.
3) A. G. Renfrew, P. C. Piatt, and L. H. Cretcher, *J. Org. Chem.*, **17**, 467 (1952).
4) Y. Iwanami, *Nippon Kagaku Zasshi*, **82**, 778, 780 (1961).
5) Y. Iwanami, *ibid.*, **83**, 100, 161, 316, 593, 597 (1962); H. Sasaki, H. Sakata, and Y. Iwanami, *ibid.*, **85**, 704 (1964).
6) Y. Iwanami, Y. Kenjo, K. Nishibe, M. Kajiura, and S. Isoyama, This Bulletin, **37**, 1740 (1964); Y. Iwanami, S. Isoyama, and Y. Kenjo, *ibid.*, **37**, 1745 (1964).
7) Y. Iwanami, *Nippon Kagaku Zasshi*, **82**, 632, 634 (1961); **83**, 600 (1962).

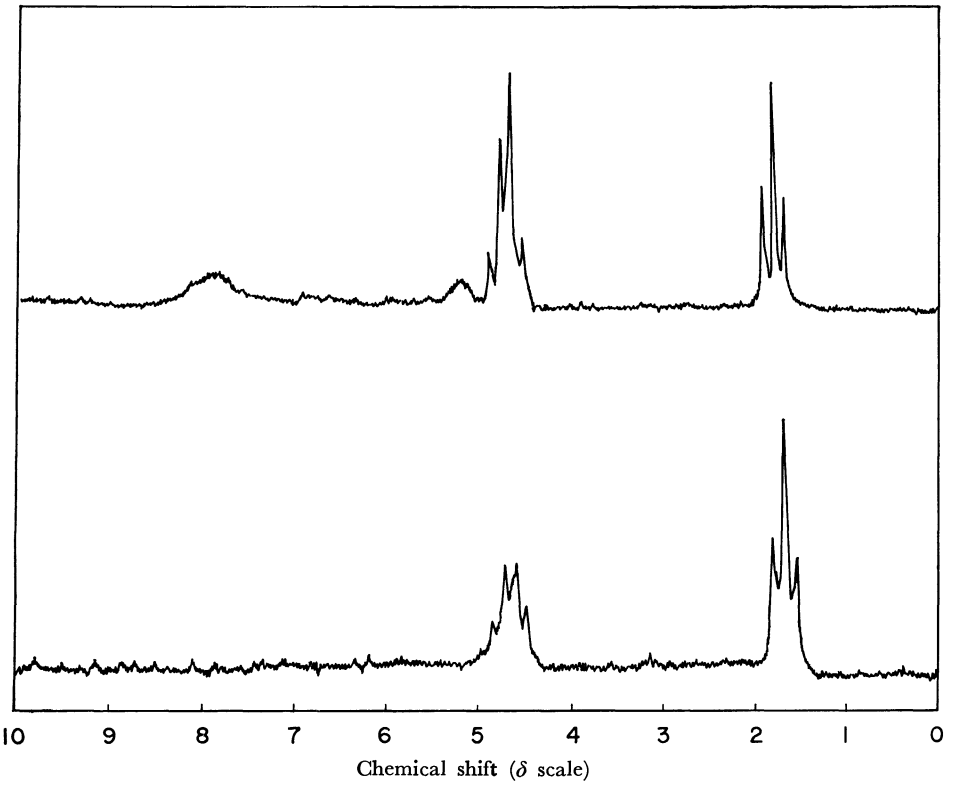

Fig. 1. NMR spectra (60 MHz) of ethyl isoxanthopterin-6-acetate (IIIa) in sulfuric acid (above) and deuteriosulfuric acid (below).

carbonylmethylene-5,6-dihydroisoxanthopterin (IVa).

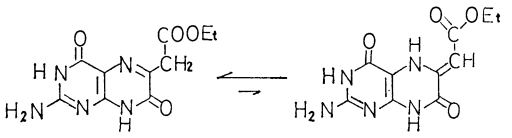

IIIa IVa

However, tautomerization between IIIa and IVa is not excluded as shown by the fact that the methylene protons adjacent to the ring are exchangeable with deuterium of the solvent. This exchange is fully explained by tautomerization which causes direct and repeated additions of deuterium to the carbon bearing an olefinic proton in another tautomeric (enamine) form or replacements occuring stepwise to exchange an amino proton with deuterium and then to transfer it onto olefinic carbon, in deuteriosulfuric acid.

Thus, the structure of III in solution and crystalline state has been estableished by NMR and IR spectra, respectively.

Indication of imine-enamine tautomerism is given only when the spectrum in sulfuric acid is compared with that in deuteriosulfuric acid. This was the only successful experiment to detect tautomerism. Unfortunately, we could not see whether or not the interconversion of imine to enamine occurs in inert solvents, because of low solubility. On the basis of our previous observation,[1] however, we deduce that III would exclusively exist in the imine form under ordinary circumstances (for example, in crystalline state or in an inert solvent). When III is dissolved in sulfuric acid or other protic solvents, protonation by the acids would cause the interconversion of imine to enamine as follows:

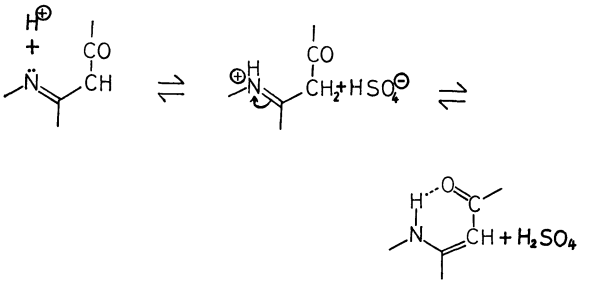

This mechanism is well explained by the above deuterium exchange. Probably, concerted reaction[1] of the solvent cation and anion equilibrate both tautomeric forms.

It is of interest that an isomer of IIIa, ethyl xanthopterin-7-acetate,[8] exists in the enamine form[9] in deuteriodimethyl sulfoxide, in contrast to III, while the compound exists as a 1 : 1 mixture of imine and enamine forms in trifluoroacetic acid. The tautomerism occurring in trifluoroacetic acid can also be accounted for the above hypothetical mechanism.

8) L. Merlini, W. von Philipsborn, and M. Viscontini, *Helv. Chim. Acta*, **46**, 2592 (1963).

9) Recently, we have examined the structures of 6-phenacylisoxanthopterines and 7-phenacylxanthopterins, which possess β-carbonyl groups in their side chains as do III and above mentioned ethyl xanthopterin-7-acetate.[8] It was found that both phenacylpterins exist in the enamine form, and the interconversion of enamine to imine is evidenced by NMR spectra in deuteriosulfuric acid. The results will be reported elsewhere.

Experimental

IR spectra were measured for potassium bromide disks on a Nippon Bunko DS-301 spectrophotometer. NMR spectra were determined with a Hitachi H-60 spectrometer and recorded in δ values with tetramethylsilane as external standard.

Ethyl Isoxanthopterin-6-acetate (IIIa). Into a suspension of IIa sulfate (0.4 g) in an aqueous solution (10 m*l*) of sodium acetate (0.8 g), a solution of Ia (0.35 g) in ethanol (10 m*l*) was added dropwise with stirring at room temperature. After the mixture was stirred for further 3 hr, it was allowed to stand overnight. The precipitated crystals (0.5 g) were collected by filtration and recrystallized repeatedly from dimethyl sulfoxide. The crystals were washed well with water and ethanol successively on a glass filter and kept *in vacuo* over phosphorus pentoxide at an elevated temperature (100°C) for a few hours in order to eliminate completely the solvent to give IIIa as dark yellow powders; mp>300°C.

Found: C, 41.08; H, 4.55; N, 23.45%. Calcd for $C_{10}H_{11}O_4N_5 \cdot 3/2H_2O$: C, 41.12; H, 4.79; N, 23.94%.

Methyl Isoxanthopterin-6-acetate (IIIb). In a similar manner to IIIa, the crude product of IIIb (0.15 g) from IIa sulfate (0.2 g) and Ib (0.15 g) was recrystallized from dimethyl sulfoxide to afford IIIb; mp>300°C.

Found: C, 39.10; H, 4.10; N, 25.22%. Calcd for $C_9H_9O_4N_5 \cdot 3/2H_2O$: C, 38.87; H, 4.32; N, 25.10%.

Ethyl 2,4-Diamino-7(8H)-pteridinone-6-acetate (IIIc). Similarly, the crude product of IIIc (0.56 g) from IIb sulfate (1.2 g) and Ia (0.85 g) was recrystallized from dimethyl sulfoxide. The crystals collected on a glass filter were washed with a 1:1 mixture of dimethyl sulfoxide and 50% sulfuric acid, water, and ethanol, successively, and then kept *in vacuo* to give IIIc; mp>300°C.

Found: C, 40.97; H, 4.46; N, 28.71%. Calcd for $C_{10}H_{12}O_3N_6 \cdot 1/4H_2SO_4 \cdot 1/4H_2O$: C, 40.95; H, 4.47; N, 28.66%.

Methyl 2,4-Diamino-7(8H)-pteridinone-6-acetate (IIId). The crude product of IIId (0.73 g) from IIb sulfate (1.20 g) and Ib (1.14 g) was recrystallized from dimethyl sulfoxide; mp>300°C.

Found: C, 41.98; H, 4.47; N, 32.59%. Calcd for $C_9H_{10}O_3N_6 \cdot 1/2H_2O$: C, 41.70; H, 4.28; N, 32.42%..

I am indebted to Mr. T. Inagaki, Central Research Laboratories, Nitto Chemical Industry Co., for his determination of the NMR spectra, and to Mr. A. Norose for his technical assistance.

BULLETIN OF THE CHEMICAL SOCIETY OF JAPAN, VOL. 44, 1316—1321(1971)

Heterocycles Structurally Influenced by a Side Chain. I. 3-Phenacyl-2(1*H*)-quinoxalinones and 3-Phenacyl-2*H*-1,4-benzoxazin-2-ones[1)]

Yasuo IWANAMI and Taketsugu SEKI*
Sasaki Institute, Kanda-Surugadai, Chiyoda-ku, Tokyo
Takeshi INAGAKI
Central Research Laboratories, Nitto Chemical Industry Co., Ltd., Daikoku-cho, Tsurumi-ku, Yokohama

(Received March 17, 1970)

Seven phenacyl derivatives of 2(1*H*)-quinoxalinone and 2*H*-1,4-benzoxazin-2-one (IV and V) have been synthesized to introduce a common structural element $-CH_2-CO-$ into their 3-positions. Their structures are compared with those of the related compounds described previously. The main purpose of the present study was to see whether or not their ring double bonds (–N=C–) have ever been displaced onto the side chains, constituting an enamine so as to form =CH–CO–, the carbonyl of which is hydrogen bonded with the secondary amino group of the rings thereby formed. Consequently, existence as the enamine form, facilitated by an intramolecular hydrogen bonding, has been evidenced by IR and NMR spectral data. It is, therefore, fitting to call them by the more practical expression "3-phenacylidene-3,4-dihydro-2(1*H*)-quinoxalinone" (IVa), and so on. Hydrolysis of IV gave the corresponding 3-methyl-2-(1*H*)-quinoxalinones (VI) and benzoic acid (VII), while that of V afforded the starting substances, *o*-aminophenols (III) and benzoylpyruvic acid (VIII) which had been partially decomposed into pyruvic acid (IX) and VII.

One of the authors reported[2–7)] in and after the year of 1961 that many nitrogen-containing heterocycles having a β-carbonyl on their side chains introduced onto the carbon adjacent to the nitrogen atom tend to isomerize so that the carbon-nitrogen double bond is displaced onto the side chain to form an α,β-unsaturated carbonyl group. Isomerization is facilitated by the resulting intramolecular hydrogen bonding[3)] between the carbonyl and the secondary amino group thus newly formed.

1) Presented in part at the Autumn Allied Meeting of the Chemical Society of Japan, Sendai, October, 1968.
* Present address: Research Laboratories, Nikken Chemicals Co., Ltd., Ohmiya, Saitama.
2) Y. Iwanami, *Nippon Kagaku Zasshi*, **82**, 778, 780 (1961); **83**, 100, 161, 316, 590, 597 (1962).
3) Y. Iwanami, *ibid.*, **83**, 593 (1962).
4) H. Sasaki, H. Sakata, and Y. Iwanami, *ibid.*, **85**, 704 (1964).
5) Y. Iwanami, Y. Kenjo, K. Nishibe, M. Kajiura, and S. Isoyama, This Bulletin, **37**, 1740 (1964).
6) Y. Iwanami, S. Isoyama, and Y. Kenjo, *ibid.*, **37**, 1945 (1964).
7) Y. Iwanami, *ibid.*, **44**, 1311 (1971).

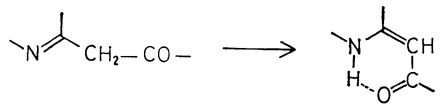

imine enamine

However, we recently encountered[8] an exceptional case of alkyl isoxanthopterin-6-acetates, which exist in the imine form indicating a converse predominance.

We have, therefore, extended our study to 3-phenacyl-2(1*H*)-quinoxalinones (IV) and 3-phenacyl-2*H*-1,4-benzoxazin-2-ones (V).

Condensation of ethyl benzoylpyruvates (I) with *o*-phenylenediamine (IIa), *o*-aminophenol (IIIa) and some of their derivatives (IIb, c, and IIIb—d) gave the corresponding 3-phenacyl-2(1*H*)-quinoxalinones (IVa—c) and 3-phenacyl-2*H*-1,4-benzoxazin-2-ones (Va—d). Five of the products except IVa and Va are new compounds.

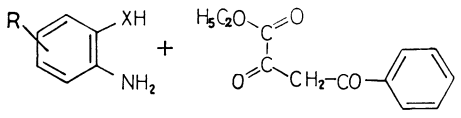

IIa: R=H, X=NH
IIb: R=4-Cl, X=NH
IIc: R=Benzo[*d*], X=NH
IIIa: R=H, X=O
IIIb: R=4-CH_3, X=O
IIIc: R=4-Cl, X=O
IIId: R=Benzo[*c*], X=O

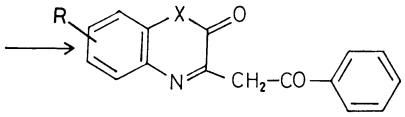

IVa: R=H, X=NH
IVb: R=7-Cl, X=NH
IVc: R=Benzo[*g*], X=NH
Va: R=H, X=O
Vb: R=6-CH_3, X=O
Vc: R=6-Cl, X=O
Vd: R=Benzo[*f*], X=O

IR spectra of these compounds were measured for KBr disks. The absorption bands of carbonyls and carbon-carbon double bonds (both in the side chains) are shown in all cases (Table 1). The results suggest that a nitrogen-carbon double bond in the ring is just visionary and the double bond has ever been displaced onto the side chain. Moreover, the carbonyl bands are not in the region 1670—1663 cm^{-1} expected[9] for an α,β-α',β'-unsaturated ketone, but in a lesser wavenumber region 1623—1620 cm^{-1}. This lower frequency shift is probably accounted for an intramolecular hydrogen bonding of the carbonyl with the amino group of the ring. The secondary amino group can not occur unless the imaginary nitrogen-carbon double bond has been displaced onto the side chain. Thus, these compounds exist in the enamine form, which is

Table 1. IR absorption bands of the products (cm^{-1})

Compound	$\nu_{C=O}$			$\nu_{C=C}$
	Lactone	Lactam	Ketone	
IVa		1689	1622	1613
IVb		1690	1622	1613
IVc		1693	1620	1610
Va	1755		1620	1611
Vb	1755		1621	1613
Vc	1757		1623	1612
Vd	1750		1620	1613

All spectra were measured for KBr disks.

attributable to the internal hydrogen bond by the analogy of a number of their related compounds.[2-7]

The enamine structure is further evidenced by NMR spectra determined for dimethyl sulfoxide-d_6 solutions (the solubilities of these compounds in the usual solvents are not high enough for spectroscopy). The NMR spectra of IVa and Vb are shown in Fig. 1. In the spectrum of IVa (above), no signals appear in the region between 6.91 and 0 ppm, except for those due to protons of the solvent, but a singlet appears at 6.91 ppm (δ scale). Therefore, we can conclude that IVa does not involve methylene but a methine group in its structure. Bands at lower fields are due to aromatic protons, and the carbonyl adjacent to the phenyl ring would displace the signals due to the *ortho* protons down-field giving the band at *ca.* 8.07. Consequently, the carbonyl group does not exist as an enol in IVa. The two broad signals at 12.09 and 13.88 ppm are due to amino protons. Existence of amino protons is also proper only to the enamine form. Hydrogen bonding between the carbonyl and amino groups is suggested by the lowest-field position of the amino proton signal. The structure consistent with these chemical shifts is designated as "3-phenacylidene-3,4-dihydro-2(1*H*)-quinoxalinone."

This is not exceptional to the existing forms of many other related compounds.[2-7]

Similarly, Vb showed a methine, an amino, and aromatic *ortho* (to a carbonyl) proton signal (Fig. 1, below). In this case, Vb possesses a methyl group attached to the benzoxazine ring, and the corresponding signal appears at 2.32 ppm. The relative intensity of the methine singlet represents exactly one proton when compared to three protons of another singlet due to the ring methyl group. Presence of the methine group in Vb is thus satisfactory from this quantitative point of view. The customary name of V, 3-phenacyl-2*H*-1,4-benzoxazin-2-one, is not fitting, and the most practical designation would be "3-phenacylidene-3,4-dihydro-2*H*-1,4-benzoxazin-2-one."

The NMR spectra of the other products (IVb and Va,c,d), except for that of IVc sparingly soluble in dimethyl sulfoxide-d_6, are essentially the same as those of IVa and Vb described above. The broad amino proton signals of Vc and Vd are indistinctly observed because of their insufficient solubility. The δ values of the methine, amino benzoyl *ortho* protons are listed in Table 2. The IR spectra were measured for potas-

8) Y. Iwanami, This Bulletin, **44**, 1314 (1971).
9) L. J. Bellamy, "The Infrared Spectra of Complex Molecules," Methuen and Co., London (1958), p. 132.

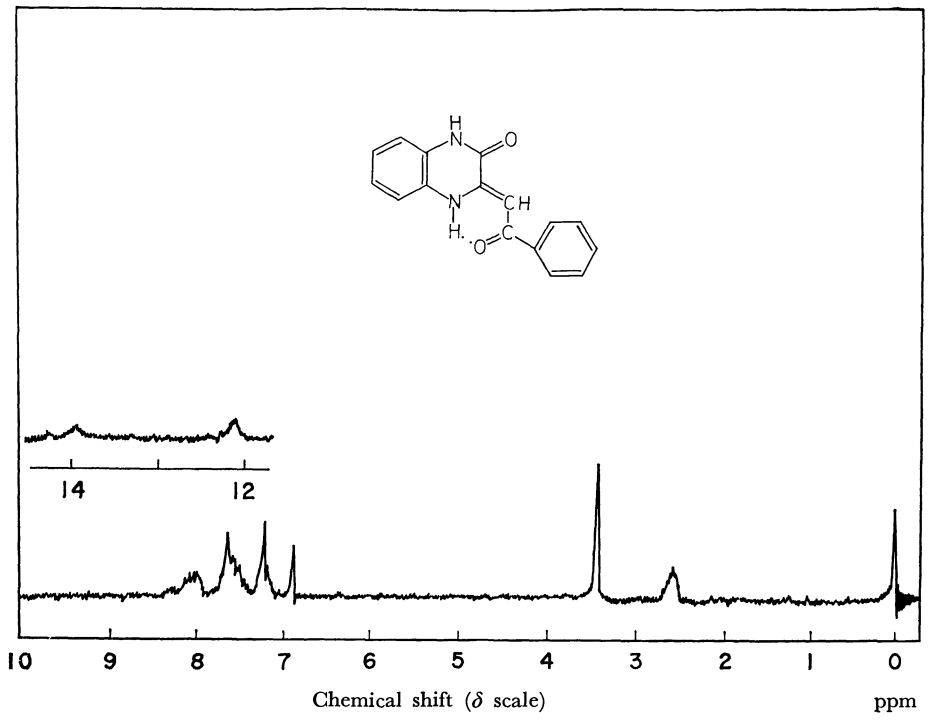

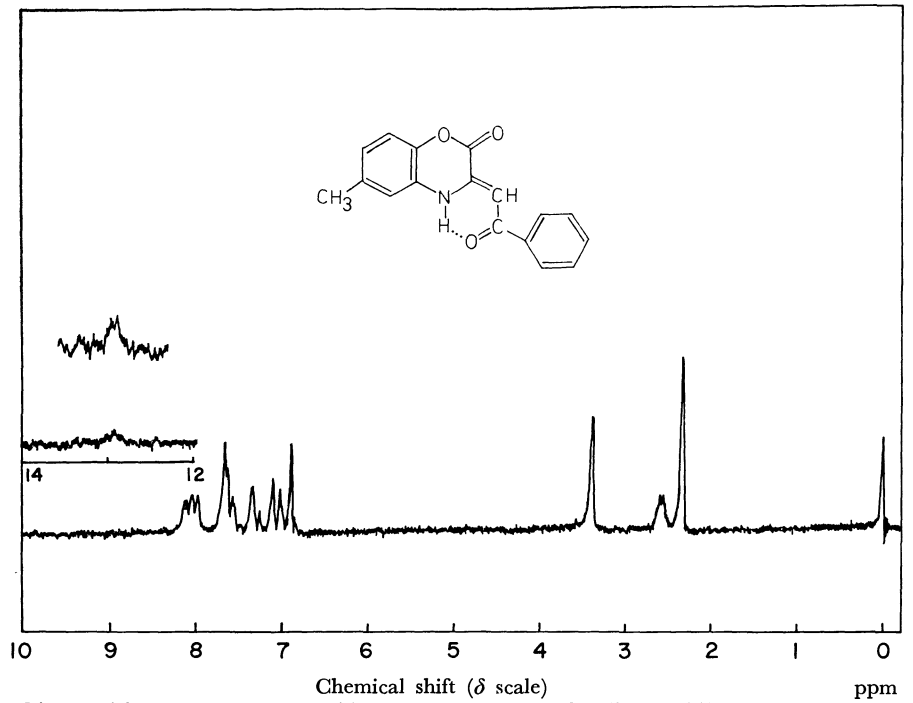

Fig. 1. NMR spectra (60 MHz) of 3-phenacylidene-3,4-dihydro-2(1*H*)-quinoxalinone (IVa) (above), and 6-methyl-3-phenacylidene-3,4-hydro-2*H*-1,4-benzoxazin-2-one (Vb) (below) in DMSO-d_6 (internal TMS).

sium bromide disks (Table 1) and the NMR spectra for dimethyl sulfoxide-d_6 solutions (Table 2). Structure in solution or crystalline state has, therefore, been confirmed to be the same (the enamine form) by both spectroscopies.

Profiles of the NMR spectra, measured for trifluoroacetic acid solutions, were greatly different. Three or four singlets appeared in the region 6.98—4.39 ppm (Table 2). This probably accounted for the tautomerism as follows:

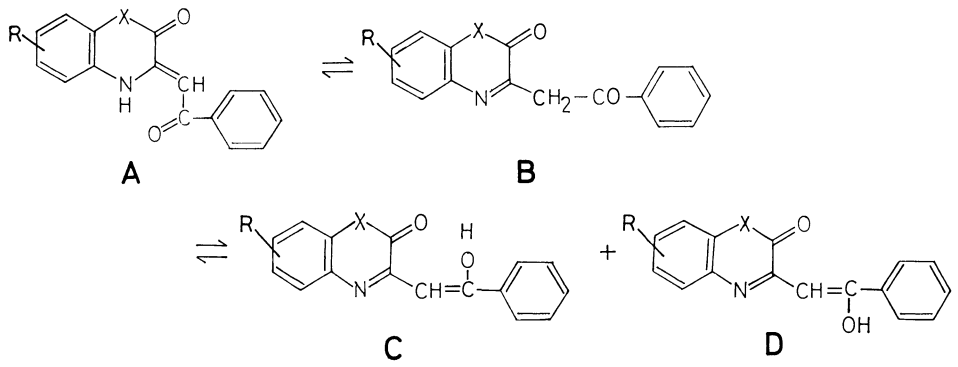

Table 2. Chemical shifts of the products

Compound	DMSO-d_6			CF_3COOH	
	=CH	Benzoyl(*ortho*)	NH	=CH	CH_2
IVa	6.91	*ca.* 8.07	13.88 12.09	6.59 5.70	4.79
IVb	6.92	*ca.* 8.10	13.68 12.12	6.78 6.43 5.54	4.39
IVc	—	—	—	6.98 6.55 5.69	4.79
Va	6.98	*ca.* 8.13	12.97	6.26 5.35	4.53
Vb	6.89	*ca.* 8.05	12.92	6.65 6.45 5.55	4.65
Vc	7.07	*ca.* 8.19	(12.02)	6.44 5.56	4.65
Vd	7.11	*ca.* 8.13	(12.18)	6.97 6.43 5.56	4.69

Values are on δ scale, unmeasurable: —, and indistinct: ( ).

In crystalline state or in dimethyl sulfoxide, these compounds exist as A, as already mentioned. In a strongly ionizing solvent like trifluoroacetic acid, however, the solvent forces them to tautomerize between A and B, B and C (or D), and possibly A and C (or D). This effect of the ionizing solvent would be due to solvation with proton and the anion. The mechanism can be explained by a simultaneous attack (concerted reaction) of an anion and a proton,[10] analogous to similar phenomena observed[7,8] on the related compounds in trifluoroacetic acid or sulfuric acid.

The interconversions are supported by the following interpretations and experiments. In trifluoroacetic acid, a methylene ($-CH_2-$) proton signal (Table 2) is shown in every case. This is satisfactory for B. Although no direct evidences are given to the presence of both tautomers C (*cis*) and D (*trans*), occurrence of three methine (=CH–) ptoron signals (Table 2) can be interpreted as that one methine belongs to A and the two others to C and D. Since intramolecular hydrogen bonding possibly occurs as well in C as in A, a couple of the signals both fallen in a range 6.98—6.43 ppm would be attributable to the methines of A and C. Thus, the remaining signal in the higher field 5.70—5.35 ppm is likely to be that of D (when only two methine signals appear, one form may be minimized or two of the three signals overlapped). Moreover, the typical benzoyl (*ortho*) proton signals observed in dimethyl sulfoxide-d_6 are weakened in trifluoroacetic acid. Enolized forms C and D explain this felicitously.

On the other hand, the spectra determined in trifluoroacetic acid-*d* exhibit no methylene nor methine proton signals, *i.e.* all hydrogens on the aliphatic carbon have been replaced with deuterium. As an example, two of the possible exchange mechanisms would be as

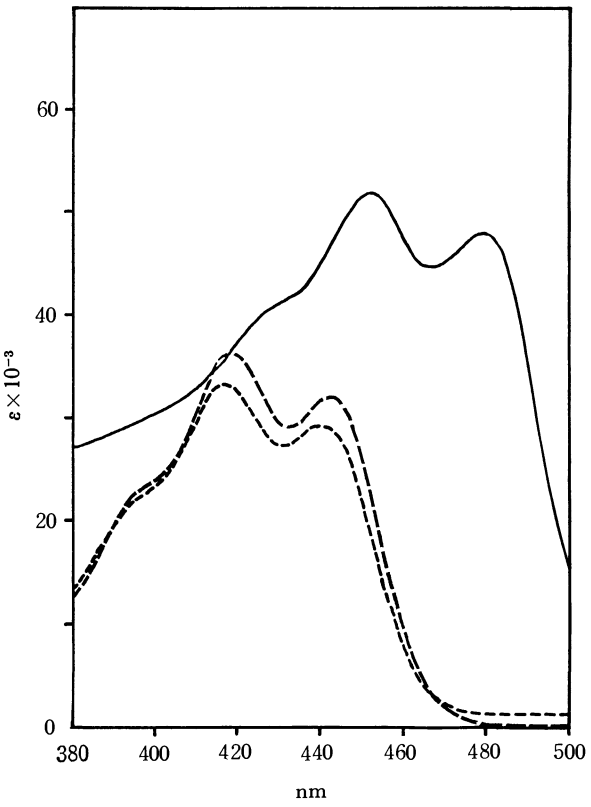

Fig. 2. Electronic absorption spectra of 3-phenacylidene-3,4-dihydro-2(1*H*)-quinoxalinone (IVa); in EtOH: ------, in DMSO: ——, and in CF_3COOH: ——.

10) E. S. Gould, "Mechanism and Structure in Organic Chemistry," Henry Holt and Co., Inc., London (1960), p. 385.

follows:

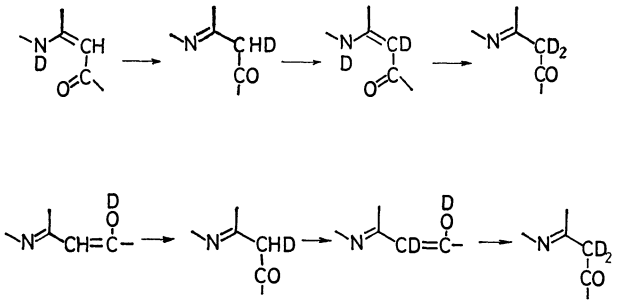

Besides the interconversion between A and B[7] (above), the keto-enol tautomerism involving B, C, and D (below) probably contributes to the deuterium exchange. At least, disappearance of the signals is consistent with the above tautomerisms forced by the acid.

In addition to these supports,[11] another evidence for C and D is obtained from electronic absorption. The spectra of IVa are shown in Fig. 2. The absorptions in ethanol and in dimethyl sulfoxide are almost the same, whereas that in trifluoroacetic acid shows a bathochromic shift. This is consistent with the enol forms C and D, since the enol double bond connects two aromatic rings so as to intensify the resonance through this new conjugated double bond.

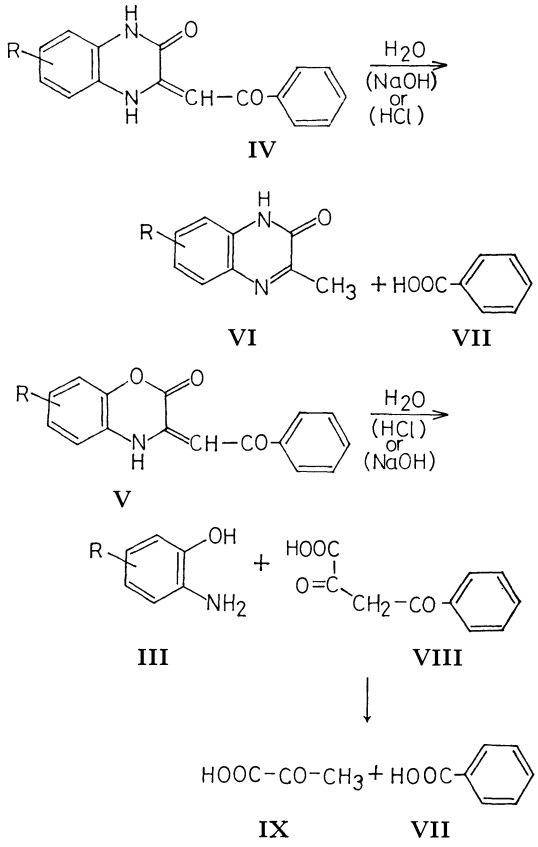

Hydrolysis of IV gave the corresponding 3-methyl-2(1*H*)-quinoxalinones (VI) and benzoic acid (VII), while that of V afforded the starting substances, *o*-aminophenols (III) and benzoylpyruvic acid (VIII) which had been partially decomposed into pyruvic acid (IX) and VII.

The reasons why V gave starting materials whereas IV preserved its quinoxaline ring would be exactly the same as those given for their analogues.[5]

Experimental

IR spectra were measured for KBr disks with a Nippon Bunko DS-301 spectrophotometer, NMR spectra were determined on a Hitachi H-60 spectrometer, and electronic absorption spectra were taken on a Hitachi 124 spectrophotometer.

The starting material, ethyl benzoylpyruvate (I), was prepared according to the method of Beyer and Claisen.[12] All melting points are uncorrected.

3-Phenacylidene-3,4-dihydro-2(1H)-quinoxalinone (*IVa*). Preparation was essentially the same as that reported.[13] Yield 95%. Recrystallization from acetone gave IVa as yellow needles; mp 268—269°C (lit.[13,14] mp 267—268°C). Found: C, 72.84; H, 4.64; N, 10.38%.

7-Chloro-3-phenacylidene-3,4-dihydro-2(1H)-quinoxalinone (*IVb*). Into a solution of IIb (0.7 g) in ethanol (20 m*l*), a solution of sodium salt of I (1.4 g) 50% acetic acid (25 m*l*) was dropped with stirring. After the mixture had been stirred for further 2 hr, it was allowed to stand overnight. The precipitated crystals (84% yield) were recrystallized from hot dimethyl sulfoxide to give IVb as yllow prisms; mp 323°C.

Found: C, 64.58; H, 3.88; N, 9.37%. Calcd for $C_{16}H_{11}O_2N_2Cl$: C, 64.34; H, 3.68; N, 9.38%.

The other compounds were synthesized in a similar manner.

3-Phenacylidene-3,4-dihydro-2(1H)-benzo[g]quinoxalinone (*IVc*). Yield 61%. Orange-yellow needles from dimethyl sulfoxide; mp 343°C.

Found: C, 76.62; H, 4.59; N, 9.27%. Calcd for $C_{20}H_{14}O_2N_2$: C, 76.42; H, 4.49; N, 8.91%.

3-Phenacylidene-3,4-dihydro-2H-1,4-benzoxazin-2-one (*Va*). Yield 72%. Orange-yellow prisms from acetone; mp 200—201°C (lit.[15,16] mp 201°C). Found: C, 72.65; H, 4.20; N, 5.60%.

6-Methyl-3-phenacylidene-3,4-dihydro-2H-1,4-benzoxazin-2-one (*Vb*). Yield 86%. Yellow prisms from acetone; mp 174.5—175°C.

Found: C, 73.40; H, 4.81; N, 5.31%. Calcd for $C_{17}H_{13}O_3N$: C, 73.11; H, 4.69; N, 5.02%.

6-Chloro-3-phenacylidene-3,4-dihydro-2H-1,4-benzoxazin-2-one (*Vc*). Yield 74%. Yellow prisms from acetone; mp 212—213°C.

Found: C, 64.25; H, 3.42; N, 4.80%. Calcd for $C_{16}H_{10}O_3NCl$: C, 64.12; H, 3.36; N, 4.67%.

3-Phenacylidene-3,4-dihydro-2H-naphtho[2,1-b]-1,4-oxazin-2-one (*Vd*). Yield 89%. Orange fibers from acetone; mp 200—200.5°C.

Found: C, 75.90; H, 4.15; N, 4.72%. Calcd for $C_{20}H_{13}O_3N$: C, 76.18; H, 4.16; N, 4.44%.

11) IR spectral data also support a lactam structure of IV, as shown in the structurel formulae, but not lactim. This partial structure is the same in dimethyl sulfoxide-d_6, as proved by NMR spectroscopy. In spite of a reasonable interpretation of the NMR spectra in trifluoroacetic acid, the possibility of decomposition in the acid may not be ruled out because of the variety of signals.

12) C. Beyer and L. Claisen, *Ber.*, **20**, 2181 (1887).

13) S. Fatutta and A. Stener, *Gazz. Chim. Ital.*, **88**, 89 (1958).

14) Reported as 3-phenacyl-2(1*H*)-quinoxalinone.

15) E. Biekert, D. Hoffmann, and F. J. Meyer, *Chem. Ber.*, **94**, 1664 (1961).

16) Reported as 3-phenacyl-2*H*-1,4-benzoxazin-2-one.

Hydrolysis of IVa. A suspension of IVa (0.75 g) in 2 N sodium hydroxide (25 m*l*) was refluxed for 1 hr. The reaction mixture soon turned into a solution upon heating. Into the solution, after cooling, 6 N hydrochloric acid was dropped with stirring until it remained slightly alkaline. The hydrolysate was repeatedly extracted with chloroform. From the combined extracts, the solvent was removed *in vacuo*, and the residue was recrystallized from ethanol to give 3-methyl-3, 4-dihydro-2(1*H*)-quinoxalinone (VIa) (0.28 g) as colorless needles; mp 243—244°C, undepressed on admixture with a sample which had been prepared.[2] Found: N, 17.57%.

The aqueous layer was acidified with 6 N hydrochloric acid, and extracted with ether repeatedly. Ether was removed from the combined extracts, and the residue was recrystallized from ethanol to afford benzoic acid (VII) (0.29 g) as colorless plates; mp 122—122.5°C, undepressed on admixture with a commercial sample. The product VII was UV-spectroscopically identical with the sample.

Hydrolysis of Va. A solution of Va (1.20 g) in a mixture of acetic acid (40 m*l*) and 6 N hydrochloric acid (20 m*l*) was refluxed for 2 hr. After it had been cooled, the hydrolysate was extracted with benzene three times. The combined extracts were dried over anhydrous sodium sulfate, and the solvent was removed. The residue (0.61 g) was recrystallized from ether to give benzoylpyruvic acid (VIII) as yellowish prisms; mp 155—156°C. (lit.[11] mp 155—156°C), undepressed on admixture with a sample prepared according to literature. Its identity was also proved by UV spectroscopy. The acidity of the aqueous layer was reduced to pH 5 by adding sodium hydrogencarbonate powder, and the aqueous solution was extracted with ether three times. The combined extracts were dried over anhydrous sodium sulfate, and ether was removed. The residue was recrystallized from ethanol to afford *o*-aminophenol (IIIa) (0.48 g); mp 172—174°C, undepressed on admixture with a commercial sample used for the synthesis of Va. UV spectra proved its identity.

From the mother liquors, small amounts of VII and pyruvic acid (IX) were isolated (IX was precipitated as its 2,4-dinitrophenylhydrazone). They were identified by mixed melting points and UV spectroscopy. When Va was refluxed with 6 N hydrochloric acid for 3 hr, the yields of VII and IX which were probably derived from the partial hydrolysis of VIII, increased.

Hydrolyses of the Other Compounds. The hydrolyses of IVb, c and Vb–d were performed in a similar manner to that described above. The corresponding 3-methyl-2(1*H*)-quinoxalinones (VIb,c) were obtained from IVb,c in similar yields and were identical with the respective samples prepared[3] by the mixed melting points and by comparison of their UV spectra. From Vb–d, the corresponding *o*-aminophenols (IIIb–d) and VIII were formed, and their identity with those used for the syntheses of Vb–d was similarly checked by means of melting points and UV spectra.

Similar results were obtained from the hydrolyses of IVa–c with hydrochloric acid and those of Va–d with sodium hydroxide.

BULLETIN OF THE CHEMICAL SOCIETY OF JAPAN, VOL. 44, 1321—1327(1971)

The Oligomerization of Butadiene with Nickel Complexes Produced by Means of the Electrolysis of Nickel(II) Chloride

Takayuki OHTA, Keisuke EBINA, and Noboru YAMAZAKI
Tokyo Institute of Technology, Ookayama, Meguro-ku, Tokyo

(Received April 23, 1970)

The oligomerization of butadiene has been found during the electrolysis of solutions containing nickel(II) chloride and electron donors. The oligomerization was affected by the nature of the electron donors used. When the ethanolic solutions of tetrakis(pyridine)nickel(II) chloride or nickel(II) chloride and pyridine with tetra-*n*-butyl ammonium perchlorate or methanolic solutions without the perchlorate were electrolyzed in the presence of butadiene, a number of linear and dihydrogenated oligomers, with small amounts of branched oligomers, were obtained. The main oligomers were identified as *n*-octadiene, *n*-dodecatriene, and *n*-hexadecatetraene. By adding triphenylphosphine to the reaction system in place of pyridine, *n*-octatriene and alkoxyoctadiene were catalytically produced instead of hydrooligomers, accompanied by tetrakis(triphenylphosphine)nickel(0). A mechanism involving π-allyl intermediates was proposed for the oligomerization.

It has been known that butadiene is oligomerized selectively to cyclic dimers and trimers with various catalyst systems containing lower-valency transition-metal compounds. Recently, several reports on the linear dimerization of butadiene by cobalt,[1] iron,[2] rhodium,[3] palladium,[4] and nickel[5] catalysts have been

1) E. W. Duck, D. K. Jenkins, J. M. Locke, and S. R. Wallis, *J. Chem. Soc., C*, **1969**, 227; S. Otsuka, T. Taketomi, and T. Kikuchi, *Kogyo Kagaku Zasshi*, **66**, 1094 (1963); T. Saito, T. Ono, Y. Uchida, and A. Misono, *ibid.*, **66**, 1099 (1963); D. H. Wittenberg, *Angew. Chem.*, **75**, 1124 (1963); S. Tanaka, K. Mabuchi, and N. Shimazaki, *J. Org. Chem.*, **29**, 1626 (1964); M. Iwamoto, K. Tani, H. Igaki, and S. Yuguchi, *ibid.*, **32**, 4148 (1967).

2) H. Takahashi, S. Tai, and M. Yamaguchi, *J. Org. Chem.*, **30**, 1661 (1965); M. Hidai, Y. Uchida, and A. Misono, This Bulletin, **38**, 1243 (1965); A. Carbonaro, A. Greco, and G. Dall, Asta, *Tetrahedron Lett.*, **1967**, 2037.

3) T. Alderson, E. L. Jenner, and R. V. Lindsey, Jr., *J. Amer. Chem. Soc.*, **87**, 5638 (1965).

4) a) S. Takahashi, T. Shibano, and N. Hagihara, *Tetrahedron Lett.*, **1967**, 2451; S. Takahashi, T. Shibano, and N. Hagihara, This Bulletin, **41**, 454 (1968); b) E. J. Smutny, *J. Amer. Chem. Soc.*, **89**, 6793 (1967).

5) H. Muller, D. Wittenberg, H. Seibt, and E. Scharf, *Angew. Chem., (Intern. Ed.)*, **4**, 327 (1965); H. Seibt and N. V. Kutepow, *Belg. Pat.* 635483 (1964), *Chem. Abstr.*, **61**, 11891 (1964).

presented.

In a previous paper,[6] we reported that dihydrogenated linear dimers, trimers, and tetramers of butadiene were obtained with catalysts composed of nickel (II) chloride, electron donors, and lithium aluminum hydride or sodium borohydride. In the course of our studies of the synthesis of oligoolefin-metal complexes by means of the electrolytic reduction of metal salts, a novel tetramer of butadiene has been found.[7] We have also studied the oligomerization of butadiene in detail. This paper will deal with the results of butadiene oligomerizations by means of the electrolysis of alcoholic solutions containing nickel(II) chloride and electron donors, and with the identification of the oligomers obtained.

Experimental

Materials. Methyl and ethyl alcohols were purified and dried with the corresponding magnesium alkoxides according to the method by Lund and Bjerrum.[8] Ethyl ether was dried over Na and then with $LiAlH_4$, and distilled under a nitrogen stream. Butadiene was dried with $LiAlH_4$ and freshly distilled before use. Triphenylphosphine was recrystallized from ethyl alcohol. Pyridine, piperidine, and triethylamine were distilled over sodium hydroxide under nitrogen. Nickel(II) chloride, tetrakis(pyridine)nickel(II) chloride, and tetra-*n*-butylammonium perchlorate were prepared according to the known procedures and were purified by the usual methods.[9]

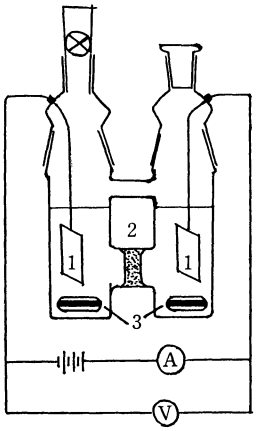

Fig. 1. Electrolysis cell.

A, ammeter; V, voltameter; 1, electrode; 2, sintered glass disk; 3, magnetic stirring bar

Electrolyses. The electrolyses were carried out in the modified H-type glass cell shown in Fig. 1. In a typical experiment, a cell equipped with a stopcock and containing 25 mmol of tetrakis(pyridine)nickel(II) chloride and magnetic stirring bars was dried under a vacuum. The atmospheric pressure was then restored using purified nitrogen. Under a blanket of nitrogen, 180 m*l* of methyl alcohol was transferred to the cell, which was then cooled in a dry ice-methyl alcohol bath and degassed on a vacuum system. Under a vacuum, butadiene was introduced *via* the trap-to-trap method. The stopcock connecting the cell to the vacuum line was then closed, and the electrolyte was warmed to the room temperature. The electrolysis was performed at ambient temperature, with the terminal voltage maintained at about 50 V for 20—40 hr; during this time, an amount of electricity of 2 Faradays per mol of nickel(II) chloride, as calculated from the current and time, was passed through the solution. The current was almost constant throughout the electrolysis, being 30 mA in ethyl alcohol and about 70 mA in methyl alcohol.

After electrolysis, the catholyte was treated with dilute hydrochloric acid in order to destroy the produced nickel complexes, which consisted of an oligoolefin, pyridine, and nickel. A mixture of the butadiene oligomers formed was extracted with diethyl ether, followed by washing with water and drying over anhydrous sodium sulfate, and concentrated under reduced pressure. Then the oligomers were fractionated by distillation.

Analyses. The amounts of all the oligomers obtained herein were calculated from the calibration curve for cyclododeca-1,5,9-triene, assuming that the molar responses of the dimers, trimers, and tetramers of butadiene to cyclododeca-1,5,9-triene are 1.25, 1, and 0.8 respectively, (It has been observed that the molar responses of 1-octene and hexadeca-1,6,10,14-tetraene to cyclododeca-1,5,9-triene are 1.25 and 0.8 respectively). The yields of the oligomers were based on the amounts of butadiene introduced. Each oligomer was isolated by fractional distillation and or by preparative gas chromatography, and their structures were verified by IR, NMR, and mass spectrometries and by elemental analyses.

A gas chromatograph (Shimadzu Seisakusho Ltd., GC-4APT) fitted with a copper tube (3 mm × 3 m) packed with Apiezon grease-L on Diasolid was employed to detect and determine dimeric, trimeric, and tetrameric isomers. The gas chromatograph was operated under the following conditions: for the analyses of the dimers of butadiene, the temperatures of the column and the injection part were 120 and 200°C respectively, and the hydrogen flow rate was 60 m*l*/min. For trimers and tetramers, the temperatures of the column and the injection part were 180 and 200°C respectively, and the hydrogen flow rate was 120 m*l*/min. In order to isolate the respective oligomers, a gas chromatograph (Ohkura-Rikagaku) fitted with a copper tube (4 mm × 2 m) packed with Apiezon grease-L or polydiethylene glycol succinate on Diasolid was used under the same conditions as those presented above.

The infrared spectra were recorded on a Jasco IR spectrophotometer, Model IR-G, as a liquid film, the UV and visible spectra, on a Shimadzu Model SV-50A spectrophotometer, the NMR spectra, at 60 MHz on a JEOL Model C-60 in a carbon tetrachloride solution, with tetramethylsilane as the internal standard, and the mass spectra, on a Hitachi Model RMU-5B.

Identification of Oligomers. The results of the IR and NMR spectra, the elemental analyses, and the molecular-weight measurements of each oligomer of butadiene are shown in Table 1. On the basis of these results, the four oligomer fractions, 3-MOD, 1-MOD, 3-EOD, and 1-EOD, were confirmed to be 3-methoxyocta-1,7-diene, 1-methoxyocta-2,7-diene, 3-ethoxyocta-1,7-diene, and 1-ethoxyocta-2,7-diene respectively. On the contrary, to the other oligomer fractions, P-6, P-7, P-9, P-10, and P-11, many isomeric structures

6) N. Yamazaki and T. Ohta, *J. Macromol. Sci.*, **A3**, 1571 (1969).

7) N. Yamazaki and S. Murai, *Chem. Commun.*, **1968**, 147.

8) H. Lund and J. Bjerrum, "Technique of Organic Chemistry. VII." Organic Solvents, Arnold Weissberger, Interscience Publisher, New York (1955), p. 334.

9) A. R. Pray, "Inorganic Synthesis. V," J. C. Bailar, Jr., Mcgrow-Hill Book Company, New York (1953), p. 153.

which give essentially identical IR and NMR spectra can be derived from the results of their spectrometric analyses. However, in view of the formation mechanism of the oligomers described in a following section, the structures of P-6, P-7, P-9, P-10, and P-11 of the oligomer fractions may be assumed to be 5-vinyldeca-2,8-diene, 3-methylundeca-1,5,10-triene, 1-methoxydodeca-2,6,11-triene, 5-vinyltetradeca-1,8,13-triene, and *n*-hexadeca-1,6,10,15-tetraene respectively (Table 2).

The other oligomers, *n*-octa-1,6- and -1,7-diene, *n*-octa-1,3,7-triene, and *n*-dodeca-1,6,10-triene, were identified by vpc. The identification by vpc was conducted by comparing the retention times with those of authentic samples, which were prepared by the previously-described reactions.[6]

Table 1. Elemental analysis and spectrometric, and molecular weight measurements of the oligomers

Fraction number	Empirical formula	Elemental[a] analysis %	Molecular[a] weight	IR Frequency cm^{-1}	IR Vibration mode	NMR τ value[b]	NMR Intensity ratio	NMR Assignment
3-MOD,	$C_9H_{16}O$	C, 77.13 (77.09) H, 12.05 (11.50)	140[c] (140.2)	1643	unconjugated ν C=C	3.90—4.75(m)	2	=CH-
						4.75—5.35(m)	4	$=CH_2$
				1380	δ CH_3	6.45—6.80(m)	2	-C-CH-C- (O)
				1101	ν C-O(OCH_3)			
				990	δ CH_2(-CH=CH_2)	6.85 (s)	3	$-OCH_3$
				925		7.70—8.30(m)	2	=C-CH_2-C-
				910		8.30—8.80(m)	4	-C-CH_2-C-
1-MOD,	$C_9H_{16}O$	C, 77.12 (77.09) H, 11·80 (11.50)	140[c] (140.2)	1670	unconjugated ν C=C(internal)	4.00—4.75(m)	3	=CH-
						4.75—5.40(m)	2	$=CH_2$
				1638	ν C=C(terminal)	6.30 (d)	2	-O-CH_2-C=
				1360	δ CH_3	6.85 (s)	3	$-OCH_3$
				1115	ν C-O(-OCH_3)	7.70—8.30(m)	4	=C-CH_2-
				991	δ CH_2(-CH=CH_2)	8.30—8.70(m)	2	-C-CH_2-C-
				970	δ CH(*trans*-CH=CH-)			
				910	δ CH_2(-CH=CH_2)			
3-EOD,	$C_{10}H_{18}O$	C, 78.00 (77.90) H, 11.35 (11.75)	154[c] (154.3)	1643	unconjugated ν C=C	3.80—4.75(m)	2	=CH-
						4.75—5.35(m)	4	$=CH_2$
				1373	δ CH_3	6.20—7.15(m)	3	-O-CH_2-CH_3
				1095	ν C-O(-OCH_3)			-C-CH-C- (O)
				1000	δ CH_2(-CH=CH_2)			
				925		7.65—8.20(m)	2	=C-CH_2-C-
				915		8.40—8.75(m)	4	-C-CH_2-C-
						8.85 (t)	3	-CH_2-CH_3
1-EOD,	$C_{10}H_{18}O$	C, 77.88 (77.90) H, 11.62 (11.75)	154[c] (154.3)	1670	unconjugated ν C=C(internal)	3.80—4.70(m)	3	=CH-
						4.70—5.80(m)	2	$=CH_2$
				1638	ν C=C(terminal)	6.25 (d)	2	-O-CH_2-CH=
				1375	δ CH_3	6.65 (q)	2	-O-CH_2-CH_3
				1105	ν C-O(-OC_2H_5)	7.70—8.30(m)	4	=C-CH_2-C-
				990	δ CH_2(-CH=CH_2)	8.30—8.75(m)	2	-C-CH_2-C-
				970	δ CH(*trans*-CH=CH-)			
				910	δ CH_2(-CH=CH_2)	8.87 (t)	3	-CH_2-CH_3
P-6,	$C_{12}H_{20}$	C, 87.30 (87.75) H, 12.55 (12.25)	—	1643	unconjugated ν C=C	3.80—4.85(m)	5	=CH-
						4.85—5.40(m)	2	$=CH_2$
				1380	δ CH_3	7.65—8.28(m)	5	=C-CH_2-
				996	δ CH_2(-CH=CH_2)			=C-CH- (I)
				970	δ CH(*trans*-CH=CH-)			
				910	δ CH_2(-CH=CH_2)	8.28—8.53(m)	6	=C-CH_3
						8.53—8.90(m)	2	-C-CH_2-C-
P-7,	$C_{12}H_{20}$	C, 87.27 (87.75) H, 12.41 (12.25)	168[d] (164.3)	1643	unconjugated ν C=C	4.00—4.85(m)	4	=CH-
						4.85—5.35(m)	4	$=CH_2$
				1375	δ CH_3	7.65—8.30(m)	7	=CH-CH_2-
				995	δ CH_2(-CH=CH_2)			=C-CH- (I)
				970	δ CH(*trans*-CH=CH-)			
				910	δ CH_2(-CH=CH_2)	8.53—8.90(m)	2	-C-CH_2-C-
						9.02 (d)	3	-CH-CH_3

TABLE 1. Continued

P-9,	$C_{13}H_{22}O$	—	—	1643	unconjugated	4.00—4.85(m)	5	=CH-
					ν C=C	4.85—5.50(m)	3	$=CH_2$
				1375	δ CH_3	6.25 (d)	2	$-O-CH_2CH=$
				1110	ν C-O($-OCH_3$)	6.80 (s)	3	$-OCH_3$
				990	δ CH_2($-CH=CH_2$)	7.70—8.30(m)	8	$=C-CH_2-$
				965	δ CH(*trans*-CH=CH-)	8.30—8.90(m)	2	$-C-CH_2-C-$
				910	δ CH_2($-CH=CH_2$)			
P-10,	$C_{16}H_{26}$	C, 87.71 (88.00) H, 12.29 (12.00)	225[d] (218.4)	1640	unconujgated	3.85—4.85(m)	5	=CH-
					ν C=C	4.85—5.35(m)	6	$=CH_2$
				990	δ CH_2($-CH=CH_2$)	7.70—8.30(m)	9	$=C-CH_2-$
				970	δ CH(*trans*-CH=CH-)			=C-CH-
				910	δ CH_2($-CH=CH_2$)	8.30—8.90(m)	6	$-C-CH_2-C-$
P-11,	$C_{16}H_{26}$	C, 87.99 (88.00) H, 12.01 (12.00)	228[d] (218.4)	1640	unconjugated	3.90—4.80(m)	6	=CH-
					ν C=C	4.80—5.35(m)	4	$=CH_2$
				990	δ CH_2($-CH=CH_2$)	7.70—8.30(m)	12	$=C-CH_2-$
				965	δ CH(*trans*-CH=CH-)	8.40—8.80(m)	4	$-C-CH_2-$
				908	δ CH_2($-CH=CH_2$)			

a) A value in parentheses shows a calculated value for the respective compound.
b) Symbols in parentheses show: m, multiplet; d, doublet; s, singlet; q, quintet.
c) Determined by mass spectrometry (parent peak m/e).
d) Determined by cryoscopic method in benzene.

TABLE 2. CHEMICAL STRUCTURES OF OLIGOMERS

Fraction number	Compound	Constitutional formula
3-MOD	3-methoxyocta-1,7-diene	$CH_2=CHCH(OCH_3)CH_2CH_2CH_2CH=CH_2$
1-MOD	1-methoxyocta-2,7-diene	$CH_3OCH_2CH=CHCH_2CH_2CH_2CH=CH_2$
3-EOD	3-ethoxyocta-1,7-diene	$CH_2=CHCH(OC_2H_5)CH_2CH_2CH_2CH=CH_2$
1-EOD	1-ethoxyocta-2,7-diene	$C_2H_5OCH_2CH=CHCH_2CH_2CH_2CH=CH_2$
P-6 (5-VDD)	5-vinyldeca-2,8-diene	$CH_3CH=CHCH_2CH_2CH(CH=CH_2)CH_2CH=CHCH_3$
P-7 (3-MUDT)	3-methylundeca-1,5,10-triene	$CH_2=CHCH(CH_3)CH_2CH=CHCH_2CH_2CH_2CH=CH_2$
P-9 (1-MODT)	1-methoxydodeca-2,6,11-triene	$CH_3OCH_2CH=CHCH_2CH_2CH=CHCH_2CH_2CH_2CH=CH_2$
P-10 (5-VTDT)	5-vinyltetradeca-1,8,13-triene	$CH_2=CHCH_2CH_2CH(CH=CH_2)CH_2CH_2CH=CHCH_2CH_2CH_2CH=CH_2$
P-11 (NHDT)	hexadeca-1,6,10,15-tetraene	$CH_2=CHCH_2CH_2(CH_2CH=CHCH_2)_2CH_2CH_2CH=CH_2$

Results and Discussion

On the electrolysis of the alcoholic solutions containing nickel(II) chloride and electron donors in the presence of butadiene, the initial blue or yellow color of nickel(II) ion in the solution changed to a dark brown-red, which color disappeared in air. Using pyridine as an electron donor, a number of linear and dihydrogenated oligomers were obtained, plus small amounts of branched oligomers. By adding triphenylphosphine to the reaction system in place of pyridine, *n*-octatriene and alkoxyoctadiene were catalytically produced instead of hydrooligomers, accompanied by tetrakis(triphenylphosphine)nickel(0). In neither case were cyclic oligomers produced. The yields and selectivities of the oligomers were affected by the nature of the electron donors and solvents used (Tables 3 and 4). The current efficiency of the nickel(0) complex was about 75%, based on the 2e process.

Effects of Electron Donors on the Oligomerization of Butadiene. (I) Effects of Pyridine: When pyridine was used as the electron donor, an air-sensitive and dark brown-red solution containing oligoolefin-nickel (0) complexes was produced. The properties and structures of the complexes will be reported in a following paper. Most of the oligomers obtained by decomposing the complexes with dilute hydrochloric acid were found to be linear and dihydrogenated dimers, trimers, and tetramers. No oligomers higher than tetramers could be detected by gas chromatography or gel-permeation chromatography. A programmed-temperature gas chromatogram of a mixture of the oligomers is indicated in Fig. 2. Oligomers at the peak numbers of 6, 7, 8, 9, 10, and 11 were isolated by means of preparative gas chromatography with Apiezon grease-L and polydiethyleneglycol succinate; they were spectrometrically analyzed (Table 1). Their structures may be characterized as in Table 2. Although dimeric butadiene isomers at the peak numbers of 2 and 3 could not be separated with any of the columns employed (Apiezon grease-L, polydiethyleneglycol succinate, dioctylsebacate, and squalene), they were identified as octa-1,6- and -1,7-diene respectively by comparing the retention times with those of authentic samples. In the same way, oligomers corresponding to the peak numbers of 4 and 5 have also been found to be 3-methoxyocta-1, 7-diene and 1-methoxyocta-2,7-diene respectively.

A gas chromatogram of a mixture of those oligomers

Table 3. Oligomerization of butadiene with nickel complexes produced by means of electrolysis of nickel(II) chloride and electron donor in protic solvents

Expt. No.	$NiCl_2$ mmol	Butadiene mmol	Electron donor (mmol)	Solvent[a]	Amount of current $\times 10^2$ F	Yield[c] %	Produced oligomers, % Dimers	Trimers	Tetramers
014	23	400	—	EtOH	5	0			
E-029	20	220	—	MeOH	5	1.4	53	7	40
104	20	250	Pyridine (80)	MeOH	4	25.6	60	27	13
103	10	250	HMPA[b] (80)	MeOH	4	7.45	95	5	0
083	10	300	Triphenylphosphine (20)	MeOH and Benzene	2	45.6	>95		
012	25	300	Triphenylphosphine (50)	EtOH	5	47.3	>95		
100	20	250	Acetonitrine (80)	MeOH	4	0			
101	20	250	Piperidine (80)	MeOH	4	0			
112	20	250	Triethylamine (80)	MeOH	4	0			

a) 90 m*l* of the solvent (containing 1.7 g of Bu_4NClO_4 in the case of ethyl alcohol) in each compartment of the electrolysis cell.
b) Hexamethylphosphoramide.
c) Based on the mole of butadiene introduced.

Table 4. Dimers of butadiene formed with electrolysis of nickel (II) chloride in the presence of triphenyl phosphine in methyl alcohol and ethyl alcohol

Expt. No.	Yield,[c] %	Components dimer mixture, % NOT[d]	3-MOD	1-MOD	3-EOD	1-EOD
083[a]	45.6	27.4	28.8	43.8	—	—
082[b]	28.1	33.3	22.2	44.5	—	—
012[a]	47.3	83.7	—	—	2.80	9.50
011[b]	47.2	71.6	—	—	2.50	10.0

a) PPh_3/Ni(II), 2; b) PPh_3/Ni(II), 4.
c) Based on the mole of butadiene introduced.
d) Octa-1,3,7-triene.

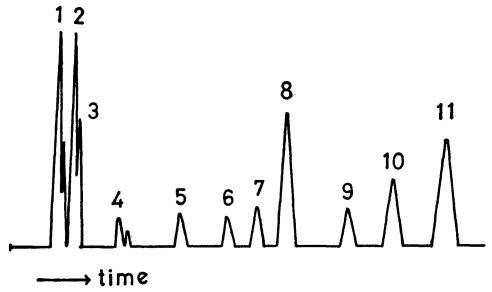

Fig. 2. A programmed temperature gas chromatogram of a mixure of oligomers obtained by means of electrolysis of $NiCl_2 4NC_5H_5$.
Oligomers corresponding to peak numbers: 2, octa-1,6-diene; 3, octa-1,7-diene; 4, 3-methoxyocta-1,7-diene; 5, 1-methoxyocta-2,7-diene; 6, 5-vinyldeca-2,8-diene; 7, 3-methylundeca-1,5,10-triene; 8, dodeca-1,6,10-triene; 9, 1-methoxydodeca-2,6,11-triene; 10, 5-vinyltetradeca-1,8,13-triene; 11, hexadeca-1,6,10,15-tetraene.
Conditions: initial temperature, 80°C; final temperature, 180°C; rate of temperature increase, 2°C/min; column, Apiezon grease-L (3 mm × 3 m); hydrogen flow rate, 120 m*l*/min.

was very close to that of the oligomers obtained by reducing tetrakis(pyridine)nickel(II) chloride with lithium aluminum hydride or sodium borohydride in the presence of butadiene.[6] This finding might suggest a similarity in mechanisms for the oligomerization in these reaction systems. For the oligomerization by the catalysts participated with the chemical reducing agents, we previously proposed a mechanism involving bis-π-allylic $C_8H_{12}Ni$ and $C_{12}H_{18}Ni$ complexes as intermediates.[6]

The yields of the oligomers were affected by the molar ratios of pyridine to nickel(II) chloride, but not by the amounts of the electric current when it was passed over two Faradays to mol of nickel(II) chloride. The maximum yield was obtained at the molar ratio two of pyridine to nickel(II) chloride.[10]

(II) Effects of triphenylphosphine: On the electrolyses of ethanolic solutions containing nickel(II) chloride, a four-fold excess of triphenylphosphine in place of pyridine, and the supporting electrolyte, the initial yellow color of the catholyte changed to a dark brown-red, and at the end of the electrolysis a brown solid precipitated. The dark brown-red color of the cathodic solution faded when it was exposed to the air.

From the cathodic solution, octa-1,3,7-triene was obtained catalytically, plus small amounts of 3-ethoxyocta-1,7-diene and 1-ethoxyocta-2,7-diene. From the anolyte were obtained small amounts of the oligomers. Probably, the oligomers formed in the catholyte were transferred through the glass filter of the cell to the anodic compartment. When methyl alcohol containing a small amount of benzene to dissolve triphenylphosphine was substituted for ethyl alcohol as a reaction medium, approximately equimolar amounts of octa-1, 3,7-triene, 3-methoxyocta-1,7-diene, and 1-methoxyocta-2,7-diene were obtained (Table 4).

The brown precipitate described above was filtered, washed with ethyl alcohol, and dried under a vacuum

10) T. Ohta, K. Ebina, and N. Yamazaki, unpublished data.

TABLE 5. DIMERIZATION OF BUTADIENE WITH TETRAKIS(TRIPHENYLPHOSPHINE)-NICKEL (0) IN METHYL ALCOHOL AND ETHYL ALCOHOL[a)]

Expt. No.	$Ni(PPh_3)_4$, mmol	Butadiene, mmol	Solvent, (ml)	Yield,[b)] %	Component of dimer mixture, %				
					NOT[c)]	3-MOD,	1-MOD,	3-EOD,	1-EOD
102	1.35	100	MeOH (20) and Benzene (10)	16.5	28.2	32.3	39.5	—	—
113	1.40	180	EtOH (30)	100	83.0	—	—	3.5	8.7

a) Dimerization of butadiene was carried out in a 100-ml glass tube at 20—30°C for 48 hr
b) Based on the mole of butadiene introduced.
c) Octa-1,3,7-triene.

at room temperature. The compound was assumed to be a tetrakis(triphenylphosphine)nickel(0) complex from elemental analysis (Calcd for $C_{72}H_{60}P_4Ni$: C, 78.06; H, 5.45; Ni, 5.30. Found: C, 76.35; H, 5.05; Ni, 5.25); the yield was 87% based on nickel(II) chloride. When this complex was used separately as a catalyst for the dimerization of butadiene in ethyl or methyl alcohol containing benzene, octa-1,3,7-triene 3-alkoxyocta-1,7-diene, and 1-alkoxyocta-2,7-diene were formed; their proportions were similar to those of the oligomers produced by electrolysis in each case (Table 5). These results led us to assume that nickel (II) chloride, in the presence of triphenylphosphine, was electrochemically reduced to the tetrakis(triphenylphosphine)nickel(0), and that the resulting complex in alcohol reacted with butadiene to give, catalytically, octa-1,3,7-triene and alkoxyoctadiene. It is noteworthy that tetrakis(triphenylphosphine)nickel(0) was prepared by means of the electrolytic reduction of nickel(II) chloride in the presence of triphenylphosphine in ethyl alcohol.

Octa-1,3,7-triene and alkoxyoctadienes have also been obtained with palladium-complex catalysts or other metal complexes of the VIII group (*e.g.*, Ru and Pt).[4b)] These oligomers may be produced through a π-allyl intermediate analogous to that proposed by Wilke.[11)]

(III) Effects of Other Electron Donors: Differently from the cases of pyridine and triphenylphosphine, the addition of acetonitrile, piperidine, or triethylamine to the electrolysis system resulted in a change in the color of neither the catholyte nor oligomers, but a large amount of metallic nickel was deposited on the cathodic electrode, as in the absence of electron donors. The absence of a color change in the catholyte on electrolysis indicates that no nickel complexes were produced. The use of hexamethylphosphoramide as an electron donor gave a small amount of the oligomers, composed predominantly of the dimers.

Pyridine and triphenylphosphine have both σ-donor and π-acceptor properties and can stabilize lower-valency transition-metal complexes by a combination of the two properties. On the other hand, acetonitrile, piperidine, and triethylamine, which lack suitable low-lying empty orbitals, act only as donors and formed less robust metal complexes than pyridine and triphenylphosphine. The above facts suggest that nickel(II) chloride, in the presence of pyridine and triphenylphosphine, is electrochemically reduced to yield lower-valency nickel-electron donor complexes and that the butadiene oligomers are produced on the complexes.

Electrochemical Reduction Process of Nickel(II) Chloride In the present electrolysis systems, three components, Ni^{2+} salt, the electron donor, and butadiene, can be reduced, and three probable modes of reduction can be visualized: (1) a direct electron transfer from the cathode to the nickel ion; (2) the reduction of the nickel(II) ion with the anion radicals (or dianions) formed by the reduction of the electron donors,[12,13)] and (3) the reaction of the nickel(II) ion with the anionic species produced by direct-electron transfer from the cathode to butadiene.

It was previously reported that the electron was preferably transferred from the cathode to butadiene, followed by the initiation of anionic polymerization in the *n*-Bu_4NClO_4-dimethoxyethane system.[14)] However, in protic solvents, neither polymers nor oligomers could be obtained. The addition of nickel(II) chloride and electron donors to the electrolysis system gave a variety of linear oligomers of butadiene. Probably, the anionic species produced by path (3) would react with the solvent prior to reacting with nickel(II) chloride.[15)] These results may exclude path (3). In the absence of electron donors, small amounts of oligomers were obtained, plus a large amount of metallic nickel. This indicates that nickel(II) chloride was electrochemically reduced through path (1). A half-wave potential of $Ni(pyridine)_4^{2+}$, -0.78 V *vs.* SCE (1 M KCl, 0.5 M pyridine)[16)] is less negative than those of butadiene ($E_{1/2}=-3.27$ V *vs.* SCE in dimethoxyethane).[14)] pyridine ($E_{1/2}=-2.48$ V or less in pyridine),[12)] and triphenylphosphine ($E_{1/2}=-2.70$ V in dimethylformamide);[13)] this finding also supports path (1).

On the basis of these results, we assume that path (1) is predominant for the primary electrode process, although path (2) cannot be ruled out.

11) G. Wilke, *Angew. Chem.*, **75**, 10 (1963); G. Wilke, B. Bogdanovic, P. Hardt, P. Heimbach, W. Kiem, M. Kröner, W. Oberkirch, K. Tanaka, E. Steinrücke, D. Walter, and H. Zimmermann, *ibid.*, **78**, 157 (1966).

12) S. N. Bhadani and G. Parravano, *J. Polym. Sci., A-1*, **8**, 225 (1970).

13) K. S. V. Santhanam and A. J. Bard, *J. Amer. Chem. Soc.*, **90**, 1118 (1968).

14) N. Yamazaki, I. Tanaka, and S. Nakahama, *J. Macromol. Sci.*, **A2**, 1121 (1968).

15) E. de Boer, "Advances in Organometallic Chemistry," Vol. 2, ed. by F. G. A. Stone and R. West, Academic Press, New York (1964), p. 115.

16) Chemical Society of Japan, "Kagakubinran (basic part)," Maruzen Co., Ltd., Tokyo, Japan (1966), p. 1377.

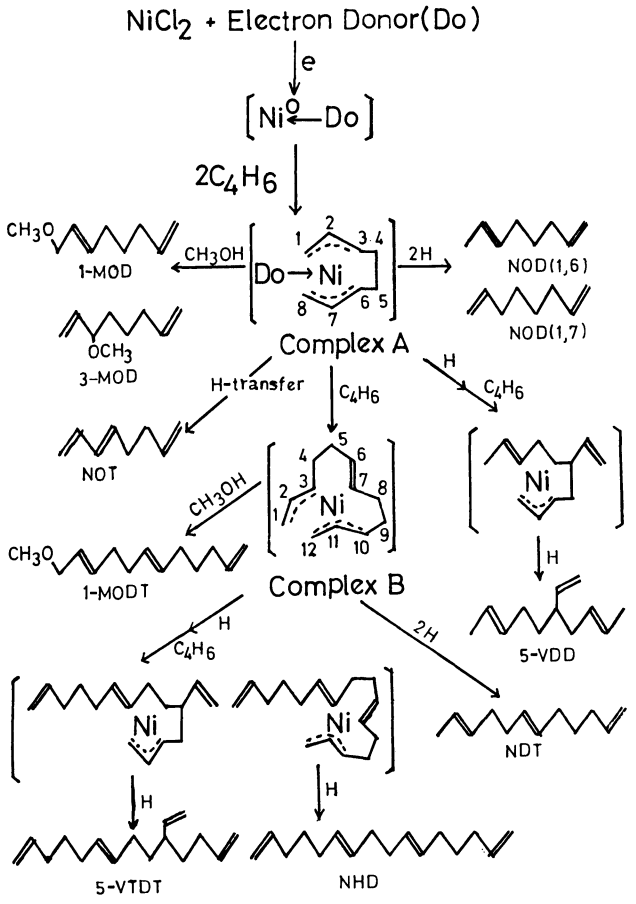

Fig. 3. A scheme for the oligomerization.

Mechanism of Oligomerization. The dark brown-red solution produced on the electrolysis of tetrakis(pyridine)nickel(II) chloride in the presence of butadiene was concentrated by evaporating methyl alcohol, unreacted butadiene, and free pyridine. The resulting dark brown-red compound was soluble in benzene and methyl alcohol to give brown-red solutions which were air-sensitive and which gradually decomposed to nickel metal and the corresponding oligomers at room temperature. The UV and visible spectra of the compound in *n*-hexane showed the maximum absorptions at 290—295 mμ ($\varepsilon \sim 3.2 \times 10^3$) and 422 m$\mu$ ($\varepsilon \sim 5.9 \times 10^2$); these absorptions disappeared in air. In its infrared spectrum, absorptions at 1000, 910, and 965 cm^{-1} due to terminal and trans-internal double bonds were observed. A far-infrared spectrum of the compound gave two air-sensitive absorptions at 530 and 305 cm^{-1} and showed two air-sensitive absorptions at 630 and 430 cm^{-1} due to pyridine coordinated to nickel. These results led us to assume that nickel complexes bonded with π-allylic structure of oligoolefins, such as octa-2,6-diene-1,8-diyl(pyridine)nickel(0), complex A, and dodeca-2,6,10-triene-1,12-diylnickel(0), complex B, shown in Fig. 3, were produced in the catholyte. When triphenylphosphine was used instead of pyridine, the resulting complex, tetrakis(triphenylphosphine)nickel (0), has been found to catalyze the dimerization of butadiene to *n*-octatriene and alkoxyoctadiene (Table 4).

On the basis of these findings, a mechanism for the oligomerization of butadiene by means of the electrolysis of alcoholic solutions containing nickel(II) chloride, electron donors, and butadiene may be proposed to be as follows. Nickel(II) chloride is electrochemically reduced to give electron donor-nickel(0) complexes, and butadiene is reacted with the complexes to yield complexes A and B (Fig. 3); then the 1,6- or 3,6-carbon of C_8H_{12} in complex A and the 1,10-carbon of $C_{12}H_{18}$ in complex B are hydrogenated or alkoxylated to octa-1,6- and -1,7-diene, and dodeca-1,6,10-triene or 1-alkoxyocta-2,7-diene, 3-alkoxyocta-1,7-diene, and 1-alkoxydodeca-2,6,11-diene respectively. In the formation of a linear tetramer and a branched trimer and tetramer, one hydrogen atom attacks the 1-carbon of a π-allylic group of complex A and the 3-carbon of a π-allylic group of complex B to destroy a rare gas structure of nickel atom and activate the other π-allylic groups of complexes A and B. Then one molecule of butadiene is inserted in the bond between the nickel atom and the 6-carbon of complex A or the 10- or 12-carbon of complex B, and the $C_{12}H_{19}$ or $C_{16}H_{25}$ produced on the nickel atom is hydrogenated to 5-vinyldeca-2,8-diene, and 5-vinyltetradeca-1,8,13-triene or hexadeca-1,6,10,15-tetraene.

It has been reported that cyclic dimers were formed *via* $C_8H_{12}NiPR_3$, similar to complex A in the reaction of butadiene with $Ni(CO)_2(PR_3)_2$ in benzene,[11] whereas octa-1,3,7-triene, accompanied by small amounts of octa-2,6-diene and acetone, were formed in isopropyl alcohol and monodeutrated octa-1,3,7-triene in C_6H_5OD.[17] In the IR spectra of a mixture of dimers obtained by means of electrolysis, an absorption at 1740 cm^{-1} due to the aldehyde group was observed. These facts suggest that the octa-1,3,7-triene obtained herein may be produced by the hydrogen transfer of C_8H_{12} in a complex with alcohol, and that hydrogen required for the hydrooligomerizations may originate from the alcohol used as a solvent.

17) J. Feldman, O. Frampton, B. Saffer, and M. Thomas, *Amer. Chem. Soc. Chicago Meeting, Div. Petrol. Chem.*, Preprints, **9**, (4), A55 (1964).

The Zinc Bromide-catalyzed Rearrangement of Pulegone Oxide and Piperitone Oxide

Hajime WATANABE, Jun KATSUHARA, and Noriyuki YAMAMOTO
Sun Star Dentifrice Company, Research Laboratory, Takatsuki, Osaka
(Received July 29, 1970)

The rearrangement of (+)-*cis*- (I) and (−)-*trans*-pulegone oxide (II) was effected by the catalysis of zinc bromide in boiling benzene to give the same (−)-2,2,5-trimethylcyclohepta-1,3-dione (III), with a retention of the optical activity. The structure of (−)-III with the expanded 7-membered ring was confirmed by the chemical transformation into 1,1,4-trimethyl-cycloheptane(IV), which was identical with that derived from eucarvone(V). Piperitone oxide(VIII) was also converted into diosphenol(X) in the same manner as in pulegone oxides.

Reusch[1] has recently reported that both (+)-*cis*- (I) and (−)-*trans*-pulegone oxide (II), upon gas-phase pyrolysis at 200°C, yielded the same crystalline solid melting at 50—51°C; its structure was suggested to be 2,2,5-trimethylcycloheptane-1,3-dione on the basis of the IR and NMR spectra alone.

We also have obtained a colorless crystal (III), mp 55—56°C, by treating I or II with zinc bromide in boiling benzene according to the Settine procedure.[2] A comparison of the elemental analysis and the NMR, IR, and mass spectra of III with those of the Reusch compound described in the literature[1] has shown the identity of these two compounds, although there is a slight difference in their melting points. No description has been reported for the optical activity of the Reusch compound; however, levo-rotation is found for III in the present work.

We now wish to describe the confirmation of the structure proposed by Reusch and the stereochemistry of this compound, as determined by means of unambiguous chemical transformation.

Eucarvone (V) (semicarbazone, mp 184°C) was hydrogenated over palladium charcoal to give the corresponding tetrahydro-compound (VI), which was converted into the tosylhydrazone (VII) and then reduced with lithium aluminum hydride to yield 1,1,4-trimethylcycloheptane (IV).

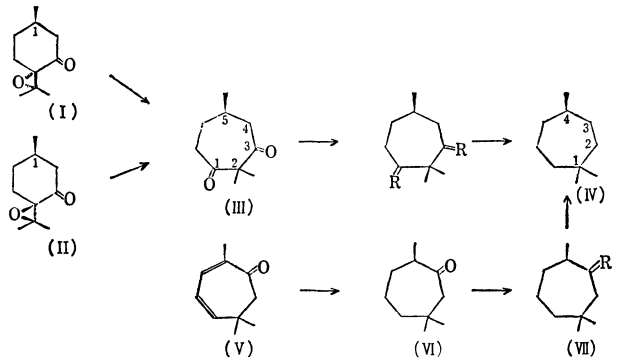

Scheme 1

On the other hand, (−)-III was converted, *via* its ditosylhydrazone, into IV. The identity of these two oily products (IV), obtained by different transformations, was shown by a comparison of their physical properties and IR and NMR spectra. This conversion provides further convincing evidence for the 2,2,5-trimethylcycloheptane-1,3-dione structure of the Reusch dione as well as for that of the (−)-III obtained by the present authors. Since the configuration at C-5 of the rearrangement product, (−)-III, must be the same as that (R-) at the C-1 of the parent compounds, (+)-*cis*-I and (−)-*trans*-II, the R-configuration can safely be assigned to the C-5 of (−)-III.

Piperitone oxide (VIII), upon treatment with zinc bromide in boiling benzene, gave diosphenol (X).

The zinc bromide-catalyzed rearrangements of I, II, and VIII in the present work seem to proceed *via* ionic intermediates; this is contrast to the thermal and photochemical rearrangements,[1,3-5] which have been looked upon as proceeding through radical pathways and which may be reasonably interpreted in terms of anionotropy.[6]

By Lewis-acid catalysis, the oxirane ring of piperitone oxide (VIII) undergoes heterolytic fission so as to form the most stable inoic intermediate (IX), in which the positive charge resides on the tertiary carbon, 1; there follows the 1,2-hydride shift (anionotropy), which fulfils the electron deficiency of the carbonium center, as is shown in Scheme 2. The same mechanism can be given for the formation of III (Scheme 3).

Under the same circumstances, the epimeric pule-

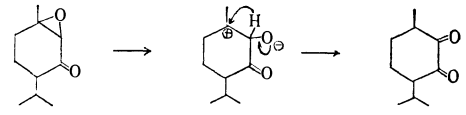

Scheme 2

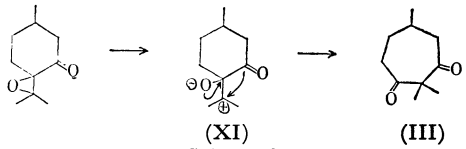

Scheme 3

1) W. Reusch, D. F. Anderson, and C. K. Johnson, *J. Amer. Chem. Soc.*, **90**, 4988 (1968).
2) R. L. Settine, G. L. Parks, and G. L. K. Hunter, *J. Org. Chem.*, **29**, 616 (1964).
3) H. Wehrli, C. Lehmann, K. Schaffner, and O. Jeger, *Helv.*, **47**, 1336 (1964).
4) O. Jeger, K. Schaffner, and H. Wehrli, *Pure Appl. Chem.*, **9**, 555 (1964).
5) C. K. Johnson, B. Dominy, and W. Reusch, *J. Amer. Chem. Soc.*, **85**, 3894 (1963).
6) C. D. Gutsche, "Organic Reaction," Vol. **8**, John Wiley & Sons, Inc., N.Y. (1954).

gone oxides, (+)-I and (−)-II, are converted into the transient polar-state intermediate (XI in Scheme 3), which then spontaneously rearranges with the anionoid migration of the carbonyl group (C-3) bearing the more negative charge. This mode of rearrangement can reasonably be preferred to that involving the migration of the C-5 methylene residue with the less negative charge. The intermediate (XI) should also be preferred, on the same basis, to an alternative which would lead to XII, the product obtained by the photo-induced rearrangement.[3-5]

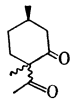

(XII)

It should be noted that the ground-state reaction under the acid catalysis of both epimeric epoxides (I) and (II) produced exclusively (−)-III, with an expanded carbocycle resulting from the anionotropy of the carbonyl group, while the photo-induced rearrangement (excited-state reaction) afforded the isomeric diketone (XII),[3-5] which resulted from the rather unusual methyl migration, and the pyrolysis gave a mixture of the two.[1]

Experimental

Zinc Bromide-catalyzed Rearrangement of Pulegone Oxide. (+)-*cis*-Pulegone oxide (mp 59°C, $[\alpha]_D^{20}$ +46.6° (*c* 0.3, methanol), 6.4 g: 0.038 mol) was boiled with zinc bromide (3.2 g: 0.014 mol) in dry benzene (200 m*l*) for 6 hr. After this period, water was added to the reaction mixture and it was extracted with ether. The combined extract was dried and the solvent was removed to give a crude crystalline product, III-a, (5.8 g, 90%), which melted at 55—56°C after several recrystallizations from petroleum ether.

Found: C, 71.23; H, 9.61%. Calcd for $C_{10}H_{16}O_2$: C, 71.37; H, 9.59%. $[\alpha]_D^{25}$ −81.6° (*c* 1.15, ethanol). IR spectrum: 1690 (cm^{-1}), 1730, 1370, 1355. NMR spectrum: τ 8.99 doublet 3H (-CH_3). τ 8.79 singlet 6H (-C(CH_3)$_2$). CD: mμ ([θ] in methanol) 342(0), 313.5(−8170), 240(0), 212 (+11100); mμ ([θ] in isooctane) 345(0), 325(−7830), 321(−7030), 315(−9790), 307(−7680), 304(−4900), 240—225(0), 210(+15500).

(−)-*trans*-Pulegone oxide (II: mp 54—55°C; $[\alpha]_D^{20}$ −18.8° (*c* 2.4, ethanol); 0.4 g; 0.0024 mol) was treated with zinc bromide (0.2 g, 0.0089 mol) in benzene (25 m*l*) in exactly the same manner as has been described above and then worked up to give III-b (mp 55—56°C 0.32 g, 80%). The melting point of this crop was not depressed by the admixture of III-a. The IR- and NMR spectroscopical comparisons, as well as the polarimetrical comparisons, corroborated the identity of these two crops, III-a and III-b, from different sources.

Reduction of 2,2,5-Trimethylcycloheptane-1,3-dione (III). According to the usual procedure in the literature,[7] (−)-III was converted into ditosylhydrazone (mp 262°C); a 2-g portion was then reduced with lithium aluminum hydride (1.2 g) to yield an oily product (IV) after purification by means of preparative vpc; yield, 0.1 g (14%). The optical activity of this compound was substantially null at the wavelength of sodium D-line, but it seemed to possess a feeble dextrorotation in the shorter-wavelength region.

Reduction of Eucarvone (V). Eucarvone (V; its semicarbazone, mp 184°C) was hydrogenated over palladium charcoal (150 mg) to yield tetrahydroeucarvone (VI; its semicarbazone, mp 190°C; yield, 1.8 g (90%). The tosylhydrazone of VI (mp 262°C; 0.3 g, 0.0009 mol) was reduced with lithium alminium hydride (0.46 g) and then worked up as usual[7] to yield a liquid, 1,1,4-trimethylcycloheptane (0.11 g, 84%). The IR and NMR spectra of this compound were identical in every respect with those of IV.

Zinc Bromide-catalyzed Rearrangement of Piperitone Oxide. In the same manner as with pulegone oxides (*vide supra*), (−)-piperitone oxide (3 g, 0.0178 mol) was treated with zinc bromide (1 g) in benzene (200 m*l*) and then worked up to give crude diosphenol (1.8 g, 60%), which, after washing with a 3% sodium bicarbonate solution and recrystallizations, melted at 82—83°C. The melting point was not depressed at all by the admixture of the authentic specimen prepared from menthone.

The authors wish to thank Professor Yuzo Inouye of Kyoto University, and Dr. Hitoshi Minato and Dr. Kaoru Kuriyama of the Shionogi Research Laboratory for many helpful discussions during the course of this work. Thanks are also due to Dr. Shigeru Muraki of the Takasago Perfumery Co. for his measurements of the NMR and mass spectra.

7) L. Caglioti and P. Grasselli, *Chem. Ind.*, **1964**, 153; L. Caglioti and M. Magi, *Tetrahedron*, **19**, 1127 (1963).

Asymmetric Hydrogenation of C=O Double Bond with Modified Raney Nickel. XVIII

Yoshiharu IZUMI and Kazuo OHKUBO

Division of Organic Chemistry, Institute for Protein Research, Osaka University, Kita-ku, Osaka

(Received September 7, 1970)

The asymmetric activities of the catalysts modified with L-α-amino and L-α-hydroxy acids, which have two asymmetric centers on α, β and α, γ-carbons were studied, and the participation of the β- and γ-configurations to the asymmmetric activity of the catalyst was made clear. It was found that the S:β-configuration and the S:γ-configuration increase the asymmetric activity of the + and − directions respectively.

The asymmetric hydrogenation with a modified Raney nickel catalyst has been widely studied by our research group on the basis of the relationship between the stereochemical structures of the modifying reagents and the asymmetric activities of the modified catalyst.[1] The studies have mainly been done using α-amino or α-hydroxy acids which have one α-asymmetric carbon; it was found that the catalysts modified with L-α-amino and L-α-hydroxy acids predominantly give (−) and (+)-3-hydroxybutyrate respectively in the asymmetric hydrogenation of methyl acetoacetate.[2,3]

In order to elucidate the participation of the β- or the γ-asymmetric center of the modifying reagents to the asymmetric activities of the catalysts and to make clear the relationship between the diastereoisomeric structures of the modifying reagents and the asymmetric activities of the catalysts, the asymmetric activities of the catalysts modified with α-amino or α-hydroxy acids, which have two asymmetric centers, have been studied in the present investigation.

Moreover, the effect of the configuration of the β-methoxyl group was also investigated using the diastereomers of *O*-methylthreonine and compared with that of the β-ethyl group of the diastereoisomers of isoleucine.

Experimental

Materials. Modifying Reagents: The optical rotations of the modifying reagents used in this study are listed in Table 1.

Preparation, Modification and Measurement of the Asymmetric Activities of the Catalysts. The preparation of the R-Ni catalyst, the hydrogenation of methyl acetoacetate, and the measurement of the asymmetric activities of the catalysts were carried out by the procedures described in the previous paper.

The catalysts were modified with 1% aqueous solutions of modifying reagents at isoelectric points for the amino acids, and at pH 2.9 for the hydroxy acids, by the procedure described in the previous paper.

Results and Discussion

Asymmetric Activity of the Catalyst Modified with Diasymmetric Amino and Hydroxy Acid. The asymmetric activities of the catalysts modified with diastereomers of L-isoleucine, L-β-methylnorleucine and L-β-methylleucine are listed and compared with that of the one modified with valine in Table 2.

As can be seen in Table 2, the asymmetric activities

TABLE 1. THE OPTICAL ROTATION OF MODIFYING REAGENT

Modifying reagent	Optical rotation $[\alpha]_D^{20}$	Value in literature
L-(2S:3S)-β-Methylleucine	+38.6 (*c* 1.2, 6NHCl)	
L-(2S:3R)-β-Methylleucine	+40.6 (*c* 1.0, 6NHCl)	
L-(2S:3S)-β-Methylnorleucine	+30.4 (*c* 1.5, 6NHCl)	
L-(2S:3R)-β-Methylnorleucine	+46.7 (*c* 1.5, 6NHCl)	
L-(2S:4S)-γ-Methylnorleucine	+21.0 (*c* 1.9, 6NHCl)	
L-(2S:4R)-γ-Methylnoreucine	+19.0 (*c* 1.0, 6NHCl)	
L-(2R:3S)-*O*-Methylthreonine	+29.4 (*c* 1.8, 6NHCl)	+30.5 (5NHCl)[a]
L-(2R:3R)-*O*-Methylthreonine	−12.7 (*c* 1.5, 6NHCl)	−13.5 (5NHCl)[a]
L-(2S:3S)-2-Hydroxy-3-methylvaleric acid	+3.9 (*c* 2.5, water)	+3.9 (water)[b]
L-(2S:3R)-2-Hydroxy-3-methylvaleric acid	+3.7 (*c* 2.2, water)	
L-(2S:3S)-2-Hydroxy-3-methylisocaproic acid	+6.44 (*c* 3.3, C_2H_5OH)	
L-(2S:3R)-2-Hydroxy-3-methylisocaproic acid	+11.33 (*c* 3.5, C_2H_5OH)	
L-(2S:3S)-2-Hydroxy-3-methylcaproic acid	+ 8.8 (*c* 5, C_2H_5OH)	
L-(2S:3R)-2-Hydroxy-3-methylcaproic acid	+14.5 (*c* 4.1, C_2H_5OH)	
L-(2S:4S)-2-Hydroxy-4-methylcaproic acid	−10.0 (*c* 5, C_2H_5OH)	
L-(2S:4R)-2-Hydroxy-4-methylcaproic acid	− 9.6 (*c* 5.3, C_2H_2OH)	

a) J. P. Greenstein and M. Winitz, *Chemistry of Amino Acid*, **3**, 2252. (1961).
b) M. Winitz, L. Bloch-Frankental, N. Izumiya, S. M. Birnbaum, C. G. Baker, and J. P. Greenstein, *J. Amer. Chem. Soc.*, **78**, 2433 (1956).

1) Part XV: T. Tanabe, T. Ninomiya, and Y. Izumi, This Bulletin, **43**, 2276 (1970).
2) Y. Izumi, M. Imaida, H. Fukawa, and S. Akabori, *ibid.*, **36**, 155 (1963).
3) S. Tatsumi, M. Imaida, Y. Fukuda, Y. Izumi, and S. Akabori, *ibid.*, **37**, 846 (1964).

Table 2. Modifications with L-α,β-diasymmetric amino acids and L-valine

Modifying conditions: Reagent R–CH(NH_2)–CO_2H R	Configuration	Absolute configuration α-carbon	Absolute configuration β-carbon	pH	Temp. °C	$[\alpha]_D^{25}$ of Methyl 3-hydroxybutyrate
$-CH(C_2H_5)(CH_3)$	Erythro	S	S	5.94	0	−1.95
					100	−2.63
	Threo	S	R	5.94	0	−2.13
					100	−3.04
$-CH(CH_2CH_2CH_3)(CH_3)$	Erythro	S	S	6.12	0	−1.81
					100	−2.66
	Threo	S	R	6.10	0	−2.42
					100	−3.40
$-CH(CH(CH_3)_2)(CH_3)$	Erythro	S	S	5.77	0	−2.18
					100	−2.72
	Threo	S	R	5.97	0	−2.50
					100	−3.30
$-CH(CH_3)_2$	—	S	—	5.96	0	−1.72
					100	−2.30

Table 3. Modifications with L-α,β-diasymmetric hydroxy acids

Modifying conditions: Reagent R-CH(OH)-CO_2H R	Configuration	Absolute configuration α-carbon	Absolute configuration β-carbon	pH	Temp. °C	$[\alpha]_D^{25}$ of Methyl 3-hydroxybutyrate
$-CH(C_2H_5)(CH_3)$	Erythro	S	S	2.9	0	+0.68
					70	+1.07
	Threo	S	R	2.9	0	−0.22
					70	−0.22
$-CH(CH_2CH_2CH_3)(CH_3)$	Erythro	S	S	2.9	0	+0.67
					70	+0.75
	Threo	S	R	2.9	0	+0.22
					70	+0.25
$-CH(CH(CH_3)_2)(CH_3)$	Erythro	S	S	2.9	0	+0.17
					70	+0.24
	Threo	S	R	2.9	0	−0.20
					70	−0.23

of the catalysts modified with these amino acids at 100°C are higher than those of the catalysts modified at 0°C, and the catalysts modified with threo-isomers have higher asymmetric activities than with corresponding erythro-isomers, whether the modifying temperature is 0°C or 100°C.

Furthermore, the asymmetric activity of the catalyst modified with valine was slightly lower than those of the catalysts modified with erythro-isomers, which are less active than the threo-isomers.

In the cases of modifications with diasymmetric L-2-hydroxy-3-methylvaleric acid, L-2-hydroxy-3-methylcaproic acid, and L-2-hydroxy-3-methylisocaproic acid, scarcely no simple correlation was observed between the asymmetric activities of the catalysts and the diastereomeric configurations of the modifying reagents, and, in some cases, the asymmetric direction of the catalysts was inverted, as is shown in Table 3.

As has been mentioned above, a considerably strong effect of the β-configuration of the modifying reagent on the asymmetric activity of the catalyst is observed in the cases of modifications with both amino and hydroxy acids, and the effect of the β-configuration of hydroxy acid often overcomes that of the α-configuration. The mode of the contribution of the β-configuration of the modifying reagent to the asymmetric activity of the catalyst can ben concluded from the results shown in Tables 2 and 3; the S:β-configuration brings the asymmetric activity of the + direction[4] to the catalyst, and the R:β-configuration brings the asymmetric activity of the − direction, without regard to the kind of modifying reagent, whether amino or hydroxy acid.

The effect of the γ-asymmetric center of the modifying reagent on the asymmetric activity of the catalyst was

4) Asymmetric direction of the catalyst. The asymmetric activity consists of two factors; one is presented as the value of the optical purity of the product of the asymmetric hydrogenation, and the other is presented by the sign + or − and correlates with the absolute configuration of the product. In usual discussions, the asymmetric activity of the catalyst is discussed only in connection with the former factor. However, in a special case, the second factor has to be discussed as the problem of the "asymmetric direction of the catalyst."

Table 4. Modifications with L-norvaline, L-leucine, L-norleucine, L-methylnorleucine, and L-2-hydroxy-4-methylcaproic acid

Modifying conditions: R–CH(X)–CO_2H R	X	Absolute configuration α-carbon	Absolute configuration β-carbon	pH	Temp. °C	$[\alpha]_D^{25}$ of Methyl 3-hydroxybutyrate
$-CH_2-CH(C_2H_5)(CH_3)$	NH_2	S	S	5.95	0	−1.08
					100	−1.51
		S	R	5.98	0	−0.73
					100	−0.89
$-CH_2-CH_2-CH_2-CH_3$	NH_2	S	—	6.08	0	−1.14
					100	−1.52
$-CH_2-CH(CH_2)(CH_3)$	NH_2	S	—	5.98	0	−1.08
					100	−1.64
$-CH_2-CH_2-CH_3$	NH_3	S	—	6.04	0	−0.95
					100	−1.62
$-CH_2-CH(C_2H_5)(CH_3)$	OH	S	S	2.9	0	0
					70	+0.03
		S	R	2.9	0	−0.05
					70	−0.08

investigated using L-(2S:4S)-γ-methylnorleucine, L-(2S:4R)-γ-methylnorleucine, L-(2S:4S)-2-hydroxy-4-methylcaproic acid, and L-(2S:4R)-2-hydroxy-4-methylcaproic acid as the modifying reagents, while the asymmetric activities of the catalysts modified with these α,γ-diasymmetric amino acids or hydroxy acids were compared with those with norvaline, leucine and norleucine.

The difference between the asymmetric activities of the catalysts modified with L-(2S:4S)-γ-methylnorleucine and those modified with L-norvaline, L-leucine and L-norvaline can be hardly observed in Table 4. However, when the asymmetric activities of the catalysts modified with two diastereoisomers of γ-methylnorleucine were compared, the effect of the γ-asymmetric center was observed; the catalyst modified with L-(2S:4S)-diastereoisomer has a higher asymmetric activity than the one with L-(2S:4R)-diastereoisomer.

From those results, it seems that the S:γ-methyl group of the amino acid used as a modifying reagent does not increase the asymmetric activity of the catalyst. On the other hand, the R:γ-methyl group of the modifying reagent considerably decreases the asymmetric activity of the catalyst; that is, the R-configuration of γ-carbon brings the asymmetric activity of the + direction and has an effect on the asymmetric activity of the catalyst opposite to that of the R:β-configuration.

On the other hand, in the cases of the modifications of the diastereoisomer of the hydroxy acids, the asymmetric activities of the catalysts modified with these hydroxy acids were too low for us to discuss the exact role of the γ-asymmetric center in the asymmetric activities of the catalysts.

As is shown in Table 5, *threo-O*-methylthreonine has less ability as a modifying reagent than does *erythro-O*-

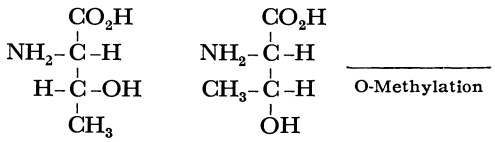

L-Threonine

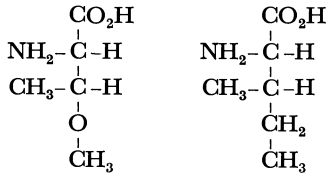

L-Isoleucine

L-*threo*-O-Methylthreonine

Fig. 1

Table 5. Modifications of diastereoisomers of L-*O*-methylthreonine

Modifying conditions: Reagent R–CH(NH_2)–CO_2H R	Configuration	Absolute configuration α-carbon	Absolute configuration β-carbon	pH	Temp. °C	$[\alpha]_D^{25}$ of Methyl 3-hydroxybutyrate
$-CH(OCH_3)(CH_3)$	Erythro	S	S	5.90	0	−0.12
					100	−0.38
	Threo	S	R	5.90	0	0
					100	−0.06

methylthreonine, contrary to the results obtained in the cases of the modifications with α,β-diasymmetric amino acids. Furthermore, the asymmetric activities of the catalysts modified with the two diastereoisomers of *O*-methylthreonine are both considerably lower than those of catalysts modified with isoleucine isomers:

These results can be understood as follows. If the CH_3-C-C-COOH structure is replaced by CH_3-O-C-C-COOH as the main chain in *O*-methylthreonine, as is shown by the Fischer diagram in Fig. 1, because the methoxyl group is bulkier than the methyl group, the L-threo-isomer corresponds with L-isoleucine and the L-erythro-isomer corresponds with L-alloisoleucine. Accordingly, the relationship between the asymmetric activities of the catalyst and the configurations of the α,β-diasymmetric amino acid used as the modifying reagent is also established in the case of *O*-methylthreonine.

BULLETIN OF THE CHEMICAL SOCIETY OF JAPAN, VOL. 44, 1333—1336(1971)

Asymmetric Hydrogenation of C=O Double Bond with Modified Raney Nickel. XX. The Effect of Additives on the Asymmetric Activity

Fukuji HIGASHI,* Toshio NINOMIYA, and Yoshiharu IZUMI

Division of Organic Chemistry, Institute for Protein Research, Osaka University, Kita-ku, Osaka

(Received October 24, 1970)

The effects of various additives in methyl acetoacetate were tested in the asymmetric hydrogenation reaction. Among them, water has a particular effect on the asymmetric activities of the catalysts; in the presence of a certain amount of water, the catalysts modified with L-Glu, L-Val, and L-Ala hydrogenated methyl acetoacetate to methyl $L_S(+)$3-hydroxybutyrate, while, without the addition of water, the catalysts promoted the hydrogenation to yield methyl $D_S(-)$3-hydroxybutyrate. The catalyst modified with L-Ala at pH 6.0 and the catalyst modified with L-Glu at pH 5.0 and 100°C were especially sensitive to water, and both catalysts showed (+) asymmetric activity when a trace of water was also present. Even in the hydrogenation without the addition of water, the recovered catalysts modified with L-Glu, L-Val, and L-Ala from the hydrogenation in the presence of water gave results similar to those in the hydrogenation in the presence of water. The effect of water as an additive was discussed, and it was concluded that the water affects the asymmetric site of the catalyst rather than the keto-enol equilibrium of the substrate.

In the previous reports of this series on asymmetric hydrogenation with a Raney nickel catalyst modified with optically active amino acid or hydroxy acid, the asymmetric activity of the catalyst has been demonstrated to be affected by the structure of the modifying reagent, and by the pH and temperature in the modifying procedures.[1)]

The present paper will report on the effects of various additives in the hydrogenation system on the asymmetric activity of the catalyst modified with L-amino acid. As modifying reagents, L-glutamic acid (L-Glu), L-valine (L-Val), and L-alanine (L-Ala) were used because the effect of the modifying temperature on the asymmetric activity of the catalyst is quite different in each case, as was shown in a previous paper.[2)]

The present paper will also discuss the particular effect of water on the asymmetric activity of the catalyst modified with L-amino acid and will refer to the irregular asymmetric activity of the catalyst modified with L-Ala at pH 6.0 and 0°C reported in the previous paper.[2)]

Experimental

The preparation and modification of the Raney nickel catalyst, the hydrogenation of methyl acetoacetate, and the measurement of the asymmetric activity of the catalyst were carried out in the manner described in a previous paper.[3)]

The Addition of the Additives. The additive was introduced into the autoclave with methyl acetoacetate and the catalyst at the same time.

Recovery of the Catalyst and the Recovered Catalyst. After the asymmetric hydrogenation of methyl acetoacetate to methyl 3-hydroxybutyrate, the hydrogenation product was removed by decantation; then the catalyst was washed three times with a small amount of methanol. The catalyst thus obtained, served as the recovered catalyst in the hydrogenation of methyl acetoacetate.

Results and Discussion

Table 1 shows the asymmetric activity of the catalyst modified with L-Glu in the hydrogenation of methyl acetoacetate (MAA) in the presence of various additives. As Table 1 shows, water caused a (+) asymmetric activity of the catalyst, while other additives caused a (−) asymmetric activity of the catalyst. A similar tendency

* Present address: Laboratory of Polymer Chemistry, Tokyo Institute of Technology, Ookayama, Meguro-ku, Tokyo.

1) Part XV: T. Tanabe, T. Ninomiya, and Y. Izumi, This Bulletin, **43**, 2276 (1970).

2) Y. Izumi, M. Imaida, H. Fukawa, and S. Akabori, *ibid.*, **36**, 155 (1963).

3) Y. Izumi, T. Harada, T. Tanabe, and K. Okuda, This Bulletin, **44**, 1418 (1971).

TABLE 1. THE EFFECT OF ADDITIVES ON THE ASYMMETRIC ACTIVITY OF THE CATALYST MODIFIED WITH L-Glu (pH 5.0) AT 0°C

Additive	m*l*	$[\alpha]_D^{20}$ of Methyl 3-hydroxybutyrate
n-hexane	18	−3.90
EtOEt	18	−3.44
MAA	18	−3.35
AcOH	18	−1.65
H_2O	18	+0.80

TABLE 2. THE EFFECT OF ADDITIVES ON THE ASYMMETRIC ACTIVITY OF THE CATALYST MODIFIED WITH L-Val(pH 6.0) AT 0°C

Additive	m*l*	$[\alpha]_D^{20}$ of Methyl 3-hydroxybutyrate
n-hexane	18	−2.25
EtOH	18	−2.01
MAA	18	−2.55
AcOH	18	−1.90
H_2O	18	+0.48

TABLE 3. THE EFFECT OF ADDITIVES ON THE ASYMMETRIC ACTIVITY OF THE CATALYST MODIFIED WITH L-Ala (pH 6.0) AT 0°C

Additive	m*l*	$[\alpha]_D^{20}$ of Methyl 3-hydroxybutyrate
MAA	18	−0.08
AcOH	10	−0.14
H_2O	18	+0.34

was also observed with the catalysts modified with L-Val and L-Ala (Tables 2 and 3).

It is well known that the acetoacetic ester exists in the keto-enol mixture and that the proportion of the keto form of ethyl acetoacetate increases in the following order of the solvents: *n*-hexane (enol form 46.4%) < diethyl ether (27.1%) < ethanol (12%) < ethyl acetoacetate (7.7%) < methanol (6.9%) < acetic acid (5.7%) < water (0.4%).[4]

Therefore, in the case of MAA (94% keto form in the pure state), the proportion of the keto form of MAA in the above solvents can be considered to increase in the same order.

However, the asymmetric activity of each catalyst does not change regularly with the increase in the proportion of the keto form of the substrate, as is shown in Tables 1,2, and 3. Thus the change in the asymmetric activity of the catalyst in the presence of additives can not be explained only by the shift of the keto-enol equilibrium of MAA from the one side to the other.

On the basis of the above discussion, water seems to have a specific effect on the catalyst. Hence, the effect of water was examined in detail. The effect of water on the asymmetric activities of the catalysts modified with L-Glu, L-Val, and L-Ala at 0°C and 100°C was studied; the results are summarized in Figs. 1 and 2.

The increase in the amount of water added brought about a depression not only in the (−) asymmetric activity, but also in the (+) asymmetric activity relative to the catalysts modified with the above three amino acids, and the amount of water which caused the inversion of the asymmetric direction[5] of the catalyst from (−) to (+) was different in each catalyst.

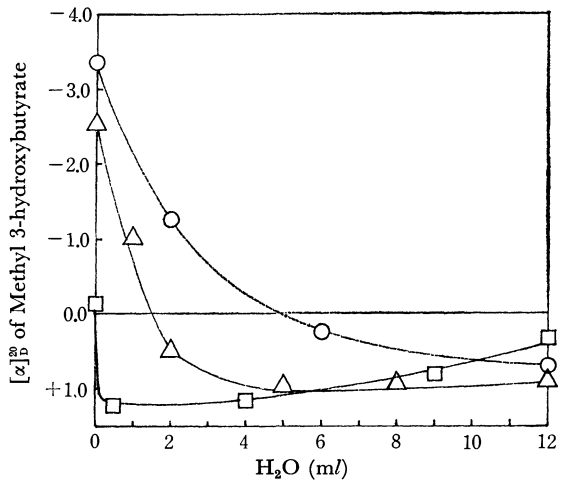

Fig. 1. Effect of water on the asymmetric activities of the catalysts modified at 0°C.
○ L-Glu (at pH 5.0)
△ L-Val (at pH 6.0)
□ L-Ala (at pH 6.0)

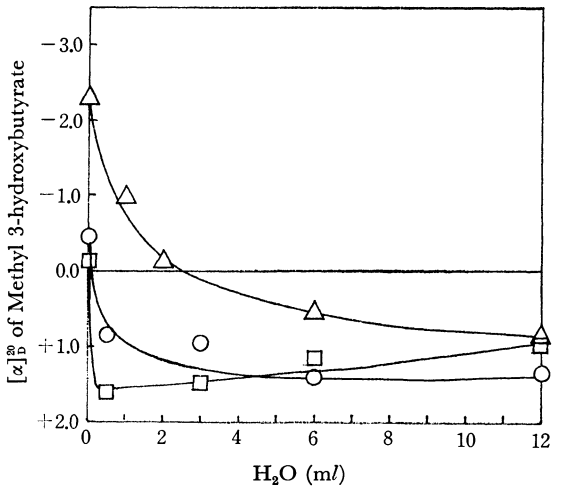

Fig. 2. Effect of water on the asymmetric activities of the catalysts modified at 100°C.
○ L-Glu (at pH 5.0)
△ L-Val (at pH 6.0)
□ L-Ala (at pH 6.0)

These facts indicate that the degree of the influence of water on the catalyst is characteristic of the modifying reagent. It may be concluded that water affects the asymmetric site of the catalyst, while it does not affect the keto-enol equilibrium of MAA; if the water affected the equilibrium, the degree of the influence of water on each catalyst would be similar.

Figures 3, 4, and 5 show the symmetric activities of the catalysts modified with L-Glu, L-Val, and L-Ala at 0°C in the hydrogenation with the addition of

4) K. H. Meyer, *Ann.*, **380**, 212 (1911).

5) The asymmetric direction of the catalyst is represented by the optical rotatory sign (+ or −) of the reductive product, methyl 3-hydroxybutyrate.

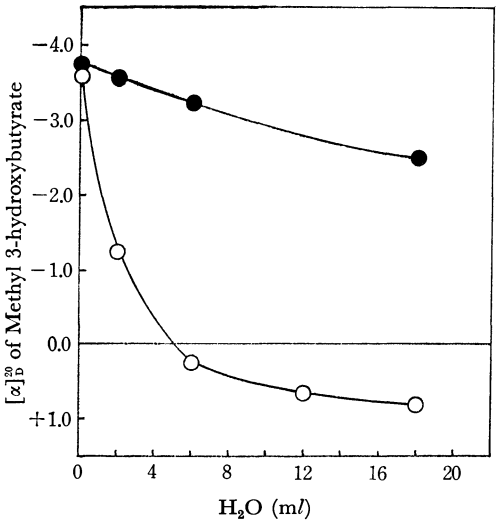

Fig. 3. Asymmetric activities of the catalyst modified with L-Glu at 0°C and of its recovered catalyst.
○ Asymmetric activity of the catalyst in the hydrogenation with addition of water.
● Asymmetric activity of the recovered catalyst under the standard hydrogenation conditions.

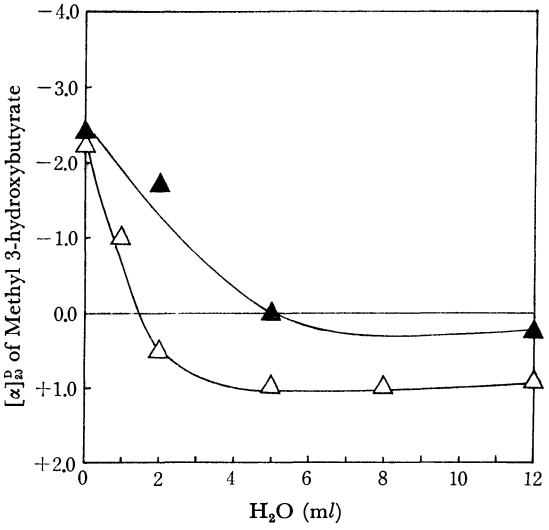

Fig. 4. Asymmetric activities of the catalyst modified with L-Val at 0°C and of its recovered catalyst
△ Asymmetric activity of the catalyst in the hydrogenation with addition of water.
▲ Asymmetric activity of the recovered catalyst under the standard hydrogenation conditions.

water and those of the recovered catalyst in the hydrogenation under the standard conditions.[6]

The catalysts recovered from the hydrogenation of MAA containing water show considerably lower (−) asymmetric activities in the standard hydrogenation of methyl acetoacetate than do the catalysts modified with L-GIu, L-Val, and L-Ala in the hydrogenation under the standard conditions. On the other hand, it has been established that both catalysts modified with these amino acids at 0°C and the recovered catalysts

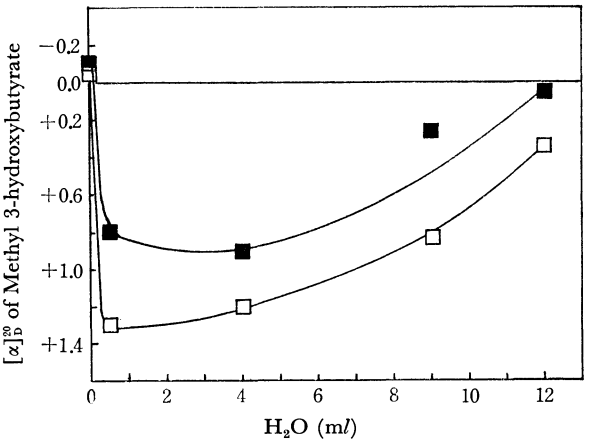

Fig. 5. Asymmetric activityes of the catalyst modified with L-Ala at 0°C and of its recovered catalyst.
□ Asymmetric activity of the catalyst in the hydrogenation with addition of water.
■ Asymmetric activity of the recovered catalyst under the standard hydrogenation conditions.

show the same asymmetric activities in the hydrogenation of MAA alone. These facts suggest that the asymmetric site of each catalyst is greatly affected by water and that water affects the recovered catalyst. If the water had no effect on the symmetric site of the catalyst, the recovered catalyst would show the same asymmetric activity as the catalyst used first under the standard conditions.

The Catalyst Modified with L-*Glu.* As has been described previously, the catalyst modified with L-Glu at 0°C shows (−) asymmetric activity, while on the other hand, the one modified at 100°C shows(+) asymmetric activity The catalyst modified with L-Glu at 100°C was studied with the expectation that the (+)asymmetric activity of the catalyst would be produced by the water absorbed during the modification.

In Fig. 6, the asymmetric activities of the catalyst modified at 100°C and those of the recovered catalyst are plotted against the number of repeated recoveries under the standard conditions.

The asymmetric activities of the recovered catalyst

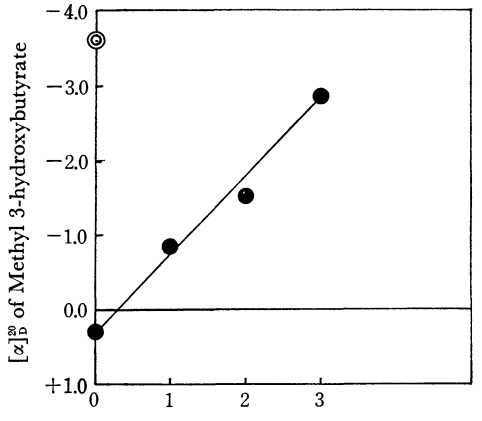

Fig. 6. Asymmetric activity of the catalyst modified with L-Glu at 100°C.
vs. Number of repeating of recovery procedure.

6) The standard hydrogenation conditions are the conditions of the hydrogenation of methyl acetoacetate alone, without any additives.

modified at 100°C gradually approaches that of the catalyst modified at 0°C. This finding suggests that the asymmetric site of the catalyst modified at 100°C is unstable and that it gradually becomes similar to the state of that modified at 0°C through the recovery procedure.

The Catalyst Modified with L-*Val.* It has been reported in a previous paper[1] that (−) asymmetric activity of the catalyst modified with L-Val does not change with the modifying temperature. However, the addition of water causes the (+) asymmetric activity in the catalyst as is shown in Figs. 1 and 2. These facts indicate that the catalyst modified with L-Val, which seems to show only (−) asymmetric activities, also include a factor inducing (+) asymmetric activity.

The Catalyst Modified with L-*Ala.* The catalyst modified with L-Ala is the most sensitive to water among the catalysts modified with the amino acids investigated, as is shown in Fig. 1. From the above fact it can be supposed that the considerably high (+) asymmetric activity of the catalyst modified with L-AIa reported in the previous paper[2] is due to the effect of the contaminant water on the catalyst surface.

As it seemed to be difficult to prevent perfectly the inclusion of water in the hydrogenation system in the ordinary modification procedure described above, it seems that the constant values of the asymmetric activities can be obtained only with difficulty with the catalysts modified with L-Ala at 0°C and 100°C, and with L-Glu at 100°C, by the standard method.

BULLETIN OF THE CHEMICAL SOCIETY OF JAPAN, VOL. 44, 1336—1338(1971)

Intramolecular Interaction between Hydroxyl Group and π-Electrons. XXIV.[1] The Interaction Involving the Cyano Group

Michinori Ōki and Takashi Yoshida

Department of Chemistry, Faculty of Science, The University of Tokyo, Hongo, Tokyo

(Received September 14, 1970)

The infrared O–H stretching spectra of various 1- and 2-cyano alcohols have been measured, and the presence of intramolecular O–H···π interaction has been detected. Some discussion of the confirmation of such alcohols is given.

Various olefins and aromatics are known to behave as proton acceptors to establish interaction between the hydroxyl group and π-electrons. Since we have reported in a previous paper[1] that the π-electrons of the carbonyl group, which involves the hetero atom, can act as proton acceptors, we have now naturally extended the work to the π-electrons of the carbon-nitrogen system. Although the intramolecular interaction between the hydroxyl group and π-electrons of the cyano group was briefly treated by Allerhand and Schleyer,[2] and although the possibility of such an interaction was implied by Casadevall *et al.*,[3] more precise work has been clearly needed. The purpose of this paper is to present the results of our investigation.

Experimental

Materials. All the cyano alcohols used in this study were known compounds and were prepared according to the published methods. The purity of the sample was checked prior to use.

Infrared Spectra. The spectra were recorded on a Perkin Elmer 112 G grating spectrophotometer. The samples were dissolved in carbon tetrachloride to make up a 3—6 mmol/*l* concentration. The absorption bands due to the hydroxyl group of the 1-cyano alcohols were either completely symmetric or slightly unsymmetric. Thus, no effort was made to divide these bands into their components. On the other hand, 2-cyano alcohols showed two-peaked bands which were divided into symmetric curves, as has been described previously.[4]

Results and Discussion

1-Cyano Alcohols. The O–H stretching (ν_{O-H}) absorptions of 1-cyanocyclohexanol are given in Fig. 1.

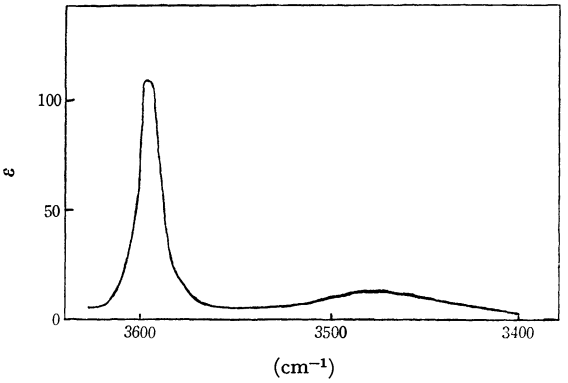

Fig. 1. The ν_{O-H} absorption of 1-cyanocyclohexanol.

1) M. Ōki, H. Iwamura, J. Aihara, and H. Iida, This Bulletin, **41**, 176 (1968).

2) A. Allerhand and P. von R. Schleyer, *J. Amer. Chem. Soc.*, **85**, 866 (1963).

3) E. Casadevall, M. Lasperas, and L. Mion, *Tetrahedron Lett.*, **1970**, 1525.

4) M. Ōki, H. Iwamura, T. Murayama, and I. Oka, This Bulletin, **42**, 1986 (1969).

It will be seen that 1-cyanocyclohexanol shows a broad and weak absorption at *ca.* 3480 cm^{-1} and a sharp and strong absorption at *ca.* 3600 cm^{-1}. This feature is generally observed with 1-cyano alcohols. Since the intramolecular O–H···N distance is too far to form a hydrogen bond, the absorption at the lower frequency may be attributed to the presence of the intermolecular hydrogen bond. Indeed, when the concentration of 1-cyano alcohol is increased, the absorption at the lower wave number increases in its intensity. The presence of the intermolecular hydrogen bond at the concentration where other ordinary alcohols exist solely as monomers may be attributed to the larger proton-donating ability of the hydroxyl group as a result of the electronic effect of the cyano group. In the following discussion, it is assumed that the effect of the absorption band resulting from the intermolecular hydrogen bond on the monomeric absorption is negligible, and so only the data on the monomeric band are given.

Table 1. The ν_{O-H} data of 1-cyano alcohols derived from ketones [RR'C(OH)CN]

R	R'	ν_{OH} (cm^{-1})
CH_3	CH_3	3601
CH_3	C_2H_5	3602
CH_3	$CH_3(CH_2)_2$	3602
CH_3	$(CH_3)_2CH$	3605
$(CH_2)_5$		3594

The data concerning the ν_{O-H} absorption of 1-cyano alcohols derived from ketones are given in Table 1. It will be seen that 1-cyano alcohols prepared from ketones show only one symmetric absorption, the location of which is fairly low when compared with the cases of normal tertiary alcohols (*ca.* 3616 cm^{-1}). The results can be interpreted in either of the following two ways: 1) All the hydroxyl groups are free; in other words, the hydroxyl group does not interact with the cyano group. The shift of the band to the lower frequency is caused by the high electronegativity of the cyano group.[5] 2) All the hydroxyl group interacts with the cyano groups, and the lower shift of the ν_{O-H} is to be ascribed to the interaction.

A comparison of the data with those of the corresponding ethynyl compounds may throw light on this problem.

Since propargyl alcohol is known from microwave spectroscopy[6] to exist solely as a conformation in which the hydroxyl group is close to the π-electrons, it is natural to assume that propargyl alcohol takes a similar conformation in solution with a nonpolar solvent. Indeed, propargyl alcohol has been reported to show only one ν_{O-H} band, at 3620 cm^{-1}, in a carbon tetrachloride solution[7]; its conformation has been suggested to be as such that the hydroxyl group and π-electrons interact because of the lower location of the band.

1-Ethynylcyclohexanol shows only one symmetric ν_{O-H} band, at 3607 cm^{-1}. Although this location could be ascribed to the ordinary tertiary alcohol, because 1-adamantanol and 1-hydroxybicyclo [2.2.2]-octane are known to give bands at 3605 and 3608 cm^{-1} respectively,[8] it is also known that other non-rigid tertiary alcohols never give the ν_{O-H} band below 3610 cm^{-1}.[9] Therefore we choose to attribute the lower location of the ν_{O-H} band of 1-ethynylcyclohexanol to the presence of the O-H···π interaction. Then, the rather large shift of the ν_{O-H} absorption of 1-cyanocyclohexanol to 3594 cm^{-1} is in the direction to be expected from the electronegativity.

Table 2. The ν_{O-H} data of 1-cyano alcohols derived from aldehydes [RCH(OH)CN]

R	ν_{OH}(cm^{-1})	β/α
CH_3	3607	1.0
C_2H_5	3611	1.44
$CH_3(CH_2)_2$	3609	1.87
$(CH_3)_2CH$	3614	1.48
$(CH_3)_3C$	3612	2.0

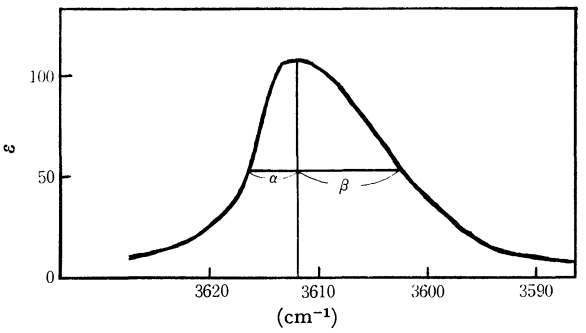

Fig. 2. The ν_{O-H} absorption of α-cyanoneopentyl alcohol, showing the notation of α and β.

Considering these factors, it is most probable to assume that the 1-cyano alcohols shown in Table 1 give only one ν_{O-H} absorption because of the sole presence of a conformer in which the hydroxyl group and π-electrons of the cyano group interact with each other.

On the other hand, 1-cyano alcohols derived from aldehydes show unsymmetric ν_{O-H} bands, as is shown in Table 2. The α and β in Table 2 are the values proposed by Rader and Aaron[10], as is shown in Fig. 2. That is, the line corresponding to the half-band-width is cross-cut by a straight line corresponding to the maximum absorption. The α value is, then, the section of the higher-frequency side, and β, that of the lower-frequency side. If the β/α value is larger than unity, it can be interpreted as that there is a small peak on the lower-frequency side. As may be seen in Table

5) In phenol derivatives, if a compound carries an electron-withdrawing substituent at the *m*- or *p*-position, the ν_{O-H} band appears at the lower frequency. See, for example, P. J. Stone and H. W. Thompson, *Spectrochim. Acta*, **10**, 16 (1957).

6) E. Hirota, *J. Mol. Sepctry.*, **26**, 335 (1968); K. Bolton, N. L. Owen, and J. Sheridan, *Nature*, **217**, 164 (1968).

7) P. von R. Schleyer, D. S. Trifan, and R. Bacskai, *J. Amer. Chem. Soc.*, **80**, 6691 (1958).

8) L. Joris, P. von R. Schleyer, and E. Ōsawa, *Tetrahedron*, **24**, 4759 (1968).

9) M. Ōki and H. Iwamura, This Bulletin, **32**, 950 (1959).

10) H. S. Aaron and C. P. Rader, *J. Amer. Chem. Soc.*, **85**, 3046 (1963); H. S. Aaron, C. P. Ferguson, and C. P. Rader, *ibid.*, **89**, 1431 (1967).

2, all the cyano alcohols derived from aldehydes except acetaldehyde give ν_{O-H} absorptions which possess β/α values larger than 1.

These results can also be interpreted in two ways. The two bands could arise from the free and the interacting forms of the cyano alcohols, or, the reason could be the presence of the two interacting conformations. Either way is possible, but the present authors wish tentatively to ascribe the phenomena to the second reason in consideration of the results with ketone-cyanohydrin and propargyl alcohol.

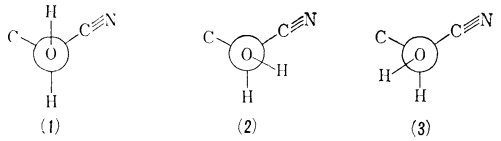

(1) (2) (3)

Three conformations, **1**, **2**, and **3**, are possible for the aldehyde-cyanohydrins concerning the rotation about the C–O axes. Since it has been assumed that all the molecules are intramolecularly O–H···π interacting species, the conformation **3** may be neglected in the following discussion. The hydroxyl proton and the cyano group are too far separated to interact with each other, and the geometry is not favorable for the interaction. There are, then, clearly two conformations in which O–H and π-systems can interact, and these conformations may be reflected in the ν_{O-H} absorptions.

Next, the question may be raised as to which conformation corresponds to the absorption at a higher frequency. There is no definite answer to this question. However, from the analogous consideration in secondary alcohols[9], the O–H absorption at the higher frequency may be assigned to the conformation **2**, since the conformation **4** of secondary alcohols is known to give rise to absorptions at higher freqencies than does the conformation **5**.

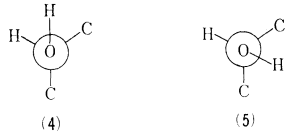

(4) (5)

To a question why aldehyde-cyanohydrins having the bulkier alkyl group give large β/α values, we wish to attribute this tentatively to the shift to the lower freqencies of absorption corresponding to the conformation **1** because of the stronger interaction caused by the proximity of the two groups due to the buttressing effect of the alkyl group. A similar effect was also observed with cyano alcohols derived from alkyl methyl ketones, where alkyl is a bulky group.

Table 3. The data of 2-cyano alcohols $RR'C(OH)CH_2CN$

R	R′	ν_h[a]	ν_l[a]	intensity ratio[b]
H	H	3634	3615	0.99
H	CH_3	3625	3607	1.83
CH_3	CH_3	3611	3593	0.69

a) The suffixes *h* and *l* refer to absorptions at higher and lower frequencies, respectively.
b) The intensity ratios were obtained by taking the ratio of the products of molecular extinction coefficients and the half-band widths after graphical separation, corresponding to the A_l/A_h value.

That is, a slightly unsymmetrical ν_{O-H} band is observed for those compounds, although it is hard to estimate the difference from unity in the β/α value because of the low degree of unsymmetrv.

2-Cyano Alcohols. The ν_{O-H} data of several 2-cyano alcohols are given in Table 3. Apparently these alcohols give two ν_{O-H} absorptions, the two maxima being separated by *ca.* 18 cm^{-1}. Although the shifts are observed with the bands at higher frequencies, they are located at the ordinary positions for the free hydroxyls when the class of the alcohols is considered. Therefore, those at the higher wave numbers are assigned to the free hydroxyl group.

The separation of the two bands at the higher and the lower frequencies, namely, *ca.* 18 cm^{-1}, is a little too large to attribute its origin to the presence of the second conformer of the alcohol. The intensity ratios are also too small to attribute to the conformational heterogeneity of the alcohols.[8,9,11] These facts together with a consideration of the molecular models, which reveals that the hydroxyl group can come close to the π-electron system, lead to the conclusion that the band at the lower wave number should be assigned to the O–H···π interacting species, although it could include absorption due to the free hydroxyl group of the second conformer in the cases of primary and secondary alcohols.

The higher intensity ratios for propylene cyanohydrin may be attributed to the steric effect between the cyano and the methyl groups, through which the conformation with the hydroxyl group and the cyano group in the gauche relation is relatively favored. However, no explanation of the results with isobutylene cyanohydrin is possible using this idea. Clearly, further study is needed to understand these numerical values.

11) The separation of the two peaks and the intensity ratio (A_l/A_h) due to the conformational heterogeneity of secondary alcohols are usually 10—14 cm^{-1} and 3—5 respectively.[8,9]

The Polymerizations of 2-Vinyl-4-acryloxy-1,3-dioxolane and 2-Vinyl-4-methacryloxy-1,3-dioxolane

Tatsuro OUCHI, Kaneyuki YOKOI, Kenzi YOSHIMURA, and Masayoshi OIWA

Department of Applied Chemistry, Faculty of Engineering, Kansai University, Senriyama, Suita-shi, Osaka

(Received September 16, 1970)

The polymerizations of 2-vinyl-4-acryloxy-1,3-dioxolane(VADO) and 2-vinyl-4-methacryloxy-1,3-dioxolane (VMDO), and the copolymerizations of those divinyl cyclic acetals with styrene (St) and acrylonitrile(AN), have been carried out at 60°C, using 2,2′-azobisisobutyronitrile as the initiator. They were discussed kinetically. The following results were obtained: 1) The polymerizations of the above cyclic acetals containing allylidene and vinyl groups proceeded primarily on the acryl or methacryl group, and the allylidene group was extinguished a little by means of cyclization; the ratios of the rate constant of the unimolecular cyclization reaction to that of the bimolecular propagation reaction of the uncyclized radical were 0.065 mol/*l* (VADO) and 0.114 mol/*l*(VMDO). 2) The following monomer reactivity ratios were obtained at 60°C: VADO(M_1)-St(M_2) $r_1=0.22$, $r_2=0.81$; VADO(M_1)-AN(M_2) $r_1=0.89$, $r_2=0.95$; VMDO(M_1)-St(M_2) $r_1=0.51$, $r_2=0.49$. The Q and e values of the two monomers were calculated from these values: VADO, $Q=0.41$, and $e=0.65$; VMDO, $Q=0.81$ and $e=0.38$.

In previous papers, the polymerizations of cyclic acetal compounds containing two equivalent functional groups were kinetically investigated, but the difference in reactivity between allylidene and vinyl groups has not been discussed in detail.[1-4]

In the present experiment, the polymerization of 2-vinyl-4-acryloxy-1,3-dioxolane (VADO) was carried out; by employing the kinetic equation derived in a previous paper,[2] we will kinetically discuss our results in view of the difference in reactivity between the allylidene and acryl groups.

The polymerization of 2-vinyl-4-methacryloxy-1,3-dioxolane (VMDO) was further carried out; we will investigate the influence of the α-methyl group on the vinyl group.

The copolymerizations of the above divinyl cyclic acetals with styrene (St) or acrylonitrile (AN) were also carried out, and the reactivity ratios were estimated.

Experimental

Materials. The oxochlorides were prepared by the reactions of acrylic and methacrylic acids with benzoyl chloride in the presence of anthraquinone, according to the procedure of Stempel *et al*:[5]

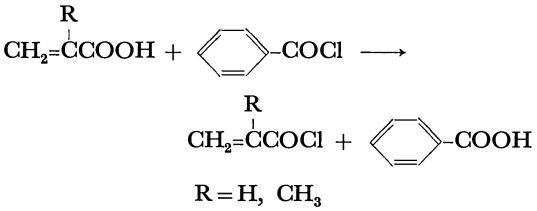

R = H, CH_3

The oxochlorides (1 mol) were slowly dropped into a mixture of 1 mol of 2-vinyl-4-hydroxymethyl-1,3-dioxolane (VHDOL), 1 mol of trimethylamine as a catalyst, 0.1 wt% anthraquinone as an inhibitor, and benzene (1500 m*l*) as a solvent at 0—3°C over a 5-hr period; the mixtures were then washed with water to remove any unreacted VHDOL, oxochlorides, and the ($(C_2H_5)_3N\cdot HCl$) salt.

The products remaining in the benzene layer were separated, dried over calcium carbonate, and then distilled *in vacuo*; VADO bp 87—89°C/2mmHg, VMDO bp 95—98°C/3mmHg. The yields were 20—25%.

The final products were confirmed to be the new monomers of VADO and VMDO by a determination of the infrared spectrum, the molecular weight (MW), the saponification value (SV), and the bromine value (BV).

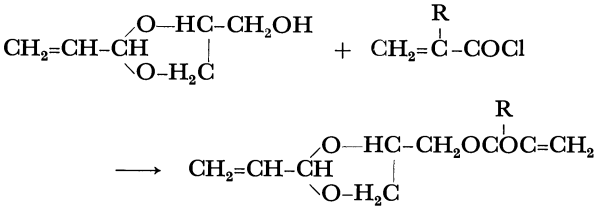

R = H, CH_3

VADO Found: C, 57.89; H, 6.31%; MW, 184.6; BV, 172.2; SV, 302.5. Calcd for $C_9H_{12}O_4$: C, 58.69; H, 6.57%; MW, 184.2; BV, 173.5; SV, 304.6.

VMDO Found: C, 60.67; H, 7.21%; MW, 200.1; BV, 159.8; SV, 281.8. Calcd for $C_{10}H_{14}O_4$: C, 60.60; H, 7.12%; MW, 198.2; BV, 161.2; SV, 283.1.

The St, AN, 2,2′-azobisisobutyronitrile (AIBN), benzene, and dimethylformamide (DMF) used as the solvents were purified by conventional methods.

Polymerization Procedure. A glass ampoule was charged with the prescribed amount of each monomer, a solvent, and AIBN; it was then degassed, sealed off under a vacuum, and set in a thermostatted water bath at 60±0.1°C. The reaction solution was poured into a large amount of methanol, and the polymer thus separated was filtered and then dried *in vacuo* until it reached a constant weight. The conversion was less than 10%. The homopolymers of these divinyl acetals were purified from benzene-methanol.

The copolymers obtained on VADO or VMDO-St and VADO-AN systems were also reprecipitated from benzene-methanol and DMF-methanol respectively.

Analyses of the Polymer and Copolymer. The overall residual double bonds of the polymer and the copolymer

1) T. Ouchi and M. Oiwa, *Kogyo Kagaku Zasshi*, **72**, 746 (1969).
2) T. Ouchi, Y. Imase, and M. Oiwa, This Bulletin, **43**, 2863 (1970).
3) Y. Minoura and M. Mitoh, *J. Polym. Sci., Part A-1*, **3**, 2149 (1965).
4) S. G. Matsoyan, *ibid.*, **52**, 189 (1961).
5) G. H. Stempel, R. P. Cross, and R. P. Mariella, *J. Amer. Chem. Soc.*, **72**, 2299 (1950).

(allylidene+acryl) were calculated by means of the bromine values measured by the method of Siggia (BV_{a+v});[6] the residual allylidenic double bonds were then calculated by means of those determined according to the usual bromite-bromate method (BV_a).[7]

The composition of the copolymer was determined by C, H, and N elementary analyses.

The infrared spectra were measured on a Shimadzu infrared spectrophotomerte, Model IR-27.

The infrared spectra of the resulting monomer and polymer are shown in Fig. 1. The absorption peaks at 1598, 1740, and 1200—1040 cm^{-1} may be assigned to C=C, >C=O, and cyclic acetal respectively.

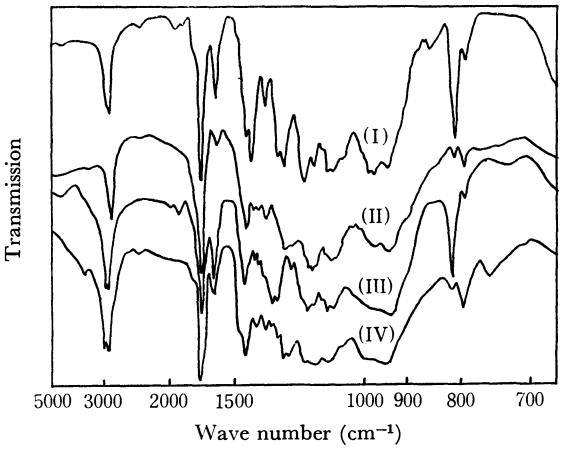

Fig. 1. Infrared spectra of VADO, VMDO monomer and polymer.
(I) VADO monomer, (II): VADO polymer, (III): VMDO monomer, (IV): VMDO polymer

Results and Discussion

Homopolymerization. The VADO and VMDO polymerizations were carried out under different initiator and monomer concentrations at 60°C. The results are given in Tables 1 and 2, in which the values of BV_{a+v} and BV_a are estimated by extrapolating to zero at yield.

As can be seen from Tables 1 and 2, the residual unsaturation of the polymer, $2R_{us}$, is not equal to 1.00, and it does not depend on the initiator concentration, but decreases with a decrease in the monomer concentration. Accordingly, the polymerizations of these monomers may proceed by a mechanism of cyclopolymerization such as that of DβMPP.[2] Since the value of BV_a is nearly equal to that of BV_{a+v}, it may be considered that the pendant double bonds in the polymer almost corresponded to the allylidene groups; since the reactivity of acryl is larger than that of allylidene, it can be pointed out that the usual propagation is assumed to be related to the acryl and that the cyclization is related to the acryl and the allylidene.

Table 1. Polymerization of VADO at 60°C

(I) ($\times 10^{-3}$ mol/l)	(M) (mol/l)	R_p ($\times 10^{-4}$ mol/l·sec)	$BV^{a)}_{a+v}$	$BV^{a)}_a$	$2R^{b)}_{us}$
0.61	2.01	0.633	84.07	84.06	0.969
1.22	2.01	2.60	84.11	84.07	0.970
1.83	2.01	3.48	84.06	84.05	0.969
2.44	2.01	4.02	84.09	84.09	0.969
3.66	2.01	4.92	84.05	84.02	0.969
1.83	1.15	1.93	82.15	82.13	0.947
1.83	1.34	2.26	82.76	82.72	0.954
1.83	1.61	2.74	83.45	83.44	0.962
1.83	2.68	4.69	84.75	84.71	0.977

Table 2. Polymerization of VMDO at 60°C

(I) ($\times 10^{-3}$ mol/l)	(M) (mol/l)	R_p ($\times 10^{-4}$ mol/l·sec)	$BV^{a)}_{a+v}$	$BV^{a)}_a$	$2R^{b)}_{us}$
1.22	2.01	2.54	76.47	76.45	0.948
1.83	2.01	3.40	76.42	76.40	0.947
2.44	2.01	3.92	76.45	76.41	0.947
3.66	2.01	4.81	76.43	76.42	0.947
4.88	2.01	5.55	76.48	76.41	0.948
1.83	1.15	1.87	73.36	73.35	0.909
1.83	1.34	2.21	74.57	74.55	0.924
1.83	1.61	2.68	75.45	75.43	0.935
1.83	2.68	4.65	77.39	77.33	0.959

a) The values were obtained by extrapolating to zero for the conversion.
b) $2R_{us}=BV_{a+v}/BV_{fd}$.

The results of these homopolymerizations were then analyzed by the kinetic equations according to the following reaction scheme:

		Rate const.
Decomposition of initiator	$I \rightarrow 2R\cdot$	k_d
Initiation	$R\cdot + M \rightarrow M\cdot$	k_i
Cyclization	$M\cdot \rightarrow M_c\cdot$	k_c
Propagation	$M\cdot + M \rightarrow M\cdot$	k_p
	$M_c\cdot + M \rightarrow M\cdot$	k_{cp}
Termination	$M_c\cdot + M_c\cdot \rightarrow P_c$	$\alpha^2 k_t$
	$M_c\cdot + M\cdot \rightarrow P_c'$	$\alpha\beta k_t$
	$M\cdot + M\cdot \rightarrow P$	$\beta^2 k_t$

(1)

If a steady-state condition is assumed, Eqs. (2)—(6) can be obtained.

When the monomer concentration is kept constant, the relation of the rate of polymerization, R_p, to the initiator concentration, (I), can be written by Eq. (2):

$$R_p/(I)^{1/2} = A(I)^{1/2} + B \tag{2}$$

where:

$$\left.\begin{aligned} A &= (k_{cp}/k_c)(2fk_d)(k_p/k_{cp}-\beta/\alpha)(M) = \text{const.} \\ B &= (k_{cp}/\alpha)(2fk_d/k_t)^{1/2}(M)\{(k_p/k_{cp}-\beta/\alpha) \\ &\quad \times (k_{cp}/k_c)(M)+1\} = \text{const.} \end{aligned}\right\} \tag{3}$$

Similarly, when the initiator concentration is kept constant, the relation between R_p and the monomer concentration, (M), can be written by Eq. (4):

$$R_p/(M) = C(M) + D \tag{4}$$

where:

6) S. Siggia, "Quantitative Organic Analysis *via* Functional Groups," 3rd ed., J. Wiley & Sons, New York and London (1963), p. 301.

7) I. P. Losev and O. Y. Fedotoba, "Praktikum po Khimii Vysokopolimernykh Soedinenii," Gosudarstvennoe Nauchno-Tekhnicheskoe Izdatelstvo Khimicheskoi Literatury, Moskova.

$$\left.\begin{aligned} C &= (k_{cp}/\alpha)(2fk_d/k_t)^{1/2}(k_p/k_{cp}-\beta/\alpha) \\ &\quad \times (k_{cp}/k_c)(\mathrm{I})^{1/2} = \text{const.} \\ D &= (k_{cp}/k_c)(2fk_d)(k_p/k_{cp}-\beta/\alpha)(\mathrm{I}) \\ &\quad + (k_{cp}/\alpha)(2fk_d/k_t)^{1/2}(\mathrm{I})^{1/2} = \text{const.} \end{aligned}\right\} \quad (5)$$

On the other hand, the residual unsaturation of the polymer, $2R_{us}$, is given by:

$$(1-2R_{us})^{-1} - (1+E(\mathrm{I})^{1/2}/(\mathrm{M}))^{-1} = \frac{k_p}{k_c}(\mathrm{M}) \quad (6)$$

where:

$$E = \alpha(2fk_dk_t)^{1/2}/k_{cp}$$

Influence of the Initiator and Monomer Concentrations on the Rate of Polymerization. When the monomer concentration is varied, it may be kinetically expected from Eq. (2) that the plots of $R_p/(\mathrm{I})^{1/2}$ *vs.* $(\mathrm{I})^{1/2}$ will have straight lines. Similarly, if the initiator concentration is kept constant and the monomer concentration is varied, a linear relationship between $R_p/(\mathrm{M})$ and (M) may be expected on the basis of Eq. (4). The results are plotted in Fig. 2, in which the fit of the experimental data to the linear relationship is fairly good. From the slopes and intercepts of the straight lines shown in Fig. 2, the *A*, *B*, *C*, and *D* of VADO

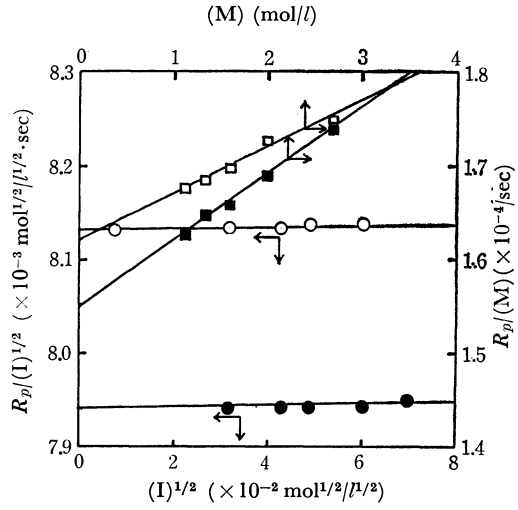

Fig. 2. Plots of $R_p/(\mathrm{I})^{1/2}$ *vs.* $(\mathrm{I})^{1/2}$ and R_p (M) *vs.* (M).
○, □: VADO; ●, ■, VMDO

were estimated to be 5.97×10^{-6}, 8.13×10^{-3}, 4.90×10^{-6}, and 1.62×10^{-4} respectively; the corresponding values of VMDO were found to be 3.05×10^{-6}, 7.94×10^{-3}, 6.94×10^{-6}, and 1.55×10^{-4} respectively. Accordingly, the ratios of the rate constant, as calculated from the above values, are shown in Table 3.

Table 3. The parameters of polymerization

Monomer	$2fk_d$ ($\times10^{-5}$ sec^{-1})	$k_{cp}/k_t^{1/2}$ ($\times10^{-1}$ mol$^{1/2}$/$l^{1/2}$·sec$^{1/2}$)	$(k_p/k_{cp}-\beta/\alpha)(k_{cp}/k_c)$ ($\times10^{-2}l$/mol)	E ($\times10^{-2}l^{1/2}$/mol$^{1/2}$)
VADO	9.34	3.92	3.18	2.47
VMDO	3.39	6.22	4.48	9.36×10^{-1}
DβMPP	6.95	0.57×10^{-1}	2.26	1.46×10^{2}

Here, the $2fk_d$ value of the order of 10^{-5} seems to be pertinent when AIBN is used as an initiator.

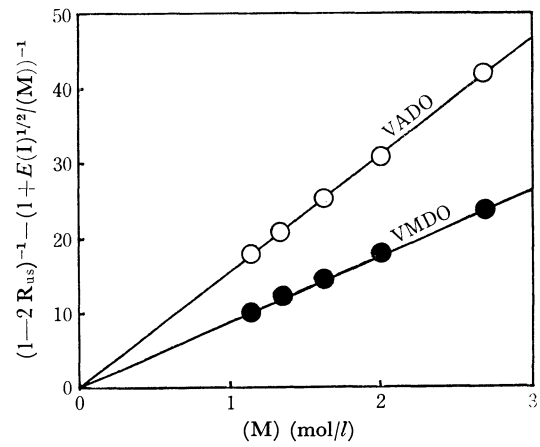

Fig. 3. Plots of $\{(1-2R_{us})^{-1}-(1+E(\mathrm{I})^{1/2}/(\mathrm{M}))^{-1}\}$ *vs.* (M).

On the other hand, the $k_{cp}/\alpha k_t^{1/2}$ values of VADO and VMDO were larger than that of DβMPP; the termination between the two $M_c\cdot$ values in the polymerizations of VADO and VMDO might be slower than that of the DβMPP polymerization.

The Residual Unsaturation. The plots of $\{(1-2R_{us})^{-1}-(1+E(\mathrm{I})^{1/2}/(\mathrm{M}))^{-1}\}$ *vs.* (M) are shown in Fig. 3; there is a good linear relationship, as was predicted by Eq. (6). The ratios of the rate constant of the unimolecular cyclization reaction to that of the bimolecular propagation of the uncyclized radical, k_c/k_p, were estimated to be 0.065 mol/*l*(VADO), and 0.114 mol/*l*(VMDO) from the slopes of the straight lines. The results show that the pendant double bonds in polymers are almost not cyclized at all because the acryl double bond is more active than the allylidene double bond. The difference between VADO and VMDO could not be seen in these polymerizations; the influence of methyl groups could not be observed, either.

Therefore, although VADO and VMDO both undergo cyclopolymerization, they act as monofunctional monomers rather than as bifunctional monomers.

Copolymerization. The composition and the unsaturation of polymer as functions of the monomer

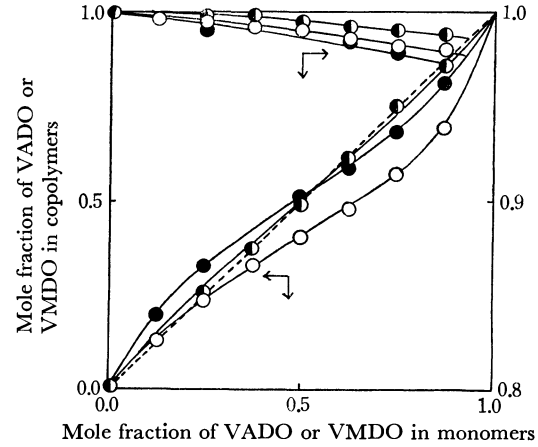

Fig. 4. Relation of the copolymer composition and the residual unsaturation to the monomer composition.
○: [VADO+St] = 3.49 mol/*l*, ◑: [VADO+AN] = 6.10 mol/*l*, ●: [VMDO+St] = 3.49 mol/*l*, —: calculated curve

composition are shown in Fig. 4. It may be seen in the figure that the residual unsaturations of the copolymer thus obtained decreased slightly with an increase in the comonomer composition until they became nearly constant at 1.0. Accordingly, the cyclization may be approximately negligible, the ratio being obtainable by the well-known Fineman-Ross method; the results are summarized in Table 4.

Table 4. Reactivity ratios for VADO or VMDO (M_1)-monovinyl compounds(M_2) systems

M_1	M_2	r_1	r_2	Q_1[10]	e_1[10]	Q_2	e_2
VADO	St	0.22	0.81	1.00	−0.80	0.43	0.51
VADO	AN	0.89	0.95	0.60	1.20	0.39	0.79
VMDO	St	0.51	0.49	1.00	−0.80	0.80	0.30

In Fig. 4 the theoretical solid curves as calculated from the resulting reactivity ratios agreed well with the results of the experimental measurements.

The average values of Q and e for VADO, VMDO were estimated as follows: VADO, $Q=0.41$, and $e=0.65$; $Q=0.80$, and $e=0.30$.

These values are not equal to Q, e values of diallylidene cyclic acetals[8-9] but those of DβMPP,[2] methyl acrylate[10] and methyl methacrylate.[10] Consequently, VADO and VMDO may be suggested to be polymerized as same as monoacryl and methacryl esters.

The Q value for VMDO was larger than that for VADO; it might be influenced by the hyperconjugation of methyl group.

On the other hand, the e value of VMDO was more negative than that of VADO; it might be contributed to the methyl group which was a proton donor.

8) T. Ouchi, S. Yamamoto, Y. Akao, Y. Nagaoka, and M. Oiwa, *Kogyo Kagaku Zasshi*, **71**, 1078 (1968).
9) T. Ouchi, S. Tatasuno, T. Nakayama, and M. Oiwa, *ibid.*, **73**, 607 (1970).
10) J. Brandrup and E. H. Immergut, "Polymer Handbook," J. Wiley & Sons, New York (1966).

BULLETIN OF THE CHEMICAL SOCIETY OF JAPAN, VOL. 44, 1342—1345(1971)

The Reaction of Ethyl Alkylchloropyruvate with Sodiomalonate and Sodioacetoacetate[1)]

Akira TAKEDA, Satosi WADA, Masatosi FUJII, Isao NAKASIMA, and Shoiti HIRATA
Department of Synthetics Chemistry, School of Engineering, Okayama University, Tusima, Okayama

(Received October 1, 1970)

The reaction of alkylchloropyruvate (**1**) with sodiomalonate gave γ-alkyl-α,β-dialkoxycarbonyl-$\Delta^{\beta,\gamma}$-butenolide (**2**), which led to γ-ketocarboxylic acid (**3**). The reaction of **1** with sodioacetoacetate gave 2-alkyl-5-methylfuran-3,4-dicarboxylate (**6**) *via* the intermediate 2-alkyl-3-hydroxy-5-methyl-2,3-dihydrofuran-3,4-dicarboxylate (**5**). It has been shown unambiguously that the carbanions of both sodiomalonate and sodioacetoacetate attack the carbonyl carbon of **1** predominantly.

Reichstein *et al.* disclosed in 1933 that bromopyruvic ester reacted with sodiooxaloacetate to yield 2,3,4-furantricarboxylic ester.[2)] Dunlop and Hurd[3)] assumed that the cyclization process involved the formation of 3-hydroxy-2,3-dihydrofurantricaboxylate as the intermediate. Cantlon *et. al.* later discussed and confirmed its structure by means of NMR data.[4)] We reported that the reaction of ethyl chlorophenylpyruvate with diethyl sodiomalonate gave γ-phenyl-α,β-diethoxycarbonyl-$\Delta^{\beta,\gamma}$-butenolide, which on hydrolysis and subsequent decarboxylation afforded γ-benzoylpropionic acid.[5)]

Since the mode of reactions of carbanions such as sodiomalonate and sodioacetoacetate with alkylhalopyruvate has not been investigated, it appears to us worthwhile to elucidate the structures of intermediates as well as products in reactions, which lead to 2,5-dialkyl-3,4-dialkoxycarbonylfurans, or to γ-alkyl-α,β-dialkoxycarbonyl-$\Delta^{\beta,\gamma}$-butenolides. The facility of

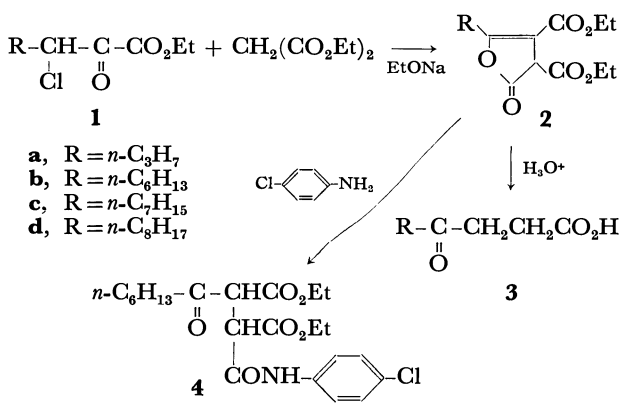

Scheme 1

1) Presented in part at the Annual Meetings of the Chemical Society of Japan, April 1, 1967 (Tokyo) and April 4, 1969 (Tokyo).

2) T. Reichstein, A. Grussner, K. Schindler, and E. Hardmeyer, *Helv. Chim. Acta*, **16**, 276 (1933).

3) A. P. Dunlop and C. D. Hurd, *J. Org. Chem.*, **15**, 1160 (1950).

4) I. J. Cantlon, W. Cocker, and T. B. H. McMurry, *Tetrahedron*, **15**, 46 (1961).

5) A. Takeda, S. Wada, and T. Uno, *Mem. School Eng., Okayama Univ.*, **2**, 80 (1967).

Table 1. γ-Alkyl-α,β-diethoxycarbonyl-$\Delta^{\beta,\gamma}$-butenolides (**2**)

Compound	R	Yield %	Bp °C/mmHg	n_D^{25}	Found, % C	Found, % H	Calcd, % C	Calcd, % H
2a	n-C_3H_7	43	133—135/3	1.4564	57.83	6.93	57.77	6.71
2b	n-C_6H_{13}	46	155—157/3	1.4551	61.26	8.05	61.52	7.74
2c	n-C_7H_{15}	42	164—168/3	1.4571	62.35	8.29	62.56	8.03
2d	n-C_8H_{17}	32	160—163/1	1.4565	63.62	8.40	63.51	8.29

obtaining alkylchloropyruvic esters (**1**)[6] also prompted us to study these reactions in order to find new synthetic routes to 2,5-dialkylfurans and γ-oxoalkanecarboxylic acids.

This paper deals with the preparation of four γ-alkyl-α,β-diethoxycarbonyl-$\Delta^{\beta,\gamma}$-butenolides (**2a—d**), which were readily converted to γ-ketocarboxylic acids (**3a—d**), together with the preparation of three 2-alkyl-5-methylfuran-3,4-dicarboxylates (**6b—d**), which were converted to 2-alkyl-5-methylfurans (**8b—d**). These furans were finally transformed to the corresponding 1,4-diketones (**9b—d**). The intermediate 2-alkyl-3-hydroxy-5-methyl-2,3-dihydrofuran-3,4-dicarboxylates (**5b—d**) also were isolated and characterized.

The reaction of **1** with sodiomalonate gave the product (**2**) in a 40—50% yield, which was separated as a colorless oil and purified by vacuum distillation. The structure of **2** was confirmed by elemental analyses and IR spectra (lactone C=O 1835, 1820 cm^{-1}; ester C=O 1750, and conjugated ester C=O 1725 cm^{-1}; C=C 1665 cm^{-1}). Further evidence to support the $\Delta^{\beta,\gamma}$-butenolide structure of **2** was provided by the fact that the treatment of **2b** with p-chloroaniline gave N-(p-chlorophenyl)-2,3-diethoxycarbonyl-4-oxocapramide (**4**) in 95% yield. The acid hydrolysis of **2** and the subsequent decarboxylation yielded γ-ketocarboxylic acids (**3a—d**) in good yield (Scheme 1). IR spectra of **3** exhibited a characteristic band at 1695 cm^{-1} due to C=O and were identical with those of the authentic sample.[7] A series of γ-alkyl-α,β-diethoxycarbonyl-$\Delta^{\beta,\gamma}$-butenolides (**2a—d**) and γ-keto acids (**3a—d**) derived in this way are listed in Tables 1 and 2, respectively.

Table 2. Preparation of γ-keto acids (**3**) from $\Delta^{\beta,\gamma}$-butenolides (**2**)

Compound	R	Yield, %	Mp, °C
3a	n-C_3H_7	51	48—49[a]
3b	n-C_6H_{13}	59	66—67[b]
3c	n-C_7H_{15}	74	78—78.5[c]
3d	n-C_8H_{17}	55	78—79[d]

a) Mp 48.5—49.5°C: A. S. Perlin and C. B. Purves, *Can. J. Chem.*, **31**, 227 (1953).
b) Mp 66—67°C: H. Reinheckel, K. Haage, and R. Gensike, *Angew. Chem.*, **77**, 810 (1965).
c) Mp 77—79°C: I. Ernest, H. Jelinkova, *Collect. Czech. Chem. Commun.*, **24**, 3341 (1959); *Chem. Abstr.*, **54**, 4375 (1958).
d) Mp 78°C: H. Reinheckel *et. al*, *loc. cit.*

6) A. Takeda, S. Wada, M. Fujii, and H. Tanaka, This Bulletin, **43**, 2997 (1970).
7) A. Takeda, K. Takahasi, S. Torii, and T. Moriwake, *J. Org. Chem.*, **31**, 616 (1966).

The reaction of **1** with ethyl sodioacetoacetate was carried out in dry ethanol. Ethyl 3-chloro-2-oxononanoate (**1b**) gave ethyl 2-n-hexyl-3-hydroxy-5-methyl-2,3-dihydrofuran-3,4-dicarboxylate (**5b**) as the condensation product in 73% yield. Treatment of **5b** with sulfuric acid effected the dehydration to afford ethyl 2-n-hexyl-5-methylfuran-3,4-dicarboxylate (**6b**) in quantitative yield. The structural assignment of **5b** was based on IR spectra (OH 3490 cm^{-1}; ester C=O 1735, 1706 cm^{-1}; C=C 1640 cm^{-1}) and NMR spectra ($CDCl_3$) (τ 7.74, s, 3H, $-\overset{}{\underset{}{C}}(=O)-CH_3$; τ 7.58, s, 1H, OH). When treated with alcoholic potassium hydroxide solution, **5b** underwent both dehydration and hydrolysis to give 2-n-hexyl-5-methylfuran-3,4-dicarboxylic acid (**7b**) in good yield. **7b** was transformed into dimethyl ester (**11**) with diazomethane and identified. While **1b** (R=n-C_6H_{13}) gave only **5b** as the major product, **1c**(R=n-C_7H_{15}) and **1d** (R=n-C_8H_{17}) afforded

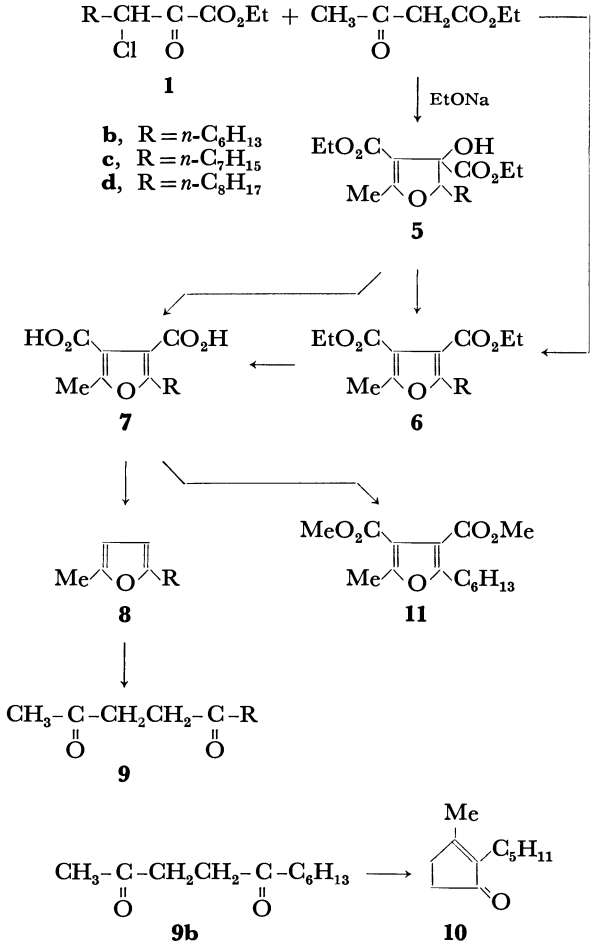

Scheme 2

TABLE 3. 1,4-DIKETONES (**9**) AND THE INTERMEDIATES (**5,6,7,8**)

Compound	R	Yield %	Bp °C/mmHg (Mp, °C)	n_D^{25}	Found, %		Calcd, %	
					C	H	C	H
5b	n-C_6H_{13}	73	158—161/3	1.4649[a]	62.16	8.59	62.18	8.59
5c	n-C_7H_{15}	b)	183—185/6[c]	1.4639	63.07	8.78	63.14	8.83
5d	n-C_8H_{17}	b)	180—182/2.5[c]	1.4659	64.43	9.05	64.02	9.05
6b	n-C_6H_{13}	99	150—152/2	1.4705[a]	66.18	8.56	65.78	8.44
6c	n-C_7H_{15}	b)	183—185/6[c]	1.4680	66.70	8.83	66.64	8.70
6d	n-C_8H_{17}	b)	180—182/2.5[c]	1.4688	67.69	9.10	67.43	8.93
7b	n-C_6H_{13}	99[d]	(120—121)		61.62	7.14	61.41	7.14
7c	n-C_7H_{15}	e)	(105)		62.87	7.64	62.67	7.51
7d	n-C_8H_{17}	e)	(112.5)		64.01	7.89	63.81	7.85
8b	n-C_6H_{13}	77	101—103/29[f]	1.4538	79.83	10.71	79.46	10.91
8c	n-C_7H_{15}	46	113—114/22[g]	1.4522	80.05	10.98	79.94	11.18
8d	n-C_8H_{17}	55	128—129/21[h]	1.4538	80.07	11.64	80.35	11.41
9b	n-C_6H_{13}	79	(34)[i]		72.04	10.77	71.70	10.94
9c	n-C_7H_{15}	54	(43)[j]		72.47	11.36	72.68	11.18
9d	n-C_8H_{17}	57	(48—49)		73.17	11.49	73.54	11.39

a) Measured at 27°C. b) Obtained as a mixture. Separation into the components was by tlc (Experimental). c) Temperature range at which the mixture distilled. d) Yield from **6b**. e) The mixture of **5** and **6** was used as the starting material (Experimental). f) Bp 102—105°C/30 mmHg.[8] g) Bp 107—110°C/16 mmHg.[8] h) Bp 95—97°C/11 mmHg.[8] i) Mp 33°C.[9] j) Mp 40.5°C.[9]

the mixtures of the corresponding intermediate (**5c, 5d**) and the dehydrated product (**6c, 6d**). These mixtures were used without fractionation for the preparation of **7c** as well as **7d** by means of alkaline hydrolysis. Decarboxylation of acids **7b—d** carried out in quinoline by heating with copper powder, afforded 2-alkyl-5-methylfurans (**8b—d**). IR spectra and the boiling point of the furans (**8b—d**) were identical with those of the authentic samples, which were obtained in the alternative way.[8] The ring-opening of **8b—d** to give the 1,4-diketones (**9b—d**) was effected by heating with aqueous acetic acid containing a small amount of sulfuric acid. The sequence of these reactions is shown in Scheme 2. Table 3 shows the yields, physical properties, and analytical data of three 1,4-diketones obtained in this experiment and their intermediates. Diketone **9b** was converted to 2-n-pentyl-3-methyl-2-cyclopenten-1-one (**10**) by the usual method.

Since substrate (**1**) has two reactive positions, α and β, in the molecule, there are possibilities of forming two kinds of ring skeleton for both reactions described in Schemes 1 and 2. The formation of **3** from **2** and that of **8** from **5** unambiguously indicate that the carbanions of sodiomalonate and sodioacetoacetate have attacked the carbonyl carbon of **1** predominantly.

Experimental[10]

All boiling points and melting points are uncorrected. Thin layer chromatography was carried out on silica gel G (E. Merck AG, Darmstadt), where the spots of materials were detected by spraying with sulfuric acid solution of potassium permanganate (7: 3 in wt.). Infrared spectra were determined on a Hitachi IR EPI-S2 spectrophotometer.

Ethyl alkylchloropyruvates (**1**) other than **1a** used in this experiment were prepared by the Darzens type condensation of the appropriate aldehydes and ethyl dichloroacetate.[6] Ethyl 3-chloro-2-oxohexanoate (**1a**) was obtained as a pure product by direct chlorination of ethyl 2-oxohexanoate[11] with sulfuryl chloride.

The followings are typical of the experiments to derive **2, 3, 5, 6, 7, 8,** and **9**.

*Ethyl 3-Chloro-2-oxohexanoate (**1a**).* To a stirred solution of ethyl 2-oxohexanoate (7.9 g, 0.05 mol) was added dropwise 7.0 g (0.052 mol) of sulfuryl chloride at 25—30°C. The reaction mixture was stirred at room temperature for additional 60 hr. Distillation of the crude product gave 7.3 g (76%) of **1a**: bp 98—100°C/16 mmHg; n_D^{25} 1.4387; IR (cm^{-1}, liquid) 1755 (ketone C=O) and 1735 (ester C=O).

Found: C, 50.18; H, 6.83%. Calcd for $C_8H_{13}ClO_3$: C, 49.88; H, 6.80%.

*γ-n-Hexyl-α,β-diethoxycarbonyl-$\Delta^{\beta,\gamma}$-butenolide (**2b**).* Diethyl malonate (20.0 g, 0.125 mol) and ethyl 3-chloro-2-oxononanoate (**1b**)[6] (11.7 g, 0.05 mol) were added to 60 m*l* of anhydrous ethanol in which 2.3 g (0.1 g-atom) of sodium was dissolved. The mixture was heated for 7 hr at 65—70°C with stirring and allowed to stand overnight. The reaction mixture was acidified with 10% aqueous sulfuric acid and taken up in ether. The ethereal extract was washed with aqueous sodium bicarbonate and then with water, dried over anhydrous magnesium sulfate, and concentrated. Distillation of the residual oil afforded 7.2 g (46%) of **2b**; bp 155—157°C/3 mmHg; IR (cm^{-1}, liquid) 1835, 1820 (lactone C=O), 1750 (ester C=O), 1725 (conjugated ester C=O), and 1665 (C=C).

*4-Oxodecanoic Acid (**3b**).* A mixture of 3.0 g (0.01 mol) of **2b**, 60 m*l* of sulfuric acid, and 90 m*l* of water was stirred for 10 hr at 170°C in an oil bath. The reaction mixture was cooled, extracted with ether. The ethereal layer was shaken with 5% aqueous sodium hydroxide. The aqueous layer was acidified and then taken up in ether. The extract was

8) Office de Recherches Industrielles de Laboratoire, French 1186346 (1959); *Chem. Abstr.*, **56**, 455 (1962).

9) H. Hunsdiecker, *Ber.*, **75**, 452 (1942).

10) Elementary analyses were carried out by Mr. Eiichiro Amano of our laboratory. We are indebted to Dr. Akira Suzuki and Mr. Sigezo Simokawa, both of Hokkaido University, Sapporo, for NMR measurements.

11) M. Igarasi and H. Midorikawa, *J. Org. Chem.*, **29**, 2082 (1964).

dried over anhydrous magnesium sulfate and the solvent was removed. The residual solid was recrystallized from *n*-hexane to give 1.1 g (59%) of **3b**: mp 66—67°C.

N-(p-*Chlorophenyl*)-*2,3-diethoxycarbonyl-4-oxodecanamide (4)*. A mixed solution of **2b** (0.6 g, 0.002 mol) and *p*-chloroaniline (0.25 g, 0.002 mol) in 2 m*l* of chloroform was stirred at room temperature for 1 hr. After evaporation of the solvent 0.6 g (95%) of **4** was obtained: mp 80—81°C; IR (cm^{-1}, Nujol) 3300 (amide NH), 1730 (ester C=O), 1715 (ketone C=O), and 1665 (amide C=O).

Found: C, 59.94; H, 7.11; N, 3.33%. Calcd for $C_{22}H_{30}ClNO_6$: C, 60.06; H, 6.87; N, 3.18%.

Ethyl 2-n-Hexyl-3-hydroxy-5-methyl-2,3-dihydrofuran-3,4-dicarboxylate (5b). To a solution of ethyl sodioacetoacetate, prepared from sodium (2.3 g, 0.1 g-atom), anhydrous ethanol (100 m*l*), and ethyl acetoacetate (26.0 g, 0.2 mol), was added 23.5 g (0.1 mol) of **1b**. The mixture was heated at 60—65°C with stirring for 7 hr. After being kept standing overnight at room temperature, the reaction mixture was acidified with 20% aqueous sulfuric acid and taken up in ether. The ethereal extract was washed with water, dried over anhydrous sodium sulfate, and concentrated. Distillation of the residue yielded 24.4 g (73%) of **5b**: bp 158—161°C/3 mmHg; R_f 0.54.[12]

Ethyl 2-n-Hexyl-2-methylfuran-3,4-dicarboxylate (6b). Sulfuric acid (50 m*l*) was added dropwise to 10.0 g (0.03 mol) of **5b** in an ice bath. After being heated for 5 min at 50°C, the reaction mixture was poured into 50 m*l* of ice water and extracted with ether. The ethereal layer was washed with water and subsequently with 10% sodium carbonate solution. After being dried over anhydrous sodium sulfate, the solvent was removed. Distillation of the residue under diminished pressure gave 9.1 g (99%) of **6b**: bp 150—152°C/2 mmHg; R_f 0.73;[12] IR (cm^{-1}, liquid) 1720 (ester C=O) and 1590 (C=C).

2-n-Hexyl-5-methylfuran-3,4-dicarboxylic Acid (7b).

(a) From 6b: To a solution of potassium hydroxide (1.0 g, 0.018 mol) in 10 m*l* of 50% aqueous ethanol, 1.0 g (0.003 mol) of **6b** was added. The reaction mixture, after being refluxed for 6 hr, was acidified with 10% aqueous sulfuric acid, and extracted with ether. The ethereal extract, which was treated in the usual manner, gave 0.75 g (99%) of acidic material. The crude product was recrystallized from *n*-hexane - benzene to yield pure sample of **7b**: mp 120—121°C; IR (cm^{-1}, Nujol) 1685, 1630, and 1570.

(b) From 5b: A mixture of **5b** (1.4 g, 0.005 mol) and the solution of potassium hydroxide (5.0 g, 0.09 mol) in 10 m*l* of aqueous 50% ethanol was refluxed for 6 hr. The crude product of **7b** was isolated in the same manner as described in the foregoing experiment. Recrystallization from *n*-hexane - benzene gave 0.8 g (63%) of the prdouct: mp 120—121°C; IR (cm^{-1}, Nujol) 1685, 1630, and 1570.

Reaction of Ethyl 3-Chloro-2-oxodecanoate (1c) with Ethyl Acetoacetate. Ethyl 3-chloro-2-oxodecanoate[6] (37.0 g, 0.15 mol) was added to a solution of ethyl sodioacetoacetate, prepared from 3.4 g (0.15 g-atom) of sodium, 38.7 g (0.3 mol) of ethyl acetoacetate, and 100 m*l* of anhydrous ethanol. The stirred mixture was heated at 60—65°C for 7 hr and allowed to stand overnight at room temperature. After being acidified with 20% aqueous sulfuric acid, the reaction mixture was extracted with ether. The extract was washed with water, dried over anhydrous sodium sulfate, and concentrated. Distillation of the resudie yielded 27.3 g of the liquid, which was collected at 183—185°C/6 mmHg. For analysis and spectral determination, the liquid was fractionated to **5c** and **6c** by means of preparative thin layer chromatography. R_f values[13] were 0.30 for **5c** and 0.56 for **6c**. From 0.4 g of the mixture 0.3 g of **5c** and 0.1 g of **6c** were obtained. IR spectra (cm^{-1}, liquid): **5c**, 3490 (OH), 1735(ester C=O), 1705(conjugated ester C=O), and 1640 (C=C); **6c**, 1720 (ester C=O), and 1590 (C=C).

2-n-Heptyl-5-methylfuran-3,4-dicarboxylic Acid (7c). The liquid mixture (25.0 g) obtained in the foregoing experiment was refluxed with much excess of potassium hydroxide dissolved in 50% aqueous ethanol for 6 hr. It gave 11.0 g of the crude product (**7c**): mp 105°C (from *n*-hexane - benzene); IR (cm^{-1}, Nujol) 1685, 1630, and 1570.

Reaction of Ethyl 3-Chloro-2-oxoundecanoate (1d) with Ethyl Acetoacetate. Condensation was carried out in the same manner as that of **1c**. The following reactants were used: 23.5 g (0.09 mol) of **1d**; 23.4 g (0.18 mol) of ethyl acetoacetate; 2.1 g (0.09 g-atom) of sodium which was dissolved in 100 m*l* of anhydrous ethanol before use. Distillation afforded 30.5 g of the liquid which was collected at 180—182°C/2.5 mmHg. The liquid was fractionated to **5d** and **6d** by preparative tlc. R_f values[13] were 0.22 for **5d** and 0.43 for **6d**. IR spectra (cm^{-1}, liquid): **5d**, 3490 (OH), 1735 (ester C=O), 1705 (conjugated ester C=O), and 1640 (C=C); **6d**, 1720 (ester C=O) and 1590 (C=C).

2-n-Octyl-5-methylfuran-3,4-dicarboxylic Acid (7d). The liquid mixture (17.8 g) obtained in the above experiment, gave 8.4 g of the crude product (**7d**) on the alkaline hydrolysis: mp 112.5°C (from benzene); IR (cm^{-1}, Nujol) 1685, 1630, and 1570.

2-n-Hexyl-5-methylfuran (8b). A mixture of **7b** (10.0 g, 0.039 mol) and quinoline (25 m*l*) was refluxed for 5 hr in the presence of copper powder (5.0 g). After filtration, the mixture was extracted with ether. The extract, washed with water, diluted hydrochloric acid, then with water, was dried over anhydrous sodium sulfate. The fraction distilling at 101—103°C/29 mmHg was collected: yield 5.0 g (77%), IR (cm^{-1}, liquid) 1570.

2,5-Undecanedione (9b). A mixture of **8b** (3.0 g, 0.018 mol), glacial acetic acid (7 m*l*), water (2.5 m*l*), and a few drops of sulfuric acid was refluxed for 2 hr. The mixture was poured into 10 m*l* of water and taken up in ether. The ethereal layer was separated, washed with saturated sodium bicarbonate and water, and dried over anhydrous sodium sulfate. Removal of the solvent yielded crystals. Recrystallization of the crude product from methanol gave 2.6 g (79%) of **9b**: mp 34°C; IR (cm^{-1}, Nujol) 1715 (ketone C=O).

2-n-Pentyl-3-methyl-2-cyclopentene-1-one (10). Dione **9b** (0.7 g, 0.04 mol) was heated with 3% aqueous sodium hydroxide (7 m*l*) at reflux temperature for 7 hr with vigorous stirring. The mixture was taken up in ether, washed with water and dried over anhydrous sodium sulfate. Removal of the solvent gave 0.4 g (61%) of **10**. The 2,4-dinitrophenylhydrazone of **10**, mp 119—120°C, was identical with the authentic sample.[14]

Metyl 2-n-Hexyl-5-methylfuran-3,4-dicarboxylate (11). When treated with diazomethane, **7b** was transformed into its methyl ester **11**: bp 145—148°C (bath)/3 mmHg;[15] n_D^{25} 1.4755; IR (cm^{-1}, liquid) 1720 (ester C=O) and 1590 (C=C); NMR (τ, $CDCl_3$) 7.56 (s, 3H, CH_3), and 6.18 (s, 6H, $2CH_3$-OCO).

Found: C, 64.15; H, 7.59%. Calcd for $C_{15}H_{22}O_5$: C, 63.81, H, 7.85%.

12) Conditions of tlc: support, silica gel G (E. Merck AG, Darmstadt), 0.3 mm; developer, *n*-hexane - acetone (3:1 v/v).

13) Conditions of preparative tlc: support, silica gel G (E. Merck AG, Darmstadt), 0.8 mm; developer, *n*-hexane - acetone (5:1 v/v); eluent, acetone.

14) C. Rai and S. Dev, *Experientia*, **11**, 114 (1955).

15) The temperature of the oil bath at which **9** was distilled under diminished pressure (3 mmHg).

Conformational Changes in Heterocyclic Analogs of Metaparacyclophane

Sadatoshi AKABORI, Kengo SHIOMI, and Takeo SATO*

Department of Chemistry, Faculty of Science, Toho University, Narashino-shi, Chiba
**Department of Chemistry, Faculty of Science, Tokyo Metropolitan University, Setagayaku, Tokyo*

(Received October 2, 1970)

Sulfur analogs of [2.2]metaparacyclophane, II, III, and IV were prepared and their NMR spectra were examined. Of the three possible inversion mechanism, the one which involves the inversion of the *m*-phenylene unit is proposed.

The unique features of [2.2]metaparacyclophane (I) system[1-5] resulting from the crowding of two aromatic rings give rise to interesting physical and chemical properties. They include anomalies in the ultraviolet[4] and nuclear magnetic resonance spectrum.[3,5]

In a paper[2] dealing with the NMR spectra of I, it was shown that inversion of the 11-membered ring occurred at temperatures higher than 187°C. In order to study the inversion mechanism further, 2,9-dithia[2.2]metaparacyclophane (II) and its derivative III were prepared and their NMR spectra were examined.

Compound II was prepared according to the procedure of Vögtle[3] by the reaction of *m*-benzenedithiol with 1,4-bis(bromomethyl)benzene under high dilution conditions. A colorless amorphous compound, mp 99—100°C was obtained. A 22-membered tetrathia compound IV[6] was isolated in 3.4% yield by the condensation between two moles each of the halide and the dithiol. When the reaction was carried out in THF only IV was formed even under high-dilution conditions.

The NMR spectrum[7] of II in CCl_4-CS_2 (1:1) at room temperature shows absorptions at δ 5.73 and 7.39 (broad signal, A_2B_2 pattern, $C_{12,13}$ and $C_{15,16}$ aryl protons), δ 6.90—7.40 (AB_2 pattern, $C_{4,5,6}$ aryl protons), δ 6.22 (triplet, C_8 aryl proton) and at δ 3.87 and 3.90 (broad absorption, AB pattern, methylene protons). The spectrum was essentially similar to that of Vögtle.[3] The C_8 and half-side of *p*-phenylene aryl protons exhibited unusual high field shifts due to the ring current effects of the opposite benzene ring. No such upfield shift was observed with the larger ring compound IV, which in DMSO-d_6 showed absorptions at δ 4.06 (singlet, methylene protons), δ 7.00 (singlet, *p*-phenylene unit aryl protons), δ 7.10 and 7.20 (AB_2 pattern, outer *m*-phenylene protons) and at δ 7.39 (inner *m*-phenylene protons). The peak for methylene protons of compound IV was a sharp singlet, which suggests that the comformation of cyclic compound is flexible, with no fixation.

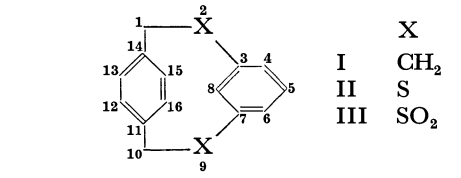

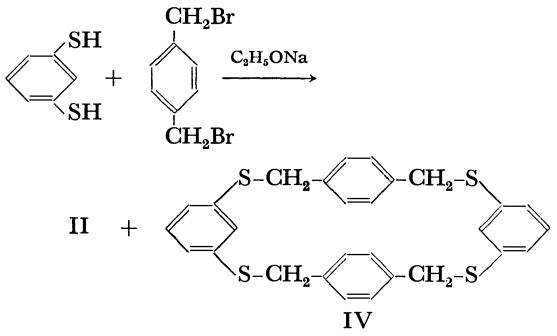

Oxidation of II with 30% hydrogen peroxide in acetic acid gave III as colorless high-melting needles.

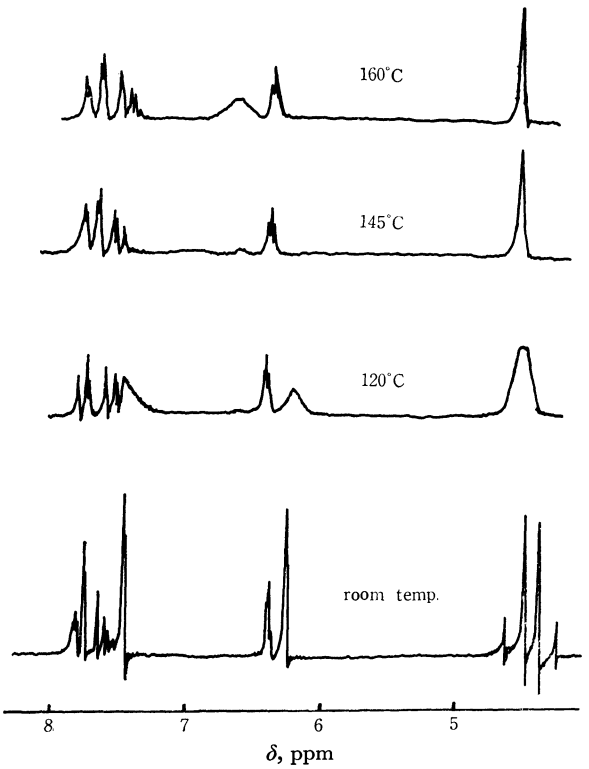

Fig. 1. NMR spectra of III in DMSO-d_6 (100 MHz).

1) T. Hylton and V. Boekelheide, *J. Amer. Chem. Soc.*, **90**, 6887 (1968).
2) S. Akabori, S. Hayashi, M. Nawa, and K. Shiomi, *Tetrahedron Lett.*, **1969**, 3727.
3) F. Vögtle, *Chem. Ber.*, **102**, 3077 (1969).
4) D. J. Cram, R. C. Helgeson, D. Lock, and L. A. Singer, *J. Amer. Chem. Soc.*, **88**, 1324 (1966).
5) D. T. Hefelfinger and D. J. Cram, *ibid.*, **92**, 1073 (1970).
6) Parent peak, *m/e* 488. The spectrum was recorded on a Hitachi RMU-6 spectrometer.
7) The spectra were recorded on a JNM-4H-100 spectrometer TMS as a reference.
8) H. S. Gutowsky and C. H. Holm, *J. Chem. Phys.*, **25**, 1228 (1956).

The structure was supported by elemental analysis and spectral data. As shown in Fig. 1, the NMR spectrum of III in DMSO-d_6 shows absorptions at δ 7.50 and 7.82 (AB_2 pattern, $C_{4,5,6}$ aryl protons), δ 6.28 and 7.48 (A_2B_2 pattern, $C_{12,13,15,16}$ aryl protons), δ 6.40 (triplet, C_8 aryl proton) and at δ 4.34 and 4.54 (AB pattern, J=13 Hz, methylene protons). Downfield shift (0.18 ppm) of C_8 aryl proton of III compared with that of II could be attributed mainly to the anisotropy effects of two sulfone groups. With the rise of temperature of the solution individual signals of A_2B_2 pattern collapse to a broad signal at about 145°C as shown in Fig. 1.

Temperature dependence of the A_2B_2 pattern is in line with the exchange between $C_{12,13}$ and $C_{15,16}$ proton environments resulting from the ring inversion among conformers A and B. Based on the chemical shift at 23°C ($\Delta\nu$=120 Hz) and temperature of coalescence (T_c=145°C), the energy barrier to interconversion is calculated to be $\Delta G_c^{\ddagger}$=20.0±0.3 kcal/mol.[8,9] Inversion energy was calculated to be $\Delta G_c^{\ddagger}$=20.1±0.4 kcal/mol from methylene proton signals (T_c=118°C, $\Delta\nu$=20 Hz). The energy barrier for II,[10] however, was found to be as low as $\Delta G_c^{\ddagger}$=14.8±0.4 kcal/mol (calculated from methylene protons, $\Delta\nu$=20 Hz, T_c= 23.0°C).[10] The difference is attributable mainly to the bulkiness and rigidness of sulfone groups as compared with bivalent sulfur groups.

There are three types of possible inversion mechanisms, (a), (b), and (c). In (a), inversion of the *m*-phenylene ring occurs through the rotation of C_1–C_2 and C_9–C_{10} bonds. In (b), rotation of *p*-phenylene unit occurs similarly about C_1–C_{14} and C_{10}–C_{11} bonds. In (c), rotation of the meta-ring occurs in a concerted fashion. Examination of molecular model[11] of I indicates that the para-ring is more strained that the meta-ring and inversion of the latter occurs more easily. By similar consideration (c) can be ruled out by steric hindrance of internal aryl protons. If the inversion was due to (b), one might not expect the coalescence of methylene protons of II and III at higher temperatures. At higher temperatures, however, II and III showed a sharp singlet due to methylene protons and a downfield shift of C_8 aryl protons. This suggests that the inversion may occur by (a).

9) S. Glasstone, K. J. Laidler, and H. Eyring, "The Theory of Rate Processes," McGraw-Hill, Inc., London, 1941, Chapt. 1.

10) In Ref. 3, a value of $\Delta G_c^{\ddagger}$ was calculated as 14.7 kcal/mol based on the aryl protons of A_2B_2 pattern and as 14.9 kcal/mol based on the methylene signals of AB pattern.

11) R. H. Boyd, *J. Chem. Phys.*, **49**, 2574 (1968).

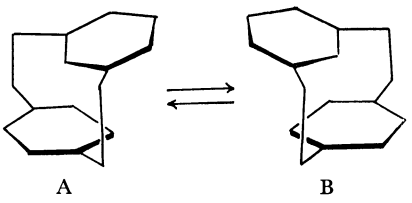

Experimental

2,9-Dithia[2.2]metaparacyclophane (II). 1, 4-Bis(bromomethyl)benzene in 250 m*l* of dried tetrahydrofuran and solution of 7.1 g (0.05 mol) of *m*-benzenedithiol in 250 m*l* of 75% ethanol containing 5 g of sodium hydroxide were added separately drop by drop through a modified Hershberg dropping funnel to 1.5 *l* refluxing ethanol during the course of 48 hr. Stirring was carried out throughly during the addition. When it was complete, the resulting mixture was filtered for removal of sodium bromide. The filtrate was dissolved in benzene, washed with water. The benzene solution was then dried, concentrated and subjected to column chromatography on alumina using benzene as an eluent. From the first elute a colorless solid was isolated. By recrystallization from chloroform-benzene II was obtained in a 6.9% yield, mp 99—100°C, lit,[3] 99—100°C.

Found: C, 68.50; H, 4.64; S, 26.45%. Calcd for $C_{14}H_{12}S_2$: C, 68.85; H, 4.83; S, 26.27%.

From the second elute IV was isolated. It was recrystallized from chloroform to give 0.25 g (3.4% yield) of colorless solid, mp 218—220°C.

Found: C, 68.32; H, 4.88; S, 26.50%. Calcd for $C_{28}H_{24}S_4$: C, 68.85; H, 4.83; S, 26.27%.

When a solution of 10 g (0.07 mol) of *m*-benzenedithiol in 320 m*l* absolute ethanol containing 5 g of sodium hydroxide and a solution of 18.5 g (0.07 mol) of 1,4-bis(bromomethyl)-benzene in 320 m*l* of dried tetrahydrofuran were added to 200 m*l* of tetrahydrofuran in the course of 98 hr at room temperature. A 5.7% yield of IV, mp 218—220°C, was obtained.

2,9-Dithia[2.2]metaparacyclophane-2,2,9,9-tetroxide(III). A mixture of 2.25 g of II dissolved in 30 m*l* glacial acetic acid containing 30% hydrogen peroxide was put to stand at room temperature overnight. It was concentrated *in vacuo* to give white crystals, which were dissolved in chloroform and subjected to silica gel column chromatography using chloroform as an eluent. Compound III was obtained as colorless needles, recrystallized from chloroform, mp >300°C, in an 8% yield, ν_{max} 1310 and 1150 cm^{-1}.

Found: C, 54.67; H, 3.76%. Calcd for $C_{14}H_{12}S_2O_4$: C, 54.55; H, 3.92%.

We wish to thank the Ministry of Education for financial support.

Kinetics of Liquid-phase Hydrogenation of Aliphatic α,β-Unsaturated Aldehyde over Raney Cobalt Catalyst

Kazuhiko HOTTA and Teruo KUBOMATSU

The Osaka Municipal Technical Research Institute, Kita-ku, Osaka

(Received October 6, 1970)

Kinetic studies on the hydrogenation of 2-methyl-2-pentenal (UD) over the Raney cobalt catalyst were performed at temperatures ranging from 10 to 40°C in *n*-hexane. The products were found to be 2-methylpentan-1-ol (SA), 2-methyl-2-penten-1-ol (UA) and 2-methylpentanal (SD). The initial rates of the formation of SA(r_{SA}), SD(r_{SD}), and UA(r_{UA}) were determined in the concentrations of UD(C_{UD}), 0.026—0.263 mol/*l*. It was found by kinetic analysis that ($r_{SA}+r_{SD}$) was represented by a Langmuir-type rate equation and r_{UA} by another one. The rate equations which fitted the rate data are as follows.

$$r_{SA}+r_{SD}=\frac{1.1\times10^{10}e^{-15200/RT}C_{UD}}{(1+4.4\times10^{5}e^{-7500/RT}C_{UD})^2}$$

$$r_{UA}=\frac{1.2\times10^{8}e^{-13500/RT}C_{UD}}{(1+9.3\times10^{3}e^{-5600/RT}C_{UD})^2}$$

A mechanism in which the formation of SA and SD and that of UA proceed through different types of adsorbed UD was proposed. The adsorbed species in enol form and that in keto form were considered with respect to the formation of SA and SD. Activation energies for the formation of SA plus SD and of UA were determined to be 7.7 and 7.9 kcal/mol, respectively. The selectivity defined as the ratio of r_{SA} to ($r_{SA}+r_{SD}$) was found to increase with the increase of the surface coverage of hydrogen.

The vapor phase hydrogenation of 2-ethyl-2-hexenal over the supported copper catalyst was studied by Tanaka and Yada.[1] It was found that each reaction order with respect to the carbon-carbon double bond and the aldehyde group was unity. The hydrogenation of crotonaldehyde over the Raney copper-cadmium catalyst has also been kinetically studied in the vapor phase by Yada and Kudo.[2] In order to determine the rate constant, they assumed that the reaction order with respect to the reactant was unity, and neglected to consider the adsorption factor.

We have studied the liquid phase hydrogenation of α,β-unsaturated aldehydes over the Raney nickel catalyst with or without modifiers and have found that the products were saturated aldehydes and alcohols and that unsaturated alcohol was not produced.[3] Over the Raney cobalt catalyst, on the other hand, unsaturated alcohol was found to be formed with saturated aldehyde and alcohol. There have been only few kinetic studies on such a complicated reaction system in the liquid phase, consisting of both parallel and successive reactions.

It is the purpose of this paper to elucidate the kinetic behavior of the hydrogenation of 2-methyl-2-pentenal over the Raney cobalt catalyst in *n*-hexane. The kinetics was found to be best fitted to the rate equation based on the Langmuir-Hinshelwood mechanism. A detailed discussion is also made on the mechanism of the reactions.

Experimental

Catalyst. A commercial Raney cobalt-aluminum alloy (Co:50 wt%) was developed with a 15% sodium hydroxide solution at 50°C for 1 hr. The sample was washed with minimum volume of distilled water until the washings became neutral, then 5 times with 2-propanol, and 10 times with *n*-hexane in a hydrogen atomsphere. *n*-Hexane was then evaporated with hydrogen stream. The resulting catalyst, 540 mg (Co: *ca.* 500 mg), in dry form was weighed and stored in *n*-hexane under a hydrogen atmosphere. Decrease in the activity of the catalyst could be ignored within 4 weeks after the preparation.

Apparatus and Procedure. The catalyst, 540 mg, and *n*-hexane were put into a glass reaction vessel with a rubber-stoppered branch tube, and then the reaction vessel was equipped with a metal flange with three needle valves and with a mechanically sealed stirrer. After replacing air with hydrogen by making use of valve(1), the reactor was immersed in a constant temperature water bath controlled to ±0.05°C. Hydrogen was bubbled into the catalyst-solvent system through valve (2). In order to carry out the reaction under normal pressure, hydrogen was exhausted through valve (3) to atmosphere through a bubble counter. The catalyst-solvent system was stirred with 500 rpm in the hydrogen flow to saturate the catalyst with hydrogen. The reactant to be hydrogenated was then injected to this system. The total volume of the reactant and the solvent was kept to 50 m*l*. When the reactant was injected to the catalyst-solvent-hydrogen system, rapid absorption of hydrogen took place. The rate dropped to almost constant after 30 sec. Thus, the reaction was considered to reach the steady state within 30 sec after the injection of the reactant.

The total rate of the formation of the products was found to increase and become saturated with increased stirring. Hydrogenation was carried out under the conditions where the rate is independent of stirring. The maximum of the apparent activation energy observed in this study is 10 kcal/mol, indicating that diffusional process plays no important role under the conditions adopted.

The reaction mixture was sampled from the branch tube through a rubber stopper and the composition of the liquid phase was determined by glc employing a column packed with 20% PEG 6000/C-22.

Materials. *n*-Hexane was purified by hydrogenating reducible impurities. Cylinder hydrogen and 2-propanol were used without further purification. 2-Methyl-2-pentenal, pre-

1) T. Tanaka and S. Yada, *Kagaku Kogaku*, **21**, 721 (1957).
2) S. Yada and S. Kudo, *Shokubai*, **6**, 85 (1964).
3) K. Hotta and T. Kubomatsu, Preprints for the 20th Annual Meeting of the *Chem. Soc. Japan* (Tokyo, 1967), No. 11303.

pared from propionaldehyde and stored in portions of (0.2—1.8) m*l*, in sealed glass ampoules under a nitrogen atmosphere at −15°C, was 99% up pure.

Results

Determination of the Initial Rate. A representative of the change in product pattern as a function of reaction time of the hydrogenation of 2-methyl-2-pantenal (UD) over the Raney cobalt catalyst is shown in Fig. 1. The plots shown by the symbol ♁ are from a catalyst prepared in one batch and those by the symbol ♀ from a catalyst in another batch. Reproducibility in the rate measurement is satisfactory.

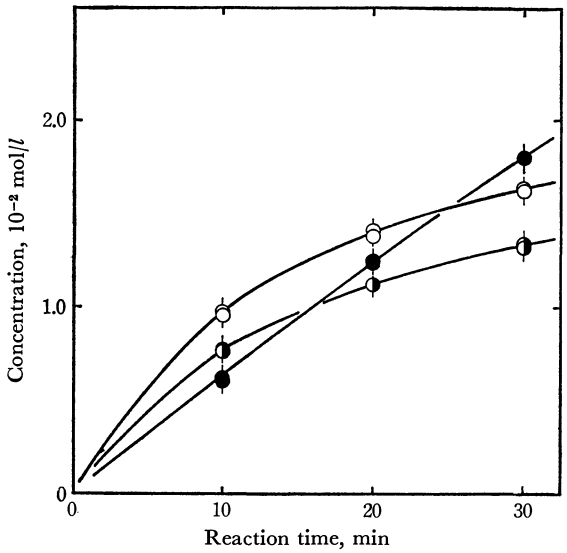

Fig. 1. Product concentration-time curves at 40°C, C_{UD}, 0.105 mol/*l*; SD, ○; SA, ●; UA, ◑

The rate of formation of the saturated aldehyde, 2-methylpentanal (SD), and that of the unsaturated alcohol, 2-methyl-2-penten-1-ol (UA), decrease gradually with reaction time. The rate of formation of the saturated alcohol, 2-methylpentan-1-ol (SA), is practically constant. It was also observed that the rate of formation of SA, however, showed a negative order dependence at higher concentration of UD and at lower reaction temperature. This indicates that (i) the hydrogenation of UD consists of a consecutive reaction which proceeds *via* SD or/and UA, and (ii) SA is the terminal product.

Isomerization from UA to SD and the dehydrogenation of SA and UA were not observed.

It was found that each product concentration-time curve could be represented by the third order equation as shown by the solid line in Fig. 1:

$$C = Xt^3 + Yt^2 + Zt \qquad (1)$$

where C denotes the concentration of a product at the reaction time t, and X, Y, Z are constants. The rate at t is given by differentiating Eq. (1) with respect to t, *viz.*,

$$\frac{dC}{dt} = 3Xt^2 + 2Yt + Z \qquad (2)$$

Thus the initial rate is given by

$$\left(\frac{dC}{dt}\right)_{t=0} = Z$$

Therefore the initial rate is the rate at the reaction time $t=0$, obtained by extrapolation from the rate of formation-time curve experimentally determined in the period in which the reaction proceeds in steady state. The kinetic analysis is made with the assumption that the reaction proceeds in steady state even at the reaction time $t=0$.

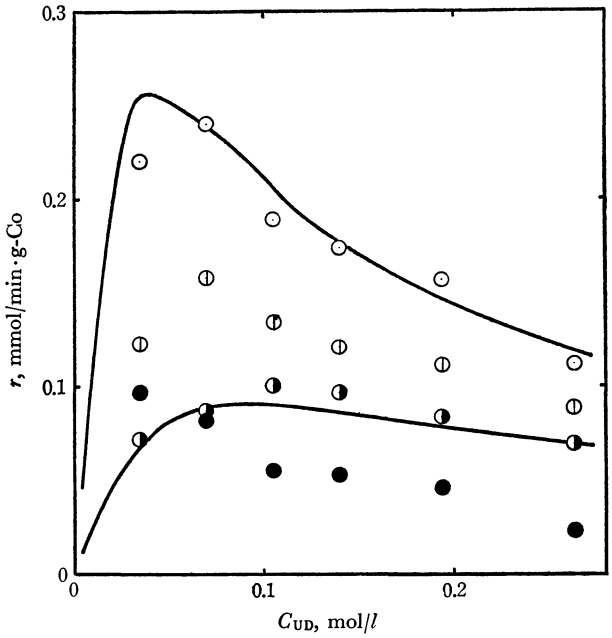

Fig. 2. Concentration dependence of the initial rate of the formation of, SD, ⦶; SA, ●; SA+SD, ○; UA, ◑, at 40°C.

Concentration Dependence of the Initial Rate: The initial rate of formation of SA, SD, and UA were plotted against the concentration of UD in Fig. 2. The curves for SD and UA have maxima, while the one for SA showed a progressive decrease with increasing the concentration of UD. This suggests that the reaction proceeds by the Langmuir-Hinshelwood mechanism, in which hydrogen and UD are adsorbed competitively. The rate equation corresponding to the mechanism is

$$r = k\theta_H\theta_{UD} \qquad (3)$$

where k denotes the rate constant of the surface reaction, θ_H, the surface coverage of hydrogen, and θ_{UD}, that of UD. The following equation can be derived from Eq. (3) as has been reported by Kishida and Teranishi[4]

$$r = \frac{kbC_{UD}}{(1+bC_{UD})^2} \qquad (4)$$

where C_{UD} denotes the concentration of UD, and b the ratio of the adsorption equilibrium constant of UD to that of hydrogen, divided by the liquid phase concentration of hydrogen, *i.e.* $b=K_{UD}/K_H\cdot C_H$, and called adsorption coefficient. When the rate measurement is carried out under a constant pressure of hydrogen, and the solubility of hydrogen is considered to be independent of the composition of reaction mixture

4) S. Kishida and S. Teranishi, *J. Catal.*, **12**, 90 (1968).

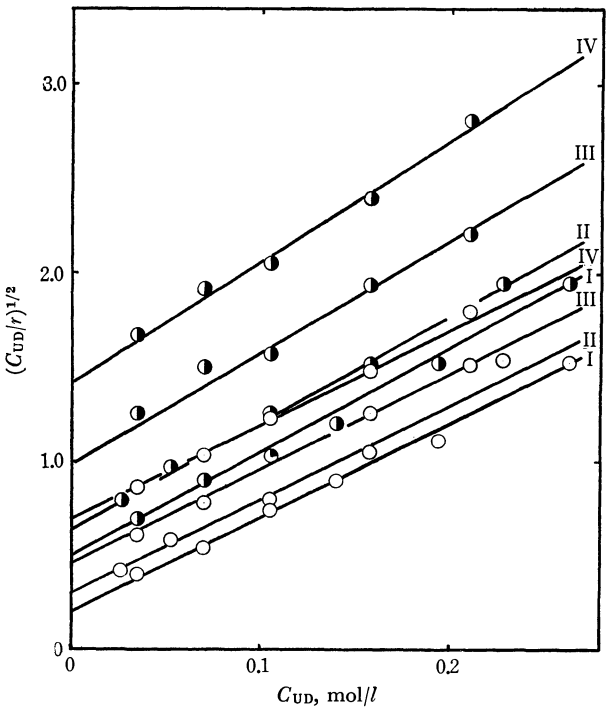

Fig. 3. $(C_{UD}/r)^{1/2}$ *vs.* C_{UD} plots for, $r_{SA}+r_{SD}$, ○; r_{UA}, ◑ at 40°C, I; 30°C, II; 20°C, III; 10°C, IV.

the adsorption coefficient b has a constant value at a given temperature. The adsorption of *n*-hexane as a solvent is neglected. The re-adsorption of products can be neglected in the initial rate treatment performed in this study.

Rearranging Eq. (4), we obtain

$$\left(\frac{C_{UD}}{r}\right)^{1/2} = \frac{1}{(kb)^{1/2}} + \left(\frac{b}{k}\right)^{1/2} \cdot C_{UD} \qquad (5)$$

This gives a linear relation between $(C_{UD}/r)^{1/2}$ and C_{UD}. In Fig. 3, plots of $(C_{UD}/r_{UA})^{1/2}$, and $(C_{UD}/(r_{SA}+r_{SD}))^{1/2}$ *vs.* C_{UD} are shown, where r_{UA}, r_{SA}, and r_{SD} denote the initial rates of formation of UA, SA, and SD, respectively. These plots obvioulsy give straight lines. We see that the plot of $(C_{UD}/r_{SA})^{1/2}$ *vs.* C_{UD} deviates from a straight line. This trend of plots can be interpreted as indicating that SA and SD were formed through the same adsorbed species. The kinetic parameters k and b were determined from the plots in Fig. 3, and are given in Table 1. The behavior of the concentration dependence of the initial rate of formation of SA plus SD and that of UA, employing such values of k and b, reveal satisfactory agreement between the experimental data and the calculated values, as shown by solid lines in Fig. 2.

Table 1. Kinetic parameters

Temperature (°C)	With respect to the formation of SA+SD: k (mmol/min·g-Co)	b (l/mol)	UA: k	b
40	1.0	25	0.38	11
30	0.68	17	0.28	9.0
20	0.44	11	0.17	6.1
10	0.29	7.1	0.11	4.5
Temperature coefficient (kcal/mol)	7.7	7.5	7.9	5.6
Frequency factor (mmol/min·g-Co)	2.5×10^4	—	1.3×10^4	—
Pre-exponential factor (l/mol)	—	4.4×10^5	—	9.3×10^3

The activation energies for the formation of SA plus SD and of UA were 7.7 and 7.9 kcal/mol, respectively. The values are considered to the reasonable compared with those reported by other workers.[5,6] The temperature coefficients of b were also determined to be 7.5 and 5.6 kcal/mol, for SA plus SD and for UA,

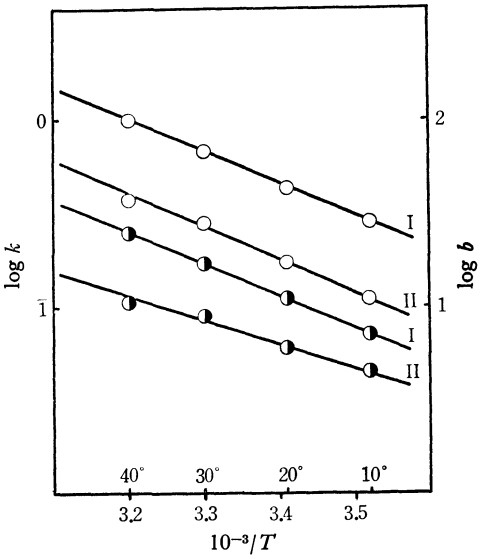

Fig. 4. Arrhenius plots, ○, for the formation of SA+SD, I; UA, II, and log b *vs.* $(1/T)$ plots, ◑, for the formation of SA+SD, I; UA, II.

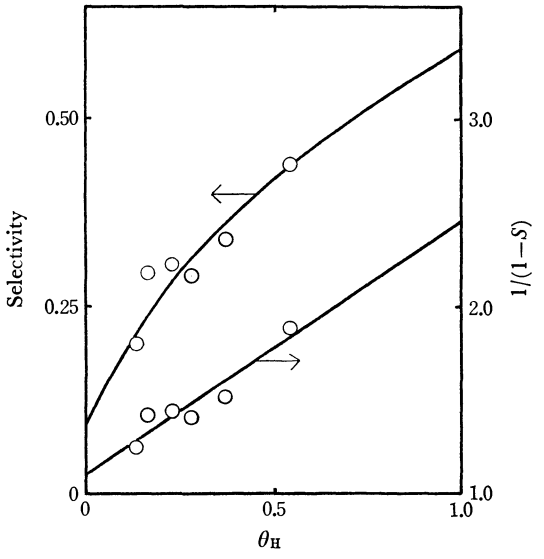

Fig. 5. Relations between the selectivity (S), $1/(1-S)$, and the surface coverage of hydrogen at 40°C.

5) E. B. Maxted and C. H. Moon, *J. Chem. Soc.*, **1935**, 1190.
6) C. C. Oldenburg and H. F. Rase, *J. Amer. Inst. Chem. Eng.*, **3**, 462 (1957).

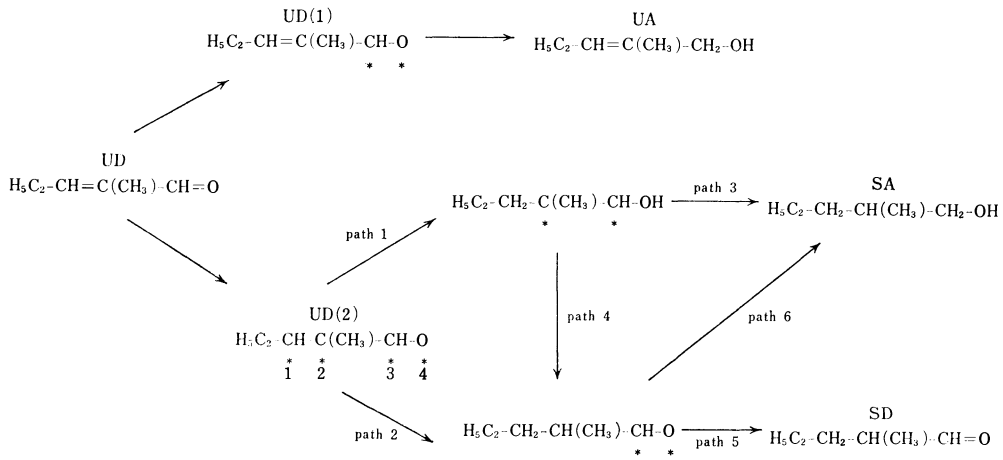

Fig. 6. Scheme of the hydrogenation mechanism.

respectively. This indicates that hydrogen is adsorbed more strongly than UD. The frequency factors of the rate constants for SA plus SD and for UA were determined to be 2.5×10^4 and 1.3×10^4 mmol/min·g-Co, respectively. The pre-exponential factors of the adsorption coefficients for SA plus SD and for UA were also determined to be 4.4×10^5 and 9.3×10^3 l/mol, respectively. Plots of the logarithm of k and b *vs.* the reciprocal of absolute temperature are shown in Fig. 4.

The relation between selectivity and surface coverage of hydrogen can be calculated employing the kinetic parameters obtained above. Selectivity S is defined as the ratio of r_{SA} to $(r_{SA}+r_{SD})$ and the surface coverage of hydrogen is calculated by the equation $\theta_H = 1/(1+bC_{UD})$. The result at 40°C is shown in Fig. 5. It is found that selectivity increases with the increase of hydrogen coverage.

Discussion

The hydrogenation mechanism which is considered to be consistent with the experimental results above mentioned is shown in Fig. 6. Two different types of adsorbed UD are considered in the mechanism. Formation of UA proceeds through UD (1), and that of SA and SD occurs through UD (2). The adsorbed species UD (2) is hydrogenated by 1,2 addition (path 2) to form the adsorbed species in keto form and by 1,4 addition (path 1) to form that in enol form. The reaction mechanism which involves both 1,2 and 1,4 additions of hydrogen has been proposed by McQuillin *et al.*[7] The adsorbed enol species is hydrogenated to SA or isomerized to the adsorbed keto species, while the isomerization from the latter to the former does not occur as reported by Badin and Pacsu.[8]

If UD is adsorbed competitively as UD (1) and UD(2) on the same catalyst site and reacts with adsorbed hydrogen, the rate equations for the formation of UA and of SA plus SD can be derived as follows.

$$r_{UA} = \frac{k_{UD(1)}b_{UD(1)}C_{UD}}{\{1+(b_{UD(1)}+b_{UD(2)})C_{UD}\}^2} \quad (6)$$

$$r_{SA}+r_{SD} = \frac{k_{UD(2)}b_{UD(2)}C_{UD}}{\{1+(b_{UD(1)}+b_{UD(2)})C_{UD}\}^2} \quad (7)$$

where $k_{UD}(1)$ denotes the rate constant for the formation of UA, $k_{UD}(2)$ that of SA plus SD, $b_{UD}(1)$ the adsorption coefficient of UD(1), and $b_{UD}(2)$ that of UD(2). Rearranging these equations, we have

$$\left(\frac{C_{UD}}{r_{UA}}\right)^{1/2} = \frac{1}{(k_{UD(1)}b_{UD(1)})^{1/2}} + \frac{b_{UD(1)}+b_{UD(2)}}{(k_{UD(1)}b_{UD(1)})^{1/2}}\cdot C_{UD} \quad (8)$$

$$\left(\frac{C_{UD}}{r_{SA}+r_{SD}}\right)^{1/2} = \frac{1}{(k_{UD(2)}b_{UD(2)})^{1/2}} + \frac{b_{UD(1)}+b_{UD(2)}}{(k_{UD(2)}b_{UD(2)})^{1/2}}\cdot C_{UD} \quad (9)$$

which give linear relations between $(C_{UD}/r_{UA})^{1/2}$, $(C_{UD}/(r_{SA}+r_{SD}))^{1/2}$ and C_{UD}. Then relations between the slopes and the intercepts of the plots of Eqs. (8) and (9) are obtained as follows.

$$x_1/y_1 = b_{UD(1)} + b_{UD(2)}$$

$$x_2/y_2 = b_{UD(1)} + b_{UD(2)}$$

where x_1 denotes the slope of the plot for r_{UA}, y_1 the intercept of that for r_{UA}, x_2 the slope of the plot for $(r_{SA}+r_{SD})$, and y_2 the intercept of that for $(r_{SA}+r_{SD})$. This indicates that the ratio of the slope and the intercept of the Langmuir-plots for r_{UA} and for $(r_{SA}+r_{SD})$ have the same value. It was found, however, from the plots in Fig. 3 that the values of the term, x/y, were not identical for both lines. This suggests that the part of the catalyst surface on which UD(1) is hydrogenated differs from that on which UD(2) is hydrogenated, and the formation of UA and that of SA plus SD can be treated seperately.

Following discussion is made to analyze semi-quantitatively the result shown in Fig. 5 on the basis of the mechanism assumed. According to the mechanism, the rate of the formation of SA and SD can be written as

$$r_{SA} = k_6\theta_H\theta_{keto} + k_3\theta_H\theta_{enol} \quad (10)$$

$$r_{SD} = k_5\theta_{keto} \quad (11)$$

where k_i denotes the rate constant whose subscript i represents each reaction path shown in Fig. 6, and θ the surface coverage. Equating the rates of the formation and the removal of the adsorbed enol species and those of the adsorbed keto species, we get

7) F. J. McQuillin, W. O. Ord, and P. L. Simpson, *J. Chem. Soc.*, **1963**, 5996.

8) E. J. Badin and E. Pacsu, *J. Amer. Chem. Soc.*, **66**, 1963 (1944).

$$k_1\theta_H\theta_{UD(2)} = k_3\theta_H\theta_{enol} + k_4\theta_{enol}$$
$$k_2\theta_H\theta_{UD(2)} + k_4\theta_{enol} = k_6\theta_H\theta_{keto} + k_5\theta_{keto}$$

where the re-adsorption of products were neglected in the "initial rate" treatment, and the fraction of the surface coverage of the adsorbed enol species and that of the adsorbed keto species are obtained:

$$\theta_{enol} = \frac{k_1\theta_H\theta_{UD(2)}}{k_3\theta_H+k_4} \quad (12)$$

$$\theta_{keto} = \frac{k_2(k_3\theta_H+k_4)+k_1k_4}{(k_6\theta_H+k_5)(k_3\theta_H+k_4)}\cdot\theta_H\theta_{UD(2)} \quad (13)$$

Substituting Eqs. (12) and (13) into Eq. (10), the rate of formation of SA is obtained as

$$r_{SA} = \left[\frac{k_1k_3\theta_H}{k_3\theta_H+k_4} + \frac{k_2k_6\theta_H(k_3\theta_H+k_4)+k_1k_4k_6\theta_H}{(k_3\theta_H+k_4)(k_6\theta_H+k_5)}\right] \times \theta_H\theta_{UD(2)} \quad (14)$$

The rate of formation of SA is divided into three terms. The first term represents it through the reaction path 1—3 *via* the adsorbed species in enol form, the second term through the path 2—6, and the third term through the path 1—4—6. Equation (14) is then rewritten as

$$r_{SA} = (r_{SA})_{1-3} + (r_{SA})_{2-6} + (r_{SA})_{1-4-6} \quad (15)$$

Addition of Eqs. (10) and (11) leads to

$$r_{SA} + r_{SD} = (k_6\theta_H+k_5)\cdot\theta_{keto} + k_3\theta_H\theta_{enol} \quad (16)$$

Insertion of Eqs. (12) and (13) into Eq. (16) gives, after rearrangement.

$$r_{SA} + r_{SD} = (k_1+k_2)\cdot\theta_H\theta_{UD(2)} \quad (17)$$

Selectivity S is also derived as follows.

$$S = \frac{r_{SA}}{r_{SA}+r_{SD}} = \frac{k_1k_3\theta_H(k_6\theta_H+k_5)+k_1k_4k_6\theta_H+k_2k_6\theta_H(k_3\theta_H+k_4)}{(k_3\theta_H+k_4)(k_6\theta_H+k_5)(k_1+k_2)} \quad (18)$$

Equation (18) can be rearranged as

$$S = 1 - \frac{\left(\frac{k_2\theta_H}{k_1+k_2}+\frac{k_4}{k_3}\right)\cdot\frac{k_5}{k_6}}{\left(\theta_H+\frac{k_5}{k_6}\right)\left(\theta_H+\frac{k_4}{k_3}\right)} \quad (19)$$

After rearrangement, Eq. (19) can be reduced as follows. (i) If $k_4/k_3=0$, then

$$\frac{1}{1-S} = \frac{k_6}{k_5}\cdot\frac{k_1+k_2}{k_2}\cdot\theta_H + \frac{k_1+k_2}{k_2} \quad (20)$$

and (ii) if $k_2/(k_1+k_2)=1$, then

$$\frac{1}{1-S} = \frac{k_6}{k_5}\cdot\theta_H + 1 \quad (21)$$

A linear relation between $1/(1-S)$ and θ_H was experimentally found as shown in Fig. 5. The values of the slope and the intercept determined by the least square method were 1.36 and 1.10, respectively. Thus we have from Eq. (20) $k_2/(k_1+k_2)=1/1.10$, $k_5/k_6=1.10/1.36$. Hence $k_1=0.1k_2$.

As the rate constant of 1,2 addition (k_2) is much larger than that of 1,4 addition (k_1), and the rate constant of reaction path 4 is negligibly small compared with that of reaction path 3, SD is considered to be formed through the adsorbed keto species *via* path 2—5.

Employing the values of the rate constants, the three terms in Eq. (15) can be calculated referring to Eq. (14). The first and second term are reduced as

$$(r_{SA})_{1-3} = 0.1k_2\cdot\theta_H\theta_{UD(2)}$$
$$(r_{SA})_{2-6} = k_2\theta^2_H\theta_{UD(2)}/(\theta_H+0.81)$$

The third term is negligibly small since k_4 is zero. Thus a fraction of $(r_{SA})_{2-6}$ over r_{SA} is

$$(r_{SA})_{2-6}/r_{SA} = 0.91\theta_H/(\theta_H+0.073) \quad (22)$$

It is found from Eq. (22) that the contribution of paths 2—6 to the formation of SA increases with the increase of hydrogen coverage. It can therefore be said that the formation of SA occurs dominantly through the adsorbed enol species *via* paths 1—3 at lower hydrogen coverage and through the adsorbed keto species *via* paths 2—6 at higher hydrogen coverage.

The fact that the selectivity, $r_{SA}/(r_{SA}+r_{SA})$, increases with the increase of hydrogen coverage as shown in Fig. 5 can be interpreted as due to the increase of the fraction of adsorbed keto species consumed for the formation of SA.

Reactions of Allenes. IV.[1] New Palladium Complexes Having a Bridged Allene Trimer Ligand

Tadashi OKAMOTO

Institute for Chemical Research, Kyoto University, Gokasho, Uji

(Received October 6, 1970)

Di-μ-acetato-[2,2′-(1-methyleneethylene)bis-π-allyl]dipalladium (I) was obtained (18%) by the reaction of allene and palladium acetate. Its structure was estimated from the data of elemental analysis, molecular weight, hydrogenolysis reaction, IR, and NMR. Complex I was synthesized otherwise by the reaction of allene with di-μ-acetato-2,2′-bi-π-allyldipalladium. The insertion mechanism for the latter reaction was confirmed by the product of the reaction using allene-d_4, $Pd_2(C_9H_8D_4)(CH_3COO)_2$. It was found that this insertion reaction was by far faster than analogous reactions with bis(acetylacetonato)-2,2′-bi-π-allyldipalladium or di-μ-acetato-bis-(π-allyl palladium). The observed acceleration was assumed to be due to strain in the substrate. From NMR data of I and other π-allylpalladium complexes already published, it was shown that the difference in chemical shifts between *syn* and *anti* protons of π-allyl complexes is dependent on the substituents on the central carbon; the non-conjugated substituents give smaller values (0,9—1.01 ppm for μ-chloro complexes), and α,β-unsaturated substituents give larger values (1.27 − 1.28 ppm for μ-chloro complexes). Chloro and acetylacetonato derivatives of I, and the activation energy for spin exchange of saturated methylene protons in I are also described.

It is well known that an allenic compound produces various stable σ-, π-, and π-allyl complexes by the reaction with transition metal compounds.[2] This suggests that some organometallics affording information on catalytic reactions might be obtained, by the reaction of allene with transition metal compounds which are useful as catalysts in organic syntheses.

On this assumption, the author examined the reaction of allene with palladium acetate, and obtained some new π-allyl complexes.[3,4] This paper deals with a full description of the formation and the structure of the palladium complexes having a new bridging ligand of allene trimer, 2,2′-(1-methyleneethylene)bis-π-allyl. Results are given also on the NMR of the μ-acetato complex with variation of temperature and the fast insertion of allene into a strained π-allyl complex.[4]

Results and Discussion

Isolation and the Structure of Di-μ-acetato-[2,2′-(1-methyleneethylene)bis-π-allyl]dipalladium. Palladium acetate and allene were stirred in benzene overnight. Subsequent separation of the resulting solution with a silica-gel column gave a yellow crystal, di-μ-acetato-[2,2′-(1-methyleneethylene)bis-π-allyl]dipalladium (I). Analytical data and the molecular weight determination showed that the complex had a molecular formula $Pd_2C_{13}H_{18}O_4$. Presence of acetate ligands was estimated by the carboxylate stretching absorptions of its IR spectrum (1570 and 1410 cm^{-1}) and the absorption of acetyl protons (2.0 ppm) on the NMR spectrum. The IR spectrum further showed absence of an ester carbonyl group. This was confirmed by the NMR spectrum of chloro complex VI. Hydrogenolysis of I made it clear that five moles of hydrogen were necessary for complete hydrogenation, and the organic ligand had the carbon framework of 2,3,5-trimethylhexane. At this stage, I was formulated as $Pd_2(C_9H_{12})(CH_3COO)_2$. Further studies of the structure were carried out with the aid of NMR spectra. The spectra are shown in Fig. I. The broad absorptions observed at ambient temperature became sharp at elevated temperatures and the relative intensities of the absorptions became clear; corresponding to the absorptions in the order of decreasing δ value, relative intensities are 1H, 1H, 2H, 2H, 2H, 2H, 2H, and 6H. The spectra are interpreted as consisting of the absorptions by one vinylidene, two π-allyls, and one saturated methylene group from their chemical shifts.[2i,2j,5]

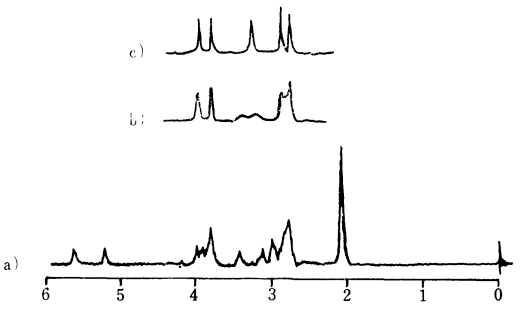

Fig. 1. NMR Spectra of I.
a) in $CDCl_3$ at −28°C.
b) in CD_3COOD at 40°C.
c) in CD_3COOD at 70°C.

1) Part III: T. Okamoto, S. Kunichika, and Y. Sakakibara, *Bull. Inst. Chem. Res., Kyoto Univ.*, **48**, 96 (1970).

2) For π-complexes: a) J. A. Osborn, *Chem. Commun.*, **1968**, 1231. b) R. Ben-Shoshan and R. Pettit, *J. Amer. Chem. Soc.*, **89**, 2231 (1967). c) P. Racanelli, G. Pantini, A. Immirzi, G. Allegra, and L. Porri, *Chem. Commun.*, **1969**, 361. d) K. Vrieze, H. C. Volger, and A. P. Praat, *J. Organometal. Chem.*, **21**, 467 (1970). For σ-complexes: e) M. Green, N. Mayne, and F. G. A. Stone, *Chem. Commun.*, **1966**, 755. f) R. Ben-Shoshan and R. Pettit, *ibid.*, **1968**, 247. g) S. Otsuka, A. Nakamura, and K. Tani, *J. Organometal. Chem.*, **14**, p 30 (1968). And a). For π-allyl complexes: h) A. Nakamura, This Bulletin, **39**, 543 (1966). i) R. G. Schultz, *Tetrahedron*, **20**, 2809 (1964). j) M. S. Lupin, J. Powell, and B. L. Shaw, *J. Chem. Soc., A*, **1966**, 1687. k) R. P. Hughes and J. Powell, *J. Organometal. Chem.*, **20**, p 17 (1969). l) T. Susuki and J. Tsuji, This Bulletin, **41**, 1954 (1968). And f).

3) T. Okamoto, Y. Sakakibara, and S. Kunichika, This Bulletin, **43**, 2658 (1970).

4) T. Okamoto, *Chem. Commun.*, **1970**, 1126.

5) K. Nukada, O. Yamamoto, and T. Suzuki, *Anal. Chem.*, **35**, 1892 (1963).

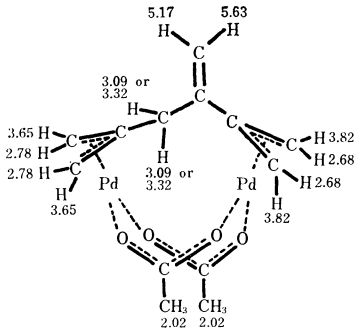

Formula. Structure and NMR Assignment of I (δ value in CD_3COOD at 40°C).

They were supported also by the spectra of the deuterated complex. The structure elucidated from the NMR spectra and their assignments are shown in Formula. The assignments of four absorptions of two π-allyl groups are of interest. An interpretation that the deshielding effect caused by a neighboring unsaturated bond gives higher δ values for the π-allyl group adjacent to a carbon-carbon double bond is not correct. For complex I, the absorptions by the isolated π-allyl appear inside the two absorptions by the π-allyl adjacent to an unsaturated bond. In other words, the difference in chemical shifts between the absorptions by *syn* and *anti* protons of a π-allyl group,

$$\Delta\delta = \delta_{syn} - \delta_{anti}$$

is larger for the π-allyl group adjacent to an unsaturated bond than for the isolated π-allyl. This seem to be the general rule at least for palladium complexes. For di-μ-chloro dipalladium complexes, an isolated π-allyl gives the $\Delta\delta$ value from 0.90 to 1.01 ppm for 5 examples in $CDCl_3$, and a conjugated π-allyl gives the value of 1.28 or 1.27 in three cases (Table 1). Di-μ-acetato complexes also follow this rule. The results are interpreted as follows. The electronic effect of a substituent on the central carbon of a π-allyl group delivered through the carbon-carbon bond is nearly equal for *syn* and *anti* protons of a π-allyl group, and is cancelled in the remainder of the subtraction of their chemical shifts. The $\Delta\delta$ value is, therefore, nearly constant for isolated π-allylic palladium complexes having the same anion ligands. For π-allyls adjacent to unsaturated bonds, however, magnetic anisotropy of the unsaturated carbons influences *syn* and *anti* protons unequally, and gives different $\Delta\delta$ values from those of isolated π-allyl groups. The spectra of I, in which ring formation hinders the rotation of bonds, show that the *syn* proton of a π-allyl suffers a deshielding effect by an adjacent unsaturated carbon and the *anti* proton suffers more shielding.

Table 1. NMR Data of π-allylic palladium complexes

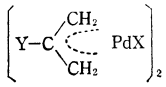

(in $CDCl_3$, ppm down-field from TMS)

Complex	δ_{anti}	δ_{syn}	$\Delta\delta$	Literature
X=Cl				
Y=H–	3.09	4.07	0.98	6
Y=Cl–	3.26	4.27	1.01	2j
Y=CH_3–	2.88	3.85	0.97	6
Y=CH_3COO–	3.10	4.00	0.90	2l
Y=CH_3CH_2COO–	3.12	4.04	0.92	2l
Y=CH_2=C(CH_2-Cl)–	2.87	4.15	1.28	
Y=CH_2=C(CH_2-OCH_3)–	2.83	4.10	1.27	2i
Y=CH_2=C(CH_2-$OCOCH_3$)–	2.90	4.18	1.28	
X=CH_3COO				
Y=H–	2.85	3.88	1.03	6
Y=CH_3–	2.71	3.70	0.99	6
Y=$C_3H_4C(=CH_2)$-CH_2–[a]	2.78	3.65	0.87	
Y=CH_2=C(CH_2-$OCOCH_3$)–	2.62	3.93	1.31	
Y=CH_2=C-($CH_2C_3H_4$)–[a]	2.68	3.82	1.14	

a) The values for complex I.

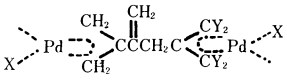

I: X=CH_3COO Y=H
III: X=CH_3COO Y=D
VI: X=Cl Y=H
VII: X=$CH_3COCHCOCH_3$ Y=H

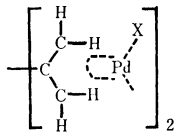

II: X=CH_3COO
V: X=$CH_3COCHCOCH_3$

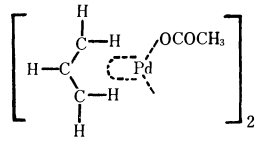

IV

Synthesis of Complex I from Di-μ-acetato-2,2'-bi-π-allyldipalladium and Allene. Complex I was also synthesized in a high yield by bubbling allene into a dichloromethane solution of di-μ-acetato-2,2'-bi-π-allyldipalladium (II).

$$Pd_2(C_3H_4)_2(CH_3COO)_2 + C_3H_4 \longrightarrow Pd_2(C_3H_4)_3(CH_3COO)_2$$
(II) (I)

The reaction proceeded almost quantitatively. when allene-d_4 was used for this reaction, $Pd_2(C_9H_8D_4)(CH_3COO)_2$ (III) was obtained. NMR spectra of III are shown in Fig. 2. The spectra show that two absorptions at δ 3.65 and 2.78 ppm in the corresponding complex I have disappeared. The structure of tetradeutero complex III clearly indicates that this complex is formed *via* insertion of allene between the bridged bi-π-allyl and palladium. The coupling of newly coordinated allenes with replacement of π-allyl ligands,

6) S. D. Robinson and B. L. Shaw, *J. Organometal. Chem.*, **3**, 367 (1965).

Table 2. Comparison of the raectivity for insertion of allene

CH_2Cl_2, 20 ml; complex, 0.222 mmol; allene, 100 ml; room temperature, 15 hr

Complex	Product (%)	
$Pd_2(C_3H_4)_2(CH_3COO)_2$ (II)	$Pd_2(C_3H_4)_3(CH_3COO)_2$	(93.5)
$Pd_2(C_3H_4)_2(CH_3COCHCOCH_3)_2$ (V)	recovered	(86.6)
$Pd_2(C_3H_5)_2(CH_3COO)_2$ (IV)	recovered	(99.9)
$Pd_2(C_3H_4)_3(CH_3COO)_2$ (I)	recovered	(87.5)

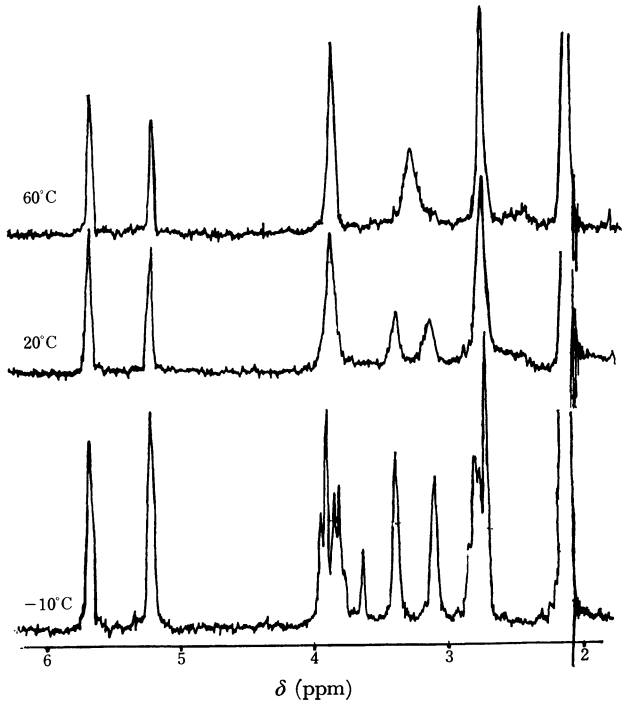

Fig. 2. Temperature-dependent NMR spectra of III (in $CDCl_3$).

observed by the reaction of allene with acetylacetonato-π-allylpalladium,[2k] did not take place in this case.

Such a bridge elongation by insertion has not yet been reported and suggests that there is some allowance in length of the ligand bridging two palladium metals combined with μ-acetato ligands. The result is interesting from the fact that palladium acetate acts as a catalyst for dimerization[7,8] or co-dimerization[9] of ethylenic compounds and arenes.

Concerning insertion, the reaction was found to be an assisted one. Experimental results are listed in Table 2. Under the same conditions as in the reaction of allene and II, di-μ-acetato-bis(π-allylpalladium) (IV) and bis(acetylacetonato)-2,2'-bi-π-allyldipalladium (V) did not insert allene, and the substrates were recovered almost quantitatively. Thus, it is clear that the acceleration observed for II is not simply due to the presence of μ-acetato ligands or a bi-π-allyl ligand. Hughes and Powell reported that there is some strain in complex II on the basis of its NMR spectra of a lower symmetry than C_{2v} and that rigid μ-acetato bridges impart the strain.[2k] Temperature-independent spectra from −100°C to 60°C suggest that no exchange of the μ-acetato ligand occurs in this complex at least faster than NMR time scale. Temperature-dependent NMR spectra of I and simple inspection of a scaled model suggest there is less strain in this complex.

The insertion of allene might be explained to occur easily by the relief of the strain in the substrate complex. This is a new factor besides steric repulsion and electronic factors[10] controlling the insertion into a π-allyl-metal bond.

Derivatives of I. When I was treated with an aqueous sodium chloride solution, it exchanged all acetate ligands for chloride ions, and a yellowish gray complex, dichloro-[2,2'-(1-methyleneethylene) bis-π-allyl]dipalladium (VI), was precipitated. Complex I was regenerated from VI by treatment with silver acetate in acetone. An acetylacetonato complex, bis-(acetylacetonato)-[2,2'-(1-methyleneethylene) bis-π-allyl]dipalladium (VII), was obtained from VI as usual with thallium acetylacetonate.[2j] The NMR spectrum of VII was similar to the spectra of I at high temperatures.

Temperature-dependent NMR Spectra of I and III. I shows temperature-dependent NMR spectra and the spectra at low temperatures are very complicated due to the overlap of absorptions. In the case of tetradeutero complex III, however, interpretation of the spectra became simple. At −10°C, two saturated methylene protons of complex III exhibited AB type couplings with a coupling constant of 15.5 Hz. This value is reasonable for the coupling constant of geminal methylene protons on a sufficiently large ring. It shows that the ring is fixed at the temperature. With the rise of temperature, the AB quartet changed into a broad doublet at room temperature, and finally coalesced

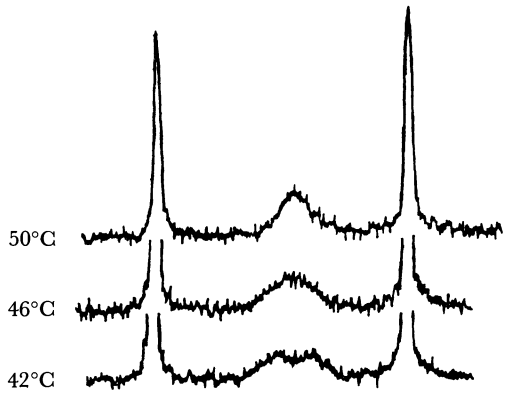

Fig. 3. Coalescence of the AB quartet of III.

7) C. F. Kohll and R. van Helden, *Rec. Trav. Chim. Pays-Bas*, **86**, 193 (1967).

8) J. M. Davidson and C. Triggs, *Chem. Ind.* (London), **1966**, 457.

9) Y. Fujiwara, I. Moritani, S. Danno, R. Asano, and S. Teranishi, *J. Amer. Chem. Soc.*, **91**, 7166 (1969).

10) Y. Takahashi, S. Sakai, and Y. Ishii, *J. Organometal. Chem.*, **16**, 177 (1969).

into a singlet at 46°C (Fig. 3). As the origin of the dynamic nuclear magnetic resonance observed, two factors might be considered, the molecular fluctuation of the complex, and the dissociation of the μ-acetato bridge followed by the rotation of the organic ligand. A rough estimate of the activation energy from the coalescence temperature[11] with the assumption that the frequency factor is 10^{12},[12] gave 14.5 kcal/mol, which might be too large for the energy of the former mechanism.

For π-allyl parts, the spectra of I and III are also dependent on temperature (Figs. 1 and 2). At −10°C *syn* and *anti* protons of III were each separated into two doublets with coupling constants 1.0 and 1.5 Hz, respectively. The separation between the doublets was greater for *syn* protons, as can be seen from inspection of a scaled model. Coalecsence of both doublets starts almost at the same temperature as that for saturated methylene protons, suggesting that these processes occur by the same mechanism. Contrary to what has been reported for IV,[13] the magnetic unequality in I and III would arise from the difference in a stereochmical situation against the bridging 1-methyleneethylene group.

The exchange of *syn* and *anti* protons was not detected at least until 100°C in acetic acid-d_4, indicating that no terminal CH_2 rotation is present in these complexes.

Experimental

All reagents were obtained commercially and used without further purification unless otherwise stated. Melting points were determined with a Yanagimoto melting point apparatus. IR spectra were measured as KBr pellets using a Perkin-Elmer 521 spectrometer; NMR spectra, on a Varian A-60 spectrometer for dilute solutions in the specified solvents. The chemical shifts were expressed in δ value (ppm) relative to TMS used as the internal standard. The temperature of measurement was 40°C unless otherwise specified. Mass spectra were obtained with a JMS-01SG spectrometer; the molecular weight was determined with a vapor pressure osmometer of Mechrolab-301. A gas chromatograph of Yanagimoto GCG 220 type was used for both analytical and preparative purposes.

Formation of Complex I from Allene and Palladium Acetate. Into a solution of palladium acetate[14] (5.0 g) in benzene (250 m*l*) was introduced allene gas (6.7 *l*); stirring was continued overnight at ambient temperature. After addition of hexane (250 m*l*), the resulting solution was chromatographed on silica-gel (Wako-gel C200). Stepwise elution with diethyl ether and ethyl acetate afforded complex I as an ethyl acetate solution. After evaporating the solvent, recrystallization of the residue from dichloromethane-hexane gave a pure product as a yellow crystal (0.92 g, 18.3%), mp 148—150°C (dec).

Found: C, 34.63; H, 4.10%; mol wt (benzene, 37°C), 466. Calcd for $Pd_2(C_9H_{12})(CH_3COO)_2$: C, 34.58; H, 4.11%; mol wt, 451. IR: 1620(C=C), 1570(COO^-), 1468, 1410(COO^-), 1340, 1042, 1020, 945, 932, and 760 cm^{-1}. NMR(in $CDCl_3$): 5.63 (1H, $=CH_2$), 5.17 (1H, $=CH_2$), 3.82 (2H, π-allyl), 3.65 (2H, π-allyl), 3.32 and 3.09 (2H, $-CH_2-$), 2.78 (2H, π-allyl), 2.68 (2H, π-allyl), and 2.02 ppm (6H, CH_3CO).

Hydrogenolysis of I. Complex I (0.78 mmol) was dissolved in chloroform and hydrogen was fed from a gas buret after evacuation with dry-ice cooling. A rapid gas absorption ceased in 65 min with consumption of 3.55 mmol of hydrogen.[15] The products were palladium metal, acetic acid, and hydrocarbons. The hydrocarbons were found to be a mixture of three compounds by gas chromatography (VPC, PEG 6000) with a relative ratio[16] of 37:14:50 in the order of retention time. Absence of C_3 hydrocarbons was confirmed by VPC (β,β'-oxydipropionitrile, 25°C). The three hydrocarbons were separated by gas chromatography using the same column (PEG 6000). The first effluent was identified as 2,3,5-trimethylhexane by peak to peak correspondence with the standard NMR chart (API 214). The other two products were identified as 2,3,5-trimethyl-2-hexene and 2,4,5-trimethyl-2-hexene by their NMR spectra, and mass spectra of the brominated products.

2,3,5-trimethyl-2-hexene; NMR(in CCl_4): 0.85 (d, 6H), 1.60 (s, 9H), and 1.88 ppm (s, 2H). The mass spectrum for the brominated product; m/e^+ 285 $(M-1)^+$.

2,4,5-trimethyl-2-hexene; NMR(in CCl_4): 0.7—0.9 (m, 9H), 1.4—1.6 (m, 1H), 1.57 (d, 3H), 1.67 (d, 3H), 2.03 (m, 1H), and 4.92 ppm (d, 1H), The mass spectrum for the brominated product; m/e^+ 285 $(M-1)^+$.

Calculation of the theoretical amount of hydrogen based on the molecular formula and the ratio of the three hydrocarbons above gave 3.62 mmol, which is in good accordance with the experimental value.

Synthesis of I from Di-μ-acetato-2,2'-bi-π-allyl-dipalladium. Allene gas (100 m*l*) was introduced into the dichloromethane solution (20 m*l*) of complex II[2k] (0.222 mmol), and the mixture was stirred at ambient temperature overnight. When the solvent was distilled off, a yellow crystal was obtained. Recrystallization from dichloromethane-hexane afforded I (0.207 mmol, 93.5%). Under the same conditions, tetradeutero complex III was obtained using allene-d_4,[18] mp 150—152°C (dec).

Found: C, 34.57; H, 5.06%. Calcd for $Pd_2(C_9H_8D)_4(CH_3COO)_2$: C, 34.31; H, 4.87%. IR: 1570, 1410, 1340, 1040, 1020, 940, 930, and 672 cm^{-1}. NMR(in $CDCl_3$): 5.63 (s, 1H), 5.17 (s, 1H), 3.80 (s, 2H), 3.30 and 3.08 (each broad s, sum 2H), 2.68 (s, 2H), and 2.02 ppm (s, 6H); (in $CDCl_3$, −10°C): 5.60 (s), 5.15 (s), 3.85 (d, J=1.5 Hz), 3.77 (d, J=1.0 Hz), 3.43 and 2.93 (AB, J=15.5 Hz), 2.72 (d, J=1.0 Hz), 2.65 (d, J=1.5 Hz), and 2.05 ppm (s).

Comparison of Various Complexes for Insertion of Allene. Di-μ-acetato-bis(π-allylpalladium) (IV) was prepared by the method of Robinson and Shaw.[6]

Bis(acetylacetonato)-2,2'-bi-π-allyldipalladium (V) was prepared by the method of Hughes and Powell[1c] as a white crystal, mp 187—190°C (dec).

11) G. Binsch, in "Topics in Stereochemistry," Vol. 3, ed. by E. L. Eliel and N. L. Allinger, Interscience Publishers, New York, N. Y. (1968), p.97.

12) Selection of this value is arbitrary. However, from the fact that the value is in the same order as that of the interconversion of cyclohexane and the valence isomerization of bullvalene,[11] this would be a reasonable selection.

13) J. Powell, *J. Amer. Chem. Soc.*, **91**, 4311 (1969).

14) T. A. Stephenson, S. M. Morehouse, A. R. Powell, J. P. Heffer, and G. Wilkinson, *J. Chem. Soc.*, **1965**, 3632.

15) To avoid the error caused by the adsorption of hydrogen by palladium, hydrogen feeding was stopped when the rapid absorption of gas was over.

16) It was assumed that the relative response per gram of these hydrocarbons was equal. Values in literature[17] suggest that the error caused by this assumption is within 5%.

17) A. E. Messner, D. M. Rosie, and P. A. Argabright, *Anal. Chem.*, **31**, 230 (1959).

18) A. T. Morse and L. C. Leitch, *J. Org. Chem.*, **23**, 990 (1958).

Found: C, 39.06; H, 4.44%. Calcd for $Pd_2(C_6H_8)(CH_3COCHCOCH_3)_2$: C, 39.05; H, 4.50%.

The reaction conditions for insertion were the same as described above. The results are shown in Table 2.

Syntheses of Derivatives of Complex I. Dichloro-[2,2'-(1-methyleneethylene)bis-π-allyl]dipalladium (VI). To a benzene solution (20 m*l*) of I (0.100 g) was added an aqueous sodium chloride (0.035 g) solution (0.1 m*l*) and the mixture was stirred for an hour at ambient temperature. The resulting precipitate was washed with dichloromethane, acetone, and water. Recrystallization from dimethylsulfoxide-methanol gave a yellowish gray complex (0.067 g, 75%), mp 221—223°C (dec)

Found: C, 27.08; H, 3.06%. Calcd for $Pd_2C_9H_{12}Cl_2$: C, 26.76; H, 2.99%. IR: 1625, 1465, 1430, 1410, 1355, 1320, 965, 940, 850, 780, 758, 746, and 688 cm^{-1}. NMR(in DMSO-d_6): 5.73 (s, 1H), 5.37 (s, 1H), 4.38 (s, 2H), 4.18 (s, 2H), 3.23 and 3.38 ppm (m, 6H).

Complex I (0.072 g, 96%) was regenerated from VI (0.067 g) by treating with silver acetate (0.067 g) in dry acetone.

Bis(acetylacetonato)-[2,2'-(1-methyleneethylene)bis-π-allyl]dipalladium (VII). Thallium(I) acetylacetonate (0.169 g) and VI (0.112 g) were stirred in benzene (30 m*l*) overnight. The resulting precipitate of thallium chloride was removed by filtration, and the filtrate was evaporated to give VII. Recrystallization from dichloromethane-hexane gave a pure product as a white crystal (0.115 g, 78%), mp 150—151°C (dec).

Found: C, 42.74; H, 4.80%. Calcd for $Pd_2(C_9H_{12})(CH_3COCHCOCH_3)_2$: C, 42.94; H, 4.90%. IR: 1570, 1525, 1512, 1440, 1391, 1357, 1259, 1018, 773 cm^{-1}. NMR (in $CDCl_3$): 5.59 (s, 1H), 5.35 (d, 2H), 5.29 (m, 1H), 3.88 (s, 2H), 3.72 (s, 2H), 3.40 (s, 2H), 2.83 (s, 2H), 2.70 (s, 2H), and 1.98 ppm (s, 12H).

The author is grateful to Professor Sango Kunichika and Dr. Yasumasa Sakakibara for their helpful discussions and encouragement.

BULLETIN OF THE CHEMICAL SOCIETY OF JAPAN, VOL. 44, 1357—1361 (1971)

Thiocyanoacetate. I. Reactions of Thiocyanoacetic Esters with Aldehydes[1)]

Satoshi KAMBE,
Toshio HAYASHI,* Heinosuke YASUDA,*[2)] and Hiroshi MIDORIKAWA*
Oyama Technical College, Oyama, Tochigi
**The Institute of Physical and Chemical Research, Wako-shi, Saitama*

(Received October 8, 1970)

Thiocyanoacetic esters (I) and aldehydes reacted in the presence of potassium fluoride or carbonate to give α,β-unsaturated ester as a major product and an unexpected solid product (II) as a minor one, which was determined to be *N*-carbamoyl-2-imino-5-substituted 1,3-oxathiolane-4-carboxylic esters.

The thiocyanato group which is often referred to as "pseudohalogen," is strongly electron-attractive. The thiocyanoacetic esters (I) would thus be expected to have an active methylene group.[3)] I is structurally similar to chloroacetic and cyanoacetic esters, which easily react with carbonyl compounds. However, little is known so far about the reactions of **I** with carbonyl compounds. This might be ascribed to the fact that the thiocyanato group is extremely sensitive to the bases usually used as a catalyst, giving cyclization compounds[4)] or resinous matters. However, if a suitable catalyst is found, I is expected to react with carbonyl compounds. The purpose of this investigation is to find the possibility of I as an active methylene compound.

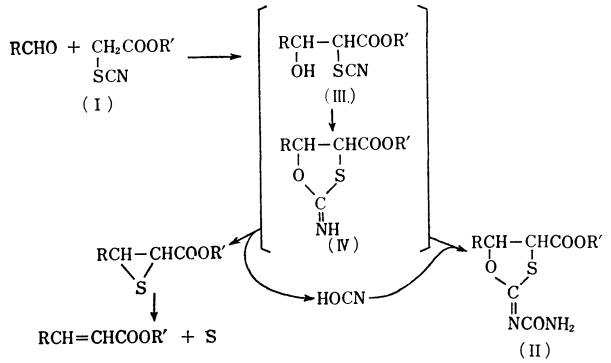

Scheme 1

Results and Discussion

Equimolecular reactions of thiocyanoacetic ester (I) with an aldehyde in the presence of potassium fluoride or carbonate were carried out in moist ether at low temperatures. The reaction consistently gave liquid products as major ones, and an unexpected, solid product (II) as a minor one and elemental sulfur. Glpc analysis and NMR spectra showed that the liquid products contain a stereoisomeric mixture of *cis*- and *trans*- α,β-unsaturated esters and two other components which could not be identified. In the case of the

1) Presented in part at the 22nd Annual Meeting of the Chemical Society of Japan, Tokyo, April 2nd, 1969.
2) Present address: Chemical Laboratory, Department of Education, Utsunomiya University.
3) D. J. Cram, "Fundamentals of Carbanion Chemistry," Academic Press, New York, N. Y. (1955), p. 55.
4) Unpublished Results.

TABLE 1. PROPERTIES OF THE PRODUCTS

Compound	R	R	Mp °C[a]	Yield % b)	Yield % c)	Formula	Analysis % Found (Calcd) C	H	N	S
IIa	C_6H_5	C_2H_5	190—191	18	42	$C_{13}H_{14}O_4N_2S$	52.42 (53.06)	4.87 (4.76)	9.50 (9.52)	10.88 (10.88)
IIb	C_6H_5	CH_3	188—189	13	26	$C_{12}H_{12}O_4N_2S$	53.46 (53.43)	4.21 (4.14)	9.63 (9.59)	11.04 (10.94)
IIc	*p*-$CH_3OC_6H_4$	C_2H_5	179—180	17	31	$C_{14}H_{16}O_5N_2S$	51.97 (51.85)	4.95 (4.97)	8.66 (8.64)	9.82 (9.86)
IId	*p*-$CH_3OC_6H_4$	CH_3	161—162	14	29	$C_{13}H_{14}O_5N_2S$	50.43 (50.35)	4.58 (4.55)	9.07 (9.03)	10.11 (10.31)
IIe	CH_3	C_2H_5	128—129	13	27	$C_8H_{12}O_4N_2S$	41.37 (41.37)	5.19 (5.17)	12.02 (12.06)	13.81 (13.79)
IIf	C_2H_5	C_2H_5	147—148	15	32	$C_9H_{14}O_4N_2S$	43.82 (43.90)	5.60 (5.69)	11.49 (11.39)	13.02 (13.00)
IIg	*n*-C_3H_7	C_2H_5	176—177	12	20	$C_{10}H_{16}O_4N_2S$	46.80 (46.15)	5.97 (6.15)	10.78 (10.76)	12.06 (12.30)
IIh	*iso*-C_3H_7	C_2H_5	149—150	9	13	$C_{10}H_{16}O_4N_2S$	46.00 (46.15)	6.26 (6.15)	10.81 (10.76)	12.23 (12.30)
IIi	*n*-C_4H_5	C_2H_5	218—219	8	10	$C_{11}H_{18}O_4N_2S$	48.00 (48.17)	6.59 (6.62)	10.25 (10.21)	11.60 (11.58)

a) All melting points are uncorrected.
b) Potassium fluoride was used as a catalyst.
c) Potassium carbonate was used as a catalyst.

TABLE 2. IR DATA OF PRODUCT II (cm^{-1})

Compd	NH stretching				C=O stretching		C=N and carbamoyl C=O stretching		NH deformation
a	3300m		3180m		1743s		1681s		1575s
b	3320m	3290m	3220m	3190m	1752s	1737s	1680s	1660m	1580s
c	3450m	3390m	3242m	3200m	1748s		1687s	1620m	1587s
d	3300m		3190m		1748s		1688s	1620m	1587s
e	3450m	3370m	3280m	3200m	1737sh	1730s	1680s	1645m	1586s
f	3360m	3290m	3240m	3200m	1738sh	1731s	1678s		1573s
g	3300m		3180m		1724s		1676s	1615m	1578s
h	3420m		3200m		1743s		1676s	1630m	1570s
i	3310m		3180m		1740s		1680s		1580s

All spectra were measured in KBr pellets.

TABLE 3. NMR DATA OF PRODUCT II (ppm downfield from TMS)

Compd	H_α[a]	H_β[a]	*J*	COOR		NH_2		Other signals	
a	4.83	5.97	6.3	0.72[b]	3.96[c]	7.02	7.30	7.40[d]	
b	4.87	5.97	6.3	3.25[e]		7.04	7.30	7.40[d]	
c	4.76	5.89	6.3	0.78[b]	3.75[c]	not located		3.75[f]	
d	4.76	5.88	6.3	3.28[e]		not located		3.74[f]	
e	4.41	4.95	6.0	1.19[b]	4.14[c]	6.93	7.16	1.37[g]	
f	4.40	4.88	6.0	1.21[b]	4.15[c]	6.91	7.16	1.78[g]	
g	4.44	4.70	6.0	1.20[b]	4.15[c]	6.93	7.16	0.93[g]	1.64[h]
h	4.45	4.74	6.0	1.20[b]	4.15[c]	6.93	7.18	0.94[g]	near 2.00[l]
i	4.45	4.77	6.0	1.20[b]	4.16[c]	6.90	7.15	0.93[g]	1.60[h]
j[j]	4.46	4.78	6.0	3.80[e]		6.75	6.93	0.95[g]	1.64[h]
e[l]	4.20	4.88	6.3	1.29[b]	4.24[c]	5.75		1.56[g]	

All spectra were measured in DMSO-d_6 solution.
a) The proton on α-position to ester group is denoted by H_α, and that on β-position by H_β.
b) Methyl protons of the ethoxy carbonyl group.
c) Methylene protons of the ethoxy carbonyl group.
d) Aromatic protons.
e) Methyl protons of the methoxycarbonyl group.
f) Methoxyl protons.
g) Methyl group.
h) Methylene group.
i) Methine group.
j) Methyl *N*-carbamoyl-2-imino-1,3-oxathiolane-5-ethyl-4-carboxylate.
l) Measured in a $CDCl_3$ solution.

reaction between ethyl thiocyanoacetate and benzaldehyde, the liquid products were found to be only a mixture of *cis*- and *trans*-cinnamic esters (*cis*:*trans*= 25:75).

The structural elucidation of the solid product (II) is based on elemental analysis, spectral studies, and chemical reactivity. Product (IIa), for example, was white needles having a structural formula $C_{13}H_{14}N_2O_4S$, *m/e* 294, and mp 190—191°C. All the solid product (II) obtained have the general formula $RC_4H_5N_2O_2COOR'$ which corresponds formally to an addition compound between β-substituted β-hydroxy

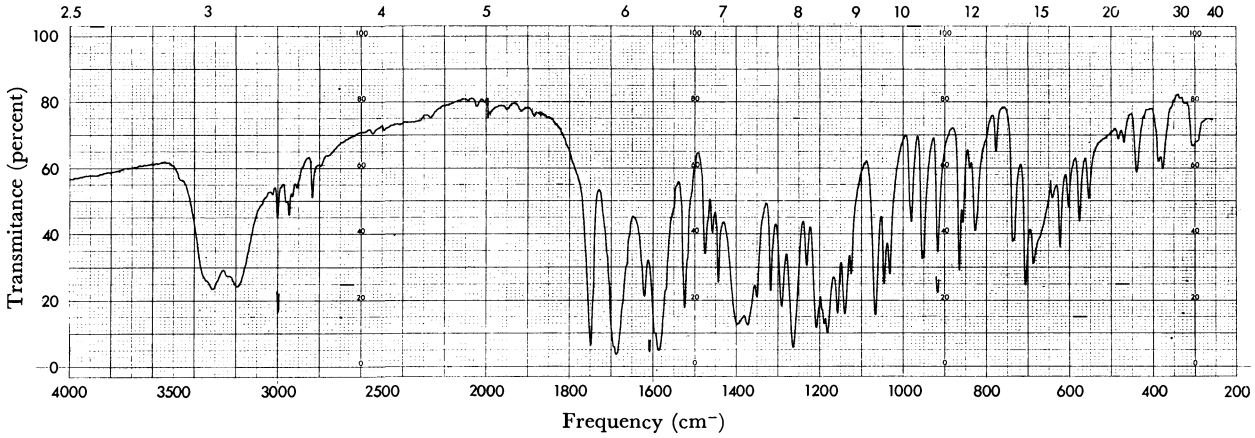

Fig. 1. IR spectrum of IIc (KBr pellet).

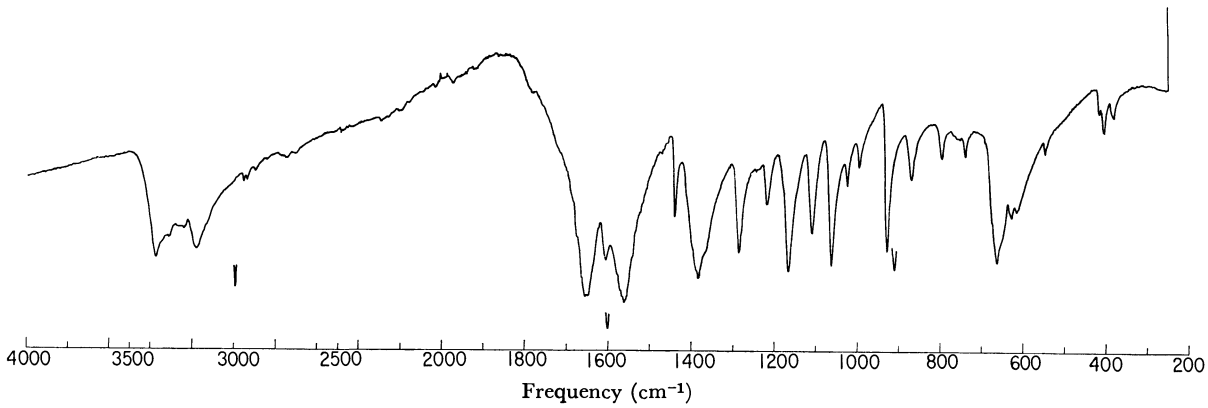

Fig. 2. IR spectrum of *N*-carbamoyl-2-imino-1,3-oxathiolane.

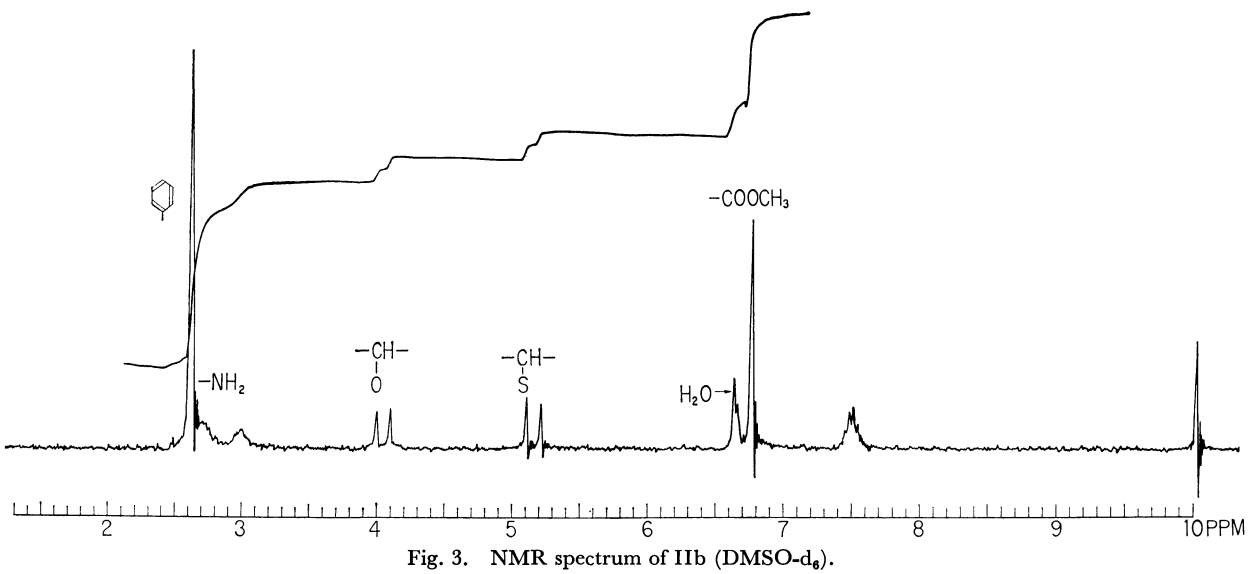

Fig. 3. NMR spectrum of IIb (DMSO-d_6).

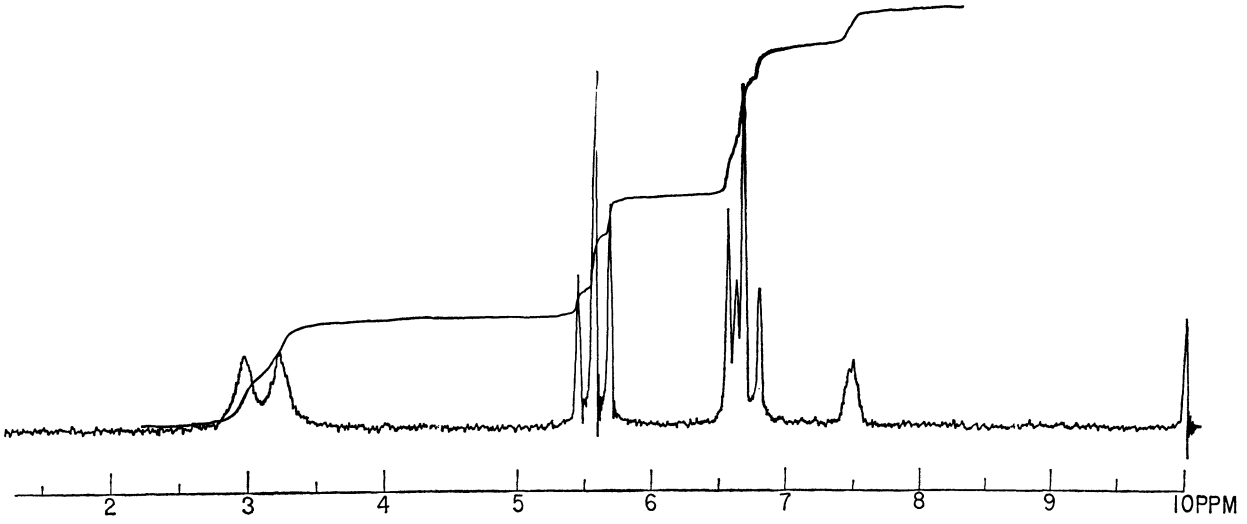

Fig. 4. NMR spectrum of *N*-carbamoyl-2-imino-1,3-oxathiolane (DMSO-d_6).

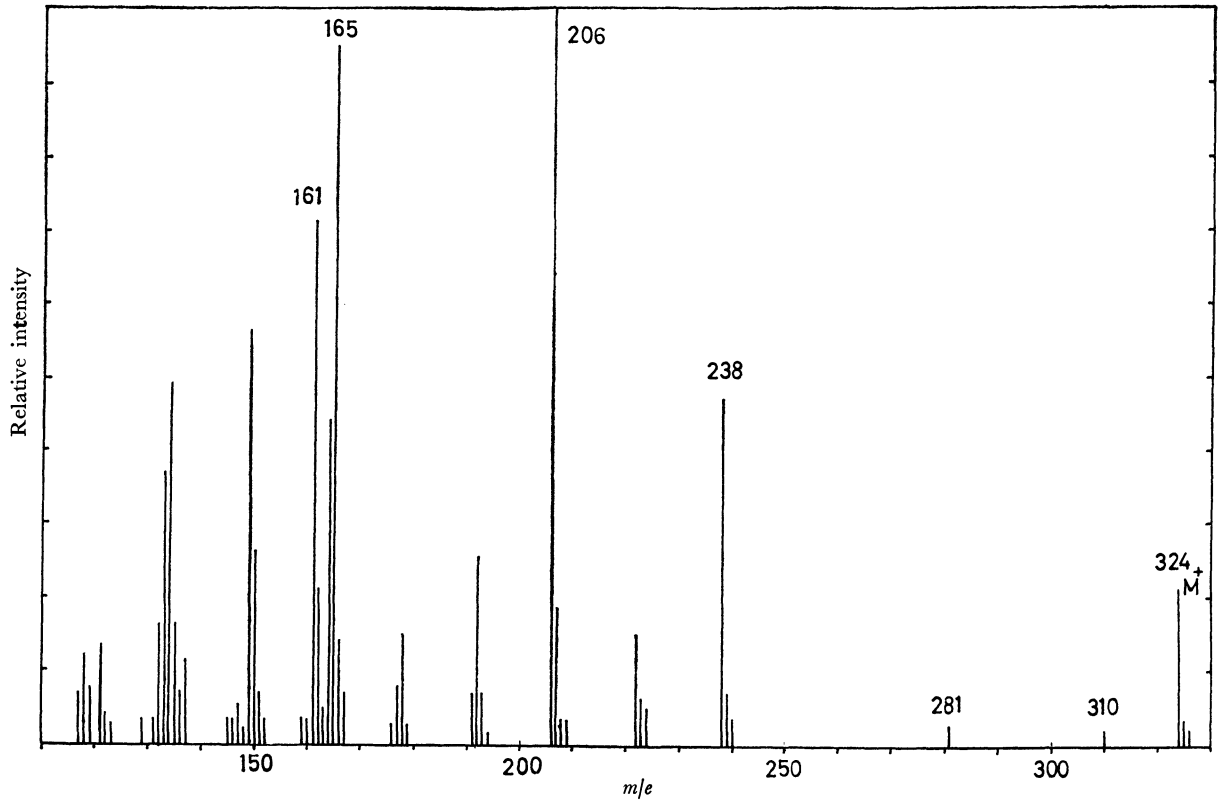

Fig. 5. Mass spectrum of IIc.

α-thiocyano-propionic ester (III) and cyanic acid. II, when treated with ethanol solution of sodium hyroxide, gives rise to α,β-unsaturated ester. We see from Table 2 that the IR spectra of II (KBr pellet) exhibit broad stretching bands in the range 3450—3180 cm^{-1}, the ester C=O band near 1740 cm^{-1}, and the C=N and carbamoyl C=O bands in the range 1688—1615 cm^{-1}. As shown in Figs. 1 and 2, the spectra in the region between 1700 and 1550 cm^{-1} are very similar in position and shape to those of *N*-carbamoyl-2-imino-1,3-oxathiolane. The NMR spectra of II (DMSO-d_6) also revealed that the signals of the NH_2 protons in II are similar in position and shape to those of the carbamoyl NH_2 protons in *N*-carbamoyl-2-imino-1,3-oxathiolane (Figs. 3 and 4). The doublet of the NH_2 protons near 7.00 ppm in a DMSO-d_6 solution coalesces into one broad signal near 5.75 ppm in a $CDCl_3$ solution (Table 3). However, the reason why the NH_2 signal splits into doublet in a DMSO-d_6 solution, could not be elucidated. The mass spectra of II also suggested the presence of *N*-carbamoyl-2-imino-1,3-oxathiolane system (Figs. 5

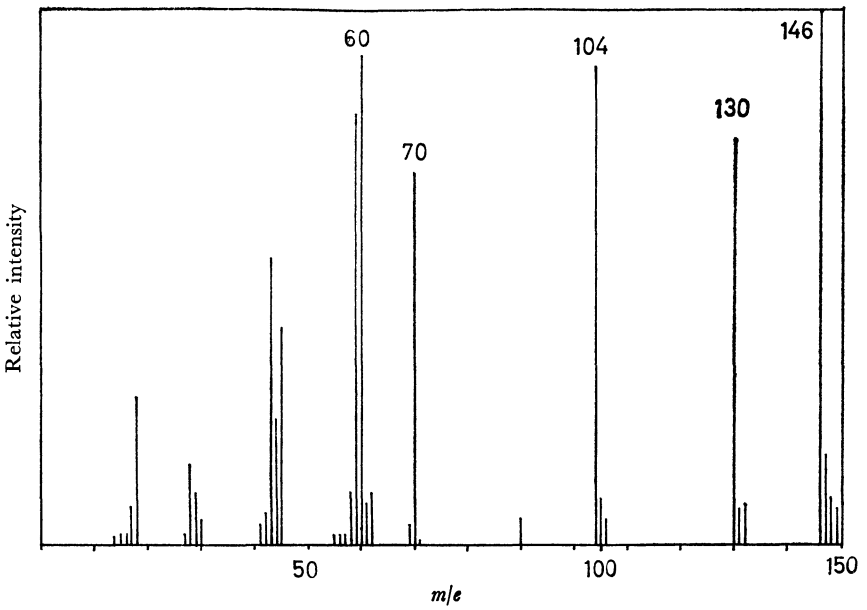

Fig. 6. Mass spectrum of *N*-carbamoyl-2-imino-1,3-oxathiolane.

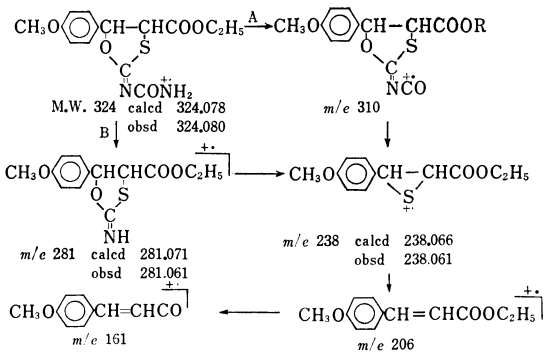

Scheme 2

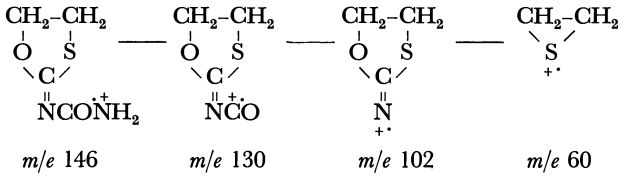

Scheme 3

and 6, and Scheme 2). Although the fragmentation of II proceeds in two ways A and B as shown in Scheme 3, route A is similar to the fragmentation of the oxathiolane. We have determined the structure of II to be *N*-carbamoyl-2-imino-5-substituted 1,3-oxathiolane-4-carboxylic ester.

A plausible reaction pathway is postulated in Scheme 1. Wagner-Jauregg *et al.*[5] and Price and Kirk[6] found that 2-thio-cyanoethanols are slowly converted into thiirane and *N*-carbamoyl-2-imino-1,3-oxathiolane at room temperature. Intermediate III which is produced initially from I and aldehyde, would be converted into II and thioglycidic ester by the same mechanism. Owen *et al.*[7] reported that the thioglycidic esters are unstable and lose sulfur, forming unsaturated esters. The reason why II is obtained as a minor product might be ascribed to slowness of reaction by which liberated cyanic acid is added to III, because II once formed is stable against potassium carbonate in ether.

NMR spectra suggest that II obtained in the present work is all in the same configuration. However, without isolation of any isomeric form, the configuration cannot be determined by means of NMR technique.

Experimental

NMR spectra were obtained on a JNM-C-60 high-resolution NMR spectrometer at temperatures 19—20°C. Tetramethylsilane was used as an internal reference standard. IR spectra were determined in the KBr pellet using a Perkin-Elmer 521 spectrophotometer. Mass spectra were measured with a JMS-01S instrument operating at 75 eV.

Reaction of Thiocyanoacetic Ester (I) with Aldehyde. General Procedure. Thiocyanoacetic ester (0.05 mol) was added dropwise below 10°C to a mechanically stirred solution of potassium carbonate or fluoride (0.05 mol) and aldehyde (0.05 mol) in 20 m*l* of moist ether. Stirring was continued for 10 hr, and the solution was allowed to stand overnight. The catalyst was removed by filtration, and the precipitated solid product was collected on a filter, washed with a small amount of water and then dried. Repeated recrystallization yielded pure *N*-carbamoyl-2-imino-5-substituted 1,3-oxathiolane-4-carboxylic ester (II). The filtrate was subjected to Glpc analysis.

Conversion of IIa into Ethyl Cinnamate. A solution which contained 1.0 g of IIa and 1.0 g of sodium hydroxide in 15 m*l* of ethanol was refluxed for an hour. After ethanol was removed with a vacuum evaporator, the remaining liquid was subjected to glpc and NMR analysis.

5) Th. Wagner-Jauregg, *Ann. Chem.*, **561**, 87 (1949): H. D. Hogelsang, Th. Wagner-Jauregg, and R. Rebling, *ibid.*, **569**, 183 (1950); Th. Wagner-Jauregg and M. Maring, *Helv. Chim. Acta*, **41**, 377 (1958).

6) C. C. Price and P. F. Kirk, *J. Amer. Chem. Soc.*, **75**, 2396 (1953).

7) T. C. Owen, C. L. Gladys, and L. Field, *J. Chem. Soc.*, **1962**, 656.

Formation of Ketenimines by the Reaction of Thioamides with Diethyl Azodicarboxylate and Triphenylphosphine

Oyo MITSUNOBU, Koki KATO, and Makoto WADA

Department of Chemistry, College of Science and Engineering, Aoyama Gakuin University, Megurisawa-cho, Setagaya-ku, Tokyo

(Received October 14, 1970)

The reaction of diphenylacetothioanilide with diethyl azodicarboxylate and triphenylphosphine gave rise to the formation of diphenylketene(*N*-phenyl)imine. Similarly, the reaction of *N*-(*p*-tolyl)diphenylacetothioamide gave diphenylketene(*N*-*p*-tolyl)imine. On treatment with diethyl azodicarboxylate in the presence of sodium ethoxide, diphenylacetothioanilide afforded bis(*N*-phenylbenzalimidoyl) disulfide in a good yield. The intermediate of the formation of the ketenimines is also discussed.

Ketenimines have attracted considerable attention because of their importance as versatile reagent. Their use as condensing agents in the preparation of peptides[1] and nucleotides[2] has been examined. The preparation of ketenimines has been accomplished in various ways, 1) the interaction of phosphinimine and ketene,[3] 2) the reaction of diazomethane with nitriles,[4] 3) dehydrochlorination or dechlorination of imino chlorides,[5] 4) dehydration of amides,[6] 5) the Beckmann rearrangement,[7] 6) the reaction of α-haloxime with triphenylphosphine,[8] 7) photolysis of diphenyldiazomethane in the presence of isonitrile,[9] and 8) ring opening of isoxazolium salts.[10]

A new approach to the synthesis of disubstituted carbodiimides from *N,N'*-disubstituted thioureas using diethyl azodicarboxylate (**1**) and triphenylphosphine (**3**) was described in the preceding paper.[11] The reaction proceeds through the initial formation of an 1:1 adduct (**2**) of the thiourea and **1**. Formation of the carbodiimide couples to a redox system.

Since thioamides (**6**) are similar in structure to thioureas, **6** would be expected to react with **1** giving an 1:1 adduct (**7**). In view of the reactivity of **2**, we might expect that the **7** is desulfurized by **3** to give the corresponding ketenimine (**8**), diethyl hydrazodicarboxylate (**4**) and triphenylphosphine sulfide (**5**).

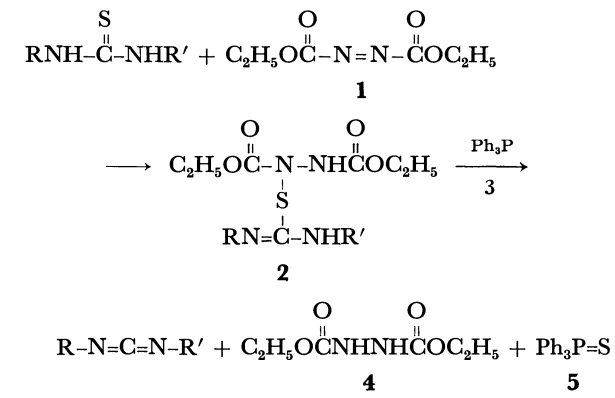

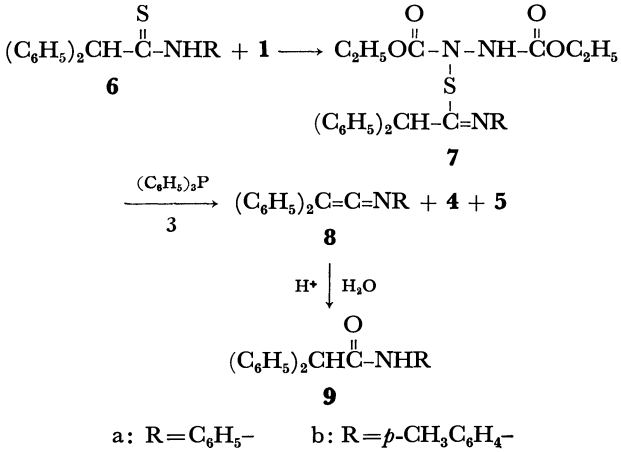

a: R=C_6H_5– b: R=*p*-$CH_3C_6H_4$–

Equimolar amounts of **1** and diphenylacetothioanilide (**6a**) in tetrahydrofuran (THF) were allowed to react for 4 hr, and then an equimolar amount of **3** was added. After the solution was kept standing for 7 days, the solvent was removed to give a yellow syrup. The infrared spectrum of the syrup shows a strong absorption at 2000 cm^{-1} which is attributed to N=C=C of the ketenimine. From the syrup, however, diphenylketen(*N*-phenyl)imine (**8a**) could not be isolated in pure state. In a repetition of the above experiment, the resulting yellow syrup was therefore treated with 2N hydrochloric acid to convert the **8a** into diphenylacetanilide (**9a**). The mixture was separated by column chromatography on silica gel to give **9a**, **4**, **5**, and triphenylphosphine oxide (**12**) in 35.5%, 98.0%, 36.1%, and 60.0% yields, respectively, and 63.0%

1) a) R. B. Woodward, R. A. Olofson, and H. Mayer, *J. Amer. Chem. Soc.*, **83**, 1010 (1961). b) R. B. Woodward and D. J. Woodman, *J. Org. Chem.*, **34**, 2742 (1969). c) D. S. Kemp and S. W. Chien, *J. Amer. Chem. Soc.*, **89**, 2743 (1967).

2) a) F. R. Atherton, A. L. Morrison, R. J. Cremlyn, G. W. Kenner, A. R. Todd, and R. F. Webb, *Chem. Ind.* London, **1955**, 1183. b) R. J. Cremlyn, G. W. Kenner, and A. R. Todd, *J. Chem. Soc.*, **1960**, 4511. c) T. M. Jacob and H. G. Khorana, *J. Amer. Chem. Soc.*, **86**, 1630 (1964).

3) H. Staudinger and E. Hauser, *Helv. Chim. Acta*, **4**, 887 (1921).

4) R. Dijkstra and H. J. Backer, *Rec. Trav. Chim. Pays-Bas*, **73**, 575, 695 (1954).

5) a) C. L. Stevens and J. C. French, *J. Amer. Chem. Soc.*, **75**, 657 (1953). b) C. L. Stevens and J. C. French, *ibid.*, **76**, 4398 (1954).

6) C. L. Stevens and G. H. Singhal, *J. Org. Chem.*, **29**, 34 (1964). b) H. J. Bestmann, J. Lienert, and L. Mott, *Ann. Chem.*, **718**, 24 (1968).

7) S. Hüng and W. Rehder, *Angew. Chem.*, **80**, 314 (1968).

8) M. Masaki, K. Fukui, and M. Ohta, *J. Org. Chem.*, **32**, 3564 (1967).

9) J. A. Green and L. A. Singer, *Tetrahedron Lett.*, **1969**, 5093.

10) R. B. Woodward and D. J. Woodman, *J. Amer. Chem. Soc.*, **88**, 3169 (1966).

11) O. Mitsunobu, K. Kato, and F. Kakese, *Tetrahedron Lett.*, **1969**, 2473.

of **6a** was recovered. This indicates that up to 35.5% of **8a** was formed by the present procedure. Similarly, diphenylketene(*N*-*p*-tolyl)imine was formed in a 42.5% yield. The formation of **12** can be explained as follows. The addition reaction of **6a** to **1** is a time consuming step and on treatment the reaction mixture with **3**, unreacted **1** forms a quaternary phosphonium salt (**11**)[12] which is hydrolyzed to **4** and **12**. In fact, thin layer chromatography (tlc) of the solution resulting from the reaction of **1** and **6a** showed that the starting materials survived even after 7 days.

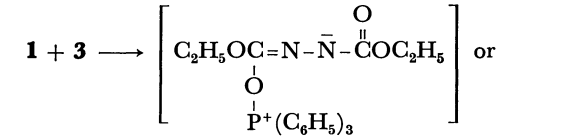

11a

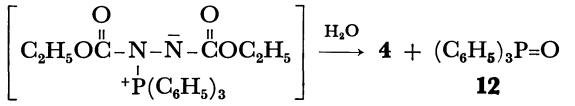

11b

It was therefore considered desirable to accelerate the reaction of **1** with **6** for preparation of **8**. Thus, ethanol was used as solvent in place of THF. As expected, the reaction of **1** with **6a** in ethanol was shown to proceed more faster than in THF, namely, **1** and **6a** were consumed within 1 day as indicated by tlc. After treatment with **3**, followed by treatment with 2N hydrochloric acid, the products were separated by column chromatography. The yield of **8a** increased to a 61.2% and **5** was isolated in a 91.2% yield, although a small amount of **12** was still isolated.

Other attempts to promote the reaction met with no success. For example, when *p*-toluensulfonic acid or benzoyl peroxide was used as a catalyst, the starting materials remained in considerable extent after one day as indicated by tlc. On the other hand, when sodium ethoxide was used as a catalyst, the reaction proceeded in an unexpected direction. When one half of **1** was added to **6a** in THF in the presence of sodium ethoxide, the color of the solution immediately faded. However, when the remaining half was added, disappearance of the orange red of **1** was no longer observed. Thus, **1** was allowed to react with 2 mol of **6a** at room temperature and bis(*N*-phenylbenzalimidoyl) disulfide (**13**) was obtained in a 97% yield. The structure of **13** was confirmed by elementary analysis and infrared spectrum.

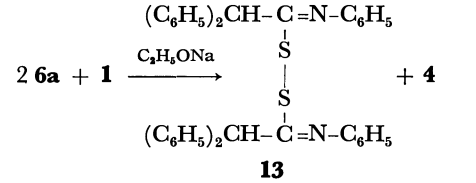

13

Concerning the intermediate of the present reaction, two possibilities could be considered, the initial formation of **7** and the formation of bis(*N*-arylbenzalimidoyl) disulfide (**13**).[13] In order to confirm the reaction path, the reaction of **1** with an equimolar amount of **6a** in THF was followed by infrared absorption spectrum. The spectrum indicated that the intensity of the C=O absorption of **1** gradually decreased and new absorptions appeared at 1740 cm^{-1} (C=O) and 1645 cm^{-1} (C=N) with the progress of reaction. The tlc of the solution revealed a new spot[15] which disappeared, on treatment of the solution with **3**, and the spot of the ketenimine was observed. That the disulfide is not an intermediate was further proved by a separate experiment in which **13** was treated with an equimolar amount of **3**. No **8a** was formed as indicated by tlc.

An attempt was made to isolate the proposed intermediate, **7**. However, from the reaction solution of **1** and **6a**, only a yellow oily substance was obtained which could not be purified.

The present procedure is unique since the reaction is coupled to a redox system, namely, triphenylphosphine is oxidized to triphenylphosphine sulfide and diethyl azodicarboxylate is reduced to diethyl hydrazodicarboxylate.

Experimental

Solvents were purified and dried in the usaual way. Tri phenylphosphine was of commercial grade and was used after recrystallization from ethanol. Diphenylacetic acid[16] and diethyl azodicarboxylate[17] were prepared according to published procedures. IR spectra were recorded on a Nippon Bunko IR-G spectrometer and measured as KBr disk. IR spectra of the reaction solution were measured in a 0.05 cm matched cell (NaCl). Tlc were carried on silica gel (Wako Gel B-O) plates with benzene as the solvent and spots were developed with iodine vapor.

Diphenylacethyl Chloride. A modification of the procedure used for the preparation of glutarimide-*β*-acetyl chloride[18] was used. A mixture of diphenylacetic acid (30 g) and thionyl chloride (26 g) was heated at 100°C for 15 min. On being cooled to room temperature, 3 drops of dimethylformamide were added to the solution and refluxed for 15 min during which time vigorous evolution of HCl and SO_2 took place. Diphenylacethyl chloride was isolated by distillation; 26 g, 80%, bp 121—122°C/3mmHg.

Diphenylacetothioanilide and N-*(p-Tolyl)diphenylacetothioamide.* A modification of the procedure in literature[19] was used.

12) a) D. C. Morrison, *J. Org. Chem.*, **23**, 1072 (1958). b) V. A. Ginsburg, M. N. Vasiléva, S. S. Dubov, and A. Y. Yakubovich, *Zh. Obshch. Khim.*, **30**, 2854 (1960); *Chem. Abstr.*, **55**, 17477 (1961). c) E. Brunn and R. Huisgen, *Angew. Chem.*, (*Int. Ed. Engl.*), **8**, 513 (1969).

13) Oxidation of thioamides was investigated and, in certain cases, corresponding disulfides were obtained.[14]

14) a) F. Hodosan and N. Serban, *Bull. Soc. Chim. Fr.*, **1959**, 507. b) K. Heyns and W. V. Benbenburg, *Chem. Ber.*, **89**, 1303 (1956). c) H. Rivier and J. Zeltner, *Helv. Chim. Acta*, **20**, 691 (1937). d) J. R. Schaeffer, C. T. Goodhue, H. A. Risley, and R E. Stevens, *J. Org. Chem.*, **32**, 392 (1967).

15) A small amount of bis(*N*-arylbezalimidoyl) disulfide was formed at the same time.

16) C. S. Marvel, F. D. Hager, and E. C. Caudle, "Organic Syntheses," Coll. Vol. I, p. 224 (1956).

17) J. C. Kauer, "Organic Syntheses," Coll. Vol. IV, p. 411 (1962).

18) Y. Egawa, M. Suzuki, and T. Okuda, *Chem. Pharm. Bull.* (Tokyo), **11**, 589 (1963).

19) a) W. Walter, J. Curts, and H. Pawelzik, *Ann.*, **643**, 29 (1961); *Chem. Abstr.*, **55**, 24652 (1961). b) L. F. Fieser and M. Fieser, "Reagents for Organic Syntheses," John Wiley & Sons, Inc., New York (1967), p. 333.

Twenty grams of diphenylacetanilide and 35 g of phosphorus pentasulfide were suspended in 150 m*l* of dioxane and stirred for 30 min at 80°C. The material was then extracted with dioxane and the combined extract was evaporated to dryness *in vacuo*. The residue was crystallized from xylene and diphenylacetothioanilide amounted to 17 g (78%), mp 187—188°C. In a similar way, *N*-(*p*-tolyl)diphenylacetothioamide was obtained in an 80% yield, mp 190—191°C.

*Preparation of Bis(*N*-phenylbenzalimidoyl) Disulfide (**13**).* To a solution of 0.303 g (0.001 mol) of diphenylacetothioanilide and a catalytic amount (one heaping of spatula) of sodium ethoxide in 14 m*l* of tetrahydrofuran (THF) was added dropwise to 0.087 g (0.0005 mol) of diethyl azodicarboxylate in 6 m*l* of THF. The color of the reaction mixture immediately faded. The solution was then evaporated under reduced pressure and the residue was chromatographed on silica gel (2.3 cm × 15 cm) to separate the products. Elution with benzene gave bis(*N*-phenylbenzalimidoyl) disulfide (0.29 g, 97%) which was dissolved in THF and precipitated with petroleum ether to give a pure sample, mp 169—170°C.

Found: N,4.39%. Calcd for $C_{40}H_{32}N_2S_2$:N,4.63%. IR(KBr) 1625 cm^{-1}(C=N) ; no N–H absorption.

Elution next with methanol gave diethyl hydrazodicarboxylate(0.087 g, 98%, mp 130—131°C).

Reaction of N-*(*p*-Tolyl)diphenylacetothioamide with Diethyl Azodicarboxylate and Triphenylphosphine.* To a stirred solution of 0.317 g (0.001 mol) of *N*-(*p*-tolyl)diphenylacetothioamide and 0.262 g (0.001 mol) of triphenylphosphine in 18 m*l* of THF was added 0.174 g (0.001 mol) of diethyl azodicarboxylate in an atmosphere of nitrogen at room temperature. After the solution was kept standing for 7 days at room temperature, it was evaporated *in vacuo*. The residue was dissolved in 10 m*l* of acetone and 4 m*l* of 2N hydrochloric acid and allowed to stand overnight to convert the diphenylketene-*N*-(*p*-tolyl)imine to *N*-(*p*-tolyl)diphenylacetamide. On being concentrated to dryness, the products were chromatographed on silica gel (2.3 cm × 50 cm). Elution with benzene gave two unknown substances (0.007 g and 0.002 g), recovered *N*-(*p*-tolyl)diphenylacetothioamide (0.148 g, 46.7%), triphenylphosphine sulfide (0.157 g, 53.4%), *N*-(*p*-tolyl)diphenylacetamide (0.128 g, 40.4%), diethyl hydrazodicarboxylate (quantitative) and triphenylphosphine oxide (0.135 g, 46.0%).

Reaction of Diphenylacetothioanilide with Diethyl Azodicarboxylate and Triphenylphosphine. *a) THF as Solvent.* To a solution of diphenylacetothioanilide (0.303 g, 0.001 mol) and triphenylphosphine (0.262 g, 0.001 mol) in THF (14 m*l*) was added dropwise diethyl azodicarboxylate (0.174 g, 0.001 mol) in THF (6 m*l*). After the solution had been kept standing for 7 days and subjected to the same work-up, diphenylacetanilide, diethyl hydrazodicarboxylate, triphenylphosphine sulfide, and triphenylphosphine oxide were obtained in 35.5%, 98.0%, 36.1%, and 60.0% yields, respectively, along with a small amount of an unknown product. Sixty three percent of diphenylacetothioanilide was recovered unchanged.

A change in the order of the addition does not affect the yield of the amide. The reaction also proceeds at 0°C. Triphenylphosphine in THF was added to diphenylacetothioanilide and diethyl azodicarboxylate in THF at 0°C. After the solution was allowed to stand in a refrigerator for 7 days and subjected to the same work-up, diphenylacetanilide was obtained in a 40.8% yield.

b) Ethanol as Solvent. To a stirred solution of 0.303 g (0.001 mol) of diphenylacetothioanilide in 5 m*l* of ethanol was added dropwise 0.174 g (0.001 mol) of diethyl azodicarboxylate in 6 m*l* of ethanol at 40°C. After 1 day at 40°C, diphenylacetothioanilide and diethyl azodicarboxylate were consumed as indicated by tlc and then the reaction mixture was evaporated *in vacuo* to give a yellow oily substance. Triphenylphosphine (0.262 g, 0.001 mol) was added and it was then dissolved in 6 m*l* of THF and kept standing for 7 days at room temperature. On being evaporated and treated with dilute hydrochloric acid in a similar manner as described above, the products were separated by columm chromatography (eluate: benzene) on silica gel to give an unknown compound (0.016 g), bis(*N*-phenylbenzalimidoyl) disulfide (0.011 g), triphenylphosphine sulfide (0.268 g, 91.2%), diphenylactanilide (0.176 g, 61.2%), diethyl hydrazodicarboxylate (0.166 g, 94.3%) and triphenylphosphine oxide (0.022 g, 8%).

The Reactions of Aroyl Peroxides with Grignard Reagents. III. On the Structure and the Reaction of the Complex Containing Benzoyl Peroxide[1]

Masao Ōkubo, Kazuhiro Maruyama,* and Jirō Ōsugi*
Government Industrial Research Institute, Nagoya, Kita-ku, Nagoya
**Department of Chemistry, Faculty of Science, Kyoto University, Sakyo-ku, Kyoto*
(Received October 17, 1970)

The orange-colored complex which is formed in the reaction of benzoyl peroxide with Grignard reagent was studied by infrared spectra, and the reaction of the complex with Grignard reagent was also examined. In this complex, the structure of BPO was still maintained by coordinating with magnesium atom through the peroxidic as well as the carbonyl oxygen atoms. Reaction products of this complex with phenylmagnesium bromide were benzoic acid(as Mg-salts), phenyl benzoate, benzophenone, triphenylcarbionol, and bromobenzene. The heterolytic mechanism on the formation of bromobenzene was proposed. The molar ratio of products depended seriously upon the mode of addition of Grignard reagents. The exclusive formation of bromobenzene and Mg-salts of benzoic acid without phenyl benzoate under an experimental condition was explained by assuming the electron-transfer process through the coordinating bond in the complex.

The two complexes were isolated in the reaction of benzoyl peroxide (BPO) with Grignard reagents, and analytical data of their components were reported previously.[2] The mechanism of the first stage of this reaction has been proposed on the basis of the relative reactivities of several peroxides.[3] In this paper, the detailed studies on the second stage of the reaction, which was found to proceed more slowly than the first stage,[3] will be reported.

Results and Discussion

Structure of the Complex II. The white complex, which has been named as the Complex I, is produced when the molar ratio [PhMgBr]:[BPO] is 1.33: 1.0, and this was found to be the same structure with the carbonated PhMgBr. Another orange-colored complex, which is named as the Complex II, is obtained when the molar ratio is 0.66:1.0,[3] and this is obtained also by mixing 2 mol of the Complex I with 1 mol of BPO.[2] In order to confirm the previous and tentatively proposed formulae for these complexes, they were submitted to infrared spectroscopy. The tetrahydrofuran (THF) solutions of the Complex I and II have very similar absorption bands with one another as shown in Figs. 1 and 2. The solution of BPO shows a quite different spectrum, which has three intense absorption bands at 1792, 1770, and 1214 cm^{-1} (Fig. 3). If these data were solely taken into consideration, one may arrive at an erroneous conclusion that the peroxide linkage, which had been proposed to be maintained in the Complex II, has already been broken. However, the Complex II produces phenyl benzoate if it is allowed to react with PhMgBr. Considering that phenyl benzoate is the primary product of the reaction of BPO with PhMgBr and that PhCOOMgBr reacting with PhMgBr does produce benzophenone, benzoyl peroxide is concluded to be alive in the Complex II.

The IR spectra of the Complex I and II have two main absorption bands at 1640 and 1415 cm^{-1}, both of which are poorly resolved triplets. The Complex I, reacts with PhMgBr to produce benzophenone and triphenylcarbinol in the similar manner to phenyl benzoate, though the reaction is remarkably slow. This fact means that the grouping –CO–O–MgBr in the Complex I has substantially an ester character. Thus, the absorption band at 1640 cm^{-1} can be assigned mainly to the C=O stretching vibration, which

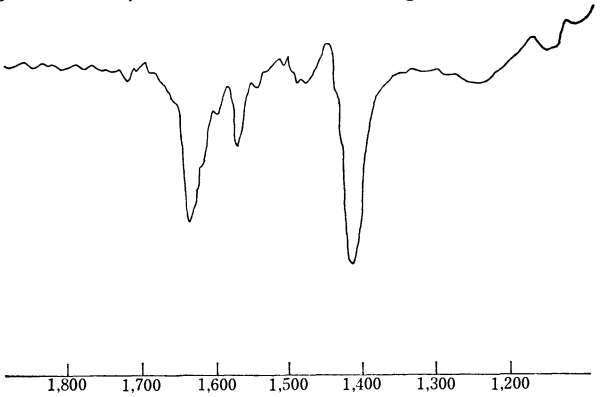

Fig. 1. IR spectrum of the complex I in THF. (cm^{-1})

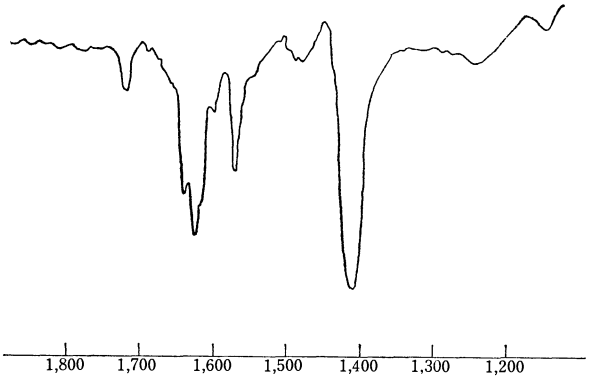

Fig. 2. IR spectrum of the complex II in THF. (cm^{-1})

1) The main part of this work was done at Department of Chemistry, Faculty of Science, Kyoto University.
2) M. Ōkubo, K. Maruyama, and J. Ōsugi, This Bulletin, **42**, 1162 (1969).
3) M. Ōkubo, K. Marayama, and J. Ōsugi, *ibid.*, in press.

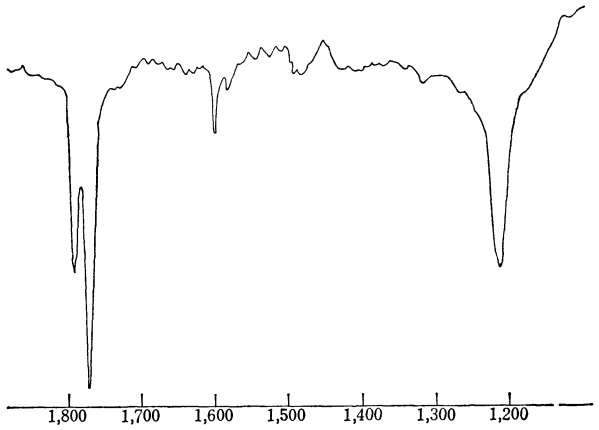

Fig. 3. IR spectrum of BPO in THF. (cm^{-1})

appears at 1770 and 1792 cm^{-1} in the case of free BPO(the difference is about -140 cm^{-1}). The other band at 1415 cm^{-1} can be assigned mainly to the C–O stretching vibration, which appears at 1214 cm^{-1} in the case of free BPO(the difference is about $+200$ cm^{-1}). These shifts(-140 and $+200$ cm^{-1}) are considered to correspond to reasonable changes of bonding energies which are about -0.4 and $+0.6$ kcal/mol. Taking account of analytical data of the Complex I[1] and of the fact that the coordination number of magnesium can be varied between four and six, the Complex I would exist as dimeric state which is depicted in Fig. 4.

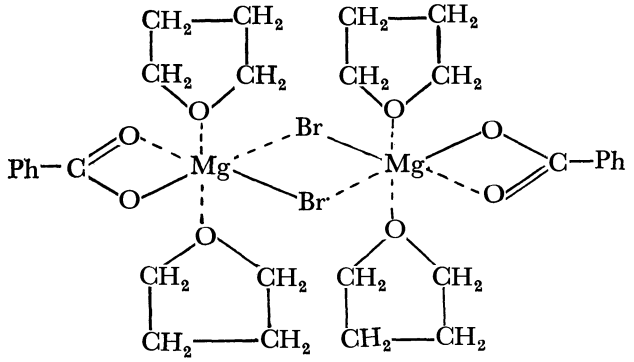

Fig. 4. Structure of the complex I.

Benzoyl peroxide in the Complex II, which shows the quite similar IR spectrum to that of the Complex I, must have almost the same structure as the PhCOO-grouping in the Complex I. Taking account of analytical data of the Complex II[2] and of the coordination number of magnesium, the structure of the Complex II may be depicted as Fig. 5.

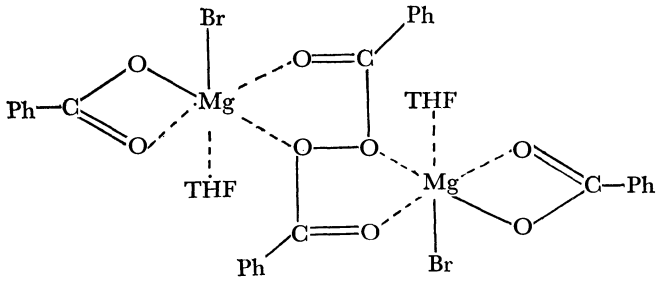

Fig. 5. Structure of the complex II.

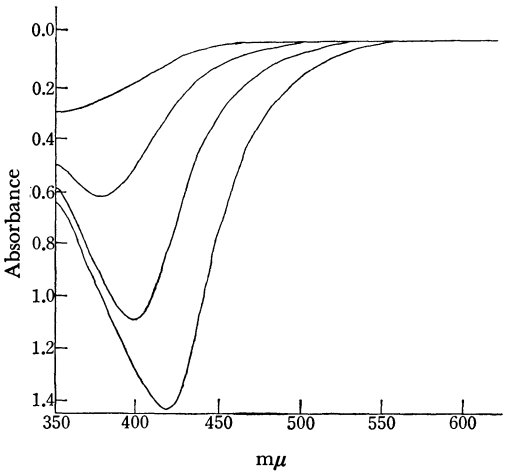

Fig. 6. Visible absorption spectra of the complex II in THF concentration; 10^{-4}—10^{-5} mol/*l*.

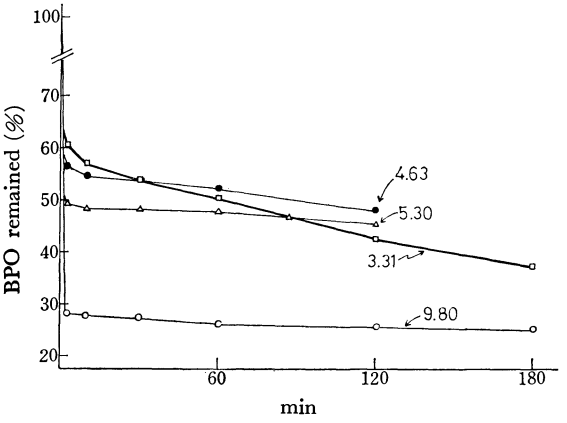

Fig. 7. Effect of concentration on the decomposition of BPO.
Molar ratio [PhMgBr]:[BPO]=1:1
Numbers in the Fig. : Molar concn. $\times 10^3$ mol/*l*

The visible absorption spectra of Complex II in THF was found to be dependent on the concentration as shown in Fig. 6. As the concentration is higher, the absorption maximum is shifted to longer wavelengths. This fact may be explained by considering the change of the degree of aggregation of this complex with the change of concentration. This suggestion is borne out by the examination of the effect of the concentration on the rate of the decomposition of BPO with PhMgBr when the molar ratio is 1:1 (Fig. 7). The second stage of the reaction is remarkably slow,[3] and the main reaction of this stage is apparently concerned with the reaction of the Complex II with remaining PhMgBr. It is noted that the curve for the second stage in Fig. 7 becomes steeper as the concentration of the initial reactants is lower though the crease of the curve falls down as the concentration is higher. This fact may be the result that the lower aggregates which might exist in diluted solutions react faster with the remaining Grignard reagent. Thus, the Complex II is considered to exist as aggregated state in the more concentrated solution.

Reaction of the Complex II For the purpose of clarification of the second stage of the reaction, the reaction of the Complex II with PhMgBr must be

Table 1. Reactions of the complex II with PhMgBr

Expt. No.	Molar ratio[a] [PhMgBr]/[Complex II]	Time for addn. hr	Yields[c] % PhBr	PhH	PhCOOH	PhCOOPh	PhCOPh	Ph_3COH
1	2	0	26.6	—	135	36.6	17.8	10.3
2	1 + 1[b]	0[b]	28.5	—	142	36.0	17.0	11.5
3	2	2.5	30.9	—	184	small amount	trace	non
4	2	4.0	31.5	found	192	non	non	—
5	1.5	2.5	39.0[d]	found	187	non	non	non

a) 0.00570 mol of PhMgBr in 30 m*l* of THF (0.19M) was added to 0.00285 mol of the Complex in 50 m*l* of THF.
b) 0.00570 mol of PhMgBr in 30 m*l* of THF was divided into two portions. The first portion was added at once, and the second portion was also added at once after 2 hr.
c) Yields were calculated based on PhMgBr used ([PhMgBr]/[Complex II]=2).
d) The yield is calculated bassd on PhMgBr used ([PhMgBr]/[Complex II]=1.5).

examined.[4] If the twice moles of Grignard reagent were added at once to the THF solution of the Complex II at 0°C, the orange color of the solution disappeared immediately and the peroxide was found to be consumed almost completely. Bromobenzene (26.6%), phenyl benzoate (36.0%), benzophenone (17.8%), and triphenylcarbinol (10.3%) were obtained from the neutral part. The latter three products obviously come from the reaction of PhMgBr with BPO in the Complex II. The formation of the appreciable amount of bromobenzene must be the result of the attack on the Mg-Br linkage in the Complex II by the phenyl group of the Grignard reagent. The question, whether the Mg–Br bond in the complex is broken heterolytitcally or homolytically, is then to be solved.

The molar ratio of the products was found to be affected remarkably by the mode of addition of PhMgBr solution. The results were summarized in Table 1. In the experiment No. 1, two molar equivalents of PhMgBr were added at once to BPO solution. In No. 2, a first equivalent of PhMgBr is added to BPO solution at once and the second equivalent was also added at once after 2 hr. In No. 3, two molar equivalents were added dropwise as slow as the orange color of the solution did not fade during the addition, using an ordinary dropping funnel. In No. 4 and No. 5, 2 and 1.5 equivalents were added in very small drops by using a burette, respectively, and slowly in the similar manner to No. 3. It is to be noted that the amounts of bromobenzene and benzoic acid gradually increased and those of phenyl benzoate, benzophenone and triphenylcarbinol decreased remarkably as the rate of addition is slowed down and as the size of a drop of PhMgBr solution becomes small. This result can be interpreted by the following discussion. The localized high PhMgBr concentration which may appear in the reaction systems of No. 1 and No. 2, will cause a number of Grignard molecules to make attack on the several sites of the Complex II. Thus, bromobenzene is formed if the Mg–Br bond is attacked, and phenyl benzoate is formed if BPO is attacked when it is dissociated as the Complex II is decomposed. On the other hand, if PhMgBr is added slowly and in very small drops, the Mg–Br bond is attacked exclusively

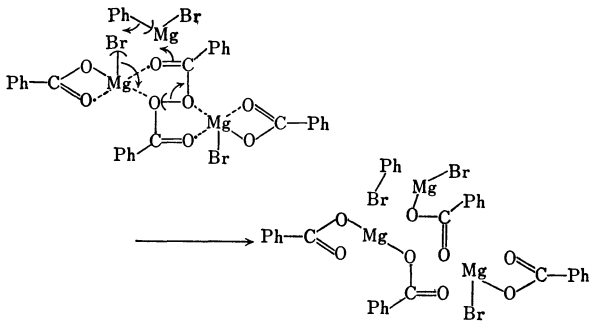

as the result of the electron-transfer process which leads to the selective formation of bromobenzene and magnesium salts of benzoic acid probably according to the following mechanism: This electron–transfer process must be fairly slow though the most reactive site of the Complex II is the one of the Mg–Br bonds, since the exclusive formation of bromobenzene and benzoic acid salts is effected only if the Grignard reagent is added very slowly. It is shown in Table 1 that the slow addition causes the yield of benzoic acid to approach 200%, and this fact is also explained by the above mechanism.

The recovery of the phenyl group of PhMgBr is about 100% in the experiments No. 1 and No.2(50% based on PhMgBr), and as low as about 30—39% in the experiments No. 3, No. 4, and No. 5. As benzene was detected in No. 4 and No. 5, the Complex I which is reproduced in the reaction may coordinate to the unreacted PhMgBr and may stabilize this.[5] However, the important fact is that the yield of bromobenzene increases as the rate of addition is slowed down but does not exceed 50% based on the Complex II.[6] This

4) The solution of the Complex II was prepared by adding a half equivalent of BPO to a completely carbonated PhMgBr solution.[2] See experimental section.

5) The coordination of PhMgBr to PhCOOMgBr is reasonable, since the Complex I can react with PhMgBr at higher temperatures to produce benzophenone and finally triphenylcarbinol. But this reaction is very slow at 0°C as stated in the preceding section.

6) In No. 4, the orange color of the reaction mixture disappeared before the total volume of the PhMgBr solution was added. In No. 5, the orange color of the Complex II was just found to disappear when 1.5 molar equivalents of PhMgBr solution were added. On this base, the yield of bromobenzene is 49%. Since two molar equivalents of the Complex I are reproduced from one molar equivalent of the Complex II according to the above-proposed mechanism, one molar equivalent of PhMgBr is consumed to produce bromobenzene, and the remaining molar equivalent may be coordinated by the reproduced Complex I at 0°C.

may be illustrated by considering that only one bromine atom in the Complex II reacts as bromonium cation to afford bromobenzene from PhMgBr.

Different behaviors of the Complex II in the three solvents, namely tetrahydrofuran, ethyl ether, and water, would provide a key to solve this problem. The Complex II is remarkably soluble in THF without any decomposition, but it does not dissolve in ethyl ether.[2] In water, this complex decomposes with release of molecular bromine.[2] The similar complex containing peroxide is not obtained from the reaction in ethyl ether. Since ethyl ether is more weakly basic than THF,[7] the complex containing BPO, if it is formed in ethyl ether, may have a lower electron density around the Mg–atom than in the case of the Complex II itself and may thus make easier the Br–atom to be detached as cationic bromonium ion. The stability of the Complex II itself may thus be ascribed to the strong coordination of THF to Mg–atoms. Another fact that a heavy precipitate appears easily when the ethyl ether solution of PhMgBr is carbonated, can also be ascribed to the easier disproportionation of PhCOOMgBr into $(PhCOO)_2Mg$ and $MgBr_2$ because of the lower coordinating ability of ethyl ether. Thus the complex similar to the Complex II is hard to exist in such a system. The easy releasing of molecular bromine upon treatment of the Complex II with water may be the result that the water molecule replaces the THF molecules and makes stronger the polarity of the Mg–Br bond and finally expels the bromine as bromonium ion. Thus, the different behaviors of the Complex II in the three solvents can be illustrated if the Mg–Br bond in the Complex II is considered to be broken heterolytically to produce bromonium ion.

Another observation which supports the consideration clearly is the fact that reaction of the Complex II with cyclohexene produces 1,2-dibromocyclohexane in the yield as high as more than 85%. Thus, the olefine may be attacked by the bromonium ion, which is produced through the slow electron-transfer process, to give 2-bromocyclohexyl carbonium ion, and this carbonium ion attacks another Mg–Br bond to afford 1,2-dibromide. Therefore, the formation of bromobenzene may be the result of the nucleophilic attack of phenyl anion on the Mg–Br bond. The oxidation of one of the two Mg–Br linkages through the slow electron-transfer process may thus be the characteristic mechanism of the Complex II.

Experimental

Reagents. All the reagents were prepared and/or obtained in the same manner with those used in the preceding paper.[3]

Measurements of Spectra. IR spectra were measured as Nujol-mulls and as THF solutions with Nihon Bunko IR-S-type and DS-401-type spectrometers. Visible absorption spectra were measured with Perkin–Elmer 202-type spectrometer.

Preparation of the Solution of the Complex II. Ten mililiters of stocked solution of PhMgBr in THF (0.57 M) was pipetted into the N_2-purged flask and 20 m*l* of THF was added. The three-way glass-cock was turned and dried CO_2 was introduced with vigorous stirring. The stirring was continued for 30 min after the absorption of CO_2 was completed. The flask was then warmed up to about 50°C for 30 min to expel the excess CO_2 completely with slow nitrogen stream. After the solution was cooled to 0°C, 0.690 g of BPO (0.00285 mol) and 20 m*l* of THF were added successively with gentle stirring. The mixture was stirred at 0°C for 30 min and at room temperature for 90 min. The orange–colored solution of 0.00285 mol of the Complex II in THF (50 m*l*) was thus prepared and was used for the next reaction.

Reaction of the Complex II with PhMgBr. Ten mililiters of PhMgBr solution (0.57 M) was diluted to 30 m*l* and added to the solution of the Complex II prepared above. In the experiments No. 1 and No. 2, the mixing apparatus described in the preceding paper[3] was used. In No. 3, a pressure-equalized dropping funnel was used. In No. 4 and No. 5, a burette equipped with a pressure-equalizing tube was used. All the experiments were conducted under nitrogen stream.

Product Analysis. The reaction mixtures were concentrated to a small volume under reduced pressure, treated with aqueous ammonium chloride, extracted with ethyl ether and washed with aqueous sodium hydrogencarbonate. The ether extracts were dried over anhydrous magnesium sulfate and concentrated for vpc analysis. The ether solution of neutral products was analyzed with Yanagimoto GCG-55A-type and GCG-2-type vapor fractometers. The water extracts were acidified, and the precipitated benzoic acid was extracted with ether, evaporated to dryness and weighed.

Reaction of the Complex II with Cyclohexene. To a 90 m*l* of the orange-colored solution of the Complex II (0.00546 mol), the same moles of cyclohexene in 10 m*l* of THF was added at once at room temperature. One mililiter portions of the reaction mixture were pipetted out at definite time intervals, and titrated with thiosulfate solution according to Wibaut.[8] After about 4 hr, the thiosulfate euqivalent comes down to a value to about 10% of used peroxide, and the color of the reaction mixture faded almost completely. The solution was evaporated to a small volume under reduced pressure, ethyl ether was added, and the pale-yellow crystals were removed by filtration. The filtrate was treated as usual manner, and the neutral part was analyzed again by vpc technique using hexachloroethane as the inner reference. Any product other than 1,2–dibromocyclohexane was not detected.

7) H. E. Wirth and P. I. Slick, *J. Phys. Chem.*, **66**, 2277 (1962).

8) J. P. Wibaut, H. B. van Leewen, and B. van der Wal, *Rec. trav. Chim. Pays-Bas*, **73**, 1033 (1954).

The Elimination Orientation in the Fluoride-promoted Olefin Formation. A Comparison with the Alkoxide-promoted Eliminations[1]

Noboru Ono

Department of Chemistry, Faculty of Science, Kyoto University, Sakyo-ku, Kyoto

(Received October 20, 1970)

When the 2-butyl and 2-pentyl derivatives were treated with tetraethylammonium fluoride in acetonitrile, an olefin-forming elimination took place and an overwhelming Saytzeff orientation was observed. The relative yield of 1-olefin was little affected by changes in the leaving group and β-alkyl group. These results were compared with the results of the eliminations with the conventional base-solvent systems (EtO^- in EtOH, t-BuO^- in t-BuOH, and t-BuO^- in DMSO).

Directive effects in elimination reactions have been well documented.[2] Recently, the transition state of the E2 reaction has attracted the interest of many workers. Brown[3] has shown that the Hoffmann-rule product increases with an increase in the steric requirements of the attacking base, of the alkyl group in the incipient double bond, or of the leaving group. Some results contradicting Brown's explanation have also been presented.[4-8] Bunnett[4-6] has explained the orientation rule by the variable-transition-state theory. According to this theory, a positional orientation correlates with the relative degree of the breaking of the C_β-H and C_α-X bonds in the transition state.

Nearly all of the results cited above have been obtained in studies where alkoxides were used as the base. A thorough investigation of other base-solvent effects is worthwhile in order to elucidate the fine aspects of the mechanism of the olefin-forming elimination reaction.

In previous papers,[9-12] it has been reported that tetraethylammonium fluoride behaves as a strong base in dipolar aprotic solvents, and that styrene and substituted styrenes were produced in high yields in the E2 reaction of 2-arylethyl halides. The fluoride-induced eliminations were considered to proceed through a very tight transition state where the β-proton is less than half transferred to the base.[11] This fact indicates that the fluoride ion plays an interesting role in the β-eliminations from 2-alkyl derivatives. In the present paper, the orientation of the fluoride-induced eliminations from 2-alkyl derivatives will be determined, and the results will be compared with those of alkoxide-induced reactions.

Results and Discussion

The reactions were carried out at 50°C with a base that has a molar ratio to the substrate of two to one. To prevent the isomerization of the olefinic products during the eliminations, a constant stream of dry nitrogen was bubbled through the reaction mixture and the products were collected at −76°C in a cold trap containing a few milliliters of dimethylformamide. Using gas-liquid partition chromatography (glpc), the relative proportions of the isomeric olefins obtained in the eliminations from 2-alkyl derivatives (Eq. (1)) have been determined.

$$RCH_2\underset{\displaystyle X}{\underset{|}{C}}HCH_3 \longrightarrow RCH_2CH{=}CH_2 + \underset{H}{\overset{R}{\diagdown}}C{=}C\underset{CH_3}{\overset{H}{\diagup}} + \underset{H}{\overset{R}{\diagdown}}C{=}C\underset{H}{\overset{CH_3}{\diagup}} \qquad (1)$$

R = Me, Et X = Cl, Br, I, OTs

The results, together with the results for the reactions with ethoxide in ethanol, t-butoxide in t-butanol, and t-butoxide in dimethylsulfoxide (DMSO), are summarized in Table 1. Most of the data with alkoxide ions are taken from earlier papers. For convenience in comparing these results, these data are presented graphically in Figs. 1—4. The changes in the 1-olefin/2-olefin ratio in the eliminations from 2-butyl and 2-pentyl derivatives are plotted *versus* the change in the leaving group (X) in Figs. 1 and 2. Similar plots for 2-alkyl bromides and tosylates *versus* the change in the alkyl group (R) attached to the β-position to the leaving group are shown in Figs. 3 and 4. The scales of the abscissae are arbitrary, but are chosen so that the straight line is obtained for the reaction with ethoxide in ethanol.

A previous report[11] from this laboratory showed that the 2-arylethyl derivatives underwent fluoride-induced E2 reaction in the acetonitrile solvent. For example, the reaction of 2-arylethyl chloride followed second-order kinetics, first-order in tetraethylammonium fluoride and first-order in the substrate. The Hammett $\sigma\rho$ relation was established with ρ equal to 2.033, k_0

1) Presented at the 23rd Annual Meeting of the Chemical Society of Japan, Tokyo, April, 1970.

2) a) C. K. Ingold, "Structure and Mechanism in Organic Chemistry 2nd Edition," Cornell Univ. Press, Ithaca, New York (1969), p. 649. b) D. V. Banthorpe, "Elimination Reaction," Elsevier Publishing Co., London (1963).

3) H. C. Brown and R. L. Kilimisch, *J. Amer. Chem. Soc.*, **88**, 1425 (1966), and preceding papers.

4) R. A. Bartsch and J. F. Bunnett, *ibid.*, **90**, 408 (1968).

5) R. A. Bartsch and J. F. Bunnett, *ibid.*, **91**, 1376 (1969).

6) R. A. Bartsch and J. F. Bunnett, *ibid.*, **91**, 1382 (1969).

7) D. H. Froemsdorf and M. E. McCain, *ibid.*, **87**, 3983 (1965).

8) D. H. Froemsdorf, M. E. McCain, and W. W. Wilkison, *ibid.*, **87**, 3984 (1965).

9) J. Hayami, N. Ono and A. Kaji, *Tetrahedron Lett.*, **1968**, 1385.

10) J. Hayami, N. Ono, and A. Kaji, *ibid.*, **1970**, 2727.

11) J. Hayami, N. Ono, and A. Kaji, This Bulletin, 44 (1971) in Press.

12) J. Hayami, N. Ono, and A. Kaji, *Nippon Kagaku Zasshi*, **92**, 87 (1971).

being 3.89×10^{-3} *l*/mol sec at 25°C. The kinetic isotope effect was also determined, k_H/k_D being 3.99. In the present instances, no butene was obtained in the reaction of 2-butyl iodide in the acetonitrile solvent, even in the presence of tetraethylammonium perchlorate. There is little possibility that the El mechanism is operative in the present instances of the olefin-forming eliminations.

The outstanding features of the fluoride-induced elimination reaction are clearly shown in Figs. 1—4. The changes in the leaving groups and alkyl groups had essentially no effect upon the orientation of elimination from 2-alkyl derivatives. These is a definite predominance of the Saytzeff orientation, the ratio of the 1-olefin to 2-olefin ranging from 0.10 to 0.16. Bartsch[16] has reported the orientation in the elimination from 2-alkyl halides induced with halide ions in demethylformamide and DMSO. He has reported the Saytzeff orientation in the reaction of 2-butyl halides with fluoride, but his fluoride is not free of water, and, therefore, there may be trouble in discussing the nature of the base-solvent system. As has been reported earlier,[9,12] the presence of two molar equivalents of water in the fluoride-acetonitrile system reduced the reactivity drastically.

The explanations that have been postulated for the base-solvent effect upon the orientation of the elimination reaction fall into two categories. One is that the size of the attacking bases affects the orientation of

Table 1. Products from the eliminations of RCH_2CHXCH_3

R	X	Base	Solvent	Temp. C°	Olefin composition %		
					1-olefin	*trans*-2	*cis*-2
CH_3	I	F^-	CH_3CN	50	10.3	71.2	18.5
CH_3	Br	F^-	CH_3CN	50	11.6	68.9	19.5
CH_3	Cl	F^-	CH_3CN	50	11.6	67.7	20.7
CH_3	OTs	F^-	CH_3CN	50	13.7	55.4	30.9
CH_3	I	EtO^-	EtOH	reflux	9.9	65.3	24.8
CH_3	Br	EtO^-	EtOH	reflux	18.0	61.1	20.9[a]
CH_3	Cl	EtO^-	EtOH	reflux	23.8	58.5	17.7
CH_3	OTs	EtO^-	EtOH	55	35	43	22[b]
CH_3	I	*t*-BuO^-	DMSO	25	19.6	62.4	18.0[c]
CH_3	Br	*t*-BuO^-	DMSO	25	31.5	54.1	14.4[c]
CH_3	Cl	*t*-BuO^-	DMSO	25	41.2	47.2	11.6[c]
CH_3	OTs	*t*-BuO^-	DMSO	55	61	28	11[b]
CH_3	I	*t*-BuO^-	*t*-BuOH	50	33.8	44.3	21.9[d]
CH_3	Br	*t*-BuO^-	*t*-BuOH	50	53.4	27.7	18.9[d]
CH_3	Cl	*t*-BuO^-	*t*-BuOH	50	68.3	17.7	13.8[d]
C_2H_5	I	F^-	CH_3CN	50	10.3	76.5	13.2
C_2H_5	Br	F^-	CH_3CN	50	12.4	74.1	13.5
C_2H_5	Cl	F^-	CH_3CN	50	12.8	70.8	16.4
C_2H_5	OTs	F^-	CH_3CN	50	14.2	55.6	30.2
C_2H_5	I	EtO^-	EtOH	reflux	19.3	65.2	15.5[e]
C_2H_5	Br	EtO^-	EtOH	reflux	24.2	58.9	16.9[f]
C_2H_5	Cl	EtO^-	EtOH	reflux	36.2	51.6	13.6[e]
C_2H_5	OTs	EtO^-	EtOH	55	42	38	20[b]
C_2H_5	I	*t*-BuO^-	DMSO	50	23.6	60.7	15.7
C_2H_5	Br	*t*-BuO^-	DMSO	50	43.5	46.8	9.7[g]
C_2H_5	OTs	*t*-BuO^-	DMSO	50	70.1	22.9	7.0[h]
C_2H_5	I	*t*-BuO^-	*t*-BuOH	50	55.0	33.8	9.2
C_2H_5	Br	*t*-BuO^-	*t*-BuOH	50	81.2	12.0	6.8[g]

a) Ref. 8 gives 19%, 62%, 19%.
b) Data from Ref. 7.
c) Data from Ref. 13.
d) Data from Ref. 3.
e) Data from Ref. 14.
f) Ref. 14 gives 24.6%, 59.0%, 16.4%.
g) Data from Ref. 15.
h) Ref. 7 gives 72%, 21.4%, 6.6%.

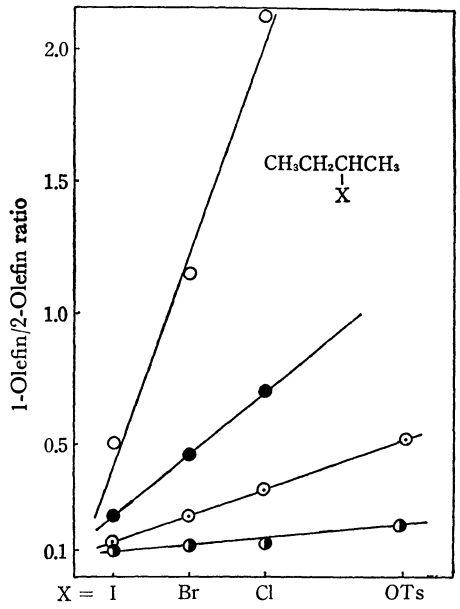

Fig. 1. 1-Olefin/2-Olefin ratio in the eliminations from 2-butyl derivatives.
○ *t*-BuO^- in *t*-BuOH, ● *t*-BuO^- in DMSO, ⊙ EtO^- in EtOH ◑, F^- in CH_3CN

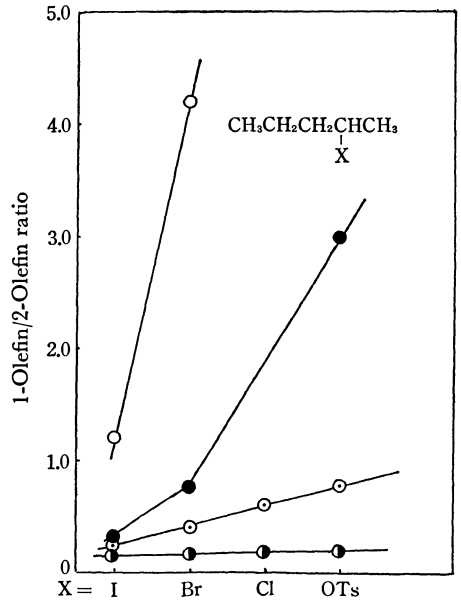

Fig. 2. 1-Olefin/2-Olefin ratio in the eliminations from 2-pentyl derivatives.
○ *t*-BuO^- in *t*-BuOH, ● *t*-BuO^- in DMSO, ⊙ EtO^- in EtOH, ◑ F^- in CH_3CN

13) D. L. Griffith, D. L. Meges, and H. C. Brown, *Chem. Commun.*, **1968**, 90.
14) W. H. Saunders, Jr., S. R. Fahrenholtz, E. A. Caress, J. P. Lowe, and M. Schreiber, *J. Amer. Chem. Soc.*, **87**, 3401 (1965).
15) R. A. Bartsch, *J. Org. Chem.*, **35**, 1334 (1970).
16) R. A. Bartsch, *ibid.*, **35**, 1023 (1970).

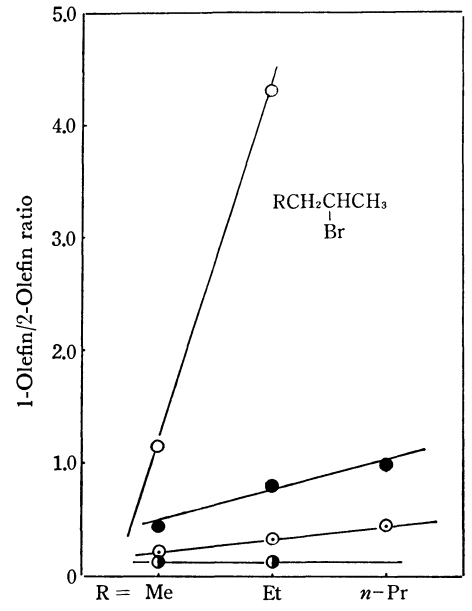

Fig. 3. 1-Olefin/2-Oelefin ratio in the eliminations from 2-alkyl bromides.
○ t-BuO$^-$ in t-BuOH, ● t-BuO$^-$ in DMSO, ⊙ EtO$^-$ in EtOH, ◑ F$^-$ in CH_3CN
R=n-Pr: from Refs. 5 and 6

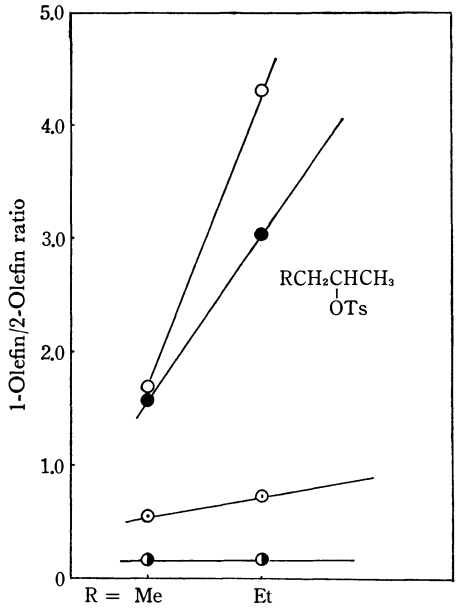

Fig. 4. 1-Olefin/2-Olefin ratio in the eliminations from 2-alkyl tosylates.
○ t-BuO$^-$ in t-BuOH, ● t-BuO$^-$ in DMSO, ⊙ EtO$^-$ in EtOH ◑ F$^-$ in CH_3CN

the elimination, and the other is that the base strength affects the orientation of the elimination. Brown[3] has proposed that, in the absence of significant steric interaction, the reaction proceeds to form the more stable of the two possible olefins; however, an increase in the steric requirement of the attacking base and the environment should tend to shift the course of the reaction from the Saytzeff toward the Hoffmann elimination. On the other hand, Bunnett[5] and also, Froemsdorf[7,8] have proposed that an increase in the Hoffmann elimination is attributable to the carbanion character in the transition state induced by an increase in the base strength, the "poorer" leaving group also assisting the carbanion character.

The explanation based on the base strength is not adequate to explain the present results in the light of the following facts. First, the variations in the olefin proportion in each of the figures (Figs. 1—4) are smallest for the elimination with the fluoride ion in acetonitrile and are intermediate for the reactions with ethoxide in ethanol, and with t-butoxide in DMSO, and are largest for the reaction with t-butoxide in t-butanol. These orders scarcely correlate at all with the reactivity of the base.[17] Second, in the eliminations from 2-alkyl derivatives with t-butoxide in t-butanol, more 1-olefin is produced than in the same reactions with the stronger base, t-butoxide in DMSO. Third, as Saunders[19] has pointed out, in a reaction of 2-arylethyl-ammonium bromides, the kinetic isotope effect and the substituent effect indicate a distinctly less carbanion character for the reaction with t-butoxide in t-butanol than for that with ethoxide in ethanol, although the relative yield of 1-olefin increases on the change from ethoxide in ethanol to t-butoxide in t-butanol for the reactions of 2-alkyl derivatives. It may be concluded, therefore, that the change in the apparent base strength does not play any major role in altering the olefin proportion in the present reactions.

In explaining the present results, the role of the steric requirements of the entities attacking the substrate should be taken into account. As Brown[3] has pointed out, solvation, both of the attacking base and of the leaving group, must be considered in estimating their steric requirements and their influence on the direction of elimination. Considering the anion solvation, it is quite plausible that the fluoride ion in acetonitrile has the smallest steric requirement, and that the t-butoxide ion in t-butanol has the largest steric requirement, among the four base-solvent systems.[20] The largest change in the 1-olefin/2-olefin ratio is observed in the reactions induced by t-butoxide in t-butanol, because this base-solvent system has the largest steric requirement. When the steric requirements of the attacking entities become smaller, the attacking entities should become less sensitive to smaller changes in the steric requirements of the environment (the leaving group the alkyl group, and solvation), and *vice versa*. As a result of this steric interrelation, the more stable Saytzeff-type product definitely predominates and the changes

17) The relative reactivity of the base increases from the alkoxide ion in alcohol to the fluoride ion in acetonitrile to the alkoxide ion in DMSO. Tetraethylammonium fluoride in acetonitrile is about 800 times as effective as sodium ethoxide in ethanol in promoting the E2 reaction from 2-phenylethyl chloride at 25°C,[10,11] and t-butoxide in DMSO is several times stronger than fluoride in acetonitrile.[18]

18) A. F. Cockerill, S. Rottschaefer, and W. H. Saunders, Jr., *J. Amer. Chem. Soc.*, **89**, 901 (1967).

19) W. H. Saunders, Jr., D. G. Bushman, and A. F. Cockerill, *ibid.*, **90**, 1775 (1968).

20) It is uncertain which has the larger steric requirement, the ethoxide ion in ethanol or the t-butoxide ion in DMSO; however, the results in Figs. 1—4 are suggestive and can be correlated with steric requirements better than with the reactivities of the attacking entities.

in the leaving groups and alkyl groups have little effect on the orientation in the fluoride-induced eliminations.

The data in Table 1 also reveal interesting changes in the *trans*-2-olefin/*cis*-2-olefin ratios with the solvents. High *trans*/*cis* ratios of about 4—5 are observed in dipolar aprotic solvents; on the contrary, smaller *trans*/*cis* ratios of about 1—2 are observed in *t*-butanol. Bartsch and Bunnett have reported similar results.[6] A high *trans*/*cis* ratio of about 5 was observed in the reaction of 2-hexyl halides with *t*-butoxide in DMSO, and a *syn*-elimination stereochemistry was postulated. However, the possibility of the intervention of *syn*-elimination has been ruled out recently by an experiment with erythro-3-deutero-2-bromobutane.[21] The *trans*/*cis* ratios have been interpreted as indicating the extent of the double-bond character in the transition states.[5,6]. However, at present no direct relationship between the 1-olefin/2-olefin ratio and the *tran*/*cis* ratio has been found for the reactions discussed above.[6,22] The reason for the high *trans*/*cis* ratio in dipolar aprotic solvents is hard to find and needs to be studied further.

Experimental

Materials. *2-Alkyl Halides*: The 2-butyl halides were either commercial samples or were prepared from alcohols by the usual method. 2-Pentyl iodide was prepared analogously to the procedure used for Coe[23]: 2-pentanol (25 g) was added, drop by drop, to triphenylphosphite diiodide (from 76 g of iodine and 100 g of triphenyl phosphite); the mixture was then kept at room temperature for 30 min. Two distillations gave 2-pentyl iodide (11 g, 20%); bp 55°C/50mmHg (lit,[24] 139—142°C). 2-Pentyl bromide was prepared by a procedure similar to that used for 2-pentyl iodide except that bromine was used instead of iodine. 2-Pentyl chloride was prepared by the method of Whitmore and Karnatz[25] from 2-pentanol, pyridine, and thionyl chloride. Two distillations gave a material with a bp of 94—96°C (lit,[14] 96°C). These 2-pentyl halides were shown to be free of isomers by glpc.

2-Alkyl Tosylates: The tosylates were prepared in the usual fashion[26] by treating the alcohols with freshly-recrystallized *p*-tolueneuslfonyl chloride in dry pyridine. After having been stored in a refrigerator for one day, the mixture was poured onto ice and dilute sulfuric acid, and extracted with methylene chloride. After washing and drying, the solvent was replaced by hexane and the solution was treated with charcoal. The hexane was then removed at reduced pressure, leaving a pale yellow liquid.

Base and Solvent. The solvents were purified by the usual method. The tetraethylammonium fluoride was prepared by a method reported previously.[12]

Elimination Products from Reactions of 2-Alkyl Derivatives. The reactions of 2-alkyl derivatives with Et_4NF in acetonitrile were performed as follows. In a typical case, 2-butyl iodide (1.8 g, 0.01 mol) was treated with 3 g (0.02 mol) of Et_4NF in 30 ml of acetonitrile at 50.0°C. Volatile products were bubbled out of the reaction vessel with a slow nitrogen stream in order to minimize the isomerization of the olefins. The products were then collected at −76°C in a cold trap containing a few milliliters of dimethylformamide and were then analyzed by glpc. Gas-liquid partition chromatographic analyses were performed with a Yanagimoto GCG-5DH instrument. Activated alumina was used as the solid support; the three isomers of butene or pentene were thus successfully separated at an ambient temperature on a 6 m×3 mm dimethylformamide column (40%).

The author is indebted to Professor Aritsune Kaji for helpful discussions. Special thanks are due to Dr. Jun-ichi Hayami who has always encouraged the author and also has given him invaluable suggestions and advices to this work.

21) R. A. Bartsch, *Tetrahedron Lett.*, **1970**, 297.

22) Bartsch has recently found the same trend in several dipolar aprotic solvents, high *trans*/*cis* ratios of 3.0—4.0, which are independent of the percentage of 1-olefin, but no reasonable explanation of it has been found (R. A. Bartsch, private communication).

23) D. G. Coe, S. R. Landauer, and H. N. Rydon, *J. Chem. Soc.*, **1954**, 2281.

24) H. C. Brown and O. H. Wheeler, *J. Amer. Chem. Soc.*, **78**, 2199 (1956).

25) F. C. Whitmore and F. A. Karnatz, *ibid.*, **60**, 2536 (1938).

26) R. S. Tipson, *J. Org. Chem.*, **9**, 235 (1944).

Peptide Synthesis by Oxidation-Reduction Condensation. II.[1] The Use of Disulfide as an Oxidant

Rei MATSUEDA, Hiroshi MARUYAMA, Masaaki UEKI, and Teruaki MUKAIYAMA
Laboratory of Organic Chemistry, Tokyo Institute of Technology, Ookayama, Meguro-ku, Tokyo
(Received October 23, 1970)

A peptide synthesis starting from free *N*-protected amino acid and free amino acid ester by the use of triphenylphosphine, an oxygen acceptor, and disulfide, a hydrogen acceptor, was studied. The oxidation-reduction condensation reaction affords peptides with high optical purity in excellent yields by simple procedure.

In the preceding report,[2] it was shown that *N*-*o*-nitrophenylsulfenyl(NPS)-amino acid, in which NPS group is generally known as a protecting group of amino component in peptide synthesis, affords a new peptide linkage by one step procedure when it was treated with triphenylphosphine and carboxyl component. During this peptide forming reaction, phosphine is used as an oxygen acceptor and sulfenyl group of the amide is reduced to accept a hydrogen.

In the present experiment, a direct peptide synthesis by the oxidation-reduction condensation starting from free *N*-protected amino acid and free amino acid ester was tried by the use of disulfide as an oxidant.

In the model reaction of carboxamide formation, *N*-*n*-butylhexanamide was obtained in 62% yield from hexanoic acid and *n*-butylamine by the use of *p*,*p*′-dichlorodiphenyl disulfide as an oxidant and cupric chloride as a mercaptan scavenger according to the following equation.

$$n\text{-}C_5H_{11}COOH + n\text{-}C_4H_9NH_2 + Ph_3P + (p\text{-}ClC_6H_4S)_2 + CuCl_2 + 2Et_3N \xrightarrow[\text{in } CH_2Cl_2]{\text{room temp., 3hr}} n\text{-}C_5H_{11}CONH(n\text{-}C_4H_9) + Ph_3P{=}O + (p\text{-}ClC_6H_4S)_2Cu + 2Et_3NH^+Cl^-$$

In this reaction, a small amount (2% yield) of thiohexanoic acid *S*-*p*-chlorophenyl ester was isolated along with *N*-*n*-butylhexanamide. The thiolester did not react with *n*-butylamine in methylene chloride when they were allowed to stand for 3 hr, indicating that the thiolester is not an intermediate of this reaction. The result shows that the reaction may proceed through an initial formation of phosphonium salt I, which in turn reacts with carboxylic acid to form the salt II; this subsequently, is transfomed into III, conceivably by way of an internal nucleophilic displacement. The active intermediate of acyloxyphosphonium mercaptide III has two possible pathways of decomposition: namely, (1) the formation of amide by nucleophilic attack of amine on carboxyl carbon and (2) the formation of thiolester by an intramolecular nucleophilic attack of mercapto anion on carboxyl carbon as shown in Scheme 1.

In order to minimize the undesirable formation of thiolester in the above experiment, the effects of various kinds of metal compounds were examined with the assumption that pathway (2) would be skipped when soft metallic compounds are used as mercaptan scavengers. The mercapto anion (soft base) in the intermediate of acyloxyphosphonium salt is expected to react readily with soft metallic cation (soft acid) as predicted by Pearson's principle.[3] Expectedly, the results showed a good agreement with the Pearson's principle and thiolester formation was completely prevented when mercuric chloride and silver chloride were used (see Table 1).

Then, the reaction was applied to peptide synthesis by using mercuric chloride as a metal component. First, the synthesis of benzyloxycarbonyl (Z)-L-phenylalanylglycine ethyl ester which has an optical active amino acid as a carboxyl component was tried and the dipeptide was obtained in 89% yield without racemization.

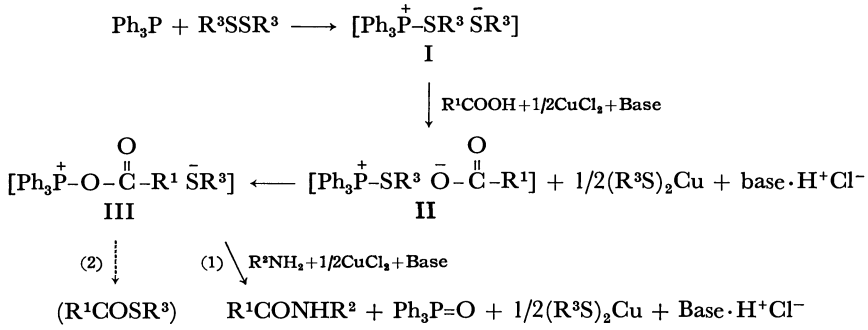

Scheme 1. Reaction pathway for the formation of amide from acid, amine, phosphine, and disulfide in the presence of $CuCl_2$ and base.

1) Preliminary communications: T. Mukaiyama, M. Ueki, H. Maruyama, and R. Matsueda, *J. Amer. Chem. Soc.*, **90**, 4490 (1968); T. Mukaiyama, R. Matsueda, H. Maruyama, and M. Ueki, *ibid.*, **91**, 1554 (1969); T. Mukaiyama, R. Matsueda, and H. Maruyama, This Bulletin, **43**, 1271 (1970).

2) M. Ueki, H. Maruyama, and T. Mukaiyama, Submitted for publication in This Bulletin.

3) R. G. Pearson, *J. Amer. Chem. Soc.*, **84**, 16 (1962); *ibid.*, **85**, 3533 (1963).

TABLE 1. EFFECTS OF METAL COMPONENTS ON THE PREVENTION OF THIOLESTER FORMATION

Metal compound	n-$C_5H_{11}CONH$-(n-C_4H_9) Yield, %	n-$C_5H_{11}COS$-C_6H_4Cl-p Yield, %
AgCl	72	0
$HgCl_2$	66	0
HgCl	62	0
CdI_2	57	0
$HgSO_4$	47	0
$CuCl_2$	62	2
$PdCl_2$	60	3
$PbCl_2$	54	2
$NiCl_2$	42	9
CuCl	43	8
$ZnCl_2$	38	6
$CoCl_2$	23	8

Z-L-Phe-OH + H-Gly-OEt + Ph_3P + (o-$NO_2C_6H_4S)_2$ + $HgCl_2$ + $2Et_3N$ ⟶ Z-L-Phe-Gly-OEt + Ph_3P=O (89% yield) + (o-$NO_2C_6H_4S)_2Hg$ + $2Et_3NH^+Cl^-$

Next, the synthesis of Z-Gly-L-Phe-OEt which has an optical active amino acid as an amino component was tried and the dipeptide was obtained in 91% yield as an oil by column chromatography on silica gel. This oily substance was identified to be an optical pure dipeptide by the subsequent saponification to Z-Gly-L-Phe-OH.

The results show that the peptide forming reaction is applicable for a stepwise elongation of peptide chain.

Next, the racemization was further studied in order to know the applicability of this reaction to the fragment condensation which is very sensitive to racemization.

In the synthesis of peptides, the complete retention of optical activity is an important though rarely achieved goal. Recent work[4] has established that oxazolone is an essential intermediate for the racemization of most of the activated species in the peptide synthesis. In order to check the racemization in the fragment condensation, the above mentioned new reaction was further examined by the Young test[5] (benzoyl(Bz)-L-leucylglycine ethyl ester synthesis) which is known to be the most sensitive racemization test. The authentic samples of the L and DL peptides were synthesized according to Young's report[5] and it was found that the infrared spectra of the two peptides were different to each other as shown in Table 2.

TABLE 2. INFRARED SPECTRA OF L AND DL Bz-Leu-Gly-OEt (KBr pellets)

	L Peptide (cm^{-1})	DL Peptide (cm^{-1})
NH stretching absorption	3300 (singlet)	3275, 3330 (doublet)
	1024 (singlet)	1039, 1024 (doublet)

Since the L peptide was observed to be more soluble in solvent than the DL peptide, the procedure of Young test in this reaction was determined to measure a specific rotation of an unrecrystallized crude product which is isolated by dry column chromatography[6] or a preparative layer chromatography on silica gel. By this procedure, azide method gave the value of $[\alpha]_D^{20}$ −32.6° (c 3.1 EtOH), L-isomer 96%.[5] While the oxidation-reduction condensation reaction carried out in methylene chloride at room temperature gave a poor result as shown in the following equation.

Bz-L-Leu-OH + 3H-Gly-OEt + Ph_3P + (o-$NO_2C_6H_4S)_2$ + $HgCl_2$ ⟶ Bz-Leu-Gly-OEt + Ph_3P=O (76% yield) $[\alpha]_D^{20}$ −7.6° (c 3.1, EtOH), L isomer 22%[6] + (o-$NO_2C_6H_4S)_2Hg$ + $2Cl^-H^+$·H-Gly-OEt

As to the Young test, the racemization intermediate is known to be 4-isobutyl-2-phenyloxazolone whose formation is catalyzed by bases.[7] A base-catalyzed enolization mechanism which involves two proton abstraction steps from the amide hydrogen and from the oxazolone hydrogen was also reported by Kemp and his associates.[8]

In the above reaction, hydrochloric acid is produced along with the peptide by the reaction of the supposed key intermediate of acyloxyphosphonium salt, ($Ph_3\overset{+}{P}$-O-COR^1) $\bar{S}$R^2, ethyl glycinate and mercuric chloride. Therefore, tertiary amine must be used in order to scavenge hydrochloric acid produced at the same time.

In order to eliminate the basic substances as tertiary amine from the reaction system, the reactions were tried by using various kinds of organo-mercuric compounds. These mercuric compounds were classified into two groups through the mercuric mercaptide formation reaction: class a) mercuric salts of urea, succinimide, p-nitrophenol, *etc.* which yield mercuric mercaptide by the reference anion exchange of the phosphonium mercaptide, ($Ph_3\overset{+}{P}$-SR) $\bar{S}$R, with mercuric compounds; class b) di-p-methoxyphenylmercury and p-methoxyphenylmercuric bromide which yield mercuric mercaptide through the protonation of mercaptan to mercuric compounds, but not by the reference anion exchange. The results of the Young test by employing class a) compounds are shown in Table 3.

In these cases, the acyloxyphosphonium mercaptide readily reacts with the metal compounds (MX) to produce metal mercaptides and the second acyloxy phosphonium salts, ($Ph_3\overset{+}{P}$-O-COR^1)X$^-$, by the reference anion exchange. The X$^-$ anion involved in the salt would be expected to have a significant effect on racemization and in accordance with this expectation, the optical purity increased as the X$^-$ anion stability

4) M. Goodman and K. C. Steuben, *J. Org. Chem.*, **27**, 3409 (1962); M. Goodman and L. Levine, *J. Amer. Chem. Soc.*, **86**, 2918 (1964); M. W. Williams and G. T. Young, *J. Chem. Soc.*, **1964**, 3701.

5) M. W. Williams and G. T. Young, *ibid.*, **1963**, 881. L-Isomer % was calcualted from Young's equation ($[\alpha]_D/-34\times 100$).

6) B. Loev and K. M. Snaper, *Chem. Ind.* (London), **1965**, 15; B. Loev and M. M. Goodman, *ibid.*, **1967**, 2026.

7) M. W. Williams and G. T. Young, *J. Chem. Soc.*, **1964**, 3701.

8) D. S. Kemp and S. W. Chien, *J. Amer. Chem. Soc.*, **89**, 2746 (1967).

Table 3. The Young test by the use of class a) compounds

Metal compounds MX_2	pK_a value of HX	Additives	$(RS)_2$	Crude Bz-Leu-Gly-OEt	
				Yield, %	L isomer, %
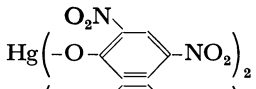	4.0	—	(p-$ClC_6H_4S)_2$	92	73
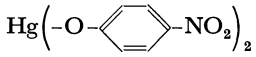	7.2	—	(p-$ClC_6H_4S)_2$	82	51
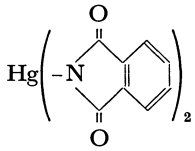	8.3	—	(p-$ClC_6H_4S)_2$	85	47
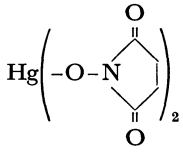	9.4	—	(p-$ClC_6H_4S)_2$	89	59
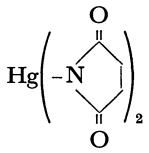	9.5	—	(p-$ClC_6H_4S)_2$	91	46
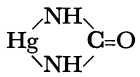	13.8	—	(p-$ClC_6H_4S)_2$	81	23
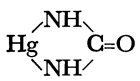	13.8	Pivalic acid (pKa 5.0)	(p-$ClC_6H_4S)_2$	76	60
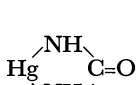	13.8	(pKa 9.4)	(p-$ClC_6H_4S)_2$	89	92

Table 4. The young test by the use of class b) compounds

Metal compounds MX_2	$(RS)_2$	Reaction Period, day	Crude Bz-Leu-Gly-OEt		
			Yield, %	$[\alpha]_D^{20}$ (c 3.1 EtOH)	L isomer, %
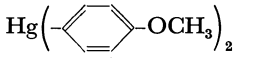	(p-$ClC_6H_4S)_2$	3	88	−30.5°	90
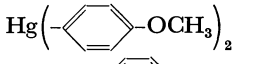	(o-$O_2NC_6H_4S)_2$	2	92	−32.4°	95
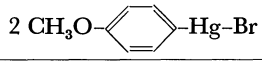	(o-$O_2NC_6H_4S)_2$	2	92	−32.0°	94

increased except in the case of *N*-hydroxysuccinimide. To investigate the characteristic effect of *N*-hydroxysuccinimide which is well known to give a favorable result in the dicyclohexylcarbodiimide method,[9] the reactions using mercuric salt of urea in the presence of acidic substances were studies. *N*-hydroxysuccinimide gave a better result than pivalic acid which has a smaller pK_a value. On the other hand, the more favorable results were obtained s shown in Table 4 when class b) compounds were used.

In these cases, the intermediate, acyloxyphosphonium salt, is attacked only by ethyl glycinate to produce the peptide and mercaptan. The mercaptan is in turn scavenged by the reaction with bis(p-methoxyphenyl)-mercury to yield mercuric mercaptide and anisole as shown in the following Scheme 2.

Since anisole is produced directly through the protonation of mercaptan to the mercuric compound, p-methoxyphenyl anion would not be produced during this mercaptide formation reaction and oxazolone formation can be prevented. The reaction by using bis(p-methoxyphenyl)mercury was further studied in various kinds of solvents and the results are shown in Table 5.

The reaction was found to proceed in all the solvents examined, but a partial racemization was observed in polar solvents as acetonitrile and *N*,*N*-dimethylformamide; while addition of *N*-hydroxysuccinimide also gave an improved result. As described above, peptides with high optical purity are produced in excellent

9) J. E. Zimmerman and G. W. Anderson, *J. Amer. Chem. Soc.*, **89**, 7151 (1967). Special character of preventing racemization of *N*-hydroxysuccinimide is also reported by H. Goodman, *Chem. Eng. News*, **1968**, 40.

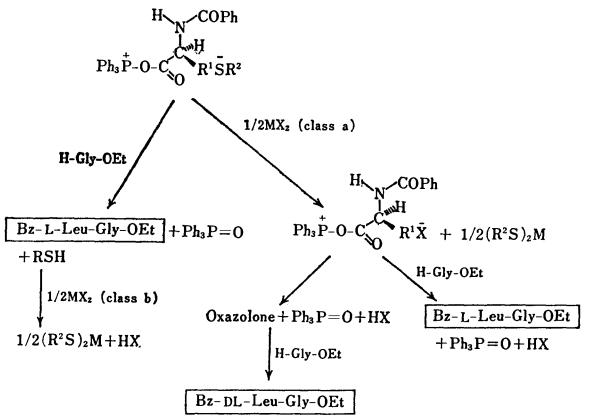

Scheme 2. Reaction pathways for the formation of L-and DL-Bz-Leu-Gly-OEt from Bz-L-Leu-OH, H-Gly-OEt, Ph_3P, and $(o\text{-}NO_2C_6H_4S)_2$ in the presence of either class a) or class b) metallic compound.

TABLE 5. EFFECTS OF SOLVENTS ON RACEMIZATION BY THE YOUNG TEST

Solvent	Dielectric constant	Crude Bz-Leu-Gly-OEt Yield %	L isomer %
Benzene	2.2	91	95
Dioxane	2.3	89	89
$CHCl_3$	4.9	96	96
AcOEt	6.0	94	90
THF[1]	7.0	91	89
CH_2Cl_2	9.9	92	95
$ClCH_2CH_2Cl$	10.5	94	88
DMF[2]	37.0	86	37
CH_3CN	37.5	88	66
CH_3CN + HO-N(succinimide)	37.5	87	86

1) THF: tetrahydrofuran
2) DMF: *N,N*-dimethylformamide

yields in solution by stepwise synthesis but also by the model reaction of fragment condensation (Young test) when mercuric compounds, mercaptan scavenger, are used in this oxidation-reduction condensation.

In recent years, the potential utility of the solid phase method in peptide synthesis has been extended. With respect to this problem, insoluble metal mercaptides, produced at the same time in the above mentioned reaction, seem to be troublesome problem when it is applied to the solid phase method. Then, various kinds of non-metallic mercaptan scavengers were investigated in an attempt to purge the insoluble mercaptide from the reaction system.

First, the reaction was tried by the use of olefins as mercaptan scavengers since some olefins such as 2,3-dihydropyran is known to react readily with cysteine in the presence of Lewis acid,[10] and good results were obtained. When the Young test was carried out in methylene chloride by using 2,3-dihydropyran and zinc chloride as catalyst, Bz-L-Leu-Gly-OEt was obtained in 92% yield, $[\alpha]_D^{20}$ −32.9° (*c* 3.1 EtOH), L-isomer 97%. Good result was also obtained in the case when *n*-butyl vinyl ether is employed (90% yield, L-isomer 95%).

Next, the reaction was further examined by the Young test with sulfenate esters which can behave as both oxidant and mercaptan scavenger (see Table 6).

Bz-L-Leu-OH + H-Gly-OEt + Ph_3P + $2R^1S\text{-}OR^2$
⟶ Bz-L-Leu-Gly-OEt + Ph_3P=O + $(R^1S)_2$ + $2R^2OH$

TABLE 6. THE YOUNG TEST BY THE USE OF SULFENATE ESTERS AS BOTH OXIDANT AND MERCAPTAN SCAVENGER

Sulfenate ester	Crude Bz-Leu-Gly-OEt Yield %	L isomer %
$o\text{-}O_2NC_6H_4SOCH_3$	84	55
$2,4\text{-}(O_2N)_2C_6H_3SO^tBu$	85	78
$2,4\text{-}(O_2N)_2C_6H_3SO^tBu$ + HO-N(succinimide)	84	95

Partial racemization observed in these reactions may be due to the basic character of alkoxy anion of the intermediate phosphonium salt which is produced by the reaction of triphenylphosphine and sulfenate ester, but a favorable result was also obtained in the presence of 1 equivalent of *N*-hydroxysuccinimide.

It is known that some of thiols such as mercaptopyridine, mercaptopurine, *etc.*, which bear a mercapto group α or γ with respect to a ring nitrogen exist in solution predominantly in the thione form.[11] This fact indicates that by employing 2,2′-dipyridyl disulfide as a disulfide component, the peptide forming reaction can be carried out in the absence of a mercaptan scavenger with the consideration that 2-mercaptopyridine produced along with peptide would isomerize to the stable thione form. The reaction by the Young test in methylene chloride was completed within 30 min at room temperature and the peptide was obtained in 91% yield, $[\alpha]_D^{20}$ −32.6° (*c* 3.1 EtOH), L-isomer 96%, according to the following equation.

Bz-L-Leu-OH + H-Gly-OEt + Ph_3P + $\left(\text{N}\!\!\diagup\!\!\diagdown\text{S-}\right)_2$
⟶ Bz-L-Leu-Gly-OEt + Ph_3P=O + 2 N,S-heterocycle (H)

In conclusion, it is noted that peptide with high optical purity is produced in excellent yield from free *N*-protected amino acid, free amino acid ester, phosphine (an oxygen acceptor), and disulfide (a hydrogen acceptor) during oxidation-reduction process.

Experimental

All melting points are uncorrected. Infrared spectra were determined on a Hitachi Model EPI-G2 Spectrophotometer

10) G. F. Holland and L. A. Cohen, *J. Amer. Chem. Soc.*, **80**, 3765 (1958).

11) R. A. Jones and A. R. Katritzky, *J. Chem. Soc.*, **1958**, 3610.

and optical rotation was determined on a Perkin-Elmer Model 141 Polarimeter.

Reagents. Mercuric salts of urea,[12] succinimide and phthalimide, *p*-methoxyphenylmercuric bromide[13] and bis(*p*-methoxyphenyl)mercury[14] were prepared by the literature procedures. Mercuric salt of *N*-hydroxysuccinimide was prepared by the following procedure: A solution of 9.45 g(30 mmol) of mercuric acetate in ethanol (100 m*l*) was added with vigorous stirring to a solution of 6.09 g (60 mmol) of *N*-hydroxysuccinimide in ethanol. The white precipitate was collected by filtration, washed with ethanol and dried, 11.59 g (90%), mp 194—195°C (dec).

Found: C, 22.26; H, 2.18; N, 6.69%. Calcd for $C_8H_8N_2O_6Hg$: C, 22.41; H, 1.88; N, 6.69%. Mercuric salts of *p*-nitrophenol and 2,4-dinitrophenol were prepared by the same procedure in aqueous solution.

Methyl *o*-nitrobenzenesulfenate[15] and *t*-butyl 2,4-dinitrobenzenesulfenate[16] were prepared by the method described in the literature. 2-Mercaptopyridine was prepared by the method in the literature[11] with some modification: A solution of 2-chloropyridine 45.2 g (0.4 mol), thiourea 30.4 g (0.4 mol), and iodine 0.3 g in ethanol (120 m*l*) was refluxed for 6 hr. After cooling, 60 m*l* of concentrated aqueous ammonia (*d* 0.88) was added and the solution was kept standing for 5 days at room temperature. After evaporation of ethanol, the aqueous solution was acidified by acetic acid to pH 3 and extracted with chloroform. The chloroform layer was dried over sodium sulfate and evaporated to dryness. Crude material was recrystallized from benzene to give pure 2-mercaptopyridine, 27.7 g (62%), mp 124—126°C. 2,2′-Dipyridyl disulfide was obtained quantitatively by potassium ferricyanide oxidation of the 2-mercaptopyridine.[17]

Reaction of Hexanoic Acid, n-Butylamine, Triphenylphosphine (IV), and p,p′-Dichlorodiphenyl Disulfide in the Presence of Cupric Chloride and Triethylamine (TEA). To a mixture of hexanoic acid 1.16 g (10 mmol), cupric chloride 1.34 g (10 mmol), and *p,p′*-dichlorodiphenyl disulfide 2.87 g (10 mmol) in methylene chloride (20 m*l*) were added with ice cooling TEA 2.02 g (20 mmol), IV 2.62 g (10 mmol), and *n*-butylamine 0.73 g (10 mmol) in methylene chloride (10 m*l* each) in this order. The resultant solution was stirred for 4 hr at room temperature. After filtration off of the precipitated copper mercaptide, the solution was washed with water, N HCl, water, 5% $NaHCO_3$ solution and water and dried. The solvent was evaporated off and from the residue *N-n*-butylhexanamide was obtained by chromatography on silica gel, 1.06 g (62%), bp 115—118°C (2 mmHg).

Found: C, 69.94; H, 12.25; N, 8.08%. Calcd for $C_{10}H_{21}NO$: C, 70.12; H, 12.36; N, 8.18%. In addition, a small amount of thiohexanoic acid *S-p*-chlorophenyl ester was isolated, 0.05 g (2%), bp 138—140°C (2 mmHg).

Found: C, 59.67; H, 6.18; Cl, 14.52; S, 13.27%. Calcd for $C_{12}H_{15}ClOS$: C, 59.38; H, 6.19; Cl, 14.64; S, 13.20%.

The yields of amide obtained when various kinds of metallic compounds were used in place of cupric chloride in the above reaction are shown in Table 1.

Reaction of Z-L-Phe-OH, H-Gly-OEt, IV, and o,o′-Dinitrodiphenyl Disulfide(V) in the Presence of Mercuric Chloride and TEA. To a stirred mixture of Z-L-Phe-OH 2.99 g (10 mmol), mercuric chloride 2.71 g (10 mmol), and V 3.08 g (10 mmol) in methylene chloride (20 m*l*) was added successively with ice cooling TEA 2.02 g (20 mmol), IV 2.62 g (10 mmol), and H-Gly-OEt 1.03 g (10 mmol) in 10 m*l* each of the same solvent. The resultant mixture was stirred for 3 hr at room temperature and the precipitated mercury mercaptide was filtered off. The filtrate was washed with water, N HCl, water, 5% $NaHCO_3$ solution, water and dried over sodium sulfate. The solvent was evaporated *in vacuo* and from the residue Z-L-Phe-Gly-OEt was obtained by dry column chromatography[6] on silica gel using methylene chloride as solvent, 3.43 g (89%), mp 110—110.5°C, $[\alpha]_D^{20}$ −17.1° (*c* 2 EtOH). [lit,[18] mp 110—113°C, $[\alpha]_D^{25}$ −16.6° (*c* 2 EtOH)].

Found: C, 65.83; H, 6.53; N, 7.42%. Calcd for $C_{21}H_{24}N_2O_5$: C, 65.61; H, 6.29; N, 7.29%.

Reaction of Z-Gly-OH, H-L-Phe-OEt, IV, and V in the Presence of Mercuric Chloride and TEA. Substitution of Z-L-Phe-OH for Z-Gly-OH and H-Gly-OEt for H-L-Phe-OEt in the above reaction gave Z-Gly-L-Phe-OEt in 91% yield as an oil [lit.[19] oil]. This oily material (0.97 g) was saponified by N NaOH in aqueous dioxane by the literature procedure[19] to yield Z-Gly-L-Phe-OH, 0.74 g (83%), mp 125—126°C, $[\alpha]_D^{25}$ 36.2° (*c* 2 acetone). [lit,[18] mp 125—126°C, $[\alpha]_D^{25}$ 37° (*c* 2 acetone)].

Found: C, 64.04; H, 5.64; N, 7.66%. Calcd for $C_{19}H_{20}N_2O_5$: C, 64.03; H, 5.66; N, 7.86%.

The Test for the Racemization in This Type of Reactions by Young's Method.[5] Authentic samples of L- and DL-Bz-Leu-Gly-OEt were prepared by the azide method in the Young's report. Since the solubilities of L and DL peptides were observed to be different to each other, general isolation procedure was determined to be made by dry column chromatography or preparative layer chromatography on silica gel and $[\alpha]_D$ values of crude peptides were determined without recrystallization. By this procedure, Bz-L-Leu-Gly-OEt was obtained in 68% yield, $[\alpha]_D^{20}$ −32.6° (*c* 3.1 EtOH), L-isomer 96%,[5] according to the azide method carried out in ether.

Reaction of Bz-L-Leu-OH, H-Gly-OEt, IV, and V in the Presence of Mercuric Chloride and TEA. To an ice cooled mixture of Bz-L-Leu-OH 2.35 g (10 mmol), V 3.08 g (10 mmol), and mercuric chloride 2.71 g (10 mmol) in methylene chloride (30 m*l*) was added with strirring a solution of IV 2.62 g (10 mmol) and H-Gly-OEt 3.03 g (30 mmol) in 20 m*l* of the same solvent. Stirring was continued for 4 hr at room temperature and the precipitated mercury mercaptide was filtered off. The filtrate was washed with water, N HCl, water, 5% $NaHCO_3$ solution and water, dried and evaporated *in vacuo*. The residue was separated by preparative layer chromatography on silica gel by developing with ethyl ether. Zone corresponding to the peptide was scraped and eluted by methylene chloride and methanol (10:1). The eluate was evaporated to dryness and the residue was dissolved in methylene chloride, washed with water, and dried over sodium sulfate. After evaporation of the solvent, Bz-L-Leu-Gly-OEt was washed with petroleum ether (30—50°C) and collected by filtration, 2.58 g (81%), mp 144—147°C, $[\alpha]_D^{20}$ −7.9° (*c* 3.1 EtOH), L-isomer 23%.

Found: C, 63.99; H, 7.38; N, 8.98%. Calcd for $C_{17}H_{24}N_2O_4$: C, 63.73; H, 7.55; N, 8.74%.

Reactions of Bz-L-Leu-OH, H-Gly-OEt, IV, and V in the Presence of Organomercuric Compounds. (General Procedure) Each 10 mmol of H-Gly-OEt and IV in methylene chloride

12) N. V. Subba Rao and T. R. Seshadri, *Proc. Indian Acad. Sci., Sect. A*, **10**, 1 (1939).
13) F. Challenger and S. A. Miller, *J. Chem. Soc.*, **1938**, 894.
14) A. Michaels and J. Rabinerson, *Ber.*, **23**, 2343 (1890).
15) T. Zincke and F. Farr, *Ann. Chem.*, **391**, 57 (1912).
16) N. Kharasch, D. P. McQuarrie, and C. M. Buess, *J. Amer. Chem. Soc.*, **75**, 2658 (1953).
17) H. Kubota and T. Akita, *Yakugaku Zasshi*, **81**, 5111 (1961).
18) R. W. Young, K. H. Wood, R. T. Joyce, and G. W. Anderson, *J. Amer. Chem. Soc.*, **78**, 2126 (1956).
19) S. Goldschmidt and K. K. Gupta, *Chem. Ber.*, **98**, 2381 (1965).

(20 ml) was added at room temperature to vigorously stirred mixture of equimolar amounts of Bz-L-Leu-OH, V, and organomercuric compound in the same solvent (30 ml). The reaction mixture was stirred for a few hours in the case of class a) compounds, and for a few days in the case of class b) compounds. The peptide was isolated by dry column chromatography or preparative layer chromatography as described above. Results is are shown in Tables 3 and 4.

Reactions of Bz-L-Leu-OH, H-Gly-OEt, IV, and V in the Presence of Olefins. To a mixture of Bz-L-Leu-OH 1.17 g (5 mmol), V 1.54 g (5 mmol), 2,3-dihydropyran 1.68 g (20 mmol), and zinc chloride 0.68 g (5 mmol) in methylene chloride (30 ml) was added with ice cooling a solution of IV 1.31 g (5 mmol) and H-Gly-OEt 0.52 g (5 mmol) in the same solvent. The resultant mixture was stirred for 6 hr at room temperature, washed with 5% $NaHCO_3$ solution and water and dried. After evaporation of the solvent, the residue was chromatographed on silica gel. A fraction eluted by benzene gave *o*-nitrophenyl 2-tetrahydropyranyl sulfide, 2.04 g (85%), mp 60—61°C.

Found: C, 55.50; H, 5.49; N, 5.97; S, 13.58%. Calcd for $C_{11}H_{13}NO_3S$: C, 55.21; H, 5.47; N, 5.86; S, 13.40%. Bz-L-Leu-Gly-OEt was obtained by elution with ether, 1.47 g (92%), $[\alpha]_D^{20}$ −32.9° (*c* 3.1 EtOH), L-isomer 97%.

Substitution of 2,3-dihydropyran for *n*-butyl vinyl ether gave the peptide in 90% yield with 95% L-isomer content.

Reactions of Bz-L-Leu-OH, H-Gly-OEt, IV, and Sulfenate Esters. A solution of H-Gly-OEt (5 mmol) and IV (5 mmol) in methylene chloride was added to a solution of Bz-L-Leu-OH (5 mmol) and sulfenate ester (10 mmol) and the mixture was stirred for a few hours. Work up was done as above and the results are shown in Table 6.

Reaction of Bz-L-Leu-OH, H-Gly-OEt, IV, and 2,2′-Dipyridyl Disulfide. A solution of IV 1.31 g (5 mmol) and H-Gly-OEt 0.52 g (5 mmol) in methylene chloride (20 ml) was added drop by drop at room temperature to a stirred solution of Bz-L-Leu-OH 1.17 g (5 mmol) and 2,2′-dipyridyl disulfide 1.10 g (5 mmol) in the same solvent (30 ml). Stirring was continued for 30 min and the solution was washed with N HCl, water, 5% $NaHCO_3$ solution and water, and dried over sodium sulfate. Work up as mentioned above gave Bz-L-Leu-Gly-OEt, 1.46 g (91%), mp 148—152°C, $[\alpha]_D^{20}$ −32.6° (*c* 3.1 EtOH), L-isomer 96%.

BULLETIN OF THE CHEMICAL SOCIETY OF JAPAN, VOL. 44, 1378—1381 (1971)

Liquid Phase Chlorination of Olefins with Cupric Chloride. III. Effect of Additives and Kinetics

Takashi KOYANO and Osamu WATANABE

Central Research Laboratory, Toa Nenryo Kogyo Co., Oi-machi, Iruma-gun, Saitama

(Received October 23, 1970)

Chlorination of 1-octene with cupric chloride has been investigated in methanol at 110—130°C. The yield of 1,2-dichlorooctane (I) increased by addition of lithium chloride in the reaction mixture, while that of 1-chloro-2-methoxyoctane (II) decreased. Addition of water and cuprous chloride markedly retarded the reaction. The initial rates of formation of I and II could be expressed as $v=k[\text{octene}]_0\,[CuCl_2]_0^{1.6}$ and $v=k[\text{octene}]_0\,[CuCl_2]_0$, respectively. These results can be explained as an initial formation of a complex between olefin and cupric chloride molecule, followed by competitive attack on the complex by chloride ion and methanol. In the less polar reaction media containing more octene, the ratio of I/II increased. This may be ascribed to the steric effect of cupric chloride in the intermediate.

In our previous investigations on the mechanism of chlorination of olefins with cupric chloride in liquid phase, the initial formation of an open-type cationic intermediate by electrophilic addition of cupric chloride to the olefin and the succeeding competitive attacks on the intermediate by the second chlorinating species and the solvent have been suggested.[1,2] However, the nature of this second chlorinating agent has not been clarified and we have continued the study in order to understand the reaction thoroughly. This paper reports the effect of additives on product composition and the kinetic results for the reaction of octene in methanol.

Results

All reactions were carried out by a sealed tube technique. Octene was selected as the olefin because of its relatively low vapor pressure at the reaction condition and convenience in analysis of the products by gas chromatography. The products consised of 1,2-dichlorooctane (I) and 1-chloro-2-methoxyoctane (II). Effects of reaction medium and added lithium chloride on the product composition are shown in Table 1.

The product composition is subject to the influence of cupric chloride concentration and the products ratio I/II decreases as the reaction progresses.[1] This can be predicted from the different rate orders in cupric chloride for the formations of I and II. Therefore, the data should be compared at the same conversion of cupric chloride, when the effects of environment on the products ratio are discussed. The rate of methanolysis of I or II is sufficiently small even in the presence of cupric chloride under the reaction conditions and can be ignored.

1) T. Koyano, This Bulletin, **43**, 1439 (1970).
2) T. Koyano, *ibid.*, **43**, 3501 (1970).

Table 1. Effect of additives

MeOH (vol%)	Octene (vol%)	Solvent (vol%)	LiCl (mol/l)	Time (hr)	Conversion ($CuCl_2$ %)	Products ratio I/II
90	10			1	8.4	1.29
				1.5	11.4	1.16
				2	13.6	1.07
				2.5	15.6	0.96
				3	17.3	0.86
98	2			3	8.9	1.11
95	5			3	13.3	0.99
85	15			1.5	13.3	1.17
80	20			1	11.1	1.36
75	25			1	13.6	1.40
90	5	H_2O 5		3	12.4	1.25
90	5	n-C_7H_{16} 5		3	11.5	1.16
90	10		0.1	3	32.8	2.95
			0.2	3	43.4	10.63
			0.4	3	54.7	34.71
			0.6	3	59.5	61.50
0	10	EtOH 90		3	17.1	1.32[a]

$CuCl_2$ 0.20 mol/l, 125°C
a) ratio of dichloride/ethoxychloride

Increase of octene content in the reaction solution increased the portion of I in the products. However, the conversion was not increased linearly in proportion to the octene content, probably due to marked retardation effect of cuprous chloride formed as well as to instability of the intermediate cationic complex in less polar media. Partial replacement of octene by heptane reduces the rate but the ratio I/II is the same as that in the case of octene without heptane. Thus, the effect of octene except for the action as a reactant resembles that of heptane, which means that it seems to be related to polarity of the solution.

Addition of water retarded the reaction. In discussing the product composition of this case, a possibility of nucleophilic attack of water may also have to be taken into account, although no apparent peaks of hydroxylic compounds were observed in the gas chromatogram and no hydroxylic products have been reported in the reactions with styrene in the presence of hydrated or added water.[3-5]

A comparatively large I/II ratio in ethanol solvent reaction can be attributed to its low polarity, although steric disadvantage of ethanol as an attacking agent at the reaction center should also be duly considered. It should be noted that steric inhibition is not important in the chlorination of ethylene.[6]

When lithium chloride was added in the reaction system, both the conversion of cupric chloride and the ratio I/II increased considerably with the amount of the salt. It is noteworthy that, in contrast to the striking increase in yield of I, that of II decreased; *i.e.*, on additions of lithium chloride in 0, 0.1, 0.2, 0.4, and 0.6 mol/l, the yields of II were 9.3, 8.3, 3.7, 1.5, and 1.0% on the basis of cupric chloride.

The reaction was followed by titrating cuprous chloride formed. Since the reaction was inhibited significantly by the presence of cuprous chloride, the rates were expressed by initial rates in order to avoid complication as made by Walling[7] and Uemura *et al.*[5] The results are given in Table 2.

Table 2. Rate of reaction

Temp. (°C)	Octene (mol/l)	$CuCl_2$ (mol/l)	Additive (mol/l)	$v_1 \times 10^6$	$v_2 \times 10^6$
110	0.200	0.305		0.44	0.23
		0.500		0.92	0.36
		0.692		1.54	0.53
120	0.191	0.085		0.09	0.13
		0.100		0.13	0.16
		0.202		0.44	0.34
		0.497		1.79	0.80
		0.619		2.78	1.11
	0.212	0.195	n-C_8H_{18} 0.394	0.40	0.28
	0.401	0.195	n-C_8H_{18} 0.200	0.68	0.51
	0.600	0.195		1.02	0.77
	0.597	0.256		1.36	0.80
		0.325	CuCl 0.063	0.28	0.84
		0.325	CuCl 0.063	0.82	0.94
			LiCl 0.061		
		0.323		1.78	0.98
125	0.204	0.119		0.35	0.41
		0.201		0.80	0.71
		0.484		3.28	1.58
130	0.204	0.110		0.61	0.74
		0.208		1.81	1.27
		0.480		6.17	2.48
		0.658		9.72	3.58

v_1: initial rate of formation of I (mol/l sec)
v_2: initial rate of formation of II (mol/l sec)

In changing octene concentration, a suitable amount of n-octane was added to compensate the change of solvent polarity. The rate of formation of I was approximately 0.9 th order and that of II was 1st order in octene. Hence the initial rates may be expressed by the following equations, where v_1 and v_2 are the initial rates for I and II, respectively, and k_1 and k_2 are the corresponding rate constants.

$$v_1 = k_1[\text{octene}]_0[CuCl_2]_0^m \quad (1)$$

$$v_2 = k_2[\text{octene}]_0[CuCl_2]_0^n \quad (2)$$

Terms concerned with cuprous chloride, water and other additives can be excluded from these equations when these materials are not present in the initial step of reaction. Plots of log v_1 and log v_2 *vs.* log $[CuCl_2]_0$ show straight lines at each temperature. From the slopes of the lines m and n were calculated and the results are summarized in Table 3 together with the corresponding k_1, k_2, and entropies of activation. Energies of activation were calculated to be 29.9 kcal/mol for I and 29.0 kcal/mol for II.

3) K. Ichikawa, S. Uemura, T. Hiramoto, and Y. Takagaki, *Kogyo Kagaku Zasshi*, **71**, 1657 (1968).
4) S. Uemura, T. Hiramoto, Y. Takagaki, and K. Ichikawa, *ibid.*, **72**, 2390 (1969).
5) S. Uemura, Y. Takagaki, and K. Ichikawa, *ibid.*, **72**, 2577 (1969).
6) T. Koyano, K. Kaneko, and O. Watanabe, *ibid.*, **74**, 211 (1971).
7) A. Lorenzini and C. Walling, *J. Org. Chem.*, **32**, 4008 (1967).

TABLE 3. KINETIC RESULTS

Temp. (°C)	m	n	$k_1\times10^5$ (l^m/mol^m·sec)	$k_2\times10^5$ (l/mol·sec)	ΔS_1 (e.u.)	ΔS_2 (e.u.)
110	1.6	1.0	1.32	0.38	−3.3	−8.2
120	1.7	1.1	3.23	0.98	−3.6	−8.2
125	1.6	1.0	5.04	1.55	−3.7	−8.3
130	1.6	0.9	9.29	2.56	−3.4	−8.2

ΔS_1: entropy of activation for formation of I
ΔS_2: entropy of activation for formation of II

Discussion

The decrease in absolute yield of II which took place when lithium chloride was added strongly suggests that the amount of certain active species responsible for formation of II decreased in the reaction mixture. Since the concentration of methanol did not change practically in these instances, another factor, *viz.*, the concentration of cupric chloride molecule integrated over the reaction time, must have decreased. Nevertheless, the yield of I increased. Thus, it should be assumed that the second chlorinating species for I differs from cupric chloride molecule and increases on addition of lithium chloride. Chloride ion might be such a reactive species. If this is true, the reactions are represented by the following rate equations.

$$v_1 = k_1[\text{octene}][CuCl_2][Cl^-] \quad (3)$$

$$v_2 = k_2[\text{octene}][CuCl_2][MeOH] \quad (4)$$

Cupric chloride molecule exists probably as a distorted octahedral complex in methanol solution, and replacement of the coordinating methanol with the olefin is indispensable for initiation of the reaction. However, addition of water decreases the concentration of cupric chloride molecule by substituting chlorine in the complex as a result of its high coordinating power.[8] Water can also substitute the coordinating methanol. Since water is not so readily replaced by an olefin, a much weaker ligand, initial formation of the reaction intermediate complex should be seriously hindered.

$$CuCl_2(MeOH)_4 \overset{\text{olefin}}{\rightleftharpoons} [CuCl_2\cdot\text{olefin}](MeOH)_3 \longrightarrow \text{reaction}$$

$$\uparrow \downarrow H_2O$$

$$[CuCl(H_2O)(MeOH)_4]^+Cl^- \text{ (inactive)}$$

$$CuCl_2(H_2O)(MeOH)_3 \text{ (less active)}$$

When the solution becomes less polar by increasing addition of octene, dissociation of cupric chloride should become less favorable and the concentration of chloride ion smaller. However, experimental results were contrary to those predicted from the chloride ion concentration. Therefore, in these cases, the ratio of k_1 to k_2 must have changed and overshadowed the change of chloride ion concentration.[11] A possible interpretation is that the charge separation between Cl–CuCl is disadvantageous in less polar solvents and Cl–CuCl bond becomes tighter, that is, more bulky around the cationic center in the intermediate complex.

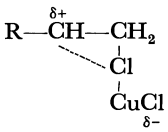

This assumption is in line with the explanation for stereochemical behavior in the chlorination of inner olefins by cupric chloride.[2] Then, the attack of methanol is more restricted than that of chloride ion. The smaller entropy of activation, although the difference was not remarkable, favors the view that the activation complex for the formation of II is more crowded than the one for the formation of I and the attack of methanol is more sensitive to steric factors.

The formation of I was 1.6th order in cupric chloride added while that of II followed 1st order kinetics. The lower rate order for II indicates that major part of II was not formed by methanolysis of I, but directly through a different route. This kinetic observation is another evidence for the competitive reactions.

It is interesting that Uemura *et al.* reported the rate order in chlorination of styrene was 1.8th order in cupric chloride in 1-propanol solution.[5] If the chlorination takes place by the action of one mole of cupric chloride molecule and one mole of chloride ion, the reaction order must be much smaller than 2 in cupric chloride added, $[CuCl_2]_0$. On the other hand, the rate would be approximately proportional to $[CuCl_2]_0^2$, if two moles of cupric chloride molecules participate in the reaction. This may be evident when the concentrations of cupric chloride molecule and chloride ion are expressed in terms of $[CuCl_2]_0$, and Eqs. (3) and (5), are rewritten:[12]

8) According to the spectrochemical series,[9] ligand field splitting increases in the following order. In fact, the order of ligand field strength toward Cu^{2+} has been shown to be EtOH $<$ H_2O[10]

$$Cl^- < ROH < H_2O$$

9) L. E. Orgel, "An Introduction to Transition Metal Chemistry (Ligand Field Theory)," Methuen Co., London (1960), p. 96.

10) N. J. Friedman and R. A. Plane, *Inorg. Chem.*, **2**, 11 (1963).

11) If the formation of I is explained by the attack of 2 moles of cupric chloride molecules, the tendency can be understood by considering the change in concentration of cupric chloride molecule. However, this possibility can be denied for several reasons given in this paper.

12) For the sake of simplification, assume that the dissociation of $CuCl_2$ in methanol is only of the type

$$CuCl_2 \rightleftharpoons CuCl^+ + Cl^-$$

$$K = \frac{[CuCl_2]}{[CuCl^+][Cl^-]}$$

Concentrations of $[Cl^-]$ and $[CuCl_2]$ are calculated to be

$$[Cl^-] = \frac{1}{2K}(\sqrt{4KC_0+1}-1)$$

$$[CuCl_2] = \frac{1}{4K}(\sqrt{4KC_0+1}-1)^2$$

where C_0 is the formal concentration of $CuCl_2$.
Then,

$$v_1' = k'[CuCl_2][Cl^-] = \frac{k'}{8K^2}(\sqrt{4KC_0+1}-1)^3$$

$$v_1'' = k''[CuCl_2]^2 = \frac{k''}{16K^2}(\sqrt{4KC_0+1}-1)^4$$

From the fact that the formation of II is lst order in $[CuCl_2]_0$, $(\sqrt{4KC_0+1}-1)$ could be simplified as $\sqrt{4KC_0}$. Then, we have as first approximation

$$v_1' \propto C_0^{3/2}, \qquad v_1'' \propto C_0^2$$

$$v_1 = k_1'[\text{octene}][CuCl_2]^2 \quad (5)$$

Our results seem to fit the former case. Thus, we presume that the chlorination occurs mostly by attack of chloride ion[13] on the intermediate complex formed between cupric chloride molecule and olefin. Possibility of participation of other anionic species such as $CuCl_3^-$ and $CuCl_4^{2-}$ can not strictly be ruled out. However, such species are supposed to be less nucleophilic because of their anionic charge dispersion over large molecules and also sterically less advantageous as compared to chloride ion. Then, the overall reaction sequence is represented by the following scheme, the second steps being rate-determining.

$$R\text{-}CH{=}CH_2 + CuCl_2 \longrightarrow [\overset{\delta+}{R}CHCH_2Cl \cdots \overset{\delta-}{Cu}Cl]$$

$$\xrightarrow{Cl^-} RCHClCH_2Cl$$

$$\xrightarrow[MeOH]{} RCH(OMe)CH_2Cl$$

Addition of cuprous chloride suppressed the reactions significantly. If all the added cuprous chloride form one to one complexes with cupric chloride[14] and the complexes are inert or at least far less reactive than cupric chloride itself,[7] active cupric chloride concentration would be 0.262 mol l in our experiment. Therefore, v_1 should be larger than that in the case of cupric chloride concentration at 0.256 mol/l. However, v_1 was five times smaller while v_2 was slightly larger than those expected. These results indicate that the main reason for the decrease of v_1 is other than the decrease of cupric chloride molecule. A plausible explanation is that chloride ion plays an important role in the formation of I and the concentration of chloride ion decreased by complex formation with cuprous chloride. Although the complex Cu_2Cl_3 may actually exist in the reaction solution, the predominant cuprous chloride complexes would still be $CuCl_2^-$ and $CuCl_3^{2-}$.[14]

The fact that existence of oxygen is disadvantageous for the formation of dichloride has been interpreted by the same sort of consideration, *i.e.*, the decrease of chloride ion.[6]

Addition of lithium chloride together with cuprous chloride did not compensate the retardation completely. A fairly large portion of lithium chloride seems to exist undissociated in the reaction solution.

Experimental

Materials. 1-Octene (Schuchardt, München) was dried over Na_2SO_4 and distilled under N_2 before use, which was gas-chromatographically pure. Methanol (GR, Koso Chemical Co.) was distilled from $Mg(OMe)_2$ under N_2. Anhydrous cupric chloride and lithium chloride were of GR grade (Koso). Cuprous chloride was prepared by the reduction of cupric chloride with sodium sulfite under N_2[15]. 1,2-Dichlorooctane was prepared by the chlorination of 1-octene with sulfuryl chloride in the presence of benzoyl peroxide[16] (bp 67—68°C/4 mmHg). 1-Chloro-2-methoxyoctane was synthesized by the action of *t*-butyl hypochlorite on 1-octene in methanol.[17]

Analytical Methods. Cupric chloride was determined by iodometry.[1] Cuprous chloride was titrated with 0.1 N ceric ammonium sulfate solution using ferroin as an indicator.[18,19] The reaction products were analyzed by gas chromatography. Conditions (apparatus, column, temperature and carrier gas): (A). Shimadzu GC-4APT, Apiezon L on Chromosorb W, 150°, He; (B). Shimadzu GC-5F, Silicone DC-200 on Diasolid L, 160°, N_2.

Procedure. In each 15 ml sealed tube was placed 10 ml of the prescribed reaction mixture under N_2. After an appropriate period of heating in a constant temperature bath ($\pm$0.05°C) the sealed tube was taken out and cooled in ice-water. The reaction solution was subjected to gas chromatography. All the solution was then poured into 10 ml of 0.1 M ferric ammonium sulfate solution (in 3 M H_2SO_4) and the cuprous ion was titrated with a standard ceric solution. Since the products practically consisted of only I and II, the amount of consumed cupric chloride was divided between I and II in the proportion of the analytical result by gas chromatography, and the amounts of formation were calculated.[20] The rate of reaction was very sensitive to retardation caused by the products. Therefore, the initial rate of formation was conveniently calculated by reading the reaction time at 2% conversion from the time-conversion plot.

Methanolysis of I. A 10 ml solution of I (0.114 mol/l) with $CuCl_2$ (1.0 mol/l) in MeOH was heated at 120°C in a 15 ml glass sealed tube. After 13 hr a trace of II was detected in the solution, and after 19.5 hr 1.6% of I was converted to II.

The authors wish to thank Professor Naoki Inamoto, Dr. Keinosuke Suzuki and Dr. Ken'ichi Takeuchi for valuable discussions and suggestions.

13) or a loosely connected ion pair, *e.g.*, a solvent separated ion pair.

14) H. McConnell and N. Davidson, *J. Amer. Chem. Soc.*, **72**, 3168 (1950).

15) R. N. Keller and H. D. Wycoff, "Inorganic Syntheses," Vol. II, ed. by W. C. Fernelius, McGraw-Hill Book Co., New York (1946), p. 1.

16) M. S. Kharasch and A. F. Zavist, *J. Amer. Chem. Soc.*, **73**, 964 (1951).

17) C. F. Irwin and G. F. Hennion, *ibid.*, **63**, 858 (1941).

18) I. M. Kolthoff and R. Belcher, "Volumetric Analysis," Vol. III, Interscience, New York (1957), p. 121.

19) L. F. Hatch and R. R. Estes, *Ind. Eng. Chem., Anal. Ed.*, **18**, 136 (1946).

20) One mole of either product is assumed to be formed by the consumption of two moles of cupric chloride.

Studies on Reactions of Isoprenoids. XIV.[1] Facile Lactone Formations from 2-*endo*-Cyano-, 2-*endo*-Cyanomethyl-, and 2-*endo*-Carboxymethyl-5-norbornenes

Tadashi SASAKI, Shoji EGUCHI, and Michio SUGIMOTO

Institute of Applied Organic Chemistry, Faculty of Engineering, Nagoya University, Furo-cho, Chikusa-ku, Nagoya

(Received October 29, 1970)

Treatment of 2-*endo*-cyano-5-norbornene (I) with polyphospholic acid (PPA) at 60°C afforded 6-*endo*-hydroxybicyclo[2.2.1]heptane-2-*endo*-carboxylic acid lactone (V) in 40—46% yields, while 2-*endo*-cyanomethyl-5-norbornene (IV) prepared from 2-*endo*-methoxycarbonyl-5-norbornene (II) *via* the corresponding alcohol (III) gave 3-*exo*-hydroxybicyclo[2.2.1]heptane-2-*exo*-acetic acid lactone (VIII) in 25% yield by a similar treatment with PPA. With sulfuric acid, IV gave only intractable polymeric materials. However, under milder conditions using a sulfuric acid-acetic acid mixture, IV afforded 2-*exo*-cyanomethyl- (VI) and 2-*exo*-carbamoylmethyl-6-*exo*-acetoxynorbornane (VII) in 69 and 2% yields, respectively. On the other hand, iodolactonization of the carboxylic acid (IX) derived from IV afforded 5-*exo*-iodo-6-*endo*-hydroxybicyclo[2.2.1]heptane-2-*endo*-acetic acid lactone (X) in 68% yield. The formation of VIII from IV was explained by the successive Wagner-Meerwein rearrangement, 3,2- and 6,2-hydride shifts, followed by cyclization.

Although a number of cyclizations in the 2-*endo*-substituted 5-norbornene (*i.e.*, bicyclo[2.2.1]hept-5-ene) system have been extensively studied recently,[2] no reports seem to have been given on the cyclization reactions under the Ritter reaction conditions. Only a limited number of intramolecular Ritter reactions of acyclic-, monocyclic-, and bicyclic unsaturated nitriles[3] have been reported in contrast to numerous examples of intermolecular reactions.[4] From an interest in the synthesis of cage compounds like adamantane,[5] we investigated the chemical behaviors of 2-*endo*-cyano-5-norbornene (I) and 2-*endo*-cyanomethyl-5-norbornene (IV) under several Ritter reaction conditions,[6] and the iodolactonization of bicyclo[2.2.1]hept-5-enyl-2-*endo*-acetic acid (IX).

Preparation of Starting Materials

Starting nitriles, I and IV, and carboxylic acid IX were prepared by a sequence of reactions summarized in Scheme 1. The Dieles-Alder reaction of acrylonitrile with cyclopentadiene at 160°C produced only a 1:1 mixture of 2-*exo*- and -*endo*-cyano-5-norbornene. The reaction was carried out by mixing acrylonitrile cooled to 0°C with freshly prepared cyclopentadiene trapped at −73°C. The 1:1 adduct thus obtained was confirmed to be the desired 2-*endo*-cyano-5-norbornene (I) on the basis of IR and NMR spectral data, though vpc analysis revealed some (*ca.* 10%) contamination with *exo*-isomer.

The Diels-Alder reaction of methyl acrylate with cyclopentadiene proceeded more stereospecifically under similar conditions and afforded 2-*endo*-methoxycarbonyl-5-norbornene (II) in 79% yield, the vpc analysis of which showed *ca.* 3% contamination of the *exo*-isomer. II could be converted to the corresponding alcohol III by means of lithium aluminum hydride reduction. The tosylate of III was treated with sodium cyanide in dimethyl sulfoxide at 90—95°C to afford 2-*endo*-cyanomethyl-5-norbornene (IV) in 33% overall yield from II. The structure of IV was confirmed by analytical and spectral data. Vpc analysis showed only one peak.

Alkaline hydrolysis of IV afforded the corresponding carboxylic acid IX in 86% yield, and the structure was confirmed by analytical and spectral data.

Results and Discussion

Treatment of I with concd. sulfuric acid (98%, sp. gr., 1.84) under common Ritter reaction conditions[3,6] produced a solid material which was purified by sublimation to give colorless crystals (V), mp 155—157°C, in 41% yield. The IR spectrum (KBr) exhibited a strong absorption band at 1770 cm^{-1} (γ-lactone) but no amide bands. The NMR spectrum ($CDCl_3$) gave signals at τ 5.32 (1H, d, d, J=6.0 and 4.5 Hz, C_{6x}–H),[7] 6.85 (1H, broad t, J=*ca.* 5 Hz, C_{2x}-H), 7.30—7.70 (2H, broad s, C_1–H and C_4–H), 7.90—8.50 (6 H, m, other ring protons), suggesting

1) Part XIII: T. Sasaki, S. Eguchi, and H. Yamada, *J. Org. Chem.*, **36**, No. 6 (1971), in press.

2) a) For halolactonizations, see G. I. Oxer and D. Wege, *Tetrahedron Lett.*, **1969**, 3513 and references cited therein; b) For oxymercurations, see A. Factor and T. G. Traylor, *J. Org. Chem.*, **33**, 2607 (1968) and references cited therein; c) For intramolecular photocycloadditions, see R. R. Sauers and K. W. Kelly, *ibid.*, **35**, 498 (1970); d) For photocyclizations, see P. J. Kroop and H. J. Krauss, *J. Amer. Chem. Soc.*, **91**, 7466 (1969); e) For carbene and nitrene additions, see A. Nickon, H. Kwasnik, T. Swartz, R. O. Williams, and J. B. DiGiorgio, *ibid.*, **87**, 1615 (1965); I. Brown, O. E. Edwards, J. M. McIntosh, and D. Vocelle, *Can. J. Chem.*, **47**, 2751 (1969).

3) For the Ritter reaction of bicyclo[3.3.1]non-6-ene-3-carbonitrile, see J. G. Korsloot and V. G. Keizer, *Tetrahedron Lett.*, **1969**, 3517.

4) For a recent review, *cf.* L. I. Krimen and D. J. Cota, "Organic Reactions," Vol. 17, John Wiley and Sons, Inc., New York, N. Y. (1969), pp. 213—325.

5) For example, T. Sasaki, S. Eguchi, and T. Toru, *Chem. Commun.*, **1970**, 1239, and preceeding papers.

6) For the Ritter reaction of camphene which afforded the corresponding products after the Wagner-Meerwein rearrangement of the ring system, *cf.* T. Sasaki, S. Eguchi, and T. Oyobe, This Bulletin, **43**, 1252 (1970).

7) The subscripts x and n refer to *exo*-and *endo*-configurations, respectively.

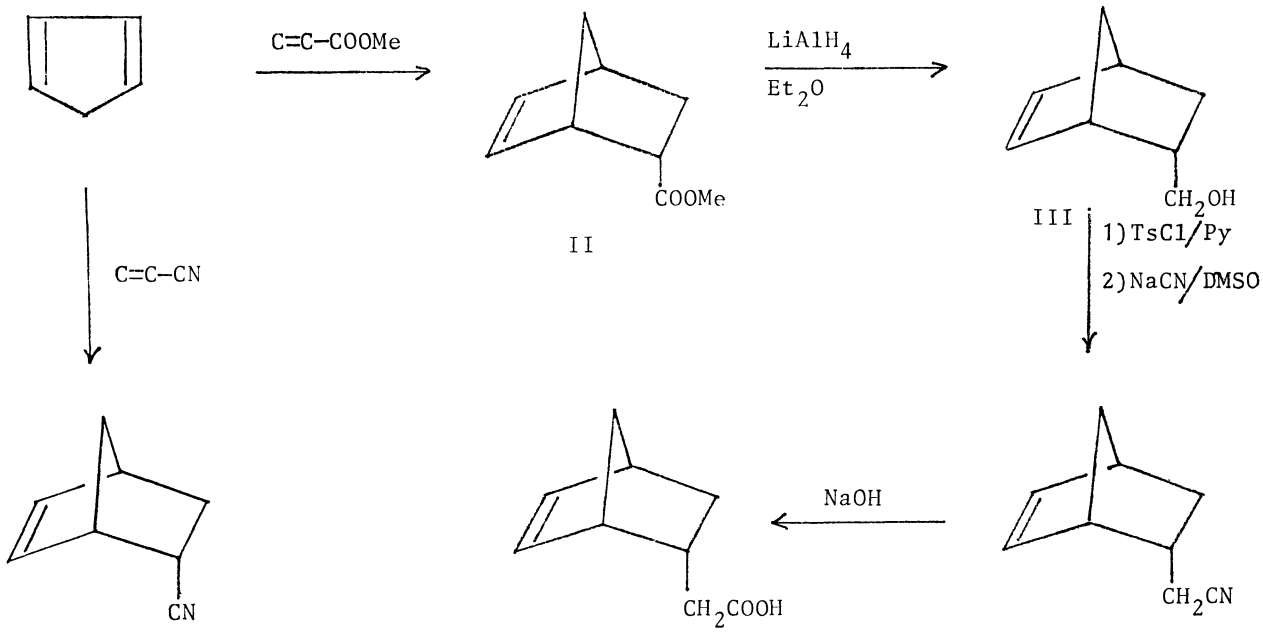

Scheme 1

V to be 6-*endo*-hydroxybicyclo[2.2.1]heptane-2-*endo*-carboxylic acid lactone. The assignment was confirmed by means of mixed melting point determination and complete superimposable IR spectrum with an authentic sample.[8]

Since no intramolecular Ritter reaction products were obtained under the above conditions, PPA was used instead of sulfuric acid. When I was stirred into about 5 times excess PPA (*ca.* 85%), an exothermic reaction took place and the mixture raised the temperature up to *ca.* 60°C, at which temperature the stirring was continued for a day. The product was taken up in chloroform after dilution with water. Chromatography on a silica gel column afforded a semisolid which was purified by sublimation to give the γ-lactone V in 46% yield, together with oily products in *ca.* 10% yield which was still a mixture of at least two compounds as confirmed by tlc and IR (neat) spectrum (γ_{max} 1730 and 1705 cm^{-1}). Further purification of the oily products was unsuccessful.

The results indicate that the normal intramolecular Ritter reaction of I is not favored and cyclization to C_6-position is preceded by the solvolytic reactions of nitrile. This might be ascribed to the steric remoteness

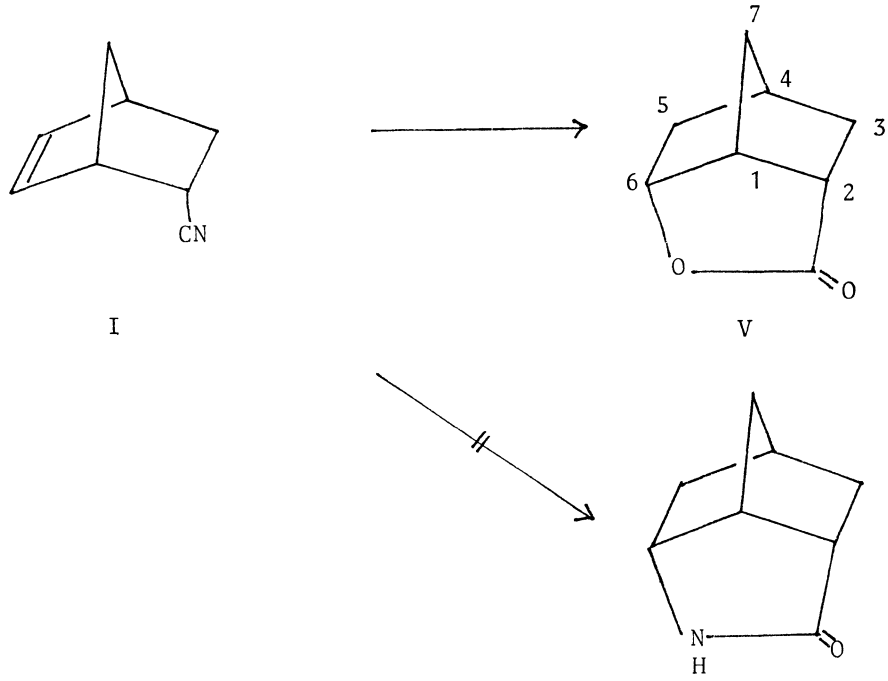

8) S. Beckmann and H. Geiger, *Chem. Ber.*, **94**, 48 (1961).

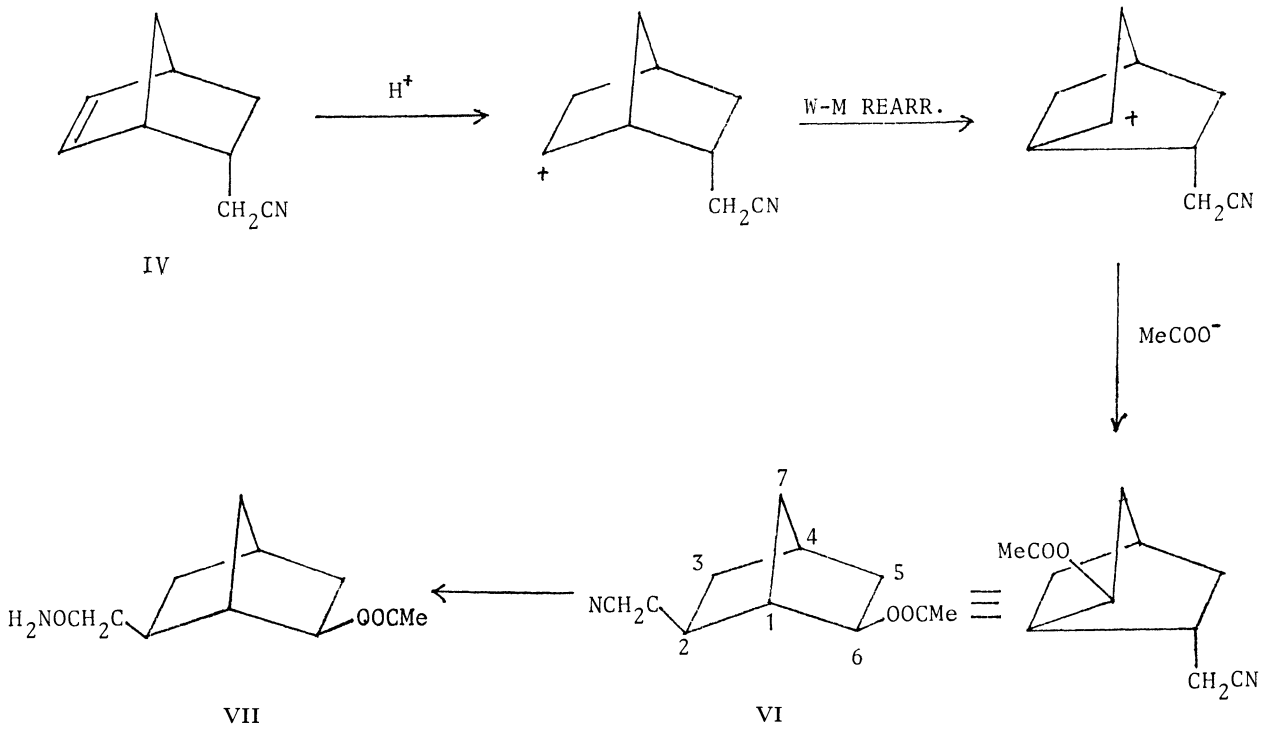

Scheme 2

of the nitrogen atom from C_6-position.

Treatment of 2-*endo*-cyanomethyl-5-norbornene (IV) with concd. sulfuric acid afforded very insoluble polymeric materials, but treatment of IV with a sulfuric acid-acetic acid mixture (1:10 vol/vol) at room temperature gave an oily acetate VI in 69% yield together with a crystalline acetate VII, mp 122—125°C in 2% yield after chromatography on a silica gel column. In the same reaction at 55—60°C, VI and VII were obtained in 13.8 and 44.2% yields, respectively. However, their structures turned out to be 2-*exo*-cyanomethyl- and 2-*exo*-carbamoylmethyl-6-*exo*-acetoxybicyclo[2.2.1]heptane, respectively, on the basis of analytical and spectral data and mechanistic considerations:[9] VI exhibited IR absorption bands (neat) at 2260 ($\nu_{C\equiv N}$), 1720 ($\nu_{C=O}$), 1245, and 1025 (ν_{C-O}) cm^{-1}, and NMR signals ($CDCl_3$) at τ 5.45 (1H, d, d, d, J=6.7, 3.0, and 2.3 Hz, C_{6n}–H), 7.48—7.90 (4H, m, CH_2CN and C_1–H and C_4–H), 8.00 (3 H, s, $OCOCH_3$), and 8.10—9.60 (7 H, m, other ring protons). VII had IR absorption bands (KBr) at 3320, 3180 (ν_{NH}), 1720 ($\nu_{C=O}$), 1245 and 1020 (ν_{C-O}) cm^{-1}, and NMR signals ($CDCl_3$) at τ 3.50—4.35 (2 H, s, disappeared on deuteration, NH_2), 5.20—5.50 (1 H, m, C_{6n}–H), 7.20—8.12 (7 H, m, other ring protons). Although the stereochemistry of both VI and VII was not conclusive from NMR data, we were led to assign their structures as given in Scheme 2 from the well-established Wagner-Meerwein rearrangement proclivity of the system under the employed conditions[9] and from the fact that no lactone or lactam was produced in the above reaction.

When IV was stirred into PPA in about 5 times excess amount, exothermic reaction (temperature rise to *ca.* 60°C) took place. After being kept at 60°C for a day, the mixture was worked up as above to give an oily product which was purified by chromatography. The major product VIII was obtained as an oil in *ca.* 25% yield. VIII exhibited a strong IR absorption band (neat) at 1770 (δ-lactone) cm^{-1}, indicating that VIII is a γ-lactone derivative but not amide or lactam. Microanalysis indicated a molecular formula of $C_9H_{12}O_2$ and the NMR spectrum ($CDCl_3$) gave signals at τ 5.50 (1 H, d, d, d, J=5.5, 2.0 and 1.0 Hz, C_{3n}–H), 6.80—8.06 (5 H, m, other ring protons); appearance of a signal at τ 5.50 excluded the possibility of 1-hydroxybicyclo[2.2.1]heptane-2-*exo*- or -*endo*-acetic acid lactone for VIII. Finally VIII was confirmed to be 3-*exo*-hydroxybicyclo[2.2.1]heptane-2-*exo*-acetic acid lactone. Possibility of the existence of its *endo*-isomer was excluded since the observed coupling constant 5.5 Hz for the signal due to C_3–H was in the range of the generally accepted value[10] for $J_{3n,2n}$ but not for $J_{3x,2x}$ (9—10 Hz) as shown in Fig. 1. The observed signal pattern was also compatible with the expected one from the dihedral angles.

Several other minor products were also produced in the reaction of IV with PPA. However, their purification by chromatography on a silica gel column was unsuccessful.

9) T. G. Traylor, *Accounts Chem. Res.*, **2**, 152 (1969).

10) However, the value should be considered as a guide, since it varies according to substituents as well as to the presence of another ring. For example, V exhibited 6 Hz as $J_{6X,5X}$ which is apparently affected by γ-lactone, *cf.* L. M. Jackman and S. Sternhell, "Applications of Nuclear Magnetic Resonance Spectroscopy in Organic Chemistry," 2nd Ed., in "International Series of Monographs in Organic Chemistry," ed. by D. H. R. Barton and W. Doering, Pergamon Press, New York, N. Y. (1969), p. 289, and references cited therein.

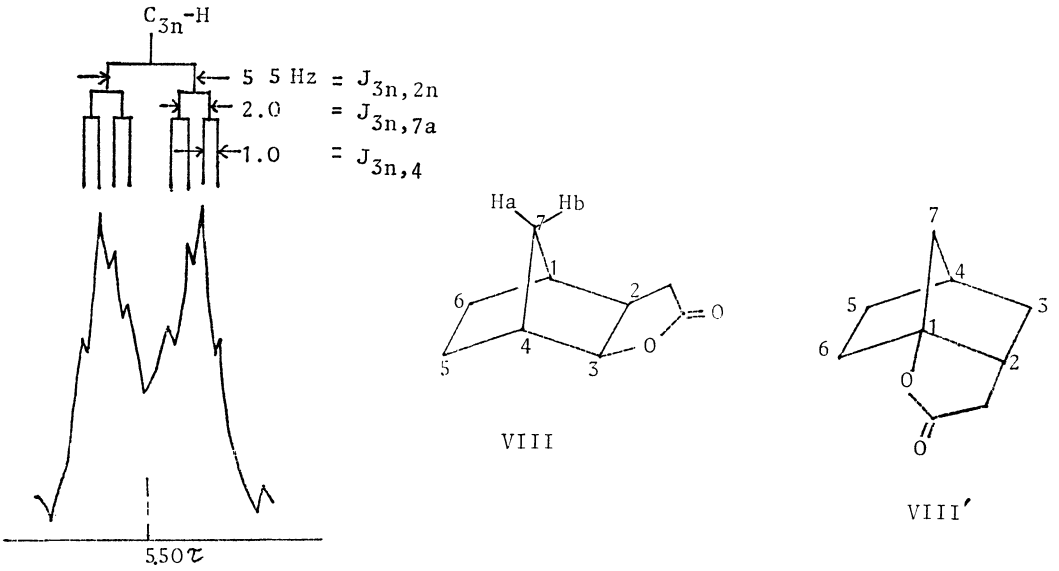

Fig. 1

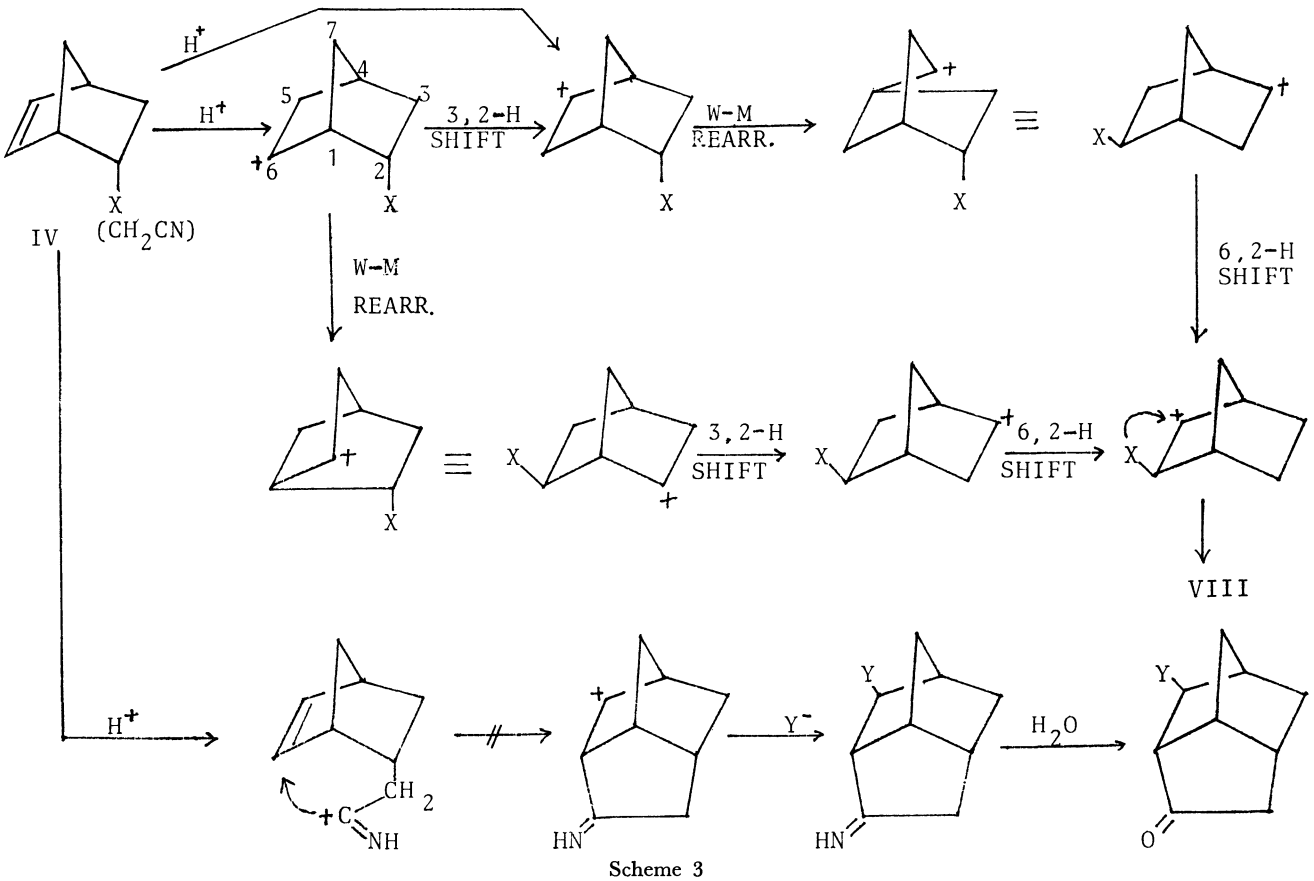

Scheme 3

Formation of VIII from IV could be explained by assuming the reaction paths involving a protonation at C_6 followed by the Wagner-Meerwein rearrangement and a 6,2-H shift, and/or a protonation at C_5 followed by a 3,2-H shift, the Wagner-Meerwein rearrangement and a 6,2-H shift, and/or followed by the Wagner-Meerwein rearrangement, a 3,2-H shift and a 6,2-H shift as explained in Scheme 3. The rearrangement might provide another example of the 6,2-H shift and also the 3,2-H shift in the norbornene ring system in addition to recently reported data.[11]

Iodolactonization of bicyclo[2.2.1]hept-5-ene-2-*endo*-acetic acid (IX), a derived carboxylic acid from IV,

11) *Cf.* C. C. Lee, B-S. Hahn, and L. K. M. Lam, *Tetrahedron Lett.*, **1969**, 3049 and references cited therein, and R. D. Hughes and J. K. Stille, Abst. Paper, The 159th Amer. Chem. Soc. National Meeting (Houston, Texas, Feb., 1970), ORGN 125.

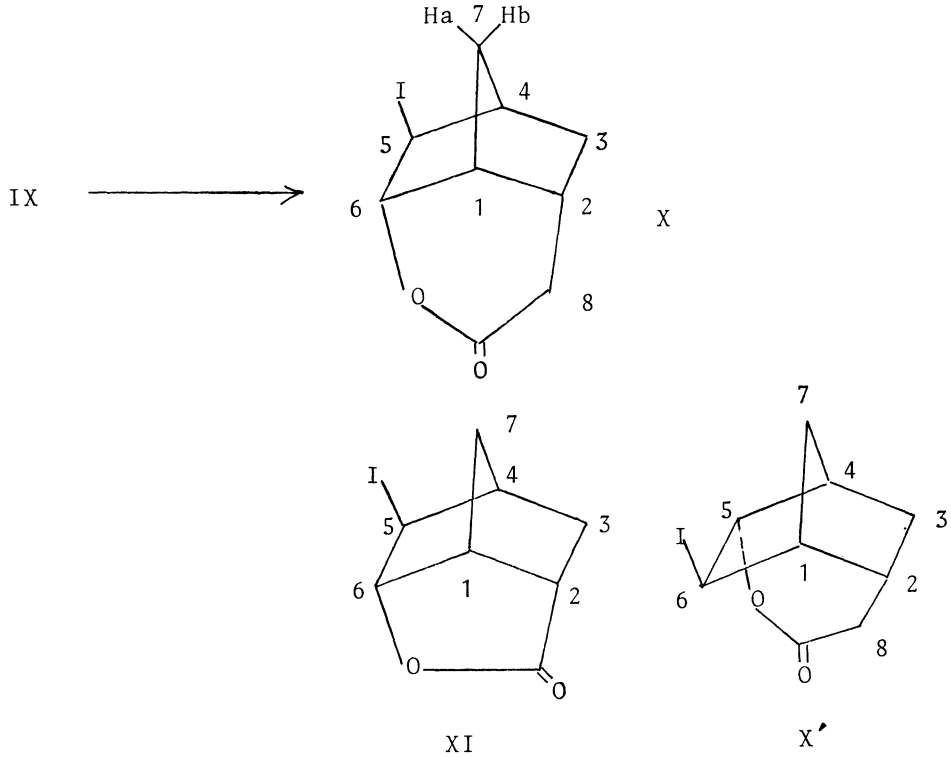

was examined since IV did not produce the corresponding δ-lactone cyclized at C_6-position but afforded a novel γ-lactone (VIII) on treatment with PPA, while I gave a γ-lactone (V) under the same conditions. IX gave crystalline iodolactone X, mp 93—95°C in 68% yield by the standard iodolactonization procedure.[2a] X gave a strong IR absorption band (KBr) at 1737 (δ-lactone) cm^{-1} and NMR signals ($CDCl_3$) at τ 4.75 (1 H, d, m, J=4.5 and *ca.* 1 Hz, C_{6x}–H), 6.22 (1 H, d, d, J=3.0 and 1.5 Hz, C_{5n}–H), 7.20—7.93 (7 H, m, other protons), 8.23 (1 H, d, d, J=10.5 and 3.0 Hz, each peak was further split into m with J=*ca.* 1 Hz, C_{7b}–H), and 8.85 (1 H, d, d, J=11.5 and 2.3 Hz each peak was further split with J=*ca.* 1 Hz, C_{3n}–H). On irradiation of the signal at τ 8.23, the signal at τ 6.22 changed into a doublet with J=1.5 Hz, while the signal at τ 4.75 remained unchanged. Irradiation of the signal at τ 4.75 caused a simplification of the signal at τ 6.22 to a doublet with J=3.0 Hz. From the above spectral data and the analogy of the iodolactonization of bicyclo[2.2.1]hept-5-ene-2-*endo*-carboxylic acid,[2a] the structure of X was assigned to 5-*exo*-iodo-6-*endo*-hydroxybicyclo[2.2.1]heptane-2-*endo*-acetic acid lactone.[12] The chemical shifts and the coupling were very similar to those reported for 5-*exo*-iodo-6-*endo*-hydroxybicyclo[2.2.1]heptane-2-*endo*-carboxylic acid lactone (XI). Only a slight difference is observed between X and XI; X had a larger $J_{5n,6x}$ (1.5 Hz) than XI ($J_{5n,6x}$=*ca.* 0.3 Hz) as was demonstrated by the double resonance experiments.

It should be mentioned that the formation of VIII from IV is the result of the extensive Wagner-Meerwein rearrangement and hydride shifts. No trace of 5-membered ketonic product expected from the Houben-Hoesch type cyclization[4] was found in the reaction of IV (Scheme 3). This also indicates the preference of the above rearrangement and the hydride shifts in this system.

Experimental[13]

2-endo-*Cyano-5-norbornene (I).* Freshly prepared cyclopentadiene collected at *ca.* −73°C was added to an equimolar amount of cooled acrylonitrile (*ca.* 0°C) with stirring. Stirring was continued for one day, keeping the temperature below 0°C for the first several hours, and then at an ambident temperature. The product was distilled under reduced pressure to give I as a colorless oil in 73.6% yield: bp 98—101°C/37 mmHg; n_D^{20} 1.4910 (lit,[14] bp 84—89°C/13 mmHg; n_D^{25} 1.4934); IR (neat) 2260 ($\nu_{C\equiv N}$) cm^{-1}; NMR ($CDCl_3$) τ 3.63 (1, H, d, d, J=6.5 and 3.0 Hz, C_5-H), 3.85 (1 H, d, d, J=6.5 and 3.0 Hz, C_6–H), 6.72 and 6.91 (each 1 H, broad s, C_1–H and C_4–H), 7.15 (1 H, d, d, J=9.0 and 3.0 Hz, each signal was further split with J=*ca.* 0.5 Hz, C_{2x}–H), 7.55—8.20 (2 H, m, C_3-protons), and 8.24—8.82 (2 H, m, C_7-protons).

Found: C, 80.69; H, 7.62; N, 11.69%. Calcd for C_8H_9N: C, 80.63; H, 7.61; N, 11.76%.

Vpc revealed two peaks in *ca.* 9:1 ratio.

2-endo-*Cyanomethyl-5-norbornene (IV).* The Diels-Alder reaction of cyclopentadiene with methyl acrylate under similar

12) Further chemical studies would be necessary for the absolute exclusion of an alternative structure X', though there seem to be no reasons for IX producing the electronically and sterically unfavored product (X') preferentially.

13) All melting points were determined on a Yanagimoto micro-melting point apparatus and are uncorrected. Microanalyses were carried out on a Perkin-Elmer 240 Elemental Analyzer. Infrared spectra were recorded on a JASCO Model IR-S infrared spectrometer and NMR spectra were obtained with a JEOL Model JMN-C-60HL NMR spectrometer using TMS as an internal standard. Vpc analyses were performed on a K-23 Hitachi gas chromatograph.

14) K. Alder, H. Krieger, and H. Weiss, *Ber.*, **88**, 144 (1955).

conditions afforded *ca.* 97% pure 2-*endo*-methoxycarbonyl-5-norbornene (II) in 79% yield as a colorless oil: bp 96—99°C/36 mmHg; n_D^{19} 1.4750 (lit,[14] bp 63.5°C/5.2 mmHg; n_D^{25} 1.4718); the structure was confirmed by IR and NMR data.

Lithium aluminum hydride reduction of II afforded 2-*endo*-hydroxymethyl-5-norbornene (III) in 74.5% yield as an oil: n_D^{19} 1.4988 (lit,[16] n_D^{20} 1.5028).

III was treated with a small excess amount of *p*-toluenesulfonyl chloride in pyridine at room temperature for 1 day. Work-up in the usual way afforded the corresponding tosylate as an oil, n_D^{19} 1.5340, which was treated with an equimolar amount of sodium cyanide in dry dimethyl sulfoxide at 90—95°C for 2 hr. The product was taken in benzene after dilution with water. Removal of the solvent and distillation afforded 2-*endo*-cyanomethyl-5-norbornene (IV) in 33% overall yield from II as a colorless oil: bp 80—82°C/12 mmHg; n_D^{19} 1.4868; IR (neat) 2240 ($\nu_{C\equiv N}$) cm^{-1}; NMR ($CDCl_3$) τ 3.70—4.18 (2 H, complex m, C_5–H and C_6–H), 7.12 (2 H, broad and unsymmetrical s, C_1–H and C_4–H), 7.40—8.85 (6 H, m, other protons), and 9.40 (1 H, d split to m, $J=13.5$ Hz, C_{3n}–H).

Found: C, 81.55; H, 8.24; N, 10.20%. Calcd for $C_9H_{11}N$: C, 81.16; H, 8.33; N, 10.52%.

Vpc showed a single peak.

Treatment of I with Sulfuric Acid. To ice-cooled concd. sulfuric acid (40 m*l*) was added slowly I (14.0 g) with stirring which was continued for 1 day at room temperature. The mixture was poured onto ice-water (*ca.* 400 m*l*) and then extracted with chloroform after neutralization with 10% aq. sodium hydroxide. The combined chloroform extracts were dried (Na_2SO_4) and the solvent was removed to give a yellowish residue which on sublimation at 60—80°C/30 mmHg afforded a colorless solid (6.63 g, 40.7%) of 6-*endo*-hydroxybicyclo[2.2.1]heptane-2-*endo*-carboxylic acid lactone (V), mp 150—153°C. Recrystallization from aq. ethanol raised mp to 155—157°C (lit,[7] 157—158°C).

Treatment of I with PPA. To PPA (*ca.* 25 g) was added I (4.8 g) with stirring. Stirring was continued for several minutes to produce a homogeneous viscous solution (temperature rise to *ca.* 60°C due to heat generation), which was kept at the same temperature for 1 day with occasional stirring. The product was taken in chloroform by extraction after dilution with water and the crude product was purified on a silica gel column eluting with dichloromethane-methanol system. The major product was γ-lactone V (45.8%) and the minor product was a mixture of unidentified amides (*ca.* 10%)

Treatment of IV with Acetic Acid-Sulfuric Acid Mixture. To an ice-cooled mixture of concd. sulfuric acid (0.5 m*l*) and glacial acetic acid (5 m*l*) was added slowly IV (0.5 g) with stirring which was continued for 12 hr at room temperature. The product was taken in chloroform by extraction after dilution of the mixture with water and neutralization with 10% aq. sodium hydroxide. The combined chloroform extracts were dried (Na_2SO_4) and the solvent was removed to give an oily residue (0.76 g) which was chromatographed on a silica gel column eluting with dichloromethane-methanol system. The first fraction afforded 0.51 g (68.9%) of 6-*exo*-acetoxy-2-*exo*-cyanomethylbicyclo[2.2.1]heptane (VI) as an oil, n_D^{17} 1.4816.

Found: C, 68.76; H, 7.81; N, 7.18%. Calcd for $C_{11}H_{15}O_2N$: C, 68.37; H, 7.87; N, 7.25%.

The second fraction gave 0.15 g (2.0%) of 6-*exo*-acetoxy-2-*exo*-carbamoylmethylbicyclo[2.2.1]heptane (VII) as colorless crystals, mp 122—125°C.

Found: C, 62.76; H, 8.13; N, 6.39%. Calcd for $C_{11}H_{17}O_3N$: C, 62.54; H, 8.11; 6.63%.

A similar treatment of IV at 55—60°C for 12 hr and work-up as above gave VI and VII in 13.1 and 44.2% yield, respectively.

Treatment of IV with PPA. A mixture of PPA (*ca.* 7 g) and IV (1.4 g) was stirred manually to give a homogeneous viscous solution (temperature rise to *ca.* 60°C) which was kept at 60°C for 1 day with occasional stirring. The product was taken up in chloroform by extraction after dilution with water. The chloroform extract was dried and evaporated to give an oily residue (1.1 g) which was chromatographed on a silica gel column eluting with dichloromethane-methanol system. The first fraction afforded 0.35 g (25%) of 3-*exo*-hydroxybicyclo[2.2.1]heptane-2-*exo*-acetic acid lactone (VIII) as an oil, n_D^{17} 1.5032.

Found: C, 71.24; H, 7.90%. Calcd for $C_9H_{12}O_2$: C, 71.02; H, 7.95%.

The second fraction was an oil (*ca.* 0.3 g) which was still a mixture of several unidentified products.

Bicyclo[2.2.1]hept-5-ene-2-endo-*acetic Acid (IX).* A mixture of IV (1.5 g) and 20% aq. sodium hydroxide was stirred at room temperature for 1 day to afford a clear solution. The solution was washed once with benzene and neutralized with 10% sulfuric acid, and extracted with benzene (20 m*l*×5). The combined extracts were dried (Na_2SO_4) and evaporated to dryness affording a colorless oil (1.47 g, 85.7%) of IX: n_D^{21} 1.4958; IR (neat) 3000—2500 (ν_{OH}), 1710 ($\nu_{C=O}$), and 1410 (ν_{C-O}, δ_{OH}) cm^{-1}.

Found: C, 71.31; H, 7.86%. Calcd for $C_9H_{12}O_2$: C, 71.62; H, 7.95%.

Iodolactonization of IX. To a solution of IX (0.5 g, 3.3 mmol) in aq. sodium carbonate (*ca.* 3%, 100 m*l*) was added slowly a mixture of iodine (1.3 g, 4.9 mmol) and potassium iodide (1.2 g, 6.9 mmol) in water (50 m*l*) with stirring. After stirring was continued for 5 hr, sodium hydrogen sulfite was added until the decolorization was complete. The mixture was then extracted with chloroform (20 m*l*×5). The combined extracts were washed with 3% aq. sodium bicarbonate and dried (Na_2SO_4). Removal of the solvent and work-up with *n*-hexane gave colorless crystals (0.6 g, 68%) of 5-*exo*-iodo-6-*endo*-hydroxybicyclo[2.2.1]heptane-2-*endo*-acetic acid lactone (X), mp 93—95°C.

Found: C, 38.93; H, 3.93%. Calcd for $C_9H_{11}O_2I$: C, 38.87; H, 3.99%.

The Beilstein test was positive.

The authors wish to thank Miss T. Ikushima for NMR measurements and Mr. M. Okada for elemental analyses.

15) J. D. Roberts, F. R. Trumbull, Jr., W. Bennett, and R. Armstrong, *J. Amer. Chem. Soc.*, **72**, 3116 (1950).

16) K. Alder and E. Windermuth, *Ber.*, **71**, 1939 (1938).

The Synthesis of Methylacetylene by the Pyrolysis of Propylene. VI. The Pyrolysis of Allyl Iodide

Sango KUNICHIKA, Yasumasa SAKAKIBARA,* and Mamoru TANIUCHI

Institute for Chemical Research, Kyoto University, Gokashō, Uji

* *Chemical Laboratory of Textile Fibers, Kyoto University of Industrial Arts and Textile Fibers, Kyoto*

(Received November 6, 1970)

Allyl iodide has been pyrolyzed in a flow system over a wide range of conditions (temperature, 800—1100°C; contact time, $1.44\times10^{-4}-14.0\times10^{-4}$ sec; concentration, 1.8—6.5 mol%; pressure, atmospheric pressure) in order to find suitable conditions for producing methylacetylene and allene and in order to elucidate the reactions of the allyl radical with iodine or the iodine atom at high temperatures. In addition, a study of the mechanism of the pyrolysis of allyl iodide at high temperatures (800—1100°C) has been made. A total yield of allene and methylacetylene of 10 mol per 100 mol of allyl iodide pyrolyzed was obtained under suitable conditions. In the pyrolysis, little cleavage of the C–C bonds of allyl iodide occurred, and propylene, allene, methylacetylene,diallyl, benzene, and an unidentified product were found to be the main products. By means of the zero-conversion method, diallyl alone has been found to be the major product in the early stage of the pyrolysis, while propylene, allene, methylacetylene, and benzene have been found to be the chief products at higher conversions. On the basis of the observed results, a free-radical mechanism has been proposed for the main reactions. It has further been concluded that the pyrolysis is a radical decomposition initiated by the $C_3H_5I \rightarrow C_3H_5\cdot+I$ reaction and that the overall mechanism in the early stage of the pyrolysis may be represented essentially by the $2C_3H_5I \rightarrow C_6H_{10}+I_2$ reaction.

In previous papers, the present authors reported the synthesis of methylacetylene by the pyrolysis of propylene[1] and allyl halides.[2] Since the C–I bond dissociation energy of allyl iodide[3] (43.5 kcal/mol) is considerably lower than that of the α(C–H) of propylene[3] (87.5 kcal/mol), the pyrolysis of allyl iodide may be expected to bring about better results under moderate conditions and to give information about the reactions of the allyl radical with iodine and the iodine atom at high temperatures. It was further found, by the pyrolysis of allyl halides,[2b] that iodine or the iodine atom has a catalytic effect in converting the allyl radical into allene. Therefore, the pyrolysis of allyl iodide was investigated with the aim of producing methylacetylene and allene and elucidating the catalytic action of iodine on the allyl radical.

Although several papers[2b,4-7] have been published on the pyrolysis of allyl iodide, the investigations have been generally concerned with the strength of the C–I bond and have been carried out at low temperatures, except for our own study[2b] and that of Lossing, Ingold, and Henderson.[6] With the exception of our study,[2b] product analyses have been limited and little is known about the decomposition products. Diallyl alone was positively identified in the pyrolysis products; there was no data for the identification of other pyrolysis products. Of course, methylacetylene and allene were not found in the products. The reaction products reported by previous investigators are summarized in Table 1.

TABLE 1. SUMMARY OF PREVIOUS INVESTIGATIONS

	Reference	Temperature range (°C)	Product
4)	Szwarc	a)	diallyl
6)	Lossing, Ingold and Henderson,	750 to 915	diallyl
7)	Benson	a)	C_6H_{10} [b]
2b)	Kunichika, Sakakibara and Taniuchi	800 to 1100	propylene, allene, methylacetylene, diallyl, and benzene

a) No accurate information was obtained about the temperature range of the pyrolysis.

b) Benson says that the C_6H_{10} is undoubtedly cyclohexene or methylcyclopentene.[7]

Butler and Polanyi[5] first studied the pyrolysis of allyl iodide kinetically. From the kinetics of the pyrolysis, Szwarc[4] and Benson[7] proposed a simple radical mechanism involving an initial dissociation of allyl iodide into the iodine atom and the allyl radical. Lossing *et al.*[6] found that the production of the allyl radical appeared to be almost quantitative in the high-temperature pyrolysis of allyl iodide, the only hydrocarbon product of any importance being the dimerization product, diallyl.

The purpose of the present investigation is to determine suitable conditions for the production of methylacetylene and allene by the pyrolysis of allyl iodide, and to obtain data on the distribution of the pyrolysis products. On the basis of the observed experimental results, an effort will be made to clarify the reaction mechanism for the pyrolysis at high temperatures (800—1100°C) and the reactions of the allyl radical with iodine and the iodine atom.

1) a) Y. Sakakibara, This Bulletin, **37**, 1262 (1964); S. Kunichika and Y. Sakakibara, *Bull. Inst. Chem. Res., Kyoto Univ.*, **42**, 270 (1964). b) Y. Sakakibara, This Bulletin, **37**, 1268 (1964). c) S. Kunichika, Y. Sakakibara, and M. Taniuchi, *Bull. Inst. Chem. Res., Kyoto Univ.*, **43**, 469 (1965).

2) S. Kunichika, Y. Sakakibara, and M. Taniuchi, a) This Bulletin, **42**, 1082 (1969); b) *Bull. Inst. Chem. Res., Kyoto Univ.*, **47**, 437 (1969).

3) S. W. Benson, "Thermochemical Kinetics," John Wiley & Sons, Inc., New York·London Sydney (1968), p. 215.

4) M. Szwarc, *Chem. Rev.*, **47**, 75 (1950).

5) E. T. Butler and M. Polanyi, a) *Nature*, **146**, 129 (1940); b) *Trans. Faraday Soc.*, **39**, 19 (1943).

6) F. P. Lossing, K. U. Ingold, and I. H. S. Henderson, *J. Chem. Phys.*, **22**, 621 (1954).

7) S. W. Benson, *ibid.*, **38**, 1945 (1963).

Table 2. Pyrolysis of allyl iodide at various temperatures

Run No.	20	3	18	4	9	17	28	29
Temp., °C	800	800	900	900	1000	1000	1100	1100
Contact time, 10^{-4} sec	3.89	12.3	2.49	6.59	1.81	2.86	1.44	1.60
Composition of reactant gas, mol%								
Nitrogen	95.9	96.5	95.5	96.9	96.3	96.3	97.1	96.7
Allyl iodide	4.1	3.5	4.5	3.1	3.7	3.7	2.9	3.3
Rate of expansion	0.984	0.995	0.994	0.980	0.968	0.995	1.00	1.00
Conversion, %	12.8	27.6	14.5	32.2	15.7	34.8	33.5	37.2
Yield, mol/100 mol of allyl iodide pyrolyzed								
Propylene	14.5	41.4	24.8	41.4	26.9	38.2	38.2	39.9
Allene		4.6	3.7	5.2	5.5	6.8	10.2	9.4
Methylacetylene								
Diallyl	39.4	9.7	26.7	10.8	27.9	9.4	4.5	5.5
Unidentified product		6.4		6.1		7.2	4.6	5.1
Benzene	3.2	5.6	4.6	8.9	6.4	6.4	6.8	7.0
Total yield of methylacetylene and allene		4.6	3.7	5.2	5.5	6.8	10.2	9.4
Percentage of hydrogen and carbon accounted for in products								
Hydrogen	100.0	94.7	91.6	98.2	99.9	92.3	80.4	85.0
Carbon	99.5	89.4	91.0	98.1	101.0	91.0	80.0	84.6

Experimental

Materials. The allyl iodide was prepared from allyl chloride.[8] Bp 101—102°C; n_D^{22}1.5540. Cylinder nitrogen of a 99.9 mol% purity was used as diluent and carrier gas.

Apparatus and Procedure. The apparatus and the technique were essentially the same as had been used previously for the pyrolytical study of allyl chloride,[2a] except for the use of toluene as an absorbent. In order to prevent the reactions of unsaturated hydrocarbon products (especially, allene and methylacetylene) with hydrogen iodide or residual iodine after emergence from the reaction tube, the gaseous effluent, after passage through a water trap, was bubbled through a 200-m*l* portion of an aq. 2 N NaOH solution which had been put in two washing bottles. The alkaline solution was extracted twice with 50-m*l* portions of toluene, and then a portion of the toluene extract was taken up as has been described previously.[2a]

Analysis. The analytical method for the pyrolysis products was essentially the same as that described previously.[2a]

Results

Some of the experimental results are shown in Tables 2 and 3. In the pyrolysis, little cleavage of the C–C bonds of allyl iodide occurred. Consequently, all the decomposition products possessed C_3 and C_6 skeletons derived from the allyl and iodoallyl radicals; the C_1, C_2, and C_4 hydrocarbons were detected in only small amounts. Propylene, allene (A-C_3H_4), methylacetylene (M-C_3H_4), diallyl, benzene, and an unidentified product were found to be the main products. Except for the products mentioned above, no other products, not even hydrogen, were detected in any considerable amount. The kinds of the decomposition products were appreciably fewer than those in the pyrolyses of allyl chloride and bromide.[2b] In addition, larger amounts of propylene and diallyl were obtained, but smaller amounts of benzene were found.

The Effect of the Temperature on the Product Yields. The results obtained in the conversion range from 13 to 16% are shown in Table 2 and Fig. 1. As the temperature was increased, the yield of allene gradually increased to reach 6 mol at 1000°C, and that of propylene increased from 15 mol at 800°C to 27 mol at 1000°C. The yield of diallyl decreased from 39 mol to 28 mol, while that of benzene increased slowly from 3 mol to 6 mol. At a higher conversion range from 27 to 34%, the yield of allene increased from 5 mol at 800°C to 10 mol at 1100°C, while that of propylene decreased from 41 mol to 38 mol. The yield of diallyl

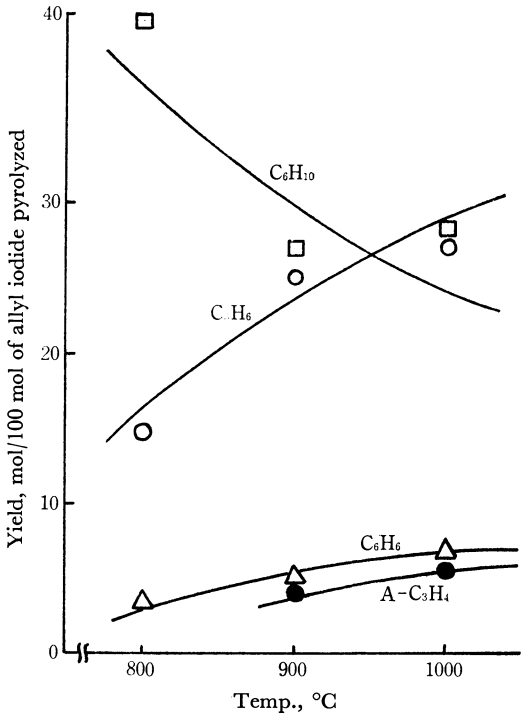

Fig. 1. Effect of temperature on product yields. conversion, 13—16%

8) R. L. Letsinger and J. G. Traynham, *J. Amer. Chem. Soc.*, **70**, 2818 (1948).

TABLE 3. PYROLYSIS OF ALLYL IODIDE AT VARIOUS CONVERSIONS AND CONCENTRATIONS

Run No.	8	13	23	22	14	26	16	25
Temp., °C	1000	1000	1000	1000	1000	1000	1000	1000
Contact time, 10^{-4} sec	1.48	2.24	3.06	3.11	6.95	3.06	2.97	3.18
Composition of reactant gas, mol%								
Nitrogen	97.0	95.5	94.2	96.4	96.3	98.1	96.3	93.5
Allyl iodide	3.0	4.5	5.8	3.6	3.7	1.9	3.7	6.5
Rate of expansion	0.979	0.967	0.984	0.990	0.980	0.994	0.985	0.974
Conversion, %	10.8	21.8	50.2	58.0	68.4	40.2	40.5	40.4
Yield, mol/100 mol of allyl iodide pyrolyzed								
Propylene	21.7	34.5	39.4	43.6	44.4	30.9	39.4	42.0
Allene	3.9	6.3	5.9	9.4	7.1	9.5	6.7	6.7
Methylacetylene			0.8	trace	2.6			
Diallyl	33.3	19.2	2.0	2.0	6.3	5.2	7.1	3.5
Unidentified product			4.3	4.7	4.6	6.6	6.8	6.4
Benzene	4.1	7.1	7.7	6.3	5.7	5.7	5.0	8.4
Total yield of methylacetylene and allene	3.9	6.3	6.7	9.4	9.7	9.5	6.7	6.7
Percentage of hydrogen and carbon accounted for in products								
Hydrogen	100.0	93.3	74.4	80.7	80.5	75.2	86.4	85.5
Carbon	100.0	93.2	74.0	79.0	77.9	75.5	84.0	85.0

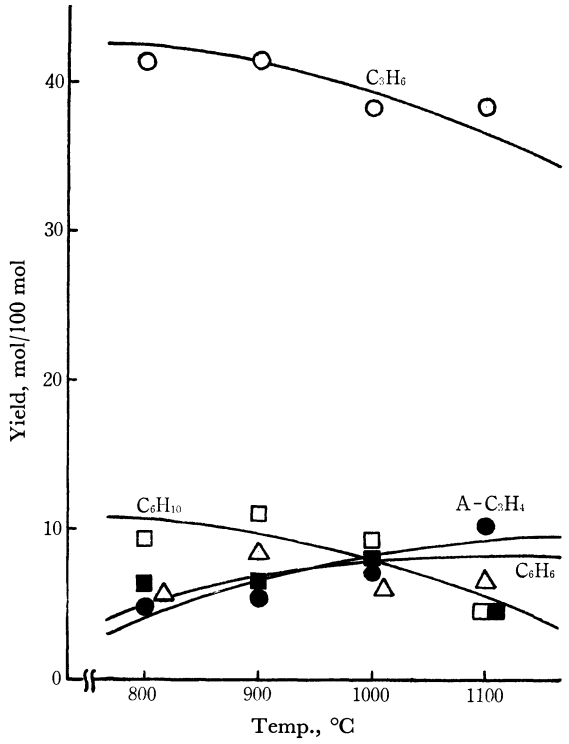

Fig. 2. Effect of temperature on product yields.
conversion, 27—34%
■: unidentified product

decreased from 10 mol to 5 mol. On the contrary, the yield of benzene was almost constant at 7 mol (Fig. 2).

The yield of methylacetylene was very small over the conversion range studied, and so the effect of temperature on its yield could not be examined. The carbon and hydrogen balance became remarkably worse at higher temperatures as a result of the increase in tarry and carbonaceous products (Table 2).

The Relation between the Conversion and the Yields. The results of the pyrolysis at 1000°C are shown in Table 3 and Fig. 3. The total yields of methylacetylene and allene increased with an increase in the conversion, ranging from 4 mol at 10% conversion to 10 mol at 70% conversion. As the conversion was increased, the yield of allene increased from 4 mol at 10% conversion to 7 mol at 70% conversion, while that of methylacetylene increased slowly in the 50—70% conversion range, reaching 2 mol at 70% conversion. The yield of propylene increased from 22 mol

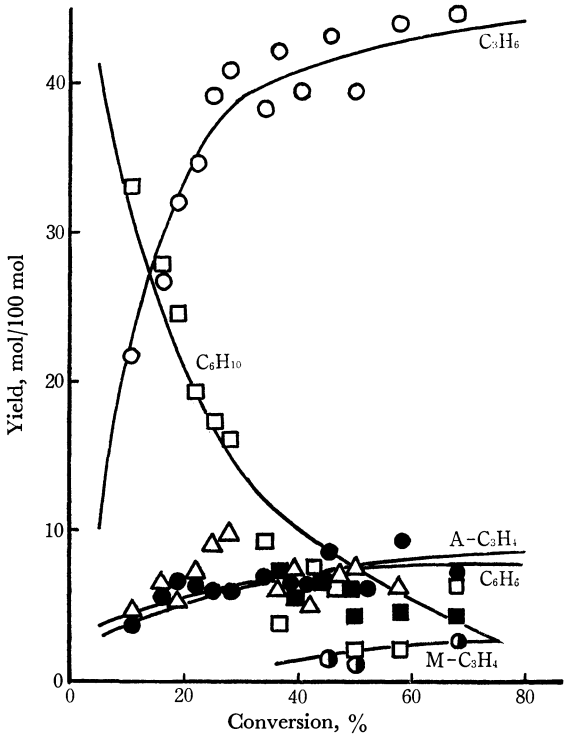

Fig. 3. Relation between conversion and product yields.
temp., 1000°C
■: unidentified product

at 10% conversion to 44 mol at 70% conversion. Although its yield increased rapidly at lower conversions, the increase was much slower at higher conversions (ranging from 30% conversion to 70% conversion). The yield of diallyl, on the other hand, decreased from 33 mol at 10% conversion to 6 mol at 70% conversion. Though its yield decreased quickly at lower conversions, the decrease was much slower at higher conversions. Thus, the tendency of change in diallyl was found to be nearly the reverse of that in propylene. The yield of benzene increased from 4 mol at 10% conversion to 7 mol at 70% conversion. The yield of an unidentified product increased in the 30—70% conversion range, reaching 5 mol at 70% conversion. The amount of tarry and carbonaceous products increased with the increasing conversion to make the material balance remarkably worse, as is described in Table 3. Moreover, it was determined by the zero-conversion method that the major product in the early stage of the pyrolysis was diallyl, as is shown in Fig. 3.

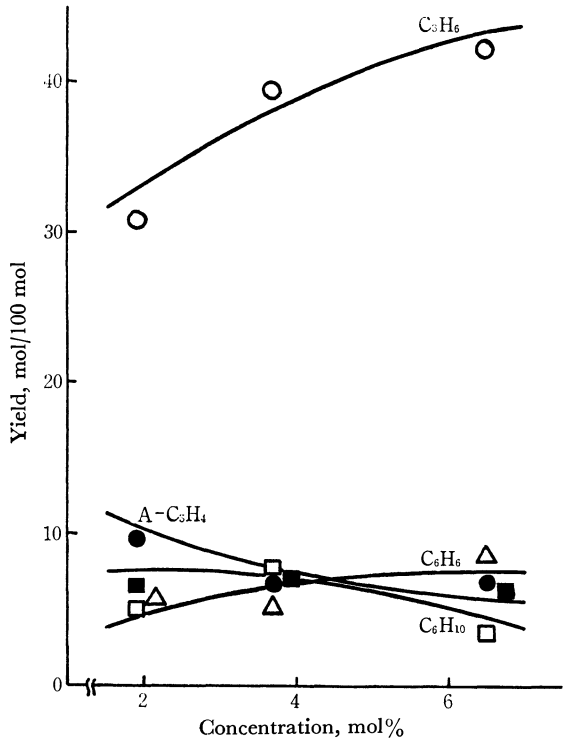

Fig. 4. Effect of concentration on product yields. conversion, *ca.* 40%
■: unidentified product

The Effect of the Concentration on the Yields. The yields of products obtained in a concentration range from 2 to 7 mol% at 1000°C are shown in Fig. 4 (also in Table 3). As the concentration was increased, the yield of propylene gradually increased from 31 mol to 42 mol, while that of allene slowly decreased from 10 mol to 7 mol. The yield of benzene increased from 6 mol to 8 mol, and that of diallyl decreased from 6 mol to 4 mol. The yield of an unidentified product was almost constant at about 6 mol over the concentration range studied.

In closing, it is worthy of special mention that all the decomposition products possess C_3 and C_6 skeletons derived from the allyl and iodoally radicals. It was further found that the amount of propylene was approximately equal to the sum of the amounts of allene, methylacetylene, and four times the amounts of benzene (Fig. 3 and Table 3).

Discussion

Mechanism. On the basis of the experimental results, a mechanism for the pyrolysis of allyl iodide may be proposed. The heats of reaction for the reactions mentioned below are also given when available. The values of the heats of formation of the various materials used in their computation are shown in Table. 4.

Table 4. Heats of formation of gases at 298°K and 1 atm(kcal/mol)

C_3H_5I[9a]	21.5	I_2[9b]	14.9
C_3H_6[9b]	4.9	HI[9c]	6.2
A-C_3H_4[9b]	45.9	I[9b]	25.5
M-C_3H_4[9c]	44.3	C_3H_5·[9b]	40.6
C_6H_{10}[9d]	17.8	H[9b]	52.1

A possible explanation may be offered for the formation of allene and methylacetylene in the pyrolysis of allyl iodide.

$$C_3H_5I \longrightarrow C_3H_5\cdot + I \qquad \Delta H = 44.6 \qquad (1)$$

$$I + C_3H_5I \longrightarrow C_3H_5\cdot + I_2 \qquad \Delta H = 8.5 \qquad (2)$$

$$I + C_3H_5I \longrightarrow HI + \cdot C_3H_4I \qquad (3)$$

$$C_3H_5\cdot + C_3H_5I \rightleftharpoons C_6H_{10} + I \qquad \Delta H = -18.8 \qquad (4)$$

$$C_3H_5\cdot + C_3H_5I \longrightarrow C_3H_6 + \cdot C_3H_4I \qquad (5)$$

$$C_3H_5\cdot + HI \longrightarrow C_3H_6 + I \qquad \Delta H = -16.4 \qquad (6)$$

$$C_3H_5\cdot + I \longrightarrow C_3H_4 + HI \qquad \Delta H = -14.0 \qquad (7)$$

$$C_3H_5\cdot + I_2 \longrightarrow C_3H_4 + HI + I \qquad \Delta H = 22.1 \qquad (8)$$

$$2C_3H_5\cdot \longrightarrow C_6H_{10} \qquad \Delta H = -63.4 \qquad (9)$$

$$2\dot{C}_3H_4I \longrightarrow C_6H_6 + 2HI \qquad (10)$$

$$A\text{-}C_3H_4 + I \longrightarrow M\text{-}C_3H_4 + I \qquad \Delta H = -1.6 \qquad (11)$$

$$2I + M \longrightarrow I_2 + M \qquad \Delta H = -36.1 \qquad (12)$$

Reactions (1) to (12) are the main reactions in the pyrolysis. Reaction (1) is the initiation step, which features the dissociation of allyl iodide into the allyl radical and the iodine atom. All the main products—propylene, allene, diallyl, benzene, and methylacetylene— except for an unidentified product, are formed largely by subsequent reactions— (5) and (6), (7) and (8), (4), and (9), (10), and (11) respectively. As the formation step of allene, the unimolecular decomposition of the allyl radical[1,10] is also considered, but the

9) a) A. S. Rodgers, D. M. Golden, and S. W. Benson, *J. Amer. Chem. Soc.*, **88**, 3194 (1966); b) See Ref. 3, p. 195; c) S. W. Benson, "The Foundations of Chemical Kinetics," McGraw-Hill Book Company, Inc., New York, Toronto, London (1960), p. 662; d) R. J. Akers and J. J. Throssell, *Trans. Faraday Soc.*, **63**, 124 (1967).

10) M. Szwarc, *J. Chem. Phys.*, **17**, 284 (1949); K. J. Laidler and B. W. Wojciechowski, *Proc. Poy. Soc., Ser. A*, **259**, 257 (1960); A. Amano and M. Uchiyama, *J. Phys. Chem.*, **68**, 1133 (1964).

activation energy of Reaction (13) (*ca.* 62 kcal/mol)[2a]

$$C_3H_5\cdot \longrightarrow C_3H_4 + H \qquad (13)$$

is fairly high compared to that of Reaction (1). Therefore, Reaction (13) may be discounted energetically. Thus, two possible alternatives, Reactions (7) and (8), may be considered as the formation reactions of allene. The ΔH value of the overall process for Reaction (8) is *ca.* 22 kcal/mol. Although Reaction (7) should have a high specific rate in view of its exothermicity (*ca.* 14 kcal/mol), Reaction (8) may also be considered in view of the high ratio of molecular iodine to atomic iodine.[11] The pathway of Reaction (8) can probably be written as follows:[12]

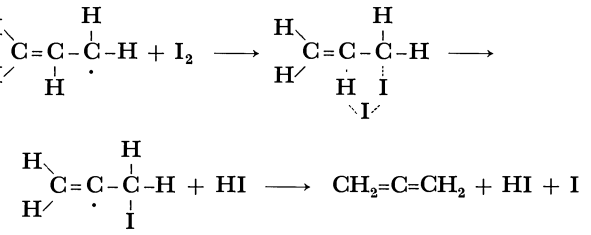

The values of the activation energy for hydrogen abstraction from propane by the allyl radical and the iodine atom have been reported to be *ca.* 25 kcal/mol in both cases.[13] It may, therefore, be presumed that the allyl radical and the iodine atom show almost the same reactivity for hydrogen abstraction. In addition, the corresponding value for an allylic hydrogen in propylene by the iodine atom has been estimated to be 18 kcal/mol.[14] Consequently, assuming that the α (C–H) bond energies of propylene and allyl iodide are essentially the same, it may be considered that an allylic hydrogen in allyl iodide would be abstracted easily by the allyl radical (Reaction (5)) and the iodine atom (Reaction (3)) under the present conditions. Reactions (2) and (3) of the iodine atom with allyl iodide are in competition with each other since, although Reaction (2) is better than Reaction (3) from an energetic point of view, the latter reaction may also play an important role at higher temperatures. Reactions (4) and (5) of the allyl radical with allyl iodide will proceed competitively. In addition, Reactions (4) and (9) involving the allyl radical, leading to diallyl, will be competitive reactions under our reaction conditions.[7] In Reaction (10), benzene would arise *via* the combination and cyclization of two iodoallyl radicals, formed by the α-hydrogen (allylic hydrogen) abstraction of allyl iodide, as in the cases of the other allyl halides.[2,15] The isomerization of allene to methylacetylene (Reaction (11)) would proceed through the same mechanism as the iodine-catalyzed, positional isomerization of butene.[16]

Figure 3 shows that the only major product in the early stage of the pyrolysis is diallyl. Hence, the stoichiometry of the reaction in the early stage is very well represented by the $2C_3H_5I \rightarrow C_6H_{10} + I_2$ reaction. This is fitted to the mechanism proposed by Szwarc[4] and Benson[7] in the pyrolysis of allyl iodide. It can, therefore, be presumed that Reactions (2) and (4) may play an important role in the early stage of the pyrolysis.[4,7] From the relationship between the yield and the conversion (Fig. 3), diallyl in the pyrolyzed gas appears to reach an equilibrium state in the early stage of the pyrolysis and to exist thereafter in an equilibrium concentration. Thus, Reaction (4) is presumed to be an equilibrium.

As the temperature increases (Fig. 1), the yields of propylene and allene increase, while that of diallyl decreases. This may be explained by the following two reasons. First is temperature effect on the reaction rates; generally, subtituent reactions prevail over addition reactions at higher temperatures.[17] Therefore, Reaction (5) would be relatively favored over Reaction (4) with an increase in the temperature. Thus, the yield of propylene increases, while that of diallyl decreases. Second is the temperature effect on the equilibrium constant of Reaction (4); the heat of formation of the forward reaction of Reaction (4) is negative. Consequently, the equilibrium constant of Reaction (4) decreases with an increase in the temperature. This leads to a decrease in the formation of diallyl, while an increase in the formation of propylene and allene results from Reactions (5) and (6), and (7) and (8), respectively, these being reactions consuming allyl radical. In the higher conversion range, from 27 to 34% (Fig. 2), more amounts of iodine and the iodine atom are considered to exist at an equilibrium concentration in the pyrolysis system than is the case with a lower conversion. Thus, the allyl radical formed is apt to be converted into allene through Reactions (7) and (8) in the higher conversion range with an increase in the temperature. Thus, the yield of propylene seemingly decreases, but the total yield of propylene and allene increases with an increase in the temperature.

As the conversion proceeds (Fig. 3), the yields of propylene and allene increase, while that of diallyl decreases. This may be explained by considering Reaction (4) to be a rapid equilibrium reaction; because its equilibrium constant is invariable with respect to the conversion, diallyl becomes the major product in the early stage of the pyrolysis. Thus, after the equilibrium was attained in the early stage of the pyrolysis, the yields of propylene and allene are increased by Reactions (5) and (6), and by Reactions (7) and (8), but that of diallyl decreases.

11) J. W. Mellor, "A Comprehensive Treatise on Inorganic and Theoretical Chemistry," Voll. II, Longmans, Green and Co. Ltd., London, New York, Tronto (1927), p. 49.

12) J. H. Raley, R. D. Mullineaux, and C. W. Bittner, *J. Amer. Chem. Soc.*, **85**, 3174 (1963).

13) a) H. Tominaga, S. Abiko, and T. Kunugi, *Sekiyu Gakkai Shi*, **10**, 190 (1967); b) P. S. Nangia and S. W. Benson, *J. Amer. Chem. Soc.*, **86**, 2773 (1964); J. H. Knox and R. G. Musgrave, *Trans. Faraday Soc.*, **63**, 2201 (1967).

14) D. M. Golden, A. S. Rodgers, and S. W. Benson, *J. Amer. Chem. Soc.*, **88**, 3196 (1966).

15) a) A. Maccoll, *J. Chem. Soc.*, **1955**, 965; b) L. M. Porter and F. F. Rust, *J. Amer. Chem. Soc.*, **78**, 5571 (1956); L. J. Hughes and W. F. Yates, *J. Phys. Chem.*, **64**, 1789 (1960).

16) S. W. Benson and A. N. Bose, *J. Amer. Chem. Soc.*, **85**, 1385 (1963).

17) N. N. Semenoff, "Some Problem in Chemical Kinetics and Reactivity," (translated into Japanese) Vol. I, Moscow (1954), p. 43.

Besides, the amount of propylene is approximately equal to the sum of the amounts of allene, methylacetylene, and four times the amount of benzene, and the amount of hydrogen is very small. These experimental results may be well explained by the mechanism mentioned above.

Assuming that almost all the hydrogen iodide is consumed by Reaction (6), we obtain the following stoichiometric relations:

From Reactions (5), (10) and (6):

$$4C_3H_5\cdot + 2C_3H_5I \longrightarrow 4C_3H_6 + C_6H_6 + 2I$$

Similarly, from Reactions (3), (10), and (6):

$$4C_3H_5\cdot + 2C_3H_5I \longrightarrow 4C_3H_6 + C_6H_6 + 2I$$

From Reactions (7) and (6):

$$2C_3H_5\cdot \longrightarrow C_3H_6 + C_3H_4$$

From Reactions (8) and (6):

$$2C_3H_5\cdot + I_2 \longrightarrow C_3H_6 + C_3H_4 + 2I$$

Therefore, when 1 mol of benzene is formed, 4 mol of propylene is formed. In addition, when 1 mol of allene (methylacetylene) is formed, 1 mol of propylene is formed. The experimental data seem to confirm this (Fig. 3 and Table 3). Thus, it can be concluded that propylene is formed nearly exclusively by Reactions (5) and (6), and that the rate of Reaction (6) is very rapid, since the amount of hydrogen is very small.

As the conversion increases (Fig. 3), the yield of benzene increases, while that of diallyl decreases. As a result, it may be presumed also that benzene will be formed to some extent through diallyl.[7,18] With the increasing conversion, the pyrolysis reaction would become more complex, since the participation of hydrogen abstraction by the allyl radical or the iodine atom in secondary reactions increases remarkably. Consequently, it is difficult to account for the experimental results at higher conversions.

18) R. D. Mullineaux and J. H. Raley, *J. Amer. Chem. Soc.*, **85**, 3178 (1963).

BULLETIN OF THE CHEMICAL SOCIETY OF JAPAN, VOL. 44, 1393—1399 (1971)

Studies of the Thiocarbonyl Compounds. III. The Mechanism of the Thermal Rearrangement of Aryl Thionocarboxylates[1)]

Aritsune KAJI, Yoshiaki ARAKI, and Koshin MIYAZAKI*

Department of Chemistry, Faculty of Science, Kyoto University, Sakyo-ku, Kyoto

* *Chemical Research Laboratory, Nippon Soda Co., Ltd., Kōzu, Odawara-shi, Kanagawa*

(Received November 17, 1970)

The thermal rearrangement of aryl thionocarboxylates was kinetically investigated in diphenyl ether. The rate constants of the rearrangement of aryl *N,N*-dimethylthionocarbamates were well correlated with the σ^- values, but the plots of the electron-releasing *para*-substituents deviated slightly on the lower side of the *meta* correlation line. A good linear free-energy relationship existed between the rearrangement of aryl *N,N*-dimethylthionocarbamates and the bimolecular nucleophilic reaction of 4- or 5-substituted 1-chloro-2-nitrobenzenes with piperidine. By the use of the substituent constants obtained from the latter reaction for the electron-releasing *para*-substituent constants, a fairly good ρ-σ^- relationship was obtained. Linear free-energy relationships also existed between the rearrangements of aryl *N,N*-dimethylthionocarbamates and aryl thionobenzoates, and between the rearrangements of aryl *N,N*-dimethylthionocarbamates and *O*-aryl *S*-phenyl dithiocarbonates. The order of the reaction constants was in accord with that of the inductive effects of the α-substituents of the thiocarbonyl group, so the electron-releasing conjugative effects of the α-substituents of the thiocarbonyl group did not play important roles in the rate-determining step. The present results indicate that the thermal rearrangement of aryl thionocarboxylates is an intramolecular S_N–Ar which involves a four-membered cyclic transition state formed by a nucleophilic attack of the lone-pair electrons of the thiocarbonyl sulfur atom on the migrating aromatic ring.

Since Schönberg and his co-workers reported the thermal rearrangement of diaryl thionocarbonates (I) to diaryl thiolcarbonates (II)[2,3)] (the so-called Schönberg rearrangement), a number of thermal rearrangements have been reported regarding the intramolecular 1,3 aryl migration from oxygen to sulfur. Tarbell and his co-workers reported that the Schönberg rearrangement proceeds by a nucleophilic attack of the thiocarbonyl sulfur atom on the aromatic ring, with a four-membered cyclic transition state.[4,5)]

Recently we reported the rearrangement of *O,S*-diaryl dithiocarbonates (III) to *S,S*-diaryl dithiocarbonates (IV)[6)] and the rearrangement of aryl thionobenzoates (V) to aryl thiolbenzoates (VI).[7)] These rearrange-

1) Presented at the 23rd Annual Meeting of the Chemical Society of Japan, Tokyo, April, 1970.

2) A. Schönberg and L. Vargha, *Ber.*, **63**, 178 (1930).

3) A. Schönberg, L. Vargha, and W. Paul, *Ann. Chem.*, **483**, 107 (1930).

4) H. R. Al-Kazimi, D. S. Tarbell, and D. Plant, *J. Amer. Chem. Soc.*, **77**, 2479 (1955).

5) D. H. Powers and D. S. Tarbell, *ibid.*, **78**, 70 (1956).

6) Y. Araki, This Bulletin, **43**, 252 (1970).

7) Y. Araki and A. Kaji, *ibid.*, **43**, 3214 (1970).

ments are facilitated by an electron-withdrawing group on the migrating aromatic ring and proceed *via* a four-membered cyclic transition state through the intramolecular nucleophilic attack of the thiocarbonyl sulfur atom on the migrating aromatic ring. Since a good linear free-energy relationship exists between these rearrangements, the existence of hetero-atoms directly bound to the thiocarbonyl group is not essential for the rearrangements with intramolecular 1,3 aryl migration from oxygen to sulfur.

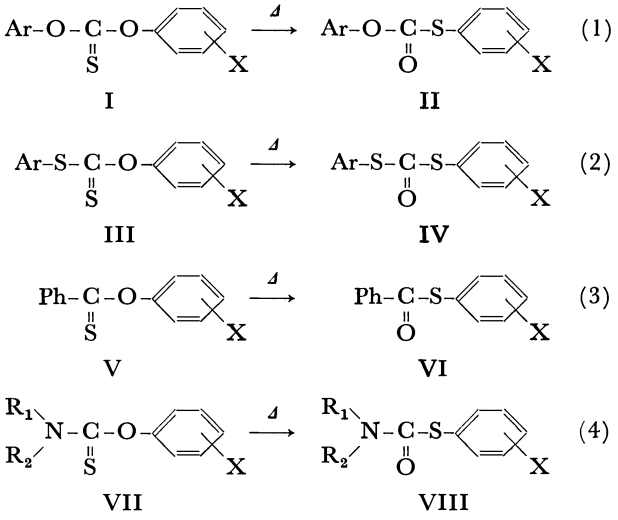

Aryl *N,N*-disubstituted thionocarbamates (VII) were also found to rearrange to aryl *N,N*-disubstituted thiolcarbamates (VIII).[8] A kinetical investigation in the absence of any solvent showed that this rearrangement proceeds by the intramolecular mechanims just as in the above rearrangements. It was also reported that ordinary Hammett plots of log k against σ^- do not give a satisfactory linear relationship (the correlation coefficient is 0.982), and that, by assuming that $r=1.60$ in the Yukawa-Tsuno equation,[9] the plots between log k and $\sigma^0+r\Delta\sigma_R$ give a better straight line (the correlation coefficient is 0.987). It is noteworthy that this value of r is extraordinary large. On the other hand, Relles and Pizzolato, in their study of the substituent effect of the same rearrangement in dipheny ether, reported that, when the log k values are plotted against Hammett σ values, the correlation coefficient is only 0.839, but when the log k values are plotted against the σ^- values, the correlation coefficient is 0.954,[10] which is inferior to the correlation coefficient reported by Miyazaki. However, they did not report the effects of the *meta*-substituents and of the strongly electron-withdrawing *para*-substituents.

It is obvious that all of the Schönberg-type rearrangements proceed *via* a four-membered cyclic transition state through an intramolecular nucleophilic attack of the thiocarbonyl sulfur atom on the migrating aromatic ring. However, as for the substituent effects, many obscure points remain. Therefore, we studied kinetically the thermal rearrangements of the various *meta*- or *para*-substituted aryl *N,N*-dimethylthionocarbamates and diaryl thionocarbonates in diphenyl ether and compared them with other Schönberg-type rearrangements.

This paper will discuss a detailed mechanism of the Schönberg-type rearrangements.

Results and Discussion

The various aryl *N,N*-dimethylthionocarbamates (VIIa—o) were synthesized by the reaction of dimethylamine with an aryl chlorothionoformate (Eq. (5)) and/or by the reaction of *N,N*-dimethylthiocarbamoyl chloride with an appropriate phenol (Eq. (6)).

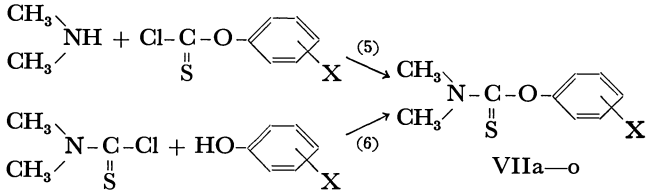

The various aryl *N,N*-dimethylthiolcarbamates (VIIIa—o) were obtained by heating the corresponding compounds VII. The compounds VIII were identified by a mixed-melting-point test and by a comparison of the infrared spectra with those of the corresponding authentic samples, which were prepared by the reaction of *N,N*-dimethylcarbamoyl chloride with an appropriate thiophenol (Eq. (7)) and/or by the reaction of dimethylamine with an aryl chlorothiolformate (Eq. (8)).

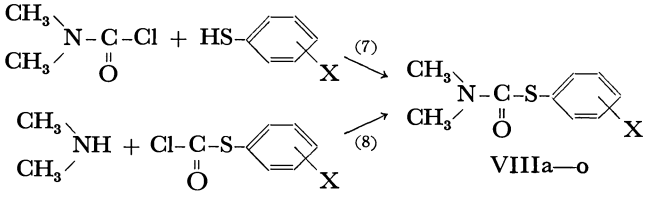

In order to clarify the substituent effects, the kinetics of the thermal rearrangement of aryl *N,N*-dimethylthionocarbamates were investigated at 200.5±0.1°C in diphenyl ether. The reactions were followed by the ampoule techniques, and the rates were determined by ultraviolet spectrophotometric measurements. As has been noted previously,[8,10] this rearrangement obeyed fairly good first-order kinetics. The first-order rate constants were derived from the slopes of the straight lines obtained by plotting ln[VII]/([VII]+[VIII]) against the time; the results are summarized in Table 1. The rates of the rearrangement are much faster for the electron-withdrawing substituents than for the electron-releasing substituents.

The logarithms of the rate constants can be plotted against the σ^- values[11] to give a straight line (Fig. 1). By means of the method of least-squares, the ρ value was calculated to be 1.97 (the correlation coefficient is

8) K. Miyazaki, *Tetrahedron Lett.*, **1968**, 2793. A preliminary report of this work was presented in part at the 18th Annual Meeting of the Chemical Society of Japan, Osaka, April, 1965.

9) Y. Yukawa, Y. Tsuno, and M. Sawada, This Bulletin, **39**, 2274 (1966).

10) H. M. Relles and G. Pizzolato, *J. Org. Chem.*, **33**, 2249 (1968).

11) J. Clark and D. D. Perrin, *Quart. Rev.* (London), **18**, 295 (1964).

Table 1. First-order rate constants of the thermal rearrangement of aryl *N,N*-dimethylthionocarbamates (VII) in diphenyl ether at 200.5±0.1°C

Compd. No.	X	$k \times 10^6$ (sec^{-1})
VIIa	*p*-OCH_3	0.813
VIIb	*p*-CH_3	2.22
VIIc	H	5.92
VIId	*p*-Cl	9.40
VIIe	*p*-Br	13.1
VIIf	*m*-$COCH_3$	16.8
VIIg	*m*-Cl	24.8
VIIh	*m*-Br	28.5
VIIi	*m*-CF_3	31.6
VIIj	*m*-NO_2	72.1
VIIk	*p*-CO_2CH_3	137
VIIl	*p*-$CO_2C_2H_5$	142
VIIm	*p*-$COCH_3$	148
VIIn	*p*-CN	372
VIIo	*p*-NO_2	1210

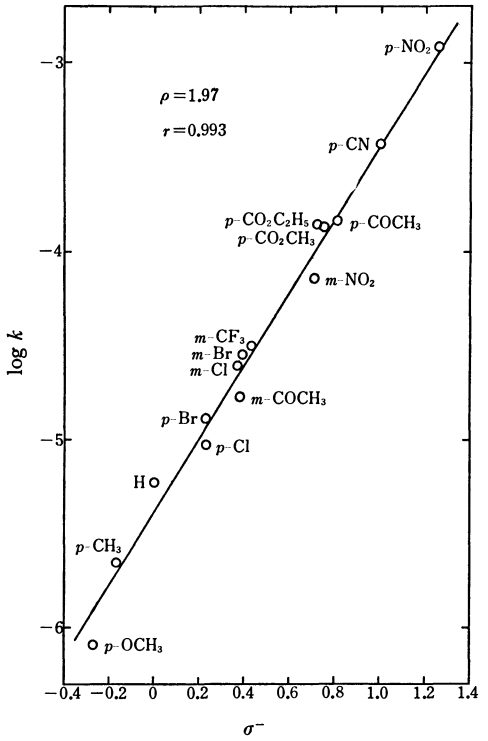

Fig. 1. Hammett plot for the rates of the thermal rearrangement of aryl *N,N*-dimethylthionocarbamates (VII) in diphenyl ether at 200.5±0.1°C.

0.993). These results establish that this rearrangement is an intramolecular nucleophilic aromatic substitution reaction and that the additional delocalization by the resonance of the negative charge produced at the reaction site occurs in the transition state in diphenyl ether. The good correlation coefficient shows that it is sufficient if the *r* value in the Yukawa-Tsuno equation is 1.00 for this rearrangement in diphenyl ether. On the other hand, the *r* value of 1.60 has been obtained in the absence of any solvent.[8] It is clear that the solvent affects the rates of this rearrangement. In the absence of any solvent, the substrates themselves behave as solvents; these solvent effects, "self-solvent effects," presumably vary in parallel with the variation in the substituents on the materials, so that *r* in Yukawa-Tsuno equation may become as large as 1.60.

The Hammett plots of the electron-releasing *para*-substituents deviate slightly on the lower side of the *meta* correlation line (Fig. 1). The electron-releasing *para*-substituents may be expected to cause an additional resonance between the substituent and the reaction center in a manner similar to that of the electron-withdrawing *para*-substituents. However, such a resonance is ordinarily found to be very minor and negligible. Consequently, with regard to the electron-releasing *para*-substituents, the Hammett σ values are usually used instead of σ^- values in such nucleophilic reactions. However, the electron-releasing *para*-substituents of aryl *N,N*-dimethylthionocarbamates obviously exert a higher retardation of the rearrangement than would be anticipated from the ρ—σ^- relationship. It is necessary to give suitable σ^- values for the electron-releasing *para*-substituents instead of the Hammett σ values in this case. With respect to the σ^- value of the *para*-methoxy group, values of −0.11 for the reactions of phenols and −0.25 for the reactions of anilines have been provided,[12] but these values are very unsatisfactory for correcting the above Hammett plots.

The bimolecular nucleophilic aromatic substitution reactions[13] are reactions very similar to the Schönberg-type rearrangements. These nucleophilic aromatic substitution reactions do not correlate with the Hammett σ values, σ^n values[14] and σ^0 values,[15] but correlate well with the σ^- values.

Brieux and his co-workers, in their study of the substituent effects on the nucleophilic aromatic substitution reactions, calculated the *para*-substituent constants by using ρ values obtained from the *meta*-substituent series.[16,17] These *para*-substituent constants are very similar to the σ^- values. Two series are available. They are the $\sigma_{C_6H_5S}^-$ values obtained from the reactions of 4- or 5-substituted 1-chloro-2-nitrobenzenes with sodium thiophenoxide, and the $\sigma_{C_5H_{10}NH}$ values obtained from the reactions of the same compounds with piperidine. When the logarithms of the rate constants in Table 1 were plotted against $\sigma_{C_6H_5S}^-$ instead of the σ^- values, a rather unsatisfactory correlation was obtained (the correlation coefficient was 0.980) (Fig. 2). However, a very good linear relationship was observed against $\sigma_{C_5H_{10}NH}$ instead of the σ^- values (the correlation coefficient was here 0.994)

12) P. R. Wells, *Chem. Rev.*, **63**, 171 (1963).
13) For reviews on the subject, see a) J. F. Bunnett, *Quart. Rev.* (London), **12**, 1 (1958); b) S. D. Ross, "Progress in Physical Organic Chemistry," Vol. 1, ed. by S. G. Cohen, A. Streitwieser, Jr., and R. W. Taft, Interscience Publishers, New York, N. Y. (1963), p. 31; c) E. Buncel, A. R. Norris, and K. E. Rusell, *Quart. Rev.* (London), **22**, 123 (1968).
14) H. van Bekkum, P. E. Verkade, and B. M. Wepster, *Rec. Trav. Chim. Pays-Bas*, **78**, 815 (1959).
15) R. W. Taft, Jr., *J. Phys. Chem.*, **64**, 1805 (1960).
16) W. Greizerstein, R. A. Bonelli, and J. A. Brieux, *J. Amer. Chem. Soc.*, **84**, 1026 (1962).
17) A. M. Porto, L. Altieri, A. J. Castro, and J. A. Brieux, *J. Chem. Soc., B*, **1966**, 963.

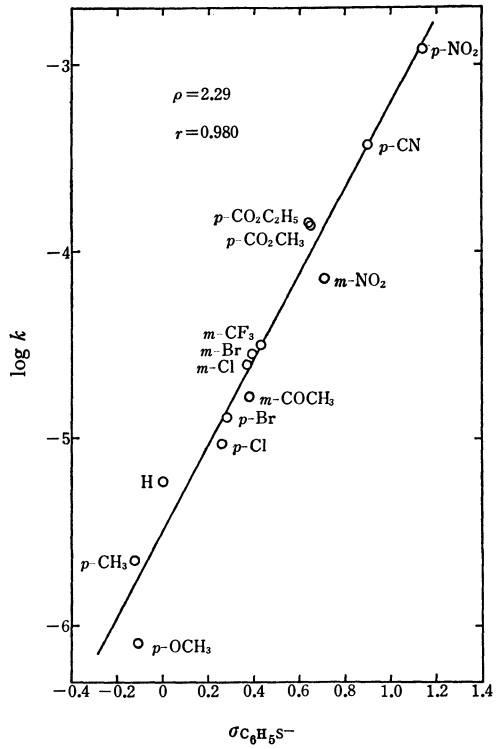

Fig. 2. Plot of the rates of the thermal rearrangement of aryl *N,N*-dimethylthionocarbamates (VII) in diphenyl ether at 200.5±0.1°C against $\sigma_{C_6H_5S^-}$.

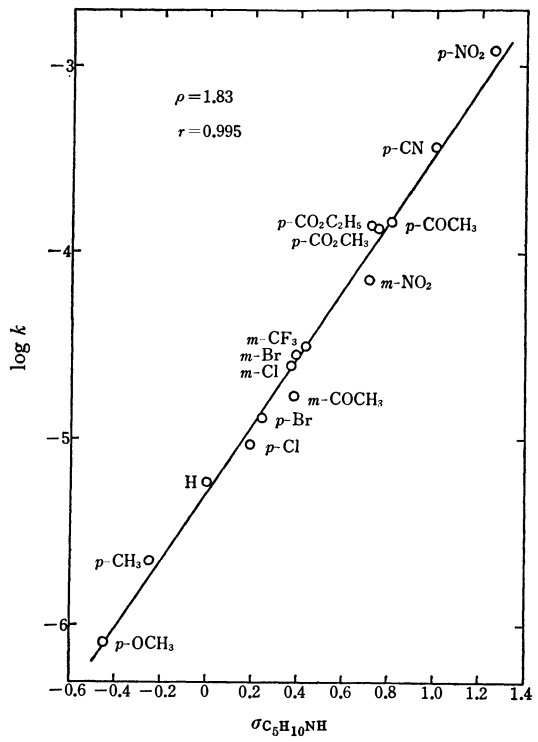

Fig. 3. Plot of the rates of the thermal rearrangement of aryl *N,N*-dimethylthionocarbamates (VII) in diphenyl ether at 200.5±0.1°C against $\sigma_{C_5H_{10}NH}$.

(Fig. 3).

Then, by the use of $\sigma_{O_5H_{10}NH}$ for the electron-releasing *para*-substituent constants, a linear free-energy correlation between log k from Table 1 and the σ^- values was established. This was the best correlation (Fig. 4). The ρ value calculated using the method of least squares is 1.83, and the correlation coefficient is 0.995.

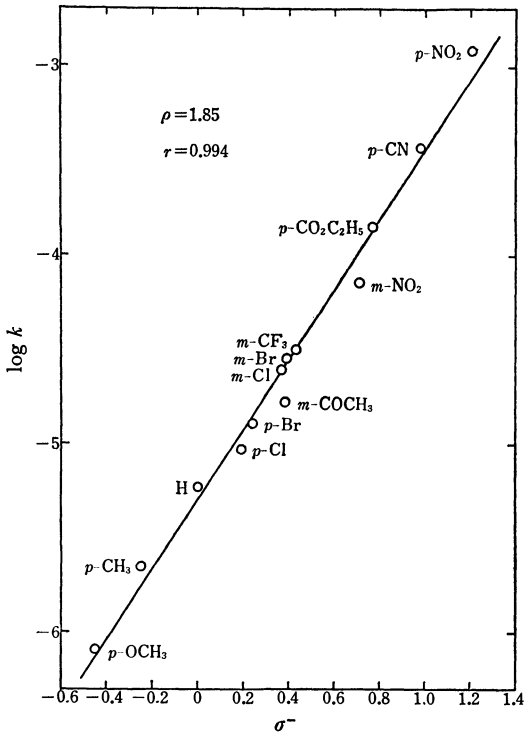

Fig. 4. Plot of the rates of the thermal rearrangement of aryl *N,N*-dimethylthionocarbamates (VII) in diphenyl ether at 200.5±0.1°C against σ^-, using $\sigma_{C_5H_{10}NH}$ for the electron-releasing *para*-substituent constants.

A very good linear free-energy relationship was observed in diphenyl ether between the rearrangements of aryl *N,N*-dimethylthionocarbamates and aryl thionobenzoates and also between the rearrangements of aryl *N,N*-dimethylthionocarbamates and *O*-aryl *S*-phenyl dithiocarbonates (the correlation coefficients were 0.999).

These results and the previously-reported results show that all of the Schönberg-type rearrangements probably proceed by the same mechanism in diphenyl ether. Therefore, on the rearrangements of aryl thionobenzoates[7] and *O*-aryl *S*-phenyl dithiocarbonates,[6] linear free-energy correlations between log k and the σ^- values were examined, using $\sigma_{C_5H_{10}NH}$ as the electron-releasing *para*-substituent constants. The ρ values calculated using the method of least squares and the correlation coefficients, r, are listed in Table 2.

TABLE 2. REACTION CONSTANTS AND CORRELATION COEFFICIENTS OF THE THERMAL REARRANGEMENT OF

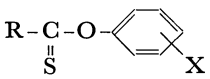

IN DIPHENYL ETHER AT 200.5±0.1°C

R	ρ	r
$(CH_3)_2N$	1.83	0.995
C_6H_5	1.33	0.997
C_6H_5S	1.19	0.995
C_6H_5O	1.06	—

From the foregoing discussion, it is evident that all of the Schönberg-type rearrangements are intramolecular nucleophilic aromatic substitution reactions. Therefore, it is very plausible that the Schönberg-type rearrangements proceed by an addition-elimination mechanism, in analogy with the intermolecular nucleophilic aromatic substitution reactions.

The rates of the thermal rearrangements of diphenyl thionocarbonate and *p*-nitrophenyl phenyl thionocarbonate[18] at 200.5±0.1°C in diphenyl ether were determined by the same method as was used for that of aryl *N,N*-dimethylthionocarbamates. Their first-order rate constants are 1.04×10^{-6} sec^{-1} (the half-value of the observed rate constant) and 2.34×10^{-5} sec^{-1} respectively. From these data, the ρ value was calculated (Table 2).

As is shown in Table 2, the order of the ρ values of the Schönberg-type rearrangements is as follows: aryl *N,N*-dimethylthionocarbamates>aryl thionobenzoates>*O*-aryl *S*-phenyl dithiocarbonates>aryl phenyl thionocarbonates. This order is in accord with that of the inductive effects of the α-substituents of the thiocarbonyl group.[19] This indicates that the proportions of the negative charge on aromatic rings in the transition state are governed by the inductive effects of the α-substituents of the thiocarbonyl group. According to Hammond's postulate,[20] it may be expected that, in endothermic steps, the transition states will resemble the products. Since the activation energies of the Schönberg-type rearrangements are highly positive values,[5-7,10] it may be expected that the transition state of the Schönberg-type rearrangements will closely resemble the intermediate. Therefore, the Schönberg-type rearrangements may proceed *via* an intermediate, as is shown in Scheme 1.

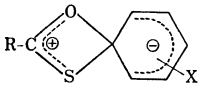

Scheme 1

Moreover, the rate constants of *p*-nitrophenyl *N,N*-dimethylthionocarbamate, *p*-nitrophenyl thionobenzoate,[7] *O*-*p*-nitrophenyl *S*-phenyl dithiocarbonate,[6] and *p*-nitrophenyl phenyl thionocarbonate in diphenyl ether at 200.5±0.1°C are 1.21×10^{-3} sec^{-1}, 1.18×10^{-4} sec^{-1}, 1.06×10^{-4} sec^{-1}, and 2.34×10^{-5} sec^{-1}, respectively. Since the Schönberg-type rearrangements may be governed by the enthalpy of activation at temperatures near 200°C[7], this order will not change under any possible conditions. It is suprising that this order is not in accord with that of the electron-releasing conjugative effects, but is in accord with that of the inductive effects of the α-substituents of the thiocarbonyl group. If the electron-releasing conjugative effects of the α-substituents of the thiocarbonyl group play important roles in the rate-determining step, as Newman and Karnes suggested with regard to the rearrangement of aryl *N,N*-disubstituted thionocarbamates[21] (Scheme 2), the rate constants should decrease in the order of: *p*-nitrophenyl *N,N*-dimethylthionocarbamate>*p*-nitrophenyl phenyl thionocarbonate>*p*-nitrophenyl thionobenzoate>*O*-*p*-nitrophenyl *S*-phenyl dithiocarbonate.[22]

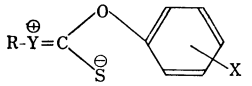

Scheme 2

From these results and the fact that the Schönberg-type rearrangements unsatisfactorily correlate the reactions of 4- or 5-substituted 1-chloro-2-nitrobenzenes with sodium thiophenoxide, but well correlate the reactions of the same compounds with piperidine, it is plausible that the Schönberg-type rearrangements are intramolecular S_N–Ar which involve a four-membered cyclic transition state formed by the nucleophilic attack of the lone-pair electrons of the thiocarbonyl sulfur atom on the migrating aromatic ring, as is shown in Scheme 3:

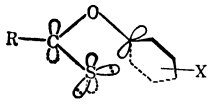

Scheme 3

If the π electron of the thiocarbonyl sulfur atom attacks the migrating aromatic ring, there will necessarily be considerable extra strain because of the necessity of the rotation of the thiocarbonyl sulfur atom to permit the overlap between a *p* orbital initially perpendicular to the plane of the four-membered ring and a *p* orbital of the migrating aromatic ring initially on the plane of the four-membered ring.

Experimental[23]

Materials. The *N,N*-dimethylcarbamoyl chloride was prepared according to the method reported by Sugasawa and Deguchi.[24] The *N,N*-dimethylthiocarbamoyl chloride was prepared by the procedure recorded for the synthesis of the diethyl-analogue;[25] mp 40—41°C (lit,[26] mp 41°C). The aryl chlorothionoformates were prepared by a known method:[27] *m*-acetylphenyl-, light yellow oil, bp 148—149°C/8.5 mmHg (Found: C, 50.28; H, 3.10; Cl, 16.41%. Calcd for $C_9H_7ClO_2S$: C, 50.35; H, 3.27; Cl, 16.55%). *p*-Cyanophenyl-, colorless needles (from ligroin), mp 65—67°C

18) This compound certainly rearranges only to *O*-phenyl *S*-*p*-nitrophenyl thiolcarbonate, but it is very probable that any other unsymmetrical thionocarbonate can rearrange to two products.

19) The Hammett σ_m values of $(CH_3)_2N$, C_6H_5, C_6H_5S, and C_6H_5O are −0.21, 0.06, 0.18, and 0.25 respectively.

20) G. S. Hammond, *J. Amer. Chem. Soc.*, **77**, 334 (1955).

21) M. S. Newman and H. A. Karnes, *J. Org. Chem.*, **31**, 3980 (1966).

22) The $(\sigma_p^+-\sigma_m^+)$ values of $(CH_3)_2N$, C_6H_5O, C_6H_5, and C_6H_5S are −1.49, −0.75, −0.29, and 0.11, respectively. The σ_m^+ values of $(CH_3)_2N$ and C_6H_5O are not available; accordingly, σ_m values were used in place of σ_m^+ values. The σ^+ values of C_6H_5S are not available, either; therefore, the $(\sigma_p-\sigma_m)$ value was used in place of the $(\sigma_p^+-\sigma_m^+)$ value.

23) All the boiling and melting points are uncorrected.

24) S. Sugasawa and Y. Deguchi, *Yakugaku Zasshi*, **76**, 968 (1956).

25) R. H. Goshorn, W. W. Levis, Jr., E. Jaul, and E. J. Ritter, "Organic Syntheses," Coll. Vol. IV, p. 307 (1963).

26) E. Lieber and J. P. Trivedi, *J. Org. Chem.*, **25**, 650 (1960).

27) M. H. Rivier, *Bull. Soc. Chim. Paris*, [3] **35**, 837 (1906).

(Found: C, 48.48; H, 1.79; N, 6.80%. Calcd for $C_8H_4ClNO_3S$: C, 48.60; H, 2.02; N, 7.08%). *m*-(Trifluoromethyl)phenyl-, light yellow oil, bp 98—99°C/19 mmHg (Found: C, 39.50; H, 1.89%. Calcd for $C_8H_4ClF_3OS$: C, 39.90; H, 1.66%). The physical properties for the other aryl chlorothionoformates were reported in an earlier paper.[28,29] The *p*-acetylphenyl chlorothiolformate was prepared from *p*-(acetyl)thiophenol and phosgene by a general method reported previously:[6] colorless needles (from *n*-hexane), mp 73—74.5°C (Found: C, 50.40; H, 3.02; Cl, 16.66%. Calcd for $C_9H_7ClO_2S$: C, 50.35; H, 3.27; Cl, 16.55%).

Aryl N,N-*Dimethylthionocarbamates (VIIa—o).* The following general methods were employed for the preparation of the compounds VII.

TABLE 3. ARYL *N,N*-DIMETHYLTHIONOCARBAMATES

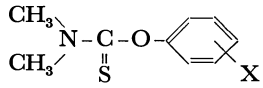

Compd. No.	X	Appearance	Mp[a] °C (lit)	Method	Yield[b] %
VIIa	*p*-OCH_3	colorless prisms[c]	85—85.5 (82—84)[d]	A B	72.5 67.6
VIIb	*p*-CH_3	colorless needles[c]	95—96[e] (86—88)[f]	A	66.7
VIIc	H	colorless needles[g]	29.5—30.5[h] (30—30.4)[i]	A B	63.5 54.7
VIId	*p*-Cl	colorless prisms[g]	58—59[e]	A B	75.0 71.4
VIIe	*p*-Br	colorless prisms[c]	87.5—88.5 (84—86)[f]	A	67.5
VIIf	*m*-$COCH_3$	colorless needles[c]	66—67	A	79.8
VIIg	*m*-Cl	colorless prisms[c]	92.5—93.5	A B	74.0 61.1
VIIh	*m*-Br	colorless prisms[c]	98—99	A	70.8
VIIi	*m*-CF_3	colorless plates[c]	64—65 (64—65)[d]	A B	65.0 63.7
VIIj	*m*-NO_2	colorless plates[j]	148—150 (153—155)[d]	A	65.8
VIIk	*p*-CO_2CH_3	colorless prisms[c]	102—103 (100—102)[d]	A	69.7
VIIl	*p*-$CO_2C_2H_5$	colorless needles[k]	81.5—82.5	A	53.5
VIIm	*p*-$COCH_3$	colorless needles[c]	102.5—103.5[e] (99—103)[d]	A B	73.1 60.8
VIIn	*p*-CN	colorless prisms[c]	116—117	A B	71.0 66.1
VIIo	*p*-NO_2	colorless plates[j]	146.5—147.5 (150—153)[d]	A	81.8

a) All melting points are uncorrected.
b) Yield of the pure product.
c) Recrystallized from methanol.
d) Ref. 21.
e) A. Kaji, This Bulletin, **34**, 254 (1961).
f) Ref. 10.
g) Recrystallized from ligroin.
h) bp, 120 °C/3 mmHg.
i) Ref. 27.
j) Recrystallized from acetone-ethanol.
k) Recrystallized from ethanol.

28) A. Kaji and K. Miyazaki, *Nippon Kagaku Zasshi*, **87**, 272 (1966).
29) K. Miyazaki, This Bulletin, **42**, 1697 (1969).

Method A (Eq. (5)): To a solution of 15 g (0.10 mol) of 30%-dimethylamine in 50 m*l* of acetone was added, drop by drop, 0.05 mol of aryl chlorothionoformate under agitation at 5—10°C over a period of 10 min. After the addition had been completed, the mixture was warmed to 40—50°C for 5 min. It was then cooled to room temperature and poured into *ca.* 150 m*l* of cold water; the desired product was thereby obtained as a pale yellow oil and crystallized spontaneously on standing. Recrystallization from a suitable solvent gave pure crystals. The data are shown in Table 3.

Method B (Eq. (6)): To a solution containing 0.05 mol of an appropriate phenol and 2 g (0.05 mol) of sodium hydroxide in 50 m*l* of aqueous acetone (90%) was added, all at once, 6.2 g (0.05 mol) of *N,N*-dimethylthiocarbamoyl chloride. The mixture was heated under reflux for 30 min and then cooled to room temperature. Thereafter, the reaction mixture was worked up in the same manner as has been described in Method A. The date are also shown in

TABLE 4. ARYL *N,N*-DIMETHYLTHIOLCARBAMATES

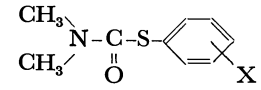

Compd. No.	X	Appearance	Mp[a] °C (lit)	Method	Yield[b] %
VIIIa	*p*-OCH_3	colorless needles[c]	94—95 (94—96)[d]	D	77.0
VIIIb	*p*-CH_3	colorless prisms[e]	36—37 (31—33)[f]	D	75.0
VIIIc	H	colorless prisms[e]	43—44	D	78.0
VIIId	*p*-Cl	colorless needles[g]	80.5—81	C(16)[h] D	30.0 66.5
VIIIe	*p*-Br	colorless prisms[i]	87—87.5 (81—83)[f]	C(15) D	33.0 62.5
VIIIf	*m*-$COCH_3$	colorless needles[e]	78—79	C(9) D	44.0 44.5
VIIIg	*m*-Cl	colorless needles[e]	47—48	C(16) D	50.5 65.0
VIIIh	*m*-Br	colorless needles[e]	53—54	C(9) D	50.5 56.0
VIIIi	*m*-CF_3	colorless needles[e]	31—32[j]	C(10) D	30.5 53.5
VIIIj	*m*-NO_2	colorless needles[i]	120—121 (117—120)[d]	C(6) D	68.5 68.0
VIIIk	*p*-CO_2CH_3	colorless needles[k]	93—94 (91—93)[d]	C(5) D	56.0 32.0
VIIIl	*p*-$CO_2C_2H_5$	colorless prisms[l]	55—56.5	C(3) D	55.0 38.7
VIIIm	*p*-$COCH_3$	colorless needles[i]	107—108 (106—109)[d]	C(3) E	63.0 61.0
VIIIn	*p*-CN	colorless needles[l]	103—104	C(3)	75.0
VIIIo	*p*-NO_2	colorless needles[i]	119—120 (122—124)[d]	C(0.5) D	85.0 57.5

a) All melting points are uncorrected.
b) Yield of the pure product.
c) Recrystallized from *n*-hexane.
d) Ref. 21.
e) Recrystallized from ligroin.
f) Ref. 10.
g) Recrystallized from aqueous methanol.
h) Heating time (hr).
i) Recrystallized from methanol.
j) Ref. 21.; bp, 100—103/0.2 mmHg.
k) Recrystallized from benzene-*n*-hexane.
l) Recrystallized from benzene-ligroin.

Table 3. The compounds VIIf, VIIg, VIIh, VIIl, and VIIn are new compounds. VIIf, Found: C, 59.05, H, 5.35; N, 6.02%. Calcd for $C_{11}H_{13}NO_2S$: C, 59.20; H, 5.44; N, 5.86%. VIIg, Found: C, 49.87; H, 4.40; N, 6.33%. Calcd for $C_9H_{10}ClNOS$: C, 50.15; H, 4.64; N, 6.50%. VIIh, Found: C, 41.70; H, 3.67; N, 5.18%. Calcd for $C_9H_{10}BrNOS$: C, 41.55; H, 3.85; N, 5.38%. VIIl, Found: C, 56.70; H, 6.06; N, 5.76%. Calcd for $C_{12}H_{15}NO_3S$: C, 56.95; H, 5.93; N, 5.53%. VIIn, Found: C, 58.30; H, 4.91; N, 13.52%. Calcd for $C_{10}H_{10}N_2OS$: C, 58.30; H, 4.86; N, 13.60%.

Aryl N,N-*Dimethylthiolcarbamates (VIIIa—o).* The following general methods were employed for the preparation of the compounds VIII.

Thermal Rearrangement of VII, Method C (Eq. (4)): The apparutus used for this method consisted of a 5 m*l*, round-bottomed flask. About 500 mg of VII was placed in the flask and kept at 205—210°C in an oil bath for the desired period, nitrogen being passed into the flask at a slow rate throughout the heating. The flask was then cooled to room temperature, and the contents were scratched in an ice bath to induce crystallization. The product thus obtained was recrystallized from a suitable solvent. The results are summarized in Table 4.

Method D (Eq. (7)): The reaction conditions of *N,N*-dimethylcarbamoyl chloride with an appropriate thiophenol to give VIII correspond to those of the Method B used in the preparation of VII. The data are shown in Table 4.

Method E (Eq. (8)): The reaction conditions of dimethylamine with the aryl chlorothiolformate to give VIII are nearly identical with those described for the Method A used in the preparation of VII. The results are listed in Table 4. The compounds VIIIc, VIIId, VIIIf, VIIIg, VIIIh, VIIIl, and VIIIn are new compounds. VIIIc, Found: C, 59.33; H, 5.84; N, 7.70%. Calcd for $C_9H_{11}NOS$: C, 59.64; H, 6.12; N, 7.73%. VIIId, Found: C, 50.19; H, 4.29; N, 6.61%. Calcd for $C_9H_{10}ClNOS$: C, 50.12; H, 4.67; N, 6.49%. VIIIf, Found: C, 59.25; H, 5.87; N, 6.26%. Calcd for $C_{11}H_{13}NO_2S$: C, 59.20; H, 5.44; N, 5.86%. VIIIg, Found: C, 50.35; H, 4.37; N, 6.66%. Calcd for $C_9H_{10}ClNOS$: C, 50.15; H, 4.64; N, 6.50%. VIIIh, Found: C, 41.45; H, 3.96; N, 5.60%. Calcd for $C_9H_{10}BrNOS$: C, 41.55; H, 3.85; N, 5.38%. VIIIl, Found: C, 56.80; H, 5.81; N, 5.49%. Calcd for $C_{12}H_{15}NO_3S$: C, 56.95; H, 5.93; N, 5.53%. VIIIn, Found: C, 57.90; H, 5.05; N, 13.38%. Calcd for $C_{10}H_{10}N_2OS$: C, 58.30; H, 4.86; N, 13.60%.

Aryl Phenyl Thionocarbonates (I). The method of preparing diphenyl thionocarbonate was previously reported.[6] *p*-Nitrophenyl phenyl thionocarbonate was prepared by the reaction of phenol and *p*-nitrophenyl chlorothionoformate[6] with triethylamine in a manner similar to that described in an earlier paper.[6] Colorless plates (from acetone-ethanol), mp 184—185°C (lit,[4] 181—182°C).

O-*Phenyl* S-*Aryl Thiolcarbonates (II).* These compounds were prepared by the reactions of phenol and aryl chlorothiolformate with triethylamine in a manner similar to that described in an earlier paper.[6] Phenyl-: colorelss needles (from *n*-hexane), mp 53.5—54°C (lit,[2] 57°C). *p*-Nitrophenyl-: colorless needles (from *n*-hexane), mp 76.5—77.5°C (lit,[4] mp 65—67°C).

Kinetic Measurements. The rates were followed by the ampoule technique and were determined by ultraviolet spectrophotometric measurements in a manner similar to that described in an earlier paper.[6]

The authors wish to express their sincere thanks to Dr. Jun-ichi Hayami for his invaluable discussions.

The Synthesis of the Polymer Containing the Si-O-phenylene Bond, using Transition Metal Salts as Catalysts[1]

Yoshio IWAKURA, Keikichi UNO, Fujio TODA, Kenjiro HATTORI, and Minoru ABE*

Department of Synthetic Chemistry, Faculty of Engineering, The University of Tokyo, Bunkyo-ku, Tokyo

(Received November 20, 1970)

Various transition metals were found to be effective as catalysts in the dehydrocondensation of phenols and silanes.

$$R_3SiH + PhOH \xrightarrow{\text{metal salt}} R_3SiOPh + H_2$$

The effective species were $PdCl_2$, $H_2PtCl_6 \cdot 6H_2O$, $PtCl_2$, $RhCl_3$, $NiCl_2$, silane-treated $NiCl_2$, PtI_2, PtS, Raney Ni, Pd-black, Pt-black, Au-black, $FeCl_3$, $ZnCl_2$, $CuSO_4$, CuCl, Cu–Cr, $Cu(CH_3CO_2) \cdot CuO$, the methyl ethyl ketoxime complex of Pd, $Pt(OX)_3$, and $Pd(OX)_2$. The ineffective species were metal mirrors of Pd, Au, Ag, Pt, and Cu, and the acetylacetonato complex of Ni, Co(II), Co(III), and Cu. The reaction was then extended to the preparation of polymers containing a Si–O–phenylene linkage in the main chain. Dihydricphenols, *e.g.*, bisphenol A, hydroquinone, 4,4′-dihydroxydiphenyl gave high-molecular-weight polymers with an equimolar amount of a dihydrosilane, *e.g.*, diphenylsilane, *p*-toluylmethylsilane and *p*-bisdimethylsilylphenylene, in bulk or in a solvent at temperatures above 150°C. The polymer obtained began to flow above 100°C.

It has been known that Group VIII metals and metal halides catalyze the reaction of an organosilane with compounds containing a hydroxy group:[2-7]

$$R_3SiH + ZOH \xrightarrow{\text{cat.}} R_3SiOZ + H_2$$

Z = H, alkyl, aryl, acyl, *etc.*

Dolgov *et al.*[7] reported that the dehydrocondensation of trialkylsilanes with alcohols and mono- or polyhydric phenols proceeded smoothly at the temperature of 100°C and that gave alkoxy- and phenoxysilanes in almost quantitative yields in the presence of a catalytic amount of colloidal nickel prepared from $NiCl_2$.

We now wish to report in the catalytic activity of various transition metals, especially the salts of Ni, Pd, and Pt, in the reactions of organosilanes and phenols. Among these catalysts, several metal salts, such as $PdCl_2$ and the Pd complex of methyl ethyl ketoxime, initiated the reaction, even at room temperature. Such a reation was used in the preparation of polymers containing siloxane linkage in the main chain from difunctional phenols and difunctional silanes.

Polyaryloxysilanes have been reported to be obtained from difunctional phenols and dianilino- or diphenoxysilanes through a melt-polycondensation reaction procedure at temperatures above 200°C and under reduced pressure.[8,9] Here, a similar polymer was prepared under much milder conditions.

Experimental

Materials. 4,4′-Dihydroxydiphenyl was prepared by the hydrolysis of a diazonium compound derived from commercial 4,4′-benzidine according to the usual method. Recrystallization from dioxane gave pure 4,4′-dihydroxydiphenyl; mp 277—278°C. All the other phenols were commercially available, and they were recrystallized before use. The phenyldimethylsilane, *p*-toluylmethylsilane,[10] diphenylsilane,[11] and *p*-bis(dimethylsilyl)-benzene[12] were prepared by methods previously reported. The purity of the silanes was ascertained by gas chromatography, using dioctyl phthalate (D.O.P.) or thermol-3 as the liquid phase.

The Reaction of Silane with Phenol. To a mixture of 3.0 g of phenyldimethylsilane and 2.35 g of phenol, were added 0.02 g of metal salt. In the case of a very active catalyst, $PdCl_2$, for example, a vigorous exothermic reaction occurred, hydrogen gas evolved immediately after the addition of the catalyst at room temperature, and the solution turned dark. In the case of a catalyst with a mild activity, such as $NiCl_2$, an exothermic reaction occurred when the bath temperature was 110°C. After the reaction, the catalyst was removed by filtration and the product was distilled under reduced pressure to give phenoxysilane. The identity of the product was confirmed by infrared spectroscopy and gas chromatographs. The evolved gas was analysed by gas chromatography using a Molecular Sieve 13X column.

Polycondensation. The polymerization was carried out by heating a mixture of 5.00 g of bisphenol A and 4.03 g of diphenylsilane with 0.02 g of $PdCl_2$ at 150—160°C for 10 hr. The resulting polymer was purified by reprecipitation from THF-*n*-hexane and dried. The powdery polymer thus obtained was submitted to elemental analysis and other analyses. The other polymers were prepared by a similar method. The viscosity was determined by the use of an Ubellohde viscosimeter at 30°C in a tetrahydrofuran solution and in a concentration of 0.5 g/d*l*.

* Present address: Department of Synthetic Chemistry, Faculty of Technology, Gumma University, Kiryu, Gumma.

1) Presented in part at the meeting of Chemical Society of Japan, Sendai, Oct., 1968.

2) B. N. Dolgov, N. P. Kharitonv, and M. G. Voronkov, *Zh. Obsch. Khim.*, **24**, 1178 (1954).

3) B. N. Dolgov, "Chemistry and Practical Use of Organosilicon Compounds. No. 1," Leningrad (1958), p. 18.

4) A. D. Petrov, V. F. Mironov, V. A. Ponomarenko, and E. A. Chernyshev, "Synthesis of Organosilicon Monomers," Consultant Bureau, New York (1964), pp. 411—413.

5) L. H. Sommer and J. E. Lyons, *J. Amer. Chem. Soc.*, **89**, 1521 (1967).

6) K. Yamamoto, M. Kumada, I. Nakajima, K. Maeda, and N. Imaki, *J. Organometal. Chem.*, **13**, 329 (1968).

7) B. N. Dolgov, Yu. I. Khudobin, and N. P. Kharitonov, *Izvest. Akad. Nauk. SSSR*, **1958**, 113.

8) J. E. Curry and J. D. Byrd, *J. Appl. Polymer Sci.*, **9**, 295 (1965).

9) W. R. Dunnavant, R. A. Markle, P. B. Stickney, J. E. Curry, and J. D. Byrd, *J. Polymer Sci., Part A-1*, **5**, 707 (1967).

10) M. Maienthal, M. Helman, C. P. Haber, L. A. Hymo, S. Carpenter, and A. J. Carr, *J. Amer. Chem. Soc.*, **76**, 6392 (1954).

11) I. E. Baines and C. Eaborn, *J. Chem. Soc.*, **1956**, 1436.

12) R. West and E. G. Rochow, *J. Org. Chem.*, **18**, 303 (1953).

13) Pt complex of 8-hydroxyquinoline.

Results and Discussion

Activity of Catalyst in the Reaction of Silane and Phenol.

The reaction of phenyldimethylsilane with phenol and bisphenol-A was carried out in the presence of a metal salt as a catalyst. The reaction products were confirmed to be siloxanes by elemental analysis, as is shown in Table 1.

Table 1. Reaction between silane and phenol with $PdCl_2$ as catalyst

Product	Bp °C/mmHg	Yield %	Elemental analysis Found (Calcd) C%	H%	Si%
$PhMe_2SiOPh$	94—95/0.3	93	74.19 (74.68)	7.26 (7.02)	12.9 (12.3)
O-$SiMe_2$Ph / CMe_2 / O-$SiMe_2$Ph	220—223/0.2	92	74.63 (74.95)	7.32 (7.30)	11.1 (11.3)

Table 1. The yield of the products was almost quantitative, and the gas evolved was found to be composed of hydrogen and a trace of methane. From these results, therefore, the reaction was considered to proceed as is shown in Eqs. (1) and (2):

$$PhMe_2SiH + PhOH \xrightarrow{cat.} PhMe_2SiOPh + H_2 \quad (1)$$

$$PhMe_2SiH + HO\text{-}C_6H_4\text{-}CMe_2\text{-}C_6H_4\text{-}OH \xrightarrow{cat.}$$

$$PhMe_2SiO\text{-}C_6H_4\text{-}CMe_2\text{-}C_6H_4\text{-}OSiMe_2Ph + 2H_2 \quad (2)$$

The infrared spectra of phenyldimethylphenoxysilane, phenyldimethylsilane, and phenol are summarized in Fig. 1. In this figure, the absorptions around 3300, 2100, 920, and 880 cm^{-1} were identified as the absorptions of OH(3300), SiH(2100, 880), and Si-O-  (920) respectively. When the reaction proceeded, the absorptions of OH and SiH diminished and the appearance of a new absorption of Si-O- 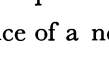 was observed. The rates of the reactions using various kinds of metal derivatives as catalysis were estimated by the volumetry of the hydrogen gas evolved and by infrared spectroscopy. The order of the rates thus obtained may be attributed to the order of the activity of the catalysis used, because all the reactions were carried out under the same conditions. The orders of the activity of catalysts used were as follows:

1) For metal halide:

$$PdCl_2 > H_2PtCl_6 \cdot 6H_2O > PtCl_2 > RhCl_3 > NiCl_2$$

2) For metal black:

Pd-black > Pt-black ≈ Raney Ni (W_2) > Au-black

3) For other metal salts:

PtI_2, PtS, $Pt(OX)_3$,[13] $Pd(OX)_2$, methyl ethyl ketoxime of Pd, $CuSO_4$, CuCl, Cu–Cr, $Cu(CH_3CO_2)CuO$, $FeCl_3$, $ZnCl_2$

The metal mirrors of Pd, Au, Ag, Pt, and Cu showed little activity. We tried to use acetylacetonato complexes of Ni, Cu, Co(II), and Co(III) as homogeneous catalysts, but they provoked no reaction. As is shown in Table 2, all the metals which are active as catalysts in the reactions of phenols and silanes were found to be transition metals.

Table 2. The catalytic metals in periodic table of the reaction between phenols and silanes

VIa	VIIIb			Ib	IIb
Cr	Fe	Co	Ni	Cu	Zn
Mo	Ru	Rh	Pd	Ag	
W			Pt	Au	Hg

■: highly active; □: active; ⬚: slightly active.

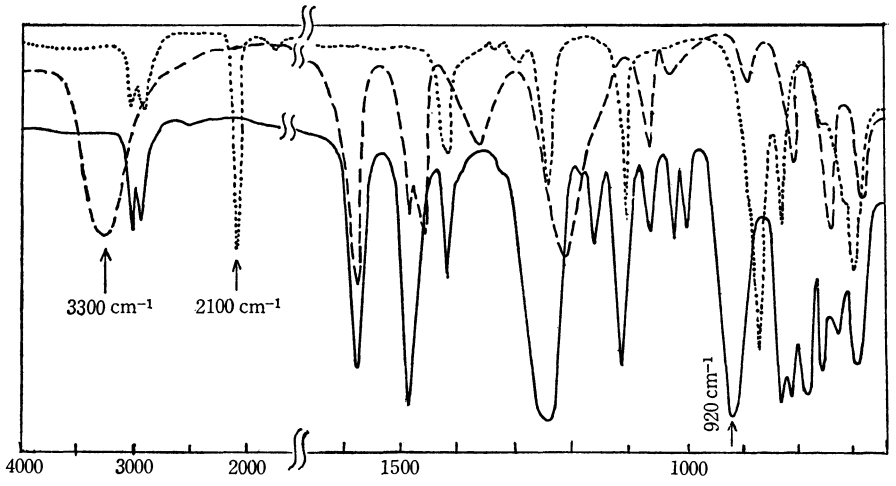

Fig. 1. Infrared spectra of phenyldimethylsilane, phenol, and phenyldimethylphenoxysilane.

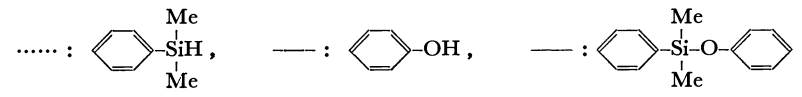

TABLE 3. BULK OR SOLUTION POLYMERIZATION OF DIHYDRIC AND DIHYDROSILANES

Dihydric phenol	Dihydro silane	Polymerization condition (in N_2) cat. $PdCl_2$			η_{inh} in THF at 30 °C	Elemental analysis		
		temp (°C)	time (hr)	solvent		C% Found (Calcd)	H% Found (Calcd)	Si% Found (Calcd)
B.P.A.	TMS	110	20	none	(0.100) [b]	75.84 (76.62)	6.84 (6.71)	7.77 (7.79)
B.P.A.	DPS	150	10	diglyme	0.122	78.41 (79.37)	6.22 (5.92)	6.47 (6.88)
HQ.	DPS	150	10	diglyme	0.079	71.55 (74.45)	4.66 (4.86)	9.35 (9.67)
DHDP.	DPS	210	1.5	none	0.079	74.77 (78.65)	5.46 (4.95)	7.10 (7.65)
DHDP.	BDMSP	210	1.5	none	0.103	68.39 (68.02)	6.22 (6.80)	15.1 (15.0)
DHDP.	BDMSP	160[a]	12	THF	(0.090) [b]	67.96 (68.02)	6.44 (6.80)	15.4 (15.0)

B.P.A. bisphenol A T.M.S. *p*-toluylmethylsilane
HQ. hydroquinone D.P.S. diphenylsilane
DHDP. 4,4′-dihydroxydiphenyl BDMSP. *p*-bis-dimethylsilylphenylene
a) cat: $Pt(OX)_3$ b) in toluene

In these reactions, the reaction mixtures turned dark when heated, and the formation of colloidal metal was observed in the reactions, using almost all of the metal salts. The metal salts seemed to be reduced by silane; the colloidal metal black thus formed had a high catalytic activity in the reaction of silane and phenol. The results will be presented in detail in the following paper.

Polycondensation. The polycondensation reactions of various phenols and dihydrosilanes were carried out in bulk (or in solution); the results are shown in Table 3. These polymers tend to flow above 100°C as a consequence of the chain mobility of the silicon-oxygen bond.

The authors are grateful to the Shinetsu Chem. Ind. Co. for the supply of the chlorosilanes used in this experiment.

BULLETIN OF THE CHEMICAL SOCIETY OF JAPAN, VOL. 44, 1402—1407 (1971)

Radikalische aromatische *m*-Nitrierung bei Umsetzung von Benzoylperoxyd mit Stickstoffdioxyd und bei Umsetzung von *p*-Chlorperoxybenzoesäure mit Stickstoffoxyd in Toluol

Tadashi SUEHIRO, Mikio HIRAI, und Takehira KANEKO
Chemisches Institut der Gakushuin Universität, Mejiro, Tokio

(Eingegangen am 7. Dezember, 1970)

Die radikalische Nitrierung des Toluols findet bei der Umsetzung von Benzoylperoxyd mit Stickstoffdioxyd bei 60—100°C in 4—15% Ausbeute und bei der Umsetzung von *p*-Chlorperoxybenzoesäure mit Stickstoffoxyd bei 20—80°C in 30—50% Ausbeute statt. In beiden Umsetzungen waren die Isomeren-Verhältnisse der gebildeten Nitrotoluole *o*/*m*/*p*=6—25/75—91/0—3. Daß diese *m*-orientierende Nitrierung über das Zwischenprodukt, Aroyloxycyclohexadienyl-Radikal, abläuft, wurde sichergestellt aufgrund der Isomeren-Verhältnisse der Nitrotoluole im Vergleich zu denen der Benzoesäureester von Kresolen aus der konkurrierenden Benzoyloxylierung (*o*/*m*/*p*=40—54/13—16/33—45) und aufgrund der relativen Reaktivität des Toluols (2—4) gegenüber Benzol bei der Nitrierung und der Benzoyloxylierung.

In den früheren Mitteilungen[1-3] haben wir den Mechanismus der homolytischen Tritylierung bei der Umesetzung von Trityl-Radikal mit Benzoylperoxyden in Aromaten klar gemacht. Die Reaktion läuft über das Zwischenprodukt, Benzoyloxycyclohexadienyl Radikal (I), ab, dann folgen die Additions- und Spaltungsreaktionen, (2) und (3), in die substituierten Tetraphenylmethane.

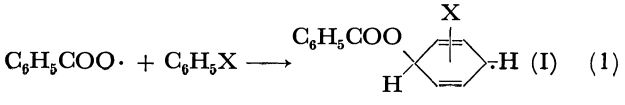

$$C_6H_5COO\cdot + C_6H_5X \longrightarrow C_6H_5COO(X)H \text{ (I)} \quad (1)$$

1) T. Suehiro, A. Kanoya, T. Yamauchi, T. Komori, und S. Igeta, *Tetrahedron*, **24**, 1551 (1968).
2) T. Suehiro, S. Igeta, O. Kuwabara, und M. Hirai, ebenda, **26**, 963 (1970).
3) T. Suehiro, S. Igeta, O. Kuwabara, M. Hirai, M. Ishida, und J. Yamazaki, Dieses Bulletin, **43**, 3303 (1970).

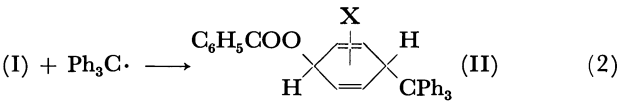

$$(II) \longrightarrow XC_6H_4CPh_3 + C_6H_5COOH \quad (3)$$

Diese Reaktionen lassen darauf schließen, daß Trityl-Radikal, wenn es auch außerordentlich stabil ist, doch noch in die Reaktion eingehen kann, wenn I als Zwischenprodukt auftritt, und dessen Addukt II in die stabilen Produkte zerfällt. Dies weist auf eine neue Möglichkeit der aromatischen Substitution mittels stabilen Radikals in Gegenwart des bestimmten Radikal-Startmittels hin.

Der Mechanismus der Tritylierung ist eigenartig: Im Gegensatz zu der üblichen radikalischen aromatischen Substitution von *o*- und *p*-Orientierung[4] fällt die Tritylierung als *m*-Orientierung auf. Wenn also eine Nitrierung des Toluols durch Stickstoffdioxyd oder durch Stickstoffoxyd in Gegenwart von Benzoyloxy-Radikal stattfindet, kann *m*-Nitrotoluol als Hauptprodukt gebildet werden. Dies wurde in der Tat verwirklicht und darüber wollen wir hier berichten.

System Benzoylperoxyd - Stickstoffdioxyd

Es ist bekannt, daß Stickstoffdioxyd und Stickstoffoxyd oft als Radikal-Abfänger verwendet werden können.[5] Gill und Williams[6] nahmen Interesse an der Reaktion von Benzoylperoxyd in Gegenwart von Stickstoffdioxyd und untersuchten die Produkte des Zerfalls vom Peroxyd in Tetrachlorkohlenstoff und in Benzol in der Stickstoffdioxyd-Atmosphäre, wobei sie Nitrobenzol in mäßiger Ausbeute isolierten. Weil Nitrobenzol durch die Kombination von Phenyl-Radikal aus dem Peroxyd mit Stickstoffdioxyd gebildet wird, und weil die Autoren nur in begrenzten Sorten von Lösungsmitteln die Umsetzung durchführten, konnten sie die Rolle des Benzoyloxycyclohexadienyl-Radikals nicht ausfindig machen.

Wir haben die Umsetzung in der Absicht durchgeführt, das Auftreten des Benzoyloxycyclohexadienyl-Radikals zu untersuchen. Wir wählten infolgedessen Toluol oder dessen Mischung als Lösungsmittel und ermittelten die Isomeren-Verhältnisse der Nitrierungs- und Benzoyloxylierungsprodukte. Die Umsetzung von Benzoylperoxyd in Toluol in Gegenwart von Stickstoffdioxyd ist sehr kompliziert: Die Oxydation des Toluols durch Stickstoffdioxyd unter Bildung von ω-Nitrotoluol, Benzylnitrit, Benzaldehyd und Salpetrigesäure, der thermische Zerfall vom Peroxyd und dessen Folgereaktionen in Gegenwart von Stickstoffdioxyd und die radikalische und auch vielleicht die heterolytische Zersetzung vom Peroxyd durch Salpetrigesäure usw. laufen nebeneinander. Obwohl der richtige Reaktionsmechanismus unter diesen Umständen der Umsetzung sehr schwer herauszufinden ist, nahmen wir unter den Produkten Rücksicht besonders auf Nitroaromate und Benzoesäureester von Phenolen und bestimmten die rationalen Verhältnisse.

Wenn das Zwischenprodukt III mit Stickstoffdioxyd kombiniert und das Addukt IV zerfällt, müssen Nitroaromaten und Benzoesäure einerseits (Reaktion (7)) und Benzoesäureester von Phenolen und Salpetrigesäure andererseits (Reaktion (8)) entstehen.

$$(C_6H_5COO)_2 \longrightarrow 2\ C_6H_5COO\cdot \quad (4)$$

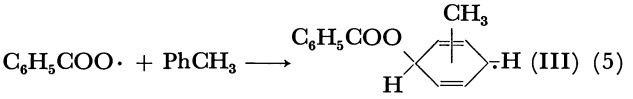

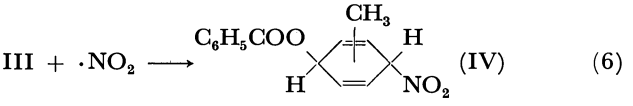

$$IV \longrightarrow CH_3C_6H_4NO_2 + C_6H_5COOH \quad (7)$$

$$IV \longrightarrow C_6H_5COOC_6H_4CH_3 + HNO_2 \quad (8)$$

Es kann bei der Reaktion (6) auch Alkylnitrit entstehen. Dies, zusammen mit ω-Nitrotoluol und Benzylnitrit aus Toluol und Stickstoffdioxyd, kann man durch Waschen mit Alkali oder durch Hydrolyse beseitigen. Die Isomeren-Verhältnisse gemäß der Reaktion (5)—(8) müssen bei Nitrotoluol *m*-orientierend sein und bei Benzoesäureestern von Kresolen *o*- und *p*-orientierend. Das Verhältnis $(m)/(o+p)$ in Nitrotoluol muß mit

Tabelle 1. Abhängigkeit der Ausbeute an Nitroaromaten von der Konzentration des Stickstoffdioxyds

Benzoyl-peroxyd mMol	Sitckstoffdioxyd		Nitrobenzol		Nitrotoluol				
					mg				
	m*l*	mMol	mMol	% auf Peroxyd	*o*-	*m*-	*p*-	Gesam. mMol	% auf Peroxyd
0.535	0.10	3.26	0.0676	12.6	1.92	9.85	0	0.086	14.4
0.614	0.10	3.26	0.0678	11.0	1.93	11.8	0	0.100	13.6
0.534	0.02	0.65	0.0113	2.1	0.101	8.53	0	0.063	7.3
0.464	0.02	0.65	0.0200	4.3	0.753	8.93	0	0.072	9.8
0.488	0.01	0.33	0.0059	1.2	0.736	2.48	0.11	0.024	5.0
0.435	0.01	0.33	0.0044	1.0	0.977	2.65	0.16	0.028	6.3

a) Die Umsetzungen wurden im Einschlußrohr im Vakuum bei 100°C in 6.0 m*l* reinem Toluol durchgeführt. Die Reaktionszeit 5 Stunden.

4) z. B. Bei Arylierung siehe R. Ito, T. Migita, N. Morikawa, und O. Simamura, *Tetrahedron*, **21**, 955 (1965).

5) z. B. Artikel von Y. Ree und G. H. Williams, "Advances in Free Radical Chemistry," Ediert von G. H. Williams, Band 3. Logos Press (1968), S. 199; J. F. Tilney-Bassett und W. A. Waters, *J. Chem. Soc.*, **1957**, 3129.

6) G. B. Gill und G. H. Williams, ebenda, **1956**, 5756.

TABELLE 2. AUSBEUTE AN I) NITRO-VERBINDUNGEN UND II) BENZOESÄUREESTERN BEI DER UMSETZUNG VON BENZOYLPEROXYD MIT STICKSTOFFDIOXYD[a)]

Temp. °C	Reaktions-zeit, Std.	Reaktions-bedingung[b)]	Nitro-benzol	Nitrotoluol		
				o-	*m*-	*p*-
I)						
60	260	A	1.4	0.26	2.4	0.08
80	50	A	3.1	0.58	4.02	0.25
80	50	B	0	0.016	0.21	0.16
80	50	C	1.1	—	—	—
100	5	A	2.8	0.66	2.04	0.10
100	5	C	1.1	1.37	4.07	0.22

Temp. °C	Reaktions-zeit, Std.	Reaktions-bedingung[b)]	Benzoe-säure-phenyl-ester	Benzoesäureester von Kresolen		
				o-	*m*-	*p*-
II)						
60	260	A	4.3	5.3	1.5	3.9
80	50	A	7.5	6.9	2.2	4.7
80	50	C	2.3	—	—	—
100	5	A	9.5	10.9	3.4	11.6
100	5	C	2.0	—	—	—

a) Die Ausbeute, %, bezogen auf Peroxyd. Die Umsetzungen wurden im Einschlußrohr in Stickstoff-Atmosphäre durchgeführt. Benzoylperoxyd 0.62 mMol, Stickstoffdioxyd 0.33 mMol.

b) Reaktionsbedingung A: In einer Mischung von 3 m*l* Toluol und 3 m*l* Benzol; B: Kein Benzoylperoxyd in einer Mischung von 3 m*l* Toluol und 3 m*l* Benzol; C: In reinem Toluol 6 m*l*.

TABELLE 3. ISOMEREN-VERHÄLTNISSE DER NITROTOLUOLE UND DIE RELATIVE REAKTIVITÄT DES TOLUOLS BEI DER NITRIERUNG IM SYSTEM BENZOYLPEROXYD-STICKSTOFFDIOXYD

Temp. °C	Nitrotoluole Isomeren-Verhältnisse, %			k_{PhCH_3}/k_{PhH}
	o-	*m*-	*p*-	
60	9[b)]	88[b)]	3[b)]	2.30[b)]
80	13	85	2	2.70
100	24[b)]	73[b)]	3[b)]	1.95[b)]

a) Die Konzentration des Stickstoffdioxyds war 0.33 mMol/6 m*l* Lösung.

b) Ohne Korrektur mit dem Nitrotoluol, der bei der Umsetzung von Toluol mit Stickstoffdioxyd bei Abwesenheit vom Peroxyd gebildet wird.

TABELLE 4. ISOMEREN-VERHÄLTNISSE DER BENZOESÄUREESTER VON KRESOLEN UND DIE RELATIVE REAKTIVITÄT DES TOLUOLS BEI DER BENZOYLOXYLIERUNG IM SYSTEM BENZOYL-PEROXYD-STICKSTOFFDIOXYD

Temp. °C	Benzoesäureester von Kresolen Isomeren-Verhältnisse, %			k_{PhCH_3}/k_{PhH}
	o-	*m*-	*p*-	
60	54	13	33	2.96[b)]
80	50	16	34	3.16
100	42	13	45	4.12

a) Die Konzentration des Stickstoffdioxyds war 0.33 mMol/6 m*l* Lösung.

b) Ohne Korrektur mit dem Benzoesäurephenylester, der aus Benzoyloxyd allein in 2.0—2.4% Ausbeute gebildet wird.

dem $(o+p)/(m)$ von Benzoesäureestern übereinstimmen und die relative Reaktivität des Toluols zu Benzol in beiden Substitutionen dieselbe sein.

Die Umsetzungen wurden im Einschlußrohr im Vakuum oder in Stickstoff-Atmosphäre durchgeführt, und die Ergebnisse sind in den Tabellen 1—4 wiedergegeben. In Gas-Chromatogramm findet man die Produkte in der Reihenfolge: Lösungsmittel, Benzaldehyd, Benzylalkohol, Nitrobenzol, eine unbekannte Verbindung, *o*-, *m*-, und *p*-Nitrotoluole, Biphenyl und Methylbiphenyle, und Benzoesäureester von Phenol und Kresolen. Wie aus der Tabelle 1 ersichtlich ist, wird Nitrobenzol auch bei Abwesenheit von Benzol gebildet. Phenyl-Radikal aus dem Peroxyd kann durch Kombination mit Stickstoffdioxyd Nitrobenzol geben. Durch dieses Nitrobenzol muß die Ausbeute bei der Umsetzung in der Benzol-Toluol-Mischung korrigiert werden.

Bei der Konzentration vom Stickstoffdioxyd 0.01—0.1 m*l*/6 m*l* Lösung nimmt die Ausbeute an Nitrobenzol und auch an Nitrotoluolen mit der Konzentration des Stickstoffdioxyds zu, d.h. die Reaktion (6) bestimmt die Geschwindigkeit der Bildung der Nitrotoluole. Stickstoffdioxyd ist unter diesen Bedingungen wahrscheinlich nicht wirksam genug als Radikal-Abfänger. Die Isomeren-Verhältnisse müssen infolgedessen von dem Standpunkt aus verwertet werden, daß die Reaktion (5) eine rapide umkehrbare Reaktion ist. Das gilt auch bei der Verwertung der relativen Reaktivität des Toluols. Bei der Konzentration des Stickstoffdioxyds höher als 0.1 m*l*/6 m*l* Lösung wurde die Ermittlung von Nitroaromaten durch Nebenprodukte, Benzaldehyd und Benzylalkohol, erschwert und wir mußten darauf verzichten, unter den Bedingungen die Umsetzung durchzuführen, in denen die Hinreaktion (5) die Geschwindigkeit bestimmt.

In der Tabelle sieht man weiter einen deutlichen Unterschied zwischen den Zunahmen der Ausbeute an Nitrobenzol und an Nitrotoluolen: Nitrobenzol nimmt *ca.* 10 mal so viel zu mit der Zunahme des Stickstoffdioxyds, während Nitrotoluole *ca.* 2 mal so viel zunehmen. Wenn Nitrobenzol durch die Kombination von Stickstoffdioxyd und Phenyl-Radikal gebildet wird (Weg A), muß die Zunahme der Ausbeute an Nitrobenzol genau so groß oder kleiner sein wie die von Nitrotoluolen je nachdem, ob die Reaktion (5) geschwindigkeits-bestimmend ist oder ob es eine umkehrbare Reaktion ist. Die Ergebnisse sind diesen Vorstellungen entgegen, das hat zur Folge, daß Nitrobenzol auch auf einem anderen Weg B gebildet wird. Es

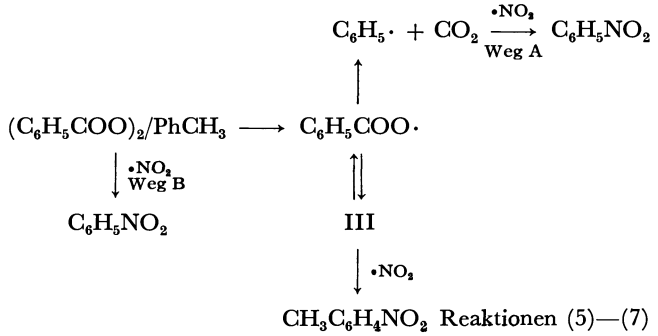

scheint doch sehr gut möglich, daß der Weg B über Phenyl-Kation läuft.

Beim Umsetzen des Toluols allein mit Stickstoffdioxyd von der Konzentration 0.01 m*l*/6 m*l* Lösung werden Nitrotoluole in einer Ausbeute von 0.4% gebildet, deren Isomeren-Verhältnisse bei 80°C *o*/*m*/*p*=4/53/43 sind. Wenn aber Benzoylperoxyd zugesetzt wird, steigt die Ausbeute 10 mal so hoch und die Isomeren-Verhältnisse wechseln in die *m*-Orientierung (*o*/*m*/*p*=13/85/2). In der Berechnung haben wir den Effekt von Nitrotoluolen, die bei Abwesenheit vom Peroxyd gebildet werden, vernachlässigt. Die Isomeren-Verhältnisse liegen sehr nahe denen der Tritylierung (*o*/*m*/*p*=10/81/9).[2] Die Ausbeute der Nitroaromate waren aber wesentlich kleiner (6—14%).

Die Benzoyloxylierung des Toluols bei 80°C (*o*/*m*/*p*=50/16/34) verläuft wie bei der Umsetzung vom Benzoylperoxyd in Gegenwart von Kupfer(II)chlorid[7] (*o*/*m*/*p*=56/18/26) bzw. in Gegenwart von Jod[8] (*o*/*m*/*p*=53/16/31).

Die relative Reaktivität des Toluols bei der Nitrierung, 2.0—2.7, kann mit der bei der Benzoyloxylierung, 3.0—4.1, mit der bei der Benzoyloxylierung im System Benzoylperoxyd-Kupfer(II)chlorid,[7] 2.51, bzw. im System Peroxyd-Jod,[8] 2.85, und mit der bei Tritylierung,[2] 2.82, verglichen werden. Diese Ergebnisse können am besten mit dem Schema der Reaktionen (4)—(8) erklärt werden.

Die Ausbeute an Nitroaromaten relativ zu Benzoesäureester 6/19 bei 80°C zeichnet sich als die relative Geschwindigkeit der Reaktion (7) zu (8) aus. Die Reaktion im System Benzoylperoxyd-Stickstoffdioxyd ist in dem Sinne von Bedeutung, daß sie die Nitrierung und die Benzoyloxylierung über ein gemeisames Zwischenproduct III veranlaßt.

System *p*-Chlorperoxybenzoesäure-Stickstoffoxyd

Die radikalische *m*-Nitrierung in besserer Ausbeute findet man im System Peroxybenzoesäure-Stickstoffoxyd. Hydroperoxyde wie *t*-Butylhydroperoxyd und Peroxybenzoesäure können durch Stickstoffoxyd zertzt werden.[9] Wenn *p*-Chlorperoxybenzoesäure durch Stickstoffoxyd zersetzt wird, wird *p*-Chlorbenzoyloxy-Radikal frei gesetzt (Reaktion(9)), das sich dann an den aromatischen Doppelbindungen anlagert. In Gegenwart von Stickstoffoxyd-Überschuß wird das Aroyloxycyclohexadienyl-Radikal von Stickstoffoxyd abgefangen. Das Nitroso-Addukt VI kann auf zwei Wege zerfallen: Es entstehen Nitrosoaromate und Chlorbenzoesäure einerseits (Reaktion (12)) und Chlorbenzoesäureester und HNO (falls vorhanden) andererseits (Reaktion (13)). Obwohl die Nitroso-Verbindung an sich ein Radikal-Abfänger ist, wird sie leicht durch Peroxycarbonsäure in die Nitro-Verbindung übergeführt.

$$ClC_6H_4COOOH + NO\cdot \longrightarrow ClC_6H_4COO\cdot + HONO \quad (9)$$

$$ClC_6H_4COO\cdot + PhCH_3 \longrightarrow$$

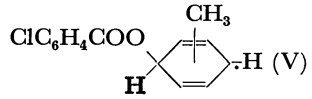

(V) (10)

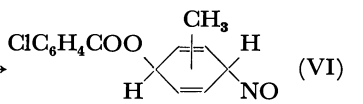

(VI) (11)

$$VI \longrightarrow CH_3C_6H_4NO + ClC_6H_4COOH \quad (12)$$

$$VI \longrightarrow ClC_6H_4COOC_6H_4CH_3 + HNO \quad (13)$$

$$HNO + ClC_6H_4COOOH \longrightarrow HONO + ClC_6H_4COOH \quad (14)$$

$$HONO + ClC_6H_4COOOH \longrightarrow HONO_2 + ClC_6H_4COOH \quad (15)$$

$$CH_3C_6H_4NO + ClC_6H_4COOOH \longrightarrow CH_3C_6H_4NO_2 + ClC_6H_4COOH \quad (16)$$

Die Oxydation des Nitrosobenzols zum Nitrobenzol durch Peroxycarbonsäure ist gut untersucht worden.[10] Bei höheren Temperaturen wie z.B. 50°C läuft die Oxydation zum Nitrobenzol quantitativ. Auf diese Weise oxydiert *p*-Chlorperoxybenzoesäure Nitrosobenzol bei 50°C sehr schnell ($\tau_{1/2}$ 30 Min.). Bei niedrigen Temperaturen wird aber *p*-Nitrosodiphenylhydroxylamin erzeugt.[10] Die Oxydationsgeschwindigkeiten der isomeren Nitrosoaromaten zu Nitroaromaten sind verschieden voreinander, und dieser Unterschied kann einen Fehler in der Ermittelung der Isomeren-Verhältnisse und auch in der relativen Reaktivität herbeiführen. Um diesen Fehler möglichst zu unterdrücken, ließen wir die Reaktionsmischung nach dem Einleiten des Stickstoffoxyds eine halbe Stunde bei 50°C oder höheren Temperaturen stehen, damit die Oxydation der Nitroso-Verbindung verfertigen wird.

Die Umsetzung wurde auf folgender Weise durchgeführt: Man leitet in die Lösung von *p*-Chlorperoxybenzoesäure in Toluol oder dessen Mischung in Stickstoff-Atmosphäre in 15 Minuten einen Überschuß Stickstoffoxyd bei 20—80°C. Man hält die Mischung eine weitere halbe Stunde unter Stickstoff-Leitung bei 50°C oder höheren Temperaturen. Die Produkte wurden nach der Gas-Chromatographie ermittelt. Die Ergebnisse sind in den Tabellen 5 und 6 aufgestellt.

Man findet im Chromatogramm außer Nitrobenzol und Nitrotoluole nur wenig Benzaldehyd (~4%), keinen Benzylalkohol, Spuren von *p*-Nitrochlorbenzol und Biphenylen, und keine *p*-Chlorbenzoesäureester von Phenolen: Die Umsetzung von Peroxybenzoesäure mit Stickstoffoxyd verläuft viel einfacher als die vom Benzoylperoxyd mit Stickstoffdioxyd. *p*-Chlorbenzoyloxy-Radikal lagert sich an die aromatische Doppelbindung genau so an wie das nicht substituierte Benzoyloxy-Radikal, wenn man die Reaktivität des

7) M. E. Kurz und P. Kovacic, *J. Org. Chem.*, **33**, 1953 (1968).
8) S. Hashimoto, W. Koike, und M. Yamamoto, gelesen vor der 10. Diskussionstagung der Chemischen Gesellschaft, Japan, über Organische Radikalische Reaktion, Osaka, Oktober 1969, Vordruck S. 17.
9) J. R. Shelton und R. F. Kopczewski, *J. Org. Chem.*, **32**, 2908 (1967).
10) J. H. Boyer und S. E. Ellzey, Jr., ebenda **24**, 2038 (1959); E. Koubek, ebenda, **28**, 2157 (1963).

TABELLE 5. AUSBEUTE AN NITROAROMATEN IM SYSTEM *p*-CHLORPEROXYBENZOESÄURE-STICKSTOFFOXYD[a)]

Reakt. Nr.	Temp. °C	Peroxycarbonsäure, umgesetzt %	Nitrobenzol		Nitrotoluol				
			mg	mMol	mg *o*-	mg *m*-	mg *p*-	Gesam. mMol	Ausb. auf Peroxycarbonsäure, %
1	20	100[b)]	41.9	0.341	7.52	117.2	0	0.91	44
2	20	60[c)]	30.6	0.249	9.30	77.8	0	0.64	49
3	50	93[d)]	30.2	0.245	12.9	68.0	0	0.59	31
4	50	84[d)]	26.4	0.215	9.1	62.0	0	0.52	29
5	80	100[d)]	14.4	0.117	5.6	18.4	0	0.175	10
6	80	100[d)]	15.7	0.128	8.6	22.1	0	0.224	12

a) Die Umsetzungen wurden in Stickstoff-Atmosphäre mit *ca.* 3 mMol *p*-Chlorperoxybenzoesäure in einer Mischung von 15 m*l* Benzol und 15 m*l* Toluol durchgeführt. Man leitet Stickstoffoxyd 30 mMol in 15 Minuten.
b) Nach dem Einleiten von Stickstoffoxyd hält man die Mischung eine halbe Stunde bei 70°C.
c) Nach dem Einleiten von Stickstoffoxyd hält man die Mischung eine halbe Stunde bei 50°C.
d) Nach dem Einleiten von Stickstoffoxyd hält man die Mischung eine halbe Stunde bei der Reaktionstemperatur.

TABELLE 6. ISOMEREN-VERHÄLTNISSE DER NITROTOLUOLE UND RELATIVE REAKTIVITÄT DES TOLUOLS BEI DER NITRIERUNG IM SYSTEM *p*-CHLORPEROXYBENZOESÄURE-STICKSTOFFOXYD

Reakt. Nr.	Isomeren-Verhältnisse, %			k_{PhCH_3}/k_{PhH}
	o-	*m*-	*p*-	
1	6.0	94.0	0	3.19
2	10.6	89.4	0	3.05
3	15.9	84.1	0	2.89
4	12.8	87.2	0	2.90
5	23.4	76.6	0	1.78
6	28.0	72.0	0	2.09

Radikals aus der Orientierung bei Tritylierung entnimmt.[2)] Die Nitrierung im System Peroxybenzoesäure-Stickstoffoxyd läuft *m*-orientierend. Wenn man die Möglichkeit in Betracht zieht, daß zwei bis drei Mole Peroxycarbonsäure je nach dem Ablauf der Reaktion (15) verbraucht werden, dürfte die oberflächliche Ausbeute von 30—50% bei 20—50°C befriedigend hoch sein. Auf Grund der Produkten-Analyse scheint die Reaktion (13) nicht merklich abzulaufen. Das kommt wahrscheinlich aus der unbeständigen Natur von HNO her: die Stabilität des Endproduktes aus dem Addukt VI übt eine entscheidende Wirkung auf den Verlauf der Reaktion aus.

Die Isomeren-Verhältnisse von Nitrotoluolen (*o*/*m*/*p*=15/85/0) bei 50°C stimmen mit denen bei der Nitrierung im System Benzoylperoxyd-Stickstoffdioxyd (*o*/*m*/*p*=13/85/2) überein. So ist auch das Verhältnis mit der relativen Reaktivität des Toluols, 2.90, zu der bei der Benzoyloxylierung im System Benzoylperoxyd-Kupfer(II)chlorid,[7)] 2.51, und zu der bei der Tritylierung,[2)] 2.82. Daß die Isomeren-Verhältnisse und die relative Reaktivität des Toluols mit der Temperatur-Erhöhung ausgeglichen zu werden scheinen, ist sehr auffallend. Weil es noch nicht bestimmt wurde, daß die Reaktion (10) die Geschwindigkeit bestimmende Stufe der Nitrierung ist, kann man darüber noch nicht diskutieren.

Die aromatische *m*-Substitution nach dem Mechanismus wie die Reaktionen (1) bis (3) ist sehr selten berichtet worden, außer der Tritylierung[1,2)] und der radikalischen *m*-Nitrierung in dieser Arbeit. Ein Beispiel in der elektrophilen Substitution haben Kovacic und andere[11)] bei der *m*-Aminierung mitgeteilt. Ein anderes Beispiel einer vielleicht radikalischen Reaktion wurde von Heslop und Robinson[12)] gezeigt, wo Anisol durch eine saure Mischung von Wasserstoffperoxyd-Salpetrigesäure in 2-Nitro-4-methoxy-phenol übergeführt wird und Toluol in Nitrotoluol verwandelt wird, die Struktur des letzteren allerdings nicht geklärt wurde.

Beschreibung der Versuche

a) Nitrierung und Benzoyloxylierung im System Benzoylperoxyd-Stickstoffdioxyd. Die Reaktion wurde im Einschlußrohr im Vakuum oder in Stickstoff-Atmosphäre durchgeführt. Man stellt Stickstoffdioxyd durch Erhitzen von Bleinitrat im Stickstoff-Strom dar und sammelt es als Abfall bei der Temperatur vom festen Kohlenstoffdioxyd-Methanol. Man ermittelt die Menge an Stickstoffdioxyd aus dessen Volumen im flüssigen Zustand bei −9°C und destilliert das Oxyd in die Lösung vom Benzoylperoxyd in Toluol oder dessen Mischung im Vakuum ein und schließt die Mischung im Vakuum oder in Stickstoff-Atmosphäre ein.

Die Bestimmung von Nitrobenzol, *o*-, *m*-, und *p*-Nitrotoluolen erfolgte mit der Gas-Chromatographie an Kolonne Apiezon L 25% auf Shimalite, 3 m, bei 155°C mit Helium 15 m*l*/15 Sek oder an Kolonne UCON-Öl LB550-X auf C-22 (mit Salzsäure gewaschen und erhitzt), 3 m, bei 185°C mit Helium 15 m*l*/8 Sek. Der innere Standard war *p*-Nitrochlorbenzol.

Die Ermittlung von Benzoesäureestern von Phenolen wurde auch gas-chromatographisch an Kolonne Apiezon L auf Shimalite bei 215°C durchgeführt.

Die Reaktionsmischung wäscht man zunächst mit Alkali so lange, bis die wäßrige Lösung sich nicht mehr orange färbt, und dann mit Wasser, und man bringt die neutrale Lösung zur Bestimmung von Benzoesäureestern. Für die Analyse der Nitro-Verbindungen destilliert man die neutrale Lösung mit Wasserdampf ab und nimnt das Destillat in Methylenchlorid auf.

b) Nitrierung im System p-*Chlorperoxybenzoesäure-Stickstoffoxyd.*

11) P. Kovacic, C. T. Goralski, J. J. Hiller, Jr., J. A. Levsky, und R. M. Lange, *J. Amer. Chem. Soc.*, **87**, 1261 (1965); P. Kovacic und J. A. Levsky, ebenda, **88**, 1000 (1966); P. Kovacic und A. K. Harrison, ebenda, **89**, 32 (1967).
12) R. B. Heslop und P. L. Robinson, *J. Chem. Soc.*, **1954**, 1271.

Man stellt Stickstoffoxyd aus Kaliumjodid und Salpetrigesäure in 50%iger Schwefelsäure her und wäscht mit konz. Schwefelsäure und dann mit Alkali und trocknet bei der Temperatur vom festen Kohlenstoffdioxyd-Methanol. Zu einer Mischung aus 15 m*l* Benzol und 15 m*l* Toluol gibt man 3 mMol durch Sublimation gereinigte *p*-Chlorperoxybenzoesäure, Schmp. 123°C (Zers.) im Einschlußrohr, und leitet in die Lösung in Stickstoff-Atmosphäre einen Überschuß Stickstoffoxyd, 30 mMol, in einer Geschwindigkeit von 2 mMol/Minute ein. Nach dem Einleiten des Stickstoffoxyds spült man die Mischung durch Durchleiten von Stickstoff und hält die Mischung eine halbe Stunde bei 50°C oder bei der Reaktionstemperatur. Dann bestimmt man titrimetrisch den Überschuß von Peroxycarbonsäure, wäscht die Mischung mit Alkali und destilliert mit Wasserdampf ab, um die Nitro-Verbindungen zu reinigen.

Die Ermittelung der Nitro-Verbindungen erfolgte gaschromatographisch wie oben beschrieben. Der innere Standard war *o*-Dichlorbenzol.

BULLETIN OF THE CHEMICAL SOCIETY OF JAPAN, VOL. 44, 1407—1410(1971)

The Synthetic Intermediate of Pyridoxine. II.[1] The Thermal Cyclization of Ethyl α-Isocyanopropionate to 5-Ethoxy-4-methyloxazole[2]

Itsutoshi MAEDA, Kazushi TOGO, and Ryonosuke YOSHIDA
Central Research Laboratories, Ajinomoto Co., Inc., Suzuki-cho, Kawasaki

(Received December 9, 1970)

The thermal cyclization of ethyl α-isocyanopropionate (I) was performed to 5-ethoxy-4-methyloxazole (II) as an intermediate for the synthesis of pyridoxine. The similar reaction of several new alkyl esters of α-isocyanocarboxylic acid to the corresponding 5-alkoxy-4-substituted oxazole was also carried out. The reaction products of the thermal cyclization of I were investigated. When the cyclization was carried out at 180°C for 5 hr, the maximum yield of the main product, II, was 20%; unreacted I (30%), ethyl α-cyanopropionate (20%), and dimer of I (5%) were also obtained. The α-hydrogen of ethyl α-isocyanosuccinate (X) can be more easily removed than that of I, so X may be expected to be more readily converted to 5-ethoxy-4-ethoxycarbonylmethyloxazole (XI), which is also an intermediate of pyridoxine. The yield of XI from X did not exceed 30% because of the side reaction.

By Firestone *et al*,[3] 5-ethoxy-4-methyloxazole, an important intermediate for the synthesis of pyridoxine by the Diels-Alder reaction with dienophiles, has been prepared from ethyl *N*-formylalaninate and phosphorus pentoxide. Recently, as a modification[4] of this procedure, it has been reported that ethyl *N*-formylalaninate was converted to its boron trifluoride complex, after which the complex was treated with phosphorus pentoxide to prepare 5-ethoxy-4-methyloxazole. However these methods have the defect that the reaction mixture forms a hard or powderlike mass which is difficult to remove from the vessel.

The present investigation was undertaken in an attempt to prepare this oxazole without the use of phosphorus pentoxide. This paper will present our findings on the thermal cyclization of ethyl α-isocyanopropionate to produce 5-ethoxy-4-methyloxazole.

Results and Discussion

Ethyl *N*-formylalaninate was converted to ethyl α-isocyanopropionate (I) following the methods of Ugi *et al.* for the synthesis of the derivatives of isonitrile.[5] Several new alkyl esters of α-isocyanocarboxylic acid were synthesized from the alkyl esters of *N*-formylamino acid. The results are listed in Table 1. In order to examine the possibility of the thermal cyclization of I, the solution of I was kept at 170°C. Upon being heated, the solution gradually turned brown-red. In order to analyze the reaction products, the resulting solution was submitted to gas chromatography. Various kinds of 5-alkoxy-4-substituted oxazoles were obtained through the cyclization of the alkyl esters of α-isocyanocarboxylic acid by external heating. The yield of 5-alkoxy-4-substituted oxazoles was calculated on the basis of the area of each peak in a gas chromatograph after a usual calibration using authentic samples; the results are listed in Table 2.

The thermal cyclization from ethyl α-isocyanopropionate (I) to 5-ethoxy-4-methyloxazole (II) was carried out at various temperatures in order to determine the temperature at which the maximum conversion can be obtained. The set of curves in Fig. 1 is presented to show; (A) the conversion of I to II; (B) the decrease in I, and (C) the residue of II at various temperatures. The maximum conversion of I to II, obtained by

1) Part I of this series: I. Maeda, M. Takehara, K. Togo, S. Asai, and R. Yoshida, This Bulletin, **42**, 1435 (1969).

2) Presented in part at the 22nd Annual Meeting of the Chemical Society of Japan, Tokyo, April, 1969.

3) R. A. Firestone, E. E. Harris, and W. Reuter, *Tetrahedron* **23**, 943 (1967).

4) F. Hoffmann-La Roche and Co., Neth. Appl. 6508673 (1966); *Chem. Abstr.*, **64**, 14193 (1966).

5) I. Ugi, W. Betz, U. Fetzer, and K. Offermann, *Chem. Ber.*, **94**, 2814 (1961).

TABLE 1. ALKYL ESTERS OF α-ISOCYANOCARBOXYLIC ACID

RCHCOOR′ NC		Bp °C/mmHg	n_D(°C)	Yield %	Elementary analysis					
					Calcd %			Found %		
R	R′				C	H	N	C	H	N
CH_3	CH_3	77—79/19	1.4100 (30)	69.4	53.09	6.24	12.38	53.06	6.32	12.58
CH_3	C_2H_5	85—86/20	1.4105 (30)	70.4	56.58	7.14	11.02	56.65	7.39	11.36
CH_3	$CH(CH_3)_2$	86—87/20	1.4076 (30)	71.5	59.55	7.85	9.92	59.59	7.98	9.86
CH_3	C_4H_9	105—108/20	1.4190 (30)	76.9	61.91	8.44	9.03	61.54	8.24	8.95
$(CH_3)_2CHCH_2$	C_2H_5	88—90/10	1.4268 (22)	55.9	63.88	8.94	8.28	63.66	9.21	8.28
H	C_2H_5	89—91/20	1.4180 (22)	50.5	53.09	6.24	12.38	52.44	6.56	12.27
$C_6H_5CH_2$	C_2H_5	118—123/1	1.5000 (29)	74.2	70.91	6.45	6.89	70.77	6.17	6.89
CH_3SCH_2	CH_3	100—113/1	1.4783 (27)	71.0	48.55	6.40	8.09	48.76	6.53	8.01
CH_3OOCCH_2	C_2H_5	114—115/3	1.4369 (22)	58.8	54.26	6.58	7.03	54.54	7.00	7.09

TABLE 2. 5-ALKOXY-4-SUBSTITUTED OXAZOLES

RC=C(OR′)–O / N=CH		Reaction		Yeild (%)
		Temp.	Time	
R	R′	(°C)	(hr)	
CH_3	CH_3	160	3	15.6
CH_3	C_2H_5	170	3	16.6
CH_3	$CH(CH_3)_2$	180	3	22.1
CH_3	C_4H_9	180	3	28.2
H	C_2H_5	150	3	5.1
$(CH_3)_2CHCH_2$	C_2H_5	180	3	21.2

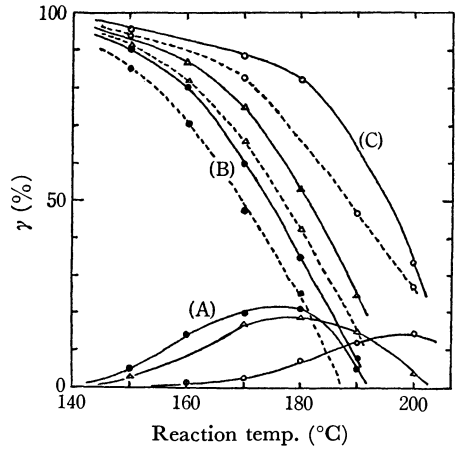

Fig. 1. The thermal cyclization from ethyl α-isocyanopropionate (I).
(A) conversion of I to II ——
(B) decrease of I ——
(C) residue of II ——
Reaction time; ○—○ 1 hr, △—△ 3 hr, ●—● 5 hr

keeping the compound I for 5 hr at 180°C was 21.4%. The results suggest that the compound II first formed from compound I is decomposed by further subsequent reactions and that the thermal conversion of I to II is accompanied by a side reaction. In order to investigate the side-reaction products compound I (30 g) was heated at 180°C for 5 hr and then distilled. The results are shown Table 3. The products of each fraction were identified by gas chromatography, NMR, and IR-spectra analyses. The gas chromatograms of fraction 2 (low-boiling materials) and fraction 5 (high-boiling materials) are shown in Fig. 2. Compounds I and II were identified as ethyl α-isocyanopropionate and 5-ethoxy-4-methyloxazole respectively by comparing their retention times with those of authentic samples. Compound I and III were observed in fraction 3 by gas chromatography. The IR spectrum of fraction 3 showed bands at 2270 cm^{-1} ($\nu_{C\equiv N}$), 2180 cm^{-1} ($\nu_{N\equiv C}$) and 1750 cm^{-1} ($\nu_{C=O}$), while the NMR spectrum exhibited peaks at 8.70τ (triplet 6H, $CH_2\underline{CH_3}$), 8.48τ (doublet 3H, $C\underline{H_3}CH$), 8.38τ (doublet 3H, $C\underline{H_3}CH$), 6.36τ (quartet, 1H, $CH_3C\underline{H}$) 5.88τ (quartet, 4H, $CH_3C\underline{H_2}$), and 5.62τ (quartet, 1H, $CH_3C\underline{H}$). These facts show that the fraction 3 was a mixture of I and ethyl α-cyanopropionate (III). The compound V in fractions 4 and 5 was identified as ethyl *N*-formylalaninate by a comparison of its retention time with that of an authentic sample. For the identification of the unknown product, compound VI, each of the components of fractions 4 and 5 was collected by preparative

TABLE 3. EACH FRACTION OF THE DISTILLATE

Fraction	Bp °C/mmHg	Weight g
1	64—80/20	7.4
2	80—88/20	7.3
3	88—92/20	5.7
4	92—142/6	0.9
5	142—170/6	3.1
6	residue	3.7

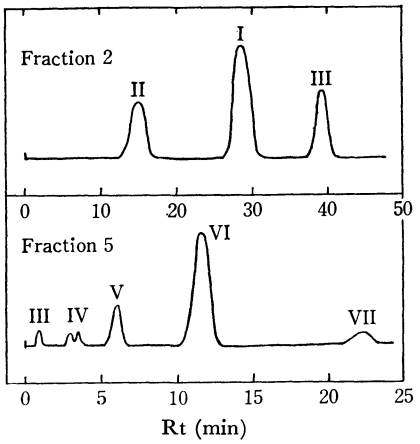

Fig. 2. The gas chromatograms of fraction 2 (low boiling materials) and fraction 5 (high boiling materials).

gas chromatography. The mass spectrum of compound VI showed a molecular ion peak at *m/e* 254, supporting the molecular formula of $C_{12}H_{18}N_2O_4$ (mol wt 254.28) obtained by elementary analysis. The IR spectrum of compound VI showed bands at 2270 cm^{-1} ($\nu_{C\equiv N}$), 1740 cm^{-1} ($\nu_{C=O}$), 1670 cm^{-1} ($\nu_{C=O}$), and 1600 cm^{-1} ($\nu_{C=C}$, $\nu_{C=O}$). The NMR spectrum showed peaks at 8.70τ (double triplet, 6H, $CH_2C\underline{H}_3$), 8.50τ (doublet, 3H, $CHC\underline{H}_3$), 8.00τ (singlet, 3H, $C\underline{H}_3C=$), 5.80τ (double quartet, 4H, $C\underline{H}_2CH_3$), 5.75τ (quartet, 1H, $C\underline{H}CH_3$), and 1.73τ (broad doublet, 1H, NH). The UV spectrum indicated a maximum absorption at 316 mμ. Futhermore, compound VI was hydrolyzed by heating it at 180°C for 30 min with an aqueous solution of sodium hydroxide. The resulting compound was identified as alanine by paper chromatography. On the basis of these data, compound VI was identified as ethyl *N*-(3-cyano-2-ethoxy-2-butenoyl)-alaninate. The amount of each product was determined by the usual gas-chromatography method using authentic samples. The results are shown in Table 4 and Scheme 1.

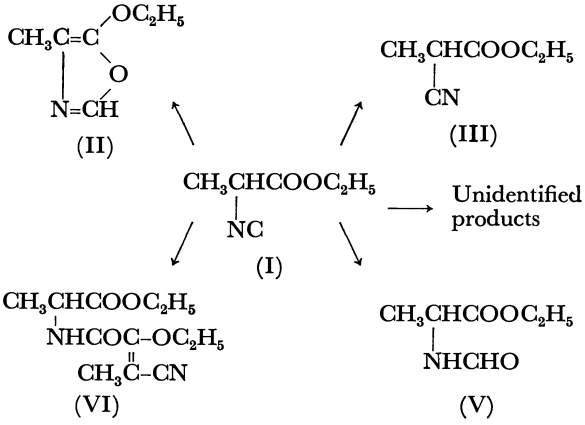

Scheme 1. Thermal reaction products of ethyl α-isocyanopropionate.

Table 4. The amount of the thermal cyclization products

Product number	Fraction	Per cent based on I
II	1, 2	20.4 mol%
I(unreacted)	1, 2, 3	30.4
III	1, 2, 3, 4	18.7
IV	4, 5	—
V	4, 5	0.9
VI	4, 5	5.0
VII	5	—
residue		12.3 wt%

The oxazole derivative (IX) seems to be formed by α-hydrogen abstraction from isocyano derivatives (VIII).

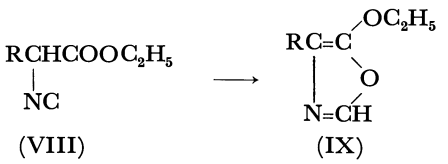

The facility of the cleavage of the α-carbon–hydrogen linkage depends on the electron density around the α-carbon. An electrophilic effect of R, such as $CH_2COOC_2H_5$, can reduce the electron density around the α-carbon. Therefore, diethyl α-isocyanosuccinate ($R=CH_2COOC_2H_5$) may be expected to be more readily converted to an oxazole derivative than ethyl α-isocyanopropionate ($R=CH_3$). At various temperatures diethyl α-isocyanosuccinate (X) was converted to 5-ethoxy-4-ethoxycarbonylmethyloxazole (XI), which is an intermediate for the synthesis of pyridoxine. The results are shown in Fig. 3. The rate of decrease in the starting material, X, was larger than that of I, though the rate of decrease in the residue of XI was similar to that of II. This indicates that the side reaction of X to XI occurs much more than that of I to II. Therefore, the maximum conversion of X to XI did not exceed 30% in spite of the facility of the cleavage of the αC–H linkage.

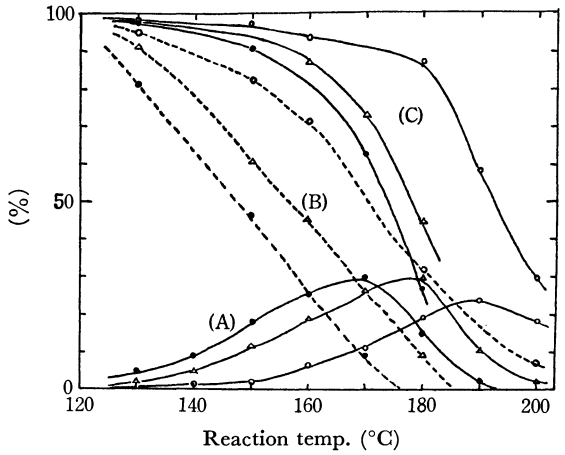

Fig. 3. The thermal cyclization from ethyl α-isocyanosuccinate (X)
(A) conversion of X to XI ——
(B) decrease of X ——
(C) residue of XI ——
Reaction time; ○—○ 1 hr, △—△ 3 hr, ●—● 5 hr

Experimental[6]

Ethyl α-Isocyanopropionate (I). Ethyl *N*-formylalaninate (43.5 g, 0.3 mol) and 100 m*l* of triethylamine were dissolved in 50 m*l* of chloroform. To the solution, 238 g of a chloroform solution containing phosgene (30 g, 0.3 mol) was added, drop by drop under ice-cooling at 25°C over a 1 hr period. The reaction mixture was stirred a further 30 min at room temperature and then washed with 160 m*l* of water to remove triethylamine hydrochloride. The chloroform layer was dried over anhydrous magnesium sulfate, and the solvent was evaporated *in vacuo*. The residue was distilled to give ethyl α-isocyanopropionate (bp 85—86°C/20 mmHg; yield; 26.8 g, 70.4%). Similarly, alkyl esters of α-isocyanocarboxylic acids were synthesized from alkyl esters of *N*-formyl amino acids, as is shown in Table 1.

The Thermal Cyclization of Alkyl Esters of α-Isocyanocarboxylic Acids to 5-Alkoxy-4-substituted Oxazoles. The alkyl ester of α-isocyanocarboxylic acid (2 g) was poured into a 10-m*l* ampoule. The ampoule was then sealed and placed in an oil bath equipped with a thermometer. The temperature was maintained as is shown in Table 2. The resulting liquid

6) All the boiling points are uncorrected.

TABLE 5. GAS CHROMATOGRAPHIC ANALYSIS OF OXAZOLE DERIVATIVES

R	R′	Column[a] length (m)	Column[a] temp. (°C)	Flow rate of He (ml/min)	Type[b]	Internal standard
CH_3	CH_3	1.5	85	75	1C	diethyleneglycol diethyl ether
CH_3	C_2H_5	2.25	85	60	1C	isoamyl acetate
CH_3	$CH(CH_3)_2$	2	90	75	2B	isoamyl acetate
CH_3	C_4H_9	1.5	100	75	1C	diethyleneglycol diethyl ether
H	C_2H_5	2	85	75	2B	isoamyl acetate
$(CH_3)_2CHCH_2$	C_2H_5	1.5	110	75	1C	diethyleneglycol diethyl ether

a) 5% Dinonyl phthalate on Chromosorb T b) 1C (2mmϕ) 2B (4mmϕ)

was analyzed by gas chromatography. Gas chromatography was carried out on a model GC-2B and 1C compact chromatographic analysis unit of Shimadzuseisakujo, Ltd. The operation conditions are shown in Table 5. The authentic samples were prepared, using the technique for 5-ethoxy-4-methyloxazole from ethyl *N*-formylalaninate, using phosphorus pentoxide.[3] All of the above authentic samples were confirmed by gas-chromatographic analysis to have no impurity affecting the results.

5-Ethoxy-4-methyloxazole from Ethyl α-Isocyanopropionate. Ethyl α-isocyanopropionate (1 g) was added to an ampoule. The ampoule was then sealed and placed in an oil bath. The reaction was carried out at 140—190°C at intervals of 10°C for 1, 3, and 5 hr. After the reaction, the contents of the ampoule were diluted with benzene to 50 m*l*; then, the 5-ethoxy-4-methyloxazole and the unreacted ethyl α-isocyanopropionate were analyzed by gas chromatography, using a stainless-steel column packed with 5% dinonyl phthalate on Chromosorb T (2 mmϕ×3.75 m; column temperature: 85°C; flow rate of He: 20 m*l*/min; internal standard: isoamyl acetate). The curves (A) and (B) in Fig. 1 were thus drawn. Similarly, 5-ethoxy-4-methyloxazole (1 g) was heated under the above reaction conditions and analyzed; the curve (C) in Fig. 1 was thus drawn.

The Products of the Thermal Cyclization of Ethyl α-Isocyanopropionate. Ethyl α-isocyanopropionate (30 g) was put into a dried autoclave with a 100 m*l* capacity by means of a magnetic stirrer. The autoclave was kept at 180°C by electrical heating for 5 hr and then it was chilled. The reaction mixture was distilled under reduced pressure. The fractions of the distillate shown in Table 3 were thus obtained. Each fraction of the distillate was analyzed by gas chromatography; the compounds shown in Table 4 were identified by comparing their retention times with those of authentic samples. The yields of the compounds I, II, V, and VI were calculated from the total weight of the mixture on the basis of the calibration curves of the gas chromatography for an authentic sample. The authentic samples were prepared as follows: 5-ethoxy-4-methyloxazole (II) was prepared from ethyl *N*-formylalaninate with phosphorus pentoxide. Ethyl *N*-formylalaninate (V) was prepared from ethyl alaninate hydrochloride and formic acid. Compound VI was separated from the fractions 4 and 5 by preparative gas chromatography (10% Carbowax 20 M on Diasolid L; 8 mmϕ×3 m; column temperature, 190°C; flow rate of He, 75 m*l*/min); it was shown to be $C_{12}H_{18}N_2O_4$ by elementary analysis.

Found: C, 56.77; H, 7.35; N, 10.76%. Calcd: C, 56.68; H, 7.14; N, 11.02%.

The yield of ethyl α-cyanopropionate (III) was calculated from the calibration curves of compound I.

5-Ethoxy-4-ethoxycarbonylmethyloxazole from Diethyl α-Isocyanosuccinate. The reaction and analysis of 5-ethoxy-4-methyloxazole from ethyl α-isocyanopropionate were similar to those described above except that gas chromatography was carried out with 3% Silicone XE-60 on Chromosorb T (4 mmϕ× 1.875 m glass column; column temperature, 140°C; flow rate of He, 70 m*l*/min; internal standard, dibenzyl ether).

The authors wish to thank Professor Dr. M. Matsui of Tokyo University and Professor Dr. Y. Nakatani of Ochanomizu University for their many helpful discussions and suggestions.

Studies on Aminosugars. XXVI. A New Method for the Simultaneous Protection of Amino and Hydroxyl Groups in Aminosugars and Aminocyclitols[1]

Sumio UMEZAWA, Yasushi TAKAGI, and Tsutomu TSUCHIYA

Department of Applied Chemistry, Faculty of Engineering, Keio University, Koganei-shi, Tokyo

(Received December 11, 1970)

2-Deoxystreptamine-1,6:3,4-dicarbamate (II), methyl 2-amino-2-deoxy-α-D-glucopyranoside-2,3-carbamate (VIII) and methyl 6-amino-6-deoxy-α-D-glucopyranoside-4,6-carbamate (X) were prepared by utilizing *p*-nitrophenoxycarbonyl chloride or phenoxycarbonyl chloride.

The simultaneous protection of amino and hydroxyl groups is useful in synthetic chemistry, and this has been performed in case of *cis* amino and hydroxyl groups in cyclic compounds as well as in adjacent amino and hydroxyl groups in open-chain compounds by protection in the form of oxazolidine,[2] 2-oxazoline,[3] and 2-oxazolidone.[4] However, since natural aminosugars and aminocyclitols often have *trans*-equatorial substituents, the simultaneous protection of *trans*-diequatorial amino and hydroxyl groups or *trans*-diequatorial aminomethyl (or hydroxymethyl) and hydroxyl (or amino) groups are often desired.

Recently, Miyai and Gross[5] prepared the 2,3-carbamate derivative of benzyl 2-amino-4,6-*O*-benzylidene-2-deoxy-β-D-glucopyranoside by use of *N,N'*-carbonyl-diimidazole in absolute tetrahydrofuran. In the course of our investigation[6] of synthesis of aminoglycosides we have found a successful protection of the above-described couples of amino and hydroxyl groups by utilizing *p*-nitrophenoxycarbonyl chloride (NPCC) or phenoxycarbonyl chloride (PCC). Brief report of some of our findings has been published earlier.[1] The characteristic features of our method lie in that 1) the protection is performed in one-step procedure in good yields, 2) in a medium containing water which is a requisite condition in dealing with aminosugars or aminocyclitols, and 3) couples of amino and hydroxyl groups are selectively protected in the presence of other hydroxyl groups.

As typical examples, we here described the preparation of 2-deoxystreptamine-1,6:3,4-dicarbamate (II), methyl 2-amino-2-deoxyl-α-D-glucopyranoside-2,3-carbamate (VIII), and methyl 6-amino-6-deoxy-α-D-glucopyranoside-4,6-carbamate (X) from 2-deoxystreptamine (I), methyl 2-amino-2-deoxy-α-D-glucopyranoside, and methyl 6-amino-6-deoxy-α-D-glucopyranoside, respectively.

An aqueous solution of deoxystreptamine (I) was treated with a cold solution of NPCC in acetone in the presence of appropriate amount of anion exchange resin (OH form) and subsequent solvent extraction followed by column chromatography gave a cyclic dicarbamate derivative (II) in a yield of 73%. Structural proof of II was performed on the basis of its elemental analysis, IR (Chart I) and NMR spectra. The absence of the absorption peak at ~1550 cm^{-1} (amide II) indicated the cyclic amide structure and the chair conformation as shown in Chart 2 was confirmed by the splitting pattern of H-2,2' signals in its NMR spectrum. Further confirmation was obtained from its mono-*O*-acetyl derivative (III), which gave *m/e* 256 (molecular ion) by mass spectroscopy and, in the NMR spectrum, large coupling constants (J=9.4—11.2 Hz) between H_1–H_{2a}(H_3–H_{2a}), H_3–H_4(H_1–H_6), and H_4–H_5(H_5–H_6)

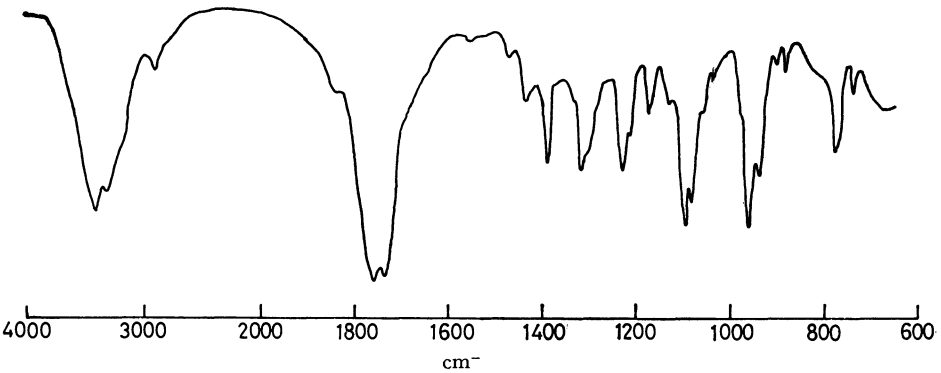

Chart 1. IR spectrum of 2-deoxystreptamine-1,6:3,4-dicarbamate (II).

1) Preliminary communication: S. Umezawa, T. Tsuchiya, Y. Takagi, This Bulletin, **43**, 1602 (1970).

2) See for example: E. D. Bergmann, *Chem. Rev.*, **53**, 309 (1953); G. E. McCasland and E. C. Horswill, *J. Amer. Chem. Soc.*, **73**, 3744, 3923 (1951); "Chemistry of Carbon Compounds," ed. by E.H. Rodd, Elsevier Publishing Co. (1957), IV-A, p. 372.

3) See for example: R. H. Wiley and L. L. Benett, Jr., *Chem. Rev.*, **44**, 447 (1949); W. M. zu Reckendorf, *Chem. Ber.*, **98**, 93 (1965); E.H. Rodd, *loc. cit.*, IV-A, p. 361; *ibid.*, I-F, p. 470 (1967).

4) See for example: P. H. Gross, K. Brendel, and H. K. Zimmerman, *Ann. Chem.*, **680**, 159 (1964); **681**, 225 (1965); K. Miyai, H. K. Zimmerman, and P. H. Gross, *J. Org. Chem.*, **34**, 1635 (1969); E.H. Rodd, *loc., cit.*, IV-A, p. 372.

5) K. Miyai and P. H. Gross, *J. Org. Chem.*, **34**, 1638 (1969).

6) Y. Nishimura, T. Tsuchiya, and S. Umezawa, This Bulletin, **43**, 2960 (1970).

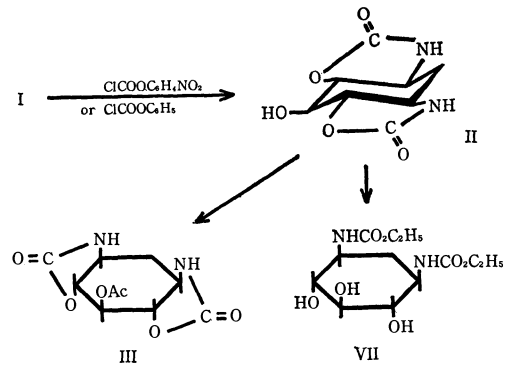

Chart 2

indicated the presence of all *trans*-axial protons. Compound II could also be prepared from I and PCC in the presence of anion-exchange resin or sodium carbonate, but the reaction required a longer period than that by NPCC.

When, however, I and PCC were brought into reaction in the presence of sodium hydrogen carbonate for a short period, *N,N'*-diphenoxycarbonyl-2-deoxystreptamine (IV) was formed. The spectroscopic data of its tri-*O*-acetyl derivative (V) and 4,5,6-tri-*O*-acetyl-*N,N'*-diacetyldeoxystreptamine (VI) support the structure for IV. When the solution of the compound IV in aqueous acetone was treated with a small amount of anion-exchange resin, IV was converted to a cyclic dicarbamate (II) in one hour in a yield of 81%. This result indicates that the reaction intermediate to II is IV, not an *O*-phenoxycarbonyl derivative.[7] Since *N*-ethoxycarbonyl derivative[6] (VII) of I could not be cyclized under the similar conditions, electron-withdrawing properties of phenyl and nitrophenyl groups may facilitate the cyclization.

We have found the properties of the cyclic carbamate group useful for synthetic purposes. When II was treated with barium hydroxide at 100°C, the carbamate groups were broken to give I; whereas, when II was refluxed in ethanol with a catalytic amount of sodium it was converted to VII in a yield of 77% (Chart 2). Thus, the protected hydroxyl group in a cyclic carbamate group could be made free leaving the amino group still protected.

By the similar treatment of methyl 2-amino-2-deoxy-α-D-glucopyranoside[8] with NPCC, a cyclic carbamate (VIII) was obtained in a yield of 78%. The structure was proved from its elemental analysis and spectroscopic data, and also from those of its di-*O*-acetyl derivative (IX) (Chart 3): The absence of any absorption peak near 1550 cm^{-1} in VIII and IX and the large coupling constants ($J_{2,3}$, $J_{3,4}$, and $J_{4,5}$=9—12Hz) of these compounds showed that both are cyclic carbamates of CI conformation, and these results exclude the pos-

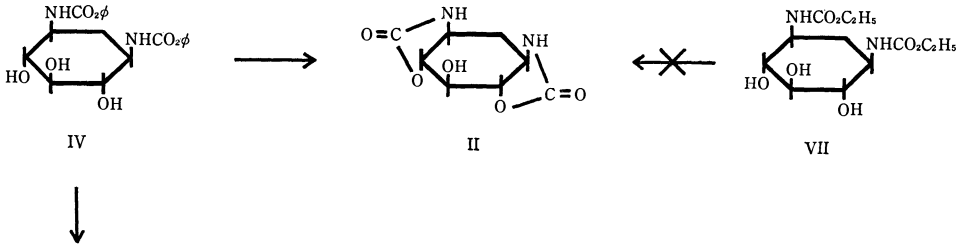

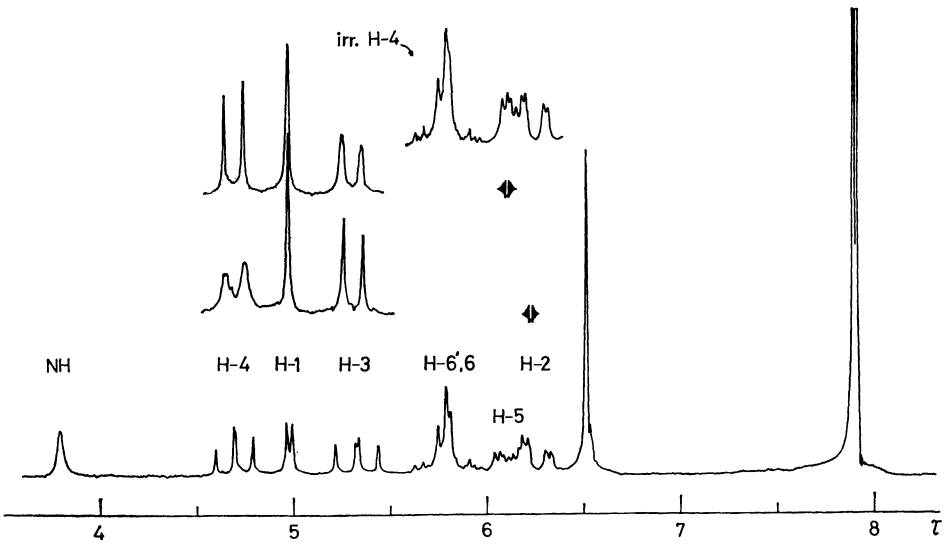

Chart 3. NMR spectrum of methyl 4,6-di-*O*-acetyl-2-amino-2-dexoy-α-D-glucopyranoside-2,3-carbamate (IX) in $CDCl_3$ at 100 MHz.

7) *Cf.* Ref. 5.

8) P. W. Austin, F. E. Hardy, J. G. Buchanan, and J. Baddiley, *J. Chem. Soc.*, **1963**, 5350.

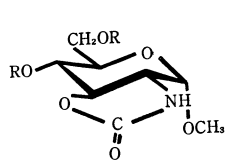

Ⅷ R=H
Ⅸ R=Ac

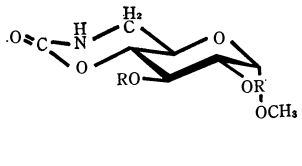

Ⅹ R=H
Ⅺ R=Ac

sibility of a 2,4-cyclic carbamate structure for the carbamate.

When similarly treated with NPCC, methyl α-D-glucopyranoside gave no reaction indicating that NPCC does not come into reaction with any hydroxyl group under a similar condition. This result also precludes the possibility of formation of an *O*-phenoxycarbonyl intermediate.

Methyl 6-amino-6-deoxy-α-D-glucopyranoside[9] was converted to 4,6-cyclic carbamate (X) in a yield of 78%. The structure was proved by its elemental analysis and spectroscopic data, and also from those of its di-*O*-acetyl derivative (XI), the CI conformation of these compounds being confirmed. These results exclude the possibility of 3,6-cyclic carbamate for the carbamate.

In glucopyranosides, the 2-*O*-, 3-*O*-, and 2,3-di-*O*-substituted derivatives was readily prepared *via* corresponding 4,6-*O*-benzylideneglucopyranosides, but the protecting method was not applicable in such case as 6-amino-6-deoxy-glucopyranosides. The above described cyclic carbamate method gives a solution for this problem.

Experimental

Thin-layer chromatography (tlc) was performed by the use of silica gel and the chromatograms were visualized by spraying with sulfuric acid. The NMR spectra were recorded with Varian A-60D and HA-100D spectrometers. Tetramethylsilane (τ 10.00; for the solutions other than deuterium oxide) and sodium 4,4′-diemthyl-4-silapentane-1-sulfonate (τ 10.00; for the solutions of deuterium oxide) were used as the internal standards.

2-Deoxystreptamine-1,6 : 3,4-dicarbamate (II). a) From 2-Deoxystreptamine (I) and p-Nitrophenoxycarbonyl Chloride (NPCC) in the Presence of Dowex Resin: To an ice-cold mixture of an aqueous solution (1 m*l*) of I (104 mg, 0.64 mmol) and wet Dowex 1×2 resin (OH form, 3.5 m*l*), a cold solution of NPCC (340 mg, 1.7 mmol) in acetone (3.4 m*l*) was added under stirring within several minutes and the mixture was stirred at that temperature for 1 hr. A weakly acidic yellow slurry resulted. Another Dowex resin (3.5 m*l*) and NPCC (340 mg) in acetone (3.4 m*l*) was added and stirring was continued for 1 hr in the cold. On tlc with acetone-ethyl acetate (2:1), three spots (R_f 0.95, 0.5, and 0) appeared; the first is a mixture of NPCC, *p*-nitrophenol, and some derivatives originated from NPCC, and the last a by-product, which gave R_f 0.35 on tlc with DMF. The mixture was extracted with ether to remove the first mixture (R_f 0.95) and the residual mixture was filtered off, washed with hot aqueous acetone (1:2). The combined filtrate and the washings were then evaporated to give a yellow solid (109 mg). The solid was chromatographed on a column of silica gel (1.4×18 cm) with DMF and the fraction containing II (R_f 0.5 with acetone-ethyl acetate 2:1) was evaporated to give a colorless solid (100 mg, 73%), which was recrystallized from aqueous methanol (1:1); mp >285°C.

Found: C, 41.14; H, 5.30; N, 12.35%. Calcd for $C_8H_{10}O_5N_2 \cdot H_2O$: C, 41.38; H, 5.21; N, 12.07%.

IR spectrum: 3410 (s), 3300, 2920 (w), 1760 (s), 1735 (s), 1470 (w), 1435, 1390, 1315, 1230, 1210, 1175, 1130 (w), 1095, 1085, 960 (s), 935, 905 (w), 885 (w), 775, 740 cm^{-1}. NMR spectrum (in DMSO-d_6 at 60 MHz): τ : 2.3 (2H s., disappeared on deuteration, NHCO), 4.0 (1H short-range multiplet, disappeared on deuteration, OH), 5.6—6.7 (5H m., H-1,3,4,5,6), 7.80 (1H double triplets H-2_e), 8.40 (1H q., H-2_a); $J_{1,2a}=J_{3,2a}=J_{2a,2e}=11$ Hz, $J_{1,2e}=J_{3,2e}=3$ Hz.

b) From I and Phenoxycarbonyl Chloride (PCC) in the Presence of Dowex Resin: To an ice-cold mixture of an aqueous solution (2 m*l*) of I (108 mg, 0.67 mmol) and wet Dowex 1×2 resin (OH form, 4.1 m*l*), a cold solution of PCC (470 mg, 3.0 mmol) in acetone (4.2 m*l*) was added under stirring within several minutes, whereupon the resultant mixture became weakly acidic (pH 6) and gave a precipitate, which was proved to include compound II. After continuation of stirring at room temperature overnight followed by ice-cooling, Dowex resin (2.2 m*l*) and a cold solution of PCC (227 mg) in acetone (2 m*l*) were added successively, and the mixture (pH 5) was stirred at room temperature overnight. The resultant mixture (pH 6.5) gave almost no precipitation. On tlc with ethyl acetate-methanol (10:1), a spot (R_f 0.34, major) was accompanied with weak spots at R_f 0.56 and 0; the latter was ninhydrin-positive and the former faded as the reaction proceeded. Incidentally, compound II and the *N*, *N*′-diphenoxycarbonyl derivative (IV) of I gave almost identical R_f value with several developing solvent mixtures, and this made the determination of the reaction period by monitoring the tlc patterns difficult. The mixture was filtered and the resin was washed with hot aqueous acetone (1:2). On combining the filtrate and the washings, some solid precipitated. After filtration, the solution was treated with ether until the ethereal solution became negative for DQC reagent.[10] The aqueous suspension was concentrated to give a solid which was filtered off, washed with water until the washing became negative for ninhydrin reagent. Colorless solid (86 mg, 60%) was obtained and was identical with II obtained by method a) in its IR and NMR spectra.

c) From I and PCC in the Presence of Sodium Carbonate: To an ice-cold solution (5 m*l*) of I (200 mg 1.23 mmol) and sodium carbonate (160 mg), a cold solution of PCC (427 mg, 2.73 mmol) in acetone (8 m*l*) was added under stirring and the resultant suspension (pH ~8) was stirred at room temperature overnight, whereupon a clear solution (pH ~7.5) resulted. On tlc with ethyl acetate-methanol (10:1), a spot (R_f 0.34, major) appeared accompanied with minor spots of R_f 0.56 and 0. Sodium hydrogencarbonate (30 mg) was added and the mixture was again stirred overnight. The reaction mixture was treated with ether until the ethereal solution became negative for DQC reagent; the aqueous solution gave a precipitate. Filtration and washings with water gave II (193 mg, 73%).

d) From N,N′-Diphenoxycarbonyl-2-deoxystreptamine (IV) in the Presence of Dowex Resin: To a solution of IV (102 mg) in aqueous acetone (1:3, 10 m*l*), Dowex 1×2 resin (OH form, 0.1 m*l*) was added and the mixture was stirred at room tem-

9) F. Cramer, H. Otterbach, and H. Springmann, *Chem. Ber.*, **92**, 384 (1959).

10) This reagent was used for the detection of phenol liberated. A tlc plate spotted with a solution containing phenol is sprayed with 0.2% solution of 2,6-dichloroquinone chlorimide (DQC) in ethanol and the plate is exposed to the vapour of ammonia. Blue color appears.

perature for 1 hr. After neutralization with hydrochloric acid, the mixture was heated to 45°C to dissolve the precipitate, filtered, and the filtrate was evaporated to give a residue which was washed with ether and then with water to give a colorless solid (II) 43.5 mg (81%).

N N'-*Diphenoxycarbonyl-2-deoxystreptamine (IV).* To an ice-cold solution of I (508 mg, 3.13 mmol) and sodium hydrogencarbonate (658 mg, 7.82 mmol) in water (11 m*l*), a solution of PCC (1.22 g, 7.80 mmol) in acetone (18 m*l*) was dropped under stirring in 10 min and the mixture was stirred for more 30 min. After neutralization with hydrochloric acid the precipitate was filtered off, washed thoroughly with ether and with water to give a solid (IV), 716 mg (57%); mp > 295°C, R_f 0.33 (tlc with ethyl acetate - methanol 10:1).

Found: C, 59.57; H, 5.68; N, 6.83%. Calcd for $C_{20}H_{22}O_7N_2$: C, 59.69; H, 5.51; N, 6.96%.

IR spectrum: 3400, 3330, 3050 (w), 2930 (w), 2870 (w), 1710 (s, NH*C*O*O*), 1595 (w, phenyl), 1540 (s, amide II), 1495 (phenyl), 1340 (w), 1305, 1285, 1215 (s), 1150, 1115, 1075, 1030, 985, 960, 910, 855, 840, 790, 765, 715, 690 cm^{-1}. NMR spectrum (in DMSO-d_6 at 60 MHz): τ : 2.1—3.0 (12 H m., phenyl and N*H*CO).

This compound was unstable and attempted recrystallization from aqueous methanol caused partial convertion to II.

Preparation of N,N'-*Bis(ethoxycarbonyl)-2-deoxystreptamine (VII) from II.* To a suspension of II (78.4 mg) in dry ethanol (1.6 m*l*), 0.01 N sodium ethoxide in ethanol (1 m*l*) was added and the mixture was refluxed for 1.5 hr. On tlc with ethyl acetate - methanol (10:1), starting material (R_f 0.34) had disappeared and VII (R_f 0.23) and a product (R_f 0) appeared. When the solution was then allowed to stand at room temperature overnight, the product of R_f 0 almost disappeared and crude VII precipitated. The product was collected by centrifuge, washed with cold ethanol and then dissolved in water (0.7 m*l*) Additon of acetone (14 m*l*) gave some precipitates, which were removed by centrifuge, and the solution was evaporated to give a solid (VII), 86 mg (77%). The IR and NMR spectra of the product were superimposable with those of the authentic sample.[6] The product did not depress the melting point (218°C) when mixed with the authentic sample.

5-O-*Acetyl-2-deoxystreptamine-1,6:3,4-dicarbamate (III).* To a suspension of II (158 mg) in pyridine (3 m*l*) acetic anhydride (0.15 m*l*) was added and the mixture was stirred at room temperature for 3 hr. After addition of a drop of methanol, the clear solution was evaporated to give a residue, which was washed with cold water to give a chromatographically homogeneous solid, 143 mg (76%), R_f 0.57 (tlc with acetone - ethyl acetate 2:1). Recrystallized from aqueous acetone (1:2); mp 276°C (decomp.); molecular weight 256 (M^+, by mass spectrum).

Found: C, 47.03; H, 5.07; N, 10.46%. Calcd for $C_{10}H_{12}O_6N_2$: C, 46.88; H, 4.72; N, 10.93%.

IR spectrum: 3300 (νNH), 2930 (w), 1770 (s), 1735, 1475 (w), 1415, 1395, 1380, 1340, 1295, 1245 (acetyl ester), 1225, 1105, 1070, 1040, 980, 955, 925, 895, 870, 800, 775, 745 cm^{-1}. NMR spectrum (in DMSO-d_6 at 60 MHz): τ : 2.2 (2H s., N*H*CO), 4.45 (1H t., H-5), 5.91 (2H q., H-4,6), 6.30 (2H double triplets, H-1,3), 7.85 (1H double triplets, H-2$_e$), 7.90 (3H s., OAc), 8.40 (1H q., H-2$_a$); $J_{1,2a}=J_{3,2a}=J_{2a,2e}=11$ Hz, $J_{1,2e}=J_{3,2e}=3.2$ Hz, $J_{3,4}=J_{1,6}=11$ Hz, $J_{4,5}=J_{5,6}=9.4$ Hz. Irradiation at τ 5.91 caused the signals at τ 4.45 (H-5) to collapse to a singlet.

4,5,6-*Tri*-O-*acetyl*-N,N'-*diphenoxycarbonyl-2-deoxystreptamine (V).* To a solution of IV (74.3 mg) in pyridine (1.5 m*l*), acetic anhydride (0.21 m*l*) was added and the solution was allowed to stand overnight. After a slight precipitate was removed by filtration, the solution was coevaporated with toluene to give a solid, which was washed thoroughly with water to give a chromatographically homogeneous solid, 81.1 mg (83%), mp 192.5—194.5°C, R_f 0.52 (tlc with ether).

Found: C, 59.07; H, 5.31; N, 5.40%. Calcd for $C_{26}H_{28}O_{10}N_2$: C, 59.08; H, 5.34; N, 5.30%.

IR spectrum: 3420, 3350, 3080 (w), 2960 (w), 1760 (s), 1730, 1600 (w, phenyl), 1545 (sh, amide II), 1525 (amide II), 1500 (phenyl), 1385, 1365, 1310, 1260, 1235, 1205 (s), 1170 (w), 1065, 1030, 980, 920 (w), 895 (w), 845 (w), 790, 765, 720, 695 cm^{-1}. NMR spectrum (in DMSO-d_6 at 60 MHz): τ: 1.9—3.0 (12 H m., phenyl and NHCO), 7.99 (6H s., O(4,6)Ac), 8.03 (3H s., O(5)Ac).

4,5,6-*Tri*-O-*acetyl*-N,N'-*diacetyl-2-deoxystreptamine (VI).* This substance was prepared by the usual way from acetic anhydride and pyridine, mp >300°C (lit,[11] 340—350°C)

Found: C, 51.96; H, 6.80; N, 7.53%. Calcd for $C_{16}H_{24}O_8N_2$: C, 51.60; H, 6.50; N, 7.52%.

IR spectrum: 1750 (s); 1655 (s, sh), 1640 (s)(amide I); 1555 cm^{-1} (amide II). NMR spectrum[11,12] (in methanol-d_4 - D_2O at 60 MHz): τ: 8.02 (9H s., OAc), 8.13 (6H s., NAc).

*Methyl 2-Amino-2-deoxy-α-*D*-glucopyranoside-2,3-carbamate (VIII).* To a solution of methyl 2-amino 2-deoxy-α-D-glucopyranoside (base, 616 mg, 3.19 mmol) in water (8 m*l*), wet Dowex 1×2 resin[13] (OH form, 100—200 mesh, 15.5 m*l*) was added and the mixture was ice-cooled. A cold solution of NPCC (1.63 g, 8.07 mmol) in acetone (16 m*l*) was added under vigorous stirring for 10 min, when the mixture became a viscous yellow slurry. After gentle stirring for 1 hr at room temperature, the slurry (pH ~7) was washed with ether and the resultant aqueous suspension was filtered and the residual mass was washed with hot water. The filtrate and the washings were combined and made acidic (pH ~3) by the addition of hydrochloric acid. The solution was extracted with ether to remove *p*-nitrophenol accompanied until the ethereal solution gave no yellow color when sodium hydroxide solution was added. The aqueous solution was then neutralized with Dowex 1×2 resin (OH form), filtered, and evaporated to give a solid (~650 mg). Since the solid still contained an impurity (tlc, R_f 0 with ethyl acetate - methanol 5:1), chromatography on a small column of silica gel (16 g) with ethyl acetate - methanol (5:1) was carried out and the fraction containing the carbamate (VIII, R_f 0.54) was evaporated and the residue was dried by coevaporation with ethanol and benzene. Hygroscopic solid was obtained; 542 mg (78%); $[\alpha]_D^{21}+110°$ (*c* 0.5, water).

Found: C, 43.76; H, 5.70; N, 6.61%. Calcd for $C_8H_{13}O_6N$: C, 43.83; H, 5.98; N, 6.39%.

IR spectrum: 3350 (s, broad), 2940, 1760 (s, broad), 1455, 1400 (broad), 1335, 1290, 1205, 1185, 1140, 1105, 1065, 1040, 1005, 945, 915, 785 cm^{-1}. NMR spectrum (in D_2O at 60 MHz): τ: 4.86 (1H d., H-1), 5.40 (1H q., H-3), 5.93 (1H t., H-4), 6.22 (1H q., H-2), 6.5 (3H s., OCH_3); $J_{1,2}=3$ Hz, $J_{2,3}=12$ Hz, $J_{3,4}=9.3$ Hz, $J_{4,5}=\sim 9$ Hz. Irradiation at τ 4.86 (H-1) caused the quartet at τ 6.22 (H-2) to collapse to a doublet ($J=\sim 12$ Hz).

*Methyl 4,6-Di-O-acetyl-2-amino-2-deoxy-α-*D*-glucopyranoside-2,3-carbamate (IX).* To a solution of VIII (202 mg) in

11) F. W. Lichtenthaler, *Chem. Ber.*, **96**, 2047 (1963).

12) M. Nakajima, A. Hasegawa, and N. Kurihara, *Ann. Chem.*, **689**, 235 (1965).

13) The aqueous suspension of the resin in a cylinder was set aside for a while and the volume of the resin was measured under pressing with a glass rod with a flat top having the same diameter with that of the cylinder.

pyridine (4 ml), acetic anhydride (0.3 ml) was added and the mixture was allowed to stand at room temperature overnight. On tlc, a single spot (R_f 0.67, with ethyl acetate) appeared. After a drop of water was added, the solution was evaporated and the residue was dissolved in chloroform. The solution was washed successively with potassium hydrogensulfate solution, water, sodium hydrogencarbonate solution and water, dried over sodium sulfate and coevaporated with benzene to give a hygroscopic solid, 219 mg (78%); $[\alpha]_D^{21}$ +94° (*c* 0.5, chloroform).

Found: C, 47.34; H, 5.77; N, 4.32%. Calcd for $C_{12}H_{17}O_8N$: C, 47.52; H, 5.65; N, 4.62%.

IR spectrum: 3400 (νNH), 2960, 1780 (s), 1750 (s), 1455, 1375, 1245 (s, ester), 1185, 1140, 1110, 1045 (s), 1005 (s), 940, 785, 755 cm^{-1}. NMR spectrum (in $CDCl_3$ at 100 MHz): τ: 3.8 (1H s., NHCO), 4.70 (1H q., H-4), 4.98 (1H d., H-1), 5.33 (1H q., H-3); 5.76 (H-6′) and 5.81 (H-6) (each 1H quartet forming in total the AB part of an ABX system); 6.10 (1H m., H-5), 6.25 (1H q., H-2), 6.52 (3H s., OCH_3), 7.90 and 7.92 (each 3H s., OAc); $J_{1,2}$=3 Hz, $J_{2,3}$=11.8 Hz, $J_{3,4}$=10 Hz, $J_{4,5}$=9.2 Hz, $J_{5,6}$=~3 Hz, $J_{5,6'}$=~4.5 Hz, $J_{6,6'}$=12.4 Hz. Irradiation at τ 5.33 (H-3) caused the quartet of H-2 to collapse to a doublet (J=~3 Hz) and the quartet of H-4 to a doublet (J=~9 Hz). Irradiation at τ 6.25 (H-2) caused the quartet of H-3 to collapse to a doublet (J=10 Hz), the doublet of H-1 to a singlet and the quartet of H-4 to an incomplete doublet. Irradiation at τ 6.10 (H-5) caused the quartet of H-4 to collapse to a doublet (J=10 Hz). Irradiation at τ 4.70 (H-4) caused the multiplet of H-5 to collapse to a quartet (J=~3 and ~4.5 Hz).

Methyl 6-Amino-6-deoxy-α-D-glucopyranoside-4,6-carbamate (X). To a solution of methyl 6-amino-6-deoxyl-α-D-glucopyranoside hydrochloride (715 mg, 3.11 mmol) in water (7 ml), wet Dowex 1×2 resin (OH form, 100—200 mesh, 18 ml, the volume was measured under pressing) was added and the mixture was ice-cooled. A cold solution of NPCC (1.63 g, 8.07 mmol) in acetone (16 ml) was added to the mixture under vigorous stirring for 40 min, when a viscous yellow slurry (pH~6) resulted. On tlc, a spot (R_f 0.85 with acetone-methanol 3:1) appeared. The slurry was made acidic (pH ~3) with hydrochloric acid and extracted with ether several times. The aqueous suspension was filtered, and the residual mass was washed with hot water. The combined filtrate and washings were neutralized with Dowex 1×2 resin (OH form), filtered, and evaporated to give a solid (~690 mg). This was dissolved in water (1.4 ml), filtered and concentrated almost to dryness. Addition of acetone gave colorless cystals, 529 mg (78%), mp 233—236°C, $[\alpha]_D^{25}$ +38.1° (*c* 0.7, water).

Found: C, 44.14; H, 6.01; N, 6.36%. Calcd for $C_8H_{13}O_6N$: C, 43.83; H, 5.98; N, 6.39%.

IR spectrum: 3430 (s), 3300, 2950 (w), 2900 (w), 1725 (s), 1660, 1495, 1460, 1405, 1385, 1370, 1320, 1280 (s), 1210, 1135, 1110, 1090, 1065, 1050, 1015, 995 (s), 945, 895, 855, 765 (s), 745, 710, 660 cm^{-1}. NMR spectrum (in D_2O at 60 MHz): τ: 5.09 (1H d., H-1), 6.54 (3H s., OCH_3); $J_{1,2}$= 3.2 Hz.

Methyl 2,3-Di-O-acetyl-6-amino-6-deoxy-α-D-glucopyranoside-4,6-carbamate (XI). To a solution of X (224 mg) in pyridine (5 ml), acetic anhydride (0.5 ml) was added and the mixture was allowed to stand at room temperature overnight. On tlc, a single spot (R_f 0.42 with ethyl acetate) appeared. Hereafter the solution was treated likewise as in the preparation of IX and a colorless solid (300 mg, 97%) was obtained. Recrystallization from chloroform-petroleum ether or from ethanol; mp 207—209°C, $[\alpha]_D^{21}$ +61.4° (*c* 0.8, chloroform).

Found: C, 47.80; H, 5.73; N, 4.68%. Calcd for $C_{12}H_{17}O_8N$: C, 47.52; H, 5.65; N, 4.62%.

IR spectrum: 3430 (w, NH), 2950 (w), 1760 (s), 1740 (s), 1715 (s), 1490, 1460, 1400, 1375 (s), 1270, 1240 (s, ester), 1220 (s, ester), 1195, 1180, 1160, 1145, 1095, 1075, 1055, 1000, 945, 920, 885, 850, 765, 755, 735, 680 cm^{-1}. NMR spectrum (in $CDCl_3$ at 100 MHz): τ: 3.2 (1H broad doublet in appearance, J=~3.5 Hz, NHCO), 4.42 (1H t., H-3), 5.03 (1H d., the signal in the higher field being strong, H-1), 5.13 (1H q., at τ 5.07, 5.11, 5.17, and 5.21, the signals at 5.07 and 5.17 being strong, H-2), 5.8—6.05 (2H m., H-4 and H-5 ?), 6.35—6.85 (2H m., H-6,6′ ?), 6.55 (3H s., OCH_3), 7.91 (6H s., OAc); $J_{1,2}$=3.5 Hz, $J_{2,3}$=9.7 Hz, $J_{3,4}$=~9.5 Hz. Irradiation at τ 3.2 caused the signals at τ 6.35—6.5 to change. Irradiation at τ 4.42 (H-3) caused the signals at τ 5.13 (H-2) to collapse to a doublet (J=~3.5 Hz) and the multiplet at τ 5.8—6.05 (which contained H-4) to change. Irradiation at τ 5.07 (H-1 and 2) or at τ 5.92 caused the signals at τ 4.42 (H-3) to collapse to a doublet (J=~9 Hz), respectively.

We are grateful to Dr. Hiroshi Naganawa of Institute of Microbial Chemistry for the measurements of NMR spectra at 100 MHz and to Mr. Saburo Nakada of our Laboratory for the elemental analysis.

NOTES

BULLETIN OF THE CHEMICAL SOCIETY OF JAPAN, VOL. 44, 1416—1417 (1971)

Asymmetric Hydrogenation of C=O Double Bond with Modified Raney Nickel Catalyst. XVI

Yoshiharu IZUMI, Shinichi YAJIMA,* Kazuo OKUBO, and Kirill K. BABIEVSKY**
Division of Organic Chemistry, Institute for Protein Research, Osaka University, Kita-ku, Osaka
(Received June 8, 1970)

In the course of the investigation of the asymmetrically modified R-Ni catalyst, it was found that catalysts modified with α-amino or α-hydroxy dicarboxylic acids have higher asymmetric hydrogenation activities than do those modified with α-amino or α-hydroxy monocarboxylic acids. That is, the asymmetric activity of the catalyst modified with aspartic acid, glutamic acid, or malic acid is higher than that of the catalyst modified with alanine, butyrine, norvaline, or lactic acid.[1-6]

The expectation that the excellent property of α-amino or α-hydroxy dicarboxylic acid as a modifying reagent will greatly depend on the ω-carboxyl group is also supported by the fact that the optimum asymmetric activity of the catalyst modified with α-amino or α-hydroxy dicarboxylic acid is produced by the modification at pH 5, which is the point where the ω-carboxyl group is neutralized. The contribution of the ω-carboxyl group to the increase in the asymmetric activity of the catalyst may be ascribable to its ionic and steric effects and to its electronegativity. Therefore, it can be expected that more acidic, more electronegative, and bulkier substituents than the carboxyl group, such as the sulfonyl group, will increase the asymmetric activity of the catalyst.

In the present work, the abilities of L-α-hydroxy-β-sulfopropionic acid, L-homocysteic acid, and L-cysteic acid as modifying reagents were tested at various modifying pH values in order to test the expectation mentioned above. The results are shown in Figs. 1 and 2, where they are compared with those obtained with aspartic acid and malic acid.

As may be seen in Figs. 1 and 2, unexpected results were obtained. The asymmetric activities of the catalyst modified with the sulfonic acids were considerably lower than those of the catalysts modified with

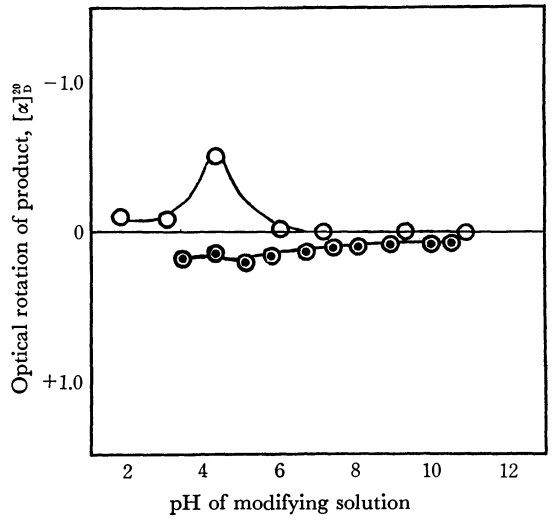

Fig. 1. Modifications with L-cysteic acid and L-homocysteic acid (Modified at 0°C).
—⊙— L-Cysteic acid $HO_3SCH_2CHCO_2H$ (NH_2)
—○— L-Homocysteic acid $HO_3SCH_2CH_2CHCO_2H$ (NH_2)

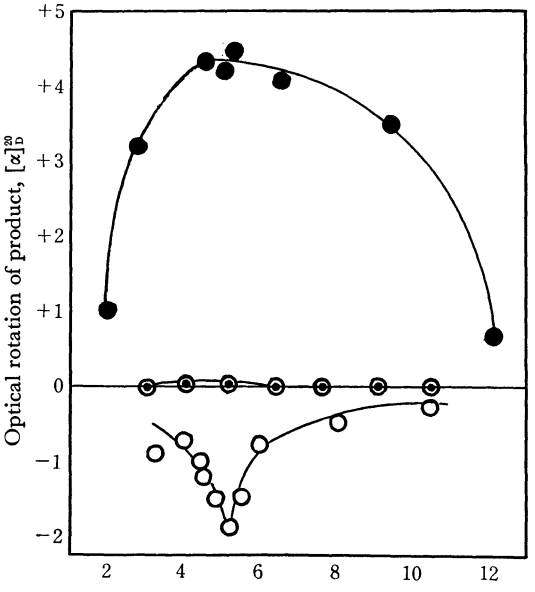

Fig. 2. Modifications with L-malic acid and L-aspartic acid and L-α-hydroxy-β-sulfopropionic acid.
-●- L-malic acid $HOOCCH_2CHCO_2H$ (OH)
-○- L-aspartic acid $HOOCCH_2CHCO_2H$ (NH_2)
-◎- L-α-hydroxy-β-sulfopropionic acid $HO_3SCH_2CHCO_2H$ (OH)

* Present address: Kawaken Fine Chemicals Co., Ltd., Tokyo.
** Present address: Institute of Heteroorganic Compounds, Academy of Sciences of the USSR, Moscow, USSR.

1) Y. Izumi, M. Imaida, H. Fukawa, and S. Akabori, This Bulletin, **36**, 21 (1963).
2) Y. Izumi, M. Imaida, H. Fukawa, and S. Akabori, *ibid.*, **36**, 155 (1963).
3) Y. Izumi, S. Tatsumi, and M. Imaida, *ibid.*, **39**, 2223 (1966).
4) Y. Izumi, T. Tanabe, S. Yajima, and M. Imaida, *ibid.*, **41**, 941 (1968).
5) Y. Izumi, K. Matsunaga, S. Tatsumi, and M. Imaida, *ibid.*, **41**, 2515 (1968).

the α-amino or α-hydroxy dicarboxylic acids. Scarcely no effect of the modifying pH is found in the case of modifications with cysteic acid and α-hydroxy-β-sulfopropionic acid, although a slight effect was found in the case of modification with homocysteic acid.

The asymmetric directions of the catalysts modified with L-homocysteic acid and L-α-hydroxy-β-sulfopropionic acid come under the general rule of the relation between the absolute configuration of the modifying reagent and the asymmetric direction of the catalyst —the catalysts modified with L-α-amino acids or D-α-hydroxy acids at 0°C produce predominantly methyl D-3-hydroxybutyrate in the hydrogenation of methyl acetoacetate. However, cysteic acid gives a catalyst which has an asymmetric direction, contrary to the general rule, as was also found in the case of the catalyst modified with serine, cysteine, and threonine.[7]

From the results described above, the regular correlations between the asymmetric activities of the catalysts modified with sulfonic acids and the ones modified with amino dicarboxylic acids were difficult to be found, from the simple view point of ionic effect, electronegativity or steric hindrance of the β- or γ-substituent.

As it was reported in the previous paper that the modifying reagent might be adsorbed on the catalyst surface with the chelate formation,[8] the contribution of the sulfonyl group to the chelate formation must be discussed. In connection with the sulfonyl group, however, it is generally known that, as the dissociation constant of the sulfonic acid is much larger than that of the carboxylic acid, the ability of the chelate formation with the metal ion is considerably weaker than that of the carboxyl group.

Accordingly, it is hard to accept the idea that the unexpected results obtained with the catalysts modified with the β- or γ-sulfonyl substituted amino and hydroxy acids are brought about by the different types of adsorption of the modifying reagent.

Therefore, it can be expected that the amino acids or hydroxy acids which have a sulfonyl group on the β- or γ-carbon are adsorbed by amino and carboxyl groups or by hydroxy and carboxyl groups.

As a conclusion of the present work, it was made clear that the electronegativity and bulkiness of the sulfonyl group on the β- or γ-carbon of the amino or hydroxy acid did not simply affect the asymmetric activity of the catalyst, and that the other new effect of the sulfonyl group overcame the effects of the electronegativity and bulkiness of the sulfonyl group.

The new effect of the substituent will be discussed in detail in This Bulletin in the near future.

The L-α-hydroxy-β-sulfopropionic acid was prepared from L-cysteic acid and was successively purified as benzidine and dicyclohexylamine salts.

Experimental

The asymmetric activity of the catalyst was measured by a method reported in a previous paper.[6]

Preparation of the Dicyclohexylamine Salt of L-α-Hydroxy-β-sulfopropionic Acid. In 150 m*l* of 10% hydrochloric acid, 18.7 g of L-cysteinic acid monohydrate was dissolved. Into this solution, 50 m*l* of isoamyl nitrite was vigorously stirred, drop by drop, at room temperature, and then the reaction mixture was stirred continuously overnight. The isoamyl alcohol thus separated was removed, and the aqueous layer was washed thoroughly with ether. The aqueous solution was evaporated to a syrup, and the resulting syrup was taken up in a small amount of water and again evaporated. This syrup gave, quantitatively, benzidine salt in an alcohol solution; mp 260°C.

Found: C, 50.54; H, 4.71; N, 7.88%. Calcd for $C_{15}H_{18}O_6N_2S$: C, 50.85; H, 5.12; N, 7.91%.

To 17 g of syrup dissolved in 100 m*l* of acetone, was added 35 g of dicyclohexylamine, drop by drop, with ice cooling. The dicyclohexylamine salt thus precipitated was collected and washed with acetone. Two recrystallizations from ethanol-ether (1:5) gave 29.5 g (53.6%); mp 260°C.

Found: C, 58.83; H, 9.59; N, 5.22%. Calcd for $C_{27}H_{54}O_7N_2S[HSO_3CH_2CH(OH)\cdot CO_2H\cdot 2$ 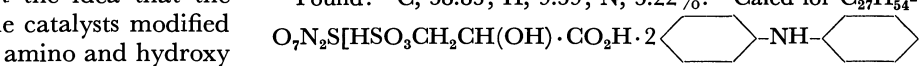 $\cdot H_2O]$: C, 59.00; H, 9.82; N, 5.09%. $[\alpha]_D$ −8.57 (*c* 2.3 EtOH).

Preparation of a Modifying Solution of L-α-Hydroxy-β-sulfopropionic Acid. In 30 m*l* of water, 5.36 g of the dicyclohexylamine salt was dissolved. The dicyclohexylamine was removed using a column of Amberite IR 120(400—600 mesh, 1×18 cm), and with water. The total volume of the eluted solution was adjusted to 100 m*l*. The specific rotation $[\alpha]_D$ −13.3 (*c* 1.65, H_2O) for L-α-hydroxy-β-sulfopropionic acid was calculated from the α_D of the solution obtained. An attempt to isolate the free acid failed.

The authors wish to express their thanks to Professor Shōichirō Yamada and Professor Yōichi Shimura, Osaka University, for their helpful discussions, and to the Ajinomoto Co., Ltd., Tokyo, for the gift of L-homocysteic acid.

6) Y. Izumi, S. Tatsumi, and M. Imaida, *ibid.*, **42**, 2373 (1969).

7) Proline, hydroxyproline, and alanine all produced catalysts which have an asymmetric direction, thus contradicting the general rule. However, proline and hydroxyproline are special amino acids which have a pyrrole ring, and the modification with alanine is very sensitive to the modifying condition, so such results are reasonable even according to the general rule. The details of the asymmetric activity of the catalyst modified with alanine will be discussed in This Bulletin in the near future.

8) Y. Izumi and T. Ninomiya, This Bulletin, **43**, 579 (1970).

BULLETIN OF THE CHEMICAL SOCIETY OF JAPAN, VOL. 44, 1418—1419 (1971)

Asymmetric Hydrogenation of C=O Double Bond with Modified Raney Nickel. XVII

Yoshiharu IZUMI, Tadao HARADA, Tadashi TANABE, and Kazuo OKUDA

Division of Organic Chemistry, Institute for Protein Research, Osaka University, Kita-ku, Osaka

(Received June 8, 1970)

In the course of our studies of the asymmetric hydrogenation catalyst, it was found that the Raney nickel catalysts modified with various optically-active compounds catalyze asymmetrically the hydrogenation of methyl acetoacetate to methyl 3-hydroxybutyrate; the relationship between the structure of the modifying reagent and the asymmetric activity of the catalyst has been studied in detail.[1] From the facts that *N*-substituted amino acids, *N*-cyanoethyl, *N*-benzoyl, and *N,N*-dimethyl derivatives of L-glutamic acid and L-aspartic acid, produce catalysts with much lower asymmetric activities than the original amino acids, it was concluded that a primary amino residue of amino acid is necessary for an effective modifying reagent.[2]

However, the role of the α-carboxyl group of the amino acid or hydroxy acid used as a modifying reagent for the asymmetric activity of the catalyst has not yet been made clear.

In the present paper, the asymmetric activities of the catalysts modified with optically-active 2-amino alcohols, R-C*H(NH_2)CH_2OH, are examined in order to investigate the role of the α-carboxyl group.

The activities of the catalysts modified with amino alcohols are shown in Table 1, where they are compared with those of the catalysts modified with the corresponding amino acids. Also, the results of the adsorption-stability test of the modifying reagent on the catalyst are shown in Table 2.

Table 1. Asymmetric activities of the catalysts modified with optically active 2-amino alcohols, and 2-amino acids

Modifying reagent	Modifying conditions		$[\alpha]_D$ of methyl 3-hydroxybutyrate
	pH	Temp. °C	
L-Alaninol	11.6	0	−0.04
L-Leucinol	11.4	0	−0.25
L-Valinol	11.4	0	−0.15
L-Alanine	6.1	0	+0.45
L-Leucine	6.0	0	−1.65
L-Valine	5.9	0	−2.64

Table 2. The asymmetric activities of the catalysts after the contact with the substrate before use

Modifying reagent	Modifying temp., °C	$[\alpha]_D$ of methyl 3-hydroxybutyrate
L-Leucine	0	−1.40
L-Leucinol	0	−0.08

As is shown in Table 1, the catalyst modified with 2-amino alcohol has a lower asymmetric activity than that modified with the corresponding amino acid, and so it is evident that it is desirable for the modifying reagent to have an α-carboxyl group.

Moreover, the Raney nickel catalysts modified with L-leucine and L-leucinol were employed in the hydrogenation of methyl acetoacetate after contact with the substrate before use in order to study the adsorption stabilities of the modifying reagents on the catalysts in the presence of the substrate. As may be found in Table 2, the process of the contact with the substrate reduced the asymmetric activity of the catalyst modified with L-leucinol to about 30%, while the process did not result in any remarkable change in that of the catalyst modified with L-leucine. These facts show that the displacement of a carboxyl group by a hydroxymethyl group results in a considerable decrease in the adsorption stability on the catalyst, and that this poor adsorption stability of the amino alcohol in the presence of methyl acetoacetate causes the considerably lower asymmetric activity of the catalyst.

Materials

2-Amino Alcohols. These compounds were synthesized from the corresponding optically-active 2-amino acid ethyl esters by the method of Karrer and Naik.[3]

Experimental

Preparation of the Modified Raney Nickel Catalyst. Into a solution of 4.5 g of sodium hydroxide in 20 m*l* of deionised water, 1.5 g of Raney nickel alloy (Ni:Al=4:6) was added, in small portions, and then the solution was allowed to stand for 1 hr at 100°C. Then, the catalyst was washed with water until the pH of the washing was about neutral. The catalyst so obtained was added a 1—2% aqueous solution of the modifying reagent, and the mixture was allowed to stand at the specified temperature, with occasional shaking, for 1.5 hr. After the subsequent removal of the modifying solution by decantation, the catalyst was washed once with water and three times with methanol.

Hydrogenation. Methyl acetoacetate (17.5 m*l*, The Nippon Syntehtic Chemical Industry Co., Ltd.) was hydrogenated with a modified Raney nickel catalyst prepared from 1.5 g of the alloy under an initial hydrogen pressure of about 90 kg/cm² at 60°C in a shaking autoclave.

Adsorption-stability Test. The catalysts modified with L-leucine and L-leucinol, prepared by the procedure described above, were placed in contact with 20 m*l* of methyl aceto-

1) Part XIV: Y. Izumi, and T. Ninomiya, This Bulletin, **43**, 579 (1970). Part XV: T. Tanabe, T. Ninomiya, and Y. Izumi, *ibid.*, **43**, 2276 (1970). Part XVI: Y. Izumi, S. Yajima, K. Okubo, and K. K. Babievsky, *ibid.*, **44**, 1416 (1971).

2) Y. Izumi, M. Imaida, H. Fukawa, and S. Akabori, *ibid.*, **36**, 155 (1963).

3) P. Karrer and A. R. Naik, *Helv. Chim. Acta*, **31**, 1617 (1948).

acetate at room temperature for 30 min, and then washed three times with methanol. The resulting catalyst was used for the hydrogenation of methyl acetoacetate.

Measurement of the Asymmetric Activity of the Catalyst. After the removal of the catalyst by filtration, the hydrogenation products were distilled under reduced pressure (bp 61—62°C/12 mmHg). The optical rotatory power of the distilled product was measured by a conventional polarimeter in a 1 dm tube without dilution. The optical rotatory power of methyl D-3-hydroxybutyrate, prepared by esterification with diazomethane of D-3-hydroxybutyric acid ($[\alpha]_D^{20} = -25.1$, *c* 10, H_2O), is $[\alpha]_D^{16}$ −22.05; literature value,[4] $[\alpha]_D^{20}$ −20.9.

4) P. A. Levene and H. L. Haller, *J. Biol. Chem.*, **65**, 51 (1925).

BULLETIN OF THE CHEMICAL SOCIETY OF JAPAN, VOL. 44, 1419—1420(1971)

Asymmetric Hydrogenation of C=O Double Bond with Modified Raney Nickel.[1] XIX

Tadao HARADA, Masami IMAIDA,* and Yoshiharu IZUMI

Division of Organic Chemistry, Institute for Protein Research, Osaka University, Kita-ku, Osaka

(Received October 20, 1970)

In the previous papers of this series,[2] it has been reported that, in the presence of the Raney nickel catalyst modified with optically-active α-amino or α-hydroxy acid, methyl acetoacetate is asymmetrically hydrogenated to methyl 3-hydroxybutyrate. Thereafter, the correlation of the asymmetric activity of the catalyst and the chemical and steric structures of the modifying reagent was studied.

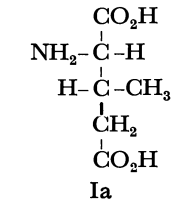

Ia

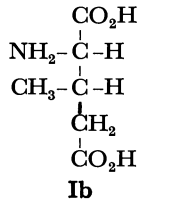

Ib

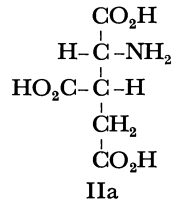

IIa

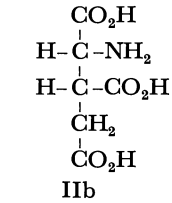

IIb

In the present paper, the asymmetric activities of catalysts modified with optically-active 3-methylglutamic acid[3] (Ia, Ib) and 2-aminotricarballylic acid[4] (IIa, IIb) are described, and the effect of the β-substituent of the modifying reagent on the asymmetric activity of the catalyst and the relationship between the asymmetric activities of the catalysts modified with the *thero* and the *erythro* isomers are discussed.

TABLE 1. OPTICAL ROTATIONS OF MODIFYING REAGENTS

Modifying reagent		Optical rotation, $[\alpha]_D$
3-Methylglutamic acid	Ia (2S, 3R)	+22 (*c* 2.2, 4N HCl)
	Ib (2S, 3S)	+42 (*c* 3, 4N HCl)
2-Aminotricarballylic acid	IIa (2R, 3S)	−49 (*c* 1, 5N HCl)
	IIb (2R, 3R)	−36 (*c* 1, 5N HCl)

Experimental

The preparation of the modified Raney nickel catalyst, the hydrogenation of methyl acetoacetate, and the measurement of the asymmetric activity of the catalyst were done as described in a previous paper.[5]

Results and Discussion

Measurements were made of the asymmetric activities of the catalysts modified with aqueous solutions of L-*threo*-3-methylglutamic acid (Ia), L-*erythro*-3-methylglutamic acid (Ib), D-2-aminotricarballylic acid ((2R, 3S), IIa), and D-2-aminotricarballylic acid ((2R, 3R), IIb), the pH of which had been adjusted to specified values with a sodium hydroxide solution; the results are shown in Figs. 1 and 2.

Correlation of the Asymmetric Activity of the Catalyst and the β-Configuration of the Modifying Reagent. As has been reported in the previous papers of this series, the direction of the optical rotation of the hydrogenation product, methyl 3-hydroxybutyrate, is decided by the α-configuration of the modifying reagent (for example, in the hydrogenation with the catalysts modified with D-glutamic acid and L-glutamic acid, the directions of

1) Presented in part at the 20th Annual Meeting of the Chemical Society of Japan, Tokyo, April, 1967.

* Present address: Osaka Prefectural Institute of Public Health, Morimachi, Higashinari-ku, Osaka.

2) Part XV: T. Tanabe, T. Ninomiya, and Y. Izumi, This Bulletin, **43**, 2276 (1970). Part XVI: Y. Izumi, S. Yajima, K. Okubo, and K.K. Babievsky, *ibid.*, **44**, 1416 (1971). Part XVII: Y. Izumi, T. Harada, T. Tanabe, and K. Okuda, *ibid.*, **44**, 1418 (1971). Part XVIII: Y. Izumi, and K. Okubo, *ibid.*, **44**, 1330 (1971).

3) The diastereomeric mixture was obtained by the procedure of Morrison. [D. C. Morrison, *J. Amer. Chem. Soc.*, **77**, 6072 (1955).] The details of its separation into the diastereomers and the optical resolution of the isomers will be reported in This Bulletin, later.

4) The optically-active isomers were prepared by the procedure of Greenstein *et al.*, while the configurations of their α- and β-carbons were assigned by Kaneko *et al.* [J. P. Greenstein, N. Izumiya, M. Winitz, and S. M. Birnbaum, *J. Amer. Chem. Soc.*, **77**, 707 (1955). T. Kaneko, Y. Ariyoshi, S. Andō, and H. Katsura, This Bulletin, **37**, 324 (1964).]

5) Y. Izumi, T. Harada, T. Tanabe, and K. Okuda, This Bulletin, **44**, 1418 (1971).

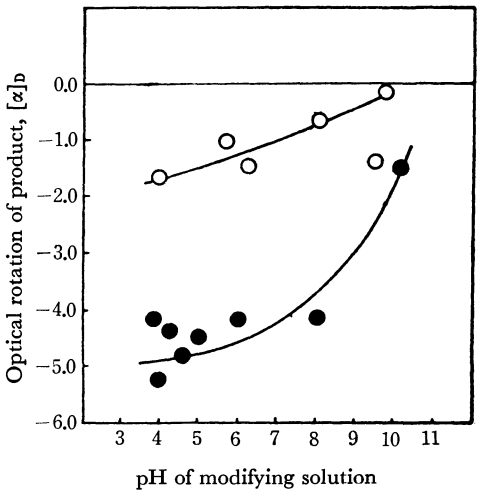

Fig. 1. Asymmetric activities of the catalysts modified with L-*threo*- and L-*erythro*-3-methylgulamic acids.
○ L-*erythro*-3-methylgutamic acid
● L-*threo*-3-methylglutamic acid

the optical rotations of the hydrogenation product were (+) and (−) respectively), and the β-configuration of the α,β-diasymmetric amino or hydroxy acid used as a modifying reagent greatly affects the asymmetric activity of the catalyst (for example, the asymmetric activity of the catalyst modified with the *threo* isomer of α,β-diasymmetric amino acid (2R, 3S) or (2S, 3R)) is higher than that of the catalyst modified with the corresponding *erythro* isomer ((2R, 3R) or (2S, 3S))). These differences in the asymmetric activities of the catalysts modified with the *erythro* and the *threo* isomers are ascribable to the disagreement of the β-configuration, which is distinguished mainly in terms of the bulkiness of the two β-alkyl substituents. As can be seen in Figs. 1 and 2, the catalyst modified with the *threo* isomer (1a or IIa) had a higher asymmetric activity than the one modified with the corresponding *erythro* isomer (Ib or IIb). Accordingly, the similarlity between α,β-diasymmetric monoamino monocarboxylic acids and these β-substituted glutamic acids, in the correlation of the β-configuration of the modifying reagent and the asymmetric activity of the catalyst, suggests that the effect of the β-configuration of 3-methylglutamic acid and 2-aminotricarballylic acid is also due to the differences in bulkiness between a β-carboxymethyl group and either a methyl or a carboxyl group.

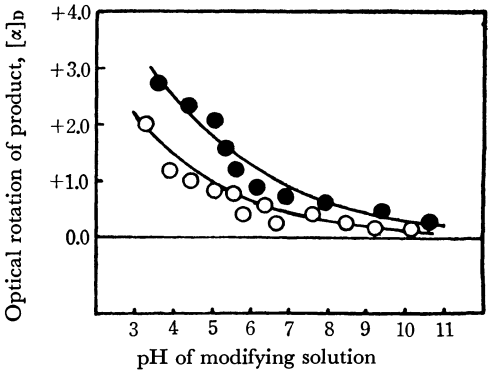

Fig. 2. Asymmetric activities of the catalysts modified with isomeric 2-aminotricarballylic acids.
● D-2-aminotricarballylic acid (2R, 3S)
○ D-2-aminotricarballylic acid (2R, 3R)

Correlation of the Asymmetric Activity of the Catalyst and the β-Substituent of the Modifying Reagent. As is shown in Figs. 1 and 2, the catalysts modified with Ia (*threo*) and Ib (*erythro*) had higher asymmetric activities than those modified with IIa (*threo*) and IIb (*erythro*) respectively.

As has been reported in a previous paper,[6] the asymmetric activity of the catalyst modified with monoasymmetric amino acid increases with an increase in the bulk of the α-alkyl substituent (R–CH–COOH), while that of the catalyst modified with monoasymmetric hydroxy acid decreases with an increase in the bulk of the α-alkyl substituent. From the facts that both *threo*- and *erythro*-3-methylglutamic acids are more effective asymmetric modifying reagents than the corresponding 2-aminotricarballylic acids, although a carboxyl group is bulkier than a methyl group, it seems that the asymmetric activity of the catalyst depends not only on the bulk of the β-substituent of the modifying reagent, but also on the electronic factor of the β-substituent. Similar effects of the β-substituents on the asymmetric activities of the catalysts can be found in the asymmetric activities of the catalysts modified with serine and threonine.[7]

6) Y. Izumi, T. Tanabe, S. Yajima, and M. Imaida, This Bulletin, **41**, 941 (1968).
7) Y. Izumi, M. Imaida, H. Fukawa, and S. Akabori, *ibid.*, **36**, 155 (1963).

BULLETIN OF THE CHEMICAL SOCIETY OF JAPAN, VOL. 44, 1421 (1971)

Retention Index in Programmed Temperature Gas Chromatography

Isao TAKEMURA

Quality Control Laboratory, Max Factor Co., Ltd., Nishi-Gotanda, Shinagawa-ku, Tokyo

(Received July 23, 1970)

Linear programmed temperature gas chromatography (PTGC) can be applied to simultaneous analysis of mixtures consisting of many ingredients with a wide range of boiling points. However, fundamental data of ingredients under the same conditions, such as retention temperature and relative retention values, should be collected prior to qualitative or quantitative analysis of unknown samples. Recently the data on ingredients of many stationary liquids in isothermal gas chromatography (IGC) have been summarized systematically by many workers. If the data in IGC could be applied to PTGC, the complexity in PTGC would be reduced considerable.

For a linear PTGC with constant flow rate, the author has presented the following linear relationship between logarithmic relative retention value (α^{IT}) of IGC and relative retention value (α^{PT}) of PTGC.[1]

$$\log \alpha^{IT} = m(\alpha^{PT} - 1) \tag{1}$$

where m is a constant dependent upon the column temperature in IGC, the evaporation potential of internal standard material, the program rate, the flow rate of carrier gas, the initial temperature and the column length in PTGC.[2] If the operating conditions do not change, Eq. (1) holds in different homologous series on both polar and nonpolar columns.[3]

The Kovats index system[4] is widely accepted in IGC. In this system, the relative retention is referred to the series of normal paraffin hydrocarbons as standard substances. Retention indices I_{IT} are calculated by means of the relation

$$I_{IT} = 100\frac{\log \alpha_{X,N}}{\log \alpha_{N+1,N}} + 100N \tag{2}$$

where $\alpha_{X,N}$ is the relative retention value of unknown compound X compared to the n-paraffin with N carbon atoms, and $\alpha_{N+1,N}$ the relative retention value of the two n-paraffins with $N+1$ and N carbon atoms. Van den Dool and Kratz[5] and also Kaiser[6] have shown that for PTGC the retention indices can be calculated by means of the following relation and that the values are equal to those calculated by Eq. (2) for IGC provided that the indices measured are independent of temperature.

$$I_{PT} = 100\frac{T_r(X) - T_r(N)}{T_r(N+1) - T_r(N)} + 100N \tag{3}$$

where $T_r(X)$, $T_r(N)$, $T_r(N+1)$ are retention temperatures of unknown compound and n-paraffins of carbon number N and $N+1$, and $T_r(N) \leq T_r(X) \leq T_r(N+1)$. Guiochon[7] realized that, when the column temperature in IGC was 0.92 times the retention temperature of unknown compound X in PTGC, the retention index for IGC was approximately the same as that for PTGC.

In this paper, it is shown that Eq. (3) can be obtained from Eqs. (1) and (2).

The retention index for IGC gives the relative retention values for PTGC obtained from Eqs. (1) and (2):

$$I_{IT} = 100\frac{\alpha^{PT}_{X,N} - 1}{\alpha^{PT}_{N+1,N} - 1} + 100N \tag{4}$$

The relative retention value of n-paraffin of carbon number $N+1$ in PTGC is given by

$$\alpha^{PT}_{N+1,N} = \frac{\{T_r(N+1) - T_0\}/r - t_0}{\{T_r(N) - T_0\}/r - t_0} \tag{5}$$

It follows that

$$\alpha^{PT}_{N+1,N} - 1 = \frac{T_r(N+1) - T_r(N)}{T_r(N) - (T_0 + rt_0)} \tag{6}$$

where T_0 is the initial temperature, r is the program rate and t_0 is the time of air peak from the starting point. Similarly, for unknown compound X, we get

$$\alpha^{PT}_{X,N} - 1 = \frac{T_r(X) - T_r(N)}{T_r(N) - (T_0 + rt_0)} \tag{7}$$

Substituting Eqs. (6) and (7) into Eq. (4), the same equation as Eq. (3) is obtained:

$$I_{IT} = 100\frac{T_r(X) - T_r(N)}{T_r(N+1) - T_r(N)} + 100N \tag{8}$$

This is the equation of retention index for IGC related with retention temperature in PTGC. It may indicate that retention index for PTGC is the same as that for IGC.

1) I. Takemura, *Bunseki Kagaku*, **19**, 39 (1970).
2) I. Takemura, *ibid.*, **19**, 1174 (1970).
3) I. Takemura, *ibid.*, in press.
4) E. Kovats, *Helv. Chim. Acta*, **41**, 1915 (1958).
5) H. van den Dool and P. D. Kratz, *J. Chromatogr.*, **11**, 463 (1963).
6) R. Kaiser, *Internal Symposium G. D. Ch.*, Gesellschaft Deutscher Chemiker, Munich, Sept. 1963. Discussion contribution.
7) G. Guiochon, *Anal. Chem.*, **36**, 661 (1964).

BULLETIN OF THE CHEMICAL SOCIETY OF JAPAN, VOL. 44, 1422—1423 (1971)

The Coupling Reaction of Phenylmagnesium Bromide with Mn(III) or Co(III) Tris(acetylacetonate)

Tadao NAKAYA, Hideo ARABORI, and Minoru IMOTO

Department of Applied Chemistry, Faculty of Engineering, Osaka City University, Sugimoto-cho, Sumiyoshi-ku, Osaka

(Received September 14, 1970)

It is well known that aryl Grignard reagents give the corresponding diaryls with suitable metallic halides, such as $CoCl_2$, $CuCl_2$, $NiBr_2$, and AgBr.[1,2] However, no report has appeared concerning the coupling reaction of aryl Grignard reagents by means of the salts of Mn(III) or Co(III).

This note will deal with the coupling reaction of phenylmagenesium bromide with Mn(III) or Co(III) tris(acetylacetonate).

Results and Discussion

Into an ethereal solution of phenylmagnesium bromide under nitrogen we stirred, drop by drop, on cooling a dry benzene solution of a 0.8 molar equivalent of Mn(III) tris(acetylacetonate) to give mainly biphenyl, together with a small amount of acetophenone. The reaction conditions and yields are indicated in Table 1. During the course of the reaction, a precipitate was formed which had Mn(II) bis(acetylacetonate) as its main ingredient[3]; acetylacetone was never detected. When the mole ratio of Mn(III) tris (acetylacetonate) to phenylmagnesium bromide was decreased to 1:3, the relative yield of biphenyl was reduced, whereas that of acetophenone was considerably increased. The increasing yields of acetophenone were probably due to the reaction[4-6] of the excess of phenylmagnesium bromide with the acetylacetonate ion[5,7] liberated from Mn(III) tris(acetylacetonate) in the reaction mixture, though the exact reaction route remains obscure. When Mn(II) bis(acetylacetonate) was used as a coupling agent, only biphenyl was obtained in a low yield. A similar reaction using manganous chloride afforded a relatively high yield of biphenyl.[8]

TABLE 1. REACTIONS OF PHENYLMAGNESIUM BROMIDE WITH VARIOUS METAL SALTS IN THE PRESENCE AND ABSENCE OF α-METHYLSTYRENE

PhMgBr mol	Metal salt	mol	α-Methylstyrene mol	Time min	Products: Biphenyl mmol (Yield, %)[a]	Products: Acetophenone mmol
0.025	$Mn(Acac)_3$	0.02	—	60	12.0 (98)	0.4
0.03	$Mn(Acac)_3$	0.01	—	60	7.0 (47)	6.9
0.03	$Mn(Acac)_3$	0.01	0.015	60	6.7 (45)	6.5
0.03	$Mn(Acac)_2$	0.01	—	60	2.3 (15)	0
0.03	$MnCl_2$	0.01	—	60	4.1 (27)	0
0.06	$Co(Acac)_3$	0.01	—	60	15.5 (52)	0
0.04	$Co(Acac)_2$	0.01	—	60	5.0 (25)	0

a) Based on reacted PhMgBr.

In order to obtain information concerning the nature of the coupling reaction by Mn(III) tris(acetylacetonate), the reaction was carried out in the presence of α-methylstyrene, which would be expected to be a radical acceptor.[9] As can be seen in Table 1, the presence of the radical acceptor does not affect the yields of the products. Accordingly, it may be said that the reaction does not involve free radical steps. The finding that Mn(II) bis(acetylacetonate) is relatively unreactive toward phenylmagnesium bromide may be ascribed to the fact that it is a stable metal complex.[3,10]

On the other hand, the slow addition of a suspension of Co(III) tris(acetylacetonate) in benzene to a ethereal solution of phenylmagnesium bromide gave the relatively good yield of biphenyl. No other products were detected. Thus, the result suggests a useful method for the coupling of aryl Grignard reagents. Co(II) bis(acetylacetonate) was similarly, but much less effective than Co(III) tris(actylacetonate).

Experimental

Reagent. The bromobenzene and α-methylstyrene were purified by distillation. The Co(II) bis(acetylacetonate), Co(III) tris(acetylacetonate), Mn(II) bis(acetylacetonate), and manganous chloride were of all of a special reagent grade and were used without further purification. The Mn-(III) tris(acetylacetonate) was prepared by the method of Charles.[11] The phenylmagnesium bromide solution was prepared according to the procedure of Kharasch and Fields.[12]

Small portions of the Grignard solution were taken out with a pipet, hydrolyzed by cold 1 N hydrochloric acid, and

1) M .S. Kharasch and O. Reinmuth, "Grignard Reaction of Nonmetallic Substances," Prentice-Hall, New York (1954), pp. 116—137.

2) C. Walling, "Free Radicals in Soultion," John Wiley & Sons, New York (1957), pp. 588—589.

3) M. J. S. Dewar and T. Nakaya, *J. Amer. Chem. Soc.*, **90**, 7134 (1968).

4) J. English, Jr., and F. V. Brutcher, Jr., *ibid.*, **74**, 4279 (1952).

5) J. P. Freeman, *ibid.*, **80**, 1926 (1958).

6) P. Canonne and H. Bilodeau, *Can. J. Chem.*, **44**, 2849 (1966).

7) T. Nakaya, H. Arabori and M. Imoto, This Bulletin, **43**, 1888 (1970).

8) M. S. Kharasch, F. L. Lambert, and W. H. Urry, *J. Org. Chem.*, **10**, 298 (1945).

9) Fo-Sun Van, B. A. Dolgoplosk, and B. L. Erusalimskiĭ *Izvest. Akad. Nauk SSSR, Otdel. Khim. Nauk*, **1960**, 469; *Chem. Abstr.*, **54**, 22335 (1960).

10) F. A. Cotton and G. Wilkinson, "Advanced Inorganic Chemistry," Interscience-Publishers, John Wiley & Sons, New York (1962), pp. 694—698.

11) R. G. Charles, "Inorganic Syntheses," Vol. Vll, ed. by J. Kleinberg, McGraw-Hill Book Co., New York, N. Y. (1963), p. 183.

12) M. S. Kharasch and E. K. Fields, *J. Amer. Chem. Soc.*, **63**, 2316 (1941).

analysed with a Yanagimoto Model GCG-550-EP-type gas chromatograph, with columns packed with Silicone SE 30, in order to determine the quantity of biphenyl present in the Grignard solution.

General Procedure for the Reaction of Phenylmagnesium Bromide with Metal Salts. An outline of one reaction follows, while the general results are presented in Table 1. Into an anhydrous ethereal solution of 0.03 mol of phenylmagesium bromide, we stirred, drop by drop, and on cooling, 0.01 mol of Mn(III) tris(acetylacetonate) in a dry benzene solution, keeping the temperature at 10°C for 30 min. The reaction mixture was stirred at room temperature for another 30 min. The mixture was quickly filtered through a glass filter, and the precipitate was washed with benzene. The filtrate was hydrolysed by cold 1 N hydrochloric acid, and the hydrochloric acid layer was extracted with benzene. After separation, the combined organic layers were dried over sodium sulfate, and the solvent was removed under reduced pressure. The residue was submitted to gas-liquid partition chromatography (glpc). The yield data were obtained by glpc, with *n*-dodecane used as the internal standard. The products were identified by a comparison of their gas chromatograms and IR spectra with those of authentic samples obtained commercially.

The yields of biphenyl listed in Table 1 are freed from t hose formed in the preparation of the Grignard reagents.

BULLETIN OF THE CHEMICAL SOCIETY OF JAPAN, VOL. 44, 1423—1424 (1971)

ESR Studies of the $(RO)_2PSS$ Radicals in UV-Irradiated *O,O'*-Dialkyl Dithiophosphate Glasses

Mitsuo SATO, Michiyasu YANAGITA, Yuzaburo FUJITA, and Takao KWAN
Faculty of Pharmaceutical Sciences, The University of Tokyo, Bunkyo-ku, Tokyo

(Received October 22, 1970)

ESR studies have been reported on γ-irradiated phosphate crystals such as KH_2PO_4, where the formation of the phosphate radical, PO_4^{2-}, was observed, and its electronic nature has been discussed.[1-3] For example, according to Subramanian *et al.*,[3] the phosphate radical showd an isotropic ^{31}P ($I=1/2$) hyperfine splitting in the range of 20—40 gauss, leading one to suggest that 0.6—1.1% spins are localized on the phosphorus 3*s* orbital.

We have investigated the UV-irradiation of *O,O'*-dialkyl dithiophosphate glasses and found that dithiophosphate radical species are formed. The radical showed electronic characteristics quite similar to those of the phosphate radicals, the results will be reported in this note.

Experimental

Four kinds of *O,O'*-dialkyl dithiophosphate $(RO)_2PSSH$, where R is CH_3, C_2H_5, *n*-C_3H_7, or *n*-C_4H_9 were synthesized by the reaction of phosphorus pentasulfide with the corresponding alkyl alcohols; they were purified by subsequent distillation under reduced pressure.

Each sample was placed in a quartz tube, 4 mm id, carefully degassed, and then immersed in a quartz Dewar vessel filled with liquid nitrogen. The sample was then irradiated at the temperature of liquid nitrogen with the light of a low-pressure mercury lamp (Ushio Electric Co. UL-200W). After the irradiation, the sample was transferred, without warming, to a Dewar vessel kept inside the microwave cavity; electron-spin resonance measurements were then made with an X-band spectrometer (JES P-10) operated at 100 kHz field modulation.

Results and Discussion

Upon the UV irradiation of *O,O'*-dialkyl dithiophosphates, the ESR signals of the radical species shown in Fig. 1 were observed, along with that of

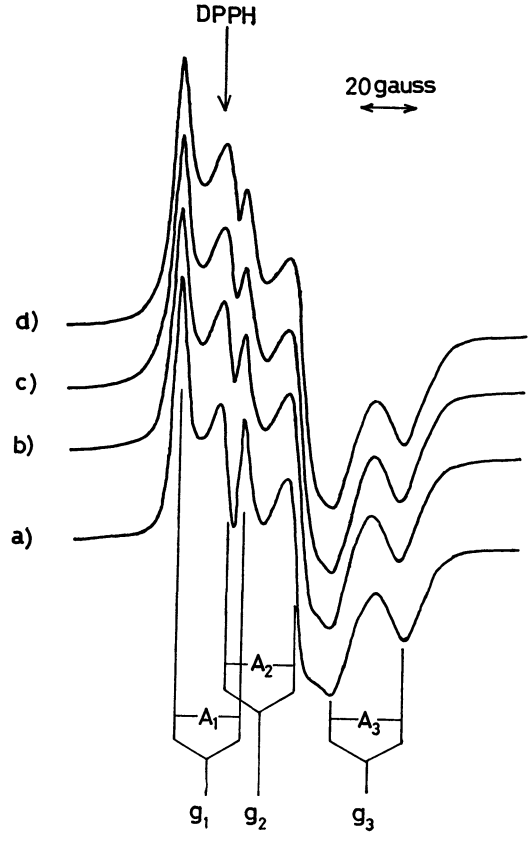

Fig. 1. ESR spectra of dialkyl dithiophosphate radicals. (a) $(CH_3O)_2PSS$, (b) $(C_2H_5O)_2PSS$, (c) $(n\text{-}C_3H_7O)_2$-PSS, (d) $(n\text{-}C_4H_9O)_2$ PSS

1) W. E. Hughes and W. G. Moulton, *J. Chem. Phys.*, **39**, 1359 (1963).
2) R. A. Serway and S. A. Marshall, *ibid.*, **45**, 4098 (1966).
3) S. Subramanian, M. C. R. Symons, and H. W. Wardale, *J. Chem. Soc., A.*, **1970**, 1239.

Table 1. ESR constants of dithiophosphate radicals

Radical species	g_1	g_2	g_3	A_1 (gauss)	A_2 (gauss)	A_3 (gauss)
$(CH_3O)_2PSS\cdot$	2.0027	2.0147	2.0407	24.7	25.8	26.1
$(C_2H_5O)_2PSS\cdot$	2.0023	2.0150	2.0400	24.0	26.2	26.1
$(n\text{-}C_3H_7O)_2PSS\cdot$	2.0026	2.0154	2.0397	24.3	27.1	25.8
$(n\text{-}C_4H_9O)_2PSS\cdot$	2.0022	2.0149	2.0397	24.0	26.2	25.8

hydrogen atoms. The spectra were almost identical for all the compounds employed, and the signal intensities increased with the time during 20 minutes' irradiation with little variation in the line shape. Thus, it can be considered that a very similar sort of radical was produced by the liberation of hydrogen atoms. No other photolytic reactions were detectable at least under our experimental conditions.

In the light of the ESR informations on sulfur radicals[4-7] and on phosphate radicals,[1-3] each spectrum in Fig. 1 can be readily interpreted as due to the $(RO)_2$-PSS radical: a triplet due to the anisotropy in the g factor splits to doublets as a result of the action of three canonical components of a hf tensor. The observed g-values and hf coupling constants are listed in Table 1.

It is shown in Table 1 that the g-values are almost identical for all the compounds within the limits of experimental error, and that the g-value shifts (Δg) from that of a free spin (2.0023) are $\Delta g_1=0.000$, $\Delta g_2=0.013$, and $\Delta g_3=0.038$ for g_1, g_2, and g_3 respectively. Generally speaking, this kind of g-value shift depends upon the magnitude of the spin-orbit coupling of an atom with an unpaired electron and increases rapidly with the atomic number. Also, it depends upon the energy separations between the ground state and excited states of the radical. For example, in carbon radicals, including alkyl and aromatic radicals, the g-value shift is relatively small and usually lies within 0.002. On the contrary, much larger shifts have been observed for sulfur radicals[4-7] ($\Delta g_1=0.001$, $\Delta g_2=0.020$—0.030, $\Delta g_3=0.040$—0.60), and for phosphate radicals,[3] most of which exhibit anisotropy with an axial symmetry ($\Delta g_1=\Delta g_2=0.002$—$0.005$, $\Delta g_3=0.010$—0.050).

The unpaired electron of the dithiophosphate radical may not be involved in the alkyl group, because the observed spectra did not show any hf structure due to protons in the alkyl groups (R), irrespective of the variation in R from the methyl to the n-butyl group. Instead, the hf splitting shown in the spectra may be interpreted most reasonably as that of $^{31}P(I=1/2)$, which is common to all the compounds investigated. The hf coupling constant is almost isotropic, in contrast to the g-factor, and its isotropic component of 25.5 gauss is too small for an unpaired electron to be localized on the phosphorus atom, as will be discussed below.

If the unpaired electron is localized on the oxygen atom, one may expect hf splitting or unresolved hf-line broadening due to the protons in the adjacent alkyl group, as in the case of alkoxy radicals.[8] Since the observed spectra do not show any appreciable change with R, it seems very likely that the unpaired electron is localized mainly on the sulfur atom.

It is assumed that the radical is formed by the scission of the S–H bond and that unpaired electrons are confined mainly on the sulfur atom. The structure of the radical is, then, one with C_{2v} symmetry where two P–S bonds are equivalent, and the orbital for the unpaired electron is a non-bonding $3p(\pi)$-orbital of the sulfur atom with a_2 symmetry.[9]

Although the a_2 orbital of the sulfur atom occupied by the unpaired electron does not give the spin density on the phosphorus atom in the first approximation, it is well known that some spin density arises in the $3s$ orbital of the phosphorus atom *via* the mechanism of spin-polarization[10] or that of configurational interaction of P–S σ-electrons.

The isotropic ^{31}P hf coupling constant (A_p) of 25.5 gauss (72.1 MHz) corresponds to the following spin density (f_{3s}) in the $3s$ orbital of the phosphorus atom:

$$f_{3s}=\frac{A_P}{A_P^\circ}=\frac{72.1\ (\mathrm{MHz})}{10178\ (\mathrm{MHz})}\simeq 0.7\%$$

where A_P° (10178 MHz) is the calculated hf coupling constant for an electron in the phosphorus $3s$ orbital.[11] As is shown above, the calculated spin density, f_{3s}, for the dithiophosphate radical nearly coincides with those for phosphate radicals (0.6—1.1%[3,12]).

The value of f_{3s} may reflect the extent of the spin polarization and the $3s$ character of phosphorus in the P–S σ-orbital.[10] Thus, it may be suggested that the extent of spin-polarization and the $3s$ character of phosphorus are nearly the same in both dithiophosphate and phosphate radicals.

4) J. J. Windle, A. K. Wirsema, and A. L. Tappel, *J. Chem. Phys.*, **41**, 1996 (1964).
5) Y. Kurita and W. Gordy, *ibid.*, **34**, 282 (1961).
6) D. A. Stiles, W. J. R. Tyerman, O. P. Strausz, and H. E. Gunning, *Can. J. Chem.*, **44**, 2149 (1966).
7) M. Yanagita, Y. Fujita, and T. Kwan, *Nippon Kagaku Zasshi*, **91**, 898 (1970).
8) L. H. Piette and W. C. Landgraf, *J. Chem. Phys.*, **32**, 1107 (1960).
9) P. W. Atkins and M. C. R. Symons, "The Structure of Inorganic Radicals," Elsevier, Amsterdam (1967).
10) H. M. McConnell and D. B. Chesnut, *J. Chem. Phys.*, **28**, 107 (1958).
11) J. R. Morton, *Chem. Rev.*, **64**, 453 (1964): G. W. Chantry, A. H. Horsfield, J. R. Morton, J. R. Lowlands, and D. H. Wiffen, *Mol. Phys.*, **5**, 233 (1962).
12) T. F. Hunter and M. C. R. Symons, *J. Chem. Soc., A*, **1967**, 1770.

BULLETIN OF THE CHEMICAL SOCIETY OF JAPAN, VOL. 44, 1425—1427(1971)

Notiz zur charakteristischen Färbung der mit farblosen Anionen, OH^-, J^- und S^{2-}, beladenen, starkbasischen Anionenaustauscherharze schwacher Eigenfarbe durch Messungen der diffusen Reflexionsspektren[1]

Masatoshi FUJIMOTO und Tadayoshi SUGA*

II. Chemisches Institut der Naturwissenschaftlichen Fakultät der Universität Hokkaido, Sapporo

(Eingegangen am 22. Oktober 1970)

Im Anschluß an die Harztüpfelmethode[2] beobachteten wir häufig charakteristische Färbung, die die starkbasischen Anionenaustauscherharze schwacher Eigenfarbe auch beim Beladen der farblosen anorganischen Anionen wie Hydroxid-, Jodid- oder Sulfidionen annehmen. Die sind nämlich schmutziger Ocker bzw. Hellbraun an der Hydroxidform, Zitronengelb bzw. Hellgelb an der Jodidform und Grünlichhellgelb bzw. Hellgrün mit Stich ins Dunkelblau an der Sulfidform.[3] Aus dem Interesse für äußerliche Ähnlichkeit zwischen den Farbtonen betreffender Harzphase und denjenigen schwerlöslicher Salze entsprechender Anionen mit den sog. weichen Säuren wie Silber(I), Quecksilber(II) sowie Blei(II) usw. vermuteten wir zuerst unbekannte besondere Wechselwirkungen zwischen hydrophoben Haftgruppen und stark polarisierbaren Gegenanionen in der äußerst hochkonzentrierten Ionenatmosphäre an gequollener Polyelektrolytphase. Diese Vermutung wurden doch durch Messungen der diffusen Reflexionsspektren der Harzphase fast ausgeschlossen, und dadurch kommt eine andere unerwartete und wichtige Tatsache in Rede, die beim dauernden Anwenden der Anionenaustauscherharze auf die Harztüpfelmethode immer in Betracht zu ziehen ist, worauf wir unten zurückkommen.

Experimentelles

Es wurden die folgenden handelsüblichen kugelförmigen Anionenaustauscherharze auf Styrolbasis geprüft: Dowex 1 (X1～X16), Dowex 2 (X1～X8), Diaion SA ♯100 (analytischer Grad, mittelmäßig vernetzt), Diaion PA (304～320 sowie 404～420). Dielet zten zwei sind sog. Popcorn-Harze[4] verschiedener Vernetzungsgrade aber fast unverändert weitmaschiger schwammartiger Struktur und besonders weiß an Untergrundfarbe (vgl. dazu Abb. 1). Die Harze wurden vor Gebrauch zweimal mit 0.5 M Salzsäure, 2 M Natronlauge und daran anschließend mit 2 M und 0.5 M Salzsäure[5] nacheinander umbeladen bis zur Abwesenheit der Spuren Eisen(III)-ionen im Ablauf, mit entionisiertem Wasser völlig ausgewaschen und luftgetrocknet. Die so behandelten Harze wurden beim Versuch erneut über Hydroxid- oder Chloridform in die genannte Form umbeladen (s.u.). In Tabelle 1 steht der Aschengehalt an einigen der angewendeten Harzproben in der Chloridform, zusammen mit dem der nicht raffinierten käuflichen Harzproben.

TABELLE 1. ASCHENGEHALT AN EINIGEN DER BENUTZTEN ANIONENAUSTAUSCHERHARZE (mg Asche als Oxide, bezogen auf 1 g lufttrockenes Harz in der Cl-Form)

Harz	nicht raffinierte käufliche Probe	völlig raffinierte Harzprobe
Dowex 1-X10	— (—)	0.2_7 (bräunlich)
Diaion PA-310	0.3_0 (dunkelgrün)	0.0_0 (bräunlich?)
Diaion PA-410	0.6_0 (bräunlich)	0.0_4 (braunlich)

Zur Herstellung der Meßproben des Harzes wurde immer die frisch hergestellte wäßrige Lösung des p.a.-Reagens benutzt, damit unerwünschte Verunreinigung streng auszuschalten ist. Der Schwefelwasserstoff wurde aus Eisensulfid und dest. Salzsäure hergestellt. Das entwickelte Gas wurde zur Entfernung eventuell spurenweise vorhandenen Staubs durch zwei Waschflasche mit entionisiertem Wasser nacheinander geleitet, und dann ins entionisierte Wasser geleitet. Die so frisch hergestellte Lösung des Schwefelwasserstoffs wurde sogleich zur Umbeladung des Harzes verwendet. Das handelsübliche Natriumsulfid, in dem sich beim Aufbewahren etwas intensiv gelbe Polysulfide bildeten, wurde angewendet entweder ohne weitere Reinigung oder nach dem Durchlaufen der wäßrigen Lösung durch Anionenaustauschersäule bis zur Entfärbung; die gelben Polysulfidionen wurden am oberen Teile der Säule sicher und leicht beseitigt.

Zur Messung der Reflexionsspektren wurde das Hitachi-Registrierende Spektralphotometer EPS-3T mit Quarzoptik und Remissionsansatz R-10 benutzt. Zur Vorbereitung der Meßproben wurde etwa 1 g frisch umbeladener Anionenaustauscher durch ein quantitatives Filterscheibchen abfiltriert, dreimal mit je 1 m*l* entionisiertem Wasser gewaschen und im Dunkeln stehengelassen. Die fast getrockneten Proben wurden in den etwa 3 mm tiefen und mit Quarzscheibe versehenen Probenteller eingefüllt und glatt gewalzt und gegen das gleich behandelte Harz in der Chloridform gemessen, um eventuelle reguläre Reflexionsanteil auszuschalten.[6] Bei der Sulfidform wurde die frisch hergestellte Meßprobe gleich nach kurzem Absaugen in den Meßteller fest einge-

1) Vorgetragen vor der 23. Hauptversammlung der Japanischen Chemischen Gesellschaft in Tokio, 4. April 1970.

* Die jetzige Adresse: Sanken Kako G.m.b.H., Higashinada-ku, Kobe.

2) M. Fujimoto, *Chemist-Analyst*, **49**, 4 (1960); **54**, 58, 92 (1965).

3) Y. Nakatsukasa und M. Fujimoto, *Microchem. J.*, **9**, 465 (1965).

4) Bei dieser Reihe der Harze bedeutet die erste Ziffer ‚3' od. ‚4' den Typus-I od. II der Haftgruppe, und daran anschließende zwei wie ‚04' bzw. ‚20' den Vernetzungsgrad. Diese wurden uns aus dem Zentralforschungsinstitut der Mitsubishi Kasei G.m.b.H., Kawasaki, freundlich angeliefert, wofür wir ihm zu herzlichem Dank verpflichtet sind.

5) K. A. Kraus und G. E. Moore, *J. Amer. Chem. Soc.*, **75**, 1460 (1953).

6) M. Fujimoto und G. Kortüm, *Ber. Bunsenges. Physik. Chem.*, **68**, 488 (1964).

schlossen, um unerwünschte Luftoxidation möglichst zu vermeiden. Die $F(R_{\infty,\text{Probe}})$-Werte für typische Farbkurven wurden nach der Methode von Fujimoto und Kortüm[6] aus der gemessenen Kurve des Reflexionsvermögens umgerechnet.

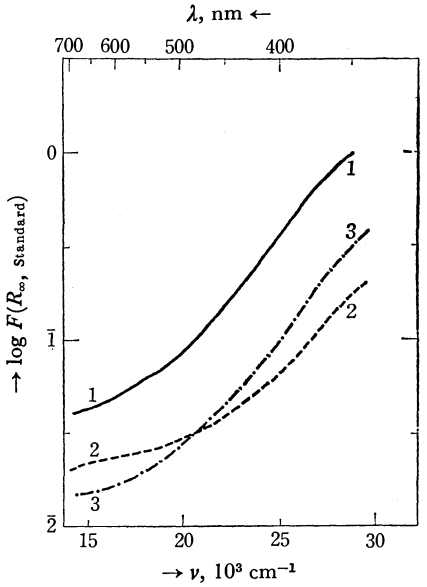

Abb. 1. Typische Farbkurven einiger der benutzten Anionenaustauscherharze in der Cl-Form, gemessen gegen MgO.
Kurve 1 (——): Dowex 1-X10 (200~400 mesh), 2 (——): Diaion PA-310 (20~50 mesh), und 3 (·····): Diaion PA-410 (20~50 mesh).

Meßergebnisse und Diskussion

Abb. 1 zeigt die typische Eigenfarbkurve einiger der als Standard benutzten Harzproben in der Chloridform. In Abb. 2 werden die diffusen Reflexions-

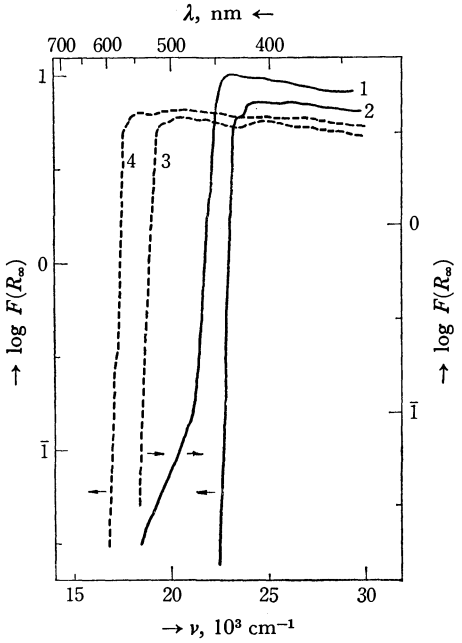

Abb. 3. Typische Farbkurven der zermahlten Kriställchen der Jodide, gemessen gegen MgO.
Kurve 1: TlJ (gelb), 2: AgJ (gelb), 3: PbJ_2 (chromgelb), und 4: HgJ_2 (gelblichrot).

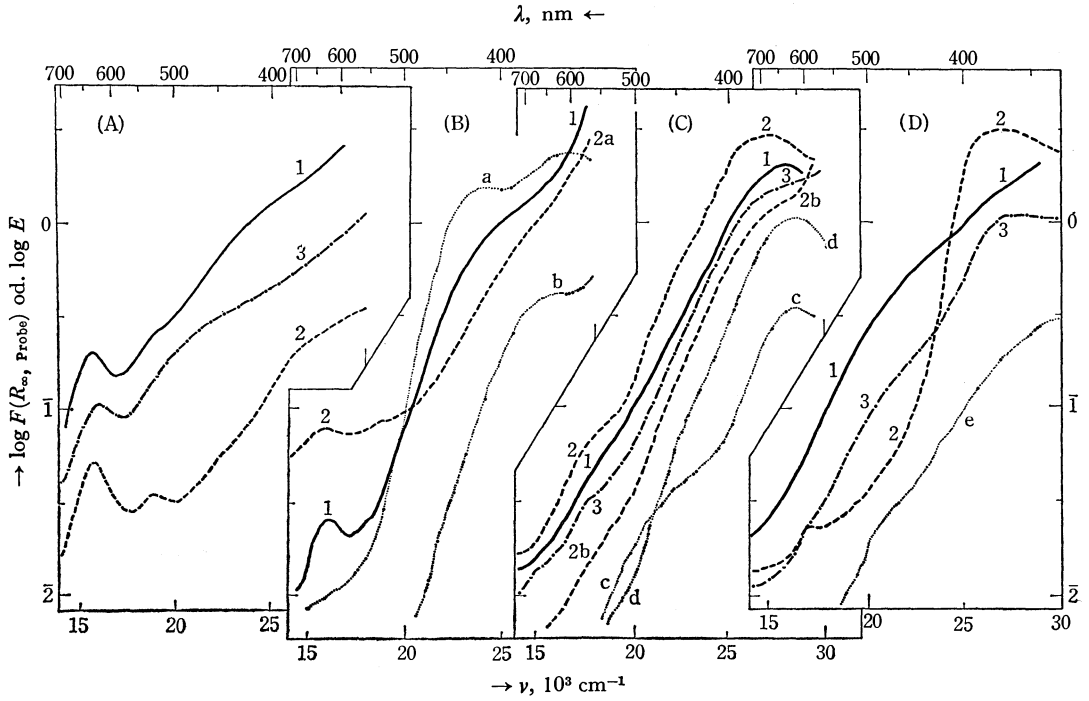

Abb. 2. Diffuse Reflexionsspektren der starkbasischen Anionenaustauscher in verschiedenen Formen, zusammen mit einigen Durchsichtspektren der wäßr. Lsgg.
Sulfidform aus ROH+H_2S (A) und aus RCl+Na_2S (B) [Kurve 2a: aus RCl+farbloser Na_2S-lsg.]; Jodidform aus ROH+KJ (C) [Kurve 2b: aus RCl+KJ]; und Hydroxidform aus RCl+NaOH (D). Dünne Punktlinien zeigen die Durchsichtspektren: Kurven a und b: 1 M und 0.1 M benutzte Na_2S_{1+x}-lsg.; c: 1×10^{-4} M J_2 in 4×10^{-4} M KJ; d: 1×10^{-4} M J_2 in 1 M KJ; und e: kolloide Suspension des $Fe(OH)_3$ aus ca. 1.5×10^{-4} M Fe^{3+}. Kurve 1 (——): Dowex 1-X10, 2 (——): Diaion PA-310, und 3 (·····): Diaion PA-410.

spektren der genannten Harze in der Sulfid-, Jodid- und Hydroxidform wiedergegeben. Dabei zur Deutung der Meßdaten ist der Einfluß der unterschiedlichen Quellung an den völlig umbeladenen Harzproben auf den Streukoeffizienten der Kügelchen nicht gefährlich, obwohl er nicht so vollständig auszuschalten ist, daß man die typische Farbkurve einwandfrei zeichnen könnte. In Abb. 3 stehen die zum Vergleich gemessenen typischen Farbkurven der zermahlten Kriställchen der schwerlöslichen Jodide besonders charakteristischer Farbe, die jedoch ganz anders sind als diejenigen der Harzproben in der Jodidform.

Die bei der Jodidform sogar mit reinstem Kaliumjodid immer deutlich hervorgerufenen gelblichen Farben an Harzphase sind aber durch Zusatz von Natriumsulfit langsam verschwunden. Überdies deutet die bedeutende Ähnlichkeit der betreffenden Farbkurve mit der Absorptionskurve der wäßrigen Trijodidionen wie in Abb. 2C ursprüngliche Anwesenheit der Spuren etwaiger Oxidationsmittel in der völlig raffinierten Harzphase an. Weitere Beweise dafür werden dadurch geführt, daß die aus dem Schwefelwasserstoff und ROH[7] sowie aus der durch Harzsäule farblos gereinigten Natriumsulfidlösung und RCl[7] sorgfältig hergestellten Harzproben auch, sehr langsam aber nach lang dauerndem Durchlauf der Lösung immer mehr oder weniger dunkelgrünliche Farbe annehmend, mindestens ein deutliches Maximum bei etwa 630 nm und manchmal zusätzliche Maxima bzw. Schulter bei 530 und etwa 440 nm zeigen. Diese drei Maxima bei 630, 530 und 440 nm entsprechen also genau den Absorptionsmaxima der grünen alkalischen Lösung aus Eisen(II)- bzw. Eisen(III)-ionen und überschüssigen Sulfidionen wie in Abb. 4.[8] Aus der bei den Harztüpfelnachweisen berichteten Erfassungsgrenze für Eisen(III)[9,10] schätzen wir den Höchstgehalt an Eisen in ein paar Körnchen des starkbasischen Anionenaustauschers wie Dowex 1 auf wesentlich weniger als 1 ng ab.[11] Daß das genannte Absorptionsmaximum bei etwa 630 nm auch bei sorgfältig raffinierten Harzproben so deutlich wie in

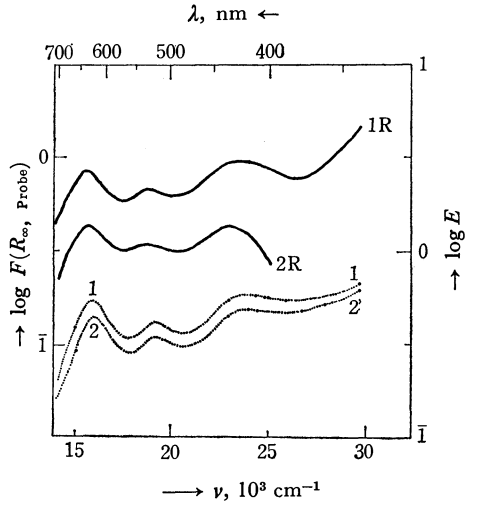

Abb. 4. Typische Farbkurven der an Anionenaustauscher angereicherten grünen Komplexe aus Eisensalzen und Natriumsulfide, gegenübergestellt mit Durchsichtspektren. Kurve 1: Durchsichtspektrum der dunkelgrünen Lsg. aus Mohrschem Salze, und Na_2S (pH=11.60) und Kurve 2: dasjenige aus Ammoniumeisenalaun und Na_2S (pH=11.72) [Beide Lsgg. enthalten $[Fe]_{total}=1.5\times10^{-4}$ M und $[S]_{total}=4\times10^{-3}$ M]. Die Kurven 1R und 2R: typische Farbkurven der an Dowex 1-X10 angereicherten grünen Komplexe 1 und 2 [1.00 g RCl+5 m*l* Lsg.-1 od. 2].

der Kurve 2a der Abb. 2B erkennbar ist, weist uns ursprüngliche Anwesenheit der Spuren des dreiwertigen Eisens selbst in den völlig gereinigten Harzproben.

Die dauerhaft grünen Komplexe, die sich aus Überschuß von Sulfidionen und Eisen(II) oder Eisen(III) in der alkalischen wäßrigen Lösung bilden, lassen sich an Anionenaustauscherharze in der Chloridform schnell anreichern und färben die Harzphase gleichmäßig schwach smaragdgrün bzw. grünlichocker (vgl. Abb. 4). Die werden an Kationenaustauscher in der Natriumform gar nicht angereichert. Die grünliche Farbe an Anionenaustauscher ist aber bei niedrigerer Konzentration an Sulfidionen luftempfindlich. Die klingt beim Trocknen an der Luft ziemlich schnell ab.

Wir haben aus den Messungen der diffusen Reflexionsspektren der Harzproben festgestellt die ursprüngliche Anwesenheit der Spuren Eisens und zwar des Eisens-(III) selbst in sehr sorgfältig raffinierten Anionenaustauschern. Diese Tatsache muß man daher beim Anwenden genannter Anionenaustauscher zu genauen Messungen oder auf die Harztüpfelanalyse besonders bei allzu langem Aufbewahren der Harzkügelchen in der Versuchslösung wie 24 Std immer sehr vorsichtig in Betracht ziehen.

7) RX bedeutet den Anionenaustauscher in der X-Form.

8) Unabhängig davon wurde eine Anwendung der genannten Absorption auf die Bestimmung geringer Menge des Eisens berichtet; vgl. dazu T. Fukazawa, M. Iwatsuki and H. Asakawa, Vortrag Nr. 20442 der 23. Hauptversammlung der Japanischen Chemischen Gesellschaft in Tokio, 4. April 1970.

9) M. Fujimoto, Dieses Bulletin, **29**, 776 (1956).

10) M. Fujimoto and Y. Nakatsukasa, *Anal. Chim. Acta*, **26**, 427 (1962).

11) Der so hoch abgeschätzte höchste Eisengehalt wie 1 ng in 10 Kügelchen der 200 mesh (etwa 70 μm Durchmesser) gequollenen Harze entspricht etwa 0.5 mg Eisen pro Gramm Harz.

BULLETIN OF THE CHEMICAL SOCIETY OF JAPAN, VOL. 44, 1428—1429(1971)

The NMR Spectra of Several *N*-(2-Biphenylyl)carboxamides

Mamoru Ohashi, Kazuo Tsujimoto, Akira Yoshino, and Teijiro Yonezawa
Department of Hydrocarbon Chemistry, Faculty of Engineering, Kyoto University, Kyoto
(Received October 24, 1970)

During the course of an investigation of the structures of the photochemical decomposition products of several 1-acylbenzotriazoles,[1] it was discovered that the NMR spectrum of *N*-(2-biphenylyl)-pivalamide exhibited two signals farther downfield than usual aromatic protons. In connection with this finding, we examined the NMR spectra of several *N*-(2-biphenylyl) carboxamides and found that the two peaks were observed for all the spectra so far studied.

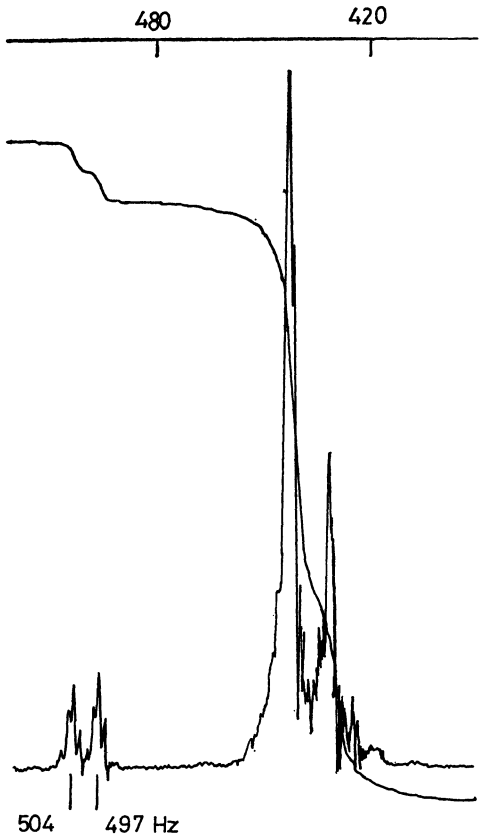

Fig. 1. The partial 60 MHz NMR spectrum of *N*-(2-biphenylyl)-pivalamide ($CDCl_3$) at room temperature.

Figure 1 shows the lower region of the spectrum of *N*-(2-biphenylyl)pivalamide. The two signals at 497 and 504 Hz from TMS at 60 MHz seemed assignable to the protons on the nitrogen atom of two geometrical isomers, **Ia** and **Ib**; this is in accord with the well-documented hindered rotation of amides.[2] Similar signals were also observed in the spectra of *N*-(2-biphenylyl) benzamide (II, 508 and 515 Hz) and *N*-(2-biphenylyl) acetamide (III, 490 and 497 Hz).

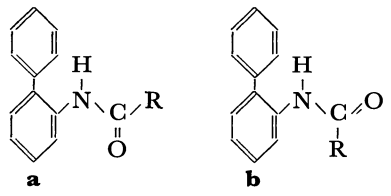

I R=C(CH$_3$)
II R=ph
III R=CH$_3$

Two conformations, **a** and **b**, were conceivable for the amide[2] from the viewpoint of steric factors, and the relative intensity of the two signals might reflect the relative abundance of the isomers (1:1). When the spectrum of I was measured in dimethyl sulfoxide-d_6, the two signals collapsed to a broad singlet which appeared at 519 Hz. This seemed to indicate that, in dimethyl sulfoxide, one of the two conformers became predominant and a strong hydrogen bonding between N–H and the solvent made the N–H signals deshielded.

On the other hand, no temperature dependence was observed for the spectrum of I in carbon tetrachloride in the range from room temperature to 150°C. Furthermore, the 220 MHz NMR spectrum of I (Fig. 2) exhibited the same intervals between the two signals as in the case of 60 MHz, suggesting that the two signals are caused by coupling. These phenomena were, however, inconsistent with the aforementioned assumption. Therefore, we carried out a decoupling experiment in order to clarify the cause of the two signals. When the aromatic protons at 435 Hz were irradiated, the two signals collapsed to singlet peak. Similarly, the shape of signals of aromatic protons markedly changed on irradiation at the center of the signals. These facts clearly demonstrated that the lowfield proton couples with the aromatic protons, the coupling constant being 7.2 Hz. Although a great number of works on long-range coupling, including a favourable coupling path in a planar zig-zag arrangement,[3] have been reported, only a few reports have been concerned with couplings between the proton on the nitrogen atom and the other protons across more than four bonds.[3-5] However, such a large coupling constant as 7.2 Hz has never been reported.

The presence of a five-bond coupling to the N–H proton seemed so unlikely that we looked for other explanations. One possibility was that the signals at

1) M. Ohashi, K. Tsujimoto, and T. Yonezawa, *Chem. Commun.*, **1970**, 1089.

2) a) J. A. Pople, W. G. Schneider, and H. J. Bernstein, "High-resolution Nuclear Magnetic Resonace," McGraw-Hill Book Co., New York (1959), p. 365. b) T. H. Siddall, III, and C. A. Prohaska, *J. Amer. Chem. Soc.*, **88**, 1172 (1966).

3) S. Sternhell, *Pure and Appl. Chem.*, **14**, 15 (1964).

4) R. F. Abraham and H. F. Bernstein, *Can. J. Chem.*, **37**, 1056 (1969).

5) S. Sternhell, *Quart. Rev.*, **23**, 236 (1969).

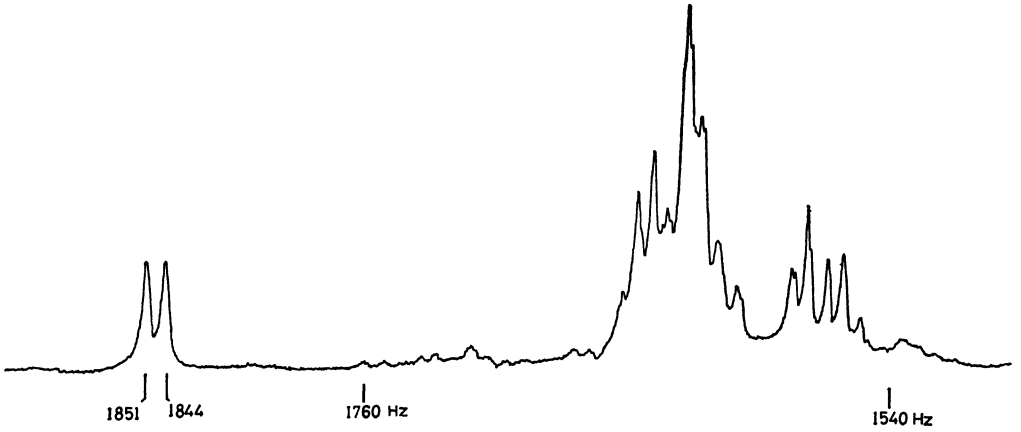

Fig. 2. The partial 220 MHz NMR spectrum of *N*-(2-biphenylyl)-pivalamide ($CDCl_3$) at room temperature.

497 and 504 Hz were due to one of the aromatic protons. In order to clarify this point, deuterium exchange was carried out. The sample recrystallized from methanol-d_4 - deuterium oxide showed a strong N–D absorption at 2400cm^{-1} in its IR spectrum; its NMR spectrum exhibited the two unchanged signals at the same positions, but the shapes of the signals of the usual aromatic protons changed markedly. This result indicated that the N–H proton which was obscured by the intense signals of the aromatic protons and that the two distinct signals at the downfield is probably due to an aromatic proton.

Since neither *N*-phenylbenzamide nor *N*-(4-biphenylyl)-carboxamides shows such spectral features, steric factors in *N*-(2-biphenylyl) carboxamides must be responsible for this remarkable deshielding effect.

On the basis of the aforementioned facts, it was deduced that the pivaloylamino group must lay on the same plane as that of the phenyl ring and that the anisotropy of the carbonyl group[6] might cause such a big deshielding effect on the proton at the ortho position to the amino group.[7] Steric effects and intramolecular π-NH hydrogen bonding were conceivable as factors fixing the conformation of the amino group as **a** in the scheme.

The spectrum of II was measured in a $CDCl_3$ solution to which a few drops of dimethyl sulfoxide has been added. The spectrum's two signals and the N–H signal moved up- and down-field respectively. Finally, the spectrum measured in dimethyl sulfoxide did not exhibit the two signals, but showed a broad singlet at 595 Hz which disappeared on deuterium exchange. These phenomena can be explained on the basis of the aforementioned conclusion; that is, the strong hydrogen bonding between the solvent and N–H proton would destroy the coplanarity of the carbonyl group, and hence the negative anisotropy effect on the ortho-proton would disappear to give the signals in the usual aromatic region.

Experimental

All the melting points are uncorrected. The NMR spectra were measured on JEOL JNM-3H60 or Varian HR 220-MHz spectromerters in a ca. 20% solution in either chloroform-*d* ($CDCl_3$) or dimethyl sulfoxide-d_6, with TMS as the internal standard.

N-(2-Biphenylyl)pivalamide (I). A solution of pivaloyl chloride (3.0 g) in methylene chloride (30 m*l*) was stirred, drop by drop, into a solution of *o*-biphenylamine (4.2 g) in methylene chloride (20 m*l*) and cooling with ice-water. To the reaction mixture we then added a solution of triethylamine (3.0 m*l*) in methylene chloride, after which the mixture was stirred for half an hour at room temperature. The mixture containing precipitates was washed with water (100 m*l*) three times and dried over anhydrous sodium sulfate. The subsequent evaporation of the solvent gave *N*-(2-biphenylyl) pivalamide (3 g). After recrystalization from ethanol, it had a mp of 69.7—70.1°C.

Found: C, 80.45; H, 7.44; N, 5.61%. Calcd for $C_{17}H_{19}ON$: C, 80.57; H, 7.56; N, 5.53%.

IR(KBr) 3260(NH), 1640(C=O), 770, 740, 700 cm^{-1} (benzene ring)

N-(2-Biphenylyl)benzamide(II) and N-(2-Biphenylyl)acetamide(III). The same experimental technique was used as that reported for *N*-(2-biphenylyl)pivalamide. The identification was made by a comparison of IR spectra of these products with the standard IRDC cards.[10]

N-(2-biphenylyl)benzamide mp 86.7—87.0°C (lit, 85—86°C).[8]

N-(2-biphenylyl)acetamide mp 116°C (lit, 117°C.)[9]

The authors wish to express their hearty thank to Dr. Isao Morishima for his helpful discussions and encouragement.

6) P. T. Narasimhan and M. T. Rogers, *J. Phys. Chem.*, **63**, 1388 (1959).
7) L. Crombie and J. W. Lown, *J. Chem. Soc.*, **1962**, 775.
8) A. Pictet and A. Hubert, *Ber.*, **29**, 1182 (1896).
9) von C. Graebe and A. S. Rateance, *Ann. Chem.*, **279**, 266 (1894).
10) IRDC cards, No. 6552 and 1551. Nankodo, Tokyo (1961).

BULLETIN OF THE CHEMICAL SOCIETY OF JAPAN, VOL. 44, 1430—1434 (1971)

Electron-accepting Properties of 2,3-Dicyano-1,4-benzoquinone and 2,3-Dichloro-5,6-dicyano-1,4-benzoquinone

Yôichi IIDA

Department of Chemistry, Faculty of Science, Hokkaido University, Sapporo

(Received November 11, 1970)

Various methods are available for determining the electron affinities of electron-acceptor molecules.[1] The 7,7,8,8-tetracyanoquinodimethane (TCNQ), 2,3-dicyano-1,4-benzoquinone (p-H_2QCy_2), and 2,3-dichloro-5,6-dicyano-1,4-benzoquinone (p-Cl_2QCy_2) molecules are known to be strong electron acceptors and to form stable anion radical salts with some diamagnetic counter cations.

Several years ago, we reported on the preferred electron transfer reaction between anion radicals in solution.[2] When p-X_2QCy_2, (X=H or Cl), was added to an acetonitrile solution of the sodium salt of the TCNQ anion radical, the oxidation-reduction reaction was found to take place simply through a one-electron transfer from the TCNQ anion radical to p-X_2QCy_2. This reaction was expressed by the following oxidation-reduction equilibrium:

$$Na^+TCNQ^- + p\text{-}X_2QCy_2 \rightleftharpoons TCNQ + Na^+p\text{-}X_2QCy_2^-, \quad (1)$$

where X=H or Cl. The equilibrium constant in acetonitrile at 20±1°C was determined spectroscopically as $K=30$ for the case of X=H, while it was $K \geq 2\times10^3$ for the case of X=Cl. As for this oxidation-reduction equilibrium, the observed equilibrium constant at temperature, T, is expressed as:

$$-RT\ln K = E(TCNQ) - E(p\text{-}X_2QCy_2) + \Delta\Delta G^0_{solv}(TCNQ, TCNQ^-) - \Delta\Delta G^0_{solv}(p\text{-}X_2QCy_2, p\text{-}X_2QCy_2^-), \quad (2)$$

where E(A) is the electron affinity of the neutral A molecule and $\Delta\Delta G^0_{solv}$(A,A$^-$), the difference in the free energy of solvation between the molecule and its anion radical. Therefore, if one assumes $\Delta\Delta G^0_{solv}$(TCNQ, TCNQ$^-$)$\approx\Delta\Delta G^0_{solv}$($p$-$X_2QCy_2$, p-$X_2QCy_2^-$), one can obtain:

$$-RT\ln K = E(TCNQ) - E(p\text{-}X_2QCy_2). \quad (3)$$

From the observed values of K, the difference in the electron affinities between TCNQ and p-H_2QCy_2 was estimated to be $E(p\text{-}H_2QCy_2)-E(TCNQ)=0.09$ eV, while that between TCNQ and p-Cl_2QCy_2 was $E(p\text{-}Cl_2QCy_2)-E(TCNQ)\geq0.19$ eV.

On the other hand, TCNQ, p-H_2QCy_2, and p-Cl_2QCy_2 form charge-transfer complexes with many electron donor molecules in solution. It has been known, in general, that the energy of the charge-transfer band of a molecular complex, $h\nu_{CT}$ (D,A), can be described as:

$$h\nu_{CT}(D, A) = I(D) - E(A) - C + P, \quad (4)$$

where I(D) is the ionization potential of the donor, D, and E(A), the electron affinity of the acceptor, A; C is the coulombic energy of the dative-bond structure, and P is the difference between all the other energy quantities in the dative-bond and no-bond structures with both partners at their equilibrium internuclear separation in the complex.[3] This relation has often been used for the estimation of the electron affinity.[1] In the present paper, the difference in the electron affinities, $E(p\text{-}X_2QCy_2)-E$(TCNQ), where X=H or Cl, was estimated from the difference in the charge-transfer energies between $h\nu_{CT}$ (D, p-X_2QCy_2) and $h\nu_{CT}$ (D, TCNQ). We shall examine how these values of $E(p\text{-}X_2QCy_2)-E$(TCNQ) correspond to those evaluated previously from the oxidation-reduction equilibria.

The charge-transfer complexes of TCNQ, p-H_2QCy_2, and p-Cl_2QCy_2 were examined in an ethylene dichloride solution. Various aromatic hydrocarbons were employed as the electron donors. The charge-transfer spectra were measured by means of a Beckman DK-2A spectrophotometer. Table 1 shows the observed maximum positions of the charge-transfer absorptions under investigation.[4]

As for the complexes containing TCNQ, p-H_2QCy_2, or p-Cl_2QCy_2 as an acceptor, the I(D) value is constant for a common donor. In these cases, the great variation will occur in E(A). It is assumed that the other quantities are more or less constant, since the molecular sizes and the shapes of the acceptors are all similar. In this case, the energy difference of the charge-transfer bands, $h\nu_{CT}$ (D, TCNQ)–$h\nu_{CT}$ (D, p-X_2QCy_2), where X=H or Cl, can be approximately written as:

$$h\nu_{CT}(D, TCNQ) - h\nu_{CT}(D, p\text{-}X_2QCy_2) = E(p\text{-}X_2QCy_2) - E(TCNQ). \quad (5)$$

1) G. Briegleb, *Angew. Chem.*, **76**, 326 (1964).

2) Y. Iida and H. Akamatu, This Bulletin, **40**, 231 (1967).

3) S. P. McGlynn, *Chem. Rev.*, **58**, 1113 (1958); G. Briegleb, "Elektronen-Donator-Acceptor Komplexe," Springer-Verlag, Berlin-Göttingen-Heidelberg (1961).

4) Two charge-transfer bands were observed for the complex containing naphthalene, 2,3-dimethylnaphthalene, acenaphthene or pyrene as a donor, and p-H_2QCy_2 or p-Cl_2QCy_2 as an acceptor. We can see that the energy difference of the complex between the first and the second charge-transfer bands remains nearly constant for a given donor; the value of this energy difference was found to be $(5.05\pm0.15)\times10^3$ cm^{-1} for the naphthalene complexes, $(3.95\pm0.05)\times10^3$ cm^{-1} for the 2,3-dimethylnaphthalene complexes, $(7.45\pm0.05)\times10^3$ cm^{-1} for the acenaphthene complexes, and $(6.75\pm0.15)\times10^3$ cm^{-1} for the pyrene complexes. This means that these two charge-transfer bands can be attributed to the transitions from the highest and the next occupied orbitals of the donor to the lowest vacant orbital of the acceptor. The energy difference between the highest and the next occupied orbitals of the donor is approximated by that between the first and the second charge-transfer bands. See, for example, H. Kuroda, T. Kunii, S. Hiroma, and H. Akamatu, *J. Mol. Spectrosc.*, **22**, 60 (1967).

Table 1. The data on the maximum positions of the charge-transfer bands (in unit of 10^3 cm^{-1})[a)]

Donor	Acceptor		
	TCNQ	p-H_2QCy_2	p-Cl_2QCy_2
Benzene	—	25.9	24.2
Toluene	—	24.1	22.5
p-Xylene	—	21.1	19.4
Naphthalene	18.6	17.9	15.9
		22.8	21.1
2,3-Dimethylnaphthalene	17.0	16.8	14.7
		20.7	18.7
Acenaphthene	15.4	14.9	13.2
		22.4	20.6
Phenanthrene	19.5	19.0	17.1
Pyrene	13.7	13.7	11.8
		20.6	18.4

a) They were measured in ethylene dichloride solution at room temperature, although benzene, toluene, or p-xylene was used as a solvent as well as a donor.

When the complexes showed two charge-transfer absorptions, the maximum positions of the first charge-transfer bands were employed for $h\nu_{CT}$(D, A). Unfortunately, the maximum positions for the complexes of TCNQ with benzene, toluene, and p-xylene were not determined, because the absorption due to TCNQ hindered the observation of their charge-transfer bands. Therefore, the data on the charge-transfer bands for the complexes of p-H_2QCy_2 or p-Cl_2QCy_2 with the same donor molecules were not available for comparison. We used, then, the values of $h\nu_{CT}$(D, A), where D is naphthalene, 2,3-dimethylnaphthalene, acenaphthene, phenanthrene, or pyrene, and where A is TCNQ, p-H_2QCy_2, or p-Cl_2QCy_2. These values were taken from Table 1. By the use of Eq. (5), $E(p\text{-}X_2QCy_2)-E$(TCNQ), where X=H or Cl, was evaluated for each common donor. For the above five donors, the average value of $E(p\text{-}H_2QCy_2)-E$(TCNQ) was estimated to be $(0.4\pm0.4)\times10^3$ cm^{-1} (*i.e.*, 0.05 ± 0.05eV), while that of $E(p\text{-}Cl_2QCy_2)-E$(TCNQ) was estimated to be $(2.3\pm0.4)\times10^3$ cm^{-1} (*i.e.*, 0.29 ± 0.05 eV). If the standard value is once given to the electron affinity for TCNQ, $E(p\text{-}H_2QCy_2)$ and $E(p\text{-}Cl_2QCy_2)$ will be determined from these relations. When E(TCNQ) $=1.7$ eV is taken as a reference,[5)] $E(p\text{-}H_2QCy_2)$ and $E(p\text{-}Cl_2QCy_2)$ are estimated to be 1.75 ± 0.05 eV and 1.99 ± 0.05 eV respectively. These values are found to be in good accordance with $E(p\text{-}H_2QCy_2)=1.79$ eV and $E(p\text{-}lC_2QCy_2)\geq1.89$ eV respectively; these latter values were determined from the method of the oxidation-reduction equilibrium between the anion radicals by using the same standard value of E(TCNQ)$=1.7$ eV.[2)] It is interesting to note that the introduction of the chlorine substituents into p-H_2QCy_2 increases the value of the electron affinity by at least 0.1—0.2 eV.

Judging from these results, the previous estimation of the $E(p\text{-}H_2QCy_2)$ and $E(p\text{-}Cl_2QCy_2)$ values from the method of oxidation-reduction equilibrium is strongly supported by the present method of the charge-transfer spectra. Therefore, it may be concluded that the application of the oxidation-reduction equilibrium between anion radicals in solution is a new method for determining the electron affinities of acceptor molecules generally. However, we should keep in mind that, in this method, the E(A) values include some uncertainties, since the $\Delta\Delta G^0_{solv}$(A, A^-) value does not remain constant for each of the acceptor molecules.

5) Although Briegleb reported E(TCNQ)$=1.7$ eV,[1)] no definite value has yet been determined for E(TCNQ).

BULLETIN OF THE CHEMICAL SOCIETY OF JAPAN, VOL. 44, 1431—1432 (1971)

The Novel Synthesis of Halodeoxy Sugars

Saburo INOKAWA, Kuniaki SEO,* Hiroshi YOSHIDA, and Tsuyoshi OGATA

Department of Synthetic Chemistry, Faculty of Engineering, Shizuoka University, Johoku, Hamamatsu

**Department of Applied Chemistry, College of Technology, Ooka, Numazu*

(Received December 3, 1970)

The halodeoxy sugars are important synthetic intermediates,[1] but their preparation is often an involved process. This paper will describe a facile method for the formation of halodeoxy sugars by the reaction of cyclic phosphite or phosphonite derivatives of sugars with methyl iodide. The usefulness of this reaction is demonstrated by the conversion of 1,2-*O*-isopropylidene-α-D-glucofuranose (**1**) into 6-deoxy-6-iodo-1,2-*O*-isopropylidene-3,5-*O*-(methylphosphonate)-α-D-glucofuranose (**3**) *via* the intermediate 1,2-*O*-isopropylidene-3,5,6-*O*-(phosphite)-α-D-glucofuranose (**2**). No evidence for the presence of another iodo isomer was obtained. To explore the scope of this facile reaction, 5-deoxy-5-iodo-3-*O*-(methylphenylphosphinate)-α-D-xylofuranose (**6**) was prepared *via* the 1,2-*O*-isopropylidene-3,5-(phenylphosphonite)-α-D-xylofuranose (**5**) from 1,2-*O*-isopropylidene-α-D-xylofuranose (**4**). The structures of the products were determined by studying the NMR spectra and by elementary analyses.

1) For reviews of halodeoxy sugars see: a) S. Hanessian, *Advan. Carbohyd. Chem.*, **21**, 142 (1966); b) J.E.G. Barnett, *ibid.*, **22**, 177 (1967).

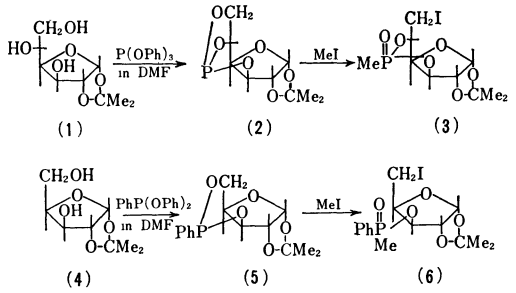

Experimental

The nuclear magnetic resonance spectra were taken at 60 MHz on a Hitachi-Perkin-Elmer R-20 spectrometer, using tetramethylsilane as the internal reference. The thin-layer chromatograms were run on a silica-layer G;[2] phosphorus compounds were detected by spraying the plates with a cobalt chloride solution[3] and by then heating them. Periodic sampling and examination by thin-layer chromatography (tlc) permitted the determination of the most suitable reaction conditions for the preparation runs.

Materials. The 1,2-*O*-isopropylidene-α-D-glucofuranose (**1**)[4] and 1,2-*O*-isopropylidene-α-D-xylofuranose (**4**)[5] were prepared in the usual way. The triphenyl phosphite was used after the vacuum distillation of a commercial substance. The diphenyl phenylphosphonite[6] (bp 174—176°C/2 mmHg) was prepared by the reaction of an excess of phenol and phenylphosphonous dichloride.[7]

1,2-O-Isopropylidene-3,5,6-O-(phosphite)-α-D-glucofuranose (2). A solution of 5.0 g of **1** and 8.0 g of triphenyl phosphite in 30 m*l* of dimethylformamide (DMF) with 0.1 g of sodium ethoxide was allowed to stand at room temperature for 15 hr. The solution was then concentrated *in vacuo*; the residue was sublimated twice *in vacuo* at 120°C/2 mmHg to give, in an 80% yield (4.5 g), colorless needles; mp 155°C; $[\alpha]_D^{25}$ −24.3° (*c* 10, DMF); tlc upper (petroleum ether - ethyl acetate 4:1).

Found: C, 43.2; H, 5.25%. Calcd for $C_9H_{13}O_6P$: C, 43.6; H, 5.28%.

The PMR data (chloroform-*d*) were as follows: τ 3.88 (one-proton doublet, $J_{1,2}$=4.0 Hz, H_1), 5.47 (one-proton doublet, $J_{2,3}\fallingdotseq 0$ Hz, H_2), 5.6—6.2 (four-proton multiplets, $H_{3,4,5,6}$), and 8.54, 8.71 [six-proton singlets, $C(CH_3)_2$].

6-Deoxy-6-iodo-1,2-O-isopropylidene-3,5-O-(methylphosphonate) α-D-glucofuranose (3). A solution of 2 g of **2** in 15 m*l* of methyl iodide, with a small amount of copper powder, was heated at 100°C for 20 hr in a sealed tube. The solution was then filtered and concentrated *in vacuo*; the residue was dissolved in chloroform, washed with a sodium carbonate aqueous solution and water, dried over sodium sulfate, and concentrated *in vacuo* to give, in an 80% yield (2.5 g), colorless needles; mp 176—177°C (from methanol); $[\alpha]_D^{25}$ +15.2° (*c* 10, chloroform); tlc medium (petroleum ether - ethyl acetate, 4:1).

Found: C, 30.8: H, 4.17%. Calcd for $C_{10}H_{16}O_6PI$: C, 30.8; H, 4.13%.

The PMR data (chloroform-*d*) were as follows: τ 4.00 (one-proton doublet, $J_{1,2}$=4.0 Hz, H_1), 5.09 (one-proton multiplet, H_3), 5.33 (one-proton doublet, $J_{2,3}\fallingdotseq 0$ Hz, H_2), 5.5—5.9 (two-proton multiplets, $H_{4,5}$), 6.45 (two-proton doublet, $J_{5,6}$=7.0 Hz, H_6), 8.40 (three-proton doublet, $J_{P,CH}$=18.0 Hz, P-CH_3), and 8.49, 8.66 [six-proton singlets, $C(CH_3)_2$].

5-Deoxy-5-iodo-3-O-(methylphenylphosphinate)-α-D-xylofuranose (6). A solution of 7 g of **4** and 12 g of diphenyl phenylphosphonite in 40 m*l* of DMF with 0.1 g of sodium ethoxide was allowed to stand at room temperature for 20 hr. The solution was then concentrated *in vacuo*, and the resulting oil was fractionally distilled *in vacuo* to give 4.0 g of crude **5** contaminated with small amounts of phenol and diphenyl phenylphosphonite at 160—162°C/2mmHg; tlc medium (petroleum ether-ethyl acetate, 9:1). The crude **5** obtained above, without further purification, was dissolved in 15 m*l* of methyl iodide; then solution was heated with a small amount of copper powder at 100°C for 4 hr in a sealed tube. The solution was then filtered and concentrated *in vacuo*. Fractional high-vacuum distillation gave, in a 20% yield (3.1 g) based on **4**, a thick colorless sirup at 120°C/10^{-2}—10^{-3} mmHg; $[\alpha]_D^{20}$=−23° (*c* 3.04, carbon tetrachloride); tlc upper (petroleum ether - ethyl acetate, 1:4).

Found: C, 41.3; H, 4.65%. Calcd for $C_{15}H_{20}O_5PI$: C, 41.1; H, 4.60%.

The PMR data (carbon tetrachloride) were as follows: τ 2.0—2.8 (five-proton multiplets, C_6H_5), 4.25 (one-proton doublet, $J_{1,2}$=4.0 Hz, H_1), 5.20 (one-proton d. doublet, $J_{2,3}\fallingdotseq$O Hz, $J_{3,4}$=2.0 Hz. $J_{P,CH}$=9.0 Hz, H_3), 5.42 (one-proton doublet, H_2), 5.65 (one-proton broad doublet, H_4), 6.81 (two-proton doublet, $J_{4,5}$=7.0 Hz, H_5), 8.26 (three-proton doublet, $J_{P,CH}$=14.5 Hz, P-CH_3), and 8.60, 8.83 [six-proton singlets, $C(CH_3)_2$].

Results and Discussion

When a solution of **1** and triphenyl phosphite (1:1.2 molar ratio) in DMF was allowed to stand in the presence of sodium ethoxide at room temperature, **1** was transformed almost quantitatively into the product, **2**, as the tlc showed one major spot. When the solution was evaporated *in vacuo*, the sublimation of the resulting residue gave colorless needles in an 80% yield. The structure of **2** was established by elementary analysis and by studying the NMR spectrum.

The treatment of **2** with methyl iodide in a sealed tube at 100°C afforded **3** as colorless needles (from methanol) in an 80% yield. The structure of **3** was established by elementary analysis and by a study of the NMR spectrum. The appearance of the two-proton doublet at τ 6.45, shifted from 5.6—6.2 in the NMR spectrum of **1**, shows that **3** is a 6-deoxy-6-iodo compound, while the appearance of the three-proton doublet with a large coupling constant (J=18.0 Hz) at τ 8.40 shows that a CH_3 group is bonded to the phosphorus atom.

Similarly, the compound **6** was prepared by the reaction of **4** and diphenyl phenylphosphonite, followed by treatment with methyl iodide, in a poor yield (20%). Although the tlc showed that the reaction was rather clear, the poor yield seems to be due to difficulty in separation by fractional distillation.

This reaction may be effected to provide convenient and widely-usable route to halodeoxy sugars.

2) Nakarai Chemicals, Ltd., Kyoto.

3) R. Donner and K. Lohs, *J. Chromatogr.*, **17**, 349 (1965).

4) O. Th. Schmidt, "Methods in Carbohydrate Chemistry," Vol. II, ed by R. L. Whistler and M. L. Wolfrom, Academic Press, New York and London (1963), p. 318.

5) P. A. Levene and A. L. Raymond, *J. Biol. Chem.*, **102**, 317 (1933).

6) A. E. Arbusov, G. Kamai, and L. V. Nesterov, *Chem. Abstr.*, **51**, 5720 (1957).

7) B. Buchner and L. B. Lockhart, Jr., "Organic Syntheses," Coll. Vol. IV, p. 784 (1963).

BULLETIN OF THE CHEMICAL SOCIETY OF JAPAN, VOL. 44, 1433—1434 (1971)

The X-Ray Powder Diffraction Pattern of Tetrasulfur Tetranitride

Shuichi HAMADA, Akira TAKANASHI, and Toshiaki SHIRAI

Department of Chemistry, Faculty of Science, Science University of Tokyo, Kagurazaka, Shinjuku-ku, Tokyo

(Received December 11, 1970)

Tetrasulfur tetranitride, S_4N_4, is an eight-membered ring molecule, one which involves four coplanar nitrogen atoms. The molecular symmetry and the crystal system of tetrasulfur tetranitride have been reported to be $\bar{4}2\,m(D_{2d})$[1] and monoclinic[2-4] respectively. On the basis of an X-ray analysis on the single crystal, Clark[5] verified the unit cell dimensions and the space group reported by Buerger[4] to be as follows: $a_0=8.75$, $b_0=7.16$, $c_0=8.65$ Å, $\beta=92.5°$, and space group, $P2_1/n(C_{2h}^5)$. However, studies of X-ray powder diffractometry on tetrasulfur tetranitride have been reported only by Garcia-Fernandez,[6,7] and the Miller indices were not assigned in his reports.

In this work, a reexamination and an assignment of the Miller indices on the X-ray powder diffraction peaks will be attempted.

Experimental

Materials. The tetrasulfur tetranitride was prepared by the method reported by Villena-Blanco and Jolly.[8] A crude product was extracted with dry dioxane. When the dioxane solution was cooled to room temperature, tetrasulfur tetranitride crystallized out as orange-yellow crystals. These crystals were filtered off and dried in a paper-box contained silica-gel, and so a sample for tetrasulfur tetranitride was obtained without further purification.

Procedure. An infrared spectrophotometer, Model DS-403G, from the Japan Spectroscopic Company was used to obtain the infrared spectra of a carbon disulfide solution of the sample at wave numbers ranging from 2400 to 3600 cm^{-1}, and from 600 to 1000 cm^{-1}.

An Olympus reflecting microscope, Model STS, was used to determine the melting point of the sample in a heating block at the heating rate of 0.5°C/min. The temperatures of the heating block were calibrated by using materials with known melting points.

The thermal gravimetric analysis and the differential thermal analysis of the sample were carried out at a heating rate of 5°C/min in a nitrogen atmosphere using a Thermoflex, Model 8002, from the Rigaku Denki Company.

An X-ray diffractometer, Model JDX-5P, from the Japan Electron Optics Laboratory was used to obtain X-ray powder diffraction intensity diagrams; a goniometer and Cu$K\alpha$ radiation were also used. The diffraction angles were calibrated by using silicon.

Results and Discussion

The IR Spectra of the Sample. Only the characteristic absorption bands[9,10] of tetrasulfur tetranitride at 938 and 700 cm^{-1} were observed in the spectra of the carbon disulfide solution of the sample.

The Melting Point of the Sample. The melting point of the sample was estimated to be 182.0°C. The melting points for tetrasulfur tetranitride have been reported to range from 176°C to 187.5°C.[11-19] The value of the melting point for tetrasulfur tetranitride, which was prepared by the Jolly method,[8] was found to be 178—179°C.[20] However, by repeated recrystallization from benzene, or by purification on an alumina chromatographic column, tetrasulfur tetranitride with a melting point as high as 187—187.5°C has been obtained.[19] Therefore, the sample obtained in this work was considered to be pure enough for us to obtain a good diffraction pattern for tetrasulfur tetranitride from the results of the IR spectra and the melting point of the sample.

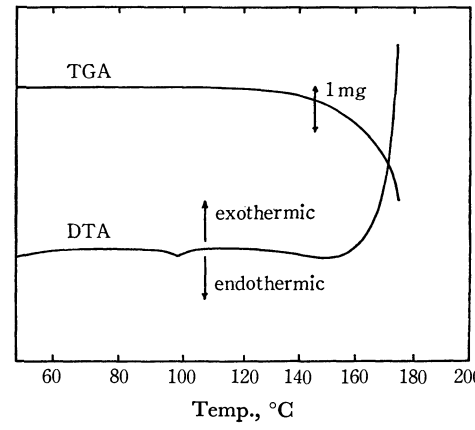

Fig. 1. TGA and DTA curves of sample.

1) C. S. Lu and J. D. Donohue, *J. Amer. Chem. Soc.*, **66**, 818 (1944).
2) E. Artini, *Z. Krist.*, **42**, 68 (1907).
3) G. F. H. Smith, *Miner. Mag.*, **16**, 97 (1911).
4) J. M. Buerger, *Amer. Min.*, **21**, 575 (1936).
5) D. Clark, *J. Chem. Soc.*, **1952**, 1615.
6) H. Garcia-Fernadez, *Compt. Rend.*, **250**, 3181 (1960).
7) H. Garcia-Fernandez, *Bull. Soc. Chim. Fr.*, **1961**, 1021.
8) M. Villena-Blanco and W. L. Jolly, "Inorganic Syntheses," Vol. IX, ed. by S. Y. Tyree, Jr., *et al.*, McGraw-Hill, New York (1967), p. 98.
9) H. Garcia-Fernandez, *Compt. Rend.*, **260**, 6107 (1965).
10) H. G. Heal, "Inorganic Sulfur Chemistry," ed. by G. Nickless, Elsevier, Amsterdam (1968), p. 464.
11) A. G. McDiarmid, *J. Amer. Chem. Soc.*, **78**, 3871 (1956).
12) C. G. R. Nair and A. R. V. Murthy, *J. Inorg. Nucl. Chem.*, **25**, 453 (1963).
13) O. Glemser, A. Haas, and H. Reinke, *Z. Natruforsch.*, **20b**, 809 (1965).
14) Y. Sasaki and F. P. Olsen, *Inorg. Nucl. Chem.*, **3**, 351 (1967).
15) O. Ruff and E. Geisel, *Ber.*, **38**, 2659 (1905).
16) M. Goehring, *Quart. Rev.*, **10**, 437 (1956).
17) P. S. Braterman, *J. Chem. Soc.*, **1965**, 2297.
18) M. H. M. Arnold, J. A. C. Hugill, and J. M. Hutson, *ibid.*, **1936**, 1645.
19) M. Villena-Blanco, *U. S. Atom. Energy Commun.*, **1963**, UCRL 11081.
20) W. L. Jolly, "The Synthesis and Characterization of Inorganic Compounds," Prentice-Hall, Englewood Cliffs, N. J. (1970), p. 502.

However, there is some doubt whether or not the observed melting point shows the proper melting point of tetrasulfur tetranitride. Figure 1 shows the results of the thermal gravimetric analysis and the differential thermal analysis of the sample. An abrupt weight loss near the melting point was found to be due to exothermic change in the sample. Moreover, an explosive decomposition occurred just after the measurements stopped. Judging from the standard heat of formation, ΔH^0, of tetrasulfur tetranitride (110±2 kcal/mol),[21] the thermal decomposition was considered to dominate the sublimation near the melting point. Therefore, the fusion of tetrasulfur tetranitride must accompany the thermal decomposition. Goehring and Voigt[22] have reported that tetrasulfur tetranitride decomposed into its elements at approximately 130°C.

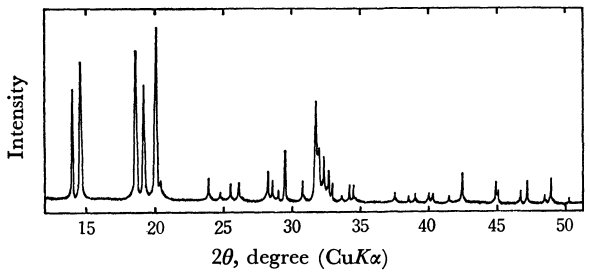

Fig. 2. X-Ray powder diffraction pattern of tetrasulfur tetranitride.

The X-Ray Powder Diffraction Pattern of Tetrasulfur Tetranitride. The X-ray powder diffraction pattern was obtained over the 2θ range from 13° to 50°, as is shown in Fig. 2. The observations in the 2θ range over 50° were omitted. The diffraction peak, d=5.06 Å, reported by Garcia-Fernandez was not observed in the sample, but this peak was observed in a residue of the dioxane solution. Therefore, the peak was considered to be due to a by-product, although the by-product was not identified.

The Miller indices were assigned to the corresponding observed d values as is shown in Table 1, since the observed d values agreed well with those calculated from the lattice constants reported by Clark.[5]

The observed relative intensities of diffraction peaks did not agree with the intensities which were calculated by using the structure factors reported by Sharma and Donohue.[23] The relative intensities were apt to change with the conditions of the sample in spite of a good agreement in the d values. The crystallization rate from the dioxane solution affected the relative intensities; decreases in the intensities of the ($\bar{1}11$), (111), and (200) peaks, and increases in the intensities of the (101) and (202) peaks were observed at a rapid crystallization, for example, while the pulverizing condition scarcely affected the intensities of the same sample at all.

Table 1. The d values and the relative intensities of tetrasulfur tetranitride

$h\,k\,l$	Calcd		This work		Garcia-Fernandez	
	d, Å	I/I_0	d, Å	I/I_0	d, Å	I/I_0
$\bar{1}\,0\,1$	6.29	40.4	6.28	64	6.32	33—80
1 0 1	6.01	42.6	6.02	81	6.06	33—80
					5.06	15—33
$\bar{1}\,1\,1$	4.72	100	4.73	88	4.76	80—100
1 1 1	4.61	80.9	4.61	69	4.61	80—100
2 0 0	4.37	67.7	4.38	100	4.39	33—80
0 0 2	4.32	12.7	4.34	11		
0 1 2	3.70	15.8	3.71	11	3.70	15—33
0 2 0	3.58	15.3	3.58	5	3.61	15—33
$\bar{2}\,1\,1$	3.47	7.5	3.48	9		
2 1 1	3.38	6.8	3.39	10		
$\bar{2}\,0\,2$	3.14	8.4	3.15	17		
$\bar{1}\,2\,1$	3.11	20.6	3.11	12		
1 2 1	3.08	8.9	3.08	5		
2 0 2	3.01	15.2	3.02	29	3.02	1—15
$\bar{2}\,1\,2$	2.88	12.0	2.89	11	2.88	15—33
$\bar{3}\,0\,1$	2.80	47.4	2.81	58		
2 1 2	2.77	22.2	2.78	31	2.77	80—100
$\bar{1}\,0\,3$	2.77	12.6				
2 2 0	2.77	5.8				
0 2 2	2.76	43.7	2.76	26		
3 0 1	2.73	22.4	2.73	18		
1 0 3	2.70	17.3	2.71	10		
$\bar{2}\,2\,1$	2.66	3.9	2.66[a]	3		
$\bar{1}\,2\,2$	2.65	3.1				
1 2 2	2.61	8.8	2.61	9	2.61	33—80
$\bar{3}\,1\,1$	2.61	2.5				
$\bar{1}\,1\,3$	2.59	5.3	2.59	8		
$\bar{2}\,2\,2$	2.36	7.9	2.37	6	2.36	15—33
$\bar{3}\,1\,2$	2.33	0.8	2.33[a]	4		
$\bar{2}\,1\,3$	2.32	2.5				
2 2 2	2.30	3.7	2.31	6		
0 2 3	2.24	27.2	2.25	6	2.24	15—33
2 1 3	2.24	3.9				
$\bar{1}\,3\,1$	2.23	7.0	2.23[a]	6		
1 3 1	2.22	5.0				
$\bar{3}\,2\,1$	2.20	4.3				
3 2 1	2.17	4.2	2.17	4		
$\bar{3}\,0\,3$	2.09	12.1	2.10	16	2.10	15—33
0 3 2	2.09	2.7				
0 1 4	2.07	4.3	2.08	2		
$\bar{3}\,1\,3$	2.01	4.5	2.01	12	2.02	15—33
$\bar{4}\,0\,2$	1.99	2.8	2.00	4		
3 1 3	1.93	6.9	1.94	7		
4 0 2	1.92	4.8	1.92[a]	13	1.92	15—33
$\bar{4}\,1\,2$	1.91	9.7				
2 0 4	1.90	4.0				
4 2 0	1.87	4.1	1.87	5	1.87	15—33
4 1 2	1.85	3.9	1.86	13		
0 2 4	1.85	2.5				
$\bar{1}\,3\,3$	1.81	6.9	1.82	2	1.81	15—33

a) assignments are uncertain

21) C. K. Baker, A. W. Cordes, and J. L. Margrave, *J. Phys. Chem.*, **69**, 334 (1965).
22) M. Goehring and D. Voigt, *Z. Anorg. Allgem. Chem.*, **285**, 181 (1956).
23) B. D. Sharma and J. Donohue, *Acta Crystallogr*, **16**, 891 (1963).

BULLETIN OF THE CHEMICAL SOCIETY OF JAPAN, VOL. 44, 1435—1436 (1971)

The Thermochromism of Molybdenum(V) in Hydrochloric Acid Solutions

Yukichi Yoshino, Iwao Taminaga, and Shin Uchida

Department of Chemistry, College of General Education, The University of Tokyo, Komaba, Meguro-ku, Tokyo

(Received December 14, 1970)

During a systematic study of the autoxidation of molybdenum(V) in aqueous solutions,[1] it was found that the color of the hydrochloric acid solutions of molybdenum(V) changes remarkably with a rise in temperature. It was established that the change is prominent in the concentration range of 4—6 molar HCl, and is reversible between room temperature and 100°C. These observations have been explained on the basis of temperature dependence of the monomer-dimer equilibrium[2]

$$(MoOCl_4)_2O^{4-} + 2HCl \rightleftarrows 2MoOCl_5^{2-} + H_2O$$

Experimental

Molybdenum(V) solutions were prepared by dissolution of $(NH_4)_2MoOCl_5$[3] in an appropriate concentration of hydrochloric acid. Thrice distilled water was used throughout the experiment. The absorbance measurements were carried out by an Ito model QU-3 spectrophotometer using 1-cm stoppered quartz cells. The temperatures were controlled by circulating ethylene glycol from a Haake thermostat.

Results and Discussion

Figure 1 shows the effect of temperature on the visible spectra at 5 molar HCl. The molybdenum(V) solution has two absorption maxima at 450 mμ (I) and at 720 mμ (II), both of which are assigned to *d–d* transition in $4d^1$ electronic configuration.[4] It will be seen that the absorbance at 450 mμ decreases strikingly with a rise in temperature, while at 720 mμ absorbance remains almost unchanged. The net result is that the solution is yellow at room temperature but turns to light green at higher temperatures.

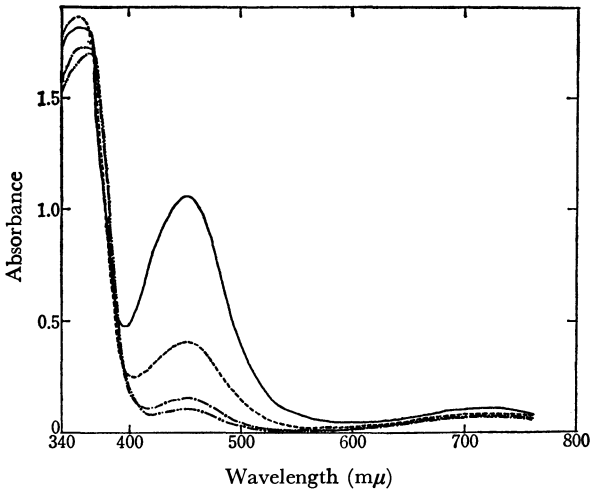

Fig. 1. The spectrum of 5×10^{-3} M $(NH_4)_2MoOCl_5$ in 5M HCl at various temperatures.
a) —— 33.5°C, b) —— 57.5°C, c) ----- 78.6°C, d) -·-·-· 94.0°C

It was established that, when the hot solution is allowed to cool to room temperature, the original pattern of spectra is recovered with slight decrease of absorbance. It was noted that the patterns of spectra at lower and higher temperatures are quite similar to those observed at lower and higher concentration ranges of hydrochloric acid.[2]

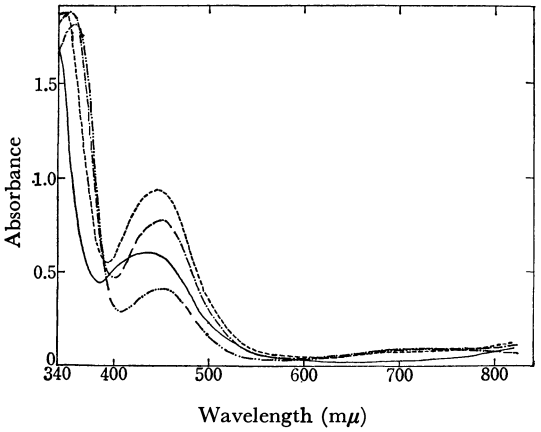

Fig. 2. The spectrum of 5×10^{-3} M $(NH_4)_2MoOCl_5$ in 4 M HCl at various temperatures.
a) —— 25.7°C, b) —— 58.6°C, c) ----- 78.2°C, d) -·-·-· 93.2°C

In a 6 molar HCl solution, the color of the solution is light green at room temperature, but with a temperature rise a slight decrease in absorbance is still observable at 450 mμ.

As shown in Fig. 2, when the concentraton of HCl is kept at 4 molar, the absorption maximum (I) decreases and shifts to shorter wave length at room temperature. When the temperature is raised, the absorption maximum (I) at first shifts to 450 mμ and increases in intensity, and then begins to decrease. By comparing such a change to that in a 5 molar HCl solution, it is suggested that another form of polymeric species (D_2) exists in the 4 molar HCl solution at room temperature, and that with a rise in temperature this species at first changes into yellow dimer (D_1), and then to green species (M). Moreover, it was confirmed that the spectral change is reversible with respect

1) Y. Yoshino, T. Takeuchi, H. Kinoshita, and S. Uchida, This Bulletin, **41**, 765 (1968); *Sci. Pap. Coll. Gen. Educ. Univ. Tokyo*, **19**, 71 (1969).
2) J. P. Haight, Jr., *J. Inorg. Nucl. Chem.*, **24**, 663 (1962).
3) W. G. Palmer, "Experimental Inorganic Chemistry," Cambridge University Press, Cambridge, England (1954), p. 408.
4) H. B. Gray and C. R. Hare, *Inorg. Chem.*, **1**, 363 (1962).

to temperature.

To summarize the above observations, it may be concluded that the thermochromism of molybdenum(V) in approximately 5 molar HCl solution is due to the shift of equilibria between monomeric and dimeric species of molybdenum(V), and is the same sort of change observed in varying concentrations of hydrochloric acid. On this basis, the apparent equilibrium constants, K of the monomer (M)-dimer (D_1) equilibria,

$$D_1 \rightleftarrows 2M$$

were calculated according to Haight's approach.[2] The results are summarized in Table 1.

Table 1. Apparent equilibrium constants for dimer-monomer equilibria at various temperatures

6M HCl		5M HCl		4M HCl	
t°C	$K\times10^3$, M	t°C	$K\times10^3$, M	t°C	$K\times10^3$, M
23.8	3.18	33.5	0.368	25.7	(0.853)
56.3	14.9	57.5	1.37	58.6	(0.442)
75.5	30.0	78.6	5.78	78.2	5.79
92.5	54.2	94.0	12.1	93.2	1.37

Total concentration of molybdenum(V): 5×10^{-3}M.

Using these values, $-\log K$ was plotted against the reciprocal absolute temperature; the plots are shown in Fig. 3.

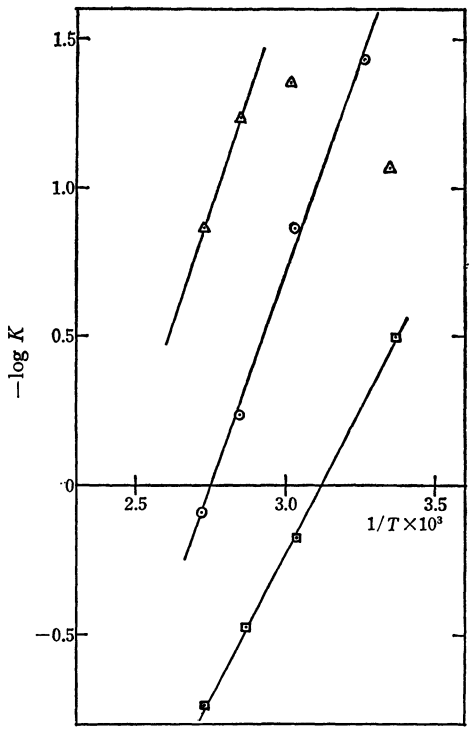

Fig. 3. The plots of $-\log K$ against $1/T$.
5×10^{-3} M Mo(V) in 4 M (△), 5 M (⊙), 6 M HCl (⊡)

Linear relations were found to hold in the cases of 6 and 5 molar HCl solutions over the temperature range studied, and this confirms the existence of monomer-dimer equilibria in these solutions. In the case of 4 molar HCl solution, however, the linear relation no longer holds in the lower temperature range as would be expected from the above-mentioned experiments.

From the slopes of the straight lines, the values of enthalpy change, ΔH, were evaluated as 8.9, 13.3, and 14.3 kcal/mol for 6, 5 and 4 molar HCl solutions respectively. These values are somewhate larger than Haight's, $\Delta H=6.0\pm0.2$ kcal/mol in 5 molar HCl solutions. The variation of the enthalpy values seems understandable in light of the possible overlapping of further hydrolytic equilibria in a relatively low concentration range of acid such as 4 to 6 molar HCl.

BULLETIN OF THE CHEMICAL SOCIETY OF JAPAN, VOL. 44. 1436—1438 (1970)

The Charge-transfer Complexes of Metal Chelates of 8-Hydroxyquinoline with 2,5-Diazido-3,6-dichloro-1,4-benzoquinone and 2,5-Diazido-3,6-dibromo-1,4-benzoquinone

Shigeo KOIZUMI and Yôichi IIDA

Department of Chemistry, Faculty of Science, Hokkaido University, Sapporo

(Received December 14, 1970)

Charge-transfer complexes made from electron donors and acceptors have been studied extensively.[1] However, there are few donor molecules that are known to be composed of organic metal chelates. In 1965 Bailey *et al.* prepared the charge-transfer complexes of 8-hydroxyquinoline and its copper, palladium, and nickel chelates with various electron acceptors.[2] Bis(8-hydroxyquinolinato)palladium(II) ($Pd(Ox)_2$) and bis(8-hydroxyquinolinato)copper(II) ($Cu(Ox)_2$) are known to form stable crystalline (1:1) complexes with *p*-chloranil and *p*-bromanil.

On the other hand, the electron-accepting properties of 2,5-diazido-3,6-dichloro-1,4-benzoquinone (*p*-$Q(N_3)_2Cl_2$), one of the derivatives from *p*-chloranil, have been recently reported by Koizumi and Matsunaga.[3] In the present experiment, we found that $Pd(Ox)_2$ and Cu-

1) G. Briegleb, "Elektronen-Donator-Acceptor Komplexe," Springer-Verlag, Berlin-Göttingen-Heidelberg (1961).

2) A. S. Bailey, R. J. P. Williams, and J. D. Wright, *J. Chem. Soc.*, **1965**, 2579.

3) S. Koizumi and Y. Matsunaga, This Bulletin, **43**, 3010 (1970).

Table 1. The elementary analysis data on the charge-transfer complexes used for this study

Donor	Acceptor	Found (%)			Calcd[a] (%)		
		C	H	N	C	H	N
$Pd(Ox)_2$	p-$Q(N_3)_2Cl_2$	43.20	1.85	17.96	44.01	1.85	17.14
$Cu(Ox)_2$	p-$Q(N_3)_2Cl_2$	47.16	2.31	18.10	47.14	1.98	18.32
$Pd(Ox)_2$	p-$Q(N_3)_2Br_2$	37.92	1.70	14.16	38.82	1.62	15.09
$Cu(Ox)_2$	p-$Q(N_3)_2Br_2$	41.12	2.04	15.29	41.19	1.73	16.01

a) The value calculated for the (1:1) complex.

$(Ox)_2$ can also form stable crystalline (1:1) charge-transfer complexes with p-$Q(N_3)_2Cl_2$ and p-$Q(N_3)_2Br_2$.[4] We shall examine the solid-state spectra of these complexes in order to study the charge-transfer interaction between $M(Ox)_2$ and p-$Q(N_3)_2X_2$, where M=Pd or Cu and where X=Cl or Br. The charge-transfer spectra of these complexes are interesting in comparison with those of the complexes of the same metal chelates with p-chloranil or p-bromanil.

Experimental

Four crystalline complexes were prepared according to a method similar to that described by Bailey *et al.*.[2]; $Pd(Ox)_2$-p-$Q(N_3)_2Cl_2$, $Cu(Ox)_2$-p-$Q(N_3)_2Cl_2$, $Pd(Ox)_2$-p-$Q(N_3)_2Br_2$, and $Cu(Ox)_2$-p-$Q(N_3)_2Br_2$. For each of these compounds, the mole ratio of the donor to the acceptor was determined to be (1:1) on the basis of the elementary analysis; the results of this analysis are given in Table 1.

The complexes were pulverized and diluted with sodium chloride. The diffuse reflection spectra of these complexes were recorded as the difference in reflectance between the mixture and pure sodium chloride by means of a Beckman DK-2A spectroreflectometer. The solid-state spectra were then obtained by plotting the diffuse reflection spectra using the Kubelka-Munk equation, $f(R)=(1-R)^2/2R$, in which R is the reflectance.

Results

The p-$Q(N_3)_2Cl_2$ *Complexes.* The solid-state spectrum of the $Pd(Ox)_2$-p-$Q(N_3)_2Cl_2$ complex (Fig. 1, Curve a) shows band peaks at 29.0 kK, 22.6 kK, and 14.7 kK. The high-energy bands at 29.0 kK and 22.6 kK arise mostly from the absorptions due to the component molecules, while the band at 14.7 kK appears in the low-energy region where neither of the component molecules absorbs. The value for this low-energy band was found almost to coincide with that for the band at 14.8 kK of the $Pd(Ox)_2$-p-Chloranil complex, which Bailey *et al.* assigned to the charge-transfer transition from $Pd(Ox)_2$ to p-chloranil.[2] Therefore, the band at 14.7 kK for the $Pd(Ox)_2$-p-$Q(N_3)_2Cl_2$ complex is attributable to the charge-transfer transition from $Pd(Ox)_2$ to p-$Q(N_3)_2Cl_2$. Judging from these results, the electron affinity for p-$Q(N_3)_2Cl_2$ seems to be essentially the same as that for p-chloranil. Since the molecular sizes and the shapes of these acceptors are almost alike, the crystal structure of the $Pd(Ox)_2$-p-$Q(N_3)_2Cl_2$ complex may be similar to that of the Pd-

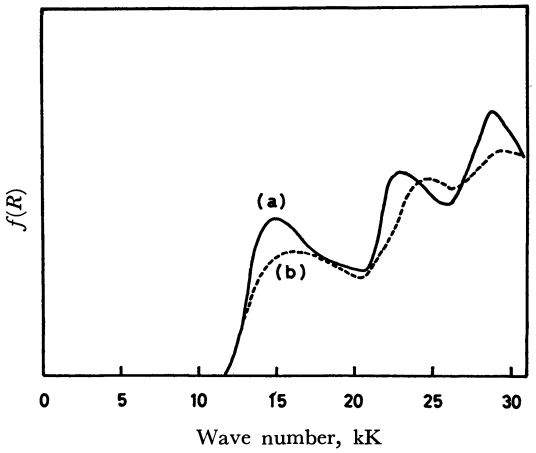

Fig. 1. The solid-state spectra of (a) $Pd(Ox)_2$-p-$Q(N_3)_2Cl_2$ and (b) $Cu(Ox)_2$-p-$Q(N_3)_2Cl_2$.

$(Ox)_2$-p-Chloranil complex as determined by Kamenar *et al.*[5]

On the other hand, the solid-state spectrum of the $Cu(Ox)_2$-p-$Q(N_3)_2Cl_2$ complex (Fig. 1, Curve b) shows band peaks at 29.3 kK, 24.6 kK, and 16.0 kK. The low-energy band at 16.0 kK can also be assigned to the charge-transfer transition from $Cu(Ox)_2$ to p-$Q(N_3)_2Cl_2$; this energy value was found to be close to the 15.9 kK value for the $Cu(Ox)_2$-p-Chloranil complex.[2] It is

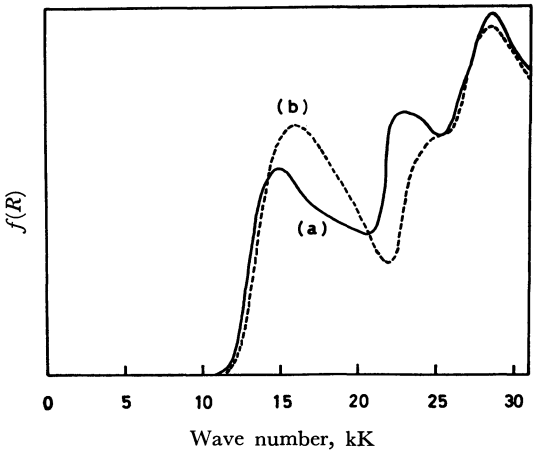

Fig. 2. The solid-state spectra of (a) $Pd(Ox)_2$-p-$Q(N_3)_2Br_2$ and (b) $Cu(Ox)_2$-p-$Q(N_3)_2Br_2$.

4) The acceptor of 2,5-diazido-3,6-dibromo-1,4-benzoquinone is abbreviated as p-$Q(N_3)_2Br_2$.

5) According to an X-ray diffraction study by Kamenar *et al.*, the crystal structure of the $Pd(Ox)_2$-p-Chloranil complex has the triclinic symmetry. The planar $Pd(Ox)_2$ and p-chloranil molecules, which are alternately stacked, are arranged in planes approximately parallel to the crystallographic (111) plane. See B. Kamenar, C. K. Prout, and J. D. Wright, *J. Chem. Soc.*, 4851 (1965).

important to note that the charge-transfer energy for the $Cu(Ox)_2$-*p*-$Q(N_3)_2Cl_2$ complex is larger than that for the $Pd(Ox)_2$-*p*-$Q(N_3)_2Cl_2$ complex by 1.3 kK. For a common acceptor, the great variation in the charge-transfer energy will arise from a difference in the ionization potentials of the donors. Therefore, the ionization potential of $Cu(Ox)_2$ seems to be higher than that of $Pd(Ox)_2$ by about 1.3 kK.

The p-$Q(N_3)_2Br_2$ *Complexes.* The solid-state spectrum of the $Pd(Ox)_2$-*p*-$Q(N_3)_2Br_2$ complex (Fig. 2, Curve a) shows high-energy bands at 28.6 kK and 22.9 kK, and a low-energy charge-transfer band at 14.8 kK. It is interesting to see that the charge-transfer energy for this complex coincides with that of 14.8 kK for the $Pd(Ox)_2$-*p*-Bromanil complex.[6] This leads to a value of the electron affinity for *p*-$Q(N_3)_2Br_2$ close to that for *p*-bromanil.

The $Cu(Ox)_2$-*p*-$Q(N_3)_2Br_2$ complex gives a solid-state spectrum (Fig. 2, Curve b) composed of a high-energy band at 28.3 kK, a shoulder at 25.0 kK, and a low-energy charge-transfer band at 15.9 kK. The energy difference in the charge-transfer transitions between the $Cu(Ox)_2$-*p*-$Q(N_3)_2Br_2$ and $Pd(Ox)_2$-*p*-$Q(N_3)_2Br_2$ complexes was found to be 1.1 kK, which is in good accordance with the 1.3 kK value for the energy difference in the charge-transfer transitions between the $Cu(Ox)_2$-*p*-$Q(N_3)_2Cl_2$ and $Pd(Ox)_2$-*p*-$Q(N_3)_2Cl_2$ complexes.

Discussion

The above-mentioned results on the solid-state spectra clearly indicate that the electron affinities of *p*-$Q(N_3)_2Cl_2$ and *p*-$Q(N_3)_2Br_2$ are essentially the same as those of *p*-chloranil and *p*-bromanil respectively. The azido group thus appears to be as effective as the chlorine or bromine substituent in improving the acceptor strength of *p*-benzoquinone. This conclusion is in good agreement with that given previously by Koizumi and Matsunaga.[3]

On the other hand, the ionization potential of a metal chelate of 8-hydroxyquinoline is very much affected by the species of the central metal ion. This was shown as an appreciable difference in the ionization potentials of $Cu(Ox)_2$ and $Pd(Ox)_2$. Moreover, we examined what kind of metal chelates of 8-hydroxyquinoline can form charge-transfer complexes with *p*-$Q(N_3)_2X_2$, where X=Cl or Br. The preparation of the charge-transfer complexes of $Cd(Ox)_2$, $Hg(Ox)_2$, $Mn(Ox)_2$, and $Ni(Ox)_2$ with *p*-$Q(N_3)_2X_2$ in various solvents was attempted for this purpose. However, no such crystalline compounds could be obtained from these metal chelates.[7] In view of these results, we can see that, for the metal chelates of 8-hydroxyquinoline, not only the magnitude of the ionization potential but also the ability of the formation of the charge-transfer complexes is strongly dependent on the species of the central metal ions.

6) Y. Iida, unpublished work.

7) Although a slight complex formation was detected with $Ni(Ox)_2$, the pure solid charge-transfer complex was not isolated, presumably because of the very poor solubility of $Ni(Ox)_2$ in the suitable solvents.

BULLETIN OF THE CHEMICAL SOCIETY OF JAPAN, VOL. 44, 1439 (1971)

Conformational Factors Affecting the NMR Chemical Shifts of Nuclear Protons in Some Diarylmethanes

G. MONTAUDO, S. CACCAMESE, P. FINOCCHIARO, and F. BOTTINO
Institutes of Industrial and Organic Chemistry of the University, v.le A.Doria, Catania, Italy

(Received October 12, 1970)

We have been interested in the study of conformational properties of diphenylmethanes (DPM) and have proposed[1] that a number of tri-*ortho*-substituted DPM exist predominantly in a conformation (I) where the *ortho* aromatic hydrogen lies below the adjacent ring.

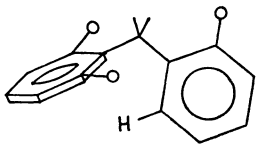

(I)

NMR data provide useful information on the conformation. In fact the shielding on the *ortho* positions, due to the ring current[2] of the adjacent nucleus, is a function of molecular conformation.[1] Some NMR data on variously substituted DPM, which appeared recently in this Journal,[3] can be interpreted as a further support of our previous results.

In Table 1 are collected the NMR chemical shifts of *ortho* aromatic protons for a number of tri-*ortho*-substituted DPM derivatives taken from Suzuki's work[3] together with our data. In tri-*ortho*-substituted DPM the *ortho* nuclear proton appears sensibly shielded with respect to the mono-substituted derivatives (Table 1, compounds 1 and 2). This can be accounted for by assuming that the tri-*ortho*-substituted compounds exist predominantly in form I where the *ortho* aromatic hydrogen lies below the adjacent ring. Other conformations become disfavored in this case because of the repulsive interaction between the *ortho* substituents and the π-electron cloud of phenyl ring.

The magnitude of the shielding effect observed for tri-*ortho*-substituted compounds (0.5—0.8 ppm) compares fairly well with the theoretical shielding value calculated for conformer I through the Johnson and Bovey tables.[2] Considerably lower shielding values are calculated for other (skew) conformations. The shielding effect could be calculated as the difference between the chemical shift values of *ortho* and *para* nuclear protons since the latter are unperturbed from the adjacent ring diamagnetic current. However, this is not always possible for the compounds in Table 1 and the shielding has been computed taking the pentamethylbenzene nuclear proton as reference. The new data[3] seem to be in substantial agreement with ours and appear to support our interpretation.

TABLE 1. CHEMICAL SHIFTS OF *ortho* AND *para* NUCLEAR PROTONS IN DPM DERIVATIVES

		Chem. shift (δ, CCl_4)		Δ[a] (ppm)	Ref.
	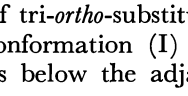	H_{ortho}	H_{para}		
1	2-Me	7.12	7.12		b
2	2-Cl	7.15	7.15		b
3	2,3,5,6-Me	7.08	7.08		b
4	2,6-Cl,2′-Me	6.20	6.92	0.63	b
5	2,3,5,6,2′-Me	6.42	7.00	0.41	1
6	2,4,6,2′,5′-Me	6.28	6.97	0.55	1
7	2,3,5,6,2′5′-Me	6.22	6.92	0.61	1
8	2,4,6,2′,3′,4′,5′-Me	6.00		0.83	3
9	2,3,4,6,2′3′,4′,5′-Me	6.01		0.82	3
10	2,3,5,6,2′,3′,4′,5′-Me	5.99	6.80	0.84	3
11	2,3,4,5,2′,3′,4′,5′,6′-Me	6.06		0.77	3
12	2,3,4,6,2′,3′,4′,5′-Me,5-Cl	6.04		0.79	3
13	2,3,5,6,2′,3′,4′,5′-Me,4-Cl	6.00		0.83	3
14	2,3,5,6,2′,4′,5′-Me,4-Cl	6.15		0.67	3
15	2,4,5,2′,3′,4′,6′-Me,3,5′-Cl	6.23		0.60	3
16	3,4,5,2′,3′,5′,6′-Me,2,4′-Cl	6.14		0.69	3

a) calculated as the difference between H_{ortho} value and the chemical shift of pentamethylbenzene nuclear proton (6.83 δ).
b) this work.

1) G. Montaudo, S. Caccamese, P. Finocchiaro, and F. Bottino, *Tetrahedron Lett.*, **1970**, 877.
2) C. E. Johnson and F. A. Bovey, *J. Chem. Phys.*, **29**, 1012 (1958).
3) H. Suzuki, This Bulletin, **42**, 2618 (1969).

SHORT COMMUNICATIONS

Hydration of 2-Cyanopyridine with Metal Chelates

Sigeo KOMIYA, Shinnichiro SUZUKI, and Ken-ichi WATANABE

Department of Chemistry, Faculty of Science, Tokyo Metropolitan University, Setagaya-ku, Tokyo

(Received January 9, 1971)

It has been reported[1,2] that 2-cyanopyridine is hydrated with nickel(II) chloride or copper(II) chloride to afford the metal chelates of 2-pyridinecarboxamide. On the other hand, 2-cyanopyridine is hydrated into 2-pyridinecarboxamide by the catalytic action of metal chelates, *viz.* nickel(II) or copper(II) chealtes of picolinic acid and its amide.[1]

In this paper, we report that some other ordinary metal chelates are also effective for the hydration of 2-cyanopyridine to give only 2-pyridinecarboxamide. The metal chelates used as catalysts were $[Ni(en)_3]Cl_2 \cdot 2H_2O$, $[Cu(en)_2]Cl_2 \cdot 2H_2O$, $[Co(en)_3]Cl_2$, $Ni(piaH)_2Cl_2 \cdot 2H_2O$, and $Co(piaH)_2Cl_2 \cdot 2H_2O$ (en: ethylenediamine, piaH: 2-pyridinecarboxamide).

As a preliminary test, the hydration of 2-cyanopyridine was carried out without catalysts (60°C, 5 hr). It was found that no hydration took place in the pH range 5.5—8.5. Thus, the aqueous solution of 2-cyanopyridine (0.0471 M) containing each metal chelate (0.0058 M) was kept at 60°C in the pH range 5.5—8.5, and then a definite quantity of the reaction mixture was sampled every hour. The samples were charged into ion exchange column (Dowex 50 H-Type×2) and developed with water. Thus, 2-cyanopyridine unreacted was separated completely from the reaction mixture. Then the decrease in amount of the starting material was followed spectrophotometrically at 272 mμ, and the yield of reaction product, 2-pyridnecarboxamide, was calculated.

It was confirmed that the reaction product was only the 2-pyridinecarboxamide and the chelates used for the reaction were recovered without any change. The results are given in Fig. 1. The chelates of copper(II), nickel(II), and cobalt(II) have a catalytic activity, but not cobalt(III) chelate.

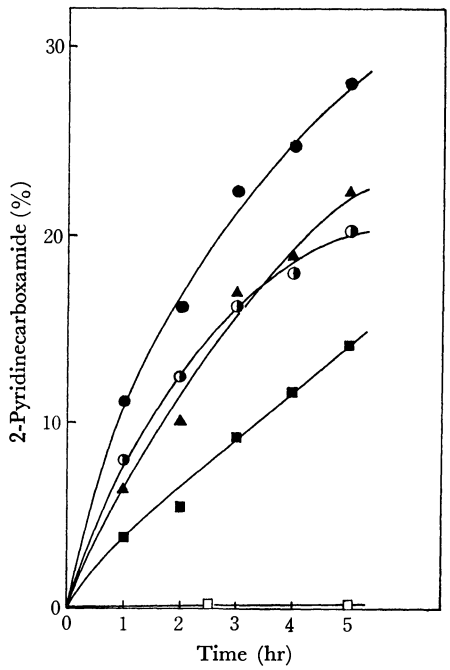

Fig. 1. Hydration of 2-cyanopyridine in the presence of metal chelates.
0.0471 M 2-cyanopyridine, 0.00578 M metal chelate, at 60°C.
■ $[Ni(en)_3]Cl_2 \cdot 2H_2O$ (pH 8.0)
◑ $[Cu(en)_2Cl_2 \cdot 2H_2O$ (pH 7.0—8.0)
● $Ni(piaH)_2Cl_2 \cdot 2H_2O$ (pH 6.0)
▲ $Co(piaH)_2Cl_2 \cdot 2H_2O$ (pH 6.9—6.8)
□ $[Co(en)_3]Cl_3$ (pH 6.9)
2-Pyridinecarboxamide (%)=
100−2-Cyanopyridine (%) (unreacted)

It is known that the former are labile complexes and the latter is an inert complex. Such characters of chelates were in accord with catalytic activity of the hydration. It is assumed that the hydration proceeds through the combination of the ligand exchange and the reaction of coordinated ligands.

1) K. Sakai, T. Ito, and K. Watanabe, This Bulletin, **40**, 1660, (1967).
2) P. F. B. Barnard, *J. Chem. Soc., A*, **1969**, 2140.

The Reaction of Bis(2-cyanopyridine)copper(II) Chloride with Amines in Methanol

Shinnichiro SUZUKI, Masayoshi NAKAHARA,* and Ken-ichi WATANABE

Department of Chemistry, Faculty of Science, Tokyo Metropolitan University, Setagaya-ku, Tokyo

**Department of Chemistry, Faculty of Science, Rikkyo University, Nishi-ikebukuro, Toshima-ku, Tokyo*

(Received January 9, 1971)

It has been reported [1] that 2-cyanopyridine is alcoholized with transition metal ions (*e.g.* Cu(II), Ni(II) and Co(II)) in alcohols to afford complexes of *O*-alkyl pyridine-2-carboximidate, Type I. It is assumed that the nitrile group of 2-cyanopyridine is activated by chelation with the metal ion and therefore the attack of the nucleophiles (*e.g.* OR^- or OH^- [2]) on it is promoted. To develop this idea, a test of amination to the nitrile group in chelates was made with various amines. We obtained not the expected complexes but new ones (Types II and III).

When ammonia, methylamine, dimethylamine, ethylamine, or benzylamine was used for the reaction, the chelates of Type II were obtained. On the other hand, when trimethylamine, diethylamine, or triethylamine was used, only the chelate of Type III was obtained. The methanol solution of bis(2-cyanopyridine)copper(II) chloride[1] and that of amines (1—2 mol to the complex) were mixed at 0°C and the reaction mixture was stirred for 45—60 min. The precipitate of the complex was then obtained by addition of ether, and was recrystallized from methanol-ether mixture at room temperature.

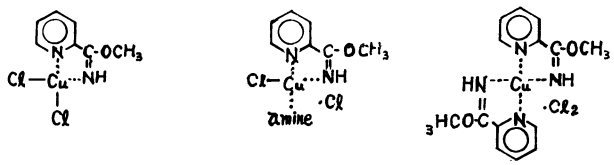

(MeOpy)$CuCl_2$ (I)[1] (MeOpy)(amine)$CuCl_2$ (II) (MeOpy)$_2CuCl_2$ (III)

The results of elementary analysis and spectroscopic measurements of the chelates are given in Tables 1 and 2. In Table 1, the chelates of Type II are 1)—5). The chelate of Type III is 6). The ultraviolet and the visible spectra of 6) differ from those of the chelates of Type II, which suggests the structural difference between the chelates of these two types. The formation of the chelate of Type III seems to be due to the steric hindrance of bulky alkyl groups in the amines.

Table 1. Analytical data of complexes

Compound	No.	Cu, %		C, %		H, %		N, %	
		Found	Calcd	Found	Calcd	Found	Calcd	Found	Calcd
(MeOpy)$(NH_3)CuCl_2$	1)	22.56	22.09	29.07	29.23	3.75	3.86	14.59	14.61
(MeOpy)$(CH_3NH_2)CuCl_2$	2)	21.06	21.06	32.07	31.85	4.32	4.35	13.40	13.93
(MeOpy)$[(CH_3)_2NH]CuCl_2$	3)	19.95	20.13	34.24	34.24	4.58	4.80	13.07	13.31
(MeOpy)$(CH_3CH_2NH_2)CuCl_2$	4)	19.9	20.13	34.33	34.24	4.85	4.80	13.20	13.31
(MeOpy)$(\langle\bigcirc\rangle CH_2NH_2)CuCl_2$	5)	16.70	16.82	44.35	44.51	4.32	4.54	11.18	11.13
(MeOpy)$_2CuCl_2$	6)	15.72	15.62	40.67	41.33	4.06	3.97	13.33	13.78

Table 2. Color, absorption maxima and infrared absorption maxima of complexes

No.	Color	ν_{max} max in cm^{-1} and log ε (in parentheses) in methanol		C–N str.	C–O–C (cm^{-1}) antisym. str.
1)	pale blue	36600 (3.85)	14900 (1.89)	1655	1388
2)	blue green	36600 (3.85)	14700 (1.93)	1646	1382
3)	light green	36600 (3.85)	14600 (1.92)	1644	1386
4)	blue green	36600 (3.85)	15000 (1.85)	1646	1385
5)	deep blue	36600 (3.85)	14600 (1.95)	1655	1381
6)	pale blue	36600 (4.06)	12900 (2.02)	1646	1398

1) P. F. B. Barnard, *J. Chem. Soc., A*, **1969**, 2140.

2) K. Sakai, T. Ito, and K. Watanabe, This Bulletin, **40**, 1660, (1967).

The Anomeric Configuration of 6-Methyl-3-D-glycosyluracil

Naotaka YAMAOKA, Hiroshi SUGIYAMA,* and Katsura TUZIMURA

*Faculty of Agriculture and *Chemical Research Institute of Non-Aqueous Solution, Tohoku Univerisity, Sendai*

(Received January 21, 1971)

Recent papers[1,2] in which Lemieux's PMR method was applied to determine the anomeric configuration of pyrimidine nucleosides prompt us to suggest the limitations of the method. The use of a seeming coupling constant in high-resolution PMR might be a mistake for the assignment of the anomeric proton of acylated ribofuranosyl nucleosides without consideration of the half-height width of the absorption peak,[3] since two heavily overlapped broad peaks seem to be one broad peak. We wish now to report the anomeric proton assignment of 6-methyl-3-D-glycosyluracils (Ia, b, and II) synthesized by the condensation of 6-methyluracil with acylglycosyl halide in nitromethane containing a hydrogen halide acceptor.[4]

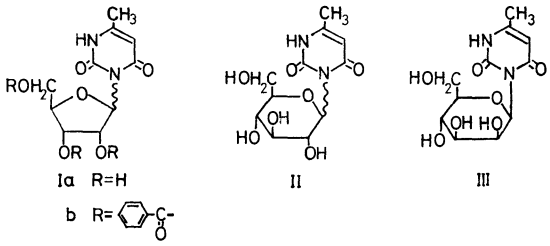

6-Methyl-3-D-ribofuranosyluracil (Ia) [$[\alpha]_D^{22} = -18°$ (c 0.083, H_2O), $\lambda_{max}^{H_2O}$=266, $\lambda_{min}^{H_2O}$=234 mμ (Found: C, 46.56: H, 5.59; N, 11.08; Calcd for $C_{10}H_{14}N_2O_6$: C, 46.51; H, 5.47; N, 10.85; mol wt, 258.23): NMR data (DMSO-d_6) δ 6.10 (d, $J_{1',2'}$=3.7 Hz, H-1')] and 6-methyl-3-(tri-*O*-benzoyl-D-ribofuranosyl)uracil (Ib) [NMR data (DMSO-d_6) δ 6.55 (s, half-height width 3 Hz, H-1')] seemed to be pure β anomer judging from the NMR data.[1,2] 6-Methyl-3-D-glucopyranosyluracil [II, mp 196—200°C, $[\alpha]_D^{22}$=0° (c 0.091, H_2O), $[M]_{350}^{22}$ =0° (c 0.0032 M, H_2O), $\lambda_{max}^{H_2O}$=266 (ε 9370), $\lambda_{min}^{H_2O}$= 234 mμ (ε 2036): (Found: C, 45.48; H, 5.64; N, 9.52; Calcd for $C_{11}H_{16}N_2O_7$: C, 45.83; H, 5.59; N, 9.72; mol wt 288.25): NMR data (D_2O) δ 5.65 (d, $J_{1',2'}$=9.67 Hz, H-1'), 5.76 (d, $J_{1',2'}$=9.33 Hz, H-1'), 5.62 (q, $J_{5,6}$=0.7 Hz, H-5)] was an anomeric mixture. In order to prepare the pure anomer to give clear data, II was converted into 6-methyl-3-β-D-mannopyranosyluracil (III) [mp 237—238°C, $[\alpha]_D^{22}$ =−32.8° (c 0.091, H_2O), $\lambda_{max}^{H_2O}$=267, $\lambda_{min}^{H_2O}$=235 mμ: (Found: C, 45.83; H, 5.59; N, 9.79; Calcd for $C_{11}H_{16}N_2O_7$: C, 45.83; H, 5.60; N, 9.72; mol wt 288.25): NMR data (D_2O) δ 6.08 (d, $J_{1',2'}$=0.6 Hz, H-1')] in several steps.

The optical rotatory dispersion of the dialdehydes formed from a 0.01 mol solution of the free nucleosides (Ia, II, and III) containing excess sodium metaperiodate[5] gave the following data:

Ia, $[M]_{589}^{22} = -80°$, $[M]_{350}^{22} = -410°$
II, $[M]_{589}^{22} = -85°$, $[M]_{350}^{22} = -400°$
III, $[M]_{589}^{22} = -25°$, $[M]_{350}^{22} = -230°$

The anomeric configuration of furanosyl nucleoside could not be assigned only from the seeming PMR coupling constant of less than 1 Hz without a consideration of the broad half-height width of the absorption peak of the anomeric proton.

1) M. W. Winkley and R. K. Robins, *J. Org. Chem.*, **33**, 2822 (1968).
2) R. S. Klein, I. Wempen, K. A. Watanabe, and J. J. Fox, *ibid.*, **35**, 2330 (1970).
3) R. U. Lemieux and D. R. Lineback, *Ann. Rev. Biochem.*, **32**, 155 (1963).
4) N. Yamaoka, K. Aso, and K. Matsuda, *J. Org. Chem.*, **30**, 149 (1965).
5) B. Lythgoe, H. Smith, and A. R. Todd, *J. Chem. Soc.*, **1947**, 355.

Polarographic Investigation of Copper(II)-Poly(α, L-Glutamic Acid) Complex in the Helix-Coil Transition Region

Senkichi INOUE, Kiwamu YAMAOKA,* and Masaji MIURA*

*Department of Chemistry, Faculty of General Education, and *Department of Chemistry, Faculty of Science, Hiroshima University, Higashisenda-machi, Hiroshima*

(Received January 25, 1971)

We wish to report results of a polarographic study of the aqueous solution of cupric chloride in the presence of poly (α,L-glutamic acid) in the pH range 3.0—6.0 where the polymer alone is known to undergo conformational transitions. The purpose of this investigation is to obtain electrochemical data for a better understanding of the mechanism of the pH induced helix-coil transition of synthetic polyamino acids with ionizable side chains. This can be achieved by adding, as a structural probe, a small amount of any polarographically reducible metallic ion which can form a stable complex with polymer but does not perturb polymer conformation.

The cupric ion, which is known to bind to poly (α, L-glutamic acid),[1] could be reduced at the dropping mercury electrode either in the presence or absence of the polymer in the pH range examined. The variation of the limiting current of Cu(II) in the Cu(II)-polymer solution with pH (i_l-pH curve) was affected most by the nature of supporting electrolyte. The paralellism between the i_l-pH curve and helix-coil transition curves obtained with other methods such as viscosity[2] and optical rotation[2] became apparent only when the concentration of the supporting electrolyte so decreased that it was comparable with the concentration of the polymer. The polarographic limiting currents were determined in two extreme sets of supporting electrolytes. The concentration of cupric ions was 1×10^{-4} M and the mean residue weight concentration of the polymer was 1.6×10^{-3} M, the ratio of the monomer unit of the polymer to cupric ion being 16 in the Cu(II)-polymer solution. The limiting current of Cu(II) could be attributed to the diffusion-controlled current (i_d)[3] both in the presence and absence of the polymer in the solution containing either of the two supporting electrolytes, since a strict linear relationship, which could be extrapolated to intercept the origin, was obtained between the observed current and the product of $m^{2/3}\cdot t^{1/6}$, where m is the flow rate of mercury and t the drop time. This relation also held for the Cu(II)-polymer solution at pH 3.5 or 6.5, where the complex is in helical or random-coil conformation, thus ruling out the contribution of migration current to i_l.

Without the polymer, Cu(II) was reduced at a half-wave potential $E_{1/2}=0.05$ V *vs.* SCE in the entire pH region and the diffusion current did not significantly decrease at pH 3.0—6.0 in either of the two supporting electrolytes. In the presence of the polymer, however, Cu(II) was reduced at $E_{1/2}=0.00$ V *vs.* SCE, while the diffusion current sharply decreased with increase in pH between 4 and 5. In Fig. 1 the data are expressed in terms of the ratio of diffusion current of Cu(II) with the polymer to that without it, $(i_d)_p/(i_d)_o$, in each supporting electrolyte system. Based on the fact that the electrode mechanism of the reduction of Cu(II) is invariant, the ratio of the two diffusion constant (D_p/D_o) was also calculated with the aid of Ilkovic's equation and is plotted in Fig. 1. On the assumption that two electrons are transferred from each Cu(II), the diffusion constants at pH 3.8 and 5.0 were calculated to be 6.3×10^{-6} and 0.97×10^{-6} (cm²/sec), respectively, for the Cu(II)-polymer solution in 1.5×10^{-3} M NaCl at 25°C.

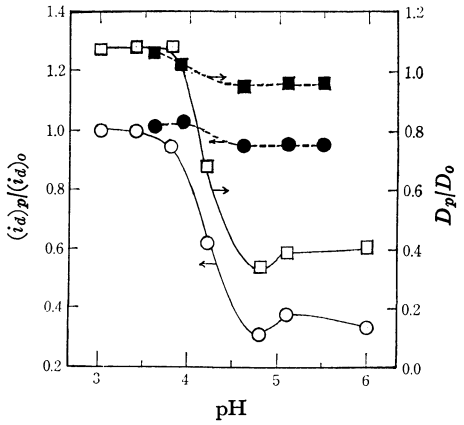

Fig. 1. The pH dependence of polarographic diffusion currents and diffusion constants of the Cu(II)-poly(α,L-glutamic acid). ●,■:$(i_d)_p/(i_d)_o$ and D_p/D_o in 0.2M acetic acid-sodium acetate buffer, ○,□: $(i_d)_p/(i_d)_o$ and D_p/D_o in 1.5×10^{-3}M sodium chloride. Polarographic currents were memeasured manually on a Yanagimoto Model P-8 polarograph.

The curves in acetate buffer indicate that cupric ions interact with acetate ions more strongly than with ionized polymer molecules, or that the electrode process is independent of the conformation of Cu(II)-polymer complex. On the other hand, the interaction between Cu(II) and polymer primarily controls the electrode reduction process in low sodium chloride concentration. The decrease in $(i_d)_p/(i_d)_o$ values at higher pH may be assumed to result from the formation of both electrostatic ion-pairs and inter- and/or intramolecular chelate complexes with the amide and carboxyl groups of the polymer. In conclusion, polarographic methods can be utilized in elucidating the mechanism of the helix-coil transition of ionizable polyamino acids.

1) H. Takesada, H. Yamazaki, and A. Wada, *Biopolymers*, **4**, 713 (1966).

2) P. Doty, A. Wada, J. T. Yang, and E. R. Blout, *J. Polym. Sci.*, **23**, 851 (1957).

3) I. M. Kolthoff and J. J. Lingane, "Polarography," Interscience Publishers, New York, N. Y. (1952), p. 83.

Satellite X-Ray Scattering by TCNQ-Phenothiazine Complex and Diffuse Scattering by TCNQ-*N*-Methylphenothiazine Complex

Hayao KOBAYASHI and Yoshihiko SAITO

The Institute for Solid State Physics, The University of Tokyo, Roppongi, Minato-ku, Tokyo

(Received February 15, 1971)

1:1 complexes formed between 7,7,8,8-tetracyanoquinodimethane (TCNQ) and two electron donors, phenothiazine (PHT) and *N*-methylphenothiazine (*N*-MePHT were investigated by X-ray diffraction method. The black PHT-TCNQ complex crystallizes in the form of needles elongated along the *a* axis It is monoclinic with space group $C2/c$ or Cc and has a super lattice structure with transverse phase modulation. The cell constants of fundamental lattice are: $a=7.04$, $b=25.38$, $c=10.51$ Å and $\beta=92.1°$. Crystals of *N*-MePHT-TCNQ are monoclinic with space group $C2/m$ and $a=10.90$, $b=13.32$, $c=7.09$ Å, $\beta=91.9°$, $Z=2$. General features of intensity distributions of both complexes indicate that the two structures are similar in a broad sense.

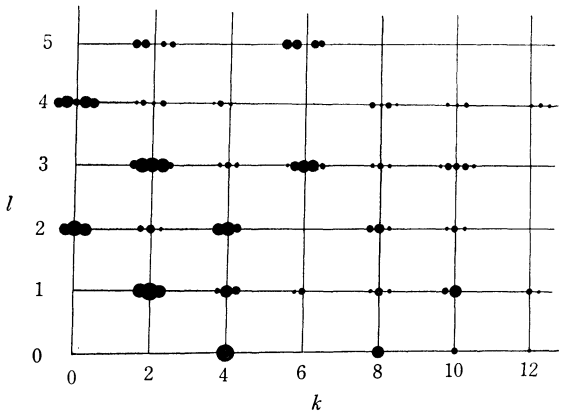

Fig. 1. Distribution of satellite scatterings around $(0,k,l)$ Bragg reflections from PHT-TCNQ. Magnitude of a circle is drawn in proportion to the intensity of X-ray reflection.

In the case of PHT-TCNQ complex, satellite reflections appear in reciprocal space at $(h, k\pm m\delta, l)$, where h, k, and l are Miller indices, $m=1, 2, 3$, and 4 and $\delta=0.232\pm0.015$ at room temperature. Distribution of satellites around $(0,k,l)$ reflections is schematically shown in Fig. 1. The general features of the satellite reflections are similar to those observed in the crystals of ferroelectric thiourea.[1] The observed diffraction patterns can be explained on the basis of the lattice with transverse phase modulation. That is, the lattice points are sinusoidally distorted. The position of the nth lattice point is approximately given by

$$\boldsymbol{r} = n_1\boldsymbol{a} + n_2\boldsymbol{b} + n_3\boldsymbol{c} + (p\boldsymbol{a}/a + q\boldsymbol{c}/c)\sin(2\pi n_2\delta),$$

where $(n_1\boldsymbol{a}, n_2\boldsymbol{b}, n_3\boldsymbol{c})$ is the position of the nth lattice point, p and q are 0.85 Å and 0.75 Å, respectively, and $1/\delta$ is the period of modulation and is equal to 4.3. The donor and acceptor molecules seem to be stacked alternately forming columns parallel to the *a* axis. The origin of this sinusoidal structure seems to be particularly interesting, because such a modulation may arise owing to the delicate balance of various interactions in the crystal, such as charge-transfer interaction, repulsion between non-bonding atoms, hydrogen-bonding, dipole-dipole interaction, *etc.* Detailed analysis is now under way.

The structure of *N*-MePHT-TCNQ complex was deduced from packing consideration and refined to an *R*-value of 0.096. The donor and acceptor molecules are alternately stacked face to face forming columns parallel to the *c* axis. Unlike PHT complex, diffuse scattering associated with strong Bragg reflections is observed. In fact, the orientation of *N*-MePHT molecule is disordered and the apparent molecular asymmetry is D_{2h}. The intermolecular spacing between *N*-MePHT and TCNQ is 3.43 Å. The molecular dimension of TCNQ is intermediate between those of $TCNQ^0$ [2] and $TCNQ^{-1/2}$ [3,4] where $TCNQ^0$ and $TCNQ^{-1/2}$ represent the neutral TCNQ molecule and TCNQ with formal charge of $-1/2$, respectively.

1) H. Futama, Y. Shiozaki, A. Chiba, E. Tanaka, T. Mitsui, and J. Furuichi, *Phys. Lett.*, **25A**, 8 (1967); Y. Shiozaki, private communication

2) R. E. Long, R. A. Sparks, and K. N. Trueblood, *Acta Crystallogr.*, **18**, 932 (1965).

3) P. Goldstein, K. Seff, and K. N. Trueblood, *ibid.*, **B24**, 778 (1968).

4) A. W. Hanson, *ibid.*, **B24**, 768 (1968).

Studies of the Coordination Bonding and Stability of the Mixed-ligand Complexes of Copper(II)

Hiroshi Yokoi, Masaki Otagiri, and Taro Isobe

Chemical Research Institute of Non-aqueous Solutions, Tohoku University, Katahira, Sendai

(Received February 27, 1971)

In recent years, many studies of the stability of mixed-ligand complexes have been carried out; the importance of the chemical behavior of the complexes have received increasing attention from the viewpoint of its relationship to fundamental concepts in inorganic and biological chemistry.[1-3] More quantitative studies, however, seem to be necessary for determining definitely the factors governing the mixed-ligand complex formation.[3] We wish to report here on our new results concerning the coordination bonding and stability for the mixed-ligand complex written in the following equilibrium (the results were obtained by the use of ESR and optical absorption techniques):

$$CuA_2 + CuB_2 \rightleftharpoons 2\,CuAB \qquad (1)$$

$$K = \frac{[CuAB]^2}{[CuA_2]\,[CuB_2]} \qquad (2)$$

Here, two different bidentate ligands of ethylenediamine, its alkyl derivatives, trimethylenediamine, and various amino acids are represented as A and B, and an equivolume mixture of water and methanol was used as the solvent.

The observed ESR line shapes showed that the symmetry of the ligand field of all the mixed-ligand complexes employed is as axial as that of the parent complexes. It was found that the $g_{//}$ and $g_{\perp}$ values of almost all the mixed-ligand complexes are intermediate between those of the corresponding two parent complexes, as is shown in Fig. 1, for example, with regard to the $g_{//}$ value; furthermore, the wavelengths and intensities of the visible absorption maximum of the mixed-ligand complexes are intermediate. It may be concluded from these experimental facts that the mixed-ligand complexes are intermediate in the degree of covalency of the coordinate bond between the corresponding two parent complexes.[4]

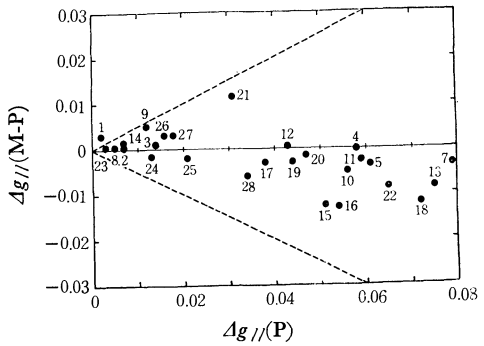

Fig. 1. A plot of $\Delta g_{//}$(M-P) against $\Delta g_{//}$(P) for 28 mixed ligand complexes.
$\Delta g_{//}(\text{M-P}) = g_{//}^{M} - (1/2)(g_{//}^{P_1} + g_{//}^{P_2})$
$\Delta g_{//}(\text{P}) = |g_{//}^{P_1} - g_{//}^{P_2}|$
where $g_{//}^{M}$, $g_{//}^{P_1}$, and $g_{//}^{P_2}$ are the $g_{//}$ values of a mixed ligand complex and its two parent complexes, P_1 and P_2, respectively.

Table 1. The value of log K[a]

Temperature	System[b]		
(°C)	I	II	III
50	1.38±0.02	0.80±0.03	0.15±0.03
20	1.44±0.02	0.78±0.04	0.14±0.03
ca. −100[c]		0.79±0.10	−0.45±0.15

a) The K values at 20 and 50°C were determined spectrophotometrically according to the Kida's method,[2] and the K values at *ca.* −100°C were determined from the X-band ESR spectra measured at 77°K by resolving the absorption lines into three components.
b) I: A=en, B=L-Ala, II: A=en, B=β-Ala, III: A=en, B=dmg (dmg: *N,N*-dimethylglycine anion, other abbreviations are the ones ordinarily used).
c) the assumed freezing point.

Table 2. Thermodynamic constants

	System		
	I	II	III
ΔG^0_{293}(kcal/mol)	−1.93±0.03	−1.05±0.06	−0.19±0.04
ΔH (kcal/mol)	−0.86±0.58	0.01±0.20	1.02±0.31
ΔS (e.u.)	3.65±0.21	3.62±0.09	4.12±1.20

The K values and the thermodynamic constants were determined for several equilibrium systems (A: ethylenediamine, B; amino acid) in order to estimate the factors governing the equilibrium; the data are listed in Tables 1 and 2. These results indicate that the entropy term plays a main role in determining the equilibrium, but that the differences in the K values are due to small differences in the enthalpy change. The fact that the enthalpy changes are small seems to be in agreement with the average of the Cu-A and Cu-B bond strengths in the mixed-ligand complexes, as has been mentioned above.

The details will soon be published elsewhere.

1) H. Sigel, Proc. 3rd Symp. "Coordination Chemistry," Debrecen, Hungary, 1970, Vol. 1, ed. by M. T. Beck, Akádémiai Kiado, Budapest (1970), p. 191.
2) S. Kida, This Bulletin, **29**, 805 (1956).
3) Y. Marcus and I. Eliezer, *Coordin. Chem. Rev.*, **4**, 273 (1969).
4) B. R. McGarvey, "Transition Metal Chemistry," Vol. 3, ed. by R. L. Carlin, Marcel Dekker, New York (1967), p. 89.

Triplet Dimers Observed for Several β-Diketone Chelate Complexes of Copper(II) in Toluene

Hiroshi Yokoi and Taro Isobe
Chemical Research Institute of Non-aqueous Solutions, Tohoku University, Katahira, Sendai
(Received March 9, 1971)

We wish to report here on the new experimental fact that triplet dimers are formed at very high concentrations in the toluene solutions of several 1:2 β-diketone chelate complexes of copper(II). In this study, the following representative β-diketone chelate complexes were employed: $Cu(Etacest)_2$, $Cu(Meacest)_2$, $Cu(acac)_2$, and $Cu(bzac)_2$, where Etacest, Meacest, acac, and bzac are the anions of ethyl acetoacetate, methyl acetoacetate acetylacetone, and benzoylacetone respectively. The X-band ESR spectrum of $Cu(Etacest)_2$ in toluene as measured at 77°K is shown as an example in Fig. 1.

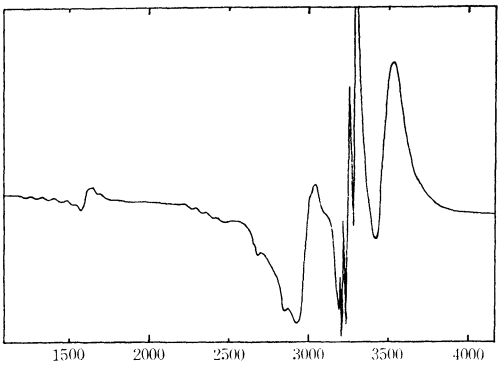

Fig. 1. The X-band ESR Spectrum of $Cu(Etacest)_2$ in toluene (c^0: 5×10^{-3} mol/l, measured at 77°K).

This spectrum clearly consists of two kinds of spectra superposed upon each other; one of them is due to monomer species (M), and the other, to triplet dimer species (D). The line shape of the latter spectrum is a typical one for magnetically-coupled Cu(II)–Cu(II) systems in the triplet state.[1-4]

It seemed that it would be very interesting to see whether or not the following type of equilibrium is established in the solution:

$$2\,M \rightleftharpoons D, \quad K=\frac{[D]}{[M]^2} \qquad (1)$$

When the observed intensity ratio between a particular ESR absorption line due to D and a particular line due to M is expressed as R, the following equation can be derived:

$$2R^2 + rR = Krc^0 \qquad (2)$$

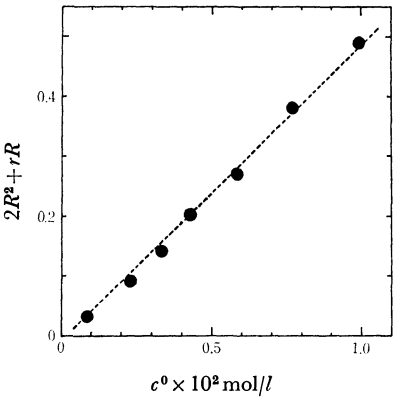

Fig. 2. A plot of $(2R^2+rR)$ against c^0 for $Cu(Etacest)_2$ in toluene

where c^0 is the initial concentration of a complex and r, the proportionality constant between R and the actual concentration ratio of D to M. The values of $(2R^2+rR)$ were plotted against c^0 for $Cu(Etacest)_2$ in toluene by putting $r=0.072$, which was the approximate value evaluated graphically from one of its ESR spectra, assuming that the actual ratio of [D] to [M] is proportional to the totally-integrated intensity ratio of the ESR absorptions of D to M. The existence of a linear relationship between them, as is shown in Fig.2, clearly indicates that the above-described equilibrium is held in the solution; accordingly, the K value could be calculated from its slope to be $(1.0\pm0.2)\times10^4$. Similarly, the K values of $Cu(Meacest)_2$, $Cu(acac)_2$, and $Cu(bzac)_2$ in toluene could be estimated to be $(6.0\pm2.0)\times10^3$, $(9.0\pm2.0)\times10^3$, and $(1.1\pm0.2)\times10^3$ respectively. The magnetic parameters determined for these systems (assuming the axial field) are listed in Table 1. The details will soon be published elsewhere, together with a discussion of these magnetic data in connection with the structures of the dimers.

Table 1. Magnetic parameters[a]

Copper(II) complex	Monomer $g_{//}$	Monomer $g_\perp$	Monomer $A_{//}\times10^3$ cm^{-1}	Monomer $A_\perp\times10^3$ cm^{-1}	Dimer $g_{//}$	Dimer $g_\perp$	Dimer D cm^{-1}
$Cu(Etacest)_2$	2.29	2.05	18	2.5	2.31	2.07	0.043 ±0.004
$Cu(Meacest)_2$	2.28	2.04	18	2.5	2.30	2.07	0.040 ±0.005
$Cu(acac)_2$	2.26	2.05	19	2.5	2.29	2.06	0.018 ±0.005

a) The data of $Cu(bzac)_2$ were omitted here because of some difficulty in determining the accurate ones of its dimer species from its ESR spectra.

1) J. F. Boas, R. H. Dunhill, J. R. Pilbrow, R. C. Srivastava, and T. D. Smith, *J. Chem. Soc., A*, **1969**, 94; J. R. Pilbrow, A. D. Toy, and T. D. Smith, *ibid.*, **1969**, 1029.
2) G. F. Kokoszka, M. Linzer, and G. Gordon, *Inorg. Chem.*, **7**, 1730 (1968).
3) N. D. Chasteen, and R. L. Belford, *ibid.*, **9**, 169 (1970).
4) W. E. Hatfield, J. A. Barnes, D. Y. Jeter, R. Whymann, and E. R. Jones, Jr., *J. Amer. Chem. Soc.*, **92**, 4982 (1970).

On the Planar Structure of the Bis(dimethylglyoximato)cobalt(I) Complex

Nobufumi MAKI

Department of Chemistry, Faculty of Engineering, Shizuoka University, Johoku, Hamamatsu

(Received March 16, 1971)

The bis(dimethylglyoximato)cobalt(III) complexes with a trans-configuration cited below have all been found to be reduced to the cobalt(I) state in non-aqueous solvents such as a DMSO (dimethyl sulfoxide); no further reduction to the metal takes place over the potential range between 0 and −2.70 V (*vs.* SCE): $H[CoCl_2(dgH)_2]$,[1] $Na[Co(NO_2)_2(dgH)_2]\cdot H_2O$, $H[Co(NCS)_2(dgH)_2]$, $H[Co(CN)(dgH)_2Cl]\cdot 4H_2O$, $(NH_4)_2[Co(CN)(dgH)_2(SO_3)]\cdot 4H_2O$, $[Co(CN)(dgH)_2(OH_2)]\cdot 3H_2O$,[2] $[Co(CN)(dgH)_2(NH_3)]\cdot \frac{1}{2}H_2O$, $[Co(dgH)_2(NH_3)_2]ClO_4$, $[Co(dgH)_2(py)(NH_3)]$,[1] $[Co(dgH)_2(OH_2)_2]ClO_4$,[2] $[Co(dgH)_2(OH_2)(NH_3)]OCOCH_3$, $[CoX(dgH)_2(NH_3)]$ (X=I, Br, Cl, F[2]), $Na[Co(CN)_2(dgH)_2]\cdot 2H_2O$.

The most striking feature of this result is that the liberation of the fifth and the sixth ligand occurs at the cobalt(I) state during the reduction, except for the case of cyanide ligands. The anodic wave of free ligand ions released from the complex was detected to exist by using a Kalousek commutator. Therefore, it seems likely that the contribution of the two ligands located above and below the $[Co(dgH)_2]$structure need not be accounted for in determining whether or not the cobalt(I) state can exist during the reduction. That is, the resulting cobalt(I) complex would take a planar structure of the $[Co^I(dgH)_2]$ type with a pair of hydrogen bonds, as is indicated in the following;

$$trans\text{-}[Co^{III}X_2(dgH)_2]^{n-} \xrightarrow{2e} [Co^I(dgH)_2]^- + 2X^{m-}.$$

In contrast to this behavior with a trans-configuration, the tris(dimethylglyoximato)cobalt(III) complex[3] was found to be reduced to the metal *via* the cobalt(II) complex in the DMSO containing 0.1 M $[(C_2H_5)_4N]ClO_4$ at the dropping mercury electrode:

$$[Co^{III}(dgH)_3] \xrightarrow{e} [Co^{II}(dgH)_3]^- \xrightarrow{2e} Co(metal).$$

No cobalt(I) state was found upon the reduction. This is consistent with the prediction that the $[Co^I(dgH)_2]^-$ anion with a planar structure could not be formed from the reduction of the cobalt(III) complexes with a *cis*-configuration, since it is not likely that the rearrangement of ligands, *viz.*, the isomerization, takes place in DMSO. Inversely, this result can be invoked to emphasize the importance of the planarity of the bis(dimethylglyoximato)cobalt(I) complex from the standpoint of the electronic structure.

Figure 1 illustrates the current-potential curves for the *trans*-$[Co^{III}F(dgH)_2(NH_3)]$ and $[Co(dgH)_3]\cdot 2.5H_2O$ complexes measured under the same experimental conditions. In the figure, the wave-height is approximately proportional to the number of electrons participating in the electrode processes, since the limiting current of both the waves is diffusion-controlled.

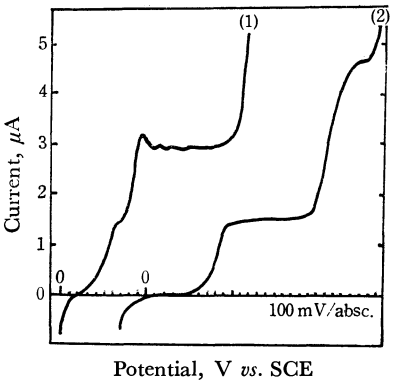

Fig. 1. Typical current-potential curves obtained at the concentration of 10^{-3}M under the same conditions (25°C): (1) *trans*-$[CoF(dgH)_2(NH_3)]$; (2) $[Co(dgH)_3]\cdot 5/2\ H_2O$ in the DMSO containing 0.1M$[(C_2H_5)_4N]ClO_4$.

TABLE 1. HALF-WAVE POTENTIALS OF *trans*- AND *cis*-BIS(DIMETHYLGLYOXIMATO)COBALT(III) COMPLEXES IN DMSO CONTAINING 0.1M$[(C_2H_5)_4N]ClO_4$(25°C)

Compound	lst Wave	2nd Wave
trans-$[CoF(dgH)_2(NH_3)]$	−0.59 ($Co^{III}\rightarrow Co^{II}$)	−0.81 ($Co^{II}\rightarrow Co^{I}$)
trans-$[CoCl(dgH)_2(NH_3)]$	−0.58 ($Co^{III}\rightarrow Co^{II}$)	−0.81 ($Co^{II}\rightarrow Co^{I}$)
trans-$H[CoCl_2(dgH)_2]$	——[a] ($Co^{III}\rightarrow Co^{II}$)	−0.81 ($Co^{II}\rightarrow Co^{I}$)
trans-$[Co(dgH)_2(NH_3)_2]ClO_4$	−0.74 ($Co^{III}\rightarrow Co^{I}$)	
$[Co(dgH)_3]\cdot 5/2H_2O$	−0.81 ($Co^{III}\rightarrow Co^{II}$)	−2.11 ($Co^{II}\rightarrow Co^{0}$)
cis-$[Co(dgH)_2en]ClO_4\cdot 1/3H_2O$	−0.87 ($Co^{III}\rightarrow Co^{II}$)	−2.29 ($Co^{II}\rightarrow Co^{0}$)
cis-$[Co(dgH)_2(NH_3)_2]ClO_4\cdot 7H_2O$	−0.82 ($Co^{III}\rightarrow Co^{II}$)	−2.04 ($Co^{II}\rightarrow Co^{0}$)

a) The 1st wave lies at positive region of potential. V *vs.* SCE

Table 1 presents some examples of the electrode processes and their half-wave potentials. Thus, the cis- *vs.* trans-distinction has been clearly demonstrated polarographically with regard to the stability of the cobalt(I) complex in DMSO; a similar differentiation was shown to be possible for the *cis*- and *trans*- tetracyano cobalt(III) complexes in aqueous solutions.[4] This method of distinguishing steric isomers is more promising than that based on the spectra,[5] because the latter is more complicated; its interpretation and assignment is based on the infrared spectra.

1) Abbreviations used: dg=$CH_3\cdot C(NO)C(NO)\cdot CH_3$; py=pyridine.

2) Novel complexes, which have not yet been reported.

3) A. Nakahara, This Bulletin, **27**, 560 (1954).

4) N. Maki and K. Yamamoto, This Bulletin, **43**, 2450 (1970).

5) R. D. Gillard and G. Willkinson, *J. Chem. Soc.* ,**1963**, 6041.

The Synthesis of Lanthanide(III) Complexes with Schiff Bases Obtained from Salicylaldehyde

Shoichiro YAMADA, KUNIKO YAMANOUCHI, and Hiro KUMA
Institute of Chemistry, College of General Education, Osaka University, Toyonaka, Osaka
(Received March 22, 1971)

There have been only a few papers available on lanthanide(III) complexes with Schiff bases as ligands.[1-3] Complexes with *N*-*n*-alkylsalicylideneiminates (I,

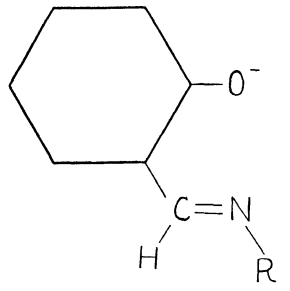

I

abbreviated as SAL·R) have not been reported in literature. With *N*,*N*′-ethylenebis(salicylideneiminate) (II, abbreviated as SALen), complexes of types $Ln_2(SALen)_3$ and $Ln_2(SALen)_3 \cdot nL$ were previously reported, L being H_2O and C_2H_5OH, and Ln a lanthanide(III)

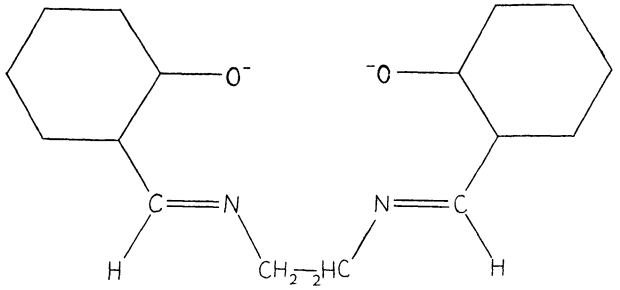

II

ion. However, some properties, such as colour, solubility and melting point, widely differ from those of the complexes of a similar composition obtained in the present work. The method of preparation employed in the previous work differs from the present one, and recrystallization was not possible in the previous work, whereas the complexes were purified by recrystallization from organic solvents in our case. The present communication deals with tris(*N*-methylsalicylideneiminato)- and *N*,*N*′-ethylenebis(salicylideneiminato)-lanthanide(III) complexes.

Complexes of the type $Ln(SAL \cdot CH_3)_3 \cdot nH_2O$ were synthesized in the following way. To preformed *N*-methylsalicylideneimine (0.033 mol) was added lanthanide(III) chloride hydrate (0.01 mol), and the mixture was ground for about 1 hr, until it nearly solidified. No solvent was used in this process. The powder obtained was recrystallized from methanol or ethanol. They are soluble in methanol and ethanol, and slightly soluble in acetone and chloroform. The cerium(III) and neodymium(III) complexes are brownish orange and yellowish orange, respectively.

TABLE 1. ANALYTICAL DATA OF THE COMPLEXES OF THE TYPES $Ln(SAL \cdot CH_3)_3 \cdot nH_2O$ (COMPLEX I) AND $Ln_2(SALen)_3 \cdot nH_2O$ (COMPLEX II)

Ln	*n*	mp °C	Found, %			Calcd, %		
			C	H	N	C	H	N
Complex I								
Ce	4	159—161	46.40	5.05	6.55	46.90	5.25	6.84
Nd	3	259—261	48.21	4.94	6.90	47.98	5.03	6.99
Complex II								
Nd	4	227—229	46.61	4.54	6.44	46.81	4.75	6.83
Sm	4	275—277	45.56	4.53	7.14	46.35	4.70	6.76
Eu	4	164—166	45.98	4.50	6.22	46.23	4.69	6.74
Tb	3	167—169	47.37	4.33	6.71	47.07	4.44	6.86
Er	3	178—180	45.88	4.32	7.10	46.40	4.38	6.76

The complexes of the type $Ln_2(SALen)_3 \cdot nH_2O$ were prepared as follows. To a solution of *N*,*N*′-ethylenebis(salicylideneimine) (0.005 mol) in ethanol (10 ml) was added lanthanide(III) chloride hydrate (0.015 mol), and the resulting solution was stirred for 1 hr at about 40°C. The precipitate was filtered off and purified by recrystallization from methanol or ethanol. The complexes are soluble in methanol and ethanol, but slightly soluble in chloroform and acetone. They are yellow and show melting points as given in Table 1. The complexes reported previously melted with decomposition above 300°C, and were not soluble in common organic solvents.

Analytical data of the complexes are shown in Table 1.

1) N. K. Dutt and K. Nag, *J. Inorg. Nucl. Chem.*, **30**, 2493 (1968).
2) T. Isobe, S. Kida, and S. Misumi, This Bulletin, **40**, 1862 (1967).
3) S. Yamada, K. Yamanouchi, and H. Kuma, *Synth. Inorg. Metalorg. Chem.*, **1**, 9 (1971).

The Photo-erasable Memory Effect Associated with a "Conductive Path" Formed in Ag-doped Chalcogenide Glasses

Hiraku SAKUMA, Isamu SHIMIZU, Hiroshi KOKADO, and Eiichi INOUE
Imaging Science and Engineering Laboratory, Tokyo Institute of Technology, Ookayama, Meguro-ku, Tokyo
(Received April 2, 1971)

We previously reported the rapid metal diffusion into chalcogenide glasses induced by light irradiation,[1] and also the remarkable increase in electrical conductivity in the metal-doped areas.[2] The conductivity of the metal-doped areas was about 10^6 times higher than that of the undoped areas. It has been pointed out that the differences in the chemical and electrical properties between the metal-doped and the undoped areas can be used for a new type of photo-imaging materials.

During the investigation of the electrical properties, a photo-erasable memory effect was found in the silver-doped chalcogenide glasses. The sample was prepared as follows. About a 1000 Å-thick layer of silver was doped with light[1] into the evaporated film of $As_{24}S_{70}$-Te_6 (atomic %). The surface-type cell shown in Fig. 1 (a) was made by the vacuum deposition of gold electrodes on the sample surface. The spacing between the electrodes was 1 mm. The cell showed two stable states in electrical conductivity—the low conductive state (1) and the high conductive state (2), as indicated in Fig. 1 (b). The cell changed from the (1) state to the (2) state at an applied voltage of over 20 V in this experiment. This high-conductive state easily changed back to the (1) state within half a minute upon light irradiation from a 250 W Hg high-pressure lamp. The ratio of the electrical conductivities of the (1) state to the (2) state was over the order of magnitude of 10^3.

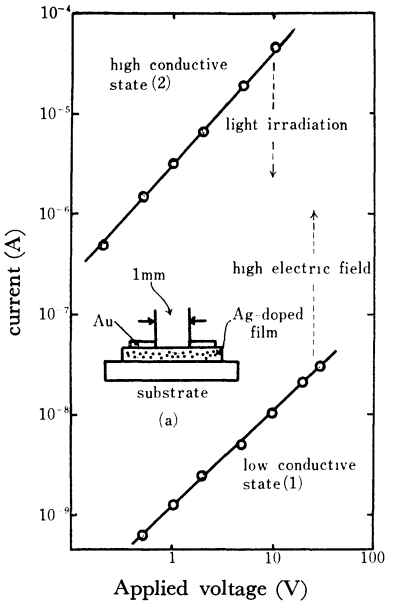

Fig. 1. (a) The structure of the surface type cell
(b) I-V characteristics of the Ag doped chalcogenide film

From observation with a microscope, the high-conductive state was found to be attained by the formation of a "conductive path" between the electrodes. When a high voltage was applied to the cell in the (1) state, the boundary of the negative electrode and the glass film began to darken, and then "branchlike" paths began to grow from the electrode. A microscopic photograph of the path is shown in Fig. 2. These paths stretched

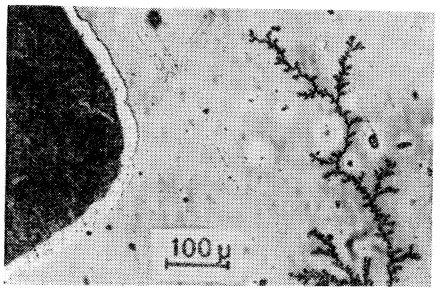

Fig. 2. The microphotograrh of condutive path formed in the surface of the Ag-doped chalcogenide glassfilm (black region on the left-hand is the positive electrode)

toward the positive electrode; high-conductive state (2) was attained when one of the paths reached the positive electrode. Upon the light irradiation, the path faded away and, at the same time, the electrical conductivity returned to the lower state (1). These results indicate that the formation and the disappearance of the "conductive path" caused the memory effect.

This photo-erasable memory effect is similar to the memory effects in chalcogenide glasses reported in other papers recently,[3-5] but the doped Ag is thought to play an important role in this case. At the present stage, the mechanism of the formation of conductive path is not clear in detail, but ionic process (such as the reduction of Ag^+, which is supposed to exsist in the chalcogenide glass) is suggested by the fact that the conductive path always grows from the negative electrode. The path is expected to have an Ag or Ag-rich composition. Its disappearance upon light irradiation can be considered to be connected with the optical diffusion of Ag into chalcogenide glasses.

1) I. Shimizu, H. Sakuma, H. Kokado, and E. Inoue, This Bulletin, **44**, 1173 (1971).
2) H. Sakuma, I. Shimizu, H. Kokado, and E. Inoue, *ibid.*, to be published.
3) S. R. Ovshinsky, *Phys. Rev. Lett.*, **21**, 1450 (1968).
4) A. D. Pearson, *IBM J. Res. Develop.* **13**, 510 (1969).
5) H. Fritzsch , *ibid.*, **13**, 515 (1969).

Electrochemiluminescence of 9,10-Dichloroanthracene and 9,10-Dibromoanthracene

Tamotsu MATSUMOTO, Masanori SATO, Satoshi HIRAYAMA, and Shigeru UEMURA
Faculty of Textile Science, Kyoto Technical University, Matsugasaki, Sakyo-ku, Kyoto
(Received February 17, 1971)

Recent investigations on the electrochemiluminescence (ECL) of organic compounds have revealed that in most cases the emission spectra coincide with the fluorescence spectra of the corresponding compounds. However, in some compounds such as anthracene, the ECL spectra have components which cannot be assigned to fluorescence,[1] and their assignments are still in question. We recently found from an investigation of the ECL of 9,10-dichloroanthracene (9,10-di-Cl-A) and 9,10-dibromoanthracene (9,10-di-Br-A) that the ECL of the former was composed of two main components which were clearly distinguishable, while the ECL of the latter had only one component. In this communication we wish to elucidate the difference in ECL of these compounds.

Synthesized 9,10-di-Cl-A and 9,10-di-Br-A were purified by sublimation. In a *N,N*-dimethylformamide (DMF) solution containing potassium perchlorate as a supporting electrolyte, the ECL of both compounds was examined at a platinum wire electrode of 0.05 cm in diameter and 3 cm in length. A 40-Hz square-wave potential (less than 6V) was applied to the working electrode with a function generator. Dried nitrogen gas was passed through the solution during the measurements.

The results[2] obtained at room temperature are shown

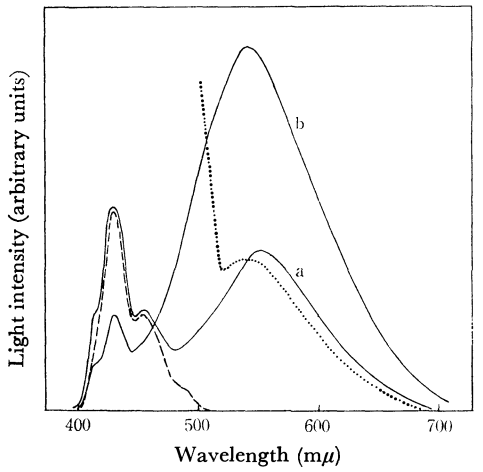

Fig. 1. Emission spectra of 9,10-di-Cl-A.
Solid line a: ECL (7×10^{-4} M)
b: ECL of 9,10-di-Cl-A (7×10^{-4} M) containing anthracene (10^{-3} M)
Broken line: Fluorescence (7×10^{-4} M)
Dotted line: Emission observed on the saturated DMF solution of 9,10-di-Cl-A (Irradiation at 366 mμ)

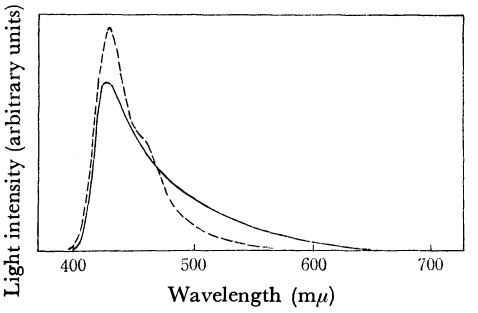

Fig. 2. Emission spectra of 9,10-di-Br-A.
Solid line: ECL (5×10^{-4} M)
Broken line: Fluorescence (5×10^{-4} M)

in Figs. 1 and 2 for 9,10-di-Cl-A (7×10^{-4}M) and 9,10-di-Br-A (5×10^{-4}M), respectively. Fluorescence spectra measured under the same conditions as those of ECL measurements are also given. Ordinate scales are arbitrary for ECL and fluorescence, hence their intensities cannot be compared with each other.

The ECL of 9,10-di-Br-A agrees with its fluorescence. However, the ECL of 9,10-di-Cl-A has a second component in the longer wavelength region, differing from its fluorescence component. The same ECL spectrum is also observed in methylene chloride instead of DMF. The long-wavelength component agrees with the excimer emission observed with a saturated DMF solution of 9,10-di-Cl-A (dotted line in Fig. 1).[3] When a small amount of anthracene (*ca.* 10^{-3}M) was added to the solution of 9,10-di-Cl-A, the long-wavelength ECL component was strongly enhanced as shown by curve b in Fig. 1. The observed spectral change was not due to the ECL of anthracene, because it had a maximum near 405 mμ.[1] Similar phenomena were also observed on addition of 9,10-dimethyl-A. However, the addition of 9,10-di-Br-A and 9,10-diphenyl-A, known to form an excimer or an exciplex with difficulty, caused no change in the ECL spectrum of 9,10-di-Cl-A.

On the other hand, the ECL spectrum of 9,10-di-Br-A did not change with the addition of anthracence and the observed emission was merely a superposition of each ECL spectrum.

To understand these behaviors the report by Chandross and Ferguson[3] that an excimer emission was observed on 9,10-di-Cl-A but no measurable one on 9,10-di-Br-A should be noted. They also found an exciplex emission of 9,10-di-Cl-A and anthracene.

Thus, the present results indicate conclusively that the long-wavelength component in 9,10-di-Cl-A ECL can be attributed to an excimer emission.

1) T. C. Werner, J. Chang, and D. M. Hercules, *J. Amer. Chem. Soc.*, **92**, 763 (1970).
2) Photomultiplier used; EMI 9558QB.
3) E. A. Chandross and J. G. Ferguson, *J. Chem. Phys.*, **45**, 3554 (1966).

The Solvent Effect on the Catalytic Activity of Benzonitrile-Alkali Ion Salt Solutions for the Hydrogen Exchange Reactions

Masaru ICHIKAWA and Kenzi TAMARU

Sagami Chemical Research Center, Onuma, Sagamihara, Kanagawa

The Department of Chemistry, The University of Tokyo, Hongo, Bunkyo-ku, Tokyo

(Received February 25, 1971)

Recently it has been reported that the activation of hydrogen takes place by means of some electron donor-acceptor (EDA) complexes of aromatic compounds with alkali metals in their solutions as well as in the solid state.[1] It was previously shown that the hydrogen absorption and the hydrogen exchange reaction proceeded homogeneously at room temperature in the anthracene dianion complex solutions,[2] much as on their films.[3] We would like to report here a marked solvent effect on the catalytic activity by the benzonitrile-alkali ion radical salt solutions for the hydrogen exchange reactions, especially, there is a strong inhibition of alkali cations by chelating solvents.

Benzonitrile-alkali ion radical salts were prepared in solution by a reaction between benzonitrile (10^{-4}—10^{-2} mol) and each of the alkali metals in *ca.* 80 cc of dry THF (tetrahydrofuran), MDE (monoethylene glycol dimethyl ether), DED (diethylene glycol dimethyl ether), TED (triethylene glycol dimethyl ether) and benzonitrile, much as has been described previously.[4] The composition of the complexes was confirmed by a study of their electronic spectra. Each of the complex solutions was introduced into a reaction vessel (*ca.* 270 cc) through a glass filter in order to remove an excess of the unreacted metal. When D_2 (10—45 cm Hg) was introduced to the complex solution, which was strongly stirred, the gaseous deuterium was reversibly exchanged with the hydrogen of the complex molecule in the temperature range from −20 and 50°C; a small amount of hydrogen was absorbed[5] at the same time in the benzonitrile-sodium or -lithium solution. The initial rates (in the first-order kinetics) or HD formation in the D_2–HZ (HZ=PhCN$^-$M$^+$; M=Li, Na, K, and Rb) exchange reaction are given in Table 1. It was demonstrated by the NMR spectrometry[6] that the PhCN$^-$K$^+$ complex was deutrated at the *p*-position of benzonitrile. The kinetics of the D_2–HZ exchange reaction was also investigated by changing the D_2 pressure and the concentration of the PhCN$^-$K$^+$ in THF (1.2×10^{-2}—2.8×10^{-3} mol):

TABLE. 1

Complex(HZ) (1.2×10^{-3} mol)	Solvent (80 cc)	D_2–HZ exchange reaction K_{HD}(cc/hr)	E(kcal/mol)
PhCN$^-$Li$^+$	THF	0.1	16
PhCN$^-$Na$^+$	THF	4.8	10
PhCN$^-$K$^+$	THF	10.0[a]	6
PhCN$^-$Rb$^+$	THF	0.3	—
PhCN$^-$K$^+$	MED	2.0	—
PhCN$^-$K$^+$	DED	0.58	—
PhCN$^-$K$^+$	TED	0.32	—
PhCN$^-$K$^+$	PhCN	>0.001	—
PhCN$^-$K$^+$	THF (9×10^{-3} mol; PhCN)	>0.2	—

a) The HD formation in the D_2–HZ exchange reaction took place homogeneously to reach nearly a monodeuteration of PhCN$^-$K$^+$ complex:

$$\frac{N_{exch.}}{(PhCN^-K^+)} = 0.87\ (25°C)$$

Where $N_{exch.}$ denotes the total number of the hydrogen exchanged with deuterium gas.

$$V_{HD} = kP_{D_2}(PhCN^-K^+)^2$$

It was interesting to note in Table 1 that the activity of the PhCN$^-$M$^+$ solution decreased strikingly when strong chelating solvents were used with alkali cations, such as DED, TED, or benzonitrile. When a small amount of benzonitrile (0.9×10^{-2} mol) was added to the THF solution of the benzonitrile – K stoichiometric complex, the exchange rates decreased; they were retarded completely by the addition of an excess.

The D_2–HZ and H_2–D_2 exchange reactions exhibited wide varieties of activities in solution; this was in contrast to the reactions over their complex films under similar reaction conditions.[7] The characteristic behaviour of such chelating solvents might be attributed to the solvation to alkali cations, which brings about a wide separation between anion and cation centers[8] in the complex molecule, thus preventing the development of favorable circumstances for the hydrogen activation.

A similar behavior of the different solvents was observed for the hydrogen exchange reaction and hydrogen absorption in their complex solutions, such as anthracene dianion, naphthalene monoanion and cyanonaphthalene dianion with alkali cations.

1) M. Ichikawa, M. Soma, T. Onishi, and K. Tamaru, This Bulletin, **43**, 3672 (1970), references therein.

2) M. Ichikawa and K. Tamaru, *J. Amer. Chem. Soc.*, in press.

3) M. Ichikawa, S. Tanaka, S. Naito, M. Soma, T. Onishi, and K. Tamaru, *Trans. Faraday Soc.*, submitted for publication.

4) M. Ichikawa, S. Tanaka, S. Naito, M. Soma, T. Onishi, and K. Tamaru, *Trans. Faraday Soc.*, **66**, 981 (1970).

5) It was shown by the NMR and UV spectrometry that the PhCN$^-$Na$^+$ and PhCN$^-$Li$^+$ were decomposed very slowly at room temperature in the presence of hydrogen gas to produce benzonitrile and metal hydride (NaH and LiH).

6) After deuteration and the removal of the solvent, the PhCN$^-$K$^+$ complex was oxidized to neutral PhCN by dry oxygen gas at 25°C as measured by mass and NMR spectrometry.

7) M. Ichikawa, M. Soma, T. Onishi, and K. Tamaru, *Trans. Faraday Soc.*, **63**, 997 (1967); M. Tsuda and H. Inokuchi, This Bulletin, **43**, 3410 (1970).

8) M. Szwarc, *Prog. Phys. Org. Chem.*, **6**, 323 (1969); T. E. Hogen-Esch and J. Smid, *J. Amer. Chem. Soc.*, **88**, 307, 318 (1966).

New Finding of Glassy Liquid Crystal – a Non-equilibrium State of Cholesteryl Hydrogen Phthalate

Kazuhiro Tsuji, Michio Sorai, and Syûzô Seki
Department of Chemistry, Faculty of Science, Osaka University, Toyonaka, Osaka
(Received March 25, 1971)

The ordinary glassy state is realized for many liquids when they are supercooled below their glass transition points without crystallization. This type of glassy state, however, can be established by other procedures, *e.g.* condensation of vapor,[1] precipitation process,[2] or thermal decomposition.[3] Recently we reported also the possible existence of glassy state of crystalline materials as a non-equilibrium state of many plastic crystals.[4] In this communication, we should like to report the new finding of the glassy state for liquid crystal of cholesteryl hydrogen phthalate (abbrebiated as CHP).

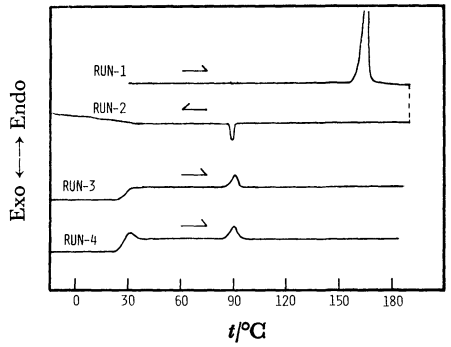

Fig. 1. DSC curves of cholesteryl hydrogen phthalate.

CHP obtained from Tokyo Kasei Kogyo Co., was recrystallized twice from ethanol. Thermal analysis was carried out for this specimen with a differential scanning calorimeter (Perkin-Elmer DSC-1B) as shown in Fig. 1. Run-1 shows a heating curve of crystalline CHP from room temperature to 190°C with the heating rate of 5°C/min. The crystalline CHP melted directly into an isotropic liquid at 160°C. Run-2 shows a cooling curve of the isotropic liquid with cooling rate of −5°C/min. The isotropic liquid was transformed into a liquid crystalline state at 90°C and no other thermal anomaly was observed between 90 and −100°C except for a slight baseline shift around 27°C. This implies that there exists only one liquid crystalline phase for CHP in contrast to the results by Barrall II *et al.*,[5] who reported two liquid crystalline states obtainable through monotropic transitions on cooling the isotropic liquid. Observation under polarizing microscope revealed a focal-conic texture for the present liquid crystal, but identification of its type has not been made. Run-3 shows a heating curve of the supercooled liquid crystal thus obtained. The DSC curve showed two thermal anomalies; a conspicuous stepwise anomaly at *ca.* 27°C which bears close resemblance to usual glass transition, and a phase transition at 90°C from liquid crystal to isotropic liquid.

Run-4 shows a heating curve of the supercooled liquid crystal annealed for 2 hr at 23°C just below the apparent glass transition point and then cooled down to −20°C before heating. It gave a stepwise curve with a small peak which corresponds to the enthalpy relaxation usually observed in an ordinary glass transition phenomenon. These facts confirm the view that the thermal anomaly at about 27°C might be considered to be a glass transition of the liquid crystalline state in CHP.

In order to examine more precisely the nature of this glass transition, activation enthalpy was determined according to McMillan's method.[6] Figure 2 shows the activation plot, from which the activation enthalpy was found to be 76.6 ± 3 K J mol^{-1}.

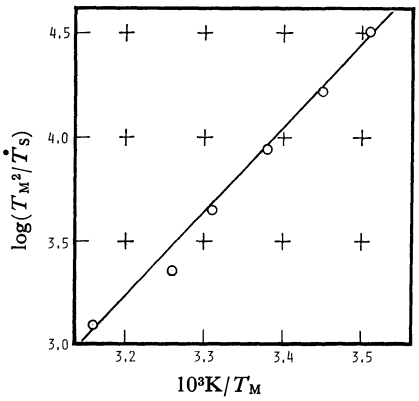

Fig. 2. Activation plot for glass transition of cholesteryl hydrogen phthalate (T_M, Inflection point; $\dot{T}_S$, Heating rate).

The glass transition temperature (T_g) was determined to be 22°C from the heat capacity measurements by use of an adiabatic calorimeter and the characteristic heat capacity jump at T_g, ΔC_p, was found to be 180 J K^{-1} mol^{-1}. The details of the present results of the heat capacity measurements will be given in due course.

From these results it can be concluded that the glassy state of liquid crystal has been established for the first time in the present study and we propose to designate this state as "**glassy liquid crystal**".

1) M. Sugisaki, H. Suga, and S. Seki, This Bulletin, **41**, 2581, 2591 (1968).
2) N. Onodera, H. Suga, and S. Seki, *J. Non-Cryst. Solids*, **1**, 331 (1969).
3) N. Onodera, H. Suga, and S. Seki, This Bulletin, **41**, 2222 (1968).
4) K. Adachi, H. Suga, and S. Seki, This Bulletin, **41**, 1073 (1968); **43**, 1916 (1970); **44**, 78 (1971).
5) E. M. Barrall II, J. S. Porter, and J. F. Johnson, *Mol. Cryst. and Liq. Cryst.*, **8**, 27 (1969).
6) J. A. McMillan, *J. Chem. Phys.*, **42**, 3497 (1965).

Infrared Longitudinal Bands in Crystalline Carbon Dioxide

Haruka YAMADA, Arata KIMOTO, and Kazuo SANNABE
Department of Chemistry, Kwansei Gakuin University, Nishinomiya

(Received March 31, 1971)

Recently two absorption peaks at 678.3 cm^{-1} and 2383.0 cm^{-1} were reported for the cubic crystal of carbon dioxide. They appeared at non-normal incidence and disappeared at normal incidence.[1] An attempt[1,2] has been made to interpret them as the longitudinal modes of ν_2 and ν_3 vibrations by means of the Haas-Hornig equation.[3] Assignment of these bands, however, still seems uncertain, because of the uncertainty of the value $d\mu/dQ$ used in the Haas-Hornig equation.

We have remeasured the absorption spectra of polycrystalline CO_2 films deposited fairly rapidly (60~90 sec) at liquid nitrogen temperature, the thickness being 1.8—2.8 μ. Spectra of each film were run at normal incidence, 0°, and at angles up to 30° from normal. The results are completely in agreement with those reported by Parker and Eggers.[1] The peaks at 678.0 cm^{-1} and 2379 cm^{-1} are angle-dependent, but the others do not shift or change significantly with the angle of incidence. We have further tried to confirm the longitudinal modes by a direct polarization measurement at non-normal incidence. As shown in Figs. 1 and 2, the peak at 678.0 cm^{-1} in the ν_2 region observed at non-normal incidence appears strongly in the *p*-polarized component of the radiation, where the electric vector is parallel to the incident plane, disappearing in the *s*-polarized radiation where the electric vector is perpendicular to the incident plane. The absorption curve observed at normal incidence shows no difference in *p*- and *s*- polarizations. The same holds for the peak at 2379 cm^{-1} in the ν_3 region.

Since the peaks occur only in the *p*-polarization, this strongly supports their assignment to the longitudinal optical modes.

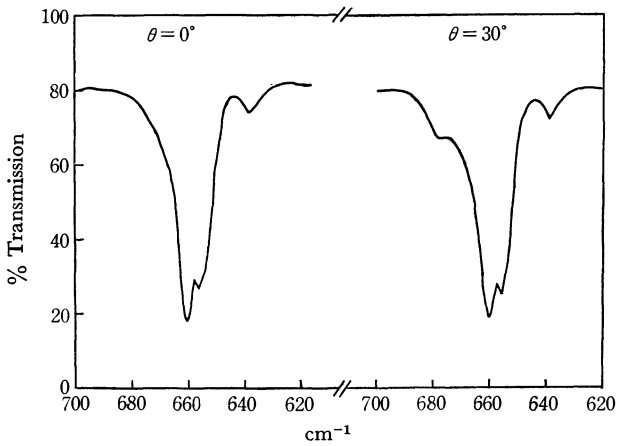

Fig. 1. Infrared absorption spectra of CO_2 crystal in the ν_2 region, at normal and non-normal incidence (unpolarized).

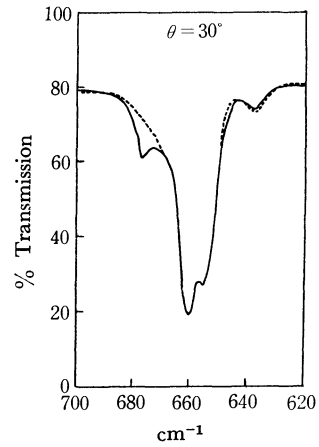

Fig. 2. Polarized absorption spectra of CO_2 crystal in the ν_2 region at non-normal incidence;
—— *p*-polarized, ------ *s*-polarized.

1) M.A. Parker and D. F. Eggers, *J. Chem. Phys.*, **45**, 4354 (1966).
2) D. C. McKean, *ibid.*, **52**, 6451 (1970).
3) C. Haas and D. F. Hornig, *ibid.*, **26**, 707 (1967).

Spatial Distribution of Potassium Atoms Scattered from the (001) Surfaces of Lithium Fluoride

Shinji TOMODA, Isao KUSUNOKI, and Kumasaburo KODERA
Department of Chemistry, Faculty of Science, Kyoto University, Sakyo-ku, Kyoto
(Received March 19, 1971)

Investigation of gas-solid interactions by means of molecular beams has recently attracted a great deal of attention.[1] The object of the study is to make clear the gas-surface interaction from the scattering of rare gases or hydrogen from clean surfaces of metals.[2] On the scattering of metal atoms from alkali halide crystals, however, few papers have been published during the past thirty years.

In earlier studies on the scattering of metal atoms from alkali halide surfaces, three types of patterns were reported; one which corresponds to specular reflection,[3] a second which obeys the cosine law,[4] and the third which is called "quasi-specular" or broad lobular pattern.[5] The results reported by different authors do not seem to be consistent with each other. Thus, more complete information on the phenomena is desiable. Concerning the technique of thin film growth on solid surfaces, work in this field might be important for clarifying the initial process of sticking of metal atoms on the surfaces.

In the present work, scattering patterns of the potassium beam from the surface of lithium fluoride were measured at several angles of incidence between 55° and 70° (measured from the surface normal). To determine the angular distribution of the flux of scattered atoms, a surface ionization detector was rotated around the target crystal. The thermal beam of potassium (cross section: 0.46 mm × 11.7 mm) was produced by effusion from an oven. Background pressure with the beam on was 2×10^{-7} Torr. Targets with lithium fluoride (001) surface prepared in different ways were used, one with a surface made by cleaving a crystal in air and the other was made optically flat by polishing with corundum powder suspended in water. The crystal was heated in a vacuum at about 470°K before it was exposed to the beam. The measurements were carried out at several temperatures from 170°K to 470°K.

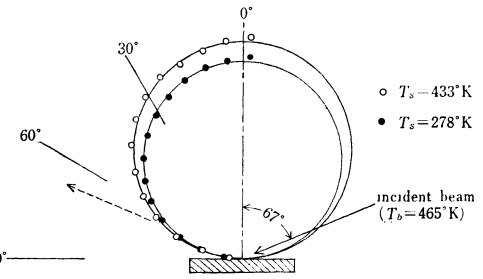

Fig. 1. Angular distribution of potassium atoms scattered from the cleavage surface of lithium fluoride (001). The solid curve indicates the cosine law. The broken line represents the specular direction. T_s and T_b are the surface temperature and the beam temperature, respectively.

Two different scattering patterns were obtained corresponding to the preparation of the surface. As is shown in Fig. 1, the spatial distribution from the cleavage surface closely follows the cosine law. This pattern indicates diffuse scattering and agrees with the results of Taylor.[4] Figure 2 shows the patterns from the polished surface. The peaks correspond approximately to the specular positions. The results give no definite conclusion but suggest that the molecules of water on the polished surface have some effect on the scattering pattern.

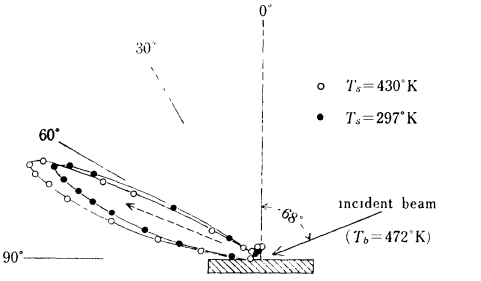

Fig. 2. Angular distribution of potassium atoms scattered from the polished surface of lithium fluoride (001). The broken line represents the specular direction. T_s and T_b are the surface temperature and the beam temperature, respectively.

Above room temperature, the scattering patterns and the scattered fluxes did not change significantly with the target temperature, while at temperatures below 250°K, the scattered fluxes decreased markedly and the patterns showed different directional features compared with those at high temperatures. The scattered flux attenuated rapidly with the time of exposure to the beam. This indicates the condensation of potassium atoms on the surface and the increase of the sticking probability. It is still difficult to explain the behavior of the two different surfaces.

1) *Cf. e.g.* "Fundamentals of Gas-Surface Interactions," ed. by H. Saltsburg, J. N. Smith, Jr., and M. Rogers, Academic Press (1967); "Rarefied Gas Dynamics," 5th symp., Vol. 1, ed. by C. L. Brundin, Academic Press (1967); *ibid.*, 6th symp., Vol. 2, ed. by L. Trilling and H. Y. Wachman (1969).

2) *Cf. e.g.* D. L. Smith and R. P. Merrill, *J. Chem. Phys.*, **53**, 3588 (1970); A. G. Stoll, D. L. Smith, and R. P. Merrill, *ibid.*, **54**, 163 (1971).

3) A. Ellett, H. F. Olson, and H. A. Zahl, *Phys. Rev.*, **34**, 493 (1929).

4) J. B. Taylor, *ibid.*, **35**, 375 (1930).

5) R. R. Hancox, *ibid.*, **42**, 864 (1932).

A Chlorine NQR Study of Trichlorides of Group V Elements

Masao HASHIMOTO, Toshiaki MORIE, and Yoshifumi KATO

Department of Chemistry, Faculty of Science, Kobe University, Nada-ku, Kobe

(Received June 19, 1970)

The NQR frequency of ^{35}Cl has been observed in polycrystalline PCl_3, $POCl_3$, $AsCl_3$, and $SbCl_3$ at 77°K and above. In all cases, the resonance frequency decreases at higher temperatures. The temperature coefficient of the resonance frequency is analyzed according to a modified Bayer-type treatment. A qualitative examination of the experimental results, including Robinson's results for $BiCl_3$ at 83 and 299°K, reveals that the strength of the intermolecular interactions in the solids of these trichlorides decreases in this order: $BiCl_3 > SbCl_3 > AsCl_3 > PCl_3$. The resonance was found to "fade-out" at temperatures below the melting point for the solids of PCl_3 and $POCl_3$, while the resonance was observed up to the melting point for the other compounds. The origin of this phenomenon is discussed.

As to the nuclear quadrupole resonance (NQR) of chlorine in trichlorides of the Group V elements, there have already been a number of investigations by several workers.[1-7] In the earlier studies, however, the measurements were made at only a few temperatures. Recently, though, Chihara *et al.*[8] measured almost continuously the NQR frequencies of chlorine and antimony in solid antimony trichloride in the range from 20°K to about 150°K.

The first theoretical elucidation of the temperature variation of resonance frequencies was given by Bayer,[9] who attributed the phenomenon to the influence of lattice vibration on the electric-field gradient tensor under a simple model with a one-dimensional torsional mode. This theory was later extended generally by Kushida[10] and Wang[4] separately. According to these treatments, the NQR frequencies are connected to the mean square amplitude of each normal vibration through both the electric-field gradient tensor and the asymmetry parameter. On the assumption that the mean energy of a normal mode is equal to that of the corresponding Planck oscillator, the resonance frequency may be said to be related explicitly to the temperature and the moment of inertia for the vibration concerned. Kushida *et al.*,[11] furthermore, discussed the dependence of the NQR frequency on the pressure as well as on the temperature.

In this investigation, the measurements of the NQR frequencies of ^{35}Cl in phosphorous, phosphoryl, arsenic, and antimony trichloride were carried out at 77°K and above at intervals of a few degrees. No reference to the temperature dependence of the NQR frequency of ^{35}Cl in phosphorous and phosphoryl trichloride has been found in previous works.

In all the compounds studied in this paper, the principal axes of the electric-field gradient tensor at a chlorine nucleus do not coincide with those of the moment of inertia of the molecule concerned. A treatment generalized for such a case is applied to the analysis of the temperature dependence of the NQR frequencies of ^{35}Cl in phosphorous trichloride. Some discussions of the torsional motions and the intermolecular interactions in the solid are given on the basis of the experimental results.

Experimental

The NQR frequencies of ^{35}Cl were measured with a super-regenerative spectrometer which was externally quenched and frequency-modulated.[12] For the frequency modulation, a 80 Hz sine wave was used. The quenching frequency was varied from 35 KHz to 70 KHz. The resonance frequencies were measured visually; that is, an NQR signal was compared directly on an oscilloscope screen with that from a standard frequency generator (National VP-828A), which was itself calibrated by means of a digital frequency counter (National VP-415 M). The accuracy of the frequency measurements is considered to be ±2 KHz.[13] Although the super-regenerative spectrometer used was not well suited for observing linewidths, the linewidths were estimated by recording the signals through a lock-in amplifier.

The resonance frequencies were measured at 77°K and above in liquid nitrogen and in various liquid baths. The temperature was determined by using two copper-constantan thermocouples, each in contact with the upper or the lower side of the sample tube. The accuracy of the temperature measurements may be considered to be better than ±1°K.[14]

Commercial compounds (Wako Pure Chemical Industries, Ltd.) were used without further purification. They were packed in glass tubes with an outside diameter of 18 mm.

Results

Phosphorous Trichloride. The resonance frequencies of ^{35}Cl due to two nonequivalent chlorine sites

1) R. Livingston, *Phys. Rev.*, **82**, 289 (1951).
2) H. G. Dehmelt and H. Krüger, *Z. Phys.*, **130**, 385 (1951).
3) R. Livingston, *J. Phys. Chem.*, **57**, 496 (1953).
4) T. C. Wang, *Phys. Rev.*, **99**, 566 (1955).
5) H. G. Robinson, *ibid.*, **100**, 1731 (1955).
6) S. Ogawa, *J. Phys. Soc. Jap.*, **13**, 168 (1958).
7) G. E. Peterson, Thesis, University of Pittsburgh, (1962).
8) H. Chihara, N. Nakamura, and H. Okuma, *J. Phys. Soc. Jap.*, **24**, 306 (1968).
9) H. Bayer, *Z. Phys.*, **130**, 227 (1951).
10) T. Kushida, *J. Sci. Hiroshima Univ.*, **A19**, 327 (1955).
11) T. Kushida, G. B. Benedek, and N. Bloembergen, *Phys. Rev.*, **104**, 1364 (1956).

12) T. P. Das and E. L. Hahn, "Nuclear Quadrupole Resonance Spectroscopy," Solid State Physics, Suppl. 1, Academic Press, New York (1958), p. 90.

13) By comparing our measurements with those already reported, we estimated the accuracy of our frequency measurements.

14) In Ref. 8, Chihara *et al.* tabulated the resonance frequencies of ^{35}Cl in antimony trichloride in the low-temperature region (from 21.5°K to 178°K). By comparing our data with theirs, we deduced the accuracy of our temperature measurements.

(designated as ν_1 and ν_2) were measured at temperatures above 77°K. The signals could be observed up to about 165°K. Above this temperature, the resonance was found to fade out, while this compound melts at 179°K. The temperature dependences of ν_1 and ν_2 are shown in Fig. 1. The line-width of ν_2 was almost constant between 77°K and about 150°K. Above this temperature, though, the width increased rapidly.

Phosphoryl Trichloride. Although the compound melts at 272°K, two NQR signals (designated as ν_1 and ν_2) were found to fade out at temperatures above about 200°K. By immersing the sample in chlorobenzene bath (228°K), the NQR signals were searched for over the frequency region of 20 MHz to 33.5 MHz. No signals was found under these conditions. As is shown in Fig. 2, ν_1 and ν_2 decrease parallel with an increase in the temperature. The linewidth of the ν_2 was found to increase gradually as the temperature increased. The width at 187°K was about three times as large as that at 77°K.

Arsenic Trichloride. Three resonance frequencies of ^{35}Cl (designated as ν_α, ν_β, and ν_γ) could be measured at temperatures between 77°K and the melting point of the compound (257°K). Their temperature dependences are shown in Fig. 3.

Antimony Trichloride. The resonance frequencies of ^{35}Cl due to two nonequivalent chlorine sites (designated as ν_1 and ν_2) could be measured up to the melting point of the compound (346°K). Our data were in good agreement with those of Chihara *et al.*[8] The linewidths of the ν_1 and ν_2 at 77°K were found to be almost equal to the corresponding values at room temperature.

Bismuth Trichloride. We could not observe the NQR signals of ^{35}Cl in this compound. The reason for our failure might perhaps be traced to the purity of the sample.

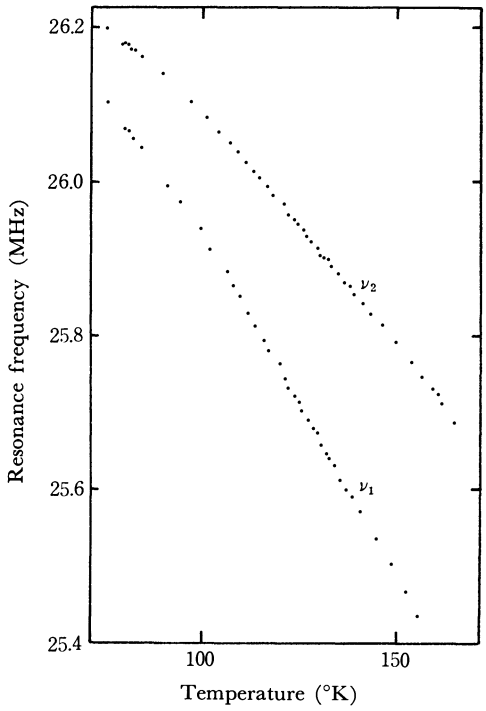

Fig. 1. Temperature dependence of ν_1 and ν_2 in PCl_3.

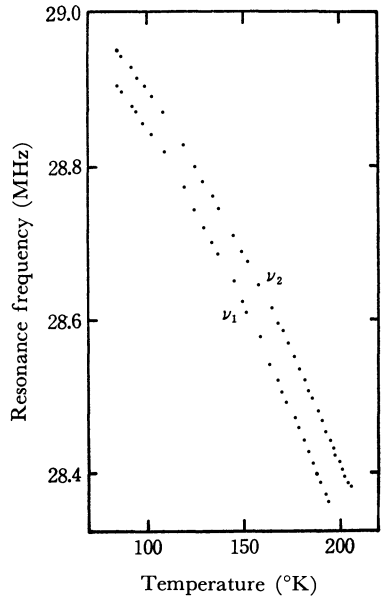

Fig. 2. Temperature dependence of ν_1 and ν_2 in $POCl_3$.

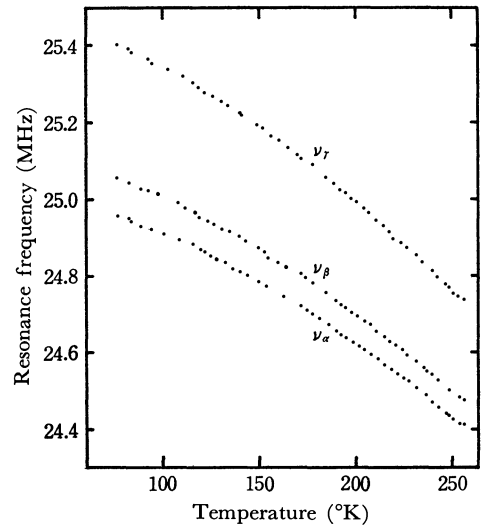

Fig. 3. Temperature dependence of ν_α, ν_β, and ν_γ in $AsCl_3$.

Theoretical

When the principal axes of the field gradient (x, y, and z) coincide with the inertial axes (X, Y, and Z) around which the torsional motions may take place, the z component of the field gradient seen at a nucleus in the vibrating molecule (q) can be related to that in the static molecule (q_0) by Wang's expression;[15]

$$q = q_0\{1 - \tfrac{3}{2}(\langle\theta_X^2\rangle + \langle\theta_Y^2\rangle) + \tfrac{1}{2}\eta(\langle\theta_Y^2\rangle - \langle\theta_X^2\rangle)\}, \quad (1)^{16}$$

where $\langle\theta_i^2\rangle$ is the average square torsional displace-

15) T. C. Wang, *Phys. Rev.*, **99**, 566 (1955).

16) As has already been pointed out by Chihara *et al.* (Ref. 8), a slight correction must be made in the right-hand side of Wang's original expression.

Table 1. The frequency (ω_i) and the mean square amplitude ($\langle\theta_i^2\rangle$) of the torsional motion in phosphorous trichloride

T (°K)	ω_1	ω_2 (cm^{-1})	ω_3	$\langle\theta_1^2\rangle$	$\langle\theta_2^2\rangle$ (10^{-3} rad^2)	$\langle\theta_3^2\rangle$
93	57±7	29±1	39±5	3.8±1.9	13.6±1.0	4.5±1.0
143	50±6	27±1	35±5	7.5±1.7	24·5±1.0	8.4±2.3

ment about an axis, i, and η, the asymmetry parameter. This expression can not be applied immediately to the analysis of the field gradient at the chlorine nucleus in an MCl_3 molecule in the absence of the coincidence between the principal axes of the field gradient and inertial axes. Therefore, one must modify Eq. (1) to obtain an expression valid for such a situation.[17]

Now, let q' represent the field gradient at the chlorine nucleus along an M–Cl bond direction (designated as the z axis of the field-gradient tensor) in an MCl_3 molecule. For the sake of simplisity, the field gradient is assumed to be axially symmetric (*i.e.*, $\eta=0$) and the symmetry of the MCl_3 molecule is assumed to be C_{3v}. As the principal axes of the moment of inertia, we take the system of axes (X_1, X_2, and X_3) shown in Fig. 4, in which the X_3 axis is chosen perpendicular to the plane of three chlorine atoms, and the X_2 axis, parallel with the Cl(2)–Cl(2) direction.

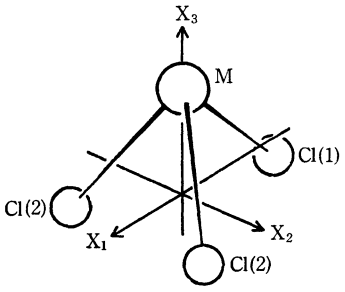

Fig. 4. The orientation of the coordinate system in the MCl_3 molecule.

A torsional motion around an X_i axis makes the z axis fluctuate by an angle of $c_i\theta_i$, where θ_i is a torsional displacement around the X_i axis, and c_i, a constant specified by the molecular geometry. As a first-order approximation, the total effect of the torsional motions around three inertial axes (X_i) on the field gradient at a chlorine nucleus may be written as follows:

$$q' = q_0'\{1 - 3/2 \sum_i \sin^2 \alpha_i \langle\theta_i^2\rangle\}, \quad (2)$$

where α_i is the angle between X_i and the z axis. Hence, the temperature-dependent frequency (ν') is related to the frequency of the stationary molecule (ν_0') by:

$$\nu' = \nu_0'\{1 - 3/2 \sum_i \sin^2 \alpha_i \langle\theta_i^2\rangle\}. \quad (3)$$

If the torsional motion is approximated by a quantum mechanical harmonic oscillator, the mean square displacement ($<\theta_i^2>$) is;

$$\langle\theta_i^2\rangle = \hbar/A_i\omega_i[1/2 + 1/\{\exp(\hbar\omega_i/kT) - 1\}], \quad (4)$$

where ω_i is the torsional frequency, and A_i, the moment of inertia associated with the torsional motion about the X_i axis.

The asymmetry parameter of the field gradient at a chlorine nucleus in $SbCl_3$ was found to be large,[18] and that in $BiCl_3$ seems likely to be large because of a strong intermolecular bond formation to be discussed later. In $AsCl_3$ there are three kinds of resonance frequencies; this make it difficult to regard the symmetry of the molecule as trigonal. Therefore, the assumptions included in the derivation of Eq. (2) or (3) are not valid for the cases of $SbCl_3$, $BiCl_3$, and $AsCl_3$ because of the large asymmetry parameter or the destruction of the trigonal symmetry. Since, however, as will be discussed later, the inter-molecular interactions in the solid of PCl_3 seem to be quite weak, the assumptions mentioned above may be valid for the case of this molecule.

The results of the analysis of the temperature dependence of ν_1 and ν_2 in PCl_3 according to Eqs. (3) and (4) are shown in Table 1. Unfortunately, we could not determine all the parameters definitely, although their values are considered to be reasonable.

Discussion

Although the crystal structure of the compounds studied in this work are, for the most part, unknown, here, we shall attempt a qualitative discussion of the intermolecular interactions in their crystals.

Two or three resonance frequencies are observed in each compound studied. The separation ($\Delta\nu$) between the multiple lines in each compound is shown in Table 2. According to Robinson's results,[5] the separation ($\Delta\nu$)

Table 2. The frequency separation ($\Delta\nu$) between non-equivalent sites in MCl_3 molecules at 77°K

Compound	$\Delta\nu$ (MHz)
$POCl_3$	0.05
PCl_3	0.10
$AsCl_3$	0.40[a]
$SbCl_3$	1.61
$BiCl_3$	3.68[b]

a) A separation between the highest resonance frequency and the mean of the lower two.
b) See Ref. 5.

17) I. Tatsuzaki and Y. Yokozawa, *J. Phys. Soc. Jap.*, **12**, 802 (1957).

18) T. Okuda, A. Nakao, M. Shiroyama, and H. Negita, This Bulletin, **41**, 61 (1968).

found for $BiCl_3$ is about 3.68 MHz at 83°K. A less drastic splitting occurs in $SbCl_3$. The separation ($\Delta\nu$) found for this compound is about 1.61 MHz at 77°K. Allen[19] pointed out that splittings greater than 0.5 MHz must be attributed to a different type of chemical bonding to the chlorine atoms. In fact, Peterson,[7] in his X-ray study of $SbCl_3$, found that one of the Sb–Cl bond lengths within a molecule is 2.30 Å, and the other two, 2.325 Å. Futhermore, the two nearest intermolecular Sb–Cl distances are 3.41 Å, which is smaller than the van der Waals distance (4 Å). Chihara *et al.* reasonably explained both the large separation ($\Delta\nu$) and the difference in the temperature dependence of the two lines of $SbCl_3$ in terms of this intermolecular-bond formation. That is, the intermolecular-bond formation mentioned above diminishes the electron density of the p_x or p_y orbitals of chlorine atoms participating in the bond formation and, therefore, their resonance frequencies. The decreases in this electron density and the resonance frequency due to the intermolecular-bond formation are proportional to the degree of the intermolecular overlap, which should tend to decrease as the molecular librations increase in amplitude at higher temperatures. The direct temperature effect, which tends to decrease the resonance frequency at higher temperatures, counteracts the above effect; their compromise determines the actual temperature coefficient of the resonance frequency.

If the formation of intermolecular covalent bonds similar to that found in $SbCl_3$ is possible in the crystal of $BiCl_3$, it accounts for the large separation ($\Delta\nu$) and the positive temperature coefficient found for $BiCl_3$. Both the fact that the separation ($\Delta\nu$) of $BiCl_3$ is considerably larger than that of $SbCl_3$ and the fact that one of the two lines in $BiCl_3$ exhibits a positive temperature coefficient suggest that the strength of the intermolecular covalent bonds in $BiCl_3$ is stronger than that in $SbCl_3$.

Because of the intermolecular interactions, the quadrupole coupling constant (eQq) of the solid determined from the pure quadrupole spectra may differ as much as 10% from that of gas determined from the hyperfine structure of the rotational spectra in the microwave region. Comparisons between the eQq values of PCl_3 and $POCl_3$ in the gaseous and solid states are given in Table 3, together with the values of some other molecules.

TABLE 3. COMPARISON OF eQq IN GAS AND SOLID

Compound	eQq gas (MHz)	eQq solid (MHz)	r(gas/solid)	Ref.
PCl_3	53.3	52.40	1.017	20
$POCl_3$	55.4	57.97	0.955	20
CH_3Cl	75.13	68.40	1.098	19
CH_2Cl_2	78.3	72.42	1.081	19
CF_3Cl	78.05	77.58	1.006	19

19) H. C. Allen Jr., *J. Phys. Chem.*, **57**, 501 (1953).
20) C. R. Nave, T. L. Weatherly, and Q. Williams, *J. Chem. Phys.*, **49**, 1413 (1968).

Since the difference in the eQq values in Table 3 and the $\Delta\nu$ values in Table 2 are rather small for PCl_3 and $POCl_3$, the intermolecular interactions in their solid states are considered to be weak.

The three M-Cl bonds within an MCl_3 molecule may be equivalent in its gaseous state, while in its solid state the intermolecular interactions destroy the equivalence. Therefore, the separation ($\Delta\nu$) between multiple lines may be a measure of the intermolecular interactions. In general, the melting point of a crystal reflects the degree of the intermolecular interactions. The relation between the melting point and the $\Delta\nu$ among these trichlorides is shown in Fig. 5. An expected correlation between them is found;

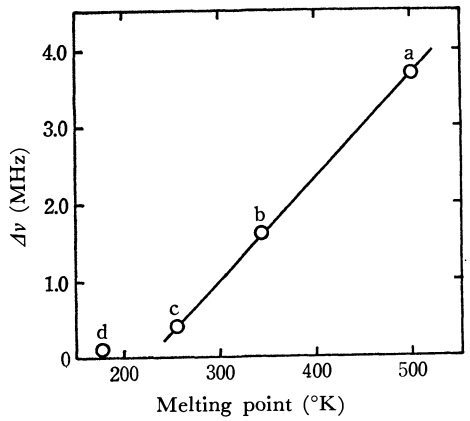

Fig. 5. Melting point versus $\Delta\nu$ plots: (a), $BiCl_3$; (b), $SbCl_3$; (c), $AsCl_3$; (d), PCl_3.

this indicates that the strength of the intermolecular interactions decreases in this order: $BiCl_3 > SbCl_3 > AsCl_3 > PCl_3$.

As the strength of the intermolecular interactions becomes weaker, the magnitude of the mean-square amplitudes ($<\theta_i^2>$) increases; consequently, the absolute values of their temperature coefficients ($|d<\theta_i^2>/dT|$) may be expected to increase. Furthermore, it may

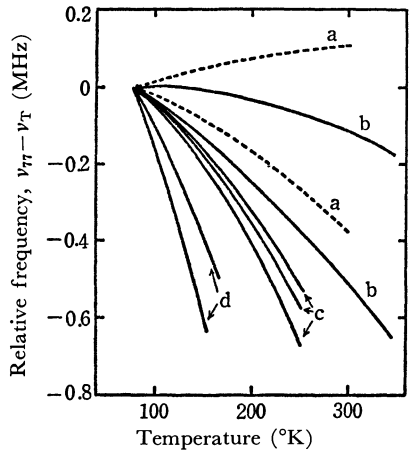

Fig. 6. Relative frequency (difference between the resonance frequency at 77°K (ν_{77}) and that at higher temperature (ν_T)) of ^{35}Cl in MCl_3 molecule as a function of temperature: (a), $BiCl_3$ (Estimated from the data at 83° and 299°K reported by Robinson.); (b), $SbCl_3$; (c), $AsCl_3$; (d), PCl_3.

be seen from Eqs. (1) and (2) that the absolute value of the temperature coefficient of the resonance frequency ($|d\nu/dT|$) is proportional to that of the mean-square amplitudes ($|d<\theta_t^2>/dT|$). Therefore, if the strengths of intermolecular interactions are assumed to become weaker from material to material in this order: $BiCl_3>SbCl_3>AsCl_3>PCl_3$, it seems reasonable that the absolute values of the mean temperature coefficient of the resonance frequency of chlorine in the MCl_3 molecule increase in this order: $PCl_3>AsCl_3>SbCl_3>BiCl_3$, as may be seen from Fig. 6.

A fade-out phenomenon analogous to that found for PCl_3 and $POCl_3$ has been observed for some other solids[21-23] which had phase transitions associated with internal or molecular reorientations in the solids. From the fact that the fade-out apparently occurred only in a solid where internal or molecular rotation was either definitely known to occur or was very likely, it had been considered that such motions were responsible for the fade-out.[22] Although no reference to such motions in the solids of PCl_3 and $POCl_3$ has been found in previous works, the fade-out found for them may be due to molecular rotation, which is expected to occur as a result of the weak intermolecular interactions. One of the mean-square amplitues of torsional motions found for the solid PCl_3 is about 13.6×10^{-3} rad^2 at 93°K. According to Chihara *et al.*,[8] that of the solid $SbCl_3$ is about 10×10^{-3} rad^2 at the same temperature. This indicates a rather high degree of torsional motion in solid PCl_3 at lower temperatures.

Structual information on the solid triiodides of the Group V elements is available.[24] From a structural point of view, it is impossible to regard the solid of the triiodide of arsenic, antimony, or bismuth as a molecular crystal; this is because of a layer-structure formed by the sharing of the edges of the MI_6 octahedra. On the other hand, in the solid of PI_3 the existence of the intermolecular bonds is not expected from its crystal structure. It is not unreasonable to consider that this trend in the triiodide series occurs also in the trichloride series. This confirms the above conclusion that, in the solid of PCl_3, the strength of the intermolecular forces is quite weak, whereas Lucken[25] estimated that the phosphorous trichloride was isomorphous with the antimony trichloride, in which the strong intermolecular forces exist. If $BiCl_3$ crystalizes with the BiI_3 structure, it is difficult to explain the large separation ($\Delta\nu$) found for $BiCl_3$, because in the BiI_3 structure all the metal-halogen bonds are expected to be equivalent. Therefore, it is tempting to conclude from the similarity of the resonance spectra and their temperature dependence that $BiCl_3$ and $SbCl_3$ are isostructural with each other.

The authors wish to express their thanks to Professor Mikio Takeyama and Dr. Yoshio Kamishina for their valuable discussions and suggestions on the fabrication of the equipment. One of the authors (M.H.) also wishes to Professor Ryôiti Kiriyama for his continual encouragement and interest.

21) H. C. Allen, Jr., *J. Amer. Chem. Soc.*, **74**, 6074 (1952).
22) H. S. Gutowsky and D. W. McCall, *J. Chem. Phys.*, **32**, 548 (1960).
23) H. C. Meal and H. C. Allen, Jr., *Phys. Rev.*, **90**, 348 (1953).
24) R. W. G. Wyckoff, "Crystal Structures", **2**, Chap. VB.
25) E. A. C. Lucken, "Nuclear Quadrupole Coupling Constants", Academic Press, New York (1969), p. 274.

The Catalytic Oxidation of Carbon Monoxide on Titanium Dioxide; Anatase and Rutile

Yoshito Onishi

Department of Chemistry, Faculty of Industrial Arts, Kyoto Technical University, Matsugasaki, Sakyo-ku, Kyoto

(Received July 18, 1970)

For the purpose of examining the surface state of titanium dioxide during the catalytic oxidation of carbon monoxide, the electric conductivities of anatase and rutile at 350—800°C, the amount of active oxygen on the catalyst surface at 400—600°C, and oxygen deficiency during the reaction were measured. The temperature-dependence of electric conductivities are represented by the formula $\sigma = A \cdot e^{-E/RT}$ in narrow temperature ranges. The amounts of active oxygen per unit surface area of rutile were 3—5 times as much as those of anatase at same temperatures, and 1—3% of them desorbed during the reaction. When the coverage fraction of active oxygen on the catalyst, θ, is assumed to be equal to 1 in oxygen, the following equation can express the relation between the rate constant of the reduction of titanium dioxide by carbon monoxide, k_{CO}, and that of the oxidation of reduced titanium dioxide by oxygen k_{O_2}, during the oxidation of carbon monoxide:

$$k_{CO} \cdot P_{CO} \cdot \theta = 2k_{O_2} \cdot P_{O_2} \cdot (1-\theta)^2 .$$

In the preceding paper,[1] the following results have been reported: the rate constant of oxidation of carbon monoxide on titanium dioxide is proportional to P_{CO} and it does not depend upon P_{O_2} nor P_{CO_2}, the rate-determining step is the reaction between the surface oxygen on the catalyst and carbon monoxide, and the difference between activation energies of the uptake of surface oxygen atoms by carbon monoxide from anatase and rutile is about 10 kcal/mol. Several papers[2-5] have discussed an amount of surface oxygen, oxygen defect, and active sites on the catalyst in the oxidation of carbon monoxide on metallic oxide catalysts. For the titanium dioxide, the oxygen defect is formed on its surface during the reaction, and there are surface oxygen which react easily with carbon monoxide, *i.e.*, active oxygen.[1]

In this paper, the amount of active oxygen and its deficient amount during the oxidation of carbon monoxide on the surface of two crystal forms will be determined. The relation between the amount of active oxygen and the rate constants of the reduction of titanium dioxide by carbon monoxide and the oxidation of the reduced titanium dioxide by oxygen will be studied.

Experimental

The samples used were anatase (A) and rutile (R). The latter was obtained by heating A at 1150°C for 3 hr.[1] The apparatus and the preparation of the reactant gas were described in the preceding paper.[1] The sample was evacuated and treated with a circulating oxygen at 600°C for 3 hr in the reaction system before the measurements.

The electric conductivity of the sample was calculated from the observed current under a constant D.C. voltage applied to a pair of gold electrodes which were pressed to the sample with a definite weight.

Results and Discussion

Dependence of Electric Conductivity of the Catalyst upon Temperature. The electric conductivity of the catalyst pretreated in oxygen at 600°C for 3 hr was determined in oxygen under pressure of 70 mmHg or in circulating mixed gas with a composition of $CO/O_2 = 2/1$ under pressure of 70 mmHg[6] at a constant temperature. The temperature-dependence of electric conductivities for anatase and rutile determined at 350—800°C are shown in Figs. 1 and 2. The measured points at 600°C and lower are almost linear for two samples and the conductivity σ can be represented

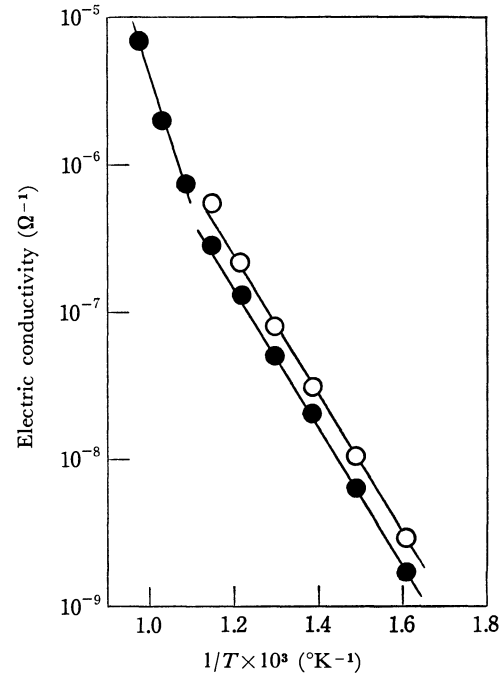

Fig. 1. Effect of temperature on electric conductivity of anatase.
●: in O_2 ○: in $CO/O_2 = 2/1$

1) Y. Onishi and T. Hamamura, This Bulletin, **43**, 996 (1970).
2) G. Parravano, *J. Amer. Chem. Soc.*, **75**, 1448 (1953).
3) E. R. S. Winter, *J. Chem. Soc.*, **1955**, 2726.
4) F. S. Stone, *Advan. Catal.*, **13**, 1 (1962).
5) K. Tarama, S. Teranishi, and A. Yasui, *Kogyo Kagaku Zasshi*, **60**, 1222 (1957).
6) In this case, carbon dioxide formed was condensed in the liquid nitrogen trap and the total pressure gradually decreased, but the electric conductivity did not change.

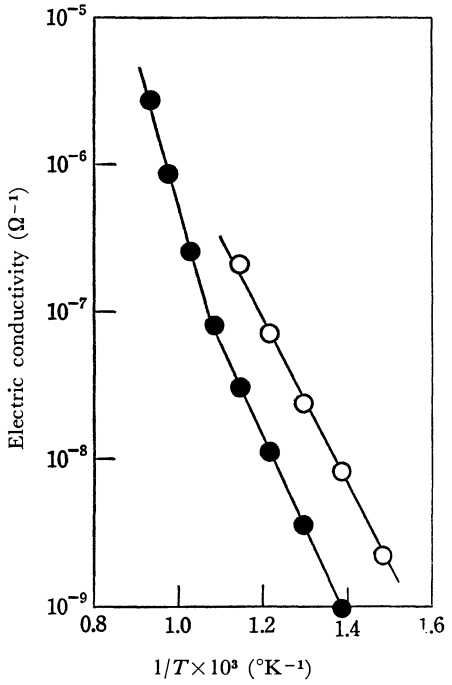

Fig. 2. Effect of temperature on electric conductivity of rutile.

●: in O_2 ○: in $CO/O_2=2/1$

by the following equation:

$$\sigma = A\cdot e^{-E/RT} \quad (1)$$

where A is a constant, and E an activation energy, respectively. The plots at higher temperatures than 600°C gradually deviate upward from linear lines, but in narrow temperature ranges, Eq. (1) may be applied. The obtained values of E are listed in Table 1.

Table 1. Activation energies for electric conductivities of catalysts

Temp. (°C)	350—600 $CO/O_2=2/1$	350—600 O_2	600—800 O_2
Anatase (kcal/mol)	21.3	21.3	38.5
Rutile (kcal/mol)	25.7	29.5	46.9

The value of rutile determined under temperatures lower than 600°C in oxygen almost agrees with that of Gorelik,[7] and the value above 600°C, with those of Earle,[8] Cronemeyer,[9] and Hauffe.[10] The conductivity in the mixed gas is larger than that in oxygen for both anatase and rutile because of the reduction with carbon monoxide, and this fact shows that titanium dioxide is an n-type oxide semi-conductor.

Amount of Active Oxygen of the Catalyst. When the catalyst pretreated in oxygen at 600°C for 3 hr was cooled, their conductivities were function of the temperature, and these values almost unchanged upon the evacuation. Therefore, it is considered that the catalyst surface is clean and stable by this treatment, and the catalyst thus treated will be called its starting state hereafter.

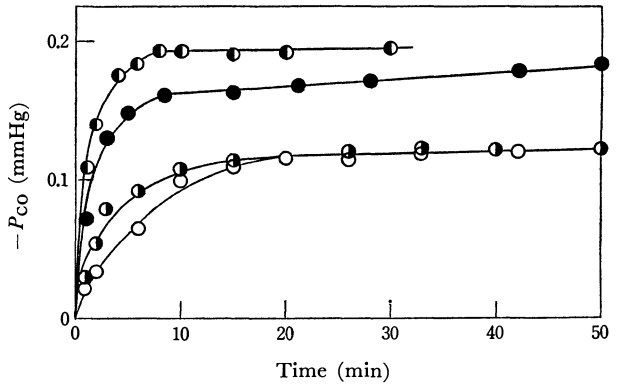

Fig. 3. Amounts of carbon monoxide reacted *vs.* time curves on anatase.

◐: $P_{CO}=149$ mmHg at 550°C
◑: $P_{CO}=75$ mmHg at 500°C
●: $P_{CO}=16$ mmHg at 550°C
○: $P_{CO}=14$ mmHg at 500°C

When titanium dioxide of the starting state was exposed to carbon monoxide under pressures of 10—150 mmHg at 400—600°C, carbon dioxide formed was condensed in the liquid nitrogen trap, and the CO pressure decreased, but the rate of decrease fell down with the time as is shown in Fig. 3. The total amount of carbon dioxide condensed was almost equal under the different initial pressure of carbon monoxide at the same temperatures. If a limited amount of the surface oxygen of the catalyst (it may be the oxygen of both crystal-lattice point and adsorbed one) is assumed to react easily with carbon monoxide (these oxygen will be called active oxygen hereafter), the amount of the active oxygen can be estimated from the amount of carbon dioxide condensed. The number of the active oxygen atoms per unit surface area, and its percentage to the surface lattice oxygen assuming that the surface is (011) for anatase and (110) for rutile,[11] are listed in Table 2.

Table 2. Numbers of active oxygen atoms and their percentages to surface lattice oxygen on anatase and rutile

	Temp. (°C)	600	550	500	450	400
A	Numbers $\times10^{-17}$ (atoms/m^2)	5.14	3.26	2.07	1.25	0.66
	%	4.63	2.94	1.87	1.13	0.60
R	Numbers $\times10^{-17}$ (atoms/m^2)	16.2	11.3	8.35	5.66	—
	%	15.6	10.8	8.01	5.44	

Deficient Amount of thr Active Oxygen during the Oxidation of Carbon Monoxide. When titanium dioxide of the starting state is exposed to carbon monoxide

7) S. I. Gorelik, *Zhur. Eksptl. i Teoret. Fiz.*, **21**, 826 (1951); *Chem. Abstr.*, **49**, 1395f (1955).
8) M. D. Earle, *Phys. Rev.*, **61**, 56 (1942).
9) D. C. Cronemeyer, *ibid.*, **87**, 876 (1952).
10) K. Hauffe, "Reaktionen in und an festen Stoffen," Springer, Berlin (1955), p. 136.
11) A. N. Winchell and H. Winchell, "Elements of Optical Mineralogy, Part II," John Wiley and Sons Inc., New York (1951), pp. 66, 69.

under a pressure of about 10^{-2} mmHg at a definite temperature, it is reduced by carbon monoxide and its conductivity increases with the time. Therefore, the amount of the reduction product CO_2 formed until the conductivity becomes the same value in the mixed gas shows the deficient amount of the active oxygen during the reaction. The number of the deficient active oxygen sites and its ratio to total active oxygen atoms, $(1-\theta)$, are listed in Table 3; θ represents the coverage fraction of active oxygen on the catalyst and θ is equal to 1 at the starting state.

Table 3. Deficiencies of active oxygen atoms during the oxidation of carbon monoxide on anatase and rutile

	Temp. (°C)	600	550	500	450
A	Deficiency $\times 10^{-15}$ (atoms/m^2)	8.61	5.93	3.98	2.47
	$(1-\theta)\times 10^2$	1.68	1.82	1.92	1.98
R	Deficiency $\times 10^{-16}$ (atoms/m^2)	2.09	1.98	1.89	1.78
	$(1-\theta)\times 10^2$	1.29	1.75	2.26	3.14

Relation between Reduction Rate and Oxidation Rate of Titanium Dioxide. If the reduction starts from its starting state ($\theta=1$) in the above case, the value of θ at any point can be calculated by measuring the amount of carbon monoxide consumed. Therefore, the rate of decrease of carbon monoxide at any θ value can be estimated by measuring the CO pressure as a function of time. Similarly, when oxygen is introduced over the reduced titanium dioxide, it is oxidized by oxygen (some of the oxygen may be adsorbed on it), and the O_2 pressure decreases. Therefore, the oxidation rate of titanium dioxide of any θ value can be estimated by measuring the O_2 pressure. From these measurements, the following equations are obtained:

$$-\mathrm{d(CO)}/\mathrm{d}t = k_{CO}\cdot P_{CO}\cdot\theta \quad (2)$$

$$-\mathrm{d(O_2)}/\mathrm{d}t = k_{O_2}\cdot P_{O_2}\cdot(1-\theta)^2 \quad (3)$$

where k_{CO} and k_{O_2} are the rate constants of reduction and oxidation of titanium dioxide, respectively. The values of k_{CO} and k_{O_2} are listed in Table 4; k_{CO} are the same values shown in Fig. 3 of the preceding paper[1] in which they have been shown as k'. The oxidation rate of titanium dioxide by oxygen (the adsorption rate of oxygen) is far faster than the reduction rate by carbon monoxide.

Table 4. Estimated values of k_{CO} and k_{O_2}

Temp. (°C)	600	550	500	450
$k_{CO}\times 10^5$ (CO_2 mmol/min·cmHg·m^2)				
Anatase	7.50	3.96	1.76	0.896
Rutile	30.1	22.4	18.3	13.6
$k_{O_2}\times 10$ ($-O_2$ mmol/min·cmHg·m^2)				
Anatase	2.35	1.20	0.55	0.25
Rutile	18.0	7.50	3.40	1.33

The values of $k_{CO}\cdot\theta$ and $k_{O_2}\cdot(1-\theta)^2$ calculated from Eqs. (2) and (3) using the values in Tables 3 and 4 are listed in Table 5. The following relation is obtained at 450—600°C for both anatase and rutile during the catalytic oxidation of carbon monoxide using the mixed gas with the composition of $CO/O_2=2/1$:

Table 5. Calculated values of $k_{CO}\cdot\theta$ and $k_{O_2}\cdot(1-\theta)^2$

Temp. (°C)	600	550	500	450
$k_{CO}\cdot\theta\times 10^5$ (CO_2 mmol/min·cmHg·m^2)				
Anatase	7.38	3.90	1.73	0.87
Rutile	29.7	22.0	17.8	13.1
$k_{O_2}\cdot(1-\theta)^2\times 10^5$ ($-O_2$ mmol/min·cmHg·m^2)				
Anatase	6.70	4.00	2.03	0.98
Rutile	29.8	23.0	17.4	13.1

$$k_{CO}\cdot P_{CO}\cdot\theta = 2k_{O_2}\cdot P_{O_2}\cdot(1-\theta)^2 . \quad (4)$$

Above equation shows that the present reaction consists of both the reduction and the oxidation processes of the catalyst by carbon monoxide and oxygen.

The author wishes to express his deep thanks to Professor Takuya Hamamura of Kyoto Technical University and Professor Kumasaburo Kodera of Kyoto University for their kind advices and discussions.

An Adiabatic Calorimeter for Heat Capacity Measurements in the Temperature Range from 80 to 550 K. Heat Capacities of α-Alumina (Sapphire) and Anhydrous Magnesium Acetate

Natsuo Onodera,* Arata Kimoto,** Minoru Sakiyama, and Syûzô Seki
Department of Chemistry, Faculty of Science, Osaka University, Toyonaka, Osaka
(Received September 12, 1970)

An adiabatic calorimeter for the measurements of heat capacities of solid and liquid in the temperature range 80—550 K and the automatic temperature control system are described. The working platinum resistance thermometer is calibrated against a standard thermometer. The measurements of heat capacity of α-Al_2O_3 prove the precision to be $\pm 0.3\%$ and give an accuracy of $\pm 0.6\%$. By means of this calorimeter, heat capacities of anhydrous magnesium acetate have been measured for its glassy and crystalline states around the glass transition point.

Adiabatic calorimetry of the intermittent-heating type[1] determines most accurately heat capacities of solid and liquid below room temperature. If this method is carried out ideally, the adiabatic shield is always maintained at the same temperature as that of the sample container it surrounds so that there is no heat exchange between them. Hence the heat capacity of sample (including the container) is calculated from the electrical energy supplied to the sample and the consequent temperature rise. At elevated temperatures, however, heat transfer due to radiation becomes more significant with temperature rise and this makes it difficult to maintain adiabatic conditions during the measurement. Mainly for this reason, isothermal calorimetry (drop method) has been employed above room temperature. In this method, enthalpies at various temperatures relative to a reference temperature, $H(T)-H(T_0)$, are measured in high precision and heat capacity is calculated by differentiating the enthalpy function. Nevertheless, high temperature adiabatic calorimetry is more suitable for investigations of the anomalous thermal effects taking place in a narrow temperature range such as phase transitions or for the studies on non-equilibrium states, annealing effect, *etc.*

As already mentioned, the problem of heat exchange must be considered for adiabatic calorimetry at high temperatures.[2] Limitation in the choice of construction materials also offers a serious problem. For these reasons, an adiabatic calorimeter has not been used frequently in a high temperature region for heat capacity measurements of substances with poor thermal conductivities, as compared with one used in a low temperature region. However, in recent years, several calorimeters with high accuracy up to 500 K or 1000 K have been reported by West and Ginnings,[3] Trowbridge and Westrum,[4] Karasz and O'Reilly,[5] Grønvold,[6] and Leadbetter,[7] in which great attention was paid to the establishment of adiabaticity and the selection of construction materials. In our laboratory, two kinds of adiabatic calorimeters for low temperatures, from 1 to 20 K and 11 to 300 K, have been constructed[8,9] and studies carried out with them on various solid and liquid samples have been reported. We intended to extend our studies to the more elevated temperature region, since there are many substances indicating interesting thermal behavior above room temperature in view of the changes in state of aggregation or of chemical thermodynamics.

This paper describes an adiabatic calorimeter with an automatic control system which has been used for heat capacity measurements of solids and liquids in the temperature range 80—550 K. Although there was no essential alteration in the structure of this calorimeter in comparison with that[8] for low temperatures, some considerations for high temperature operation were made in the choice of construction materials. Heat capacity measurements of α-Al_2O_3 showed that the precision was within $\pm 0.3\%$ and the accuracy within $\pm 0.6\%$, which were sufficient for our purpose. The apparatus is employed mainly to study phase transitions in polyatomic ionic, ferroelectric, or liquid crystals and thermal behaviors in polymers, amorphous solids, or glasses and also to provide useful chemical thermodynamical data when combined with the measurements with low temperature calorimeters. Heat capacities of anhydrous magnesium acetate have been measured at 300—500 K for the glassy and crystalline states. The glass transition (T_g) of this substance[10] was also studied in detail.

---

* Present address: Japan Information Center of Science and Technology, Nagata-cho, Chiyoda-ku, Tokyo.

** Present address: Musashi Works, Hitachi Ltd., Kodaira, Tokyo.

1) For a detailed review and discussion of adiabatic calorimetry, see "Experimental Thermodynamics," Vol. 1, ed. by J. P. McCullough and D. W. Scott, Butterworths, London (1968).

2) E. D. West, *J. Res. Natl. Bur. Stand.*, **67A**, 331 (1963). Also see Chap. 4 by D. C. Ginnings and E. D. West and Chap. 9 by E. D. West and E. F. Westrum, Jr., in Ref. 1.

3) E. D. West and D. C. Ginnings, *J. Res. Natl. Bur. Stand.*, **60**, 309 (1958).

4) J. C. Trowbridge and E. F. Westrum, Jr., *J. Phys. Chem.*, **67**, 2381 (1963); J. C. Trowbridge, Doctoral Dissertation, Univ. of Michigan (1963).

5) F. E. Karasz and J. M. O'Reilly, *Rev. Sci. Instr.*, **37**, 255 (1966).

6) F. Grønvold, "Thermodynamics," Vol. 1, International Atomic Energy Agency, Vienna (1966).

7) A. J. Leadbetter, *J. Phys. C, Ser.* 2, **1**, 1481 (1968).

8) H. Suga and S. Seki, This Bulletin, **38**, 1000 (1965).

9) M. Sorai, H. Suga, and S. Seki, *ibid.*, **41**, 312 (1968).

10) N. Onodera, H. Suga, and S. Seki, *ibid.*, **41**, 2222 (1968).

Construction of the Calorimeter

The cross sectional view of the calorimeter is shown in Fig. 1. The main body of the calorimeter consists of a sample container A, an adiabatic jacket C which is separated into three parts C_a (side), C_b (top), and C_c (bottom), an upper block D, an outer jacket E, and a vacuum vessel H. The sample container A is suspended by three thin constantan wires from the top portion of the adiabatic jacket. The adiabatic jacket is in turn suspended from the copper upper block D, which serves together with the copper outer jacket E for attenuating the thermal effects from their surroundings and for making favorable adiabatic conditions in the inner system by controlling each heater current.

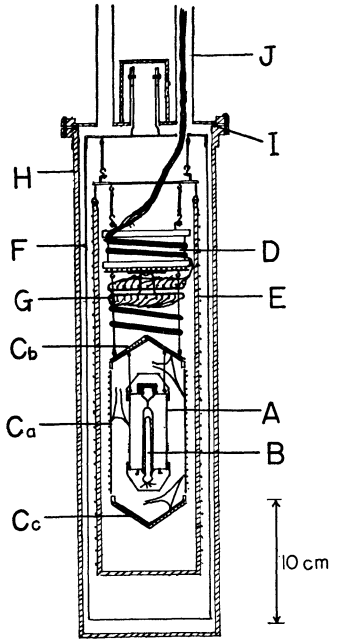

Fig. 1. Cross sectional view of the calorimeter.
A: Sample container B: Thermometer C_a, C_b, and C_c: Adiabatic jackets D: Upper block E: Outer jacket F: Radiation shield G: Terminals H: Vacuum vessel I: Gasket J: Stainless steel pipe

The sample container, whose schematic drawing is shown in Fig. 2, is made of copper, 0.3 mm thick and chromium-plated, with a central reentrant well for setting a combined thermometer-heater. Eight radial fins N silver-soldered to the well and to the inside wall of the container provide good thermal contact of the sample with the container assembly. The size of the main body of the container is 3 cm in diameter and 6 cm long. The total weight of the container is about 70 g and its effective capacity is *ca.* 35 cm^3. A sample entrance at the center of the top of the container is 8 mm in inner diameter. It is crucial to select a suitable seal in order to keep the container gas-tight at all temperatures. A silicone rubber disc-shaped gasket L cut from a sheet 1 mm thick was eventually found to be useful at least up to 550 K. A copper lid is screwed down tightly to the entrance by hand.

The container is equipped with a Leeds & Northrup

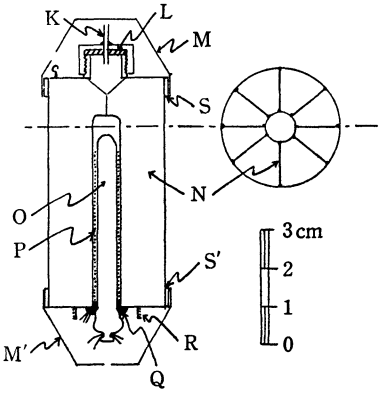

Fig. 2. Cross sectional view of the sample container.
K: Cu tubing L: Gasket M, M': Caps N: Radial fins O: Platinum resistance thermometer P: Heater Q: Beryllia cement R: Spool S, S': Cu bands

capsule type (type 8164) platinum resistance thermometer O, for the temperature measurement of the sample. Around the thermometer, approximately 70 ohms of doubly glass-wound B. & S. #36 constantan wire (Driver-Harris Co.) P is wound non-inductively and as closely as possible, which serves as the calorimeter heater for supplying energy to the sample container. Although the well is machined so as to be well fitted with the combined thermometer-heater, it was necessary to fill the gap with a beryllia cement Q at the entrance portion of the well in order to reduce the temperature gradient in the container assembly. It was confirmed that this device suppressed the temperature distribution to within 0.2 K in the container assembly even in the heating process at 550 K. All the lead wires from the combined thermometer-heater are wound several times around a spool R at the bottom of the container.

Since the outlines of the surface of the top and the bottom of the container are not completely uniform, it is very likely that a significant temperature distribution will arise in these parts particularly during the course of heating. To reduce this, two copper caps M and M' (0.5 mm thick and chromium plated) are closely fitted mechanically to copper bands S and S' soldered to the top and the bottom of the container.

The adiabatic jacket is also of chromium-plated copper and is made as thin as possible (0.5 mm) in order to get quick thermal response. Each part of the jacket, C_a, C_b, and C_c, is equipped with a separate heater: a glass-insulated B. & S. #36 constantan wire wound non-inductively. Adiabatic condition is maintained by adjusting the current in each heater independently. Around C_a are also wound the lead wires from the sample container and those of the thermocouples which detect the temperature differences between A and C_a, C_a and C_b, and C_a and C_c. All the wires are fixed and insulated with silicone varnish or Teflon tapes, aluminum foils being wrapped over them.

Temperature difference between the outer surface of the container and the inner surface of C_a is detected by a six junction (in series) copper-constantan thermocouple. Temperatures of C_b and C_c are also detected differentially against that of C_a by a similar method. The junctions of these thermocouples are insulated with

small, thin pieces of mica, protected with aluminum foils, and inserted tightly into stainless steel bands and pockets set on the sample container and the jacket, respectively. These thermocouples provide an error voltage of about 240 μV per degree of differential at 300 K.

Temperatures of D and E are controlled to an appropriate level lower than that of the adiabatic jacket depending on the operating temperature so that adiabaticity of the interior system may be best maintained.

For measurements in an elevated temperature region (higher than 100°C), another radiation shield F of nickel-plated brass is installed, which remarkably decreases the heat loss due to radiation toward the outside.

All the lead wires employed are Polyflon-coated B. & S. #38 copper wires prepared by immersing the cotton-wound copper wires in Daikin Polyflon dispersion D-1, and then decomposing cotton and sintering the adhered Polyflon at 380°C in a vacuum.[11] All the lead wires are brought to a copper terminal G, wound around the upper block, and then taken out of the calorimeter assembly through one of three stainless pipes J which suspend the assembly, and through a Picein seal. The lead wires are soldered to G by a Kyowa Shôji NEIS 105 silver solder which is composed of silver-cadmium alloy and has a relatively low melting point (*ca.* 380°C).

The interior of the brass vacuum vessel H, which is immersed in a liquid nitrogen or ice temperature Dewar vessel, is kept in high vacuum of 10^{-5} to 10^{-6} Torr by a seal fitted in a rectangular groove (3 mm in width and 1 mm in depth). For the seal a rectangular cross-sectional lead gasket or a neoprene rubber *O*-ring I is found to be suitable in liquid-nitrogen or ice temperatures respectively. It is difficult to attain a vacuum higher than 5×10^{-4} Torr at temperatures higher than 500 K, probably due to some decomposition of silicone varnish used as an insulating adhesive.

Temperature Measurements and Calibration of the Thermometer

Resistance of the platinum resistance thermometer is measured by a Leeds & Northrup type G-2 Mueller Bridge, a Riken high sensitivity galvanometer, and a telescope-scale system in which the distance between the galvanometer and the scale is *ca.* 5 m. This arrangement enables us to measure the temperature to 2×10^{-4} deg in the range 80—550 K.

The working thermometer was calibrated in the conventional manner against a standard thermometer of a similar type calibrated at the National Bureau of Standards (NBS), U.S.A., based on the International Temperature Scale of 1948. The relation between the difference in the resistances of the working and standard thermometers ΔR and the resistance of the standard thermometer R_s can be expressed as follows:

$$\left.\begin{aligned} \Delta R \times 10^5 &= 84.857R_s - 112.5, \\ &\text{for } 4.8 < R_s \leqq 24 \text{ (80—260 K)}, \\ \Delta R \times 10^5 &= 84.857R_s - 112.5 - 0.244(R_s - 24)^2, \\ &\text{for } 24 \leqq R_s < 53 \text{ (260—550 K)}, \end{aligned}\right\} \quad (1)$$

where both R_s and ΔR are in ohm. The accuracy of temperature measurements is estimated to be within ±0.01 deg in absolute value and within ±0.0001 deg in relative value.

Energy Measurements

The circuit for supplying and measuring the electrical energy to the calorimeter heater is nearly the same as the one reported.[8] The calorimeter heater is powered by three 6 V storage batteries in series and the current is adjusted with a six-dial decade resistor (0 to 111, 111.1 ohm). The current and the potential drop across the calorimeter heater are measured in the conventional way with an Otto-Wolff type KDE-3 five-dial potentiometer in conjunction with a Shimadzu galvanometer (type R, class C). Correction is made for the current passing through the by-pass resistors (1 and 100 kΩ) in computing the net current flowing through the calorimeter heater.

To avoid a correction for the small amount of heat generated in the current lead between the sample container and the adiabatic jacket, one of the potential leads terminates just near the container and another just near the jacket, as suggested by Ginnings and West.[12]

The energy input is started and stopped automatically with an electronic timer synchronized with a transistor clock and the heating interval is measured and presented on a digital counter with an accuracy of 0.05% or better.[8]

Adiabatic Control System

Detection of temperature differences for the maintenance of adiabaticity are carried out by use of thermocouples between C_a and A (temperature difference ΔT_1), between C_a and C_b (ΔT_2), between C_a and C_c (ΔT_3), between C_a and D (ΔT_4), and also between C_a and E (ΔT_5). The error signal given as thermal electromotive force of the thermocouples is fed into each servo-circuit, which controls the heater current of each portion of the jacket by on-off control mode.

The error voltage corresponding to ΔT_1 is amplified with an Ohkura AM-1001 microvoltmeter ($\pm10\,\mu$V in full scale) by a factor of 2000 and the output voltage is recorded on an Ohkura electronic recorder, while a cum connected with the pen-drive-motor shaft actuates two micro-switch relays and controls the heater current of C_a. The half-span of the recorder is 1 mV, which corresponds to 2×10^{-3} deg at 300 K. The error voltage due to ΔT_2 is amplified with a Tôa type AD-4 DC amplifier and then with a DC difference amplifier which uses a 12AX7. The output voltage is fed into a grid of 6AQ5. which actuates a microswitch for the control of the heater current for C_b. The error signals due to ΔT_3 and ΔT_5 are transformed into deflection of the mirrors of Shimadzu galvano-

11) Polyflon coated wires were inevitably used, as more favorable glass-wound thin copper wires could not be obtained at the time of construction.

12) D. C. Ginnings and E. D. West, *Rev. Sci. Instr.*, **35**, 965 (1964).

meters (type R, class C). Light beams which have passed through optical choppers are reflected by the mirrors and detected with the photoelectric tubes of electronic photo-relays, which actuate microswitches for the control of heater current. The temperature difference ΔT_4 is detected by an Ohkura type AM-101 microvoltmeter ($\pm 25\ \mu V$ in full scale) and is controlled manually, since the temperature of the upper block little influences the inner system.

Measurements of Heat Capacity

After the specimen was packed into the sample container, a small amount of helium gas, which facilitates attainment to thermal equilibrium in the container, is introduced through a narrow copper tube K. The tube is then pinched off to keep it gas-tight.

The temperature of the sample is measured at approximately one minute intervals for about ten minutes after adiabaticity and internal equilibrium are nearly established. Temperature drift was found to be within 3×10^{-4} deg·min^{-1} below room temperature, but gradually increases with temperature rise ultimately to 3×10^{-3} deg·min^{-1} at 550 K.

The electric power produced in the calorimeter heater is obtained by measuring the heater current at 0.21 τ and 0.79 τ and the voltage at 0.50 τ according to the Giauque method,[13] where τ is the heating interval (usually 1000 sec in our experiments). The energy supply is adjusted so that the temperature elevation in this heating period can be 4—6 deg in the empty case and 2.5—4 deg in the loaded one. For these heating rates, internal equilibrium in the sample container is attained within 5 min after heating was stopped.

When the automatic adiabatic control works normally, the temperature difference ΔT_1 is kept, in the equilibration period within $\pm7\times10^{-4}$ deg below room temperature and within $\pm3\times10^{-3}$ deg at 550 K, and in the heating period within $\pm4\times10^{-3}$ deg and within $\pm1\times10^{-2}$ deg, respectively. The ΔT_2 and ΔT_3 are controlled at least within 0.15 deg even in the heating period at 550 K.

Calibration of the Calorimeter

The reliability of the present calorimeter was examined by the measurements of heat capacity of the Calorimetry Conference standard sample of α-Al_2O_3 (synthetic sapphire).[14] Approximately 70 g of this sample was used for calibration. The heat capacity of the sample corresponds to about 70% of the total heat capacity above room temperature (including the container), while only about 30% at the lowest temperature employed.

The heat capacity of the sample was given by subtracting the smoothed heat capacity data of the empty cell (r.m.s.: 0.21%) from the total heat capacity. In Table 1 are tabulated the observed and smoothed molar heat capacities of α-Al_2O_3. As shown in Fig. 3 most of the observed points fall within $\pm0.3\%$ in relative deviation from the smoothed curve. The r.m.s. deviation is 0.25%. The difference of our smoothed values from those of Furukawa *et al.*[15] falls almost within $\pm0.6\%$ from 80 to 550 K. This agreement is sufficient for our present purpose.

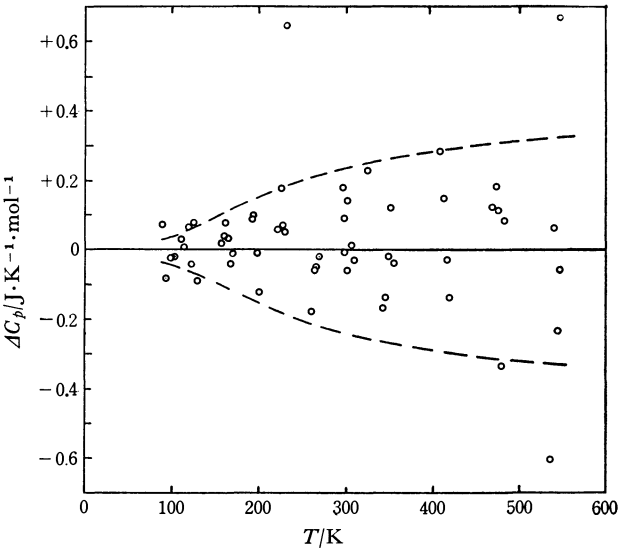

Fig. 3. Deviations of experimental heat capacities ΔC_p of α-Al_2O_3 from a smooth curve. Dashed curves show $\pm0.3\%$ of C_p.

Analysis of Errors

In order to account for the scattering of the experimental points as well as the possible occurrence of some systematic errors, the order of magnitude of errors due to the following instrumental and operational sources was estimated.

(1) Temperature Measurements. Errors in reading the resistance values do not exceed 0.5×10^{-3} deg in terms of temperature even at elevated temperatures where increase in the resistance with temperature reduces the sensitivity of the galvanometer. Therefore, this error source is not of primary importance. However, arbitrariness in drawing the drift straight line to the midpoint of the heating period, on a resistance *vs.* time curve, permits $\pm0.15\%$ error at the highest temperature.

(2) Energy Measurements. Total contribution to the error from instruments such as the potentiometer, the timer, and the standard resistances is estimated to be within $\pm0.05\%$.

(3) Heat Transfer due to Non-adiabaticity. Erroneous heat transfer may arise from or to the sample container owing to the transient non-adiabaticity which reveals itself as the error voltage of the thermocouples. This is significant just after the beginning and the end of the heat supply. This error can be estimated by evaluating various heat transfer coefficients between the container and the adiabatic jacket, which are subdivided as follows.

13) W. F. Giauque and C. J. Egan, *J. Chem. Phys.*, **5**, 45 (1937).

14) This sample was synthesized by the NBS and obtained through their courtesy.

Table 1. Experimental and smoothed values of the molar heat capacity of the calorimetry conference standard sample of α-Al_2O_3 (Sapphire)

T (K)	C_p (exptl) ($J \cdot K^{-1} \cdot mol^{-1}$)	C_p (smoothed) ($J \cdot K^{-1} \cdot mol^{-1}$)	T (K)	C_p (exptl) ($J \cdot K^{-1} \cdot mol^{-1}$)	C_p (smoothed) ($J \cdot K^{-1} \cdot mol^{-1}$)
89.43	9.770	9.696	269.29	72.53	72.55
94.31	11.035	11.119	295.00	78.85	78.67
98.86	12.523	12.547	298.20	79.44	79.35
103.12	13.942	13.963	298.49	79.40	79.41
111.33	16.899	16.868	301.88	80.27	80.13
115.07	18.265	18.257	301.95	80.08	80.14
118.64	19.682	19.617	305.53	80.89	80.88
122.08	20.92	20.96	309.15	81.58	81.61
125.38	22.35	22.27	324.64	84.79	84.56
128.57	23.46	23.55	341.81	86.96	87.13
157.34	35.02	35.00	345.19	87.52	87.66
160.08	36.13	36.09	348.55	88.17	88.19
162.76	37.22	37.14	351.88	88.83	88.71
165.39	38.20	38.17	355.20	89.18	89.22
167.97	39.18	39.22	408.21	96.93	96.65
170.50	40.20	40.21	411.96	97.28	97.13
192.72	48.70	48.61	415.69	97.56	97.59
195.42	49.75	49.65	419.41	97.91	98.05
198.08	50.59	50.60	469.44	103.67	103.55
200.69	51.38	51.50	472.26	104.01	103.83
221.60	58.64	58.58	475.07	104.21	104.10
224.59	59.74	59.56	477.86	104.02	104.36
227.54	60.60	60.53	480.63	104.70	104.62
230.46	61.53	61.48	534.99	108.33	108.94
233.33	63.05	62.40	538.97	109.26	109.20
259.23	69.73	69.91	542.94	109.21	109.45
262.62	70.74	70.80	546.85	109.63	109.69
265.97	71.61	71.66	550.77	110.60	109.93

a) Heat Transfer by Lead-Wire Conduction: This includes the conduction through the lead wires of the combined thermometer-heater, the thermocouples brought to the container, and the constantan wires suspending the container. These are found to contribute below 2×10^{-3} W·deg^{-1} to heat transfer coefficient.

b) Heat Transfer by Gas Conduction: Thermal conductivity of gas is independent of the pressure if the mean free path of the gas λ is much smaller than the size of space in consideration L, and is proportional to the pressure if $\lambda \gg L$, where L is $\sim$1 cm in the present case. Below 500 K, the latter condition holds so sufficiently that heat transfer coefficient is easily evaluated to give approximately 1×10^{-5} W·deg^{-1}. Above 500 K, however, estimation becomes very difficult because λ gets nearer to L owing to the deterioration of vacuum. However, this value probably does not exceed 5×10^{-3} W·deg^{-1}.

c) Heat Transfer by Radiation: This effect becomes rapidly important with increase in temperature. Although the geometrical shape in the present apparatus is rather complicated, the standard equation for the radiative heat transfer[2] is sufficient for rough calculation. If we assume 0.1 both for the emissivities of two parallel planes with small temperature difference (the value is overestimated for polished metal surfaces), heat transfer coefficient by radiation amounts to 3×10^{-3} W·deg^{-1} at 300 K and 15×10^{-3} at 500 K.

Thus, the summation of all these effects give 5×10^{-3} W·deg^{-1} at 300 K and 2×10^{-2} W·deg^{-1} at 500 K. These values explain that under ordinary experimental conditions errors in measured heat capacity caused by transient non-adiabaticity may become $\pm 0.05\%$ at 300 K and $\pm 0.25\%$ at 500 K in maximum estimate. At higher temperatures, therefore, considerable part of the actual errors can be attributed to this source. In practice, fluctuation in the observed heat capacity is not so strongly dependent on temperature as expected from the preceding estimate (see Fig. 3). This may be due to the overestimate of the values for emmissivity.

(4) Heat Transfer due to Thermal Inhomogeneities. Important systematic errors arise frequently from the thermal inhomogeneities on the outer surface of the container or the inner surface of the adiabatic jacket. In the most probable case, heat exchange is caused by generation of temperature distribution on the surface of the container during the heating period. The greater part of this error is compensated if the temperature gradients in the empty and the loaded measurements are alike. Generally, however, the dif-

ference in thermal conductivity, heat capacity, and density in the container between the two cases prevents this situation.[2)]

This error is so difficult to estimate that great care must be taken about the design of the container to avoid the generation of the surface temperature gradient. We confirmed experimentally that the beryllia cement as a thermal conducting adhesive between the body of the container and the combined thermometer-heater as well as the two caps on the top and the bottom parts of the container served this purpose. Indeed, an agreement of our data with those of Furukawa *et al.*[15)] and also with those of other workers[3-7)] is regarded as an evidence showing that the sources of systematic error are sufficiently eliminated in the construction of the present apparatus.

Heat Capacities of Anhydrous Magnesium Acetate

Anhydrous magnesium acetate was prepared by dehydration of magnesium acetate tetrahydrate in a vacuum (10^{-3} Torr) at *ca.* 50°C for 7 days. Further dehydration was carried out in the sample container in a high vacuum (10^{-5} Torr) at 310 K for 20 hr. The dehydrated salt has been found to be in the glassy state.[10)] Heat capacities of the glassy sample are given in Table 2 and Fig. 4. The glass transition temperature is found to be located at *ca.* 470 K. The glassy sample crystallizes abruptly when it is heated above 475 K. The heat capacities of the crystalline sample thus formed are also given in Table 2 and Fig. 4. From the temperature drift curves during the measurements and the temperature elevation due to crystallization, the heat of crystallization was estimated to be *ca.* 11.4 kJ mol.$^{-1}$

Table 2. Heat capacity of glassy and crystalline magnesium acetate (MW = 142.397)

T (K)	C_p ($J \cdot K^{-1} \cdot mol^{-1}$)	T (K)	C_p ($J \cdot K^{-1} \cdot mol^{-1}$)
Glassy		463.29	30.349
310.02	20.452	466.56	34.065
315.42	20.671	469.22	36.691
320.78	20.887	471.23	38.533
326.06	21.109	473.47	39.194
331.32	21.235		
336.54	21.457	Crystalline	
341.71	21.641	348.14	21.613
346.83	21.813	354.39	21.909
366.21	22.578	361.35	22.226
371.25	22.700	368.99	22.591
376.25	22.981	376.56	22.858
381.37	23.223	383.92	23.110
386.83	23.359	391.28	23.429
392.23	23.681	398.56	23.746
397.60	23.923	405.75	24.089
402.92	24.007	417.35	24.485
409.12	24.384	424.33	24.773
415.18	24.732	431.24	25.027
421.22	24.963	444.20	25.612
427.27	25.219	450.87	26.097
433.36	25.379	457.46	26.114
439.70	25.974	464.84	26.359
445.55	26.139	472.31	26.685
451.39	27.082	479.72	26.834
452.04	26.633	487.00	27.213
456.54	26.995	494.19	27.421
459.94	28.158	501.28	27.823

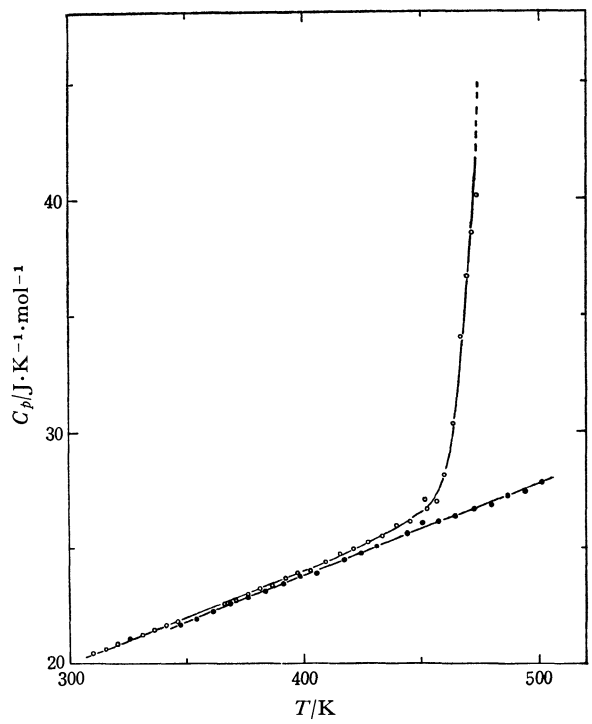

Fig. 4. Molar heat capacities of anhydrous magnesium acetate.
○: glassy state ●: crystalline state

Summary

An adiabatic calorimeter for the heat capacity measurements of solid or liquid sample in the temperature range 80—550 K was constructed with the main purpose of investigating various interesting thermal behaviors of substances demonstrated above room temperature. Most of the temperature control systems to keep an adiabatic condition are semi-automatic and thus need only one operator. The working platinum resistance thermometer was calibrated against a standard one calibrated by the NBS. The reliability of this apparatus was demonstrated through the measurements of heat capacity of the Calorimetry Conference sample of α-Al_2O_3. The results show that the relative errors in heat capacity values are almost within ±0.3% and the smoothed curve values agree with those of Furukawa *et al.* almost within ±0.6% over the whole temperature range available. The non-systematic errors are to some extent explainable in terms of the order of magnitude estimation based on the experiments. Heat capacities of amorphous and crystalline magnesium acetate were measured at 300—500 K. Glass transition phenomenon was observed at *ca.* 470 K. Heat of crystallization was also estimated to be 11.4 kJ·mol^{-1}.

15) G. T. Furukawa, T. B. Douglas, R. E. McCoskey, and D. C. Ginnings, *J. Res. Natl. Bur. Stand.*, **57**, 67 (1956); D. C. Ginnings and G. T. Furukawa, *J. Amer. Chem. Soc.* **75**, 522 (1953).

The Dichroic Spectra of Hydroxy Derivatives of Naphthalene, Anthracene, and Phenanthrene in Polyvinylalcohol Sheets[1]

Hiroyasu INOUE, Takio NAKAMURA,* and Tetsutaro IGARASHI

Department of Applied Chemistry, Faculty of Technology, Kanagawa University, Kanagawa-ku, Yokohama

(Received October 1, 1970)

The dichroic spectra of 1,4-dihydroxynaphthalene, 9-hydroxyanthracene, sodium 9,10-dihydroxyanthracene-2-sulfonate, and 9,10-dihydroxyphenanthrene, which were usually unstable in a liquid solution, were measured in stretched polyvinylalcohol sheets. From a comparison of the results of the dichroic spectra with those of the MO calculations, the polarizations of the electronic bands were determined, and the bands were assigned in terms of the relevant bands of the corresponding unsubstituted aromatic compounds.

The electronic spectra of some hydroxy derivatives of naphthalene and of anthracene have been investigated theoretically and experimentally.[2-4] There have, however, been few reports on the electronic spectra of 1,4-dihydroxynaphthalene, 9-hydroxyanthracene, and 9,10-dihydroxyanthracene. This is also the case for 9,10-dihydroxyphenanthrene. The reason for such a situation is probably that these compounds are very unstable in a liquid solution and it is difficult to determine their absorption spectra by the usual procedure.

It has been well known that these unstable hydroxy aromatic compounds are temporarily formed when 1,4-naphthoquinone, anthrone, anthraquinone, and 9,10-phenanthrenequinone are irradiated by ultraviolet light in solutions. In these cases, the products are very sensitive to oxidation by dissolved oxygen in solution and, hence, change immediately to the original compounds. We have found, however, that the above-mentioned hydroxy aromatic compounds are fairly stable in polyvinylalcohol (PVA) sheets when they are produced in the sheets by photochemical reactions.[5]

Accordingly, in the present paper, the electronic spectra of these compounds will be presented and the assignment of the near-ultraviolet absorption bands will be confirmed by analyses of the dichroic spectra and by theoretical calculations.

Experimental

Materials. All the materials used here were obtained commercially. 1,4-Naphthoquinone and 9,10-phenanthrenequinone were purified by repeated recrystallizations from ethanol. Sodium anthraquinone-2-sulfonate was used in place of anthraquinone, because the latter has poor permeability into PVA sheets. Sodium anthraquinone-2-sulfonate was purified by repeated recrystallizations from an aqueous solution. Anthrone was purified by zone melting using a Shimadzu Zone Refiner CZ-1. The PVA powder used for the preparation of the sheets was used without further purification, and its mean degree of polymerization was 1500.

Preparation of Sample Sheets. To obtain the sample sheets, dried PVA sheets (0.2 mm thick) containing quinones or anthrone in a concentration of 10^{-2}—10^{-3} M were irradiated using a low-pressure mercury lamp as a light source. The quinones and anthrone were completely converted to hydroxy aromatic compounds after a few minutes' photoirradiation. For the measurement of the dichroic spectra, the PVA sheets were stretched prior to the photoirradiation.

Dichroic Spectra. The measurement and analysis of the dichroic spectra were carried out following the method developed by Tanizaki.[6] The spectra were measured with a Shimadzu Spectrophotometer QV-50 equipped with a Glan-Thomson-type calcite polarizer. The notations used in the figures of the dichroic spectra were as follows[4]:

$D_{\parallel}$ and $D_{\perp}$: Absorbances measured for incident light polarized, respectively, parallel and perpendicular to the stretched direction of a PVA sheet.

R_d: Ratio between $D_{\parallel}$ and $D_{\perp}$, $D_{\parallel}/D_{\perp}$.

R_s: Degree of stretching of a sheet.

θ: Orientation angle for the moment of the absorption band. From this, the angle between the transition moments of different bands can be obtained.

MO Calculations

We have used the semi-empirical ASMO SCF CI method, including a variable β approximation.[7] One-center repulsion integrals were evaluated by the Pariser-Parr approximation,[8] in which the ionization potentials and the electron affinities were taken as 11.42 and 0.58 eV respectively for the carbon atom, and as 33.00 and 11.47 eV for the oxygen atom. The two-center repulsion integrals were evaluated by means of the Mataga-Nishimoto equation.[9] All singly-excited configurations associated with the transitions between each of the five highest occupied levels and each of the five lowest vacant levels were included in the CI calculation.

Results and Discussion

1,4-Dihydroxynaphthalene. 1,4-Dihydroxynaphthalene was obtained from 1,4-naphthoquinone by

1) Presented in part at the 23rd Annual Meeting of the Chemical Society of Japan, Tokyo, April, 1970.

* Present address: Shinsei Teppan Co., Ltd., Edogawa-ku, Tokyo.

2) K. Nishimoto and R. Fujishiro, This Bulletin, **37**, 1660 (1964).

3) H. Baba and S. Suzuki, *ibid.*, **35**, 683 (1962).

4) Y. Tanizaki and S. Kubodera, *J. Mol. Spectry.*, **24**, 1 (1967).

5) The products are almost unchanged as long as the PVA sheets are kept dry.

6) Y. Tanizaki and N. Ando, *Nippon Kagaku Zasshi*, **78**, 542 (1957); Y. Tanizaki, This Bulletin, **32**, 75 (1959); Y. Tanizaki, T. Kobayashi, and N. Ando, *ibid.*, **32**, 1362 (1959); Y. Tanizaki, *ibid.*, **38**, 1798 (1965).

7) K. Nishimoto and L. S. Forster, *Theoret. Chim. Acta*, **3**, 407 (1965); **4**, 155 (1966).

8) R. Pariser and R.G. Parr, *J. Chem. Phys.*, **21**, 767 (1953).

9) N. Mataga and K. Nishimoto, *Z. Physik. Chem., Neue Folge*, **13**, 140 (1957).

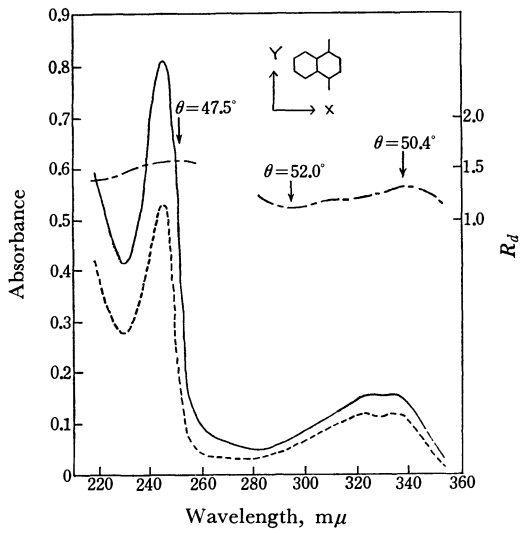

Fig. 1. Dichroic spectra of 1,4-dihydroxynaphthalene. R_s=10, ——: $D_{\parallel}$, ----: $D_{\perp}$, ——·——: $R_d(=D_{\parallel}/D_{\perp})$

photoirradiation in a PVA sheet. The dichroic spectra are shown in Fig. 1. The features of the absorption curve were similar to that measured previously by Spruit.[10]

The intense band at 246 mμ has the highest R_d value; hence, the transition moment of this band is considered to be inclined to the stretched direction of the sheet (hereafter, such a band will be denoted as "a ∥ band", and the band whose transition moment is perpendicular to the ∥ band will be denoted as "a ⊥ band"). The R_d values in the region of 280—360 mμ were relatively small and varied to some extent, having a maximum and a minimum. From this behavior of the R_d curve, it may be deduced that there are two bands closely overlapping in this wavelength region. The tendency of the R_d value to increase with an increase in the wavelength indicates that the longer-wavelength one of the overlapped bands is a ∥ band, while the shorter-wavelength one is a ⊥ band.

According to the consideration of the symmetry of this molecule, an isolated band should be polarized along the *X*- or *Y*-axis of the molecule, so the sum of the orientation angles of two differently polarized bands can be expected to give a right angle if the bands are not overlapped with other bands. However, the observed orientation angles of the ∥ band at 246 mμ and of the ⊥ band at around 300 mμ were 47.5° and 52.0° respectively, and their sum (99.5°) was too large for the orthogonality of the direction of polarizations. This non-orthogonality is attributable to the large value of the apparent orientation angle of the 246 mμ band. A weak ⊥ band can, therefore, be predicted to be hidden under the 246 mμ band. However, the presence of this ⊥ band is not detected from the absorption curve.

Next, let us compare the experimental results described above with the calculated electronic transitions. The results of the calculations are presented in Table 1. The observed 246 mμ (∥) band can be

10) C. J. T. Spruit, *Rec. Trav. Chim.*, **68**, 309 (1949).

Table 1. The result of the MO calculation on the electronic transition of 1,4-dihydroxynaphthalene

	Transition energy, eV (mμ)[a]	Polarization[b]	Oscillator strength
I	3.53 (351)	X	0.1007
II	3.61 (344)	Y	0.2013
III	4.83 (257)	X	0.5051
IV	5.04 (246)	Y	0.1324
V	5.44 (228)	Y	0.0148
VI	5.49 (226)	X	0.8593

a) Only the transitions appeared above 220 mμ were listed.
b) The molecular axes were shown in Fig. 1.

safely said to correspond to the III transition (X-polarized). Hence, the ∥ and ⊥ band in the dichroic spectra can be said to be polarized along the *X*- and *Y*-axes of the molecule respectively. Therefore, the ∥ and the ⊥ bands observed in the long wavelength region are due to the I (X) and II (Y) transitions respectively. The ⊥ band hidden under the 246mμ band may correspond to the IV transition (Y).

By the use of Platt's notation, we can assign the observed bands as follows. The 246 mμ band is the ^1B_b band, and the ∥ band and the ⊥ band appearing in the region of 280—360 mμ are the ^1L_b and the ^1L_a bands respectively. Consequently, the order of the positions of the bands for 1,4-dihydroxynaphthalene (the ^1B_b, ^1L_a, and ^1L_b bands as the wavelengths increase) is same as those for the other hydroxynaphthalenes studied by Tanizaki and Kubodera.[4] However, the ^1B_b and the ^1L_a bands of 1,4-dihydroxynaphthalene appeared at longer wavelengths than the corresponding bands of the other α-hydroxynaphthalenes (1-, 1,5-1,8-derivatives),[4] and it was remarkable that the fine structure disappeared in the ^1L_a and the ^1L_b bands of 1,4-dihydroxynaphthalene.

9-Hydroxyanthracene. 9-Hydroxyanthracene was obtained from anthrone by photoinduced tautomeriza-

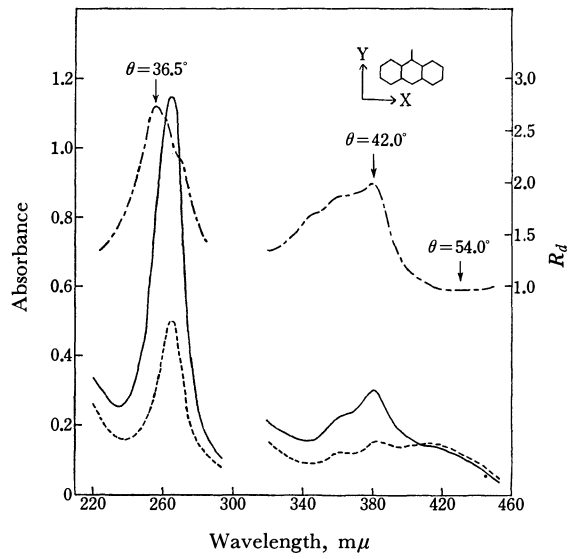

Fig. 2. Dichroic spectra of 9-hydroxyanthracene. R_s=9.8, ——: $D_{\parallel}$, ----: $D_{\perp}$, ——·——: $R_d(=D_{\parallel}/D_{\perp})$

tion.[11] Its absorption spectrum in a PVA sheet closely resembles that measured by Baba and Takemura[12] with a rapid-scan spectrophotometer in the region above 320 mμ. The dichroic spectra of 9-hydroxyanthracene are shown in Fig. 2. It may be seen in the figure that the intense 266 mμ band has a large R_d value, so it is a ∥ band. On the other hand, the relatively weak bands with three peaks appearing in the region of 340—460 mμ have medium and small R_d values, so it is clear that there are two bands in this region; the longer-wavelength one is a ⊥ band, and the shorter-wavelength one is a ∥ band. Since the sum of the orientation angles of this ⊥ band at 420 mμ and the ∥ band at 266 mμ is 90.5°, the orthogonality of the transition moments between these bands is almost satisfied. Thus, the absorption band in the region above 410 mμ consists of the pure ⊥ band. On the other hand, the band in the region of 340—410 mμ consists of this ⊥ band and a ∥ band, because the R_d values in this wavelength region are too small in comparison with that of the 266 mμ band to be that of a pure ∥ band.

Consequently, it was found that 9-hydroxyanthracene showed three absorption bands above 220 mμ; these bands may be interpreted as those of anthracene shifted to red by hydroxy groups. Concerning the electronic transitions of anthracene, the polarizations of the bands have already been investigated by Zimmermann and Joop,[13] and Craig and Hobbins.[14] According to their results, the intense 250 mμ band is polarized to the long axis of the molecule (X-axis) and assigned to the ^1B_b band, while the relatively weak band at longer wavelength is polarized to the short axis (Y-axis) and assigned to the ^1L_a band. The ^1L_b band of anthracene was not appreciably observed, but this band is considered to be hidden under the ^1L_a band. The absorption bands of 9-hydroxyanthracene can easily be interpreted on the basis of this assignment. At first, the 266 mμ band (∥) can be said to correspond to the ^1B_b band of anthracene (X-axis); consequently, the polarization of a ∥ band is determined to be along the long axis of the molecule (X-axis). Therefore, the ⊥ band in the region of 340—460 mμ is polarized to the short axis of the molecule (Y-axis); hence, this band can be said to correspond to the ^1L_a band of anthracene. Furthermore. it is apparent that the X-polarized ^1L_b band is present in the region of 340—410 mμ.

These experimental results are compared with the results of the MO calculations in Table 2. The V transition (265 mμ) can be said to correspond unequivocally to the observed 266 mμ band. There are four transitions (I—IV) in the longer wavelength region of the V transition; however, two of them correspond to the observed ^1L_a and ^1L_b bands. From a consideration of the position, the polarization, and the oscillator strength, the I and II transitions may be said to correspond to the ^1L_a and the ^1L_b bands respectively.

Table 2. The result of the MO calculation on the electronic transition of 9-hydroxyanthracene

	Transition energy, eV (mμ)[a]	Polarization[b]	Oscillator strength
I	3.22 (385)	Y	0.2900
II	3.38 (367)	X	0.0520
III	4.08 (304)	X	0.0221
IV	4.65 (267)	Y	0.0002
V	4.67 (265)	X	2.0347
VI	4.75 (261)	X	0.2683
VII	5.05 (246)	Y	0.0106
VIII	5.32 (233)	Y	0.0045

a) Only the transitions appeared above 220 mμ were listed.
b) The molecular axes were shown in Fig. 2.

Sodium 9,10-Dihydroxyanthracene-2-sulfonate. This was obtained from sodium anthraquinone-2-sulfonate by a photochemical reduction.[15,16] Since a sodium sulfonate group has only a slight influence on the electronic spectrum of an aromatic compound, the observed dichroic spectra shown in Fig. 3 may be regarded as those of 9,10-dihydroxyanthracene. The patterns of the absorption curve and of the R_d curve were very similar to those of 9-hydroxyanthracene; hence, each band can be assigned like that of 9-hydroxyanthracene. That is, the intense band at 272 mμ is the ^1B_b band and is polarized along the X-axis, and the longer- and the shorter-wavelength parts of the relatively weak band in the region of 340—460 mμ are determined to be the ^1L_a and the ^1L_b bands respectively.

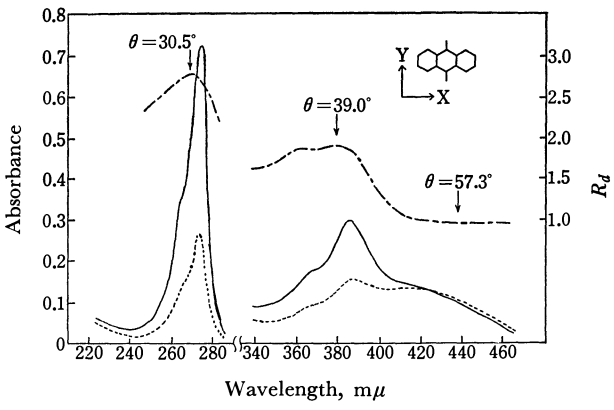

Fig. 3. Dichroic spectra of sodium 9,10-dihydroxyanthracene-2-sulfonate.
R_s=4.5, ——: $D_{\parallel}$, ----: $D_{\perp}$, —·—: $R_d(=D_{\parallel}/D_{\perp})$

The results of the MO calculations for 9,10-dihydroxyanthracene are shown in Table 3. The observed ^1L_a, ^1L_b, and ^1B_b bands can be said to correspond to the I, II, and V transitions respectively.

9,10-Dihydroxyphenanthrene. This was obtained from 9,10-phenanthrenequinone by photochemical

11) N. Kanamura and S. Nagakura, *J. Amer. Chem. Soc.*, **90**, 6905 (1968).
12) H. Baba and T. Takemura, *Tetrahedron*, **24**, 4779 (1968); T. Takemura and H. Baba, *ibid.*, **24**, 5311 (1968).
13) H. Zimmermann and N. Joop, *Z. Elektrochem.*, **66**, 342 (1962).
14) D. P. Craig and P. C. Hobbins, *J. Chem. Soc.*, **1955**, 539.
15) C. L. Wells, *Trans. Faraday Soc.*, **57**, 1703 (1961).
16) J. L. Bolland and H. R. Cooper, *Proc. Roy. Soc.*, **A225**, 405 (1954).

Table 3. The result of the MO calculation on the electronic transition of 9,10-dihydroxyanthracene

	Transition energy, eV (mμ)[a]	Polarization[b]	Oscillator strength
I	2.96 (419)	Y	0.2820
II	3.22 (385)	X	0.1831
III	3.63 (342)	forbidden	
IV	4.58 (271)	forbidden	
V	4.61 (269)	X	1.8888
VI	4.87 (255)	Y	0.0760
VII	4.93 (251)	forbidden	
VIII	5.23 (237)	Y	0.0018
IX	5.37 (231)	forbidden	
X	5.63 (220)	X	0.3625

a) Only the transitions appeared above 220 mμ were listed.
b) The molecular axes were shown in Fig. 3.

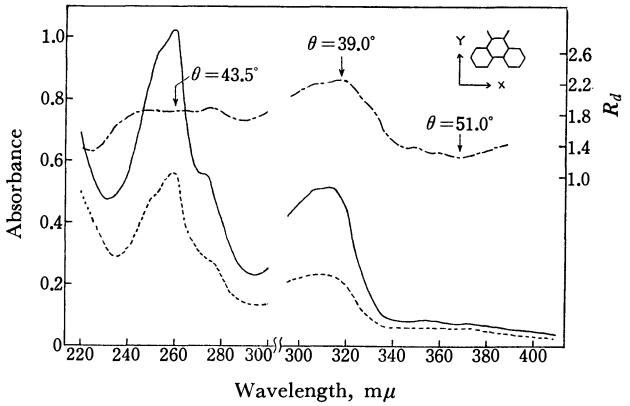

Fig. 4. Dichroic spectra of 9,10-dihydroxyphenanthrene. R_s=9.0, ——: $D_{\parallel}$, ----: $D_{\perp}$, —·—: $R_d(=D_{\parallel}/D_{\perp})$

reduction.[17] The dichroic spectra are shown in Fig. 4. From the behavior of the R_d curve, it can be deduced that the bands at 260 mμ and at 314 mμ are polarized in the same direction (∥ bands). However, the R_d values of the 260 mμ band are somewhat smaller than those of the 314 mμ band. This suggests the presence of a ⊥ band near the 260 mμ band.

A very weak band appears above 340 mμ. The polarization of this band is perpendicular to the transition moment of the 314 mμ band, because the sum of the orientation angles of these band makes a right angle; that is, this weak band is a ⊥ band.

These experimental results are compared with the theoretical results in Table 4. The most intense ∥ band, at 260 mμ, undoubtedly corresponds to the calculated transition VI, which is polarized along the X-axis of the molecule and which has the largest oscillator strength in the region above 220 mμ. Therefore, the ∥ bands may be considered to be polarized to the X-axis. Although there is no transition around

17) P. C. Carapellucci, H. P. Wolf, and K. Weiss, *J. Amer. Chem. Soc.*, **91**, 4635 (1969).

Table 4. The result of the MO calculation on the electronic transition of 9,10-dihydroxyphenanthrene

	Transition energy, eV (mμ)[a]	Polarization[b]	Oscillator strength
I	3.32 (374)	Y	0.0459
II	3.58 (346)	X	0.4001
III	4.35 (285)	Y	0.0676
IV	4.44 (280)	X	0.0160
V	4.64 (267)	Y	0.4000
VI	4.78 (259)	X	1.1400
VII	5.11 (243)	X	0.0452
VIII	5.42 (229)	Y	0.0823
IX	5.59 (222)	X	0.4076

a) Only the transitions appeared above 220 mμ were listed.
b) The molecular axes were shown in Fig. 4.

314 mμ in the present calculation, the II transition presumably corresponds to the observed 314 mμ band, judging from the direction of the polarization and the oscillator strength. Between the II and VI transition, there are two Y-polarized transitions, III (f= 0.0676) and V (f=0.400), at 285 mμ and 267 mμ. The lower R_d values of the 260 mμ band as compared with those of the 314 mμ band are ascribable to the presence of the Y-polarized bands corresponding to the III and V transitions. However, it can not be decided in the present study whether the shoulder at about 275 mμ corresponds to the V transition or whether it is the vibrational structure of the 260 mμ band. The ⊥ band appearing above 340 mμ may be considered to be due to the I transition, judging from its position, its intensity, and its polarization.

The results obtained above were compared with those on the absorption bands of phenanthrene. The electronic spectrum of phenanthrene has been studied in detail.[18–20] The two bands at 258 mμ and at 300 mμ have been found to be polarized along the X-axis and have been assigned to the ^1B_b and the ^1L_a bands respectively. Thus, the 260 mμ and the 314 mμ bands of 9,10-dihydroxyphenanthrene may be considered to be the ^1B_b and the ^1L_a bands respectively. The very weak band of phenanthrene around 330 mμ ($\log \varepsilon$= 2.2) may be interpreted as being due to the symmetry-forbidden ^1L_b transition. In the case of 9,10-dihydroxyphenanthrene, the ⊥ band appearing above 340 mμ (the I transition) may correspond to the ^1L_b band of phenanthrene. In contrast to the case of phenanthrene, the I transition of 9,10-dihydroxyphenanthrene is symmetry-allowed, f=0.0459.

The authors wish to thank Dr. T. Hoshi of Aoyama Gakuin University for his help in the MO calculations.

18) D. S. McClure, *J. Chem. Phys.*, **22**, 1256 (1954); **25**, 481 (1956).
19) H. Zimmermann and N. Joop, *Z. Elektrochem.*, **65**, 66 (1961).
20) T. Azumi and S. P. McGlynn, *J. Chem. Phys.*, **37**, 2413 (1962).

Studies on Intermolecular Complex Formation. I. Between Nucleotide Bases and Organic Compounds

Chihiro TAMURA, Noriko SAKURAI, and Sadao SATO

The Central Research Laboratories of Sankyo Co., Ltd., Hiromachi, Shinagawa-ku, Tokyo

(Received October 30, 1970)

The present investigation was focussed on a survey of the chemical compounds which are capable of binding with nucleotide bases. X-Ray powder patterns show that adenine and cytosine have a strong tendency to interact with many organic compounds having a carboxyl group and cyclic alternant CONH groups. A few compounds bind with thymine and uracil.

In view of the structure and function of DNA, many single crystal analyses of the complexes between the nucleotide bases have been analyzed.[1-7] Several types of base-pairing were found, and in these complexes the principal binding force is due to complementary hydrogen bonds. We had expected that complexes exist not only between the nucleotide bases themselves but also between nucleotide bases and other organic compounds having some characteristic structure. By infrared spectrum, Kyogoku *et al.* studied some biologically active compounds which interact with nucleotide bases in solution.[8]

The X-ray powder method was applied in surveying these compounds with respect to their ability to form complexes with nucleotide bases. A large number of combinations was found to give rise to a change in diffraction patterns which might indicate the formation of complex. Some of them were obtained in the form of single crystal and we succeeded in determining their crystal structures.[9,10] New types of intermolecular hydrogen bonding were found, the details of which will be published elsewhere. In the present paper we will describe the results of the survey and discuss the structural characteristics of the molecules which can form the complexes.

Experimental

The experimental procedure was as follows: equivalent moles (*ca.* 100 mg) of organic substance and the base were added to 70% aqueous ethanol (*ca.* 15 cc). The mixture was warmed on a water-bath until dissolution was complete and then allowed to stand for several days in a refrigerator. A glass holder with a depth of 0.2 mm was filled with crystalline material thus obtained, and X-ray diffractions were recorded up to $2\sin\theta=50°$ with a Rigakudenki model D6C diffractometer. Spacings of diffraction peaks are listed in Table 4, the height of the maximum peaks being normalized to one hundred.

The formation of new crystalline species was verified by comparing their diffraction patterns with those of components. An example of such comparison is shown in Fig. 1. All component samples were recrystallized by use of the same solvent in order to avoid an erroneous conclusion due to polymorphism of the components. The mass and infrared spectra of such crystals were sometimes useful in confirming the formation of new complexes. The stability of each crystal was examined by taking diffraction patterns of the same sample at intervals of several hours. Any changes in these patterns indicate that the substance is unstable at room temperature and humidity. Subsequently such samples were kept during measurements at a low temperature and at the same humidity as that in the refrigerator.

Some of the complexes showed only a small number of new peak superimposed over those of the diffraction patterns of the components. In such cases, the diffraction patterns were recorded repeatedly more than three times to confirm their reproducibility.

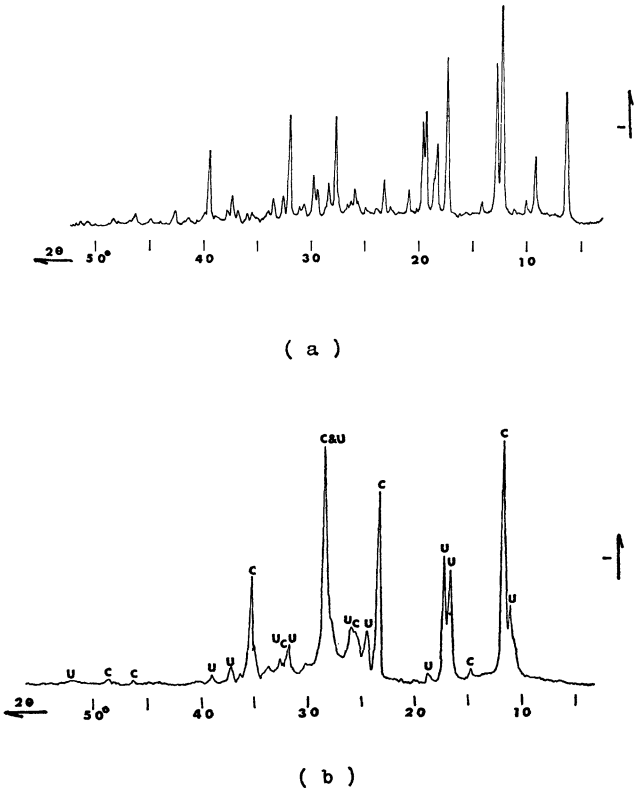

Fig. 1. X-ray powder pattern of the complex of uracil-cytosine (a), the pattern of a mechanical mixture of uracil (U) and cytosine (C), the original components, (b). $\lambda=1.5418$.

1) F. S. Mathews and A. Rich, *J. Mol. Biol.*, **8**, 89 (1964).
2) L. Katz, K. Tomita, and A. Rich, *ibid.*, **13**, 340 (1969).
3) A. E. V. Hashemeyer and H. M. Sobell, *Acta Cryst.*, **18**, 525 (1965).
4) E. J. O'Brien, *ibid.*, **23**, 92 (1967).
5) H. M. Sobell, K. Tomita, and A. Rich, *Proc. Natl. Acad. Sci. U.S.*, **40**, 885 (1963).
6) A. E. Hashemeyer and H. M. Sobell, *Nature*, **202**, 969 (1964).
7) K. Hoogsteen, *Acta Cryst.*, **12**, 822 (1959); *ibid.*, **16**, 907 (1963).
8) Y. Kyogoku, R. C. Lord, and A. Rich, *Nature*, **218**, 69 (1968).
9) C. Tamura, N. Sakurai, and S. Sato, The Proceeding of the Conference of Chemical Society of Japan, p. 423 (1970).
10) *Ibid.*, p. 424 (1970).

Results and Discussion

The results of the experiments, in part, are shown in Tables 1 and 2. A + sign denotes the formation of a new crystalline species and a 0 designates that no change for a pair was observed under these conditions. The sign ± indicates that only a few new diffraction peaks were observed in addition to the original peaks. Some of the new crystalline species were established as being due to complex formation by means of single crystal analysis, and some were suggested to be complexes by infrared spectra or mass spectra. Therefore, it

TABLE 1. INTERMOLECULAR COMPLEX FORMATION BETWEEN SOME ACIDS AND NUCLEOTIDE BASES
With thymine and uracil all are not interactive

	Adenine	Cytosine		Adenine	Cytosine
benzoic acid	+	+	anisic acid	+	0
cyclohexanecarboxylic acid	+	+	3,4-dichlorobenzoic acid	+	+
o-tuluic acid	+	+	*p*-toluic acid	+	0
m-toluic acid	+	+	*p*-*tert*-butylbenzoic acid	+	±
p-toluic acid	+	0	*p*-cyanobenzoic acid	+	+
salicylic acid	+	+	*p*-aminosalicylic acid	+	+
m-hydroxybenzoic acid	+	+	*p*-nitrobenzoic acid	+	+
p-hydroxybenzoic acid	+	+	picolinic acid	+	+
anthranilic acid	+	0	nicotinic acid	+	+
m-aminobenzoic acid	+	0	isonicotinic acid	0	+
p-aminobenzoic acid	+	0	pyradinic acid	+	+
o-fluorobenzoic acid	+	+	oxalic acid	+	+
m-fluorobenzoic acid	+	+	succinic acid	+	+
p-fluorobenzoic acid	+	+	maleic acid	+	+
o-chlorobenzoic acid	+	+	fumaric acid	+	+
m-chlorobenzoic acid	+	+	palmitic acid	±	0
p-chlorobenzoic acid	0	±	stearic acid	±	0
o-bromobenzoic acid	+	+			
m-bromobenzoic acid	+	+			
p-bromobenzoic acid	0	0			

Table 2. Intermolecular complex formation between nucleotide bases and related compounds of nucleotide bases

With thymine and uracil all are not interactive

	adenine	cytosine		adenine	cytosine
 uracil	±	+	 benzoylene urea	+	0
 thymine	+	0	 phthalazine-1,4-dione	0	0
 5-bromouracil	+	+	 2-3-dihydroxyquinoxaline	0	0
 5-nitrouracil	+	+	 1-(2*H*)-phthalazinone	+	+
 4-amino-1,3-dimethyl-uracil	0	0	 4-ketobenzotriazine	0	0
 alloxane	+	+	 isatonicanhydride	0	0
 barbituric acid	+	+	 phthalimide	0	0
 barbital	+	0	 3-indazolinone	0	0
 cyanuric acid	+	0	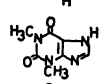 theophylline	+	+
 orotic acid	+	+	 theobromine	+	0
 4,6-dihydroxy-2-mercapto-pyrimidine	+	+	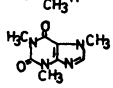 caffeine	0	0
 2-amino-4-hydroxy-6-methylpyrimidine	0	+	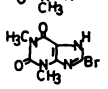 8-bromotheophylline	0	0
 2-amino-4-hydroxy-5,6-dimethylpyrimidine	+	0	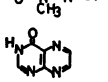 4-hydroxypteridine	0	+
 3,6-dioxohexahydro-1,2,4,5-tetrazine	0	0			

seems most probable to assume that the new crystalline-species correspond to those of the complexes, but not another modification of the components. Table 3 shows the number of substances forming complexes and the total number examined; they can be classified into six categories. It has been observed that adenine and cytosine form complexes with many organic compounds, while thymine and uracil form hardly any such complexes with those examined. Guanine was not included because of its poor solubility. The spacings listed in Table 4 are for the complexes and their components.

Table 3. Complex-formation ability of organic compounds with adenine and cytosine

number of substances forming complexes / total number of substances examined

	Category	For adenine		For cytosine	
1	Containing -COOH	33/36	91.8%	28/36	77.8%
2	Containing -CH(NH$_3^{\oplus}$)-COO$^{\ominus}$	0/18	0.0	0/18	0.0
3	Containing -CONH$_2$	1/17	5.9	0/17	0.0
4	Linear molecules containing CO & NH	0/10	0.0	0/10	0.0
5	Cyclic molecules containing CO & NH	6/39	15.4	5/39	12.8
6	Cyclic molecules containing -CONHCONH-	11/12	91.6	5/12	41.6

Carboxylic Acids. Table 3 shows that 92% of the carboxylic acids examined can bind with adenine and 78% with cytosine. Even long chain fatty acids, which are structurally different from the planar molecule of adenine, form the complexes as shown in Table 1. The structure of single crystal analysis,[9] in which the combination of the acid and base is of the type (acid$_4$-base$_2$) through the NH–O and OH–N hydrogen bonds is shown in Fig. 2. It seems that most of the other acid-adenine complex crystals are of a similar type.

It should be noted that many *p*-substituted benzoic acid derivatives do not form the complexes.

Aminoacids. In biological processes some interactions are expected to exist between nucleic acids

TABLE 4. POWDER DATA OF COMPLEXES AND THEIR COMPONENTS

ADENINE-A *

D	INT
3.198	100
6.758	80
5.574	63
3.770	54
2.998	21
5.401	16
3.969	15
5.155	15
2.780	12
3.562	10
2.912	7
4.928	5
2.103	4
2.338	4
1.985	3

ADENINE-B *

D	INT
8.672	100
6.194	73
3.100	62
7.830	50
3.267	48
3.209	34
3.132	32
4.004	32
5.471	25
2.823	20
3.590	18
2.722	16
3.900	11
3.493	10
1.957	9
2.156	9
2.894	9
2.988	9
3.440	9
4.332	9
2.585	7
3.351	7
2.276	6
6.657	6
2.386	5
2.522	5
3.739	5
1.863	4
2.062	4
3.389	4
4.575	4

ADENINE-C *

D	INT
6.657	100
3.198	48
13.392	43
3.278	38
4.439	28
3.619	24
3.028	22
6.109	22
2.921	19
2.959	19
5.906	14
2.212	13
2.501	13
2.867	9
4.647	8
3.363	7
3.770	6
2.023	5
2.442	5
2.730	5
2.321	4
2.607	4

CYTOSINE

D	INT
7.628	100
3.834	68
2.550	41
3.187	26
8.425	9
6.067	7
3.520	5
2.495	4
2.823	3
4.230	3
1.884	2
2.238	1
2.430	1
3.038	1

THYMINE

D	INT
12.450	100
13.810	72
6.237	49
6.970	28
2.321	14
4.152	6
2.998	5
3.480	4
2.644	3
3.121	3
4.745	3
15.237	3
1.989	2
2.780	2
4.647	2
2.045	1
2.080	1
2.858	1
7.695	1

URACIL

D	INT
5.340	100
3.153	68
7.971	55
5.155	41
3.220	30
3.110	20
2.411	15
4.770	13
3.850	12
3.440	9
2.557	8
2.659	8
3.648	8
3.493	7
2.747	5
2.979	5
2.515	4
2.823	4
4.247	3
2.023	2
2.071	2
2.321	2
3.969	2
5.906	2

ALLOXANE

D	INT
7.500	100
6.067	27
3.708	25
4.022	17
2.969	14
2.979	14
3.132	14
2.468	11
2.921	11
2.755	10
2.840	10
3.326	9
3.900	9
2.652	6
5.539	6
1.855	5
2.171	5
4.291	5
5.340	5
5.680	5
2.281	4
4.822	4
8.346	4
2.304	3
2.607	3
2.085	2

O-AMINO-BENZOIC ACID

D	INT
7.971	100
5.829	98
4.004	73
3.351	62
3.786	19
2.840	9
3.453	9
2.912	8
2.607	5
2.998	5
2.196	4
2.675	4
3.048	4
6.417	4
2.002	3
2.141	3
2.238	3
4.720	3
1.929	2
2.045	2
2.315	2
2.449	2
8.845	2
1.969	1
4.439	1

M-AMINO-BENZOIC ACID

D	INT
5.185	100
10.402	37
3.590	26
3.633	20
3.453	16
2.529	14
2.287	13
3.414	13
3.754	13
3.818	13
2.049	12
2.386	12
3.314	9
2.468	8
2.423	7
3.143	7
3.187	7
4.291	6
2.002	5
2.755	4
1.933	3
2.338	2
5.791	2

P-AMINO-BENZOIC ACID

D	INT
5.754	100
6.371	40
4.040	28
3.985	28
9.213	16
2.501	10
2.998	10
2.885	8
2.652	6
4.647	5
3.267	4
2.222	3
2.259	3
2.127	2
2.380	2
3.100	2
3.520	2
1.852	1
1.922	1
3.389	1
3.693	1

2-AMINO-4-METHYL-6-HYDROXY-PYRIMIDINE

D	INT
10.653	100
3.278	40
6.758	22
5.309	10
5.372	9
5.946	5
2.667	2
2.979	2
3.604	2
8.425	2
2.706	1
5.039	1

P-AMINO-SALICYLIC ACUD

D	INT
5.216	100
6.067	93
3.038	71
6.758	68
4.058	50
11.946	48
3.427	35
2.032	18
2.259	16
3.209	13
2.488	10
3.604	9
2.436	8
5.754	8
6.970	8
2.592	7
2.969	7
2.080	6
3.723	6
2.380	4
2.550	4
2.614	4
3.493	4
7.447	4
4.484	1

ANISIC ACID

D	INT
5.505	100
5.246	70
3.534	29
2.468	17
3.934	16
2.501	14
2.481	12
3.079	12
9.309	10
3.351	8
2.755	6
6.707	6
1.945	5
2.040	4
3.723	4
2.304	3
2.350	3
2.522	3
2.714	2
6.109	2
8.425	2
2.797	1

8-AZAADENINE

D	INT
5.405	100
6.607	44
3.153	39
6.970	39
3.619	22
3.453	20
10.782	19
3.110	12
3.302	7
4.152	7
4.506	7
4.874	7
2.969	6
3.048	6
5.754	6
6.194	6
2.867	5
2.659	4
5.985	4
2.344	3
2.706	3
2.171	2
1.922	1
2.080	1
2.222	1

BARBITAL

D	INT
11.051	100
5.539	90
3.693	44
2.763	26
5.340	12
1.845	4
2.212	3
5.011	3
2.536	2
6.067	2

BARUBITJRIC-ACID

D	INT
3.121	100
5.068	68
2.675	17
3.255	5
4.439	5
2.023	4
3.453	4
2.797	3
4.745	3
2.062	2
2.550	2
2.747	2
3.648	2
5.609	2
1.828	1
2.186	1
2.374	1
2.462	1
2.614	1
1.977	0
2.281	0

BENZOIC ACID

D	INT
10.782	100
5.405	65
5.155	30
3.739	23
3.440	13
2.969	11
3.209	10
2.730	9
2.578	8
4.623	8
3.633	7
2.298	4
3.326	3
2.117	2
2.181	2
2.321	2
2.404	2
4.191	2
2.858	1

BENZOLENE-UREA

D	INT
10.526	100
5.340	93
3.562	21
5.829	20
2.894	11
3.351	11
3.480	9
5.039	9
3.633	5
3.058	3
3.754	3
8.425	3
11.787	3
2.667	2
3.132	2
2.222	1
2.321	1

O-BROMO-BENZOIC ACID

D	INT
2.867	100
3.834	90
5.717	65
3.576	29
2.508	24
2.578	14
4.311	13
11.632	12
3.648	10
1.918	8
3.278	8
6.559	8
2.287	7
2.067	5

M-BROMO-BENZOIC ACID

D	INT
12.450	100
6.326	63
4.230	49
3.834	32
3.079	28
2.176	23
4.848	23
5.867	22
1.814	19
3.153	18
3.934	16
1.873	12
2.585	12
2.959	12
2.117	11
2.137	10
3.376	9
3.440	9
2.495	8
2.529	8
3.018	8
2.629	6
2.071	5
2.233	4
2.392	4
2.763	4
2.805	4
2.876	4
3.590	4

5-BROMO-URACIL

D	INT
7.081	100
3.562	58
3.209	57
2.380	28
2.475	21
4.928	18
1.784	16
2.637	10
3.900	10
4.171	9
2.940	8
3.100	8
1.998	7
2.858	7
2.099	4
2.550	4
3.453	4
5.644	4
2.122	3
1.814	2
2.332	2
2.196	2
2.249	2
2.780	2
4.375	2
4.720	2

O-CHLORO-BENZOIC ACID

D	INT
5.829	100
2.940	55
3.917	54
11.632	40
3.243	37
2.430	29
4.758	27
3.770	26
3.604	19
3.678	17
3.187	16
2.557	15
3.453	15
3.143	11
2.265	10
5.068	10
2.380	9
7.138	9
3.018	7
3.089	7
4.171	7
1.965	6
2.222	5
7.762	5
2.094	3
2.788	3
1.981	2
4.695	2

M-CHLORO-BENZOIC ACID

D	INT
6.417	100
3.818	67
3.232	64
4.770	49
2.449	15
4.506	14
2.411	13
2.659	11
3.069	11
3.363	10
3.969	10
3.576	9
2.161	7
1.993	6
2.270	6
9.025	4
2.113	3
2.714	3
2.763	3
5.539	3
2.040	2
2.607	2
1.929	1

P-CYANO-BENZOIC ACID

D	INT
12.810	100
5.754	64
3.187	56
6.371	31
4.332	30
3.576	17
3.648	15
7.138	15
3.255	10
2.254	9
2.309	9
3.058	5
2.675	4
2.714	4
2.867	4
2.912	4
2.217	3
3.363	3
3.427	3
2.161	2

CYANURIC-ACID

D	INT
2.988	100
5.574	44
4.210	18
2.080	4
2.675	4
3.302	4
5.246	4
2.622	3
3.520	3
2.151	1
2.380	1
4.462	1
6.194	1

CYCLOHEXANE-CARBOXYLIC-ACID

D	INT
4.623	100
4.955	50
4.396	40
5.405	37
4.095	35
8.043	32
3.314	16
3.900	12
3.708	8
3.440	6
3.018	5
6.916	5
2.592	3
3.100	3
2.206	2
2.309	2
2.417	2
1.945	1
2.688	1
2.367	1
2.683	1
2.823	1
2.921	1

CYCLOSERINE

D	INT
4.418	100
3.883	81
2.940	30
8.845	30
3.038	16
3.401	15
3.278	14
8.117	14
7.437	11
3.708	9
3.648	8
5.068	8
2.691	7
2.368	4
2.404	4
2.442	4
4.901	4
2.222	3

3,4-DICHLORO-BENZOIC ACID

D	INT
5.405	100
3.883	43
3.153	40
3.232	33
3.100	30
4.901	30
2.212	25
3.028	25
2.780	23
3.708	19
6.194	19
3.278	18
15.504	15
5.185	14
2.386	11
5.829	11
2.578	10
2.698	10
4.004	9
3.507	7

4,6-DIHYDROXY 2-MERCAPTO-PYRIMIDINE

D	INT
9.213	100
3.089	24
2.321	14
3.480	7
3.255	6
3.619	6
4.770	6
3.376	5
1.981	4
2.455	3
3.164	3
3.314	3
2.217	2
2.495	2
2.788	2
2.988	2
7.375	2
10.282	2
2.132	1

O-FLUORO-BENZOIC ACID

D	INT
6.109	100
12.109	50
3.079	39
5.405	39
4.095	35
6.559	14
2.176	12
2.462	12
3.153	12
2.058	11
3.290	11
2.488	8
3.663	8
3.018	8
3.232	8
3.633	6
1.866	5
4.983	3
2.368	2
2.698	2
3.440	1
3.802	1

M-FLUORO-BENZOIC ACID

D	INT
4.077	100
12.109	87
5.405	75
3.834	58
2.036	46
5.039	28
2.462	23
2.156	22
2.522	17
6.109	14
6.417	12
1.845	11
2.212	10
3.232	9
3.633	9
3.314	8
2.368	4
2.578	4
2.698	4
2.315	3
3.028	3
2.797	2

P-FLUORO-BENZOIC ACID

D	INT
5.155	100
12.999	71
3.590	51
3.232	47
3.278	45
4.599	42
6.559	42
5.754	22
2.940	21
2.254	17
2.675	15
2.298	12
2.600	10
3.739	8
2.449	7
2.876	7
2.392	6
3.008	6
1.848	5
2.730	5
4.077	5
6.237	5
1.895	4
2.090	4
2.132	3
3.427	3
2.166	2

FUMARIC ACID

D	INT
3.089	100
3.900	85
3.028	61
2.374	38
2.327	33
3.466	22
3.604	22
3.326	14
3.209	13
2.141	10
3.153	8
4.796	8
2.113	7
2.714	7
2.501	6
2.536	6
2.265	5
2.858	5
1.903	3
1.989	3
2.763	3
2.222	2

HYDANTOIN

D	INT
3.232	100
4.575	50
2.950	17
3.520	12
2.309	8
2.495	5
6.109	5
3.058	4
2.141	2
2.201	2
2.722	2

M-HYDROXY-BENZOIC ACID

D	INT
3.339	100
3.739	98
5.277	89
4.552	64
3.590	58
11.334	57
3.132	50
2.876	38
2.903	26
2.276	24
4.353	22
5.717	20
2.481	19
3.818	18
1.922	16
3.028	14
1.981	13
2.127	13
2.398	9
1.807	7
2.067	7
2.637	7
4.332	7
1.873	6
2.691	6
9.408	6
2.032	5
2.739	5
2.151	4

P-HYDROXY-BENZOIC ACID

D	INT
3.619	100
5.011	71
2.979	54
3.314	54
4.552	27
4.004	16
3.427	14
2.080	13
3.038	12
2.404	10
2.270	9
2.675	9
2.488	7
2.564	7
2.233	6
2.529	5
3.739	5
2.171	4
9.309	4
2.356	3
2.823	3
6.326	3
1.838	2
1.895	2
1.957	2
2.036	2
2.780	1

4-HYDROXY-PTERIDINE

D	INT
6.707	100
6.194	73
6.511	51
5.609	49
3.326	27
3.934	19
3.008	17
5.216	14
12.277	11
3.619	10
3.243	9
3.267	9
4.114	9
2.543	8
2.667	8
3.414	8
4.396	8
2.338	7
4.210	7
5.906	7
11.946	6
2.315	5
3.089	5
2.462	3
3.507	3

ISONICOTINIC-ACID

D	INT
3.401	100
5.340	84
3.187	80
2.233	28
2.392	25
3.619	21
3.100	18
2.254	15
4.484	11
4.095	8
2.659	6
5.717	6
2.094	5
2.931	5
3.723	5
2.876	4
6.151	4
1.884	3
2.468	3
2.449	2
2.529	2
2.714	2

MALEIC ACID

D	INT
3.175	100
3.121	19
3.339	12
3.520	12
3.576	11
3.969	10
2.788	9
5.068	8
2.691	7
5.340	7
2.227	5
2.374	5
2.529	5
2.652	5
2.292	4
2.921	3
4.040	3

NICOTINIC-ACID

D	INT
5.754	100
3.326	74
4.353	74
3.427	60
3.187	52
3.590	49
4.191	38
2.181	28
2.629	23
2.350	19
2.201	12
2.259	11
2.515	9
3.058	9
2.771	7
2.921	7
2.876	6
3.739	6
2.014	5
1.961	3
2.298	3
6.371	3
1.989	2
2.049	2
2.979	2

P-NITRO-BENZOIC ACID

D	INT
5.246	100
3.209	40
3.243	35
10.526	35
2.085	9
1.945	6
2.644	6
2.309	6
2.614	4
2.894	4
2.141	3
2.495	3
3.534	3
4.114	2
5.791	2
6.417	2

5-NITRO-URACIL

D	INT
3.058	100
4.332	29
4.506	29
2.481	25
5.096	25
2.755	24
4.623	23
3.952	22
3.480	21
2.840	20
2.374	19
5.539	16
2.614	15
2.894	13
3.678	13
3.562	10
2.254	9
2.049	8
2.522	8
2.959	8
1.881	7
2.298	6
3.209	5
2.171	4
3.278	4

OROTIC ACID

D	INT
3.110	100
4.529	75
3.018	27
4.928	26
4.022	20
2.270	18
6.371	18
2.023	17
2.315	16
3.209	16
3.917	16
2.885	15
2.411	14
2.417	14
3.401	14
3.427	13
4.848	10
2.564	9
3.576	9
3.818	9
5.680	8
2.108	7
4.114	7
1.841	6
5.155	6
9.118	4

OXALIC ACID

D	INT
3.079	100
5.985	33
5.829	16
4.745	9
3.453	6
2.265	5
2.436	4
1.937	3
1.989	3
2.374	3
2.404	3
2.607	3
2.885	3
2.940	3
2.564	2

PARMITIC ACID

D	INT
11.946	100
7.138	92
18.034	77
5.126	54
1.989	52
2.243	39
9.025	33
28.500	32
3.590	30
2.988	26
4.484	21
2.564	19
3.986	13
13.392	12
2.108	10
9.612	9
1.888	7
3.739	4
5.717	4
7.971	4
2.392	3
4.152	3

1-(2H)-PHTHALAZINONE

D	INT
5.680	100
9.213	75
3.100	36
6.916	31
2.831	20
3.708	16
3.453	14
3.548	14
3.048	13
3.376	13
2.298	8
2.442	7
6.281	7
2.571	5
3.969	5
2.040	4
4.506	4
4.623	4
2.062	3
2.698	3
2.522	1

PICOLINIC-ACID

D	INT
5.039	100
4.822	74
3.363	72
4.332	50
10.048	47
6.511	46
3.187	40
6.607	37
3.678	36
2.217	33
2.276	32
3.562	30
4.928	22
2.683	21
2.652	18
2.885	18
3.290	18
2.090	11
2.171	11
2.814	11
2.191	10
2.430	10
2.488	10
2.771	9
3.079	9
2.309	8
2.959	8
1.941	7
12.628	7
12.999	7
1.998	5
2.103	5
2.127	5
4.114	5
2.374	4
1.910	3
1.961	3
2.027	3
5.574	3

PYRADINIC-ACID

D	INT
6.237	100
3.232	47
4.484	21
3.693	9
2.298	5
3.089	5
2.867	4
2.442	3
3.507	3
2.058	2
2.127	1
2.652	1
2.797	1
2.998	1

PYRADINAMIDE (ALPHA)

D	INT
5.011	100
5.754	54
5.609	47
3.243	37
11.191	29
3.363	22
2.508	21
6.417	15
2.259	12
3.754	10
3.058	9
4.332	7
3.633	6
2.146	4
2.350	4
4.647	4
1.755	3
2.108	3
2.430	3
2.788	3
2.823	3
2.885	3
3.986	3
1.834	1
1.884	1

PYRADINAMIDE (BETA)

D	INT
6.970	100
3.507	70
5.277	60
4.671	50
2.338	44
2.805	22
13.810	14
3.220	9
2.675	8
3.187	8
3.278	7
5.011	7
7.762	7
2.309	6
5.791	6
4.848	5
2.912	4
3.339	4
2.019	3
2.722	3
3.883	3
2.108	1

DL-2-PYRRORIDONE-5-CARBOXYRIC-ACID

D	INT
4.040	100
3.739	59
3.314	53
3.867	49
2.386	33
4.375	33
6.026	32
5.539	30
2.894	29
2.113	23
2.515	19
4.139	16
2.644	14
2.998	14
2.304	13
2.706	12
2.455	10
2.356	9
3.576	9
3.648	8
1.866	7
2.747	7
1.949	6
2.006	6
2.254	6
2.780	6
3.164	6
1.845	5
4.484	5
2.287	4

SALICYLIC-ACID

D	INT
5.155	100
8.043	97
3.520	29
3.175	22
5.754	22
3.100	14
2.912	13
5.609	8
8.845	6
2.259	4
2.368	3
2.529	3
2.659	3
2.797	3
4.506	3
1.926	2
2.571	2
6.371	2
1.941	1
2.053	1
2.730	1

STEARIC ACID

D	INT
13.392	100
8.043	42
20.082	22
5.754	15
2.002	13
2.227	10
4.152	7
10.048	7
3.339	5
3.708	5
4.004	5
4.462	5
2.867	4
2.508	3
5.011	2
2.113	1

SUCCINIC ACID

D	INT
4.439	100
3.414	74
2.849	52
2.222	18
3.351	7
4.928	5
1.907	3
4.058	1

P-TERT-BUTYL-BENZOIC ACID

D	INT
4.770	100
4.462	77
4.447	67
10.402	51
8.425	37
3.969	29
4.375	22
4.230	17
8.758	17
3.770	15
3.507	13
9.100	12

Table 4. continue

3.278	12
5.539	12
3.232	11
5.277	11
6.151	10
3.427	6
2.265	5
2.940	5
3.376	5
5.754	5
2.108	4
2.998	4
7.375	4
2.304	3
2.659	3
6.511	3
2.683	2
2.722	2

THEOPHYLLINE

D	INT
6.067	100
10.048	80
3.302	71
6.657	67
3.326	65
7.695	65
4.796	33
3.376	32
4.983	32
3.834	18
3.708	13
4.210	11
3.018	10
2.571	9
2.763	8
2.592	7
1.926	5
2.171	5
2.675	5
4.418	5
11.051	5
3.520	4
2.338	3
2.392	3
2.495	3
2.522	3
2.867	3
2.894	3
3.576	3
8.506	3
1.817	2
2.222	2
2.249	2
5.309	2
1.841	1
2.281	1

2-THIO URACIL

D	INT
3.187	100
5.791	84
2.894	45
3.376	30
4.506	24
3.453	23
2.600	13
4.077	12
1.804	10
2.543	9
1.941	8
3.018	8
2.380	7
2.780	7
2.979	7
5.068	7
2.755	5
2.254	4
2.449	3
2.481	3
2.002	2
2.287	2
1.973	1
2.132	1

O-TOLUIC ACID

D	INT
11.787	100
3.480	77
5.471	50
3.232	45
3.969	41
3.693	24
6.463	22
3.850	18
2.885	14
5.717	12
3.376	11
3.770	10
5.126	10
4.375	8
7.375	8
3.576	6
2.023	5
2.206	4
2.265	4
2.374	4
2.430	4
2.481	4
2.600	4
4.874	4
1.929	3
2.698	3
4.210	3
1.892	2
2.304	2
1.866	1
4.647	1

M-TOLUIC ACID

D	INT
6.371	100
3.548	18
3.232	12
10.402	12
5.068	8
5.906	8
4.250	7
4.439	6
3.802	5
4.152	4
2.600	3
3.883	3
3.986	3
2.287	2
2.969	2
3.079	2
7.081	2
2.356	1
2.436	1
2.495	1
2.747	1
2.858	1
7.500	1
8.268	1

P-TOLUIC ACID

D	INT
5.126	100
3.339	51
3.562	25
6.026	21
6.371	7
2.564	5
3.018	4
3.934	3
5.680	3
1.831	2
2.462	2
3.069	2
3.198	2

2,4,6-TRIAMINO-1,3,5-TRIAZINE

D	INT
6.707	100
3.363	88
3.466	69
5.011	63
3.100	42
4.095	23
4.040	19
3.302	13
2.455	12
2.998	12
5.906	12
2.683	5
2.940	5
2.243	4
2.344	4

ADENINE + THYMINE

D	INT
11.946	100
5.946	69
3.326	65
6.657	50
8.845	46
3.255	42
5.680	41
4.720	28
11.334	27
4.152	24
2.969	23
3.100	20
5.126	12
3.969	11
2.858	10
3.110	10
2.637	9
2.763	9
4.396	5

CYTOSINE + URACIL

D	INT
5.096	100
7.196	97
4.529	83
3.232	79
4.848	70
2.797	64
6.916	62
2.281	43
9.612	36
13.810	35
2.404	34
3.143	31
2.998	30
3.834	25
4.250	19
2.876	16
3.028	16
2.667	15
8.845	15
3.427	13
2.739	10
2.912	10
6.281	10
1.957	9
7.900	9
3.480	8
7.695	7
2.380	6
2.622	6
2.122	5
2.181	5
2.536	5
3.723	5
2.495	4
1.884	3

ADENINE + ALLOXANE

D	INT
3.351	100
3.187	95
23.251	50
3.548	43
5.680	36
4.623	29
3.723	26
6.810	26
4.439	25
2.921	24
5.906	21
13.598	20
4.822	19
7.628	18
8.588	17
9.408	17
4.928	16
4.291	15
6.194	13

CYTOSINE + ALLOXANE

D	INT
3.255	100
6.511	61
3.986	29
6.970	24
4.396	18
4.647	17
4.552	16
6.707	14
3.153	13
3.440	13
4.270	11
2.392	10
3.376	10
5.438	10
8.117	8
2.350	7

2.014	5
1.870	4
3.079	4
3.604	2

ADENINE + O-AMINO-BENZOIC ACID

D	INT
5.791	100
4.901	81
3.187	77
11.481	52
7.314	50
3.255	45
7.971	45
5.574	40
6.559	38
6.707	37
3.562	33
3.754	32
4.506	30
9.118	25
3.633	22
10.282	21
3.069	20
4.077	17
2.885	16
3.414	16
14.489	16
2.739	15
2.979	15
5.155	15
2.763	14
3.867	11
22.655	9
4.210	8
2.117	6
2.462	6
1.977	4

ADENINE + M-AMINO-BENZOIC ACID

D	INT
3.351	100
3.453	60
5.680	52
5.829	52
3.232	50
3.534	46
11.191	28
6.810	25
6.371	24
3.834	22
3.028	21
3.110	21
6.657	21
2.950	20
3.900	19
4.928	15
2.840	13
4.230	13
4.484	13
8.845	11
12.810	9
5.340	8
9.408	7
2.747	6
8.043	5

ADENINE + P-AMINO-BENZOIC ACID

D	INT
8.268	100
6.194	81
2.771	74
4.152	55
3.302	35
3.466	16
6.916	15
3.220	13
4.983	13
2.969	11
2.233	8
3.934	8
2.080	6
3.069	5
2.176	4
2.698	4
2.831	4
2.921	4
2.058	3
9.118	3
2.495	2
2.543	2

CYTOSINE + 2-AMINO-4-METHYL-6-HYDROXY-PYRIMIDINE

D	INT
6.326	100
6.916	49
3.267	43
8.043	39
4.004	33
4.058	32
12.628	23
3.164	16
3.466	15
2.108	7
3.619	7
2.867	6
2.287	5
2.315	5
3.028	5
4.210	5
4.529	5
5.609	5
1.824	3
2.196	3
2.436	3
2.529	3
2.667	2
5.039	2
2.739	1

ADENINE + P-AMINO-SALICYLIC ACID

D	INT
6.281	100
3.267	91
3.376	46
7.025	23
6.511	15
5.039	14
5.717	14

2.979	12
8.425	9
2.417	8
2.885	8
3.121	8
4.822	8
4.040	7
2.667	6
3.480	6
4.210	6
5.155	6
2.166	4
3.619	4
5.246	4
2.099	3
2.137	3
2.522	3
2.217	2
2.747	2
2.780	2
1.841	1
1.918	1
2.023	1
2.062	1
2.287	1
2.592	1
3.754	1
10.048	1

CYTOSINE + P-AMINO-SALICYLIC ACID-A

D	INT
9.118	100
6.463	96
4.552	48
3.028	39
2.805	20
7.437	17
3.534	8
3.723	8
2.449	7
2.495	7
2.292	6
2.212	5
3.132	5
2.132	4
3.302	4
5.309	4
10.048	4
10.526	4
1.985	3
2.094	3
2.607	3
3.187	3
3.339	3
3.986	3
7.081	3
2.858	2
4.210	2
2.380	1
2.644	1
2.714	1
5.039	1

CYTOSINE + P-AMINO-SALICYLIC ACID-B

D	INT
10.915	100
3.389	94
3.708	93
9.509	75
6.657	71
4.796	64
11.334	64
3.326	46
3.198	42
3.818	32

ADENINE + ANISIC ACID

D	INT
5.471	100
10.915	36
4.210	30
3.663	16
6.371	16
2.747	15
3.255	7
2.592	6
3.100	6
3.562	6
3.363	5
6.067	4
2.321	3
2.931	3

ADENINE + 8-AZAADENINE

D	INT
6.970	100
3.243	78
5.471	46
3.453	37
3.048	25
3.648	20
5.185	16
6.109	15
2.805	14
4.396	11
2.592	9
11.051	7
2.027	6
2.315	6
3.867	4
2.141	3
4.133	3
7.900	3
9.309	3

THYMINE + 8-AZAADENINE

D	INT
6.862	100
5.471	85
3.232	29
12.450	25
3.648	20
3.427	18
13.810	17
5.155	16
6.026	16
3.018	15
11.051	12
4.375	11
2.788	8

ADENINE + BARBITAL

D	INT
5.906	100
11.787	58
3.401	49
3.232	17
2.950	16
3.562	15
5.539	15
2.979	14
3.110	14
4.439	12
4.671	9
5.185	9
3.900	8
2.196	5
2.380	5
2.622	5
2.698	5
3.754	5
7.762	5
2.309	4
2.788	4

ADENINE + BARBITURIC-ACID

D	INT
6.281	100
3.232	98
5.155	73
3.058	70
3.604	65
3.562	61
3.633	59
3.143	57
7.196	55
2.814	42
4.955	33
2.730	26
2.564	23
2.637	18
5.946	18
3.834	15
4.004	15
2.449	14
4.575	14
2.146	12
2.270	12
2.227	6
4.396	5

CYTOCINE + BARBITURIC-ACID

D	INT
3.267	100
14.255	58
5.216	36
4.004	22
4.040	22
3.453	20
4.506	20
3.389	17
7.081	17
2.921	15
3.678	13
2.698	12
8.425	12
4.230	11
2.404	9

ADENINE + BENZOIC ACID

D	INT
13.810	100
3.363	59
3.121	32
3.453	29
6.916	25
5.405	18
4.745	17
3.243	14
3.818	14
5.906	14
4.133	11
4.671	11
5.277	11
3.058	10
3.187	9
4.171	9
4.332	9
2.771	7
7.695	7
9.718	6
2.298	5
11.051	5
2.840	4
2.998	4
4.040	4
6.371	4
1.977	3
2.714	3
3.723	3
1.884	2
2.049	2
2.374	2
2.436	2
2.501	2

CYTOSINE + BENZOIC ACID

D	INT
21.551	100
5.574	93
3.198	61
10.782	56
3.255	36
4.462	35
5.405	32
7.628	31
4.191	28
2.797	21
3.739	19
4.040	18
7.375	18
3.326	14
6.109	14
2.350	12
2.607	12
2.488	11
3.100	11
3.834	11
2.543	10
2.714	10
2.831	10
2.998	9
3.520	8
3.648	8
2.298	7

2.950	6
3.401	6
4.848	6
4.955	5
1.937	4
2.238	4
1.961	2
2.161	2

ADENINE + BENZOLENEURFA

D	INT
5.372	100
10.782	95
7.437	90
12.999	74
6.463	73
7.138	48
3.326	35
3.576	30
3.100	29
6.109	28
3.466	26
3.708	26
14.979	19
3.663	18
4.311	15
3.232	14
3.018	11
5.867	11
2.903	9
2.156	8
2.468	8
4.671	7
5.068	6
2.108	5
2.667	5
4.770	5
8.672	5
2.515	4
8.192	4
4.114	3

ADENINE + O-BROMO-BENZOIC ACID

D	INT
3.326	100
5.068	20
5.754	18

CYTOSINE + O-BROMO-BENZOIC ACID

D	INT
5.791	100
3.867	94
3.401	82
2.903	73
3.678	71
5.471	69
3.018	38
3.220	38
4.058	35
3.339	32
3.562	28
2.780	23
5.277	22
3.058	21
2.667	20
2.805	19
10.915	17
4.874	16
9.509	15
6.151	14
11.481	12
2.515	11
2.404	10
5.126	10
2.585	8
1.941	7
2.040	7
2.156	7
4.484	7
2.327	6
1.866	5
2.249	5
1.903	4

ADENINE + M-BROMO-BENZOIC ACID

D	INT
3.302	100
3.663	41
4.133	34
4.745	30
3.507	28
4.623	24
3.175	23
3.363	22
4.484	19
2.998	16
2.564	15
5.574	15
5.155	14
5.471	14
2.196	13
3.739	13
6.810	13
2.171	11
2.921	11
3.867	11
4.270	10
2.814	8
1.929	7
6.326	7
2.127	6
2.380	6
2.404	6
3.969	6
1.981	5
2.067	5
2.730	5
8.845	5
2.032	4
7.314	3

CYTOSINE + M-BROMO-BENZOIC ACID

D	INT
4.396	100
4.745	88
2.714	62
4.058	62
4.171	43
3.562	31
3.678	31
2.040	24

2.442	23
5.906	22
2.529	19
5.277	19
2.222	17
2.380	17
3.100	16
2.151	15
3.818	14
12.277	13
23.879	13
2.356	12
3.493	12
6.237	12
2.592	11
2.931	10
1.881	8
2.780	8
8.346	8
4.848	8
3.278	7
3.326	7
4.874	6
7.138	6
9.213	6
3.187	5
1.941	4
2.814	4

ADENINE + 5-BROMO URACIL

D	INT
3.255	100
2.979	54
3.187	43
3.058	38
5.829	35
3.770	33
5.539	32
6.607	32
2.564	28
2.600	28
2.805	26
3.143	26
3.590	26
9.025	26
2.622	23
3.867	23
3.401	21
12.628	21
18.409	21
10.782	19
4.171	18
4.848	18
7.437	18

CYTOSINE + 5-BROMO URACIL

D	INT
3.232	100
3.427	83
6.810	73
4.874	65
2.950	59
3.590	52
3.917	52
2.867	51
2.637	43
2.481	37
2.356	34
3.110	33
2.417	32
3.290	32
11.632	32
7.138	26
9.826	25
4.623	24
3.770	22
2.797	20
2.747	18
8.117	18
2.006	17
2.564	16
7.695	13
2.171	12
4.375	12
5.906	12
2.201	10
2.132	9
2.254	9

THYMINE + 5-BROMO URACIL

D	INT
3.278	100
11.946	77
3.243	61
4.077	35
2.876	33
2.629	28
2.931	24
3.507	24
6.067	24
1.989	18
2.032	18
2.045	18
2.722	18
3.934	17
4.745	16
2.578	15
3.562	15
2.362	14
2.398	14
5.680	11

ADENINE + O-CHLORO-BENZOIC ACID

D	INT
6.371	100
18.801	33
3.187	18
9.509	16
3.401	5
2.132	4
2.755	4
2.931	4
3.754	4
3.834	4
5.096	3
5.539	2
7.081	2
2.259	1

CYTOSINE + O-CHLORO-BENZOIC ACID

D	INT
3.376	100
5.471	70

3.198	52
3.648	46
2.979	27
2.747	26
2.652	21
5.906	18
4.022	13
3.934	10
3.818	8
4.848	8
10.782	8
2.141	7
5.155	7
2.564	6
2.032	5
2.508	5
11.946	4
1.957	3
1.863	2

ADENINE + M-CHLORO-BENZOIC ACID

D	INT
6.151	100
4.418	82
3.604	49
5.829	34
3.739	21
2.508	20
3.100	19
4.770	19
3.326	16
6.916	15
9.213	15
3.038	14
4.623	14
7.830	14
3.198	13
3.883	13
2.979	9
3.466	9
7.437	9
11.632	9
2.858	8
2.912	8
2.404	6
2.356	5
2.629	5
2.227	4
17.673	4
2.067	3
2.156	3
2.201	3
2.691	3

CYTOSINE + M-CHLORO-BENZOIC ACID

D	INT
4.353	100
4.720	80
3.986	63
5.867	54
2.667	52
5.309	33
3.648	31
2.515	28
3.018	28
7.025	27
3.520	23
4.152	21
6.151	20
2.010	19
2.350	19
3.058	19
2.117	15
22.655	15
2.249	13
2.321	12
2.380	12
2.564	12
2.404	10
2.156	9
2.903	9
3.243	9
3.802	8
6.463	7
2.455	6
1.910	3
1.929	3
1.949	3

ADENINE + CYANURIC ACID

D	INT
3.243	100
8.425	39
9.025	20
4.983	14
3.028	10
4.230	4
5.405	4

ADENINE + CYCLOHEXANE-CARBOXYLIC-ACID

D	INT
18.409	100
4.291	35
4.671	34
3.969	30
3.290	29
6.194	28
3.648	15
5.867	15
3.187	14
3.708	12
11.632	12
2.667	10
5.216	8
2.912	7
2.959	7
3.401	7
4.955	7
3.534	6
4.484	6
5.574	4
6.758	4
8.845	4
9.309	4
2.831	2

CYTOSINE + CYCLOHEXANE-CARBOXYLIC-ACID

D	INT
12.999	100

4.439	91
7.563	33
3.834	31
3.648	20
4.152	17
3.187	15
4.004	12
4.770	11
5.867	10
3.326	9
2.607	8
4.623	8
2.557	7
3.520	7
3.278	6
4.901	5
5.068	5
2.227	4
2.344	4
6.151	4
2.488	3
2.921	3
3.028	3
8.346	3
2.675	2
5.372	2

ADENINE + CYCLOSERINE

D	INT
3.220	100
3.187	83
6.707	51
7.081	51
5.126	36
5.574	34
3.739	31
3.493	29
3.867	17
3.376	16
3.314	15
2.979	14
7.762	13
3.058	11
2.417	7
4.396	7
2.797	6
4.291	6
4.575	4
6.151	2

ADENINE + 3,4-DICHLORO-BENZOIC ACID

D	INT
3.278	100
6.326	37
7.138	25
6.237	23
7.255	23
5.505	20
3.633	17
3.754	14
2.780	12
4.720	12
4.848	12
2.867	9
4.114	4

CYTOSINE + 3,4-DICHLORO-BENZOIC ACID

D	INT
5.096	100
2.814	36
3.326	31
4.040	29
8.506	26
12.628	19
4.955	18
3.164	16
2.488	15
2.298	13
3.058	13
3.255	13
3.619	13
4.484	13
6.194	12
2.344	10
3.427	10
2.156	8

ADENINE + 4,6-DIHYDROXY-2-MERCAPTO-PYRIMIDINE

D	INT
10.526	100
9.408	64
3.480	50
2.607	47
3.302	28
3.110	23
5.216	21
2.442	15
3.220	15
2.071	14
2.332	12
2.557	12
3.187	12
4.077	10
5.068	10
3.351	8
2.233	6
2.998	6
7.437	6
1.973	5
2.675	5
2.771	4
3.619	4
1.998	3
2.040	3
2.108	3
2.191	3
2.858	3

CYTOSINE + 4,6-DIHYDROXY-2-MERCAPTO-PYRIMIDINE

D	INT
3.302	100
4.901	87
3.278	72
6.067	65
9.309	65
4.040	63
3.917	44
9.826	40
4.647	37

5.680	34
2.885	26
2.557	24
2.356	22
3.453	22
4.695	21
5.126	21
2.840	20
2.979	19
6.862	18
2.622	16
3.089	15
5.011	14
2.315	13
3.209	13
3.414	13
3.633	13
1.993	12
2.442	12
3.143	11
1.957	9
2.076	8
2.501	8
2.683	8
3.008	8
1.937	7
2.730	7
12.109	7
2.201	6
2.763	6
2.238	5
2.411	5
7.695	5
2.040	4
4.353	4

ADENINE + O-FLUORO-BENZOIC ACID

D	INT
4.529	100
7.255	81
3.187	49
4.095	49
6.194	43
9.718	39
6.326	36
12.810	36
3.619	32
5.309	31
5.216	30
2.423	29
3.466	26
2.233	21
3.466	15
2.276	14
2.831	14
2.309	13
3.562	13
2.771	11
1.817	10
2.108	10
1.870	9
2.578	9
2.667	9
2.885	9
2.931	9
2.969	9
2.049	7
2.600	6
3.038	6
3.754	6
2.181	5
2.515	5
4.291	5
3.900	4
17.673	4

CYTOSINE + O-FLUORO-BENZOIC ACID

D	INT
7.081	100
3.132	86
3.232	86
4.671	53
4.250	49
3.562	48
5.185	33
4.040	32
2.309	21
6.511	17
6.281	16
3.058	13
2.350	9
9.309	9
2.592	8
3.867	6
1.918	4
2.099	4
2.243	4
2.462	4
1.941	3
2.156	3
2.501	3

ADENINE + M-FLUORO-BENZOIC ACID

D	INT
3.243	100
13.392	40
6.237	35
3.187	34
3.351	27
3.548	25
20.082	25
5.754	24
3.507	22
6.463	19
6.758	19
3.723	18
6.657	17
4.552	14
5.216	13
10.048	12
8.043	11
4.671	9
5.539	9
4.928	8
2.706	6
4.462	6
2.858	5
4.396	5
4.171	4
2.233	3
2.780	3

CYTOSINE + M-FLUORO-BENZOIC ACID

D	INT
3.255	100

Table 4. continue

3.164	42
4.311	53
3.185	53
6.511	52
4.114	48
4.647	36
3.590	29
6.237	25
7.138	21
9.408	18
2.321	17
3.493	17
5.505	14
5.906	14
2.374	13
2.629	13
3.644	13
3.900	13
7.375	8
2.141	7
2.481	7
2.739	7
2.797	7
3.786	7
2.265	6
2.592	6
18.409	6

ADENINE
+
P-FLUORO-
BENZOIC ACID

D	INT
3.314	100
5.405	71
7.375	69
3.453	34
2.840	30
6.109	27
8.758	19
3.678	18
2.912	14
3.100	13
2.755	12
10.402	10
14.730	9

CYTOSINE
+
P-FLUORO-
BENZOIC ACID

D	INT
5.906	100
6.916	45
3.187	41
17.327	35
3.255	33
4.874	29
3.389	27
4.439	27
3.507	26
5.505	18
13.810	13
3.850	10
2.780	8
3.028	8
2.730	6
2.578	5
9.826	5
2.959	1

ADENINE
+
FUMALIC ACID

D	INT
6.463	100
3.376	41
4.874	30
4.462	25
11.051	21
5.340	19
6.916	18
3.708	17
4.077	17
13.392	17
2.578	15
3.648	14
4.210	13
4.270	13
2.227	12
2.592	12
2.442	11
5.867	10
2.714	9
5.609	9
2.550	8
2.969	8
3.069	8
3.209	8
3.453	8
5.539	8
2.287	6
3.100	6
3.562	6
8.425	6
9.408	6
2.386	4
7.830	3

CYTOSINE
+
FUMALIC ACID

D	INT
4.770	100
3.267	56
3.376	43
3.850	41
3.048	35
7.695	22
6.511	19
2.998	17
2.404	12
3.562	11
14.255	9
2.849	8
2.380	7
2.233	5
5.906	4
2.141	3
2.270	3

ADENINE
+
HYDANTOIN

D	INT
3.278	100
4.332	16
7.900	16
4.848	13
6.237	12
6.511	9
4.623	7
3.028	6
2.270	5
3.889	4

ADENINE
+
M-HYDROXY-
BENZOIC ACID

D	INT
3.363	100
3.220	85
5.096	74
3.414	62
3.534	56
7.255	55
3.604	54
6.026	46
5.372	44
3.069	40
4.822	30
3.708	26
2.912	21
2.550	17
8.672	16
2.730	14
2.780	14
2.344	11
2.404	10
2.058	8
2.191	8
2.006	7

CYTOSINE
+
M-HYDROXY-
BENZOIC ACID

D	INT
4.353	100
4.484	72
5.068	66
3.883	60
5.309	50
3.648	44
3.576	43
18.034	41
5.906	40
6.026	40
8.672	38
3.548	36
3.339	32
2.940	28
2.600	25
6.237	24
3.038	22
2.529	21
2.894	21
13.598	20
3.079	19
4.191	19
3.232	15
2.398	12
2.417	11
2.243	10
2.511	10
2.006	9
2.667	7
2.755	7

ADENINE
+
P-HYDROXY-
BENZOIC ACID

D	INT
3.326	100
5.609	93
3.198	87
3.480	58
2.969	51
5.372	51
2.805	42
7.255	33
3.110	27
4.901	25
3.850	23
4.191	19
5.096	17
8.506	15
11.632	15
6.326	12
2.151	11
10.782	11

CYTOSINE
+
P-HYDROXY-
BENZOIC ACID

D	INT
4.770	100
7.196	18
14.029	14
2.398	10
3.590	10
2.867	9
3.363	8
3.048	7
3.534	6
3.198	5
3.802	3
4.133	3
2.667	2
5.277	2
6.109	2
6.417	2
7.695	2

CYTOSINE
+
4-HYDROXY-
PTERIDINE

D	INT
5.906	100
3.427	85
5.754	77
3.132	66
6.707	40
4.822	31
9.826	30
4.623	22
7.138	22
3.850	20
2.840	16
3.232	13
3.986	13
11.632	11
7.762	10
2.637	8
2.287	6
2.392	6
2.706	6
2.156	5
2.755	5

CYTOSINE
+
ISONICOTINIC-
ACID

D	INT
17.327	100
3.290	63
5.791	59
3.401	57
3.986	53
5.309	48
3.175	44
4.353	37
2.495	30
6.916	29
3.480	28
2.903	27
4.720	25
8.672	18
3.089	17
2.238	13
2.386	11
2.979	11

ADENINE
+
MALEIC ACID

D	INT
3.209	100
6.326	44
3.069	37
9.408	37
2.931	33
4.506	31
3.351	28
8.268	28
3.576	26
3.883	25
3.440	24
5.539	18
2.508	13
4.874	13
2.132	12
2.259	11
2.332	10
2.171	8
2.430	8
2.014	5
2.053	5
5.906	5

CYTOSINE
+
MALEIC ACID

D	INT
3.164	100
4.874	61
7.471	23
3.678	19
5.216	19
3.786	18
2.959	16
3.917	16
3.326	15
2.667	13
3.187	11
2.849	11
2.515	10
2.430	9
2.488	9
3.038	8
2.455	7
2.755	7
3.507	6
1.953	5
2.049	5
2.108	5
2.176	5
2.062	4
6.511	3
2.243	2

ADENINE
+
NICOTINIC ACID

D	INT
7.138	100
5.277	45
4.755	17
3.934	13
3.110	12
3.018	11
3.220	11
3.619	11
7.695	11
2.062	4
2.571	8
11.632	7
2.849	6
2.249	5
6.067	5

CYTOSINE
+
NICOTINIC ACID

D	INT
5.405	100
4.575	91
14.255	83
2.867	81
2.362	72
4.152	68
7.138	64
2.571	42
8.346	34
11.051	31
4.770	26
2.979	25
2.032	23
2.181	23
3.290	18
2.488	14
3.633	14
2.771	13
3.164	12
6.446	11
3.389	9
2.132	8
2.298	7
2.430	5
2.076	4
2.503	4
1.953	3
2.249	3

ADENINE
+
P-NITRO-
BENZOIC ACID

D	INT
5.438	100
3.209	40
6.417	28
2.722	8
3.267	7
3.389	7
4.311	7
6.026	6
3.548	5
4.575	5
6.862	5
3.008	4
2.156	3
2.117	2
2.356	2

CYTOSINE
+
P-NITRO-
BENZOIC ACID

D	INT
5.438	100
6.326	44
3.267	36
4.250	31
6.237	25
3.507	17
4.171	14
2.921	10
3.339	9
4.695	9
3.143	7
4.955	7
2.411	6
3.008	6
2.254	5
2.122	4
2.722	4
3.648	3
4.484	3
5.126	3
12.450	3
1.922	2

ADENINE
+
5-NITRO URACIL

D	INT
3.363	100
3.132	87
5.754	61
5.471	59
3.314	57
3.039	53
3.018	45
3.548	38
2.831	24
2.747	20
4.077	20
4.114	19
2.204	18
6.067	17
2.176	13
4.291	13
6.607	12
4.623	9
3.818	8

CYTOSINE
+
5-NITRO URACIL

D	INT
3.121	100
6.194	97
4.874	57
3.520	40
5.505	35
3.187	32
3.389	30
5.277	29
3.018	24
3.339	24
2.571	20
2.722	18
10.526	18
2.921	17
2.270	13
8.192	11
3.802	8
2.249	6
2.831	6
3.986	6
2.201	5
2.368	5

ADENINE
+
OROTIC ACID

D	INT
3.164	100
3.493	61
4.623	61
4.874	31
3.648	29
8.043	27
6.067	21
2.858	20
2.959	20
2.332	18
2.831	18
3.351	18
4.004	18
3.038	12
4.529	10
2.405	9
2.206	8
2.067	7
2.683	7
3.818	6
4.291	5
2.423	4
6.810	4

CYTOSINE
+
OROTIC ACID

D	INT
13.598	100
3.164	72
6.810	47
5.680	34
3.314	32
4.506	25
4.040	21
2.508	20
2.298	19
2.356	17
2.462	17
3.770	16
6.511	16
3.850	15
2.959	13
4.671	13
2.876	12
5.216	12
9.213	11
11.191	11
2.233	10
3.534	10
10.526	9
5.126	8
6.026	8
16.994	8
2.667	7
2.714	6
4.270	6
5.438	6
2.430	5
2.191	4
7.563	4
1.910	2
2.132	2

ADENINE
+
OXALIC ACID

D	INT
3.220	100
4.955	71
3.802	30
5.717	27
7.375	26
3.153	23
3.326	22
3.600	15
3.401	12
2.894	10
3.534	9
2.201	8
2.722	8
2.522	7
4.191	6
5.405	6
5.946	6
7.830	6
8.346	6
3.883	5
2.374	4
4.040	4
2.151	3
1.888	2
2.019	2
2.067	2

CYTOSINE
+
OXALIC ACID

D	INT
5.754	100
5.155	92
4.671	84
4.484	61
7.762	54
2.332	49
3.440	39
3.903	38
10.402	36
5.906	34
2.998	31
3.089	30
2.814	29
3.376	29
2.876	25
2.578	23
2.515	19
2.259	18
2.950	18
5.068	17
2.869	16
2.386	15
3.326	14
3.867	13
2.212	12
2.675	11
2.141	10
2.607	9
1.918	8
3.255	7
3.934	7
2.103	6
3.132	6
2.085	5
1.957	4
2.747	4
4.114	3

ADENINE
+
PARMITIC ACID

D	INT
14.029	100
21.038	71
3.648	55
4.770	32
4.529	30
3.278	27
3.302	24
4.439	19
8.425	19
10.526	17
3.187	16
3.969	16
7.025	15
4.191	13
6.026	12
6.707	8
4.983	7
5.246	7
2.103	6
2.309	6
9.509	6
2.592	4

ADENINE
+
1-(2H)-
PHTHALAZINONE

D	INT
17.327	100
5.155	83
3.302	75
8.672	52
3.079	46
4.332	37
3.562	36
3.453	31
7.563	28
2.876	20
2.683	13
5.754	12
3.209	10
2.508	9
3.648	9
3.834	5
2.212	4
6.417	4
2.137	3

CYTOSINE
+
1-(2H)-
PHTHALAZINONE

D	INT
8.425	100
8.506	98
4.022	86
2.637	48
3.326	14
6.067	9
9.509	9
6.607	8
2.304	7
3.693	7
1.945	4
2.931	4
1.929	3
4.484	3
10.402	2

ADENINE
+
PICOLINIC ACID

D	INT
6.810	100
5.717	85
4.529	50
7.437	45
8.845	37
10.782	27

CYTOSINE
+
PICOLINEC ACID

D	INT
18.801	100
3.209	89
4.599	86
6.607	86
5.216	83
7.900	77
3.314	67
5.039	67
4.796	64
3.786	61
3.952	61
4.210	61
4.695	61
4.928	61
2.797	56
2.885	52
3.440	52
10.048	52
12.109	49
8.672	44
9.509	43
2.362	37
2.730	35
2.449	34
2.622	32
3.633	32
6.067	29
2.386	28

CYTOSINE
+
PYRADINIC ACID

D	INT
13.810	100
4.671	99
5.216	40
3.175	33
2.423	23
6.970	23
2.644	22
5.985	17
3.739	15
3.562	14
2.137	13
2.368	12
2.912	12
2.805	10
4.004	10
2.276	7
2.698	7
3.480	7
2.006	6
2.067	6
2.522	6
2.969	6
2.191	5
3.900	5
1.926	4

ADENINE
+
PYRADINAMIDE
(BETA)

D	INT
7.830	100
8.672	67
6.194	57
3.883	39
3.959	36
5.277	34
4.004	24
7.025	20
5.438	17
2.814	13
1.945	12
2.585	9
3.590	8
2.722	7
3.507	7
4.695	7
2.151	6
2.683	6
3.739	6
2.876	4
4.311	4
2.344	3
3.243	3
3.389	3
2.002	2
2.062	2
2.309	2
9.509	2
2.113	1
2.281	1
2.398	1

ADENINE
+
DL-2-PYRRORID-
ONE-5-CARBOXY-
LIC ACID

D	INT
12.810	100
22.655	53
15.781	50
3.290	25
7.628	22
5.155	21
13.598	18
3.187	17
14.730	15
5.644	14
3.754	12
4.040	12
2.959	11
3.153	11
4.396	11
4.901	11
3.818	10
2.622	9
3.089	9
3.548	9
2.747	7
4.599	7
6.758	7
7.138	7
2.903	6
4.270	6
5.340	6
10.164	6
2.823	5
6.026	4
2.315	3
2.362	3

CYTOSINE
+
DL-2-PYRRORID-
ONE-5-CARBOXY-
LIC ACID

D	INT
3.480	100
4.439	55
3.100	41
3.633	16
4.077	15
5.791	14
8.192	10
11.632	9
2.622	5
4.575	5
7.138	5
3.867	4
2.885	3
5.438	3
6.326	3
2.321	2
2.557	2

ADENINE
+
SALICYLIC ACID
-A

D	INT
7.500	100
5.039	41
5.246	27
5.609	27
3.187	26
14.979	26
3.480	24
8.043	23
4.462	22
3.220	21
6.417	20
3.153	18
10.526	15
20.549	11
3.986	9
3.278	7
3.008	6
3.708	6
2.797	5
1.933	3
2.233	3
2.321	2
2.191	1
2.014	1

ADENINE
+
SALICYLIC ACID
-B

D	INT
3.278	100
17.673	83
3.934	58
6.237	58
5.644	52
3.187	42
5.867	41
6.067	40
3.739	35
2.721	22
5.039	21
3.389	20
8.588	20
4.418	16
4.796	16
5.126	15
2.921	13
3.132	13
2.988	11
3.520	11
5.216	11
2.585	9
2.823	8
4.114	8
6.916	8
2.321	6
3.633	6
7.025	6
8.934	6
2.019	5
2.094	5
2.392	5
2.206	4
2.265	4
2.691	4
10.282	3

CYTOSINE
+
SALICYLIC ACID

D	INT
3.209	100
3.121	90
4.311	69
5.216	65
7.196	52
4.004	29
3.900	25
4.191	19
2.309	17
3.069	15
4.506	13
3.534	12
3.590	12
6.237	11
2.747	9
2.287	8
6.511	8
2.637	7
4.575	7
1.973	5
2.475	5
2.607	5
2.814	5
2.564	4
2.053	3
2.156	3
2.430	3
3.453	3
5.754	3
8.934	3
2.495	2
28.500	2
4.770	2
6.758	11
3.453	9
3.590	9
4.133	8
5.096	8
3.058	7
2.831	6
2.903	5
2.805	4
4.353	4
2.755	3
4.529	3

ADENINE
+
STEARIC ACID

D	INT
16.365	100
15.237	27
24.543	24
23.251	10

ADENINE
+
SUCCINIC ACID

D	INT
3.290	100
4.623	18
3.376	17
3.507	13
4.770	11
5.829	11
5.445	10
3.453	8
3.619	7
3.969	7
5.505	7
8.845	6
2.730	5
2.629	4
2.292	3
2.840	3
4.353	3
2.550	2

CYTOSINE
+
SUCCINIC ACID

D	INT
3.267	100
5.717	75
4.770	32
4.848	21
4.955	16
3.079	15
2.141	14
3.414	14
5.277	14
3.834	13
5.985	13
2.386	12
3.153	12
3.576	12
2.206	11
2.858	10
3.351	10
3.028	9
14.255	9
4.210	7
4.599	7
6.559	7
2.430	6
2.675	5
3.678	5
2.321	4
2.959	4
1.989	3
2.607	3
2.730	3
3.952	3
7.138	2

ADENINE
+
P-TERT-BUTYL-
BENZOIC ACID

D	INT
13.810	100
4.270	39
3.562	38
5.277	34
4.647	30
4.133	28
3.038	25
3.453	25
12.109	25
4.004	23
4.077	21
6.511	16
6.970	15
6.067	13
4.418	11
2.849	6
5.754	6
3.100	5
11.051	5
2.931	4

CYTOSINE
+
P-TERT-BUTYL-
BENZOIC ACID

D	INT
22.089	100
7.695	64
4.529	57
5.505	33
3.850	20
3.376	16
4.983	13
2.840	12
2.495	10
3.663	10
3.143	9
4.095	8
4.822	8
2.259	6
2.780	6
3.562	6
4.210	6
2.270	5
2.543	5
3.209	5
4.270	5
4.396	5
5.309	5
6.109	5
6.970	4
2.298	3
5.754	3

ADENINE
+
THEOBROMINE

D	INT
11.481	100
8.672	35
6.194	28
5.609	21
3.723	18
5.340	18
3.290	17
8.192	17
3.187	14
6.559	14
2.979	11
3.351	11
10.402	8
4.482	6
2.780	5
3.917	4
2.659	2
2.449	1

CYTOSINE
+
M-TOLUIC ACID

D	INT
13.192	100
6.281	94
3.534	64
3.187	48
4.822	42
3.132	40
4.311	36
7.628	35
3.089	34
2.495	25
10.402	25
3.290	23
6.026	23
4.133	22
3.786	19
2.998	16
3.440	16
3.850	15
3.969	15
2.739	13
2.698	11
4.484	11
2.823	10
3.648	10
2.238	8
2.386	8
2.940	8
6.758	8
2.430	7
5.039	7
2.292	6
2.644	6
2.006	2

ADENINE
+
P-TOLUIC ACID

D	INT
3.267	100
15.237	56
6.417	30
3.175	22
3.562	18
6.916	17
7.900	17
3.693	16
3.401	15
3.969	14
5.096	11
4.928	10
5.340	10
5.680	10
3.069	9
4.418	9
5.906	9
2.940	8
4.270	7
4.623	6
2.176	5
2.840	5
10.282	4
2.468	3
2.659	3

THYMINE
+
2+4+6-TRIAMINO
1+3+5-TRIAZINE

D	INT
8.192	100
3.326	82
3.039	31
2.536	24
4.745	23
3.401	21
3.100	20
3.232	15
4.114	15
5.185	13
5.985	11
6.758	11
2.156	10
2.747	9
2.814	9
2.998	9
3.507	9
5.405	9
4.040	8
11.632	8
2.362	7
3.648	7
9.118	5

URACIL
+
2+4+6-TRIAMINO
1+3+5-TRIAZINE

D	INT
7.375	100
3.164	72
8.672	50
3.778	22
2.338	21
5.039	20
2.771	19
2.921	18
3.326	18
4.270	18
4.623	18
2.468	15
3.220	15
2.629	12
3.255	12
3.493	12
4.375	12
2.137	11
2.309	9
1.852	8
1.895	8
2.032	8
2.113	8
3.058	8
6.970	8
7.971	8
2.522	7
2.840	7
3.619	7
6.109	6
1.873	5
2.222	5
2.585	5
2.722	5

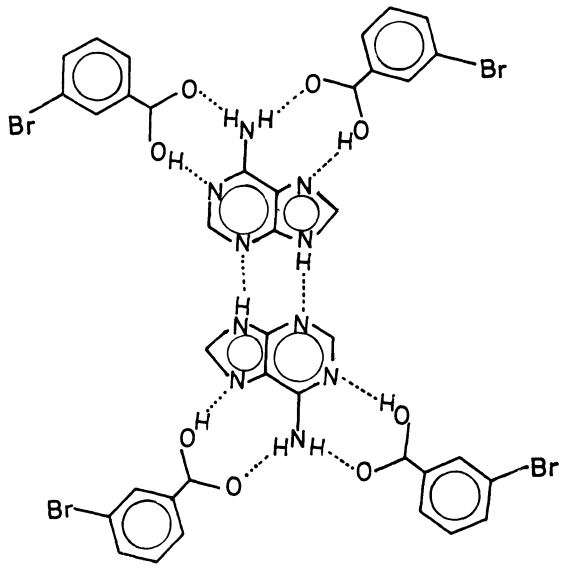

Fig. 2. The hydrogen bonding system of the complex crystal between *m*-bromobenzoic acid and adenine.

and amino acids. However, no amino acids were found to interact with these bases under the present conditions. The zwitter-ion form of amino acid might be related to this inertness. The substances tested in the present study were glycine, α-alanine, β-alanine, L-serine, L-threonine, L-valine, L-leucine, L-isoleucine, L-asparatic acid, L-histidine, L-proline, arginine, tryptophan, phenylalanine, methionine, cystein, creatine, and aminocapronic acid.

Acid Amides and Lactams. In view of complex-forming ability, acid amides and lactams could be classified into four categories (3 to 6) as shown in Table 3. Acid amides are inert; compounds tested are benzamide, *o*-, *m*-, and *p*-toluamide, *o*-, *m*-, and *p*-hydroxy benzamide, *o*-, *m*-, and *p*-chlorobenzamide, picolinamide, nicotinamide, and isonicotinamide. The only exception in amide group is pyrazinamide which can bind with adenine. Lactam group are inactive; the compounds tested are butyrolactam, valerolactam, ε-caprolactam, 2-azacyclononanone, tetrahydro-2-pyrimidone, succinamide, maleimide, phthalimide, glycinanhydride, 1,3-dimethylurea, acetylurea, 1-acetyl-3-methylurea, 1-phenyl-3-acetylurea. 1,3-diphenylurea, phenylurea, benzylurea, benzoylurea, and acetanilide.

Although the linear molecules containing CO and NH groups (category 4) do not interact with the bases, the corresponding atomic arrangement in cyclic molecules bind with adenine and/or cytosine; examples are benzoylurea/benzoyleneurea, and acetylurea/hydantoin. However even in cyclic molecules containing CO and NH groups, *e.g.*, anhydroglycine I, 3,6-dioxohydro-1,2,4,5-tetrazine II, 2,3-dihydroxyquinoxaline III and phthalazine-2,4-dione IV, binding

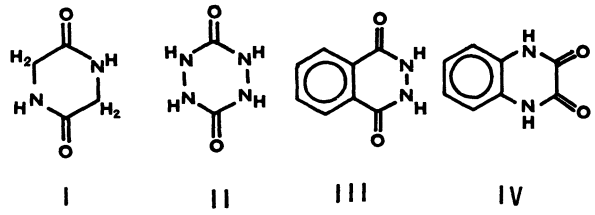

I II III IV

was not observed with these bases. This indicates that the atomic arrangement required for binding with adenine and cytosine would be cyclic alternant –CONH– groups. It should be noted that uracil[11] and thymine are regarded as typical members of category 5. In such a system, the proton donor and acceptor groups will be in the proper orientation with those in the bases to reinforce individual hydrogen bonds. In fact, the hydrogen bond system in the adenine-phenobarbital complex solved by Kim and Rich[13] is just the case as shown in Fig. 3.

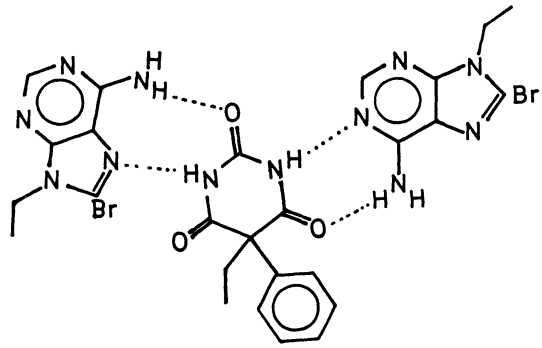

Fig. 3. The hydrogen bonding system of the complex crystal between phenobarbital and 8-bromo-9-ethyladenine, by Kim and Rich.

There are some other compounds which also bind with adenine and cytosine: 1-(2*H*)-phthalazinone, cycloserine, and 4,6-dihydroxy-1-mercaptopyrimidine. However, it is difficult to recognize any common features among them.

Amino and Nitrogen Heterocycles: A few compounds were found to bind with uracil and/or thymine; these are 1,3,5-triamino-2,4,6-triazine, azaadenine, and bromouracil. But many other related compounds, such as 2-methyl-4-amino-5-carbinopyrimidine, 2-aminopyridine, 2-aminopyrimidine, and 3-amino-1,2,4-triazole, do not form complexes.

We thank Professor Yoshio Sasada of Tokyo Institute of Technology for his valuable discussions and suggestions.

11) The complex of cytosine-uracil was found in this survey and its structure was determined by means of single crystal analysis.[10] The non-Watson-Crick pairing of uracil-cytosine found is almost the same as that of 5-fluorouracil-cytosine complex reported by Voet and Rich.[12]

12) D. Voet and A. Rich, *J. Amer. Chem. Soc.*, **91**, 3069 (1969).
13) S. Kim and A. Rich, *Proc. Natl. Acad. Sci. U.S.*, **60**, 402 (1969).

Studies of the Alkaline Earth Complexes in Various Solutions. VI. The Extraction and Complex Formation of Beryllium(II) in Sodium Perchlorate Media Containing Some Univalent Inorganic Anions

Tatsuya SEKINE, Yū KOMATSU, and Mitsuo SAKAIRI

Department of Chemistry, Science University of Tokyo, Kagurazaka, Shinjuku-ku, Tokyo

(Received November 2, 1970)

The distribution of beryllium(II) between methylisobutylketone containing TTA (thenoyltrifluoroacetone) and aqueous 4.0 M sodium perchlorate constant ionic media has been measured by using a carrier-free beryllium-7 tracer. The distribution behavior, determined as a function of the TTA and the hydrogen ion concentration, was explained in terms of the extraction of the $Be(TTA)_2$, the $Be(ClO_4)_2$ and the mixed species $Be(TTA)(ClO_4)$, and their extraction constants were determined. Then, the stability constants for the chloride, bromide, and nitrate complexes were determined from the decrease in the TTA extraction when some of the perchlorate ions in the aqueous phase were replaced by the ligand anions. Those of the thiocyanate complexes, on the other hand, were determined from the extraction of $Be(SCN)_2$ species with TBP (tributylphosphate) in hexane. It was concluded that the stabilities of these complexes are very low; the values β_1 and β_2 range between 1 and 0.1, but still these complexes should be taken into account in any discussion of the chemical behavior under some experimental conditions.

Although much has been reported on the complex formation of beryllium(II) with the fluoride ion in aqueous solutions, few seem to have studied those with other halide anions.[1]

In the present investigation, the authors have determined the distribution of beryllium(II) between aqueous sodium perchlorate media containing chloride, bromide, iodide, nitrate or thiocyanate ions and methylisobutylketone (MIBK) containing thenoyltrifluoroacetone (TTA) or hexane containing tributylphosphate (TBP). The distribution data were explained in terms of the complex formation, and the stability constants were determined by a graphic method. It was also found that the extraction of beryllium(II) mixed complexes with perchlorate and TTA anion or the beryllium(II) perchlorate should be taken into account in order to explain the distribution behavior of this metal ion under some experimental conditions.

Experimental

Tracer and Reagents. All of the reagents were of a reagent grade. Carrier-free beryllium-7 was used as the tracer. Sodium perchlorate was prepared from sodium carbonate and perchloric acid, and was recrystallized three times from water. MIBK and TBP were washed with 0.1 M perchloric acid, water, and 0.1 M sodium hydroxide, and then several times with water. The other reagents were used without further purification. The concentration of the stock perchlorate or nitrate solution was determined by weighing the residues after a certain amount of the solution had been dried in an air-bath at 120°C. The concentration of the chloride, bromide, iodide or thiocyanate stock solution was determined by titration with standard solutions of silver nitrate.

Procedures. Most of the procedures carried out were similar to those described in the previous paper.[2] MIBK containing TTA or hexane containing TBP was used as the organic phase. The aqueous phase was kept at 4.0 M (ClO_4) throughout the experiments, and when it was necessary, an acetate buffer (0.01 M initially) was added to the solution. The procedures were always carried out in a thermostatted room at 25°C. The hydrogen ion concentration in the aqueous phase was measured potentiometrically by using a standard solution containing 0.0100 M perchloric acid and 3.99 M sodium perchlorate as the standard of $-\log[H^+]=2.000$ in the 4.0 M ionic media.

Statistical Treatment

In the present work, the net distribution ratio, D, was defined and measured as follows:

$$D = [\mathrm{Be(II)}]_{org.total}/[\mathrm{Be(II)}]_{total}$$

In this paper, the chemical species in the organic phase are denoted by the subscript "org", while those in the aqueous phase have no subscript.

$$D = \frac{\gamma\text{-count-rate per ml of the org. phase}}{\gamma\text{-count-rate per ml of the aq. phase}} \quad (1)$$

1. Extraction of Be(II) in Perchlorate Solutions into MIBK Containing TTA. The equilibria for the extraction of beryllium(II) in a perchlorate medium with an acidic HA are generally described as follows:

$$Be^{2+} + 2HA(org) \rightleftarrows BeA_2(org) + 2H^+ \quad (2)$$

$$Be^{2+} + HA(org) + ClO_4^- \rightleftarrows BeAClO_4(org) + H^+ \quad (3)$$

$$Be^{2+} + 2ClO_4^- \rightleftarrows Be(ClO_4)_2(org) \quad (4)$$

When the perchlorate concentration in the aqueous phase is kept constant, the equilibrium constants can be described as:

$$K_{ex_0} = [BeA_2]_{org}[H^+]^2/[Be^{2+}][HA]^2_{org} \quad (5)$$

$$K_{ex_1} = [BeAClO_4]_{org}[H^+]/[Be^{2+}][HA]_{org} \quad (6)$$

$$K_{ex_2} = [Be(ClO_4)_2]_{org}/[Be^{2+}] \quad (7)$$

When we assume that only the Be^{2+} species is present in the aqueous perchlorate media, whereas the BeA_2, $BeAClO_4$ and $Be(ClO_4)_2$ species are all present in the organic phase, the net distribution ratio may be described as:

$$D = \frac{[BeA_2]_{org} + [BeAClO_4]_{org} + [Be(ClO_4)_2]_{org}}{[Be^{2+}]} \quad (8)$$

1) L. G. Sillén and A. E. Martell, "Stability Constants," the Chemical Society, spec, pub. **17** (1964).

2) T. Sekine and M. Sakairi, This Bulletin, **40**, 261 (1967).

Equation (8) can be also written from Eqs. (5), (6), and (7) as:

$$D = K_{ex_0}([HA]_{org}/[H^+])^2 + K_{ex_1}([HA]_{org}/[H^+]) + K_{ex_2} \quad (9)$$

or

$$D([H^+]/[HA]_{org})^2 = K_{ex_0} + K_{ex_1}([H^+]/[HA]_{org}) + K_{ex_2}([H^+]/[HA]_{org})^2 \quad (10)$$

Equation (9) shows that the value K_{ex_2} can be determined from the distribution ratio when the organic phase contains no HA, and Eq. (10) shows that the value $D([H^+]/[HA]_{org})^2$ should be constant at any $[H^+]/[HA]_{org}$ when the organic phase contains, practically, only the BeA_2 species, while it will increase with the increase in $[H^+]/[HA]_{org}$ when an extraction of metal species containing perchlorate ions into the organic phase occurs.

The above statistical treatments were made on the assumption that the ion-pairs, $Be(ClO_4)_2$ and $BeA\text{-}ClO_4$, undergo no dissociation in the organic phase. However, when there is a dissociation of perchlorate ions in the solvating polar solvent, MIBK, the organic concentration of beryllium(II) should be described as:

$$[Be(II)]_{org.\ total} = [BeA_2]_{org} + [BeAClO_4]_{org} + [BeA^+]_{org} + [Be(ClO_4)_2]_{org} + [BeClO_4^+]_{org} + [Be^{2+}]_{org} \quad (11)$$

and the following dissociation constants for the organic species should also be determined:

$$K_{diss.1(org)} = \frac{[BeA^+]_{org}[ClO_4^-]_{org}}{[BeAClO_4]_{org}} \quad (12)$$

$$K_{diss.2,1(org)} = \frac{[BeClO_4^+]_{org}[ClO_4^-]_{org}}{[Be(ClO_4)_2]_{org}} \quad (13)$$

$$K_{diss.2,2(org)} = \frac{[Be^{2+}]_{org}[ClO_4^-]_{org}}{[BeClO_4^+]_{org}} \quad (14)$$

The following equation are then obtained:

$$[BeAClO_4]_{org} + [BeA^+]_{org} = [BeA(ClO_4)]_{org}(1 + K_{diss.1(org)}/[ClO_4^-]_{org}) \quad (15)$$

$$[Be(ClO_4)_2]_{org} + [BeClO_4^+] + [Be^{2+}]_{org} = [Be(ClO_4)_2]_{org}(1 + K_{diss.2,1(org)}/[ClO_4^-]_{org} + K_{diss.2,1(org)} \times K_{diss.2,2(org)}/[ClO_4^-]^2_{org}) \quad (16)$$

The organic perchlorate ion concentration can be described as follows (disregarding the A^- ion and hydroxide ion):

$$[ClO_4^-]_{org} = [Na^+]_{org} + [H^+]_{org} + [BeA^+]_{org} + [BeClO_4^+]_{org} + 2[Be^{2+}]_{org} \quad (17)$$

Equation (17) shows that the perchlorate ion concentration in the organic phase is dependent not only on the sodium and hydrogen ion concentrations, but also on the concentrations of the cationic beryllium species in the organic phase. Consequently, if the total beryllium concentration is changed, or when the hydrogen ion or the extractant concentration is changed, the total organic perchlorate ion concentration in Eq. (17) which will be introduced into Eqs. (15) and (16) should be changed.

Fortunately such a consideration seems to be unnecessary. According to the results previously obtained by our laboratory,[3] the distribution ratio of sodium perchlorate between MIBK and an aqueous solution is 1.4×10^{-2}, thus, an MIBK phase in an equilibrium with 4.0 M sodium perchlorate should contain about 5×10^{-2} M sodium perchlorate. Furthermore, the extraction of perchloric acid from the aqueous phase will not be very large[4] and the perchlorate ion concentration in the organic phase should not be considerably changed even when the hydrogen ion concentration in the aqueous phase is changed within the range studied in this paper. For these reasons, even when the dissociation of the ion-pair species in the organic phase occurs, the expressions in Eqs. (6) to (10) can be used to describe the distribution behavior in the present system. However, when the aqueous sodium perchlorate concentration is much lower and/or the beryllium concentration is much higher, the possibility of the effect of the dissociation in the organic phase should be considered.

2. TTA Extraction and Complex Formation of Be(II). Under conditions where only the extraction of BeA_2 species is assumed, the following equation can be used instead of Eq. (10):

$$K_{ex_0} = D_0[H^+]^2[HA]^{-2}_{org} \quad (18)$$

where D_0 denotes the distribution ratio when the aqueous phase contains no complex forming ligands, that is, $D_0=[BeA_2]_{org}/[Be^{2+}]$.

When the Be^{2+} species associates with a uninegative ligand, L^-, the over-all stability constants for the n-th complex is defined as:

$$\beta_n = [BeL_n^{2-n}]/[Be^{2+}][L^-]^n \quad (19)$$

and the total aqueous concentration of beryllium(II) can be described as:

$$[Be(II)]_{total} = [Be^{2+}](1 + \sum \beta_n[L^-]^n) \quad (20)$$

The distribution ratio can then be described as:

$$D = [BeA_2]_{org}/[Be^{2+}](1 + \sum\beta_n[L^-]^n) \quad (21)$$

From Eqs. (18) and (21), the following equation is obtained:

$$D[H^+]^2[HA]^{-2}_{org}Ke\times0^{-1} = (1 + \sum\beta_n[L^-]^n)^{-1} \quad (22)$$

3. TBP Extraction of Neutral Complexes. When the neutral complex of beryllium(II) with L^- is extracted with e molecules of an organophilic adduct-forming extractant, E, the extraction can be described as:

$$BeL_2 + eE(org) \rightleftarrows BeL_2E_e(org) \quad (23)$$

$$K'_{DM} = [BeL_2E_e]_{org}/[BeL_2][E]^e_{org} \quad (24)$$

When the concentration of the extractant, E, is kept at a constant value, c_1, the following constant can be employed instead of that in Eq. (24):

$$K_{DM} = [BeL_2]_{org}/[BeL_2] \quad (\text{at } [E]_{org} = C\text{M}) \quad (25)$$

The net distribution ratio of beryllium(II) can then be described as:

$$D = \frac{[BeL_2]_{org}}{[Be^{2+}] + [BeL^+] + [BeL_2] + \cdots} \quad (26)$$

3) Y. Hasegawa, T. Ishii, and T. Sekine, This Bulletin, **44**, 275 (1971).

4) T. Sekine, T. Fukushima, and Y. Hasegawa, *ibid.*, **43**, 2638 (1970).

or

$$D[L^-]^{-2} = K_D\beta_2/(1 + \sum \beta_n[L^-]^n) \quad (27)$$

4. Graphic Determination of the Stability Constants. The equilibrium constants in these equations can be determined graphically from the experimental results as follows. When the D in Eq. (9) is denoted by $-y$, and the $[HA]_{org}/[H^+]$, by v, or when the $D[H^+]^2 \cdot [HA]_{org}^{-2}K_{ex_0}^{-1}$ or $D[L^-]^{-2}$ term in Eq. (22) or Eq. (27) is denoted by y, and the $[L^-]$ in these equations, by v, the equations can generally be described as:

$$\log y = \log c - \log(a_0 + a_1v + a_2v^2 + \cdots) \quad (28)$$

By plotting $\log y$ *vs.* $\log v$, the constants, a_0, a_1, a_2, $\cdots$, are determined by the "curve-fitting" method presented in previous papers.[5,6]

Results

Figure 1 shows the extraction of beryllium(II) in sodium perchlorate solutions at $-\log[H^+]$ 2.00 into MIBK. As no anionic species other than perchlorate ions is present in the aqueous phase, the extracted species should be the ion-pair $Be^{2+}(ClO_4^-)_2$ and the extraction can be given by Eq. (4). Although no control of the activity was made in these experiments, the slope of the plot is +2 between 1 M to 3 M sodium perchlorate, as can be expected from Eq. (4). The deviation of the data at the higher salt concentrations may be due to the change in the activities.

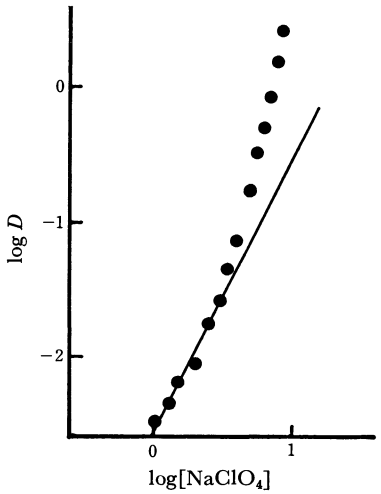

Fig. 1. Distribution of beryllium(II) between MIBK and aqueous sodium perchlorate at $[H^+]=10^{-2}$ M. The straight line shows the slope +2.

Figure 2 gives the $\log D$ *vs.* $\log[HA]_{org}/[H^+]$ plot for the distribution of beryllium(II) between MIBK containing TTA at various concentrations and 4 M sodium perchlorate solutions at various hydrogen ion concentrations. The distribution ratio of beryllium(II) in 4 M perchlorate media at $-\log[H^+]$ 2.00 into MIBK containing no TTA was found to be 6.9×10^{-2}, as may be seen from Fig. 1. This value gives the K_{ex_2} in Eq. (9). The distribution ratio increases with the increase in $[HA]_{org}/[H^+]$, and the slope of

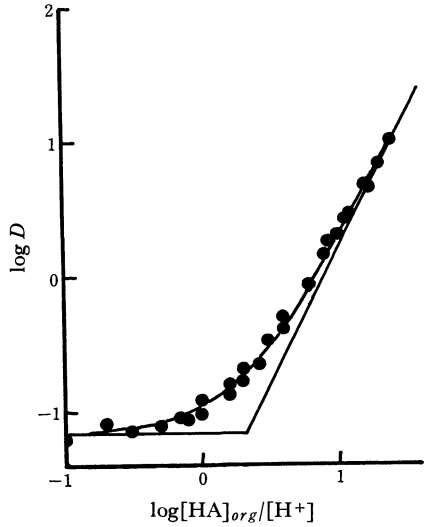

Fig. 2. Distribution ratio of beryllium(II) between MIBK containing TTA and 4 M (H, Na)ClO_4 as a function of $[HA]_{org}/[H^+]$. The two straight lines are $Y=-1.16$ and $Y=2X-1.80$. The solid curve gives $Y=\log(1.6\times10^{-2}X^2+2.3\times10^{-2}X+6.9\times10^{-2})$. Here $Y=\log D$ and $X=\log[HA]_{org}/[H^+]$.

the plot increases from zero to two. This can be explained as follows. In the lowest $[HA]_{org}/[H^+]$ region, where the slope is zero, beryllium(II) is extracted as the $Be(ClO_4)_2$ species, and in the highest region, where the slope is two, it is extracted as the BeA_2 species, while in the region where the slope is between zero to two, extracted beryllium species in the organic phase should be mixtures of $Be(ClO_4)_2$, $BeAClO_4$, and BeA_2. The plot in Fig. 2 was analyzed by the curve-fitting method; the equilibrium constants thus obtained are given in Table 1. The solid curve in Fig. 1 is the extraction curve calculated from these constants.

Figure 3 gives the $\log D[H^+]^2[HA]_{org}^{-2}K_{ex_0}^{-1}$ *vs.*

TABLE 1. EQUILIBRIUM CONSTANTS FOR THE EXTRACTION OF THE BERYLLIUM COMPLEXES

(a) TTA extraction from 4 M $NaClO_4$ into MIBK phase.

$\log K_{ex_0}$	$\log K_{ex_1}$	$\log K_{ex_2}$
−1.80	−1.64	−1.16

$$Be^{2+} + nClO_4^- + (2-n)HA(org) \rightleftarrows BeA_{2-n}(ClO_4)_n(org) + (2-n)H^+$$

$$K_{ex_n} = \frac{[BeA_{2-n}(ClO_4)_n]_{org}[H^+]^{2-n}}{[Be^{2+}][HA]_{org}^{2-n}}$$

(from 4 M $NaClO_4$)

(b) TBP extraction of $Be(SCN)_2$ complex in 4 M Na(SCN, ClO_4)

$\log K_{DM}$	$\log K_{DM'}$
1.71	3.81

$$Be(SCN)_2 + 3TBP(org) \rightleftarrows Be(SCN)_2(TBP)(org)$$

$$K_{DM} = \frac{[Be(SCN)_2]_{or}}{[Be(SCN)_2]} \quad ([TBP]_{org} = 0.2\ M)$$

$$K_{DM'} = \frac{[Be(SCN)_2(TBP)_3]_{org}}{[Be(SCN)_2][TBP)]_{org}}$$

5) T. Sekine and M. Ono, This Bulletin, **38** 2087 (1965).
6) T. Sekine, M. Sakairi, and Y. Hasegawa, *ibid.*, **39** 2141 (1966).

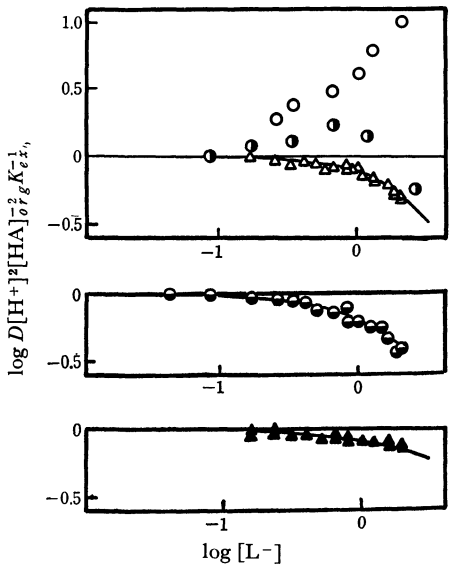

Fig. 3. Change in the extraction of beryllium(II) in 4 M Na(L, ClO_4) as a function of the ligand concentration. In the figure, L^- is Cl^-(◒), Br^-(△), I^-(◑), NO_3^-(▲), or SCN^-(○). The organic phase was MIBK containing 0.01 M TTA for the thiocyanate system and 0.2 M TTA for the others. The hydrogen ion concentration in the aqueous phase is $10^{-3.2}$ M for the thiocyanate system and $10^{-2.0}$ M for the others. The solid curves are $Y=-\log(1+a[L^-]+b[L^-]^2)$ where $a=0.44$ and $b=0.19$ for Cl^-, $a=0.13$ and $b=0.18$ for Br^- and $a=0.22$ and $b=0$ for NO_3^-. The constants for the iodide and thiocyanate systems were not determined by the reasons given in the text.

log [L^-] plot when the ligand anion in 4.0 M Na(ClO_4) was chloride, bromide, or nitrate ions. In these experiments, the TTA concentration in MIBK was 0.2 M, and the $-\log[H^+]$ in the aqueous phase was 2.00 or 2.53.

As may be seen from Fig. 2, the slope of the plot is practically +2 when $\log[HA]_{org}/[H^+]$ is 1.3 or 1.8. It has been observed that the extraction was practically proportional to $([HA]_{org}/[H^+])^2$ even when the concentration of chloride, bromide, or nitrate ions in the aqueous phase was 2.0 M. Thus, it may be concluded that the extraction of metal species containing the ligand, MAL or ML_2, is negligible and that only the BeA_2 species is extracted into the organic phase when the ligand concentration is less than 2.0 M. From these facts, we may see that Eq. (22) is valid for the calculation of the stability constants from these data. The constants thus determined are given in Table 2. The solid curves in Fig. 3 are the extraction curves calculated from the stability constants in Table 1 and the value $K_{ex_2}=10.^{-1.80}$

Table 2. Stability constants of beryllium(II) complexes in 4 M Na(ClO_4) at 25°C

$\beta_n = [BeL_n^{2-n}]/[Be^{2+}][L^-]^n$

ligand	$\log\beta_1$	$\log\beta_2$
Cl^-	−0.85	−0.70
Br^-	−0.70	−0.80
NO_3^-	−0.63	—
SCN^-	−0.16	−0.60

Beryllium(II) in 4.0 M perchlorate media containing iodide or thiocyanate ions was also extracted with TTA in MIBK. However, the results were complicated, as can also be seen in Fig. 3; the addition of the ligand even increases the extraction in some ligand concentration regions. This was assumed to be due to the extraction of the complex formed, BeL_2, or of the mixed complexes with TTA, BeAL, into MIBK. Thus, it was not possible to obtain the stability constants of the beryllium(II) iodide or thiocyanate complexes by the TTA-extraction method.

Beryllium(II) in 4.0 M sodium perchlorate containing one of these five ligands was also extracted into hexane containing TBP. It was observed that the distribution ratio is always very low (about 10^{-2} or less) when the aqueous phase contains chloride, bromide, iodide, or nitrate ions at various concentrations and when the organic phase contained 0.2 M TBP in hexane. However, when the aqueous phase contained thiocyanate ions, a remarkable extraction of beryllium(II) was observed.

Figure 4 gives the log D *vs.* log[SCN^-] plot when the organic phase is hexane containing 0.2 M TBP and when the aqueous phase is 4.0 M Na(SCN, ClO_4) at $-\log[H^+]$ values between 3.5 and 4.0. It may be seen from Fig. 4 that the distribution increases with the increase in the thiocyanate concentration and that the slope $d\log D/d\log[SCN^-]$ decreases from 2 to about 1 or less. Assuming that only the $Be(SCN)_2$ species is extracted with TBP, the results were analyzed using Eq. (27). Figure 5 gives the $\log D/[SCN^-]^2$ *vs.* log [SCN^-] plot. The constants were determined from Fig. 5 by the curve-fitting method; they are given in Tables 1 and 2. The solid curve in Fig. 5 is the curve calculated from these constants. When the thiocyanate concentration is lower than 0.1 M, the data deviate from the statistically expected curve based on Eq. (27).

In order to see the effect of the hydrogen ion concentration on the TBP extraction of beryllium thio-

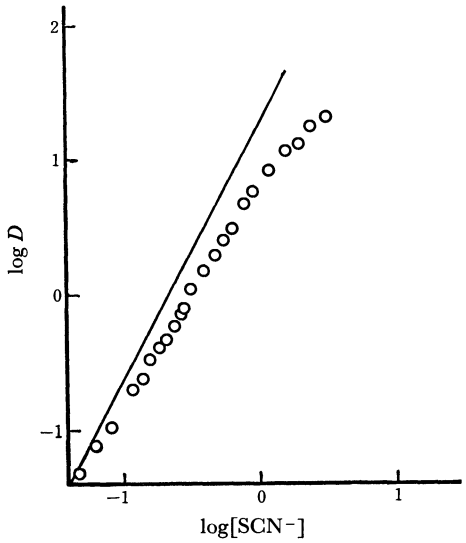

Fig. 4. Extraction of beryllium(II) from 4 M Na(SCN, ClO_4) at $[H^+]=10^{-4}$ M into hexane containing 0.2 M TBP as a function of the thiocyanate concentration. The straight line shows the slope of +2.

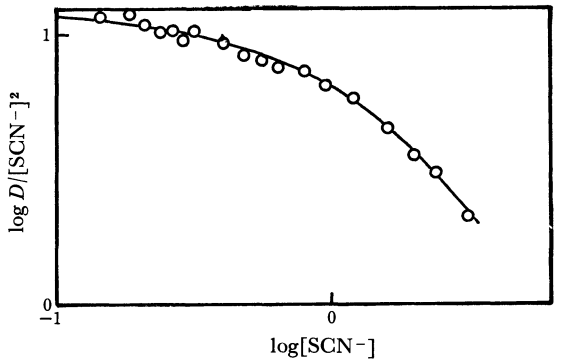

Fig. 5. Determination of the stability constants of the thiocyanate complexes by the curve fitting. The data in Fig. 4 were plotted as $\log D[SCN^-]^2$ *vs.* $\log[SCN^-]$ and were fitted with the curve $Y=\log c-\log(1+a[SCN^-]+b[SCN^-]^2)$ were a is $\beta_1(=0.69)$, b is $\beta_2(=0.25)$ and c is $K_D\beta_2(=12.6)$.

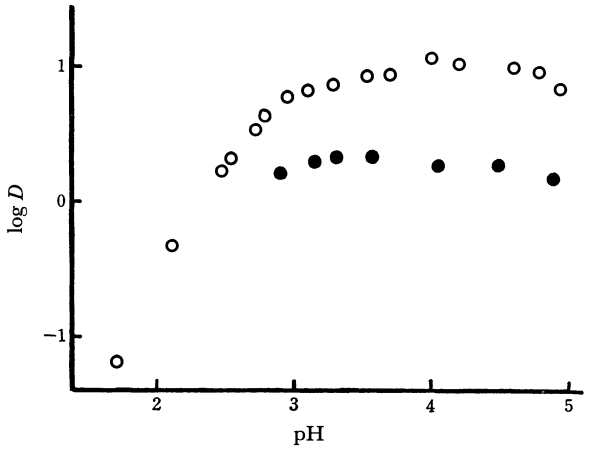

Fig. 6. Hydrogen ion concentration dependence of the extraction of beryllium thiocyanate complex.
Organic phase: Hexane containing 0.2 M TBP.
Aqueous phase: 2 M NaSCN+2 M $NaClO_4$ (open circles), 0.4 M NaSCN+3.6 M NaClO (closed circles).

cyanate, the distribution ratio was determined as a function of $-\log[H^+]$ when the TBP concentration was 0.2 M and when the thiocyanate concentration was 2.0 M or 0.4 M. The results are given in Fig. 6. As may be seen from Fig. 6, the distribution ratio is practically independent of the hydrogen ion concentration when it is between $10^{-3.5}$ and $10^{-4.5}$.

Figure 7 shows the distribution of beryllium(II) in the aqueous phase containing 3.0 M sodium perchlorate and 1.0 M sodium thiocyanate at a $-\log[H^+]$ value of about 4.0 into hexane as a function of the organic TBP concentrations. In Fig. 7, it may be seen that the slope of the plot is +3; thus, the extraction equilibrium can be described by the following equation:

$$Be(SCN)_2 + 3TBP(org) \rightleftarrows Be(SCN)_2(TBP)_3(org)$$

As has been described, two different solvent extraction methods were used for the determination of the beryllium complexes in the present study. The metal TTA chelate extraction method is applicable only to the chloride, bromide, and nitrate complexes, whereas the TBP adduct neutral complex extraction method

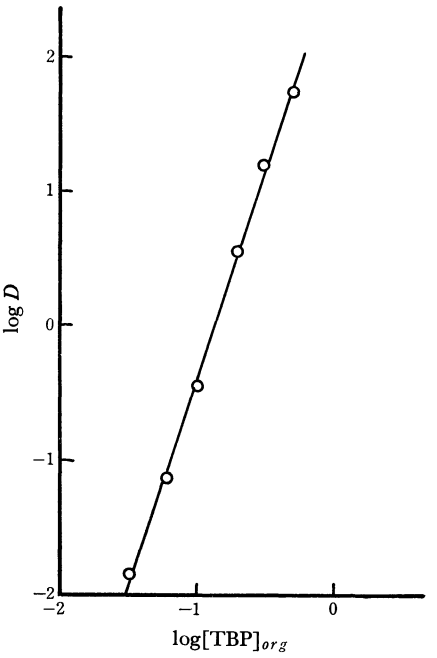

Fig. 7. TBP dependence of the beryllium thiocyanate extraction. Organic phase: hexane containing TBP. Aqueous phase: 3 M $NaClO_4$+1 M NaSCN and $[H^+]$ is about 10^{-4} M.

was applicable to the thiocyanate complexes. Neither of them was suitable for the iodide complexes.

Discussion

In a previous paper,[2] a deviation of the log D of beryllium(II) *vs.* $-\log[H^+]$ plot from the slope +2 was observed when the organic phase was MIBK containing 0.03 M TTA and when the aqueous phase was 1.0 M sodium perchlorate (Fig. 1 in Ref. 2). In that study, however, the deviation was too small to allow a reasonable analysis of the coextraction of the perchlorate or mixed TTA-perchlorate complex into MIBK (it may be seen from Fig. 1 in the present paper that the K_{ex_2} from 1.0 M perchlorate media is 3×10^{-3}). As may also be seen from Fig. 1, the beryllium perchlorate extraction increases with an increase in the aqueous sodium perchlorate concentration and in the extraction of beryllium(II) in 4.0 M sodium perchlorate into MIBK in Fig. 2, even in the absence of TTA; this can be explained in terms of the beryllium perchlorate extraction. The change in the slope of the extraction curve, log D *vs.* $\log[HA]_{org}/[H^+]$, can also be understood in terms of perchlorate extraction, as can be seen from the calculated curve in Fig. 2 based on the constants already given.

As has been pointed out,[7] the extraction constant of the mixed complex can be calculated from the extraction constants of the two other species:

$$K_{ex_1}(stat.) = 2(K_{ex_2} \times K_{ex_0})^{1/2} = 10^{-1.18}$$

This statistical value is about three times the experimentally observed value ($10^{-1.64}$); thus, the mixed complex is somewhat less stable than the statistical

7) T. Sekine and D. Dyrssen, *J. Inorg. Nucl. Chem.*, **26**, 2013 (1964).

value. The slope of the extraction curve is almost +2 when $\log[HA]_{org}/[H^+]$ is kept above 1.1; that is, the distribution ratio generally given by Eq. (8) in that range can be described as $D_0=[BeA_2]_{org}/[Be^{2+}]$. As all the determination of the stability constants by the TTA extraction is carried out in this $[HA]_{org}/[H^+]$ range, the analysis of the data based on Eq. (22) should be reasonable.

The use of Eq. (22) for the analysis of the data in Fig. 3 seems also to be reasonable because it was observed that the distribution ratio is proportional to the square of $[HA]_{org}/[H^+]$, even in the systems where some of the perchlorate ions were replaced by chloride, bromide, or nitrate ions.

As may be seen from Fig. 5, the experimental data well fit the solid line calculated from the constants based on Eq. (27). This seems to show that the distribution behavior of beryllium is represented by Eq. (27). It is remarkable that the stability of the extractable complex, $Be(SCN)_2$, is relatively low, but its extraction is high in the higher ligand concentration region. For example, when the thiocyanate concentration is 1.0 M, 13 percent of the aqueous beryllium(II) is in the form of $Be(SCN)_2$, but still about 86 percent of the initial aqueous beryllium is extracted into the organic phase. This is due to the high distribution constant of this complex. The extraction should be much higher at the higher TBP concentration.

Although the stabilities of the beryllium complexes given in Table 2 are not large, these very weak complexes are still important in order to understand the chemical behavior of this metal ion under certain experimental conditions, as we have seen in the TBP extraction of its thiocyanate.

The stability constants of beryllium(II) chloride and nitrate complexes were determined in 0.5 M perchlorate media at 18°C by Kolosova and Belyavskaya[8]; they were reported to be $\log\beta_1=1.11$, $\log\beta_2=0.30$, and $\log\beta_3=1.40$ for chloride complexes, and $\log\beta_1=-0.60$ and $\log\beta_2=1.62$ for nitrate complexes. These previous stability constants are much higher than the present data shown in Table 2, even if the lower ionic concentration is taken into account. No report seems to have been published on the stability constants for the beryllium(II) complexes with bromide or thiocyanate ions. Biermann and McCorkell[9] have studied the extraction of beryllium thiocyanate into MIBK, 1-hexanol, 2-octanol, and isoamylacetate when the initial aqueous beryllium concentration is rather high (above 0.1 M in the initial aqueous phase). They reported a remarkable pH dependence of the extraction; the percent extraction increases from pH 0.5 to 2.0, it is almost constant between pH 2.0 and 3.0, and then it decreases above pH 3.0. They explained it in terms that an increase of pH in the lower pH region causes the back extraction of the undissociated thiocyanic acid into the aqueous phase and increases the thiocyanate ion concentration. At the same time, the decrease in the thiocyanic acid in the organic phase increases the activity of the solvent. They also explained the decrease in the extraction in the higher pH region in terms of the hydrolysis of beryllium, which forms $BeOH^+$. They also assumed that the only beryllium species in the aqueous phase besides the above $BeOH^+$ is the Be^{2+} (no complex formation in the aqueous phase) and concluded that the extraction is given by the equation $D_{Be}=0.3[SCN^-]^2$ where $D_{Be}=[Be(SCN)_2]_{org}/[Be^{2+}]$.

As can be seen from Fig. 6, in the present study we have not observed such a drastic decrease in D above pH 4.0 as they reported. Thus, from the results in Fig. 6 and from the hydrolysis constants in the literature,[1] we have concluded that the hydrolysis around pH 4.0 is very small. Moreover, we can not accept the assumptions that the formation of the thiocyanate complex in the aqueous phase is negligible and that the slope of the $\log D$ *vs.* $\log[SCN^-]$ plot is two, as can be seen from the results in Fig. 4. The complex formation of alkaline earth metal ions with these ligand anions has not been studied very much because of the instability of the complexes, but, as is seen in this study, beryllium(II) shows some tendency to form complexes; this is probably due to the small ionic size of the Be^{2+}.

A part of this work has been carried out in the Laboratory of Nuclear Chemistry, Institute of Physical and Chemical Research. The authors are grateful to Professor Nobufusa Saito, the head of the Laboratory. They are also grateful to Mr. Akira Kaneko for his experimental aid.

8) I. F. Kolosova and T. A. Belyavskaya, *Vestik Moskov Univ. Khim.*, **18**, No. 152 (1963).

9) W. J. Biermann and R. McCorkell, *Can. J. Chem.*, **40** 1368 (1962); **41** 112 (1963); **45** 2846 (1967).

Measurement of Negative Ions Formed by Electron Impact. VIII. Ionization Efficiency Curves of Negative Ions from Methyl and Ethyl Cyanides

Satoru TSUDA, Akira YOKOHATA, and Toshikatsu UMABA

Department of Chemistry, Faculty of Engineering, Hiroshima University, Senda-machi, Hiroshima

(Received November 9, 1970)

The ionization efficiency (I.E) curves of *m/e* 26(CN^-), 27(HCN^-), 38(C_2N^-) and 39($CHCN^-$) ions from methyl and ethyl cyanides, besides 40(CH_2CN^-) ions from methyl cyanide, and 50(C_3N^-) ions from ethyl cyanide were measured to the extent of about 25 eV electron energies under the pressure of $\sim 10^{-6}$ mmHg by a Hitachi RMU-6D mass spectrometer. Schemes of plausible reactions expected to appear at each onset value observed in the respective IE curves were sought thermochemically by using ΔH_f values of the reactants and products. The estimation method of unknown ΔH_f values is described also. It should be noted that for CN^- ions one process (probably, $R+CN^-$) was observed in lower energies than 2 eV; C_2N^- ions are expected to be formed with excess energy; also, for CN^- and HCN^- ions rather strange phenomena of the decrement of their signal intensities with increasing electron energies were observed in the range of higher energies. Moreover, the IE curves of C_3N^- ions in the higher energy region were well interpreted in terms of the overlapping phenomena of dissociative capture process with ion pair formation process. It was found from this work that EA(HCN) $\gtrsim$1 eV, $\Delta H_f(CHCN^-) \sim 3.2$ eV, EA(CHCN) $\gtrsim$1.1 eV and EA(CH_2CN) $\gtrsim$1.6 eV. For the electron affinity of C_2N a value $\gtrsim$2.3 eV is tentatively introduced on the basis of EA(C_3N)=2.4 eV, EA(C_5N)=2.3 eV, and EA(CN)=3.4 eV.

Recently, several studies have been reported on the measurement of negative ion mass spectra by the electron impact method.[1-6] However, they were restricted to a limited number of compounds. Data on the ionization efficiency (IE) curves of negative ions are limited[7-12] and hardly any detailed discussions are given.

The authors reported the measurement results of the IE curves of NO_2^-, O^-, $CH_2NO_2^-$, CN^-, and CNO^- ions from nitroalkanes,[13] of O^- and OH^- ions from *n*-propyl and isopropyl alcohols,[14] O^-, C_2H^-, and C_2HO^- ions from tetrahydrofuran,[15] and Cl^- ions from alkyl chlorides,[16] and discussed plausible reaction schemes expected to appear at respective onset values from a thermochemical viewpoint. The work was extended to methyl and ethyl cyanides.[17] Emphasis was placed on the measurements of the IE curves of CN^-, HCN^-, C_2N^-, and $CHCN^-$ ions from both compounds, and CH_2CN^- ions from methyl cyanide and C_3N^- ions from ethyl cyanide.

Experimental

Experiments were performed on a Hitachi RMU-6D mass spectrometer equipped with the T-2M ion source having a rhenium filament. The ion detection circuit consisted of a ten stage electron multiplier and a Faraday collector. All measurements were made with a total emission current of 20 μA, an accelerating voltage of 3.6 kV and an electron multiplier voltage of 2.8 kV, under a pressure of $\sim 10^{-6}$ mmHg in the source. The ionizing current then varied from 10.5 μA at above 10 eV to 6.4 μA at $\sim$3 eV.[16] The energy scale was calibrated in every measurement by the vanishing current method as compared with the appearance potential of *m/e* 16(O^-) ions from carbon monoxide, carbon dioxide and oxygen, as described previously.[16] The repeller voltage was adjusted to the best condition for collecting the ions. The chemicals used were of research grade.

Results and Discussion

IE curves. *CN^- Ions*: Figure 1 shows the IE curves of *m/e* 26 (CN^-) ions[18] obtained from methyl and ethyl cyanides. It can be seen that in every case at least two processes contribute to their formation. The first process appears at the energies lower than 2 eV and the second processes[19] do at $\sim$5.3 eV and

1) C. E. Melton, "Mass Spectrometry of Organic Ions," ed. by F. W. McLafferty, Academic Press, New York, N. Y. (1963), p. 163.
2) E. W. McDaniel, "Collision Phenomena in Ionized Gases," John Wiley & Sons Inc., New York (1964), p. 368.
3) F. Fiquat-Fayard, *Actions Chim. Biol. Radiations*, **8**, 31 (1965).
4) R. T. Aplin, H. Budzikieweiz, and C. Djerassi, *J. Am. Chem. Soc.*, **87**, 3180 (1965).
5) C. E. Melton and P. S. Rudolf, *J. Chem. Phys.*, **47**, 1771 (1967).
6) D. F. Munro, J. E. Ahnell, and W. S. Koski, *J. Phys. Chem.*, **72**, 2682 (1968).
7) L. G. Christophorou, R. N. Compton, G. S. Hurst, and P. W. Reinhardt, *J. Chem. Phys.*, **45**, 536 (1966).
8) L. G. Christophorou and R. N. Compton, *Health Physics*, **13**, 1277 (1967).
9) R. N. Compton and L. G. Christophorou, *Phys. Rev.*, **154**, 110 (1967).
10) T. Sugiura, T. Seguchi, and K. Arakawa, This Bulletin, **40**, 2992 (1967).
11) W. T. Nalf and C. D. Cooper, *J. Chem. Phys.*, **49**, 2784 (1968).
12) R. N. Compton, J. A. Stockdale, and P. W. Reinhardt, *Phys. Rev.*, **180**, 111 (1969).
13) S. Tsuda, A. Yokohata, and M. Kawai, This Bulletin., **42** 614, 1515 (1969).
14) S. Tsuda, A. Yokohata, and M. Kawai, *ibid.*, **42**, 2514 (1969).
15) S. Tsuda, A. Yokohata, and M. Kawai, *ibid.*, **42**, 3115 (1969).
16) S. Tsuda, A. Yokohata, and M. Kawai, *ibid.*, **43**, 1649 (1970).

17) A report was recently made on the measurement of methyl cyanide in which the isotope effect and mechanism of formation of CH_3CN^- ions were mainly discussed. Hardly any detailed discussions were given on fragment negative ions. (T. Sugiura and K. Arakawa. The 22nd Annual Meeting of Chemical Society of Japan, Tokyo (1969)).
18) The possibility of $C_2H_2^-$ for *m/e* 26 ions can be excluded because of few signals of $C_2H_2^-$ ions from hydrocarbons.[1]
19) Since the tailing from the 1st process may overlap with the appearance of the 2nd process, it is generally difficult to determine exactly the appearance potential of the latter. In this case, however, it was not so difficult.

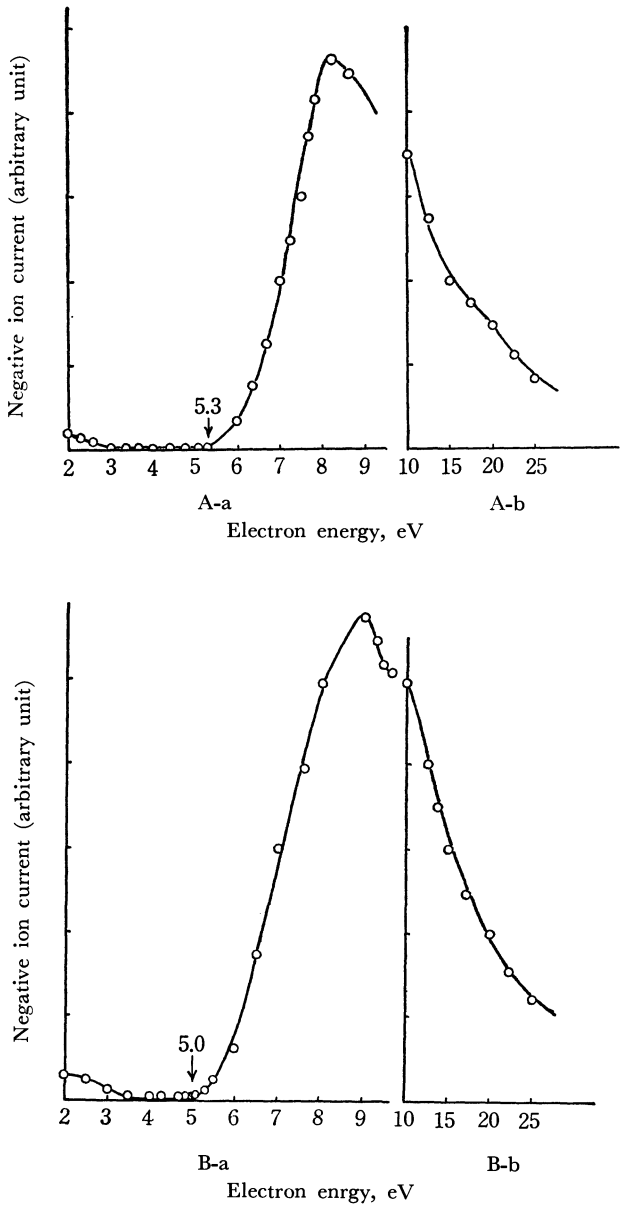

Fig. 1. Ionization efficiency curves of *m/e* 26(CN^-) ions from CH_3CN and C_2H_5CN.
A: CH_3CN B: C_2H_5CN

~5.0 eV, respectively, being of almost the same shape as the IE curves. They suggest dissociative electron capture processes except for the part in a higher energy region in which there is the possibility of an ion pair formation process.

The appearance potential (AP) of reaction (1) can be expressed by Eq. (2), if the kinetic energies of fragments are ignored and the ions formed are in ground state.

$$XYZ + e^- \rightarrow X^- + YZ \quad (1)$$

$$AP_{calc} = \Delta H = \Delta H_f(X^-) + \Delta H_f(YZ) - \Delta H_f(XYZ) \quad (2)$$ [20]

In the case of ion pair formation ($YZ \rightarrow YZ^+$), the following equation holds.

$$AP_{calc} = \Delta H = \Delta H_f(X^-) + \Delta H_f(YZ^+) - \Delta H_f(XYZ) \quad (3)$$

The schemes of plausible reactions expected to appear at each onset value (AP_{obs}) observed in the IE curves were sought thermochemically from Eqs. (2) and (3). For the first process, the following reactions might be assigned.

$$CH_3CN + e^- \rightarrow CN^- + CH_3 \quad (AP_{calc} = 1.08\ eV) \quad (4)$$

$$C_2H_5CN + e^- \rightarrow CN^- + C_2H_5 \quad (AP_{calc} = 1.08\ eV) \quad (5)$$

In the estimation of AP_{calc}, the values of $\Delta H_f(CH_3\text{-}CN) = 0.78$ eV,[21] $\Delta H_f(C_2H_5CN) = 0.49$ eV, $\Delta H_f(CH_3) = 1.39$ eV, $\Delta H_f(C_2H_5) = 1.10$ eV and $\Delta H_f(CN^-) = 0.47$ eV[22] were used.

The correspondence of AP_{calc} values to AP_{obs} values (below 2 eV) suggests the possibility of reactions (4) and (5). However, the cross section of these reactions seems to be very small. McDowell and Warren[23] failed to detect CN^- signals in this region, but this would probably be due to the fact that their detection method was not so improved as in the present time.

For the second process, although complicated, the following reactions might be considered.

$$CH_3CN + e^- \rightarrow CN^- + CH_2 + H \quad (AP_{calc} \simeq 4.45\ eV) \quad (6)$$

$$CH_3CN + e^- \rightarrow CN^- + CH + H_2 \quad (AP_{calc} \simeq 5.85\ eV) \quad (7)$$

$$C_2H_5CN + e^- \rightarrow CN^- + C_2H_3 + H_2 \quad (AP_{calc} \simeq 2.6\ eV) \quad (8)$$

$$C_2H_5CN + e^- \rightarrow CN^- + C_2H_4 + H \quad (AP_{calc} \simeq 2.78\ eV) \quad (9)$$

$$C_2H_5CN + e^- \rightarrow CN^- + C_2H_2 + H + H_2 \quad (AP_{calc} \simeq 4.59\ eV) \quad (10)$$

Estimation of each AP_{calc} value was made by use of values of $\Delta H_f(CH_2) = 2.5$ eV, $\Delta H_f(H) = 2.26$ eV, $\Delta H_f(CH) = 6.16$ eV, $\Delta H_f(C_2H_3) = 2.83$ eV, $\Delta H_f(C_2H_4) = 0.54$ eV and $\Delta H_f(C_2H_2) = 2.35$ eV.[24] Although the consistency of AP_{calc} values with AP_{obs} values is not so good, reactions (6) and (10) would probably correspond to each onset value. In these cases, the difference of 0.8—0.4 eV between AP_{calc}

20) $\Delta H_f(X)$: heat of formation of X.

21) By combining $D(CH_3\text{-}CN) = 4.48$ eV with $\Delta H_f(CH_3) = 1.39$ eV and $\Delta H_f(CN) = 3.87$ eV, a value of 0.78 eV for $\Delta H_f(CH_3\text{-}CN)$ can be estimated. Also, by assuming $D(CH_3\text{-}CN) = D(C_2H_5\text{-}CN)$, and using $\Delta H_f(C_2H_5) = 1.10$ eV, a value of $\Delta H_f(C_2H_5CN) = 0.49$ eV is obtained. (T. L. Cottrell, "The Strengths of Chemical Bonds," London, Butterworths (1958), p. 197. R. R. Bernecker and F. A. Long, *J. Phys. Chem.*, **65**, 1565 (1961). C. A. McDowell and J. W. Warren, *Trans. Faraday Soc.*, **48**, 1084 (1952).

22) To be estimated from $EA(CN) = 3.4$ eV and $\Delta H_f(CN) = 3.87$ eV (refer to (13)). EA(CN): electron affinity of CN.

23) C. A. McDowell and J. W. Warren, *Trans. Faraday Soc.*, **48**, 1084 (1952).

24) refer to Bernecker's paper in Ref. 21. The use of another value (4.23 eV) of $\Delta H_f(CH)$, as described in Ref. 25, gives $AP_{calc} = 3.92$ eV for the occurrence of reaction (7). However, the possibility of reaction (7) accompanied with the formation of H_2 due to the rearrangement would be probably smaller than that of reaction (6).

values (4.45 eV and 4.59 eV) and AP_{obs} values (5.3 eV and ~5.0 eV) might be assessed to the excess kinetic energy of fragments. Although McDowell and Warren[23] reported the value of ~5.6 eV for the appearance of CN^- ions from methyl cyanide, it might be interpreted to correspond to the second process in this work. However, they failed to detect the CN^- signals in the range below ~5.6 eV and no discussions were made in detail for CN^- ions from methyl cyanide. If a value of ~5.6 eV corresponds to the reaction of (CH_3+ CN^-), the excess kinetic energy of fragments seems to be too high. It would be reasonable to expect the occurrence of reaction (6). It is possible at least energetically.

Reasons for the existence of a long tail extending to the range from ~10 eV to the higher energies are not well known. Even if the overlapping of ion pair formation (reaction (11) or (12)) with reactions (6) or (10) is taken into consideration, the decrement of signal intensity with an increasing electron energy is a little strange. The possibility of the ion pair formation could be excluded.

$$CH_3CN + e^- \rightarrow CN^- + CH_3^+ + e^- \quad (AP_{calc} = 10.92\ eV) \quad (11)$$

$$C_2H_5CN + e^- \rightarrow CN^- + C_2H_5^+ + e^- \quad (AP_{calc} = 9.78\ eV) \quad (12)$$

HCN^- Ions: Figure 2 shows the IE curves of *m/e* 27 ions from methyl and ethyl cyanides. The possibility of $C_2H_3^-$ ions might be excluded from the fact that there is no occurrence of $C_2H_3^-$ ions from ethyl alcohol, propyl alcohol,[1] and tetrahydrofuran.[15] The two cyanides gave curves similar to each other. We see that the first process appears at ~2 eV for methyl cyanide and below 2 eV for ethyl cyanide, and the second process at ~6.0 eV and ~5.0 eV, respectively.

The appearance potential of reactions (13) and (14) can be estimated to be AP_{calc}=3.02 eV and AP_{calc}= 1.45 eV by using $\Delta H_f(HCN)$=1.30 eV[23]

$$CH_3CN \rightarrow HCN + CH_2 \quad (AP_{calc} = \Delta H_{calc} = 3.02\ eV) \quad (13)$$

$$C_2H_5CN \rightarrow HCN + C_2H_4 \quad (AP_{calc} = \Delta H_{calc} = 1.45\ eV) \quad (14)$$

Combining of AP_{calc}=3.02 eV with AP_{obs} ≃2 eV leads to EA(HCN) ≃1 eV.[25] Then, the appearance potential of the reaction containing HCN^- ion in (14) can be estimated to be ≲0.45 eV.

For the second process, reactions (15) and (16) might be expected, where a value of ΔH(CH)=4.23 eV[26] and a value of $\Delta H_f(HCN^-)$=0.3 eV are used.

$$CH_3CN + e^- \rightarrow HCN^- + CH + H \quad (AP_{calc} \simeq 6.01\ eV) \quad (15)$$

$$C_2H_5CN + e^- \rightarrow HCN^- + C_2H_3 + H \quad (AP_{calc} \simeq 4.90\ eV) \quad (16)$$

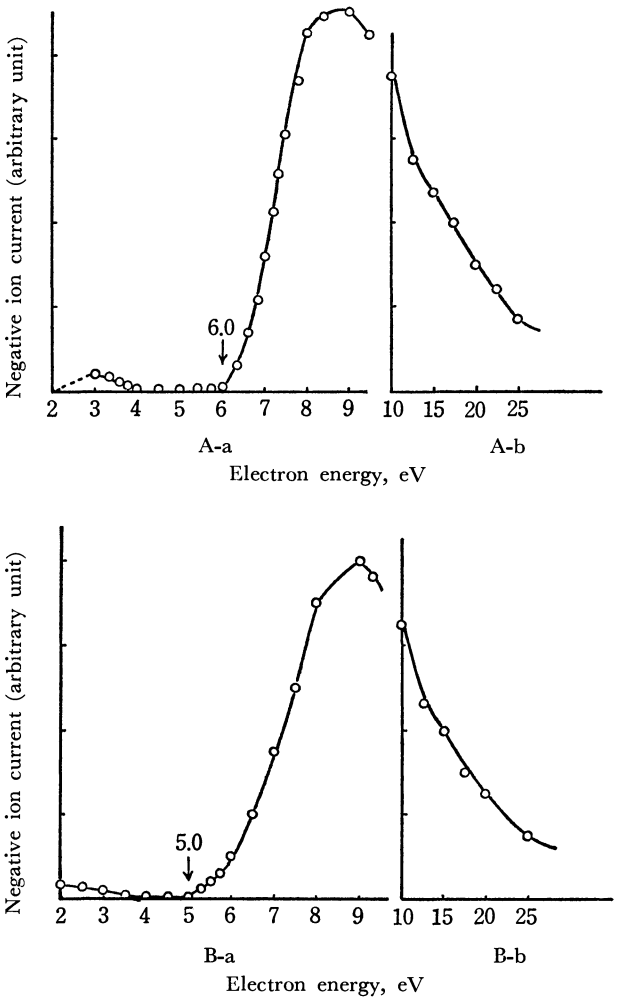

Fig. 2. Ionization efficiency curves of *m/e* 27(HCN^-) ions from CH_3CN and C_2H_5CN.
A: CH_3CN B: C_2H_5CN

The AP_{calc} values are in good agreement with the AP_{obs} values (~6.0 eV and ~5.0 eV).

Let us discuss the possibility of $C_2H_3^-$ ions. On the basis of ΔH_f(N)=4.9 eV,[27] the AP_{calc} value of reaction (17) can be estimated as follows.

$$CH_3CN \rightarrow C_2H_3 + N \quad (AP_{calc} = \Delta H_{calc} = 6.95\ eV) \quad (17)$$

Thus, if an electron affinity of C_2H_3 is assumed to be ~0.95 eV, the value of AP_{obs} ≃6.0 eV can be reasonably interpreted. If so, AP_{calc} of reaction (18) is given as ~5.2 eV which is almost consistent with AP_{obs} ≃5.0 eV.

$$C_2H_5CN + e^- \rightarrow C_2H_3^- + H_2 + CN \quad (AP_{calc} \simeq 5.2\ eV) \quad (18)$$

However, no formation of $C_2H_3^-$ ions from ethyl alcohol, propyl alcohol, and tetrahydrofuran would exclude the possibility of this ion. Moreover, the difficulty of interpretation of the first process by $C_2H_3^-$ ions affords additional evidence for their exclusion.

C_2N^- Ions: Figure 3 shows that we have

25) Since the ions might be formed with an excess kinetic energy, this shows the lowest value.

26) To be estimated from D(CH–H)=3.99 eV, ΔH_f(H)=2.26 eV and $\Delta H_f(CH_2)$=2.5 eV (refer to Cottrell's article Ref. 21, p. 174).

27) V. I. Vedeneyev, L. V. Gurvich, V. N. Kandrat'yev, V. A. Medvedev, and Ye. L. Frankevich, "Bond Energies, Ionization Potentials and Electron Affinities," Bulter Tranner Ltd., London (1966), p. 118.

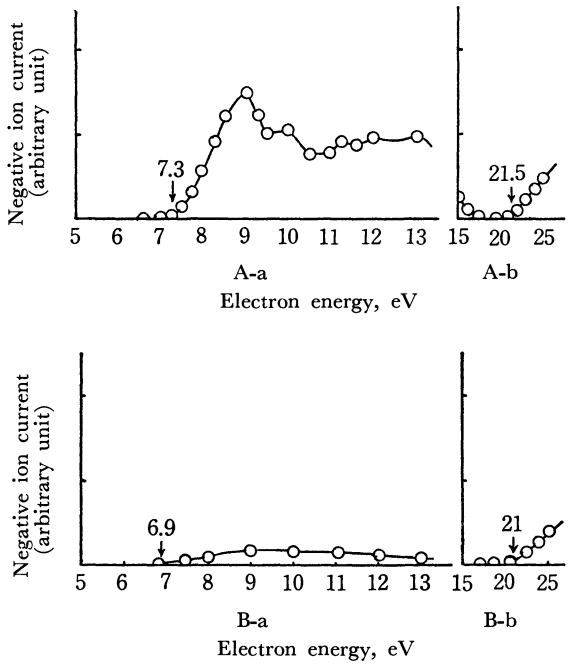

Fig. 3. Ionization efficiency curves of m/e 38(C_2N^-) ions from CH_3CN and C_2H_5CN.
A: CH_3CN B: C_2H_5CN

$AP_{obs} \simeq 7.3$ eV for the first process and $AP_{obs} \simeq 21.5$ eV for the second process in methyl cyanide, and $AP_{obs} \simeq 6.9$ eV and $AP_{obs} \simeq 21$ eV for the respective processes in ethyl cyanide. The IE curves from methyl cyanide show a relatively complicated shape for the first process, and a simple shape for that in ethyl cyanide. For the first process, we have

$$CH_3CN + e^- \rightarrow C_2N^- + H_2 + H \quad (AP_{calc} \leq 4.48\ eV) \quad (19)$$

$$CH_3CN + e^- \rightarrow C_2N^- + 3H \quad (AP_{calc} \leq 9.00\ eV) \quad (20)$$

$$C_2H_5CN + e^- \rightarrow C_2N^- + CH_3 + H_2 \quad (AP_{calc} \leq 3.90\ eV) \quad (21)$$

$$C_2H_5CN + e^- \rightarrow C_2N^- + CH_4 + H \quad (AP_{calc} \leq 3.99\ eV) \quad (22)$$

$$C_2H_5CN + e^- \rightarrow C_2N^- + CH_2 + H_2 + H \quad (AP_{calc} \leq 7.25\ eV) \quad (23)$$

$$C_2H_5CN + e^- \rightarrow C_2N^- + CH_3 + 2H \quad (AP_{calc} \leq 8.42\ eV) \quad (24)$$

In the estimation of AP_{calc}, a value of $\Delta H_f(C_2N^-) \leq 3$ eV was used which can be computed from $\Delta H_f(C_2N) = 5.3$ eV[28] and $EA(C_2N) \geq 2.3$ eV assumed tentatively. Evidently, we have no value of EA(C_2N) while EA(C_3N) and EA(C_5N) are known to be 2.4 eV and 2.3 eV,[28] being EA(CN) = 3.4 eV. Here, a value of ≥ 2.3 eV was assigned tentatively for EA(C_2N).

If reaction (19) is assumed to correspond to the first process, the difference (≥ 2.8 eV) between AP_{obs} ($\simeq 7.3$ eV) and AP_{calc} ≤ 4.48 eV might be ascribed to the excess kinetic energy of fragments. In the same way, the assignment of reaction (21) or (22) for the first process in ethyl cyanide may give a value ≥ 3 eV as the excess kinetic energy of fragments. In the present stage, however, this is still open to question.

For the second process, we have

$$CH_3CN + e^- \rightarrow C_2N^- + H^+ + H_2 + e^- \quad (AP_{calc} \leq 18.08\ eV) \quad (25)$$

$$C_2H_5CN + e^- \rightarrow C_2N^- + CH_3^+ + H_2 + e^- \quad (AP_{calc} \leq 13.70\ eV) \quad (26)$$

$$C_2H_5CN + e^- \rightarrow C_2N^- + H^+ + CH_4 + e^- \quad (AP_{calc} \leq 17.59\ eV) \quad (27)$$

The assignment of reactions (25) and (27) seems also to require a kinetic energy ≥ 3.5 eV for the fragments.

$CHCN^-$ Ions: The IE curves (Fig. 4) show that three processes in methyl cyanide and two processes in ethyl cyanide contribute to the formation of m/e 39 ($CHCN^-$) ions, where in the former the first process appears at $\sim$2.3 eV, the second process at $\sim$7.0 eV and the third process at $\sim$20 eV; in the latter the respective processes appear at $\sim$6.5 eV and $\sim$16.5 eV.

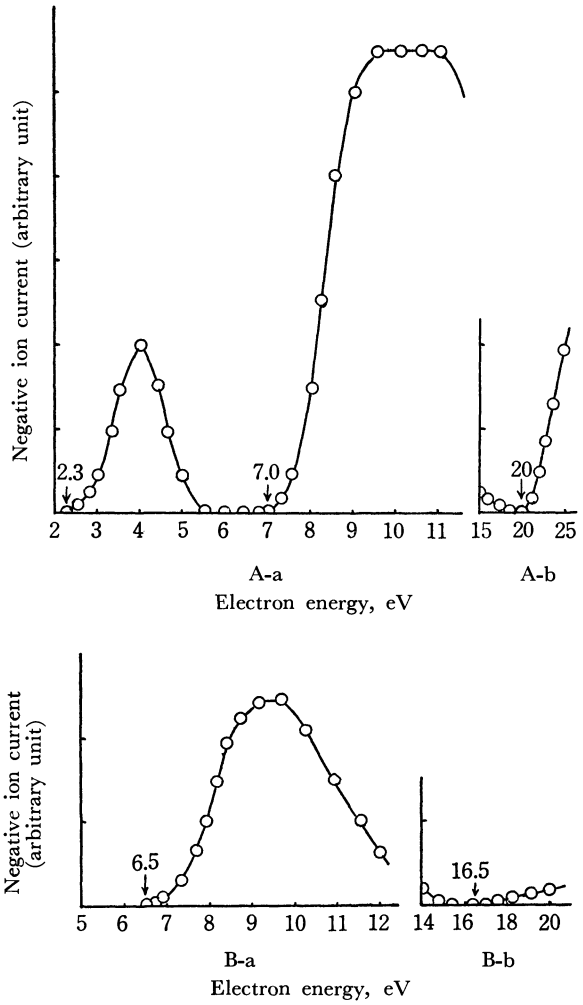

Fig. 4. Ionization efficiency curves of m/e 39 ($CHCN^-$) ions from CH_3CN and C_2H_5CN.
A: CH_3CN B: C_2H_5CN

28) V. H. Dibeler, R. M. Reese, and J. L. Franklin, *J. Amer. Chem. Soc.*, **83**, 1813 (1961).

Since the ΔH_f(CHCN) and EA(CHCN) values are not known, it is impossible to estimate AP_{calc} values of the reactions assigned for each process. By setting $\Delta H_f(CHCN^-) = \Delta H_f(CHCN) - EA(CHCN) = X$ (eV), let us estimate the AP_{calc} values of the reactions to be assigned for each onset value in the IE curves.

For the first process in methyl cyanide,

$$CH_3CN + e^- \rightarrow CHCN^- + H_2$$
$$(AP_{calc} = X - 0.78 \text{ (eV)}) \quad (28)$$

For the second process in methyl cyanide and the first process in ethyl cyanide,

$$CH_3CN + e^- \rightarrow CHCN^- + 2H$$
$$(AP_{calc} = X + 3.74 \text{ (eV)}) \quad (29)$$
$$C_2H_5CN + e^- \rightarrow CHCN^- + CH_3 + H$$
$$(AP_{calc} = X + 3.16 \text{ (eV)}) \quad (30)$$

Combining these values with AP_{obs} values (2.3 eV, 7.0 eV, and 6.5 eV) we obtain the results 3.08 eV, 3.26 eV, and 3.34 eV for X; $\bar{X}$=3.23 eV. Then the AP_{calc} values of reactions expected for the last process can be estimated as follows.

For the third process in methyl cyanide and the second process in ethyl cyanide.

$$CH_3CN + e^- \rightarrow CHCN^- + H^+ + e^-$$
$$(AP_{calc} = 20.56 \text{ eV}) \quad (31)$$
$$C_2H_5CN + e^- \rightarrow CHCN^- + CH_3^+ + H + e^-$$
$$(AP_{calc} = 16.23 \text{ eV}) \quad (32)$$

The consistency of the AP_{calc} values with the AP_{obs} values ($\sim$20 eV and $\sim$16.5 eV) is relatively good. In other words, the assignment of each reaction and a value of $\Delta H_f(CHCN^-) \simeq 3.2$ eV might be reasonable.

Next, let us estimate a value of ΔH_f(CHCN). The appearance potential of reaction (33) gives the value of $\Delta H_f(CHCN^+) \simeq 15.9$ eV.[29] An estimation of ΔH_f(CHCN) is needed for the value of IP(CHCN)[30] but it is not known.

$$CH_3CN \rightarrow CHCN^+ + H_2 + e^- \quad (AP = 15.1 \text{ eV}) \quad (33)$$

According to Mulliken's assignment, the values of $IP(C_2H_6)$ (=11.65 eV[31]) and the onset ($\sim$11.7 eV)[32] in the IE curves of $C_2H_5OH^+$ ions from ethyl alcohol are considered to correspond to the removal of an electron from the C–C orbital. On the other hand, the removal of an electron from the C–H π orbital requires a value of about 13 eV.[33] Thus, let us assign tentatively IP(CHCN)$\simeq$11.7 eV, the energy required for the removal of an electron from the C–C orbital. We can then get a value of 4.2 eV for ΔH_f(CHCN). If so, a value of $\Delta H_f(CH_2CN) = 1.96$ eV[34] would lead to D(H–CHCN)$\simeq$4.5 eV. Judging from the usual C–H bond energy, this value seems to be reasonable.

Thus, EA(CHCN) could be estimated by combining the values of ΔH_f(CHCN) and $\Delta H_f(CHCN^-)$. Since the fragment ions may be formed with an excess kinetic energy, the following procedure is preferable. Let us assume EA(CHCN)=Y (eV) and excess kinetic energy=Z (eV). Then, the AP_{calc} of reaction (34) is estimated as follows.

$$CH_3CN + e^- \rightarrow CHCN^- + H_2$$
$$(AP_{calc} = 3.4 - Y + Z) \quad (34)$$

By combining this value with $AP_{obs} \simeq 2.3$ eV, we can get a value of EA(CHCN)$\gtrsim$1.1 eV.

CH_2CN^- Ions: The IE curves (Fig. 5) represent the typical dissociative electron capture process. We have $AP_{obs} \simeq 1.8$ eV.

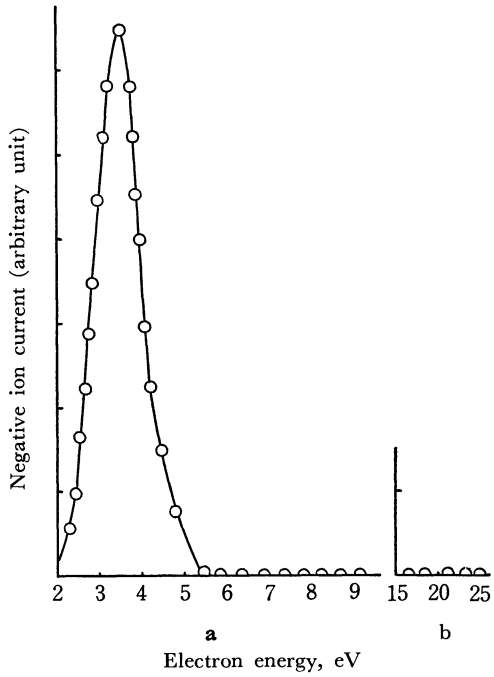

Fig. 5. Ionization efficiency curves of *m/e* 40 $(CH_2CN)^-$ ion from CH_3CN.

The appearance potential of reaction (35)[34] has been reported to be 3.44 eV which gives a value of $\Delta H_f(CH_2CN) = 1.96$ eV.

$$CH_3CN \rightarrow CH_2CN + H$$
$$(AP_{calc} = \Delta H_{calc} = 3.44 \text{ eV}) \quad (35)$$

The value EA(CH_2CN)$\geq$1.64 eV is obtained by combining AP_{calc} (=3.44 eV) with AP_{obs} (1.8 eV).

For the ion pair formation the following reaction is expected.

$$CH_3CN + e^- \rightarrow CH_2CN^- + H^+ + e^-$$
$$(AP_{calc} = 15.4 \text{ eV}) \quad (36)$$

However, few signals in the range of energies from $\sim$5.4 eV to 25 eV appear to exclude the possibility of ion pair formation.

C_3N^- Ions: Figure 6 shows that the first process appears at $\sim$9.4 eV and the second process at $\sim$13.9 eV, although their cross sections are small.

On the basis of $\Delta H_f(C_3N) = 131$ kcal/mol[28] and EA(C_3N)=55 kcal/mol,[28] the AP_{calc} values of reac-

29) F. H. Field and J. L. Franklin, "Electron Impact Phenomena," Academic press, New York, N. Y. (1957), p. 274.
30) IP(X): ionization potential of X.
31) R. S. Mulliken, *J. Chem. Phys.*, **3**, 519 (1935).
32) S. Tsuda and W. H. Hamill, *Advan. Mass Spectry.*, **3**, 249 (1965).
33) C. A. McDowell and B. C. Cox, *J. Chem. Phys.*, **22**, 946 (1954).
34) R. F. Pottie and F. P. Lossing, *J. Amer. Chem. Soc.*, **83**, 4737 (1961).

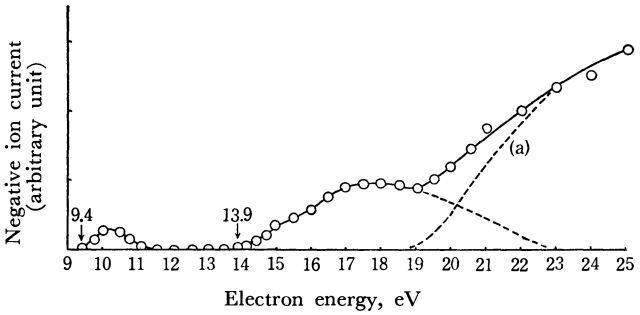

Fig. 6. Ionization efficiency curves of m/e 50(C_3N^-) ions from C_2H_5CN.

tions (37), (38), (39), and (40) can be estimated as follows:

$$C_2H_5CN + e^- \rightarrow C_3N^- + 2H_2 + H \quad (AP_{calc} = 5.09\,eV) \quad (37)$$

$$C_2H_5CN + e^- \rightarrow C_3N^- + H_2 + 3H \quad (AP_{calc} = 9.59\,eV) \quad (38)$$

$$C_2H_5CN + e^- \rightarrow C_3N^- + 5H \quad (AP_{calc} = 14.09\,eV) \quad (39)$$

$$C_2H_5CN + e^- \rightarrow C_3N^- + 2H_2 + H^+ + e^- \quad (AP_{calc} = 18.69\,eV) \quad (40)$$

Relatively good consistencies of AP_{calc} values (9.59 and 14.09 eV) with AP_{obs} values ($\sim$9.4 and $\sim$13.9 eV) suggest the possibility of reactions (38) and (39). Reaction (37) could be excluded.

The shape of the IE curve in the energy region higher than $\sim$18.7 eV can be well interpreted in terms of the overlapping due to the ion pair formation (reaction (40)) appearing at 18.69 eV. The IE curves expected from the ion pair formation process are expressed by a dotted curve, (a) in Fig. 6, which is consistent with the usual picture presumed for the ion pair formation.

BULLETIN OF THE CHEMICAL SOCIETY OF JAPAN, VOL. 44, 1491—1496 (1971)

The Hybridization Effect on the Equilibrium Distance. III[1]

Tomoo MIYAZAKI, Tsunehisa SHIGETANI, and Hiroyuki SHINODA

Department of Applied Chemistry, Faculty of Science and Engineering, Waseda University, Nishi-Ohkubo, Shinjuku-ku, Tokyo

(Received November 30, 1970)

In order to re-examine the unexpected conclusion previously reported that the hybridization effect is unimportant in determining the C–C single bond length, a more reliable calculation involving the configuration interaction treatment and more elabolate calculations by the NDDO and unrestricted INDO methods have been performed. The results of the INDO-CI and unrestricted INDO calculations were in good agreement with those which were obtained by the previous calculations. According to the NDDO calculations, however, the equilibrium distances of different kinds of C–C single bonds were found to increase with the decreased *s* character in hybrids, although this effect was not very significant. The effect of interaction between non-adjacent atomic orbitals in determining the bond length has been discussed in full detail.

The object of the present paper is to explore the relative importance of the pi electron resonance and hybridization in the shortening of the single-bond length of conjugated hydrocarbons. During the past several years, many discussions have been presented concerning this problem.[4–6] Mulliken commented on this situation that it was rather necessary, and proper, to place considerable reliance on a theory, provided it was a reliable theory, since it was difficult to decide experimentally between hybridization and electron delocalization as causes of bond shortening.[7] In those days, however, there was no appropriate and direct method for calculating the equilibrium distance. At the present time, though, the interatomic distance can be calculated by such semi-empirical, self-consistent molecular orbital methods as the CNDO/2,[8–10] INDO,[11] NDDO[8] and MINDO[12] methods, in all of which all the valence electrons are taken into account. They have been developed mainly with the object of calculating the ground-state properties of molecules.

In a previous paper,[2] the CNDO/2 method was used to calculate the C–C and C–H equilibrium distances of the saturated and unsaturated simple hydrocarbons and those molecules which have broken pi bonds. The equilibrium distances of different types of C–C single and double bonds which are usually considered tri-tri, di-di single and di-di double bonds

1) The previous paper[2] (1969) and communication[3] (1970) are regarded as Part I and Part II of this series respectively.

2) T. Miyazaki and H. Ohbayashi, This Bulletin, **42**, 2767 (1969).

3) T. Miyazaki, *Tetrahedron Lett.*, **16**, 1363 (1970).

4) M. J. S. Dewar and A. N. Schmeising, *Tetrahedron*, **5**, 166 (1959).

5) R. S. Mulliken, *ibid.*, **6**, 68 (1959).

6) "An Epistologue on Carbon Bonds," *ibid.*, **17**, 123—266 (1962).

7) R. S. Mulliken, *ibid.*, **17**, 247 (1962).

8) J. A. Pople, D. P. Santry, and G. A. Segal, *J. Chem. Phys.*, **43**, S 129 (1965).

9) J. A. Pople and G. A. Segal, *ibid.*, **43**, S 136 (1965).

10) J. A. Pople and G. A. Segal, *ibid.*, **44**, 3289 (1966).

11) J. A. Pople, D. L. Beveridge, and P. A. Dobosh, *ibid.*, **47**, 2027 (1967).

12) M. J. S. Dewar and E. Haselbach, *J. Amer. Chem. Soc.*, **92**, 590 (1970).

were not much different from the te-te single and tri-tri double bond distances respectively. Moreover, it was found that the equilibrium distances are dependent upon the interaction between non-adjacent atomic orbitals.

In a previous communication,[3] the INDO method was used to determine the effect of the introduction of the one-center exchange integrals into the calculation of the C–C equilibrium distance. Both the INDO and CNDO/2 methods seemed to indicate that the hybridization effect is unimportant in the shortening of the C–C single bond length.

In view of the above results, a more reliable calculation involving configuration interaction (CI) treatment and more elabolate calculations by the NDDO and unrestricted INDO methods will be used in this paper to determine the normal and hypothetical C–C equilibrium distances. The effect of interaction between non-adjacent atomic orbitals in determining the bond length has been discussed in full detail. This is because these electronic interactions are appreciably effective in determining the C–C equilibrium distance.

Methods of Calculation

Calculation of the sp^2–sp^2 Single Bond Length. The calculation is illustrated schematically in the energy curve of Fig. 1. The equilibrium distance of the sp^2–sp^2 C–C single bond was estimated by minimizing an energy (E^+) with respect to the interatomic distance

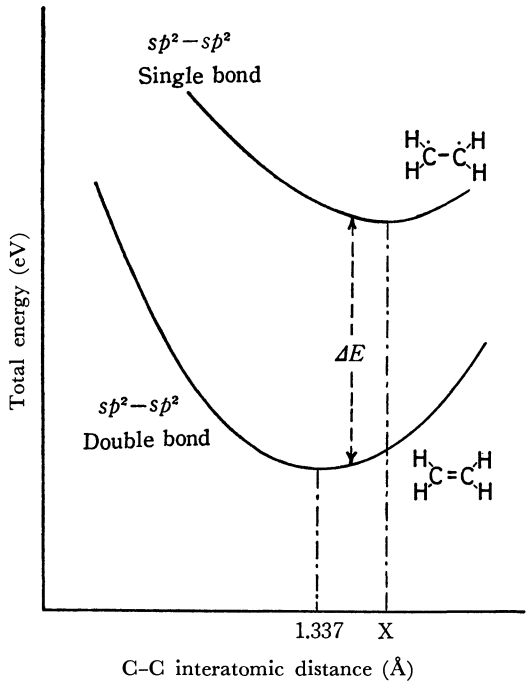

Fig. 1. Total energy as a function of C–C bond length. X is the equilibrium distance of sp^2–sp^2 single bond.

considered. The energy (E^+) was defined by the following equation:

$$E^+ = E_{\text{total}} - \Delta E \tag{1}$$

$$E_{\text{total}} = E_{\text{elec}} + E_{\text{repul}} \tag{2}$$

$$\Delta E = \frac{1}{4}\sum_{\mu}^{\pi}(P^{\pi}{}_{\mu\mu})^2\gamma_{\mu\mu} + \frac{1}{2}\sum_{\substack{\mu,\nu \\ (\mu\neq\nu)}} {}^{\pi}P^{\pi}{}_{\mu\nu}(H_{\mu\nu}{}^{\pi}+F^{\pi}{}_{\mu\nu})$$

$$= \frac{1}{4}\sum_{\mu}^{\pi}(P^{\pi}{}_{\mu\mu})^2\gamma_{\mu\mu} + 2P^{\pi}{}_{\mu\nu}\beta^{\pi}{}_{\mu\nu} - \frac{1}{2}(P^{\pi}{}_{\mu\nu})^2\gamma_{\mu\nu} \tag{3}$$

where E_{elec} is the total electronic energy of ethylene as determined by the molecular orbital calculation, where E_{repul} is the sum of the repulsion energy between cores, which is approximated by a point charge model, where $\sum^{\pi}$ describes the summation over the pi system, where $P^{\pi}{}_{\mu\mu}$ is the pi orbital charge density, where $P^{\pi}{}_{\mu\nu}$ is the pi bond order, where $\gamma_{\mu\mu}$ and $\gamma_{\mu\nu}$ are one-center and two-center electron-electron repulsion integrals respectively, and where $\beta_{\mu\nu}$ is the resonance integral between the atomic orbitals, χ_{μ} and χ_{ν}. The equilibrium distance was calculated by the variation of the interatomic distance, while the other bonds in the molecule were held fixed at their observed equilibrium distances.

The equilibrium distances of the *sp*–*sp* single and double bonds can be estimated in the same manner as has been described above.

The INDO and Other Methods. The intermediate neglect of the differential overlap (INDO) method employed in the present calculation is based upon an SCF treatment of all the valence electrons and is regarded as an improvement over the CNDO/2 method used to determine the equilibrium distance of the C–C bond in the previous investigation. In the INDO method, all two-electron integrals involving differential overlap are neglected except for one-center integrals of $(\mu\nu|\mu\nu)$ type; the other one-center integrals involving orbital overlap vanish through symmetry. The one-center repulsion integrals are written in terms of the Slater-Condon parameters, which are known from analyses of the multiplet energy splitting for the free atoms. The values of these terms used in the INDO method has been listed by Pople *et al.*[11] The monatomic core integrals differ somewhat from those of the CNDO/2 method because of the introduction of these parameters.

The molecular orbitals and their energies can be obtained by solving the set of secular equations and the corresponding secular matrix consisting of the Fock elements. The expressions for the Fock matrix elements and the details of the method can be found in Pople's original paper.[8–11]

The NDDO method disregards differential overlap only for atomic orbitals on different atoms. At this level of approximation, $(\mu_A\nu_A|\lambda_B\sigma_B)$ type integrals are taken into account. All the electronic repulsions are theoretically evaluated according to the formulas listed by Roothaan,[13] and the approximation where all the electron repulsion integrals are calculated as Coulomb integrals involving a valence *s* function is avoided.

A more reliable method of calculation for determining the equilibrium distance uses a configuration interaction (CI) treatment. The hypothetical bond length of a molecule, including the broken pi bonds,

13) C. C. J. Roothaan, *J. Chem. Phys.*, **19**, 1445 (1951).

can be calculated by the corrected total energy considering the interaction of the ground state with doubly-excited configurations (^1A_g) for the sigma system. All the doubly-excited configurations were taken into account for ethylene and acetylene, but the CI calculation was restricted to the 30 doubly-excited states for ethane.

The configurations of the molecules including the broken pi bonds are all open-shell. In applying the unrestricted INDO method to the calculation of these molecules, calculations for different types of spin multiplicity are possible. However, the spin multiplicity of the hypothetical molecule discussed in this work may be considered to be a singlet state.

In order to investigate the effect of electronic interaction between non-adjacent atomic orbitals in determining the bond length, the equilibrium distance has been determined from the total energy, neglecting some interactions between atomic orbitals. The invariance property of the INDO method under a simple transformation, such as the replacement of the s and p orbitals by hybrids, is effective for this investigation.

Through the similarity transformation by some appropriate matrix, the energy ($H'_{\mu\nu}$ and $F'_{\mu\nu}$) and population ($P'_{\mu\nu}$) matrices, with reference to the carbon hybrids, can be obtained from the results of the INDO calculation. The interactions (E^*) between non-adjacent hybrids are given by:

$$E^*_{\mu\nu} = P'_{\mu\nu}(H'_{\mu\nu}+F'_{\mu\nu}) . \quad (4)$$

Results and Discussion

The C–H equilibrium distances of ethane, ethylene, and acetylene calculated by both the CNDO/2 and INDO methods are shown in Table 1. In Table 2, the C–C equilibrium distances of C_2-hydrocarbons calculated by a variety of methods are collected. The distances obtained by the INDO-CI treatment of the present work are in complete agreement with those obtained by the CNDO/2 and INDO methods of the previous paper. Generally, the equilibrium distances calculated by the INDO and INDO-CI methods are slightly longer than those obtained by the CNDO/2 calculation. The C–C equilibrium distances calculated by the NDDO method were shorter than those obtained by the INDO and CNDO/2 calculations. The calculated interatomic distances of the tri-tri, di-di single, and di-di double bonds by the INDO-CI treatment are substantially in agreement with the results of the CNDO/2 calculation, the simplest form of calculation. The results of the unrestricted INDO calculations for the equilibrium distances in different types of spin states are listed in Table 3. They did not differ from one another in the calculated equilibrium distance.

However, a tendency for the bond length to decrease with an increased s character of the hybrid was found in the results of the NDDO calculations for the hypothetical tri-tri and di-di single and di-di double bond lengths. This is a noteworthy fact, but the difference between the te-te and tri-tri single bonds is negligible. The result obtained by the NDDO method must be due to the fact that all the electronic repulsions are theoretically calculated; that is, the usual approximation, in which they are assumed to depend only on the atoms and not on the actual type of orbital, is unnecessary in this calculation.

From the results of the NDDO calculation, it follows that the C–C single bond length is certainly affected by the types of the hybridization of the carbon atom, but this hybridization effect is not so large as has previously been believed.

The problem in this paper should be re-examined by the modified CNDO/2[14] and MINDO[15] methods, in which the off-diagonal bonding parameters are given by the different types of approximation. This is true because the off-diagonal bonding parameter

Table 1. Carbon-hydrogen equilibrium distances

Molecule	C-H Equilibrium distance (Å)		
	CNDO/2[a]	INDO	Obsd[b]
Ethane	1.117	1.120	1.093
Ethylene	1.106	1.113	1.086
Acetylene	1.088	1.095	1.058

a) The result of the CNDO/2 method was published in the previous paper.[2]
b) "Interatomic Distances," Supplement, Special Publication, No. 18, The Chemical Society (London).

Table 2. Carbon-carbon equilibrium distances

Type of C-C bond	C-C Equilibrium distance (Å)				
	CNDO/2[a]	INDO[a]	INDO-CI	NDDO	Obsd[b]
te-te single	1.471	1.472	1.472	1.460	1.534
tri-tri single	1.475	1.479	1.480	1.456	
di-di single	1.476	1.479	1.480	1.447	
tri-tri double	1.317	1.319	1.328	1.305	1.337
di-di double	1.323	1.325		1.301	
di-di triple	1.198	1.200	1.210	1.181	1.205

a) The results of the CNDO/2 and INDO methods were published in the previous paper[2] and communication.[3]
b) "Interatomic Distances," Supplement, Special Publication, No. 18, The Chemical Society (London).

14) J. D. Bene and H. H. Jaffé, *J. Chem. Phys.*, **48**, 1807 (1968).

15) For example, M. J. S. Dewar, and E. Haselbach, *J. Amer. Chem. Soc.*, **92**, 590 (1970).

TABLE 3. CARBON-CARBON EQUILIBRIUM DISTANCES BY THE UNRESTRICTED INDO CALCULATION

Type of C-C bond	C-C Equilibrium distance (Å)		
	Singlet	Triplet	Quintet
te-te single	(1.472)		
tri-tri single	1.483	1.479	
di-di single	1.479[a]		1.483
di-di single	1.485[b]		
di-di single	1.482[c]		

Electron spins are assigned as illustrated below.

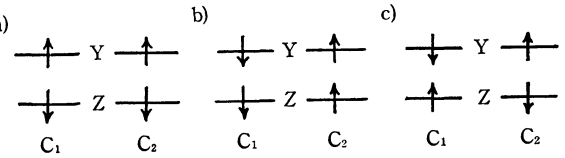

(β_A^0) is given the same value for resonance integrals between sigma orbitals and those between pi orbitals in the CNDO/2 and INDO methods. In the modified CNDO/2 method proposed by Bene and Jaffé, the $\beta_{\mu\nu}^{\sigma}$, where μ and ν are sigma orbitals, is distinguished from the $\beta_{\mu\nu}^{\pi}$, where μ and ν are pi orbitals, by introducing a empirical parameter, k, as follows:

$$\beta_{\mu\nu}^{\sigma} = \frac{1}{2} S_{\mu\nu}(\beta_A^0 + \beta_B^0) \tag{5}$$

$$\beta_{\mu\nu}^{\pi} = \frac{1}{2} k S_{\mu\nu}(\beta_A^0 + \beta_B^0) \tag{6}$$

Also, in the MINDO method proposed by Dewar *et al.*, the resonance integrals are approximated by the following equation:

$$\beta_{\mu\nu} = \frac{1}{2} k' S_{\mu\nu}(I_\mu + I_\nu) \tag{7}$$

where k' is a constant and where I_μ and I_ν are valence-state ionization potentials for the atomic orbitals, χ_μ and χ_ν respectively. However, the energies and orbitals obtained using the approximation (Eq. (7)) will not be invariant to hybridization of the atomic-orbital basis set.

The results of the NDDO calculation indicate the hybridization effect on the equilibrium distance should be discussed by the use of the calculations presented above.

The effect of the interaction between non-adjacent atomic orbitals for determining the interatomic distance can be made clear by the use of Tables 4—6. The magnitude of the absolute value of Δr in Tables 4—6 proves the extent of the effect of non-adjacent atomic orbital interaction (E^*) in determining the equilibrium distance. It should be emphasized that the most effective factor in determining the interatomic distance is the gradient of the variation of the interaction energy (E^*) with the change in the interatomic distance rather than the magnitude of its absolute value.

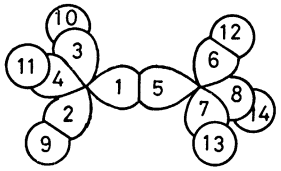

Fig. 2. The numbering of atomic orbital. (Ethane)

TABLE 4. THE EFFECT OF INTERACTION BETWEEN NON-ADJACENT ATOMIC ORBITALS[a] FOR DETERMINING THE EQUILIBRIUM DISTANCES

Neglected atomic orbital interaction[b]	Ethane, C-H (1.120 Å), C-C (1.472 Å)[a]	
	Δr (Å)[c,d]	
	C-H	C-C tri-tri single
(9—10), (9—11), (10—11), (12—13), (12—14), (13—14)	+0.001	−0.003
(9—12), (9—13), (9—14), (10—12), (10—13), (10—14), (11—12), (11—13), (11—14)	−0.001	+0.001
(2—12), (2—13), (2—14), (3—12), (3—13), (3—14), (4—12), (4—13), (4—14), (6—9), (6—10), (6—11), (7—9), (7—10), (7—11), (8—9), (8—10), (8—11)	−0.001	+0.008
(2—10), (2—11), (3—9), (3—11), (4—9), (4—10), (6—13), (6—14), (7—12), (7—14), (8—12), (8—13)	0	+0.010
(1—9), (1—10), (1—11), (5—12), (5—13), (5—14)	+0.003	−0.028
(1—12), (1—13), (1—14), (5—9), (5—10), (5—11)	+0.007	+0.034
(1—2), (1—3), (1—4), (2—3), (2—4), (3—4), (5—6), (5—7), (5—8), (6—7), (6—8), (7—8)	−0.007	−0.024
(1—6), (1—7), (1—8), (5—2), (5—3), (5—4)	−0.007	+0.058
(2—6), (2—7), (2—8), (3—6), (3—7), (3—8), (4—6), (4—7), (4—8)	−0.007	+0.123

a) The equilibrium distances were calculated by the INDO method.
b) The orbital numbers are indicated in Fig. 2.
c) The Δr is difference between the equilibrium distance and the bond length calculated from the total energy neglecting the non-adjacent atomic orbital interaction.
d) The plus and minus signs refer to the lengthening and shortening of distance, respectively.

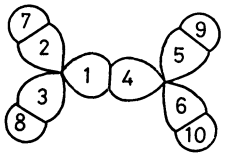

Fig. 3. The numbering of atomic orbital. (Ethylene sigma system)

Fig. 4. The numbering of atomic orbital. (Acetylene sigma system)

Conclusion

The unexpected conclusion reported previously that the C–C bond length is little affected by the types of the hybridization of the carbon atom has been re-examined by the INDO-CI, NDDO and unrestricted INDO methods.

The conclusion from the INDO-CI and unrestricted INDO calculations has agreed with that obtained previously by the CNDO/2 calculation. However, a tendency for the bond length to decrease with an increase in the *s* character in hybrids was found in the results of the NDDO calculations for the hypothetical tri-tri and di-di single, and the di-di double bond

Table 5. The effect of interaction between non-adjacent atomic orbitals for determining[a] the equilibrium distance

Ethylene, C-H (1.113 Å), C=C (1.319 Å), C-C (1.479 Å)[a]			
Neglected atomic orbital interaction[b]	Δr (Å)[c,d]		
	C-H	C=C tri-tri double	C-C tri-tri single
(7—8), (9—10)	−0.001	0	0
(7—9), (8—10)	−0.001	−0.003	−0.004
(7—10), (8—9)	0	+0.010	+0.005
(1—2), (1—3), (2—3), (4—5), (4—6), (5—6)	−0.019	−0.019	−0.031
(1—5), (1—6), (4—2), (4—3)	−0.009	+0.052	+0.036
(2—5), (3—6)	−0.003	+0.028	+0.025
(2—6), (3—5)	−0.006	+0.043	+0.040
(1—7), (1—8), (2—8), (3—7), (4—9), (4—10), (5—10), (6—9)	0	−0.007	−0.011
(1—9), (1—10), (4—7), (4—8)	+0.008	+0.012	+0.009
(2—9), (3—10), (5—7), (6—8)	−0.001	+0.003	+0.002
(2—10), (3—9), (5—8), (6—7)	0	+0.001	−0.011

a) The equilibrium distances were calculated by the INDO method.
b) The orbital numbers are indicated in Fig. 3.
c) The Δr is difference between the equilibrium distance and the bond length calculated from the total energy neglecting the non-adjacent atomic orbital interaction.
d) The plus and minus signs refer to the lengthening and shortening of distance, respectively.

Table 6. The effect of interaction between non-adjacent atomic orbitals for determining the equilibrium distance

Acetylene, C-H (1.095 Å), C≡C (1.200 Å), C=C (1.325 Å), C-C (1.479 Å)[a]				
Neglected atomic orbital interaction[b]	Δr (Å)[c,d]			
	C-H	C≡C di-di triple	C=C di-di double	C-C di-di single
(5—6)	0	+0.001	−0.003	+0.001
(1—4), (3—2)	−0.006	+0.023	+0.008	−0.001
(2—4)	−0.002	+0.009	+0.002	+0.004
(1—2), (3—4)	−0.019	−0.013	−0.023	−0.032
(1—5), (3—6)	+0.004	0	−0.005	−0.003
(1—6), (3—5)	+0.001	−0.001	−0.005	−0.005
(2—6), (4—5)	0	0	−0.003	0

a) The equilibrium distances were calculated by the INDO method.
b) The orbital numbers are indicated in Fig. 4.
c) The Δr is difference between the equilibrium distance and the bond length calculated from the total energy neglecting the non-adjacent atomic orbital interaction.
d) The plus and minus signs refer to the lengthening and shortening of distance, respectively.

lengths. The tendency was, however, very small in comparison with those generally found.

It has been noted that the equilibrium distances are largely dependent on some electronic interactions between non-adjacent atomic orbitals.

A more extensive study of this problem by methods using different types of approximation for estimating the resonance integral will be the subject of a subsequent paper.

Our thanks are offered to Professor K. Higasi for his continuous interest and encouragement. The calculations were carried out on the IBM-7040 computer at the Computation Center of Waseda University. We would like to thank I.B.M. Japan, Ltd., for lending this computer to the university.

BULLETIN OF THE CHEMICAL SOCIETY OF JAPAN, VOL. 44, 1496—1503 (1971)

The Protonation of Aromatic Hydrocarbon Radical Anions. I. A Comparison of Methods and a Study of the Mechanism[1)]

Shigeo HAYANO and Masamichi FUJIHIRA

Institute of Industrial Science, The University of Tokyo, Roppongi, Minato-ku, Tokyo

(Received November 30, 1970)

The protonation mechanism of the aromatic hydrocarbon radical anions, such as biphenyl, naphthalene, phenanthrene, anthracene, 1,2-benzanthracene, and pyrene, in dimethylformamide (DMF) and water mixtures was studied. Three methods of measuring the concentration of the radical anions, *i.e.* polarography and ESR and UV absorption spectroscopy, were compared with each other by making simultaneous measurements of the same anthraquinone radical anion solution. A good linear relation of the polarographic anodic diffusion current to the UV absorbance was found, while the ESR signal intensity had linear relations with neither of the others in the system which contained an excessive number of parent molecules, 2×10^{-3} M. The change in the visible absorption spectra of the aromatic hydrocarbon radical anions as a function of the time suggested that all the aromatic hydrocarbon radical anions decay by a first-order reaction. As a result, the radical anions were considered to decay through the following sequence:

$$R^{\cdot-} + H_2O \xrightarrow{k} RH\cdot + OH^-,\ RH\cdot + R^{\cdot-} \rightleftarrows RH^- + R,\ \text{and}\ RH^- + H_2O \xrightarrow{k'} RH_2 + OH^-.$$

The electrochemical reduction of aromatic hydrocarbons in aprotic solvents has been the subject of a number of studies.[2,3)] These investigations have elucidated the mechanism of the reduction and the correlation between the polarographic half-wave potentials with electron affinities, ultraviolet absorption frequencies, or parameters of Hückel molecular orbital (HMO) calculations.[2-6)] In such aprotic media, aromatic hydrocarbons[7,8)] undergo reversible one-electron transfers at cathodes, yielding radical anions. Most radical anions undergo further reduction, at potentials half a volt more negative, to dianions, which are then usually rapidly protonated to carbanions, which themselves may then be protonated to the dihydro compounds. That is, the aromatic hydrocarbons usually give two one-electron waves in their polarograms. It was found, however, that on the addition of proton donors such as water,[7)] hydrogen iodide,[7)] and phenol,[8)] the first wave increased in height at the expense of the second wave. Hoijtink[7)] was the first to show that this phenomenon could be explained by means of the HMO theory; that is, for alternant aromatic hydrocarbons the radical, RH·, formed by the protonation of the radical anion, $R^{\cdot-}$, has a higher electron affinity than the parent molecule. The RH· radical can, therefore, be reduced without the necessity of further change in the electrode potential. Although the mechanisms have been studied extensively by polarography, very few investigations[9,10)] have made direct measurements of the mechanism and kinetics of protonations of radical anions.

The aims of this investigation were to examine the methods of measuring the radical anion concentrations and then to study the mechanism of the protonation of aromatic hydrocarbon radical anions in dimethylformamide (DMF) and water mixtures where radical anions were electrochemically generated by controlled potential electrolysis.

Experimental

Materials. All the organic reagents were obtained commercially. E.P.-grade anthraquinone, phenanthrene,

1) Parts of this work were presented at the 23rd Annual Meeting of the Chemical Society of Japan, Tokyo, April, 1970, and at the 16th Symposium of Polarography, Kyoto, Oct., 1970.

2) M. E. Peover, "Electroanalytical Chemistry," Vol. 2, ed. by A. J. Bard, Marcel Dekker, Inc., New York, N. Y. (1967), p. 1.

3) G. J. Hoijtink, "Advances in Electrochemistry and Electrochemical Engineering," Vol. 7, ed. by P. Delahay and C. W. Tobias, Interscience Publishers, New York, N. Y. (1970), p. 221.

4) A. Maccoll, *Nature*, **163**, 178 (1949).

5) F. A. Matsen, *J. Chem. Phys.*, **24**, 602 (1956).

6) G. J. Hoijtink, *Rec. Trav. Chim.*, **74**, 1525 (1955).

7) G. J. Hoijtink, J. van Schooten, E. de Boer, and W. Y. Aalbersberg, *Rec. Trav. Chim.*, **73**, 355 (1954).

8) P. H. Given and M. E. Peover, *J. Chem. Soc.*, **1960**, 385.

9) K. Umemoto, This Bulletin, **40**, 1058 (1967).

10) T. Fujinaga, K. Izutsu, K. Umemoto, T. Arai, and K. Takaoka, *Nippon Kagaku Zasshi*, **89**, 105 (1968).

and naphthalene were purified by recrystallization from ethanol, ethanol, and methanol respectively. E.P.-grade anthracene was purified by sublimation. G.R.-grade pyrene and 1,2-benzanthracene were used without further purification. E.P.-grade biphenyl was also used without further purification.

Tetraethylammonium iodide (TEAI) and tetraethylammonium perchlorate (TEAP) were prepared according to the methods of Given *et al.*[11] and Fujinaga[12] *et al.*; these reagents showed no polarographic wave in a DMF solution in their accessible potential ranges of −0.6 V to −2.8 V and +0.4 V to −2.8 V, respectively, *vs.* SCE. Commercially-available G.R.-grade tetraethylammonium bromide (TEAB) was wet because of its deliquescent property and was consequently purified by recrystallization[13] from ethanol; then it was dried at 100°C for 12 hr in a vacuum and stored in a desiccator over silica gel. The TEAB also showed no polarographic wave in DMF in its accessible potential range, −0.5 V to −2.8 V *vs.* SCE.

The solvents used were purified in the usual manner,[12] the commercial, G.R. grade dimethylformamide (DMF) was dried over anhydrous K_2CO_3 for a few days with occasional shaking and then vacuum-distilled twice under nitrogen gas, and the water content of the DMF was determined to be 0.02% by Karl Fischer titration.

Polarography. An aqueous saturated calomel electrode was connected to the cell by a 1 N KNO_3-agar bridge[14] or a 1 N TEAB-agar bridge, the outlet of which was positioned just above the dropping mercury electrode. The 1 N KNO_3-agar bridge is adapted for measurements of the potential range of +0.4 V to −2.0 V *vs.* SCE, as in the case of anthraquinone, while the 1 N TEAB-agar bridge is adapted for measurements of the potential range of −0.5 V to −2.8 V *vs.* SCE, which was used for aromatic hydrocarbons; the bridges prevent the contamination of bromide or potassium ions from the TEAB- and KNO_3-bridges respectively. In order to lower the contamination of water from the bridge, one end of the bridge was aged in an aliquot of the supporting electrolyte solution for at least a day. The solution which contained a small amount of a depolarizer and 0.1 N of a supporting electrolyte was deaerated by bubbling pure nitrogen gas[15] for 15—20 min. No correction for the liquid-junction potential was taken into account. All the measurements were carried out at 25°C. The polarograph used was a Yokogawa Denki model POL-11.

The Simultaneous Measurements of Polarograms and UV and ESR Spectra of Anthraquinone Radical Anions. A solution containing 2×10^{-3} M of anthraquinone and 0.1 N of TEAP as the supporting electrolyte was placed in the electrolysis cell, as is shown in Fig. 1, and was deaerated for 20—30 min by bubbling pure nitrogen gas, which came through a flow-type 10-mm quartz cell for the absorption spectra and which came through a glass capillary for the ESR measurements. Then the bubbling was stopped and the nitrogen gas overflowed the catholyte by means of the cock, C_1, in Fig. 1; the DC polarogram of the base solution was recorded against the SCE (RE), which was also used in the controlled potential electrolysis as the reference electrode. Again, nitrogen bubbling was started and the solution was electrolyzed at the constant potential on the first plateau of the polarogram. The concentration of the radical anion could be controlled roughly by the length of the electrolysis time. After the electrolysis, the nitrogen gas again overflowed the catholyte, the solution in the center and in the anodic chamber was removed to prevent backflow, and then a DC polarogram was recorded. After that, the solution was introduced into the 10-mm quartz cell used for the UV spectrometry and the glass capillary used for the ESR spectrometry.

All the measurements were carried out at 20°C. A Japan Electron Optics Laboratory ESR spectrometer model JES-ME-3X, a Shimadzu recording spectrophotometer model MPS-50L, a Shimadzu polarograph model RP-50, and a Hokuto Denko potentiostat model PS-500B, were used.

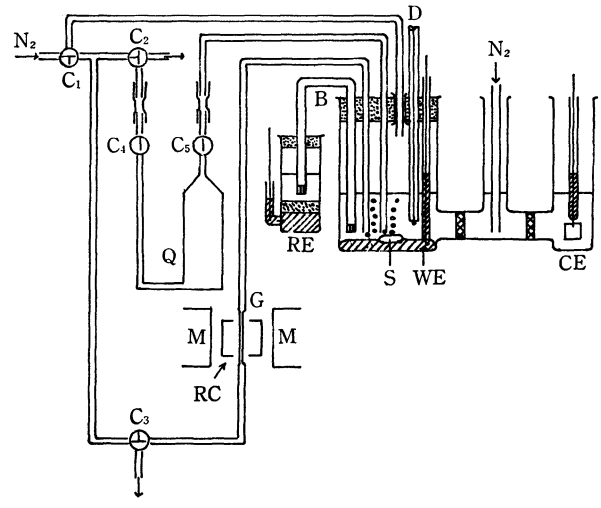

Fig. 1. Apparatus for simultaneous measurements of radical anions. N_2, pure nitrogen; C, cock; Q, UV quartz cell; M, magnet; G, glass capillary for ESR measurements; RC, resonant cavity; B, agar bridge; S, magnetic stirrer; RE, reference electrode (SCE); WE, mercury pool cathode; CE, Pt anode; D, d. m. e.

Visible Absorption Spectroscopy of Aromatic Hydrocarbon Radical Anions. The apparatus was almost identical with that used for the simultaneous measurements described above (Fig. 1). The following improvements were made, however: the 10-mm quartz cell and the electrolysis cell were kept at a constant temperature by means of a thermostat in order to make it possible to change the temperature. One more electrolysis cell, in which a DMF solution containing 5×10^{-3} M of the same aromatic hydrocarbon as was measured and 0.1 N of TEAB was placed, was connected to the line before the cock, C_1, in Fig. 1. After pure nitrogen had been bubbled in for 10—15 min, the solution in this cell was electrolyzed at the potential on the first diffusion plateau and the electrolysis was continued throughout each experiment. By this procedure, pure nitrogen gas was purified much more; the reduction potentials of the aromatic hydrocarbons are so negative that the oxygen is practically completely absorbed by the reaction with the radical anion.[16-18]

11) P. H. Given, M. E. Peover, and J. Schoen, *J. Chem. Soc.*, **1958**, 2674.

12) T. Fujinaga, K. Izutsu, and K. Takaoka, *J. Electroanal. Chem.*, **12**, 203 (1966).

13) C. K. Mann, "Electroanalytical Chemistry," Vol. 3, ed. by A. J. Bard, Marcel Dekker, Inc., New York, N. Y. (1969), p. 132.

14) M. E. Peover and J. D. Davies, *J. Electroanal. Chem.*, **6**, 46 (1963).

15) Pure nitrogen is purified by passing it through four alkaline pyrogallol solutions, concentrated sulfuric acid, and sodium hydroxide.

16) D. L. Maricle and W. G. Hodgson, *Anal. Chem.*, **37**, 1562 (1965).

17) K. S. V. Santhanam and A. J. Bard, *J. Amer. Chem. Soc.*, **88**, 2669 (1966).

18) D. L. Maricle, *Anal. Chem.*, **35**, 683 (1963).

The main electrolysis was started after the nitrogen bubbling had continued for 45 min, and it was continued for 10 min. When the water content was small, the decay was slow enough to record the change in the spectra, but in the case of fast decay by the addition of considerable water, the absorbance against time must be recorded at the absorption maximum of the radical anions.

Results and Discussion

Controlled-Potential Electrolysis of Anthraquinone and Polarography of the Radical Anion of Anthraquinone. The polarographic reduction of anthraquinone (AQ) in DMF showed two well-defined waves with half-wave potentials of −0.90 V and −1.54 V *vs.* SCE (Fig. 2); these waves correspond to the formation of radical anions and dianions respectively:

$$AQ + e \rightleftharpoons AQ^{\cdot-} \qquad \text{1st wave} \qquad (1)$$

$$AQ^{\cdot-} + e \rightleftharpoons AQ^{2-} \qquad \text{2nd wave} \qquad (2)$$

However, the controlled potential electrolysis of anthraquinone at the potential (B), which was a little more negative than that of the second wave, gave radical anions as in the electrolysis at the potential (A) on the diffusion plateau of the first wave, but the rate of formation of the radical anions was double that of the latter. This is because a dianion, AQ^{2-}, reacts with a neutral AQ in solution to give two radical anions, as is shown below:

$$AQ^{2-} + AQ \rightleftharpoons 2AQ^{\cdot-} \qquad (3)$$

The equilibrium constant of this reaction:

$$K = \frac{[AQ^{\cdot-}]^2}{[AQ^{2-}][AQ]} \qquad (4)$$

is obtained[19] from Eq. (5):

$$E_{1/2}(1st) - E_{1/2}(2nd) = \frac{RT}{F} \ln K \qquad (5)$$

where $E_{1/2}(1st)$ and $E_{1/2}(2nd)$ are the half-wave potentials of the first and second waves respectively, where R is the gas constant, where T is the absolute temperature, and where F is the Faraday constant. The value of K is calculated to be 10^{11}; therefore, the equilibrium of Reaction (3) lies almost completely to the right. Thus, we can obtain the various concentrations of the radical anions of anthraquinone by changing the length of the electrolysis time of the controlled potential electrolysis at the potential on the first palteau (A), and when we want to generate the radical anions rapidly and in large quantities, electrolysis at the potential on the second plateau (B) is useful.

The polarogram (Fig. 2) for the solution containing $AQ^{\cdot-}$ which was prepared by the controlled potential electrolysis at either the potential on the first (A) or the second plateau (B) described above, shows an anodic wave with a large maximum (C) which suddenly drops at −0.4 V *vs.* SCE and which has a diffusion plateau at more positive potential (D). The shape of this anodic wave is very similar to that found by Santhanam and Bard[17] for the anodic oxidation of

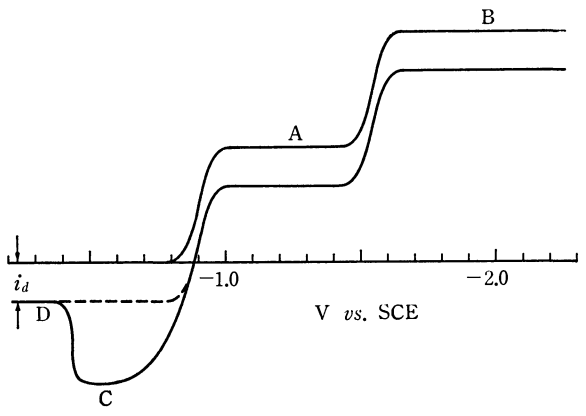

Fig. 2. DC polarograms of anthraquinone.

9,10-diphenylanthracene radical anions, and it probably can be explained by a similar mechanism. The base currents before electrolysis and anodic currents after electrolysis were measured with the various heads of the dropping mercury electrode (d.m.e.). From these data, we obtained the anodic currents, i_d, of $AQ^{\cdot-}$ in the anodic plateau (D) with the various heads of the d.m.e.; we found that this anodic current, i_d, varied as the square-root of the head of the d.m.e. (Fig. 3). Therefore, this anodic current may be diffusion-controlled and may be proportional to the concentration of $AQ^{\cdot-}$. Furthermore, this anodic diffusion current showed no change with time; *i.e.*, the radical anion $AQ^{\cdot-}$ was found to be stable[9,10,20] in DMF.

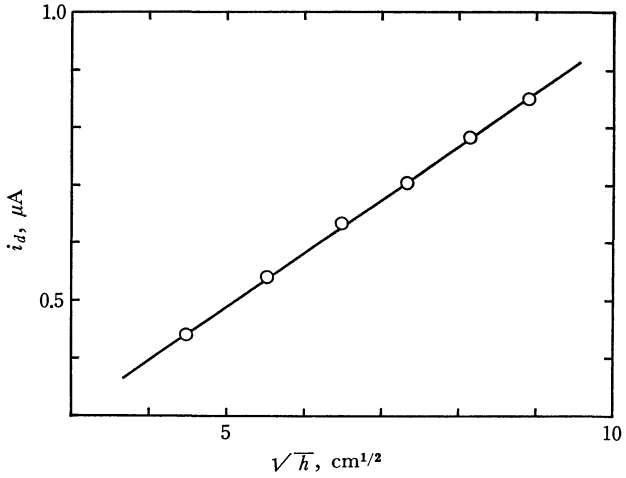

Fig. 3. Dependence of anodic current i_d on the square-root of the mercury head.

UV Absorption Spectra. The UV absorption spectra of radical anions and dianions of anthraquinone will be reported in detail in this Bulletin. The parent molecule, AQ, has an absorption band at the λ_{max} of 325 mμ in DMF, which itself has strong absorptions at wavelengths shorter than 270 mμ. The catholyte by controlled potential electrolysis had absorption bands at the λ_{max} of 390, 410, and 553 mμ in the visible region; these results are consistent with the absorption spectra of the anthraquinone radical anion reported

19) J. Heyrovsky and J. Kuta, "Principle of Polarography," Academic Press, New York, N. Y. (1966), p. 181.

20) W. Sakai, I. Matsuo, K. Miyata, and F. Hori, *Denki Kagaku*, **37**, 618 (1969).

by other authors.[10,21,22] The intensity of the maxima showed no change with time. As a result of this observations, the AQ^- radical anion was found to be not only stable in DMF, but also completely free from oxygen in the UV cell.

ESR Spectra. The ESR spectra of anthraquinone radical anions in DMF solutions containing 1×10^{-4} M, 2×10^{-3} M, and 5×10^{-3} M of anthraquinone before controlled potential electrolysis, which were carried out at -1.20 V *vs.* SCE for 15 min, 45 sec, and 30 sec respectively, are given in Fig. 4. The hyperfine coupling constants obtained from the ESR spectrum of the solution containing 1×10^{-4} M of anthraquinone before electrolysis are $a_{H_1}=0.3$ gauss and $a_{H_2}=1.0$ gauss; these values almost agree with those in the literature.[9,21,23] As is shown in Fig. 4, the more parent molecules were present, the broader were the spectra obtained. This behavior can be explained as a result of rapid intermolecular electron-exchange[24] between the parent anthraquinone molecules and the radical anions:

$$AQ^- + AQ \rightleftharpoons AQ + AQ^- \qquad (6)$$

It can be said also that the radical anions were free from the oxygen throughout the measurements, for the ESR spectra showed no change with time.

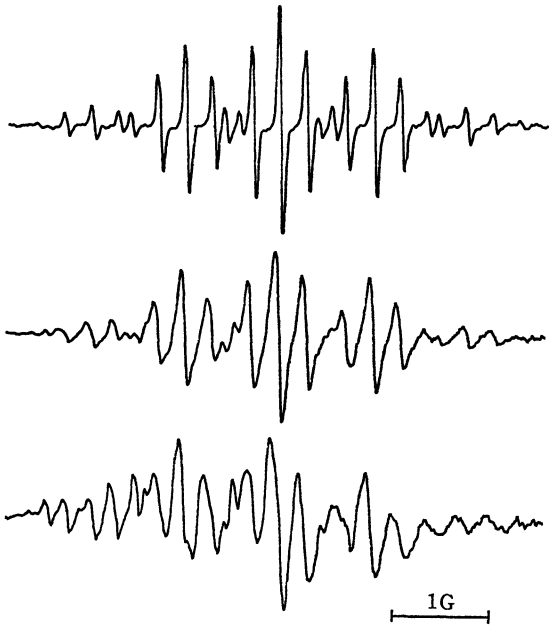

Fig. 4. ESR spectra of anthraquinone radical anions in DMF: above, 1×10^{-4}M; center, 2×10^{-3}M; below, 5×10^{-3}M of anthraquinone contained before partial reduction.

Comparison of Methods. It has been shown above from the measurements of polarograms and the UV and ESR spectra, that anthraquinone radical anions are stable in DMF and are free from oxygen. Therefore, the anthraquinone radical anions are suitable for the simultaneous measurements of the same solution by the three different methods; this can make clear the correlation of the measured quantities. The correlation between the anodic diffusion current, i_d, the absorbance, A, and the ESR signal intensity, I, of the derivative absorption curve are shown in Fig. 5. There exist a good linear relation between the diffusion currents and the absorbance, while the ESR signal intensity has no linear relation either with the diffusion currents or the absorbance. As the diffusion currents and the absorbance are usually proportional to the concentration, the above result leads to the conclusion that the ESR signal intensity of anthraquinone radical anions has no linear dependence on the concentration.

As the diffusion coefficients of the radical anion and the parent molecule are assumed to be approximately equal, the concentration of radical anions in Fig. 5 could be estimated from the i_d values to vary over the range of 2×10^{-5}—2×10^{-4} M; therefore, the molar extinction coefficient (at 553 mμ) of anthraquinone radical anions may be 1.2×10^4 M^{-1} cm^{-1}.

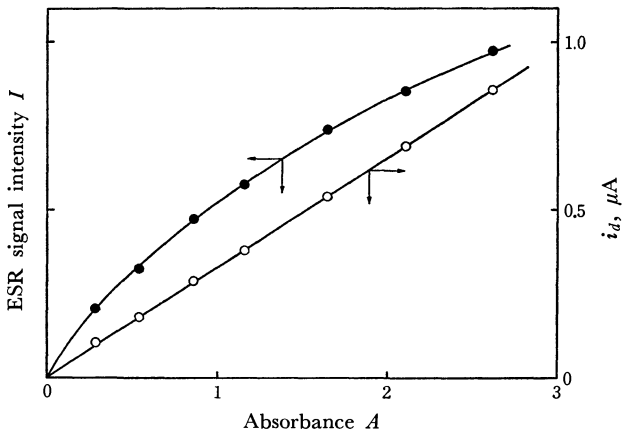

Fig. 5. Correlation between anodic diffusion current i_d, absorbance A and ESR signal intensity of the derivative absorption spectra I.

In the present system, it can be assumed, according to Weissman,[24] that the lines of ESR are close to Lorentzian and that the contributions to the line width from individual broadening mechanisms are additive. Then the line width of a line can be written as follows:

$$\Delta H_{p-p} = \Delta H_0 + \Delta H_e + \Delta H_s$$
$$= \Delta H_0 + h_e[R] + h_s[R^-] \qquad (7)$$

where ΔH_{p-p} is the line width as measured between points of extreme slope, *i.e.*, from peak to peak of the derivative spectrum, where ΔH_e is the contribution to the width from the electron-exchange reaction with the parent molecule, where ΔH_s is the contribution to the width from the intermolecular spin exchange reaction, and where ΔH_0 is the width in the absence of these two contributions, or when there is little such contributions. As is written in Eq. (7), these two contributions are known[24,25] to be proportional to the concentration of the parent molecule and the radical

21) W. Sakai, K. Miyata, and F. Hori, *ibid.*, **37**, 688 (1969).
22) T. Osa and T. Kuwana, *J. Electroanal. Chem.*, **22**, 389 (1969).
23) J. Gendell, J. H. Freed, and G. K. Fraenkel, *J. Chem. Phys.*, **37**, 2832 (1962).
24) R. L. Ward and S. I. Weissman, *J. Amer. Chem. Soc.*, **79**, 2086 (1957).
25) A. Hudson and G. R. Luckhurst, *Chem. Rev.*, **69**, 191 (1969).

anions respectively. Furthermore, the rate constants of these reactions are related to the line brodening by $k_e = 1.52 \times 10^7 h_e$ M^{-1} sec^{-1} or $k_s = 1.52 \times 10^7 h_s$ M^{-1} sec^{-1}. The sum of the concentrations of the parent molecules and the radical anions were kept constant, 2×10^{-3} M, in the above experiment. Hence:

$$\Delta H_{p-p} = (h_s - h_e)[\mathrm{AQ}^-] + \text{const.}$$

The plot of ΔH_{p-p} against $[\mathrm{AQ}^-]$ gave a straight line (Fig. 6). The direct measurements of ΔH_{p-p} from the ESR spectra are not so accurate. Therefore, ΔH_{p-p} was determined from $\sqrt{[\mathrm{AQ}^-]/I}$, since $I \times (\Delta H_{p-p})^2$ is proportional to the concentration of the radical anions.[26] The value of $(h_s - h_e)$ was determined from the slope of the straight line and was 140± 10 gauss M^{-1}. Similarly, the value of h_e could be determined from experiments where the concentrations of the radical anions were kept constant and where only the concentrations of parent molecules were varied; it was 10±5 gauss M^{-1} and the rate constants, k_e and k_s, were $(1.5 \pm 0.8) \times 10^8$ M^{-1} sec^{-1} and $(2.3 \pm 0.2) \times 10^9$ M^{-1} sec^{-1} respectively. These values are comparable to those of others.[25]

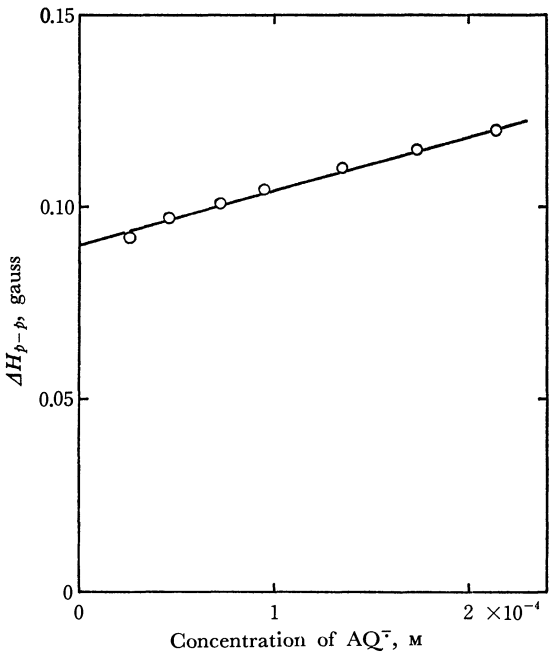

Fig. 6. Dependence of ΔH_{p-p} on $[\mathrm{AQ}^-]$ where the sum of the concentrations of parent molecules and radical anions were kept constant, 2×10^{-3} M.

As has been described above, the nonlinear dependence of the ESR signal intensity on the concentration of the radical anions was found to be due to the broadening caused by the rapid intermolecular spin exchange, even if the concentration of the parent molecule is constant. However, the ESR measurement is very useful for studying the mechanism of the protonation of radical anions, because it can detect only radicals. As the quantitative method, UV absorption spectroscopy is more appropriate than polarography because of its accuracy and simplicity, unless the absorption maxima of the radical anions overlap those of the parent molecule and other compounds produced during the reaction.

The Decay of Aromatic Hydrocarbon Radical Anions in DMF-Water Mixtures. The radical anions of aromatic hydrocarbons in a DMF solution which contains small amounts of water are considered to decay by this protonation mechanism:

$$\mathrm{R}^- + \mathrm{H_2O} \xrightarrow{k} \mathrm{RH}\cdot + \mathrm{OH}^- \quad (8)$$

$$\mathrm{RH}\cdot + \mathrm{R}^- \underset{}{\overset{k_{12}}{\rightleftharpoons}} \mathrm{RH}^- + \mathrm{R} \quad (9)$$

$$\mathrm{RH}^- + \mathrm{H_2O} \xrightarrow{k'} \mathrm{RH_2} + \mathrm{OH}^- \quad (10)$$

If the radical anions decay only through the sequence described above, the changes of the concentration of the radical anions with time are as given by Umemoto[9]:

$$\frac{\mathrm{d}[\mathrm{R}^-]}{\mathrm{d}t} = -2k[\mathrm{H_2O}][\mathrm{R}^-] \quad (11)$$

Equation(11) can be deduced from the facts that the reaction of Eq. (8) is slow, but the electron transfer reaction of Eq. (9) is very fast, and that, furthermore, the equilibrium of Eq. (9) lies completely to the right.[27]

26) However, the proportional constant must be determined from at least one direct measurement.

27) These facts are confirmed as follows. The equilibrium constant of Eq. (9) can be estimated by Eq. (14) if the half-wave potentials of Eq. (12) and Eq. (13) are known:

$$\mathrm{R} + \mathrm{e} \rightleftharpoons \mathrm{R}^- \quad (12)$$

$$\mathrm{RH}\cdot + \mathrm{e} \rightleftharpoons \mathrm{RH}^- \quad (13)$$

$$E_{1/2}(\mathrm{RH}\cdot \rightarrow \mathrm{RH}^-) - E_{1/2}(\mathrm{R} \rightarrow \mathrm{R}^-) = \frac{RT}{F} \ln K \quad (14)$$

The Hückel theory predicts that the protonated radicals, RH·, derived from alternant hydrocarbons should have the same half-wave potentials, about −1.1 V *vs.* SCE, since the highest occupied orbital into which a further electron is uptaken is the non-bonding molecular orbital. This fact was ascertained experimentally by Dietz and Peover[28] using rapid sweep cyclic voltammetry at a platinum electrode. Among the aromatic hydrocarbons used in the present work, anthracene shows the lowest half-wave potential; its value is −1.95 V *vs.* SCE. Therefore, the equilibrium constant of Eq. (9) is greater than 10^{14} in the present study.

The rate constants of such a rapid intermolecular electron exchange of aromatic hydrocarbon radical anions as Eq. (15) have been determined by studying the line broadening of the ESR spectra[29,30]:

$$\mathrm{R}^- + \mathrm{R} \underset{}{\overset{k_{11}}{\rightleftharpoons}} \mathrm{R} + \mathrm{R}^- \quad (15)$$

they are about 10^8 M^{-1} sec^{-1} in DMF and 10^7 M^{-1} sec^{-1} in DMF containing 10% of water.[29] The rate constants of Eq. (16) may also be the same order as Reactions (6) and (15):

$$\mathrm{RH}^- + \mathrm{RH}\cdot \underset{}{\overset{k_{22}}{\rightleftharpoons}} \mathrm{RH}\cdot + \mathrm{RH}^- \quad (16)$$

According to Marcus,[31] the rate constant of the forward reaction of Eq. (9) can be estimated as follows:

$$k_{12} \simeq (k_{11}k_{22}Kf)^{1/2} \quad (17)$$

where:

$$\ln f = (\ln K)^2/4 \ln (k_{11}k_{22}/Z^2) \quad (18)$$

In the present system, k_{12} is calculated to be $10^{10.94}$ M^{-1} sec^{-1} when k_{11} and k_{22} are 10^7 M^{-1}sec^{-1}, Z is 10^{11} M^{-1} sec^{-1} and K is 10^{14}. Thus, the k_{12} is nearly equal to the collision frequency of the hypothetical uncharged species in solution, Z.

28) R. Dietz and M. E. Peover, *Trans. Faraday Soc.*, **62**, 3535 (1966).

29) T. P. Layloff, T. Miller, R. N. Adams, H. Fäh, A. Horsfield, and W. G. Proctor, *Nature*, **205**, 382 (1965).

30) M. T. Jones and S. I. Weissman, *J. Amer. Chem. Soc.*, **84**, 4269 (1962). P. J. Zandstra and S. I. Weissman, *ibid.*, **84**, 4408 (1962).

31) R. A. Marcus, *J. Phys. Chem.*, **67**, 853 (1963).

Table 1. The visible absorption spectra of aromatic hydrocarbon radical anions

Hydrocarbon anion	a) in mμ	b) in mμ	c) in mμ	d) in mμ
(Biphenyl)$^{\cdot-}$	407	405	402	
	610	617	625	
	648	637		
(Naphthalene)$^{\cdot-}$	368	366	366	369
	437	437	433	437
	466	465	463	
	775	735		735
(Phenanthrene)$^{\cdot-}$	383	395	379	392
	421	415	415	417
	452	444	446	444
	665	654	637	649
(Anthracene)$^{\cdot-}$	364**	369		
	400**	401	403	400
	510			513
	548	549	546	546
	595	599	595	595
	638		637	
	656	662	654	662
	693		694	
	725	714	725	719
(1,2-Benz-anthracene)$^{\cdot-}$	**			388
	**			397
	415			422
	475			
	505			503
	538			541
	588			592
	758			
	792			
(Pyrene)$^{\cdot-}$	365	366	364	
	385	385	383	385
	450	455	450	455
	496	493	490	493
	742	719	735	730

a) Our results. b) See Ref. 32. c) See Ref. 33. d) See Ref. 34.
** The parent molecules have absorption bands in the same region.

Equation (11) suggests that the radical anions will decay by a first-order reaction when the concentration of water is much greater than that of the radical anions. These predictions can be confirmed by a study of the change in the absorbance of the radical anions with time. The positions of the electronic absorption bands of the aromatic hydrocarbon radical anions obtained are given in Table 1, where the spectra of other authors[32-34] are compared with our results. These results show a fairly good agreement, though the measurements were carried out with different solvents.

The parent molecules, R, used, except for anthracene and 1,2-benzanthracene and their dihydroderivatives, RH_2, have no strong absorption bands in the range of 350—750 mμ, but the carbanions, RH^-, formed by Eq. (9) or by the monoprotonation of the dianions Eq. (20) have absorption maxima in a visible region.[35,36] Furthermore, the spectra of the RH^- carbanion were found to be similar to that of the carbonium ion, RH^+.[37]

However, the spectra corresponding to the RH^- carbanion were not found during the decay of the radical anions. These results mean that the rate constant of the protonation of RH^- in Eq. (10) is much greater than that of $R^{\cdot-}$ in Eq. (8). The absorbances of all the radical anions in the present study decayed exponentially with time; that is, the $\log A$ against time plots gave straight lines, which means a first-order decay of the radical anions as expected from Eq. (11).

Now that the radical anions of the aromatic hydrocarbons investigated in this study have been shown to decay through the Eq. (8)—Eq. (10) sequence, let us consider the reason why the aromatic hydrocarbon radical anions do not decay through this sequence:

$$2R^{\cdot-} \rightleftharpoons R^{2-} + R \tag{19}$$

$$R^{2-} + H_2O \xrightarrow{k''} RH^- + OH^- \tag{20}$$

$$RH^- + H_2O \xrightarrow{k'} RH_2 + OH^- \tag{10}$$

First, let us consider the case in which the disproportionation reaction Eq. (19) is the rate-determining step. The rate constants are assumed to be given approximately by the theory of Marcus[38] even in a system where the standard free energy of the reaction, ΔG°, is very large, as follows:

$$k = Z \exp(-\Delta G^*/RT) \tag{21}$$

where Z is the collision number in the solution and where ΔG^* is as given by Eqs. (22)—(24):

$$\Delta G^* = e_1^* e_2^*/D_s r + m^2\lambda \tag{22}$$

where:

$$2m + 1 = -[\Delta G^\circ + (e_1 e_2 - e_1^* e_2^*)/D_s r]/\lambda \tag{23}$$

and:

$$\lambda = \left(\frac{1}{2a_1} + \frac{1}{2a_2} - \frac{1}{r}\right)\left(\frac{1}{D_{op}} - \frac{1}{D_s}\right)(\Delta e)^2 \tag{24}$$

In these equations, the notations are the same as those of Marcus.[38] In a disproportionation reaction such as Eq. (19), the work of bringing reactants tagether, $e_1^* e_2^*/D_s r$, is not neglected, but the work for the products, $e_1 e_2/D_s r$, is neglected, since one product is uncharged. The solvent reorganization parameter, λ, is assumed to be almost the same as that of the reaction of Eq. (15), and λ=13.1 kcal/mol, obtained from

32) P. Balk, G. J. Hoijtink and W. H. Schreurs, *Rec. Trav. Chim.*, **76**, 813 (1957).
33) E. de Boer and S. I. Weissman, *ibid.*, **76**, 824 (1957).
34) A. G. Evans and B. J. Tabner, *J. Chem. Soc.*, **1963**, 5560.
35) C. N. R. Rao, V. Kalyanaraman, and M. V. George, "Applied Spectroscopy Reviews," Vol. 3, ed. by E. G. Brame, Jr., Marcel Dekker, Inc., New York, N. Y. (1970), p. 153.
36) N. H. Velthorst and G. J. Hoijtink, *J. Amer. Chem. Soc.*, **87**, 4529 (1965).
37) H. H. Perkampus, "Advances in Physical Organic Chemistry," Vol. 4, ed. by V. Gold, Academic Press, New York, N.Y. (1966), p. 195.
38) R. A. Marcus, *J. Chem. Phys.*, **24**, 966 (1956).

TABLE 2. HALF-WAVE POTENTIAL DIFFERENCES, STANDARD FREE ENERGIES AND RATE CONSTANTS OF DISPROPORTIONATION REACTION

Hydrocarbon	$-E_{1/2}$ (1st)	$-E_{1/2}$ (2nd)	$\Delta E_{1/2}$	ΔG°	ΔG^*	k_d
	V *vs.* SCE		V	kcal/mol		$M^{-1}\,sec^{-1}$
1,2-Benzanthracene	2.02	2.42	0.40	9.3	9.7	6.2×10^3
Pyrene	2.08	2.57	0.49	11.3	11.4	3.1×10^2
Anthracene	1.95	2.45	0.50	11.6	11.7	1.9×10^2
Biphenyl	2.60					
Naphthalene	2.54					
Phenanthrene	2.47					
Benzophenone[a)]	1.75	2.06	0.31	7.2	8.1	9.3×10^4

a) See Ref. 9.

Eq. (24) by taking $a_1=a_2=6$Å, was used for the calculation of k_d.

The standard free energy of the disproportionation reaction, ΔG°, is also determined from the experimental results, the half-wave potentials of the first and second waves of aromatic hydrocarbons, by the following equation:

$$E_{1/2}(R^- \rightarrow R^{2-}) - E_{1/2}(R \rightarrow R^-) = \frac{RT}{F} \ln K \qquad (25)$$

which is an inverse of Eq. (5). The difference in the half-wave potentials, $\Delta E_{1/2}$, the standard free energy, ΔG°, and the calculated values of the rate constants, k_d, of the disproportionation reaction are given in Table 2. The differences in the half-wave potentials of biphenyl, naphthalene, and phenanthrene can not be obtained, since these compounds do not give the second wave in the accessible potential region. These differences, however, may not be smaller than those of the others obtained, because the electrostatic repulsion of the pair of electrons in the antibonding orbital, ϕ_{n+1}:

$$E_{rep} = \iint \phi_{n+1}(1)\phi_{n+1}(2)\frac{e^2}{r}\phi_{n+1}(1)\phi_{n+1}(2)d\tau_1 d\tau_2$$

is larger in the case of smaller molecules, such as biphenyl, naphthalene and phenanthrene[39]; furthermore, the values of $\Delta E_{1/2}$ were found[40] to have a linear dependence on E_{rep}.

Hence, if the forward reaction of Eq. (19) is rate-determining, the decay of the radical anion by the sequence of Eqs. (19), (20), and (10) is given by:

$$\frac{d[R^-]}{dt} = -k_d[R^-]^2$$

As the concentrations of the radical anions are of the order of 10^{-4} M in the initial period, the products, $k_d[R^-]$, are $10^{-1}-10^{-2}\,sec^{-1}$ and are comparable to the apparent first-order rate constants, $2k[H_2O]$, in Eq. (11), the values of which are $10^{-1}-10^{-3}\,sec^{-1}$ in the present system.

As the present work has shown that the radical anion obeys the first-order decay, the rate-determining reaction may be the protonation reaction of dianions, Eq. (20), if the calculated order for k_d is correct.

At present, however, k_d is not obtained experimentally; furthermore, attempts to test the theory of Marcus for the dependence of ΔG^* on ΔG° have beem made[41,42] for the system, where ΔG° is not so large, 2—3 kcal/mol, but have never been made for the system where ΔG° is as large as 10 kcal/mol in the aromatic hydrocarbon radical anion disproportionation reaction. The values of ΔG° calculated from $\Delta E_{1/2}$ as Table 2 shows, are, however, possibly smaller than the true values, because $E_{1/2}$ (2nd) may be shifted to a positive potential by the rapid protonation of dianions, as is ascertained from the fact that AC polarography almost did not give the second wave. For the calculation of k_d, $10^{11}\,M^{-1}\,sec^{-1}$ was used as the value of Z, but 10^9—$10^{10}\,M^{-1}\,sec^{-1}$ may be more appropriate as the collision number between radical anions in solution, because the rate constants of spin exchange described before are considered[25] to be diffusion-controlled. Considering these factors, the disproportionation reaction itself is possibly slower than the protonation reaction of radical anions, Eq. (8), in the present system.

It is very interesting that the decay of benzophenone radical anions is known[9] to consist of the contributions of a first- and second-order reaction for radical anion concentrations. This is explained by the smaller ΔG° of benzophenone (in Table 2), as has been discussed by Fujinaga *et al.*[9,10]

The protonation reactions through either the Eqs. (8), (9), and (10) sequence or the Eqs. (19), (20), and (10) sequence lead to an increase in the first wave height at the expense of the second wave, because the reducible substance, *i.e.*, RH or R, is regenerated at the potential of the first plateau by these sequences, which are examples of ECE mechanisms. However, the radical anion and dianion of anthraquinone are not protonated in the DMF-alkaline water system.[43] Therefore, by the addition of water, no increase in the first wave height is found, although the second wave shifts to the positive potential and the two waves approach each other. This is because the strong solvation of the dianion by hydrogen bonding with water lowers the standard free energy of disproportionation

39) N. S. Hush and J. Blackledge, *J. Chem. Phys.*, **23**, 514 (1955).
40) Y. Matsui and Y. Date, presented at the 16th Symposium of Polarography, Kyoto, Oct., 1970.
41) L. M. Dorfman, *Accounts Chem. Res.*, **3**, 224 (1970).
42) K. Suga and S. Aoyagi, presented at the 9th Symposium of ESR, Tokyo, Oct., 1970.
43) S. Hayano and M. Fujihira, presented at the 15th Symposium of Polarography, Sendai, Oct., 1969.

reaction, $\Delta G°$. As a result, R is reproduced to some extent and may be reduced at the potential of the first plateau, but at the same time R^{2-} is generated equally. The latter may be oxidized and may compensate for the reduction of neutral species.

The authors wish to thank Dr. M. Senō, Dr. T. Osa and Dr. M. Sukigara for their helpful discussions. The authors also wish to thank Mr. H. Saito and Mr. I. Yamashita for their assistance in the simultaneous measurements.

BULLETIN OF THE CHEMICAL SOCIETY OF JAPAN, VOL. 44, 1503—1506 (1971)

The Solubilization of Orange OT in Anionic Surfactant Solutions: A Polarographic Study

Shigeo HAYANO and Noriko SHINOZUKA

Institute of Industrial Science, The University of Tokyo, Roppongi, Minato-ku, Tokyo

(Received December 1, 1970)

Orange OT (1-*o*-tolyl-azo-β-naphthol) solubilized in sodium dodecyl sulfate (SDS) and sodium dodecylbenzene sulfonate (SDBS) solutions showed a well-defined irreversible polarographic wave. The proportionality of the limiting current to the square root of the mercury height and to the dye concentration indicates the wave to be diffusion-controlled. It is noted that the anionic surfactants showed the waves due to the adsorption-desorption and reorientation of the surfactant molecules on the electrode. The apparent diffusion coefficients of the solubilized dye calculated from the polarographic data were in good agreement with those of the anionic surfactant micelle with electrolyte. We may conclude that the polarographic diffusion coefficient of the solubilized dye is equal to that of the micelle of the solubilizer surfactant. The marked surfactant concentration dependence of the diffusion coefficient was observed with both surfactants and was attributed to the interaction of the micelles. The transfer coefficient of the electrode reaction of Orange OT increased with an increase in the concentration of the surfactant. This tendency is different from the effect of the surface-active agents on the transfer coefficient in the reduction of inorganic ions. From the experimental observations, it seems that the electrode reaction of the solubilized dye is little effected by the charged micelles.

The preceding papers[1,2] described the polarographic behavior of the solubilized dye in nonionic surfactant solutions. The solubilized neutral dyes (anthraquinone derivatives) showed well-defined, diffusion-controlled polarographic waves, and the diffusion constants calculated from the polarographic data were in good accordance with those for the micelles of the nonionic surfactants. This means that the solubilized dye diffused from the bulk solution to the electrode with micelles of the surfactant and that the dye was reduced polarographically where the surfactant micelles seemed to have little effect on the reduction process of the dye.

In this paper, we shall report the polarographic results of the solubilized dye (Orange OT), which showed a well-defined, irreversible, diffusion-controlled wave in anionic surfactant solutions and shall conclude that the diffusion coefficient of the dye is equal to that of the micelle of the surfactant.

Experimental

Materials. Orange OT (1-*o*-tolyl-azo-β-naphthol) was recrystallized twice from ethanol. Sodium dodecylbenzene sulfonate (SDBS) was obtained through the courtesy of the Lion Oil and Fats Co. and was recrystallized from petroleum ether. Sodium dodecyl sulfate (SDS) made by the Kao-Atlas Co., Ltd., was extracted from ether and was recrystallized from ethanol.

Procedure. Orange OT was solubilized in an anionic surfactant solution containing a 0.1 M sodium acetate-acetic acid buffer solution (pH=4.62) as a supporting electrolyte. The solution was stored for a week at 25°C. The excess dye was removed by filtration through a G4 glass filter. The concentration of the filtrates were rechecked by their solid contents on the filter, which had been determined by the measurement of the spectroscopic absorbancy.

The polarographic measurements were carried out at 25°C with Yokogawa POL-11 and POL-21 polarographs. The DME had the following characteristics: $m=2.075$ mg/sec (in pure water without applied potential) and $t=3.58$ sec (in a 10^{-2} M SDBS buffer solution at -0.5 V *vs.* SCE). The height of the mercury head was 75.5 cm.

Results

Orange OT in the Ethanol-water Solution. The polarogram of Orange OT in an 40% ethanolic solution showed pH-dependent waves. In an alkaline solution a maximum of the first kind was observed, while in an acidic solution the wave was well-defined and the current was proportional to the square root of the mercury-column height. (Fig. 1) From the log-plots of the waves, a value of $n\alpha=1.22$ (α being the transfer coefficient) was obtained in a solution of pH=4.6. Supposing that the reduction of Orange OT proceeds with a two-electron transfer,[3] the diffusion coefficient of the dye in an ethanolic solution at pH=4.6 was calculated to be 3.8×10^{-6} cm²/sec.

1) S. Hayano and N. Shinozuka, This Bulletin, **42**, 1469 (1969).
2) S. Hayano and N. Shinozuka, *ibid.*, **43**, 2083 (1970).
3) I. F. Wladimirzew and I. J. Posstowski, *Ber. Akad. Wiss. USSR*, **83**, 855 (1952).

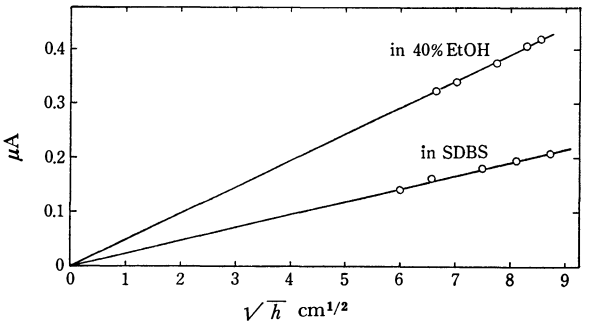

Fig. 1. Dependence of current of Orange OT on mercury height.

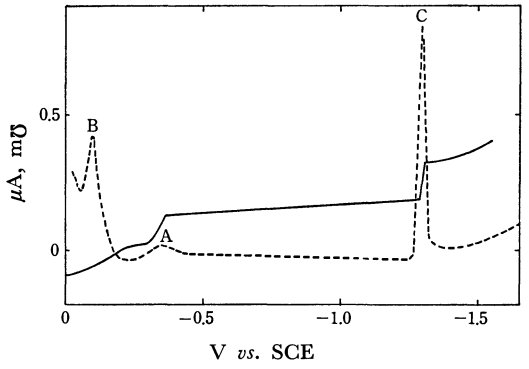

Fig. 2. DC and AC polarograms of the solubilized Orange OT in SDBS solution.

Orange OT Solubilized in SDBS Solution. Orange OT solubilized in a SDBS solution showed a well-defined, irreversible wave in DC polarograms; the AC polarographic peak was very small and round (Fig. 2). In the polarograms of the solubilized dye in anionic surfactant solutions, there appear waves due to the adsorption-desorption of the surfactant molecules on the electrode. In Fig. 2, the A wave is attributed to the reduction of Orange OT, while the B and C waves are adsorption and desorption waves respectively of SDBS molecules. These waves were of course observed with the base solution containing no Orange OT.

The relation of the limiting current to the mercury height shown in Fig. 1 indicates the diffusion-controlled character of the current. A linear line between the current and the dye concentration was also obtained. From these experimental results, the limiting current of Orange OT may be thought to be diffusion-controlled.

TABLE 1. DEPENDENCE OF POLAROGRAPHIC PARAMETERS ON SDBS CONCENTRATION

SDBS concn. (M)	$-E_{1/2}$ (V)	i_d (μA)	D ($\times 10^{-6}$ cm²/sec)	$n\alpha$
10^{-2}	0.380	0.182	1.77	0.72
3×10^{-2}	0.375	0.166	1.35	0.71
5×10^{-2}	0.392	0.152	1.14	—
8×10^{-2}	0.410	0.120	0.71	0.80
10^{-1}	0.400	0.104	0.53	0.81

Dye concn. 5.78×10^{-5} M

Table 1 summarizes the effects of the SDBS concentration on $E_{1/2}$, i_d, D, and $n\alpha$ of the dye.

The half-wave potential of the dye reduction became more negative with the increase in the SDBS concentration, but the change in $E_{1/2}$ was small compared with the potential shift when the complex formation occurred. The 3rd column of Table 1 shows a marked effect of the concentration of SDBS upon the current; this indicates that the diffusion coefficient of the dye decreased with the increase in the SDBS concentration.

The change in $n\alpha$ values with the surfactant concentration is shown in the 5th column of Table 1. It is evident that the $n\alpha$ value increased with the SDBS concentration.

The effects of the solubilized dye concentration upon $E_{1/2}$, D, and $n\alpha$ were also investigated, but the changes in these factors were very small.

Orange OT Solubilized in the SDS Solution. The polarogram of Orange OT solubilized in a SDS solution is shown in Fig. 3, where the A wave is the diffusion current of Orange OT. The B, C, D, and E waves were observed without Orange OT and were due to the adsorption phenomena of SDS molecules on the electrode. The change in the peak potentials of these waves with the SDS concentration is shown in Fig. 4. The behavior of the C and D waves, which were attributed to the reorientation of the surfactant

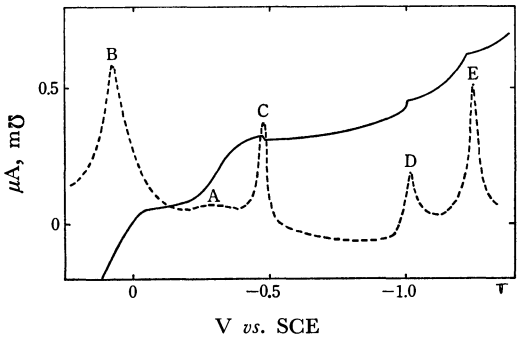

Fig. 3. DC and AC polarograms of the solubilized Orange OT in SDS solution.

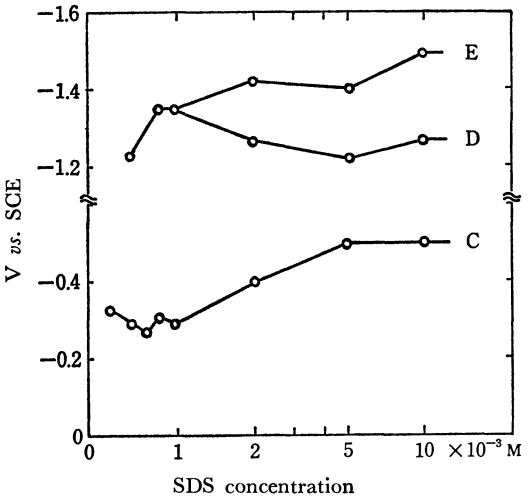

Fig. 4. Changes of peak potential of C, D, and E waves with SDS concentration.

molecules by Eda,[4] was carefully observed in order to evaluate the limiting current of Orange OT; the overlap of these waves with the limiting current of Orange OT may cause considerable error. The B and E waves may be adsorption and desorption waves respectively. The details of these nonfaradaic currents will be published elsewhere.

The effects of the SDS concentration on $E_{1/2}$, i_d, D, and $n\alpha$ are given in Table 2. $E_{1/2}$ was almost constant throughout the SDS concentrations used in this study, and in this case the complex formation was also negligible. The apparent diffusion coefficient of the dye was markedly decreased with the increase in the SDS concentration in a way similar to that in SDBS solutions. The value of $n\alpha$, which was larger than that for SDBS solutions, increased with the SDS concentration.

Table 2. Dependence of polarographic parameters on SDS concentration

SDS concn. (M)	$-E_{1/2}$ (V)	i_d (μA)	D ($\times 10^{-6}$ cm^2/sec)	$n\alpha$
2×10^{-2}	0.295	0.170	2.18	1.13
3×10^{-2}	0.303	0.150	1.80	1.14
5×10^{-2}	0.301	0.115	1.06	1.23
7×10^{-2}	0.295	0.108	0.935	1.25
9×10^{-2}	0.303	0.085	0.580	1.25

Dye concn. 5.0×10^{-5} M

Discussion

Diffusion Coefficient of the Solubilized Dye. The apparent diffusion coefficients of the solubilized dye, as calculated from the polarographic data, were in good agreement with those of the anionic surfactant micelle with the electrolyte reported in the literature. Mankowich[5] calculated the molecular weight to be about 20,000 for a SDBS micelle in a 1% SDBS solution with 0.1 N Na_2SO_4. This molecular weight corresponds to a D value of about 8.7×10^{-7} cm^2/sec. Mysels' values[6] of the self-diffusion coefficient for 1.7—10.1×10^{-2} M SDS with 0.1 N NaCl were between 0.92 and 0.82×10^{-6} cm^2/sec. Although our results are somewhat larger than the above values, on the whole, there seems to be no great discrepancy. This fact indicates the diffusing particle to be the micelle solubilizing the dye in it.

The marked surfactant concentration dependence of D could be due to a large growth of the micelle, to the interaction with other micelles, or to the diffusion of the dye not solubilized in the micelle at the lower surfactant concentrations. Schott[7] has reported, that in SDS solutions, only one dye molecule was solubilized per micelle above the critical micelle concentration and that the aggregation number of SDS in the presence of 0.1 M NaCl was 131. With the present dye/surfactant ratio (below 1/170), all the dye molecules were solubilized in micelles. As to the size of the micelle reported in the literature[8], no drastic change appears throughout the experimental range; SDS concentration was 10^{-2}—10^{-1} M, and the dye concentration, 10^{-5}—1.5×10^{-4} M, in the presence of the 0.1 M acetate buffer. Therefore, it is the interaction with other micelles that must be responsible for the concentration dependence of D.

The empirical plots of $1/D$ *vs.* the square roots of the surfactant concentration suggested by Stigter *et al.*[6] are shown for SDBS in Fig. 5. The extrapolated value to the cmc (approximately 10^{-3} M) is 2.8×10^{-6} cm^2/sec, which is rather large compared with that in the literature.[5] The bending point of the line may be attributed to the change in the interaction of the micelles, but it cannot be interpreted in detail.

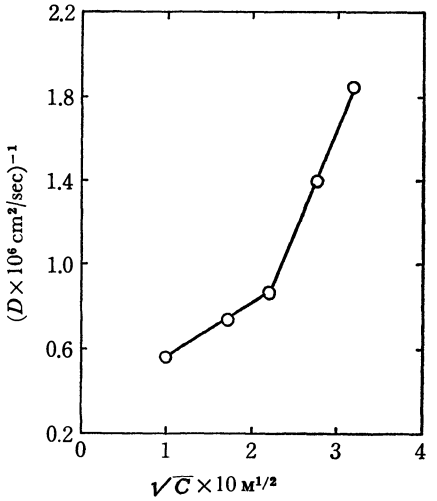

Fig. 5. Relation of the reciprocal of D to the square root of the SDBS concentration.

The value of D for SDS at 7×10^{-2} M, 0.935×10^{-6} cm^2/sec, is somewhat different from the value of Stigter *et al.*[6] at 7×10^{-2} M SDS, 0.858×10^{-6} cm^2/sec (with 0.1 M NaCl), but these values may be thought to be equal considering the difference in methods.

The Change in the Transfer Coefficient. The change in $n\alpha$ values with the surfactant concentration indicates the effect of the surfactant molecules on the electrode process. Kuta and Smoler[9] have been studied the transfer coefficient of TiO_2^+ and the vanadyl ion with surface-active substances such as polyvinyl alcohol and tribenzyl amine; they concluded that the α on the covered surface is usually less than that on the free surface. In this study, the transfer coefficient increases with an increase in the concentration of the surfactant, and the value for SDS is greater than that for SDBS. The latter fact can be interpreted by the fact that SDS is adsorbed in the micelle-like form at the potential of Orange OT reduction.[4] In 5×10^{-2} M SDS, $n\alpha$ is 1.23; this is comparable with the value of $n\alpha=1.22$ in 40% ethanolic solution. The change in the transfer coefficient with the surfactant and its

4) K. Eda, *Nippon Kagaku Zasshi*, **80**, 349 (1959).
5) A. M. Mankowich, *Ind. Eng. Chem.*, **47**, 2175 (1955).
6) D. Stigter, R. J. Williams, and K. J. Mysels, *J. Phys. Chem.*, **59**, 330 (1955).
7) H. Schott, *J. Phys. Chem.*, **70**, 2966 (1966).
8) J. N. Phillips and K. J. Mysels, *J. Phys. Chem.*, **59**, 325 (1955).
9) J. Kuta and I. Smoler, *Z. Elektrochem.*, **64**, 285 (1960).

concentration is now under investigation in our laboratory.

The Effect of the Surfactant Adsorption on the Reduction of the Solubilized Dye. The adsorption-desorption waves of the SDBS and SDS molecules show that, at the potential of Orange OT reduction, the anionic surfactant molecules are adsorbed on the electrode. Therefore, an effect from the anionic-charged particles may be expected. The dye is reduced at the potential of the positively-charged DME range; however, the dye gives a diffusion-controlled wave and remains unaffected by the anionic surfactant. These results, and the large α value obtained with a large surfactant concentration, suggest that the electrode reaction proceeds as if there were no effect of charged micelles near the electrode.

BULLETIN OF THE CHEMICAL SOCIETY OF JAPAN, VOL. 44, 1506—1510 (1971)

Proton Spin-Lattice Relaxation Studies of Intermolecular Interactions in the Mixtures of Chloroform and Proton-Acceptor Solvents

Kazuo SATO and Atsuo NISHIOKA

Department of Polymer Engineering, Tokyo Institute of Technology, Ookayama, Meguro-ku, Tokyo

(Received December 11, 1970)

Proton spin-lattice relaxation measurements were carried out on chloroform in carbon tetrachloride, benzene, pyridine, acetone, and dimethylsulfoxide (DMSO) in order to investigate the effect of the intermolecular interaction on the spin-lattice relaxation time, T_1, of chloroform. It was found that the order of the effects of solvents on T_1 is as follows: DMSO>acetone, pyridine>benzene, carbon tetrachloride; this order corresponds to that of the association constant of chloroform with these solvents. The T_1 values of benzene and acetone were also determined on chloroform-benzene and chloroform-acetone mixtures. On the basis of the results obtained on these solutions together with the results on the T_1 of chloroform in various solvents, we estimated the lifetimes of the chloroform-benzene complex and of the chloroform-acetone hydrogen-bonding complex. We tried to keep the proton-density constant throughout the solutions, in order to avoid an ambiguity arising from its change, by adopting the corresponding deuterated compounds.

Proton magnetic resonance (PMR) relaxation studies are an important and useful tool for the study of the microdynamic behavior of liquids.[1,2] Giulotto, Lanzi, and Tosca[3] studied the hydrogen-bonded molecular clusters of phenol in carbon tetrachloride, and showed that the proton spin-lattice relaxation is sensitive to the molecular clustering. Recently Anderson and Fryer[4] and Anderson[5,6] examined both theoretically and experimentally the effect of molecular association on the rotatory motions of molecules in the liquid state; they concluded that the molecular association moved as a unit whose lifetime is longer than the molecular rotational correlation time, τ_c, (for most molecular liquids, τ_c is of the order of 10^{-11}—10^{-12} sec) should affect the spin-lattice relaxation considerably.

Huntress[7,8] studied the quadrupolar relaxation experiments on chloroform and chloroform-*d* and on equimolar mixtures of chloroform-*d*—benzene and chloroform—benzene-d_6, and calculated the rotational diffusion constants from the relaxation times obtained. Huntress interpreted the change in the reorientation of chloroform molecules between neat and benzene solutions in terms of the formation of a complex between chloroform and benzene. However, Anderson showed that the proton spin-lattice relaxation time, T_1, of benzene in chloroform-*d* is equal to those in benzene-d_6 and in carbon tetrachloride. He concluded that the complex between chloroform and benzene is a weak one and does not move as a unit.

In this paper, we will present the experimental results of our proton spin-lattice relaxation studies of mixtures of chloroform and various proton-acceptor solvents (basic solvents), including a chloroform-benzene mixture, and will discuss the intermolecular association and microdynamic behavior of molecules.

It has been well established that the chloroform proton is active and possesses the ability of forming hydrogen bonding, and various chloroform solutions have been studied extensively by means of various experimental techniques.[9-12] So far, PMR chemical shift measurements[11-17] have often been made on mix-

1) A. Abragam, "The Principles of Nuclear Magnetism," chap. VIII, Clarendon, Oxford, England (1961).
2) H. G. Hertz, Progr. NMR Spectry., **3**, chap. 5. (1967).
3) L. Giulotto, G. Lanzi, and L. Tosca, *J. Chem. Phys.*, **24**, 632 (1956).
4) J. E. Anderson and P. A. Fryer, *ibid.*, **50**, 3784 (1969).
5) J. E. Anderson, *ibid.*, **47**, 4879 (1967).
6) J. E. Anderson, *ibid.*, **51**, 3578 (1969).
7) W. T. Huntress, Jr., *J. Phys. Chem.*, **73**, 103 (1969).
8) W. T. Huntress, Jr., Adv. Magnetic Resonance **4**, chap. 1, (1970).
9) G. C. Pimental and A. L. McClellan, "The Hydrogen Bond," W. H. Freeman and Company, San Francisco, California (1960), p. 197.
10) M. D. Magee and A. Walker, *J. Chem. Phys.*, **50**, 1019 (1969).
11) P. Laszlo, Progr. NMR Spectry., **3**, chap. 6 (1967).
12) J. C. Davis, Jr., and K. K. Deb Adv. Magnetic Resonance, **4**, chap. 4, (1970).
13) C. M. Huggins and G. C. Pimentel, *J. Chem. Phys.*, **23**, 1244 (1955).
14) C. J. Creswell and A. L. Allred, *J. Phys. Chem.*, **66**, 1469 (1962).
15) B. B. Howard, C. F. Jumper, and M. T. Emerson, *J. Mol. Spectrosc.*, **10**, 117 (1963).
16) A. L. McClellan, S. W. Nicksic, and J. C. Guffy, *J. Mol. Spectrosc.*, **11**, 340 (1963).
17) W. Lin and S. Tsay, *J. Phys. Chem.*, **74**, 1037 (1970).

tures of chloroform and several basic solvents, such as dimethyl sulfoxide (DMSO), acetone, triethylamine, pyridine, acetonitrile, some ethers and ketones, and aromatic solvents. The results have been interpreted in terms of hydrogen-bonding formation or in terms of the formation of a complex between chloroform and solvents, and the association constant has been estimated by means of various procedures.

The greatest advantage of the PMR relaxation study may be its sensitivity to the molecular microdynamic motions and the change in molecular motions due to intra- or intermolecular interactions. We consider that information obtained through T_1 measurements, together with the results of the chemical shift and infrared absorption measurements, should lead us to understand in detail the nature of intermolecular interaction.

We therefore carried out PMR relaxation measurements on the following chloroform solutions: chloroform — chloroform-*d* — carbon tetrachloride, chloroform — chloroform-*d* — benzene-d_6, benzene — benzene-d_6 — chloroform-*d*, chloroform — chloroform-*d* — acetone-d_6, acetone — acetone-d_6 — chloroform-*d*, chloroform — chloroform-*d* — pyridine-d_5, and chloroform — chloroform-*d* — DMSO-d_6. In order to avoid the ambiguity arising from the variation in the proton density, we tried to keep the proton density of the solutions constant by adopting a deuterated analogue.

Experimental

Materials The chloroform and benzene were reagent-grade samples purchased from the Tokyo Kasei Co., Ltd., and were distilled by the usual procedures before use. The acetone and carbon tetrachloride were spectroscopic-grade samples from the Tokyo Kasei Co., Ltd., and were used without further purification. The chloroform-*d*, benzene-d_6, acetone-d_6, DMSO-d_6, and pyridine-d_5 were provided by E, Merck AG, Darmstadt, and were also used without further purification.

The atmospheric oxygen dissolved in the sample was carefully removed by several freeze-pump-thaw cycles in a NMR tube, then, under a vacuum, the sample tube was sealed. After sealing, the sample was used for the experiment immediately.

NMR measurements. The NMR spectrometer used in this study was JNM-C-60H spectrometer of Japan Electron Optics. Lab. operated at 60 MHz. The T_1 measurements were made at 25±1°C by the adiabatic rapid-passage and saturation-recovery methods with sampling. The experimental errors were within ±3%. The chemical shifts were measured by the usual side-band technique, with cyclohexane as the internal standard. The solution viscosities were measured at 25±0.1°C with a Cannon-Ubbelohde viscometer.

In the viscosity measurements, however, deuterated analogues were not used because the isotopic effects of deuterium on the viscosity are considered to be small.

Results and Discussion

The results of the chemical-shift and T_1 measurements of five chloroform solutions are shown in Figs. 1 and 2 respectively.

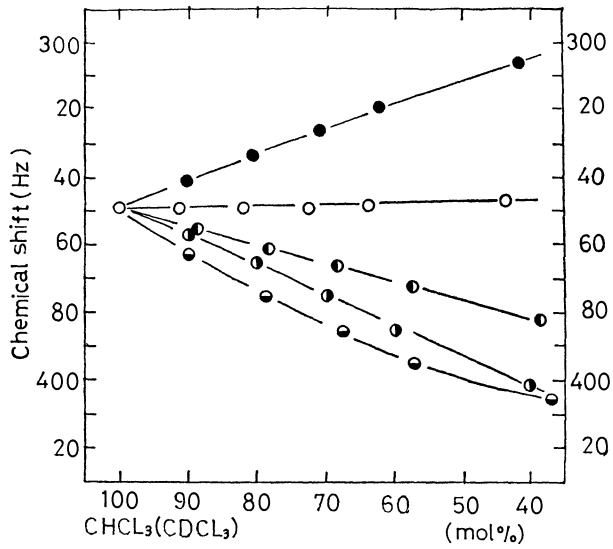

Fig. 1. Plots of chemical shifts of chloroform proton in various solvents *vs.* apparent mole fraction of chloroform.
solvent; benzene-d_6 (●), carbontetrachloride (○), acetone-d_6 (◐), pyridine-d_5 (◑), DMSO-d_6 (◒).
The number of chloroform proton per unit volume is constant; $N=29.8\times10^{20}$.
Apparent mole fraction of chloroform was varied by addition of chloroform-*d*.

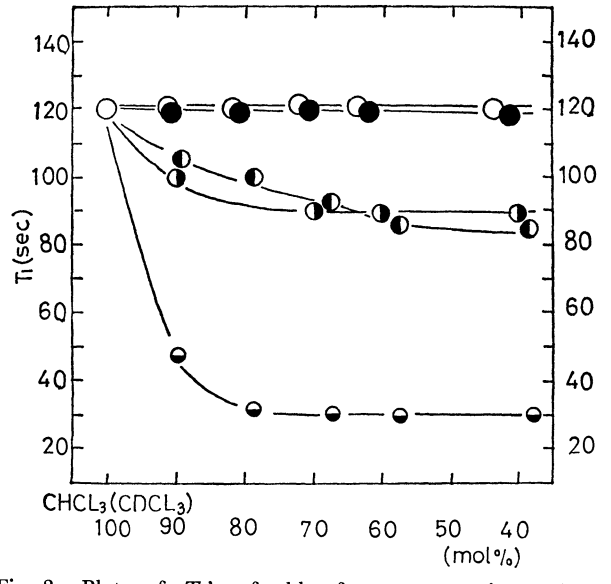

Fig. 2. Plots of T_1's of chloroform proton in various solvent *vs.* apparent mole fraction of chloroform.
solvent; benzene-d_6 (●), carbontetrachloride (○), acetone-d_6 (◐), pyridine-d_5 (◑), DMSO-d_6 (◒).
The number density of chloroform proton is constant; $N=29.8\times10^{20}$.
Apparent mole fraction of chloroform was varied by addition of chloroform-*d*.

Before proceeding to a discussion of each solution, we should like to make several remarks. Strictly speaking, the solutions studied are systems of three components which contain two deuterated analogues. We examined the PMR chemical shift of the chloroform of all solutions in order to test whether or not isotopic effects on the intermolecular interaction between chloroform and basic solvents are negligible.

It is clear from Fig. 1 that the concentration dependence of the chemical shift is almost identical with the literature data.[11-17] Therefore, it may be considered that the isotopic effects on the intermolecular interaction are negligible.

Secondly, we must consider the proton relaxation mechanism of chloroform. Winter[1,18] proposed that, in addition to the dipolar relaxation, the scalar coupling between a proton and chlorine nuclei modulated by the rapid quadrupolar relaxation of the latter may become another relaxation mechanism. On the other hand, Pritchard and Richards[19] proposed that the spin-rotation interaction is another important relaxation mechanism and that the scalar coupling may be unimportant.

In any case, it may be reasonable to assume that the dipolar relaxation mechanism is predominant for the chloroform proton; this assumption is supported by the experimental fact that the T_1 value of the chloroform proton changes from 80 sec for neat chloroform[20] to 120 sec for 40% chloroform in chloroform-*d*. Because the scalar coupling and the spin-rotation mechanisms should not be unchanged by deuterated dilution, this change in T_1 value may be due to the predominant intermolecular dipole-dipole interaction. Moreover, because of the small gyromagnetic ratio, deuteron and chlorine are considered to contribute negligibly to the relaxation of chloroform in this study.

Thirdly, let us consider the effect of the self-association of chloroform.[7,8,21,22] Jumper, Emerson, and Howard,[21] from the PMR chemical shift, estimated the self-association constant of chloroform to be $K=0.16\pm 0.006$ $(\mathrm{m\cdot f})^{-1}$. This value of K is roughly of an order of magnitude smaller than the association constant found for the association of chloroform to basic solvents studied in this paper. Jumper *et al.* found also that, in carbon tetrachloride, the fraction of chloroform participating in the self-association decreases. The T_1 values measured in carbon tetrachloride do not change over the experimental concentration range of chloroform, so we may conclude that the self-association of chloroform is not so strong as to affect the proton spin-lattice relaxation of chloroform in solution. Therefore, the change in T_1 accompanied by dilution with basic solvents may really be due to the effect of intermolecular chloroform-solvent interaction.

Finally, the effect of the macroscopic solution viscosity on T_1 must be considered. According to the Debye-B.P.P. theory,[1,23] the spin-lattice relaxation rate, $1/T_1$, is proportional to the solution viscosity, η. However, it has been well recognized that the B.P.P. theory gives τ_c values of an order of magnitude larger than those estimated from the experiment.[24,25] The proportionality between $1/T_1$ and η is considered to be doubtful. Bull and Jonas[26] studied the pressure dependence of T_1 on benzene and acetone, and showed that the proportionality between $1/T_1$ and η does not hold.

In this study, for example, the η of a carbon tetrachloride solution of chloroform (the mole fraction of chloroform is 40%) is about 1.3 times that of neat chloroform. Nevertheless, T_1 does not change entirely. Therefore, we did not carry out the corrections of the solution viscosity on T_1 in this study.

Now, we should like to turn our attention to the results obtained. It is clear from Fig. 2 that we can classify the solutions studied into three groups. The first group, in which the T_1 values of chloroform are not affected by the presence of solvents, includes chloroform-carbon tetrachloride and chloroform-benzene solutions. Especially, it is interesting that the π-complex between chloroform and benzene does not affect the spin-lattice relaxation of chloroform greatly. Several interpretations of the molecular microdynamics of the π-complex will be shown in the successive discussion in connection with the results of Huntress and Anderson.

The second group, in which T_1 values of chloroform are affected to some extent through the intermolecular interaction with basic solvents, includes chloroform-acetone and chloroform-pyridine solutions. In these solutions, the intermolecular interactions are due to the hydrogen bonds, which is considered to be stronger than the π-complex. Indeed, Abraham[27] pointed out that the complex between chloroform and benzene is essentially similar to other hydrogen bonds; that is, it is essentially electrostatic in character, but because of the weak ionic character of the C–H bond, it is considerably less stable than the more common hydrogen bonds.

The chloroform-DMSO solution is classified in the third group, in which T_1 values of chloroform are affected considerably by the strong intermolecular interaction. In this solution, the spin-lattice relaxation rate of chloroform increases by a factor of about 4 as a result of the presence of a small amount of DMSO. Anderson has also shown that the T_1 value of DMSO protons is affected by the presence of chloroform. Therefore, it may be concluded that the intermolecular interaction between chloroform and DMSO is the strongest, and that the associated species should move as a unit with a lifetime longer than the rotational or translational correlation times of DMSO and chloroform.

The order of the affinity of solvents in associating with chloroform is found to be as follows: DMSO> acetone, pyridine>benzene, carbon tetrachloride. This order corresponds well to that of the association constants between chloroform and solvents described above, obtained through the chemical shift measure-

18) J. Winter, *Comp. Rend.*, **249**, 1346 (1959).
19) A. M. Pritchard and R. E. Richards, *Trans. Faraday Soc.*, **62**, 2014 (1966).
20) K. Sato and A. Nishioka, This Bulletin, to be published.
21) C. F. Jumper, M. T. Emerson, and B. B. Howard, *J. Chem. Phys.*, **35**, 1911 (1961).
22) R. Kaiser, *Can. J. Chem.*, **41**, 430 (1963).
23) N. Bloembergen, E. M. Purcell, and R. V. Pound, *Phys. Rev.*, **73**, 679 (1948).
24) W. B. Moniz and H. S. Gutowsky, *J. Chem. Phys.*, **38**, 1155 (1963).
25) W. B. Moniz, W. A. Steele, and J. A. Dixon, *ibid.*, **38**, 2418 (1963).
26) T. E. Bull and J. Jonas, *ibid.*, **52**, 4553 (1970).
27) R. J. Abraham, *Mol. Phys.*, **4**, 369 (1961).

ment.[11-17] Thus, in addition to the information about the microdynamic molecular motion, the strength of the association can be estimated through PMR relaxation measurements. Moreover, if the rotational or translational correlation times of each component molecule are known, the order of the lifetimes of the association can also be presumed.

Hubbard[28] has derived an equation for the intermolecular relaxation time which takes account of both the rotational and translational molecular motions:

$$(1/T_1)\text{inter} = (\pi\hbar^2\gamma^4 N/10r^3)\tau_t[1 + 0.233\ (b/r)^2 + 0.15(b/r)^4 + \cdots] \quad (1)$$

where N is the number of spins per unit of volume, r is the molecular radius, b is the distance of the nucleus from the center of the molecule, and τ_t is the translational correlation time, and where all other notations represent their ordinary meanings. We assume, as has been described above, that for the chloroform proton the intermolecular dipole-dipole relaxation is predominant over the other relaxation mechanisms within the experimental conditions in this study. Therefore, Eq. (1) is applicable in calculating τ_t of chloroform in solutions. The following values of r and b were used in the calculation: r=2.81 Å, b=1.10 Å. The radius was obtained by assuming hexagonal closed packing, and b was taken to be equal to the C–H bond length.[29]

In Figs. 3 and 4 respectively, the T_1 values of benzene — benzene-d_6 — chloroform-d, and acetone — acetone-d_6 — chloroform-d solutions are shown. The result of T_1 measured in carbon tetrachloride is also shown in Fig. 3. The T_1 values of both benzene and acetone are affected by the presence of chloroform, but not the T_1 of benzene in carbon tetrachloride. These results imply that the molecular motions of

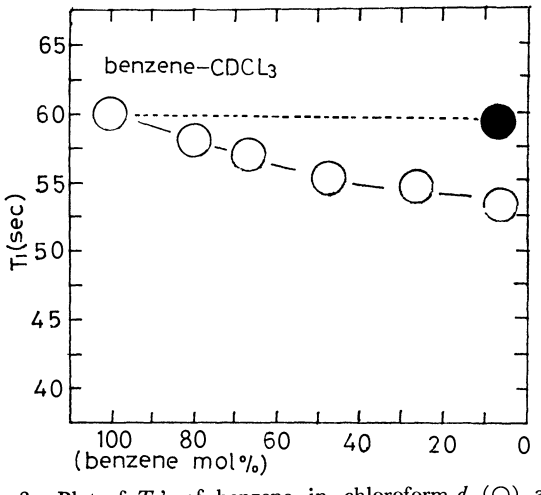

Fig. 3. Plot of T_1's of benzene in chloroform-d (○) and carbontetrachloride (●) *vs.* apparent mole fraction of benzene.
The number density of benzene proton is constant; N= 40.5×10^{20}.
Apparent mole fraction of benzene was varied by addition of benzene-d_6.

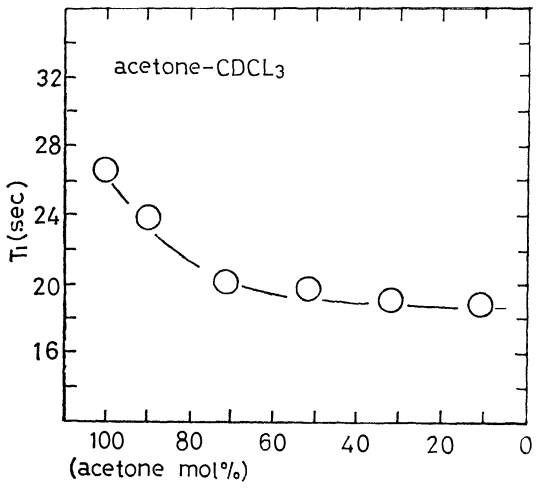

Fig. 4. Plot of T_1's of acetone in chloroform-d *vs.* apparent mole fraction of acetone.
The number density of acetone proton is constant; N= 48.8×10^{20}.
Apparent mole fraction of acetone was varied by addition of acetone-d_6.

benzene and acetone are influenced to some extent by the intermolecular interaction with chloroform, the former due to the π-complex, and the latter, to the hydrogen bond. These results do not, however, coincide with the those of Anderson. We speculate that this discrepancy may arise from the difference in the experimental temperature (Anderson made his experiment at 35°C).

It is reasonable to assume that the intramolecular dipole-dipole relaxation is predominant for both benzene and acetone protons because of their small fractions in the present study. As will be shown later, this assumption is supported by the fact that the τ_c values of benzene and acetone calculated by this assumption correspond to those of Bonera and Rigamonti.[30,2] We calculate τ_c using the following expression:[1,23]

$$(1/T_1)\text{intra} = 3/2\hbar^2\gamma^4 \sum \langle r_{ij}^{-6}\rangle \cdot \tau_c \quad (2)$$

where r_{ij} is the hydrogen-hydrogen interatomic distance. For benzene and acetone, the values of r_{ij} were taken from Zeidler's work.[31]

Chloroform-Benzene Solution. In Table 1, the (T_1) inter, τ_t of chloroform and the (T_1)intra, τ_c of benzene are shown at various solution compositions. The order of the magnitude of τ_t roughly agrees with Hertz's result[2]: 1.1×10^{-10} sec. The values of (T_1) intra and τ_c in neat benzene also agree with those of Bonera and Rigamonti. It may easily be seen that the translational motion of chloroform is not influenced by the π-complex with benzene, but that the rotational motion of benzene is influenced slightly. On the basis of this experimental fact, we conclude that the π-complex does move as a unit, but that its lifetime is short, probably of the order of 10^{-12} sec. According to the theory of Anderson, it is reasonable to consider

28) P. S. Hubbard, *Phys. Rev.*, **131**, 275 (1963).
29) "Table of Interatomic Distances and Configuration in Molecules and Ions," M 106, ed. by L. E. Sutton, Chem. Soc., London (1958).
30) G. Bonera and A. Rigamonti, *J. Chem. Phys.*, **42**, 171 (1965).
31) M. D. Zeidler, *Ber. Bunsenges. Physik. Chem.*, **69**, 659 (1965).
32) E. R. Andrew and R. G. Eades, *Proc. Roy. Soc.* (London), **A218**, 537 (1953).

Table 1. The values of (T_1)inter, τ_t (chloroform) and (T_1)intra, τ_c (benzene) of chloroform-benzene solution

Chloroform -benzene mole ratio	Chloroform		Benzene	
	(T_1)inter (sec)	$\tau_t \times 10^{10}$ (sec)	(T_1)intra (sec)	$\tau_c \times 10^{12}$ (sec)
100 : 0	120	2.9		
90 : 10	120	2.9	54	2.1_8
50 : 50	120	2.9	56	2.1_0
0 : 100			60	1.9_6

τ_t and τ_c were calculated by using Eqs. (1) and (2), respectively.

that the association whose lifetime is of the order of 10^{-12} sec does not modulate the molecular motion, the correlation time of which is about 10^{-10} sec. The slight influence on the rotational motion of benzene may be due to the fact that the C_6 rotation (the C_6 axis of benzene coincides with the C_3 axis of chloroform) in the π-complex is almost free. Indeed, Andrew and Eades[32] have found that benzene molecules reorient quite freely about the C_6 axis even in a solid.

The conclusion we proposed above does not conflict with that of Huntress that the tumbling motion of of chloroform is slowed by a factor of 4 by complexing with benzene. That is, the correlation time of the tumbling motion of chloroform is of the order of 10^{-12} sec, sufficiently short to be affected by π-complexing. Anderson has shown experimentally that the intramolecular spin-lattice relaxation of benzene is not affectedgreatly through π-complexing with chloroform at 35°C, and he has suggested that the molecular rotation of benzene about the C_2 axis takes place by large-angle jumps rather than by small diffusive steps. However, in the present study, no such insensibility of the spin-lattice relaxation of benzene to π-complexing was found. It seems necessary to reexamine this problem over a wide range of experimental conditions.

Chloroform-Acetone Solution. In Table 2, the (T_1)inter, τ_t and (T_1)intra, τ_c of chloroform and acetone respectively are shown. The values of (T_1)-intra and τ_c of acetone in neat acetone agree with those of Bonera and Rigamonti. It is clear from the table that both the translational motion of chloroform and the rotational motion of acetone in solution are affected to a certain degree by the intermolecular hydrogen-bonding interaction. Therefore, we may conclude that the hydrogen bond is moderately strong, and that its lifetime is of the order of 10^{-11} sec. One may consider that the association whose lifetime is of the order of 10^{-11} sec should reduce the molecular motion of acetone to a greater extent. According to Debye-B.P.P., τ_c is proportional to the third power of the radius of the molecule. Thus, if the association between chloroform and acetone is rigid and if its lifetime is much longer than the correlation time, the τ_c of acetone in the associated complex may be several times larger than that of acetone in the neat liquid. However, the chloroform-acetone association seems not so rigid as in a single molecule, and the C_3 rotation of the methyl group of acetone in the association is considered to be relatively free. From their line-width measurements Gutowsky and Pake[33] have found that the methyl groups rotate even in solid acetone. Because of these two situations, the τ_c of acetone might not become so large as expected.

Table 2. The values of (T_1)inter, τ_t (chloroform) and (T_1)intra, τ_c (acetone) of chloroform-acetone solutions

Chloroform -acetone mole ratio	Chloroform		acetone	
	(T_1)inter (sec)	$\tau_t \times 10^{10}$ (sec)	(T_1)intra (sec)	$\tau_c \times 10^{12}$ (sec)
100 : 0	120	2.9		
90 : 10	105	3.5	$18._7$	0.9_3
50 : 50	85	4.4	$19._6$	0.9_1
0 : 100			$26._5$	0.6_7

τ_t and τ_c were calculated by using Eqs. (1) and (2), respectively.

We expect that the lifetime of the chloroform-pyridine complex may be of the same order as that of the chloroform-acetone complex, and that the chloroform-DMSO complex may have the longest lifetime of all the solutions studied in this paper. A more detailed consideration of these solutions is possible, the spin-lattice relaxation measurements being made of pyridine and DMSO protons.

33) H. S. Gutowsky and G. E. Pake, *J. Chem. Phys.*, **18**, 162 (1950).

The Liquid-phase γ-Radiolysis of Benzene-Nitrous Oxide Mixtures

Shun-ichi HIROKAMI, Seishi SHISHIDO, and Shin SATO

Department of Applied Physics, Tokyo Institute of Technology, Ookayama Meguro-ku, Tokyo

(Received December 12, 1970)

The γ-radiolysis of the benzene-nitrous oxide liquid mixtures has been studied at room temperature and at 0°C, the mixing ratios covering almost all the range from pure benzene to pure nitrous oxide. Phenol was found to be one of the main products; its G-value is about a half of that of nitrogen at the lower concentration of nitrous oxide. Kinetic analysis shows that the G-values of electrons from benzene are 3.2 ± 0.2. An empirical equation for expressing the G-value of nitrogen from the benzene solution of nitrous oxide proposed by Hentz and Sherman (*J. Phys. Chem.*, **73**, 2676 (1969).) was examined. The agreement was very poor at higher concentrations of nitrous oxide. Possible reasons were discussed.

In recent years there has been much interest in the formulation of quantitative descriptions of the non-homogeneous kinetics of charge scavenging in the liquid-phase radiolysis.[1-4] Warman, Asmus, and Schuler proposed an empirical equation for the charge scavenging and adduced much experimental evidence for the validity of this equation, especially in connection with the radiolysis of cyclohexane:[5]

$$G_s = G_{fi} + G_{gi}\frac{\sqrt{\alpha S}}{1+\sqrt{\alpha S}} \qquad \text{(I)}$$

Here, G_s is the 100 eV yield of electrons or cations scavenged by an additive, the molarity of which is denoted by S. G_{fi} is the yield of free ion pairs; *i.e.*, these pairs escape from their mutual Coulombic field. G_{gi} is the yield of geminate-ion pairs, which are restrained in their mutual Coulombic field. The α parameter can be considered to be proportional to the specific rate of the charge-scavenging reaction. When nitrous oxide is used as an electron scavenger and when the G-value of nitrogen from the solution is used as a measure of the electron scavenging, Eq. (I) has to be modified, because the production of nitrogen from a hydrocarbon solution is believed to consist of two steps.[6] Hentz and Sherman discussed four possible mechanisms for the formation of nitrogen in a benzene solution.[7] The mechanism they preferred was the following:

$$e^- + N_2O \rightarrow N_2O^- \qquad (1)$$

$$N_2O^- + C_6H_6 \rightarrow N_2 + C_6H_6O^- \qquad (2)$$

$$C_6H_6O^- + N_2O \rightarrow N_2 + \text{residue} \qquad (3)$$

In any mechanism, however, the formation of nitrogen has two origins, such as the reactions (2) and (3), both of which complete with neutralization. Therefore, if we use Eq. (I) as an analogy, the empirical equation for $G(N_2)$ should have the following form:

$$G(N_2) = 2G_{fi} + G_{gi}\frac{\sqrt{\alpha S}}{1+\sqrt{\alpha S}}\left(1+\frac{\sqrt{\beta S}}{1+\sqrt{\beta S}}\right) \qquad \text{(II)}$$

Here, G_{fi}, G_{gi}, and S have the same meanings as in Eq. (I). The β parameter is for the reaction (3), the analog of α in the reaction (1). Hentz and Sherman used this equation to analyze their experimental results on the radiolysis of the benzene solution of nitrous oxide and thus estimated the values of G_{gi}, α, and β.

When comparing the radiolyses of cyclohexane and benzene solutions of nitrous oxide, the most remarkable difference observed is in the G-value of nitrogen; the $G(N_2)$ from the cyclohexane solution is more than twice that from the benzene solution at the same concentrations of nitrous oxide up to 0.5 mol/l.[8] A possible explanation of this is that the G-value of the electrons from benzene might be much smaller than that of those from cyclohexane. However, this is not likely because the W-values of these two compounds in the gas phase are believed to be not very different. Another explanation is that the ratio between the rate of the recombination reaction of geminate-ion pairs and the rate of the electron-scavenging reaction of nitrous oxide is much larger in benzene than in cyclohexane. If this is the case, the $G(N_2)$ from the benzene solution should approach the value obtained from the cyclohexane solution with an increase in the concentration of nitrous oxide to more than 0.5 mol/l.

Experimental

Tokyo Pure Chemical Co. benzene (spectro grade) was used as supplied. Since the G-values of the hydrogen (0.04) and biphenyl (0.08) were in good agreement with the reported values, further purification was not made. Nitrous oxide (Matheson Co. pure grade) was distilled bulb-to-bulb, and the head and tail fractions were rejected.

All the mixtures were sealed into small sampling glass tubes (about 3 ml) with a breakable seal attached. The amount of benzene was measured by a small pippet or a micro syringe, and that of nitrous oxide, volumetrically. The nitrous oxide concentrations at room temperature were calculated by using the Ostwald solubility coefficient of 3.8. At this temperature, more than 4 mol/l could not be attained because of the fragility of the breakable seal. At 0°C, however, almost all the mixing ratios could be obtained. At concentrations lower than 0.2 mol/l, the solution was crystallized. Several runs were made at the temperature of a dry

1) A. Mozumder, "Advances in Radiation Chemistry," Vol. 1, ed. by M. Burton and J. L. Magee, Wiley-Interscience, New York (1969), p. 1.
2) J. M. Warman, K. -D. Asmus, and R. H. Schuler, *Adv. Chem. Ser.*, **82**, 25 (1968).
3) G. R. Freeman, *Rad. Res. Rev.*, **1**, 1 (1968).
4) S. Sato, This Bulletin, **41**, 304 (1968).
5) J. M. Warman, K. D. Asmus, and R. H. Schuler, *J. Phys. Chem.*, **73**, 931 (1969).
6) G. Scholes and M. Simic, *Nature*, **202**, 895 (1964).
7) R. R. Hentz and W. V. Sherman, *J. Phys. Chem.*, **73**, 2676 (1969).
8) S. Sato, R. Yugeta, K. Shinsaka, and T. Terao, This Bulletin **39**, 156 (1966).

ice-methanol mixture. In this case, solid benzene floated in the liquid nitrous oxide.

Samples were irradiated at their respective temperatures by ^{60}Co γ rays with a dose rate of 0.88×10^6 R/hr, usually for 4 hr. To analyze the gases noncondensable at the liquid-nitrogen temperature, the irradiated sample tubes were used to a conventional vacuum line, and after had been broken the seal, the gas in the two liquid nitrogen traps was collected by a Toepler pump and placed in a gas buret connected to a cuprous oxide furnace in order to combust the trace of hydrogen produced. In order to analyze the products in the solution, the seal was broken in the atmosphere, and a micro syringe was used to inject a small amount of the solution into the gas chromatographs (a 1-m dioctyl-phthalate column at 130°C and a 0.5-m alkyl-benzene-sulfonic-acid-sodium-salt column at 125°C). The quantitative estimation was made by comparing the peak areas with those of the prepared solutions. To ascertain the formation of phenol, a Millon reagent was also used. The yield calculated from the absorbance at 400 nm was in fair agreement with that estimated by gas chromatography.

Results

Tables 1 and 2 summarize the results obtained at room temperature. The G-value of nitrogen increased with the increase in the concentration of nitrous oxide, reached 6.74 at the highest concentration examined, and still showed a tendency to increase. The yields of phenol and biphenyl also increased with the increase in the nitrous-oxide concentration, but the yield of an unspecified product (probably hydrogenated biphenyl) stayed constant.

The results obtained at 0°C are summarized in Tables 3 and 4. In these cases, the concentration was expressed by the mole fraction, because the liquid volume was substantially affected by the amount of nitrous oxide.

Table 1. G-Value of nitrogen from the γ-radiolysis of benzene solution of nitrous oxide at room temperature[a)]

N_2O mol/l	$G(N_2)$	N_2O mol/l	$G(N_2)$
0.118	1.37	1.30	4.30
0.119	1.26	1.37	4.41
0.203	1.87	1.54	4.82
0.313	2.16	1.70	4.95
0.615	3.16	1.81	5.01
0.965	3.70	2.01	5.00
1.01	3.92	3.04	6.06
1.27	4.28	4.64	6.74

a) Within experimental error, the G-values of nitrogen coincide with the following relation. $G(N_2)=3.78\sqrt{[N_2O]}$.

Table 2. G-Values of phenol, biphenyl, and unspecified products[a)] from the γ-radiolysis of benzene solution of nitrous oxide at room temperature

N_2O mol/l	G-Value		
	Phenol	Biphenyl	Unspecified
0	0	0.08	0.06
0.366	1.50	0.51	0.11
0.568	1.48	0.33	0.09
0.753	2.10	0.57	0.13
0.955	1.82	0.42	0.08
1.15	2.00	0.47	0.08
1.70	2.46	0.68	0.10
2.09	2.56	0.63	0.08
3.37	3.96	0.91	0.09
4.52	4.00	0.99	0.05

a) The elution time on the gas-chromatograph corresponds to that of hydrogenated biphenyls.

Table 3. G-Value of nitrogen from the γ-radiolysis of benzene-nitrous oxide liquid mixtures at 0°C

N_2O mol%	$G(N_2)$	N_2O mol%	$G(N_2)$
15.4	3.75	63.0	7.18
15.5	4.13	72.5	7.78
28.4	4.91	81.0	8.33
32.9	5.00	90.3	9.14
40.2	6.07	92.7	9.74
46.2	6.77	94.4	10.2
51.3	7.26		

Table 4. G-Values of phenol, biphenyl, and unspecified products from the γ-radiolysis of benzene-nitrous oxide liquid mixtures at 0°C

N_2O mol/l	G-Value		
	Phenol	Biphenyl	Unspecified
19.4	2.07	0.40	0.05
21.8	2.30	0.38	0.05
28.8	2.26	0.49	0.04
41.6	2.91	0.55	0.05
45.9	3.01	0.54	0.05
52.3	2.92	0.50	0.03
54.7	3.01	0.48	0.02
61.1	2.94	0.48	0.02
66.9	2.78	0.48	0.02
68.7	2.96	0.48	0.02
70.9	2.96	0.41	0.02

In Fig. 1, the G-values of nitrogen and phenol are plotted as a function of the electron density of nitrous oxide. The G-value of nitrogen obtained at the temperature of dry ice-methanol is also plotted; it shows a linear dependence on the electron density of nitrous oxide.

Discussion

Formation of Phenol. In the study of the gas phase radiolysis of benzene-nitrous oxide mixtures, Rzad and Warman observed a very high yield of phenol formation ($G\sim40$).[9)] They proposed a chain mechanism involving the electron transfer from $C_6H_6O^-$ to nitrous oxide, a mechanism which corresponds

9) S. J. Rzad and J. M. Warman, *J. Phys. Chem.*, **72**, 3013 (1968).

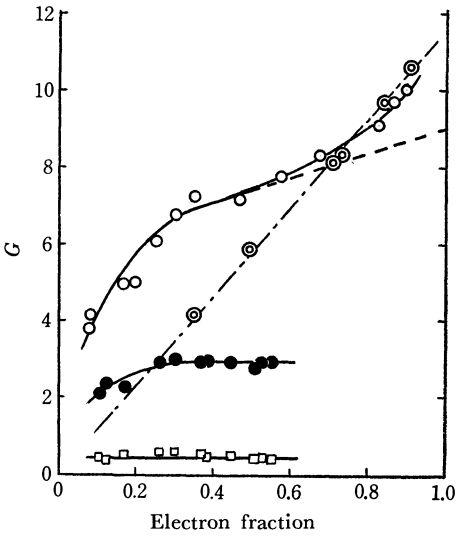

Fig. 1. G-Value of nitrogen (○), phenol (●), and biphenyl (□) obtained at 0°C and G-value of nitrogen (◎) at dry-ice temperature as a function of the electron density of nitrous oxide. Dashed line was tentatively drawn by connecting the G-value of nitrogen at around 0.5 in the electron density with $G_0=9$, which is the average used for the calculation of $g(N_2)$.

to the reaction (3) presented in the Introduction. To explain the present results, the chain mechanism is obviously not necessary. In place of the electron transfer, we tentatively assumed the following reactions:

$$C_6H_6O^- + N_2O \rightarrow N_2 + C_6H_6O_2^- \quad (3)$$

$$C_6H_6O_2^- + C_6H_6^+ \rightarrow C_6H_5OH + C_6H_6O \quad (4)$$

Here, C_6H_6O stands for the intermediate product of the reaction between benzene and an oxygen atom.

Boocock and Cvetanović investigated the reactions of oxygen atoms with benzene in the gas phase, using the mercury photosensitized decomposition of nitrous oxide as the source of oxygen atoms; they found that the yield of phenol formation is very much smaller than that expected from the yield of nitrogen.[10] The ratio in the yield of phenol to nitrogen formation was about 0.06. For the rest of the oxygen atoms, they found that carbon monoxide and polymers were formed. In the present study, carbon monoxide could not be observed. This may be attributed to the fact that the present experiment was performed in a liquid. The intermediate product, C_6H_6O, therefore, probably gives rise to only polymers. In fact, the formation of yellowish-white polymers was observed, though it was not analyzed.

As is shown in Tables 2 and 4, the yield of biphenyl increased with the increase in the concentration of nitrous oxide. This increase may be explained by the following reactions:

$$C_6H_6O^* \rightarrow C_6H_5 + OH \quad (5)$$

$$2\,C_6H_5 \rightarrow C_6H_5\text{-}C_6H_5 \quad (6)$$

Here, the asterisk denotes the excited state which is the precursor of C_6H_6O in the reaction (4).

10) G. Boocock and R. J. Cvetanović, *Can. J. Chem.*, **39**, 2436 (1961).

Formation of Nitrogen. The gas-phase radiolysis of nitrous oxide has been investigated by many groups of investigators, but the mechanism of the formation of nitrogen has not yet been established in detail.[11,12] For the liquid phase, only one report by Robinson and Freeman could be found in the literature.[13] According to their tentative reaction mechanism, the G-value of ionization is 3.0, and that of excitation, which results in the decomposition into N_2 and O, is 6.4. Our present results are compatible with their mechanism. As may be seen in Fig. 1, when the electron fraction of nitrous oxide is in the range from 0.6 to 0.9, the G-values of nitrogen obtained at 0°C are a little smaller than those obtained at the dry-ice temperature. At this temperature, benzene and nitrous oxide probably decompose independently, because the system is not homogeneous. The deviation of $G(N_2)$ from the linearity obtained at the dry-ice temperature may be explained by the charge-transfer reaction from N_2O^+ to benzene. The ionization potential of nitrous oxide in the gas phase has been reported to be 12.9 eV, and that of benzene, to be 9.5 eV. This type of charge transfer may be completed at electron densities down to 0.6 in Fig. 1. If this reasoning is correct, the formation of nitrogen below 0.6 in the electron density of nitrous oxide should be explained by the following two types of reactions. One is the reaction initiated by the electron scavenging of nitrous oxide, which has already been discussed in the Introduction; the other is the non-ionic reaction of nitrous oxide, which may be described as follows:

$$N_2O \rightsquigarrow N_2 + O \quad (7)$$

The oxygen atoms produced in this reaction may react with benzene and produce a polymer, as has been discussed. This mechanism matches the observation that the G-value of phenol becomes saturated as the concentration of nitrous oxide increases, while in the same range of nitrous oxide concentration the G-value of nitrogen still has a tendency to increase.

Another possible non-ionic reaction forming nitrogen is the benzene sensitized decomposition of nitrous oxide. In this respect, we have recently examined the benzene-photosensitized decomposition of nitrous oxide in a cyclohexane solution. The light source used was a low-pressure mercury lamp. The quantum yield of the decomposition was very small (about 0.005). This result does not necessarily mean that the benzene-sensitized decomposition is negligibly small in the radiolysis, because highly excited states of benzene, which may be formed in the radiolysis but not in the photolysis, might play a role in the decomposition of nitrous oxide. This possibility, therefore, cannot be completely ruled out by the present experiment.

Nitrogen Resulting from the Electron Scavenging of Nitrous Oxide. In order to apply the empirical equation

11) J. A. Hearne and R. W. Hummel, *Rad. Res.*, **15**, 254 (1961).
12) S. Takao, S. Shida, Y. Hatano, and H. Yamazaki, This Bulletin **41**, 2221 (1968).
13) M. G. Robinson and G. R. Freeman, *J. Phys. Chem.*, **72**, 1394 (1968).

(II) to the present data, we have to discriminate the G-value of the nitrogen produced by the electron scavenging from the value of that produced by other processes. A tentative calculation has been made by using the following relation:

$$G(N_2) = \varepsilon_B g(N_2) + \varepsilon_{N_2O} G_0$$

Here, $g(N_2)$ is the G-value of nitrogen resulting from the reaction initiated by the energy absorbed by benzene, and G_0 is the G-value of nitrogen from pure liquid nitrous oxide, excluding the contribution of N_2O^+. ε_B and ε_{N_2O} are the electron densities of benzene and nitrous oxide respectively. As the value of G_0, we had to take a wide range of values, from 8 to 10, because of the inaccuracy of the data, as is shown in Fig. 1. However, the calculated $g(N_2)$ values were not so scattered, as is shown in Fig. 2. The asymptotic value obtained at high concentrations of nitrous oxide ranges from 6.2 to 6.8. If the contribution from the benzene-sensitized decomposition can be disregarded, this value should be equal to twice that of the G-value of the electrons from benzene.

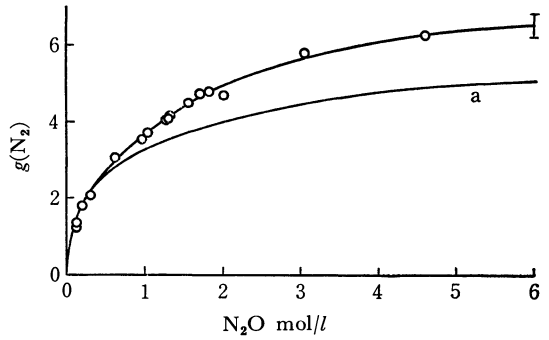

Fig. 2. G-Value of nitrogen formation initiated by the energy absorbed by benzene at room temperature as a function of the concentration of nitrous oxide. The curve a) is drawn by using Eq. (II).

The curve a) in Fig. 2 was drawn by using Eq. (II), with $G_{gi}=3.9$, $\alpha=0.7$ l/mol, and $\beta/\alpha=50$, according to the method of Hentz and Sherman.[7] The agreement was obviously very poor. We tried various combinations of the values for G_{gi}, α, and β, but as long as Eq. (II) was used, a successful adjustment could not be made. If Eq. (II) correctly expresses the result of the electron scavenging of nitrous oxide, the disagreement might be due to a neglect of the benzene-sensitized decomposition of nitrous oxide. However, the G-value of electrons estimated above, 3.2 ± 0.2, is a little smaller than that to be expected from the W-value of benzene in the gas phase ($\sim$25 eV); *i.e.*, as far as the G-value of nitrogen is concerned, it is not necessary to take the contribution of the benzene-sensitized decomposition of nitrous oxide into account.

In connection with the G-value of electrons from benzene, the G-value of phenol at 0°C is suggestive; it does not exceed 3, even at the highest concentration of nitrous oxide examined. If the mechanism of the formation of phenol is that proposed above, the G-value of phenol should be nearly equal to that of the electrons scavenged by nitrous oxide. This, however, is not conclusive, either, because of the uncertainty of the reaction mechanism.

Although the validity of Eq. (I) is evidenced by many experimental results,[14] this equation itself has shortcomings when it is applied to higher concentrations of scavengers; experimentally, the value of $[S]$ cannot exceed that of the pure state, which is usually less than 10 mol/l for most of the solutes. Therefore, since α is 0.7 l/mol in the case of benzene, the $\sqrt{\alpha S}(1+\sqrt{\alpha S})^{-1}$ fraction is less than 0.8. Even in the case of $\alpha=16$ l/mol, which has been reported in the study of the electron scavenging of methyl bromide in the radiolysis of cyclohexane[2], the above fraction is 0.93. In other words, the G_{gi} estimated by using Eq. (I) or (II) can never be observed experimentally.

In the formulation of the non-homogeneous kinetics of charge scavenging, it is usually assumed, for the convenience of the theoretical treatment, that only one ion pair exists in a spur. Even Eq. (I) is based on the same assumption, though it is very empirical.[4] However, it is well known that the formation of multi-ion pairs in a spur is not negligibly small.[15] Therefore, when a high concentration of scavenger is used, the contribution of such ion pairs cannot be ignored. The large deviation of the experimental data from the empirical equation shown in Fig. 2 might be due to such a neglect. For a complete interpretation, further investigation is obviously desired.

14) S. J. Rzad, P. P. Infelta, J. M. Warman, and R. H. Schuler, *J. Chem. Phys.*, **52**, 3971 (1970).
15) W. J. Beekman, *Physica*, **15**, 327 (1949).

Test for Validity of Constant Ionic Medium Principle. Variation of the Activity Coefficient of Hydrogen Ion in Various Compositions of Medium Cations with 3 M Perchlorate Ions

Hitoshi OHTAKI and Georg BIEDERMANN*

Department of Electrochemistry, Tokyo Institute of Technology, Ookayama, Meguro, Tokyo

* *Department of Inorganic Chemistry, The Royal Institute of Technology, Stockholm, Sweden*

(Received December 15, 1970)

Potential changes of cells with a glass electrode and a hydrogen electrode in combination with a reference half-cell were measured in solutions of various compositions of cations at constant concentrations of hydrogen and total perchlorate ions. Measurements were carried out for the systems $LiClO_4$-$NaClO_4$, $LiClO_4$-$AgClO_4$, $NaClO_4$-$AgClO_4$, $NaClO_4$-$TlClO_4$, $LiClO_4$-$Mg(ClO_4)_2$, $LiClO_4$-$Ba(ClO_4)_2$, $NaClO_4$-$Ba(ClO_4)_2$, $AgClO_4$-$Ba(ClO_4)_2$, and $LiClO_4$-$La(ClO_4)_3$. In some cases a remarkable potential change was observed. Part of the change was due to the variation of the liquid junction potential at the interface of a test solution and a solution in a salt bridge. However, the change was attributed in greater part to the electrostatic free energy change of the transfer of hydrogen ion from a ($3/m$ M A^{m+}, 3M ClO_4^-) solution to a (xM A^{m+}, yM B^{n+}, 3M ClO_4^-) solution (where $mx+ny=3$). Variation of the composition of electrolytes gives rise to a significant change of the dielectric constant of a solution, so that the activity coefficient of hydrogen ions varies in different solutions at a constant concentration of perchlorate ions. Potential changes are additive in $A_1(ClO_4)_{m_1}$-$B_1(ClO_4)_{n_1}$, $A_1(ClO_4)_{m_1}$-$B_2(ClO_4)_{n_2}$ and $B_2(ClO_4)_{n_2}$-$B_1(ClO_4)_{n_1}$ solutions for a given replacement of cations in solutions, where A_1, B_1, and B_2 denote cations with charges of m_1, n_1, and n_2, respectively.

When we apply the constant ionic medium principle to reactions in electrolyte solutions, it is essential to choose what variable must be kept constant in the course of the reactions. Often the formal ionic strength is taken as the variable. Sometimes the total equivalent concentration of all ions is chosen, and sometimes the concentration of "inert" cation or anions. A historical review on the application of ionic media and merits of the use of the high concentration of medium salts have been described by Biedermann and Sillén.[1] The assumption of constant ionic activities in a constant ionic medium, however, has not been rigorously tested. The present study was undertaken to examine this by testing the validity of the ionic medium principle by means of emf measurements of cells containing solutions in which concentrations of perchlorate and hydrogen ions were kept constantant and those of "inert" cations were varied.

Experimental

Reagents. All reagents used were prepared from relevant carbonates or oxides and perchloric acid. They have been used for studies of hydrolytic reactions of metal ions in the Laboratory of Inorganic Chemistry of the Royal Institute of Technology, Stockholm.

Apparatus. *Glass electrodes*: Beckman glass electrodes (No. 40498) were used.

Hydrogen electrodes were prepared by the method described by Bates.[2] Emf values obtained were corrected to those at one atmospheric pressure.[3]

Silver chloride electrodes were prepared by Brown's method.[4]

The "Wilhelm" type of half-cell described by Forsling, Hietanen, and Sillén[5] was used as the reference half-cell.

A Leeds and Northrup Type K-3 Universal Potentiometer for measurements with hydrogen electrodes and *a Radiometer PHM 4 pH Meter* with glass electrodes were used. Emf's were read to 0.01 mV with the former and 0.1 mV with the latter.

A Coulometric Analyzer (Leeds and Northrup Co., Philadelphia) was used for coulometric reduction of hydrogen ions.

Hydrogen gas, free from oxygen and carbon dioxide, was preequilibrated with a solution of 3 M perchlorate and was then introduced into a hydrogen electrode. A titration vessel was filled with nitrogen gas, free from carbon dioxide and preequilibrated with a 3 M perchlorate solution, instead of hydrogen gas when we used only glass electrodes for measurements. No essential difference has been found in results obtained with hydrogen and glass electrodes.

Procedure for Potentiometric Measurements. All potentiometric measurements were performed at 25.00±0.01°C in a paraffin oil thermostat which was placed in a room thermostated at 25±2°C. In the course of emf measurements the total concentration of perchlorate ion was kept constant at 3 M. The hydrogen ion concentration was also kept constant at 0.01 M except in the case of $NaClO_4$-$TlClO_4$ solutions in which the total concentration of perchlorate ion was 3 M but the concentrations of hydrogen ion were 0.01 and 0.1 M.

The titration procedure was as follows: Into a solution S_1 titrant S_2 was added. The composition of S_1 was ($3-0.01$)/m M A^{m+}, 0.01 M H^+, 3 M ClO_4^-, and that of S_2 was ($3-0.01$)/n M B^{n+}, 0.01 M H^+, 3 M ClO_4^-. All metal ions used were not hydrolyzed in such acid solutions. Titration was performed up to a point where A^{m+} ions of more than half of the total equivalent were replaced with B^{n+} ions, and then the reverse titration, *i.e.*, titration of the S_2 solution with the S_1 solution was carried out with the same set of electrodes. Data obtained with these two titrations were combined by the use of data in the overlapped region.

Emf's of cells

$$\text{Ref}\,|\,\text{Solution}\,|\,\text{GE} \qquad (A)$$

and

$$\text{Ref}\,|\,\text{Solution, H}_2\,|\,\text{Pt} \qquad (B)$$

were determined, where the solution has the general com-

1) G. Biedermann and L. G. Sillén, *Arkiv Kem.*, **5**, 425 (1953).

2) R. G. Bates, "Electrometric pH Determinations," J. Wiley and Sons, New York (1954).

3) W. R. Hainsworth, H. J. Rowley, and D. A. MacInnes, *J. Amer. Chem., Soc.*, **46**, 1437 (1924).

4) A. S. Brown, *ibid.*, **56**, 646 (1934).

5) W. Forsling, S. Hietanen, and L. G. Sillén, *Acta Chem. Scand.*, **6**, 901 (1952).

position

$$|x\text{M } A^{m+},\ y\text{M } B^{n+},\ 0.01000\text{ M } H^+,\ 3.000\text{ M } ClO_4^-|$$
$$(mx + ny + 0.01 = 3) \qquad (C)$$

and Ref denotes the reference half-cell

$$\text{Ag-AgCl}|(3-0.01)/m\text{ M } A(ClO_4)_m,$$
$$0.01\text{ M } AgClO_4|3/m\text{ M } A(ClO_4)_m| \qquad (D)$$

The value of the emf measured, E, may be given by the following equation at 25°C;

$$E = E^\circ + \frac{RT}{F}\ln a_H + E_j$$
$$= E^\circ + 59.15\log[H^+] + 59.15\log f_H + E_j(H, A, B) \qquad (1)$$

where E° is a constant and a_H and f_H denote the activity and the activity coefficient of hydrogen ion, respectively. E_j represents the liquid junction potential at the junction

$$3/m\text{ M } A(ClO_4)_m|\text{Solution} \qquad (E)$$

which is a function of concentrations of H^+, A^{m+}, and B^{n+} at the 3 M perchlorate ions, the junction potential at the junction, $(3-0.01)/m$ M $A(ClO_4)_m$, 0.01 M $AgClO_4/3/m$ M $A(ClO_4)_m$, in the salt bridge in the reference half-cell being assumed constant during the emf measurements.

Equation (1) can be rewritten as

$$E - 59.15\log[H^+] = E^\circ + 59.15\log f_H + E_j(H, A, B) \qquad (2)$$

Since E° is a constant ΔE, the difference of $E-59.15\log[H^+]$ values in a solution, $(3-0.01)/m$ M A^{m+}, 0.01 M H^+, 3 M ClO_4^-, and in a solution, xM A^{m+}, yM B^{n+}, 0.01 M H^+, $(mx+ny+0.01=3)$, depends on the variation of f_H and E_j with the composition of cations in a solution at the constnat perchlorate and hydrogen ion concentrations.

Results and Discussion

Variation of potentials with compositions of electrolytes in a solution can be given by

$$\Delta E = \frac{RT}{F}\Delta\ln f_H + \Delta E_j$$
$$= 59.15\Delta\log f_H + \Delta E_j(H, A, B) \qquad (3)$$

where $\Delta\log f_H$ and ΔE_j represent differences of $\log f_H$ and E_j, respectively, in solutions, $(3-0.01)/m$ M A^{m+}, 0.01 M H^+, 3 M ClO_4^- and xM A^{m+}, yM B^{n+}, 0.01 M H^+, 3 M ClO_4^- $(mx+ny+0.01=3)$. Values of ΔE were determined in nine sets of various combinations of $A(ClO_4)_m$ and $B(ClO_4)_n$. Results are graphically shown in Figs. 1 and 2.

Each ΔE could be expressed by an approximate linear function of $[B^{n+}]$, but in some cases in which ΔE varies markedly, it could be better described with a quadratic function of $[B^{n+}]$ than a linear function. Equations for variations of ΔE as a function of $[B^{n+}]$ in various systems of $A(ClO_4)_m$-$B(ClO_4)_n$ are summarized in Table 1. Solid lines in Figs. 1 and 2 show curves drawn on the basis of equations for ΔE in Table 1.

Liquid junction potentials have been determined in some solutions containing 3 M perchlorate as ionic media. In 3 M $LiClO_4$ solution, E_j has been evaluated as $-16[H^+]$ mV/M[6] and in 3 M $NaClO_4$, $E_j = -16[H^+]$ mV/M[1] or $-17[H^+]$ mV/M.[7] When the concentration of hydrogen ion increases, a quadratic function with respect to the hydrogen ion concentration may be more adequate to describe the variation of

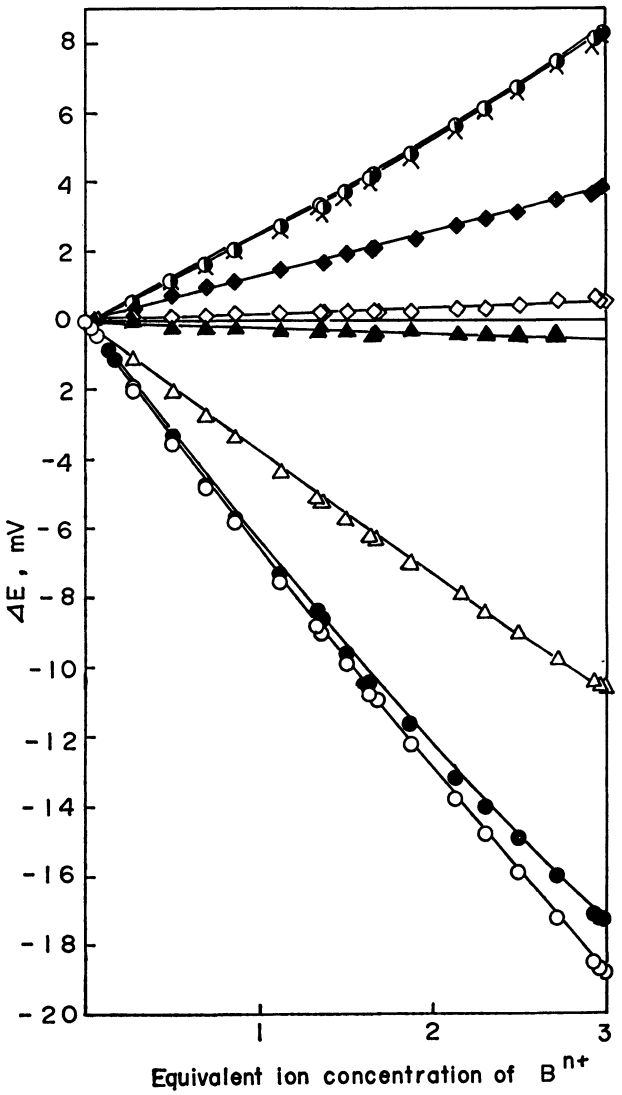

Fig. 1. ΔE in various sets of metal perchlorate media at $[H^+]=0.010$ M. ◑, $NaClO_4$-$Ba(ClO_4)_2$; ×, $AgClO_4$-$Ba(ClO_4)_2$; ◆, $LiClO_4$-$Mg(ClO_4)_2$; ◇, $LiClO_4$-$La(ClO_4)_3$; ▲, $NaClO_4$-$AgClO_4$; △ $LiClO_4$-$Ba(ClO_4)_2$; ●, $LiClO_4$-$AgClO_4$; ○, $LiClO_4$-$NaClO_4$

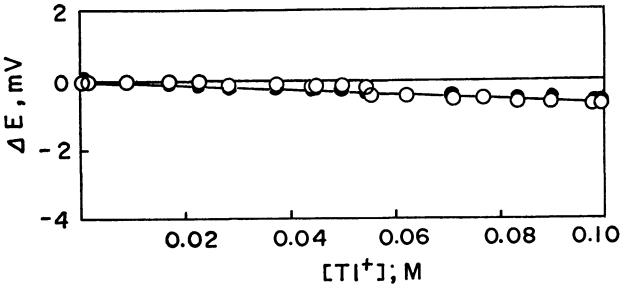

Fig. 2. ΔE in $NaClO_4$-$TlClO_4$ solutions: ○, $[H^+]=0.010$ M; ●, $[H^+]=0.100$ M.

6) H. Ohtaki and H. Kato, *Inorg. Chem.*, **6**, 1935 (1967).
7) N. Ingli, G. Lagerström, M. Frydman, and L. G. Sillén, *Acta Chem. Scand.*, **11**, 1034 (1957).

Table 1. Variation of ΔE as a function of the composition of electrolytes in the solution

$A(ClO_4)_m$-$B(ClO_4)_n$	$\Delta E=\alpha[B^{n+}]+\beta[B^{n+}]^2$, mV	ΔE at 1 equiv. $[B^{n+}]$, mV
$NaClO_4$-$Ba(ClO_4)_2$	$\Delta E=4.6[Ba^{2+}]+0.6[Ba^{2+}]^2$	2.6
$AgClO_4$-$Ba(ClO_4)_2$	$\Delta E=4.5[Ba^{2+}]+0.6[Ba^{2+}]^2$	2.5
$LiClO_4$-$Mg(ClO_4)_2$	$\Delta E=2.5[Mg^{2+}]$	1.3
$LiClO_4$-$La(ClO_4)_3$	$\Delta E=0.6[La^{3+}]$	0.2
$NaClO_4$-$AgClO_4$	$\Delta E=-0.2[Ag^+]$	−0.2
$LiClO_4$-$Ba(ClO_4)_2$	$\Delta E=-7.6[Ba^{2+}]+0.3[Ba^{2+}]^2$	−3.7
$LiClO_4$-$AgClO_4$	$\Delta E=-6.7[Ag^+]+0.3[Ag^+]^2$	−6.4
$LiClO_4$-$NaClO_4$	$\Delta E=-6.8[Na^+]+0.2[Na^+]^2$	−6.6
$NaClO_4$-$TlClO_4$	$\Delta E=-7[Tl^+]$ $([Tl^+]\leq 0.1M]$	−7

E_j.[1] About −0.2 mV may be estimated for the liquid junction potential caused by the diffusion of hydrogen ions at the junction (E), which is in the same order of magnitude with the experimental uncertainty of a measurement with a pH meter.

Correction of the junction potential caused by migration of hydrogen ions in solutions were examined in the following way. From a solution containing 3 M $LiClO_4$ and a trace amount of hydrogen ions, the hydrogen ions were removed coulometrically and values of $E-59.15\log[H^+]$ were extrapolated to $[H^+]=0$.[8] The value obtained by extrapolation is denoted as E', which may be given by

$$E' = E^\circ + 59.15\log f_H + E_j(\mathrm{Li}, 0) \quad (4)$$

Since E' was determined in a solution in which concentrations of hydrogen and sodium ions ($Na^+=B^{n+}$ in this case) were zero, E_j is denoted as $E_j(0, \mathrm{Li}, 0)$ or simply $E_j(\mathrm{Li}, 0)$ as in Eq. (4). The composition of electrolytes in the solution was then changed by the addition of the solution S_2 (only a trace amount of hydrogen ions was contained without removing electrodes from the solution, and the value of E'

$$E' = E^\circ + 59.15\log f_H + E_j(\mathrm{Li}, \mathrm{Na}) \quad (5)$$

was determined with the same procedure as before. The current passed in the course of coulometric titrations was so small that variation of composition of the solution by electrolysis was negligible, $\Delta E'$, the difference of E' values in 3 M $LiClO_4$ and in 3 M $(Li^+, Na^+)ClO_4^-$ solutions, differed from ΔE by only negligible amounts in the whole range of compositions of solutions, as seen in Fig. 3.

Different mobilities of lithium and sodium ions give rise to a liquid junction potential, $E_j(\mathrm{Li}, \mathrm{Na})$ at the junction (E). The liquid junction potential may be estimated by Henderson's equation,[9] which can be simplified as[1]

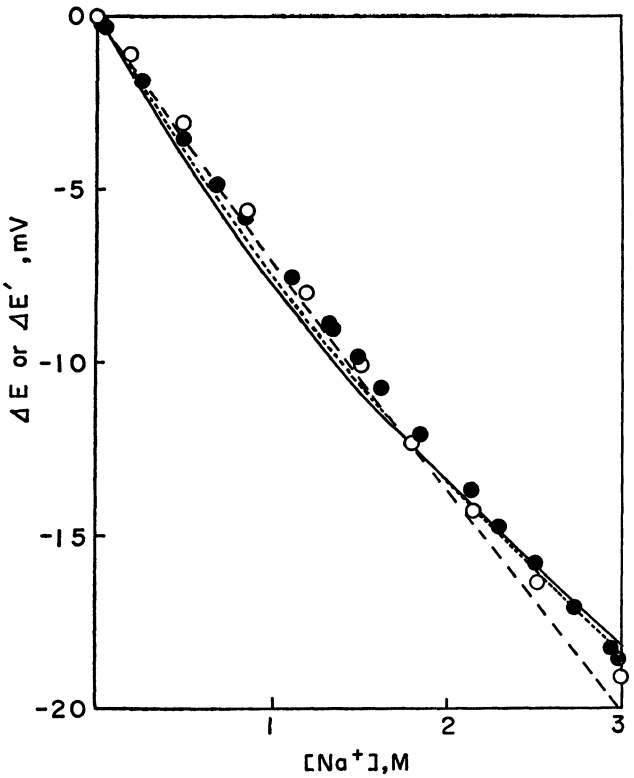

Fig. 3. Relationship between ΔE (●) or $\Delta E'$ (○) and $[Na^+]$. ----, calculated ΔE values by the use of Eq. (13); —— calculated ΔE values by the use of Eq. (13); calculated ΔE_{corr} values by the use of (16) with $r_H=7.0$Å and $\delta_{ClO_4}=-9.0$; ···, calculated ΔE_{corr} by Eq. (16) with $r_H=4.0$Å and $\delta_{ClO_4}=-6.7$.

$$E_j(\mathrm{A}, \mathrm{B}) = -59.15\log\left(1 + \frac{n d_{B(A)}[B^{n+}]}{3}\right) \quad (6)$$

in 3 equiv./l perchlorate solutions, where $d_{B(A)}$ denotes

$$d_{B(A)} = \frac{\Lambda_{B(ClO_4)_n} - \Lambda_{A(ClO_4)_m}}{\Lambda_{A(ClO_4)_m}} \quad (7)$$

and Λ represents the equivalent conductivity of the relevant electrolyte.

Equation (6) may be approximated as

$$E_i(\mathrm{A}, \mathrm{B}) \simeq -19.72 n d_{B(A)}[B^{n+}] \quad (8)$$

The value of $d_{B(A)}$ in a 3 M $(Li^+, Na^+)ClO_4^-$ solution may be evaluated from data of Λ in 3 M $LiClO_4$ and in 3 M $NaClO_4$. It can be estimated from data

$$-19.72 d_{H(Li)} \simeq -16^{6)} \text{ or } d_{H(Li)} = 0.81 \quad (9)$$

and

$$-19.72 d_{H(Na)} \simeq -17^{7)} \text{ or } d_{H(Na)} = 0.86 \quad (10)$$

Since $d_{Na(Li)}$ is derived from Eqs. (9) and (10) as

$$d_{Na(Li)} = \frac{\Lambda_{NaClO_4} - \Lambda_{LiClO_4}}{\Lambda_{LiClO_4}} = \frac{d_{H(Li)}+1}{d_{H(Na)}+1} - 1 = -0.027 \quad (11)$$

provided that Λ_{HClO_4} remains unchanged in 3 M $LiClO_4$ and 3 M $NaClO_4$ solutions, the liquid junction potential, $E_j(\mathrm{Li}, \mathrm{Na})$ is obtained as

$$E_j(\mathrm{Li}, \mathrm{Na}) = -19.72 d_{Na(Li)}[Na^+] = 0.53[Na^+] \quad (12)$$

Thus, ΔE values obtained experimentally may be corrected by the liquid junction potential $E_j(\mathrm{Li}, \mathrm{Na})$:

8) G. Gran, *Analyst*, **77**, 661 (1952).
9) P. Henderson, *Z. phys. Chem.* (Leipzig), **59**, 118 (1907); *ibid.*, **63**, 325 (1908).

$$\Delta E_{corr} = 59.15\Delta \log f_H = \Delta E - E_j(\mathrm{Li, Na})$$
$$\simeq -7.3[\mathrm{Na^+}] \quad (13)$$

Calculation of Eq. (8) may be oversimplified with neglection of higher terms of $[B^{n+}]$ and, therefore, the term with $[Na^+]^2$ is dropped in Eq. (13). The value -17 in Eq. (10) for E_j(H, Na) may be the upper limit of the $-19.72d_{H(Na)}$ value, so that ΔE_{corr} estimated by Eq. (13) may give the lower limit of ΔE_{corr}. Since no essential difference has been observed in the measurements with hydrogen and glass electrodes, the sodium effect on glass electrodes is negligible. In Fig. 3 values of ΔE_{corr} calculated by Eq. (13) are plotted by a broken line.

Liquid junction potentials have not been determined in other solutions but it can be expected that the liquid junction potentials may not be so large that the contribution of the variation of the potentials to ΔE values becomes significant, because most ions have similar equivalent conductivities in aqueous solutions except for hydrogen and hydroxyl ions. Thus, it is concluded that the change of the activity coefficient of hydrogen ion is attributed to ΔE with varying compositions of electrolytes in solutions.

Reactions of hydrogen ions with metal ions and perchlorate ions are denied from the fact that no association and hydrolytic reactions have been observed in these solutions. Association of lithium or sodium ions with perchlorate ions has not been detected in 3 M solutions. If no association reaction occurs in lithium perchlorate-sodium perchlorate solutions, variation of the activity coefficient of hydrogen ions may be caused by the free energy change of transfer of hydrogen ions from a 3 M $LiClO_4$ solution to a $LiClO_4$-$NaClO_4$ mixture.

According to Hasted, Ritson, and Collie,[10] the dielectric constant of a solution decreases with increasing concentration of an electrolyte. The variation of the dielectric constant is proportional to the concentration of an electrolyte and the contributions of a cation and an anion, δ, to the variation are additive.

$$\varepsilon = \varepsilon_0 + (\delta_c + \delta_a)C \quad (14)$$

where ε and ε_0 represent dielectric constants of a solution and the pure solvent, respectively, and C the molar concentration of an electrolyte, and values of δ are evaluated to be -11 ± 1 for Li^+ and -8 ± 1 for Na^+. However, no value has been given for δ_{ClO_4}. Equation (14) holds for solutions containing about 2—2.5 equiv./l cations and anions, and its application to 3 M solutions should not give rise to serious error making the following discussion worthless. Free energy changes of transfer of ions from one solution to another may be calculated by the simple Born's equation or, more adequately, by other equations with more realistic models of hydrated ions.[11,12] Stokes[11] has calculated hydration energies of various ions with models of hydrated ions taking into consideration the dielectric saturation effect of water in hydration shells. Ohtaki[13] has modified Stokes' model and applied it to hydrated hydronium ion in order to interprete variation of dissociation constants of acids in mixed solvents. Ohtaki assumed a "naked" hydronium ion having an ionic radius of 1.4 Å, the ion being surrounded by the first and the second hydration shells each with thickness of 2.8 Å. In the following considerations, a simple approximation is applicable where the dielectric constants in the first and second hydration shells of a hydronium ion in 3 M $LiClO_4$ solution are the same as those in 3 M $NaClO_4$ and 3 M (Li^+, Na^+)-ClO_4^- mixtures, and dielectric constants of bulk solutions are given by Eq. (14). With these approximations the electrostatic free energy changes of transfer of 1 mol of hydronium ion from 3 M $LiClO_4$ to a 3 M (Li^+, Na^+)ClO_4^- mixture can be given by

$$\mu_H^\circ(m) - \mu_H^\circ(s) = \boldsymbol{R}T\{\ln f_H(m) - \ln f_H(s)\} = \boldsymbol{R}T\Delta \ln f_H$$
$$= \frac{Ne^2}{2r_H}\left(\frac{1}{\varepsilon(m)} - \frac{1}{\varepsilon(s)}\right) \quad (15)$$

where μ_H^0 denotes the standard chemical potential of the hydronium ion and m and s in parentheses represent quantities in a 3 M (Li^+, Na^+) ClO_4^- mixture and 3 M $LiClO_4$, respectively as follows. Since ΔE_{corr} is given by $\boldsymbol{R}T\boldsymbol{F}^{-1}\Delta \ln f_H$, ΔE_{corr} can be represented

$$\Delta E_{corr} = \frac{Ne^2}{2\boldsymbol{F}r_H}\left(\frac{1}{\varepsilon(m)} - \frac{1}{\varepsilon(s)}\right) \quad (16)$$

$$\left.\begin{aligned} &\text{and} \quad \varepsilon(s) = \varepsilon_0 + 3(\delta_{Li} + \delta_{ClO_4}) \\ &\varepsilon(m) = \varepsilon_0 + x\delta_{Li} + y\delta_{Na} + 3\delta_{ClO_4} \quad (x+y=3) \end{aligned}\right\} \quad (17)$$

If we assume that the radius of the hydrated hydronium ion is 7.0 Å (1.4 Å for the naked hydronium ion and 2.8 Å for each hydration shell), satisfactory agreements were found between ΔE_{corr} (or even ΔE) values observed and calculated using Eq. (16) when we choose $\delta_{ClO_4} = -9$. Values of ΔE_{corr} in mV unit thus calculated were plotted by a solid line in Fig. 3. Application of the Hepler's model[12] gave similar results (shown by a dotted line in Fig. 3) with $r_H = 4$ Å and $\delta_{ClO_4} = -6.7$. $r_H = 7$ Å may be a better assumption than $r = 4$ Å in these calculations because Hasted *et al.*[10] estimated the minimum hydration number of 10 for a proton in their treatment and these hydrated water molecules may possibly be included in the first and second hydration shells.[14] The value $\delta_{ClO_4} = -9$ assumed in calculations with Stokes' model seems to be reasonable in comparison with values of $\delta_{Cl} = -3$, $\delta_I = -7$ and $\delta_{OH} = -13$, and the results show that electrostatic free energy changes caused by the variation of bulk dielectric constants of solutions may play the most important role in variation of the activity coefficient of hydrogen ions.

For magnesium, barium, and lanthanum ions, values of δ have been found to be -24, -22, and -35, respectively.[10] Application of the above arguments to (A^+, B^{n+})ClO_4^- solutions leads to the following conclusions. Replacement of lithium ions with corresponding equivalent quantities of these ions contributes to variation of dielectric constants of solu-

10) J. B. Hasted, D. M. Ritson, and C. H. Collie, *J. Chem. Phys.*, **16**, 1 (1948).
11) R. H. Stokes, *J. Amer. Chem. Soc.*, **86**, 979 (1964).
12) L. G. Hepler, *Austr. J. Chem.*, **17**, 587 (1964).
13) H. Ohtaki, This Bulletin, **42**, 1573 (1969).
14) R. Grahn, *Arkiv Kem.*, **21**, 13 (1962).

tions to a less extent than that with sodium ions. In Li^+–La^{3+} mixtures, the potential variation may be fairly small and in Na^+–Ba^{2+} solutions ΔE varies in the opposite direction with that found in Li^+–Na^+ solutions. Variation of ΔE in Li^+–Ba^{2+} and Li^+–Mg^{2+} solutions may be smaller than that in Li^+–Na^+ solutions.

Experimental results support these considerations. Thus, it can be said that the main part of the variation of potentials measured in this study is interpreted in terms of electrostatic free energy changes of transfer of hydrogen ions from one salt medium to another, the main factor of the variation being caused by the change of the bulk dielectric constant of solutions with varying compositions of medium salts.

This conclusion is supported by the fact that the variation of potential is additive. Potential variations occurring at 1 equivalent-ion replacement of a cation are shown in the last column of Table 1. The equivalent replacement of a highly hydrated cation, such as lithium ion, with strongly hydrated bi- or tervalent cations might be expected to introduce only a small violation of the ionic medium principle of the solution. Replacement of strongly hydrated cations with less hydrated cations, on the other hand, results in a larger variation of activity coefficients of reacting species in the medium. From the viewpoint of δ values, activity coefficients of reacting species may vary to a much larger extent when an anion such as ClO_4^- of a medium salt is replaced by another kind of anion, *e.g.*, Cl^- ion.

BULLETIN OF THE CHEMICAL SOCIETY OF JAPAN, VOL. 44, 1519—1522 (1971)

The Water Structure Model of Narten *et al.* and the Pressure Effect on Sound Absorption in Water

Otohiko NOMOTO*,** and Harumi ENDO*

**Department of Applied Physics, Defence Academy, Yokosuka*

***Kobayashi Institute of Physical Research, Kokubunji, Tokyo*

(Received December 18, 1970)

The mechanism of the temperature dependence of ultrasonic absorption in water under atmospheric pressure has hitherto been studied by means of the two-state-model theory of water. For an explanation of the pressure dependence of ultrasonic absorption by the two-state model, however, we are obliged to adopt the contradictory assumption that the open-packed structure of water has a higher energy than the more close-packed one. In order to avoid this contradictory assumption inherent in the two state-model theory, we have here employed the water model recently proposed by Narten *et al.* on the basis of X-ray scattering analysis. Although the calculation based on the Narten-model succeeds in explaining the pressure dependence of the ultrasonic absorption without the above-mentioned contradictory assumption, the structual compressibility (β_{st}) thus obtained is about two times larger than the most reasonable value. The origin of this discrepancy seems to be that the Narten model of water considers the framework of the ice-1 lattice to be of infinite extent, without any boundary. By assuming the cluster-structure to be of a finite size, we can reduce β_{st} to a reasonable value in agreement with the experimental results. The water cluster is found to be about eight molecules in diameter at 4°C.

The ultrasonic absorption (α) in water is known to be higher than the classical value (α_{cl}) due to the shear viscosity (η) and the heat conductivity (k). As α_{cl} is proportional to the square of frequency (f), it is usual to write:

$$\frac{\alpha_{cl}}{f^2} = \frac{(2\pi)^2}{\rho V^3}\left(\frac{2}{3}\eta + \frac{1}{2}\frac{\gamma-1}{\gamma}\frac{k}{C_v}\right) \tag{1}$$

Here, ρ is the density; V, the sound velocity; C_v, the specific heat at a constant volume, and $\gamma(=C_p/C_v)$, the ratio of the specific heats. As $\gamma \cong 1$ in water, the term due to heat conduction can be omitted in this case. The difference being ascribed to the bulk viscosity (κ), the total absorption (α/f^2) becomes:

$$\frac{\alpha}{f^2} = \frac{(2\pi)^2}{\rho V^3}\left(\frac{2}{3}\eta + \frac{1}{2}\kappa\right) \tag{2}$$

It is known, from hypersonic measurements, that (α/f^2) in water is independent of the frequency up to the GHz ($=10^9$ Hz) range. This means that, in the general formula of relaxational viscosity absorption:

$$\alpha = \frac{2}{3}\frac{\eta}{\rho V^3}\frac{\omega^2}{1+\omega^2\tau_1^2} + \frac{1}{2}\frac{\kappa}{\rho V^3}\frac{\omega^2}{1+\omega^2\tau_2^2} \tag{3}$$

and dispersion:

$$V^2 = V_0^2 + \frac{4}{3}\frac{G}{\rho}\frac{\omega^2\tau_1^2}{1+\omega^2\tau_1^2} + \frac{K'}{\rho}\frac{\omega^2\tau_2^2}{1+\omega^2\tau_2^2} \tag{4}$$

the relaxation time for the shear viscisity (τ_1) and that for the bulk viscosity (τ_2) are sufficiently small ($\omega\tau_1 \ll 1$, $\omega\tau_2 \ll 1$ where $\omega = 2\pi f$), even in the GHz range. Here, G is the shear modulus, and K', the relaxational part of the bulk modulus related to η and κ by Maxwell's relations:

$$\eta = G\tau_1 \text{ and } \kappa = K'\tau_2 \tag{5}$$

There being relations

$$\frac{1}{\beta_0} = K_0, \quad \frac{1}{\beta_\infty} = K_\infty \tag{6}$$

between the static and instantaneous compressibilities (β_0 and β_∞), and the corresponding bulk modulus (K_0 and K_∞), we obtain as the relaxational modulus, K',

and the structual (or relaxational) compressibility, β_{st}:

$$K = K_0 + K' \text{ and } \beta_0 = \beta_\infty + \beta_{st} \quad (7)$$

The mechanism of ultrasonic absorption in water has been studied by Hall,[1] by Smith and Lawson,[2] and by Davis and Litovitz.[3] They applied the two-state-model theory of water to explain the bulk viscosity and relaxational compressibility. Hall's theory, based on the monomer-dimer model, explained the temperature dependence of sound absorption using suitably adjusted parameters to fit the experimental results (*cf.* also Davis and Litovitz[3]). In Hall's paper, it is assumed that the open-packing state of water is the lower energy state. For the explanation of the pressure dependence of the ultrasonic absorption, however, Litovitz and Carnevale,[4] calculating by means of a modification of Hall's two-state-model theory, were obliged to adopt the assumption that the open-packing structure of water has a higher free energy than the close-packing state, in contradiction to the usual physico-chemical concepts as to the structure of liquid water (*cf.* also Herzfeld and Litovitz[5]). To interpret the pressure dependence of ultrasonic absorption in water without introducing these contradictory assumptions in the two-state-model theory, we employed the water model recently proposed by Narten *et al.*[6] on the basis of their X-ray scattering analysis.

Water Structure Model Proposed by Narten *et al.* (Interstitial Model)

Samoilov[7] has proposed an interstitial model of the liquid water structure so as to explain the radial distribution function obtained from the X-ray data. Narten *et al.*, building on Samoilov's idea, formulated a model, consisting of a framework of the extended ice-1 structure, with some non-hydrogen-bonded water molecules filling some of the cavities of the network. This framework structure is very open, with ample spaces or cavities to accommodate non-hydrogen-bonded water molecules. The positions to accommodate the water molecules in the interstices are on the triad axis. The accommodated water molecules in the cavity interact with the framework molecules with less specific, although by no means negligible, force. In this model, the ice-1 framework is anisotropically extended, and both vacant lattice sites and the occupancy of the interstices by water molecules are permitted, although the vacant lattice site of the framework is practically absent up to 100°C. Accordingly, liquid water can be said to consist of two species forming both the framework and the interstitial molecules. This model, however, considers the lattice of the extended ice-1 framework to be infinite, without boundary, no cluster-structure being taken into account. Narten *et al.* found that the calculated radial distribution functions agree with the experimental results up to very high temperatures (*ca.* 200°C).

Theoretical

Acoustic pressure in an associated liquid accompanies two sorts of compression: *a*) the compression of the intermolecular distance, and *b*) the breakdown of intermolecular bonds accompanying the destruction of the open structure. The former is represented by the instantaneous compressibility, β_∞, while the latter is the origin of the structual compressibility, β_{st}. In this calculation, we assume the volume of the liquid water to be proportional to the number of framework lattice sites. This means that the dimensions of the framework remain the same, independent of whether the cavity sites are vacant or not. On this assumption, the molar volume (v) can be given by the following relations:

$$v = \frac{W}{f_1} v_{fr} \quad (8)$$

$$W = \frac{f_1 + z f_2}{f_1} \quad (9)$$

where

v_{fr}: the volume per mole of H_2O of framework
W: the fraction of water molecules in the framework positions
f_1: the occupancy of the framework sites (f_1 is 100% up to 100°C; *cf.* Narten *et al.*[6])
f_2: the occupancy of the interstitial sites
z: the number of interstitial sites per framework site

In this calculation, we will limit the temperature range at up to 100°C. Then, we obtain $f_1=1$ in Eqs. (8) and (9) from the experimental results of Narten *et al.*[6]

By substituting Eq. (8) into

$$\beta_{st} = -\frac{1}{v}\left(\frac{\partial v}{\partial p}\right)_T \quad (10)$$

we obtain:

$$\beta_{st} = W z \left(\frac{\partial f_2}{\partial p}\right)_T \quad (11)$$

where z is kept constant.

On the other hand, Narten *et al.* found both the entropy of mixing and the molar Gibbs free energy of the model from their statical thermodynamic consideration of the interstitial water model. Further, they obtained, as the free-energy change associated with the transformation of the interstitial molecule into the framework:

$$\Delta G_I^0 = RT\left[\ln \frac{f_2}{1-f_2} - z \ln (1-f_2)\right] \quad (12)$$

We obtain from Eq. (11):

$$\left(\frac{\partial f_2}{\partial p}\right)_T = W f_2 (1-f_2) \Delta v_I^0 / RT \quad (13)$$

1) L. Hall, *Phys. Rev.*, **73**, 775 (1948).
2) A. Smith and A. Lawson, *J. Chem. Phys.*, **22**, 351 (1954).
3) C. Davis and T. Litovitz, *ibid.*, **42**, 2563 (1965).
4) T. Litovitz and E. Carnevale, *J. Appl. Phys.*, **26**, 816 (1955).
5) K. Herzfeld and T. Litovitz, "Absorption and Dispersion of Ultrasonic Waves," Academic Press, New York and London, (1959) p. 438.
6) H. Narten, M. Danford, and H. Levy, *Discuss. Faraday Soc.*, **43**, 97 (1967).
7) O. Samoilov, "Ion no Suiwa" (Translation from Russian by W. Uehira), Chijin Shokan, Tokyo (1967).

Then, the structural compressibility is given by

$$\beta_{st} = zW^2 f_2(1-f_2)\Delta v_I^0/RT \quad (14)$$

Here $\Delta v_I^0=(\partial G_I^0/\partial p)_T$ becomes v_{fr}, because we assume that the interstitial water molecule has no effective volume. Therefore, by substituting Eq. (10), we obtain the relation:

$$\beta_{st} = \frac{zv_{fr}}{RT}\frac{f_2(1-f_2)}{(1+zf_2)^2} \quad (15)$$

It is easy to show that Eq. (15) is equivalent to the result obtained by Frank and Quist[8] on Pauling's water model:[9]

$$\beta_{st} = \frac{v_{fr}}{RT}(1-W)[W-v(1-W)] \quad (16)$$

where $v=1/z$.

We can find the temperature (t) dependence of the parameters (f_2 and W) from the data of Narten *et al.*, represented as graphs in their paper:

$$W = -4.59\times10^{-4}\ (t-4) + 0.82$$

In their paper, however, f_2 is so random that we can not find any definite relation with the temperature. We calculated f_2 from Eq. (9), by assuming z (=1/2) to be independent of the temperature.

Results of Calculations

Figure 1 shows the temperature dependence of β_{st} as obtained from Eq. (15). The results of other authors[1-4] are also shown for the sake of comparison. As may be seen, the present result gives nearly the same slope of the $\beta_{st}(t)$-curve as in previous investigations, but the value of β_{st} is about two times any previous finding (such as that of Hall *et al.*).

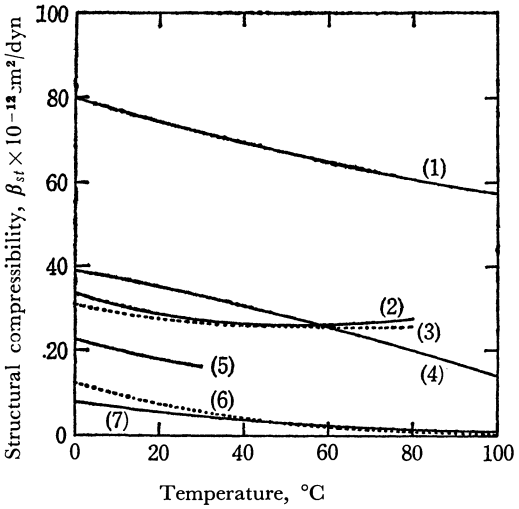

Fig. 1. Structual compressibility as function of temperature.

(1) Present study
(2) Hall
(3) Davis and Litovitz
(4) Smith and Lawson
(5) Frank and Quist
(6) Eucken[10]
(7) Némethy and Scheraga[11]

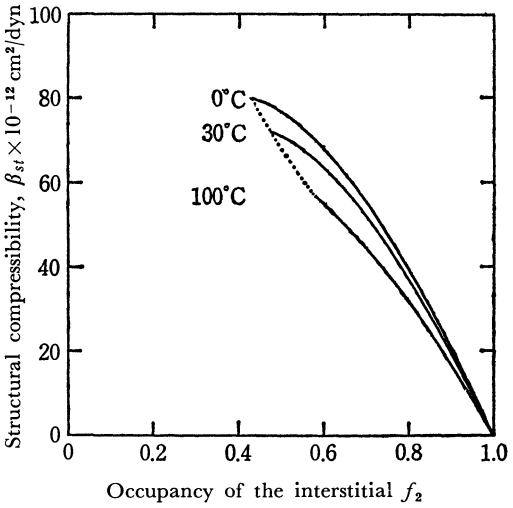

Fig. 2. β_{st} dependence of f_2 at various temperature.
---- Temperature dependence of f_2 under the atmospheric pressure.

Figure 2 shows the f_2 dependence of β_{st} at 0, 30, and 100°C. As the framework-structure part of water is destroyed with an increase in the pressure, we have to expect a monotonous increase in the occupancy of the cavity (f_2) with an increase in the pressure. On the other hand, the dotted line shows the temperature dependence of f_2 under atmospheric pressure.

Considerations and Discussion

Our results at 4°C are shown in Table 1, together with the previous ones. An obvious difference is that our value of $\beta_{st}=78.9\times10^{-12}$ cm²/dyne is much larger than that, $\beta_0(=\beta_\infty+\beta_{st})=50.2\times10^{-12}$ cm²/dyne, in water. It is necessary to remove this contradiction. If we assume a reasonable value (*cf.* Hall[1]) to be $\beta_{st}=32.2\times10^{-12}$ cm²/dyne at 4°C, which is in accordance with ultrasonic absorption measurements, we find from Eq. (16) that the apparent value, z', is 0.284 on the condition that $w=0.820$ remains the same (here we assume Eq. (17)). Then, we obtain from Eq. (9) $f_2=0.773$.

Table 1

Temp. 4°C	Present results: Narten model	Present results: Cluster model	Frank-Quist (Pauling model)	Two state model
V_{fr}	22.0	22.0	22.0	
W	0.820	0.820	0.818	
z	0.500	0.284	0.261	
f_2	0.439	0.773	(0.858)	
$\beta_{st}\times10^{-12}$	78.9	32.2	21.0	32.2[1]
				30.0[3]

The radial distribution function determined by Narten *et al.* from the X-ray scattering data is based on the lattice model up to a distance of about 10 Å,

8) H. Frank and A. Quist, *J. Chem. Phys.*, **34**, 604 (1961).
9) L. Pauling, "The Nature of the Chemical Bond," Cornell University Press, Ithaca, New York, (1960) 3er. Ed.. p. 472.
10) A. Eucken, Nachr. Akad. Wiss. Göttingen, Math-Physik. Kl. p. 38 (1946); *Z. Electrochem.* **52**, 255 (1948); **53**, 102 (1949) (*cf.* Refs. 3 and 5).
11) G. Némethy and H. Scheraga, *J. Chem. Phys.*, **36**, 3382 (1962).

further distances being averaged out. It is probable that water consists of clusters of finite sizes larger than 10 Å in radius.

Here we assume that the water structure consists of clusters containing n^3 water molecules, the structure inside the cluster being the same as the Narten model. As the number of interstitices are reduced to $[(n-1)/n]^3$ times, we find that z apparently becomes $[(n-1)/n]^3$ times as large as the infinite model. Further, we assume in this cluster model that the average intermolecular distance between clusters is not affected, so the density in this model does not change. The space between the clusters is assumed not to accommodate the non-hydrogen-bonded molecules. Considering the above conditions, we obtain the following relation:

$$\left(\frac{n-1}{n}\right)^3 z = z' \tag{18}$$

where z $(=1/2)$ is the number of interstitial sites per framework site, corresponding to the Narten model without considering the cluster. If we choose $z'=0.284$, so as to bring the calculated β_{st} value in Table 1 (column (2)) into agreement with the observed value, we obtain $n=5.81$ from Eq. (18). Assuming the cluster to be spherical, the diameter of the cluster becomes about eight molecules at 4°C. In performing the above calculations at various temperatures, we find the radius (n_r) of the spherical cluster (expressed in the number of water molecules) to be dependent on the temperature as is plotted in Fig. 3. As may be seen, n_r increases with an increase in the temperature. Although this is rather unexpected, we cannot place too much weight on it, considering the very approximate nature of our hypothesis.

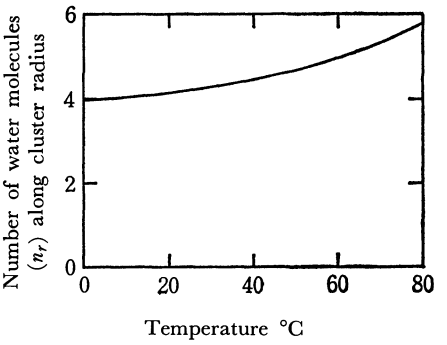

Fig. 3. n_r in dependence on temperature.

BULLETIN OF THE CHEMICAL SOCIETY OF JAPAN, VOL. 44, 1522—1526 (1971)

ESR Measurement and Irradiation at Variable Temperatures below 77°K

Machio IWASAKI, Keichi NUNOME, Takahisa ICHIKAWA,* and Kazumi TORIYAMA

Government Industrial Research Institute, Nagoya, Hirate-machi, Kita-ku, Nagoya

(Received December 26, 1970)

An apparatus for irradiation and subsequent ESR measurements at variable temperatures below 77°K was constracted by combining an ESR spectrometer, and an X-ray irradiator, and a laboratory scale low temperature refrigerator operating at the temperature region between 77 and 4.2°K. A device for rotating the single crystal specimen was made to measure the angular dependence of the ESR spectra. The lowest specimen temperature achieved was estimated to be 6°K and the precision of the temperature control was less than ±0.5°K for a period of several hours. The apparatus makes it possible to irradiate samples and to measure ESR spectra at any temperature in the range between 77 and 6°K. Some applications for irradiation and ESR measurements at low temperatures are also described. An unstable radical which disappears at about 60°K was found in an irradiated single crystal of L-cystine dihydrochloride. Experimental evidence for the quantum tunnelling of the methyl group in polymethylmethacrylate radical was also found by the temperature dependence of the spectra observed at temperatures lower than 77°K.

ESR measurements at a temperature region lower than 77°K are usually carried out at 4.2°K by using liquid helium. In some cases, even lower temperatures can be achieved by rapid pumping of liquid helium. It is not easy, however, to maintain intermediate temperatures between 4.2 and 77°K (liquid nitrogen temperature), especially for a fairly long period. For example, in the measurements of the orientation dependence of the ESR spectra of single crystals, a constant temperature with a fairly high precision has to be maintained for at least several hours. In addition, for the study of the primary process of radiation-induced reactions, the irradiation is to be made at temperatures lower than 77°K, because of instability of the produced radicals. This kind of experiment can not be easily carried out by using liquid helium. Besides, liquid helium is not always available and is not easy to handle. If low temperatures could be obtained without the use of liquid helium, a number of laborious processes required for experiments at a temperature region lower than 77°K might be considerably reduced.

Recently a laboratory scale refrigerator which can be operated by using a compressed helium gas from commercial cylinders has been developed and it provides a fairly simple way to obtain any intermediate temperatures between 77 and 4.2°K. We have applied

* Present address: Department of Applied Chemistry, Faculty of Engineering, University of Hiroshima, Senda-cho, Hiroshima.

this sort of equipment for irradiation and subsequent ESR measurements at low temperature and obtained fairly successful results. This paper describes our apparatus built mainly for the measurements of the angular dependence of the ESR spectra of irradiated single crystals.

In this method the crystals are cooled by thermal conduction through the contact with a cryogenic tip of the refrigerator so that a number of checks have to be made to ascertain the real temperature of the specimens. Performance of our equipment will be described together with some results obtained for the NO radical in a single crystal of hydroxylamine hydrochloride, irradiated single crystals of *N*-acetylalanine and L-cystine dihydrochloride, and irradiated polymethylmethacrylate films.

Apparatus

The refrigerator is a Cryo-Tip system AC-3L-110 supplied by Air Products and Chemicals Inc. The alignment of an ESR spectrometer, X-ray irradiator, and the refrigerator is shown in Fig. 1. The movable mount of the refrigerator was designed and built to make it possible to shift the refrigerator horizontally from the X-ray irradiator to the sample cavity for prompt ESR measurements after irradiation. Besides this horizontal movement, the mount performs vertical movement for inserting the specimen holder into the X-ray irradiator or the sample cavity, and the rotational movement for changing the crystal orientations to the magnetic field. The mount has also a cross leader for the fine adjustment of the sample position in the cavity. A device for adjusting the vertical axis of the refrigerator is also added to make sure that the rotational axis of the crystal is perpendicular to the magnetic field. A sketch of the refrigeraaor mount is shown in Fig. 2.

Hydrogen and helium gases from cylinders are led to the liquid nitrogen dewar where the gases are precooled down to 77°K. Hydrogen and helium gases are then expanded successively and liquefied at the tip

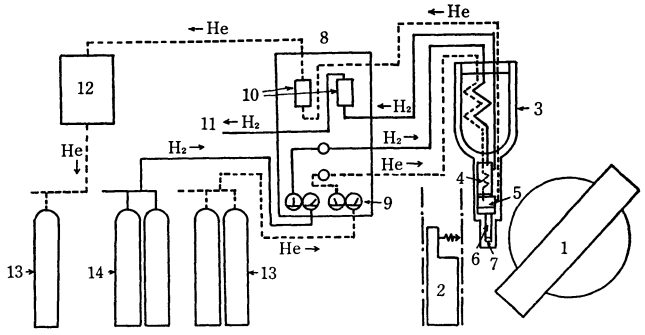

Fig. 1. Block diagram of the apparatus for irradiation and subsequent ESR measurements at variable temperatures lower than 77°K: 1. ESR magnet; 2. X-ray tube; 3. liquid nitrogen Dewar; 4. hydrogen liquefying chamber; 5. helium liquefying chamber; 6. specimen holder; 7. specimen; 8. control panel; 9. pressure regulator; 10. flow meter; 11. vent for hydrogen gas; 12. apparatus for restoring helium gas; 13. helium cylinder; 14. hydrogen cylinder.

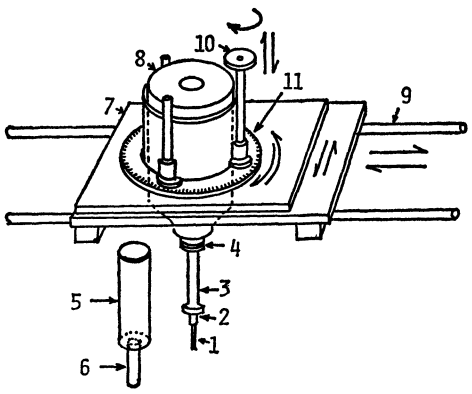

Fig. 2. Sketch of the refrigerator and its movable mount: 1. specimen holder; 2. heat exchanger; 3. radiation shield; 4. O-ring for vacuum shroud; 5. vacuum shroud; 6. spectrosil tube; 7. refrigerator holder; 8. Dewar vessel of liquid nitrogen; 9. guide rail for horizontal shift; 10. handle for vertical shift; 11. indicator for rotational angle. Although the mechanisms are not shown in the figure, the positions in the horizontal plane are adjustable to two perpendicular directions by fine adjustment knobs. The vertical axis for rotation is also adjustable.

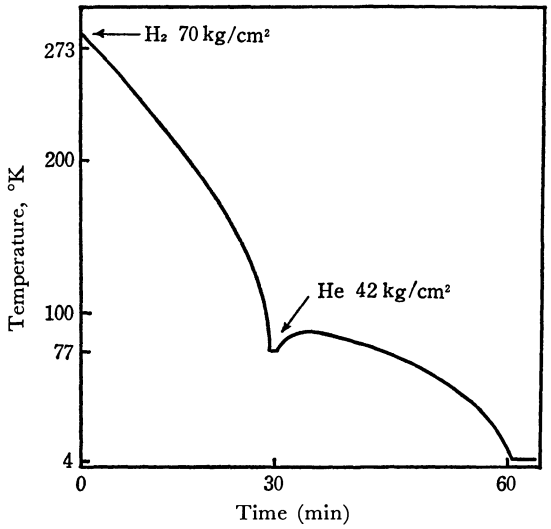

Fig. 3. Cooling curve for normal operation of the refrigerator.

of the refigerator. Figure 3 shows a cooling curve measured with a chromel-constantan thermocouple attached to the tip of the refrigerator. After the low pressure purge at 7—14 kg/cm² for 20 min, the hydrogen pressure was raised to 70 kg/cm². This is taken as an origin of the time scale in the abscissa of Fig. 3. After 30 min needed for liquefying hydrogen gases, the hedlium pressure was increased to 42 kg/cm² and another 30 min were required to liquefy helium gases. The tip temperature is easily controlled in the range from 77° to 4.2°K by adjusting the flow rate of the gases. It is easy to maintain any intermediate temperature, say 40°K, for several hours with an accuracy of less than ±0.5°K.

A vent pipe of the used hydrogen gas is led to the roof, while the helium gas is restored to the cylinders by a compressor through a liquid nitrogen trap with

active charcoal.

Specimens for ESR measurements are attached to the sample holder of a sapphire or a copper rod (3 mmϕ × 80mm) connected to the tip of the refrigerator surrounded by an aluminum vacuum shroud (Fig. 2). The length of the specimen holder depends on the dimension of the ESR cavity into which part of the specimen holder is inserted. The part of the specimen holder is surrounded by a Spectrosil tube of 10 mmϕ, the inside of which is evacuated through the vacuum shroud for maintaining thermal insulation. The ESR measurements are easily carried out by inserting the Spectrosil tube into a cavity with a TE_{011} mode. Adjustment of the orientation of the specimen to the magnetic field can be achieved by simply rotating the refrigerator mount around the vertical axis. This method is entirely free from the bubble noise inherent to the method using liquid coolants. Since the surface of the Spectrosil tube is maintained at room temperature, there is no variation of the Q-value of the sample cavity even though the temperature of specimen changes.

Irradiation of the specimen at low temperatures is also easily carried out by inserting the Spectrosil tube into the irradiation chamber in which an X-ray tube is installed The X-ray irradiator is placed in front of an ESR magnet at a distance of about 1 m to make it easier to transfer the refrigerator promptly to the ESR cavity right after irradiation. The ESR signal due to color centers produced at room temperature in the Spectrosil tube by X-irradiation is a sharp singlet having the g-factor close to the free spin value and its intensity is not so strong that the central part of the signal of the specimen is masked.

Temperature Measurements

Although the temperature of the tip of the refrigerator is maintained at 4.2°K when helium gas is liquefied, there should be thermal gradient along the rod of the specimen holder in such a way that the specimen is cooled by the thermal conduction through a long rod. The temperature difference between the tips of the refrigerator and the sapphire or copper rods measured by an Au doped Co–Pt thermocouple was about 6 and 4°K, respectively, when the Cryo-Tip system was operated with full power. The temperature rise through the rod is reduced to 2—1°K when the temperature of the tip of the refrigerator is raised to 70°K. Figure 4 shows the correction curve for the temperature rise at the sample position of the rod. The ordinate represents the temperature rise through the rod and the abscissa the temperature at the tip of the refrigerator.

The main cause of the temperature rise through the rod seems to be the radiation from the Spectrosil tube which is kept at room temperature. The vacuum in the Spectrosil tube is extremely high because the residual air is completely trapped on the surface of the heat exchanger, the temperature of which is very much lower than the freezing points of oxygen and nitrogen. Therefore, the conduction through the residual gases from the Spectrosil tube may be negligible. It is not possible, however, to use a radiation shield of silver mirror inside the Spectrosil tube as in the Dewar vessel because it lowers the Q-value of the sample cavity. When the Spectrosil tube was dipped into a liquid nitrogen dewar, the temperature rise became negligibly small and the liquid helium temperature was attained. Therefore, the cold nitrogen gas from the Dewar vessel of liquid nitrogen was introduced into the sample cavity to lower the temperature of the surface of the Spectrosil tube. By this device the temperature rise through the rod is reduced to about 2°K when the copper rod is used at the full operation of the refrigerator. The lowest possible specimen temperature obtained by our apparatus is about 6°K.

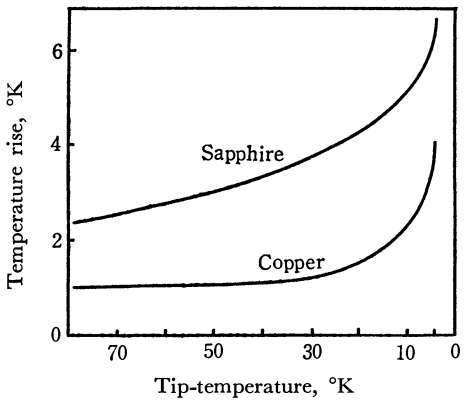

Fig. 4. Correction curve for the temperature rise along the sample rod *vs.* temperature of the cryogenic tip of the refrigerator.

The temperature rise during X-irradiation was found to be 2—3°K under operating conditions of 30 mA and 40 kV. The distance from the X-ray target to the specimen holder is about 30 mm.

The temperature of the sample itself attached to the rod is very difficult to measure, because of the small size of the crystal or film. In order to avoid the thermal gradient inside the specimen, it is necessary to use a very thin, say 0.1—0.2 mm, crystal or film. In this case, the temperature of the sample was confirmed by the ESR measurements.

ESR Measurements

According to Gamble and Miyagawa, the ESR spectrum of the radical CH_3–$\dot{C}R_1R_2$ formed in an irradiated single crystal of *N*-acetylalanine shows a remarkable temperature dependence in the region between 4—20°K due to the quantum mechanical effect on the hindered oscillation of methyl group.[1] Temperature changes of the spectral features they observed at 4.2, 12.5, and 17.5°K are so sensitive to the observed temperature that it may provide a good test sample for checking the real temperature of the specimen. We have also measured the temperature dependence of the same sample by using our apparatus with a copper rod as a sample holder. The spectra obtained at 12.5 and 17.5°K, which were estimated from the correction curve in Fig. 4, are in very good

1) W. L. Gamble and I. Miyagawa, *Phys. Rev. Lett.* **20**, 415 (1968).

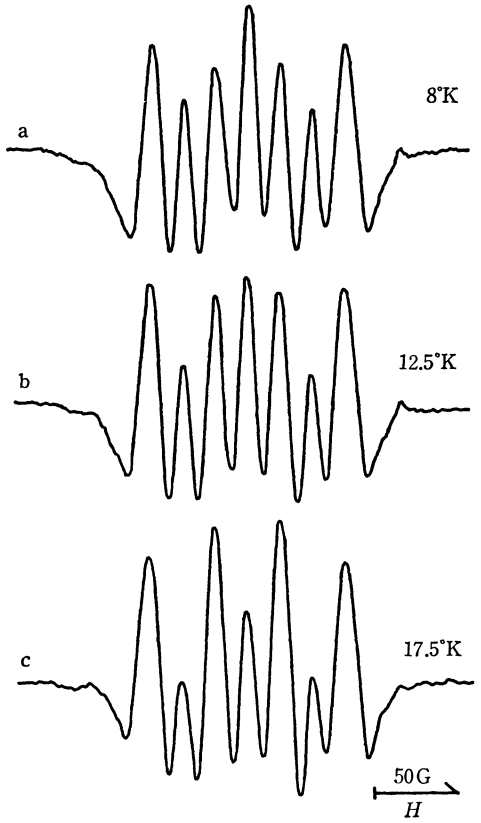

Fig. 5. ESR spectra of an irradiated single crystal of *N*-acetylalanine measured at (a) 8°K, (b) 12.5°K, and (c) 17.5°K. The magnetic field is applied along the *c*-axis.

agreement with their spectra as shown in Figs. 5(b) and (c). This means that the specimen temperature is practically the same as that of the copper rod. Figure 5(a) gives a spectrum observed at 8°K which is the lowest temperature obtained by our apparatus without aid of cold nitrogen gas flow into the sample cavity. The spectral feature of Fig. 5(a) is in between their spectra observed at 4.2 and 12.5°K. The splendid agreement between the two independent measurements may ensure the estimates of the specimen temperature in both the experiments.

In the temperature region higher than 20°K, the spectral change of this radical is so gradual that it is of no use to check the specimen temperature. Therefore another check was made by using the Curie law, *viz.*, the linear relation of the ESR intensity to reciprocal temperature. For this purpose one has to use the sample, the signal of which is hard to saturate at the low temperature region. The NO radical found by Ohigashi and Kurita[2] in an irradiated single crystal of hydroxylamine hydrochloride has extremely short T_1 and it may be expected that the signal is not saturated in a fairly wide range of low temperature. Figure 6 shows the relative intensity of the ESR spectra of the NO radical plotted against the reciprocal temperature estimated from the correction curve in Fig. 4. In this experiment, the sapphire rod was used for the specimen holder. As is seen in Fig. 6, a good linear relation was obtained in the temperature range between 25 and 60°K.

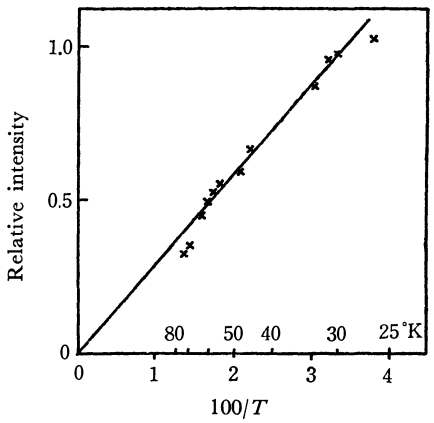

Fig. 6. Plots of the ESR intensities *vs.* reciprocal temperatures for the NO radical trapped single crystal of hydroxylamine hydrochloride.

It is concluded that the specimen temperature is practically the same as that of the sample rod in the wide range of low temperature achieved by our apparatus.

Applications

Irradiation at low Temperature. In some cases irradiation has to be made at temperature lower than 77°K, since the primary species produced by irradiation are sometimes unstable at 77°K. For example, the cation radical formed in an irradiated single crystal of L-cystine dihydrochloride[3] is known to be unstable at 77°K.[4] Irradiation at temperatures lower than

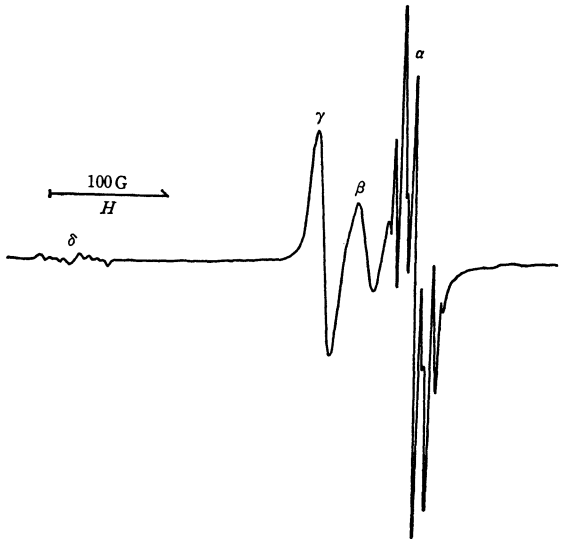

Fig. 7. ESR spectra of a single crystal of L-cystine dihydrochloride irradiated and measured with our system. The magnetic field is applied along the *c'*-axis.

2) H. Ohigashi and Y. Kurita, *J. Phys. Soc. Jap.* **24,** 654 (1968).

3) H. C. Box, H. G. Freund, K. T. Lilga, and E. E. Budzinski, *J. Phys. Chem.*, **74,** 40 (1970).

4) According to the recent study of Akasaka *et al.* (13th Symposium on Radiation Chemistry, Tokyo, Oct. 9, 1970), the spectrum of the cation is observable even at 77°K if the observation is made in the dark.

77°K is desirable for studying the primary process of radiation-induced reactions.

Our system was applied in the irradiation of a single crystal of L-cystine dihydrochloride. A typical spectrum measured right after irradiation is shown in Fig. 7. Both the cation (α in Fig. 7) and the anion (β in Fig. 7) are stably trapped. In addition, a new signal δ with an extremely large g-anisotropy and a small hyperfine structure was found at lower magnetic field side of the spectra due to the cation and anion. The signal disappeared irreversibly when the temperature was elevated to about 60°K. Figure 8 shows an angular dependence of this signal measured in the ac′ plane. The variation of the g-value in this plane is from 2.26 to the free spin value. Although the magnetically non-equivalent site of this signal is one in the ac' plane, there are two sites in both the ab and bc' planes. This means that the radical responsible to this signal does not possess symmetry of the mother molecule. From this together with the large positive g-shift the signal may be assigned to a sort of sulfur radical produced by the scission of the S–S bond.

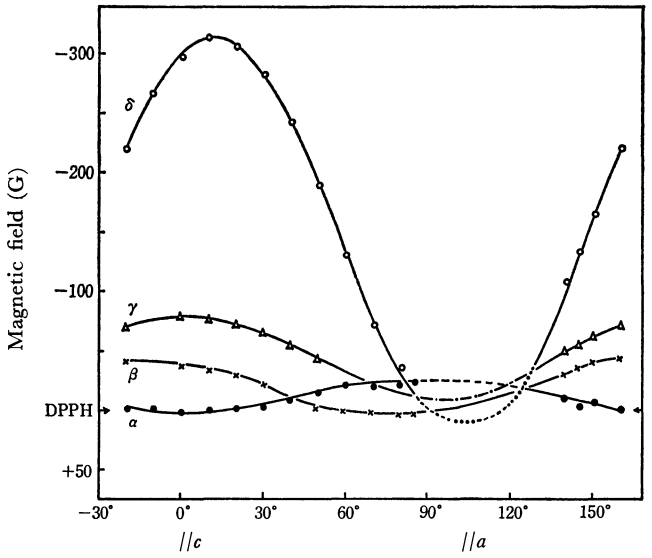

Fig. 8. Angular dependence of the ESR spectra of a single crystal of L-cystine dihydrocholide irradiated and measured with our system. The magnetic field is applied in the ac′ plane.

This experiment shows that our system is applicable to the irradiation at temperatures lower than 77°K and the subsequent ESR measurements.

Measurements of ESR Temperature Dependence. In some cases, the temperature dependence of the ESR spectra in a temperature region lower than 77°K is required to be measured. As an example, it is reported that the ESR spectrum of polymethylmethacrylate radical, RCH_2–$\dot{C}(CH_3)COOMe$ measured at 4.2°K exhibits a remarkable difference from that at 77°K.[5] Interpretation of this difference is not possible because of the lack of information on the spectral change at intermediate temperatures. By means of our system the temperature dependence of the spectra was successfully measured in the range between 77 and 6°K. The results are shown in Fig. 9. As described in our paper,[6] the spectrum observed at 77°K is interpreted on the assumptions of the freely rotating methyl group and the distribution of the conformational angle of the two C–H_β bonds to the half filled $2p$ orbital. The spectral change observed at temperatures lower than 77°K can be interpreted by the quantum mechanical effect on the hindered oscillation of the methyl group as is the case of the radical, CH_3–$\dot{C}R_1R_2$, in irradiated *N*-acetylalanine.[1] The spectra observed at 6°K is well reproduced by the seven-line spectrum due to the quantum tunnelling of the methyl group[7] and further splittings due to the two β-proton couplings. The temperature dependence observed by our system gave the experimental evidence for the quantum tunnelling of the methyl group in the polymethylmethacrylate radical. Details will be given elsewhere.

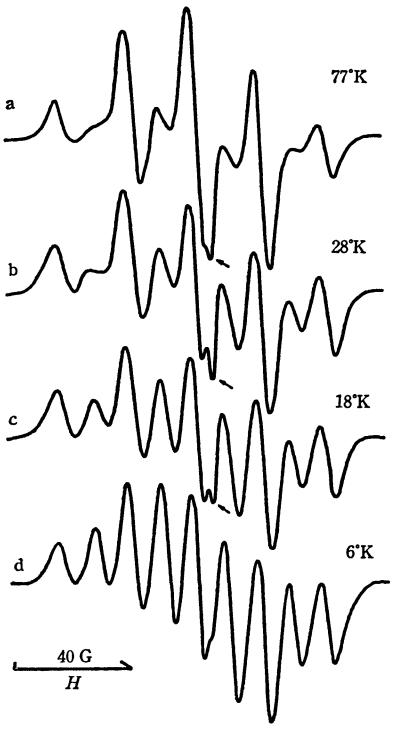

Fig. 9. Temperature dependence of the ESR spectra of polymethylmethacrylate radical measured at (a) 77°K, (b) 28°K, (c) 18°K, and (d) 6°K. The arrows indicate the signal due to the color center of the Spectrosil tube.

The authors wish to thank Drs. Y. Kurita and H. Ohigashi of Basic Research Laboratory, Toray Industries, Inc. for their helpful cooperation in measuring the ESR signal of the NO radical trapped in an irradiated single crystal of hydroxylamine hydrochloride.

5) D. W. Ovenall, *Nature*, **184**, 181 (1959).

6) M. Iwasaki and Y. Sakai, *J. Polymer Sci.*, *A*-1, **7**, 1537 (1969).

7) J. H. Freed, *J. Chem. Phys.*, **43**, 1710 (1965).

Studies on Triplet Energy Transfer by Means of an Emission-Absorption Flash Technique. II. Mixed Triplet-Triplet Annihilation in Ethanol

Koichi KIKUCHI, Hiroshi KOKUBUN, and Masao KOIZUMI

Department of Chemistry, Faculty of Science, Tohoku University, Katahira, Sendai

(Received December 28, 1970)

The mixed delayed fluorescence due to the processes, $A^T+B^T \xrightarrow{p_M{}^A k_{MTT}} A^*+B$ in the following systems in ethanol solutions have been quantitatively investigated. a) 1) 9-methylanthracene-anthracene, 2) 9-phenylanthracene-anthracene, 3) 9-methylanthracene-9-phenylanthracene, 4) anthracene-acridine, 5) 9-methylanthracene-acridine, 6) 9-phenylanthracene-acridine. b) 7) eosin-anthracene, 8) proflavine-anthracene, 9) eosin-acridine. It has been found that for class a) in which the separations of singlet excited levels of A and B are less than a few times of kT, the delayed fluorescence of both components occur and the value of $(p_M{}^A+p_M{}^B)$ is close to that of the efficiency of a simple p-type delayed fluorescence, p^A or p^B. The delayed mixed excimer fluorescence also occurs in most cases. For class b) in which the level differences largely exceed kT, only the delayed fluorescence of the lower level component occurs. It has also been established that the delayed excimer fluorescence in a single component system increases in intensity from anthracene through 9-methyl- to 9-phenylanthracene. The $p_M{}^A/p_M{}^B$ values are discussed for systems (1), (2), and (3).

Delayed fluorescence due to T–T annihilation has been studied extensively by Parker[1] and Birks[2] since its discovery by Parker and Hatchard.[3] It seems that the recent work of Birks *et al.*[4] has terminated the debates upon its mechanism. Their conclusion is that T–T annihilation occurs according to the dual paths

(I) $A^T+A^T \rightarrow A_2{}^{**} \rightarrow A_2{}^* \rightarrow 2A + h\nu$ (excimer fluorescence)
$\qquad\qquad\qquad\quad \rightarrow A^* + A \rightarrow 2A + h\nu'$ (monomer fluorescence)

(II) $A^T + A^T \rightarrow A^* + A$

in which process (I) goes through encounter whereas (II) proceeds by a long range interaction. This scheme is essentially the same as the one proposed earlier by Parker.[5] Birks *et al.* and Parker also agree on the point that process (I) is temperature dependent while (II) is not, the former predominating at room temperature.

One purpose of the present work is to compare the efficiency of *mixed T–T annihilation* with that of simple type T–T annihilation at room temperature assuming that process (I) is predominant. Since the discovery of mixed T–T annihilation by Parker,[6] no quantitative investigation seems to have been made. Although there is no doubt that in the anthracene (donor)-naphthacene (acceptor) system,[7] the delayed fluorescence of the latter is brought about by $D^T+A^T \rightarrow D+A^*$, there is some ambiguity as to the mechanism of the enhanced delayed fluorescence in the eosin-anthracene system.[8] Parker's observation gave no quantitative information as to what extent the enhanced delayed fluorescence of both eosin (D) and anthracene (A) occurs *via*

(III) $D^T + A^T \rightarrow D^* + A$ (M-type 1)
$\qquad\qquad\qquad\quad \rightarrow D + A^*$ (M-type 2)

or

$D^T + D^T \rightarrow D^* + D$
$A^T + A^T \rightarrow A^* + A$ (P-type)

We developed a method of separating M-type from P-type using the flash technique involving absorption and emission measurements.[9] By means of this method, we established that (M-1) occurs very efficiently and that (M-2) does not occur at all in the alcoholic solution of eosin and anthracene. In the present work, the proflavine-anthracene and eosin-acridine systems have been studied. They are similar with respect to the singlet energy separation between donor and acceptor. Further, systems consisting of donor and acceptor with almost the same singlet excited levels have been studied. As such compounds, we have chosen anthracene and its substituted compounds which are well known to give only very weak excimer fluorescence. It is expected that the dependence of the relative fluorescence yield of donor and acceptor (processes (M-1) and (M-2)) on the singlet energy levels of the two components can be studied more easily with such compounds. In connection with the mixed T–T annihilation, quantitative investigations on the simple type T–T annihilation of the component compounds and on the delayed excimer fluorescence have been performed. The intensities of the mixed delayed excimer fluorescence (MDE-Fl) have been compared with those of

1) C. A. Parker, "Photoluminescence of Solutions," Elsevier, Amsterdam (1968), Chap. 2. D.

2) J. B. Birks, "Photophysics of Aromatic Molecules," Wiley-Interscience, New York (1969), Chap. 8.

3) C. A. Parker and C. G. Hatchard, *Proc. Chem. Soc.*, **1962**, 147.

4) J. B. Birks, B. N. Srinivasan, and S. P. McGlynn, *J. Mol. Spectrosc.*, **27**, 266 (1968). G. F. Moore and I. H. Munro, *Spectrochim. Acta*, **23A**, 1291 (1967). J. B. Birks, *Chem. Phys. Letters*, **2**, 417 (1968).

5) C. A. Parker, *Nature*, **200**, 331 (1963).

6) C. A. Parker and C. G. Hatchard, *Proc. Chem. Soc.*, **1963**, 62.

7) C. A. Parker, *Proc. Roy. Soc.* (London), **A276**, 125 (1963).

8) C. A. Parker, C. G. Hatchard, and T. A. Joyce, *Nature*, **205**, 1282 (1965).

9) K. Kikuchi, H. Kokubun, and M. Koizumi, *Z. Physik. Chem. N. F.*, **62**, 79 (1968).

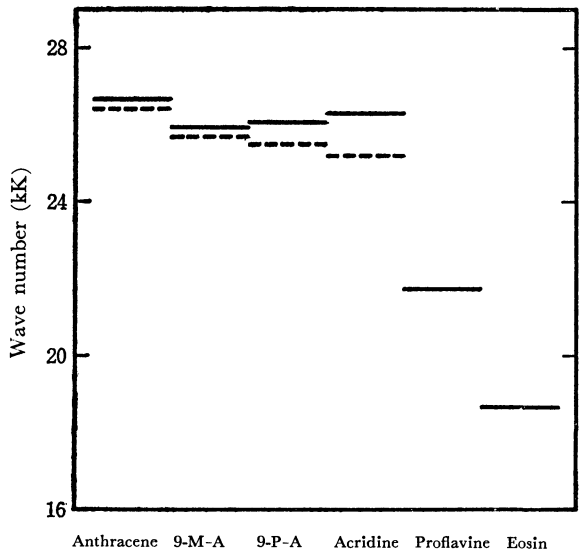

Fig. 1. 0-0 bands of absorption (solid line) and fluorescence (broken line).

the delayed excimer fluorescence (DE–Fl) of the components.

Figure 1 gives the energy levels of the lowest singlet excited states for the compounds studied, as evaluated from the 0–0 band of absorption and emission in ethanol.

Method of Analysis

Our method consists of the measurements of the time dependence of both T–T absorption and D–Fl under the same conditions by means of a flash apparatus.[10] For a solution containing a single component A or B which exhibits P-type D–Fl, the following relations

$$^3A + {}^3A \xrightarrow{p_A k_{TT}^A} {}^1A^* + A \quad \text{(i)}$$
$$\searrow^{q_A k_{TT}^A} (AA)^* \quad \text{(v)}$$
$$^3B + {}^3B \xrightarrow{p_B k_{TT}^B} {}^1B^* + B \quad \text{(ii)}$$
$$\searrow^{q_B k_{TT}^B} (BB)^* \quad \text{(vi)}$$

hold exactly between the measured D–Fl intensity I_{DF} and the measured optical density of the T–T absorption D_T.

$$I_{DF}^A(P, \lambda_1) = \alpha^A(\lambda_1)\phi_F^A(p^A k_{TT}^A[^3A]^2) = \alpha^A(\lambda_1)\phi_F^A p^A k_{TT}^A\left(\frac{D_T^A(\lambda_1')}{\varepsilon_T^A(\lambda_1')d}\right)^2 \quad (1)$$

$$I_{DF}^B(P, \lambda_2) = \alpha^B(\lambda_2)\phi_F^B(p^B k_{TT}^B[^3B]^2) = \alpha^B(\lambda_2)\phi_F^B p k_{TT}^B\left(\frac{D_T^B(\lambda_2')}{\varepsilon_T^B(\lambda_2')d}\right)^2 \quad (2)$$

where k_{TT} and p are respectively the rate constant for the encounter of two triplet molecules and the efficiency of T–T annihilation, and α is a parameter depending on the spectral distribution of the fluorescence and on the experimental conditions. ϕ_F is a quantum yield of fluorescence and d, the cell length, is 10 cm. The wavelengths λ_1 and λ_2 are chosen in a suitable way as described below in the region where DE–Fl is negligible.

For a solution containing both A and B, the mixed T–T annihilation, should be taken into account. In

$$^3A + {}^3B \xrightarrow{p_M^A k_{MT}} {}^1A^* + B \quad \text{(iii)}$$
$$\xrightarrow{p_M^B k_{MT}} {}^1B^* + A \quad \text{(iv)}$$
$$\xrightarrow{q_M k_{MT}} (AB)^* \quad \text{(vii)}$$

this case D–Fl intensity of A (or B) at given triplet concentrations of A and B, is a sum of P-type D–Fl given by (1) (or (2)) and MD–Fl, (3) (or (4)).

$$I_{DF}^A(M, \lambda_1) = \alpha^A(\lambda_1)\phi_F^A p_M^A k_{MT}[^3A][^3B] = \alpha^A(\lambda_1)\phi_F^A p_M^A k_{MT}\frac{D_T^A(\lambda_1')D_T^B(\lambda_2')}{\varepsilon_T^A(\lambda_1')\varepsilon_T^B(\lambda_2')d^2} \quad (3)$$

$$I_{DF}^B(M, \lambda_2) = \alpha^A(\lambda_2)\phi_F^B p_M^B k_{MT}[^3A][^3B] = \alpha^B(\lambda_2)\phi_F^B p_M^B k_{MT}\frac{D_T^A(\lambda_1')D_T^B(\lambda_2')}{\varepsilon_T^A(\lambda_1')\varepsilon_T^B(\lambda_2')d^2} \quad (4)$$

In most systems, however, both D–Fl and the T–T absorption of the components overlap each other. The measured D–Fl intensity at λ_1, for example, consists of the components due to A and B species. Thus

$$I_{DF}(\lambda_1) = I_{DF}^A(P, \lambda_1) + I_{DF}^A(M, \lambda_1) + I_{DF}^B(P, \lambda_1) + I_{DF}^B(M, \lambda_1) \quad (5)$$

A similar equation holds for $I_{DF}(\lambda_2)$. In an analogous way, the optical density for λ_1' is given by

$$D_T(\lambda_1') = D_T^A(\lambda_1') + D_T^B(\lambda_1') = \varepsilon_T^A(\lambda_1')[^3A]d + \varepsilon_T^B(\lambda_1')[^3B]d \quad (6)$$

Hence we have to divide the measured quantity $I_{DF}(\lambda_1)$ (or $I_{DF}(\lambda_2)$) into the components $I_{DF}^A(\lambda_1)$ and $I_{DF}^B(\lambda_1)$ (or $I_{DF}^A(\lambda_2)$ and $I_{DF}^B(\lambda_2)$) and similarly $D_T(\lambda_1')$ (or $D_T(\lambda_2')$) into $D_T^A(\lambda_1')$ and $D_T^B(\lambda_1')$ (or $D_T^A(\lambda_2')$ and $D_T^B(\lambda_2')$). This is done successfully by means of the following equations, if λ_1, λ_2 and λ_1', λ_2' are chosen properly.

$$D_T^A(\lambda_2') = \{D_T(\lambda_1') - [\varepsilon_T^B(\lambda_1')/\varepsilon_T^B(\lambda_2')] \times D_T(\lambda_2')\}/\{[\varepsilon_T^A(\lambda_1')/\varepsilon_T^A(\lambda_2')] - [\varepsilon_T^B(\lambda_1')/\varepsilon_T^B(\lambda_2')]\} \quad (7)$$

$$D_T^B(\lambda_1') = \{D_T(\lambda_2') - [\varepsilon_T^A(\lambda_2')/\varepsilon_T^B(\lambda_1')] \times D_T(\lambda_1')\}/\{[\varepsilon_T^B(\lambda_2')/\varepsilon_T^B(\lambda_1')] - [\varepsilon_T^A(\lambda_2')/\varepsilon_T^A(\lambda_1')]\} \quad (8)$$

$$I_{DF}^A(\lambda_1) = \{I_{DF}(\lambda_2) - [\alpha^B(\lambda_2)/\alpha^B(\lambda_1)] \times I_{DF}(\lambda_1)\}/\{[\alpha^A(\lambda_2)/\alpha^A(\lambda_1)] - [\alpha^B(\lambda_2)/\alpha^B(\lambda_1)]\} \quad (9)$$

$$I_{DF}^B(\lambda_2) = \{I_{DF}(\lambda_1) - [\alpha^A(\lambda_1)/\alpha^A(\lambda_2)] \times I_{DF}(\lambda_2)\}/\{\alpha^B(\lambda_1)/\alpha^B(\lambda_2) - \alpha^A(\lambda_1)/\alpha^A(\lambda_2)\} \quad (10)$$

In order to carry out the above procedure, it is necessary to measure ε_T at various wavelengths and also to know the shape of the delayed fluorescence.

The above analysis enables us to compare the magnitude of $I_{DF}^A(\lambda_1)$ in the mixed system with that of $I_{DF}^A(\lambda_1)$ in the solution containing only A, both at various $D_T^A(\lambda_2')$ values; then the excess of the former is attributed to the mixed T–T annihilation given by Eqs. (3) and (4). A similar analysis can be applied to MDE–Fl, at least in principle. In this case the wavelengths of emission have to be chosen in the region of excimer fluorescence. In practice, however, the dif-

10) K. Kikuchi, H. Kokubun, and M. Koizumi, This Bulletin, **41**, 1545 (1968).

Table 1. Molar extinction coefficient of T-T absorption in ethanol

Compound	Molar extinction coefficients ($\times 10^4$ M^{-1} cm^{-1})							
	420 nm	421 nm	424 nm	426 nm	428 nm	440 nm	550 nm	580 nm
Anthracene	4.9	5.2	3.6	2.1		0.23		
9-Methylanthracene	2.4		4.3	3.7_4		0.28		
9-Phenylanthracene			1.2_5		1.3_5	0.9_1		
Acridine			0.8_9			1.8_5		
Eosin								0.9_4
Proflavine							1.1	

ficulty in obtaining the exact spectrum of DE–Fl prohibits a complete analysis of the data.

Experimeutal

Details of the apparatus and manipulation have been reported.[10] All the reagents were purified by standard methods. For the studies on the mixed T–T annihilation, β-acetonaphthone was used as a triplet energy sensitizer in order to produce a large quantity of the two species in the triplet state to be investigated. The scattering light longer than 400 nm was removed by means of a Hoya-U2 filter. Ethanol solutions were used. The concentrations of the solutes were usually chosen for a species with a higher T-level as 10^{-5} M and for the other, 10^{-6} M. The concentration of β-acetonaphthone was always 5×10^{-4} M. A set of five deaerated solutions were prepared simultaneously and two of them were used for the measurement of T–T absorption at two wavelengths and the remaining for the measurement of D–Fl at three wavelengths. It was confirmed that the fluctuation in the flash intensity was less than a few percent.

The molar absorption coefficient of T–T absorption at a certain wavelength was determined in the following way. Using eosin or proflavine as a T-energy donor, the optical density of T–T absorption of a given substance (acceptor) directly after flashing (energy donor only, excited) was measured under conditions of a complete energy transfer. The concentration of T-state was evaluated from the decrease of the ground state donor immediately after flashing in the absence of an acceptor, taking into consideration a correction factor determined from the ratio between the fluorescence intensities of a donor in the presence and absence of an acceptor. (In the presence of an acceptor, triplet donor quickly returns to the ground state and causes a corresponding increase in the absorption of light.) It was confirmed that the optical-densities taken at time t on the decay curves measured at various wavelengths remain constant in ratio with each other irrespective of the choice of t. This implies the non-participation of intermediates other than the triplet state. The molar absorption coefficients obtained are in satisfactory agreement with the data in literature. Some necessary data are listed in Table 1.

Results

Studies on the Delayed Fluorescence of a Solution Containing One Species. In order to analyse the data of the two component systems according to the method described above, it is necessary to prepare beforehand some data of the single component systems. Among them the p-values and the intensities of the excimer fluorescence of anthracene derivatives are considered to be of value since they have not yet been reported.

Measurement of D–Fl was made by using β-acetonaphthone as a sensitizer. The spectral shape was determined by plotting the intensities at the same time-points on the decay curves measured at various wave lengths. It was confirmed that the shape remains constant irrespective of the time points on the intensity decay curves. The spectral shapes for anthracene, 9-methylanthracene, 9-phenylanthracene, and acridine are given in Figs. 2, 3, 4, and 5. They were corrected for the instrumental factors. The intensities of D–Fl are weaker than those of normal fluorescence in the 0–0 band region due to the reabsorption but appreciably stronger in the longer wavelength region.

The latter result is attributed to DE–Fl which increases in the order, anthracene<9-methylanthracene<9-phenylanthracene. It is notable that the DE–Fl of acridine is apparent. The plots of $\sqrt{I_{DF}(\lambda)}$

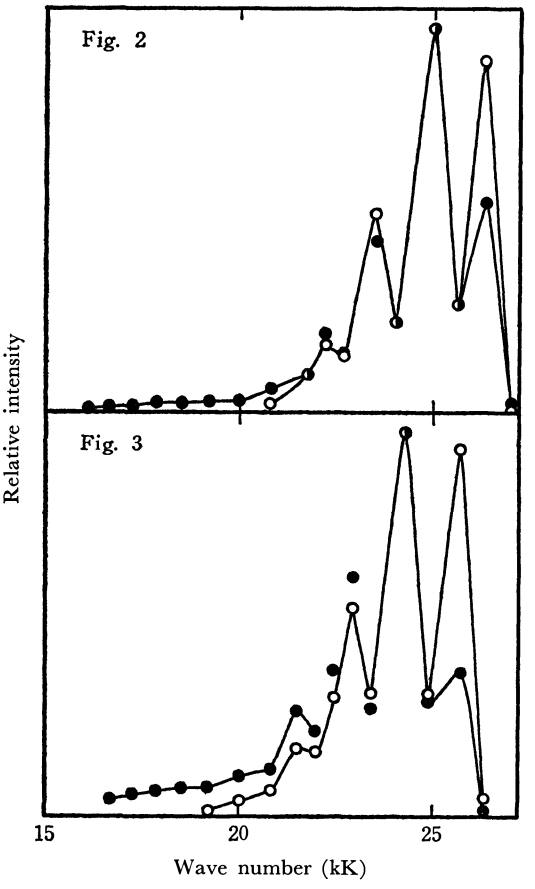

Fig. 2, 3. Normal fluorescence (○) and delayed fluorescence (●) spectra; Fig. 2, anthracene, Fig. 3, 9-methylanthracene.

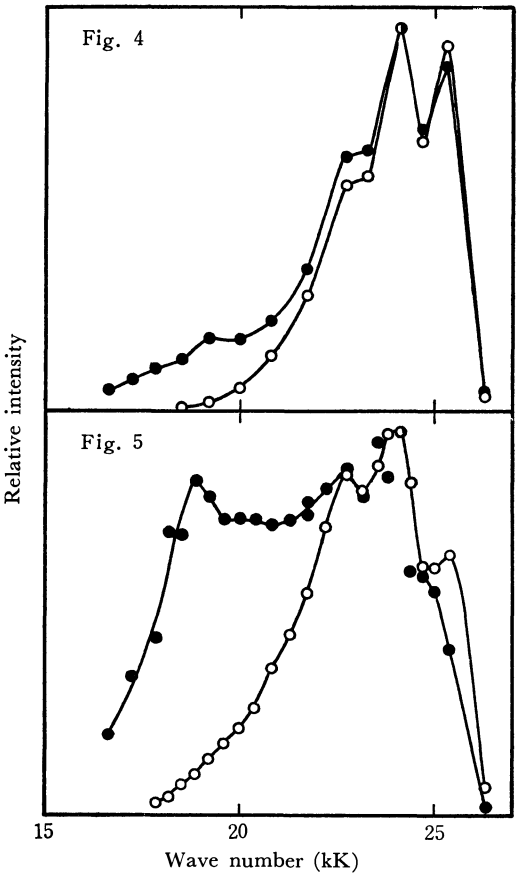

Fig. 4, 5. Normal fluorescence (○) and delayed fluorescence (●) spectra; Fig. 4, 9-Phenylanthracne, Fig. 5, acridine.

against D_T were found to be satisfactorily linear for anthracenes and acridine substantiating the view that the delayed fluorescence of these compounds are of P-type. These are the most important relations for the study of the mixed T–T annihilation. A few example for anthracene are shown in Fig. 6. The D–Fl spectra of eosin and proflavine both of E-type were not measured since the intensities were very weak. Some data necessary for the analysis of the mixed T–T annihilation are listed in Table 2.

From the results listed in Tables 1 and 2, we can evaluate the values of $\alpha(\lambda)\phi_F p k_{TT}$ by means of Eqs. (1) and (2). The values of p have been obtained by the method reported already.[10] k_{TT}-values can be evaluated from the decay curves of T–T absorption and the ε_T-values listed in Table 1. The values of ϕ_{ST}, p, and k_{TT} for anthracene, 9-methyl- and 9-phenyl-

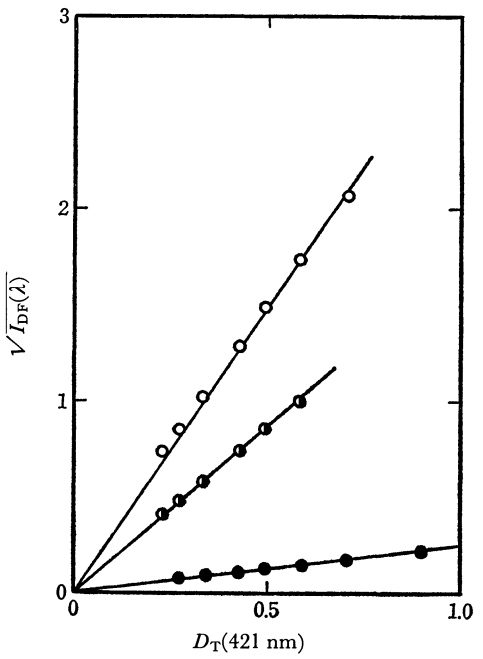

Fig. 6. The plots of $\sqrt{I_{DF}(\lambda)}$ against $D_T(421)$ for anthracene; ○ 400 nm, ◑ 412 nm, ● 540 nm.

anthracene, and acridine are compiled in Table 3.

A similar analysis can be carried out on the DE–Fl to the step of evaluating the $\beta\phi_{EF}qk_{TT}$ values, which are also listed in Table 3.

Studies on a Solution Dissolving Two Aromatic Compounds. In the studies of mixed T–T annihilation, it is most interesting to evaluate the $p_M{}^A$- and $p_M{}^B$-values (see processes (iii) and (iv)). The procedure both experimental and theoretical will be described in some detail for one system, anthracene (B) and 9-methylanthracene (A). For other systems, only significant findings will be described. All the data evaluated are listed in Table 4. A and B denote the species respectively with lower and higher 0–0 emission band. β-acetonaphthone was used as a sensitizer. For 9-methylanthracene(A)-anthracene(B), decays of T–T absorption were measured at 420 and 426 nm from 100 μsec after flashing because the triplet β-acetonaphthone was found to disappear almost completely during this time interval. The decays were analysed according to Eqs. (7) and (8).

Similarly the decays of D–Fl were measured at 400, 412, and 540 nm. The relation between D–Fl and T–T absorption for anthracene and for 9-methylanthracene obtained by the above analysis is shown in

Table 2. Relationship between delayed fluorescence and T-T absorption

Compound	Relation	Wavelength dependence of D-Fl intensity		
		400 nm	412 nm	540 nm
Anthracene	$\sqrt{I_{DF}}(400)=3.0\times D_T(421)$	1.00	0.32	0.0056
9-Methylanthracene	$\sqrt{I_{DF}}(412)=4.6\times D_T(424)$	0.33	1.00	0.018
9-Phenylanthracene	$\sqrt{I_{DF}}(412)=13\times D_T(424)$	0.76	1.00	0.042
Acridine	$\sqrt{I_{DF}}(412)=1.9\times D_T(440)$	0.75	1.00	0.18
Eosin	$I_{DF}(570)=1.1\times D_T(580)$*			
Proflavine	$I_{DF}(500)=2.0\times D_T(550)$*			

Table 3. Values of ϕ_{ST}, p, k_{TT}, and $\beta\phi_{EF}q$

	ϕ_{ST}	p	k_{TT} ($M^{-1}sec^{-1}$)	$\beta\phi_{EF}q$
Anthracene	0.070	0.77	2.9×10^9	2.6
9-Methylanthracene	0.65	0.05_3	2.4×10^9	$11._5$
9-Phenylanthracene	0.50	0.07_4	1.8×10^9	54
Acridine	0.27[a]	0.14	3.3×10^9	5.4

a) *cf.* This Bulletin, **43**, 3435 (1970).

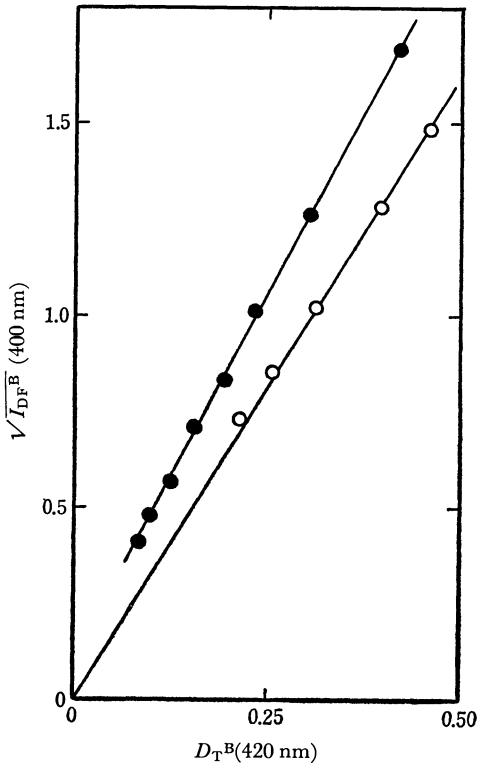

Fig. 7. The relation between D-Fl and T-T absorption for anthracene.

Figs. 7 and 8. Straight lines are the reference plots for the simple P-type delayed fluorescence corresponding to the relations in Table 2. The excesses over the reference lines are clearly due to the mixed T–T annihilation, I_{DF}^A(M, 412) and I_{DF}^B(M, 400). Figure 9 shows that these two quantities are in excellent proportionality to the product of D_T^B (420) and D_T^A (426) as is expected from Eqs. (3) and (4). Thus it is certain that the excess D–Fl is due to the mixed T–T annihilation. From the values of slope in Fig. 9 one can evaluate the value of $\alpha^B(400)\phi_F^B p_M^B k_{MT}/[\varepsilon_T^B(420)\varepsilon_T^A(426)d^2]$ and the corresponding value of A.

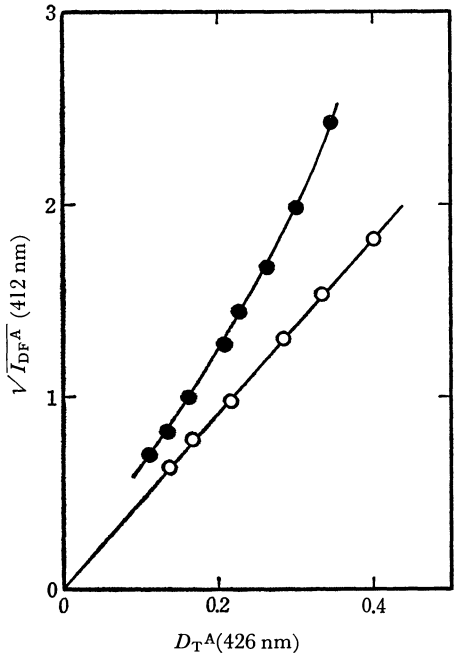

Fig. 8. The relation between D-Fl and T-T absorption for for 9-methylanthracene.

It is convenient to introduce a factor f defined as follows to compare the efficiency of the mixed type and pure P-type D–Fl.

$$f^A = p_M^A k_{MT}/p^A k_{TT}^A \qquad f^B = p_M^B k_{MT}/p^B k_{TT}^B \tag{11}$$

By combining Eqs. (1), (2) and Eqs. (3), (4) one can easily evaluate the f^A and f^B values as well as the $p_M^A k_{MT}$ and $p_M^B k_{MT}$ values given in Table 4.

As seen in Fig. 2 and Fig. 3, DE–Fl of anthracene and 9-methylanthracene exists although very weak.

Table 4. Summary of mixed T-T annihilation

Compounds A	Compounds B	f^A	f^B	$p_M^A k_{MT}$	$p_M^B k_{MT}$	$(p_M^A+p_M^B)k_{MT}$ ($M^{-1}sec^{-1}$)	p_M^A/p_M^B	$R_0^{B\to A}$ (Å)	$R_0^{A\to B}$ (Å)	$e^{-\Delta E/RT}$	$\beta_M(540)\times\phi_{EF}^M q^M k_{MT}$
9-Methylanthracene	Anthracene	$1._4$	0.5_4	$1._7\times10^8$	$1._2\times10^8$	$2._9\times10^8$	$1._4$	14.5	7.4	0.028	0
9-Phenylanthracene	Anthracene	$2._3$	0.3_3	3×10^8	0.7×10^8	$3._7\times10^8$	$4._1$	15.0	7.6	0.009	4×10^{11}
9-Phenylanthracene	9-Methylanthracene	$1._6$	0.5_3	2×10^8	0.6×10^8	$2._6\times10^8$	$3._3$	13.8	13.8	0.32	2×10^{11}
Acridine	Anthracene	0.7_5	0.4_8	$3._5\times10^8$	$1._1\times10^8$	$4._6\times10^8$	$3._2$				2×10^{10}
Acridine	9-Methylanthracene	0.5	0.3_4	$2._3\times10^8$	0.4×10^8	$2._7\times10^8$	$5._7$				8×10^9
Acridine	9-Phenylanthracene	—	0.2_4	—	0.3×10^8	—	—				—
Eosin	Anthracene	—	0	$5._5\times10^8$	0	$5._5\times10^8$					—
Proflavine	Anthracene	—	0	$4._4\times10^8$	0	$4._4\times10^8$					—
Eosin	Acridine	—	0	$3._2\times10^8$	0	$3._2\times10^8$					—

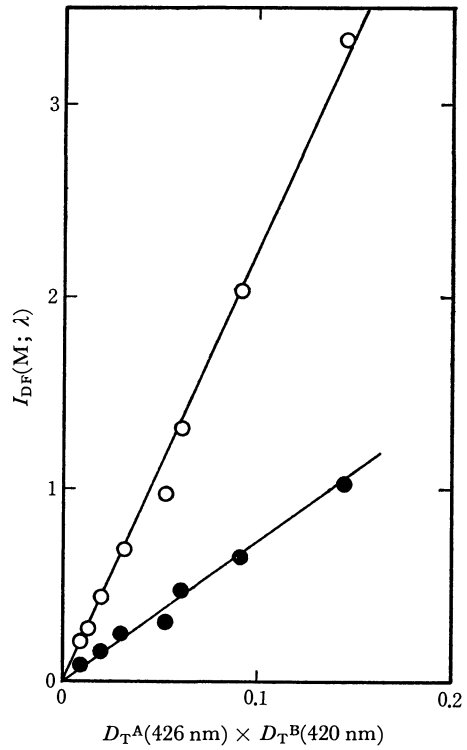

Fig. 9. The plots of $I_{DF}(M; \lambda)$ *vs.* $D_T^A(426) \times D_T^B(420)$ for 9-methylanthracene(A)-anthracene(B) system; ○ A at 412 nm, ● B at 400 nm.

Since D–Fl of monomer is negligible at 540 nm, D–Fl at this wavelength consists of the P-type and the mixed type DE–Fl, $I_{EF}(P, 540)$ and $I_{EF}(M, 540)$.

$$I_{DF}^A(P, 540) = I_{EF}^A(P, 540) + I_{EF}^A(M, 540)$$
$$= \beta^M \phi_{EF}^M q^M k_{MT} \frac{D_T^A(\lambda_1')D_T^B(\lambda_2')}{\varepsilon_T^A(\lambda_1')\varepsilon_T^B(\lambda_2')d^2}$$
$$+ \beta^A(540)\phi_{EF}^A q^A k_{TT}[D_T^A(\lambda)/\varepsilon_T^A(\lambda)d]^2 \quad (12)$$

The analysis can be made as in the case of monomer D–Fl, but in this case it was found that MDE–Fl is negligible.

For anthracene(B)-9-phenylanthracene(A), Fig. 10 shows the relation between the MDE-Fl intensity I_{DF}^E at 540 nm and the product of $D_T^A(440)$ and $D_T^B(421)$, obtained as a result of the above analysis. Although the linearity is not very good, there is no doubt that MDE–Fl occurs in this system.

System, 9-phenylanthracene(A) and 9-methylanthracene(B) also gives MDE–Fl.

In acridine(A)-anthracene(B), the fluorescence yield of acridine is one order less than that of anthracene derivatives and the triplet lifetime is much smaller; hence the measurement and analysis could not be performed accurately. However, the analysis clearly showed that both components exhibit MD–Fl as shown in Fig. 11. There is scarcely any doubt that MDE–Fl also occurs as seen from Fig. 12. For acridine(A)-9-methylanthracene(B), the results are qualitatively similar to those of the above system.

In acridine(A)-9-phenylanthracene(B), D–Fl spectra of the two components greatly resemble each other and

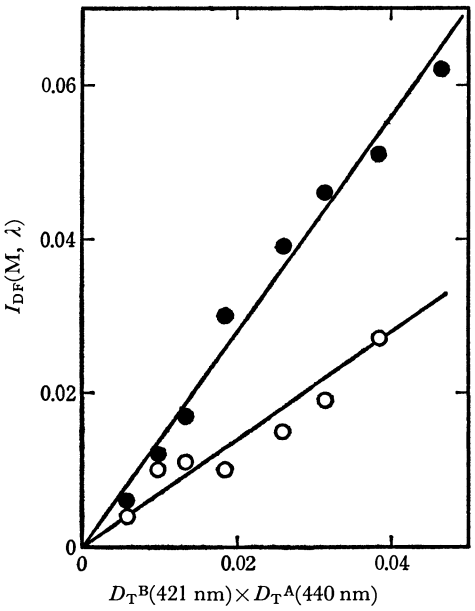

Fig. 11. The plots of $I_{DF}(M; \lambda)$ *vs.* $D_T^B(421) \times D_T^A(440)$ for acridine(A)-anthracene(B) system; ○ A at 400 nm, ● B at 412 nm.

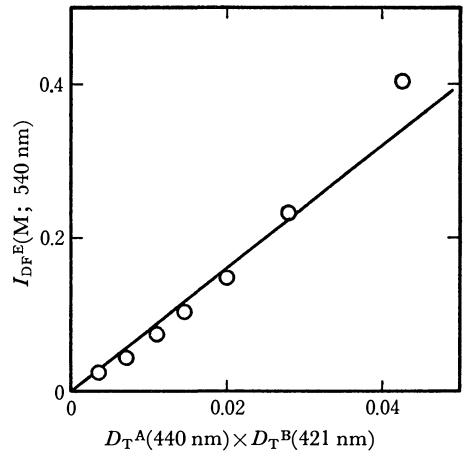

Fig. 10. The relation between $I_{DF}^E(M; 540)$ and $D_T^A(440) \times D_T^B(421)$ for anthracene(B)-9-phenylanthracene(A) system.

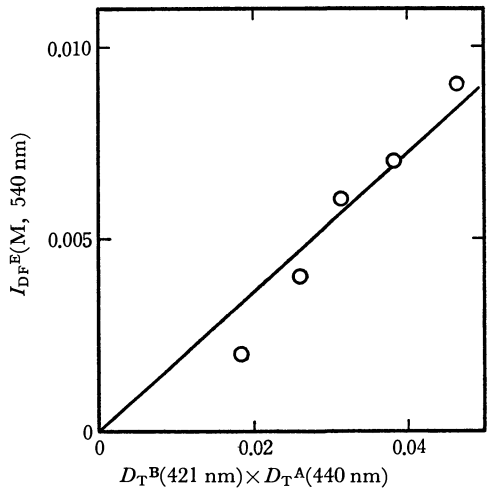

Fig. 12. The relation between $I_{DF}^E(M, 540)$ and $D_T^B(421) \times D_T^A(440)$ for acridine(A)-anthracene(B) system.

the fluorescence yield of the latter is considerably larger than that of the former. Therefore D–Fl could not be divided into two components. However, since D–Fl from acridine is very weak, the approximate values of f^B and $p_M{}^B k_{MT}$ could be estimated. The analysis at 540 nm also gave evidence for the occurrence of MDE–Fl.

Studies on Two Species with Quite Different Excited Singlet Levels. As is well known, D–Fl of eosin and of proflavine (both, A) is of E-type and is expressed by

$$I_{DF}{}^A(E, \lambda) = \alpha^A(\lambda)\phi_F{}^A k_T[{}^3A] \qquad (1')$$

of Eqs. (1) and (2). Accordingly, the expression for instead MD–Fl $I_{DF}(M, \lambda)$ has to be modified as follows.

$$I_{DF}{}^A(M, \lambda) = \alpha^A(\lambda)\phi_F{}^A p_M{}^A k_{MT}[{}^3A][{}^3B] + \alpha^A(\lambda)\phi_F{}^A k_T[{}^3A]$$

Apart from these two points, the method of analysis is essentially the same as in P-type D–Fl.[10] In eosin(A)-anthracene(B),[9] only D–Fl of eosin is increased remarkably by mixed T–T annihilation while that of anthracene scarcely shows any increase.

In proflavine(A)-anthracene(B), D–Fl of proflavine under ordinary conditions is of E-type and a similar analysis to that for the above system gave essentially the same result; D–Fl of proflavine largely increases by mixed T–T annihilation while that of anthracene is scarcely affected (Fig. 13).

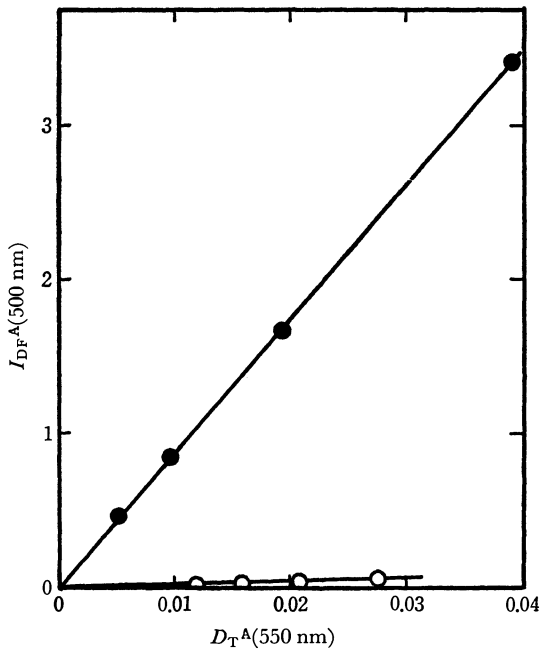

Fig. 13. The relation between $I_{DF}{}^A(500)$ and $D_T{}^A(550)$ for proflavine(A)-anthracene(B) system; ○[B]=0 M, ●[B]=2×10^{-6} M.

For eosin(A)-acridine(B), the results are similar to those of the above two systems.

For the last three systems MDE–Fl could not be investigated.

Discussion

In the present investigation, mixed T–T annihilation of anthracene derivatives have been studied quantitatively. Since the concentrations of both components are less than 10^{-5} M, no process in the initially excited singlet state participates, for instance, A*+B→A+B* and A*+B→(AB)*, *etc.* Accordingly the present results are concerned only with T–T annihilation of various types. The method of analysis leaves nothing doubtful at least in principle. Although errors may become considerable in some cases owing to experimental difficulties, the following general conclusions can be drawn.

1) When the singlet excited levels of A and B differ a few times of kT, D–Fl of both components occur.

2) When the level differences largely exceed kT, only D–Fl of the component with a lower level occurs.

3) MD-Fl occurs generally in case 1).

4) The efficiency of MDE–Fl ($p_M{}^A+p_M{}^B$) is equal to that of P-type D–Fl (p^A or p^B) at least in the order of magnitude.

For the mixed excimer fluorescence Birks and Christophorous[11] in classifying two types, stated that it occurs with a diffusion controlled rate in the systems composed of like compounds such as anthracene and its derivatives, while it does not occur at all in a pair of molecules with different aromatic cores. It has been established that similar situations hold also in mixed T–T annihilation.

It is very interesting that the value of $p_M{}^A/p_M{}^B$ is always larger than unity, *i.e.*, the component with a lower singlet excited level emits more efficiently when the 0–0 band of fluorescence is adopted as an excited level. Since the mixed T–T annihilation at room temperature occurs according to the following scheme as has been well established,[4]

$$B^T + A^T \rightarrow (B\cdots A)^{**} \xrightarrow{k_M{}^B} B^* + A$$
$$\xrightarrow{k_M{}^A} A^* + B$$
$$\rightarrow (B\cdots A)^* \text{ (mixed excimer)}$$

the value of $p_M{}^A/p_M{}^B$ is nothing but the ratio of the rate constants $k_M{}^A$ and $k_M{}^B$.

At present, the microscopic mechanism of a simple type delayed fluorescence as well as of a mixed one is unknown; $(B\cdots A)^{**}$ merely denotes an encounter state of unknown character. Birks suggested that the intermediate in the case of a simple type one may experience a quintet, triplet, or singlet state.[12] Such a change in spin states may occur in the early stage of encounter, but in mixed T–T annihilation, differing from the simple T–T annihilation, the two components A* and B or B* and A produced may still have a chance of transforming to each other. Thus it is necessary to take the following three possibilities into consideration as the molecular processes determining the $p_M{}^A/p_M{}^B$ value.

A) A^T and B^T approach close enough to interact and change their electronic states yielding ultimately (A*+B) or (B*+A) (bracket denotes that the two components still exist in the encounter state) in a certain proportion as determined by a specific electronic or vibronic interaction.

11) J. B. Birks and L. G. Christophorous, *Nature*, **196**, 33 (1962); p. 423 in Ref. 2.

12) J. B. Birks, *Chem. Phys. Letters*, **1**, 561 (1968).

B) The possibility may exist that in the encounter state, the Boltzmann distribution is approached between A* and B* due to electronic exchange interaction.

C) During the diffusion apart, there is another possibility that a long range dipole-dipole interaction causes a mutual transformation. This is thought to be possible because the distance to which the two components separate during the lifetime of the excited state $\sim 10^{-8}$ sec is estimated to be 10—100 Å. If the R_0-value in Förster's theory[13] is suitable, then $A+B^* \rightleftharpoons B+A^*$ may occur during the lifetime.

From the above viewpoint, the values of the Boltzmann factor $e^{-\Delta E/RT}$ (ΔE, difference of 0–0 band of fluorescence) and of R_0 for $B^*+A \rightleftarrows B+A^*$ are added in Table 4. The values of p_M^A/p_M^B change from 3 to 5 except for system (1). Putting aside the results for the systems involving acridine which are less reliable, only the p_M^A/p_M^B values for (1), (2), and (3) will be discussed. It is evident that these values are not well related with either the values of R_0 or of $e^{-\Delta E/RT}$. It may be said from the R_0 values that the energy transfer due to Förster's mechanism does not occur so efficiently in the present systems. Although the value of p_M^A/p_M^B for system (3) well agrees with the value of $e^{-\Delta E/RT}$, it may be judged that this is rather a mere coincidence in view of large discrepancies in (1) and (2). Thus in the present systems, it seems likely that the p_M^A/p_M^B values are determined mainly by the ratio of the two processes $(A\cdots B)^{**} \rightarrow (A^*\cdots B)$ and $(A\cdots B^*)$. The two components in the encounter state may then separate quickly with any noticiable chance of transforming to each other. When the levels of A* and B* are far apart, it is reasonable to consider that only the emission of the lower component occurs.

A few remarks will be added to the DE–Fl of anthracene derivatives. Birks and Aladekomo[14] reported that anthracene does not exhibit the excimer fluorescence while 9-methylanthracene does. He states[15] that anthracene with a great tendency of forming a stable photodimer does not give excimer fluorescence, while 9-methylanthracene with less tendency of dimerization due to a little steric hindrance will emit the excimer fluorescence. He expects that 9-phenylanthracene which does not dimerize will be more liable of forming excimer. However, no experimental data were given for the latter two compounds. The present results have verified his argument for the first time. Thus the values of $\beta\phi_{EF}q$ measured at 540 nm listed in Table 3 increase five times from anthracene to 9-methylanthracene and also from 9-methylanthracene to 9-phenylanthracene. In spite of some uncertainty in β-value, there is scarcely any doubt that these great differences reflect the differences in their excimer formation tendencies.

13) Th. Förster, *Ann. Physik.*, **2**, 55 (1948).

14) J. B. Birks and J. B. Aladekomo, *Photochem. Photobiol.*, **2**, 415 (1963).

15) p. 321 in Ref. 2.

BULLETIN OF THE CHEMICAL SOCIETY OF JAPAN, VOL. 44, 1534—1538 (1971)

Nature of the Acid Sites on the Surface of Silica-alumina. II. The Relation between the Acid Property of the Sites and the Photo-ionization of Polyacenes Adsorbed on the Surfaces

Kazuto TAKIMOTO and Masaji MIURA

Department of Chemistry, Faculty of Science, Hiroshima University, Higashisenda-machi, Hiroshima

(Received January 8, 1971)

The ESR and diffuse reflection spectra of the polyacenes adsorbed on the surfaces of silica gel, alumina, and silica-alumina were measured. The amount of the cation radicals generated on the surfaces was enhanced upon irradiation with UV light. This was interpreted in terms of the photo-ionization accomplished *via* a charge-transfer state by an absorption of $h\nu_{CT}$, which was expected to vary with the strength of the Lewis-acid sites. The rate of the radical formation was not the first order, and that of the annihilation was the second order only in the initial stage. These phenomena are discussed in connection with the heterogeneity of the acid properties on the surfaces.

It is well known that such polyacenes as anthracene and perylene cause an electron transfer and a proton transfer on the surface of silica-alumina, even in the absence of ultraviolet (UV) irradiation. This phenomenon is interpreted in terms of the interaction of these polyacenes with the strong Lewis-acid sites and the Brönsted-acid sites on the surface of silica-alumina. A number of studies of the acidity, activity, and structure of the acid sites have been done in connection with catalysis by such techniques as infrared, ESR, diffuse reflection, and gas adsorption.[1-4] From these studies, we know that some strong acid sites on the surface interact with the polyacenes even in the ground state;

1) E. P. Parry, *J. Catalysis*, **2**, 371 (1963); G. Fabbri and G. Farne, *Ann. Chim.* (Rome), **56**, 309 (1966).

2) D. N. Stamires and J. Turkevich, *J. Amer. Chem. Soc.*, **86**, 749 (1964); G. M. Muha, *J. Phys. Chem.*, **71**, 633 (1967); B. R. T. Garrett, I. R. Leith, and J. J. Rooney, *Chem. Commun.*, **1969**, 222.

3) A. N. Terenin, V. A. Barachevskii, E. I. Kotov, and V. Kholmogorov, *Spectrochim. Acta*, **19**, 1797 (1963).

4) A. J. de Rosset, C. G. Finstron, and C. J. Adams, *J. Catalysis* **1**, 244 (1962).

the cation radical is formed by an electron transfer from the polyacenes to the surface, and the carbonium ion is generated by a proton transfer from the surface to the polyacenes. Terenin and his co-workers have found that the formation of the cation radical on the surface is enhanced by UV irradiation.[5] This may show that the electron transfer occurs even on the weaker acid sites upon irradiation with UV light. As has previously been reported,[6] the acid properties of silica-alumina, alumina, and silica gel have been fairly well revealed. It is, therefore, of great interest to study the photo-ionization of polyacene adsorbed on the surfaces in connection with their acid properties.

The polyacene adsorbed on the surface can be regarded as a surface complex. We take into consideration the charge-transfer state in order to explain the transition from a nonbonding type, D···A, to a cation and anion type, $D^+ + A^-$, by UV irradiation, where D and A are a donor and an acceptor respectively. It is significant that the energy corresponding to the charge-transfer absorption band, $h\nu_{CT}$, caused by the interaction of the polyacene with the acid site varies with the strength of the acid site. The purpose of this work is to reveal; (1) the relation between the radical formation by UV irradiation and the acid property of the surface, and (2) the mechanism of the annihilation of the radical.

Experimental

Naphthalene and anthracene were purified by the sublimation method. Guaranteed perylene obtained from the Tokyo Kasei Co. was used without further purification. *n*-Hexane was purified by distillation, with several pieces of metallic sodium added to remove any moisture. The 12% silica-alumina, alumina, and silica gel were the same as those used in the preceding work.[6]

The polyacenes were adsorbed from their vapor phases or from the oxygen-free *n*-hexane solutions onto the surfaces of the silica-alumina, alumina, and silica gel. The source of UV light was an 1-kW high-pressure mercury arc. The ESR spectra were obtained by using a spectrometer described elsewhere.[7] The rate of the radical formation was determined from the increase in the relative intensity of the ESR signal on UV irradiation. The diffuse reflection spectra were measured by using a Hitachi-Perkin-Elmer 139 spectrophotometer, equipped with an attachment to measure diffuse reflection.

Results

ESR Spectra. When the surface coverage of polyacene was low and the coloration was just discernible, an ESR spectrum with nine well-resolved peaks was observed, as may be seen in Fig. 1; the hyperfine coupling constant and the *g*-value of the spectrum were 3.4 gauss and 2.0025 respectively. The spectrum was the same as that of the cation radical of polyacene, as was found by comparing the spectrum with that measured in a strongly oxidizing reagent.[8]

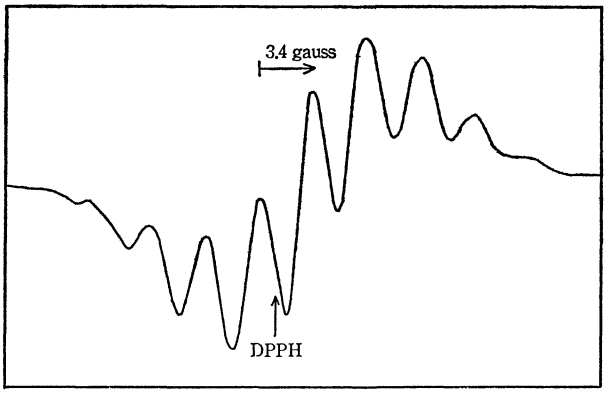

Fig. 1. ESR spectrum of the perylene cation radical adsorbed on the surface of 12% silica-alumina.

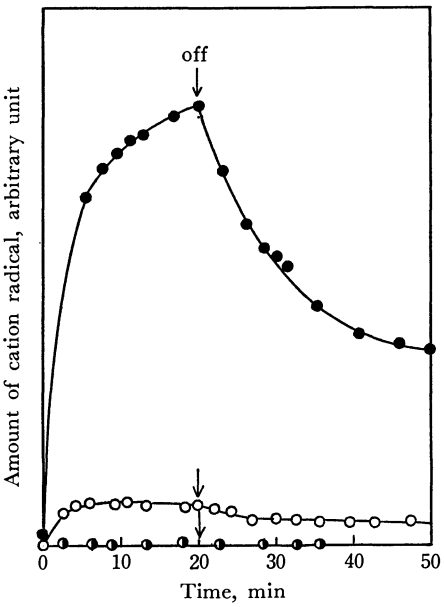

Fig. 2. Rates of the radical formation from naphthalene adsorbed on the surfaces of silica-alumina, alumina, and silica gel with UV irradiation.
●: 12% silica-alumina (G 320)
○: alumina (G 1400)
◑: silica gel (G 1400)

Figure 2 shows the rate of the radical formation from the naphthalene adsorbed on the surfaces of the silica-alumina, alumina, and silica gel which were treated at 300°C for 8 hr *in vacuo*. In the absence of UV irradiation, the cation radical of the naphthalene was formed only on the surface of the silica-alumina. Upon UV irradiation, the cation radical was generated also on the surface of the alumina, though it was not formed on the surface of the silica gel. The rates of radical formation by UV irradiation and its annihilation on the surface of the silica-alumina were faster than those on the alumina. The rate of the radical annihilation was considerably slower than that of the radical formation. The rates of the formation and annihilation of the radicals from the anthracene and perylene are

5) V. A. Barachevskii and A. N. Terenin, *Opt. i Spectroskopiya*, **17**, 304 (1964).
6) M. Miura, Y. Kubota, T. Iwaki, K. Takimoto, and M. Muraoka, This Bulletin, **42** 1476, (1969).
7) A. Hasegawa and M. Miura, *ibid.*, **40**, 2553 (1967).
8) W. I. Aalbergsberg, G. J. Hoijtink, E. L. Mackor, and W. P. Weijland, *J. Chem. Soc.*, **1959**, 3055.

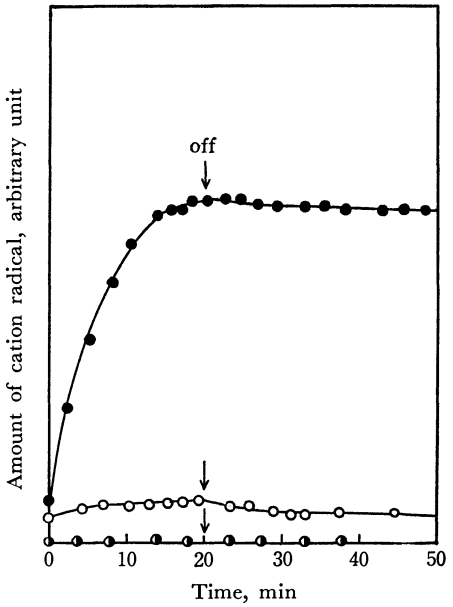

Fig. 3. Rates of the radical formation from anthracene adsorbed on the surfaces of silica-alumina, alumina, and silica gel with UV irradiation.
●: 12% silica-alumina (G 140)
○: alumina (G 1400)
◑: silica gel (G 1400)

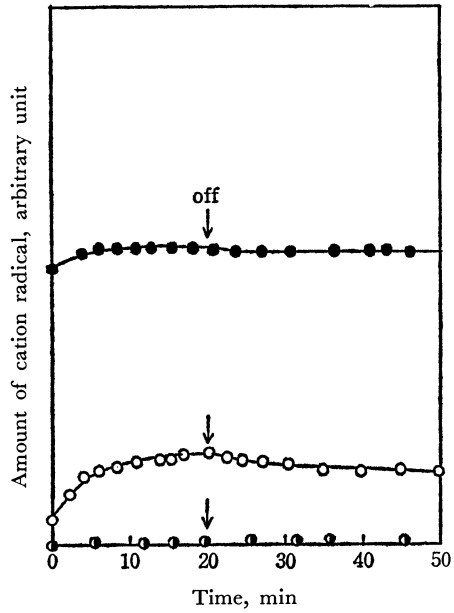

Fig. 4. Rates of the radical formation from perylene adsorbed on the surfaces of silica-alumina, alumina, and silica gel with UV irradiation.
●: 12% silica-alumina (G 10)
○: alumina (G 1400)
◑: silica gel (G 1400)

shown in Figs. 3 and 4 respectively. The formation rates of the radicals of these two polyacenes were faster than that of naphthalene. However, the ratios of the rates of the annihilation to those of the formation were small in comparison with that of naphthalene.

Diffuse Reflection Spectra. Figure 5 shows the diffuse reflection spectrum of the naphthalene adsorbed on the surface of the silica-alumina. Intense visible

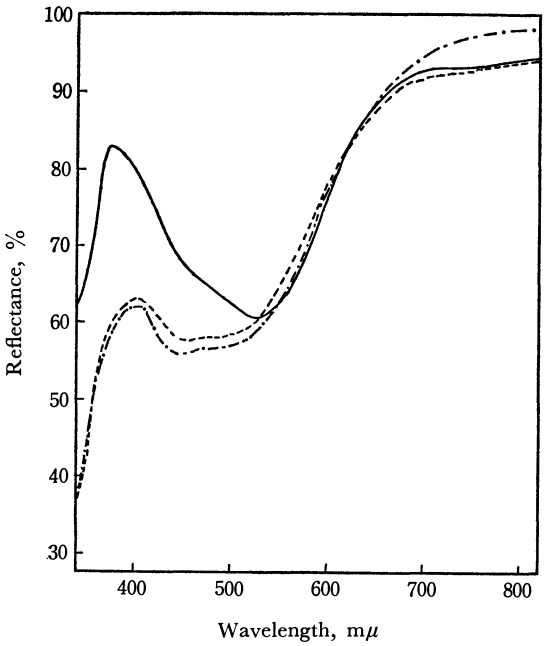

Fig. 5. Diffuse reflection spectra of naphthalene adsorbed on the surface of 12% silica-alumina.
—— in the absence of UV irradiation
---- UV irradiation for 30 min
·—· keeping in a dark room for a day after UV irradiation

bands at 440 and about 530 mμ, and a feeble band at 760 mμ were observed. Upon UV irradiation for 30 min, the absorption band at 440 mμ was remarkably enhanced, while the bands at 530 and 760 mμ scarcely changed. According to several authors,[9] the band at 430 mμ, corresponding to that at 440 mμ in this work, is to be ascribed to the carbonium ion, naphthalene·H^+. On the other hand, the band at 530 mμ arises from the cation radical, naphthalene$^+$. The band at 760 mμ is attributable to the anion radical, naphthalene$^-$, which, in theory, must have the same band as that of the cation radical.[10] The structured bands below 320 mμ belong to physically-adsorbed naphthalene molecules. After the sample had been allowed to stand in a dark room for a day, the absorption maxima at 440 and 530 mμ increased a little, while the bands at wavelengths longer than 680 mμ slightly decreased.

The spectrum of the anthracene adsorbed on the surface of silica-alumina is shown in Fig. 6. The absorption bands appeared at 420, 560, 620, 660, and 720 mμ. The absorption maxima at 420 and 720 mμ may be assigned to the carbonium ion and the cation radical of the anthracene respectively.[9] The species for the weak absorption bands at 560, 620, and 660 mμ are not certain. The structured bands below 380 mμ arise from physically-adsorbed anthracene molecules. The absorption spectrum of the perylene adsorbed on the surface of the silica-alumina is shown in Fig. 7. The absorption bands are situated at 540, 610—620, and 730 mμ. After UV irradiation, the

9) V. Gold and F. D. Type, *J. Chem. Soc.*, **1952**, 2172.
10) H. Kon and M. S. Blois, *J. Chem. Phys.*, **28**, 743 (1958).

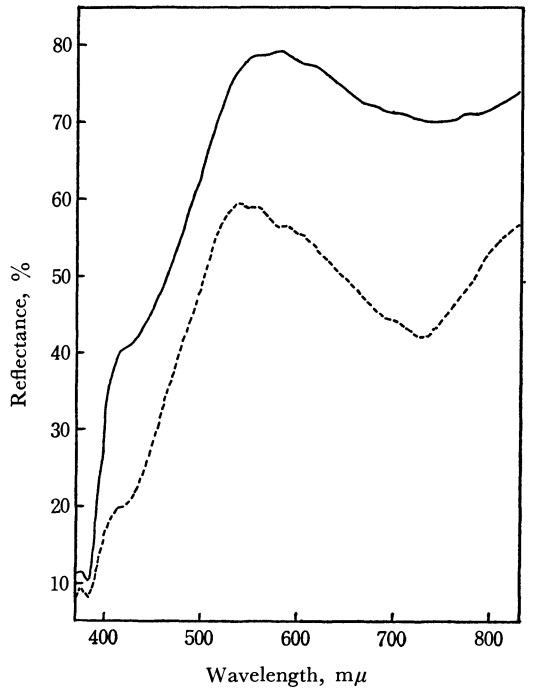

Fig. 6. Diffuse reflection spectra of anthracene adsorbed on the surface of 12% silica-alumina.
—— in the absence of UV irradiation
---- UV irradiation for 30 min

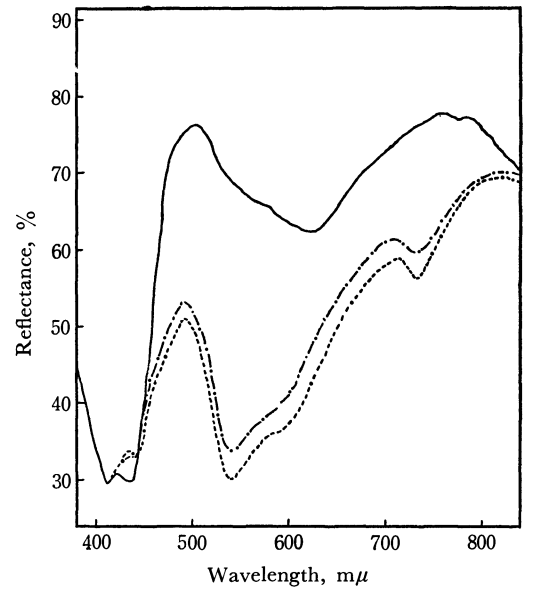

Fig. 7. Diffuse reflection spectra of perylene adsorbed on the surface of 12% silica-alumina.
—— in the absence of UV irradiation
---- UV irradiation for 30 min
·—· keeping in a dark room for a day after UV irradiation

maximum at 540 mμ increased significantly, while that at 730 mμ did so fairly much. These bands may be ascribed to the perylene cation radical. The bands below 450 mμ are due to physically-adsorbed perylene molecules.

Discussion

According to Mulliken's theory,[11] the wave functions of a surface complex may be represented by the following formulas:

$$\Psi_G^{(i)} = a^{(i)}\phi_{D\cdots A}^{(i)} + b^{(i)}\phi_{D^+\cdots A^-}^{(i)}$$
$$\Psi_E^{(i)} = a^{*(i)}\phi_{D\cdots A}^{(i)} + b^{*(i)}\phi_{D^+\cdots A^-}^{(i)}$$

where $\Psi_G^{(i)}$ and $\Psi_E^{(i)}$ are the ith wave functions in the ground state and the excited state respectively, and $\phi_{D\cdots A}^{(i)}$ and $\phi_{D^+\cdots A^-}^{(i)}$ are the ith wave functions of the nonbonding type and the charge-transfer type respectively, among many wave functions of the complex which result from the heterogeneity in the strength of the Lewis-acid site on the surface.

When a polyacene was adsorbed on the surface of silica-alumina, the cation radical was formed even in the absence of UV irradiation. This indicates the presence of a considerable amount of the surface complex, whose coefficient, $|b^{(i)}|$, in $\Psi_G^{(i)}$ is much larger than $|a^{(i)}|$. In other words, a large number of the strong Lewis-acid sites are present on the surface of silica-alumina. As the ionization potential of polyacene decreases, the amount of the cation radical generated on the surface in the ground state increases, as may be seen in Figs. 2, 3, and 4. This is due to an increase in the number of the charge-transfer-type functions, accompanied by a decrease in the ionization potential of polyacene.

The charge-transfer band corresponding to the transition from Ψ_G to Ψ_E could not be detected. This may be due to the band-broadening caused by the fact that the coefficients, $|a|$ and $|b|$, in Ψ_G can take various values. The energy of the charge transfer, $h\nu_{CT}$, decreases as the electron affinity of the Lewis-acid site increases and as the ionization potential of polyacene decreases. The photo-ionization of the polyacene adsorbed on the site, the electron affinity of which has a low value as compared with that of the ionization potential of the polyacene, may be accomplished *via* a charge-transfer state by the absorption of $h\nu_{CT}$. Thus, when polyacene adsorbed on the surface of silica-alumina was irradiated with UV light, the cation radical was formed even in the weak-acid site on the surface where it could not be produced in the absence of UV irradiation.

In the case of the alumina, the perylene and naphthalene adsorbed on the strong Lewis-acid sites are ionized by the transfer of the electron to the surface, while those adsorbed on the comparatively weak acid sites are also ionized *via* a charge-transfer state by means of UV irradiation. The amount of the radicals formed by the photo-ionization is, however, affected by the acid property of the surface. The difference between the amounts of the radicals produced on the surfaces of the alumina and the silica-alumina results not from the difference in the distribution of the acid sites, but from that in their number.[6,12] On the other hand, the naphthalene and perylene adsorbed on the surface of the silica gel were scarcely

11) R. S. Mulliken, *J. Phys. Chem.*, **56**, 801 (1952); *J. Amer. Chem. Soc.*, **74**, 811 (1958); *J. Chim. Phys.*, **61**, 20 (1963).

12) M. R. Basila, J. R. Kantner, and K. H. Rhee, *J. Phys. Chem.*, **68**, 3197 (1964).

ionized even with UV irradiation. This may be due to the lack of Lewis-acid sites on the surface.

When the energy level of a nonbonding type, D···A, rises to over the barrier or a charge-transfer state, the cation radical is generated. Its stability becomes higher as the electron affinity of the Lewis-acid site increases because the photo-ejected electron is stabilized on the site.

The rate of the radical formation was not the first order. However, the rate of the formation may be expected to be the first order, since the radical is formed by UV irradiation through the following process:

$$D\cdots A \xrightarrow{h\nu} D^+\cdots A^- \xrightarrow{\text{stabilization}} D^+ + A^-$$

The deviation of the formation rate from the first order may be caused by the heterogeneity of the surface. The sites on the surface have a wide range of acidity and acid strength. Such a distribution of the acid sites may complicate the rate of the radical formation.

On the other hand, when the UV light was put off, the annihilation of the radical occurred. Two mechanisms for the annihilation may be considered:

(1) $D^+ + A^- \xrightarrow{\text{reaction}}$ other products

(2) $D^+ + A^- \xrightarrow{\text{recombination}} D\cdots A + h\nu$

When the sample was kept for a day after UV irradiation and again irradiated, the amount of the radical was restored almost to the initial value. Hence, the (2) mechanism seems to be predominant. The rate of the annihilation was the second order in the initial stage, while it became the first order in the later stage. The annihilation rate seems to be the second order, since the recombination of the cation radical with the trapped electron predominantly contributes to the rate process. The fact that the rate of the radical annihilation in the later stage is apparently the first order may be due to the distribution of the Lewis-acid sites. That is, the rate constant of the recombination may be different according to the strength of the Lewis-acid sites; the rate of the recombination of the radical with the photo-ejected electron becomes faster as the Lewis-acid site is weaker, and also as the ionization potential of polyacene is higher. As a result, the rate of the annihilation seems to deviate from the second order as the reaction proceeds. This may also explain why the rate of the annihilation of the radical is slow in comparison with that of the formation, and why the ratio of the rate of the annihilation to that of the formation is least for perylene among these three polyacenes.

The authors wish to express their thanks to Dr. Akinori Hasegawa for his helpful discussions.

BULLETIN OF THE CHEMICAL SOCIETY OF JAPAN, VOL. 44, 1538—1543 (1971)

The Reactions of Photogenerated Solvated Electrons in Methanolic Solutions of Potassium Iodide

Hiroshi SEKI and Masashi IMAMURA

The Institute of Physical and Chemical Research, Wako, Saitama

(Received January 22, 1971)

Hydrogen formation from UV-irradiated potassium iodide solutions was studied using CH_3OH and CH_3OD as the solvents and nitrous oxide and acids as the solvated-electron scavengers. The maximum quantum yield of the solvated electron in CH_3OH was found to be 0.6 both in nitrous oxide and in acid solutions. It was concluded that the solvated electron produces hydrogen in pure methanol through Reaction (1), $e^-_{solv} \rightarrow H + CH_3O^-$, with a quantum yield of 0.35 at 25°. The rate constant of this reaction is 5.4×10^5 sec^{-1}, corresponding to a half-life of 1.3 μsec. From the results obtained with acid solutions, it was also concluded that nitrous oxide reacts with a solvated electron to produce one molecule of nitrogen in neutral methanol.

Solvated electrons are produced in aqueous solutions and many other polar liquids by the irradiation of ionizing radiations. The reactions of these solvated electrons, particularly of hydrated electrons, have been extensively studied by many investigators.[1] Solvated electrons have also been known to be produced by the UV irradiation of aqueous and alcoholic solutions of several inorganic[2] and organic compounds,[3] and, by the flash-photolysis technique, they have been shown to give an absorption spectra identical with those produced by ionizing radiations.[4-7]

Jortner *et al.*[8] studied the photochemical formation of solvated electrons using an electron scavenger in 0.15 M iodide solutions in methanol, ethanol, and isopropanol, and reported the quantum yields of 0.6—0.7 for the solvated electrons in these alcohols. Whereas they failed to observe the hydrogen formation from these solutions, Dainton *et al.*[9] observed it from an

1) See a recent review by E. J. Hart and M. Anbar, "The Hydrated Electron," Wiley-Interscience, New York (1970).
2) G. Stein, *Adv. Chem. Ser.*, **50**, 230 (1965).
3) L. I. Grossweiner and H. Joschek, *ibid.*, **50**, 279 (1965).
4) M. S. Matheson, W. A. Mulac, and J. Rabani, *J. Phys. Chem.*, **67**, 2613 (1963).
5) R. Devonshire and J. J. Weiss, *ibid.*, **72**, 3815 (1968).
6) L. I. Grossweiner, E. F. Zwicker, and G. W. Swenson, *Science*, **141**, 1180 (1963).
7) G. Dobson and L. I. Grossweiner, *Radiat. Res.*, **23**, 290 (1964).
8) J. Jortner, M. Ottolenghi, and G. Stein, *J. Phys. Chem.*, **67**, 1271 (1963).
9) F. S. Dainton, G. A. Salmon, and P. Wardman, *Proc. Roy. Soc.* (London), **A 313**, 1 (1969).

UV-irradiated methanolic solution of lithium ferrocyanide.

In the γ-radiolysis of methanol, on the other hand, free solvated electrons are produced with $G=2.0$ and are believed to be a precursor of the product hydrogen.[10] Two possible pathways for the hydrogen formation from solvated electrons in radiation-irradiated methanol have been supposed:

$$e^-_{solv} \rightarrow H + CH_3O^- \quad (1)$$

$$CH_3OH_2^+ + e^-_{solv} \rightarrow H + CH_3OH \quad (2)$$

The pulse radiolysis studies showed that the decay of solvated electrons in alcohols is represented by the first-order kinetics,[11,12] indicating that they react principally with alcohol molecules. The rate constant of this decay reaction has been determined not only by the pulse-radiolysis technique, but also by steady-irradiation experiments.[13–15] However, there seem to be disagreements among these values larger than can be accounted for by experimental errors.

In contrast to the earlier result,[8] we observed the formation of hydrogen from UV-irradiated methanolic solutions of potassium iodide, and chose this system as an appropriate one for investigating the reaction of a solvated electron with a methanol molecule free from the interference of the competing reaction (Reaction (2)). This paper will report on the results of Reaction (1) as well as on the reaction of the solvated electron with nitrous oxide.

Experimental

Chemicals. Reagent-grade methanol supplied by the Wako Pure Chemical Co. was purified by distillation from a dinitrophenylhydrazine-H_2SO_4 solution. Deuterated methanol, CH_3OD(>99 atom%D), was obtained from CIBA, Ltd., and was purified similarly by using a small spinning-band distillation apparatus. The isotopic purity of the distilled CH_3OD was determined by NMR and was found to be usually ~99%.

The potassium iodide and hydrochloric and sulfuric acids were of a reagent grade from Wako and were used without further purification. Nitrous oxide and carbon dioxide, standard gases from the Takachiho Trading Co., were purified by distillation *in vacuo*.

Sample Preparation. A weighed amount of potassium iodide was degassed thoroughly in an irradiation ampoule before transferring degassed methanol into the ampoule by distillation on a vacuum line. When an acid solution was prepared, a small amount of acid was degassed beforehand and then added to the degassed methanolic solution through a break-seal. A such meticulous care was necessary to prevent the coloration due to iodine liberation in the solutions prepared.

Nitrous oxide and carbon dioxide were added to the solution volumetrically, their concentrations being calculated from the solubility data.[16]

Irradiation. The light source was an Ushio ULO-6DQ low-pressure mercury lamp, which was operated at 38V AC and 0.15 A with a voltage stabilizer. A 254-nm light was isolated by the use of an interference filter.[17] The methanolic solution of potassium iodide has a CT spectrum, with its peak at 220 nm extending to nearly 270 nm. The irradiation ampoule was a quartz cylinder, 2 cm in i.d. and 10 cm in length. All the photolyses were conducted at room temperature (~25°).

The light intensity and the quantum yields were determined by using a potassium ferrioxalate actinometer; the potassium ferrioxalate had been prepared according to the method described by Calvert and Pitts.[18] The concentration of the ferrous ions formed was determined by the *o*-phenanthroline method, and the quantum yield was taken to be $\Phi(Fe^{2+})=1.25$ at 254 nm.[18] The light intensity was in the range of $(2.7—8.3)\times10^{-9}$ einstein l^{-1} sec^{-1}.

Analytical Procedures. The hydrogen was determined by combustion on cuprous oxide using a micro gas-analyzer.[19] The amount of nitrogen produced from nitrous oxide solutions was determined from the residual gas volume after complete combustion, followed by absorption on magnesium perchlorate and Ascarite in the gas-analyzer. The formaldehyde was determined by the chromotropic-acid method.[19] The isotopic compositions of the hydrogen produced from CH_3OD samples were determined by mass-spectrometric analysis.[20]

Flash Photolysis. The details of the flash-photolysis apparatus have been described previously.[21] Briefly, the photolysis flash consisted of two Ushio xenon lamps. The operating characteristics of the lamps were 100 joule of energy per flash and 10 μsec for flash duration to a 50% peak. The reaction vessel was a quartz cylinder, 10 mm in i.d. and 10 cm in length, with flat plates sealed on either end.

Pulse Radiolysis. The rate constant of the reaction between solvated electron and nitrous oxide in methanol was determined by the pulse-radiolysis technique using a 3 MV Van de Graaff accelerator; the details will be published elsewhere.[22]

Results

Iodide Solutions in CH_3OH. Potassium iodide solutions (0.05—0.1 M) in CH_3OH produce hydrogen as a gaseous product upon UV irradiation. In the absence of potassium iodide, the UV irradiation produces no detectable hydrogen. A typical result is shown in Fig. 1, from which the quantum yield for hydrogen formation can be calculated to be 0.35 at 25°.

Another stable product from methanol is formalde-

10) H. Seki and M. Imamura, *J. Phys. Chem.*, **71**, 870 (1967).
11) I. A. Taub, D. A. Harter, M. C. Sauer, Jr., and L. M. Dorfman, *J. Chem. Phys.*, **41**, 979 (1964).
12) F. S. Dainton, J. P. Keene, T. J. Kemp, G. A. Salmon, and J. Teply, *Proc. Chem. Soc.*, **1964**, 265.
13) K. N. Jha and G. R. Freeman, *J. Chem. Phys.*, **48**, 5480 (1968).
14) W. V. Sherman, *J. Phys. Chem.*, **71**, 4245 (1967).
15) R. A. Basson and H. J. van der Linde, *J. Chem. Soc., A*, **1967**, 28.
16) a) N_2O: A. Seidell, "Solubilities of Inorganic and Metal Organic Compounds," **2**, 4th Ed., American Chemical Society, Washington, D.C. (1965), p. 802. b) CO_2: *ibid.*, **1**, p. 479.
17) The interference filter obtained from Nippon Shinku Kogaku Co. had $\lambda_{max}=256$ nm with a half-width of 18 nm.
18) J. G. Calvert and J. N. Pitts, Jr., "Photochemistry," John Wiley & Sons, Inc., New York (1966), p. 783.
19) M. Imamura, S. U. Choi, and N. N. Lichtin, *J. Amer. Chem. Soc.*, **85**, 3565 (1963).
20) Massspectrometric determination was carried out at Tokyo Metropolitan Isotope Center and at Tokyo Institute of Technology.
21) A. Kira and K. Nishi, *Rep. Inst. Phys. Chem. Res.*, **44**, 56 (1968).
22) A. Kira, S. Arai, and M. Imamura, *ibid.*, to be published.

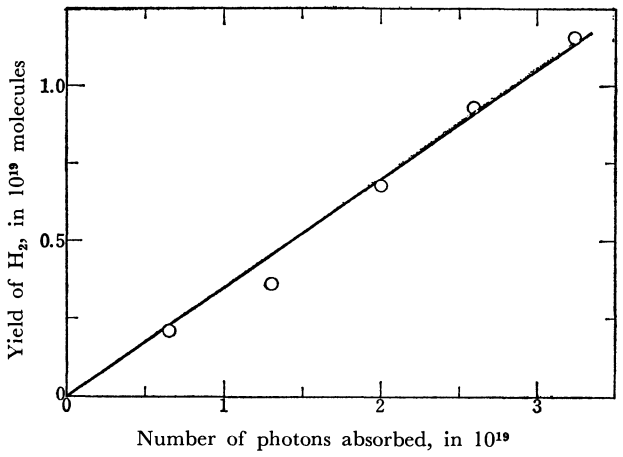

Fig. 1. Formation of hydrogen from UV-irradiated methanolic solution of potassium iodide. [KI]=0.1 M.
UV irradiation was carried out through an interference filter (see Ref. 17) at room temperature. $\Phi(H_2)$ is calculated to be 0.35.

hyde, which was determined after removing iodide from the irradiated solution by distillation *in vacuo*. The average quantum yield for formaldehyde is 0.3 at 25°, which is approximately the same as the value for $\Phi(H_2)$ from an iodide solution without a scavenger.

The quantum yields for hydrogen and formaldehyde were found to be independent of the iodide concentration within the range studied; most of the experiments were carried out at 0.1 M KI.

A flash photolysis study revealed the transient formation of I_2^-, which has absorption maxima at about 390 and 750 nm and which decays with a half-life of about 100 μsec at 420 nm; neither spectrum nor decay of the solvated electron could be observed because of the relatively long resolution time of the apparatus used. The absorption spectrum of I_2^- in methanol resembles those observed in aqueous[5] and ethanolic solutions.[7]

Effect of Electron Scavengers. N_2O. Nitrous oxide has been known as an effective solvated-electron scavenger, and its solution in methanol, in the absence of iodide, has been confirmed not to produce nitrogen upon UV irradiation. However, when nitrous oxide was added to the iodide solution in methanol, it produced nitrogen and the hydrogen yield was reduced. The quantum yields of nitrogen as well as hydrogen are plotted in Fig. 2 as a function of the nitrous oxide concentration.

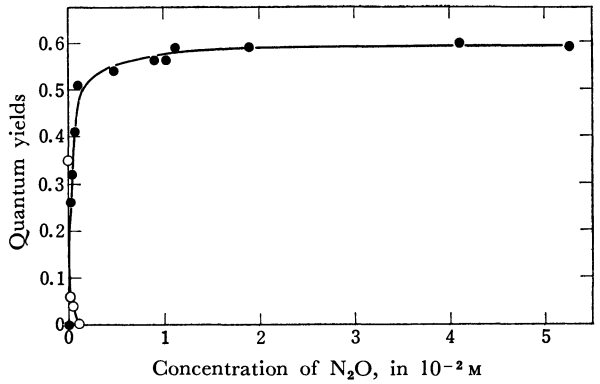

Fig. 2. Dependence of quantum yields for nitrogen and hydrogen on the concentration of nitrous oxide. [KI]=0.1 M.
●, N_2; ○, H_2

The quantum yield of nitrogen reaches a plateau value of 0.59 above 1.2×10^{-2} M N_2O, independent of the iodide concentration within the range investigated. This limiting yield is in good agreement with the value obtained by Jortner *et al.* (0.6).[8] With an increase in the concentration of nitrous oxide, the yield of hydrogen decreases rapidly, no hydrogen being detected at nitrous oxide concentrations as low as 5×10^{-4} M. In the presence of nitrous oxide, a small amount of I_3^- was found to be produced; this was not detected in the absence of nitrous oxide.

CO_2. Carbon dioxide, a solvated-electron scavenger, reduces $\Phi(H_2)$, no hydrogen being detected at concentrations as low as 10^{-3} M.

H^+. Hydrochloric or sulfuric acid was also added as a solvated-electron scavenger. As is shown in Fig. 3, the quantum yield for hydrogen increases with an increase in the concentration of acid, the plateau value being 0.57 for each acid. The plateau value of the quantum yield is in agreement with the plateau value of $\Phi(N_2)$ in nitrous oxide solutions.

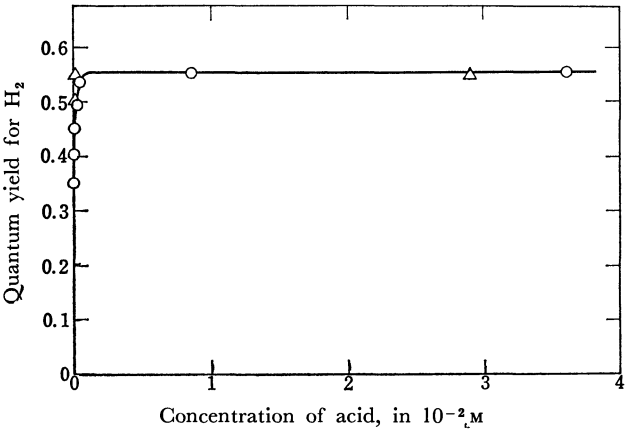

Fig. 3. Dependence of the quantum yield for hydrogen on the concentration of acids. [KI]=0.1 M.
○, H_2SO_4; △, HCl

Iodide Solutions in CH_3OD. Hydrogen was found to be produced by the UV irradiation also from iodide solutions in CH_3OD. The quantum yield for hydrogen, however, is considerably lower than that in CH_3OH, about 1/20 for the 0.1 M KI solution. The isotopic composition of hydrogen produced from 0.1 M KI solutions in CH_3OD was determined to be H_2: HD : D_2=16 : 84 : 0. As the purified CH_3OD contained ~1% CH_3OH, the observed isotopic compositions of hydrogen were subjected to corrections for the low rate of hydrogen production and the isotopic purity of the solvent. The result is that the fractions of HD should be very close to 100% if the 100% CH_3OD is used as a solvent. In the presence of nitrous oxide, however, the plateau value of $\Phi(N_2)$ (0.72) is substantially higher than that in CH_3OH (0.59). Similar

results have also been reported with H_2O and D_2O by Jortner *et al.*[8]

Although the quantum yield for hydrogen is very low in the 0.1 M KI solution in CH_3OD, it showed a steady increase with a decrease in the concentration of iodide, and, simultaneously, the fraction of H_2 in the product hydrogen was found to increase. However, the limiting quantum yield for nitrogen from CH_3OD solutions containing nitrous oxide is independent of the iodide concentration, as in the CH_3OH solutions. This apparently interesting phenomenon is being subjected to further study.

Rate Constant of the $e^-_{solv}+N_2O$ Reaction in Methanol. The rate constant of the reaction between the solvated electron and nitrous oxide in methanol was determined by the pulse-radiolysis technique. The decay of the solvated electron obeys the second-order kinetics, and its rate constant was found to be 1.3×10^{10} $M^{-1}sec^{-1}$, which is in fair agreement with the previous value (1.3×10^{10} $M^{-1}sec^{-1}$) obtained by us from the competition kinetics in the γ-radiolysis of methanol.[10] This value also agrees with that of $(1.4\pm0.4)\times10^{10}$ $M^{-1}sec^{-1}$ obtained by Dainton *et al.* from competition kinetics using nitrous oxide and benzyl chloride in methanol.[9]

Discussion

Photochemical studies of aqueous solutions of potassium iodide have been carried out extensively, and the primary processes seem to be relatively well understood.[2] Some difficulties in the interpretation of differences in the peak wavelengths of negatively-charged transients produced by the flash irradiation of several aqueous inorganic solutions[23] have been eliminated by the results from novel flash-photolysis experiments carried out by Devonshire and Weiss.[5] They succeeded in showing that the transient species produced from UV-irradiated aqueous solutions of several inorganic salts have absorption spectra identical with that of the hydrated electron obtained in the pulse radiolysis of aqueous systems.

Scavengers added to aqueous solutions react with hydrated electrons, not with the excited iodide ions,[24,25] and may compete with the secondary diffusive recombination. Recent results by Czapski, Ogdan, and Ottolenghi,[25] who investigated the photochemistry of aqueous solutions of iodide and bromide in the presence of high concentrations of nitrous oxide, have revealed that the "cage effect" takes place in the iodide system.

Similar results have been obtained for methanolic and ethanolic solutions of iodide,[6-8] no elaborate discussions of the primary processes taking place in UV-irradiated iodide solutions being required at the present stage. The primary processes for iodide ions are assumed here to be:

$$I^-_{solv} + h\nu \rightarrow I^-{}^*_{solv} \quad (3)$$

$$I^-{}^*_{solv} \rightarrow I^-_{solv} + \text{energy} \quad (4)$$

$$I^-{}^*_{solv} \rightarrow (I_{solv} + e^-_{solv}) \begin{cases} \nearrow I_{solv} + e^-_{solv} & (5a) \\ \searrow I^-_{solv} & (5b) \end{cases}$$

The parentheses in the above scheme mean that I_{solv} and e^-_{solv} are formed in a pair; Reaction (5b) represents the secondary recombination process.

In the present study, in the absence of an electron scavenger, the UV irradiation produces hydrogen with $\Phi(H_2)=0.35$ at 25°. Hydrogen may reasonably be assumed to form from the solvated electrons produced by Reaction (5a). The solvated electron has an absorption spectrum extending to short wavelengths.[1] We compared the quantum yield obtained by the use of an interference filter with that obtained by the use of a glass filter that transmits longer wavelengths, and found no significant difference in the $\Phi(H_2)$ between the two cases. This experiment may rule out the possibility of the participation of photo-excited solvated electrons in producing hydrogen, as has been suggested for rigid matrices at 77°K.[26]

The results on the isotopic composition of hydrogen from the UV-irradiated CH_3OD solutions indicate that hydrogen arises *via* Reaction (1), which results in the rupture of the hydroxyl hydrogen of methanol. Since the abstraction of the hydrogen atom by another hydrogen atom or by free radicals in liquid methanol takes place principally at the α-position,[27,28] the nearly 100% HD production after corrections for the isotopic purity of CH_3OD used and for the lower yield of hydrogen in the CH_3OD solution can be explained satisfactorily by assuming Reaction (1). It should be noted here that, in the nitrous oxide solutions in CH_3OD, the plateau value of $\Phi(N_2)$ is as high as 0.72, substantially higher than that in CH_3OH, indicating that most of the solvated electrons produced are recaptured, probably by iodine atoms, before forming hydrogen in CH_3OD.

The fact that, despite the higher $\Phi(N_2)$ in CH_3OD than in CH_3OH, the quantum yield for hydrogen is lower in CH_3OD than in CH_3OH, may be explained in terms of the isotope effect on the O–H (O–D) bond rupture. A similar isotope effect has been observed in the reactions of hydrated electron with H_2O[29] and D_2O:[30] $k(e^-_{aq}+H_2O)=16$ M^{-1} sec^{-1} and $k(e^-_{aq}+D_2O)=1.25$ M^{-1} sec^{-1}.

As a necessary consequence of the formation of solvated electrons, iodine atoms are produced (Reaction 5a), followed by the transient formation of I_2^-. Iodine atoms or I_2^- are expected to oxidize CH_2OH radicals produced by the $H+CH_3OH\rightarrow H_2+CH_2OH$ reaction to give formaldehyde:

23) J. J. Weiss in "The Chemistry of Ionization and Excitation," G. R. A. Johnson and G. Scholes, Ed., Taylor & Francis, Ltd., London (1967), p. 17.
24) F. S. Dainton and S. R. Logan, *Proc. Roy. Soc.* (London), **A 287**, 281 (1965).
25) G. Czapski, J. Ogdan, and M. Ottolenghi, *Chem. Phys. Lett.*, **3**, 383 (1969).
26) T. Shida and W. H. Hamill, *J. Amer. Chem. Soc.*, **88**, 3689 (1966).
27) J. H. Baxendale and G. Hughes, *Z. Physik. Chem.*, **14**, 323 (1958).
28) R. Nagai and M. Imamura, unpublished results.
29) E. J. Hart, S. Gordon, and E. M. Fielden, *J. Phys. Chem.*, **70**, 150 (1966).
30) E. J. Hart and E. M. Fielden, *ibid.*, **72**, 577 (1968).

$$I(\text{or } I_2^-) + CH_2OH \rightarrow CH_2O + I^-(2I^-) + H^+ \quad (6)$$

Some of the iodine atoms capture solvated electrons to form iodide ions. This reaction sequence is supported quantitatively by the experimental fact that the quantum yield for formaldehyde, $\Phi(CH_2O)$, is approximately the same as $\Phi(H_2)$. The second-order decay of the transiently-formed I_2^- and the non-formation of I_3^- as a stable product also support the above argument. Dobson and Grossweiner[7] have assumed similar reactions of I or I_2^- as well as the decay of solvated electrons in ethanolic solutions.

Upon the addition of nitrous oxide, solvated electrons are efficiently scavenged and nitrogen is formed:

$$e^-_{solv} + N_2O \rightarrow N_2 + O^- \quad (7)$$

As may be seen from Fig. 2, at the nitrous oxide concentration of 1×10^{-2} M, $\Phi(N_2)$ reaches a plateau value of 0.59, higher than $\Phi(H_2)$ in the absence of electron scavengers, and $\Phi(H_2)$ diminishes to zero at concentrations as low as 5×10^{-4} M N_2O. These facts indicate that hydrogen is not produced by the reaction between the photo-excited iodide ion and methanol, and that, in the concentration range studied, nitrous oxide competes not only with hydrogen formation and the reaction with iodine, but also with the secondary recombination for solvated electrons. Other modes of nitrogen formation by the $N_2O+O^-\rightarrow N_2+O_2^-$ reaction, sometimes assumed in the radiolysis of organic systems and by the reaction with the photo-excited iodide ion can be ruled out by the results with acid solutions, as will be mentioned below. It was shown previously[10] that reactions of nitrous oxide with H atoms or CH_2OH radicals do not give rise to nitrogen formation.

Carbon dioxide also scavenges the solvated electron efficiently. At the concentration of 10^{-3} M, the formation of neither hydrogen nor formaldehyde could be detected; a lack of information on the reaction of CO_2^- limits any realistic evaluation of the observation that formaldehyde is not formed.

The addition of acid increases $\Phi(H_2)$ to a plateau value that is equal to the plateau value of $\Phi(N_2)$ in the nitrous oxide solution (Fig. 3). This result can be explained in terms of the efficient reactivity of the hydrogen ion towards the solvated electron:

$$e^-_{solv} + CH_3OH_2^+ \rightarrow H + nCH_3OH \quad (8)$$

It also has an important implication for the reaction between nitrous oxide and solvated electrons. If, as has been mentioned above, nitrous oxide reacts also with O^- to form an additional nitrogen, the $\Phi(H_2)$ in the acid solution should be lower than $\Phi(N_2)$ in the nitrous oxide solution. The rate constants of Reactions (7) and (8) are both in the order of 10^{10} M^{-1} sec^{-1}, and no hydrogen-producing pathways other than Reaction (8) can be supposed for acid solutions. Therefore, we can conclude from the present results that nitrous oxide reacts with one solvated electron to produce one molecule of nitrogen in neutral methanolic solutions. The possibility of producing nitrogen by the reaction between the photo-excited ioide ion and nitrous oxide can also be ruled out from this viewpoint.

The same conclusion regarding the reaction between the solvated electron and nitrous oxide has been obtained by Jha and Freeman[13] from the radiolysis results with acid and nitrous oxide solutions in methanol and by Jortner *et al.*[8] from the photochemical study of aqueous iodide solutions as well. This has been assumed in our previous study carried out to determine the solvated-electron yield in methanol by the use of nitrous oxide as a solvated-electron scavenger.[10]

In the presence of nitrous oxide in low concentrations, the hydrogen formation will compete with the reactions of solvated electrons with nitrous oxide, iodine, and an impurity (if any), and hydrogen and nitrogen are produced simultaneously. Under these conditions, therefore, the ratio of $\Phi(N_2)$ to $\Phi(H_2)$ is expressed by:

$$\frac{\Phi(N_2)}{\Phi(H_2)} = \Phi(e^-_{solv}) \times \frac{k_7[N_2O]}{k_1 + k_7[N_2O] + k_x[X]} \Big/ \Phi(e^-_{solv}) \times \frac{k_1}{k_1 + k_7[N_2O] + k_x[X]} = k_7[N_2O]/k_1$$

Here, $\Phi(e^-_{solv})$ is the assumed quantum yield for the free solvated electron competing among the reactions mentioned above; its value is not determined experimentally, however. $k_x[X]$ is the overall expression for the reaction rate of the reactants other than nitrous oxide. As the two quantum yields were determined simultaneously from the same solution, the above conventional expression may be pertinent.

Figure 4 shows the linear relationship between $\Phi(N_2)/\Phi(H_2)$ and $[N_2O]$ in the concentration range of $(1—5)\times10^{-4}$ M. According to the above equation,

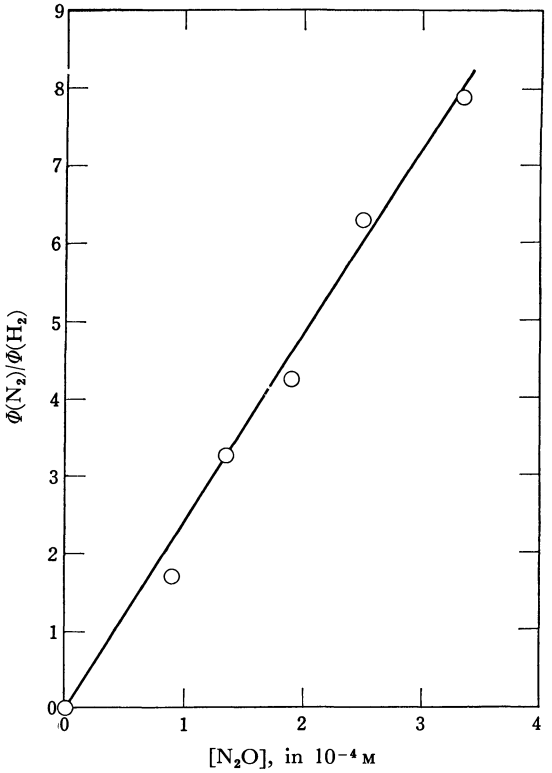

Fig. 4. A plot of $\Phi(N_2)/\Phi(H_2)$ *vs.* $[N_2O]$ for UV-irradiated solutions of low nitrous oxide concentrations. [KI]=0.1 M.

the slope of the straight line gives $k_7/k_1=2.4\times10^4$ M^{-1}. Taking $k_7=1.3\times10^{10}$ M^{-1} sec^{-1}, one can obtain a first-order rate constant of $k_1=5.4\times10^5$ sec^{-1}, which corresponds to a half-life of 1.3 μsec.

The present k_1-value of 5.4×10^5 sec^{-1} seems close to some literature values obtained directly by the pulse-radiolysis technique, 3.7×10^5 sec^{-1} (20°),[12] or indirectly by the competition kinetics, 4.6×10^5 sec^{-1} (25°),[13] with due consideration taken of the experimental errors involved in the preparation of samples of low nitrous oxide concentrations in this study; a much higher half-life of 7.5 μsec, corresponding to the lower rate constant of 0.9×10^5 sec^{-1}, has also been reported from a competition-kinetics study.[15]

Finally, it is interesting to compare the rate constant for Reaction (1) with that for the reaction of the hydrated electron with methanol in aqueous solutions. The rate constant for the latter reaction has recently been obtained by Hickel and Schmidt with photogenerated hydrated electrons in a hydrogen-saturated solution of sodium hydroxide as $k(e_{aq}^- + CH_3OH) \leq 400$ M^{-1} sec^{-1}.[31] Although this reaction is essentially different from Reaction (1) that is the decomposition of the solvated electron, the comparison of these rate constants may have some relevance to the structure and reactivity of solvated electrons; no discussion can be made here, however.

Conclusion. The photochemical formation of solvated electrons from aqueous or alcoholic solutions of potassium iodide is not a novel subject. However, this system has been shown, according to circumstances, to be convenient for studying the reactions of solvated electrons, which all play an important role in the radiation chemistry of polar liquids.

In this study, it was concluded that the solvated electron forms hydrogen in methanol through Reaction (1), in which the hydroxyl hydrogen is dissociated. The rate constant of this reaction was determined explicitly. We have assumed that hydrogen is formed in neutral solutions from solvated electrons, escaping the primary and secondary recombinations (geminate recombination),[32] and that the scavengers used compete with the hydrogen-formation process in the lower concentration range and can compete with the secondary recombination in the higher concentration range. Although it is not essential for the present study whether or not nitrous oxide competes with the secondary recombination at higher concentrations, the linear dependency of $\Phi(N_2)$ on the square root of the nitrous oxide concentration[25,32] observed at these concentrations may support the above assumption.

It has also been shown that the reaction of the solvated electron with nitrous oxide yields one molecule of nitrogen in neutral methanolic solutions.

The authors wish to acknowledge the assistance of Mr. Hiro Ishida in a part of this study of acid solutions. They also wish to express their thanks to Dr. Shigeyoshi Arai and Dr. Akira Kira for their helpful suggestions in carrying out the flash-photolysis and the pulse-radiolysis experiments.

31) B. Hickel and K. H. Schmidt, *ibid.*, **74**, 2470 (1970).

32) R. M. Noyes, *J. Amer. Chem. Soc.*, **77**, 2042 (1955).

The Activity of Dilute Sodium in Liquid Au-Na Alloy

Kazushi HIROTA and Takashi KATSURA

Department of Chemistry, Tokyo Institute of Technology, Ohokayama, Meguro-ku, Tokyo

(Received March 23, 1970)

The electromotive force of the cell;

Au–Na alloy $|Na_2CO_3|$ $CO_2 + O_2$, Pt-Rh,

was determined as a function of the temperature and the concentration of sodium in the alloy. The results were consistent with the activity values determined previously by the equilibrium method. The overpotential due to the current passing through the Au–Na alloy surface is less than 1 mV per mA/cm^2 of the current density at 1400°K. The activity of sodium, referred to the pure liquid standard state, was calculated from the electromotive force of this cell. The activity coefficient of sodium in Au–Na alloy is:

$$\log \gamma_{Na} = -2.55/T \cdot 10^{-3} + 0.39 \pm 0.05$$

in the temperature range from 1250°K to 1500°K and in the concentration range of less than 10 atom%Na.

In connection with construction of a sodium electrode adequate for use at high temperatures, the determination of the activity of sodium in an Au–Na alloy was undertaken. The large difference in ionization energies between Au and Na may result in the large negative value of the partial molar heat of mixing, and in the low value of the activity coefficient of the sodium in the alloy. Liquid metallic gold, therefore, is suitable as a solvent of sodium to reduce the vapor pressure and the reactivity of sodium.

Only a few thermochemical measurements have been performed on the Au–Na alloy. These are the calorimetric determination of the heat of the reaction of Au(s) with Na(l) at 403°K and at the concentration of 96.7 atom% Na by Oriani and Webb,[1] and the equilibrium determination among the Au-Na alloy, the Na_2CO_3 melt, and the CO_2+CO gas mixture at 1400°K.[2]

In the following, the electromotive force of the cell, Au–Na|Na_2CO_3|CO_2+O_2, Pt–Rh, will be determined. From the results of the measurements, the properties of the Au–Na electrode will be ascertained, and the activity coefficient of the sodium in the Au–Na alloy will be calculated by the use of the standard free energy of the formation of Na_2CO_3.

Experimental

The construction of the sodium electrode is given in Fig. 1. The Au–Na alloy was placed at the bottom of the alumina tube. The potential of this alloy was led to the outside of the furnace by an iridium wire, which was protected from gas and from the Na_2CO_3 melt with an alumina tube in order to prevent it from acting as a gas electrode.

The Au–Na alloy was made by means of an electrolysis of the Na_2CO_3 melt, *i.e.*, by the charge of the cell shown schematically in Fig. 1. At room temperature, the Au–Na alloy does not react with water when the concentration of sodium in the alloy is less than 20 atom%. The chemical composition of the alloy was determined by a method reported previously.[2]

The sodium carbonate melt dissolves alumina slightly under every set of experimental conditions. At the working conditions of 1400°K, about 5 mg/1 g Na_2CO_3 of alumina was found to dissolve in the sodium carbonate in the saturated state.

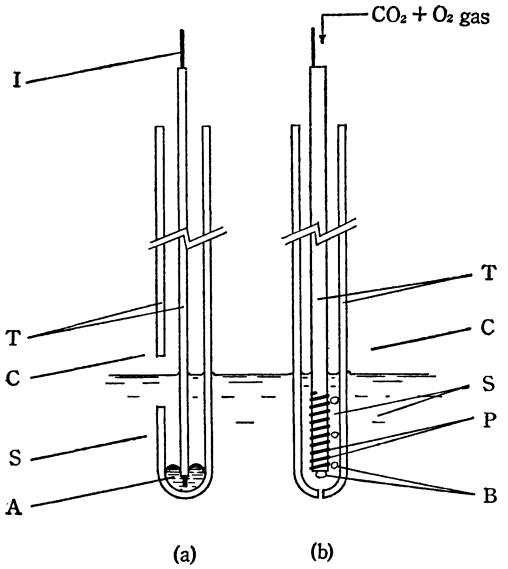

Fig. 1. Construction of the cell, Au-Na alloy|Na_2CO_3|CO_2 +O_2, Pt-Rh.
(a) Au-Na alloy electrode. (b) CO_2+O_2 gas electrode. A, Au-Na alloy; B, bubbles of CO_2+O_2 gas mixture; C, CO_2 gas; I, Iridium wire; P, platinum wire; S, sodium carbonate melt; T, alumina tubes.

Figure 1b shows the construction of the gas electrode used as the reference electrode. The composition of the gas was 80 vol%CO_2 and 20 vol%O_2, within an error of ±0.5 vol%.

These electrodes were immersed in the sodium carbonate in an alumina crucible placed in a vertical tube furnace. CO_2 gas flowed upward through the furnace. The temperature of the system was kept constant within ±5°C. The electromotive force obtained was corrected for the thermoelectromotive force.

Results and Discussion

The cell investigated has the following characteristics:

Au-Na|Na_2CO_3|CO_2(0.8 atm) + O_2(0.2 atm), Pt-Rh.

When every part of this cell is kept at sufficient equilibrium conditions, the electromotive force values are equal to that associated with the free energy change of the following reaction:

1) R. A. Oriani and M. B. Webb, *Acta Met.*, **7**, 63 (1959).
2) K. Hirota and T. Katsura, This Bulletin, **43**, 94 (1970).

Table 1. Comparison of experimental values at 1400°K with the calculated by Eq. (5)

Atom fraction of Na	Measured e.m.f. (in mV)	Calculated by Eq. (5) E_{calc} (in mV)	Difference (in mV)
0.0036_7	771	775	−4
0.0060_5	825	835	−10
0.0062_2	834	838	−4
0.022_3	984	992	−8
0.022_7	985	994	−9
0.031_7	1022	1035	−13
0.049_0	1081	1087	−6
0.052_3	1082	1095	−13
0.055_3	1089	1102	−13

$$CO_2(g) + (1/2)O_2(g) + 2Na(\text{in Au-Na alloy}) = Na_2CO_3(l) \quad (1)$$

The electromotive forces determined in the present experiment are given in Tables 1 and 2.

Comparison with the Equilibrium Experiment. The principal experimental criterion for the reliability of the electrode is that the potential is in agreement with the thermodynamic calculations. In a previous paper,[2] the activity coefficient of sodium in Au–Na alloy has been determined at 1400°K by the use of equilibrium between the Au–Na alloy and the Na_2CO_3 melt in contact with the CO_2+CO gas mixture.

The results for the $CO(g)+Na_2CO_3(l)=2Na(g)+2CO_2(g)$ reaction in the concentration range from 0.02 to 0.2 wt%Na are as follows at 1400°K:

$$\Delta G^\circ/4.606\,\boldsymbol{R}T + \log(P_{Na}/N_{Na}) = 2.44 \pm 0.03 \quad (2)$$

where $\Delta G^\circ = 2\Delta G_f^\circ(CO_2) - \Delta G_f^\circ(Na_2CO_3) - \Delta G_f^\circ(CO)$, where the ΔG_f°s are the standard free energies of the formation of each compound, and where N_{Na} and P_{Na} are the atom fraction of sodium in the alloy and the partial pressure of monatomic sodium in equilibrium with the alloy respectively.

The calculated electromotive force, E_{calc}, associated with the free energy change in Reaction (1) is given by;

$$E_{calc} = [\Delta G_f^\circ(CO_2) - \Delta G_f^\circ(Na_2CO_3)]/2\boldsymbol{F} - (\boldsymbol{R}T/2\boldsymbol{F}) \ln (a_{Na_2CO_3}/P^2_{Na} \cdot P_{CO_2} \cdot P_{O_2}{}^{1/2}) \quad (3)$$

where $\boldsymbol{F}$ is Faraday's constant and $a_{Na_2CO_3}$ is the activity of the liquid Na_2CO_3 referred to the pure liquid Na_2CO_3. From Eqs. (2) and (3), we obtain at 1400°K:

$$E_{calc} = [\Delta G_f^\circ(CO) - \Delta G_f^\circ(CO_2)]/2\boldsymbol{F} - (\boldsymbol{R}T/2\boldsymbol{F}) \ln (a_{Na_2CO_3}/N^2_{Na} \cdot P_{CO_2} \cdot P_{O_2}{}^{1/2}) + (11.24 \pm 0.14)\boldsymbol{R}T/2\boldsymbol{F} \quad (4)$$

When $a_{Na_2CO_3}=1$, $P_{CO_2}=0.8$, and $P_{O_2}=0.2$, i.e., under the working conditions of the cell, Eq. (4) yields:

$$E_{calc} = 277.8 \log N_{Na} + 1{,}451 \pm 9 \text{ (mV)} \quad (5)$$

where the values of the standard free energy of the formation of CO and CO_2 are taken from "JANAF Thermochemical Tables."[3]

3) The standard free energy of the formation values used in the present calculation are taken from "JANAF Thermochemical Tables" PB168 370, U. S. Department of Commerce/National Bureau of Standards (1965).

Table 2. Electromotive force of the cell at 1250°K, 1300°K, 1350°K, 1450°K and 1500°K, as a function of sodium concentration in Au-Na alloy

Temp. °K	Atom fraction of Na in Au-Na alloy	Measured e.m.f. (in mV)	$[\Delta G_f^\circ(CO_2) - \Delta G_f^\circ(Na_2CO_3)]/2.2.303\boldsymbol{R}T + \log(P_{Na}/N_{Na})$
1250	0.097_8	1377	6.79
	0.124	1403	6.79
	0.145	1426	6.81
	0.20_0	1491	6.93
	0.20_6	1497	6.95
	0.22_6	1520	7.00
1300	0.047_4	1209	6.24
	0.053_4	1227	6.25
	0.097_2	1291	6.24
	0.123	1326	6.28
	0.135	1354	6.34
	0.137	1354	6.33
	0.161	1375	6.35
	0.192	1405	6.39
	0.21_1	1427	6.43
	0.24_2	1468	6.54
	0.25_9	1502	6.64
	0.31_3	1541	6.71
	0.33_2	1592	6.88
1350	0.0137	1001	5.82
	0.021_2	1059	5.85
	0.024_4	1068	5.82
	0.038_2	1119	5.82
	0.053_1	1159	5.83
	0.079_2	1205	5.83
	0.105	1244	5.85
	0.138	1287	5.89
	0.186	1339	5.95
	0.21_0	1372	6.02
	0.25_2	1412	6.09
	0.27_0	1432	6.14
	0.33_5	1489	6.26
	0.34_9	1524	6.37
1450	0.0135	854	5.06
	0.022_2	918	5.07
	0.037_5	984	5.07
	0.062_3	1045	5.06
	0.103	1111	5.08
	0.115	1131	5.10
	0.156	1183	5.14
	0.22_4	1252	5.23
	0.27_7	1306	5.32
	0.28_7	1322	5.36
	0.32_7	1358	5.43
1500	0.0139	787	4.73
	0.027_3	880	4.75
	0.046_3	943	4.73
	0.068_4	992	4.72
	0.103	1057	4.76
	0.144	1107	4.79
	0.20_6	1166	4.83
	0.24_2	1210	4.91

The experimental values found by electromotive force measurements of the cell were compared with the corresponding E_{calc} values calculated by Eq. (5), substituting the sodium concentration found in the alloy by chemical analysis. The values of the standard free energy of the formation of CO and CO_2 are known to be highly reliable. The accuracy of Eq. (5), therefore, depends only on that of the equilibrium experiment.

The values given in Table 1 exhibit an approximate agreement between the results of the equilibrium experiment and the present electromotive force measurement. The difference between these values, the calculated and the measured, is about 10 mV; this indicates the approximate magnitude of the error in the present method of electromotive force measurement.

The Overpotential at the Au–Na Alloy Electrode. The electrode potential as a function of current density was determined by this cell;

$$\begin{array}{lll} CO_2 + O_2 \mid & & \text{, Ir wire} \quad (1) \\ & Na_2CO_3 \mid \text{Au-Na alloy} & \\ CO_2 + O_2 \mid & & \text{, Ir wire} \quad (2) \end{array}$$

Two gas electrodes and one Au–Na alloy electrode were immersed in the same sodium carbonate melt, and two iridium wire were connected at the alloy electrode. The potential difference between one of the gas electrodes and an iridium wire was measured at 1400°K as a function of the current passed through the other gas-electrode iridium-wire pair. The results are shown in Fig. 2.

The overpotential determined by this method was 0.9 mV per mA/cm² of the current density at 0.5 atom% Na; this overpotential value decreased with an increase in the concentration of sodium in the alloy.

Estimation of Probable Error. The Au–Na alloy in the sodium electrode at working conditions slowly loses sodium even if the external current is zero. When the concentration of sodium in the alloy was low, the rate at zero external current was 1.0—0.5 mA/cm² in terms of the current density at the steady state of the system; it was almost independent of the sodium concentration.

However, when the partial pressure of sodium is about 10 mmHg or more, the escaping rate of sodium at zero external current increases rapidly with the concentration of sodium in the alloy. The rate, estimated by the time dependency of the electromotive force, was 20—10 mA in terms of the equivalent charging current at the concentration of about 30 atom%Na and at 1400°K. This rate depends also on the dimensions of the electrode tube and is a function of the convectional flow of the sodium carbonate melt.

The partial reduction of alumina in contact with Au–Na alloy results also in the loss of sodium. At a relatively high concentration of sodium, the alumina in contact with the alloy turned grey. Sodium is lost at a high rate at first, and then it slowly becomes a low rate as time elapses.

This loss of sodium results in the gradient of the sodium concentration at the surface of the Au–Na alloy, and leads to a depression of the electromotive force of the cell. The estimation of the magnitude of this depression in electromotive force can be obtained roughly by the use of Fig. 2.

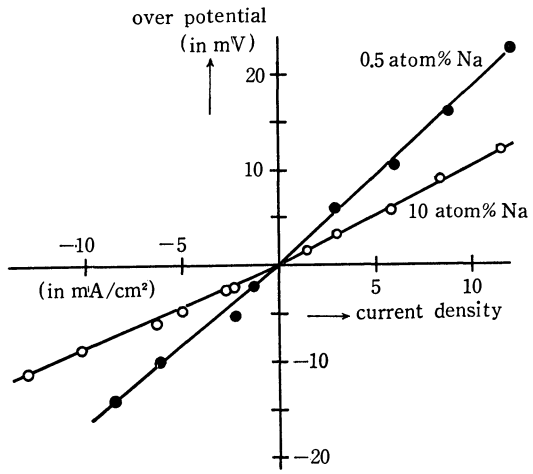

Fig. 2. Overpotential of Au-Na alloy electrode at 1400°K as a function of current density.

In the measurement of the electromotive force, the rate of the decrease in the sodium concentration was kept within 20 mA/cm². Therefore, the depression in the electromotive force values does not exceed about 20 mV in the present measurement. No correction was made for this depression in electromotive force values, since the phenomena have a complex nature.

The gas electrode used was highly reliable in spite of the fact that it has much kinetic resistance. The accuracy of this electrode in this temperature range seems to be better than that in the range from 800 to 600°C in which Borucka and Sugiyama made their measurements.[4]

It is known that Na_2CO_3 decomposes partly into Na_2O and CO_2 gas at a high temperature.[5] On the surface of the Au–Na alloy, a large part of the CO_2 molecules may be reduced to CO molecules by sodium, and the fugacity of CO_2 in the sodium carbonate melt may be low in comparison with that in the gas phase.

At the equilibrium of these reactions, it is obvious that:

$$-\boldsymbol{R}T \ln (a_{Na_2CO_3} \cdot P^2_{Na}/a^2_{Na_2O} \cdot P_{CO}) = \Delta G_f^\circ(Na_2CO_3) - 2\Delta G_f^\circ(Na_2O) - \Delta G_f^\circ(CO) \quad (6)$$

When the concentration of sodium in the alloy is high, it is also obvious that $a_{Na_2CO_3} < 1$ and that $P_{CO} \fallingdotseq 1$. Therefore, we obtain, for the temperature range between 1300°K and 1500°K:

$$\log a_{Na_2O} < \log P_{Na} - 1.9 \quad (7)$$

Therefore, the decomposition of the Na_2CO_3 melt may be disregarded under the present experimental conditions.

Activity Coefficient of Sodium at an Infinite Dilution. Equation (3) may be rearranged in the following form:

$$[\Delta G_f^\circ(CO_2) - \Delta G_f^\circ(Na_2CO_3)]/2.303\boldsymbol{R}T + \log(P_{Na}/N_{Na}) = \boldsymbol{F}E/2.303\boldsymbol{R}T - \log(N_{Na} \cdot P_{CO_2}^{1/2} \cdot P_{O_2}^{1/4}) \quad (8)$$

4) A. Borucka and C. M. Sugiyama, *Electrochim. Acta*, **14**, 871 (1969).

5) M. Schenke, G. H. J. Broers, and J. A. A. Ketelaar, *J. Electrochem. Soc.*, **113**, 404 (1966).

The right-hand side of Eq. (8) consists of directly measurable quantities in the present measurements. By the use of the right-hand side of Eq. (8), the left-hand side was calculated; the values thus obtained are given in Table 2.

When the concentration of sodium is lower than 10 atom%Na, the right-hand side of Eq. (8) does not depend on the sodium concentration within the range of experimental uncertainty. For this concentration range, the experimental values can be written in the form:

$$[\Delta G_f^\circ(CO_2) - \Delta G_f^\circ(Na_2CO_3)]/2\cdot2.303\boldsymbol{R}T + \log(P_{Na}/N_{Na}) = 15.0/T\cdot10^{-3} - 5.3 \pm 0.05 \quad (9)$$

By the use of the values of the standard free energy of formation[3] it is found that:

$$\log(P_{Na}/N_{Na}) = 7.5/T\cdot10^{-3} - 4.61 \pm 0.05 \quad (10)$$

When we choose pure liquid as the standard state for the activity of sodium, a_{Na}, the activity coefficient, $\gamma_{Na}=a_{Na}/N_{Na}$, can be obtained from Eq. (9), and the standard free energy of the condensation of monatomic sodium gas into the pure liquid sodium[3]:

$$\log \gamma_{Na} = -2.55/T\cdot10^{-3} + 0.39 \pm 0.05 \quad (11)$$

The relative partial molar excess free energy of sodium in the Au–Na alloy, referred to the pure liquid state defined by $\Delta\bar{G}^E_{Na}=\Delta\bar{G}_{Na}-\boldsymbol{R}T\ln N_{Na}=\boldsymbol{R}T\ln\gamma_{Na}$, is:

$$\Delta\bar{G}^E_{Na} = -11.7 + 1.78\cdot10^{-3}\cdot T \pm 0.15 \text{ (kcal/mole)} \quad (12)$$

From this value, the relative partial molar excess entropy and the relative partial molar heat of the mixing of sodium is obtained by the relation $\Delta\bar{G}^E_{Na}=\Delta\bar{H}^M_{Na}-T\cdot\Delta\bar{S}^E_{Na}$:

$$\Delta\bar{S}^E_{Na} = -1.8 \pm 1.0 \text{ (cal/mol·deg)},$$
$$\Delta\bar{H}^M_{Na} = -11.7 \pm 0.15 \text{ (kcal/mol)} \quad (13)$$

The values given in Eqs. (9), (10), (11), and (13) are valid in the concentration range lower than 10 atom%Na and in the temperature range between 1300° and 1500°K.

The Activity of Sodium as a Function of the Concentration up to 30 atom%Na. At concentrations of sodium higher than 10 atom%Na, the right-hand side of Eq. (8) does not remain constant, but increases with the sodium concentration. When we plot the right-hand side of Eq. (8) against $(1-N_{Na})^2$, a rather pronounced curvature is obtained. However, when we plot these values against N^2_{Na}, the values seems to fall on straight lines. The Au–Na alloy, therefore, is not a regular solution. The results are given in Fig. 3.

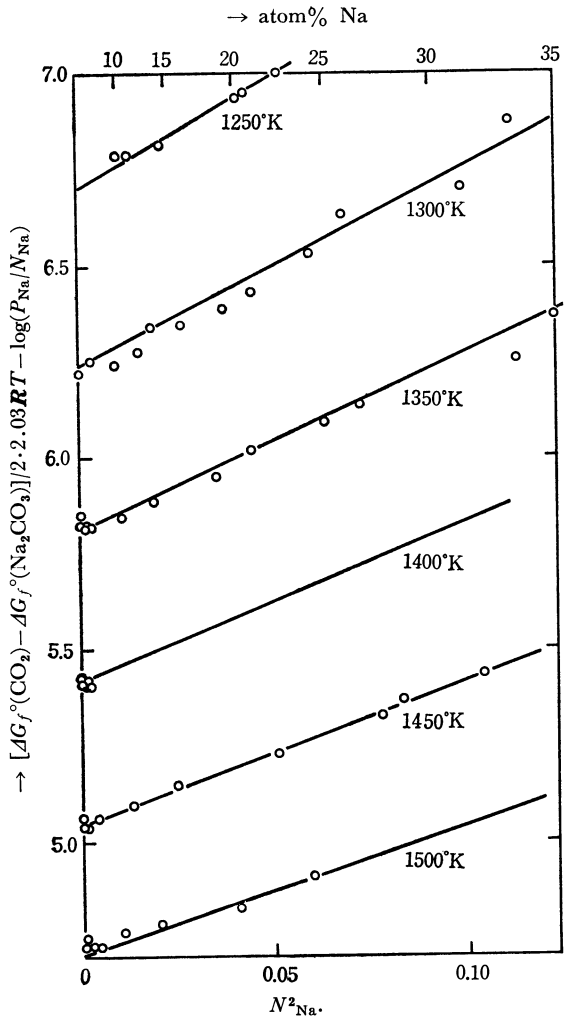

Fig. 3. A linear relation between the right hand side of Eq. (8) and N^2_{Na}. Eq. (14) is given as solid lines.

If we dare to give an algebraic expression for these results, we obtain the following equation, Eq. (14), for the range of sodium concentration lower than 30 atom%Na:

$$[\Delta G_f^\circ(CO_2) - \Delta G_f^\circ(Na_2CO_3)]/2\cdot2.303\boldsymbol{R}T + \log(P_{Na}/N_{Na}) = 15.0/T\cdot10^{-3} - 5.3 + 23\cdot N^2_{Na}/(T\cdot10^{-3})^3 \pm 0.1 \quad (14)$$

This equation is shown as solid lines in Fig. (3).

Preparation of Chromium(III) and Cobalt(III) Complexes with *d,l*-α-Phenylalanine-*N,N*-diacetic Acid[1]

Akira UEHARA, Eishin KYUNO, and Ryokichi TSUCHIYA
Department of Chemistry, Faculty of Science, Kanazawa University, Kanazawa

(Received April 28, 1970)

The following chromium(III) and cobalt(III) complexes with PADA (*d,l*-α-phenylalanine-*N,N*-diacetic acid) were prepared: $K[Cr(OH)pada(H_2O)]\cdot 5H_2O$ (violet) (I), $K[Cr(OH)pada(H_2O)_2]\cdot 3H_2O$ (green)(II), $(enH_2)_{1/2}[Cr(OH)pada(H_2O)_2]$ (green) (III), [Cr pada(*o*-phen)]·H_2O (brown) (IV), $K_2[Cr(ox)pada]\cdot 2H_2O$ (violet) (V), $K[Co(OH)pada(H_2O)]\cdot 5H_2O$ (blue-violet) (VI), and $K_2[Co_2(OH)_2(pada)_2]$ (brown-pink) (VII). On the basis of electronic spectra in both aqueous solution and solid state, it was found that PADA behaves toward central metal as a quadridentate ligand in complexes I, IV, V, VI, and VII; in other words, unlike the case of nitrilotriacetic acid (NTA), nitriloisopropionicdiacetic acid (NIPDA) and *l*-leucine-*N,N*-diacetic acid (LDA), PADA did not give different coordinating structures to the respective complexes in solid state and aqueous solution. From thermal analysis with derivatograph in the reaction processes of complex VI, it was found that the complex liberates one mole of coordinating water at about 170—180°C, resulting in the formation of the diol complex VII.

The authors have studied the preparation and properties of the chromium(III) and cobalt(III) complexes with NTA,[2,3] NIPDA,[4] LDA,[5] NPDA,[6] and AEDA.[7] Continuing these studies, we tried to prepare the corresponding complexes with PADA. The rational formulas of the chelating agents concerned are given in Table 1. In spite of a similar frame in these agents, the coordinating behaviors somewhat differ from each other due to differences in the fine structures and in the chemical properties such as acid dissociation constants. For instance, the ligands forming three five-membered chelate rings such as NTA, NIPDA, and LDA act toward metals as either $N\text{–}O_3$, $N\text{–}O_2$, or O_3 type, whereas the ligands forming two five- and one six-membered chelate rings such as NPDA and AEDA do not act as O_3 type.

If one of hydrogen atoms in a methylene group in NTA is substituted by a more bulky radical such as benzyl group, it is expected that the coordinating behaviors considerably differ from NTA, NIPDA, and LDA probably due to the stronger steric effect of the ligand substituted as above. The main purpose of the present work is to prepare PADA and the complexes therewith in order to confirm the above expectation.

When the ligands NTA and its analogues act as a quadridentate toward metal, the remaining *cis* sites are occupied by H_2O and OH^- in an aqueous medium. Therefore, an olation process expressed by the following scheme is expected in appropriate thermal conditions:

$$2[M(OH)L(H_2O)]^- \xrightarrow[-2H_2O]{} [L\ M(OH)_2M\ L]^{2-},$$

where M and L denote central metals such as chromium(III) or cobalt(III) and the quadridentate ligands, analogues of NTA, respectively. Another purpose of this study is to find a consistency between the diol complex thermally obtained as above and that directly prepared.

Table 1. Rational formula and abbreviation of chelating agents

Rational formula	Chelate ring	R	Chelating agent
N(CHRCOOH)(CH$_2$COOH)(CH$_2$COOH)	5, 5, 5	H	NTA[a]
		CH_3	NIPDA[a]
		$CH_2\cdot CH(CH_3)_2$	LDA[a]
		$CH_2\cdot C_6H_5$	PADA[a]
N(CH$_2$CH$_2$·R)(CH$_2$COOH)(CH$_2$COOH)	5, 5, 6	COOH	NPDA[a]
		SO_3H	AEDA[a]

a) NTA, Nitrilotriacetic Acid;[2] NIPDA, Nitriloisopropionicdiacetic Acid;[4] LDA, *l*-Leucine-*N,N*-diacetic Acid;[5] PADA, *d,l*-α-Phenylalanine-*N,N*-diacetic Acid; NPDA, Nitrilopropionicdiacetic Acid;[6] AEDA, β-Aminoethylsulfonic-*N,N*-diacetic Acid.[7]

Experimental

Preparation of d,l-α-*Phenylalanine*-N,N-*diacetic Acid.* Sixteen grams of *d,l*-α-phenylalanine was dissolved in 100 m*l* of water containing 7 g of potassium hydroxide, and 100 m*l* of aqueous solution containing 19 g of monochloroacetic acid was dropwise neutralized with 20 g of potassium hydrogen carbonate. The latter solution should be added gently and carefully, or else the deposition of *d,l*-α-phenylalanine takes place. The mixed solution was heated on a water bath, 30 m*l* of water containing 12 g of potassium hydroxide being added. Heating was continued for one hour in order to complete the condensation reaction. After the resulting solution was cooled to room temperature, the pH of the solution was adjusted to 2—3 by adding concentrated hydrochloric acid. White powdered crystals were easily obtained. Recrystallization of the crude product was carried out by dissolving it in potassium hydrogen carbonate solution and by adjusting the pH of the solution to 2—3. Yield 10 g.

Found: N, 4.99; C, 55.55; H, 5.85%. Calcd for N-$(CH(CH_2C_6H_5)COOH)(CH_2COOH)_2$: N, 4.80; C, 55.13; H, 5.89%.

Preparation of Complexes. Preparative procedures of the complexes are schematically shown in Table 2.

1) Presented in part at the 22nd Annual Meeting of the Chemical Society of Japan, Tokyo, March, 1969.
2) A. Uehara, E. Kyuno, and R. Tsuchiya, This Bulletin, **40**, 2317 (1967).
3) *Idem., ibid.*, **40**, 2322 (1967).
4) *Idem., ibid.*, **41**, 2393 (1968).
5) *Idem., ibid.*, **43**, 414 (1970).
6) *Idem., ibid.*, **41**, 2385 (1968).
7) *Idem., ibid.*, **42**, 2835 (1969).

Table 2. Preparative scheme for chromium(III) and cobalt(III) PADA complexes

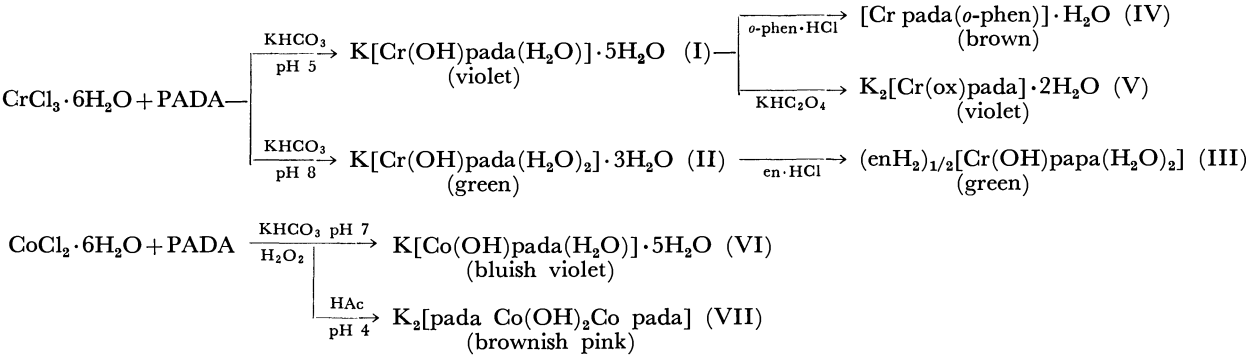

Potassium Hydroxo-d,l-*α-phenylalanine*-N,N-*diacetatoaquochromate(III) Pentahydrate, K[Cr(OH)pada(H$_2$O)]·5H$_2$O (I)*: Two hundred milliliters of water containing 14 g of PADA was neutralized with 6 g of potassium hydroxide. The solution was added to 100 m*l* of water containing 13 g of chromium(III) chloride hexahydrate, and the mixture was heated on a water bath until the color of the solution turned violet. After the pH of the solution was carefully adjusted to 5, the solution was concentrated to about 200 m*l* and left to stand in a refrigerator. Violet crystals were obtained which were recrystallized from water. Yield 4 g.

Found: N, 2.84; C, 31.60; H, 5.06%. Calcd for K-[Cr(OH)pada(H$_2$O)]·5H$_2$O: N, 2.96; C, 31.91; H, 4.83%.

Potassium Hydroxo-d,l-*α-Phenylalanine*-N,N-*diacetatodiaquochromate(III) Trihydrate, K[Cr(OH)pada(H$_2$O)$_2$]·3H$_2$O (green) (II)*: The preparative procedure was the same as for complex I until the violet solution was obtained. When the pH of the solution was carefully adjusted to 8, the color turned green. The resulting solution was left to stand in a refrigerator. Green crystals were obtained which were recrystallized from water. Yield 1.5 g.

Found: N, 2.94; C, 32.78; H, 4.83%. Calcd for K-[Cr(OH)pada(H$_2$O)$_2$]·3H$_2$O: N, 3.10; C, 32.90; H, 5.13%,

Ethylenediammonium Hydroxo-d,l-*α-phenylalanine*-N,N-*diacetatodiaquochromate(III), (enH$_2$)$_{1/2}$[Cr(OH)pada(H$_2$O)$_2$] (green) (III)*: Four and a half grams of complex II was dissolved in 100 m*l* of water containing 4 g of ethylenediamine hydrochloride. A gradual concentration on a water bath soon produced green crystals which were recrystallized from water. Yield 2.5 g.

Found: N, 3.39; C, 40.61; H, 5.31%. Calcd for (en-H$_2$)$_{1/2}$[Cr(OH)pada(H$_2$O)$_2$]: N, 3.12; C, 40.67; H, 5.72%.

d,l-*α-Phenylalanine*-N,N-*diacetato*-o-*phenanthrolinechromium(III) Monohydrate, [Cr pada(o-phen)]·H$_2$O (brown) (IV)*: Five grams of complex I was dissolved in a 200 m*l* of water, and then 2 g of *o*-phenanthroline was added to the solution. The pH of the solution was adjusted to *ca.* 5, and the solution was warmed on a water bath until the color turned brown. From the cooled solution brown crystals were obtained which were recrystallized from water. Yield 2 g.

Found: N, 7.96; C, 55.83; H, 4.10%. Calcd for [Cr pada(*o*-phen)]·H$_2$O: N, 7.61; C, 56.16; H, 3.92%.

Potassium Oxalato-d,l-*α-phenylalanine*-N,N-*diacetatochromium-(III) Dihydrate, K$_2$[Cr(ox)pada]·2H$_2$O (violet) (V)*: Five grams of complex I was dissolved in 100 m*l* of water containing 0.5 g of potassium hydroxide and 1.5 g of oxalic acid. When the solution was heated on a water bath, the color gradually turned from violet to bright violet. The solution was left to stand in a refrigerator for several days. Violet crystals were obtained which were recrystallized from water. Yield 1 g.

Found: N, 2.64; C, 33.83; H, 3.01%. Calcd for K$_2$-[Cr(ox)pada]·2H$_2$O: N, 2.83; C, 33.41; H, 2.82%.

Potassium Hydroxo-d,l-*α-phenylalanine*-N,N-*diacetatoaquocobaltate(III) Pentahydrate, K[Co(OH)pada(H$_2$O)]·5H$_2$O (blue-violet) (VI)*. Seven grams of PADA was dissolved in 200 m*l* of water containing 6 g of potassium hydroxide. Six grams of cobalt(II) chloride hexahydrate was dissolved in 50 m*l* of water. The latter was added little by little under magnetic stirring. The two solutions must not be mixed in the reverse order, otherwise the deposit of PADA is formed. The pH of the mixed solution was carefully adjusted to 6—7, and a few milliliters of hydrogen peroxide solution was added in order to oxidize cobalt(II) ion. As soon as the solution turned violet, it was stored in a refrigerator. Bluish-violet crystals were obtained. Since the solution sometimes turned from violet to brownish pink when the pH was not adequately adjusted, it had to be kept violet in order to obtain the desired complex. Recrystallization was carried out from water. Yield 1.5 g.

Found: N, 2.82; C, 30.11; H, 5.10%. Calcd for K-[Co(OH)pada(H$_2$O)]·5H$_2$O: N, 2.79; C, 31.17; H, 5.03%.

*Potassium μ-Dihydroxobis(*d,l-*α-phenylalanine)*-N,N-*diacetatodicobaltate(III), K$_2$[pada Co(OH)$_2$Co pada] (brown-pink) (VII)*: The compound was prepared from the filtrate after the crystals of complex VI were removed as precipitate. After the pH of the filtrate was adjusted to 3—4, the resulting solution was gently heated on a water bath until the color of the solution turned brownish pink. On cooling, brownish pink crystals were obtained. Purification of the crystals was carried out from water. Yield 1 g.

Found: N, 3.60; C, 39.84; H, 3.33%. Calcd for K$_2$-[pada Co(OH)$_2$Co pada]: N, 3.56; C, 39.73; H, 3.33%.

Instruments. The instruments used in the present work are the same as described previously.[6]

Results and Discussion

IR Spectra. IR spectra for the complexes were measured in a Nujol-mull state. It is known that characteristic bands for free and coordinated carboxylic acid generally appear at ~1750 and ~1640 cm^{-1}, respectively, in aminopolycarboxylic acid complexes.[8] Since the complexes prepared in the present work showed a band near ~1640 cm^{-1}, it is obvious that the carboxylate groups in the complexes are all coordinated.

Molar Conductivity and Magnetic Moment. Molar

8) D. H. Bush and J. C. Bailar, Jr., *J. Amer. Chem. Soc.*, **75**, 4574 (1953).

conductivities were measured in an aqueous solution at 25°C in order to find the type of electrolytes for the complexes. Magnetic moments were evaluated from the magnetic susceptibilities measured by the Gouy method. The results are given in Table 3.

Table 3. Molar conductivity (λ), magnetic moment (μ_{eff}) and coagulation value (mF)

Complex	λ[a] mho cm^{-1}	mF[b]	μ_{eff} B.M. (°K)
I	125.6		3.83 (296)
II	121.3		3.86 (295)
III	148.9		3.78 (296)
IV	5.2		3.91 (296)
V	254.3		3.85 (296)
VI	121.2	5.7	dia. (295)
VII	154.8	0.5	dia. (295)

a) 10^{-3} mol/l aqueous solution was used at 25°C.
b) $Fe(OH)_3$ sol was used.

The values of the molar conductivities for the complexes I, II, III, and VI fairly support the view that they are 1 : 1 type electrolyte. The values for the complexes IV and V indicate that the former is a non-electrolyte and the latter, 1 : 2 type electrolyte, respectively. On the other hand, the value for complex VII may be somewhat smaller than that expected for 1 : 2 type electrolyte as $K_2[Co_2(OH)_2pada_2]$. However, the fact that the coagulation value for VII measured by using ferric oxide hydrosol was 0.5 milliformol will support 1 : 2 type for VII.

The values of the magnetic moments for complexes I—V were in the region of 3.8—3.9 B.M., while the magnetic susceptibilities for complexes VI and VII showed that they are diamagnetic. This indicates that the central metals chromium and cobalt in complexes are both tervalent.

Electronic Spectra. It has often been pointed out that the ligands NTA,[2] NIPDA,[4] and LDA,[5] forming three five-membered chelate rings can act as a terdentate ligand of O_3 and $N\text{–}O_2$ as well as a quadridentate ligand of $N\text{–}O_3$ type. Though PADA also has three five-membered chelate rings as in the above three ligands, how does it behave toward metals?

Figure 1 shows the spectra for complex I in aqueous solution and solid state together with those for the corresponding NTA complex $K[Cr(OH)nta(H_2O)]\cdot 2H_2O$. The former two spectra closely resemble that for NTA-complex in solid state but not in aqueous solution, indicating that the coordinating structure of complex I is the same as that for NTA-complex in solid state. It has been assigned that NTA, NIPDA, and LDA act as a quadridentate ($N\text{–}O_3$) in a solid and as a terdentate (O_3) in a solution. In the case of PADA, no such phenomenon could be detected.

Figure 2 contains the spectra for complexes II and III in aqueous solution, together with that for the corresponding NTA complex, $K[Cr(OH)nta(H_2O)_2]\cdot 3H_2O$. Since their spectra are substantially similar, it will be accepted that PADA acts as a terdentate ligand in complexes II and III. Though PADA can

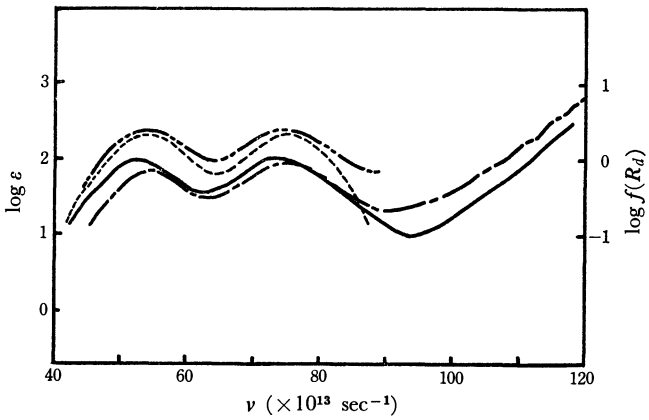

Fig. 1. Electronic spectra for complex I in an aqueous solution (———), in a solid state (– – –) and $K[Cr(OH)nta(H_2O)]\cdot 2H_2O$ in an aqueous solution (——), in a solid state (----).

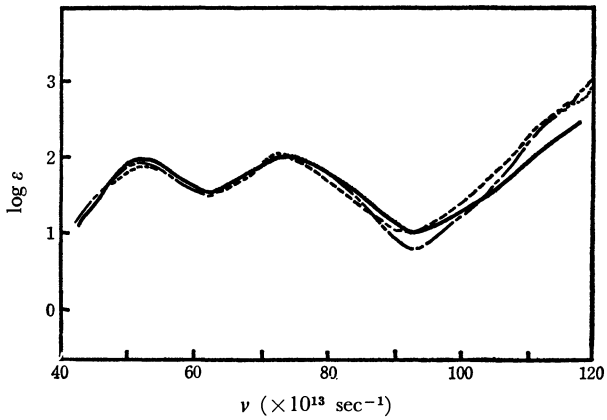

Fig. 2. Electronic spectra for complexes II (----), III (– – –) and $K[Cr(OH)nta(H_2O)_2]\cdot 3H_2O$ (——).

act toward metals as both a quadridentate and terdentate, as seen in complexes I, II, and III, the coordinating manner does not change as extensively as that in NTA, NIPDA, or LDA. This may be due to the stronger steric hindrance by a large radical (benzyl radical) in PADA.

The absorption spectra for complexes VI and VII in aqueous solution are given in Fig. 3. Inamura

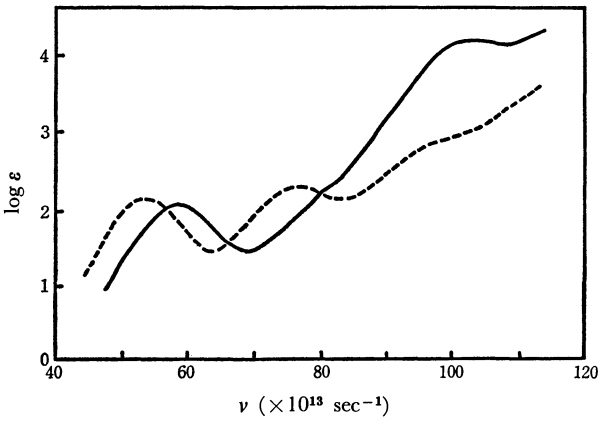

Fig. 3. Electronic spectra for complexes VI (----) and VII (——).

and Kondo[9] have reported that the spectra for the ol-ammine cobalt(III) complexes containing bridged OH groups show no distinct second d-d band, but a band due to bridged OH groups at $90—100\times10^{13}$ (c/s). As an example, it can be shown that K_2[nta-$Co(OH)_2Co$ nta] gives a band at near 100×10^{13} (c/s).[10] As seen from the figure, complex VII does now show such a distinct second band as in the case of complex VI, but a band at 100×10^{13} (c/s) appears predominantly. From these results, complex VII is considered to be a diol complex.

The derivatogram for complex VI is given in Fig. 4.[11] Two steps corresponding to the loss of 4 moles and one mole of water are observed in the temperature ranges of 40—90 and 90—110°C, respectively. The

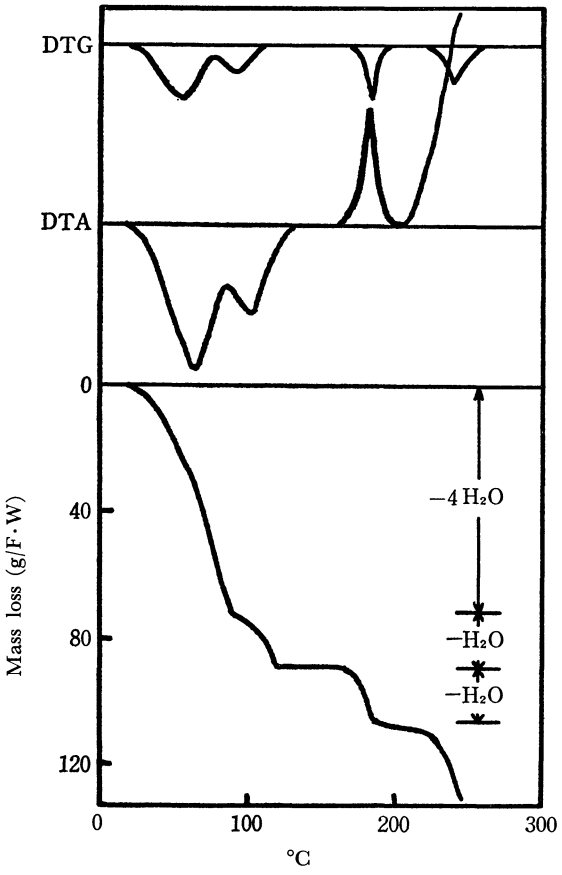

Fig. 4. Derivatogram for complexes VI.

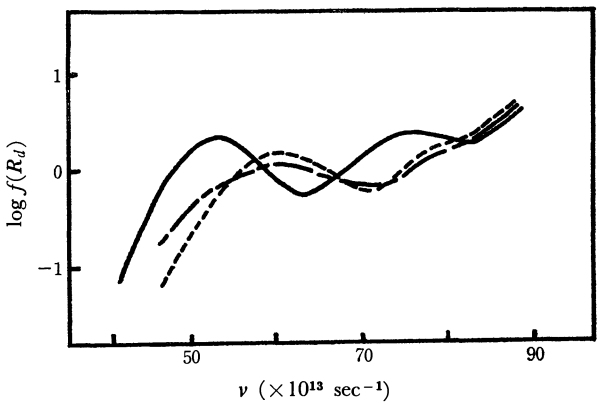

Fig. 5. Electronic spectra for complex VI (——), complex VII (----) and the sample of complex VI picked up at 180°C during heating (—-—).

Table 4. Absorption maxima

Complex	ν_1 (log ε_1)	ν_2 (log ε_2)	Complement
I	53.38 (1.86)	73.53 (1.98)	
II	52.17 (1.81)	73.35 (1.89)	
III	51.46 (1.93)	72.64 (1.95)	
IV	56.07 (1.98)	75.64 (2.19)	86.21 (2.97)[a] 109.1 (4.21)[a]
V	54.05 (1.89)	74.26 (1.92)	
IV	53.48 (2.19)	76.53 (2.35)	
VII	59.41 (2.09)	b)	~105 (~4.10)[c]

a) The specific bands due to the coordinating *o*-phenanthlorine.
b) The band can not be clearly detected because of the strong overlap owing to the specific band of the bridging OH groups.
c) The specific band due to the bridging OH groups. The band is not clearly detected because of its broadening.

DTA curve in the above two steps shows the endothermic reaction. Although the mass loss corresponding to one mole of water is also detected at 170—180°C, the reaction is shown to be exothermic in spite of liberation of water. At this step, the color of the sample turned from bluish violet to brownish pink. The spectrum for complex VI picked up at 180°C in the intermediate course of the derivatograph is given in Fig. 5, together with those for complexes VI and VII. The spectrum observed for the sample obtained in the thermal process is found to be similar to that of complex VII. It is also deduced from the results that the diol complex was formed by heating complex VI.

The authors wish to thank the Ministry of Education for the financial support granted for this research.

9) Y. Inamura and Y. Kondo, *Nippon Kagaku Zasshi*, **74**, 627 (1953).
10) M. Mori, M. Shibata, E. Kyuno, and Y. Okubo, This Bulletin, **31**, 940 (1958).
11) R. Tsuchiya, A. Uehara, and E. Kyuno, This Bulletin, **44**, 701 (1971).

Preparation of Hydroxoaquo- and Diol-Type Cobalt(III) Complexes with Analogues of Nitrilotriacetic Acid[1)]

Akira UEHARA, Eishin KYUNO, and Ryokichi TSUCHIYA

Department of Chemistry, Faculty of Science, Kanazawa University, Kanazawa

(Received April 30, 1970)

The following hydroxoaquo- and diol-type cobalt(III) complexes were prepared: K[Co(OH)(α-abda)-$(H_2O)]\cdot 2H_2O$ (I), K[Co(OH)(vda)$(H_2O)]\cdot 1.5\,H_2O$ (II), K[Co(OH)pgda(H_2O)] (III), K_2[nipda $Co(OH)_2$-Co nipda]$\cdot 2H_2O$ (IV), K_2[(α-abda) $Co(OH)_2$Co (α-abda)]$\cdot 3H_2O$ (V), K_2[vda $Co(OH)_2$Co vda]$\cdot 3H_2O$ (VI), K_2[*l*da $Co(OH)_2$Co *l*da]$\cdot 2H_2O$ (VII) and K_2[pgda $Co(OH)_2$Co pgda]$\cdot 2H_2O$ (VIII), where α-abda, vda, pgda, nipda and *l*da are the abbreviations of *d,l*-α-amino-*n*-butyric-*N,N*-diacetate, *l*-valine-*N,N*-diacetate, *d*-α-phenylglycine-*N,N*-diacetate, nitriloisopropionicdiacetate and *l*-leucine-*N,N*-diacetate ions, respectively. From the measurements of electronic spectra, conductivities and coagulation values and the results of derivatography, it was found that the diol complexes IV—VIII were also formed from the correspoindng hydroxoaquo complexes in the thermal reaction process.

Studies on the preparation and the properties of chromium(III) and cobalt(III) complexes with some analogues of nitrilotriacetic acid (NTA) have been reported.[2-4)] When these chelating agents coordinate to metals in the hydroxoaquo-type complexes, $[M(OH)L(H_2O)]^-$, where M is cobalt (III) or chromium(III) and L is a quadridentate analogue of NTA, the ligands, OH^- and H_2O, should inevitably be situated in *cis*-positions. It is well known that a hydroxoaquo complex may liberate the coordinating water, resulting in the formation of the corresponding diol complexes under certain conditions. Such examples were found in the complexes $[Co(OH)(NH_3)_4(H_2O)]X_2$[5,6)] and $[Cr(OH)en_2(H_2O)]Cl_2$[7)] for the first time. Studies[2,3)] concerning diol-formation from K[Co(OH)nipda$(H_2O)]\cdot 2H_2O$ and K[Co(OH)*l*da$(H_2O)]\cdot H_2O$ were recently carried out in our laboratory.

In order to extend the study on diol-formation, the present work was undertaken (1) to prepare several hydroxoaquo complexes as the starting material and their corresponding diol complexes, and (2) to find the consistency between the diol complexes thermally obtained and those directly prepared.

For the sake of convenience, the general, rational formula and the abbreviations of chelating agents used in the present work are given in Table 1.

Experimental

Preparation of Hydroxoaquo Complexes. The general paths for the preparation of the hydroxoaquo and the diol complexes are given in Table 2, where L denotes one of the analogues of nitrilotriacetate ion.

*1) Potassium Hydroxo-*d,l*-α-amino-*n*-butyric-*N,N*-diacetato-aquocobaltate(III) Dihydrate, K[Co(OH)(α-abda)$(H_2O)]\cdot 2H_2O$ (I)*: Ten grams of *d,l*-α-amino-*n*-butyric acid was dissolved in 30 m*l* of water containing 6 g of potassium hydroxide. 19 g of monochloroacetic acid was dissolved in 200 m*l* of water, and then gradually neutralized with 20 g of potassium hydrogen carbonate. The two solutions were mixed together and heated on a water bath. After the temperature of the solution reached 70—80°C, 12 g of potassium hydroxide was added. An exothermic reaction took place. Heating was continued for about one hour in order to complete the reaction. When the resulting solution was cooled in a refrigerator, potassium chloride was precipitated. After the precipitate was removed by filtration, the filtrate was used as the starting material.

To the filtrate, 300 m*l* of water containing 20 g of cobalt(II) chloride hexahydrate was gradually added under magnetic stirring, since rapid addition often produced undesirable sediments such as cobalt hydroxide. The pH of the solution was adjusted to 6—7 by means of potassium hydrogen carbonate or acetic acid, and then 5 m*l* of hydrogen peroxide solution was dropped in order to oxidize cobalt(II) salt. Bluish violet crystals were obtained from the cooled solution. The crude products were recrystallized from aqueous solution. Yield about 5 g.

Found: N, 3.55; C, 25.07; H, 4.31%. Calcd for K[Co(OH)(α-abda)$(H_2O)]\cdot 2H_2O$: N, 3.63; C, 24.96; H, 4.45%.

*2) Potassium Hydroxo-*l*-valine-N,N-diacetatoaquocobaltate(III) Sesquihydrate, K[Co(OH)vda$(H_2O)]\cdot 1.5H_2O$ (II)*: This

Table 1. Rational formula and abbreviation of chelating agents

Rational formula	R	Full name	Abbreviation
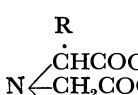	$-CH_3$	Nitriloisopropionicdiacetic acid	NIPDA
	$-CH_2\cdot CH_3$	*d,l*-α-Amino-*n*-butyric-*N,N*-diacetic acid	α-ABDA
	$-CH(CH_3)_2$	*l*-Valine-*N,N*-diacetic acid	VDA
	$-CH_2CH(CH_3)_2$	*l*-Leucine-*N,N*-diacetic acid	LDA
	$-C_6H_5$	*d*-α-Phenylglycine-*N,N*-diacetic acid	PGDA

1) Presented at the 23rd Annual Meeting of Chemical Society of Japan, Tokyo, April, 1970.

2) A. Uehara, E. Kyuno, and R. Tsuchiya, This Bulletin, **43**, 414 (1970).

3) M. Tachibana, A. Uehara, E. Kyuno, and R. Tsuchiya, *ibid.*, **43**, 1061 (1970).

4) A. Uehara, E. Kyuno, and R. Tsuchiya, *ibid.*, **44**, 1548 (1971).

5) A. Werner, *Ber.*, **40**, 4434 (1907).

6) W. W. Wendlandt and J. K. Fisher, *J. Inorg. Nucl. Chem.*, **24**, 1685 (1962).

7) H. Pfeiffer, *Z. Anorg. Allg. Chem.*, **56**, 261 (1907).

TABLE 2. A GENERAL PATH FOR PREPARATION OF COMPLEXES

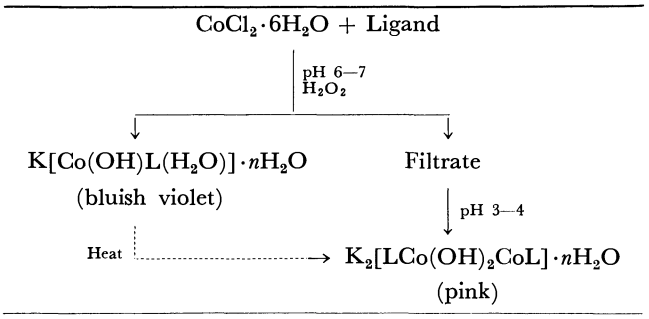

complex was prepared by a similar procedure to that for α-ABDA except that 12 g of *l*-valine was used as the starting material in stead of *d,l*-α-amino-*n*-butyric acid. The crystals were also bluish violet. Recrystallization was carried out from water. Yield 7 g.

Found: N, 3.46; C, 27.81; H, 4.40%. Calcd for K-[Co(OH)vda(H_2O)]·1.5H_2O: N, 3.59; C, 27.72; H, 4.65%.

*3) Potassium Hydroxo-*d*-α-phenylglycine-*N,N*-diacetatoaquocobaltate(III), K[Co(OH)pgda(H_2O)] (III)*: Five grams of d-α-phenylglycine was dissolved in 10 m*l* of water containing 2 g of potassium hydroxide. Nine grams of monochloroacetic acid was dissolved in 30 m*l* of water and gradually neutralized with 20 g of potassium hydrogen carbonate. Further procedure for obtaining the solution containing the desired ligand material was the same as that for α-ABDA except that 4 g of potassium hydroxide was added to the warmed solution on a water bath.

6.5 g of cobalt(II) chloride hexahydrate was dissolved under magnetic stirring in the solution obtained after the above procedure. After the pH of the solution was adjusted to 7—7.5, a few milliliters of hydrogen peroxide solution was added. The solution turned violet. In this case, the violet solution often turns pink as a result of the partial formation of the diol complex, and it is important to take care to keep the pH value of the solution in the desired range as exact as possible. From the rapidly cooled solution, bluish violet crystals were obtained. Recrystallization was carried out from water. Yield about 0.5 g.

Found: N, 3.31; C, 34.31; H, 3.80%. Calcd for K-[Co(OH)pgda(H_2O)]: N, 3.37; C, 34.73; H, 3.64%.

Preparation of Diol Complexes. 4) Potassium μ-Dihydroxobis(nitriloisopropionicdiacetato)dicobaltate(III) Dihydrate, K_2[nipda Co(OH)$_2$Co nipda]·2H_2O (IV): Five grams of NIPDA[8] was dissolved in 100 m*l* of aqueous solution containing 6 g of cobalt(II) chloride hexahydrate. The solution was heated on a water bath and neutralized with 5 g of potassium hydrogen carbonate. After the pH of the solution was adjusted to 6—7, a few milliliters of hydrogen peroxide was dropped into the solution in order to oxidize cobalt(II) salt, when bluish violet crystals of K[Co(OH)nipda(H_2O)]·H_2O[3] were obtained. After the crystals were separated, the pH of the filtrate was adjusted to 3—4 with acetic acid. The solution was warmed gently until the color turned from violet to pink. Pink crystals were obtained from the cooled solution after several days. They were recrystallized from water. Yield 0.5 g.

Found: N, 4.14; C, 25.64; H, 3.45%. Calcd for K_2-[nipda Co(OH)$_2$Co nipda]·2H_2O: N, 4.18; C, 25.10; H, 3.31%.

*5) Potassium μ-Dihydroxobis(*d,l*-α-amino-*n*-butyric-*N,N*-diacetato)dicobaltate(III) Trihydrate. K_2[(α-abda) Co(OH)$_2$Co (α-abda)]·3H_2O*: This was crystallized from the filtrate after the removal of complex I in its preparation. After the pH of the filtrate was adjusted to 3—4 with acetic acid, the solution was warmed gently on a water bath until it turned pink. On cooling for several days, pink crystals were obtained which were recrystallized from water. Yield about 0.6 g.

Found: N, 3.92; C, 26.80; H, 3.77%. Calcd for K_2-[(α-abda) Co(OH)$_2$Co (α-abda)]·3H_2O: N, 3.91; C, 26.84; H, 3.94%.

*6) Potassium μ-Dihydroxobis(*l*-valine-*N,N*-diacetato)dicobaltate(III) Trihydrate, K_2[vda Co(OH)$_2$Co vda]·3H_2O (VI)*: This was crystallized from the filtrate in the preparation of complex II by a procedure similar to that for complex V. Pink crystals were recrystallized from water. Yield about 1 g.

Found: N, 3.71; C, 29.04; H, 4.61%. Calcd for K_2-[vda Co(OH)$_2$Co vda]·3H_2O: N, 3.76; C, 29.06; H, 4.33%.

*7) Potassium μ-Dihydroxobis(*l*-leucine-*N,N*-diacetato)dicobaltate(III) Dihydrate, K_2[lda Co(OH)$_2$Co lda]·2H_2O (VII)*: This complex was prepared by a similar procedure to that for complex IV except that six grams of *l*-leucine-*N,N*-diacetic acid (LDA)[2] was used as a starting ligand in place of NIPDA. The complex was pink as in the case of complex IV. Recrystallization was carried out from water. Yield 0.5 g.

Found: N, 3.65; C, 31.48; H, 4.31%. Calcd for K_2-[lda Co(OH)$_2$Co lda]·2H_2O; N, 3.71; C, 31.86; H, 4.54%.

*8) Potassium μ-Dihydroxobis(d-α-phenylglycine-*N,N*-diacetato)-dicobaltate(III) Dihydrate, K_2[pgda Co(OH)$_2$Co pgda]·2H_2O (VIII)*: This was prepared in a procedure similar to that for complex V except that the filtrate in the preparation of complex III was used. It was also recrystallized from water. In the preparation of the pgda-complex, the diol salt was more easily formed as compared with the corresponding hydroxoaquo salt, whereas in the case of the other complexes, hydroxoaquo salts were more readily produced than the corresponding diol salts. Yield 0.5 g.

Found: N, 3.61; C, 35.97; H, 3.19%. Calcd for K_2-[pgda Co(OH)$_2$Co pgda]·2H_2O: N, 3.53; C, 36.30; H, 3.30%.

Apparatus. The apparatus used in the present study is the same as reported previously.[9]

Results and Discussion

Electronic Spectra. A striking difference in features between the hydroxoaquo and the diol complexes is that the former is bluish violet, whereas the latter is pink. Spectra for all the complexes were obtained but only representative examples in a pair of VDA complexes, II and VI, are shown in Fig. 1. Complex II gives the first and the second bands at 53.57 and 76.53×10^{13} sec^{-1} respectively. Complex VI does not show the second band distinctly, but a new band at $\sim 100 \times 10^{13}$ sec^{-1}. All the complexes, IV, V, VII, and VIII exhibit the same features in their spectra as those of complex VI.

It is known[10] that the ol-ammine complexes show the specific band due to the bridged OH group at

8) A. Uehara, E. Kyuno, and R, Tsuchiya, This Bulletin, **41**, 2393 (1968).

9) A. Uehara, E. Kyuno, and R. Tsuchiya, This Bulletin, **41**, 2385 (1968).

10) Y. Inamura and Y. Kondo, *Nippon Kagaku Zasshi*, **74**, 627 (1953).

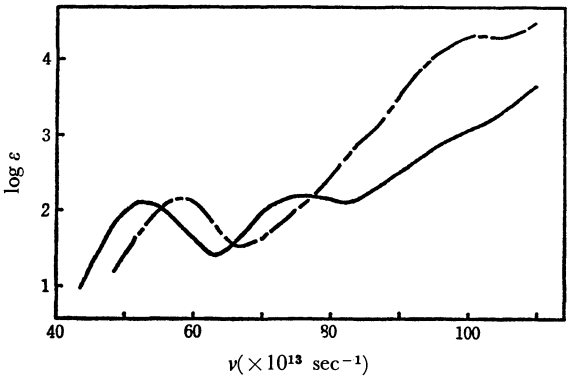

Fig. 1. Electronic spectra for complexes II (——) and VI (– – –).

Table 3. Absorption maxima

Complex	ν_1 (log ε_1)	ν_2 (log ε_2)[a]	Complement[b]
I	53.10 (2.15)	75.38 (2.35)	
II	53.38 (2.09)	76.34 (2.26)	
III	53.10 (2.13)	76.73 (2.29)	
IV	59.76 (2.11)		~100 (~4.2)
V	59.64 (2.13)		~100 (~4.3)
VI	59.06 (2.16)		~100 (~4.2)
VII	59.76 (2.18)		~100 (~4.3)
VIII	59.29 (2.18)		~105 (~4.6)

a) The second bands of complexes IV to VIII can not be clearly detected because of the overlap with the specific band due to the bridging OH groups.
b) These values show the specific bands due to the bridging OH groups. The band can not be clearly detected because of its broadening.

about 100×10^{13} sec^{-1}. In some cases the second band does not appear due to being concealed by the strong specific band. Such a difference[11] may propose one evidence that VI is a diol and II a hydroxoaquo complex. The numerical values of absorption maxima for all the complexes prepared in the present work are summarized in Table 3.

Conductivity and Coagulation Value. To determine the type of electrolytes for the complexes, the molar conductivities and coagulation values were measured in an aqueous solution at 25°C. The numerical data are shown in Table 4. All the complexes show a molar conductivity of the same order. Accordingly, no distinction could be detected between the hydroxoaquo and the diol complexes by this method. However, it is known that the average coagulation values for uni- and bivalent complex anions are 6.6 mF and 0.48 mF, respectively.[12] The values measured with an iron(III) hydroxide sol for the complexes I to III was 5—6 mF, while for complexes IV to VIII, 0.6—0.8 mF, indicating that the former three are 1 : 1 type (hydroxoaquo complex anion) and the latter four 1 : 2 type electrolytes (diol complex anion).

11) M. Mori, M. Shibata, E. Kyuno, and Y. Okubo, This Bulletin, **31**, 940 (1958).
12) A. Nakahara, K. Nakamoto, and R. Tsuchida, *Nippon Kagaku Zasshi*, **74**, 488 (1953).

Table 4. Molar conductivity (λ) and coagulation value (mF)

Complex	λ[a] mho cm^{-1}	mF
I	113.1	6
II	117.6	6
III	123.1	5
IV	121.2	0.6
V	145.6	0.8
VI	162.3	0.7
VII	153.2	0.6
VIII	132.5	0.7

a) 10^{-3} mol/l aqueous solution was used.

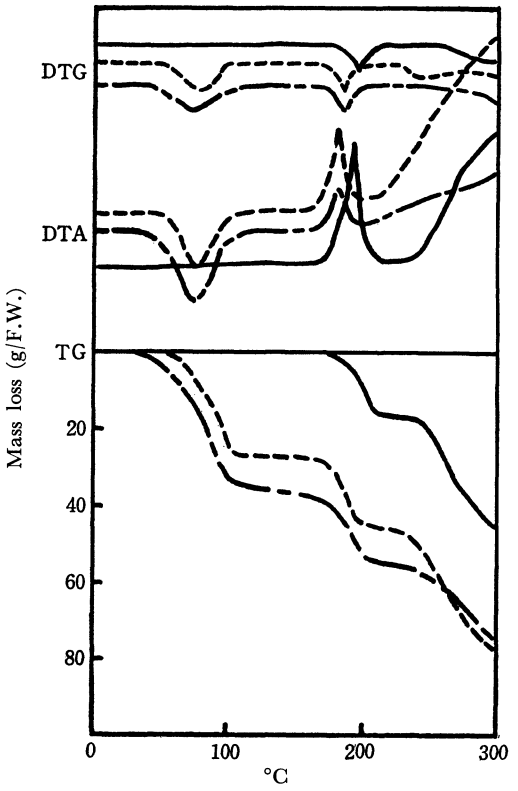

Fig. 2. Derivatograms for complexes I(– – –), II(----), and III (——).

Change from Hydroxoaquo- to Diol-Complex in the Thermal Reaction Process. The hydroxoaquo complexes in the solid phase are expected to liberate the coordinating water upon heating, forming the corresponding diol complexes as suggested by a broken arrow in Table 2. The thermal reaction for the complexes was measured with a derivatograph.[13] Figure 2 shows the derivatograms for complexes I, II, and III. Five hundred milligrams of the samples was used in each run in a constant nitrogen stream with a heating rate of 1°C/min. As seen from TG and DTA curves, complexes I and II are observed to liberate two moles of water at 50—110 and one and a half moles of water at 80—130°C, respectively, with endothermic

13) R. Tsuchiya, Y. Kaji, A. Uehara, and E. Kyuno, This Bulletin, **42**, 1881 (1969).

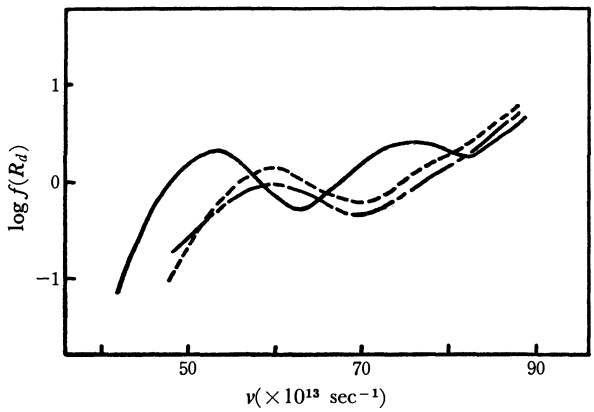

Fig. 3. Electronic spectra for complexes II (——), VI (----) and the sample II picked up at 190°C (—·—).

reactions. It is further found that one mole of coordinated water is liberated from the complexes I, II, and III at 185—200, 175—190, and 190—215°C, respectively, with exothermic reactions. At these steps, the color of the samples changed from bluish violet to pink as in the case of the corresponding NIPDA,[3] LDA,[2] and PADA (*d,l*-Phenylalanine-*N,N*-diacetic Acid)[4] complexes.

Figure 3 gives the electronic spectra measured by the diffuse reflectance method for complexes II, VI and for the sample of complex II picked up at this heating step (190°C). The spectrum for the last sample resembles that for complex VI, suggesting that the structure of the sample picked up at this step is similar to that of complex VI. Accordingly, the fact that the diol complex is formed by heating the corresponding hydroxoaquo complex may be successfully verified by the above experimental results.

The authors wish to express their thanks to the Ministry of Education for the financial support granted this research.

BULLETIN OF THE CHEMICAL SOCIETY OF JAPAN, VOL. 44, 1555—1560 (1971)

The Chromium(III) Complexes with Natural α-Amino Acids[1]

Hisayuki MIZUOCHI,[2] Akira UEHARA, Eishin KYUNO, and Ryokichi TSUCHIYA
Department of Chemistry, Faculty of Science, Kanazawa University, Kanazawa

(Received October 6, 1970)

The following chromium(III) complexes with natural α-amino acids were prepared: $[Cr(\alpha\text{-ambut})_3]\cdot 2H_2O$ (red) (I), $(-)_{546}$-$[Cr(l\text{-leu})_3]\cdot 2H_2O$ (red) (II), $(+)_{546}$-$[Cr(l\text{-leu})_3]\cdot 2H_2O$ (red) (III), $[Cr(l\text{-glu})_3]\cdot 2H_2O$ (red) (IV), $(+)_{546}$-$[Cr(l\text{-lys})_2(H_2O)_2]Cl\cdot 3H_2O$ (red) (V), $[Cr(OH)(\alpha\text{-ambut})_2(H_2O)]\cdot H_2O$ (light purple) (VI), $[Cr(OH)(l\text{-val})_2(H_2O)]\cdot H_2O$ (light purple) (VII), $[Cr(OH)(l\text{-leu})_2(H_2O)]\cdot H_2O$ (light purple) (VIII) and $[Cr(OH)(l\text{-glu})_2(H_2O)]\cdot H_2O$ (light purple) (IX), where α-ambut, *l*-leu, *l*-glu, *l*-lys, and *l*-val are the basic forms of α-amino-n-butyric acid, *l*-leucine, *l*-glutamine, *l*-lysine and *l*-valine, respectively. From the results of electronic and infrared absorption spectra, molar conductivities and behaviors toward ion exchangers, the composition and structures of the complexes were determined. The striking information obtained is that the complexes (I)—(IV) are considered to have all the β-form unlike the corresponding cobalt(III) complexes having both α- and β-forms. On the basis of ORD and CD measurements, the complexes (II), (III), and (V) were found to be optically active.

A number of transition metal complexes with various amino acids are already known. Within the limits of chromium(III) as a central metal ion, the complexes with synthetic amino acids such as NTA (nitrilotriacetic acid)[3] and IDA (iminodiacetic acid)[4] and their derivatives[5–8] have been prepared, their chemical properties and structures being investigated.

Of the natural amino acids, however, studies on the complexes are rare except for the tris-type complexes containing glycine[9,10] α-alanine,[11–15] asparagine[16], or *l*-aspartic acid.[17] In the present work, attempts were made to prepare chromium(III) complexes with various natural α-amino acids in tris- or bis-type and to investigate which type of complex can be successfully synthesized in each natural α-amino acid and which form of complex can be obtainable in two geometrically possible isomers.

1) Presented in part at the 18th Symposium on Coordination Chemistry, Kyoto, October, 1968 and at the 22nd Annual Meeting of the Chemical Society of Japan, Tokyo, April, 1969.
2) Present address: Yamanouchi Rubber Industries Co., Ltd., Hirakata, Osaka.
3) A. Uehara, E. Kyuno, and R. Tsuchiya, This Bulletin, **40**, 2317, 2322 (1967).
4) K. Yamasaki and S. Ito, *Proc. Japan Acad.*, **42**, 1077 (1966); H. Mizuochi, S. Shirakata, E. Kyuno, and R. Tsuchiya, This Bulletin, **43**, 397 (1970).
5) A. Uehara, E. Kyuno, and R. Tsuchiya, *ibid.*, **41**, 2385, 2393 (1968); **42**, 2835 (1969).
6) T. Tomita, E. Kyuno, and R. Tsuchiya, *ibid.*, **42**, 947 (1969).
7) Y. Fujii, E. Kyuno, and R. Tsuchiya, *ibid.*, **43**, 786 (1970).
8) D. W. Cooke, *Inorg. Chem.*, **5**, 1141 (1966).
9) H. Ley and H. Winkler, *Ber.*, **45**, 380 (1912).
10) L. M. Volshtein and V. P. Molosnova, *Doklady Aka. Nauk. S. S. S. R.*, **92**, 479 (1952).
11) L. Tchougaeff and E. Serbin, *Compt. rend.*, **151**, 1361 (1910).
12) L. Hugounenq and A. Morel, *ibid.*, **154**, 119 (1912).
13) H. Ley and K. Ficker, *Ber.*, **45**, 377 (1912).
14) L. M. Volshtein, *Compt. rend. acad. sci. (S. S. S. R.)*, **54**, 321 (1946).
15) R. W. Green and K. P. Ang., *J. Amer. Chem. Soc.*, **77**, 5482 (1955).
16) L. M. Volshtein and V. P. Molosnova, *Zh. Neorg. Khim.*, **4**, 1995 (1959).

Experimental

Preparation of Chromium(III) Complexes. Preparation of the chromium(III) complexes with natural α-amino acids carried out in the present work was classified into the following three methods depending upon the kinds of chromium(III) salts used as the starting material.

1. *Method using Chromium(III) Hydroxide*: This is essentially the same as the method by Ley and Winkler.[9] To a solution of *l*-glutamine (45 g, 0.3 mol) was added a slight excess of freshly prepared chromium(III) hydroxide (12 g, 0.12 mol), and the mixture was heated on a water bath until a reddish violet solution was obtained. This was filtered at once to remove unreacted hydroxide. The filtrate was evaporated to a half volume and cooled to room temperature. After adding a small amount of ethanol, the mixture was kept in a refrigerator overnight in order to precipitate the unreacted amino acid. After being filtered, the filtrate was kept to stand at room temperature for two or three days. Pink crystals were gradually precipitated.

The yield was about 10%. Found: C, 34.33; H, 6.03; N, 15.92%. Calcd for $[Cr(l\text{-glu})_3]\cdot 2H_2O$ (*l*-glu=*l*-glutamine): C, 34.38; H, 5.92; N, 16.05%.

By applying the same method as described above, the corresponding complexes with glycine, *d,l*,α-alanine and *l*-asparagine were prepared in better yields (about 30%) than in *l*-glutamine.

2. *Method using Chromium(III) Chloride*: This is similar to the method reported by Green and Ang,[15] and by Volshtein and Molosnova.[16] To a solution of α-amino-*n*-butyric acid (30 g, 0.3 mol), for example, was added an aqueous solution of chromium(III) chloride hexahydrate (27 g, 0.1 mol), and the mixture was heated on a water bath until it turned to violet. The color changed again to reddish violet by the dropwise addition of potassium hydrogen carbonate (30 g, 0.3 mol). On heating the solution, pink crystals began to appear on the wall of the evaporating dish. The filtrate was cooled to room temperature and kept standing overnight. Fine pink crystals were obtained.

The yield was about 10%. Found: C, 36.51; H, 7.10; N, 10.65%. Calcd for $[Cr(\alpha\text{-ambut})_3]\cdot 2H_2O$ (α-ambut=α-amino-*n*-butyric acid): C, 37.02; H, 6.90; N, 10.71%.

The yields for the complexes with glycine, *d,l*-α-alanine, and *l*-asparagine prepared by applying this method were all 30%.

The complex with *l*-lysine obtained by the same method was bis-type. Found: C, 30.79; H, 7.67; N, 12.52%. Calcd for $[Cr(l\text{-lys})_2(H_2O)_2]Cl\cdot 2H_2O$ *l*-lys=*l*-lysine: C, 30.80; H, 7.77; N, 11.98%.

By using a similar method except that 0.2 moles of the desired amino acid, instead of 0.3 moles, were employed as a starting material and the mixed solution was kept standing at room temperature for about one week instead of overnight after the addition of potassium hydrogen carbonate, the bis-type complexes with *l*-glutamine, α-amino-n-butyric acid, *l*-leucine, and *l*-valine were obtained as light purple crystals. For *l*-glutamine complex, Found: C, 31.21; H, 6.11; N; 13.49%. Calcd for $[Cr(OH)(l\text{-glu})_2(H_2O)]\cdot H_2O$: C, 30.36; H, 5.82; N, 14.17%. For α-amino-n-butyric acid complex, Found: C, 32.38; H, 6.63; N, 9.34%. Calcd for $[Cr(OH)(\alpha\text{-ambut})_2(H_2O)]\cdot H_2O$: C, 31.05; H, 6.79; N, 9.06%. For *l*-leucine complex, found: C, 41.39; H, 7.94; N, 7.91%. Calcd for $[Cr(OH)(l\text{-leu})_2(H_2O)]\cdot H_2O$ (*l*-leu=*l*-leucine): C, 40.75; H, 7.69; N, 7.92%. For *l*-valine complex, Found: C, 35.75; H, 6.81; N, 8.34%. Calcd for $[Cr(OH)(l\text{-val})_2(H_2O)]\cdot H_2O$ (*l*-val=*l*-valine): C, 35.60; H, 6.89; N, 8.31%.

The chromium(III) complex with leucine in tris-type was prepared by a different method from that mentioned above, though chromium(III) chloride was used as starting material in the same manner. 26.6 g (0.1 mol) of chromium(III) chloride hexahydrate in 200 m*l* of 80% methanol and 39.3 g (0.3 mol) of *l*-leucine were mixed and the mixture was heated in a round flask equipped with a reflux condenser. As the reaction proceeded, the color of the solution turned from green to violet. After the reaction was completed, a mixture of methanol and aqueous ammonia (0.3 mol) was gradually added dropwise to the solution, whereby its color became reddish. The solution was filtered and cooled to room temperature. A small amount of methanol having been added, the mixture was kept in a refrigerator for two days to let ammonium chloride precipitate. The filtrate was evaporated to half its volume under reduced pressure and was kept standing at room temperature after repeated filtration. Pink crystals were obtained, soluble in methanol. After removal of the crystals, the filtrate was kept at room temperature for a long time. Another crop of crystals was obtained, insoluble in methanol but soluble in *N,N*-dimethylformamide (DMF). In spite of this difference in solubility, the chemical composition of the two complexes obtained above is expressed by $[Cr(l\text{-leu})_3]\cdot 2H_2O$.

Soluble in methanol: Found: C, 44.09; H, 7.57; N, 8.45%.

Soluble in DMF: Found: C, 45.39; H, 8.73; N, 8.52%. Calcd for $[Cr(l\text{-leu})_3]\cdot 2H_2O$: C, 45.17; H, 8.42; N, 8.78%.

Preparation of Cobalt(III) Complexes. In order to compare the UV and IR spectra of the chromium(III) complexes with those of the corresponding cobalt(III) ones, the latter were also prepared by known methods.[18,19]

Apparatus. The molar conductivities and UV spectra were measured with a Yokogawa Universal Bridge BV-Z-12A and with a Hitachi EPS Spectrophotometer, respectively. The IR spectra were measured with a JASCO DS-301 and a JASCO Model IR-E Infrared Spectrophotometers both in KBr disk and in nujol mull. The optical rotatory dispersion (ORD) and circular dichroism (CD) curves were recorded with a JASCO Optical Rotatory Dispersion Recorder, Model UV-S attached with a CD recorder. The quantity of crystalline water contained in these compounds was estimated from the TG curve measured with a Shimadzu TM-1A Thermanobalance and a MOM Derivatograph Typ-OD-102.

Results and Discussion

UV Absorption Spectra. The UV absorption spectra of the chromium(III) complexes with amino acids in tris-type, together with those in bis-type with glycine or *l*-lysine, were measured in 20% perchloric acid solution except for that of tris-*l*-leucinatochromium(III) complexes measured in methanol and DMF and that of the corresponding cobalt(III) complexes measured in 60% perchloric acid solution. The numerical data of their maxima are summarized in Table 1. The spectra of tris(*l*-leucinato)chromium(III) and tris(*l*-glutaminato)chromium(III) are shown in Figs. 1 and 2, respectively, together with

17) L. M. Volshtein, *Zh. Neorg. Khim.*, **1**, 2378 (1956).

18) M. Mori, M. Shibata, E. Kyuno, and M. Kanaya, This Bulletin, **34**, 1837 (1961).

19) M. Shibata, H. Nishikawa, and Y. Nishida, *ibid.*, **39**, 2310 (1966); *Inorg. Chem.*, **7**, 9 (1968).

Table 1. Absorption maxima of the chromium(III) and cobalt(III) complexes

	Cr(III)		Co(III)	
	ν_1(log ε)	ν_2(log ε)	ν_1(log ε)	ν_2(log ε)
gly[11]			57.7(2.16)	79.6(2.06)
α-ala[16]	56.0(1.85)	75.4(1.75)	58.0(2.22)	80.4(2.21)
l-glu	56.1(1.95)	76.0(1.84)	57.0(2.32)	79.2(2.30)
α-ambut	55.8(1.87)	75.0(1.79)	57.3(2.35)	79.8(2.30)
l-leu	57.8(1.67)	76.9(1.79)	58.0(2.27)	80.4(2.26)
gly[a]	57.3(1.64)	76.7(1.57)		
l-lys[a]	57.5(1.56)	78.7(1.58)		

a) Bis-type complexes. Others: tris-typecomplexes.

those of the corresponding cobalt(III) complexes of β-form.

It is known that there are two geometrical isomers in tris-type amino acid complexes, *i.e.*, *mer* (*cis*, *trans*) and *fac* (*cis*, *cis*) type with respect to the nitrogen or oxygen atoms coordinating to central metal, the former called α-form (violet) and the latter β-form (red).

It was pointed out[20] that the main difference between the absorption curves in these two isomers appears predominantly in the first band; *viz.*, the first band of the α-form isomer shows some splitting, while that of the β-form isomer does not. Although the positions giving the maximum absorbancies for these chromium(III) complexes are shifted to a somewhat lower frequency region compared with those for the corresponding cobalt(III) complexes, the shapes of the bands for the chromium(III) complexes prepared

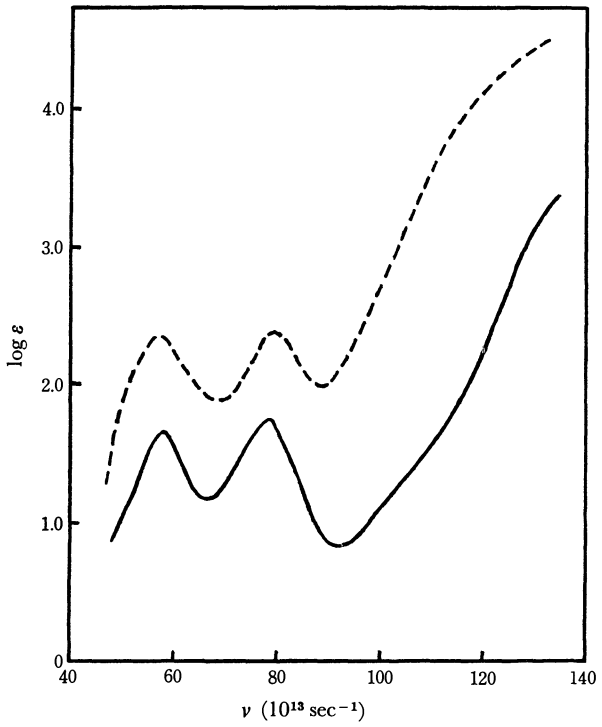

Fig. 1. Electronic absorption spectra of [Cr(*l*-leu)$_3$] in methanol (——) and of β-[Co(*l*-leu)$_3$] in 60% perchloric acid solution (----).

20) J. Hidaka, Y. Shimura, and R. Tsuchida, This Bulletin, **35**, 567 (1962).

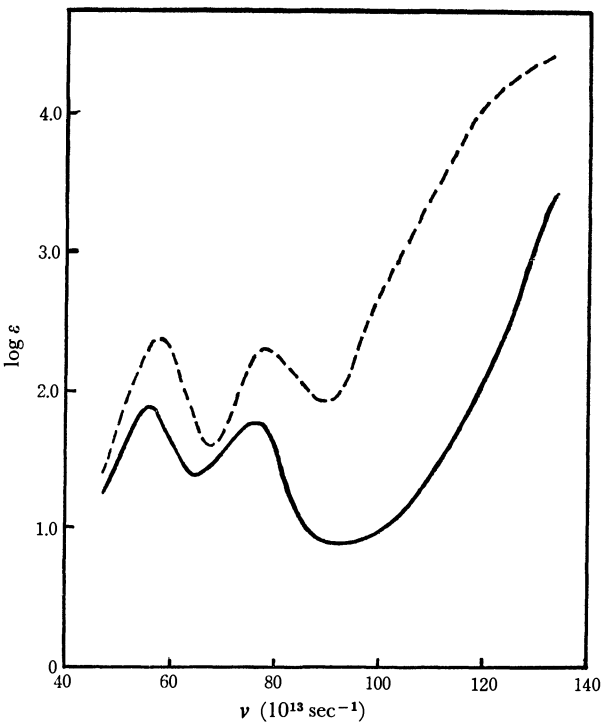

Fig. 2. Electronic absorption spectra of [Cr(*l*-glu)$_3$] in 20% perchloric acid (——) and of β-[Co(*l*-glu)$_3$] in 60% perchloric acid solutions (----).

in the present work are nearly the same as those for the corresponding cobalt(III) ones assigned to β-form. This suggests that the chromium(III) complexes in tris-type have also the β-form.

The spectra of bis(*l*-lysinato)- and bisglycinatodiaquochromium(III) complexes are shown in Fig. 3. In bis(*l*-aminato)diaquochromium(III) complexes, five geometrically possible isomers are considered, which are given in Fig. 4. It is obvious from Fig. 3 that the first absorption band not only gives a higher molar absorption coefficient than the second band but also shows no splitting. This leads us to presume the coordinating structure of these bisaminatodiaquo complexes to be (e) in Fig. 4, which is not trans structure with respect to nitrogen or oxygen atoms.

Since the absorption spectra could not be measured in aqueous solution owing to much smaller solubility in water, those for hydroxobisaminatoaquo complexes, $[Cr(OH)Am_2(H_2O)]\cdot H_2O$, where Am=*l*-

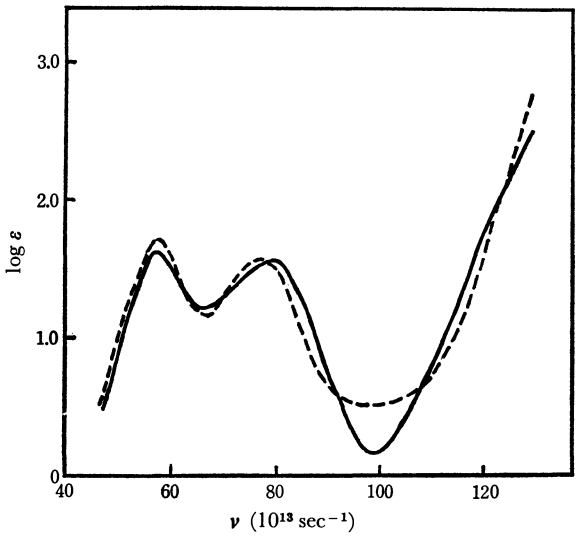

Fig. 3. Electronic absorption spectra of $[Cr(l\text{-lys})_2(H_2O)_2]Cl$ (——) and of $[Cr(gly)_2(H_2O)_2]NO_3$ (----) in aqueous solutions.

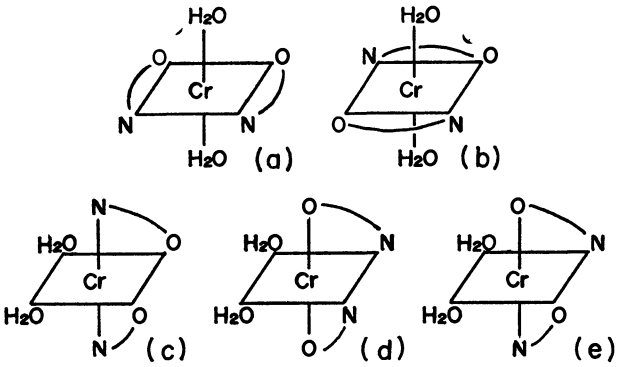

Fig. 4. Five geometrically possible isomers for $[CrL_2(H_2O)_2]^+$, where L denotes bidentate amino acid.

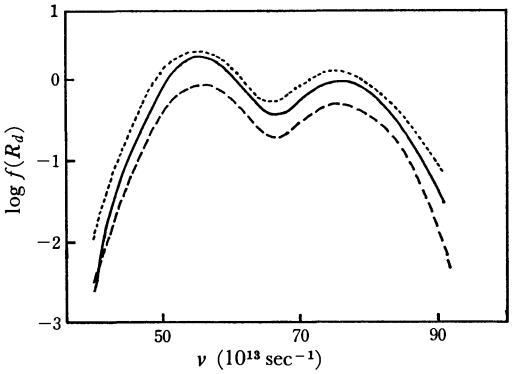

Fig. 5. Absorption spectra of $[Cr(OH)(\alpha\text{-ambut})_2(H_2O)]$ (——), $[Cr(OH)(l\text{-leu})_2(H_2O)]$ (— —) and $[Cr(OH)(l\text{-val})_2(H_2O)]$ (----) by the diffuse reflectance method.

glutamine, α-amino-*n*-butyric acid, *l*-leucine, or *l*-valine, were obtained by the diffuse reflectance method. The representative spectra for the chromium(III) complexes with α-amino-*n*-butyric acid, *l*-leucine and *l*-valine are shown in Fig. 5.

The first absorption peaks appear at 55, 56, and $55 \times 10^{13}\,sec^{-1}$ and the second peaks appear at 76, 75.5, and $75.5 \times 10^{13}\,sec^{-1}$ for α-amino-*n*-butyric acid, *l*-leucine and *l*-valine, respectively, as seen in Fig. 5. From the features of the absorption curves in this figure, where the first absorption bands do not show appreciable splitting, having higher absorption coefficients than the second bands, the hydroxobisaminato-aquochromium(III) complexes seem to have (e) structure in Fig. 4, containing OH and H_2O ligands in *cis* sites.

IR spectra. Infrared absorption spectra were measured over the range of 4000—700 cm^{-1}. The spectra of the chromium(III) complexes with glycine,

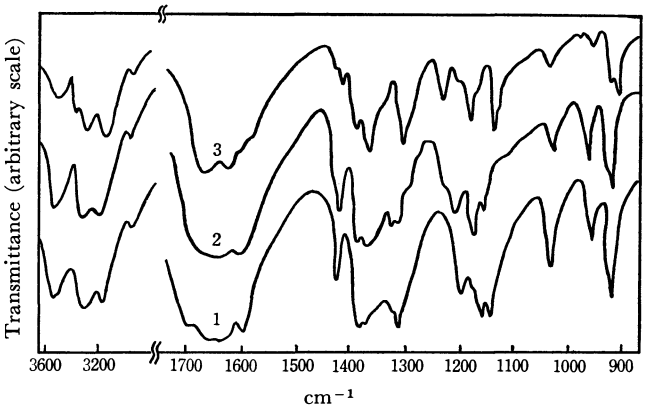

Fig. 6. IR spectra of $[Cr(gly)_3]$ (1), β-$[Co(gly)_3]$ (2), and α-$[Co(gly)_3]$ (3).

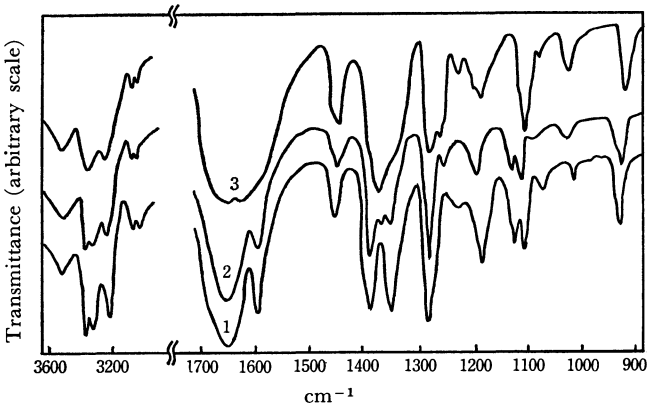

Fig. 7. IR spectra of $[Cr(\alpha\text{-ala})_3]$ (1), β-$[Co(\alpha\text{-ala})_3]$ (2), and α-$[Co(\alpha\text{-ala})_3]$ (3).

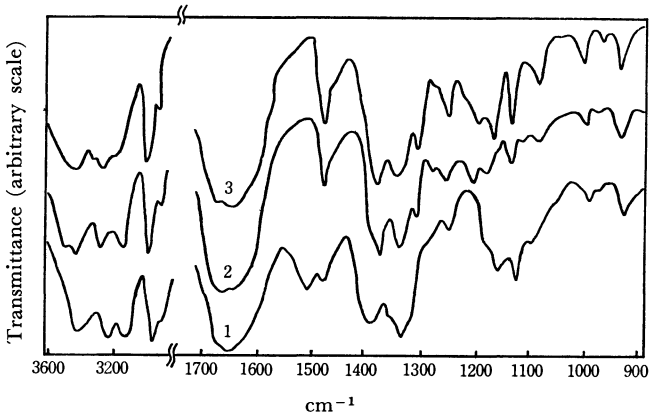

Fig. 8. IR spectra of $[Cr(l\text{-leu})_3]$ (1), β-$[Co(l\text{-leu})_3]$ (2), and α-$[Co(l\text{-leu})_3]$ (3).

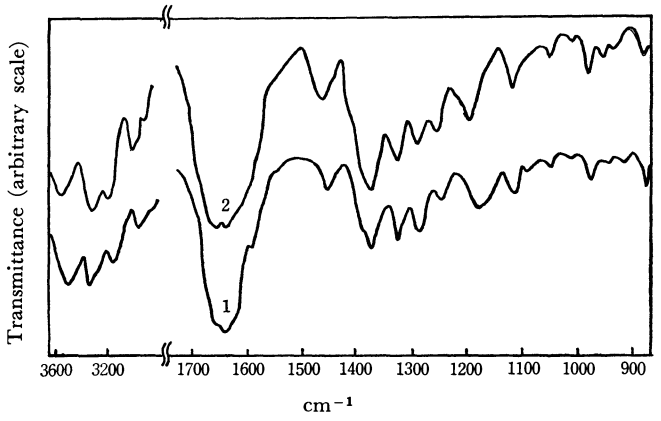

Fig. 9. IR spectra of [Cr(α-ambut)$_3$] (1) and β-[Co(α-ambut)$_3$] (2).

d,l-α-alanine, *l*-leucine, α-amino-*n*-butyric acid, and *l*-glutamine in tris-type are shown in Figs. 6—10, together with those of the corresponding cobalt(III) complexes in both α- and β-forms, though the α-forms of cobalt(III) complexes with α-amino-*n*-butyric acid and with *l*-glutamine could not be found.

The spectral curves for the chromium(III) complexes are extremely analogous to those for the corresponding cobalt(III) complexes in β-form rather than those in α-form, especially in several wave number regions, 3180—3400 cm^{-1} (NH_2 stretching), 1600—1650 cm^{-1} (NH_2 bending), 1350—1420 cm^{-1} (COO^- stretching) and 1100—1200 cm^{-1} (CH_2 deformation). It can be assumed from IR spectra that the tris-type of chromium(III) complexes have the same β-structure as the corresponding cobalt(III) complexes.

Behaviors toward Ion Exchangers and Molar Conductivity. Bisglycinatodiaquochromium(III) nitrate and bis(*l*-lysinato)diaquochromium(III) chloride were adsorbed by Cl^--form exchanger and their molar conductivity data measured in 1×10^{-3} mol/*l* were 69.5 and 202.4 mho cm^{-1}, respectively. This suggests that the above two complexes are 1 : 1 valency type, the complex cation being univalent as expected.

On the other hand, hydroxoaminatoaquochromium(III) complexes were adsorbed by neither cation nor anion exchangers and their conductivities could not be measured owing to insolubility in water. This is in line with the behavior of their non-electrolytes.

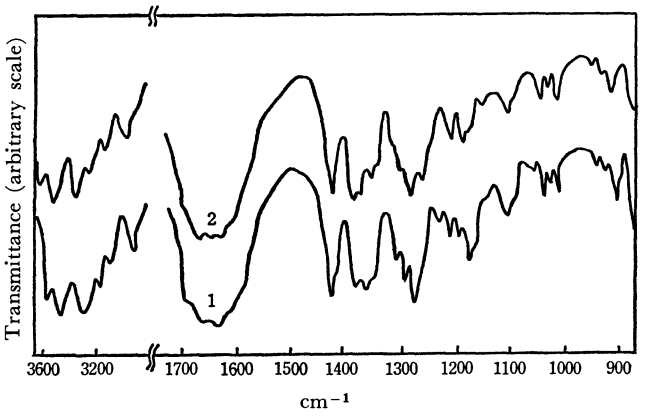

Fig. 10. IR spectra of [Cr(gly)$_3$] (1) and β-[Co(gly)$_3$] (2).

ORD and CD Spectra. The optical rotatory dispersion, circular dichroism, and absorption curves for tris(*l*-leucinato)chromium(III) soluble in methanol and in DMF and those for bis(*l*-lysinato)diaquochromium(III) chloride measured in water are given in Figs. 11 and 12, respectively. The molar rotations for two tris(*l*-leucinato)chromium(III) complexes were $[M]_{546}=-3496$ and $+5932$ respectively, and

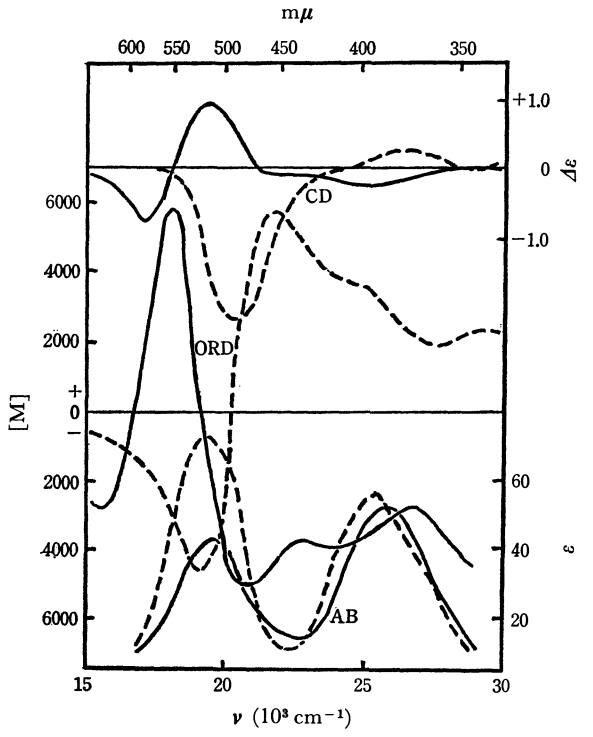

Fig. 11. Absorption, ORD and CD spectra of [Cr(*l*-leu)$_3$] $2H_2O$ measured in methanol (——) and those measured in DMF (----).

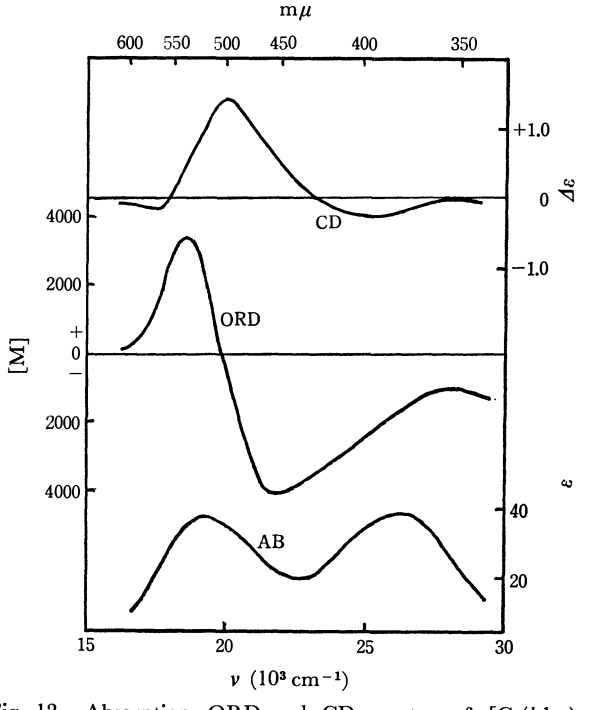

Fig. 12. Absorption, ORD and CD spectra of [Cr(*l*-lys)$_2$-$(H_2O)_2$]Cl·3H_2O.

Table 2. Chromium(III) complexes with α-amino acids prepared

Amino acid	$[CrL_3]$	$[CrL_2(H_2O)_2]X$	$[Cr(OH)L_2(H_2O)]$
Glycine	○	○	○
α-Alanine	○		○
l-Aspartic acid	○		
l-Asparagine	○		
α-Aminobutyric acid	◑		◑
l-Leucine	◑		◑
l-Glutamine	◑		◑
l-Lysine		◑	
l-Valine			◑

○: Complexes already prepared
◑: Complexes prepared in this work

that for bis(*l*-lysinato)diaquochromium(III) chloride was $[M]_{546}=+2867$.

The chromium(III) complexes with various amino acids in the types, $[CrL_3]$, $[CrL_2(H_2O)_2]X$ and $[Cr(OH)L_2(H_2O)]$, where L denotes amino acid and X denotes Cl^- or NO_3^-, were synthesized, and they are summarized in Table 2 together with those reported.

The tris-type chromium(III) complexes were all of β(*fac*)-structure, though in the corresponding cobalt(III) complexes both α- and β-forms have been found. The reason why α-form can not be obtained as crystals in the preparative conditions of the chromium(III) complexes with natural amino acids is not clear as yet.

An attempt to prepare the α-form of the chromium(III) complexes may be examined with the following ideals. Since the isomers (a) and (b), two of the bisaminatodiaquochromium(III) complexes depicted in Fig. 4, have *trans*-structure, the introduction of the third chelation of amino acid into them is impossible without the movement of chelating ligands already coordinated. On the contrary, in the *cis*-isomers (c), (d), and (e), the probability of the formation of the α-form complexes will amount to 5/6 by introducing the third chelation.

As an example, the preparation of a α-form chromium(III) complex in crystalline state was attempted by using *d,l*-α-alanine as the third bidentate ligand to be introduced into bisglycinatodiaquochromium(III) nitrate, and violet crystals were obtained. Taking account of the color of the crystals, the complexes are considered to have α-form structure and the starting bisglycinato complex to have cis-structure of either (c), (d), or (e).

BULLETIN OF THE CHEMICAL SOCIETY OF JAPAN, VOL. 44, 1560—1562 (1971)

Spectrophotometric Determination of Benzethonium with Tetrabromophenolphthalein Ethyl Ester

Masahiro TSUBOUCHI

Faculty of Education, Tottori University, Tottori

(Received August 1, 1970)

A spectrophotometric method is proposed for the determination of benzethonium. The method is based on solvent extraction of the ion-pair formed between benzethonium and colored tetrabromophenolphthalein ethyl ester, into 1,2-dichloroethane. The extract has a maximum absorbance at 615 mμ, and follows Beer's law with good precision up to 4×10^{-6} M in aqueous solution. The absorbance of the extract is constant in the pH range 7—11. Organic cations interfere.

Tetrabromophenolphthalein ethyl ester (TBPE) has been used as a pH indicator. In a previous paper,[1] this reagent was shown to be useful for the colorimetry of diphenhydramine by solvent extraction. In the course of this study, various amines or organic cations were extracted with TBPE into dichloroethane. The colors of the extracts were found to be classified into the following three categories. (1) Red-violet which is developed by the presence of diphenhydramine, *N*,*N*-dimethylpiperazine, papaverine, triethanolamine, pilocarpine, or eserine. (2) Blue which is extracted by the presence of benzethonium, spartein, neostigmine, tetraethylammonium, acetylcholine, or thiamine. (3) Yellow which is the same color as reagent blank for the presence of aniline, acetonitrile, 3-aminoquinoline, pyridine, *N*,*N*-dimethylformamide, EDTA, or NTA.

This paper deals with the determination of benzethonium with TBPE. The proposed method has a very good reproducibility and a high sensitivity. The titrimetric method[2] has been used for the determination of benzethonium which is widely used as disinfectant.

Experimental

Apparatus. Spectrophotometric measurements were carried out with a Shimadzu QR-50 spectrophotometer, with 10-mm cuvettes. An Iwaki Model KM shaker with a time switch was used for the extraction. The pH measurements were carried out with a Toa Denpa Model HM-5 pH meter.

Reagents. *Tetrabromophenolphthalein Ethyl Ester (TBPE) Solution*: Weighed amounts of tetrabromophenolphthalein

1) M. Tsubouchi, This Bulletin, **43**, 3164 (1970).

2) Japanese Pharmacopoeia, VII-1, Part II, Nankodo (1965), p. 214.

ethyl ester potassium salt were dissolved in ethyl alcohol.

Standard Benzethonium Solution: A stock solution was prepared by dissolving 4.661 g of benzethonium chloride (dried at 105°C) and diluting to 1 *l* with water to make the solution 1.0×10^{-2} M. The stock solution was used to prepare the standard solution with desired concentration.

Buffer Solution: The pH 8.5 buffer was prepared by mixing 0.5 M potassium dihydrogen phosphate solution and 0.15 M sodium borate solution.

All the chemicals were of reagent grade and the water used was passed through an ion-exchange resin.

Procedure. Take 5 m*l* of benzethonium solution (less than 2×10^{-5} M), 2 m*l* of TBPE solution (10^{-3} M) and 5 m*l* of the buffer solution into a 10 -m*l* separating funnel. Dilute the mixture to 25 m*l* with water and shake the solution for 2 min with 10 m*l* of 1,2-dichloroethane. After separation of the two layers, run off the extract into a glass tube through a filter paper to remove droplets of water. Measure the absorbance of the extract at 615 mμ using a reagent blank as a reference.

Results and Discussion

Absorption Spectra. Figure 1 shows the visible absorption spectra of benzethonium extracts with TBPE. It can be seen that the presence of benzethonium in aqueous solution leads to a considerable increase in the extraction. The absorbance maximum of the extracts is at 615 mμ. The same absorption spectra as in Fig. 1 were obtained for spartein, tetraethylammonium, acetylchlorine, or thiamine. The blue color in the organic layer can be attributed to the ion pair formation between the TBPE and the cations.

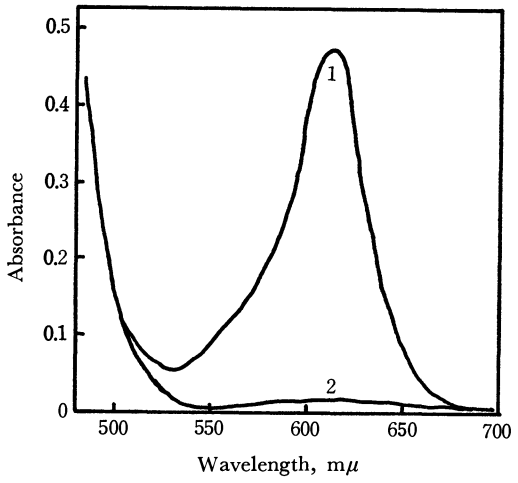

Fig. 1. Absorption spectra.
1: Spectrum of organic phase extracted from the aqueous solution (25 m*l*) containing 2×10^{-6} M of benzethonium, 8×10^{-5} M of TBPE and 5 m*l* of pH 8.5 buffer solution.
2: Spectrum of organic phase extracted from the aqueous solution (25 m*l*) containing the same component as that of curve 1 but benzethonium is absent.
Reference: Water

Effect of pH. The effect of pH on extraction was studied by extracting benzethonium from a series of aqueous solutions buffered at various pH values. As shown in Fig. 2, the absorbance of the extract was constant when the pH of the aqueous phase was in the range 7—11.

The extreme pH dependence was observed for the determination of quinine[3] or thiamine[4] with bromophenol blue or bromothymol blue. Similarly, no constant absorbance in any pH range could be obtained, when bromophenol blue or bromocresol green was used as extracting agent for benzethonium.

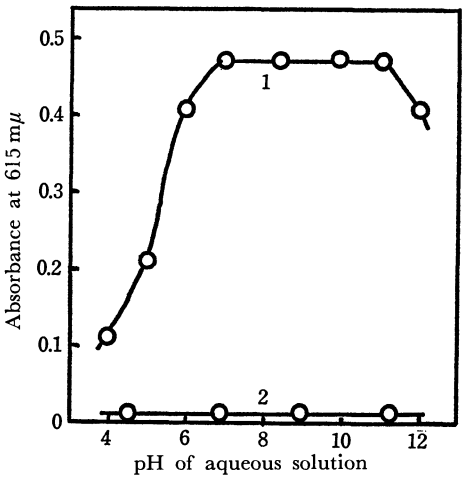

Fig. 2. Effect of pH.
1: Extract with 2×10^{-6} M benzethonium
2: Extract without benzethonium
Reference: Water

Effect of Reagents. The influence of TBPE concentration on extraction is illustrated in Fig. 3. It is apparent that the concentration of TBPE should be maintained greater than 10-fold molar excess over benzethonium to obtain a constant extraction. Excess amounts (2—10 m*l*) of the buffer solution used in the procedure had no influence on the absorbance of the

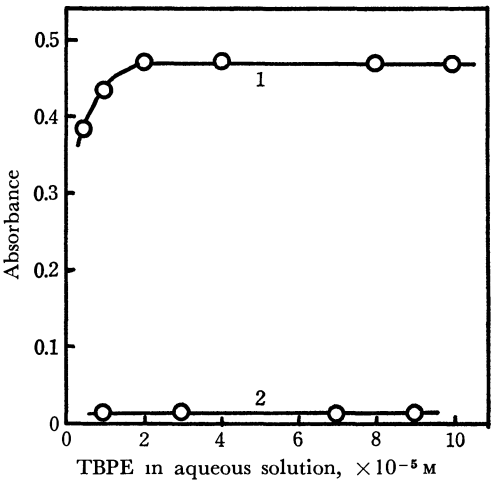

Fig. 3. Effect of the amount of TBPE.
1: Extract with 2×10^{-6} M benzethonium
2: Extract without benzethonium
Reference: Water

3) M. Tatsuzawa, S. Nakayama, and A. Okawara, *Bunseki Kagaku*, **19**, 761 (1970).
4) V. D. Gupta and D. E. Cadwallader, *J. Pharm. Sci.*, **57**, 112 (1968).

extract. When the addition of the buffer solution was less than 2 m*l*, no effective separation of the two layers was observed.

Solvent for Extraction. The behavior of various solvents in the extraction was studied. Solvents were found to be classified into the following three categories. (1) Those with which the presence of benzethonium leads to a considerable increase in the extraction of blue TBPE: *e.g.* chloroform, 1,2-dichloroethane. (2) Those which do not extract the blue TBPE even in the presence of benzethonium: *e.g.* monochlorobenzene, toluene, *n*-hexane, cyclohexane, carbon tetrachloride. (3) Those with which the blue TBPE is extractable even without benzethonium: *e.g.* methyl isobutyl ketone, nitromethane, nitrobenzene, butyl acetate, ethyl acetate, ether, isoamylalcohol.

1,2-Dichloroethane was found to be most suitable for the extraction of a TBPE-benzethonium system.

Other Variables. Full color development required about 1 min shaking. Continued shaking up to 5 min produced no further change in absorbance. The color intensity of dichloroethane extracts remains constant for 1 hr. Fluctuation of room temperature (16—27°C) gave no measurable effect on absorbance.

Calibration and Precision. The system followed Beer's law up to 4×10^{-6} M of benzethonium in aqueous layer, with molar absorptivity of 9.00×10^{4} mol^{-1} cm^{-1} liter at 615 mμ.

The reproducibility of the proposed method was estimated from the results of ten sample solutions, each with a final benzethonium concentration of 2.0×10^{-6} M. The mean absorbance was 0.450 with a standard deviation of 0.005 absorbance unit.

Percentage of Extraction and Composition of the Colored Species. A sample (25 m*l*) containing 4.0×10^{-6} M of benzethonium was extracted with 10 m*l* of dichloroethane at pH 8.5. The amounts of benzethonium in the aqueous layer and organic layer were then determined according to the proposed method. The percentage of extraction was about 5% in the absence and 99% in the presence of TBPE.

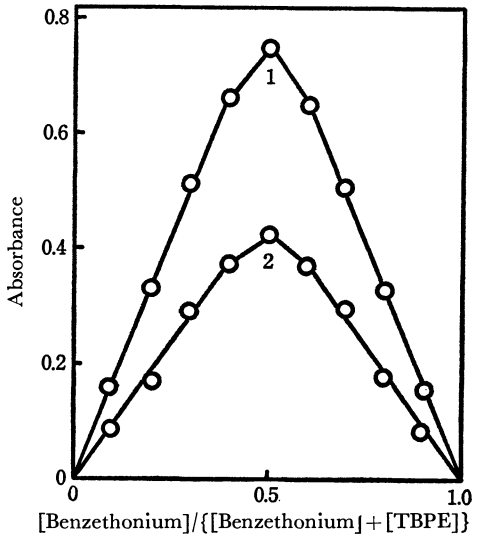

Fig. 4. Continuous variation curves.
Extraction was done from the aqueous solutions in which the total concentration of benzethonium plus TBPE was 8×10^{-6} M.
Reference: Reagent blank extracted from an aqueous solution without benzethonium
1: 615 mμ, 2: 590 mμ

Figure 4 shows the continuous variation curve for benzethonium. It might be suggested that a 1 : 1 ion-pair compound is formed in the dichloroethane phase between TBPE and benzethonium.

These results are characteristic of benzethonium as compared with diphenhydramine[1] in the extraction system.

Effect of Diverse Substances. Table 1 shows the effect of diverse substances on the determination of benzethonium. Organic cations interfere.

Table 1. Effect of diverse substances

Added extraneous substance	Ratio of extraneous substance over benzethonium, mol/mol	Error expressed by % recovery
Ammonium sulfate	3000	101
Calcium chloride	3000	100
Sodium carbonate	3000	100
Sodium chloride	3000	100
Sodium nitrate	3000	100
Potassium bromide	3000	100
Antipyrine	40	109
Benzyl alcohol	30000	100
Caffeine	30	111
o-Cresol	30000	100
Ethyl alcohol	30000	100
Glucose	30000	100
Lactose	30000	100
Nicotinamide	100	110
Papaverine	10	108
Phenol	30000	99
Sodium acetate	30000	100
Sodium citrate	30000	100
Sodium salicylate	30000	99
Sodium tannate	30000	100
Spartein	0.1	110
Tetraethylammonium bromide	0.1	110
Triethylamine	70	104
Starch (0.4%)	—	100

Benzethonium taken: 2×10^{-6} M

Analysis of Practical Samples. Waste Water: The method was applied to a waste water containing benzethonium which had been used as a disinfectant solution for cupboard and plate basket. The sample solution was diluted or concentrated, and then analyzed by the proposed method or titrimetric method.[2] The result was 3.97×10^{-4} M of benzethonium by the proposed method, and 3.95×10^{-4} M by the titrimetric method.

Pharmaceutical Preparation: A commercially available disinfectant solution obtained was treated in the same manner as the waste water. The result was 0.220 M of benzethonium by the proposed method, and 0.218 M by the titrimetric method.

The author expresses appreciation to Professor Y. Yamamoto of Hiroshima University for valuable advice.

Studies on Cobaloxime Compounds. IV. The Polarography of Cobaloximes

Yorikatsu HOHOKABE and Noboru YAMAZAKI

Department of Polymer Science, Faculty of Engineering, Tokyo Institute of Technology, Ookayama, Meguro-ku, Tokyo

(Received August 19, 1970)

Various types of cobaloximes, *e.g.*, *Co*-alkyl derivatives with different bases as an axial ligand and polymeric cobaloximes with the general formula of $Co(OH)(DH)_2$(Copoly—AM-VPy) (DH: dimethylglyoximato monoanion) in which Copoly—AM-VPy is a low-molecular-weight copolymer of acrylamide and 4-vinylpyridine, were prepared, and their half-wave potentials in cathodic reduction were compared to each other and to those of a few vitamin B_{12} compounds. All of them showed a single irreversible cathodic wave. Methyl- and cyanocobaloximes were reduced at more negative potentials than the corresponding methylcobalamin and cyanocobalamin(vitamin B_{12}). The half-wave potential of methylcobaloxime shifted in the direction of the more negative potentials as the donating strength of the axial base increased. This was correlated with the charge-transfer transition energies of those cobaloximes as determined from their electronic spectra. The polymeric cobaloximes were reduced at less negative potentials than the others.

The cobaloxime compounds have properties quite similar to those of vitamin B_{12} compounds in their chemical reactivity, as have been established especially by Schrauzer *et al.*[1] The oxidation and reduction of cobalt in those complexes are the most important steps in many of the reactions. The polarographic reduction is a useful means inasmuch as the half-wave potentials can be considered as resulting solely from the ease of the reduction of each complex itself, since mercury cathode has a common reducing power which can be controlled in any way; this is different from the reduction with other chemical reducing reagents, that is, the result of two reactants, *i.e.*, the complex and a reagent.

The polarographic behavior of cobaloximes has been studied extensively by Maki[2] and by Schrauzer *et al.*[3] Maki reported that $K[Co(CN)_2(DH)_2]\cdot 3/2H_2O$[4] showed a single irreversible wave at −1.105 V *vs.* SCE in 0.5 M Na_2SO_4; they attributed this wave to a two-electron reduction from Co(III) to Co(I). Schrauzer *et al.* reported the half-wave potentials of several cobaloximes. For example, $CoCl(DH)_2$(py) yields three cathodic waves, at −0.10, −1.0, and −1.27 V, *vs.* the Ag/AgCl electrode at 25°C in a 50% aqueous ethanolic solution, while there were four waves, at −0.67, −1.44, −2.42, and −3.06 V *vs.* Ag/0.10 M $AgNO_3$ at 25°C in acetonitrile. The first wave corresponds to the reduction of Co(III) to Co(II); the second, to Co(II)—Co(I), and the third, to Co(I)—Co(0), whereas the fourth is due to the reduction of pyridine. They have also reported the polarographic reduction of some alkylcobaloximes, which show two irreversible waves in acetonitrile. For instance, $CH_3Co(DH)_2(H_2O)$ yields two cathodic waves, at −1.7 and −2.42 V *vs.* Ag/0.10 M $AgNO_3$. From a comparison between these alkylcobaloximes and $CoCl(DH)_2$(py), they have deduced that the organocobaloximes are complexes of Co(II).

In this work, various types of cobaloximes, *e.g.*, *Co*-methyl derivatives with different axial bases and *Co*-alkylcobaloximes with pyridine as a common axial base were synthesized. The half-wave potentials of these cobaloximes were determined under the same conditions and were compared to each other and also to those of other several cobaloximes and vitamin B_{12} derivatives. The dependence of the ease of reduction upon the kind of the axial ligand was discussed. The results will be described below.

Experimental

Materials. All the alkylcobaloximes were synthesized mostly by the methods of Schrauzer and have been reported in previous publications.[5-7] The cyanocobalamin and methylcobalamin were kindly supplied by the Eisai Co. All the other reagents used in the measurements were of a G. R. grade and were obtained from commercial sources.

Measurements. The polarographic measurements were made with a Yanagimoto potential-controlled Polarograph (model PA102) at 25°C. All the complexes were dissolved in a 0.1 N K_2SO_4 aqueous solution. Before each determination, nitrogen gas was bubbled through the solution for 10 min. Two ppm of a copolymer of acrylamide and 4-vinylpyridine (Copoly—AM-VPy, AM : VPy molar ratio= 14.5, M_n=1500) were added to each solution in order to diminish the maximum wave. The characteristics of the capillary used were as follows: m=0.684 mg/sec and t= 4.55 sec, the values of which were measured in a 0.1 N K_2SO_4 aqueous solution.

Results and Discussion

All the cobalt complexes examined in this work showed a single irreversible cathodic wave under these conditions. These results were in good agreement with those on $K[Co(CN)_2(DH)_2]\cdot 3/2H_2O$ obtained by Maki, and not with those on the cobaloxime derivatives obtained by Schrauzer. According to Maki's results, which were obtained under conditions more similar to ours, this wave can be attributed to Co(III)—

1) *E. g.*, G. N. Schrauzer and J. Kohnle, *Chem. Ber.*, **97**, 3056 (1964); G. N. Schrauzer, *Accounts Chem. Res.*, **1**, 97 (1968).

2) N. Maki, *Kagaku*, **16**, 202 (1961); *Nature*, **188**, 227 (1960).

3) G. N. Schrauzer, R. J. Windgassen, and J. Kohnle, *Chem. Ber.*, **98**, 3324 (1965); G. N. Schrauzer and R. J. Windgassen, *J. Amer. Chem. Soc.*, **88**, 3738 (1966).

4) DH means the dimethylglyoximato monoanion.

5) N. Yamazaki and Y. Hohokabe, *Chem. Commun.*, **1968**, 829.

6) N. Yamazaki and Y. Hohokabe, This Bulletin, **44**, 63 (1971).

7) N. Yamazaki and Y. Hohokabe, submitted to this Bulletin.

Co(I) reduction. Most of the cobaloximes were reduced at more negative potentials than $Co(H_2O)_6^{2+}$, probably as a result of a strong interaction of dimethylglyoxime ligands with cobalt.

Many alkyl derivatives, especially hydroxypropyl and methyl derivatives, have been synthesized as model vitamin B_{12} compounds,[6] and their electronic and infrared absorption spectra, and also the effect on a B_{12}-dependent enzymatic reaction, have been reported.[6-8]

The reduction waves of these analogs and vitamin B_{12} compounds under the same conditions are compared in Table 1. Methylcobalamin or cyanocobalamin was reduced at a less negative potential than the corresponding methyl- or cyanocobaloximes. For example, methyl(pyridine)cobaloxime was reduced at a potential more negative by −0.11 V than that of methylcobalamin. Planary-coordinating-dimethylglyoxime ligands in cobaloximes seem to charge more electrons to cobalt atoms than does corrin in cobalamin.

TABLE 1. HALF-WAVE POTENTIALS OF METHYL- AND CYANO-COBALOXIMES, AND -COBALAMINS

Each material was dissolved in 0.1 N K_2SO_4 at the concentration of 3.0×10^{-4} M, unless indicated. Measurement was done at 25°C. Estimated errors were ±0.01 unless indicated.

Material[a]	$E_{1/2}$ (V *vs.* SCE)	$n\alpha$[d]
$Co(CN)(DH)_2(py)$[b]	−1.19[d]	0.33
Cyanocobalamin[c]	−1.09	0.41
$CH_3Co(DH)_2(H_2O)$	−1.26	0.31
$CH_3Co(DH)_2$(nico)	−1.28	0.29
$CH_3Co(DH)_2$(tolu)	−1.28	0.30
$CH_3Co(DH)_2$(py)	−1.31	0.33
$CH_3Co(DH)_2$(pico)	−1.33	0.35
$CH_3Co(DH)_2$(imd)	−1.40	0.27
Methylcobalamin[c]	−1.20	0.25
$[Co(H_2O)_6]Cl_2$	−1.21	0.37

a) py; pyridine. nico; nicotinamide. tolu; *p*-toluidine. pico; *γ*-picoline. imd; imidazole.
b) 0.6×10^{-4} M. c) 1.0×10^{-4} M. d) ±0.02.

The half-wave potentials of *Co*-methylcobaloximes are affected by another axial ligand. As the electron-donating power of the axial base increases, the potential shifts to more negative potentials. The relationship between the pK_a of the axial base and the half-wave potential of the cobaloxime is shown in Fig. 1. The order of the ease of reduction coincided with that of the spectrochemical shift of methylcobaloximes;[7] *i.e.*, the charge-transfer transition energies of methylcobaloximes decreased in this order: (imidazole)-, (*γ*-picoline)-, (pyridine)-, (*p*-toluidine)-, (nicotinamide)-, and aquocobaloxime. Therefore, the half-wave potentials measured in this experiment are considered to be a measure of the reducibility of the Co atom in these complexes.

8) Y. Hohokabe and N. Yamazaki, This Bulletin, **44**, 798 (1971).

Generally, in the polarographic reduction, the electron from the mercury cathode is transferred to the lowest vacant orbital of the reductant. According to molecular orbital theory, non-bonding orbitals (d_{xy}, d_{yz}, d_{zx}) are filled with 6 electrons in the case of an octahedral Co(III) complex, and the antibonding orbital (σ^*) is the lowest vacant one which is formed with the formation of the corresponding bonding orbital (σ) by the interaction of the d_{z^2} orbital of the central metal with suitable orbitals of axial ligands. Therefore, the potential at which the reduction of the complex occurs probably depends directly upon the absolute energy level of the lowest vacant orbital, and not necessarily upon the energy difference between σ and σ^*. Since the stronger interaction of the axial-base component causes increasing negative potentials of the reduction, as has been mentioned above, it is considered that a strong interaction of the base results in raising the absolute energy level of σ^*. If the absolute energy level of σ is assumed to be less affected by the formation of molecular orbitals between cobalt and ligands than that of σ^*, the energy difference between σ and σ^*, *i.e.*, ν_I, which can be determined by studying the electronic spectrum, should increase with the interaction of the ligands in the complex.

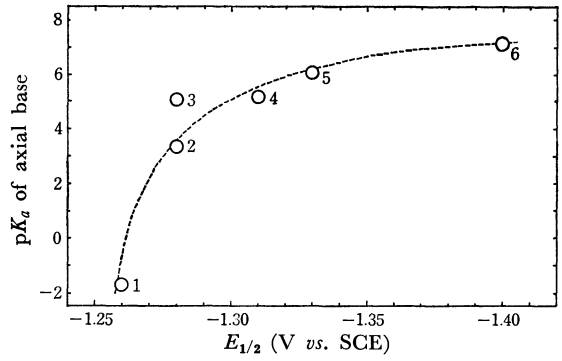

Fig. 1. The relationship between pK_a of the axial base and the half-wave potential of the methylcobaloxime, $CH_3Co(DH)_2B$.
B: 1, H_2O; 2, nicotinamide; 3, *p*-toluidine; 4, pyridine; 5, *γ*-picoline; 6, imidazole.

In short, $\Delta E_{1/2}$ which is the difference between a half-wave potential of methylcobaloxime and that of a given cobaloxime as a criterion, and $\Delta\nu_I$, which is the difference in charge-transfer transition energy between them, are expected to be correlated. Using as a criterion methylaquocobaloxime, in which coordinating water is considered to be the weakest ligand among the ligands examined in this work, we could obtain the correlation between $\Delta\nu_I$ and $\Delta E_{1/2}$; it is illustrated in Fig. 2. Methyl(imidazole)cobaloxime is not included here because its ν_I is obscurely shown as a shoulder band on its electronic spectrum. As is shown in Fig. 2, there is clearly a relationship between $\Delta\nu_I$ and $\Delta E_{1/2}$, supporting the argument just presented. In other words, as has been discussed above, a strongly-interacting ligand raises the σ^* orbital, while the level of σ is less affected, resulting in making the reduction potential more negative and in raising

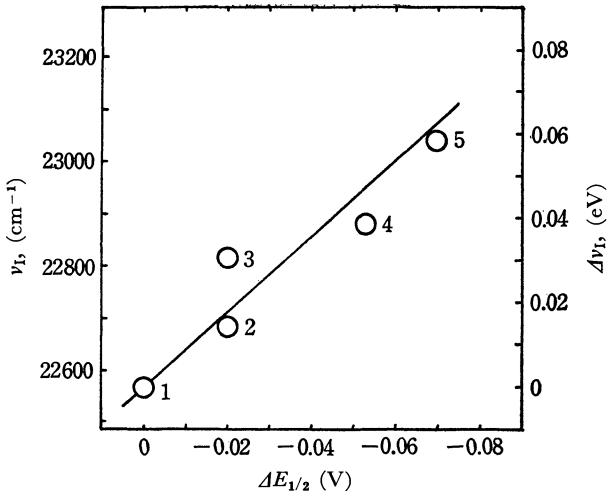

Fig. 2. The correlation between $\Delta\nu_I$ and $\Delta E_{1/2}$ of methylcobaloximes.
The data of methylaquocobaloxime were adopted as a standard for the calculation of $\Delta\nu_I$ and $\Delta E_{1/2}$. ν_I is the lowest charge-transfer transition energy which had been obtained directly from electronic spectral data.[7]
1, H_2O; 2, nicotinamide; 3, *p*-toluidine; 4, pyridine; 5, *γ*-picoline.

the charge-transfer transition energy ($\sigma\rightarrow\sigma^*$). This is well supported by the fact that the slope of the $\Delta\nu_I$ *vs.* $\Delta E_{1/2}$ plots is around 0.9; this shows that the differentiations are of the same degree in both series.

Many (pyridine)cobaloximes with various kinds of another axial ligand were also examined; the results are shown in Table 2. Simple alkyl derivatives were reduced at nearly the same potential, while benzyl and hydroxypropyl derivatives were at less negative potentials. The argument which has just described in the case of methylcobaloximes, *i.e.*, that a strongly coordinating ligand raises the level of the antibonding orbital, could not be ascertained in (pyridine)-cobaloximes with a different axial ligand, such as Cl, CN, and alkyl, because the low solubility of chloro- and cyano-cobaloximes in water prevented us from determining their spectrochemical sequences in those (pyridine)cobaloxime series. However, speaking only of alkyl derivatives, the relationship between ν_I and $E_{1/2}$ was not observed. Benzyl and hydroxyalkyl ligands have substituents of different natures, such as the aromatic ring and the hydroxy group respectively, so that the affinity of the complex to the electrode might differ from those of simple alkyl derivatives.

The ease of the reduction depends, of course, on the electron affinity of the cobalt atom in the complex. In addition, it is known that the half-wave potential is governed by the rate of the reduction reaction at the cathode in the irreversible reduction; *i.e.*, the higher the rate of reduction reaction, the less negative the potential. The higher rate of the reduction reaction will be attained by the larger value of the rate constant of the electrode reaction. This is probably the consequence of the closer distance between the cathode and the reactant (Co atom), and of the electron affinity of the cobalt atom in the complex.

It is expected that a strongly electron-attractive ligand facilitates the reduction of the complex. Since the Hammett σ constants are considered to be a measure of the electronic properties of the ligand, the half-wave potentials of (pyridine)cobaloximes are correlated with the constants of their axial ligands in Figs. 3 and

Table 2. Half-wave potentials of various (pyridine)cobaloximes: $CoX(DH)_2$(pyridine), or $RCo(DH)_2$(pyridine)

Each material was dissolved in 0.1 N K_2SO_4 at the concentration of 3.0×10^{-4} M, unless indicated. Measurement was done at 25°C. Estimated errors were ±0.01 unless indicated.

Material X or R	$E_{1/2}$ (V *vs.* SCE)	$n\alpha$[d]
CN[a]	−1.19[d]	0.33
$C_6H_5CH_2$[b]	−1.20[d]	0.74[e]
$CH_3CH(OH)CH_2$	−1.24[d]	0.35
$HOCH_2CH(OH)CH_2$	−1.26	0.27
$HOCH_2CH(CH_3)$	−1.27[d]	0.28
Cl[c]	−1.28	0.31
$CH_3CH_2CH_2$	−1.30	0.33
$CH_3CH(CH_3)$	−1.30	0.31
CH_3	−1.31	0.33
CH_3CH_2	−1.31	0.32

a) 0.6×10^{-4} M. b) 1.0×10^{-4} M. c) 1.5×10^{-4} M.
d) ±0.02. e) ±0.05.

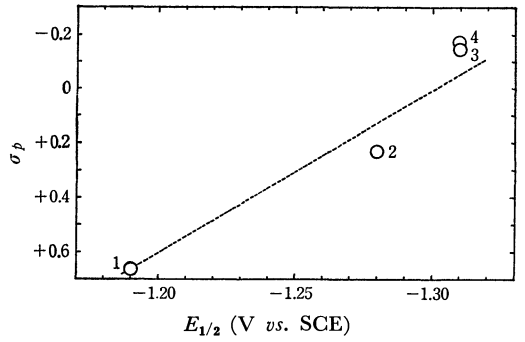

Fig. 3. The relationship between the Hammett constant σ_p and the half-wave potential of (pyridine)cobaloximes: $CoX(DH)_2$(pyridine).
X: 1, CN; 2, Cl; 3, CH_3CH_2; 4, CH_3.

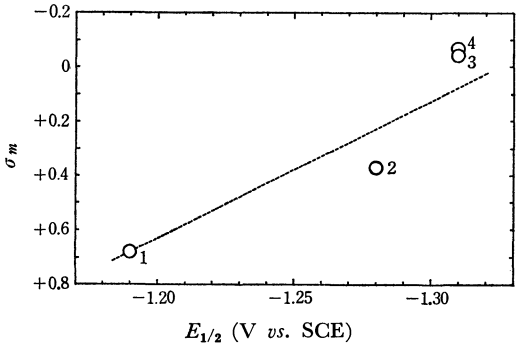

Fig. 4. The relationship between the Hammett constant σ_m and the half-wave potential of (pyridine)cobaloximes: $CoX(DH)_2$ (pyridine).
X: 1, CN; 2, Cl; 3, CH_3CH_2; 4, CH_3.

Table 3. Half-wave potentials of polymeric cobaloximes and others

Measurement was done in 0.1 N K_2SO_4 at 25°C. Copoly—AM-VPy means a copolymer of acrylamide (AM) and 4-vinylpyridine (VPy). The molecular weight and AM : VPy molar ratio are: a, 1400 and 13.7; b, 3000 and 11.9, respectively.[4] The concentration was: a, b, 2.0×10^{-4} M (Co); c, 3.0×10^{-4} M. Estimated errors were: d, ±0.01; e, ±0.02; f, ±0.04.

Material	$E_{1/2}$ (V *vs.* SCE)	$n\alpha$[e]
$Co(OH)(DH)_2$(Copoly—AM-VPy)[a]	−1.15[e]	0.70
$Co(OH)(DH)_2$(Copoly—AM-VPy)[b]	−1.16[d]	0.60
$CoCl(DH)_2(H_2O)$[c)]	−1.22[f]	0.36
$Co(OH)(DH)_2(H_2O)$[c]	−1.26[d]	0.25

4. The complex with an electron-attractive ligand is reduced at a less negative potential, as has been expected. However, it was found, from an investigation of the infrared spectra of cobaloximes,[6] that the electron-attractive ligand in the sixth position causes stronger interaction between Co and the fifth ligand, *i.e.*, the axial base, in turn resulting in an increase in the electron density of the equatorial moiety in the cobaloxime. The observation of the polarographic behavior seems to be inconsistent with that of the infrared spectra. It is also expected, however, that the electron from the mercury cathode is transferred to Co through an electron-attractive ligand, such as CN or Cl; this facilitates the reduction of the central cobalt atom, irrespective of the electron density of the Co in the complex.

The polymeric cobaloximes have also been prepared and described previously.[5,9] They are reduced at less negative potentials than other, analogous monomeric cobaloximes, as is shown in Table 2. The half-wave potentials of polymeric cobaloximes were expected to be more negative than that of hydroxo-aquocobaloxime. Nevertheless, the reduction of the former was observed to take place at a less negative potential than that of the latter. This might be due to a polymer effect, by which the existence of amide groups in the neighborhood of the Co moiety facilitated the electron-transfer from the cathode to the complex. The addition of the same copolymer to the other monomeric cobaloximes did not change their half-wave potentials, but only diminished the maximum wave which was generally observed in the absence of a surface-active agent. Since polyacrylamide is known as a surface-active agent, the facilitating effect of the polymeric ligand on the reduction of the polymeric cobaloxime may be attributed to the strong adhesion of polymeric cobaloxime to the dropping mercury cathode, thus facilitating reduction reaction by the electron of mercury cathode. The half-wave potential was not affected by a change in the molecular weight of the polymeric ligand.

9) The half-wave potentials of polymeric cobaloximes reported previously had more negative values, but they may have been incorrectly standardized.

The Crystal Structure of κ'-Al_2O_3, the New Intermediate Phase

Masataro Okumiya and Goro Yamaguchi

Department of Industrial Chemistry, Faculty of Engineering, The University of Tokyo, Hongo, Tokyo

(Received August 24. 1970)

A structure model of κ'-Al_2O_3 has been obtained by means of X-ray powder diffraction data. An hexagonal unit cell with $a=5.544$ and $c=9.024$ Å and containing $5\frac{1}{3}$ Al_2O_3 was assumed. The oxygen arrangement is the same close packed structure as that of tohdite, and $10\frac{2}{3}$ aluminium atoms are statistically distributed over several octahedral and tetrahedral positions. The R factor for the reflection intensity is 0.13 for 115 reflections.

The first investigation of the dehydration of tohdite $5Al_2O_3 \cdot H_2O$ was performed by Krischner in 1966 using the electron diffraction method.[1] In 1970, a more detailed investigation[2] was performed by the present authors using electron diffraction, X-ray powder diffraction, thermogravimetric measurement, differential thermal analysis, and the measurement of the density; the following transformation series were thus established:

$$\text{tohdite} \xrightarrow{\text{dehyd.}} \kappa'\text{-}Al_2O_3 \rightarrow \kappa\text{-}Al_2O_3 \rightarrow \alpha\text{-}Al_2O_3$$

The κ'-Al_2O_3 was found to be a new unstable intermediate phase and was easily produced by heating tohdite(F)[2] in a high vacuum at just the dehydration temperature. It seems necessary, for a further discussion of the transformation series, to elucidate the atomic arrangement of this unstable phase. The present work has been performed in order to elucidate the atomic arrangement and to confirm the conclusion of the previous discussion. For this purpose, the structure analysis was made by the X-ray powder diffraction method.

Experimental Procedure

The specimen of κ'-Al_2O_3 (from tohdite) used in this work was prepared as follows. Tohdite obtained by treating gibbsite hydrothermally with AlF_3 was heated in a high vacuum (10^{-4} mmHg) up to the temperature of complete dehydration (750°C) and then cooled rapidly to room temperature. This was performed in a high-vacuum TGA instrument[2] in order to check the dehydration percentage. The κ'-Al_2O_3 (from tohdite) was obtained as hexagonal plates with a micron-order size and containing about 0.3% of fluorine as an impurity; this specimen was denoted as κ'-Al_2O_3 (from tohdite(F)) in the previous paper.[2] In the present X-ray intensity calculation, the small amount of fluorine was neglected.

The X-ray powder diffraction diagram was obtained by means of Ni-filtered Cu$K\alpha$ radiation using a Rigaku Denki diffractometer equipped with a scintillation counter and a pulse-height discriminator. The diffraction intensities relative to the (202) intensity were obtained by measuring the peak areas. 41 peaks were measured up to $\sin\theta/\lambda=0.621$ Å^{-1}. No correction was made for the preferred orientation effect on the intensity.

Structure Determination

In the previous paper,[2] κ'-Al_2O_3(from tohdite) was assumed to have a hexagonal unit cell of almost the same size as that of tohdite $5Al_2O_3 \cdot H_2O$. The cell dimensions calculated from the powder diffraction data are $a=5.544\pm0.001$ and $c=9.024\pm0.001$ Å. Density measurement showed that this unit cell contains about $5\frac{1}{3}$ of Al_2O_3, namely, 16 oxygen atoms and $10\frac{2}{3}$ aluminium atoms.

On the basis of this unit cell, the X-ray powder diffraction pattern can be indexed. The systematic absences among the observed reflections of κ'-Al_2O_3 (from tohdite) are the same as those of tohdite: *hhl* with $l=2n+1$. The possible space groups are $P\bar{3}1c$, $P31c$, $P6_3mc$, $P\bar{6}2c$, and $P6_3/mmc$.

It was found that the intensity distribution of the reflections of κ'-Al_2O_3 (from tohdite) resembles that of the corresponding reflections of tohdite (especially that of the reflections at $2\theta>40°$) (Fig. 1). Therefore, we considered κ'-Al_2O_3 (from tohdite) to have a structure similar to that of tohdite. We attempted to derive a structure model of κ'-Al_2O_3 (from tohdite) from the structure of tohdite as determined from the X-ray powder diffraction data.[3,4] The space group of κ'-Al_2O_3 (from tohdite) was assumed to be the same as that of tohdite, $P6_3mc$.

The structure factors are obtained from the X-ray powder diffraction intensities. The intensities of the overlapping peaks were separated into the ratio of the calculated intensities of the corresponding reflections of tohdite. A three-dimensional Fourier synthesis was made using these structure factors and the phases of the corresponding reflections of tohdite.

After a several-cycle refinement of Fourier synthesis, the outline of the structure of κ'-Al_2O_3 (from tohdite) was obtained as follows: The arrangement of oxygen atoms was revealed to be the same as that of tohdite, ABAC closed packing. As for the positions of the aluminium atoms, it was found that the aluminium atoms are distributed over several octahedral and tetrahedral positions, including aluminium positions in tohdite, and that some of their occupancies are less than 1. These occupancy factors were refined by the least-squares method. The least-squares analysis program was written for the HITAC 5020E computer, in which the occupancy factors of aluminium atoms were varied so as to minimize $R_I'=\sum(I_o-I_c)^2$, where:

I_o=integrated intensity

$I_c=K \cdot I_p \cdot \sum_i m_i \cdot |F_c|^2$, where:

$\sum_i$=the sum over overlapping peaks

1) H. Krischner, *Ber. Deut. Keram. Ges.*, **39**, 1366 (1966).

2) M. Okumiya, G. Yamaguchi, O. Yamada, and S. Ono, *bid.*, **44**, 418 (1971).

3) G. Yamaguchi, H. Yanagida, and S. Ono, *ibid.*, **37**, 752 (1964).

4) G. Yamaguchi, M. Okumiya, and S. Ono, *ibid.*, **42**, 2247 (1969).

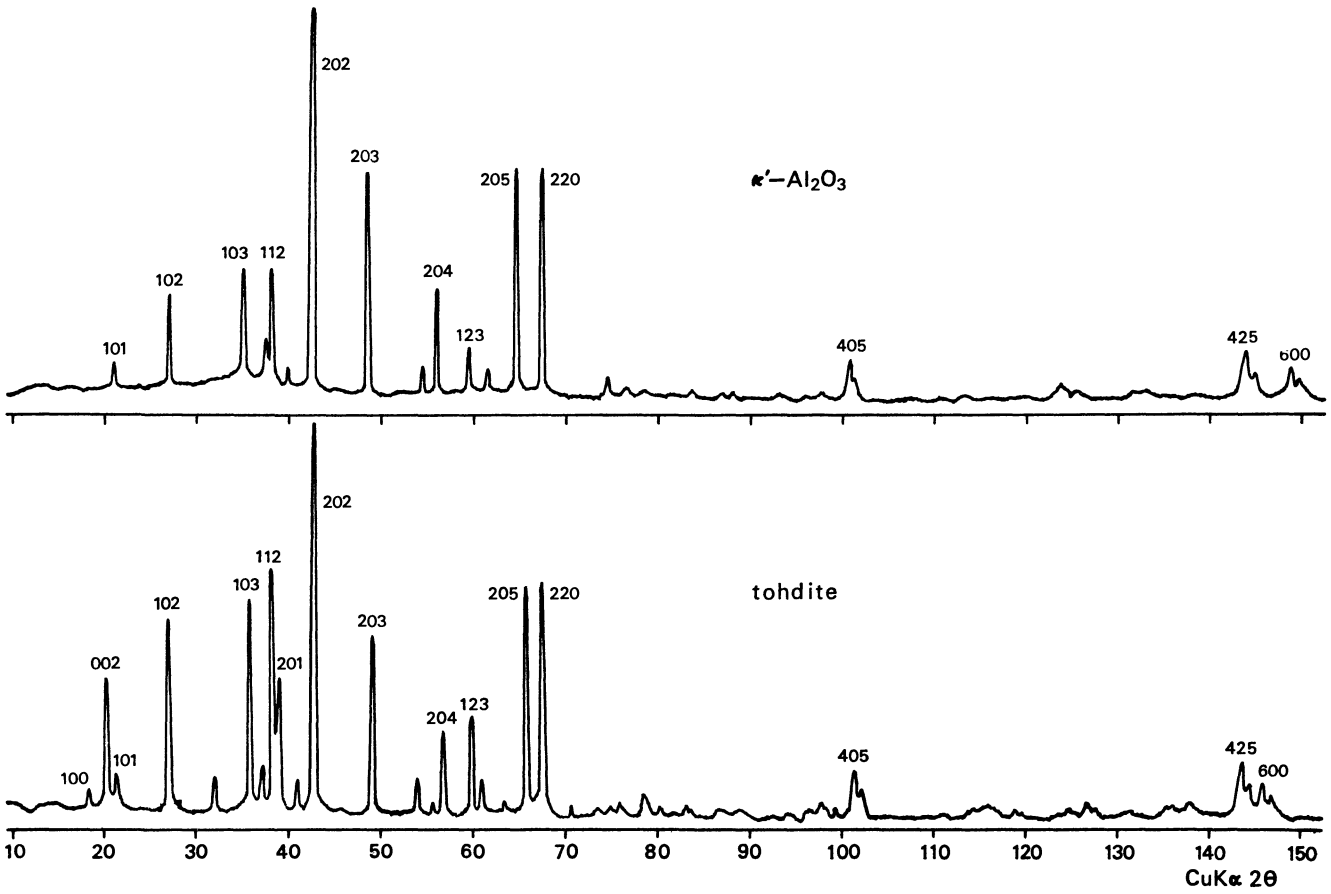

Fig. 1. X-Ray powder diffraction pattern of κ'-Al_2O_3 and tohdite.

K=scale factor
m_i=multiplicity
L_p=Lorentz and polarization factor

The structure factor, F_c, is presented as:
$F_c=\sum_j p_i \cdot f_j \cdot \exp 2\pi i(hx_j+ky_j+lz_j)$, where:
p_j=occupancy factor

In the calculation of the structure factor, an overall isotropic temperature factor was used. Six occupancy factors were varied independently, while the restrictive condition, $\Sigma p=10\frac{2}{3}$, was neglected. The occupancy factors of oxygen atoms were fixed as 1.0. The final occupancy factors and their standard deviations, as estimated from the diagonal element of the inverse to the least-squares matrix, are listed in Table 1, together with the atomic coordinates.

Table 1. Atomic coordinates and occupancy factors with their standard deviations ($\times 10^2$)

Position	x	y	z	p	Number of equivalent positions
O(1)	0	0	0	1.0	2
O(2)	0.500	$-x$	0.006	1.0	6
O(3)	0.832	$-x$	0.256	1.0	6
O(4)	1/3	2/3	0.254	1.0	2
Al(1)	1/3	2/3	0.056	0.51(2)	2
Al(2)	0.833	$-x$	0.061	0.08(1)	6
Al(3)	2/3	1/3	0.148	0.98(5)	2
Al(4)	0.156	$-x$	0.118	0.34(1)	6
Al(5)	0.169	$-x$	0.363	0.67(3)	6
Al(6)	0.884	$-x$	0.448	0.12(2)	6

Overall isotropic temperature factor 0.72 (0.05)Å^2

The calculated intensities for the parameter of Table 1 are listed in Table 2. The $R_I=\Sigma|I_o-I_c|/\Sigma I_o$ factor is 0.13.

Discussion

The results of this structure calculation confirmed the previous conclusions that the oxygen sub-lattice is preserved during the transformation from tohdite to κ'-Al_2O_3 (from tohdite) and that aluminium atoms are randomly distributed over the octahedral and tetrahedral positions. The distribution of the aluminium atoms of Table 1 is illustrated in Fig. 2. The total number of aluminium atoms in the unit cell is calculated as 10.2 ($\sigma=0.3$). This is in fairly good agreement with the ideal, $\Sigma p_j=10\frac{2}{3}$.

Between the second and the third layers of oxygen atoms, aluminium atoms are distributed over the octahedral positions, Al(5), and the tetrahedral positions, Al(6). The obtained occupancy factor for the Al(5) positions of 0.67 is considered to be 2/3; this means that three Al(5) positions are occupied randomly by two aluminium atoms, while in the structure of tohdite the corresponding positions are fully occupied by three aluminium atoms. The Al(6) positions are partly occupied, with an occupancy factor of 0.12, while the

TABLE 2. X-RAY POWDER PATTERN DATA FOR κ'-Al_2O_3 (from tohdite)

h	k	l	d_{obs}	d_{cal}	I_o	I_c	h	k	l	d_{obs}	d_{cal}	I_o	I_c
1	0	0		4.801	0	0	2	1	7	(1.051)	1.051		5
0	0	2		4.512	0	0	4	1	0		1.048	5	0 7
1	0	1	4.233	4.239	7	7	1	1	8		1.045		2
1	0	2	3.284	3.288	24	24	4	1	1		1.041	0	0
1	1	0		2.772	0	2	3	2	3		1.034	2	4
1	0	3	2.546	2.549	37	36	2	0	8		1.021		0
2	0	0	2.399	2.401	12	12	4	1	2	1.021	1.021	4	4 5
1	1	2	2.360	2.362	32	33	2	2	6		1.020		1
2	0	1		2.320	0	3	3	0	7		1.004	0	0
0	0	4	2.255	2.256	6	5	4	0	5	0.999	0.999	17	16
2	0	2	2.118	2.119	100	101	1	3	6		0.997	0	0
1	0	4		2.042	0	0	2	3	4		0.990	0	0
2	0	3	1.876	1.876	61	58	4	1	3		0.989	0	1
1	2	0		1.815	0	1	1	0	9		0.981	0	0
1	2	1		1.779	0	0	5	0	0		0.960	0	0
1	1	4		1.750	0	1	2	1	8		0.958	1	1
1	2	2	1.683	1.684	8	9	5	0	1		0.955	0	0
1	0	5		1.689	0	1	1	4	4		0.950	0	0
2	0	4	1.643	1.644	28	33	3	2	5		0.940	0	0
3	0	0		1.600	0	0	5	0	2		0.939	0	1
3	0	1		1.576	0	1	4	0	6		0.938	3	2
1	2	3	1.553	1.554	14	14	3	1	7		0.926		3
3	0	2	1.507	1.508	7	8	2	0	9		0.925	9	3 8
0	0	6		1.504	0	0	3	3	0		0.924		0
2	0	5	1.442	1.443	76	73	3	0	8		0.922		2
1	0	6		1.435	0	0	5	0	3		0.915	2	1
1	2	4		1.414	0	0	4	2	0		0.907		1
3	0	3		1.413	0	0	4	1	5		0.906		0
2	2	0	1.386	1.386	72	75	3	3	2		0.905	8	1 6
1	3	0		1.332	0	0	4	2	1		0.903		2
2	2	2		1.325	0	0	0	0	10		0.902		1
1	1	6		1.322	0	1	4	2	2	(0.889)	0.890		7
1	3	1		1.317	0	1	3	2	6		0.889	6	0 7
3	0	4		1.305	0	0	1	0	10		0.887		0
1	2	5		1.280	0	1	5	0	4		0.884	0	0
1	3	2		1.227	0	2	4	0	7		0.878	0	0
2	0	6	1.274	1.275	11	8	2	1	9		0.878	0	0
1	0	7	1.245	1.245	6	4	2	2	8	0.875	0.875	14	17
1	3	3	1.218	1.218	7	8	4	2	3	0.869	0.869	9	9
4	0	0	1.200	1.200	2	2	5	1	0		0.862	0	0
3	0	5		1.197	0	0	3	1	8		0.861	0	1
4	0	1		1.190	1	2	4	1	6		0.860		1
2	2	4		1.181	0	3	5	1	1		0.858	3	0 2
4	0	2	1.160	1.160	4	5	1	1	10		0.858		1
1	2	6		1.158	0	1	3	3	4		0.855	0	0
1	3	4		1.147	0	0	3	0	9		0.850	0	0
2	0	7		1.136	0	0	5	0	5		0.848	0	0
0	0	8	1.128	1.128	5	4	5	1	2		0.847	0	1
4	0	3	1.115	1.115	5	7	2	0	10	0.845	0.845	16	9 19
2	3	0		1.101	0	0	4	2	4	0.842	0.842		10
1	0	8		1.098		1	3	2	7		0.837	6	4
3	0	6		1.096	1	0 1	5	1	3		0.829	3	3
2	3	1		1.093		0	4	0	8		0.822	0	0
3	1	5		1.072	0	1	4	1	7		0.813	0	0
3	2	2		1.070	0	1	4	2	5	0.811	0.811	40	38
4	0	4	1.060	1.060	4	6	5	0	6		0.809	0	1
							5	1	4		0.805	0	0
							6	0	0	0.800	0.800	27	26
							6	0	1		0.797	0	0

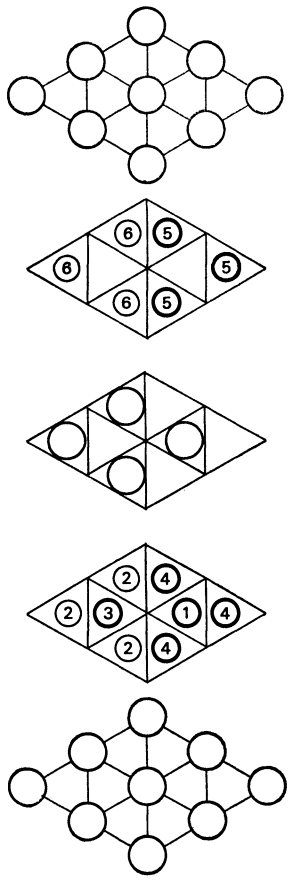

Fig. 2.

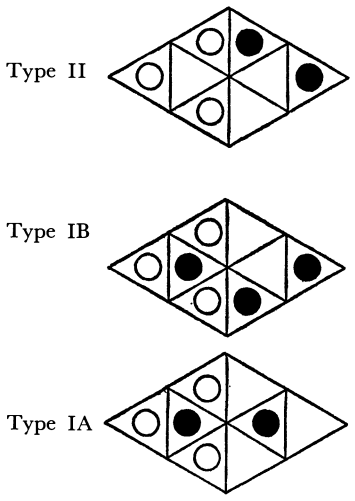

Fig. 3. Arrangement of aluminium atoms in the 1st (type IA, IB) and the 2nd (type II) aluminium layers of κ'-Al_2O_3 (from tohdite).

corresponding positions of tohdite are vacant. This type of cation arrangement is denoted as Type II; one of the three possible arrangements is illustrated in Fig. 3.

Between the first and the second oxygen layers aluminium atoms are distributed over octahedral, Al(3) and Al(4), and tetrahedral, Al(1) and Al(2), positions. The obtained occupancy factors, 0.98 for Al(3), 0.34 for Al(4), and 0.51 for Al(1), are considered to be 1, 1/3, and 1/2 respectively. The distribution of aluminium atoms between these oxygen layers could be explained as the average of two types of cation arrangement: Type IA: the Al(3) and Al(1) positions are fully occupied, and Al(2) is partly (12%) occupied. If we overlook the atoms in Al(2), this type is found in tohdite between the corresponding oxygen layers. Type IB: Al(3) is fully occupied, the three Al(4) positions are occupied by two aluminium atoms, and the Al(2) positions are partly (8%) occupied.

There are two types of combinations of adjacent aluminium layers, *i.e.*, IA-II and IB-II. In the former type, there is no face-shared contact between oxygen polyhedra around aluminium atoms. In the latter type, some of the oxygen octahedra have to share contact faces along the *c*-axis.

Considering that the occupancy factors for Al(6) and Al(2) are rather small and that the unstable κ'-Al_2O_3 (from tohdite) might not be described as a definite unit cell, but as a statistical structure average, it is possible that other octahedral and tetrahedral positions (Fig. 4) are also occupied by aluminium atoms with small occupancy factors. However, no other highly occupied aluminium positions should exist except those listed in Table 1, since the structure proposal of Table 1 is satisfactory enough to explain the X-ray powder pattern of κ'-Al_2O_3 (from tohdite).

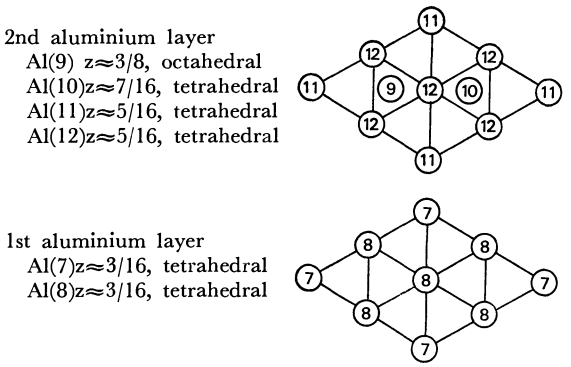

Fig. 4. Tetrahedral and octahedral positions of aluminium atoms which might be occupied with small occupancy.

According to the above-mentioned structure, κ'-Al_2O_3 (from tohdite) may be described as a partly cation-redistributed structure of tohdite and as an unstable intermediate phase in the transformation from tohdite to κ'-Al_2O_3 (from tohdite).

All the calculations were performed with HITAC 5020E computer of the Computation Center of the University of Tokyo. The calculation of the Fourier synthesis was done by the use of Universal Crystallographic Computation Program System 5020 UNICS.

Several Novel Ru(VI) and Ru(IV) Complexes Derived from [RuO_4bipy] and [RuO_3phen]$_2O$

Toshio ISHIYAMA

Radiation Center of Osaka Prefecture, Shinke-cho, Sakai, Osaka

(Received August 31, 1970)

Five novel neutral complexes of ruthenium(VI) and ruthenium(IV) with 2,2′-bipyridine and 1,10-phenanthroline, [$RuO_2(OH)_2$bipy]·$3H_2O$, [$Ru(OH)_3$phen]$_2O$, [RuO_2bipy$_2$]·$3H_2O$, [RuO_2bipy·phen]·$3H_2O$ and [RuO_2phen$_2$], were prepared and characterized by a study of their infrared, visible and ultraviolet absorption spectra, and by polarographic measurements. [$RuO_2(OH)_2$bipy] and [$Ru(OH)_3$phen]$_2O$ were obtained by the reduction of previously-reported complexes, [RuO_4bipy] and [RuO_3phen]$_2O$ respectively, with methanol, and [RuO_2bipy$_2$], [RuO_2bipy·phen] and [RuO_2phen$_2$], by the reactions of [RuO_4bipy] and [RuO_3phen]$_2O$ in methanol with 2,2′-bipyridine and 1,10-phenanthroline respectively. [RuO_2bipy·phen] and [RuO_2phen$_2$] were also obtained in methanol by the substitution reactions of [RuO_2bipy$_2$] and [RuO_2bipy·phen] with 1,10-phenanthroline respectively. The five complexes were all diamagnetic. [$RuO_2(OH)_2$bipy] was assumed to be a "ruthenyl" complex with two oxide ions coordinated at the *trans* positions, like such well-known *trans*-dioxo-ruthenyl analogues as $Cs_2[RuO_2Cl_4]$ and [$RuO_2(OH)_2(NH_3)_2$], and [$Ru(OH)_3$phen]$_2O$ was assumed to be a binuclear complex with an oxygen-bridge between ruthenium atoms. [RuO_2bipy$_2$], [RuO_2bipy·phen], and [RuO_2phen$_2$] were assumed to be mononuclear complexes with two oxide ions coordinated at the *trans* positions, and their oxidation numbers were found polarographically, to be 4.

Organic chelate compounds of "ruthenyl" and oxo-bridged binuclear ruthenium(IV) species with coordinated hydroxy groups have not been reported, since most "ruthenyl" and hydroxoruthenium species are very unstable and are easily hydrolyzed. Wagnerova[1] attempted to prepare a "ruthenyl" oxalate, $[RuO_2ox_2]^{2-}$, by the reduction of ruthenium tetroxide with oxalate ions. He reported that there was no evidence of a "ruthenyl" oxalate, $[RuO_2ox_2]^{2-}$, although the corresponding osmium(VI) species was very stable, and that $[Ruox_3]^{2-}$ might be obtained. Lott and Symons[2] and Woodhead and Fletcher[3] obtained several ruthenyl complexes formulated as $[Ru^{VI}O_2X_4]^{2-}$. They suggested that the two oxygen atoms of "ruthenyl" complexes, like their osmium analogues, could all be presumed to be *trans*, and reported that the complexes were all diamagnetic, probably because of the low symmetry of the ligand field.

Bis(2,2′-bipyridine)- and bis(1,10-phenanthroline)-ruthenium(IV) chelates, with two oxide ions coordinated at the *trans* positions in either case, have not been reported. Dwyer and his co-workers[4] prepared dichlorobis(2,2′-bipyridine)- and dichlorobis(1,10-phenanthroline)-ruthenium(II) complexes, and they denoted them as $[Ru^{II}B_2Cl_2]^0$. They reported that these neutral complexes were spin-paired and showed no tendency of disproportionation to the tris complexes under normal experimental conditions, although the bis-iron(II) chelates rapidly disproportionate in aqueous solutions, and suggested that the Ru(II) complexes isolated had *cis*-configurations.

In the present paper five new complexes, [$RuO_2(OH)_2$bipy]·$3H_2O$, [$Ru(OH)_3$phen]$_2O$, [RuO_2bipy$_2$]·$3H_2O$, [RuO_2bipy·phen]·$3H_2O$, and [RuO_2phen$_2$], are reported, they were obtained by the reduction and substitution reactions of two previously-reported complexes,[5),6)] [RuO_4bipy]·$3H_2O$ and [RuO_3phen]$_2O$, with 2,2′-bipyridine and 1,10-phenanthroline in methanol.

Experimental

Materials. Ruthenium(III) chloride monohydrate (extra pure grade) supplied by Mitsuwa Chemicals & Co. was used without further treatment. Both 2,2′-bipyridine and 1,10-phenanthroline were supplied by Yoneyama Chemicals. The former was purified by recrystallization from distilled water, and the latter, from ethanol after it had been dried by heating at 115°C for 3 hr. Commercial methanol was dried by treatment with magnesium ribbon and iodine. Lithium perchlorate (extra pure grade) supplied by Mitsuwa Chemicals & Co. was purified by recrystallization from methanol after drying.

Syntheses. (1) Dioxodihydroxo(2,2′-bipyridine)-ruthenium(VI), [$RuO_2(OH)_2$bipy]·$3H_2O$, and μ-Oxo-bis[trihydroxo-(1,10-phenanthroline)ruthenium(IV)], [$Ru(OH)_3$phen]$_2O$: A solution of 1 g of [RuO_4bipy]·$3H_2O$ or [RuO_3phen]$_2O$ in 150 m*l* of methanol was refluxed and shaken on a hot-water bath until the solution turned dark-brown. The solution was then evaporated to dryness, and the residue was recrystallized from methanol and dried *in vacuo*. Yields: dioxodihydroxo(2,2′-bipyridine)ruthenium(VI), 93.85%, and μ-oxo-bis[trihydroxo(1,10-phenanthroline)ruthenium-(IV)], 95.15%, on the basis of the starting complexes. The product complexes are insoluble in carbon tetrachloride, benzene, ether, acetone, and dioxane, but are soluble in water, methanol, ethanol, acetic acid, and dimethyl formamide. Both complexes are stable in methanol, and [$RuO_2(OH)_2$bipy] is stable in water too. However, the aqueous solution of [$Ru(OH)_3$phen]$_2O$ slowly changes from dark-brown to green, probably because of air oxidation in water. The ruthenium and water contents and the molecular weights of the complexes were measured by methods reported previously.[5)]

1) Wagnerova, D. M., *Collection Czech. Commun.*, **27**, 1130 (1962).
2) K. A. K. Lott and M. C. R. Symons, *J. Chem. Soc.*, **1960**, 973.
3) J. L. Woodhead and J. M. Fletcher, UKAEA, AERE, **R-4123**.
4) Late F. P. Dwyer, H. A. Goodwin, and E. C. Gyarfas, *Aust. J. Chem.*, **16**, 544 (1963).
5) T. Ishiyama, *Ann. Rep. Rad. Ctr. Osaka*, **8**, 40 (1967).
6) T. Ishiyama, This Bulletin, **42**, 2071 (1969).

Found: Ru, 26.58; C, 32.24; H, 4.03; N, 7.47; H_2O, 14.05%; mol wt, 330. Calcd for $[RuO_2(OH)_2(C_{10}H_8N_2)]\cdot 3H_2O$: Ru, 26.79; C, 31.83; H, 4.24; N, 7.43; H_2O, 14.24%; mol wt, 325(anhydride).

Found: Ru, 31.36; C, 41.47; H, 3.28; N, 8.24%; mol wt, 650. Calcd for $[Ru(OH)_3(C_{12}H_8N_2)]_2O$: Ru, 29.95; C, 42.28; H, 3.23; N, 8.22%; mol wt, 681.

(2) Dioxobis(2,2'-bipyridine)ruthenium(IV), $[RuO_2bipy_2]\cdot 3H_2O$, and *Dioxobis(1,10-phenanthroline)ruthenium(IV), $[RuO_2phen_2]$*: To a solution of 1 g of $[RuO_4bipy]\cdot 3H_2O$ or $[RuO_3phen]_2O$ in 15 m*l* of methanol, 5 g of 2,2'-bipyridine or 1,10-phenanthroline was added. The reaction mixture was refluxed under shaking on a hot-water bath until the solution turned orange-brown. The solution was then evaporated to dryness, and the residue was repeatedly washed with benzene and then dissolved in pure water. An insoluble product was filtered off. The solution was concentrated, and the crystals formed were recrystallized from pure water and dried *in vacuo*. Yield: dioxobis(2,2'-bipyridine)ruthenium(IV), 96.15%, and dioxobis(1,10-phenanthroline)-ruthenium(IV), 98.35%, on the basis of the starting complexes. Both complexes are insoluble in carbon tetrachloride, benzene, ether, ester, and dioxane, but are soluble in water, methanol, acetic acid, acetone, and dimethyl formamide.

Found: Ru, 20.16; C, 47.29; H, 4.22; N, 10.19; H_2O, 11.00%; mol wt, 450. Calcd for $[RuO_2(C_{10}H_8N_2)_2]\cdot 3H_2O$: Ru, 20.40; C, 48.00; H, 4.40; N, 11.20; H_2O, 10.80%; mol wt, 446(anhydride).

Found: Ru, 20.35; C, 58.43; H, 3.41; N, 11.51%; mol wt, 510. Calcd for $[RuO_2(C_{12}H_8N_2)_2]$: Ru, 20.65; C, 58.30; H, 3.25; N, 11.33%; mol wt, 494.

(3) Dioxo(2,2'-bipyridine)(1,10-phenanthroline)ruthenium(IV), $[RuO_2bipy\cdot phen]\cdot 3H_2O$: To a solution of 1 g of $[RuO_4bipy]\cdot 3H_2O$ in 150 m*l* of methanol, 5 g of 1,10-phenanthroline were added. The reaction mixture was refluxed under shaking on a hot-water bath until the solution turned orange-brown. Then we followed the procedure described in the proceding section. Yield: 84.42%, on the basis of $[RuO_4bipy]\cdot 3H_2O$. The complex is insoluble in carbon tetrachloride, benzene, ether, ester, and dioxane, but is soluble in water, methanol, ethanol, acetic acid, acetone, and dimethyl formamide.

Found: Ru, 19.14; C, 50.53; H, 4.37; N, 11.17; H_2O, 11.00%; mol wt, 510. Calcd for $[RuO_2(C_{10}H_8N_2)(C_{12}H_8N_2)]\cdot 3H_2O$: Ru, 19.16; C, 50.57; H, 4.19; N, 10.68; H_2O, 10.30%; mol wt, 470(anhydride).

(4) Tetraoxo(2,2'-bipyridine)ruthenium(VIII), $[RuO_4bipy]\cdot 3H_2O$, and μ-Oxo-bis[trioxo(1,10-phenanthroline)ruthenium(VII)], $[RuO_3phen]_2O$. These substances were synthesized according to the methods reported in previous papers.[5,6] The results of the elemental analyses and the molecular weights coincided with those reported previously.

Absorption Spectra. The infrared absorption spectra were obtained on an infrared spectrophotometer, Model IR-S of the Japan Spectroscopic Co., by the KBr disk method. The crystalline water of the complexes was removed by heating for 15 hr at 115°C. It was ascertained from the elemental analysis that the structure of the complexes is not altered by this treatment. The visible and ultraviolet absorption spectra were measured with a Beckmann Model D.U. spectrophotometer.

Magnetic Measurements. The magnetic susceptibility was measured at 25°C with a Cahn R.G. Electrobalance by the Faraday method. The five new complexes were all found to be diamagnetic.

Polarographic Measurements. The polarographic measurements were carried out with a Yanagimoto Automatic Recording Polarograph (Type PA 101). The characteristics of the capillary used were $m=0.648$ mg/sec and $t=4.63$ sec/drop in a 0.5 mol/*l* $LiClO_4$ methanol solution when the height of the mercury reservoir was 70.0 cm and when the applied potential was 0 volt *vs.* a saturated mercurous sulfate reference electrode at 25°C. A conventional H-type electrolytic cell with a potassium sulfate-saturated agar bridge and a sintered glass disk was used as the reference electrode. The experimental procedure was as follows: In order to make the solutions to be measured, four standard solutions were first prepared by dissolving crystals of $[RuO_2bipy_2]$, $[RuO_2bipy\cdot phen]$, $[RuO_2phen_2]$, and $[Ru(OH)_3phen]_2O$ in methanol; the concentrations of the complexes were all adjusted to 10^{-3} mol/*l*. Lithium perchlorate was used as the supporting electrolyte, and its concentration was adjusted to 1 mol/*l*. A 10-m*l* portions of each standard solution was transferred into a 50-m*l* Erlenmeyer flask, to which was then added 10 m*l* of a mol/*l* solution of lithium perchlorate in methanol. A part of the mixture was transferred into an electrolytic cell. The dissolved oxygen was removed by bubbling nitrogen gas in for about half an hour, and the polarograms were recorded in a flow of nitrogen gas through the surface of the solution in an electrolytic cell.

Results and Discussion

Oxidation States of the Complexes. Polarograms of the four new complexes are shown in Fig. 1. All the complexes measured are reduced polarographically in two steps. The half-wave potentials of the first waves of $[RuO_2bipy_2]$, $[RuO_2bipy\cdot phen]$, $[RuO_2phen_2]$, and $[Ru(OH)_3phen]_2O$ are −0.18, −0.19, −0.22, and −0.21 V *vs.* Hg, Hg_2SO_4 (satd.) elec. respectively in 0.5 mol/*l* $LiClO_4$ methanol solutions,

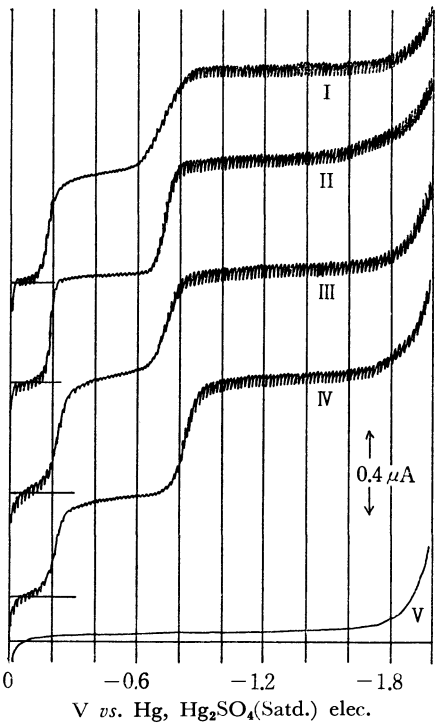

Fig. 1. Polarograms of the complexes.
I: 5×10^{-4} mol/*l* $[RuO_2bipy_2]$, II: 5×10^{-4} mol/*l* $[RuO_2bipy\cdot phen]$, III: 5×10^{-4} mol/*l* $[RuO_2phen_2]$, IV: 5×10^{-4} mol/*l* $[Ru(OH)_3phen]_2O$, V: 0.5 mol/*l* $LiClO_4$ in CH_3OH (the supporting electrolyte).

while those of the second waves are −0.71, −0.73, −0.74, and −0.82 volt respectively. The ratios of the height of the first wave to that of the second are approximately 1 : 1 for all the complexes. Consequently, the first and second waves correspond to a gain of one electron each, indicating the reduction from Ru(IV) to Ru(III), and from Ru(III) to Ru(II) states, respectively. A similar polarogram has also been reported by Niedrach and Tevebaugh[7] for ruthenium(IV) in a perchloric acid solution. They interpreted this as meaning that ruthenium(IV) was step-by-step reduced to Ru(III) and to Ru(II) states. As a result, the oxidation numbers of ruthenium in $[RuO_2bipy_2]$, $[RuO_2bipy\cdot phen]$, $[RuO_2phen_2]$, and $[Ru(OH)_3phen]_2O$ were all concluded to be 4.

Compositions of the Complexes. (1) Dioxodihydroxo(2,2'-bipyridine)ruthenium(VI) and μ-Oxo-bis[trihydroxo(1,10-phenanthroline)ruthenium(IV)]: From the results of the elemental analysis, the mole ratios of ruthenium to 2,2'-bipyridine or 1,10-phenanthroline were both found to be 1 : 1. The data of the molecular weight indicate that the oxohydroxoruthenium(VI) complex with 2,2'-bipyridine is mononuclear, and that the hydroxoruthenium(IV) complex with 1,10-phenanthroline is an oxo-bridged binuclear species.

(2) Dioxobis(2,2'-bipyridine)ruthenium(IV) and dioxobis(1,10-phenanthroline)ruthenium(IV): From the results of the elemental analysis, the mole ratios of ruthenium to 2,2'-bipyridine or 1,10-phenanthroline were both found to be 1 : 2. The data of the molecular weight indicate that both of the complexes, $[RuO_2bipy_2]$ and $[RuO_2phen_2]$, are mononuclear.

(3) Dioxo(2,2'-bipyridine)(1,10-phenanthroline)-ruthenium(IV): From the results of the elemental analysis, the mole ratio of ruthenium, 2,2'-bipyridine, and 1,10-phenanthroline seems to be 1 : 1 : 1. The observed molecular weight indicates that the complex is mononuclear, $[RuO_2bipy\cdot phen]$.

Reduction and Substitution Reactions of $[RuO_4bipy]$ and $[RuO_3phen]_2O$ with 2,2'-bipyridine and 1,10-phenanthroline in Methanol. The reactions of $[RuO_4bipy]$ and $[RuO_3phen]_2O$ are shown schematically in Fig. 2.

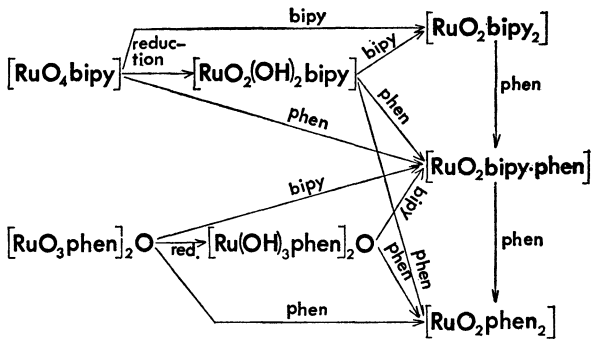

Fig. 2. Reduction and substitution reactions of $[RuO_4bipy]$ and $[RuO_3phen]_2O$ in methanol.

$[RuO_2(OH)_2bipy]$ and $[Ru(OH)_3phen]_2O$ are formed by the reduction of $[RuO_4bipy]$ and $[RuO_3phen]_2O$ respectively, with methanol. It was confirmed, by elemental analyses and by comparison of the spectra, that $[RuO_2bipy_2]$ was formed by the reactions of $[RuO_4bipy]$ or $[RuO_2(OH)_2bipy]$ with 2,2'-bipyridine, and that $[RuO_2phen_2]$ was produced by the reactions of $[RuO_3phen]_2O$ or $[Ru(OH)_3phen]_2O$ with 1,10-phenanthroline. It was also found that the mixed-ligand complex, $[RuO_2bipy\cdot phen]$, could be synthesized by the following reactions in mehtanol: (1) the reaction of $[RuO_4bipy]$ with 1,10-phenanthroline, (2) the reactions of $[RuO_3phen]_2O$ and $[Ru(OH)_3phen]_2O$ with 2,2'-bipyridine, and (3) the stoichiometric reaction between equimolar 1,10-phenanthroline and $[RuO_2(OH)_2bipy]$. In the third reaction, $[RuO_2phen_2]$ was formed if an excess of 1,10-phenanthroline was employed. $[RuO_2bipy\cdot phen]$ and $[RuO_2phen_2]$ were also obtained in methanol by the substitution reactions of $[RuO_2bipy_2]$ and $[RuO_2bipy\cdot phen]$ respectively with equimolar 1,10-phenanthroline. The structures of these bis-chelates of dioxoruthenium(IV) will be discussed later.

Air Oxidation of $[Ru(OH)_3phen]_2O$ in an Aqueous Solution. An aqueous solution of $[Ru(OH)_3phen]_2O$ changes slowly from dark-brown to green, probably because of air oxidation in water. It was confirmed from the spectral change that $[Ru(OH)_3phen]_2O$ was transformed to $[RuO_3phen]_2O$ in water.

Infrared Absorption Spectra. The main infrared absorption bands of the present complexes are shown in Table 1, together with those of free ligands. The C=N, C=C, and C–H stretching peaks are all shifted to the higher frequency side by ligation in a manner similar to the cases of $[RuO_4bipy]$ and $[RuO_3phen]_2O$.[5,6] The absorption bands at 3380 and 3390 cm^{-1} of oxo-hydroxoruthenium(VI) and oxo-bridged hydroxoruthenium(IV) complexes with 2,2'-bipyridine and 1,10-phenanthroline respectively were assigned to the O–H stretching. Similar observations have been reported for hydroxo-complexes of osmium,[8] hydroxonitrosyl ruthenium complexes,[9] and $[Re(OH)Cl_2(O\cdot COC_3H_7)]_2$.[10] The infrared spectra of the ruthenium(IV) oxide complexes with 2,2'-bipyridine and 1,10-phenanthroline contain no peaks which can be attributed to the O–H stretching frequencies, indicating that the hydroxo groups are not present in the ruthenium(IV) oxide complexes.

Electronic Absorption Spectra. The visible and ultraviolet absorption spectra of oxo-hydroxoruthenium(VI), oxoruthenium(IV), and oxo-bridged hydroxoruthenium(IV) complexes with 2,2'-bipyridine and 1,10-phenanthroline were measured in water and methanol. They are shown in Figs. 3 to 7, together with those of pure ligands in water.

Dioxodihydroxo(2,2'-bipyridine)ruthenium(VI) has six absorption bands, at 670, 560, 450, 364, 290, and 244 mμ (Fig. 3). Four of those peaks, those at 670, 560, 450, and 364 mμ, may all be assigned to the charge transfer from ligand to metal. Considerable data on the spectra of tetrahedral oxyanions, which

7) L. W. Niedrach and A. D. Tevebaugh, *J. Amer. Chem. Soc.*, **73**, 2835 (1951).
8) W. P. Griffith, *J. Chem. Soc.*, **1964**, 245.
9) D. Scargill, *ibid.*, **1961**, 4444.
10) R. Cotton, "The Chemistry of Rhenium and Technetium," Interscience Publishers, New York (1965), p. 111.

Table 1. The characteristic infrared absorption bands of oxo-hydroxoruthenium(VI), oxo-bridged hydroxoruthenium(IV) and oxoruthenium(IV) complexes with 2,2'-bipyridine and 1,10-phenanthroline (cm^{-1})

Assignments	bipy	$[RuO_2(OH)_2bipy]$	$[RuO_2bipy_2]$	phen	$[Ru(OH)_3phen]_2O$	$[RuO_2phen_2]$
ν(O-H)		3380			3390	
ν(C=N)	1582	1605	1610	1621	1625 sh	1630
ν(C=C)	1560	1565	1580	1585 1560	1600 1580 sh	1595 1565
ν(C-H)	759	775	780	762 730	770 720	770 730

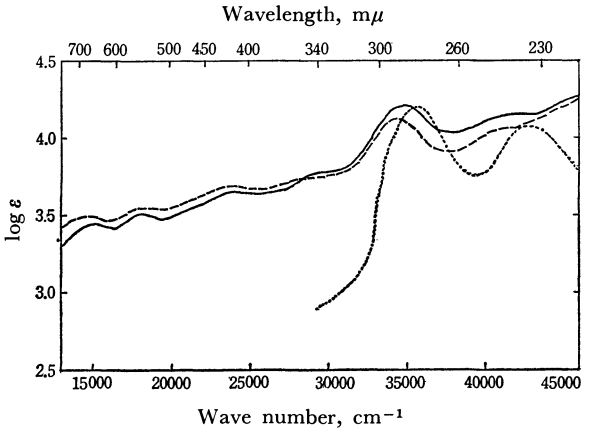

Fig. 3. Absorption spectra of $[RuO_2(OH)_2bipy]$ and 2,2'-bipyridine.
—— $[RuO_2(OH)_2bipy]$ in H_2O, ---- $[RuO_2(OH)_2bipy]$ in CH_3OH, ------ bipy in H_2O

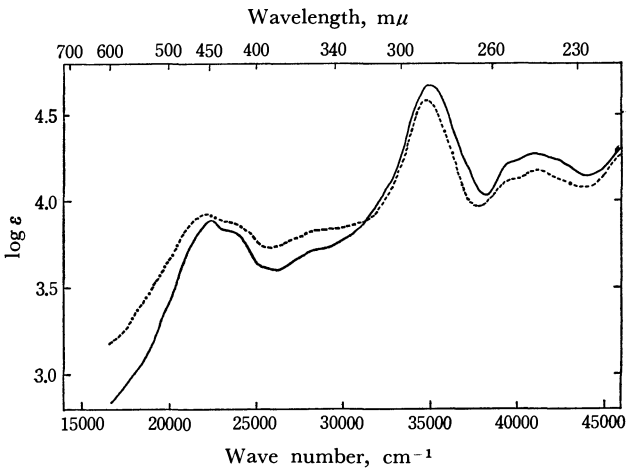

Fig. 4. Absorption spectra of $[RuO_2bipy_2]$ in water (——) and methanol (------).

have one or two *d* electrons in their ground states, were reported by Symons and his co-workers[11,12] and by Wolfsberg and Helmholz.[13] They suggested that the lowest transitions in such oxyanions as CrO_4^{3-}, MnO_4^{2-}, MnO_4^{3-}, and FeO_4^{2-} might also be interpreted as due to the charge transfer from oxygen to metal. The 290 and 244 mμ bands appear to be intraligand transitions corresponding to the two bands at 279 and 233 mμ in 2,2'-bipyridine.

Dioxobis(2,2'-bipyridine)ruthenium(IV) has five absorption bands and a shoulder at 450, 425, 350, 287, 244, and 255 mμ respectively (Fig. 4). A similar spectrum has also been reported by Fergusson and Harris[14] for tris(2,2'-bipyridine)ruthenium(II) chloride, which has six absorption bands at 452, 425, 348. 287, 250, and 245 mμ and which shows a close resemblance to those of the present complex, $[RuO_2bipy_2]$, in the intensity and the characteristic shape of each band. They suggested that the 452 and 425 mμ bands might be assigned to the charge transfer from metal to ligand ($t_{2g} \rightarrow \pi^*$ transitions), and the 348 mμ band, to the charge transfer from ligand to metal ($\pi \rightarrow e_g^*$ transition). The 450 and 425 mμ bands in the present complex, $[RuO_2bipy_2]$, may also be assigned to the charge transfer from metal to ligand, and the 350 mμ band, to the charge transfer from ligand to metal. The two peaks in the ultraviolet region appear to be intraligand transitions corresponding to the 279 and 233 mμ bands observed for free 2,2'-bipyridine.

Dioxobis(1,10-phenanthroline)ruthenium(IV) has four peaks and two shoulders at 450, 420, 265, 225, 310, and 290 mμ respectively (Fig. 5). A similar, spectrum has also been reported by Crosby, Perkins

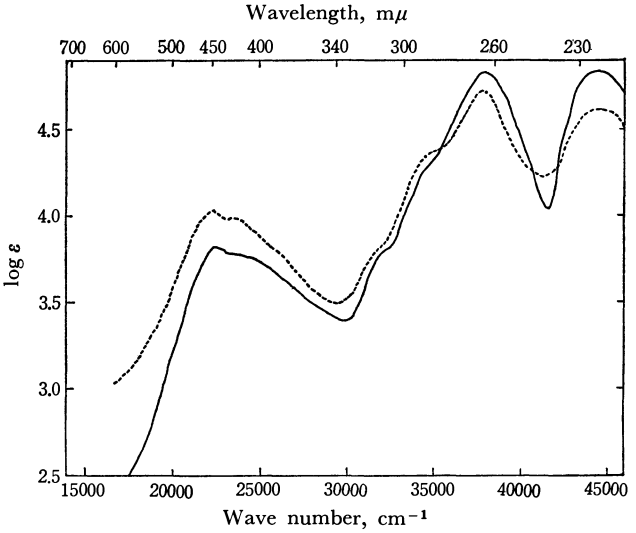

Fig. 5. Absorption spectra of $[RuO_2phen_2]$ in water (——) and methanol (------).

11) A. Carrington, D. S. Schouland, and M. C. R. Symons, *J. Chem. Soc.*, **1957**, 659.
12) A. Carrington, D. J. E. Ingram, D. S. Schouland, and M. C. R. Symons, *ibid.*, **1956**, 4710.
13) M. Wolfsberg and L. Helmholz, *J. Chem. Phys.*, **20**, 837 (1952).
14) J. E. Fergusson and (Miss) G. M. Harris, *J. Chem. Soc., A*, **1966**, 1293.

and Klassen[15] for tris(1,10-phenanthroline)ruthenium(II) chloride, which has six absorption bands at 450, 420, 315, 288, 265, and 223 mμ; this spectrum bears a remarkable resemblance to those of the present complex, $[RuO_2phen_2]$, in the intensity and the characteristic shape of each band. They suggested that the 450 and 420 mμ bands might be assigned to the charge transfer from metal to ligand. The 450 and 420 mμ bands in the present complex, $[RuO_2phen_2]$, may also be assigned to the charge transfer from metal to ligand. The two shoulders and the two peaks observed in the ultraviolet region appear to be intraligand transitions corresponding to the 320, 290, 265, and 230 mμ bands in free 1,10-phenanthroline.

Dioxo(2,2′-bipyridine)(1,10-phenanthroline)ruthenium(IV) has six peaks at 450, 425, 370, 290, 265, and 225 mμ (Fig. 6). The 450 and 425 mμ bands may both be assigned to the charge transfer from metal to ligand, and the 370 mμ band, to the charge transfer from ligand to metal. The latter charge-transfer transition (ligand-to-metal) is probably due to the coordination of the 2,2′-bipyridine molecule. A similar absorption band has been reported by Fergusson and Harris[14] for $[Ru^{II}Cl_2bipy_2]$ and $[Ru^{III}Cl_2bipy_2]Cl\cdot 3H_2O$. The three peaks observed in the ultraviolet region appear to be intraligand transitions corresponding to the 279 mμ band in 2,2′-bipyridine and to the 265 and 230 mμ bands in 1,10-phenanthroline respectively. The electronic absorption data show that this compound is a mixed-ligand complex of 2,2′-bipyridine and 1,10-phenanthroline.

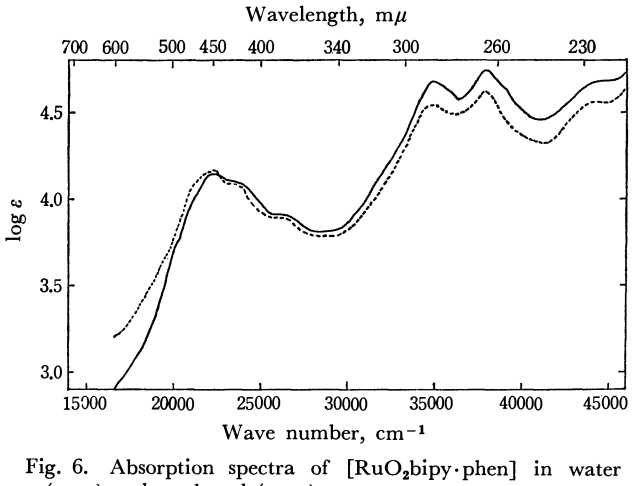

Fig. 6. Absorption spectra of $[RuO_2bipy\cdot phen]$ in water (——) and methanol (------).

μ-Oxo-bis[trihydroxo(1,10-phenanthroline)ruthenium(IV)] has four peaks and two shoulders at 450, 375, 265, 222, 315, and 290 mμ respectively (Fig. 7). The two peaks observed at 450 and 375 mμ may both be assigned to the charge transfer from metal to ligand, as in $[RuO_2phen_2]$. The charge-transfer bands for the present complex, $[Ru(OH)_3phen]_2O$, are observed in a shorter-wavelength region than those of the previous complex, $[RuO_3phen]_2O$. This fact shows that the charge-transfer transitions of $[Ru(OH)_3phen]_2O$ occur with a higher energy than those of $[RuO_3phen]_2O$. The two charge-transfer bands of $[Ru(OH)_3phen]_2O$ are diffusely observed in comparison with those of $[RuO_2phen_2]$, presumably due to an interaction between two ruthenium atoms or a low symmetry of the binuclear species. The two shoulders and two peaks observed in the ultraviolet region may all be assigned to the intraligand transitions of 1,10-phenanthroline. The spectrum of $[Ru(OH)_3phen]_2O$ which has been oxidized with air for a month in water coincides with that of the first complex, $[RuO_3phen]_2O$, showing that the present complex, $[Ru(OH)_3phen]_2O$, is transformed to $[RuO_3phen]_2O$ in water. This fact was also confirmed by the elemental analysis and by measurement of the molecular weight and the magnetic susceptibility.

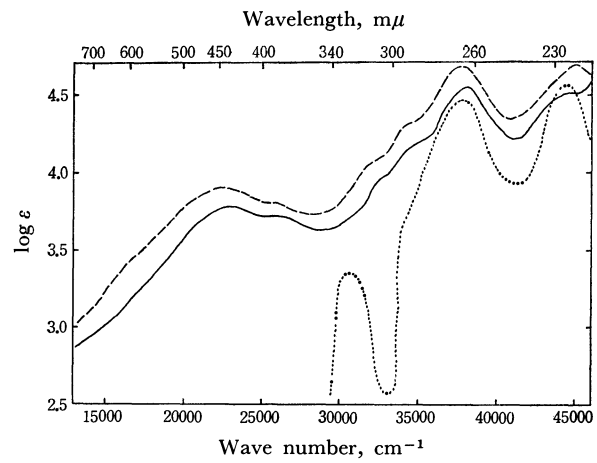

Fig. 7. Absorption spectra of $[Ru(OH)_3phen]_2O$ and 1,10-phenanthrolone.
—— $[Ru(OH)_3phen]_2O$ in H_2O, ---- $[Ru(OH)_3phen]_2O$ in CH_3OH, ------ phen in H_2O

Magnetic Properties. The observed diamagnetism of dioxodihydroxo(2,2′-bipyridine)ruthenium(VI) indicates the pairing of the two *d* electrons in Ru(VI). The complex contains the ruthenium atom octahedrally bonded one 2,2′-bipyridine, two oxide, and two hydroxide ligands. The molecular orbital treatments of $[RuO_2Cl_4]^{2-}$ and $[OsO_2(OH)_4]^{2-}$ which have been reported by Lott and Symons[2] may be applied to $[RuO_2(OH)_2bipy]$ just as to the asymmetrical "ruthenyl" complex, $[RuO_2(OH)_2(NH_3)_2]$.[16]

The diamagnetism of μ-oxo-bis[trihydroxo(1,10-phenanthroline)ruthenium(IV)] may be explained by applying the molecular orbital treatment of $K_4[Ru_2OCl_{10}]$ which has been reported by Dunitz and Orgel.[17]

The diamagnetism of dioxobis(2,2′-bipyridine)-, dioxobis(1,10-phenanthroline)-, and dioxo(2,2′-bipyridine)(1,10-phenanthroline)-ruthenium(IV) is especially interesting. Each of the present complexes, $[RuO_2bipy_2]$, $[RuO_2phen_2]$, and $[RuO_2bipy\cdot phen]$, contains the ruthenium atom octahedrally bonded to two oxide and two 2,2′-bipyridine or 1,10-phenanthroline ligands, and the four d electrons must exist as two pairs, assuming a *trans*-configuration with two

15) G. A. Crosby, W. G. Perkins, and D. M. Klassen, *J. Chem. Phys.*, **43**, 1498 (1965).

16) W. P. Griffith, "The Chemistry of the Rarer Platinum Metals," Interscience Publishers, New York (1967), p. 157.

17) J. D. Dunitz and L. E. Orgel, *J. Chem. Soc.*, **1953**, 2594.

oxide ligands. It was reported by Deguchi[18] and Nakai for $[Cu(bipy)_2(ClO_4)]ClO_4$ and $[Cu(phen)_2(H_2O)](NO_3)_2$ that the steric interference between H-atoms linked to the 3- and 3'- or 2- and 9-carbon atoms might be removed by the tetrahedral distortion of the two 2,2'-bipyridine or 1,10-phenanthroline molecules respectively. This may be assumed to be a *trans*-configuration when the above consideration is applied to the present complexes, $[RuO_2bipy_2]$, $[RuO_2phen_2]$, and $[RuO_2bipy\cdot phen]$.

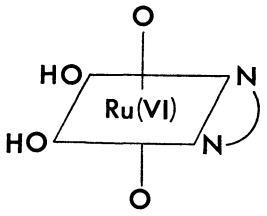

Fig. 8. The proposed structure of $[RuO_2(OH)_2bipy]$.

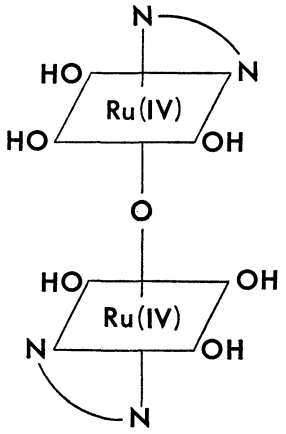

Fig. 9. The proposed structure of $[Ru(OH)_3phen]_2O$.

The structures shown in Figs. 8 and 9 seem clear possibilities for the two types of the present complexes. The oxidation number of $[RuO_2(OH)_2bipy]$ is assumed to be 6, and those of $[Ru(OH)_3phen]_2O$, $[RuO_2bipy_2]$, $[RuO_2phen_2]$ and $[RuO_2bipy\cdot phen]$, to be 4.

The author wishes to express his thanks to Professor Shinichi Kawaguchi of Osaka City University for his kind guidance and encouragement throughout this work, and to Professor Hideo Yamatera, the University of Nagoya, for his guidance in molecular orbital consideration. His thanks are also due to Dr. Tetsuo Mamuro, the chairman of the Department of Health Physics and Instrumentation of the Radiation Center of Osaka Prefecture, for his encouragement and support, to Dr. Toyokichi Kitagawa of Osaka City University for his guidance in the measurement of polarograph, and to Dr. Shichio Kawai, the University of Osaka, for his guidance in the measurement of the magnetic susceptibility.

18) Y. Deguchi and H. Nakai, Report of the 20th Symposium on the Chemistry of Metal Coordination Compd, p. 189 (1970).

The Chemical-transport Reaction of Spinel-type Oxides

Koichi NAGASAWA*, Yoshichika BANDO, and Toshio TAKADA
Institute for Chemical Research, Kyoto University, Uji
(Received September 29, 1970)

Single crystals and thin films of spinel-type oxides were prepared by a chemical-transport reaction in a closed system, using HCl gas as the transport agent. This paper will report on the preparation conditions and the reaction process of the chemical-transport reaction. The reaction process of Co_3O_4 was found to be different from that of other oxides, since Co_3O_4 was dissociated into CoO and O_2 in the closed tube. The reaction process was explained by the difference in the dissociated oxygen pressure between the source zone and the crystallization zone in the system. The chemical-transport reaction of $NiFe_2O_4$ was applied to the preparation of thin film. The single-crystal thin films were epitaxially grown on the (110) and (111) surfaces of MgO.

The growth of spinel-type oxides is very important for the fundamental investigation of their physical properties. Therefore, many investigations of the growing method, for instance, the growth from the melt or from the flux, have been made. The growing method from the melt is not suitable for the material dissociated below the melting point, and the method from the flux sometimes causes the flux to be included in the crystals.

The growing method from the gas phase has been expected not to have such defects, and so recently much interest has been directed toward this method. Takei and Takasu[1] prepared single-crystal films of $NiFe_2O_4$ $CoFe_2O_4$, and Fe_3O_4 on the MgO substrate by the decomposition of appropriate mixtures of the metal halides by water vapor. Sputtering in a glow-discharge system from a ceramic cathode of the ferrite also made it possible to prepare single-crystal films of nickel ferrite.[2] In addition, the chemical transport reaction method in a closed system, which was developed by Schäfer and his co-workers,[3] for the growth of single crystals of various solid substances, *e.g.*, Si, Ge, Cu_2O, and Fe_2O_3 is applicable to the growth of ferrite. Hauptmann[4] applied this chemical-transport reaction, using HCl gas as the transport agent, to the preparation of Fe_3O_4 single crystals. In this case, single crystals were presumably grown by this reaction:

$$Fe_3O_4(s) + 8HCl(g) \rightleftharpoons 2FeCl_3(g) + FeCl_2(g) + 4H_2O(g) \quad (1)$$

where (s) and (g) indicate the solid and gaseous states respectively. Moreover, Kleinert[5] reported the growth of $NiFe_2O_4$, $MnFe_2O_4$, and other spinel-type oxides by the same method. In these cases, the materials which were used as the sources were not dissociated in the system. As the cobaltite Co_3O_4 is dissociated into CoO and O_2 at high temperatures, the process of this chemical-transport reaction may be expected to be different from that of other oxides.

In the present investigation, single crystals of Co_3O_4 were synthesized by a chemical-transport reaction using HCl gas, and the reaction process of Co_3O_4 was compared with that of $NiFe_2O_4$. Moreover, $NiFe_2O_4$ thin films were epitaxially grown on the (110) and (111) surfaces of the MgO single crystal. Some parts of this investigation have been already reported in a short note.[6,7] This paper will present the results in detail and will discuss them.

Experimental

Source Materials and Substrates. The source materials for the chemical-transport reaction were Co_3O_4 powder, $NiFe_2O_4$ powder, and sintered $NiFe_2O_4$. The Co_3O_4 powder was obtained by the thermal decomposition of $CoCO_3$ at 700°C in air. α-Fe_2O_3 and NiO were weighed, mixed, and then calcined at 1000°C for 2 hr. Calcination was followed by crushing. This powder was pressed and fired in air at 1200°C for a day. The $NiFe_2O_4$ powder was obtained by crushing this sintered body. $CoCO_3$ and NiO were Wakoo guaranteed reagents, and α-Fe_2O_3 was a product of the Toda Industrial Co., Ltd. (99.9%). Single crystals of MgO were obtained from the New Metals Corp.; a polished (110) or (111) surface or a cleaved (100) surface was used as the substrate for the growth of $NiFe_2O_4$ thin film.

Method. The source material, Co_3O_4 or $NiFe_2O_4$

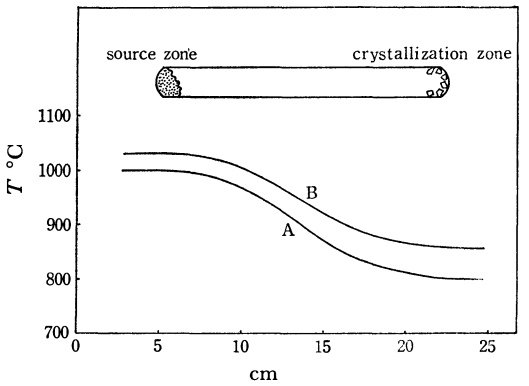

Fig. 1. Temperature gradient of the furnace and position of the closed silica tube. A is the gradient in the preparation of Co_3O_4 and $NiFe_2O_4$ single crystals and B $NiFe_2O_4$ single crystal thin films.

* Present address: Central Research Laboratory, Mitsubishi Electric Corp., Amagasaki, Hyogo.

1) H. Takei and S. Takasu, *Jap. J. Appl. Phys.*, **3**, 175 (1964).
2) W. D. Westwood, H. K. Eastwood, R. G. Poulson, and S. G. Sadler, *J. Amer. Ceram. Soc.*, **50**, 119 (1967).
3) H. Schäfer, H. Jacob, and K. Etzel, *Z. Anorg. Allg. Chem.*, **286**, 27 (1956).
4) Z. Hauptman, *Czech. J. Physics*, **12**, 148 (1962).
5) D. Kleinert, *Z. Chem.*, **3**, 353 (1968).
6) T. Takada, Y. Bando, N. Yamamoto, and K. Nagasawa, *Jap. J. Appl. Phys.*, **8**, 619 (1969).
7) K. Nagasawa, Y. Bando, and T. Takada, *ibid.*, **7**, 174 (1968).

powder, was loaded into one end of a silica tube 18 cm in length and 1.4 cm in diameter. After the tube had then been evacuated to 10^{-6} mmHg, 40 mmHg of HCl gas was admitted and the other end of the tube was sealed off. The tube was heated for 2—3 days in a furnace with a temperature gradient, as is shown in Fig. 1, and then quenched in water within a minute. The temperatures of the source zone and crystallization zone were 1000°C and 800°C respectively. The tube was then broken, and the crystals obtained in the crystallization zone were removed from the wall of the tube.

In the growth of $NiFe_2O_4$ thin films, the source material was sintered $NiFe_2O_4$, 8 mm in diameter and 3 mm thick. The silica tube used was 17 cm in length and 9 mm in diameter. In the crystallization zone, a substrate of MgO single crystal having a polished (110) or (111) surface or a cleaved (100) surface was mounted. The pressure of the HCl gas admitted was 50 mmHg. The temperature in the source zone was 1030°C, and at the substrate zone, 860°C, as is shown in Fig. 1. The tube was heated for two days, pulled out of the furnace, and cooled in air. The film grown on the surface of the substrate could be separated from the substrate by treating it in a hot 2—5% aqueous solution of nitric acid. The surface area and weight of the film were measured, and the film thickness was calculated from the density of $NiFe_2O_4$.

Analysis. The phases of the source material remaining in the source zone after the reaction, which will here after be called the "residue", and the single crystals obtained were identified by means of X-ray powder diffraction using Mn-filtered Fe-radiation. The lattice constants of the single crystals were measured by the X-ray powder pattern, using {721} reflection. A Laue photograph was taken of a face of a crystal obtained using copper radiation.

In the case of the $NiFe_2O_4$ thin film, a Laue photograph was taken by means of the transmitted diffracted lines. As an electron beam could pass through the edge of the film, the lattice constant of the films was measured by means of usual electron diffraction, using Au polycrystalline film as a standard sample. The atomic ratios of iron to nickel in the films were measured by chemical analysis.

Results and Discussion

Chemical-transport Reaction of Co_3O_4. The transport of Co_3O_4 and $NiFe_2O_4$ by HCl yielded some black and bright crystals 2—5 mm in size. Figure 2 shows photographs of representative crystals. The Laue photograph showed that the best developed faces were {111}. The {110} planes were also observed in some

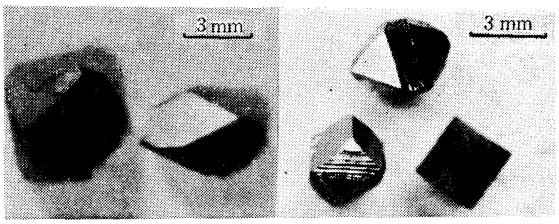

(A) (B)

Fig. 2. Photographs of (A) Co_3O_4 single crystals and (B) $NiFe_2O_4$ single crystals.

$NiFe_2O_4$ single crystals. The X-ray powder diffraction of the single crystals indicated that they had a spinel structure and that the lattice constant was 8.080 Å in Co_3O_4 and 8.352 Å in $NiFe_2O_4$ respectively. These values agreed approximately with the A.S.T.M. value.

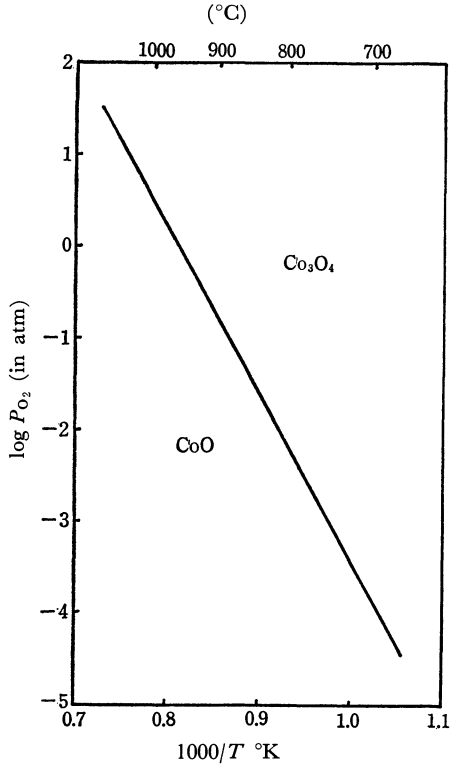

Fig. 3. Oxygen pressure in equilibrium with Co_3O_4 and CoO as a function of 1000/T°K.

TABLE 1. CONDITIONS EMPLOYED IN PREPARATION OF SPINEL-TYPE OXIDE SINGLE CRYSTALS BY CHEMICAL TRANSPORT REACTION AND RESULTS

Run No.	Source material	Weight of source material charged (g)	Phase of residues at the source zone	Phase of single crystals obtained	Admitted HCl gas (mmHg)	Reaction time (day)	Temperature gradient (°C)
1	Co_3O_4	0.40	CoO	Co_3O_4	40	2	1000—800
2	Co_3O_4	0.15	CoO	Co_3O_4	40	2	1000—800
3	Co_3O_4	0.70	Co_3O_4+CoO	Co_3O_4	40	3	1000—800
4	Co_3O_4	0.50	Co_3O_4+CoO	Co_3O_4	40	3	1000—800
5	$NiFe_2O_4$	0.15	$NiFe_2O_4$	$NiFe_2O_4$	40	3	1000—800
6	$NiFe_2O_4$	0.30	$NiFe_2O_4$	$NiFe_2O_4$	40	3	1000—800
7	$NiFe_2O_4$	0.50	$NiFe_2O_4$	$NiFe_2O_4$	40	3	1000—800

In the case of the chemical-transport reaction of Co_3O_4, the phases of the residue changed with the amount of the source material present before the reaction. Table 1 gives a survey of the growth experiments. Runs 1 and 2, in which the weights of the source material were 0.40 and 0.15 g respectively, gave only CoO as the residue. However, runs 3 and 4, in which these weights were 0.50 g and 0.70 g, gave two phases of CoO and Co_3O_4 as the residue. Such phenomena could be explained by the dissociation reaction of Co_3O_4, $Co_3O_4 \rightarrow 3CoO + 1/2O_2$. In this case, the dissociation oxygen pressure is given by the equation[8]: $\log P_{O_2} = -19150/T + 15.48$. Figure 3 shows the dissociation pressure *versus* the temperature. According to Fig. 3, the dissociation pressure of Co_3O_4 is 2.78 atm at 1000°C and 5.6×10^{-3} atm at 800°C. Co_3O_4 at the source zone is perhaps dissociated into CoO and O_2 at 1000°C until the oxygen pressure reaches 2.78 atm in the closed system. If the Co_3O_4 is assumed to be completely dissociated into CoO and O_2 in the system whose volume is estimated to be about 27 m*l*, the oxygen pressures of runs 1—4 can be calculated to be 3.2, 1.2, 4.0, and 5.5 atm respectively. The calculated dissociated pressure of run 2, 1.2 atm, is lower than the dissociation pressure, 2.78 atm, at 1000°C. Therefore, it is considered that, in run 2, the Co_3O_4 is completely dissociated into CoO and O_2, and that then $CoCl_2$ gas is prepared by the reaction of CoO and HCl in the source zone. However, in this experiment, Co_3O_4 crystals were prepared in the crystallization zone. As the oxygen pressure in the tube should be higher than the dissociation pressure of Co_3O_4 in the crystallization zone of 800°C, this reaction may occur as follows:
in the source zone of 1000°C:

$$Co_3O_4(s) \rightarrow 3CoO(s) + \frac{1}{2}O_2(g) \quad (2)$$

$$3CoO(s) + 6HCl(g) \rightarrow 3CoCl_2(g) + 3H_2O(g) \quad (3)$$

and in the crystallization zone of 800°C:

$$2CoCl_2(g) + 3H_2O(g) + \frac{1}{2}O_2(g) \rightarrow Co_3O_4(s) + 6HCl(g) \quad (4)$$

The calculated oxygen pressures of runs 3 and 4, 4.0 and 5.5 atm respectively, are much higher than 2.78 atm, and in the source zone Co_3O_4 should be partially dissociated into CoO and O_2 until the oxygen pressure amounts to 2.78 atm. Therefore, the reaction proceeds with a source material consisting of CoO and Co_3O_4. In runs 3 and 4 the following reaction may be added to the above-mentioned reaction in the source zone:

$$Co_3O_4(s) + 8HCl(g) \rightleftharpoons CoCl_2(g) + 2CoCl_3(g) + 4H_2O(g). \quad (5)$$

The reverse reaction may occur in the crystallization zone.

In run 1, the calculated oxygen pressure, 3.2 atm, is slightly higher than 2.78 atm. However, in this experiment, the residue was CoO. This can be explained by considering the following process. In the initial stage, the reaction should proceed with two phases of CoO and Co_3O_4 in the source zone, and the oxygen pressure seems to be kept at 2.78 atm in the tube. As the growth of Co_3O_4 single crystals consumes the O_2 gas in the crystallization zone, as is shown in Eq. (4), the Co_3O_4 at the source zone should be dissociated into CoO and O_2 by the quantity of Co_3O_4 prepared in the crystallization zone, thus keeping the oxygen pressure 2.78 atm. Therefore, the quantity of Co_3O_4 in the source zone should decrease with the growth of Co_3O_4 single crystals in the crystallization zone, and only CoO should come to exist as the residue in the source zone. In every case from run 1 to run 4, it is considered that Co_3O_4 single crystals grow under the oxygen pressure dissociated in the source zone.

In the case of $NiFe_2O_4$, the phases of single crystals and the residue did not change with the amount of the source before the reaction, as is shown in runs 5, 6, and 7. The chemical-transport reaction seems to proceed with source material of a single phase, according to this simple reversible reaction:

$$NiFe_2O_4(s) + 8HCl(g) \rightleftharpoons NiCl_2(g) + 2FeCl_3(g) + 4H_2O(g). \quad (6)$$

Preparation of Thin Film of $NiFe_2O_4$. Figure 4 shows the surfaces of the MgO (100), (110), and (111) substrates on which $NiFe_2O_4$ was deposited by the chemical-transport reaction. On the (100) MgO

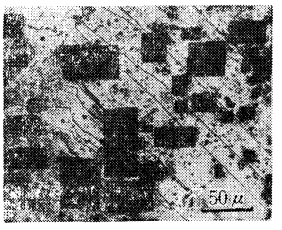

(A)

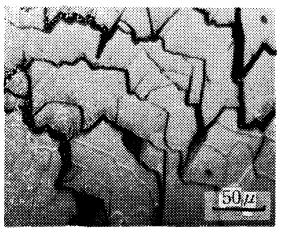

(B)

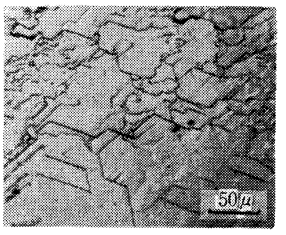

(C)

Fig. 4. Photomicrographs of (A) (100), (B) (110), and (C) (111) surface of MgO single crystals on which $NiFe_2O_4$ was deposited.

8) O. Kubaschewski and LL. Evans, "Metallugical Thermochemistry," London Pergamon Press (1956), p. 331.

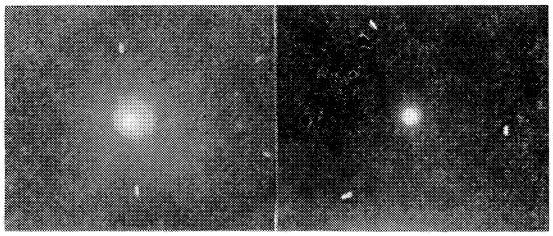

(A) (B)

Fig. 5. Laue patterns of film using copper radiation. (A) film on (110) surface of MgO. (B) film on (111) surface of MgO.

substrate, many oriented pyramid-like microcrystals were observed, as is shown in Fig. 4(A). On the contrary, thin films were observed on the (110) and (111) MgO substrates. The film was shiny and opaque brown, and it overlaid the substrate. The films removed from the substrate was composed of a ferromagnetic material. The film thickness was about 5000 Å, and the growing speeds were about 100 Å/hour. Laue patterns obtained using copper radiation are shown in Fig. 5. The pattern of the film on the (110) surface of MgO consisted of reflections with a two-fold axis; the film was a (110) plane with a cubic structure. The pattern of the film on the (111) surface of MgO corresponded to that of the single crystal film with a (111) surface with a cubic structure. The electron diffraction of the film removed from the (111) surface of MgO gave spots with a six-fold axis. The lattice constant calculated by means of the diffraction spots was 8.38 Å. This value agrees within 0.5% with the A.S.T.M. value of $NiFe_2O_4$. The atomic ratio of iron to nickel in the film was determined to be 1.97 ± 0.04 from the chemical analysis. Therefore, it may be concluded that the film was nickel ferrite deposited epitaxially on the (110) and (111) planes of MgO.

When the $NiFe_2O_4$ powder was charged as the source, thin films were not grown, and many small crystals were found on the substrate. The rate of surface reaction may be much higher in the powdered source material than in the sintered one, as the surface area of the powdered material is larger than that of the sintered one. It is considered that the high rate of surface reaction results in much transport. In this case, the great deal of transport seems to cause the overgrowth of $NiFe_2O_4$ crystals on the substrate.

The authors wish to express their thanks to Dr. N. Yamamoto for his fruitful discussions.

The Effect of Axial Pyridine Ligands on the Charge Transfer Bands of *trans*-Bis(dimethylglyoximato)Cobalt(III) and -Iron(II) Complexes

Yukio YAMANO, Isao MASUDA, and Koichiro SHINRA

Department of Applied Chemistry, Faculty of Engineering, Osaka University, Yamadakami, Suita, Osaka

(Received November 16, 1970)

The electronic absorption spectra of $[Co^{III}(dmgH)_2B_2]^+$ and $[Fe^{II}(dmgH)_2B_2]$ (dmgH=dimethylglyoximate monoanion and B=pyridine derivatives) are inspected with respect to the effect of the axial pyridine ligands on the charge-transfer bands of the complexes. The characteristic bands observed in the 275—305 mμ region for the Co(III) complexes and in the 485—555 mμ region for the Fe(II) complexes, which have been assigned to a metal→oxime charge-transfer band, are shifted to shorter wavelengths with a decrease in the basicity of the pyridine derivatives. The results have been discussed by taking into account the π-interaction of the $d_\pi(d_{xz}, d_{yz})$ orbital of the central metal ion with the empty π-orbitals of both the dimethylglyoximate and the pyridine derivatives. It is suggested that the π-interaction is stronger in the Fe(II) complexes than in the Co(III) complexes, while the σ-bond is stronger in the latter. The infrared spectral evidence that the C=N stretching frequency is dependent on the axial pyridine derivatives, and that it is observed at a lower frequency in the Fe(II) than in the Co(III) complexes, is consistent with the above results.

It was thought to be informative to investigate the nature of the bonding between axial ligands and planar transition metal complexes in order to understand the transmission of the electronic effect of the axial ligands in the complexes. When ligands such as pyridine are coordinated axially to the planar complexes, a d_π-(metal)-π^*(py) bonding may be either taken into account[1-3] or may be omitted.[4,5] In previous works, the present authors postulated a π-interaction between the central cobalt ion and the pyridine ring in the *trans*-bis(1,2-dioximato)cobalt(III) complexes on the basis of the anomalous behavior of the pyridine ligands, extensively facilitating the deprotonation reaction of the intramolecular hydrogen bridges of the complexes.[6]

In earlier publications,[7] it was reported that the electronic absorption spectra of the *trans*-bis(1,2-dioximato)cobalt(III) complexes with aniline derivatives show characteristic C-I(340—400 mμ) and C-II(300—375 mμ) bands, which can be ascribed to the charge-transfer transitions from the axial aniline derivatives to the cobalt ion, and from the cobalt ion to the dioximate ligand, respectively. It seemed that it would be interesting to elucidate the effects of the axial pyridine analogues on the charge-transfer spectra of the complexes.

In this paper, the electronic spectra of *trans*-$[Co(dmgH)_2B_2]^+$ (dmgH=dimethylglyoximate monoanion and B=pyridine derivatives) have been inspected and compared with the spectra of $[Fe(dmgH)_2B_2]$, and the data have been discussed by taking into account the π-interaction between the axial ligands and the central metal ion.

Experimental

Preparations. The cobalt(III)-dimethylglyoxime complexes with the $[Co(dmgH)_2B_2]Cl$ formula, listed in Table 2, were prepared by a method described elsewhere.[6]

The iron(II)-dimethylglyoxime complexes with the $[Fe(dmgH)_2B_2]$ formula were prepared according to the method of Miwa *et al.*[8] The procedure was carried out under a nitrogen atmosphere. To an ethanol solution of $dmgH_2$ (1.5 g, 0.013 mol), $FeSO_4 \cdot 7H_2O$ (1.5 g, 0.0065 mol) in an aqueous solution was added at room temperature; this was followed by the stirring in of pyridine or its derivatives (3—4 g, 0.03—0.04 mol) in an ethanol solution. The pH value of the solution was adjusted to about 7 by adding aqueous HCl or NaOH. Fine crystals precipitated; they were collected on a filter and washed with water, ethanol, and then ether. The analytical data are summarized in Table 1.

Measurements. The electronic absorption spectra of $[Co(dmgH)_2B_2]Cl$ were measured in an aqueous-ethanol (1 : 1) solution. As to $[Fe(dmgH)_2B_2]$, the electronic absorption spectra were measured in an ethanol solution containing an excess of the free axial ligand under a nitrogen atmosphere, since the complexes in solution are known to change upon standing in the air due to the dissociation of the axial ligand and the concomitant oxidation of the central iron ion.[9] The complexes showed little spectral change under the above conditions, and they gave a spectrum quite close to that obtained for the solid sample. A Hitachi Spectrophotometer, Model EPS-3, and a Hitachi Infrared Spectrometer, Model EPI-2G, were used for recording the spectra.

Results and Discussion

Cobalt(III) Complexes. As may be seen in Fig. 1, the electronic absorption spectra of $[Co(dmgH)_2B_2]^+$ (B=pyridine derivatives) show three intense bands in the 250—400 mμ region, the band around 250 mμ may be assigned to the intraligand(dmgH) $\pi \rightarrow \pi^*$ transition.[10] The bands at 315—370 mμ and 275—305 mμ, which will hereafter be referred to as the α- and β-bands respectively, are not well defined and

1) R. C. Elder, *Inorg. Chem.*, **7**, 1117 (1968).
2) B. C. Claude and G. Alain, *Tetrahedron Lett.*, **1969**, 4189.
3) S. J. Cole, G. C. Curthoys, and E. A. Magnusson, *J. Amer. Chem. Soc.*, **92**, 2991 (1970).
4) W. D. Horrocks, Jr., R. C. Taylor, and G. N. LaMar, *ibid.*, **86**, 3031 (1964).
5) J. A. Happe and R. L. Ward, *J. Chem. Phys.*, **39**, 1211 (1963).
6) Y. Yamano, I. Masuda and K. Shinra, *Inorg. Nucl. Chem. Lett.*, **4**, 581 (1968); *J. Inorg. Núcl. Chem.*, **33**, 521 (1971); I. Masuda, M. Sakano, and K. Shinra, This Bulletin, **42**, 2296 (1969).
7) C. Matsumoto, T. Kato, and K. Shinra, *Nippon Kagaku Zasshi*, **86**, 1266 (1965); C. Matsumoto, I. Masuda, and K. Shinra, *ibid.*, **88**, 46 (1967).
8) M. Miwa, Y. Kubota, and Y. Inamura, The 16th Symposium on Coordination Chemistry in Japan, p. 40 (1966).
9) B. A. Jillot and R. J. P. Williams, *J. Chem. Soc.*, **1958**, 462.
10) B. Roos, *Acta. Chem. Scand.*, **19**, 1715 (1965).

TABLE 1. ELEMENTAL ANALYSES OF THE COMPLEXES

Complex[a)]	Calcd, %			Found, %		
	C	H	N	C	H	N
$[Co(dmgH)_2(3\text{-}CH_3Py)_2]Cl\cdot 2H_2O$	43.90	5.84	15.39	43.69	5.84	16.14
$[Fe(dmgH)_2(4\text{-}NH_2Py)_2]\cdot H_2O$	43.90	5.73	22.75	43.74	5.53	21.40
$[Fe(dmgH)_2(3\text{-}NH_2Py)_2]$	45.58	5.53	23.63	45.36	5.65	23.25
$[Fe(dmgH)_2(4\text{-}CH_3Py)_2]\cdot H_2O$	49.00	6.17	17.13	49.15	6.07	17.66
$[Fe(dmgH)_2(3\text{-}CH_3Py)_2]\cdot H_2O$	49.00	6.17	17.13	48.82	6.08	18.96
$[Fe(dmgH)_2(Py)_2]\cdot H_2O$	46.77	5.67	18.18	46.28	5.44	18.80
$[Fe(dmgH)_2(3\text{-}CNPy)_2]\cdot 4H_2O$	42.38	5.29	19.78	41.96	4.32	19.78

a) dmgH=dimethylglyoximate monoanion and Py=pyridine.

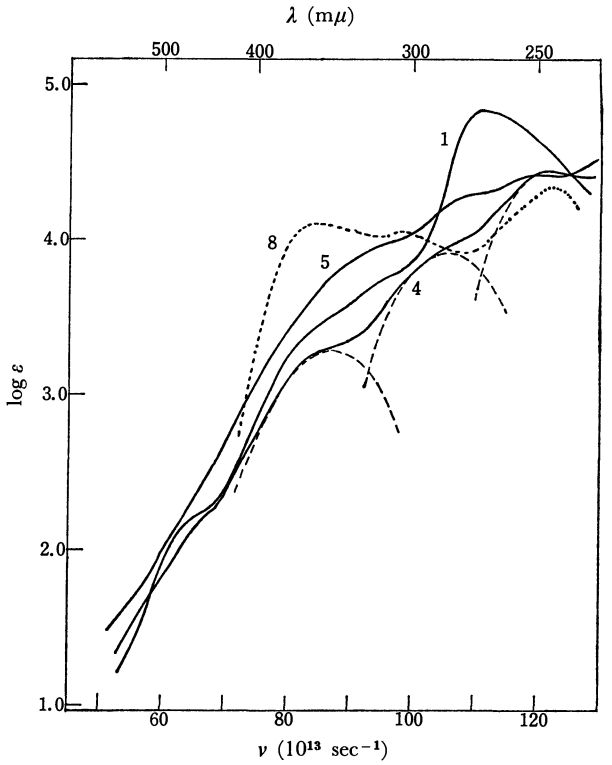

Fig. 1. Electronic absorption spectra of $[Co(dmgH)_2B_2]^+$ in aqueous-ethanol (1 : 1) solution.
1: B=4-NH_2Py, 4: B=Py, 5: B=4-CNPy, 8: B=aniline.

have lower intensities than the C-I and C-II bands of $[Co(dmgH)_2A_2]^+$ (A=aniline derivatives). The lower intense band at about 450 mμ might be due to a *d*—*d* transition. The complexes of the same type with ammonia, benzylamine, and imidazole as axial ligands show a spectral pattern similar to that of the pyridine species.[7] The absorption maxima of the α- and β-bands have been determined by the method of parabolic approximation.[11] The results obtained for $[Co(dmgH)_2Py_2]^+$ are represented in Fig. 1, while the numerical data are given in Table 2.

By plotting the frequencies (ν_{max}) of the α- and β-bands against the basicities of the free pyridine derivatives,[12–14] linear correlations have been found, as is shown in Fig. 2-α and -β. The α- and β-bands are shifted to a longer wavelength with an increase in the basicity of the pyridine derivatives. The degree of the shifts for the α-band is 1.5 times larger than that for the β-band. These shifts for the α- and β-bands caused by the nature of the axial ligands seem to be qualitatively similar to those observed for the C-I and C-II bands of $[Co(dmgH)_2A_2]^+$. In the case of this complex, the C-I band has been assigned to the charge-transfer band from the axial aniline derivatives to the cobalt ion on the basis of the fact that, with an increase in the basicity of the aniline derivatives, this band is

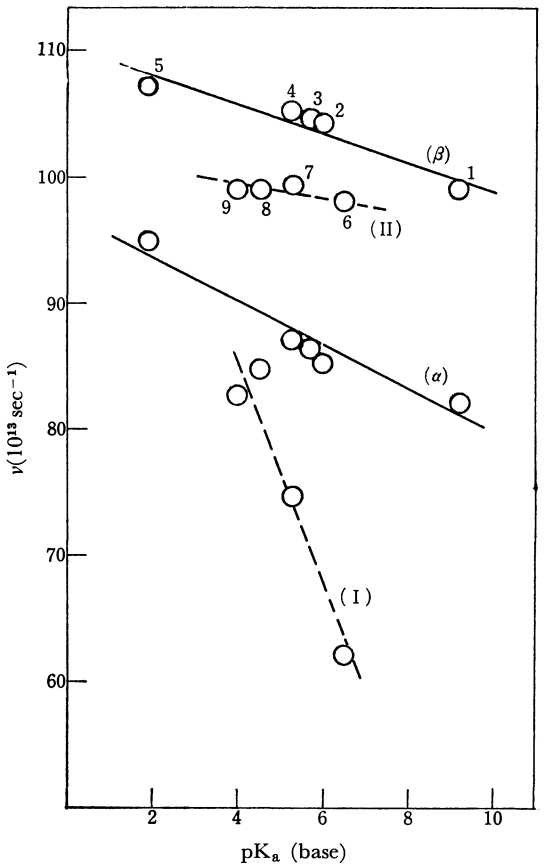

Fig. 2. Plots of the $\nu_{max.}$ of $[Co(dmgH)_2B_2]^+$ and $[Co(dmgH)_2A_2]^+$ against the pK_a values of the conjugate acids of free bases.
(α): α-band, and (β): β-band of axial pyridine complexes.
(I): C-I band, and (II): C-II band of axial aniline complexes.

11) W. Kuhn and E. Braun, *Z. Phys. Chem.* (Leipzig), **B8**, 281 (1930).
12) H. H. Jaffe and G. O. Doak, *J. Amer. Chem. Soc.*, **77**, 4441 (1955).
13) P. T. T. Wong and D. G. Brewer, *Can. J. Chem.*, **46**, 131 (1968).
14) N. F. Hall, *J. Amer. Chem. Soc.*, **52**, 5124 (1930).

TABLE 2. ELECTRONIC ABSORPTION SPECTRA OF $[Co(dmgH)_2B_2]^+$ IN AQUEOUS-ETHANOL SOLUTION

Number[a]	B	α-Band		β-Band		π→π* (dmgH) Band	
		ν_{max}	log ε_{max}	ν_{max}	log ε_{max}	ν_{max}	log ε_{max}
1	4-NH_2Py	82.00	3.30	99.00	3.80	110.65[b]	4.80
2	4-CH_3Py	85.15	3.27	104.20	3.89	121.85	4.50
3	3-CH_3Py	86.25	3.30	104.50	3.90	123.20	4.50
4	Py	87.00	3.30	105.20	3.95	121.20	4.40
5	4-CNPy	94.80	3.98	107.20	4.23	119.10	4.40
	A	C-I band[c]		C-II band		π→π* (dmgH) band	
6	*p*-$N(CH_3)_2$An[d]	62.11	3.99	98.04	3.94	121.46	4.59
7	*p*-CH_3OAn	74.63	4.09	99.34	3.88	120.19	4.36
8	An	84.63	4.12	99.01	4.02	120.48	4.33
9	*p*-ClAn	82.64	4.18	99.01	4.00	120.09	4.36

The frequency is given in 10^{13} sec^{-1}.
a) These numbers are referred in Figs. 1 and 2.
b) This band includes the π→π* bands of both dmgH and 4-NH_2Py.
c) In Ref. 7.
d) An=aniline.

shifted to a longer wavelength, although the C-II band is shifted only a little.[7] As to the C-II band, it has been assigned to the charge-transfer band from the cobalt ion to the dioximate ligand, since it is shifted to a longer wavelength with an increase in the electron-withdrawing property of the dioximate ligands for $[Co(DH)_2(p\text{-}CH_3OAn)_2]^+$ (DH=1,2-dioximate monoanion and An=aniline).[7] Judging from the above observations and the frequencies of these bands, it is reasonable to ascribe the α- and β-bands for $[Co(dmgH)_2B_2]^+$ to the charge-transfer bands from the axial pyridine derivatives to the cobalt ion, and from the cobalt ion to the dimethylglyoximate ligand, respectively.

It is significant to note that: i) the β-band in $[Co(dmgH)_2B_2]^+$ is considerably affected by the nature of the axial pyridine derivatives, whereas the C-II band in $[Co(dmgH)_2A_2]^+$ is only slightly affected, and ii) the β-band for the axial pyridine complexes is observed at a higher energy than the C-II band for the axial aniline complexes (the difference in the energies between these two bands becomes larger as the basicity of the bases decreases) (Fig. 2). In order to explain these facts, it will be necessary to consider the d_π(Co)–π*(Py) interaction in addition to the d_π-(Co)–π*(dmgH) bonding,[15] and the σ-bonding. As is shown in Fig. 5, it seems that the $d_\pi(d_{xz}, d_{yz})$–π*-(Py) interaction stabilizes the d_π-levels, thus weakening the $d_\pi(d_{xz}, d_{yz})$–π*(dmgH) bonding and stabilizing the π*(dmgH) level. The extent of the stabilization of the π*(dmgH) level would, in this case, be smaller than that of the d_π-levels. Therefore, the d_π(Co)→π*(dmgH) charge-transfer band is observed in a shorter wavelength region for the axial pyridine complexes than for the axial aniline complexes. The empty π-level of the pyridine derivatives is expected to be lowered in the order: 4-NH_2Py>Py>4-CNPy.[16,17] Therefore, the π-interaction described above will become stronger and the d_π(Co)→π*(dmgH) charge-transfer band will be shifted to a higher energy in the order; 4-NH_2Py<Py<4-CNPy. The intraligand-(dmgH)π→π* band tends to shift to a longer wavelength as the π-acceptor property of the pyridine derivatives increases. This seems to be consistent with the above considerations.

Iron(II) Complexes. $[Fe(dmgH)_2B_2]$ (B=pyridine derivatives) has often been characterized by two intense absorption bands at about 500 and 400 mμ (Fig. 3).[8,9,18,19] In this paper we will designate them as the γ- and δ-bands respectively. In the case of the complexes with axial ammine or hydrazine ligands, no absorption band corresponding to the above δ-band has been observed. The γ-band has been assigned to the d_π(Fe)→π*(dmgH) transition on

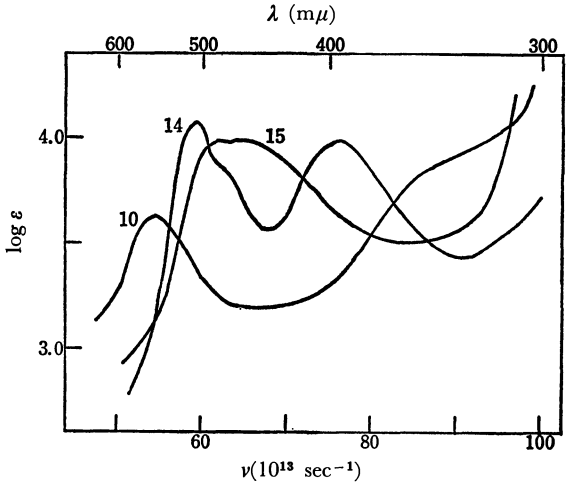

Fig. 3. Electronic absorption spectra of $[Fe(dmgH)_2B_2]$ in ethanol solution.
10: B=4-NH_2Py, 14: B=Py, 15: B=3-CNPy.

15) K. Burger and I. Ruff, *Talanta*, **10**, 329 (1963); K. Burger' I. Ruff, and F. Ruff, *J. Inorg. Nucl. Chem.*, **27**, 179 (1965).
16) H. Tsubomura, *Nippon Kagaku Zasshi*, **78**, 293 (1957).
17) M. R. Basica and D. J. Clancy, *J. Phys. Chem.*, **67**, 1551 (1963).
18) K. Sone, This Bulletin, **25**, 1 (1952).
19) C. Matsumoto, Y. Yamano, and K. Shinra, *Nippon Kagaku Zasshi*, **89**, 46 (1968).

Table 3. Electronic absorption spectra of $[Fe(dmgH)_2B_2]$ in ethanol solution and in powder reflection ($\nu_{p.r.}$)

Number[a]	B	$d\rightarrow d$ Band[b]		γ-Band			δ-Band		
		$\nu_{p.r.}$	$\nu_{p.r.}$	ν_{max}	log ε_{max}	$\nu_{p.r.}$	ν_{max}	log ε_{max}	$\nu_{p.r.}$
10	4-NH_2Py	40.68	43.50	54.15	3.62	53.86	89.85	3.86	85.47
11	4-CH_3Py	41.70	45.90	57.70	3.95	57.80	79.20	3.90	74.63
12	3-NH_2Py	41.70	45.04	57.30	3.95	57.63	79.00	3.89	74.47
13	3-CH_3Py	42.25	46.00	58.25	3.98	58.10	75.80	3.87	73.44
14	Py	42.87	46.50	59.06	4.07	58.59	75.80	3.99	73.17
15	3-CNPy	43.30	48.50	61.65	3.98	61.48	64.65	3.99	64.79

The frequency is given in 10^{13} sec^{-1}.

a) These numbers are referred in Figs. 3 and 4.

b) In the spectra of $[Fe(dmgH)_2(3\text{-}CH_3Py)_2]$ in ethanol solution, two $d\rightarrow d$ bands with lower intensity ($\log\varepsilon=2.16$ and 2.0) are observed at $\nu_{max}=46.13$ and 42.13. In the spectra of the other complexes in ethanol solution, similar bands were unsuccessfully observed for their lower solubility.

the basis of the fact that, with an increase in the electron-withdrawing property of the dioximate ligand, it is shifted to a longer wavelength, although the δ-band is shifted only a little.[19] In a recent theoretical treatment,[20] the band at 526 mμ for $[Fe(dmgH)_2(NH_3)_2]$ has been indicated to be the $d_\pi(Fe)\rightarrow\pi^*$(dmgH) charge-transfer band. As to the δ-band mentioned above, it has been proposed that it is due to the $d_\pi(Fe)\rightarrow\pi^*$(Py) charge-transfer transition, since it is shifted to a longer wavelength in the 4-cyanopyridine complex than in the pyridine complex.[9]

Our interest led us to inspect the shifts of both the γ- and δ-bands for a series of axial pyridine derivatives in connection with the shifts of the α- and β-bands for $[Co(dmgH)_2B_2]^+$. As is shown in Fig. 4, the δ-band is considerably shifted to a longer wavelength with a decrease in the basicity of the pyridine derivatives; this indicates an increase in the derivatives' π-acceptor property. Therefore, the δ-band is ascribed to the $d_\pi(Fe)\rightarrow\pi^*$(Py) charge-transfer transition. The γ-band is shifted to a shorter wavelength as the basicity of the pyridine derivatives decreases. The degree in the shift of the γ-band is almost the same as that of the β-band for $[Co(dmgH)_2B_2]^+$ (Figs. 2 and 4). This result is consistent with the above statement that the γ-band of the Fe(II) complexes, like the β-band of the Co(III) complexes, is due to the d_π(metal)$\rightarrow\pi^*$-(dmgH) charge-transfer transition.

Such an effect of the axial pyridine derivatives on the $d_\pi(Fe)\rightarrow\pi^*$(dmgH) charge-transfer band may, as has been discussed for the Co(III) complexes, reflect a contribution of the $d_\pi(Fe)$–π^*(Py) interaction to the bonding between the iron ion and the pyridine ring. That is, with an increase in the π-acceptor property of the pyridine derivatives, the $d_\pi(Fe)$–π^*(Py) bonding becomes stronger and the d_π-orbitals are further stabilized. Therefore, the $d_\pi(Fe)$–π^*(dmgH) bonding becomes weaker. The fact that the bands with lower intensities in the 610—740 mμ region, which may be attributed to $d\rightarrow d$ transitions, are shifted in the same way as the γ-band (Fig. 4) seems to support the above consideration.

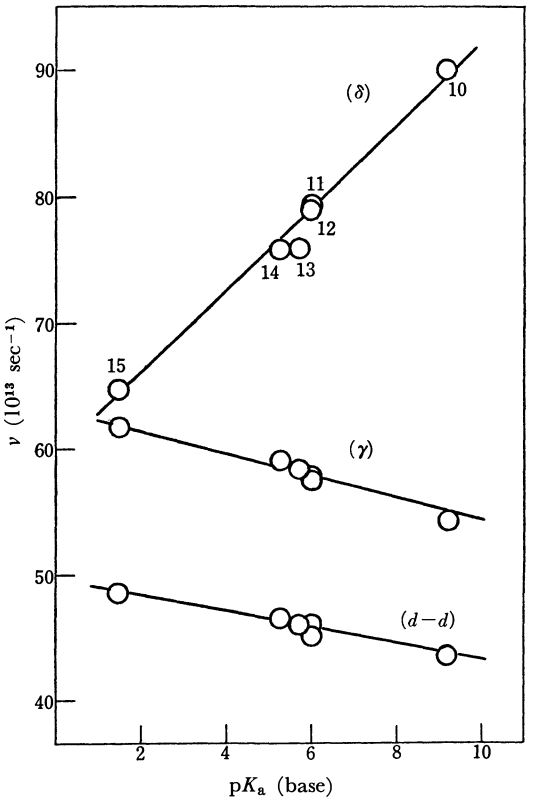

Fig. 4. Plots of the ν_{max} of $[Fe(dmgH)_2B_2]$ against the pK_a values of the conjugate acids of free bases.
(γ): γ-band, (δ): δ-band, and (d—d): $d\rightarrow d$ band.

Comparison of the Cobalt(III) and Iron(II) Complexes. The d_π(metal)$\rightarrow\pi^*$(dmgH) charge-transfer bands in the Co(III) complexes(β-band) and in the Fe(II) complexes(γ-band) are almost equally shifted to longer wavelengths as the basicity of the pyridine derivatives increases. The energy of the charge-transfer band for the Co(III) complexes is about twice that for the Fe(II) complexes (Figs. 2 and 4). One reason for this may be that, in these complexes, the ionization potential of the Fe(II) ion is lower than that of the Co(III) ion, as is shown in Fig. 5.[21] A lower ioni-

20) G. De Alti, V. Galasso, A. Bigotto, and G. Costa, *Inorg. Chim. Acta*, **3**, 533 (1969).

21) H. Basch, A. Viste, and H. B. Gray, *Theor. Chim. Acta*, **3**, 458 (1965); *J. Chem. Phys.*, **44**, 10 (1966).

TABLE 4. IR SPECTRA OF THE COMPLEXES,[a] cm^{-1}

B	$[Co(dmgH)_2B_2]^+$				$[Fe(dmgH)_2B_2]$			
	$\nu_{C=N}$	ν_{N-O}		ν_{Co-N}[b]	$\nu_{C=N}$	ν_{N-O}		ν_{Fe-N}[b]
4-NH_2Py	1529	1223	1089	518	1518	1219	1069	518
4-CH_3Py	1562	1236	1093	514	1540	1210	1078	517
3-NH_2Py					1536	1212	1068	516
3-CH_3Py	1560	1233	1093	514	1537	1206	1080	515
Py	1564	1238	1095	515	1532	1203	1081	515
4-CNPy	1568	1235	1092	514				
3-CNPy					1542	1209	1068	514
p-$N(CH_3)_2$An	1573	1242	1096	515				
p-CH_3OAn	1580	1236	1088	515				
An	1582	1236	1088	515				
p-ClAn	1578	1237	1093	512				

a) Measured in Nujol mull.
b) Metal-N(oxime) stretching frequency.

zation potential of the Fe(II) ion may also explain the different direction of the charge-transfer band between the axial ligands and the central metal ion for the Co(III) and Fe(II) complexes: from the pyridine derivatives to the cobalt ion, and from the iron ion to the pyridine derivatives, respectively.

The above facts suggest that the π-bonds between the central metal ion and the ligands are stronger in the Fe(II) complexes than in the Co(III) complexes and that the σ-bonds are stronger in the latter than in the former.

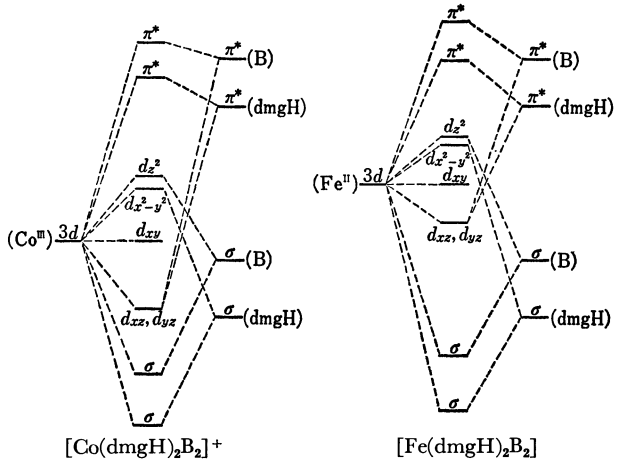

Fig. 5. Schematic orbital diagrams for $[Co(dmgH)_2B_2]^+$ and $[Fe(dmgH)_2B_2]$. By using the approximation of C_{4v} symmetry for the planar metal chelate of the complexes the axes were determined as follows; the nitrogen atoms of the dimethylglyoximate ligands lie on the x and y axes, and the cobalt ion lies on the intersection. The z axis is perpendicular to the xy plane.

IR Spectra. As is shown in Table 4, the IR spectra of the Co(III) and Fe(II) complexes show characteristic bands in the 1700—1800, 1510—1590, and 1060—1240 cm^{-1} regions; these are assigned to the O–H–O, C=N, and N–O stretching frequencies respectively.[15,22] The band observed at about 515 cm^{-1} might be attributed to the metal-N(oxime) stretching frequency on the basis of the assignment for $[Ni(dmgH)_2]$.[23] The C=N stretching frequencies of the complexes are shifted to much lower frequencies than for the free dimethylglyoxime($\nu_{C=N}=1750\ cm^{-1}$)[23] because of the existence of a d_π(metal)–π^*(dmgH) bonding.[15] The C=N stretching frequencies are dependent on the axial pyridine derivatives.

In the Co(III) complexes, it is obvious from Tables 2 and 4 that the C=N stretching frequencies are shifted to longer wavelengths as the β-band(d_π(Co)$\rightarrow\pi^*$-(dmgH)) is shifted to a longer wavelength. These results seem to suggest that, as the d_π(Co)–π^*(Py) interaction becomes stronger, the d_π(Co)–π^*(dmgH) bonding is more weakened and the C=N double bonding character is increased. The C=N stretching frequencies are lower in the Fe(II) complexes than in the Co(III) complexes, indicating that the d_π(metal)–π^*(dmgH) bonding is stronger in the former. The stretching frequency of the Co–N(oxime) is slightly lower than that of the Fe–N(oxime). This may be due to the facts that the π-bond is stronger in the Fe(II) complexes and that the σ-bond is stronger in the Co(III) complexes, as has been suggested before.

22) A. Nakahara, J. Fujita, and R. Tsuchida, This Bulletin, **29**, 296 (1956).
23) K. Torii, I. Nakagawa, and T. Shimanouchi, The 14th Symposium on Coordination Chemistry in Japan, p. 269 (1964).

Kinetics and Mechanism of the Ligand Substitution Reaction of the Mercury(II)-4-(2-pyridylazo)resorcinol Complex with 1,2-Cyclohexanediamine-*N*,*N*,*N*′,*N*′-tetraacetic Acid

Shigenobu FUNAHASHI, Masaaki TABATA, and Motoharu TANAKA

Laboratory of Analytical Chemistry, Faculty of Science, Nagoya University, Chikusa-ku, Nagoya

(Received December 7, 1970)

Kinetics and mechanism of the ligand substitution reaction of the mercury(II)-PAR complex with CyDTA were studied at 25°C in the presence of halogenide ion at an ionic strength of 0.1. The rate law can be written as

$$-\frac{d[Hg(par)_2^{2-}]}{dt} = (k_1'[H^+] + k_2' + k_{3,X}'[H^+][X^-])\frac{[Hg(par)_2^{2-}]}{[Hpar^-]}[Hcydta^{3-}]$$

where X^- refers to a halogenide ion (chloride, bromide, iodide). The rate constants k_1', k_2', and $k_{3,X}'$ were determined as: $k_1' = (2.4\pm0.1)\times10^7$ M^{-1} sec^{-1}, $k_2' = (1.9\pm0.1)\times10^{-2}$ sec^{-1}, $k_{3,Cl}' = (4.5\pm0.2)\times10^9$ M^{-2} sec^{-1}, $k_{3,Br}' = (3.2\pm0.1)\times10^{11}$ M^{-2} sec^{-1}, $k_{3,I}' = (5.6\pm0.2)\times10^{14}$ M^{-2} sec^{-1}. The rate constants for the paths involving mixed hydroxo and halogeno complexes (k_2' and $k_{3,X}'$) are quantitatively accounted for in terms of electron donation of ligands OH^- and X^-.

The ligand substitution reactions of metal complexes with multidentate ligands have been extensively studied by many authors.[1-9] Some of these studies have shown that ligands coordinated to a central metal ion affect the rate of substitution. In the reaction of monoacidopentaaquonickel(II) complex with 4-(2-pyridylazo)resorcinol (PAR) it has been shown that the ligand coordinated to nickel(II) labilizes coordinated water molecules.[7] Hunt *et al.*[8] reported that the rate of water exchange of some nickel(II) complexes became faster with increasing extent of substitution. In the ligand substitution of the Ni(II)-EDDA complex and the Ni(II)-NTA complex with PAR,[9] it has been revealed that EDDA and NTA coordinated to nickel(II) labilize water molecules attached to nickel(II).

In the present study, the kinetics and mechanism of the ligand substitution reaction of the mercury(II)-PAR complex with CyDTA (1,2-cyclohexanediamine-*N*,*N*,*N*′,*N*′-tetraacetic acid) were studied in the presence of halogenide ion. The reaction system is

$$Hg(II)\text{-}PAR + CyDTA \rightleftarrows Hg(II)\text{-}CyDTA + PAR \quad (1)$$

Primary purpose of this study is to elucidate the effect of monodentate ligands on the reaction.

Experimental

Reagents. *Mercury(II) Perchlorate*: Commercial G. R. mercury(II) oxide was dissolved in perchloric acid. Twice recrystallized sodium bicarbonate was added to the solution to obtain mercury carbonate. The mercury(II) perchlorate solution was prepared by dissolving mercury carbonate in a perchloric acid solution. The concentration of the mercury(II) solution was determined by a standard EDTA solution using xylenol orange as an indicator.

CyDTA: The acid form of CyDTA obtained from Dojindo Co., Ltd., was dissolved in a sodium hydroxide solution. CyDTA was then precipitated by addition of perchloric acid. The purified CyDTA was dissolved in 2 eq. of sodium hydroxide. The CyDTA solution was standardized complexometrically by a zinc(II) standard solution using Erio T as an indicator.

Sodium Chloride: Sodium chloride was obtained by addition of reagent grade hydrochloric acid to a saturated sodium chloride solution. Sodium chloride obtained was heated by an infrared lamp in order to expel excess hydrochloric acid.

Sodium Bromide: G. R. sodium bromide was recrystallized three times from distilled water. The bromide solution was standardized by a standard silver nitrate solution using eosine as an indicator.

Sodium Iodide: G. R. sodium iodide was recrystallized twice from distilled water. The precipitated sodium iodide was washed with ether and benzene, and then dried *in vacuo* at room temperature. The sodium iodide solution was standardized in the same way as the bromide solution.

Methods of preparation of all other reagents (sodium perchlorate, sodium hydroxide, PAR, borax and boric acid) have been described previously.[4]

Apparatus: The following instruments were used: Hitachi Perkin-Elmer 139 UV-VIS spectrophotometer, Hitachi Model QPD-53 recorder, Hirama Type 6 spectrophotometer, X-Y recorder Type UR-631 (Matsushita Communication Industrial Co., Yokohama), Radiometer PHM-4d (Copenhagen) with a Type G 202 B glass electrode and K 401 calomel electrode, Sharp Model TEB-10 thermoelectric circulating bath and a Coolnics circulator Type CTE-IB (Komatsu Solidate Co., Komatsu).

Procedure of Measurement of the Substitution Reaction Rate. Ionic strength was kept constant at 0.1 M with sodium perchlorate. A buffer solution of borate-boric acid was used. The mercury(II)-PAR solution containing PAR in excess was taken in a silica beaker with a light path of 5.3-cm or a quartz cell with a light path of 2.0-cm placed in the cell com-

1) D. W. Rogers, D. A. Aikens, and C. N. Reilley, *J. Phys. Chem.*, **66**, 1582 (1962).
2) D. B. Rorabacher and D. W. Margerum, *Inorg. Chem.*, **3**, 382 (1964).
3) W. H. Baddley and F. Basolo, *J. Amer. Chem. Soc.*, **88**, 2944 (1966).
4) M. Tanaka, S. Funahashi, and K. Shirai, *Inorg. Chem.*, **7**, 573 (1968).
5) D. L. Rabenstein and R. J. Kula, *J. Amer. Chem. Soc.*, **91**, 2492 (1969).
6) S. Funahashi, S. Yamada, and M. Tanaka, This Bulletin, **43**, 769 (1970).
7) S. Funahashi and M. Tanaka, *Inorg. Chem.*, **8**, 2159 (1969).
8) A. G. Desai, H. W. Dodgen, and J. P. Hunt, *J. Amer. Chem. Soc.*, **92**, 798 (1970), and their papers cited therein.
9) S. Funahashi and M. Tanaka, *Inorg. Chem.*, **9**, 2092 (1970).

partment thermostated at 25±0.2°C. The reaction was started by mixing the mercury(II)-PAR complex solution and the CyDTA solution. The reaction was followed automatically, the transmittance of the reaction system at 500 nm being recorded as a function of time. Molar absorption coefficients of $Hg(par)_2^{2-}$ and $Hpar^-$ at 500 nm are $\varepsilon_{Hg(par)_2}=6.50\times10^4$ and $\varepsilon_{Hpar}=1.31\times10^3$, respectively. All pH values were measured with a Radiometer PHM-4d which was carefully calibrated with a standard buffer solution (sodium borate 0.01 M) prepared as described by Bates.[10] All experiments were carried out at room temperature of 25±1°C.

Results

Substitution of the Mercury(II)-PAR Complex with CyDTA. The reaction of the mercury(II)-PAR complex with CyDTA was studied in the presence of a large excess of PAR over a pH range 8.5—9.1. Under the present experimental conditions the dominant species of CyDTA and PAR are the monoprotonated species $Hcydta^{3-}$ and $Hpar^-$, respectively, as apparent from stability constants: $K^H_{Hcydta}=10^{11.78}$, $K^H_{H2cydta}=10^{6.20}$, $K^H_{Hpar}=10^{12.31}$, $K^H_{H2par}=10^{5.48}$. The mercury(II)-PAR complex forms the 1 : 2 complex $Hg(par)_2^{2-}$. The mercury(II)-CyDTA complex is the 1 : 1 complex $Hg(cydta)^{2-}$ ($K_{Hg(cydta)}=10^{24.4}$ [11], $K^{OH}_{Hg(cydta)OH}=10^{3.2}$ [12]). Equilibrium (1) is much favored to the right so that the substitution reaction of the mercury(II)-PAR complex with CyDTA goes substantially to completion and the reverse reaction can be neglected. Thus the reaction system studied is described as

$$Hg(par)_2^{2-} + Hcydta^{3-} + H_2O \rightarrow Hg(cydta)^{2-} + 2\,Hpar^- + OH^-$$

From the measurements of the initial rate, the rate of decrease of the mercury(II)-PAR complex is found to be first-order with respect to mercury(II)-PAR and to CyDTA. Thus the rate equation can be expressed as

$$-\frac{d[Hg(par)_2^{2-}]}{dt} = k_{0(H,PAR)}[Hg(par)_2^{2-}][Hcydta^{3-}] \quad (2)$$

This equation is confirmed also from the linearity of the second order plots obtained by it. We have the following relationships

$$A_0 = \varepsilon_{Hg(par)_2}C_{Hg} + \varepsilon_{Hpar}(C_{PAR}-2C_{Hg}) \quad (3)$$

$$A_t = \varepsilon_{Hg(par)_2}[Hg(par)_2^{2-}] + \varepsilon_{Hpar}(C_{PAR}-2C_{Hg}+2[Hg(cydta)^{2-}]) \quad (4)$$

$$A_\infty = \varepsilon_{Hpar}C_{PAR} \quad (5)$$

where A_0, A_t, and A_∞ are the absorbances of the reaction system at reaction time 0, t and ∞, respectively, and C_{Hg} and C_{PAR} denote the total concentration of mercury(II) and of PAR, respectively. Substitution of Eqs. (3), (4) and (5) into the integrated form of Eq. (2) leads to

10) R. G. Bates, "Determination of pH, Theory and Practice," John Wiley & Sons, Inc., New York (1964), p. 76.
11) J. H. Holloway and C. N. Reilley, *Anal. Chem.*, **32**, 249 (1960).
12) D. L. Janes and D. W. Margerum, *Inorg. Chem.*, **5**, 1135 (1966).

Table 1. Conditional rate constants for the reaction between the mercury(II)-PAR complex and CyDTA at 25°C and μ=0.1 ($NaClO_4$)

$C_{Hg}\times10^6$ M	$C_{PAR}\times10^4$ M	$C_{CyDTA}\times10^5$, M	pH	$k_{0(H,PAR)}\times10^{-2}$ $M^{-1}sec^{-1}$
0.984	1.50	1.93	8.94	2.9
1.97	1.50	1.93	8.62	5.5
1.97	1.50	1.93	8.78	4.1
1.97	1.50	1.93	8.92	3.2
1.97	1.50	1.93	8.93	2.9
1.97	1.50	1.93	9.07	2.6
1.97	2.00	1.93	8.64	3.7
1.97	2.00	1.93	8.79	2.8
1.97	1.98	1.93	8.88	2.5
1.97	2.00	1.93	9.07	2.0
1.97	4.00	1.93	8.62	1.9
1.97	4.00	1.93	8.78	1.3
1.97	4.00	1.93	8.87	1.2
1.97	1.50	0.771	8.93	3.0
1.97	1.50	2.70	8.94	3.0
1.97	1.50	3.85	8.93	3.0
2.95	1.50	1.93	8.92	3.0

Table 2. Conditional rate constants $k_{0(H,PAR,X)}$ for the reaction of the mercury(II)-PAR complex with CyDTA in the presence of halogenide ions at 25°C and μ=0.1 ($NaClO_4$)
$C_{Hg}=1.97\times10^{-6}$ M, $C_{CyDTA}=1.93\times10^{-5}$ M, $C_{PAR}=2.00\times10^{-4}$ M

$[I^-]\times10^8$, M	pH	$k_{0(H,PAR,I)}\times10^{-2}$, $M^{-1}sec^{-1}$
2.16	8.77	3.8
2.16	8.87	3.2
2.16	8.88	3.1
2.16	9.05	2.4
4.28	8.89	3.7
8.85	8.90	5.2
10.69	8.90	5.6

$[Br^-]\times10^4$, M	pH	$k_{0(H,PAR,Br)}\times10^{-2}$, $M^{-1}sec^{-1}$
0.94	8.46	9.8
0.94	8.82	4.5
0.94	8.74	5.2
0.94	9.01	3.8
1.98	8.84	7.8
3.96	8.83	11.9
5.95	8.83	17.0
7.93	8.82	21.8

$[Cl^-]\times10^2$, M	pH	$k_{0(H,PAR,Cl)}\times10^{-2}$, $M^{-1}sec^{-1}$
1.00	8.54	12.0
1.00	8.71	8.2
1.00	8.84	6.5
1.00	8.89	5.4
0.50	8.83	4.9
1.59	8.84	8.0

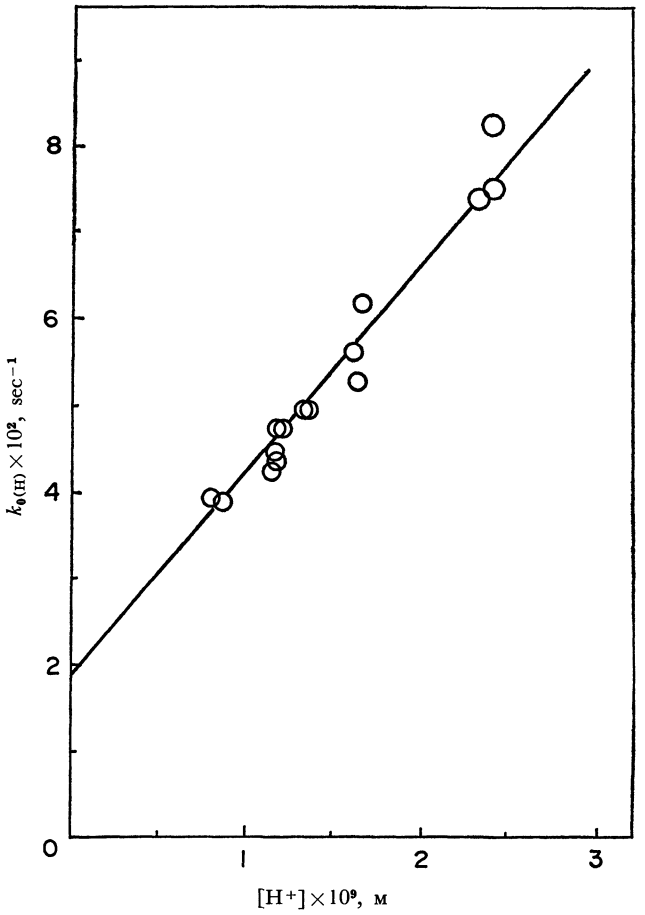

Fig. 1. Plot of $k_{0(H)}$ *vs.* $[H^+]$.
$C_{CyDTA}=(0.771-3.85)\times10^{-5}$ M, $C_{Hg}=(0.984-2.95)\times10^{-6}$ M, $C_{PAR}=(1.50-4.00)\times10^{-4}$ M, $\mu=0.1$ ($NaClO_4$), 25°C.

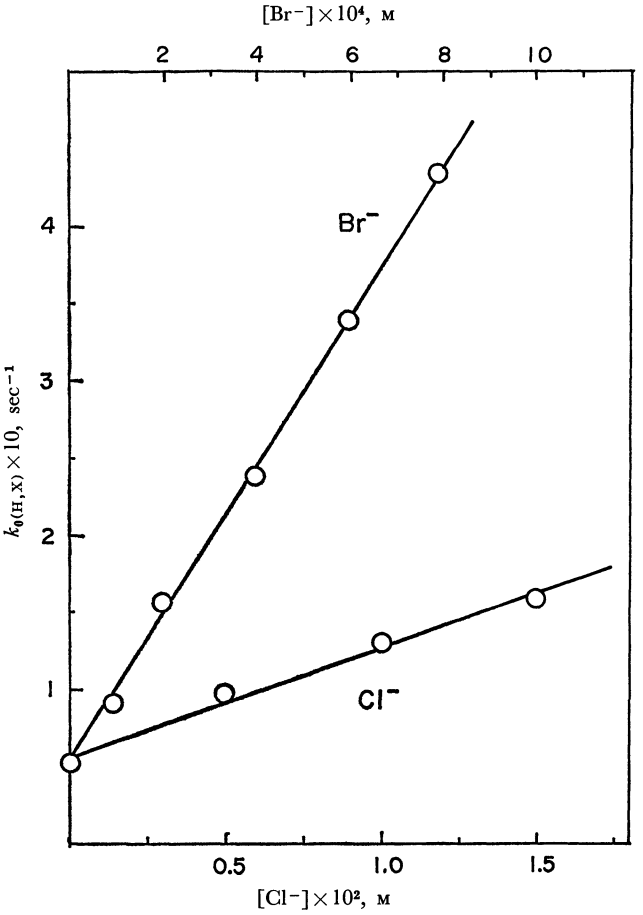

Fig. 2. Effect of the halogenide ion concentration on conditional rate constants.
$C_{Hg}=1.97\times10^{-6}$ M, $C_{CyDTA}=1.93\times10^{-5}$ M, $C_{PAR}=2.00\times10^{-4}$ M, pH=8.83±0.01, $\mu=0.1$ ($NaClO_4$), 25°C.

$$\frac{2.303}{C_{CyDTA}-C_{Hg}}\log\left\{\frac{A_0-A_\infty}{A_t-A_\infty}-\frac{C_{Hg}(A_0-A_t)}{C_{CyDTA}(A_t-A_\infty)}\right\}=k_{0(H,PAR)}t \quad (6)$$

Plots of the left-hand side of this equation *vs.* t give a straight line, of which the slope corresponds to the conditional rate constant $k_{0(H,PAR)}$. Conditional rate constants are summarized in Table 1. The data indicate the linear relationship between $k_{0(H,PAR)}$ and the reciprocal concentration of PAR with the zero intercept. Values of $k_{0(H,PAR)}[Hpar^-]$ (*i.e.* $k_{0(H)}$) are plotted against the concentration of hydrogen ion in Fig. 1, from which we can derive the following relationship:

$$k_{0(H,PAR)}[Hpar^-]=k_1'[H^+]+k_2' \quad (7)$$

The rate equation of the substitution of the mercury-(II)-PAR complex with CyDTA is

$$-\frac{d[Hg(par)_2^{2-}]}{dt}=(k_1'[H^+]+k_2')\frac{[Hg(par)_2^{2-}][Hcydta^{3-}]}{[Hpar^-]} \quad (8)$$

Substitution of the Mercury(II)-PAR Complex with CyDTA in the Presence of Halogenide Ions. A halogenide ion accelerates the substitution of the mercury(II)-PAR complex with CyDTA. Conditional rate constants $k_{0(H,PAR,X)}$ under various conditions are summarized in Table 2. The plot of $k_{0(H,X)}$ *vs.* $[X^-]$ gives a straight line with an intercept as shown in Fig. 2. The value of the intercept, corresponding to the reaction path independent of halogenide ions, is the same as that found in the reaction in the absence of halogenide at the same pH (*i.e.* $[H^+]=(1.5\pm0.1)\times10^{-9}$, see Fig. 1.). Hence, we have the following relationship:

$$k_{0(H,X)}=k_1'[H^+]+k_2'+k_{3(H)}'[X^-] \quad (9)$$

The values of conditional rate constants in the presence of iodide, bromide, and chloride are plotted against hydrogen ion concentrations in Fig. 3. It is evident that $k_{0(H,X)}$ is linearly related to the hydrogen ion concentration. Thus Eq. (9) can be written as

$$k_{0(H,X)}=k_1'[H^+]+k_2'+k_{3,X}'[H^+][X^-] \quad (10)$$

From these results we obtain the following rate equation for the ligand substitution reaction of the mercury(II)-PAR complex with CyDTA in the presence of halogenide ion:

$$-\frac{d[Hg(par)_2^{2-}]}{dt}=(k_1'[H^+]+k_2'+k_{3,X}'[H^+][X^-])\times\frac{[Hg(par)_2^{2-}][Hcydta^{3-}]}{[Hpar^-]} \quad (11)$$

The rate constants k_1', k_2', $k_{3,Cl}'$, $k_{3,Br}'$, and $k_{3,I}'$ at 25°C and $\mu=0.1$ are tabulated in Table 3.

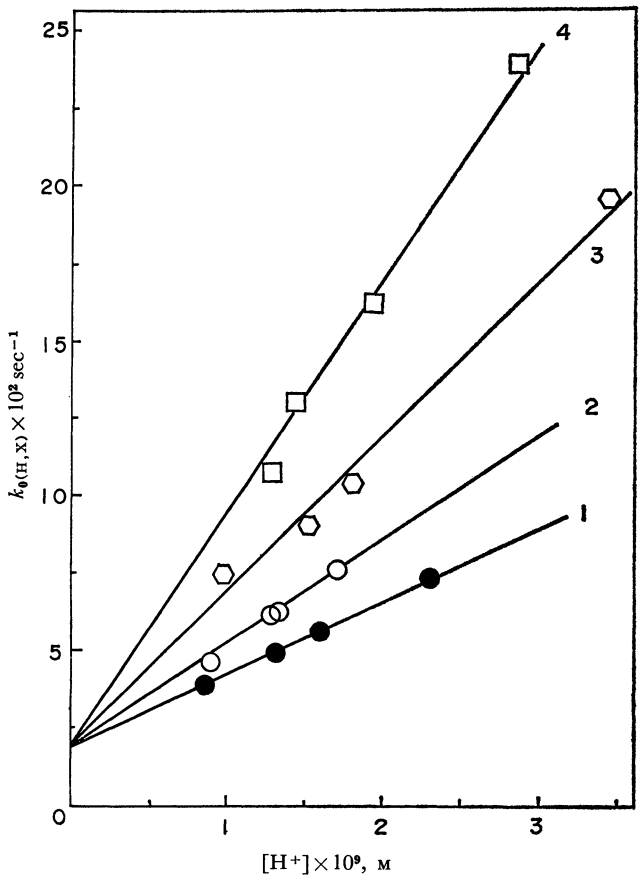

Fig. 3. Effect of the hydrogen ion concentration on conditional rate constants in the presence of halogenide ions. 1: $[X^-]=0$ M, 2: 2.16×10^{-8} M, 3: $[Br^-]=0.94\times10^{-4}$ M, 4: $[Cl^-]=1.00\times10^{-2}$ M, $C_{Hg}=1.97\times10^{-6}$ M, $C_{CyDTA}=1.93\times10^{-5}$ M, $C_{PAR}=2.00\times10^{-4}$ M, $\mu=0.1$ ($NaClO_4$), 25°C.

Table 3. Rate constants for the ligand substitution reaction of the mercury(II)-PAR complex with CyDTA in the presence of halogenide ion at 25°C and $\mu=0.1$ ($NaClO_4$)

k_1'	$(2.4\pm0.1)\times10^7$ M^{-1} sec^{-1}
k_2'	$(1.9\pm0.1)\times10^{-2}$ sec^{-1}
$k_{3,Cl}'$	$(4.5\pm0.2)\times10^9$ M^{-2} sec^{-1}
$k_{3,Br}'$	$(3.2\pm0.1)\times10^{11}$ M^{-2} sec^{-1}
$k_{3,I}'$	$(5.6\pm0.2)\times10^{14}$ M^{-2} sec^{-1}

Discussion

The rate of the reaction of the mercury(II)-PAR complex with CyDTA is suppressed by the increased PAR concentration, and is first-order with respect to the hydrogen ion concentration. The predominant species of PAR is the mono-protonated form $Hpar^-$. CyDTA can not react directly with the 1 : 2 mercury-(II)-PAR complex $Hg(par)_2^{2-}$ but with the 1 : 1 mercury(II)-PAR complex Hg(par) formed by the dissociation of a PAR. Thus it seems reasonable to consider Equilibrium (12) to precede the rate-determining step (13).

$$Hg(par)_2^{2-} + H^+ \rightleftarrows Hg(par) + Hpar^- \quad (12)$$

$$Hg(par) + Hcydta^{3-} \rightarrow Hg(cydta)^{2-} + Hpar^- \quad (13)$$

Such a predissociation equilibrium has been observed also in the ligand substitution reactions of the zinc(II)-PAR complex[4] and the copper(II)-PAR complex[6] with (ethyleneglycol)bis(2-aminoethylether)-*N*,*N*,-*N*'-tetraacetic acid. When the equilibrium constant of Reaction (12) is taken into consideration, the following equation can be derived from Eq. (11).

$$-\frac{d[Hg(par)_2^{2-}]}{dt} = \left(\frac{k_1' K^{par}_{Hg(par)_2}}{K^H_{Hpar}} + \frac{k_2' K^{par}_{Hg(par)_2}}{K^H_{Hpar}}[H^+]^{-1} + \frac{k_{3,X}' K^{par}_{Hg(par)_2}}{K^H_{Hpar}}[X^-]\right)[Hg(par)][Hcydta^{3-}] \quad (14)$$

where $K^H_{Hpar}=[Hpar^-]/[par^{2-}][H^+]$ and $K^{par}_{Hg(par)_2}=[Hg(par)_2^{2-}]/[Hg(par)][par^{2-}]$.

In the presence of halogenide ions the following equilibrium should be operative in the present ligand substitution.

$$Hg(par) + X^- \rightleftarrows Hg(par)X^- \quad (15)$$

PAR has three coordinate sites (N in pyridine, N in azo and O in resorcinol). The 1 : 1 mercury(II)-PAR complex will accept another ligand. The third term on the right-hand side of Eq. (14) corresponds to the reaction path through the mixed halogeno complex. The second term on the right-hand side of Eq. (14) involves the reciprocal concentration of hydrogen ion. This suggests a reaction path through a mixed hydroxo complex similar to the mixed halogeno complex. Protolytic reaction of mercury(II) ion is sufficiently fast, and the following equilibrium precedes the rate-determining step.

$$Hg(par) \rightleftarrows Hg(par)OH^- + H^+ \quad (16)$$

With constants for Equilibria (15) and (16), Eq. (14) is rewritten as

$$-\frac{d[Hg(par)_2^{2-}]}{dt} = \frac{k_1' K^{par}_{Hg(par)_2}}{K^H_{Hpar}}[Hg(par)] + \frac{k_2'}{K_W}\frac{K^{par}_{Hg(par)_2}}{K^{OH}_{Hg(par)OH}K^H_{Hpar}}[Hg(par)OH^-] + \frac{k_{3,X}' K^{par}_{Hg(par)_2}}{K^X_{Hg(par)X}K^H_{Hpar}}[Hg(par)X^-])[Hcydta^{3-}] = (k_1[Hg(par)] + k^{OH}[Hg(par)OH^-] + k^X[Hg(par)X^-])[Hcydta^{3-}] \quad (17)$$

Some related constants are defined as follows:

$$K_W = [H^+][OH^-] \quad (18)$$

$$K^{OH}_{Hg(par)OH} = \frac{[Hg(par)OH^-]}{[Hg(par)][OH^-]} \quad (19)$$

$$K^X_{Hg(par)X} = \frac{[Hg(par)X^-]}{[Hg(par)][X^-]} \quad (20)$$

$$k_1 = k_1'\left(\frac{K^{par}_{Hg(par)_2}}{K^H_{Hpar}}\right) \quad (21)$$

$$k^{OH} = \frac{k_2'}{K_W}\frac{1}{K^{OH}_{Hg(par)OH}}\left(\frac{K^{par}_{Hg(par)_2}}{K^H_{Hpar}}\right) \quad (22)$$

$$k^X = k_{3,X}'\frac{1}{K^X_{Hg(par)X}}\left(\frac{K^{par}_{Hg(par)_2}}{K^H_{Hpar}}\right) \quad (23)$$

The proposed reaction mechanism of the mercury-(II)-PAR complex with CyDTA in the presence of

halogenide ions is as follows:

$$Hg(par)_2^{2-} + H^+ \rightleftarrows Hg(par) + Hpar^-$$

$$Hg(par)OH^- + Hcydta^{3-} \xrightarrow{k^{OH}} Hg(cydta)^{2-} + Hpar^- + OH^-$$

$$Hg(par) + Hcydta^{3-} \xrightarrow{k_1} Hg(cydta)^{2-} + Hpar^-$$

$$Hg(par)X^- + Hcydta^{3-} \xrightarrow{k^X} Hg(cydta)^{2-} + Hpar^- + X^-$$

The equilibria between $Hg(par)_2^{2-}$ and Hg(par), and between Hg(par) and $Hg(par)X^-$ precede the rate-determining steps. CyDTA reacts with Hg(par), $Hg(par)OH^-$, and $Hg(par)X^-$ formed through the equilibrium processes.

It is necessary to determine $K^{par}_{Hg(par)_2}$, $K^{OH}_{Hg(par)OH}$ and $K^X_{Hg(par)X}$ in order to estimate the values of k_1, k^{OH}, and k^X. Unfortunately, these stability constants could not be successfully determined because of hydrolysis and precipitation of complexes. As apparent from Fig. 4, the plot of $\log(k_{3,X}'/k_{3,H_2O}')$ *vs.* E_n values of ligands (halogenide and hydroxide ions) gives a good straight line with a slope of 6.1, where k_{3,H_2O}' corresponds to $k_1'/55.5$ and E_n refers to the electron donor constant of a ligand.[13] Since $k_{3,X}'/k_{3,H_2O}' = (55.5/k_1) \times k^X K^X_{Hg(par)X}$ from Eqs. (21)—(23), $\log k^X K^X_{Hg(par)X}$ has a linear relationship with E_n's of ligands. Therefore, either $\log k^X$ or $\log K^X_{Hg(par)X}$ or both are proportional to E_n of X. In fact, the following results have been reported in some systems. In the case of the reaction between $Ni(H_2O)A^+$ and PAR there is an excellent correlation between E_n values of ligands and formation rate constants (where A denotes F^-, N_3^-, CH_3COO^-, OH^-, and H_2O[7]). For the mixed complex of Hg(cydta)X^{3-}, log stability constant $\log K^X_{Hg(cydta)X}$ is related to E_n of X by a straight line with a slope of 4.[12] The plot of $\log K^X_{HgX_4}$ *vs.* E_n gives a straight line with a slope of 1.5,[14] $K^X_{HgX_4}$ being defined as follows: $K^X_{HgX_4} = [HgX_4^{2-}]/[HgX_3^-][X^-]$. For the mixed complex of the type $Hg(CN)_3X^{2-}$, the slope of the plot of $\log K^X_{Hg(CN)_3X}$ *vs.* E_n of X^- has been found to be 2.[15] These facts being taken into account, the slope of the plot of $\log K^X_{Hg(par)X}$ *vs.* E_n is expected to be smaller than 6.1. This suggests that the rate constant (k^X) also depends on the E_n value of a ligand (X^-) coordinated to the mercury(II)-PAR complex; a ligand having larger E_n value tends to weaken the bond of mercury(II) with PAR. When a ligand coordinated to a central metal donates to a greater extent, the bond of the central metal with the leaving ligand will be weakened and more easily broken.

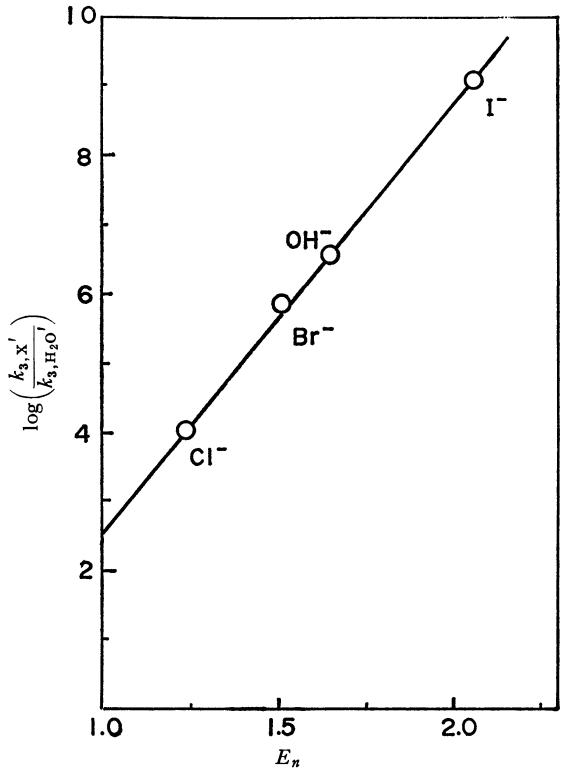

Fig. 4. Plot of $\log(k_{3,X}'/k_{3,H_2O}')$ *vs.* E_n.

The financial support given by the Ministry of Education is gratefully acknowledged.

13) J. O. Edwards, *J. Amer. Chem. Soc.*, **76**, 1540 (1954).
14) L. G. Sillén, *Acta Chem. Scand.*, **3**, 539 (1949).
15) L. Newman and D. N. Hume, *J. Amer. Chem. Soc.*, **83**, 1795 (1961).

The Extraction of the Cesium Ion with Some Nitrophenols into Nitrobenzene. I. Distribution Studies

Mutsuo KOYAMA, Osamu TOCHIYAMA, and Taitiro FUJINAGA

Department of Chemistry, Faculty of Science, Kyoto University, Sakyo-ku, Kyoto

(Received December 19, 1970)

The liquid-liquid extraction of alkali-metal nitrophenolates was studied by using nitrobenzene as the extracting solvent. Nitrophenol derivatives such as *o*-, *m*-, *p*-nitrophenols, α-dinitrophenol, and picric acid were chosen here in order to examine the effect of their steric characters and pK values on the distribution equilibrid. It was concluded that: 1) all the cesium nitrophenolates extracted into nitrobenzene were mainly in the dissociated form; 2) the extraction of *m*- and *p*-nitrophenolates proceeds by the stepwise adduct formation with free phenols, whereas little tendency of adduct formation was observed with the picrate system; 3) α-dinitrophenolate has a character between the other two; 4) the distribution of *o*-nitrophenolate is negligible. A detailed discussion is given of the phenomena in terms of ionic equilibria in both the aqueous and organic phases.

The liquid-liquid extraction of alkali metal ions has received attention not only from the viewpoint of practical analysis, but also from that of a theoretical interest in solute-solvent interaction.

In a previous paper, the present authors reported on the extraction of cesium into nitrobenzene with chromium complexes.[1] Similar extractions have been investigated by many authors using various reagents, such as tetraphenylborate,[2,3] dipicrylamine[4,5] and polyiodide.[6] In all these cases, the subject species are dissociated completely into ions in both the organic and aqueous phases.

On the other hand, Horner *et al.*[7] have shown the possibility of extracting cesium with various phenols as the reagents. Later, many alkyl derivatives of phenol were examined by Konečný and Sistkóva[8] and the extraction equilibria were discussed by Zingaro *et al.*[9] In the extraction of alkali phenolate, the extracted species are tightly-bounded ion pairs sometimes adducted with reagent acids.

Although the extraction mechanisms and the equilibria are pretty well understood in the case of chelate-extraction systems, the interpretation of the ion-pair extraction has not been completed. The distribution coefficient in the ion-pair system depends not only upon the bulk character of the solvents, such as dielectric constants and/or the solubility parameters, but also upon the particular interactions between solute and solvent, or sometimes between solutes.

The present series of studies were undertaken in order to investigate the influence of the characteristics of reagent anions on the extraction of alkali-metal ions and to estimate the relative degree of solute-solvent interactions.

In these studies, nitrobenzene was chosen as the organic solvent and cesium ions were distributed into both phases, using nitrophenol derivatives as the reagents. The nitrophenol derivatives examined were *ortho*-, *meta*-, *para*-nitrophenol (*o*-NP, *m*-NP, *p*-NP), 2,4-dinitrophenol (α-DNP), and 2,4,6-trinitrophenol (picric acid, PA); they were chosen because they have different acid dissociation constants in water and different steric effects, and are expected to have characters intermediate between those of alkyl phenols and dipicrylamine, tetraphenylborate, and others. In nitrobenzene, which is a strongly ionizing solvent, only dissociated forms are expected, and a difference in anion solvations (homoconjugation) can be observed for each nitrophenol.

The present paper is confined to a study of the ionic equilibria in the extraction processes. In the next paper,[10] the role of anions and the solute-solvent interaction will be discussed with the results obtained through the distribution and conductivity studies.

Experimental

Reagents. All the reagents used were of a reagent-grade purity. The nitrobenzene was vacuum-distilled before use. Carrier-free ^{137}Cs was supplied by the Oak Ridge National Laboratory.

Apparatus. The γ-ray measurements were performed with a single-channel pulse-height analyser (Osaka Denpa-Model LA-3T) equipped with a 1.5″ x 1.5″ NaI(Tl) well-type crystal. The absorbance measurements were carried out with an automatic recording spectrophotometer (Shimadzu-Model SV-5 A) by the use of quartz cells with a 1-cm light path. A pH meter (Horiba Model P) was used for all the pH measurements.

Procedure. In the distribution studies of nitrophenols, the pH of the aqueous phase was controlled by the addition of either a hydrochloric acid or a sodium hydroxide solution. Each nitrophenol solution of a 0.1 M concentration was prepared by dissolving the phenol in nitrobenzene. Four milliliters of the aqueous solution and the same volume of

1) T. Fujinaga, M. Koyama, and O. Tochiyama, *Anal. Chim. Acta*, **42**, 219 (1968).
2) T. Sekine and D. Dyrssen, *inid.*, **45**, 433 (1969).
3) J. Krtil, M. Fojtik, and M. Kyrš, *Collection Czechoslov. Chem. Commun.*, **27**, 2069 (1962).
4) J. Rais, M. Kyrš, and M. Pivoňková, *J. Inorg. Nucl. Chem.*, **30**, 611 (1968).
5) S. Motomizu, K. Tôei, and T. Iwachido, This Bulletin, **42**, 1006 (1969).
6) L. M. Slater, *Nucl. Sci. Eng.*, **17**, 576 (1963).
7) D. E. Horner, D. J. Crouse, K. B. Brown, and B. Weaver, *ibid.*, **17**, 234 (1963).
8) C. Konečný and N. Sistková, *Collection Czechoslov. Chem. Commun.*, **32**, 1938 (1967).
9) B. Z. Egan, R. A. Zingaro, and B. M. Benjamin, *Inorg. Chem.*, **4**, 1055 (1965).
10) T. Fujinaga, M. Koyama, and O. Tochiyama, This Bulletin, to be published.

the nitrobenzene solution were brought into contact and shaken in a glass tube for 30—60 min. at 20±1°C. The distribution ratios of nitrophenols were obtained by measuring their concentrations in the aqueous phase according to the following procedure. An appropriate aliquot of the aqueous phase was taken in a volumetric flask and diluted with a 0.1 M sodium hydroxide solution. The absorbance (*p*-NP; 402 nm, *m*-NP; 392 nm, *o*-NP; 420 nm, α-DNP; 362 nm and PA; 358 nm) was measured in order to determine the concentration of the nitrophenols. The pH of the aqueous phase after the equilibration was also measured and used for the calculation of the distribution ratios. The glass electrode pH meter was found to show pH 0.00, 1.00, 2.00, and 3.00 within an error of ±0.1 in solutions of perchloric acid of 1.0, 0.10, 1.0×10^{-2}, and 1.0×10^{-3} M respectively.

Similar procedures were employed for the distribution studies of the cesium ion. The pH of the aqueous phase, however, was adjusted with lithium hydroxide or sodium hydroxide, and the ionic strength was controlled with lithium chloride or sodium chloride.

A cesium chloride solution of an adequate concentration was added to the aqueous phase, and the distribution ratio of the cesium ion was obtained by measuring the γ-ray activities of ^{137}Cs in both the aqueous and organic phases.

Theoretical

(1) Distribution of Nitrophenols. In the extraction of nitrophenol ROH, the following equilibria can be considered in both phases:

$$(RO^-)_a + (H^+)_a \rightleftarrows (ROH)_a \quad (1)$$

$$(ROH)_a \rightleftarrows (ROH)_o \quad (2)$$

$$(RO^-)_o + (H^+)_o \rightleftarrows (ROH)_o \quad (3)$$

where the a and o subscripts refer to the aqueous and organic phases respectively. The concentration constants are expressed by the following equations:

$$K_{a,ROH} = [RO^-]_a[H^+]_a/[ROH]_a \quad (4)$$

$$K_{D,ROH} = [ROH]_o/[ROH]_a \quad (5)$$

$$K_{0,ROH} = [RO^-]_o[H^+]_o/[ROH]_o \quad (6)$$

$K_{a,ROH}$ and $K_{0,ROH}$ are the dissociation constants of ROH in the aqueous and nitrobenzene phases respectively, and $K_{D,ROH}$, the distribution coefficient of the neutral ROH.

At the distribution equilibrium between the two phases, the distribution ratio of ROH, D_{ROH}, is written as:

$$D_{ROH} = \frac{[ROH]_o+[RO^-]_o}{[ROH]_a+[RO^-]_a} \quad (7)$$

Among these chemical species, $[RO^-]_0$ can be neglected, because the dissociation of ROH in nitrobenzene is very small. Therefore,

$$D_{ROH} = \frac{[ROH]_o}{[ROH]_a+[RO^-]_a} \quad (7')$$

By combining Eqs. (2), (4), (5), and (7'), D_{ROH} is expressed as Eq. (7''):

$$D_{ROH} = \frac{K_{D,ROH}}{1+K_{a,ROH}/[H^+]_a} \quad (7'')$$

In this equation, D_{ROH} is a function of pH, that is (i) in the lower pH region:

$$D_{ROH} = K_{D,ROH} \quad (7''\text{-i})$$

and (ii) in the higher pH region:

$$D_{ROH} = K_{D,ROH}[H^+]_a/K_{a,ROH} \quad (7''\text{-ii})$$

If the curve of $\log D_{ROH}$ *vs.* pH consists of two parts which are represented by Eqs. (7''-i) and (7''-ii), $K_{D,ROH}$ and $K_{a,ROH}$ can be calculated from these equations.

The following relationship is obtained between the total concentration of nitrophenol and the concentration of undissociated nitrophenol in nitrobenzene:

$$[ROH]_{total} = [ROH]_o + [ROH]_a + [RO^-]_a$$

$$b = [ROH]_o\left(1+\frac{1}{K_{D,ROH}}+\frac{K_{a,ROH}}{K_{D,ROH}[H^+]_a}\right) \quad (8)$$

(2) Distribution of the Cesium Ion. In the experiments on the distribution of the cesium ion, the following equilibria must be considered in both the aqueous and organic phases:

$$(Cs^+)_a + (OR^-)_a \rightleftarrows (CsOR)_a \quad (9)$$

$$(CsOR)_a \rightleftarrows (CsOR)_o \quad (10)$$

$$(Cs^+)_0 + (OR^-)_o \rightleftarrows (CsOR)_o \quad (11)$$

$$(OR^-)_0 + n(ROH) \rightleftarrows (OR\cdot nROH^-)_o \quad (12)$$

$$K_{a,CsOR} = [Cs^+]_a[OR^-]_a/[CsOR]_a \quad (13)$$

$$K_{D,CsOR} = [CsOR]_o/[CsOR]_a \quad (14)$$

$$K_{0,CsOR} = [Cs^+]_o[OR^-]_o/[CsOR]_o \quad (15)$$

$$K_{Cs}^* = K_{0,CsOR}K_{D,CsOR}/K_{a,CsOR}$$
$$= [Cs^+]_o[OR^-]_o/[Cs^+]_a[OR^-]_a \quad (16)$$

$$K_n^f = [OR\cdot nROH^-]_o/[OR^-]_o[ROH]_o^n \quad (17)$$

Here, $K_{a,CsOR}$ and $K_{O,CsOR}$ represent the dissociation constants in each phase; $K_{D,CsOR}$, the distribution coefficient of the neutral CsOR; K_{Cs}^*, the distribution coefficient of fully-dissociated Cs^+ and OR^-, and K_n^f, the homoconjugation constant or the adduct formation constant in the organic phase.

When the concentration of cesium ions is sufficiently large as compared with those of other cations in the organic phase, the electrical neutrality in the phase can be written as:

$$[Cs^+]_o = [OR^-]_o + [OR\cdot ROH^-]_o + [OR\cdot 2ROH^-]_o + \cdots$$
$$= [OR^-]_o(1+\sum_n K_n^f[ROH]_o^n) \quad (18)$$

On the other hand, the distribution ratio of the cesium ion is:

$$D_{Cs} = \frac{[Cs^+]_o+[CsOR]_o}{[Cs^+]_a+[CsOR]_a} \quad (19)$$

When free cesium ions are considered to be the only chemical species of cesium in both the organic and aqueous phases, Eq. (19) can be written as:

$$D_{Cs} = [Cs^+]_o/[Cs^+]_a \quad (19')$$

By combining Eqs. (13)—(19'), D_{Cs} can be transformed into:

$$D_{Cs} = K_{Cs}^{*1/2}(1+\sum_n K_n^f[ROH]_o^n)^{1/2}\frac{[OR^-]_a^{1/2}}{[Cs^+]_a^{1/2}} \quad (20\text{-i})$$

$$= K_{Cs}^{*1/2}(1+\sum_n K_n^f[ROH]_o^n)^{1/2} \times \frac{K_{a,ROH}^{1/2}[ROH]_o^{1/2}}{K_{D,ROH}^{1/2}[Cs^+]_a^{1/2}[H^+]_a^{1/2}} \quad (20\text{-ii})$$

When most of the cesium ions are present in the form of ion pairs in both phases,

$$D_{Cs} = \frac{K_{D,CsOR}}{K_{a,CsOR}}[OR^-]_a \quad (21\text{-i})$$

$$= \frac{K_{D,CsOR}K_{a,ROH}[ROH]_o}{K_{a,CsOR}K_{D,ROH}[H^+]_a} \quad (21\text{-ii})$$

Eqs. (20) and (21) predict the difference in the dependence of D_{Cs} on $[H^+]_a$ and $[Cs^+]_a$.

Therefore, from the experimental data, whether the chemical form $(Cs^+)_o$ or $(CsOR)_o$ stands in the nitrobenzene phase can be confirmed.

When a considerable amount of NaOR or LiOR is extracted, the electrical neutrality expressed in Eq. (18) is no longer valid; the following relationship must be considered instead:

$$[M^+]_0 = [OR^-]_0 + [OR\cdot ROH^-]_0 + [OR\cdot 2ROH^-]_0 + \cdots \quad (18')$$

where M^+ denotes the competing cation, such as Li^+ or Na^+, and where

$$K_{a,MOR} = \frac{[M^+]_a[OR^-]_a}{[MOR]_a} \quad (22)$$

$$K_{D,MOR} = \frac{[MOR]_o}{[MOR]_a} \quad (23)$$

$$K_{o,MOR} = \frac{[M^+]_0[OR^-]_o}{[MOR]_o} \quad (24)$$

$$K_M^* = \frac{[M^+]_0[OR^-]_o}{[M^+]_a[OR^-]_a} \quad (25)$$

From these equations, we obtain:

$$D_{Cs} = [Cs^+]_o/[Cs^+]_a = K_{Cs}^{*1/2}\left(\frac{K_{Cs}^*}{K_M^*}\right)^{1/2}\frac{[OR^-]_a^{1/2}}{[M^+]_a^{1/2}} \times (1+\sum K_n^f[ROH]_o^n)^{1/2} \quad (26)$$

This equation shows that the D_{Cs} values are no longer the function of $[Cs^+]_a$, but the function of $[M^+]_a$, when $[Cs^+]_a \ll [M^+]_a$.

Results and Discussion

(1) Distribution of Nitrophenols. Figure 1 presents the relationship between the distribution ratios of each nitrophenol at the concentration of 0.1 M and the pH of the aqueous phase after the partition equilibrium has been attained. In these studies, the aqueous ionic strength was not fixed, because the ex-extraction of sodium nitrophenolates could be neglected.

In the figure, there are two parts, representing Eqs. (7″-i) and (7″-ii). From these curves, the $K_{a,ROH}$ and $K_{D,ROH}$ values can be obtained; these values are shown in Table 1. The $K_{a,ROH}$ values are in good agreement with those measured by other method.[11]

11) C. D. Hodgeman, "Handbook of Chemistry and Physics," 42nd Ed., Published by The Chemical Rubber Publishing Co, Cleveland, Ohio (1960).

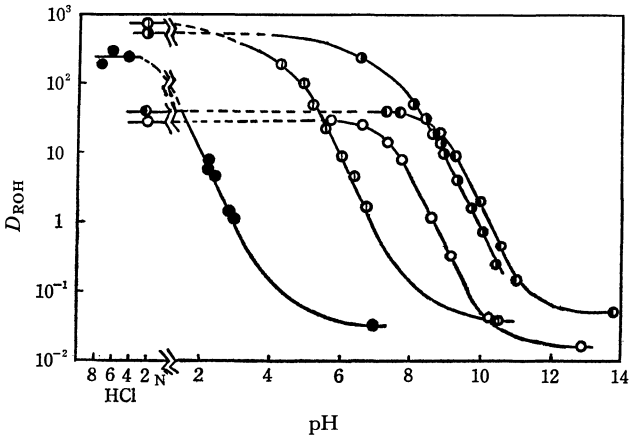

Fig. 1. Distribution of nitrophenols as the function of pH. $[ROH]_{total}=0.1$
○ *p*-NP ◐ *m*-NP ◑ *o*-NP ⓘ α-DNP ● PA

TABLE 1. DISTRIBUTION COEFFICIENTS AND DISSOCIATION CONSTANTS OBTAINED BY THE EXTRACTION METHOD

	$K_{D,ROH}$	$K_{a,ROH}$	$K_{a,ROH}$ other methods[11]
p-NP	28.4	6.1×10^{-8}	6.5×10^{-8}
m-NP	40.2	2.2×10^{-9}	5.2×10^{-9}
o-NP	599	1.1×10^{-7}	0.75×10^{-7}
α-DNP	746	0.89×10^{-4}	1.0×10^{-4}
PA	256	2.6×10^{-1}	3.8×10^{-1}

In the higher pH regions, the curves are not as linear as was expected from Eq. (7″-ii), because the extraction of NaOR can not be neglected in these regions.

From the experiment, the relationships between pH and $[ROH]_o$, which are represented by Eq. (8), were obtained and used in the calculation of the distribution of the cesium ion.

(2) Distribution of the Cesium Ion. (2-1) The Relationship between D_{Cs} and pH: In Fig. 2, the dependence of the distribution ratios of the cesium ion on the pH of the aqueous solution is presented. In this study, the total concentration of nitrophenol and the total concentration of the lithium ion were maintained at 0.4 M. However, the distribution of lithium ions in the organic phase was practically

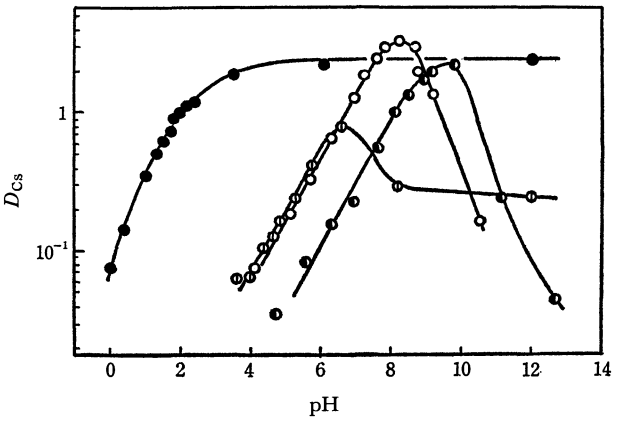

Fig. 2. Distribution of cesium ion as the function of pH. $[ROH]_{total}=0.4$, $[Li^+]_a=0.4$, $[Cs^+]_a=10^{-3}$.
○ *p*-NP ◐ *m*-NP ⓘ α-DNP ● PA

negligible, and the concentration of lithium ions in the aqueous phase was practically 0.4 M. The distribution ratios have been corrected for the constant aqueous cesium ion concentration (10^{-3} M) according to Eq. (27). This correction is based on Eq. (20), which is derived from the assumption that the chemical species in both organic and aqueous phases are fully dissociated:

$$D_{Cs}(\text{corrected}) = D_{Cs}(\text{raw})\left(\frac{10^{-3}}{[Cs^+]_a(\text{experimental})}\right)^{1/2} \quad (27)$$

Since, in the case of *o*-nitrophenol, the distribution ratios were found to be below 10^{-3} at all the pH values, no relationship is presented in the figures.

In Fig. 2, the slope of the ascending part of the curve is 1/2 in every case, and Eq. (20) applies well. In these parts, $[ROH]_o$ can be considered constant in Eq. (20-ii), because the third term in Eq. (8) can be neglected in the low pH regions, as is demonstrated in Fig. 1. In the case of picric acid, the slope deviates from 1/2 and approaches to 1 in the lower pH region. This deviation can be attributed to the increase of $[H^+]_o$ caused by the extraction of picric acid and/or of hydrochloric acid. If the hydrochloric acid is extracted and the electrical neutrality is expressed as $[H^+]_o=[Cl^-]_o$, the relation between D_{Cs} and $[H^+]_a$ can be represented by Eq. (27):

$$D_{Cs} = \frac{K_{Cs}^*}{K_H^*} K_{HCl}^{*1/2} \frac{[Cl^-]_a^{1/2}}{[H^+]_a^{1/2}} \quad (27)$$

where:

$$K_H^* = \frac{[H^+]_o[OR^-]_o}{[H^+]_a[OR^-]_a} \quad (25')$$

$$K_{HCl}^* = \frac{[H^+]_o[Cl^-]_o}{[H^+]_a[Cl^-]_a} \quad (28)$$

According to Eq. (27), the slope of the plot of log D_{Cs} *vs.* pH must remain 1/2, even in the lower pH region. If $[H^+]_o$ is mainly created by the dissociation of the picric acid extracted and if, therefore, the electrical neutrality is expressed as $[H^+]_o=[OR^-]_o$, Eq. (26'), which is derived from Eq. (26) by replacing $[M^+]$ by $[H^+]$, applies to the relation between D_{Cs} and $[H^+]_a$. This equation shows that the slope must be 1 in the lower pH region:

$$D_{Cs} = K_{Cs}^{*1/2}\left(\frac{K_{Cs}^*}{K_H^*}\right)^{1/2}(1 + \sum_n K_n^f[ROH]_o^n)^{1/2} \times \frac{K_{a,ROH}^{1/2}[ROH]_o^{1/2}}{K_{D,ROH}^{1/2}[H^+]_a} \quad (26')$$

Therefore, the increase of the slope which is observed in the lower pH region can be attributed to the extraction and dissociation of picric acid, and not to the extraction of hydrochloric acid.

The increase in pH also causes a loss of $[ROH]_o$ according to Eq. (8). In the high pH regions, the concentration of nitrophenol in nitrobenzene can be presented as:

$$[ROH]_o = [ROH]_{total}\left(1+\frac{1}{K_{D,ROH}}+\frac{K_{a,ROH}}{K_{D,ROH}[H^+]_a}\right)^{-1} = \frac{K_{D,ROH}}{K_{a,ROH}}[H^+]_a[ROH]_{total} \quad (8')$$

Therefore, Eq. (20) comes to Eq. (20'):

$$D_{Cs} = K_{Cs}^{*1/2}\frac{[ROH]_{total}^{1/2}}{[Cs^+]_a^{1/2}} \times \left\{1 + \sum_n K_n^f\left(\frac{K_{D,ROH}}{K_{a,ROH}}[H^+]_a[ROH]_{total}\right)^n\right\}^{1/2}$$

where $[ROH]_{total}$ and $[Cs^+]_a$ are constant. This equation shows that the slopes of log D_{Cs} *vs.* pH approach $-n/2$ in the high pH regions. Although few data are available for the high pH regions because the solution is not well-buffered in those regions, *p*- and *m*-nitrophenols show a decrease in D_{Cs} with an increase in the pH. In contrast, the system with picric acid shows no decrease in D_{Cs} with an increase in the pH. This means that the K_n^f value is negligibly small and that simple ion pairs are the predominant species in the extract. In the case of α-dinitrophenol, the slope of the descending part reaches zero as the pH increases. This can be explained by using Eq. (20'). In the region where D_{Cs} decreases as the pH increases, the second term:

$$\left(K_1^f\frac{K_{D,ROH}}{K_{a,ROH}}[H^+]_a[ROH]_{total}\right)$$

plays a more important role than the first term, 1. On the other hand, in the region where the slope reaches zero, the second term becomes less important. Thus with the system of α-dinitrophenol, non-conjugated ions are extracted in the higher pH region, and both conjugated and non-conjugated ions are extracted in the lower pH region.

(2-2) The Relationship between D_{Cs} and $[Cs^+]_a$: The relationship between the distribution ratios of cesium ions and the cesium-ion concentration in equilibrium is shown in Figs. 3—6. The aqueous ionic strength, which was adjusted with sodium or lithium chloride (before the equilibration), was considered to be unchanged during the extraction process. The pH of the aqueous phase was adjusted so as to be constant in each experiment.

The slope of log D_{Cs} *vs.* log $[Cs^+]_a$ is $-1/2$ unless the concentration of cesium ions is relatively small. This value shows that the cesium ion in the nitrobenzene phase is a free ion and that Eq. (20) holds quite well.

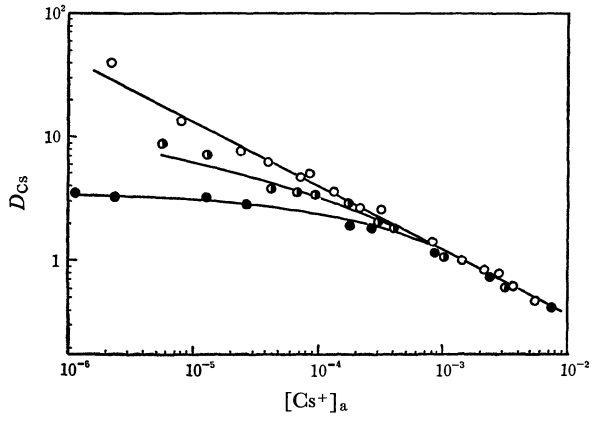

Fig. 3. Distribution of cesium ion as the function of cesium concentration (*p*-NP).
$[ROH]_{total}=0.4$, pH 7.0
○ $[Li^+]_a=0.008$, ◑ $[Li^+]_a=0.2$, ● $[Na^+]_a=0.32$

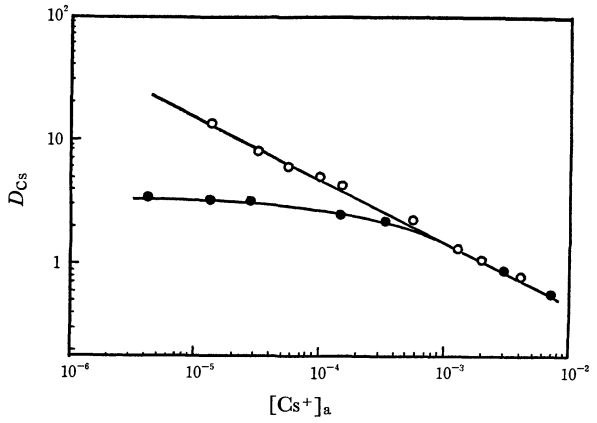

Fig. 4. Distribution of cesium ion as the function of cesium ion concentration (*m*-NP).
$[ROH]_{total}=0.4$, pH 8.7
○ $[Li^+]_a=0.02$, ● $[Na^+]_a=0.27$

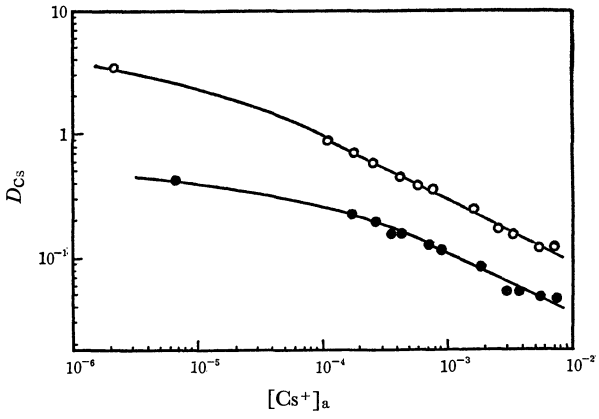

Fig. 5. Distribution of cesium ion as the function of cesium ion concentration (α-DNP).
○ $[ROH]_{total}=0.4$, pH 5.3, $[Li^+]_a=0.02$
● $[ROH]_{total}=0.2$, pH 12.5 $[Li^+]_a=0.25$

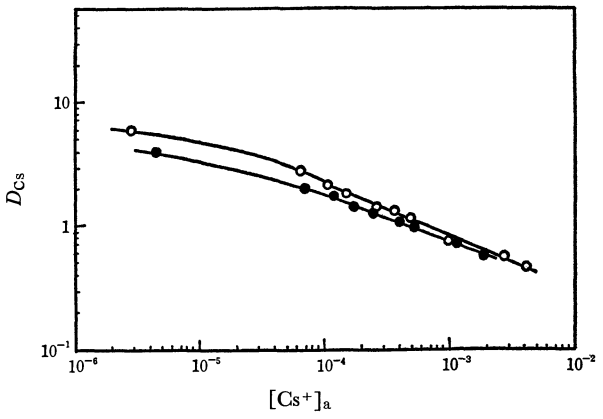

Fig. 6. Distribution of cesium ion as the function of cesium ion concentration (PA).
○ $[ROH]_{total}=0.4$, pH 1.6
● $[ROH]_{total}=0.2$, pH 12.3 $[Li^+]_a=0.25$

In Figs. 3—6, the effect of the aqueous ionic strength can be seen when the concentration of lithium or sodium ions is quite large. When the concentration of cesium ions is quite small, Eq. (26) shows the relationship between D_{Cs} and $[Cs^+]_a$. The equation indicates that D_{Cs} is no longer the function of $[Cs^+]_a$ but the function of $[M^+]_a$. The relationship between D_{Cs} and $[M^+]_a$ when the cesium-ion concentration is quite small is shown in Fig. 7. The slope of $\log D_{Cs}$ *vs.* $\log [M^+]_a$ is $-1/2$. This shows that Eqs. (18′) and (26) are valid in this case.

The extraction behavior with picric acid is shown in Fig. 6. The slope of $\log D_{Cs}$ *vs.* $\log [Cs^+]_a$ deviates a little from the slope of $-1/2$, although no metal ions are present except cesium ions. In this case, the cation competing against the cesium ion in the organic phase is a proton which is derived from the dissociation of picric acid in the organic phase (the dissociation constant, pK_o, of picric acid in nitrobenzene is 7.5[12]). From the assumption that $[H^+]_o=[OR^-]_o$ is valid, the concentration of protons in the organic phase can be calculated as *ca.* 10^{-4} M by using Eq. (6). Accordingly, in the region where the concentration of cesium ions in the organic phase is lower than 10^{-4} M, D_{Cs} is no longer dependent on $[Cs^+]_a$, but on $[H^+]_o$. With an increase in the concentration of cesium ions beyond 10^{-4} M, D_{Cs} becomes more dependent on the concentration of cesium ions.

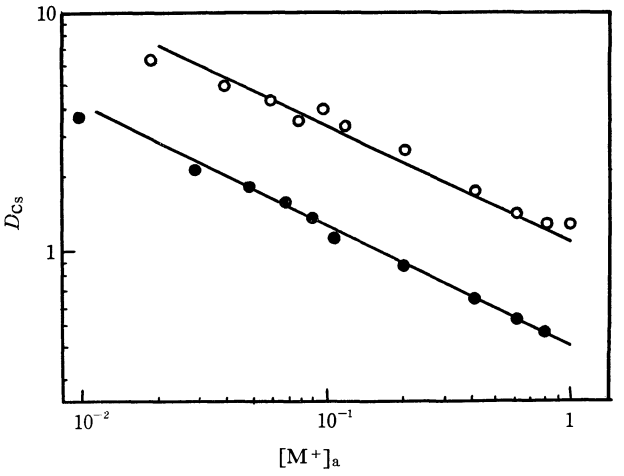

Fig. 7. Distribution of cesium ion as the function of sodium ion concentration or lithium ion concentration (*p*-NP).
$[ROH]_{total}=0.1$, $[Cs^+]_a=10^{-5}$
○ M=Li, pH 8.2, ● M=Na, pH 7.6

(2-3) The Relationship between D_{Cs} and $[ROH]_{total}$: Figure 8 shows the dependence of the distribution ratios of the cesium ion on the total concentration of nitrophenol. In this study, the experimental values have been corrected to the value at the constant pH and at the constant aqueous cesium-ion concentration. The correction has been made according to the following equation:

$$D_{Cs}(\text{corrected}) = D_{Cs}(\text{raw}) \times \left\{\frac{[Cs^+]_a(\text{corrected})[H^+]_a(\text{corrected})}{[Cs^+]_a(\text{raw})[H^+]_a(\text{raw})}\right\}^{1/2}$$

In this experiment, no cations were present in either the organic or aqueous phase except proton and cesium ions.

At a constant pH, the term

$$(1 + 1/K_{D,ROH} + K_{a,ROH}/K_{D,ROH}[H^+]_a)$$

12) I. M. Kolthoff, D. Stcoesoća, and T. S. Lee, *J. Amer. Chem. Soc.*, **75**, 1834 (1953).

TABLE 2. EXTRACTION OF CESIUM ION WITH SOME NITROPHENOLS

Reagent	Slope of log D_{Cs} plot			Principal species in org. phase	K_{Cs}* or $K_{Cs}*K_n^f$	$K_{Cs}*/K_{Na}*$
	pH	log $[Cs^+]_a$	log $[ROH]_t$			
p-NP	1/2	−1/2	3.3/2	Cs^+ $OR\cdot 2ROH^-$	$K_{Cs}*K_2^f=1.2$	2.3×10^3
m-NP	1/2	−1/2	3/2	Cs^+ $OR\cdot 2ROH^-$	$K_{Cs}*K_2^f=1.1$	1.3×10^3
o-NP	—	—	—	—	—	—
α-DNP	1/2	−1/2	2/2	Cs^+ $OR\cdot ROH^-$ Cs^+ OR^- (alkaline)	$K_{Cs}*K_1^f=2.1\times10^{-2}$ $K_{Cs}*=7.4\times10^{-5}$	1.3×10^3
PA	1/2	−1/2.4	1.3/2	Cs^+ OR^-	$K_{Cs}*=2.4\times10^{-3}$ $K_{Cs}*K_1^f=3.6\times10^{-2}$	5.0×10^3

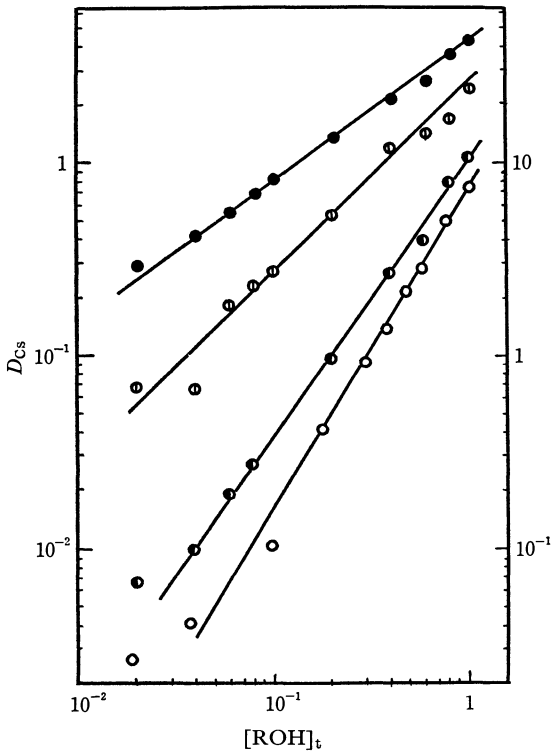

Fig. 8. Distribution of cesium ion as the function of nitrophenol concentrations.
○ *p*-NP, pH 7, $[Cs^+]_a=10^{-3}$ (right-hand scale)
◐ *m*-NP, pH 6, $[Cs^+]_a=10^{-5}$ (right-hand scale)
◑ α-DNP, pH 5, $[Cs^+]_a=10^{-5}$ (left-hand scale)
● PA, pH 2, $[Cs^+]_a=2\times10^{-4}$ (left-hand scale)

is constant in Eq. (8). Therefore, the slope of log D_{Cs} *vs.* log $[ROH]_{total}$ is the same as that of log D_{Cs} *vs.* log $[ROH]_o$. The slopes correspond to $(n+1)/2$ in Eq. (20-ii). From the experiment shown in Fig. 8, the n values obtained were 0.3 with picric acid, 1 with α-dinitrophenol, 2 with *m*-nitrophenol, and 2.3 with *p*-nitrophenol. The number, n, of the adduct molecules increases as the number of substituted nitro-groups decreases. This observation is also supported by the results shown in the experiments on the relationship between D_{Cs} and pH.

(2-4) Conclusions: The results of the above experiments are summarized in Table 2. In this table, no clear relations can be found in the case of *o*-nitrophenol, because the distribution ratios were below 10^{-3} in every experiment. The reason for this difference from the cases of *p*- and *m*-nitrophenols can not be explained by these experiments alone, though the obstruction of the formation of the CsOR ion-pair, the difficully of the formation of the conjugated ion $(OR\cdot nROH^-)_0$, and some other causes can be considered.

In all cases, the chemical form of cesium ions is concluded to be dissociated ions. The participation of free nitrophenols was observed in the distribution of cesium ions. Through distribution studies, however, no information can be obtained on whether free nitrophenols interact with anions or with cations. Nevertheless, in the present study, we assumed that free nitrophenols interact only with anions. The reason for this assumption will be discussed in the next paper,[10] which will deal with the results of the conductivity measurements. The adduct formation (homoconjugation) of free nitrophenols with anions is seen in the cases of mono- and di-substituted nitrophenols. These cases correspond with the cases of other alkyl-substituted phenols. The extraction of picrate resembles those of dipicrylaminate, tetraphenylborate, reineckate, and other ion-pairs.

The extraction constants were calculated from the data; the values were obtained; as K_{Cs}* or $K_{Cs}*K_n^f$. In the cases of picric acid and α-dinitrophenol, both K_{Cs}* and $K_{Cs}K_1^f$ were obtained, K_{Cs}*, from the data when pH is very high, and $K_{Cs}*K_1^f$, from the data when pH is low. As can be seen from the slopes of the curves of log D_{Cs} *vs.* log $[ROH]_{total}$ in Table 2, the n values can not be determined exactly. Therefore, the extraction constants obtained in this experiment include some uncertainty.

The exchange constants, $K_{Cs}*/K_M*$, are also shown in Table 2. The values were obtained from the data when $[M^+]_a \gg [Cs^+]_a$ or from the log D_{Cs} *vs.* log$[Cs^+]_a$ curves, which are shown in Figs. 3—6.

In this paper, all the experimental data are plotted as a function of the concentration, and all the constants are calculated by using the concentration, no special attention being paid to the activity coefficients in the two phases. However, the ionic strength in the aqueous phase was maintained constant in most of the experiments. No meaningful deviation is noticeable in the explanation of the experimental results.

The relationship between these extraction constants and solubilities will be discussed in the next paper.[10]

The Crystal Structure of 2,2′-Bipyridinium Tetrabromocobaltate(II)

Shigetaka KODA, Shun'ichiro OOI, and Hisao KUROYA

Department of Chemistry, Faculty of Science, Osaka City University, Sumiyoshi-ku, Osaka

(Received January 30, 1971)

The crystal structure of 2,2′-bipyridinium tetrabromocobaltate(II) has been established by successive Fourier analyses. The atomic parameters were refined by least-squares techniques, using the three-dimensional X-ray data, to an R factor of 0.127 for 1461 non-zero reflections. The complex crystallizes in the space group $P2_1/c$ with four formula units in the unit cell with dimensions of $a=8.42$, $b=14.00$, $c=12.88$ Å, and $\beta=98.7°$. The crystal consists of slightly distorted tetrahedral $[CoBr_4]^{2-}$ anions and 2,2′-bipyridinium cations, in which two pyridinium ring planes are inclined toward one another at an angle of 39°. The two N^+–H groups in the cation participate in N^+–H···Br^- type hydrogen bonds (N···Br=3.23 Å and 3.31 Å). The mean value of the four Co-Br bond lengths is 2.42 Å.

In the course of the preparation of the bromo-analogue of *trans*-$[CoCl_2(bipy)_2]Cl$,[1,2] (bipy=2,2′-bipyridine), we isolated green crystals whose color is quite similar to that of the *trans*-$[CoBr_2en_2]Br\cdot HBr\cdot 2H_2O$.[3] However, the absorption spectra and elemental analyses of the compound suggested that this salt does not contain a complex cation of *trans*-$[CoBr_2(bipy)_2]^+$, but is a novel compound with the chemical formula of $[bipyH_2]\cdot[CoBr_4]$. Subsequently, this salt could be prepared by the direct reaction of 2,2′-bipyridine with $CoBr_2\cdot 6H_2O$ in concentrated hydrobromic acid. The chloro-analogue of this compound, $[bipyH_2][CoCl_4]$, can also be obtained by a similar method. Instead of characterizing the compound by means of the usual methods, such as a study of the IR or electronic spectra, we have undertaken an X-ray crystal analysis of $[bipyH_2][CoBr_4]$. We have already presented preliminary accounts of our work;[4] here the crystal structure of this compound will be given in detail.

Experimental

1) Preparation of Complexes. a) $[bipyH_2][CoX_4]$ *(X=Cl, Br)*: Both compounds were prepared by mixing equivalent amounts of the appropriate metal halide and bipyridine in conc. hydrohalogenic acid. The products were then recrystallized from the hot conc. HX solution. They are moderately hygroscopic.

2,2′-Bipyridinium Tetrabromocobaltate(II),

Yellowish-green crystals were obtained from the deep blue solution as needles.

Found: C, 22.35; H, 1.98; N, 5.16%. Calcd for $C_{10}H_{10}N_2Br_4Co=[bipyH_2][CoBr_4]$: C, 22.35; H, 1.87; N, 5.21%.

2,2′-Bipyridinium Tetrachlorocobaltate(II),

Large blue crystals were obtained from a deep blue solution in the form of plates.

Found: C, 33.61; H, 2.93; N, 7.99%. Calcd for $C_{10}H_{10}N_2Cl_4Co=[bipyH_2][CoCl_4]$: C, 33.45; H, 2.79; N, 7.80%.

b) Pyridinium Tetrabromocobaltate(II), $[pyH]_2[CoBr_4]$ *(py=pyridine)*: This compound was prepared following the method of Percival and Wardlaw.[5]

Found: C, 23.67; H, 2.67; N, 5.65%. Calcd for $C_{10}H_{12}N_2Br_4Co=[pyH]_2[CoBr_4]$: C, 22.29; H, 2.25; N, 5.20%.

2) Electronic Spectra of Solids. Specimens of $[bipyH_2][CoBr_4]$ and $[pyH]_2[CoBr_4]$ were ground with nujol and placed between two plates of opal glass, and their transmission spectra were measured with a Hitachi EPU-2A photoelectric spectrophotometer.[6]

3) X-Ray Data Measurement. The specimens used in the present investigation were coated with vaseline in order to prevent decomposition caused by atmospheric moisture. Oscillation and Weissenberg photographs taken with Ni$K\alpha$ radiation exhibited a monoclinic symmetry with space group $P2_1/c$. The lattice parameters were obtained from ($hk0$) and ($h0l$) Weissenberg photographs on which Al wire patterns had been superimposed; then they were refined by a least-squares method. In order to collect the three-dimensional intensity data, equi-inclination Weissenberg photographs were taken with Co-filtered Ni$K\alpha$ radiation from $0kl$ to $5kl$ and from $hk0$ to $hk6$, using a multiple-film technique. The intensities were visually estimated by the use of a standard scale. Thus, 1461 independent non-zero reflections were observed. These relative intensities were corrected for Lorentz and polarization factors, a spot-shape correction being made for upper layers. An absorption correction was applied to the data around the c axis, using a cylindrical approximation, since μR is equal to about 3.5. All the intensities were then placed on a common scale by a least-squares method. The crystal data are summarized in Table 1.

TABLE 1. CRYSTAL DATA

Formula	$C_{10}H_{10}N_2CoBr_4$
monoclinic	$a=8.42\pm0.01$ Å
	$b=14.00\pm0.02$
	$c=12.88\pm0.01$
	$\beta=98.7\pm0.2°$
Space Group	$P2_1/c$
Z	4
Dx	2.38 g/cm^3
μ	190 cm^{-1} (for Ni$K\alpha$)

1) F. M. Jaeger and J. A. van Dijk, *Z. Anorg Allg. Chem.*, **227**, 273 (1936).

2) Recently it was elucidated that the Jaeger's *trans*-$[CoCl_2\cdot bipy_2]Cl$ should be formulated as *cis*-$[CoCl_2bipy_2]_2\cdot[CoCl_4]$ (J.G. Gibson, R. Laird, and E. D. McKenzie, *J. Chem. Soc., A*, **1969**, 2089).

3) S. Ooi, Y. Komiyama, Y. Saito, and H. Kuroya, This Bulletin, **32**, 263 (1959).

4) S. Koda, S. Ooi, and H. Kuroya, *ibid.*, **43**, 971 (1970).

5) E. G. V. Percival and W. Wardlaw, *J. Chem. Soc.*, **1929**, 1505.

6) K. Shibata, "Methods of Biochemical Analysis," Vol. VII, Interscience Publishers, New York, N. Y. (1959), p. 77.

Structure Determination

The coordinates of the three bromine atoms were determined by an elaborate examination of the twenty largest peaks in the three-dimensional Patterson function. The positions of all the remaining atoms (except hydrogen) were found by successive three-dimensional Fourier analyses,[7] all the atoms of the pyridine rings being assumed provisionally to be carbon atoms at this stage. The refinement of the crystal structure was carried out by a block-diagonal-matrix, least-squares method.[8] Three cycles of refinement using isotropic temperature factors for all the atoms reduced the conventional R factor to 0.16.

The atoms in the close vicinity of each bromine atom were thoroughly examined in order to pick out the nitrogen atoms among the pyridine ring atoms, for it is quite reasonable to suppose that there must be N^+–H···Br^--type hydrogen bonds in the crystal. We found two ring atoms which are in close contact, 3.23 Å and 3.31 Å, with Br(1) and Br(4) respectively. They were identified as the nitrogen atoms on the basis of close contacts as well as the favorable directions of the hydrogen atoms.

In the further refinement, the anisotropic thermal parameters were applied to the heavy atoms. Four cycles of the least-squares calculation resulted in a convergence, with R=0.127, for all the 1461 non-zero reflections.

The atomic scattering factors used were taken from the International Tables for X-ray Crystallography. The final atomic coordinates and thermal parameters are given in Tables 2(a) and (b). All the numerical calculations were carried out on a FACOM 270-30 computer of our university. Tables of the observed and calculated structure factors are preserved by the Chemical Society of Japan.[9]

Results and Discussion

The crystal consists of 2,2′-bipyridinium cations and tetrahedral $[CoBr_4]^{2-}$anions. Figures 1 and 2 show the crystal structure viewed along the a and c axes respectively. As is shown in the figures, the structure is composed of regions of anions and cations, both elongated along the c axis. The arrangement of these ions

Table 2(a). The final atomic parameters (e.s.d's in parentheses)

Atom	x/a	y/b	z/c	B(Å^2)
Br(1)	0.2365(5)	0.2281(3)	0.0051(3)	*
Br(2)	−0.0068(5)	0.3132(3)	0.2204(3)	*
Br(3)	0.2540(6)	0.0714(3)	0.2582(4)	*
Br(4)	0.4813(5)	0.3224(3)	0.2528(3)	*
Co	0.2356(8)	0.2312(5)	0.1941(5)	*
N(1)	0.1128(34)	0.6758(20)	0.0615(23)	0.9(5)
N(2)	0.3491(34)	0.8129(20)	−0.0890(23)	0.8(5)
C(1)	0.2531(41)	0.6996(24)	0.0338(28)	0.8(6)
C(2)	0.3805(47)	0.6363(28)	0.0449(32)	1.6(7)
C(3)	0.3572(51)	0.5440(30)	0.0823(35)	2.0(8)
C(4)	0.2169(49)	0.5252(28)	0.1117(34)	1.8(7)
C(5)	0.0870(51)	0.5833(30)	0.0977(34)	2.1(8)
C(6)	0.2633(42)	0.8055(24)	−0.0087(29)	0.9(6)
C(7)	0.1928(42)	0.8790(25)	0.0364(29)	0.9(6)
C(8)	0.2154(51)	0.9709(30)	−0.0079(35)	2.1(8)
C(9)	0.2977(47)	0.9769(27)	−0.0920(33)	1.6(7)
C(10)	0.3694(52)	0.9017(31)	−0.1249(36)	2.3(8)

* Anisotropic temperature factors are listed in Table 2(b).

Table 2(b). The anisotropic temperature factors in the form of $\exp(-B_{11}h^2-B_{22}k^2-B_{33}l^2-B_{12}hk-B_{13}hl-B_{23}kl)$ (e.s.d's. in parentheses)

Atom	B_{11}	B_{22}	B_{33}	B_{12}	B_{13}	B_{23}
Br(1)	0.0050(5)	0.0014(2)	0.0021(3)	0.0011(6)	0.0006(7)	0.0004(4)
Br(2)	0.0053(6)	0.0030(2)	0.0016(3)	0.0026(6)	0.0001(8)	−0.0010(4)
Br(3)	0.0106(7)	0.0007(2)	0.0038(3)	0.0007(6)	0.0035(9)	0.0016(4)
Br(4)	0.0051(6)	0.0017(2)	0.0024(3)	−0.0008(5)	−0.0008(8)	−0.0019(4)
Co	0.0097(9)	0.0020(3)	0.0045(5)	0.0004(9)	0.0018(13)	−0.0003(6)

7) The computer program used was kindly offered by Mr. Makoto Fukuyo of Osaka City University.

8) The computer program used was a modified version of HBLS-IV which was adapted for use with a FACOM 270-30 computer by Mr. Ken Hirotsu of Osaka City University.

9) The complete data of the F_o–F_c table are kept as Document No. 7107 at the office of the Chemical Society of Japan. A copy may be secured by citing the document number and by remitting, in advance, ¥150 for photoprints. Pay by check or money order payable to: The Chemical Society of Japan.

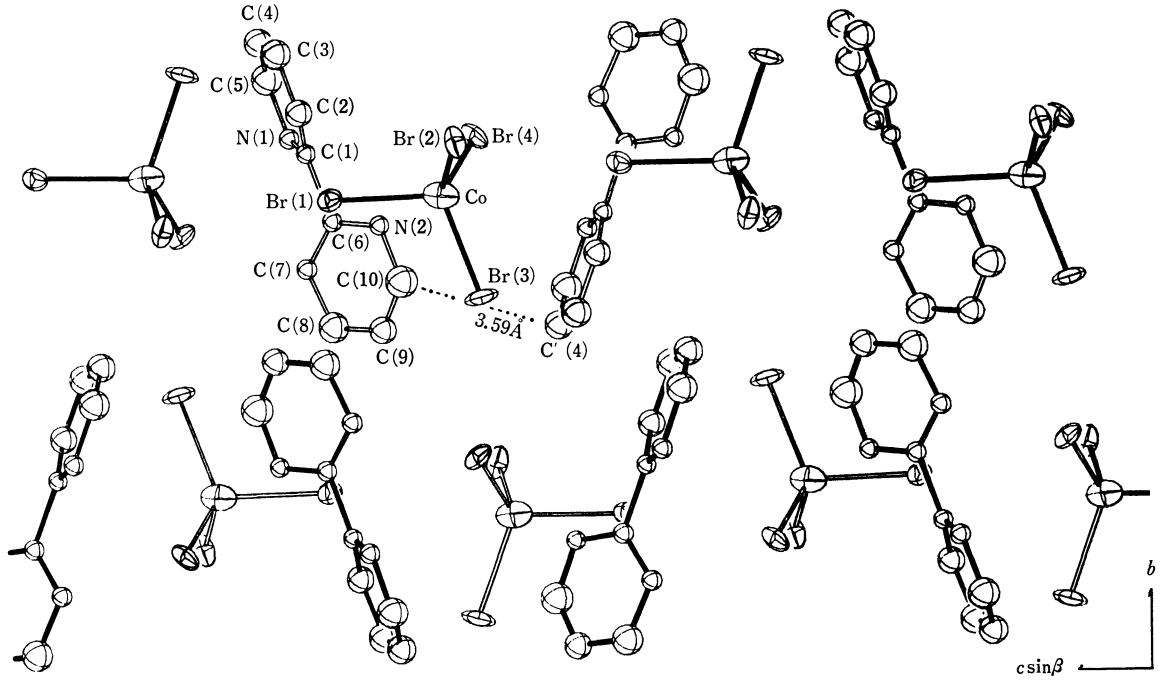

Fig. 1. The crystal structure viewed along the *a* axis.

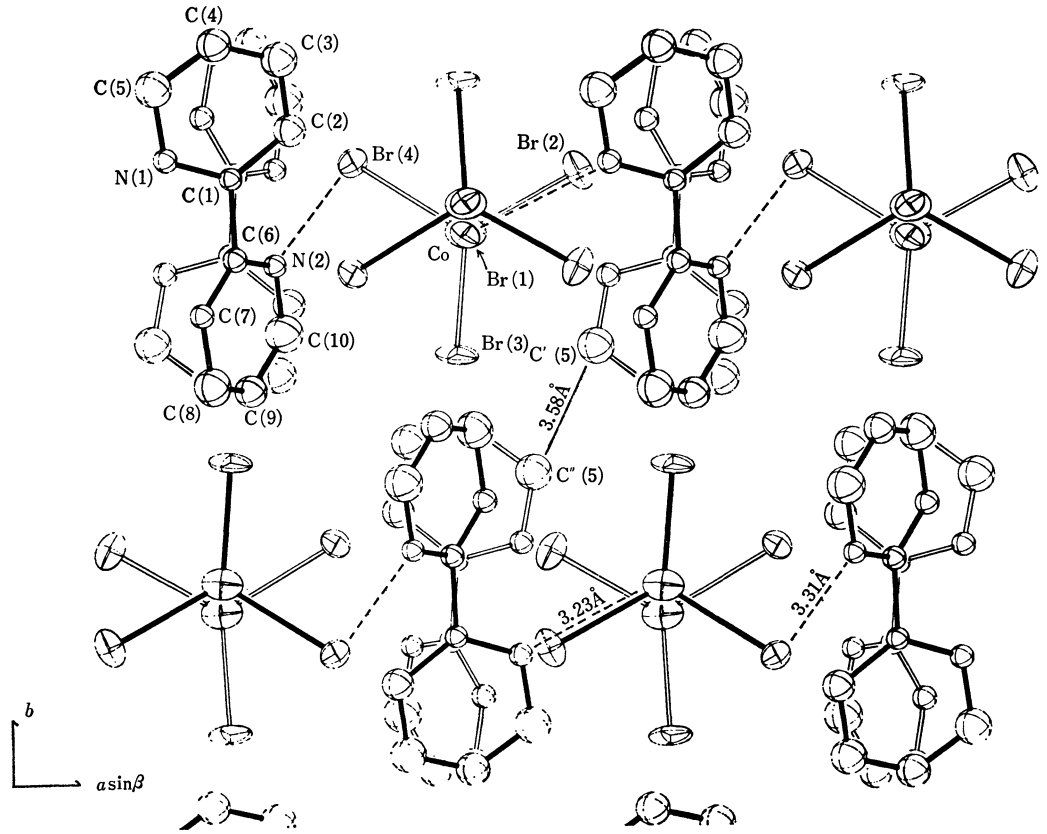

Fig. 2. The crystal structure viewed along the *c* axis.

in a checkered pattern is clearly illustrated in Fig. 2. Two-dimensional linkages are also formed by a N^+—H··· Br^--type hydrogen bonding extended along the *a* axis. These linkages are indicated by dashed lines in Fig. 2. The distances of the hydrogen bonds, 3.23 Å and 3.31Å, are in the range expected for this type. Apart from these, the closest intermolecular contacts are C′(5)··· C″(5) (=3.58 Å) and C′(4)···C(10) (=3.59 Å) (see Figs. 1 and 2). The interatomic distances and angles are listed in Tables 3(a) and (b).

It is known that the conformation of the 2,2′-bipyridine molecule is coplanar in the crystalline state, the

Table 3(a). Bond lengths (Å) and their standard deviations

Co-Br(1)=2.436(8)	Co-Br(2)=2.409(8)
Co-Br(4)=2.452(9)	Co-Br(3)=2.382(8)
C(1)-C(2)=1.38(5)	C(6)-C(7)=1.36(5)
C(2)-C(3)=1.40(6)	C(7)-C(8)=1.43(6)
C(3)-C(4)=1.32(6)	C(8)-C(9)=1.37(6)
C(4)-C(5)=1.35(6)	C(9)-C(10)=1.32(6)
C(5)-N(1)=1.41(5)	C(10)-N(2)=1.35(5)
C(1)-N(1)=1.33(5)	C(6)-N(2)=1.35(5)
C(1)-C(6)=1.59(5)	

Table 3(b). Bond angles (°) and their standard deviations

Br(1)-Co-Br(2)=106.1(5)	
Br(1)-Co-Br(3)=108.7(3)	
Br(1)-Co-Br(4)=100.9(5)	
Br(2)-Co-Br(3)=114.3(4)	
Br(2)-Co-Br(4)=113.7(3)	
Br(3)-Co-Br(4)=112.0(3)	
C(1)-N(1)-C(5)=121(3)	C(6)-N(2)-C(10)=116(3)
C(2)-C(1)-N(1)=121(3)	C(7)-C(6)-N(2)=126(3)
C(1)-C(2)-C(3)=119(4)	C(6)-C(7)-C(8)=115(4)
C(2)-C(3)-C(4)=117(4)	C(7)-C(8)-C(9)=119(4)
C(3)-C(4)-C(5)=126(4)	C(8)-C(9)-C(10)=121(4)
C(4)-C(5)-N(1)=116(4)	C(9)-C(10)-N(2)=123(4)
C(2)-C(1)-C(6)=124(3)	C(1)-C(6)-C(7)=121(3)
C(6)-C(1)-N(1)=115(3)	C(1)-C(6)-N(2)=113(3)

two nitrogen atoms being in the *trans* positions with respect to the C–C bond connecting the two pyridine rings.[10] However, this is not the case with our bipyridinium cation. As may be seen in Figs. 1 and 2, the bipyridinium cation lacks planarity. The individual pyridinium moiety is planar; the equation of the best plane through the six atoms N(1), C(1), C(2), C(3), C(4), and C(5), is:

$$0.162X + 0.332\,Y + 0.929\,Z = 3.99,$$

and that of the plane of the six atoms N(2), C(6), C(7), C(8), C(9), and C(10) is:

$$0.742\,X + 0.140\,Y + 0.655\,Z = 3.17,$$

where X, Y, and Z are the rectangular coordinates in Å units, X standing for $x+z\cos\beta$; Y, for y, and Z, for $z\sin\beta$. C(1) shows the maximum deviation of 0.04 Å from the former plane, and both C(9) and C(10) are in the maximum deviation from the latter plane by 0.04 Å. These two ring planes are inclined at an angle of 39° to each other. This dihedral angle is comparable with those found in (bipyH$_2$)SeOCl$_4$,[11] within the accuracy of the standard deviations.

The coordination around the cobalt atom is almost a regular tetrahedron. However, in the four Co–Br bonds, two of them (Co–Br(1)=2.436 Å and Co–Br(4) =2.452 Å) are longer than the other two (Co–Br(2)= 2.409 Å and Co–Br(3)=2.382 Å). The differences in the bond lengths between these two groups are possibly significant in view of the e.s.d.'s. The elongation in the former group must result from the hydrogen bonding in which the corresponding bromine atoms participate.

In the solid state, the color of [bipyH$_2$][CoBr$_4$] is green, while that of the analogous complex, [pyH]$_2$·[CoBr$_4$], is blue. As can be seen from Fig. 3, in which

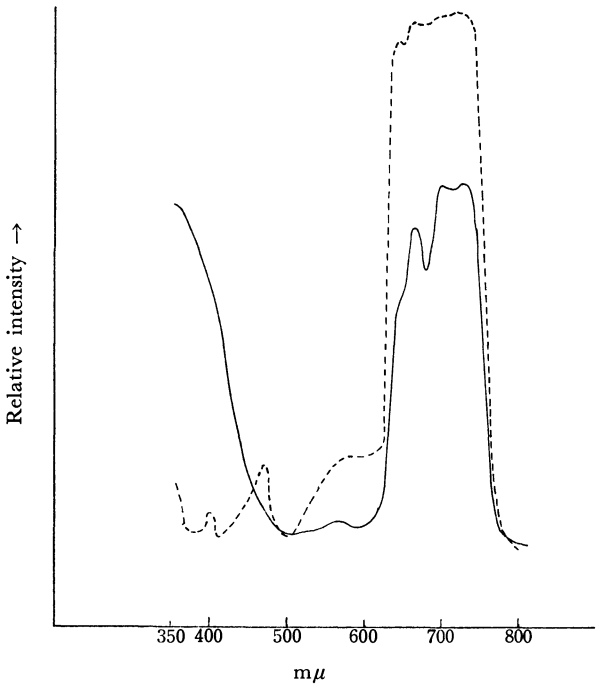

Fig. 3. Transmission spectra of [bipyH$_2$][CoBr$_4$]: —— and [pyH]$_2$[CoBr$_4$]: ----.

their transmission spectra are shown, the remarkable color difference between them is attributable to the absorption bands in the higher frequency region; a detailed discussion will be given in subsequent papers.

The authors are grateful to Dr. Akio Takenaka of Kwansei Gakuin University for providing them with the computer program for crystal structure illustration. Thanks are also due to Mr. Jun-ichi Gohda for his organic elemental analyses.

10) L. L. Merritt, Jr., and E. D. Schroeder, *Acta Crystallogr.*, **9**, 801 (1956).

11) Bi-Cheng Wang and A. W. Cordes, *Inorg. Chem.*, **9**, 1643 (1970).

Preparation and Circular Dichroism of Six Isomers of Bis(L-alaninate-*N*-monoacetato)cobaltate(III) Complexes

Ken-ichi OKAMOTO, Jinsai HIDAKA, and Yoichi SHIMURA

Department of Chemistry, Faculty of Science, Osaka University, Toyonaka, Osaka

(Received February 1, 1971)

Six isomers, two *trans(N)* and four *cis(N)*, of bis(L-alaninate-*N*-monoacetato)cobaltate(III) ions have been synthesized as their sodium or potassium salts. The isomers have been separated by ion-exchange column chromatography and their geometrical and chiral configurations determined on the basis of their absorption and circular dichroism spectra in visible and near ultraviolet regions and of proton magnetic resonance spectra. The corresponding L-prolinate-*N*-monoacetate complex has also been studied. The asymmetry of the coordinated imino nitrogen has been discussed from the analysis of the CD curves.

L-Alanine-*N*-monoacetic acid is a derivative of iminodiacetic acid and a typical O,N,O-tridentate ligand of linear type which contains one asymmetric carbon atom. The nitrogen atom of this ligand, however, becomes asymmetric by coordination to a metal ion; the circular dichroism (CD) spectrum of the complex will then be supplied from two vicinal contributions produced by the asymmetric carbon and the asymmetric nitrogen. Some isomers of cobalt(III) complexes with iminodiacetate or *N*-methyliminodiacetate, which have neither asymmetric carbon nor nitrogen atom, have been prepared and characterized by their electronic absorption[1,2] and CD spectra[3] in visible and ultraviolet regions and by PMR spectra.[2,4] Of these complexes, *cis(N)* isomer of bis(iminodiacetato) complex has a chiral configuration, and the absolute configurations of the optical isomers have been determined from comparison of their CD bands with those of a stereospecifically formed complex ion, $(+)_{546}$-[Co{$(-)_{589}$-pdta}]$^-$.[5]

In the present paper, the preparation and separation of isomers of bis(L-alaninate-*N*-monoacetato)cobaltate (III) complex will be reported with those of the corresponding L-prolinate-*N*-monoacetate complex; the geometrical and chiral configurations of these complexes will be determined by their electronic absorption, CD, and PMR spectra. The additivity of three kinds of CD contributions, one from the configurational chirality and the other two from the vicinal chiralities of the asymmetric carbon and nitrogen atoms, will be discussed.

Experimental

(1) Preparation of Ligands. A solution of 45 g of L-alanine in 125 m*l* of 4 N lithium hydroxide was added to a solution of 47.3 g of monochloroacetic acid in 125 m*l* of 4 N lithium hydroxide. To this mixture 125 m*l* of 4 N lithium hydroxide was added drop by drop with vigorous stirring at 70—80°C. The pH of the mixture was maintained in the range 8—9 during the reaction. After the addition, the mixture was heated at 90°C for about 10 min. The reaction mixture was cooled to room temperature and 120 m*l* of concentrated hydrochloric acid was added to it. The solution was concentrated in a vacuum evaporator until it became syrupy. When it was kept in a refrigerator for 24 hr, white crystals were separated out, which were collected by filtration and then washed well with ethanol. These white crystals, the desired acid hydrochloride, were contaminated with a small amount of lithium chloride. They were recrystallized from warm water. The pure crystals were washed with ethanol and ether, and then dried in a vacuum desiccator. The yield was approximately 23 g. $[\alpha]_D^{25} = +3.0°$ (*c* 5.4, water).

Found: C, 31.84; H, 5.53; N, 7.41%. Calcd for L-alamaH$_2$·HCl·1/4H$_2$O=C$_5$H$_{10}$NO$_4$Cl·1/4H$_2$O: C, 31.93; H, 5.63; N, 7.45%.

L-Proline-*N*-monoacetic acid was also prepared by a similar procedure using L-proline instead of L-alanine. $[\alpha]_D^{17} = -54°$ (*c* 1.0, water).

Found: C, 48.66; H, 6.46; N, 7.98%. Calcd for L-promaH$_2$=C$_7$H$_{11}$NO$_4$: C, 48.55; H, 6.40; N, 8.09%.

(2) Preparation of Isomeric Mixture of Lithium Bis(L-alaninate-N-monoacetato)cobaltate(III): *Li*[*Co*(L-*alama*)$_2$]·nH_2O. A solution of 8.4 g of cobalt(II) chloride hexahydrate in 10 m*l* of water was added to a solution containing 13.6 g of L-alamaH$_2$·HCl·1/4H$_2$O whose pH had been previously adjusted to 7.3 with 4 N lithium hydroxide. To this solution 10 g of lead dioxide was added and the resulting mixture was mechanically stirred at about 30°C for 2 hr. The color of the solution turned from dark red to bluish violet. Thereafter the pH was adjusted to 6.5 with 4 N lithium hydroxide and the mixture was kept for 90 min at room temperature. An excess of lead dioxide was filtered off. A large amount of methanol-ether (1 : 2) mixture was added to the filtrate. The bluish violet deposit was filtered and washed with methanol-ether (1 : 2) mixture and ether, and then dried in a vacuum desiccator. The yield was approximately 11 g.

(3) Separation of the Isomers of [*Co*(L-*alama*)$_2$]$^-$. About 8 g of the lithium salt obtained in (2) was dissolved in an appropriate amount of water and passed through a column (25 mm × 1500 mm) containing strong anion exchange resin, Dowex 1×8 (200—400 mesh, chloride form). After the column had been swept with water, the adsorbed band was eluted with 0.07 N aqueous solution of potassium chloride or sodium perchlorate at a rate of 2.5 m*l* per min. Six colored bands, a brownish red one (i), a reddish purple one (ii), and four violet ones (iii), (iv), (v) and (vi), were eluted in this order. Isomers i and ii were confirmed to be *trans(N)* ones and iii, iv, v and vi the *cis(N)* ones, by measurement of their absorption spectra. Each eluate was concentrated to dryness in a vacuum evaporator. The resulting solid isomers were contaminated with a small amount of potassium chlo-

1) J. Hidaka, Y. Shimura, and R. Tsuchida, This Bulletin, **35**, 567 (1962).
2) D. W. Cooke, *Inorg. Chem.*, **5**, 1141 (1966).
3) C. W. Van Saun and B. E. Douglas, *ibid.*, **8**, 1145 (1969).
4) J. I. Legg and D. W. Cooke, *ibid.*, **5**, 594 (1966).
5) The following abbreviations are used for the ligands; "ida" for an iminodiacetate ion, "L-alama" L-alaninate-*N*-monoacetate ion, "L-proma" L-prolinate-*N*-monoacetate ion, "edta" ethylenediaminetetraacetate ion, and "pdta" propylenediaminetetraacetate ion.

Table 1. Analytical results (in %)

Elution order	Complex salt	$\Delta\varepsilon_{589}$	C		H		N	
			Found	Calcd	Found	Calcd	Found	Calcd
i	*trans*(*N*)-RR-Na[Co(L-alama)$_2$]·2.5H$_2$O	(−)0.26	28.68	28.79	4.60	4.59	6.62	6.72
ii	*trans*(*N*)-RS-Na[Co(L-alama)$_2$]·2.5H$_2$O	(+)0.05	28.58	28.79	4.62	4.59	6.70	6.72
iii	*Δ-cis*(*N*)-RR-K[Co(L-alama)$_2$]·4H$_2$O	(−)4.62	26.42	26.09	4.93	4.82	6.14	6.09
iv	*Δ-cis*(*N*)-RS-K[Co(L-alama)$_2$]·3H$_2$O	(−)2.84	27.66	27.16	4.54	4.58	6.01	6.33
v	*Λ-cis*(*N*)-RR-K[Co(L-alama)$_2$]·4H$_2$O	(+)0.66	26.39	26.09	4.89	4.82	5.95	6.09
vi	*Λ-cis*(*N*)-RS-K[Co(L-alama)$_2$]·3H$_2$O	(+)1.75	27.09	27.16	4.67	4.58	6.32	6.33
—	*trans*(*N*)-RR-K[Co(L-proma)$_2$]·3H$_2$O	(+)0.06	33.92	34.01	4.88	4.89	5.66	5.67

ride, and were treated as follows. An aqueous solution of silver perchlorate was added drop by drop to the solution containing the crude complex and the precipitated silver chloride was filtered off. The complex desired was obtained by adding ethanol to the filtrate. The complex crystals were washed with water-ethanol (1 : 2) mixture and ethanol, and then dried in a vacuun desiccator. Isomers i and ii were isolated as sodium salts, while iii∼vi as potassium salts. Analytical results are given in Table 1.

*(4) Preparation and Separation of Potassium Bis(*L*-prolinate-*N*-monoacetato)cobaltate(III):* *K[Co(*L*-proma)$_2$]·nH_2O.* This was prepared and separated by a similar procedure to that for L-alama complex, using L-promaH$_2$ instead of L-alamaH$_2$·HCl·1/4H$_2$O. Two colored bands, a violet one and a brownish red one, were eluted in this order with 0.07 N aqueous solution of potassium chloride. The violet isomer was unstable in solution; the CD of the violet eluate decayed out with time. The violet isomer was not obtained in solid state, but the absorption and CD spectra of the solution suggested that this is the *cis(N)* isomer. The brownish red isomer was isolated as potassium salt trihydrate (Table 1), and was confirmed to be the *trans(N)* isomer by measurement of the absorption spectrum.

(5) Measurements. The electronic absorption spectra of the complexes were measured with a Beckman DU spectrophotometer. The CD spectra were recorded with a Roussel-Jouan dichrograph and a JASCO Model ORD/UV-5 spectrophotometer. All measurements were made in aqueous solutions at room temperature. The PMR spectra of the complexes in deuterium oxide were measured with a Japan Electron Optics 3H-60 spectrometer.

Results and Discussion

It has veen well established that the *trans(N)* and *cis(N)* isomers of a [Co^{III}(O)$_4$(N)$_2$]$^-$ type complexes can be identified from the splitting pattern of their first absorption bands in the visible region.[6,7] As is seen in Fig. 1 and Table 2, the first absorption bands of the two earlier eluates (isomers i and ii) of [Co(L-alama)$_2$]$^-$ and of the stable eluate of [Co(L-proma)$_2$]$^-$ exhibit a sub-peak (or shoulder) at the longer wavelength side of the major peak. On the contrary, on the absorption curves of the four later eluates (isomers iii, iv, v and vi) of [Co(L-alama)$_2$]$^-$, a vague shoulder is observed at the shorter wavelength side of the major peak. This indicates that the former group is *trans(N)* isomer and the latter *cis(N)*.

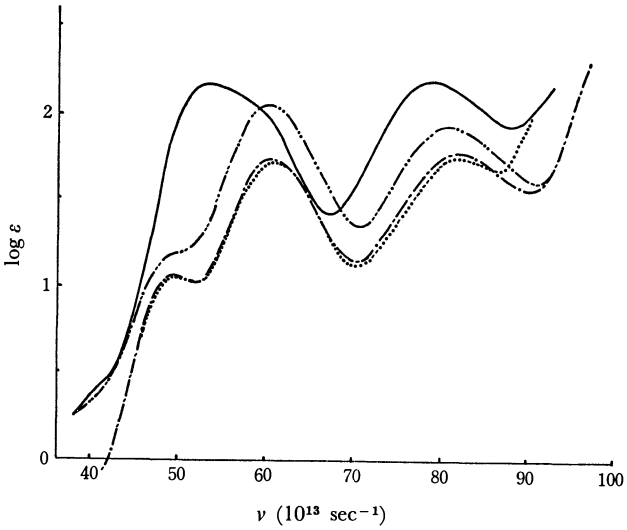

Fig. 1. Absorption curves of *trans(N)*-RR-[Co(L-alama)$_2$]$^-$ (———), *trans(N)*-RS-[Co(L-alama)$_2$]$^-$ (— — —), *trans(N)*-[Co(ida)$_2$]$^-$ (----) and *Δ-cis-(N)*-RR-[Co(L-alama)$_2$]$^-$ (——).

The *cis(N)* isomers of [Co(L-alama)$_2$]$^-$ exhibit two CD extrema in the first absorption band region as shown in Table 3. Of the four isomers the earlier eluted two isomers (iii and iv)show a negative and a positive CD band listing from longer wavelength side, whereas isomers v and vi show a positive and a negative band in the corresponding region. The absolute configuration of the isomer of *cis(N)*-[Co(ida)$_2$]$^-$, which was obtained from the less soluble diastereoisomer with (−)$_{546}$-[Co·(en)$_2$(ox)]$^+$, has been assigned to be *Λ*[8] by Van Saun and Douglas,[3] and the first absorption band of this complex shows a positive and a negative CD band listing from longer wavelength side. The *Λ*-(−)$_{546}$ isomer of [Co(edta)]$^-$ also shows a similar Cotton effect pattern in this region.[3,9] Since each of the *cis(N)* isomers in the present work has a C_2 or pseudo-C_2 symmetry, it is expected that the effective crystal field in these complexes is quite similar to those in the ida and edta complexes. Therefore it is concluded that the *cis(N)* isomers iii and iv have a *Δ* configuration and the isomers v and vi a *Λ* configuration.

In the parent complex, [Co(ida)$_2$]$^-$, four isomers are

6) a) N. Matsuoka, J. Hidaka, and Y. Shimura, This Bulletin, **40**, 1868 (1967); b) *Inorg. Chem.*, **9**, 719 (1970).

7) a) N. Koine, N. Sakota, J. Hidaka, and Y. Shimura, This Bulletin, **42**, 1583 (1969); b) *ibid.*, **43**, 1737 (1970).

8) Absolute configurations of the complexes are designated by the IUPAC tentative rule: *Inorg. Chem.*, **9**, 1 (1970).

9) B. E. Douglas, R. A. Haines, and J. G. Brushmiller, *Inorg. Chem.*, **2**, 1194 (1963).

TABLE 2. ABSORPTION MAXIMA OF [Co(O,N,O-tridentate)$_2$]$^-$ TYPE COMPLEXES

Complex ion	I Band		II Band		Ref.
	ν_{max}	($\log \varepsilon_{max}$)	ν_{max}	($\log \varepsilon_{max}$)	
trans(*N*)-RR-[Co(L-alama)$_2$]$^-$	49.6	(1.08)	82.6	(1.77)	
	60.6	(1.74)			
trans(*N*)-RS-[Co(L-alama)$_2$]$^-$	*ca.* 50	(1.2)	81.5	(1.91)	
	60.4	(2.05)			
trans(*N*)-RR-[Co(L-proma)$_2$]$^-$	*ca.* 50	(1.1)	81.3	(1.86)	
	59.3	(1.79)			
trans(*N*)-[Co(ida)$_2$]$^-$	50.0	(1.06)	83.3	(1.75)	(1)
	61.2	(1.72)			
Δ-cis(*N*)-RR-[Co(L-alama)$_2$]$^-$	53.3	(2.22)	78.8	(2.21)	
Δ-cis(*N*)-RS-[Co(L-alama)$_2$]$^-$	53.5	(2.15)	79.2	(2.15)	
Λ-cis(*N*)-RR-[Co(L-alama)$_2$]$^-$	53.2	(2.17)	78.4	(2.15)	
Λ-cis(*N*)-RS-[Co(L-alama)$_2$]$^-$	53.5	(2.15)	78.7	(2.10)	
cis(*N*)-[Co(ida)$_2$]$^-$	53.4	(2.18)	79.0	(2.13)	(1)

Frequencies are given in 10^{13} sec^{-1}.

TABLE 3. CD DATA

Complex ion		I Band		II Band	
		ν_{ext}	($\Delta\varepsilon_{ext}$)	ν_{ext}	($\Delta\varepsilon_{ext}$)
trans(*N*)-RR-[Co(L-alama)$_2$]$^-$	(i)	48.4	(−0.32)	78.9	(+0.08)
		59.7	(−1.11)		
trans(*N*)-RS-[Co(L-alama)$_2$]$^-$	(ii)	49.2	(+0.06)	80.0	(+0.18)
		61.2	(−1.04)		
trans(*N*)-RR-[Co(L-proma)$_2$]$^-$		48.6	(+0.14)	80.1	(−0.20)
		58.6	(−1.72)		
Δ-cis(*N*)-RR-[Co(L-alama)$_2$]$^-$	(iii)	50.9	(−4.62)	*ca.* 74	(−1.0)
		58.6	(+4.57)	80.5	(−1.44)
Δ-cis(*N*)-RS-[Co(L-alama)$_2$]$^-$	(iv)	51.2	(−2.86)	*ca.* 74	(−0.5)
		58.8	(+2.74)	81.9	(−0.83)
Λ-cis(*N*)-RR-[Co(L-alama)$_2$]$^-$	(v)	52.4	(+0.71)	*ca.* 74	(+0.2)
		60.1	(−1.56)	77.9	(+0.21)
Λ-cis(*N*)-RS-[Co(L-alama)$_2$]$^-$	(vi)	51.6	(+1.78)	*ca.* 74	(+0.4)
		59.9	(−2.90)	77.7	(+0.61)

Frequencies are given in 10^{13} sec^{-1}.

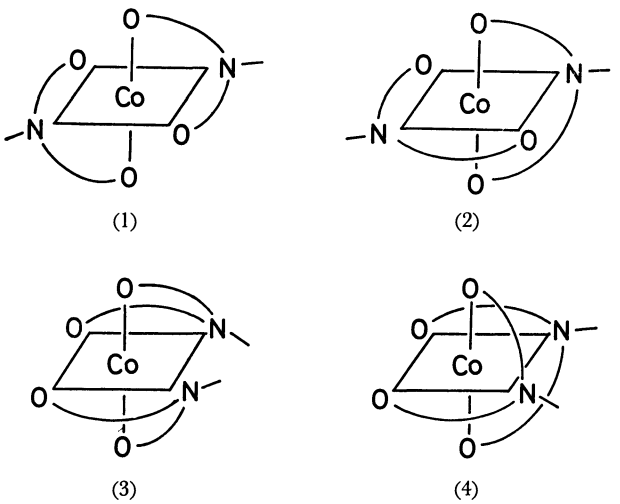

Fig. 2. Four possible isomers for a [Co(O,N,O-tridentate)$_2$] type complex: (1) facial-*trans*(*N*), (2) meridional-*trans*(*N*), (3) *Λ-cis*(*N*) and (4) *Δ-cis*(*N*).

possible as is seen in Fig. 2; so far the meridionally coordinating *trans*(*N*) isomer (2) is unknown. Such a meridional form of ida has been found only in a mixed complex with diethylenetriamine, [Co(ida)(dien)]$^+$.[4] A molecular model examination shows that the *Δ-cis*(*N*) isomer of L-proma complex can not exist because of serious steric hindrance between two pyrrolidine rings in the complex. We obtained an unstable violet colored eluate, which shows an absorption spectrum of *cis*(*N*)-[Co(O)$_4$(N)$_2$]$^-$ type and a CD spectrum similar to those of isomers v and vi of L-alama complex (with *Λ* configuration). The molecular model of the *Λ* isomer of [Co(L-proma)$_2$]$^-$ shows that the pyrrolidine ring of one ligand makes a rather short contact to the acetate methylene in another ligand, and that this may be the reason for the instability of this isomer. The stable *trans*(*N*)-[Co(L-proma)$_2$]$^-$ may be type (1) isomer in Fig. 2.

When L-alama coordinates to a cobalt(III) ion, the nitrogen atom of the ligand is optically activated (as

having R or S configuration). Accordingly three isomers, RR, RS, and SS, are possible for each of the bis(L-alama) complexes of *trans(N)*, *Δ-cis(N)* and *Λ-cis(N)* form. In the case of L-proma complex, the ligand cannot coordinate to take the S configuration of nitrogen atom; then only the RR isomer is expected for each of the *trans(N)* and *Δ-cis(N)* L-proma complexes. In fact, only one isomer was obtained by ion-exchange column chromatography for each of the *trans(N)* and *cis(N)* complexes. It has already been established that L-prolinate shows a complete stereospecific coordination of this kind; L-prolinate itself fixes the absolute configuration of the asymmetric nitrogen center to the S configuration.[10,11]

Experimentally only two isomers of possible three isomers were obtained for the *trans(N)* bis(L-alama) complex by ion-exchange column chromatography. If the nitrogen center takes S configuration, a repulsion exists between an alaninate methyl group of a coordinated L-alama ligand and a proton of the glycinate ring of the same ligand as is seen in Fig. 3(b). There is no such a repulsion in the R-form coordination (Fig. 3(a)). From this viewpoint, it is possible to assume tentatively that the two *trans(N)* isomers of bis(L-alama) complex obtained are the RR and RS forms of the type (1) isomer in Fig. 2.

The PMR spectra of the *trans(N)* bis(L-alama) complexes, i and ii, are shown in Fig. 4. The proton signals of *trans(N)* bis(L-alama) complexes consist of a group of AX_3 pattern due to $>CH-CH_3$ and another group of AB pattern due to $-CH_2-$. Only one set of AX_3 and AB patterns is expected for the RR or SS isomer and two sets for the RS isomer, since the former has C_2 symmetry and the latter C_1. As shown in Fig. 4, isomer i showed a doublet (at 1.73 ppm) in the region of methyl protons, whereas isomer ii showed two doublets (at 1.65 and 1.78 ppm) in this region. This behavior supports the view that isomer i is RR and isomer ii RS form. This was also confirmed by the result in the region of methylene and methine protons (3—5 ppm): the PMR spectrum of isomer i exhibited a pair of quartets, whereas that of isomer ii was complicated.

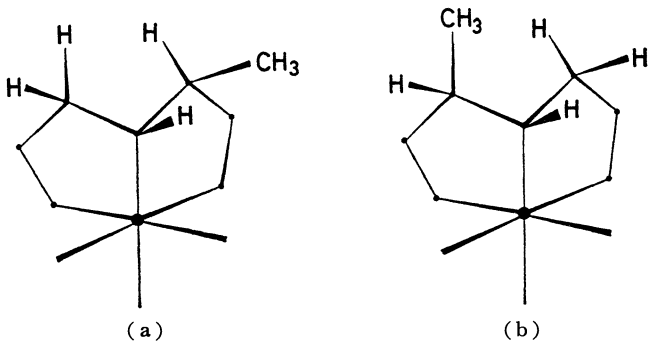

Fig. 3. Two possible configurations of the L-alama^{2-} ligand facially coordinated to a cobalt atom: (a) R from with regard to the asymmetric nitrogen atom, and (b) S form.

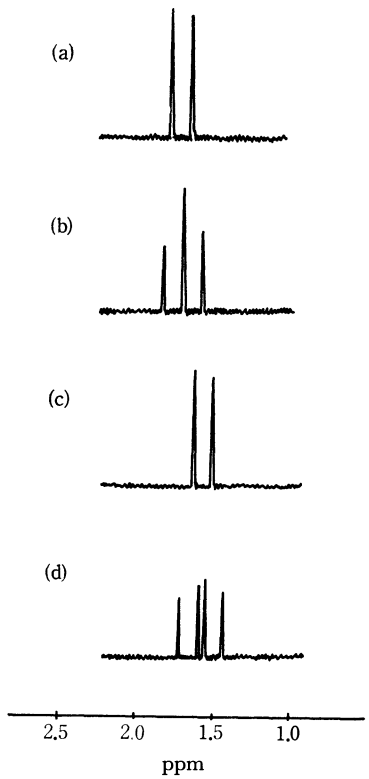

Fig. 4. The PMR spectra of bis(L-alama) complexes in D_2O. (a) isomer i (RR), (b) isomer ii (RS), (c) isomer v (RR) and (d) isomer iv (RS).

A similar conclusion was also obtained for the PMR spectra of the isomers of *cis(N)* bis(L-alama) complex. Isomer iv showed two doublets (at 1.48 and 1.66 ppm) due to two methyl groups and isomer v a doublet (at 1.56 ppm) (Fig. 4). The poor yields of isomers iii and vi did not allow measurement of the PMR spectra. However, the absorption maximum and CD extremum data in Tables 2 and 3 suggest that isomer iii corresponds to isomer v (RR) and isomer vi to iv (RS). Thus, if the possibility of the SS configuration is excluded, the four isomers obtained of *cis(N)*-[Co(L-alama)$_2$]$^-$ are assigned as follows: iii to *Δ*-RR, iv to *Δ*-RS, v to *Λ*-RR, and vi to *Λ*-RS.

It has been reported for several cobalt(III) complexes that the configurational and vicinal contributions to CD are separable and almost additive.[6b,12-14] The CD data and curves of the present complexes are shown in Table 3 and Figs. 5 and 6. The CD curve of a *cis(N)* isomer consists of a configurational contribution (*Δ* or *Λ*) and two vicinal ones due to the asymmetric nitrogen (R or S) and carbon (L) atoms. This assumption leads to the following additivity formulas:

$$\Delta\varepsilon(\text{iii}) = \Delta + 2\text{R} + 2\text{L} \qquad (1)$$

10) T. Yasui, J. Hidaka, and Y. Shimura, *J. Amer. Chem. Soc.*, **87**, 2762 (1965); T. Yasui, This Bulletin, **38**, 1746 (1965).

11) D. A. Buckingham, L. G. Marzilli, I. E. Maxwell, and A. M. Sargeson, *Chem. Commun.*, **1969**, 583.

12) C. T. Liu and B. E. Douglas, *Inorg. Chem.*, **3**, 1356 (1964); B. E. Douglas and S. Yamada, *ibid.*, **4**, 1561 (1965); B. E. Douglas, *ibid.*, **4**, 1813 (1965); J. I. Legg, D. W. Cooke, and B. E. Douglas, *ibid.*, **6**, 700 (1967); S. K. Hall and B. E. Douglas, *ibid.*, **8**, 372 (1969); C. Y. Lin and B. E. Douglas, *Inorg. Chim. Acta*, **4**, 3 (1970).

13) J. Hidaka and Y. Shimura, This Bulletin, **40**, 2312 (1967); K. Yamasaki, J. Hidaka, and Y. Shimura, *ibid.*, **42**, 119 (1969).

14) K. Ogino, K. Murano, and J. Fujita, *Inorg. Nucl. Chem. Letters*, **4**, 351 (1968).

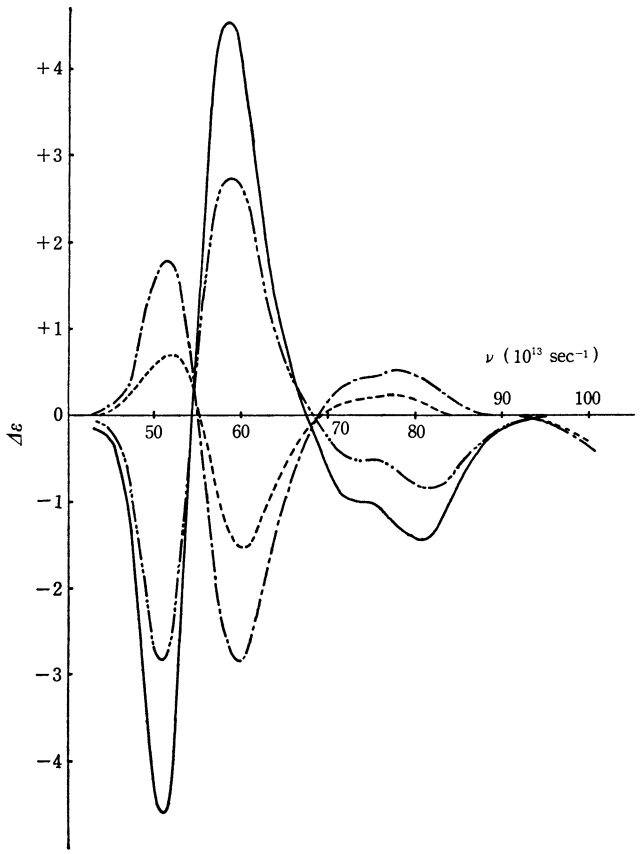

Fig. 5. CD curves of *cis(N)*-[Co(L-alama)$_2$]$^-$ isomers: *Δ-cis(N)*-RR (——), *Δ-cis(N)*-RS (— — —), *Λ-cis(N)*-RR (----) and *Λ-cis(N)*-RS (— — —).

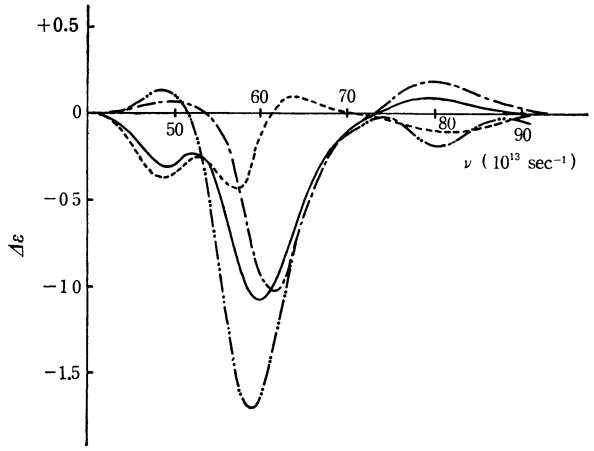

Fig. 6. CD curves of *trans(N)*-[Co(O,N,O-tridentate)$_2$] type complexes: (1) RR-[Co(L-alama)$_2$]$^-$ (——), (2) RS-[Co(L-alama)$_2$]$^-$ (— — —), (3) RR-[Co(L-proma)$_2$]$^-$ (— — — —), and (4) calculated curve (1)−(2) (----).

$$\Delta\varepsilon(\text{iv}) = \Delta + 2\text{L} \tag{2}$$

$$\Delta\varepsilon(\text{v}) = \Delta + 2\text{R} + 2\text{L} \tag{3}$$

$$\Delta\varepsilon(\text{vi}) = \Delta + 2\text{L} \tag{4}$$

where, of course, there exists the relation, $\Delta = -\Lambda$. Thus we have

$$\Delta = 1/2 \times \{\Delta\varepsilon(\text{v}) - \Delta\varepsilon(\text{iii})\} = 1/2 \times \{\Delta\varepsilon(\text{vi}) - \Delta\varepsilon(\text{iv})\} \tag{5}$$

$$2\text{R} = \Delta\varepsilon(\text{iii}) - \Delta\varepsilon(\text{iv}) = \Delta\varepsilon(\text{v}) - \Delta\varepsilon(\text{vi}) \tag{6}$$

$$2\text{L} = 1/2 \times \{\Delta\varepsilon(\text{iv}) + \Delta\varepsilon(\text{vi})\} \tag{7}$$

The curves of configurational Δ, vicinal 2R, and vicinal 2L can be calculated by applying Eqs. (5)—(7) to the observed CD curves of *cis(N)* isomers. The calculated curves are shown in Fig. 7.

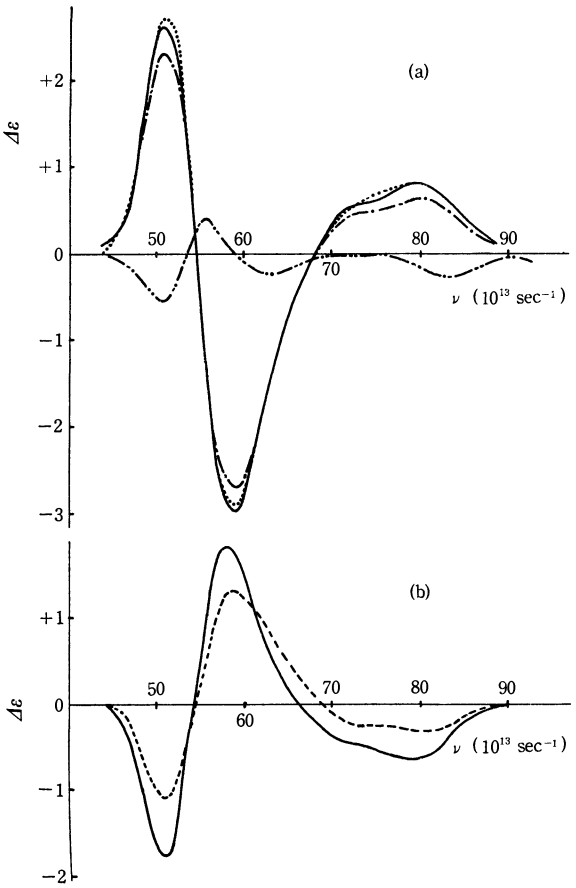

Fig. 7. Curve analyses of *cis(N)*-[Co(L-alama)$_2$]$^-$ complexes: (a) Δ configurational and 2L vicinal (carbon atom) curves; $1/2\times\{\Delta\varepsilon(\text{v})-\Delta\varepsilon(\text{iii})\}$ (——), $1/2\times\{\Delta\varepsilon(\text{vi})-\Delta\varepsilon(\text{iv})\}$ (— — —) and $1/2\times\{\Delta\varepsilon(\text{iv})+\Delta\varepsilon(\text{vi})\}$ (— — — —). Observed CD curve of *Λ-cis(N)*-[Co(ida)$_2$]$^-$ (----). (b) 2R vicinal curves (nitrogen atom); $\Delta\varepsilon(\text{iii})-\Delta\varepsilon(\text{iv})$ (——) and $\Delta\varepsilon(\text{v})-\Delta\varepsilon(\text{vi})$ (----).

The calculated configurational curve Δ (Fig. 7a), agrees well with the curve of *Δ-cis(N)*-[Co(ida)$_2$]$^-$ by Van Saun and Douglas.[3] As shown in Fig. 7b, there is also a rather good correspondence between the vicinal 2R curve which was calculated from a pair of *Δ-cis(N)* isomers and that from a pair of *Λ-cis(N)* isomers. This also supports the assignment of the configurations of the nitrogen atoms, which was made from the visible absorption and PMR spectra.

The CD spectra of the *trans(N)* bis(L-alama) isomers are also treated in a similar manner. In this case, however, there is no configurational contribution. Therefore the calculated curve, $\Delta\varepsilon(\text{i})-\Delta\varepsilon(\text{ii})$, represents the vicinal contribution 2R (Fig. 6).

Studies of the Pyrolysis of Triglycerides

Kazuo KITAMURA

Department of Chemistry, Faculty of Science and Engineering, Ritsumeikan University, Kita-ku, Kyoto

(Received April 16, 1970)

The pyrolysis of triglycerides (trilaurin and tripalmitin) in an atmosphere of nitrogen at 300—700°C has been attempted. Fatty acids, acrolein, ketones, and olefins have been identified as pyrolysis products. As intermediates of the pyrolysis, unsaturated glycol difatty acid esters and acid anhydrides were also detected. These results suggest a reaction mechanism of the pyrolysis involving the above compounds.

Numerous studies of the thermal oxidation of glycerides have been reported, but only a few papers have dealt with the pyrolysis of glycerides in the absence of air. The pyrolysis of glycerides may be expected to be different in the absence of and in the presence of air.

Crossley[1] has reported studies of the pyrolysis of glycerides with and without air, but he has not described in detail the mechanism of pyrolysis in the absence of air.

The present author has prepared pure trilaurin and tripalmitin and then pyrolyzed them in an atmosphere of nitrogen at 300—700°C. The pyrolysis products have been analyzed and indentified, and the mechanism of a series of pyrolysis reactions has elucidated.

Experimental

Pyrolysis Apparatus and Procedure. The pyrolysis apparatus used was the same as that illustrated in a previous paper.[2] When the temperature in the quartz tube reached a fixed temperature, a throughly-dried sample (about 0.5 g) in a porcelain boat was introduced to the center of the tube by means of a steel rod driven by a magnet. A slow stream of purified nitrogen (20 ml/min) was passed through the quartz tube during the pyrolysis. The products of the pyrolysis were collected in the N_1 trap (cooled by ice and salt) and in the N_2 and N_3 traps (cooled by dry ice and acetone), and were then submitted to analysis.

Preparation of Samples. Purified fatty acids were converted to acid chlorides,[3] and these were then treated with glycerol in chloroform and pyridine to give the triglycerides.[4] After repeated recrystallization from acetone, thin-layer chromatography (tlc) (coating material : silica gel G; developing solvents : petroleum ether : diethyl ether : acetic acid, 70 : 30 : 2) showed no impurities. The melting points and saponification values (S.V.) of the samples are shown in Table 1.

TABLE 1. MELTING POINTS AND SAPONIFICATION VALUES OF THE SAMPLES

Sample	Mp (°C)	S.V.
Trilaurin	45.0—45.8	263.0
Tripalmitin	65.5—65.7	207.7

Analysis of Pyrolysis Products. The pyrolysis products were dissolved in carbon tetrachloride, and were then separated into acidic and neutral fractions with 10% K_2CO_3. After the methylation of the acidic fractions, the methyl esters were analyzed by gas-liquid chromatography (glc).[5] The neutral fractions were analyzed by column chromatography, by tlc, by a study of the infrared spectrum (IR),[6] and by chemical analysis.

Results and Discussion

Acidic and Neutral Fractions. Using a 0.5-g sample each time, a series of ten pyrolyses was performed. The total weights of the acidic and neutral fractions are shown in Table 2.

TABLE 2. ACIDIC FRACTIONS AND NEUTRAL FRACTIONS

Sample	Pyrolysis temperature (°C)	Acidic fraction (g)	Acidic fraction (%)	Neutral fraction (g)	Neutral fraction (%)
Trilaurin	550	1.50	30.0	1.90	38.0
Tripalmitin	450	2.22	44.3	1.63	32.5

Fatty Acids. A part of the carbon tetrachloride solutions of the pyrolysis products were titrated with with standard alkali; the acid values (A.V.) thus obtained are shown in Fig. 1. The A.V. were most in the pyrolysis products at 550°C(trilaurin) and at 450°C (tripalmitin). At these temperature, the fatty acid yields were 46.9% (trilaurin) and 54.8% (tripalmitin).

The pyrolysis temperatures, 450°C and 550°C, are considered to be favorable for the most effective performance of the pyrolysis. Tlc showed also that no pyrolysis took place at 300°C, that at 450—550°C the spots of the pyrolysis products appeared most clearly, and that at 700°C the spots were not clear and that carbonization probably took place. Accordingly, pyrolysis can best be performed at 450—550°C.

Glc analysis of the acidic fractions in pyrolysis products showed that the main parts are the component fatty acids of the samples. In addition to these, many saturated and unsaturated lower acids were found to be present in very small amounts.

Unsaturated Glycol Difatty Acid Esters. In previous reports on the pyrolysis of ethylene glycol fatty acid esters,[2] monoglycerides[7] and diglycerides[8] in an atmosphere of nitrogen, the main decomposition

1) A. Crossley, T. D. Heyes, and B. J. F. Hudson, *J. Amer. Oil Chemists' Soc.*, **39**, 9 (1962).

2) K. Kitamura and N. Tachikawa, *J. Japan Oil Chemists' Soc.*, **14**, 250 (1965).

3) I. Imai and T. Wakabayashi, *ibid.*, **10**, 435 (1961).

4) B. F. Daubert and A. R. Baldwin, *J. Amer. Chem. Soc.*, **66**, 997 (1944).

5) A Yanagimoto GCG-2 Gas Chromatograph with a thermal-conductivity detector was used.

6) A Hitachi EPI-S_2 Infrared Spectrophotometer was used.

7) K. Kitamura, S. Kajita, A. Sasaki, and Y. Inoue, *Memoirs of the Res. Inst. of Sci. and Eng., Ritsumeikan Univ.*, **15**, 53 (1966).

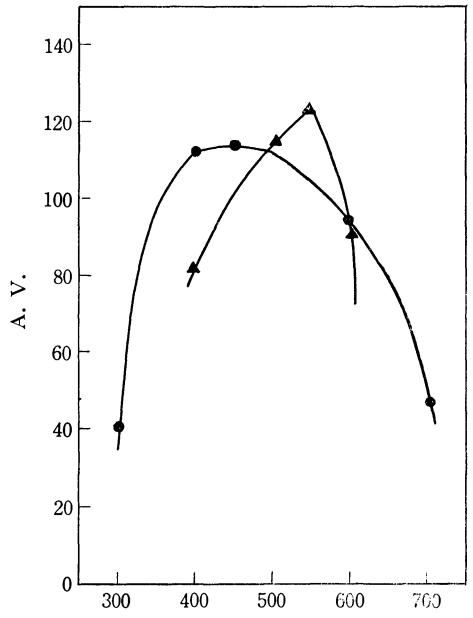

Fig. 1. Effect of the pyrolysis temperature on A.V. of the pyrolysis products.
▲: Trilaurin; ●: Tripalmitin

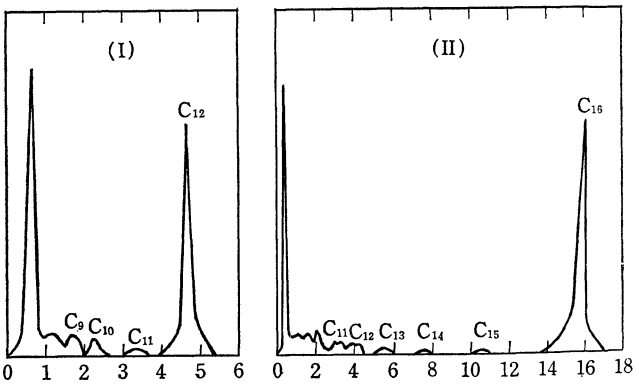

Fig. 2. Gas chromatograms of the acidic fractions (methyl esters).
(I): Trilaurin, (II): Tripalmitin, Column: Apiezon grease L, Column temperature (I): 230°C, (II): 235°C, Carrier gas: He, 40 ml/min.

reactions were the same as in the pyrolysis of fatty acid esters:

$$RCOOCH_2CH_2R' \rightarrow RC(=O\cdots H)(O\text{-}CH_2)\text{-}C(R')\text{-}H \rightarrow RCOOH + \underset{\underset{H_2}{|}}{\overset{R'}{\overset{\diagdown}{CH}}}\overset{\diagup}{C}\ ^{9)} \quad (1)$$

In the pyrolysis of ethylene glycol fatty acid esters, the pyrolysis products were obtained purely and were identified:[2]

$$\begin{matrix}CH_2OCOR\\|\\CH_2OCOR\end{matrix} \rightarrow RCOOH + \begin{matrix}CH_2\\\|\\CHOCOR\end{matrix} \quad (2)$$

8) K. Kitamura, *ibid.*, **17**, 85 (1968).

Therefore, in the pyrolysis of triglycerides (trilaurin and tripalmitin), the first decomposition process should proceed by means of the formation of fatty acids and unsaturated glycol difatty acid esters (UGDE), as is shown in the following equations:

$$\begin{matrix}CH_2OCOR\\|\\CHOCOR\\|\\CH_2OCOR\end{matrix} \rightarrow RCOOH + \begin{matrix}CH_2\\\|\\COCOR\\|\\CH_2OCOR\end{matrix} \quad (3)$$

$$\begin{matrix}CH_2OCOR\\|\\CHOCOR\\|\\CH_2OCOR\end{matrix} \rightarrow RCOOH + \begin{matrix}CHOCOR\\\|\\CH\\|\\CH_2OCOR\end{matrix} \quad (3')$$

$R = C_{11}H_{23}$ or $C_{15}H_{31}$

About 1 g of the neutral fraction of the pyrolysis product (tripalmitin) was separated by column chromatography with silica gel (50 g) as the adsorbent and with petroleum ether and ether (7:3) as developers. A substance (0.06—0.1 g), the I.V. of which was about 20.0 (halogen addition hindrance by carbonyl), was obtained from the middle part of the column. The S.V. of this substance was 170.4 (84% of the theoretical).

This substance shows IR adsorption peaks at 1780 and 1680 cm^{-1} ($-\overset{O}{\overset{\|}{C}}-O-C=C-$); 1740 cm^{-1} ($-C=O$); 1180 and 1110 cm^{-1} ($=C-O-C-$);[10] 1160 and 1110 cm^{-1} ($=C-O-C=$);[11] 870 cm^{-1} ($CH_2=C\langle$).[12]

From these results, it can be deduced that this substance has the structure of UGDE shown in Eq. (3).

In the case of trilaurin, the results obtained were almost the same.

Acid Anhydrides. In Eq. (4), because of the resonance of (iii), the pushing-out of the electron to

$$R\text{-}C(=O)\text{-}O\text{-}C=C- \ \text{(i)} \leftrightarrow R\text{-}C(=O^{\ominus})\text{-}O^{\oplus}\text{-}C=C- \ \text{(ii)} \quad (4)$$
$$\updownarrow$$
$$R\text{-}C(=O)\text{-}O^{\oplus}=C\text{-}C^{\ominus}- \ \text{(iii)}$$

the carbonyl oxygen of (ii) is considered to decrease. For this reason, the (1)-type decomposition of UGDE in Eq. (3) cannot be considered to proceed. Accordingly, the decomposition of Eq. (5) seems plausible.

$$\begin{matrix}CH_2\\\|\\COCOR\\|\\CH_2OCOR\end{matrix} \rightarrow \begin{matrix}CH_2\\\|\\C\text{-}O\\|\\CH_2\end{matrix} + \begin{matrix}RC=O\\\diagup\ O\\RC=O\end{matrix}$$
$$\searrow \quad \begin{matrix}CH_2\\\|\\C\\\|\\CHOH\end{matrix} \rightarrow \begin{matrix}CH_2\\\|\\CH\\|\\CHO\end{matrix} \quad (5)$$

$R = C_{11}H_{23}$ or $C_{15}H_{31}$

9) F. Krafft, *Ber.*, **16**, 1719, 3018 (1883); C. D. Hurd and F. H. Blunk, *J. Amer. Chem. Soc.*, **60**, 2419 (1938).
10) K. Nakanishi, "IR Absorption Spectroscopy—Practical" (in Japanese), Nankodo, Tokyo (1960), p. 100 (D.M.S. 2200).
11) K. Nakanishi *et al.*, "Jikken Kagaku Koza," Vol. 1, Maruzen, Tokyo (1957), pp. 366, 370.
12) *Ibid.*, p. 370.

On the contrary, UGDE in Eq. (3)'seems clearly not to decompose to acid anhydride and acrolein; this is supported by the fact that the yield of acrolein does not exceed about 50% of the theory.

The detection of the acid anhydrides in the neutral fractions was attempted in three ways. First, the IR spectra of the neutral fractions (pyrolysis temperature: 550°C) showed strong bands at 1810 cm^{-1} and 1740 cm^{-1}; these bands are characteristic of acid anhydrides. Secondly, the neutral fractions were analyzed quantitatively by the morpholine method;[13] the results are shown in Table 3.

Table 3. Acid anhydrides formation

Sample	Pyrolysis temperature (°C)	Acid anhydride (%)	From free acid
Trilaurin	450	4.3	
	550	6.0	2.2
Tripalmitin	450	2.7	0.8
	550	6.4	4.1

Acid anhydrides are also formed on the pyrolysis of free acids—on, for instance, the pyrolysis of lauric and palmitic acid at 550°C and 450°C respectively; the acid anhydrides from each acid are also listed in Table 3

Finally, tlc was carried out and the acid anhydrides were identified by comparing them with authentic samples.

Acrolein. In a series of ten experiments, about 0.3 m*l* of liquid was collected in the N_2 and N_3 traps; the major part of the liquid was acrolein, which was detected by glc in comparison with an authentic sample. In these cases, however, the pyrolysis products were passed directly into the 2,4-dinitrophenylhydrazine hydrochloride solution to form hydrazones (2,4-DNPH). Ketones (see below) were condensed in the N_1 trap; a small amount of acrolein was also obtained from the N_1 trap by the distillation of the carbon tetrachloride solution. This was converted to 2,4-DNPH and then added to the 2,4-DNPH obtained from the N_2 and N_3 traps. One example of these results is shown in Table 4.

Table 4. Acrolein formation

Sample (g)	2,4-DNPH (g)	Acrolein (g)	Yield (%) Found	Yield (%) Theoretical
Trilaurin 0.490	0.073	0.017	3.5	8.8
Tripalmitin 0.500	0.076	0.018	3.6	6.9

α-Olefins. Authentic samples of lauric and palmitic anhydride were pyrolyzed; they gave the corresponding acids in almost quantitative yields, which can be accounted for by the following reaction equation:

$$\begin{matrix} RCH_2C{=}O \\ \quad\quad\diagdown\!\!\diagup O \\ RCH_2C{=}O \end{matrix} \rightarrow RCH_2COOH + RCH{=}C{=}O \qquad (6)$$

$$R = C_{10}H_{21} \text{ or } C_{14}H_{29}$$

Thus, it was confirmed that acid anhydrides decomposed to acids and aldoketenes. However, as the ketenes formed seemed to be less volatile because of the long alkyl radical, and also not to be so stable because of the ketene group, they are thought to decompose during the pyrolysis as follows:[14]

$$RCH_2CH{=}C{=}O \rightarrow RCH_2CH{:} + CO \qquad (7)$$
$$\downarrow$$
$$RCH{=}CH_2$$

Using alumina as an adsorbent, the column chromatography of the pyrolysis products of triglycerides was carried out; the fractions eluted by petroleum ether showed IR spectra identical with α-olefins (1810,1645, 1420, 990, and 910 cm^{-1}).

The tlc of the pyrolysis products of triglycerides, using the pyrolysis products of alkyl ketene dimers (next paragraph) as the standard, also indicated the existence of α-olefins ($Rf \fallingdotseq 1$).

Because of the unstability of ketene, these ketene monomers have not yet been isolated.[15] Therefore, the decyl ketene dimer and the tetradecyl ketene dimer were prepared from acid chlorides and triethylamine[16] respectively: they were pyrolyzed, and the IR of the expected ketenes were measured. In these cases, however, the IR spectra were the same as those of α-olefins.

Ketones. Laurone and palmitone were detected in the pyrolysis products by tlc, and were identified by using authentic samples as the standard. Oximes of laurone (mp 36—37°C) and palmitone (mp 59—60 °C) were also obtained. In addition to these ketones, various other ketones seemed to be formed.[2]

In this experiment, laurone (from trilaurin) and palmitone (from tripalmitin) have been identified, although they were present in small amounts. Accordingly, it seems that these ketones were not formed directly from triglycerides, but that they were formed secondarily from fatty acids which were themselves originated by the decomposition of triglycerides.[2] Supposing that the ketones are formed from the triglycerides directly, Eq. (8) (Crossley[1]) has to hold:

$$\begin{matrix} CH_2OCOR \\ | \\ CHOCOR \\ | \\ CH_2OCOR \end{matrix} \rightarrow RCOOH + RCOR + CO_2 + CH_2{=}CHCHO \qquad (8)$$

$$R = C_{11}H_{23} \text{ or } C_{15}H_{31}$$

The fatty acids obtained in this experiment account for about 50%, but their the oretical yields, as calculated from Eq. (8), are about 30%. This difference is fairly

13) J. B. Johnson and G. L. Funk, *Anal. Chem.*, **27**, 1464 (1955).

14) L. Knentzel, *NASA Tech. Publ. Announcements*, **2**, 1063 (1962).

15) E. S. Rothman, *J. Amer. Oil Chemists' Soc.*, **45**, 189 (1968).

16) J. C. Sauer, *J. Amer. Chem. Soc.*, **69**, 244 (1947); I. Imai, T. Wakabayashi, M. Yoshino, and S. Komiya, *J. Japan Oil Chemists' Soc.*, **10**, 208 (1961).

Table 5. The results of pyrolysis

Pyrolysis product	Pyrolysis intermediate product	Unchanged sample	Yield (%)
Fatty acids			45.0—55.0
Acrolein			3.5—4.0
α-Olefin			small amount
Ketones			small amount
	Unsaturated glycol difatty acid esters		small amount
	Acid anhydrides		2.5—6.5
		Triglycerides	10.0

large. This fact is one of the reasons why the present author cannot accept Eq. (8).

The tlc of the neutral fractions of the pyrolysis products discussed above are shown in Fig. 3.

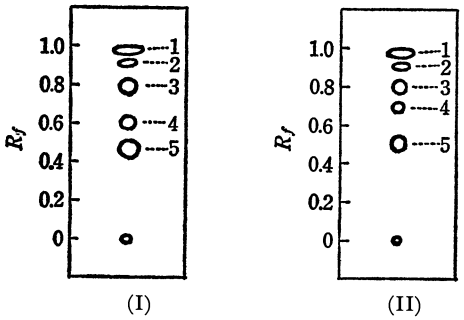

Fig. 3. Thin-layer chromatograms of the neutral fractions.
(I): Trilaurin (II): Tripalmitin
1: α-Olefins (from ketenes)
2: Ketones 3: Triglycerides
4: UGDE 5: Acid anhydrides
Coating material: Silica gel G
Developing solvents: Petroleum ether, ether and acetic acid (70 : 30 : 2)
Indicator: Sulfuric acid and charring

Conclusion

The main pyrolysis products and pyrolysis intermediate products, *etc.* discussed above, are summarized in Table 5. According to these experimental results and the discussion, the reaction mechanism of the pyrolysis of triglycerides in an atmoshere of nitrogen may be postulated to be as follows:

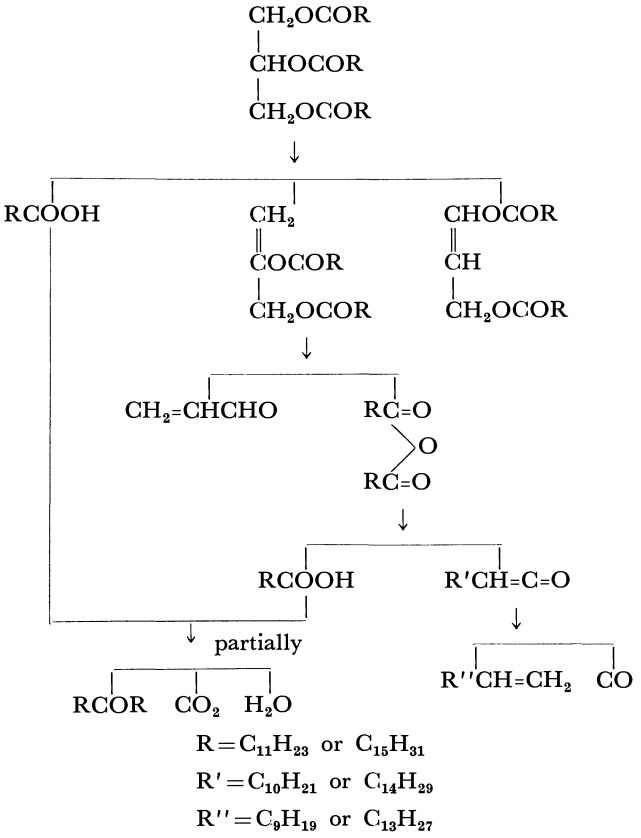

$R = C_{11}H_{23}$ or $C_{15}H_{31}$

$R' = C_{10}H_{21}$ or $C_{14}H_{29}$

$R'' = C_9H_{19}$ or $C_{13}H_{27}$

A Novel Synthesis of 4*H*-1,3-Thiazin-4-one Derivatives

Masataka YOKOYAMA

Department of Chemistry, Faculty of Science, Chiba University, Yayoi-cho, Chiba

(Received July 20, 1970)

4*H*-2,5,6-Substituted-2,3-dihydro-1,3-thiazin-4-ones were synthesized by the condensation reaction of β-alkylthio-β-mercapto-α-cyanoacrylamide with a variety of ketones and aldehydes in an acidic medium.

The monomethyl ether of enedithiols **1** proved to display different nature according to the R groups (Scheme 1). When R was carbamoyl, the resulting β-methylthio-β-mercapto-α-cyanoacrylamide (**2d**$_1$) was stable colorless needles. When R was alkoxycarbonyl, methyl β-methylthio-β-mercapto-α-cyanoacrylate (**2b**) and ethyl β-methylthio-β-mercapto-α-cyanoacrylate (**2c**) which were obtained as colorless needles, upon heating at 35—40°C, easily changed into stable yellow materials ($C_{12}H_{14}N_2S_5O_4$ for **2b** and $C_{14}H_{18}N_2S_5O_4$ for **2c**). The yellow materials were not examined in the present work. When R was cyano, a dialkyl enedithiol was obtained instead of **2a**. The ease of the complete methylation of **2a** may be due mainly to the less steric hindrance of cyano as the R group.

In view of the NMR and IR spectra of **2d**$_1$, the structure of **2d**$_1$ is probably "zwitterion"; **2d**$_1$ may be more stable than **2b** and **2c** because of this zwitterion structure.

Using the nucleophilic character of the mercapto group of β-alkylthio-β-mercapto-α-cyanoacrylamide (**2d**), the present investigation was directed to exploring the reaction of **2d** with ketones and aldehydes (**3**). Compound **2d**, in the presence of sulfuric acid, easily reacted with a series of ketones and aldehydes to give 4*H*-2,2-disubstituted-6-alkylthio-5-cyano-2,3-dihydro-1,3-thiazin-4-ones.

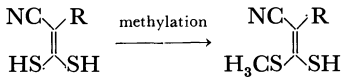

1 **2**

1a, **2a**: R=CN; **1b**, **2b**: R=CO_2CH_3;
1c, **2c**: R=$CO_2C_2H_5$; **1d**, **2d**$_1$: R=$CONH_2$

Scheme 1

The formation of **5** was considered to proceed through an intermediate **4** in the reaction of **2d** with **3**, because β,β-bis(methylthio)-α-cyanoacrylamide and **3** did not react in the presence of sulfuric acid to give *N*-addition

Table 1. Appearance, melting points, and yields

Compd.	R_1	R_2	R_3	Apperance	Mp, °C(cor)	Yield, %
5a	CH_3	R_2, R_3=$(CH_2)_5$		C. P.	227—228	93
5b	CH_3	R_2, R_3=$(CH_2)_4$		C. N.	190—191	88
5c	CH_3	CH_3	CH_3	C. N.	197—198	92
5d	CH_3	CH_3	C_2H_5	C. P.	187—188	93
5e	CH_3	H	CH_3	C. P.	212—213	90
5f	CH_3	H	C_6H_5	C. P.	225—226	92
5g	CH_3	H	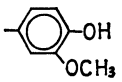	C. N.	241—242 (dec)	95
5h	CH_3	H	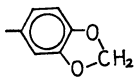	C. N.	208—209	89
5i	CH_3	H		B. Pr.	213—214 (dec)	90
5j	C_2H_5	R_2, R_3=$(CH_2)_5$		C. N.	188—189	93
5k	C_2H_5	CH_3	CH_3	C. N.	151—152	91
5l	C_2H_5	H	CH_3	C. N.	172—173	87
5m	C_2H_5	H	C_6H_5	C. N.	177—178	95
5n	C_2H_5	H		B. N.	181—182 (dec)	92
5o	$CH_2CO_2CH_3$	R_2, R_3=$(CH_2)_5$		C. N.	138—139	82
5p	$CH_2CO_2CH_3$	H	CH_3	C. N.	169—170	83
5q	$CH_2CO_2CH_3$	H	C_6H_5	C. Pr.	151—152	80
5r	$CH_2CO_2CH_3$	R_2, R_3=	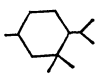	C. N.	152—153	76

C. P.: colorless plates; C.N.: colorless needles; C. Pr.: colorless prisms; B. N.: brown needles; B. Pr.: brown prisms

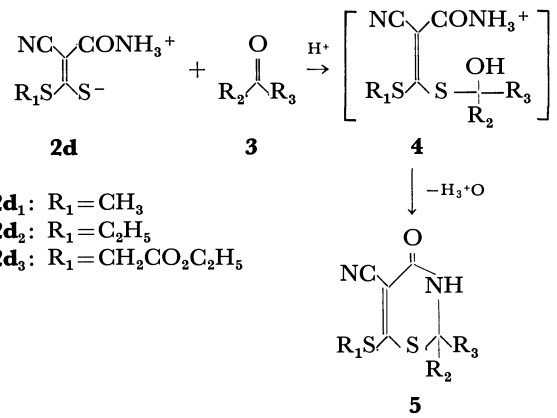

2d **3** **4**

2d$_1$: $R_1=CH_3$
2d$_2$: $R_1=C_2H_5$
2d$_3$: $R_1=CH_2CO_2C_2H_5$

Scheme 2.

TABLE 2. MASS SPECTRA FOR **5**[a], *m/e* (rel. int. %)

5c	**5d**
214 (M^+, 50)	228 (M^+, 67)
199 (42, $-CH_3$)	213 (13, $-CH_3$)
167 (92. $-SCH_3$)	199 (67, $-C_2H_5$)
157 (25, $-NHC(CH_3)_2$)	181 (100, $-SCH_3$)
110 (100)	157 (26, $-NHC(CH_3)(C_2H_5)$)
82 (33)	110 (83)
	82 (26)

5e	**5f**
200 (M^+, 93)	262 (M^+, 36)
185 (67, $-CH_3$)	215 (86, $-SCH_3$)
157 (60, $-NHCHCH_3$)	185 (15, $-C_6H_5$)
153 (67, $-SCH_3$)	157 (17, $-NHCHC_6H_5$)
110 (100)	110 (100)
82 (27)	82 (21)

5i	**5k**
252 (M^+, 44)	228 (M^+, 40)
205 (100, $-SCH_3$)	213 (100, $-CH_3$)
157 (13, $-NHCH(C_4H_3O)$)	200 (10, $-CO$)
110 (88)	171 (40, $-NHC(CH_3)_2$)
82 (25)	167 (90, $-SC_2H_5$)
	143 (40)
	110 (90)
	82 (40)

5l	**5m**
214 (M^+, 63)	276 (M^+, 62)
199 (100, $-CH_3$)	261 (13, $-CH_3$)
186 (15, $-CO$)	248 (17, $-CO$)
171 (37, $-NHCHCH_3$)	215 (100, $-SC_2H_5$)
153 (37, $-SC_2H_5$)	199 (33, $-C_6H_5$)
143 (63)	171 (70, $-NHCHC_6H_5$)
110 (63)	143 (44)
82 (17)	110 (55)
	82 (44)

a) Mass spectra were measured with a Nihon Denshi JMS-01 SG mass spectrometer. Ionizing energy was maintained at 75 eV and the total ionizing current was 200 μA.

derivatives (Scheme 2).

Table 1 shows the appearance, melting points, and yields of **5** of the present method. The structure of **5** was determined by studying the reaction process and the results of elemental analysis (Table 6) and the IR, NMR and mass spectra. In this reaction, β-ethoxycarbonylmethylthio-β-mercapto-α-cyanoacrylamide (**2d$_3$**) was treated with methanol using as solvent in the presence of acidic catalyst and converted into 4*H*-2,2-disubstituted-5-cyano-2,3-dihydro-6-methoxycarbonylthio-1,3-thiazin-4-one (**5o**—**r**) by the ester interchange.

The NMR spectra of **5m** revealed a broad peak at δ8.30 characteristic for NH, and a peak of R_2 at δ6.20 was split by the effect of NH. The mass spectra of **5** showed four characteristic fragments (Table 2); (M—NHR_2R_3), (M—CO), (M—NHR_2R_3—SR_1), and (M—NHR_2R_3—SR_1—CO). The fragments were considered to be formed by the following fragmentation.

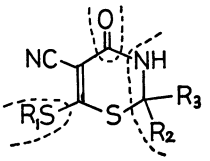

The derivatives of 4*H*-1,3-thiazin-4-one have previously been synthesized through the reaction of methyl β-thiocarbamoylthiopropionate with sulfuric acid,[1] of substituted thiosemicarbazides with dimethyl acetylenedicarboxylate,[2] and of *N*-substituted dithiocarbamic acid with propionic acid.[3] The 4*H*-1,3-thiazin-4-one derivatives hitherto reported have been 4*H*-5,6-dihydro-1,3-thiazin-4-ones. This is a new preparative method leading to 4*H*-2,3-dihydro-1,3-thiazin-4-one derivatives, which have not yet been reported. The UV spectra showed the absorption near 225 mμ corresponding to the π—π^* of the carbonyl group and near 275 mμ corresponding to the π—π^* of the double bond (Table 3).

TABLE 3. UV SPECTRA OF **5**[a]

Compd.	λ_{max}, mμ (log ε), in 99% EtOH
5a	226 (sh, 2.68), 239 (sh, 3.79), 275 (3.51), 332 (3.57)
5d	230 (sh, 3.26), 273 (3.83), 332 (3.90)
5g	230 (3.23), 285 (2.90), 343 (3.08)
5h	231 (3.96), 286.5 (3.90), 342 (4.02)
5k	225 (sh, 3.40), 276 (3.78), 330 (3.91)
5m	230 (sh, 3.92), 280.5 (3.99), 335 (4.03)
5n	225.5 (sh, 3.89), 287.5 (3.62), 335.5 (3.79)
5r	220.5 (4.26), 289 (4.08), 342 (4.47)

a) The absorbance measurements were made with a Hitachi EPS-3T type spectrophotometer.

Experimental

Microanalyses were performed at the Institute of Physical and Chemical Research. The NMR data are given in the

1) J. E. Jansen and R. A. Mathes, *J. Amer. Chem. Soc.*, **77**, 2866 (1955).
2) J. W. Lown and J. C. N. Ma, *Can. J. Chem.*, **45**, 953 (1967).
3) R. N. Warrener and E. N. Cain, *Chem. Ind.*, **1964**, 48.

order of multiplicity (s=singlet, d=doublet, t=triplet, q=quartet, and m=multiplet), integration, and assignment.

Preparation of β,β-Dimercapto-α-cyanoacrylonitrile (1a), Methyl β,β-Dimercapto-α-cyanoacrylate (1b), Ethyl β,β-Dimercapto-α-cyanoacrylate (1c), and β,β-Dimercapto-α-cyanoacrylamide (1d). Sodium salts of **1a**, **1b**, and **1c** were prepared by Gompper's method.[4] Ammonium salt of **1d** was prepared from the reaction of ethyl cyanoacetate, carbon disulfide, and aqueous ammonia.[5]

The alkylation of **1a**, **1b**, **1c**, and **1d** was worked up with dimethyl sulfate and diethyl sulfate in the usual way.

Conversion of 1d into β-Alkylthio-β-mercaptoacrylamide (2d). To a mixture of diammonium salt of **1d** (21 g, 0.11 mol) and methanol (100 m*l*) was added dimethyl sulfate (10 m*l*, 0.11 mol) slowly under stirring below 20°C. The reaction mixture was allowed to stand for 8 hr and poured into water (500 m*l*). The yellow solution was acidified with concentrated hydrochloric acid (30 m*l*). The colorless material was collected by filtration, washed with dilute hydrochloric acid, dried, and recrystallized from methanol to give ca. 18 g of colorless needles (β-methylthio-β-mercapto-α-cyanoacrylamide, **2d**$_1$): yield 95%; mp 149—150°C (dec) (reported mp 145—146°C (dec)[4]). The IR spectrum coincided with that of the compound which was prepared from potassium hydroxide, cyanoacetamide, carbon disulfide, and methyl iodide by Gompper's method.[4]

The ethylation of **1d** was worked up as mentioned in the methylation of **1d**. The crude material was recrystallized from methanol-water to give colorless needles (β-ethylthio-β-mercapto-α-cyanoacrylamide, **2d**$_2$): yield 98%; mp 116—117°C (dec); UV_{max} (99% EtOH): 227 mμ (log ε 4.16), 292.5 (3.97), 343 (4.01); Mass spectrum (75 eV) *m/e* (rel. intensity): 188 (100, M^+), 171 (20, $-NH_3$), 160 (13, –CO), 127 (73, $-SC_2H_5$); IR (KBr): 3420, 3280, 3180 (NH_3^+), 2980, 2920 (CH), 2200 (conj. CN), 1650 (CO), 1550 (conj. C=C), 1450 cm^{-1} (CH); NMR (DMSO-d_6) δ: 7.75 (broad, 3H, NH_3^+), 3.15 (q, 2H, CH_2, J=7 Hz), 1.42 (t, 3H, CH_3, J=7 Hz). Found: C, 38.19; H, 3.99; N, 14.93; S, 33.98%; mol wt (mass), 188. Calcd for $C_6H_8N_2S_2O$: C, 38.29; H, 4.25; N, 14.88; S, 34.07%; mol wt, 188.18.

The preparation of β-ethoxycarbonylmethylthio-β-mercapto-α-cyanoacrylamide (**2d**$_3$) was worked up as follows. To a mixture of potassium hydroxide (22.4 g, 0.4 mol) and methanol (120 m*l*) was added cyanoacetamide (16.8 g, 0.2 mol) and then carbon disulfide (12 m*l*) under cooling below 20°C. Ethyl bromoacetate (22 m*l*, 0.2 mol) was added slowly to the reaction mixture under cooling below 20°C. The mixture was allowed to stand for 5 min at 0°C, poured into water (500 m*l*), and acidified with concentrated hydrochloric acid (30 m*l*) to give a colorless precipitation. The crude product was collected by filtration, washed with dilute hydrochloric acid, dried, and recrystallized from methanol to give 30 g of colorless prisms: yield 65%; mp 138—139°C (dec); UV_{max} (99% EtOH): 220 mμ (sh, log ε 4.02), 277.5 (3.78), 334 (3.87); Mass spectrum (75 eV) *m/e* (rel. intensity): 246 (27, M^+), 232 (40, $-CH_2$), 215 (8, $-NH_3$), 200 (50, $-C_2H_5$, $-NH_3$), 127 (100, $-SCH_2CO_2C_2H_5$); IR (KBr): 3320, 3240, 316 (NH_3^+), 2960 (CH), 2200 (conj. CN), 1730 ($COOC_2H_5$), 1655 (CO), 1530 (conj. C=C), 1485 (CH), 1298 cm^{-1} (C–O–C). Found: C, 38.91; H, 4.04; N, 11.11; S, 26.20%; mol wt (mass), 246. Calcd for $C_8H_{10}N_2S_2O_3$; C, 39.03; T, 4.06; N, 11.37; S, 26.04%; mol wt, 246.20.

Preparation of 4H-5-*cyano*-2,3-*dihydro*-6-*methylthio*-1,3-*thiazin*-4-*one*-2-*spirocyclohexane (5a).* A mixture of cyclohexanone (5 g, 0.05 mol), β-methylthio-β-mercapto-α-cyanoacrylamide (3 g, 0.02 mol), 2% sulfuric acid (10 m*l*), and methanol (50 m*l*) was refluxed for 10 min. The crude material was collected by filtration, washed with methanol, dried, and recrystallized from acetic acid to give 4 g of colorless plates (**5a**); IR (KBr): 3280, 3160, 3040 (NH), 2900 (CH), 2220 (conj. CN), 1650 (CO), 1470 cm^{-1} (CH); NMR (CF_3CO_2H)δ: 8.30 (broad, 1H, NH), 2.78 (s, 3H, SCH_3), 2.20 (m, 4H, $2CH_2$), 1.75 (m, 6H, $3CH_2$). Found: C, 51.74; H, 5.48; N, 10.95; S, 25.19%; mol wt (mass), 254. Calcd for $C_{11}H_{14}N_2S_2O$: C, 51.96; H, 5.50; N, 11.01; S, 25.22%; mol wt, 254.23.

The preparations of **5b** to **5r** were worked up as mentioned in the isolation of **5a**. The appearance, melting

Table 4. IR (KBr) data of **5**, cm^{-1}

5d	3260, 3160, 3040 (NH), 2980, 2920 (CH), 2220 (CN), 1645 (CO), 1465 (CH)
5g	3320, 3280, 3180 (NH), 3040 (arom. CH), 2980 (CH), 2220 (CN), 1650 (CO), 1620, 1515 (benzene ring), 1470 (CH)
5h	3240, 3160, 3040 (NH, arom. CH), 2860 (CH), 2240 (CN), 1660 (CO), 1500 (benzene ring), 1480 (CH)
5k	3280, 3160, 3040 (NH), 2900 (CH), 2220 (CN), 1655 (CO), 1470 (CH)
5m	3320, 3250 (NH), 2980 (CH), 2220 (CN), 1670 (CO), 1620 (benzene ring), 1470 (CH)
5n	3300 (NH), 2970 (CH), 2220 (CN), 1670 (CO), 1620 (furan ring), 1470 (CH)
5r	3420, 3350, 3200 (NH), 2960, 2940 (CH), 2220 (CN), 1720 (CO_2CH_3), 1670 (CO)

Table 5. NMR (in CF_3CO_2H) data of **5**, δ value

5d	8.42 (broad, 1H, NH), 2.80 (s, 3H, SCH_3), 2.20 (q, 2H, CH_2CH_3, J=7 Hz), 1.85 (s, 3H, CH_3), 1.15 (*t*, 3H, CH_2CH_3, J=7 Hz)
5g	8.35 (broad, 1H, NH), 7.23 (s, 1H, C_6H_5), 7.15 (s, 2H, C_6H_5), 6.10 (s, 1H, CH), 3.95 (s, 3H, OCH_3), 2.70 (s, 3H, SCH_3)
5h	8.30 (broad, 1H, NH), 7.08 (s, 2H, CH_2), 6.98 (s, 1H, CH), 6.05 (s, 3H, C_6H_3), 2.80 (s, 3H, SCH_3)
5k	8.40 (broad, 1H, NH), 3.35 (q, 2H, CH_2CH_3, J=7 Hz), 1.90 (s, 6H, $2CH_3$), 1.50 (t, 3H, CH_2CH_3, J=7 Hz)
5m	8.30 (broad, 1H, NH), 7.50 (s, 5H, C_6H_5), 6.15 (d, 1H, H), 3.30 (q, 2H, CH_2), 1.45 (t, 3H, CH_3)
5n	8.50 (broad, 1H, NH), 7.55 (d, 1H, C_4H_3O, J=4 Hz), 6.70 (d, 1H, C_4H_3O, J_{34}=7Hz), 6.50 (q, 1H, C_4H_3O, J_{45}=4Hz, J_{34}=7Hz), 6.30 (s, 1H, CH), 3.35 (q, 2H, CH_2CH_3, J=7 Hz), 1.53 (t, 3H, CH_2CH_3, J=7 Hz)
5r	7.10 (broad, 1H, NH), 4.35 (s, 2H, C(6′)H_2), 4.30 (s, 6H, C(2′, 5′)H, C(3′, 4′)H_2), 4.20 (s, 2H, SCH_2CO_2), 4.05 (s, 9H, $3CH_3$), 3.90 (s, 3H, CO_2CH_3), 3.65 (s, 1H, CH)

4) R. Gompper and W. Töpfel, *Chem. Ber.*, **95**, 2861 (1962).
5) M. Yokoyama, This Bulletin, **43**, 2938 (1970).

TABLE 6. ANALYSES OF **5**

Compd.	Formula	Calcd (%)				Found (%)			
		C	H	N	S	C	H	N	S
5b	$C_{10}H_{12}N_2S_2O$	49.99,	5.00,	11.66,	26.69	50.18,	4.74,	11.69,	26.75
5c	$C_8H_{10}N_2S_2O$	44.86,	4.67,	13.07,	29.93	44.70,	4.77,	13.16,	29.87
5d	$C_9H_{12}N_2S_2O$	47.36,	5.26,	12.27,	28.10	47.21,	5.10,	12.37,	28.12
5e	$C_7H_8N_2S_2O$	41.99,	3.99,	13.99,	32.03	42.05,	4.03,	13.91,	31.85
5f	$C_{12}H_{10}N_2S_2O$	54.96,	3.81,	10.68,	24.45	54.81,	3.91,	10.57,	24.25
5g	$C_{13}H_{12}N_2S_2O_3$	50.65,	3.89,	9.08,	20.80	50.89,	3.93,	9.16,	20.56
5h	$C_{13}H_{10}N_2S_2O_3$	50.98,	3.27,	9.14,	20.94	50.88,	3.07,	9.02,	20.71
5i	$C_{10}H_8N_2S_2O_2$	47.62,	3.17,	11.10,	25.42	47.63,	3.11,	10.94,	25.35
5j	$C_{12}H_{16}N_2S_2O$	53.72,	5.96,	10.44,	23.90	53.68,	5.69,	10.31,	23.66
5k	$C_9H_{12}N_2S_2O$	47.36,	5.26,	12.27,	28.10	47.24,	5.10,	12.39,	27.91
5l	$C_8H_{10}N_2S_2O$	44.86,	4.67,	13.07,	29.93	44.65,	4.49,	13.14,	29.64
5m	$C_{13}H_{12}N_2S_2O$	56.52,	4.34,	10.14,	23.21	56.42,	4.71,	10.22,	23.20
5n	$C_{11}H_{10}N_2S_2O_2$	49.62,	3.76,	10.52,	24.08	49.55,	3.57,	10.47,	23.99
5o	$C_{13}H_{16}N_2S_2O_3$	50.04,	5.12,	8.97,	20.55	50.00,	5.22,	8.89,	20.51
5p	$C_8H_8N_2S_2O_3$	39.34,	3.28,	11.47,	26.26	39.25,	3.42,	11.53,	26.20
5q	$C_{13}H_{10}N_2S_2O_3$	50.98,	3.27,	9.14,	20.94	50.96,	3.18,	9.08,	20.99
5r	$C_{16}H_{22}N_2S_2O_3$	54.24,	6.21,	7.90,	18.10	54.33,	6.15,	8.03,	18.16

points, and yields of **5a** to **5r** were included in Table 1. Tables 2 and 3 showed Mass and UV spectra for the typical compounds of **5**. Compound **5**, generally, was easily soluble in concentrated sulfuric acid and acetic acid. The IR and NMR spectra for the typical compounds of **5** were shown in Tables 4 and 5.

Compounds **5** synthesized were: 4*H*-5-cyano-2,3-dihydro-6-methylthio-1,3-thiazin-4-one-2-spirocyclopentane (**5b**), 4*H*-5-cyano-2,3-dihydro-2,2-dimethyl-6-methylthio-1,3-thiazin-4-one (**5c**), 4*H*-5-cyano-2,3-dihydro-2-ethyl-2-methyl-6-methylthio-1,3-thiazin-4-one (**5d**), 4*H*-5-cyano-2,3-dihydro-2-methyl-6-methylthio-1,3-thiazin-4-one (**5e**), 4*H*-5-cyano-2,3-dihydro-6-methylthio-2-phenyl-1,3-thiazin-4-one (**5f**), 4*H*-5-cyano-2,3-dihydro-2-(3-methoxy-4-hydroxyphenyl)-6-methylthio-1,3-thiazin-4-one (**5 g**), 4*H*-5-cyano-2,3-dihydro-2-(3,4-methylenedioxyphenyl)-6-methylthio-1,3-thiazin-4-one (**5h**), 4*H*-5-cyano-2,3-dihydro-2-furyl-6-methylthio-1,3-thiazin-4-one (**5i**), 4*H*-5-cyano-2,3-dihydro-6-ethylthio-1,3-thiazin-4-one-2-spirohexane (**5j**), 4*H*-5-cyano-2,3-dihydro-2,2-dimethyl-6-ethylthio-1,3-thiazin-4-one(**5k**), 4*H*-5-cyano-2,3-dihydro-6-ethylthio-2-methyl-1,3-thiazin-4-one(**5l**), 4*H*-5-cyano-2,3-dihydro-6-ethylthio-2-phenyl-1,3-thiazin-4-one(**5m**), 4*H*-5-cyano-2,3-dihydro-6-ethylthio-2-furyl-1,3-thiazin-4-one(**5n**), 4*H*-5-cyano-2,3-dihydro-6-methoxycarbonylmethylthio-1,3-thiazin-2-spirohexane(**5o**), 4*H*-5-cyano-2,3-dihydro-6-methoxycarbonylmethylthio-2-methyl-1,3-thiazin-4-one(**5p**), 4*H*-5-cyano-2,3-dihydro-6-methoxycarbonylmethylthio-2-phenyl-1,3-thiazin-4-one(**5q**), and 4*H*-5-cyano-2,3-dihydro-6-methoxycarbonylmethylthio-1,3-thiazin-4-one-2-spiro-2′-(1-isopropyl-4-methylcyclohexane)(**5r**), respectively.

The author wishes to express his thanks to Professor Dr. Tatsuo Takeshima and Dr. Hiroshi Midorikawa for their helpful discussions and encouragement throughout the course of this work. He also wishes to thank Dr. Toshio Hayashi for his helpful advice in many respects.

The Michael Reaction of Fluoro-substituted-9,9′-Bifluorenylidenes and -Fluorenes, and the Syntheses of Some Related Compounds[1]

Masahiro MINABE, Akio TANAKA,* Masahiro WAKUI,** and Kazuo SUZUKI

Department of Industrial Chemistry, Faculty of Technology, Utsunomiya University, Ishii-cho, Utsunomiya

(Received September 3, 1970)

The Michael reaction of fluoro-substituted 9,9′-bifluorenylidenes and fluorenes was carried out; the normal addition products, fluoro-substituted tribiphenylenepropanes, were obtained, but no abnormal product was isolated. Some new fluoro-substituted-fluorenes, -9,9′-bifluorenylidenes, -9,9′-bifluorenyls and -α,δ-dibiphenylenebutadienes, were synthesized. The structures of the fluoro-substituted tribiphenylenepropanes were confirmed by the lithium-halogen interconversion reaction of 9-lithiofluorenes and 9-bromo-9,9′-bifluorenyls. The pyrolyses of fluoro-substituted tribiphenylenepropanes afforded fluoro-substituted or nonfluoro-substituted-9,9′-bifluorenylidenes, -9,9′-bifluorenyls, -fluorenes, and -fluorenones. Differential scanning calorimetry was applied to fluoro-substituted-9,9′-bifluorenyls and -tribiphenylenepropanes.

The Michael reaction[2] of 9,9′-bifluorenylidene (**4**) with 2,7-dibromofluorene gave the normal product, 2′,7′-dibromotribiphenylenepropane, together with the abnormal 2′,7′,2″,7″-tetrabromotribiphenylenepropane and tribiphenylenepropane. Also, normal 2,7,2′,7′-tetrabromotribiphenylenepropane and the abnormal 2′,7′-dibromotribiphenylenepropane, 2′,7′,2″,7″-tetrabromotribiphenylenepropane and tribiphenylenepropane were similarly obtained from 2,7,2′,7′-tetrabromo-9,9′-bifluorenylidene and fluorene (**1**). The formation of these abnormal products was explained by a combination of addition, elimination, and protonation processes in the presence of sodium hydroxide-pyridine solution. The normal products were primarily obtained in the presence of sodium ethoxide, as has previously been reported in this series.[2,3]

The present paper will deal with another Michael reaction, that of fluoro-substituted 9,9′-bifluorenylidenes and fluorenes. The experiments were designed primarily to clarify any effects due to the difference between fluoro-substitution. Secondly, the new fluoro-substituted compounds were synthesized in order to compare their properties with those of other, corresponding halogeno compounds.

The Michael reaction of **4**[4] and 2-fluorofluorene (**2**)[5] with potassium hydroxide in pyridine or with sodium ethoxide in ethanol gave 2′-fluorotribiphenylenepropane (**12**), 2-fluorofluorenone (**10**),[5] and recovered materials. The yield of **12** increased with an increase in the base concentration (see Table 1, Runs 1—6.)

When the reaction of 2,2′-difluoro-9,9′-bifluorenylidene (**6**)[5,6] with **1** was carried out under similar base conditions, 2,2′-difluorotribiphenylenepropane (**13**) and **10** were obtained (see Table 1, Runs 7—9).

An analogous reaction between **4** and 2,7-difluorofluorene (**3**)[7] yielded 2′,7′-difluorotribiphenylenepropane (**16**) exclusively (see Table 2, Runs 1—4). Further the condensation of 2,7,2′,7′-tetrafluoro-9,9′-bifluorenylidene (**8**) with **1** led to 2,7,2′,7′-tetrafluorotribiphenylenepropane (**17**) in a good yield (see Table 2, Runs 5—7).

The sequence for the formation of these addition products is shown in Scheme I. While a 9-fluorenyl carbanion (A′) is generated from (A) in the presence of a base, a new bond in carbanion (C′) can be formed by the attack of (A′) on the highly-polarized central double bond of (B). Then, (C′) may be transformed to the normal addition product (C) by protonation.

From 2- or 2,7-di-bromo-,[2] -iodo-, and -chloro-[8] derivatives, the normal and abnormal compounds were produced; however, in the corresponding fluoro derivatives, only the normal compounds were formed under the same conditions. These results can be explained in terms of the inductive effect of the fluorine atoms, which may operate on the 9′-methine carbon atom in the ion (C′); the 9′-hydrogen atom causes an increase in electron availability, and, consequently, the 9″-carbon is protonated in preference to the removal of a 9′-proton (*i.e.*, examples **12** and **16**). Likewise affected is the 9″-carbon (*i.e.*, examples **13** and **17**), so that the fission of the 9-9″ carbon-carbon bond is controlled; therefore, the 9″-carbon can be protonated with ease to form the normal compounds.

It can be assumed that the (C′) and (C″) ions could hardly attain equilibrium under such reaction conditions, so that the ions can be subjected to protonation with a fairly rapid formation of the corresponding tribiphenylenepropanes.

2,2′,2″-Trifluorotribiphenylenepropane (**15**) and 2,7,2′,7′,2″,7″-hexafluorotribiphenylenepropane (**19**) were obtained by the reaction of **6** and **2**, and by that

1) Studies on Fluorene Derivatives. XXVII. Part XXVI of this series: K. Suzuki, M. Minabe, S. Kubota, and T. Isobe, This Bulletin, **43**, 2217 (1970).

* Present address. The Saitama Institute of Public Health, Omiya.

** Present address: Department of Applied Chemistry, Faculty of Engineering, University of Osaka Prefecture, Sakai.

2) K. Suzuki, *Nippon Kagaku Zasshi*, **72**, 825, 827 (1951); K. Suzuki, M. Minabe, M. Fujimoto, and N. Nohara, This Bulletin, **42**, 1609 (1969); L. A. Pinck and G. E. Hilbert, *J. Amer. Chem. Soc.*, **68**, 2014 (1946).

3) a) K. Suzuki, *Nippon Kagaku Zasshi*, **75**, 711, 714, 793 (1954). b) K. Suzuki, *ibid.*, **75**, 795 (1954). c) K. Suzuki and M. Fujimoto, This Bulletin, **37**, 1833 (1964).

4) R. C. Fuson and H. D. Porter, *J. Amer. Chem. Soc.*, **70**, 895 (1948); J. Thiele and A. Wansheidt, *Ann. Chem.*, **376**, 278 (1910); K. Suzuki and S. Kajigaeshi, This Bulletin, **35**, 408 (1962).

5) E. D. Bergmann, H. Hoffman, and D. Winter, *Ber.*, **66**, 46 (1933).

6) E. D. Bergmann, *J. Chem. Soc.*, **1935**, 987.

7) a) T. L. Fletcher and M. J. Namkung, *Chem. Ind.* (London), **1961**, 179. b) S. Berkovic, *Israel J. Chem.*, **1**, 1 (1963).

8) Presented at the 23rd Annual Meeting of the Chemical Society of Japan, Tokyo, April, 1970; Preprints, III, p. 1739.

Table 1. Michael reaction of 2-fluoro-substituted 9,9'-bifluorenylidenes and fluorenes

Run	Reactants g: 9,9'-Bifluorenylidenes	Reactants g: Fluorenes	Reactants g: Mol. rate	React. conditions: Solvent (ml)	React. conditions: Base (%)	React. conditions: Time hr	Products g: Tribiphenylenepropanes (%)	Products g: Fluorenones	Recovered g: Acceptor	Recovered g: Donor
1	**4** 1.10	**2** 0.61	1/1	Py. 30	KOH 0.1	45	**12** 0.65 (38)	**10** 0.01	0.63	0.14
2	**4** 1.10	**2** 0.61	1/1	Py. 30	KOH 1	5.5	**12** 1.39 (81)	**10** 0.03	0.20	trace
3	**4** 1.10	**2** 0.61	1/1	Py. 30	KOH 15	0.75	**12** 1.52 (89)	**10** 0.02	0.08	trace
4	**4** 1.10	**2** 1.23	1/2	P . 30	KOH 10	0.75	**12** 1.64 (96)	**10** 0.33	0.02	0.17
5	**4** 1.10	**2** 0.61	1/1	EtOH 30	NaOEt 1	9	**12** 1.30 (76)	**10** trace	0.11	
6	**4** 1.10	**2** 0.61	1/1	EtOH 30	NaOEt 5	5	**12** 1.34 (78)	**10** trace	0.10	
7	**6** 1.21	**1** 0.55	1/1	Py. 30	KOH 0.1	75	**13** 1.19 (68)	**10** 0.03	0.19	0.16
8	**6** 1.21	**1** 0.55	1/1	Py. 30	KOH 10	2	**13** 1.55 (88)	**10** 0.02	trace	0.06
9	**6** 1.21	**1** 1.10	1/2	Py. 30	KOH 10	1.5	**13** 1.51 (86)	**10** 0.07	trace	0.65
10	**6** 1.21	**2** 0.61	1/1	Py. 30	KOH 10	2.5	**15** 1.63 (90)	**10** 0.01	0.06	0.04
11	**5** 1.15	**2** 0.61	1/1	Py. 30	KOH 10	2	**14** 1.54 (88)	**10** 0.02	0.02	0.02
12	**5** 1.15	**1** 0.55	1/1	Py. 30	KOH 10	4	**12** 1.33 (78)	**10** 0.016 **9** 0.02	0.06	0.04

a) Py.=Pyridine; EtOH=Ethanol; NaOEt=Sodium ethoxide.
b) Found for **12**: C, 91.51; H, 4.71. For **13**: C, 88.29; H, 4.53. For **14**: C, 88.43; H, 4.43. For **15**: C, 85.16; H, 3.93%.

Table 2. Michael reaction of 2,7-difluoro-substituted 9,9'-bifluorenylidenes and fluorenes

Run	Reactants g: 9,9'-Bifluorenylidenes	Reactants g: Fluorenes	Reactants g: Mol. rate	React. conditions: Solvent (ml)	React. conditions: Base (%)	React. conditions: Time hr	Products g: Tribiphenylenepropanes (%)	Products g: Fluorenones	Recovered g: Acceptor	Recovered g: Donor
1	**4** 1.10	**3** 0.67	1/1	Py. 30	KOH 0.1	60	**16** 0.61 (35)	**11** 0.05	0.56	0.31
2	**4** 1.10	**3** 0.67	1/1	Py. 30	KOH 10	1	**16** 1.30 (73)	**11** 0.21	0.10	trace
3	**4** 1.10	**3** 1.35	1/2	Py. 30	KOH 10	1	**16** 1.61 (91)	**11** 0.40	0.01	0.10
4	**4** 1.10	**3** 0.67	1/1	EtOH 30	NaOEt 10	2	**16** 1.57 (90)	**11** trace	trace	0.04
5	**8** 1.34	**1** 0.55	1/1	Py. 30	KOH 0.1	15	**17** 1.45 (77)	**11** 0.14	trace	0.10
6	**8** 1.34	**1** 0.55	1/1	Py. 30	KOH 10	2	**17** 1.41 (75)	**11** 0.06		0.05
7	**8** 1.34	**1** 1.11	1/2	Py. 30	KOH 10	2	**17** 1.60 (85)	**11** 0.10		0.58
8	**8** 1.34	**3** 0.67	1/1	Py. 30	KOH 10	2	**19** 1.77 (88)	**11** 0.14		trace
9	**7** 1.21	**3** 0.67	1/1	Py. 30	KOH 10	2	**18** 1.50 (80)	**11** 0.15		0.01
10	**7** 1.21	**1** 0.55	1/1	Py. 30	KOH 10	2	**16** 1.39 (79)	**11** 0.08 **9** 0.07	0.04	0.05

a) Py.=Pyridine; EtOH=Ethanol; NaOEt=Sodium ethoxide.
b) Found for **16**: C, 88.04; H, 4.73. For **17**: C, 82.84; H, 4.09. For **18**: C, 82.51; H, 3.79. For **19**: C, 77.61; H, 3.19%.

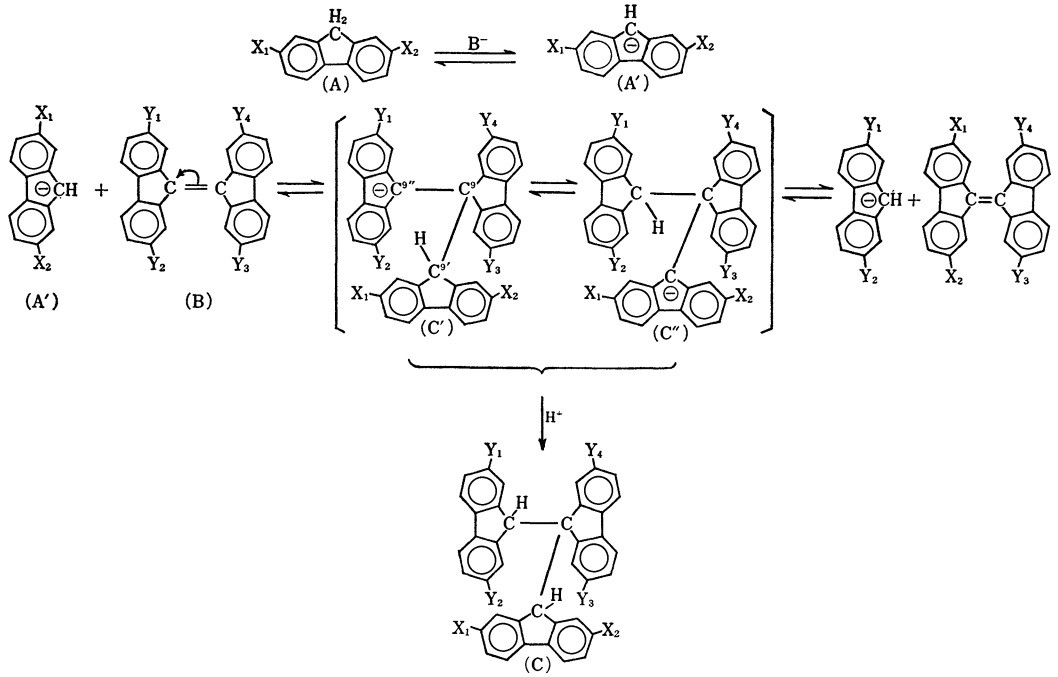

a). (A)=**1**($X_1=X_2=H$), **2**($X_1=F$; $X_2=H$) or **3**($X_1=X_2=F$).
b). (B)=**4**($Y_1=Y_2=Y_3=Y_4=H$), **5**($Y_1=F$; $Y_2=Y_3=Y_4=H$), **6**($Y_1=Y_4=F$; $Y_2=Y_3=H$), **7**($Y_1=Y_2=F$; $Y_3=Y_4=H$) or **8**($Y_1=Y_2=Y_3=Y_4=F$).
c). (C)=**12**($X_1=F$; $X_2=Y_1=Y_2=Y_3=Y_4=H$), **13**($Y_1=Y_3=F$; $X_1=X_2=Y_2=Y_4=H$), **14**($X_1=Y_1=F$; $X_2=Y_2=Y_3=Y_4=H$), **15**($X_1=Y_1=Y_3=F$; $X_2=Y_2=Y_4=H$), **16**($X_1=X_2=F$; $Y_1=Y_2=Y_3=Y_4=H$), **17**($X_1=X_2=H$; $Y_1=Y_2=Y_3=Y_4=F$), **18**($X_1=X_2=Y_1=Y_2=F$; $Y_3=Y_4=H$), **19**($X_1=X_2=Y_1=Y_2=Y_3=Y_4=F$), 2-Fluorotribiphenylenepropane($X_1=X_2=Y_1=Y_2=Y_3=H$; $Y_4=F$) or 2,7-Difluorotribiphenylenepropane ($X_1=X_2=Y_1=Y_2=H$; $Y_3=Y_4=F$).

Scheme 1.

TABLE 3. SYNTHESES AND ANALYTICAL DATA ON 9,9′-BIFLUORENYLS

9,9′-Bifluorenylidene g	9,9′-Bifluorenyl g	Mp °C	Formula	Found (%)		Calcd (%)	
				C	H	C	H
2-Fluoro- (**5**) 0.10	2-Fluoro- (**21**) 0.10	243—244	$C_{26}H_{17}F$	89.48	4.93	89.63	4.92
2,2′-Difluoro- (**6**) 0.10	2,2′-Difluoro- (**22**) 0.094	241—242	$C_{26}H_{16}F_2$	84.87	4.36	85.23	4.40
2,7-Difluoro- (**7**) 0.10	2,7-Difluoro- (**23**) 0.091	241.5—242.5	$C_{26}H_{16}F_2$	84.92	4.41	85.23	4.40
2,7,2′,7′-Tetrafluoro- (**8**) 0.10	2,7,2′,7′-Tetrafluoro- (**24**) 0.098	241—242	$C_{26}H_{14}F_4$	77.27	3.72	77.61	3.51

of **8** and **3**, respectively (see Table 1, Run 10 and Table 2, Run 8). These Michael products could be expected as normal products, but the stereoisomeric tribiphenylenepropanes[3b,9] were not isolated. The reactions of 2-fluoro-9,9′-bifluorenylidene (**5**) with **2** or **1** gave 2′,2″-difluoro-9,9′-bifluorotribiphenylenepropane (**14**) or **12** (see Table 1, Runs 11 and 12). Similarly, the reactions of 2,7-difluoro-9,9′-bifluorenylidene (**7**) with **3** or **1** afforded 2′,7′,2″,7″-tetrafluorotribiphenylenepropane (**18**) or **16** respectively (see Table 2, Runs 9 and 10).

Four fluoro-substituted 9,9′-bifluorenyls, *i.e.*, 2-fluoro- (**21**) (mp 243—244°C), 2,2′-difluoro- (**22**)[5] (mp 241—242°C), 2,7-difluoro- (**23**) (mp 241.5—242.5°C), and 2,7,2′,7′-tetrafluoro-9,9′-bifluorenyl (**24**) (mp 241—242°C), were obtained by the reduction of the corresponding 9,9′-bifluorenylidenes. Interestingly, these melting points are very close to that of 9,9′-bifluorenyl (**20**)[10] (mp 244—245°C).

The related fluoro-substituted 9-hydroxy-9,9′-bifluorenyls and 9-bromo-9,9′-bifluorenyls were synthesized in the usual way, as is shown in Table 4. Ten fluoro-substituted tribiphenylenepropanes were prepared and confirmed by the reaction of 9-lithiofluorenes and 9-bromo-9,9′-bifluorenyls, as is summarized in Table 5.

9) K. Suzuki, *Nippon Kagaku Zasshi*, **70**, 189 (1949); K. Suzuki, *Technol. Repts. Tohoku Univ.*, **19**, 63 (1955).

10) R. Weissgerber, *Ber.*, **46**, 2913 (1908).

Table 4. Characterization of 9-hydroxy-9,9'-bifluorenyls and 9-bromo-9,9'-bifluorenyls

Run	Reactants g		9-Hydroxy-9,9'-bifluorenyl (mp) °C	Yield g (%)	IR spectra (−OH) cm^{-1}	Anal (%) Found		Anal (%) Calcd
	Fluorene	Fluorenone				C	H	C H (Formula)
1	**1** 2.0	**10** 2.3	2-Fluoro- (182—184)	3.8 (89)	3300	85.47	4.60	85.69 4.70 ($C_{26}H_{17}OF$)
2	**2** 5.9	**9** 5.4	2'-Fluoro- (184—186)	10.3 (95)	3300	85.68	4.96	85.69 4.70 ($C_{26}H_{17}OF$)
3	**2** 3.0	**10** 2.8	2,2'-Difluoro- (178—180)	4.9 (85)	3290	81.42	4.29	81.66 4.22 ($C_{26}H_{16}OF_2$)
4	**1** 1.4	**11** 1.5	2,7-Difluoro- (211—212)	2.5 (93)	3570 (sharp)	81.60	4.28	81.66 4.22 ($C_{26}H_{16}OF_2$)
5	**3** 4.5	**9** 3.6	2',7'-Difluoro- (199—200.5)	4.8 (63)	3280	82.01	4.44	81.66 4.22 ($C_{26}H_{16}OF_2$)
6	**3** 3.2	**11** 3.0	2,7,2',7'-Tetrafluoro- (188—189)	5.3 (91)	3390	74.43	3.42	74.64 3.37 ($C_{26}H_{14}OF_4$)

Run	9-Bromo-9,9'-bifluorenyl (mp) °C	Yield %	Anal (%) Found C	Found H	Calcd C H (Formula)
1	2-Fluoro- (180—181; dec)	73	73.42	3.65	73.08 3.77 ($C_{26}H_{16}FBr$)
2	2'-Fluoro- (161—163; dec)	87	73.47	3.68	73.08 3.77 ($C_{26}H_{16}FBr$)
3	2,2'-Difluoro- (178—179; dec)	88	70.45	3.45	70.13 3.40 ($C_{26}H_{15}F_2Br$)
4	2,7-Difluoro- (173—174; dec)	73	70.33	3.66	70.13 3.40 ($C_{26}H_{15}F_2Br$)
5	2',7'-Difluoro- (176—177; dec)	99	70.40	3.44	70.13 3.40 ($C_{26}H_{15}F_2Br$)
6	2,7,2',7'-Tetrafluoro- (175—176; dec)	87	64.96	2.81	64.89 2.72 ($C_{26}H_{13}F_4Br$)

Table 5. Formation of fluoro-substituted tribiphenylenepropanes by lithium-halogen interconversion reaction

Reactants g: Fluorene	Reactants g: 9-Bromo-9,9'-bifluorenyl	Tribiphenylenepropane (Yield) g (%); (mp) °C	Anal (%) Found C	Found H	Calcd C H (Formula)
1 0.66	2-Fluoro- 1.28	2-Fluoro- 0.12 (8); 283—284 (dec)	91.41	5.07	91.38 4.92 ($C_{39}H_{25}F$)
2 0.74	9-Bromo-9,9'-bifluorenyl 1.23	2'-Fluoro- (**12**) 0.20 (13); 279—280 (dec)	91.61	4.83	91.38 4.92 ($C_{39}H_{25}F$)
2 0.74	2-Fluoro- 1.28	2,2'-Difluoro- (**13**) 0.34 (21); 288—289 (dec)	88.01	4.35	88.28 4.56 ($C_{39}H_{24}F_2$)
2 0.74	2'-Fluoro- 1.28	2',2''-Difluoro- (**14**) 0.18 (12); 282—283 (dec)	88.36	4.29	88.28 4.56 ($C_{39}H_{24}F_2$)
2 0.74	2,2'-Difluoro- 1.34	2,2',2''-Trifluoro- (**15**) 0.17 (10); 298—300 (dec)	Mixed Mp Determination		
1 0.58	2,7-Difluoro- 1.38	2,7-Difluoro- 0.12 (8); 279—280 (dec)	88.19	4.43	88.28 4.56 ($C_{39}H_{24}F_2$)
1 0.58	2',7'-Difluoro- 1.38	2',7'-Difluoro- (**16**) 0.35 (22); 285—286 (dec)	88.56	4.75	88.28 4.56 ($C_{39}H_{24}F_2$)
3 0.71	2,7-Difluoro- 1.38	2,7,2',7'-Tetrafluoro- (**17**) 0.17 (10); 287—288 (dec)	82.95	3.82	82.67 3.91 ($C_{39}H_{22}F_4$)
3 0.71	2',7'-Difluoro- 1.38	2',7',2'',7''-Tetrafluoro- (**18**) 0.41 (24); 293—294 (dec)	82.53	3.78	82.67 3.91 ($C_{39}H_{22}F_4$)
3 0.71	2,7,2',7'-tetrafluoro- 1.49	2,7,2',7',2'',7''-Hexafluoro- (**19**) 0.21 (12); 303.5—304 (dec)	Mixed Mp Determination		

The pyrolyses of **19**, **17**, **13**, and **12** were also carried out. The carbon-fluorine bonds being stable under such thermal conditions, fluoro-substituted- or non-fluoro-substituted- 9,9′-bifluorenylidenes, -9,9′-bifluorenyls, -fluorenes, -fluorenones, and recovered tribiphenylenepropanes were obtained. The thermal behavior was analogous to that proposed previously.[1,3a]

The thermal behavior of the 9,9′-bifluorenyls (**20**, **21**, **22**, **23**, and **24**) and the fluoro-substituted tribiphenylenepropanes (**12**, **13**, **15**, **16**, **17**, and **19**) was studied. Typical thermograms of **13** and **24** are shown in Fig. 1.

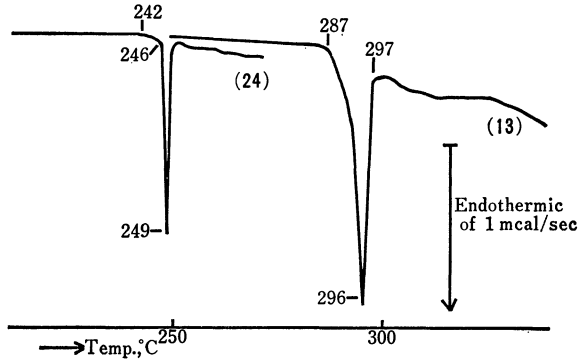

Fig. 1. Differential scanning calorimeter thermograms of **13** and **24**.

In the (**24**) thermogram, the sharp, first single peak curved slowly at 242°C and then steeply at 246°C to reach the inflection point, 249°C, of the melting endotherm, which corresponds to the melting point (241—242°C) of **24**. The peak indicates that **24** is thermally "unreactive."

The second major endothermic peak, centering at 287°C and 297°C in the thermogram (**13**), corresponds to the melting point (289—290°C (dec)), but it is relatively broader than that of **24**. This may be due to its being thermally "reactive" at the melting point. The further endothermal tendency of **13** after the melting peak indicates the formation of pyrolysates and their secondary pyrolyses. In addition, an analogous thermal behavior was observed for other compounds.

Experimental[11]

The IR spectra were recorded on KBr pellets using a JASCO model IR-G spectrophotometer (Japan Spectroscopic Co., Ltd.).

Measurements of DSC Thermograms. The instrument used in this series was a differential scanning calorimeter, Model DSC-1B (Perkin-Elmer Corp.). The experiments were run with a sensitivity of ±4 mcal/sec under an atmosphere of nitrogen, at a scan time of 8°C/min and a chart speed of 0.5 inch/min. Each sample, **24** (0.63 mg) and **13** (3.27 mg), was packed in aluminum pans with a volatile sample sealer.

Syntheses of 9-Bromofluorenes. 2-Fluoro-9-bromofluorene: a) A mixture of 2.0 g of **2**, 2.0 g of *N*-bromosuccinimide (NBS), and 10 m*l* of anhydrous benzene was refluxed for 3 hr to afford 2.1 g (75%) of colorless 2-fluoro-9-bromofluorene (mp 112—113°C) from cyclohexane. Found: C, 59.33; H, 2.69. Calcd for $C_{13}H_8FBr$: C, 59.35; H, 3.06%.

b) 2-Fluorofluoren-9-ol[12] (0.40 g; 0.002 mol) in 10 m*l* of acetic acid was saturated with hydrogen bromide at room temperature, after which the mixture was allowed to stand overnight. The removal of the solvent under reduced pressure, washing with water, and extraction with 10 m*l* of cyclohexane yielded 0.40 g (76%) of colorless needles, mp 113—114°C, identical in all respects with the product obtained by Method a.

2-Fluoro-7-nitrofluoren-9-one: A 0.92-g (0.004 mol) portion of 2-fluoro-7-nitrofluorene[7b,13] was oxidized by sodium bichromate and recrystallized from benzene; 0.79 g (86%) of ketone was obtained as yellow needles, mp 201—202.5°C. IR (>C=O): 1716 cm^{-1}.

Found: C, 64.17; H, 2.52; N, 5.55%. Calcd for $C_{13}H_6NO_3F$: C, 64.21; H, 2.49; N, 5.76%.

2,7-Difluorofluoren-9-ol: The foregoing 2,7-difluorofluorenone (**11**)[14] was subjected to reduction with zinc dust and aqueous ammonium hydroxide in ethanol, and recrystallized from aqueous methanol (25%); it gave a quantitative yield of 2,7-difluorofluoren-9-ol, mp 165.5—166°C, as fine, colorless needles. IR (-OH): 3190—3290 cm^{-1}.

2,7-Difluoro-9-bromofluorene: a) The bromination of 2,7-difluorofluoren-9-ol (5.0 g) with dry hydrogen bromide yielded 5.8 g (90%) of 2,7-difluoro-9-bromofluorene, mp 136—138°C. Found: C, 55.94; H, 2.34. Calcd for $C_{13}H_7F_2Br$: C, 55.55; H, 2.51%.

b) A 3.0-g portion of **3** was worked up with NBS; it formed 3.3 g (79%) of 2,7-difluoro-9-bromofluorene, identical in all respects with the product obtained by Method a.

*Syntheses of 9,9′-Bifluorenylidenes. 2-Fluoro-9,9′-bifluorenylidene (**5**)*: A mixture of 10.2 g of 2-fluoro-9′-hydroxy-9,9′-bifluorenyl, 400 m*l* of acetic acid, and 5 m*l* of concentrated sulfuric acid was refluxed for 30 min. The reaction mixtures was then evaporated to 50 m*l* under reduced pressure, and the precipitate was filtered off, washed with water, and extracted with 100 m*l* of acetone. Red needles (4.1 g) of **5**, mp 208—209°C, formed, while the concentration of the mother liquor yielded an additional 2.6 g of **5** (total: 6.7 g, 69%). Found: C, 90.40; H, 4.20%. Calcd for $C_{26}H_{15}F$: C, 90.15; H, 4.36%.

*2,7-Difluoro-9,9′-bifluorenylidene (**7**)*: A 0.8-g portion of 2,7-difluoro-9′-hydroxy-9,9′-bifluorenyl was worked up as in the synthesis of **5**; **7** was thus obtained (0.45 g; 59%) as red needles, mp 224—225°C.

Found: C, 86.00; H, 3.53%. Calcd for $C_{26}H_{14}F_2$: C, 85.70; H, 3.87%.

*2,2′-Difluoro-9,9′-bifluorenylidene (**6**)*. a) **6** was prepared from 2-fluoro-9-bromofluorene (1.32 g; 0.005 mol), as in the case of **4**; 0.7 g (84%); mp 226—227°C.

Found: C, 86.04; H, 3.54%. Calcd for $C_{26}H_{14}F_2$: C, 85.70; H, 3.87%.

b) A benzene (20 m*l*) solution of 1.11 g (0.0025 mol) of 2,2′-difluoro-9-bromo-9,9′-bifluorenyl was percolated through an alumina column (45 g of activated alumina: for chromatography, 300 mesh, Wako Pure Chemical Ind. Ltd.; column: 1.8 cmϕ × 18 cm). The colorless solution immediately turned red over alumina, and the red band formed was eluted with benzene. The red solution was evaporated

11) All the melting points are uncorrected.

12) G. G. Smith and R. P. Bayer, *Tetrahedron*, **18**, 323 (1962) (*Chem. Abstr.*, **57**, 8515 (1962)).

13) J. A. Miller, R. B. Sandin, E. C. Miller, and H. P. Rusch, *Cancer Res.*, **15**, 188 (1955) (*Chem. Abstr.*, **49**, 16178 (1955)).

14) H. L. Pan and T. L. Fletcher, *J. Med. Chem.*, **8**, 491 (1965).

to dryness under reduced pressure; subsequent recrystallization from acetic acid gave 0.78 g (86%) of **6** (mp 226.5—227°C).

*2,7,2',7'-Tetrafluoro-9,9'-bifluorenylidene (**8**).* An acetone (34 m*l*) solution of 3.2 g of 2,7-difluoro-9-bromofluorene was treated with potassium hydroxide-methanol (0.64 g/14 m*l*) to give 2.1 g (92%) of red **8**, mp 337—338°C (dec).

Found: C, 78.06; H, 3.10%. Calcd for $C_{26}H_{12}F_4$: C, 78.00; H, 3.02%.

Syntheses of 9,9'-Bifluorenyls. Typical Procedure: A mixture of 0.10 g of **5**, 20 m*l* of acetic acid, 1 g of zinc dust, and 1 m*l* of hydrochloric acid was refluxed for 2 hr. The reaction mixture was filtered, the filtrate was poured into cold water, and the precipritate was recrystalized from a mixture of benzene and ethanol (1 : 1) to give 0.10 g of colorless needles, **21**, mp 243—244°C.

Formation of 2,2'-Difluoro-α,δ-dibiphenylenebutadiene and 2,7,2',7'-Tetrafluoro-α,δ-dibiphenylenebutadiene. A mixture of 0.5 g of **2**, 45 m*l* of ethanol, and 2.5 g of potassium hydroxide in 5 m*l* of water was refluxed under a gentle stream of air for 24 hr. The precipitate was recrystallized from pyridine to give 0.14 g (26%) of 2,2'-difluoro-α,δ-dibiphenylenebutadiene as orange needles with a mp of 392—393°C (dec). Found: C, 86.21; H, 4.30%. Calcd for $C_{28}H_{16}F_2$: C, 86.14; H, 4.13%. In addition, 0.10 g (20%) of **2** and 0.21 g (39%) of **10** were isolated from the ethanol mother solution.

2,7,2',7'-Tetrafluoro-α,δ-dibiphenylenebutadiene was prepared by the same procedure as before. Yield, 23% of fine orange-red needles, mp 398°C (dec). Found: C, 78.85; H, 3.23%. Calcd for $C_{28}H_{14}F_4$: C, 78.87; H, 3.31%.

The Michael Reaction of 9,9'-Bifluorenylidenes and Fluorenes. Typical Procedure: A Mixture of 1.34 g (1/300 mol) of **8**, 1.11 g (1/150 mol) of **1**, 28 m*l* of pyridine, and 3 g of potassium hydroxide in 2 m*l* of water was placed in a sealed tube and heated at 93—95°C for 2 hr. During this period, the color turned from red to dark green.

The reaction mixture was poured into 40 m*l* of methanol, and the precipitate was filtered off, washed with water, recrystallized from ethyl acetate, and from a mixture of benzene and ethanol to give 1.37 g of **17**, mp 286—287°C (dec.).

The pyridine-methanol mother solution was poured into 500 m*l* of water, and the precipitate was sublimed *in vacuo* at 150°C to yield an additional 0.23 g (total 1.60 g; 85%) of **17** from the sublimation residue.

The sublimed part was extracted with 50 m*l* of cyclohexane, and the extract was chromatographed on alumina; 0.58 g of **1**, mp 110—112°C, and 0.04 g of **11**, mp 200—201°C, were thus isolated. Further, 0.06 g (total 0.10 g) of **11** was obtained from the insoluble portion.

The identities of the compounds in this series were confirmed by mixed-melting-point determinations and by a comparison of the IR absorption spectra with those of authentic samples.

Syntheses of 9-Hydroxy-9,9'-bifluorenyls and 9-Bromo-9,9'-bifluorenyls. General Procedure: The reaction was carried out in the usual way. *n*-Butyllithium was prepared from 2.8 g of *n*-butyl bromide in 20 m*l* of anhydrous ether and 0.4 g of lithium chips in 40 m*l* of anhydrous ether. 2,7-Difluoro-9-lithiofluorene was prepared by adding 3.2 g of **3** in 40 m*l* of anhydrous benzene to the *n*-butyllithium solution. To this mixture we then added 150 m*l* of anhydrous benzene containing 3.0 g of **11**. Then, the reaction mixture was worked up as usual. 2,7,2',7'-Tetrafluoro-9-hydroxy-9,9'-bifluorenyl was prepared in a good yield (5.3 g; 91%), mp 188—189°C, from cyclohexane.

A 4.6-g portion of 2,7,2',7'-tetrafluoro-9-hydroxy-9,9'-bifluorenyl in 50 m*l* of acetic acid was saturated with dry hydrogen bromide at room temperature, after which the reaction mixture was allowed to stand overnight. Crystals of 2,7,2',7'-tetrafluoro-9-bromo-9,9'-bifluorenyl (4.8 g) were thus obtained, mp 175—176°C (dec), from cyclohexane.

*Formation of 2',2''-Difluorotribiphenylenepropane (**14**) by a Lithium-halogen Interconversion Reaction.* *n*-Butyllithium was prepared from 0.69 g of *n*-butyl bromide in 10 m*l* of anhydrous ether and 0.08 g of lithium chips in 20 m*l* of anhydrous ether. Then 2-fluoro-9-lithiofluorene was formed by adding 0.74 g of **2** in 15 m*l* of anhydrous benzene to the *n*-butyllithium solution. Into this resulting mixture there were slowly stirred 40 m*l* of anhydrous benzene containing 1.28 g of 2-fluoro-9'-bromo-9,9'-bifluorenyl. After standing overnight, the reaction mixture was treated as usual to give 0.18 g (12%) of **14** from ethyl acetate, mp 282—283°C (dec).

All the syntheses of this series were carried out in a similar manner.

*Pyrolysis of 2,7,2',7',2'',7''-Hexafluorotribiphenylenepropane (**19**).* Finely-powdered **19** (2.41 g; 0.004 mol) was heated at 310—320°C for 3.5 min in a 200-m*l* Erlenmeyer flask. The red molten product was extracted with 50 m*l* of boiling cyclohexane. The extract was allowed to stand overnight, and the deposit was combined with the insoluble portion. Upon fractional crystallization from benzene and ethyl acetate, *0.28* g of **8**, mp 336—338°C (dec), *0.76* g of **24**, mp 238—239°C, and 0.84 g of recovered **19**, mp 303—304°C (dec) were separated.

The cyclohexane mother solution was chromatographed on an alumina column; 0.02 g of **3**, mp 79—81°C, and 0.05 g of **11**, mp 203—205°C, were thus obtained.

*Pyrolysis of 2,7,2',7'-Tetrafluorotribiphenylenepropane (**17**).* A 2.84-g portion of **17** was heated at 310°C for 3 min. The following compounds were separated: 0.02 g of **8**, mp 335°C (dec), 0.20 g of **24**, mp 239—241°C, 0.28 g of **23**, mp 238—240°C, 0.05 g of **11**, mp 199—201°C, and recovered **17**, mp 285—286°C (dec).

*Pyrolysis of 2,2'-Difluorotribiphenylenepropane (**13**).* A 2.66-g portion of **13** was heated at 310—320°C for 2 min. Consequently, 0.37 g of **22**, mp 239—241°C, 0.80 g of **21**, mp 240—241.5°C, 0.12 g of **20**, mp 241—243°C, 0.16 g of **6**, mp 224—226°C, 0.23 g of **5**, mp 206—207°C, 0.02 g of **4**, mp 181—182.5°C, 0.09 g of **10**, mp 112—114°C, and 0.03 g of fluorenone (**9**), mp 80—81°C, were obtained. Further, 0.15 g of **13**, mp 288—289.5°C (dec) was recovered.

*Pyrolysis of 2'-Fluorotribiphenylenepropane (**12**).* The heating of 5.13 g of **12** at 300—305°C for 3 min gave 0.48 g of **21**, mp 239—241°C, 0.80 g of **20**, mp 239—240°C, 0.02 g of **6**, mp 219—222°C, 0.26 g of **5**, mp 205—207°C, 0.23 g of **4**, mp 181—182°C, 0.004 g of **10**, mp 113—114°C, 0.02 g of **9**, mp 81—81.5°C, 0.01 g of **1**, mp 113—115°C, and 1.73 g of recovered **12**, mp 280—281.5°C (dec).

The identities of the compounds in this series were confirmed by a comparison of their melting points and IR spectra with those of authentic samples.

The authors wish to express their gratitude to Professor S. Mitsui, of Tohoku University, for his helpful discussions. They are also grateful to Drs. John and Elizabeth Weisburger of the National Institutes of Health, U.S.A., for supplying editorial assistance.

Substituents Effects on the Azo-Hydrazone Tautomerism of 4-Arylazo-2,6-di-*t*-butylphenols

Eiichiro MANDA

Government Chemical Industrial Research Institute, Tokyo, Honmachi, Shibuya-ku, Tokyo

(Received September 14, 1970)

The substituents effects on the azo-hydrazone tautomerism of 4-arylazo-2,6-di-*t*-butylphenols in carbon tetrachloride were studied by means of infrared and visible spectra. The substituents effects on their absorption spectra were discussed. The azo tautomers are predominant in the tautomeric equilibria of 3'- and 4'-substituted derivatives. Considerable participations of the hydrazone tautomers are found in the equilibria of the 2'-substituted derivatives having substituents capable of forming intramolecular hydrogen bonding with hydrazone-hydrogen atom. In the equilibria of 2',6'-disubstituted derivatives, the positions of the equilibria move somewhat to the azo side from those of the corresponding 2'-substituted derivatives.

It is well known that the hydroxyazo dyes (I) show the azo-hydrazone tautomerism:

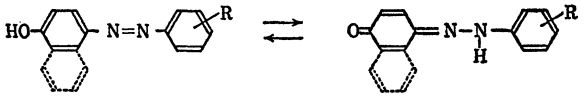

(I) - azo tautomer (I) - hydrazone tautomer

Many papers have been given on the naphthol derivatives of the dyes (I) since their tautomeric equilibria were found to show remarkable changes with their substituents and the solvents.[1-10] It has been observed that the electron-releasing substituents and the non-polar solvents favor the azo tautomers in equilibria. There are few papers on the phenol derivatives of (I). This might be due to the fact that the azo tautomers have been found predominant in equilibria. 4-Arylazo-2,6-di-*t*-butylphenols (II), which are the derivatives of hydroxyazo dyes (I), were prepared. The infrared and visible spectra of the phenols (II) in carbon tetrachloride solution showed interesting substituent effects on the tautomerism.

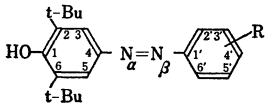

(II)

Results and Discussion

The results are summarised in Table 1.

Infrared Spectra. It has been pointed out that the dyes (I) show significant differences in their infrared spectra and that, among many absorption bands, the characteristic bands are the ν_{OH} band of the azo tautomer and the ν_{NH} and ν_{CO} bands of the hydrazone tautomer.[5,6] In this paper, each tautomer was studied by means of the ν_{OH} and the ν_{NH} bands, respectively, since the ν_{CO} bands appeared in the absorption region of the solvent.

ν_{OH} Bands: It has been reported that the ν_{OH} bands of (I) were sometimes found in the region of the ν_{NH} bands as a result of the hydrogen bondings, and some difficulties were encountered to distinguish the respective bands.[5] The infrared spectra of the azo tautomers of the phenols (II) always show sharp, monomeric ν_{OH} bands.[11] The bands are located nearly always at *ca.* 3640 cm^{-1}, while ν_{OH} bands of 4-substituted-2,6-di-*t*-butylphenols have been reported to shift within the region 3649—3626 cm^{-1} with their substituents.[12] The intensities vary with the substituents and tend to become smaller when the substituents displace the positions of the equilibria towards the hydrazone side.

ν_{NH} Bands: The bands are found in the region 3380—3280 cm^{-1} and the locations and the intensities vary not only with the substituents but also with substituting positions. Of 3'- and 4'-substituted derivatives, 4'-nitro derivative has a trace of ν_{NH} band, but no other derivative has it. Of 2'-substituted derivatives, methoxy, halogen and nitro derivatives have ν_{NH} bands, but not methyl derivative. The bands are due to the hydrazone tautomers which are favored in the equilibria by the additional stabilisation of the intramolecular hydrogen bonding between 2'-substituent and hydrazone-hydrogen atom.[6] The bands are also found in the spectra of 2',6'-dichloro, 2',6'-dibromo, 2',6'-dinitro, 2',4'-dinitro, and 2',4',6'-trinitro derivatives, in which intramolecular hydrogen bondings are also possible. The wave numbers of the ν_{NH} bands give the following order of locations:

$$2',4',6'\text{-}(NO_2)_3 - 2',6'\text{-}(NO_2)_2 - 2',4'\text{-}(NO_2)_2 - 2'\text{-}NO_2$$
$$- 2',6'\text{-}Cl_2 - 2',6'\text{-}Br_2 - 2'\text{-}Br_2 - 2'\text{-}Cl - 2'\text{-}MeO - 2'\text{-}F$$

The order might not be the order of the strengths of the intramolecular hydrogen bondings since the locations of the ν_{NH} bands have been observed to shift towards lower wave numbers with electron-attracting substituents in the unassociated 4-arylazo-1-naphthols

1) R. Kuhn and F. Bär, *Ann. Chem.*, **516**, 1431 (1935).
2) H. Shingu, *Nippon Kagaku Zasshi*, **60**, 542 (1939).
3) A. Burawoy, A. G. Salem, and A. R. Thompson, *J. Chem. Soc.*, **1952**, 4793.
4) A. Burawoy and A. R. Thompson, *ibid.*, **1953**, 1443.
5) D. Hadzi, *ibid.*, **1956**, 2143.
6) K. J. Morgan, *ibid.*, **1961**, 2151.
7) A. H. Berrie, P. Hampson, S. W. Longworth, and A. Mathias, *ibid.*, *B*, **1968**, 1308.
8) I. Saito, Y. Bansho, and A. Kakuta, *Kogyo Kagaku Zasshi*, **70**, 1715 (1967).
9) I. Saito, Y. Bansho, and Y. Shioiri, *ibid.*, **70**, 1721 (1967).
10) I. Saito, Y. Bansho, and M. Iwasaki, *ibid.*, **70**, 1725 (1967).
11) I. Brown, G. Eglinton, and M. Martin-Smith, *Spectrochim. Acta*, **19**, 463 (1963).
12) L. A. Cohen and W. M. Jones, *J. Amer. Chem. Soc.*, **85**, 3402 (1963).

Table 1. Spectral data of the phenols (II)

R of II	Infrared spectra		Visible spectra				$\frac{\varepsilon_a}{\varepsilon_a+\varepsilon_h}$
	ν_{OH} band cm^{-1}	ν_{NH} band cm^{-1}	Azo band λ_{max} mμ	ε_a	Hydrazone band λ_{max} mμ	ε_a	
2'-MeO	3643 w	3372 m	365	6.42×10^3	454	2.67×10^4	0.19
3'-MeO	3641 s	—	358	2.40×10^4	442	2.55×10^3	0.90
4'-MeO	3641 s	—	359	2.41×10^4	447	2.51×10^3	0.91
2'-Me	3643 s	—	357	2.24×10^4	450	2.22×10^3	0.91
3'-Me	3644 s	—	353	2.12×10^4	442	2.97×10^3	0.88
4'-Me	3644 s	—	354	2.27×10^4	443	1.48×10^3	0.94
Unsubstituted	3641 s	—	352	2.51×10^4	443	2.40×10^3	0.91
2'-F	3642 s	3381 vw	359	1.98×10^4	433	8.22×10^3	0.71
4'-F	3644 s	—	353	2.45×10^4	440	2.10×10^3	0.92
2'-Cl	3639 m	3365 w	370	1.15×10^4	434	1.71×10^4	0.62
3'-Cl	3639 s	—	358	2.27×10^4	437	2.84×10^3	0.89
4'-Cl	3645 s	—	360	2.93×10^4	438	2.17×10^3	0.93
2'-Br	3644 m	3358 w	368	1.47×10^4	434	1.81×10^4	0.55
4'-Br	3639 s	—	361	2.90×10^4	441	2.28×10^3	0.93
4'-COOEt	3641 s	—	369	2.61×10^4	438	7.83×10^3	0.77
2'-NO_2	—	3314 m	396	1.77×10^4	458	2.70×10^4	0.40
3'-NO_2	3639 s	—	366	1.86×10^4	434	2.22×10^3	0.89
4'-NO_2	3641 s	3363 trace	388	2.33×10^4	440	1.11×10^4	0.68
2',6'-Me_2	3642 s	—	336	2.10×10^4	442	1.59×10^3	0.93
2',6'-F_2	3640 s	—	348	1.97×10^4	426	2.40×10^3	0.89
2',6'-Cl_2	3639 s	3356 w	340	1.31×10^4	408	8.90×10^3	0.60
2',6'-Br_2	3639 s	3340 trace	341	1.75×10^4	422	2.34×10^3	0.88
2',6'-$(NO_2)_2$	3638 trace	3300 w	392	2.21×10^4	437	1.97×10^4	0.53
2',4'-$(NO_2)_2$	—	3308 m	399	3.04×10^4	438	3.51×10^4	0.46
2',4'-6'-$(NO_2)_3$	—	3283 m	—		410	3.97×10^4	0

vw, w, m, s; relative intensities

ε_a, ε_h; molar extinction coefficients of azo and hydrazone bands, respectively.

in which the intramolecular hydrogen bondings are impossible.[6] Besides, the hydrogen bondings in 2',6'-disubstitted derivatives can be disturbed by the twisting of aryl nuclei. The molecular model inspections for the hydrazone tautomers of such geometries that the quinone nuclei and the aryl nuclei are in the same plane show that the distance between α-nitrogen atom and 2'-chlorine atom is *ca.* 2.3 Å, and the distance between α-nitrogen atom and the oxygen atom of 2'-nitro group is *ca.* 1.4 Å. Thus, it is very likely that aryl nuclei are twisted as a result of large steric repulsions.

Visible Spectra. The phenols (II) have two absorption maxima in the region 340—460 mμ and substituents change their locations and the molar extinction coefficients (ε) of the absorption maxima. It is well known that the hydroxyazo dyes (I) have two absorption maxima in the region 320—480 mμ, and the absorptions at shorter wavelengths originate from azo tautomers and the absorptions at longer wavelengths from hydrazone tautomers.[1-10,13,14] It is concluded from a comparison between infrared and visible spectra that the phenols (II) follow this relation. This is also supported by the fact that untautomerising 2,6-di-*t*-butyl-*p*-benzoquinone-*N*-methylphenylhydrazone has its absorption maximum at 437 mμ.

Azo Bands: Figure 1 gives the correlation of the Hammett substitution constants[15] and the wavelengths of the absorption maxima of the azo bands of 3'- and 4'-substituted derivatives. It is observed that the substituents of larger electron-releasing or -attracting powers show larger bathochromic effects, in which an anomalously large shift is caused by 4'-nitro group, and the shift by 3'-substituents are smaller than those by 4'-substituents. The absorptions may be due to π–π^* transitions of the completely conjugated π-electron systems of azo tautomers.[16] 2'-Substituted derivatives show bathochromic shifts to 3'- and 4'-isomers although hypsochromic shifts are expected because of the steric interaction between 2'-substituents and azo group. Thus, the observed bathochromic shifts might be due to the electronic effects of 2'-substituents stronger than 3'- and 4'-substituents. 2', 6'-Disubstituted derivatives, except for dinitro derivative, have their absorption maxima at wavelengths shorter than the corresponding 3'- and 4'-substituted derivatives. The planer conformations of 2',6'-disubstituted derivatives are impossible because of the steric repulsion between azo group and substituents. The molecular model inspection for the co-planer azo tautomer of 2',6'-dichloro derivative show that the distance between α-nitrogen atom and 2'-

13) J. N. Ospenson, *Acta Chem. Scand.*, **4**, 1451 (1950).
14) J. N. Ospenson, *ibid.*, **5**, 491 (1951).
15) D. H. McDaniel and H. C. Brown, *J. Org. Chem.*, **23**, 420 (1958).

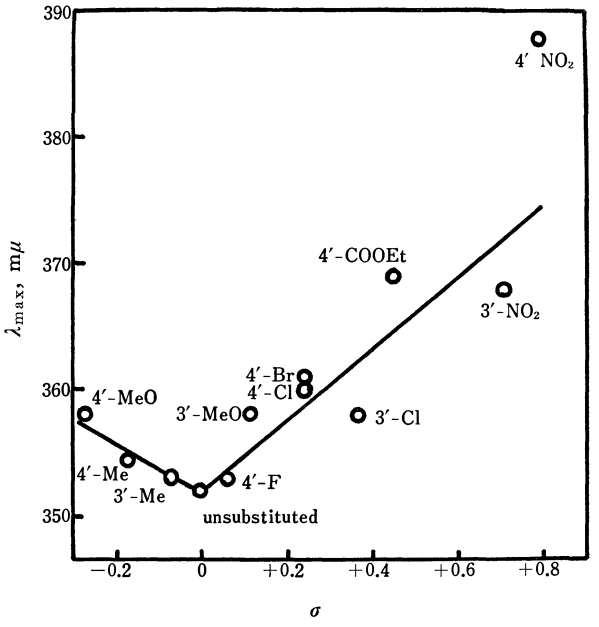

Fig. 1. The correlation of the Hammett substitution constants with the wavelength of the azo bands of 3′- and 4′-substituted phenols (II).

chlorine atom is *ca.* 2.5 Å and that between β-nitrogen atom and 6′-chlorine atom is *ca.* 2.9 Å. Thus, the twist of the aryl nuclei may exist in the actual molecules and give rise to hypsochromic shifts. The bathochromic shift of 2′,6′-dinitro derivative may be due to the overwhelming electronic effects of two nitro groups.

Hydrazone Bands: Figure 2 gives the correlation

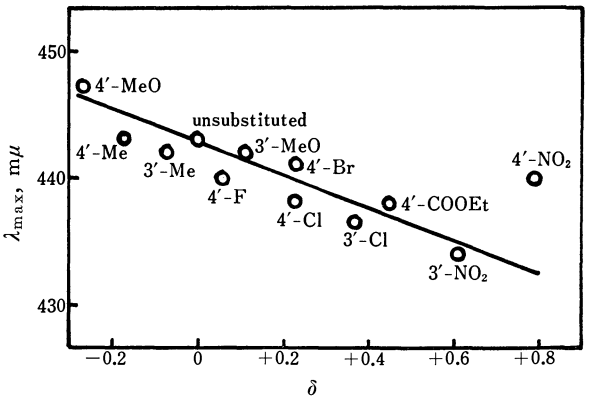

Fig. 2. The correlation of the Hammett substitution constants with the wavelength of the hydrazone bands of 3′- and 4′-substituted phenols(II).

of the Hammett substitution constants and the wavelengths of the absorption maxima of the hydrazone bands of 3′- and 4′-substituted derivatives. The electron-releasing substituents have the trend to shift the absorption maxima towards longer wavelengths and the electron-attracting substituents have the opposite trend. The same trend is observed in 2′-substituted derivatives except for 2′-nitro derivative. The bathochromic shift in 2′-nitro derivative is due to the strong intramolecular hydrogen bonding. 2′,6′-Disubstituted derivatives have the same trend as in 3′- and 4′-derivatives. But the locations of the absorption maxima are displaced to wavelengths shorter than those of the corresponding 2′-substituted derivatives owing to the twist of the aryl nuclei.

Tautomeric Equilibria. The position of the tautomeric equilibrium can be estimated with molar extinction coefficients ε at the absorption peaks in the infrared or visible spectra. The visible spectra, however, show that the disappearance of the ν_{NH} bands in the infrared spectra does not mean the absence of hydrazone tautomers. The small amount of the hydrazone tautomer will erase the weak ν_{NH} band. The position of the equilibria should be discussed by means of the molar extinction coefficients in the visible spectra when the true molar extinction coefficients of the individual tautomers are known and the location of the absorption maxima are separated sufficiently from each other.[3] On account of the above restrictions, the tautomeric equilibria of the phenols (II) can not be discussed quantitatively. The values of the ratio $\varepsilon_{\text{azo band}}/\varepsilon_{\text{azo band}} + \varepsilon_{\text{hydrazone band}}$ are caluculated in Table 1 since the values should indicate the positions of the tautomeric equilibria indirectly. The conclusions from these values and the infrared spectra are as follows. The azo tautomers are predominant in the tautomeric equilibria of 3′- and 4′-substituted derivatives. The electron-releasing substituents favor the hydrazone tautomers in equilibria. Considerable participation of the hydrazone tautomers is found in the equilibria of 2′-substituted derivatives having substituents which can form the intramolecular hydrogen bondings with the hydrazone-hydrogen atoms since the hydrazone tautomers are stabilised by intramolecular hydrogen bonding. In the equilibria of 2′,6′-disubstituted derivatives, the positions of the equilibria move somewhat to the azo side from those of the corresponding 2′-substituted derivatives. The disubstitution at 2′- and 6′-positions may disturb the intramolecular hydrogen bonding and diminish the stabilisation for hydrazone tautomers. In the equilibrium of 2′,4′,6′-trinitro derivative, however, the electronic effect is so large that the hydrazone tautomer is completely predominant.

Experimental

Phenols (II) were prepared through the condensation of 2,6-di-*t*-butyl-*p*-benzoquinone with arylhydrazine hydrochlorides or arylhydrazines (in case of dinitro and trinitro derivatives). Preparation of 4′-methyl derivative gives a typical example as follows: 2,6-di-*t*-butyl-*p*-benzoquinone (1.67 g, 0.0076 mol) was added to the ethanol solution (100 m*l*) of *p*-tolylhydrazine hydrochloride (1.45 g, 0.0091 mol), containing concentrated hydrochloric acid (5 m*l*). After the reaction mixture was kept standing for one week at room temperature, yellow crystals of 4-(4′-tolylazo)-2,6-di-*t*-butylphenol were precipitated by careful addition of water (*ca.* 30 m*l*) to the reaction mixture. The prepared phenols (II) were purified with recrystalisations from ethanol and silica gel column chromatography. The following melting points (°C) were observed for each crystal; 2′-MeO: orange plates, 163.4—164.0. 3′-MeO: yellow needles, 126.6—128.6.

16) J. W. Ledbetter, Jr., *J. Phys. Chem.*, **72**, 4111 (1968).

4′-MeO: yellow plates, 114.0—114.5. 2′-Me: orange powder, 113.5—119.5. 3′-Me: orange powder, 88.5—92.5. 4′-Me: yellowish orange needles, 135. —136.0. Unsubstituted: red needles, 98.0—99.0. 2′-F: yellowish orange needles, 101.6—103.6. 4′-F: yellowish orange needles, 106.0—107.0. 2′-Cl: reddish orange plates, 134.4—135.4. 3′-Cl: orange needles, 102.8—103.8. 4′-Cl: orange needles. 138.0—139.0. 2′-Br: orange plates, 154.0—155.5. 4′-Br: orange needles, 151.8—152.8. 4′-COOEt: yellow needles, 186.4—187.4. 2′-NO_2: red plates, 158.5—159.5. 3′-NO_2: yellowish orange needles, 162.5—163.5. 4′-NO_2: red plates, 191.0—192.5. 2′,6′-Me_2: reddish orange needles, 117.5—118.5. 2′,6′-F_2: orange plates, 123.8—125.8. 2′,6′-Cl_2: yellowish orange plates, 110.8—111.5. 2′,6′-Br_2: orange needles, 123.5—125.0. 2′,6′-$(NO_2)_2$: red needles, 156.0—157.0. 2′,4′-$(NO_2)_2$: yellow needles, 185.5—188.0. 2′,4′,6′-$(NO_2)_3$: violet plates, 202.0—203.0. 2′,6′-Di-*t*-butyl-*p*-benzoquinone-*N*-methylphenylhydrazone (red needles, mp 127.0—127.5°C) was prepared from 2,6-di-*t*-butyl-*p*-benzoquinone and α-methyl-α-phenylhydrazine by the same method. Results of elementary analyses for the prepared compounds were in good agreement with theoritical values. The infrared spectra of the phenols (II) in carbon tetrachloride solution of 4.00×10^{-3} M in 1 mm NaCl cell were recorded with Shimadzu IR-27G Grating Spectrophotometer. The visible spectra of the phenols (II) in carbon tetrachloride solution of 2.00×10^{-3} M in 0.11 mm quartz cell were recorded with Hitachi EPS-2U Recording Spectrophotometer. Be0r's law was valid for the concentration higher than 5.00×10^{-3} M.

BULLETIN OF THE CHEMICAL SOCIETY OF JAPAN, VOL. 44, 1623—1627 (1971)

The Radical Polymerization and Copolymerization of Triallylidene Sorbitol with Styrene or Acrylonitrile

Tatsuro Ouchi, Yoshikazu Yaguchi, and Masayoshi Oiwa

Department of Applied Chemistry, Faculty of Engineering, Kansai University, Senriyama, Suita-shi, Osaka

(Received September 16, 1970)

The polymerization of triallylidene sorbitol (TAS) and the copolymerization of TAS with styrene (St) or acrylonitrile (AN) have been carried out, using benzoyl peroxide as an initiator at 80°C. They were kinetically investigated in relation to the degradative or effective chain transfer by the allylidene group, and by the cyclization by three double bonds. The results can be summarized as follows: 1) the relation among the rate of polymerization, R_p, the initiator concentration, (I), and the monomer concentration, (M), can be expressed by the following equation: $((I)/R_p-a)^{-1}=A(M)+B$, where a, A, and B are constant; 2) the ratio of the rate of unimolecular cyclization to the total rate of bimolecular propagation and the chain transfer of uncyclized radical was estimated to be 0.291; 3) the degree of polymerization depends on the monomer concentration, but not on the initiator concentration; 4) the rates of copolymerization decrease markedly with an increase in the TAS or tricrotylidene sorbitol (TCS) mole fraction in monomer mixtures; and 5) the following monomer reactivity ratios were ascertained: St(M_1)-TAS(M_2) $r_1=4.60$, $r_2=0.13$, AN(M_1)-TAS(M_2) $r_1=0.70$, $r_2=0.26$, St(M_1)-TCS(M_2) $r_1=2.31$, $r_2=0.39$, AN(M_1)-TCS(M_2) $r_1=0.30$, $r_2=0.36$. The Q and e values for the functional group were calculated from the above values as 0.05 and −0.08 (TAS), and 0.10 and −0.25 (TCS) respectively.

In a previous paper,[1] the polymerization of diallylidene pentaerythritol (DAPE) was kinetically investigated in relation to the degradative or effective chain transfer by the allylidene group, and by the cyclization by two double bonds in DAPE. The monomer reactivities have also been reported in the copolymerizations of DAPE or dicrotyridene pentaerythritol (DCPE) with various monomers.[2,3]

The present paper will deal with the polymerization of triallylidene sorbitol (TAS), and the difference between triallylidene and diallylidene cyclic acetal compounds will be kinetically discussed.

The copolymeizations of TAS and triallylidene pentaerythritol (TCS) with styrene (St) or acrylonitrile (AN) were carried out; they will be discussed by using the Gibbs equation.[4]

Experimental

Monomers. The TAS was prepared from D-sorbitol and acrolein by the procedure of Fisher and Smith;[5] bp 194—196°C/8 mmHg (lit,[5] bp 149—151°C/0.9 mmHg).

Found: C, 60.82; H, 6.88%; bromine value, 159; molecular weight, 296. Calcd for $C_{15}H_{20}O_6$: C, 60.80; H, 6.80%; bromine value, 161; molecular weight, 296.

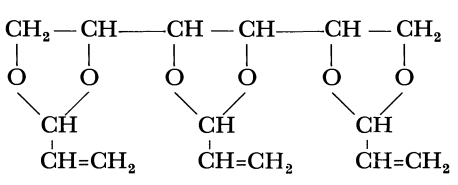

TAS

The TCS was synthesized with D-sorbitol and crotonaldehyde,[6] and was purified by extraction with light oil.

Found: C, 63.49; H, 7.78%; bromine value, 140; molecular weight, 340. Calcd for $C_{18}H_{26}O_6$: C, 63.89,

1) T. Ouchi and M. Oiwa, *Kogyo Kagaku Zasshi*, **72**, 746 (1969).
2) T. Ouchi, S. Yamamoto, Y. Akao, Y. Nagaoka, and M. Oiwa, *ibid.*, **71**, 1078 (1968).
3) T. Ouchi, S. Tatsuno, T. Nakayama, and M. Oiwa, *ibid.*, **73**, 607 (1970).
4) W. E. Gibbs, *J. Polym. Sci.*, **A-2**, 4809 (1964).
5) R. F. Fisher and C. W. Smith, *J. Org. Chem.*, **25**, 319 (1960).
6) T. G. Bonner, E. J. Bourne, and D. Lewis, *J. Chem. Soc.*, **1963**, 3375.

H, 7.75%; bromine value, 140; molecular weight, 338.

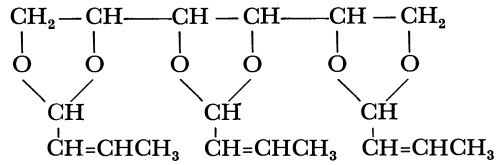

TCS

The St, AN, benzoyl peroxide (BPO), benzene, and dimethylformamide (DMF) were purified by the usual methods.

Polymerization Procedure. The polymerization was carried out using BPO as a radical initiator. Measured amounts of each monomer, initiator, and solvent were placed in an ampoule, which was then degassed twice in the usual manner and flushed with nitrogen. The ampoule was sealed under a vacuum and then set into a thermostat. After a definite reaction time, the ampoule was removed from the thermostat; the polymer was then separated by pouring the contents into a large amount of petroleum ether, followed by centrifuging.

The polymer thus obtained was then washed repeatedly with petroleum ether and dried *in vacuo* to a constant weight. The conversion of the polymer was less than 10%.

Analyses of the Polymer. The composition of the copolymer was determined by elementary analysis. The residual unsaturation of the polymer was calculated from the composition and the bromine value (BV) obtained by the bromite-bromate method.[7] The molecular weight of the polymer was measured with a vapor-pressure osmometer (Hewlett Packard Model-302), using benzene as the solvent at 37°C.

Kinetics of Homopolymerization

The initial polymerization of triallylidene cyclic acetal compounds is treated in a manner similar to that described in previous papers,[1,8] including the chain transfer and the cyclization. The kinetic equations are derived by assuming the following elementary reactions:

Decomposition of initiator	$I \rightarrow 2R\cdot$	$2k_d(I)$
Initiation	$R\cdot + M \rightarrow M\cdot$	$3k_i(R\cdot)(M)$
Cyclization	$M\cdot \rightarrow M_c\cdot$	$k_c(M\cdot)$
Propagation	$M\cdot + M \rightarrow M\cdot$	$3k_p(M\cdot)(M)$
	$M_c\cdot + M \rightarrow M\cdot$	$3k_{cp}(M_c\cdot)(M)$
Effective chain transfer	$R\cdot + M \rightarrow R' + M\cdot$	$3k_i'(R\cdot)(M)$
	$M\cdot + M \rightarrow P + M\cdot$	$3k_{tr}(M\cdot)(M)$
	$M_c\cdot + M \rightarrow P + M\cdot$	$3k_{ct}(M_c\cdot)(M)$
Degradative chain transfer	$R\cdot + M \rightarrow R' + M^*$	$3k_i^*(R\cdot)(M)$
	$M\cdot + M \rightarrow P + M^*$	$3k_{tr}^*(M\cdot)(M)$
	$M_c\cdot + M \rightarrow P + M^*$	$3k_{ct}^*(M_c\cdot)(M)$

where I denotes an initiator; R·, an initiator radical; M, a monomer; M· the uncyclized radical; $M_c\cdot$, the cyclized radical; R′, the inactive product; M*, the stable radical, and P, a polymer.

7) I. P. Losev and O. Y. Fedotoba, "Praktikum po Khimii Vysokopolimernykh Soedinenii," Gosudarstvennoe Nauchno-Tekhnicheskoe Izdatelstvo Khimicheskoi Literatury, Moskova.

8) T. Ouchi, S. Tatsuno, T. Nakayama, and M. Oiwa, This Bulletin, **43**, 2241 (1970).

The following equations can be obtained by assuming steady-state conditions.

The rate of polymerization, R_p, is given by:

$$R_p = \left(\frac{3(M) + c}{3a(M) + bc}\right)(I) \tag{1}$$

which, on rearrangement, gives:

$$(3(M) + c)(I)/R_p = 3a(M) + bc \tag{2}$$

$$\frac{1}{(I)/R_p - a} = \left(\frac{3}{b - a}\right)\left(\frac{(M)}{c} + \frac{1}{3}\right) \tag{3}$$

The residual unsaturation of the polymer, $3R_{us}$, is shown by:

$$\frac{1}{3R_{us}} - 1 = \frac{c}{3(M)} \tag{4}$$

The relation among the degree of polymerization, $\bar{P}_n$, and the monomer and initiator concentrations is represented by:

$$\frac{R_p(3a(M) + bc}{\bar{P}_n(I)} = 6a\gamma_t(k_t' + k_d/\gamma_t + k_{tr}/k_{tr})^*(M) + 3ab\gamma_t(k_i' + k_d/\gamma_t + k_{ct}/k_{ct}^*) \tag{5}$$

where: $\gamma_t = k_d(k_t + k_t')/(k_t + k_t' + k_t^*)$

$a_{tr}^* = k_{tr}^*/(k_p + k_{tr} + k_{tr}^*)$

$b_{ct}^* = k_{ct}^*/(k_{cp} + k_{ct} + k_{ct}^*)$

$a = a_{tr}^*/2\gamma_t,\ b = b_{ct}^*/2\gamma_t$

$c = k_c/(k_p + k_{tr} + k_{tr}^*)$

Results and Discussion

Polymerization of TAS. The polymerization of TAS was investigated under different initiator and monomer concentrations at 80°C. The results are given in Table 1, in which the values of the residual unsaturation and the molecular weight are estimated by extrapolating to zero for conversion.

The Residual Unsaturation. As can be seen from Table 1, the residual unsaturation is independent of the initiator concentration, but decreases with a decrease in the monomer concentration.

The plots of $(1/3R_{us}—1)$ against $1/(M)$ are shown in Fig. 1. A straight line through the point of origin was obtained, as predicted by Eq. (4). By using this slope, c was obtained as 0.873 mol/*l*.

The Rate of Polymerization. When the monomer concentration is kept constant and the initiator concentration is varied, it may be expected from Eq. (1) that R_p will give a straight line with (I). The result is shown in Fig. 2, in which the experimental data are very close to the calculated linear relationship.

By using the c value thus obtained, the a and b values were calculated by applying the method of least-squares to Eq. (2); a and b were 4.73×10^3 sec and 9.73×10^4 sec respectively (Fig. 3).

By using the a value thus obtained the plots of $((I)/R_p—a)^{-1}$ against (M) according Eq. (3) shown in Fig. 4 were obtained; they show a good linear relationship. Therefore, the a value seems to be proper.

The Degree of Polymerization. As can be seen in Table 1, the degree of polymerization, $\bar{P}_n$, is very small;

Table 1. Polymerization of TAS at 80°C

(BPO) ($\times 10^{-1}$ mol/l)	(TAS) (mol/l)	R_p ($\times 10^{-6}$ mol/l·sec)	BV	$3R_{us}$	Molecular weight
3.30	1.35	19.5	88.0	0.816	859
2.48	1.35	15.0	88.9	0.824	804
1.65	1.35	7.80	88.5	0.820	850
0.826	1.35	5.63	87.9	0.815	827
1.65	0.676	5.04	75.2	0.697	837
1.65	0.542	4.49	70.5	0.653	813
1.65	0.452	4.03	67.0	0.621	808

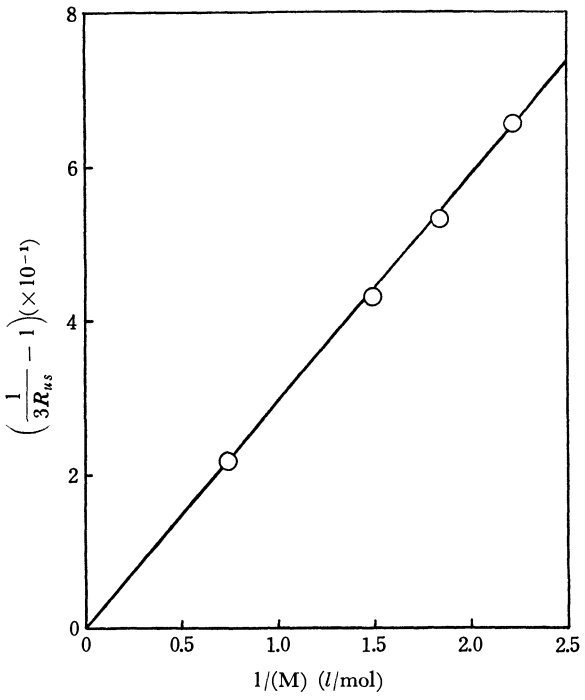

Fig. 1. Plots of $(1/3R_{us}-1)$ *vs.* 1/(M).

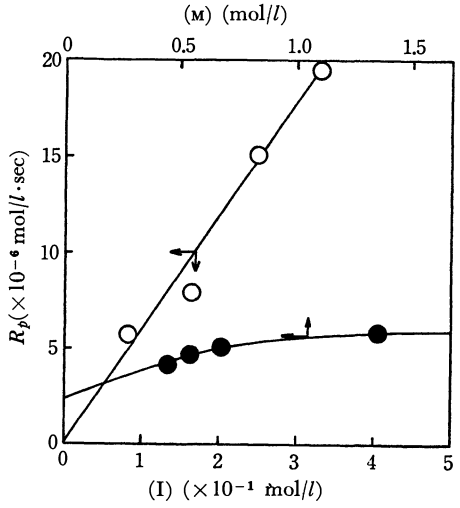

Fig. 2. Plots of rate of polymerization against the initiator and monomer concentrations.

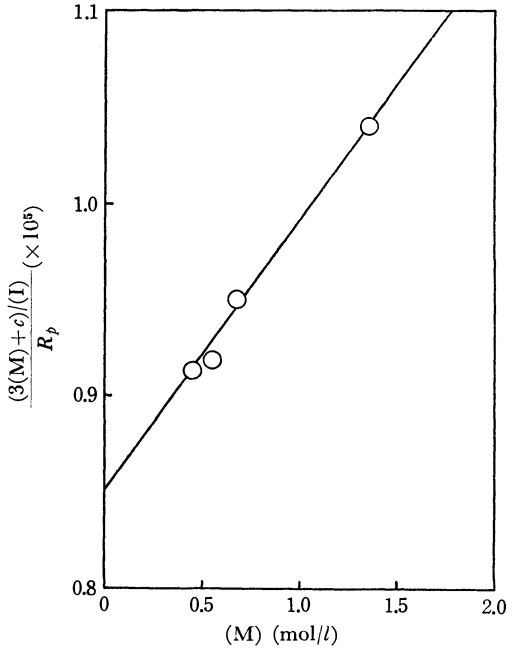

Fig. 3. Plots of $\frac{(3(M)+c)/(I)}{R_p}$ *vs.* (M).

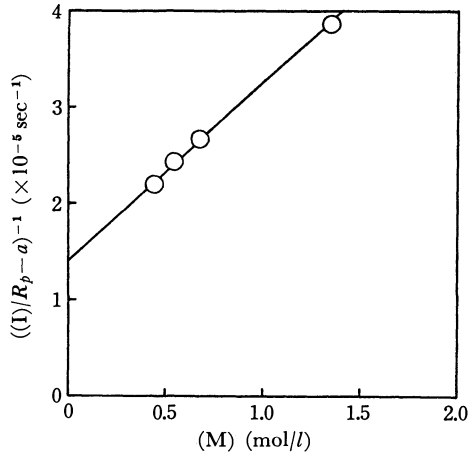

Fig. 4. Plots of $((I)R_p-a)^{-1}$ *vs.* (M).

it is independent of the initiator concentration, but increases with an increase in the monomer concentration. A similar tendency has been found on the polymerization of DAPE.[1] The plots of $R_p/\overline{P}_n$ against (I) and $(3a(M)+bc)R_p/\overline{P}_n(I)$ against (M) are shown in Fig. 5; they have a good linear relationship and satisfy Eq. (5). Accordingly, these results suggest that the a, b, and c values obtained here are justifiable on the polymerization of TAS.

Generally, k_d is of the order of about 10^{-5}—10^{-6} in

Table 2. Polymerization of parameters

Monomer	a ($\times 10^3$ sec)	b ($\times 10^4$ sec)	$\frac{k_c}{3(k_p+k_{tr}+k_{tr}^*)}$ (M)	$\frac{k_c}{2(k_p+k_{tr}+k_{tr}^*)}$ (M)
TAS	4.73	9.73	0.291	—
DAPE	2.00	2.00	—	0.276

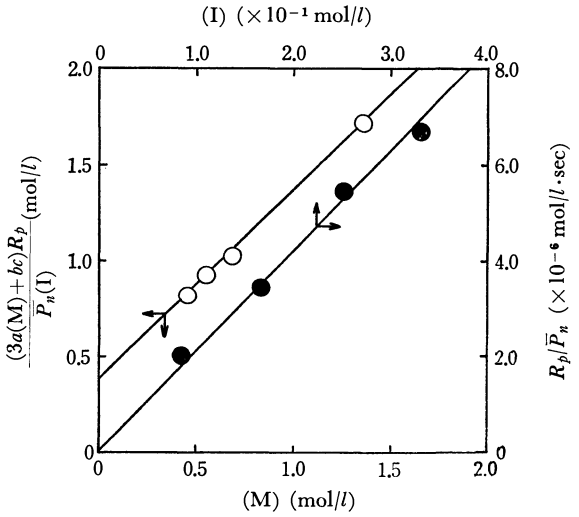

Fig. 5. Plots of $(3a(M)+bc)R_p/\bar{P}_n(I)$ *vs.* (M) and $R_p/\bar{P}_n$ *vs.* (I).

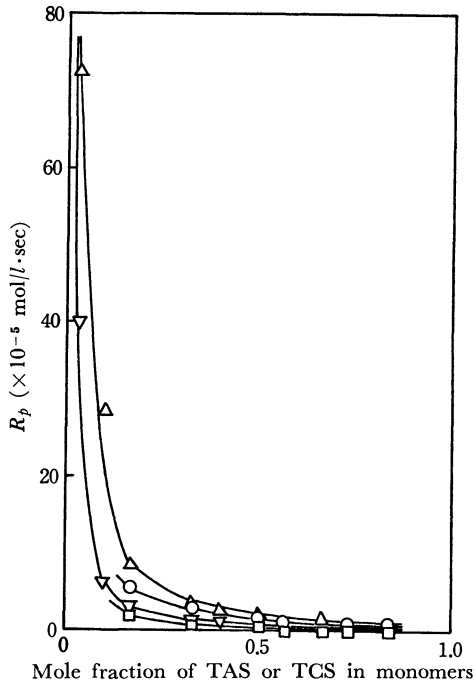

Fig. 6. Plots of the rate of copolymerization against the monomer composition at 60°C.
○: St-TAS, △: AN-TAS, □: St-TCS, ▽: AN-TCS

the case of a radical polymerization, as is well known.[9] Consequently, a_{tr}^* and b_{tr}^* were estimated to be of the order of about 10^{-2}—10^{-3} and 10^{-1}—10^{-2}; the degradative chain transfer may preferentially occur rather than the propagation.

Comparison of Parameters. The polymerization parameters for TAS and DAPE are summarized in Table 2.

It was found that the a and b of TAS were larger than those of DAPE. Consequently, the degradative chain transfer is found to occur more readily on TAS than on DAPE. This may result from the difference in the probablity of collision between diallylidene and triallylidene compounds.

On the other hand, the ratios of the rate of cyclization to the total rates of propagation and chain transfer for TAS polymerization were larger than those for DAPE; triallylidene compounds were cyclized more easily than diallylidene compounds. The difference in steric hindrance between tri- and diallylidene cyclic acetals may cause such tendency.

For investigating the effect of the temperature on polymerization, the polymerization was carried out at 60, 70, and 80°C. The overall activation energy, as calculated from the Arrhenius plot, was 17.3 kcal/mol, which was nearly equal to that of the usual radical polymerization.

Copolymerization. The dependence of the monomer composition on the rate of copolymerization at 80°C is shown in Fig. 6. The rates of copolymerization decrease markedly with an increase in the mole fraction of TAS in the monomer mixtures. This tendency may be ascribed to the degradative chain transfer by the allylidene group and to the steric hindrance by the cyclic acetal.

Monomer Reactivity Ratios. Figure 7 shows the polymer composition as a function of the monomer composition. Figure 8 shows the residual unsaturation as a function of the copolymer composition. These results mean that the residual unsaturations of the copolymers obtained decreased slightly with an increase in the TAS or TCS, and were nearly equal to 1.0. Accordingly, the cyclization may be approximately negligible on these systems of copolymerization.

The functional group reactivity ratios, r_1' and r_2', determined according to a modification of the Gibbs copolymerization equation,[4] are summarized in Table 3.

In Fig. 7 the theoretical solid curves calculated from the resulting reactivity ratios are shown to agree very closely with the experimental measurements.

The Q' and e' values for TAS and TCS, as calculated from the r_1' and r_2' values, are shown in Table 3.

The average values of Q' and e' for TAS, TCS, DAPE, and DCPE were estimated to be as follows: TAS $Q'=0.05$, $e'=-0.08$; TCS $Q'=0.10$, $e'=-0.25$; DAPE $Q'=0.03$,[2] $e'=0.0$;[2] DCPE $Q'=0.01$,[3] $e'=-0.32$.[3]

9) J. Brandrup and H. E. Immergut, "Polymer Handbook," John Wiley & Sons, New York (1965).

10) G. E. Ham, "Copolymerization," Intersci. Pub., New York (1964), p. 845.

TABLE 3. REACTIVITY RATIOS FOR TAS OR TCS(M_2)-MONOVINYL COMPOUNDS (M_1) SYSTEMS

M_1	M_2	Monomer		Functional group		Q_1[10]	e_1[10]	Q_2'	e_2'
		r_1	r_2	r_1'*	r_2'*				
St	TAS	4.60	0.13	13.8	0.04_3	1.00	−0.80	0.04	−0.06
AN	TAS	0.70	0.26	2.10	0.08_7	0.60	1.20	0.06	−0.10
St	TCS	2.31	0.39	6.93	0.13	1.00	−0.80	0.09	−0.21
AN	TCS	0.30	0.36	0.90	0.12	0.60	1.20	0.11	−0.29

* $r_1'=3r_1$, $r_2'=r_2/3$.

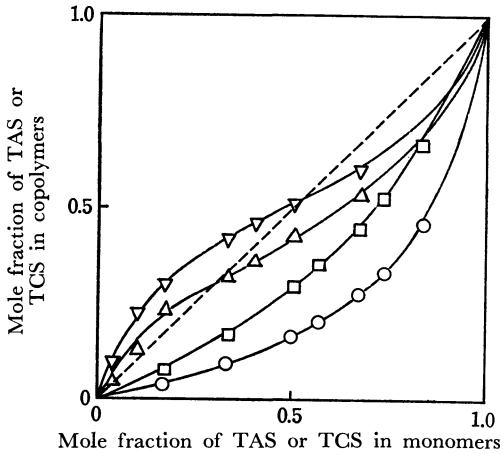

Fig. 7. Monomer-polymer composition curves.
○: St-TAS, △: AN-TAS, □: St-TCS, ▽: AN-TCS,
——: logical curve

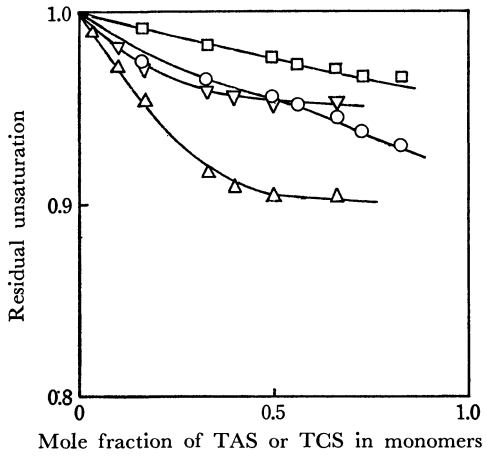

Fig. 8. Plots of residual unsaturation against the monomer composition.
○: St-TAS, △: AN-TAS, □: St-TCS, ▽: AN-TCS

No difference in Q' and e' values between tri- and diallylidene cyclic compounds could be recognized. This suggests that the TAS are unconjugate and neutral monomers just the same as the DAPE.

The Q' values for TCS were slightly larger than those for TAS; they might be influence by the hyperconjugation of the methyl group. On the other hand, the e' values of TCS were more negative than those of TAS; they must be contributed to the methyl group, which is a proton donor.

Elimination Reactions Promoted by Fluoride Ion in Acetonitrile. Elimination Reaction from 2-Arylethyl Derivatives[1]

Jun-ichi HAYAMI,[2] Noboru ONO, and Aritsune KAJI
Department of Chemistry, Faculty of Science, Kyoto University, Kyoto
(Received September 21, 1970)

Rates of bimolecular elimination have been determined for the reaction of 2-arylethyl bromides, chlorides, and tosylates with anhydrous tetraethylammonium fluoride in acetonitrile. The rates of elimination reactions in this new base system were much faster than those in conventional base systems (alkoxide-alcohol). The Hammett ρ values were found to be $\rho=2.033$ (X=Cl) at 25.0°C and $\rho=1.879$ (X=Br) at 5.0°C for *p*-Y-$C_6H_4CH_2$-CH_2X. Kinetic deuterium isotope effects were determined using 2-phenylethyl-2,2-d_2 bromide and chloride to be $k_H/k_D=3.99$ (X=Cl) and 5.03 (X=Br). These data and the low k_{OTs}/k_{Br} ratio suggest that fluoride-ion-promoted elimination reaction proceeds through a very tight transition state where β-proton is less than half transferred to the base.

Recent works on the transition state of the bimolecular elimination invoked interesting problems. Bunnett proposed the theory of the variable E2 transition state—a continuous spectrum between pane-carbonium extreme through central to pane-carbanion extreme of the transition state.[3] Parker and co-workers proposed the theory of a variable transition state in the spectrum between E2C—E2H extreme with the concept of variable "looseness" or "tightness".[4] Hoffmann's view[5] may be in close agreement with the latter interpretation.

Some examples of the halide ion promoted bimolecular elimination reactions were explored to establish a criterion of the theory. Halide ion, especially the halide ion in a dipolar aprotic solvent, is a weak hydrogen but a strong carbon nucleophile. A study of the bimolecular elimination in a dipolar aprotic solvent promoted by a strong hydrogen nucleophile might be of use in order to establish a better understanding of the reaction.

In previous papers[6] the authors reported that tetraethylammonium fluoride behaves as a strong base and that styrene was produced in an excellent yield in the reaction of 2-phenylethyl bromide. Under similar conditions tetraethylammonium chloride and bromide underwent solely the substitution reaction.

Substitution reactions and elimination reactions by chloride, bromide, and iodide ion are well-known and the mechanism of these reactions have been studied extensively.[4] However, there are few reports on fluoride ion promoted bimolecular reactions, and no quantitative kinetic data are available.[7] This may be due to the difficulty in finding the electrolyte soluble in pure dipolar aprotic solvents to secure fluoride anion in a homogeneous reaction system. This difficulty has been overcome by use of tetraethylammonium fluoride in a dipolar aprotic solvent.

In the present communication the authors report the characteristics of the elimination reaction from 2-phenylethyl derivatives promoted by the new base system and suggest a structure for the transition state.

Results and Discussion

Kinetic measurements of the elimination reactions of the series of the para-substituted 2-phenylethyl bromide and chloride were undertaken using the base system of tetraethylammonium fluoride in acetonitrile. Similar experiments with several of the para-substituted 2-phenylethyl tosylates were undertaken. The general formula is as follows.

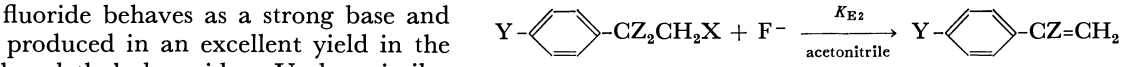

$$Y\text{-}C_6H_4\text{-}CZ_2CH_2X + F^- \xrightarrow[\text{acetonitrile}]{k_{E2}} Y\text{-}C_6H_4\text{-}CZ{=}CH_2 \quad (1)$$

Y = CH_3O, CH_3, H, Cl
Z = H, D
X = Cl, Br, OTs

Reaction rates were determined by following the appearance of styrene or substituted styrenes spectrophotometrically. With a large excess of the base, first order (pseudo-first-order) kinetics held for every run. A typical example is given in Table 5. Second order rate constants were calculated by dividing the pseudo-first-order rate coefficients by the pertinent tetraethylammonium fluoride concentrations. The concentration of the fluoride ion was determined by titration with thorium nitrate.[8] The results are given in Table 1. The olefin-forming elimination was accompanied by the bimolecular substitution to some extent,[6] and olefin was obtained in the yield of 75% for the elimination from tosylates. In other cases olefin was obtained almost quantitatively as is shown in Table 1 (see Experimental).

A four-fold variation in base concentration caused no

1) Presented at the 22nd Annual Meeting of the Chemical Society of Japan, Tokyo, April 1969.

2) To whom correspondence should be addressed.

3) a) J. F. Bunnett, *Angew. Chem.*, **74**, 731 (1962). b) J. F. Bunnett, *Surv. Prog. Chem.*, Vol. 5, Academic Press, New York, N. Y. (1969), p. 53. c) D. J. McLennan, *Quart. Revs.*, **21**, 490 (1967). d) Z. Rappoport, *Tetrahedron Lett.*, **1968**, 3601.

4) a) A. J. Parker, M. Raune, G. Biale, and S. Winstein, *ibid.*, **1968**, 2113. b) D. J. Lloyd and A. J. Parker, *ibid.*, **1968**, 5183. c) R. Alexander, E. F. C. Ko, A. J. Parker, and T. J. Broxton, *J. Amer. Chem. Soc.*, **90**, 5049 (1968). d) E. F. C. Ko and A. J. Parker, *ibid.*, **90**, 6447 (1968). e) G. Biale, A. J. Parker, I. D. R. Stevens, and S. Winstein, *ibid.*, **92**, 115 (1970).

5) G. M. Fraser and H. M. R. Hoffmann, *J. Chem. Soc., B*, **1967**, 265.

6) a) J. Hayami, N. Ono, and A. Kaji, *Tetrahedron Lett.*, **1968**, 1385. b) J. Hayami, N. Ono, and A. Kaji, *Nippon Kagaku Zasshi*, **92**, 87 (1971).

7) a) L. Rand and M. J. Albinak, *J. Org. Chem.*, **25**, 1837, (1960). b) J. T. Maynard, *ibid.*, **28**, 112 (1963). c) J. F. Normant and H. Deshayes, *Bull. Soc. Chim. Fr.*, **1967**, 2455.

8) W. Selig, *Analyst*, **93**, 118 (1968).

Table 1. Rate constants for eliminations from p-Y-$C_6H_4CZ_2CH_2X$ with Et_4NF in CH_3CN

Y	Z	X	Temp.[a] (°C)	$[F^-]\times10^2$ (mol/l)	$k_{E2}\times10^3$ [b] (l/mol sec)	Olefin yield[c] (%)
Cl	H	Cl	35	2.12	29.7	100
Cl	H	Cl	25	1.26	11.0	100
Cl	H	Cl	15	2.56	3.48	100
H	H	Cl	35	2.12	10.7	100
H	H	Cl	25	2.16	3.89	100
H	H	Cl	15	2.02	1.26	100
CH_3	H	Cl	35	2.12	5.57	100
CH_3	H	Cl	25	2.50	1.75	100
CH_3	H	Cl	25	5.00	1.78	100
CH_3	H	Cl	25	10.00	1.80	100
CH_3O	H	Cl	35	2.12	3.55	100
CH_3O	H	Cl	25	2.16	1.06	100
H	H	Br	5	2.05	29.9	100
CH_3	H	Br	15	2.38	38.7	100
CH_3	H	Br	5	2.05	15.4	100
CH_3O	H	Br	15	2.56	26.3	100
CH_3O	H	Br	5	2.05	9.30	100
CH_3	H	OTs	15	2.09	1.04	75
CH_3O	H	OTs	15	2.09	0.710	75
H	D	Cl	35	1.84	2.68	100
H	D	Cl	25	1.84	0.888	100
H	D	Br	5	2.09	5.94	100

a) Bath temperature was controlled to ±0.1°C or better.
b) Pseudo-first-order rate constants were determined spectrophotometrically and converted to second-order rate constants. Usual conditions were [substrate]=*ca.* 1.0×10^{-3} mol/l, [base]=*ca.* 2×10^{-2} mol/l.
c) The olefin yields were determined spectrophotometrically from the values of A_∞ for rate determinations. The values contain errors of 1—2%.

significant change in the second order rate constants. Thus the elimination reactions promoted by fluoride ion should follow the second-order rate law, first order in the substrate and also first order in the fluoride. The rate data were fitted to log k_{E2} *vs.* $1/T$ plots and enthalpies and entropies of activation were calculated. These values are shown in Table 2.

Table 2. Activation parameters for eliminations from p-Y-$C_6H_4CH_2CH_2Cl$ with Et_4NF in CH_3CN

Y	$\Delta H^{\neq}$ [a] (kcal/mol)	$\Delta S^{\neq}$ [a] (e. u.)
Cl	17.7	−7.4
H	19.0	−7.1
CH_3	21.3	−2.2
CH_3O	22.4	−0.2

a) $\Delta H^{\neq}$, $\Delta S^{\neq}$: at 25°C

The Hammett ρ-values were derived by the least-squares procedure of Jaffé[9] from the rate constants of the 2-phenylethyl derivatives with para substituents, methoxy, methyl, hydrogen and chlorine. These calculations together with results of elimination reactions in ethanol and t-butyl alcohol are summarized in Table 3. The kinetic deuterium isotope effects with 2-phenylethyl-2,2-d_2 bromide and chloride were determined, the results are also given.

9) H. H. Jaffé, *Chem. Revs.*, **53**, 191 (1953).

Kinetic data show that tetraethylammonium fluoride in acetonitrile is about 800 times as effective as sodium ethoxide in ethanol in promoting the E2 reaction from 2-phenylethyl chloride, k_{E2} being 3.89×10^{-3} and 4.5×10^{-6} l/mol sec at 25°C.[10] The activation parameters in Table 2 fall in a reasonable range for typical E2 reactions.

Second order kinetics and the activation parameters show that the E1 mechanism can be excluded for the present cases. Of the two mechanisms E2 and E1cB, compatible with the kinetics, E1cB should be excluded since the ρ-values and the k_H/k_D ratios, both obtained in the present communication, are against criteria for E1cB.

Recently, McLennan[3c] and also Rappoport[3d] reviewed the criteia for E1cB. They suggested that E1cB should show a very high positive value of ρ (which should be greater than 3.7 obtained in the E2 reaction of 2-arylethyl-trimethylammonium salt) and the k_H/k_D ratio of unity. In certain cases of "Type II" E1cB, E1cB with negative ρ-values are suggested.

In the present cases, the ρ-values are positive but the values in the neighborhood of 2 seem to be too small and the k_H/k_D ratios of more than 3 are too high for the

10) The value for sodium ethoxide was calculated by extrapolation from other temperatures, using the experimental data of DePuy *et al.*[11] They have reported that k_{E2} is 24.1×10^{-5} at 60°C and 185×10^{-5} at 80°C.

11) C. H. DePuy and C. A. Bishop, *J. Amer. Chem. Soc.*, **82**, 2535, (1960).

TABLE 3. HAMMETT CORRELATIONS AND DEUTERIUM ISOTOPE EFFECTS FOR ELIMINATIONS FROM p-Y-$C_6H_4CZ_2CH_2X$

X	Temp. °C	Base	Solvent	ρ[a]	r[b]	k_H/k_D
Cl	35	F^-	CH_3CN	1.851	0.999	3.99
Cl	25	F^-	CH_3CN	2.033	0.998	4.38
Br	5	F^-	CH_3CN	1.879[c]	0.986	5.03
Cl	30	EtO^-	EtOH	2.61[d]		
Br	30	EtO^-	EtOH	2.154[e]	0.987	7.11[f]
Br	30	t-BuO^-	t-BuOH	2.08[g]	0.999	7.89[f]
Br	30	t-BuO^-	t-BuOH	2.529[h]	0.999	8.16[h]
Cl	60	$^{36}Cl^-$	CH_3CN	0.57[i]	0.991	

a) Calculated by the method of least squares. b) Correlation coefficient.
c) Based on p-MeO, p-Me and H only (p-Cl; rate was too high to be measured).
d) Ref. 11 e) Ref. 12 f) Ref. 13 g) Ref. 14 h) Ref. 15 i) ρ-value for substitution reaction. (Ref. 18)

E1cB mechanism to be operative (Table 3).

Interesting features of the fluoride promoted elimination from substituted 2-phenylethyl derivatives can be characterized by the small ρ values, low k_H/k_D ratios and very diminished ratios of k_{OTs}/k_{Br} although they are not at all out of the range of the expected magnitude for the E2 reaction.

As is shown in Table 3, the k_H/k_D ratio of 5 for 2-phenylethyl bromide at 5°C is smaller than the k_H/k_D ratios for the same compound with a conventional base, which gives the k_H/k_D ratios sometimes exceeding 7. The k_H/k_D ratios for the E2 reaction generally decrease with the increase in reaction temperature. An example can be found in reports by Saunders[13,15] as well as in Table 3. This implies that the k_H/k_D ratio for the 2-phenylethyl bromide might decrease to a certain amount and more diminished ratios would be anticipated at higher temperatures. Smaller k_H/k_D ratios were also obtained for 2-phenylethyl chloride.

The positive ρ value with k_H/k_D less than the theoretical maxima (*ca.* 7)[16] may suggest the pane-carbanion transition state in which the proton is more than half transferred.

The other characteristics of the fluoride promoted E2 reaction, however, are strongly against the pane-carbanion interpretation. According to Hoffmann,[5] the small value of the leaving group selectivity coefficient, the rate ratio k_{OTs}/k_{Br}, is a good criterion for the little C-X (C_α-leaving group) bond-breaking together with the little C–H (C_β-hydrogen) bond-breaking in the bimolecular reaction. The k_{OTs}/k_{Br} ratio of 0.027 obtained is one of the smallest values (Table 4).[17] Rho (ρ) value of 1.8 or less (anticipated at higher temperatures) for the 2-arylethyl bromide seems too low for a pane-carbanion transition state but may be compatible with the "central" synchronous process.

TABLE 4. RATIOS k_{OTs}/k_{Br} FOR ELIMINATIONS FROM p-Y-$C_6H_4CH_2CH_2X$

Y	Base	Solvent	k_{OTs}/k_{Br}
CH_3	F^-	CH_3CN	0.027
CH_3O	F^-	CH_3CN	0.027
CH_3O	EtO^-	EtOH	0.1[a]
CH_3O	t-BuO^-	t-BuOH	0.15[a]
H	EtO^-	EtOH	0.1[a]
NO_2	t-BuO^-	t-BuOH	1.57[a]

a) Ref. 5.

Taking into account the very low k_{OTs}/k_{Br} ratio and the diminished Hammett ρ value, the present authors suggest that in the fluoride promoted E2 reaction, β-proton is less than half transferred in the transition state. In other words, a very tight and reactant-like transition state should be ascribed to this E2 reaction where both the C–H and C–X bond-breaking are not far advanced.

It might be interesting to discuss a plausible mechanism in the light of E2C—E2H spectrum. As Parker[4] has pointed out, the tight transition state such as proposed in the present study is against the E2C mechanism. Another kinetic result in authors' laboratory[18] is also against the E2C mechanism. The E2C transition state should be much like an SN2 transition state, and the ρ value for the E2C reaction of 2-arylethyl chloride may be expected to be similar or slightly higher than the ρ value for the SN2 reaction of the same compounds. The ρ value (*ca.* 2) obtained in the present study is substantially higher than the ρ value found in the SN2 reaction of 2-arylethyl chloride with radioactive chloride ion in acetonitrile ($\rho=0.57$)[18] and is in a reasonable range for normal E2H reactions. This conclusion is consistent with the "principle of hard and soft acids and bases" which predicts that hard fluoride ion is liable to attack a hard proton while the soft halide ion (Cl^-, Br^-, or I^-) can attack relatively soft carbon.[19]

12) W. H. Saunders, Jr., and R. A. Williams, *J. Amer. Chem. Soc.*, **79**, 3712, (1957).
13) W. H. Saunders, Jr., and D. H. Edison, *ibid.*, **82**, 138 (1960).
14) C. H. DePuy and C. A. Bishop, *ibid.*, **82**, 2532 (1960).
15) A. F. Cockerill, S. Rottschaefer, and W. H. Saunders, Jr., *ibid.*, **89**, 901 (1967).
16) F. H. Westheimer, *Chem. Revs.*, **61**, 265 (1961).

17) The smaller k_{OTs}/k_{Br} for the reaction in acetonitrile compared to the one in the protic solvent may be rationalized in terms of the lack of the solvation stabilization of the leaving group (anion) in a dipolar aprotic solvent. In a protic solvent, assistance by the solvation may give rise to a relatively looser transition state that reflects upon slightly enhanced k_{OTs}/k_{Br} ratios.

18) J. Hayami, N. Tanaka, S. Kurabayashi, Y. Kotani, and A. Kaji, Abstracts of Papers, III-1323, 23rd Annual Meeting of Chemical Society of Japan, Tokyo, April 1970.
19) R. G. Pearson and J. Songstad, *J. Amer. Chem. Soc.*, **89**, 1827 (1967).

The idea of the tight transition state is not incompatible with the Swain-Thornton rule,[20] which postulates a more reactant-like transition state for a more reactive base. The tight transition state in the fluoride promoted elimination can be rationalized in terms of the very small steric requirement of the fluoride ion in a dipolar aprotic solvent and the high proton affinity of the fluoride which is the reflection of the intrinsically high electronegativity of fluorine.

The results clearly show that the fluoride promoted elimination from 2-arylethyl derivatives is a typical E2 reaction, and the characteristics of the reaction suggest features of the tight transition state. Utility of the fluoride ion in a dipolar aprotic solvent is promising. Features of the elimination reaction including the orientation rule in the olefin-formation from secondary alkyl derivatives were given in a previous paper.[21]

Experimental[22]

Materials. 2-Arylethyl *p*-toluenesulfonates were prepared in the usual way from the corresponding 2-arylethanols and were recrystallized from ethanol.

2-Phenylethyl tosylate, mp 38.5—39.0°C (lit,[23] 38.5—39.0°C); 2-*p*-chlorophenylethyl tosylate, mp 79.0—79.3°C (lit,[24] 79.5—80.1°C); *p*-tolylethyl tosylate, mp 68.0—69.0°C (lit,[24] 68.6—69.3°C); *p*-anisylethyl tosylate, mp 58.5—59.0°C (lit,[24] 58.3—59. °C); 2-phenylethyl-2,2-d_2 tosylate, mp 38.5—39. °C (lit,[13] 37.4—38.0°C).

2-Arylethyl Chlorides: 2-Arylethyl chlorides were prepared by heating to reflux arylethyl tosylates with excess of tetraethylammonium chloride in acetonitrile. In a typical example, 2-phenylethyl-2,2-d_2 tosylate (12.0 g, 0.044 mol) and tetraethylammonium chloride (16.5 g, 0.1 mol) were dissolved in 100 m*l* of acetonitrile and the solution was heated under gentle reflux for 24 hr. The solution was cooled and poured into 100 m*l* of water and the organic layer was taken out with pentane. After washing and drying the extracts, pentane was carefully removed and the product was distilled to give 4.8 g (86%) of 2-phenylethyl-2,2-d_2 chloride, bp 84.0°C/16 mmHg. On the NMR spectra of the deuterated compound, the signal due to β hydrogen (7.1 τ) completely vanished. Boiling points of the chlorides are as follows; 2-phenylethyl chloride, bp 90°C/25 mmHg;[11] 2-*p*-chlorophenylethyl chloride, bp 84°C/4 mmHg[11]; 2-*p*-anisylethyl chloride, bp 95°C/4 mmHg; 2-*p*-tolylethyl chloride, bp 67°C/4 mmHg.

2-Arylethyl Bromide: 2-Arylethyl bromides were prepared in a procedure analogous to that for the preparation of the 2-arylethyl chlorides using sufficient acetonitrile to dissolve tetraethylammonium bromide at a reflux temperature. Boiling points of the bromides are as follows: 2-phenylethyl bromide, bp 90°C/11 mmHg[12]; 2-phenylethyl-2,2-d_2 bromide, bp 95°C/16 mmHg[13]; 2-*p*-anisylethyl bromide, bp 124°C/4 mmHg[12]; 2-*p*-tolylethyl bromide, bp 101°C/10 mmHg.

Solvent and Base. Acetonitrile was purified as previously reported.[25] Preparation of tetraethylammonium fluoride was reported.[6] Fluoride reagent should be prepared freshly before use, as it is very hygroscopic and liable to decompose slowly to form triethylamine and ethylene even at room temperature. Hydrogen fluoride evolved seemed to deteriorate the specimen by forming tetraethylammonium acid fluoride. Tetraethylammonium fluoride stored for a month in a vacuum desiccator showed a greatly diminished rate of elimination reactions, sometimes about one hundredth of a fresh specimen.

Determination of Amount of Substitution Reactions. The amount of 2-arylethyl fluorides arising from substitution reactions of 2-arylethyl chlorides, bromides, and tosylates with fluoride in acetonitrile was determined by glc analysis. A solution in acetonitrile containing 0.2 M of tetraethylammonium fluoride and 0.1 M of a 2-phenylethyl derivative was allowed to react to completion. The resulting solution was poured into water and extracted with pentane. The extracts were dried and concentrated by careful fractionation of pentane. The concentrate was analyzed on a column of TG-3000 on Celite 545 at 110°C. Glc analysis showed that the fluorides were formed from the corresponding halides in 4% yield while the tosylates gave fluorides in 25% yield.

Kinetic Measurements. The reactions in acetonitrile were carried out in a thermostat kept within ±0.1°C of the stated temperature. Reaction rates were followed by analysis of styrene or substituted styrene spectrophotometrically. The reaction mixture was placed in a 50 m*l* volumetric flask, and after an appropriate time 1 m*l* aliquots of the solution were withdrawn at intervals and the reaction was quenched by the addition of 0.05 N nitric acid. The time of the first withdrawal was taken as "time-zero". Thus $\log A_\infty/(A_\infty - A_t)$ *vs.* t plot gave a good straight line with a negative time intercept. About 20-fold excess of fluoride was used and pseudo-first-order rate constants were determined from the slope of a plot of $\log A_\infty(A_\infty - A_t)$ against time, where A_t is the absorbance at time t and A_∞ is the absorbance after at least ten half-lives. The last values, A_∞, showed that the olefins were produced essentially in quantitative yield except for tosylates where a fair amount of the substitution was accompanied by elimination. The absorbance was meas-

Table 5. Reaction of 2-(*p*-chlorophenyl)ethyl chloride with Et_4NF in CH_3CN at 25.0°C

Time (min)	A_t	$\log A_\infty/(A_\infty - A_t)$	$k_1 \times 10^3$ a) (min^{-1})
5	0.180	0.04386	
10	0.250	0.05928	8.36
15	0.320	0.08027	8.80
20	0.378	0.09621	8.43
25	0.450	0.1173	8.41
30	0.504	0.1339	8.50
	1.900		Av. 8.50b)

$[ArCH_2CH_2Cl]_0 = 1.02 \times 10^{-3}$ mol/*l*, $[F^-] = 1.26 \times 10^{-2}$ mol/*l*.
a) Corrected for zero intercept of $[\log A_\infty/(A_\infty - A_t)]_0 = 0.023$.
b) From the slope of the best fit straight line.

20) C. G. Swain and E. R. Thornton, *ibid.*, **84**, 817 (1962).
21) N. Ono, This Bulletin, **44**, 1393 (1971). Part of the work was published in a preliminary form: J. Hayami, N. Ono, and A. Kaji, *Tetrahedron Lett.*, **1970**, 2727.
22) Melting points were determined on a Yanagimoto hot stage apparatus and were uncorrected. NMR spectra were determined with a Jeolco 3H-60 spectrometer using tetramethylsilane as an internal standard, and UV spectra with a Hitachi Perkin-Elmer 139 spectrophotometer. Glc analyses were performed with a Yanagimoto GCG-5DH gas-chromatograph.
23) C. H. DePuy and D. H. Froemsdorf, *J. Amer. Chem. Soc.*, **79**, 3710 (1957).
24) W. H. Saunders, Jr., D. G. Bushman, and A. F. Cockerill, *ibid.*, **90**, 1775 (1968).
25) R. U. Lemieux and J. Hayami, *Can. J. Chem.*, **43**, 2162 (1965).

ured at the absorption maximum of styrene or substituted styrene. Molar extinction coefficients are as follows: styrene λ_{max}, 248 mμ ($\varepsilon=1.46\times10^4$); *p*-chlorostyrene λ_{max}, 253 mμ ($\varepsilon=1.86\times10^4$); *p*-methylstyrene λ_{max}, 252 mμ ($\varepsilon=1.69\times10^4$); *p*-methoxystyrene λ_{max}, 259 mμ, ($\varepsilon=1.69\times10^4$). Initial concentration in the reaction mixture was 2×10^{-2} mol/l in fluoride and 1×10^{-3} mol/l in 2-arylethyl compounds unless otherwise stated. A typical example is shown in Table 5.

BULLETIN OF THE CHEMICAL SOCIETY OF JAPAN, VOL. 44, 1632—1638 (1971)

The Hofmann Rearrangement. I. Kinetic Substituent Effects of *ortho*-, *meta*-, and *para*-Substituted *N*-Bromobenzamides[1]

Tsuneo IMAMOTO, Yuho TSUNO, and Yasuhide YUKAWA

The Institute of Scientific and Industrial Research, Osaka Univervity, Yamadakami, Suita, Osaka

(Received September 25, 1970)

The kinetic substituent effects on the Hofmann rearrangements of *ortho*-, *meta*-, and *para*-substituted *N*-bromobenzamides were studied in an aqueous sodium hydroxide solution. The rate constants of the *meta*- and *para*-derivatives were correlated by means of our equation:

$$\log k/k_0 = -2.39(\sigma^0+0.41\Delta\bar{\sigma}_R^+) + 0.002$$

The reaction rates of *ortho*-derivatives were found to be 2—20 times faster than those of the corresponding *para*-derivatives. The reaction mechanism of this rearrangement was discussed in terms of LFER, the *ortho*/*para* rate ratios, and the activation parameters; as a result, the concerted mechanism (the participation of the phenyl group in electron-deficient nitrogen at the transition state) was favored rather than the two-step mechanism. The similarity of the reaction mechanism of the Hofmann to the Lossen rearrangement was also shown on the basis of LFER.

The Hofmann reaction, the conversion of amide into primary amine uncontaminated with secondary amine, is one of the most useful reactions for organic syntheses.[2] The course of this reaction has already been demonstrated, as in the following scheme by isolating reaction intermediates:

$$R\text{-}CONH_2 \xrightarrow{OX^-} R\text{-}CO\bar{N}^-\text{-}X \xrightarrow{-X^-} R\text{-}NCO \xrightarrow{H_2O} R\text{-}NH_2$$

The rearrangement step, where the conjugate base of *N*-haloamide is converted accompanying the release of the halide ion into isocyanate, is the most important stage in the course of the Hofmann reaction. This rearrangement is well-known to be intramolecular from the results of many stereo-chemical and isotopic studies.[2,3] As for further details of the mechanism, however, only a few kinetic studies have been reported. Hauser and his co-worker,[4,5] in their kinetic study of substituted *N*-bromobenzamides, showed that electron-releasing substituents in the phenyl group accelerated the rate of the rearrangement and that electron-attracting substituents retarded it. Joshi *et al.*[6] reported the kinetic results of the rearrangements of three aliphatic *N*-bromoamides. In spite of these insufficient data, it has been formally speculated that the rearrangement proceeds through a two-step mechanism;[7] the release of the halide ion from the conjugate base of *N*-haloamide takes place in the first step, and the unstable univalent nitrogeneous intermediate thus formed rearranges immediately into isocyanate. Wright and Fry[8] recently investigated the isotope effect of this rearrangement using phenyl-1-^{14}C labeled *N*-bromobenzamide and suggested a concerted mechanism; the release of the halide ion and the migration of the phenyl group to nitrogen took place simultaneously. Joshi *et al.* also presented a similar mechanism in their paper. It appears, however, that the amount of data reported hitherto is not sufficient to support strongly the concerted mechanism, and the two-step mechanism has not yet been definitely excluded.

In order to elucidate the reaction mechanism more precisely, we have extensively studied kinetic substituent effects on the Hofmann rearrangement of substituted *N*-bromobenzamides.

Experimental

Materials. Various substituted *N*-bromobenzamides were prepared by a modification of Hauser's method.[4]

Finely-pulverized amide (0.1 mol) was added to an ice-cold hypobromite solution, freshly prepared from 0.2 mol of bromine, 0.5 mol of sodium hydroxide, and 300—800 m*l*

1) This paper is dedicated to Emeritus Professor Munio Kotake in commemoration of his 75th birthday.

2) E. S. Wallis and J. F. Lane, "Organic Reactions," Vol. III, John Wiley and Sons Inc., New York (1946); M. Matsuno, *J. Soc. Org. Synth. Chem. Japan, sp. ed.*, **29**, 563 (1968).

3) T. J. Prosser and E. L. Eliel, *J. Amer. Chem. Soc.*, **79**, 2544 (1957).

4) C. R. Hauser and W. B. Renflow, Jr., *ibid.*, **59**, 121 (1937).

5) C. R. Hauser and S. W. Kantor, *ibid.*, **72**, 4284 (1950).

6) K. M. Joshi and K. K. Shah, *J. Indian Chem. Soc.*, **43**, 481 (1966).

7) C. K. Ingold, "Structure and Mechanism in Organic Chemistry," Cornell University Press, Ithaca and London (1969), p. 748; J. D. Roberts and M. C. Caserio, "Basic Principle of Organic Chemistry," Benjamin Inc., New York (1964), p. 655; D. J. Cram and G. S. Hammond, "Organic Chemistry," McGraw-Hill, New York (1969), p. 459.

8) A. Fry, private communication; J. C. Wright and A. Fry, *J. Chem. Eng. News*, **1968**, No. 1, p. 28.

Table 1. Substituted *N*-bromobenzamides

Subst.	Mp °C (lit[3])	Analysis (Calcd)				
		C%	H%	N%	Br%	Active Br%
p-CH_3O						33.09 (34.73)
p-*t*-C_4H_9	117—118	51.46 (51.58)	5.49 (5.51)	5.61 (5.47)	31.07 (31.20)	31.07 (31.20)
p-CH_3	136.0—137.5 (131—133)	45.01 (44.89)	3.67 (3.77)	6.60 (6.54)	37.28 (37.33)	36.50 (37.33)
p-C_2H_5	93—94	46.66 (47.39)	4.25 (4.42)	6.07 (6.14)	34.40 (35.02)	33.87 (35.02)
p-Ph	159—161	56.30 (56.55)	3.53 (3.65)	4.92 (5.07)	28.99 (28.94)	29.70 (28.94)
Unsubst.	132.5—134.5 (129—131)	42.24 (42.03)	2.73 (3.02)	6.96 (7.00)	39.80 (39.95)	39.48 (39.95)
p-F	168—170	38.60 (38.56)	2.39 (2.31)			36.95 (36.65)
p-Cl	181—184 (170—174)	36.00 (35.86)	2.17 (2.15)	6.10 (5.97)		33.52 (34.08)
p-Br	184—185	30.41 (30.14)	1.71 (1.81)	5.08 (5.02)	57.21 (57.29)	27.86 (28.65)
p-NO_2	223—226 (198—202)	34.61 (34.31)	1.91 (2.06)	11.77 (11.43)		31.58 (32.61)
m-CH_3	60—62	45.33 (44.89)	3.77 (3.77)	6.55 (6.54)	37.60 (37.33)	34.36 (37.33)
m-Cl	111—113 (102—105)	36.02 (35.86)	2.03 (2.15)	6.03 (5.97)		33.82 (34.08)
m-Br	126.5—127.5 (122—126)	30.44 (30.14)	1.70 (1.81)	5.11 (5.02)		28.11 (28.65)
m-CF_3	120—121	35.64 (35.83)	1.90 (1.88)			29.34 (29.82)
m-NO_2	183.0—186.5 (173—176)	34.03 (34.31)	2.24 (2.06)	11.62 (11.43)	32.72 (32.61)	31.96 (32.61)
o-CH_3	101—102	45.39 (44.89)	3.76 (3.77)	6.75 (6.54)	37.08 (37.33)	36.44 (37.33)
o-Cl	105.5—107.0 (104—105)	36.09 (35.86)	1.99 (2.15)	6.07 (5.97)		33.24 (34.08)
o-Br	130—133	30.29 (30.14)	1.60 (1.81)	5.13 (5.02)	57.02 (57.29)	27.98 (28.65)
o-NO_2	176—178 (170—176)	34.61 (34.31)	1.86 (2.06)	11.77 (11.43)	32.50 (32.61)	31.55 (32.61)

of water. After vigorous stirring for 2—15 min, the reaction mixture was filtered rapidly with a suction into a solution of 30 m*l* of acetic acid in 70 m*l* of ice water. The *N*-bromoamide thus precipitated was collected, washed successively with 5% aqueous acetic acid and water, and dried at room temperature. The yields of the crude products were generally 80—90%. Unsubstituted, *p*-methyl, *p*-fluoro, *p*-phenyl, and *m*-chloro derivatives were recrystallized from dichloroethane; *m*-nitro and *p*-nitro derivatives, from acetic acid; *p*-chloro and *p*-bromo derivatives, from methanol; the *o*-nitro derivative, from dichloroethane-DMF (4 : 1), and the *m*-trifluoromethyl derivative, from dichloroethane-*n*-hexane (5 : 1). Better results were obtained in every case by recrystallization at a temperature lower than 60°C.

However, the acidification of the reaction mixture in the cases of *m*-methyl, *o*-methyl, *p*-methoxy, *p*-ethyl, and *p*-*t*-butyl derivatives did not give the precipitates, but a pasty mass. This was redissolved in a 3% sodium hydroxide solution at −5—0°C and filtered into cold aqueous acetic acid containing ice to give almost colorless precipitates of the corresponding *N*-bromoamide. This solid material was collected, washed with water, pressed to dry, and dissolved in chloroform or dichloroethane. Into this saturated solution, *n*-hexane was added until turbidity just appeared, and then the solution was cooled. *N*-Bromoamides containing more than 96% of the theoretical amount of active bromine could be obtained by this method.

These *N*-bromoamides were kept cold, away from the light.

The analytical data and melting points for *N*-bromoamides are listed in Table 1.

The *o*-methoxy- and *m*-methoxy-*N*-bromobenzamides were very unstable compounds, and the corresponding pure materials could not be obtained. In the cases of *p*-ethoxy- and *p*-phenoxybenzamides, because of accompanying bromination on the benzene ring, the compounds isolated were not the expected ones, but *m*-bromo-*p*-ethoxy- and *p*-(*p*′-bromophenoxy)-*N*-bromobenzamides.

Kinetic Measurements. The reaction rates were measured by titrating the residual amount of unrearranged *N*-bromoamide with a standardized sodium thiosulfate solution.[9] In a measuring flask we placed 200 m*l* of a standardized aqueous sodium hydroxide solution and immersed in a constant-temperature water bath (accuracy ±0.01°). A

9) Van Dam, *Rec. Trav. Chim. Pays-Bas*, **18**, 408 (1899); Van Dam and J. H. Aberson, *ibid.*, **19**, 318 (1900).

certain amount of *N*-bromoamide was weighed accurately into a 300-m*l* Erlenmeyer flask and immersed in the bath. After standing for one hour, the sodium hydroxide solution was transferred into the Erlenmeyer flask, and shaken vigorously until all of the *N*-bromobenzamide had been dissolved. The course of the reaction was followed by titrating a residual amount of active bromine with a sodium thiosulfate solution at moderate intervals; a 10-m*l* portion of the solution was pipetted out and transferred into 100 m*l* of an ice-cold 0.5 N HCl solution to which 2 m*l* of 20% aqueous solution of potassium iodide had been added just before; the iodine thus liberated was titrated with a 0.025 N $Na_2S_2O_3$ solution to the starch-iodide end-point.

In the cases of *m*-methoxy- and *o*-methoxy-benzamides, from which corresponding *N*-bromoamides could not be isolated, the kinetic measurements were carried out as follows. A hypobromite solution (0.025 mol/*l*, $f=0.996$) was prepared by the drop-by-drop addition of bromine to an ice-cold 0.5 N NaOH solution ($f=1.000$). Finely-pulverized pure amide (0.0055 mol) was added to 200 m*l* of this hypobromite solution at the reaction temperature, the mixture was shaken vigorously for a few minutes, and then the reaction was followed by the above procedure.

Results and Discussion

Effect of the Concentration. In order to examine the effects of the concentrations of *N*-bromoamide and sodium hydroxide on the reactivity, kinetic measurements of unsubstituted- and *m*-chloro-*N*-bromobenzamides were made in respect to:

A. Changing the concentration of *N*-bromoamide in a 1 N NaOH solution;

B. Changing the concentration of sodium hydroxide, but keeping that of *N*-bromoamide constant (0.05 mol/); and

C. Changing the overall concentration, with the concentration ratio of *N*-bromoamide to sodium hydroxide kept at 1 : 20.

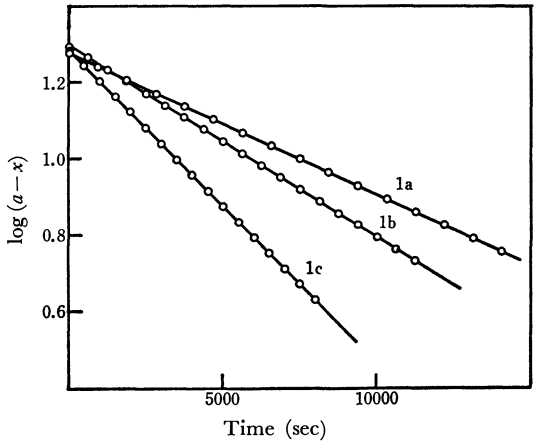

Fig. 1. Typical first-order plots.
1a: *m*-Cl; 0.05 mol/*l*, NaOH; 2 N, at 30.00°C.
1b: H; 0.025 mol/*l*, NaOH; 0.5 N, at 20.00°C.
1c: H; 0.1 mol/*l*, NaOH; 2 N, at 20.00°C.

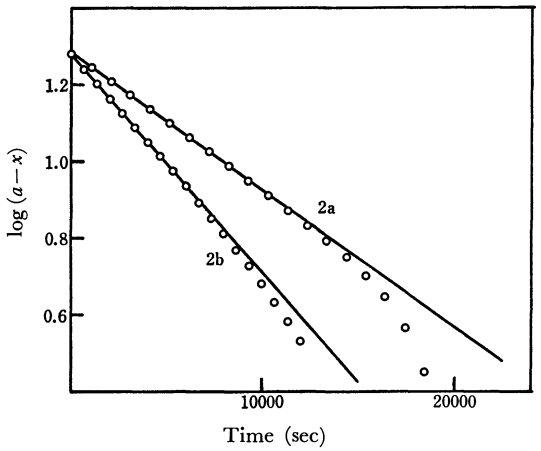

Fig. 1. First-order plots.
2a: *m*-Cl; 0.05 mol/*l*, NaOH; 0.1 N, at 30.00°C.
2b: H; 0.05 mol/*l*, NaOH; 0.1 N, at 20.00°C.

TABLE 2. EFFECT OF THE CONCENTRATIONS OF *N*-BROMOAMIDE AND NaOH

	Conc. of amide (mol/*l*)	Conc. of NaOH (N)	H ($k_1\times10^4$ sec^{-1}) 20.00°C	*m*-Cl $k_1\times10^4$ (sec^{-1}) 30.00°C	$\frac{k_1(\text{H, 20°C})}{k_1(m\text{-Cl, 30°C})}$
Case A	0.100	1.000	1.582±0.003	9.76±0.09	1.62
	0.0500	1.000	1.579±0.003	9.56±0.02	1.65
	0.0250	1.000	1.548±0.002	9.52±0.01	1.63
	0.0125	1.000	1.540±0.002	9.44±0.01	1.63
	0.00625	1.000	1.534±0.003	9.34±0.03	1.64
Case B	0.0500	2.000	1.932±0.002	11.63±0.01	1.66
	0.0500	1.000	1.579±0.002	9.56±0.02	1.65
	0.0250	1.000	1.548±0.002	9.52±0.01	1.63
	0.0500	0.500	1.409±0.001	8.81±0.01	1.60
	0.0250	0.500	1.401±0.002	8.52±0.02	1.64
	0.0500	0.250	1.361±0.001	8.39±0.008	1.62
	0.0500	0.100	1.33 ±0.006	8.3 ±0.02	1.60
Case C	0.100	2.000	1.958±0.004	11.81±0.01	1.66
	0.0500	1.000	1.579±0.002	9.56±0.02	1.65
	0.0250	0.500	1.401±0.002	8.52±0.02	1.64
	0.0125	0.250	1.319±0.002	8.20±0.02	1.61
	0.00500	0.100	1.301±0.002	7.96±0.03	1.63
	0.	0.	1.29[a)]	7.85[a)]	1.64

a) Extrapolated value.

The concentration factor for *N*-bromoamide and sodium hydroxide was 1.000±0.003 in every case. The reaction temperatures were 20.00±0.01°C for unsubstituted amide and 30.00±0.01°C for *m*-chloro amide. The first-order rate constants were calculated by the least-squares method according to Eq. (1):

$$k \times t = 2.303 \times \log (a/a-x) \quad (1)$$

where t is the reaction time and where $a-x$ is the concentration of *N*-bromoamide at time t. Almost all the cases obeyed first-order kinetics, at least to 80% completion of the reaction (see Fig. 1). The observed rate constants are listed in Table 2.

In the case A, a very small rate enhancement was observed despite the increase in the concentration of *N*-bromoamide from 0.00625 to 0.1 mol/*l*. On the other hand, in the case B, the rate constant considerably depended on the concentration of sodium hydroxide, but tended to converge to a constant value as it approached an infinite dilution. The extremely small concentration of sodium hydroxide, however, gave an anomaly. In the case B with 0.1 N NaOH, the solution was gradually darkened as the reaction proceeded, and the dark brown precipitates appeared after the reaction was about half completed. The reaction rate increased with the progress of reaction (see Fig. 2).[10] The reaction involves a preequilibrium between *N*-bromoamide and its conjugate base, as is indicated by the following scheme. The relatively low concentration

$$X\text{-}C_6H_4\text{-}CONHBr + OH^- \rightleftharpoons X\text{-}C_6H_4\text{-}CON^-\text{-}Br + H_2O$$

ratio of sodium hydroxide to *N*-bromoamide releases a small amount of the *N*-bromoamide reactant, which then reacts rapidly with the rearranged products to lose its active bromine. The dark brown precipitates are considered to be the reaction products of *N*-bromoamide with amine or isocyanate.

From the above observations, it appears necessary to keep the initial concentration ratio [NaOH]/[Amide] at least *ca.* 10 to obtain a good kinetic result. The case C indicates the rates measured under reaction conditions in which the concentration ratio of *N*-bromo-

Table 3. Rate constants of the Hofmann rearrangement of substituted *N*-bromobenzamides

Subst.	Temp. °C	$k_1 \times 10^4$ (sec^{-1})	Subst.	Temp. °C	$k_1 \times 10^4$ (sec^{-1})
p-CH_3O	13.00	4.81 ±0.02	*m*-CH_3	23.00	4.120 ±0.006
	10.00	2.92 ±0.01		15.00	1.064 ±0.002
	5.00	1.275 ±0.001		8.00	0.3147 ±0.0009
		1.251 ±0.003[a]	*m*-CH_3O	30.00	4.09 ±0.004[a]
	2.00	0.771 ±0.001		20.00	0.847 ±0.001[a]
p-*t*-C_4H_9	20.00	3.63 ±0.01		15.00	0.361 ±0.001[a]
	13.00	1.121 ±0.003		10.00	0.1503 ±0.0002[a]
	5.00	0.274 ±0.001		0.00	0.02447±0.00010[a]
p-CH_3	18.00	3.148 ±0.004	*m*-Cl	38.00	3.06 ±0.004
	14.00	1.626 ±0.002		30.00	0.852 ±0.002
	10.00	0.819 ±0.001		23.00	0.2789 ±0.0005
	3.71	0.2682 ±0.0008	*m*-Br	38.00	3.318 ±0.006
p-C_2H_5	20.00	4.05 ±0.02		30.00	0.929 ±0.002
	13.00	1.263 ±0.002		23.00	0.2997 ±0.0005
	5.00	0.308 ±0.001	*m*-CF_3	45.00	4.278 ±0.009
p-Ph	25.00	4.28 ±0.01		35.00	0.946 ±0.0006
	18.00	1.40 ±0.004		30.00	0.4266 ±0.0005
	10.00	0.366 ±0.002		23.00	0.1341 ±0.0002
				15.00	0.03214±0.00004
Unsubst.	25.00	3.13 ±0.005	*m*-NO_2	55.19	4.79 ±0.02
	20.00	1.401 ±0.002		50.00	2.30 ±0.009
		1.370 ±0.001[a]		45.00	1.13 ±0.003
	10.00	0.250 ±0.0004	*o*-CH_3O	5.00	7.37 ±0.02[a]
	0.00	0.0391 ±0.0001		0.00	3.04 ±0.01[a]
p-F	30.00	3.51 ±0.004	*o*-CH_3	5.00	7.36 ±0.02
	23.00	1.15 ±0.01		3.00	5.19 ±0.01
	15.00	0.300 ±0.002		2.00	4.30 ±0.005
p-Cl	35.00	4.346 ±0.002		0.00	2.976 ±0.011
	30.00	2.029 ±0.004	*o*-Cl	25.00	3.78 ±0.003
	20.00	0.4053 ±0.0007		18.00	1.144 ±0.002
p-Br	35.00	3.97 ±0.007		10.00	0.273 ±0.0004
	30.00	1.834 ±0.003	*o*-Br	25.00	4.444 ±0.005
	25.00	0.830 ±0.001		18.00	1.368 ±0.001
	20.00	0.365 ±0.0004		10.00	0.3268 ±0.0007
p-NO_2	55.00	4.85 ±0.02	*o*-NO_2	50.00	3.74 ±0.10
	50.00	2.49 ±0.01		45.00	1.83 ±0.02
	45.00	1.18 ±0.01		40.00	0.871 ±0.001

a) Measured by using sodium hypobromite solution.

10) The rate constant under this reaction conditions was calculated from the first-order plots of the initial stage of the reaction.

amide to sodium hydroxide kept at 1:20. The observed rate constants appeared to be given by the combined results of the concentration effects of *N*-bromoamide (case A) and sodium hydroxide (case B).

The rate constants independent of the initial concentration can be obtained by the extrapolation of the observed rate constants to an infinite dilution. However, they are only approximate and are not as precise as those measured directly. It is very noticeable that the rate ratios of the unsubstituted derivative to the *m*-chloro derivative are almost the same under these conditions. This indicates that any reaction conditions within the limits examined may be employed to ascertain the relative change in the rates of various substituted *N*-bromobenzamides. Practically, fixed conditions with the respective concentrations of *N*-bromoamide and sodium hydroxide being 0.025 mol/*l* and 0.5 N were employed throughout the series of runs as the most suitable standard from the experimental point of view.

Substituent Effects. The rates of the release of the bromide ion from the conjugate bases of various substituted *N*-bromobenzamides were determined at various temperatures. The initial concentrations of *N*-bromoamides and sodium hydroxide were maintained at 0.025 mol/*l* and 0.5 N (f=1.000±0.003) respectively throughout the series. Plots of the log $(a-x)$ against time t gave an excellent straight line, covering over 75% of the reaction, for almost all derivatives. In the cases of *p*-phenyl, *p*-fluoro, *p*-*t*-butyl, and *o*-nitro derivatives, the reaction rates were gradually increased as the reaction proceeded; thus, the rate constants were calculated from the plots of the initial state of the reaction. The *m*-nitro and *p*-nitro derivatives behaved peculiarly; the first-order plots provided a good straight line at temperatures over 45°C, but not at 30°C. Rate measurements of unsubstituted and *p*-methoxy derivatives were made not only by the general method but also by the conventional modification used for *o*-methoxy and *m*-methoxy derivatives (see the Experimental section). The disagreement between the two methods did not exceed *ca.* 2% of the rate constant. The obtained rate constants are listed in Table 3. The rate constants at 30.00°C and the activation parameters derived are also shown in Table 4.

TABLE 4. KINETIC RESULTS OF THE HOFMANN REARRANGEMENT OF SUBSTITUTED *N*-BROMOBENZAMIDES

Subst.	$k_1\times10^4$ (sec^{-1}) 30.00°C	$\Delta H^{\neq}$ (kcal/mol)	$\Delta S^{\neq}$ (e.u.)
p-CH_3O	62.8[a]	25.48±0.09	15.4 ±0.3
p-*t*-C_4H_9	17.6[a]	27.34±0.06	19.0 ±0.2
p-CH_3	20.9[a]	27.03±0·03	18.36±0.11
p-C_2H_5	19.6[a]	27.25±0.11	18.9 ±0.4
p-Ph	9.22[a]	26.93±0.08	16.4 ±0.3
Unsubst.	6.96[a]	27.83±0.04	18.77±0.14
p-F	3.51	27.90±0.11	17.7 ±0.4
p-Cl	2.029	27.79±0.03	16.23±0.10
p-Br	1.834	27.95±0.04	16.57±0.13
p-NO_2	0.121[a]	28.6 ±0.39	13.4 ±1.3
m-CH_3	12.5[a]	27.78±0.09	19.8 ±0.3
m-CH_3O	4.09	27.52±0.05	17.7 ±0.2
m-Cl	0.852	28.6 ±0.2	17.1 ±0.7
m-Br	0.929	27.95±0.04	16.57±0.13
m-CF_3	0.4266	29.03±0.09	17.2 ±0.3
m-NO_2	0.113[a]	28.8 ±0.29	13.7 ±0.9
o-CH_3O	397[a]	26.2 ±0.45	21.3 ±1.5
o-CH_3	439[a]	26.8 ±0.16	23.6 ±0.5
o-Cl	8.56[a]	28.8 ±0.15	22.4 ±0.5
o-Br	10.0[a]	28.60±0.04	22.10±0.14
o-NO_2	0.185[a]	28.6 ±0.36	14.2 ±1.2

a) Extrapolated from data at other temperatures.

The present authors[11] have previously pointed out that the Linear Aromatic Substituent-Reactivity relationship (LArSR relationship, Eq. (21)) is one of the most useful tools for speculating on the reaction mechanism:

$$\log k/k_0 = \rho(\sigma^0 + r\Delta\bar{\sigma}_R^+) \qquad (2)$$

where σ^0 is the normal substituent constant, where r is a constant depending on the resonance requirement in the reaction, and where $\Delta\bar{\sigma}_R^+$ measures the capacities of the substituents to supply electrons by resonance. It is of interest to discuss the reaction mechamism of the Hofmann rearrangement in terms of the above equation. First, the logarithms of the rate constants have been plotted against Hammett's σ constants in order to examine the applicability of the original Hammett equation, $\log k/k_0=\rho\sigma$ to our data. A good overall linear relation with a ρ-value of −2.52 is observed with the correlation coefficient of 0.994, while *p*-methoxy and *p*-*t*-butyl derivatives deviate a little. There is no reason to consider that the deviation of the *p*-methoxy group

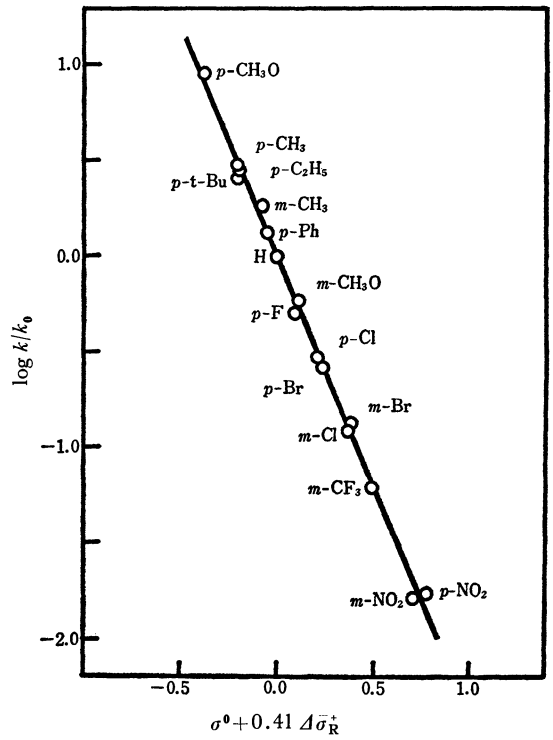

Fig. 3. Application of the LArSR relationship.

11) Y. Yukawa, Y. Tsuno, and M. Sawada, This Bulletin, **39**, 2274 (1966); Y. Yukawa and Y. Tsuno, *Nippon Kagaku Zasshi*, **86**, 873 (1965).

is attributable to the experimental error. It would be more reasonable to refer the deviation to the strongly electron-releasing conjugative ability of the methoxy group. That is, the Hofmann rearrangement may be considered to be a slightly more σ^+-characteristic reaction than the dissociation of benzoic acids, from which the Hammett's σ constants are derived. The use of Eq. (2) gives a better linearity, including the *p*-methoxy group, with a correlation coefficient of 0.997, as is shown in Fig. 3.

$$\log k/k_0 = -2.39(\sigma^0 + 0.41\,\Delta\bar{\sigma}_R^+) + 0.002 \qquad (3)$$

For the interpretation of the above derived parameters, especially of the resonance parameter, *r*, it will be very useful to consider the effect of the conjugation in the initial and the transition states.

In the conjugations applicable for the initial state, the *dπ–pπ* conjugation on the N–Br bond (I) may be considered to be important as the factor influencing the reactivity; the contribution of this conjugation leads to an increase in the bond-order of the N–Br bond and makes it more difficult to release the bromide ion from the reactant molecule (the Bond-energy Effect). The degree of this conjugation can be affected by the substituent on the migrating phenyl group, especially by electron-releasing conjugative groups at the *para*-position, For instance, the *p*-methoxy group, a typical electron-releasing conjugative group, will produce a considerable increase in the above conjugation effect through the cross conjugation of the carbonyl group. As is indicated by Formula (II), the methoxy group particularly strengthens the conjugation of the carbonyl group with the phenyl group, while it weakens the conjugation of the carbonyl group with the nitrogen orbital, resulting in a relative increase in the *dπ–pπ* conjugation on the N–Br bond. Therefore, if the present reaction is controlled solely by the *dπ–pπ* conjugation effect at the initial state, the resonance parameter, *r*, in the LArSR relationship Eq. (2) may be expected to be negative, as has been observed in the Curtius rearrangement

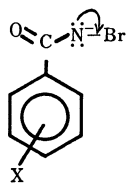

(I)

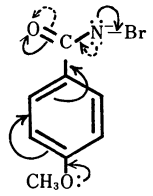

(II)

in toluene ($r=-1.04$)[12] and in the Wolff rearrangement ($r=-1.7$).[13] In the present Hofmann rearrangement, however, comparatively large positive *r*-value (0.41) has been obtained. This result clearly indicates that the bond-energy effect mentioned above is not necessarily a predominant factor in influencing the reactivity of the Hofmann rearrangement.

On the other hand, the following two models may be assumed as probable structures of the transition state. The (III) model corresponds to the two-step mechanism,

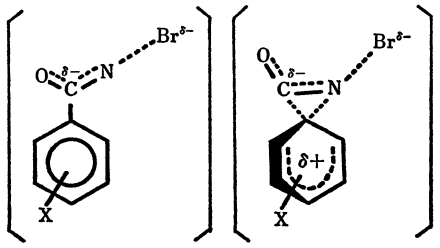

(III) (IV)

where the release of the bromide ion takes place at the first step and the univalent nitrogeneous intermediate formed rearranges immediately into isocyanate. The other model (IV) corresponds to the concerted mechanism (or the one-step mechanism), where the release of the bromide ion and the migration of the phenyl group to the nitrogen are simultaneous processes. In the former model, the substituent effect on the stabilization of this state is expected to afford a small positive *r*-value (a value of the same order as for σ, $r=0.27$), since its electronic nature resembles closely that of the benzoate anion. On the other hand, in the latter model, a strongly electron-releasing conjugation is required for the partial bond formation between the phenyl group and nitrogen, and thus a large positive *r*-value should be observed, as in the Beckmann rearrangement of acetophenone oximes ($r=0.60$—0.65). The observed *r*-value (0.41), however, appears too large for the (III) model and, on the contrary, too small for the (IV) model. Its *r*-value does not entirely support either of the above two models without considering the effect of the conjugation at the initial state. It is a rather plausible explanation for the present data that the large positive *r*-value due to the electrophilic conjugative effect at the transition state (IV) may be somewhat compensated for by the negative *r*-value resulting from the *dπ–pπ* conjugation on the N–Br bond at the initial state.

It is also of interest to discuss the effect of *ortho*-substituents with regard to the reaction mechanism. The polar effect of the *ortho*-substituent is generally recognized to be nearly equal to that of *para*-substituent;[14] thus, the rate ratio and the relative value of the activation parameters of *ortho*- to *para*-substituent can be taken as

Table 5. Effects of *ortho*-substituents

Subst.	Rel. rate[a]	k^o/k^p[b]	$\Delta\Delta H^{\neq}$ (kcal/mol)	$\Delta\Delta S^{\neq}$ (e.u.)
H	1.	1.	0.	0.
o-CH_3O	57.0	6.3	+0.7±0.5	+5.9±1.8
o-CH_3	63.1	21.0	−0.2±0.2	+5.2±0.6
o-Cl	1.23	4.2	+1.0±0.2	+6.2±0.6
o-Br	1.44	5.5	+0.7±0.1	+5.5±0.3
o-NO_2	0.027	1.5	0.0±0.8	+0.8±2.5

a) Relative rate at 30.00°C to the unsubstituted *N*-bromoamide.
b) The *ortho*/*para* rate ratio at 30.00°C.

12) Y. Yukawa and Y. Tsuno, *J. Amer. Chem. Soc.*, **79**, 5530 (1957); Y. Yukawa and Y. Tsuno, *ibid.*, **80**, 6346 (1958).
13) Y. Yukawa, Y. Tsuno, and T. Ibata, This Bulletin, **40**, 2613 (1967).
14) R. W. Taft, Jr., "Steric Effects in Organic Chemistry," John Wiley and Sons Inc., New York (1956), p. 556.

measures of *ortho* effects reflecting the reaction mechanism. The *ortho*/*para* rate ratios and relative value of activation parameters are summarized in Table 5. It may be noted that comparatively large *ortho*/*para* rate ratios are observed, and that these values depend mainly on the difference in the entropy of activation, except for the case of the nitro group. The introduction of an *ortho*-substituent restricts the rotation of the phenyl ring and lessens the entropy in the initial state more than dose that of the corresponding *para*-substituent. If the reaction proceeds by the two-step mechanism, the difference in the entropy of the *ortho*- and *para*-derivatives in the initial state will not have any effect on the relative value of the entropy of activation. However, in the case of the concerted mechanism, the entropy of activation of the *para*-derivative is lowered below that of corresponding *ortho*-derivative by the restriction of the motion of the phenyl ring on proceeding from the reactant to the transition state; therefore, it can be expected that the relative value of the entropy of activation, $\Delta\Delta S^{\neq}$, depends considerably on the difference in entropy in the initial state. The observed value of $\Delta\Delta S^{\neq}$ can be qualitatively interpreted by the above considerations. On the other hand, the following explanation of the *ortho* rate effects is also probable. The through-conjugation between carbonyl and phenyl groups is weakened by reduced co-planarity due to the introduction of the *ortho* group. This effect increases the conjugation of the carbonyl group with the nitrogen orbital, but decreases the $d\pi$–$p\pi$ conjugation on the N–Br bond. The smaller $d\pi$–$p\pi$ conjugation may play a role in bringing about the rate acceleration.

Hauser and Renflow had measured the rates of eight *meta*-, *para*-, and two *ortho*-substituted *N*-bromobenzamides in a 1N aqueous sodium hydroxide solution at 30°C. Logarithms of our rate constants have been plotted against theirs. An excellent correlation results, with a correlation coefficient of 0.9999 and a slope of 1.000 except for nitro and *p*-methoxy derivatives, which are attended with large experimental uncertainty in Hauser's data. This fact indicates that the mechanism of this reaction is little affected by a minor change in the reaction conditions.

The Lossen rearrangement, of which the leaving group is carboxylates as a substitute for halide, is expected to be analogous to the Hofmann rearrangement with respect to the reaction mechanism. Hauser and his co-worker[15] had reported the kinetic results of the decomposition of potassium dihydroxamates (R–CON–OCOR′)$^-$K$^+$, where R and R′ were various substituted phenyl groups. As is shown in Table 6, the

Table 6. Comparison with the Lossen rearrangement
X-C_6H_4-CON^--OCO-C_6H_4-Y

Subst. (Y)	Slope	Corr. coeff.	n[a]
o-NO_2	0.98	1.000	3
m-NO_2	1.15	1.000	3
m-F	1.25	1.000	2
o-Cl	1.06	0.999	5
H	1.15	0.999	5

a) The number of the species of substituent X.

LFER between the Lossen rearrangement and the Hofmann rearrangement is excellent regardless of the different leaving groups. These satisfactory linear relationships suggest that the mechanisms of the two reactions are almost the same. It is conceivable that the contribution of the homo-conjugation (Formula V), which may be compared with the $d\pi$–$p\pi$ conjugation in the Hofmann rearrangement, on the depression of the reactivity should not be neglected.

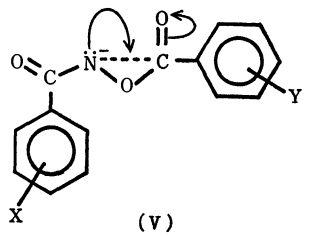

(V)

15) W. B. Renflow and C. R. Hauser, *J. Amer. Chem. Soc.*, **59**, 2308 (1937); R. D. Bright and C. R. Hauser, *ibid.*, **61**, 618 (1939).

The Hofmann Rearrangement. II. Kinetic Substituent Effects of *ortho-*, *meta-*, and *para*-Substituted *N*-Chlorobenzamides

Tsuneo IMAMOTO, Yuho TSUNO, and Yasuhide YUKAWA

The Institute of Scientific and Industrial Research, Osaka University, Yamadakami, Suita, Osaka

(Received September 25, 1970)

The reaction rates of the Hofmann rearrangement of *ortho-*, *meta-*, and *para*-substituted *N*-chlorobenzamides were measured under the same reaction conditions as were used for the preceding *N*-bromo series. The rate constants of the *N*-chloroamides were found to be slightly larger than those of the *N*-bromoamides. The relative values of the activation entropy and the activation enthalpy of *N*-chloro- and *N*-bromo-derivatives were approximately −4 e.u. and −1.3 kcal/mol respectively. The LFER between the two series was excellent, indicating that the reaction mechanism was almost the same for both series. The effects of the leaving group on the reactivity of *ortho*-substituents were discussed in terms of the *ortho/para* rate ratios and the relative values of the activation parameters of *ortho-* and *para*-substituents.

As has been described in the preceding paper,[1] the kinetic substituent effects on the Hofmann rearrangement of substituted *N*-bromobenzamides were studied in order to elucidate the mechanism precisely. The results appeared to suggest that this rearrangement proceeded through a concerted-type transition state; the dissociation of the nitrogen-bromine bond and the migration of the phenyl group to nitrogen took place simultaneously. Furthermore, the results indicated that the contribution of the $d\pi$–$p\pi$ conjugation to the nitrogen-bromine bond in the initial state was also an important factor in depressing the reactivity.

It remained necessary to examine whether or not these qualities of the rearrangement are changed by the substitution of the leaving group, bromide, for chloride. In the present study, the substituent effects of substituted *N*-chlorobenzamides have thus been determined, and the results are discussed in terms of the effects of the leaving group on the reactivity.

Experimental

Materials. Various substituted *N*-chlorobenzamides, but not *m-* and *p*-methoxy and *p*-ethoxy derivatives, were prepared by a modification of Elliott's method.[2] Ten grams of pure amide was dissolved in 10% hydrochloric acid, and chlorine gas was passed into this solution for one hour. The *N*-chloroamide thus precipitated was collected, washed with water, and dried *in vacuo*. The yields of the crude products were generally 70—80% of the theoretical amounts.

In the cases of *m-* and *p*-methoxy and *p*-ethoxy benzamides, chlorination on the benzene ring was also present and the corresponding pure *N*-chloroamides could not be isolated by the above method. However, these *N*-chloroamides could be obtained by the application of the method of Altenkirk and Israelstam.[3] Ten grams of pure amide and 0.4 g of borax were dissolved in methanol, and into this solution an equimolar quantity of *t*-butyl hypochlorite was added at room temperature. After standing in the dark for *ca.* 15 hr, the reaction mixture was diluted with water to twice the original volume. The *N*-chloroamide thus precipitated was collected, washed with water, and dried *in vacuo* (yield 50—70%).

The crude *N*-chloroamides were recrystallized from dichloroethane or from a mixed solvent of methanol and dichloroethane. The analytical data and melting points for *N*-chlorobenzamides are listed in Table 1.

Kinetic Measurements. The rates of the rearrangement of the substituted *N*-chlorobenzamides except those of the *m*-methyl derivative were measured by the same method as was previously used for *N*-bromobenzamides.[1] The initial concentrations of *N*-chloroamide and sodium hydroxide were 0.025 mol/*l* and 0.5 N respectively.

In the case of *m*-methyl benzamide, from which the corresponding *N*-chloro derivative could not be isolated,[4] the kinetic measurements were carried out as follows. Finely-pulverized amide (0.0055 mol) was added at the reaction temperature to 200 m*l* of a hypochlorite solution (0.025 mol/*l*, $f=1.000$), freshly prepared by passing chlorine gas into an ice-cold 0.5 N ($f=1.000$) NaOH solution. The mixture was shaken vigorously for a few minutes, and then the reaction was followed by titrating the residual active chlorine with a 0.025 N $Na_2S_2O_3$ solution.

In order to compare the two rate constants, that obtained by the usual method and that obtained by the conventional modification applied to the *m*-methyl derivative, the rates of the *m*-chloro derivative were measured at 30°C by both the above methods. The rate constant obtained by the latter method was, at most, *ca.* 2% smaller than the constant obtained by the former method.

Results and Discussion

The rates of the release of the chloride ion from the conjugate bases of substituted *N*-chlorobenzamides were measured under the same reaction conditions as were used for the previous *N*-bromo series. All the runs strictly obeyed first-order kinetics, at least to 75% completion of the reaction, except for those of the *m*-methyl derivative. Some examples of first-order plots are shown in Fig. 1. In the case of the *m*-methyl derivative, the rates of which were measured by using a hypochlorite solution, a short induction period was observed when the reaction was about 15% complete (see Fig. 1),[5] and the rate constants were calculated from the first-order plots, excluding the induction period. The reproducibility of the rate constant obtained from repeated runs was within 0.7%, and the plots of $\log k/T$ *vs.* $1/T$ gave an excellent straight line in every case. The ob-

1) T. Imamoto, Y. Tsuno, and Y. Yukawa, This Bulletin, **44**, 1632 (1971).

2) G. R. Elliott, *J. Chem. Soc.*, **121**, 203 (1922).

3) B. Altenkirk and S. S. Israelstam, *J. Org. Chem.*, **27**, 4532 (1962).

4) Chlorination with chlorine gas gave solely a pasty mass.

5) The induction period may be caused by the *N*-chlorination of the amide with hypochlorite at the initial stage of the reaction.

TABLE 1. SUBSTITUTED *N*-CHLOROBENZAMIDES

Subst.	Mp °C (lit[3])	Analysis (Calcd)				
		C%	H%	N%	Cl%	Active Cl%
p-CH_3O	142—143 (142—143)	51.77 (51.77)	4.40 (4.34)	7.47 (7.55)	18.94 (19.10)	19.00 (19.10)
p-C_2H_5O	128.0—129.0	54.04 (54.15)	5.08 (5.05)	6.88 (7.02)	17.91 (17.76)	17.69 (17.76)
p-CH_3	153.5—154.5 (147)	56.87 (56.65)	4.60 (4.75)	8.38 (8.26)	20.79 (20.90)	20.52 (20.90)
p-C_2H_5	106.5—107.0	58.49 (58.86)	5.41 (5.49)	7.69 (7.63)	19.18 (19.31)	19.23 (19.31)
Unsubst.	117.0—118.0 (117—118)	53.93 (54.04)	3.67 (3.89)	9.00 (9.00)	22.98 (22.79)	22.48 (22.79)
p-F	178—180	48.28 (48.44)	3.02 (2.90)			20.13 (20.43)
p-Cl	196—198 (194—195)	44.05 (44.24)	2.58 (2.65)	7.46 (7.37)	37.48 (37.31)	18.46 (18.66)
p-Br	198—199	35.86 (35.86)	2.01 (2.15)	5.99 (5.97)		15.00 (15.12)
p-NO_2	230—233 (200—202)	41.99 (41.92)	2.19 (2.51)	13.78 (13.97)	17.70 (17.68)	16.98 (17.68)
m-CH_3O	103.0—103.5 (165—166)	51.90 (51.77)	4.29 (4.34)	7.55 (7.55)	19.27 (19.10)	18.86 (19.10)
m-Cl	121—122 (119—120)	44.14 (44.24)	2.54 (2.65)	7.60 (7.37)	37.37 (37.31)	18.30 (18.66)
m-Br	127.0—127.5	35.81 (35.86)	2.08 (2.15)	6.00 (5.97)		14.85 (15.12)
m-NO_2	188—189 (184)	42.21 (41.92)	2.37 (2.51)	14.02 (13.97)	17.82 (17.68)	17.41 (17.68)
o-CH_3	87.0—88.5 (88—89)	56.28 (56.65)	4.63 (4.75)	8.14 (8.26)	20.80 (20.90)	20.54 (20.90)
o-Cl	107.0—107.5 (105—106)	44.10 (44.24)	2.46 (2.65)	7.55 (7.37)	37.20 (37.31)	18.44 (18.66)
o-Br	149.0—150.5 (151—152)	36.00 (35.86)	1.96 (2.15)	6.02 (5.97)		14.98 (15.12)
o-NO_2	172—173	41.89 (41.92)	2.22 (2.51)	14.30 (13.97)	17.82 (17.68)	17.45 (17.68)

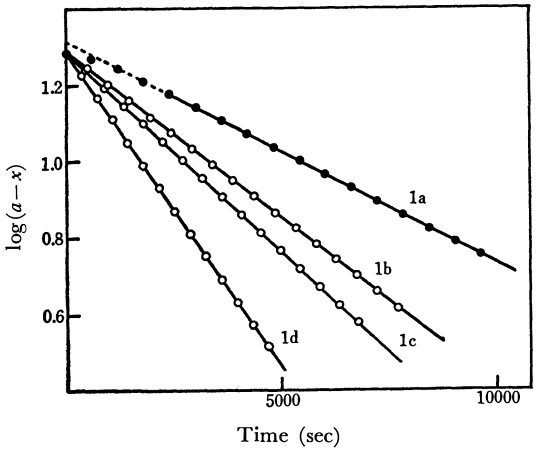

Fig. 1. Typical first-order plots.
1a: *m*-CH_3, at 15°C; 1b: *p*-F, at 25°C
1c: *p*-Cl, at 30°C; 1d: H, at 25°C.

served rate constants are listed in Table 2. The rate constants at 30°C and the derived activation parameters are summarized in Table 3.

The rate constant at 30°C is found to be slightly larger than that of the corresponding *N*-bromoamide, and the chloride/bromide rate-ratio is calculated to be *ca.* 1.2 in every substituent. It should be noted that the observed rate-ratio is considerably different from that of the usual alkyl halide reported hitherto in various nucleophilic substitution reactions and elimination reactions. That is, an alkyl chloride reacts 10—1000 times slower than the corresponding bromide,[6] whereas in the Hofmann rearrangement the *N*-chloroamide is slightly more reactive than the *N*-bromoamide. This result might possibly be referred to the fact that the bond-breaking of the nitrogen-halogen bond does not take place in the rate-determining step, but this possibility is entirely obviated by the kinetic results on the Lossen rearrangement. Hauser *et al.*[7] had studied the kinetic substituent effect on the Lossen rearrangement of dihydroxamates (I), and obtained a comparatively large positive ρ-value (+1.0). This result evidently indicates that the rate-determining step involves the bond-cleavage of the nitrogen-oxygen bond. From the similarity of the reaction mechanism of the Lossen

6) A. Streitwieser, Jr., "Solvolytic Displacement Reactions," McGraw-Hill Book Company, Inc., New York (1962), p. 29; C. K. Ingold, "Structure and Mechanism in Organic Chemistry," Cornell University Press, Ithaca and London (1969), p. 453.

7) W. B. Renflow and C. R. Hauser, *J. Amer. Chem. Soc.*, **78**, 5002 (1937); R. D. Bright and C. R. Hauser, *ibid.*, **61**, 618 (1939).

Table 2. Rate constants of the Hofmann rearrangement of substituted *N*-chlorobenzamides

Subst.	Temp. °C	$k_1 \times 10^4$ (sec^{-1})	Subst.	Temp. °C	$k_1 \times 10^4$ (sec^{-1})
p-CH_3O	13.00	5.456 ± 0.001		40.00	0.5807 ± 0.0001
	10.00	3.414 ± 0.009		30.00	0.1218 ± 0.0002
	5.00	1.507 ± 0.003			
	0.00	0.6492 ± 0.0009	*m*-CH_3	15.00	1.341 ± 0.002[a]
				10.00	0.5852 ± 0.0005[a]
p-C_2H_5O	13.00	5.826 ± 0.007		5.00	0.2487 ± 0.0005[a]
	10.00	3.629 ± 0.008			
	5.00	1.619 ± 0.002	*m*-CH_3O	30.00	4.999 ± 0.008
	0.00	0.7000 ± 0.0019		25.00	2.355 ± 0.002
				20.00	1.085 ± 0.0008
p-CH_3	15.00	2.364 ± 0.004		15.00	0.4812 ± 0.0002
	10.00	1.041 ± 0.002			
	5.00	0.4448 ± 0.0007	*m*-Cl	38.00	3.500 ± 0.001
	0.00	0.1843 ± 0.0003		30.00	1.061 ± 0.0006
					1.043 ± 0.002[a]
p-C_2H_5	20.00	5.091 ± 0.006		20.00	0.2181 ± 0.0003
	15.00	2.302 ± 0.002			
	10.00	1.012 ± 0.001	*m*-Br	38.00	3.728 ± 0.001
	5.00	0.4333 ± 0.0004		30.00	1.139 ± 0.001
				20.00	0.2331 ± 0.0002
Unsubst.	30.00	8.045 ± 0.008			
	25.00	3.789 ± 0.004	*m*-NO_2	50.00	2.524 ± 0.002
	20.00	1.749 ± 0.001		45.00	1.258 ± 0.001
	15.00	0.7754 ± 0.0007		40.00	0.6026 ± 0.0005
				30.00	0.1272 ± 0.0002
p-F	30.00	4.297 ± 0.004			
	25.00	2.013 ± 0.001	*o*-CH_3	5.00	12.3 ± 0.07
	20.00	0.9200 ± 0.0008		0.00	5.23 ± 0.010
	15.00	0.4075 ± 0.0004			
			o-Cl	20.00	2.619 ± 0.003
p-Cl	35.00	5.083 ± 0.006		15.00	1.139 ± 0.001
	30.00	2.428 ± 0.002		10.00	0.4794 ± 0.003
	25.00	1.132 ± 0.001		5.00	0.1964 ± 0.0010
	20.00	0.5129 ± 0.0004			
			o-Br	20.00	3.096 ± 0.003
p-Br	35.00	4.633 ± 0.003		15.00	1.345 ± 0.001
	30.00	2.219 ± 0.002		10.00	0.5667 ± 0.0004
	25.00	1.021 ± 0.001		5.00	0.2313 ± 0.0006
	20.00	0.4654 ± 0.0005			
			o-NO_2	50.00	4.740 ± 0.001
p-NO_2	50.00	2.464 ± 0.003		45.00	2.309 ± 0.002
	45.00	1.217 ± 0.001		40.00	1.095 ± 0.001
				30.00	0.2258 ± 0.0002

a) Measured by using sodium hypochlorite solution.

Table 3. Kinetic results of the Hofmann rearrangement of substituted *N*-chlorobenzamides

Subst.	$k_1 \times 10^4$ (sec^{-1}) 30.00°C	$\Delta H^{\neq}$ (kcal/mol)	$\Delta S^{\neq}$ (e. u.)
p-CH_3O	67.4[a]	24.89±0.03	13.61±0.10
p-C_2H_5O	70.9[a]	24.75±0.01	13.26±0.04
p-CH_3	23.64[a]	26.04±0.02	15.33±0.08
p-C_2H_5	23.00[a]	26.04±0.01	15.27±0.05
Unsubst.	8.045	26.45±0.05	14.55±0.15
p-F	4.297	26.65±0.02	13.97±0.06
p-Cl	2.428	26.83±0.02	13.43±0.05
p-Br	2.219	26.88±0.08	13.37±0.28
p-NO_2	0.1218	28.66±0.06	13.52±0.21
m-CH_3	13.67[a]	26.27±0.02	15.01±0.06
m-CH_3O	5.008	26.49±0.03	13.73±0.11
m-Cl	1.061	27.35±0.03	13.49±0.09
m-Br	1.139	27.31±0.10	13.51±0.33
m-NO_2	0.1272	28.48±0.08	13.00±0.28
o-CH_3	575.[a]	25.2 ±0.20	18.9 ±0.66
o-Cl	12.78[a]	27.41±0.02	18.64±0.05
o-Br	15.16[a]	27.45±0.01	19.09±0.04
o-NO_2	0.2258	29.01±0.04	15.89±0.14

a) Extrapolated from data at other temperatures.

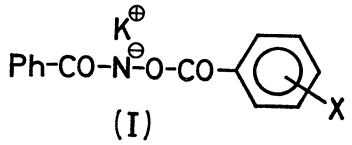

(I)

to that of the Hofmann rearrangement, it is also clear that the dissociation of the nitrogen-halogen bond in the Hofmann rearrangement takes place in the rate-determining step. The data on the relative reactivities of the *N*-chloro and *N*-bromo derivatives can be rather reasonably interpreted by considering the effect of solvation at the initial and the transition states. The reactant molecule, the conjugate base of *N*-haloamide, is strongly solvated by the hydrogen bond with the amide group, at which a large negative charge is acquired. Both *N*-chloro and *N*-bromo derivatives, however, will be subjected to almost the same degree of the solvation, since this solvation is controlled for the most part by the large acquired negative charge at the amide group, with a minor influence by the halogen atom. On the other hand, at the transition state the solvent water molecule is strongly hydrogen-bonded with a large negative charge on the halogen atom. Therefore, the degree of the solvation is proportional

to the ion potential of the halide ion itself; the *N*-chloro derivative is more solvated than the *N*-bromo derivative. The difference in the solvation effect in the transition state can be estimated to be one of the main factors in increasing the reactivity of *N*-chloroamide relative to that of *N*-bromoamide. This consideration is supported by the fact that the relative values of the activation entropy and the activation enthalpy have been found to be approximately −4 e.u. and −1.3 kcal/mol respectively.

In addition to the solvation effect, the effect of the $d\pi$–$p\pi$ conjugation on the relative rate effect can not be neglected. As has been described in the preceding paper, the $d\pi$–$p\pi$ conjugation on the nitrogen-halogen bond seems to be an important factor in depressing the reactivity. Therefore, if the $d\pi$–$p\pi$ conjugation on the N–Br bond is stronger than that of the N–Cl bond, the reactivity of the *N*-bromoamide will be relatively more depressed than that of the *N*-chloroamide. The above assumption regarding the relative strength of the $d\pi$–$p\pi$ conjugation on the nitrogen-halogen bond may be supported by the data on the $d\pi$–$p\pi$ conjugation of the carbon-halogen bond.[8] This might lead to a subsequent conclusion that, in the Hofmann rearrangement, the effects of the solvation and the $d\pi$–$p\pi$ conjugation on the relative reactivity are so important as to overcome the effects of the polarization and the σ-bond strength of the nitrogen-halogen bond.

The application of LFER to the present data will provide valuable information on the effect of the leaving group on the reactivity as well as on the more precise reaction mechanism of this rearrangement. In a preceding study of the substituent effect of the *N*-bromoamides, it has been inferred that the most important factors characterizing the Hofmann rearrangement are the $d\pi$–$p\pi$ conjugation on the N–Br bond in the initial state and the participation of the phenyl group migrating to electron-deficient nitrogen in the transition state.

These two factors can be influenced by the substituent on the migrating phenyl group, especially by the electron-releasing conjugative substituent at the para-position. In the initial state, such a substituent increases the $d\pi$–$p\pi$ conjugation on the nitrogen-bromine bond by the aid of the cross conjugation effect of the carbonyl group, as is indicated in Formula (II), and

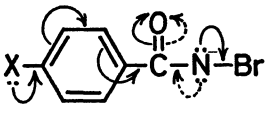

(II)

makes it more difficult to release the bromide ion from the reactant molecule. On the other hand, in the transition state, the same electron-releasing conjugative substituent facilitates the additional conjugation of the phenyl group with electron-deficient nitrogen, with a considerable stabilization of the transition state, and promotes the rate acceleration.

It is one of the purposes of the present study to examine the effect of the leaving group on the conjugation effects mentioned above. The logarithms of the relative rate constants of *meta*- and *para*-substituted *N*-chlorobenzamides have been plotted against those of *N*-bromoamides. An excellent linear relation has been observed except for the nitro group,[9] as shown in Fig. 2. The slope of the correlation line and its correlation coefficient are calculated as 0.97 and 0.9999 respectively.

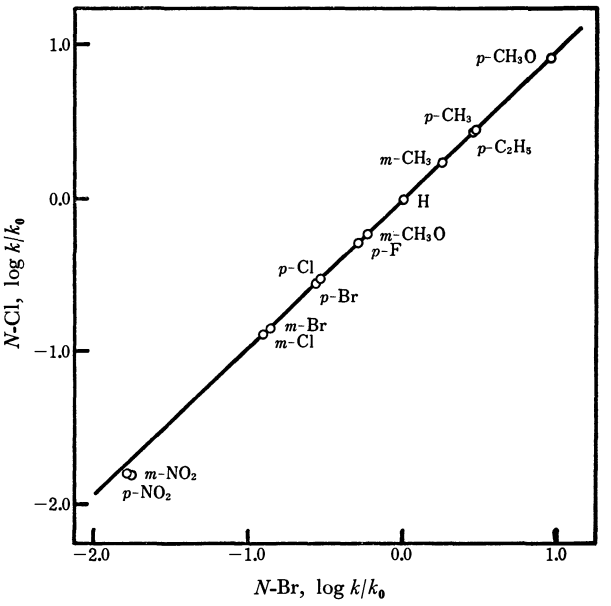

Fig. 2. Comparison of *N*-chloro with *N*-bromo derivatives.

Furthermore, as may be anticipated from the above results, the application of the Linear Aromatic Substituent-Reactivity relationship (LArSR relationship; $\log k/k_0=(\sigma^0+r\Delta\bar{\sigma}_R^+)$) to the present data gives almost the same values of the reaction constant, ρ, and of the resonance parameter, r, as those of the *N*-bromo series.

$$\log k/k_0 = -2.43(\sigma^0+0.41\Delta\bar{\sigma}_R^+) + 0.02$$

These results obviously indicate that the conjugation effects in both the initial and the transition states are also important factors for the reaction of *N*-chloroamides; furthermore, it may be concluded that the substituent effect for each conjugation effect is almost the same for both the *N*-chloro and *N*-bromo series. This conclusion does not conflict with the earlier estimation of the relative strength of the $d\pi$–$p\pi$ conjugation of N–Cl and N–Br bonds; such a small difference in the strength of the $d\pi$–$p\pi$ conjugation will not be so sensitively reflected in the substituent effect as to give a certain trend to the correlation plots.

It is also of interest to discuss the effect of the leaving group on the *ortho* effect. The *ortho*/*para* rate ratios for several substituents observed in Hofmann, Lossen and Curtius rearrangements are listed in Table 4. In

8) Although the data on the relative strength of the $d\pi$-$p\pi$ conjugation on the nitrogen-halogen bond have not yet been reported, its relative strength may be presumed to be the order, F$\ll$Cl$<$Br$<$I, from that of $d\pi$-$p\pi$ conjugation on the carbon-halogen bond; J. Hine and P. D. Langford, *J. Amer. Chem. Soc.*, **78**, 5002 (1956); J. Hine, N. W. Burske, M. Hine, and P. D. Langford, *ibid.*, **79**, 1406 (1957).

9) The deviations of the nitro groups are attributable to the uncertainty of the rate constants of the nitro-*N*-bromobenzamides.

Table 4. *ortho/para* rate ratios

$X\text{-}C_6H_4\text{-}CO\text{-}N^-\text{-}Y$

X/Y	Br	Cl	CO_2-	Cl CO_2-	NO_2 CO_2-	N_2
CH_3O	6.3		8.5			150.
CH_3	21.0	24.3				131.
Cl	4.2	5.3		5.9		208.
Br	5.5	6.8		8.0		277.
NO_2	1.5	1.9			2.2	70.

Table 5. Relative values of activation parameters of *ortho-* to *para*-derivatives

	N-Br		N-Cl		$N\text{-}N_2$	
	$\Delta\Delta H^{\neq}$ (kcal/mol)	$\Delta\Delta S^{\neq}$ (e. u.)	$\Delta\Delta H^{\neq}$ (kcal/mol)	$\Delta\Delta H^{\neq}$ (e. u.)	$\Delta\Delta H^{\neq}$ (kcal/mol)	$\Delta\Delta S^{\neq}$ (e. u.)
CH_3O	+0.7±0.5	+5.9±1.8				
CH_3	−0.2±0.2	+5.2±0.6	−0.8±0.2	+3.6±0.7	−5.0±0.3	−6.4±0.8
Cl	+1.0±0.2	+6.2±0.6	+0.6±0.0	+5.2±0.1	−5.4±0.6	−6.8±1.9
Br	+0.7±0.1	+5.5±0.3	+0.6±0.1	+5.7±0.3	−5.5±0.2	−4.1±0.7
NO_2	0.0±0.8	+0.8±2.5	+0.4±0.1	+2.4±0.4	−3.1±0.2	−1.7±0.5

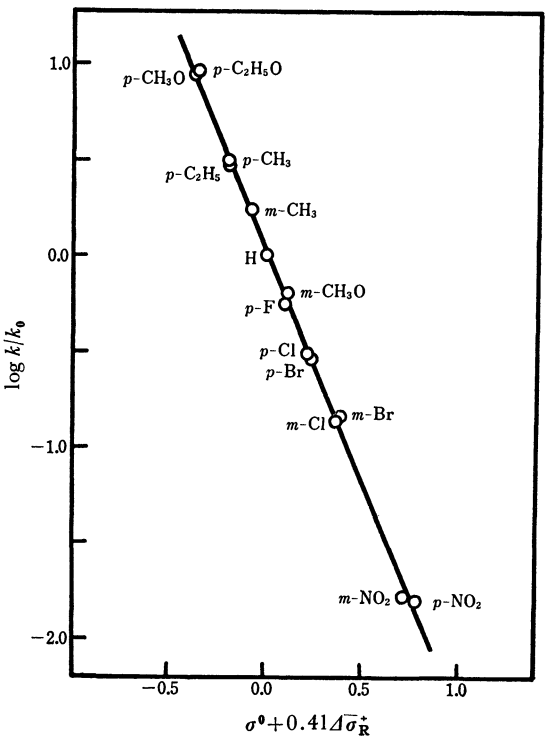

Fig. 3. Application of the LArSR relationship.

the case of the *N*-bromo series, the *ortho/para* rate ratio varies over a considerably wide range, depending on the substituent, but it tends to decrease with an increase of the electron-attracting character of the substituent except for the methoxy group. This tendency appears also in the present *N*-chloro series and in the Lossen rearrangement. Another noticeable fact is the relative value of the activation parameters of *ortho-* and *para*-substituents. In both the *N*-chloro and *N*-bromo series, similar values of $\Delta\Delta H^{\neq}$ and $\Delta\Delta S^{\neq}$ are observed in a given substituent except for nitro groups,[10] as is shown in Table 5. These facts apparently indicate that the *ortho* effects in the Hofmann and the Lossen rearrangements are almost the same in every leaving group.

On the other hand, the Curtius rearrangement, of which leaving group is a nitrogen molecule, is expected to be considerably different from the Hofmann and the Lossen rearrangements with respect to the reaction mechanism. The structure of the transition state of the Curtius rearrangement is considerably closer to that of the initial state, since, in this rearrangement, a stable nitrogen molecule is released in the rate-determining step. The reactivity, therefore, depends greatly on the strength of the $N\text{-}N_2$ bond.[11] In the case of an *ortho*-substituent, the bond-order of the $N\text{-}N_2$ bond is reduced by the steric restriction of the through conjugation of the phenyl group with the carbonyl group with an elevation in the reactivity. The exclusive significancy of this bond-energy effect on the Curtius rearrangement is evidently reflected in the *ortho* effects—the quite large *ortho/para* rate ratios and the enthalpy dependency of their rate ratios (see Tables 4 and 5). It is especially to be noted that the *ortho* effects on the Curtius rearrangement are in marked contrast to those on the Hofmann and the Lossen rearrangements, which are caused both by the bond-energy effect in the initial state and by the participation of the phenyl group migrating to nitrogen in the transition state.

10) The comparatively large disagreement of the nitro groups is caused by the uncertainty of the activation parameters of *N*-bromoamides. The *p*-nitro-*N*-bromobenzamide did not obey first-order kinetics at 30°C due to accompanying hydrolysis of the reactant molecule itself, and the reaction rates were measured at 45—55°C where satisfactory first-order plots were obtained. The narrow temperature range and the side reaction may afford considerable uncertainty to the derived values of activation parameters. In the case of *o*-nitro-*N*-bromobenzamide the reaction rate gradually increased as the reaction proceeded, and the rate constants were calculated from the initial stage of the reaction. Therefore, the activation parameters of this derivative may be also attended with large uncertainty.

11) Y. Yukawa and Y. Tsuno, *J. Amer. Chem. Soc.*, **79**, 5530 (1957); Y. Yukawa and Y. Tsuno, *ibid.*, **80**, 6346 (1958).

The Hofmann Rearrangement. III. Kinetic Substituent Effects of 4- and 5-Substituted 2-Chloro-*N*-chlorobenzamides

Tsuneo IMAMOTO, Yuho TSUNO, and Yasuhide YUKAWA

The Institute of Scientific and Industrial Research, Osaka University, Yamadakami, Suita, Osaka

(Received September 25, 1970)

The kinetic measurements of the Hofmann rearrangement of 2,4-, 2,5- 2,6-, and 3,5-disubstituted *N*-chlorobenzamides were carried out. The rate constants of 4- and 5-substituted 2-chloro-*N*-chlorobenzamides were applicable to the LArSR relationship:

$$\log k/k_0 = -2.21(\sigma^0+0.69\Delta\bar{\sigma}_R^+) + 0.03$$

indicating that the reactivity of the 2-chloro series was subjected to a larger additional conjugation effect than that of the 2-unsubstituted series. The detailed discussion of the reaction mechanism on the basis of these results supported strongly the concerted mechanism.

As has been described in the preceding papers,[1,2] kinetic studies of the Hofmann rearrangement of *mono*-substituted *N*-bromo- and *N*-chloro-benzamides were carried out with a view to elucidating its precise reaction mechanism. From the results, we concluded that both the bond-energy effect in the initial state and the participation of the migrating phenyl group in electron-deficient nitrogen in the transition state were important factors in characterizing the rearrangement.

In order to establish the existence of the above two factors, a kinetic study of the rearrangement of 4- and 5-substituted 2-chloro-*N*-chlorobenzamides has undertaken, and a further attempt has been made to evaluate each of them semi-quantitatively on the basis of LFER.

In this paper we will report these kinetic results, along with those of a few other disubstituted *N*-chlorobenzamides, and will discuss the reaction mechanism of the Hofmann rearrangement.

Experimental

Materials. *Disubstituted benzamides* were prepared by the usual methods and were identified by elementary analysis. The melting points of these amides are listed in Table 1.

Disubstituted N-chlorobenzamides were prepared by the methods described in the preceding paper. The melting points and the analytical data of these *N*-chloroamides are listed in Table 1.

Kinetic Measurements. The reaction rates were deter-

Table 1. Disubstituted benzamides and their *N*-chloro-derivatives

Subst.	Amides Mp °C	*N*-Chloroamides Mp °C (lit [a])	Analysis (Calcd) C%	H%	N%	Cl%	Act. Cl%
2-Cl-4-CH_3O	161.5—162.5	128.5—129.0	43.63 (43.67)	3.33 (3.21)	6.29 (6.37)	32.33 (32.22)	16.28 (16.11)
2-Cl-4-CH_3	180—181	119—120	47.06 (47.09)	3.45 (3.46)	6.84 (6.86)	34.58 (34.75)	17.21 (17.37)
2-Cl-5-CH_3	185.5—186.0	121—122	46.88 (47.09)	3.39 (3.46)	6.83 (6.86)	34.62 (34.75)	17.13 (17.37)
2,4-di-Cl	193—194	136—137	37.41 (37.46)	1.71 (1.80)	6.13 (6.24)	47.20 (47.38)	15.79 (15.79)
2,5-di-Cl	160.0—160.5	158.0—158.5	37.29 (37.46)	1.77 (1.80)	6.00 (6.24)	47.20 (47.38)	15.64 (15.79)
2-Cl-4-NO_2	171.0—171.5	190—200 (184—185)	35.97 (35.77)	1.67 (1.72)	12.19 (11.92)	30.24 (30.17)	14.56 (15.08)
2,6-di-Cl	202—203	190—192	37.52 (37.46)	1.87 (1.80)	6.42 (6.33)	47.50 (47.38)	15.64 (15.79)
3,5-di-Cl	161—162	198—200	37.59 (37.46)	1.71 (1.80)	6.33 (6.33)	47.20 (47.38)	15.44 (15.79)
3,5-di-Br	187—188	212—214	26.75 (26.83)	1.23 (1.29)	4.26 (4.47)		11.38 (11.31)
3,5-di-NO_2	183—184	176—177 (168)	34.26 (34.23)	1.44 (1.64)	17.28 (17·11)	14.31 (14.44)	14.16 (14.44)
2,5-di-Cl-4-CH_3 [b]		171—173	40.14 (40.29)	2.30 (2.54)	5.85 (5.87)	44.45 (44.59)	14.77 (14.86)

a) B. Altenkirk and S. S. Israelstam, *J. Org. Chem.*, **27**, 4532 (1962).

b) This *N*-chloroamide was obtained by the treatment of 2-chloro-4-methylbenzamide with chlorine gas under the same reaction condition as applied for the other amides.

1) T. Imamoto, Y. Tsuno, and Y. Yukawa, This Bulletin, **44**, 1632 (1971).

2) T. Imamoto, Y. Tsuno, and Y. Yukawa, *ibid.*, **44**, 1639 (1971).

mined according to the procedure described in the preceding paper. The initial concentrations of *N*-chloroamide and sodium hydroxide employed were 0.025 mol/*l* and 0.5 N respectively.

Results and Discussion

The rates of the release of the chloride ion from the conjugate bases of *multi*-substituted *N*-chlorobenzamides were measured under the same reaction conditions as those used in connection with the preceding kinetics of *mono*-substituted *N*-chlorobenzamides. All the runs except those of the 3,5-dinitro derivative strictly obeyed first-order kinetics, at least to 75% completion of the reaction.[3] The reproducibility of the rate constant from repeated runs was within 0.7%, and the plots of log k/T *vs.* $1/T$ gave an excellent straight line in every case. The observed first-order rate constants are listed in Table 2. The rate constants at 30.00°C and the derived activation parameters are summarized in Table 3.

Table 2. Rate constants of the Hofmann rearrangement of *multi*-substituted *N*-chlorobenzamides

Subst.	Temp. °C	$k_1 \times 10^4$ (sec^{-1})
2-Cl-4-CH_3O	6.00	6.52 ± 0.02
	4.00	4.680 ± 0.013
	0.00	2.366 ± 0.004
2-Cl-4-CH_3	17.00	6.478 ± 0.016
	13.00	3.358 ± 0.006
	10.00	2.021 ± 0.005
	5.00	0.8459 ± 0.0016
	0.00	0.4995 ± 0.0011
2-Cl-5-CH_3	20.00	4.495 ± 0.008
	15.00	1.976 ± 0.002
	10.00	0.8443 ± 0.0016
	0.00	0.3495 ± 0.0003
2,4-di-Cl	30.00	5.446 ± 0.001
	25.00	2.502 ± 0.002
	20.00	1.118 ± 0.002
	15.00	0.4822 ± 0.00004
2,5-di-Cl	35.00	4.406 ± 0.003
	30.00	2.059 ± 0.001
	25.00	0.9309 ± 0.0005
	20.00	0.4089 ± 0.0007
2-Cl-4-NO_2	45.00	2.755 ± 0.006
	40.00	1.311 ± 0.002
	35.00	0.5979 ± 0.0006
	30.00	0.2675 ± 0.0003
2,6-di-Cl	35.00	6.191 ± 0.007
	30.00	2.829 ± 0.002
	25.00	1.259 ± 0.0009
	20.00	0.5453 ± 0.0003
	15.00	0.2270 ± 0.0002
3,5-di-Cl	50.00	3.274 ± 0.005
	45.00	1.634 ± 0.001
	40.00	0.7902 ± 0.0007
	30.00	0.1715 ± 0.0002
3,5-di-Br	50.00	3.924 ± 0.004
	45.00	1.952 ± 0.002
	40.00	0.9545 ± 0.0008
	30.00	0.2084 ± 0.0003
2,5-di-Cl-4-CH_3	30.00	7.23 ± 0.01
	25.00	3.354 ± 0.004
	20.00	1.518 ± 0.002
	15.00	0.6620 ± 0.0009

Table 3. Kinetic results of the Hofmann rearrangement of *multi*-substituted *N*-chlorobenzamides

Subst.	$k_1 \times 10^4$ (sec^{-1})	$\Delta H^{\neq}$ (kcal/mol)	$\Delta S^{\neq}$ (e. u.)
2-Cl-4-CH_3O	253[a]	25.05±0.14	16.8 ±0.47
2-Cl-4-CH_3	48.8[a]	26.57±0.03	18.52±0.11
2-Cl-5-CH_3	21.46[a]	27.02±0.01	18.37±0.03
2,4-di-Cl	5.446	27.44±0.04	17.04±0.14
2,5-di-Cl	2.059	27.86±0.05	16.48±0.16
2-Cl-4-NO_2	0.2675	29.19±0.06	16.82±0.21
2,6-di-Cl	2.829	28.55±0.04	19.39±0.12
3,5-di-Cl	0.1715	28.10±0.04	12.33±0.14
3,5-di-Br	0.2084	27.94±0.03	12.20±0.11
2,5-di-Cl-4-CH_3	7.226	27.04±0.05	16.29±0.15

a) Extrapolated from data at other temperatures.

As a result of the previous kinetic studies of the Hofmann rearrangement of *mono*-substituted *N*-bromo- and *N*-chloro-benzamides, it was suggested that the bond-energy effect in the initial state and the participation of the phenyl group in electron-deficient nitrogen were important factors in controlling the reactivity. The most interesting point in connection with these two factors consists in the effects of the *para*-substituted electron-releasing conjugative groups on the reactivity. In the transition state these substituents facilitate the additional conjugation of the phenyl group with electron-deficient nitrogen, with a considerable stabilization of its state. In the inital state, however, such substituents increase the bond-order of the nitrogen-halogen bond through the cross-conjugation of the carbonyl group with the phenyl group and with the nitrogen orbital, and lead to a rate retardation with a stabilization of the initial state. The former conjugation effect is expected to give a comparatively large positive value of the reasonance parameter, r, of the LArSR relationship, whereas the latter effect will rather afford a negative r-value. The resonance parameter (r=0.41) for the rearrangement of *mono*-substituted *N*-chlorobenzamides can be qualitatively interpreted in terms of the mutual compensation of the conjugation effects in the initial and the transition states.

In order to establish these theories, it is necessary to ascertain the substituent effect in a system where the amide group is sufficiently hindered from conjugating with the phenyl group in the initial state, and so the kinetic study of 4- and 5-substituted 2-chloro-*N*-chlorobenzamides has been undertaken. The chloro group at the *ortho*-position has been chosen as the most suitable group in satisfying the following requirements: sufficient steric effect to restrict the through-conjugation of the amide group with the phenyl group in the initial state, measurable rates, and the easily-

3) In the case of 3,5-dinitro derivative excellent first-order plots were not obtained especially at the temperature lower than 45°C. This anomaly is presumably caused by accompanying the hydrolysis of the reactant conjugate base of *N*-chloroamide.

available amides.

The logarithms of the relative rate constants of the present 2-chloro series have been plotted against those of the preceding 2-unsubstituted series. As is illustrated in Fig. 1, all the *meta*-substituents and the *para*-nitro substituent form an excellent strainght line with a slope of 0.930 and a correlation coefficient of 0.9999, whereas the electron-releasing conjugative substituents at the *para*-position deviate upward from the correlation line. Each deviation, however, appears to be proportional to electron-releasing conjugative ability of its substituent. In fact, the least-mean-square calculation using the values of the electron-releasing conjugative ability ($\Delta\bar{\sigma}_R^+$)[4] gives an excellent straight line with a correlation coefficient of 0.9999, including all the *para*-substituents, as is shown in Fig. 2. The slope of the correlation line is 0.930, which is the same as that calculated from all the *meta*-substituents and the *para*-nitro substituent. This fact evidently indicates that the reactivity of the 2-chloro series is subjected to a larger additional conjugation effect than that of the 2-unsubstituted series. The application of the LArSR relationship to the present data gives a good linearity, as is shown in Fig. 3. Although the calculated reaction

$$\log k/k_0 = -2.21(\sigma^0+0.69\Delta\bar{\sigma}_R^+) + 0.03$$

constant ($\rho=-2.21$) is nearly equal to the value of the 2-unsubstituted series ($\rho=-2.43$), the resonance parameter ($r=0.69$) is considerably larger than that of the 2-unsubstituted series ($r=0.41$).

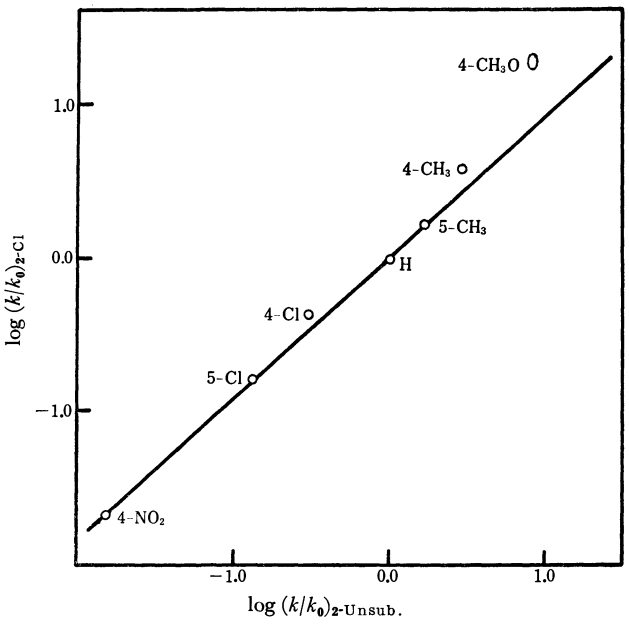

Fig. 1. Comparison with 2-unsubstituted derivatives.

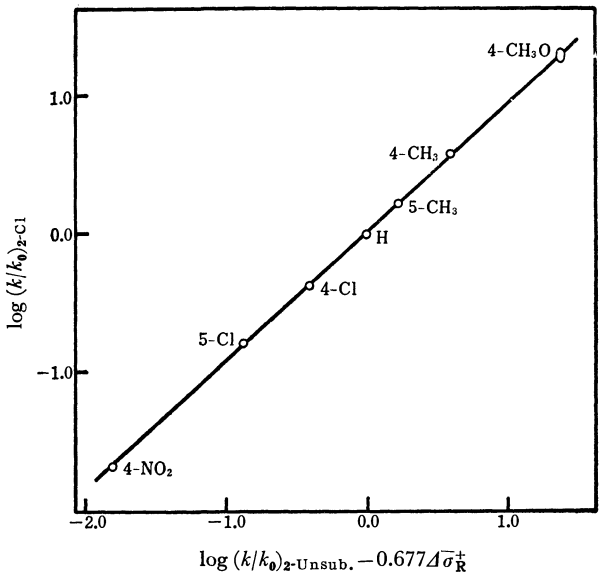

Fig. 2. Comparison with 2-unsubstituted derivatives with the application of the LArSR relationship.

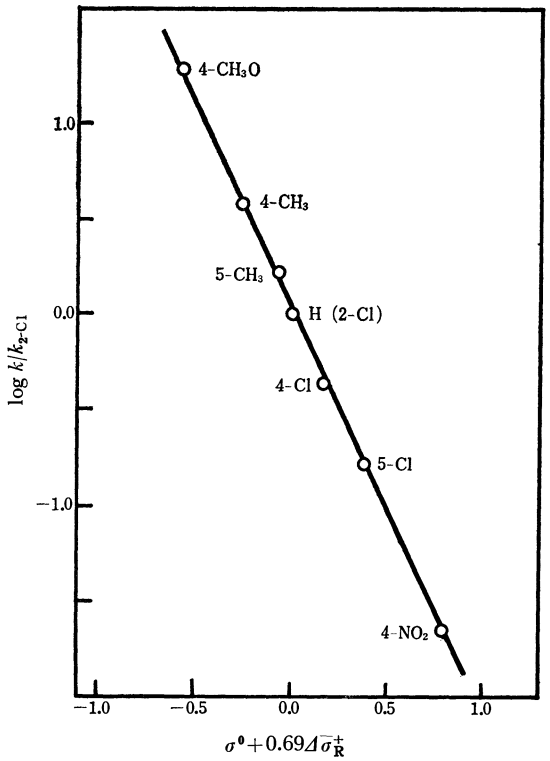

Fig. 3. Application of the LArSR relationship.

The conjugations applicable to the initial state are visualized in Formulae (I) and (II). The through-conjugation of the carbonyl group with the phenyl

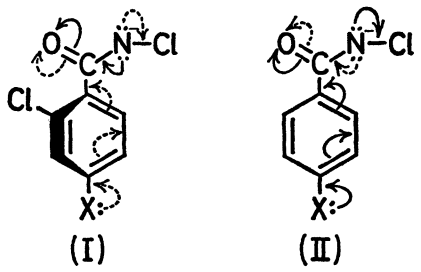

group is remarkably restricted in the 2-chloro system (I), while it is not in the 2-unsubstituted system (II). The substituent effect on this conjugation *effect* in the 2-chloro series, therefore, is expected to be

4) Y. Yukawa, Y. Tsuno, and M. Sawada, This Bulletin, **39**, 2274 (1966).

smaller than that in the 2-unsubstituted series.

On the other hand, in the transition state the degree of the conjugation in both series depends on the reaction mechanism (or on the structure of the transition state). In the two-step mechanism, the conjugation of phenyl group with the amide group is restricted in the 2-chloro system (III), but not in the 2-unsubstituted system (IV). On the contrary, in the concerted mechanism the degree of the conjugation may be expected to be almost the same for both the 2-chloro and 2-unsubstituted systems (V and VI), since in this state the phenyl ring is twisted almost at a right angle to the amide group due to the effective overlap of orbitals.

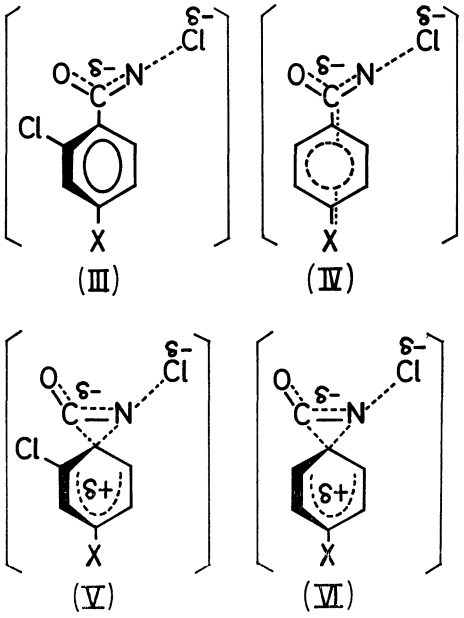

If the reaction proceeds through the two-step mechanism, the reactivity of the 2-chloro series should be considerably affected by the steric restriction of the conjugation in both the initial and transition states. The substituent effect of the conjugation effect on the 2-chloro series is expected to be smaller than that on the 2-unsubstituted series; the r-value of the 2-chloro series should be smaller than the value (0.41) of the 2-unsubstituted series. On the other hand, if the reaction proceeds through the concerted mechanism, the r-value to be observed on the 2-chloro series will be larger than the value of the 2-unsubstituted series, since the effect of the conjugation in the transition state is almost the same for both the 2-chloro and 2-unsubstituted series; further, the substituent effect on the conjugation effect in the initial state is reduced for the 2-chloro series more than for the 2-unsubstituted series. The comparatively large positive r-value (0.69) resulting in the 2-chloro series strongly supports the concerted mechanism rather than the two-step mechanism.

It is of interest to discuss the effect of the introduction of the chlorine atom into the *ortho*-position in relation to the above discussion of the substituent effect of

Table 4.

k_{2-Cl}/k_H	= 1.6
$k_{2,6\text{-di-Cl}}/k_H$	= 0.35
$k_{2,6\text{-di-Cl}}/k_{2\text{-Cl}}$	= 0.22
$k_{2\text{-Cl}}/k_{4\text{-Cl}}$	= 5.3
$k_{2,6\text{-di-Cl}}/k_{2,4\text{-di-Cl}}$	= 0.52

4- and 5-substituted 2-chloro-*N*-chlorobenzamides. The relative reactivities among unsubstituted, 2-chloro, 4-chloro, 2,4-dichloro, and 2,6-dichloro derivatives are listed in Table 4. The first introduction of the chlorine atom at the *ortho*-position effects a small rate acceleration ($k_{2-Cl}/k_H=1.6$), where as the second one at another *ortho*-position effects rather a rate retardation ($k_{2,6-diCl}/k_{2-Cl}=0.22$). The steric rate effect of the *ortho*-substituent can be qualitatively evaluated by means of the *ortho*/*para* rate ratios, since the polar effect of the *ortho*-substituent is generally recognized to be nearly equal to that of the corresponding *para*-substituent. The k_{2-Cl}/k_{4-Cl} value of the present reaction is calculated to be 5.3, indicating considerable steric rate acceleration due to the first introduction of the *ortho*-chloro substituent. The value of $k_{2,6-diCl}/k_{2,4-diCl}$, which corresponds to the steric rate effect due to the other *o*-chloro substituent, is calculated to be 0.52, indicating that the steric effect of the other *o*-chloro substituent affords a rather small rate retardation.

From these results, it would be reasonable to consider that the first introduction of the chloro substituent at the *ortho*-position effects a large steric effect to restrict the conjugation of the phenyl group with the carbonyl group considerably. The observed value of the resonance parameter of the 2-chloro series, therefore, may be attributed for the most part to the conjugation effect in the transition state. This value can be compared with the r-value of the Beckmann rearrangement, the reaction mechanism of which is estimated to be a concerted one. The r-value of the Beckmann rearrangement under various conditions has been calculated to be *ca.* 0.65. If the substituent effect on the conjugation in the transition state of the Hofmann rearrangement has an r-value of about 0.7, the effect of the $d\pi$-$p\pi$ conjugation in the initial state in the 2-unsubstituted series might be estimated to be *ca.* −0.3 as a resonance parameter by the subtraction of the value of 0.7 from the observed r-value (0.41) of the 2-unsubstituted series. This estimated r-value of the bond-energy effect due to the $d\pi$-$p\pi$ conjugation of the nitrogen-chlorine bond is reasonable as compared with the observed r-values of the Curtius and the Wolff rearrangements, which are characterized exclusively by the bond-energy effect of the $N-N_2$ bond.[5]

It is also of interest to discuss the substituent effects on the Hofmann rearrangement in terms of the derived activation parameters. The plots of $\Delta H^{\neq}$ *vs.* $\Delta S^{\neq}$ are

5) The r-values of the Curtius rearrangement in toluene and of the Wolff rearrangement in toluene are −1.04 and −1.7, respectively; Y. Yukawa and Y. Tsuno, *J. Amer. Chem. Soc.*, **79**, 5530 (1957); Y. Yukawa and Y. Tsuno, *ibid.*, **80**, 6346 (1958); Y. Yukawa, Y. Tsuno, and T. Ibata, This Bulletin, **40**, 2613 (1967); Y. Yukawa, Y. Tsuno, and T. Ibata, *ibid.*, **40**, 2618 (1967).

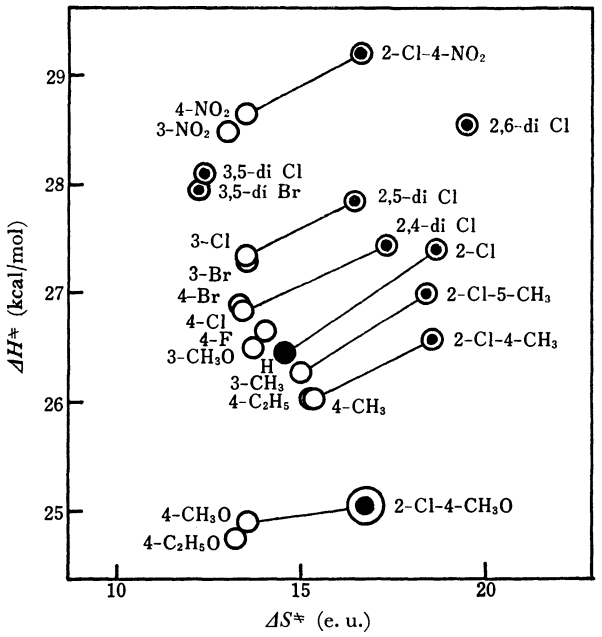

Fig. 4. $\Delta H^{\ddagger}$ *vs.* $\Delta S^{\ddagger}$ for the Hofmann rearrangement.

shown in Fig. 4, along with those of the *meta*- and *para*-substituents of the 2-unsubstituted series studied previously. In the case of the 2-unsubstituted series the enthalpy of activation varies from *ca.* 24.5 to *ca.* 28.5 kcal, although the entropy of activation varies merely from *ca.* 13 to *ca.* 15 e.u. This enthalpy dependency of the substituent effect on the reactivity is presumably caused both by the bond-energy effect in the initial state and by the additional conjugation effect of the phenyl group in the transition state, rather than by the solvation effect. The solvation effect is surely considered to play an important role in the reactivity; however, the substituent effect on it appears to be almost the same throughout the series. Another noticeable fact is shown by the plots of the 2-chloro series, which form a pattern similar to that of the 2-unsubstituted series, though they deviate in parallel fashion by *ca.* 3 e.u. and *ca.* 0.5 kcal from the corresponding plots of the 2-unsubstituted series. This fact shows that the reaction mechanism of the 2-unsubstituted and 2-chloro series are substantially the same. In the 3,5-dichloro and 3,5-dibromo derivatives, excellent additivities are found not only in the free energy of activation but also in the entropy and the enthalpy of activation. These additivities also indicate that the reaction mechanism of this rearrangement does not change with the change in the polar effect, at least not in the cases examined. The 2,6-dichloro derivative, however, does not retain any additivity. The failure of the additivity in the free energy of activation may be attributed to the entropy of activation, as is indicated in Fig. 4. The entropy gain caused by the concerted mechanism is perhaps saturated by the first introduction of the chlorine atom. The second introduction will afford rather rate retardation because of the additional polar effect.

Synthesis and Spectral Properties of Chloro-substituted Triptycenes

Ikuko MORI, Tadao KADOSAKA,* Yoshiteru SAKATA, and Soichi MISUMI

The Institute of Scientific and Industrial Research, Osaka University, Suita, Osaka

(Received October 22, 1970)

A series of 2-, 7-, 10-, and 11-chloro-substituted triptycenes were prepared by means of the addition of benzyne or 3-chlorobenzyne to anthracene and its derivatives for studying the effect of chloro-substituent on electronic and NMR spectra. It was found that the intensity of the longest wavelength bands in the chlorotriptycenes could be explained in terms of superposition of three benzenoid chromophores, and that the calculated value of chloro-group on magnetic anisotropy was in good agreement with the values reported.

Owing to its rigid cage structure which enables σ-type overlap between three isolated π-electron systems, triptycene has been given much attention since the first synthesis by Bartlett *et al.*[1] Thereafter many derivatives have been synthesized[2] for the investigation of electronic, NMR, and CD spectral properties.

A stepwise introduction of a particular substituent at 2-, 10-, and 11-positions of triptycene (I) is interesting

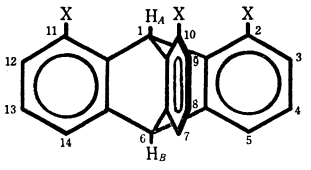

I

for the study of the effect of the substituent on the electronic absorption spectrum of triptycene. Such derivatives are suitable for exploring the magnetic anisotropy of the substituent by comparison of the chemical shift of bridgehead proton H_A with that of the other one H_B.

In the present paper we will report on the synthesis and the spectral, electronic and NMR properties of several chlorotriptycenes.

Results and Discussion

Synthesis The synthesis of mono-, di-, and trichlorotriptycenes was carried out according to the reaction sequence shown in Chart 1. Chloro-substituted anthracenes, III, IV, and V, were prepared from the corresponding anthraquinone derivatives by reduction with zinc and aqueous ammonia.[3] The mono- and di-chlorotriptycenes were obtained in two ways, by the reaction of the corresponding chloroanthracenes with benzyne generated from anthranilic acid according to the procedure of Friedman,[4] and by the reaction of anthracene and 1-chloroanthracene with 3-chlorobenzyne generated from 6-chloroanthranilic acid. The fact that both methods give identical products, 2-chloro-

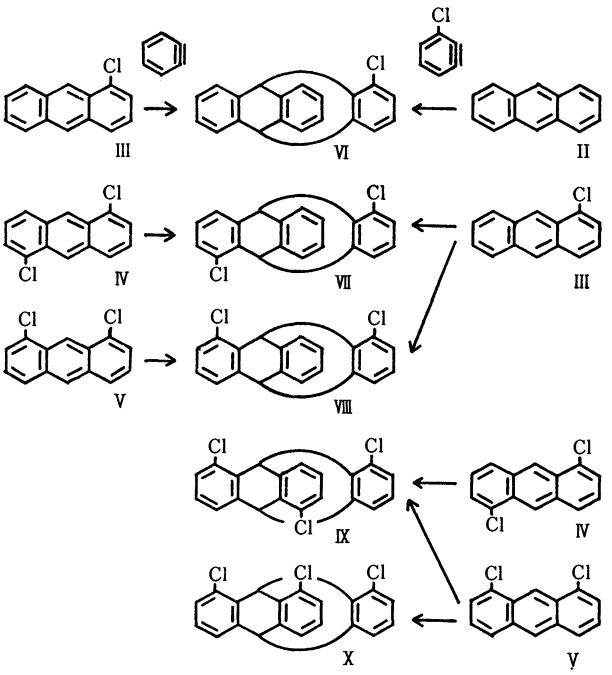

Chart 1

triptycene (VI) and dichlorotriptycenes (VII and VIII), indicates intermediary formation of 3-chlorobenzyne from 6-chloroanthranilic acid. 2,7,11-Trichlorotriptycene (IX) was prepared by the addition of 3-chlorobenzyne to 1,5-dichloroanthracene (IV), while an isomer, 2,10,11-trichlorotriptycene (X) was obtained along with IX by use of 1,8-dichloroanthracene (V) in place of IV. The properties and yields of the above chlorotriptycenes are summarized in Table 5.

In general, a mixture of two isomeric triptycenes, quasi-*trans* and quasi-*cis*, is obtained by the reaction of 3-chlorobenzyne with the substituted anthracenes devoid of center of symmetry, *i.e.*, III, V, and XI; for example, a mixture of quasi-*trans* (XII) and quasi-*cis* (XIII) from XI as follows.

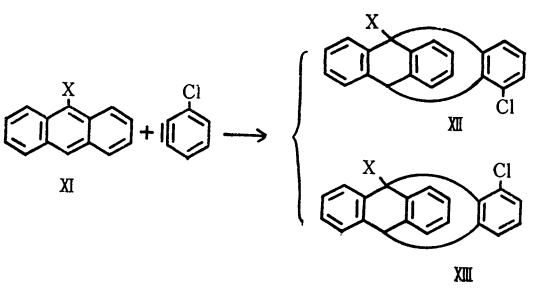

* Present address: Osaka Customs, Minato-ku, Osaka.

1) P. D. Bartlett, M. J. Ryan, and S. G. Cohen, *J. Amer. Chem. Soc.*, **64**, 2649 (1942).

2) For review, see B. H. Klanderman, *Org. Chem. Bull.*, **37**, No. 1 (1965).

3) H. Schilling, *Ber.*, **46**, 1066 (1913).

4) L. Friedman and F. M. Logullo, *J. Amer. Chem. Soc.*, **85**, 1549 (1963); *J. Org. Chem.*, **34**, 3089 (1969).

As the isomers are distinguishable from the chemical shifts (Table 4) of the bridgehead protons in NMR spectra, the ratio of the isomers can be determined by comparison of their peak areas. The ratios obtained are shown together with those of 9-substituted anthracenes in Table 1. It is difficult to attribute these ratios to steric requirement of substituents. The inductive effect of the substituents would be mainly operative in determining the ratios.

Table 1. Ratios of isomeric triptycenes yielded by the reaction with 3-chlorobenzyne

Anthracene	Triptycene derivative quasi-*trans*/quasi-*cis*
1-Chloro- (III)	1
1,8-Dichloro- (V)	1.9
9-Chloro- (XI)	1.9
9-Methyl- (XI)	1
9-Ethyl- (XI)	1
9-*i*-Propyl- (XI)	0.8

Electronic Spectra Two different interpretations have been given on the electronic spectra of triptycene and its derivatives up to the present. On the basis of appreciable spectral difference between triptycene and triphenylmethane, Bartlett and Lewis ascribed the difference to the intramolecular charge transfer in the former.[5] On the other hand, Wilcox, Jr., and Craig gave the explanation that the electronic spectrum of triptycene could be regarded as the superposition of three benzenoid chromophores on the ground of crude MO calculation.[6]

The spectra of chloro-substituted triptycenes are shown along with those of the parent compound triptycene in Fig. 1 and Table 2. They show that all the longest wavelength bands of chlorotriptycenes appear at the same position, but the intensity of the bands at 260—280 mμ decreases with the increase of the number of chloro-substituent. It seems that this phenomenon can be explained by Platt's quantitative approach to the intensities of the ^1L_b band in polysubstituted benzenes.[7] He assigned to each substituent a quantity

Table 2. Absorption maxima and intensity of triptycene and chlorotriptycenes in dioxane

	λ_{max} mμ (ε)
I: X=H	220.5(28300), 256.5(3010), 263[a](2640), 271(3870), 278.5(4740)
VI	224(32500), 273(2280), 280(2820)
VII	224(43800), 269(1280), 274(1550), 278(1600), 282(1600)
VIII	224(42500), 278(1580), 282(1460)
IX	221(76000), 273(960), 281.5(1000)
X	221(80200), 273.5(925), 282(975)

a) Inflection

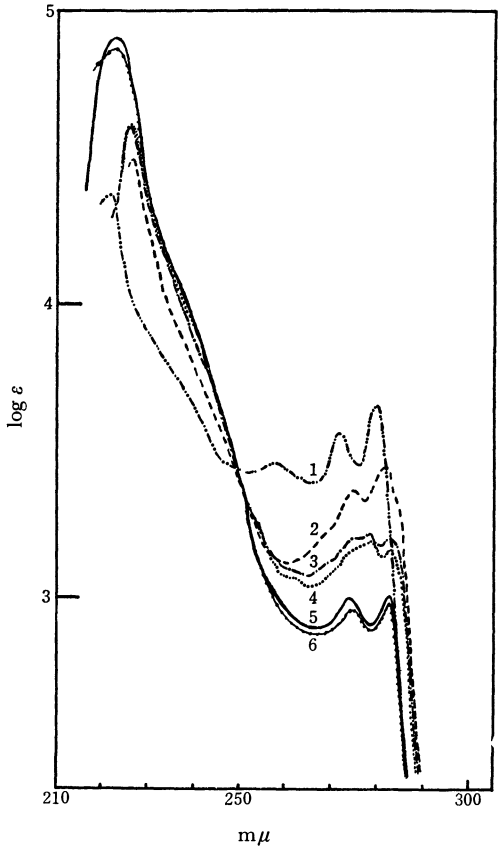

Fig. 1. Electronic spectra of triptycene and chlorotriptycenes in dioxane.
1, Triptycene(Tr); 2, 2-Cl-Tr(VI); 3, 2,7-Cl_2-Tr(VII); 4, 2,10-Cl_2-Tr(VIII); 5, 2,7,11-Cl_3-Tr(IX); 6, 2,10,11-Cl_3-Tr(X)

called the spectroscopic moment m, which has units of (centimeter moles/liter)$^{1/2}$ and from which the increase or the decrease in the maximum extinction ε can be calculated by the following vector-addition formula for two substituents.

$$\varepsilon - \varepsilon_0 \sim m_i^2 + m_j^2 - 2m_i m_j \cos\theta \qquad (1)$$

where ε_0 is the vibrational intensity of benzene itself and θ is the angle between the axes through each substituent and bisecting the ring.

To calculate the intensity, triptycene is divided into three *o*-xylene chromophores, and 2-chlorotriptycene is divided into one 3-chloro-*o*-xylene and two *o*-xylene chromophores in the same manner. Then the relative intensities of *o*-xylene and 3-chloro-*o*-xylene are res-

Table 3. Calculated and observed values for the intensity of the longest wavelength absorption bands of chlorotriptycenes

Triptycene	ε-Value	
	Calcd	Obsd
2-Cl- (VI)	3339	2820
2,7-Cl_2- (VII)	1938	1600
2,10-Cl_2- (VIII)	1938	1460
2,7,11-Cl_3- (IX)	537	1000
2,10,11-Cl_3- (X)	537	975

5) P. D. Bartlett and E. S. Lewis, *J. Amer. Chem. Soc.*, **72**, 1011 (1950).
6) C. F. Wilcox, Jr., *J. Chem. Phys.*, **33**, 1874 (1960); C. F. Wilcox, Jr., and A. C. Craig, *J. Org. Chem.*, **26**, 2491 (1961).
7) J. R. Platt, *J. Chem. Phys.*, **19**, 263 (1951).

pectively 49 and 1, estimated by Eq. (1) and the moments of methyl and chlorine groups (7 and 6).[7] Assuming the ε-values of *o*-xylene chromophore is one third of ε-value of triptycene (ε=4740) and ε_0 is 150,[7] $\varepsilon-\varepsilon_0$ value of 3-chloro-*o*-xylene is $(4740/3-150)\times 1/49$. Thus the ε-value of the longest wavelength bands of chlorotriptycenes were calculated as shown in Table 3.

The calculated values also show the decreasing tendency of the intensities with the number of chloro-substituent. A moderately good agreement between observed and calculated values was obtained. The small difference between both values is possibly due to the replacement of the spectroscopic moment of bridgehead carbon simply by that of methyl group.

Consequently, we suppose that the intensity of ^1L_b bands of chlorotriptycenes can be accounted for in terms of the superposition of three benzenoid chromophores, which supports Wilcox, Jr.'s interpretation on the UV spectra of triptycene.

NMR Spectra The NMR spectra of triptycene and its derivatives were first reported by Theilacker *et al.*[8] and later analyzed in detail by Smith and Shoulders,[9] and Kidd *et al.*[10] The spectrum of triptycene in carbon disulfide reveals an $A'_2B'_2$ pattern of aromatic protons centered at 2.96 τ and a singlet of two bridgehead tertiary protons at rather low field of 4.79 τ. Supposing that a substituent is introduced at 2- or 3-position of triptycene, bridgehead proton should shift to higher or lower field owing to the anisotropy of the substituent. Thus the magnitude of such shifts will allow us to estimate the shielding effect of the substituent by comparison with the other bridgehead proton as in structure (I). Table 4 shows the chemical shifts of bridgehead

Table 4. Chemical shifts (δ) of bridgehead protons of chlorotriptycenes in $AsCl_3$ and average internal chemical shift per chlorine atom

Triptycene	No. of Cl				$\Delta\sigma$/Cl
	0	1	2	3	
2-Cl- (VI)	5.49	5.90			−0.41
2,7-Cl_2 (VII)		5.92			
2,10-Cl_2- (VIII)	5.52		6.37		−0.43
2,7,11-Cl_3- (IX)		5.93	6.38		−0.45
2,10,11-Cl_3- (X)	5.53			6.89	−0.45
				average	−0.43

protons of chlorotriptycenes. The spectra of chlorotriptycenes (VI—X) were all measured in arsenic trichloride because of poor solubility of trichloroderivatives (IX and X) in the usual organic solvents. The table reveals that with the increase of the number of chlorine atoms the resonance position of the bridgehead proton regularly shifts to lower field by average 0.43 ppm.[11]

A difference in net shielding, or the internal chemical shift $\Delta\sigma$, between two protons H_A and H_B in a molecule can generally be expressed by the equation

$$\Delta\sigma = \sigma_A - \sigma_B = \Delta\sigma_d + \Delta\sigma_w + \Delta\sigma_e \quad (2)$$

where $\Delta\sigma_d$ is magnetic anisotropy effect, $\Delta\sigma_w$ is the van der Waals effect and $\Delta\sigma_e$ is electric field effect. In reference to the X-ray analysis[12] the geometry of chlorotriptycenes was drawn from which the distance r between a bridgehead proton nearer to chlorine atom and the midpoint of C–Cl bond, the distance R between the proton and the chlorine atom, and the angle θ given by the line represented as r and C–Cl bond axis were measured, as shown in Fig. 2.

The electric field effect $\Delta\sigma_e$ in Eq. (2) is calculated by the equation of Buckingham[13]

$$\Delta\sigma_e = -2\times 10^{-12}E_z - 10^{-18}E^2, \quad (3)$$

and the electric field term E is estimated by the following equation, assuming the point charge.

$$E = \mu/R^2\cdot l, \quad (4)$$

where μ is the dipolemoment of chlorobenzene (1.56 D) and l is the distance between chlorine atom and the center of the benzene ring (Fig. 2).

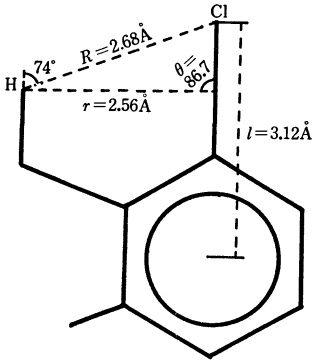

Fig. 2. Measured distances (R, r, and l) and angles in chlorotriptycenes.

The steric compression effect $\Delta\sigma_w$ is estimated from the following equation which was presented by Bothner-By and modified by Nakagawa.[14]

$$\Delta\sigma_w = (-[R]/R^6)\times 7 \quad (5)$$

where [R] is atomic refraction. The value $\Delta\sigma_d$ (−0.03 ppm) which is left in substracting $\Delta\sigma_e$ (−0.29 ppm) and $\Delta\sigma_w$ (−0.11 ppm) from the observed value $\Delta\sigma$ may be ascribed to the long range shielding due to the magnetic anisotropy of the substituent. $\Delta\sigma_d$ is related with the measured values of θ and r by the following McConnell equation.[15]

8) W. Theilacker, K. Albrecht, and H. Uffmann, *Chem. Ber.*, **98**, 428 (1965).

9) W. B. Smith and B. A. Shoulders, *J. Phys. Chem.*, **69**, 2022 (1965).

10) K. G. Kidd, G. Kotowycz, and T. Schaefer, *Can. J. Chem.*, **45**, 2155 (1967).

11) Because of difficulty in quantitative evaluation for solvent effect, the value in arsenic trichloride will be taken in the following calculations.

12) K. Ozeki, N. Sakabe, and J. Tanaka, Symposium on Molecular Structure held by The Chemical Society of Japan, Summary 3B25, Tokyo, October 1968; K. J. Palmer and D. H. Templeton, *Acta Crystallogr.*, **B24**, 1048 (1968).

13) A. D. Buckingham, *Can. J. Chem.*, **38**, 300 (1960).

14) A. A. Bothner-By, *J. Mol. Spectrosc.*, **5**, 52 (1960); N. Nakagawa, "Interpretation of NMR Spectra," Kyoritsu, Tokyo (1966), p. 98.

15) H. J. McConnell, *J. Chem. Phys.*, **27**, 226 (1957).

Table 5. Analytical data, solvents in reaction and yields of chlorotriptycenes

Triptycene	Formula	Anal Calcd % C	H	Cl	Found % C	H	Cl	Mp °C	Recryst. Solvent	Yield %	Reaction solvent
2-Cl- (VI)	$C_{20}H_{13}Cl$	83.19	4.54	12.28	83.12	4.27	12.37	225.0—225.5[a]	C_2H_5OH	1) 30 2) 16	1) CH_2Cl_2-THF[c] 2)
3-Cl-	$C_{20}H_{13}Cl$	83.19	4.54	12.28	83.12	4.54	12.12	167.5—168.0[b]	Pet. ether	1) 2	1) DME[c]
2,7-Cl_2- (VII)	$C_{20}H_{12}Cl_2$	74.32	3.74	21.94	74.00	3.54	21.70	258.0—258.5[a]	C_2H_5OH	1) 42 2) 8	1) CH_2Cl_2-THF[c] 2) DME[c]
2,10-Cl_2- (VIII)	$C_{20}H_{12}Cl_2$	74.32	3.74	21.94	74.13	3.54	21.77	299.5—300.0[a]	C_6H_6	1) 75 2) 8	1) CH_2Cl_2-THF[c] 2) DME[c]
2,7,11-Cl_3- (IX)	$C_{20}H_{11}Cl_3$	67.16	3.10	29.74	66.80	3.47	29.98	303—307[a]	C_2H_5OH	1) 9 2) 16	1) DME[c] 2) DME[c]
2,10,11-Cl_3- (X)	$C_{20}H_{11}Cl_3$	67.16	3.10	29.74	67.72	3.14	29.41	413—415[a]	C_6H_{12}		

a) in sealed tube. b) lit[4] mp 168—169°C. c) THF=tetrahydrofuran; DME=dimethoxyethane.
1) benzyne method. 2) chlorobenzyne method.

$$\Delta\sigma_d = (1/3r^3)\Delta\chi(1-3\cos^2\theta) \quad (6)$$

A calculated value of $\Delta\chi$, -1.6×10^{-30} cm^3/molecule, is in good agreement with the values reported by Schaeffer and Yonemoto[16] (5×10^{-30} cm^3/molecule) and by Flautt[17] (1.5×10^{-30} cm^3/molecule).

Two bridgehead protons of 3-chlorotriptycene show a singlet peak, or no internal chemical shift, probably due to the smaller difference of distances between both protons and the substituent in 3-substituted triptycene than in 2-substituted one.

These results imply that our assumption is reasonable, and that the triptycene derivatives are fairly suitable compounds for the study of magnetic anisotropy, due to the presence of appropriate reference proton in the rigid molecular structure.

Experimental

All melting points are uncorrected. The IR and UV spectra were measured on a Jasco autorecording spectrometer DS-402G and on a Hitachi EPS-3T, respectively. The NMR spectra were measured on a Hitachi Perkin-Elmer R-20 spectrometer (60 MHz) using TMS as an internal standard. A frequency counter was used to measure the frequency separation between signals.

Mono-, Di-, and Tri-chlorotriptycenes. Preparation of mono-, di-, and tri-chlorotriptycenes was carried out using the Diels-Alder reaction of anthracene derivatives with benzyne or 3-chlorobenzyne, generated from anthranilic or 6-chloroanthranilic acid respectively (Chart 1). All the reactions were carried out according to the procedure of Friedman and Logullo.[4] 3-Chlorotriptycene was synthesized by the reaction of anthracene with 4-chlorobenzyne generated from 5-chloroanthranilic acid.

2-Chlorotriptycene (VI) obtained by two methods shows an identical melting point and spectral properties. The reaction of 1-chloroanthracene with 3-chlorobenzyne gave a mixture of dichlorotriptycenes, VII and VIII. Attempts to separate VII and VIII from the mixture were unsuccessful. However, the chromatography on alumina of the reaction mixture of 1,8-dichloroanthracene (V) with 3-chlorobenzyne resulted in the separation of the trichlorotriptycenes, IX and X. An early benzene fraction was evaporated and recrystallized from alcohol to give 2,7,11-trichlorotriptycene (IX). Crystals obtained from the latter fraction were treated with cyclohexane to remove IX from slightly soluble isomer, 2,10,11-trichlorotriptycene (X) and were recrystallized from cyclohexane to give pure X.

The analytical data, melting points and yields of several chlorotriptycenes obtained are summarized in Table 5.

Reaction of 3-Chlorobenzyne with 9-Alkyl- and 9-Chloro-anthracenes. All reactions of 3-chlorobenzyne with 9-alkyl- and 9-chloro-anthracenes were undertaken according to the general procedure[18] described in the following case of 9-methylanthracene.

To a solution of 9-methylanthracene[19] (2.0 g, 10 mmol) and *i*-amyl nitrite (2.0 m*l*, 15 mmol) in dimethoxyethane (20 m*l*) was dropwise added a solution of 6-chloroanthranilic acid (2.6 g, 15 mmol) in dimethoxyethane (10 m*l*) for 30 min under refluxing and stirring. After further reflux for 10 min and addition of *i*-amyl nitrite (2 m*l*), an additional solution of 6-chloroanthranilic acid (2.6 g) in dimethoxyethane (10 m*l*) was added dropwise to the mixture for 30 min under reflux. The mixture was refluxed for 20 min with stirring to complete the reaction and cooled, and the solvent was removed *in vacuo*. The residue obtained was treated with maleic anhydride (2.0 g) in xylene (25 m*l*) under reflux for 1 hr. After evaporation of xylene the residue was chromatographed on alumina (50 g) with benzene. A part (150 m*l*) of the effluent (700 m*l*) was evaporated to dryness in a vacuum and the residue was dissolved in deuterochloroform to measure NMR spectrum. The ratio of quasi-*trans*/quasi-*cis* in the product was determined from half-width of bridgehead proton signals in both isomers.

The authors wish to express their appreciation to Professor Masazumi Nakagawa of Osaka University for his continued encouragement through this work.

16) T. Schaeffer and T. Yonemoto, *Can. J. Chem.*, **42**, 2318 (1964).
17) T. J. Flautt and W. F. Erman, *J. Amer. Chem. Soc.*, **85**, 3212 (1963).
18) *Cf.* L. F. Fieser, "Organic Experiments," 3rd Ed., D. C. Heath Co., Boston (1964), p. 314.
19) A. Sieglitz and R. Marx, *Ber.*, **56**, 1619 (1923).

The Cyclization Products from Acetone with Cyanoacetic Esters

Minoru IGARASHI*,** and Hiroshi MIDORIKAWA**

*Department of Chemistry, Faculty of Science, Ibaraki University, Mito, Ibaraki

**The Institute of Physical and Chemical Research, Wako, Saitama

(Received October 28, 1970)

The structure of the cyclization product from acetone with the cyanoacetic ester has been established as 3-alkoxycarbonyl(cyano)methylene-6-cyano-5,5-dimethyl-1-cyclohexene-1-ol by means of infrared and NMR spectroscopic determinations and by successive degradations.

A cyclic compound, $C_{14}H_{16}O_3N_2$, regarded as 4,6-dicyano-4-ethoxycarbonyl-3,5,5-trimethyl-$\Delta^{2,6}$-cyclohexadien-1-ol (I), was first obtained by Gardner and Haworth[1] by the condensatioln of acetone with a sodium derivative of ethyl cyanoacetate. The reaction course was inferred to be as follows.

$$(CH_3)_2CO + 2CH_2(CN)COOC_2H_5 \xrightarrow{NaOC_2H_5}$$

$$(CH_3)_2C(CH(CN)COOC_2H_5)_2 \xrightarrow{(CH_3)_2CO}$$

$$(CH_3)_2C\begin{matrix}\diagup CH(CN)COCH_2COCH_3 \\ \diagdown CH(CN)COOC_2H_5\end{matrix} \xrightarrow{(HCl)}$$

$$(CH_3)_2C\begin{matrix}\diagup C(CN)=\!=\!=\!=\!=C(OH)\diagdown \\ \diagdown CH(CN)COOC_2H_5 \quad HO(CH_3)C\diagup\end{matrix}CH \xrightarrow{-H_2O}$$

$$(CH_3)_2C\begin{matrix}\diagup C(CN)=\!=\!=\!=\!=C(OH)\diagdown \\ \diagdown C(CN)(COOC_2H_5)\text{-}C(CH_3)\diagup\end{matrix}CH \qquad (I)$$

They claimed that the product afforded a benzoyl derivative, but no rigorous proof for the structure was presented. The same product was obtained by us from acetone with ethyl cyanoacetate in the presence of potassium fluoride.[2] In view of the existing uncertainty of the structure of the product and our interest in the analogous cyclization reaction, it seemed worth while to reinvestigate the condensation product of acetone and cyanoacetic ester.

We prepared a compound, $C_{13}H_{14}O_3N_2$, by the condensation of acetone with methyl cyanoacetate in the presence of anhydrous potassium fluoride. After purification by recrystallizations, the product was obtained as pale yellow plates, mp 175°C, which were turned green by the action of ferric chloride in an alcoholic solution and which dissolved readily in an aqueous sodium carbonate solution. The reaction of the product with an excess of alcoholic 2,4-dinitrophenylhydrazine gave no precipitates, but the product became slightly reddish-yellow after standing for several days. These results indicated the structure of the product to be the enol-form rather than the tautomeric keto-form.

The infrared spectrum (Nujol) (Fig. 1) of the product showed an OH stretching band at 3110 cm^{-1} and a band located at 3530 cm^{-1} in an acetone solution. Other prominent bands were observed at 2270 cm^{-1} (very weak) and 2220 cm^{-1} (strong), corresponding to the presence of unconjugated and conjugated nitrile groups respectively. Absorption bands characteristic of the carbonyl group (1720 cm^{-1}) and the C=C group (1590 cm^{-1}) were observed. These infrared spectrum data render the formula I untenable and suggest that formula II or III is more plausible:

$$NC\diagdown \overset{4}{C}H_2\text{-}\overset{5}{C}(CH_3)_2\diagdown{}^{6} \quad \text{(II)}$$
$$\quad {}^{3}C=C \qquad\qquad CHCN$$
$$CH_3OOC\diagup \quad \diagdown CH=C(OH)\diagup$$
$$\qquad\qquad {}_{2} \quad {}_{1}$$

$$CH_3OOC\diagdown \quad \diagup CH_2\text{-}C(CH_3)_2\diagdown \quad \text{(III)}$$
$$\quad C=C \qquad\qquad CHCN$$
$$NC\diagup \quad \diagdown CH=C(OH)\diagup$$

The structure could also be deduced from the NMR spectrum, and a complete assignment could be made in terms of a mixture of two geometrical isomers, II and III.

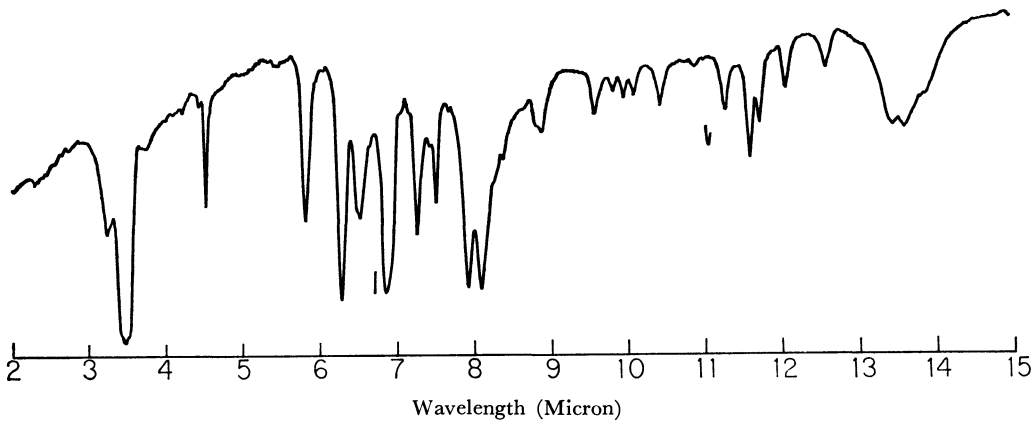

Fig. 1. The IR spectrum of 6-cyano-5,5-dimethyl-3-methoxycarbonyl(cyano)methylene-1-cyclohexene-1-ol.

1) H. D. Gardner, Jr., and W. N. Haworth, *J. Chem. Soc.*, **95**, 1955 (1909).

2) M. Igarashi, H. Midorikawa, and S. Aoyama, *J. Sci. Res. Inst.*, **52**, 105 (1958).

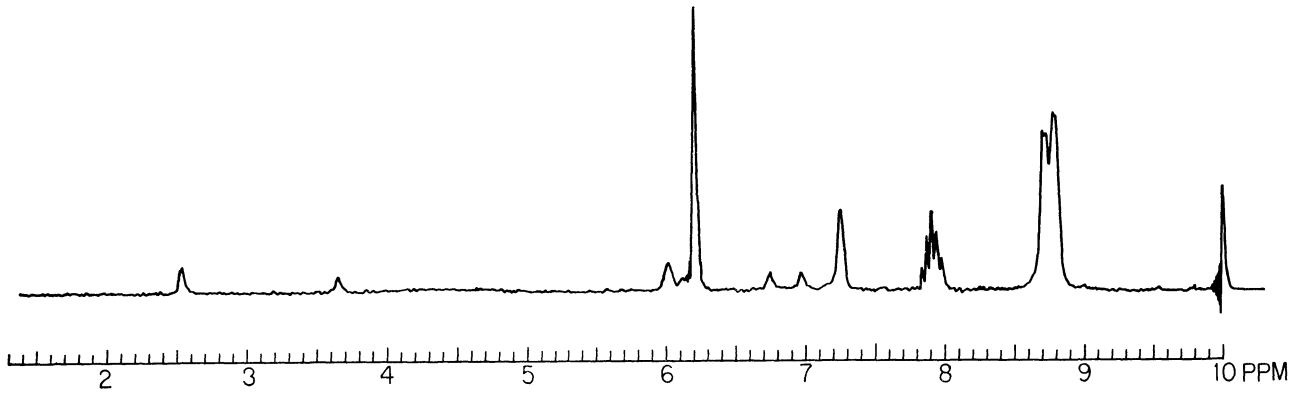

Fig. 2. The NMR spectrum of 6-cyano-5,5-dimethyl-3-methoxycarbonyl(cyano)methylene-1-cyclohexene-1-ol.

The spectrum (deuterioacetone) (Fig. 2) contained two doublets, (each 3H) at 1.22 and 1.29 ppm, which can be ascribed to the C5–dimethyl groups. The methylene group gave rise to a singlet and a doublet at 2.75 and 3.14 ppm respectively. C4–(axial)H and (equatorial)H of the III isomer would be expected to give more separated signals than those of the II isomer because of the marked interaction with the ester carbonyl group. Molecular-model considerations supported this effectation. On the basis of this assumption, the singlet was assigned to the C4–H_2 protons of the II isomer, and the doublet, to those of the III isomer. In both isomers, the O–CH_3 signal of the ester group appeared at 3.80 ppm as a sharp singlet. The singlet (1H) at 4.00 ppm was assignable to the C6–H since it would be expected to appear at a higher field than the olefinic C2–H. Two signals (1H), at 6.35 and 7.46 ppm, were assigned to the C2–H proton. One of these (7.46 ppm) was indicative of C2–H in the II isomer, since the isomeric composition estimated on the basis of the integration of the area under this signal was consistent with that estimated on the basis of a signal at 2.75 ppm, which has been assigned to C4–H_2 of the II isomer. From the NMR spectrum, the composition of the mixture was estimated to be: II isomer, 60%, and III isomer, 40%.

Substantially the same result was obtained from the condensation product, $C_{14}H_{16}O_3N_2$, mp 135°C, of acetone with ethyl cyanoacetate under similar conditions. In this case, the isomer ratio was 50:50.

6-Cyano-5,5-dimethyl-3-methoxycarbonyl(cyano)-methylene-1-cyclohexene-1-ol (containing the II and III isomers) was hydrolyzed with aqueous sodium hydroxide for 3 hr to give 6-cyano-3-cyanomethyl-5, 5-dimethyl-2-cyclohexene-1-one (IV) (85% yield).

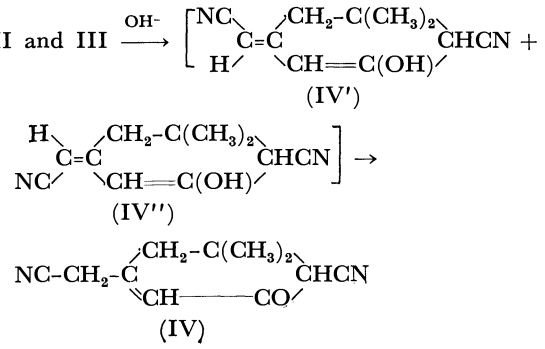

We had expected to obtain a mixture of two isomeric compounds, IV′ and IV″. However, the product obtained gave no evidence of being a mixture (tlc, IR, and NMR). The structure of IV was confirmed as follows.

The product readily afforded the corresponding hydrazone, in contrast to the case when the starting materials were II and III, when it was treated with 2, 4-dinitrophenylhydrazine in ethanol. The infrared spectrum of the product revealed a band at 2270 cm^{-1} characteristic of the unconjugated nitrile group, and none due to the conjugated one. Other prominent bands observed at 1680 and 1640 cm^{-1}, which may be assigned to the stretchings of C=O (conjugated) and C=C (conjugated) groups respectively, suggest the presence of the keto-form structure, IV.

The NMR spectrum (deuteriochloroform) showed signals at 1.19 and 1.33 ppm (singlets) due to the two methyl groups. The singlet at 2.45 ppm (2H) was assignable to the ring methylene protons (C4–H_2), and the singlet at 3.35 ppm (2H), to the side-chain protons (C3–CH_2–CN), because the latter disappeared completely when IV was converted into V. Two signals were observed for the methine protons. We attribute the signal at 3.45 ppm to the C6–H proton, and the signal at 6.30 ppm to the C2–H proton, on the general ground that the olefinic proton is more deshielded than the paraffinic proton.

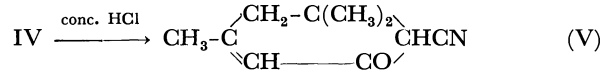

(V)

The hydrolysis and subsequent decarboxylation of IV yielded a ketone (yield 80%). Microanalysis supported the formula of $C_{10}H_{13}ON$. The infrared spectrum revealed a band at 2270 cm^{-1} attributable to a unconjugated nitrile group, a strong carbonyl band at 1675 cm^{-1}, and a conjugated C=C band at 1635 cm^{-1}.

The NMR spectrum (Fig. 3) of the product showed three singlets (each 3H), at 1.08, 1.23, and 1.98 ppm. The two higher-field singlets were ascribed to the C5–dimethyl groups by analogy with those of compounds II—IV. Then, the remaining lower field singlet was ascribed to the C3–methyl group. The methylene protons in the ring (C4–H_2) gave a singlet at 2.35 ppm; this was consistent with that of the compound IV. The singlets at 3.38 (1H) and 5.88 (1H) ppm were

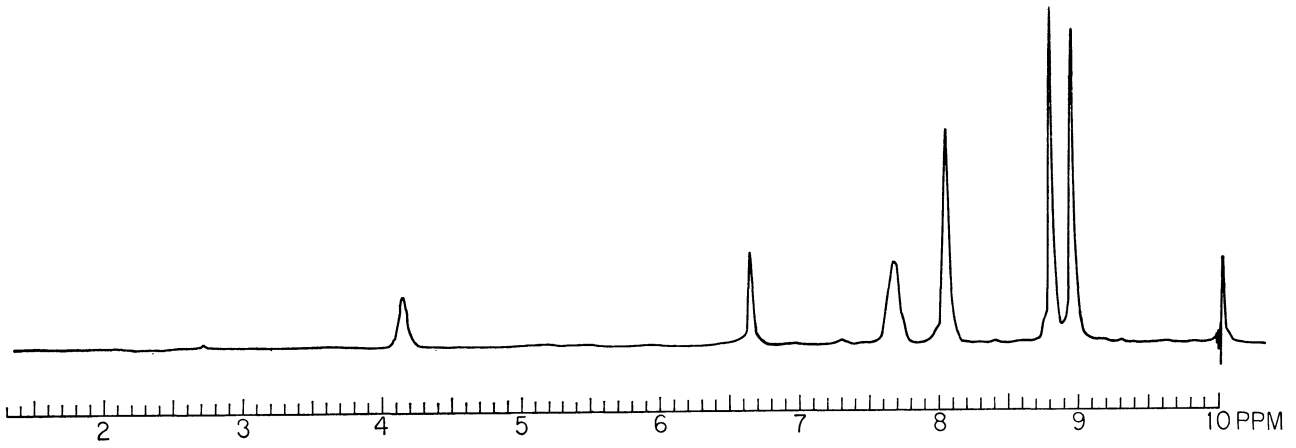

Fig. 3. The NMR spectrum of 6-cyanoisophorone.

assigned to the C6–H and C2–H protons respectively by a comparison with those of the other, known 2-cyclohexene-1-one systems.[3]

From the above data, we assign the product to the V structure, 6-cyanoisophorone.

6-Cyanoisophorone (V) was converted into 6-carbamoylisophorone (VI) with 75% sulfuric acid at 70—80°C for 2 hr. The infrared spectrum of the product showed the two bands at 3355 and 3135 cm^{-1} characteristic of the NH_2 group. The remainder of the spectrum was consistent with the presence of a $CONH_2$ group. These bands disappeared from the spectrum when the compound was hydrolyzed and subjected to decarboxylation.

Finally, the hydrolysis of the amide VI with 75% sulfuric acid at 130—150°C for 3 hr yielded isophorone (VII). The infrared spectrum and the mp (144°C) of its 2,4-dinitrophenylhydrazone were identical with those of an authentic sample.

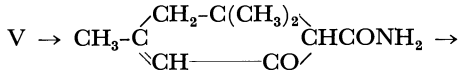

(VI)

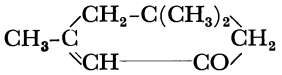

(VII)

From the facts that the cyclic products (II and III) were obtained from only the isopropylidenecyanoacetic ester and that its dimer was isolated as the intermediate,[2] the reaction course may be concluded to be as shown in Scheme I.

Experimental

The infrared spectra were recorded on a Shimadzu model IR-27G infrared spectrophotometer. The NMR spectra were measured on a JNM-60 high-resolution NMR spectrometer operating at 60 MHz. The chemical shifts are given as ppm downfield from tetramethylsilane as the internal standard.

6-Cyano-5,5-dimethyl-3-methoxycarbonyl(cyano)methylene-1-cyclohexene-1-ol. The condensation was carried out according to the method previously used.[2]

Acetone (11.6 g) and methyl cyanoacetate (9.9 g) were mixed, and then anhydrous potassium fluoride (5.8 g) was added to the mixture. After refluxing for 10 hr on a water bath, the reaction mixture was cooled, dissolved in water, acidified with hydrochloric acid, and extracted with ether. The ethereal solution was washed several times with water and shaken with an aqueous sodium carbonate solution. When the alkaline solution was acidified with hydrochloric acid, a yellowish oil separated. After a while, the oil solidified to a hard cake. The yield was 13.6 g (55%). It was crystallized from acetone - water to slight yellow needles melting at 177—178°C (decomp).

The compound dissolved readily in an aqueous sodium carbonate solution, and it gave a green coloration with ferric

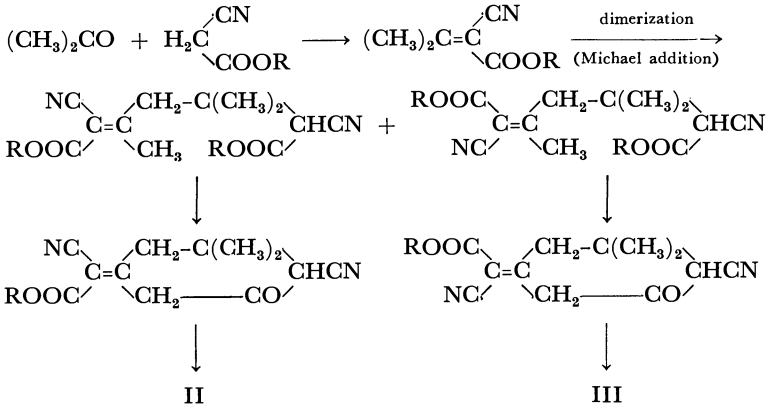

Scheme I

3) H. A. Szymanski and R. E. Yelin, "NMR Band Handbook," Plenum, New York (1968), p. 33.

chloride in an alcoholic solution. The reaction of the product with 2,4-dinitrophenylhydrazine in an ethanolic solution gave no crystalline material; it only turned slightly reddish-yellow after standing for several days.

Found: C, 63.60; H, 5.72; N, 11.48%; mol wt, 242. Calcd for $C_{13}H_{14}O_3N_2$: C, 63.40; H, 5.73; N, 11.38%; mol wt, 246.

IR(Nujol): 3110 (OH), 2270 (very weak) (unconjugated CN), 2220 (strong) (conjugated CN), 1725 (CO), 1590 (side chain C=C), 1540 (ring C=C) cm^{-1}.

NMR (deuterioacetone): 1.22 (doublet) (CH_3), 1.29 (doublet) (CH_3), 2.75 (singlet) and 3.15 (doublet) (CH_2), 4.00 (singlet) (C6–H), 6.35 (singlet) and 7.46 (singlet) (C2-H) ppm.

6-Cyano-3-cyanomethyl-5,5-dimethyl-2-cyclohexene-1-one (IV). A mixture of the unsaturated ester (II and III) (0.1 mol) and a 0.2 N sodium hydroxide solution (0.2 mol) was allowed to saponify for 3 hr on a water bath. The alkaline solution was cooled. When it was acidified with dilute hydrochloric acid, a yellowish oil separated from the aqueous solution. The oil solidified when it was allowed to stand in an ice-box. The yield was 83%. Recrystallizations from water gave slightly yellow needles; mp 111—113°C.

Found: C, 69.85; H, 6.56; N, 14.93%. Calcd for $C_{11}H_{12}ON_2$: C, 70.18; H, 6.43; N, 14.88%.

IR (Nujol): 2270 (CN), 1680 (C=O), 1640 (C=C) cm^{-1}.

NMR (deuteriochloroform): 1.19 (singlet) (CH_3), 1.33 (singlet) (CH_3), 2.45 (singlet) (C4–H_2), 3.35 (singlet) (C3–CH_2–CN), 3.45 (singlet) (C6–H), 6.30 (singlet) (C2–H) ppm.

2,4-Dinitrophenylhydrazone. Mp 212°C.

Found: C, 55.44; H, 4.06; N, 22.99%. Calcd for $C_{17}H_{16}O_4N_6$: C, 55.43; H, 4.38; N, 22.82%.

6-Cyanoisophorone (V). A mixture of IV (4.2 g) and concentrated hydrochloric acid was refluxed for one hour. The reaction mixture was then dissolved in water and extracted with ether. The ether extract on evaporation left an oil distilling at 163—164°C/12 mmHg. The oil solidified when it was allowed to stand overnight in an ice-box. The yield was 2.8 g (77%). Recrystallizations from chloroform-petroleum ether gave colorless plates; mp 56—57°C.

Found: C, 73.51; H, 7.90; N, 8.56%. Calcd for $C_{10}H_{13}ON$: C, 73.59; H, 8.03; N, 8.58%.

IR (Nujol): 2270 (CN), 1670 (C=O), 1635 (C=C) cm^{-1}.

NMR (carbon tetrachloride): 1.08 (singlet) (C5–CH_3), 1.23 (singlet) (C5–CH_3), 1.98 (singlet) (C3–CH_3), 2.35 (singlet) (C4–H_2), 3.38 (singlet) (C6–H), 5.88 (singlet) (C2–H) ppm.

2,4-Dinitrophenylhydrazone. Mp 230°C.

Found: N, 20.24%. Calcd for $C_{16}H_{17}O_4N_5$: N, 20.40%.

6-Carbamoylisophorone (VI). To a solution of 95% sulfuric acid (10 g) and water (2 g), 6-cyanoisophorone (3 g) was added, and then the mixture was heated at 70—80°C for 2 hr. After being cooled, the solution was poured into ice water and extracted with ether. The ethereal solution was repeatedly washed with water, and then the ether was removed. The oily residue solidified when it was allowed to stand overnight in an ice-box. Recrystallizations from methanol gave colorless plates; mp 139—140°C (yield, 75%).

Found: C, 66.05; H, 8.09; N, 7.68%. Calcd for $C_{10}H_{15}O_2N$: C, 66.27; H, 8.34; N, 7.73%.

Isophorone VII. A mixture of 75% sulfuric acid (2 m*l*) and 6-carbamoylisophorone (0.6 g) was heated at 150—160°C for 3 hr. After cooling, the reaction mixture was poured into ice water and extracted with ether. The ethereal solution was washed, dried, and then evaporated. The distillation of the residue gave isophorone; bp 95—100°C/2 mmHg (lit,[4] bp 109°C/32 mmHg).

IR: 1670 (C=O), 1640 (C=C) cm^{-1}.

2,4-Dinitrophenylhydrazone. Mp 144—145°C (lit,[4] mp 146°C).

Found: N, 17.70 %. Calcd for $C_{15}H_{18}O_4N_4$: N, 17.60%.

The authors wish to express their hearty thanks to Professors Taro Hayashi and Tatsuo Takeshima for their kind advice and encouragement, and to Dr. Haruo Homma and his staff for their microanalyses.

4) A. W. Fort, *J. Org. Chem.*, **26**, 332 (1961).

The Independent Isolation of a Primary Enamine and the Tautomeric Imine[1]

Chung-gi SHIN

Laboratory of Organic Chemistry, Faculty of Technology, Kanagawa University, Rokkakubashi, Kanagawa-ku, Yokohama

and Mitsuo MASAKI,* and Masaki OHTA

Laboratory of Organic Chemistry, Tokyo Institute of Technology, Ookayama, Meguro-ku, Tokyo

(Received October 30, 1970)

Isolation of a primary enamine and its tautomeric imine has been described and their dimerization discussed. Reduction of ethyl 3-methyl-2-nitro-2-butenoate with aluminum amalgam afforded ethyl 2-amino-3-methyl-2-butenoate (I) (enamine form), while treatment of ethyl 3-methyl-2-oxobutanoate with triphenylphosphinimine gave ethyl 2-imino-3-methylbutanoate (II) (imino form). The enamine and its tautomeric imine dimerized to give 3,6-diisopropylidene-2,5-dioxopiperazine (VII) and 2-ethoxycarbonyl-2,5-diisopropylimidazolid-4-one (IX), respectively. However, individual acylation of both the enamine and the imine gave the same acyl compound.

It has been postulated that α-imino acids are important intermediates in the transformation between α-amino acids and α-keto acids.[2] However, there has been no report on the tautomerism between imino acid and enamino acid. Previous investigations on the enamine had dealt almost exclusively with secondary and tertiary enamines.[3]

In a previous paper,[4] the authors reported briefly that a primary enamine (ethyl 2-amino-3-methyl-2-butenoate: I) could be isolated as a reduction product of the corresponding α,β-unsaturated α-nitrocarboxylic ester, and the tautomeric imine (ethyl 2-imino-3-methylbutanoate: II) from a reaction mixture of the corresponding α-oxocarboxylic ester with triphenylphosphinimine. The acylation of both I and II, however, gave the same acyl enamine derivative and the dimerization of I and II gave dioxopiperazine (VII) and imidazolidone derivative (IX), respectively. The isomerization between I and II, however, was unsuccessful.

On the other hand, in the case of the reaction of α-oxocarboxylic esters with *N*-phenyltriphenylphosphinimine, secondary enamine (III) and the tautomeric imine (IV) were obtained as an equilibrium mixture.

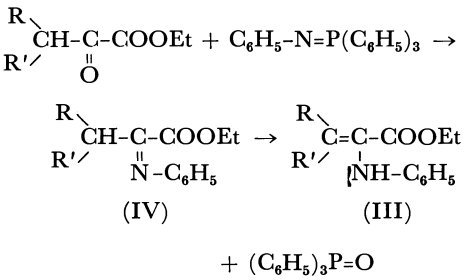

Scheme 1

On the basis of the IR and NMR data, it has been found that the isomerization of IV to III occurred and the composition of the reaction mixture was evaluated.[5] So far, however, a complete enamine-imine interconversion between III and IV has been unsuccessful.[5] In the case of ethyl pyruvate, the reaction mixture (III and IV; R=R′=H) dimerized to give 3-anilino-5-ethoxycarbonyl-5-methyl-1-phenyl-Δ^3-pyrrolin-2-one (VI) *via* ethyl 2,4-dianilino-4-ethoxycarbonyl-2-pentenoate (V) as an intermediate.[5]

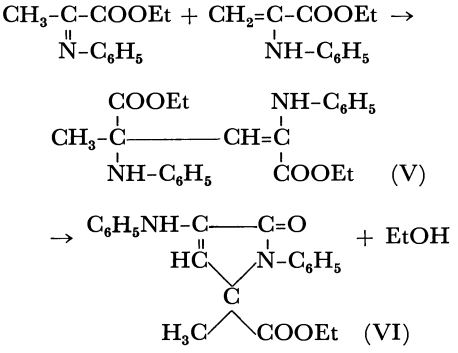

Scheme 2

This paper reports the synthesis of ethyl 2-imino-3-methylbutanoate (II) through the reaction of ethyl 3-methyl-2-oxobutanoate with triphenylphosphinimine by the method of Appel and Hauss,[6] as well as the dimerization and chloroacetylation of I and II, respectively.

Results and Discussion

According to the method of Tatsuoka *et al.*[7] ethyl 2-amino-3-methyl-2-butenoate (I) was prepared in a 56% yield as a pale yellow oil from ethyl 3-methyl-2-nitro-2-butenoate with aluminum amalgam in ether under reflux.[8] Appel and Hauss reported the reaction of methyl pyruvate with triphenylphosphinimine to give methyl 2-iminopropionate, though the structure of the

1) A part of this paper was presented at the 21st Annual Meeting of the Chemical Society of Japan, Tokyo, April, 1968.

* Present address: Polymer Research Laboratory, Ube Industries, Ltd., Goi, Ichihara City, Chiba.

2) a) F. Knoop and H. Oesterlin, *Z. Phys. Chem.*, **148**, 294 (1925); *ibid.*, **170**, 186 (1927). b) E. F. Gale, *Chem. Ind.*, **1948**, 131. c) S. Sakurai, *J. Biochem.*, **43**, 851 (1956); *ibid.*, **44**, 47, 557 (1957); *ibid.*, **45**, 379 (1958).

3) A. G. Cook, "Enamines: Synthesis, Structure and Reactions," Marcel Dekker, New York and London (1969).

4) M. Masaki, C. Shin, H. Kurita, and M. Ohta, *Chem. Commun.*, **1968**, 1447.

5) C. Shin, H. Ando, and J. Yoshimura, This Bulletin, **44**, 474 (1971).

6) R. Appel and A. Hauss, *Z. Anorg. Chem.*, **311**, 290 (1961).

7) S. Tatsuoka, M. Murakami, and T. Tamura, *Yakugaku Zasshi*, **70**, 230 (1950).

8) C. Shin, M. Masaki, and M. Ohta, *J. Org. Chem.*, **32**, 1860 (1967).

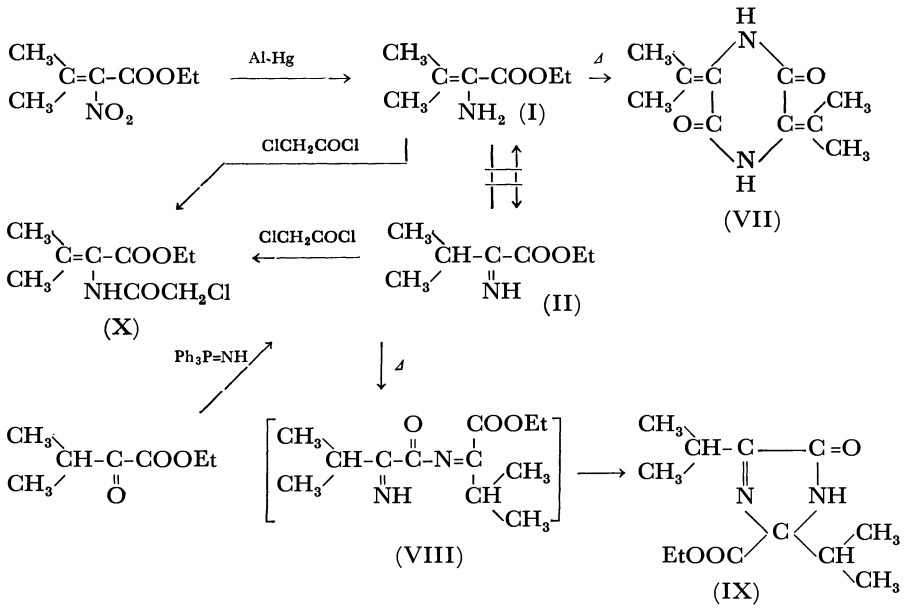

Scheme 3

product was not clarified since the product could not be isolated and its characterization was deduced only by hydrogenation into (±)-alanine.[6] However, treatment of ethyl 3-methyl-2-oxobutanoate with triphenylphosphinimine in anhydrous acetonitrile for 2 hr under reflux afforded a pale yellow oil as an analytical pure product in a 40% yield, and the product was identified as ethyl 2-imino-3-methylbutanoate (II), the tautometric isomer of I. The infrared spectrum of II showed an intense ester carbonyl band at 1730 cm^{-1} and a medium band attributable to C=N stretching vibration at 1640 cm^{-1}, while that of I showed two intense absorption bands at 1730 cm^{-1} and 1690 cm^{-1} and medium bands at 1640 and 1600 cm^{-1} as shown in Figs. 1A and 1B.

The NMR spectrum of I showed peaks at τ 5.72 (q, $-C\underline{H}_2CH_3$, 2H), 6.82 (broad s, $-NH_2$, 2H), 7.91 (s, $-CH_3$, 3H), 8.22 (s, $-CH_3$, 3H), and 8.67 (t, $-CH_2C\underline{H}_3$, 3H), while that of II showed peaks at τ 0.00 (broad s,

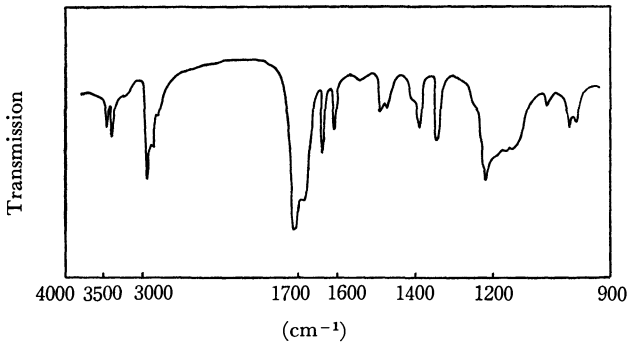

Fig. 1A. Infrared spectrum of I in NaCl.

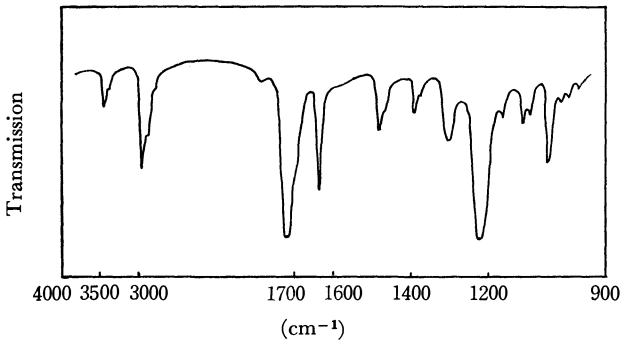

Fig. 1B. Infrared spectrum of II in NaCl.

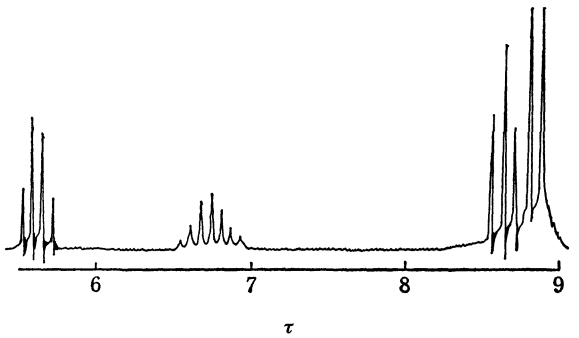

Fig. 2A. NMR spectrum of ethyl 3-methyl-2-oxobutanoate in $CDCl_3$.

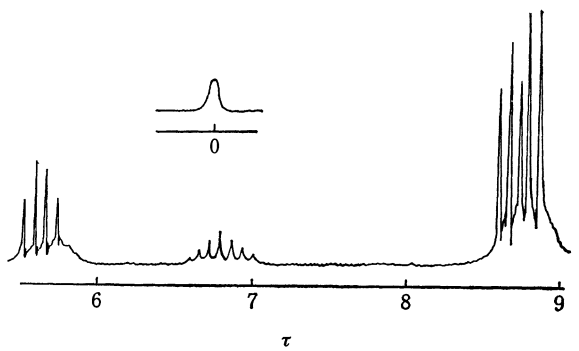

Fig. 2B. NMR spectrum of II in $CDCl_3$.

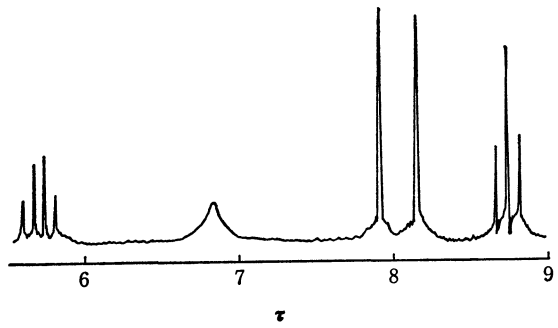

Fig. 2C. NMR spectrum of I in $CDCl_3$.

one imino proton), 5.67 (q, $-C\underline{H}_2CH_3$, 2H), 6.87 (m, methine proton, 1H), 8.65 (t, $-CH_2C\underline{H}_3$, 3H), and 8.80 (d, two $-CH_3$, 6H) as shown in Figs. 2B and 2C. The pattern is essentially the same as that of parent α-keto ester except that, in the latter, no signal lower than 5.0 was observed and the one proton multiplet shifted to τ6.72 (Fig 2A). The NMR spectrum of I showed no signal lower than τ5.0 (Fig 2C).

When enamine (I) was treated with chloroacetyl chloride in aqueous sodium hydrogencarbonate with vigorous stirring at room temperature, ethyl 2-(2-chloroacetamido)-3-methyl-2-butenoate (X) was obtained in a 47% yield, which was also obtained in a 30% yield from II by reaction with chloroacetyl chloride in ether in the presence of triethylamine. The ester (X) was synthesized by the hydrolysis of 2-chloromethyl-4-isopropylideneoxazol-5-one followed by the esterification of the resulting *N*-(chloroacetyl) dehydrovaline, and the acetyl enamine structure (X) was confirmed with NMR spectrum by Kurita *et al.*[9]

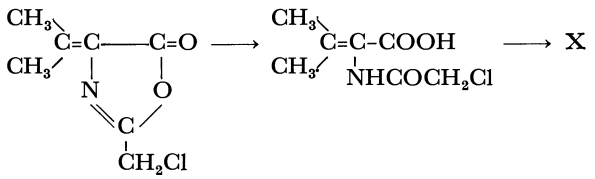

When α-imino ester (II) was allowed to stand for a week at room temperature and then redistilled, 2-ethoxycarbonyl-2,5-diisopropylimidazolid-4-one (IX) was obtained in a 79% yield. α-Amino ester (I) was heated in a sealed tube at 180—190°C for 48 hr to give the dioxopiperazine (VII). The structure of X was derived from its elemental and spectroscopic analyses (see Experimental). It has been found that the above three dimerization courses (Schemes 2 and 3) were different. Thus it seems that the interconversion between I and II can not be carried out under the experimental conditions mentioned above, although the conversion of III to IV occurred at room temperature. Attempt to isomerize enamine or imine conversely by alkali was unsuccessful.

Experimental

All boiling and melting points are uncorrected. The IR spectrum was recorded with a Hitachi EPI-S2 Spectrometer. The NMR spectrum was measured with a JNM-4H-100 Spectrometer (Japan Electron Optics Laboratory Co., Ltd.) at 100 MHz.

Materials. Triphenylphosphinimine hydrobromide was prepared by the reaction of triphenylphosphine dibromide with ammonia in the presence of triethylamine by the method of Horner and Oediger[10] Mp 240—242°C (decomp.). The acetonitrile used was distilled from phosphorous pentoxide and dried over calcium hydride.

Ethyl 2-Amino-3-methyl-2-butenoate (I). The procedure was modified from the method of Tatsuoka *et al.*[7] A solution of ethyl 3-methyl-2-nitro-2-butenoate (22 g) in ether (150 m*l*) was added drop by drop to aluminum amalgam (from 13 g of aluminum) placed in ether (300 m*l*) with vigorous stirring at room temperature. After a few minutes, the ether began to reflux. During the addition of the above solution, a few drops of water was added at 10-min intervals to maintain refluxing. After addition of the solution was completed, the stirring was continued for 2 hr. The mixture was extracted thoroughly several times with ether. The combined ethereal extract was dried over anhydrous sodium sulfate and then evaporated. Distillation of the residual oil afforded a pale yellow oil (6.9 g, 56%), bp 65—72°C/9 mmHg.

Found: C, 58.51; H, 9.03; N, 9.79%. Calcd for $C_7H_{13}NO_2$: C, 58.72; H, 9.15; N, 9.78%.

Ethyl 2-Imino-3-methylbutanoate (II). To a solution of triphenylphosphinimine (from triphenylphosphinimine hydrobromide (10.74 g) and sodium hydride (1.3 g)) in acetonitrile (150 m*l*), ethyl 3-methyl-2-oxobutanoate (4 g) was added and heated on a steam bath with stirring. After 30 min, the solution began to reflux. After stirring was continued for more 5—10 min, the solution was allowed to stand at room temperature with stirring and then acetonitrile was evaporated. Dry ether was added to the residual oil and then substance precipitated was filtered off. The ethereal solution was concentrated again, and then the residual oil was extracted with dry petroleum ether three times (each 50 m*l*). After concentrating the solution, the resulting oil was distilled under reduced pressure to afford a pale yellow oil (1.6 g, 40%), bp 65—67°C/15 mmHg.

Found: C, 58.68; H, 9.37; N, 9.56%. Calcd for $C_7H_{13}NO_2$; C, 58.72; H, 9.15; N, 9.78%.

3,6-Diisopropylidene-2,5-piperazinedione (VII). The reaction was carried out using the technique of Fischer for 3,6-dialkyl-2,5-piperazinedione.[11] Compound I (0.5 g) was heated in a sealed tube at 180—190°C for 48 hr. Into the reaction mixture was added a small quantity of ethanol. The crystalline product was collected and recrystallized from ethanol to afford colorless needles (0.14 g, 20.5%), mp 264—265°C (decomp.), undepressed on admixture with the authentic sample.[8]

2-Ethoxycarbonyl-2,5-diisopropylimidazolid-4-one (IX). Compound II (1.2 g) was allowed to stand for a week at room temperature. Distillation under reduced pressure, was unsuccessful. The residual syrup gradually crystallized at room temperature. Redistillation of the crystalline syrup gave a pale yellow oil (0.8 g, 80%), bp 116—117°C/0.07 mmHg (mp 48—49°C). NMR ($CDCl_3$): τ 0.77 (broad s, NH), 5.71 (q, $-C\underline{H}_2CH_3$, 2H), 6.94 (m, methine proton, 1H), 7.22 (m, methine proton, 1H), 8.71 (t, $-CH_2C\underline{H}_3$, 3H), 8.72 (d, two $-CH_3$, 6H), 8.96 (d, $-CH_3$, 3H), 9.26 (d, $-CH_3$, 3H). IR (KBr): 3107, 1750, 1630, 1275, 1200 cm^{-1}.

9) H. Kurita, Y. Chigira, M. Masaki, and M. Ohta, This Bulletin, **41**, 2759 (1968).

10) L. Horner and H. Oediger, *Ann. Chem.*, **627**, 142 (1959).

11) E. Fischer, *Ber.*, **34**, 433 (1901).

Found: C, 59.85; H, 8.21; N, 11.76%. Calcd for $C_{12}H_{20}N_2O_3$: C, 59.98; H, 8.39; N, 11.66%.

Ethyl 2-(2-Chloroacetamido)-3-methyl-2-butenoate (X).

A) From I: Chloroacetyl chloride (0.8 g) was added drop by drop, with vigorous stirring, to I (1 g) suspended in a solution of sodium hydrogencarbonate (0.6 g) in water (15 m*l*) at room temperature. After stirring for 30 min, a crystalline product precipitated. The crystals were collected, washed well with water, and recrystallized from 50% ethanol to afford colorless needles (0.7 g, 47%), mp 117—118°C, undepressed on admixture with the authentic sample.[9] NMR ($CDCl_3$): τ 2.07 (broad s, NH), 5.77 (q, $-C\underline{H}_2CH_3$, 2H), 5.86 (s, $-COCH_2-$, 2H), 7.80 (s, $-CH_3$, 3H), 8.15 (s, $-CH_3$, 3H), 8.72 (t, $-CH_2C\underline{H}_3$, 3H). IR (KBr): 3200, 1720, 1665, 1535 cm^{-1}.

B) From II: A solution of chloroacetyl chloride (0.58 g) in dry ether (30 m*l*) was added drop by drop, with stirring, to a solution of II (0.7 g) in dry ether (30 m*l*) in the presence of triethylamine (0.5 g) in an ice-salt bath. After stirring overnight at room temperature, triethylamine hydrochloride precipitated was filtered off, and then the ethereal solution was concentrated to give residual oil. Heated at 70°C under reduced pressure (2 mmHg), the oil immediately converted into crystals. Recrystallization from di-*n*-butyl ether afforded colorless needles (0.32 g, 30%), mp 118.5—119°C, undepressed on admixture with the sample obtained by procedure *A*.

Further Studies of the Chemical Cleavage of the Tryptophyl Bond by Ozonization-hydrazine Treatment[1,2]

Fumio SAKIYAMA and Shin-ichiro SAKAI*

Institute for Protein Research, Osaka University, Kita-ku, Osaka

(Received November 2, 1970)

The second step (hydrazine treatment) in the chemical cleavage of the tryptophyl bond according to the scheme proposed previously was further studied under mild conditions using a model *N'*-formylkynurenyl peptide, carbobenzoxy-L-alanyl-*N'*-formyl-L-kynurenyl-L-leucine. The reaction of the model compound with an excess of hydrazine acetate at 25—30°C for 24—48 hr gave rise to the selective cleavage of the kynurenyl bond together with a concomitant tetrahydropyridazone formation. The maximum cleavage was 80—90%. It was then suggested that the incomplete cleavage of the tryptophyl bond in synthetic oligopeptides by means of ozonization-hydrazine treatment was mainly due to insufficient conversion of the indole nucleus into *N'*-formylanthranyl grouping in the first step (ozonization).

A new principle for the chemical cleavage of the tryptophyl bond has previously been proposed.[3,4] According to the reaction scheme, the tryptophyl residue in the peptide chain is first oxidized selectively by ozone to the *N'*-formylkynurenyl residue, which serves the γ-carbonyl function: a subsequent reaction with hydrazine results in 2,3,4,5-tetrahydropyridazone formation, with a concomitant cleavage of the peptide bond acylated by the tryptophyl residue (Fig. 1). On the basis of the experiments performed on model compounds, the cleavage reaction of several synthetic tryptophyl peptide derivatives was carried out, and fairly good results were obtained.[1] However, on the reaction of the ozonized hen's egg-white lysozyme with hydrazine under the same conditions, the expected cleavage reaction was accompanied by a considerable non-selective hydrolysis of other peptide bonds.[5]

Sin e the oxidation step is free from such hydrolytic cleavage, it was quite obvious that the reaction temperature in the second step with hydrazine was too high to exclude undesirable hydrolysis. A similar disadvantage is expected in other chemical reactions reported in the literature aiming at effecting the cleavage of a kynurenyl bond.[6-8] For instance, the intramolecular participation of the γ-carbonyl or the γ-hydroxy group in the preferential hydrolysis of the peptide linkage involving the kynurenine is effectively accomplished only on heating at 100°C in a weakly alkaline or a diluted hydrochloric acid solution. Thus, it is desirable to establish milder conditions for the selective cleavage of the kynurenyl bond with hydrazine. In the present report, the authors will deal

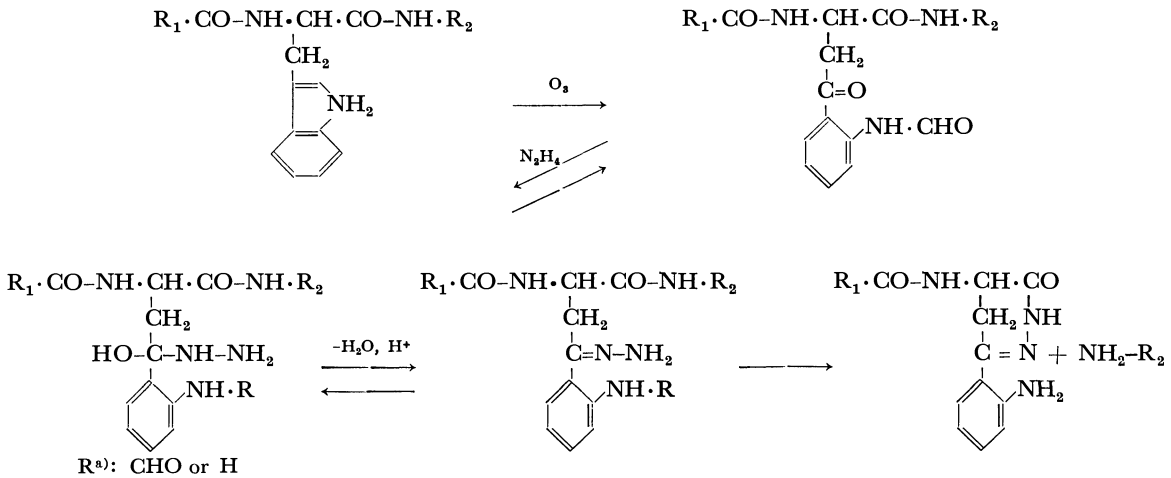

Fig. 1. The chemical cleavage of the tryptophyl bond *via* the *N'*-formylkynurenyl peptide derivative.
a) The stage at which the formyl group is eliminated has not been clarified yet in the direct reaction of the model peptide with hydrazine acetate.

* Present address: Faculty of Pharmaceutical Sciences, Chiba University, Chiba.

1) The Non-Enzymatic Cleavage of Peptide Bonds. Part III. Part II, M. Morishita and F. Sakiyama, This Bulletin, **43**, 524 (1970); M. Morishita, F. Sakiyama, and K. Narita, *ibid.*, **40**, 433 (1967).

2) A part of the investigation was presented at the Symposium of Protein Structure, Tokyo, October 1968.

3) F. Sakiyama, M. Morishita, T. Sowa, and K. Narita, This Bulletin, **39**, 631 (1966).

4) M. Morishita, T. Sowa, F. Sakiyama, and K. Narita, *ibid.*, **40**, 632 (1967).

5) K. Narita, F. Sakiyama, and M. Morishita presented at the 7th International Congress of Biochemistry held at Tokyo in August, 1967.

6) A. Previero, M. A. Coletti-Previero, and P. Jollès, *Biochem. Biophys. Res. Commun.*, **22**, 17 (1966).

7) A. Previero, M. A. Coletti-Previero, and P. Jollès, *Biochim. Biophys. Acta*, **124**, 400 (1966).

8) F. M. Veronese, E. Boccu', C. A. Benassi, and E. Scoffone, *Z. Naturforsch.*, **24b**, 294 (1969).

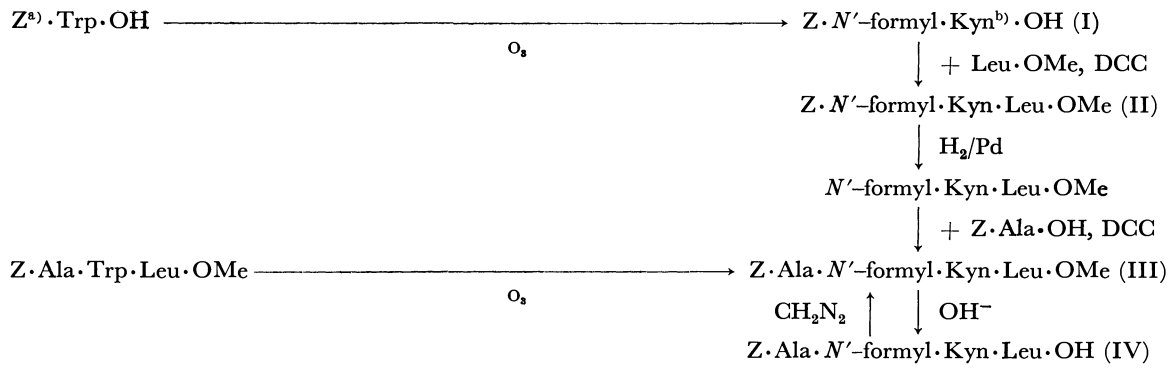

Fig. 2. Synthesis of carbobenzoxy-L-alanyl-*N'*-formyl-L-kynurenyl-L-leucine.
a) Z: carbobenzoxy b) Kyn: kynurenine

with the preparation of a model peptide derivative containing *N'*-formylkynurenine and its reaction with hydrazine, and with the application of the improved method to the cleavage of the tryptophyl bond in several oligopeptides and gramicidin A.

Results and Discussion

Synthesis of a Model Peptide Derivative. The synthesis of peptide derivatives containing *N'*-formylkynurenine has previously been reported by Previero and his colleagues,[9] who utilized the ozonolysis of the corresponding tryptophyl peptide derivatives in the presence of resorcinol.[10] As a model peptide derivative, the carbobenzoxy derivative of alanyl-*N'*-formylkynurenylleucine was chosen. Two routes of synthesizing the tripeptide derivative were examined; one was a step-by-step elongation of the peptide chain, starting from the carboxyl-terminal leucine, while the other was a direct ozonization of carbobenzoxyalanyltryptophylleucine or its methyl ester (Fig. 2).

For the step-by-step procedure, it was necessary to prepare the *N*-α-protected derivative of *N'*-formylkynurenine. Since a conventional *t*-butyloxycarbonyl substituent was not suitable for the present purpose,[11] the classical carbobenzoxy residue was used. The *N*-α-carbobenzoxy derivative of tryptophan was ozonized without resorcinol; in order to isolate crystalline carbobenzoxy-*N'*-formylkynurenine, the crude material had to be purified by chromatography on a silicic-acid column. The formation of the kynurenyl bond was then attempted either by the *p*-nitrophenyl-ester method or by the dicyclohexylcarbodiimide (DCC) method.[12] The conversion of carbobenzoxy-*N'*-formylkynurenine into its *p*-nitrophenyl-ester was performed by means of interesterification with trifluoracetyl *p*-nitrophenolate;[13] though the active ester thus obtained was subjected to reaction with the leucine methyl ester, no fruitful results were obtained. Then, the carbobenzoxy-*N'*-formylkynurenylleucine methyl ester was prepared by the DCC method without any considerable difficulties. The formation of the alanyl bond was similarly achieved by the coupling of carbobenzoxy alanine with the *N'*-formylkynurenylleucine methyl ester which had been prepared by the catalytic hydrogenation of its carbobenzoxy derivative. By a comparison of the melting points and by a study of the infrared spectrum and the chromatographic behavior, the carbobenzoxy tripeptide ester was found to be identical with that prepared by the direct ozonization of the carbobenzoxyalanyltryptophylleucine methyl ester.[14]

The protected tripeptide ester was then submitted to usual hydrolysis in aqueous alkaline media. However, the ester group was not quantitatively hydrolyzed, and the ultraviolet spectrum of the reaction mixture revealed an anomalous absorption at 332 mμ, indicating that a certain unexpected reaction occurred during this treatment.[15] On the other hand, the alkaline hydrolysis in an aqueous pyridine solution reduced such an unfavorable side reaction; finally, the repeated recrystallization of the hydrolysate yielded the pure carbobenzoxytripeptide, which reverted to the parental tripeptide methyl ester on esterification by diazomethane.

The direct ozonization of the carbobenzoxy derivative of alanyltryptophylleucine into the corresponding *N'*-formylkynurenyl derivative was a less favorable procedure for the present purpose because it was difficult to purify the ozonization product, as is also observed in the preparation of carbobenzoxy *N'*-formylkynurenine.

Reaction of Carbobenzoxy-L-Alanyl-N'-Formyl-L-Kynurenyl-L-Leucine with Hydrazine. The results of the experiments on the cleavage of the tryptophyl bond in lysozyme under the conditions reported in a previous paper[1] suggested that one of the major defects to be improved was the non-specific hydrolysis of the peptide bonds during the reaction of the ozonized protein with hydrazine. From this point of view, the cleavage reaction was again investigated at room temperature using

9) A. Previero and M. A. Coletti-Previero, *C. R. Acad. Sci. Paris, Ser. C.*, 633 (1967).
10) A. Previero, A. Signor, and S. Bezzi, *Nature*, **204**, 687, (1964); A. Previero and E. Bordignon, *Gazz. Chim. Ital.*, **94**· 630 (1964).
11) The *t*-butyloxycarbonyl group could be removed by the action of formic acid in which the tryptophan residue was usually ozonized. B. Halpern and D. E. Nitecki, *Tetrahedron Lett.*, **1967**, 3031.
12) J. C. Sheehan and G. P. Hess, *J. Amer. Chem. Soc.*, **77**, 1067 (1955).
13) S. Sakakibara and N. Inukai, This Bulletin, **38**, 1979 (1965).
14) For preparation of the methyl ester of the model peptide, the ozonization method of the corresponding tryptophyl peptide derivative was more useful than the stepwise method involving the protected *N'*-formylkynurenine.
15) As one of possible side reactions, a heteroring formation such as 4-quinolone might be suggested from the spectroscopic data, but no further study was carried out.

the model peptide derivative. However, on the reaction of carbobenzoxy-L-alanyl-*N'*-formyl-L-kynurenyl-L-leucine in an aqueous hydrazine-acetate buffer at pH 4.0, neither leucine nor alanine was released, even after 72 hr. On the other hand, on the incubation of the above reaction mixture at 100°C for 3.5 hr, leucine was detected with an apparent increase in the absorption around 350 mμ due to the formation of the expected tetrahydropyridazone derivative.

When the reaction scheme presented in Fig. 1 is considered, it is rational to assume that, if the hydrazone is once formed, the intramolecular condensation of the amino group in it with the adjacent α-carbonyl function takes place and that the cleavage of the peptide linkage concerned is accomplished by a concomitant heterocyclic ring formation. Therefore, the formation of the hydrazone of the (*N'*-formyl-) kynurenine must be a key reaction in the present cleavage of the peptide bond. Since the hydrazone is formed by an equilibrium reaction through an intermediate tetrahedral hydroxyhydrazino (carbinolamine) derivative (Fig. 1), the higher the hydrazine concentration, the more efficient the formation of the hydrazone. In addition, it must be noted that the hydrazone formation consists of a successive reaction, addition of hydrazine, and subsequent elimination of water, which is usually catalyzed with either an acid or a base. Therefore, the reaction of the tripeptide derivative with 80% hydrazine hydrate was attempted in order to convert quantitatively its carbonyl function into hydrazone. In fact, a marked decrease in the characteristic absorption at 322 mμ due to the *N'*-formylkynurenyl residue was observed within five minutes of mixing the *N'*-formylkynurenyl peptide derivative and hydrazine base at room temperature. This fact indicates that the addition of hydrazine to the carbon-oxygen double bond in the kynurenyl residue takes place effectively.

When the hydrazine-treated tripeptide derivative was incubated in aqueous media at pH 4.0 at room temperature after the excess of hydrazine hydrate had been removed, leucine could be liberated in a 30% yield after 72 hr. During this reaction, white precipitates were separated and identified as 4-carbobenzoxyalanylamino-6-(*o*-aminophenyl)-2,3,4,5-tetrahydropyridaz-3-one. This fact shows that, in an aqueous solution, the hydroxyhydrazino (carbinolamine) intermediate was dehydrated to the hydrazone, and that the intramolecular hydrazinolysis of the peptide bond subsequently took place on the carboxyl side of the kynurenyl residue.

The release of leucine from the hydrazine-treated model peptide derivative under various conditions was determined; the results are summarized in Table 1. In the reaction in aqueous media, the extent of the cleavage was estimated to be 30—45%. When dioxane was added in the reaction media, more leucine was released and the course of the cleavage could also be followed by means of ultraviolet spectroscopy. On the other hand, when the reaction solvent was replaced by glacial acetic acid, the leucine released was similar in extent with that released in aqueous media.[16] Even after treatment with hydrazine hydrate, the cleavage reaction with a large excess of hydrazine was more effective than that without the cleaving reagent. This finding suggests that, under those conditions, the retro-reactions of the hydroxyhydrazino (carbinolamine) derivative and the hydrazone by equilibrium are prevented, and that enough hydrazone for the effective cleavage of the kynurenyl bond is always produced during the reaction.

Table 1. Release of leucine by the reaction of carbobenzoxy-L-alanyl-*N'*-formyl-L-kynurenyl-L-leucine with hydrazine after pretreatment with the binucleophile

Concentration of the model peptide derivative (mM)	Concentration of hydrazine (M)	Reaction: Media	Reaction: Temp.	Reaction: Period (hr)	Yield of leucine released (%)	Yield of tetrahydropyridazone formed (%)
2.00[a]	0	aq. soln (pH. 3.8)	r.t.	72	30	—
2.00[a]	0	aq. soln (pH. 3.8)	r.t. then 100°C	72 3	47	—
2.00[a]	0.02	aq. soln (pH. 1.8)	r.t.	30	36	—
1.78[a]	0.05	aq. soln (pH. 3.6)	40°C	5 25 48	40 45 44	— — —
1.34[b,c]	0	aq. soln (pH. 3.65) - dioxane (4:1 by vol.)	r.t.	43 120	— 71	51 53
1.26[b,d]	0	gl. acetic acid	r.t.	120	51	—
1.38[b]	1.6	gl. acetic acid	r.t.	47 120	— 77	79 81
1.15[b,e]	1.6	gl. acetic acid	r.t.	47 120	— 55	45 56

a,b) The pre-treatmet with 80% hydrazine hydrate was carried out at room temperature for 2 min (a) or for half an hour (b).
c) The residual material after evaporation of hydrazine and water was allowed to stand overnight at room temperature.
d) Distinct absorption maximum at 353 mμ was not obtained, but a shoulder was observed.
e) After treatment with hydrazine, removal of the excess reagent was omitted.

The cleavage reaction was subsequently simplified into a single procedure because the hydrazone formation and subsequent cleavage of the peptide bond could then be achieved under the same circumstances as in the present case. When the model peptide derivative was subjected to a reaction with a large excess of hydrazine in glacial acetic acid at room temperature, the absorption at 322 mμ was gradually decreased and a new absorption at 353 mμ emerged. The ninhydrin assay of the reaction mixture showed the liberation of the amino acid, which increased parallel with the increase in the absorption at 353 mμ (Fig. 3). As is shown in Table 2, the extent of the cleavage reaction for 48—50 hr at room temperature was estimated to be 73—92% on the basis of the absorbance of the tetrahydropyridazone derivative formed. By amino acid analysis,

16) Incubation of the hydrazine-treated tripeptide derivative in glacial acetic acid brought about liberation of leucine without the heteroring formation (see Table 1). This liberation of the amino acid may be due to a different mechanism from the present scheme.

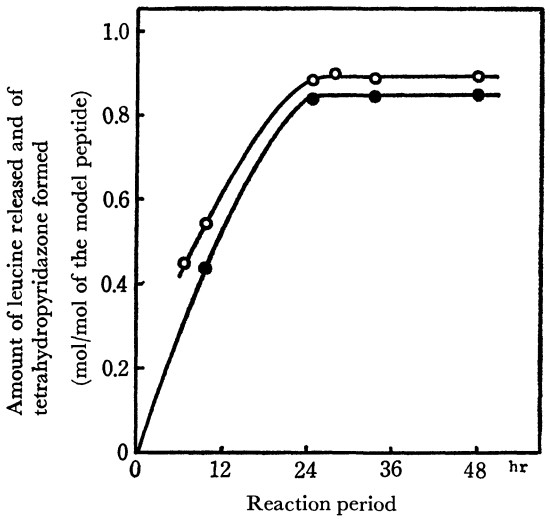

Fig. 3. Relationship between the tetrahydropyridazone formation (—○—) and liberation of leucine (—●—) by the reaction of the model *N'*-formyl-kynurenyl peptide (IV, 1.32 mM) with hydrazine (0.66M) in glacial acetic acid at room temperature.

TABLE 2. RELEASE OF LEUCINE BY THE DIRECT REACTION OF CARBOBENZOXY-L-ALANYL-*N'*-FORMYL-L-KYNURENYL-L-LEUCINE WITH HYDRAZINE ACETATE IN GLACIAL ACETIC ACID[a]

Concentration of		Yield of	
the model peptide derivative(mM)	hydrazine (M)	leucine released	tetrahydropyridazone derivative
6.18	5.0	—	74
2.41	2.0	—	91
1.60	1.6	81(81)	91(84)
1.19–1.39	0.5–1.2	78–87	82–90
0.59	1.6	78(80)	92(86)
0.57	0.5	—	84
0.27	1.6	113[b](86)	73(67)
0.12	0.1	—	no maximum

a) The formation of the tetrahydropyridazone derivative was estimated after 48—50 hr at room temperature and analysis of the amino acid was done after 120 hr. The yield after 24 hr was presented in parentheses.
b) See b) in Table 4.

it was also confirmed that leucine was the sole amino acid liberated during the cleavage reaction for 120 hr and that about 78—87% of the theoretical amount of the amino acid was present.[17] A study of the ultraviolet spectrum showed another reaction product to be identical with the expected 4-L-(*N*-carbobenzoxy-L-alanylamino)-6-(*o*-aminophenyl)-2,3,4,5-tetrahydropyridaz-3-one (Table 3). Table 4 shows the results of the cleavage reaction of the tryptophyl bond by ozonization and subsequent hydrazine treatment under the same conditions. The over-all reaction yielded the corresponding amino acid in a 30—50% yield on the basis of the parent peptide, but the second step directly causing the cleavage of the peptide chain could be

17) Removal of the β-benzoylpropionyl grouping as a substituent in the nucleotide synthesis was carried out with 0.5 M hydrazine in pyridine-water (R. L. Letsinger and P. S. Miller, *J. Amer. Chem. Soc.*, **91**, 3356 (1969)).

TABLE 3. SPECTRAL IDENTIFICATION OF THE TETRAHYDROPYRIDAZONE DERIVATIVE OBTAINED IN THE REACTION OF Z-ALA-*N'*-FORMYLKYN-LEU-OH WITH HYDRAZINE.

	Ratio of the absorbance against that at 283 mμ		
	250 mμ	283 mμ	353 mμ
4-L-(*N*-carbobenzoxy-L-alanyl-amino)-6-(*o*-aminophenyl)-2,3,4,5-tetrahydropyridaz-3-one[a]	1.50	1.0	0.76
A sample obtained by base treatment and subsequent reaction in aq. media[b]	1.46	1.0	0.67
A sample obtained by direct cleavage reaction in glacial acetic acid[c]	1.44	1.0	0.71

a) Part II, p. 530 in Ref. 1).
b) Compound V in Experimental part.
c) The sample was isolated on reaction of carbobenzoxy-L-alanyl-*N'*-formyl-L-kynurenyl-L-leucine (1.91 mM) with hydrazine acetate (1.2 M) in glacial acetic acid at room temperature for 48 hr.

TABLE 4. THE CHEMICAL CLEAVAGE OF THE TRYPTOPHYL BOND IN SEVERAL SYNTHETIC PEPTIDES AND GRAMICIDIN A[a]

Peptide derivative	Ozonization yield determined as		Yield of the over-all cleavage reaction determined by	
	N'-formyl-Kyn	Kyn	tetrahydro-pyridazone formation	amino acid analysis
Z·Trp·Gly·OH	47	41	42	34
Z·Trp·Leu·OH	45	51	50	65[b]
Z·Trp·Phe·OH	47	57	56	40
Z·Gly·Trp·Gly·OH	49	39	38	30
Z·Ala·Trp·Leu·OH	48	54	44	56[b]
Gramicidin A	86	43	46	—

a) The data presented were given by duplicate experiments except ozonization of gramicidin.
b) These yields were probably over-estimated according to low resolution between the leucine and a byproduct (possibly acetylhydrazine, eluted just before leucine in analysis on a Mitamura Amino Acid Analyzer (a column used for analysis, 0.9×50 cm, Aminex A-4)). Flow rate of the developing buffer (0.2 N citrate buffer, pH 3.25) was 50 ml/hr.

carried out to an extent similar to that in case of the model compound. From this result it must again be emphasized that, in the cleavage of the tryptophyl bond, the complete conversion of the tryptophan into the (*N'*-formyl-) kynurenine is necessary for the quantitative scission of the peptide linkage.

Propionic or butyric acid can be utilized as a reaction solvent in place of the glacial acetic acid, but formic acid, which is a good solvent for proteins, can not. Moreover, hydrazine acetate only must be used as the cleaving reagent; it is not replaceable by hydrazine dihydrochloride or sulfate.

In conclusion, the cleavage of the kynurenyl bond can be achieved by the aid of hydrazine under such mild conditions that no other peptide bond is affected. The hydrazine treatment can be carried out by two methods; one is the direct reaction of the kynurenyl

residue with hydrazine, while the other involves the preformation of the carbinolamine intermediate by treatment with the binucleophile in basic media. Though the cleavage of the tryptophyl bond in oligopeptides is possible to a similar extent by either procedure, the latter method may also be useful for that of the peptide bonds in proteins.

Experimental

All the melting points were uncorrected. The amino-acid analyses were performed on a Beckman amino acid analyzer model MS unless otherwise specified. The absorption spectra were measured by a Beckman spectrophotometer, type DB. The examination of the synthetic peptide by mass spectrometry was done by means of a Hitachi Mass Spectrograph, type RMU-6D. Ozone was generated from oxygen by a generator manufactured by the Nippon Ozone Co., Ltd., type 0-3-2. The formic acid (98—100%) was purchased from Merck AG and was used without purification.

The Cleavage Reaction of the N′-Formylkynurenyl Bond in the Model Peptide by Hydrazine. A typical procedure for the present reaction will be described below. About 2.8 mg (5 μmol) of carbobenzoxy-L-alanyl-*N′*-formyl-L-kynurenyl-L-leucine was dissolved in 80% or 100% hydrazine hydrate (0.2 m*l*); after this mixture had stood at room temperature for half an hour, the hydrazine and water were evaporated *in vacuo* by the same procedure as was used with lyophilization.[18] The residual substance was then dissolved in glacial acetic acid containing hydrazine acetate (1.6 M) (3 m*l*), and the reaction vessel, equipped with a stopper, was kept at 25—27°C on a water bath equipped with a thermostat. Portions (0.2 m*l*) of the acetic acid solution were withdrawn at suitable intervals and diluted with ethanol (3 m*l*). The ethanol solution was submitted to spectrometry at ranges from 450/400 mμ to 300 mμ or from 400 mμ to 230 mμ, with dilution to a suitable concentration, if necessary. The progress of the cleavage reaction could be followed in terms of the tetrahydropyridazone formation, and the extent of the cleavage reaction was determined from the absorbance at 353 mμ ($\varepsilon_{353m\mu}=8.13\times10^3$).

When the pretreatment by hydrazine was omitted, the model peptide was directly subjected to the reaction with hydrazine acetate in glacial acetic acid.

For the determination of the amino acid released, about 0.1 μmol (a theoretical amount when the reaction occurred quantitatively) was pipetted, diluted immediately with a 0.2 M citrate buffer at pH 2.2, frozen, and kept in a freezer (−20°C) until analysis has been performed by means of an amino-acid analyzer.

Isolation and Characterization of the 4-L-(N-Carbobenzoxy-L-alanylamino)-6-(o-aminophenyl)-2,3,4,5-tetrahydropyridaz-3-one (V) Formed on the Reaction of the Model Peptide with Hydrazine. The carbobenzoxy-L-alanyl-*N′*-formyl-L-kynurenyl-L-leucine (113 mg, 0.2 mmol), dissolved in 80% hydrazine hydrate (2 m*l*), was allowed to stand at room temperature for 5 min; then, the excess hydrazine was evaporated *in vacuo* to dryness over concentrated sulfuric acid (overnight). The residue was dissolved in water (15 m*l*), and the pH of the aqueous solution was adjusted to 3.8 with 4M acetic acid. At this stage, a large amount of an insoluble material was separated, but the suspension, after dilution to 100 m*l* with water, changed to an almost clear solution on standing at room temperature for 2 hr. After 24 hr, white precipitates which had separated were collected; they amounted to 23 mg. Additional precipitates (6 mg) were obtained after 72 hr. The white precipitates were combined and crystallized from methanol-water. Mp 200—204°C (lit,[1] 197.5—198°C). Molecular weight (mass spectrometry), Found: 409. Calcd for $C_{21}H_{23}O_4N_5$: 409. R_f (TLC, SiO_2) 0.69 (ethyl acetate: acetic acid= 5:1 by volume). λ_{max}; 353 mμ, 283 mμ and 250 mμ (in ethanol).

Cleavage Reaction of the Tryptophyl Bond in Several Tryptophyl Peptide Derivatives and Gramicidin. The tryptophyl peptide derivative (10 μmol) was dissolved in 98—100% formic acid (2 m*l*) and oxidized by approximately 0.01% ozone at 7—8°C until the increase of the absorption at 320 mμ reached its maximum. An aliquot (0.1 m*l*) was withdrawn, evaporated to dryness *in vacuo* over sodium hydroxide pellets, and used for amino-acid analysis after acid hydrolysis. Another portion (0.5 m*l*) was similarly evaporated and then dissolved in a glacial acetic acid (2 m*l*) containing hydrazine acetate (1.6 M). The acetic acid solution was kept at 25—27°C on a water bath for 48—50 hr, and then the liberated amino acid was determined. The progress of the cleavage was also followed by the spectrometric method, which has been described previously.

Carbobenzoxy-N′-formyl-L-kynurenine (I). Carbobenzoxy-L-tryptophan (1.38 g) was dissolved in a 98—100% formic acid (50 m*l*), and ozone in oxygen was bubbled at 5—10°C into the formic acid solution until a maximal absorption at 320 mμ was obtained. The solvent was then replaced by chloroform, and the insoluble materials were filtered off. The clear chloroform solution was shaken with 1N sodium carbonate, and the aqueous alkaline solution was acidified to pH about 1 after mixing with chloroform. The acidified solution was shaken with chloroform, and the sirupy ozonization product (854 mg) obtained on the evaporation of the chloroform was purified by chromatography on a silicic-acid (20 g) column. On the concentration of the first fraction from the column (300 m*l*, developing with chloroform containing 5—10% methanol), an amorphous substance (669 mg)[19] resulted. The crude carbobenzoxy-*N′*-formyl-L-kynurenine was obtained by repeating extraction and back-extraction between chloroform and aqueous acid or an alkaline solution as has been described above. The pure sample (246 mg, 16%) was obtained by recrystallization from methanol; mp 145—146°C. $[\alpha]_D^{25}=+23.1$ (*c* 0.73, in methanol). R_f (TLC, SiO_2) 0.85 (ethyl acetate: acetic acid=10:1 by volume). Molecular weight (mass spectrometry), Found: 370. Calcd: 370. λ_{max} (ethanol): 320 mμ and 258 mμ. ν(KBr): 3320, 3200, 1748, 1685, 1642, 1598, 1580, 1520, 1442 and 1407 cm^{-1}.

Found: C, 61.46; H, 4.68; N, 7.73%. Calcd for $C_{19}H_{18}O_6N_2$: C, 61.61; H, 4.90; N, 7.56%.

Carbobenzoxy-N′-formyl-L-kynurenyl-L-leucine Methyl Ester (II). Carbobenzoxy-*N′*-formyl-L-kynurenine (222 mg) and L-leucine methyl ester (88 mg) were dissolved in chloroform (2 m*l*), and dicyclohexylcarbodiimide (124 mg) was added to the chloroform solution under cooling with ice water. After 2 hr at 0°C and then 1 hr at 20°C, the insoluble dicyclohexylurea was filtered off. A crystalline material (280 mg) resulted on the evaporation of the chloroform; it was recrystallized from methanol. Yield, 205 mg

18) If evaporation of the aqueous hydrazine was omitted, the cleavage took place less effectively.

19) In another experiment, a crystalline material (mp 177—184°C, browning with gas evolution) was isolated. λ_{max} (methanol) 263 mμ and 325 mμ. Found: C, 58.03: H, 4.16; N, 7.14; ash 8.1%. Since this compound showed identical properties with the *N′*-formylkynurenine derivative after alkali-acid treatment, the crystalline sample was throught to be an adduct with silicic-acid used for chromatography.

(69%); mp 146—147°C (sintered at 139°C). $[\alpha]_D^{25} = -15.2$ (*c* 0.94, in methanol). Molecular weight (mass spectrometry), Found; 497. Calcd; 497.

Found: C, 62.67; H, 6.46; N, 8.35%. Calcd for $C_{26}H_{31}O_7N_3$: C, 62.76; H, 6.28; N, 8.45%.

Carbobenzoxy-L-alanyl-N′-formyl-L-kynurenyl-L-leucine Methyl Ester (III). *i) By Step-by-step Synthesis from the Leucine Methyl Ester*: The carbobenzoxy-*N′*-formyl-L-kynurenyl-L-leucine methyl ester (876 mg) was dissolved in methanol (70 m*l*) containing glacial acetic acid (106 mg) and hydrogenated on palladium-charcoal for 5 hr at room temperature. After the filtration of the catalyst, the clear methanol solution was passed through a Dowex 1 (OH-form) column and the effluent was evaporated to dryness. The residue (676 mg), solidified in crystals, was coupled with carbobenzoxy-L-alanine (394 mg) by dicyclohexylcarbodiimide (363 mg) in chloroform (10 m*l*) for 2 hr under cooling with ice water. After the chloroform solution freed from the resulting urea derivative was washed with diluted alkali, diluted acid, and water successively, the crude tripeptide derivative (863 mg) was obtained on the evaporation of the solvent. The crude product was then purified by silicic-acid chromatography. The fraction (60 m*l*) eluted with 5% methanol in chloroform after the column had been washed with chloroform (300 m*l*) was evaporated. Pure crystals (320 mg, mp 142—144°C) resulted on treatment with methanol. From the mother liquor, an additional product (130 mg, mp 143°C) was isolated by chromatographic purification. Total yield, 450 mg; 45%. The sample for analysis was further purified by recrystallization from methanol; mp 143—144°C (sintered at 140°C). By admixing with the carbobenzoxy-*N′*-formyl-L-kynurenyl-L-leucine methyl ester (II), the melting temperature dropped to 134—144°C. $[\alpha]_D^{18} = +27.1$ (*c* 1.4, in chloroform). λ_{max} (ethanol), 322 mμ. Molecular weight (mass spectrometry), Found, 568. Calcd: 568.

Found: C, 61.47; H, 6.33; N, 9.76%. Calcd for $C_{29}H_{30}O_8N_4$: C, 61.25; H, 6.38; N, 9.85%.

ii) By the Ozonization of the Carbobenzoxy-L-alanyl-L-tryptophyl-L-leucine Methyl Ester. The carbobenzoxy-L-alanyl-L-tryptophyl-L-leucine methyl ester[1] (5.37 g) was dissolved in formic acid (30 m*l*) and oxidized by ozone for 70 min under cooling with ice water. Then the solvent was replaced with chloroform, and the chloroform solution was washed with a diluted sodium carbonate solution. On the evaporation of the solvent, a neutral substance (5.35 g) was obtained; it was similarly chromatographed on a silicic-acid column. From the fraction eluted with chloroform containing 2—3% methanol, the crystalline, protected tripeptide derivative (1.84 g) was obtained by the evaporation of the solvent and by subsequent treatment with methanol. An additional ozonization product was obtained by repeated chromatography of the mother liquor after the first crystalline materials had been collected. The total yield of the crude products (2.22 g, mp 139—141°C) was 39%. The sample for analysis was again recrystallized from methanol; mp 143—144°C (after sintered at 139°C). $[\alpha]_D^{18} = +26.8$ (*c* 1.4, in chloroform). No depression of the melting point of the pure sample was observed after admixing with the sample obtained by the (i) procedure.

Carbobenzoxy-L-alanyl-N′-formyl-L-kynurenyl-L-leucine (IV). The protected tripeptide ester (III) (142 mg) was dissolved in pyridine (3 m*l*), and after 1N sodium hydroxide (0.5 m*l*) had been added to the pyridine solution, the aqueous pyridine solution was stirred for 40 min under cooling with ice water. After the methyl ester (III) was no longer detected (thin layer chromatography), dry ice and water were added successively. The hydrolysate was then shaken twice with chloroform (30 m*l* each), and the chloroform solution was dried with anhydrous sodium sulfate and concentrated under reduced pressure. The resulting crystalline material was washed with ether and recrystallized from methanol-water. Yield, 100 mg (70%). Mp 138—140°C (sintered at 136°C). The ultraviolet spectrum showed a small shoulder at 332 mμ. Recrystallization from the same solvent was repeated. The pure crystals thus prepared showed no absorption at 332 mμ; mp 140°C (foam after sintered at 136°C). $[\alpha]_D^{25} = -29.7$ (*c* 0.77, in methanol). The crystals showed a higher melting point at 159—162°C (dec., sintered at 132°C) after having been dried at 50°C for 5 hr under reduced pressure (10 mmHg) for analysis.

Found: C, 59.40, 59.34; H, 6.20, 6.28; N, 9.98, 9.90%. Calcd for $C_{28}H_{34}O_8N_4 \cdot 1/2H_2O$; C, 59.67; H, 6.26; N, 9.94%. The protected *N′*-formylkynurenyl peptide (IV) (87 mg), dissolved in methanol (1 m*l*), was treated with an excess of diazomethane in an ethereal solution. The methylation was continued for half an hour at room temperature, and the solution was concentrated to a sirup giving a crystalline product by treatment with methanol. The pure esterification product (55 mg, mp 140—142°C) obtained by recrystallization from methanol showed no depression of the melting point after admixture with compound (III).

The infrared absorption spectrum of the esterification product also showed a good agreement with that of compound (III).

The authors wish to express their thanks to Professor Kozo Narita for his advice during the present investigation. They also wish to thank Misses Yoshiko Yagi and Yuriko Sako for carrying out the amino-acid analyses.

Photochemical Reaction of 3,4-Diphenylsydnone[1]

Yoshiharu HUSEYA, Akiko CHINONE, and Masaki OHTA

Department of Chemistry, Faculty of Science, Tokyo Institute of Technology, Ookayama, Meguro-ku, Tokyo

(Received November 6, 1970)

In a recent communication,[2] we proposed 1*H*-1,3-diphenyldiazirine for the photolysis product of 3,4-diphenylsydnone. However, it was found later that the product was identical with the already known 2,4,5-triphenyl-1,2,3-triazole. In this paper, details of the photolysis of 3,4-diphenylsydnone and identification of the product are described. The formation of triazole derivative by the photolysis of 3,4-diphenylsydnone seems to be interesting. The reaction mechanisms are discussed.

Recently, much interest has been focussed upon the photolysis of mesoionic compounds due to their peculiar structures and 1,3-dipolar character. Krauch *et al.*[3] reported that the photolysis of 3-phenylsydone gave 4-phenyl-1,3,4-oxadiazoline-5-one, presumably *via* fused three-membered intermediate, 1*H*-diazirine derivative or nitrile imine. Kato[4] is working on photolysis of various mesoionic compounds with a view to investigating their photolysis in terms of a fused three-membered intermediate. In anticipation of the isolation of the intermediate having three-membered ring structure, we have been studying the photolysis of 3,4-disubstituted sydnone.

We reported that photolysis of 3,4-diphenylsydnone **(1)** gave a product of mp 119—120°C, which was considered, though not conclusively, to be 1,3-diphenyl-2-azirine **(3)**, on the basis of elementary analysis and mass spectroscopic analysis. However, on further examination, it was found that several behaviors of the compound could not be explained satisfactorily by the proposed structure.

Molecular weight determination of photolysis product (A) by the Rast method or by vapor pressure osmometer gave the value 310 and as an alternative formula, $C_{20}H_{15}N_3$ is possible which is consistent with this molecular weight and elementary analysis. For this empirical formula, three isomers of triphenyltriazoles are possible. It was found that 2,4,5-triphenyl-1,2,3-triazole **(6)** synthesized by Auwers *et al.*[5] has the same melting point and chemical properties as (A). Comparison with authentic sample revealed that (A) was identical with (**6**).

The mass spectroscopic results which caused us to deduce an incorrect structure can be explained by considering that the major peak at *m/e* 194 was due to a fragment $C_6H_5CNNC_6H_5$ derived from **6**. Both **3** and **6** have no proton except that of phenyl. Thus, NMR data are not sufficiently informative for determination of the structure, and some ambiguity was encountered in analyzing the NMR absorption spectrum due to phenyl proton. However, the results can be explained by means of both **3** and **6**.

Further evidence for excluding the diazirine structure (**3**) for A is provided by the fact that product A shows no infrared absorption at about 1740 cm^{-1} due to strained C=N linkage, and that attempts to reduce A by lithium aluminum hydride or catalytic hydrogenation with palladium-charcoal were unsuccessful.

The photolyses of 3-*p*-chlorophenyl-4-phenylsydnone and 4-phenyl-3-*p*-tolylsydnone were carried out under the same conditions to give corresponding 1,2,3-triazole derivatives.

The unexpected formation of **6** is unusual and some considerations are given on the mechanism of this

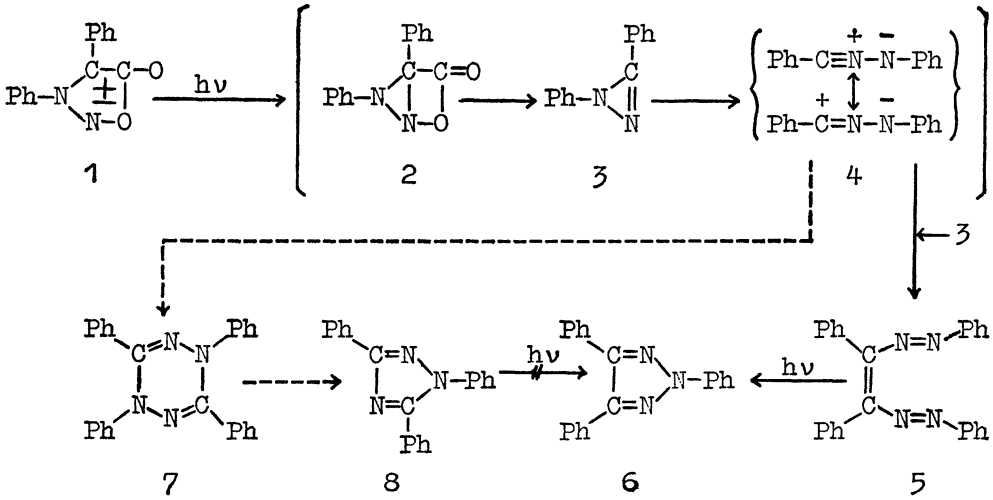

1) Studies of mesoionic compounds, XXXV. Part XXXIV: A. Chinone, S. Sato, and M. Ohta, This Bulletin, **44**, 826 (1971).

2) A. Chinone, Y. Huseya, and M. Ohta, *ibid.*, **43**, 2650 (1970).

3) C. H. Krauch, J. Kuhls, and H. J. Piek, *Tetrahedron Lett.*, **1966**, 4043.

4) Hiroshi Kato, Private communication.

5) a) K. Auwers and V. Meyer, *Ber.*, **22**, 540 (1889). b) K. Auwers and M. Siegfeld, *ibid.*, **26**, 792 (1893).

reaction. Similar to the photolysis of 3-phenylsydnone, the intermediacy of 1*H*-1,3-diphenyldiazirine (**3**) or diphenylnitrile imine (**4**) is probable in the photolysis of **1**. It was reported that diphenylnitrile imine produced from 2,5-diphenyltetrazole by thermolysis gave 1,3,4,6-tetraphenyl-1,2,4,5-tetrazine (**7**) by head-to-tail dimerization.[6] On the contrary, Scheiner and Dinda[7] stated that the formation of **6** from 2,5-diphenyltetrazole by photolysis proceeds *via* 1,2-bisphenylazo-1,2-diphenylethylene (**5**), and suggested that **5** is formed by photodimerization involving tetrazole-tetrazole association and not by head-to-head dimerization of 1,3-dipolar nitrile imine (**4**). The head-to-tail thermal dimerization of **4** should afford 1,2,4,5-tetrazine (**7**). As it is known that irradiation of some heterocyclic five membered rings yields rearranged products,[8] the formation of **6** from **7** *via* 1,3,5-triphenyl-1,2,4-triazole (**8**) seems to be probable. However, photolysis of authentic sample of **8**[9] resulted in the recovery of starting material. Thus, if the formation of **6** by photolysis of **1** proceeds *via* **5**, it would be unreasonable to consider that **6** is derived exclusively from nitrile imine.

Krauch *et al.*[3] reported that 1,3-dipolar cycloaddition of 3-phenylsydnone did not take place by photolysis. Our attempt on this reaction using dicyclopentadiene as a dienophile was also unsuccessful. While thermal 1,3-dipolar cycloaddition to 3-phenylsydnone is well known,[10] the same reaction by photolysis has not been realized. For the purpose of intercepting the intermediate nitrile imine, we have attempted the photolysis of 3,4-diphenylsydnone in the presence

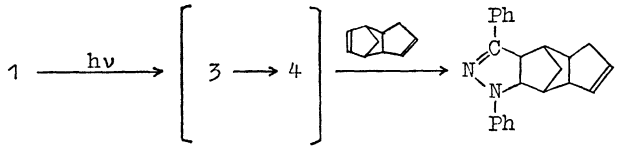

9

of dicyclopentadiene as a dipolarophile. The irradiation of a suspension of 3,4-diphenylsydnone in dicyclopentadiene gave a product to which tetracyclic structure (**9**) may be assigned, on the basis of elementary analysis, the same melting point as reported by Huisgen *et al.*[11] and spectroscopic data, indicating that the cycloaddition of dicyclopentadiene to **4** (or 1,3-position of **3**) occurred and addition of dicyclopentadiene to 2,3-position of **3** did not occur. These results show that the photolysis of 3,4-diphenylsydnone is not similar to thermal 1,3-dipolar cycloaddition observed in sydnone, which occurs at 2,4-position of sydnone. The thermal 1,3-dipolar cycloaddition of **1** was tried in dicyclopentadiene at 165°C to give intractable oil.

Thus, it is most likely that the reaction may proceed through the sequence indicated below.[12,13]

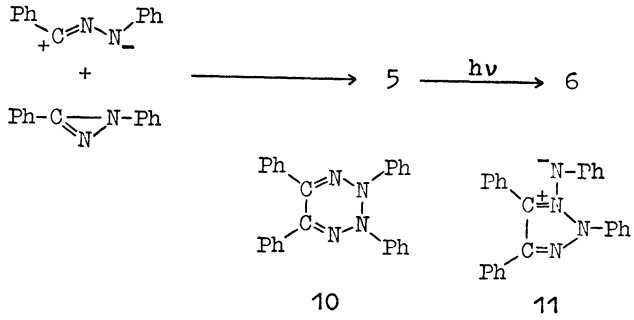

10 11

Experimental

All melting points were determined on a hot stage, and were not corrected.

Photolysis of 3,4-diphenylsydnone. A solution of 3.0 g of 3,4-diphenylsydnone[15,16] in 300 m*l* of dioxane was placed in a Pyrex vessel, purged with nitrogen for 0.5 hr, and irradiated with a high-pressure mercury lamp (100W) under nitrogen. The reaction ended after 30 hr. The solvent was evaporated under reduced pressure, and the residue was chromatographed over alumina. Elution with benzene gave 0.45 g (24%) of **6**, mp 119—120°C, IR ν(KBr) 3050, 1595, 1493, 970, 775, 700 cm^{-1}. The identity of **6** was established by comparison (IR and mixed mp) with an authentic sample. The same procedures were employed with two other sydnones.

Irradiation of 4-phenyl-3-*p*-tolysylsydnone[16] gave 4,5-diphenyl-2-*p*-tolyl-1,2,3-triazole (23%), mp 114—116°C, IR ν(KBr) 3050, 1510, 975, 825, 770 cm^{-1}.

Found: N, 13.32%. Calcd for $C_{21}H_{17}N_3$: N, 13.50%.

Irradiation of 3-*p*-chlorophenyl-4-phenylsydnone[16] gave 2-*p*-chlorphenyl-4,5-diphenyl-1,2,3-triazole (21%), mp 99—101°C, IR ν(KBr) 3050, 1490, 975, 825, 770, 700 cm^{-1}.

Found: N, 12.64%. Calcd for $C_{21}H_{17}N_3Cl$: N, 12.86%.

Photolysis of 3,4-diphenylsydnone with dicyclopentadiene. A suspension of 2.0 g of **1** in 300 m*l* of commercial dicyclopentadiene was irradiated with a high-pressure mercury lamp for 20 hr. Removal of the solvent under reduced pressure and recrystallization of the residue from ethanol gave 0.55 g of 1,3-diphenyl-4,8-methane-3a,4,4a,7a,8,8a-hexahydroindeno[5,6-*c*]pyrazole, mp 178—179°C (lit,[11] mp 173—174°C).

6) R. Huisgen, J. Sauer, and M. Seidel, *Chem. Ber.*, **94**, 2503 (1961).

7) P. Scheiner and J. F. Dinda, *Tetrahedron*, **26**, 2619 (1970).

8) a) P. Beak and W. Messer, *ibid.*, **25**, 3287 (1969). b) H. Wynberg, R. M. Kellogg, H. Driel, and G. E. Beekhuis, *J. Amer. Chem. Soc.*, **89**, 3501 (1964).

9) Engelhardt, *J. Prakt. Chem.*, [2] **54**, 153 (1897).

10) a) R. Huisgen, R. Grashey, H. Gotthardt, and R. Schmidt, *Angew. Chem.*, **74**, 29 (1962). b) R. Huisgen, H. Gotthardt, and G. Grashey, *ibid.*, **74**, 30 (1962).

11) R. Huisgen, M. Siedel, G. Wallbillich, and H. Knupfer, *Tetrahedron*, **17**, 3 (1962).

12) Compound **5** has been prepared by the oxidation of β-benzyl phenylosazone, to which 1,2,3,4-dihydrotetrazine structure (**10**) was assigned by Spasov *et al.*[14] and the open chain structure (**5**) by Scheiner and Dinda[7].

13) Scheiner and Dinda[7] suggested the intermediacy of azomethine imine (**11**) in the conversion of **5** to **6**.

14) A. V. Spasov, D. Elenkov, and St. Rovev, *Bulgarska Akad. Nauk., Otdel. Geol.-Geograf Khim. Nauk., Izvest. Khim. Inst.*, **1**, 229 (1951); *Chem. Abstr.*, **47**, 2153 g (1953).

15) E. Knoevenagel, *Ber.*, **37**, 4073 (1904).

16) W. Baker, W. D. Ollis, and V. D. Poole, *J. Chem. Soc.*, **1949**, 307.

Mechanism and Reactivity of Hydrolysis of Aliphatic Sulfonate Esters

Akira MORI, Masuzo NAGAYAMA, and Hiroshi MANDAI

Research Department, Lion Fat & Oil Co., Ltd., Hirai, Edogawa-ku, Tokyo

(Received November 7, 1970)

It was shown with a five-membered sultone that the hydrolysis of aliphatic sultones in water proceeds substantially by $B_{AL}1$-E1 mechanism, and that it is a nucleophilic substitution reaction caused by hydroxyl ion and water. We carried out a kinetic experiment on the hydrolysis of 1,4-butanesultone and ethyl ethanesulfonate, both in water and in water - acetone mixed solvent. It was found that these aliphatic sulfonate esters were hydrolyzed substantially by $B_{AL}1$-E1 mechanism as in the case of a five-membered sultone, and in particular, ethyl ethanesulfonate was hydrolyzed by complete $B_{AL}1$-E1 mechanism. The results seem to be justified by a tracer experiment with $H_2{}^{18}O$. Namely, the ratios of the C–O fission to the S–O fission in 1,3-propanesultone and ethyl ethanesulfonate were 85.6:14.4 and 100:0, respectively. In strong alkaline solutions and approtic solvent - water systems, the S_N2 reaction involving attack of the nucleophile on sulfur atom took place partly in sultones, but practically not in linear sulfonate esters. On the other hand, the ratio of relative reaction rates of a five-membered sultone, a six-membered sultone, and a linear sulfonate ester in water is 37:1:7. Since E_a is nearly the same for these three compounds, the contribution of strain in the molecular structure to the reactivity is small, and in consequence the above ratio seems to be attributed to ΔS^*.

We reported[1,2] that aliphatic five-membered and six-membered sultones are obtained from sulfonation of long chain alpha olefins with sulfur trioxide and that these sultones are converted into an useful detergent by hydrolysis the mechanism of which is ascribed substantially to $B_{AL}1$-E1. Kinetic data of the hydrolysis in D_2O suggested that the reaction is a nucleophilic substitution reaction by hydroxyl ion and water ($k_H/k_D=1.03$).[2] However, the sultones used in the tracer experiments on the hydrolysis with $H_2{}^{18}O$ were long chain aliphatic sultones, which gave a mixture of hydroxy alkane sulfonates and alkene sulfonates by hydrolysis, and in consequence, an accurate result could not be expected because of difficulty in purification of the products. In this study, therefore, 1,3-propanesultone which yields only one product by hydrolysis was used in the $H_2{}^{18}O$ tracer experiment, and the previous results were reinvestigated.

Sulfonation of long chain alpha-olefins with sulfur trioxide gives six-membered sultones in addition to five-membered sultones which seem to differ from each other. Studies were thus made on the structural effect on the mechanism of hydrolysis and the reactivity of aliphatic sulfonate esters.

Hydrolysis of linear alkyl sulfonate esters was carried out in $H_2{}^{18}O$, and the results were compared with those obtained in the kinetic study.

Experimental

Materials. Commercial *1,3-propanesultone* (c.p.grade) was distilled under reduced pressure before use:bp 113.0—114.5°C/3 mmHg.

1,4-butanesultone was prepared from tetrahydrofuran according to the method of Truce and Hoerger.[3]: bp 112°C/1.5 mmHg, n_D^{25}1.437.

Found: C, 35.27; H, 5.64; S, 23.33%. Calcd for $C_4H_8SO_3$; C, 35.28; H, 5.92; S, 23.55%.

Ethyl ethanesulfonate was prepared from ethylsulfonyl chloride and ethyl alcohol according to the method of Sekera and Marvel[4]: bp 43°C/1 mmHg and n_D^{25}1.4229.

Found: C, 34.90; H, 7.40; S, 23.11%. Calcd for $C_4H_{10}SO_3$: C, 34.77; H, 7.29; S, 23.20%.

All the solvents used in kinetic experiments were purified by distillation.

Commercial *sodium perchlorate* (c.p.grade) was used.

Water enriched with ^{18}O was obtained from the Yeda Research and Development Co., Ltd. (Israel) and the atomic percentage of ^{18}O was 1.742.

Sodium hydroxide enriched with ^{18}O was prepared in an authentic manner from sodium ethoxide and water enriched with ^{18}O.

Measurement of the Rate of Hydrolysis. 1,4-Butanesultone and ethyl ethanesulfonate were hydrolyzed in water and in 65 vol% of aqueous acetone at room temperature under the following conditions, the pH being kept constant with a pH-stat (manufactured by Toa Electronic Ltd., Model HS-1B). The amount of sultones decomposed was calculated from that of sodium hydroxide required for counterbalancing the decrease of the pH by sulfonic acids formed by the decomposition of sultones.

Hydrolysis was carried out in an atmosphere of nitrogen to eliminate the effect of carbon dioxide in air. Sodium perchlorate was added to maintain the ionic strength of the reaction system constant.

Conditions of Hydrolysis. Concentration of the samples: 0.04 mol/*l*; Solvents: Water and aqueous acetone (65 vol%); Ionic strength: 0, 0.5 and 0.8; Temperatures: 25.0—55.0°C; pH: 3.0—11.3.

Determination of the Reaction Rate Constant (k_1). Using a linear equation, logs $S/(S-S')$ was plotted *versus* time t(sec), where S is the initial amount of sultone and S' is amount of sultone decomposed in time t(sec). k_1 was obtained from the slope of the plots.

Hydrolysis in $H_2{}^{18}O$. Hydrolysis of 1,3-Propanesultone: 1,3-Propanesultone (1.954 g, 1.6×10^{-2} mol) was dissolved in a solution containing 750 mg (1.8×10^{-2} mol) of $Na^{18}OH$ in 10 m*l* of $H_2{}^{18}O$, and the solution was heated on a water bath at 70°C for 2.5 hr. The pH of the reaction mixture was greater than 12 at the end of the reaction. The unreacted sultone was removed by extraction with 5 m*l* of petroleum

1) M. Nagayama, H. Okada, and S. Tomiyama, *Kogyo Kagaku Zasshi*, **72**, 2248 (1969).

2) A. Mori, M. Nagayama, and H. Mandai, *ibid.*, **74**, 715 (1971).

3) W. E. Truce and F. D. Hoerger, *J. Amer. Chem. Soc.*, **76**, 5357 (1954).

4) V. C. Sekera and C. S. Marvel, *ibid.*, **55**, 345 (1933).

ether carried out four times. The aqueous layer was neutralized with N/10 HCl, and the solvent was evaporated to leave crude sulfonate behind. Recrystallization from 95% ethyl alcohol gave 1.80 g of needles of pure sulfonate. NMR spectral analysis showed that the sulfonate thus obtained contained only sodium 3-hydroxypropanesulfonate.

Pure sulfonate (1 g) was treated with 3 m*l* of dimethylformamide and 40 m*l* of thionyl chloride to give chlorosulfonyl chloride according to the method of Bosshard *et al.*[5] The product was purified by distillation under reduced pressure: yield, 100 mg, bp 65.0°C/3 mmHg; IR spectra, strong SO_2–Cl absorption was observed at 1380 and 1165 cm^{-1}.

The atomic percentage of excess ^{18}O in the sulfonate and chlorosulfonyl chloride was measured according to the method of Rittenberg and Ponticorvo[6] and the ratio of the C–O fission to the S–O fission was determined.

Hydrolysis of Ethyl Ethanesulfonate: To a solution of 750 mg (1.8×10^{-2} mol) of $Na^{18}OH$ in 10 m*l* of $H_2{}^{18}O$ was added 2.211 g (1.6×10^{-2} mol) of ethyl ethanesulfonate, and the hydrolysis was carried out with stirring at 80°C for 2 hr on a water bath. The pH of the reaction mixture at the end of the reaction was greater than 12. The unreacted ethyl ethanesulfonate was extracted with ethyl ether, the aqueous layer was neutralized with N/10 hydrochloric acid, the solvent was removed, and NaCl was separated to yield crude sulfonate. Recrystallization from 95% ethanol gave 1.50 g of needles of pure sulfonate. The ratio of the C–O fission to the S–O fission was determined from the atomic percentage of excess ^{18}O in the sulfonate thus obtained and ^{18}O enriched aqueous sodium hydroxide solution used for the hydrolysis.

Results and Discussion

Kinetic Studies of Hydrolysis. Hydrolysis of 1,4-Butanesultone: The relationship between log K_1 and pH in the hydrolysis of 1,4-butanesultone in 65 vol % of aqueous acetone and in water is shown in Fig 1. It is apparent that a six-membered sultone undergoes exactly the same type of reaction as a five-membered sultone. A first-order reaction takes place in water, but in a mixed system consisting of an aprotic solvent and water, a rise is observed in the curve and this tendency becomes slightly less pronounced than in the case of the five-membered sultone on the alkaline side. However, from the rise observed in the curve, it seems that an S_N2-E2 reaction takes place to some extent, although a $B_{AL}1$-E1 reaction predominates.

The effect of the ionic strength in 65 vol % of aqueous acetone on the alkaline side, where the reactivity of the S_N2-E2 reaction is large, is shown in Table 1. Here again, the positive salt effect is observed as before, and the increase of electron charge in the transition state, namely the cause of the monomolecular reaction, is detected.

Table 1. Effect of ionic strength on the K_1 value of hydrolysis of C_4 1,4-sultone (at 50°C, pH 9 in 65 vol % Acetone)

Ionic strength	$6+\log K_1$
0	0.629
0.5	0.696
0.8	0.788

Hydrolysis of Ethyl Ethanesulfonate: The relationship between log K_1 and pH in the hydrolysis of ethyl ethanesulfonate in 65 vol % of aqueous acetone and in water is shown in Fig. 2. A clean first-order reaction is observed both in the aqueous acetone and in water. This suggests that, in contrast to sultones, ethyl ethanesulfonate is hydrolyzed completely by the $B_{AL}1$-E1 reaction to the exclusion of the S_N2-E2 reaction. This will be examined later with reference to the analysis of ^{18}O contained in the products of the hydrolysis of ethyl ethanesulfonate in ^{18}O enriched water.

As shown in Fig. 2, the effect of the ionic strength was partly at pH 4 and 10, but only a weak salt effect was observed.

Kinetic Constants of 1,4-Butanesultone and Ethyl Ethanesulfonate: The Arrhenius plots for the hydrolysis of

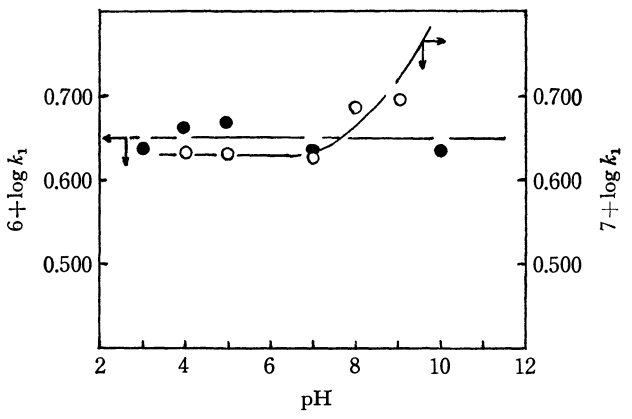

Fig. 1. log k_1 *vs.* pH in the hydrolysis of C_4 1,4-sultone.
○ in 65 vol % acetone, at 50°C, ionic strength 0.5
● in water, at 45°C, ionic strength 0.5

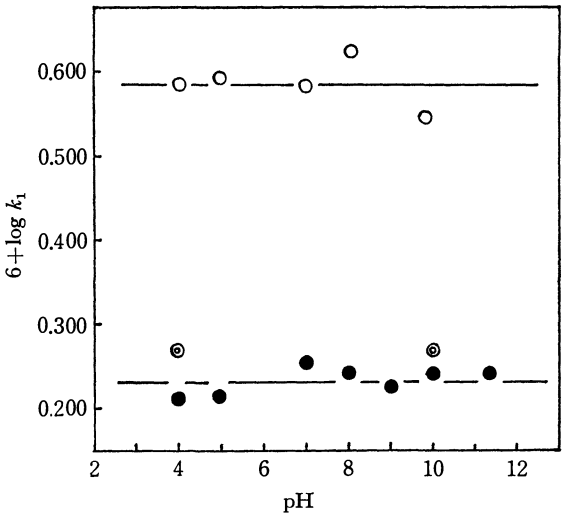

Fig. 2. log k_1 *vs.* pH in the hydrolysis of ethyl ethane sulfonate and effect of ionic strength on the k_1 values.
● in 65 vol % acetone, at 45°C, ionic strength 0.5
◎ in 65 vol % acetone, at 45°C, ionic strength 0.8
○ in water, at 25°C, ionic strength 0.5

5) H. H. Bosshard, R. Mory, M. Schmid, and Hch. Zollinger, *Helv. Chim. Acta*, **42**, 1653 (1959).

6) D. R. Rittenberg and L. Ponticorvo, *J. Appl. Rad. Isotopes*, **1**, 208 (1956).

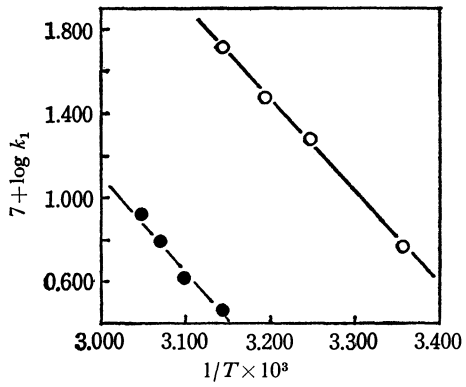

Fig. 3. Arrhenius plots for the C_4 1,4-sultone hydrolysis at pH 7, ionic strength 0.5.
● in 65 vol % acetone ○ in water

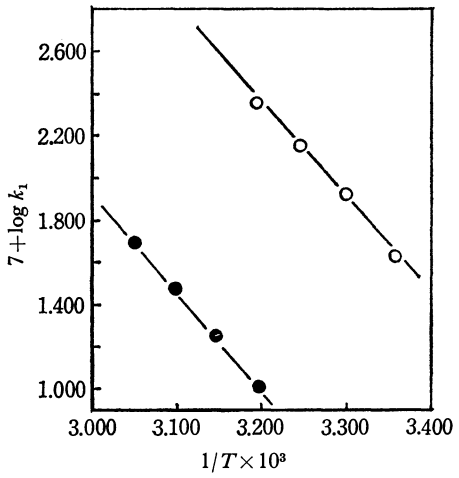

Fig. 4. Arrhenius plots for the ethyl ethane sulfonate hydrolysis at pH 7, ionic strength 0.5.
● in 65 vol % acetone ○ in water

1,4-butanesultone and ethyl ethanesulfonate in 65 vol % of aqueous acetone and in water at pH 7 and ionic strength 0.5 are shown in Figs. 3 and 4, respectively. Table 2 was prepared from these results. For comparison, the data on 1,3-propanesultone reported previously[2] are also shown.

Table 2. Kinetic constants (in 65 vol % of aqueous acetone at 25°C, and ionic strength 0.5)

	$K_1\times10^7$ (sec^{-1})	E_a (Kcal/mol)	ΔS^* (e u)
CH_2–CH_2–CH_2 O———SO_2	18.8	20.2	−17.1
	215[a]		
	130[b] (at 20°C)	20.4±0.1[b]	−13.8[b] (at 40°C)
CH_2–CH_2–CH_2–CH_2 O———SO_2	0.316	20.5	−24.0
	5.76[a]	20.0[a]	−20.0[a]
CH_3–CH_2–SO_2O– CH_2–CH_3	1.88	21.3	−17.9
	42.3[a]	20.9[a]	−13.2[a]

a) in water
b) Bordwell's Data[7] in water

7) F.G. Bordwell, C.E. Osborne, and R.D. Chapman, *J. Amer. Chem. Soc.*, **81**, 2698 (1959).

As shown in Table 2, the ratio of relative reaction rates of a five-membered sultone, a six-membered sultone, and a linear alkyl sulfonate ester in water at pH 7 is 37:1:7. This ratio seems to be the relative rate *via* $B_{AL}1$-E1 mechanism, because in the relationship between log K_1 and pH the values of log K_1 are constant below pH 10. Since E_a is nearly the same, these compounds can be regarded to undergo practically the same type of reaction. On the other hand, the strain in the ring should depend on the enthalpy term.[8,9] This term, however, is nearly the same, *viz.*, the difference in free energy of strain between a five-membered ring and a six-membered ring is slight. Consequently, contribution of the strain to the reactivity in the hydrolysis of sultones seems to be small and the reactivity is controlled practically by the entropy term (ΔS^*) alone.

Hydrolysis in $H_2{}^{18}O$. The hydrolysis of sultones and ethyl ethanesulfonate proceed mostly by $B_{AL}1$-E1 mechanism, but the results of kinetic studies suggest that S_N2-E2 reaction also occurs in the case of sultones. For the sake of confirmation, hydrolysis was carried out in $H_2{}^{18}O$ in a strongly alkaline medium (pH>12), and the atomic percentage of excess ^{18}O in the aqueous sodium hydroxide, hydrolysis products and its chlorinated compound were measured to determine the ratios of the C–O fission to the S–O fission in sultones and ethyl ethanesulfonate.

A previous kinetic study[2] indicates that both long chain substituted 1,3-sultones and unsubstituted 1,3-sultones undergo the same types of reactions and the ratios of the C–O fission to the S–O fission are nearly the same for the two groups. The samples of long chain substituted sultones for the analysis of ^{18}O present technical problems with respect to purification. Unsubstituted sultones which yield a single component, and are easily purified, seem to give more accurate values for the C–O and S–O fission. Thus, the ratio of the C–O fission to the S–O fission in 1,3-propanesultone seems to be applicable to aliphatic five-membered sultones.

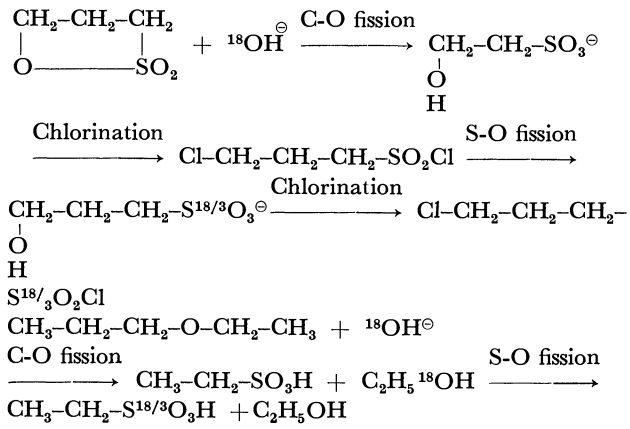

The ratios of the C–O fission to the S–O fission in 1,3-propanesultone and ethyl ethanesulfonate are shown in Table 3.

8) F.S. Dainton, T.R.E. Devlin, and P.A. Small, *Trans. Faraday Soc.*, **51**, 1710 (1955).
9) P. A. Small, *ibid.*, **51**, 1717 (1955).

Table 3. Atomic percentage of excess ^{18}O and the ratios of the C-O fission to the S-O fission in the hydrolysis of 1,3-propanesultone and ethyl ethanesulfonate

Condition of Hydrolysis / Sample	1,3-propanesultone at 70°C, for 2.5 hr above pH 12	Ethyl ethanesulfonate at 80°C, for 2 hr above pH 12
$Na^{18}OH$-$H_2{}^{18}O$	1.459 (atom %)	1.503 (atom %)
Resulted Sulfonate	0.351	0.002
Chlorosulfonyl-chloride	0.101	—
C-O fission	85.6 (%)	100 (%)
S-O fission	14.4	0

The hydrolysis of a five-membered sultone occurs *via* scission of the S–O linkage even in water in a strongly alkaline medium. Since the S–O fission *via* monomolecular cleavage is difficult to conceive, the S_N2 reaction seems to be possible. This is reasonable if one considers that $OH^{\ominus}$, a hard base, tends to attack $-^{\oplus}SO_2$ more readily than $C^{\oplus}$ since $-^{\oplus}SO_2$ is a harder acid.

The S_N2 reaction tends to occur in aliphatic sultones when the activity of hydroxyl ion is increased such as in a strong alkaline medium or in a system consisting of an aprotic solvent and water.

On the other hand, in the hydrolysis of ethyl ethanesulfonate not the S_N2 reaction but the $B_{AL}1$-E1 reaction *via* the C–O fission occurs exclusively, both in a strong alkaline medium and in an aprotic solvent-water system. This result agrees with the kinetic results.

The S_N2 reaction seems to occur in six-membered sultones to a slightly less extent than in five-membered sultones, since a rise in the plot of log K_1 *versus* pH in the former sultone in 65 vol % of aqueous acetone is slightly less pronounced.

It is obvious that the hydrolysis of sultones proceeds by $B_{AL}1$-E1 mechanism. It is considered that in ordinary hydrolysis systems, where the activity of hydroxyl ion is not very high, only the $B_{AL}1$-E1 reaction occurs as in the case of ethyl ethanesulfonate.

Consequently, the ratio of K_1 of a five-membered sultone, a six-membered sultone, and ethyl ethanesulfonate in water at pH 7 shows the relative reactivity of hydrolysis by the $B_{AL}1$-E1 reaction.

We thus conclude that in the reactions of hydrolysis of aliphatic alkyl sulfonate esters which proceed by the $B_{AL}1$-E1 reaction *via* the cleavage of C–O bond, the contribution of a ring strain to reactivity is very small, and the reactivity seems to be decided essentially by the entropy term ($\Delta S^{\neq}$).

The S_N2 reaction which follows a fission of S–O bond only occurs when the sultones are reacted in a solvent where the activity of hydroxyl ion is very high. This reaction seems to occur more easily in a five-membered sultone than a six-membered sultone.

However, in straight chain alkyl sulfonate ester which has no ring strain, the S_N2 reaction was not observed. It is obvious that in this reaction, contribution of the ring strain to the reactivity is very large. This tendency is consistent with the observation by Kaiser *et al.*[10] on aliphatic five-membered, six-membered and straight chain alkyl sulfates.

It is very interesting to compare these observations with the study by Müller *et al.*[11] with regard to the reactions of hydrolysis of aromatic sultones, in which only the S_N2 reaction can occur. Even in this case, contribution of the ring strain is also very large.

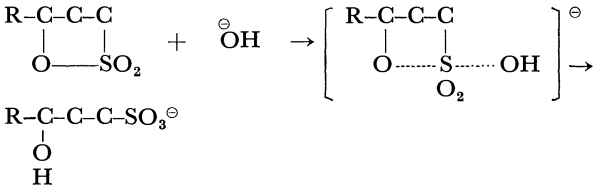

The authors are grateful to Dr. Shinichi Tomiyama, the Senior Managing Director of Lion Fat & Oil Co., Ltd. They also wish to express their thanks to Professer Dr. Shigeru Oae, Osaka City University and Professor Dr. Waichiro Tagaki, Gunma University, for many helpful discussions and suggestions during this work.

10) E. T. Kaiser, M. Panar, and F. H. Westheimer, *J. Amer. Chem. Soc.*, **85**, 602 (1963).

11) P. Müller, D. F. Mayers, O. R. Zaborsky, and E. T. Kaiser, *ibid.*, **91**, 6732 (1969).

The Preparation of Deoxyguanosine Oligomers on an Insoluble Polymer Support

Takeo SHIMIDZU and Robert L. LETSINGER*

Faculty of Engineering, Kyoto University, Kyoto

**Department of Chemistry, Northwestern University, Evanston, Illinois, U.S.A.*

(Received December 4, 1970)

The syntheses of deoxyguanosine-containing oligonucleotides, deoxyguanylyldeoxyguanylyldeoxyguanosine (d-GpGpG), deoxyguanylyldeoxyguanylyldeoxyguanylyldeoxyguanosine (d-GpGpGpG) and deoxyguanylyldeoxyguanylyldeoxyguanylylthymidine (d-GpGpGpT) have been described. Those nucleotidic materials were synthetized on an insoluble polymer support; the polymer was a copolymer of styrene, *p*-vinylbenzoic acid, and divinylbenzene. The blocking group used at the *N*-position of deoxyguanosine was di-*p*-methoxytrityl.

Since Letsinger and his co-worker[1] used a polymer support technique to synthetize an oligonucleotide, many similar investigations have been made.[2-9] The most striking characteristic of the polymer support technique is the simplicity of its treatment and reaction-controlling of the intermediary products of nucleotidic materials, as in the Merrifield method[10] used in the synthesis of oligopeptide. However, in polymer support techniques used to synthetize a polypeptide with a higher molecular weight at a higher degree of condensation reaction, there is a limitation which results from a failure of sequence in the synthetized polypeptide, which can not be isolated from the desired product.[11] That is, in the polymer support techniques in polypeptide and polynucleotide syntheses, by-products resulting from an incompleteness of condensation steps accumulate until there is a cleavage of the product from the polymer support. Still, this technique is useful for the synthesis of a oligonucleotide unless the separation and isolation of the desired oligonulceotide is impossible. Table 1 shows the results of several syntheses of oligonucleotides by the polymer support technique. These procedures give higher yields than would a conventional homogeneous method.

In a preceding paper,[9] we described the synthesis of deoxyguanylyldeoxyguanosine on an insoluble polymer support; on it the 5'-OH of deoxyguanosine was bound as an anchor group. In this paper, the application of this method to the syntheses of trinucleotide, tetranucleotides, and their derivatives will be described. That is, deoxyguanylyldeoxyguanylyldeoxyguanosine (d-GpGpG), deoxyguanylyldeoxyguanylyldeoxyguanyl-

TABLE 1. SUMMARY OF OLIGONUCLEOTIDE SYNTHESES BY POLYMER SUPPORT TECHNIQUES[a]

Ⓟ—COCl					Ⓟ—ϕ(OCH$_3$)$_2$—C(Cl)—ϕ		Ⓟ—NH$_2$
St-DVB[3]	St-DVB[9,10]		AN-AA[12]	DMBD-VBA	St[6]	St[7]	St[8]
6'-NH$_2$	5'-OH		5'-OH	5'-OH	5'-OH	5'-OH	5'-Phosphate
d(CT) 77% (55)	(TT)	82% (80)	(TT) 72%	(TT) 68%	(TT) 54%	(TT) 96%	p(TT) 40%
d(CTT) 34% (18)	d(TA)	70% (64)			(TTT) 38%	d(TC) 88%	p(TTT) 5%
d(CTTT) 15% (8)	d(TC)	72% (60)			(TTTT) 37%	d(TG) 94%	
d(CTA) 26%	(TTT)	56% (40)			d(ATT) 30%	(TTT) 84%	
	d(GG)	60% (48)	Shape of Anchorage				
	d(GGG)	22% (7)					
	d(GGGG)	7%					
	d(GGGT)	18%					
			6'NH$_2$[3]	5'-OH[1,4,8]	5'-OH[6,7]		5'-Phosphate[8]

% shows overall yield ( ) shows overall yield by conventional homogeneous methods.

a) A new polymer support technique using a polymer containing 2-pyridineethanol has been published during contribution: W. Freist and F. Cramer, *Angew. Chem. (Intl. Ed.)*, **9**, 368 (1970).

1) R. L. Letsinger and M. J. Kornet, *J. Amer. Chem. Soc.*, **85**, 3045 (1963).

2) R. L. Letsinger, M. J. Kornet, V. Mahadevan, and D. M. Jerina, *ibid.*, **86**, 5163 (1964).

3) R. L. Letsinger and V. Mahadevan, *ibid.*, **87**, 5326 (1965); **88**, 5319 (1966).

4) F. Cramer, R. Helbig, H. Hettler, K. H. Scheit, and H. Siegler, *Angew. Chem.*, **78**, 640 (1966).

5) R. L. Letsinger, D. M. Jerina, and M. H. Caruthers, *Biochemistry*, **6**, 1397 (1967).

6) L. R. Melby and D. R. Strobach, *J. Amer. Chem. Soc.* **89**, 450 (1967); *J. Org. Chem.*, **35**, 421 (1969).

7) H. Hayatsu and H. G. Khorana, *J. Amer. Chem. Soc.*, **89**, 3880 (1967).

8) G. M. Blackburn, M. J. Brown, and M. R. Harris, *J. Chem. Soc.*, **1967**, 2438; **1969**, 676.

9) T. Shimidzu and R. L. Letsinger, *J. Org. Chem.*, **33**, 708 (1968).

10) R. B. Merrifield, *J. Amer. Chem. Soc.*, **85**, 2149 (1963).

11) E. Bayer, H. Eckstein, K. Hägele, W. A. König, W. Brüning, H. Hagenmaier, and W. Parr, *ibid.*, **92**, 1735 (1970).

12) T. Shimidzu, *J. Syn. Org. Chem., Jap.*, **28**, 581 (1970).

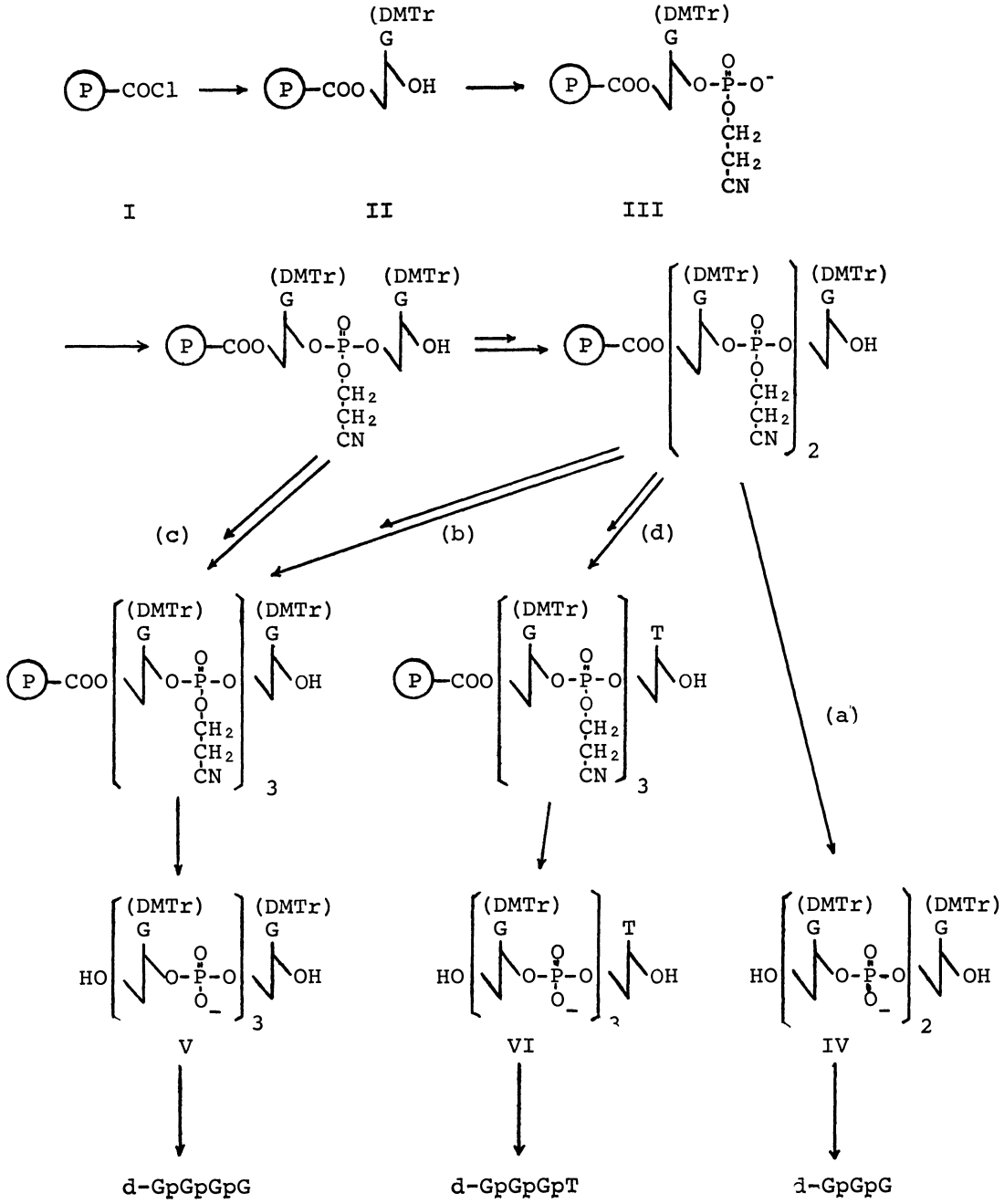

Fig. 1. Synthetic path of oligonucleotides.[13]

yldeoxyguanosine (d-GpGpGpG), deoxyguanylyldeoxyguanylyldeoxyguanylylthymidine (d-GpGpGpT), and their *N'*-di-*p*-methoxytrityl-substituted derivatives are synthetized. As the blocking group at the *N*-position[13] of deoxyguanosine, di-*p*-methoxytrityl (DMTr) is used.

These nucleotides were synthetized by the phosphodiester route on insoluble polymer supports like those described in the preceding paper.[9] The course of the synthesis is shown in Fig. 1.

The polymer supports used are tabulated in Table 2. The selectivity in the position of the anchorage of the hydroxy group in *N*-di-*p*-methoxytrityl deoxyguanosine[14] ((DMTr)d-G) depends on the crosslinkage of the polymer. A lower degree of crosslinkage gave a low selectivity of the 5'–0 anchorage, although the reac-

Table 2. Composition of polymer supports

	I	II	III	IV
Styrene	57.5	57.5	57.5	50.0 mmol
p-Divinylbenzene	0.040	0.064	0.012	0.063 mmol
p-Vinylbenzoic acid	6.36	6.90	6.35	12.5 mmol
% COCl	10	11	10	20
% Crosslinkage	0.06	0.1	0.02	0.1

13) For convenience the di-*p*-methoxytrityl group is represented on the amino group, though the exact position it occupies in the guanine ring has not been established with certainty: W. E. Razzell and H. G. Khorana, *J. Biol. Chem.*, **234**, 2105 (1959).

14) H. Schaller, G. Weimann, B. Lerch, and H. G. Khorana, *J. Amer. Chem. Soc.*, **85**, 3821 (1963).

Table 3. Additions of di-*p*-methoxytrityldeoxyguanosine on polymer supports

	Ⓟ–COCl (g)	Nucleoside (g)	Pyridine (ml)	Reaction time (hr)	Nucleoside anchored (mmol/g·pol.)(g)		Selectivity (5′O-linkage) (%)
I	1.0	1.28	25	48	0.120	0.23	
	1.0	1.28	40	48	0.129	0.25	100
	1.0	1.28	40	72	0.118	0.22	
II	6.0	4.56	50	12	0.410	0.11	
	6.0	4.00	50	24	0.855	0.23	100
	5.0	3.42	40	48	1.395	0.44	
III	1.0	1.28	40	48	0.180	0.34	85
IV	1.0	2.00	40	48	0.340	0.30	95

Table 4. Overall yield of d-GpGpG

Polymer Support	I	IV
Overall yield	22%	12%

tion rate was faster. When the COCl content in the polymer support reaches 20%, the yield of the oligonucleotide decreases. These results are tabulated in Tables 3 and 4.

The synthetized *N*-substituted oligonucleotides were finally separated using a Sephadex LH-20 column. When gel filtration with Sephadex LH-20, for example, is used, the limited separation capacity of the column must be considered. It can be seen from Fig. 2 that the upper limit of the molecular size of water-insoluble nucleotidic material which can be applied to the Sephadex LH-20 column is between five and six in the degree of condensation. In general, the separation and purification of oligonucleotide using an ion-exchange cellulose or an ion-exchange gel column is easier than that using a gelfiltration column when the oligonucleotide is soluble in water.

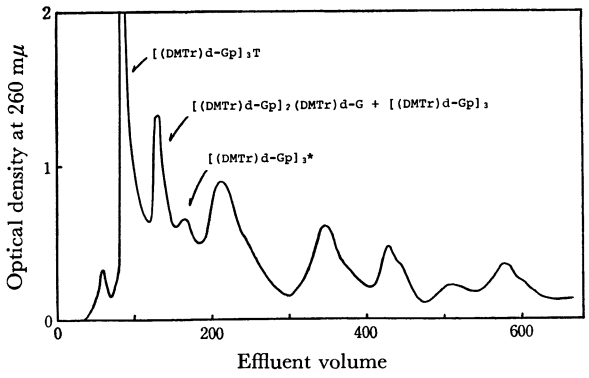

Fig. 2. Isolation of [(DMTr)d-Gp]$_3$T, VI, by sephadex LH 20 column.
*) (DMTr) is partly cloven.

The overall yields of these nucleotides were 22% (for d-GpGpG), 7% (for d-GpGpGpG *via* (b)), 17.5% (for d-GpGpGpG *via* (c)), and 18% (for d-GpGpGpT).

Experimental

Polymer Support, p–*COCl*. As is shown in Table 2, definnite amounts of freshly-distilled styrene, *p*-divinylbenzene, and *p*-vinylbenzoic acid[15] were placed, with a few seeds of the popcorn polymer and 0.5 mg of benzoyl peroxide, in an Erlenmeyer flask which had been well purged with nitrogen. Polymerization and chlorination were performed by the method described in the preceding paper.[9]

Di-p-*methoxytrityldeoxyguanosine*. Prepared by the procedure of Schaller *et al.*,[14] mp 167—168°C.

Paperchromatography was performed by the descending technique using Toyo Roshi No. 53 paper. The solvents were: A, isopropyl alcohol - concentrated ammonia - water (7:1:2); C, ethyl alcohol - 1M ammonium acetate at pH 7.35 (7:3). The phosphate buffer solution used in the electrophoreses was a mixture of 1/15M KH_2PO_4 and 1/15M Na_2HPO_4 (1:17).

The selectivity in the position of the anchorage of the hydroxy group in (DMTr)d-G was determined after the first phosphorylation of the anchored (DMTr)d-G. The selectivity (5′-0 linkage) was defined as [d-Gp/(d-Gp+pd-G)]×100.

N-*Di*-p-*methoxytrityldeoxyguanosine Trimer* (*IV*). *N*-Di-*p*-methoxytrityldeoxyguanosine (1.2 g) was treated with 1.0 g of the polymer support (I) in 20 ml of dry pyridine for 48 hr. Then, 10 ml of methanol was added to esterify any remaining acid chloride groups, and the mixture was stirred for 12 hr. Then, the polymer was collected by filtration and washed completely with methanol in an Soxhlet extractor until no residual *N*-di-*p*-metoxytrityldeoxyguanosine was found in the extract. The polymer was then dried under a vacuum over phosphorus pentoxide. The weight of the polymer was 1.170 g, from which value the amount of the *N*-di-*p*-methoxytrityldeoxyguanosine bound to the polymer support was estimated to be about 0.170 g.

The polymer-deoxyguanosine derivative (II) was added to a mixture of *β*-cyanoethylphosphate[16,17] (1 mmol) and mesitylenesulfonyl chloride[18] (2 mmol) in 20 ml of dry pyridine, and the mixture was stirred for 50 hr. Then, the solids were separated and kept at 50° with a 50% aqueous solution of pyridine for 30—40 min in order to hydrolyze a condensed phosphate. Finally, the solids, consisting of the polymer (III), were washed with methanol and dried under a vacuum over phosphorus pentoxide.

Prior to the addition of the second nucleosidic material, the activation of the terminal phosphate was achieved with mesitylenesulfonyl chloride. The polymer (III) was suspended in 20 ml of dry pyridine, after which a 2 mmol portion of mesitylenesulfonyl chloride was added. The reaction mixture was stirred for 24 hr. Then a solid was allowed to settle and the supernatant liquid was withdrawn. The solid was washed three times with dry pyridine to remove the major portion of mesitylenesulfonyl chloride, moisture being

15) J. R. Leebrick and H. E. Ramsden, *J. Org. Chem.*, **23**, 935 (1958).

16) P. T. Gilham and G. M. Tener, *Chem. Ind.* (London), 542 (1959).
17) G. M. Tener, *J. Amer. Chem. Soc.*, **83**, 159 (1961).
18) C. H. Wang and S. G. Cohen, *ibid.*, **79**, 1924 (1957).

kept off meanwhile. Then 1.0 g of *N*-di-*p*-methoxytrityldeoxyguanosine was added to the solid along with 20 m*l* of dry pyridine. The reaction was carried out under stirring for 3 days. Then, 20 m*l* of methanol were added. After 3 hr's stirring, the mixture was filtered, and the solid was washed with pyridine, methanol, and ether successively.

With the 1.0 g portion of the solid, such phosphorylation and the addition of nucleosidic material were repeated using appropriate amounts of the reagents.

After the addition of the third nucleosidic material, *N*-di-*p*-methoxytrityldeoxyguanosine, 0.2 g of the resulting solid was treated with a mixture of 1 m*l* of 2N NaOH, 2 m*l* of ethanol, and 2 m*l* of dioxane for 12 hr in order to cleave a nucleotide from the polymer support. The polymer was collected by filtration and washed with ethanol several times. The alkaline filtrate, together with ethanol washes of the polymer, was neutralized with Dowex 50 resin (pyridinium form). After the removal of the Dowex resin, the addition of ethanol to the solution and evaporation were repeated 2 times; the resulting material was made up with 1 m*l* of an ethanol solution. The solution was placed in a Sephadex LH-20 column (1 cm × 70 cm) and eluted with 90% ethanol at the rate of 0.5 m*l*/min. After a small peak, the major peak (160—220 m*l*) appeared. The third peak partly overlapped the second. The major elution part, the second peak, was concentrated and was then placed in the column again. A major peak (168—260 m*l*) was found just after a small peak (158—167 m*l*). The elution of the major peak was concentrated and kept in a refrigerator after a small amount of ether had been added. A pale yellow precipitate was collected and dried under reduced pressure over phosphorus pentoxide. A soft powdery material was thus obtained (13 mg). This material was homogeneous in the solvent A (R_f 0.75—78). The ultraviolet characteristics in an ethanol solution were: λ_{max}, 278 mμ (55,000), 263 mμ (56,200), 237 mμ (78,400); λ_{min}, 274 mμ (51,700), 252 mμ (53,400), 225 mμ (70,900).

Found: C, 60.50; H, 5.01; N, 11.29%. Calcd for $C_{93}H_{89}O_{22}N_{15}P_2$: C, 61.01; H, 4.90; N, 11.48%; for $C_{93}H_{91}O_{23}N_{15}P_2$ (monohydrate): C, 60.42; H, 4.96; N, 11.36%; for $C_{93}H_{93}O_{24}N_{15}P_2$ (dihydrate): C, 59.84; H, 5.02; N, 11.26%.

Deoxyguanylyldeoxyguanylyldeoxyguanosine (d-GpGpG). From 0.2 g of the solid, the nucleotidic materials were cloven as has been described above. The neutralized solution was made up to 1 m*l*. Then 3 m*l* of 80% acetic acid was added to the solution, and the mixture was kept for 5 hr. The acetic acid was evaporated under reduced pressure at room temperature. Then 20 m*l* of dilute ammonium hydroxide was added, the mixture was centrifuged, and the supernatant was concentrated to 5 m*l*. The supernatant solution was then adjusted to pH 9.5 with a very small amount of acetic acid. The supernatant was applied to the top of a DEAE-cellulose (carbonate form) column (2 cm × 20 cm). The column was washed with 0.02M NH_4HCO_3 until no ultraviolet-absorbing material was eluted. Further elution was carried out using a linear gradient of ammonium bicarbonate. The mixing vessel and the reservoir contained 1 *l* of 0.02M salt and an equal volume of 0.3M salt. The main peak ranged from the elution volume of 700 to that of 1120 m*l*. The total optical density was 240 O.D. The elution was repeated to dryness by adding water, and finally lyophilized.

Thus, 11.2 mg of the desired product, d-GpGpG, was obtained. The material was homogeneous in electrophoresis at pH 8.0 (1/15M phosphate buffer). The electrophoretic mobility, compared with that of deoxyguanosine 5′-phosphate, was 0.15. The ultraviolet absorption characteristics in water were: λ_{max}, 255 mμ (23,900); λ_{min}, 224 mμ (10,100); $\lambda_{shoulder}$, 268 mμ. R_f in the solvent A was 0.01. A venom phosphodiesterase preparation[19] was added to a small amount of the product, and the mixture was incubated at 37° for 12 hr. When paper electrophoresis was then carried out at pH 8.0, three spots were obtained: mobility 0 (2.4 O.D.), mobility 0.15 (0.1 O.D.), and mobility 1.0 (5.1 O.D.). Those spots corresponded to deoxyguanosine, an undegraded material, and deoxyguanosine 5′-phosphate. The optical densities were determined from the differences between the absorbances of the eluted solutions of the spots and those of the elutions of the appropriate blanks. From these results, the material was identified as deoxyguanylyldeoxyguanylyldeoxyguanosine, d-GpGpG.

N-Di-p-methoxytrityldeoxyguanosine Tetramer (V) and (VI). The residual polymer was divided in half. Each polymer was phosphorylated with an appropriate amount of β-cyanoethylphosphate and mesitylenesulfonyl chloride, as has been described above. Then the phosphorylated polymers were activated, and *N*-di-*p*-methoxytrityldeoxylguanosine and thymidine (in appropriate amounts) respectively were added. On the other hand, 0.15 g of the solid that contained (*N*-di-*p*-methoxytrityldeoxyguanosine dimer was phosphorylated and then activated with appropriate amount of the reagents. Then, 0.07 g of *N*-di-*p*-methoxytrityldeoxyguanylyl-*N*-di-*p*-methoxytrityl)deoxyguanosine was added (route (c)). The procedures of the cleaving of the nucleotidic materials and purifications were the same as above.

The material (V) (*via* (b)) appeared in the elution of 95—130 m*l* after a small peak of an ultraviolet-absorbing material when the Sephadex LH-20 column and 95% ethanol were used just as above. Also, the material (V) (*via* (c)) appeared in the elution of 97—143 m*l* in another run. The material (VI) appeared in the elution of 81—121 m*l* (Fig. 2). When these materials were precipitated in the way mentioned above and dried, we obtained 16 mg of the nucleotidic material (V) (*via* (b)), 20 mg of the nucleotidic material (V) (*via* (c)), and 36 mg of the nucleotidic material (VI). Each material was dissolved homogeneously in the solvent A; the R_fs were 0.54—0.56 for the nucleotidic material (V) and 0.48—0.51 for the nucleotidic material(VI), respectively. The ultraviolet characteristics in ethanol solutions of the material(V) were: λ_{max}, 278 mμ (73,800), 264 mμ (74,100), 238 mμ (105,000); λ_{min}, 274 mμ (68,400), 253 mμ (71,200), 226 mμ (93,100): and of the material(VI), λ_{max}, 277 mμ (60,000), 260 mμ (61,200), 232 mμ (83,000); λ_{min}, 270 mμ (59,200), 250 mμ (59,000).

Found: C, 60.00; H, 4.91; N, 11.20%. Calcd for the material(V) (*via* (b)): $C_{124}H_{117}O_{30}N_{20}P_3$: C, 60.54; H, 4.80; N, 11.39%: for $C_{124}H_{121}O_{32}N_{20}P_3$ (dihydrate): C, 59.66; H, 4.89; N, 11.22: for $C_{124}H_{123}O_{33}N_{20}P_3$ (trihydrate): C, 59.23; H, 4.93; N, 11.14%.

Found: C, 57.01; H, 4.91; N, 10.83%. Calcd for the material(VI): $C_{103}H_{102}O_{29}N_{17}P_3$: C, 57.97; H, 4.78; N, 11.16%; for $C_{103}H_{106}O_{31}N_{17}P_3$ (dihydrate): C, 57.01; H, 4.88; N, 10.97%; for $C_{103}H_{108}O_{32}N_{17}P_3$ (trihydrate): C, 56.54; H, 4.93; N, 10.88%.

A comparison of the syntheses of the *N*-di-*p*-methoxytrityldeoxyguanosine tetramer shows that the conversion of each additional reaction was 40—50%, regardless of the length of the additional nucleosidic or nucleotidic materials.

The residual unreacted portions in the addition reaction were found to be nucleotidic materials which lacked the desired sequences, such as [(DMTr)d-Gp]$_2$(DMTr)d-G, [(DMTr)d-Gp]$_3$, and [(DMTr)d-Gp]$_2$T. They were ob-

19) 500 units of the phosphodiesterase in 2.5 m*l* of 0.3M Tris buffer at pH 8.85.

tained in considerable amounts, as is shown in Fig. 2. Those materials were identified and determined after the cleavage of the respective blocking groups, as will be described below.

Deoxyguanylyldeoxyguanylyldeoxyguanylyldeoxyguanosine (d-GpGpGpG). Eight mg of the nucleotidic material(V) (*via* (c)) were treated with 1 m*l* of 80% acetic acid for 5 hr at room temperature. The acetic acid was then evaporated in a vacuum. To the resulting materials, 10 m*l* of dilute ammonium hydroxide was added; the mixture was then centrifuged, and the supernatant was concentrated to 3 m*l*. The supernatant solution was made up to 5 m*l* with 0.2M ammonium bicarbonate. The solution was then placed in a DEAE-cellulose column, just has been described above. The column was washed with 0.02M NH_4HCO_3 until no further ultraviolet-absorbing material was eluted. Then, further elution was carried out using the linear gradient of ammonium bicarbonate described above. The major peak (the 1060—1280 m*l*-portion) was collected and lyophilized. The d-GpGpGpG thus obtained (4.1 mg) was homogeneous in paper electrophoresis at pH 8 (the relative mobility was 0.09 for d-pG=1.0).

The ultraviolet absorption characteristics in water were: λ_{max}, 257 mμ (18,000); λ_{min}, 224 mμ (12,500); $\lambda_{shoulder}$, 268 mμ; in 1M NaCl were: λ_{max}, 256 mμ (26,400); λ_{min}, 224 mμ (12,300) $\lambda_{shoulder}$, 267 mμ.

A portion of the material was incubated at 37° for 12 hr with 0.1 m*l* of the venom phosphodiesterase preparation. Three spots were obtained on chromatography in the solvent C; the R_fs were 0—0.04, 0.35 and 0.69, corresponding to an undegraded material (d-GpGpGpG or d-GpGpG), deoxyguanosine 5′-phosphate, and deoxyguanosine, respectively. The optical density units found on eluting these spots were 0.2, 6.7, and 2.1, respectively. Those results show that the material was d-GpGpGpG and that 98% of the tetranucleotide was degraded; d-pG/d-G=3.2.

Deoxyguanylyldeoxyguanylyldeoxyguanylylthymidine (d-GpGpGpT). Ten mg of the nucleotidic material(VI) was trated with acetic acid by the procedure described in the preceding section. The major peak (1100—1290 m*l* portion) was collected and lyophilized. Thus, d-GpGpGpT was obtained (5.7 mg); it was homogeneous in paper electrophoresis at pH 8 (the relative mobility was 0.11—0.12 for d-pG=1.0). The ultraviolet absorption characteristics in water were: λ_{max}, 263 mμ (30,000); λ_{min}, 230 mμ (18,900); $\lambda_{shoulder}$, 240 mμ: in 1M NaCl were: λ_{max}, 261 mμ (29,200); λ_{min}, 229 mμ (18,700); $\lambda_{shoulder}$, 238 mμ.

The enzymatic hydrolysis by the venom phosphodiesterase yielded 1.0 optical density unit of deoxyguanosine, 2.1 optical density units of thymidine 5′-phosphate, 0.8_5 optical density unit of thimidine 5′-phosphate, and 0.1 optical density unit of deoxyguanylyldeoxyguanosine; *i.e.*, 79% of d-GpGpGpT was hydrolyzed (neglecting the hypochromic effect of degraded nucleotides). Also, the enzymatic degradation by spleen phosphodiesterase was achieved. In this case, 2.0 optical density units of deoxyguanosine 3′-phosphate, 0.6 optical density unit of thymidine, and 0.1_5 optical density unit of undegraded material were yielded. These results confirmed that the resulting tetranucleotide was d-GpGpGpT.

Isolation of By-products, d-GpGpG, d-GpGpGp, and d-GpGpT. The elutions of the peaks (120—155 m*l*, 155—185 m*l*, and 185—300 m*l*) shown in Fig. 2 were concentrated and treated with 80% acetic acid to cleave the blocking group; then they were placed in a DEAE-cellulose column in a way similar to that described above.

From the first portion, two major nucleotidic materials (elutions at 0.120—1.130M NH_4HCO_3 (39 optical density units) and at 0.135—0.165M NH_4HCO_3 (18 optical density units)) were obtained. From the second portion a single major nucleotidic material (elution at 0.130—0.155M NH_4HCO_3 (20 optical density units)), and form the third portion, another single nucleotidic material (elution at 0.125—0.135M NH_4HCO_3 (112 optical density units)) from three ultravioletabsorbing materials, were obtained. These materials were identified as d-GpGpG, d-GpGpGp, d-GpGpGp, and d-GpGpT, respectively by means of enzymatic hydrolyses and electrophoreses.

From the result that d-GpGpGp was found in both the first and the second portions in the Sephadex LH-20 column separation, it might be concluded that a partial cleaving of the blocking group takes place in the course of the synthesis. The greater quantity of d-GpGpT comparing with those of d-GpGpG and d-GpGpGp is believed to be due to one of two routes in the synthesis; one is the route skipping over the first coupling step, and the other is that skipping over the second coupling step.

BULLETIN OF THE CHEMICAL SOCIETY OF JAPAN, VOL. 44, 1677—1682 (1971)

Substituted Benzopyranopyridine and Pyrimidine Ring Syntheses by the Ternary Condensation of Ethyl Cyanoacetate, Salicylaldehyde, and Certain Aldehydes in the Presence of Ammonium Acetate

Akio SAKURAI, Hiroshi MIDORIKAWA, and Yasuo HASHIMOTO*

The Institute of Physical and Chemical Research, Wako-shi, Saitama

**Tokyo Electrical Engineering College, Nishikicho, Chiyoda-ku, Tokyo*

(Received December 5, 1970)

Various 1-substituted benzopyranopyridines were readily prepared by the condensation of ethyl cyanoacetate and salicylaldehyde (or 3-methoxysalicylaldehyde) with aliphatic aldehydes (propion, *n*-butyl, *n*- and isovaleraldehyde) in the presence of ammonium acetate. On the other hand, condensation with aromatic aldehydes such as benzaldehyde and *o*-, *m*-, or *p*-substituted benzaldehydes gave 2-aryl-benzopyranopyrimidines.

In a previous paper,[1] the synthesis of 2- or 1,2-disubstituted benzopyranopyridines by the condensation of ethyl cyanoacetate, salicylaldehyde, and ketones in the presence of ammonium acetate has been reported.

1) A. Sakurai, H. Midorikawa, and Y. Hashimoto, This Bulletin, **43**, 2925 (1970).

The present paper will deal with the syntheses of 1-alkylbenzopyranopyridines (from aliphatic aldehyde) and 2-arylbenzopyranopyrimidines (from aromatic aldehyde) by the reaction of ethyl cyanoacetate and salicylaldehyde or 3-methoxysalicylaldehyde with various aldehydes in the presence of ammonium acetate.

The reaction of ethyl cyanoacetate and salicylaldehyde or 3-methoxysalicylaldehyde with aliphatic aldehydes was carried out by refluxing a mixture of the ester, salicylaldehyde, aliphatic aldehyde, and ammonium acetate (molar ratio 1:1:1:1-1.5) in ethanol. In this case, the condensation of the amino group of 3-amidinocoumarin[1] (I) with the carbonyl group of the aldehyde, cyclization between the methylene group adjacent to the aldehyde carbonyl and the 4-position of the coumarin ring, and subsequent dehydrogenation took place to form 1-alkyl-4-amino-5-oxo-[1]-benzopyrano[3,4-*c*]pyridines (II).

However, when isobutyraldehyde was employed as the aldehyde reactant, the corresponding product of the type II was not obtained. The NMR spectrum (in CF_3CO_2H) of IIa (from propionaldehyde) showed only a methyl singlet at 2.9 ppm, while IIb (from *n*-butyraldehyde) showed a methyl triplet at 1.55 ppm and a methylene quartet at 3.35 ppm in a higher field than the aromatic-ring region. These facts indicated that the methylene group adjacent to the aldehyde carbonyl was involved in this cyclization. On the other hand, the condensation with aromatic aldehydes (benzaldehyde or its derivatives) gave 2-aryl-4-amino-5-oxo-[1]benzopyrano[4,3-*d*]pyrimidines (IV). In this case, 1 mol each of ethyl cyanoacetate, salicylaldehyde, and benzaldehyde (or its derivatives) reacted with 2 mol of ammonia to give IV, with the elimination of 1 mol of ethanol and 2 mol each of water and hydrogen. The compound IVa was also obtained by the condensation of 3-amidinocoumarin or 3-cyanocoumarin with benzaldehyde in the presence of ammonium acetate

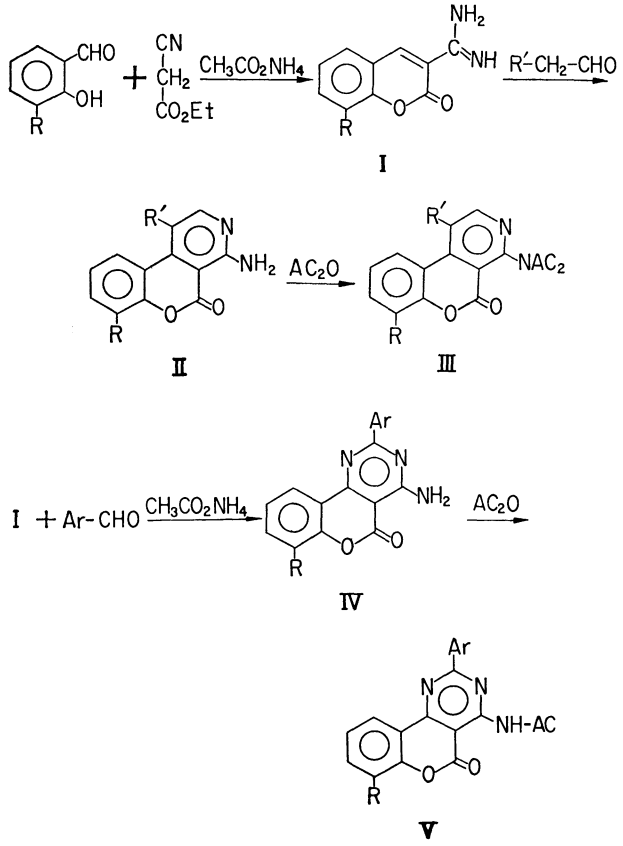

Scheme 1

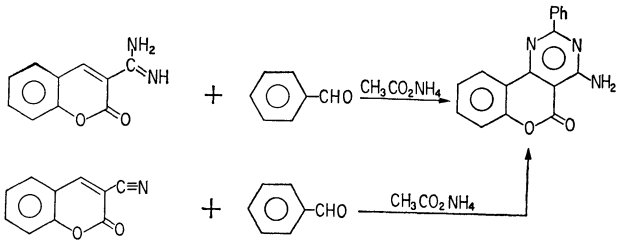

Scheme 2

Table 1
1-Alkyl-4-amino-5-oxo-[1]benzopyrano[3,4-C]pyridine (II)

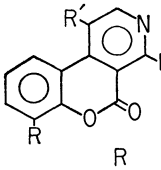

	R	R′	MP,°C	Yield,%	Formula	Calcd,% C	H	N	Found,% C	H	N
IIa	H	CH_3	221–222	34	$C_{13}H_{10}O_2N_2$	69.01	4.46	12.38	68.93	4.66	12.36
b	H	C_2H_5	207–209	19	$C_{14}H_{12}O_2N_2$	69.99	5.03	11.66	69.92	5.07	11.66
c	H	n-C_3H_7	186–187	20	$C_{15}H_{14}O_2N_2$	70.85	5.55	11.02	70.32	5.57	10.80
d	H	i-C_3H_7	176–177	5	$C_{15}H_{14}O_2N_2$	70.85	5.55	11.02	70.87	5.41	11.16
e	H	n-C_4H_9	173–174	20	$C_{16}H_{16}O_2N_2$	71.62	6.01	10.44	71.74	5.93	10.42
f	OCH_3	CH_3	212–215	35	$C_{14}H_{12}O_3N_2$	65.62	4.72	10.93	65.37	4.50	10.96
g	OCH_3	C_2H_5	214–215	19	$C_{15}H_{14}O_3N_2$	66.65	5.22	10.37	66.40	5.24	10.30
h	OCH_3	n-C_3H_7	200–202	20	$C_{16}H_{16}O_3N_2$	67.59	5.67	9.85	67.57	5.69	9.71
i	OCH_3	i-C_3H_7	211–212	12	$C_{16}H_{16}O_3N_2$	67.59	5.67	9.85	67.10	5.64	9.78
j	OCH_3	n-C_4H_9	181–182	19	$C_{17}H_{18}O_3N_2$	68.44	6.08	9.39	68.29	6.03	9.29

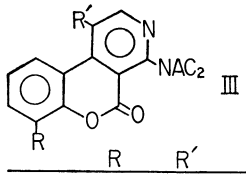

III

Table 2
1-Alkyl-4, 4-diacetamino-5-oxo-[1] benzopyrano [3,4-C] pyridine (III)

	R	R′	MP, °C	Yield, %	Formula	Calcd, % C	H	N	Found, % C	H	N
IIIa	H	CH_3	176–179	55	$C_{17}H_{14}O_4N_2$	65.80	4.55	9.03	65.50	4.64	9.21
b	H	C_2H_5	132–135	86	$C_{18}H_{16}O_4N_2$	66.66	4.97	8.64	66.96	5.02	8.86
c	H	n-C_3H_7	104–108	88	$C_{19}H_{18}O_4N_2$	67.44	5.36	8.28	67.66	5.28	8.42
d	OCH_3	CH_3	228–230	45	$C_{18}H_{16}O_5N_2$	63.52	4.74	8.23	63.40	4.69	8.37
e	OCH_3	C_2H_5	177–180	89	$C_{19}H_{18}O_5N_2$	64.40	5.12	7.91	64.48	5.33	8.05
f	OCH_3	n-C_3H_7	160–163	90	$C_{20}H_{20}O_5N_2$	65.21	5.47	7.61	65.54	5.52	7.92

Table 3. Infrared spectral data for the compounds II

	ν NH_2	ν C=O	δ NH_2	Aromatic ring	δ CH
IIa	3430, 3270, 3150	1700	1625	1610, 1590, 1570, 1545	760
b	3420, 3260, 3130	1690	1620	1610, 1590, 1565, 1540	755, 745
c	3410, 3270, 3130	1700	1625	1610, 1590, 1570, 1545	765, 750
d	3420, 3260, 3120	1720	1630	1610, 1590, 1565, 1545	765, 750
e	3410, 3260, 3120	1700	1630	1610, 1570, 1550	770
f	3420, 3270, 3140	1695	1620	1610, 1590, 1570, 1550	780
g	3410, 3260, 3130	1700	1625	1610, 1590, 1570, 1550	785
h	3410, 3260, 3140	1695	1620	1610, 1570, 1545	785
i	3400, 3260, 3150	1695	1620	1610, 1590, 1565, 1540	780
j	3410, 3260, 3140	1700	1625	1610, 1590, 1570, 1550	785

Table 4. Infrared spectral data[a] for the compounds III

	ν O–C=O	ν N–C=O	Aromatic ring	δ CH
IIIa	1725	1700,	1610, 1590, 1575, 1540	770
b	1735	1715, 1700	1600, 1590, 1570, 1540	770
c	1735	1720, 1695	1610, 1590, 1570, 1540	770
d	1725	1705	1610, 1590, 1575, 1545	785
e	1730	1685	1610, 1590, 1570, 1540	790, 785
f	1725	1695, 1680	1610, 1580, 1570, 1540	785

a) All spectra were taken in potassium bromide disks; cm^{-1}

(Scheme 2).

The infrared spectra of IV revealed slightly lower shifted absorption bands for a primary amino group at about 3400 and 3300 cm^{-1} and at about 1700 cm^{-1} for a coumarin-type carbonyl group. This shows the presence of intramolecular C=O···H_2N bonding, as is shown in the compounds obtained by condensation with ketones.[1] When heated with acetic anhydride in pyridine, type IV compounds were converted to their corresponding monoacetylated derivatives (V). On

Table 5. NMR spectral data[a] for the compounds II and III

	CH_3	OCH_3	CH_2	–CH–	Ring –CH=
IIa	2.9 (s, 3H)				7.5–8.2 (m, 4H), 8.6–8.8(m, 5H)
b	1.55(t, 3H)		3.35(q, 2H)		7.5–8.8 (m, 5H)
c	1.2 (t, 3H)		1.9 (sx, 2H), 3.25 (t, 2H),		7.5–8.8 (m, 5H)
g	1.5 (t, 3H)	4.1 (s, 3H)	3.3 (q, 2H)		7.5–7.7, 8.0–8.3 (m, 2H eaeh)
h	1.2 (t, 3H)	4.12(s, 3H)	1.95(sx, 2H), 3.25(t, 2H)		7.5–7.7, 8.0–8.3 (m, 2H each)
i	1.5 (d, 6H)	4.1 (s, 3H)		3.7–4.3(m, 1H)	7.4–7.8, 7.9–8.4 (m, 2H each)
IIIb	1.6 (t, 3H) 2.4, 2.7 (s, 3H each)	2.7 (s, 3H each)	3.5 (q, 2H)		7.5–8.1, 8.4–8.8 (m, 5H)

a) Parts per million downfield from tetramethylsilane in CF_3CO_2H; s=singlet, d=doublet, t=triplet, q=quartet, sx=sextet, m=multiplet

the other hand, type II compounds gave diacetylated derivatives (III) under the same reaction conditions. In the infrared spectra of III, carbonyl stretching bands shifted to frequencies higher by from 20 to 30 cm^{-1} than those of the compounds II. However, the carbonyl bands of V appeared in the region nearly the same as or slightly lower than those of the compounds IV, and the imino stretching band always appeared at 3250 cm^{-1}. These data, therefore, can reasonably be explained by the presence of intramolecular hydrogen bonding in the compounds II and IV.

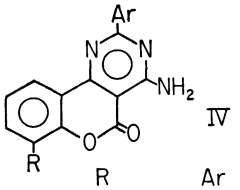

Table 6
2-Aryl-4-amino-5-oxo-[1]benzopyrano[4,3-d]pyrimidine (IV)

	R	Ar	MP, °C	Yield, %	Formula	Calcd, % C	Calcd, % H	Calcd, % N	Found, % C	Found, % H	Found, % N
IVa	H	Ph	266–268	20	$C_{17}H_{11}O_2N_3$	70.58	3.83	14.53	70.33	4.01	14.47
b	H		277–280	13	$C_{18}H_{13}O_2N_3$	71.27	4.32	13.86	71.06	4.10	13.68
c	H		211–213	8	$C_{18}H_{13}O_3N_3$	67.70	4.11	13.16	67.81	4.04	13.34
d	H		262–264	11	$C_{18}H_{13}O_3N_3$	67.70	4.11	13.16	67.77	4.12	13.11
e	H		229–231	17	$C_{20}H_{17}O_2N_3$	72.49	5.17	12.68	72.36	4.98	12.56
f	H		318–321	17	$C_{19}H_{14}O_3N_4 \cdot 1\frac{1}{2}H_2O$	61.12	4.55	15.01	61.34	4.40	15.20
g	H		254–256	6	$C_{19}H_{16}O_2N_4$	68.66	4.85	16.86	68.42	4.51	16.89
h	H		254–257	25	$C_{17}H_{10}O_4N_4$	61.08	3.02	16.76	61.82	3.27	16.62
i	H		225–228	10	$C_{19}H_{15}O_4N_3$	65.32	4.33	12.03	65.14	4.27	11.98
j	H		247–248	12	$C_{19}H_{15}O_4N_3$	65.32	4.33	12.03	65.47	4.23	12.29
k	H		185–186	13	$C_{21}H_{19}O_4N_3$	66.83	5.07	11.14	66.80	4.55	11.18
l	H		322–324	13	$C_{17}H_9O_3N_3Br_2$	44.09	1.96	9.07	44.18	2.19	8.96
m	OCH_3	Ph	283–284	20	$C_{18}H_{13}O_3N_3$	67.70	4.11	13.16	67.43	3.97	13.06
n	OCH_3		263–265	15	$C_{19}H_{15}O_3N_3$	68.46	4.54	12.61	68.07	4.55	12.35
o	OCH_3		234–236	15	$C_{21}H_{19}O_3N_3$	69.79	5.30	11.63	69.50	5.11	11.48
p	OCH_3		300-303	40	$C_{18}H_{12}O_5N_4$	59.34	3.32	15.38	59.30	3.24	15.83
q	OCH_3		327–330	12	$C_{20}H_{17}O_5N_3$	63.32	4.52	11.08	62.52	4.24	11.59
r	OCH_3		251–253	28	$C_{20}H_{17}O_5N_3$	63.32	4.52	11.08	63.06	4.38	11.30
s	OCH_3		222–225	26	$C_{22}H_{21}O_5N_3$	64.85	5.20	10.31	64.91	5.17	10.46

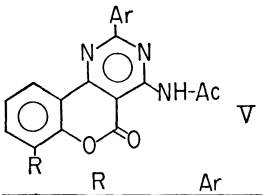

Table 7
2-Aryl-4-acetamino-5-oxo-[1]benzopyrano[4,3-d]pyrimidine (V)

	R	Ar	MP,°C	Yield,%	Formula	Calcd.% C	Calcd.% H	Calcd.% N	Found.% C	Found.% H	Found.% N
Va	H	Ph	252-253	87	$C_{19}H_{13}O_3N_3$	68.87	3.96	12.68	68.80	3.48	12.78
b	H		257-260	88	$C_{20}H_{15}O_4N_3$	66.47	4.18	11.63	66.44	4.23	11.53
c	H		330-332	77	$C_{21}H_{16}O_4N_4$	64.94	4.15	14.43	64.22	4.51	14.48
d	H		260-263	88	$C_{19}H_{12}O_5N_4$	60.64	3.21	14.89	59.95	3.45	15.05
e	H	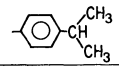	235-237	89	$C_{22}H_{19}O_3N_3$	70.76	5.13	11.25	70.79	4.99	11.45
f	OCH_3	Ph	267-268	70	$C_{20}H_{15}O_4N_3$	66.47	4.18	11.63	66.19	4.45	11.75
g	OCH_3		303-305	89	$C_{20}H_{14}O_6N_4$	59.11	3.47	13.79	58.69	3.71	13.85
h	OCH_3	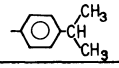	238-239	91	$C_{23}H_{21}O_4N_3$	68.47	5.25	10.42	68.94	5.21	10.60

Table 8. Infrared spectral data[a] for the compounds IV

	ν NH_2	ν C=O	δ NH_2	Aromatic ring	δ CH
IVa	3480, 3360	1705	1630	1615, 1595, 1555, 1535	765, 700
b	3430, 3330	1695	1630	1615, 1605, 1580, 1550, 1540	825, 770
c	3400, 3260	1710		1615, 1600, 1555, 1540	770, 765
d	3430, 3330	1695	1625	1615, 1600, 1580, 1540	830, 775
e	3430, 3330	1695	1625	1610, 1575, 1550, 1535	825, 775, 770
f	3420, 3290, 3200	1710, 1680	1640	1615, 1600, 1550, 1530	825, 775
g	3420, 3345	1700	1625	1615, 1600, 1565, 1545	820, 775
h	3450, 3340	1705	1625	1610, 1600, 1555, 1545	770, 750, 710
i	3470, 3410, 3290	1690	1625	1615, 1605, 1555, 1540, 1520	825, 765
j	3420, 3290	1705	1630	1615, 1605, 1590, 1555, 1540	820, 770
k	3420, 3300	1700	1630	1615, 1605, 1585, 1555, 1540	815, 770
l	3480, 3380	1705	1625	1610, 1590, 1560, 1535,	770
m	3510, 3370	1700		1615, 1595, 1555, 1535	785, 740
n	3450, 3340	1715	1630	1615, 1565, 1540	825, 795
o	3470, 3350	1715	1620	1610, 1565, 1555, 1535	830, 800
p	3430, 3350	1715	1620	1610, 1565, 1555, 1535	790, 750
q	3460, 3330	1695	1630	1615, 1605, 1570, 1540	790, 735
r	3420, 3290	1705	1635	1600, 1570, 1540, 1525	795
s	3430, 3310	1700	1625	1615, 1600, 1585, 1565, 1535	790

a) All spectra were taken in potassium bromide disks; cm^{-1}

Table 9. Infrared spectral data for the compounds V

	ν NH	ν O-C=O, NH-C=O	Aromatic ring	δ CH
Va	3250	1700, 1685	1610, 1600, 1590, 1570, 1550	765, 700
b	3250	1680	1610, 1600, 1590, 1570, 1545, 1520	825, 780
c	3360, 3250	1700, 1680	1615, 1600, 1580, 1550, 1530	830, 775
d	3250	1700, 1690	1610, 1590, 1575, 1550, 1535	830, 780, 770
f	3250	1695, 1685	1615, 1605, 1590, 1580, 1555	795, 750
g	3250	1690	1610, 1590, 1580, 1555, 1530	805, 745, 705

TABLE 10. NMR SPECTRAL DATA[a] FOR THE COMPOUNDS IV AND V

	CH_3	OCH_3	CH_2	-CH-	Ring -CH=	NH
IVa					7.55–8.9(m, 10H)	9.75(br, 1H)
c		4.4 (s, 3H)			7.2–8.3, 8.7–8.9(m, 9H)	9.48(br, 1H)
d		4.05(s, 3H)			7.15–8.7(m, 9H)	9.6 (br, 1H)
e	1.35(d, 6H)			2.75–3.4(m, 1H)	7.5–8.8(m, 8H)	8.5, 9.6(s, 1H each)
f	2.52(s, 3H)				7.6–8.8(m, 9H)	9.3, 9.7(s, 1H each)
g	3.6 (s, 6H)				7.6–8.1, 8.5–8.8(m,9H)	9.8 (br, 1H)
j		4.12(d, 6H)			7.2–8.8(m, 8H)	9.65(br, 1H)
k	1.55(t, 6H)	4.4 (q, 4H)			7.1–8.8(m, 8H)	9.6 (br, 1H)
m		4.1 (s, 3H)			7.4–8.3(m, 8H)	8.45, 9.5(br, 1H each)
o	1.35(d, 6H)	4.1 (s, 3H)		2.7–3.4(m, 1H)	7.4–7.8, 8–8.4(m, 7H)	8.45, 9.6(br, 1H each)
r		4.1 (s, 9H)			7.2–8.2(m, 6H)	8.6, 9,6(br, 1H each)
s	1.6 (t, 6H)	4.15(s, 3H)	4.45(q, 4H)		7.1–8.7(m, 7H)	9.65(br, 1H)
Va	2.73(s, 3H, $CO-CH_3$)				7.5–8.95(m, 9H)	12.22(br, 1H)
e	1.4(d, 6H)2.7 (s, 3H, $CO-CH_3$)			2.8–3.4(m, 1H)	7.5–9(m, 8H)	12.25(br, 1H)
f	2.74(s, 3H, $CO-CH_3$)	4.17(s, 3H)			7.6–8.6(m, 8H)	12.27(br, 1H)
h	1.4(d, 6H) 2.7(s, 3H, $CO-CH_3$)	4.1 (s, 3H)		2.8–3.4(m, 1H)	7.5–8.6(m, 7H)	12.2 (br, 1H)

a) Parts per million downfield from tetramethylsilane in CF_3CO_2H; s=singlet, d=doublet, t=triplet, q=quartet, m=multiplet, br=broad

Experimental

All the melting points are uncorrected. The infrared spectra were determined by means of potassium bromide disks. The NMR spectra were determined in trifluoroacetic acid at 60 Mc, using tetramethylsilane as the internal standard. The chemical shifts are reported as parts per million downfield from TMS.

Reaction of Ethyl Cyanoacetate and Salicylaldehyde or 3-Methoxysalicylaldehyde with Aldehydes. A mixture of ethyl cyanoacetate (0.03 mol), salicylaldehyde or 3-methoxysalicylaldehyde (0.03 mol), aldehyde (0.03 mol), and ammonium acetate (0.04 mol) in ethanol (10 m*l*) was refluxed for 0.5—1.5 hr. A pale yellow crystalline matter precipitated out during the reaction. The experimental results and spectral data are summarized in Tables 1,3,5,6,8, and 10.

Reaction of 3-Amidinocoumarin (1) and Benzaldehyde. A mixture of 1 (2.82 g), benzaldehyde (1.59 g), and ammonium acetate (1.54 g) in ethanol (5 m*l*) was refluxed for 0.5 hr. A crystalline precipitate was formed during the reaction; this was collected, and washed with ethanol and then with water. Recrystallization from pyridine afforded 0.9 g of pale yellow crystals; mp 265—267°C. By their infrared spectra and the results of elemental analyses, this compound was identified with IVa.

Reaction of 3-Cyanocoumarin and Benzaldehyde. A mixture of 3-cyanocoumarin (2.55 g), benzaldehyde (1.59 g), and ammonium acetate (1.54 g) in pyridine (5 m*l*) was heated for 1 hr. The pale yellow crystals which precipitated were then recrystallized from pyridine to give 0.8 g of almost white crystals; mp 262—264°C. This compound was proved to be identical with IVa by a study of their infrared spectra.

Reaction of the II and IV Compounds and Acetic Anhydride. To a solution of II or IV (0.001 mol) dissolved in pyridine (3—5 m*l*), acetic anhydride (5—8 m*l*) was added, the mixture was then refluxed for 2—4 hr. After standing overnight at room temperature, the crystalline precipitate thus formed was washed with dilute methanol. The experimental results and spectral data are summarized in Tables 2,4,7,9, and 10.

The authors wish to express their thanks to Dr. Taro Hayashi and Dr. Tatsuo Takeshima for their kind advice. Thanks are also due to Dr. Haruo Homma and his staff for their microanalyses, to Mr. Jun Uzawa for his measurements of the NMR spectra, and to Mr. Hironori Ogawa for his measurements of the IR spectra.

Nuclear Magnetic Resonance Study of the Effect of the Hydrogen Bond on the Internal Rotation of Biphenyls

Michinori Ōki, Kageyasu Akashi, Gaku Yamamoto, and Hiizu Iwamura
Department of Chemistry, Faculty of Science, The University of Tokyo, Hongo, Tokyo
(Received December 8, 1970)

Internal rotation about the pivot bond of several biphenyl derivatives has been studied by means of the nuclear magnetic resonance technique using non-identical chemical shifts of the two methyls in the isopropyl group which is located close to the center of dissymmetry. The results with the 2-methoxy and 2-hydroxy derivatives are compared. The solvent effect is marked in 2-hydroxy derivatives. These results, together with the substituent effect, indicate that the fact that the energy of activation for rotation about the pivot bond of the 2-hydroxy derivatives is a little higher than the corresponding methyl ether may be attributed to the stabilization of the ground state resulting from the presence of intramolecular O–H···π interaction. The infrared data agree with the above conclusion.

In recent years it has become very common to use the nuclear magnetic resonance technique in investigating the internal rotation. Originally, a biphenyl derivative had to be resolved into optical isomers in order to investigate the rotation about the pivot bond, because polarimetry was a sole method for the investigation. Nowadays, however, it is also possible to study the internal rotation of biphenyls by means of NMR,[1-5] and it has been confirmed that the process which is observed by polarimetry and that studied by NMR are the same.[5,6] These investigations have revealed that the solvent effect on the internal rotation in biphenyl is very small, if present at all.[4,5,7]

However, a paper[8] from this laboratory has shown that a distinct solvent effect was observed in the internal rotation of 1-hydroxy-5,7-dihydro[*c*,*e*]oxepin (**1**). This compound shows an energy of activation for the internal rotation in dimethyl sulfoxide smaller by *ca.* 1 kcal/mol than that in deuteriochloroform. This phenomenon is not observed with the corresponding methyl ether (**2**). Thus, the hydrogen bond must be playing an important role in decreasing the energy of activation for **1**.

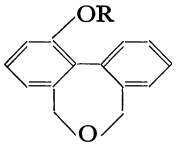

(**1**): R=H
(**2**): R=CH_3

Two possibilities may be pointed out with regard to the decrease in energy of activation by the formation of the hydrogen bond. The first is the possibility that the transition state of the inversion of biphenyls is stabilized in dimethyl sulfoxide because of the decrease in the electronegativity of oxygen on formation of the hydrogen bond, with a concomittant increase in the electron density at the position 1 or with an increase in the contribution of the resonance structure (**3**). The second is the stabilization of the ground state due to the presence of the intramolecular O–H···π interaction, which may be very little in dimethyl sulfoxide because of the strong proton-accepting ability of the sulfoxide. The first possiblity will lower the transition state in dimethyl sulfoxide relative to that in deuteriochloroform, whereas the second possibility will lower the ground state in deuteriochloroform relative to that in dimethyl sulfoxide. In either case, the energy of activation will be lowered.

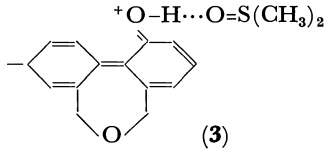

(**3**)

In the above discussion, the effect of the intermolecular hydrogen bond in **1** is disregarded, though it could be important at the concentration used for the NMR study. However, as will be seen later, the IR study indicates that the effect may be disregarded.

We wish here to report on the effect of the substituents on the internal rotation of biphenyls as studied by NMR, and to present a basis on which it can be concluded that the internal O–H···π interaction is an important factor in lowering the energy of activation for rotation about the pivot bond.

Syntheses

After several attempts at synthesizing some substituted derivatives of **1**, it was found that introducing a desired substituent at a desired position of **1** was very difficult. Therefore, we decided to use some isopropyl derivatives which have been shown[9] to give rise to magnetically non-equivalent methyl groups when the rotation about the pivot bond is slow on the NMR time scale.

The syntheses of many of the necessary methoxy

1) M. Ōki, H. Iwamura, and N. Hayakawa, This Bulletin, **36**, 1542 (1963); *ibid.*, **37**, 1865 (1964).
2) W. L. Meyer and R. B. Meyer, *J. Amer. Chem. Soc.*, **85**, 2170 (1963).
3) R. J. Kurland, M. B. Rubin, and W. B. Wise, *J. Chem. Phys.*, **40**, 2426 (1964).
4) I. O. Sutherland and M. V. J. Ramsay, *Tetrahedron*, **21**, 3401 (1965).
5) M. Ōki and H. Iwamura, *ibid.*, **24**, 2377 (1967).
6) A. Mannschreck, A. Mattens, and G. Rissmann, *J. Mol. Spectrosc.*, **23**, 15 (1967).
7) B. M. Graybill and J. E. Leffler, *J. Phys. Chem.*, **61**, 1461 (1959).
8) M. Ōki, H. Iwamura, and T. Nishida, This Bulletin, **41**, 656 (1968).
9) M. Ōki and G. Yamamoto, *ibid.*, **44**, 266 (1971).

compounds have previously been reported.[9] In such cases, the methoxy compounds (**4**) were demethylated by refluxing in acetic acid with hydrogen bromide to give the corresponding hydroxybiphenyl derivatives (**5**):

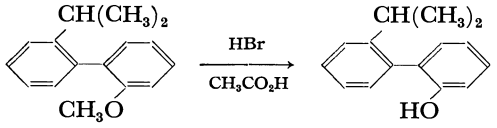

(**4**) (**5**)

Treating 2-isopropyl-5-nitroiodobenzene (**6**) and 2-methoxyiodobenzene (**7**) under the Ullmann conditions yielded 2-isopropyl-5-nitro-2′-methoxybiphenyl (**8**), which was then demethylated as above to give **9**:

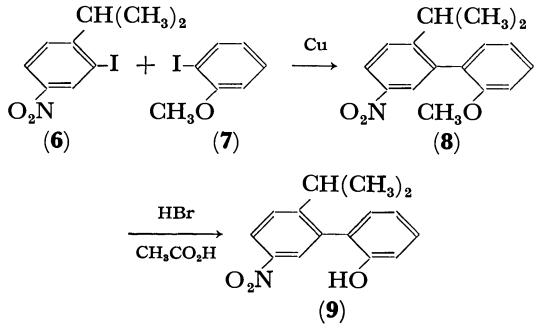

(**6**) (**7**) (**8**) (**9**)

Experimental

Measurements. The NMR spectra were measured on a spectrometer, either a Japan Electron Optics JNM C-60H and JNM C-60HL, a Hitachi R 20A, or a Varian Associates A-60 spectrometer. The solvents were dimethyl-d_6 sulfoxide or tetrachloroethane, and the concentration was *ca.* 0.3 mol/*l* or *ca.* 8% (w/w). Cyclooctane was used as the internal standard. The calibration of the coalescence temperature was determined by studying the chemical-shift difference between methylene and hydroxyl protons of ethylene glycol. This calibration was applied to the other range of temperature, and the error was estimated to be ±2°C.

In cases where the coupling constant is smaller than the chemical shift at the lower temperature, the quartets due to the magnetically non-equivalent methyls in isopropyl group coalesce when the temperature is raised, the chemical shift gradually decreases, and a broad single-peaked curve is obtained at the coalescence temperature (T_c). When the temperature is raised by 1°C from the T_c, two broad peaks are observable, indicating that the T_c is fairly dependable. On the other hand, in the cases where the coupling constant is larger than the chemical shift, the two peaks in the higher field and the two peaks in the lower field coalesce when the temperature is raised.

Various approximating methods have been presented to derive the kinetic data from the temperature-dependent NMR information. In this study, the following two equations were used to obtain the data:

$$\frac{1}{\tau} = \frac{\pi(\delta\nu_0)}{2(w-w_0)} \quad (1)$$

where τ is the average half-life time; $\delta\nu_0$, the difference in chemical shifts when the exchange is negligible; w, the half-band width at a given temperature, and w_0, the half-band width when the exchange is fast.

$$\frac{1}{\tau} = \frac{\pi(\delta\nu_0)}{\sqrt{2}} \quad (2)$$

Equation (2) is applicable at the coalescence temperature.

The effect of the population of the conformers with respect to the isopropyl group on the difference in chemical shift was calibrated by extrapolating the linear part of the $\delta\nu_0$ *vs.* temperature correlation at low temperatures.

The half-band width of cyclooctane, which was added as an internal standard, was used as w_0 by carefully adding a definite amount of cyclooctane to the solution.

The infrared spectra were obtained on a Perkin-Elmer 112 G single-beam grating spectrophotometer. Data obtained with *ca.* 1 mmol/*l* solution in carbon tetrachloride are given in Table 5. The spectra were also obtained with a tetrachloroethane solution, the concentration being *ca.* 0.3 mol/*l*, in order to obtain data which should be useful in discussing the NMR results.

Syntheses of the Materials. The Ullmann Reaction: When a mixture of 20 g (0.1 mol) of 2-methoxyiodobenzene, 15 g (0.05 mol) of 2-isopropyl-5-nitroiodobenzene, and 15 g of copper bronze was heated at 180°C, the reaction set in; the temperature was then raised to 260°C. After it had then been cooled, 20 more grams of copper bronze was added, and the mixture heated at *ca.* 200°C for 1 hr. The mixture was cooled and extracted with acetone in a Soxhlet apparatus. The extract was concentrated and chromatographed on alumina to give 1.5 g of 2-methoxy-2′-isopropyl-5′-nitrobiphenyl, mp 84—85°C. NMR (δ from TMS in CCl_4): 1.05 (3H, d J=7); 1.15 (3H, d J=7); 2.60 (1H, septet); 3.82 (3H, s); 6.9—8.4 (7H, m).

Found: C, 70.83; H, 6.32; N, 5.13%. Calcd for $C_{16}H_{17}NO_3$: C, 70.83; H, 6.32; N, 5.16%.

2-Methoxy-5-nitro-2′-isopropylbiphenyl, mp 107°C, was similarly prepared from 2-methoxy-5-nitroiodobenzene and 2-isopropyliodobenzene, the yield being 14%. NMR (δ from TMS in CCl_4): 1.05 (3H, d J=7); 1.10 (3H, d J=7); 2.83 (1H, septet); 3.72 (3H, s); 6.8—8.3 (7H, m).

Found: C, 70.87; H, 6.55; N, 4.99%. Calcd for $C_{16}H_{17}ON_3$: C, 70.83; H, 6.32; N, 5.16%.

Demethylation of the Methyl Ethers. To a solution of 1 g of the biphenyl derivative in 10—20 m*l* of acetic acid, 15—20 m*l* of 47% aqueous hydrogen bromide and *ca.* 5 m*l* of acetic anhydride were added, after which the mixture was heated for *ca.* 5 hr. The mixture was then poured onto ice water and extracted. The recrystallization of the acidic part gave the desired 2-hydroxy-2′-isopropylbiphenyl derivative. The data are given in Table 1.

Table 1. 2-Hydroxy-2′-isopropylbiphenyls

Substituent	mp (°C)	Anal.[a] (Found)		
		C	H	N
none	55—56	85.03	7.89	
4-NO_2	81—82	70.07	5.58	5.52
5-NO_2	94	70.07	5.82	5.77
4′-NO_2	128—129	70.07	6.17	5.70
5′-NO_2	90—91	70.36	5.72	5.58

a) Calculated values for 2-hydroxy-2′-isopropylbiphenyl are C 84.87 and H 7.60%. Calculated values for the nitro derivatives are C 70.02, H 5.88, and N 5.44%.

Results

Attempts at obtaining the energy and the entropy of activation from the Arrhenius plot of the data obtained by the method described in the Experimental section revealed that a considerable amount of error cannot be

Table 2. Coalescence temperature and various data at the T_c for 2-hydroxy-2′-isopropylbiphenyls[a)]

Substituent	Solvent	T_c (°C)	$\delta\nu_0$ (Hz)	k_c (sec^{-1})	$\Delta G^{\ddagger}_c$ (kcal/mol)
none	DMSO[b)]	58±2	6.9±0.3	15.4±0.5	17.8±0.2
	TCE[b)]	77	2.8	6.2	19.3
4-NO_2	DMSO	58	8.1	17.8	17.6
	TCE	76	3.7	8.2	19.1
5-NO_2	DMSO	49	8.3	18.5	17.0
	TCE	65	2.5	5.6	18.7
4′-NO_2	DMSO	60	6.4	14.0	17.8
	TCE	57	5.8	12.9	17.7
5′-NO_2	DMSO	42	7.7	17.1	16.7
	TCE	55	6.1	13.4	17.6

a) The subscript c denotes the value at coalescence temperature.
b) DMSO and TCE stand for dimethyl sulfoxide and tetrachloroethane, respectively.

avoided. This error may come from the facts that the signal of cyclooctane was chosen as the standard of the half-band width and that the chemical shifts of the methyl groups change according to the change in population with the temperature, in addition to the methods of approximation used in this study. However, it is possible to minimize the error if we limit the data of the half-band width to a fairly large value and limit the temperature to a small range. Thus, we decided to use a single temperature, the highest coalescence temperature among those of the compounds studied. Table 2 shows the coalescence temperatures and the pertinent data of the phenols; in Table 4 only the rates of the internal rotation of the methyl ethers in tetrachloroethane are given, because those in dimethyl sulfoxide are quite similar. The solvent effects on the rates of internal rotation and the free energies of activation for the hydroxy compounds are given in Table 3. The errors other than the systematic are estimated to be ±0.2 kcal/mol.

Table 3. Rates and energies of activation for internal rotation about the pivot bond of 2-hydroxy-2′-isopropylbiphenyls at 77°C

Substituent	in Dimethyl sulfoxide		in Tetrachloroethane	
	k(sec^{-1})	$\Delta G^{\ddagger}$(kcal/mol)	k(sec^{-1})	$\Delta G^{\ddagger}$(kcal/mol)
none	35	18.1	6	19.3
4-NO_2	45	17.9	8	19.1
5-NO_2	95	17.4	9	19.0
4′-NO_2	35	18.1	33	18.1
5′-NO_2	90	17.4	33	18.1

Table 4. Kinetic data of 2-methoxy-2′-isopropylbiphenyls in tetrachloroethane

Substituent	T_c (°C)	$\delta\nu_0$ (Hz)	k_c (sec^{-1})	$\Delta G^{\ddagger}_c$ (kcal/mol)	k_{86} (sec^{-1})	$\Delta G^{\ddagger}_{86}$ (kcal/mol)
none	86	7.2	16.0	19.2	16	19.2
4-NO_2	86	7.1	15.8	19.2	16	19.2
5-NO_2	70	6.3	14.0	18.4	32	18.7
4′-NO_2	79	7.2	16.0	18.8	23	18.9
5′-NO_2	69	7.7	17.1	18.3	50	18.4

Discussion

Since we have obtained only the free energy of activation, it will be safer to compare some corresponding compounds rather than to discuss the absolute values. A comparison of the data obtained with the hydroxy compounds with those of the methoxy derivatives will be made. Since it was pointed out in a previous paper[9)] that two factors—electron density and through conjugation—must be considered in discussing the internal rotation of biphenyls about the pivot bond, it is not safe to compare the data of compounds which have different substituents or which have the same substituents at different positions.

The data in Tables 2 and 3 suggest that the energies of activation for rotation of the hydroxylic compounds are not much different in dimethyl sulfoxide. Indeed, the differences are within the range of error. If the intermolecular hydrogen bonding between the phenols and dimethyl sulfoxide played an important role in lowering the energy of activation, compound **12** should show a smaller value of the energy of activation than the other compounds because the resonance structure (**12a**) is favored on forming the hydrogen bond. The experimental data, however, show an increasing tendency, although small. Therefore, the lowering of the electronegativity of the oxygen in the hydroxyl group due to the formation of the hydrogen bond is negligibly small.

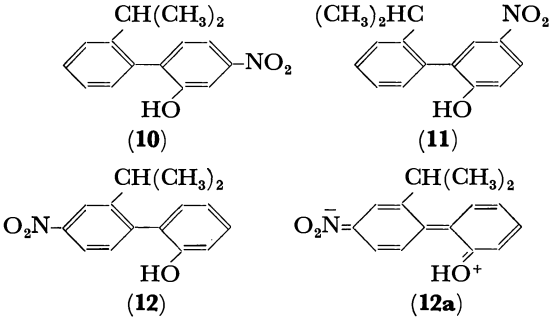

From the results shown in Tables 2—4, together with the fact that the $\Delta G^{\ddagger}$'s for rotation about the pivot bond of 2-methoxybiphenyl derivatives in dimethyl sulfoxide are not very different from those in chlorinated hydrocarbons (see reference 8 and the Results of this paper), it is clear that there are some compounds which give similar $\Delta G^{\ddagger}$ values irrespective of the nature of the substituent (hydroxy or methoxy), whereas some compounds show a fairly large difference in $\Delta G^{\ddagger}$'s and k's. The methoxy compounds belong to the first category, and, among the hydroxy compounds, those which possess a nitro group in the ring not having a hydroxyl group are classified in the first category, and the others in the second. These phenomena may best be understood when the effect of the O–H···π interaction is considered.

Since those compounds which have a nitro group at the ring having a hydroxyl group may be expected to be more acidic, the intramolecular interaction is fairly strong. On the other hand, the nitro group attached to the benzene ring which is to be the proton acceptor will decrease the basicity of the π-electron system. Thus, the O–H···π interaction will be stronger and the

ground state will be more stabilized with compounds **10** and **11** than with compounds **9** and **12**. The difference in the energy of activation between these two groups is *ca.* 1 kcal/mol; this is in good agreement with the data obtained by the infrared method with 4-nitro-2-hydroxybiphenyl and 2-hydroxy-4'-nitrobiphenyl.[10]

It is an interesting phenomenon that compound **5** shows a tendency similar to that of compounds **10** and **11**. We have no good explanation for this, but wish tentatively to attribute it to the steric effect of the isopropyl group. That is, because of the steric requirement of the isopropyl group, the biphenyl derivatives studied here will have two benzene rings almost perpendicular to each other, the conformation favoring the intramolecular O–H···π interaction. Thus it may be considered that, unless the π-system is unfavorable for accepting the proton, almost all the molecules will be of the intramolecularly interacting species, leveling the effect of the O–H···π interaction to the same order of magnitude as compounds **5**, **10**, and **11**.

Table 5. Infrared spectral data of 2-hydroxy-2'-isopropylbiphenyls

Substituent		ν_{OH}(cm^{-1})	A(mol$^{-1}\cdot l\cdot$cm^{-2})
none	i[a]	3553.7	1.0×10^4
	f[a]	—	—
4-NO_2	i	3541.8	1.35
	f	—	—
5-NO_2	i	3530.0	1.4
	f	—	—
4'-NO_2	i	3570.0	0.2
	f	3602.8	1.3
5'-NO_2	i	3571.1	0.3
	f	3602.8	1.3

a) i and f denote O–H···π interacting and free species, respectively.

Support for this postulate may be obtained from the data given in Table 5. As may be seen, even the compound **5** does not show any O–H stretching absorption due to the free hydroxyl group. This indicates that introducing the isopropyl group at the 2'-position favors the intramolecular O–H···π interaction compared with 2-hydroxybiphenyl, which has shown absorption due to the free hydroxyl group.[11] Indeed, even 4-nitro-2-hydroxybiphenyl showed some free hydroxyl groups, the presence of which made the calculation of the interaction energy possible.[10] The shift (*ca.* 10 cm^{-1}) of the absorption band to a lower frequency than in the corresponding compounds lacking the isopropyl group also suggests that the O–H···π interaction is favored in the isopropyl compounds.

It may be argued that, at the concentration suitable for the NMR study, the inter- rather than the intramolecular hydrogen bond is important. Therefore, in order to justify the above discussion, infrared spectral study at that concentration is needed. The infrared absorptions in the 3μ region of compounds **5**, **9**, **11**, and **12** were thus measured at a 0.3 mol/l concentration in tetrachloroethane. Although there remains some ambiguity because of the solvent absorption, the results indicate that these compounds have no absorption below 3500 cm^{-1}; this suggests that they exist as, at least mainly, monomers. The compounds **5** and **11** have only one absorption, at *ca.* 3530 and *ca.* 3540 cm^{-1} respectively, which may be attributed to the intramolecularly interacting (O–H···π) molecular species.[12]

On the other hand, compounds **9** and **12** have two absorptions at the same wave numbers (3580 and 3560 cm^{-1}), the intensity being larger with the latter band. The band at the higher frequency may be attributed to the free form because it is at too high a frequency to be assigned to the dimer.[13] The band at the lower frequency may be assigned to the O–H···π interacting species, because the 20 cm^{-1} shift to a lower frequency is quite normal for the interaction. Thus the infrared spectral data support the above conclusion drawn from the NMR results.

There are many points to be clarified with regard to the substituent effect on the energy of activation for the internal rotation about the pivot bond of biphenyls. For example, it is not at all clear why the nitro group at the 5- or 5'-position lowers the energy of activation. We have intentionally omitted some discussions familiar to stereochemists, such as those of the buttressing effect and the difference in the sizes of hydroxyl and methoxyl groups, since the data presented here can not be discussed in detail. However, we believe that, as a first approximation, the intramolecular O–H···π interaction is an important factor in governing the energy of activation for the internal rotation of 2-hydroxybiohenyl derivatives.

10) M. Ōki, H. Iwamura, and Y. Urushibara, *ibid.*, **31**, 770 (1958).

11) M. Ōki and H. Iwamura, *ibid.*, **34**, 1395 (1961).

12) The O–H stretching absorption of the O–H···π interacting species at a 3×10^{-3} mol/l concentration in carbon tetrachloride is located close to 3550 cm^{-1}. See Table 5.

13) The absorption due to the dimer of hydroxy compounds is considered to be at *ca.* 3490 cm^{-1}.

Reactions of *p*-Benzoquinone Derivatives with Ethylenediamine

Teruzo ASAHARA, Manabu SENŌ, and Takuma TESHIROGI

Institute of Industrial Science, The University of Tokyo, Roppongi, Minato-ku, Tokyo

(Received December 12, 1970)

From the reaction results of *p*-benzoquinone derivatives with various amino compounds, it becomes clear that chloranil reacts with ethylenediamine to afford an unexpected product. The spectroscopic analyses of the product show that this is an addition compound with some contribution of charge-transfer structures. Bromanil gives a similar product upon reaction with ethylenediamine.

It is well known that *p*-benzoquinones react with amine derivatives. For example, *p*-benzoquinone (BQ) and 2,5-dimethoxy-*p*-benzoquinone (DMQ) react with ethanolamine (EtA) to afford 2,5-bis(2-hydroxyethylamino)-*p*-benzoquinone, and chloranil (CA) reacts with EtA to give 2,5-bis(2-hydroxyethylamino)-3,6-dichloro-*p*-benzoquinone.

Harley-Mason and Laird[1] reported the successful formation of 1,2,3,4-tetrahydro-1,4,5,8-tetraazaanthracene (I) through the reaction of 2,5-dihydroxy-*p*-benzoquinone (DHQ) with ethylenediamine (EDA) by passing air into the aqueous reaction mixture. During the investigation to extend these synthetic processes to other amine derivatives, we have found that chloranil and bromanil do not afford products with the expected structures by the reaction with EDA. The present report will deal with these reactions.

Results and Discussion

It was found that 2,5-bis(2-aminoethylamino)-*p*-benzoquinone (II) was obtained when a dispersion of DMQ and EDA in ethanol was kept overnight at room temperature. This indicates that EDA reacts with DMQ in the same way as EtA does. As II is unstable at elevated temperature, it was identified as the adduct with phenyl isocyanate.

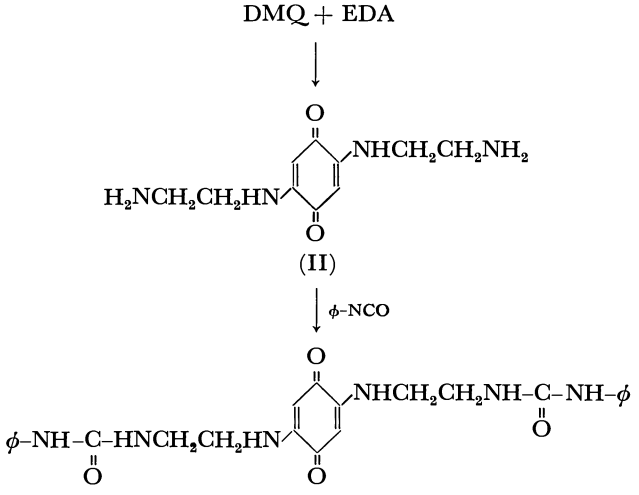

A yellow product was obtained by heating II in water for several hours. This compound was identified as the tetraazaanthracene derivative, I, which was also prepared by Harley-Mason through another route,[1] by IR and elementary analysis and by a study of its electronic spectrum. The following reaction scheme may be supposed:

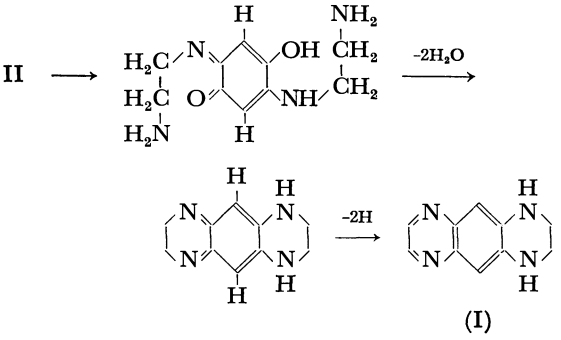

That is, II is tautomerized to an *ortho*-quinone derivative, followed by dehydration to a ring-closed product. This is unstable and is oxidized by oxygen in air to I.

Next, the reaction of CA with amines was investigated. CA reacts easily with monoacetylethylenediamine (AcEDA) to afford 2,5-bis(2-acetoaminoethylamino)-3,6-dichloro-*p*-benzoquinone. This product is hydrolyzed easily to chloranic acid in concentrated hydrochloric acid; therefore, the structure could be determined.

CA was dissolved homogeneously in hot benzene, and into this solution one or two equivalents of EDA in benzene were added, drop by drop. A green product(IIIa) was obtained by adding one molar equivalent of EDA, and a yellow product(IIIb) was obtained by adding two molar equivalents of EDA. These reactions were traced by means of the electronic spectra of the reaction mixtures. The CA solutions in acetone with a definite concentration were mixed with the EDA solutions in acetone in various concentrations; after the mixtures had stood for half an hour, their electronic spectra were recorded at around 380 mμ. The details of the experimental conditions and the results are listed in Fig. 1. CA has a peak at 323 mμ, and only the tail is shown in Fig. 1(No. 1). When EDA is added, a peak appears at 373 mμ; its intensity becomes greater with an increase in the concentration of EDA and attains a maximum with a slightly bathochromic effect, (5 mμ) at a molar ratio EDA/CA of unity (No. 4). By a further increase in the EDA concentration, this peak decreases in intensity and shifts to a lower wavelength, but the peak increases again in intensity at a molar ratio EDA/CA of two (No. 5).

The spectroscopic properties of the two products, IIIa and IIIb, were examined. The infrared spectra of IIIa and IIIb are similar to one another. The

1) J. Harley-Mason and A. H. Laird, *Tetrahedron*, **7**, 70 (1959).

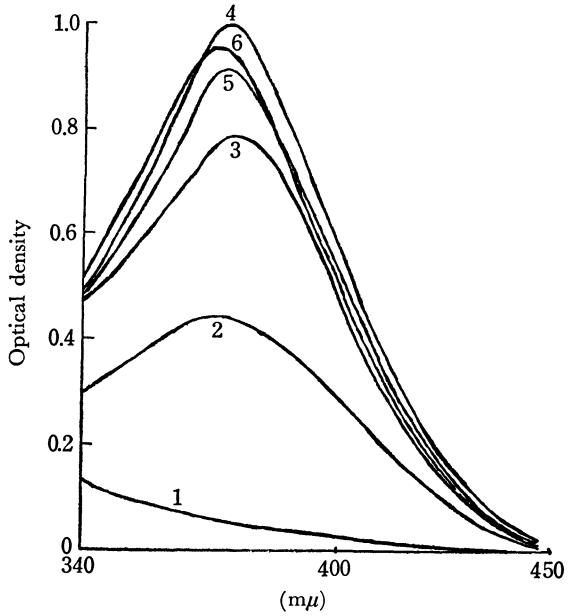

Fig. 1. Electronic spectra of the reaction of CA with EDA.

Run No.	CA(mol/l) $\times 10^4$	EDA(mol/l) $\times 10^4$
1	1.8	0
2	1.8	0.6
3	1.8	1.2
4	1.8	1.8
5	1.8	3.6
6	1.8	4.2

peaks assigned to the stretching vibrations of the $-NH_2$ and $-CH_2-$ groups and the deformation vibration of the $-CH_2-$ groups are found at 3300, 2900, and 1420 cm^{-1} respectively, but no peak assigned to >C=O is clearly found.

The proton NMR spectra of EDA, IIIa, and IIIb were obtained at 60 MHz in dimethyl sulfoxide-d_6, with reference to tetramethylsilane as the internal standard. The peaks of protons of the $-CH_2-$ and $-NH_2$ groups of EDA are found at 2.50 and 1.30 ppm; those of IIIa, at 3.27 and 7.68 ppm, and of IIIb at 2.82 and 6.13 ppm, respectively. The peaks of $-NH_2$ were determined by adding deuterium oxide. The intensity ratio of the $-NH_2$ to the $-CH_2-$ group, however, is not equal in the spectra of IIIa and IIIb, probably because of the presence of a small amount of water in the solvent.

In the mass spectrum of IIIa, the *m/e* value of the parent ion is 246; this is equal to the value referred to CA, and the spectrum pattern is similar to that of CA. In the mass spectrum of IIIb, the parent ion is *m/e* 248 and the spectrum pattern is very similar to that of tetrachlorohydroquinone (TCHQ).

Moreover, the following result was obtained. IIIb reacts with acetic anhydride in the presence of pyridine as a catalyst to afford tetrachlorohydroquinone diacetate. It is clear from IR and elementary analysis that this product is the same as the compound obtained by the acetylation of TCHQ with acetyl chloride in pyridine.

Similar behavior was observed for bromanil (BA). That is, while BA reacts with AcEDA to give 2,5-bis(2-acetoaminoethylamino)-3,6-dibromo-*p*-benzoquinone, it does not react with EDA to afford the expected product; instead, IVb is obtained from the mixture. This product reacts with acetic anhydride to afford tetrabromohydroquinone diacetate, as in the case of CA.

These investigations lead to the following interesting conclusion. While CA and BA react easily with aliphatic and aromatic amines, they react with EDA to afford unexpected addition products. The structures of these addition compounds, IIIb and IVb, could not be definitely determined from these results, but they might be similar to those of the reaction intermediates in reactions of CA and aromatic amines examined by Nagakura *et al.*[2] The reaction properties of CA described above are in accord with the result that the reaction of CA and *o*-phenylenediamine does not give a well-defined product, unlike the reactions with *m*- and *p*-phenylenediamine.

Experimental

2,5-Bis(2-aminoethylamino)-p-*benzoquinone (II).* Four grams of DMQ and 16 g of EDA were dispersed in 200 m*l* of ethanol, and the mixture was then left standing overnight. By filtration, a red-violet solid was obtained as the product (II); yield, 6 g. The product (0.3 g) was dissolved in 50 m*l* of DMF, then after which 1 m*l* of phenyl isocyanate was added. The reaction mixture was heated at 100°C for one hour, and then cooled and poured into water. The dispersed solid was collected, dried, and recrystallized from acetic acid; mp 254°C.

Found: C, 62.05; H, 5.77; N, 18.07%. Calcd for $C_{24}H_{26}N_4O_6$: C, 62.33; H, 5.67; N, 18.17%.

1,2,3,4-Tetrahydro-1,4,5,8-tetraazaanthracene (I). One gram of II was dispersed in 300 m*l* of water, and the mixture was refluxed for ten hours. Water was removed under reduced pressure, and the yellow residue was recrystallized from nitrobenzene to afford yellow needles.

Found: C, 64.46; H, 5.29; N, 30.04%. Calcd for $C_{10}H_{10}N_4$: C, 64.50; H, 5.41; N, 30.09%.

2,5-Bis(2-acetoaminoethylamino)-3,6-dichloro-p-*benzoquinone.* A mixture of 10 g of CA and 20 g of AcEDA in 200 m*l* of ethanol was refluxed for five hours. After cooling, the dispersed solid was collected by filtration and dried; crude yield, 15 g (98%). It was recrystallized from a mixture of pyridine and water. mp 246°C.

Found: C, 44.77; H, 4.70; N, 14.88%. Calcd for $C_{14}H_{18}N_4Cl_2O_4$: C, 44.56; H, 4.77; N, 14.85%.

The Reaction Product from CA and One Mole Eqivalent of EDA (IIIa). Five grams of CA were dissolved in 100 m*l* of hot benzene, and into the resulting solution 2.44 g of EDA in 50 m*l* of benzene were added, drop by drop. Green solids separated out immediately. The hot mixture was filtered to collect a solid product, which was then dried under reduced pressure; yield, 6.5 g.

Found: C, 20.99; H, 2.19; N, 8.00; Cl, 40.48%.

The Reaction Product from CA and Two Mole Equivalents of EDA (IIIb). Five grams of CA and 4.88 g of EDA were mixed in a way similar to that used in the case of IIIa; yield, 9.2 g.

Found: C, 33.39; H, 3.43; N, 15.00; Cl, 36.00%. Calcd for $C_{10}H_{16}N_4Cl_4O_2$: C, 32.81; H, 4.41; N, 15.31; Cl, 38.74%.

2) T. Nogami, K. Yoshihara, H. Hosoya, and S. Nagakura, *J. Phys. Chem.*, **73**, 2670 (1969).

The Reaction Product from BA and Two Mole Equivalents of EDA (IVb). Into 8.6 g of BA in 120 m*l* of hot benzene, 4.88 g of EDA in 50 m*l* of benzene were added; yield, 6.5 g.

Found: C, 22.55; H, 2.37; N, 8.11; Br, 56.84%. Calcd for $C_{10}H_{16}N_4Br_4O_2$: C, 22.02; H, 2.97; N, 10.30; Br, 58.77%.

Tetrachlorohydroquinone Diacetate. One gram of IIIb and a few drops of pyridine were added to 10 m*l* of acetic anhydride, and the mixture was heated at 40°C for three hours. The reaction mixture was poured into water, and the precipitates were collected by filtration and recrystallized from a mixture of dioxane and water; mp, 247°C (lit. 252°C).

Found: C, 36.30; H, 1.53; Cl, 42.52%. Calcd for $C_{10}H_6Cl_4O_4$: C, 36.14; H, 1.81; Cl, 42.77%.

Tetrabromohydroquinone Diacetate. This was prepared from IVb and acetic anhydride and was recrystallized from acetic acid; mp 284°C (lit. 283°C).

Found: C, 23.88; H, 0.89; Br, 61.88%. Calcd for $C_{10}H_6Br_4O_4$: C, 23.56; H, 1.19; Br, 62.69%.

BULLETIN OF THE CHEMICAL SOCIETY OF JAPAN, VOL. 44, 1689—1691 (1971)

A Synthesis of Thyrotropin-Releasing Factor

Ken INOUYE, Keiko NAMBA, and Hideo OTSUKA

Biochemistry Division, Shionogi Research Laboratory, Shionogi & Co., Ltd., Fukushima-ku, Osaka

(Received December 25, 1970)

A procedure is given for the synthesis of thyrotropin-releasing factor (TRF), a tripeptide L-pyrogultamyl-L-histidyl-L-proline amide. Benzyloxycarbonyl(Z)-glutaminyl-histidyl-proline amide (III) is obtained as an intermediate by the coupling of Z-glutamine *p*-nitrophenyl ester with histidyl-proline amide which is derived from the crystalline Z-dipeptide amide. Deprotection of III and the subsequent cyclization produce TRF in a moderate yield. Compound III and the corresponding N^{α}-acetyl derivative have little or no TRF activity.

Recently the structure of thyrotropin-releasing factor (TRF, or thyrotropin-releasing hormone, TRH), isolated from porcine[1] and ovine hypothalami,[2] has been elucidated to be a tripeptide L-pyroglutamyl-L-histidyl-L-proline amide. Both a synthetic preparation of the tripeptide amide and natural TRF (porcine) have been shown to be active in man.[3] This important finding as well as the fact that porcine and ovine hormones are chemically identical suggests that TRF is not species-specific among a wide variety of mammals. Because of its very minute occurrence in nature, it seems difficult to isolate TRF from natural sources in quantities sufficient for biochemical investigations and for clinical use. A chemical synthesis of this tripeptide amide will, therefore, become of extreme importance to meet such requirements. Some syntheses have appeared already.[4] We also wish to report a simple procedure for synthesizing the hormone. The present synthesis consists of a step-by-step elongation from C-terminal of the peptide chain, using a benzyloxycarbonyl group for N^{α}-protection, to obtain glutaminyl-histidyl-proline amide which undergoes facile transformation into the corresponding pyroglutamyl peptide (TRF). The procedure is outlined in Fig. 1.[5]

Benzyloxycarbonyl-proline amide, derived from the corresponding acid by a mixed anhydride method, was converted into the crystalline free base of proline amide (I) by catalytic hydrogenolysis. Coupling of I with benzyloxycarbonyl-histidine azide[6] yielded a crystalline dipeptide, benzyloxycarbonyl-histidyl-proline amide (II), in 85 per cent yield. Compound II was treated with hydrogen bromide in acetic acid, followed by coupling with benzyloxycarbonyl-glutamine *p*-nitrophenyl ester[7] to give benzyloxycarbonyl-glutaminyl-histidyl-proline amide (III). A crude preparation of compound III was partially purified by chromatography on a silica gel column with methanol-chloroform (1:3) as solvent. Further purification was performed on a column of carboxymethyl(CM) cellulose using an ammonium acetate buffer with a linear concentration gradient. The effluent solution was monitored at 245 mμ in order to detect the peptide emerging from the column. The pure preparation of III thus obtained was submitted to deprotection with hydrogen bromide in acetic acid. The resulting hydrobromide of glutaminyl tripeptide (IV) was converted into the acetate by passing through a column of an anion-exchange resin (acetate form). The final step leading to the formation of the desired

1) a) J. Bøler, F. Enzmann, K. Folkers, C. Y. Bowers, and A. V. Schally, *Biochem. Biophys. Res. Commun.*, **37**, 705 (1969); b) R. M. G. Nair, J. F. Barrett, C. Y. Bowers, and A. V. Schally, *Biochemistry*, **9**, 1103 (1970); c) K. Folkers, F. Enzmann, J. Bøler, C. Y. Bowers, and A. V. Schally, *Biochem. Biophys. Res. Commun.*, **37**, 123 (1969).

2) a) R. Burgus, T. F. Dunn, D. Desiderio, D. N. Ward, W. Vale, and R. Guillemin, *Nature*, **226**, 321 (1970); b) R. Burgus, T. F. Dunn, D. M. Desiderio, D. N. Ward, W. Vale, and R. Guillemin, *Endocrinology*, **86**, 573 (1970).

3) C. Y. Bowers, A. V. Schally, D. S. Schalch, C. Gual, A. J. Kastin, and K. Folkers, *Biochem. Biophys. Res. Commun.*, **39**, 352 (1970).

4) a) D. Gillessen, A. M. Felix, W. Lergier, and R. O. Studer, *Helv. Chim. Acta*, **53**, 63 (1960); b) C. M. Baugh, C. L. Krumdieck, J. M. Hershman, and J. A. Pittman, Jr., *Endocrinology*, **87**, 1015 (1970); c) G. Flouret, *J. Med. Chem.*, **13**, 843 (1970).

5) All amino acid residues are of the L-configuration. The abbreviated designation of amino acids, peptides and their derivatives is in accordance with the proposal of the IUPAC-IUB Commission of Biochemical Nomenclature, which appeared in *Biochemistry*, **5**, 2485 (1966); *ibid.*, **6**, 362 (1967).

6) R. W. Holley and E. Sondheimer, *J. Amer. Chem. Soc.*, **76**, 1326 (1954).

7) M. Bodanszky and V. du Vigneaud, *ibid.*, **81**, 5688 (1959).

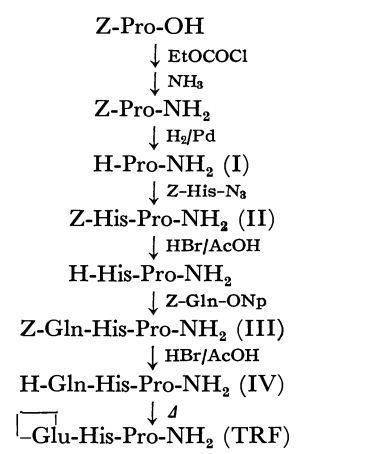

Fig. 1. Synthesis of pyroglutamyl-histidyl-proline amide (TRF).[5]

pyroglutamyl peptide (TRF) is a brief heat treatment of IV (acetate) in acetic acid. The reaction was followed by thin-layer chromatography (silica gel); IV and TRF have R_f values of 0.05 and 0.24, respectively, in methanol-chloroform (1:1) as solvent. Purification of crude TRF was easily achieved by chromatography on a CM cellulose column using an ammonium acetate buffer. The TRF preparation thus obtained was found to be homogeneous to Pauly reagent in thin-layer chromatography (E. Merck Cellulose F, in *n*-butanol:acetic acid:pyridine:water=30:6:20:24, BAPW) and its $[\alpha]_D$ was identical with a literature value[4a] within the error of measurement. The elemental and the amino acid analyses were also in good accordance with the theoretical values.

TABLE 1. THYROTROPIN-RELEASING ACTIVITY OF SYNTHETIC TRF AND RELATED COMPOUNDS[10]

Method	Compound[a] and dose	Number of animals	TRF activity (%increase in blood radioactivity)
A[8]	Saline	4	111.3±24.0
	TSH standard 0.2 mU	6	131.7±14.7
	TSH standard 0.4 mU	6	144.8±17.4
	Synthetic TRF 2 ng	5	153.0± 9.8
	III 2 ng	7	95.0± 5.3
	V 2 ng	7	89.6± 5.4
B[9]	Saline	6	99.5±10.4
	TSH standard 0.4 mU	5	244.0±25.0
	Synthetic TRF 20 ng[b]	7	328.4±27.7

a) TSH=Thyrotropin, III=Z-Gln-His-Pro-NH_2, V=Ac-Gln-His-Pro-NH_2
b) Dose per 100 g body weight

The synthetic TRF was then subjected to biological assays. An in vivo thyrotropin-releasing activity in mice was assayed by the method of Schally *et al.*,[8] and the effect of elevating the blood levels of TSH in rats was estimated by the McKenzie method.[9] Some results are presented in Table 1, in which the data on compound III and acetyl-glutaminyl-histidyl-proline amide (V), derived from IV by acetylation in aqueous pyridine, are also shown.[10] A level as low as 2 ng of the present TRF preparation can release thyrotropin (TSH) in mice, whereas both III and V are devoid of activity at least at the same level. These data as well as those of the chemical characterization are likely to provide evidence for the identity of our synthetic TRF with the natural hormone.

Experimental

All melting points were uncorrected.

Benzyloxycarbonyl-proline Amide. A solution of benzyloxycarbonyl-proline (24.9 g, 0.1 mol) and triethylamine (15.3 m*l*, 0.11 mol) in anhydrous tetrahydrofuran (250 m*l*) was chilled in an ice-salt bath (below −10°C) and to this was added dropwise ethyl chloroformate (10.5 m*l*, 0.11 mol). The mixture was stirred for 10 min, and then concentrated aqueous ammonia (28%, 19.2 m*l*) was introduced. After the mixture had been stirred at room temperature for 30 min, the solvent was removed by evaporation *in vacuo*. To the residue were added ethyl acetate (30 m*l*) and water (30 m*l*), and the mixture was shaken vigorously. The organic phase was further washed with N hydrochloric acid, 5% sodium bicarbonate and water, dried over sodium sulfate and evaporated *in vacuo* to give an oily residue which crystallized from ethyl acetate-petroleum ether; yield 20.1 g (81%), mp 90—91° C, $[\alpha]_D^{27}$ −35.0±0.4° (*c* 2.06, ethanol). Lit,[11] mp 94°C, $[\alpha]_D^{23}$ −33.8° (*c* 2, ethanol).

Found: C, 63.17; H, 6.55; N, 11.53%. Calcd for $C_{13}H_{16}N_2O_5$: C, 62.89; H, 6.50; N, 11.28%.

Benzyloxycarbonyl-histidyl-proline Amide (II). Benzyloxycarbonyl-proline amide (2.2 g, 9 mmol) was hydrogenolyzed over palladium in methanol for 1.5 hr. Removal of the solvent yielded *proline amide (I)* as a sirupy residue which crystallized upon addition of ether; wt. 1.24 g, mp 101—102°C, $[\alpha]_D^{23}$ −86.5±1.2° (*c* 1.08, methanol).

An ethyl acetate solution of benzyloxycarbonyl-histidine azide (derived from 4.1 g (13.5 mmol) of the hydrazide in the usual manner)[6] was added to compound I (1.2 g) obtained above and the mixture was kept at 4°C overnight. Removal of the solvent by evaporation *in vacuo* yielded a sirupy residue which was crystallized from methanol-water. After recrystallization from water the product amounted to 2.95 g (85%); mp 102—104 °C, $[\alpha]_D^{24}$ −40.7±0.7° (*c* 1.13, methanol).

Found: C, 58.56; H, 6.10; N, 17.48%. Calcd for $C_{19}H_{23}N_5O_4 \cdot 1/4H_2O$: C, 58.52; H, 6.07; N, 17.96%.

Benzyloxycarbonyl-glutaminyl-histidyl-proline Amide (III). Compound II (1.54 g, 4 mmol) was dissolved in saturated hydrogen bromide in acetic acid (15 m*l*) and the mixture was allowed to stand at room temperature for 40 min, followed by the addition of ether to yield fine precipitates. The precipitates (1.98 g) were dissolved in dimethylformamide (25 m*l*) and to this was added triethylamine (1.68 m*l*, 12 mmol). The hydrobromide of triethylamine which separated was filtered off and benzyloxycarbonyl-glutamine *p*-nitrophenyl ester (1.61 g, 4 mmol)[7] was added to the filtrate. The

8) a) A. V. Schally, C. Y. Bowers, and T. W. Redding, *Endocrinology.*, **78**, 726 (1966); b) T. W. Redding, C. Y. Bowers and A. V. Schally, *ibid.*, **79**, 229 (1966).
9) J. M. McKenzie, *ibid.*, **63**, 372 (1958).
10) The assays were performed by Dr. Masahiro Sakoda, Kobe University School of Medicine. We thank Dr. Sakoda for permission to include these data in the present communication.
11) D. Hamer and J. P. Greenstein, *J. Biol. Chem.*, **193**, 81 (1951).

mixture was kept at 4°C for 65 hr and evaporated *in vacuo*. The sirupy residue was triturated with ethyl acetate and the mixture was filtered off to collect precipetates which were washed with ethyl acetate and ether and dried *in vacuo* (2.65 g) The precipitates were dissolved in methanol-chloroform (1:3 by vol.) and the solution was submitted to a column of silica gel (E. Merck, 0.05—0.2 mm, 90g) which had been prepared with methanol-chloroform (1:3). The same solvent system was used for elution. Fractions which gave a single component (R_f=0.35, sulfuric acid charring) on thin-layer chromatography (Silica gel G, methanol-chloroform (1:2) as solvent) were pooled and evaporated *in vacuo* to afford a residue which solidified upon treatment with ethyl acetate (1.98 g). The partially purified material (0.80 g) was chromatographed for further purification on a column (1.7×53 cm) of carboxymethyl cellulose (Serva, 0.56 meq/g) using an ammonium acetate buffer (pH 5.0, 2000 m*l*) with a linear concentration gradient of 0.005—0.1 M. Ten-m*l* fractions were collected and their absorptivity at 245 mμ was recorded. Fractions (tubes 41—52) corresponding to a major peak were pooled, evaporated and lyophilized; wt. 0.49 g (53%), $[\alpha]_D^{25}$ −60.4 ±1.1° (*c* 0.88, water), −46.1±0.9° (*c* 0.98, methanol).

Found: C, 52.70; H, 6.00; N, 17.00%. Calcd for $C_{24}H_{31}N_7O_6 \cdot 1/2CH_3COOH \cdot 3/2H_2O$: C, 52.62; H, 6.36; N, 17.18%.

Pyroglutamyl-histidyl-proline Amide (Thyrotropin-releasing Factor, TRF). To compound III (0.20 g) was added saturated hydrogen bromide in acetic acid (*ca.* 5 m*l*) and the mixture was kept at room temperature for 60 min, followed by precipitation by the addition of ether. The resulting precipitates were filtered off, washed with ether and dried *in vacuo* to give *glulaminyl-hislidyl-proline amide hydrobromide (IV)*; wt. 0.26 g, $[\alpha]_D^{25}$ −13.8±0.5° (*c* 0.98, methanol).

Found: C, 30.91; H, 5.03; N, 15.64%. Calcd for $C_{16}H_{25}N_7O_4 \cdot 3/2HBr \cdot 2H_2O$: C, 31.11; H, 5.14; N, 15.87%.

The hydrobromide (IV) obtained above (0.25 g) was dissolved in water and the solution was passed through a column (1.2×10 cm) of Amberlite CG—400 (acetate form); the column was washed with portions of water. The aqueous solutions were combined and evaporated *in vacuo* at a bath temperature of 50°C. The residue was dissolved in glacial acetic acid (20 m*l*) and the solution was heated at 95°C for 15 min. After removal of the solvent by evaporation *in vacuo* the residue was subjected for purification to chromatography on a column (1.7×30 cm) of carboxymethyl cellulose (Serva, 0.56 meq/g) using an ammonium acetate buffer (pH 5.0, 1440 m*l*) with a linear concentration gradient of 0.005—0.1 M. Fractions (7.5 m*l*/tube) were collected and their absorptions at 245 mμ were recorded. There were two peaks, I (tubes 8—10) and II (31—42), on the chromatogram and the tubes corresponding to peak II were pooled and evaporated *in vacuo*. The resulting glassy residue was dried *in vacuo* and then precipitated from acetic acid-ether to yield pure TRF as hygroscopic colorless powder; wt. 0.11 g, $[\alpha]_D^{25}$ −43.4±0.8° (*c* 1.01, 95% acetic acid). Lit,[4a] $[\alpha]_D^{25}$ −44.8° (*c* 1, 95% acetic acid). Homogeneous on thin-layer chromatography (Cellulose F, E. Merck) to Plauy reagent; R_f=0.47 (BAPW). Amino acid ratios in acid hydrolysate:[12] His 1.00, Glu 0.90, Pro 1.14, NH_3 1.01.

Found: C, 50.63; H, 6.56; N, 20.78%. Calcd for $C_{16}H_{22}N_6O_4 \cdot 1/2CH_3COOH \cdot 1/2H_2O$: C, 50.86; H, 6.28; N, 20.94%.

Acetyl-glutaminyl-histidyl-proline Amide. Cmopund IV (0.156 g) was dissolved in 90% pyridine (4 m*l*) at 0°C, and to this solution was added acetic anhydride (0.1 m*l*) and the mixture was kept at 0°C for 90 min. After addition of water (2 *ml*) the mixture was evaporated *in vacuo*. The residue was dissolved in water and the solution was passed through a column (1.2×9 cm) of Amberlite CG-400 (acetate); the column was washed with portions of water. The aqueous solutions were combined and evaporated *in vacuo* to give a residue which was reprecipitated from acetic acid-ether; yield 0.098 g (80%), $[\alpha]_D^{25}$ −50.5±0.8° (*c* 1.11, methanol). Thin-layer chromatography (Cellulose F, F. Merck); R_f=0.45 (BAPW).

Found: C, 46.55; H, 6.40; N, 19.65%. Calcd for $C_{18}H_{27}N_7O_5 \cdot 1/2CH_3COOH \cdot 2H_2O$: C, 46.81; H, 6.82; N, 20.11%.

Grateful acknowledgement is made to Dr. Masahiro Sakoda, Kobe University School of Medicine, for performing biological assays. We also thank Dr. Mitsuo Ebata and his staff for amino acid analysis, Dr. Kaoru Kuriyama and his staff for optical rotation measurements, and members of our microanalysis laboratory for elemental microanalysis.

12) D. H. Spackman, W. H. Stein, and S. Moore, *Anal. Chem.*, **30**, 1190 (1958).

Aroyloxy-Radikal. Die Aktivierungsenergien bei der Kohlendioxyd-Abspaltung und bei der Anlagerung an Benzol-Doppelbindung

Tadashi SUEHIRO und Mototoshi ISHIDA
Chemisches Institut der Gakushuin Universität, Mejiro, Tokio

(Eingegangen am 11. Januar, 1971)

Bei der Einwirkung von Trityl-Radikal auf Benzoylperoxyd-carbonyl-^{14}C, *p*-Chlorbenzoylperoxyd-carbonyl-^{14}C bzw. auf *p*-Methoxybenzoylperoxyd-carbonyl-^{14}C in Benzol bei 25°C und 45°C wurde die Ausbeute an Kohlendioxyd, Tetraphenylmethan und an Benzoesäure-trityl-ester nach der Isotopen-Verdünnungsmethode bestimmt. Aus der Abhängigkeit der Ausbeute von Temperatur wurden die relativen Aktivierungsenergien der Aroyloxy-Radikale bei der Kohlendioxyd-Abspaltung ($E_{1,r}$) und bei der Anlagerung an die Benzol-Doppelbindung ($E_{4,r}$) im Vergleich zu der bei der Kombination mit Trityl-Radikal (E_5) errechnet. Die relativen Aktivierungsenergien waren wie folgt: Bei Benzoyloxy-Radikal $E_{1,r}=12.9$ Kcal/Mol und $E_{4,r}=6.3$ Kcal/Mol; bei *p*-Chlorbenzoyloxy-Radikal $E_{1,r}=13.5$ Kcal/Mol und $E_{4,r}=6.2$ Kcal/Mol; bei *p*-Methoxybenzoyloxy-Radikal $E_{1,r}=14.7$ Kcal/Mol und $E_{4,r}=6.1$ Kcal/Mol.

Die Reaktivität des freien Radikals mit der Aktivierungsenergie der betreffenden Reaktionen zu bewerten ist von Bedeutung. Viele Forscher[1-4] nahmen Interesse an der Zersetzlichkeit des Aroyloxy-Radikals, darunter haben Bevington und seine Mitarbeiter[1] mit Hilfe der Vinyl-Polymerisationstechnik die Aktivierungsenergie vom Benzoyloxy-Radikal bei der Kohlendioxyd-Abspaltung (Reaktion (1)) auf 14 Kcal/Mol[1c] geschätzt. Die Unsicherheit ihrer Bestimmung besteht darin, dass sie statt der Aktivierungsenergie des Benzoyloxy-Radikals bei der Anlagerung an die Äthylen-Doppelbindung des Styrols (Reaktion (2)) die der Kettenwachstumsreaktion[5] von 7 Kcal/Mol, d. h. die der Anlagerung des Polymer Radikals an Olefin-Doppelbindung angenommen haben. Die Ergebnisse der anderen Forscher enthalten eine Aktivierungsenergie der entsprechenden Referrenz-Reaktion. Wir haben auf anderem Wege die Messungen der Aktivierungsenergie von Aroyloxy-Radikal bei der Kohlendioxyd-Abspaltung (Reaktion (1)) und bei der Anlagerung an Benzol (Reaktion (4)) vorgenommen, darüber wir hier berichten wollen.

$$ArCOO\cdot \longrightarrow Ar\cdot + CO_2 \quad (1)$$

$$ArCOO\cdot + PhCH{=}CH_2 \longrightarrow PhCHCH_2OCOAr \quad (2)$$

Experimentelle Methode und Ergebnisse

Wir haben uns mit der Einwirkung von Trityl-Radikal auf Benzoylperoxyd in aromatischen Lösungsmitteln beschäftigt,[6] dabei haben wir festgestellt, dass das Aroyloxy-Radikal, das aus Peroxyd durch Einwirkung von Trityl-Radikal erzeugt wird (Reaktion (3)), konkurrierend sich an den aromatischen Ring anlagert (Reaktion (4)) und sich mit Trityl-Radikal vereinigt (Reaktion (5)). Nebenbei läuft Reaktion (1) in geringerem Masse ab. Die Reaktion (4) führt weiter zur Bildung von Tetraphenylmethan (Reaktion (6)). Man kann daraus ersehen, dass die Reaktionen (1), (4), (5) und (6) zusammen die Reaktion von Benzoyloxy-Radikal in Aromaten in Gegenwart des Radikal-Abfängers Trityl-Radikals darstellen. Dass die Reaktion (4) die geschwindigkeits-bestimmende Stufe der Tetraphenylmethan-Bildung ist, ist ebenfalls bewiesen worden.[6c] Wenn man infolgedessen die Mengenverhältnisse von Kohlendioxyd und Tetraphenylmethan bezüglich auf Benzoesäure-trityl-ester aus der Reaktion (5) in ihrer Temperatur-Abhängigkeit bestimmt, so erhält man die Aktivierungsenergien der Reaktionen (1) und (4) relativ zu (5).

$$(ArCOO)_2 + Ph_3C\cdot \longrightarrow ArCOOCPh_3 + ArCOO\cdot \quad (3)$$

$$ArCOO\cdot + PhH \longrightarrow ArCOOPhH\cdot \quad (4)$$

$$ArCOO\cdot + Ph_3C\cdot \longrightarrow ArCOOCPh_3 \quad (5)$$

$$ArCOOPhH\cdot + Ph_3C\cdot \longrightarrow (ArCOOPhHCPh_3) \longrightarrow ArCOOH + PhCPh_3 \quad (6)$$

Obwohl die Aktivierungsenergie der Reaktion (5) noch nicht ermittelt wurde, lässt sie sich sicherlich als 0—3 Kcal/Mol verwerten, darüber wird nachher berichtet.

Wir haben bei 25°C und 45°C die Ausbeute an Kohlendioxyd und an Tetraphenylmethan bei der Einwirkung von Trityl-Radikal auf Benzoylperoxyd-carbonyl-^{14}C, *p*-Chlorbenzoylperoxyd-carbonyl-^{14}C und auf *p*-Methoxybenzoylperoxyd-carbonyl-^{14}C in Benzol ermittelt und daraus die Temperatur-Abhängigkeit der Geschwindigkeit der Reaktionen (1) und (4) bezüglich auf die Reaktion (5) errechnet. Die Ergebnisse sind in den Tabellen (1), (2) und (3) wiedergegeben.

Die Ausbeute an Benzoesäure-trityl-ester aus der Reaktion (5) wurde durch Abziehen der Ausbeute der Reaktionen (1) und (4) aus 100% erhalten. Die gute Ausbeute wurde mit der Isotopen-Verdünnungsmethode der gesamten Trityl-Gruppe von den Produkten Tetraphenylmethan und Benzoesäure-trityl-ester beim Um-

1) a) J.C. Bevington, *Proc. Roy. Soc., Ser. A*, **239**, 420 (1957); b) J. C. Bevington, *Trans. Faraday Soc.*, **53**, 997 (1957); c) J. C. Bevington und J. Toole, *J. Polym. Sci.*, **28**, 413 (1958); d) J. C. Bevington, J. Toole, und L. Trossarelli, *Trans. Faraday Soc.*, **54**, 863 (1958); e) J. C. Bevington, J. Toole, und L. Trossarelli, *Makromol. Chem.*, **28**, 237 (1958).

2) L. Jaffe und E. J. Prosen, *J. Chem. Phys.*, **27**, 416 (1957).

3) C. D. Cook und C. B. Depatie, *J. Org. Chem.*, **24**, 1144 (1959).

4) A. Yamamoto, N. Inamoto, N. Morikawa, und O. Simamura, gelesen vor der 19. Jahrestagung der Chem. Gesellschaft, Japan, April, 1966 in Tokio. Abstrakt III. Seite 113.

5) M. S. Matheson, E. E. Auer, E. B. Bevilacqua, und E. J. Hart, *J. Amer. Chem. Soc.*, **73**, 1700 (1951).

6) a) T. Suehiro, A. Kanoya, T. Yamauchi, T. Komori, und S. Igeta, *Tetrahedron*, **24**, 1551 (1968); b) T. Suehiro, S. Igeta, O. Kuwabara, und M. Hirai, *ibid.*, **26**, 963 (1970); c) T. Suehiro, S. Igeta, O. Kuwabara, M. Hirai, M. Ishida, und J. Yamazaki, Dieses Bulletin, **43**, 3303 (1970).

Tabelle 1. Die ausbeute an tetraphenylmethan, kohlendioxyd und benzoesäuretritylester bei der einwirkung von trityl-radikal auf benzoylperoxyd-carbonyl-^{14}C in benzol[a)]

Temp. °C	Ph_6C_2 mMol	Ph_4C-^{14}C: Zugabe d. markiert. Ph_4C, mg	Ph_4C-^{14}C: Isoliert. Ph_4C-^{14}C c/m/mg	Ph_4C-^{14}C: Isoliert. Ph_4C-^{14}C mMol	Ph_4C-^{14}C: Isoliert. Ph_4C-^{14}C Ausb.%	CO_2-^{14}C: Zugabe d. nicht markiert. CO_2, mMol	CO_2-^{14}C: Isoliert. Benzoesäure-phenacyl-ester c/m/mMol	CO_2-^{14}C: Isoliert. Benzoesäure-phenacyl-ester Ausb.%	Benzoesäure-trityl-ester Ausb.[b)] %
25	0.821	49.63	1247±9.2	0.374	45.6	2.336	40310±913	1.99	52.4
	0.810	43.56	1128±5.6	0.370	45.7	2.162	41540±517	1.92	52.4
45	0.822	50.88	1281±9.4	0.368	44.8	1.712	101150±1201	3.69	51.5
	0.803	48.42	1253±9.2	0.362	45.1	1.956	96940±1153	4.12	50.8

a) Die Ausbeute sind auf Mol Hexaphenyläthan bezogen.
b) Die Ausbeute vom Trityl-ester ist von der Reaktion 5.

Tabelle 2. Die ausbeute an tetraphenylmethan, kohlendioxyd und benzoesäuretritylester bei der einwirkung von trityl-radikal auf *p*-chlorbenzoylperoxyd-carbonyl-^{14}C in benzol[a)]

Temp. °C	Ph_6C_2 mMol	Ph_4C-^{14}C: Zugabe d. markiert. Ph_4C, mg	Ph_4C-^{14}C: Isoliert. Ph_4C-^{14}C c/m/mg	Ph_4C-^{14}C: Isoliert. Ph_4C-^{14}C mMol	Ph_4C-^{14}C: Isoliert. Ph_4C-^{14}C Ausb.%	CO_2-^{14}C: Zugabe d. nicht markiert. CO_2, mMol	CO_2-^{14}C: Isoliert. Benzoesäure-phenacyl-ester c/m/mMol	CO_2-^{14}C: Isoliert. Benzoesäure-phenacyl-ester Ausb.%	Benzoesäure-trityl-ester Ausb.[b)] %
25	0.803	33.97	820.1±4.1	0.437	54.4	2.350	15640±437	0.63	45.0
	0.806	32.39	791.7±5.3	0.435	54.0	2.509	15340±449	0.66	45.4
45	0.800	41.02	965.4±4.8	0.429	53.6	2.613	35650±464	1.61	44.8
	0.804	30.04	746.3±5.0	0.434	54.0	3.084	24620±541	1.30	44.7

a) Die Ausbeute sind auf Mol Hexaphenyläthan bezogen.
b) Die Ausbeute an Trityl-ester ist von der Reaktion 5.

Tabelle 3. Die ausbeute an tetraphenylmethan, kohlendioxyd und benzoesäuretritylester bei der einwirkung von trityl-radikal auf *p*-methoxybenzoylperoxyd-carbonyl-^{14}C in benzol[a)]

Temp. °C	Ph_6C_2 mMol	Ph_4C-^{14}C: Zugabe d. markiert. Ph_4C, mg	Ph_4C-^{14}C: Isoliert. Ph_4C-^{14}C c/m/mg	Ph_4C-^{14}C: Isoliert. Ph_4C-^{14}C mMol	Ph_4C-^{14}C: Isoliert. Ph_4C-^{14}C Ausb.%	CO_2-^{14}C: Zugabe d. nicht markiert. CO_2, mMol	CO_2-^{14}C: Isoliert. Benzoesäure-phenacyl-ester c/m/mMol	CO_2-^{14}C: Isoliert. Benzoesäure-phenacyl-ester Ausb.%	Benzoesäure-trityl-ester Ausb.[b)] %
25	0.801	33.57	1068.2±4.6	0.315	39.3	3.031	3263±221	0.20	60.5
	0.808	34.46	1077.4±4.7	0.320	39.6	3.240	4170±257	0.24	60.2
45	0.804	35.93	1124.7±4.8	0.315	39.2	2.993	9701±269	0.53	60.3
	0.807	35.50	1109.1±4.7	0.317	39.3	2.492	11826±278	0.54	60.2

a) Die Ausbeute sind auf Mol Hexaphenyläthan bezogen.
b) Die Ausbeute an Trityl-ester ist von der Reaktion 5.

setzen von Benzoylperoxyd, 96—97% bezogen auf 2 mal Mol Hexaphenyläthan festgestellt.

Die Bestimmung der Ausbeute an Kohlendioxyd und an Tetraphenylmethan wurde nach der Isotopen-Verdünnungsmethode durchgeführt. Das entwickelte Kohlendioxyd-^{14}C wurde zunächst durch die Grignard-Reaktion in Benzoesäure-carbonyl-^{14}C übergeführt und als Benzoesäure-phenacyl-ester ermittelt. Der Isotopie-Effekt bei der Grignard-Reaktion kann rechnerisch vernachlässigt werden, weil die Reaktion in guter Ausbeute (75—78% nach der Reinigung durch Sublimation) verläuft und der Fehler höchstens nur wenige Prozent beträgt.

Die Geschwindigkeit der Kohlendioxyd-Abspaltung (Reaktion (1)) bei 25°C relativ zu der Ester-Bildung (Reaktion (5)) kann man wie folgt ausdrücken:

$$[d(CO_2)/dt/d(\text{Trityl-ester})/dt]_{25} = k_{1,25}(ArCOO\cdot)_{25}/k_{5,25}(ArCOO\cdot)_{25}(Ph_3C\cdot)_{25} \quad (7)$$

Auf gleiche Weise erhält man für 45°C die Gleichung (8):

$$[d(CO_2)/dt/d(\text{Trityl-ester})/dt]_{45} = k_{1,45}(ArCOO\cdot)_{45}/k_{5,45}(ArCOO\cdot)_{45}(Ph_3C\cdot)_{45} \quad (8)$$

Die Temperatur-Abhängigkeit der relativen Geschwindigkeit, Reaktion (1) gegenüber Reaktion (5), kann man folgenderweise formulieren:

$$\frac{k_{1,45}/k_{5,45}(Ph_3C\cdot)_{45}}{k_{1,25}/k_{5,25}(Ph_3C\cdot)_{25}} = \frac{[d(CO_2)/dt/d(\text{Trityl-ester})/dt]_{45}}{[d(CO_2)/dt/d(\text{Trityl-ester})/dt]_{25}} \quad (9)$$

Wenn Hexaphenyläthan in derselben Konzentration verwendet wird, kann man die Konzentration bei 45°C, $(Ph_3C\cdot)_{45}$, im Vergleich zu der Konzentration bei 25°C aus den Dissoziationskonstanten, $K_{25}=5.72\times10^{-4}$ und $K_{45}=20.9\times10^{-4}$ Mol/l[7)], als $1.92=(20.9/5.72)^{1/2}$ er-

TABELLE 4. AKTIVIERUNGSENERGIEN DER AROYLOXY-RADIKALE (Kcal/Mol)

Substituent vom Benzoylperoxyd	Kohlendioxyd-Abspaltung	Anlagerung an Benzol-Doppelbinding	Kombination mit Trityl-Radikal
(H)	$12.9+E_5$ (± 0.9)	$6.3+E_5$ (± 0.1)	(E_5 $=2.0$)
p-Cl	$13.5+E_5'$ (± 1.5)	$6.2+E_5'$ (± 0.1)	(E_5' $=1.5$)
p-CH_3O	$14.7+E_5''$(± 0.8)	$6.1+E_5''$(± 0.1)	($E_5''$$=1.5$)

rechnen. Weiter bei Ersetzen
$[d(CO_2)/dt/d(\text{Trityl-ester})/dt]$ durch $[(CO_2\%)/(\text{Trityl-ester}_{\text{Reakt.5}}\%)]$
erhält man folgende Gleichung:

$$\frac{(k_1/k_5)_{45}}{(k_1/k_5)_{25}} = \frac{1.92\times[(CO_2\%)/(\text{Trityl-ester}\%)]_{45}}{[(CO_2\%)/(\text{Trityl-ester}\%)]_{25}} \quad (10)$$

Beim Auftragen von log (k_1/k_5) gegen $1/T$ erhält man $E_1-E_5=12.9$ Kcal/Mol für Benzoyloxy-Radikal, 13.6 Kcal/Mol für *p*-Chlorbenzoyloxy-Radikal und 14.7 Kcal/Mol für *p*-Methoxybenzoyloxy-Radikal.

Auf gleiche Weise errechnet man für $E_4-E_5=$ 6.3 Kcal/Mol für Benzoyloxy-Radikal, 6.2 Kcal/Mol für *p*-Chlorbenzoyloxy-Radikal und 6.1 Kcal/Mol für *p*-Methoxybenzoyloxy-Radikal. Sie sind in Tabelle 4 zusammengestellt.

Diskussion

Die genaue zahlenmässige Verwertung von E_5, E_5' und E_5'' ist schwierig. Man hat dazu als Vergleichswert 0—2 Kcal/Mol bei Kombination zweier kleiner Alkyl-Radikale[8] und 1—5 Kcal/Mol bei den grösseren und polymeren Alkyl-Radikalen[9]. Ungefähr 7 Kcal/Mol findet man für die Kombination zweier Trityl-Radikale.[7b] Wir nehmen vorläufig einfach $E_5=$ 2.0 Kcal/Mol an, weil man bei der Annahme des geometrischen Mittelwerts der Reaktionsgeschwindigkeit der Kreuz-Kombination eine Aktivierungsenergie von 3.5 Kcal/Mol[10] erhält und weil die Kombination wegen der polaren Eigenschaften der Reaktionspartner beschleunigt werden kann.[11] E_5' ist wahrscheinlich kleiner als E_5, weil *p*-Chlorbenzoyloxy-Radikal elektronegativer als Benzoyloxy-Radikal ist. Den Unterschied, $E_5-E_5'=0.5$ Kcal/Mol ziehen wir aufgrund der Differenz der Aktivierungsenergie von 1.2 Kcal/Mol zwischen den durch Trityl-Radikal induzierten Zersetzungen von Benzoyl- und *p*-Chlorbenzoylperoxyden[7a] vor. Ähnlicherweise nehmen wir an $E_5-E_5''=$ 0.5 Kcal/Mol.[7a]

Unter dieser Annahme erhält man $E_1=15$ Kcal/Mol für Benzoyloxy- und *p*-Chlorbenzoyloxy-Radikale und 16.2 Kcal/Mol für *p*-Methoxybenzoyloxy-Radikal. Weiter errechnet man $E_4=8.3$ Kcal/Mol für Benzoyloxy-Radikal, $E_4'=7.7$ Kcal/Mol für *p*-Chlorbenzoyloxy-Radikal und $E_4''=7.6$ Kcal/Mol für *p*-Methoxybenzoyloxy-Radikal.

Der Wert 15 Kcal/Mol für E_1 steht in guter Übereinstimmung mit dem von 14 Kcal/Mol von Bevington und anderen.[1c] Simamura und andere[4] berichteten den Unterschied von 10 Kcal/Mol zwischen den Aktivierungsenergien bei der Kohlendioxyd-Abspaltung von Benzoyloxy- und Acetyloxy-Radikalen. Nimmt man den Wert 6.6 Kcal/Mol[12] für Acetyloxy-Radikal an, so rechnet man für E_1 16.6 Kcal/Mol, der auch dem anderen Wert nahekommt. Unser Ergebnis $E_1''=$ 16.2 Kcal/Mol steht auch im Einklang mit dem 17 Kcal/Mol von Bevington und anderen.[1d] Der *p*-Chlor-Substituent übt keine merkliche Wirkung auf die Aktivierungsenergie bei der Zersetzung von Aroyloxy-Radikal in Aryl-Radikal und Kohlendioxyd aus, dagegen erhöht der *p*-Methoxy-Substituent die Aktivierungsenergie.

Die erhaltenen Ergebnisse von der Aktivierungsenergie der Reaktion (4) sind plausibel klein, wenn man auf die schnelle umkehrbare Anlagerung des Aroyloxy-Radikals an die aromatische Doppelbindung[13] Rücksicht nimmt. Für die rapide Anlagerungsreaktion des Aroyloxy-Radikals an die Benzol-Doppelbindung konnten wir keinen Einfluss der Substituenten *p*-Methoxy-, H und *p*-Chlor- auf die Aktivierungsenergie differenzieren. Man kann sich hier nur qualitativ vorstellen, dass Aroyloxy-Radikal mit negativen Substituenten sich schneller an die Doppelbindung anlagert als das Radikal mit positiven Substituenten.

Beschreibung der Versuche

Die typische Durchführung der Versuche ist folgende: Man löst im Dunkeln in der Stickstoff-Atmosphäre 399.07 mg (0.821 mMol) Hexaphenyläthan und 223.67 mg (0.924 mMol) Benzoylperoxyd-carbonyl-^{14}C (24046±43 c/m/mg) in je 20 m*l*

7) a) T. Suehiro, A. Kanoya, H. Hara, T. Nakahama, M. Omori, und T. Komori, Dieses Bulletin, **40**, 668 (1967); b) K. Ziegler und L. Ewald, *Ann.*, **473**, 163 (1929). Der Wert bei 45°C wurde durch Extrapolation erhalten.

8) F. Moseley und J. C. Robb, *Proc. Roy. Soc., Ser. A*, **243**, 119 (1957); G. O. Pritchard und J. R. Dacery, *Can. J. Chem.*, **38**, 182 (1960); A. Shepp und K. O. Kutschke, *J. Chem. Phys.*, **26**, 1020 (1957); G. O. Pritchard, Y. P. Hsia, und G. H. Miller, *J. Amer. Chem. Soc.*, **85**, 1568 (1963); Priv. Mitt. zitiert in H. W. Melville, J. C. Robb, und R. C. Tutton, *Discuss. Faraday Soc.*, **14**, 150 (1953).

9) W. I. Bengough und H.W. Melville, *Proc. Roy. Soc., Ser. A*, **230**, 429 (1955); M. S. Matheson, E. E. Auer, E. B. Bevilacqua, und E. J. Hart, *J. Amer. Chem. Soc.*, **71**, 497 (1949); M. S. Matheson, E. E. Auer, E. B. Bevilacqua, und E. J. Hart, *ibid.*, **73**, 5395 (1951); N. Grassie und E. Vance, *Trans. Faraday Soc.*, **52**, 727 (1956).

10) Wir nehmen den Wert 0 Kcal/Mol für die Aktivierungsenergie der Kombination zweier Benzoyloxy-Radikale an, dazu haben wir als Vergleichswert 0 Kcal/Mol für *t*-Butoxy-Radikal (D. J. Carlsson und K. U. Ingold, *J. Amer. Chem. Soc.*, **89**, 4891 (1967)).

11) Die Geschwindigkeit der Kombination von Trichlormethyl-Radikal mit 2-Trichlormethylcyclohexyl-Radikal ist 7 mal oder noch grösser als die Kombination zweier Trichlormethyl-Radikale oder zweier 2-Trichlormethylcyclohexyl-Radikale (H. W. Melville, J. C. Robb, und R. C. Tutton, *Discuss. Faraday Soc.*, **14**, 150 (1953)). Wenn man annimmt, dass die Beschleunigung aus der Verminderung der Aktivierungsenergie herkommt, beträgt sie *ca.* 1.5 Kcal/Mol.

12) W. Braun, L. Rajbenbach, und F. R. Eirich, *J. Phys. Chem.*, **66**, 1591 (1962).

13) T. Nakata, K. Tokumaru, und O. Simamura, *Tetrahedron Lett.*, **1967**, 3303.

Sauerstoff freiem reinem Benzol und stellt sie gesondert in eine umgekehrt U-förmige Reaktionsapparatur. Nach dem Kühlen der beiden Lösungen mit flüssigem Stickstoff evakuiert man die Apparatur und schliesst sie im Vakuum ab. Man erwärmt im Dunkeln die Apparatur in einem Thermostat von 25°C solange, bis die Lösungen die Temperatur erreichen und sich vermischen und lässt sie im Thermostat 4 Stunden stehen. Man kühlt die Mischung mit flüssigem Stickstoff ab und verbindet die Apparatur mit einem Vakuum-System, das von einer Ampulle mit 2.53 mMol Phenylmagnesiumbromid in 5 m*l* Äther und von einem Reservoir mit nicht radioaktivem Kohlendioxyd eingerichtet ist. Man destilliert das Kohlendioxyd, das bei der Umsetzung von Trityl-Radikal mit Peroxyd entwickelt wurde, in die Grignard-Lösung ein, während man die Mischung der Umsetzung bei Raumtemperatur und das Grignard-Reagens bei der Temperatur des flüssigen Stickstoffs hält. Aus dem Kohlendioxyd-Reservoir destilliert man 2.336 mMol von nicht markiertem Kohlendioxyd in zwei Portionen zunächst in die Umsetzungsmischung von Trityl-Radikal und Peroxyd ein und anschliessend von dort aus in das Grignard-Reagens über. Man schmilzt dann die Grignard-Mischung im Ampulle ein und lässt die Mischung über Nacht bei Raumtemperatur einwirken. Man zersetzt die Mischung der Grignard-Reaktion mit 6N Salzsäure, reinigt die rohe Benzoesäure durch Vakuum-Sublimation und führt sie in den Phenacyl-ester. Man reinigt den Ester zunächst durch Chromatographie an Aluminiumoxyd mit Essigester als Laufmittel und dann durch Kristallisation aus Isopropanol, bis der konstante Schmelzpunkt von 119—119.5°C erreicht wird (Probe für die Analyse des Phenacyl-esters). Zu der Reaktionsmischung vom Trityl und Peroxyd fügt man 49.63 mg des markierten Tetraphenylmethan (4245±15 c/m/mg), zersetzt den Überschuss vom Peroxyd durch Natriumjodid in Aceton, trennt Benzoesäure ab, und chromatographiert die neutralen Produkte an Aluminiumoxyd mit Benzol-*n*-Hexan als Laufmittel. Das eluierte rohe Tetraphenylmethan-^{14}C reinigt man durch Vakuum-Sublimation bei 200°C und durch mehrmalige Umkristallisation aus Benzol, bis der Schmelzpunkt 286—286.5°C (im Einschlussrohr) erreicht wird (Probe für die Analyse des Tetraphenylmethans).

Die Bestimmung der Radioaktivität erfolgte mit einem Gerät von Beckman LS-200 Szintirationszähler mit PO-POP-PPO in Toluol. Für diese Bestimmung danken wir Herrn Dr. N. Morikawa von der Universität Tokio vielmals.

BULLETIN OF THE CHEMICAL SOCIETY OF JAPAN, VOL. 44, 1695—1697 (1971)

Nucleoside Analogs. II. A Synthesis of 9-Adenyl-deoxyinositols

Tetsuo SUAMI, Yasushi FUKAI, Yukio SAKOTA, Makoto KARIMOTO, Nobuo TAKOI, and Yoko TSUKAMOTO

Department of Applied Chemistry, Faculty of Engineering Keio University, Koganei-shi, Tokyo

(Received January 30, 1971)

Four 9-adenyl-deoxyinositols were prepared by a reaction between 4-amino-6-chloro-5-nitropyrimidine (**1**) and inosamines (**2a**, **2b**, **2c**, and **2d**), followed by a reduction and a cyclization. In the present article, 1-(6′-amino-9′-purinyl)-1-deoxy-*scyllo*-inositol (**5a**), 1-(6′-amino-9′-purinyl)-1-deoxy-*muco*-inositol (**5b**), 2-(6′-amino-9′-purinyl)-2-deoxy-*epi*-inositol (**5c**), and 2-(6′-amino-9′-purinyl)-2-deoxy-*myo*-inositol (**5d**) were described. These compunds exhibited an inhibitory effect against *piricularia oryzae*.

An alternation of a ribose moiety in naturally occurring adenosine may yield a biologically active nucleoside analog. Along this consideration, dihydroxycyclohexane analogs of the nucleoside have been described in a previous paper.[1)]

In connection with the previous paper of this series,[1)] four biologically active 9-adenyl-deoxyinositols (**5a**, **5b**, **5c**, and **5d**) have been prepared by a reaction between 4-amino-6-chloro-5-nitropyrimidine (**1**)[2)] and inosamines (**2a**, **2b**, **2c**, and **2d**), followed by reduction of a nitro group and cyclization of an imidazole ring, which will be described in the present article.

When a mixture of **1** and *scyllo*-inosamine (**2a**),[3,4)] was heated in 2-methoxyethanol under reflux for 20 hr, 1-(4′-amino-5′-nitro-6′-pyrimidinylamino)-1-deoxy-*scyllo*-inositol (**3a**) was obtained in 78% yield. Reduction of **3a** with zinc powder in boiling water afforded 1-(4′,5′-diamino-6′-pyrimidinylamino)-1-deoxy-*scyllo*-inositol (**4a**) in 87% yield, which was used for a successive synthesis without any further purification. Cyclization of **4a** was carried out by heating in formamide to give 1-(6′-amino-9′-purinyl)-1-deoxy-*scyllo*-inositol (**5a**) in a yield of 52%. The compound **5a** showed an ultraviolet absorption characteristic of an adenine at 263 mμ.[5)]

An analogous reaction beginning with *muco*-inosamine-1 (**2b**)[4)] and **1** afforded 1-(6′-amino-9′-purinyl)-1-deoxy-*muco*-inositol (**5b**) in 25% yield.

Reactions between *epi*-inosamine-2 (**2c**)[3,6,7)] and **1**

1) T. Suami, Y. Sato, Y. Fukai, and Y. Sakota, *J. Heterocycl. Chem.*, **6**, 663 (1969).
2) W. R. Boon, W. G. M. Jones, and G. R. Ramage, *J. Chem. Soc.*, **1951**, 99.
3) H. E. Carter, R. K. Clark, Jr., B. Lytle, and G. E. McCasland, *J. Biol. Chem.*, **175**, 683 (1948).
4) T. Suami, F. W. Lichtenthaler, and S. Ogawa, This Bulletin, **39**, 170 (1966).
5) R. K. Robins, K. J. Dille, C. H. Willits, and B. E. Christensen, *J. Amer. Chem. Soc.*, **75**, 263 (1953).
6) E. L. May and E. Mosettig, *J. Org. Chem.*, **14**, 1137 (1947).
7) T. Suami, S. Ogawa, Y. Nakashima, and H. Sano, This Bulletin, **40**, 2958 (1967).

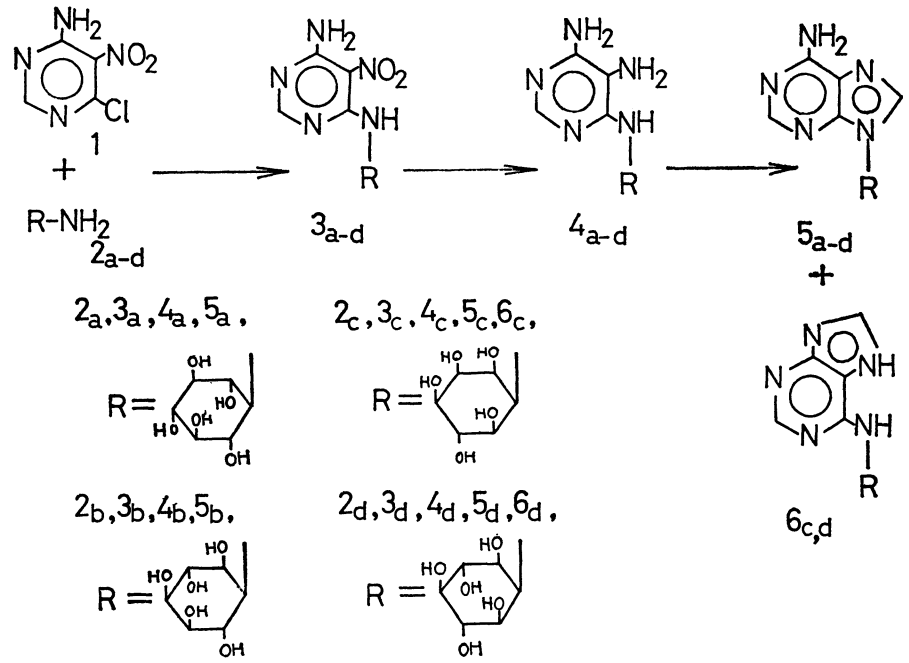

and between *myo*-inosamine-2 (**2d**)[3,8,9] and **1** yielded 2-(6′-amino-9′-purinyl)-2-deoxy-*epi*-inositol (**5c**) and 2-(6′-amino-9′-purinyl)- 2-deoxy-*myo*-inositol (**5d**) respectively by an analogous after-treatment. In these reactions, besides the compounds **5c** and **5d**, 2-(6′-purinylamino)-2-deoxy-*epi*-inositol (**6c**) and 2-(6′-purinylamino)-2-deoxy-*myo*-inositol (**6d**) were obtained. These structural assignments were agreeable with their ultraviolet absorption maxima.[10–12]

The biological activities of 9-adenyl-deoxyinositols against *piricularia oryzae* will be reported elsewhere.

Experimental

Melting points were determined on a Mitamura Riken micro hot stage and uncorrected. The infrared spectra were determined in a potassium bromide disc with a Hitachi EPI-2 spectrometer. The ultraviolet absorption spectra were determined in water with a Hitachi EPS-2 spectrometer.

4-Amino-6-chloro-5-nitropyrimidine (1). The compound was prepared by the method of Boon and coworkers.[2]

Scyllo-*Inosamine (2a).* The compound was prepared by the method of Suami and coworkers.[4]

1-(4′-Amino-5′-nitro-6′-pyrimidinylamino)-1-deoxy-scyllo-*inositol (3a).* A mixture of 1.75 g of **1** and 1.79 g of **2a** in 200 m*l* of 2-methoxyethanol was heated under reflux in a presence of a small amount of triethylamine for 20 hr. After the mixture was settled overnight at room temperature, crystals were collected by filtration and washed with water to give 2.48 g (78% yield) of the product, mp above 300°C.

Found: C, 37.87; H, 4.90; N, 21.71%. Calcd for $C_{10}H_{15}N_5O_7$: C, 37.86; H, 4.77; N, 22.08%.

1-(4′,5′-Diamino-6′-pyrimidinylamino)-1-deoxy-scyllo-*inositol (4a).* To a suspension of 60 g of zinc powder in 600 m*l* of boiling water, 1.0 g of **3a** was added with a mechanical agitation. The mixture was heated under reflux for 6 hr, and then it was filtered. The filtrate was evaporated under reduced pressure to a 100 m*l* volume. The residual solution was settled at room temperature to give pale yellow crystals. Crystals were collected by filtration to give 0.79 g (87% yield) of the product, mp 281—283°C (dec.).

1-(6′-Amino-9′-purinyl)-1-deoxy-scyllo-*inositol (5a).* A 0.5 g-portion of **4a** was heated with 10 m*l* of formamide under reflux for 40 min. After the mixture was settled overnight at room temperature, crystals were collected by filtration to give 0.39 g of a crude product. The product (200 mg) was dissolved in boiling water (200 m*l*) and the solution was decolorized with active charcoal. After cooling, the solution gave 0.14 g (53% yield) of crystals which were collected by filtration, mp above 300°C. UV λ_{max} (pH 1) 258; (pH 7) 263; (pH 13) 263 mμ.

Found: C, 44.42; H, 5.44; N, 23.81%. Calcd for $C_{11}H_{15}N_5O_5$: C, 44.44; H, 5.09; N, 23.56%.

muco-*Inosamine-1 (2b).* Hexaacetyl *muco*-inosamine-1 was prepared by the method of Suami and coworkers.[4] A 6.0 g-portion of the hexaacetyl derivative was hydrolyzed in 6N hydrochloric acid and then treated with Amberlite IRA-400 to give 2.03 g (81% yield) of **2b**, mp 184—200°C (dec.).

1-(4′A-mino-5′-nitro-6′-pyrimidinylamino)-1-deoxy-muco-*inositol (3b).* A mixture of 0.49 g of **1** and 0.54 g of **2b** was heated in 2-methoxyethanol (40 m*l*) for 3 hr under reflux with a small amount of triethylamine. The mixture was evaporated *in vacuo* and the residue was crystallized in water. The crystals were collected by filtration and washed with chloroform to give 0.68 g (77% yield) of **3b**, mp 260—261°C.

Found: C, 37.77; H, 4.88; N, 21.88%. Calcd for $C_{10}H_{15}N_5O_7$: C, 37.86; H, 4.77; N, 22.07%.

1-(4′,5′-Diamino-6′-pyrimidinylamino)-1-deoxy-muco-*inositol (4b).* A 1.0 g-portion of **3b** was reduced by analogous procedures as described in **4a** to give 0.73 g (81% yield) of **4b**, mp 166—171°C.

1-(6′-Amino-9′-purinyl)-1-deoxy-muco-*inositol (5b).* A

8) G. E. McCasland and E. C. Horswill, *J. Amer. Chem. Soc.*, **75**, 4020 (1953).

9) T. Suami, S. Ogawa, and M. Uchida, This Bulletin, **43**, 3577 (1970).

10) T. Okano, S. Goya, A. Takadate, and Y. Ito, *J. Pharm. Soc. Jap.* **86**, 649 (1966).

11) G. B. Elion, E. Burgi, and G. H. Hitchings, *J. Amer. Chem. Soc.*, **74**, 411 (1952).

12) J. A. Montgomery and L. B. Holum, *ibid.*, **80**, 404 (1958).

0.5 g-portion of **4b** was heated in formamide (10 ml) for 30 min. The mixture was treated analogously by the method as described in **5a** to give 0.27 g of a crude product. Recrystallization from water afforded 0.21 g (41% yield) of **5b**, mp 287—288.5°C. UV λ_{max} (pH 1) 259; (pH 7) 260; (pH 13) 261 mμ.

Found: C, 44.34; H, 5.35; N, 23.31%. Calcd for $C_{11}H_{15}N_5O_5$: C, 44.44; H, 5.09; N, 23.56%.

epi-*Inosamine-2 (**2c**)*. *epi*-Inosamine-2 hydrochloride was prepared by the method of Suami and coworkers.[7] The hydrochloride was treated with Amberlite IRA-400 to give **2c** in 90% yield. Mp 195—200°C (dec.).

2-(4'-Amino-5'-nitro-6'-pyrimidinylamino)-2-deoxy-epi-*inositol (**3c**)*. A mixture of **1** (1.40 g) and **2c** (2.16 g) was heated in 2-methoxyethanol for 3 hr as described in **3a** to give 2.57 g of a crude product. Recrystallization from water afforded 2.36 g (93% yield) of **3c**, mp 264—265°C.

Found: C, 37.77; H, 4.90; N, 21.80%. Calcd for $C_{10}H_{15}N_5O_7$: C, 37.86; H, 4.77; N, 22.08%.

2-(4',5'-Diamino-6'-pyrimidinylamino)-2-deoxy-epi-*inositol (**4c**)*. (A) **3c** (1.54 g) was reduced with zinc powder (10 g) in boiling water (100 ml) analogously as described in **4a** to give 1.07 g of a crude product. Recrystallization from water afforded 0.87 g (62% yield) of **4c**, mp 165—170°C. (B) To a mixture of ferrous sulfate (8.9 g) and barium hydroxide (10.6 g) in 100 ml of water, **3c** (1.0 g) was added with agitation and the mixture was heated at 90°C for 30 min. The warm mixture was filtered and the filtrate was evaporated under reduced pressure to 20 ml. The residual solution was settled in a refrigerator to give 0.73 g (81% yield) of **4c** as pale yellow crystals, mp 166—171°C.

2-(6'-Amino-9'-purinyl)-2-deoxy-epi-*inositol (**5c**) and 2-(6'-purinylamino)-2-deoxy*-epi-*inositol (**6c**)*. **4c** (0.70 g) was heated in formamide (10 ml) for 30 min under reflux. The mixture was evaporated *in vacuo* and the residue was warmed in 0.4 N hydrochloric acid (14 ml) for 30 min at 50°C. The solution was passed through a column (1.5 cmφ) of Amberlite CG-120 (H^+ form) and subsequently the column was washed with water. The product was eluted from the column with 2.5N ammonia (100 ml) and the eluate was decolorized with active charcoal. The solution was evaporated under reduced pressure to a small volume, and the residue was settled in a refrigerator to give 0.38 g of a crude product. The product was recrystallized from water to give 0.11 g (15% yield) of **5c** as needle crystals, mp 282—283°C. UV λ_{max} (pH 1) 261; (pH 7) 262; (pH 13) 263 mμ.

Found: C, 44.50; H, 5.37; N, 23.70%. Calcd for $C_{11}H_{15}N_5O_5$: C, 44.44; H, 5.09; N, 23.56%.

From the mother liquor of **5c**, another crop of crystal was obtained. Recrystallization from water afforded 0.19 g (26% yield) of crystals, mp above 310°C. The product was identified to be **6c**. UV λ_{max} (pH 1) 275; (pH 7) 268; (pH 13) 275 mμ.

Found: C, 44.64; H, 5.53; N, 23.38%. Calcd for $C_{11}H_{15}N_5O_5$: C, 44.44; H, 5.09; N, 23.56%.

myo-*Inosamine-2 (**2d**)*. Hexaacetyl *myo*-inosamine-2[3] was prepared by the method of Suami and coworkers[9] beginning with pentaacetyl 1-bromo-1-deoxy-*scyllo*-inositol.[8] **2d** was obtained from the hexaacetyl compound by an analogous method used for **2b**. Mp 263—265°C (dec.).

2-(4'-Amino-5'-nitro-6'-pyrimidinylamino)-2-deoxy-myo-*inositol (**3d**)*. A mixture of **1** (0.35 g) and **2d** (0.40 g) was heated in 2-methoxyethanol for 3 hr as described in **3a** to give 0.57 g (90% yield) of crystals, mp 302—304°C (dec.).

Found: C, 37.76; H, 4.91; N, 21.98%. Calcd for $C_{10}H_{15}N_5O_7$: C, 37.86; H, 4.77; N, 22.07%.

2-(4',5'-Diamino-6'-pyrimidinylamino)-2-deoxy-myo-*inositol (**4d**)*. A 1.0 g-portion of **3d** was reduced with zinc powder as described in **4a** to give 0.67 g (74% yield) of the product as pale yellow needles, mp 294—304°C (dec.).

2-(6'-Amino-9'-purinyl)-2-deoxy-myo-*inositol (**5d**) and 2-(6'-purinylamino)-2-deoxy*-myo-*inositol (**6d**)*. A 2.5 g-portion of **4d** was heated in formamide (70 ml) for 1 hr in a nitrogen atomosphere. The reaction mixture was treated analogously as described in **5c** to give 0.82 g of a crude product. Recrystallization from water afforded 0.41 g (16% yield) of needles of mp 257—258.5°C (dec.), which was identified to be **6d**. UV λ_{mxa} (pH 1) 266; (pH 7) 270; (pH 13) 276 mμ.

Found: C, 44.44; H, 4.77; N, 23.81%. Calcd for $C_{11}H_{15}N_5O_5$: C, 44.44; H, 5.09; N, 23.56%.

From the mother liquor, 0.15 g (6% yield) of crystals were obtained, which was identified to be **5d**. Mp 325—327°C (dec.). UV λ_{max} (pH 1) 260; (pH 7) 261; (pH 13) 262 mμ.

Found: C, 44.46; H, 5.20; N, 23.73%. Calcd for $C_{11}H_{15}N_5O_5$: C, 44.44; H, 5.09; N, 23.56%.

The authors are grateful to professor Sumio Umezawa for his helpful advice and Mr. Saburo Nakada for his elementary analyses. This research has been supported financially in part by a grant of the Japanese Ministry of Education, to which the authors' thanks are due.

NOTES

BULLETIN OF THE CHEMICAL SOCIETY OF JAPAN, VOL. 44, 1698—1699 (1971)

Synthetic Studies of the Flavone Derivatives. XXII.[1] The Synthesis of Eupatoretin and Eupatin

Kenji FUKUI, Takashi MATSUMOTO, and Sachihiko IMAI

Department of Chemistry, Faculty of Science, Hiroshima University, Higashi-sendamachi, Hiroshima

(Received December 7, 1970)

Recently, Kupchan *et al.*[2] reported the isolation of two new cytotoxic flavonols, eupatoretin and eupatin, from *Eupatorium semiserratum*. On the bases of chemical and spectral studies, they proposed that the structures of these flavonols were 3,3′-dihydroxy-4′,5,6,7-tetramethoxyflavone (I) for eupatoretin and 3,3′,5-trihydroxy-4′,6,7-trimethoxyflavone (II) for eupatin. In a previous paper,[3] we reported the synthesis of 3,4′,5-trihydroxy-3′,6,7-trimethoxyflavone (III), an isomer of eupatin, the structure of which had earlier been assigned to chrysosplenetin.[4]

For the structural confirmation of these natural pigments, we have now studied the syntheses of flavonols, I and II. By the method of Hörhammer *et al.*,[5] 3-benzyloxy-2′-hydroxy-4,4′,5′,6′-tetramethoxychalcone (IV) was converted into 3′-benzyloxy-3-hydroxy-4′,5,6,7-tetramethoxyflavone (V) in an 18% yield under improved reaction conditions without chromatographic purification (lit.[5]:10% yield after chromatography). The catalytic debenzylation of V in ethanol in the presence of Pd-C (10%) gave I, mp 150—151°C, which was shown to be identical with natural eupatoretin by a mixed-melting-point determination and by a spectral comparison. The synthetic I was further characterized by the preparation of its diacetate (VI), mp 151—152°C. Subsequently, the selective demethylation[3] of the C_5-methoxyl group in I with anhydrous aluminum chloride in dry nitrobenzene was carried out; the demethylated flavonol II was thus obtained as golden yellow needles, mp 244.5—245.5°C, which then gave triacetate (VII), mp 218—220°C. The synthetic II was also found to be identical with natural eupatin by a direct comparison.

The structures of eupatoretin and eupatin are thus confirmed to be I and II respectively.

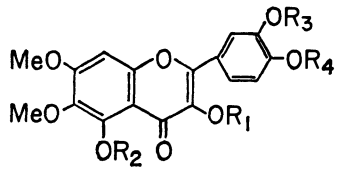

I $R_1=R_3=H$, $R_2=R_4=Me$
II $R_1=R_2=R_3=H$, $R_4=Me$
III $R_1=R_2=R_4=H$, $R_3=Me$
V $R_1=H$, $R_2=R_4=Me$, $R_3=Bz$
VI $R_1=R_3=Ac$, $R_2=R_4=Me$
VII $R_1=R_2=R_3=Ac$, $R_4=Me$

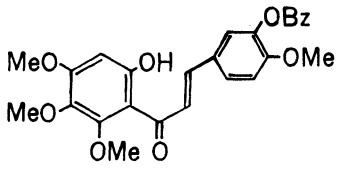

IV

Experimental[6]

3′-Benzyloxy-3-hydroxy-4′,5,6,7-tetramethoxyflavone (V). To a hot solution of IV (830 mg) in methanol (83 ml), we added hydrogen peroxide (30%: 3.5 ml) and an aqueous potassium hydroxide solution (20%: 13 ml). The mixture was refluxed for 1 min, poured into a mixture of ice and water (300 ml), and then immediately acidified with dilute hydrochloric acid. The yellow precipitates were collected, washed with water, and then recrystallized from ethanol to give V as yellow needles, mp 146—148°C, which gave a brown ferric chloride reaction in ethanol; yield, 150 mg (18%) (lit.[5] mp 142—143°C, yield 10%). UV λ_{max}^{EtOH} mμ (log ε); 235[7] (4.35), 254.5 (4.37), 360 (4.36).

3,3′-Dihydroxy-4′,5,6,7-tetramethoxyflavone (I). A solution of V (145 mg) in ethanol (50 ml) was submitted to catalytic hydrogenolysis at *ca.* 30°C in the presence of Pd-C (10%: 75 mg). After the catalyst had been filtered off, the filtrate was evaporated and the residue was recrystallized from benzene to give I as bright yellow plates, mp 150—151°C, which gave a brown ferric chloride reaction in ethanol; yield, 75 mg (62%). The mixed melting point with natural eupatoretin (mp 150—152°C[8]) was 150—152°C. UV: λ_{max}^{EtOH} mμ (log ε); 256 (4.34), 361 (4.29).

Found: C, 60.96; H, 4.72%. Calcd for $C_{19}H_{18}O_8$: C, 60.96; H, 4.85%.

3,3′-Diacetoxy-4′,5,6,7-tetramethoxyflavone (VI). A mixture of I (30 mg), acetic anhydride (0.4 ml), and dry pyridine (0.6 ml) was refluxed for 1 hr. The crude product was

1) Part XXI: M. Nakayama, K. Fukui, T. Horie, Y. Shimizu, and M. Masumura, *Nippon Kagaku Zasshi*, **91**, 1174 (1970).

2) S. M. Kupchan, C. W. Sigel, J. R. Knox, and M. S. Udayamurthy, *J. Org. Chem.*, **34**, 1460 (1969).

3) K. Fukui, T. Matsumoto, and S. Tanaka, This Bulletin, **42**, 1398 (1969).

4) M. Shimizu and N. Morita, *Chem. Pharm. Bull.* (Tokyo), **16**, 2310 (1968).

5) L. Hörhammer, H. Wagner, H. Rösler, E. Graf, and L. Farkas, *Chem. Ber.*, **97**, 2857 (1964).

6) All melting points were uncorrected.

7) Schoulder.

8) Observed in this laboratory.

recrystallized from benzene containing *n*-hexane to give the diacetate (VI) as colorless needles, mp 151—152°C, which gave a negative ferric chloride reaction in ethanol; yield, 27 mg (73%). UV: λ_{max}^{EtOH} mμ (log ε); 232[7](4.33), 264.5 (4.25), 319(4.42). Lit.[2] mp 145—147°C, UV: λ_{max}^{EtOH} mμ (ε); 235(28300), 263(25000), 316(31000).

3,3′,5-Trihydroxy-4′,6,7-trimethoxyflavone (II). The flavonol I (50 mg) was added to a mixture of anhydrous aluminum chloride (0.5 g) and dry nitrobenzene (5.0 m*l*). The mixture was allowed to stand at room temperature for 5 hr and then poured into a mixture of ice (10 g) and concentrated hydrochloric acid (3.0 m*l*) with stirring and cooling. After the removal of the nitrobenzene by steam distillation, the residual precipitates were collected, washed with water, and then recrystallized from methanol to give II as yellow needles, mp 244.5—245.5°C, which gave a dark green ferric chloride reaction in ethanol; yield, 18 mg (37%). The mixed melting point with natural eupatin (mp 244.5—245.5°C[8]) was 244.5—245.5°C. UV: λ_{max}^{EtOH} mμ (log ε); 259(4.34), 272[7](4.19), 294[7](3.83), 368(4.33).

Found: C, 60.04; H, 4.41%. Calcd for $C_{18}H_{16}O_8$: C, 60.00; H, 4.48%.

3,3′,5-Triacetoxy-4′,6,7-trimethoxyflavone (VII). A mixture of II (12.5 mg), acetic anhydride (0.2 m*l*), and dry pyridine (0.3 m*l*) was refluxed for 2 hr. The crude product was then recrystallized from benzene containing *n*-hexane to give the triacetate (VII) as colorless needles, mp 218—220°C, which gave a negative ferric chloride reaction; yield, 10 mg (60%). UV: λ_{max}^{EtOH} mμ (log ε); 260(4.19), 319(4.44).

Found: C, 59.22; H, 4.47%. Calcd for $C_{21}H_{22}O_{11}$: C, 59.26; H, 4.56%.

The authors are grateful to Professor S. Morris Kupchan, Universty of Virginia, for his gifts of natural eupatoretin and eupatin.

BULLETIN OF THE CHEMICAL SOCIETY OF JAPAN, VOL. 44, 1699—1701 (1971)

The Reactions of Hexafluoropropylene with Arylamines and the Preparation of *N*-(2,3,3,3-Tetrafluoropropyl)arylamines

Nobuo ISHIKAWA and Takayoshi MURAMATSU

Department of Synthetic Chemistry, Faculty of Engineering, Tokyo Institute of Technology, Meguro-ku, Tokyo

(Received December 12, 1970)

Nucleophilic additions of alkylamines to fluoroolefins are well known.[1] For instance, alkylamines react exothermally with tetrafluoroethylene or chlorotrifluoroethylene to give acetamidines (**2**) *via* imidylfluorides (**1**):[2]

$$RNH_2 + CF_2{=}CFX \longrightarrow \underset{\mathbf{1}}{R\text{-}N{=}CFCHFX} + HF$$

$$RNH_2 + \mathbf{1} \longrightarrow \underset{\mathbf{2}}{R\text{-}N{=}C(NH\text{-}R)\text{-}CHFX} + HF$$

As arylamines are less basic than alkylamines, they are less reactive to fluoroolefins, and little is known about the reactions of arylamines with perfluoroolefins. The early work of Knunyants and his co-workers[3] revealed that aniline and perfluoroisobutene in ether gave the condensed product **3**, which could then be hydrolyzed by sulfuric acid into an amide **4**.

$$PhNH_2 + CF_2{=}C(CF_3)(CF_3) \longrightarrow \underset{\mathbf{3}}{PhNHCF{=}C(CF_3)(CF_3)} + HF$$

$$\mathbf{3} + H_2O \longrightarrow \underset{\mathbf{4}}{PhNH\text{-}C(=O)\text{-}CH(CF_3)(CF_3)} + HF$$

On the other hand, England and his co-workers[2] reported that aniline reacted with 0.25 mol of tetrafluoroethylene at 135°C to give difluoroacetamidine (**5**) in an 85% yield:

$$PhNH_2 + CF_2{=}CF_2 \longrightarrow \underset{\mathbf{5}}{PhN{=}C(NHPh)\text{-}CHF_2}$$

We carried out the reactions of aromatic amines with hexafluoropropylene, using dimethylformamide as the solvent. They reacted even at room temperature, and two kinds of products were obtained, depending upon the relative concentration.

As an example, when a dilute solution (about 10%) of *p*-toluidine in dimethylformamide was allowed to react with 2 mol of hexafluoropropylene, a compound with a mp of 93.5—94°C was obtained. From the IR, NMR, and mass spectra, the structure of this compound was found to be *N*-*p*-tolyl-α,β,β,β-tetrafluoropropionamide (**6**). In the IR spectrum, the presence of the –CONH group was shown by strong bands at 1675 (C=O) and 3340 (N-H) cm^{-1}, and in the mass spectrum the parent peak of *m/e* 235 and other reasonable fragment peaks appeared. In the NMR spectra, two kinds of fluorine atoms (CF_3 and CHF) and four kinds of hy-

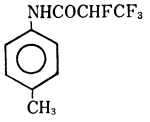

6

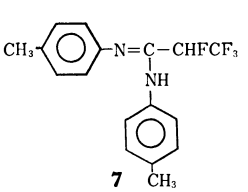

7

1) R. D. Chambers and R. H. Mobbs, "Advances in Fluorine Chemistry," Vol. 4, ed. by M. Stacey *et al.*, Butterworth Scientific Publications, London (1965), p. 62.

2) D. C. England, L. R. Melby, M. A. Dietrich, and R. V. Lindsey, Jr., *J. Amer. Chem. Soc.*, **82**, 5116 (1960).

3) I. L. Knunyants, L. S. German, and B. L. Dyatkin, *Izv. Akad. Nauk, SSSR., Otd. Khim. Nauk*, **1956**, 1353.

Table 1. Preparations of tetrafluoropropionarylides [A] and tetrafluoropropylarylamines [B]

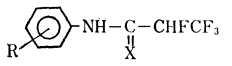

[A] (X=O) [B] (X=H_2)

R	[A] Yield (%)	[A] Mp (°C)	[A] F Anal (%) Obsd	[A] F Anal (%) Calcd	[B] Yield (%)	[B] Bp (°C/mmHg)	[B] F Anal (%) Obsd	[B] F Anal (%) Calcd
H	78.1	83.5—84	36.1	35.9	89.8	97—98/19	36.2	36.7
2-CH_3	44.5	93 —95	32.4	32.3	86.4	114—115/29	30.9	34.4
3-CH_3	75.5	66 —66.5	32.7	32.3	79.9	97—99/11	34.2	34.4
4-CH_3	85.2	93.5—94	32.5	32.3	74.7	108—109/17	34.1	34.4
2,4-$(CH_3)_2$	46.4	110 —110.5	30.2	30.5	74.4	120—121/28	32.4	32.3

drogen atoms (NH, aromatic 4H, CHF and CH_3) appropriately appeared.

When a rather concentrated solution (about 22%) of *p*-toluidine was allowed to react with 1.5 mol of hexafluoropropylene in the same manner, we obtained another compound with a mp of 87—88.5°C. The absorption spectra of this compound were quite different from those of **6**, and we confirmed that this compound is the condensed product of 2 mol of *p*-toluidine and 1 mol of hexafluoropropylene, *i.e.*, *N,N'*-di-*p*-tolyltetrafluoropropionamidine (**7**). The IR spectrum had no C=O band, and the mass spectrum showed an appropriate parent peak (*m/e* 324) and fragment peaks. Two kinds of fluorine atoms (CF_3, CHF) and four kinds of hydrogen atoms (Me_2, (aromatic 4H)$_2$, NH, and CHF) were present in the NMR spectra.

The scheme of the above reactions seems to be as follows. The reaction of arylamine and hexafluoropropylene gives the imidylfluoride (**8**) first. When the reaction mixture is then treated with water, this **8** is hydrolyzed into the propionamide (**9**), but if an excess arylamine is present in the reaction system, **8** reacts with it further to give the propionamidine (**10**):

$$ArNH_2 + CF_2{=}CFCF_3 \longrightarrow ArNHCF_2CHFCF_3$$

$$\downarrow -HF$$

$$ArN{=}CFCHFCF_3 \quad \mathbf{8}$$

$$\xrightarrow{H_2O,\ (-HF)} ArNHCCHFCF_3 \quad \mathbf{9}$$

$$\xrightarrow{ArNH_2} ArN{=}CCHFCF_3 \quad \mathbf{10}$$

In addition to *p*-toluidine, we reacted aniline, *o*- and *m*-toluidines, and 2,4-xylidine with hexafluoropropylene at a low arylamine concentration; in each case, we could obtain the corresponding tetrafluoropropionarylide in a good yield (Table 1).

Because of the strong electronegativity of the fluorine atom, these tetrafluoropropionarylides were not stable to alkali, and when heated in a dilute aqueous sodium hydroxide solution they were readily hydrolyzed to arylamine and tetrafluoropropionic acid. Therefore, we carried out the reduction of the carbonyl groups of these amides with lithium aluminum hydride and thus obtained stable *N*-(tetrafluoropropyl)arylamines. The physical properties of these amines are listed in Table 1.

Experimental

N-p-*Tolyl-α,β,β,β-tetrafluoropropionamide (6).* A solution of 2.14 g (0.02 mol) of *p*-toluidine in 20 m*l* of dimethylformamide was put into an autoclave (100 m*l*) and cooled to about −40°C. 0.04 Mol of liquefied perfluoropropylene was then added to the autoclave, and the temperature of the reaction vessel was allowed to rise to room temperature (20°C), whereupon the mixture was agitated magnetically at this temperature for six hours. Then the reaction mixture was thrown into water; after it had been stirred for a while, an oily matter solidified and a pale yellow crystalline mass separated out. This was filtered off, washed, and dried to give 4.04 g of (85.2%) the crude product. After recrystallization from dilute methanol, colorless crystals with a mp of 93.5—94°C were obtained. IR: 3340 (N–H), 1675 (C=O), 1145, 1188 (C–F) cm^{-1}. NMR (in $CDCl_3$): ^1H τ 7.72 (CH_3, s), 4.88 (CHF, dq), 2.47—3.07 (arom–H, dd), 1.72 (NH, br); ^{19}F δ −3.0 (CF_3, dd), +122.8 (CHF, m) from external CF_3CO_2H. MS: *m/e* 91 ($C_6H_5CH_2$), 106 ($CH_3C_6H_4NH$), 134 ($CH_3C_6H_4NHCO$), 235 ($C_{10}H_9ONF_4$).

The reactions with other arylamines were run similarly, and the products (Table 1) gave similar IR and NMR spectra.

N,N'-*Di*-p-*tolyl-α,β,β,β-tetrafluoropropionamidine (7).* A solution of 4.28 g (0.04 mol) of *p*-toluidine in 15 m*l* of dimethylformamide was allowed to react with 0.06 mol of hexafluoropropylene in the same manner as in the above reaction. After five hours, the reaction mixture was treated with water; 4.72 g (72.8%) of yellow crystals were thus obtained. This crude product was dissolved in benzene, and the solution was chromatographed on an activated alumina column. The yellow band was eluted with benzene, the solvent was evaporated, and the residue was recrystallized from dilute methanol, thus giving colorless crystals with a mp of 87—88.5°C

Found: F 23.1%, Calcd for $C_{17}H_{16}F_4N_2$: F 23.4%. IR: 3240 (N–H), 1133, 1183 (C–F) cm^{-1}. NMR (in $CDCl_3$): ^1H τ 7.78 (CH_3, s), 4.42 (CHF, m), 2.85—3.70 (arom–H, dd), 2.62 (NH, br); ^{19}F δ −3.3 (CF_3, dd), +124.4 (CHF, m) from external CF_3CO_2H. MS: *m/e* 65 (C_5H_5), 91 ($C_6H_5CH_2$), 107 (C_7H_7NH+H), 218 ($C_7H_7N{=}C{-}CHFCF_3$), 324 ($C_{17}H_{16}N_2F_4$).

N-*(2,3,3,3-Tetrafluoropropyl)*-p-*tolylamine.* A solution of 1.52 g (0.04 mol) of lithium aluminum hydride in 50 m*l* of diethyl ether was cooled in an ice-salt bath and then a solution of 4.70 g (0.02 mol) of **6** in 15 m*l* of diethyl ether was

stirred mechanically in at 0—5°C. After the addition, stirring was continued for three hours at room temperature; the solution was then allowed to stand for one day. Into the reaction mixture a small amount of ethyl acetate and water was then added cautiously in order to decompose the excess lithium aluminum hydride; the ether layer was evaporated, and then the residue was distilled out in a vacuum. A colorless liquid with a bp of 108—109°C/17 mmHg which weighed 3.30 g (74.7%) was thus obtained. IR: 3440 (N–H), 1150, 1186 (C–F)cm^{-1}. NMR: ^{1}H τ 7.89 (CH_3, s), 6.98 (NH, br), 6.59 (CH_2, m), 5.55 (CHF, m), 3.02—3.90 (arom–H, m); ^{19}F δ +0.01 (CF_3, dd), +125.8 (CHF, m) from external CF_3CO_2H.

The other tetrafluoropropionarylamides were also reduced in the same manner (Table 1): their products gave similar IR and NMR spectra.

BULLETIN OF THE CHEMICAL SOCIETY OF JAPAN, VOL. 44, 1701—1702 (1971)

A Cleavage of a Furan Derivative Observed during the Curtius Reaction

Takao YOSHIDA, Hakuji KATSURA, and Takeo KANEKO

Department of Chemistry, Faculty of Science, Osaka University, Toyonaka, Osaka

(Received December 14, 1970)

It is well known that furfuryl alcohol derivatives are easily attacked by acidic reagents to afford γ-diketones, γ-ketoacids, or γ-lactones. In this paper a conversion of a furfuryl alcohol derivative to a γ-valerolactone derivative in the absence of acidic reagent during the Curtius reaction is reported.

Furfuryl alcohol (I) was converted to 2-hydroxymethylfuran-3,4-dicarboxylic acid dimethylester (II) by the Alder-Rickert reaction.[1] 2-Acetoxymethylfuran-3,4-dicarboxylic acid (IV), which was obtained by alkaline hydrolysis of dimethylester (II) followed by acetylation with acetic anhydride-pyridine, was treated with thionyl chloride to give 2-acetoxymethylfuran-3,4-dicarbonylchloride (V). Diacyl azide (VI), which was prepared from the reaction of acyl chloride (V) with sodium azide, was subjected to the Curtius reaction in ethanol or benzyl alcohol-benzene solution.

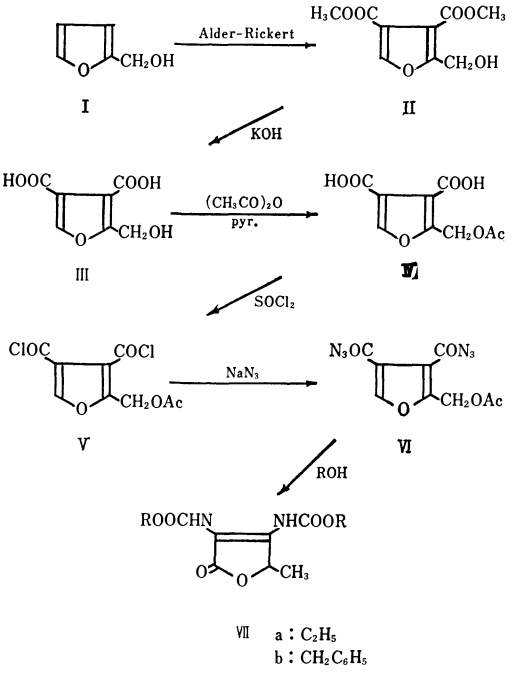

Fig. 1.

The structures of the products separated by means of silica gel column chromatography were elucidated from IR, NMR, and UV spectroscopic studies. When diacyl azide (VI) was heated in ethanol, the product showed the absorption at 1780, 1690, 1190 cm^{-1} in IR spectrum which indicated the presence of α,β-unsaturated γ-lactone. In NMR spectrum signals of a three proton doublet at δ1.55 (J=6.5 Hz) and one proton quartet at δ 5.70 (J=6.5 Hz) appeared. This showed the presence of structure of $>CH-CH_3$ in the molecule. UV spectrum also showed λ_{max} at 267.5 mμ (ε, 15.500). From these results as well as from elemental analysis and molecular weight measurement, the structure of the product was confirmed to be α,β-dehydro-α,β-dicarbethoxyamino-γ-valerolactone (VII, a). When benzyl alcohol was used on the Curtius reaction, the product which showed similar spectra to those of VIIa in IR and NMR was confirmed to have the structure of α,β-dehydro-α,β-dicarbobenzyloxyamino-γ-valerolactone (VII, b).

Experimental

All melting points are uncorrected. IR, NMR, and UV were measured by use of Jasco IR-S, Varian A-60, and Hitachi EPS-3 spectrometers, respectively.

2-Hydroxymethylfuran-3,4-dicarboxylic Acid Dimethylester (II). A mixture of furfuryl alcohol (1) (4.9g, 0.05 mol), acetylenedicarboxylic acid dimethylester (7.2 g, 0.05 mol) and anhydrous dioxane (20m*l*) was heated under reflux for 5 hr. After dioxane was removed, the residue was dissolved in ethyl acetate (50m*l*). The solution was subjected to hydrogenation with 10% palladium on charcoal under atmospheric pressure at room temperature. When one equivalent (0.05mol) of hydrogen was absorbed, the catalyst was filtered off and the filtrate was evaporated to remove ethyl acetate. The residue was heated to 200°C under reduced pressure of about 100 mmHg until the generation of ethylene stopped. Subsequent distillation at 2 mmHg afforded 2-hydroxymethylfuran-3,4-dicarboxylic acid dimethylester (II) (9.0 g, 84%), bp 140—141°C/2 mmHg. IR (neat): 3450, 1730, 1600, 1200, 1080, 770 cm^{-1}. NMR ($CDCl_3$): δ 3.83, 3.87 (7H, s-s), 4.73 (2H, s), 7.87 (1H, s).

Found: C, 49.80; H, 4.74%. Calcd for $C_9H_{10}O_6$: C, 50.47; H, 4.71%.

1) K. Alder and H. F. Rickert, *Ber.*, **70**, 1354 (1937); K. Hofmann, *J. Amer. Chem. Soc.*, **67**, 421, 738 (1945).

2-Hydroxymethylfuran-3,4-dicarboxylic Acid (III). 2-Hydroxymethylfuran-3,4-dicarboxylic acid dimethylester (II) (12.9 g, 0.06 mol) was dissolved in methanol (60 ml). To this solution sodium hydroxide aqueous solution (8.4 g in 20 ml) was added dropwise with cooling, and the reaction mixture was allowed to stand for 18 hr at room temperature. After evaporating methanol under reduced pressure, the residual solution was acidified with concentrated hydrochloric acid (14.5 ml). Precipitated crystals were collected on a funnel and washed with a small amount of cold water. Recrystallization from water gave 2-hydroxymethylfuran-3,4-dicarboxylic acid (III) (7.7 g, 16%), mp 173°C (dec). IR (Nujol): 3300, 1720, 1620, 1015, 765 cm^{-1}.

Found: C, 44.98; H, 3.19%. Calcd for $C_7H_6O_6$: C, 45.17; H, 3.25%.

2-Acetoxymethylfuran-3,4-dicarboxylic Acid (IV). A mixture of 2-hydroxymethylfuran-3,4-dicarboxylic acid (20 g, 0.11 mol), acetic anhydride (40 ml) and pyridine (80 ml) was stirred for 10 min until disolution was complete. After the increase in temperature of the solution stopped, the solution was gradually heated and kept at about 100°C for 4 hr. The crystalline product obtained after the reaction mixture had been cooled was collected and dissolved in water (100 ml). The solution was acidified with concentrated hydrochloric acid to precipitate crude product. Recrystallization from ethyl acetate gave 2-acetoxymethylfuran-3,4-dicarboxylic acid (IV) (12.5 g, 51%), mp 156.5—157°C. IR (Nujol): 1725, 1200, 1050, 770 cm^{-1}.

Found: C, 47.22; H, 3.53%. Calcd for $C_9H_8O_7$: C, 47.38; H, 3.53%.

2-Acetoxymethylfuran-3,4-dicarbonyl Chloride (V). A mixture of 2-acetoxymethylfuran-3,4-dicarboxylic acid (IV) (4 g, 0.018 mol) and thionyl chloride (10 ml) was heated under reflux for 1 hr. After evaporating excess of thionyl chloride, distillation of the residual oil afforded 2-acetoxymethylfuran-3,4-dicarbonyl chloride (V) (4.4 g, 95%) bp 128°C/1 mmHg. IR (neat): 1750—1790, 1600, 1220, 750 cm^{-1}.

Found: Cl, 25.77%. Calcd for $C_9H_6O_5Cl_2$: Cl, 26.75%.

α,β-Dehydro-α,β-dicarbethoxyamino-γ-valerolactone (VII,a). To a solution of sodium azide (2.2 g, 0.034 mol) in water (10 ml), which was cooled with ice-salt bath, was added a solution of 2-acetoxymethylfuran-3,4-dicarbonyl chloride (V) (4.4 g, 0.017 mol) in anhydrous ether (20 ml) during 30 min with vigorous stirring. The reaction mixture was then stirred for an additional 3 hr at below 0°C. The ethereal layer was washed well with cooled saturated sodium bicarbonate solution and cooled water, and dried over anhydrous magnesium sulfate. Ether was removed under reduced pressure at room temperature. Crude acyl azide (VI) (5.3 g) thus obtained was dissolved in ethanol (20 ml), and the ethanol solution was heated gradually under nitrogen atmosphere. After the first vigorous evolution of gas ceased, the reaction mixture was refluxed for an additional 2 hr. Ethanol was removed under reduced pressure and residual oil was subjected to column chromatography on silica gel (Kieselgel, 0.02—0.5 mm, 50 g). The fraction eluted with carbon tetrachloride-chloroform (1:1, 600 ml) afforded 1.3 g of crude product. Recrystallization from methanol gave α,β-dehydro-α,β-dicarbethoxyamino-γ-valerolactone (VII,a) (710 mg, 16%) mp 120—121°C. IR (Nujol): 3350, 3100, 1780, 1740, 1690, 1570, 1270, 1190, 1050 cm^{-1}. NMR ($CDCl_3$): δ 1.30 (6H, t), 1.55 (3H, d, J=6.5 Hz), 4.21, 4.23 (4H,q,q), 5.70 (1H,q, J=6.5 Hz) UV: λ_{max}^{EtOH} 267.5 mμ (ε=15.500).

Found: C, 48.45; H, 5.85; N, 10.26%; mol wt (Rast), 268. Calcd for $C_{11}H_{16}O_6N_2$: C, 48.52; H, 5.92; N, 10.29%; mol wt, 272.

α,β-Dehydro-α,β-dicarbobenzyloxyamino-γ-valerolactone (VII,b). The crude acyl azide (VI), prepared from 2-acetoxye methylfuran-3,4-dicarboxylic acid (4.5 g, 0.017 mol) by the same procedure as described above, was heated under reflux with benzyl alcohol (3.9 g, 0.036 mol) in benzene (20 ml) for 2.5 hr. After evaporating benzene, the residual oil was subjected to column chromatography on silica gel (Kieselgel, 0.02—0.5 mm, 50 g). The fraction eluted with chloroform-carbon tetrachloride (1:1, 300 ml) afforded α,β-dehydro-α,β-dicarbobenzyloxyamino-γ-valerolactone (VII, b) (770 mg, 11%) mp 115—116°C (recrystallized from methanol). IR (Nujol): 3350, 1750, 1735, 1700, 1570, 1270, 1190, 1030 cm^{-1}. NMR ($CDCl_3$): δ 1.50 (3H,d, J=6 Hz), 5.17 (4H, s), 5.70 (1H,d, J=6 Hz), 7.35 (10H, s).

Found: C, 63.71; H, 5.14; N, 7.08%. Calcd for $C_{21}H_{20}O_6N_2$: C, 63.63; H, 5.09; N, 7.07%.

BULLETIN OF THE CHEMICAL SOCIETY OF JAPAN, VOL. 44, 1703—1704 (1971)

Deuteron Quadrupole Interactions in Two Modifications of Oxalic Acid Dihydrate Crystal

Takehiko CHIBA and Gen SODA*

Department of Chemistry, Nihon University, Sakurajosui, Setagaya-ku, Tokyo

**Department of Physical Chemistry, Faculty of Science, Osaka University, Toyonaka, Osaka*

(Received December 21, 1970)

A brief account has been previously published of the deuteron quadrupole interactions in the α and β modifications of the deuterated oxalic acid dihydrate crystal, $C_2O_4D_2 \cdot 2D_2O$, in relation to their structures.[1] In this note, the details of the results of deuteron magnetic resonance and a discussion with reference to the structures, as determined by recent extensive diffraction studies,[2] will be given.

As is to be expected from the similarities in their structures, the deuteron resonance spectra of the α-form have features similar to those of the β-form, which have been measured previously.[3] The water deuterons showed spectra characteristic of a 180°-flip motion of D_2O: lines of stationary deuterons at low temperatures, fast-motion-averaged lines at high temperatures, and broadened-out lines in the intermediate temperature range. The values of the deuteron quadrupole coupling (eqQ/h), the asymmetry parameter (η), and the direction cosines of the principal axes of the field gradient tensors are listed in Table 1[4] ($|q_{zz}| \geq |q_{yy}| \geq |q_{xx}|$ assumed). The values listed for the β-form are those revised by the computor processing[5] of the previous experimental results[3] by including some additional new data.

The two empirical relations[1,5] that 1) the z principal axis is in the bond direction, and that 2) the y principal axis is perpendicular to the plane formed by the D–X–Y, are examined. In view of the structure determined by the neutron diffraction studies,[2] as is shown in Table 2, the deviation angles from these relations, θ_z and θ_y, are within the range usually found, namely, $\theta_z \lesssim 3°$ and $\theta_y \lesssim 10°$, providing other evidence of the usefulness of determining bond directions from the deuteron resonance.

The eqQ *vs.* r(O···O) (the hydrogen bond length)-plot generally fits well to the smooth curve relation

TABLE 1. DEUTERON QUADRUPOLE COUPLING eqQ/h, ASYMMETRY PARAMETER, η, AND THE DIRECTION COSINES OF z AND y PRINCIPAL AXES IN α- AND β-FORM $C_2O_4D_2 \cdot 2D_2O$ CRYSTALS

	Temperature (°C)	eqQ/h (kHz)	η (%)				
α-Form					a	b	c^*
D_1^{α}	−82	107.1±0.5	13.3±0.5	z	−0.587	±0.247	0.771
	25	118.0±1.1	11.3±1.1	y	0.399	±0.917	0.010
D_2^{α}	−82	229.4±1.8	10.2±1.0	z	0.563	±0.266	0.783
				y	−0.603	±0.780	0.169
D_3^{α}	−82	237.2±0.7	10.8±0.4	z	0.699	±0.650	−0.300
				y	−0.620	±0.759	0.200
D_2^{α}, D_3^{α} (Motion-averaged)	25	125.6±1.3	89.0±1.9	z	−0.633	±0.759	0.153
				y	0.766	±0.584	0.268
β-Form					a^*	b	c
D_1^{β}	−70	134.7±0.5	10.8±0.6	z	−0.655	∓0.152	0.740
	25	139.1±0.3	9.3±0.5	y	0.581	±0.524	0.623
	67	140.4±0.4	10.2±0.5				
D_2^{β}	−70	232.2±1.0	6.4±0.5	z	−0.171	∓0.497	0.851
				y	0.615	±0.621	0.486
D_3^{β}	−70	223.9±0.8	8.5±0.5	z	−0.668	±0.729	−0.150
				y	0.589	±0.642	0.491
D_2^{β}, D_3^{β} (Motion-averaged)	67	120.5±0.4	92.8±0.6	z	−0.286	±0.732	−0.619
				y	0.543	±0.656	0.525

Principal directions for D_1's listed are the room temperature values. The values at other temperatures are substantially unchanged.

1) T. Chiba and G. Soda, "Magnetic Resonance and Relaxation," Proc. 14th Colloque Ampère, Ljubljana, North-Holland Publ. Co., Amsterdam (1966), p. 722.

2) R. G. Delaplane and J. A. Ibers, *Acta Crystallogr.* **B25**, 2423 (1969); P. Coppens and T. M. Sabine, *ibid.*, 2442 (1969).

3) T. Chiba, *J. Chem. Phys.*, **41**, 1352 (1964).

4) The hydrogen atoms are differently numbered by various authors. In this note we adopt the numbering of Ref. 2: D_1 (acid), D_2 (water) incorporated in the *ac*-plane hydrogen-bond network, and D_3 (water) incorporated in the screw hydrogen-bond network in the *b*-axis direction. The crystal form is indicated by a superfix, α or β.

5) G. Soda and T. Chiba, *J. Chem. Phys.*, **50**, 439 (1969).

Table 2. Deviation angles of the z principal axes from the O-D direction, θ_z, and those of the y principal axes from the COD or D_2O plane normals, θ_y

	D_1^α	D_2^α	D_3^α	D_1^β	D_2^β	D_3^β
θ_z	0.9°	2.8°	1.4°	1.0°	3.0°	1.5°
θ_y	8.9°	2.0°	1.7°	4.3°	4.4°	2.7°

previously presented (Fig. 1).[3,5,6] Small systematic deviations for the water deuterons need to be mentioned, however. The D_3^α and D_2^β points above the curve of the eqQ *vs.* r(O···O)-plot are from bent hydrogen bonds (156° and 157°), while the D_2^α and D_3^β points are from nearly straight hydrogen bonds (168° and 170°). The fitting to a smooth curve is perfect if eqQ is plotted against r(O···O), as in Fig. 1. This seems reasonable because, in a weak hydrogen bond, the strength of the bond must primarily be determined by the electrostatic interaction between the H and the hydrogen-bond-acceptor atom. This is also consistent with the good correlation of eqQ-r(O···D) as given in the form of an empirical equation.[5] The O–D distance, which reflects the hydrogen bond strength, should have primary importance in determining the eqQ. The correlation between eqQ and r(O–D) is, however, not very satisfactory (Fig. 1), (see also Fig. 5 of Ref. 7).

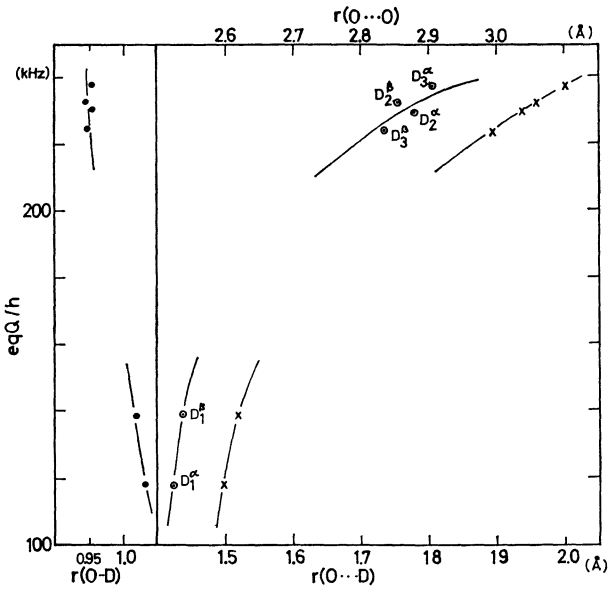

Fig. 1. Deuteron quadrupole coupling values in α- and β-$C_2O_4D_2 \cdot 2D_2O$ plotted against r(O...O) (⊙), r(O...D) (×), and r(O–D) (●).

The dependence of the eqQ on the r(O···O) or on r(O···D) is so apparent that it seems reasonable to ascribe the origin of the marked positive temperature dependence of the eqQ of the D_1^α to the temperature variation of the r(O···O) or r(O···D). If the r(O···O) dependence of eqQ is estimated from a comparison of the D_1^α and D_1^β data at room temperature, an increase in the eqQ of D_1^α from 107.1 kHz at 191°K to 118.0 kHz at 298°K must be caused by the 0.008 Å increase in the r(O···O). The maximum thermal expansion in the *ac* plane of the α-form crystal is reported to be in the direction nearly parallel to the O–D_1···O and O–D_3···O, with a coefficient of 0.0114 for a 90—290°K change.[8] This amounts to a lengthening of 0.079 Å for each pair of O–D_1···O and O–D_3···O bonds if we assume this expansion to be shared by these two hydrogen-bond systems. Actually, the expansion is accompanied by the deformation of various parts, and the fraction shared by the O–D_1···O bond is not known, but the increase in the O–D_1···O length by 0.008 Å from 191° to 298°K is small enough to be well explained by the thermal expansion.

The large amplitudes of a torsional oscillation approximately perpendicular to the plane of the oxalic acid molecule and a translational oscillation about the axis approximately parallel to the C–C bond were concluded to exist in these crystals from the large thermal parameters observed in the structure analyses.[2] This may be another possible cause of the positive temperature dependence of eqQ. These oscillations force the OD_1 group to oscillate in the direction perpendicular to the O–D_1···O bond, thus tending to increase the average D_1···O separation. The total mean-square amplitude at room temperature of these two oscillations for the OD_1 group is 0.060 Å^2 ((0.24 Å)^2). As a rough estimate, if these oscillation frequencies are assumed to be less than 50 cm^{-1}, a decrease in the average D···O distance by more than 0.0067 Å can be expected for a 298° to 191° K change. The assumed frequency range may not be unreasonable for the type of oscillations considered here, and this mechanism can explain most of the required change in the D···O distance. Other effects, such as the bending vibration of the OD bond, which lead to a (normal) negative temperature variation of the eqQ may also be present, and the observed temperature dependence of eqQ is actually a sum of various contributions.

A similar but smaller positive temperature dependence of eqQ for acid deuteron is observed for the β-form crystal (5.7 kHz for −70°—67°C) and in potassium binoxalate, KDC_2O_4 (6.1 kHz for −37.3°—137.7°C).[7] These phenomena may also be due to the mechanisms of the types considered above. For deuterons in weaker hydrogen bonds, the lengthening of the hydrogen-bond distance by thermal expansion or by oscillation makes a smaller contribution to the temperature dependence of eqQ. This is probably the reason why temperature dependence of the eqQ of water deuterons can often be well explained by the simple Bayer theory.[9,10]

A change in the strength of the O–D···O bond indicated by the positive temperature dependence of eqQ would imply a decrease in the OH vibration frequency with the temperature. In this respect, the

6) The correlation of the eqQ values of water deuterons for reduction by a torsional motion, as in Fig. 5 of Ref. 3, is not made.

7) J. W. McGrath, *J. Chem. Phys.*, **48**, 5549 (1968).

8) J. M. Robertson and A. R. Ubbelohde, *Proc. Roy. Soc.*, **A170**, 241 (1939).

9) H. Bayer, *Z. Physik.*, **130**, 227 (1951).

10) T. Chiba, *J. Chem. Phys.*, **39**, 947 (1963); T. Chiba and G. Soda, This Bulletin, **41**, 1524 (1968).

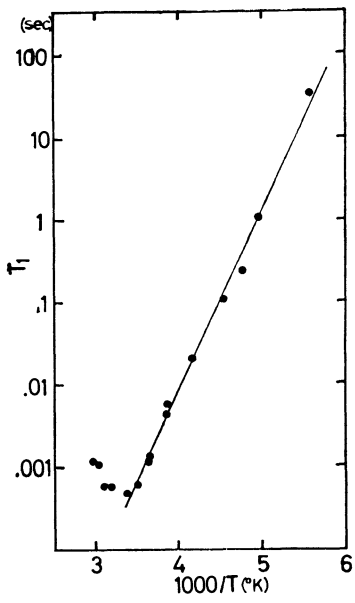

Fig. 2. Temperature dependence of T_1 of water deuterons in α-form $C_2O_4D_2 \cdot 2D_2O$.

temperature dependence of the vibration spectra in these crystals is of interest.

Because data on the line-width change with the temperature in the α-form crystal were rather poor, we estimated the barrier height of the flip motion of the D_2O to be 9.7 kcal/mol from the temperature dependence of the spin-lattice relaxation time, T_1 (Fig. 2.) This value is less than 10.7 kcal/mol (a revised value of the previous measurement[3,11]) for the β-form; this is consistent with the fact[5] that the hydrogen bonds linking the water molecule are slightly longer in the α-form than in the β-form.

Experimental

The α-form $C_2O_4D_2 \cdot 2D_2O$ crystals were grown from a saturated solution, whose deuterium content was controlled to about 90%, by gradual cooling. The angular dependence of the quadrupole splittings when the magnetic field was rotated about the *a*, *b*, and *c** axes was measured at various temperatures; the quadrupole coupling tensors were then determined by the method described previously.[5] The T_1 of D was measured by the pulse method using the 180°—90° pulse sequences at 10 MHz.[11] The magnetic field was applied in a direction (nearly parallel to the *c* axis) on the *ac* plane where quadrupole splittings of the water deuterons are sufficiently small to give a single-valued T_1. In this setting, D_1 lines are about 40 kHz apart and need not be considered.

The measurement of the deuteron resonance and the computor analysis of the data were done at the Institute for Solid State Physics, The University of Tokyo. We wish to thank Professor Y. Kakiuchi of the Institute for his interest in this work and for providing the facilities. We also wish to thank Messrs. A. Suetaka and T. Kataoka for their assistance in the experiment.

11) T. Chiba and Y. Kakiuchi, This Bulletin, **41**, 828 (1968).

BULLETIN OF THE CHEMICAL SOCIETY OF JAPAN, VOL. 44, 1705—1707 (1971)

Enthalpy of Vaporization of Some Organic Substances at 25.0°C and Test of Calorimeter

Kazuhito KUSANO and Ingemar WADSÖ*

Faculty of Engineering, Miyazaki University, Miyazaki

**Thermochemistry Laboratory, University of Lund, Chemical Center, Lund, Sweden*

(Received December 21, 1970)

In the course of the calibration of ebulliometers at around 200°C, some recommended standard substances,[1] such as aniline, methyl benzoate, and nitrobenzene, were carefully purified. For these compounds, no calorimetric data of the enthalpy of vaporization (ΔH_v) at 25.0°C have been found in the literature. On the other hand, there is some doubt whether or not it is possible to measure the ΔH_v for compounds having such a high boiling temperature by means of a calorimeter which is constructed so as to pass an inert carrier gas through its cavities in order to evaporate the substance.

An attempt was made to examine the possibilities of determining the ΔH_v-values for these low-vapor-pressure compounds and, if possible, to compare the ΔH_v-values with those calculated from their vapor pressure–temperature relations.

Experimental

Materials. Aniline, methyl benzoate, nitrobenzene, and diethylene glycol diethyl ether were employed in this investigation. All of these compounds were obtained from commercial sources and were of a puris grade (B.D.H.). Prior to the purifications, diethylene glycol diethyl ether was dried over metallic sodium,[2] whereas the standard substances were treated by shaking them over molecular sieves (4A). The compounds were purified by repeated fractional distillations under a regulated reduced pressure so as to distil the compounds at around 100°C. The best fractions collected

1) A. Weissberger, Ed., "Technique of Organic Chemistry," 2nd Ed., Vol. VI. Interscience Publishers Inc., New York (1954). p. 189.

2) E. R. Alexander and A. G. Pinkus, *J. Amer. Chem. Soc.*, **71**, 1787 (1949).

Table 1. Some physical ccnstants of compounds

Compound	Boiling point (°C)	d^{25} Observed	d^{25} Reference	n_D^{25} Observed	n_D^{25} Reference
Aniline	184.00[c] 184.32[a] 184.40[b]	1.0175	1.0173[d] 1.0175[c] 1.01750[a]	1.5837	1.58364[a] 1.5840[d] 1.5855(20°)[c] 1.58318[k]
Methyl benzoate	199.35[a] 199.50[b]	1.0839	1.08377[a]	1.5147	1.51457[a]
Nitrobenzene	210.85[a,b]	1.1983	1.19805[f] 1.1982[a] 1.19864[e]	1.5500	1.55006[a]
Diethylene glycl diethyl ether	181—189[g] 186.0[j] 188.9[i] 187.4 (observed)	0.9043	0.9063(20°)[h]	1.4094	1.4155(20°)[h]

a) International Bureau of Standards. Ref. 4., Dreisbach, Ref. 15. b) Weissberger, Ref. 1. c) Deshpande *et al.*, Ref. 5. d) Average value calculated from data at 20° and 30°C, Summer *et al.*, Ref. 6. e) Walden *et al.*, Ref. 7. f) Bowden *et al.*, Ref. 8. g) Doolittle, Ref. 9. h) Value at 20°C. Vogel, Ref. 10. i) Othmer *et al.*, Ref. 11. j) Wikoff *et al.*, Ref. 12; Kotera *et al.*, Ref. 13. k) Dreisbach *et al.*, Ref. 14.

Table 2. Enthalpy of vaporization of some organic substances at 25.0°C

Exp. No.	Amount of substance evaporated (mg)	Evaporation time (sec)	Electric current supplied (mA)	Electrical energy supplied (J)	Apparent enthalpy of vaporization (kJ/mol)	Zero effect correction (kJ/mol)	Enthalpy of vaporization This work (kJ/mol)	Enthalpy of vaporization Literature value (kJ/mol)
				Aniline				
1	40.52	1213.3	20.116	24.425	56.134	−0.207	55.927	54.28[a]
2	40.40	1207.6	20.115	24.308	56.028	−0.207	55.821	
3	40.30	1205.5	20.117	24.271	56.082	−0.208	55.874	58.1[b]
4	40.33	1204.1	20.120	24.250	55.994	−0.208	55.786	
5	40.15	1206.3	20.114	24.280	55.898	−0.207	55.691	46.2[d]
6	40.19	1203.6	20.107	24.209	56.095	−0.208	55.887	
7	40.19	1202.3	20.112	24.194	56.061	−0.208	55.853	
							55.834±0.029	
				Methyl benzoate				
1	32.74	1195.6	15.028	13.435	55.869	−0.301	55.568	55.84[a]
2	32.79	1198.9	15.033	13.479	55.965	−0.305	55.660	
3	48.73	1197.5	18.304	19.960	55.764	−0.201	55.563	52.5[b]
4	49.16	1204.1	18.306	20.074	55.651	−0.197	55.454	
5	33.06	1205.6	15.037	13.562	55.898	−0.305	55.593	51.4[c]
							55.568±0.039	
				Nitrobenzene				
1	35.62	1201.7	16.397	16.074	55.551	−0.498	55.053	55.19[a]
2	35.76	1204.9	16.398	16.119	55.488	−0.498	55.990	
3	36.05	1213.0	16.396	16.223	55.555	−0.494	55.061	57.2[b]
4	38.33	1803.5	13.830	17.161	55.551	−0.502	55.049	
5	25.67	1216.2	13.830	11.593	55.497	−0.494	55.003	
							55.013±0.018	
				Diethylene glycol diethylether				
1	40.59	1217.1	15.603	14.744	58.933	−0.629	58.304	
2	39.94	1202.5	15.595	14.552	59.105	−0.639	58.466	
3	39.90	1200.2	15.599	14.532	59.091	−0.640	58.451	
4	39.97	1201.2	15.600	14.564	59.030	−0.639	58.391	
							58.403±0.037	

a) Dreisbach, Ref. 15. b) Calculated from the data of Stull, Ref. 18. c) Dreisbach *et al.*, Ref. 14. d) Calculated from the ΔH_v-values at 20° and 60°C. Arich *et al.*, Ref. 19.

were dried again over the respective desiccant and then distilled into dried 5-m*l* glass ampoules placed in a small Brühl apparatus containing Drierite on its bottom. The ampoules filled with the substances were flushed with dry nitrogen and then sealed. The purity of the samples, judged by glc, was, in all cases, shown to be 99.9 mol% or better; besides, the water content, also analysed by glc,[3] was estimated to be less than 0.015 wt%. Some physical properties of these compounds are listed in Table 1.

Calorimeter and Calorimetric Procedures. Main part of the calorimeter is made up of a hollow cylindrical silver vessel. Details of the construction of the calorimeter and of the calorimetric procedures have been described elsewhere.[16-18]

In the course of the experimental determinations of methyl benzoate and aniline, the electrical energy supplied to the calorimeter and/or the evaporation time has been altered in order to determine whether or not the ΔH_v-values observed are affected by such experimental conditions. However, the influence of neither the electrical energy nor the evaporation time was observed in any cases, as may be seen in Table 2.

Results and Discussion

The results of the calorimetric determinations are summarised in Table 2. Since the uncertainties accompanying the average values of ΔH_v, given by the standard deviations, are found to be less than 40 J/mol, the reproducibility of each experimental run is considered to be quite satisfactory. However, in the present cases, since the correction terms,[16-18] most of which consist of an zero-effect correction which is estimated to contain a error of more than 10% in itself, amount to several hundred joules at the highest, the uncertainty caused by the correction terms serves to decrease the accuracy of each observed ΔH_v-value. In addition to this, since some systematic errors decrease the accuracy, it is advisable to round the last significant figures in each average ΔH_v-value.

The observed ΔH_v-values for methyl benzoate and for nitrobenzene gave an excellent agreement with the respective literature values compiled by Dreisbach;[15] on the contrary, for aniline, a result higher than the literature value[15] by 1.55 kJ/mol was observed. The ΔH_v-values evaluated from the vapor pressure-temperature relation,[20] using data compiled by Stull,[21] gave poor agreement in all cases. No ΔH_v datum for diethylene glycol diethyl ether could be found in the literature, but that determined in this investigation is acceptable since the plot of the ΔH_v-value *versus* the normal boiling temperature falls on a point to be expected from the same relations of 1,2-dialkoxyethanes and 2-alkoxyethyl acetates[17] and of a homologous series of $C_2H_5(OCH_2)_nCH_3$.[22]

From the experimental results, it can be concluded that a calorimeter of this type can be used for the determination of the enthalpy of vaporization at 25.0°C for compounds with normal boiling temperature up to 210°C.

One of the author (K.K.) wishes to thank Mrs. Kyôko Nakahara for her kind suggestions and the Ministry of Education (Japan) for an award of a grant for an Oveseas Research Visitor (42-甲-91).

3) O. L. Hollis and W. V. Hayes, *J. Gas Chromatogr.*, **4**, 235 (1966); P. Sellers, *J. Chem. Thermodynamics*, **2**, 211 (1970).
4) International Bureau of Standards, Brusseles, *J. Chim. Phys.*, **32**, 501, 189 (1935).
5) D. D. Deshpande and M. V. Pandya, *Trans. Faraday Soc.*, **61**, 1858 (1965).
6) K. M. Sumer and A. R. Thompson, *J. Chem. Eng. Data*, **12** 489 (1967).
7) P. Walden and E. J. Birr, *Z. Physik. Chem.*, **(A) 163,** 281 (1933).
8) S. T. Bowden and E. T. Butler, *J. Chem. Soc.*, **1939,** 79.
9) A. K. Doolittle, *Ind. Eng. Chem.*, **27,** 1169 (1935).
10) A. I. Vogel, *J. Chem. Soc.*, **1948,** 618.
11) D. F. Othmer, S. A. Savitt, A. Krasner, A. M. Goldberg, and D. Markowits, *Ind. Eng. Chem.*, **41,** 572 (1949).
12) H. L. Wikoff, B. R. Cohen, and M. I. Crossman, *Ind. Eng. Chem., Anal. Ed.*, **12**, 93 (1940).
13) A. Kotera, K. Suzuki, K. Matsumura, T. Nakano, T. Oyama, and O. Kambayashi, This Bulletin, **35**, 797 (1962).
14) R. R. Dreisbach and R. A. Martin, *Ind. Eng. Chem.*, **41**, 2875 (1949).
15) R. R. Dreisbach, "Physical Properties of Chemical Compounds," Vol. 1. Amer. Chem. Soc., Advance in Chemistry Series No. 15 (1955).
16) I. Wadsö, *Acta Chem. Scand.*, **20**, 536 (1966).
17) K. Kusano and I. Wadsö, *ibid.*, **24**, 2037 (1970).
18) K. Kusano and I. Wadsö, *ibid.*, in press.
19) G. Arich, G. Tagliavini, and M. Miankani, *Chem. e ind.*, (Milan) **38**, 937 (1956); *Chem. Abstr.*, **39,** 517 (1947).
20) R. C. Reid and T. K. Sherwood, "The Properties of Gases and Liquids," 2nd Ed., McGraw-Hill Inc., New York (1966), p. 114.
21) D. R. Stull, *Ind. Eng. Chem.*, **39,** 517 (1947).
22) M. Månsson, *J. Chem. Thermodynamics*, **1,** 141 (1969).

BULLETIN OF THE CHEMICAL SOCIETY OF JAPAN, VOL. 44, 1708—1709 (1971)

The Reaction of Cyclohepta-2,6-dienone with Amines

Toshiya SATO, Kenji SATO, and Toshio MUKAI
Department of Chemistry, Faculty of Science, Tohoku University, Sendai

(Received December 22, 1970)

Cyclohepta-2,6-dienone (I) was found to react with primary amines or secondary amines to afford tropinone-type adducts (II) or a 1:2 adduct such as III in good yields. We wish to describe the results here, including those of the reactions of I with some carbonyl reagents.

First of all, we attempted to synthesize oxime (IV: Y=OH), tosylhydrazone (IV: Y=NHTs), and hydrazone (IV: Y=NH_2) in order to form cyclohepta-2,6-dienylidene (V) or its precursor, the diazo compound.[1] However, the reaction of I with the corresponding carbonyl reagents resulted in the formation of resinous products, and we failed to isolate the expected product. An inspection of the IR and NMR spectra of the products indicates the absence of the C=C bond and an olefinic proton. This means an amino group of the reagents is added to the dienone system of I. For comparison with this behavior, the reactions of other amines with I were also investigated.

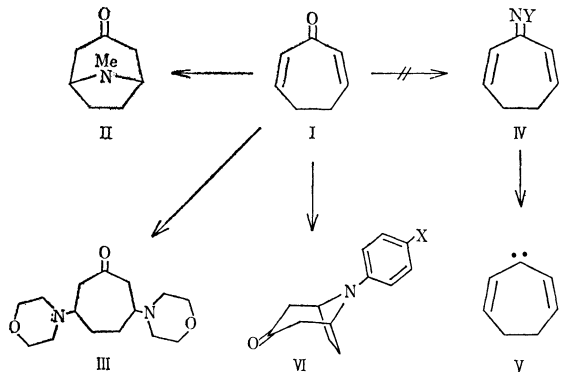

Y=OH, $NHTs$, NH_2

When cyclohepta-2,6-dienone (I) was treated with aqueous methylamine in an alcoholic solution, tropinone (II) could be obtained; this had been reported by Horák who, however, identified the formation of II by paper chromatography.[2] Although this method was suggested by Robinson in 1917,[3] it is a method of preparing tropinone in addition to variant methods discovered by Robinson,[3] Willstätter,[4] Schöpf,[5] and Turro.[6] The similar reaction of I with arylamines afforded *N*-arylnortropionone derivatives (VI) in fairly good yields, which are shown in Table 1. The structure of the products could be elucidated on the basis of elemental analysis and a study of the IR, UV, and NMR spectra (see Table 1 and Experimental section). Derivatives which possess an ethyl, isopropyl, benzyl or β-hydroxyethyl group at the *N*-position were synthesized by Robinson's method,[7] whereas so far *N*-aryl derivatives have not been synthesized. Thus, the reaction of I with arylamines is a unique method for the synthesis of the *N*-arylnortropinones.

TABLE 1. *N*-ARYL DERIVATIVES OF NORTROPINONE

X in VI	Mp (°C)	Yield (%)	IR(C=O) in KBr cm^{-1}	UV in EtOH nm (log ε)	
OMe	134	93	1709	250(4.14)	308(3.20)
Me	96	68	1701	252(4.14)	293(3.17)
H	103	91	1704	250(4.14)	287(3.22)
Cl	155	73	1709	258(4.16)	300(3.18)
NO_2	202	45	1712	231(3.58)	392(4.13)

When even 1 equivalent of morpholine was reacted with I at room temperature, a 2:1 adduct (III) was formed. As expected, the yield of III was increased by the use of 2 equivalents of the amine. The structure of III was proved by elemental analysis and by a study of the spectral data (see Experimental section).

The addition reaction of cross-conjugated α,β-unsaturated ketones with amines has been known for a long time.[8] Recently, it was found that, under irradiation, alcohols and acids added to I.[9] In addition, the photochemical addition of diethylamine to cycloheptenone or cyclooctenone has also been reported.[10] However, our experiment clarified that amines added readily to the enone system of I in the dark reaction, as had been reported before.[8]

Experimental

Tropinone (II). A 40% aqueous solution of methylamine (7 g, 90 mmol) was gradually added, under ice-cooling, to a solution of I (9.73 g, 90 mmol) dissolved in ethanol (15 m*l*). After the reaction mixture had been allowed to stand at a room temperature for 2 hr, it was extracted with ether. The evaporation of the ethereal extract, followed by the distillation of the residual oil, afforded an oil (bp 79—89°C/7 mmHg, 6.9 g, 55%) which partially crystallized on standing. The recrystallization of the crystalline part from cyclohexane provided needles, mp 41—42°C, which were identical with tropinone (lit, mp 42°C).[3] It also afforded quaternary ammonium iodide, mp 266°C (lit, mp 265°C)[11] in a quantitative yield when treated with methyl iodide in acetone.

N-Arylnortropinone (VI). To a solution of I (432 mg,

1) W. Kirms, "Carbene Chemistry," Academic Press, New York (1964).
2) V. Horák, *Coll. Czechoslov. Chem. Commun.*, **28**, 1614 (1963).
3) R. Robinson, *J. Chem. Soc.*, **111**, 762 (1917).
4) R. Willstätter and M. Bommer., *Ann. Chem.*, **422**, 15 (1921).
5) C. Schöpf and G. Lehmann, *ibid.*, **518**, 5 (1935).
6) N. J. Turro, S. S. Edelson, J. R. Williams, T. R. Darling, and W. B. Hammond, *J. Amer. Chem. Soc.*, **91**, 2283 (1969).
7) L. C. Keagle and W. H. Hartung, *ibid.*, **68**, 1608 (1946).
8) J. Guareschi, *Ber.*, **28**, 160 (1895).
9) R. Noyori and M. Kato, *Tetrahedron Lett.*, **1968**, 5075.
10) R. Noyori, A. Watanabe, and M. Kato, Abstract of the 22nd Annual Meeting of the Chem. Soc. Japan, Vol. 3, p. 1326 (1969).
11) R. Willstätter, *Ber.*, **29**, 393 (1896).

4 mmol) dissolved in ether (20 m*l*), we added aniline (372 mg, 4 mmol); the resulting mixture was allowed to stand at room temperature for 3 hr, during which period some crystals deposited. Filtration, followed by recrystallization from cyclohexane, provided needles (VI: X=H), mp 103°C (444 mg). The chromatography of a benzene-solution of a non-crystallized part on an alumina column afforded needles, mp 103°C (285 mg). The combined yield was 91%. The NMR spectrum in $CDCl_3$ (60 MHz) showed τ 2.33—3.26 (5H, multiplet), 5.30 (2H, broad singlet), and 7.1—8.2 (8H, multiplet).

Other derivatives (VI: X=OMe, Me and Cl) could be obtained in a similar way, that is, by treating I with the corresponding base in an ethanolic solution. For the synthesis of the *p*-nitrophenyl derivative (VI: X=NO_2), however, it was necessary to reflux the ethanolic solution containing I and *p*-nitroaniline (each 4 mmol in 10 m*l*) for 15 hr. The results of elemental analyses of the products are shown in Table 2.

Table 2. Elemental analyses of *N*-arylnortropinones (VI)

	X=	OMe	Me	H	Cl	NO_2
C (%)	Found	72.69	78.05	77.78	66.52	63.31
	Calcd	72.70	78.10	77.58	66.24	63.40
H (%)	Found	7.51	8.25	7.81	6.14	5.95
	Calcd	7.41	7.96	7.51	5.99	5.73
N (%)	Found	6.16	6.24	7.39	5.99	11.39
	Calcd	6.06	6.51	6.96	5.94	11.38

3,6-Dimorpholinocycloheptanone (III). Morpholine (1.74 g, 20 mmol) was gradually added under ice-cooling, to a solution of I (1.08 g, 10 mmol) dissolved in ethanol (5 m*l*). After standing for 12 hr at room temperature, the reaction mixture, then containing crystals deposited, was filtered to give pale yellow crystals, mp 109—117°C (956 mg). The concentration of the filtrate afforded other crystals, mp 122—123°C (890 mg) as a second crop. The chromatography of the non-crystallized portions on an alumina column provided crystals, mp 120°C (504 mg) (from petroleum-ether benzene fractions). Recrystallization from ethanol afforded III as colorless prisms, mp 124°C (2.08 g, 74%). IR in KBr for C=O, 1695 cm^{-1}: NMR spectrum in $CDCl_3$ (60 MHz); τ 6.36 (8H, quartet), 7.33 (6H, broad singlet), 7.53 (8H, quartet), and 7.8—8.3 (4H, multiplet).

Found: C, 63.60; H, 9.27; N, 9.87%. Calcd for $C_{15}H_{26}O_3N_2$: C, 63.80; H, 9.28; N, 9.92%.

The authors are indebted to the Sankyo Co. for partial financial support.

BULLETIN OF THE CHEMICAL SOCIETY OF JAPAN, VOL. 44, 1709—1710 (1971)

Partial Molar Heats of Solution of Hydrated Electrolytes in Saturated Solutions

Haruo NAKAYAMA

Department of Chemistry, Faculty of Engineering, Yokohama National University, Ooka-machi, Minami-ku, Yokohama

(Received December 23, 1970)

Partial molar heats of solution of several hydrated electrolytes in saturated solutions ($\Delta H_s(sat) \equiv \bar{H}_2(sat) - H_2^s$) have been determined calorimetrically. From the results obtained, the following two subjects have been discussed: (1) the correlation between the values of $\Delta H_s(sat)$ and the dissolution process of hydrated electrolytes, and (2) the legitimacy of calculating a derivative $(\partial \ln \gamma_\pm / \partial \ln m)_{T,P}$ in a saturated solution from the value of $\Delta H_s(sat)$ and the temperature dependence of the solubility.

A solid sample of a hydrated electrolyte, sealed in an ampoule, was dissolved into 45 m*l* of a solvent, which consisted of an aqueous solution of the same electrolyte, the concentration of which was greater than 60% of its solubility. For each salt, $\Delta H_s(sat)$ has been obtained by extrapolating the observed heats of solution to saturation solubility. These values are listed in the second column of Table 1. They may be in error by as much as 3—4%.

Generally, for a hydrated electrolyte with the formula of $A_{\nu_+}X_{\nu_-} \cdot nH_2O$, the solubility in water, m'_{sat},[1] is expressed by the following equation:[2]

$$-\nu \boldsymbol{R} \ln\left(\frac{m'_{sat}}{m'_{sat}+M/(n+\nu)}\right) - n\boldsymbol{R} \ln\left(\frac{m'_{sat}+M/n}{m'_{sat}+M/(n+\nu)}\right) = \frac{\Delta H_s(sat)}{T} - \Delta S_m{}^F + \Delta C_p \ln\left(\frac{T_m}{T}\right) - S^E \qquad (1)$$

where $\nu = \nu_+ + \nu_-$, $\boldsymbol{R}$ is the gas constant, ΔS_m^F is the molar entropy of fusion at the melting point (T_m), ΔC_p is the difference in molar-heat capacities at a constant pressure between a liquid (fused) state and a solid state, and S^E is the entropy of mixing of a liquid (fused) electrolyte other than the cratic term (the left-hand side of Eq. (1)).

For $CaCl_2 \cdot 6H_2O$, for which all the experimental data are available,[3,4] the terms of the above equation become, at 25°C:

$$-\nu \boldsymbol{R} \ln\left(\frac{m'_{sat}}{m'_{sat}+M/(n+\nu)}\right) - n\boldsymbol{R} \ln\left(\frac{m'_{sat}+M/n}{m'_{sat}+M/(n+\nu)}\right) = 0.048\boldsymbol{R},$$

1) m' is molality suitable for a hydrated electrolyte; *i.e.*, an m′ solution of the hydrated electrolyte with a general formula $A\nu_+X\nu_- \cdot nH_2O$ contains $m'\nu_+$ moles of cation A, $m'\nu_-$ moles of anion X, and $m'n$ moles of water in 1000 g of solvent (water). Hence $m' = m/(1 - nm/M)$, where m is usual molality and $M = 55.51$.

2) H. Nakayama, *Bull. of the Faculty of Engineering, Yokoyama National University*, **19**, 29 (1970). The derivation of Eqs. (1) and (2) is briefly given in appendix.

3) "Solubilities of Inorganic and Organic Compounds," Vol. 1, ed. by H. Stephen and T. Stephen, Pergamon Press, London (1963).

4) "International Critical Tables of Numerical Data, Physics, Chemistry and Technology," McGraw-Hill Book Comp., New York (1928).

$\Delta H_s(sat)/T=15.16\boldsymbol{R}$ (this work, Table 1), $\Delta S_m^E=14.81\,\boldsymbol{R}$, $\Delta C_p\ln(T_m/T)=0.41\boldsymbol{R}$; consequently, from Eq. (1), $S^E=0.71\,\boldsymbol{R}$. A notable feature of this example is that the terms having significant values are $\Delta H_s(sat)/T$ (entropy of solution in a saturated solution) and ΔS_m^E, and that these two terms are of approximately the same magnitude. This situation is typical of aqueous solutions of hydrated electrolytes for the following reasons.

Thermodynamically, the dissolution of a solid solute may be divided into two processes: (1) the melting of a solid solute, and (2) the mixing of the melt with a solvent. In the case of an aqueous solution of a hydrated electrolyte, the change in entropy (and also in enthalpy) due to the latter mixing process will be small since the melt of a hydrated electrolyte already contains considerable amounts of water.[5] The $\Delta C_p\ln(T_m/T)$ term in Eq. (1) will also be small because of the low melting point of the hydrated electrolyte. Consequently, it may be concluded that the dissolution process of a hydrated electrolyte is essentially specified by the melting process of a solid state.

On the other hand, $\Delta H_s(sat)$ is connected with the temperature dependence of the solubility $(\partial\ln m'_{sat}/\partial(1/T))_P$ by the following equation:[2]

$$\Delta H_s(sat) = -\nu\boldsymbol{R}\left(1-\frac{nm_{sat}}{M}\right)^2 \times\left(1+\left(\frac{\partial\ln\gamma_\pm}{\partial\ln m}\right)_{sat,T,P}\right)\cdot\left(\frac{\partial\ln m'_{sat}}{\partial(1/T)}\right)_P, \quad (2)$$

where $\gamma_\pm$ is the mean activity coefficient based on the m unit. From this relation, we may expect that the derivative $(\partial\ln\gamma_\pm/\partial\ln m)_{T,P}$ in a saturated solution can be calculated from the thermal data $(\Delta H_s(sat)$ and $(\partial\ln m'_{sat}/\partial(1/T))_P)$ only. In Table 1, the values of $(\partial\ln\gamma_\pm/\partial\ln m)_{sat,T,P}$ obtained in this procedure are compared with those obtained by the graphical differentiation of the existing $\gamma_\pm - m$ data. They are in good agreement within the limits of experimental accuracy. This proposed method may also be applied to other electrolytes.

Experimental

The calorimeter used was a twin-type micro-calorimeter manufactured by Ōyōdenki Kenkyujo (CM-502). The hydrated electrolytes, which were separated from their saturated solutions at 25°C, were left in an atmosphere of a constant vapor pressure of water (the dissociation pressure of each salt) until no more change in weight was observed.

Appendix

If we choose the pure liquid (fused) state as the standard state, the activity of a solid solute, a_2^s, may be given by the following equation:[6]

$$\boldsymbol{RT}\cdot\ln a_2^s = -\Delta H_m^F(1-T/T_m) + \Delta C_p(T_m-T-T\cdot\ln(T_m/T)). \quad (A\text{-}1)$$

On the other hand, when a solid solute is in equilibrium with its saturated solution, $\boldsymbol{RT}\cdot\ln a_2^s$ can be expressed as:

$$\boldsymbol{RT}\cdot\ln a_2^s = (\bar{H}_2(sat)-H_2^l) - T(\bar{S}_2(sat)-S_2^l), \quad (A\text{-}2)$$

Table 1. The partial molar heats of solution of hydrated electrolytes in saturated solutions at 25°C. And the comparison of the values of $(\partial\ln\gamma_\pm/\partial\ln m)_{sat,T,P}$ calculated from thermal data and those observed directly

Electrolytes	ΔH_s (sat) (kcal/mol)	$(\partial\ln\gamma_\pm/\partial\ln m)_{sat,T,P}$ Calcd from Eq. (2)[a]	Observed[b]
$BaCl_2\cdot2H_2O$	4.35	+0.30	+0.39[7]
$NaBr\cdot2H_2O$	3.15	+0.78	+0.62[8]
$MgCl_2\cdot6H_2O$	2.85	+5.50	+5.02[9]
$CaCl_2\cdot6H_2O$	8.98	+2.42	+2.55[10]
$Na_2SO_4\cdot10H_2O$	14.90	−0.40	−0.40[11]

a) The slope $(\partial\ln m'_{sat}/\partial(1/T))_P$ is obtained by graphical differentiation of the solubility data.[3]
b) The values obtained by graphical differentiation using $\gamma_\pm$ data cited.

where the superscript l stands for a liquid state. We may rewrite the enthalpy term of Eq. (A-2) as:[6]

$$\bar{H}_2(sat)-H_2^l = (\bar{H}_2(sat)-H_2^s)-\Delta H_m^F+\Delta C_P(T_m-T) = \Delta H_s(sat)-\Delta H_m^F+\Delta C_P(T_m-T). \quad (A\text{-}3)$$

The entropy term of Eq. (A-2) can be expressed as:

$$\bar{S}_2(sat)-S_2^l = -\boldsymbol{R}\left\{\nu_+\ln\left(\frac{X_+^{sat}}{X_+^l}\right)+\nu_-\ln\left(\frac{X_-^{sat}}{X_-^l}\right)+n\ln\left(\frac{X_{H_2O}^{sat}}{X_{H_2O}^l}\right)\right\}+S^E, \quad (A\text{-}4)$$

with

$$X_+^{sat}=\frac{\nu_+m'_{sat}}{M+m'_{sat}(n+\nu)},\quad X_+^l=\frac{\nu_+}{n+\nu},$$

$$X_-^{sat}=\frac{\nu_-'m_{sat}}{M+m'_{sat}(n+\nu)},\quad X_-^l=\frac{\nu_-}{n+\nu},$$

$$X_{H_2O}^{sat}=\frac{M+nm'_{sat}}{M+m'_{sat}(n+\nu)},\quad X_{H_2O}^l=\frac{n}{n+\nu},$$

where X^{sat} and X^l represent the mole fraction in a saturated solution and in a liquid (fused) state respectively. By combining these four equations, we finally get Eq. (1).

The entropy of solution of a solid solute is connected with the temperature dependence of the solubility by the following equation:[6]

$$\bar{S}_2(m')-S_2^s=\left(\frac{\partial(\mu_2(m')-\mu_2^s)}{\partial\ln m'}\right)_{T,P}\cdot\left(\frac{\partial\ln m'_{sat}}{\partial T}\right)_P. \quad (A\text{-}5)$$

The chemical potential of a hydrated electrolyte ($A\nu_+X\nu_-\cdot n H_2O$) becomes:

$$\mu_2(m')=\mu^{0'}(T,P)+\boldsymbol{RT}\ln(m\gamma_\pm)+n\boldsymbol{RT}\ln a_1, \quad (A\text{-}6)$$

in which a_1 is the activity of water. By inserting Eq. (A-6) into Eq. (A-5) and using the Gibbs-Duhem relation, $M\mathrm{d}\ln a_1+m\mathrm{d}\ln a_2=0$, we obtain for a saturated solution:

$$\bar{S}_2(sat)-S_2^s=\nu\boldsymbol{RT}\left(1-\frac{nm_{sat}}{M}\right)^2\cdot\left\{1+\left(\frac{\partial\ln\gamma_\pm}{\partial\ln m}\right)_{sat,T,P}\right\}\times\left(\frac{\partial\ln m'_{sat}}{\partial T}\right)_P. \quad (A\text{-}7)$$

This equation is identical with Eq. (2), since $\Delta H_s\,(sat)=T(\bar{S}_2(sat)-S_2^s)$.

5) For instance, for $CaCl_2\cdot6H_2O$ the water content is 49.3% in the melt and 54.7% in the saturated solution (at 25°C).

6) J. H. Hildebrand and R. L. Scott, "Regular Solutions," Prentice-Hall Inc., Englewood Cliffs, New Jersey (1962).

7) R. A. Robinson, *Trans. Faraday Soc.*, **36,** 735 (1940).

8) L. L. Makarov, Yu. G. Vlasov, and V. A. Azarko, *Zh. Fiz. Khim.*, **40,** 1134 (1966).

9) G. N. Lewis and M. Randall, revised by K. S. Pitzer and L. Brewer, "Thermodynamics," McGraw-Hill Book Comp., New York (1961).

10) R. H. Stokes, *Trans. Faraday Soc.*, **41,** 637 (1945).

11) R. A. Robinson, J. M. Wilson, and R. H. Stokes, *J. Amer. Chem. Soc.*, **63,** 1011 (1941).

BULLETIN OF THE CHEMICAL SOCIETY OF JAPAN, VOL. 44, 1711—1712 (1971)

The Chemical Behavior of the ^{72}As Formed by the EC Decay of ^{72}Se in an Organic Solvent

Takeshi SOTOBAYASHI, Toshio SUZUKI, and Tomohiko NODA
Department of Chemistry, Faculty of Science, University of Niigata, Niigata

(Received December 24, 1970)

Many papers have been published on the chemistry of a hot atom formed as a result of isomeric transition with internal conversion or negative beta decay.[1-6] Since, however, little information is available on the chemical behavior of an EC-decay product, we attempted to study the chemical behavior of 26-h ^{72}As, an EC-decay product of 8.4-d ^{72}Se, in an organic solvent. In the present work, some organic-solvent solutions of two selenium compounds of different chemical natures (selenocyanate complex and selenium tetrabromide) were prepared by a liquid-liquid extraction method, and the separation of ^{72}As from the solvent solution and the oxidation state of the separated ^{72}As were studied.

TABLE 1. THE NUCLEAR PROPERTIES OF ^{72}As AND PROTON-INDUCED SELENIUM ISOTOPES

Type of production	Nuclide	Half-life	Mode of decay	Major γ-radiations (keV)
—	^{72}As	26 h	EC, β^+	510, 835
p,4n	^{72}Se	8.4d	EC	46
p,3n	^{73}Se	42m, 7.1m	EC	359, 685
p,2n	^{74}Se	stable	—	—
p, n	^{75}Se	120 d	EC	120, 136, 265, 280, 401

An arsenic trioxide target was irradiated with 30-MeV protons in the frequency-modulated cyclotron of the Institute for Nuclear Study of the University of Tokyo. Table 1 shows the nuclear properties of ^{72}As and proton-induced selenium isotopes. The ^{72}Se and ^{75}Se were γ-spectrometrically identified in the target two weeks after the irradiation. The target was dissolved in 6M hydrochloric acid, together with a selenium carrier (SeO_2). Elemental selenium was precipitated by passing sulfur dioxide through the target solution. The precipitate was separately dissolved in 0.1M potassium cyanide and 4M hydrobromic acid, and then converted into potassium selenocyanate and selenium tetrabromide respectively. From these two radioselenium solutions (0.1 mg Se/m*l*), two kinds of organic solutions of purified radioselenium were prepared by the following two procedures. All the radioactivities were γ-spectrometrically measured by using a 3 in $\times$3 in NaI(Tl) scintillation detector coupled with an 800-channel pulse-height analyzer.

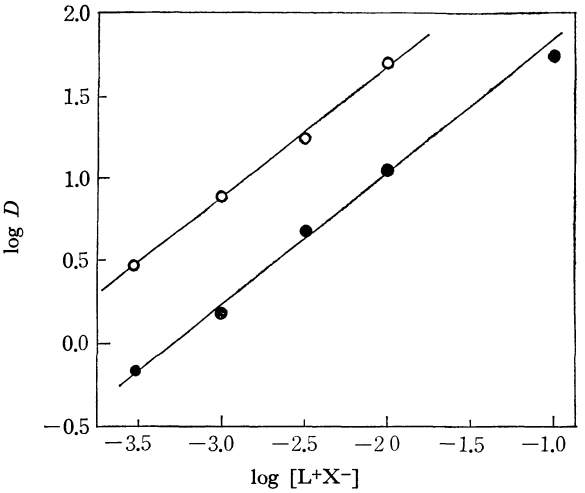

Fig. 1. log D *vs.* log (L^+X^-) plot.
L^+X^-: TPA or TAMA,
—●—: Extraction of $Se^{72,75}$ with TPA in chloroform,
—○—: Extraction of $Se^{72,75}$ with TAMA in chloroform.

First, radioselenium was extracted from the 0.1M potassim cyanide solution into a chloroform solution of 0.01—0.001M tetraphenylarsonium chloride (TPA) or 0.1—0.01M trialkylmethylammonium chloride (TAMA),[7] which had been pre-equilibrated with a 0.1M potassium cyanide solution. Figure 1 shows the extraction behavior of radioselenium with TPA or TAMA in chloroform; the logarithm of the distribution ratio, (D), is plotted against that of the concentration of the extracting reagent (TPA or TAMA). These log-log plots, with an equal slope of about 0.82, suggest that the extracted species with TPA and TAMA were, as expected, $Ph_4As^+SeCN^-$ and $R_3MeN^+SeCN^-$ [7] respectively. Secondly, radioselenium was quantitatively extracted into benzene containing 1 *w*/*v* % phenol from a 4M hydrobromic acid solution. The chemical form of the extracted selenium species is believed to be $SeBr_4$.[8] These two sample solutions (chloroform and benzene) were allowed to stand in a glass vessel for more than one day to obtain a sufficient amount of ^{72}As growing from ^{72}Se. Thereafter, each organic solution was transferred to a second vessel. The inner walls of the emptied vessel were carefully washed with a small portion of the respective solvent

1) S. Wexler and G. R. Anderson, *J. Chem. Phys.*, **33**, 850 (1960).
2) S. Wexler, *ibid.*, **36**, 1992 (1962).
3) J. F. Duncan and F. G. Thomas, *J. Inorg. Nucl. Chem.*, **29**, 869 (1969).
4) T. Shiokawa, H. Kudo, and T. Omori, This Bulletin, **38**, 1340(1965).
5) T. Shiokawa and T. Omori, *ibid.*, **42**, 696(1969).
6) M. Haissinsky, "Nuclear Chemistry and Its Application," (English ed.), Addison-Wesley Pub. Co. Inc., London (1964).
7) An alkyl group, R, refers to $C_nH_{2n+1}(n=8-10)$.
8) T. McGee, U. Lynch, and G. G. Boswell, *Talanta*, **15**, 1435 (1968).

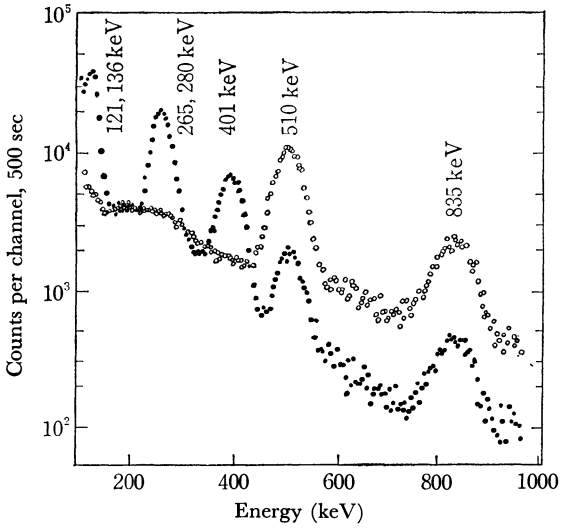

Fig. 2. A set of γ-spectra for an organic phase (TPA, —●—) and its corresponding hydrochloric acid solution containing the deposited fraction of ^{72}As (—○—).

solution, and subsequently with a few milliliters of concentrated hydrochloric acid.

Figure 2 shows the set of γ-spectra for organic and aqueous solutions in the 110– to 1000-keV range. As is shown in Fig. 2, most of the radioselenium proved to remain in the organic solution. Most ^{72}As freshly growing from its parent during equilibration was found in the hydrochloric acid — on the vessel walls. The respective activity fractions of ^{72}As on the walls and in the organic solution were determined by measuring the photopeak areas at 835 keV. The results are summarized in the third column of Table 2.

It should be noted that ^{72}As showed a similar depositing behavior on the vessel walls for the two extracted selenium compounds of different chemical natures. The deposited fraction of ^{72}As seems to decrease with the increase in the concentration of the complexing reagent (TPA). Further, it was found that the fraction of ^{72}As on the walls varied with the ratio of the area in contact with the organic solution to the total volume of the organic solution; the ^{72}As fraction on the walls increased by a factor of 1.5 when the ratio changed from 3.8 to 7.4 cm^2/m*l*. A further examination was carried out in order to determine the percentage abundances in the oxidation state of the deposited ^{72}As obtained in the same way as in the above experiments. As^{3+} and As^{5+} were separated by a conventional hydrochloric acid-benzene extraction method.[9] The results are presented in the last column of Table 2. It may clearly be seen from Table 2 that about 75% of the ^{72}As recovered on the walls existed in the 3+ oxidation state, regardless of the difference in chemical nature of the extracted selenium compound.

Table 2. Deposited fraction of ^{72}As on vessel walls and oxidation state of deposited ^{72}As

Extracting reagent	Aqueous phase	Fraction on vessel walls of ^{72}As (%)	Relative abundance As^{3+} (%)	Relative abundance As^{5+} (%)
TPA, 10^{-3}M	0.1M KCN	81—90	73	27
TPA, 10^{-2}M	0.1M KCN	41—56	75	25
TAMA, $2\cdot10^{-2}$M	0.1M KCN	53	73	27
Benzene[a)]	4M HBr	64—77	78	22

a) The benzene phase contained 1 *w/v* % phenol.

From the present observations, it can be said that the effects of an EC decay process, followed by the bond rupture of the ^{72}Se-tagged compounds, probably play a major role in determining the deposition behavior of ^{72}As.

The authors wish to express their appreciation to Prof. Kazumasa Miyano of the Nuclear Physics Laboratory for his helpful discussions.

9) G. O. Brink, P. Kafas, R. A. Sharp, E. L. Lewis, and J. W. Irvine, Jr., *J. Amer. Chem. Soc.*, **79**, 1303 (1957).

BULLETIN OF THE CHEMICAL SOCIETY OF JAPAN, VOL. 44, 1712—1714 (1971)

Effect of Pressure on Graphitization of Carbon. VIII. Effect of Water on the Graphitization of Carbon under High Pressure

Kanichi KAMIYA* and Michio INAGAKI

Faculty of Engineering, Nagoya University, Furo-cho, Chikusa-ku, Nagoya

(Received December 24, 1970)

It has been reported[1-3] that the graphitization of carbon is promoted remarkably by pressurizing and that the heterogeneous graphitization, in which one domain in coke or char particle is completely graphitized and the other part remains ungraphitized, is observed under high pressure. The pyrophyllite, $Al_2O_3 \cdot 4SiO_2 \cdot H_2O$, which has been used as a pressure transmitting material, begins to be dehydrated around 400°C.[4] The water derived from pyrophyllite was found to accelerate the graphitization of carbon under pressure in the presence of calcite or

* On leave of absence from Toyoda Physical and Chemical Research Institute, Showa-ku, Nagoya.

1) T. Noda and H. Kato, *Carbon*, **3**, 289 (1965).

2) T. Noda, K. Kamiya, and M. Inagaki, This Bulletin, **41**, 485 (1968).

3) K. Kamiya, M. Inagaki, M. Mizutani, and T, Noda, *ibid.*, **41**, 2169 (1968).

4) C. O. Hulse and R. B. Craft, *J. Appl. Phys.*, **36**, 1593 (1965).

calcium carbonate.[5]

In the present work, the effect of water on graphitization of carbon under pressure was investigated by comparing results obtained in experiments of dry system in which calcined pyrophyllite was used as a pressure transmitting material and those in a wet system in which a small amount of water was added to carbon specimen.

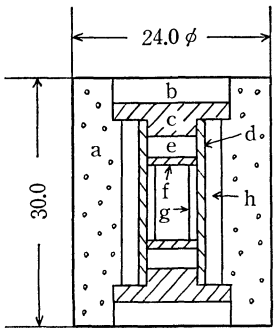

Fig. 1. Pressure cell arrangement
a. pyrophyllite
b. metal disk
c. graphite plate
d. graphite heater
e. pyrophyllite disk
f. graphite plate
g. glass-like carbon
h. boron nitride

Pressurizing of the specimen was carried out by using a piston-cylinder type vessel. The details on experimental apparatus and procedure were reported previously.[2,3] The high pressure cell arrangement used is shown in Fig. 1. In the experiments of dry system, calcined pyrophyllite disks were inserted into the artificial graphite heater (e, in Fig. 1) in place of raw pyrophyllite disks which had been used in previous works. Calcination of pyrophyllite was performed at 970°C in air. The completion of dehydration was confirmed by measuring ignition loss (about 6.2%). The mechanical strength of pyrophyllite was found to increase rapidly when calcined above 1000°C.[4] Pyrophyllite calcined at 970°C maintained the original texture, but was a little harder than the raw material. The other parts of cell arrangement were exactly the same as in the previous one. The sample used was a typical soft carbon, the polyvinyl chloride coke, PV-7, carbonized to 680°C. Heat treatment temperature of specimen (HTT) was determined from the consumed electric input-power by using the relation between temperature and consumed power established beforehand. Heat treatments were carried out at several temperatures between 1200°C and 1800°C for various residence times under 5 kbar. The carbons heat-treated under pressure showed a composite profile of (00 l) diffraction lines. The content of the graphitic component G_S was evaluated for the heat-treated carbon by the same procedure as reported in details previously.[1-3]

The variation of content of G_S with HTT for a constant residence time of 60 min is shown in Fig. 2a). In comparison with results of experiments where raw pyrophyllite disks were used in the graphite heater, the development of the component G_S with respect

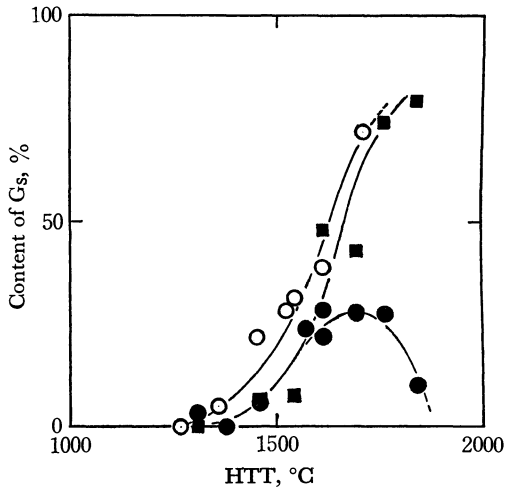

Fig. 2a. Variation of content of the component G_s with HTT for 60 min under 5 kbar.
○ with raw pyrophyllite
● with calcined pyrophyllite
■ with calcined pyrophyllite and water of 20 mg.

to HTT was found to be depressed in the present experiments where calcined pyrophyllite disks were used. Above 1700°C, content of G_S decreased with the increase in HTT. The decrease in the content of G_S was assumed to be due to the fact that, above this HTT, homogeneous graphitization occurred more easily than the heterogeneous one.[6] The variation of content of G_S with residence time at 1800°C under

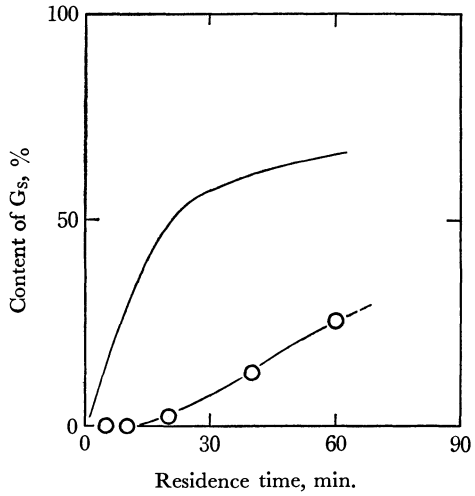

Fig. 2b. Variation of content of the component G_s with residence time at 1590°C under 5 kbar.
— with raw pyrophyllite
○ with calcined pyrophyllite

5 kbar is shown in Fig. 2b). The variation of content of G_S in the case where raw pyrophyllite has been used is also shown. It is clear that heterogeneous graphitization was depressed without any water which originated from the dehydration of pyrophyllite. Even though the pyrophyllite disks in the heater were calcined, there remains the possibility that water might

5) S. Hirano, Théses (March, 1970) Nagoya University.

6) K. Kamiya, M. Inagaki, H. Saito, and T. Noda, This Bulletin, **43**, 926 (1970).

come into the specimen through a boron nitride sleeve from the pyrophyllite cylinder surrounding the graphite heater. In order to eliminate the possibility, the whole pyrophyllite cylinder was calcined at 970°C. Since it became harder with calcination, a part of applied load may have been supported by the cylinder and the pressure in the specimen might be much lower than expected. No exact value of pressure was figured out in this case. The heterogeneous graphitization, however, seemd to occur because a small amount of the graphitic component could be detected on (004) diffraction profile.

In the experiments of wet system, distilled water of about 20 mg was added to the sample and the heat treatments were carried out by using the same pressure cell arrangement as that shown in Fig. 1. The amount of water corresponded roughly to that derived from the complete dehydration of two disks of raw pyrophyllite in the graphite heater and was about 20 weight percent of carbon specimen. Almost the same results as those with raw pyrophyllite were obtained with this arrangement as shown in Fig. 2a).

From the results, it can be said that water accelerates heterogeneous graphitization under pressure, but has nothing to do with the occurrence of heterogeneous graphitization. Heterogeneous graphitization or two-phase graphitization, was found to be possibly caused by the stress-concentration at the contacts between the coke particles.[7)]

The authors wish to thank Dr. T. Noda, president of Mie University, for his valuable discussion and perusal of the paper, and Prof. S. Naka of the Faculty of Engineering, Nagoya University, for his encouragement and valuable discussions.

7) K. Kamiya, M. Inagaki, and T. Noda, *Carbon*, in press.

BULLETIN OF THE CHEMICAL SOCIETY OF JAPAN, VOL. 44, 1714—1716 (1971)

The Dehydration of Alcohols to Ethers or Olefins with Triphenyl[(phenylcarbamoyl)methyl]phosphonium Inner Salt[1]

Suketaka Ito and Shigetsugu Sugiura

Department of Industial Chemistry, Faculty of Engineering, Shinshu University, Wakasato, Nagano

(Received December 31, 1970)

An equilibrium has been set up between benzylidenetriphenylphosphorane with alcohol and the corresponding phosphonium alkoxide, and the equilibrium mixture has been shown to undergo the Wittig reaction successfully.[2,3]

It has been reported, however, by Grayson and Keough[4] that phosphonium salts containing a benzyl group react with ethanolic sodium ethoxide (or butanolic sodium butoxide) to give toluene, ether, and tertiary phosphine oxide, and that the same products are obtained from the corresponding phosphorane and alcohol. In another report, by Speziale and Ratts,[5] dichloromethylenetriphenylphosphorane has been shown to react with *t*-butanol to afford isobutene, along with dichloromethane and phosphine oxide. In these investigations, the reactivities of other types of alcohols have not been studied.

In this paper we wish to describe the reaction of several alcohols, including a diol, and phenol with the title phosphonium inner salt.

Results and Discussion

Triphenyl[(phenylcarbamoyl)methyl]phosphonium Inner Salt (Ia). Ia could be obtained in a 80—90% yield by the treatment of triphenyl[(phenylcarbamoyl)methyl]-phosphonium chloride(VIII) with sodium hydride in benzene containing a small amount of dimethyl sulfoxide. Although Trippett and Walker[6] postulated the ylide form of Ia as the intermediate in the reaction of methylenetriphenylphosphorane with two molecules of phenyl isocyanate, the IR and the NMR spectrum of Ia exhibit no N–H peak; therefore, Ia exists in the inner salt form, that is, the betaine form, in which the negative charge can be more delocalized by resonance than in the ylide form:

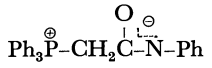

Ia

Reaction of Ia with Alcohols. When Ia was allowed to react with alcohol in benzene or excess alcohol under refluxing in a slow stream of nitrogen, an ether and/or an olefin were observed as the volatile products. All the olefins except cyclohexene were allowed to be absorbed in a bromine-dichloromethane solution, and were determined as dibromides. The diethyl ether and cyclohexene were condensed in a cold trap, and the

1) Partly presented at the 23rd Annual Meeting of the Chemical Society of Japan, Tokyo, April, 1970.

2) G. Wittig and W. Haag, *Chem. Ber.*, **88**, 1654 (1955).

3) For a review about the Wittig Reaction, see S. Trippett, "Advances in Organic Chemistry, Methods and Results," Vol. 1, ed. by R. A. Raphael, E. C. Taylor, and H. Wynberg, Interscience Publishers, Inc., New York, 1960, pp. 83—102.

4) M. Grayson and K. W. Keough, *J. Amer. Chem. Soc.*, **82**, 3919 (1960).

5) A. J. Speziale and K. W. Ratts, *ibid.*, **84**, 854 (1962).

6) S. Trippett and D. M. Walker, *J. Chem. Soc.*, **1959**, 3874.

Table 1. The ethers and the olefins obtained by the reaction of alcohols with triphenyl[(phenylcarbamoyl)methyl]phosphonium inner salt (Ia)

Alcohol (m*l*)	mmol of Ia	Reflux time (hr)	Ether (Yield, %)	Olefin (Yield, %)
EtOH (50)	20	1	Et_2O (16)	Ethylene (trace)
EtOH (50)	20	3	Et_2O (54)	Ethylene (trace)
n-BuOH (20)	5	1	Bu_2O (60)	1-Butene (trace)
Iso-PrOH (20)	5	3	$(Iso\text{-}Pr)_2O$ (0)	Propene (9)
t-BuOH (20)	5	3	*t*-Bu_2O (0)	Isobutene (0.4)
 -OH (20)	5	3	$_2$O (0)	Cyclohexene (13)
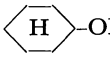 -OH (10)+EtOH (10)	5	3	Et_2O (18)+Et-O- (0)	Ethylene (trace) +Cyclohexene (1)
Allyl-OH (20)	5	1	$(Allyl)_2O$ (57)	
n-BuOH (20)	5	a)	Bu_2O (3)	1-Butene (—)
Allyl-OH (20)	5	a)	$(Allyl)_2O$ (11)	
n-BuOH[b]	5	3	Bu_2O (2)	1-Butene (0)
$PhCH_2OH$[b]	5	3	$(PhCH_2)_2O$ (29)	
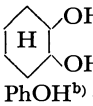 (*trans*)[b]	5	3	O (9)	
PhOH[b]+MeOH (1)	5	1+1	PhOMe (22)	

a) The temperature of the mixture was maintained at 20°C for 24 hr.
b) A portion of 20 mmol of alcohol in 20 m*l* of benzene was used.

Table 2. The reaction of triphenyl[(phenylcarbamoyl)methyl]phosphonium chloride (VIII) with sodium alkoxide in alcohol[a]

Alcohol (m*l*)	mmol of VIII	Reflux time (hr)	Ether (Yield, %)	Olefin (Yield, %)
EtOH (50)	20	1	Et_2O (29)	Ethylene (trace)
EtOH (50)	20	3	Et_2O (73)	Ethylene (trace)
Iso-PrOH (20)	5	3	$(Iso\text{-}Pr)_2O$ (0)	Propene (13)
n-BuOH (20)	5	1	Bu_2O (74)	1-Butene (trace)
n-BuOH (20)	5	3	Bu_2O (82)	1-Butene (trace)
t-BuOH (20)	5	3	*t*-Bu_2O (0)	Isobutene (0.4)

a) The amount of sodium alkoxide was 10 percent excess to VIII.

other ethers were detected directly from the reaction mixtures by means of GLC.

Acetanilide (VIa) and triphenylphosphine oxide (VII) were also obtained; for example, the yields of VIa and VII in the reaction of ethanol for 3 hr were 77 and 74% respectively.

The treatment of Ia with phenol in refluxing benzene gave acetanilide; no volatile products were observed in this case. When methanol was added to the above reaction mixture (Ia+phenol), anisole was obtained. The alcohols, the ethers, and the olefins obtained are summarized in Table 1. The reaction of alcohols with Ia can be illustrated as follows:

The final step of this reaction may be analogous to the second step of the Michaelis-Arbusov reaction. On account of the steric hindrance, the secondary and tertiary alcohols are less reactive and gave olefins exclusively in poor yields. The primary alcohols afforded ethers in fairly good yields, and those containing an eliminatable hydrogen atom in the β-position generated olefins as a by-product, whereas no ethylenic product was obtained in the reaction of ethanol or butanol with benzylidenetriphenylphosphorane.[4] The high reactivity of allyl and benzyl alcohol is reasonable and parallel with the observation in the reaction of monobromocyanoacetamide and triethyl phosphite with these alcohols.[7]

Reaction of Phosphonium Chlorides with Alcoholic Sodium Alkoxides. Table 2 shows the yields of ethers and olefins in the reactions of the corresponding phosphonium chloride (VIII) with sodium alkoxide in alcohol. The yields of ethers are higher in the reactions of VIII than in those of Ia, probably because of the relative stability of Ia in alcohol. Table 3 shows the results of the reactions of the related phosphonium salts with butanolic sodium butoxide. In Scheme 1, the driving force for the collapse of III to IV is attributed to a weakening of the P–C bond, because the negative

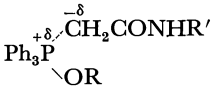

charge of the leaving group can be delocalized. Therefore, if the R′ of the leaving group is electron-attractive, III can probably alter to IV with ease.[8] On the other hand, the electron-attractive ability of R′ may facili-

7) T. Mukaiyama, O. Mitsunobu, and T. Obata, *J. Org. Chem.*, **30**, 101 (1965).

8) Grayson and Keough[4] observed the decreased reactivity of the unsubstituted benzyltriphenylphosphonium chloride compared to the *p*-nitro homolog and the inertness of the butyltriphenylphosphonium salt in the ether-formation reaction.

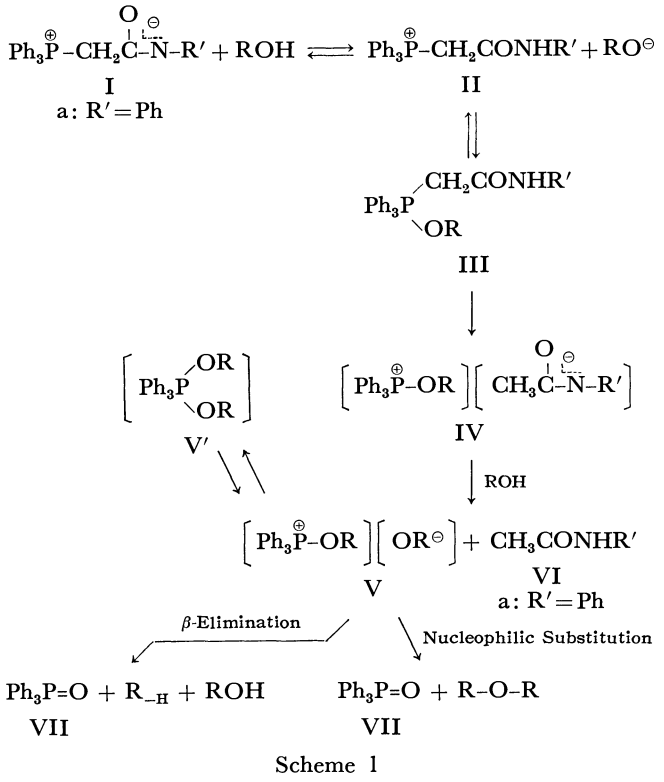

Scheme 1

TABLE 3. THE REACTION OF PHOSPHONIUM CHLORIDE, $Ph_3{}^{\oplus}CH_2CONHR'\ Cl^{\ominus}$ WITH SODIUM BUTOXIDE IN *n*-BUTANOL[a)]

-R'	Yield of Bu_2O (%)
-Ph	74
$-C_6H_4$-Me(-*p*)	47
$-C_6H_4$-OMe(-*p*)	35
$-C_6H_4$-Cl(-*p*)	62
$-CH_2Ph$	58
-H	46

a) A portion of 5 mmol of the phosphonium chloride was allowed to react with 5.5 mmol of sodium butoxide in 20 m*l* of refluxing butanol for 1 hr.

tate the abstraction of the amido proton by a base and may also cause the stabilization of I. In view of these opposite effects, it may be difficult to obtain an unequivocal relationship between the nature of the *N*-substituents of the phosphonium chlorides and their reactivity in this reaction.

Experimental[9)]

Triphenyl[(phenylcarbamoyl)methyl]phosphonium Inner Salt (Ia). A mixture of 12.9 g (0.03 mol) of triphenyl (phenylcarbamoyl)-methyl phosphonium chloride(VIII) and 80 m*l* of dry benzene was refluxed under a nitrogen atmosphere for 2 hr with 1.1 g (0.033 mol) of dispersed sodium hydride in mineral oil (72%) and 2 g of dimethyl sulfoxide. The reaction mixture was then cooled, and a small amount of precipitates was removed by decantation. Crystallization was then induced by scratching the flask containing the solution. After standing for 2 hr, the resulting crystalline precipitate was filtered, washed with two 10-m*l* portions of benzene, and dried *in vacuo*. The yield of Ia was 10.4 g (87%). The recrystallization of Ia from benzene gave pale yellow needles; mp 122—125°C.

Found: C, 79.11; H, 5.67; N, 3.13%; mol wt (MS), 395
Calcd for $C_{26}H_{22}NOP$: C, 78.97; H, 5.61; N, 3.54%; mol wt 395.5.

The treatment of Ia with gaseous hydrogen chloride in benzene afforded the starting quaternary phosphonium salt quantitatively.

Reaction of Ia with Ethanol.[10)] A mixture of 7.91 g (0.02 mol) of Ia and 50 m*l* of absolute ethanol was refluxed for 3 hr in a slow stream of nitrogen. In a cold trap (−70°C) connected to the reaction flask through a condenser, was condensed diethyl ether (54%), which was determined by means of GLC using a 2.25-meter polyethylene glycol-6000 column at 50°C. The reaction mixture was cooled, concentrated, and then chromatographed on 40 g of 100-mesh silica gel (2.2×30 cm; benzene-ether, and benzene-ethanol) to give 2.08 g (77%) of acetanilide(VIa, mp 114—115°C) 4.11 g (74%) of triphenylphosphine oxide(VII, mp 156—157°C). VIa (82%) could be detected also directly from the reaction mixture by means of GLC using a 2.25-meter silicone grease DC-550 column at 200°C.

Reaction of Triphenyl[(phenylcarbamoyl)methyl]phosphonium Chloride (VIII) and Related Compounds with Alcoholic Sodium Alkoxide. Phosphonium Chlorides. These compounds were prepared from triphenylphosphine (0.2 mol) and the corresponding halides (0.2 mol) by a modification of the procedure of Fuerst and his associates[11)] by treatment in refluxing ethanol (50—70 m*l*) for 3—4 hr. Yields: 80—90% (except one example). Triphenyl[(benzylcarbamoyl)methyl]phosphonium chloride: colorless prisms; mp 230—233°C; yield, 80%.

Found: C, 72.38; H, 5.78; N, 3.08%. Calcd for $C_{27}H_{25}$-NOP: C, 72.74; H, 5.65; N, 3.14%. Triphenyl[(*p*-nitrophenylcarbamoyl)methyl]phosphonium chloride: pale yellow prisms; mp 212—213°C;[12)] yield, 24%. (Found: C, 65.38; H, 4.77; N, 5.79%).

Reaction of VIII with Sodium Butoxide in Butanol.[13)] A mixture of 2.16 g (0.005 mol) of VIII and 20 m*l* of *n*-butanol containing 0.0055 mol of sodium butoxide was refluxed for 1 hr in a stream of nitrogen. The 1-butene thus generated was allowed to be absorbed in a bromine—dichloromethane solution in a trap connected to the reaction flask through a condenser. The reaction mixture was cooled, and then dibutyl ether (74%) in butanol was detected by means of GLC using a 2.25-meter silicone grease DC-550 column at 80°C.

9) Melting points are uncorrected. The yields of the products are shown in mole percentage. For the micro-analysis, a Perkin-Elmer Elemental Analyzer Model 240, and a Shimadzu Gas Chromatograph Model GC-2C for the GLC determination were employed.

10) The reactions of Ia with alcohols were represented by this example.

11) H. Fuerst, G. Wetzke, W. Berger, and W. Schubert, *J. Prakt. Chem.*, **17**, 299 (1962).

12) Fuerst *et al.*[11)] reported the melting point of this compound to be 79°C.

13) The reactions of the phosphonium chlorides with alcoholic sodium alkoxides were represented by this example.

BULLETIN OF THE CHEMICAL SOCIETY OF JAPAN, VOL. 44, 1717 (1971)

Syntheses and Reactions of Functional Polymers. LVII. Synthesis and Polymerization of Isopropenyl-1,3,4-oxadiazolin-5-ones

Takeshi ENDO, Takeshi INOUE, and Makoto OKAWARA

Research Laboratory of Resources Utilization, Tokyo Institute of Technology, Ookayama, Meguro-ku, Tokyo

(Received January 7, 1971)

It has been reported[1] that 2-alkyl-1,3,4-oxadiazolin-5-ones are obtained by the reaction of hydrazides with phosgene, but the synthesis of 2-isopropenyl-1,3,4-oxadiazolin-5-ones is not known. We found that 2-isopropenyl-1,3,4-oxadiazolin-5-ones I-III were obtained easily by the reaction of corresponding hydrazides with phosgene.

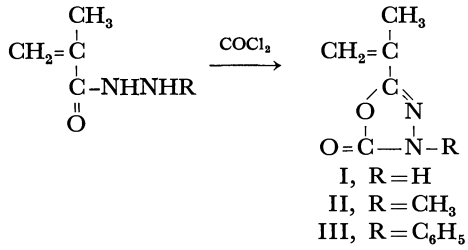

I, R=H
II, R=CH_3
III, R=C_6H_5

II was also obtained by the reaction of sodium salt of I with methyl iodide.

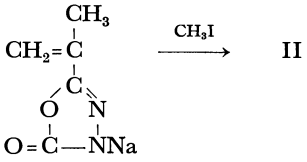

The structures of I-III were confirmed by IR spectrum and elementary analysis. The results are given in Table 1. IR spectra indicate three characteristic absorption bands.

Radical polymerization of I-III was carried out in bulk to give new type polymers containing oxadiazolone group in the side chain.

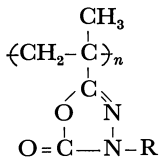

P-I, R=H
P-II, R=CH_3
P-III, R=C_6H_5

The results are shown in Table 2. The absorption attributable to double bond (C=C) in the polymers disappeared, and the absorption of C=N shifted to a higher wave number as compared with monomer due to the absence of conjugation with double bond (C=C). The polymers obtained were soluble in dipolar aprotic solvents such as dimethylformamide (DMF), dimethyl sulfoxide and methylpyrrolidone, but insoluble in common solvents such as water, alcohol and benzene.

TABLE 1. SYNTHESES OF 2-ISOPROPENYL-1,3,4-OXADIAZOLIN-5-ONES

Compounds	Yield (%)	Melting point °C	IR (cm^{-1}) C=C	IR (cm^{-1}) C=N	IR (cm^{-1}) C=O	Elementary analysis (%)			
I	50	83—84	1640	1570	1770	Calcd	C 47.62,	H 4.80,	N 22.22
						Found	C 47.27,	H 4.74,	N 22.40
II	50	49—50	1637	1565	1775	Calcd	C 51.42,	H 5.75,	N 19.99
						Found	C 50.90,	H 5.80,	N 19.96
III	100	103—104	1635	1565	1765	Calcd	C 65.33,	H 4.98,	N 13.86
						Found	C 65.54,	H 4.92,	N 13.87

TABLE 2. POLYMERIZATION OF 2-ISOPROPENYL-1,3,4-OXADIAZOLIN-5-ONES

Compounds	Time (hr)	Temp. (°C)	Yield (%)	$[\eta]$[a]	IR (cm^{-1}) C=N	IR (cm^{-1}) C=O	Form of polymers
I	4	100	64.3	0.34	1600	1765	brown powder
II	4	100	47.0	0.22	1605	1780	white powder
III	3	110	54.3	0.20	1620	1785	white powder

Catalyst: azobisisobutyronitrile (AIBN) 3 mol% for monomers.
a) Measured at 30°C in DMF.

1) W. R. Sherman, *J. Org. Chem.*, **26**, 88 (1961).

BULLETIN OF THE CHEMICAL SOCIETY OF JAPAN, VOL. 44, 1718—1719 (1971)

Synthese Einiger 6-Substituierten 9-Vinylpurine

Kiichi TAKEMOTO, Fumio KAWAKUBO, und Koichi KONDO

Abteilung für Petrochemie, Technische Fakultät der Universität Osaka, Suita, Osaka

(Eingegangen am 5. Februar, 1971)

Im Zusammenhang mit einer Reihe von Untersuchungen über Vinylverbindungen der Nucleinbasen[1] haben wir einige 6-substituierten 9-Vinylpurine (II) neu hergestellt. Als Homologe sind bisher 9-Vinyladenin[2,3], 9-Vinylhypoxanthin[4] und 6-Chlor-9-vinylpurin (I)[5] bekannt, und die Polymerisation sowie

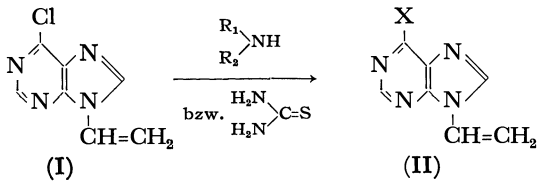

(I) (II)

($R_1=R_2=CH_3$ od. C_2H_5)

die Eigenschaften der erhaltenen Polymeren wurden näher untersucht.[6] Nach einem einfacheren Prinzip stellten wir einige noch unbekannten 9-Vinylpurine ausgehend von 6-Chlor-9-vinylpurin (I) dar: 6-Dimethylamino-9-vinylpurin (II, $X=N(CH_3)_2$) wurde aus I in wäßriger Dimethylaminlösung nach 4-stündigem Rühren bei Raumtemperatur, 6-Diäthylamino-9-vinylpurin (II, $X=N(C_2H_5)_2$) wurde aus I in wäßriger Diäthylaminlösung nach 2-stündigem Rückflüß, 6-Hydrazino-9-vinylpurin (II, $X=NHNH_2$) wurde aus I in Hydrazinhydrat nach 30-minutenlangem Rühren bei Raumtemperatur, und 6-Mercapto-9-vinylpurin (II, X=SH) wurde aus I unter Einwirkung von äquimolarem Thioharnstoff in Äthanollösung nach zweistündigem Rückfluß gewonnen. IR und NMR-Spektren bestätigen die Konstitutionen der Produkte. Die Verbindungen mit Dimethylamino- sowir Diäthylaminogruppen sind in Wasser, Benzol und Alkohol löslich, und die 6-Hydrazino-9-vinylpurin ist in Wasser löslich, in Benzol und Äthanol aber sehr schwer löslich. Im Gegensatz zu diesen Vertretern ist 6-Mercapto-9-vinylpurin sowohl in Wasser als in allen gewöhnlichen Lösungsmitteln unlöslich, nur in wäßriger NaOH-Lösung aber löslich.

Unter den hergestellten Vinylpurinen lassen sich nur 6-Dimethylamino- und 6-Hydrazinoderivate unter der radikalischen Bedingung polymersieren: der Polymerisationsumsatz beträgt bei jenem Vertreter 32%, und bei diesem Vertreter wenig, wenn die Polymerisation in Dimethylsulfoxid bei 80°C in 8 Stunden in Gegenwart von 10^{-3} Mol/*l* Azobisisobuttersäuredinitril durchgeführt wird. In der gleichen Versuchsbedingung beträgt der Umsatz bei 6-Chlor-9-vinylpurin 88%. Die Polymere sind farbloses Pulver, enthalten nicht mehr Vinylgruppe, sind in allgemeinen in Wasser und Methanol löslich, in Äther aber unlöslich. Die Synthese der anderen neuen 9-Vinylpurine, sowie die Versuche über die Eigenschaften der hergestellten monomeren und polymeren 9-Vinylpurine in bezug auf ihre 6-ständigen Substituenten sind im Gange.

Beschreibung der Versuche

6-Chlor-9-vinylpurin (I). 6-Chlor-9-vinylpurin wird aus 6-Chlorpurin bei der Umsetzung mit Vinylacetat in Anwesenheit von Quecksilber(II)-salz hergestellt.[5]

6-Dimethylamino-9-vinylpurin (II, $X=N(CH_3)_2$). 0.50 g (2.8 mMol) I wird in 20 m*l* wäßr. 50%iger Dimethylaminlösung 4 Stde. bei Raumtemperatur gerührt. Die Lösung wird dann eingeengt und der Rückstand aus Petroläther umkristallisiert. Ausbeute 0.45 g (86% d. Th.), farblose Nadeln.

6-Diäthylamino-9-vinylpurin(II, $X=N(C_2H_5)_2$). 0.50 g (2.8 mMol) I wird in 20 m*l* wäßr. 50%iger Diäthylaminlösung 2 Stde. unter Rückfluß gekocht. Die Lösung wird dann eingeengt, der gebliebene Rückstand dreimal mit je

TABELLE 1. DARGESTELLTE 6-SUBSTITUIERTN 9-VINYLPURINE (II)

X	Schmp.	% Ausb.	Summenformel (Mol. -Gew.)		Analysenwerte C(%)	H(%)	N(%)
$-N(CH_3)_2$	146—147°C[a]	86	$C_9H_{11}N_5$	Ber.	57.14	5.82	37.04
			(189.2)	Gef.	56.89	5.74	37.32
$-N(C_2H_5)_2$	80.5—81.5°C	58	$C_{11}H_{15}N_5$	Ber.	60.83	6.91	32.26
			(217.3)	Gef.	60.81	6.95	32.18
$-NHNH_2$	165—167°C[a]	85	$C_7H_8N_6$	Ber.	47.73	4.54	47.73
			(176.2)	Gef.	47.60	4.28	48.09
-SH	298°C[b]	75	$C_7H_6N_4S$	Ber.	47.19	3.37	31.46
			(178.2)	Gef.	47.18	3.12	31.53

a) sublimiert b) zersetzt

1) M. Imoto und K. Takemoto, *Synthesis*, **1970**, 173.
2) N. Ueda, K. Kondo, M. Kono, K. Takemoto, und M. Imoto, *Makromol. Chem.*, **120**, 13 (1968).
3) H. Kaye, *Polym. Lett.*, **7**, 1 (1969).
4) K. Kondo, H. Iwasaki, N. Ueda, K. Takemoto, und M. Imoto, *Makromol. Chem.*, **125**, 298 (1969).
5) J. Pitha und P.O.P.Tso, *J. Org. Chem.*, **33**, 1341 (1968).
6) K. Kondo, H. Iwasaki, K. Nakatani, N. Ueda, K. Takemoto, und M. Imoto, *Makromol. Chem.*, **125**, 42 (1969).

30 m*l* Äther extrahiert, und das so extrahierte Produckt nach Einengen in Wasser umgefallen. Ausbeute 1.35 g (58% d. Th.), farblose Nadeln.

6-Hydrazino-9-vinylpurin(II, X=NHNH$_2$). 0.50 g (2.8 mMol) I wird in 20 m*l* Hydrazinhydrat 30 Minuten bei Raumtemperatur gerührt. Der gebildete Niederschlag wird dann abfiltriert, und aus Wasser-Äthanol-Gemisch (1:1) umkristallisiert. Ausbeute 0.50 g (85% d.Th.), farblose Nadeln.

6-Mercapto-9-vinylpurin(II, X=SH). 0.50 g (2.8 mMol) I wird mit äquimolarer Menge Thioharnstoff in 20 m*l* Äthanol 2 Stde. gerührt. Das niedergeschlagene Produkt wird dann abfiltriert, in 1 N-NaOH-Lösung gelöst, und mit Essigsäure umgefällt. Ausbeute 0.37 g (75% d.Th.), hellgelbes amorphes Pulver.

SHORT COMMUNICATIONS

Chronopotentiometric Oxidation of Biferrocenyl in Anhydrous Acetonitrile and in Methylene Chloride[1)]

Tamotsu MATSUMOTO, Masanori SATO, and Akio ICHIMURA[2)]

Laboratory of Analytical and Inorganic Chemistry, Faculty of Textile Science, Kyoto Technical University, Matsugasaki, Sakyo-ku, Kyoto

(Received January 21, 1971)

It is well known from voltammetric studies that ferrocene as well as its substituted derivatives generally shows a reversible one electron oxidation wave in non-aqueous solvents.[3)] By using chronopotentiometry at the bright platinum anode, we found that biferrocenyl which consists of two equivalent ferrocenyls shows two step waves, each corresponding to one electron oxidation.

The current reversal chronopotentiograms of biferrocenyl in both solvents are shown in Figs. 1 and 2. Results of the current reversal at the first oxidation step show the oxidation proceeds reversibly in both solvents, because the ratio of transition time τ (A)/τ (A') equals 3/1, and $E_{0.25\,\tau(A)}$ equals approximately $E_{0.22\tau(A)}$. On the contrary, the second oxidation step seems completely irreversible in acetonitrile, since no reduction wave is shown by the current reversal at the second oxidation step (ABA' in Fig. 1). Nevertheless the reduction wave corresponding presumably to the reduction of the oxidized product in the case of the current reversal at the first oxidation step remains unchanged. The product at the second oxidation step is more stable in methylene chloride than in acetonitrile. As is shown in Fig. 2, the reduction wave (B') of the oxidized product at the second oxidation step appears in spite of its irreversible character. In curve ABB'A', Fig. 2, the ratio of transition times, τ(A):τ(B):τ(B'):τ(A'), is equal to 1.0:2.5:0.3:0.9, which is approximately equal to the theoretical value[4)]; 1.0:3.0:0.29:1.05.

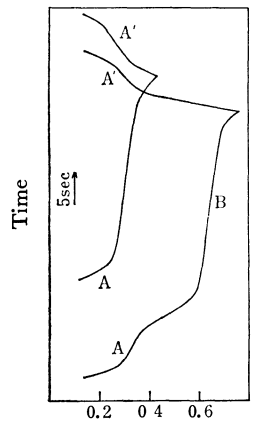

V *vs.* SCE

Fig. 1

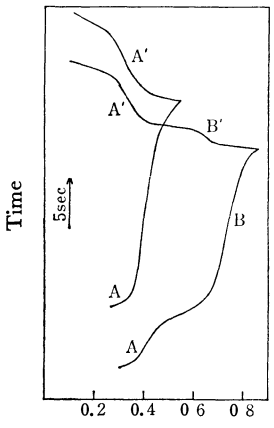

V *vs.* SCE

Fig. 2

Figs. 1 and 2. Current reversal chronopotentiograms of biferrocenyl in acetonitrile (Fig. 1) and in methylene chloride (Fig. 2).

$$\mathrm{Fc\text{-}Fc} \underset{+e}{\overset{-e}{\rightleftarrows}} \mathrm{Fc^+\text{-}Fc}, \quad (A/A') \qquad \mathrm{Fc^+\text{-}Fc} \underset{+e}{\overset{-e}{\rightleftarrows}} \mathrm{Fc^+\text{-}Fc^+}. \quad (B/B')$$

Biferrocenyl: 0.406 mmol/*l* (Fig. 1); 0.144 mmol/*l* (Fig. 2). Supporting electrolyte: 0.1M-Et_4NClO_4 (Fig. 1); 0.05M-Bu_4NClO_4 (Fig. 2).

Concerning the mechanism of the electrochemical oxidation of the biferrocenyl, it seems that in analogy to the oxidation of ferrocene derivatives each ferrocenyl group in a biferrocenyl molecule is oxidized at different potentials (Table 1). Denoting $(C_5H_5)Fe(C_5H_4)$- by Fc–, the following oxidation scheme can hold in both solvents.

$$\mathrm{Fc\text{-}Fc} - \mathrm{e} = \mathrm{Fc^+\text{-}Fc} \quad \text{(1st wave)}$$

$$\mathrm{Fc^+\text{-}Fc} - \mathrm{e} = \mathrm{Fc^+\text{-}Fc^+} \quad \text{(2nd wave)}$$

The reason for the splitting of the oxidation step can be understood by considering that for the first oxidation of one ferrocenyl group the other ferrocenyl group in a same molecule acts as an electron donating substituent group. Consequently the quarter wave potential is shifted to a more negative direction compared with that of ferrocene. Contrary to this, at the second oxidation step, the oxidized form of one ferrocenyl group acts as an electron withdrawing substituent group to the other ferrocenyl group. Thus, the characteristic potential of the second wave is shifted to the more positive potential compared with that of ferrocene. As for the second oxidation step in acetonitrile solvent, it seems that the product reacts chemically with an unoxidized biferrocenyl causing disproportionation to give Fc$^+$–Fc, which is identical with the product at the first oxidation step.

TABLE 1. CHARACTERISTIC POTENTIALS[a)] OF BIFERROCENYL AND FERROCENE (25°C)

Compound \ Solvent	Acetonitrile (0.1M Et_4NClO_4)	Methlyene chloride (0.05M Bu_4ClO_4)
Biferrocenyl		
1st wave	+0.286	+0.380
2nd wave	+0.635	+0.715
Ferrocene	+0.385	+0.440

a) $E_{0.25\tau(A)}$ (1st wave) and $E_{0.42\tau(B)}$ (2nd wave); V *vs.* SCE

1) Presented at the 22nd Annual Meeting of the Chemical Society, Tokyo, April 1969, and at the 16th Symposium on Polarography and Electroanalytical Chemistry, Kyoto, September 1970.

2) Present address: Faculty of Science, Osaka City University, Sumiyoshi-ku, Osaka.

3) T. Kuwana, D. E. Bublitz, and G. Hoh, *J. Amer. Chem. Soc.*, **82**, 5811 (1960).

4) H. B. Herman and A. J. Bard, *Anal. Chem.*, **36**, 971 (1964).

On the Composition of the Pentacyanocobaltate(I) Complex

Nobufumi MAKI and Yukio ISHIUCHI
Department of Chemistry, Faculty of Engineering, Shizuoka University, Johoku, Hamamatsu
(Received February 16, 1971)

The question of the composition and structure of the pentacyanocobaltate(I) ion formed by the reduction of pentacyano-cobaltate(II) and -cobaltate(III) complexes still remains in a controversial state in spite of a number of works done on this problem.[1] Nowadays, however, the $[Co^{I}(CN)_5H]^{3-}$ formula has been widely accepted and used as the most possible structure since Griffith and Wilkinson[2] proposed it on the basis of the proton NMR spectrum. In addition, it has already been established that the reaction between $[Co^{I}(CN)_5]^{4-}$ and H^+ can proceed in water.[3]

In the present study, the stoichiometric relation between $[Co^{I}(CN)_5]^{4-}$ and H^+ was determined to be always 2:1, suggesting a dimeric configuration of the pentacyanocobaltate(I) complex in solution. That is, the findings that both the polarographic reductions of Co(III)→Co(I) and of $2H^+ \rightarrow H_2$ can take place simultaneously at −1.75 V (*vs.* SCE) at the dropping mercury electrode (DME)[4] suggested to us the idea of employing the diffusion currents of both waves to follow the reaction between $[Co^{I}(CN)_5]^{4-}$ and H^+ by means of amperometric titrations.

The titrations of the parent complexes, $K_m[Co(X)(CN)_5]$, were carried out with 0.2 N HCl under a stream of nitrogen at the constant potential (−1.75 V) at which the current had reached a limiting plateau, indicating the formation of the $[Co^{I}(CN)_5]^{4-}$ ion at the DME, where the ligand, X, denotes the ion, $S_2O_3^{2-}$, SO_3^{2-}, N_3^-, NO_2^-, SCN^-, I^-, Br^-, or Cl^-, or the molecule, OH_2. The neutral solution to be titrated was prepared by dissolving the crystals of the complex at 10^{-2} M in a 0.5 M Na_2SO_4 solution which had been deaerated by nitrogen. As one example, Figure 1 illustrates the titration of the $[Co^{I}(CN)_5]^{4-}$ ion formed by the reduction of the $K_4[Co(S_2O_3)(CN)_5]$ complex with 0.2 N HCl. At the beginning of titration, the current remains constant while the H^+ ions are being consumed by the $[Co^{I}(CN)_5]^{4-}$ to be titrated. The end-point is indicated by the beginning of an increase in the reduction wave of H^+ ions; the new current corresponds to the reduction of excess hydrogen ions. The following reaction schemes are considered to be the most plausible:

$$2[Co^{III}(S_2O_3)(CN)_5]^{4-} \xrightarrow{2e} 2[Co^{I}(S_2O_3)(CN)_5]^{6-}$$
$$\downarrow$$
$$2[Co^{I}(CN)_5]^{4-} + 2S_2O_3^{2-}$$
$$\downarrow$$
$$[Co^{I}(CN)_5\text{-}H\text{-}Co^{I}(CN)_5]^{7-}.$$

A blank test was carried out, in advance, individually for 0.5 M Na_2SO_4, 0.01 M $Na_2S_2O_3$[5], 0.01 M NaBr[5], and so on, but a straight line without a break was obtained for each solution; the $(2H^+ \rightarrow H_2)$ current increased linearly at −1.75 V when 0.2 N HCl (0—1.5 m*l*) was added, indicating that no reaction of capturing H^+ ions takes place between them.

The sixth ligand, such as $S_2O_3^{2-}$, was confirmed by using a Kalousek commutator[6] to be released from the $[Co^{I}(X)(CN)_5]^{n-}$ ion at the DME.

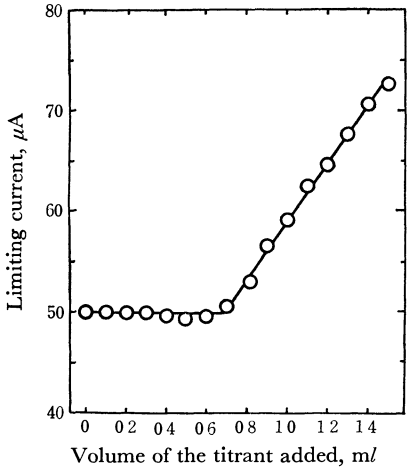

Fig. 1. Amperometric titration curve of the $[Co(S_2O_3)(CN)_5]^{4-}$ ion (35 m*l*) with 0.2N HCl (f=1.173) at −1.75 V (*vs.* SCE). The concn. of the complex: 10^{-2}M in 0.5M Na_2SO_4 (25°C).

TABLE 1. RESULTS OF AMPEROMETRIC TITRATIONS

Compound	Volume of HCl added at equiv. point m*l*	Mole of HCl consumed at equiv. point	Ratio of $[Co^{I}(CN_5)]^{4-}$/H^+ at equiv. point
$K_4[Co(S_2O_3)(CN)_5]$	0.69	1.62×10^{-4}	2.16
$K_4[Co(SO_3)(CN)_5]\cdot3H_2O$	0.70	1.64×10^{-4}	2.13
$K_3[Co(N_3)(CN)_5]\cdot2H_2O$	0.71	1.67×10^{-4}	2.11
$K_3[CoBr(CN)_5]$	0.67	1.57×10^{-4}	2.22

Table 1 summarizes some of the results. Thus, the molar ratio of the $[Co^{I}(CN)_5]^{4-}$ ion to H^+ was approximately 2:1, irrespective of the kind of the ligand, X. This result, combined with the evidence [2] of the existence of a direct linkage between the metal and H^+, suggests that the pentacyanocobaltate(I) complex takes a dimeric structure through a cobalt-hydrogen linkage, such as has been mentioned above.

1) *E.g.*, J. Kwiatek, "Catalysis Review," Vol. 1, ed. by H. Heinemann, Marcel Dekker, New York, N. Y. (1968), pp. 38—152.
2) W. P. Griffith and G. Wilkinson, *J. Chem. Soc.*, **1959**, 2757.
3) J. Hanzlík and A. A. Vlček, *Chem. Commun.*, **1969**, 47.
4) N. Maki, J. Fujita, and R. Tsuchida, *Nature*, **183**, 458 (1959).
5) The ionic strength was adjusted to a unit by adding Na_2SO_4.
6) M. Kalousek, *Collect. Czech. Chem. Commun.*, **13**, 105 (1948).

Infrared Study on Interaction between Porphyrin and Divalent Metal Ion

Hisanobu Ogoshi and Zen-ichi Yoshida
Department of Synthetic Chemistry, Kyoto University, Yoshida, Kyoto
(Received March 3, 1971)

In contrast to the NMR, ESR, and electronic spectra of metalloporphyrins, their infrared spectra have not been understood because of complication. Although only empirical assignment has been done for some observed infrared bands of the naturally occurring porphyrin complexes,[1,2] no systematic band assignment has been made for metalloporphyrins. However, the highly symmetrical metalloporphyrin enables us to assign some characteristic absorptions. Here we reprot the interaction between aromatic ligand and metal ion in the ground state in terms of the aromatic C–H bending vibrations.

The aromatic meso protons of porphyrins are easily exchanged with deuterium in D_2O–D_2SO_4. The band at 835 cm^{-1} of metal-free octaethylporphyrin has been assigned to the meso C–H out-of-plane bending vibration since it disappears on deuteration.[3] It was found that three absorptions for Zn(II)-octaethylporphyrin at 3110, 1220, and 836 cm^{-1} were found to disappear upon deuteration. They are assigned to the C–H stretching (ν(C–H)), in-plane bending (δ(C–H)), and out-of-plane bending (π(C–H)) vibrations, respectively. Zn(II)-octaethylporphyrin-d_4 shows three new bands at 2260, 942, and 638 cm^{-1}. Similarly the bands at 3040, 1227, and 836 cm^{-1} of Zn(II)-octamethylporphyrin are shifted to 2245, 916, and 638 cm^{-1} upon deuteration.

The δ (C–H) and π (C–H) frequencies of various divalent metal complexes of cotaethylporphyrin are listed in Table 1. The stronger coordination between aromatic ligand and metal ion results in the higher frequency shift in the order Pd>Ni>Co>Cu>Zn>Mg. The δ (C–H) frequency is more dependent on the nature of the metal ion than the π (C–H) frequency. The order of the frequency shift is similar to that of the metal sensitive vibration around 1000 cm^{-1} [1,4] and vibrations appearing in the far-infrared region.[1,5] Thus, the frequency shifts of the δ (CH) and π (CH) show clearly the effect of metal ion on aromatic ligand. The order found for the frequency shift is the same as that for the stability replacement reaction,[6] for the one electron-oxidation potential[7] and for the hypsochromic shift in electronic spectrum.[5,7] The shifts of the δ (C–H) and π (C–H) might be related to the changes of the electronic structure of the porphyrin ring. The higher electronegativity of the metal ion or the less ionic character of the metal-porphyrin bond causes the larger shift towards higher frequencies.

Table 1. Frequencies of the in-plane and out-of-plane bending vibrations of the aromatic C–H bond[a]

Complex	In-plane (cm^{-1})	Out-of-plane (cm^{-1})
Mg(II)-OEP	1217	834
Zn(II)-OEP	1220	836
Cu(II)-OEP	1223	837
Co(II)-OEP	1228	837
Ni(II)-OEP	1229	837
Pd(II)-OEP	1229	839

a) Spectra were measured for KBr pellets and frequencies were calibrated with polystyrene.

1) L. J. Boncher and J. J. Katz, *J. Amer. Chem. Soc.*, **89**, 1340 (1967).
2) W. S. Caughey, J. O. Alben, W. Y. Fujimoto, and L. J. York, *J. Org. Chem.*, **31**, 2631 (1966).
3) R. Bonnett, A. D. Gale, and G. F. Stephenson, *J. Chem. Soc., C*, **1967**, 1168.
4) D. W. Thomas and A. E. Martell, *J. Amer, Chem. Soc.*, **81**, 5111 (1959).
5) H. Ogoshi, N. Masai, Z. Yoshida, J. Takemoto, and K. Nakamoto, This Bulletin, **44**, 49 (1971).
6) J. N. Philips, *Rev. Pure Appl. Chem*, **10**, 35 (1960).
7) J. H. Fuhrhop and D. Mauzerall, *J. Amer, Chem. Soc.*, **91**, 4147 (1969).

Pyrolysis of Allethrin

Yasuo NAKADA, Yasuo YURA, and Keisuke MURAYAMA
Central Research Laboratories, Sankyo Co., Ltd., Hiromachi, Shinagawa-ku, Tokyo
(Received March 11, 1971)

Pyrolyses of pyrethroidal compounds have been described by Murayama *et al.*,[1,2] but no work has been done in isolation and structure. We have obtained five compounds by pyrolysis of allethrin, the structures of which are reported in this communication.

Pyrolysis of allethrin was carried out in a pyrex glass tube at 400°C under nitrogen. A typical gas chromatograph of the reaction products is shown in Fig. 1. The reaction products were separated into two fractions and a residue by distillation.

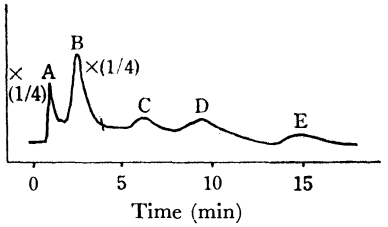

Fig. 1. Gas chromatograph of reaction products. Column: 15%-Silicone XE-60, 191°C.

The first fraction, bp 50—60/38 mmHg, corresponding to peak A, mainly consisted of one compound purified by preparative gas chromatography. Identification of this compound (I) as 2,6-dimethylhepta-2,4-diene was based on the following; *m/e* 124 (M^+) and 109 (M-15); IR, ν_{max} cm^{-1}: 2910; UV, λ_{max}^{EtOH} mμ (log ε): 238 (3.56); NMR[3]: four methyls at 9.07 (d, 3H), 8.95 (d, 3H), 8.28 (s, 3H), and 8.22 (s, 3H), a proton at 7.70 (m, 1H) and olefinic protons at 4.0—4.9 (m, 3H).

The second fraction, bp 90—120/6 mmHg, peak B, consisting of two compounds, II and III, was identified as pyrocin[4] and crysanthemic acid respectively by comparison with authentic samples.

The distillation residue, with peaks C, D, and E in Fig. 1, was separated into three compounds IV, V, and VI by column chromatography on silica gel. Identification of compound IV, corresponding to peak C, as 2,7-diallyl-3,6-dimethyl-1-indanone was based on the following; *m/e* 240 (M^+), 225 (M-15), and 199 (M-41); IR, ν_{max} cm^{-1}: 1710 and 821 (1,2,3,4-tetra-substituted phenyl); UV, λ_{max}^{EtOH} mμ (log ε): 252 (4.11) and 315 (3.44); NMR[5]: a doublet methyl at 8.64 (3H, J=3.5 Hz), a singlet methyl at 7.70 (3H), an allylic methylene as a doublet at 6.56 (2H, J=3.2 Hz), two multiplet vinyl singals at 4.8—5.2 (4H) and 4.0—4.4 (2H), and two doublet protons centered at 2.88 (1H, J=4.0 Hz) and 2.76 (1H, J=4.0 Hz) corresponding to the aromatic protons.

The mass, IR, UV, and NMR spectral data of compound V were very similar to those of compound IV; *m/e* 240 (M^+), 225, and 199; IR, ν_{max} cm^{-1}: 1718 and 830; UV, λ_{max}^{EtOH} mμ (log ε): 262 (4.15) and 293 (3.49); NMR[5]: 8.71 (d, 3H; J=3.7 Hz), 7.67 (s, 2H), 6.55 (dd, 2H; J=2.3 and 1.0 Hz), 4.8—5.3 (m, 4H), 2.88 (d, 1H; J=4.0 Hz) and 2.59 (d, 1H; J=4.0 Hz). An aromatic proton of compound V was found at a lower field than that of compound IV. Thus we concluded that compound V was 2,4-diallyl-3,5-dimethyl-1-indanone, an isomer of compound IV. Compound VI was identified as allethrin by comparison with the retention time (*glc*) and IR spectrum of an authentic sample.

We postulate the reaction mechanism for the pyrolysis of allethrin as shown in Scheme 1.

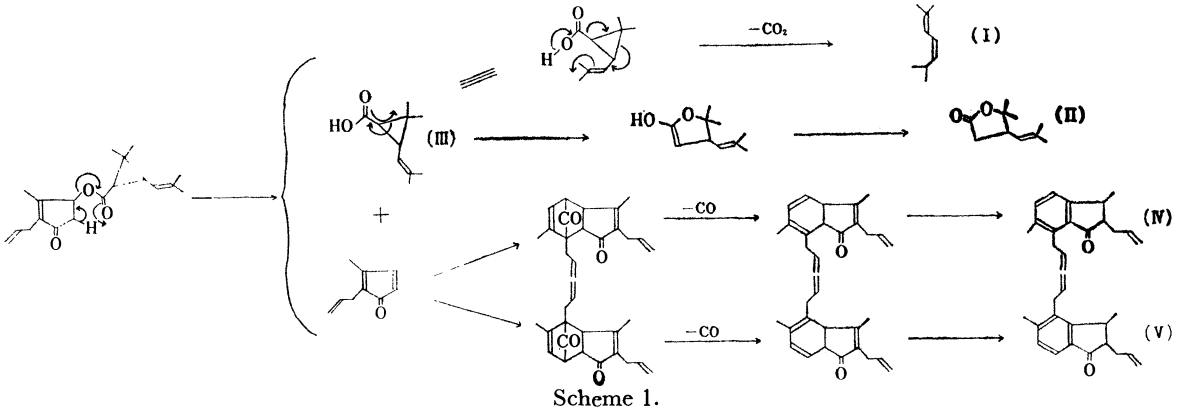

Scheme 1.

1) H. Murayama, K. Kyogoku, T. Iguchi, and H. Yamaguchi, *J. Agr. Chem. Soc. Jap.*, **44**, 532 (1970).
2) N. C. Brown, D. Hollinshead, R. F. Phipers, and M. C. Wood, *Pyrethrum Post*, **4**, 13 (1957).
3) NMR spectra were determined at 60 MHz in CCl_4 and chemical shift is expressed in τ from internal TMS.
4) L. Crombie and S. H. Harper, *J. Chem. Soc.*, **1954**, 470.
5) NMR spectra were determined at 100 MHz in CCl_4.

Partial Ion-Association Constant for Contact Ion-Pairs in Aqueous $[Co(NH_3)_6]^{3+}$-I^- Systems

Haruhiko YOKOYAMA and Hideo YAMATERA

Department of Chemistry, Faculty of Science, Nagoya University, Chikusa-ku, Nagoya

(Received March 31, 1971)

It has been known for many years that ion-pairs can be classified into several classes with different structures and properties; partial ion-association constants for each class of ion-pairs have been reported only in rare cases.[1] Classifying the ion-pair $[Co(NH_3)_6]^{3+}I^-$ into two classes, *contact ion-pairs* and *separated ion-pairs* (those separated by *one or more* solvent molecules), we give partial ion-association constants for each class of ion-pairs.

The spectrophotometric study was made at 25.0± 0.1°C on aqueous systems of a constant ionic strength of 0.062 containing $[Co(NH_3)_6](ClO_4)_3$, KI, and $NaClO_4$. An absorption band which appears near 37 kK on the addition of iodide to an aqueous solution of hexamminecobalt(III) perchlorate is known to be due to the $[Co(NH_3)_6]^{3+}I^-$ ion-pair.[2] Except for the iodide ion (hydrated) and the metal complex ion, no other species absorb light in the wave number range of interest (30—45 kK). The absorbance, D, of the solution can thus be expressed as:

$$D = \varepsilon_M[M]+\varepsilon_A[A]+\varepsilon_{M\cdot\cdot A}[M\cdot\cdot A]+\varepsilon_{M\cdot A}[M\cdot A] \quad (1)$$

where ε symbolizes the molar extinction coefficient and where M, A, M··A, and M·A represent the metal complex ion, the anion (iodide ion), the separated ion-pair, and the contact ion-pair respectively. Equation (1) can be modified to give:

$$\Delta D = (\varepsilon_{M\cdot A(CT)}-\varepsilon_A)[M\cdot A] \quad (2)$$

with $\Delta D = D-\varepsilon_M c_M-\varepsilon_A c_A$, if the following assumptions are made: (i) $\varepsilon_{M\cdot\cdot A}=\varepsilon_M+\varepsilon_A$, and (ii) $\varepsilon_{M\cdot A}=\varepsilon_{M\cdot A(CT)}+\varepsilon_M$. The symbol c denotes the analytical concentration of each species, and $\varepsilon_{M\cdot A(CT)}$ is the molar extinction coefficient of the iodide-to-complex charge transfer absorption in the contact ion-pair. Assumption (i) is equivalent to defining the separated ion-pair as the class of ion-pairs that were not spectrophotometrically distinguished from the bulk of ions in the experiment. According to assumption (ii), iodide-to-complex charge transfer absorption occurs in the contact ion-pair in place of iodide-to-solvent charge transfer absorption, whereas the absorption due to transitions in the metal complex remains unaffected.

The values for ΔD were obtained by comparing the absorbance at each wave number of a solution containing the complex and iodide ions with those of two solutions containing each ion separately. Figure 1 shows three series of results obtained with different concentrations of the complex ion, but with the same iodide concentration. An isosbestic point exists at ν=40.7± 0.1 kK and ΔD=0. Here, $\varepsilon_{M\cdot A(CT)}$ is equal to ε_A, which was measured to be 1600± 150. This observation implies that the above-mentioned assumptions are a good approximation.

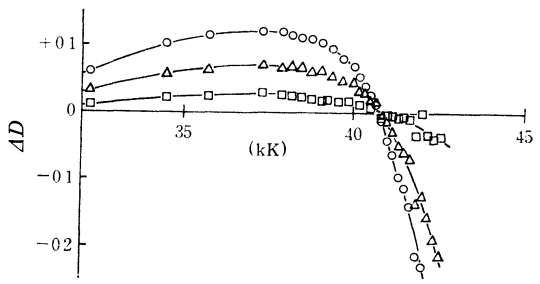

Fig. 1. ΔD for $[Co(NH_3)_6]$ $(ClO_4)_3$-KI-$NaClO_4$ solutions of ionic strength of 0.062. c_A=0.002M; c_M=0.002M(□), 0.006M(△) and 0.010M(○)

Assuming different values of [M·A] and using the observed ε_A values, we calculated $\varepsilon_{M\cdot A(CT)}$ for each wave number and drew hypothetical absorption curves. Only certain values of [M·A] within a narrow range gave absorption curves of a reasonable shape. Thus, we obtained 2300±300 for the $\varepsilon_{M\cdot A(CT)}$ value at 37.3 kK, where the charge transfer band has its maximum, and 1150± 150 at 32.3 kK, where measurements were made for the determination of the ion-association constants, as will be described below.

We define the *partial ion-association constants* for the separated and contact ion-pairs as well as the *total ion-association constant* as follows:

$$K_{sep} = \frac{[M\cdot\cdot A]}{[M][A]}, \quad K_{cont} = \frac{[M\cdot A]}{[M][A]}$$

$$K = K_{sep} + K_{cont} = \frac{[M\cdot\cdot A]+[M\cdot A]}{[M][A]} = \frac{x}{(c_M-x)(c_A-x)}$$

where x is the total molar concentration of ion-pairs. Combining these equations with Eq. (1), one has:

$$\frac{c_M c_A}{\Delta D} = \frac{K(c_M+c_A-x)}{K_{cont}(\varepsilon_{M\cdot A(CT)}-\varepsilon_A)} + \frac{1}{K_{cont}(\varepsilon_{M\cdot A(CT)}-\varepsilon_A)}$$

Plots of the observable quantity on the left-hand side *vs.* c_M+c_A-x (where x is a small correction to be considered in successive approximations) will give the total ion-association constant, K, as (slope)/(intercept). Actually, from spectrophotometric measurements at 32.3 kK on aqueous $[Co(NH_3)_6]$ I_3-KI systems of a constant ionic strength of 0.06, we obtained 9.0±0.6 for K and 2.41×10^{-4} for the intercept, $1/\{K_{cont}(\varepsilon_{M\cdot A(CT)}-\varepsilon_A)\}$. The latter, in combination with the $\varepsilon_{M\cdot A(CT)}$ value given above, leads to the values of the partial ion-association constants: 3.6±0.5 for K_{cont} and, accordingly, 5.4±0.8 for K_{sep}.

1) M. Eigen, *Discuss. Faraday Soc.*, **24**, 25 (1957); T. R. Griffiths and C. R. Symons, *Mol. Phys.*, **3**, 90 (1960); G. Atkinson and S. K. Kor, *J. Phys. Chem.*, **69**, 128 (1965), **71**, 673 (1967).

2) M. Linhard, *Z. Electrochem.*, **50**, 224 (1944); M. G. Evans and G. H. Nancollas, *Trans. Faraday Soc.*, **49**, 363 (1953); T. Kubota, *Nippon Kagaku Zasshi*, **75**, 552 (1954); N. Tanaka, Y. Kobayashi, and M. Kamada, This Bulletin, **40**, 2839 (1967).

The α-Chlorination of Sulfoxides with *N*-Chlorosuccinimide

Gen-ichi TSUCHIHASHI and Katsuyuki OGURA
Sagami Chemical Research Center, Ohnuma, Sagamihara, Kanagawa
(Received April 10, 1971)

Dimethyl sulfoxide, the only sulfoxide that is industrially produced, has been frequently used as a solvent and a reagent.[1] It is very significant that this sulfoxide is further utilized by its transformation into other useful sulfoxides; chloromethyl methyl sulfoxide seems to be an important intermediate for this purpose.[2] Although many efforts have been exerted on the α-chlorination of sulfoxides,[3] it has been difficult to isolate the monochloro derivative in a high yield by the chlorination of dimethyl sulfoxide because of the formation of such by-products as bis(chloromethyl) sulfoxide, and dichloromethyl methyl sulfoxide.[4] In this communication, we wish to report on the chlorination of sulfoxides with *N*-chlorosuccinimide (NCS), with which dimethyl sulfoxide reacts to give only chloromethyl methyl sulfoxide in an excellent yield.

$$CH_3SOCH_3 \xrightarrow[\text{base}]{\text{NCS}} CH_3SOCH_2Cl \quad 87\text{—}90\%$$

To a stirred solution of dimethyl sulfoxide (3.91 g) in dichloromethane (30 m*l*), we added NCS (7.00 g) and potassium carbonate (2.0 g) at room temperature. Stirring was then continued for 15 min. After the subsequent addition of dichloromethane (50 m*l*), the solution was filtered and the filtrate was fractionally distilled. A colorless oil (5.01 g, 90% yield) was thus obtained; it was confirmed to be pure chloromethyl methyl sulfoxide by spectroscopic and tlc analyses: bp 90°C/4 mmHg; $n^{24°}$ 1.5051; the NMR spectrum (in $CDCl_3$): δ 2.69 s (3H) and 4.38 s (2H); the IR spectrum (film): ν_{SO} 1058 cm^{-1}. Found: C, 21.51; H, 4.66; S, 28.47%. Calcd for C_2H_5ClOS: C, 21.34; H, 4.48; S, 28.48%.

A similar treatment of dimethyl sulfoxide with NCS in the presence of pyridine afforded chloromethyl methyl sulfoxide in a 87% yield, but this reaction required a longer period of time than that in the presence of potassium carbonate.

Similarly the reactions of methyl phenyl sulfoxide, dibenzyl sulfoxide, and thiolane 1-oxide with NCS in the presence of pyridine gave the corresponding α-chlorosulfoxides in 89, 91, and 60% yields respectively. Benzyl methyl sulfoxide (I) also reacted with NCS in the presence of pyridine to afford α-chlorobenzyl methyl sulfoxide (II) and benzyl chloromethyl sulfoxide (III) in 51 and 34% yields respectively. When potassium acetate was used as the base, II was obtained in a 77% yield, while III was not detected in the reaction mixture. This result may suggest that two mechanisms are operative in the α-chlorination of sulfoxides with NCS; *i.e.*, the reaction is

$$\underset{\text{I}}{PhCH_2SOCH_3} \xrightarrow[\text{base}]{\text{NCS}} \underset{\text{Cl}\quad\text{II}}{PhCHSOCH_3} + \underset{\text{III}}{PhCH_2SOCH_2Cl}$$

(a) mainly ionic in the presence of pyridine and (b) radicalic in the presence of such insoluble bases as potassium carbonate and potassium acetate. This consideration is supported by the following observations: (1) an induction period clearly exists in the reaction of dimethyl sulfoxide with potassium carbonate; (2) the addition of hydroquinone changes the amount of II produced by the chlorination of I with NCS in the presence of pyridine, but the yield of III remains unchanged (Table 1).

Table 1. Chlorination of I with NCS[a]

HO-⟨⟩-OH	Distribution[b]			II/III
	I	II	III	
0	9.1	52.4	38.9	1.36
0.3 eq.	37.7	29.3	33.0	0.88
1.0 eq.	36.5	28.3	35.3	0.80
0[c]	27.1	20.2	52.6	0.38
0[d]	7.9	72.1	20.1	3.59

a) I, 150 mg; pyridine, 0.5 m*l*; CCl_4, 10 m*l*.
b) Determined by a NMR analysis.
c) A mixture of $PhCD_2SOCH_3$, $PhCDHSOCH_3$, and $PhCH_2SOCH_3$ (90.6:8.9:0.5).
d) A mixture of $PhCH_2SOCD_3$, $PhCDHSOCD_3$, and $PhCH_2SOCD_2H$ (84.0:5.6:10.5).

Kinetic isotope effects were examined by using two deuterio derivatives of I, *i.e.*, $PhCD_2SOCH_3$ and $PhCH_2SOCD_3$. The results are shown in Table 1. The deuterium isotope effects (k_H/k_D) for both benzyl and methyl positions were calculated to be within the range of 3.0—3.5. This magnitude of isotope effects implies that proton transfer is the rate-determining step for the ionic path of the reaction.

Studies of the detailed mechanism of this reaction are now being undertaken.

1) For a recent review; see T. Durst, "Advances in Organic Chemistry," Vol. 6, ed. by E. C. Taylor and H. Wynberg, Interscience Publishers, New York, N. Y. (1969), p. 285.
2) We have already reported on the nucleophilic substitution of chloromethyl methyl sulfoxide: K. Ogura and G. Tsuchihashi, *Chem. Commun.*, **1970**, 1689.
3) G. Tsuchihashi, K. Ogura, S. Iriuchijima, and S. Tomisawa, *Synthesis*, No. 2, 89 (1971), and the references cited therein.
4) D. Martin, A. Berger, and R. Peschel, *J. Prakt. Chem.*, **312**, 684 (1970).

The Differential Thermal Analysis of Potassium Oxalate[1)]

Tatsuo HIGASHIYAMA and Shigeo HASEGAWA*

College of Liberal Arts, Okayama University, Tsushima, Okayama

* *Research Laboratory for Surface Science, Okayama University, Tsushima, Okayama*

(Received September 17, 1970)

From the differential thermal and thermogravimetric analyses of potassium oxalate together with the X-ray diffraction studies, three crystallographic modifications of the anhydrous salt were found. When potassium oxalate monohydrate crystals were dehydrated at, *e.g.*, 140°C, phase II, which is stable below 381°C, appears. The crystal in phase II has an orthorhombic unit cell ($a=10.9$, $b=6.11$, and $c=3.44$ Å at 17°C) and transforms at 381°C into phase I, which is stable above 381°C up to the temperature where the decomposition begins. The crystals in phase I belong to the tetragonal system ($a=7.01$ and $c=7.53$ Å at 404°C). The transition between phases II and I is not reversible in an exact sense, and when cooled phase I endures down to 215°C, where it transforms (reversibly) into phase III. Phase III can exist at room temperature. When heated, phase III transforms into phase I at 215°C (often accompanied by a partial transformation to phase II). The resulting phase then transforms into phase II. At all temperatures below 381°C phases I and III are metastable with respect to phase II, and they transform into phase II. The decomposition of potassium oxalate in an oxygen-free atmosphere seems to proceed in two stages.

The thermal decomposition of potassium oxalate complexes of di- and tri-valent metal in the solid state has been studied by several investigators,[2-6)] and it has been reported that in many cases potassium oxalate or potassium hydrogen oxalate results as an intermediate decomposition product; this may affect the further decomposition processes of those materials. Many of the reports, however, do not seem to have referred in detail to the thermal behavior of potassium oxalate itself. Studies of the decomposition of potassium oxalate have been made by thermogravimetric analysis (TGA),[6,7)] but no differential thermal analysis (DTA) of the material seems to have been reported yet.

In the course of DTA studies of potassium tetroxalate,[8)] we found that potassium oxalate has two crystallographically-different phases, I[9)] and II[9)]. To obtain further information about potassium oxalate, the thermal behavior of the material was studied in more detail by means of DTA, TGA, and X-ray diffraction methods, and another new phase of the anhydrous salt was found. Some features of the decomposition and transitions of potassium oxalate will be reported in this paper.

Experimental

Materials. The potassium oxalate monohydrate was prepared from commercial guaranteed-grade oxalic acid and potassium carbonate and was recrystallized five times from water. The potassium oxalate anhydrate ($K_2C_2O_4$) was obtained by dehydrating the hydrous salt at about 125°C for more than 4 hours.

Procedures. The DTA and TGA curves were obtained using a "High-temperature-type Differential Thermal and Thermogravimetric Analyser" (Rigaku Denki Co.). Pt-Pt·Rh (13%) thermocouples were used as the temperature detectors, and α-alumina was used as the reference material. The sample material was powdered in an agate motar (powder size smaller than 200 meshes), and about 400 mg of the material was charged in a platinum cell in the manner shown in Fig. 3(f) by tapping the botton of the cell. These procedures were conducted in an dry-air atmosphere when the specimen was the anhydrous salt. When necessary, the specimen was dried again in the DTA-TGA apparatus by evacuation. In most thermal measurements, the heating and cooling rate was about 2.5°C/min unless otherwise specified.

The X-ray diffraction studies at high temperatures were made on a diffractometer equipped with a modified specimen heating apparatus (Rigaku Denki Co.). In X-ray measurements, the heating rate was about 2.5°C/min and the cooling rate was 5—10°C/min. After attaining a given temperature, the specimen was kept at that temperature for about 10 min and diffraction patterns were taken at the scanning speed of 1°/min.

Results and Discussion

Figures 1(a) and (a′) show the simultaneously-recorded DTA and TGA curves of potassium oxalate monohydrate. The endothermic peak, P_1, which is associated with the dehydration of the water of crystallization appears at 135°C (peak temperature, PT). No other peak appears up to 381°C, where the second endothermic peak P_2 (PT 391°C) begins to appear. The TGA curve shows a gradual weight loss from around 426°C, indicating the decomposition of $K_2C_2O_4$. The pattern of the DTA curve accompanying this decomposition is strongly affected by the atmospheric conditions. When measurements were made in an atmosphere of flowing dry air (Fig. 1(a)), where a sufficient supply of oxygen gas to the specimen would be expected, the specimen shows two exothermic

1) Partly presented at the Chūgoku-Shikoku Meeting of Chemical Society of Japan, Okayama, October, 1967.

2) N. Tanaka and M. Nanjo, This Bulletin, **40**, 330 (1967).

3) D. Broadbent, D. Dollimore, and J. Dollimore, "Thermal Analysis," Vol. 2, ed. by R. F. Schwenker, Jr., and P. D. Garn, Academic Press, New York, London (1969), p. 739.

4) W. W. Wendlandt, T. D. George, and K. V. Krishnamulty, *J. Inorg. Nucl. Chem.*, **21**, 69 (1961).

5) W.W. Wendlandt and E.L. Simmons, *ibid.*, **27**, 2317 (1965); **27**, 2325 (1965).

6) *Chem. Abstr.*, **64**, 10741 *b*.

7) *Ibid.*, **48**, 12522 *i*; **51**, 9273 *g*; **55**, 20929 *h*.

8) T. Higashiyama and S. Hasegawa, *Rep. Res. Lab. for Surface Science, Okayama University*, **2**, 295 (1966).

9) In Ref. 8, phase II in this paper is referred to as phase I and phase I in this paper, as phase II.

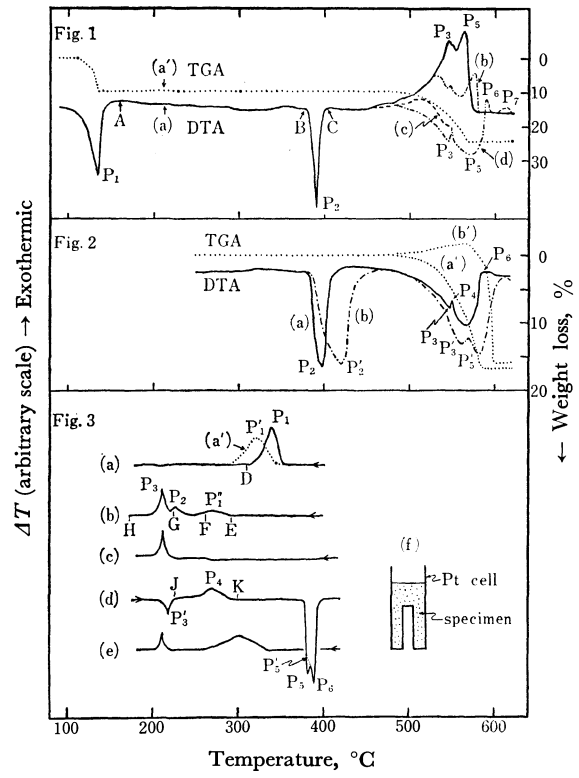

Figs. 1 and 2. Simultaneously recorded DTA and TGA curves of potassium oxalate. 1(a): $K_2C_2O_4 \cdot H_2O$, in air with flow; 1(b): in air with no flow; 1(c): in N_2 gas with no flow; 1(d): in N_2 gas with flow.
2(a): $K_2C_2O_4$ *in vacuo*; 2(b): *in vacuo*, heating rate 5°C/min.
Fig. 3. Cooling DTA of $K_2C_2O_4$ ((d): heating DTA).

peaks, P_3 and P_5, probably due to the combustion of the carbon monoxide gas produced by the decomposition. When the heating rate was 1°C/min, the separation of these two peaks was less clear. After thermal measurements up to about 612°C the resulting solid substance was potassium carbonate. Figure 1(b) is the DTA thermogram when the measurement was made in dry air at 1 atm with no flow. The exothermicity of the decomposition is decreased compared with the case of a flowing atmosphere, and the temperature of completion of the decomposition becomes higher. Figure 1(d) shows the DTA curve when the measurement was made in dry nitrogen gas with a flow at 1 atm. In this case, two endothermic peaks, P_3 and P_5 (PT 547 and 570°C respectively), appear corresponding to the decomposition of $K_2C_2O_4$. When the measurement was made in N_2 gas at 1 atm with no flow, the thermogram (c) in Fig. 1, which is rather similar to Fig. 1(b), was obtained. The (b) and (c) curves have features intermediate between the former two cases (Figs. 1(a) and 1(d)).

Figure 2(a) shows the DTA thermogram for the measurement in the vacuum of the order of 10^{-2} mmHg. This curve, showing endothermic peaks of P_3 and P_5, is quite similar to the (d) curve in Fig. 1 except that the shape of the P_2 peak is deformed more broadly and its peak temperature is shifted to the higher side because of the smaller thermal conductivity of the specimen in a vacuum. The apparent exothermic peak, P_4, at 555°C, appears clearly in a flowing N_2 gas atmosphere and *in vacuo*, but we could find, by the X-ray diffraction method, no evidence for it as a real peak. The TGA curve in Fig. 2 indicates that the apparent peak, P_4, is accompanied by a clear change in the decomposition rate; this is supported by X-ray diffractometry and pressure measurement of the evolved gases. Figure 2(b) shows the thermogram obtained *in vacuo* when the heating rate was 5°C/min. The curve is displaced to the higher-temperature side as a whole as a result of the increase in the heating rate. The TGA curve (b') shows an apparent weight increase accompanying the endothermic peak, P'_3, instead of showing a weight loss. This phenomenon may be due to the proper jetting of the resulting gases, which might be effective in a vacuum.

In the case of the measurements in N_2 gas and *in vacuo*, the temperature of the completion of the decomposition becomes higher and an exothermic peak, P_6, in Figs. 1 and 2 sometimes appears just before the completion of the decomposition. (Otherwise, P_7 in Fig. 1 often appears). The weight change accompanying P_6 is small; this might suggest that P_6 in Figs. 1 and 2 corresponds to the improvement of the crystallinity of the K_2CO_3 resulting from the decomposition process. The decomposition products in these cases were gray or dark gray, indicating the presence of carbon.

From these findings, it might be said that the supply of O_2 gas or the ease of carrying off the resultant gases plays an important role in the decomposition mechanism, and that the decomposition of $K_2C_2O_4$ in an O_2-free atmosphere proceeds through two stages. The first stage might be associated mainly with the $K_2C_2O_4 \rightarrow K_2CO_3 + CO$ reaction, and the second one, with $2\,K_2C_2O_4 \rightarrow 2\,K_2CO_3 + C + CO_2$.

The TGA curve (a') in Fig. 1 shows that there is no weight change accompanying the P_2 endothermic peak (PT 391°C), which begins to appear from 381°C. When the specimen was once heated up to 408°C (over the P_2 peak) and then submitted at once to the cooling DTA, the thermogram shown in Fig. 3(a) was obtained. A broad exothermic peak, P_1 (PT 341°C), appears from around 360°C, but no other peak appears below the peak temperature. As the period of heat-treatment increases, the peak which corresponds to P_1 in Fig. 3(a) shifts to the lower-temperature side and its peak area decreases (Fig. 3(a')). When the original specimen was heated to a temperature above *ca.* 410°C, treated for a longer time (*e.g.*, 1 hr), and then subjected to the cooling DTA, the thermogram shown in Fig. 3(b) was obtained. A very broad exothermic peak, P''_1 (PT 267°C), in Fig. 3(b) appears from around 304°C, and two other exothermic peaks, P_2 and P_3, appear at 226 and 212°C (PT) respectively. The P_3 peak is less displaced than P_2 when the cooling rate is changed. If the specimen is heat-treated at 420°C for 1 hr (TGA shows that about 0.6% of the specimen is decomposed by this heat-treatment), the broad peak, P''_1, in Fig. 3(b) almost disappears. When the specimen which had undergone the thermal-treatment heating above 390°C and cooling below 210°C was further heat-treated above *ca.* 410°C for a long enough time (*e.g.*, 1 hr), the peak which cor-

responds to P_2 in Fig. 3(b) did not appear (Fig. 3(c)).

After the original specimen had been heat-treated at, *e.g.*, 420°C for a longer time (1 hr), it was cooled to around 145°C and then heated again for the heating DTA (Fig. 3(d)). There thereupon appeared an endothermic peak, P'_3 (PT 219°C), which corresponds to the exothermic peak, P_3, in Fig. 3(b), and a broad exothermic peak at around 265°C. The endothermic peak at around 390°C, which may correspond to P_2 in Fig. 1, appears as a clear double peak. When this specimen was submitted again to the cooling DTA just after attaining 420°C, the thermogram (e) in Fig. 3 was obtained. It should be noted that the peaks which correspond to P_1 in Fig. 3(a) and P_3 in Fig. 3(b) appear, but not the peak which corresponds to P_2 in Fig. 3(b). On the other hand, when the specimen which has shown the thermogram in Fig. 3(d) was submitted from the K point to the cooling DTA, it did not show any peak.

The specimen once heated to 408°C and quickly cooled to, *e.g.*, 360°C does not show in the heating DTA the endothermic peak which corresponds to P_2 in Fig. 1, indicating that the change associated with the peak is not reversible. This peak does appear, however, if the specimen once heated to 408°C and then quickly cooled to 360°C is kept there for a longer time. This is true even for the specimen heat-treated at higher temperatures (*e.g.*, 370°C). The lower the temperature, and the longer the heat-treatment, the larger the peak area of the endothermic peak which corresponds to P_2 in Fig. 1.

When the specimen once heated around or above 408°C is cooled quickly below 351°C, it often shows, in the heating DTA, an endothermic shoulder peak, P'_5 (PT 388°C) in Fig. 3(d), in addition to the peak which corresponds to P_2 in Fig. 1. It seems interesting that the temperature of 351°C coincides with that where the broad exothermic peak P_1 in Fig. 3(a) begins to appear. When the specimen once heated to 400°C was quenched to 0°C, kept there for about 2 min, and quickly heated (to 310°C in 14 min, then to 400°C at 2.5°C/min), it showed the shoulder peak. When this specimen was further heat-treated at 400°C for 1 hr, quickly cooled to 273°C, and then heated as before, it shows a clear double peak. By the repetition of the heating, cooling, and heat-treatment descrived above, the shoulder peak P_5 (or P'_5) in Fig. 3(d) becomes the main peak, while the original main peak, P_6, becomes the shoulder. Similar phenomena were observed for the specimen heat-treated at other temperatures. The shoulder peak, P_5 (or P'_5), in Fig. 3(d) disappears if the specimen so treated as to show the peak is further heat-treated at 360°C for 12 hr, though it does not disappear upon heat-treatment at 306°C for 1 hr.

The X-ray diffraction method was employed to elucidate what phenomena or changes these peaks correspond to.

Figure 4(a) shows the X-ray powder diffraction pattern of $K_2C_2O_4$ at room temperature for the Cu-$K\alpha$ radiation. The crystallographic data of the $K_2C_2O_4$ crystal have not yet been reported. One may index the diffraction lines assuming that $K_2C_2O_4$ crystal has an orthorhombic unit cell with cell constants of $a=10.90$, $b=6.11$, and $c=3.44$ Å at 17°C. From the observed density data (2.381 g/cc at 25°C) of the material, a unit cell can be said to contain 2 chemical units.

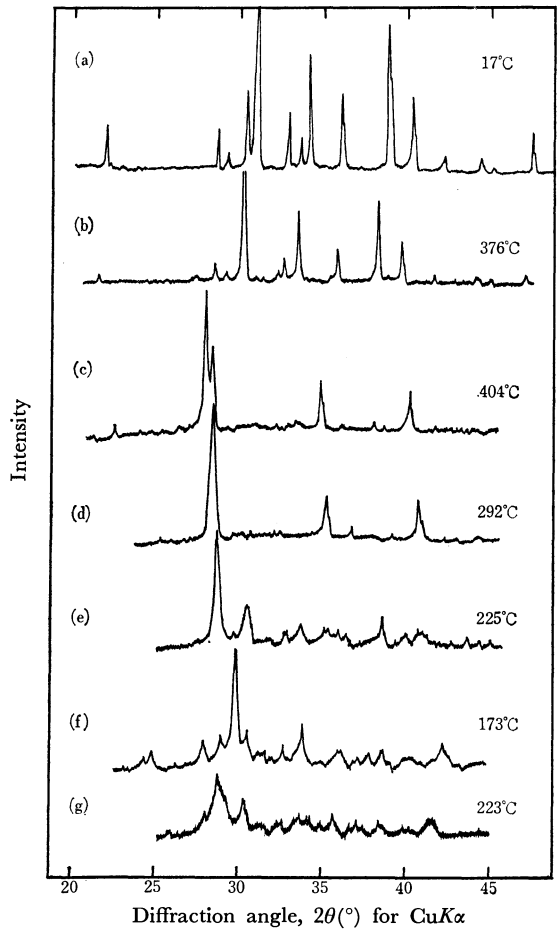

Fig. 4. X-Ray diffraction patterns of $K_2C_2O_4$. (d)—(f): in cooling process.

When $K_2C_2O_4$ crystals were heated in the X-ray high-temperature apparatus up to 376°C (B in Fig.1), the specimen shows the diffraction pattern shown in Fig. 4(b). We may index the diffraction lines in this pattern assuming that $K_2C_2O_4$ crystals have lattice parameters of $a=11.01$, $b=6.16$, and $c=3.56$ Å. When the specimen was heated to 404°C and treated there (C in Fig. 1), it showed the diffraction pattern shown in Fig. 4(c). This pattern has no similarity with the pattern (b) in Fig. 4. One may index the diffraction lines assuming that the crystals have a tetragonal unit cell with cell constants of $a=7.01$ and $c=7.53$ Å. From these facts, it may be concluded that the endothermic peak, P_2, in Fig. 1 corresponds to the polymorphic transition of potassium oxalate anhydrate crystals. As has been stated above, this transition does not occur reversibly in an exact sense. We shall refer to the phase stable below 381°C as phase II, and to that phase stable above 381°C, as phase I.

When the $K_2C_2O_4$ specimen is once heated to 410°C, kept for a rather short time—until the diffraction lines which belong to phase II disappear, and cooled to 310°C (D in Fig. 3(a)), extra lines which seem to belong

to phase II are observed in the diffraction pattern. Figure 4(d) shows the diffraction pattern when the specimen which has been heat-treated at 410°C for a long enough time, is cooled to 292°C (E in Fig. 3(b)). No extra line is seen in this pattern. When a similarly heat-treated specimen is cooled to 225°C (G in Fig. 3(b)), some extra diffraction lines appear (Fig. 4(e)) in addition to the lines in Fig. 4(d). If the specimen which had experienced a transformation history such as II →I→III (see below)→II→I is heat-treated at 410°C for a long enough time and then cooled to 310°C, it gives the diffraction lines of phase I only. When this specimen is cooled to 263°C (F in Fig. 3(b)), some extra diffraction lines appear (prominently at $2\theta=30.4°$). These new peaks disappear when this specimen is cooled to 231°C. When this specimen is further cooled to and kept for a long time at 226°C, it gives a pattern similar to Fig. 4(e). At 225°C, we may index the original diffraction lines assuming that the specimen has lattice constants of $a=$ 6.94 and $c=7.45$ Å.

Thus, the broad exothermic peak, P'_1, in Fig. 3(b) as well as the P_1 peak in Fig. 3(a) may be regarded as the peaks accompanying the transformation from phase I to phase II. The cause for the appearance of the P_2 peak in Fig. 3(b) is not clear. This peak might also correspond to the I→II transformation. However, the findings with respect to the peak seem to be more favorably explained if we say that the peak is due to rearrangement of the molecules in the lattices with less regularity, which might exist in phase I or which might have resulted from the I→II transformation at a lower temperature (*e.g.*, 250°C), to a structure more stable at the temperatures which the peak covers.

When the specimen heat-treated well at above 410°C is cooled down to H in Fig. 3(b) (173°C), it gives the diffraction pattern shown in Fig. 4(f), which is not at all similar to the (d) or (e) patterns in Fig. 4 or to that of the original specimen at the same temperature. Thus, the sharp exothermic peak, P_3, in Fig. 3 (b)is due to the second phase transition. We call this new phase as phase III. In a dry-air atmosphere, phase III is fairly stable at room temperature, especially when it has been properly prepared. It seems interesting that when the specimen completely transformed into phase I is quenched to 0°C, phase I still remains (though it is only a small portion)and the main portion is not phase III but phase II.

When the specimen which gives the diffraction pattern of phase III is heated again to 223°C (J in Fig. 3(d)) it gives the pattern shown in Fig. 4(g). The presence of the diffraction lines of phase I indicates that the transition between phases III and I occurs (at least partly) reversibly; this is supported by the DTA findings. We can also find in Fig. 4(g) many diffraction lines which belong to phase II; this means that the transition from phase III to phase II occurs to a considerable extent. As may be seen from Fig. 4(g), the crystallinity of the resultant phases is poor. If we heat this specimen up to K (*e.g.*, 300°C) over the peak, P_4 (PT 265°C), in Fig. 3(d), it gives a diffraction pattern of phase II with an improved crystallinity. Thus, the exothermic peak, P_4, in Fig. 3(d) may correspond both to the transformation of $K_2C_2O_4$ from phase I to phase II and to the improvement of the crystallinity of the resulting phase II.

As has already been stated, the heating DTA of the specimen which is in phase III gives an endothermic double peak at around 390°C. If, however, we heat-treat the specimen in phase III at, *e.g.*, 360°C for 12 hr, it shows a single peak. The double peak may then be explained as follows. The first endothermic peak (P_5 in Fig. 3(e)) may correspond to the transformation into phase I of the poor-crystalline or amorphous part of the specimen resulting from a transformation history such as II→I→III→II, rather than be due to the presence of another new phase, II′. The poor-crystalline part may be more easily and completely transformed into phase I than the crystalline part of phase II. The second endothermic peak corresponds to the transformation from phase II to phase I.

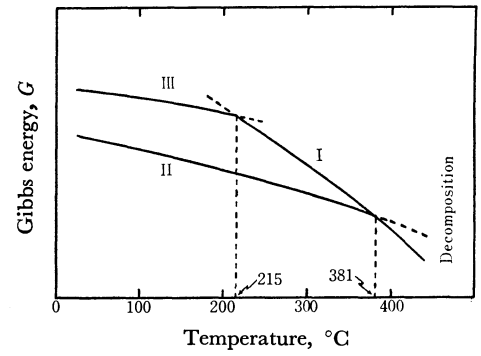

Fig. 5. Schematic representation of phase diagram of $K_2C_2O_4$.

The results discussed above may be summarized schematically as is shown in Fig. 5. Phase II is stable below 381°C, and phase I is stable above that temperature. When crystals in phase I are cooled, phase I endures down to 215°C, where phase III appears and exists below that temperature. At all temperatures below 381°C, phase I and III are meta-stable with respect to phaseII.

The Crystal Structure of Bis(pyridine-2-acetamide)copper(II) Perchlorate

Masao SEKIZAKI, Fumiyuki MARUMO,* Kazuo YAMASAKI, and Yoshihiko SAITO*

Department of Chemistry, Faculty of Science, Nagoya University, Chikusa-ku, Nagoya

**The Institute for Solid State Physics, The University of Tokyo, Roppongi, Minato-ku, Tokyo*

(Received October 22, 1970)

The crystal structure of bis(pyridine-2-acetamide)copper(II) perchlorate, $Cu(paaH)_2(ClO_4)_2$, was determined from three-dimensional X-ray photographic data and refined by block-diagonal least-squares methods, using 1698 independent reflections to give $R=0.12$. The crystals are monoclinic with a space group of C2/c. There are four formula units in a unit cell with dimensions of: $a=10.957$, $b=12.178$, $c=15.566$ Å, and $\beta=108.7°$. The complex is centrosymmetric and square-planar, with two ligand molecules coordinating to the copper atom in *trans* positions through the amide-oxygen and the ring-nitrogen atoms. Two perchlorate ions coordinate weakly to the central copper atom through one of the four oxygen atoms from the top and bottom of the plane containing copper, amide-oxygen, and ring-nitrogen atoms.

In the course of studies of the bivalent metal complexes of acid amides,[1-7] X-ray crystal analyses of $[Ni(H_2O)_2(piaH)_2]Cl_2$[3] and $[Ni(pia)_2]2H_2O$[4] have revealed that the former has a structure with octahedral coordination through the amide-oxygen and ring-nitrogen atoms of the ligand, while that the latter has a structure with square-planar coordination through the amide-nitrogen and ring-nitrogen atoms, where piaH denotes pyridine-2-carboxamide. On the basis of these results and also on the basis of spectral and magnetic studies, the structures of several complexes with other acid amides have been assigned.[5-7] The copper complex of pyridine-2-acetamide (abbreviated as paaH), $Cu(paaH)_2(ClO_4)_2$, has been assigned a structure similar to $[Ni(H_2O)_2(piaH)_2]Cl_2$, *e.g.*, an octahedral structure with coordination through amide-oxygen and ring-nitrogen atoms.[7] The fifth and sixth positions of the octahedron are presumably occupied by two perchlorate ions. To confirm the assigned structure, this complex was subjected to X-ray crystal analysis.

Experimental

The crystals of the complex, $Cu(paaH)_2(ClO_4)_2$, were obtained by letting a mixture of aqueous solutions of one mole of copper perchlorate and two moles of pyridine-2-acetamide stand overnight, as has been reported previously.[7] The blue prismatic crystals were elongated along the *c*-axis. The unit-cell dimensions were determined from the higher-order reflections of Weissenberg photographs ($CuK\alpha_1$, $\lambda=1.5405$ Å). The systematic absences were *hkl* for $h+k$ odd and *h0l* for *h* and *l* odd. Hence, the space group was $C2/c$ or Cc. The former was tentatively assumed, but it was indeed verified at a later stage of the structure analysis by the calculation of the structure factors. The crystal data are given in Table 1. Equi-inclination Weissenberg photographs were taken about [010] and [1$\bar{1}$0] up to the tenth and second layers respectively. The multiple-film technique was employed, and $CuK\alpha$ radiation was used. The cross section of the specimen used for intensity measurements was about 0.3×0.2 mm. A total of 1698 independent reflections were collected. The intensities were estimated visually and were converted to $|F|$ by applying the Lorentz, polarization,and spot-shape corrections. Absorption and extinction corrections were not made.

TABLE 1. CRYSTAL DATA

trans-Bis(pyridine-2-acetamide)copper(II) perchlorate	
$Cu(C_5H_4NCH_2CONH_2)_2(ClO_4)_2$	F.W. 534.76
Monoclinic	$a=10.957\pm0.003$ Å
	$b=12.178\pm0.006$
	$c=15.566\pm0.004$
	$\beta=108.74\pm0.02°$
	$U=1967$ Å^3
Space group	$C2/c$
$Z=4$	
$D_x=1.80$ g·cm^{-3}	
$D_m=1.79$ g·cm^{-3}	

Solution and Refinement of the Structure

The general positions are eightfold for the space group $C2/c$. The copper atoms must lie on a set of fourfold special positions, since there are only four formula units in the unit cell. The complex is thus required to have a center of symmetry or a twofold axis of rotation. The coordinates of the copper and chlorine atoms were determined from the prominent peaks in the Patterson function. The copper atoms were found to lie on the centers of symmetry. A three-dimensional electron density map was then calculated with all the terms, the signs of which were calculated on the basis of the copper and the chlorine atoms. The resulting maps showed the positions of all the lighter atoms except three oxygen atoms of a perchlorate ion. One more Fourier synthesis of the electron density gave the positions of the three remaining atoms.

At this stage it appeared that the ligand coordinates to the central atom through the ring-nitrogen and one atom of the amide group. However, it was not pos-

1) M. Sekizaki and K. Yamasaki, *Nippon Kagaku Zasshi*, **87**, 1053 (1966).
2) M. Sekizaki and K. Yamasaki, *Spectrochim. Acta*, **25A**, 475 (1969).
3) A. Masuko, T. Nomura, and Y. Saito, This Bulletin, **40**, 511 (1967).
4) Y. Nawata, H. Iwasaki, and Y. Saito, *ibid.*, **40**, 515 (1967).
5) M. Sekizaki and K. Yamasaki, *Revue de Chimie minérale*, **6**, 255 (1969).
6) M. Sekizaki, M. Tanase, and K. Yamasaki, This Bulletin, **42**, 399 (1969).
7) M. Sekizaki and K. Yamasaki, *Inorg. Chim. Acta*, **4**, 296 (1970).

TABLE 2. FINAL ATOMIC PARAMETERS AND THEIR ESTIMATED STANDARD DEVIATIONS

Positional parameters are expressed as fractions of the lattice parameters. The estimated standard deviations are in parentheses and refer the last decimal positions of the respective values.
Thermal parameters are in the form: $\exp[-(h^2\beta_{11}+k^2\beta_{22}+l^2\beta_{33}+hk\beta_{12}+hl\beta_{13}+kl\beta_{23})]$

Atom	x	y	z	β_{11}	β_{22}	β_{33}	β_{12}	β_{13}	β_{23}
Cu	0.2500	0.2500	0.0000	0.0027(02)	0.0005(02)	0.0022(01)	−0.0008(03)	0.0006(02)	0.0008(02)
Cl	0.2156(03)	0.2968(03)	0.2268(02)	0.0105(04)	0.0023(03)	0.0021(02)	−0.0033(04)	0.0047(04)	−0.0008(03)
O(1)	0.4280(07)	0.1929(07)	0.0480(06)	0.0030(07)	0.0014(06)	0.0037(04)	−0.0009(10)	0.0004(08)	0.0019(08)
O(2)	0.2322(20)	0.2357(12)	0.1569(10)	0.0469(38)	0.0085(13)	0.0074(09)	−0.0013(36)	0.0323(33)	−0.0031(17)
O(3)	0.0841(16)	0.3463(15)	0.1851(17)	0.0144(21)	0.0117(18)	0.0238(24)	0.0114(31)	−0.0010(35)	0.0109(33)
O(4)	0.1961(11)	0.2326(09)	0.2985(07)	0.0149(14)	0.0062(10)	0.0053(06)	0.0053(18)	0.0112(15)	0·0060(12)
O(5)	0.2771(20)	0.3905(12)	0.2475(12)	0.0374(36)	0.0059(13)	0.0096(11)	−0.0220(34)	0.0054(31)	−0.0005(18)
C(1)	0.2475(10)	0.0088(09)	0.0304(07)	0.0045(10)	0.0007(09)	0.0024(05)	−0.0022(13)	0.0031(12)	0.0020(10)
C(2)	0.1962(13)	−0.0976(10)	0.0114(09)	0.0083(14)	0.0009(10)	0.0042(07)	−0.0016(17)	0.0047(16)	0.0003(12)
C(3)	0.0866(12)	−0.1178(10)	−0.0642(09)	0.0057(11)	0.0021(11)	0.0037(07)	−0.0037(16)	0.0037(14)	−0.0022(12)
C(4)	0.0272(12)	−0.0294(10)	−0.1185(08)	0.0068(12)	0.0002(09)	0.0029(06)	−0.0022(14)	0.0030(13)	−0.0008(10)
C(5)	0.0792(11)	0.0707(10)	−0.0969(08)	0.0047(11)	0.0038(11)	0.0024(06)	−0.0023(16)	0.0006(12)	0.0005(11)
C(6)	0.3634(11)	0.0306(09)	0.1094(07)	0.0056(11)	0.0001(09)	0.0022(05)	−0.0016(13)	0.0003(12)	0.0016(09)
C(7)	0.4585(10)	0.1064(10)	0.0902(07)	0.0031(09)	0.0031(10)	0.0020(05)	0.0011(14)	−0.0003(11)	0.0004(10)
N(1)	0.1833(08)	0.0954(07)	−0.0248(05)	0.0046(09)	0.0006(07)	0.0013(04)	0.0003(11)	0.0014(09)	−0.0008(07)
N(2)	0.5795(10)	0.0764(09)	0.1201(09)	0.0043(10)	0.0024(09)	0.0064(08)	0.0004(13)	−0.0018(14)	0.0028(12)

sible to distinguish between the oxygen and nitrogen atoms of the amide group. Therefore, the atomic scattering factor of oxygen was applied to these atoms in the initial block-diagonal least-squares refinement. The R-value obtained was 0.32; the coordinating atom of the amide group showed a reasonable isotropic temperature factor compared with those of the other atoms of the ligand, whereas the atom of the amide group not bonded to the copper atom showed about four times as large a temperature factor as the other atoms in the ligand. Therefore, it is not appropriate to assign oxygen to the non-coordinating atom of the amide group, and subsequent refinements have been continued on the assumption of the amide-oxygen coordination.

After six cycles of block-diagonal least-squares refinements with isotropic thermal parameters, the R-value decreased to 0.22; further refinements with anisotropic thermal parameters finally reduced the R-value to 0.12. The final results show that the distance between the carbon atom, C(7), and the coordinating atom is 1.23 Å, and that the distance between C(7) and the other atom attached to C(7) is 1.31 Å (Fig. 1 and Table 3). These values correspond, respectively, to the C=O and C–N bond distances found in the related molecules.[3,4,8,9] This fact proves that the assumption of the amide-oxygen coordination is correct and that the ligand coordinates to the copper atom through the ring-nitrogen and amide-oxygen atoms. This result is in agreement with that presumed from the infrared spectral data.[7]

The final three-dimensional electron density map showed more ill-defined and lower peaks at the atomic positions of the perchlorate ion than at those of the complex cation. Moreover, the temperature factors of the atoms of the perchlorate ion are several times larger than those of the others (Table 2). These facts indicate a larger thermal motion and/or positional disorder for the former. Clearly the uncertainty in atomic positions of the perchlorate ion is responsible for the comparatively high R-value. The atomic scattering factors used for the calculations were taken from the "International Tables for X-ray Crystallography." The calculations were carried out on the FACOM 270-30 computer at the Institute for Solid State Physics, the University of Tokyo, and on the HITAC 5020E computer at the Computing Center of the University of Tokyo, using the programs of the UNICS System. The final atomic parameters are listed in Table 2. The table of the observed and calculated structure factors is kept by the Chemical Society of Japan.[10]

Description of the Structure and Discussion

The interatomic distances and angles are listed in Tables 3 and 4. The structures of the complex ion and the perchlorate ion are illustrated in Figs. 1 and 2, together with the interatomic diatances and angles. The atomic arrangement in the crystal is shown in Fig. 3 in projection along the b-axis. The complex is centrosymmetric, having two ligand molecules in *trans* positions. The copper atom is surrounded by a distorted octahedron of six coordinating atoms, four of which are the amide-oxygen atoms and the ring-nitrogen atoms of the pyridine-2-acetamide molecules. These four coordinating atoms lie on the same plane with the central copper atom. The other two weakly

8) T. Takano, Y. Sasada, and M. Kakudo, *Acta Crystallogr.*, **21**, 514 (1966).

9) R. E. Long, H. Maddox, and K. N. Trueblood, *ibid.*, **B25**, 2083 (1969).

10) The F_o-F_c table is kept as Document No. 7108 at the office of the Bulletin of the Chemical Society of Japan. A copy may be secured by citing the document number and by remitting, in advance, ¥200 for photoprints. Payment may be made by check or money order payable to: Chemical Society of Japan.

Table 3. Interatiomic distances and angles

The estimated standard deviations are in parentheses and refer to the last decimal positions of the respective values.

Cu–O(1)	1.98(1) Å	Cu–N(1)–C(1)	120.5(6)
Cu–N(1)	2.01(1)	Cu–N(1)–C(5)	121.7(7)
Cu–O(2)	2.52(2)	C(2)–C(1)–C(6)	121.2(10)
N(1)–C(1)	1.40(2)	C(1)–C(6)–C(7)	114.4(10)
C(1)–C(6)	1.48(2)	C(6)–C(7)–O(1)	123.3(10)
C(6)–C(7)	1.49(2)	C(6)–C(7)–N(2)	116.7(10)
C(7)–O(1)	1.23(2)	O(1)–C(7)–N(2)	120.0(11)
C(7)–N(2)	1.31(2)	Cu–O(1)–C(7)	124.7(8)
C(1)–C(2)	1.41(2)	C(5)–N(1)–C(1)	117.8(9)
C(2)–C(3)	1.41(2)	N(1)–C(1)–C(2)	118.5(10)
C(3)–C(4)	1.39(2)	C(1)–C(2)–C(3)	120.9(11)
C(4)–C(5)	1.34(2)	C(2)–C(3)–C(4)	118.6(11)
C(5)–N(1)	1.35(1)	C(3)–C(4)–C(5)	118.2(11)
Cl–O(2)	1.38(2)	C(4)–C(5)–N(1)	125.9(11)
Cl–O(3)	1.50(2)	Cu–O(2)–Cl	143.1(10)
Cl–O(4)	1.43(1)	O(2)–Cl–O(3)	103.1(10)
Cl–O(5)	1.31(2)	O(2)–Cl–O(4)	114.3(9)
		O(2)–Cl–O(5)	118.4(10)
N(1)–Cu–O(1)	89.9(3)°	O(3)–Cl–O(4)	101.1(8)
N(1)–Cu–O(2)	89.1(5)	O(3)–Cl–O(5)	95.9(10)
O(1)–Cu–O(2)	89.1(5)	O(4)–Cl–O(5)	118.5(9)

Table 4. Intermolecular contacts less than 3.5 Å

Molecule	I at	x,	y,	z
	II	$1/2+x$,	$-1/2+y$,	z
	III	$1/2-x$,	$1/2+y$,	$1/2-z$
	IV	x,	$-y$,	$1/2+z$
	V	$1-x$,	y,	$1/2-z$
	VI	$1/2+x$,	$1/2-y$,	$1/2+z$
$C(6)^{I}$–$O(3)^{II}$	3.23(2) Å			
$N(2)^{I}$–$O(3)^{II}$	2.97(2)			
$N(2)^{I}$–$O(5)^{II}$	3.31(2)			
$N(2)^{I}$–$O(4)^{V}$	3.04(2)			
$O(4)^{I}$–$C(2)^{III}$	3.49(2)			
$O(4)^{I}$–$C(3)^{IV}$	3.10(2)			
$O(5)^{I}$–$C(4)^{VI}$	3.32(2)			
$O(5)^{I}$–$C(5)^{VI}$	3.45(2)			

coordinating atoms are the oxygen atoms of the perchlorate ions, which lie on the normal through the copper atom. This general feature of the structure is completely coincident with that presumed from the spectral and magnetic data in the previous paper.[7] The equations of the coordination plane and the best-plane through the pyridine ring and the deviations of various atoms therefrom are given in Table 5. The six-membered chelate ring is not planar, but is in a boat form, a methylene carbon atom (C(6)) being off the coordination plane at 1.33 Å. On the contrary, the five-membered chelate ring and the pyridine ring in $[Ni(H_2O)_2(piaH)_2]Cl_2$, which has no methylene group, are almost perfectly coplanar.[3] The pyridine ring in the present complex does not lie on the coordination plane, but is tilted at an angle of about 33° with respect to the coordination plane in the Cu–N(1)–C(3) direction. This distortion of the ligand molecule is

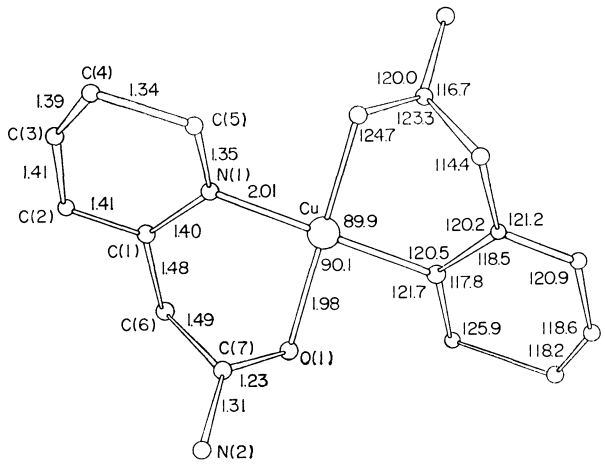

Fig. 1. Atomic arrangement, bond distances and angles of the complex ion.

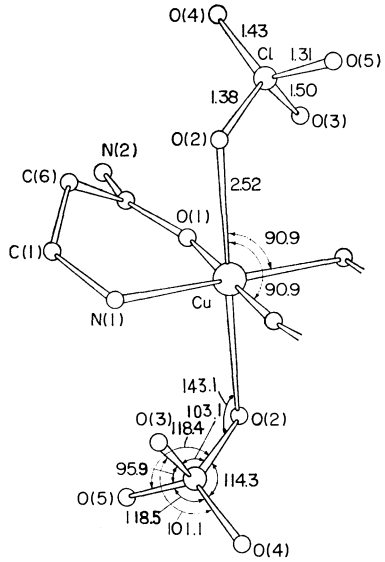

Fig. 2. Atomic arrangement, bond distances and angles of the perchlorate ion.

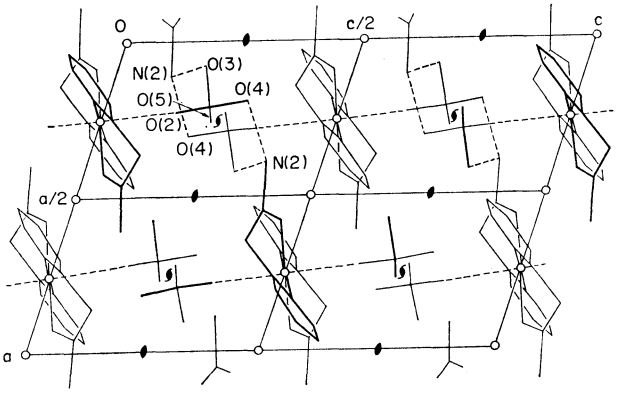

Fig. 3. Projection of the structure along the *b*-axis.

certainly due to an additional methylene group. The coordinate bond distances of this complex (Cu–O, 1.98; Cu–N, 2.01 Å) are not very different from those observed in $[Ni(H_2O)_2(piaH)_2]Cl_2$ (Ni–O, 2.045; Ni–N, 2.022 Å).[3]

The perchlorate ion forms a distorted tetrahedron with Cl–O distances of 1.31—1.50 Å and O–Cl–O

Table 5. Equations for the coordination plane and the best plane of the pyridine ring and the deviations of the atoms from them

(A) Coordination plane
$0.39881X+0.04916Y-0.91571Z=1.24215$
(B) The best-plane of the pyridine ring
$0.80595X-0.14657Y-0.57735Z=1.77402$
where $X=ax+cz\cos\beta$, $Y=by$ and $Z=cz\sin\beta$; x, y, and z are the fractional coordinates referred to the crystal axes.

	Deviations from (A)	Deviations from (B)
Cu	0.00 Å	—
O(1)	0.00	—
N(1)	−0.00	0.02
C(1)	0.63	−0.02
C(2)	0.62	0.01
C(3)	−0.06	−0.00
C(4)	−0.69	0.00
C(5)	−0.65	−0.01

angles of 95.9—118.5° (Fig. 2 and Table 3). One of the oxygen atoms, O(2), lies on a line through the copper atom and almost perpendicular to the coordination plane. The Cu–O(2) distance is 2.52 Å, which is comparable with the distances found for the other complexes in which a tetrahedral anion coordinates weakly as a unidentate ligand, *e.g.*, Cu–O, 2.60 Å for $Cu(en)_2(ClO_4)_2$,[11] Cu–F, 2.56 Å for $Cu(en)_2(BF_4)_2$,[12] and Cu–O, 2.62 Å for $Cu(histamine)_2(ClO_4)_2$[13]. These values support the weak coordination of the perchlorate ion in this case. Consequently, it may be appropriate to express this complex as $[Cu(ClO_4)_2(paaH)_2]$ rather than as $[Cu(paaH)_2](ClO_4)_2$. Such a weak coordination is sometimes called "semi-coordination," which means an intermediate between bonding and non-bonding states. This result supports the presence of interaction between the perchlorate ion and the copper atom presumed in the infrared spectral studies previously reported.[7]

All the complex entities are oriented in a O(2)···Cu ···O(2) direction nearly parallel to the plane (010). The short contacts between N(2) and O(3) and between N(2) and O(4) are 2.97 and 3.04 Å respectively (Fig. 3 and Table 4). These contacts appear to be intermolecular hydrogen bonds of the N–H···O type. No other strong interaction seems to be present between the perchlorate and the complex ions. All the complex entities are linked with each other by these hydrogen bonds, forming layers parallel to the plane (102). These layers are connected with the semi-coordination bond of Cu–O(2).

Part of the expenses of the present study was met by a Scientific Research Grant of the Ministry of Education, to which the authors' thanks are due.

11) A. Pajunen, *Suomen Kemistilehti*, **B40**, 32 (1967).
12) D. S. Brown, J. D. Lee, and B. G. A. Melsom, *Acta Crystallogr.*, **B24**, 730 (1968).
13) J. J. Bonnet and Y. Jeannin, *ibid.*, **B26**, 318 (1970).

BULLETIN OF THE CHEMICAL SOCIETY OF JAPAN, VOL. 44, 1734—1739 (1971)

Configuration Interaction Studies on Contact Shift and Contact Nuclear Spin-Spin Coupling in Paramagnetic Transition Metal Complexes

Hajime KATÔ and Hiroshi KATO*

Department of Chemistry, Faculty of Science, Kobe University, Nada-ku, Kobe

** Department of General Education, Nagoya University, Chikusa-ku, Nagoya*

(Received October 23, 1970)

The magnitude of the contact shift for hydrogen nuclei is directly related to the unpaired electron density, ρ_H, on the proton. The mechanism by which the unpaired electrons transfer from the transition metal *d*-orbitals to the ligand orbitals is studied on the basis of the method of intergroup (ligand and metal) configuration interaction. The ρ_H is given as a sum of two terms, ρ_H^P and ρ_H^D, due to the spin-polarization mechanism and the spin-delocalization mechanism respectively. When the interaction between metal and ligand is restricted to a localized bond N–M, such as nickel(II)-benzylamine, $\rho_H^P \simeq -(C_M^m)^2|\chi_H^{(0)}|^2\pi_{HN}\langle NM|NM\rangle/3 \simeq 0.001-0.0001$ (Here π_{HN} is the mutual atom(H)-atom(N) polarizability.). When the interaction between metal and ligand is not restricted to a special localized bond, as in metalocene, $\rho_H^P \simeq -(C_M^m)^2|\chi_H^{(0)}|^2\ \pi_{HH}\langle HM|HM\rangle/3 \simeq 0.01-0.001$. The spin delocalization term has the order of magnitude of: $\rho_H^P \simeq -(C_M^m)^2(\beta_{MN})^2|\chi_H^{(0)}|^2(P_{HN})^2/2(\delta E)^2$ (Here P_{HN} is the bond order between the H and N atomic orbitals.). If the proton H is not directly bonded to the atom N, $\rho_H^D \simeq 0.0001$. If the proton H is directly bonded to the atom N, $\rho_H^D \simeq 0.001$. By disregarding the contributions smaller than the order of magnitude $O(S^2)$, the formulation of the contact nuclear spin-spin coupling constant is derived. The most dominant term is identical with the formula which was derived by Pople and Santry for singlet free-ligand molecules.

The purpose of this paper is to report a study of the contact shift and the contact nuclear spin-spin coupling in paramagnetic transition metal complexes. The unpaired electrons which are formally in *d* orbitals of the transition metal are partly delocalized to the ligands. The mechanism by which the spin reaches

the nuclei on the ligand is closely related to the geometry of the complex and the details of the metal-ligand bonding. Hence, a study of the mechanism of the contact shift and the contact nuclear spin-spin coupling will give us information about the metal-ligand bonding. The present study is based on the method of intergroup (ligand and metal) configuration interaction. This method has the advantage of fixing the attention on the dominant mechanism of the transfer of the unpaired electrons.

The effects of paramagnetism on nuclear resonance shifts have been recognized since the discovery of the nuclear magnetic resonance(NMR).[1] Resonance shifts in paramagnetic molecules can arise from certain electron-nucleus interactions.[2-4] The shifts in the NMR arising from electron spin-nuclear spin coupling are called contact shifts. The pseudocontact shift can arise when the complex is not magnetically isotropic.[2,3] We shall ignore the pseudocontact contribution for the sake of simplicity. The isotropic contact shift arises principally from the Fermi contact term,[5] which is proportional to the odd electron density at the nucleus.[6-8] The magnitude of the contact shift for hydrogen nuclei is thus directly related to the unpaired electron density in the hydrogen 1*s* orbital. For a paramagnetic system of spin, *S*, contact interactions between the spin of the unpaired electron and the nuclear spin of the proton lead to the shift of the NMR frequency given by[9,10]

$$\frac{\delta \mathbf{H}_{\mathrm{H}(i)}}{\mathbf{H}} = -A_{\mathrm{H}(i)} \frac{\gamma_e}{\gamma_{\mathrm{H}}} \frac{g\beta S(S+1)}{3kT}, \qquad (1)$$

where $A_{\mathrm{H}(i)}$ is the electron spin-nuclear spin coupling constant for the *i*th hydrogen atom. A_{H} is related to the unpaired spin density, ρ_{H}, by[11]:

$$A_{\mathrm{H}} = a \times \rho_{\mathrm{H}} \qquad (\text{here } a = 1596[\text{gauss}])$$

In Eq. (1), **H** is the resonance field, $\delta \mathbf{H}_{\mathrm{H}(i)}$ is the resonance field shift for the *i*th proton, γ_e and γ_{H} are, respectively, magnetogyric ratios of the electron and the resonating proton, *g* is the electronic *g* factor, and β is the Bohr magneton.

Intergroup Configuration Interaction

In paramagnetic-transition-metal complexes, the unpaired electrons which are formally located in the transition metal are partly delocalized to the ligands. The discussion below is based on the method of intergroup (ligand and metal) configuration interaction. We will consider the self-consistent-field molecular orbitals (SCF MO's) for an individual group.

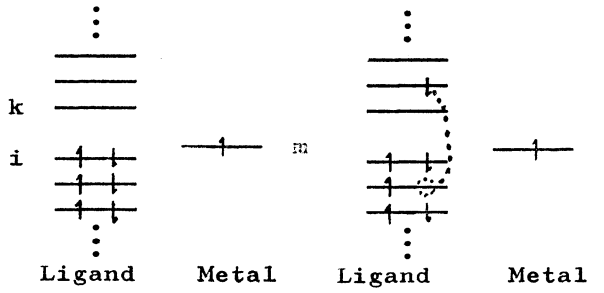

Fig. 1 Fig. 2

Fig. 1. Configuration diagram for the lowest energy configuration.
Fig. 2. Configuration diagram for spin polalization mechanism.

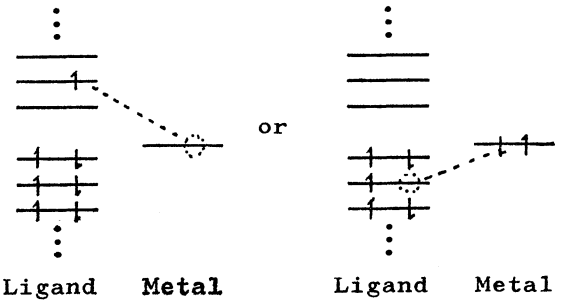

Fig. 3. Configuration diagrams for spin delocalization mechanism.

As an approximation to the configuration interaction problem for the paramagnetic transition metal complexes, we take the lowest energy state to be as shown in the configuration diagram (Fig. 1). The normalized wavefunction for this state is represented by:

$$\Phi_0 = |i\,\bar{i}\,m|, \qquad (2)$$

where *i* denotes the occupied ligand orbitals and where *m* denotes the metal orbitals, hereafter, *k* denotes the vacant ligand orbitals. In these approximations, the charge-transferred states,

$$\Phi_{im} = |i\,\bar{m}\,m|, \qquad (3)$$

$$\Phi_{mk} = |i\,\bar{i}\,k|, \qquad (4)$$

and the singly-excited doublet states:

$$\Phi_{ik}(1) = (2|i\,k\,\bar{m}| - |i\,\bar{k}\,m| - |\bar{i}\,k\,m|)/\sqrt{6}, \qquad (5)$$

$$\Phi_{ik}(2) = (|i\,\bar{k}\,m| - |\bar{i}\,k\,m|)/\sqrt{2}, \qquad (6)$$

arise the delocalization of the unpaired electrons and spin polarization in the ligand. The doublet-state functions, Φ_o, Φ_{im}, Φ_{mk}, $\Phi_{ik}(1)$, and $\Phi_{ik}(2)$, are taken here as the basis of a variational calculation of the wavefunctions.

By the first-order perturbation approximation, the ground state wavefunction, ${}^2\Phi_g$ is found to be:

$${}^2\Phi_g = \Phi_0 + \sum_i^{occ} \lambda_{im}\Phi_{im} + \sum_k^{vac} \lambda_{mk}\Phi_{mk} + \sum_i^{occ}\sum_k^{vac} \lambda_{ik}^{(1)}\Phi_{ik}(1) + \sum_i^{occ}\sum_k^{vac} \lambda_{ik}^{(2)}\Phi_{ik}(2), \qquad (7)$$

where:

1) N. Bloembergen, E. M. Purcell, and R. V. Pound, *Phys. Rev.*, **73**, 679 (1948).
2) N. Bloembergen and W. C. Dickenson, *ibid.*, **79**, 179 (1950).
3) H. M. McConnell and D. B. Chesnut, *J. Chem. Phys.*, **28**, 107 (1958).
4) H. M. McConnell and R. E. Robertson, *ibid.*, **29**, 1361 (1958).
5) E. Fermi, *Z. Physik*, **60**, 320 (1930).
6) S. I. Weissman, *J. Chem. Phys.*, **25**, 890 (1956).
7) H. M. McConnell, *ibid.*, **24**, 764 (1956).
8) A. J. Freeman and R. E. Watson, *Phys. Rev. Lett.*, **6**, 343 (1961).
9) T. W. Swift and R. E. Connick, *J. Chem. Phys.*, **37**, 307 (1962).
10) N. Bloembergen, *ibid.*, **27**, 595 (1957).
11) R. S. Drago and H. Deterson, *J. Amer. Chem. Soc.*, **89**, 5774 (1967).

TABLE 1. THE MATRIX ELEMENTS OF $\langle {}^2\Phi_g|\rho_H|{}^2\Phi_g\rangle$ AND THE ORDER OF MAGNITUDE (O) ON S

Matrix elements	:the order of magnitude O
$\langle\Phi_0\|\rho_H\|\Phi_0\rangle=\langle m\|\rho_H\|m\rangle$	$:O(0)$
$\langle\Phi_0\|\rho_H\|\Phi_{im}\rangle=-\langle i\|\rho_H\|m\rangle$	$:O(S_{im})$
$\langle\Phi_0\|\rho_H\|\Phi_{mk}\rangle=\langle m\|\rho_H\|k\rangle$	$:O(S_{mk})$
$\langle\Phi_0\|\rho_H\|\Phi_{ik}^{(1)}\rangle=2\langle i\|\rho_H\|k\rangle/(6)^{1/2}$	$:O(1)$
$\langle\Phi_0\|\rho_H\|\Phi_{ik}^{(2)}\rangle=0$	$:O(0)$
$\langle\Phi_{im}\|\rho_H\|\Phi_{mk}\rangle=-S_{mk}\langle m\|\rho_H\|i\rangle+S_{mi}\langle m\|\rho_H\|k\rangle$	$:O(S_{mi}S_{mk})$
$\langle\Phi_{im}\|\rho_H\|\Phi_{i'm}\rangle=\langle i\|\rho_H\|i'\rangle$	$:O(1)$
$\langle\Phi_{im}\|\rho_H\|\Phi_{ik}^{(1)}\rangle=-\langle m\|\rho_H\|k\rangle/(6)^{1/2}$	$:O(S_{mk})$
$\langle\Phi_{im}\|\rho_H\|\Phi_{ik}^{(2)}\rangle=-\langle m\|\rho_H\|k\rangle/(2)^{1/2}$	$:O(S_{mk})$
$\langle\Phi_{mk}\|\rho_H\|\Phi_{mk'}\rangle=\langle k\|\rho_H\|k'\rangle$	$:O(1)$
$\langle\Phi_{mk}\|\rho_H\|\Phi_{ik}^{(1)}\rangle=\langle i\|\rho_H\|m\rangle/(6)^{1/2}$	$:O(S_{im})$
$\langle\Phi_{mk}\|\rho_H\|\Phi_{ik}^{(2)}\rangle=-\langle i\|\rho_H\|m\rangle/(2)^{1/2}$	$:O(S_{im})$
$\langle\Phi_{i'k'}^{(1)}\|\rho_H\|\Phi_{ik}^{(1)}\rangle$: $(i'=i,\ k'\neq k)$ $=2\langle k'\|\rho_H\|k\rangle/3$	$:O(1)$
: $(i'\neq i,\ k'=k)$ $=2\langle i'\|\rho_H\|i\rangle/3$	$:O(1)$
: $(i'=i,\ k'=k)$ $=2(\langle i\|\rho_H\|i\rangle+\langle k\|\rho_H\|k\rangle)$	$:O(1)$
: $(i'\neq i,\ k'\neq k)$ $=0$	$:O(0)$
$\langle\Phi_{i'k'}^{(1)}\|\rho_H\ \Phi_{ik}^{(2)}\rangle$: $(i'=i,\ k'\neq k)$ $=\langle k'\|\rho_H\|k\rangle/(3)^{1/2}$	$:O(1)$
: $(i'\neq i,\ k'=\ )$ $=-\langle i\|_H\|i\rangle/(3)^{1/2}$	$:O(1)$
: $(i'=i,\ k'=k)$ $=(\langle k\|\rho_H\|k\rangle-\langle i\|\rho_H\|i\rangle)/(3)^{1/2}$	$:O(1)$
: $(i'\neq i,\ k'\neq k)$ $=0$	$:O(0)$
$\langle\Phi_{i'k'}^{(2)}\|\rho_H\ \Phi_{ik}^{(2)}\rangle$: $(i'=i,\ k'\neq k)$ $=0$	$:O(0)$
: $(i'\neq i,\ k'=k)$ $=0$	$:O(0)$
: $(i'=i,\ k'=k)$ $=0$	$:O(0)$
: $(i'\neq i,\ k'\neq k)$ $=0$	$:O(0)$

$$\lambda_{im}=\frac{\langle\Phi_{im}|H|\Phi_0\rangle}{\delta E_{im}},\quad \lambda_{mk}=\frac{\langle\Phi_{mk}|H|\Phi_0\rangle}{\delta E_{mk}},$$

$$\lambda_{ik}^{(1)}=\frac{\langle\Phi_{ik}^{(1)}|H|\Phi_0\rangle}{\delta E_{ik}},\quad \lambda_{ik}^{(2)}=\frac{\langle\Phi_{ik}^{(2)}|H|\Phi_0\rangle}{\delta E_{ik}}.$$

Here,

$$\delta E_{im}=\langle\Phi_{im}|H|\Phi_{im}\rangle-\langle\Phi_0|H|\Phi_0\rangle, \tag{8}$$

$$H=H_L+H_M+H_{LM}. \tag{9}$$

H_L and H_M are Hamiltonians in an average effective field, which are due to the electrons in the ligand and the metal respectively. Since the wavefunctions, (φ_i, φ_k) and (φ_m, $\varphi_{m'}$), are taken to be SCF MO for H_L and H_M respectively, the molecular integrals, $\langle i|H_L|k\rangle_{i\neq k}$ and $\langle m|H_M|m'\rangle_{m\neq m'}$, are equal to zero. H_{LM} represents the term corresponding to the electron-electron and electron-core interaction over the ligand and the metal.

Contact Shifts and Unpaired Electron Distribution.

The present formulation is primarily intended for the estimation of the contact shift of the transition-metal complexes. Since the contact shifts are proportional to the unpaired electron density at the proton, it is necessary to evaluate the molecular integral $\langle {}^2\Phi_g|\rho_H|{}^2\Phi_g\rangle$. ρ_H is the spin density operator at the ligand proton, H. The orders of the magnitude of λ_{im}, λ_{mk}, λ_{ik}, and λ_{ik}, are $O(S_{mi})$, $O(S_{km})$, $O(S_{km}S_{mi})$ and $O(S_{km}S_{mi})$ respectively.[12] The other matrix elements in $\langle {}^2\Phi_g|\rho_H|{}^2\Phi_g\rangle$ have also been evaluated; they are shown in Table 1. By disregarding the contributions smaller than the $O(S^3)$ order, we obtain

$$\rho_H=\langle {}^2\Phi_g|\rho_H|{}^2\Phi_g\rangle=\rho_H{}^P+\rho_H{}^D, \tag{10}$$

where:

$$\rho_H{}^P=\frac{4}{\sqrt{6}}\sum_i^{occ}\sum_k^{vac}\lambda_{ik}^{(1)}\langle i|\rho_H|k\rangle, \tag{11}$$

and

$$\rho_H{}^D=(-2\sum_i^{occ}\lambda_{im}\langle i|\rho_H|m\rangle+2\sum_k^{vac}\lambda_{mk}\langle m|\rho_H|k\rangle+\sum_i^{occ}\sum_{i'}^{occ}\lambda_{im}\lambda_{i'm}\langle i|\rho_H|i'\rangle+\sum_k^{vac}\sum_{k'}^{vac}\lambda_{mk}\lambda_{mk'}\langle k|\rho_H|k'\rangle). \tag{12}$$

ρ_H^P is the contribution due to the spin-polarization mechanism (see Fig. 2), while ρ_H^D is the contribution due to the spin-delocalization mechanism (see Fig. 3).

Spin-polarization Mechanism. In this section, we will discuss the spin-polarization mechanism. The (ik)-element of the spin polarization term in Eq. (10) is:

$$(\rho_H{}^P)_{ik}=\frac{4}{\sqrt{6}}\lambda_{ik}^{(1)}\langle i|\rho_H|k\rangle. \tag{13}$$

The molecular orbital, $|i\rangle$, is expressed as a linear combination of atomic orbitals:

$$|i\rangle=\sum_\mu C_\mu{}^i\chi_\mu. \tag{14}$$

Since the one-center term is the most dominant in $\langle i|\rho_H|k\rangle$, $(\rho_H^P)_{ik}$ is, approximately:

$$(\rho_H{}^P)_{ik}=\frac{4}{\sqrt{6}}\lambda_{ik}^{(1)}C_H{}^iC_H{}^k|\chi_H^{(0)}|^2, \tag{15}$$

where:

12) K. Fukui and H. Fujimoto, This Bulletin, **41**, 1989 (1968).

$$\lambda_{ik}^{(1)} = -\frac{2}{\sqrt{6}}\sum_{\mu,\nu} C_\mu{}^k C_\nu{}^i \frac{\langle \mu m | \nu m\rangle}{\delta E_{ik}}. \quad (16)$$

Hence,

$$(\rho_H{}^P)_{ik} = -\frac{4}{3}\frac{1}{\delta E_{ik}}\sum_{\mu,\nu} C_\mu{}^k C_\nu{}^i C_H{}^k C_H{}^i |\chi_H^{(0)}|^2 \langle \mu m | \nu m\rangle. \quad (17)$$

Let us denote the atomic orbitals of the transition metal, of the adjacent atom in the ligand, of the ligand proton, H, and of the proton-attached nucleus as M, N, H, and C respectively. Then, the spin density at the proton H due to the spin polarization mechanism, ρ_H^P, may be writtern as:

$$\begin{aligned}\rho_H{}^P &= \sum_i^{occ}\sum_k^{vac} (\rho_H{}^P)_{ik} \\ &= -\{(C_M{}^m)^2/3\}(\pi_{HN}\langle NM|NM\rangle + \pi_{HH}\langle HM|HM\rangle \\ &\quad + \sum_{t\neq N,H}\pi_{Ht}\langle tM|tM\rangle + \sum_{t,u(t\neq u)}\pi_{H,tu}\langle tM|uM\rangle), \end{aligned} \quad (18)$$

where $\pi_{NN}{}'$ is completely analogous to the mutual atom-atom polarizability associated with the atoms N and N'[13]:

$$\pi_{NN'} = 4\sum_i^{occ}\sum_j^{vac}\frac{C_N{}^i C_N{}^i C_{N'}{}^j C_{N'}{}^j}{\delta E_{ij}}, \quad (19)$$

χ_N is an atomic orbital at the nucleus, N, and $\pi_{H,tu}$ is the atom-bond-polarizability defined by:

$$\pi_{H,tu} = 2\sum_i^{occ}\sum_j^{vac}\frac{C_H{}^i C_H{}^j (C_u{}^i C_t{}^j + C_t{}^i C_u{}^j)}{\delta E_{ij}}. \quad (20)$$

When the interaction between metal and ligand is restricted to the localized bond N–M:

$$\pi_{HN}\langle NM|NM\rangle > \pi_{HH}\langle HM|HM\rangle \gtrsim \pi_{Ht}\langle tM|tM\rangle.$$

Thus ρ_H^P may be written as:

$$\rho_H{}^P \simeq -\frac{1}{3}(C_M{}^m)^2 |\chi_H^{(0)}|^2 \pi_{HN}\langle NM|NM\rangle. \quad (21)$$

That is, the order of magnitude of $\langle AM|AM\rangle$ (A= N, H, t) is $(S_{AM})^2$, $(S_{NM})^2 \gg (S_{HM})^2 \simeq (S_{tM})^2$ in the above N–M localized bond. The order of magnitude is $C_M^m \simeq 1$, $\chi_H(0) \simeq 1$, $\pi_{HN} \simeq -(0.1)^2/10[(eV)^{-1}]$, and $\langle NM|NM\rangle \simeq 3$ [eV]. Accordingly, ρ_H^P is of the order of magnitude of 0.001—0.0001. The contact shifts for the amino proton of the nickel(II)-benzylamine complex[14] can be explained by this mechanism (Table 2*a*). The alternative character of spin density (the change in the sign of the spin density) can be explained by the alternative character of $\pi_{NN'}$. Further, Eq. (21) shows that the sign of ρ_H^P is the same as the sign of J_{NH} (the I–I coupling constant between N and H AO.) of a free molecule, because $J_{NH} \propto \pi_{NH}$ and $\langle NH|NH\rangle > 0$.

When the interaction between metal and ligand is not restricted to a special localized bond, $\pi_{HH}\langle HM|HM\rangle \geq \pi_H\langle tM|tM\rangle$. Accordingly, ρ_H^P may be written as:

$$\rho_H{}^P \simeq -\frac{1}{3}(C_M{}^m)^2 |\chi_H^{(0)}|^2 \pi_{HH}\langle HM|HM\rangle. \quad (22)$$

The order of magnitude is $C_M^m \simeq 1$, $\chi_H^{(0)} \simeq 1$, $\pi_{HH} \simeq 1/10$ [$(eV)^{-1}$], and $\langle HM|HM\rangle \simeq 0.1$ [eV]. Accordingly, ρ_H^P is of the order of magnitude of 0.01—0.001. The large contact shifts and the hyperfine coupling constants for paramagnetic metallocene[15,16] can be explained by this mechanism (Table 2*b*).

Spin-delocalization Mechanism. In this section, we will discuss the spin-delocalization mechanism. In the LCAO form, the spin delocalization term in Eq. (10) is:

$$\begin{aligned}\rho_H{}^D \simeq &\Big(\sum_i^{occ}\sum_{i'}^{occ}\lambda_{im}\lambda_{i'm}C_H{}^i C_H{}^{i'} + \sum_k^{vac}\sum_{k'}^{vac}\lambda_{mk}\lambda_{mk'}C_H{}^k C_H{}^{k'}\Big)|\chi_H^{(0)}|^2 \\ &- \Big(2\sum_i^{occ}\lambda_{im}C_H{}^i C_M{}^m - 2\sum_k^{vac}\lambda_{mk}C_M{}^m C_H{}^k\Big)\chi_H^{(0)}\chi_M^{(0)}, \end{aligned} \quad (23)$$

where $\chi_M^{(0)}$ is the value of the metal orbital at the proton H. The value of the metal orbital at the proton H is insignificant (the order of the magnitude of $\chi_H^{(0)}\chi_M^{(0)}$ is calculated to be 0.001[17]), so it will be omitted. λ_{im} and λ_{mk} may be approximated in the order of magnitude as follows:

$$\lambda_{im} \simeq \frac{C_M{}^m C_N{}^i \beta_{MN}}{\delta E_{im}}, \quad \lambda_{mk} \simeq \frac{C_M{}^m C_N{}^k \beta_{MN}}{\delta E_{mk}},$$

where β_{MN} is the core-resonance integral between the atomic orbitals M and N. Then,

Table 2. Spin density on the ligand proton calculated from the observed contact shift referenced against diamagnetic ligand by Eq. (1)—(3)

a) $[Ni\ (bz)_6]^{2+}$ ($bz = C_6H_5CH_2NH_2$):
$\rho^{NH_2} = -0.0003$, $\rho^{CH_2} = +0.0001$, $\rho^{H_{ortho}} = -0.000004$, $\rho^{H_{meta}} = +0.000004$, $\rho^{H_{para}} = -0.000004$.

b) Ni $(C_5H_4\text{-}CH_3)_2$:
$\rho^H = -0.0008$, $\rho^{CH_3} = +0.0006$.
Cr $(C_5H_4\text{-}CH_3)_2$:
$\rho^H = +0.002$, $\rho^{CH_3} = -0.0005$.

c) (bipyridine)$_3$ $FeCl_3$:
$\rho^{2H} = +0.0005$, $\rho^{3H} = +0.0001$, $\rho^{4H} = +0.00006$, $\rho^{5H} = +0.00001$.

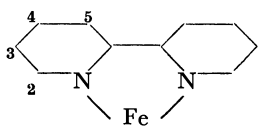

a) Ref. 14, b) Ref. 16, c) Ref. 18

13) C. A. Coulson and H. C. Longuet-Higgins, *Proc. Roy. Soc.*, **A191**, 39 (1947); *ibid.*, **A193**, 447 (1948).
14) R. J. Fitzgerald and R. S. Drago, *J. Amer. Chem. Soc.*, **89**, 2879 (1967); *ibid.*, **90**, 2523 (1968).
15) M. F. Retting and R. S. Drago, *ibid.*, **91**, 1361, 3432 (1969).
16) R. Prins, *J. Chem. Phys.*, **50**, 4808 (1969).
17) S. E. Anderson and R. S. Drago, *J. Amer. Chem. Soc.*, **91**, 3656 (1969).

$$\rho_H^D \simeq (C_M^m)^2\beta_{MN}^2|\chi_H^{(0)}|^2\left\{\left(\sum_i^{occ}\frac{C_H^iC_N^i}{\delta E_{im}}\right)^2+\left(\sum_k^{vac}\frac{C_H^kC_N^k}{\delta E_{mk}}\right)^2\right\}. \quad (24)$$

Taking the mean excitation energy (δE) approximation, one obtains:

$$\rho_H^D \simeq (C_M^m)^2\beta_{MN}^2|\chi_H^{(0)}|^2(P_{HN})^2/2(\delta E)^2, \quad (25)$$

where:

$$P_{HN} = 2\sum_i^{occ} C_H^iC_N^i.$$

The order of magnitude is $C_M^m \simeq 1$, $\beta \simeq 5$ [eV], $P_{HN} \simeq 0.1$, and $\delta E \simeq 10$[eV], so ρ_H^D is of the order of magnitude of 0.0001. Thus, if the proton H is not directly bonded to the atom N, the spin-delocalization mechanism is not important. However, if the proton H is directly bonded to the atom N, $P_{HN} \simeq 0.5$ and ρ_H^D is of the order of magnitude of 0.001—0.0001. Therefore, the spin-delocalization mechanism is not negligible in this case. The bipyridine proton contact shift in α,α'-bipyridine chelates of Fe(III)[18] can be explained by this mechanism (Table 2*c*). Further, if only the integral $\langle i|H|m\rangle$ is not equal to zero, $\rho_H^D \simeq (\beta_{NH}/E_{im})^2 \times (P_{HN}^i)^2$; that is the partial bond order $(P_{HN}^i)^2$ is proportional to the spin densities of the related atoms. The total amount of odd electrons transferred to the ligand is estimated by means of the values of $(\beta_{NM}/\delta E_{im}) \simeq 0.1$.

Contact Nuclear Spin-Spin Coupling

Ramsey[19] has shown by the perturbation therory that the contact nuclear spin-spin coupling constant, $J_{NN'}$ between the nuclei N and N' can be written as:

$$J_{NN'} = -\frac{2}{3h}\left(\frac{16\pi\beta h}{3}\right)^2\gamma_N\gamma_{N'} \times\sum_n\frac{\langle\Phi_0|\sum_k\delta(\mathbf{r}_{kN})\mathbf{S}_k|\Phi_n\rangle\langle\Phi_n|\sum_j\delta(\mathbf{r}_{jN'})\mathbf{S}_j|\Phi_0\rangle}{\delta E_{n0}}, \quad (26)$$

where Φ_0 denotes the ground state MO and where Φ_n represents the nth excited state MO. A theory of spin-spin coupling for a singlet molecule has been given by Pople and Santry[20] and the contact nuclear spin-spin coupling constant has been represented by:

$$J_{NN'} = -\frac{1}{4h}\left(\frac{16\pi\beta h}{3}\right)^2\gamma_N\gamma_{N'}|\chi_N^{(0)}|^2|\chi_{N'}^{(0)}|^2\pi_{NN'}. \quad (27)$$

Let us assume Eq. (7) as the ground-doublet-state wavefunction. In the evaluation of the proton-proton coupling constant of the ligand molecule, the molecular integrals $\langle i|\rho_N|m\rangle$ are insignificant and will be omitted. Neglecting any contributions smaller than the $O(S^2)$ order, we obtain:

$$J_{NN'} = -\frac{2}{3h}\left(\frac{16\pi\beta h}{3}\right)^2\gamma_N\gamma_{N'}(A+B+C+D), \quad (28)$$

where:

$$A = \sum_{i'}^{occ}\frac{1}{\delta E_{i'm}}(\sum_i^{occ}\lambda_{im}\langle i|\rho_N|i'\rangle)(\sum_i^{occ}\lambda_{im}\langle i'|\rho_{N'}|i\rangle), \quad (29)$$

$$B = \sum_{k'}^{vac}\frac{1}{\delta E_{mk'}}(\sum_k^{vac}\lambda_{mk}\langle k|\rho_N|k'\rangle)(\sum_k^{vac}\lambda_{mk}\langle k'|\rho_{N'}|k\rangle). \quad (30)$$

$$C = \sum_{i'}^{occ}\sum_{k'}^{vac}\frac{1}{\delta E_{i'k'}}\frac{2}{3}\langle i'|\rho_N|k'\rangle\langle k'|\rho_{N'}|i'\rangle, \quad (31)$$

$$D = \sum_{i'}^{occ}\sum_{k'}^{vac}\frac{1}{\delta E_{i'k'}}\frac{4}{3\sqrt{6}} \times\{\langle i'|\rho_N|k'\rangle[\sum_{k\neq k'}^{vac}\langle k'|\rho_{N'}|k\rangle\lambda_{i'k}^{(1)}+\sum_{i\neq i'}^{occ}\langle i'|\rho_{N'}|i'\rangle\lambda_{ik'}^{(1)} +\frac{2}{3}(\langle i'|\rho_{N'}|i'\rangle+\langle k'|\rho_{N'}|k'\rangle\lambda_{i'k'}^{(1)}] +\langle k'|\rho_{N'}|i'\rangle[\sum_{k\neq k'}^{vac}\langle k|\rho_N|k'\rangle\lambda_{i'k}^{(1)}+\sum_{i\neq i'}^{occ}\langle i|\rho_N|i'\rangle\lambda_{ik'}^{(1)} +\frac{2}{3}(\langle i'|\rho_N|i'\rangle+\langle k'|\rho_N|k'\rangle)\lambda_{i'k'}^{(1)}]\}. \quad (32)$$

Only the third term, C, in Eq.(28) is of the order of magnitude of $O(1)$; the other terms, A, B, and D, are of the order of magnitude of $O(S^2)$. Accordingly, Eq. (28) may be written approximately by only the C-term. Then;

$$J_{NN'} = -\frac{1}{h}\left(\frac{16\pi\beta h}{3}\right)^2\gamma_N\gamma_{N'} \times\sum_{i'}^{occ}\sum_{k'}^{vac}C_N^iC_N^kC_{N'}^iC_{N'}^k|\chi_N^{(0)}|^2|\chi_{N'}^{(0)}|/\delta E_{i'k'} = -\frac{1}{4h}\left(\frac{16\pi\beta h}{3}\right)^2\gamma_N\gamma_{N'}\pi_{NN'}|\chi_N^{(0)}|^2|\chi_{N'}^{(0)}|^2, \quad (33)$$

where we have considered the contribution from only the atomic orbital of the nucleus N in the evaluation of the molecular integral, $\langle k'|\rho_N|k\rangle$. Eq. (33) is identical with Eq. (27), which was derived by Pople and Santry for a singlet free molecule.[20] From this result, we can conclude that: the proton-proton coupling constant of the ligand molecule in paramagnetic transition metal complexes is approximately identical with that of a singlet free ligand molecule and that the effect of a paramagnetic metal on $J_{NN'}$ is of the order of magnitude of $(S_{LM})^2$. The spin-spin couplings observed for the ligand quinoline of the nickel(II) aminotropone-imineate[21] is $J_{23}=4.0\pm0.2$ Hz, $J_{34}=7.9\pm0.2$ Hz, and $J_{78}=7.9\pm0.2$ Hz, and for a free quinoline[22] $J_{23}=4.1\pm0.2$ Hz, $J_{34}=8.5\pm0.3$ Hz, and $J_{78}=8.2\pm0.3$ Hz. These observed results are in good agreement with the above conclusion.

Summary

When the interaction between metal and ligand is restricted to the localized bond N–M, as in nickel(II)-benzylamine,

$$\rho_H^P \simeq -(C_M^m)^2|\chi_H^{(0)}|^2\pi_{HN}\langle NM|NM\rangle/3 \simeq 0.001—0.0001.$$

When the interaction between metal and ligand is not restricted to a special localized bond, as in metallocene,

$$\rho_H^P \simeq -(C_M^m)^2|\chi_H^{(0)}|^2\pi_{HH}\langle HM|HM\rangle/3 \simeq 0.01—0.001.$$

The spin-delocalization term has the order of magnitude of $\rho_H^D \simeq -(C_M^m)^2(\beta_{MN})^2|\chi_H^{(0)}|^2(P_{HN})^2/2(\delta E)^2$. If the proton H is directly bonded to the atom N, $\rho_H^D \simeq 0.001$. If

18) G. N. La Mar and G. R. Van Hecke, *J. Amer. Chem. Soc.* **91**, 3442 (1969).
19) N. F. Ramsey, *Phys. Rev.*, **91**, 303 (1953).
20) J. A. Pople and D. P. Santry, *Mol. Phys.*, **8**, 1 (1964).
21) D. R. Eaton, A. D. Josey, W. D. Phillips, and R. E. Benson, *Discuss. Faraday Soc.*, **34**, 77 (1962).
22) C. T. Ford, F. E. Dickson, and I. I. Bezman, *Inorg. Chem.*, **3**, 177 (1964).

the H proton is not directly bonded to the atom N, $\rho_H^D \simeq$ 0.0001. The mechanism by which the spin reaches the nuclei on the ligand is closely related to the geometry of the complex and the details of the metal-ligand bonding. The magnitude of the contact shift gives us information about the mechanism and the metal-ligand bonding.

The most dominant term in $J_{NN'}$ derived for a transition metal complex, is identical with the formula which was derived for a singlet free-ligand molecule by Pople and Santry.[20] This implies that the proton-proton coupling constant of the ligand molecule in paramagnetic-transition metal complexes is nearly equal to that of the singlet free-ligand molecule and that the effect of the paramagnetic metal on $J_{NN'}$ is of the order of magnitude of $(S_{LM})^2$.

The authors wish to thank Professor Teijiro Yonezawa for his generous support of this work. They also wish to thank Dr. Isao Morishima for his helpful discussions.

BULLETIN OF THE CHEMICAL SOCIETY OF JAPAN, VOL. 44, 1739—1742 (1971)

Dehydration and Dehydrogenation of Alcohols over Acid-Base Bifunctional Catalysts

Hiroo NIIYAMA and Etsuro ECHIGOYA

Department of Chemical Engineering, Tokyo Institute of Technology, Ookayama, Meguro-ku, Tokyo

(Received November 12, 1970)

Alkaline earth silicates having both acidic and basic sites can be considered as acid-base bifunctional catalysts. Dehydration and dehydrogenation of alcohols over these catalysts were carried out. Correlation between the selectivity and acid-base properties of alcohols and the catalysts was studied. It was found that acid-base properties of both the catalysts and the alcohols were cooperative in determining the selectivity of reaction.

The dehydration and dehydrogenation of alcohols over oxide catalysts have been studied by many investigators. Some oxides particularly tend to promote dehydration, whereas others have mainly dehydrogenating effects. Several hypotheses[1] were proposed concerning the cause of selectivity; *i.e.*, (1) a geometric factor of the surface structure,[2] (2) type of semiconductor,[3] (3) acidic and basic characters,[4] and (4) some other special parameters, *e.g.*, $\eta \equiv$(cation radius)^3/(mol volume per cation) (charge of cation) proposed by Eucken[5] and Wicke.[6] These attempts were partially successful. However, the relation between the surface properties and reaction mechanism or the nature of the active sites is still obscure. It was the object of this study to clarify the cause of selectivity using acid-base bifunctional catalysts.

Experimental

Preparation of Catalysts. Colloidal silica (Nissan Chem. Co., Snowtex O) was kneaded with equal moles of an alkaline earth hydroxide ($Mg(OH)_2$, $Ca(OH)_2$, $Sr(OH)_2$, $Ba(OH)_2$) for 3 hr and calcined at 100°C for 24 hr. It was then heated at 290°C for 24 hr in an autoclave with aqueous ammonia under 80—90 kg/cm^2 pressure. Products were washed several times with ion-exchanged water and then calcined at 600°C for 3 hr.

Measurements of Acidity and Basicity. A titration method in an aprotic medium was employed. Before the measurement, samples were heated at 550°C for 1 hr under air and then degassed at 300°C under 10^{-5}mmHg pressure. *n*-Butylamine (0.02N) and benzoic acid (0.02N) in benzene were used for titration in acidity and basicity measurements, respectively. The following indicators were used; neutral red ($pK_a+6.8$), methyl red ($pK_a+4.8$), dimethyl yellow ($pK_a+3.3$), benzeneazodiphenylamine ($pK_a+1.5$), benzalacetophenon ($pK_a-5.6$), and phenolphtalein ($pK_a+9.3$).

Preparation of Deutrated n-*Propanol* (C_3H_7OD).[7] 200 ml of *n*-propanol was subjected to reaction with 5 g of metallic sodium. Unreacted *n*-propanol was removed by vacuum distillation and then 3 g of D_2O were introduced. Produced *n*-C_3H_7OD was trapped with liquid nitrogen. Deutrium concentration was estimated by IR spectroscopy from OD and OH absorption bands and the amount of *n*-C_3H_7OH was confirmed to be negligible.

Reaction Apparatus. The usual fixed bed flow type reactor was employed. A reactant was kept in an evaporator maintained at a constant temperature and introduced into the catalyst bed with hydrogen as the carrier gas. In front of the reactor, a sample inlet made of rubber was attached in order to inject poisonous materials.

All the system was heated to prevent the condensation of reactant or products. Vaporous products were taken out by a sampling cock and analyzed by gas chromatography.

Results and Discussion

Acid-base properties of the catalysts. The properties of the catalysts are given in Table 1. All the catalysts

1) P. Mars, "The Mechanism of Heterogeneous Catalysis," Elsevier Pub. Co., Amsterdam, (1960), p. 49.
2) A. A. Ballandin, "Advances in Catalysis," Vol. 10, Academic Press, New York (1958).
3) Z. G. Szabo and F. Solimosi, *Z. Anorg. Allg. Chem.*, **301**, 225, (1959).
4) K. Tanaka and K. Tamaru, This Bulletin, **37**, 1862 (1964).
5) A. Eucken, *Naturwissenschaften*, **36**, 48 (1949).
6) E. Wicke, *Z. Elektrochem.*, **53**, 279 (1949).
7) A. Murray and D. L. Williams, "Organic Synthesis with Isotopes," Vol. 2, Interscience Pub. Inc., New York (1958), p. 1340.

Table 1. Structure and surface properties of the catalyst

Catalyst	Structure	Surface area (m^2/g)	Maximum acid strength(H_0)	Acidity [a] (10^{-7} eq/m^2)	Basicity [b] (10^{-7}eq/m^2)
$MgO \cdot SiO_2$	Speolite	194	−5.6	22.4	[c]
$CaO \cdot SiO_2$	Xonotlite	46	+3.3	7.5	13.7
$SrO \cdot SiO_2$	Strontium metasilicate	9.0	+3.3	3.3	18.9
$BaO \cdot SiO_2$	Barium metasilicate	2.0	+4.8	0	30.3

a) Measured at $H_0=3.3$ b) Measured at $H_0=9.3$ c) Abnormal color was observed.

except for $MgO \cdot SiO_2$ showed fine patterns in X-ray diffraction. The order of acidic nature (acidity and acid strength) was as follows. $MgO \cdot SiO_2 > CaO \cdot SiO_2 > SrO \cdot SiO_2 > BaO \cdot SiO_2$.

The acidic nature of $MgO \cdot SiO_2$ was attributed to the unsaturation of the bond which was produced by the replacement of four coordinated silicon with magnesium.[8] The degree of unsaturation decreases with the increase of ionic radius of the replaced cation and also with the decrease of electronegativity of metal. Thus the sequence of acidic nature can be explained.

On the other hand, the order of basicity was as follows. $BaO \cdot SiO_2 > SrO \cdot SiO_2 > CaO \cdot SiO_2 > MgO \cdot SiO_2$. This was the complete reverse of the order of acidic nature but the same as that of basic nature of the corresponding alkaline earth oxides (BaO>SrO>CaO>MgO).[9] Thus the basicity could be attributed to the small electronegativity of the alkaline earth metals. The amount of uncombined alkaline earth oxides unavoidably present before the progress of chemical reaction in the solid phase, was very small and confirmed to be negligible.[10] It is concluded that these silicates have basic sites as well as acidic sites.

Dehydration and dehydrogenation of alcohols. $CaO \cdot SiO_2$, which showed both acidic and basic natures in comparable degree was chosen as the catalyst in the selectivity studies of this reaction. It showed both dehydration and dehydrogenation activities.

Addition of acidic and basic materials. Figures 1 and 2 show the effects of pyridine and phenol addition on

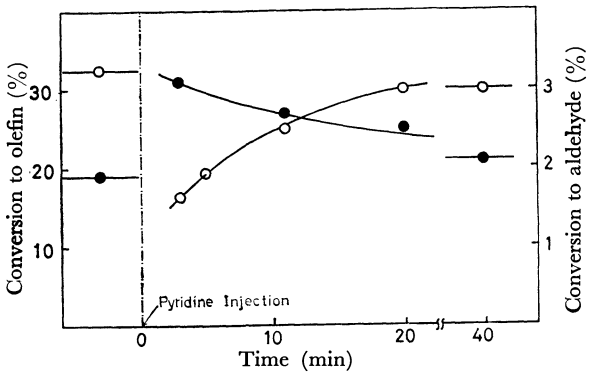

Fig. 1. The effect of pyridine injection on the decomposition of *n*-Butanol over $CaO-SiO_2$.
—○— butene
—●— butylaldehyde
Reaction temperature; 340°C W/F; 1.49 g-hr/mol Pressure of alcohol; 0.0116 atm.

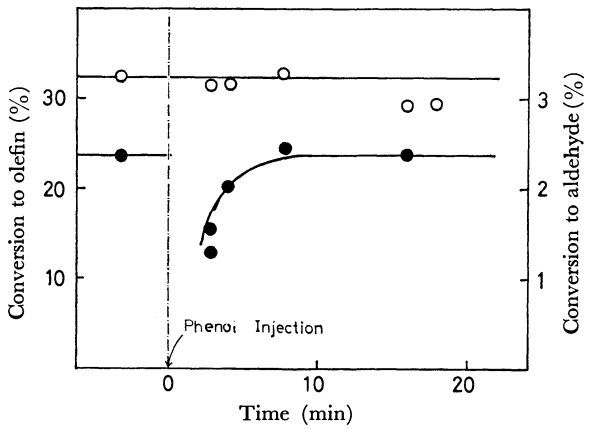

Fig. 2. The effect of phenol injection on the decomposition of *n*-butanol over $CaO \cdot SiO_2$.
—○— butene
—●— butylaldehyde
Reaction temperature; 340°C W/F; 1.49 g-hr/mol Pressure of alcohol; 0.0116 atm

the decomposition of *n*-butanol. These poisons gave no reaction products. 10 μl of the substances were introduced into the system as a pulse. Addition of pyridine brought a decrease in the dehydration activity with considerable increase in dehydrogenation activity. On the other hand, phenol inhibited the dehydrogenation reaction and gave no effect on dehydration. The effects were reversible. Thus it was concluded that dehydration took place on acidic sites and dehydrogenation on basic sites.

The promoter action of pyridine can be attributed to the inductive effect of adsorbed pyridine. Because of high electron donating ability of pyridine, adjacent sites become rich in electron density and these sites act as basic sites. This hypothesis was confirmed.

Isotope effects on both reaction rates. Either *n*-C_3H_7OH or *n*-C_3H_7OD was introduced into the reactor alternatively. Reaction rates were estimated in the steady state. Experiments were repeated several times and the mean values are given in Table 2. No isotope

Table 2. Isotope effects on both reaction rates over $CaO \cdot SiO_2$

	Conversion(%)		Isotope effects k_D/k_H
	n-PrOH	*n*-PrOD	
Dehydration	1.58	1.51	0.96
Dehydrogenation	1.11	0.59	0.53

Reaction temperature 340°C
Partial pressure of alcohol: 0.1atm
Feed rate of carrier gas: 0.134mol/hr
Weight of catalyst: 1.0g

8) C. L. Thomas, *Ind. Eng. Chem.*, **41**, 2564 (1949).
9) J. Take, S. Kikuchi, and Y. Yoneda, *Syokubai*, **10**, 127 (1968).
10) E. E. Pressler, B. Brunauer, and D. L. Kantro, *Anal. Chem.*, **28**, 896 (1956).

TABLE 3. DEHYDRATION AND DEHYDROGENATION OF FIVE ALCOHOLS OVER $CaO \cdot SiO_2$

Reactant	Reaction temperature	Reaction product	Rate of reaction (mol/g hr)		Activation energy (kcal/mol)	
			Dehydration	Dehydrogenation	Dehydration	Dehydrogenation
Ethanol	320—360°C	Ethylene, Ether Acetaldehyde	7.0×10^{-5} [b]	1.8×10^{-4}	35[b]	14
n-Propanol	290—320°C	Propylene Propionaldehyde	8.6×10^{-5}	6.2×10^{-5}	29	19
n-Butanol	310—350°C	*n*-Butene Butylaldehyde	1.7×10^{-4}	1.5×10^{-5}	26	23
Isopropanol	290—240°C	Propylene Acetone	1.5×10^{-3}	3.5×10^{-6}	23	17
t-Butanol	150—190°C	Isobutene	1.3		33	

a) Sum of the ethylene and ether formation.
b) Activation energy of ethylene formation. Activation energy of (ethylene+ether) formation was 30 kcal/mol.

effect was found in the dehydration reaction while the value 0.53 was obtained for k_D/k_H in the dehydrogenation. This value was close to 0.34 which was obtained by calculation[11] on the assumption that an isotope effect comes from the difference of the zero point energy of reactants. It was concluded that OH rupture was the rate determining step in the dehydrogenation reaction.

Decomposition of five Alcohols. Dehydration and dehydrogenation of five alcohols were carried out. Experimental conditions and the results are given in Table 3. In the dehydration of ethanol, ethylene, and ether were found in the products. Ethylene formation and ether formation took place competitively in the low conversion region. The activation energy shown in Table 3 and Fig. 4 was calculated from the rate of ethylene formation because the reaction paths differed from each other. The reaction rate at 310°C under 55 mmHg of alcoholic pressure was taken as an index of the reactivity of alcohol.

Correlation between the reactivity and Taft's σ^*[12] which represents the electron donating ability of the aliphatic group attached to OH group is shown in Fig. 3. Negative correlation for dehydration and a positive one for dehydrogenation were obtained.

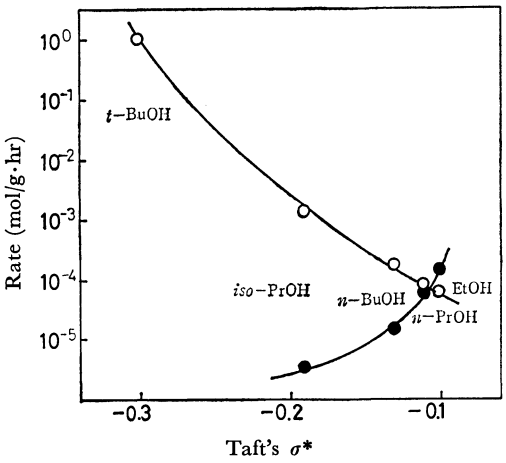

Fig. 3. Correlation between Taft's σ^* and reactivity of alcohols.
—○— dehydration rate
—●— dehydragenation rate

The heat of carbonium ion formation (ΔHc_+) could also be an index of electron donating ability.[13] The larger the ΔHc_+, the more unstable the carbonium ion and thus, the smaller the electron donating ability. Figure 4 shows the correlation between ΔHc_+ and reactivity. Almost the same correlation were obtained.

The activation energies for primary alcohols are also plotted in Fig. 4. Good correlation between ΔHc_+ and the activation energy of primary series indicates that this reactivity sequence can be referred to an energetic factor.

Both horizontal axes in the figures can also be considered to express electron density of OH group, or acid-base properties of alcohol. Therefore, it is concluded that dehydration tend to take place as the basicity of alcohol increases and dehydrogenation becomes predominant as the acidity of the alcohol increases.

The reactivity sequence of alcohols over this catalyst is quite different from that observed over metal catalysts. Over the copper catalyst which is commonly used in the dehydrogenation of alcohols, ethyl, *n*-propyl, and *n*-butyl alcohol have almost the same reactivity,

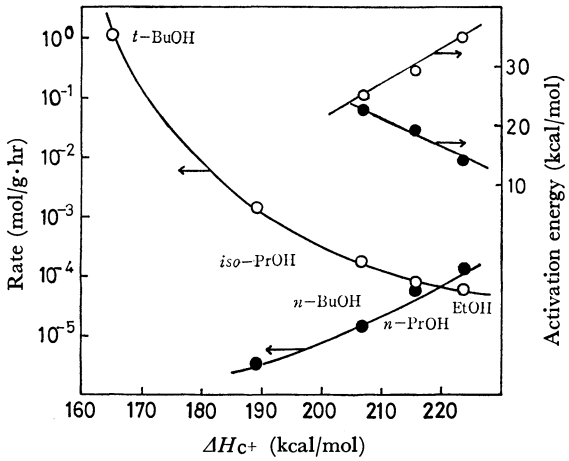

Fig. 4. Correlation between ΔHc_+ and reactivity of alcohols.
—○— dehydration
—●— dehydrogenation

11) L. Melander, "Isotope Effects on Reaction Rates," Ronald Press, (1960), p. 17
12) M. S. Newman, "Steric Effects in Organic Chemistry," John Wiley & Sons Inc., New York (1956).
13) I. Mochida and Y. Yoneda, This Bulletin, **40**, 2711 (1967).

Table 4. Catalytic activity of various alkaline earth silicates

Silicates	Dehydration rate		Dehydrogenation rate		Selectivity[c]
	mol/g·hr	mol/meq·hr [a]	mol/g·hr	mol/meq·hr[b]	
$MgO \cdot SiO_2$	65×10^{-3}	147×10^{-3}	——	——	0
$CaO \cdot SiO_2$	2.8×10^{-3}	82×10^{-3}	0.18×10^{-3}	2.9×10^{-3}	0.06
$SrO \cdot SiO_2$	0.018×10^{-3}	12×10^{-3} [d]	0.015×10^{-3}	0.88×10^{-3}	0.45
$BaO \cdot SiO_2$	0.0097×10^{-3}	——	0.0065×10^{-3}	1.1×10^{-3}	0.40

a) Rate per unit acidity (H_0 +3.3)
b) Rate per unit basicity
c) Selectivity is defined as dehydrogenation rate/total rate.
d) Acidity measured was below 0.003, and the value 0.0015 was assumed for the acidity.

and isopropanol reactivity five times higher than that of primary alcohols.[14] This suggests that the hydrogen release from carbinol carbon is the rate determining step over metal catalysts.

Eucken showed that the dehydrogenation selectivity increased over various oxides in the decomposition of ethanol could be correlated well with η[5]. Selectivity increased as η became greater. They considered that the matal atom was exposed on the surface of the oxide as the ionic radius, as well as η, increased. They proposed the following mechanism. If the dehydrogenation activity of this catalyst is attributed to the hydride ion affinity of metal, the reactivity sequence would differ from the one obtained.

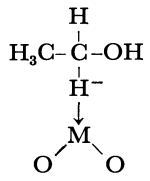

Tanaka *et al.*[4] pointed out that the physical meaning of η is acid-base properties of the surface. This coincides with our results.

Reaction mechanisms. Reaction mechanisms for both reactions (for example, ethanol decomposition) can be expressed as follows.

Dehydration

$$CH_3CH_2OH + H^+A \xrightarrow{I} CH_3CH_2\text{-}OH \xrightarrow{II} \underset{H^+\cdots A}{}$$

$$\underset{A}{CH_3\text{-}CH_2^+} + H_2O \xrightarrow{III} CH_2{=}CH_2 + H_2O + H^+A$$

The reactivity sequence suggests that either process I or II is rate determining.

Dehydrogenation

$$CH_3CH_2OH + B \xrightarrow{I} CH_3CH_2O^- \cdots H^+B \xrightarrow{II}$$

$$CH_3CH\text{-}O \xrightarrow{III} CH_3CHO + H_2 + B$$
$$H^- \cdots H^+B$$

H^+A; acidic site B; basic site

The reactivity sequence and existence of an isotope effect suggest that process I is the rate determinig step.

Activity and Selectivity of the Various Alkaline Earth Silicates. Decomposition of *n*-butanol over alkaline earth silicates with various acidity and basicity was studied. No dehydrogenation reaction was found over $MgO\cdot SiO_2$, while both reactions were observed over $CaO\cdot SiO_2$, $SrO\cdot SiO_2$, $BaO\cdot SiO_2$. Reaction rates at 350°C are given in Table 4. Selectivity was defined as dehydrogenation rate/total consumption rate.

Selectivity increased with the increase of the basic nature of the catalyst. Dehydration rate per unit acidity showed no specific value. It increased with the increase of acid strength. Besides acidity, acid strength also plays a role in the dehydration of alcohols. On the other hand, dehydrogenation rate per unit basicity remained constant.

14) W. G. Palmer and F. H. Constable, *Proc. Roy. Soc.*, **107A**, 255 (1925).

Electronic Spectra of Biphenyl and Fluorene

Toshihiko Hoshi, Hiroyasu Inoue*, Junko Shiraishi, and Yoshie Tanizaki**

Department of Chemistry, College of Science and Engineering, Aoyama Gakuin University, Meguriswa-cho, Setagaya-ku, Tokyo

**Department of Applied Chemistry, Faculty of Technology, Kanagawa University, Kanagawa-ku, Yokohama*

***Department of Chemistry, Faculty of Science, Tokyo Institute of Technology, Meguro-ku, Tokyo*

(Received November 17, 1970)

The ultraviolet absorption spectrum of diprotonated-2,7-diaminofluorene has been divided into two components polarized along the long and the short axes of the molecule by using the results of the dichroic spectra in the stretched PVA sheet. By a comparison of the experimental results with those calculated by means of a semi-empirical LCAO-ASMO-SCF-CI approximation including a variable β method the assignment of the absorption bands has been made. It has been found that the compound has five absorption bands above 210 mμ. The existence of the additional 300 mμ band of fluorene has been explained theoretically by increasing the ionization potentials of the 9- and 10-carbon atoms by 3 eV from the usual value (11.42 eV).

Biphenyl shows a structureless intense absorption band at 247 mμ in a non-polar solvent. On the other hand, fluorene, which is formed by bridging a methylene group at the 9- and 10-carbon atoms of biphenyl, has a band with a well-defined fine structure at about 300 mμ in addition to the 261 mμ band, which corresponds to the 247 mμ band of biphenyl.

Many theoretical and experimental investigations of the electronic spectrum of biphenyl have been published. For instance, Gondo[1] has calculated the electronic transition energies of biphenyl, in which the effects of twisting the 1–1′ bond in biphenyl are taken into account. Berlman and Steingraber[2] have determined the fluorescence lifetime of biphenyl and found a hidden band on the longer-wavelength side of the intense 247 mμ band.

On the other hand, only a few papers have reported on the spectrum of fluorene. Momicchioli and Rastelli[3] have calculated the transition energies and oscillator strengths for fluorene by the method of PPP with variable electronegativity, taking into account the small shortening of the 1–1′ distance and slight parameter changes.

In this paper, the absorption spectrum of diprotonated-2,7-diaminofluorene above 220 mμ has been divided into two kinds of absorption curves which are polarized along the short axis (C_2-axis) and the long axis of the molecule, by using the results of the dichroic spectra in the stretched PVA sheet.[4] We call these divided absorption curves "divided spectra." Using the divided spectra, we have determined a number of the absorption bands and the polarization directions. Furthermore, semi-empirical LCAO-ASMO-SCF-CI calculations including a variable β approximation for the above compound have been made. By a comparison of the experimental and the calculated results, the assignment of each band has been clarified.

Experimental

Materials. Diprotonated-2,7-diaminofluorene was used in place of fluorene, because the saturated concentration of fluorene in a PVA sheet was too small for the dichroic spectra to be measured. Since the absorption spectrum of diprotonated-2,7-diaminofluorene is almost identical with that of fluorene, the results obtained from the former can be regarded as representing the results from the latter.

The 2,7-diaminofluorene used here was obtained commercially and was purified by repeated recrystallizations from alcohol. The PVA powder used for the preparation of the sheets was a commercial product (mean degree of polymerization=1500, Nippon Gosei Co., Ltd., NM-14); it was used without further purification.

Measurements. The dichroic spectra using stretched PVA sheets were determined by a method described elsewhere.[5]

Divided Spectra. The method of obtaining the divided spectra has already been described[5]; that is, the relation between R_d and R_s is represented by:

$$2r^2 = \frac{2(T-1)+(T+1)R_d}{2T+(T-1)R_d} \tag{1}$$

where

$$T = \frac{R_s^2}{(R_s^2-1)}[1-\{\pi/2-\tan^{-1}(R_s^2-1)^{-1/2}\}(R_s^2-1)^{-1/2}]$$

R_d is the dichroic ratio ($R_d=D_{//}/D_{\perp}$), R_s is the stretching ratio of the PVA sheet, and r is a parameter whose inverse cotangent, $\cot^{-1}r$, indicates the angle between a transition moment and the orientation axis of a molecule.

In the case of a planar molecule having at least one C_2 symmetry axis, the absorption spectrum is divided into two kinds of absorption curves whose transition moments are parallel (x) and perpendicular (y) to the symmetry axis by the use of the dichroic spectra.

From Eq. (1), $R_{d\infty}$ is represented as:

$$R_{d\infty} = 2r^2 \tag{2}$$

where $R_{d\infty}$ is the dichroic ratio for stretching the PVA sheet to infinity. The observed optical density, D, in the unstretched PVA sheet and the ratio of D_x and D_y are given by:

$$D = D_x + D_y \tag{3}$$

$$\frac{D_x}{D_y} = \frac{2-R_{d\infty}\cot^2\varphi}{R_{d\infty}-2\cot^2\varphi} \tag{4}$$

where D_x and D_y are the optical densities whose transition moments are along the x- and y-axes respectively, and where φ is the angle between the x-axis and an orientation axis of a

1) Y. Gondo, *J. Chem. Phys.*, **41**, 3928 (1964).

2) I. B. Berlman and O. J. Steingraber, *ibid.*, **43**, 2140 (1965).

3) F. Momicchioli and A. Rastelli, *J. Chem. Soc., B*, **1970**, 1353.

4) H. Inoue and Y. Tanizaki, to be published.

5) Y. Tanizaki and S. Kubodera, *J. Mol. Spectry.*, **24**, 1 (1967).

molecule. Hence, by using Eqs. (2), (3), and (4), D can be divided into D_x and D_y.

Method of Calculation

The Pariser-Parr-Pople approximation[6] including a variable β method[7] was employed. The one-center repulsion integrals were obtained from the valence-state ionization potentials $I(r)$ and the electron affinities $A(r)$, $(rr|rr)=I(r)-A(r)$. The two-center repulsion integrals were evaluated by using the Nishimoto and Mataga equation, $(rr|ss)=14.397/(a_{rs}+R_{rs})$, where a_{rs} is a parameter determined from the equation:

$$14.397/a_{rs}=\{(rr|rr)+(ss|ss)\}/2.$$

The resonance integrals, β_{rs}'s, were adjusted at every iteration of the SCF calculations by means of the $\beta_{rs}=-1.84\ -0.51P_{rs}$ relation, where P_{rs} is the bond order of the r–s bond.

The valence-state ionization potential and the electron affinity for each carbon atom were taken as 11.42 eV and 0.58 eV respectively. The geometry and the numbering of the atoms used here are shown in Fig. 1.

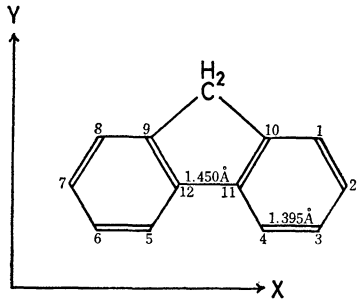

Fig. 1. Geometry of fluorene.

Results and Discussion

In Fig. 2 the absorption spectra of biphenyl, fluorene, and diprotonated-2,7-diaminofluorene are shown. As may be seen from this figure, the absorption curve of diprotonated-2,7-diaminofluorene is almost the same with that of fluorene; therefore, it seems reasonable to regard the results obtained from diprotonated-2,7-diaminofluorene as representing those of fluorene.

Biphenyl shows only one absorption maximum, at 257 mμ, above 210 mμ, whereas fluorene has an additional band at 300 mμ besides the 262 mμ band, which corresponds to the 247 mμ band of biphenyl. Figure 3 shows the "divided spectra" of diprotonated-2,7-diaminofluorene. From this figure, it is clear that the additional band at 300 mμ is polarized to the x-axis. The polarization of the intense 263 mμ band is along the x-axis, but a weak band polarized along the y-axis is hidden under this intense band. The absorption tail at around 220 mμ consists of two kinds of bands (x- and y-polarization). Thus, it may be concluded that fluorene has five absorption bands above 210 mμ.

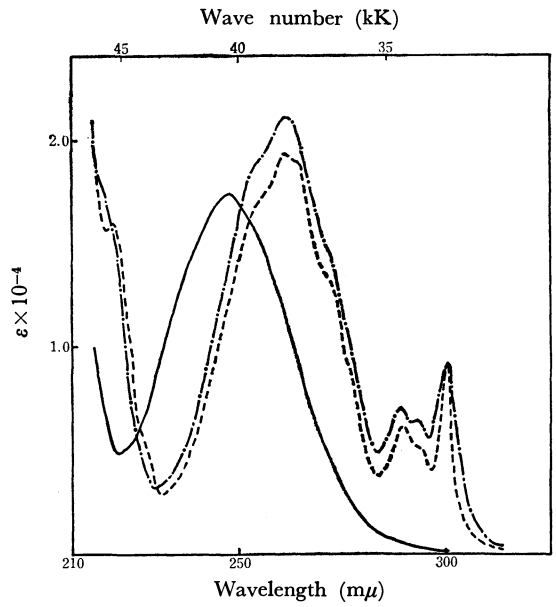

Fig. 2. Absorption spectra of biphenyl (——, in ethanol), fluorene (----, in ethanol), and diprotonated-2,7-diaminofluorene (—·—, in 80% ethanol).

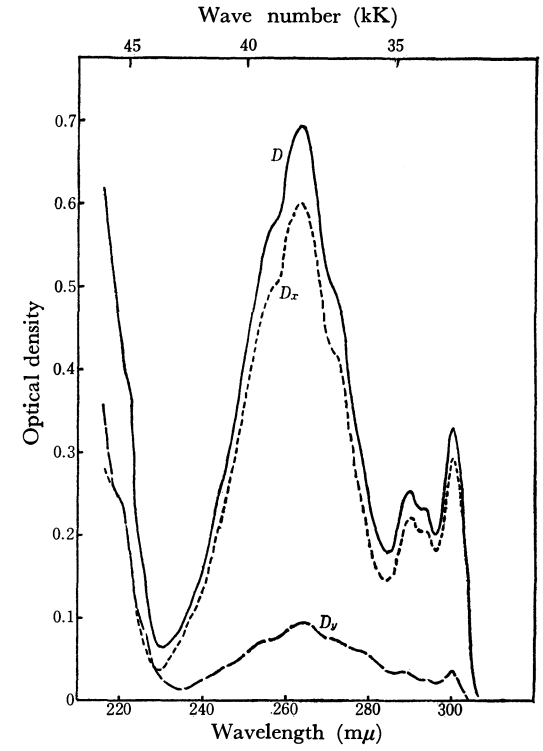

Fig. 3. Divided spectra of diprotonated-2,7-diaminofluorene.
D: The absorption spectrum in the non-stretched PVA sheet.
D_x: The x-component of D. D_y: The y-component of D.

According to Platt,[8] the additional 300 mμ band of fluorene may be interpreted as corresponding to the hidden band of biphenyl (^1L_b). This is not consistent with the present experimental results, because the ^1L_b band should be polarized to the short axis (y-axis) of the molecule. According to the calculated results obtained by Momicchioli *et al.*,[3] fluorene has five transitions below 6 eV; the lowest transition is of

6) R. Pariser and R. G. Parr, *J. Chem. Phys.*, **21**, 466, 767 (1953); J. A. Pople, *Proc. Phys. Soc.*, **68**, 81 (1955).

7) K. Nishimoto and L. S. Forster, *Theoret. Chim. Acta* (Berlin), **3**, 407 (1965).

8) J. R. Platt, *J. Chem. Phys.*, **19**, 101 (1951).

TABLE 1. A COMPARISON OF THE EXPERIMENTAL AND CALCULATED RESULTS FOR FLUORENE ($I(9)=I(10)=14.42$ eV)

	Transition energy Calcd eV (mμ)	Obsd eV (mμ)	Ocsillator sterngth Calcd	Polarization Calcd	Obsd	Symmetry
I	4.17 (297)	4.13 (300)	0.2982	x	x	B_1
II	4.25 (292)	4.71 (263)	0.0051	y	y	A_1
III	4.67 (266)	4.71 (263)	0.5389	x	x	B_1
IV	5.72 (217)	5.64 (220)	0.0781	y	y	A_1
V	5.83 (213)		0.1359	x	x	B_1

$^1A_1 \rightarrow {}^1A_1$ while the other four transitions are of $^1A_1 \rightarrow {}^1B_1$ type. These calculated results are also not sufficient to explain the results of the "divided spectra, since the polarizations of the four calculated transitions are along the x-axis (in the "divided spectra", two y-polarized bands are found); besides, the oscillator strength of the transition which may correspond to the 300 mμ band is too small. Therefore, in order to explain the results of the "divided spectra," we carried out MO calculations.

Commonly, there are two concepts for interpreting the effects of a methylene group on the π-electron system; one is that of hyperconjugation, and the other, an inductive concept. In the present paper, the effects of the methylene group in fluorene were treated as inductive; we calculated the state energies and the excited-state wave functions, increasing the ionization potentials of the carbon atoms at the 9 and 10 positions of biphenyl.[9] The results of the calculations are shown in Fig. 4. The results when the ionization potentials of the two carbon atoms are 14.42 eV agree well with those of the "divided spectra." The results calculated for biphenyl are also shown in Fig. 4a. In this case, four forbidden transitions are found at 34.1 kK (293 mμ), 34.5 kK (290 mμ), 45.8 kK (218 mμ), and 46.4 kK (216 mμ). A weak absorption band corresponding to the forbidden transition at 34.1 or 34.5 kK has been observed at 33.6 kK (298 mμ) in crystal and in solution at low temperatures.[10–13]

The four forbidden transitions of biphenyl become allowed transtions when the ionization potentials of the carbon atoms at the 9 and 10 positions are increased, and the four forbidden transitions at 34.1, 34.5, 45.8, and 46.4 kK are changed to the y-, x-, x-, and y-polarized transitions respectively. This may be due to the fact that, when the ionization potentials are increased, the symmetry of the π-electron system of biphenyl skeleton is reduced from D_{2h} to C_{2v}, in which the biphenyl skeleton is assumed to be a plane. By assuming that the two benzene rings of biphenyl are not coplanar, the symmetry of the π-electron system is also reduced from D_{2h} to D_2; however, Gondo[1] has indicated that the forbidden transitions of biphenyl are not changed into allowed transitions by this treatment.

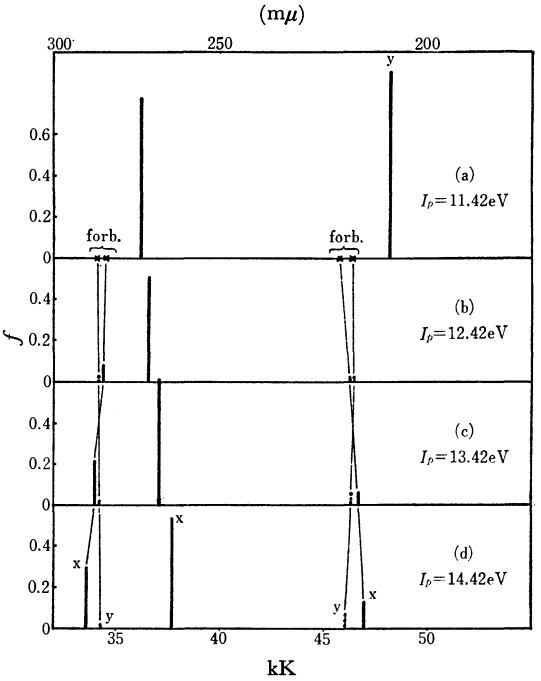

Fig. 4. Changes in the transition energies of biphenyl for the variation of the ionization potentials of the 9- and 10-carbon atoms.

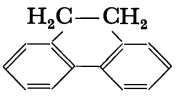

9,10-dihydrophenanthrene

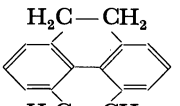

4,5-dimethyl-9,10-dihydrophenanthrene

Mislow *et al.*[14] have observed an additional band at 300 mμ in the case of 9,10-dihydrophenanthrene, as in the case of fluorene. This may be explained just as in the case of fluorene. However, the additional 300 mμ band disappears upon the introduction of two methyl groups at the 4- and 5-carbon atoms of 9,10-dihydrophenanthrene.[14] This may be attributed to the fact that the approximate symmetry of the π-electron system again becomes D_{2h} (4,5-dimethyl-9,10-dihydrophenanthrene) from C_{2v} (9,10-dihydrophenanthrene) upon the introduction of the two methyl groups.

In Table 1 the calculated results of fluorene ($I(9)=I(10)=14.42$ eV) are summarized and compared with the results of the "divided spectra."

9) K. Inuzuka and T. Yokota, *J. Mol. Spectry.*, **21**, 272 (1966).
10) A. R. Deb, *Indian. J. Phys.*, **27**, 305 (1953).
11) R. Coffman and D. S. McClure, *Can. J. Chem.*, **36**, 48 (1958).
12) D. S. McClure, *ibid.*, **36**, 59 (1958).
13) M. Nakamizo and Y. Kanda, *Spectrochim. Acta*, **19**, 1235 (1963).
14) K. Mislow, M. A. W. Glass, H. B. Hopps, E. Simon, and G. H. Wahl, Jr., *J. Amer. Chem. Soc.*, **86**, 1710 (1964).

The Effect of Benzene on the Reaction of the Recoil Bromine Atom with Ethyl Bromide[1)]

Takanobu SHIOKAWA, Toshiro SATO,* and Kenjiro KONDO**

Department of Chemistry, Faculty of Science, Tohoku University, Kotohiracho, Sendai

(Received December 17, 1970)

An attempt was made to estimate the effect of benzene on the recombination reactions of the recoil bromine atoms activated by the $^{81}Br(n,\gamma)^{82m}Br \xrightarrow{I.T} {}^{82}Br$ and $^{81}Br(n,2n)^{80m}Br$ reactions in ethyl bromide and benzene mixtures. It seems to be reasonable to conclude, from the consideration of the parent yield, that the reactions leading to the formation of parent molecules in the thermal and high-energy regions can be classified into two reaction types. Judging from the results of the $^{81}Br(n,\gamma)^{82m}Br \xrightarrow{I.T} {}^{82}Br$ reaction, approximately 53% of the parent yield from the high energy reactions in the pure ethyl bromide system is formed through the de-excitation process of the excited ethyl bromide labelled by the direct substitution reaction of the energetic recoil atom, while 47% is formed by the reaction of the recoil atom with ethyl radicals in the cage. The reaction of ethylene with hydrogen bromide, which is produced by the decomposition of the labelled excited ethyl bromide, contributes about 51% of the parent yield from the thermal energy reaction; the rest is formed by the other thermal reactions. Furthermore, no essential difference was observed between the recombination reactions of the recoil ^{82}Br and ^{80m}Br atoms produced by the $^{81}Br(n,\gamma)^{82m}Br \xrightarrow{I.T} {}^{82}Br$ and $^{81}Br(n,2n)^{80m}Br$ reactions respectively.

Many investigations have been carried out into the chemical effects associated with the nuclear transformations of bromine atoms in organic bromide systems, with emphasis laid especially on the recombination processes of recoil bromine atoms in the pure organic bromide systems.

Recently, binary and ternary mixtures of the organic bromides and hydrocarbons, such as benzene or cyclohexane, have been employed in order to evaluate precisely the recombination processes of the recoil bromine atoms in the high- and thermal-energy regions.[2-8a)] However, most of these studies have been made in terms of overall organic yields.

It has now been attempted to estimate the individual yields of labelled products and to make more detailed interpretations of the recombination processes of recoil bromine atoms.

The individual yields resulting from the $^{81}Br(n,\gamma)^{82m}Br \xrightarrow{I.T} {}^{82}Br$ and $^{81}Br(n,2n)^{80m}Br$ reactions in the mixtures of benzene and ethyl bromide were examined. Important information was obtained from the correlation between the parent yields from the high- and the thermal-energy reactions upon the addition of benzene, and from the isotope effects between ^{80m}Br and ^{82}Br recoil atoms.

Experimental

Materials. E.P.-grade ethyl bromide and G.R.-grade benzene, supplied by the Junsei Chemical Co., Ltd., were purified with the ordinary method described in Ref. 8, and their purities were checked by means of a gas chromatograph. The contents of the impurities in the ethyl bromide and benzene used for the experiments were less than 0.025% and 0.001% respectively. The bromine used was the highest grade available.

Irradiation. About 0.3—0.5 m*l* portions of the mixtures of ethyl bromide and benzene or bromine was sealed into a quartz ampoule. Thermal neutron irradiations were made 3—5 min in a pneumatic tube of JRR-1 of the Japan Atomic Energy Research Institute at room temperature at a neutron flux of 3×10^{11}n/cm^2/sec, with a concomitant gamma ray dose rate of 10^4R/hr. In the case of the $^{81}Br(n,2n)^{80m}Br$ reaction, all the irradiations were made for 2 hr with 14 MeV neutrons at a flux of 10^6n/cm^2/sec resulting from the $^3H(^2H,n)^4He$ reaction, where the effect of thermal neutrons and γ-dose on the organic yield was neglected.

Determination of Organic Yields. The irradiated samples were separated into organic and inorganic fractions by using the ordinary extraction method,[8)] and the overall organic yield was determined as a ratio of the activity in the organic fraction to the total activity. All the extraction procedures were performed after the irradiated samples had been allowed to stand long enough for the $^{78}Br(t_{1/2}$: 6.5m) produced by the $^{79}Br(n,2n)^{78}Br$ reaction in the fast neutron experiment and the $^{80m}Br(t_{1/2}$:4.38hr) produced by the $^{79}Br(n,\gamma)^{80m}Br$ reaction in the thermal neutron experiment to decay out. The organic fraction was then divided into two aliquots: one (Aliquot I) was used as the standard, and the other (Aliquot II) was submitted to gas chromatographic separation after the addition of various organic bromides as carriers. Each fraction of the organic bromides was collected in a coiled glass tube cooled in a dry-ice ethanol bath at the outlet of the column. The various products were separated by means of a gas chromatograph in a temperature-programmed all-stainless-steel column (0.6 cm in diameter and 3 m long), using tricresyl phosphate or silicone DC 703 as

1) Presented at "The International Symposium on Chemical Effects of Nuclear Transformations," Cambridge, July, 1969.

* Present addresses: Miyagi University of Education, Aramaki, Sendai.

** Present address: Laboratory of Nuclear Science, Tohoku University, Tomizawa, Sendai.

2) P. F. D. Shaw and J. E. C. Macrae, *Radiochim. Acta*, **2**, 76 (1963).

3) P. F. D. Shaw and J. E. C. Macrae, *J. Inorg. Nucl. Chem.*, **24**, 1327 (1962).

4) P. F. D. Shaw, *ibid.*, **24**, 1337 (1962).

5) M. Milman, *J. Phys. Chem.*, **67**, 537 (1963).

6) S. S. Kontis, P. Sanitowangs, and M. Weston, "Chemical Effects of Nuclear Transformations," Vol. 1, Vienna (1963), p. 333.

7) E. S. Filatov, An. N. Nesmeyanov, and Yu. B. Chepyzhev, *Vest. MGU. Ser. Khim.*, **6**, 46 (1963).

8) a) T. Shiokawa, T. Sato, K. Kondo, and K. Sato, *Nippon Kagaku Zasshi*, **87**, 922 (1966); b) T. Shiokawa, T. Sato, G. Izawa, K. Kondo, and K. Sato, *ibid.*, **86**, 1006 (1965).

staionary phase and helium as the eluent gas. Furthermore, the collected ethyl bromide and the Aliquot I mentioned above were each allowed to completely react with the sodium metal by using ethanol as the solvent; then the concentration of bromine present in these fractions was determined by the Volhard method. The parent (P) and other product yields (Q) are given by the following formulas:

$$P = \frac{A_p}{A_o} \times \frac{S_o}{S_p} \times R\,(\%)$$

$$Q = \frac{A_q}{A_p} \times P\,(\%)$$

R: overall organic yield
A_p: activity of the collected ethyl bromide fraction
A_o: activity of the Aliquot I
A_q: activity of the product
S_o: concentration of bromine of the Aliquot I
S_p: concentration of bromine in the collected ethyl bromide fraction

The higher-boiling-point products, which were inseparable by means of the gas chromatograph, were observed in this system, so these procedures were necessary to obtain the absolute yields of the organic products. Only the products having boiling points lower than that of dibromobenzene were investigated; no attempt to obtain the yields of the various products other than ethyl bromide was made in the (n, 2n) experiment.

Activity Measurements. The activities of the ^{82}Br from the $^{81}Br(n,\gamma)^{82m}Br \xrightarrow{I.T} {}^{82}Br$ reaction and of the ^{80m}Br from the $^{81}Br(n,2n)^{80m}Br$ reaction were meaured by using a sodium iodide crystal scintillation counter. The experimental error arising from the activity measurements were of the following magnitudes: (1) for overall organic yields: ±2—3%, and (2) for the product yield: ±3—15%. No correction was made for the ^{82}Br formed by (n,γ) on ^{81}Br, which accounts for 7% of the total ^{82}Br activity.[9]

Results

In order to estimate the contribution of the thermal reaction (scavenger sensitive reaction) and the high-energy reaction (scavenger insensitive reaction) to the product yields in ethyl bromide and benzene mixtures, it is necessary to establish the scavenger curves for a number of mixtures of ethyl bromide and benzene. As a typical example, Fig. 1 indicates the scavenger curve of each product obtained in the mixture of ethyl bromide (0.87 mf: mole fraction)-benzene (0.13 mf) in the $^{81}Br(n,\gamma)^{82m}Br \xrightarrow{I.T} {}^{82}Br$ reaction and of ethyl bromide (0.89 mf)-benzene (0.11 mf) in the $^{81}Br(n,2n)^{80m}Br$ reaction. Although, in this experiment, the organic yields were not corrected for the ^{82}Br directly formed by the $^{81}Br(n,\gamma)^{82}Br$ reaction, which accounts for about 7% of the total ^{82}Br,[9] it can be expected that its contribution to the organic yields is very small, since the overall organic yields for the ^{82}Br formed by the $^{81}Br(n,\gamma)^{82}Br$ and $^{81}Br(n,\gamma)^{82m}Br \xrightarrow{I.T} {}^{82}Br$ processes were almost the same as those for the ^{80m}Br and ^{80}Br produced by (n,γ) on ^{79}Br in the pure ethyl bromide.[8a,10]

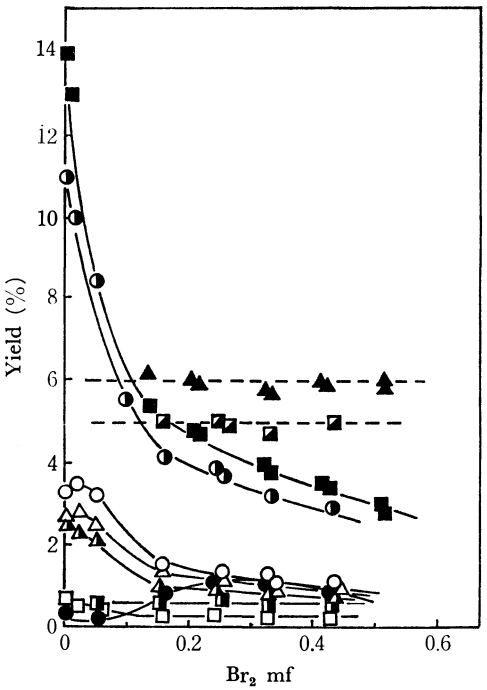

Fig. 1. Scavenger curves of various products obtained in the systems of ethyl bromide (0.87 mf)-benzene (0.13- mf) in the $^{81}Br(n,\gamma)^{82m}Br \xrightarrow{I.T} {}^{82}Br$ reaction and ethyl bromide (0.89 mf)-benzene (0.11 mf) in the $^{81}Br(n,2n)^{80m}Br$ reaction.
a) $^{81}Br(n,\gamma)^{82m}Br \xrightarrow{I.T} {}^{82}Br$
▲: C_6H_5Br △: $1.1\text{-}C_2H_4Br_2$ ○: $1.2\text{-}C_2H_4Br_2$
●: $C_6H_4Br_2$ □: CH_2Br_2 ◨: CH_3Br
◑: C_2H_5Br ◪: parent yield normalized by $(1-C)/(1+C)$
b) $^{81}Br(n,2n)^{80m}Br$
■: C_2H_5Br ▲: parent yield normalized by $(1-C)/(1+C)$

The fraction of the high-energy-reaction yield for each labelled product is given as an intercept on the coordinate axis by extrapolating each scavenger curve to zero scavenger concentration. The scavenger curve for dibromobenzene shows a minimum at a bromine concentration of 0.05 mf, and the yield gradually increases at higher bromine concentrations. The value of 0.23% at 0.05 mf of bromine was employed as the approximate yield due to the high-energy reaction.

The scavenger curves of 1,1- and 1,2- dibromoethane were very similar to the results previously reported by Shaw *et al.*[11] for their recoil study of the ^{80m}Br produced by (n,γ) on ^{79}Br in the pure ethyl bromine system; it showed almost a $(1-C)$ dependency at bromine concentrations higher than 0.15 mf (C: mole fraction of bromine). On the other hand, the parent scavenger curve showed a $(1-C)/(1+C)$ dependency at bromine concentrations higher than 0.15 mf. and the parent yield due to the high-energy reactions was obtained by the normalization by $(1-C)/(1+C)$. The experimental data for each product due to the thermal and the high-energy reactions obtained in this way are summarized in Figs. 2 and 3, together with the total yields from both the thermal and high-energy reactions in the $^{81}Br(n,\gamma)^{82m}Br \xrightarrow{I.T} {}^{82}Br$ reaction. The total organic

9) J. F. Emery, *J. Inorg. Nucl. Chem.*, **27**, 903 (1965).
10) a) M. Milman and P. F. D. Shaw, *J. Chem. Soc.*, **1957**, 1303. b) B. Knight, G. E. Miller, and P. F. D. Shaw, *J. Inorg, Nucl. Chem.*, **23**, 15 (1961).
11) A. J. Cole, M. D. Mia, G. E. Miller, and P.F.D. Shaw, *Radiochim. Acta*, **6**, 150 (1961)

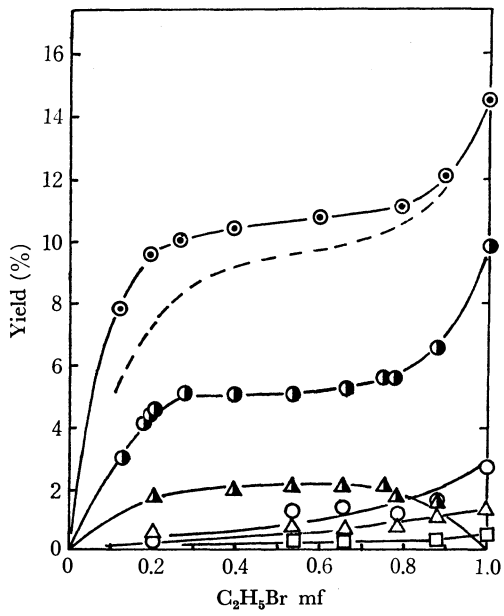

Fig. 2. Yields of various products due to the thermal energy reactions resulting from the $^{81}Br(n,\gamma)\ ^{82m}Br \xrightarrow{I.T} {}^{82}Br$ reaction in ethyl bromide and benzene mixtures as a function of ethyl bromide concentration.
⊙: total organic yields
---: sum of individual yields
Other symbols are listed in caption for Fig. 1.

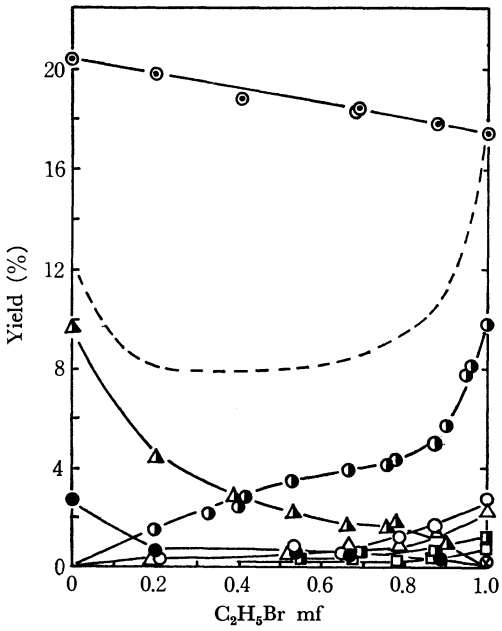

Fig. 3. Yields of various products due to the high energy reactions resulting from the $^{81}Br(n,\gamma)\ ^{82m}Br \xrightarrow{I.T} {}^{82}Br$ reaction in ethyl bromide and benzene mixtures as a function of ethyl. bromide concentration
⊙: total organic yield
⊗: $CHBr_3$
—: sum of individual yields
Other symbols are listed in caption for Fig. 1.

yields obtained in the (n,2n) experiment were shown in Ref. 8a.

For the systems in which the overall organic yield were not obtained experimentally, the overall organic yields, as estimated graphically, were used for the calculation.

The most interesting aspect of the results shown in Figs. 2 and 3 is that the parent yields from the thermal and the high-energy reactions are affected similarly by the addition of benzene. This suggests that there is a close correlation between the formations of the labelled parent molecules in both the reaction regions. The sum of the product yields in the two reaction regions in the $^{81}Br(n,\gamma)^{82m}Br \xrightarrow{I.T} {}^{82}Br$ reaction is given by a dotted line in Figs. 2 and 3. Here, the yields of other products, such as tetra-bromomethane, tri- and tetra-bromoethane, were less than 0.2 percent at most and are not included in Figs. 1, 2, and 3.

As is shown in Fig. 2, the total organic yield from the thermal energy reaction was very close to the sum of the yields of the individual products obtained experimentally. On the other hand, Fig. 3 shows that the sum of each product yield from the high-energy reactions was very low, compared with the total organic yield; especially, it was only about 40—60% of the total organic yield at benzene concentrations higher than 0.2 mf. This difference corresponds to the yields of the higher-boiling-point products which were not analyzed in this experiment. Furthermore, the sharp increase in the yields of higher-boiling-point products from the high-energy reactions at 0—0.2 mf of benzene can be practically accounted for as compensation for the decrease in both parent yields due to the thermal and the high-energy reactions as is shown in Fig. 4. This definitely suggests that, in the presence of benzene, there are some reaction

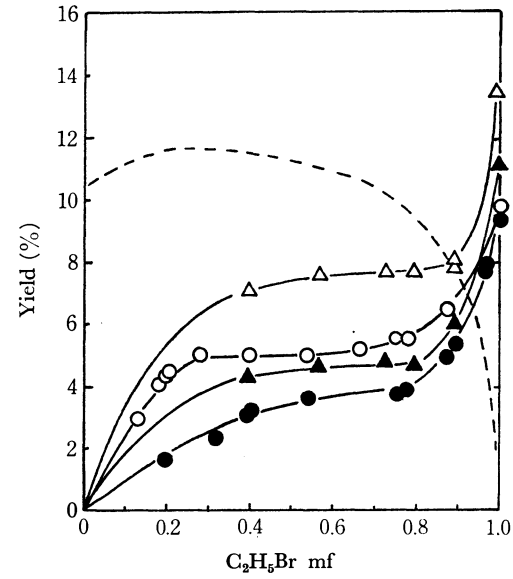

Fig. 4. Parent yields in both energy regions in ethyl bromide and benzene mixtures as a function of ethyl bromide concentration
a) $^{81}Br(n,\gamma)\ ^{82m}Br \xrightarrow{I.T} {}^{82}Br$
○: yield due to the thermal energy reactions
●: yield due to the high energy reactions
---: yield of the higher boiling point products due to the high energy reactions
b) $^{81}Br(n,2n)\ ^{80m}Br$
△: yield due to the thermal energy reactions
▲: yield due to the high energy reactions

paths interrupting the formation of the labelled parent molecules from the thermal and the high-energy reactions. On the other hand, the yields of CH_3Br, CH_2Br_2, $CHBr_3$, 1,1- and 1,2-$C_2H_4Br_2$ decreased gradually as the benzene concentration became higher; however there were no remarkable effects on the formation of these labelled molecules by the addition of benzene. The parent yields from the thermal and the high-energy reactions are approximately 0.5—3.9 percent higher in the $^{81}Br(n,2n)^{82m}Br$ reaction than those in the $^{81}Br(n,\gamma)^{82m}Br \xrightarrow{I.T} {}^{82}Br$ reaction, as is shown in Fig. 4. However, the parent-yield curves very similar tendency for the addition of benzene in both nuclear transformations.

Discussion

Recombination Reactions of Recoil ^{82}Br and ^{80m}Br Atoms. It appears from Fig. 4 that, in the presence of 0—0.2 mf of benzene, the parent yields from the thermal and the high-energy reactions in the $^{81}Br(n,\gamma)^{82m}Br \xrightarrow{I.T} {}^{82}Br$ reaction decreased abruptly in a similar fashion, and that, furthermore, this decrement in both the parent yields was almost equal to the increase in the yields of the higher-boiling-point products due to the high-energy reactions. This suggests that a part of the recoil bromine atoms react with ethyl bromide during the slowing-down process, thus contributing to the formation of some excited species labelled with ^{82}Br, and that, in the presence of benzene, higher-boiling-point products are produced by the reactions of those exicted species with benzene.

These trends can be explained by assuming that a part of the recoil atoms can undergo the substitution reaction with the bromine atom of ethyl bromide by means of billiard ball-type elastic collisions, or inelastic collisions with ethyl bromide molecules, thus forming a labelled excited ethyl bromide. As is illustrated in Fig. 5, the labelled excited ethyl bromide should be partially de-excited by the interaction with neighbouring molecules, and it gives the parent yield from the high-energy reaction through the path 2. The residual is decomposed to give ethylene and hydrogen bromide through the path 1 by the analogy with the pyrolysis of ethyl bromide.[12] Then, the radioactive hydrogen bromide formed through the path 1 reacts thermally with the ethylene which is produced either through path 1 or by the pyrolitic decomposition of ethyl bromide molecules at the near site of recoil events, thus contributing to the formation of the labelled ethyl bromide due to the thermal reactions, as is shown in Eq. (1). Ethylene produced by a reaction other than path 1 also reacts with the radioactive bromine molecule and contributes to the formation of labelled 1,2-dibromoethane by means of the thermal reactions shown in Eq. (2);

$$CH_2{=}CH_2 + H^*Br \longrightarrow CH_3CH_2{}^*Br \quad (1)$$

$$CH_2{=}CH_2 + {}^*Br_2 \longrightarrow CH_2BrCH_2{}^*Br \quad (2)$$

It may be reasonable to assume that the reaction (1) of ethylene with hydrogen bromide will be predominant over the reaction (2) from the viewpoint of radiolysis and pyrolysis. However, in the presence of a bromine scavenger, ethylene will be immediately scavenged, and both the reactions, (1) and (2), are suppressed. Meanwhile, it is conceivable that, in the presence of benzene, these labelled excited ethyl bromide molecules may react instantaneously with benzene molecules through the path 3 in Fig. 5, thus contributing to the formation of higher-boiling-point products due to the high-energy reactions. The reaction mechanisms for the path 3 are not clear because these higher-boiling-point products have not been identified experimentally. However, it may be presumed that these excited ethyl bromide molecules have sufficient energies in excess of the activation energy required for the path 3.[13]

$$C_2H_5{}^*Br \longrightarrow CH_2CH_2 + H^*Br \quad \cdots\cdots(1)$$

$$\downarrow +C_6H_6 \searrow \quad C_2H_5{}^*Br \quad \cdots\cdots(2)$$

$$\text{Higher boiling point products} \quad \cdots\cdots(3)$$

Fig. 5. Reaction paths of the excited ethyl bromide

Similarly, Rowland *et al.*[14–16] indicated that the decomposition and the de-excitation of the tritiated parent molecules in the excited state play an important role in determining the distribution of the yields of the various labelled products in the gas-phase reactions of recoil tritium with alkyl chlorides and hydrocarbons. Since little attention has been paid to the analysis of higher-boiling-point products, only the yields of thep roducts separated by gas chromatography were discussed. The authors have found that a considerable portion of the overall organic yields in the systems containing benzene, such as $C_6H_6+Br_2$ and $C_6H_6+C_6H_5Br$ systems, consists of higher-boiling-point products.

On the other hand, several radicals should be produced during the slowing-down processes of the energetic recoil bromine atoms, and a part of the recoil atoms which have escaped from the direct substitution reaction will recombine with such radicals in both the energy regions. In the cage, the recombination reactions of the recoil atoms with these radicals take place before the radicals start diffusing away, and consequently, contribute to the yields due to the high-energy reaction (immediate recombination reaction).

The recoil bromine atom which has escaped from the cage reacts with radicals or other reactants (C_2H_5Br, *etc.*) and thus contributes to the formation of labelled products in the thermal-energy region. The parent yield from the recombination reaction in the cage depends on the concentration of ethyl radicals, which will gradually be diminished by the addition of benzene because of the decrease in the collision probability of the recoil atom with the ethyl bromide molecule. Thus, the fact that the parent yield from the high-energy reactions shows a gradual decrease at benzene concentrations of more than 0.2 mf may be ascribed to the gradual

12) N. N. Semenov, "Some Problems of Chemical Kinetics and Reactivity," Pergamon Press, London (1958), p. 228.

13) Path 3 will probably involve the reaction of the excited ethyl bromide with C_6H_5 or C_6H_7 radicals formed in the recoil site.

14) F. S. Rowland, Y. M. Tang, and E. K. C. Lee, *J. Amer. Chem. Soc.*, **86**, 1280 (1964).

15) E. K. C. Lee and F. S. Rowland, *ibid.*, **84**, 3027 (1962).

16) R. S. Rowland and Y. M. Tang, *ibid.*, **87**, 3304 (1965).

decrease in the recombination reaction of the recoil bromine atom with the ethyl radical in the case. If it is assumed that the parent yield from the recombination reaction in the cage at 0—0.2 mf of benzene shows a dependence on the benzene concentration in the same manner as that obtained at about 0.2—0.8 mf of benzene, it is possible to divide the parent yield from the high-energy reaction in the pure ethyl bromide system into two parts by extrapolating the yield curve to zero mole fraction of benzene in Fig. 4.

The parent yield from the recombination reaction in the cage is estimated to be about 47% from the intercept of the yield curve in Fig. 4; the remaining 53% results from the de-excitation of the excited ethyl bromide molecules formed by the substitution reactions (path 2 in Fig. 5). Similarly, the parent yield from the thermal energy reactions can be classified into two parts by extrapolating the plateau of the yield curve at 0.2—0.8 mf of benzene in Fig. 4. It may be presumed that approximately 49% of the parent yield from the thermal energy reaction is formed by the reactions indicated by Eqs. (3), (4), and (5), while about 51% arises from the reactions of ethylene with the labeled hydrogen bromide produced through the path 1 in Fig. 5. The reaction shown in Eq. (5) may be disregarded because its activation energy is 25 kcal/mol,[17] too high for the thermal atoms to be involved.

$$C_2H_5 + {}^*Br \longrightarrow C_2H_5{}^*Br \quad (3)$$

$$C_2H_5 + {}^*Br_2 \longrightarrow C_2H_5{}^*Br + Br \quad (4)$$

$$C_2H_5Br + {}^*Br \longrightarrow C_2H_5{}^*Br + Br \quad (5)$$

The active bromine atoms escaped from the site of recoil events normally form inorganic compounds such as H*Br, as has already been shown.[18,19] The scavenger curve of 1, 2-dibromoethane in Fig. 1 shows a slight increase in the yield at low bromine concentrations. This fact indicates that there are $CH_2CH_2{}^{82}Br$ radicals formed by the reaction of ^{82}Br with CH_3CH_2Br in the high-energy region, as was postulated by Shaw *et al.*[11] in their study of the recombination reaction of the ^{80m}Br produced by the (n,2n) reaction of ^{81}Br in the pure ethyl bromide system. Another explanation would be possible for the sharp fall of the parent yield at 0—0.2 mf of benzene in Fig. 3 if the $CH_2CH_2{}^{82}Br$ radical could be considered a labeled excited species instead the labelled excited ethyl bromide. However, this explanation is not acceptable since there is no correlation between the parent and 1,2-dibromoethane yields upon the addition of bromine, as is illustrated in Fig. 1.

As is shown in Fig. 2, the parent and the total organic yields from the thermal-energy reactions show quite different features at 0.2—0.8 and at 0.8—1.0 mf of benzene. This can be understood by considering that, at high benzene concentrations, the reaction of recoil bromine atoms with hydrogen radicals resulting from Eq. (6) becomes predominant and contributes to the sharp decrease in the parent and the total organic yields from the thermal reactions. Similar reactions have been postulated by Shaw[4] to account for the overall organic yield obtained in the solution of ethyl iodide and iodine in benzene. As to the yields of the other products, such as dibromomethane, 1,1- and 1,2-dibromoethane, no remarkable effect was observed in either energy region on the addition of benzene, indicating that benzene acts almost as a diluent.

$$C_6H_6 + C_6H_5 \longrightarrow C_6H_5C_6H_5 + H \quad (6)$$

Isotope Effect between the $^{81}Br(n,2n)^{80m}Br$ and $^{81}Br(n,\gamma)^{82m}Br \xrightarrow{I.T} {}^{82}Br$ Reaction. In the case of the $^{81}Br(n,\gamma)^{82m}Br \xrightarrow{I.T} {}^{82}Br$ reaction, various products labelled with ^{82m}Br, such as $H^{82m}Br$, $CH_3{}^{82m}Br$, $Br^{82m}Br$, and $C_2H_5{}^{82m}Br$, undergo further isomeric transition to the ground state of ^{82}Br. As a consequence of the isomeric transition, followed by the Auger electron emission, ^{82}Br should have a high positive charge. It is postulated that this highly positive charge is partially neutralized by electron transfer from the remainder of the molecule or the neighbouring molecule, and that the recoil ^{82}Br obtains a considerable recoil energy ($\sim$10eV) resulting from Coulombic repulsion.[20] The individual product yields resulting from the $^{81}Br(n,\gamma)^{82m}Br \xrightarrow{I.T} {}^{82}Br$ reaction in the pure ethyl bromide were almost equal to those previously reported by other investigators for the $^{79}Br(n,\gamma)^{80}Br$ and $^{79}Br(n,\gamma)^{80m}Br$ reaction.[10,11] The absence of any isotope effect between these nuclear transformations seems reasonable, since the chemical fate of the recoil atom must be determined after it has lost most of its energy and can thus be expected not to be influenced by the slight difference in the initial energy.

However, in the case of the $^{81}Br(n,2n)^{80m}Br$ reaction with a recoil energy about 1000 times greater than that of the $^{81}Br(n,\gamma)^{82}Br$ reaction, an energy dependency of the organic yield might be expected. The parent yields due to the thermal and the high-energy reactions from the $^{81}Br(n,2n)^{80m}Br$ reaction were a little higher than those in the $^{81}Br(n,\gamma)^{82m}Br \xrightarrow{I.T} {}^{82}Br$ reaction, as is illustrated in Fig. 4.

However, the yield curve in Fig. 4 indicates a very similar dependence on the benzene concentration in both nuclear transformations. These results suggest that there is no essential difference in the mechanisms between these nuclear transformations. The differences between the parent yields for ^{82}Br and ^{80m}Br at 0—0.2 mf of benzene can be explained mainly in terms of the different probability of the formation of labeled excited ethyl bromide because of the low collision probability of ^{82}Br with a lower recoil energy in comparison with ^{80m}Br. Furthermore, it can be understood that a much higher recoil energy, causing disturbance over a wide range in the system, serves to enhance the parent yields resulting from the reactions in the cage and thermal recombination reactions after the recoil atoms have diffused away.

17) B. Liberator and F. Wiig, *J. Chem. Phys.*, **8**, 349 (1940).
18) S. Goldharber and J. E. Willard, *J. Amer. Chem. Soc.*, **74**, 318 (1952).
19) J. C. Roy, R. R. Williams, and W. H. Hamill, *ibid.*, **76**, 3274 (1954).
20) A. R. Kazanjian and W. F. Libby, *J. Chem. Phys.*, **42**, 2778 (1965).

The Emission Spectra of Hydrogen Atoms Produced from Methanol by Electron Impact

Iwao FUJITA, Motoyoshi HATADA,* Teiichiro OGAWA,[1] and Kozo HIROTA*

Department of Chemistry, Faculty of Science, Osaka University, Toyonaka, Osaka

* *Osaka Laboratory for Radiation Chemistry, Japan Atomic Energy Research Institute, Mii, Neyagawa, Osaka*

(Received December 25, 1970)

The emission spectra of several fragmental species, especially of hydrogen atoms, produced by the electron impact (energy: 240 eV) of gaseous methanol and deuteromethanols have been investigated. The intensity ratios of the Balmer-β lines of the H and D atoms are *ca.* 2.9:1 for CH_3OD and *ca.* 1:1.8 for CD_3OH, indicating that the excited hydrogen atoms result from the O–H bond scission, as well as from the C–H bond scission, of the parent methanol molecules. The ratio of the scission probability of a C–H bond to that of the O–H bond is calculated to be 0.8, taking into account the correction of the isotope effect. It was concluded that the excited hydrogen atoms are produced by the primary process of fragmentation *via* a superexcited species.

The emission spectra of simple molecules under electron impact have been studied extensively by several investigators,[2–5] and information has been obtained on the lifetime of the excited species thus produced by the use of the spectrophotometric method.[6–8] However, few studies have dealt with the emission spectra of organic molecules.[9]

In the radiation-chemical reaction of methanol, the primary process is generally considered[10] to be the split-off of a hydrogen atom from the methyl group of a methanol molecule, Eq. (1a). This conception is based on various pieces of

$$CH_3OH \begin{cases} \nearrow \dot{C}H_2OH + H & (1a) \\ \searrow CH_3\dot{O} + H & (1b) \end{cases}$$

evidence; *e.g.*, the $\dot{C}H_2OH$ radical was found in irradiated solid methanol by the ESR method,[11] and the peak of the CD_2OH^+ ion appeared abundantly in the mass spectrum of CD_3OH.[12] Contradicting the above conclucion, however, one critical experiment[13] reported that, in the γ-ray radiolysis of CH_3OD, the amount of HD in the produced hydrogen reached 60%, and also a little D_2 appeared. This finding can be easily explained if the scission of the C–H and the O–H bonds is assumed to occur with the same probability in the primary process of fragmentation, but the result was later understood in terms of an ion-molecule reaction.[12] Most methods hitherto used identify only the products which have already been stabilized. Unlike these indirect methods, however, emission spectra under electron impact may give direct information as to the excited hydrogen atoms produced by electron impact.

In the present investigation, the emission spectra of the fragmental species produced from methonal and deuteromethanols by electron impact were observed, and the origin of excited hydrogen atoms was discussed on the basis of the isotopic ratio of the hydrogen produced.

Experimental

The electron-impact apparatus was described in a previous paper.[14] The acceleration voltage of the electrons was 240 V and the electron current was between 20 and 300 μA. The gas pressure was estimated at about 10^{-2}mmHg by the use of a Pirani gauge attached near the collision chamber.

The photoemission was observed in the direction perpendicular to the electron beam, and the gas flow, through a quartz window by means of a Shimadzu GE 100 grating monochromator equipped with an EMI-6256B photomultiplier.

The CH_3OH was obtained from Nakarai Chemicals, and the CD_3OD and CH_3OD, from Merck. The CD_3OH was prepared from CD_3OD *via* $(CD_3O)_2Mg$, and was distilled in a vacuum four times. In order to eliminate the mixing of hydrogen occluded in the wall of the apparatus, the sample gas was introduced into the reservoir and collision chamber and then removed by evacuation. This procedure was repeated until a constant spectrum was obtained.

Results

Figure 1 shows the emission spectrum obtained by the electron impact of CH_3OH in the region from 350 to 500 nm. Similar spectrum can be observed from CD_3OD. No bands of the excited methanol molecule, the CH_3 radical, the CH_2 radical, or their ions are found in the same wavelength region. The intense peaks in the spectrum belong to the Balmer series of the H atom and the comet-tail band system of the CO^+ ion. The Balmer-α (656.3 nm) was not observed because of the low sensitivity of the photomultiplier in the longer-

1) Present address: Faculty of Engineering, Kyushu University, Hakozaki, Fukuoka.

2) A.G. Koval', V.T. Koppe, and Ya. M. Fogel', *Soviet Astronomy*, **10**, 165 (1966).

3) R. F. Holland, *J. Chem. Phys.*, **51**, 3940 (1969).

4) J. F. M. Aarts and F. J. De Heer, *ibid.*, **52**, 5354 (1970).

5) D. J. Burns, F. R. Simpson, and J. W. McConkey, *J. Phys. B, Ser. 2*, **2**, 52 (1969).

6) W. H. Smith, *J. Chem. Phys.*, **51**, 3410 (1969).

7) T. Sawada and H. Kamada, This Bulletin, **43**, 325 (1970).

8) J. E. Hesser and K. Dressler, *J. Chem. Phys.*, **45**, 3149 (1966).

9) D. A. Vroom and F. J. De Heer, *ibid.*, **50**, 573 (1969).

10) G. Meshitsuka, *Hoshasen Kagaku*, **2**, No. 3, 3 (1967).

11) F. S. Dainton, F. R. S., G. A. Salmon, and J. Teplý, *Proc. Roy. Soc., Ser. A*, **286**, 27 (1965).

12) T. Yamamoto, Y. Shinozaki, and G. Meshitsuka, *Shitsuryo Bunseki*, **12**, 93 (1964).

13) G. Meshitsuka, K. Ouchi, K. Hirota, and G. Kusumoto, *Nippon Kagaku Zasshi*, **78**, 129 (1957); G. Meshitsuka and M. Burton, *Radiat. Res.*, **8**, 285 (1958).

14) T. Ogawa, I. Fujita, M. Hatada, and K. Hirota, This Bulletin, **44**, 659 (1971).

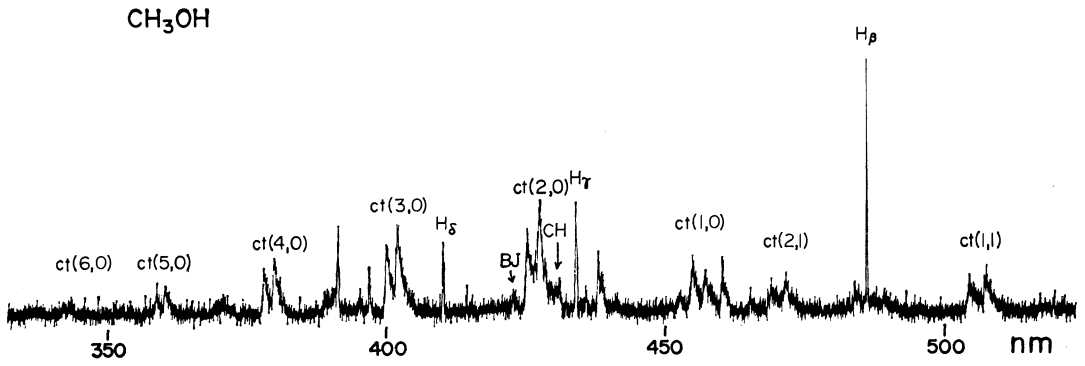

Fig. 1. Emission spectrum observed by electron impact of CH_3OH.
Acceleration voltage of electron: 240 V
H_β, H_γ, H_δ: Balmer series of hydrogen atoms
ct: CO^+ comet-tail bands
BJ: CO^+ Baldet-Johnson band

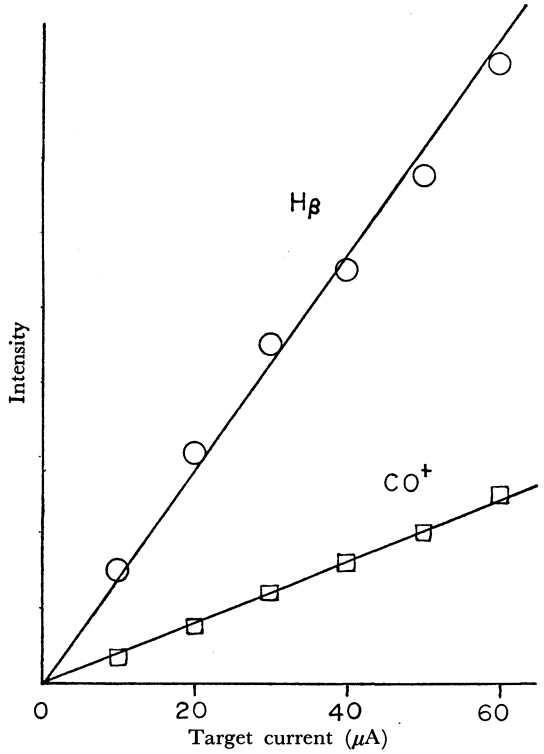

Fig. 2. Dependency of intensities of the H_β and the comet-tail (2,0) band on the target current; the pressure in the reservoir: 3 mmHg.

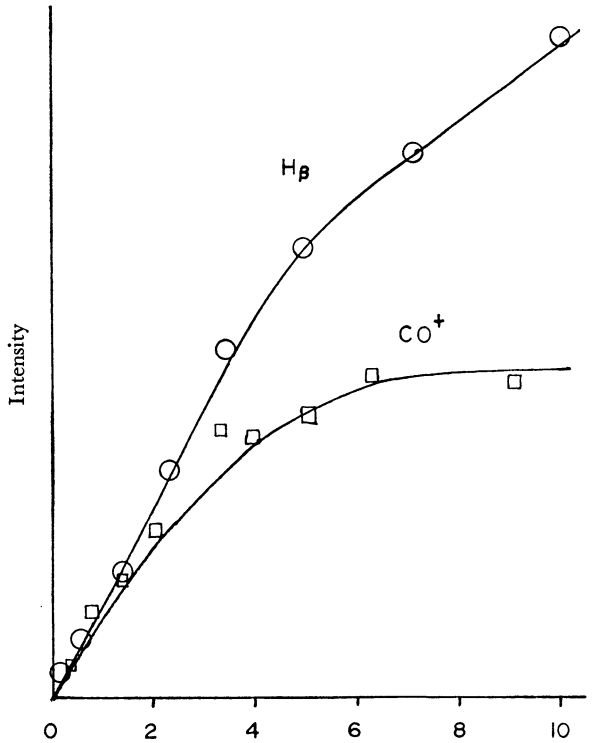

Fig. 3. Dependency of intensities of the H_β and the comet-tail (2,0) band on the gas pressure; the target current: 50 μA.

wavelength region, whereas Balmer-β (486.1 nm), Balmer-γ (434.0 nm), Balmer-δ (410.2 nm), and Balmer-ε (397.0 nm) were clearly observed. The "ct" sign in Fig. 1 represents the comet-tail band (CO^+ A $^2\Pi \longrightarrow$ X $^2\Sigma^+$), while the two numbers in parentheses following represent the vibrational quantum numbers of the upper and lower electronic states respectively. Furthermore, the Baldet-Johnson band (CO^+ $B^2\Sigma^+ \longrightarrow$ A $^2\Pi$) and the 430 nm band of the CH radical (A $^2\Delta \longrightarrow$ X $^2\Pi$) are found.

The linear dependency of the intensities of the Balmer-β line and the comet-tail (2,0) band on the target current, as shown in Fig. 2, indicates that the excited species are produced primarily by a collison of a parent molecule with an electron. The dependency of the intensities of these peaks on the pressure in the gas reservoir is shown in Fig. 3. The pressure in the collision chamber was estimated to be higher than one seven-hundredth of the pressure in the gas reservoir. The intensities of the Balmer-β line and the comet-tail (2,0) band increase linearly with an increase in the gas pressure up to a certain pressure, but they increase more slowly above this pressure. The levelling-off of the intensities at higher gas pressures may be due to the collisional deactivation of the excited species, and not to the self-absorption of the emission. Similar behavior has also been reported for the emission spectrum of carbon monoxide by Rothe and McCaa,[15] who

15) D. E. Rothe and D. J. McCaa, Technical Report CAL No. 165 (1968).

observed that the intensities of the emission bands of CO^+ increase rapidly up to *ca.* 5×10^{-2} mmHg in pressure and thereafter increase gradually, while the neutral CO bands (Herzberg and Angstrom) increase rapidly with an increase in the carbon monoxide pressure.

In order to find the absolute cross-section of the Balmer-β line from methanol, a mixture of a known composition of CD_3OD and CH_4 was bombarded by electrons, and the intensities of the Balmer-β emissions of the H and D atoms, which are separated by 1.3 Å, were measured. The cross-section of the Balmer-β emission from CD_3OD is determined to be *ca.* 4×10^{-19} cm^2 by normalization to the absolute cross-section of the Balmer-β line from CH_4 reported by Vroom and De Heer,[9] although the present cross-section may involve some error because of the relatively high pressure.

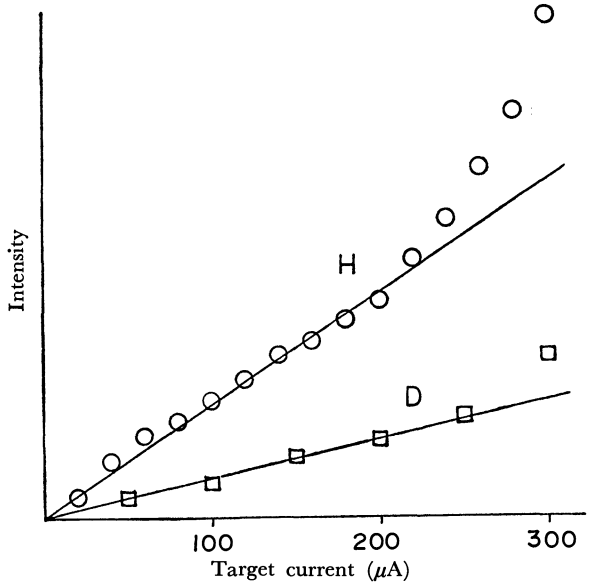

Fig. 4. Intensity of Balmer-β emission of H and D from CH_3OD; the pressure in the gas reservoir: 10 mmHg.

In order to determine the emission probabilities of the Balmer-β radiation of hydrogen atoms from the methyl group and the hydroxyl group separately, the intensity ratios of the Balmer-β emissions of the H and D atoms from CH_3OD and CD_3OH were determined. Figure 4 shows the intensities of the Balmer-β emissions of H and D from CH_3OD against the target current. The curves deviate upwards from the linear lines above a certain target current, indicating the contribution of some excited hydrogen atoms produced by collisions with two or more electrons. The intensity ratio of the Balmer-β line of H to that of D resulting from the bombardment of CH_3OD is about 2.9 in the linear part of Fig. 4, whereas that of D to that of H from CD_3OH is about 1.8. The disagreement of the above ratios for CH_3OD and CD_3OH indicates the existence of an isotope effect.

Assuming that the bond scissions of the methyl and hydroxyl groups are independent of each other, and that their isotope effect is equal in size in both groups, the following two conclusions can be drawn from the above results. First, the emission probability of D is less than that of H by *ca.* 20%, a value which is comparable to the isotope effect observed for CH_4 and CD_4.[9] Second, the probability of the production of the excited hydrogen atom from the methyl group is less by *ca.* 20% than that from the hydroxyl group per each hydrogen atom, taking into account the correction of the isotope effect.

Discussion

In the radiolysis of methanol, it was previously concluded, as has been mentioned above, that the primary process of fragmentation is a C–H bond scission.[10] This conclusion, supported by several experimental results, seems reasonable on the basis of the difference in the bond energies of the C–H and O–H bonds, the former having the smaller bond energy by 7.5 kcal/mol.[16] Nevertheless, the present measurement of the production of excited hydrogen atoms shows that a bond scission of the O–H bond is as probable as that of a C–H bond. However, this study is concerned only with the production of the excited hydrogen atom, and not with that of the hydrogen in the ground state. Therefore, the contribution of the excited hydrogen atoms to the overall production of hydrogen atoms is not established by the present experiment.

The emission probabilities of hydrogen atoms from the methyl and hydroxyl groups are of nearly the same magnitude; those from methanol and methane are also found to be comparable. These findings are interesting with regard to the result on some hydrocarbons that the number of excited hydrogen atoms produced in a particular energy level is practically independent of the hydrocarbons.[9]

Table 1. Energies for reactions

Reaction	Energy (eV)	Ref.
$CH_3OH \longrightarrow CH_3\dot{O}+H$	4.3	16
$CH_3OH \longrightarrow \dot{C}H_2OH+H$	4.0	16
$CH_3OH \longrightarrow CH_3OH^+ + e$	10.83	19
$H\,(n=1) \longrightarrow H\,(n=4)$	12.75	

The excited hydrogen atom must be produced *via* a superexcited methanol molecule, as was pointed out by Platzman *et al.*,[17,18] because the sum of the bond energy of the C–H or O–H bond and the excitation energy of a hydrogen atom is greater than the ionization energy of methanol, as is shown in Table 1. The autoionization and dissociation of the superexcited molecule compete, and the isotope effect exists only in the dissociation process, which is affected by the nuclear mass difference. Hence, the superexcited molecule containing a heavier isotope has, in general, a smaller probability of dissociation. The isotope effect of the Balmer emission from methanol mentioned above is, therefore, reasonable.

Since the intensity ratio of the Balmer line of H to

16) P. Gray and A. Williams, *Chem. Rev.*, **59**, 239 (1959).
17) R. L. Platzman, *Vortex*, **23**, 372 (1962).
18) W. P. Jesse, *J. Chem. Phys.*, **38**, 2774 (1963).
19) M. I. Al-Joboury and P. W. Turner, *J. Chem. Soc.*, **1964**, 4434.

that of D had to be measured at pressures as high as 10^{-2} mmHg because of the weak intensity of the lines, the secondary effects which affect the intensity ratio, such as collisional deactivation or self-absorption, might occur in the present system. However, further discussion along these lines could not be made because of the present lack of quantitative data on these effects.

Conclusion

By the electron impact of methanol, various excited fragments, such as the H atom, the CO^+ ion, and the CH radical, were produced, but no larger excited fragments, no excited parent molecule, and none of the corresponding ions could be found in the spectral range from 350 to 500 nm.

It was concluded that the excited hydrogen atom resulted from the scission of the O–H bond as well as from that of the C–H bond, and that the probabilities per bond of the above two processes were of nearly the same magnitude, if the isotope effect is considered. It is not certain, however, if this process is as important as the one which produced the hydrogen atom in the ground state, so that the present finding may not contribute much to clarifying the total split-off processes of the hydrogen atom from methanol.

By a comparison of the Blamer-β emission for CH_3OD and CD_3OH, an isotope effect of about 20% was preliminarily estimated for the dissociative excitation for the H and D in the molecules, the former having the larger cross-section. This effect can be explained by a process including superexcitation.

We should like to express our gratitude to Professors S. Ikeda and Y. Yokoyama for allowing us to use a Shimadzu GE 100 monochromator and various accessories in their laboratory.

BULLETIN OF THE CHEMICAL SOCIETY OF JAPAN, VOL. 44, 1754—1758 (1971)

Studies of the Surface of Titanium Dioxide. I. The Effect of Reduction by Hydrogen on the Heat of Immersion in Water

Toru IWAKI and MASAJI MIURA

Department of Chemistry, Faculty of Science, Hiroshima University, Higashisenda-machi, Hiroshima

(Received December 28, 1970)

The reduced state of the surface of titanium dioxide was studied by the measurement of the heat of immersion in water. When the titanium dioxide was reduced by hydrogen at 500°C, the heat value decreased appreciably with an increase in the pressure of hydrogen, in contrast to the increase in the heat value due to the reduction by an organic contaminant. The heat value was not restored to the original state even after oxygen had been introduced at 500°C to the reduced sample, while the color of the sample returned to white from bluish gray. These phenomena were interpreted by examining the adsorption of water, the reduced amount, and the reflectance spectrum.

It is well known that titanium dioxide is subject to a change in color from its initial white state to gray or bluish gray when heated *in vacuo* from 300 to 500°C. This color change has been considered to be caused by a removal of oxygen atoms from the surface. Such a reduction of titanium dioxide has been regarded as attributable to organic compounds which come from stopcock grease, diffusion pump oil, *etc.* in a vacuum system, and which are also occluded in titanium dioxide during its preparation.[1,2] When heated at a high temperature, these organic compounds are oxidized, resulting in the removal of oxygen atoms on the surface.

Titanium dioxide is also reduced easily by contact with a reducing gas, such as hydrogen or carbon monoxide, at a high temperature.[3] The removal of one oxygen atom from titanium dioxide produces two electrons which reside in the oxygen vacancy or the titanium ion. Reduced titanium dioxide is also well known to be an *n*-type semiconductor and to play an important role as a catalyst for such chemical reactions as the Fisher-Tropsch synthesis. Therefore, the investigation of the reduction of titanium dioxide is of interest in connection with the nature of the defect structures of solid surfaces. A number of studies of the bulk properties of reduced titanium dioxide have been performed for rutile modification by various methods,[4] but scarcely none have been done for anatase.

In the present study, the effect of an organic contaminant on the surface properties of anatase treated under several conditions was examined by measuring the heat of immersion in water. Further, in order to investigate the properties of the defect structure of the surface, the heat of immersion in water, the adsorption of water vapor, the weight change caused by the reduction, and the reflectance spectra were measured on anatase samples which were reduced by hydrogen

1) J. Gebhardt and K. Herrington, *J. Phys. Chem.*, **62**, 120 (1958).
2) C. M. Hollabaugh and J. J. Chessick, *ibid.*, **65**, 109 (1961).
3) T. J. Gray, C. C. McCain, and N. G. Masse, *ibid.*, **63**, 472 (1959).
4) F. A. Grant, *Rev. Modern Phys.*, **31**, 646 (1959).

and reoxidized by oxygen.

Experimental

Material. Titanium dioxide supplied by Teikoku Kako Co., Ltd., was purified by the method described in a previous paper.[5] X-ray analysis showed well-crystallized anatase for the sample outgassed at 500°C.

The titanium dioxide was treated under the following several sets of conditions in order to investigate the effect of the organic contaminant on the heat of immersion:

(1) Outgassing at 500°C for 5 hr at 10^{-5} mmHg.

(2) Outgassing at 500°C for 5 hr with a liquid nitrogen trap just before the sample in order to prevent the effect of the vapor of the stopcock grease.

(3) After the (1) treatment, introducing oxygen gas through a liquid nitrogen trap for 2 hr at a pressure of 0.5 atm and 500°C and then outgassing at room temperature for 0.5 hr.

(4) After the (2) treatment, introducing oxygen in the manner described above.

(5) After the condensation of diffusion pump oil on the surface of titanium dioxide, outgassing as in the (1) treatment.

(6) After the (2) treatment, introducing hydrogen gas through a liquid nitrogen trap at 0.5 atm and 500°C for 2 hr and then outgassing at 500°C for 0.5 hr.

Further, in order to examine the reduced state of the surface brought about by the reduction with hydrogen, titanium dioxide was treated under the following conditions:

(7) After the (2) treatment, introducing hydrogen gas at various pressures, ranging from about 0.01 to 1 atm, in the same way as in (6).

(8) After the (6) treatment, introducing oxygen gas through a liquid nitrogen trap for 0.5 hr at 0.5 atm and room temperature or 500°C, and then outgassing for 0.5 hr at room temperature.

Heat of Immersion. The heat of immersion was measured at 25°C by using a calorimeter, as was described previously.[6] The detection limit of the temperature difference was $\pm 1.7 \times 10^{-5}$°C, and the heat evolved in the calorimeter could be measured within ±1%. The heat of breaking of a vacant ampoule was found to be 0.3±0.05 J; this was calibrated for the heat-of-immersion data.

Surface Area. The surface area of the sample was determined by nitrogen adsorption at 77°K using the BET method; the area of a nitrogen molecule was assumed to be 16.2 Å^2 at that temperature. The surface area of each sample was 144 m^2/g, independent of the treatment, except for a sample treated with oxygen at 500°C after reduction with hydrogen (treatment (8)); the surface area of that sample was 139 m^2/g.

Adsorption of Water Vapor. The adsorption isotherms of water vapor on several samples were measured volumetrically at 25°C.

Reduced Amount. The amounts of titanium dioxide reduced by hydrogen at 500°C for 2 hr were obtained with a Cahn RG electrobalance.

Reflectance Spectrum. The reflectance spectrum was measured at 25°C with a Hitachi Perkin-Elmer 139 spectrophotometer over the wavelength range from 300 to 900mμ.

5) M. Miura, H. Naono, and T. Iwaki, *J. Sci. Hiroshima Univ. Ser. A-II*, **30**, 57 (1966).

6) M. Miura, H. Naono, T. Iwaki, T. Kato, and M. Hayashi, *Kogyo Kagaku Zasshi*, **69**, 1623 (1966).

Table 1. Heat of immersion of titanium dioxide in water

	Treatment	ΔH, erg/cm^2	Color
(1)	500°C, no trap	726	white or brown
(2)	trap	715	white
(3)	O_2	695	white
(4)	trap, O_2	695	white
(5)	oil	731	brown
(6)	H_2 (0.5 atom)	558	bluish gray

Results and Discussion

Effect of Organic Contamination on the Heat of Immersion. The values of the heat of immersion of titanium dioxide treated under the several sets of conditions are represented in Table 1. As is obvious by comparison of the (1) treatment with (2), the heat value is lowered slightly by using the liquid nitrogen trap. The sample became slightly brownish in the case of (1), but did not color in the case of (2). By the (3) or (4) treatment, the heat value was further decreased slightly as a result of the elimination of the organic contaminant by oxidation. Since the heat value was not so remarkably affected by the organic contaminant in the above cases, minute quantities of diffusion-pump oil were condensed on the sample. The results obtained by the treatment are shown in (5) of Table 1; the results indicate that the heat value increased by about 5% as compared with that of the (4) treatment. These results show that the heat of immersion is not influenced by the organic contaminant so remarkably as in the case of rutile reported by Hollabaugh and Chessick; in the latter case, the heat value increased by 120 erg/cm^2. The high value of the immersional heat is considered to arise from the reduced state of the rutile surface.[2] Therefore, the hydrogen gas was admitted to the sample at 500°C as in the (6) treatment in order to produce the reduced state to a considerable degree. In contrast to our expectations, the heat value for the surface decreased appreciably. Moreover, the sample was tinged bluish gray, different from the color caused by an organic contaminant. It seems that the surface state produced by the reduction with hydrogen is different from that produced with an organic contaminant. No further details of the effect of an organic contaminant on the surface properties were examined. Instead, the effect of reduction by hydrogen on the surface state will hereinafter be described.

Reduced State of Titanium Dioxide. In general, the surface of titanium dioxide is covered with hydroxyl groups. When the titanium dioxide is heated *in vacuo* at a high temperature, the surface hydroxyl groups may be removed as follows:

$$2OH^- \longrightarrow H_2O + O^{2-} \quad (1)$$

The resulting oxygen anion may be displaced from its original position to form a bridge, Ti–O–Ti. On the contrary, when dehydrated titanium dioxide is rehydrated, hydroxyl groups are again formed on the surface.

When a hydrogen molecule is introduced to the titanium dioxide at a high temperature, it removes the

oxygen anion as a water molecule, producing a defect structure according to the reaction:

$$O^{2-} + H_2 \longrightarrow H_2O + \square + 2e^- \quad (2)$$

where $\square$ is an oxygen vacancy.

In many studies of reduced rutile by examinations of the electric conductivity, the paramagnetic resonance, the dielectric relaxation, *etc.*, some results favor the oxygen vacancy as a dominant defect, some favor the interstitial titanium ion, and some favor a combination of the two.[7] At a high temperature, there are interstitial titanium ions, which may form the Magnéli interfaces as a result of the diffusion of oxygen vacancies.[8] Barbanel *et al.* have recently reported, from the measurement of the density of rutile, that the interstitial Ti^{3+} ion appeared when a rutile was heated above 750°C *in vacuo*.[9] In the present study, the reduction of the sample by hydrogen did not occur at 400°C, but it proceeded gradually at 500°C. Therefore, the oxygen vacancies produced may be present for the most part on the surface rather than in the bulk. The surface area of the sample may be expected to be changed by the reduction, but the nitrogen adsorption experiments showed no appreciable change in the surface area, even under the treatment with hydrogen at 1 atm.

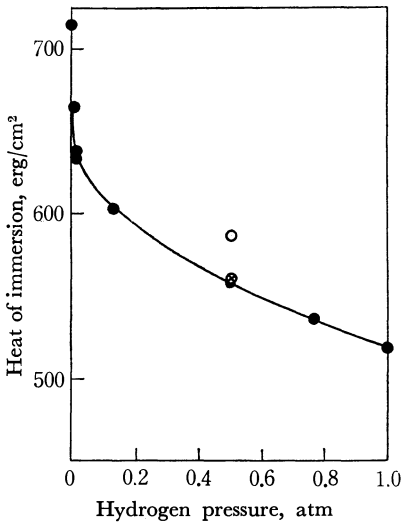

Fig. 1. Heat of immersion of titanium dioxide as a function of the pressure of hydrogen.
●, reduced at 500°C; ⊗, reoxidized at room temperature; ○, reoxidized at 500°C

Effect of Reduction on the Heat of Immersion and Adsorbed Amount of Water Vapor. The values of heat of immersion are shown in Fig. 1 as a function of the pressure of hydrogen, the pressures ranging from 0.01 to 1 atm. The heat value decreased with an increase in the pressure of hydrogen, rapidly in the lower pressure region and gradually in the higher one. The possibility of the removal of hydroxyl groups on the surface by the reduction is present in this case. Morimoto *et al.* have ascertained the water content of anatase treated at 500°C to be *ca.* 0.3 hydroxyl groups per 100Å.[2,10] If the decrease in the heat value by the reduction were responsible only for the removal of hydroxyl groups on the surface, the heat value might decrease by *ca.* 30 erg/cm². The heat of the immersion of the sample in dry benzene was measured to be 155 erg/cm²; this was not altered by the reduction. Therefore, the decrease in the heat may be caused mainly by the reduced state of the surface structure rather than by the hydroxyl groups.

Then, titanium dioxide reduced with hydrogen at 0.5 atm and 500°C was reoxidized by oxygen at 0.5 atm and room temperature or 500°C (treatment (8)). The values of the heat of immersion for the two samples in water are indicated in Fig. 1. In the former case the heat value was not varied at all, while in the latter case it was slightly increased.

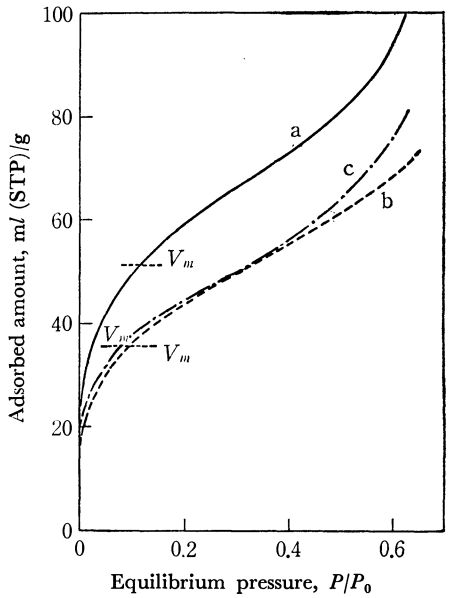

Fig. 2. Adsorption isotherms of water vapor on the surface of titanium dioxide; (a) outgassed at 500°C, (b) reduced with hydrogen at 0.5 atm, and (c) reoxidized at 500°C.

Table 2. Monolayer volume and surface area of water adsorbed on the surface of titanium dioxide

Treatment	V_m, ml (STP)/g	S_{H_2O}, m²/g	S_{H_2O}/S_{N_2}
(a) 500°C	50.7	147	1.02
(b) H_2 (0.5 atom)	36.3	105	0.73
(c) H_2–O_2 (500°C)	36.2	105	0.76

Figure 2 shows the adsorption isotherms of water vapor on the following three kinds of surfaces of titanium dioxide: outgassed at 500°C (a), reduced by 0.5 atm of hydrogen (b), and reoxidized by oxygen at 500°C (c). Table 2 lists the amount of water adsorbed on the surface corresponding to the monolayer obtained by the BET method, the surface area, S_{H_2O} being determined

7) L. A. K. Dominik and R. K. MacCrone, *Phys. Rev.*, **163**, 756 (1967).
8) J. S. Anderson and B. G. Hyde, *J. Phys. Chem. Solids*, **28**, 1393 (1967).
9) V. I. Barbanel, V. N. Bogomolov, and S. A. Borodim, *Fiz. Tverd. Tela*, **11**, 537 (1969).
10) T. Morimoto, M. Nagao, and T. Omori, This Bulletin, **42**, 943 (1969); T. Omori, J. Imai, M. Nagao, and T. Morimoto, *ibid.*, **42**, 2198 (1969).

by assuming the cross-sectional area of water molecule to be 10.8 Å², and the ratio of the area to the area being obtained from nitrogen adsorption, S_{H_2O}/S_{N_2}. In the case of (a), the monolayer of water covers the entire surface obtained from nitrogen adsorption because S_{H_2O}/S_{N_2} is nearly one, whereas in the cases of (b) and (c), the surface shows a somewhat hydrophobic character. The number of sites for water to be adsorbed on the surface may be altered by the reduction.

Reduced Amount. The change in the weight of titanium dioxide by the reduction with hydrogen at 500°C is given in Fig. 3 as a function of the pressure of hydrogen. The value at 0.006 atm of hydrogen was obtained by the volumetric method, because it is difficult to get the exact value at pressures lower than 0.05 atm by the gravimetric method because of a thermomolecular effect.

If the composition of titanium dioxide evacuated at 500°C is stoichiometric, the amount of oxygen atoms removed by the reduction with hydrogen at 0.5 atm is calculated from Fig. 3 to be 0.3% of all the oxygen atoms of titanium dioxide; the composition of $TiO_{1.994}$ can thus be obtained. Among all the oxygen ions, those on the surface layer are calculated to be 13.3% for the (001) plane, 10.6% for the (100) plane, and 9.9% for the (101) plane. These planes are the cleavage faces of anatase.[11] If the elimination of oxygen atoms from titanium dioxide is limited to the surface oxygen atoms, which account for 11.3% of the total, the oxygen atoms removed should become 2.7%, resulting in the composition of $TiO_{1.946}$ for the surface layer. Thus, the oxygen vacancies per surface area should become 0.32/100 Å². The real surface of reduced titanium dioxide, however, may have fewer oxygen vacancies than the values calculated above since the reduction may occur also in the bulk.

The relationship between the reduced amount and the hydrogen pressure in Fig. 3 resembles fairly well that between the heat of immersion and the hydrogen pressure in Fig. 1. The decrease in the heat of immersion per reduced weight takes a constant value, 210 erg/cm² per mg of oxygen vacancy, in the pressure range higher than 0.05 atm. This means that hydrogen atoms eliminate the oxygen atoms on the surface which are active to the water molecule. The weight of the reduced titanium dioxide could not be restored completely to the original weight by oxidation even at 500°C; about three quarters of the weight loss was recovered.

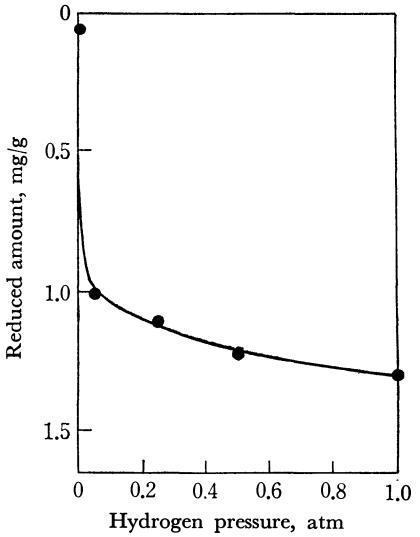

Fig. 3. Reduced amount of titanium dioxide as a function of the pressure of hydrogen.

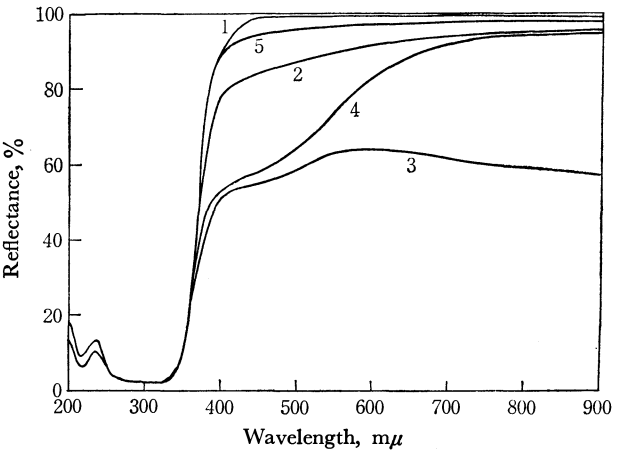

Fig. 4. Reflectance spectra of titanium dioxide; (1) unreduced, (2) outgassed at 500°C, (3) reduced with hydrogen at 0.5 atm, (4) reoxidized at room temperature, and (5) reoxidized at 500°C.

Color Changes by Reduction and Reoxidation. Titanium dioxide reduced by hydrogen was tinged with a bluish-gray color. It showed a brown color after being oxidized by oxygen at room temperature, but it became white when oxidized at 500°C. The reflectance spectra for these samples are shown in Fig. 4. An absorption in the ultraviolet region with an absorption edge of 360 mμ is caused by a transition from the valence band, the $2p$ state of O^{2-}, to the upper conduction band, the $3d$ state of Ti^{3+}, which is the fundamental absorption.[12] For the reduced sample, other absorption bands emerged in the longer-wavelength range: a shoulder at 440 mμ and a broad absorption band with a maximum above 900 mμ. The latter band disappeared when oxygen was introduced to the reduced surface at room temperature, while both bands disappeared after coming into contact with oxygen at 500°C, whereupon the spectrum was similar to the original one. The differences between the reflectances of the reduced samples and that of the unreduced sample are shown in Fig. 5. The increase in intensity of the absorption bands at both 440 mμ and above 900 mμ with an increase in the degree of reduction indicates that these bands are caused by irregularities in the lattice.

The former band is similar to a band resulting from indirect transition which is observed in germanium and silicon.[13] This forbidden transition from valence band to conduction band may be made possible by

11) L. G. Berry and B. Mason, "Mineralogy," W. H. Freeman and Co., San Francisco (1959), p. 377.

12) G. V. Schultz, *Z. Phys.*, **179**, 473 (1964).

13) W. C. Dash and R. Newman, *Phys. Rev.*, **99**, 1151 (1955).

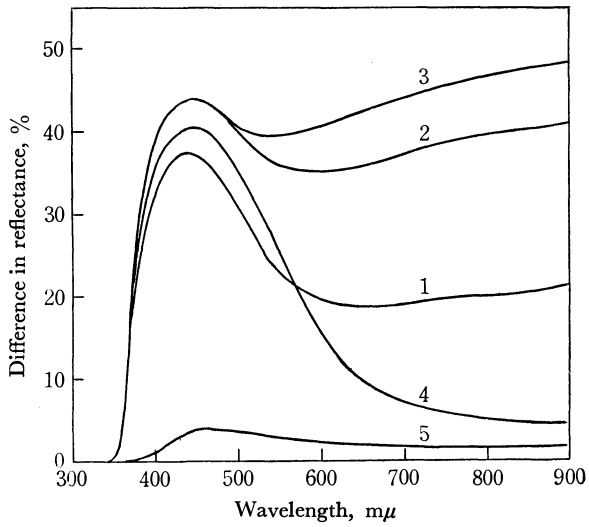

Fig. 5. Differences between reflectance of unreduced sample and those of the samples treated as follows: (1) reduced with hydrogen at 0.1 atm, (2) reduced with hydrogen at 0.5 atm, (3) reduced with hydrogen at 1 atm, (4) reoxidized at room temperature, and (5) reoxidized at 500°C.

crystal imperfections. The latter band may be responsible for the bluish-gray coloration. In a reduced sample of rutile, this coloration is considered to be caused by an excitation of electrons from the donor state as well as from the conduction band to the additional conduction band (absorption band mixiumum at $h\nu$= 1 eV).[14] However, the excitation of electrons may be made impossible by the adsorption of oxygen on the reduced surface at room temperature. The adsorbed oxygen molecules become O_2^- [15] by drawing electrons from the donor state and the conduction band, resulting in the formation of a depletion layer near the surface. Oxygen admitted to the reduced sample at 500°C may be incorporated into the crystal lattice as O^{2-} to reproduced a considerably less irregular lattice near the surface.

Conclusion. From the results of the heat of immersion in water, the weight change, and the color change, it may be considered that titanium ions are present, in a considerable part, around oxygen vacancies on the surface when titanium dioxide is reduced. Such a surface may weakly interact with water, since a certain number of active oxygen ions, which strongly attract water molecules to form surface hydroxyl groups, are removed from the surface. When the surface is reoxidized at 500°C, the electronic state of the surface can return to the original unreduced state, but the interaction of the surface with water can not be restored. Even though oxygen is incorporated on the reduced surface as O^{2-}, it may no longer be such an active oxygen ion as that on the unreduced surface.

14) J. H. Becker and W. R. Hosler, *J. Phys. Soc. Jap.*, **18**, Suppl. II, 152 (1963).
15) J. H. C. VAN Hoff, *J. Catal.*, **11**, 277 (1968).

BULLETIN OF THE CHEMICAL SOCIETY OF JAPAN, VOL. 44, 1758—1763 (1971)

The Crystal Spectra of Molecular Compounds of 1,6-Diaminopyrene

Takako AMANO,[1] Haruo KURODA, and Hideo AKAMATU

Department of Chemistry, Faculty of Science, The University of Tokyo, Hongo, Tokyo

(Received January 13, 1971)

Polarized absorption spectra were observed on the single crystals of molecular compounds which involve 1,6-diaminopyrene as electron donor and *p*-chloranil, *p*-bromanil, *p*-iodanil, and tetracyano-*p*-quinodimethane as electron acceptor. It is shown that, in spite of the low ionization potential of diaminopyrene 6.56 eV, its solid molecular compounds with chloranil, bromanil, and iodanil are of non-ionic type, and their crystal spectra exhibit the general features characteristic of a typical charge-transfer molecular compound composed of neutral molecules. The diaminopyrene-TCNQ compound was found to be of ionic type. Although the bromanil and iodanil compounds of diaminopyrene exhibit two charge-transfer bands, in the region below 10 kK and at about 20 kK respectively, the chloranil compound does not show the near-infrared charge-transfer band corresponding to the charge transfer from the highest occupied orbital of the donor to the lowest vacant orbital of the acceptor. A discussion is given for this phenomenon from the overlap between the donor and acceptor orbitals.

The solid molecular compounds of 1,6-diaminopyrene with chloranil and bromanil have been reported to be organic semiconductors of relatively good electrical conductivity.[2-6] The visible absorption spectra of the crystalline powders of these molecular compounds were first examined by Kronick *et al.* and Scott *et al.* by using the KBr-pellet method.[7,8] They concluded from the observed spectra that a considerable fraction of the constituent molecules are in ionic states at room temperature, and estimated the ionic fraction as 90

1) Present address: Department of Chemistry, Faculty of Science, Kyushu University, Hakozaki, Fukuoka.

2) M. M. Labes, R. Sehr, and M. Bose, *J. Chem. Phys.*, **33**, 868 (1960).

3) P. L. Kronick and M. M. Labes, *ibid.*, **35**, 2016 (1961).

4) M. Schwartz, D. W. Davies, and B. J. Dobriansky, *ibid.*, **40**, 3257 (1964).

5) W. H. Bentry and H. G. Drickamer, *ibid.*, **42**, 1573 (1965).

6) Y. Matsunaga, *Nature*, **211**, 183 (1966).

7) P. L. Kronick, H. Scott, and M. M. Labes, *J. Chem. Phys.*, **40**, 890 (1964).

percent in the chloranil compound and 30 percent in the bromanil compound.

The spectra of these molecular compounds were re-examined later by Matsunaga.[9] He applied the method of diffuse reflectance spectroscopy on the crystalline powder of these molecular compounds, and obtained results considerably different from those reported by the previous workers. He suggested that both molecular compounds are of an essentially nonionic type.

In view of the considerable discrepancies found between the spectra reported by the two groups, it seems worthwhile to examine the single crystal spectra of these molecular compounds. In the present paper, we will report on the polarized absorption spectra of the single crystals of the 1,6-diaminopyrene compounds which involve *p*-chloranil, *p*-bromanil, *p*-iodanil, and tetracyano-*p*-quinodimethane (TCNQ) as electron acceptor.

Experimental

TCNQ and 1,6-diaminopyrene were synthesized by the methods described in literatures.[10,11] Chloranil was obtained commercially, and purified by recrystallization and sublimation *in vacuo*. Bromanil and iodanil were kindly supplied by Prof. T. Handa of Science University of Tokyo. The crystals of all molecular compounds except that of diaminopyrene-TCNQ were prepared from benzene or toluene solutions containing appropriate amounts of the donor and acceptor. The crystal of the diaminopyrene-TCNQ was prepared from an acetonitrile solution.

The composition of each molecular compound was determined by elemental analysis of crystals. Polarized absorption spectra of the 10—35 kK region were measured on single crystals of microscopic size with a microspectrophotometer.[12] The edges of a prominent face of the crystal were tentatively chosen as the directions of the polarization of light in the measurement of the polarized absorption spectra.

Results

Diaminopyrene-Chloranil. This compound crystallizes from a benzene solution as brown needles or parallelepiped crystals.[13] The mole ratio of the donor to the acceptor was found to be 1:1. The crystal exhibits a marked dichroism when observed under a polarizing microscope.

The polarized absorption spectra observed on a thin parallelepiped crystal are shown in Fig. 1. We will denote the two edges of the crystal by *X*- and *Y*-directions. The spectra were observed for light polarization parallel and perpendicular to the *X*-direction, which we will call the $//X$ and $\perp X$ spectra, respectively. The results are shown in Fig. 1(a). A broad absorption band with a maximum of 18—19 kK and a sharper peak at 24.5 kK appear in the $//X$ spectrum. The intensity is larger in the former and smaller in the latter in the $//X$ spectrum as compared with the $\perp X$ spectrum. The difference of polarization direction in the above two absorption bands can be seen much more clearly in the $//Y$ and $\perp Y$ spectra, shown in Fig. 1(b). The first band appears only in the $//Y$ spectrum with a maximum at 18.5 kK, while the 24.5 kK peak appears only in the $//Y$ spectrum.

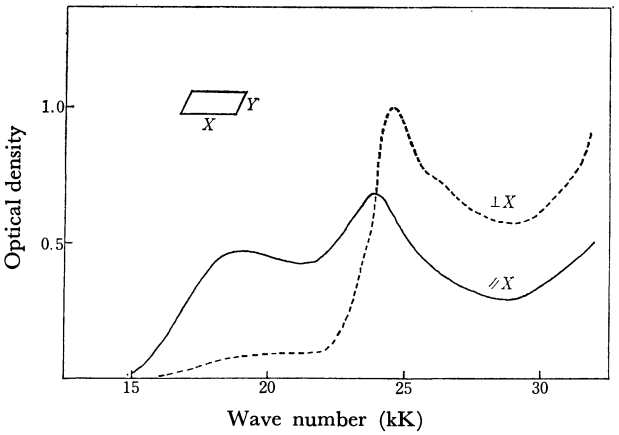

Fig. 1(a). Polarized absorption spectra of diaminopyrene-chloranil crystal: $//X$ and $\perp X$ spectra

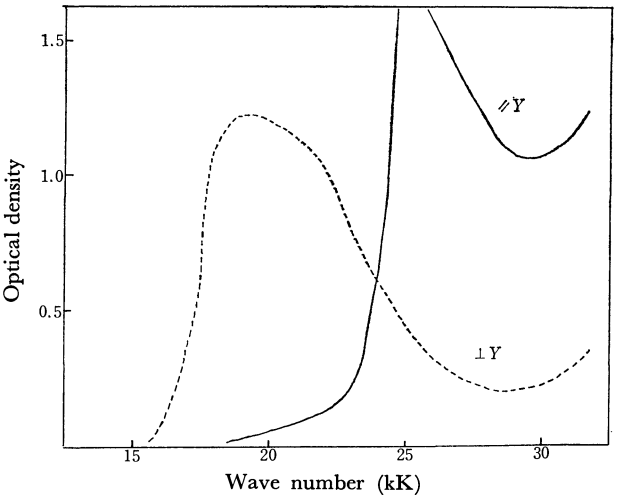

Fig. 1(b). Polarized absorption spectra of diaminopyrene-chloranil crystal: $//Y$ and $\perp Y$ spectra

In order to confirm the polarization direction of these absorption bands, we observed the variations of the optical densities at 18.5, 23.5, and 25 kK as a function of the direction of light polarization. The results are shown in Fig. 2, which shows clearly, first, that the principal axis of absorption at 18.5 kK is perpendicular to that at 25 kK, and, second, that the former makes an angle of about 30° with respect to *X*-direction.

8) H. Scott, P. L. Knonick, P. Charige, and M. M. Labes, *J. Phys. Chem.*, **69**, 1740 (1965).
9) Y. Matsunaga, *Nature*, **211**, 183 (1966).
10) H. Vollman, H. Becker, M. Correll, and H. Streek, *Ann.*, **531**, 1 (1937).
11) D. S. Acker and W. R. Hertler, *J. Amer. Chem. Soc.*, **84** 3370 (1962).
12) H. Kuroda, T. Kunii, S. Hiroma, and H. Akamatu, *J. Mol. Spectry.*, **22**, 60 (1967).
13) It has been reported by Matsunaga[9] that there are two crystalline forms, brown and green. From the benzene solution, we could obtain only the brown crystal which seems to correspond to Matsunaga's brown form. However, when chloroform or diethyl ether was used as solvent, we noticed that a small amount of green crystals were formed besides the brown crystals. The former exhibited an absorption spectrum quite different from the latter. The nature of the green crystal is not clear, but seemingly it is associated with some oxidation products of diaminopyrene.

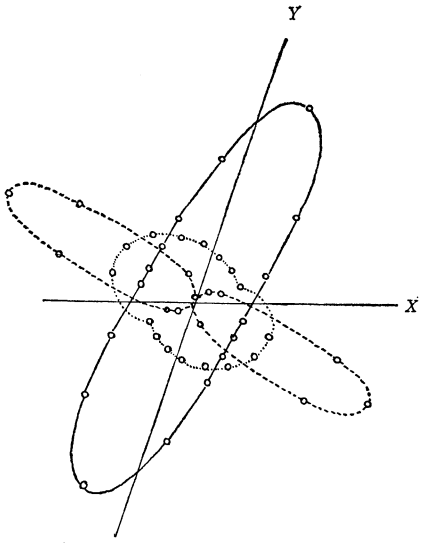

Fig. 2. Dependence of optical density on the direction of light polarization observed on a prominent face of diaminopyrene-chloranil crystal.
------: 18.5 kK ·····: 23.5 kK ——: 25.0 kK

It was not possible to obtain an accurate absorption spectrum of a needle crystal, but the main features of the spectra obtained for the light polarizations parallel and perpendicular to the elongated axis, were found to be similar to the $\perp Y$ and $/\!/ Y$ spectra of a parallelepiped crystal, shown in Fig. 1.

Our results for the brown crystal agree with the results reported by the previous workers as regards the locations of the above two bands, but we find no peak corresponding to the sharp peak at 17.5 kK reported by Kronick *et al.*,[7] who attributed it to the monopositive ion of diaminopyrene, neither we find any band corresponding to the 8 and 15 kK ones reported by Matsunaga.[9,14]

The infrared spectrum of the crystalline powder of this compound can be explained by assuming that the crystal is essentially composed of neutral molecules of the donor and acceptor as suggested by Matsunaga.[9,15] The powder was found to be diamagnetic around room temperature. Although a very weak paramagnetic resonance absorption was detectable, it was most likely to be associated with the presence of a trace of impurities or some oxidation products. All these data suggest that the brown form of diaminopyrene-chloranil crystal has an essentially non-ionic ground state.

The absorption spectra of the diaminopyrene and that of the diaminopyrene cation are reproduced in Fig. 3. If we assume a non-ionic structure for the diaminopyrene-chloranil compound, we can assign the strong absorption band in the 23—30 kK region of the crystal spectrum to the one associated with the lowest π–π^* transition of diaminopyrene. In the 10—22 kK region, we can not expect any local excitation band associated with an intramolecular transition of the donor or acceptor. Thus the 18.5 kK band should be considered as a charge-transfer band. Apparently the above interpretations are consistent with observed polarizations of the absorption bands in the crystal spectrum.

It should be noted, however, that the 1:1 complex formed between diaminopyrene and chloranil in a chloroform solution exhibits two charge-transfer bands in the visible region, the maxima of which are located respectively at 9.9 and 19.0 kK. It is hard to expect that the first charge-transfer band appearing at 9.9 kK in the solution is shifted to a higher energy as much as 10 kK in the crystal. In fact, the corresponding charge-transfer band does appear at about 7 kK in the crystal spectra of the bromanil or iodanil compounds of diaminopyrene. Therefore, we should assign the 18.5 kK band of the diaminopyrene-chloranil to one corresponding to second or third charge-transfer excitation, and not

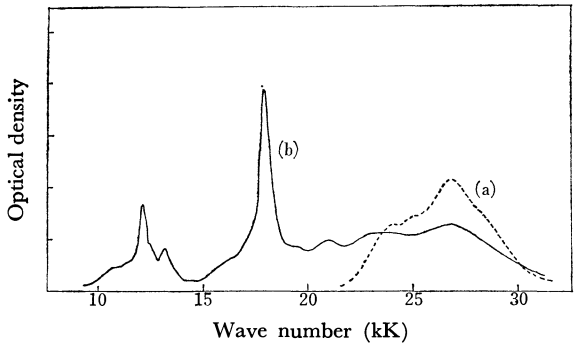

Fig. 3. Absorption spectra of diaminopyrene (a) and its monopositive ion (b) in ethanol. The ion was prepared from the interaction of chloranil in the ethanol solution.

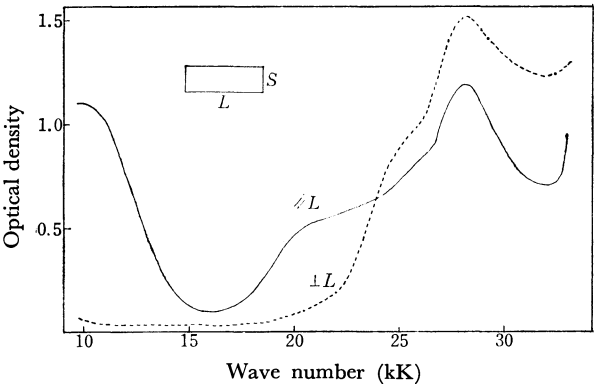

Fig. 4. Polarized absorption spectra of diaminopyrene-bromanil crystal.

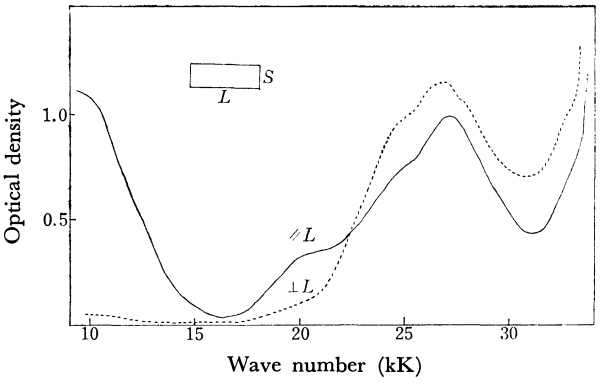

Fig. 5. Polarized absorption spectra of diaminopyrene-iodanil crystal.

14) We found absorption maxima at 8 and 15 kK in the spectra of the green crystal.
15) Y. Matsunaga, *Nature*, **205**, 72 (1965).

to one associated with the lowest charge-transfer excitation.

Diaminopyrene-Bromanil and Diaminopyrene-Iodanil. Both these compounds crystallized as dark-brown needle crystals, and the mole ratio of donor to acceptor was found to be 1:1.

We observed the polarized absorption spectra of the crystals for light polarizations parallel and perpendicular to the elongated axis of a needle crystal, which we will call the L-axis of the crystal.

The observed spectra are shown in Fig. 4 and Fig. 5. As can be seen, the crystal spectra of the two molecular compounds are quite similar to each other. Both show a strong near-infrared absorption band[16] polarized exclusively in the L-axis direction, and another strong band of different polarization in the 24—32 kK region, which exhibits an appreciably higher intensity in the $\perp L$ spectrum than in the $/\!/L$ spectrum. Besides these two absorption bands, there is one weak band of $/\!/L$ polarization around 20 kK, which appears as a shoulder at the tail of the strong ultraviolet band.

Table 1. Charge-transfer bands of 1,6-diaminopyrene-haloanil molecular compounds
(kK units)

Acceptor	1st CT band		2nd CT band	
	$CHCl_3$ soln.	cryst.	$CHCl_3$ soln.	cryst.
Chloranil	9.9_0	—	*ca* 19	19.2
Bromanil	9.2_6	<10	*ca* 19	~20
Iodanil	9.5_2	<10	*ca* 19	~20

The 1:1 molecular complex formed in a chloroform solution between diaminopyrene and bromanil exhibits two charge-transfer bands, the first located at 9.26 kK and the second at 19 kK. In the case of the diaminopyrene-iodanil complex in a chloroform solution, the first charge-transfer band is at 9.52 kK and the second at 19 kK. Since there is no absorption band of diaminopyrene in the region below 22 kK, it is most likely that the first two absorption bands of $/\!/L$ polarization found in the crystal spectra of the bromanil and iodanil compounds of diaminopyrene are associated with the charge transfer from a donor molecule to a neighboring acceptor molecule, and the ultraviolet band is a local-excitation band associated with the intramolecular transitions of diaminopyrene. The general features of the crystal spectra mentioned above are in accord with the behaviors usually found for the crystal spectrum of a typical charge-transfer molecular compound composed of neutral molecules. On the other hand, it is impossible to understand the observed crystal spectra of the bromanil and iodanil compounds of diaminopyrene if we assume an ionic structure for their ground state. Their infrared spectra are also quite similar to each other, which can be understood by assuming that they are composed of neutral molecules of the components.

Diaminopyrene-TCNQ. This compound crystallizes as a dark-brown parallelepiped crystal. The mole ratio in the crystal is again 1:1. The polarized absorption spectra are shown in Fig. 6. The general features of the crystal spectra are quite different from those of the preceeding three molecular compounds. Although this compound also exhibits an intense near-infrared absorption band polarized parallel to the longer edge of the crystal (the X-direction), its maximum is located at considerably low energy as compared with the corresponding bands of other molecular compounds. The absorption in the visible and ultraviolet region is strongly polarized in the $\perp X$ direction, where we find three absorption maxima located at about 13, 19, and 23 kK, respectively.

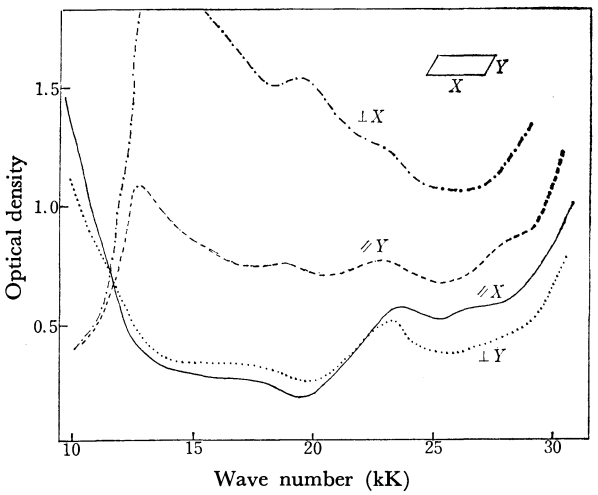

Fig. 6. Polarized absorption spectra of diaminopyrene-TCNQ crystal.

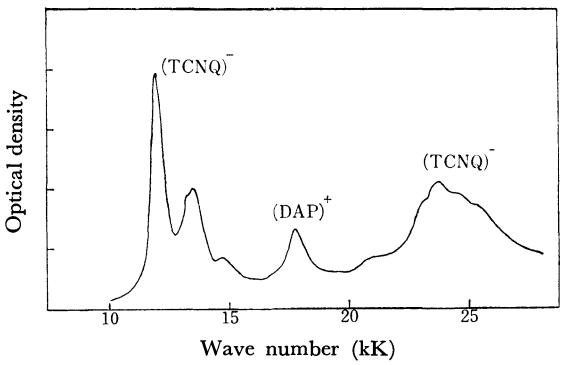

Fig. 7. Absorption spectrum of the acetonitrile solution of diaminopyrene-TCNQ.

The absorption spectrum of an acetonitril solution of the diaminopyrene-TCNQ is shown in Fig. 7, which corresponds to the superposition of the spectrum of the monopositive ion of diaminopyrene and that of the mononegative ion of TCNQ. Although both ions have their first absorption bands in the 10—15 kK region, the peaks in this region of the solution spectrum are almost entirely due to the TCNQ ion. The 17.8 kK sharp peak is due to the second band of the diaminopyrene ion, and the broad band in the 22—27 kK region

16) We were unable to determine the wavenumber of the absorption maximum from the observation of the single crystal spectrum, due to the inapplicability of our microspectrophotometer to this region. From observation of the powder spectra of these molecular compounds, the maximum was found to be at about 7kK in both cases.

is due to the TCNQ ion.

If we compare the crystal spectrum of the diaminopyrene-TCNQ with its solution spectrum, we note that all absorption bands in the crystal spectrum except the near-infrared one which is polarized in the $//X$ direction, can be understood as the local-excitation bands associated with the transitions of the diaminopyrene ion or those of the TCNQ ion. Presumably, the 12.5 kK strong band is mainly associated with the lowest π–π^* transition of the TCNQ ion, and the 19.5 kK weak band is due to the 17.8 kK transition of the diaminopyrene ion. They are considerably broadened and shifted as compared with the corresponding bands in the solution spectrum. The absorption band of the TCNQ ion in the 22—27 kK region is known to be composed of two transitions,[17] one strong transition with the transition moment parallel to the long axis of the TCNQ ion, and one weak one with the transition moment parallel to the short axis. We could attribute the weak band found at 24.6 kK in the $//X$ spectrum of the crystal to the one associated with the short-axis polarized transition of the TCNQ ion. Seemingly, the absorption band associated with the long-axis polarized transition of the TCNQ ion is markedly shifted to higher energy in the crystal. We could attribute the steep rise of absorption above 28 kK to the tail of this absorption band.

The infrared spectrum of the crystalline powder of the diaminopyrene-TCNQ suggests also that TCNQ is, in fact, in the ionic state in this molecular compound. Interestingly, however, the intensity of the paramagnetic resonance absorption is so small that the spin concentration estimated from the observed intensity corresponds to only 6.6 percent of the value expected when each ion provides one independent spin center. This suggests the presence of a strong interaction between neighboring radical ions. The appearance of a very strong charge-transfer band in the crystal spectrum is in accord with this interpretation.

Discussion

From the energy of the first charge-transfer band of the diaminopyrene-chloranil complex in solution, the ionization potential of diaminopyrene can be estimated as 6.54 eV.[18] The value estimated from the energy of the corresponding band of the diaminopyrene-bromanil complex is 6.57 eV.[19] Thus the average value is 6.56 eV.

We carried out the calculation of π-orbitals of diaminopyrene by the *variable-β* modification of the Pariser-Parr-Pople method.[20] The occupied molecular orbitals thus obtained are given in the appendix.

From the result of such a calculation, we can predict the ionization potential of diaminopyrene as 6.51 eV, which is in good agreement with the experimentally estimated values mentioned above.

Thus we believe that the ionization potential of diaminopyrene is 6.5—6.6 eV, which is smaller than the ionization potential of tetramethyl-*p*-phenylenediamine (TMPD). It should be noted that, in spite of this low ionization potential of diaminopyrene, the solid molecular compounds of diaminopyrene with chloranil, bromanil and iodanil, are of the non-ionic type, whereas TMPD forms an ionic compound with chloranil.[22]

The electron affinity has been estimated by Briegleb as 1.37, 1.40, 1.36, and 1.7 eV respectively for chloranil, bromanil, iodanil, and TCNQ.[23] Thus, the difference between the ionization potential of the donor, I_D, and the electron affinity of the acceptor, A_A, is about 5 eV for the chloranil, bromanil, and iodanil compounds of diaminopyrene, and below 5 eV for the diaminopyrene-TCNQ. This means that the lower limit of $I_D - A_A$ that gives a non-ionic crystal is located below 5 eV when the electron donor is diaminopyrene. This seems to be markedly low as compared with the molecular compounds of various other amines. A similar situation can be found, however, in the molecular compounds of tetramethylbenzidine. Presumably this is associated with the effect of molecular size of the donor on the Coulomb energy term which is to have significant contribution to the stability of the ionic structure.

Another problem to be considered is the absence of the first charge-transfer band in the crystal spectrum of the diaminopyrene-chloranil. As shown in the appendix, the diaminopyrene molecule has two closely spaced occupied levels of the symmetries, b_g and a_u at about 1.6 eV below the highest occupied orbital of the symmetry of b_g. In the bromanil and iodanil compounds of diaminopyrene, the first charge-transfer band must be associated with the charge transfer from the highest occupied orbital of a diaminopyrene molecule to the lowest vacant orbital of the neighboring acceptor molecule, and the second charge-transfer band at 19 kK must be associated with the charge transfer from either one of the second or third occupied orbitals, or with those from both of them. The energy difference between the first and second charge-transfer bands is nearly equal to the difference of the orbital energies.

In the case of diaminopyrene-chloranil, we were unable to find any absorption band corresponding to the first charge transfer bands of the bromanil and iodanil compounds. We must attribute the charge-transfer band found at 18.5 kK in the crystal spectrum of the diaminopyrene-chloranil to the one corresponding to the 19 kK charge-transfer band found for the diamino-

17) S. Hiroma, H. Kuroda, and H. Akamatu, This Bulletin, **44**, 9 (1971).

18) We have newly established the empirical relation
$$h\nu_{CT} = 0.87 I_D - 4.46 \text{ (eV)}$$
between the frequency of the charge-transfer band of a chloranil complex and the ionization potential of the donor. The equation was used to the estimate the ionization potential of diaminopyrene.

19) Here we assumed the relation
$$h\nu_{CT} = 0.928 I_D - 4.95 \text{ (eV)}$$
cf. M. Kinoshita, This Bulletin, **35**, 1609 (1962).

20) Refer to Ref. 21, for the details of calculation and the procedure of estimating the ionization potential.

21) T. L. Kunii and H. Kuroda, *Theoret. Chim. Acta*, **11**, 97 (1968).

22) T. Amano, H. Kuroda, and H. Akamatu, This Bulletin, **41**, 83 (1968).

23) These values seem to be too small to be taken as the absolute values of the electron affinities. In fact, Lyons has recently given the following values: chloranil 2.05 eV, TCNQ 2.46 eV (L. E. Lyons, private communication). The essential point of the discussion given here is unaffected by taking these values, but we have to reduce the value of $I_D - A_A$ by about 0.7 eV for all molecular compounds discussed here.

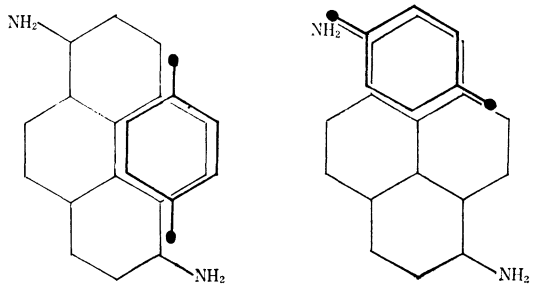

Model A Model B

Fig. 8. Models for the stacking of molecules of diaminopyrene-quinone.

pyrene-bromanil and the diaminopyrene-iodanil.

At present, we have no information on the relative arrangement of the donor and acceptor in these molecular compounds. We therefore took two models of the molecular arrangement illustrated in Fig. 8, and estimated the overlap between the donor and acceptor orbitals. The results indicate that model A is favorable for the charge transfer from the a_u orbital of diaminopyrene, but not for that from the b_g orbitals, while model B is favorable for the charge transfer from the latter orbitals and not for that from the former orbital. This suggests that the charge-transfer bands associated with charge transfer from the highest and second highest occupied orbitals of the symmetry b_g could appear when the relative arrangement of the donor and acceptor molecules in the crystal is the one illustrated by model B. On the other hand, these bands, would be almost absent and the charge-transfer band observable with a moderate intensity would be the one associated with the charge-transfer from the third highest occupied orbital of the symmetry a_u, if the molecular arrangement is of the type of model A. Presumably, diaminopyrene-chloranil corresponds to the latter case and diaminopyrene-bromanil and diaminopyrene-iodanil to the former.

Appendix. Occupied molecular orbitals of 1,6-diaminopyrene[a)]

Symmetry	Orbital energy [eV]	Coefficeients in the molecular orbitals[b)]								
		$x_1 \pm x_{10}$	$x_2 \pm x_{11}$	$x_3 \pm x_{12}$	$x_4 \pm x_{13}$	$x_5 \pm x_{14}$	$x_6 \pm x_{15}$	$x_7 \pm x_{16}$	$x_8 \pm x_{17}$	$x_9 \pm x_{18}$
a_u	−13.87173	0.18129	0.29800	0.28595	0.18155	0.16969	0.24316	0.16575	0.32409	0.20778
b_g	−13.24957	0.11337	0.26402	0.41082	0.25140	0.15980	0.10693	−0.01117	0.11012	0.36911
a_u	−12.25836	−0.11929	−0.02926	0.31809	0.13671	−0.04981	−0.24194	−0.18075	−0.25483	0.45433
b_g	−11.99341	−0.29458	−0.12997	−0.05603	0.13446	0.28501	0.37631	0.36963	0.08451	−0.09220
b_g	−10.85024	−0.30456	−0.28218	0.06516	−0.09654	−0.16860	−0.14942	0.14033	−0.17521	0.46142
a_u	−10.59088	0.21598	0.25399	0.00588	−0.35525	−0.43795	−0.20186	0.04791	0.12538	0.10972
a_u	−9.89864	0.38584	−0.06410	−0.00548	0.04713	0.04248	0.00148	0.40655	−0.42114	0.01781
a_u	−9.19109	−0.10654	−0.28805	−0.20186	−0.26803	0.01473	0.27886	0.14872	0.08314	0.43137
b_g	−9.17829	−0.02194	−0.27505	0.05560	0.41566	0.26421	−0.21694	−0.20689	−0.27279	−0.11794
b_g	−7.56899	0.25707	−0.21237	−0.29894	−0.14506	0.26295	0.24020	−0.23842	0.02330	0.30689

a) The SCF·MO's calculated by the procedure described in Ref. 12

b) $x_i + x_j$ for a_u, $x_i - x_j$ for b_g

Positron-lifetime Measurements in Polymerizing Organic Solids

Yasuo Ito, Kouji Okuda, and Yoneho Tabata

Department of Nuclear Engineering, Faculty of Engineering, The University of Tokyo, Hongo, Tokyo

(Received January 23, 1971)

The measurement of the e^+ lifetime in solid monomers during polymerization has been carried out. The mechanism of solid-state polymerization can be analyzed by the measurement of the lifetime of positrons and the amounts of positronium formed. This method was applied to the solid-state polylmerization of acrylamide. It was found from the experiments that the lifetime spectrum changes remarkably in the induction period of polymerization. The decrease in the annihilation rate λ_2 was interpreted in terms of the formation of a larger free volume during polymerization. The intensity of the slow component was also observed to decrease in the induction period of polymerization. The accumulation of active species which capture positrons and the decrease in the number of free volumes were suggested as explanations of the phenomena.

During the last 20 years, the positron annihilation in matter has been studied extensively, and most of the experimental results have been collected.[1-3] Although the experimental data have as yet a qualitative character, it is expected that positron annihilation can be used as a probe in the study of solid materials. A positron can capture an electron in a medium in which it is slowing down, and form a bound state which is called positronium (Ps). There are two ground states of Ps: the triplet state Ps, with total spin $S=1$, and the singlet state Ps, with total spin $S=0$. The lifetime of the singlet Ps (s-Ps) is so short ($\tau=0.125$ nsec) that its component is not separable from the component of the free annihilation of positrons in condensed media. The intrinsic lifetime of the triplet Ps (t-Ps) is 140 nsec, but the lifetime is considerably reduced in condensed media, since t-Ps can possibly be annihilated with electrons of the surrounding molecules *via* the following several processes:

(1) The e^+ in t-Ps can sample electrons of the surrounding molecules and be annihilated rapidly. This process is called "pick-off" annihilation. The lifetime is related to the size of the free volumes in which t-Ps can reside. The smaller the free volume in a medium, the shorter the lifetime of t-Ps.[4,5]

(2) If t-Ps can react with impurities in the medium and form a bound-state "positronium compound", the lifetime of t-Ps is reduced, because the positron is situated in a dense electron cloud and may be annihilated rapidly.[6]

(3) If the impurity molecule has an unpaired electron, t-Ps is converted into s-Ps upon collision with it and is annihilated rapidly. This process is called "triplet-to-singlet conversion" or "exchange collision." Most of the annihilation by these processes is followed by the emission of two photons of 0.51 MeV in opposite directions.

In most organic solids, the lifetime spectrum of positrons is composed of two or three components. The slow component of the lifetime spectrum may, in general, be attributed to the decay of t-Ps through the processes mentioned above.

The intensity of the slow component (I_2) is thought to be equal to the ratio of the quantity of positrons which form t-Ps and then annihilated with a slow pick-off rate compared to that of the total of positrons. If there is a certain quantity of impurities in the system which can trap positrons, I_2 is decreased.

All these features of positron annihilation in condensed media may make it possible to obtain some useful information about the structure of the solids and active species trapped in them. Some experimental results on positron annihilation in irradiated organic solids have been already reported.[7-9]

For several years, we have been studying the positron annihilation phenomena in various monomer solids which can be polymerized by irradiation.[10] The polymerizing solids are one of the most interesting systems in which to apply the annihilation method to study the reaction mechanism, because a remarkable structural change occurs during polymerization. The present paper will report the results of the lifetime measurements of solid acrylamide and related compounds as a function of the irradiation dose.

Experimental

Acrylamide (AA) and propionamide (PA) were used for the experiment. AA was purified by sublimation, and the PA was recrystallized from methanol. A position source, about 15μ Ci of ^{22}NaCl enveloped in a thin nickel foil (5μ thick), was placed in the center of glass ampoule. The powdered monomer was introduced into the ampoule, which was then sealed off under a vacuum (1×10^{-4} mmHg). The internal radius of the ampoule was 12 mm, and the packing density of AA powder was about 0.6 g/cm^3. Under such conditions, only a negligible portion of positrons annihilated in the wall of the glass ampoule.

The lifetime of the positron in the solid monomers was measured before and after γ-ray irradiation with a ^{60}Co

1) J. Green and S. Lee,"Positronium Chemistry" Academic Press (1964).
2) "Positron Annihilation," ed. by A. T. Stewart and L. O. Roelling, Academic Press, New York (1967).
3) V. I. Goldanskii, *Atomic Energy Revies*, **6**, 3(1968).
4) R. K. Wilson, P. O. Johnson, and R. Stump, *Phys. Rev.*, **129**, 2091 (1963).
5) W. Brandt, *ibid.*, **120**, 1289 (1960).
6) A. M. Cooper, G. J. Laidlaw, and B. G. Hogg, *J. Chem. Phys.*, **46**, 2441 (1967).
7) G. Chandra, V. G. Kulkarni, R. G. Lagu, and B. V. Thosar, *Physics Lett.*, **16**, 40 (1965).
8) G. Fabri and E. Germagnole, *IL NUOVO CIM.*, **23**, 572 (1962).
9) J. H. Green and S. J. Tao, *Brit. J. Appl. Phy.*, **16**, 981 (1965).
10) Y. Tabata, Y. Ito, and K. Oshima, Paper presented at Symp. on Organic Solid State Chem., BNL., Mar. 1968.

source at 30°C. The dose rate was 2×10^5 R/hr. Since it took about 2 days to obtain a time spectrum with good statistics of the coincidence-counting rate, the samples were preserved at −78°C during the lifetime measurements. Therefore the post-polymerization of the irradiated solid monomers does not proceed during the lifetime measurement.

The lifetime was measured using a Weisberg-type time-to-amplitude converter[11] which had been constructed in our laboratory. Two $1\phi\times1$ in. Naton 136 scintillators coupled to Phillips 56 AVP photomultipliers were used as the detectors of γ-rays. The output pulse from the time-to-amlitude converter was analyzed by a 200-channel pulse-height analyzer. The resolution of the lifetime measurement, $W_{1/2}$, the full width at half maximum of the time spectrum of prompt γ-rays from a ^{60}Co source, was 0.7 nsec.

A FORTRAN IV program which can decompose a time spectrum into several components was made, and each time spectrum was analyzed with it by means of an electronic computor HITAC 5020, being thus decomposed into two components. The value of I_2 was calculated by the method of Green and Bell.[12] All attempts to decompose the spectra into three components were unsuccessful.

On the other hand, the polymerization of AA was followed by measuring the conversion of monomers to polymers. The polymers were isolated by dissolving the monomers in methanol. The irradiation of monomers was carried out under conditions similar to those in the case of the lifetime measurement, except that a positron source was not introduced with monomers in the ampoule. Furthermoer, the volume change of monomers during γ-ray irradiation was measured by dilatometry. For the experiment, the powdered monomer was pressed to make a tablet. The packing density was 0.85 g/cm^3, and the tablet was put into a dilatometer capsule.

Results and Disscussion

The powdered monomers were irradiated with a dose rate of 2×10^5 R/hr at 30°C. The annihilation rate λ_2, and the intensity, I_2, of the slow component as a function of the irradiation does are shown in Fig. 1. The kinetic curve of polymerization is shown in Fig. 2, together with the results of dilatometry. The kinetic curve is a typical S-shaped one composed of induction (0—1 Mrad), proparation (1—2 Mrad), and saturation (3 Mrad) periods.

The volume of the monomer decreases during polymerization, since the density is higher in the amorphous-polymer phase than in the crystalline monomer. The value of I_2 in the monomer crystal ($I_2=20.8\pm3.2\%$) is largest among several monomers examined by us.[10] A crystallographic study of the AA crystal[13] had shown that molecules form a layer through hydrogen bonding, and that the distance between adjacent layers is large. Therefore, we can expect there to be large free volumes between these layers. It would be expected that t-Ps can diffuse or jump into the large free volume in the AA crystals and be annihilated with a slow pick-off rate. On the other hand, there are several cases where t-Ps cannot encounter large free volumes in densely-packed crystals. In such cases, slow components can not be

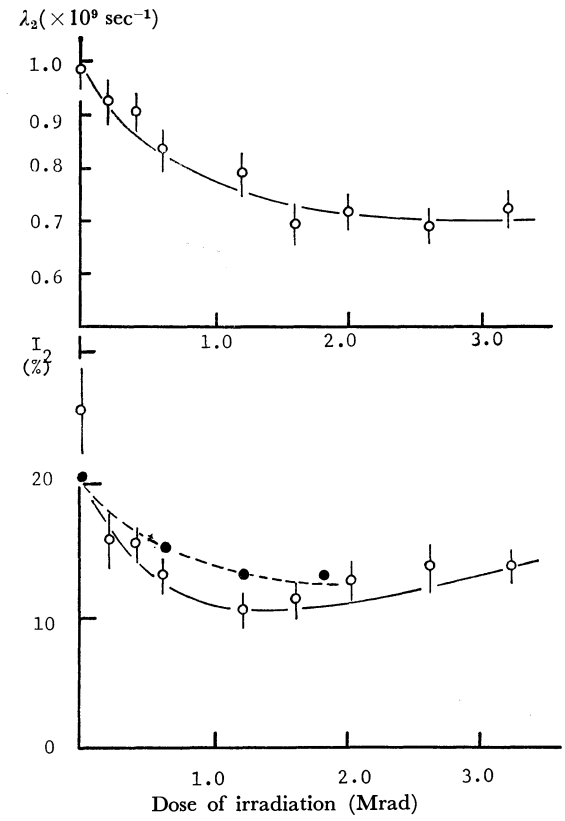

Fig. 1. λ_2 and I_2 in irradiated solid acrylamide as a function of irradiation dose. Irradiation was carried out at 30°C (-○-) and −78°C (--●--) with a dose rate of 2×10^5 R/hr. The bars at each point indicate the statistical average deviation of the counting rate.

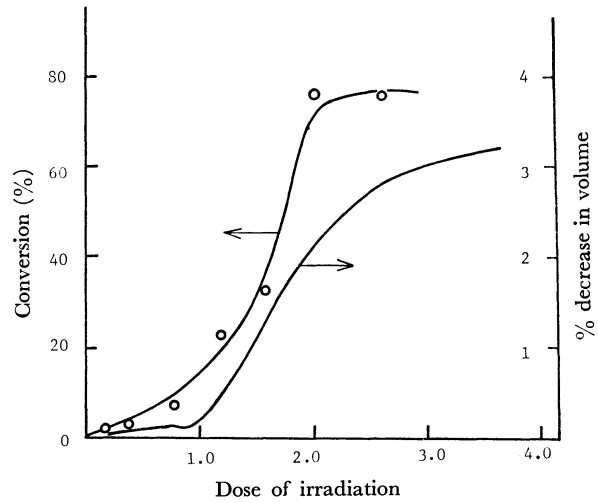

Fig. 2. Kinetic curve of polymerization in powdered AA(curve a) and result of dilatometry of AA tablet during polymerization. Dose rate: 2×10^5 R/hr. Temperature of irradiation: 30°C.

observed due to the rapid pick-off annihilation. Examples of the latter case are the monomer crystals of dimethylitaconate,[10] crystalline polyethylene,[14] and crystalline polytetrafluoroethylene.[15] In these solids, the

11) H. Weisberg, *Nucl. Instr. Method.*, **32**, 133 (1965).
12) R. E. Green and R. E. Bell, *Can. J. Phys.*, **35**, 398 (1957).
13) I. Nitta, I. Taguchi, and Y. Chatani, *Sen'iken Nenpo (Annual Report of Fiber Research)*, **12** 89 (1959).
14) S. J. Tao and J. H. Green, *Proc. Phys. Soc.*, **85**, 463 (1965).
15) W. Brandt and I. Spirn, *Phys. Rev.*, **142**, 231 (1966).

value of I_2 decreases with an increase in the crystallinity.

It must be noted that decreases in λ_2 and I_2 are observed in the induction period of polymerization. In the induction period, the conversion is still low, and the decrease in the overall volume of the solid is small, as is shown in Fig. 2. The decrease in λ_2 must be related mainly to the formation of a larger free volume, because any other annihilation processes of t-Ps, such as Ps compound formation or exchange collision, may only lead to an increase in λ_2.

It is known, as a result of the crystallographic study of the monomer, that the monomer molecules are closely aggregated in layers parallel to *bc* plane, and that there are 10 other double bonds within a distance of 5 Å from a double bond.[13] Therefore, the polymerization can be expected to proceed within a layer at the initial stage of polymerization, and the polymer phase produced can be expected to be separated from the monomer phase. Vacancies should then be produced around the polymer chains, and they make the free volumes larger by combining with original free volumes in the crystals. T-Ps can stay stable in such large free volumes and be annihilated at a lower pick-off rate. This may be the reason for the decrease in λ_2 during the induction period.

Figure 3 shows the results of the lifetime measurements of AA and PA irradiated at −78°C. Since PA is a saturated analogue of AA, it does not polymerize upon irradiation. Therefore, it is quite reasonable that λ_2 does not decrease on irradiation in the case of PA. On the other hand, λ_2 also decreases in AA irradiated at

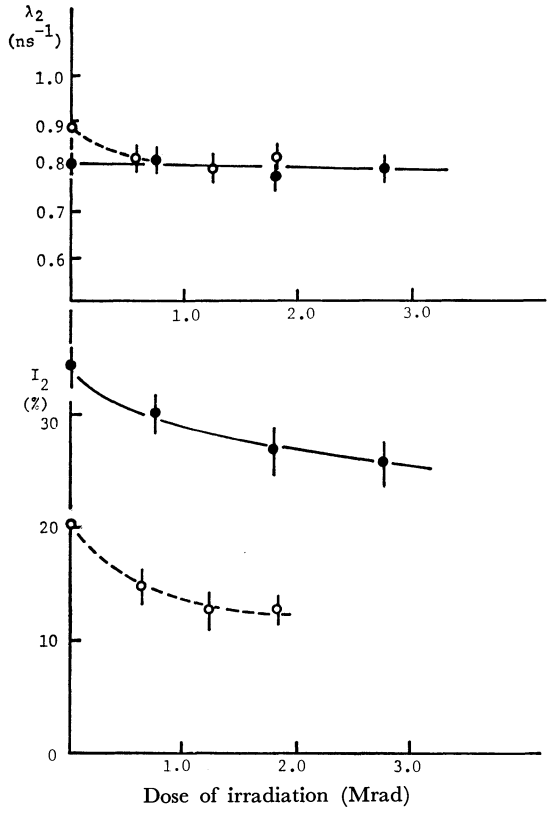

Fig. 3. λ_2 and I_2 in irradiated AA (--●--) and PA (-○-) as a function of irradiation dose. Irradiation was carried out at −78°C with a dose rate 2×10^5 R/hr.

−78°C. No polymer was detectable gravimetrically after irradiation at that temperature. However, there is an evidence that the oligomer is produced at low temperatures. For example, the ESR spectrum of AA irradiated at −196°C indicates the presence of the initiating radical species, but it changes to the spectrum of the propagating one when the temperature is raised above −94°C.[16] Therefore, the oligomer must be formed in AA irradiated at −78°C; in this case, larger free volumes are formed near the oligomer chains by a mechanism similar to that already explained.

It is interesting that λ_2 decreases to a small extent in the propagation period, in which the most remarkable change in the structure of the solid monomers must be taking place. This suggests that no free volume larger than that formed in the induction period is produced in the propagation period. As is shown in Fig. 1, the value of I_2 decreases in the induction period of the polymerization of AA. Since the decrease in I_2 was also observed in the irradiated PA (Fig. 3), the decrease in I_2 may not be directly correlated to the polymerization process. One possible explanation is that active species or impurities produced by γ-ray irradiation can capture positrons to form positron compound. Anothar explanation is that the quantity of free volumes which are responsible for the long-lifetime component in the AA solid monomer decreases gradually due to the polymerization in the crystal. Since I_2 decreases faster in a polymerizing AA solid at 30°C than in AA or PA irradiated at −78°C (Figs. 1 and 3), the decrease in the quantity of free volumes, together with the positron-compound formation, should occur in the polymerizing AA solid.

The value of I_2 is slightly increased in the later stage of polymerization (Fig. 1). This might be due to the effect of irradiation on the polymer produced. In order to determine whether or not this assumption is good, the lifetime of positrons in irradiated poly-AA was measured. Poly-AA was obtained by the radiation polymerization of the solid monomer. The procedure of sample preparation was the same as has already been described. Since the lifetime spectrum in poly-AA was complicated, we have not succeeded in decomposing it into several components. However, the lifetime spectrum did not practically change up to the irradiation dose of 2 Mrad, and at 3 Mrad the slow component apparently decreased. This result contradicts with the assumption made above, and the small increase in I_2 in the later stage of polymerization can not be attributed to the secondary effect of irradiation on the polymer produced.

Another possible explanation is that some active species which can capture positrons have disappeared due to annealing or recombination in the later stage of polymerization. This assumption seems to be supported by the following experimental results. The AA solid monomer, pre-irradiated to 2 Mrad at −78°C, was thermally treated, and the lifetime measurements were made. The variations in λ_2 and I_2 are indicated in Table 1, together with the conversion of post-polymerization. I_2 decreases with the irradiation dose at −78°C,

16) I. Nitta, S. Onishi, and T. Tanei, Paper presented at the 11th Annual Meeting of the Polymer Sci. (1962).

Table 1. Post-polymerization of acrylamide and lifetime measurement during the polymerization

	$\lambda_2 \times 10^9$ sec^{-1}	I_2 (%)	Conversion (%)
Before irradiation	0.883±.0033	20.8±3.2	—
After irradiation at −78°C(2Mrad)	0.861±0.039	13.1±1.9	trace
Kept for 2.5 hr at room temperature	0.796±0.047	14.9±2.3	4.2
Kept for 2.0 hr at 50°C	0.766±0.032	14.9±1.4	8.5
Further irradiation at−78°C(0.5 Mrad)	0.764±0.034	13.7±1.3	—

in agreement with the results presented in Fig. 3. However, it is slightly increased as post-polymerization proceeds. Therefore, a certain amount of active species which can capture positrons may have disappeared during the thermal treatment of the solid.

Conclusion

The lifetime spectrum has shown a remarkable change in the induction period of polymerization, and the decrease in λ_2 has been interpreted in terms of the formation of a larger free volume during polymerization. Such a free volume is also formed when oligomers are produced by the irradiation at low temperatures; the lifetime spectra have shown evidence of this.

I_2 also decreases in the induction period of polymerization, but this decrease may not be directly related to the polymerization process. Two possible explanations, that is, the accumulation of active species which capture positrons and the decrease in the number of free volumes, have been suggested. The former process may occur at least in the case of solid PA.

From these experiments, it has been clearly demonstrated that important information about the induction period can be obtained by the lifetime measurement of the positrons in solid monomers.[10] We expect that a detailed study of this kind may offer useful information concerning the mechanism of solid-state polymerization.

We should like to acknowledge the continuing encouragement of Prof. K. Oshima. We are also indebted to Dr. K. Hasegawa and Mr. K. Okawa for the instruction in constructing the time-analyzing equipment.

BULLETIN OF THE CHEMICAL SOCIETY OF JAPAN, VOL. 44, 1767—1771 (1971)

Radiotracer Studies on Adsorption of Surface Active Substance at Aqueous Surface. III. The Effects of Salt on the Adsorption of Sodium Dodecylsulfate

Kazuo Tajima

Department of Chemistry, Faculty of Science, Tokyo Metropolitan University, Setagaya, Tokyo

(Received January 25, 1971)

The adsorbed amounts were measured on the surface of aqueous solutions containing tritiated sodium dodecylsulfate (TSDS) and varying amounts of NaCl by the direct radiotracer method. The surface tensions were also measured for the same solutions by the drop-volume method. The Gibbs adsorption isotherm, derived without assuming the adsorption of the chloride ion, was applied, and the amounts of adsorption were calculated for both dodecylsulfate and chloride ions. The observed amounts of dodecylsulfate adsorption were confirmed to be in good agreement with those calculated, and the calculated amounts of chloride adsorption turned out to be nearly zero or slightly negative, which is usually theoretically assumed because of the ionic repulsion due to the adsorbed dodecylsulfate. Further, the adsorption of the dodecylsulfate ion attained a constant and saturate value beyond a certain concentration (SAC) below the critical micelle concentration (CMC). The logarithms of SAC were found to vary linearly with the logarithms of CMC for the range of salt concentration studied. The value of SAC being in a close relation with the surface phenomena is considered to be another measure of the surface activity of surfactants.

There have been many studies to check the validity of the Gibbs adsorption isotherm.[1-5] By a radiotracer method, we have also experimentally confirmed that the adsorption of the ionic surfactants on an aqueous surface from their solution takes place in accordance with the Gibbs equation both in the absence of and in the presence of in an excess amount of an inorganic salt having a cation in common.[6,7] However, there has no paper dealing with the direct measurement of adsorption at the air-solution interface of the ionic surfactant as a function of the concentration of the coexisting salt. Matijevic and Pethica,[8] though, derived a Gibbs ad-

1) J. W. McBain and L. A. Wood, *Proc. Roy. Soc.* (London), **A174**, **286** (1940).
2) A. P. Brady, *J. Phys. Chem.*, **53**, 56 (1949).
3) J. T. Davies, *Trans. Faraday Soc.*, **48**, 1052 (1952).
4) B. A. Pethica, *ibid.*, **50**, 413 (1954).
5) R. Matuura, H. Kimizuka, S. Miyamoto, and R. Shimozawa, This Bulletin, **31**, 532 (1958).
6) K. Tajima, M. Muramatsu, and T. Sasaki, *ibid.*, **43**, 1991 (1970).
7) K. Tajima, *ibid.*, **43**, 3063 (1970).
8) E. Matijevic and B. A. Pethica, *Trans. Faraday Soc.*, **54**, 1382 (1958).

sorption isotherm which can be applied to the solution of sodium dodecylsulfate (SDS) in the presence of sodium chloride, and calculated the adsorbed amount of the dodecylsulfate ion from the surface-tension concentration relation of the solution. In their derivation of the adsorption equation, they assumed that the excess of the chloride ion at the surface is negligible in amount. This assumption, although acceptable from the theoretical viewpoint,[9] has not been confirmed experimentally.

In the present paper, the Gibbs adsorption isotherm is applied from a more general viewpoint, with no preliminary assumption of the adsorbed amount of solute ions in the solution and with activity in place of concentration. The validity of the adsorption equation thus derived is confirmed by the direct measurement of the amount of adsorption by a radio-tracer method.

Theoretical

The Gibbs adsorption isotherm[10] is written, in a general form, as:

$$-\mathrm{d}\gamma = RT\sum\Gamma_i \,\mathrm{d}\ln a_i \tag{1}$$

where γ represents the surface tension, and Γ_i and a_i, the surface excess and the activity of the ith ionic species in solution respectively. Assuming that the bulk solution is electrically neutral as a whole and that surface hydrolysis is absent (bulk hydrolysis was confirmed to be absent, as judged from the pH being unaffected by the dissolution of SDS), Eq. (1) is rewritten for the SDS solution containing sodium chloride as:

$$-\mathrm{d}\gamma = RT\Gamma_{\mathrm{Na}^+}\mathrm{d}\ln a_{\mathrm{Na}^+} + RT\Gamma_{\mathrm{D}^-}\mathrm{d}\ln a_{\mathrm{D}^-} + RT\Gamma_{\mathrm{Cl}^-}\mathrm{d}\ln a_{\mathrm{Cl}^-} \tag{2}$$

where the three subscripts Na^+, D^-, and Cl^- denote sodium, dodecylsulfate, and chloride ions respectively. Using the activity coefficient and the concentration instead of the activity, and differentiating Eq. (2) with respect to C_{D^-}, while keeping the concentration of NaCl constant (therefore, $\mathrm{d}\,C_{\mathrm{Na}^+}=\mathrm{d}\,C_{\mathrm{D}^-}$), we obtain the following equation:

$$-\left(\frac{\mathrm{d}\gamma}{RT\,\mathrm{d}\ln C_{\mathrm{D}^-}}\right)_{\mathrm{NaCl}} = \Gamma_{\mathrm{Na}^+}\frac{C_{\mathrm{D}^-}}{C_{\mathrm{Na}^+}} + \Gamma_{\mathrm{D}^-} + 2\Gamma_{\mathrm{Cl}^-}\frac{\mathrm{d}\ln f_{\pm}^{\mathrm{NaCl}}}{\mathrm{d}\ln C_{\mathrm{D}^-}} + 2\Gamma_{\mathrm{D}^-}\frac{\mathrm{d}\ln f_{\pm}^{\mathrm{NaD}}}{\mathrm{d}\ln C_{\mathrm{D}^-}} \tag{3}$$

where C's denote the concentration of the ions specified and $f_{\pm}^{\mathrm{NaCl}}$ and $f_{\pm}^{\mathrm{NaD}}$, the mean activity coefficients of NaCl and SDS respectively. Similarly, differentiating Eq. (2) with respect to C_{Cl^-} while keeping the concentration of NaD constant, we obtain:

$$-\left(\frac{\mathrm{d}\gamma}{RT\,\mathrm{d}\ln C_{\mathrm{Cl}^-}}\right)_{\mathrm{NaD}} = \Gamma_{\mathrm{Na}^+}\frac{C_{\mathrm{Cl}^+}}{C_{\mathrm{Na}^+}} + 2\Gamma_{\mathrm{D}^+}\frac{\mathrm{d}\ln f_{\pm}^{\mathrm{NaCl}}}{\mathrm{d}\ln C_{\mathrm{Cl}^-}} + 2\Gamma_{\mathrm{Cl}^-}\frac{\mathrm{d}\ln f_{\pm}^{\mathrm{NaD}}}{\mathrm{d}\ln C_{\mathrm{Cl}^-}} \tag{4}$$

Putting

$$\frac{\mathrm{d}\ln f_{\pm}^{\mathrm{NaCl}}}{\mathrm{d}\ln C_{\mathrm{D}^-}} = \frac{\mathrm{d}\ln f_{\pm}^{\mathrm{NaD}}}{\mathrm{d}\ln C_{\mathrm{D}^-}} \equiv \alpha$$

$$\frac{\mathrm{d}\ln f_{\pm}^{\mathrm{NaCl}}}{\mathrm{d}\ln C_{\mathrm{Cl}^-}} = \frac{\mathrm{d}\ln f_{\pm}^{\mathrm{NaD}}}{\mathrm{d}\ln C_{\mathrm{Cl}^-}} \equiv \beta$$

and using the notations:

$$\frac{C_{\mathrm{D}^-}}{C_{\mathrm{Na}^+}} = a, \qquad \frac{C_{\mathrm{Cl}^-}}{C_{\mathrm{Na}^+}} = b \tag{5}$$

$$\left.\begin{aligned} -\left(\frac{\mathrm{d}\gamma}{RT\,\mathrm{d}\ln C_{\mathrm{D}^-}}\right)_{\mathrm{NaCl}} &= I_{\mathrm{Cl}^-} \\ -\left(\frac{\mathrm{d}\gamma}{RT\,\mathrm{d}\ln C_{\mathrm{Cl}^-}}\right)_{\mathrm{NaD}} &= I_{\mathrm{D}^-} \end{aligned}\right\} \tag{6}$$

Eqs. (3) and (4) are then rewritten as:

$$I_{\mathrm{Cl}^-} = \Gamma_{\mathrm{Cl}^-}(a+2\alpha) + \Gamma_{\mathrm{D}^-}(1+a+2\alpha) \tag{7}$$

$$I_{\mathrm{D}^-} = \Gamma_{\mathrm{D}^-}(b+2\beta) + \Gamma_{\mathrm{Cl}^-}(1+b+2\beta) \tag{8}$$

From the condition of electric neutrality at the surface of the solution, we further obtain:

$$\Gamma_{\mathrm{Na}^+} = \Gamma_{\mathrm{D}^-} + \Gamma_{\mathrm{Cl}^-} \tag{9}$$

by combining Eqs. (7), (8), and (9), we have:

$$\Gamma_{\mathrm{Na}^+} = \frac{1}{2(1+\alpha+\beta)}(I_{\mathrm{D}^-}+I_{\mathrm{Cl}^-}) \tag{10}$$

$$\Gamma_{\mathrm{D}^-} = \frac{1}{2(1+\alpha+\beta)}[I_{\mathrm{Cl}^-}(1+b+2\beta) - I_{\mathrm{D}^-}(a+2\alpha)] \tag{11}$$

$$\Gamma_{\mathrm{Cl}^-} = \frac{1}{2(1+\alpha+\beta)}[I_{\mathrm{D}^-}(1+a+2\alpha) - I_{\mathrm{Cl}^-}(b+2\beta)] \tag{12}$$

Estimating the activity coefficient of NaCl and SDS by using the limiting law of the Debye-Hückel theory, as in the previous paper,[7] the values of α and β are given as:

$$2\alpha = -aA\sqrt{C_{\mathrm{Na}^+}} \tag{13}$$

$$2\beta = -bA\sqrt{C_{\mathrm{Na}^+}} \tag{14}$$

where A is the constant in the Debye-Hückel limiting equation, which takes the value of 1.18 at 25°C. By substituting Eqs. (13) and (14) into Eqs. (10), (11), and (12), we obtain:

$$\Gamma_{\mathrm{Na}^+} = \frac{1}{1+i}(I_{\mathrm{Cl}^-}+I_{\mathrm{D}^-}) \tag{15}$$

$$\Gamma_{\mathrm{D}^-} = \frac{1}{1+i}[I_{\mathrm{Cl}^-}(1+bi) - I_{\mathrm{D}^-}ai] \tag{16}$$

$$\Gamma_{\mathrm{Cl}^-} = \frac{1}{1+i}[I_{\mathrm{D}^-}(1+ai) - I_{\mathrm{Cl}^-}bi] \tag{17}$$

where:

$$i = 1 - A\sqrt{C_{\mathrm{Na}^+}} \tag{18}$$

expresses the activity coefficient of the uni-univalent ion at a sufficiently dilute solution and is equal to unity when the mean activity coefficient is unity. It is worth noting that Γ_{D^-} and Γ_{Cl^-} can be separately calculated by Eqs. (16) and (17), if i is calculated according to Eq. (18), and that I_{Cl^-}, I_{D^-}, a and b are calculated from the γ *vs.* C_{NaCl} or γ *vs.* C_{NaD} curves (Eq. (5)) and from Eq. (6). The validity of Eq. (16) can be checked by comparing the value of Γ_{D^-} thus calculated with that measured directly by a radiotracer method for the solutions containing both SDS and NaCl. Further, by putting $\Gamma_{\mathrm{Cl}^-}=0$ and $i=1$, Eqs. (16) and (17) give the same

9) E. J. W. Verwey and J. Th. G. Overbeek., "Theory of the Stability of Lyophobic Colloids," Elsevier Publishing Co., Amsterdam (1948).

10) E. A. Guggenheim, "Thermodynamics, " North Holland Publishing Co., Amsterdam (1949).

equation as Matijevic and Pethica's. Here, we are in a position to check experimentally whether or not the theoretical assumption of $\Gamma_{Cl^-}=0$ in their derivation of the equation is valid.

Experimental

The tritiated sodium dodecylsulfate (TSDS) and sodium chloride were the same substances as those used in a previous paper.[7] The surface tension of solutions containing NaCl and SDS was measured by the drop-volume method, and Harkins and Brown's correction[11] was applied. The value of Γ_{D^-} was also measured directly by a radiotracer method using a sheet scintilation counter. The details of the measurements were the same as those described in preceding paper.[6,7] The pH of the bulk solutions was controled at 6±0.2 (25.0°C).

Results and Discussion

Adsorption Isotherm. Figure 1 shows the adsorption isotherms of SDS measured by the radiotracer method at the surface of an aqueous solution containing various concentrations of sodium chloride. Figures 2 and 3 show the curves of γ *vs.* log C_{D^-}, with C_{Cl^-} kept constant for the former and of γ *vs.* log C_{Cl^-}, with C_{D^-} kept constant for the latter. In Figs. 4a, b, and c, the observed values of Γ_{D^-} and those calculated by applying Eqs. (16) and (17) to the data of Figs. 2 and 3 are shown as circles and solid lines respectively. The broken lines in these figures show the values of Γ_{D^-}, which are calculated by assuming $i=1$ in Eq. (16). It may be seen in these figures that the values of Γ calculated from Eqs. (16) and (17) (solid lines) are, as a whole in good agreement, with the observed values except for the adsorption at low concentrations of SDS and NaCl. The broken lines ($i=1$) gradually deviate from both solid lines and observed Γ_{D^-} values in the region of a large concentration of SDS. As for the deviation of solid lines from the observed values of adsorption in a dilute solution of SDS, a similar tendency was also observed in the case of the salt-free SDS solution, where the surface tension used for the calculation was also measured by a drop-volume method. It should be noted that different surface tension values are obtained for the salt-free SDS solution when it is measured by the drop-volume and Wilhelmy plate methods. Therefore, in the case of a low NaCl concentration, such as in Fig. 4a, we should use the surface tension data, as measured by the Wilhelmy plate method to be described below. Unfortunately, the γ *vs.* C_{D^-} relation measured by the Wilhelmy plate method is lacking for the SDS solution with a 1×10^{-3} mol/l NaCl concentration. It can, however, be obtained graphi-

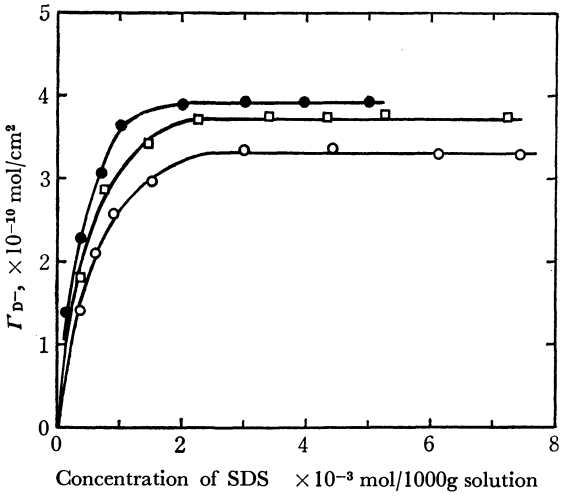

Fig. 1. Adsorption isotherms of SDS solutions in the presence of NaCl at 25°C.
—○—: 1.0×10^{-3} M NaCl
—□—: 5.0×10^{-3} M NaCl
—●—: 10.0×10^{-3} M NaCl

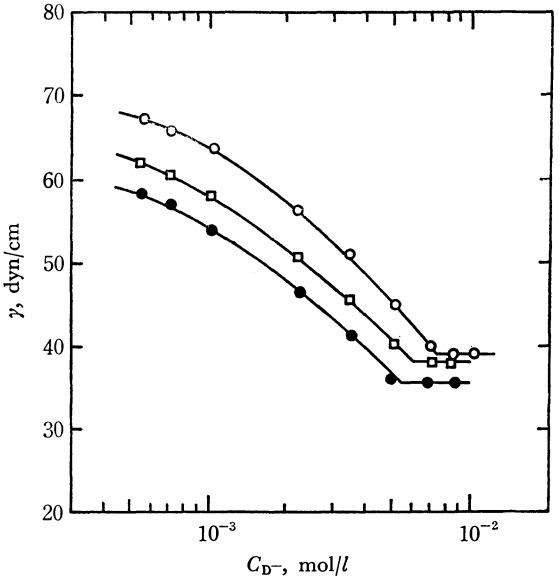

Fig. 2. Surface tensions of SDS solutions in the presence of NaCl at 25°C.
—○—: 1.0×10^{-3} M NaCl
—□—: 5.0×10^{-3} M NaCl
—●—: 10.0×10^{-3} M NaCl

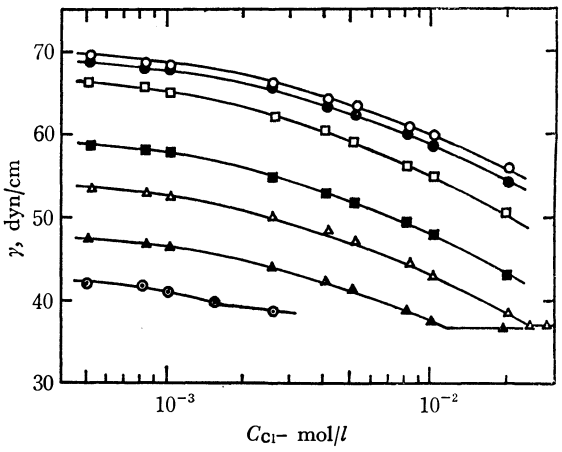

Fig. 3. Surface tensions of NaCl solutions in the presence of SDS at 25°C.
—○—: 0.545×10^{-3} M SDS
—●—: 0.698×10^{-3} M SDS
—□—: 1.01×10^{-3} M SDS
—■—: 2.21×10^{-3} M SDS
—△—: 3.48×10^{-3} M SDS
—▲—: 5.01×10^{-3} M SDS
—⊙—: 6.65×10^{-3} M SDS

11) W. D. Harkins and F. E. Brown, *J. Amer. Chem. Soc.*, **41**, 4499 (1919).

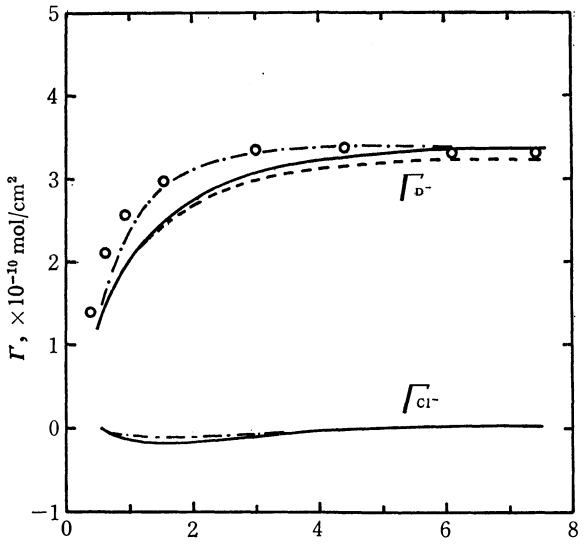

Fig. 4 a: 1.0×10^{-3} M NaCl

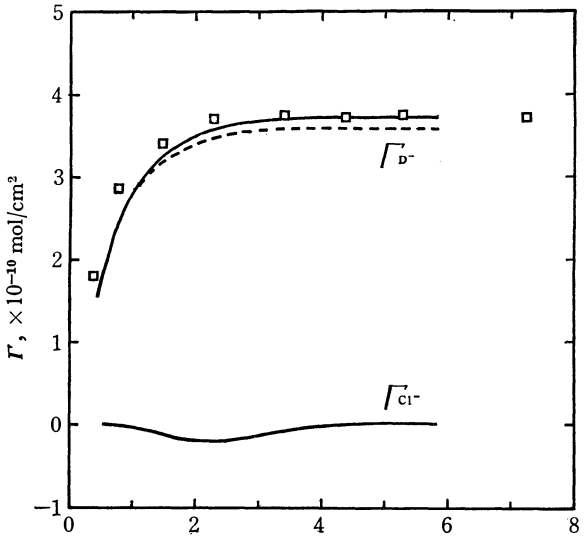

Fig. 4 b: 5.0×10^{-3} M NaCl

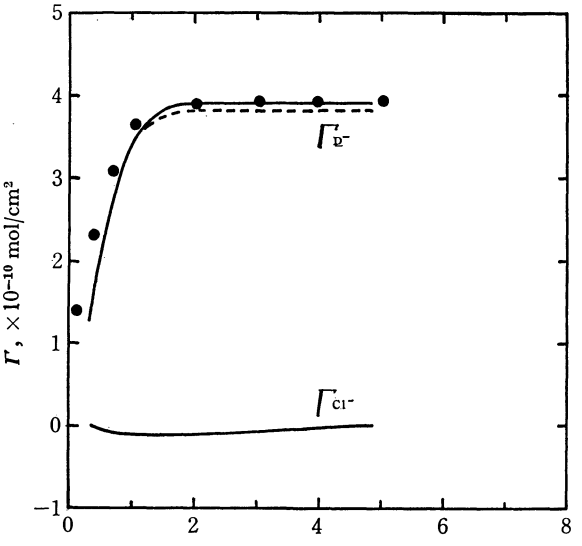

Fig. 4 c: 10.0×10^{-3} M NaCl

Fig. 4. Adsorption isotherms of Γ_{D^-} and Γ_{Cl^-} at the surface of aqueous solutions containing SDS and NaCl.
——: calculated from Eqs. (16) and (17)
— — —: calculated from Eq. (16) putting $i=1$
-·-·-: calculated by interpolation (see text)
○, □, ●: observed values

cally by an interpolation, of the γ *vs.* C_{D^-} data for the SDS solution measured by the Wilhelmy plate method, reported in a previous paper.[6] From the γ *vs.* log-C_{D^-} relation thus obtained and from the γ *vs.* logC_{Cl^-} relation similarly obtained, Γ_{D^-} and Γ_{Cl^-} can be calculated by applying Eqs. (16) and (17). The results are shown by a chain line in Fig. 4a. It is evident that the chain line is in better agreement with observed values than a solid line would be. Thus, it is confirmed that the Wilhelmy plate method always offers correct values of the surface tension for the calculation of the amount of adsorption, while the drop-volume method gives incorrect values, the error becoming smaller at ionic strengths larger than about 10×10^{-3} mol/*l*. This may be due to the rapid surface aging at a higher ionic concentration, which makes it possible to obtain an almost equilibrium value of the surface tension at a relatively short time of measurement.

Now, it should be noted that, although the non-adsorption of the chloride ion at an aqueous surface can be theoretically anticipated for aqueous solution containing SDS and NaCl, the experimental evidence has been lacking. The results of the present studies empirically confirm the almost zero value or a slightly negative value of Γ_{Cl^-} as is shown in Figs. 4a, b, and c, although the values of Γ_{Cl^-} in the solution with a lower SDS concentration involve some uncertainties similar to those of Γ_{Cl^-} in dilute solutions. It may be seen that the values of Γ_{D^-} (broken lines) calculated from Eq. (16), assuming $i=1$, agree closely within the limits of experimental error with those obtained by the Matijevic and Pethica equation, which assumes $\Gamma_{Cl^-}=0$ ($i=1$). This agreement confirms the $\Gamma_{Cl^-}=0$ assumption to be valid as far as the calculation of Γ_{D^-} according to Matijevic and Pethica equation is concerned. However, as for the calculation of Γ_{Cl^-}, small but distinct negative values are indicated, and Eqs. (16) and (17) are better applied to the calculation of the adsorption from the solution of two mixed surfactants containing a common cation, although the additional measurements shown in Fig. 3 are required for the calculation of Γ_{Cl^-} and Γ_{D^-}. In this connection, it may be inferred that Dixon *et al.*[12] made a mistake in calculating the amounts of the adsorption of Aerosol OT and Aerosol OTN at the surface of their mixed solution. They treated the two solutes as independent of each other and used simply:

$$\Gamma_{OT} = I_{OTN}, \quad \Gamma_{OTN} = I_{OT} \tag{19}$$

where Γ_{OTN}, I_{OTN}, *etc.* denote the corresponding quantities shown in Eq. (6), with D and Cl replaced by OT and OTN respectively. However, since the system

12) J. K. Dixon, C. M. Judson, and D. J. Salley, "Monomolecular Layers," H. Sobotka, Ed., p. 81, Am. Assoc, Advsn. Sci., Washington, D. C. (1954).

Table 1. Γ_s and A values for saturated adsorption on aqueous NaCl solution (25°C)

C_{NaCl} $\times 10^3$ M	CMC $\times 10^3$M	SAC $\times 10^3$M	Γ_s $\times 10^{10}$mol/m^2	A A^2/molec.
0[a]	8.12	3.1	3.19	52.0
1.0	7.50	3.0	3.31	50.2
5.0	5.80	2.6	3.75	44.3
10.0	5.10	2.0	3.90	42.6
115.0[b]	1.62	0.50	4.33	38.4

a) Ref. 6
b) Ref. 7

contains the Na^+ ion in common, we must use equations with the form of Eqs. (16) and (17) instead of Eq. (19).

Saturated Adsorption. The values of the saturated adsorption, Γ_S, of the dodecylsulfate ion in various concentrations of coexisting sodium chloride, together with the corresponding value of the molecular area, are shown in Table 1. A decrease in the molecular area, A, due to the increase in the concentration of sodium chloride is seen; it can be qualitatively interpreted as the effect of added salt on diffuse double layers of the adsorbed ion. The value of SAC, which is the bulk concentration beyond which Γ_S shows a constant and saturate value, is listed in the third column of Table 1. This SAC, which is smaller than the CMC (critical micelle concentration), was determined more accurately by the isotherm (Fig. 1) obtained by the radiotracer method. The correlation between SAC and CMC gives a good linearity, as is shown in Fig. 5. This linearity is expressed as;

$$\log \text{SAC} = 1.16 \log \text{CMC} - 0.04 \qquad (20)$$

The value of SAC is confirmed to be about 30—40% of the CMC for all the concentrations of NaCl studied in the present experiments. Van Voorst Vader[13] has reported that the adsorption amount of the ionized surfactant in the aqueous solution is approximately constant within the concentration range of 20—30% of the CMC when the inorganic salt is present. Further, even in another report[14] which insists on a continuous increase in the surfactant adsorption up to the CMC in the presence of salt, the surface tension *vs.* log concentration relation for the surfactant solution does not deviate appreciably from the linear relationship in the range of 30% of the CMC. Accordingly, a constant adsorption is more likely than a gradual increase in the amount of adsorption up to the CMC.

It is considered that, if the adsorbed phase can be assumed as a two-dimensional solution, the state of

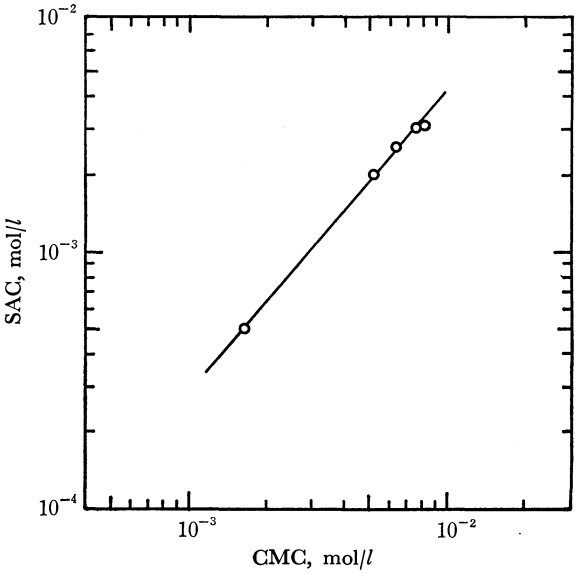

Fig. 5. Relation between SAC and CMC.

saturated adsorption at the surface may be considered as the formation of a two-dimensional micelle or a surface micelle; therefore, SAC corresponds to the concentration of the surface micellization, as in a usual micellization in the bulk solution. This similarity leads to the consideration that the surface phenomena of the surfactant solution at the air-solution interface, *e.g.*, foaming, surface viscosity, surface tension lowering and so on, may be expected to show some characteristic behavior in the vicinity of the SAC. For instance, Miles and Ross[15] and Dreger *et al.*,[16] applying the "pour test" to many sodium alkylsulfates in a foam experiment, found that the foam height first increased with the concentration and then reached a constant value at a concentration which was about 40—50% lower than the CMC. Also, Burcik[17] found the same tendency for the original foam volume of a sodium laurate solution, produced by the pouring method. Thus, the values of SAC might be used as another measure of the surface activity of the surfactant solution, which in some cases directly parallels the surface phenomena at the air-solution interface.

The author wishes to express his hearty thanks to Professor T. Sasaki for this encouragement and guidance throughout the experiments. He is grateful also to Professor M. Muramatsu for his helpful discussions and advice.

13) F. van Voorst Vader, *Trans. Faraday Soc.*, **56**, 1067 (1960).
14) H. Lange, *Kolloid-Z.*, **153**, 155 (1957).
15) G. D. Miles and J. Ross, *J. Phys. Chem.*, **48**, 280 (1944).
16) E. E. Dreger, C. L. Keim, G. D. Miles, L. Shedlovsky, and J. Ross, *Ind. Eng. Chem.*, **36**, 610 (1944).
17) J. E. Burcik, *J. Colloid Sci.*, **5**, 421 (1950).

Effects of Pressure on the Chemical Properties of Solid Surfaces. V. The Surface Acidity of the Compressed Aluminum Sulfate

Takeshi KAWAKAMI, Akihiro KONNO, and Yoshisada OGINO

Department of Chemical Engineering, Faculty of Engineering, Tohoku University, Aramaki Aoba, Sendai

(Received January 29, 1971)

In order to clarify the mechanism of the acidity change due to compression, aluminum sulfate was compressed under various pressures ranging from 0 to 4200 kg/cm² and at a temperature of 20, 65, or 80°C, and the surface acidity and the structure of these samples were measured. It was found that the acidity change due to compression was proportionate to the protonic acid. Lewis acid was made to appear only by heating the sample at temperatures higher than 90°C. Further, for the purpose of increasing the surface acidity, the compression of the sample at lower temperatures was found to be more effective than the compression at higher temperatures. In addition to the spectroscopic data, the results of DTA and TGA experiments supported the idea that the observed acidity change resulted from the distortion of the structural unit of aluminum sulfate.

In the previous works[1-3] which treated the effects of pressure on the chemical properties of solid surfaces, the present authors have found that the surface acidities of various metal sulfates vary on compression. In these works the acidity change was discussed in terms of the change in the crystal structure as well as in terms of the change in the water content in the sample. However, the discussion was only qualitative, and the details of the mechanism of the acidity change due to compression could not be clarified. Therfore, the present authors have undertaken a new series of experimental works designed to clarify the mechanism of the acidity change.

In the present work, aluminum sulfate octadecahydrate was used as a sample. The surface acidity was measured by a conventinal titration method. The structural changes due to compression were investigated by means of infrared spectroscopy, far-infrared spectroscopy, Raman spectroscopy, differential thermal analysis, and so on. In this paper, the details of the experimental results will be presented and the relation between the acidity change and the structural change will be discussed.

Experimental

Material. Commercial aluminum sulfate octadecahydrate was used as the raw material of sample.

Preparation of the Sample. The raw sulfate was compressed by the procedures described in the previous papers.[1-3] The compression was carried out under various pressures, ranging from 0 to 4200 kg/cm², and at a desired temperature of either 20, 65, 80°C. In every case, pressure was applied over a 10-min period. The resulting cyclindrical pellet, 6 mm in diameter and 2 mm in height, was pulverized in a mortar. The pulverized material was subjected to drying in vacuum for 45 min at a temperature of 18°C. The resulting dry material served as a sample for the desired measurements. In order to minimize the effects from the change in ambient conditions, compressions, pulverizings, dryings and weighings were carried out in an air-conditioned room.

For the sake of convenience, the samples which were subjected to the compression at 20, 65, and 80°C were defined as P_{20}, P_{65}, and P_{80} respectively. Then, for instance, $P_{65,4200}$ means the sample which was compressed under a pressure of 4200 kg/cm² and at a temperature of 65°C.

Surface Acidity. The surface acidity was determined by Benesi's method[4] with the following four indicators: dicinnamalacetone ($pK_a = -3.0$), benzeneazodiphenylamine ($pK_a = 1.5$), *p*-diphenylaminoazobenzene ($pK_a = 3.3$), and phenylazonaphthylamine ($pK_a = 4.0$). The acidity measurements were also carried out in the air-conditioned room.

Qualitative Tests for Lewis Acid. In order to identify Lewis acid on the sample powder, the color of the sample surface was observed by adding phenolphthalein or trithylchloride as an indicator. That is, a given amount of the sample powder was transferred to a 50-m*l* conical flask containing 10 m*l* of purified benzene. Then, several drops of a 0.1 % benzene solution of an indicator were added and color of the sample surface was observed.

Surface Areas. The specific surface area of the sample was evaluated by applying the BET theory to the adsorption data of nitrogen at −195°C.

Water Content. The content of aluminum in a given amount of the sample powder was determined by a conventional gravimetric analysis, and on the basis of these results the water content in the sample was calculated.

Differential Thermal Analysis (DTA) and Thermogravimetric Analysis (TGA). DTA and TGA runs were carried out on a Rigaku Denki Thermoflex R-8000 unit. The DTA curves and the TGA curves were obtained at a temperature programming rate of 5°C/min.

X-Ray Diffraction. Powder X-ray diffraction patterns of the sample were obtained with a Shimadzu GX-1 X-ray Diffractometer. The Cu$K\alpha$ radiation (Ni filter) at 30 kV and 15 mA was used. The sample powder was coated with a collodion film to prevent interference from air moisture.

Infrared and Far-infrared Spectroscopy. The infrared spectra for the 400—4000-cm^{-1} wave number range were obtained with Perkin-Elmer Model 125 and Perkin-Elmer Model 337 Infrared Spectrophotometers. A Hitachi FIS-3 Infrared Spectrophotometer was used to obtain spectra for the 30—400-cm^{-1} wave number range.

A nujol technique was employed in every case except when the spectra for the O–H stretching vibration was obtained. In the latter case, a chlorobutadiene technique was employed.

Raman Spectroscopy. The Raman spectra of the sample powder were obtained with a Ūkigōsei RL-II Spectroscope.

1) Y. Ogino, and T. Kawakami, This Bulletin, **38**, 972 (1965).
2) Y. Ogino, T. Kawakami, and K. Tsurumi, *ibid.*, **39**, 639 (1966).
3) Y. Ogino, T. Kawakami, and T. Matsuoka, *ibid.*, **39**, 859 (1966).
4) H. A. Benesi, *J. Phys. Chem.*, **61**, 970 (1957).

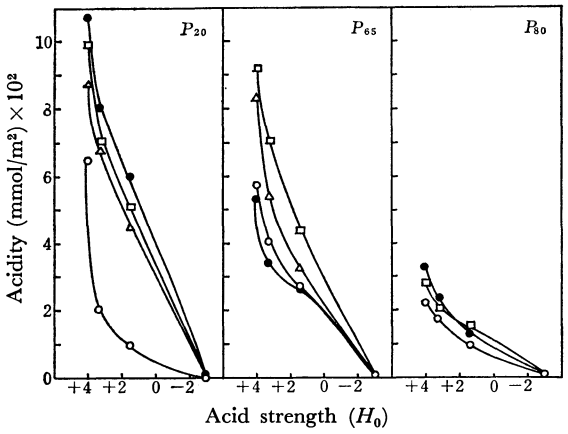

Fig. 1. Acid strength distribution curves for aluminum sulfate samples compressed under various conditions.
(○) $P_{T,0}$; (□) $P_{T,1400}$; (△) $P_{T,2800}$; (●) $P_{T,4200}$

Results

Surface Acidity. Acid-strength distribution curves for aluminum sulfate samples compressed under various conditions are given in Fig. 1, where the acidity values per unit of surface area are indicated as a function of the H_0 value. As can be seen in this figure, the surface acidity for every sample of P_{20}, P_{65}, and P_{80} increased on compression. Further, it can be said that a lower compacting temperature is preferable in order to increase the acidity value within the range of $H_0 = -3.0$—$+1.5$.

Identification of Lewis Acid. As can be seen in Table 1, none of the samples compressed at temperatures lower than 80°C showed any sign positive to the existence of Lewis Acid. Therefore, it might be concluded that only protonic acid appeared on compression. On the other hand, the color test (Table 1) against the samples which had been dehydrated at 89—104°C showed that Lewis acid appeared on the surface of the sample.[5]

Water Content. The water contents in the samples treated under various conditions are given in Fig. 2.

Table 1. Identifications for lewis acid

Compacting condition	Indicator	
	Phenolphthalein	Trithylchloride
$P_{20,0-4200}$	No color	No color
$P_{65,0-4200}$	No color	No color
$P_{80,0-4200}$	No color	No color
$T=80$	No color	
$T=90$	Pink (faint)	
$T=108$	Pink	
$T=128$	Pink (deep)	
$T=155$	Pink (deep)	

[ ] : Samples heated at various temperatures without compression. For example, $T=80$ means the sample heated at 80°C and at zero compacting pressure.

5) H. P. Leftin and W. K. Hall, "Actes Congr. Intern. Catalyse, 2e", Paris, 1960, p. 1352 (1961); G. Kortum, J. Vogel, and W. Braun, *Angew. Chem.*, **70**, 561 (1958).

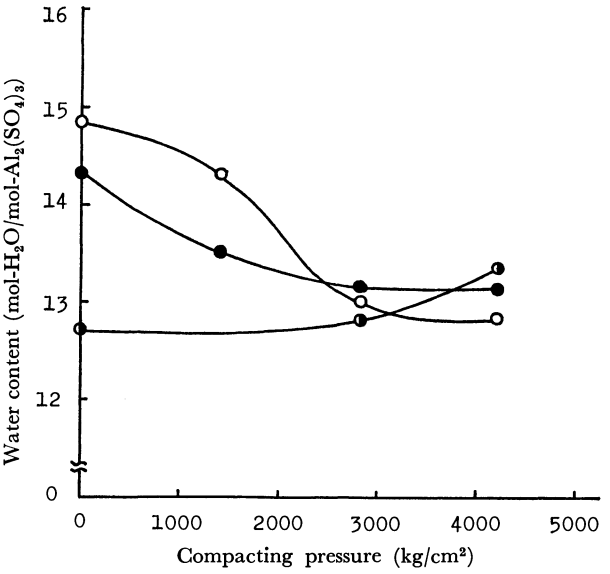

Fig. 2. Relations between the compacting pressure and the water contents in the samples compressed at various temperatures: (○), P_{20}; (●), P_{65}; (◑), P_{80}

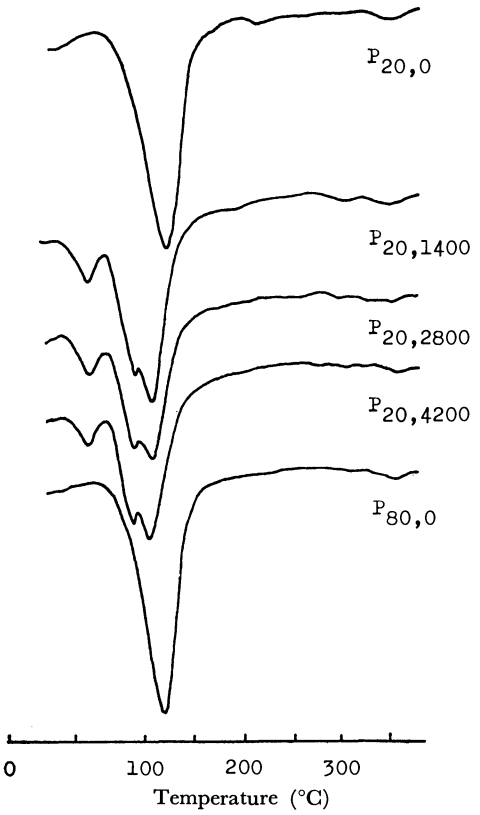

Fig. 3. DTA curves for aluminum sulfate samples compressed under various conditions.

DTA and TGA. DTA curves for several samples are given in Fig. 3. On the basis of a comparison of this figure with the results of the chemical analysis of water and the TGA data, the DTA endothermic peaks were attributed to the dehydration processes from the sample. For example, an endothermic peak appearing at 59°C for the $P_{20,0}$ sample was attributed to the desorption of the physically-adsorbed water.

Further, from the results of TGA it was found that

the amount of dehydratin at 89—104°C from each sample was as follows:

$P_{20,0}$ 12.3 mol-H_2O/mol-$Al_2(SO_4)_3$
$P_{20,1400}$ 12.3 mol-H_2O/mol-$Al_2(SO_4)_3$
$P_{20,2800}$ 12.3 mol-H_2O/mol-$Al_2(SO_4)_3$
$P_{20,4200}$ 12.3 mol-H_2O/mol-$Al_2(SO_4)_3$

It must be noted that these values were approximately equal to 12.

In addition to the above-mentioned fact, the DTA data revealed another interesting fact. A marked difference between the DTA curve for the uncompressed sample and that for the compressed sample was observed. That is, an original endothermic peak which had appeared at 89—104°C in the uncompressed sample split into two endothermic peaks in the compressed sample.

X-Ray Diffractions. The Powder X-ray diffraction patterns for the various samples are given in Fig. 4. These patterns prove that the aluminum sulfate used in this study consisted of crystals of octadecahydrate, hexadecahydrate, and tetradecahydrate. From the low intensity of the diffraction peaks for the tetrahydrate, the content of this hydrate in the sample seemed to be small.

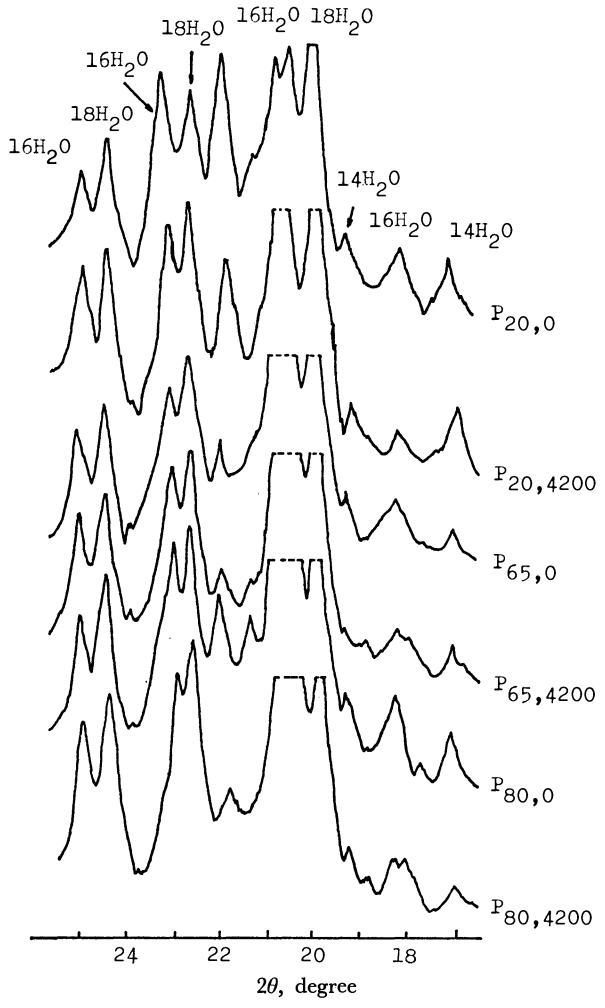

Fig. 4. X-Ray diffraction patterns for aluminum sulfate samples compressed under various conditions.

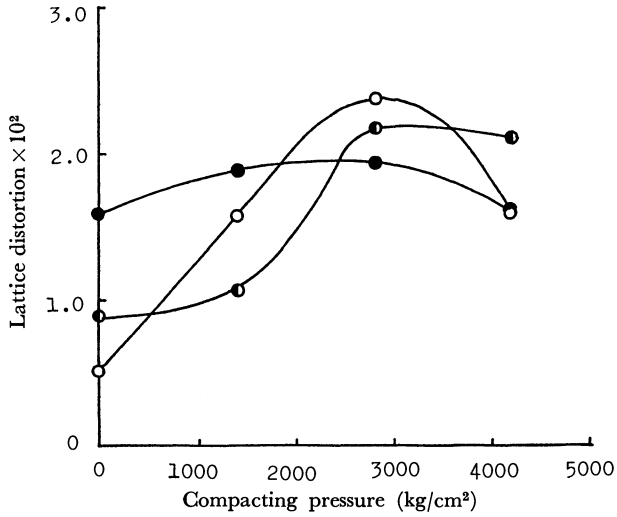

Fig. 5. Relations between the lattice distortion and the compacting pressure: (○) P_{20}; (◐) P_{65}; (●) P_{80}

The degree of lattice distortion calculated by applying Hall's method[6] to the X-ray diffraction data is given in Fig. 5. As can be seen in this figure, the degree of lattice distortion for octadecahydrate was proved to increase with the increase in the compacting pressure, except for the P_{80} sample.

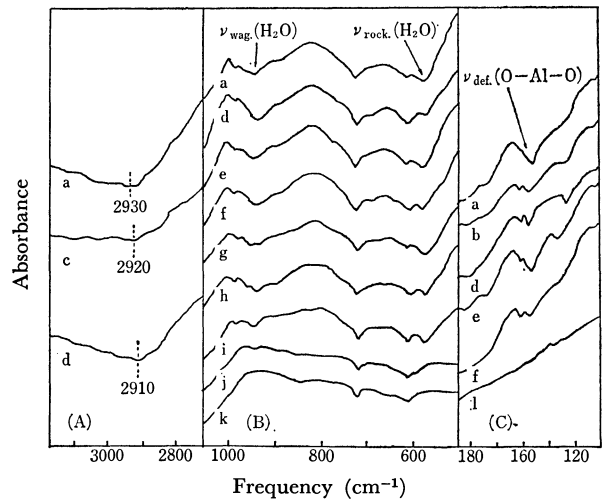

Fig. 6. Infrared and far infrared spectra for alumimun sulfate samples compressed under various conditions: ((a) $P_{20,0}$; (b) $P_{20,1400}$ (c); $P_{20,2800}$; (d) $P_{20,4200}$; (e) $P_{65,0}$; (f) $P_{65,4200}$; (g) $P_{80,0}$; (h) $P_{80,4200}$) and for the samples heated at various temperatures without compression: ((i) 90°C; (j) 130°C; (k) 155°C; (l) 105°C)

Infrared Spectra and Far-infrared Spectra. The infrared spectra of samples prepared under various conditions are given in Fig. 6. Among the absorption bands in this figure, the bands assigned to both ν_{OH} and ν_{O-Al-O} were found to vary on compression. The details of the change in the absorption spectra are given below.

i) On the compression of the sample, the peak position of a broad band ranging from 2500 cm^{-1} to 3500

6) W. H. Hall, *Proc. Phys. Soc.*, **A62**, 741 (1949).

cm^{-1}, which was assigned to the OH stretching vibration[7], shifted to lower frequencies—*i.e.* $P_{20,0}$: 2930 cm^{-1}, $P_{20,2800}$: 2920 cm^{-1}, $P_{20,4200}$: 2910 cm^{-1}.

ii) The band appearing at 155 cm^{-1} for the uncompressed sample was assigned to the O–Al–O deformation.[8] When the sample was compressed, the original 155 cm^{-1} band split into two peaks (Fig. 6); this splitting was more marked in the $P_{20,4200}$ sample than in the $P_{65,4200}$ sample.

iii) As can be seen in the Fig. 6 (i), the heating of the uncompressed sample at 90°C resulted in a decrease in the intensities of the absorption for both $\nu(H_2O)_{rock.}$ and $\nu(H_2O)_{wag.}$.

A further increase in the heating temperature resulted in the almost complete disappearance of these absorption bands (Fig. 6, j,k).

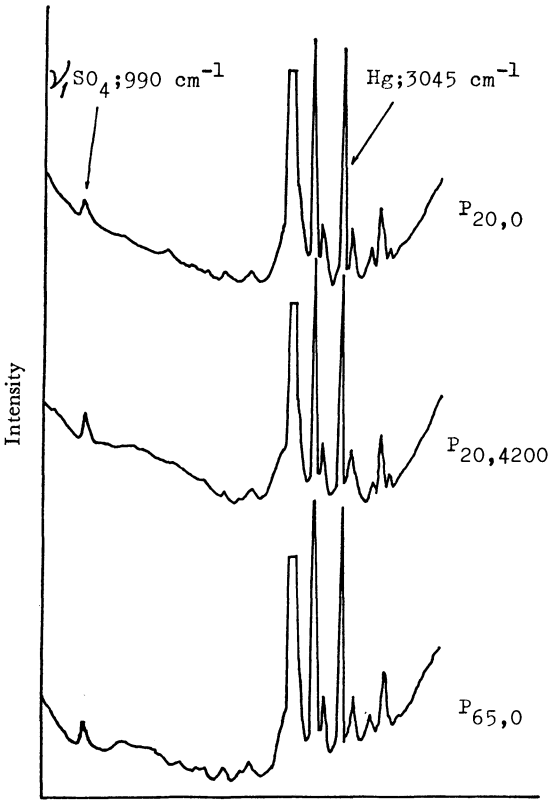

Fig. 7. Raman spectra for aluminum sulfate samples compressed under various conditions.

Raman Spectra. The Raman spectra for several samples are given in Fig. 7. The line which appeared at 990 cm^{-1} was assigned to the ν_1 vibration of sulfate ions in the sample. The relative intensity of this line against the intensity of the line for mercury (3045 cm^{-1}) is given in Table 2.

TABLE 2. RELATIVE INTENSITY OF THE RAMAN ν_1 LINE FOR SO_4^{-2}

Compacting condition	Relative intensity
$P_{20,0}$	7.0×10^{-2}
$P_{20,4200}$	12.8×10^{-2}
$P_{65,0}$	9.3×10^{-2}
$P_{65,4200}$	9.3×10^{-2}

7) I. Gamo, This Bulletin, **35**, 1055 (1962).
8) H. J. Prask and H. Boutin, *J. Chem. Phy.*, **45**, 3289 (1966).

Discussion

Acidity Change on Compression. Similar to a previous work,[1] the present reseach revealed that the surface acidity of aluminum sulfate hydrate varies on the compression of the sample. Furthermore, in the present study it was found that the degree of the acidity change due to compression was a function of the compacting temperature. This fact suggests that the surface acidity might be controlled by changing the compacting temperature as well as the compacting pressure. With respect to this point, it seems to be important that the degree of the acidity change was larger when a lower compacting temperature was employed.

The acidity which appeared on the compressed sample could not be referred to Lewis acid of a high strength, the acidity was referred to protonic acids with a strength of $H_0 \geq -3.0$. The experimental results shown in Table 1 indicate that Lewis acid was made to appear only by heating the sample to a temperature higher than 90°C. Since the compression was carried out below 80°C, it is natural to consider that the observed acidity on the compressed sample surface would have a protonic character.

Surface Areas, Water Contents, and Acidity Changes. The acidity change observed in the present study must be related to the change in the structure of the aluminum sulfate sample. However, the acidity change could not be explained by a simple structural change. For instance, the surface area of the sample varied also on compression, but this change was not proportional to the observed acidity change. That is, the surface acidity per unit of surface area varied also on compression. Moreover, the observed acidity change due to compression was not proportional to the degree of dehydration from the sample.

Crystal Structure and Acidity Changes. On the basis of the experimental results on the X-ray diffraction as well as on the water content of the sample, it was thought that the hydrates in the sample have nonstoichiometric compositions with respect to water. That is, the results of the X-ray diffraction study showed that the sample contains aluminum sulfate octadecahydrate, aluminum sulfate hexadecahydrate, and a small amount of aluminum sulfate tetradecahydrate. Therefore, the water content in the sample should be larger than 14 mol-$H_2O/Al_2(SO_4)_3$. However, as was shown in the previous section, the results of the chemical analysis showed that the water content in the sample was less than 14 mol-$H_2O/Al_2(SO_4)_3$. This discrepancy seems to show that the water content in each of the observed hydrates has a smaller value than the corresponding formular value.

The nonstoichiometric water content may produce distortions of the crystal structure of the aluminum sulfate hydrate. Indeed, the distortion of the crystal lattice of the sample was found to be considerable, as is shown in Fig. 5. Thus, the lattice distortion was suspected of causing the acidity change.

Unfortunately however, examinations based on this suspicion showed that the correlation between the observed acidity change and the degree of lattice distortion was incomplete. That is, the acidity change was found to be proportional to the degree of lattice distortion only for a series of samples made at a given compacting temperature; a change in the compacting temperature resulted in a change in the proportionality constant. Thus, the correlation was incomplete. Therefore, the observed lattice distortion can not be considered as the primary factor which determines the surface acidity.

Structural Unit for Aluminum Sulfate Hydrate. Considering the observed nonstoichiometric water content as well as the works of Gamo,[7] Prask,[8] and Taylor,[9] the model given in Fig. 8 (A) was adopted as a structural unit of aluminum sulfate hydrate. According to this model, there are 12 mol of coordinated-water (I) per unit of $Al_2(SO_4)_3$. In the present study, it was assumed that the water (I) could not be removed by compression, though the anion-water (II) could be removed by compression. Therefore, the number of moles of the anion-water (II) was thought to be variable and capable of having a value corresponding to the water content in the sample (only one water molecule is shown in Fig. 8).

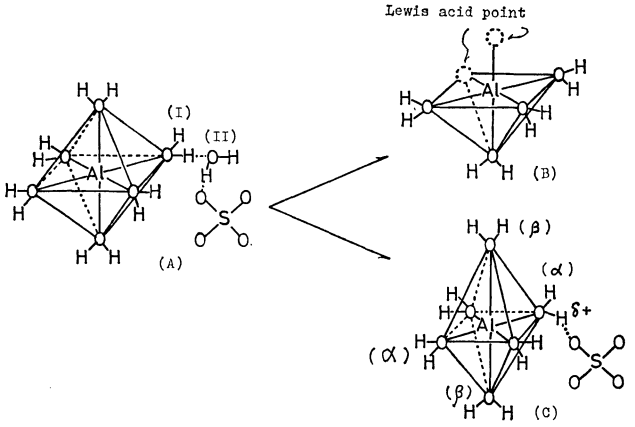

Fig. 8. A structural model for aluminum sulfate hydrate (A), the dehydrated aluminum sulfate hydrate (B) and the compressed aluminum sulfate hydrate (C).

Appearance of Lewis Acid at Higher Temperature. The proposed structural model explains the fact that Lewis acid appeared when the sample was heated to a temperature higher than 90°C. According to the results of the DTA and TGA experiments, the heating of the sample to a temperature higher than 90°C resulted in a considerable dehydration. Further, the total amount of the dehydration occurring at 90—104°C was found to be ~12 mol-H_2O/mol-$Al_2(SO_4)_3$. This means that the coordinated water (I) was removed by the heating. If any of the coordinated water is removed, vacant sites may appear around an aluminum ion (Fig. 8(B)). These vacant sites may exhibit the nature of Lewis acid.

Acidity Change on Compression. A distorted structural unit shown in Fig. 8 (C) was considered to explain the appearance of a protonic acid center in the compressed sample. As can be seen in this figure, the octahedron around an aluminum ion is deformed. That is, the distance between the central Al^{3+} ion and each of the coordinated-water is no longer equivalent, and there appear two sorts of coordinated water, *i.e.*, H_2O (α) and $H_2O(\beta)$. Now, since the distance between Al^{3+} and $H_2O(\alpha)$ is smaller than the original value, stronger interaction between Al^{3+} and $H_2O(\alpha)$ may result and the covalent character in the Al^{3+}–$H_2O(\alpha)$ may increase. Thus, some positive charges may appear on the H atom in the $H_2O(\alpha)$ molecule. This is a protonic acid center. In this manner, the increased acidity of the compressed sample can be explained by considering the increased content of the distorted structural unit.

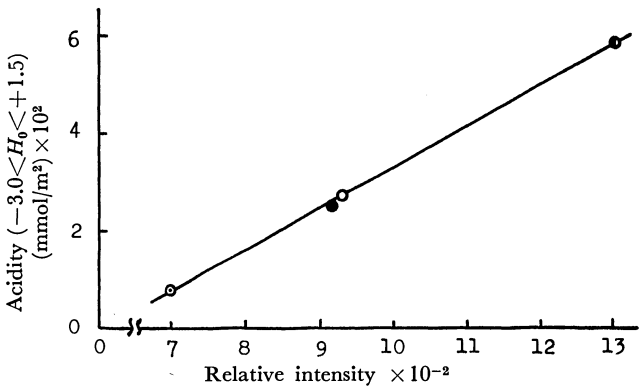

Fig. 9. Relations between the surface acidity (H_0=−3.0—+1.5) and the relative intensity of the Raman ν_1 line for SO_4^{-2}: (⊙) $P_{20,0}$; (◑) $P_{20,4200}$; (○) $P_{65,0}$; (●) $P_{65,4200}$.

In deforming the octahedral structural unit, chemical forces exerted by sulfate ions around the octahedron seem to play an important role. Since the compression results in the dehydration of anion-water (II), the sulfate ion may be displaced toward the octahedron. Therefore, the interaction between the sulfate ion and the coordinated water (α) may increase. This may promote the ionization of a H atom into $H^{\delta+}$ in the $H_2O(\alpha)$ molecule and result in the deformation of the octahedron. The experimental results shown in Fig. 9 indicate that, irrespective of the compacting pressure as well as the compacting temperature, the surface acidity of the sample can be regarded as a unique function of the relative intensity of the Raman ν_1 line of the sulfate ion. This fact indicates the intimate relation between the surface acidity and the behavior of sulfate ions in the sample.

Experimental Evidence for the Proposed Mechanism. The following experimental results also support the above described mechanism for the acidity change due to compression:

i) The existence of two kinds of coordinated water (α,β) in the compressed sample is supported by the following facts: (a) The DTA endothermic peak which corresponds to the dehydration of the coordinated water (II) was found to be a single peak for the uncompressed sample, whereas the peak for the compressed sample split into two peaks. (b) The far-in-

9) D. Taylor and H. Basset, *J. Chem. Soc.*, **1952**, 4431.

frared spectra assigned to the O–Al–O deformation in the uncompressed sample appeared at 155 cm^{-1} as a single band, whereas the O–Al–O deformation absorption for the compressed sample split into two bands.

ii) One experimental fact (i-b) mentioned above supports the supposition that the degree of the interaction between the O atom and the Al^{3+} ion in a $H_2O(\alpha)$-Al^{3+}-$H_2O(\alpha)$ group may be different from that in a $H_2O(\beta)$-Al^{3+}-$H_2O(\beta)$ group.

iii) The supposition that the interaction between the sulfate ion and the H atom in a $H_2O(\alpha)$ molecule would be increased by compression may be supported by the fact that the infrared absorption which was assigned to the O–H stretching vibration shifted toward a somewhat lower wave number as the compacting pressure of the sample was increased.

iv) The displacement of sulfate ions toward an octahedron may result in an increase in the concentration of the sulfate ion in the sample. This expectation was supported by the fact that the relative intensity of the Raman ν_1 peak of the sulfate ion increased on the compression of the sample.

BULLETIN OF THE CHEMICAL SOCIETY OF JAPAN, VOL. 44, 1777—1780 (1971)

The Electronic Spectra of the Anion Radical Salts Derived from 2,3-Dicyano-1,4-benzoquinone and 2,3-Dichloro-5,6-dicyano-1,4-benzoquinone[1)]

Yôichi IIDA

Department of Chemistry, Faculty of Science, Hokkaido University, Sapporo

(Received January 30, 1971)

The anion radical salts derived from 2,3-dicyano-1,4-benzoquinone and 2,3-dichloro-5,6-dicyano-1,4-benzoquinone were prepared. The absorption spectra in an acetonitrile solution and the solid-state spectra were examined for these anion radical salts. Unlike the absorption spectra in solution, in the solid-state spectra strong charge-transfer bands appeared and there were blue-shifts of the high-energy bands. These spectroscopic features were discussed on the basis of the charge-transfer interaction between the anion radicals. The solid-state properties of these salts were compared with those previously investigated for the anion radical salts of the halogen-substituted *p*-benzoquinones.

In general, solid ion radical salts have been a matter of great interest,[2-9)] because the ion radical molecules form, in themselves, a plane-to-plane stacking into columns so as to make a large overlap between their half-filled molecular orbitals.[10)] In this case, any individual ion radical molecule interacts through charge-transfer most strongly with one or two other radicals. In a previous paper,[7)] the solid-state properties were examined for the anion radical salts of *p*-chloranil, 2,5-dibromo-3,6-dichloro-1,4-benzoquinone, and *p*-bromanil. The electronic spectrum of the solid salt was found to be different from the monomer spectrum of the anion radical in solution and to show the intermolecular charge-transfer band. The charge-transfer interaction between the anion radicals was much affected not only by the kinds of halogen substituents in the anion radical molecules, but also by the species of the counter cations.

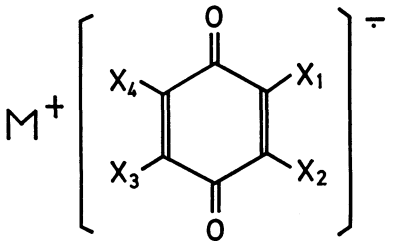

(a) ; $X_1 = X_2 = X_3 = X_4 = Cl$

(b) ; $X_1 = X_2 = X_3 = X_4 = Br$

(c) ; $X_1 = X_3 = Br$, $X_2 = X_4 = Cl$

(d) ; $X_1 = X_2 = H$, $X_3 = X_4 = CN$

(e) ; $X_1 = X_2 = Cl$, $X_3 = X_4 = CN$

Fig. 1. The anion radical salts of (a) *p*-chloranil, (b) *p*-bromanil, (c) 2,5-dibromo-3,6-dichloro-1,4-benzoquinone, (d) 2,3-dicyano-1,4-benzoquinone, and (e) 2,3-dichloro-5,6-dicyano-1,4-benzoquinone. M^+ represents a diamagnetic counter cation.

1) This work was presented at the Symposium on Molecular Structure, Sapporo, October, 1967.

2) W. J. Siemons, P. E. Bierstedt, and R. G. Kepler, *J. Chem. Phys.*, **39**, 3523 (1963).

3) R. G. Kepler, *ibid.*, **39**, 3528 (1963).

4) Y. Iida and Y. Matsunaga, This Bulletin, **41**, 2615 (1968).

5) Y. Iida, *ibid.*, **42**, 71 (1969).

6) Y. Iida, *ibid.*, **42**, 637 (1969).

7) Y. Iida, *ibid.*, **43**, 2772 (1970).

8) Y. Iida, *ibid.*, **44**, 663 (1971).

9) J. Tanaka and M. Mizuno, *ibid.*, **42**, 1841 (1969).

10) G. R. Anderson and C. J. Fritchie, Jr., Second National Meeting, Society for Applied Spectroscopy, San Diego, October, 14, Paper 111 (1963); C. J. Fritchie, Jr., *Acta Cryst.*, **20**, 892 (1966); C. J. Fritchie, Jr., and P. Arthur, Jr., *ibid.*, **21**, 139 (1966); P. Goldstein, K. Seff, and K. N. Trueblood, *ibid.*, **B24**, 778 (1968); J. Tanaka and N. Sakabe, *ibid.*, **B24**, 1345 (1968); H. Kobayashi, Y. Ohashi, F. Marumo, and Y. Saito, *ibid.*, **B26**, 459 (1970).

The present paper will describe some stable anion radical salts of cyano-substituted *p*-benzoquinones. The measurements of the solid-state spectra as well as the absorption spectra in an acetonitrile solution were attempted for the anion radical salts derived from 2,3-dicyano-1,4-benzoquinone (*p*-H_2QCy_2) and 2,3-dichloro-5,6-dicyano-1,4-benzoquinone (*p*-Cl_2QCy_2). We shall examine how the charge-transfer interaction between the anion radicals contributes to the solid-state spectra of these anion radical salts. The solid-state spectra of these salts are interesting in comparison with those of the anion radical salts of the halogen-substituted *p*-benzoquinones.[7]

Experimental

Materials. *p*-H_2QCy_2 was synthesized from *p*-benzoquinone according to the method of Thiele *et al.*,[11] while *p*-Cl_2QCy_2 was commercially available. These compounds were purified by recrystallization from ethylene dichloride.

The following four anion radical salts were prepared according to the method of Matsunaga[12]: Na^+ *p*-$Cl_2QCy_2^-$, K^+-*p*-$Cl_2QCy_2^-$, Na^+ *p*-$H_2QCy_2^-$ and K^+ *p*-$H_2QCy_2^-$. In this method, the anion radical salts were made by the one-electron reduction of the corresponding quinones with alkali metal iodides in an acetonitrile solution.

Measurements. The absorption spectra in an acetonitrile solution were measured at room temperature, using a Beckman DK-2A spectrophotometer at concentrations of the order of 10^{-4}—10^{-5} mol/*l*.

The diffuse reflection spectra of the solid salts were recorded on a Beckman DK-2A spectroreflectometer at room temperature in the range from 4.0 kK to 30.8 kK. In order to avoid cation exchange between the salt and the diluent, the sodium salts were ground and diluted with sodium chloride, while the potassium salts were similarly treated with potassium bromide. The solid-state spectra were then obtained by plotting the diffuse reflection spectra using the Kubelka-Munk equation, $f(R)=(1-R)^2/2R$, in which R is the reflectance. The experimental details were the same as those described in previous papers.[4-8]

The Absorption Spectra in Solution

Some of the absorption spectra of these anion radical salts in an acetonitrile solution are reproduced in Fig. 2. The spectra are not changed when the counter cation of the salt is replaced. Since the concentrations are so dilute, the salts seem to be completely dissociated. The obtained spectra are those of the anion radical monomer, because the counter cations of the salts are simple alkali metal cations.

The p-Cl_2QCy_2 *Anion Radical (Fig. 2, Curve a).* This anion radical in an acetonitrile solution appears reddish violet, and is quite stable at room temperature. The absorption spectrum of the anion-radical monomer has absorption peaks at 17.1 kK and 18.3 kK, a band at 21.9 kK with a shoulder around 22.9 kK, and a strong absorption at 28.7 kK. These spectroscopic features are found to be in good accordance with those

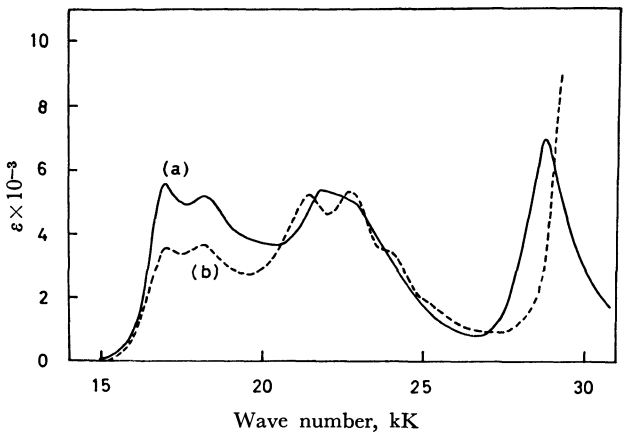

Fig. 2. The absorption spectra of (a) Na^- *p*-$Cl_2QCy_2^-$ and (b) Na^+ *p*-$H_2QCy_2^-$, in acetonitrile solution.

of the *p*-Cl_2QCy_2 anion radical previously reported by Iida and Akamatu,[13] who produced the *p*-Cl_2QCy_2 anion radical by a one-electron transfer reaction from the 7,7,8,8-tetracyanoquinodimethane anion radical to *p*-Cl_2QCy_2 in an acetonitrile solution.

The p-H_2QCy_2 *Anion Radical (Fig. 2, Curve b).* This anion radical in an acetonitrile solution appears red, and is also quite stable at room temperature. The absorption spectrum of the anion radical monomer is composed of absorption peaks at 17.1 kK and 18.2 kK and at 21.5 kK and 22.7 kK, a shoulder around 23.9 kK, and a strong absorption in the energy region higher than 29 kK. Although this absorption spectrum seems to be similar to that of the *p*-Cl_2QCy_2 anion radical, the introduction of the chlorine substituents into the *p*-H_2QCy_2 anion radical causes some shifts in their corresponding bands. Unlike as in the *p*-Cl_2QCy_2 anion radical, the splitting of the band peaks at 21.5 kK and 22.7 kK and the shoulder around 23.9 kK are noted in the case of the *p*-H_2QCy_2 anion radical.

The Solid-State Spectra

Na^+ p-$Cl_2QCy_2^-$ *(Fig. 3, Curve a).* The solid-state spectrum of this salt shows a strong absorption at 12.6 kK and high-energy bands at 21.2 kK and 25.5 kK. This spectrum was found to be different from the monomer spectrum of the *p*-Cl_2QCy_2 anion radical in solution. The band at 12.6 kK appears in the low-energy region where the anion radical monomer does not absorb. This spectroscopic feature is very similar to that for the anion radical salts of halogen-substituted *p*-benzoquinones.[7] The solid-state spectrum of Na^+ *p*-$Cl_2QCy_2^-$ can be compared with that of Na^+ *p*-Chloranil$^-$, since the *p*-Cl_2QCy_2 anion radical molecule is analogous to the *p*-chloranil anion radical. The value for the low-energy band at 12.6 kK of Na^+ *p*-$Cl_2QCy_2^-$ was found to be almost coincident with that for the band at 11.6 kK of Na^+ *p*-Chloranil$^-$, which is known, according to a previous investigation,[7] to arise from the charge-transfer transition between the *p*-chloranil anion radicals in the solid state. The intensity of the

11) J. Thiele and J. Meisenheimer, *Ber. Deut. Chem. Gesell.*, **33**, 675 (1900); J. Thiele and F. Günther, *Liebig's Ann. Chem.*, **349**, 59 (1906).

12) Y. Matsunaga, *J. Chem. Phys.*, **41**, 1609 (1964).

13) Y. Iida and H. Akamatu, This Bulletin, **40**, 231 (1967).

low-energy band for Na+ p-$Cl_2QCy_2^-$ is as strong as that for Na+ p-Chloranil$^-$. Judging from these results, the low-energy band at 12.6 kK for Na+ p-$Cl_2QCy_2^-$ seems to be attributable to the charge-transfer transition between the p-Cl_2QCy_2 anion radicals. In this case, the p-Cl_2QCy_2 anion radicals will be stacked close enough together for the π orbitals to overlap, and the π–π transitions of the monomer will be perturbed in the field of the other anion radicals. This is shown as appreciable blue-shifts of the high-energy bands at 21.2 kK and 25.5 kK for the solid-state spectrum of Na+-p-$Cl_2QCy_2^-$, compared to the monomer absorptions of the p-Cl_2QCy_2 anion radical at 17.1 kK and 21.9 kK respectively.

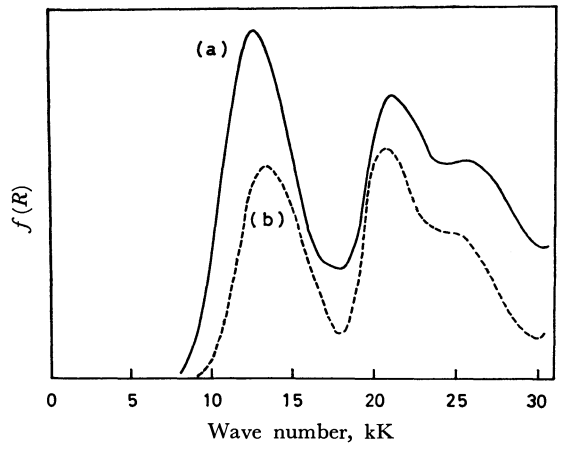

Fig. 3. The solid-state spectra of (a) Na+ p-$Cl_2QCy_2^-$ and (b) K+ p-$Cl_2QCy_2^-$.

K+ p-$Cl_2QCy_2^-$ (Fig. 3, Curve b). The solid-state spectrum of this salt shows a low-energy band at 13.3 kK and high-energy bands at 20.7 kK and 25.0 kK. The locations of the band peaks for this salt were found almost to coincide with those for Na+ p-$Cl_2QCy_2^-$. Although the intensity of the low-energy band for K+ p-$Cl_2QCy_2^-$ is somewhat weaker than that for Na+ p-$Cl_2QCy_2^-$, the electronic structures of the solid salts do not appreciably depend on the counter cations now under consideration.

Na+ p-$H_2QCy_2^-$ (Fig. 4, Curve a). This salt gives the solid-state spectrum composed of a low-energy band at 10.7 kK with a shoulder around 14.3 kK, high-energy bands at 21.2 kK and 24.5 kK, and a shoulder in the energy region higher than 30.0 kK. Unlike as in Na+ p-$Cl_2QCy_2^-$, not only the band peak at 10.7 kK but also the shoulder around 14.3 kK are noted for the charge-transfer bands of Na+ p-$H_2QCy_2^-$. The intensities of these bands are quite strong. Although these bands are not completely resolved, they consist of two prominent peaks, and the splitting is approximately 3.6 kK. The energy of the first-band peak at 10.7 kK for Na+ p-$H_2QCy_2^-$ is lower than that at 12.6 kK for Na+ p-$Cl_2QCy_2^-$. Two charge-transfer absorptions are often observed for salts in which the charge-transfer interaction between the ion radicals is remarkably strong.[14] The charge-transfer interaction for Na+ p-$H_2QCy_2^-$ appears to be stronger than that for Na+ p-$Cl_2QCy_2^-$. The high-energy bands at 21.2 kK and 24.5 kK for the solid-state spectrum of Na+ p-$H_2QCy_2^-$ can be assigned to the shifted bands of the p-H_2QCy_2 anion radical monomer at 17.1 kK and 21.5 kK respectively.

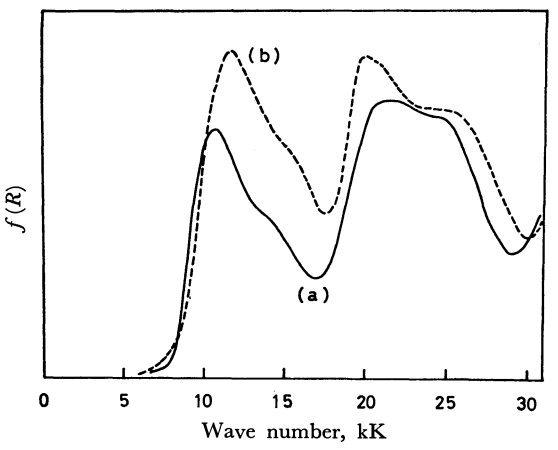

Fig. 4. The solid-state spectra of (a) Na+ p-$H_2QCy_2^-$ and (b) K+ p-$H_2QCy_2^-$.

K+ p-$H_2QCy_2^-$ (Fig. 4, Curve b). This salt shows the solid-state spectrum composed of a low-energy absorption at 11.7 kK, a shoulder around 15.4 kK, high-energy bands at 20.0 kK and 25.0 kK, and a shoulder in the energy region higher than 30.0 kK. It is interesting to see that the spectroscopic features for this salt are similar to those for Na+ p-$H_2QCy_2^-$. Therefore, the situations of the charge-transfer interaction for these substances seem to be much alike.

Discussion

The above-mentioned results of the solid-state spectra of these anion radical salts clearly show that a strong charge-transfer interaction takes place between the anion radical molecules. Therefore, the anion radical molecules can be expected to be stacked in a face-to-face manner and to form, in themselves, linear chain columns; this feature of the crystal structure has been found in a number of other ion radical salts.[10] The charge-transfer absorption characteristic of the solid salts should be ascribed to the transition of the type $\langle\cdots Q^- Q^- Q^- Q^-\cdots\rangle \longrightarrow \langle\cdots Q^- Q^0 Q^{2-} Q^-\cdots\rangle$, where Q denotes a quinone molecule. However, a question still remains as to why the broad and doublet structure of the charge-transfer absorption appears in the p-H_2QCy_2 anion radical salts. A possible explanation has been proposed by Tanaka and Mizuno.[9] According to their discussion, if there are two sites in the one-dimensional radical column in a unit cell, there are two kinds of charge-transfer states; one is from the left site to the right site, and the other is from right to left. The splitting of the charge-transfer absorption occurs when one takes into consideration the interaction term between these two states. Although

14) Two charge-transfer absorptions have also been observed for the solid-state spectra of the cation radical salts of p-phenylenediamine bromide and Würster's red bromide. In these solid salts, the charge-transfer bands are extraordinarily large, and the overlap integral between the half-filled molecular orbitals of the cation radicals is the largest in the series of Würster cation radical salts. See Refs. 4 and 9.

this off-diagonal element does not have terms proportional to the first order in the nearest neighbour electron overlap, it includes an electron-electron interaction of a dipolar type. With respect to the intermolecular separation between the anion radical molecules, the p-H_2QCy_2 anion radicals should be stacked more closely than the p-Cl_2QCy_2 anion radicals, since the latter include the bulky chlorine substituents. Therefore, the splitting of the charge-transfer absorption seems to be more important for the p-H_2QCy_2 anion radical salts than for the p-Cl_2QCy_2 anion radical salts. This is in agreement with the experimental results of the charge-transfer absorptions.

On the other hand, the charge-transfer interaction between the anion radical molecules in these anion radical salts was found to be almost independent of the species of the counter cations under consideration. This fact is in contrast to that for the anion radical salts of halogen-substituted p-benzoquinones, where the charge-transfer interaction is much reduced in the potassium salts in comparison with that in the sodium salts.[7]

In conclusion, the charge-transfer interaction between anion radical molecules was found to take place not only in the anion radical salts of halogen-substituted p-benzoquinones but also in the anion radical salts of cyano-substituted p-benzoquinones. This kind of interaction is regarded as characteristic of ion radical salts in general.

BULLETIN OF THE CHEMICAL SOCIETY OF JAPAN, VOL. 44, 1780—1783 (1971)

Ionization of Some Quinones by the Interaction with Aliphatic Amines

Tsuguo YAMAOKA* and Saburo NAGAKURA

The Institute for Solid State Physics, The University of Tokyo, Roppongi, Minato-ku, Tokyo

(Received February 8, 1971)

The interactions of alkylamines with *p*-benzoquinone and its chloro-derivatives in ethanol and ethyl ether were studied by the rapid scan spectrophotometric method. The formation of anion radicals was found spectroscopically for the *n*-butylamine-*p*-benzoquinone, *n*-butylamine-chloranil, dimethylamine-*p*-benzoquinone, and tri-*n*-butylamine-chloranil systems. The rates of ionization reactions were determined to be 0.30 sec^{-1} mol^{-1} (at 253.7°K), 0.89 $sec^{-1}mol^{-1}$ (at 222.7°K), and 1.39 $sec^{-1}mol^{-1}$ (223.2°K) for the tri-*n*-butylamine-chloranil, *n*-butylamine-chloranil, and *n*-butylamine-*p*-benzoquinone systems, respectively. The activation energy for ionization of the tri-*n*-butylamine–chloranil system in ethanol was estimated to be 0.57 kcal/mol.

The reactions of aromatic amines with *p*-benzoquinone and its derivatives are typical examples of interactions between electron donors and acceptors. Recent studies[1,2] showed that the inner (σ) and outer (π) complexes exist as reaction intermediates in this type of reactions. The reaction mechanism was clarified for the system including chloranil as electron acceptor and *m*-phenylenediamine or *s*-triaminobenzene[3] as electron donor, by detecting the intermediates spectrophotometrically at various temperatures. Another type of reaction between electron donor and acceptor may include ionization as an intermediate process. Nagakura and Tanaka[4] presented the electron-transfer theory for some aromatic substitution reactions and pointed out that ionized species may exist as intermediates for the reactions. Kosower[5] emphasized that ionization processes play an important role in various electron donor-acceptor reactions. Furthermore, in the reaction producing diethylaminovinyltrichloro-*p*-benzoquinone from triethylamine and chloranil, electron transfer was considered to be the first step of the reaction although the process was not directly observed.[6]

The existence of ionic species has been demonstrated for many systems including electron donors and acceptors.[7–12] Detailed experimental studies have been made in particular for systems including aromatic amines such as *N,N*-dimethyl- and *N,N,N',N'*-tetramethyl-*p*-phenylenediamine as electron donors.[13,14]

In spite of many works on the formation of ionic species in systems including electron donors and acceptors, kinetic studies of the ionization process are scanty. In this paper, the existence of ionic species as reaction intermediates will be demonstrated by the rapid scan spectrophotometric technique for some quinone-

* Permanent address: Department of Printing, Faculty of Engineering, Chiba University, Yayoi-cho, Chiba, Japan.

1) Z. Rappoport, *J. Chem. Soc.*, **1963**, 4498.

2) T. Nogami, T. Yamaoka, K. Yoshihara, and S. Nagakura This Bulletin, **44**, 380 (1971).

3) T. Yamaoka and S. Nagakura, *ibid.*, **43**, 355 (1970).

4) S. Nagakura and J. Tanaka, *ibid.*, **32**, 735 (1959).

5) E. M. Kosower, "Progress in Physical Organic Chemistry," Vol. 3, Interscience Publisher, New York (1965), p. 81.

6) D. Buckley, S. Dunston, and H. B. Henbest, *J. Chem. Soc.*, **1957**, 4850.

7) R. E. Miller and W. F. K. Wynne-Jones, *ibid.*, **1959**, 2375; *Nature*, **186**, 149 (1960).

8) R. Foster, *J. Chem. Soc.*, **1959**, 3508.

9) G. Briegleb, W. Liptay, and M. Cantner, *Z. Physik. Chem.* (Frankfurt), **26**, 55 (1960).

10) H. M. Buck, W. Bloemhoff, and L. J. Oosterhoff, *Tetrahedron, Lett.*, **9**, 5 (1960).

11) J. Weiss, *J. Chem. Soc.*, **1942**, 245.

12) J. W. Eastman, G. Engelsma, and M. Calvin, *J. Amer. Chem. Soc.*, **84**, 1339 (1962).

13) H. Kainer and A. Überle, *Chem. Ber.*, **88**, 1147 (1955).

14) R. Foster and T. J. Thomson, *Trans. Faraday Soc.*, **58**, 860 (1962).

aliphatic amine systems. Furthermore, the rate of ionization process will be determined by the electric conductivity measurement.

Experimental

Materials. Chloranil was recrystallized three times from acetone. *p*-Benzoquinone and 2,5-dichloro-*p*-benzoquinone were purified by vacuum sublimation. Ethanol was distilled after refluxing with magnesium ethylate. Ethyl ether was dried with sodium metal and distilled. Commercially available *n*-butylamine and tri-*n*-butylamine of GR grade were used without further purification after their purities had been checked by gas chromatography. The alcoholic or ethereal solutions of the other amines were obtained by dissolving gaseous amines which were generated by heating their hydrochlorides with sodium hydroxide.

Measurement. A Hitachi rapid scan spectrophotometer RSP-2 located at the Institute of Industrial Science, The University of Tokyo, was used to measure visible and ultraviolet spectra. The apparatus is equipped with an automatically controlled mixing cell. Spectra could be measured every 1/3 second in the wavelength range from 200 mμ to 700 mμ. The electric conductivity and its time dependence were measured with a vibrating reed electrometer and an oscilloscope.

Results and Discussion

Change in Absorption Spectra Caused by the Ionization of Quinones. Reactions of primary, secondary, and tertiary amines with *p*-benzoquinone and its chloroderivatives were investigated spectroscopically in ethanol and ethyl ether. Most reactions were so rapid that the change in visible and ultraviolet absorption spectra was pursued only by the rapid scan spectroscopic method. Concentrations of quinones were adjusted to about 10^{-4} mol/*l*, and an excess amount of amines was used in order to keep their concentrations approximately constant throughout the reaction.

First, let us describe interactions of primary amines with quinones. When *n*-butylamine is mixed with chloranil in ethanol, the spectrum rapidly changes as is shown in Fig. 1. At 1/3 second after mixing, the spectrum with a couple of peaks due to a vibrational structure appears in the region of 420—450 mμ. It is undoubtedly ascribed to the chloranil anion radical from the peak positions and shapes.[8] With the gradual disappearance of these peaks the intensity of an absorption band at 360 mμ increases. This band coincides with that of 2,5-di-*n*-butylamino-3,6-dichloro-*p*-benzoquinone observed by Buckley *et al.*[15] The result shows that an electron transfer occurs from *n*-butylamine to chloranil prior to the substitution reaction.

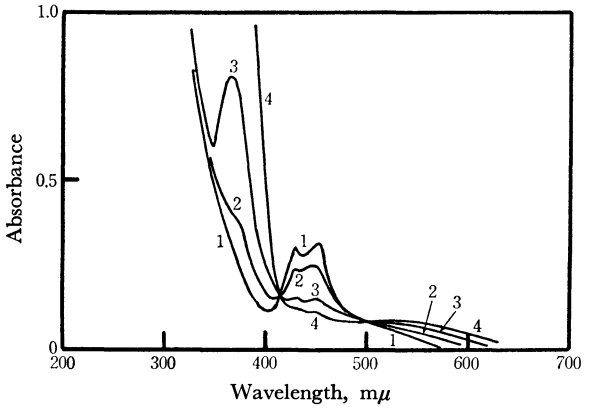

Fig. 1. The electronic absorption spectra of the *n*-butylamine - chloranil system in ethanol. Curves 1, 2, 3, and 4 are the spectra measured at 1/3 sec, 1 sec, 5 sec, and 30 sec, respectively, after the mixing.

A similar spectral change was observed for the methylamine - chloranil - ethanol system. The situation is the same for the systems including *p*-benzoquinone or 2,5-dichloro-*p*-benzoquinone instead of chloranil.

The ionization seems to be sensitive to the polarity of solvents and also the structure of electron acceptor. When *n*-butylamine and *p*-benzoquinone were mixed in ethyl ether, no absorption due to the *p*-benzoquinone anion radical was observed, only absorption bands due to the mono- and di-*n*-butylamino derivatives of *p*-benzoquinone appeared. This seems to mean that the ionic species is unstable in a weakly polar solvent like ethyl ether. When the electron affinity of the quinone is greater, the absorption of the anion radical appears even in ethyl ether. For instance,

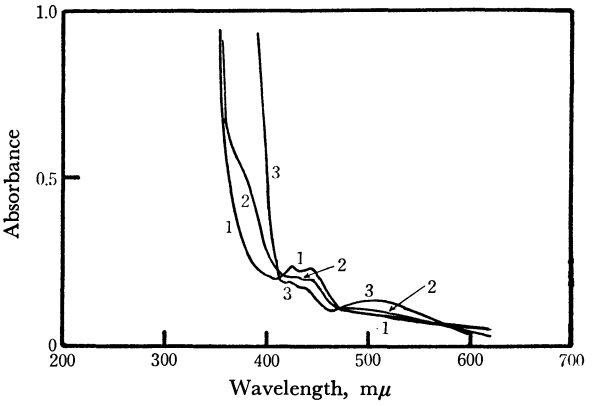

Fig. 2. The electronic absorption spectra of the *n*-butylamine - chloranil system in ethyl ether. Curves 1, 2, and 3 are the spectra measured at 1/3 sec, 1 sec, and 10 sec, respectively, after the mixing.

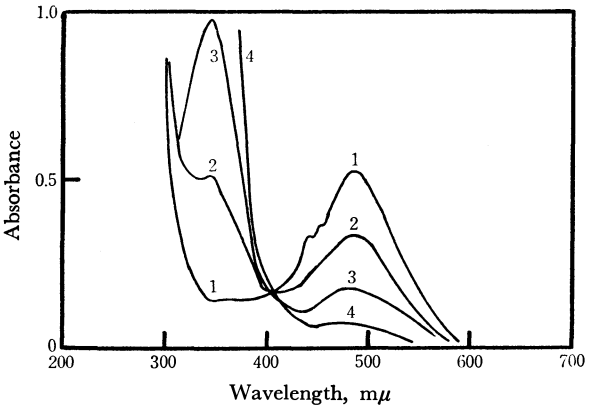

Fig. 3. The electronic absorption spectra of the dimethylamine - *p*-benzoquinone system in ethanol. Curves 1, 2, 3, and 4 are the spectra measured at 1/3 sec, 2 sec, 5 sec, and a few minutes, respectively, after the mixing.

15) D. Buckley, H. B. Henbest, and D. Slade, *J. Chem. Soc.*, **1957**, 4891.

the chloranil-*n*-butylamine system apparently shows an absorption due to the chloranil anion radical as is shown in Fig. 2, while the 2,5-dichloro-*p*-benzoquinone-*n*-butylamine system shows no such absorption.

In the interactions of secondary amines with quinones, the change in the absorption spectrum of the dimethylamine-*p*-benzoquinone-ethanol system takes place as shown in Fig. 3. At 1/3 second after mixing, an absorption band due to 2-dimethylamino-*p*-benzoquinone appears at 480 mμ for this system. Besides this band, there appears a shoulder due to the *p*-benzoquinone anion radical. This suggests that the anion exists as a precursor to 2-dimethylamino-*p*-benzoquinone. The dimethylamine-chloranil-ethanol system gives at 1/3 second after mixing, absorption peaks due to 2-dimethylamino-3,5,6-trichloro-*p*-benzoquinone but no peak due to the chloranil anion radical. It might be noted that the spectrum of the anion radical was not observed for the system containing dimethylamine as electron donor, while it was found for the system containing methylamine with the higher ionization potential. This seems to mean that the reaction rate of ionization is much lower than that of the successive process for the dimethylamine-chloranil-ethanol system.

The tri-*n*-butylamine-chloranil-ethanol system shows the absorption of the chloranil anion radical as seen in Fig. 4. In this system, the anion radical is stable and no further reaction occurs. The ionization of the system including tri-*n*-butylamine as electron donor largely depends on the electron affinity of quinone and also on the polarity of solvent. For example, in ethanol 2,5-dichloro-*p*-benzoquinone is ionized, though slowly, by the interaction with tri-*n*-butylamine but in the case of *p*-benzoquinone no ionization occurs. In ethyl ether neither quinones are ionized by the interaction with tri-*n*-butylamine.

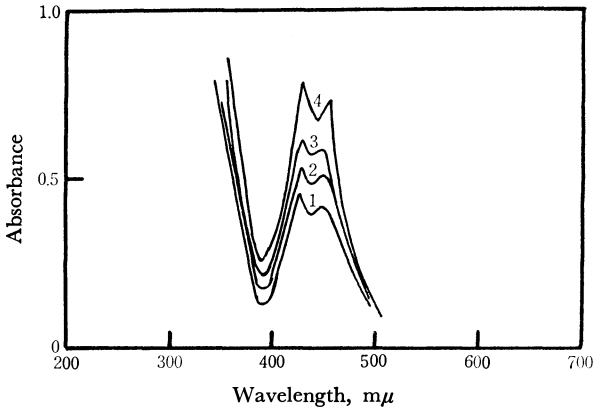

Fig. 4. The electronic absorption spectra of the tri-*n*-butylamine-chloranil system in ethanol. Curves 1, 2, 3, and 4 are the spectra measured at 1/3 sec, 1 sec, 5 sec, and a few minutes, respectively, after the mixing.

Rate of Ionization. Since the rapid scan spectrophotometric measurement could not be made at low temperatures, we undertook to use electric conductivity for the purpose of determining the rate of electron transfer from amine to quinone at various temperatures. In order to check the reliability of the measurement, the rate measured spectroscopically for the tri-*n*-butylamine-chloranil system at room temperature was compared with that obtained by aid of the conductivity measurement. The rate constants measured simultaneously by both methods coincide well with each other. Conductivity measurements were carried out at low temperatures at which the reactions succeeding the ionization actually stopped.

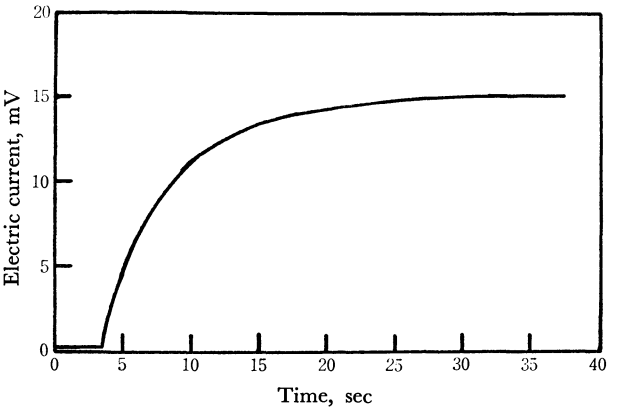

Fig. 5. Change in the electric conductivity of the ethanolic solution including tri-*n*-butylamine and chloranil.

Figure 5 shows the time dependence of conductivity of the ethanolic solution including tri-*n*-butylamine and chloranil. If the initial concentration of the amine, $[A_0]$, is excessively large compared with that of chloranil, $[Q_0]$, the electric current of the solution may change with time t as shown by the equation

$$I = \rho Q_0(1-e^{-[A_0]kt}) \qquad (1)$$

where k is the rate constant for the reaction, Amine+Quinone$\rightarrow$Amine$^+$+Quinone$^-$, and ρ is a constant determined by the electric charge and mobility of the ion, by the electrode voltage, and by the sizes of

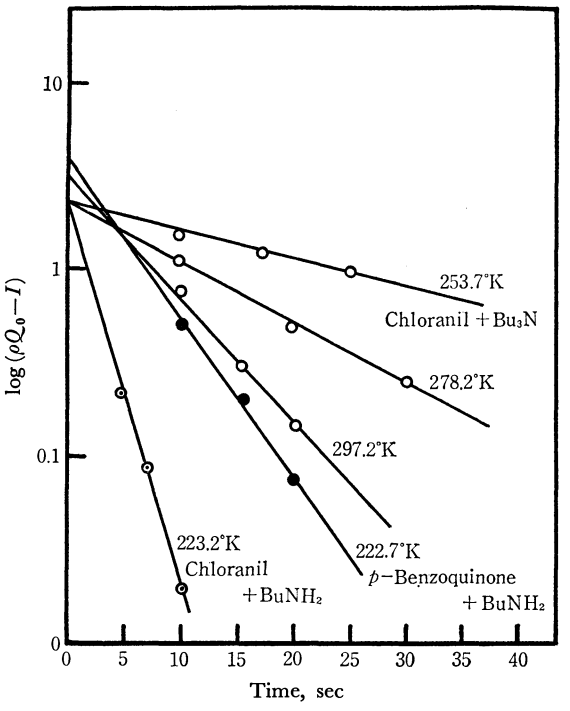

Fig. 6. Plots of log ($\rho Q_0 - I$) against the reaction time, t.

Table 1. Ionization rate constants for some aliphatic amine quinone systmes

Quinone	Amine	Rate constant ($sec^{-1}mol^{-1}$)
Chloranil	NBu_3	0.30 (253.7°K)
		0.71 (278.2°K)
		1.63 (297.2°K)
Chloranil	$BuNH_2$	0.89 (222.7°K)
p-Benzoquinone	$BuNH_2$	1.39 (223.2°K)

the electrodes. As is shown in Fig. 6, the plots of $\log(\rho Q_0 - I)$ against t give a straight line for each system. This means that the observed rate of ionization fits well into Eq. (1). The rate constant of ionization was estimated from the slope of the straight line. The results are summarized in Table 1. This table shows that the rate of ionization is the smallest for the chloranil-tri-*n*-butylamine system. This is rather unexpected because tri-*n*-butylamine has the smallest ionization potential among the amines used in the present study, and suggests that the rate of ionization is sensitive to the steric factor of the amines.

The temperature dependence of the rate constant was measured for the system containing chloranil and tri-*n*-butylamine in ethanol; the result is shown in Fig. 6. The activation energy of ionization was estimated to be 0.57 kcal/mol. The activation energies for the other primary and secondary amine systems could not be measured because the succeeding chemical reactions are rapid at higher temperatures.

We are greatly indebted to Prof. S. Hayano and Dr. M. Fujihira, The Institute of Industrial Science, The University of Tokyo, for their kindness in permitting us to use the rapid scan spectrophotometer and also for their kind advice. One of the authors (T. Y.) would like to thank Prof. T. Tsunoda, Chiba University, for continued encouragement throughout the study.

BULLETIN OF THE CHEMICAL SOCIETY OF JAPAN, VOL. 44, 1783—1788 (1971)

Structures of Bicyclo[2.2.2]octene and Bicyclo[2.2.2]octadiene as Studied by Gas Electron Diffraction

Akimichi YOKOZEKI and Kozo KUCHITSU

Department of Chemistry, Faculty of Science, The University of Tokyo, Hongo, Tokyo

(Received February 10, 1971)

Bicyclo[2.2.2]oct-2-ene and bicyclo[2.2.2]octa-2,5-diene have been investigated by gas electron diffraction. They are found to have C_{2v} symmetry in respect of the thermal-average nuclear positions. The structural parameters with estimated limits of error (the r_g bond lengths and the angles difined in the r_α structure) determined by a least-squares analysis on the molecular intensities are as follows for octene and octadiene, respectively: C(sp^3)–C(sp^3) (weighted average of the C_1–C_7 and C_7–C_8 bonds) = 1.549±0.008 and 1.553±0.017 Å, C(sp^2)–C(sp^3) = 1.509±0.015 and 1.521±0.008 Å, C(sp^2)–C(sp^2) = 1.341±0.008 and 1.339±0.005 Å, C(sp^3)–H (average) = 1.112±0.008 and 1.105±0.012 Å, ∠C–C=C = 114.2±0.6° and 113.5±0.5°, the dihedral angle θ between the C_1–C_2–C_3–C_4 and C_1–C_6–C_5–C_4 planes = 121.2±2.1° and 123.4±2.2°, ∠C=C–H = 122.4±6.0° and 125.5±4.0°, ∠H–C–H = 109.2±4.0° and 111.3±7.0°. A conformational analysis based on an empirical prescription of strain energies, similar to that of Jacob *et al.*, and a molecular-orbital analysis (CNDO/2) have accounted for the observed bond angles given above to within 1.5°.

A previous paper has reported on the structure and intramolecular motions of bicyclo[2.2.2]octane (BO) in the gas phase.[1] The weighted average of the C_1–C_2 and C_2–C_3 bond distances (r_g(average) = 1.542±0.004 Å) is similar to the C–C bond distance in cyclohexane,[2] and the C–C–C bond angles (∠C_1–C_2–C_3 = 109.7°±0.7° and ∠C_2–C_1–C_6 = 108.9°±0.6° in terms of the r_α structure[3]) are close to the tetrahedral angle. The potential function for the twisting motion around the D_{3h} symmetry axis has a broad minimum and probably has a hump of the order of 0.1 kcal/mol at the D_{3h} conformation.[4]

In connection with the above investigation, bicyclo[2.2.2]octene (BE) and bicyclo[2.2.2]octadiene (BD), in which the ethylene bridges in BO are partly replaced by vinylene bridges, are of interest in view of the influence of the double bonds on structural parameters. The observed heats of hydrogenation for these compounds,[5] which are larger than those expected from that for cyclohexene, indicate that the rings are appreciably strained. To our knowledge, however, no study of the structures of BE and BD has been reported, and even the symmetry of the molecules is uncertain.[5] Therefore, their structures have been investigated by means of gas electron diffraction.

Since these molecules have unequivalent pairs of closely-spaced C–C bond distances (C_1–C_2, C_1–C_7, and

1) A. Yokozeki, K. Kuchitsu, and Y. Morino, This Bulletin, **43**, 2017 (1970).

2) H. Kambara, K. Kuchitsu, and Y. Morino, *ibid.*, to be published.

3) K. Kuchitsu, T. Fukuyama, and Y. Morino *J. Mol. Structure*, **1**, 463 (1968).

4) E. Hirota, *J. Mol. Spectrosc.*, **38**, 367 (1971).

5) R. B. Turner, W. R. Meador, and R. E. Winkler, *J. Amer. Chem. Soc.*, **79**, 4116 (1957).

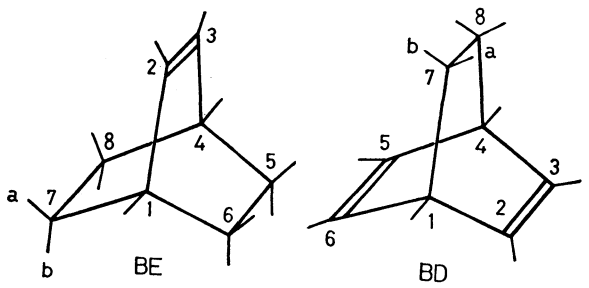

Fig. 1. The numbering of bicyclo[2.2.2]octene (BE) and bicyclo[2.2.2]octadiene (BD).

C_7–C_8), a separation of those pairs[6,7] was a serious problem in the present analysis. In order to elude the trouble, all the C(sp^3)–C(sp^3) bond distances were assumed to be equal, and the weighted average value ($\frac{1}{3}[2r_g(C_1-C_7)+r_g(C_7-C_8)]$), instead of the individual bond distances, was determined.

Experimental

Purified samples of BE and BD were supplied by courtesy of Dr. Hiroshi Tanida of Shionogi Research Laboratory. Diffraction photographs were taken at 20°C on Fuji Process Hard plates with an apparatus equipped with an r^3-sector[8]; the accelerating voltage (stabilized within 0.01%) and the bean current were about 40 kV and 0.35 μA, respectively. The pressures of the samples maintained in thermal equilibrium with their solid states were about 4 Torr for BE and 7 Torr for BD. Typical experimental conditions are listed in Table 1. Other experimental and interpretational procedures have been described in a previous paper.[1] Reduced molecular intensity and radial distribution curves are shown in Figs. 2 and 3.[9] The calculations were carried out by using the HITAC-5020E at the Computer Centre of the University of Tokyo.

Table 1. Typical experimental conditions

	Camera length (mm)	Exposure time (min)	Range of densities	Range of q values[a]
BE[b]	107.77	15	0.18—0.46	25—130
	243.24	3.5	0.11—0.35	8—60
BD[c]	107.77	10	0.16—0.51	25—130
	243.24	2.5	0.23—0.55	8—60

a) Ranges of the intensity data used for the analysis in the interval of $q=1$.
b) Bicyclo[2.2.2]octene.
c) Bicyclo[2.2.2]octadiene.

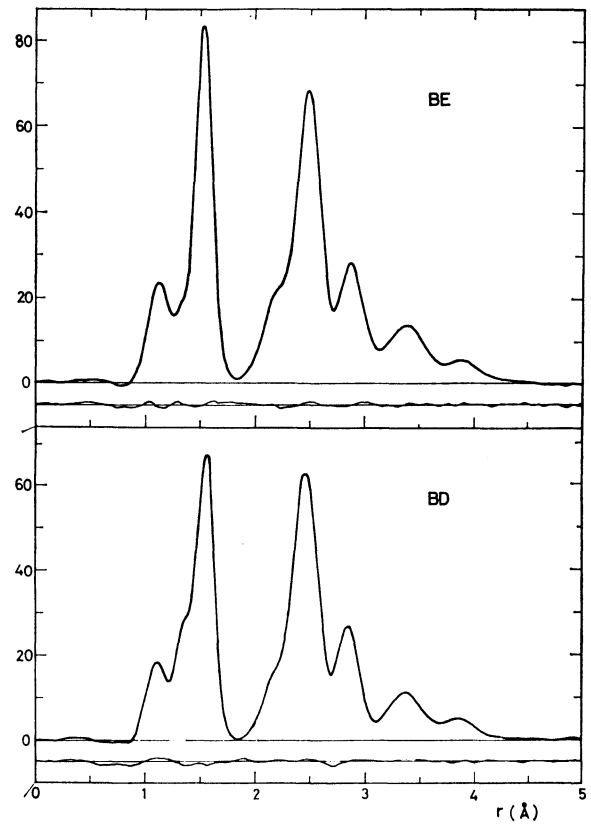

Fig. 2. Experimental radial distribution curves with the residues between the experimental and theoretical curves, damped with a function of exp(−0.00016q^2). Upper and lower curves: bicyclo[2.2.2]octene and octadiene, respectively.

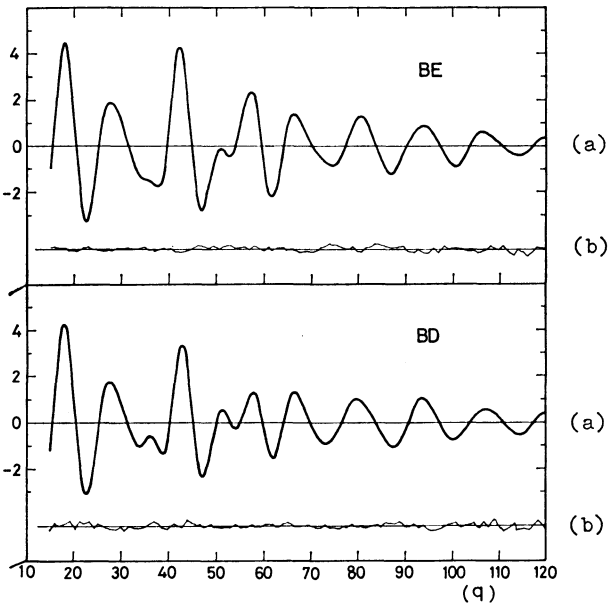

Fig. 3. Molecular intensity curves for bicyclo[2.2.2]octene (upper) and octadiene (lower). (a): best-fit theoretical, (b): experimental minus theoretical.

Analysis

Structural Parameters. The point-group symmetry of these molecules in equilibrium was not clear at the

6) Y. Morino, K. Kuchitsu, and A. Yokozeki. This Bulletin. **40**, 1552 (1967); *ibid.*, **44**, (1971), in press.
7) G. Dallinga and L. H. Toneman, *Rec. Trav. Chim.*, **87**, 795, 805 (1968); J. F. Chiang, C. F. Wilcox, Jr., and S. H. Bauer, *J. Amer. Chem. Soc.*, **90**, 3149 (1968).
8) Y. Murata, K. Kuchitsu, and M. Kimura, *Jap. J. Appl. Phys.*, **9**, 591 (1970).
9) Numerical experimental data of the leveled total intensity have been deposited with the Chemical Society of Japan (Document No. 7109). A copy may be secured by citing the document number and by remitting, in advance, ¥400 for photoprints. Payment by check or money order payable to: the Chemical Society of Japan, 5, 1-Chome, Kanda-Surugadai, Chiyodaku, Tokyo.

initial stage of the present analysis. Even though a flexible quasi-C_{2v} structure (like that observed in BO) or a rigid C_2 structure seemed to be improbable because of the presence of vinylene bridges, the C_{2v} symmetry had to be proved experimentally. If they have C_{2v} symmetry, the numbers of independent parameters sufficient to describe the geometrical arrangements are 16 and 14 for BE and BD, respectively. In this symmetry, the ethylene bridges ($-CH_2-CH_2-$) is borne to have a *cis* conformation around the C–C axis. For a C_2 symmetry with twisted conformations, the numbers of independent parameters are 28 and 25 for BE and BD, respectively. In order to facilitate the analysis and to limit the variable parameters to a reasonable number, the following assumptions about the parameters (in regard to the r_a structure[1,3]) were made.

1) All the C(sp^3)–H bond distances are equal.

2) The C(sp^3)–H bond distances are equal to that of ethylene[10] (r_a=1.0896 Å).

3) The vinylene group (C–CH=CH–C) is planar.

4) The H–C_j–H plane of the methylene group is perpendicular to the C_i–C_j–C_k plane and bisects the C_i–C_j–C_k angle, and *vice versa*.

5) The C–C–H angles at the bridgehead are equal; *i.e.*, $\angle C_2$–C_1–H=$\angle C_6$–C_1–H=$\angle C_7$–C_1–H.

Besides the above assumptions, the following constraint was introduced.

6) All the C(sp^3)–C(sp^3) bond distances are equal.

As mentioned in the introduction, this assumption was almost imperative for the present analysis. The influence of this constraint on the results is discussed in later sections. The above assumptions reduce the independent parameters for C_{2v} symmetry to eight for either molecule, while for C_2 symmetry one additional parameter is required. For either molecule the parameters to be determined are: four bond distances (weighted-average C(sp^3)–C(sp^3) and C(sp^3)–H, C(sp^2)–C(sp^3), and C=C), three bond angles ($\angle$C–C=C, $\angle$C=C–H, $\angle$H–C–H), the angle θ defined by the two straight lines connecting the center of the $C_1\cdots C_4$ with those of the C_2–C_3 and C_5–C_6 distances, and the torsional angle ϕ (the dihedral angle between the C_1–C_7–C_8 and C_4–C_8–C_7 planes). The parameter ϕ is a measure of whether the molecule has C_{2v} or C_2 symmetry in regard to the thermal-average nuclear positions.

Table 2. Estimated force constants for bicyclo [2.2.2] octene and octadiene[a]

K(C–C)	2.30	K(C–H)	4.23
K(=C–C)	3.24	K(=C–H)	4.39
K(C=C)	7.42	W(=C–H)	0.36
H(C–C–C)	0.32	F(C–C–C)	0.20
H(C=C–C)	0.29	F(C=C–C)	0.40
H(C–C–H)	0.22	F(C–C–H)	0.48
H(C=C–H)	0.16	F(C=C–H)	0.45
H(H–C–H)	0.43	F(H–C–H)	0.07
Y(C–C)	0.11	Y(C=C)	0.48

a) The estimated force constants taken from cyclohexane[12] and several olefins (butene, pentene, *etc.*).[13] The torsional (Y) and wagging (W) force constants are in md·Å units, while the others are in md/Å units.

10) K. Kuchitsu, *J. Chem. Phys.*, **44**, 906 (1966).

Calculation of Mean Amplitudes and Shrinkage Corrections. The root-mean-square vibrational amplitudes and shrinkage corrections[11] for all the atom pairs in BE and BD were calculated from a normal-coordinate analysis by using the Urey-Bradley force constants (listed in Table 2) transferred from those for cyclohexane[12] and normal olefins (butene, pentene, *etc.*).[13] The procedures have been described elsewhere.[11]

Since the force constant Y characterizing the torsional motion[1] is not known for a *cis* conformation about a C–C single bond, Y was assumed to be equal to that for the *gauche* conformation (0.11 md·Å for cyclohexane,[12] as discussed in a previous paper.[1]) The lowest twisting frequencies calculated from the above Y value for BE and BD are higher than for BO, and they depend less sensitively on Y. A change in Y from 0.11 to 0.025 md·Å leads to that in the lowest twisting frequency from 163 to 120 cm^{-1} for BE and from 203 to 170 cm^{-1} for BD, while for BO the change is from 134 to 66 cm^{-1}. Therefore, the uncertainty in the calculated mean amplitudes due to that in Y is much less than that for BO, and the ϕ parameters determined in the following analysis is essentially free from the assumption about the Y value. The uncertainties in the assumed force constants were estimated to be 10—20%, *i.e.*, three times the random standard errors quoted in the force constants determined by the Urey-Bradley analysis.[12-14] In that event, the errors in the calculated mean amplitudes caused by the above-mentioned uncertainties in the force constants were at most $\pm$5% for bonded atom pairs and less than $\pm$10% for nonbonded pairs. These

Table 3. Mean amplitudes and shrinkage corrections[a]

	l_{ij}	d_{ij}		l_{ij}	d_{ij}		l_{ij}	d_{ij}
C_2=C_3	424	32	C_7—H	798	132	$C_7\cdots H_2$	1237	25
C_1—C_2	502	11	C_1—H	794	83	$C_1\cdots H_8$	1239	22
C_1—C_7	532	14	$C_2\cdots H_3$	971	79	$C_2\cdots H_{7b}$	1035	47
C_7—C_8	523	33	$C_1\cdots H_7$	1058	69	$C_3\cdots H_1$	991	20
$C_2\cdots C_7$	723	1	$C_7\cdots H_8$	1060	89	$C_1\cdots H_3$	956	45
$C_1\cdots C_3$	586	3	$C_7\cdots H_1$	1074	29	$C_8\cdots H_1$	1024	15
$C_1\cdots C_8$	644	0	$C_1\cdots H_2$	1003	60	$C_3\cdots H_{7b}$	1056	32
$C_3\cdots C_7$	812	−9	$C_2\cdots H_1$	1044	27	$C_7\cdots H_3$	1226	17
$C_1\cdots C_4$	629	−6	$C_2\cdots H_{7a}$	1565	−10	$C_1\cdots H_4$	958	17
$C_2\cdots H$	781	126	$C_3\cdots H_{7a}$	1746	−39			
$C_6\cdots C_7$	727	8	$C_6\cdots H_{7b}$	1559	3	$C_6\cdots H_{7a}$	1049	55
$C_8\cdots C_6$	876	−12	$C_5\cdots H_{7b}$	1862	−50	$C_5\cdots H_{7a}$	1081	29
$C_2\cdots C_6$	687	1	$C_2\cdots H_6$	1169	28			
$C_2\cdots C_5$	739	−4	$C_2\cdots H_5$	1140	25			

a) Calculated mean amplitudes (l_{ij}) and shrinkage corrections (d_{ij}) in 10^{-4} Å units. The first section is common to bicyclo[2.2.2] octene and octadiene, and the second and last sections correspond to the pairs in octene and octadiene, respectively. The H···H pairs are not listed.

11) K. Kuchitsu and S. Konaka, *ibid.*, **45**, 4342 (1966).

12) H. Takahashi and T. Shimanouchi, *J. Mol. Spectrosc.*, **13**, 43 (1964).

13) T. Shimanouchi, Y. Abe, and Y. Alaki, *Polymer J.*, **2**, 199 (1971). The authors are indebted to Professor Takehiko Shimanouchi and the other authors for giving their experimental results before publication.

14) J. H. Schachtschneider and R. G. Snyder, *Spectrochim. Acta*, **19**, 117 (1963).

uncertainties were of the order of the experimental errors, which were estimated for analogous molecules (*e.g.*, triethylenediamine[15]). Therefore, the calculated values listed in Table 3 were used as constant parameters for the subsequent analysis, and the systematic errors in the structural parameters due to this procedure were estimated to be less than their random standard errors.

Least-Squares Analysis. Initial values of the structural parameters were taken from a preliminary analysis of the radial distribution curves: C=C=1.34 Å, C(sp^2)–C(sp^3)=1.51 Å, C(sp^3)–C(sp^3) (average)=1.55 Å, ∠C–C=C=114°, ∠θ=120°. C_{2v} structures ($\phi \sim 0°$) were suggested at this stage. The nine parameters mentioned above were determined for either molecule by a least-squares analysis on the molecular intensities with a preset weight function[16] and with the estimated mean amplitudes and shrinkage corrections. The most probable values and their error matrices[17] are listed in Tables 4 and 5, respectively. As a result of the above analyses, the ϕ parameters, started from 10°, converged to zero. If the molecules had double-minimum potentials in terms of ϕ, similar to that in BO, the ϕ parameters should have converged to significantly nonzero values when the above-mentioned Y values were used. (In fact, this has been observed in the case of BO, where the ϕ parameter depended on Y.) In order to further examine this problem, the dependence of the ϕ parameters on Y was investigated by the use of different sets of the mean amplitudes. Essentially zero ϕ parameters were obtained from any set used in the analysis.

In order to estimate the systematic error due to the assumption 6, the constraint 6 was released in the least-squares analysis. Strong correlation between the C_1–C_7 and C_7–C_8 distances was observed in the error matrices, and as a result, they were determined only with standard errors of about 0.014 Å, and their weighted averages deviated from those given in Table 4 by about 0.003 Å for BE and 0.005 Å for BD. At the same time, the C_1–C_2 (C(sp^2)–C(sp^3)) distances changed from those listed in Table 4 by about 0.01 Å for BE and 0.004 Å for BD, respectively. Other parameters changed only within their random standard errors. Therefore, the systematic errors from this source were taken into account in the C(sp^3)–C(sp^3) (average) and C(sp^2)–C(sp^3) parameters.

Table 4. Structural parameters[a]

	BE	BD
C–C[b]	1.549 ± 0.008	1.553 ± 0.017
=C–C	1.509 ± 0.015	1.521 ± 0.008
C=C	1.341 ± 0.008	1.339 ± 0.005
C–H[b]	1.112 ± 0.008	1.105 ± 0.012
∠C=C–C	114.2° ± 0.6°	113.5° ± 0.5°
θ	121.2° ± 2.1°	123.4° ± 2.2°
ϕ	0.4° ± 0.5°	0.1° ± 0.3°
∠C=C–H	122.4° ± 6.0°	125.5° ± 4.0°
∠H–C–H	109.2° ± 4.0°	111.3° ± 7.0°
k	1.00 ± 0.02	0.93 ± 0.03

a) The most probable values of the structural parameters (see text) for bicyclo [2.2.2] octene (BE) and octadiene (BD). The distance parameters (r_g) are in Å units and the angles are represented by the r_α structure. The index of resolution k is dimensionless. The uncertainties represent the estimated limits of error (see text).

b) Weighted average of the C(sp^3)–C(sp^3) bond distances and that of the C(sp^3)–H bond distances.

Table 5. Error matrix[a]

	C–C	=C–C	C=C	C–H	∠C=C–C	θ	ϕ	∠C=C–H	∠H–C–H	k
	11	−14	10	−2	3	−22	−21	−22	26	25
C–C	43									
		24	17	6	8	32	9	26	−43	39
=C–C	−9	8								
			26	11	8	32	14	17	−34	−28
C=C	−11	3	13							
				24	7	−5	−30	−18	42	6
C–H	−6	3	8	42						
					18	−30	−15	37	25	4
∠C=C–C	14	6	−3	5	16					
						106	32	−84	−87	−41
θ	−26	12	18	15	−1	131				
							34	28	32	−16
ϕ	−16	9	10	−8	−11	25	17			
								356	217	−39
∠C=C–H	36	10	11	−28	21	−66	42	221		
									95	84
∠H–C–H	80	−26	−20	87	29	115	48	−34	486	
										96
k	64	−15	−15	8	22	−22	−13	74	146	119

a) Error matrix ($\times 10^{-4}$) for the independent parameters (see text). The upper and lower triangles represent the elements for bicyclo [2.2.2] octene and octadiene, respectively. Units for the distances are Å, those for the angles are rad., and the index of resolution k is dimensionless.

15) A. Yokozeki and K. Kuchitsu, This Bulletin, **44**, 72 (1971).
16) Y. Morino, K. Kuchitsu, and Y. Murata, *Acta Crystallogr.*, **18**, 549 (1965).
17) K. Hedberg and M. Iwasaki, *ibid.*, **17**, 529 (1964).

Table 6. Comparison of the structures of bicyclo [2.2.2]-compounds[a)]

	BO		BE		BD	
	Obsd[b)]	Calcd[c)]	Obsd[d)]	Calcd[e)]	Obsd[d)]	Calcd[e)]
C–C[f)]	1.542	1.541	1.549		1.553	
=C–C	——		1.509		1.521	
C=C	——		1.341		1.339	
$\angle C_1$–C_2=C_3	——		114.2°	114.5°	113.5°	114.0°
$\angle C_1$–C_7–C_8	109.7°	109.9°	109.3°	109.7°	108.3°	109.6°
$\angle C_2$–C_1–C_6	108.9°	109.0°	108.0°	107.7°	106.8°	106.0°
$\angle C_2$–C_1–C_7						
$\angle C_6$–C_1–C_7			107.6°	107.3°	107.7°	106.5°
θ	(120°)	(120°)	121.2°	121.2°	123.4°	122.6°
C–H[f)]	1.107		1.112		1.105	
∠C=C–H	——		122.4°		125.5°	
∠H–C–H	110.1°		109.2°		111.3°	

a) Molecular structures of bicyclo [2.2.2] octane (BO), octene (BE), and octadiene (BD) by gas electron diffraction. The distances are represented by r_g in Å units and the angles by an r_α representation.
b) Ref. 1.
c) Ref. 21 (calculated values).
d) The present work.
e) Calculated values based on a strain-relief mechanism (see text).
f) Weighted average of the C(sp^3)–C(sp^3)bond distances and that of the C(sp^3)–H bond distances.

The limits of error in the most probable values of the structural parameters, quoted in Table 4, were estimated to be 2.5 times the random standard errors listed in Table 5 as diagonal elements plus systematic errors [those mentioned above and the experimental systematic errors (0.12% for the distance parameters due to sector imperfection, uncertainty in the electron wavelength, *etc.*[3])].

Discussion

Molecular Symmetry. The ϕ parameters determined from the analysis are essentially zero, regardless of the torsional force constant (Y) assumed in the analysis. This implies that these molecules have C_{2v} conformations in respect of the thermal-average nuclear positions and that the potentials of torsion in BE and BD have relatively sharp minima around the C_{2v} positions ($\phi=0°$). In these molecules, unlike BO, the torsional motion couples with a twist around the double bond (C_2–C_3), which demands a high cost of energy.

Bond Distances. The structural parameters determined above are compared with BO in Table 6. The weighted-average values of the C(sp^3)–C(sp^3) bond lengths are 1.542±0.004 (which is similar to that in cyclohexane[2]), 1.549±0.008 and 1.553±0.017 Å for BO, BE, and BD, respectively. The corresponding values for norbornane and norbornadiene[5] are 1.549± 0.003 and 1.573±0.014 Å. The C(sp^2)–C(sp^3) bond distances are 1.509±0.015 Å for BE (analogous to that in propylene, r_s=1.501±0.004 Å[18]), 1.521±0.008 Å for BD and 1.535±0.007 Å for norbornadiene. The above systematic differences in the C–C single bond distances, notwithstanding their relatively large limits of error, may be regarded as the influence of intramolecular strain. The double bond distances in such bicyclic compounds, on the contrary, are nearly equal to those in normal olefins (*e.g.*, 1.337 Å for ethylene[10]). This can be explained by considering that the stretching force constant for double bonds is, in general, several fold larger than that for single bonds, so that the former distance is hardly influenced by the intramolecular strain.

Bond Angles. The effect of angle strain in these bicyclic compounds is also exhibited. The deviation in the C–C–C bond angles from the tetrahedral angle increases in the sequence of BO, BE, and BD. The C=C–C bond angles are about 6° smaller than the trigonal angle, while the corresponding deformation in norbornadiene is about 12°. The C_1–C_4 distances in the three molecules are nearly equal, 2.59, 2.57, and 2.56 Å for BO, BE, and BD, respectively. On the other hand, the dihedral angle θ appears to increase as the molecules have more vinylene groups. A similar trend has been observed in norbornane and norbornadiene.

The above observation can be predicted semiquantitatively, as listed in Table 6, by a strain-relief mechanism similar to that of Jacob *et al.*[19] In the present calculation the strain energy in the molecule was constructed only in terms of angle deformations and nonbonded interactions. The force constants for the deformations of the C–C–C and C–C=C bond angles were assumed to be equal to each other, 0.687 md·Å, as estimated from the Urey-Bradley force fields for saturated hydrocarbons reported by Schachtschneider and Snyder.[14] Standard values for the C–C–C and C–C=C angle were chosen to be the tetrahedral and trigonal angles, respectively. All the nonbonded interactions among the C–C, C–H, and H–H pairs were

18) D. R. Lide, Jr., and D. Christensen, *J. Chem. Phys.*, **35**, 1374 (1961).

19) E. J. Jacob, H. B. Thompson, and L. S. Bartell, *ibid.*, **47**, 3736 (1967).

calculated by use of the functions reported by Hendrickson[20] and by Jacob *et al.*[18] The latter functions are much harder than the former, so that the latter appears to overestimate the steric interactions. In fact, a minimization of the total energy showed that the energy for BD was about 30 kcal/mol *smaller* than that for BE according to the latter function, whereas the energy for BD was about 10 kcal/mol *larger* than that for BE according to the former. In spite of the above discrepancies, the conformational analyses for bond angles were in good agreement with each other (within 0.5°). In addition, the model used in the present study gave bond angles in BO similar to those based on a more elaborate scheme by Gleicher and Schleyer[21] (within 1°).

For the purpose of comparison, another conformational analysis was made by means of a quantum-mechanical scheme known as SCF CNDO/2.[22] A program written by Segal[23] was used in the calculations. The energy was minimized by varying two independent parameters ($\angle$C–C=C and θ) systematically in step of 0.5°, while other parameters were assumed to be constant and equal to the observed values listed in Table 4. The $\angle$C–C=C and θ parameters were predicted to be 114.5° and 121.0° for BE and 115.0° and 122.5° for BD, respectively, in essential agreement with the corresponding values (Table 6) derived from the above-mentioned classical method.

The authors wish to thank Professor Yonezo Morino for his continual encouragement and Drs. Hiroshi Tanida and Kazuo Tori of the Shionogi Research Laboratory for their supply of the samples and for their stimulating discussions.

20) J. B. Hendrickson, *J. Amer. Chem. Soc.*, **83**, 4537 (1961).
21) G. J. Gleicher and P. von R. Schleyer, *ibid.*, **89**, 582 (1967).
22) J. A. Pople and G. A. Segal, *J. Chem. Phys.*, **44**, 3289 (1966).
23) G. A. Segal, "Molecular Calculations with Complete Neglect of Differential Overlap," Program 91, Quantum Chemistry Program Exchange, Indiana University, 1966. This program was rewritten at the Computer Centre of the University of Tokyo in FORTRAN-IV by Drs. Toshiyasu L. Kunii and Toshiaki Ohta, to whom the authors are indebted for allowing them to use a program CNDO/2 for HITAC-5020E.

BULLETIN OF THE CHEMICAL SOCIETY OF JAPAN, VOL. 44, 1788—1791 (1971)

The Electron-acceptor Strengths of Some Substituted Naphthoquinones

Gunzi SAITO and Yoshio MATSUNAGA

Department of Chemistry, Faculty of Science, Hokkaido University, Sapporo

(Received February 19, 1971)

The electron-acceptor strengths of the substituted naphthoquinones were compared with that of *p*-chloranil in terms of their complexing properties. The following electron affinities were estimated: 2.05 eV for 2,3-dichloro-1,4-naphthoquinone, 2.24 eV for 2,3-dichloro-5-nitro-1,4-naphthoquinone, 2.74 eV for 2,3-dicyano-1,4-naphthoquinone, and 2.78 eV for 2,3-dicyano-5-nitro-1,4-naphthoquinone.

Cyano and nitro groups are strongly electronegative, as is indicated by their large Hammett constants. Consequently, the electron-acceptor strength of aromatic molecules is much enhanced by the introduction of such substituents.[1] For example, *p*-benzoquinone is a rather weak acceptor; it is comparable in strength with *s*-trinitrobenzene. On the other hand, the 2,3-dicyano and 2,6-dinitro derivatives are among the strongest.[2] Their strengths can well be compared with those of tetracyanoethylene (TCNE) and tetracyanoquinodimethane (TCNQ). The other cyano and nitro compounds so far examined for their acceptor strengths include 2,3-dichloro-5,6-dicyano-*p*-benzoquinone (DDQ), *p*-cyananil, tetracyano-1,4-naphthaquinodimethane, trinitrophenanthrenequinone, and the nitro derivatives of fluorenemalononitrile.[2-6] However, 1,4-naphthoquinone and its derivatives have scarcely been studied. Continuing the search for a strong electron acceptor,[7] we have examined the acceptor strengths of 2,3-dicyano-1,4-naphthoquinone (DCNQ) and its 5-nitro derivative (DCNNQ) in terms of their complexing properties. In comparison with them, their precursors, 2,3-dichloro-1,4-naphthoquinone (Cl_2NQ) and its 5-nitro derivative (Cl_2NNQ), were also studied.

Experimental

Cl_2NQ and *p*-chloranil were commercially obtained. Cl_2NNQ, DCNQ, and DCNNQ were prepared starting from Cl_2NQ following the procedures of Inoue *et al.* and Wallenfels *et al.*[3,8] They were purified by recrystallization from suitable solvents. DCNQ was finally sublimed in a vacuum. The fourteen aromatic hydrocarbons, twenty-one aromatic monoamines, seven diamines, and eight other compounds listed in Table 1 were employed as electron donors. All the spectra

1) P. R. Hammond, *J. Chem. Soc.*, **1964**, 471.
2) P. R. Hammond, *ibid.*, **1963**, 3113.
3) K. Wallenfels, G. Bachmann, D. Hofmann, and R. Kern, *Tetrahedron*, **21**, 2239 (1965).
4) S. Chatterjee, *J. Chem. Soc. B.*, **1967**, 1170.
5) T. K. Mukherjee, *J. Phys. Chem.*, **71**, 2277 (1967).
6) T. K. Mukherjee, *Tetrahedron*, **24**, 721 (1968).
7) S. Koizumi and Y. Matsunaga, This Bulletin, **43**, 3010 (1970).
8) A. Inoue, Y. Nomura, N. Kuroki, and K. Konishi, *Yuki Gosei Kagaku Kyokai Shi*, **16**, 536 (1958).

were recorded at room temperature by means of a Beckman DK 2A spectrophotometer, using quartz cells with 1-cm and 5-cm path lengths. The solvent used throughout the measurements was Wako reagent-grade chloroform.

Results and Discussion

Several criteria for the electron-accepting properties of π-acceptors have been proposed by various authors.[9] The comparison of the energies at the charge-transfer (CT) absorption maxima in the molecular complexes of two acceptors with the same series of donors is one of them. The electron affinity estimated by this method may be affected, to some extent, by the kind of solvent and also by the kind of donor. Of course, we must compare the complexes of the same bond type, π–π or n–π. In the present work, we used about fifty π-donors with the hope of averaging the specific effect of the donor molecule on the energy of the CT absorption. McConnell *et al.* have proposed that the energy, $h\nu_{CT}$, observed in solution can be approximately expressed by:

$$h\nu_{CT} = I_D - E_A - C, \quad (1)$$

where I_D is the ionization potential of the donor, D, where E_A is the electron affinity of the acceptor, A, and where C represents the electrostatic energy in the dative-bond structure of the complex and also some other minor terms.[10] The difference in $h\nu_{CT}$ of the complexes of a given donor with two acceptors, 1 and 2, is, then:

$$(h\nu_{CT})_1 - (h\nu_{CT})_2 = (E_A)_2 - (E_A)_1 + (C_2 - C_1). \quad (2)$$

The last term is not necessarily zero. Batley and Lyons estimated the change to be no greater than 0.4 eV.[11] Moreover, one of the present authors has demonstrated that this term is a few kK even if the sizes and shapes of the component molecules are very different.[12] We chose *p*-chloranil for the reference, as was done in our previous work. The positions of the maxima of the CT absorption bands exhibited by the acceptors and also by the reference mixed with various donors are presented in Table 1. The linear relationships obtained by the least-squares method are as follows:

$$\begin{aligned} &Cl_2NQ && (h\nu_{CT})_1 = 1.003(h\nu_{CT})_2 + 3.285 \\ &Cl_2NNQ && (h\nu_{CT})_1 = 0.969(h\nu_{CT})_2 + 1.785 \\ &DCNQ && (h\nu_{CT})_1 = 1.034(h\nu_{CT})_2 - 2.292 \\ &DCNNQ && (h\nu_{CT})_1 = 0.977(h\nu_{CT})_2 - 2.603 \end{aligned} \quad (3)$$

The slopes found here are in good agreement with that required by Eq. (2). The intercepts may be considered as measures of the difference in the electron affinity between the naphthoquinones and the reference. The greater the electron affinity of the acceptor, the smaller the energy of the CT absorption maximum; therefore, the negative intercepts for DCNQ and DCNNQ indicate that these two are stronger electron acceptors than *p*-chloranil is. If we take the electron affinity of *p*-chloranil as 2.46 eV, following Farragher and Page,[13] those of the present acceptors are 2.05 eV in Cl_2NQ, 2.24 eV in Cl_2NNQ, 2.74 eV in DCNQ, and 2.78 eV in DCNNQ. These naphthoquinones appear to have acceptor strengths comparable with those of dichloro-*p*-xyloquinone, *p*-fluoranil, *o*-bromanil, and TCNQ respectively. It must be noted that the above-mentioned values cannot be compared directly with the affinities in the literature. Briegleb assumed the affinity of *p*-chloranil as 1.37 eV, and Batley and Lyons took the iodine molecule as their reference and estimated the affinity of *p*-chloranil as 2.59 eV. Thus, our values may be about 1 eV higher than the former estimations, but a little less than the latter.

The effect of substituents on the acceptor strength of the naphthoquinones and related compounds will now be examined in more detail. The energies of the CT absorptions in the pyrene complexes fit well the linear relationship given by Eq. (3); that is, the calculated values, 19.5 kK, 17.6 kK, 14.5 kK, and 13.2 kK for the complexes of Cl_2NQ, Cl_2NNQ, DCNQ, and DCNNQ respectively, are in excellent agreement with the observed values presented in Table 1. Therefore, the energies in the pyrene complexes will be used for the purpose of comparing the acceptor strengths in the following discussion.

The difference in energy between the Cl_2NQ complex and the DCNQ complex is 4.9 kK, while that between the Cl_2NNQ complex and the DCNNQ complex is 4.3 kK. These values are close to that of 4.5 kK evaluated for the increase in acceptor strength by the replacement of chlorine atoms with cyano groups at the 2 and 3 positions of *p*-benzoquinone. The latter was obtained on the basis of the following energies: 18.2 kK with the 2,3-dichloro derivative, 13.7 kK with the 2,3-dicyano derivative, 16.2 kK with *p*-chloranil, and 11.7 kK with DDQ given in an earlier work.[14] When a substituent is introduced to a molecule, its effect on the energy level can be correlated with the π-electron density on the carbon atom to which the substituent is to be introduced.[15] The π-electron distribution in the accepting molecular orbital, in other words, the lowest vacant molecular orbital, of a quinone molecule is, as a first approximation, given by twice the unpaired electron distribution in the semiquinone ion. By the analysis of the hyperfine structure of the electron-spin-resonance spectrum, the latter can be estimated, for the ring-proton splitting constant is approximately proportional to the unpaired electron density on the carbon atom to which the proton is attached.[16] The four equivalent protons in the *p*-benzosemiquinone ion have been reported by Adams *et al.* to show a spacing of 2.37 oersteds.[17] In the case of the 2,3-dichloro-*p*-benzosemiquinone ion examined by Venkataraman *et al.*, the splitting due to the two equivalent protons was

9) G. Briegleb, *Angew. Chem.*, **76**, 326 (1964).
10) H. M. McConnell, J. S. Ham, and J. R. Platt, *J. Chem. Phys.*, **21**, 66 (1953).
11) M. Batley and L. E. Lyons, *Nature*, **196**, 573 (1962).
12) Y. Matsunaga, This Bulletin, **42**, 2490 (1969).
13) A. L. Farragher and F. M. Page, *Trans. Faraday Soc.*, **62**, 3072 (1966).
14) Y. Matsunaga and G. Saito, This Bulletin, **44**, 958 (1971).
15) S. Nagakura and J. Tanaka, *J. Chem. Phys.*, **22**, 236 (1954).
16) H. M. McConnell, *ibid.*, **24**, 632 (1956).
17) M. Adams, M. S. Blois, Jr., and R. H. Sands, *ibid.*, **28**, 774 (1958).

Table I. Energies of the charge transfer absorption maxima (in kK)
The values in parentheses were not used in computation of Eq.(3).

Donor	*p*-Chloranil	Cl_2NQ	Cl_2NNQ	DCNQ	DCNNQ
Triphenylene	20.1	**	21.2	18.5	17.2
Fluorene	19.6	23.3	21.0	18.0	16.6
Naphthalene	20.2	23.5	21.4	18.7	17.2
Phenanthrene	20.8	24.4	21.6	19.0	17.3
p-Terphenyl	20.3	**	21.6	18.5	16.5
Chrysene	18.6	**	19.6	**	15.0
1,2-Benzanthracene	17.0	20.4	18.2	15.0	13.4
Pyrene	16.2	19.5	17.5	14.6	13.2
Anthracene	15.6	19.2	16.9	13.7	12.5
Perylene	13.2	16.8	14.5	11.7	10.5
Tetracene	12.7	**	13.9	**	**
Mesitylene	23.1	**	**	21.7	20.3
Durene	20.6	24.0	21.6	19.4	18.1
Hexamethylbenzene	19.3	22.5	20.3	18.3	16.9
1,4-Dimethoxybenzene	18.0	**	19.6	15.9	14.7
4,4′-Dimethoxybiphenyl	17.7	21.2	19.0	15.4	13.5
α-Naphthol	17.4	21.0	18.9	15.6	14.1
β-Naphthol	18.3	22.1	20.2	16.4	15.1
3,3′-Dichloro-*o*-tolidine	14.3	17.9	15.6	12.3	10.9
3,3′-Dibromo-*o*-tolidine	14.1	17.8	15.6	12.2	10.8
Benzidine	14.6	17.8	16.2	12.1	10.9
o-Tolidine	13.2	16.6	14.5	11.4	10.4
o-Dianisidine	13.4	16.3	14.8	11.3	10.3
N,N,N′,N′-Tetramethylbenzidine	11.4	14.9	13.0	9.5	9.2
	17.8	**	19.6	16.0	14.6
1,5-Diaminonaphthalene	13.3	16.4	14.3	11.7	**
Phenothiazine	12.3	16.2	13.6	(12.2)	9.9
N-Methylphenothiazine	14.0	17.4	14.8	11.7	10.5
N-Ethylphenothiazine	12.4	(16.9)	14.2	10.7	9.6
Benzo[c]phenothiazine	12.3	16.0	(12.7)	9.9	9.2
Diphenylamine	15.3	19.0	16.6	13.7	12.7
α-Naphthylamine	15.3	18.6	16.3	13.8	12.9*
Phenyl-α-naphthylamine	14.1	(19.2)	15.3	12.3	11.0
Aniline	18.6	21.8	19.4	16.8	*
N-Methylaniline	16.5	19.3	17.7	14.9*	*
N,N-Dimethylaniline	15.0	17.9	17.0	13.4	12.1*
N,N-Diethylaniline	13.0	16.4	14.5	11.8	*
o-Chloroaniline	19.1	22.4	20.4	17.4	16.3*
m-Chloroaniline	19.4	23.2	20.6	17.9	16.3*
p-Chloroaniline	18.5	22.2	19.6	16.6	15.1*
o-Toluidine	17.5	20.8	18.8	15.7	*
m-Toluidine	18.0	21.1	18.9	16.2	*
p-Toluidine	16.9	20.1	17.9	15.2	*
o-Anisidine	16.7	19.5	17.7	15.1	14.4
m-Anisidine	17.9	*	19.1	16.8*	*
o-Phenetidine	16.8	19.4	18.2	15.0	14.2*
p-Phenetidine	16.2	19.2	17.5	13.7	12.8*
2,4-Xylidine	16.1	19.3	17.5	14.7	*
N-Ethyl-*o*-toluidine	15.2	18.0	(17.9)	13.5	12.4*
N,N-Dimethyl-*m*-toluidine	14.7	17.4	*	13.1	11.6*
N,N-Diethyl-*m*-toluidine	12.7	16.0	14.0	11.6	10.0*

* These absorptions are transitory.
** The CT absorption band could not be detected.

found to be 2.319 oersteds.[18] On the other hand, the proton splitting constants in the 1,4-naphthosemiquinone ion are 3.22 oersteds at the 2 and 3 positions and 0.57 oersteds at the 5, 6, 7, and 8 positions.[17] An expected quintet with a spacing of 0.6 oersteds has been observed for the 2,3-dichloro-1,4-naphthosemiquinone ion.[19] As the present study indicated that the introduction of an electronegative substituent to the 2 position of 1,4-naphthoquinone affects the acceptor strength as much as the introduction of the same to *p*-benzoquinone does, the substituent situated on the 5 or 6 position of naphthoquinone must be less effective than that introduced to benzoquinone. The increase in the acceptor strength by a nitro group substituted at the 5 position of Cl_2NQ and that of DCNQ is in accordance with this prediction. Hammond has shown that the difference in the energy of the CT absorption maximum between the *p*-benzoquinone complex and the mononitro-*p*-benzoquinone complex is 4.0—4.4 kK, and that between the latter and the 2,6-dinitro-*p*-benzoquinone complex is 2.4 kK.[2] On the other hand, the substitution of a nitro group at the 5 position of Cl_2NQ brings about a change of 2.0 kK in the energy of the CT absorption maximum, and that at the 5 position of DCNQ, a change of 1.4 kK.

The above data clearly show that the effect of substituents on the acceptor strength is mutually dependent. The stronger the acceptor to which an electronegative substituent is introduced, the less the effect. This tendency may be considered as a kind of cumulative influence. Peover has estimated the electron affinity of unsubstituted 1,4-naphthoquinone to be 0.20 e V(1.5 kK) lower than that of *p*-benzoquinone.[20] We have found here that the Cl_2NQ complex shows a CT absorption maximum located 1.3 kK higher than that of the 2,3-dichloro-*p*-benzoquinone complex, while the CT absorption of the DCNQ complex is located only 0.9 kK higher than that of the 2,3-dicyano-*p*-benzoquinone complex. Thus, the difference in the electron affinity between a benzoquinone and the corresponding naphthoquinone becomes progressively smaller when the substituents are more electronegative. This trend sug-

18) B. Venkataraman, B. G. Segal, and G. K. Fraenkel, *J. Chem. Phys.*, **30**, 1006 (1959).
19) Y. Matsunaga, This Bulletin, **33**, 1436 (1960).
20) M. E. Peover, *Trans. Faraday Soc.*, **58**, 1656 (1963).

gests that the cumulative influence is more pronounced in the benzoquinone series than in the naphthoquinone series.

Finally, we must add that almost all the complexes between DCNNQ and monoamines were found to be transitory. However, Cl_2NNQ and DCNQ gave time-independent colored solutions when mixed with most of the donors examined.

BULLETIN OF THE CHEMICAL SOCIETY OF JAPAN, VOL. 44, 1791—1796 (1971)

Some New Oxygenated Cobalt Complexes

Megumu MUNAKATA*

Institute for Chemical Research, Kyoto University, Uji, Kyoto

(Received December 22, 1969)

Cobalt(II) complexes with ornithine, 2,4-diaminobutyric acid and 2,3-diaminopropionic acid were studied as new oxygen complexes. The former complex was reversibly, while the latter two complexes were irreversibly oxygenated at room temperature. These oxygenated complexes were diamagnetic and showed electronic absorption spectra similar to that of oxygenated cobalt histidine complex, and they were assumed to be O_2-bridged binuclear complexes, $L_2Co\text{-}O_2\text{-}CoL_2$ (L: ligand). Cobalt and O_2 of the binuclear complexes existed in the state of Co(III) and O_2^{2-}, respectively. Thermodynamic measurements showed that oxygenation was an exothermal process, and deoxygenation an endothermal one. The reversibility correlated with the reduction potential of the central cobalt(III) ion and the enthalpy change of the oxygenation. Easier deoxygenation corresponded to more positive reduction potential and to smaller enthalpy change.

Since it was found that bis(salicylaldehyde)ethylenediamine cobalt (II) reversibly combined with molecular oxygen,[1] oxygen complexes of metal chelates were noted as an interesting model for the oxygen carrying compounds such as hemoglobin and hemocyanin.[2-6] Burk *et al.*[6] reported that among histidine complexes of transition metals, only the cobalt complex possessed the ability to combine reversibly with molecular oxygen. Hearon[7] explained the results as follows. Cobalt forms octahedral complexes, while the available structure of nickel and copper complexes are tetrahedral or square planar. An unpaired electron of cobalt (II) ion accounts for the stabilization of the oxygenated complex. By the combination of cobalt histidine complex with molecular oxygen, the pairing occurs between unpaired electrons from cobalt (II) ion and molecular oxygen. The binuclear structure of peroxide form was proposed from the diamagnetic nature of the oxygenated complex,[8,9] and the reactions are expected to be

$$Co^{2+} + 2HHid \rightleftarrows Co(Hid)_2 + 2H^+ \quad (1)$$

$$2Co(Hid)_2 + O_2 \rightleftarrows [Co(Hid)_2]_2O_2 \quad (2)$$

where HHid is histidine.

In the present research, new oxygenated cobalt complexes with 2,3-diaminopropionic acid, 2,4-diaminobutyric acid and ornithine were prepared. They were identified by elemental analyses of the isolated complex salts, the uptake oxygen gas and electronic absorption spectra of the solutions. The valency states of the central cobalt ion and coordinated molecular oxygen were estimated and thermodynamic properties were obtained. From the results, the effect of ligand-field, the redox potential of the cobalt ion and the enthalpy change on the oxygenation-deoxygenation reversibility were discussed.

Experimental

Materials. 2,3-Diaminopropionic acid and 2,4-diaminobutyric acid were obtained from Sigma Chemical Company, and histidine methyl ester and *N*-acetylhistidine were obtained from Cyclo Chemical Coorporation. The other chemicals used were of reagent grade.

Preparation of Cobalt Complex. Bis(histidinate) Cobalt(II): This chelate was synthesized according to the method of Sano and Tanabe.[10]

Found: C, 37.34; H, 4.75; N, 21.90%. Calcd for $Co(C_6H_8N_3O_2)_2\cdot H_2O$: C, 37.41; H, 4.71; N, 21.82%.

Bis(2,3-diaminopropionate) Cobalt(II) and Bis(2,4-diaminobutyrato) Cobalt(II): These chelates were synthesized in the same way as in cobalt histidine chelate.

Found: C, 23.15; H, 5.76; N, 18.38%. Calcd for $Co(C_3H_7N_2O_2)_2\cdot 2H_2O$: C, 23.92; H, 5.98; N, 18.60%. Pale pink powder.

Found: C, 29.46; H, 6.57; N, 16.85%. Calcd for $Co(C_4H_9N_2O_2)_2\cdot 2H_2O$: C, 29.18; H, 6.67; N, 17.02%. Pale pink powder.

μ-Oxy-bis(Cobalt dihistidinate), $[Co(Hid)_2]_2O_2\cdot 7H_2O$: This

* Present address: Faculty of Science and Technology, Kinki University, Kowakae, Higashiosaka-shi.

1) P. Pfeiffer, E. Breith, E. Lubbe, and T. Tsumaki, *Ann. Chem. Liebigs*, **503**, 84 (1933).

2) T. Tsumaki, This Bulletin, **13**, 252 (1938).

3) M. Calvin and C. H. Barkelew, *J. Amer. Chem. Soc.*, **68**, 2267 (1946).

4) R. E. Stewart, P. A. Estep, and J. J. S. Sebarstian, U. S. Bur. Mines Inform. Circ., No. 7906 (1959).

5) A. E. Martell and M. Calvin, "Chemistry of the Metal Chelate Compounds," Prentice-Hall, Inc., Englewood Cliffs, N. J. (1952), pp. 336—357.

6) D. Burk, J. Z. Hearon, L. Caroline, and A. L. Schade, *J. Biol. Chem.*, **165**, 723 (1946).

7) J. Z. Hearon, *J. Natl. Cancer Inst.*, **9**, 1 (1948).

8) J. Z. Hearon and D, Burk, *ibid.*, **9**, 337 (1949).

9) J. Z. Hearon, *Federation Proceedings*, **6**, 259 (1947).

10) Y. Sano and H. Tanabe, *J. Inorg. Nucl. Chem.*, **25**, 11 (1963)

chelate was synthesized according to the above method.[10]

Found: C, 31.96; H, 5.16; N, 18.51%. Calcd for $[Co(C_6H_8N_3O_2)_2]_2O_2 \cdot 7H_2O$: C, 31.65; H, 5.27; N, 18.46%. Brown powder.

μ-Oxy-bis[Cobalt di(2,3-diaminopropionate)], $[Co(DAP)_2]_2O_2 \cdot 5H_2O$: A solution containing 2,3-diaminopropionic acid monohydrochloride (10 mmol) and cobalt(II) chloride 6-hydrate (5 mmol) in 10 m*l* of water was adjusted to pH 8.5 with a 1 N sodium hydroxide. After oxygen gas was passed for about 10 min at 10°C and 40 m*l* of acetone added, the solution was cooled. The resulting brown precipitate was collected on a funnel, washed successively with 60 per cent acetone, acetone and ether, and dried over calcium chloride under reduced pressure to give brown powder.

Found: C, 21.96; H, 5.71; N, 16.95%. Calcd for $[Co(C_3H_7N_2O_2)_2]_2O_2 \cdot 5H_2O$: C, 22.09; H, 5.83; N, 17.18%.

μ-Oxy-bis[Cobalt di(2,4-diaminobutyrate)], $[Co(DAB)_2]_2O_2 \cdot 6H_2O$: The same procedure as in the synthesis of $[Co(DAB)_2]_2O_2 \cdot 5H_2O$ was employed, using cobalt(II) chloride 6-hydrate and 2,4-diaminobutyric acid 2-hydrochloride. Brown powder.

Found: C, 26.54; H, 6.52; N, 15.40%. Calcd for $[Co(C_4H_9N_2O_2)_2]_2O_2 \cdot 5H_2O$: C, 26.45; H, 6.61; N, 15.43%.

The numbers of water were confirmed also by the weight loss at 40° and 100°C from the thermogravimetric curves of the complexes.

Apparatus and Procedures. Polarograms were obtained with a Yanagimoto recording polarograph, P. B.-104. Sample solutions contained 10^{-3} M cobalt(II) ion, 2×10^{-3} M chelating agent, 0.1 M potassium chloride, 0.05% gelatin, and 10^{-2} M potassium dihydrogen phosphate-disodium hydrogen phosphate buffer or 10^{-2} M ammonium chloride-ammonia buffer.

The stability constant of oxygenated complexes was determined with a Warburg manometer.[8] A solution of chelating ligand and a buffer solution were pipetted into the main room of reaction vessel and cobalt(II) chloride solution, into the sub-chamber of the vessel. The reaction volume was 2.00 m*l*, the final concentration of cobalt(II) ion was 10^{-2} M and the amount of chelating ligand was so arranged that the cobalt ion was completely converted to the chelate when two solutions were mixed. After the solutions were kept at the desired temperature (5—70°C) for a few minute in a water bath, cobalt solution was transferred into the main room and the mixture was shaken until equilibrium was attained. Oxygen consumption was then measured with a manometer, and the stability constant was calculated by the equation

$$K = \frac{[(CoL_2)_2O_2]}{[CoL_2]^2[O_2]}$$

where $[CoL_2]$ is the conentration of cobalt(II) chelate and $[O_2]$ is the solubility of oxygen gas under the conditions applied.

Results and Discussion

New Oxygenated Cobalt Complexes. The reaction

TABLE 1. REACTION BEHAVIORS OF COBALT(II) CHELATES WITH OXYGEN GAS

Ligand	pH	Visible spectrum[a] in the presence of O_2	Reaction with O_2	O_2-Uptake[b] (μ*l*)	O_2 Released[b][c] (%)	
Histidine	7.5	A	oxygenation	107	100	after 1 hr
Histidine	8.5	A	oxygenation	123	100	1 hr
Histidine	10.0	A	oxygenation	154	92	20 min
Histidine methyl ester	8.0	A	oxygenation	102	100	30 min
Histamine	9.0	C′	oxidation			
1-Methylhistidine	9.0	B	no-reaction			
N-Acetylhistidine	9.0	B	no-reaction			
Acetylacetone	9.0	B	no-reaction			
Glycine	9.0	B	no-reaction			
Alanine	9.0	B	no-reaction			
Proline	9.0	B	no-reaction			
Glutamic acid	9.0	B	no-reaction			
o-Phenanthroline	8.0	C	oxidation			
Ethylenediamine	8.0	C	oxidation			
Diethylenetriamine	8.0	C	oxidation			
Diaminopropionic acid	7.5	A	oxygenation	201	96	20 min
Diaminopropionic acid	8.5	A	oxygenation	212	85	20 min
Diaminobutyric acid	7.5	A	oxygenation	140	100	20 min
Diaminobutyric acid	8.5	A	oxygenation	182	91	20 min
Ornithine	9.0	A	oxygenation	34	100	20 min
Ornithine	10.0	A	oxygenation	93	95	20 min
Ornithine	10.0	C′				
Histidine	9.0	C′	oxidation after standing for one night at 60°C			
Diaminopropionic acid	9.0	C′				
Diaminopropionic acid	9.0	C′				

a) A: Spectra of these cobalt complexes are the same as that of oxygenated cobalt histidine complex reported by Hearon.[7]
B: Same as cobalt(II) chelate
C: Same as cobalt(III) chelate
C′: Same as cobalt(III) complex named as irreversible complex by Hearon[7]

b) Conditions of oxygen-uptake measurements;
Concentration of cobalt chelate: 10^{-2}M
Volume of the solution : 2.0 m*l*
Temperature : 30°C

c) Recovery of oxygen gas was attained by acidifying the solution after standing for the assigned time.

behaviors of various cobalt(II) chelates with oxygen gas are summarized in Table 1, which includes the three new oxygenated complexes found. Oxygen release was made by acidifying the solution, which had been contacted with air or oxygen gas for an appropriate time. As the contact time was prolonged, oxygen recovery became lower, accompanying color change. This phenomenon indicates that the oxygenated complexes are slowly oxidized to the cobalt(III) chelate. It can be deduced that if a reasonable amount of oxygen is released by acidification, the main reaction of cobalt(II) chelate by contact with oxygen gas is oxygenation, but not oxidation. Table 1 is classified according to this concept. Oxygenation, oxidation, and no-reaction could be also spectrophotometrically distinguished, because the absorption spectra of cobalt(II) chelates, cobalt(III) chelates and the oxygenated complexes differ from each other.

Cobalt(II) chelates with 2,3-diaminopropionic acid (HDAP), $NH_2 \cdot CH_2 \cdot CH < \begin{matrix} COOH \\ NH_2 \end{matrix}$, 2,4-diaminobutyric acid (HDAB), $NH_2 \cdot CH_2 \cdot CH_2 \cdot CH < \begin{matrix} COOH \\ NH_2 \end{matrix}$, and ornithine (HOrn), $NH_2 \cdot CH_2 \cdot CH_2 \cdot CH_2 \cdot CH < \begin{matrix} COOH \\ NH_2 \end{matrix}$, are readily oxygenated. The oxygen uptake behaviors are shown in Fig. 1.

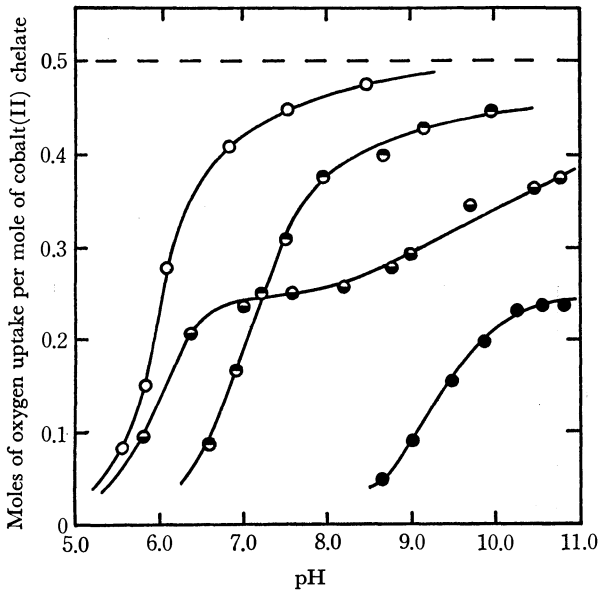

Fig. 1. Oxygen uptake of Cobalt(II) chelates.
○: $Co(DAP)_2$; ◒: $Co(Hid)_2$; ◓: $Co(DAB)_2$; ●: $Co(Orn)_2$
concentration of the chelates: 10^{-2}M
volume: 2 ml
temperature: 30°C

The reversibility of oxygenation-deoxygenation was studied by measuring the color change of solution, which occurred by aeration and thereafter by bubbling nitrogen gas. The anaerobic solutions are slightly pink, but they become deep amber in the oxygenation process. The oxygenated ornithine complex can be easily deoxygenated, but the DAP and the DAB complexes are hardly deoxygenated at room temperature. The reversibility increases in the order

$$[Co(DAP)_2]_2O_2 < [Co(DAB)_2]_2O_2$$
(partially deoxygenated)
$$\ll [Co(Orn)_2]_2O_2 < [Co(Hid)_2]_2O_2$$
(reversibly deoxygenated)

It has been considered that the imidazole ring is essential for the specific oxygenation of cobalt histidine chelate. Any oxygenated cobalt(II) chelates with amino acids, which did not have imidazole ring, were not found up to date, and further more the chelate with 1-methylhistidine, imidazole of which is blocked, is not oxygenated. However, the chelate with *N*-acetylhistidine, the amino group of which is blocked but not imidazole, does not absorb oxygen gas, and this shows that amino group is also dispensable. On the other hand, the new oxygenated complexes indicate that the imidazole ring is not always necessary. But it can be stated that the ligands having two nitrogen doners and a carboxyl or a carbonyl group are suitable. Carboxyl or carbonyl group seems to play an important role in the oxygenation reversibility, because the histidine chelate and the histidine methyl ester chelate are reversibly oxygenated, but not the histamine chelate.

Magnetic Properties and Electronic Absorption Spectra. Magnetic moments of the oxygenated cobalt complexes were obtained at 25°C with the Gouy balance. Oxygenated complexes of $Co(DAP)_2$, $Co(DAB)_2$, and $Co(Orn)_2$ showed 0.17, 0.14, and 0.15 Bohr magnetons, respectively. As reported on diamagnetic $[Co(Hid)_2]_2O_2$,[8] such small moments can be attributed to cobalt(II) chelate impurity resulting from incomplete oxygenation, and the new oxygenated complexes should be diamagnetic. Figure 2 show the electronic absorption spectra of the new oxygenated cobalt complexes. The shape

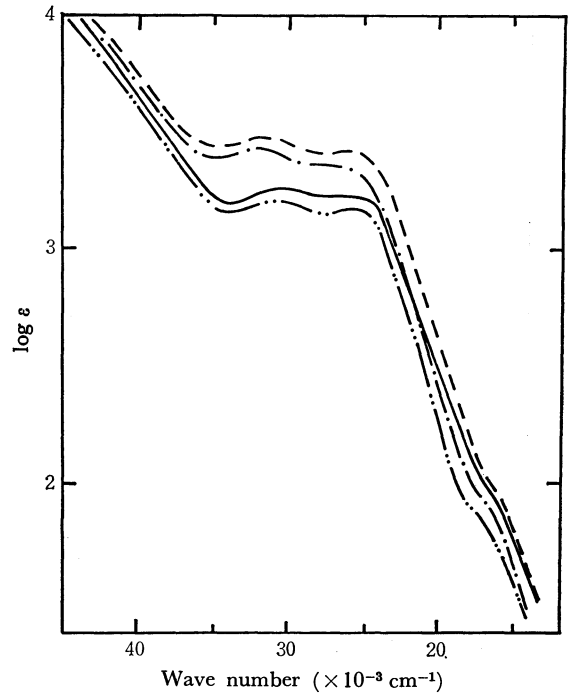

Fig. 2. Electronic absorption spectra of oxygenated cobalt complexes.
——: $[Co(Hid)_2]_2O_2$ ------: $[Co(DAP)_2]_2O_2$
- - -: $[Co(DAB)_2]_2O_2$ —·—·—: $[Co(Orn)_2]_2O_2$
pH: 9.00 (except for pH 10.00 in $[Co(Orn)_2]_2O_2$)

of the spectra resembles that of the oxygenated histidine complex, but are quite different from those of the cobalt(II) chelates (Fig. 3) and the cobalt(III) chelates[11] (Fig. 4). From these results, the new oxygenated complexes may be regarded as diamagnetic O_2-bridged binuclear cobalt complexes like the histidine complex, in which one unpaired electron from each of the cobalt(II) ions is paired with each of two unpaired electrons from molecular oxygen.

Valency States of Cobalt and Coordinated Molecular Oxygen in Oxygenated Cobalt Complexes. Figure 5 shows the polarograms obtained with cobalt(II) DAP chelate ($Co(DAP)_2$), the oxygenated complex ($[Co(DAP)_2]_2O_2$), and the cobalt(III) chelate ($[Co(DAP)_2]^+$).[12] The oxygenated complex, $[Co(DAP)_2]_2O_2$,

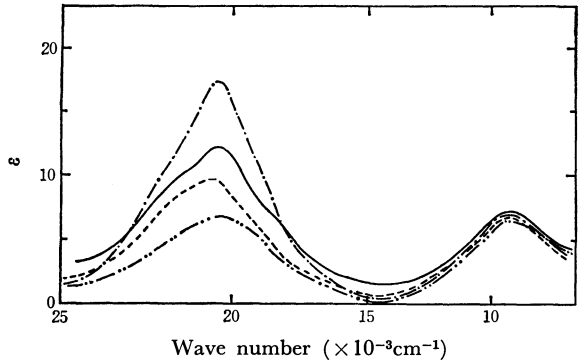

Fig. 3. Electronic absorption spectra of cobaltous chelates.
——: $Co(Hid)_2$ ------: $Co(DAP)_2$
- - -: $Co(DAB)_2$ -·-·-: $Co(Orn)_2$ pH: 9.00

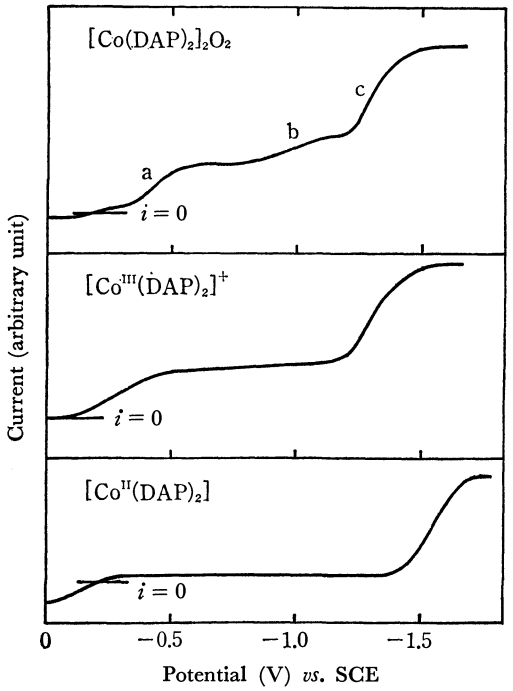

Fig. 5. Polarograms of cobalt(II) chelate, cobalt(III) chelate and the oxygenated complex with diaminopropionic acid.
pH: 8.70

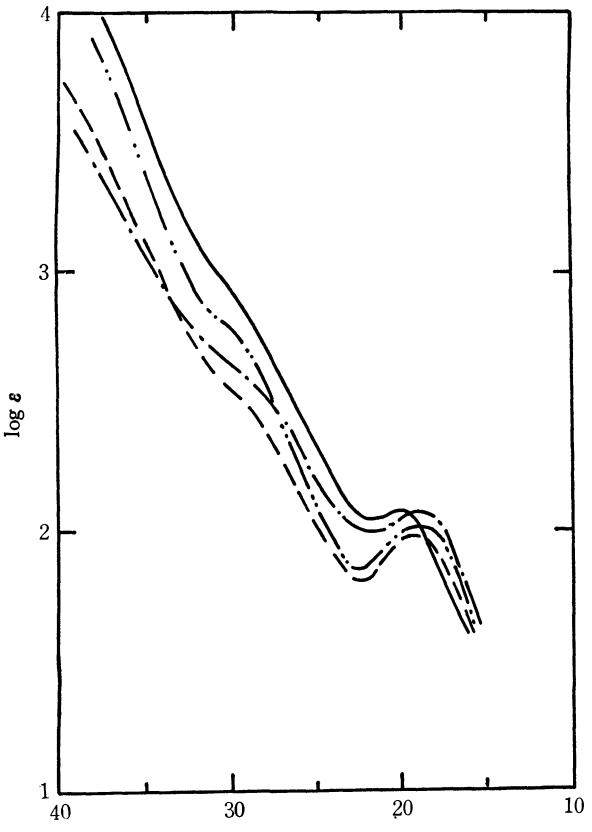

Fig. 4. Electronic absorption spectra of cobaltic chelates.
——: $[Co(Hid)_2]^+$ ------: $[Co(DAP)_2]^+$
- - -: $[Co(DAB)_2]^+$ -·-·-: $[Co(Orn)_2]^+$
pH: 9.00

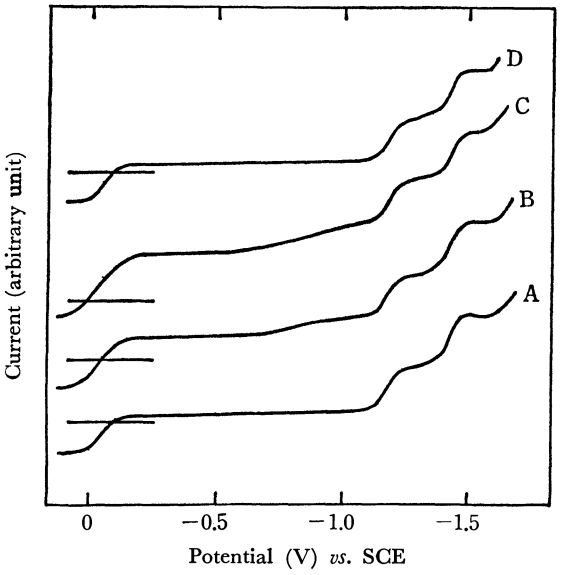

Fig. 6. Polarograms of cobalt histidine chelates.
A: solution of $Co^{II}(Hid)_2$ in the absence of air
B: after passing O_2 for 30 sec in solution A
C: after passing O_2 for 30 sec in solution B
D: after passing N_2 for 30 min in solution C
pH: 8.70

show three waves. The first wave (a) must be the reduction wave of cobalt(III) to cobalt(II), since an identical wave is observed with the cobalt(III) chelate,

11) Cobalt(III) chelate solutions were prepared by blowing oxygen gas into the cobalt(II) chelate solutions for one day at 60°C, and valency state of the cobalt (III) was confirmed by the polarograms (Ref. 12).

12) B. Jaselskins, *J. Amer. Chem. Soc.*, **80**, 1283 (1958)

Table 2. Redox potential of Co(III)/Co(II) and $H_2O_2/2H_2O$, stability constants of oxygenated cobalt complexes ($[CoL_2]_2O_2$), and enthalpy changes of oxygenation

$[CoL_2]_2O_2$	L=Hid	L=Orn	L=DAB	L=DAP
Co(III)/Co(II) (V)	−0.03	−0.15	−0.27	−0.41
$H_2O_2/2H_2O$ (V)	−0.97	−0.97	−0.97	−0.96
Stability, K[a)]	6.6×10^5	2.7×10^5	7.2×10^6	9.1×10^7
$\Delta H_{30°C}$ (kcal/mol)	−25.5	−19.6	−26.7	−29.3

pH: 8.70 (pH: 10 for Orn)
Temperature: 30°C
a) $K=\dfrac{[(CoL_2)_2O_2]}{[CoL_2]^2\,[O_2]}$

but not with the cobalt(II) chelate. The second wave (b) is observed only with oxygenated complexes. Although the exact value can not be measured, because of little overlap with wave (c), the half-wave potential (−0.96 V *vs.* SCE) is nearly equal to the reduction potential of hydrogen peroxide (−0.95 V). The potential is independent of the kind of oxygenated complexes, and wave (b) might result from hydrogen peroxide produced in the reduction process of cobalt(III) to cobalt(II):

$$[L_2Co^{III}\text{–}O_2^{2-}\text{–}Co^{III}L_2] \xrightarrow[2H^+]{2e^-} 2Co^{II}L_2 + H_2O_2$$

The last wave (c) is attributed to the reduction of cobalt(II) to metallic cobalt.

The polarograms of cobalt histidine complexes are shown in Fig. 6. The *i-E* curve is deformed by passing air or oxygen gas through the solution, but it slowly returns to the original shape by bubbling nitrogen gas. The first wave of polarograms obtained with the anaerobic solution is the oxidation wave, which might be attributed to the oxidation of cobalt(II) to cobalt(III) (A and D in Fig. 6). As oxygenation proceeds by aeration, the negative current decreases and simultaneously positive current increases (B and C in Fig. 6), but the half-wave potential remains almost constant (−0.03 V). These solutions give the second wave at the same potential (−0.97 V) as that of $[Co(DAP)_2]_2O_2$, *i.e.* the reduction potential of hydrogen peroxide. The current increases with the increase in positive current of the first wave, but the ratio of the former current to the latter is somewhat smaller than unity. This may be caused by the difference in both diffusion currents. Caglioti *et al.*[13] also reported that the polarograms of $[Co(Hid)_2]_2O_2$ showed the redox wave of cobalt(III)/cobalt(II) and the reduction wave of hydrogen peroxide. The third and fourth waves may be due to the reduction of cobalt(II) to cobalt(I) and cobalt(I) to cobalt(0), respectively. The other oxygenated complexes, $[Co(DAB)_2]_2O_2$ and $[Co(Orn)_2]_2O_2$ show a similar polarographic behavior. The reduction potentials of the central cobalt(III) ions and O_2-type oxygen are given in Table 2.

These results lead to the conclusion that the coordinated molecular oxygen accepts two electrons from two cobalt(II) ions to attain the state of O_2^{2-}, and at the same time, two cobalt(II) ions are oxidized to cobalt(III) ions.

13) V. Caglioti, P. Silvestroni, and C. Futlani, *J. Inorg. Nucl. Chem.*, **13**, 90 (1960)

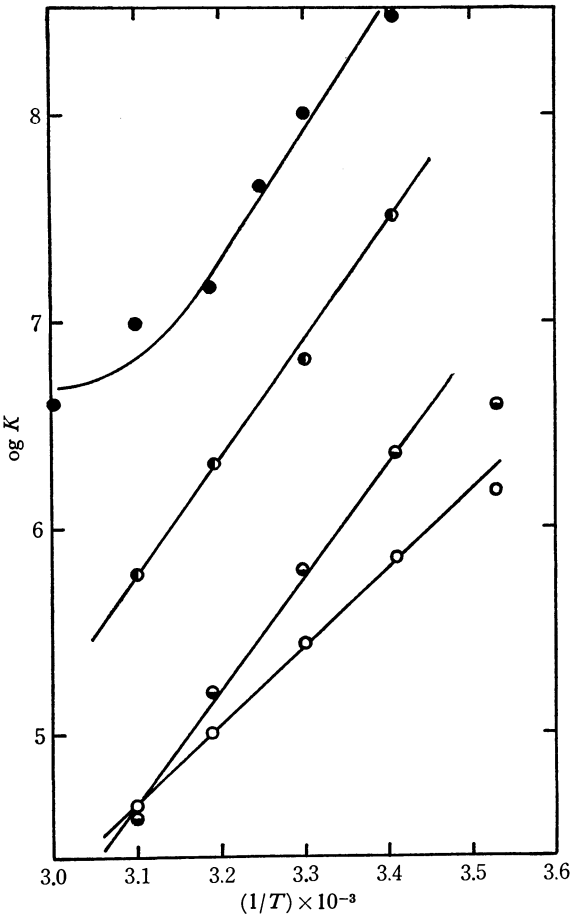

Fig. 7. Stabilities of oxygenated cobalt complexes.
○: $[Co(Orn)_2]_2O_2$; ◒: $[Co(Hid)_2]_2O_2$;
◐: $[Co(DAB)_2]_2O_2$; ●: $[Co(DAP)_2]_2O_2$;
pH=8.70 (pH=10.0 for $[Co(Orn)_2]_2O_2$)
$K=[(CoL_2)_2O_2]/[CoL_2]^2\cdot[O_2]$

Accordingly, two electrons of O_2^{2-} must be returned to the cobalt(III) ions by deoxygenations. This is confirmed by the fact that the oxygenated complexes, of which the central cobalt(III) ion gives more positive reduction potential, can be more easily deoxygenated.

Thermodynamics of Oxygenation of Cobalt Chelates. In Table 2, are presented the stability constants of the oxygenated complexes and the enthalpy changes of the oxygenation calculated from Fig. 7. Oxygenation is an exothermal process and the enthalpy change is larger in irreversible oxygenation than in the reversible one. In other words, deoxygenation, an endothermal pro-

cess, occurs when the enthalpy change of the oxygenation is small. The histidine complex is unique, because $[Co(Hid)_2]_2O_2$ is more easily deoxygenated than $[Co(Orn)_2]_2O_2$ in spite of the higher enthalpy change. This may be due to the presence of the imidazole ring, although no definite explanation can be given.

Effect of Ligand-Field on Oxygenation. Cobalt chelates with glycine, alanine, proline, and glutamic acid are neither oxygenated nor oxidized, whereas the chelates with *o*-phenanthroline (phen), ethylenediamine (en), and diethylenetriamine (dien) are oxidized immediately after oxygenation (Table 1).

From the spectrochemical series or the strength order of ligand-field,

$$\text{oxalate} < \text{glycine} < \text{en} \sim \text{dien} < \text{phen} \quad \text{(ligand)}$$

$$F^- < O < N < C \quad \text{(donor atom)},$$

it might be reasonable to consider that ligand-field of (N-O) type ligands, glycine, 1-methylhistidine, and *N*-acetylhistidine is weaker than of that (N–N) type ligands, en, dien, phen, and histamine. As observed above, ligands available to the oxygenation are (N–N) type compounds with a carboxyl or carbonyl group at the α position to an amino group. In such a situation, carboxyl or carbonyl group probably weakens the coordination power of the nitrogen atom. This anticipation is ascertained by the fact that ligand-field absorption band (20.3 kK) of cobalt(II) histidine methyl ester chelate appears at the frequency region between those of (N–N) type histamine chelate (20.5 kK) and (N–O) type glycine chelate (20.0 kK).

These results and polarographic data suggest that an important factor of oxygenation is the strength of ligand-field and at least medium strenght is favorable for reversible oxygenation.

Effect of Solvent on Deoxygenation. In aqueous solution, $[Co(DAP)_2]_2O_2$ and $[Co(DAB)_2]_2O_2$ are hardly deoxygenated, and irreversibly oxidized slowly even at room temperature and rapidly at higher temperatures (Fig. 8). However, in the solution containing more than 60 per cent ethanol, those complexes can be deoxygenated at higher temperatures. Although the experiments in other organic solvents could not be carried out, because of the low solubility of oxygenated

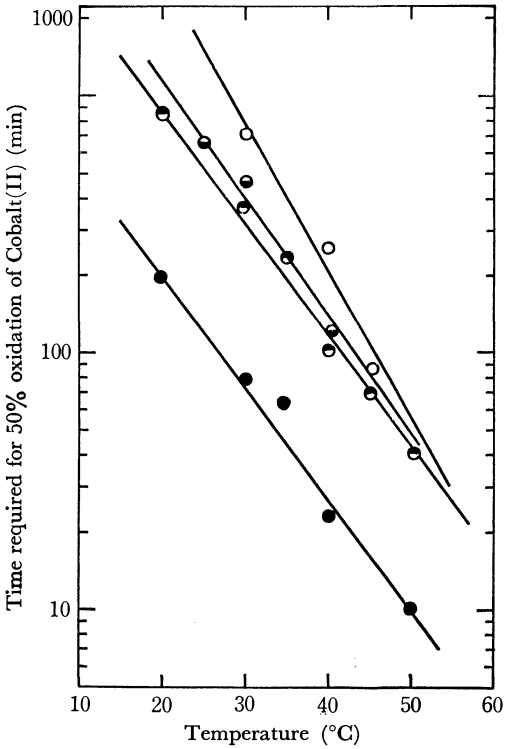

Fig. 8. Oxidation of oxygenated cobalt complexes.
○: $[Co(Hid)_2]_2O_2$ ◓: $[Co(Orn)_2]_2O_2$
◒: $[Co(DAB)_2]_2O_2$ ●: $[Co(DAP)_2]_2O_2$
pH: 8.70 (except for pH 10.00 in $[Co(Orn)_2]_2O_2$)

complexes, it can be expected that oxygenated complexes are more easily deoxygenated in nonpolar solvents than in aqueous solution.

In this paper, discussion was made mainly from the viewpoint of the ligand-field strength of the chelating agents. Changes of entropy and enthalpy might be important, because reduction potential of the central cobalt(II) ion is related to the free energy. In order to understand more closely the reversible mechanism the entropy effect must be considered.

The author wishes to express his deep gratitude to Prof. Tsunenobu Shigematsu, Dr. Masayuki Tabushi, and Dr. Masakazu Matsui for their unfailing guidance throughout the course of this work.

Electron-Transfer Reactions of Multidentate Ligand Cobalt(III) Complexes. II. The Effect of Nonbridging Ligands

Yoshimi KURIMURA and Kousaburo OHASHI*

College of General Education, Ibaraki University, Mito

**Department of Chemistry, Ibaraki University, Mito*

(Received September 24, 1970)

The specific rates for the Fe^{2+} reductions of *cis*-$Co(en)_2ACl^{2+}$ (A=methyl-, ethyl-, propyl-, butyl-, ethanol-, and propanolamine), $Co(dien)(en)Cl^{2+}$ and $Co(tetren)Cl^{2+}$ have been determined. The observed rates are relatively insensitive to the *cis*-ligand of the A. The rate constant for the *cis*-$Co(en)_2ACl^{2+}$ decreases with an increase in the size of the A ligand. In such cases as that of the aminoalcohol ligand, the rate is greater than that of the corresponding alkylamine ligand complex. The effect of chelation by nonbridging ligands has been discussed by comparing the relative effectiveness for Fe^{2+} reductions of CoN_5Cl^{2+} ($N_5=(NH_3)_5$, $(en)_2NH_3$, (dien)(en), and tetren) with that for Cr^{2+} reductions of some Co(III) complexes.

One of the most interesting points encountered in the inner-sphere electron-transfer reactions of Co(III) complexes may be the effect of nonbridging ligands on the specific rates of the reactions. It has been demonstrated that the reactivity patterens of Co(III) complexes in the electron-transfer reactions which proceed through bridged activated complexes may be much affected by the effects of the ligand-field strength of the *trans*-ligand (the a effect)[1,2] and by the energy required to stretch the *trans*-ligand away from the Co(III) center (the b effect).[3] Another explanation has been proposed by Fraser;[4] he explained the effect of chelate formation by nonbridging ligands on the reactivity of the Co(III) complexes with a CoN_5X^{n+} configuration, where X is OAc^-, Cl^-, and SO_4^{2-}, in terms of the solvation energy (the c effect).

It has been shown in the previous paper[5] that the effects of both (a) and (b) may be important in the Fe^{2+} reductions of *cis*-CoN_4XCl^{n+} ($N_4=(NH_3)_4$, $(en)_2$, and trien, $X=H_2O$ and Cl^-), since the free energy for bond stretching for the Co–N bond, in which N is the nitrogen atom located in the *trans*-position to the chloride ion, has a relatively large portion of free energy of activation.

The effect of *cis*-ligand on the rate has also been studied, and it has been demonstrated that the size of the nonbridging *cis*-ligand of B is not the most important factor in determining the reactivity of *cis*-$Co(en)_2BCl^{2+}$.[6,7]

The purposes of this study are to investigate the effect of the nonbridging ligand in the Co(III) complexes and to obtain some detailed information about the effect of the *cis*-ligand in the Fe^{2+} reductions of *cis*-$Co(en)_2ACl^{2+}$ complexes.

Experimental

Materials. *cis*-$[Co(en)_2ACl]Cl_2$,[8,9] $[Co(tetren)Cl]Cl_2$[10] (tetren=tetraethylenepentamine), and $[Co(dien)(en)Cl]Cl_2$[10] (dien=diethlenetrianime and en=ethylenediamine) were prepared by the procedures described in the references cited. The identities of these complexes were confirmed analytically and spectrophotometrically. The preparation of the iron(II) perchlorate solution and the determinations of concentrations of iron(II), the perchlorate anion, and the hydrogen ion were carried out using procedures previously reported.[5] All the other chemicals were of a reagent grade and were used without further purification. The concentrations of perchlorate and hydrogen ions in the iron(II) solution were adjusted by the addition of sodium perchlorate and perchloric acid.

Kinetic Measurements. The general procedure was to make up the reaction mixture in a Erlenmayer flask, and then to transfer the mixture to a spectrophotometer cell, which had been placed in a thermostated cell compartment of a Hitachi Model 124 spectrophotometer, using a injection syringe. The reactions were followed by observing the decrease in the absorbance of the Co(III) complexes at the wavelength in the vicinity of the first absorption maximum. The wavelengths used were 535 nm, 525 nm, and 480 nm in the cases of *cis*-$Co(en)_2ACl^{2+}$, $Co(dien)(en)Cl^{2+}$, and $Co(tetren)Cl^{2+}$ respectively. All the measurements were carried out under pseudo-first-order conditions, in which there was much more iron(II) than Co(III) complexes. The second-order rate constant for the iron(II) reduction of the Co(III) complex defined by $-d[Co(III)]/dt=k[Co(III)][Fe(II)]$ was calculated from the concentration of iron(II) and the slope of the $\log(A_t-A_\infty)$ *vs.* time plot, which is equal to $-k[Fe^{2+}]/2.303$, where A_t is the absorbance at time t; A_∞, the absorbance after all the Co(III) complex has been reduced to Co(II), and k, the rate constant. The value of A_∞ was calculated by the $A_\infty=\varepsilon[Co(II)]$ equation, where [Co(II)] is equal to the initial concentration of the Co(III) complex and where ε is the molar extinction coefficient of the aquo-cobalt(II) ion.

Results

Reductions of cis-*Co(en)$_2$ACl^{2+}.* In all cases, the $\log(A_t-A_\infty)$ *vs.* t plots were substantially linear for at

1) L. Orgel, Report of the Tenth Solvay Conference, Brussels, p. 289 (1956).
2) H. Taube, *Adv. Inorg. Chem.*, **1**, 1 (1959).
3) P. Benson and A. Haim, *J. Amer. Chem. Soc.*, **89**, 3945 (1967).
4) R. T. M. Fraser, *Inorg. Chem.*, **2**, 954 (1963).
5) Y. Kurimura, K. Ohashi, T. Ohtsuki, and H. Yamamoto, This Bulletin, **44**, 1293 (1971).
6) R. C. Patel and J. F. Endicott, *J. Amer. Chem. Soc.*, **90**, 6364 (1968).
7) R. C. Patel, R. E. Ball, J. F. Endicott, and G. Huhges, *Inorg. Chem.*, **9**, 23 (1970).
8) J. C. Bailar, Jr., and L. B. Clapp, *J. Amer. Chem. Soc.*, **67**, 171 (1945).
9) S. C. Chan and F. Leh, *J. Chem. Soc., A*, **1966**, 760.
10) R. G. Peason, C. R. Boston, and F. Basolo, *J. Phys. Chem.*, **59**, 304 (1955).

TABLE 1. RATE CONSTANTS FOR Fe^{2+} REDUCTIONS OF *cis*-$Co(en)_2ACl^{2+}$
$\sum(ClO_4^-)=1.0$M, $[H^+]=0.10$M

Exp. No.	A	[Fe(II)] M	[Co(III)] 10^{-3}M	Temp.,°C (±0.1°C)	Rate constant 10^{-5} M^{-1} sec^{-1}
1	Methylamine	0.472	6.26	25.0	2.79
2	Methylamine	0.254	6.52	25.0	2.65
3	Methylamine	0.472	6.57	35.0	6.22
4	Methylamine	0.472	6.80	44.0	12.3
5	Ethylamine	0.472	6.62	25.0	2.74
6	Ethylamine	0.254	5.60	25.0	2.65
7	Ethylamine	0.472	7.47	35.0	5.91
8	Ethylamine	0.472	6.93	44.0	11.8
9	Propylamine	0.415	6.01	25.0	2.57
10	Propylamine	0.254	6.40	25.0	2.59
11	Propylamine	0.415	5.86	35.0	5.87
12	Propylamine	0.415	6.21	44.0	11.1
13	Butylamine	0.472	5.60	25.0	2.08
14	Butylamine	0.254	5.81	25.0	1.98
15	Butylamine	0.472	4.04	34.5	4.40
16	Butylamine	0.472	4.27	44.0	9.71
17	Ethanolamine	0.415	4.18	25.0	4.63
18	Ethanolamine	0.254	5.86	25.0	4.72
19	Ethanolamine	0.415	4.04	34.5	11.0
20	Ethanolamine	0.415	5.89	44.0	19.4
21	Propanolamine	0.415	6.35	25.0	3.14
22	Propanolamine	0.254	5.51	25.0	3.07
23	Propanolamine	0.415	4.19	34.5	7.67
24	Propanolamine	0.415	4.16	44.0	13.9

TABLE 2. RATE CONSTANTS AND ACTIVATION PARAMETERS FOR Fe^{2+} REDUCTIONS OF *cis*-$Co(en)_2ACl^{2+}$ AT 25°C

A	Rate constant[a] 10^{-5} $M^{-1}sec^{-1}$	ΔF^{*}[b]	ΔH^{*}[b]	ΔS^{*} e.u.	pK_a	
NH_3	1.8[c]				9.25	
Methylamine	2.72	23.7	13.9	−32.7	10.72,[d]	10.62[h]
Ethylamine	2.70	23.7	13.8	−33.1	10.81[e]	10.63[h]
Propylamine	2.58	23.7	13.4	−34.5		10.53[h]
Butylamine	2.03	23.8	13.8	−33.7	10.71[f]	10.61[h]
Ethanolamine	4.68	23.3	13.8	−32.0	9.74[g]	9.50[h]
Propanolamine	3.11	23.6	14.5	−30.4		

a) Except for A=NH_3, average values obtained by this work at 25 ± 0.1°C.
b) Units are kcal·mol^{-1}.
c) From Ref. 3.
d) R. Yaffe and A. F. Voight, *J. Amer. Chem. Soc.*, **74**, 5043 (1952).
e) G. A. Carlson, J. P. McReynolds, and F. H. Verhoek, *J. Amer. Chem. Soc.*, **67**, 1344 (1945).
f) J. Bjerrum, *Chem. Rev.*, **46**, 381 (1950).
g) R. J. Bauehlman and F. H. Verhoek, *J. Amer. Chem. Soc.*, **70**, 1401 (1948).
h) A. Albert and E. P. Sergent, "Ionization Constants of Acid and Bases," Methuen and Co., Ltd., London (1962).

least 2 half-lives. Summeries of the kinetic measurements and activation parameters are presented in Tables 1 and 2 respectively.

Reductions of Co(dien)(en)Cl^{2+} and Co(tetren)Cl^{2+}. The second-order rate constant for the Fe^{2+} reduction of Co(dien)(en)Cl^{2+} was obtained from the slope of the $\log(A_t-A_\infty)$ plot (see Fig. 1) and the concentration of the Fe^{2+}. The $\log(A_t-A_\infty)$ plots were linear up to 1000 min in all cases, so the effect of aquations of the Co(III) complexes could be neglected. The reported rate constant for the aquation of Co(dien)(en)Cl^{2+} is 5.2×10^{-7} sec^{-1} at 35°C and pH=1.[8] Though the rate of the disappearence of the Co(dien)(en)Cl^{2+} was followed up to 1000 min, the value of A_t-A_∞ was relatively small since the reduction rate was very slow; therefore, the rate constants obtained were of poor quality. The second-order rate constants for the Fe^{2+} reduction of the Co(dien)(en)Cl^{2+} are presented in Table 3. Our attempt to determine the rate constant for the Fe^{2+} reduction of Co(tetren)Cl^{2+} by the above method failed because of the extremely slow reaction rate. The absorbance of a reaction mixture containing 0.46 M of iron(II) and 5.0×10^{-3} M of the complex at 580 nm under the conditions of $\sum[ClO_4^-]$

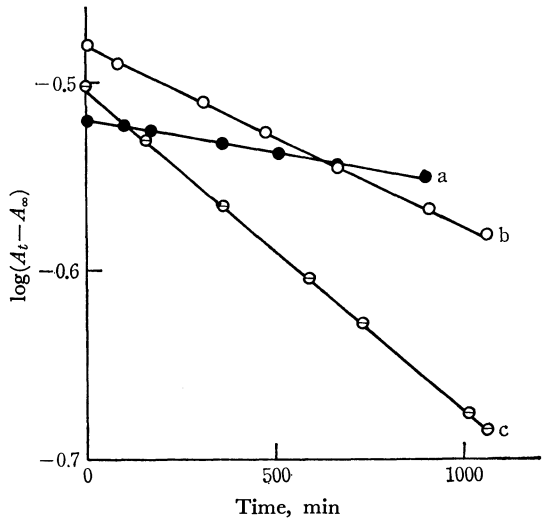

Fig. 1. Plots of $\log(A_t-A_\infty)$ *vs.* time for Fe^{2+} reduction of $Co(dien)(en)Cl^{2+}$.
a: $[Co(III)]=4.51\times10^{-3}$M, 25.0°C
b: $[Co(III)]=4.61\times10^{-3}$M, 33.0°C
c: $[Co(III)]=4.76\times10^{-3}$M, 40.0°C
$[Fe^{2+}]=0.37$M, $\sum[ClO_4^-]=1.0$M, $[H^+]=0.10$M

$=1.0$ M and $[H^+]=0.10$ M hardly decreased for 40 hr after the initiation of the reaction at 25°C. Therefore, the rate constant for the Fe^{2+} reduction of the Co(tetren)-Cl^{2+} was estimated not to exceed $10^{-8}M^{-1}sec^{-1}$ at 45°C.

Table 3. Rate constants for Fe^{2+} reduction of $Co(dien)(en)Cl^{2+}$ $\sum[ClO_4^-]=1.0$M

$[Fe^{2+}]$ M	$[Co(III)]$ 10^{-3}M	Temp., °C (±0.1°C)	Rate constant 10^{-6} M^{-1} sec^{-1}
0.13	5.57	25.0	6.2[a]
0.37	4.95	25.0	5.9[b]
0.37	4.51	25.0	6.0[b]
0.37	4.61	33.0	10[b]
0.37	4.76	40.0	16[b]

a) $[H^+]=0.10$M, b) $[H^+]=0.26$M

Discussion

Effect of the Nonbridging cis*-Ligand.* It may be reasonable to assume that all the reactions now beeing studied proceed *via* a chloride-bridged activated complex[3,5]. In such reactions of Co(III) complexes, it has been suggested that the effect of the nonbridging *cis*-ligand on the rate is of minor importance.[6] This trend also seems to be valid for the reactions of *cis*-$Co(en)_2ACl^{2+}$ with Fe^{2+} (Table 1). However, detailed information about the effect of the *cis*-ligand of the A is given by the results summarized in Table 1. The specific rate of the *cis*-$Co(en)_2NH_3Cl^{2+}$ is smaller than that of the alkylamine complexes under investigation. In such cases as the alkylamine ligands, the value of the ligand field may be slightly lowered in comparison to the ligand field for NH_3.[11,12] This may account for smaller effectiveness of the *cis*-$Co(en)_2NH_3Cl^{2+}$ than that of the *cis*-$Co(en)_2NH_2CH_3Cl^{2+}$. In the case of the alkylamine ligand, the reactivity successively decreases with an increase in the size of the amine ligand from methylamine to butylamine. Similar behavior was also observed in the case of the amino-alcohol ligand. A distinctive correlation between pK_a and the specific rate could not be found in the reactions of *cis*-$Co(en)_2ACl^{2+}$ with Fe^{2+}. A decrease in the rate with an increase in the size of the A may be due to a decrease in the stabilization of the activated state as the size of the A increases. The aminoalcohol complex is much more effective than the corresponding alkylamine complex. For example, the rate constant for the ethanolamine complex is 1.7 times that for the ethylamine complex. This suggests that the introduction of a hydroxyl group into the nonbridging *cis*-ligand facilitates the reaction rate. The presence of a hydroxyl group in the nonbridging ligand may stabilize the activated complex due to an increase in the solvation energy relative to that of the activated complex formed by the corresponding alkylamine ligand complex and Fe^{2+}.

Table 4. Rate constants for Fe^{2+} reductions of CoN_5Cl^{2+} complexes $\sum[ClO_4^-]=1.0$M, $[H^+]=0.10$M

Complex	Rate constant $M^{-1}sec^{-1}$	Ref.
$Co(NH_3)_5Cl^{2+}$	1.6×10^{-3} [a]	14
cis-$Co(en)_2NH_3Cl^{2+}$	$(1.8\pm0.1)\times10^{-5}$ [b]	3
$Co(dien)(en)Cl^{2+}$	6.0×10^{-6} [b]	this work
$Co(tetren)Cl^{2+}$	$<10^{-8}$ [b]	this work

a) 25.5°C. b) 25°C.

Effect of Chelation by Nonbridging Ligands. The relative effectiveness for Fe^{2+} reductions of the CoN_5-Cl^{2+} is appreciably decreased with an increase in the number of chelate rings in the Co(III) complex, as is shown in Table 4. The decreasing order of the effectiveness is $Co(NH_3)_5Cl^{2+}>Co(en)_2NH_3Cl^{2+}>Co$-$(dien)(en)Cl^{2+}>Co(tetren)Cl^{2+}$. Similar behavior was also observed in the Fe^{2+} reductions of *cis*-CoN_4OH_2-Cl^{2+}.[5] The effect of the *trans*-ligand on the rate of the electron-transfer reactions which proceed *via* the bridged activated complexes may be classified into: a) the ligand-field strength of the *trans*-ligand[1,2] and b) the energy required to stretch the *trans*-ligand away from the Co(III) center.[3] The relative reduction rate would be smaller if the *trans*-ligand has a stronger ligand field and/or if more energy is required to stretch the metal-ligand bond along the z axis. The relative effectiveness for Cr^{2+} reductions of CoN_5X^{n+} is decreased with an increase in the number of the chelate ring when $X=SO_4^{2-}$; however, the effectiveness is almost the same when $X=OAc^-$ and perhaps also when $X=Cl^-$.[4] The solvation effect was introduced by Fraser[4] to explain such results.

If we consider that the effects of (a) and (b) mentioned above are major factors in determining the rate of the electron-transfer reactions of the Co(III) complexes, the relative effectiveness for Cr^{2+} reductions of the CoN_5X^{n+}, whenever $X=OAc^-$, Cl^-, or SO_4^{2-}, would

11) M. Paris and N. F. Feiner, *Inorg. Nucl. Chem. Lett.*, **3**, 337 (1967).
12) S. C. Chan and K. Y. Hui, *Aust. J. Chem.*, **20**, 2529 (1967).

be changed by replacing the nonbridging ligand by an other ligand, for example, by replacing NH_3 by en or en by tetren, since the ligand-field strength may be increased in the order of NH_3<en<tetren and the energy needed for the removal of these ligand from the Co(III) center may be in the same order. On the other hand, when the solvation effect is considered to be only the predominant factor in determining the rate, the relative effectiveness for the Fe^{2+} reductions of the $Co(NH_3)_5Cl^{2+}$, $Co(en)_2NH_3Cl^{2+}$, Co(dien)(en)Cl^{2+}, and Co(tetren)Cl^{2+} would be almost the same as in the cases of Cr^{2+} reductions of the CoN_5OAc^{2+}, because the over-all charge on the Co(III) and Co(II) complexes and on the Fe(II) and Fe(III) complexes are identical, since the $FeCl^{2+}$ is the only Fe(III) species produced in the reaction:

$$CoN_5Cl^{2+} + Fe^{2+} \longrightarrow Co^{2+} + 5N + FeCl^{2+}$$

though it would dissociate into Fe^{3+} and Cl^- under the experimental conditions.[13]

Therefore, we assume that the free energies for the bond stretching of the Co–N bonds (ΔF_s) are very little in the case of CoN_5X^{n+}–Cr^{2+} reactions and large for CoN_5X^{n+}–Fe^{2+} reactions. It seems reasonably to say that the specific rates of the former reactions are hardly affected by chelate formation by nonbridging ligands if the over-all charge described above is not changed. However, the specific rates of the latter reactions are appreciably affected by the chelate formation of the nonbridging ligands, since ΔF_s may be mainly affected by the nature of the *trans*-ligand in this case. Such an assumption was reasonably accepted in the Fe^{2+} reductions of *cis*-CoN_4XCl^{n+} (N=NH_3, 0.5 en, and 0.25 trien and X=H_2O and Cl^-) in the previous work.[5] The results obtained here account for the fact that one of the most important factors in determining the rates of the electron-transfer reactions of the Co(III) complexes is the free energy for bond stretching of the Co–N bond in the Fe^{2+} reductions of *cis*-CoN_4XCl^{n+} and CoN_5Cl^{2+}. The major factors which affect the effectiveness may be: the effect of the solvation in the Cr^{2+} reductions of $CoN_5SO_4^+$, the ligand-field strength of the *trans*-ligand, and the energy required to stretch the Co–N bond in the Fe^{2+} reductions of the CoN_5Cl^{2+}, and the effect of the solvation, the ligand-field strength of the *trans*-ligand, and the stretching energy in the Fe^{2+} reductions of the *cis*-$CoN_4Cl_2^+$.

13) A. Haim and N. Sutin, *J. Amer. Chem. Soc.*, **88**, 5343 (1966).
14) H. Diebler and H. Taube, *Inorg. Chem.*, **4**, 1029 (1965).

BULLETIN OF THE CHEMICAL SOCIETY OF JAPAN, VOL. 44, 1800—1807 (1971)

The Photonuclear Reactions Leading to ^{24}Na and ^{28}Mg

Tatsuya SAITO*

Department of Chemistry, Faculty of Science, Tohoku University, Katahira-cho, Sendai

(Received November 24, 1970)

The photonuclear reaction yields of ^{24}Na and ^{28}Mg in magnesium, aluminum, silicon, phosphorus, and sulfur were obtained at energies between 20 MeV and 250 MeV by the induced radioactivity method. The ^{12}C(γ,n)^{11}C yield was used as a standard for the beam monitor. The excitation curves of the ^{27}Al→^{24}Na, ^{28}Si→^{24}Na, ^{30}Si→^{28}Mg, ^{31}P→^{24}Na, ^{31}P→^{28}Mg, ^{32}S→^{24}Na, and ^{32}S→^{28}Mg reactions were obtained from the yields by the photon-difference method. Each of these excitation functions indicates a peak in the 50—70 MeV energy range, except in the case of the sulfur target, in which the peak is due to the contribution from the compound-nucleus process. The interaction of photons with nuclei at photon energies exceeding the peak energy region probably does not lead to the formation of the compound nucleus. In the energy range from 70 MeV up to 150 MeV, the cross sections are due to the contribution from the quasi-deuteron process. At energies above 150 MeV and up to 250 MeV, the quasi-deuteron and pion production processes compete. In the high-energy photonuclear reaction mechanisms, the quasi-deuteron and pion production processes must be considered at the initial cascade process, but the evaporation process may be considered after the cascade process.

Photonuclear reactions have been studied, and detailed information has been obtained in the low-energy giant-resonance region.[1-3] Above the giant-resonance region, however, our information about the photonuclear cross sections and the reaction mechanisms is very scarce.

Many workers have investigated high-energy reactions induced by high-energy-charged particles, and the details of these mechanisms are by now well known.[4] The mechanism of high-energy nuclear reactions, the cascade evaporation process, is currently regarded as providing the proper description for reactions initiated by particles with incident energies large in comparison with the binding energies of the nucleons within the target nucleus.[5,6] A similar reaction induced by high

* Present address: Department of Applied Chemistry, Faculty of Engineering, Tohoku University, Sendai.

1) R. Montalbetti, L. Katz, and J. Goldemberg, *Phys. Rev.*, **91**, 659 (1953).
2) R. Nathans and J. Halpern, *ibid.*, **93**, 437 (1954).
3) B. L. Berman, J. T. Caldwell, R. R. Harvey, M. A. Kelly, R. L. Bramblett, and S. C. Fultz, *ibid.*, **162**, 1096 (1967).
4) J. M. Miller and J. Hudis, *Ann. Rev. Nucl. Sci.*, **9**, 159 (1959).
5) K. Chen, Z. Fraenkel, G. Friedlander, J. R. Grover, J. M. Miller, and Y. Shimamoto, *Phys. Rev.*, **166**, 949 (1968).
6) R. G. Korteling and A. A. Caretto, Jr., *ibid.*, **CI**, 1960 (1970).

energy bremsstrahlung with a maximum energy greater than 100 MeV was expected. It is an interesting problem to study the mechanisms by which the complex nucleus absorbs high-energy photons. In this fields, the following processes have been proposed to explain the photonuclear cross section data: the quasi-deuteron and the pion production processes. In order to explain the high-energy photonuclear reactions, several experiments have previously been reported on the yields and cross sections as determined by the activation method.[7-9] Debs *et al.*[7,8] irradiated several elements of medium weight by 320 MeV bremsstrahlung, thus obtaining the relative yields. By their data, the mechanism of the high-energy photonuclear reaction was explained by a model in which, after a direct process, a few particles were emitted from a struck nucleus by evaporation. Di Napoli *et al.*[10,11] irradiated carbon and iodine at energies between 300 MeV and 1000 MeV, and showed the (γ, n) excitation curves. In this energy region, these reactions result from the photopion process. Van Hise *et al.*[12] irradiated ^{32}S, ^{40}Ca, and ^{66}Zn at energies up to 300 MeV. The reactions in these experiments generally receive important contributions from both the quasi-deuteron and pion emission processes above the pion threshold. The reactions leading to ^{24}Na have already been reported. The excitation curves for the ^{27}Al→^{24}Na and ^{31}P→^{24}Na reactions up to 260 MeV have been reported by Gorbunov *et al.*[13] In addition, the yields of ^{24}Na from the ^{27}Al→^{24}Na, ^{28}Si→^{24}Na, ^{31}P→^{24}Na, ^{32}S→^{24}Na, ^{39}K→^{24}Na, and ^{40}Ca→^{24}Na reactions have been reported at energies from 100 MeV to 1200 MeV by Noga *et al.*[14]

The purpose of the present experiments is to obtain information about the character of the interaction of photons with nuclei in the energy range from 20 MeV to 250 MeV. Especially, the work reported here will improve our understanding of the high-energy photonuclear processes that occur at energies above the low-energy giant-resonance region.

Experimental

Targets and Irradiations. The target elements used in this experiment were magnesium, aluminum, silicon, phosphorus, sulfur, carbon, and gold. All of them were in their elemental form and well sufficiently pure. The impurities in these target substances were found to be negligible in amount. The irradiation sample had a weight of 100—1000 mg and was contained either in a quartz tube or in a Pyrex tube. The experimental methods were described in detail in previous papers.[15-17] The sources of electrons were obtained with the linear electron accelerator of Tohoku University from 30 MeV to 250 MeV and with that of the Japan Atomic Energy Research Institute at 20 MeV. The electron beam in the energy region from 30 MeV to 75 MeV, accelerated by the "High Current" accelerating section of the machine, produced bremsstrahlung in a 3-mm-thick platinum converter.

The sample tubes were held in alignment with the bremsstrahlung beam and were placed in a water-cooled stainless holder.

In the energy region from 100 MeV to 250 MeV, the electron beam accelerated by the "High Energy" accelerating section produced bremsstrahlung in a 0.2-mm-thick tantalum converter. All of these electrons were not converted to bremsstrahlung in a converter. The rest of the electrons were swept away with a sweeping magnet. The sample tubes were held in alignment with the bremsstrahlung beam behind the sweeping magnet and were placed in an aluminum holder.

The electron beam at 20 MeV was converted with a 2-mm-thick platinum converter. The irradiation time was 20 min—2 hr.

Radioactivity Measurement. After irradiation, the target samples were each transferred into "cold" aluminum foils. The gamma-ray spectra were measured at a suitable counting geometry by using a 36-cm^3 Ge(Li) detector coupled to a TMC 1024-channel pulse-height analyzer and a 3″ϕ×3″ NaI(Tl) crystal coupled to a Toshiba 800-channel pulse-height analyzer.

Nuclide identification for ^{24}Na, ^{28}Mg, ^{11}C, and ^{196}Au was made from the knowledge of the target nuclides,[18] the gamma-ray spectra, and the decay data. In these experiments, chemical separation was used if necessary, and gamma-ray spectrometric measurements were performed after having

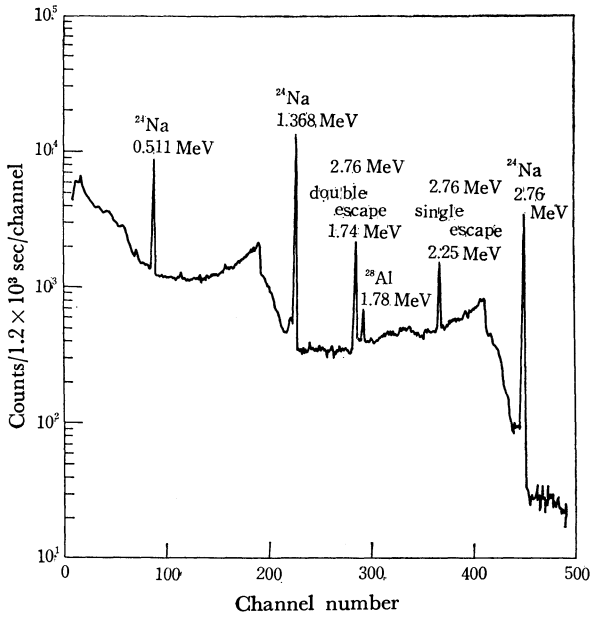

Fig. 1. Gamma-ray spectrum of sulfur target irradiated by 250 MeV bremsstrahlung measured with the 36 cm^3 Ge(Li) detector.

7) R. J. Debs, J. T. Eisinger, A. W. Fairhall, I. Halpern, and H. G. Richter, *ibid.*, **97**, 1325 (1955).
8) I. Halpern, R. J. Debs, J. T. Eisimger, A. W. Fairhall, and H. G. Richter, *ibid.*, **97**, 1327 (1955).
9) T. T. Sugihara and I. Halpern, *ibid.*, **101**, 1768 (1956).
10) V. Di Napoli, F. Dobiti, and F. Salvetti, *Nuovo Cim.*, **48 B**, 1 (1967).
11) V. Di Napoli, F. Dobiti, and F. Salvetti, *ibid.*, **55 B**, 95 (1968)
12) J. R. Van Hise, R. A. Meyer, and J. P. Hummel, *Phys. Rev.*, **139** 554 (1966).
13) A. N. Gorbunov, F. P. Denisov, and V. A. Kolotukhin, *Sov. Phys. JETP*, **11**, 783 (1960).
14) V. I. Noga, Yu. N. Ranyuk, and P. V. Sorokin, *Sov. J. Nucl. Phys.*, **9**, 673 (1969)
15) Y. Oka, T. Kato, K. Nomura, and T. Saito, This Bulletin, **40**, 575 (1966).
16) Y. Oka, T. Kato, K. Nomura, and T. Saito, *J. Nucl. Sci Technol.*, **4**, 346 (1967).
17) Y. Oka, T. Kato, and I. Nagai,. *ibid.*, **4**, 300 (1967)
18) C. M. Lederer, J. M. Hollander, and I. Perlman, "Table of Isotopes," 6th edn., J. Wiley and Sons Inc., New York, London (1968).

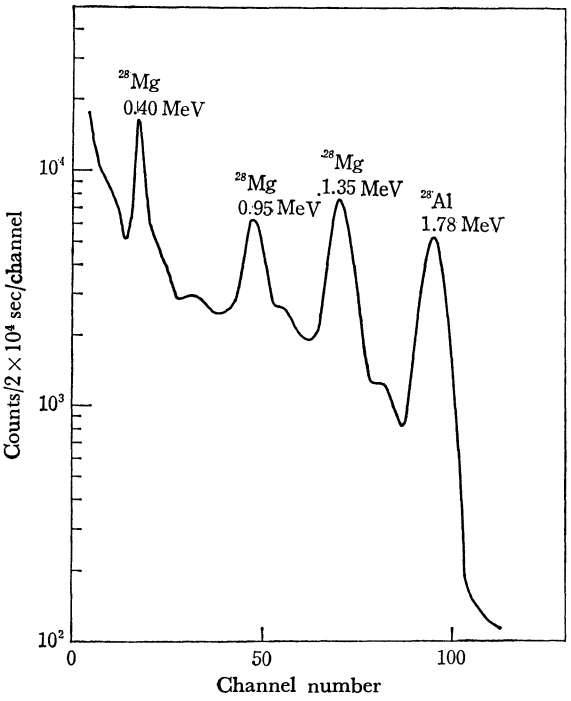

Fig. 2. Gamma-ray spectrum of magnesium fraction from phosphorus irradiated by 200 MeV bremsstrahlung with the 3″ϕ×3″ NaI(Tl) crystal.

been cooled for a time.

Typical gamma ray spectra are shown in Figs. 1 and 2.

Yield Calculation. The disintegration rate was determined by absolute calculations, *i.e.*, the chemical yield, the counting efficiencies, the branching ratio, and the internal conversion ratio. Each of these target samples was wrapped with a thin sheet of gold which was used for the determination of the relative intensity of the bremsstrahlung dose. The intensity integrated over the time of irradiation was standardized by means of the $^{12}C(\gamma,n)^{11}C$ reaction, whose absolute yield had been measured as a function of the peak bremsstrahlung energy up to 260 MeV by Barber *et al.*[19]

The yield was expressed by the following equation:[15]

$$Y(E) = \frac{D_0}{IM(1-e^{-\lambda t})}$$

where D_0 is the disintegration rate at the end of irradiation, I is the radiation dose rate, M is the amount of target nucleus expressed in atoms, and λ is the decay constant. The target elements used were not enriched ones, and it was assumed for the sake of simplicity that each of these elements consisted entirely of its most abundant isotope.

Results

The yield curves for the $^{25}Mg(\gamma, p)^{24}Na$, $^{27}Al\rightarrow{}^{24}Na$, $^{28}Si\rightarrow{}^{24}Na$, $^{31}P\rightarrow{}^{24}Na$, and $^{32}S\rightarrow{}^{24}Na$ reactions and the $^{12}C(\gamma, n)^{11}C$ curve for the monitor reaction are shown in Figs. 3 and 4, while those for the $^{30}Si(\gamma, 2p)^{28}Mg$, $^{31}P(\gamma, 3p)^{28}Mg$, and $^{32}S(\gamma, 4p)^{28}Mg$ reactions are shown in Fig. 5. The solid points in these figures represent the results obtained. The cross section curves for the $^{27}Al\rightarrow{}^{24}Na$, $^{28}Si\rightarrow{}^{24}Na$, $^{31}P\rightarrow{}^{24}Na$, $^{32}S\rightarrow{}^{24}Na$, $^{30}Si(\gamma, 2p)^{28}Mg$, $^{31}P(\gamma, 3p)^{28}Mg$, and $^{32}S(\gamma, 4p)^{28}Mg$ reactions as calculated from the photon-difference method[20] are shown in Figs. 6—12 respectively.

19) W. C. Barber, W. D. George, and D. D. Reagan, *Phys. Rev.*, **98**, 73 (1955).

Discussion

General Considerations. The wavelength of the bombarding particle energies decreases with an increase in the energy, and at energies around approximately 100 MeV it becomes smaller than the mean distance between nucleons in the nucleus, while the time of interaction of the particles with the nucleus is shorter than the characteristic nuclear time.

The characteristics of high-energy particles enable us to obtain information on nuclear characteristics not accessible to other methods. The individual production rates of a photonuclear reaction can be obtained by the measurement of the cross sections.

Investigations of the evidence of the emission of particles with $Z\geqq 2$, carried out by radiochemical methods, are of extreme importance. The particles emitted have specific characteristics. Most of the

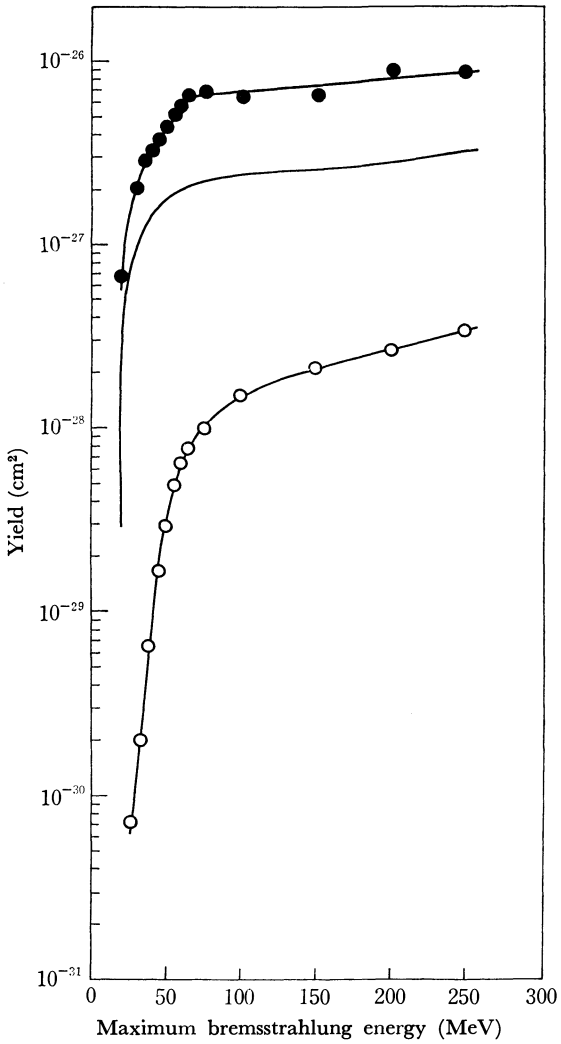

Fig. 3. The yield curves for the reactions $^{25}Mg(\gamma,p)^{24}Na$, $^{27}Al\rightarrow{}^{24}Na$, and $^{12}C(\gamma,n)^{11}C$ as a monitor.
●: $^{25}Mg(\gamma,p)^{24}Na$, ○: $^{27}Al\rightarrow{}^{24}Na$, ——: $^{12}C(\gamma,n)^{11}C$

20) A. S. Penfold and J. E. Leiss, *ibid.*, **114**, 1332 (1959).

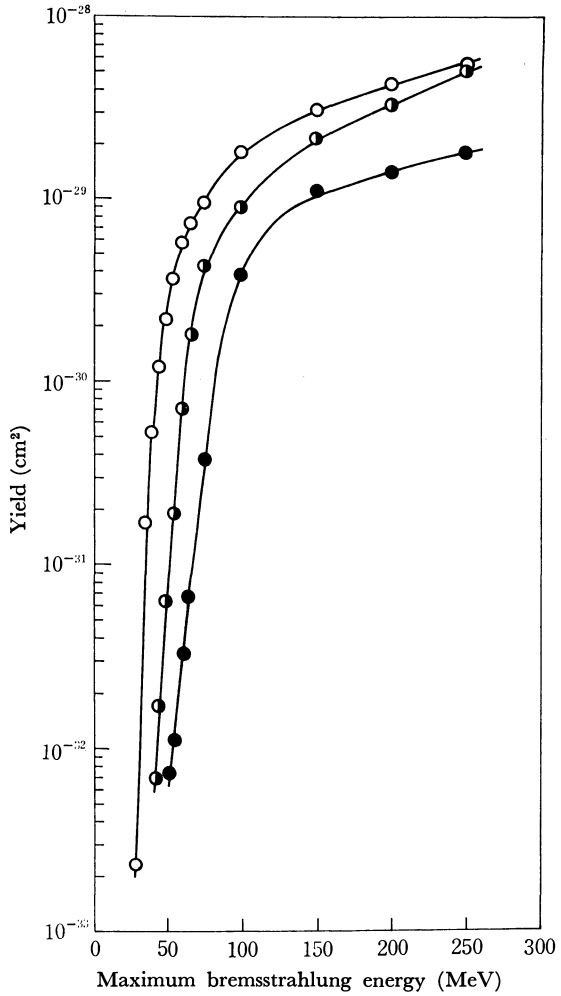

Fig. 4. The yield curves for the reactions ^{28}Si→^{24}Na, ^{31}P→^{24}Na, and ^{32}S→^{24}Na.
○: ^{28}Si→^{24}Na, ◑: ^{31}P→^{24}Na, ●: ^{32}S→^{24}Na

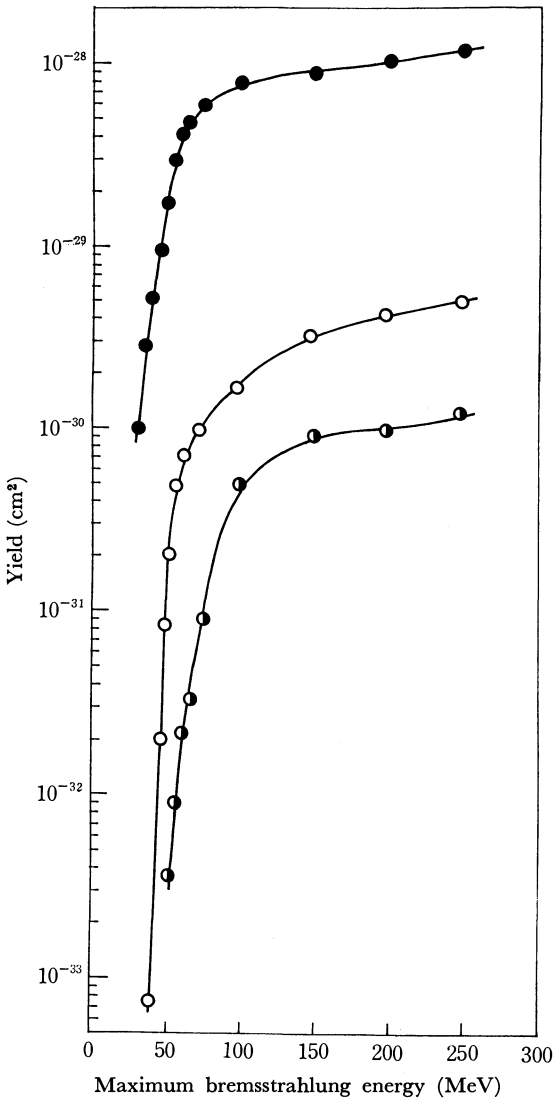

Fig. 5. The yield curves for the reactions ^{30}Si(γ,2p)^{28}Mg, ^{31}P(γ,3p)^{28}Mg, and ^{32}S(γ,4p)^{28}Mg.
●: ^{30}Si(γ,2p)^{28}Mg, ○: ^{31}P(γ,3p)^{28}Mg, ◑: ^{32}S(γ,4p)^{28}Mg

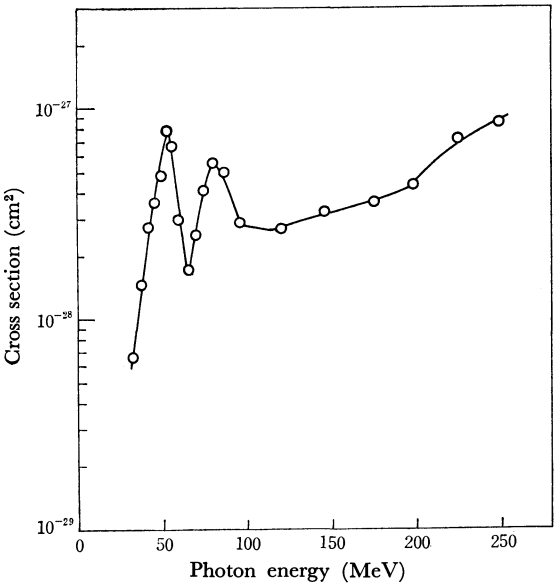

Fig. 6. The excitation function for the reaction ^{27}Al→^{24}Na.

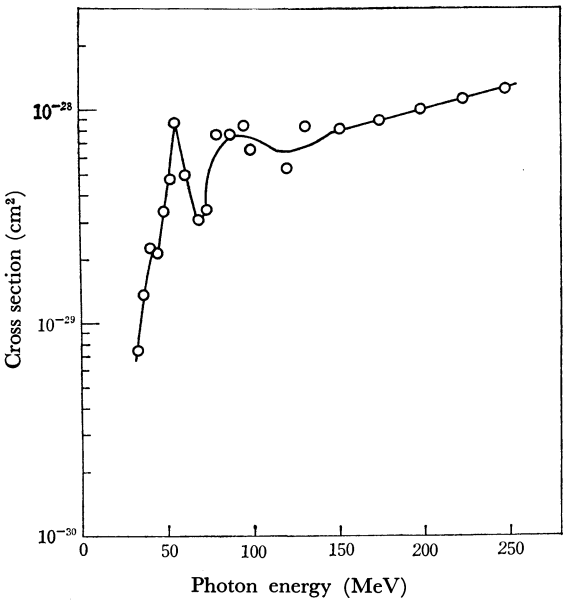

Fig. 7. The excitation function for the reaction ^{28}Si→^{24}Na.

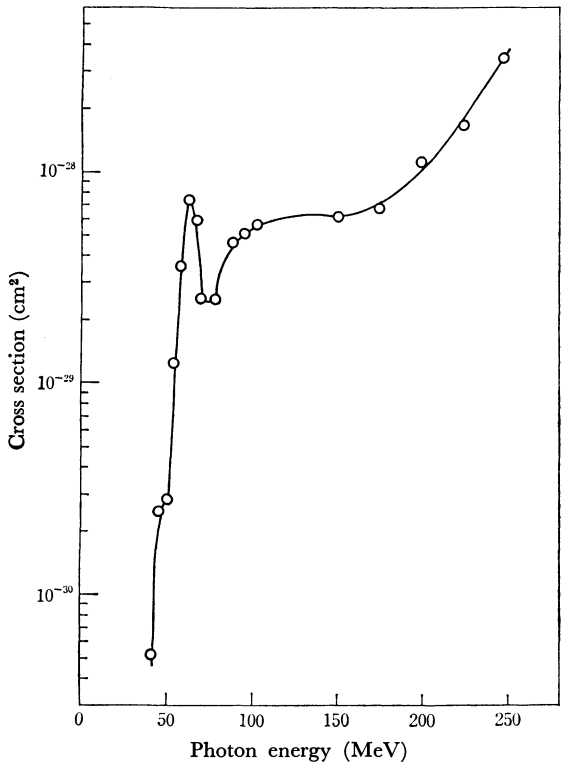

Fig. 8. The excitation function for the reaction $^{31}P \rightarrow {}^{24}Na$.

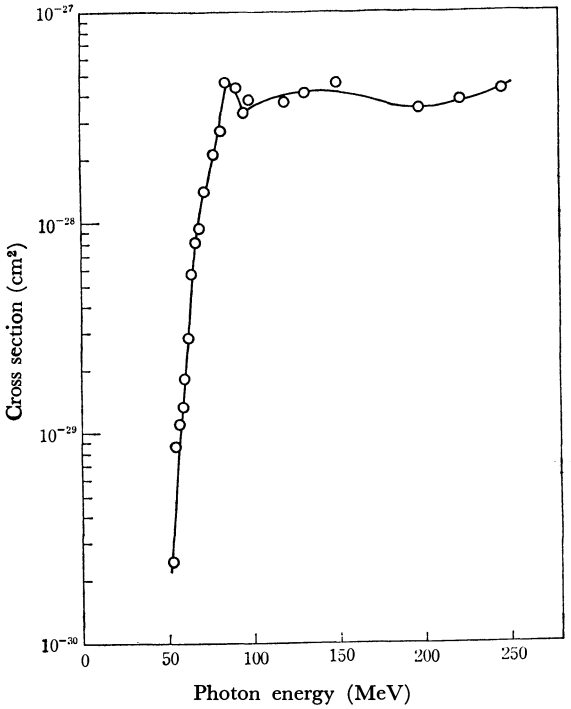

Fig. 9. The excitation function for the reaction $^{32}S \rightarrow {}^{24}Na$.

previous experiments studied high energy photonuclear reactions and involved observations of the emitted nucleons rather than observations of the residual nuclei.

However, the interpretation of a whole series of experimental data obtained in high-energy photonuclear reactions demands an understanding of the structure of the nucleus, especially with regard to the association

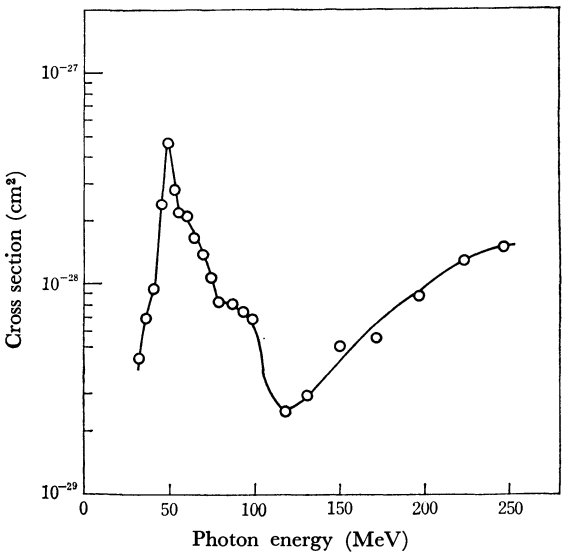

Fig. 10. The excitation function for the reaction $^{30}Si(\gamma,2p)^{28}Mg$.

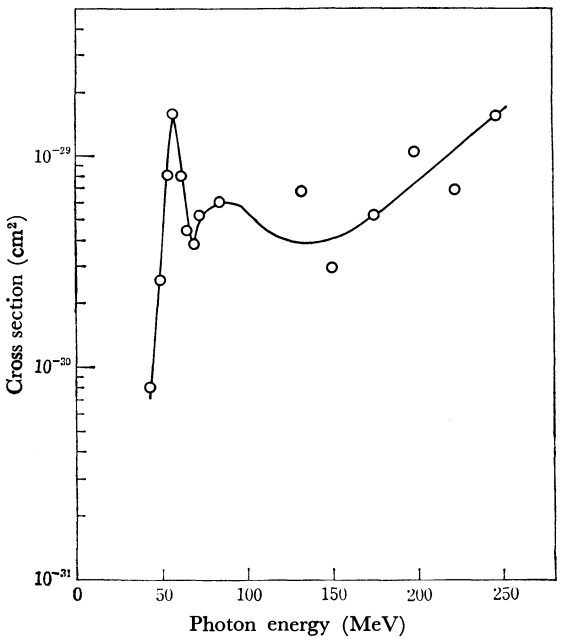

Fig. 11. The excitation function for the reaction $^{31}P(\gamma,3p)^{28}Mg$.

of nucleons within it. The study by the activation method gives important information on the activation yields for the complex nucleus by high-energy photons.

Reaction Path. For convenience in the consideration of the reaction path leading to ^{24}Na and ^{28}Mg, Tables 1 and 2 list the reaction types and the mass threshold values calculated on the basis of the mass differences.[21]

Aluminum and phosphorus are both single isotopic elements, while magnesium, silicon, and sulfur are not.

In the case of the magnesium target, the $Mg \rightarrow {}^{24}Na$ reaction was attributed to the $^{25}Mg(\gamma, p)^{24}Na$ reaction.

21) Nuclidic mass values used were those listed in G. Friedlander, J. W. Kennedy, and J. M. Miller, "Nuclear and Radiochemistry," 2nd ed., J. Wiley and Sons, New York, London (1964), p. 533.

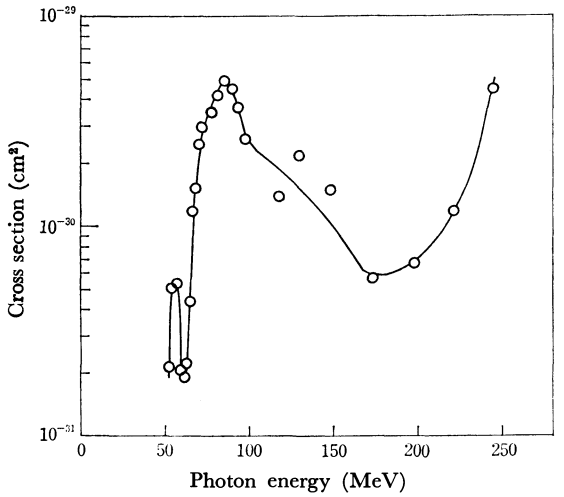

Fig. 12. The excitation function for the reaction ^{32}S(γ,4p)-^{28}Mg.

Table 1. Calculated mass thresholds leading to ^{24}Na

Target nuclide	Abundance (%)	Reaction type	$E_{th}(Q)$(MeV)
^{25}Mg	10.13	(γ, p)	12.06
^{26}Mg	11.17	(γ, pn)	25.94
		(γ, d)	20.93
^{27}Al	100	(γ, 2pn)	31.41
		(γ, dp)	29.20
		(γ, ^{3}He)	23.71
^{28}Si	92.21	(γ, 3pn)	42.99
		(γ, d2p)	40.77
^{29}Si	4.70	(γ, 3p2n)	51.47
		(γ, d2pn)	49.24
		(γ, αp)	23.19
^{30}Si	3.09	(γ, 3p3n)	62.08
		(γ, d2p2n)	59.85
		(γ, αpn)	33.80
^{31}P	100	(γ, 4p3n)	69.36
		(γ, α2pn)	41.17
		(γ, d3p2n)	67.14
		(γ, 3dp)	62.69
		(γ, ^{7}Be)	31.78
^{32}S	95.0	(γ, 5p3n)	78.22
		(γ, α3pn)	49.94
		(γ, d4p2n)	76.00
^{33}S	0.760	(γ, 5p4n)	86.86
		(γ, 2αp)	39.61
		(γ, d4p3n)	84.63
^{34}S	4.22	(γ, 5p5n)	98.27
		(γ, 2αpn)	41.71
		(γ, d4p4n)	96.05
^{36}S	0.014	(γ, 5p7n)	115.13
		(γ, 2αp3n)	58.56
		(γ, d4p6n)	113.84

The ^{27}Al→^{24}Na reaction can result from three different processes, (γ,^{3}He), (γ, dp) and (γ, 2pn), whose thresholds are 23.71, 29.20, and 31.41 MeV respectively. Since the registration of the corresponding activity from the aluminum target began at energies around the thresholds of the (γ, dp) and (γ, 2pn) reactions, it is obvious that, of the three, the latter two processes play the most substantial parts. The ^{27}Al→^{24}Na reaction was attributed to the ^{27}Al(γ, 2pn)^{24}Na reaction by Meyer *et al.*[22]

Table 2. Calculated mass thresholds leading to ^{28}Mg

Target nuclide	Abundance (%)	Reaction type	$E_{th}(-Q)$(MeV)
^{30}Si	3.09	(γ, 2p)	23.99
^{31}P	100	(γ, 3p)	31.27
^{32}S	95.0	(γ, 4p)	40.13
^{33}S	0.760	(γ, 4pn)	48.76
		(γ, d3p)	46.58
^{34}S	4.22	(γ, α2p)	31.91
		(γ, d3pn)	57.96
		(γ, 4p2n)	60.19
^{36}S	0.014	(γ, 2α)	20.48
		(γ, 4d)	68.15
		(γ, 4p4n)	77.04

Sometimes neutron backgrounds are serious enough to cause the production of ^{24}Na by the ^{27}Al(n, α)^{24}Na reaction. Since ^{24}Na activities due to the ^{27}Al(n, α)-^{24}Na reaction irradiated by 20 MeV bremsstrahlung could scarcely be measured, the (n, α) reaction is negligibly small.

The yield of the Si→^{24}Na reaction is the sum of the yields of the ^{28}Si→^{24}Na, ^{29}Si→^{24}Na, and ^{30}Si→^{24}Na reactions. With the excitation energies below 45 MeV, the ^{29}Si(γ, αp)^{24}Na and ^{30}Si(γ, αpn)^{24}Na reactions may play the most substantial part, but above 45 MeV, the yields of the ^{29}Si→^{24}Na and ^{30}Si→^{24}Na reactions are negligibly small, because the isotopic abundances of ^{29}Si and ^{30}Si are as low as 4.70% and 3.09% respectively. Therefore, the reaction product, ^{24}Na, from the ^{28}Si→^{24}Na reaction is obtained *via* the (γ, 3pn) and (γ, d2p) processes. The ^{24}Na yield from ^{31}P is the result of a large number of reactions, of which the energetically most convenient reaction (γ, ^{7}Be) has a threshold of 31.78 MeV, while the energetically least convenient reaction (γ, 4p7n) has a threshold of 69.36 MeV. The experimental threshold of the ^{24}Na yield from ^{31}P is in the neighborhood of 45 MeV. This indicates that, in those reaction processes involving the emission of complex particles, *i.e.*, α-particles, the reaction type (γ, α2pn) plays a substantial part.

The yield of the S→^{24}Na reaction is the sum of the yields of the ^{32}S→^{24}Na, ^{33}S→^{24}Na, ^{34}S→^{24}Na, and ^{36}S→^{24}Na reactions. Below 60 MeV, the ^{34}S(γ, 2αpn)^{24}Na and ^{32}S(γ, α3pn)^{24}Na reactions play the most substantial parts, but above 60 MeV, the ^{32}S(γ, 5p3n)^{24}Na and ^{32}S(γ, α3pn)^{24}Na reactions play the most substantial parts. In order to understand the results of these experiments, the existence of α-particle grouping within the nuclei must be considered.

The reaction paths leading to ^{28}Mg are the ^{30}Si(γ, 2p)^{28}Mg, ^{31}P(γ, 3p)^{28}Mg, and ^{32}S(γ, 4p)^{28}Mg reactions, if the ^{33}S→^{28}Mg, ^{34}S→^{28}Mg, and ^{36}S→^{28}Mg reactions are neglected.

22) R. A. Meyer, W. B. Walters, and J. P. Hummel, *Nucl. Phy.*, **A122**, 606 (1960).

The production yields for ^{24}Na and ^{28}Mg are actually sums of the beta decay chains for their respective masses. The contributions from the products of $Z \neq 11$ to the sodium activites and those of $Z \neq 12$ to the magnesium activities may be disregarded because the ratio of the cross sections for the production of ^{24}Ne and ^{24}Na is negligibly small for proton-induced reactions.[23]

Photonuclear Reaction Yields. In Figs. 3—5 the observed yields data for the reactions studied are plotted as 5 MeV bin width in the energy range between 30 MeV and 65 MeV. In the energy range from 100 MeV to 250 MeV, they were plotted as 50 MeV bin width. In the yield curve, the yield data at 75 MeV bremsstrahlung are added, and they are modified to an adequate smooth curve. The errors in these data are less than 20%. The systematic errors arise from absolute counting factors, beam attenuation in targets, the beam monitor, and the target position monitor. The latter two factors are the main sources of error.

The yield ratios of $Y(^{28}\mathrm{Mg})$ to $Y(^{24}\mathrm{Na})$ were computed for silicon, phosphorus, and sulfur targets, they are shown in Fig. 13.

It should be noted that the yield-ratio curve of silicon does not represent the ratio in a true sense, because not all target nuclides leading to ^{24}Na and ^{28}Mg are the same. In the case of silicon, the rapid

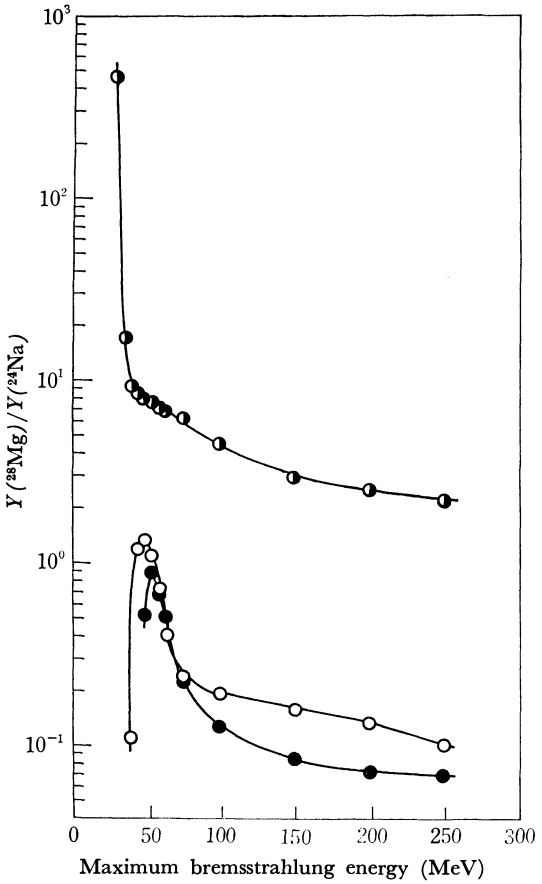

Fig. 13. Yield ratios *versus* maximum bremsstrahlung energy.
◑: $Y(^{30}\mathrm{Si}(\gamma,2\mathrm{p})\ ^{28}\mathrm{Mg})/Y(^{28}\mathrm{Si}\rightarrow^{24}\mathrm{Na})$
○: $Y(^{31}\mathrm{P}(\gamma,3\mathrm{p})\ ^{28}\mathrm{Mg})/Y(^{31}\mathrm{P}\rightarrow^{24}\mathrm{Na})$
●: $Y(^{32}\mathrm{S}(\gamma,4\mathrm{p})\ ^{28}\mathrm{Mg})/Y(^{32}\mathrm{S}\rightarrow^{24}\mathrm{Na})$

23) R. G. Korteling and A. A. Caretto, Jr., *J. Inorg. Nucl. Chem.*, **29**, 2863 (1967).

decrease up to 45 MeV of the yield ratio curve is due to the differences in the threshold energies, *i.e.* 42.99 MeV and 40.77 MeV leading to ^{24}Na and 23.99 MeV leading to ^{28}Mg. In the energy region between 45 MeV and 250 MeV, the gradual decrease in the yield ratio is independent of the difference in the threshold energy. In the peak energy region, it may be considered that the contribution of the compound nucleus process decreases, while that of the quasi-deuteron process increases.

Photonuclear Reaction Cross Sections. In Figs. 6—8, 10, and 11, the low energy peak is shown for each figure. In order to explain this, the compound nucleus model, which is in good agreement with relative low energy experimental data, is considered. In forming a compound nucleus, an incident particle is absorbed by the nucleus, and its energy is distributed among the nucleons in a nucleus. The principal and initial assumption of the theory of the compound nucleus is satisfied only if the range of the particle in the nuclear material is considerably smaller than the dimensions of the nucleus and if the excitation energy of the compound nucleus associated with one particle is considerably smaller than the energy required to separate this particle from the nucleus. For incident particle energies greater than about 50 MeV, neither of these conditions is satisfied. Nevertheless, in the energy region up to 100 MeV, the compound nucleus model is still reasonable. It is, then, not unreasonable to consider the experimental data at high energies from the point of view of this model.

At photon energies exceeding about 60—80 MeV, the energy and momentum of the photon are also absorbed by a group of nucleons which leaves the nucleus, transferring to it only a part of the energy. One such mechanism, proposed by Levinger,[24] is the quasi-deuteron mechanism. In such an interaction, it may turn out that the probability of transferring a given portion of energy to the nucleus varies little with the energy of the incident particle and that, consequently, the cross section for the production of a given isotope will also vary little.

The reaction types leading to ^{28}Mg investigated here, *i.e.*, $(\gamma, 2\mathrm{p})$, $(\gamma, 3\mathrm{p})$, and $(\gamma, 4\mathrm{p})$, do not include the emission of neutrons. On the contrary, the reaction types leading to ^{24}Na, *i.e.*, $(\gamma, 3\mathrm{pn})$, $(\gamma, 4\mathrm{p3n})$, $(\gamma, \mathrm{d2pn})$, and others, do involve the emission of neutron. After quasi-deuteron absorption, a neutron and a proton share the energy of the incoming photon and either escape from the nucleus or collide with other nucleons. In the light nuclei region, it may be very rare that a neutron or a proton collides with other nucleus. For this reason, the reaction cross sections leading to ^{28}Mg may have small values if the cross sections depend on the quasi-deuteron process. In the energy region between 70 MeV and 150 MeV, each of the cross-section data leading to ^{28}Mg is shown to have a relatively lower value compared with the peak cross section data, but that leading to ^{24}Na has almost the same value as the peak cross section data. In the energy region between 100 MeV and 150 MeV, it is difficult to explain the

24) J. S. Levinger, *Phys. Rev.*, **84**, 43 (1951).

cross section data by the compound nucleus model, but the quasi-deutron model is suitable to explain the data.

At energies above 150 MeV, which is the pion threshold energy, the quasi-deuteron and pion production processes compete. In the case of contributions to the reaction cross section from processes associated with pion production, two types of mechanisms must be considered. One involves those events in which pions are produced and emitted from the nucleus. The other involves events in which pions are produced and then re-absorption process within the nucleus. For the light nuclei, the pion re-absorption process is generally less than 10% of that for pion emission.[22] In the energy region between 150 MeV and 250 MeV, the photo-pion reaction is the sum of the productions of both charged and neutral pions. For example, to the ^{27}Al→^{24}Na reaction is now added the following photonuclear reactions. ^{27}Al(γ, $\pi^0$2pn)^{24}Na, ^{27}Al(γ, π^+p2n)-^{24}Na, ^{27}Al(γ, π^-3p)^{24}Na, *etc.* Therefore, many reaction paths must be considered for the photon absorption processes in complex nuclei, if the pion productions take part in the reaction observed. Among the high-energy photonuclear reaction mechanisms, the quasi-deuteron and pion production processes must be considered at an initial cascade process, but the evaporation process may be considered after the cascade process. According to the cascade theory, the incident photon does not transfer all its energy to the nucleus, as is assumed in the theory of the compound nucleus, but interacts with individual nuclear particles, giving them a part of its energy. Some of the nucleons which have taken part in the cascade process fly out of the nucleus, forming the experimentally observed component of high-energy nucleons, while the rest are absorbed by the nucleus, transferring their energy to the latter. The excited nucleus thus formed after the cascade process passes back to the ground state by the evaporation process. The analytical calculation of the cascade process is, even in principle, very laborious, moreover, at the present time, it is quite impossible, since a number of the cascade characteristics have no analytical expression. Hence, in order to calculate the cascade process, the Monte Carlo statistical method may be carried out with the use of a high-speed electronic computer; such calculations will be reported elsewhere.

Recoil Study. It is very difficult to obtain information about photonuclear reaction mechanisms by velocity measurements of the protons and neutrons ejected in these complex reactions. In order to gain more information, measurements of the angular distributions of emitted particles are needed. Radiochemical techniques were suitable for observations of the recoil properties of the heavy residual nuclei. The target foils used in this experiments were 3.12 mg/cm^2 magnesium and 4.57 mg/cm^2 aluminum. These were, in all cases, considerably thicker than the fragment ranges and were surrounded by recoil catchers consisting of 3.14 mg/cm^2 Mylar foils. The fraction of the ^{24}Na atoms that recoiled from the target into the Mylar catchers was measured by using a 3″ϕ×3″ NaI (Tl) crystal coupled with a 800-channel pulse-height analyzer. A number of thick-target recoil experiments were performed in the energy range from 30 MeV to 250 MeV. The results of the recoil studies are shown in Figs. 14 and 15. The listed quantities, FW and BW, are the fragments of the ^{24}Na atoms recoiling into the forward and backward fractions respectively. All of these data are shown in the laboratory system. It is assumed that the *FW/(FW+BW)* value shows the angular distribution of the ^{24}Na fragment. The ^{25}Mg (γ, p)^{24}Na reaction is due to the contribution from the compound nucleus process in the low-energy region.[25] Gorbunov *et al.*[13] assumed that, at energies above 60—80 MeV, the interaction of photons with nuclei proceeds mainly *via* photon absorption by a group to intranuclear nucleons. However, as may be seen in Figs. 14 and 15, in the energy range from 30 MeV to 60 MeV, the *FW/(FW+BW)* value of the ^{25}Mg(γ, p)-^{24}Na reaction is the same as that of the ^{27}Al→^{24}Na reaction. Therefore, it may be concluded that the low energy peak of the ^{27}Al→^{24}Na, ^{28}Si→^{24}Na, ^{30}Si→^{28}Mg, ^{31}P→^{24}Na, and ^{31}P→^{28}Mg reactions are due to the contribution from the compound nucleus process.

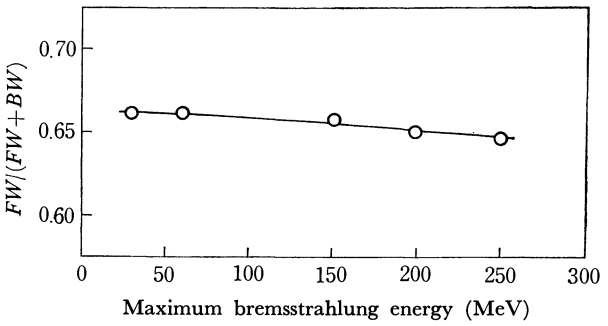

Fig. 14. Recoil fraction rate for the reaction ^{25}Mg(γ,p)^{24}Na.

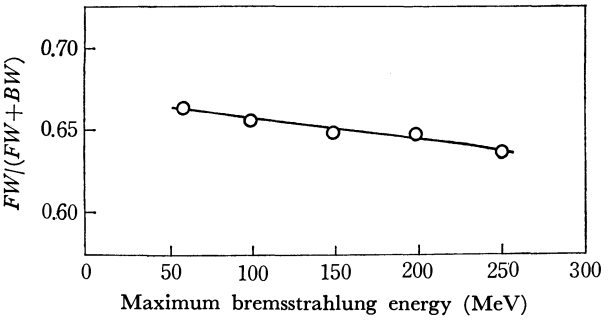

Fig. 15. Recoil fraction rate for the reaction ^{27}Al→^{24}Na.

The author wishes to express his thanks to Dr. T. Kato of Tohoku University for his continuous encouragement. The crew of the Electron Linear Accelerator in the Laboratory of Nuclear Science of Tohoku University also made possible its trouble-free operation.

25) M. E. Toms and W. E. Stephens, *ibid.*, **82**, 709 (1951).

Isotopic Fractionation in a Thermal Ion Source

Hitoshi KANNO

Department of Chemistry, Faculty of Science, The University of Tokyo, Hongo, Bunkyo-ku, Tokyo

(Received November 27, 1970)

Isotopic fractionation behavior in a thermal ion source was theroretically studied. An equation relating to the observed isotope ratio with the evaporated fraction of the sample was derived under conditions where two kinds of chemical species, atomic (atomic ions and neutral atoms) and molecular (molecular ions and molecules) species, simultaneously evaporate from the filament. It was demonstrated that integrations of all ion currents for two isotopes do not necessarily give a true ratio of the two isotopes in the sample when two evaporating chemical species are ionized at different rates. Isotopic fractionation curves for halides and elements of lithium, potassium, and rubidium are presented.

Fractionation effects in a thermal ion source are a serious problem in mass spectrometry, especially in isotope ratio measurements. In order to obtain the precise isotope ratios of samples, attempts have been made by many investigators[1,2] to estimate the degree of fractionation and to find appropriate correction methods.

The quantitative analyses of Eberhardt *et al.*[3] showed that evaporation of sample in a single filament ion source follows the Rayleigh distillation formula[4] and that atomic species (atomic ions and neutral atoms) are the only species evaporating from the filament. Their treatment, however, is insufficient in that the results can not be applied to a multiple filament ion source in which not only atomic but also molecular species (molecular ions, neutral molecules and their fragments) evaporate from the filament.

The isotopic fractionation factor in the evaporation of molecular species differs greatly from that of atomic species so that the net fractionation depends to a great extent on the molar ratio of atomic species to molecular species in the vapor leaving the filament. By taking this into account quantitative analysis seems to be helpful for clearing the extent of fractionation and improving mass spectrometric techniques and correction methods for precise isotope ratio measurements.

In this paper, variation of observed isotope ratio with percentage of the evaporated sample was theoretically calculated under conditions where both atomic and molecular species simultaneously evaporate from the filament, and it was shown that integrations of all ion currents for two isotopes do not necessarily give the true ratio of the two isotopes in the sample when two evaporating chemical species, atomic species and molecular species, are ionized at different rates.

Theoretical

When the vapor pressure of an isotopic substance is of the order of magnitude such that the chance of an evaporated atom or molecule returning to the filament is very small, the total mass of vapor escaping from the unit area of surface in unit time is given by Langmuir's equation[5]

$$\mu = p \cdot c \left(\frac{M}{2\pi RT}\right)^{1/2} \tag{1}$$

where p is vapor pressure of an evaporating isotopic substance in pure state, c, its molar concentration in a sample on the filament, M, its molecular (or atomic) weight, R, gas constant, and T, absolute temperature. Thus the number of moles N evaporating per unit area in unit time is

$$N = \mu/M = p \cdot c(2\pi MRT)^{-1/2} \tag{2}$$

For a mixture of two isotopic chemical species of masses M_1, M_2, concentrations of c_1, c_2, evaporating from a surface of filament, the numbers of moles of the two isotopes evaporating will be

$$\begin{aligned} N_1 &= p_1 \cdot c_1(2\pi M_1 RT)^{-1/2} \\ N_2 &= p_2 \cdot c_2(2\pi M_2 RT)^{-1/2} \end{aligned} \tag{3}$$

At such high temperatures as in thermal ion sources, the difference of vapor pressures between two isotopic substances will be negligibly small, so that

$$p_1 = p_2 \tag{4}$$

Hence the ratio of the molar concentrations of two isotopic species in the vaporized vapor (isotope ratio in the vapor) is given by

$$r = \frac{N_1}{N_2} = \frac{c_1}{c_2}\left(\frac{M_2}{M_1}\right)^{1/2} = \gamma \cdot R \tag{5}$$

where γ $(=(M_2/M_1)^{1/2})$ is a fractionation factor, and R $(=c_1/c_2)$ is the isotope ratio of the sample remaining on the filament. Accordingly, when some fractions of the sample on the filament are thermally decomposed into atomic species (or molecular fragments) and vaporization takes place in both atomic species A and molecules B, isotope ratios of the vapors A and B just evaporating from the filament are

$$\begin{aligned} r_a &= \alpha R \\ r_b &= \beta R \end{aligned} \tag{6}$$

where

$$\begin{aligned} \alpha &= \sqrt{\frac{MA_h}{MA_l}} \\ \beta &= \sqrt{\frac{MB_h}{MB_l}} \end{aligned} \tag{7}$$

1) S. Taniguchi, O. Toyama, and T. Hayakawa, *Mass Spectrometry*, **10**, 91 (1962).
2) M. H. Dodson, *J. Sci. Instr.*, **40**, 289 (1963).
3) A. Eberhardt, R. Delwiche, and J. Geiss, *Z. Naturforschg.*, **19a**, 736 (1964).
4) Lord Rayleigh, *Phil. Mag.*, **42**, 493 (1896).
5) I. Langmuir, *Phys. Z.*, **14**, 1273 (1913).

Here MA and MB are the molecular (or atomic) weights of vapors A and B, and the subscripts h and l denote heavy and light isotopes, respectively. In the case of lithium iodide, A and B may be either $Li^{(0,+)}$ or LiI. It is also assumed that the residual sample on the filament undergoes continuous and complete mixing and that there is no isotopic fractionation between chemical species A and B.

Now we consider the course of evaporation. If the chemical species A and B simultaneously evaporate from the filament, the material balance requires

$$dA + dB = dQ \tag{8}$$

where dA and dB are the amounts (in moles) of A and B evaporating from the filament in a time interval from t to $t + dt$, and dQ is the corresponding change (in moles) of the sample on the filament.

Let us denote the mole fractions of lighter isotopic species of the vapors A and B by n_a and n_b, and of the residual sample by n_c, respectively. Then the molar quantities of the lighter isotopic species of A and B just escaping from the filament will be given by $n_a dA$ and $n_b dB$. Thus we get

$$n_a dA + n_b dB = d(n_c Q) \tag{9}$$

and

$$r_a = \frac{n_a}{1-n_a}, \quad r_b = \frac{n_b}{1-n_b}, \quad R = \frac{n_c}{1-n_c} \tag{10}$$

For the sake of simplicity we assume that molar quantity of vapor B is always k times as much as that of vapor A throughout the course of evaporation, *viz.*,

$$dB = k dA \tag{11}$$

Combining this relation with Eqs. (6), (8), (9), and (10), we obtain the following differential equation

$$\frac{1}{k+1}\left(\frac{\alpha R}{1+\alpha R}+\frac{\beta k R}{1+\beta R}\right)dQ = \frac{R dQ}{1+R}+\frac{Q dR}{(1+R)^2} \tag{12}$$

The solution is

$$\log\left(\frac{Q}{Q_0}\right) = a\log\left(\frac{R}{R_0}\right) + \log\left(\frac{R+1}{R_0+1}\right) + b\log\left(\frac{c+dR}{c+dR_0}\right) \tag{13}$$

where

$$a = (k+1)/\{(\alpha-1) + (\beta-1)k\}$$
$$b = (\alpha-\beta)^2 k/(cd)$$
$$c = (\alpha-1) + (\beta-1)k$$
$$d = (\alpha-1)\beta + \alpha(\beta-1)k$$

and Q_0 is the initial quantity and R_0 the isotope ratio (true isotope ratio) of the sample. When $\alpha=\beta$, this equation becomes

$$(\alpha-1)\log\left(\frac{Q}{Q_0}\right) = \log\left(\frac{R}{R_0}\right) + (\alpha-1)\log\left(\frac{R+1}{R_0+1}\right) \tag{14}$$

which is the well-known Rayleigh distillation formula.

If the residence time of vapor A and B in the ion source is short enough to prevent the cross mixing of the vapors at different instances, the mean isotope ratio of the vaporized species in the ion source can be expressed in terms of α, β, k, and R as follows.

$$r_m = \frac{n_a dA + n_b dB}{(1-n_a)dA + (1-n_b)dB}$$
$$= \frac{(\alpha+\beta k)R + \alpha\beta(k+1)R^2}{(k+1)+(\beta+\alpha R k)} \tag{15}$$

Furthermore, if the ionization efficiencies[6] of the chemical species A and B have the same value, the observed isotope ratio (r_{ob}) is equal to r_m, and if the ionization efficiency of vapor A is much greater than that of B, r_{ob} is approximately equal to r_a. This is summarized as follows

$$r_{ob} = r_m \quad (\text{when } I_a = I_b)$$
$$r_{ob} = r_a \quad (\text{when } I_a \gg I_b)$$
$$r_{ob} = r_b \quad (\text{when } I_a \ll I_b)$$

where I_a and I_b are the ionization efficiencies of vapors A and B, respectively.

Calculation and Discussion

Calculations have been made for lithium, potassium and rubidium when halides of these elements are adopted as the working material. The calculated observable isotope ratios (r_{ob}) for iodides of these elements are shown in Figs. 1, 2, and 3 as a function of the fraction of the sample remaining on the filament. In these calculations it is implicitly assumed that chemical forms of vapor species are either $M^{(0,+)}$ or MI, and that ionization efficiencies of both vapor species are identical (M=Li, K, and Rb, I is iodine). As shown in Figs. 1, 2, and 3, the isotope ratio to be observed significantly deviates from the true isotope ratio when the fractions of atomic species $M^{(0,+)}$ in vaporizing substances are large and the fraction evaporated is large or small.

It is of importance to know how much is evaporated when the observed isotope ratio gives the true isotope ratio of the sample.

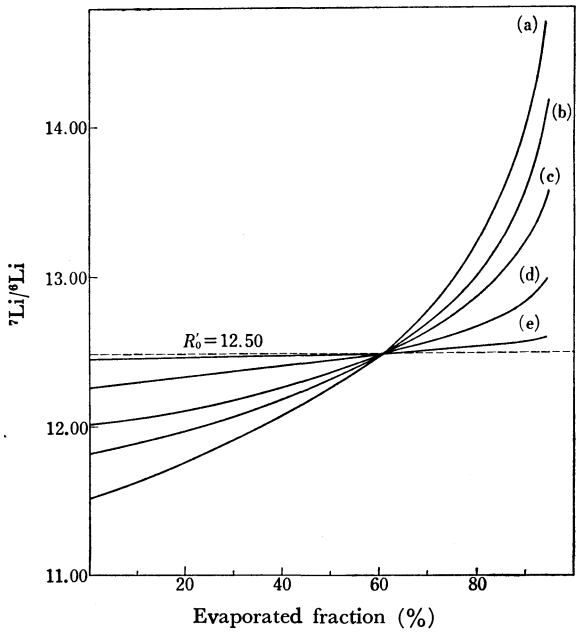

Fig. 1. Variation of $^7Li/^6Li$ with composition of vaporizing species.
(a) $k=0.00$ (b) $k=0.40$ (c) $k=1.00$ (d) $k=4.00$
(e) $k=\infty$
A: $Li^{(0,+)}$ $\alpha=1.080000$ B: LiI $\beta=1.00376$

6) Ionization efficiency is regarded as the production rate of atomic ions M^+ from vapor A or B.

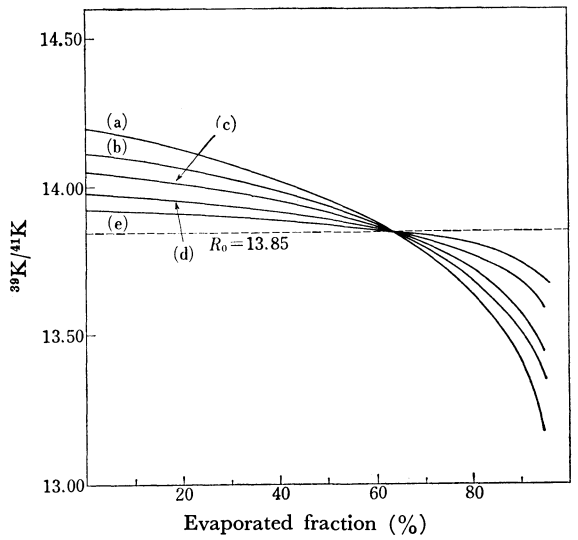

Fig. 2. Variation of $^{39}K/^{41}K$ with composition of vaporizing species.
(a) $k=0.00$ (b) $k=0.40$ (c) $k=1.00$ (d) $k=4.00$
(e) $k=\infty$
A: $K^{(0,+)}$ $\alpha=1.02532$ B: KI $\beta=1.00605$

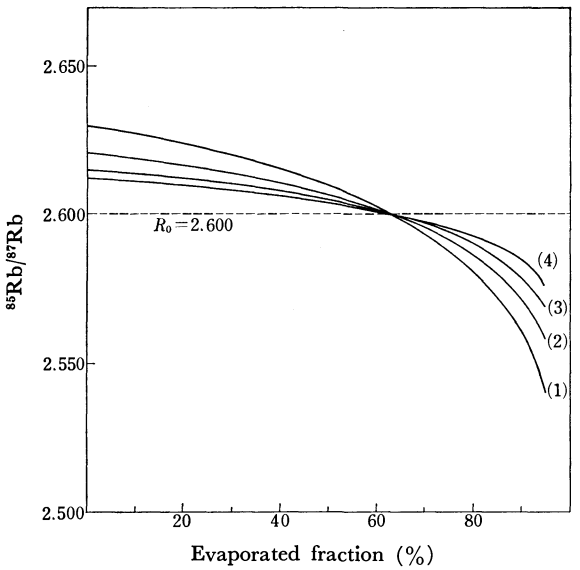

Fig. 3. Variation of $^{85}Rb/^{87}Rb$ with composition of vaporizing species.
(a) $k=0.00$ (b) $k=0.40$ (c) $k=1.00$ (d) $k=4.00$
(e) $k=\infty$
A: $Rb^{(0,+)}$ $\alpha=1.01169$ B: RbI $\beta=1.00470$

When $\alpha=\beta$, we get from Eq. (15)

$$r_{ob} = \alpha R = R_0$$

Substituting this relation into Eq. (14), we have

$$(\alpha-1)\log\left(\frac{Q}{Q_0}\right) = -\log\alpha + (\alpha-1)\log\frac{R_0+\alpha}{\alpha(R_0+1)}$$

Generally α is nearly equal to unity, *i.e.*, $\alpha=1+\varepsilon$ and $\varepsilon\ll 1$, thus

$$\frac{R_0+\alpha}{R_0+1} \approx 1, \qquad \log\alpha \approx \varepsilon$$

which leads to

$$Q = Q_0/e \approx 0.37Q_0$$

When $\alpha\neq\beta$ but $I_a=I_b$, the same result is also deduced if only α and β are nearly unity. We see that when the fraction evaporated being near 63% ($Q\approx 0.37\ Q_0$), observed isotope ratio (r_{ob}) can be regarded as the true isotope ratio (R_0) of the sample material, and that when $Q<0.37Q_0$, r_{ob} is larger than R_0 and when $Q<0.37\ Q_0$, r_{ob} is smaller than R_0. However, it should be pointed out that when $\alpha\neq\beta$ and $I_a\neq I_b$ (probably this is the usual case in a multiple filament ion source) the above relation is not realized as will be shown later.

Fractionation curves of the halides and elements of lithium, potassium and rubidium are presented in

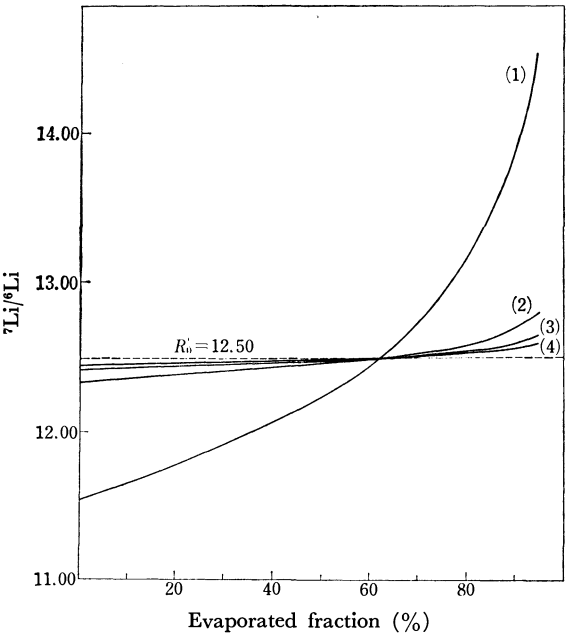

Fig. 4. Fractionation curves for lithium.
(1) ^6Li-^7Li: 1.0800 (2) ^6LiCl-^7LiCl: 1.01200
(3) ^6LiBr-^7LiBr: 1.00581 (4) ^6LiI-^7LiI: 1.00376

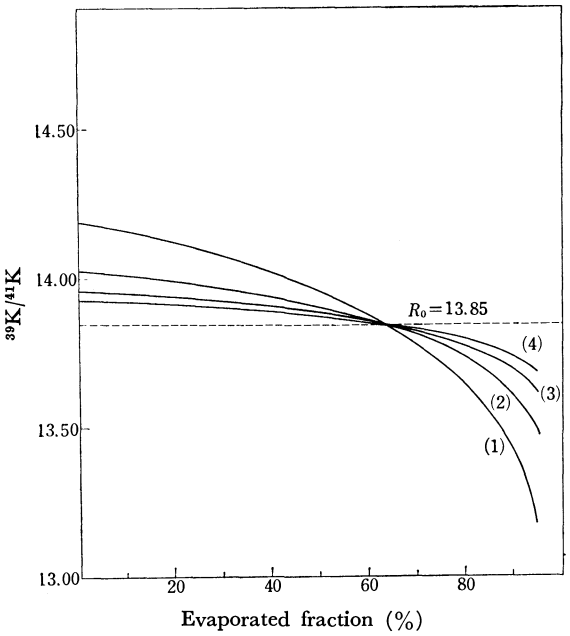

Fig. 5. Fractionation curves for potassium.
(1) ^{39}K-^{41}K: 1.02532 (2) ^{39}KCl-^{41}KCl: 1.01334
(3) ^{39}KBr-^{41}KBr: 1.00837 (4) ^{39}KI-^{41}KI: 1.00605

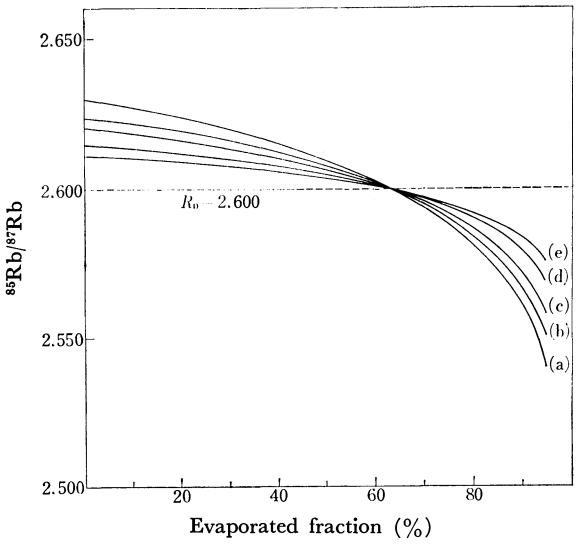

Fig. 6. Fractionation curves for rubidium.
(1) ^{85}Rb-^{87}Rb: 1.01169 (2) $^{85}RbCl$-$^{87}RbCl$: 1.00826
(3) $^{85}RbBr$-$^{87}RbBr$: 1.00604 (4) ^{85}RbI-^{87}RbI: 1.00470

Figs. 4, 5, and 6. It is apparent from these figures that fractionation of lithium iodide is the smallest. If most of the vaporizing species are molecules and molecular ions, isotopic fractionation of lithium can be reduced to minimum by adopting lithium iodide as the working material. On the other hand, in the cases of potassium and rubidium the deviations from the true isotope ratios are larger than those of lithium when the bromides or iodides of these elements are used for the isotope ratio measurements. This stems from the fact that the mass difference of potassium (or rubidium) isotopes is twice as much as that of lithium isotopes. Thus fractionation factor of lithium is more effectively decreased with the use of a heavy compound as a working material than potassium and rubidium. In other words, in the case of lithium the error from fractionation can be reduced to a considerable extent by only adopting a heavy compound as a sample and making lithium emit from the filament as a high mass molecule or molecular ion. The latter condition is practically effected by using a multiple filament ion source. This shows that elements having isotopes of large mass differences are difficult for overcoming the fractionation problem. For example, in measurements of lead where hydroxide, nitrate and sulfide are usually adopted as chemical forms of the sample, and of rare earth elements such as gadolinium and neodymium where nitrate and perchlorate are used, fractionation factors do not decrease so effectively as expected because the vaporizing species from the filament are considered to be either atomic species or decomposed molecular fragments such as $MO^{(0,+)}$ and M_2O_3. Thus in measurements of these elements we must make some other corrections for fractionation to obtain precise isotope ratios.[7,8]

As a matter of fact, the partial mixing of the successively vaporizing substances occurs in an ion source, and the actually observed deviations from the true isotope ratio may not be so large as expected from Eq. (14).

Eberhardt *et al.*[3] observed that different chemical forms and different filament materials yield differences in the observed isotope ratios, and stated that measured isotope ratios of rubidium increased in the order: sulphate on tungsten - sulfate on tantalum - chloride on tungsten - chloride on tantalum. Ozard and Russel[9] have observed in their lead isotope ratio measurement that the fractionation pattern of a rhenium filament is different from that of a tantalum filament. These observations may be partly explained by the fact that both the composition of vaporizing species and their ionization efficiencies are greatly influenced by the chemical form of the sample, condition of filament surface (temperature of filament, filament material), type of ion source (single or multiple filament ion source) and impurities in the sample and filament. It is well known that ionization of lead is significantly reduced by large alkali ions arising from contaminations.

In the calculations presented in Figs. 1, 2, and 3, ionization efficiencies of vapors A and B were assumed to be the same. However, in actual cases in a multiple filament ion source this is rare so that observed fractionation also varies with the change of ionization efficiencies of the vapors.

Table 1 shows fractionation data of lithium iodide with the conditions (a) $k=1.0$ and $I(\mathrm{LiI})=I(\mathrm{Li})$, (b) $k=1.0$ and $I(\mathrm{LiI})\gg I(\mathrm{Li})$, and (c) $k=1.0$ and

Table 1. Variation of expected isotope ratios (r_{ob}) with evaporated fraction and ionization efficiency

evaporated fraction(%)	Observed isotope ratio $^7Li/^6Li$[a]		
	$I(\mathrm{LiI})=I(\mathrm{Li})$ r'_{ob}	$I(\mathrm{LiI})\ll I(\mathrm{Li})$ r'_{ob}	$I(\mathrm{LiI})\gg I(\mathrm{Li})$ r'_{ob}
5.0	12.02_4	11.59_9	12.48_0
10.0	12.05_2	11.62_5	12.50_8
15.0	12.08_0	11.65_3	12.53_8
20.0	12.11_1	11.68_2	12.56_9
25.0	12.14_3	11.71_4	12.60_3
30.0	12.17_8	11.74_7	12.64_0
35.0	12.21_6	11.78_4	12.67_9
40.0	12.25_7	11.82_3	12.72_1
45.0	12.30_1	11.86_6	12.76_7
50.0	12.35_0	11.91_3	12.81_8
55.0	12.40_4	11.96_5	12.87_4
60.0	12.46_5	12.02_4	12.93_8
65.0	12.53_5	12.09_1	13.01_0
70.0	12.61_6	12.16_9	13.09_4
75.0	12.71_2	12.26_2	13.19_3
80.0	12.83_1	12.37_7	13.31_7
85.0	12.98_5	12.52_6	13.47_7
90.0	13.20_6	12.73_9	13.70_7
95.0	13.59_3	13.11_2	14.10_8

a) Initial isotope ratio (true isotope ratio) $^7Li/^6Li=12.50$.
$k=1.0$, A: Li $\alpha=1.08000$ B: LiI $\beta=1.00376$

7) G. W. Wetherill, *J. Geophys. Res.*, **69**, 4403 (1964).
8) J. A. Cooper, P. H. Reynolds, and J. R. Richards, *Earth Planet. Sci. Lett.*, **6**, 467 (1969).
9) J. M. Ozard and R. D. Russel, *ibid.*, **8**, 331 (1970).

$I(\mathrm{LiI}) \ll I(\mathrm{Li})$. It should be noted that when $I(\mathrm{Li}) \gg I(\mathrm{LiI})$, r'_{ob} $(=1/r_{ob})$[10] is lower than R_0' $(=1/R_0)$ in the evaporated fraction ranging from 0 to 84% and that when $I(\mathrm{Li}) \ll I(\mathrm{LiI})$, r'_{ob} is larger than R_0' from 9 to 100%. Accordingly, this suggests that integrations of all ion currents for both isotopes do not necessarily give the true isotope ratio because of the fact that non-ionized vaporization also affects observed fractionation.

In conclusion, the theory presented here, though too much idealized to give a real picture of fractionation, is adequate to give the qualitative or even semi-quantitative behavior of fractionation in a thermal ion source, and therefore, the derived results are applicable to actual cases.

The author's thanks are due to Professor Hiroshi Hamaguchi, Nobufusa Saito and Hisao Mabuchi of the University of Tokyo for their kind interest and encouragement. Numerical calculations were carried out using a HITAC 5020 computer at the computer center of the University of Tokyo.

10) Lithium isotope ratio is usually presented as $^7\mathrm{Li}/^6\mathrm{Li}$.

BULLETIN OF THE CHEMICAL SOCIETY OF JAPAN, VOL. 44, 1812—1815 (1971)

Conductometric Determination of Ion-pair Formation Constants of Tris(ethylenediamine)cobalt(III) Ion with Maleate and Fumarate Ions in Aqueous Solutions

Shunzo KATAYAMA and Reita TAMAMUSHI

The Institute of Physical and Chemical Research, Wako-shi, Saitama

(Received December 14, 1970)

The conductance behavior of mixtures was investigated for the systems tris(ethylenediamine)cobalt(III)-chloride-sodium maleate and tris(ethylenediamine)cobalt(III)chloride-sodium fumarate in aqueous solutions of various ionic strengths at 25°C. Appreciable deviation of the measured conductivity from additivity was attributed to the ion-pair formation of tris(ethylenediamine)cobalt(III) ion with maleate Ma^{2-} and fumarate Fu^{2-} ions. The concentration formation constants K_c at various ionic strengths were determined by means of computer analysis of the deviation. The thermodynamic ion-pair formation constants K at 25°C were as follows: log K= 3.60 for $[Co(en)_3]^{3+}\cdot Ma^{2-}$ and log K=2.95 for $[Co(en)_3]^{3+}\cdot Fu^{2-}$.

In a previous paper,[1] the continuous variation method was applied to the determination of the ion-pair formation constants of $[Co(NH_3)_6]^{3+}\cdot SO_4^{2-}$ and $[Co(en)_3]^{3+}\cdot SO_4^{2-}$ from the conductance measurement of $[Co(NH_3)_6]Cl_3$—Na_2SO_4 and $[Co(en)_3]Cl_3$—Na_2SO_4 mixtures. The good agreement of the results obtained with those of Jenkins and Monk[2] suggests that the conductance measurement of mixtures is a useful method for determining formation constants, particularly when applied to the systems of relatively high ionic strengths where the theoretical equations of conductance behavior lose their validity. The method is also applicable to the study of ion-pair formation in systems where a pure sample is difficult to obtain.

This paper deals with the application of the continuous variation method to the conductometric determination of ion-pair formation constants of tris(ethylenediamine)cobalt(III) ion with maleate and fumarate ions at 25°C in aqueous solutions of varying ionic strengths. The results will provide some information on the *cis-trans* isomeric effect in the ion-pair formation.

Experimental

Materials. Tris(ethylenediamine)cobalt(III)chloride was prepared according to the procedure in literature[3]; the sample was purified by two recrystallizations from its aqueous solution containing a few drops of acetic acid. Sodium maleate, Na_2Ma, of analytical reagent grade was washed by ethanol and ethyl ether, then dried at 80°C until it became constant in weight. Sodium fumarate, Na_2Fu, of analytical reagent grade was purified by recrystallization from its aqueous solution. The purity of the samples was examined by conventional chemical analysis of the components and by conductivity measurements in aqueous solutions. Chemical analysis and conductivity measurements gave the results shown in Tables 1 and 2, respectively. The limiting ionic equivalent conductivity λ^0 of $[Co(en)_3]^{3+}$ was in agreement with that reported by Jenkins and Monk,[2] and the λ^0-values

Table 1. Results of chemical analysis
(calculated values are shown in parenthesis)

Material	Component (%)					
	C	H	N	Co	Na	Cl
$[Co(en)_3]Cl_3$	20.11 (20.85)	7.02 (7.00)	23.90 (24.32)	16.82 (17.05)	—	30.16 (30.78)
$Na_2Ma\cdot H_2O$	26.96 (26.98)	2.69 (2.26)	—	—	26.13 (25.82)	—
Na_2Fu	30.07 (30.02)	1.62 (1.26)	—	—	29.06 (28.73)	—

1) S. Katayama and R. Tamamushi, This Bulletin, **43**, 2354 (1970).

2) I. L. Jenkins and C. B. Monk, *J. Chem. Soc.*, **1951**, 68.

3) W. C. Fernelius (ed), "Inorganic Syntheses," II, McGraw-Hill, New York (1946), p. 221.

Table 2. Equivalent conductivities, Λ, of $[Co(en)_3]Cl_3$, Na_2Ma and Na_2Fu in aqueous solutions of various concentrations at 25°C

10^4C (equiv./l)	Λ		
	$[Co(en)_3]Cl_3$	Na_2Ma	Na_2Fu
0.00	151.0_5 (74.7)	111.0 (60.9)	111.0 (60.9)
5.00	143.3	—	—
6.67	—	107.2	106.8
15.00	137.0	—	—
20.00	—	104.8	104.0
50.00	125.7	—	—
66.67	—	99.8	99.2
150.00	111.8	—	—
200.00	—	92.5	92.4
500.00	94.8	—	—
666.67	—	83.0	83.7

(Limiting ionic equivalent conductivities, $\lambda°$, of $[Co(en)_3]^{3+}$, Ma^{2-} and Fu^{2-} are shown in parenthesis)

of Ma^{2-} and Fu^{2-} were in fairly good agreement with the results of Topp and Davies.[4]

Preparation of Solutions. Each solution of different ionic strengths was carefully prepared by using the conductivity water of low specific conductivity ($<2\times10^{-7}$ ohm^{-1} cm^{-1}) in an atmosphere of purified nitrogen gas, and the pH-values of these solutions were adjusted to 9 with sodium hydroxide. In aqueous solutions of pH 9 the concentrations of HMa^- and HFu^- ions can be ignored.

Conductivity Measurement. The electric conductivities of mixtures were measured by mixing the solutions of same ionic strength at various volume fractions. The apparatus and the reproducibility of measurements were the same as those described previously.[1] All measurements were carried out in a water-thermostat of 25.000±0.005°C which was electrically grounded.

Results and Discussion

In tris(ethylenediamine)cobalt(III)chloride—sodium maleate and tris(ethylenediamine)cobalt(III)chloride–sodium fumarate mixtures (systems I and II, respectively), a large deviation of the measured conductivity from additivity was observed at each ionic strength. The deviation, $\Delta\kappa$, of the mixture, consisting of a C_1 molar solution of tris(ethylenediamine)cobalt(III)chloride (abbreviated as MCl_3) and a C_2 molar solution of

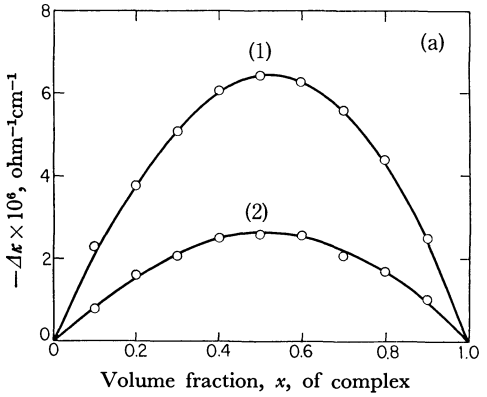

4) N. E. Topp and C. W. Davies, *J. Chem. Soc.*, **1940**, 87.

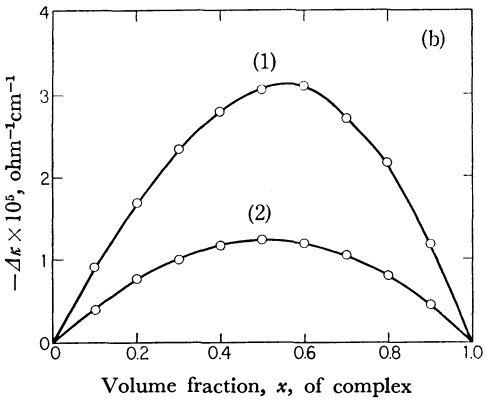

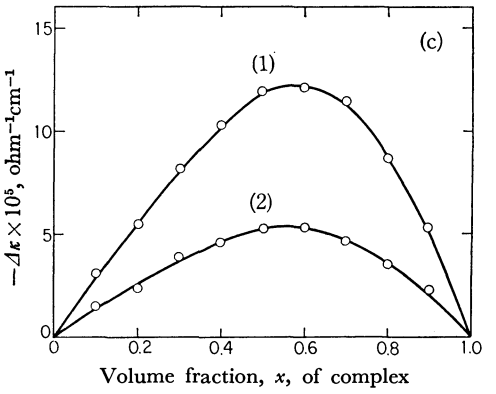

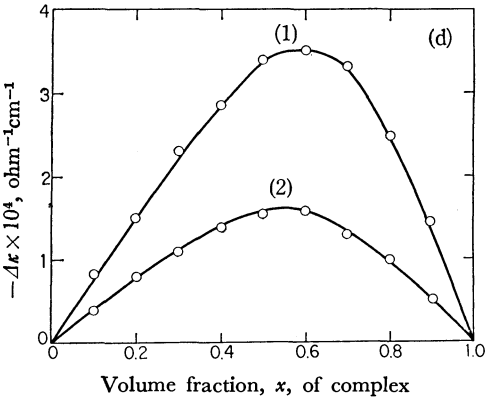

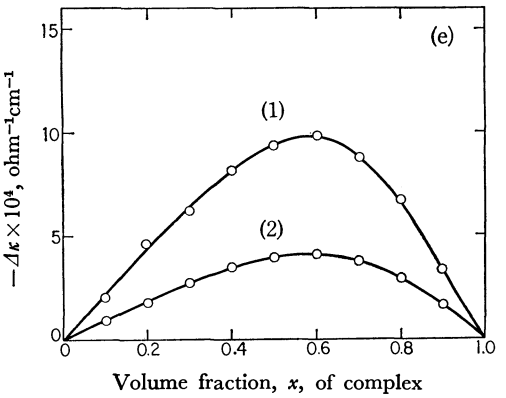

Fig. 1. Deviation of the observed conductivity from additivity, $\Delta\kappa$, as a function of the volume fraction, x, of complex (1000 Hz, 25°C).
(1) $[Co(en)_3]Cl_3$-Na_2Ma, (2) $[Co(en)_3]Cl_3$-Na_2Fu.
Ionic strength: (a) 0.001, (b) 0.003, (c) 0.01, (d) 0.03, (e) 0.1.

Na_2B (B^{2-}=Ma^{2-} or Fu^{2-}) at the volume fractions x and $(1-x)$, respectively, is given by the equation

$$10^3\Delta\kappa = 10^3\kappa - C_1 x\Lambda_m(MCl_3) - C_2(1-x)\Lambda_m(Na_2B) \quad (1)$$

where κ is the specific conductivity of the mixture, and Λ_m the molar conductivity of the species specified in parenthesis at the ionic strength of the mixture. Figures 1(a—e) show the deviation as a function of volume fraction x of the complex. The $\Delta\kappa$-values of system I were always larger than those of system II, and the deviation reached a maximum at x=0.5—0.6 in each case.

The following ion-pair formations are expected to occur in systems I and II.

$$M^{3+} + B^{2-} \rightleftarrows M^{3+}\cdot B^{2-}$$
$$M^{3+} + Cl^- \rightleftarrows M^{3+}\cdot Cl^-$$
$$Na^+ + B^{2-} \rightleftarrows Na^+\cdot B^{2-}$$

where M^{3+} represents tris(ethylenediamine)cobalt(III) cation. In the present discussion, however, the contribution of ion-pair formation of $M^{3+}\cdot Cl^-$ and $Na^+\cdot B^{2-}$ is neglected, and the deviation of the observed conductivities from additivity is assumed to be entirely due to the formation of $M^{3+}\cdot B^{2-}$. This assumption seems to be reasonable, because the formation constants of $M^{3+}\cdot Cl^-$ and $Na^+\cdot B^{2-}$ should be much smaller than those of $M^{3+}\cdot B^{2-}$.

The deviation $\Delta\kappa$ is then related to the molar concentration of ion-pair $M^{3+}\cdot B^{2-}$ by the equation

$$[M^{3+}\cdot B^{2-}] = \frac{10^3\Delta\kappa}{\alpha} \quad (2)$$

$$\alpha = |z(M^{3+}\cdot B^{2-})|\lambda(M^{3+}\cdot B^{2-}) - |z(M^{3+})|\lambda(M^{3+}) - |z(B^{2-})|\lambda(B^{2-})$$
$$= \lambda(M^{3+}\cdot B^{2-}) - 3\lambda(M^{3+}) - 2\lambda(B^{2-}) \quad (3)$$

where z is the charge number of ionic species, and λ the ionic equivalent conductivity at the ionic strength of the mixture.

The concentration formation constants K_c of $M^{3+}\cdot B^{2-}$ were determined by analysing the $\Delta\kappa$-values according to the same methods given previously.[1] In method (i) the K_c-values were obtained by estimating the values of parameter α at each ionic strength, while in method (ii) a set of K_c and α for the best fit between the observed and calculated $\Delta\kappa$-values was obtained by computer calculation. Table 3 summarizes the concentration formation constants thus determined for $[Co(en)_3]^{3+}\cdot Ma^{2-}$ and $[Co(en)_3]^{3+}\cdot Fu^{2-}$ at various ionic strengths, I.

The thermodynamic formation constants K were then determined by the extrapolation of the log K_c *vs.* $\sqrt{I}$ plots as shown in Fig. 2, and are given in the first line of Table 3. The values of log K obtained by the two methods of calculation are in relatively good agreement. The computer calculation, however, is expected to give more reliable K_c-values particularly at higher ionic strengths, because the analysis can be made without introducing arbitrariness into the estimation of parameter α.

Our study shows that the ion-pair formation constant of $[Co(en)_3]^{3+}\cdot Ma^{2-}$ is about 3 times larger than that of $[Co(en)_3]^{3+}\cdot Fu^{2-}$. A similar tendency of maleate and fumarate ions towards ion-pair formation has been reported by Topp and Davies[4] for $Ba^{2+}\cdot Ma^{2-}$, $Ba^{2+}\cdot Fu^{2-}$, $Ca^{2+}\cdot Ma^{2-}$, and $Ca^{2+}\cdot Fu^{2-}$ in aqueous solutions at 25°C, where the K-value of $Ba^{2+}\cdot Ma^{2-}$ was found to be about 5 times as large as that of $Ba^{2+}\cdot Fu^{2-}$, and the K-value of $Ca^{2+}\cdot Ma^{2-}$ to be about 3 times as large as that of $Ca^{2+}\cdot Fu^{2-}$.

TABLE 3. LOGARITHM OF CONCENTRATION FORMATION CONSTANTS, log K_c, OF ION-PAIRS $[Co(en)_3]^{3+}\cdot Ma^{2-}$ AND $[Co(en)_3]^{3+}\cdot Fu^{2-}$ AT 25°C AND AT VARIOUS IONIC STRENGTHS, I

(The values of log K, K being thermodynamic formation constant, are also included)

I	log K_c			
	$[Co(en)_3]^{3+}\cdot Ma^{2-}$		$[Co(en)_3]^{3+}\cdot Fu^{2-}$	
	Method (i)	Method (ii)	Method (i)	Method (ii)
0[a]	3.56	3.60	3.15	2.95
0.001	3.37	3.31	2.86	2.83
0.003	3.26	3.46	2.64	2.51
0.01	2.93	3.32	2.28	2.61
0.03	2.52	3.06	1.89	2.20
0.1	1.94	2.43	1.28	2.21

a) values in this line correspond to log K.

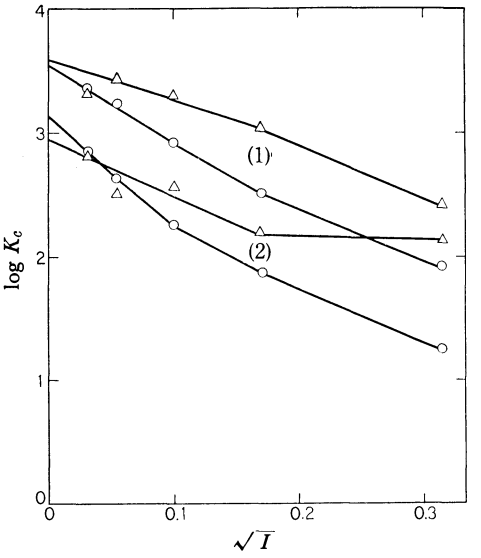

Fig. 2. Concentration formation constants of (1) ion-pair $[Co(en)_3]^{3+}\cdot Ma^{2-}$ and (2) ion-pair $[Co(en)_3]^{3+}\cdot Fu^{2-}$ as a function of ionic strength (25°C).
-○-: determined by estimating α (method (i))
-△-: determined by computer calculation (method (ii))

According to Bjerrum's theory of electrostatic interactions,[5] the ion-pair formation constant between ions i and j of opposite charge in aqueous solutions at 25°C is given by the equation

$$\log K = 0.4386 + 3\log|z_i z_j| + \log Q(b) \quad (4)$$
$$\log b = \log|z_i z_j| - 7.1468 - \log a$$

where $Q(b)$ is a function of b, and a the distance of closest approach of the ions. Introducing the values of log K given in Table 3 into Eq. (4), we obtain a=4 Å for $[Co(en)_3]^{3+}\cdot Ma^{2-}$ and a=6 Å for $[Co(en)_3]^{3+}\cdot Fu^{2-}$

5) C. B. Monk, "Electrolytic Dissociation," Academic Press, London (1961), pp. 272—275.

respectively. On the other hand, the Stokes radii of $[Co(en)_3]^{3+}$, Ma^{2-}, and Fu^{2-}, calculated from their limiting ionic equivalent conductivities, are: $r_s([Co(en)_3]^{3+})=3.7$ Å and $r_s(Ma^{2-}, Fu^{2-})=3.0$ Å. It is interesting to note that the a-value for $[Co(en)_3]^{3+}\cdot Ma^{2-}$ is significantly smaller than the sum of the Stokes radii of the ions. The result suggests that the charge distribution in ions and/or some interactions other than electrostatic attraction should be considered in the ion-pair formation between $[Co(en)_3]^{3+}$ and Ma^{2-} or Fu^{2-}.

The present work provides further evidence for the *cis-trans* isomeric effect in the ion-pair formation. However, much more information will be needed for a discussion on the isomeric effect.

We wish to thank Mrs. K. Takahashi for her kind collaboration in computer calculation.

BULLETIN OF THE CHEMICAL SOCIETY OF JAPAN, VOL. 44, 1815—1822 (1971)

Multidentate Ligand Substitution Reactions. XII. Substitution Reactions of the Nickel(II)-nitrilotriacetate Complex with Diethylenetriaminepentaacetic Acid in the Presence of Ethylenediamine and of the Nickel(II)-*N*-(2-hydroxyethyl)-iminodiacetate Complex with Ethylenediaminetetraacetic Acid and Cyclohexane-1,2-diamine-*N*,*N*,*N*′,*N*′-tetraacetic Acid

Mutsuo KODAMA, Sadatsugu KARASAWA, and Toshiyuki WATANABE

Department of Chemistry, Ibaraki University, Bunkyo, Mito, Ibaraki

(Received December 22, 1970)

The substitution reactions of the nickel(II)-nitrilotriacetate complex with diethylenetriaminepentaacetic acid in the presence of ethylenediamine and of the nickel(II)-*N*-(2-hydroxyethyl)-iminodiacetate complex with ethylenediaminetetraacetic acid and cyclohexane-1,2-diamine-*N*,*N*,*N*′,*N*′-tetraacetic acid were studied by employing the polarographic method. In the presence of ethylenediamine, the reaction of the nickel(II)-nitrilotriacetate complex with diethylenetriaminepentaacetic acid was found to proceed through the following four pathways:

$$NiX_2^{4-} \underset{\text{rapid}}{\rightleftharpoons} \begin{cases} NiX^- + \begin{cases} Z^{5-} \overset{k_1^+}{\rightleftharpoons} NiZ^{3-} + X^{3-} \\ HZ^{4-} \overset{k_2^+}{\rightleftharpoons} NiZ^{3-} + HX^{2-} \end{cases} \\ NiA^{2+} + \begin{cases} Z^{5-} \overset{k_3^+}{\rightleftharpoons} NiZ^{3-} + A^0 \\ HZ^{4-} \overset{k_4^+}{\rightleftharpoons} NiZ^{3-} + HA^+ \end{cases} \end{cases} \quad (\text{rapid: } NiXA^-)$$

where X^{3-} and Z^{5-} denote completely-deprotonated nitrilotriacetate and diethylenetriaminepentaacetate anions respectively, and A°, ethylenediamine. By comparing the rate constants of the substitution reactions of the nickel(II)-nitrilotriacetate and ethylenediamine complexes with their dissociation rate constants, the structure of the reaction intermediate was determined. From the concentration dependence of the reaction rate, the reactions of the nickel(II)-*N*-(2-hydroxyethyl)-iminodiacetate complex with ethylenediaminetetraacetic acid and with cyclohexane-1,2-diamine-*N*,*N*,*N*′,*N*′-tetraacetic acid were concluded to proceed through the following two reaction pathways:

$$\text{i)}\quad NiX_2^{2-} \underset{\text{rapid}}{\rightleftharpoons} NiX^0 + Y^{4-} \overset{k_1^+}{\rightleftharpoons} NiY^{2-} + X^{2-}$$

$$\text{ii)}\quad NiX_2^{2-} \underset{\text{rapid}}{\rightleftharpoons} NiX^0 + HY^{3-} \overset{k_2^+}{\rightleftharpoons} NiY^{2-} + HX^-$$

where X^{2-} and Y^{4-} mean completely-deprotonated *N*-(2-hydroxyethyl)-iminodiacetate and ethylenediaminetetraacetate or cyclohexane-1,2-diamine-*N*,*N*,*N*′,*N*′-tetraacetate anions. From a comparison of the rate constants for the reaction of the *N*-(2-hydroxyethyl)-iminodiacetate complex with those for the corresponding reaction of the iminodiacetate complex, it was found that the hydroxyethyl group in the *N*-(2-hydroxyethyl)-iminodiacetate anion rather accelerates the dissociation of the *N*-(2-hydroxyethyl)-iminodiacetate anion from the nickel(II) ion.

In previous papers,[1,2] we studied the substitution reaction of the nickel(II)-ethylenediaminetetraacetate (EDTA) complex with Eriochrome Black T (BT). In those papers, we mentioned that in the presence of the ammonia or thiocyanate anion the nickel(II)-EDTA

1) M. Kodama, C. Sasaki, and M. Murata, This Bulletin, **41**, 1333 (1968).

2) M. Kodama and K. Miyamoto, *ibid.*, **42**, 833 (1969).

complex shows the same kinetic behavior as in its absence, but the rate of the reaction was reducd, appreciably by increasing the concentration of the ammonia or thiocyanate anion. This was ascribed to the fact that, although the reaction proceeds only through the normal nickel(II)-EDTA complex, even in the presence of the ammonia or thiocyanate ion, its concentration is reduced by the formation of a mixed ligand complex with an ammonia or thiocyanate ion. Diethylenetriaminepentaacetic acid (DTPA) also reacts with the nickel(II)-nitrilotriacetate (NTA) complex at a measurable rate and displaces the NTA anion from its nickel(II) complex.[3] This reaction was found to proceed only through the 1:1-ratio nickel(II)-NTA complex. In the presence of ethylenediamine (EN), contrary to the observation of the effect of ammonia on the substitution reaction of nickel(II)-EDTA with BT, the substitution reaction of DTPA with the nickel(II)-NTA complex proceeds not only through the nickel(II)-NTA complex with a 1:1 ratio, but also through the nickel(II)-EN complex with a 1:1 ratio. We also studied the steric effect of the leaving group on the rate of the substitution reactions of nickel(II)-aminopolycarboxylate complexes with BT and demonstrated that the cyclohexane ring of cyclohexane-1, 2-diamine-*N*,*N*,*N*′,*N*′,-tetraacetate(CyDTA) anion slows the reaction considerably.[4] As in the case of the nickel(II)-iminodiacetate (IDA) complex,[5] the nickel(II)-*N*-(2-hydroxyethyl)-iminodiacetate (HIDA) complex also reacts with EDTA and CyDTA. Although the HIDA has the hydroxyethyl group, the reactions of the nickel(II)-HIDA complex with EDTA and CyDTA proceed much faster than would be expected for a simple glycinate mechanism. In this paper, first, we will study the substitution reaction of the nickel(II)-NTA complex with DTPA in the presence of EN and will determine the detailed reaction mechanism and rate constants. Secondly, we will deal with the substitution reactions of the nickel(II)-HIDA complex with EDTA and CyDTA, and will discuss the effect of the hydroxyethyl group of the HIDA ion on the rate of the substitution reaction.

Experimental

Reagents. The standard nickel(II) nitrate solution was prepared by dissolving a known amount of metallic nickel (99.99 %) in dilute nitric acid (1+1) and by then removing the excess nitric acid by distillation under reduced pressure. NTA, EDTA, CyDTA, and DTPA were recrystallized from their aqueous solutions by adding pure ethanol and hydrochloric acid. Their standard solutions were prepared by dissolving them in doubly-distilled water. In this study, EN purified by distillation under reduced pressure was used. The other chemicals were of analytical reagent grades and were used without further purification.

Apparatus and Experimental Procedures. All the d.c. polarograms and current-time curves were recorded by means of a Yanagimoto pen-recording polarograph, PA-102. The characteristic features of the dropping mercury electrode (DME) used in this study have been described previously.[3] For all the spectrophotometric measurements, a Hitachi EPS-3 recording spectrophotometer with a pair of 1-cm quartz cells was used. The pH was measured with a glass electrode pH-meter (a Hitachi-Horiba F-5). The rate of the substitution reaction was determined by measuring the change in the diffusion current of the anodic wave due to the decrease in the uncomplexed EDTA, CyDTA, or DTPA concentration with the time. In the kinetic study, all the measurements were conducted in solutions with an ionic strength of 0.30 ($NaClO_4$) and containing large excesses of complexed and uncomplexed EN, NTA, or HIDA over EDTA, CyDTA, or DTPA at 25°C. Therefore, all the substitution reactions could be treated as pseudo-first-order reactions. In this study, no buffer reagent was required to keep the solution's pH constant over the entire pH range covered ($7.50<pH<9.00$), because all the solutions contained a large excess of uncomplexed EN, NTA, or HIDA. All the experimental procedures employed in the kinetic study were the same as have previously been described.[3] In the spectrophotometric determination of the solution equilibrium, sample solutions with an ionic strength of 0.50 were used.

Results and Discussion

Spectrophotometric Determination of Solution Equilibria between the Nickel(II)-Nitrilotriacetate Complex and Ethylenediamine. Thermodynamically, when the product of the conditional formation constant of a 1:1 nickel(II)-NTA complex, K_{NiX}' ($=K_{NiX}/(\alpha_H)_X$), and the total concentration of the nickel(II) ion is larger than 1.0×10^6, the nickel(II) ion in the solution containing an equimolar NTA can be expected to exist exclusively in the form of NiX^-. Furthermore, when the concentration of the nickel(II)-NTA complex is nearly equal to that of uncomplexed EN and the $K_{NiX}'/(1+K_{NiA_2}^{A'}[A]_f)K_{NiA}'$ value is larger than 1.0×10^4, EN can not displace the NTA anion from its nickel(II) complex. Here, K_{NiA}' and $K_{NiA_2}^{A'}$ mean conditional first and second formation constants of nickel(II)-EN complex, and $[A]_f$, the concentration of the uncomplexed EN. Therefore, if the above conditions are fulfilled, the addition of EN to the nickel(II)-NTA complex solution will necessarily result in the formation of a mixed nickel (II)-NTA-EN complex according to the following equation:

$$NiX^- + A^0 = NiXA^-; \quad K_{NiX}^{A} = \frac{[NiXA^-]}{[NiX^-]\cdot[A_0]} \qquad (1)$$

The nickel(II)-NTA complex in an aqueous solution gives an absorption spectrum with two absorption maxima, at 395 and at 635 mμ. By the addition of EN to the nickel(II)-NTA solution, its absorbance was increased remarkably and the absorption curve's maxima were shifted to shorter wavelengths (365 and 585 mμ). These facts can be interpreted in terms of the formation of a mixed ligand complex involving an EN. As was discussed in the spectrophotometric determination of the formation constants of nickel(II)-ethylenediaminemonoacetate complexes, the following relation can be derived for the above solution equilibrium:[6]

3) M. Kodama, This Bulletin, **42**, 2532 (1969).
4) M. Kodama, C. Sasaki, and K. Miyamoto, *ibid.*, **42**, 163 (1969).
5) M. Kodama, *ibid.*, **42**, 3330 (1969).
6) M. Kodama, Y. Fujii, and T. Ueda, This Bulletin, **43**, 2085 (1970).

$$\log \frac{1}{[A]_t - \frac{A - A_{NiX}}{\varepsilon_{NiXA} - \varepsilon_{NiX}}} = \log \frac{A_{NiXA} - A}{A - A_{NiX}} + \log \frac{K^{A}_{NiX}}{(\alpha_H)_A} \quad (2)$$

where ε's and $[A]_t$ mean the molar extinction coefficients and the total concentration of EN, and where A, A_{NiXA}, and A_{NiX} are, respectively, the absorbance of the solutions in which NiX^- and $NiXA^-$ coexist, in which all the nickel(II)-NTA complex exists in the form of $NiXA^-$ and in which there is no EN. With the aid of Eq. (2), the experimental data were analyzed. The results obtained are reproduced in Fig. 1. From the $\log [1/([A]_t - (A - A_{NiX})/(\varepsilon_{NiXA} - \varepsilon_{NiX}))]$ value at $\log [(A_{NiXA} - A)/(A - A_{NiX})] =$ zero, the $\log K^{A}_{NiXA}/(\alpha_H)_A$ value was estimated to be 1.84. This corresponds to the $\log K^{A}_{NiXA}$ value of 5.84.

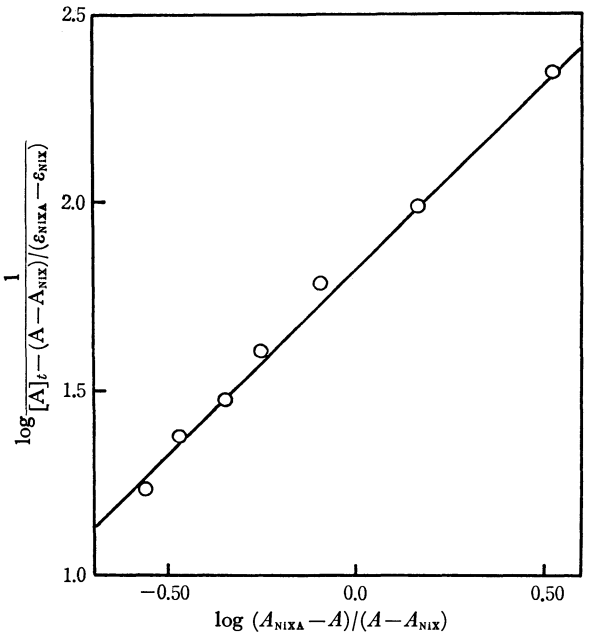

Fig. 1. The relation between $\log [1/[[A]_t - (A - A_{NiX})/(\varepsilon_{NiXA} - \varepsilon_{NiX})]]$ and $\log (A_{NiXA} - A)/(A - A_{NiX})$.
The concentration of Ni(II)-NTA complex=24.0 mM
pH=6.50, μ=0.50, λ=550 mμ
The EN concentration ranged from 30 to 300 mM

The Kinetic Study of the Substitution Reaction of the Nickel(II)-Nitrilotriacetate Complex with Diethylenetriaminepentaacetic Acid in the Presence of Ethylenediamine. As was found in the substitution reaction of the nickel(II)-NTA complex with DTPA in the absence of EN,[3] a linear relation passing through the point of origin could be obtained by plotting the $\log (i_0/i_t)$ against the time, t, in the present substitution reaction (the results are not shown here). Here, i_0 and i_t denote the wave heights of DTPA at times $t=0$ and $t=t$ respectively. When the other experimental conditions were kept constant, the slope of the above linear relation was not influenced by the addition of the nickel(II)-DTPA complex and was independent of the initial concentration of DTPA (Table 1). These facts clearly indicate that the forward reaction is much faster than the backward reaction, and that the dissociation of the nickel(II)-NTA complex is not involved in the present reaction. Therefore, the log-plot slope multiplied by 2.303 should be equal to the apparent rate constant of the forward reaction, k^{+}_{ap}. Furthermore, the log-plot slope was found to be exactly proportional to the total concentration of the nickel(II) ion (Table 2). As was shown in Fig. 2, the substitution reaction of the nickel(II)-NTA complex with DTPA in the presence of EN gave the linear relation between the log-plot slope multiplied by $(1 + K^{X'}_{NiX_2}[X]_f/K^{A'}_{NiXA}[A]_f)$ and the reciprocal of the uncomplexed EN concentration, $[A]_f^{-1}$. Here, $K^{X}_{NiX_2}$ denotes the second successive formation constant of the nickel(II)-NTA complex. By plotting the intercept of the above linear relation multiplied by the $(\alpha_H)_Z K^{X'}_{NiAX}[X]_f/[Ni]_t$ value or the slope multiplied by the $(\alpha_H)_Z K^{A'}_{NiXA}/[Ni]_t$ value against the hydrogen ion concentration, we could also obtain the straight line with the intercept of a finite value. The linear relations thus obtained are shown in Figs. 3 and 4. These facts

Table 1. The dependence of log-plot slope on the concentration of DTPA
Total Ni(II) concentration=10.0 mM, pH 7.92
Uncomplexed NTA concentration=20.0 mM, Uncomplexed EN concentration=50.0 mM

Initial concentration of DTPA, mM	Log-plot slope sec^{-1}
0.125	2.66×10^{-3}
0.250	2.71×10^{-3}
0.375	2.65×10^{-3}
0.500	2.63×10^{-3}
0.625	2.62×10^{-3}

Table 2. The dependence of log-plot slope on the concentration of nickel(II) ion
Initial concentration of DTPA=0.50 mM, pH=7.73
Uncomplexed NTA concentration=20.0 mM, Uncomplexed EN concentration=60.0 mM

Concentration of nickel(II) ion mM	Log-plot slope sec^{-1}	Concentraion ratio	Slope ratio
6.0	1.64×10^{-3}	1.00	1.00
10.0	2.77×10^{-3}	1.67	1.69
14.0	3.92×10^{-3}	2.33	2.39
18.0	4.95×10^{-3}	3.00	3.02
22.0	6.05×10^{-3}	3.67	3.69

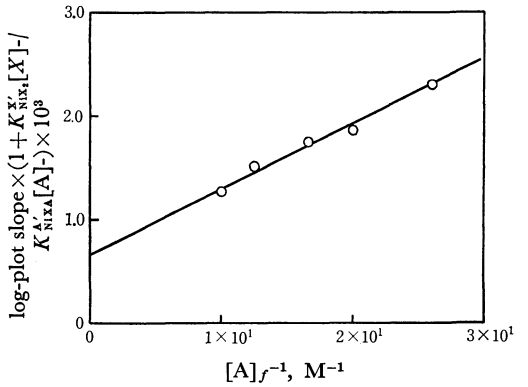

Fig. 2. The plot of log-plot slope $\times (1 + K^{X'}_{NiX_2}[X]_f/K^{A'}_{NiXA}[A]_f)$ against the reciprocal of the EN concentration.
The concentration of uncomplexed NTA=20.0 mM
The Ni(II) concentration=10.0 mM
pH=8.12, μ=0.30, 25°C

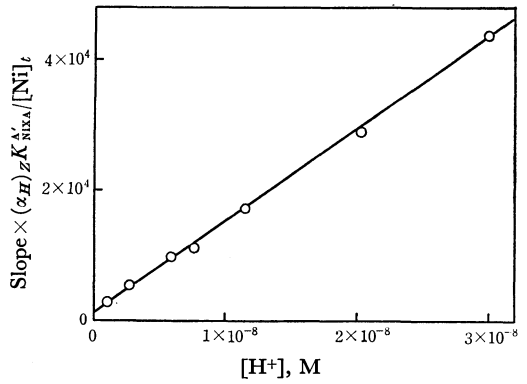

Fig. 3. The relation between the slope $\times(\alpha_H)_Z K^{A'}_{NIXA}/[Ni]_t$ and the hydrogen ion concentration.
The concentration of uncomplexed NTA =20.0 mM
The Ni(II) concentration =10.0 mM
μ=0.30, 25°C

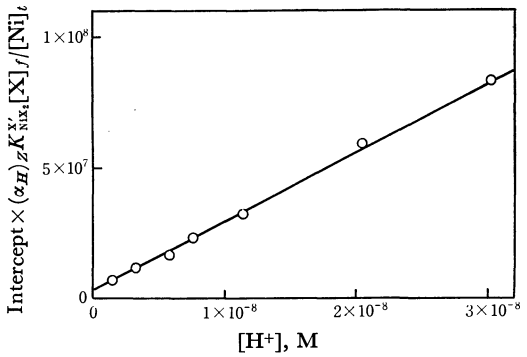

Fig. 4. The relation between the intercept $\times(\alpha_H)_Z K^{X'}_{NIX_1}[X]_f/[Ni]_t$ and the hydrogen ion concentration.
The concentration of uncomplexed NTA=20.0 mM
The Ni(II) concentration=10.0 mM
μ=0.30, 25°C

evidently imply that the substitution reaction of the nickel(II)-NTA complex with DTPA in the presence of EN proceeds through the following four reaction pathways:

$$NiX_2^{2-} \overset{\text{rapid}}{\rightleftharpoons} \begin{matrix} NiX^- \\ NiXA^- \\ NiA^{2+} \end{matrix} + \begin{cases} Z^{5-} \overset{k_1^+}{\rightleftharpoons} NiZ^{3-} + X^{3-} \\ HZ^{4-} \overset{k_2^+}{\rightleftharpoons} NiZ^{3-} + HX^{2-} \\ Z^{5-} \overset{k_3^+}{\rightleftharpoons} NiZ^{3-} + A^0 \\ HZ^{4-} \overset{k_4^+}{\rightleftharpoons} NiZ^{3-} + HA^+ \end{cases}$$

For the above reaction mechanism, k^+_{ap} is given by this relation (3):

$$k^+_{ap} = \left(\frac{k_X^+}{K^{A'}_{NIXA}[A]_f} + \frac{k_A^+}{K^{X'}_{NIXA}[X]_f}\right) \times \frac{[Ni]_t}{(\alpha_H)_Z \cdot \left(1 + \frac{K^{X'}_{NIX_1}[X]_f}{K^{A'}_{NIXA}[A]_f}\right)} \quad (3)$$

Here, k_X^+ and k_A^+ are given by (4a) and (4b) respectively.

$$k_X^+ = k_1^+ + k_2^+ \frac{[H^+]}{K_5} \quad (4a)$$

$$k_A^+ = k_3^+ + k_4^+ \frac{[H^+]}{K_5} \quad (4b)$$

where K_5 means the fifth dissociation constant of DTPA.

From the slopes and intercepts of the linear relations in Figs. 3 and 4, k_1^+, k_2^+, k_3^+, and k_4^+ were determined; they are listed in Table 3. Although the precision is not satisfactory, the k_3^+ and k_4^+ values determined in this study agree well with those obtained in the kinetic study of the substitution reaction of the nickel(II)-EN complex with DTPA (μ=0.30, $k_3^+=4\times10^6$, $k_4^+=3.5\times10^5$).[7] If the substitution reaction of the nickel(II)-NTA complex with DTPA in the presence of EN proceeds through the above four reaction pathways, the k_1^+, k_2^+, k_3^+, and k_4^+ values obtained in this study should explain satisfactorily the effect of the concentration of the uncomplexed NTA on the reaction rate. Equation (3) clearly indicates that, provided that the other experimental conditions are kept constant, a plot of the log-plot slope multiplied by the $(1+K^{X'}_{NIX_2}[X]_f/K^{A'}_{NIXA}[A]_f)$ value against the reciprocal of the uncomplexed NTA concentration, $[X]_f^{-1}$, should yield a straight line, the slope and the intercept of which are $2.303\times k_A^+[Ni]_t/$

Table 3. Rate constants (μ=0.30, 25°C) and the slope and intercept of the linear relation between $(1+K^{X'}_{NIX_1}[X]_f/K^{A'}_{NIXA}[A]_f)\times$ log-plot slope and the reciprocal of the uncomplexed NTA concentration

i) Rate constant (M^{-1} sec^{-1})

Rate constant	
k_1^+	2×10^3
k_2^+	2.4×10^2
k_3^+	3×10^6
k_4^+	4.7×10^5
k_d^{EN} [8]	0.14

ii) Slope and Intercept
Ni(II) concentration=10.0 mM, pH=8.98
Uncomplexed EN concentration=15.7 mM

Slope		Intercept	
Calcd	Obsd	Calcd	Obsd
4.3×10^{-6}	4.4×10^{-6}	$1._3\times10^{-3}$	$1._5\times10^{-3}$

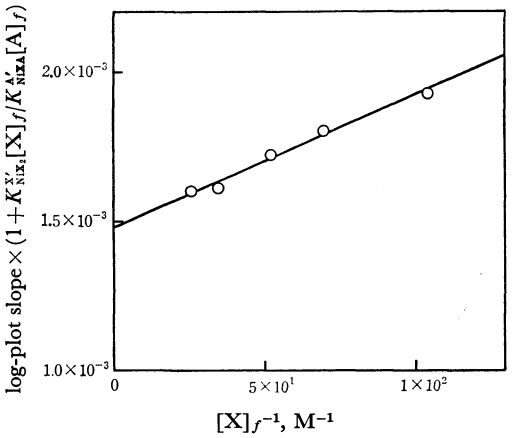

Fig. 5. The plot of log-plot slope $\times(1+K^{X'}_{NIX_1}[X]_f/K^{A'}_{NIXA}[A]_f)$ against the reciprocal of the uncomplexed NTA concentration.
The concentration of uncomplexed EN=15.7 mM
The Ni(II) concentration=10.0 mM
pH=8.98, μ=0.30, 25°C

7) The details will be described in a future report.

Table 4. The dependence of log-plot slope on the concentration of nickel(II)-HIDA complex
μ=0.30, 25°C

System	Concentration of Ni(II)-HIDA complex mM	Log-plot slope sec^{-1}	Concentration ratio	slope ratio	
EDTA	5.85	1.40×10^{-2}	1.00	1.00	Concentration of uncomplexed HIDA=18.0 mM
	9.74	2.31×10^{-2}	1.67	1.65	Initial concentration of EDTA=0.52 mM
	13.65	3.12×10^{-2}	2.33	2.23	pH=9.48
CyDTA	9.75	0.625×10^{-4}	1.00	1.00	Concentration of uncomplexed HIDA=10.0 mM
	14.6_0	1.00×10^{-4}	1.50	1.60	Initial concentration of CyDTA=0.49 mM
	19.5_0	1.26×10^{-4}	2.00	2.01	pH=8.44

$K^{X'}_{NiXA}(\alpha_H)_Z$ and $2.303 \times k^+_A[Ni]_t/K^{A'}_{NiXA}[A]_f(\alpha_H)_Z$ respectively. A typical linear relation between the product of the log-plot slope and the $(1+K^{X'}_{NiX_2}[X]_f/K^{A'}_{NiXA}[A]_f)$ and the reciprocal of the concentration of uncomplexed NTA is reproduced in Fig. 5. The slope and intercept of the above linear relation were compared with those calculated with the aid of Eq. (3) by using the k_1^+, k_2^+, k_3^+, and k_4^+ values listed in Table 3. The calculated values agreed well with those obtained (Table 3). This agreement strongly supports the reaction mechanism proposed by the present authors.

The Kinetic Study of Substitution Reactions of the Nickel(II)-N-(2-Hydroxyethyl)-Iminodiacetate Complex with Ethylenediaminetetraacetic Acid and with Cyclohexane-1,2-diamine-N,N,N',N'-tetraacetic Acid. In the substitution reaction of the nickel(II)-HIDA complex, quite similar results to those obtained in the substitution reactions of the nickel(II)-iminodiacetate (IDA) complex with EDTA and CyDTA were obtained. The plot of log-(i_0/i_t) against t invariably gave a straight line passing through the point of origin. Its slope was independent of the initial concentration of EDTA or CyDTA and was not influenced by the addition of the nickel(II)-EDTA or CyDTA complex (the results will not be given here). It was also found that the log-plot slope is exactly proportional to the concentration of the 1:1 nickel(II)-HIDA complex in solutions of a given pH (Table 4), and that the plot of the product of the log-plot slope and $2.303 \times (\alpha_H)_Y(1+K^{X'}_{NiX_2}[X]_f)/[Ni]_t$ against the concentration of the hydrogen ion gives a linear relation (Fig. 6) corresponding to the following relation:

$$\frac{k^+_{ap}(\alpha_H)_Y(1+K^{X'}_{NiX_2}[X]_f)}{[Ni]_t} = k_\alpha{}^+ + k_\beta{}^+[H^+] \qquad (5)$$

where $(\alpha_H)_Y$ denotes the (α_H) value of EDTA or CyDTA, $K^{X'}_{NiX_2}$, the conditional second successive formation constant of the nickel(II)-HIDA complex, and $[X]_f$, the concentration of the uncomplexed HIDA. Therefore, we can safely propose the following reaction mechanism for the substitution reaction of the nickel(II)-HIDA complex with EDTA or CyDTA.

i) $NiX_2{}^{2-}$
$\downarrow\uparrow$ rapid
$NiX^0 + Y^{4-} \overset{k_1^+}{\rightleftharpoons} NiY^{2-} + X^{2-}$

ii) $NiX_2{}^{2-}$
$\downarrow\uparrow$ rapid
$NiX^0 + HY^{3-} \overset{k_2^+}{\rightleftharpoons} NiY^{2-} + HX^-$

where Y^{4-} denotes the completely-deprotonated EDTA or CyDTA anion, and X^{2-}, the completely-deprotonated HIDA anion. If the reaction of the nickel(II)-HIDA complex with EDTA or CyDTA has the above reaction mechanism, k_α^+ and k_β^+ in Eq. (5) should be equal to k_1^+ and k_2^+/K_4 respectively. Here, K_4 corresponds to the fourth dissociation constant of EDTA or CyDTA. Thus, we can determine the k_1^+ and k_2^+ values for the reactions of the nickel(II)-HIDA complex with EDTA and CyDTA from the intercepts and slopes of the linear relations in Fig. 6. The k_1^+ and k_2^+ values thus determined are listed in Table 5, together with the k_1^+ and k_2^+ values of the substitution reactions of the nickel(II)-IDA complex with EDTA and CyDTA.[5]

We can mention here that the rate for the substitu-

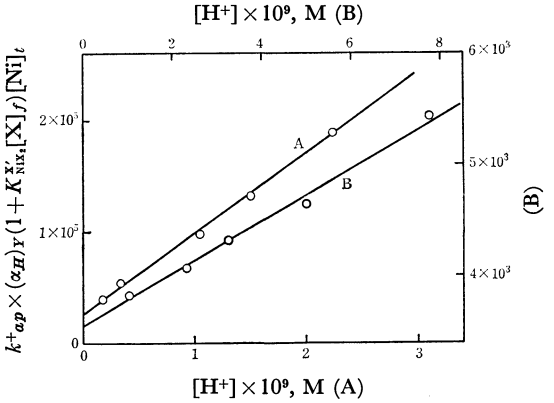

Fig. 6. The relation between $K^+_{ap}\cdot(\alpha_H)_Y(1+K^{X'}_{NiX_2}[X]_f)/[Ni]_t$ and the hydrogen ion concentration.
μ=0.30, 25°C
A) Ni(II)-HIDA—EDTA reaction
The concentration of uncomplexed HIDA=18.0 mM
The Ni(II) concentration=10.0 mM
Initial concentration of EDTA=0.52 mM
B) Ni(II)-HIDA—CyDTA reaction
The concentration of uncomplexed HIDA=10.0 mM
The Ni(II) concentration=10.0 mM
Initial concentration of CyDTA=0.49 mM

Table 5. Rate constants (μ=0.30, 25°C)
i) Substitution reaction

System	Rate constant M^{-1} sec^{-1}	EDTA	CyDTA
HIDA	k_1^+	1.7×10^4	3.7×10^3
	k_2^+	$7.3_5 \times 10^3$	0.94
IDA[5]	k_1^+	2.1×10^4	1.7×10^4
	k_2^+	$7.3_3 \times 10^3$	$3.3_3 \times 10^2$

ii) Dissociation reaction

Ni(II)-IDA complex[17]	$k_d=2.8\times10^4$ (μ=0.10, 25°C)

tion reaction of the nickel(II)-EN complex with DTPA is much larger than that for the dissociation of the nickel(II)-EN complex.[8] This can be explained in terms of the formation of the mixed ligand complex reaction intermediate involving the DTPA anion.[1,9] As was attempted in the substitution reaction of the nickel(II)-EDMA complex with DTPA,[6] we can also estimate the structure of the reaction intermediate in the substitution reaction of the nickel(II)-EN complex with DTPA by comparing its rate constant with that for the dissociation of the nickel(II)-EN complex. If the reaction of the nickel(II)-EN complex proceeds through the reaction intermediate I_a, the rate constant, k_3^+, should be about 3×10^7 times larger than the dissociation constant of a 1:1 ratio nickel(II)-EN complex. Here, we used the nickel(II)-*N*-ethyl-glycinate complex as a model. In the estimation of the relative rate constant, the electrostatic contribution to the stability of the reaction intermediate, K_{etec}, and the statistical factor were also taken into account. Similarly, when the reaction intermediate is given by I_b or I_c (Fig. 7),

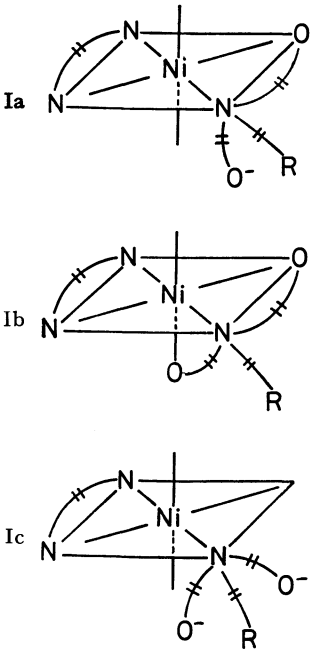

Fig. 7. Reaction intermediates for the substitution reaction of nickel(II)-EN complex with DTPA.

the ratio of the rate constant, k_3^+, to the dissociation rate constant of a 1:1 nickel(II)-EN complex should be 3×10^9 or 1×10^9. The k_3^+ and k_d^{EN} values in Table 3 clearly indicate that the reaction intermediate I_a fits best. From a comparison of the k_1^+ value with the dissociation rate constant of a 1:1 ratio nickel(II)-NTA complex, we can also estimate the structure of the reaction intermediate in the reaction of the nickel(II)-NTA complex with DTPA. The rate constant for the dissociation of a 1:1 nickel(II)-NTA complex was reported by Kimura (3.0×10^{-5} sec^{-1}, μ=0.10, 25°C).[10]

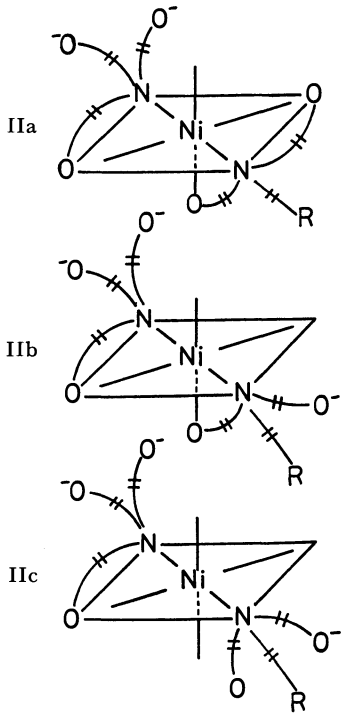

Fig. 8. Reaction intermediates for the substitution reaction of nickel(II)-NTA complex with DTPA.

As was discussed in connection with the dissociation of nickel(II)-aspartate complex,[11] by comparing this value with the rate constant calculated on the basis of the reaction intermediate proposed, we can determine the detailed structure of the reaction intermediate. The rate constant reported by Kimura agrees well only with that calculated on the basis of a glycinate reaction intermediate.[12] Consequently, the following are considered to be the possible reaction intermediate in the substitution reaction of the nickel(II)-NTA complex with DTPA (Fig. 8). The k_1^+ value determined in this study is 7.7×10^7 times larger than the dissociation rate constant of the nickel(II)-NTA complex. As is shown in Fig. 8, the rate constant ratio estimated on the basis of the reaction intermediate, II_a, agreed best with that determined experimentally. In general, the substitution reaction of the nickel(II)-aminopolycarboxylate complex proceeds through the reaction intermediate in which the attacking aminopolycarboxylate anion is bonded to the nickel(II) ion through the iminodiacetate chelate ring. Therefore, the above conclusion must be reasonable.

Previously,[2] we had reported that even in the presence of ammonia the substitution reaction of nickel(II)-EDTA complex with BT proceeds only through the normal nickel(II)-EDTA complex, NiY^{2-}. Theo-

8) A. K. S. Ahmed and R. G. Wilkins, *J. Chem. Soc.*, **1959**, 3700.
9) D. B. Rorabacher and D. W. Margerum, *Inorg. Chem.*, **3**, 382 (1964).
10) M. Kimura, *Nippon Kagaku Zasshi*, **89**, 1209 (1968).
11) M. Kodama, H. Nunokawa, and N. Oyama, This Bulletin, **44**, in Press.
12) The glycinate reaction intermediate means the reaction intermediate in which the leaving NTA anion is bonded to the nickel(II) ion through a glycinate chelate ring. The rate constant calculated with the aid of Eq. (16) in Ref. (11) was 1.6×10^{-5} sec^{-1}. In the calculation, the electrostatic contribution to the stability of the reaction intermediate and the statistical factor were also taken into consideration.

retically, the substitution reaction of the nickel(II)-EDTA complex with BT in the presence of ammonia can be expected to proceed also through the nickel(II)-ammonia complex. However, the reaction pathway which involves a mixed-ligand 1:1:1 ratio ammonia, EDTA nickel(II) complex, $NiY(NH_3)^{2-}$, is unlikely, because the mixed-ligand complex is much less favorable for the formation of a reaction intermediate, which is essentially a mixed-ligand complex involving a BT anion. On the basis of the reaction intermediate, we can estimate the contribution of the reaction pathway involving the nickel(II)-ammonia complex to the whole reaction. If we apply Eq. (5) in Ref. (13) or Eq. (17) in Ref. (9) to the substitution reaction of the nickel(II)-EDTA complex with BT, the contribution ratio of the reaction pathway involving the ammonia complex to that involving the EDTA complex can be calculated approximately by using the following relation:

$$\text{Ratio} = \frac{k_d^{NH_3} \cdot K_{Ni(NH_3)} \cdot (\alpha_H)_Y \cdot [NH_3]_f}{4 \cdot k_d^{gly} \cdot K_{Ni-gly} \cdot (\alpha_H)_{NH_3} \cdot [Y]_f}$$

where $k_d^{NH_3}$[14] and k_d^{gly}[15] are the rate constants for the dissociation of ammonia and glycinate anions respectively from the nickel(II) ion in the reaction intermediate, $[NH_3]_f$ and $[Y]_f$, the concentrations of uncomplexed ammonia and of uncomplexed EDTA, and $K_{Ni(NH_3)}$ and K_{Ni-gly}, the formation constants of 1:1-ratio nickel(II)-ammonia and -glycinate complexes respectively, and where the (α_H)'s indicate the (α_H) values of ammonia and EDTA, and 4, the statistical factor for the formation of a nickel(II)-glycinate chelate ring between the nickel(II) ion and the tetravalent EDTA anion. In the derivation of the above equation, we assumed that the nickel(II)-BT segments in the reaction intermediates of both reaction pathways have the same structure and that the reaction pathway involving the nickel(II)-EDTA complex proceeds via a glycinate reaction intermediate.[13] With the aid of the above relation, the ratio was calculated to be about 0.01 by using the reported numerical values. This small contribution ratio clearly supports the present author's explanation that the substitution reaction of the nickel(II)-EDTA complex with BT in the presence of ammonia proceeds exclusively through the normal nickel(II)-EDTA complex, NiY^{2-}. Similarly, on the basis of the proposed reaction intermediates, we can also estimate the contribution of the reaction pathway involving the normal nickel(II)-NTA complex to the whole reaction. If the reaction pathway involving the nickel(II)-EN complex proceeds through the reaction intermediate I_a, and that involving the nickel(II)-NTA complex, through II_a, under the conditions where the concentration of the uncomplexed EN is nearly identical with that of the uncomplexed NTA, the ratio of the contribution of the former reaction pathway to that of the latter reaction pathway will be given by the following relation:

$$\text{Ratio} = \frac{4 \times k_d^{EN} K'_{Ni-EN}}{6 \times k_d^{gly} K_{Ni-IDA}}$$

where 4 and 6 are statistical factors; k_d^{EN} the rate constant for the dissociation of the nickel(II)-EN complex with a 1:1 ratio,[8] and K_{Ni-EN} and K_{Ni-IDA}, the formation constants of 1:1-ratio nickel(II)-EN and -IDA complexes. The ratio calculated with the aid of the above relation was nearly equal to unity. This also supports the reaction mechanism proposed by the present authors for the substitution of the nickel(II)-NTA complex with DTPA in the presence of ethylenediamine.

As is clear from the data shown in Table 5, the k_1^+ and k_2^+ values for the substitution reaction of the nickel(II)-HIDA complex with EDTA are nearly identical with those for the corresponding substitution reaction of the nickel(II)-IDA complex. If the above two substitution reactions proceed through the reaction intermediates in which both HIDA and IDA anions are bonded to the nickel(II) ion through one nitrogen and two oxygen atoms, the k_1^+ value for the former reaction should be nearly equal to the k_1^+ value for the latter reaction, for the relative stabilities of the reaction intermediates for both reactions must be the same. Already, we have established that the substitution reaction of the nickel(II)-IDA complex with DTPA has the glycinate mechanism,[16] and also that the rate constants for the reaction of the nickel(II)-IDA complex with DTPA are nearly identical with those for the reaction with EDTA.[5] These facts clearly imply that the reaction of the nickel(II)-IDA complex with EDTA also proceeds through the reaction intermediate in which the displaced IDA anion is bonded to the nickel(II) ion through one nitrogen and one oxygen atoms (the glycinate mechanism). Thus, in the substitution reaction of the nickel(II)-IDA complex with EDTA, the reaction intermediate in which the displaced IDA anion is bonded to the nickel(II) ion through one nitrogen and two oxygey atoms should be eliminated. If the reactions of both nickel(II)-IDA and -HIDA complex with EDTA have the glycinate mechanism, the rate constant for the substitution reaction of the nickel(II)-HIDA complex should be approximately 17 times smaller than that for the reaction involving the nickel(II)-IDA complex, because the formation constant of the nickel(II)-HIDA complex with a 1:1 ratio is 17 times larger than that of the 1:1 nickel(II)-IDA complex. Therefore, the finding that the k_1^+ and k_2^+ values for the reaction of the nickel(II)-HIDA complex are nearly equal to those for the reaction of the nickel(II)-IDA complex should be ascribed to the fact that the hydroxyethyl group in the HIDA anion effectively helps the dissociation of the HIDA anion from the nickel(II) ion in the reaction intermediate. Furthermore, the k_1^+ value for the substitution reaction of the nickel(II)-IDA complex with EDTA is about 1×10^8 times larger than the rate constant for the dissociation of a 1:1-ratio nickel(II)-IDA complex.[11,17]

13) M. Kodama, C. Sasaki, and T. Noda, This Bulletin, **41**, 2033 (1968).
14) G. G. Hummes and J. I. Steinfeld, *J. Amer. Chem. Soc.*, **84**, 4639 (1962).
15) D. W. Margerum, D. B. Rorabacher, and J. F. G. Clarke, Jr., *Inorg. Chem.*, **2**, 667 (1963).
16) M. Kodama and T. Ueda, This Bulletin, **43**, 419 (1970).
17) T. J. Bydalek and A. H. Constant, *Inorg. Chem.*, **4**, 833 (1965).

If the reaction of the nickel(II)-IDA complex with EDTA proceeds through the reaction intermediate in which the EDTA anion is bonded to the nickel(II) ion through the iminodiacetate chelate ring, the ratio of the rate constant between the substitution and dissociation reactions of the nickel(II)-IDA complex should be 2.1×10^8. Here, we used the nickel(II)-HIDA complex as a model of the nickel(II)-EDTA segment. In the above calculations, the statistical factor and the electrostatic contribution were also taken into account. The rate-constant ratio calculated on the basis of the reaction intermediate in which the EDTA anion is bonded to the nickel(II) ion through the iminodiacetate chelate ring agreed well with that observed. From the above results and the discussion of them, we can safely conclude that the substitution reaction of the nickel(II)-HIDA complex with EDTA proceeds through the following reaction intermediate (Fig. 9). As is shown in Table 5, the k_1^+ and k_2^+ values for the substitution reaction of the nickel(II)-HIDA complex with CyDTA are appreciably smaller than those of the other substitution reactions studied. This may be attributed mainly to the steric hindrance resulting from the interaction between the cyclohexane

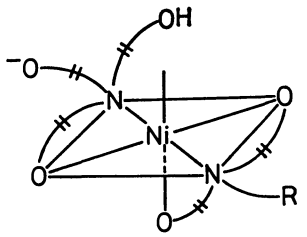

Fig. 9. Reaction intermediate for the substitution reaction of nickel(II)-HIDA complex with EDTA.

ring of CyDTA anion and the hydroxyethyl group of the HIDA anion. Finally, it should be noted that the k_2^+ value, especially, for the reaction with CyDTA is much smaller than the k_1^+ value. Since the protonation of the CyDTA anion bonded to the nickel(II) ion will reduce the electrostatic repulsion between the un-coordinated carboylate groups, and will stabilize the reaction intermediate, the above fact suggests the importance of the deprotonation of the attacking group in the formation of the reaction intermediate. In order to describe the precise nature of the effect of the protonation of the attacking group, a further, systematic investigation is necessary

BULLETIN OF THE CHEMICAL SOCIETY OF JAPAN, VOL. 44, 1822—1826 (1971)

Hydrolysis of Nickel(II) Ion in Aqueous 3 M Sodium Chloride Medium

Hitoshi OHTAKI and Georg BIEDERMANN*

Department of Electrochemistry, Tokyo Institute of Technology, Ookayama, Meguro, Tokyo

**Department of Inorganic Chemistry, The Royal Institute of Technology, Stockholm, Sweden*

(Received December 25, 1970)

The hydrolytic reaction of nickel ion was studied at 25°C in an aqueous 3M sodium chloride medium. In the range of the total nickel concentration of 0.0145—1.000M, the emf data obtained could be explained in terms of the formation of the complex $Ni_4(OH)_4$ (the charge is omitted), the formation constant of the species being found to be $\log {}^*\beta_{4,4} = -28.5_5 \pm 0.1_0$, together with some minor species NiOH ($\log {}^*\beta_{1,1} \leq -10.5$) and Ni_2OH ($\log {}^*\beta_{1,2} \leq -10.5$).

The hydrolytic reaction of nickel ion has been studied by a number of workers and the results are summarized.[1] A brief survey of these studies has been made by Burkov, Lilič, and Sillén[2] in their paper on the hydrolytic reaction of nickel ion in the 3 M sodium perchlorate medium. In addition to these studies some recent works should be mentioned.[3,4]

Most of these workers, except Burkov *et al.*,[2] reported formation of the mononuclear complex $NiOH^+$ as the main product of hydrolytic reaction. Burkov *et al.* showed that the main hydrolyzed species of nickel ion is the tetramer $Ni_4(OH)_4^{4+}$, and only negligible amounts of mononuclear complexes are formed in solutions of relatively high concentrations of nickel and perchlorate ions.

The present study deals with the hydrolytic reaction of nickel ion in the 3 M sodium chloride medium.

The hydrolytic reaction of nickel ions may, in general, be written as

$$qNi^{2+} + pH_2O + rCl^- = Ni_q(OH)_pCl_r^{(2q-p-r)+} + pH^+ \quad (1)$$

and the equilibrium constant of the reaction (1) is defined by

$${}^*\beta^\circ_{p,q,r} = [Ni_q(OH)_pCl_r^{(2q-p-r)+}][H^+]^p/[Ni^{2+}]^q[Cl^-]^r \quad (2)$$

Taking into account the formation of chloro complexes, the concentration of nickel ions which are not hydrolyzed $[Ni^{2+}]_f$, can be written as follows.

$$\begin{aligned}[Ni^{2+}]_f &= [Ni^{2+}] + \sum_m\sum_n m[Ni_mCl_n^{(2m-n)+}] \\ &= [Ni^{2+}](1 + \sum_m\sum_n m\beta_{m,n}[Ni^{2+}]^{m-1}[Cl^-]^n) \\ &= [Ni^{2+}]\alpha_{Ni(Cl)} \end{aligned} \quad (3)$$

where $\beta_{m,n}$ denotes the overall formation constant of

1) L. G. Sillén and A. E. Martell, "Stability Constants," 2nd. Ed., Chem. Soc., London (1964).

2) K. A. Burkov, L. S. Lilič, and L. G. Sillén, *Acta Chem. Scand.*, **19**, 14 (1965).

3) J. Shanker and B. C. De Souza, *Aust. J. Chem.*, **16**, 1119 (1963).

4) D. D. Perrin, *J. Chem. Soc.*, **1964**, 3644.

the complex $Ni_mCl_n^{(2m-n)+}$ and $\alpha_{Ni(Cl)}$ the side reaction coefficient of nickel ion with respect to chloride ions.

If we define $*\beta^\circ_{p,q}$ by

$$*\beta^\circ_{p,q} = [H^+]^p \sum_r [Ni_q(OH)_pCl_r^{(2q-p-r)+}]/[Ni^{2+}]^q \quad (4)$$

$*\beta^\circ_{p,q}$ is related to $*\beta^\circ_{p,q,r}$ through the equation

$$*\beta^\circ_{p,q} = \sum_r *\beta^\circ_{p,q,r}[Cl^-]^r \quad (5)$$

If we use $[Ni^{2+}]_f$, insted of $[Ni^{2+}]$ in Eq. (4), the conditional equilibrium constant $*\beta_{p,q}$ is given by

$$*\beta_{p,q} = [H^+]^p \sum_r [Ni_q(OH)_pCl_r^{(2q-p-r)+}]/[Ni^{2+}]_f^q = \alpha_{Ni(Cl)}^{-q} \sum_r *\beta^\circ_{p,q,r}[Cl^-]^r \quad (6)$$

$*\beta_{p,q}$ will be a constant in the whole range of the nickel concentrations provided that the concentration of chloride ions remains practically unchanged and that only the mononuclear chloro complexes ($m=1$) are formed.

Symbols;

- h Hydrogen ion concentration at equilibrium.
- H Analytical excess of hydrogen ions$=[Cl^-]-2B-[Na^+]$.
- B Total concentration of nickel.
- b Concentration of unhydrolyzed nickel ions.
- Z Average number of hydrogen ions set free per nickel atom$=(h-H-K_wh^{-1})/B$.
- p Number of OH groups bound to hydrolyzed species.
- q Number of nickel atoms bound to hydrolyzed species.
- r Number of chlorine atoms bound to hydrolyzed species.
- $*\beta_{p,q}$ Conditional equilibrium constant of the hydrolytic reaction of nickel ion, defined by Eq. (6).
- [ ] Concentration.
- E Emf.

Method of Measurement

Titration procedures are similar to those adopted in other systems in which cations are very weak acids and solubilities of metal hydroxides are very low.[5,6] Thus, a test solution containing nickel hydroxide precipitates was filtered, and the clear solution was titrated with an acid solution at constant B. The studied range of B values was from 0.0145 M to 1.000 M. Sodium chloride was used as an ionic medium and the total concentration of chloride ions was kept constant (3M).

Titration was performed under an atmosphere of nitrogen, which was free from carbon dioxide and was pre-equilibrated with the solvent.

The hydrogen ion concentration h was measured by means of the cell

$$\text{Ref}\,|\,\text{Solution}\,|\,\text{GE} \quad (A)$$

where GE denotes a glass electrode and Ref the reference half-cell (B):

$$\text{Ag-AgCl}\,|\,\text{3M NaCl saturated with AgCl}\,|\,\text{3M NaCl}\,| \quad (B)$$

The emf of cell (A) can be written at 25°C as

$$E = E^{\circ\prime} + 59.15 \log h + E_j \quad (7)$$

constant activity coefficient of hydrogen ions being assumed. Since pH range studied is 6—7.7, the liquid junction potential E_j is practically independent of the hydrogen ion concentration at constant concentration of total nickel and chloride ions. Thus, Eq. (7) can be rewritten in a simpler form as

$$E = E^\circ + 59.15 \log h \quad (8)$$

and E°, a constant, is determined by means of the Gran plot[7] at each titration procedure.

The average number of OH groups bound to hydrolyzed species, Z, is obtained as

$$Z = \frac{\sum_p\sum_q\sum_r p*\beta^\circ_{p,q,r}[Ni^{2+}]^q[H^+]^{-p}[Cl^-]^r}{[Ni^{2+}] + \sum_m\sum_n m\beta_{m,n}[Ni^{2+}]^m[Cl^-]^n + \sum_p\sum_q\sum_r q*\beta^\circ_{p,q,r}[Ni^{2+}]^q[H^+]^{-p}[Cl^-]^r} = \frac{\sum_p\sum_q p*\beta_{p,q}[Ni^{2+}]_f^q[H^+]^{-p}}{[Ni^{2+}]_f + \sum_p\sum_q q*\beta_{p,q}[Ni^{2+}]_f^q[H^+]^{-p}} = \frac{h - H - K_wh^{-1}}{B} \quad (9)$$

Experimental

Reagents. *Sodium chloride* (reagent grade, E. Merck Co.) was mixed with a small amount of water and hydrochloric acid and the slurry was dried and finally ignited at about 500°C in an electric oven.

Nickel chloride (reagent grade, E. Merck Co.) was recrystallized from water by addition of dried HCl gas and crystals were washed with hydrochloric acid solution. The crystals were then dried in a desiccator over potassium hydroxide pellets *in vacuo*. The crystals were dissolved in distilled water in order to prepare a stock solution of nickel chloride. pH of the stock solution was about 3.

Other chemicals were prepared by methods described elsewhere.[2,5,6]

Apparatus. *Glass electrodes*: Beckman (No. 40498) glass electrodes were used in combination with *a Radiometer PHM 4 (Copenhagen)*.

Silver-silver chloride electrodes set in *the "Wilhelm" type of half-cell*[8] were prepared according to Brown.[9]

Preparation of Test Solution. Test solutions containing hydrolyzed nickel species were prepared by means of two different methods.

(1) Thallium(I) perchlorate solution, prepared from thallium carbonate and perchloric acids, was electrolyzed in a cell in which the cathode of platinum gauze was separated from the anodic platinum foil with a sintered glass membrane. Metallic thallium was deposited on the cathode by electrolysis in an atmosphere of nitrogen. After washing thoroughly the cathode and the electrolytic cell with distilled water in a nitrogen atmosphere, the electrode and the cell vessel were dried with the stream of dried nitrogen. Slightly acid nickel

5) G. Biedermann and L. Ciavatta, *Acta Chem. Scand.*, **15**, 1347 (1961); **16**, 2221 (1962).
6) H. Ohtaki, *Inorg. Chem.*, **7**, 1205 (1968).
7) G. Gran, *Analyst*, **77**, 661 (1952).
8) W. Forsling, S. Hietanen, and L. G. Sillén, *Acta Chem. Scand.*, **6**, 901 (1952).
9) A. S. Brown, *J. Amer. Chem. Soc.*, **56**, 646 (1934).

chloride in 3M sodium chloride medium was then introduced, and oxygen gas was bubbled at the platinum gause electrode. With dissolution of metallic thallium by oxidation, pH of the solution increased to form nickel hydroxide precipitates. Thallium(I) ions thus formed were also precipitated as chloride. The amount of thallium ions remaining in the solution was so small and the thallium ions are such weak acid that the effect of thallium ions remaining in the medium on emf measurements is negligible. Nickel hydroxide and thallium chloride precipitates were filtered off through G4 glass filters with layers of finely divided platinum powder. Thus, a clear solution was obtained and used for titration.

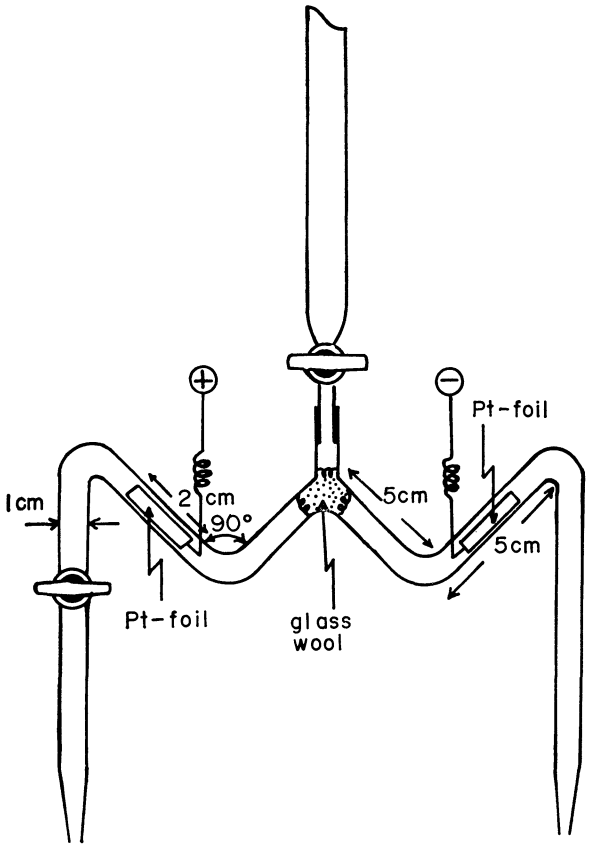

Fig. 1. Apparatus for preparation of sodium hydroxide from sodium chloride solution by electrolysis.

(2) Into the nickel chlodide solution was added a sodium hydroxide solution, prepared by electrolysis of 3M sodium chloride solution with an apparatus depicted in Fig. 1. From a buret 3M sodium chloride solution was flowed and a part of the solution was decomposed at the platinum foil cathode to sodium hydroxide and hydrogen by electrolysis. The solution was introduced to a nickel chloride solution to prepare nickel hydroxide precipitates. The flow rate of the solution was controlled by means of stop cocks. Contact of sodium hydroxide solution with glass wall of the apparatus was short (2–3 seconds), and the dissolution of any significant impurity from the apparatus could be avoided. Filtration and introduction of the solution to a titration vessel were performed in the same way as described.[5,6]

The total concentration of nickel in the test solution was determined gravimetrically by means of electrolysis and weighing as metallic nickel when the concentration of nickel was high, or as nickel dimethylglyoximate when the concentration was low.

A clear solution was titrated with an acid solution at the constant total concentration of nickel at 25.00±0.01°C in a paraffin oil thermostat, placed in a room thermostated at 25±0.2°C. Emf measurements were performed with an accuracy of ±0.1 mV at each point of measurements.

In supplementary titrations, made for testing the reversibility of the hydrolytic reaction of nickel ions, pH of a test solution was varied in the opposite direction of that in the titration described above. In these titrations a clear solution in which nickel hydroxo complexes had been present was diluted by addition of 3M sodium chloride. Thus, the total concentration of nickel *decreased*, whereas pH of the solution *increased*.

Results and Discussion

Values of Z and $-\log h$ for each value of B are represented in Fig. 2 together with those obtained by supplementary titration.

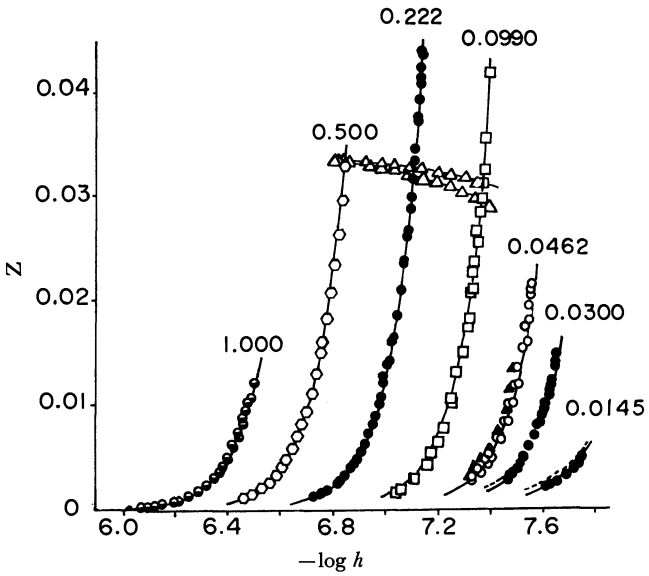

Fig. 2. Z *vs.* $-\log h$. Solid lines are those calculated with values of $\log {}^*\beta_{4,4} = -28.55$, $\log {}^*\beta_{1,1} = -10.5$, and $\log {}^*\beta_{1,2} = -10.5$. Broken lines show curves calculated with values of $\log {}^*\beta_{4,4} = -28.55$ and $\log {}^*\beta_{1,1} = -10.3$.

The concentration of hydrogen ion set free by hydrolysis, BZ, is given by the general formula as

$$BZ = \sum_p \sum_q \sum_r p {}^*\beta^{\circ}_{p,q,r} [Ni^{2+}]^q [H^+]^{-p} [Cl^-]^r$$
$$= \sum_p \sum_q p {}^*\beta_{p,q} [Ni^{2+}]_f^q [H^+]^{-p} = \sum_p \sum_q p {}^*\beta_{p,q} b^q h^{-p} \quad (10)$$

In cases where the maximum value of Z is very low, we may, without introduction of any appreciable error, simplify the preliminary calculations by employing the approximation

$$[Ni^{2+}]_f = b \simeq B \quad (11)$$

Substituting this relation into Eq. (10) and rearranging, we obtain

$$Z = \sum_p p K_p h^{-p} \quad (12)$$

where

$$K_p = \sum_q {}^*\beta_{p,q} B^{q-1} \quad (13)$$

Under an assumption of the constant chloride ion concentration, ${}^*\beta_{p,q}$ may become constant and thus K_p may also be given as a constant for a constant B.

Curves of Z plotted against $-\log h$ fitted very well

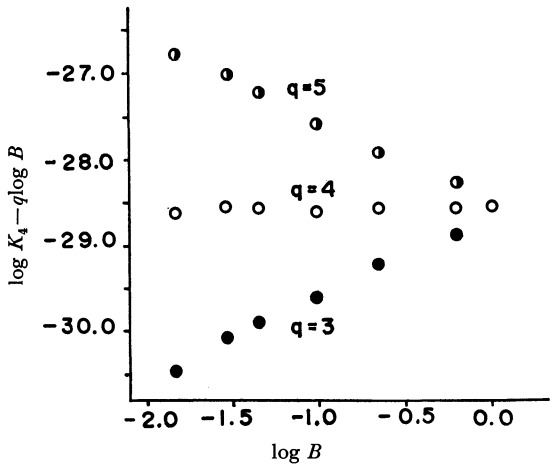

Fig. 3. Variations of log $K_4 - q\log B$ with log B at various q.

with a normalized curve, $y=px^p=f(\log x)$ with $p=4$. Values of K_4 thus found at each B were plotted against log B with various values of q. Results are shown in Fig. 3. It is seen that values of log $K_4 - q \log B$ are independent of B at $q=4$. Thus, the composition of the main species formed by hydrolysis of nickel ion and the equilibrium constant, $*\beta_{4,4}$, is evaluated. The composition of the main species may be written as $Ni_4(OH)_4Cl_r^{(4-r)+}$, although the value of r is not known.

Existence of other minor complexes was examined from data of low Z values, where small discrepancies of experimental results from the normalized curves were observed.

If the composition of minor species is written as $Ni_{q'}(OH)_{p'}Cl_{r'}^{(2q'-p'-r')+}$, Eq. (12) may be written as

$$Z = 4K_4h^{-4} + \sum_{p'} p'K_{p'}h^{-p'} \tag{14}$$

or

$$Zh^4 - 4K_4 = \sum_{p'} p'K_{p'}h^{(4-p')} \tag{15}$$

If we plot log (Zh^4-4K_4) against log h, all points would fall on a straight line with a slope of $4-p'$, provided that only homoligandic complexes are formed. The plot gave a straight line with a slope of 3, *viz.*, $p'=1$. Values of homoligandic constant K_1 at various B were plotted against log B, and are shown in Fig. 4. At $q'=1$ values of log $K_1 - \log B$ are almost independent of B, but a slight systematic deviation is observed, which can be interpreted in terms of formation of another homoligandic complex with $q'=2$, *i.e.*, $Ni_2(OH)Cl_{r''}^{(3-r'')+}$.

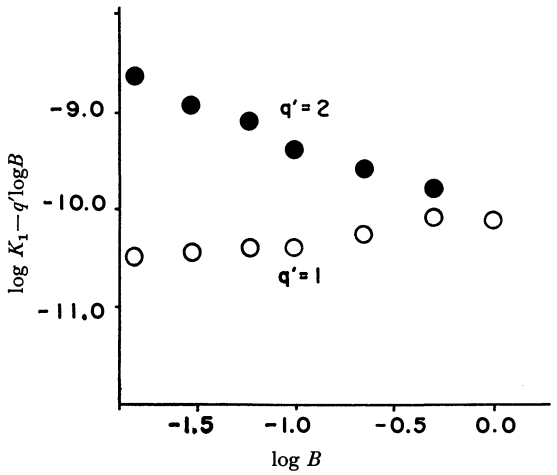

Fig. 4. Variations of log $K_1 - q'$ log B with log B at various q'.

This shows that the composition of the predominant species formed by the hydrolytic reaction of nickel ion is $Ni_4(OH)_4Cl_r$, and complexes $Ni(OH)Cl_{r'}$, and $Ni_2(OH)Cl_{r''}$ may also be formed as minor components, although no information was available for values of r.

In order to obtain more reliable information of compositions of complexes and values of $*\beta_{p,q}$, the totality of the experimental data was compared with the normalized projection maps.[10]

The computation procedure was as follows. Values of log B and $\frac{3}{4}\log B - \log h$ were calculated by graphical interpolation of Z *vs.* $-\log h$ curves at constant Z. Plots of the log B values against $\frac{3}{4}\log B - \log h$, covering the Z range from 0.002 to 0.035, have been compared with a graph of normalized functions, log $B^*(X)_{z,\gamma}$, where

$$\log B^* = \log B + \frac{1}{3}\log *\beta_{4,4} - \frac{4}{3}\log *\beta_{1,1} \tag{16}$$

$$X = \frac{3}{4}\log B - \log h + \frac{1}{4}\log *\beta_{4,4} \tag{17}$$

and

$$\log \gamma = \log *\beta_{1,2} + \frac{1}{3}(\log *\beta_{1,1} - \log *\beta_{4,4}) \tag{18}$$

The log $B^*(X)_{z,\gamma}$ functions are based on the fundamental equations

$$B = b(1 + *\beta_{1,1}h^{-1} + 2*\beta_{1,2}bh^{-1} + 4*\beta_{4,4}b^3h^{-4}) \tag{19}$$

and

$$Z = \frac{*\beta_{1,1}h^{-1} + *\beta_{1,2}bh^{-1} + 4*\beta_{4,4}b^3h^{-4}}{1 + *\beta_{1,1}h^{-1} + 2*\beta_{1,2}bh^{-1} + 4*\beta_{4,4}b^3h^{-4}} \tag{20}$$

with the assumption that complexes $Ni(OH)Cl_{r'}^{(1-r')+}$, $Ni_2(OH)Cl_{r''}^{(3-r'')+}$, and $Ni_4(OH)_4Cl_r^{(4-r)+}$ are formed.

Introducing new variables

$$\eta = *\beta_{1,1}h^{-1} \text{ and } \xi = *\beta_{4,4}^{1/3} \cdot *\beta_{1,1}^{-1/3} \cdot h^{-1}b \tag{21}$$

two of the three constants can be eliminated from Eqs. (19) and (20) which then will take the form

$$B^* = \xi\eta^{-1}(1 + \eta + 2\gamma\xi + 4\xi^3\eta) \tag{22}$$

$$Z = \frac{\eta + \gamma\xi + 4\xi^3\eta}{1 + \eta + 2\gamma\xi + 4\xi^3\eta} \tag{23}$$

Eqs. (22) and (23) show that when Z and γ are kept constant, η becomes a function of only ξ, consequently log $B^*(X)_{z,\gamma} = \log B^*(\frac{3}{4}\log B^* + \log \eta)_{z,\gamma}$ can be evaluated by assigning a series of values of ξ. If no $Ni_2(OH)Cl_{r''}^{(3-r'')+}$ complex forms, experimental data would better fit normalized curves with $\gamma=0$ than those calculated with any finite value of γ.

Solid lines in Fig. 5 show calculated curves with values of log $*\beta_{4,4} = -28.55$, log $*\beta_{1,1} = -10.5$, and log $*\beta_{1,2} = -10.5$. Broken lines show "best fitted" curves with the assumption $*\beta_{1,2}=0$. The former set of curves clearly gave better results than the latter.

Finally the data have been treated by the generalized least squares method with a computer program, "LETAGROP," in which the set of $*\beta_{1,1}$, $*\beta_{1,2}$, and

10) L. G. Sillén, *Acta Chem. Scand.*, **10**, 803 (1956).

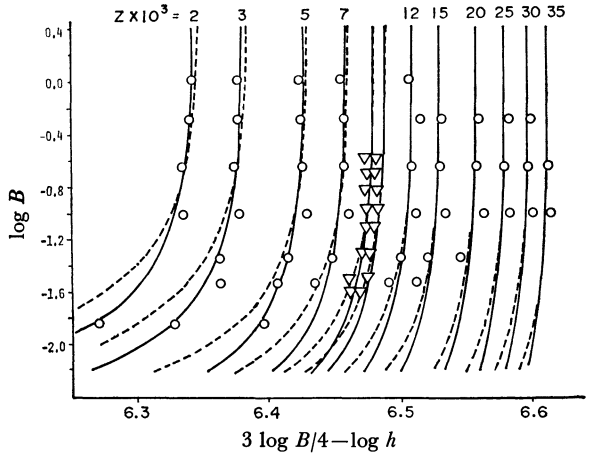

Fig. 5. Comparison of data at constant Z with normalized projection maps. Solid lines are calculated normalized projection maps with values given in (D) and broken lines are calculated "best fitted" curves with assumption of formation of only the $Ni_4(OH)_4$ and NiOH complexes.

$*\beta_{4,4}$ values were chosen to make the error square sum, $(U=\sum(Z-Z_{calc})^2)$ a minimum. Z_{calc} denotes the value of the function (20) for a particular set of the constants. The values of log $*\beta_{1,1}$, log $*\beta_{1,2}$, and log $*\beta_{4,4}$ thus calculated are

$$\left.\begin{aligned}\log *\beta_{4,4} &= -28.55 \pm 0.02\\ \log *\beta_{1,1} &= -10.5 \pm 0.1\\ \log *\beta_{1,2} &= -10.5 \pm 0.5\end{aligned}\right\} \quad (C)$$

Values of $*\beta_{p,q}$ obtained by Burkov *et al.*[2] in 3 M sodium perchlorate medium were log $*\beta_{4,4}=-27.37\pm 0.02$ and log $*\beta_{1,2}\approx -10$. Recent studies of hydrolytic reactions of nickel ion showed that log $*\beta_{1,1}=-10.12$[4] (at $\mu=0.04$, 25°C) and -10.01[3] (at $\mu=1.0$, 28°C). Funahashi and Tanaka[11] evaluated the formation constant of the $NiOH^+$ complex to be log $*\beta_{1,1}=-9.7$ (at $\mu=0.1$, 25°C) by means of a kinetic method. Agreements of our data with these results may support the formation of the $NiOH^+$ complex in 3 M sodium chloride medium, although the number of chloride atoms which may be contained in the complex is not evaluated.

Formation of chloro complexes must be taken into consideration in a chloride medium. Many workers have reported that nickel ions form the $NiCl^+$ complex[12-18] and even $NiCl_2$ in aqueous solutions. The formation constant of the latter complex is so small and even erroneous that only the former complex is taken into account in the following discussion.

If we take the value of log $\beta_{1,1}$ for the $NiCl^+$ complex as -0.55 (a simple average of spread values of log $\beta_{1,1}$ from -0.24[15] to -0.85[17]), log $\alpha_{Ni(Cl)}$ changes by 0.03 when the concentration of nickel ion varies from 0.0145 to 1.0 M, *viz.*, the value of log $*\beta_{4,4}$ possibly changes by about 0.1_2. Since about 13% of the decrease of the concentration of free chloride ions may be estimated in the solution of $B=1.0$, the conditional equilibrium constant for the formation of $Ni_4(OH)_4Cl_r^{(4-r)+}$ may decrease by 0.06 in the logarithmic unit for contribution of each chloride ion in the complex.

Calculations of conditional equilibrium constants at each B were performed by means of the "LETAGROP" computation, but no systematic trend of values of $*\beta_{p,q}$ was found. Thus, we finally propose the values of the equilibrium constants of the complex formation as follows.

$$\left.\begin{aligned}\log *\beta_{4,4} &= -28.5_5 \pm 0.1_0\\ \log *\beta_{1,1} &\leq -10.5\\ \log *\beta_{1,2} &\leq -10.5\end{aligned}\right\} \quad (D)$$

The maximum Z value at each B increases with decreasing h and then decreases after passing through the maximum at about $B=0.2$. The decrease of Z_{max} with decreasing h may be interpreted in terms of the formation of $Ni(OH)_2$ as the precipitate. If we denote the hydrogen ion concentration at Z_{max} as h_{max}, the following equation can be derived at a given B;

$$Z_{max} \simeq 4*\beta_{4,4}B^3h_{max}^{-4} \quad (24)$$

The solubility product $*K^s_{Ni(OH)_2}$ is defined as

$$*K^s_{Ni(OH)_2} = [Ni^{2+}][H^+]^{-2} \quad (25)$$

Insertion of Eq. (25) into Eq. (24) and rearrangement lead to

$$Z_{max} \simeq 4*\beta_{4,4}(*K^s_{Ni(OH)_2}\cdot\alpha_{Ni(Cl)})^3h_{max}^2 \quad (26)$$

Thus, Z_{max} may decrease with decreasing h_{max}, provided that $\alpha_{Ni(Cl)}$ remains practically unchanged.

On the other hand, the decrease of Z_{max} with increasing h_{max} in the region of higher B may be interpreted in terms of the formation of Ni(OH)Cl as the precipitate. With a similar method of calculation as that described above, the solubility product of the Ni(OH)Cl precipitate being defined as

$$*K^s_{Ni(OH)Cl} = [Ni^{2+}][H^+]^{-1}[Cl^-] \quad (27)$$

and the constant $[Cl^-]$ being assumed, the following equation can be derived;

$$Z_{max} \simeq 4*\beta_{4,4}(*K^s_{Ni(OH)Cl}\cdot\alpha_{Ni(Cl)})^3[Cl^-]^{-3}h_{max}^{-1} \quad (28)$$

and thus, Z_{max} may decrease with increasing h_{max}.

The authors wish to thank the late Professor Lars Gunnar Sillén for his valuable advice.

11) S. Funahashi and M. Tanaka, *Inorg. Chem.*, **8**, 2159 (1969).
12) R. H. Herber and J. W. Irving, Jr., *J. Amer. Chem. Soc.*, **78**, 905 (1956).
13) P. Kivalo and R. Louto, *Suomen Kem.*, **30B**, 163 (1957).
14) B. Trémillon, *Bull. Soc. Chem. Fr.*, **1958**, 1483.
15) K. B. Yatsimirskii and V. D. Korableva, *Izvest. VUZ. Khim.*, No. 4, 19 (1958).
16) K. H. Lieser, *Z. anorg. Chem.*, **304**, 296 (1960).
17) S. Tribalat and J. M. Caldero, *Compt. rend.*, **255**, 925 (1962).
18) D. A. Netzel and H. D. Droll, *Inorg. Chem.*, **2**, 412 (1963).

Solvolysis of Organic Phosphates. IV.[1] 3-Pyridyl and 8-Quinolyl Phosphates as Effected by the Presence of Metal Ions

Yukito MURAKAMI and Junzo SUNAMOTO

Department of Organic Synthesis, Faculty of Engineering, Kyushu University, Hakozaki, Fukuoka

(Received December 26, 1970)

Influence of nickel(II), copper(II), and thorium(IV) ions on the hydrolysis of 3-pyridyl and 8-quinolyl phosphates was investigated at $\mu=0.10$ in a lower pH region. The reaction in the presence of the bivalent metal ions followed apparent first-order kinetics with respect to the phosphates in homogeneous phase. The copper ion showed a positive catalytic effect only on the hydrolysis of 8-quinolyl phosphate, and such effect increased markedly as pH was raised. The nickel ion, however, did not show any significant effect on the hydrolysis of both phosphates. The requisites for effective catalysis of bivalent metals have been postulated previously: *(1) preliminary chelate formation,* and *(2) transitional chelate formation.* Accordingly, complex formation of the present phosphates with copper(II) and nickel(II) was studied by means of potentiometric measurements. The results strongly suggest the importance of (1) for yielding catalytic efficiency. The presence of the thorium ion resulted in a profound acceleration of hydrolysis of both phosphates in a relatively lower temperature range. The reaction rate did not follow the simple kinetic law although the reaction system was kept homogeneous under the present experimental conditions. The complex formation with the phosphate moiety, which would provide effective charge neutralization for the substrate, is most likely the necessary cause for the thorium-catalysis. Plausible reaction mechanisms and the corresponding potential energy correlations were postulated for the present catalysis.

The influence of metal ions on the hydrolysis reactions of phosphate monoesters has been extensively studied up to the present time in connection with the biochemical interest. Among such studies, some efforts have been made by a limited number of research groups to clarify the reaction mechanisms of catalysis which has possibly arisen through the complex-forming interaction of metal ions with organic phosphates in the transition state.

In our previous work,[2,3] the hydrolysis of pyridylmethyl phosphates was investigated in the presence of bivalent and polyvalent metal ions. Of the bivalent metal ions, only the copper ion promoted the hydrolysis rate of 2-pyridylmethyl phosphate to a considerable extent in a moderate pH range. Its presence, however, did not cause any rate enhancement for the hydrolysis of 3- and 4-pyridylmethyl phosphates. We have proposed from these studies[2-4] that the two successive interactions are required for bivalent metals to yield catalytic efficiency: (1) A metal ion must demonstrate a significant chelate-forming affinity for an organic phosphate. Both the neighboring functional group in the leaving alcohol group (*e.g.*, the pyridyl nitrogen for 2-pyridylmethyl phosphate and the carboxyl group for salicyl phosphate) and the phosphate group, in which one of the oxygen atoms may act as a donor atom, may participate in such coordination interaction. This is the requirement of the preliminary chelate formation. (2) A metal ion must demonstrate an appropriate affinity for the ester oxygen in the transition state, so that the chelate ring involving both the neighboring functional group and the ester oxygen is to be formed in the excited state. This affinity can be judged from the chelating tendency of a metal ion with the alcohol, a hydrolysis product. This may be called the requirement of the transitional chelate formation.

Among polyvalent metal ions, the thorium ion accelerated the hydrolysis of pyridylmethyl phosphates, irrespective of the difference in isomeric structures, to a remarkable extent. However, we failed to find a satisfactory explanation for the profound catalysis although the primary interaction with the phosphate moiety seems to result in such rate enhancement.

The present work as well as the subsequent investigations has been designed to accumulate kinetic and mechanistic data for the confirmation of the above requisites established for the bivalent metal catalysis.

We also intend to investigate the role of polyvalent metal ions, particularly the thorium ion, in the hydrolysis reactions from the mechanistic viewpoint. In this work, the hydrolysis of 3-pyridyl and 8-quinolyl phosphates was studied in the presence of copper(II), nickel(II), and thorium(IV) ions in aqueous media at various temperatures. The complex-forming interaction between these metal ions and the phosphates has also been investigated to obtain key information on the catalytic reaction mechanism.

Experimental

Materials. Preparation of 3-pyridyl and 8-quinolyl phosphates has been described in our previous paper.[5] Other materials of analytical grade were commercially obtained and used without further purification. The stock solutions of metal ions were prepared from their nitrate salts. These solutions were standardized by means of the usual chelatometric titration.

Kinetic Measurements. The apparatus and experimental procedures were essentially the same as those employed pre-

1) a) Contribution No. 224 from the Department of Organic Synthesis, Faculty of Engineering, Kyushu University. b) Preliminary communication: Y. Murakami, J. Sunamoto, and H. Sadamori, *J. Chem. Soc., D*, **1969**, 983. c) Part III: Y. Murakami and J. Sunamoto, This Bulletin, **44**, 1939 (1971).

2) Y. Murakami and M. Takagi, *J. Amer. Chem. Soc.*, **91**, 5130 (1969).

3) Y. Murakami and M. Takagi, This Bulletin, **42**, 3478 (1969).

4) Y. Murakami, *Nippon Kagaku Zasshi*, **91**, 185 (1970).

5) Y. Murakami, J. Sunamoto, H. Sadamori, H. Kondo, and M. Takagi, This Bulletin, **43**, 2518 (1970).

viously.[1c,2,3] In the case of the thorium-ion-catalyzed reactions, the procedure for kinetic measurements had to be slightly modified because of its extreme rate enhancement relative to the spontaneous hydrolysis. Two different aqueous solutions were initially prepared, the one containing the substrate and the other the catalyst species. A 50-m*l* solution which contained the phosphate ester, an inorganic salt for maintaining the ionic strength constant, and an appropriate amount of acid or base for adjusting the initial pH of an experimental solution was placed in a thermostated reaction cell. Another 50-m*l* solution containing a specified amount of the thorium ion and perchloric acid for minimizing a partial hydrolysis of the metal ion was placed in a thermostated bath controlled at a desired temperature. After both solutions attained an equilibrated temperature, the catalyst solution was quickly transferred into the reaction cell. The resulting solution was so controlled that the initial concentration of the substrate and the ionic strength were maintained at 2×10^{-3}M and 0.10, respectively. The subsequent procedure for kinetic measurements was essentially the same as those described previously.[2,3]

Potentiometric Measurements. A jacketed glass cell of approximately 100-m*l* capacity, which was equipped with a magnetic stirrer, nitrogen inlet and outlet tubes, a microburet delivery tube and electrodes, was adopted. A set of a Beckman glass electrode No. 39099 and a Beckman reference electrode No. 39170 was used in combination with a Horiba-Hitachi Model P pH meter for measurements at 25.0±0.1°C and the ionic strength of 0.10 (KNO_3). The initial concentration of the phosphate was maintained at 2.0×10^{-3}M, while those of the metal ions were varied in a range 1.0—2.0×10^{-3}M. Each titration was carried out under a nitrogen atomosphere and checked by duplicate or triplicate runs. The method of establishing $-\log[H^+]$ values at the constant ionic stength was the same as those employed in a series of our previous studies.

Mathematical Treatment of Equilibrium Data

Since 8-quinolyl phosphate and 3-pyridyl phosphate are tribasic acids, the acid dissociation constants are defined as follows:

$$K_{H_3L} = \frac{[H_2L][H^+]}{[H_3L^+]} \quad (1)$$

$$K_{H_2L} = \frac{[HL^-][H^+]}{[H_2L]} \quad (2)$$

$$K_{HL} = \frac{[L^{2-}][H^+]}{[HL^-]} \quad (3)$$

where H_3L^+, H_2L, HL^-, and L^{2-} refer to monocation, neutral zwitterion, monoanion, and dianion, respectively. As an example, the acid diassociation processes for 8-quinolyl phosphate are shown in Scheme 1.

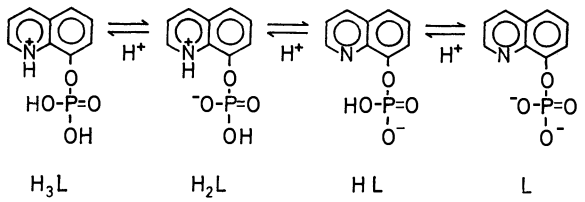

Scheme 1

These phosphate molecules have two coordination sites, an aromatic nitrogen and a phosphate group. On the basis of the results and discussion for the complex-forming interaction of 2-pyridylmethyl phosphate with various bivalent metal ions,[6] we consider that the following reaction scheme may suffice to cover the probable solution equilibria responsible for the present experimental conditions:

$$M^{2+} + L^{2-} \rightleftharpoons ML$$

$$K_1 = \frac{[ML]}{[M^{2+}][L^{2-}]} \quad (4)$$

$$M^{2+} + H^+ + L^{2-} \rightleftharpoons M(HL)^+$$

$$K_a = \frac{[M(HL)^+]}{[M^{2+}][H^+][L^{2-}]} \quad (5)$$

If these two solution equilibria take place to a significant extent, the following relationships are derived under the consideration of ionic neutrality and mass balance for ligand and metal:

$$T_M = [M^{2+}] + [ML] + [M(HL)^+] \quad (6)$$

$$T_L = [L^{2+}] + [HL^-] + [H_2L] + [H_3L^+] + [ML] + [M(HL)^+] \quad (7)$$

$$T_{OH} + [H^+] + [H_3L^+] + 2[M^{2+}] + [M(HL)^+] = [OH^-] + 2[L^{2-}] + [HL^-] + 2T_M + T_H \quad (8)$$

Then, the following two equations are derived from Eqs. (6), (7), and (8) in conjunction with Eqs. (1), (2), and (3) for the acid dissociation constants:

$$RS[L^{2-}]^2 + (T_MS + R - T_LS)[L^{2-}] - T_L = 0 \quad (9)$$

$$QS[L^{2-}]^2 + (PS + Q - T_MJ)[L^{2-}] + P = 0 \quad (10)$$

where

$$R = \frac{[H^+]^3}{K_{H_3L}K_{H_2L}K_{HL}} + \frac{[H^+]^2}{K_{H_2L}K_{HL}} + \frac{[H^+]}{K_{HL}} + 1$$

$$Q = \frac{[H^+]}{K_{HL}}\left(\frac{[H^+]^2}{K_{H_3L}K_{H_2L}} - 1\right) - 2$$

$$S = K_1 + K_a[H^+]$$

$$J = 2K_1 + K_a[H^+]$$

$$P = T_{OH} + [H^+] - [OH^-] - T_H$$

T_L, T_M, T_{OH}, and T_H refer to the total concentrations of ligand, metal ion, base, and acid added to the system, respectively. Since the concentration of the ligand dianion $[L^{2-}]$ can not become zero, the following relation is obtained through division of Eq. (10) by Eq. (9):

$$[L^{2-}] = \frac{T_M(T_LS + T_LK_1 - PS) - (PR + T_LQ)}{(PR + T_LQ)S} \quad (11)$$

Equations (9) and (10) are nonlinear with respect to equilibrium constants K_1 and K_a. In order to obtain the unknown equilibrium constants cited above, Rubin's method[7] was applied to our present system. An iterative calculation was performed to minimize the residual sum of squares (U)

$$U = \sum_{i=1}^{N}\{T_L(\text{obs})_i - T_L(\text{calc})_i\}^2 \quad (12)$$

until

$$\max_j \left|\frac{A_j^{(1)} - A_j^{(0)}}{A_j^{(0)}}\right| < \varepsilon$$

6) Y. Murakami and M. Takagi, *J. Phys. Chem.*, **72**, 116 (1968).
7) D. I. Rubin, *Chem. Eng. Progr. Symp. Ser.*, **59**, 90 (1963).

holds, where N is the number of observations and the subscript i is the observation-number index; $A_j^{(0)}$ and $A_j^{(1)}$ refer, respectively, to the approximation at one stage and to the next approximation to the jth parameter to be determined in the course of iterative calculation. The ε-value is a convergence criterion preassigned and was set at 1×10^{-4} in the present calculation.

All the calculation processes were programmed by means of the Fortran language for use with a FACOM 230-60 electronic computer of the Computation Center of Kyushu University.[8]

Results

Effects of Copper(II) and Nickel(II) Ions. The hydrolysis reactions of 8-quinolyl and 3-pyridyl phosphates were investigated in the presence of the copper(II) ion and the nickel(II) ion under various conditions. The reaction followed apparent first-order kinetics with respect to the total concentration of unreacted phosphate in homogeneous phase over the whole pH region and the metal concentration range studied. However, the nickel ion did not show any significant effect on the hydrolysis of both phosphates as can be seen in Table 1. On the other hand, the copper ion showed a positive catalytic effect only on the hydrolysis of 8-quinolyl phosphate. Such catalytic efficiency was subjected to a significant pH-dependency as shown in Table 2. The reaction rate increased markedly with the rise of pH-value of the solution. As for the concentration effect on the catalytic efficiency of the copper ion, the observed overall reaction rate was found to be consistent with Eq. (13).

$$k_{obs} = k_{H_2L}X_{H_2L} + k_{H^+}[H^+]X_{H_2L} + k_{Cu}[Cu^{2+}] \qquad (13)$$

where k_{obs} is the observed overall rate constant and X_{H_2L} is the mole fraction of the zwitterion species:

Table 1. Metal-ion-catalyzed hydrolysis of 8-quinolyl and 3-pyridyl phosphates at $\mu=0.1(KNO_3)$[a]

$-\log[H^+]$	Temp. °C	Metal ion	$k_c\times10^5$ sec^{-1}	$k_o\times10^5$ sec^{-1}	k_c/k_o
		8-Quinolyl phosphate			
2.03	80	Cu^{2+}	18.6	7.69	2.42
2.02	80	Ni^{2+}	7.75	7.69	1.01
1.88	25	Th^{4+}	12.0[b]	0.0089[c]	1×10^3
		3-Pyridyl phosphate			
2.03	70	Cu^{2+}	7.23	7.51	0.96
2.02	70	Ni^{2+}	7.45	7.49	0.99
1.88	25	Th^{4+}	36.8[b]	0.014[c]	3×10^3

a) $T_M=T_E=2.0\times10^{-3}$M, where T_M and T_E stand for the total concentrations of the metal ion and of the substrate, respectively; k_c and k_o refer to overall rate constants for the hydrolysis in the presence of metal ion and for the spontaneous reaction, respectively.
b) Deviated from the first-order plot; estimated from the initial stage of reaction.
c) Estimated using the activation energy.

8) For the detailed computational procedure: J. Sunamoto and Y. Murakami, *Kyushu Daigaku Kogaku Shuho* (Tech. Reports Kyushu Univ.), **44**, 199 (1971).

Table 2. Copper(II)-catalyzed hydrolysis of 8-quinolyl phosphate at $\mu=0.1$ (KNO_3)[a]

$-\log[H^+]$	Temp. °C	T_M/T_E	$k_c\times10^5$ sec^{-1}	$k_o\times10^5$ sec^{-1} [b]	k_c/k_o
2.03	80	2.0	30.2	7.69	3.93
2.03	80	1.0	18.6	7.69	2.42
2.01	80	0.5	13.1	7.80	1.68
2.00	80	0.2	9.95	7.80	1.28
2.00	70	1.0	6.02	2.11	2.85
2.00	60	1.0	1.75	0.717	2.44
2.76	60	1.0	29.7	0.747	3.96×10
2.26	40	1.0	0.136	0.0592	2.29
2.92	40	1.0	3.78	0.0614	6.16×10
3.21	40	1.0	13.9	0.0561	2.48×10^2
3.56	40	1.0	43.1	0.0514	8.37×10^2
3.85	30	1.0	17.4	0.107	1.62×10^3

a) $T_E=2.0\times10^{-3}$M.
b) At lower temperature, k_os were estimated using the activation energy.

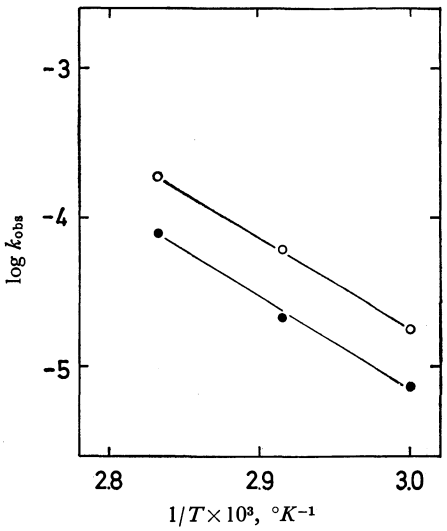

Fig. 1. Arrhenius plots of the first-order reaction rates for the hydrolysis of 8-quinolyl phosphate: ○, copper(II)-catalyzed reaction; ●, spontaneous reaction; rate constant (k_{obs}) in sec^{-1}.

k_{H_2L}, k_{H^+}, and k_{Cu} refer to the specific rate constants for the hydrolysis of zwitterion, acid catalysis, and copper-ion catalysis, respectively. The validity of this equation was checked by varying the T_M/T_E value from 0.2 to 2.0 at a particular pH-value ($-\log[H^+]=2.01\pm0.02$) as listed in Table 2. The k_{Cu} value for the hydrolysis of 8-quinolyl phosphate was estimated at 80°C and at this pH: $k_{Cu}=5.55\times10^{-2}M^{-1}$ sec^{-1}. Figure 1 illustrates the Arrhenius plots for the spontaneous and copper(II)-ion catalyzed reactions measured at 60°, 70°, and 80°C with the T_M/T_E value of 1.0, the $-\log[H^+]$ value being maintained at 2.01 ± 0.02. The temperature-dependence of the catalytic reaction rate has a close resemblance to that of the spontaneous one. Thus, the activation energy for the true catalytic reaction, which corresponds to the third term on the right hand side of Eq. (13), is almost negligible relative to that for the spontaneous reaction.

The presence of the copper(II) ion did not result in

Table 3. Copper(II)-catalyzed hydrolysis of 3-pyridyl phosphate at 70°C and $\mu=0.1$ (KNO_3)[a]

$-\log[H^+]$	T_M/T_E	$k_c\times10^5$ sec^{-1}	$k_o\times10^5$ sec^{-1}	k_c/k_o
2.00	0.5	7.03	7.70	0.91
2.02	2.0	7.67	7.70	1.00
2.03	1.0	7.22	7.68	0.94
3.45	1.0	6.03	6.10	0.99
3.82	1.0	5.33	4.80	1.11
4.07	1.0	5.00	4.13	1.21

a) $T_E=2.0\times10^{-3}$M.

any enhancement of the reaction rate in the hydrolysis of 3-pyridyl phosphate, as seen in Table 3.

Effect of Thorium(IV) Ion. The presence of the thorium(IV) ion resulted in a profound acceleration of the hydrolysis of both phosphates, although the reaction rate did not follow the simple kinetic law. During the course of reaction, formation of any insoluble materials was not detected and a good homogeneous system was maintained. Figure 2 shows the rate plots for the hydrolysis of 3-pyridyl and 8-quinolyl phosphates in terms of the first-order kinetic law under the identical experimental conditions, where the corresponding spontaneous reactions did not proceed to any appreciable extent. The extent of catalytic efficiency in both reactions is nearly the same, and thus the apparent difference in reaction rates in Fig. 2, for example,

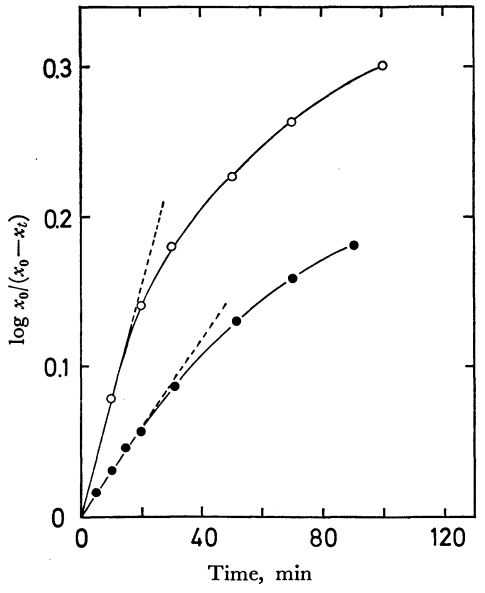

Fig. 2. Rate plots in terms of first-order kinetics for the thorium(IV)-catalyzed hydrolysis of 8-quinolyl phosphate (●) and 3-pyridyl phosphate (○) at 25°C, $-\log[H^+]=1.88$, $T_M/T_E=1.0$, and $\mu=0.10$ ($NaClO_4$). Broken lines stand for the first-order rate relation extrapolated from the initial reaction rate.

can be ascribed to the nature of the leaving alcohol groups. For both phosphates, the catalyzed reactions appear to be largely controlled by concentrations of the hydrogen ion and the thorium ion as well as the reaction temperature as illustrated in Figs. 3 and 4. The increase of these controlling factors, *i.e.*, pH, metal-concentration, and temperature, caused a significant rate enhancement. In these thorium-ion catalysis, the slow but appreciable liberation of proton was always observed before the hydrolysis proceeded to any detectable extent: this became more apparent in lower concentration of the thorium ion at lower temperature. The sluggish formation of some thorium complexes with the substrates appears to be responsible for this phenomenon. The reaction rate in the presence of the thorium ion deviated downward significantly from the first-order plot; this deviation increased as the reaction proceeded further. In order to examine whether the rate deceleration effect is due to the removal of the thorium ion from the reaction system through the complex-formation with the yielded alcohol, 3-pyridinol and 8-quinolinol were added in a half of the equimolar amount of the corresponding substrates into the corresponding reaction systems at the beginning of the reaction. However, the addition of such alcohols did not result in any significant change in reaction rate.

Potentiometric Titration. In order to obtain a

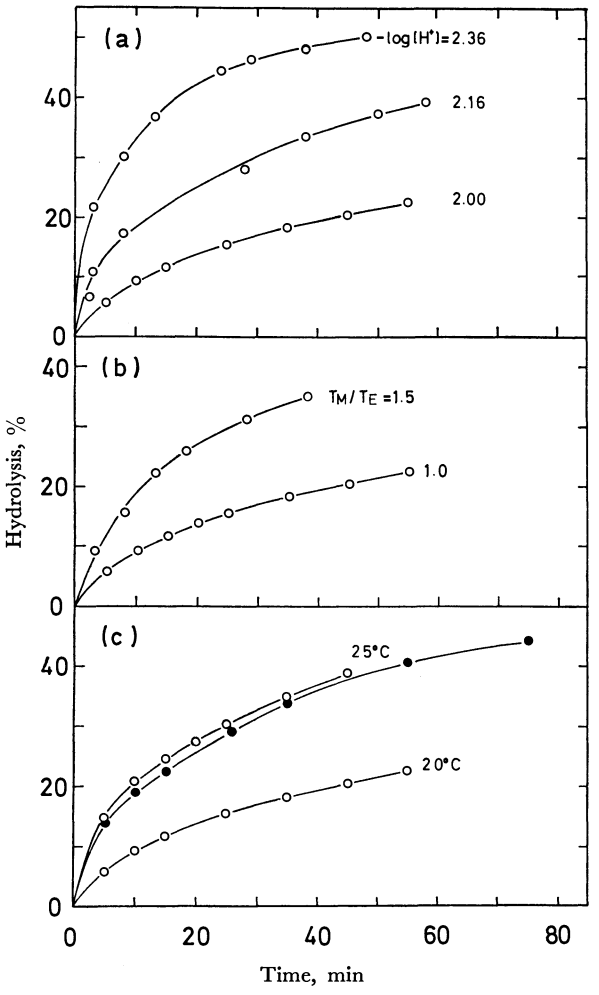

Fig. 3. Hydrolysis of 8-quinolyl phosphate in the presence of thorium(IV) ion: $T_E=2.00\times10^{-3}$M, $\mu=0.10$ (KNO_3 or $NaClO_4$); (a) 20.0°C, $T_M/T_E=1.0$; (b) 20.0°C, $-\log[H^+]=2.00$; (c) $-\log[H^+]=2.00$, $T_M/T_E=1.0$. Solid circles in (c) refer to the rate data for the presence of 8-quinolinol (1.00×10^{-3}M).

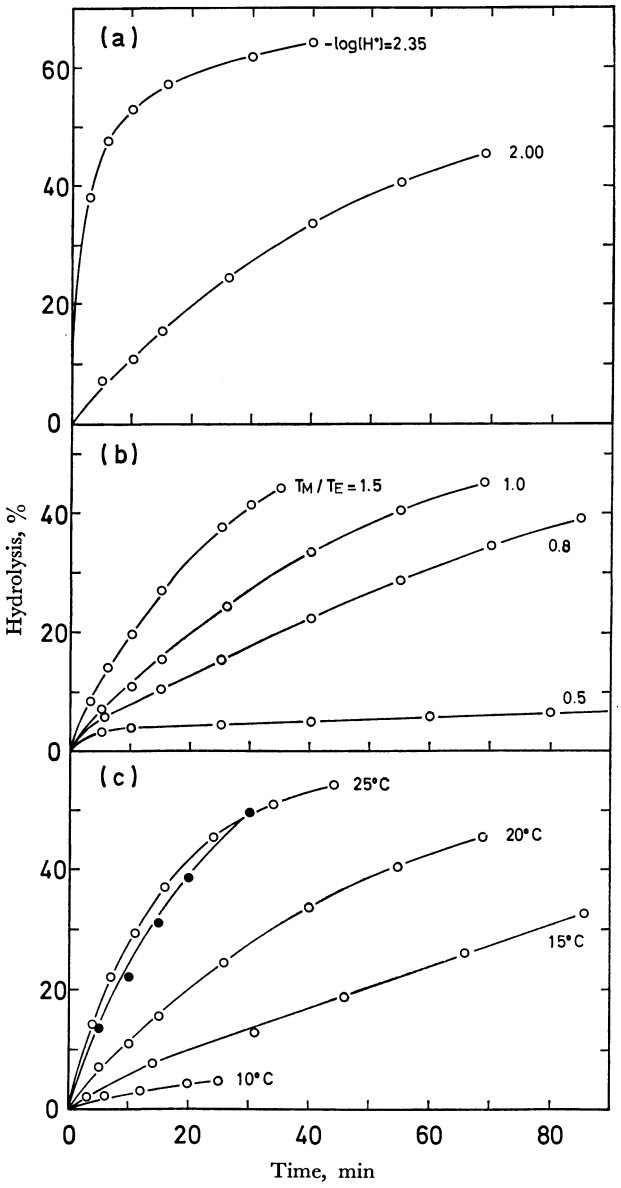

Fig. 4. Hydrolysis of 3-pyridyl phosphate in the presence of thorium(IV) ion: $T_E=2.00\times10^{-3}$M, $\mu=0.10$ (KNO_3 or $NaClO_4$); (a) 20.0°C, $T_M/T_E=1.0$; (b) 20.0°C, $-\log[H^+]=2.00$; (c) $-\log[H^+]=2.00$, $T_M/T_E=1.0$. Solid circles in (c) refer to the rate data for the presence of 3-pyridinol (1.0×10^{-3}M).

clue to understanding the catalytic mechanism in the hydrolysis of organic phosphates and to examine a correlation between the catalytic efficiency and the complex-forming tendency of metal ions with the phosphates, we have carried out potentiometric measurements of these chelate systems, in which copper(II), nickel(II), and thorium(IV) ions were included, in aqueous media at 25°C and $\mu=0.1$ (KNO_3). An attempt was made to carry out some quantitative measurements and analysis for the thorium chelate system. This was not successful, however, due to the markedly rapid hydrolysis even in a temperature range as low as 10°C. The titration curves for 8-quinolyl phosphate with copper(II) and nickel(II) are shown in Fig. 5, and for 3-pyridyl phosphate with the same metal ions in Fig. 6. Solution equilibria

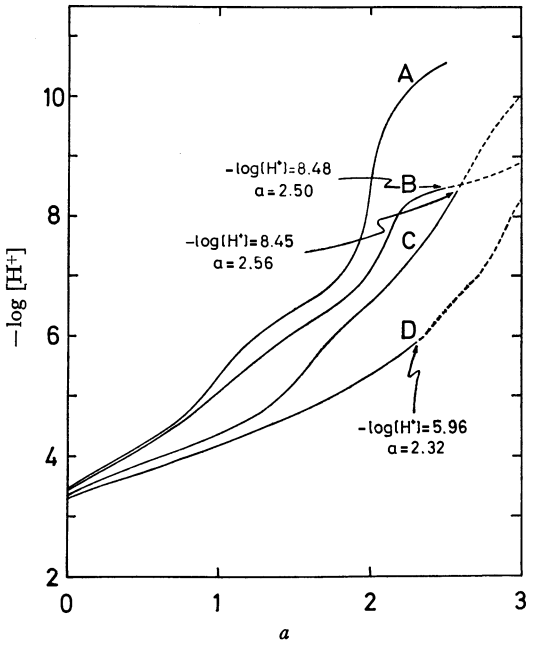

Fig. 5. Titration curves for 8-quinolyl phosphate—bivalent metal systems at 25.0°C and $\mu=0.10$ (KNO_3): A, ligand alone; B, Ni(II) system with $T_M/T_L=1.0$; C, Cu(II) system with $T_M/T_L=0.5$; D, Cu(II) system with $T_M/T_L=1.0$; initial concentration of ligand (T_L), 2.00×10^{-3}M; a=moles of base added per mole of ligand. Arrows indicate the region where pH-reading starts to become unstable on standing.

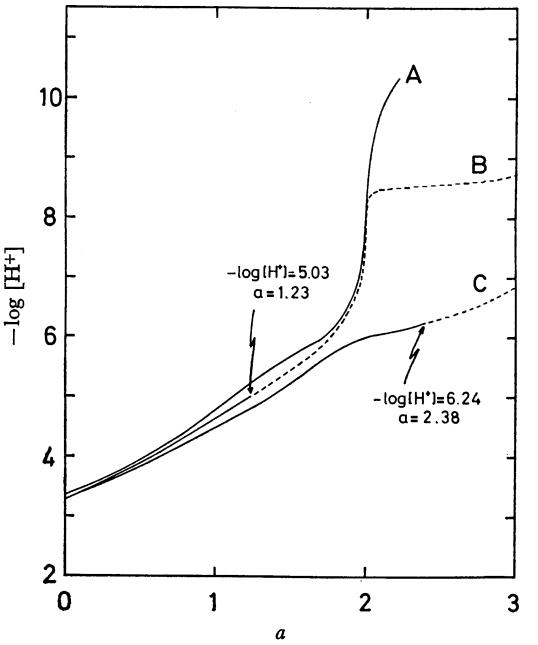

Fig. 6. Titration curves for 3-pyridyl phosphate—bivalent metal systems at 25.0°C, $\mu=0.10$ (KNO_3), and $T_M/T_L=1.0$: A, ligand alone; B, Ni(II) system; C, Cu(II) system; initial concentration of ligand (T_L), 2.00×10^{-3}M, a=moles of base added per mole of ligand. Arrows indicate the region where pH-reading starts to become unstable on standing.

were attained shortly after addition of base in a relatively low a-region (a being the degree of neutralization of the ligand). Beyond a certain a-value for each titration of the chelate systems, pH-reading became

unsteady on standing probably because of the hydrolytic tendencies of the metal ions. These non-equilibrated regions are shown in Figs. 5 and 6 by broken lines. The nickel ion obviously exhibited lower complex-forming ability toward the phosphates than the copper ion. The difference is apparent for the 8-quinolyl phosphate systems in particular. The formation of the copper complex is already appreciable in a region below $a=1.0$ while that of the nickel complex is not significant. Stability constants for metal complexes of a 1:1 ratio of ligand to metal and for the corresponding protonated complexes were calculated by means of the computational method described in the preceding section: the results are summarized in Table 4.

TABLE 4. STABILITY CONSTANTS OF METAL COMPLEXES OF SOME HETERO-AROMATIC PHOSPHATES AT 25±0.1°C AND $\mu=0.1$ (KNO_3)[a]

Metal ion	Log K_1[b]	Log K_{MHL}[c]	U[d]
2-Pyridylmethyl phosphate[e]			
	$pK_{H_3L}=1.8$	$pK_{H_2L}=4.42$	$pK_{HL}=6.30$
Cu(II)	4.44	2.23	0.1537×10^{-7}
Ni(II)	2.85	1.06	—
3-Pyridyl phosphate			
	$pK_{H_3L}=1.0$	$pK_{H_2L}=3.86$	$pK_{HL}=5.64$
Cu(II)	3.27	2.00	0.1042×10^{-4}
Ni(II)	1.93	1.99	0.2687×10^{-3}
8-Quinolyl phosphate			
	$pK_{H_3L}=1.0$	$pK_{H_2L}=4.17$	$pK_{HL}=6.42$
Cu(II)	5.29	2.43	0.7951×10^{-5}

a) Calculated from the titration data of a 1:1 molar ratio of ligand-metal.
b) $K_1=[ML]/[M^{2+}][L^{2-}]$.
c) $K_{MHL}=[MHL^+]/[M^{2+}][HL^-]$.
d) A residual sum of squares in the computational procedure; see text.
e) Previously reported.[6]

Discussion

Bivalent Metal Catalysis. In earlier papers, the effects of various metal ions on the hydrolysis of pyridylmethyl phosphates[2,3] and of salicyl phosphate[9,10] have been reported. Catalytic mechanism and efficiency for these hydrolysis reactions have been discussed from the viewpoint of complex-forming ability of metal ions at various stages of the reaction process.[2-4] 8-Quinolyl phosphate has a structural similarity to 2-pyridylmethyl phosphate although the former has a more rigid structure due to the presence of fused rings. Therefore, a comparison of the catalytic efficiency of metal ions in these phosphate hydrolyses is particularly interesting.

For the hydrolysis of 2-pyridylmethyl phosphate, only the copper ion was significantly effective among various bivalent metal ions.[2] The hydrolysis of 8-quinolyl phosphate was promoted appreciably with copper(II), but not at all with nickel(II), as shown in Tables 1 and 2. On the other hand, both metal ions were almost ineffective in the hydrolysis of 3-pyridyl phosphate as can be seen in Tables 1 and 3. Stability order among the copper complexes formed with the above three phosphates is in the following sequence (log K_1) with respect to the ligands: 8-quinolyl phosphate>2-pyridylmethyl phosphate>3-pyridyl phosphate. The former two phosphates appear to form a chelate ring for which the hetero-aromatic nitrogen and the terminal phosphate-oxygen act as donor atoms, judging from the magnitude of stability constants for 1:1 complexes.[6] The catalytic efficiency of copper(II) in terms of k_c/k_o, where k_c and k_o refer, respectively, to the overall rate constant for metal-ion-catalyzed hydrolysis and that for the spontaneous reaction, follows the sequence with respect to the phosphates: 8-quinolyl phosphate ($k_c/k_o=8.4\times10^2$; 40°C $-\log[H^+]=3.56$)>2-pyridylmethyl phosphate (1.65; 90°C, 3.67)>3-pyridylmethyl phosphate (0.96; 90°C, 3.49)~4-pyridylmethyl phosphate (1.07; 90°C, 3.59)~3-pyridyl phosphate (1.11; 70°C, 3.82). The latter three phosphates can not form a chelate ring with a metal ion but rather act as unidentate ligands, due to their structural nature. In order to clarify the correlation between the catalytic efficiency and the initial formation of metal chelate species with the substrate, the concentrations of metal species involved in the copper chelate systems, the free metal ion (M^{2+}), the 1:1 complex (ML), and its protonated complex ($M(HL)^+$), were

TABLE 5. CORRELATION BETWEEN CATALYTIC EFFICIENCY AND COMPLEX-FORMATION[a]

$-\log[H^+]$	$[M^{2+}]$, M	[ML], M	$[M(HL)^+]$, M	k_c/k_o (Temp., °C)
8-Quinolyl phosphate-Cu(II) (1:1)				
2.03	0.1982×10^{-2}	0.2051×10^{-6}	0.1734×10^{-4}	2.42 (80)
2.92	0.1934×10^{-2}	0.1213×10^{-4}	0.5337×10^{-4}	6.16×10 (40)
3.85	0.1456×10^{-2}	0.3587×10^{-3}	0.1856×10^{-3}	1.62×10^3 (30)
2-Pyridylmethyl phosphate-Cu(II) (1:1)				
3.76	0.1849×10^{-2}	0.4844×10^{-4}	0.1025×10^{-3}	1.65 (90)
4.36	0.1497×10^{-2}	0.3287×10^{-3}	0.1746×10^{-3}	1.1×10 (90)
3-Pyridyl phosphate-Cu(II) (1:1)				
2.03	0.1995×10^{-2}	0.2435×10^{-7}	0.5289×10^{-5}	0.94 (70)
3.45	0.1889×10^{-2}	0.1200×10^{-4}	0.9913×10^{-4}	0.99 (70)
4.07	0.1728×10^{-2}	0.9132×10^{-4}	0.1809×10^{-3}	1.21 (70)

a) Calculated from the acid dissociation constants of ligands and the stability constants given in Table 4; $T_M=T_L=2.0\times10^{-3}$M.

9) R. Hofstetter, Y. Murakami, G. Mont, and A. E. Martell, *J. Amer. Chem. Soc.*, **84**, 3041 (1962).

10) Y. Murakami and A. E. Martell, *J. Phys. Chem.*, **67**, 582 (1963).

calculated for the systems of 8-quinolyl, 2-pyridylmethyl, and 3-pyridyl phosphates from the data given in Table. 4. The results for the limited pH range of present interest are listed in Table 5. It is apparent that the catalytic efficiency is sensitively affected by the formation of chelate species, ML and $M(HL)^+$. With the increase of concentrations of these chelate species, a significant rate enhancement was observed accordingly for the hydrolyses of 8-quinolyl and 2-pyridylmethyl phosphates. On the other hand, 3-pyridyl phosphate does not secure a catalytic efficiency of similar trend in its hydrolysis due to the lack of chelate-ring formation. The hydrolysis of salicyl phosphate was accelerated by the presence of copper(II) as investigated previously.[10] Since this phosphate was found to form a 1:1 chelate with copper(II) (log $K_1=3.64$ at 10.0°C and $\mu=0.10$), the catalytic mechanism was considered to start with the initial formation of such a complex followed by the intramolecular rearrangement to form a chelate ring with the ester oxygen and the carboxylate group as donor groups in the transition state.[4] On the other hand, the potentiometric study on the interaction of nickel(II) with the present phosphates indicated that this metal ion does not form complexes to any detectable extent in a relatively low pH region. The difference between copper(II) and nickel(II) in such interaction is more apparent with 8-quinolyl phosphate. This is quite consistent with the inert character of nickel(II) for the hydrolysis of the phosphates.

Judging from the results obtained for the bivalent metal catalysis, the following interaction is required at the initial stage of reaction to secure an effective catalytic action of metal ions in the hydrolysis. An organic phosphate must demonstrate a significant chelate-forming tendency toward a metal ion at the initial stage. In order to make this interaction possible, a phosphate molecule must possess at least one more functional group besides the phosphate moiety, which shows a satisfactory donating affinity for a metal ion. In the present case, a hetero-aromatic nitrogen atom is considered to be such an extra donor goup. Both the phosphate group and another functional group must be situated in a molecule, so that a chelate formation becomes favored. The nitrogen atom in 3-pyridyl phosphate is not suitably oriented for chelation with a metal ion in conjunction with the phosphate moiety, while that in 8-quinolyl phosphate

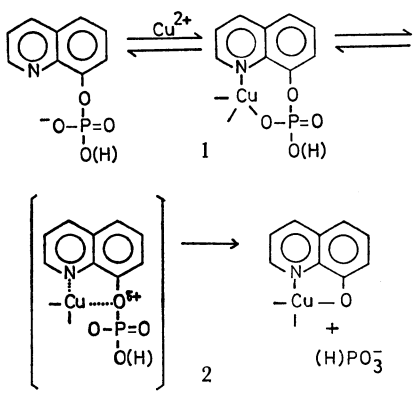

Scheme 2

is placed in a desired manner. Meanwhile, in the course of such a chelate-forming interaction the copper ion demonstrated enough coordination affinity for the nitrogen atom to secure an effective catalytic action. The nickel ion, however, does not seem to have a satisfactory affinity for the nitrogen atom as the stability data indicate. We thus invoke to postulate the reaction mechanism shown in Scheme 2 for an elucidation of significant catalytic effect of copper(II) on the hydrolysis of 8-quinolyl phosphate. This mechanism has a close similarity to that for the hydrolysis of 2-pyridylmethyl phosphate,[2] although the copper ion appears to be less active in the latter reaction.

The mechanism is also understood as an analogy to the intramolecular proton transfer mechanism in the corresponding spontaneous hydrolysis,[1c,2] since an effective metal ion for this type of reaction in general tends to act as a pseudo-proton. Chelate formation would consequently require participation of the nitrogen atom in a manner as shown by **1** and **2** (Scheme 2). If the role of a metal ion is only to neutralize the charge of the substrate as postulated for the magnesium-catalyzed hydrolysis of acyl phosphate,[11] the nitrogen atom would not necessarily be required to participate in coordination with a metal ion. As to the ground state in the copper-catalyzed hydrolysis of 8-quinolyl phosphate, the formation of the initial intermediate **1** is of no doubt judging from the relatively large stability constants listed in Table 4. Although the activation energy for the copper-catalyzed hydrolysis of 8-quinolyl phosphate is negligibly small relative to that for the spontaneous reaction as can be seen in Fig. 1, we can not eliminate the initial process of complex formation prior to the transition state for hydrolysis. Furthermore, a large negative value of apparent activation entropy ($\Delta S^{\ddagger}_{Cu}=-67$ e.u. at 80°C and $-\log[H^+]=2.01\pm0.02$) was obtained for the copper-catalyzed reaction of 8-quinolyl phosphate. This suggests that the activated complex formed in the transition state becomes considerably rigid due to the presence of the metal ion.

A similar mechanistic elucidation has been proposed to account for the copper-catalyzed hydrolysis of 8-actoxyquinoline;[12] the formation of an activated complex, either **3** or **4**, was suggested. With reference to our studies on the phosphate hydrolysis, we rather suggest that the weak interaction forming complex **3** at the initial stage is followed by the formation of complex **4** in the transition state. Hay and Edmonds[13]

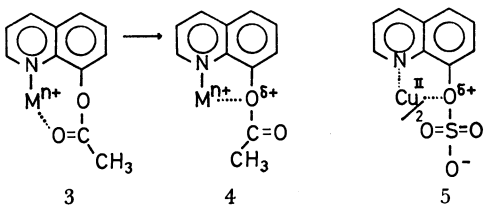

11) C. H. Oestreich and M. M. Jones, *Biochem.*, **6**, 1515 (1967).
12) R. H. Barca and H. Freiser, *J. Amer. Chem. Soc.*, **88**, 3744 (1966).
13) R. W. Hay and J. A. G. Edmonds, *J. Chem. Soc., D*, **1967**, 969.

reported that the hydrolysis of 8-hydroxyquinoline sulfate was accelerated by copper(II). They suggested the formation of complex **5** as an activated intermediate.

In case of the catalytic hydrolysis of 2-pyridylmethyl phosphate, the alcohol product (2-pyridylmethanol) forms the stable complexes only with copper(II), among various bivalent ions, upon liberation of the alcohol-proton at 1:1 and 2:1 molar ratios of ligand to metal ion;[14] thus, the copper ion has a profound affinity for the alcohol-oxygen of 2-pyridylmethanol. In the present work, 8-quinolinol, the hydrolysis product of 8-quinolyl phosphate, yields quite stable complexes with copper(II) and nickel(II): log K_1=13.49 for the copper complex and log K_1=11.44 for the nickel complex at 25°C in 50% aqueous dioxane.[15] Therefore, an affinity of these metal ions for the leaving alcohol group does not primarily control the catalytic efficiency in this instance. Rather, interaction of these metal ions with the substrate at the initial stage through pre-equilibrated complex-formation appears to be the necessary cause of the catalysis.

Thorium(IV) Catalysis. Since the extent of catalytic efficiency does not show large structural dependency, as was the case in the hydrolysis of pyridylmethyl phosphates,[3] the catalytic action must involve primarily the interaction between the thorium ion and the phosphate moiety of the substrate. The hydrolysis rate tends to level off after a while as shown in Figs. 3 and 4. Since addition of the alcohols did not result in any significant change in hydrolysis rate as mentioned in the preceding section, the rate retardation does not appear to be due to the produced alcohol but to the liberated inorganic phosphate. Judging from the relatively large stability constants for the thorium complexes formed with inorganic phosphate,[16] the potent interaction of thorium(IV) with the phosphate moiety at the initial stage of reaction and with the liberated inorganic phosphate in hydrolysis is to be expected. We observed the slow but appreciable liberation of proton at the initial stage. This finding definitely indicates the formation of certain thorium complexes in the early stage of reaction.

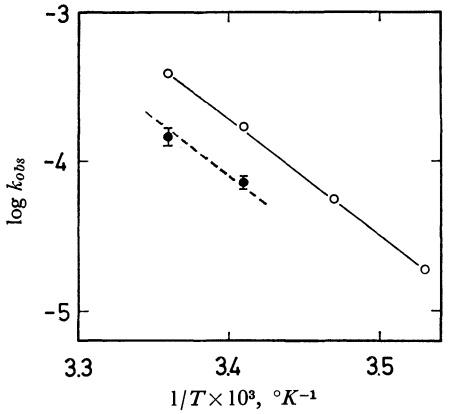

Fig. 7. Arrhenius plots of the apparent first-order reaction rates evaluated at the initial stage for the thorium(IV)-catalyzed hydrolysis of 3-pyridyl phosphate (○) and 8-quinolyl phosphate (●); rate constant (k_{obs}) in sec^{-1}.

Figure 7 shows the temperature dependence of an overall rate constant for the hydrolysis of 3-pyridyl phosphate in the presence of thorium(IV) at $-\log[H^+]=2.0$.[17] An apparent activation energy graphically estimated was 40 cal mol^{-1}. The hydrolysis reaction appears to be almost entirely due to the thorium-ion catalysis, since the spontaneous hydrolysis does not proceed to any detectable extent under these experimental conditions. This activation energy is almost in the same order of magnitude as that for the copper-catalyzed reaction described above. Therefore, a similar mechanistic elucidation may be applied to both cases: the hydrolysis reaction needs to pass through potential energy maxima forming two kinds of reaction intermediates as shown in Fig. 8.

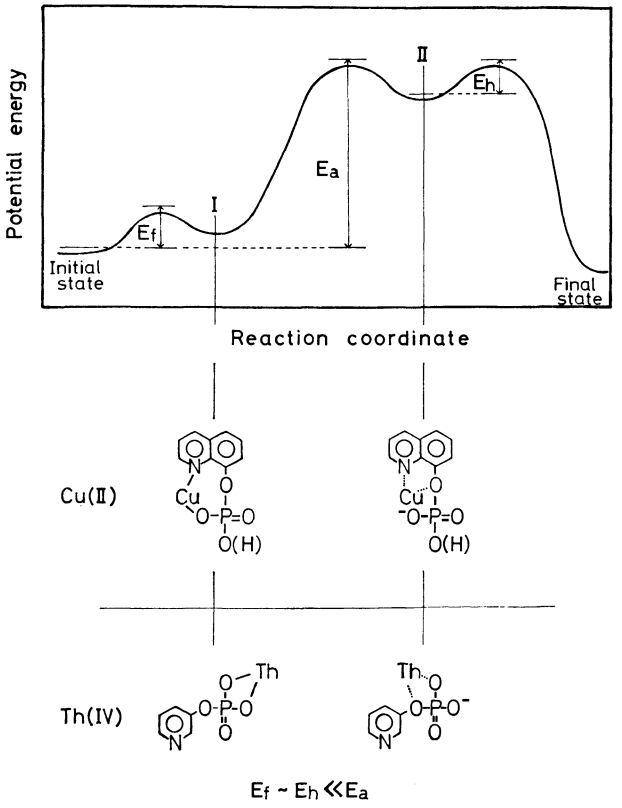

Fig. 8. Schematic representation of reaction mechanisms in terms of potential energy *vs.* reaction coordinate correlation.

In conclusion, the chelate-forming ability is the most important factor for the catalytic efficiency of bivalent metal ions, but this is not necessarily required for the thorium ion. Judging from the relatively large stability constants for the thorium(IV) complexes formed with inorganic phosphate, complex formation with the phosphate moiety is most likely the necessary cause for the catalysis. This interaction would provide effective charge neutralization for the substrate.

14) Y. Murakami and M. Takagi, This Bulletin, **38**, 828 (1965).
15) W. D. Johnston and H. Freiser, *J. Amer. Chem. Soc.*, **74**, 5239 (1952).
16) L. G. Sillén and A. E. Martell, "Stability Constants of Metal-Ion Complexes," Special Publication No. 17, The Chemical Society, London (1964).
17) When the deviation from the first-order plot was observed, the apparent first-order rate constant was evaluated from the initial part of reaction.

Studies of the Solvent Extraction of Potassium by Nitrobenzene in the Presence of Organic or Inorganic Acids

Tadashi IWACHIDO

College of Liberal Arts, Okayama University, Tsushima, Okayama

(Received December 28, 1970)

Aromatic compounds with an acidic group, such as –OH, –SH, –COOH, $-SO_3H$, >NH, >CH, and $\equiv B^-$ (tetraphenylborate) were tested as extracting agents for potassium. The first four acids showed an extractability lower by far than that of the last three. Most inorganic acids exhibited no signs of extraction. Bulky and electron-attracting substituents, such as nitro or halogen group, were proved to be effective in enhancing the extractability. The addition of iodine was also effective. A few kinds of surfactants showed considerably high extractability. Some factors influencing the extraction were speculated upon.

In recent years, the solvent extraction of alkali metals by utilizing ion-pairing agents has attracted growing attention. The first and most extensive works were carried out by researchers engaged in the treatment of radioactive fission products, especially ^{137}Cs. Tetraphenylborate,[1,2] hexanitrodiphenylamine,[3,4] and some phenols[5,6] are typical reagents. Nitrobenzene, a dipolar aprotic solvent with a high dielectric constant, has been frequently used as a solvent of these ion-pairs. However, there has been no systematic explanation of the reasons why these compounds are good for the extraction of alkali metals. This paper will establish some factors affecting potassium extraction by examining a number of organic and inorganic acids and will give some indications on how to obtain good extractions in the future.

Experimental

Reagents. The reagents used were, for the most part, commericial reagents of the purest quality; some were purified when the necessity arose. The amine derivatives were synthesized by a method described in a series of works by Tôei.[7-9] All of the potassium or sodium salts of organic and inorganic acids were dissolved in water to give a 2.5×10^{-2}M aqueous solution. Organic compounds of the acid-form were made up into either a 2.5×10^{-2}M aqueous or a 1.0×10^{-2}M nitrobenzene solution, according to the solubility of the acids. Some of the remaining organic compounds with which a high extractability was obtained were made up into a 10^{-3}M nitrobenzene solution except in a few cases (10^{-4}M).

The pH's of the aqueous solutions were adjusted when necessary by adding a 0.1M citrate buffer (pH 2 and 3), a 0.1M acetate buffer (pH 4 and 5), a 0.1M phosphate buffer (pH 6,7, and 8), or a 0.1M carbonate buffer (pH 9 and 10). The pH of the solution was also adjusted to pH 11 and 12 with 0.1M lithium carbonate and 0.1M lithium hydroxide solutions respectively. The solutions were made so that they all contained equal amounts of lithium ions.

Extraction. Into a 50-m*l* separatory funnel, 1 m*l* of a 0.1M potassium chloride solution was transferred, and then 4 m*l* of a 2.5×10^{-2}M aqueous reagent solution and 5 m*l* of water or a buffer solution were added. The resultant 10 m*l* of a 10^{-2}M potassium solution was gently shaken with 10 m*l* of nitrobenzene for 2 hr at room temperature. Some alterations were made according to the type of stock solution employed, keeping both the molar ratio of potassium to the reagent and the volume ratio of the aqueous to the organic phase at unity. In order to prevent the extraction of lithium ions with the reagent, buffers were not employed except in the cases where reagent anions were expected to hydrolyze to a great extent and where the knowledge of the dependence of the extractability on the pH was necessary for further discussions.

Determination of Potassium. After the extraction mixture had been allowed to stand for half an hour, the nitrobenzene phase was separated and subsequently subjected to atomic absorption spectrophotometry (Nippon Jarrell Ash, Type AA-1). About 0.2×10^{-6}M of potassium was detected.

Results

Extraction Curves. Figure 1 and 2 show the extraction curves obtained with several acids.

With acids having one functional group, the curve will be sigmoidal in shape, but the location of the curve shifts toward a higher or a lower pH region according to the magnitude of the acid dissociation constant and the distribution coefficient of the acid (Fig. 1).

Different types of extraction curves were obtained with acids having two or more functional groups, as is shown in Fig. 2. The form and the location of the curve may be instructive in estimating what kind of ion-pair is dominantly extractable by nitrobenzene.

Extractability. The values of the percent extractions of many kinds of acids are listed in Tables 1 to 9. The results may be summarized as follows: 1). The highest extraction of potassium was attained with the acids of amine derivatives and tetraphenylborate (8-X), as is shown in Tables 4 and 8. The values of the percent extractions of some typical acids, such as phenols, sulfonic acids, and carboxylic acids (Tables 1 to 3), were all less than 0.1, except for some nitro- or halogeno-substituted acids. Such a situation was also encountered with acids of different types, as is shown in Tables 5 to 9.

1) K. Haruyama and T. Ashizawa, *Bunseki Kagaku*, **14**, 120 (1965).
2) T. Sekine and D. Dyrssen, *Anal. Chim. Acta*, **45**, 433 (1969).
3) M. Kyrš, *Collect. Czecho. Chem. Commun.*, **27**, 2380 (1962).
4) T. Iwachido and K. Tôei, This Bulletin, **37**, 1276 (1964).
5) W. J. Ross and J. C. White, *Anal. Chem.*, **36**, 1998 (1964).
6) W. E. Keder, E. C. Martin, and L. A. Bray, "Solvent Extraction Chemistry of Metals," ed. by H.A.C. McKay, Macmillan, London (1965), p. 343.
7) K. Tôei, *Nippon Kagaku Zasshi*, **76**, 106 (1955).
8) K. Tôei, *ibid.*, **76**, 1085 (1955).
9) K. Tôei, *ibid.*, **77**, 1270 (1956).

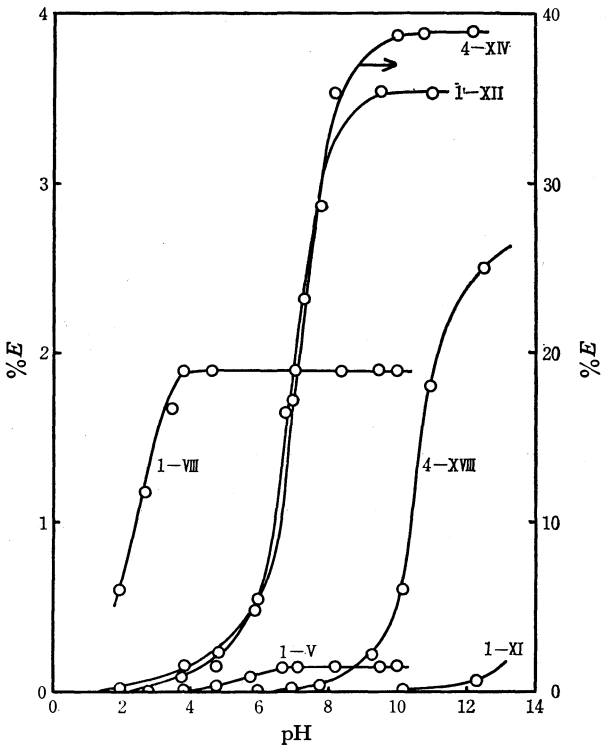

Fig. 1. The effect of pH on the extraction of potassium by some acids in nitrobenzene

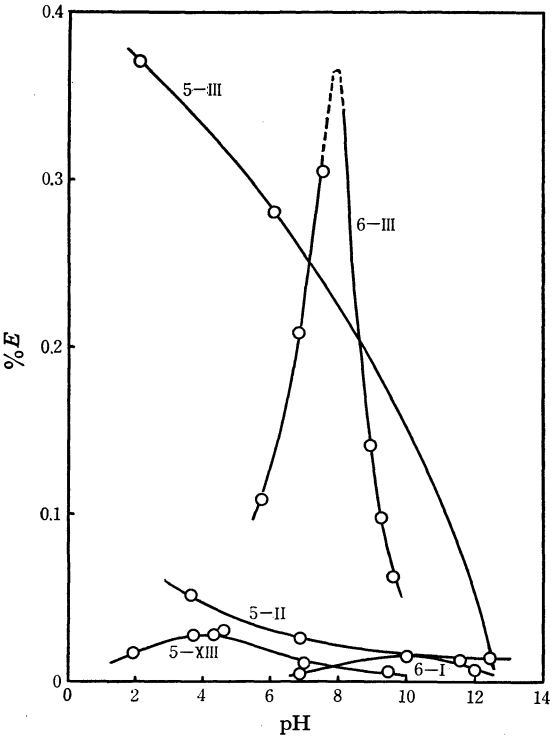

Fig. 2. The effect of pH on the extraction of potassium by some acids in nitrobenzene

It is of much interest to compare the values of percent extraction obtained with acids having a benzene or naphthalene nucleus in common: 2,4-dinitrophenol (0.150)>2,4-dinitrobenzenesulfonic acid (0.10); 1-naphthol (0.062)>1-naphthalenesulfonic acid (0.021)> 1-naphthoic acid (0.011). The sequence is the reverse

Table 1. Percent extraction of potassium with phenolates

Compound	No.	pK_a	pH	%E
Phenol	1-I	9.98	12	0
—, 2-Nitro-	1-II	7.22	12.2	0
—, 3-Nitro-	1-III	8.40	13.2	0.005
—, 4-Nitro-	1-IV	7.15	13.2	0.005
—, 2,4-Dinitro-	1-V	4.02	10.0	0.150
—, 2,5-Dinitro-	1-VI	5.32	13.2	0.060
—, 2,6-Dinitro-	1-VII	3.71	13.2	0.103
—, 2,4,6-Trinitro- (Picric acid)	1-VIII	−0.22	10.1	1.89
—, 2,4,6-Tribromo-	1-IX		13.2	0.125
—, Pentachloro-	1-X		10.5	1.05
1-Naphthol	1-XI	9.30	12.6	0.062
—, 2,4-Dinitro-	1-XII		9.50	3.54
8-Hydroxyquinoline	1-XIII	9.81	12	0.003

Table 2. Percent extraction of potassium with carboxylates

Compound	No.	pK_a	pH	%E
Benzoic acid	2-I	4.20	10.0	0
—, 2-Nitro-	2-II	3.49	10.1	0
1-Naphthoic acid	2-III	3.69	12.6	0.011
Acetic acid	2-IV	4.76	7.0	0
—, 1-Naphthyl-	2-V	4.24	12.5	0.003
Anthraquinone-2-carboxylic acid	2-VI	3.37	10.5	0.008
Methyl Red	2-VII	4.84	12.4	0.007
Nicotinic acid	2-VIII	4.81	12	0.003

Table 3. Percent extraction of potassium with sufonates

Compound	No.	pK_a	pH	%E
Benzenesulfonic acid	3-I	−0.70	1.8	0.006
—, 2,4-Dinitro-	3-II		6.90	0.10
1-Naphthalene-sulfonic acid	3-III	−0.17	6.10	0.021
2-Naphthalene-sulfonic acid	3-IV		4.3	0.035
1,2-Naphthoquinone-4-sulfonic acid	3-V		2.75	0.060
Anthraquinone-2-sulfonic acid	3-VI	−0.38	6.24	0.11

of that which can be observed between 2-naphthyl mercaptan (8-IX) and 1-naphthol (1-XI); this might be due to the hydrolysis of the former in the aqueous phase. Mercaptans (8-VII, -VIII) showed much higher extractabilities than imidazoles (8-IV, -V), although all of them are similar in size.

2) Acids having a bulky nucleus were desirable as extraction agents. This was well shown by sulfonic acids as follows: Anthraquinone-2-sulfonic acid (0.11) >2-naphthalenesulfonic acid (0.035)>benzenesulfonic acid (0.006). The same sequence was also observable with phenols and carboxylic acids (Tables 1 and 2). The insertion of a CH_2 group between the nucleus and the functional group reduced the effect, as was shown with 1-naphthylacetic acid (2-V).

3) The introduction of a bulky, electron-attracting

Table 4. Percent extraction of potassium with amine derivatives (10^{-3} M)

Compound	No.	pH	%E
Aniline	4-I	12	0[a]
—, 2-Nitro-	4-II	12.5	0[a]
—, 2,4-Dinitro-	4-III	12.5	0[a]
2,4,5,7-Tetranitroacrydone	4-IV	12.8	45.4
1,3,7,9-Tetranitrophenothiazine-5-dioxide	4-V	12.8	65.3
Phenoxazine, 1,3-Dinitro-	4-VI	12.8	0.09
—, 1,3,7,9-Tetranitro-	4-VII	11.8	3.40
1,3,6,8-Tetranitrocarbazole	4-VIII	12.8	7.30
Diphenylamine, 2,4-dinitro-	4-IX	12.5	0
—, 2,4,2′,4′-Tetranitro-	4-X	12.8	40.8
—, 2,4,6,2′,4′,6′-Hexanitro-	4-XI	13.2	58.3[b]
2-Naphthylamine, 2,4-Dinitrobenzo-	4-XII	12.8	0
—, 2,4,6-trinitrobenzo-	4-XIII	12.8	1.63
1-Naphthylamine, *N*-(2,4,6-trinitrobenzo)-2,4,-dinitro-	4-XIV	12.2	39.1[b]
2,4,6-Trinitrophenylamine, *N*-(1-anthraquinolino)-	4-XV	12.8	5.87
—, *N*-(2-nitro-1-anthraquinolino)-	4-XVI	12.8	42.7
N-(2,4,6-trinitrobenzo)-benzene-sulfamide	4-XVII	12.8	16.2
Diphenylpicrylhydrazine	4-XVIII	12.5	2.50[a]

a) The extraction of potassium was carried out with the reagent of 10^{-2}M.
b) Reagent concentration, 10^{-4}M.

substituent, such as a nitro group or halogen atoms, was highly effective in improving the extractability. In general, the extractability increases rapidly with the number of the substituents. The effect was obvious with phenols (Table 1) and amine derivatives (Table 4).

4) Compounds which have two or more functional groups in a molecule showed a characteristic extraction curve. With phthaleins (6-I, -III) and sulfonphthaleins (6-XI) we obtained a curve with a maximum at a certain pH value, and with alizalinsulfonic acid (5-III), a monotonously-descending curve. In both cases, the percent extraction begins to decrease at a somewhat higher pH value than that to be expected from the first dissociation constant of the acid. The fact may show that, among the possible species existing in the aqueous phase, the neutral ion-pair composed of equimolecular amounts of potassium and the monovalent, reagent anion is dominantly extractable by nitrobenzene. Styphnic acid (5-I) may be a good illustration. Molybdate (9-VIII) and tungstate (9-IX) may be the same.

5) The addition of iodine greatly improved the extractability (Tables 6 and 9). It is well known that the iodine combines with iodide to form a bulky I_3^- anion. Therefore, it seems likely that the KI_3, ion-pair, is extractable by nitrobenzene. For the other cases encountered, a different explanation must be given.

6) A few surfactants showed quite good results, whereas polyvinylsulfate (8-XIII) exhibited no extraction. It must be noted that the separation of the nitrobenzene phase from the aqueous phase becomes increasingly difficult as the amount of the surfactant used increases. This may prevent their practical use.

7) Many kinds of inorganic compounds were tested by varying the pH of the aqueous solution, but only a few were capable of extracting only a small amount of potassium. Bulky, monovalent peroxyacid anions were the best; divalent anions were all incapable of extracting potassium, except for a few compounds which are known as precipitants of potassium.

Extractability and Solubility. In Fig. 3 the solubility of potassium salts in water, S, is plotted against the distribution ratio, q, of these compounds between

Table 5. Percent extraction of potassium with compounds having two or more functional groups

Compound	No.	pK_a or pH Range	pH	%E
2,4,6-Trinitroresorcinol	5-I		2.4	1.73
			12.7	0
Alizalin	5-II	5.5—6.8	3.7	0.052
Alizalin-3-sulfonic acid	5-III	5.45	2.1	0.371
		11.01		
2,4-Dinitro-1-naphthol-8-sulfonic acid	5-IV		1.7	0.107
			12	0.013
4,5-Dihydroxy-2,7-naphthalenedisulfonic acid	5-V	5.36	3.9	0.003
		15.6		
2,3-Dihydroxy-6-naphthalenesulfonic acid	5-VI		2.1	0
			5.5	0
1-Nitrobenzene-3,5-disulfonic acid	5-VII		7.5	0.029
1-Naphthylamine-8-sulfonic acid	5-VIII		12	0.035
1-Napthylamine-4,8-disulfonic acid	5-IX		2.6	0.003
Tartaric aicd	5-X	3.04	4.3	0
		4.36		
Phthalic acid	5-XI	2.95	3.8	0.007
		5.41	7.0	0
Aurintricarboxylic acid	5-XII		5.2	0.059
Salicylic acid	5-XIII	2.75	3.8	0.028
		12.4		

Table 6. Percent extraction of potassium with phthaleins or sulfonphthaleins

Compound	No.	pH Range	pH	%E
Phenolphthalein	6-I	8.0—9.8	10.0	0.015
—, 3′,3″-Dimethyl-	6-II	8.2—9.8	12.5	0.017
—, 3′,3″-Dinitro-	6-III	6.8—8.2	7.5	0.305
3′,5′,3″,5″-Tetrabromophenolphthalein ethyl ester	6-IV		10.0	10
Fluorecein	6-V		8.6	0.008
—, 2,4,5,7-Tetrabromo-	6-VI		7.0	0.468
—, 2,4,5,7-Tetraiodo-	6-VII		6.7	0.23
			8.0	0.094
	(+equiv. I_2)		6.7	5.59
	(+excess I_2)		6.2	67.1
Phenolsulfonphthalein	6-VIII	6.8—8.4	7.2	0.107
			8.0	0.108
—, 3′,3″-Dimethyl-	6-IX	0.4—2.2	1.1	0.028
		7.2—8.8	8.3	0.102
—, 3′,3″-Dinitro-	6-X	2.9—4.8	4.5	0.333
			12.4	0.010
—, 3′,5′,3″,5″-Tetrabromo-	6-XI	3.0—4.6	1.2	0.270
			4.5	0.845
			9.0	0.351
—, 3′,5′,3″,5″-Tetraiodo-	6-XII		3.9	2.33
			11.6	0.047
	(+equiv. I_2)		4.9	7.43

Table 7. Percent extraction of potassium with phenyl derivatives of some oxyacids

Compound	No.	pK_a	pH	%E
Phenylarsonic acid	7-I	3.47	2.0	0
		8.48	3.8	0
			6.9	0
			8.7	0
			12.2	0
—, 2-Nitro-	7-II	3.37	1.9—12.2	0—0
		8.54		
Phenylboric acid	7-III	8.86	12.5	0

Table 8. Percent extraction of potassium with miscellaneous compounds

Compound	No.	pK_a	pH	%E
5-Nitrobarbituric acid	8-I		1.6	0.003
			12	0
Picrolonic acid	8-II		12	1.07
Phthalimide	8-III	8.3	6.5	0
Benzimidazole	8-IV	5.3	7.9	0
		12.3		
—, 2-Methyl-	8-V		7.9	0
Hexanitrotriphenylmethane	8-VI		12.8	2.58[a]
2-Mercaptobenzoxazole	8-VII		12.9	0.044
2-Mercaptobenzothiazole	8-VIII		12.9	0.125
2-Naphthyl mercaptan	8-IX		12.7	0.029
Tetraphenylboric acid	8-X		7.4	76.6[b]
Laurylbenzensulfonic acid	8-XI		6	0.43
Sodium lauryl sulfate	8-XII			1.0
Polyvinyl potassium sulfate	8-XIII		6.1	0

a) Reagent concentration, 10^{-3}M.
b) Reagent concentration, 10^{-4}M.

Table 9. Percent extraction of potassium with inorganic compounds

Anion	No.	pK_a	pH	%E
IO_4^-	9-I		6.2	0.115
ClO_4^-	9-II		6.5	0.120
MnO_4^-	9-III		7	0.331
BF_4^-	9-IV		4.0	0.045
SCN^-	9-V	−0.85	6.8	0.025
I^-	9-VI		6.2	0.012
I^- (+equiv. I_2)	9-VII		5.7	15.9
MoO_4^{2-}	9-VIII	$pK_2=6$	1.0	0.084
			4.9	0.012
			7.4	0
WO_4^{2-}	9-IX	$pK_1+pK_2=7$	1.0	0.232
			5.1	0.018
			8.0	0
$PtCl_6^{2-}$	9-X		1.0	0.004
			2.8	0.009
Uranyl Zinc Acetate	9-XI		4.6	0.021
$Co(NO_2)_6^{3-}$	9-XII		1.0	0.017
			3.9	0.014

Potassium can not be extracted by the following reagent.
IO_3^-, ClO_3^-, BrO_3^-, NO_3^-, NO_2^-, F^-, Cl^-, Br^-, N_3^-, OCN^-, CrO_4^{2-}, SO_4^{2-}, HPO_4^{2-}, SeO_4^{2-}, TeO_4^{2-}, $HAsO_4^{2-}$, CO_3^{2-}, SiF_6^{2-}, $S_2O_7^{2-}$, $S_2O_8^{2-}$, $H_2Sb_2O_7^{2-}$, $B_4O_7^{2-}$, $Cr_2O_7^{2-}$, BO_3^-, BiO_3^-, VO_3^-, AlO_2^-, AsO_2^-, $Fe(CN)_5NO^{2-}$, $Fe(CN)_6^{3-}$, $Fe(CN)_6^{4-}$

the aqueous and nitrobenzene phases. Because of the lack of the solubility data, most of the results obtained can not be shown in this figure. This figure indicates that the solubility is closely related to the extractability. It is of much interest to note that this relation holds not only for nitro compounds, which are similar in chemical constitution to nitrobenzene, the solvent, but also even for inorganic compounds. Such a correlation will be helpful for further extractions.

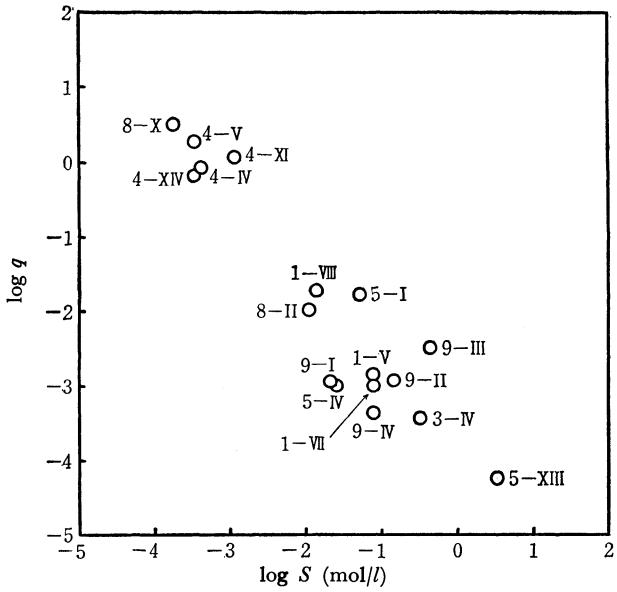

Fig. 3. The relation between the distribution ratio of potassium and the solubility of potassium salts in water
q: The distribution ratio of potassium salts
S: The solubility of potassium salts in water

Discussion

In a previous paper,[10] it has been reported that the extraction of alkali metals with organic acids into nitrobenzene can be well understood by recognizing that nitrobenzene helps the ionic dissociation of the ion-pairs extracted. The paper also has stated that the extractability of the ion-pair increases with the association constant in the aqueous phase and with the dissociation constant in nitrobenzene.

Some chemical constitutional factors influencing such equilibria will be considered below.

Ion Size. Ion association in organic solvents has been extensively studied by Kraus and his collaborators by means of conductometry.[11] As might be expected from a long-range electrostatic force, ion association generally increases with a decrease in the ion size. This may be true for a simple binary electrolyte. The estimation of the energy of charge separation, however, becomes increasingly more difficult as the structural complexity of the anions increases. In general, large anions from loosely associated ion-pairs, and the resultant ion-pairs can easily be dissociated in nitrobenzene.

On the other hand, in an aqueous solution Bjerrum's theory[12] is not always helpful for the study of ion-pairing. According to the theory, the distance of the closest approach of free ions is 3.57 Å for 1:1 electrolytes in water at 25°C. This distance roughly corresponds to that of potassium iodide. Hence, anions which are larger than iodide should not make stable ion-pairs in the aqueous solution. Diamond[13] has indicated the formation of an ion-pair of a different type between bulky and poorly hydrated ions, the distance of the separation being much greater than 3.57 Å. He also suggested that, with regard to such ion-pairs, the hydrogen-bonded structure of water enforces the association of the oppositely-charged ions to minimize the disturbance of the water structure. This type of ion-pairing or the water structure-enforced ion-pairing has a dependence on the distance of charge separation the reverse of that of the ion-pairing of the Bjerrum type. From the above considerations of the behavior of ion-pairs in both the aqueous and nitrobenzene phases, it might be expected that ion-pairing between large organic anions and a potassium cation is facilitated in the aqueous phase and suppressed in the nitrobenzene phase. Accordingly, it can be concluded that large anions favor the extraction.

Steric Factors. In tetraphenylborate (8-X), hexanitrotriphenylmethane (8-VI), and diaryl-substituted amines (Table 4), a formal, negative charge is located on the boron, carbon, and nitrogen atoms respectively, and they are all sterically hindered by large, bulky phenyl groups from coming in contact with the potassium cation. Nitro-group or halogen atoms also help to keep the oppositely-charged ions apart.

On the other hand, anions with no steric hindrance can contact the potassium cation directly, even though they have a residual bulky group. This results in a strong ion-pairing. The fact that the association constant of potassium picrate in nitrobenzene[10] is 1200, about 120-times than that of hexanitrodiphenylamine,[14] can be considered as a good illustration of the effect. Such examples may easily be seen in the remaining compounds.

Charge Dispersal. The concept of charge dispersal has been developed on the basis of the discussion of the acid-base strength. Electrons in an extended π bond are free to move anywhere within the region of the charge cloud; this promotes the delocalization of electrons through a π-molecular orbital system. Thus, the negative charge located at first on the atom from which the hydrogen atom is released as the hydrogen ion is delocalized or dispersed on the whole molecule. As a consequence, the resultant anions are stabilized by the amount corresponding to the delocalization energy. The stabilization of anions will result in the enhancement of the acidity of the corresponding conjugate acids. A similar effect might be expected as well in the case of ion-association; that is, the charge dispersion of anions weakens the interaction with cations and helps the dissociation of such ion-pairs in the organic phase. If atoms of a high electronegativity are assumed to resist the dispersion of the charge located on them, it can be expected that the anions suitable for potassium extraction by nitrobenzene are such that the negatively-charged atoms are less electronegative. The electronegativities of the atoms in question decrease in the following order: O>N>C, S>B. Therefore, the ion-pair of tetraphenylborate should strongly dissociate, and oxy-acids or phenols

10) M. Yamane, T. Iwachido, and K. Tôei, This Bulletin, **44**, 745 (1971).
11) C. A. Kraus, *J. Phys. Chem.*, **60**, 129 (1956).
12) N. Bjerrum, *K. Danske Vidensk. Selsk. (Math. fys. Medd.)* **7**, 1 (1926).
13) R. M. Diamond, *J. Phys. Chem.*, **67**, 2513 (1963).
14) S. Motomizu, K. Tôei, and T. Iwachido, This Bulletin, **42**, 1006 (1969).

in nitrobenzene should weakly dissociate. Such a sequence has already been verified with tetraphenylborate[15] and picrate.[10] The sequence may also be supported by the fact that, in liquid ammonia, the dissociation constant decreases in the following order:

$$NaSPh > NaNHPh > NaOPh,^{11}$$

where Ph denotes the phenyl radical.

Inductive Effect. The introduction of substituents which can attract electrons away from the negatively-charged atoms decreases the electron density on them. As the nitro group and halogen atoms will exert an electron-attracting inductive effect, it can be expected that, with these compounds, a highly enhanced extractability will be obtained. It is, however, difficult to discuss the effect of ion size and the inductive effect separately, because these substituents are very bulky themselves. Acrydone (4—IV) and phenothiazine (4-V) can clearly be differentiated from phenoxazine (4-VII). This fact may also suggest the inductive effect of $\geq C{=}O$, $\geq SO_2$, and $\geq O$ groups.

15) Unpublished work.

Conclusion

From the above discussion and the experimental results, it can be concluded that bulky, charge-dispersible anions with electronegative groups in adjacent positions of the functional group are the best for the extraction of potassium by nitrobenzene.

The author wishes to express his gratitude to Professor Kyoji Tôei for his guidance throughout the course of this work.

BULLETIN OF THE CHEMICAL SOCIETY OF JAPAN, VOL. 44, 1840—1843 (1971)

The Carbon-catalyzed Oxidation of Co(II)-Ethylenediaminetetraacetate by Molecular Oxygen

Akira TOMITA

Chemical Research Institute of Non-Aqueous Solutions, Tohoku University, Katahira, Sendai

(Received January 20, 1971)

The kinetics of the oxidation of a cobaltous complex of ethylenediaminetetraacetic acid (EDTA) is determined volumetrically at 50.0°C in the presence of several kinds of carbon as catalysts. One mole of oxygen was used to oxidize four Co(II) ions, and all the Co(II) ions were oxidized to Co(EDTA)$^-$ ions quantitatively. The rate of oxygen uptake was found to change from zeroth order to first order with respect to the complex ion during the course of oxidation; it was also found to be first order with the oxygen pressure and the amount of the carbon catalyst. The catalytic activity of the carbon was correlated to the quantity of surface basic oxides of the carbon. A possible mechanism which can account for the above results is proposed.

Many reactions have been known to be catalyzed by carbons or metals supported on carbon.[1] Several works[2-4] have also described the catalytic effect of the carbon on the reaction of coordination compounds, but no mechanistic details have been investigated. Recently, the functional groups on the carbon surface have been characterized by various methods. The presence of acidic oxides I[5] and basic oxides II[6] has been reported. As a first step to studying the interaction between metal complex ions and the carbon, we previously studied[7] the adsorption of a $Co(NH_3)_6^{3+}$ ion onto carbon and the base hydrolysis

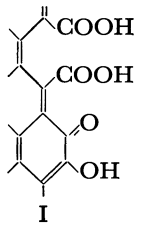

I

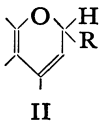

II

of the same complex ion catalyzed by the carbon. In that paper, we concluded that the active site was the acidic oxide on the carbon surface I, and suggested that the electrostatic force between the complex ion and the acidic oxides is one of the most important factors in their interaction. It then appeared of interest to investigate whether or not the active site for the reaction of complex *anions* was also the acidic oxide. The oxidation of a Co(II)-EDTA complex was undertaken for this purpose.

A Co(II)-EDTA complex ion has been known to be oxidized by various oxidants, such as H_2O_2, PbO_2,[8] and $Fe(phen)_3$.[9] It cannot be oxidized in an aqueous

1) R. W. Coughlin, *Ind. Eng. Chem. Prod. Res. Develop.*, **8**, 12 (1969).
2) J. C. Bailer, Jr., and J. B. Work, *J. Amer. Chem. Soc.*, **67**, 176 (1945).
3) F. Basolo and R. G. Pearson, "Mechanisms of Inorganic Reactions," John Wiley & Sons, New York, N. Y. (1958), p. 355.
4) B. E. Douglas and S-M. Ho, *J. Inorg. Nucl. Chem.*, **26**, 609 (1964), and references therein.
5) H. P. Boehm, *Angew. Chem.*, **76**, 742 (1964); *ibid.*, **78**, 617 (1966).
6) V. A. Garten and D. E. Weiss, *Aust. J. Chem.*, **10**, 309 (1957).
7) A. Tomita and Y. Tamai, *J. Phys. Chem.*, **75**, 649 (1971).
8) G. Schwarzenbach, *Helv. Chim. Acta*, **32**, 839 (1949).
9) R. G. Wilkins and R. E. Yelin, *J. Amer. Chem. Soc.*, **92**, 1191 (1970).

solution by bubbling oxygen or air. During the course of the previous investigation, we found the catalytic activity of the carbon for the air-oxidation of this complex ion. The catalytic effect of the carbon on the oxidation reaction has been reported in the cases of a $Co(NH_3)_6^{2+}$ ion[10] and a Fe^{2+} ion[11] with no explanation of the role of the catalyst. This paper will report the results of a kinetic study of the oxidation of the Co(II)-EDTA ion, and a tentative mechanism for the oxidation will be discussed in relation to the functional groups on the carbon surface.

Experimental

Reagents. A solution of Co(II)-EDTA was prepared from cobaltous nitrate and disodium salt of EDTA unless otherwise stated; the pH of the solution was about 0.7. The predominant chemical species under these conditions has been identified as $Co(HL)(H_2O)^-$, where L indicates the ethylenediaminetetraacetate ion.[12] The effect of the initial pH of the solution was determined in a medium with an ionic strength of 1.0 μ ($NaNO_3$). The hydrogen ion concentration was adjusted by the addition of a dilute sodium hydroxide solution.

Two kinds of carbons with different surface areas were used: a carbon black (HAF) and an active carbon (AC). These carbons were modified by the method of Boehm.[5] The surface area (N_2 adsorption) and the surface acidity (NaOH consumption) are listed in Table 1. The pretreatment of the carbon is designated by an appended "n" or "o" for oxidation by HNO_3 or O_2 respectively.

Kinetic Measurement. We used a general type of apparatus, incorporating a constant-pressure gas buret with a volume of 50 m*l* and a reaction flask with a stirrer driven magnetically. The reaction flask held 40 m*l* of the reacting solution. The flask had a side chamber containing 10 g of soda lime to absorb the carbon dioxide produced. After the aqueous solution had been saturated with oxygen and allowed to come to the desired temperature, the reaction was started by plunging the carbon catalyst under a stream of oxygen and adjusting the pressure of oxygen. The gas buret was placed in a constant-temperature bath which was held at 30.0°C, while the reactor was kept in a bath maintained at 50.0°C. They were then placed in a room which was also thermostated at 27.2°C. The rate of oxidation was measured by the amount of oxygen absorbed during the course of oxidation.

Results

Typical profiles of the oxygen absorption are shown in Fig. 1. The plateau region of these curves corresponds to 95—102% of complete oxidation calculated on the basis of:

$$4Co(HL)(H_2O)^- + O_2 \longrightarrow 4CoL^- + 6H_2O \quad (1)$$

The absorption spectrum of the solution corresponding to this stage also shows that all the cobalt ions are present as forms of the CoL^- ion. These curves were obtained in the presence of soda lime in the side compartment of the flask. Otherwise, the gas absorption curve falls again due to the evolution of carbon dioxide after the absorption of oxygen of this molarity. The evolution of carbon dioxide may be attributed to the formation of the CoL^- ion in the first step, because this phenomenon was also observed when we used the CoL^- ion instead of the $Co(HL)(H_2O)^-$ ion as the starting material. Figure 1 illustrates the effect of the initial concentration of the complex ion on the rate. The initial slopes of all the curves are equivalent, in spite of the different initial concentrations. This fact and the linearity over the initial range indicate that the reaction is of the zeroth order. Deviation from linearity occurs later, since the kinetics approaches first-order behavior.

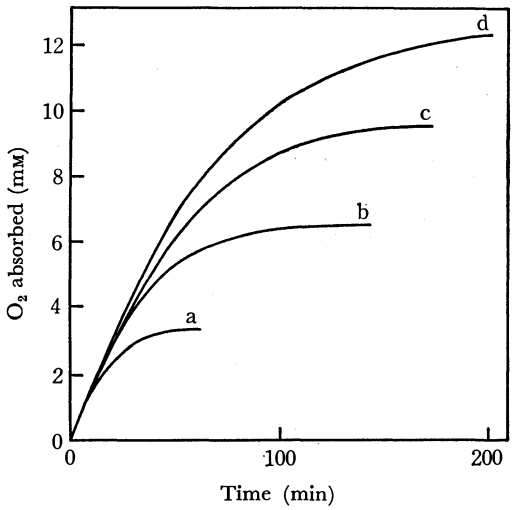

Fig. 1. Effect of initial concentration of Co(II)-EDTA: (a) 12.5 mM; (b) 25 mM; (c) 37.5 mM; (d) 50 mM. Carbon, AC 200 mg; Temperature, 50.0°C; Oxygen, 700 mmHg.

The zeroth-order rate constant as a function of the amount of the carbon was found to vary linearly in the range of 0—500 mg (Fig. 2). Such a dependence is expected for a solid catalyst, the rate being a function of the number of active sites on the surface. The rate

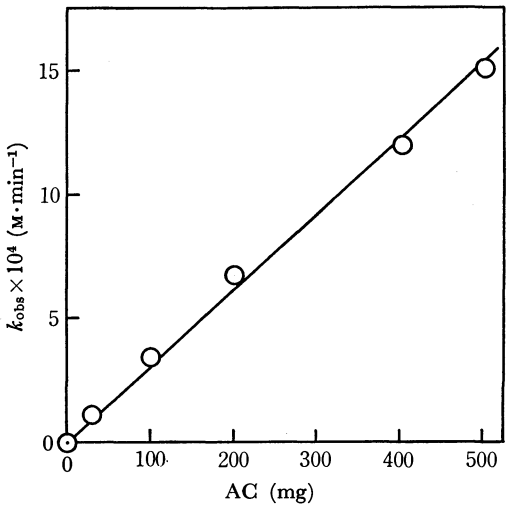

Fig. 2. Effect of the amount of AC at 50.0°C. Co(II)-EDTA, 50 mM; Oxygen, 700 mmHg.

10) J. Bjerrum and J. P. McReynolds, "Inorganic Syntheses," Vol. 2, (1946) p. 216.
11) A. M. Posner, *Trans. Faraday Soc.*, **49**, 389 (1953).
12) W. C. E. Higginson, *J. Chem. Soc.*, **1962**, 2761.

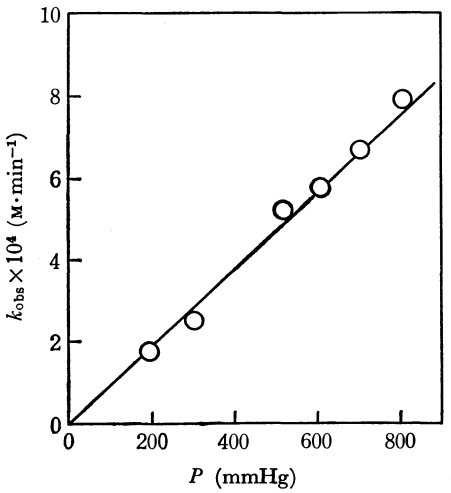

Fig. 3. Effect of the oxygen pressure at 50.0°C. Co(II)-EDTA, 50 mM; Carbon, AC 200 mg.

in the absence of the carbon was extremely low. Figure 3 shows the linear variation of the rate constant with the oxygen pressure. No oxidation was observed when the atmospheric gas was replaced by nitrogen.

The effect of the initial pH of the solution was determined in the pH region from 0.7 to 1.2, and the observed zeroth-order rate constant was represented by:

$$k_{obs} = k_a + k_b/[H^+] \quad (2)$$

and $k_a = 7 \times 10^{-4}$ (M·min^{-1}) and $k_b = 0.3 \times 10^{-4}$ (M^2·min^{-1}) are obtained at 50.0°C.

The rate constants given in Table 1 were obtained by using carbons with different surface acidities or basicities. In these runs, some experimental conditions were different from those mentioned above: cobaltous chloride was used for preparing the starting material, and the reaction temperature was 30.0°C. The catalytic activity of carbons is well correlated with the surface basicity (see also Fig. 4), but not with the surface acidity. This tendency is quite in contrast with the case of the *cationic* complex ion.[7] Under these conditions, the effect of the temperature was investigated only briefly. One oxidation run catalyzed by AC was made at 50.0°C; we found that k_{obs} was 8.6×10^{-4} (M·min^{-1}). The apparent activation energy was calculated to be about 9 kcal/mol.

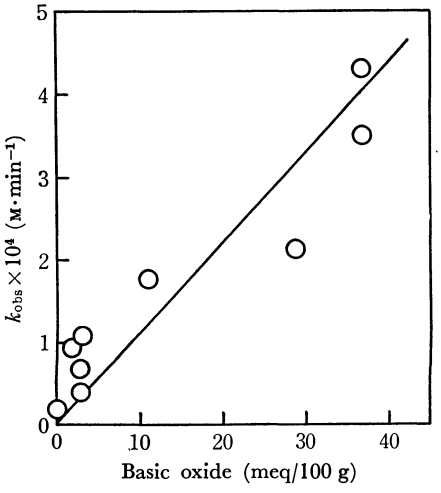

Fig. 4. Relationship between the rate constant and the basicity of the carbon surface.

Table 1. Observed rate constants for the oxidation of $Co(HL)(H_2O)^-$ catalyzed by various carbons[a]

Carbon	Surface Area (m^2/g)	Acidity[b] (meq/100g)	Basicity[c] (meq/100g)	$k_{obs} \times 10^4$ (M·min^{-1})
AC-o1	1120	38.7	37	4.3
AC	1230	32.7	37	3.5
AC-n3	—	111	29	2.1
AC-o2	1100	118	11	1.75
HAF	81	2.2	3	1.1
HAF-n3	82	5.7	2	1.0
HAF-n6	—	12.5	3	0.71
HAF-n4	71	14.7	3	0.42
HAF-o1	170	40.1	0	0.24

a) Co(II)-EDTA, 50 mM; Carbon, 200 mg; Oxygen, 700 mmHg; Temperature, 30.0°C.
b) NaOH consumption.
c) HCl consumption.

Discussion

Carbon dioxide evolution after the formation of the CoL^- ion may be considered to arise from the oxidation of carbon or from the decarboxylation of the EDTA complex. We regard the former as unlikely. Evidence in favor of the latter was adduced from the experiments in gas evolution starting from the CoL^- ion: (1) carbon dioxide was also observed to evolve under a nitrogen atmosphere, (2) the absorbance at 537 mμ corresponding to the CoL^- ion decreased upon the evolution of carbon dioxide, and (3) the amount of carbon dioxide evolved was closely related to the initial concentration of the CoL^- ion. As a more detailed mechanism is not clear from the data now available, we would like to limit our discussion to the first step of oxidation, where the side reaction is considered to be slow enough.

Any mechanism proposed for the carbon-catalyzed oxidation of a Co(II)-EDTA complex must explain, or be in accord with, the dependences of the rate on the following: (1) the amount of the carbon, (2) the oxygen pressure, (3) the initial concentration of a Co(II) complex, (4) the pH of the solution, and (5) the surface acidity or basicity of the catalysts. As there is an inverse correlation between the acidity of the carbon and the activity, the adsorption of a Co(II) complex on the acidic-surface oxides I is unlikely. Although this inverse correlation can be explained by the electrostatic repulsion between the dissociated acidic groups (*i.e.*, the -COO^- or -O^- group) and the complex anions, this interpretation is inadequate because these acidic groups are not dissociated because of the low pH value of the solution. On the other hand, the activity of carbon was well correlated with the quantity of basic surface oxides, and it seems reasonable to conclude that the active sites for this oxidation are those basic oxides (*i.e.*, with the chromene-type structure II). The following scheme may be proposed to account for the catalytic action of these functional groups:

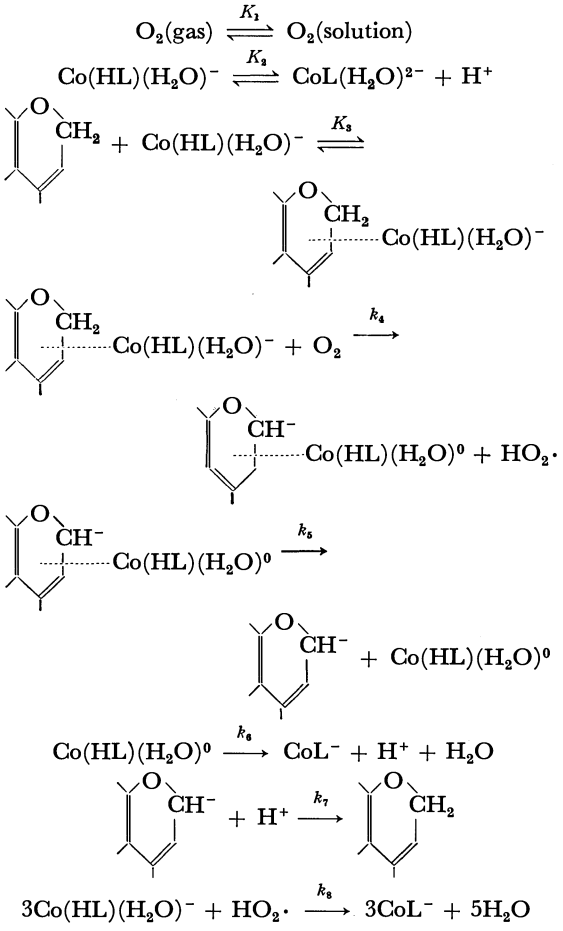

The oxidation reaction seems to proceed through two simultaneous reaction paths, one of which involves the oxidation of the protonated chelate as described above, while the other involves the oxidation of the unprotonated chelate, $CoL(H_2O)^{2-}$. The corresponding constants for $CoL(H_2O)^{2-}$ will be marked K_3', k_4', k_5', and k_6' in the following discussion. Although the presence of a sexidentate CoL^{2-} has been suggested,[9] it seems reasonable to consider only two quinquedentate anions represented by the K_2 equilibrium in a strongly acidic solution.[9,12] Letting the fraction of the surface sites covered with $Co(HL)(H_2O)^-$ and $CoL(H_2O)^{2-}$ be θ and θ', and letting the total concentration of Co(II) complexes be represented by $[Co]_T$, one obtains:

$$K_3 = \frac{\theta}{(1-\theta-\theta')\cdot[Co(HL)(H_2O)^-]} = \frac{\theta\cdot([H^+]+K_2)}{(1-\theta-\theta')\cdot[H^+]\cdot[Co]_T} \quad (3)$$

and:

$$K_3' = \frac{\theta'\cdot([H^+]+K_2)}{(1-\theta-\theta')\cdot K_2\cdot[Co]_T} \quad (4)$$

where K_3 and K_3' are the equilibrium constants for the adsorption of complex ions on the carbon. The adsorption is followed by an attack of oxygen; this is the rate-determining step, k_4 or k_4'. Assuming that the rate of $[Co(II)]_T$ consumption equals four times the rate of oxygen consumption, we can express the rate of oxidation by the above pathway as:

$$-d[Co]_T/dt = -4d[O_2]/dt = (k_4\theta+k_4'\theta')\cdot[C]\cdot K_1\cdot P \quad (5)$$

where [C] is the "concentration" of the carbon catalyst and where P is the oxygen pressure in the gas phase. Combining Eqs. (3), (4), and (5) gives:

$$-d[Co]_T/dt = \frac{(k_4\cdot K_3\cdot[H^+]+k_4'\cdot K_3'\cdot K_2)\cdot[Co]_T}{[H^+]+K_2+(K_3\cdot[H^+]+K_3'\cdot K_2)\cdot[Co]_T} \times[C]\cdot K_1\cdot P \quad (6)$$

This equation can explain the fact that the reaction is zeroth-order with respect to $[Co]_T$ at the beginning of the oxidation and is first-order at lower concentrations of the cobaltous ion. Equation (6) also shows a simple dependence of the rate of oxidation on the oxygen pressure and the amount of the carbon catalyst. The validity of this relationship may be seen by the same dependences shown in Figs. 2 and 3. The effect of the pH on the zeroth-order rate constant shown in Eq. (6) may be expressed in the form:

$$k_{obs} = K\cdot\frac{k_4\cdot K_3\cdot[H^+]+k_4'\cdot K_3'\cdot K_2}{K_3\cdot[H^+]+K_3'\cdot K_2} \quad (7)$$

where K is $[C]\cdot K_1\cdot P$, which was kept constant in these runs. In a strongly acidic solution, where $K_3'\cdot K_2$ is small compared to $K_3\cdot[H^+]$, Eq. (7) simplifies to:

$$k_{obs} = K\cdot\left(k_4+\frac{k_4\cdot K_2\cdot K_3'/K_3}{[H^+]}\right) \quad (8)$$

This theoretical equation agrees with the experimental equation (2). The dissociation constant, K_2, was reported[12] to be approximately 10^{-3}. Using this value and the constants presented in Eq. (2), we can estimate the $k_4\cdot K_3/k_4'\cdot K_3'$ ratio to be 0.023. The fact that this ratio is smaller than unity may be understood if one considers that the rate of the electron transfer to produce a pair of anions (k_4') might be faster than k_4. The oxidized complex ions may then be dissociated from the carbon surface in a fast step (k_5 and k_5'). The dehydration of the quinquedentate complex ion into the sexidentate CoL^- ion may then take place in a subsequent fast step (k_6). Considering the data reported[13] below 25°C, we can estimate the rate of this step to be very large compared to the preceeding steps. The $HO_2\cdot$ radical produced in the rate-determining step oxidizes the other three ions of Co(II)-EDTA accoring to the Weiss mechanism[14] (k_8). Thus, four ions of Co(II)-EDTA complexes are oxidized by one molecule of oxygen.

In conclusion, it should be emphasized that the catalytic behavior of the carbon in connection with the oxidation of Co (II)-EDTA was quite different from that for the adsorption or the hydrolysis of the $Co(NH_3)_6^{3+}$ ion. The active sites for the former case were surface basic oxides, II, whereas those for the latter were surface acidic oxides, I. Whether this difference has arisen from the electric charge of the complex ions, from the choice of different types of reactions, or from other reasons is not yet clear; it is advisable to investigate other reactions[15] in order to elucidate this point.

The author is grateful to Professor Yasukatsu Tamai for his helpful discussions.

13) I. A. W. Shimi and W. C. E. Higginson, *J. Chem. Soc.*, **1958**, 260.
14) J. Weiss, *J. Chim. Phys.*, **48**, C-6 (1951).
15) A. Tomita and Y. Tamai, *J. Colloid Interface Sci.*, in press.

The Fluorine, Chlorine, Bromine, and Iodine Contents of Volcanic Rocks in Japan[1]

Minoru YOSHIDA, Kazuyoshi TAKAHASHI, Norinobu YONEHARA,*
Takejiro OZAWA, and Iwaji IWASAKI[2]

Department of Chemistry, Faculty of Science, Tokyo Institute of Technology, Ookayama, Meguro-ku, Tokyo
** Department of Chemistry, Faculty of Science, Kagoshima University, Kamoike-cho, Kagoshima-shi*

(Received January 23, 1971)

The halogen contents of 49 Japanese volcanic rocks are; F: 50—1700 (average 410), Cl: 17—1220 (av. 270), Br: 0.09—8.10 (av. 0.85), I: 0.011—0.32 (av. 0.088) μg/g. The fluorine and chlorine were determined by usual photometric methods, and the bromine and iodine, by photometric methods based on their catalytic action, after decomposition and separation procedures suitable for each case. The bromine and iodine contents are appreciably lower than the values generally accepted for igneous rocks. The bromine content agrees with Sugiura's value. The frequency distribution of each halogen content shows an approximate lognormality. The chlorine and bromine contents are strongly correlated, and the Br/Cl atomic ratio is in a narrow range $(0.66—3.7)\times10^{-3}$ (av. 1.5×10^{-3}). No other correlation is observed among the halogen contents at all. Each halogen content has no marked relation to the type of rock. A regional difference is seen in the F/Cl and I/Br ratios. Three ultrabasic rocks have very low fluorine (≦20) and chlorine contents (≦50 μg/g). On the other hand, they have a slightly lower bromine content (0.15—0.34 μg/g) than, and almost the same iodine content (0.07—0.13 μg/g) as, the volcanic rocks.

Data on the halogen contents of igneous rocks are important in discussing the relation between igneous rocks and magmatic emanations. The investigation of the halogens is also interesting in connection with the "geochemical balance" of the elements. The origin of the oceans has often been discussed on the basis of the volatilization of the halogens and some other elements.[3-8] Since Correns[9] reviewed "the geochemistry of the halogens" in 1956, the fluorine and chlorine contents of igneous rocks have been reported by many investigators. The data on fluorine were compiled by Fleischer and Robinson (1963),[10] and those on chlorine, by Johns and Huang (1967),[11] although the latter authors did not quote the results of the studies by Japanese investigators.[12,13] On the other hand, data on bromine and iodine, especially those on iodine, are scarce.

Behne's results[14] of a systematic investigation of bromine in rocks were long accepted as reliable. In 1964, however, Filby[15] reported that the bromine content of two standard rock samples, G1 and W1, prepared by the U. S. Geological Survey, as determined by neutron activation analysis, was appreciably lower than Behne's average value. He confirmed this conclusion by analyzing some other standard rock samples.[16] The results of the recent determinations[17-19] of the bromine content of meteorites also show that Behne's values are too high. Recently, Sugiura[20] determined the bromine content of igneous rocks by a photometric method. His values were also lower than those of Behne; indeed, some rocks have a bromine content lower than the limits of determination of the method (0.2 ppm).

The iodine contents of igneous rocks have not yet been studied systematically so far as is known. The classical values determined titrimetrically by Fellenberg and Lunde[21] are widely used for many discussions, even at present,[7,22] in spite of doubts raised by several investigators. Noddacks' value[23] on the iodine in the earth's surface material is appreciably lower than Fellenberg's value; Urey[5] used the former value in his discussion of the concentration of certain elements at the earth's surface. Goles and Anders[24] determined

1) A part of this study was presented at the Meeting of the Volcanological Society of Japan, Fukuoka, Oct., 1968.
2) Present address: Department of Chemistry, Faculty of Science, Tōhō University, Izumi-chō, Narashino-shi.
3) V. M. Goldschmidt, *Fortschr. Mineral. Krist. Petr.*, **17**, 112 (1933); *J. Chem. Soc.*, **1937**, 659.
4) W. W. Rubey, *Bull. Geol. Soc. Am.*, **62**, 1111 (1951).
5) H. C. Urey, *Proc. Roy. Soc.*, **A219**, 281 (1953).
6) A. B. Ronov, *Geochemistry International*, **1964**, 713.
7) M. K. Horn and J. A. S. Adams, *Geochim. Cosmochim. Acta*, **30**, 279 (1966).
8) I. Iwasaki, T. Katsura, T. Ozawa, M. Yoshida, and B. Iwasaki, "The Crust and Upper Mantle of the Pacific Area," Geophysical Monograph No. 12, ed. by L. Knopf, C. L. Drake, and P. J. Hart, Am. Geophys. Union, Washington, D. C. (1968), p. 423.
9) C.W. Correns, "Physics and Chemistry of the Earth," Vol. 1, ed. by L. H. Ahrens, K. Rankama, and S. K. Runcorn, McGraw-Hill, New York (1956), p. 181.
10) M. Fleischer and W. O. Robinson, "Studies in Analytical Geochemistry," ed. by D.M. Shaw, Roy. Soc. Canada Spec. Publ. No. 6, Univ. Tronto Press (1963), p. 58.
11) W. D. Johns and W. H. Huang, *Geochim. Cosmochim. Acta*, **31**, 35 (1967).
12) I. Iwasaki, T. Katsura, N. Sakato, and M. Hirayama, *Nippon Kagaku Zasshi*, **78**, 164 (1957).
13) B. Iwasaki and T. Katsura, This Bulletin, **37**, 1827 (1964).
14) W. Behne, *Geochim. Cosmochim. Acta*, **3**, 186 (1953).
15) R. H. Filby, *Anal. Chim. Acta*, **31**, 434 (1963).
16) R. H. Filby, *Geochim. Cosmochim. Acta*, **29**, 49 (1965).
17) A. Wyttenbach, H. R. von Gunten, and W. Scherle, *ibid.*, **29**, 467 (1965).
18) G. W. Reed, Jr., and R. O. Allen, Jr., *ibid.*, **30**, 779 (1966).
19) G. G. Goles, L. P. Greenland, and D. Y. Jérome, *ibid.*, **31**, 1771 (1967).
20) T. Sugiura, This Bulletin, **41**, 1133 (1968).
21) Th. von Fellenberg and G. Lunde, *Biochem. Z.*, **175**, 162 (1926).
22) K. H. Wedepohl, "Origin and Distribution of the Elements," ed. by L. H. Ahrens, Pergamon Press, London (1968), p. 999.
23) I. Noddack and W. Noddack, *Svensk Kem. Tidskrift*, **46**, 173 (1934).
24) G. G. Goles and E. Anders, *Geochim. Cosmochim. Acta*, **26**, 723 (1962).

the iodine content of several meteorites by the neutron activation method and concluded that most of the iodine data in Fellenberg's study are systematically too high by factors of 5 to 30. Brown and Wolstenholme[25] could not detect iodine in their attempt to determine the minor components in G1 and W1 by spark-source mass spectrometry (limit of detection: 0.05 ppm). Crouch[26] investigated the applicability of a spectrophotometric method for the determination of iodine in silicate rocks and gave some data somewhat lower than Fellenberg's value, but his work has not been continued.

In our opinion, ordinary photometric methods, to say nothing of titrimetric methods, have too low sensitivities to be used in the determination of bromine and iodine in igneous rocks. The neutron activation method has, indeed, a very high sensitivity, but it requires special equipment and time-consuming procedures. The present authors have previously established photometric methods for the determination of bromine[27] and iodine[28] in silicate rocks based upon their catalytic effects on certain redox reactions. The bromine and iodine contents of about fifty volcanic rocks are here determined using these methods. Their fluorine and chlorine contents are also determined. The relations among the abundances of halogens themselves and those between the halogen contents and the other properties of rocks are discussed. The only report which has dealt with the contents of our halogens in the same rock is that of Kogarko and Gulyayeva[29] on the rocks in Lovozero alkalic massif. These rocks are, however, of a specific type and have unusually high halogen contents.

Experimental

The samples used for the present study cover various types of Japanese volcanic rocks. Three ultramafic rocks obtained from New Zealand and New Guinea were also analysed. All the samples were crushed in a steel Ellis mortar and finely pulverized in an agate mortar, with special caution taken against the contamination of the halogens.

The method of analysis will be described only briefly here; the details are given in the papers cited. The fluorine was determined as follows:[30] About 1 g of a sample was fused with sodium peroxide in a nickel crucible. After cooling, the cake was treated with a small amount of water, taking precautions against a violent reaction. The resultant solution and residue were transferred into a distillation flask. After the addition of about 30 m*l* of conc. sulfuric acid and a small amount of hydrazine sulfate, the fluorine was steam-distilled at about 140°C. The fluorine in the distillate (1 *l*) was determined by the photometric method, using zirconium and *p*-dimethylaminoazophenylarsonic acid.[31] The fluorine content of rocks can be determined with a precision of about ± 20 μg/g by this method.

The chlorine was determined by the method of Iwasaki *et al.*,[32] with some improvements.[33] About 0.2 g of a sample was fused with anhydrous sodium carbonate in a platinum crucible. After cooling, the chlorine was extracted with hot water and was determined by the photometric method, using mercuric thiocyanate. The chlorine content of rocks can be determined with a precision of about ± 10 μg/g by this method.

The bromine was determined by the method of Takahashi *et al.*[27] After 0.25—0.5 g of a sample had been fused with potassium hydroxide in a nickel crucible, the resulting cake was leached with water. The bromine in the solution was converted to the elementary form and extracted with benzene. Then, it was back-extracted into the aqueous phase by shaking it with a sodium hydroxide solution; it was determined by the photometric method on the basis of its catalytic action on the oxidation of iodine to iodate by potassium permanganate. The error in this method is about ± 0.03 μg at bromine of 0.50 μg and less at lower amounts.

The iodine was determined by the method of Yonehara *et al.*[28] After 0.5—1 g of a sample had been fused with potassium hydroxide in a nickel crucible, the resulting cake was treated with water and sulfuric acid. The iodine in the solution was converted to the elementary form and extracted with carbon tetrachloride. Then it was back-extracted into the aqueous phase by shaking it with a sodium hydroxide solution and determined by the photometric method on the basis of its catalytic action on the color-fading of a ferric thiocyanate complex. The iodine content of rocks can be determined with a precision of about ± 0.005 μg/g.

The water-soluble halogens in some rocks were determined by methods similar to that described by Iwasaki and Katsura.[13]

All the chemicals used were of analytical-reagent quality or were specially purified. Redistilled water was used throughout the analytical procedures. Blank tests were made on all the procedures of each analytical method.

Results and Discussion

Table 1 gives the results of the determination and some atomic ratios among halogens. The fluorine contents of these volcanic rocks range from 50 to 1700 μg/g; the arithmetic mean is 410 μg/g. The chlorine contents range from 17 to 1220 μg/g; the arithmetic mean is 270 μg/g. The F/Cl ratio is scattered over a wide range, from 0.43 to 45 (average 7.8). These results are consistent with those of the previous reports summarized in Table 2. The bromine contents range from 0.09 to 8.10 μg/g; the arithmetic mean is 0.85 μg/g. The Br/Cl ratio falls within a narrow range from 0.66×10^{-3} to 3.7×10^{-3} (average 1.5×10^{-3}). These values agree with those of Sugiura[20] and are lower than Behne's value.[14] The iodine contents range from 0.011 to 0.32 μg/g; the arithmetic mean is 0.088 μg/g. The

25) R. Brown and W. A. Wolstenholme, *Nature*, **201**, 598 (1964).
26) W. H. Crouch, Jr., *Anal. Chem.*, **34**, 1698 (1962).
27) K. Takahashi, M. Yoshida, T. Ozawa, and I. Iwasaki, This Bulletin, **43**, 3159 (1970).
28) N. Yonehara, M. Yoshida, and I. Iwasaki, This Bulletin, **43**, 3796 (1970).
29) L. N. Kogarko and L. A. Gulyayeva, *Geochemistry International*, **1965**, 729.
30) I. Iwasaki, "Jikken Kagaku Kōza" (Experimental Chemistry), Vol. 14, "Geochemistry" (in Japanese), ed. by The Chemical Society of Japan, Maruzen, Tokyo (1958), p. 333.
31) M. Kamada, T. Ōnishi, and M. Ōta, This Bulletin, **28**, 148 (1955); M. Kamada and T. Ōnishi, *Nippon Kagaku Zasshi*, **80**, 275 (1959).
32) I. Iwasaki, T. Katsura, and N. Sakato, *ibid.*, **76**, 1116 (1955).
33) I. Iwasaki, T. Ozawa, and M. Aoyagi, Read at the Symposium on Geochemistry of the Geochemical Society of Japan and the Chemical Society of Japan, Kanazawa, Oct. 1966.

Table 1. Halogen contents and ratio among them

No.	Sample	Content (μg/g)[a]				Atomic Ratio			
		F	Cl	Br	I	F/Cl	Br/Cl ($\times 10^{-3}$)	I/Cl ($\times 10^{-5}$)	I/Br
1	Basalt; Lava of 1950, Mihara-yama, Ô-shima, Tôkyô Metr.	110 (1.6)	310 (12)	0.83 (0.1)	0.082 (0.03)	0.66	1.2	7.4	0.062
2	Basalt; Okada, Ô-shima, Tôkyô Metr.	50	220	0.44	0.029	0.43	0.88	3.7	0.042
3	Basalt; Lava of 1962, Miyake-jima, Tôkyô Metr.	200 (3.0)	600 (14)	1.66	0.086 (0.00)	0.62	1.2	4.0	0.033
4	Basalt; Nishi-yama, Hachijô-jima, Tôkyô Metr.	70	245	1.24	0.13	0.53	2.2	15	0.066
5	Basalt; Sakasagawa, Itô, Shizuoka Pref.	250	100	0.32	0.084	4.7	1.4	24	0.17
6	Basalt; Lava of 864, Aokigahara, Fuji-san, Yamanashi Pref.	250 (40)	250 (50)	0.68	0.032	1.9	1.2	3.6	0.030
7	Basalt; Shirogane Lava, Tokachi-dake, Hokkaidô	300	430	1.38	0.072	1.3	1.4	4.7	0.033
8	Basalt; Orimoto-tôge, Shidara, Aichi Pref.	250	110	0.45	0.095	4.3	1.8	24	0.13
9	Basalt; Ôkuwa, Shidara, Aichi Pref.	400	150	0.41	0.14	5.0	1.2	26	0.20
10	Basalt; Yuto, Shidara, Aichi Pref.	210	155	0.50	0.10	2.5	1.4	18	0.13
11	Basalt; Iwano, Karatsu, Saga Pref.	370 (10)	45 (20)	0.16	0.029	15	1.6	18	0.11
12	Basalt; Taka-shima, Karatsu, Saga Pref.	420 (30)	420 (380)	1.31 (1.04)	0.046	—	—	—	—
13	Basalt; Kuniga, Nishino-shima, Oki, Shimane Pref.	1200	50	0.24	0.042	45	2.1	24	0.11
14	Basalt; Imazu, Saigô, Oki-Dôgo, Shimane Pref.	520	280	0.75	0.018	3.5	1.2	1.8	0.015
15	Basalt; Inamura-dake, Satsuma-iwô-jima, Kagoshima Pref.	190	190	1.03	0.12	1.9	2.4	18	0.073
16	Trachyandesitic Basalt; South of Ôkuwa, Shidara, Aichi Pref.	370	35	0.09	0.070	20	1.1	56	0.49
17	Nepheline basalt; Nagahama, Hamada, Shimane Pref.	1700 (10)	90 (30)	0.26	0.045	35	1.3	14	0.11
18	Dolerite; Kawai, Shidara, Aichi Pref.	330	32	0.15	0.096	19	2.1	84	0.40
19	Andesite; Lava of 1914, Sakura-jima, Kagoshima Pref.	300	n.d.	n.d.	0.082	—	—	—	—
20	Andesite; Lava of 1946, Sakura-jima, Kagoshima Pref.	350 (9.8)	330 (17)	1.45 (0.05)	0.042 (0.01)	2.0	1.9	3.6	0.018
21	Andesite; Iwô-dake, Satsuma-iwô-jima, Kagoshima Pref.	430	130	1.08	0.052	6.2	3.7	11	0.030
22	Andesite; Haha-jima, Bonin Islands, Tôkyô Metr.	200	640	2.02	0.23	0.58	1.4	10	0.072
23	Andesite; Kami-futago-yama, Hakone, Kanagawa Pref.	180	240	0.83	0.091	1.4	1.5	11	0.069
24	Andesite; Lava of 1783, Asama-yama, Gumma Pref.	240	360	1.40	0.25	1.3	1.7	19	0.11
25	Andesite; Sasshô-gawara, Kusatsu-shirane-san, Gumma Pref.	110	150	1.12	0.26	1.4	3.3	49	0.15
26	Andesite; Bomb ejected in 1962, Tokachi-dake, Hokkaidô	370	620	1.89	0.15	1.1	1.3	6.8	0.050
27	Andesite; Lava of parasitic crater (Minami Kakô), Yôtei-zan, Hokkaidô	620	220	0.60	0.022	5.3	1.2	2.8	0.023
28	Andesite; Lava of Yake-yama, Tamagawa-hotspring, Akita Pref.	420 (12)	100 (16)	0.20 (0.1)	n.d.	7.9	0.88	—	—
29	Andesite; Kuniga, Nishino-shima, Oki, Shimane Pref.	1200	90	0.18	0.064	25	0.88	20	0.22
30	Glassy andesite; Shôwa-iwô-jima, Satsuma-iwô-jima, Kagoshima Pref.	550	600	2.60	0.13	1.7	1.9	6.1	0.032
31	Dacitic andesite; Lava of young somma, Sukomogawa, Hakone, Kanagawa Pref.	230	70	0.18	0.070	6.1	1.1	28	0.25
32	Dacitic andestite; Sambe-yama, Shimane Pref.	250	160	0.48	0.032	2.9	1.3	5.6	0.042
33	Trachyandesite; Iwô-jima, Sulfur Islands, Tôkyô Metr.	750	100	0.50	0.26	14	2.2	73	0.33

TABLE 1. Continued

No.	Sample	Content (μg/g)[a]				Atomic Ratio			
		F	Cl	Br	I	F/Cl	Br/Cl ($\times 10^{-3}$)	I/Cl ($\times 10^{-5}$)	I/Br
34	Trachyte; Funakoshi, Nishino-shima, Oki, Shimane Pref.	370	100	0.20	0.036	6.9	0.88	10	0.11
35	Phonolitic trachyte; Tokage-iwa, Tsuzurao-yama, Fuse, Oki-Dôgo, Shimane Pref.	240	17	0.12	0.080	26	3.1	130	0.42
36	Dacite; Shôwa-shinzan, Usu, Hokkaidô	80	50	0.24	0.051	3.0	2.1	29	0.13
37	Dacite; Ôusu-dake, Usu, Hokkaidô	260	60	0.21	0.034	8.1	1.5	16	0.10
38	Dacite; Onigashiro, Yake-yama, Akita Pref.	530	610	2.10	0.22	1.6	1.5	10	0.066
39	Dacite; Lava of somma, Numajirigawa, Akagi-yama, Gumma Pref.	270 (3.8)	30 (7)	0.14 (0.0)	0.066 (0.01)	17	2.1	62	0.30
40	Liparite; Kôzu-shima, Tôkyô Metr.	250 (2.8)	910 (320)	2.52 (1.10)	0.073 (0.01)	0.51	1.2	2.3	0.018
41	Liparite; Nii-jima, Tôkyô Metr.	230 (20)	750	1.42	0.011	0.57	0.83	0.41	0.0049
42	Liparite; Shikine-jima, Tôkyô Metr.	220	630	1.05	0.062	0.65	0.73	2.8	0.037
43	Rhyolitic rock; Nishida, Saigô, Oki-Dôgo, Shimane Pref.	1100	50	0.10	0.026	41	0.88	15	0.16
44	Potash liparite; Manzô-yama, Shimoda, Shizuoka Pref.	50	30	0.15	0.14	3.1	2.2	130	0.59
45	Alkali rhyolite; Madara-jima, Saga Pref.	640 (40)	1220 (1150)	8.10 (7.80)	0.32	—	—	—	—
46	Obsidian; Shirataki, Hokkaidô	440 (3.4)	800 (6)	1.20 (0.00)	0.020 (0.01)	1.0	0.66	0.70	0.011
47	Obsidian; Koshi-dake, Imari, Saga Pref.	490 (6.6)	620 (7)	1.84 (0.1)	0.057 (0.01)	1.5	1.3	2.6	0.020
48	Obsidian; Hime-shima, Ôita Pref.	490 (48)	160 (3)	0.27 (0.0)	0.065 (0.04)	5.7	0.74	11	0.15
49	Glassy rock; Igo, Nakamura, Oki-Dôgo, Shimane Pref.	1000	660	2.28	0.11	2.8	1.5	4.7	0.030
50	Dunite; Dun Mountain, New Zealand	20	50	0.34	0.13	0.8	3.0	73	0.24
51	Harzburgite; Red-Hill, New Zealand	20	<10	0.15	0.078	>3.7	>6.6	>210	0.33
52	Peridotite; New Guinea	10	<10	0.24	0.070	>1.9	>10	>190	0.18

a) Numerical values in parentheses are contents of the water-soluble halogens

I/Cl ratio is scattered over a wide range, from 0.41×10^{-5} to 130×10^{-5} (average 23×10^{-5}). These values are appreciably lower than Fellenberg's value,[21] which is generally accepted. The rocks in Lovozero alkalic massif have very high halogen contents, as is shown in Table 2d.[29] The ratios among halogens are, however, in good agreement with those of the present study.

The amounts of the water-soluble halogens are usually small as compared with those of the total halogens. Some specimens (No. 12, No. 45) contain unusually large amounts of the water-soluble chlorine and bromine. They were obtained at localities near the sea and are possibly contaminated. The data on these specimens are excluded from the calculation of the ratios and the mean values. However, we do not think that all the water-soluble halogens have their origin in contamination.

The abundance of each halogen does not show any marked relationship to the type of rock, as many authors

TABLE 2. HALOGEN CONTENTS OF IGNEOUS ROCKS IN THE LITERATURE

a) F in Volcanic Rocks (mainly from Fleischer and Robinson[10])

Rock Name	No. of Samples	F (μg/g) Range	F (μg/g) Average
Basalt	268	20—2400	380
Andesite	83	0— 780	230
Rhyolitic Rocks[a]	145	0—6850	700
Phonolite, Trachyte	51	830—1490	920

a) Rhyolite, Liparite, Obsidian

b) Cl in Volcanic Rocks

Rock Name	No. of Samples	Cl (μg/g) Range	Cl (μg/g) Average
Basaltic Rocks[a,b]	279	30—890	160
Basalt[c] (Japan & North-eastern China)	84	80—890	230
Basalt[d] (Hawaii)	110	60—300	100
Andesite, Dacite[b]	109	20—3900	230
Andesite, Dacite[c] (Japan)	82	30—3900	250
Rhyolitic Rocks[b,e]	94	20—7900	550
Rhyolitic Rocks[c] (Japan)	6	240—690	550

a) Basalt, Diabase
b) All the data available including c), d); others are from Johns and Huang[11]
c) from I. Iwasaki, *et al.*[12]
d) from B. Iwasaki and Katsura[13]
e) Rhyolite, Liparite, Obsidian

c) Br in Volcanic Rocks (from Sugiura[20])

Rock Name	No. of Samples	Br (μg/g) Range	Average
Basalt	6	<0.2—2.0	0.6
Andesite[a]	9	<0.2—1.3	0.6
Dacite	6	<0.2—0.3	0.2
Glassy Rock[b]	7	0.3—5.5	2.2
Br/Cl (atomic), all	(<0.5—8)×10^{-3}	average 1.5×10^{-3}	

a) including one sample of Sanukite
b) Hyaloliparite, Obsidian, Pearlite, Pitchstone and Pyroclastic rock

d) Halogen in Lovozero Alkalic Rocks (from Kogarko and Gulyayeva[29])

	No. of Samples	Content or Ratio (atomic) Range	Average
F	21	n×10^{-3}—1.05%	0.21%
Cl	23	trace-2.75%	0.49%
Br	24	(0.02—3.28)×10^{-3}%	0.60×10^{-3}%
I	24	trace-0.13×10^{-3}%	0.06×10^{-3}%
F/Cl	21	0.02—98	8.4
Br/Cl	22	(0.09—1.8)×10^{-3}	0.60×10^{-3}
I/Cl	21	(0.2—7.0)×10^{-4}	1.4 ×10^{-4}

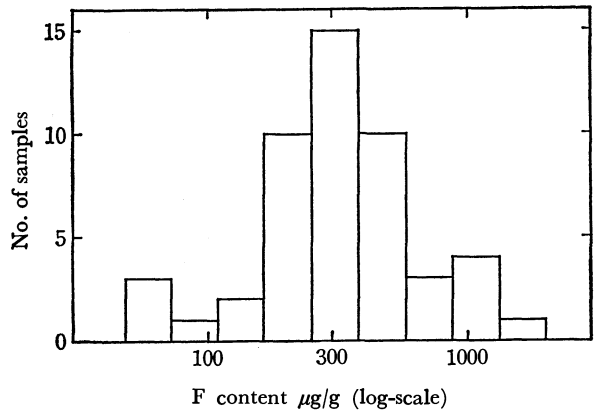

Fig. 1. Frequency distribution of fluorine content in volcanic rocks.

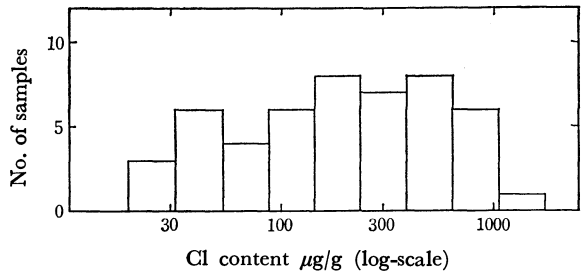

Fig. 2. Frequency Distribution of chlorine content in volcanic rocks.

have pointed out.[8-12,20] All we can say is that some glassy rocks have high chlorine and bromine contents, and that some rocks from alkaline rock provinces have high fluorine contents.

Figures 1—4 give the frequency distribution of each halogen content of the volcanic rocks analysed in this study. They show approximate lognormalities.

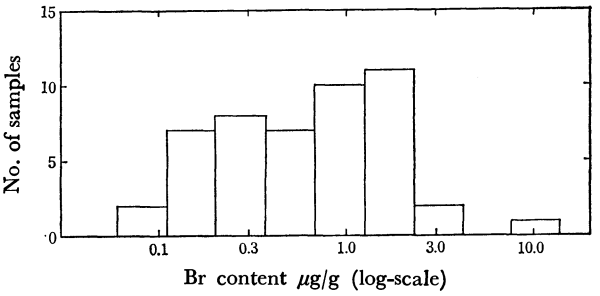

Fig. 3. Frequency distribution of bromine content in volcanic rocks.

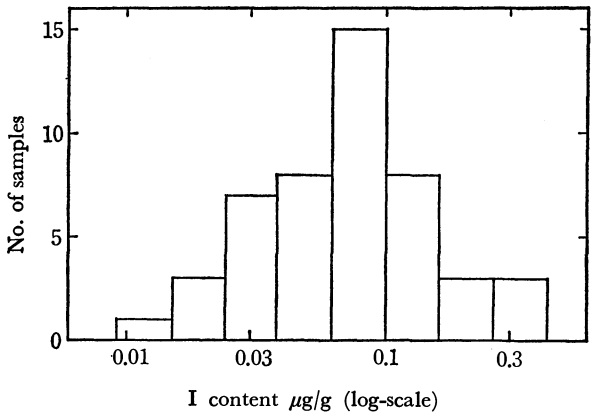

Fig. 4. Frequency distibution of iodine content in volcanic rocks.

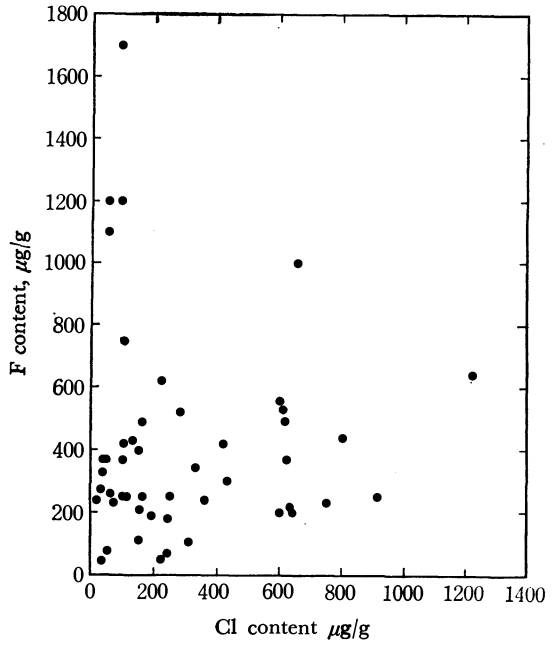

Fig. 5. Relation between chlorine content and fluorine content.

Strictly speaking, the fluorine and chlorine contents show deviations from the log-normal type distribution when they are plotted on cumulative frequency diagrams. The number of samples are, however, insufficient for a further discussion of the distribution of the halogens.

The correlations among halogens are shown in Figs. 5—9: F—Cl in Fig. 5, Br—Cl in Fig. 6, I—Cl in

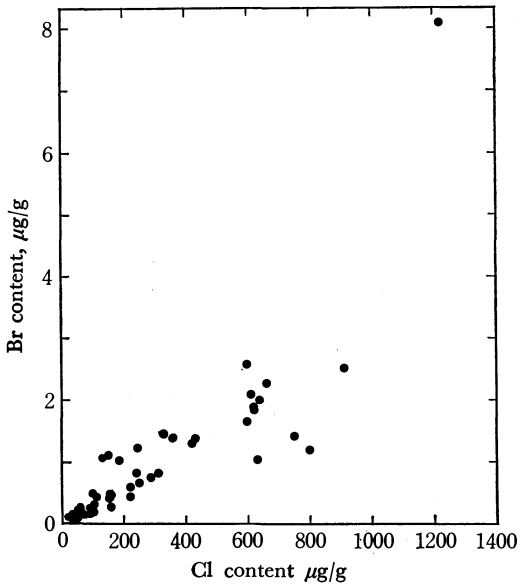

Fig. 6. Relation between chlorine content and bromine content.

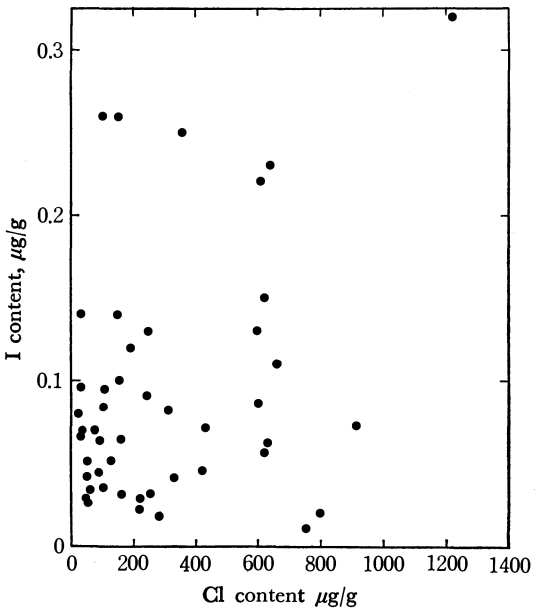

Fig. 7. Relation between chlorine content and iodine content.

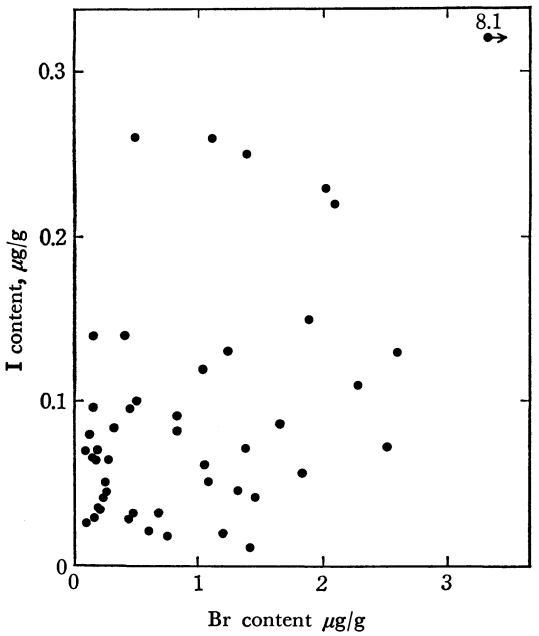

Fig. 8. Relation between bromine content and iodine content.

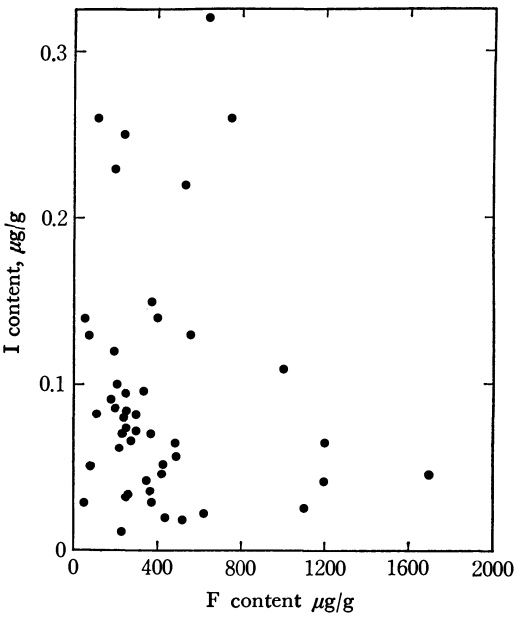

Fig. 9. Relation between fluorine content and iodine content.

Fig. 7, I—Br in Fig. 8, and I—F in Fig. 9. The chlorine and bromine contents are strongly correlated, as may be seen in Fig. 6. On the contrary, the other figures show no correlation at all. These findings indicate that in the process of the formation of volcanic rocks halogen behave in markedly different ways except for the similarity between chlorine and bromine. According to recent investigations, a primary factor governing their halogen contents is thought to be the distribution of volatile halogen compounds between the molten silicate phase and the gas phase. Kuroda and Sandell[34] stated that much of the chlorine escapes as hydrogen chloride formed by the reaction: $Cl^- + H_2O \rightleftharpoons HCl + OH^-$. Kogarko and Ryabchikov[35] discussed the relation between the fluorine and chlorine contents in gas and the chemical composition of the condensed phases in equilibrium with the gas on the basis of this reaction: $2X^-_{melt} + H_2O_{gas} = O^{2-}_{melt} + 2HX_{gas}$. Iwasaki and Katsura[36] discussed the chlorine content of volcanic rocks on the basis of the solubility of hydrogen chloride in rock melts. All the volatile components in the igneous rock have usually been regarded in the same light despite the distinctive chemical property of each of them. If the distribution of the four halogens was controlled mainly by the same mechanism

34) P. K. Kuroda and E. B. Sandell, *Bull. Geol. Soc. Am.*, **64**, 879 (1953).

35) L. N. Kogarko and I. D. Ryabchikov, *Geochemistry*, **1961**, 1192.

36) B. Iwasaki and T. Katsura, This Bulletin, **40**, 554 (1967).

Table 3. Ratios among halogens in volcanic gases

Locality	Temperature °C	No. of samples	Ratio	
			Range	Average
F/Cl				
Eleven Volcanoes in Japan[40]	95—760	23	<0.001—0.65	0.14
Satsuma-iwô-jima[39] A	350—745	23	0.050—0.44	0.14
Satsuma-iwô-jima[39] B	150—350	7	0.023—0.24	0.12
Satsuma-iwô-jima[39] C	<150	20	<0.005—13	0.99
Five Volcanoes in Japan[37]	141—813	27	<0.001—0.64	0.32
Br/Cl				
Five Volcanoes in Japan[37]	141—813	27	$(0.2—1.1)\times10^{-3}$	$0.6_2\times10^{-3}$
I/Cl				
Eight Volcanoes in Japan[38]	96—759	69	$(0.047—3.6)\times10^{-4}$	1.1×10^{-4}

the halogen contents of volcanic rocks should be intimately correlated with each other. From our results, chlorine and bromine may be taken as an illustration of this. On the other hand, the behavior of fluorine and iodine must be controlled by other factors. The ratios among halogens in natural volcanic gases are listed in Table 3.[37-40] A comparison between the data in Table 3 and the data of the present study shows that the F/Cl ratio in the gases is appreciably lower than that of volcanic rocks, as was stated in our previous reports.[39-42] The Br/Cl and I/Cl ratios in the gases are nearly equal to, or a little smaller than, those of the volcanic rocks. The same relations concerning F/Cl, Br/Cl, and I/Cl can be observed between gases evolved from volcanic rocks on heating and the original rocks used in the experiments.[40-43] The difference in behavior between fluorine and chlorine may be attributed to the formation of stable metal-fluorine complexes in rock melts, as was suggested by Kogarko *et al.*[35] Several factors which may control the distribution of iodine have been suggested: its large ionic size, its possible occurence as an elemental form, its chalcophile properties, *etc.* At present, we have no way to decide which of them is the main factor.

A regional difference is observed with regard to some ratios among halogens. The rocks from the Izu Seven Islands have low F/Cl and I/Br ratios; on the contrary, the rocks from the Circum-Japan Sea Province have high F/Cl and I/Br ratios, with a few exceptions. These two petrographic provinces have already been said to be in marked contrast to one another.[44]

The ultra-basic rocks analysed have very low chlorine and fluorine contents as compared with volcanic rocks. The results agreed with those of Stueber *et al.*[45] The bromine content is slightly lower than those of volcanic rocks, while the iodine content is almost the same as those of volcanic rocks. As a result, their Br/Cl and I/Cl ratios are appreciably higher than those of the volcanic rocks. This fact is interesting for showing the difference in the behavior of bromine and iodine from that of fluorine and chlorine duing the formation of magma in the mantle.

The authors wish to express their thanks to the Research Fund of the Kawakami Memorial Foundation for a research grant partly used in this work.

37) T. Sugiura, Y. Mizutani, and S. Oana, *J. Earth Sci. Nagoya Univ.*, **11**, 272 (1963).
38) F. Honda, Y. Mizutani, T. Sugiura, and S. Oana, This Bulletin, **39**, 2690 (1966).
39) M. Yoshida, T. Ozawa, and M. Kamada, *Nippon Kagaku Zasshi*, **90**, 163 (1969).
40) M. Yoshida, *Bull. Tokyo Inst. Technol.*, **No. 57**, 27 (1964).
41) M. Yoshida, This Bulletin, **36**, 773 (1963).
42) M. Yoshida, I. Makino, N. Yonehara, and I. Iwasaki, *ibid.*, **38**, 1436 (1965).
43) T. Sugiura, *ibid.*, **41**, 1588 (1968).
44) H. Kuno, "Volcanoes and Volcanic Rocks" (in Japanese), Iwanami, Tokyo (1954), p. 229.
45) A. M. Stueber, W. H. Huang, and W. D. Johns, *Geochim. Cosmochim. Acta*, **32**, 353 (1968).

^{55}Mn Nuclear Magnetic Resonance Studies of the Compounds with Manganese-Tin Bonds

Satoru ONAKA,* Takeshi MIYAMOTO, and Yukiyoshi SASAKI

Department of Chemistry, Faculty of Science, The University of Tokyo, Bunkyo-ku, Tokyo

(Received February 3, 1971)

The nature of Mn–Sn bonds has been studied by ^{55}Mn-NMR and IR spectroscopies of a series of compounds, $R_{3-x}X_xSn-Mn(CO)_5$, where R is C_6H_5 or CH_3 and where X is Cl or Br. Molecular orbital considerations have shown that the chemical shift of the ^{55}Mn-NMR spectra is a measure of the σ-polarity of the L–Mn bond in L–$Mn(CO)_5$-type complexes, and that the linewidth is mainly determined by the π-interaction between Mn and Sn. The π-interaction (back-donation from Mn to Sn) seems to be most pronounced in $Br_3Sn-Mn(CO)_5$ in the series of $(CH_3)_{3-x}Br_xSn-Mn(CO)_5$ compounds. The relationships among the chemical shift, the wave numbers of CO stretching modes, and the eqQ are also shown.

The aim of the present report is to ascertain, by the aid of the ^{55}Mn-NMR, the σ-character and the π-character of metal-metal bonds in the complexes, $R_{3-x}X_xSn-Mn(CO)_5$, which have been studied using Mössbauer spectroscopy,[1] where X and R stand for Cl, Br and C_6H_5, CH_3 respectively.

The L–$M(CO)_5$-type compounds, where L and M represent a ligand and a metal atom respectively, have been extensively investigated, since the octahedral symmetry around the metal atom permits the independent treatment of the σ- and the π-characteristics of the chemical bonds in these complexes.[2–9] The most successful method thus far employed to study these complexes is to measure the CO stretching frequencies in the infrared region and to interpret the data in terms of the σ- or the π-electron donation from L to M or the back donation from M to L, including cases of M–M′ bonds.[10] According to Graham,[10] these two donation powers can be quantitatively expressed by the two parameters, σ and π, which can be calculated from the CO stretching data. We have found that the NMR spectra of ^{55}Mn offer useful information concerning these two characteristics.

Some NMR data on organometallic compounds containing the Mn atom have been reported by Calderazzo, Lucken, and Williams[11] and by Miles *et al.*,[12] but no compound containing metal–metal bonds has thus far been subjected to similar study.

The NQR techniques were also introduced by Brown to the study of metal–metal bonds in cobalt complexes with a C_{3v} symmetry.[13,14]

Experimental

Materials. All the compounds except $(CH_3)Cl_2Sn-Mn(CO)_5$, $(CH_3)_2BrSn-Mn(CO)_5$, and $(CH_3)Br_2Sn-Mn(CO)_5$ were prepared by the methods of Gorsich[15] and Graham.[16] All the reactions were carried out under a dried nitrogen atmosphere.

$(CH_3)_2BrSn-Mn(CO)_5$: A solution of $NaMn(CO)_5$ was prepared from 5.9 g (0.015 mol) of $Mn_2(CO)_{10}$ in 100 m*l* of anhydrous tetrahydrofuran (THF) by stirring the mixture over an excess of 1% sodium amalgam; it was then slowly dropped into a stirred solution of 9.24 g (0.03 mol) of $(CH_3)_2SnBr_2$ in 100 m*l* of THF. The THF solution was kept overnight in a refrigerator. The organic layer separated from fine precipitates by using a centrifugal separator was condensed under reduced pressure. The yellow residue thus obtained was recrystallized from hexane at 0°C; yellow crystals were then obtained by filtration (yield, 80%).

Found: C, 19:96; H, 1.25%. Calcd for $C_7H_6O_5BrMnSn$: C, 19.84; H, 1.43%.

$(CH_3)Cl_2Sn-Mn(CO)_5$: A mixture of 2.1 g (0.005 mol) of $Cl_3Sn-Mn(CO)_5$ and an equimolar amount of $(CH_3)_2ClSn-Mn(CO)_5$ was heated at 130°C for 10 min. The crude product was recrystallized from hexane to give 2.9 g of pale yellow crystals (yield, 50%).

Found: C, 18.18; H, 0.68%. Calcd for $C_6H_3O_5Cl_2MnSn$: C, 18.03; H, 0.76%.

$(CH_3)Br_2Sn-Mn(CO)_5$: A mixture of 1.95 g (0.0035 mol) of $Br_3Sn-Mn(CO)_5$ and 0.63 g (0.00175 mol) of $(CH_3)_3Sn-Mn(CO)_5$ was heated at 130°C for an hour. The crude product was then recrystallized from hexane to give 0.71 g of yellow crystals (yield, 28%).

Found: C, 14.77; H, 0.45%. Calcd for $C_6H_3O_5Br_2MnSn$: C, 14.75; H, 0.62%.

The purities were determined by carbon and hydrogen analyses and by melting-point or decomposition-point measurements.

NMR Spectra. The ^{55}Mn-NMR spectra were registered as derivative curves at 10 KOe and 10.55 MHz on a Varian

* Present address: Department of Chemistry, Nagoya Institute of Technology, Showa-ku, Nagoya.

1) S. Onaka, Y. Sasaki, and H. Sano, This Bulletin, **44**, 726 (1971).
2) L. E. Orgel, *Inorg. Chem.*, **1**, 25 (1962).
3) J. Dalton, I. Paul, J. G. Smith, and F. G. A. Stone, *J. Chem. Soc., A*, **1968**, 1195.
4) F. A. Cotton and C. S. Kraihanzel, *J. Amer. Chem. Soc.*, **84**, 4432 (1962).
5) C. S. Kraihanzel and F. A. Cotton, *Inorg. Chem.*, **2**, 533 (1963).
6) F. A. Cotton, *ibid.*, **3**, 702 (1964).
7) R. J. Angelici, *J. Inorg. Nucl. Chem.*, **28**, 2627 (1966).
8) D. J. Darensbourg and T. L. Brown, *Inorg. Chem.*, **7**, 959 (1968).
9) S. Evans, J. C. Green, M. L. H. Green, A. F. Orchard, and D. W. Turner, *Discuss. Faraday Soc.*, **47**, 112 (1969).
10) W. A. G. Graham, *Inorg. Chem.*, **7**, 315 (1968).
11) F. Calderazzo, E. A. C. Lucken, and D. F. Williams, *J. Chem. Soc., A*, **1967**, 154.
12) W. J. Miles, Jr., B. B. Garrett, and R. J. Clark, *Inorg. Chem.*, **8**, 2817 (1969).
13) T. L. Brown, P. A. Edwards, C. B. Harris, and J. L. Kirsch, *ibid.*, **8**, 763 (1969).
14) D. D. Spencer, J. L. Kirsch, and T. L. Brown, *ibid.*, **9**, 235 (1970).
15) R. D. Gorsich, *J. Amer. Chem. Soc.*, **84**, 2486 (1962).
16) W. Jetz, P. B. Simons, J. A. J. Thompson, and W. A. G. Graham, *Inorg. Chem.*, **5**, 2217 (1966).

Table 1. ^{55}Mn-NMR chemical shift, linewidth and CO stretching frequencies

	Compound	Chemical shift (ppm±10)	Linewidth (oersted±0.01)	CO-Stretching frequencies (cm^{-1})		
				A_1^2	E	A_1^1
1.	Cl_3Sn–$Mn(CO)_5$	2024	0.18	2126	2046	2040
2.	Br_3Sn–$Mn(CO)_5$	2044	0.17	2124	2045	2038
3.	$PhCl_2Sn$–$Mn(CO)_5$	2278	0.30	2116	2033	2025
4.	$(CH_3)Cl_2Sn$–$Mn(CO)_5$	2312	0.28	2114	2032	2020
5.	$PhBr_2Sn$–$Mn(CO)_5$	2252	0.24	2116	2034	2026
6.	$(CH_3)Br_2Sn$–$Mn(CO)_5$	2256	0.25	2116	2034	2021
7.	Ph_2ClSn–$Mn(CO)_5$	2460	1.45	2104	2017	2013
8.	$(CH_3)_2ClSn$–$Mn(CO)_5$	2520	1.10	2102	2008	2016
9.	Ph_2BrSn–$Mn(CO)_5$	2468	1.70	2106	2019	2010
10.	$(CH_3)_2BrSn$–$Mn(CO)_5$	2485	1.00	2104	2010	2018
11.	Ph_3Sn–$Mn(CO)_5$	2610	3.57	2095	2004	2004
12.	$(CH_3)_3Sn$–$Mn(CO)_5$	2660	1.58	2090	1994	2002
13.	$Mn_2(CO)_{10}$	2331	<0.1			
14.	Cl–$Mn(CO)_5$[a]	1005	0.182			
15.	Br–$Mn(CO)_5$[a]	1160	0.378			
16.	I–$Mn(CO)_5$[a]	1485	0.557			
17.	CF_3–$Mn(CO)_5$[a]	1850	1.76			
18.	CF_3CO–$Mn(CO)_5$[a]	1850	1.83			
19.	CHF_2–$Mn(CO)_5$[a]	1970	2.30			
20.	CH_2F–$Mn(CO)_5$[a]	2130	2.38			
21.	CH_3–$Mn(CO)_5$[a]	2265	1.69			
22.	H–$Mn(CO)_5$[a]	2630	2.39			
23.	CH_3CO–$Mn(CO)_5$[a]	1895	2.11			
24.	$NaMn(CO)_5$[a]	2780	5.82			

a) F. Calderazzo, E. A. C. Lucken, and D. F. Williams, *J. Chem. Soc.*, *A*, **1967**, 154.

Associates VF-16 NMR spectrometer at room temperature. The manganese samples were sealed, as 0.25 mol solutions in methylene chloride, into glass tubes 8 mm in diameter under a nitrogen atmosphere. An aqueous solution of potassium permanganate (10% concentration) was used as the external standard. The linewidth, ΔH, was represented by the interval between the points of the maximum slopes.

Infrared Spectra. The spectra in the CO-stretching region were recorded with a Hitachi EPI-G2 spectrometer in hexane solutions (2—3 mg/m*l* except Cl_3Sn–$Mn(CO)_5$) with a 0.1-mm KBr liquid cell. The spectra of Cl_3Sn–$Mn(CO)_5$ were measured with a KBr variable-path-length liquid cell in a hexane solution because of its low solubility in the solvent.

All the results of the NMR and IR measurements are listed in Table 1, together with some data cited from the report by Calderazzo *et al.*[11]

Discussion

Infrared Spectra. Graphs presenting the linear relationship between the infrared wave numbers of A_1^2, A_1^1, and E modes and the chemical shift are shown in Fig. 1. The force constants, not found in the literature, of $R_{3-x}Br_xSn$–$Mn(CO)_5$ were obtained by the method of Cotton and Kraihanzel[4]; the results are listed in Table 2, along with the values of k_2, k_1, k_i and σ- and π-parameters[10] for the compounds $R_{3-x}Br_xSn$–$Mn(CO)_5$ (R is CH_3 and C_6H_5).

NMR Data. The NMR data in Table 1 show that the successive substitution of the halogen atoms on the tin atom by phenyl or methyl groups results in changes in the chemical shift of ^{55}Mn as large as 600 ppm. The chemical shift increases almost linearly with the number of the organic group on the tin atom, as

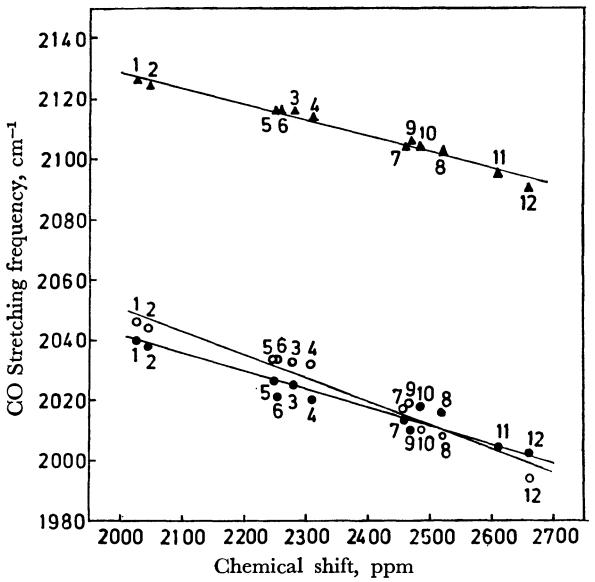

Fig. 1. Stretching frequency of A_1^2, A_1^1, and E bands *versus* ^{55}Mn-chemical shift. Upper series assigned as A_1^2 and lower series as E and A_1^1. Points labeled by ○ and ● correspond to E and A_1^1 bands respectively. The numbers in the graphs represent the compounds in Table 1.

TABLE 2. CO STRETCHING FORCE CONSTANTS AND GRAHAM'S σ- AND π-PARAMETER

Compound	Force constant, mdyn/Å			Graham's σ- and π-parameter, mdyn/Å	
	k_1	k_2	k_i	σ	π
$Br_2PhSn-Mn(CO)_5$	16.67	17.14	0.21	0.08	0.24
$Br_2(CH_3)Sn-Mn(CO)_5$	16.59	17.13	0.21	0.14	0.17
$BrPh_2Sn-Mn(CO)_5$	16.62	16.85	0.19	−0.45	0.48
$Br(CH_3)_2Sn-Mn(CO)_5$	16.60	16.80	0.24	−0.53	0.51

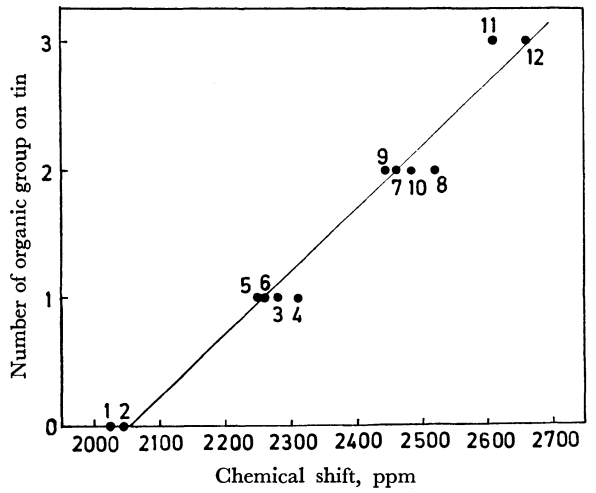

Fig. 2. Effect of organic groups on ^{55}Mn-chemical shift.

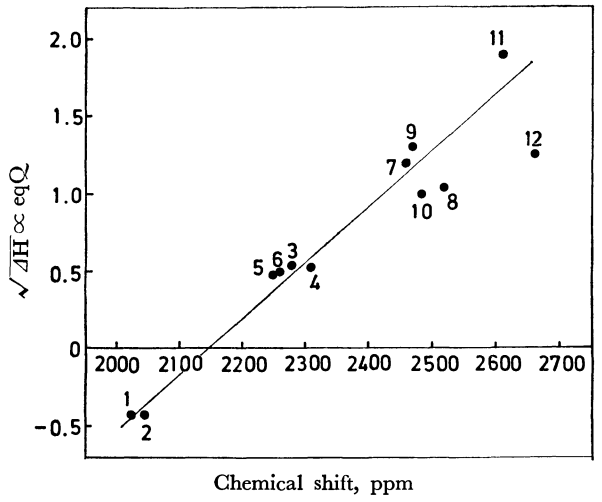

Fig. 3. The relationship between chemical shift and quadrupolar coupling constant. The signs of $\sqrt{\Delta H} \propto eqQ$ for $X_3Sn-Mn(CO)_5$ are chosen as minus signs.

is shown in Fig. 2.[17] On the other hand, the change in halogen atoms in $X_xR_{3-x}Sn-Mn(CO)_5$ from Cl to Br causes only a slight shift, as is shown in Table 1. All the NMR data can be most conveniently presented on the $\sqrt{\Delta H}$ *versus* chemical-shift graph given in Fig. 3. A remarkable feature of the graph, which is a characteristic of the compounds containing Sn–Mn bonds, is that the linewidth narrows drastically from $Ph_3Sn-Mn(CO)_5$ to $X_3Sn-Mn(CO)_5$, along with the change in the ligands on the tin atom. In the $CH_xF_{3-x}-Mn(CO)_5$ series, no such abrupt narrowing has been reported.[11] The sign of $\sqrt{\Delta H}$ is not obtained from the experiments described in this paper, but a change in the sign of the field gradient between $X_3Sn-Mn(CO)_5$ and $X_2RSn-Mn(CO)_5$ in the present series of compounds is suggested by the data shown in Fig. 3.

As we have reported previously,[1] the plotting of the NMR chemical shift of ^{55}Mn against the isomer shift of the ^{119}Sn-Mössbauer spectra suggests that the ^{55}Mn-chemical shift can be interpreted in terms of the σ-electron transfer from Mn to Sn. This finding that the ^{55}Mn-chemical shift can be interpreted in terms of the σ-character of the L–Mn bond is substantiated by the following relationship. As is shown in Fig. 4, the ^{55}Mn-chemical shift is linear to the σ-parameters[18] which are concerned with the σ-character of the L–Mn bond.[19] For these reasons, the following molecular orbital considerations are acceptable.

According to Ramsey,[21] the so-called paramagnetic shift, which mainly determines the variations in the chemical shift of transition elements, is given by the

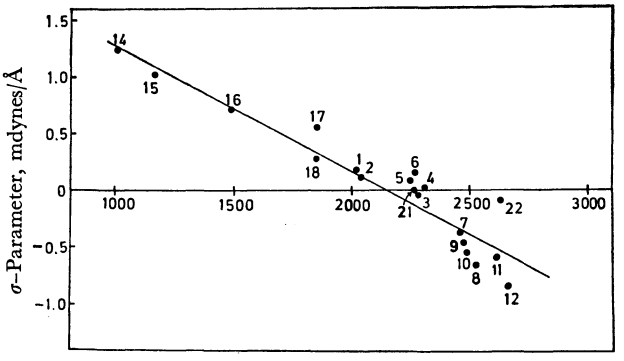

Fig. 4. The relationship between ^{55}Mn-chemical shift and Graham's σ-parameter. Graham's σ-parameters are cited from the literature, (W. A. G. Graham, *Inorg. Chem.*, **7**, 315 (1968).), and from Table 2.

17) The linearity of the chemical shift with the sum of the electronegativity of the halogen atoms on tin is also observed. The analogous linearity of the CO stretching frequencies with the sum of the electronegativity of the halogen atoms on tin has been already reported by Patmore, Thompson, and Graham in cases of the complexes $R_{3-x}X_xGe-Co(CO)_4$ and $R_{3-x}X_xSn-Mn(CO)_5$: D. J. Patmore and W. A. G. Graham, *Inorg. Chem.*, **6**, 981 (1967), J. A. J. Thompson and W. A. G. Graham, *ibid.*, **6**, 1875 (1967).

18) Graham's σ-and π-parameters are obtained by the use of these formulae: $k_1=\sigma+2\pi+c_1$, $k_2=\sigma+\pi+c_2$. He rather arbitrarily assumed that $\sigma=\pi=0$ for the $CH_3-Mn(CO)_5$ complex in order to fix the two constants c_1 and c_2.

19) The correspondence of σ-bond polarity with the "σ-parameter" calculated from infrared data has been reported for many cases.[7,17,20]

20) F. R. Dean and J. C. Green, *J. Chem. Soc.*, *A*, **1968**, 3047.

21) N. F. Ramsey, *Phys. Rev.*, **78**, 699 (1950).

expression:

$$\sigma_p = -\frac{e^2}{2m^2c^2}\sum_{n\neq 0}(E_n-E_0)^{-1}[\langle\psi_0|\sum_i l_i|\psi_n\rangle\langle\psi_n|\sum_k l_k r_k^{-3}|\psi_0\rangle + \langle\psi_n|\sum_i l_i|\psi_0\rangle\langle\psi_0|\sum_k l_k r_k^{-3}|\psi_n\rangle]$$

where ψ_0 and ψ_n denote wave functions of, respectively, the ground and excited states of the atom in question, and where l_i and r_i are angular operators and the distance from the metal nucleus to the i-th electron. Single-electron molecular energy schemes for L–Mn-$(CO)_5$ have been reported by Gray and Billing[22] and by Anderson and Brown.[23] The one-electron d-d transitions from the ground state ($^1A_1$) are:

$$b_2\ (\pi, 3d_{xy}) \longrightarrow b_1\ (\sigma^*, 3d_{x^2-y^2}),\ (^1A_1-{}^1A_1),\ \Delta E_1$$
$$b_2\ (\pi, 3d_{xy}) \longrightarrow a_1\ (\sigma^*, 3d_{z^2}),\ (^1A_1-{}^1B_2),\ \Delta E_2$$
$$e\ (\pi, 3d_{xy,yz}) \longrightarrow b_1\ (\sigma^*, 3d_{x^2-y^2}),\ (^1A_1-{}^1E_u),\ \Delta E_3$$
$$e\ (\pi, 3d_{xz,yz}) \longrightarrow a_1\ (\sigma^*, 3d_{z^2}),\ (^1A_1-{}^1E_v),\ \Delta E_4$$

The second transition does not contribute to the shift in the case of the present molecular symmetry, and ligand-charge transfer transitions from e (π, L and CO) to the upper σ-antibonding levels are disregarded because of very low values of both r^{-3} and ΔE_n^{-1}. The values of ΔE may be obtained by measuring the d-d transition spectra, but, in the present case, no data are available because of the intense charge-transfer bands in this region. When this approach is used, the following expression is obtained for the paramagnetic shift:

$$\sigma_p = -\frac{e^2\hbar^2}{2m^2c^2}\langle r^{-3}\rangle C_{a_1 g}\left[\frac{8C_{a_2}}{\Delta E_1}+\frac{4C_{E_u}}{\Delta E_3}+\frac{12C_{E_v}}{\Delta E_4}\right]$$

where C_n denotes the coefficient of the metal d-orbital in the molecular orbitals.[20,24] However, it is characteristic of the octahedral L–Mn$(CO)_5$-type compounds that the b_2 (π, $3d_{xy}$) and e (π, $3d_{xz,yz}$) levels are virtually non-bonding, so the values of ΔE_1, ΔE_3, and ΔE_4 are mainly determined by the b_1 (σ^*, $3d_{x^2-y^2}$) and a_1 (σ^*, $3d_{z^2}$) levels, which are correlated only with the σ-bonding between manganese and tin atoms or carbon atoms of carbonyl groups. As the strength of the σ-bond between Sn and Mn increases, the value of ΔE_n increases. The molecular antibonding orbital constants, C_n, increase from $Mn(CO)_5^-$ to $Mn(CO)_5^+$ through R_3Sn–$Mn(CO)_5$, X_3Sn–$Mn(CO)_5$, and X–Mn$(CO)_5$. The increase in ΔE_n causes the paramagnetic shift to decrease, while an increase in C_n causes the paramagnetic shift to increase. Thus, changes in C_n rather than in ΔE_n or in $\langle r^{-3}\rangle$ must be mainly responsible for the observed trend in the chemical shift, as has been reported in the case of platinum complexes.[22] Therefore, the following order of the values of the chemical shift may be a good measure of the σ-bond polarity of the L–Mn bonds:[11]

$Cl<Br<I<CF_3=CF_3CO<CH_3CO<CHF_2<Cl_3Sn\leqq Br_3Sn<CH_2F<PhBr_2Sn\leqq(CH_3)Br_2Sn\leqq CH_3\leqq PhCl_2Sn\leqq(CH_3)Cl_2Sn\leqq Mn(CO)_5<Ph_2ClSn\leqq Ph_2BrSn\leqq(CH_3)_2BrSn<(CH_3)_2ClSn<Ph_3Sn\leqq H\leqq(CH_3)_3Sn$

The L–Mn bond may be most ionic in $Cl^{\delta-}$—$^{\delta+}Mn(CO)_5$ and in $(CH_3)_3Sn^{\delta+}$—$^{\delta-}Mn(CO)_5$ and "covalent" at $(CO)_5Mn$–$Mn(CO)_5$.

The linewidth of the ^{55}Mn-NMR absorption is expressed by this formula:[25]

$$\Delta H = \frac{9}{500\sqrt{2}}\cdot\left(1+\frac{\eta^2}{3}\right)\cdot\left(\frac{eQ}{\hbar}\cdot\frac{\partial^2 V}{\partial z^2}\right)^2\cdot\tau_c$$

In the present type of complex, the asymmetry parameter, η, is of zero value because of the C_{4v} symmetry around the Mn nucleus. Accordingly, the linewidth of $LMn(CO)_5$ complexes is determined by two factors, the principal field gradient, $\partial^2V/\partial z^2$, and the correlation time, τ_c. However, the changes in the linewidth in a series of complexes of the $(CH_3)_{3-x}Br_xSn$–Mn-$(CO)_5$ type, as is shown in Table 1, are attributable to the change in the field gradient, because these complexes, being similar in molecular size, will give almost the same τ_c value.[26,27] Following the molecular orbital treatment of $LMn(CO)_5$ by Gray and Billing,[22] it may be deduced that the energy difference, ΔE_0, between two π-orbitals, b_2 (π, $3d_{xy}$) and e (π, $3d_{xz,yz}$) localized on Mn determines the field gradient at the Mn nucleus, or that the field gradient at the Mn nucleus is sensitive to the π-interaction between Mn and Sn. The contributions from other orbitals may be of secondary importance because of their small r^{-3} values. From the above consideration, we obtain the following order of the π-interaction between manganese and tin atoms from the linewidths:

Br_3Sn–$Mn(CO)_5>(CH_3)Br_2Sn$–$Mn(CO)_5>(CH_3)_2$-$BrSn$–$Mn(CO)_5>(CH_3)_3Sn$–$Mn(CO)_5$

The fact that the π-accepting tendency of the X_3Sn-group is stronger than that of the $(CH_3)_3Sn$-group[28] is well expressed by the larger differences in the linewidth, but Graham's π-parameters of Br_3Sn–$Mn(CO)_5$, $Br_2(CH_3)Sn$–$Mn(CO)_5$, $Br(CH_3)_2Sn$–$Mn(CO)_5$, and $(CH_3)_3Sn$–$Mn(CO)_5$ all have practically the same values within the limits of experimental error.[10] The linewidth of the ^{55}Mn-NMR spectra can, then, be thought to be a better measure of the π-interaction than the π-parameter proposed by Graham, at least in the present case.

The authors wish to express their deep gratitude to Mr. Fumikazu Yajima for his interest in this work and to Dr. Kazutaka Kawamura for his kind permission to use the NMR spectrometer. The authors are also grateful to the Ministry of Education for its financial support.

22) H. B. Gray, E. Billig, Wojcicki, and M. Farona, *Can. J. Chem.*, **41**, 1281 (1963).
23) W. P. Anderson and T. L. Brown, *Discuss. Faraday Soc.*, **47**, 37 (1969).
24) A. D. Buckingam and P. J. Stephens, *J. Chem. Soc.*, **1964**, 2747.
25) A. Abragam, "The principle of Nuclear Magnetism," Chapter VIII, Oxford (1962).
26) P. Debye, "Polar Molecules," Chapter V. Reinhold (1928).
27) According to the ^{55}Mn-NMR work on compounds of $Mn(CO)_{5-x}(PF_3)_xH$, the linewidth is mainly dependent on the eqQ value and not on τ_c.[12]
28) P. N. Brier, A. A. Chalmers, J. Lewis, and S. B. Wild, *J. Chem. Soc., A*, **1967**, 1889.

The Synthesis of Phosphonophenylazochromotropic Acids and the Stability Constants of Its Alkaline Earth Metal Chelates

Kenyu KINA, Haruo MIYATA, and Kyoji TÔEI

Department of Chemistry, Faculty of Science, Okayama University, Tsushima, Okayama

(Received February 15, 1971)

The acid dissociation constants of the three isomeric phosphonophenylazochromotropic acids and their chelate stability constants with alkaline earth metals have been measured by the pH titration method at an ionic strength of 0.10 and at 25.0±0.1°C. The stability order with respect to the ligands is as follows: *ortho-*>*meta-*>*para-*, and the stability constant of each ligand decreases in the order: Mg>Ca>Sr>Ba; this order is parallel to the reciprocal of the ionic radii of the metal ions. From a comparison between the chelate stability of *o*-phosphonophenylazochromotropic acid and that of Neo-Thorin, it has been concluded that the magnesium ion forms a more stable chelate bond with the phosphonic group than with the arsonic group.

A large number of azo compounds were synthesized and used as metal indicators. As a phenylazo derivative of chromotropic acid, Neo-Thorin, which has an arsonic group adjacent to the azo link, is well-known as a colorimetric reagent for thorium, zirconium, and uranium.

The present authors synthesized the *o*-phosphonophenylazochromotropic acid, which has a phosphonic group in place of the arsonic group of the Neo-Thorin, and two isomers (*m*-, *p*-) of this one. The structural formula for phosphonophenylazochromotropic acid disodium salt is given below:

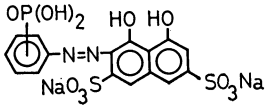

Phosphonophenylazochromotropic acid

The measurement of its chelate stability constants with alkaline earth metals was carried out by means of the pH titration method.

Experimental

Synthesis of Phosphonophenylazochromotropic Acid. Three isomeric phosphonophenylazochromotropic acids were obtained form the corresponding diazonium salt by coupling with chromotropic acid dissolved in a sodium hydroxide solution. After the coupling reaction, the reaction mixture was added, drop by drop, to well-chilled concentrated hydrochloric acid; a reddish precipitate was thus obtained. This precipitate was recrystallized several times from an acidic solution by the salting-out method. These reagents, which are obtained as disodium salt, are all fine, reddish needles. Figure 1 shows the synthetic routes of the three isomeric diazo components.

o-Aminophenylphosphonic acid has been prepared by the use of the method of Route I. Triethylphosphite (25 g) and *o*-dinitrobenzene (16.8 g) were refluxed in acetonitrile for 8 hr.[1] After releasing the solvent under reduced pressure, diethyl *o*-nitrophenylphosphonate (mp 55°C) can be obtained as yellow needles by letting it stand over-night in an ice-box; then it was hydrolyzed in boiling concentrated hydrochloric acid (5 hr).[2] The *o*-nitrophenylphosphonic acid thus obtained was reduced with the use of ferrous hydroxide. After the precipitated ferric hydroxide was removed by

I. *o*-Aminophenylphosphonic acid

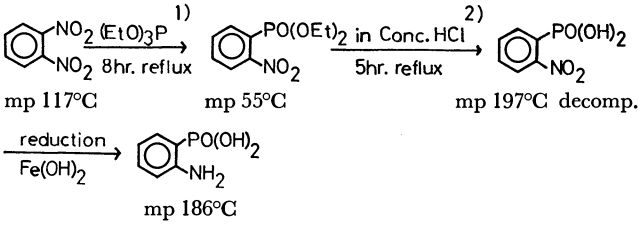

II. *m*-Aminophenylphosphonic acid

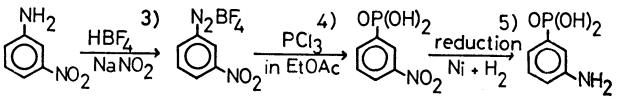

III. *p*-Aminophenylphosphonic acid was also prepared in a similar manner as above

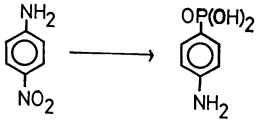

Fig. 1. Synthetic routes of diazo components.

filtration, *o*-aminophenyl-phosphonic acid, mp 186°C, rapidly crystallized as white needles when the alkaline filtrate was acidified with concentrated hydrochloric acid. Two other isomers, *m*- and *p*-aminophenylphosphonic acids, were prepared by the use of the methods of Routes II, and III; the details of the procedure have been described in a previous paper.[6]

Reagent Solutions. The stock solutions of these ligand were standardized by potentiometric titration with standard 0.10N potassium hydroxide. Carbonate-free 0.10N potassium hydroxide was prepared by the method of ion exchange and was standardized by potassium hydrogen phthalate titrimetrically. The stock solutions of the metal ion were prepared by dissolving $Mg(NO_3)_2 \cdot 6H_2O$, $Ca(NO_3)_2 \cdot 4H_2O$, $Sr(NO_3)_2$, and $Ba(NO_3)_2$ of a guaranteed reagent grade in distilled water. The concentrations of the Mg(II) and Ca(II) solutions were determined by chelatemetric titration, while the concentrations of the Ba(II) and Sr(II) solutions were determined by the usual gravimetric method.

pH Titration Method. The acid dissociation and the chelate stability constants were calculated from titration

1) J. I. G. Cadogan, *Chem. Comm.*, **1966**, 491.
2) G. M. Kosolopoff, *J. Amer. Chem. Soc.*, **71**, 4022 (1949).
3) *Org. Reactions*, **2**, 427.
4) G. O. Doak and L. D. Freedman, *J. Amer. Chem. Soc.*, **73**, 5658 (1951).
5) *ibid.*, **74**, 753, 754 (1952).
6) H. Miyata, This Bulletin, **36**, 127 (1963).

curves obtained by titrating solutions (5 m*l*) in the presence and in the absence of metal ions, with 0.10N potassium hydroxide in a double-walled glass vessel with a 5-m*l* capacity, and maintained at 25.0±0.1°C by the circulation of water from a thermostat bath. All the measurements were carried out by the use of the micro-titration apparatus, presented in Fig. 2, and the alkali was added by means of a calibrated 0.50-m*l* micrometer syringe.

Solutions under titration were kept in a nitrogen atmosphere by the circulation of carbon dioxide-free nitrogen through the titration vessel. The ionic strength was adjusted to 0.10 with potassium nitrate. The hydrogen-ion concentration was measured by means of an HRL-Model P pH meter (Horiba Instruments Co., Ltd.) with a combined glass electrode (Metrohm, EA-125 U type, Herisaw, Switzerland). The observed pH meter readings were converted into the actual hydrogen-ion concentration by comparison with the stoichiometric dissociation constant of acetic acid. The pH (−log[H+]) region above 11.0 was calibrated by measurements in the KOH solution.

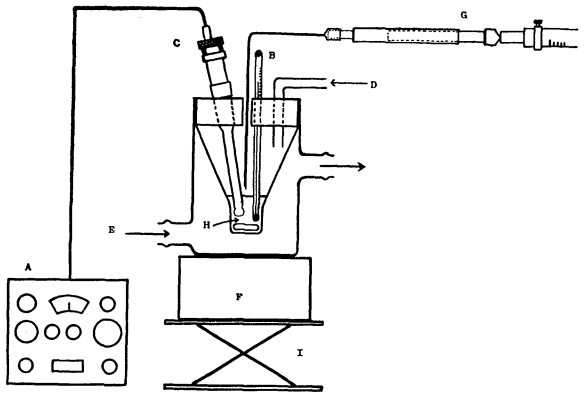

Fig. 2. Micro-titration apparatus.
A: HRL-Model P pH meter (Horiba)
B: Thermometer
C: "Metrohm" combined glass electrode
D: N_2 gas
E: 25°C water from a thermostat bath
F: Magnetic stirrer
G: Micro-meter outfit
H: Volume 5 m*l*
I: Laboratory jack

Calculation of Acid Dissociation Constants and Chelate Stability Constants. The dissociation constants of the triprotic acid are defined as follows:

$$K_{a1}=[H][H_2L]/[H_3L],$$
$$K_{a2}=[H][HL]/[H_2L],$$
$$K_{a3}=[H][L]/[HL],$$

where the ionic charge was neglected for the sake of convenience. In general, the following relationship holds among the step-by-step acid dissociation constants of the polyprotic acid:

$$\sum_{i=1}^{n}\frac{iT_L-f}{f[H]^i}K_{a1}\cdot K_{a2}\cdots K_{ai}=1,$$
$$f=T_{OH}+[H]-[OH],$$

where T_L represents the total concentration of ligand species, and T_{OH} the total concentration of the base added to the system. T_L, T_{OH}, and f are entirely of known or measurable quantities; therefore, K_{a1}, K_{a2}, and K_{a3} can be obtained by solving the simultaneous equation in principle. In practice, the ligands were treated as monoprotic acid until $a=1$, and treated as diprotic acid after $a=1$; since a clear inflection is observed, the first dissociation process can be separated from the subsequent dissociation. The chelate stability constants were calculated by the following equation:

$$K_{ML}=(T_L-F)/[L](F+T_M-T_L),$$

where:

$$[L]=(3T_L-T_{OH}-[H]+[OH])/\{[H]/K_{a3}+2[H]^2/K_{a3}K_{a2}+3[H]^3/K_{a3}K_{a2}K_{a1}\},$$
$$F=[L]\{1+[H]/K_{a3}+[H]^2/K_{a3}K_{a2}+[H]^3/K_{a3}K_{a2}K_{a1}\},$$

where T_M represents the total concentration of the metal species.

Results and Discussion

Titration Curves. The titration curves are illustrated in Figs. 3—5 for phosphonophenylazochromotropic acid in the presence and in the absence of alkaline earth metal ions. According to the results of the measurement of the pK_a of phenylphosphonic acid, the first dissociation constant was not obtained because of

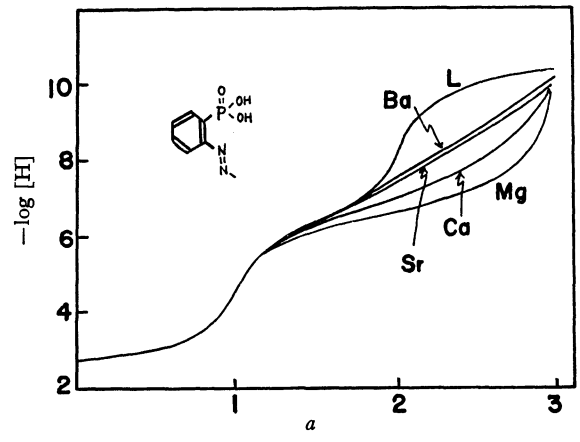

Fig. 3. Titration of *o*-phosphonophenylazochromotropic acid chelate system at 25°C, $\mu=0.10$.
L, ligand only, [Ligand]=1.338×10^{-3}M, [Mg]=2.216×10^{-3}M, [Ca]=2.256×10^{-3}M, [Sr]=2.078×10^{-3}M, [Ba]=2.048×10^{-3}M,
a=moles of base added per mole of ligand

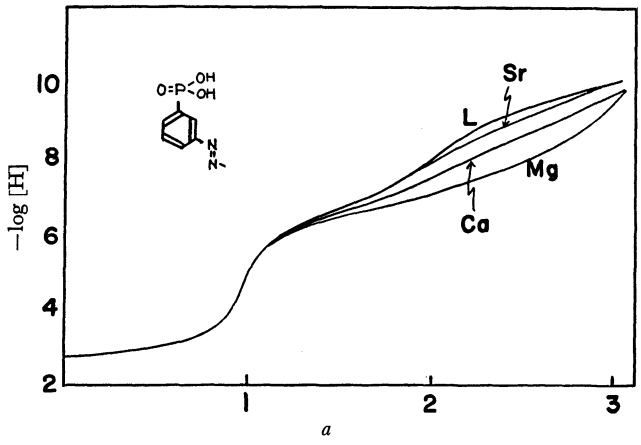

Fig. 4. Titration of *m*-phosphonophenylazochromotropic acid chelate system at 25°C, $\mu=0.10$.
L, Ligand only, [Ligand]=1.600×10^{-3}M. [Mg]=2.216×10^{-3}M, [Ca]=2.256×10^{-3}M, [Sr]=2.078×10^{-3}M, [Ba]=2.048×10^{-3}M,
a=moles of base added per mole of ligand

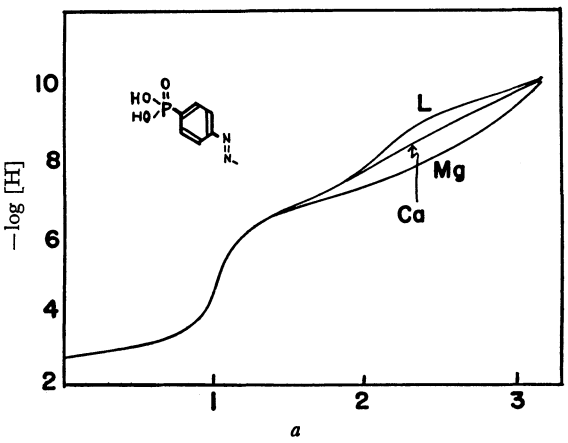

Fig. 5. Titration of *p*-phosphonophenylazochromotropic acid chelate system at 25°C, $\mu=0.10$.
L, Ligand only, [Ligand]$=1.374\times10^{-3}$M, [Mg]$=2.216\times10^{-3}$M, [Ca]$=2.256\times10^{-3}$M, [Sr]$=2.078\times10^{-3}$M,
a=moles of base added per mole of ligand

the very strong acid; however, the second dissociation constant, pK_{a2}, is 6.90. Therefore, the inflections at $a=1$ and $a=2$ on the ligand-only titration curve were identified with the dissociation of two phosphonic protons. The third dissociation step corresponds to the naphtholic hydroxyl proton.

As is shown in Figs. 3—5, a depression of the pH on the titration curves is observed in the presence of the metal ion when compared with that of the ligand only; this depression is due to the formation of a chelate. Therefore, the stability order can be judged by the extent of the pH drop. The order with respect to metal ions is as follows: Mg>Ca>Sr>Ba; that is, the stability constants, log K_{ML}, increase with a decrease in the ionic radii. Therefore, the order with respect to ligands is as follows: *ortho-*>*meta-*>*para-*. The ligand-only titration curve of *o*-phosphonophenylazochromotropic acid has a well-defined inflection at $a=2$ in comparison with those of the two isomers, and the third dissociation step is separated from the second dissociation step; therefore, the calculation of pK_{a3} can be performed like that of monoprotic acid after $a=2$.

Acid-dissociation Constants. The acid-dissociation constants of phosphonophenylazochromotropic acid are listed in Table 1. The pK_{a1} and pK_{a2} values correspond to the dissociation of the phosphonic group; the pK_{a3} value corresponds to the dissociation of the naphtholic hydroxyl group. The pK_{a1} values were not obtained in practice, because the first dissociation is almost complete, as in the case of the sulfonic group. Phenylazochromotropic acid derivatives have two naphtholic protons; however, one proton is not dissociated under ordinary conditions because of the very strong hydrogen bond between the oxygen atoms.[7] Another proton is also combined with one of the nitrogen atoms of the azo link by a hydrogen bonding; that is, in spite of the fact that the pK_a value of the naphtholic proton of chromotropic acid is 5.44,[8] those of the azo derivatives are increased to an order of magnitude of 9—10. The *o*-phosphonophenylazochromotropic acid has a higher pK_{a3} value (=10.12) than the other *m*- and *p*-isomers. This is attributed to the ortho effect of the phosphonic group. Such phenomena have been also observed with regard to *o*-sulfophenylazochromotropic acid.

Table 1. Acid-dissociation constants of phosphonophenylazochromotropic acids and stability constants of their chelates ($t=25$°C; $\mu=0.10$ by KNO_3)

Ligand	Acid-dissociation constants			Stability constants, log K_{ML}			
	pK_{a1}	pK_{a2}	pK_{a3}	Mg	Ca	Sr	Ba
ortho-	a)	6.43	10.12	5.71	4.95	4.34	4.15
meta-	a)	6.78	9.46	4.34	3.48	2.72	a
para-	a)	6.88	9.42	3.93	3.04	1.8	a
Neo-Thorin				5.57	5.20	4.39	4.22

a) not measurable owing to very strong acid or unstable chelate

Stability Constants. The chelate stability constants are also listed in Table 1. The chelate stability constants, log K_{ML}, decrease with respect to metal ions as follows: Mg>Ca>Sr>Ba. This order is parallel to the reciprocal of the ionic radii of the metal ions. *o*-Phosphonophenylazochromotropic acid forms a more stable chelate than the *m*- and *p*-isomers; this stabilization is due to the increase in the coordination number produced by the phosphonic group. The log K_{ML} values of Neo-Thorin (*o*-arsonophenylazochromotropic acid) with respect to Mg, Ca, Sr, and Ba are 5.57, 5.20, 4.39, and 4.22 respectively. The calcium, strontium, and barium chelate stability constants of Neo-Thorin are greater than those of *o*-phosphonophenylazochromotropic acid, while the magnesium chelate of *o*-phosphonophenylazochromotropic acid is more stable than that of Neo-Thorin; therefore, it may be concluded that the coordination bond of Mg with the phosphonoic group is stronger than that with the arsonic group.

7) S. Nakashima, H. Miyata, and K. Tôei, This Bulletin, **41**, 2632 (1968).
8) M. Sakaguchi, A. Mizote, H. Miyata, and K. Tôei, *ibid.*, **36**, 885 (1963).

Intramolecular Hydrogen Bonds. XVII.[1] Intramolecular Hydrogen Bonding Involving the Mercapto Group as a Hydrogen Donor

Nobuo MORI, Shinichi KAIDO, Koichi SUZUKI, Mikio NAKAMURA, and Yojiro TSUZUKI

Department of Chemistry, Science University of Tokyo, Kagurazaka, Shinjuku-ku, Tokyo

(Received October 12, 1970)

The SH stretching absorption spectra of some mercapto compounds in dilute carbon tetrachloride solutions and also in acetonitrile solutions have been measured at 20°C. Alkyl mercaptans show absorption bands which are suggestive of the rotational isomerism around the C–S bond. The spectral data indicate that benzyl mercaptan, ω-ethoxyalkyl mercaptans, and ethyl α- and β-mercaptoalkanoates form practically no intramolecular hydrogen bond between the SH group and the hydrogen-acceptor group. In thiosalicylic acid and its ethyl ester, the hydrogen-bonding to the carbonyl group is partially possible even in acetonitrile. On the other hand, the corresponding free carboxylic acids are not hydrogen-bonded between the S atom and the carboxyl group.

The mercapto group is well known[2,3] to form hydrogen bonds with oxygen, nitrogen, carbon, and sulfur atoms, and possibly with aromatic π-electrons as well, but it is apparently not capable of hydrogen bonding to such an extensive degree as occurs with the hydroxyl group. On the dilution of neat mercaptans with non-polar solvents, the stretching frequencies of the S–H bonds are only slightly shifted to the lower-frequency side and the chemical shifts of the proton magnetic resonance of the SH groups are extraordinarily small.

The literature contains scant information on the intramolecular hydrogen bonding involving the mercapto group. In ω-*N*,*N*-dialkylamino-alkyl mercaptans,[4] there is no evidence for the expected lowering of the SH-stretching frequency by hydrogen bonding. However, only a few thiols, such as ethyl β-mercapto-β-phenylacrylates,[5] *o*-amino- and *o*-hydroxy-thiophenols,[6] and ethyl thiosalicylate,[7] show relatively large spectral shifts of the bonded SH bands. More recently, Hirota and his co-workers[8] have suggested that, in *o*-substituted thiophenols, the hydrogen bonding may be indicated by an increased intensity of the SH stretching band and also by an increased downfield-shift of the SH proton resonance, even if no lowering of the SH stretching frequency is observed.

In previous papers,[9,10] it has been reported that α- and β-hydroxyalkanoic esters form an intramolecular hydrogen bond, predominantly between the hydroxyl and the ester-carbonyl groups. These results have prompted us to examine the corresponding mercapto compounds as well.

The present paper will deal with the intramolecular hydrogen bonding in benzyl mercaptan, ω-ethoxyalkyl mercaptans, ethyl α- and β-mercaptoalkanoates, and ethyl thiosalicylate, as studied by means of infrared spectroscopy. Furthermore, the SH spectra of alkyl mercaptans in dilute carbon tetrachloride solutions have also been measured, since there have been no detailed and systematic studies of them, although the SH frequencies of many thiols have been reported.[11]

Experimental

Samples. All the compounds examined were prepared in the usual manner except for commercially-available alkyl and benzyl mercaptans. The new *o*-mercaptobenzyl methyl ether was prepared form *o*-aminobenzyl methyl ether[12] by way of its diazonium salt. Their melting and/or boiling points were equal, or very close, to those previously reported, and their purity was established by gas chromatograms and/or NMR spectra. The unknown compounds had the analytical data shown in Table 1. Carbon tetrachloride and acetonitrile were fractionally distilled over phosphours pentoxide.

Infrared Measurement. This was carried out at *ca.* 20°C by the method previously described,[9] using a grating infrared spectrophotometer, Model DS-403G, of the Japan Spectroscopic Co. The concentrations used were 0.006 mol/*l* (SH spectra; cell-thickness: 5.0 cm) and 0.01 or 0.001 mol/*l* (CO spectra; cell-thickness: 1.1 or 10.0 mm), unless otherwise noted. The calculated spectral slit width was 1.5 cm^{-1} at the wave number of 1700 cm^{-1} and 0.8 cm^{-1} at 2600 cm^{-1}. Some of the unsymmetrical bands with relatively high intensities were graphically[9] divided into their components, particularly when the intensity ratios were desired.

Results and Discussion

Alkyl mercaptans. The spectra of some alkyl mercaptans in carbon tetrachloride are shown in Fig. 1, while the apparent spectral data are summarized in Table 2. The SH bands of *prim-* and *t*-alkyl mercaptans are practically symmetric, while those of *s*-alkyl mercaptans are unsymmetric; the shapes and the frequencies

1) Part XVI: N. Mori, M. Yoshifuji, Y. Asabe, and Y. Tsuzuki, This Bulletin, **44**, 1137 (1971).
2) G. C. Pimental and A. L. McClellan, "The Hydrogen Bond," W. H. Freeman and Co., San Francisco (1960), p. 201.
3) S. H. Marcus and S. I. Miller, *J. Amer. Chem. Soc.*, **88**, 3719 (1966) and the references cited therein.
4) D. Plant, D. S. Tarbell, and C. Whiteman, *ibid.*, **77**, 1572 (1955).
5) Z. Reyes and R. M. Silverstein, *ibid.*, **80**, 6367, 6373 (1958).
6) J. G. David and H. E. Hallam, *Spectrochim. Acta*, **21**, 841 (1965).
7) A. W. Wagner, H. J. Becher, and K. G. Kottenhahn, *Chem. Ber.*, **89**, 1708 (1956).
8) A. Yamashita, T. Kobayashi, R. Hoshi, and M. Hirota, presented at the 23rd Annual Meeting of the *Chem. Soc.* of Japan (Tokyo, 1970), No. 14321.
9) N. Mori, S. Omura, N. Kobayashi, and Y. Tsuzuki, This Bulletin, **38**, 2149 (1965).
10) N. Mori, Y. Asano, and Y. Tsuzuki, *ibid.*, **41**, 1871 (1968).
11) R. A. Spurr and H. F. Byers, *J. Phys. Chem.*, **62**, 425 (1958), and Ref. 16, p. 350.
12) T. Thiele and O. Dimroth, *Ann.*, **305**, 110 (1899).

Table 1. The analytical data of unknown compounds

Compound	Bp °C/mmHg	Found		Calcd	
		C%	H%	C%	H%
$(CH_3)_2C(SEt)COOEt$	83/17	54.75	9.06	54.53	9.15
$(CH_3)_2C(SEt)COOH$	128/16	48.63	8.19	48.64	8.16
$CH_2(SEt)CH_2COOEt$	102/22	51.80	8.50	51.84	8.70
$CH_2(SEt)CH_2COOH$	134/12.5	44.57	7.43	44.77	7.52
o-$C_6H_4(SH)(CH_2OCH_3)$	88/ 5.5	62.43	6.44	62.32	6.54

of the bands vary with the type of the alkyl group (R). This variation can not be due to any molecular association, since thiols are generally already monomeric even in a concentration of 0.1 mol/l in the same solvent. By analogy with the case of the corresponding alkanols,[13] it is probably attributable to the rotational isomerism around the C–S bond.

Figure 3 shows three possible steric environments around the S–H group, which are projected along the C–S bond, where C denotes an alkyl group, and X, a hydrogen atom or an alkyl group, depending on the type of R. If the molecule takes a staggered conformation, but not an eclipsed one, the mercapto-hydrogen atom of methyl and t-butyl mercaptan always exists in the environment, I or III respectively, in any rotational position about the C–S bond to be favoured. Hence, the frequency-lowering by 14 cm^{-1} of t-butyl mercaptan can be attributed to the presence of the two methyl groups *skew* to the SH. The spectral pattern of isopropyl mercaptan changed with the temperature; the intensity of the stronger band-component relative to the shoulder decreases at a higher temperature. Therefore, the band consists of at least two band-components, which can probably be assigned to the SH species in the environments, I and II respectively. The practically symmetrical bands of ethyl and n-butyl mercaptan probably consist of two bands corresponding to the two environments, I and II, because there is a possibility that they exist in these environments and also because the half-band widths are relatively wide.

Table 2. The spectral data of alkyl, benzyl and ω-ethoxyalkyl mercaptans in CCl_4

Compound	ν_{SH}, cm^{-1}	ε	$\Delta\nu_{1/2}$, cm^{-1}
CH_3SH[a]	2586	—	7
C_2H_5SH	2578	2.2	15
n-C_4H_9SH	2578	2.2	15
i-C_3H_7SH	2577 (2570)	3.0	20
s-C_4H_9SH	2577 (2570)	2.7	21
t-C_4H_9SH	2572	2.1	14
$C_6H_5CH_2SH$	2580	2.0	
$C_2H_5O(CH_2)_2SH$	2585	*ca.* 3	
$C_2H_5O(CH_2)_3SH$	2583	*ca.* 3	

a) The ε value was not determined, because the concetration was uncertain.

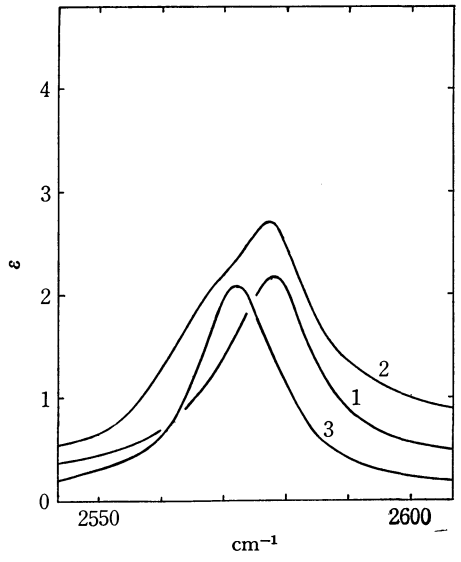

Fig. 1. The spectra of n-butyl (1), s-butyl (2), and t-butyl mercaptan (3).

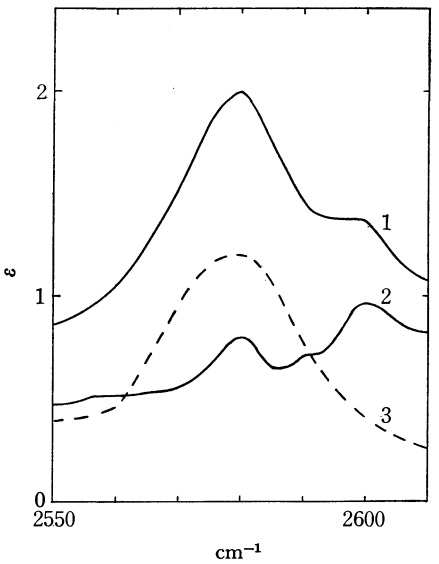

Fig. 2. The spectra of benzyl mercaptan (1) and benzyl methyl sulfide (2); (3) is the curve (2) subtrated from the curve (1).

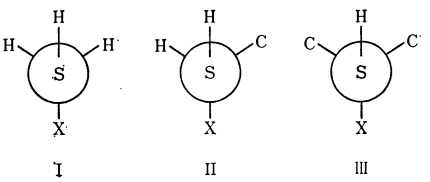

Fig. 3. Three steric environments around the SH group (X=H or C).

13) M. Ōki and H. Iwamura, This Bulletin, **32**, 950 (1959).

Benzyl mercaptan shows a complicated spectral pattern in the SH stretching region, but a simple unsymmetrical band can be obtained by subtracting the spectral curve of benzyl methyl thioether from it (Fig. 2); the peak frequency and intensity are very close to those of *prim*-alkyl mercaptans. It thus appears that the SH group is practically incapable of the interaction with the aromatic π-electrons which occurs with benzyl alcohols[14] and benzylamines.[15]

2- and 3-ethoxyalkyl mercaptans show, in carbon tetrachloride, single SH bands which are complicated by overlapping with other absorption bands on the higher-frequency side; the peak frequencies are rather close to that of methyl mercaptan, and the intensities are similar to those of alkyl mercaptans. Accordingly, the hydrogen bonding to the ethoxy group appears to be practically absent.

Furthermore, the SH frequencies of the above mercaptans are very close to those of thiophenols; hence, the electronic effects of substituents on them seem negligible. However, substituents have electronic effects on the intensities, as is indicated by the ε values of thiophenol and ethyl *p*-mercaptobenzoate (Table 5).

Ethyl α- and β-mercaptoalkanoates. Their SH spectra in carbon tetrachloride are shown in Fig. 4, while the apparent spectral data are summarized in Table 3. The bands of ethyl α-mercapto-acetate and -isobutyrate are almost symmetric, while ethyl α-mercaptopropionate shows an unsymmetric band. The frequencies and half-band widths are very close to those of the corresponding alkyl mercaptans; it thus appears that all the α-esters form no hydrogen bond. On the other hand, the high intensities, as compared with those of alkyl mercaptans, do not provide evidence for the hydrogen bond formation, because such an increase in intensity may also be caused by the electronic effects of the ethoxycarbonyl group. In order to clarify this

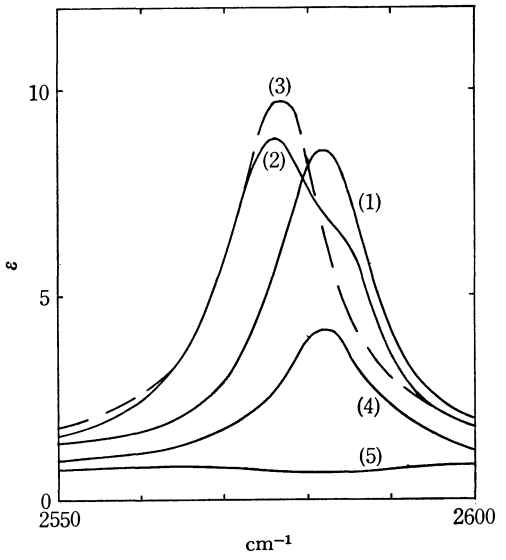

Fig. 4. The spectra of ethyl mercaptoacetate (1), α-mercaptopropionate (2), α-mercaptoisobutyrate (3), β-mercaptopropionate (4), and α-ethylthiopropionate (5).

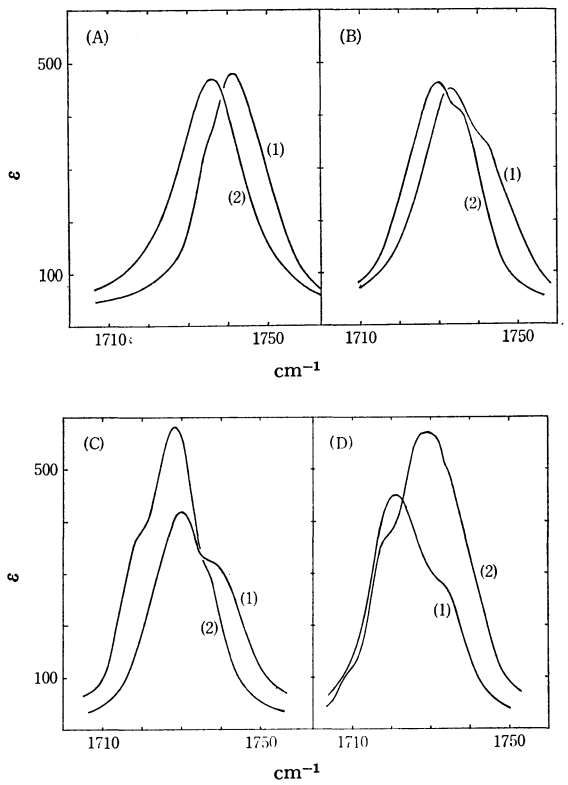

Fig. 5 (A)—(D). The CO spectra of ethyl mercaptoacetate (A) and its *S*-ethylated compound (B), α-ethylthiopropionate (C) and α-ethylthioisobutylate (D) in carbon tetrachloride (1) and acetonitrile (2).

point, the carbonyl data will be discussed further on the basis of a comparison with those of the corresponding *S*-ethylated compounds.

Ethyl α-ethylthioalkanoates show, in carbon tetrachloride, two overlapped carbonyl bands with a spacing of about 10 cm,$^{-1}$ and the intensity of the higher-frequency band increases in acetonitrile relative to that of the lower-frequency band (Fig. 5A—5D). By analogy with the cases of α-halogeno-[16] and α-alkoxycarbonyl compounds,[10,17] as well as in view of the relatively high dipole moment of a C–S bond (*cf.* μ_{C-S}: 1.2 D; μ_{C-O}: 0.9 D; μ_{C-Cl}: 1.7 D), this phenomenon can be suitably explained in terms of the rotational isomerism around the C_1–C_2 bond. Thus, the two bands can be assigned, in the usual manner, to the *cis* and *gauche* forms respectively:

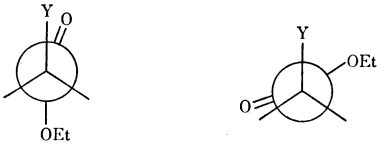

cis-Form with a higher ν_{CO} *gauche*-Form with a lower ν_{CO}

On the other hand, ethyl α-mercaptoalkanoates show, in carbon tetrachloride, a strong band, with a weak shoulder centered at a position lower by about 6 cm^{-1} than the peak position, and the frequencies of

14) For example, M. Ōki, and H. Iwamura, *ibid.*, **32**, 955 (1959).
15) M. Ōki and K. Mutai, *ibid.*, **33**, 784 (1960).
16) L. J. Bellamy, "The Infrared Spectra of Complex Molecules," Methuen and Co., London (1958), p. 400.
17) T. L. Brown, *J. Amer. Chem. Soc.*, **80**, 3513 (1958).

TABLE 3. THE APPARENT SPECTRAL DATA OF ETHYL α- AND β-MERCAPTOALKANOATES AND THEIR S-ETHYLATED COMPOUNDS[a)]

Compound	in CCl_4						in CH_3CN		
	ν_{SH}, cm^{-1}	ε	$\Delta\nu_{1/2}$, cm^{-1}	ν_{CO}, cm^{-1}	ε	$\Delta\nu_{1/2}$, cm^{-1}	ν_{CO}, cm^{-1}	ε	$\Delta\nu_{1/2}$, cm^{-1}
$CH_2(SH)COOEt$	2582	8.5	15	1742 (1737)	450 (60)	17	1736	430	21
$CH_3CH(SH)COOEt$	2576 (2584)	8.8	21	1740 (1735)	450 (60)	17			
$(CH_3)_2C(SH)COOEt$	2577	9.7	16	1735 (1727)	450 (60)	20			
$CH_2(SH)CH_2COOEt$	2582	4.1	19	1738	600	16			
$CH_2(SEt)COOEt$				1743	340	25	1736	400	25
				1733	440		1730	460	
$CH_3CH(SEt)COOEt$				1739	320	25	1728	565	25
				1730	420		1719	550	
$(CH_3)_2C(SEt)COOEt$				1733	280	20	1729	660	25
				1721	500		1719	360	
$CH_2(SEt)CH_2COOEt$				1740	490	17			

a) The values in parentheses, obtained by band reflection, are approximate.

the two band-components are close to those of their *S*-ethylated compounds. In acetonitrile (Fig. 5A), ethyl mercaptoacetate shows a single, symmetric band at the same frequency as that of the *cis* form of the corresponding *S*-ethylated compound, suggesting that the ester exists exclusively in the *cis* form. Accordingly, the two bands which appear in carbon tetrachloride can probably be associated with the same rotational isomers, *cis* and *gauche*, as has been suggested in the case of ethyl α-ethylthioalkanoates. If this is true, it should be noticed, from the relative intensities of the bands, that the proportion of the *cis* form of ethyl α-mercaptoalkanoates in carbon tetrachloride is much higher than those which have hitherto been observed in α-halogeno- and α-alkoxy-carbonyl compounds (the intensities being taken as approximately indicative of the concentrations). The equilibrium between the *cis* and the *gauche* form is considered to be determined by two factors: (1) the electrostatically repulsive interaction between the C_α–Y and C=O dipoles (Y: an electronegative atom or group), which increases with the increasing polarity of the C–Y bond,[18] and (2) the sterically repulsive interaction between the Y and carbonyl-oxygen atoms[17,19] and between the Y and alkoxy-oxygen atoms,[18] both of which increase with the increasing bulkiness of Y. Since the dipole-dipole interaction should raise the double bond character of the carbonyl group and increase the stretching frequency of the C=O group, the fact that the spacing between the two carbonyl bands of ethyl ethylthioacetate (*ca.* 10 cm^{-1}) is lower than those of ethyl halogeno- and ethoxy-acetates (*ca.* 20 cm^{-1})[17] seems to indicate that the electrostatic interaction between the C–S and the C=O dipole is lower than those in the latter esters. From this, a higher proportion of the *cis* form may be expected in the former. On the other hand, the steric repulsion of Y exerting on the C=O group in the *cis* form and also exerting on the alkoxy group in the *gauche* form should be more highly operative in the ethylthioacetate than in the ethoxyacetate, because of the larger van der Waals radius of the sulfur atom.[20] Consequently, judging from the observation that the relative intensity (*cis* to *gauche*) of ethyl ethylthioacetate (*ca.* 0.8) is lower than the 1.94 of ethyl ethoxyacetate,[17] the steric repulsion between the Y and the carbonyl group must be much more important than the other electrostatic and steric repulsions. This is consistent with the conclusion by Brown[17] that the size, rather than the polarity, of Y in acetates is the determining factor.

In the case of ethyl mercaptoacetate, the mercapto group may be expected to be equal in size to, or smaller than, the ethylthio group.[21] If it is smaller, the steric repulsion between the Y and the carbonyl group should become lower, and the proportion of the *cis* form should be higher than that of the corresponding *S*-ethylated acetate. This expectation agrees with our observation that the *cis*-to-*gauche* ratio is *ca.* 8, but this ratio seems too high to be attributable to the decreased steric repulsion only, because no such high ratio has been observed even when the Y group has a bulkiness as small as the ethoxy group or the fluorine atom. In this connection, an attractive interaction between the SH and the carbonyl group may further be considered; it is not evident, however, whether this interaction is the usual hydrogen bonding or the electrostatic attraction, but it is probably the latter because no lowering of the SH and CO frequencies is observed. In this connection, it must be mentioned that ethyl glycolate

18) S. Mizushima, T. Shimanouchi, I. Ichishima, T. Miyazawa, I. Nakagawa, and T. Araki, *ibid.*, **78**, 2038 (1956).

19) E. A. Mason and M. M. Kreevoy, *ibid.*, **77**, 5808 (1955); M. M. Kreevoy and E. A. Mason, *ibid.*, **79**, 4851 (1957).

20) The van der Waals radius (r) of an atom (Y) is approximately equal to the C–Y bond distance: r=1.40 Å for O, 1.85 for S, and 1.35 for F; O–Y distance=1.43 Å (Y:O), 1.81 (S), and 1.38 (F); hence, the r value may be considered as a function of the steric interaction.

21) In the cyclohexane system, the steric size of the SH group is close to, or somewhat lower than, that of the SCH_3 or SC_6H_5 group (*cf.* E. L. Eliel, N. L. Allinger, S. J. Angyal, and G. A. Morrison, "Conformational Analysis," Interscience Publishers, New York (1965), p. 438).

exists exclusively in the *cis* form with the hydrogen bonding between the OH and CO group; thereby, both OH and CO frequencies are very much lowered.[9,10]

Ethyl β-mercaptopropionate may be internally unbonded, since both the frequency and the intensity of the SH band are comparable to those of *prim*-alkyl mercaptans, and the carbonyl data are very close to that of the corresponding *S*-ethylated compound.

α- and β-Ethylthioalkanoic Acids. The spectral data are summarized in Table 4. The α-acids show, in carbon tetrachloride, two split carbonyl bands in the monomer region (Fig. 6). Since only one OH band of the *cis*-carboxyl structure is observed, the band-splitting is not attributable to a hydrogen bond formation between the S atom and the *trans*-carboxyl group such as occurs in α-alkoxyalkanoic acids.[22] The reason for this is not clear at the present time, but at least two reasons can be considered: (1) the Fermi resonance or other absorptions and (2) the rotational isomerism, as has been suggested above in accounting for a similar phenomenon in the corresponding esters. A further study of this problem is in progress.

β-Ethylthiopropionic acid shows only single OH and CO bands in the monomer region, both corresponding to the *cis*-carboxyl structure. These findings agree with the conclusion, confirmed in ω-methylthioalkanols,[23] that the hydrogen-accepting ability of a sulfur atom is lower than that of an oxygen atom.

Thiosalicylic Acid and Related Compounds. In carbon tetrachloride, the free SH bands of aromatic thiols generally appear near 2585 cm^{-1} (*e.g.*, thiophenol, *o*-thiocresol, and ethyl *p*-mercaptobenzoate in Table 5), indicating that the steric and electronic effects on the SH frequency are not significantly operative. Ethyl *p*-mercaptobenzoate shows two bands in the SH region (Fig. 7); the higher-frequency band can be assigned to the SH group on the basis of a comparison with the spectrum of the corresponding *S*-methylated compound. Therefore, the band (ε=20; $\Delta\nu_{1/2}$=40 cm^{-1}) at 2560 cm^{-1} of *o*-mercaptobenzyl methyl ether can be assigned to the bonded SH group,[24] but this ether shows no free SH band. This fact is very interesting which differs from the case of *o*-hydroxybenzyl methyl ether in which a weak free OH band is observed apart from a strong bonded OH band.[25] The two split bands of ethyl thiosalicylate observed in the SH region (Fig. 8) can likewise be assigned to the SH species bonded to the ethoxy- and the carbonyl-oxygen atoms respectively; this assignment is consistent with the observation of two carbonyl bands which can be assigned to the free and bonded carbonyl groups (Fig. 9A).

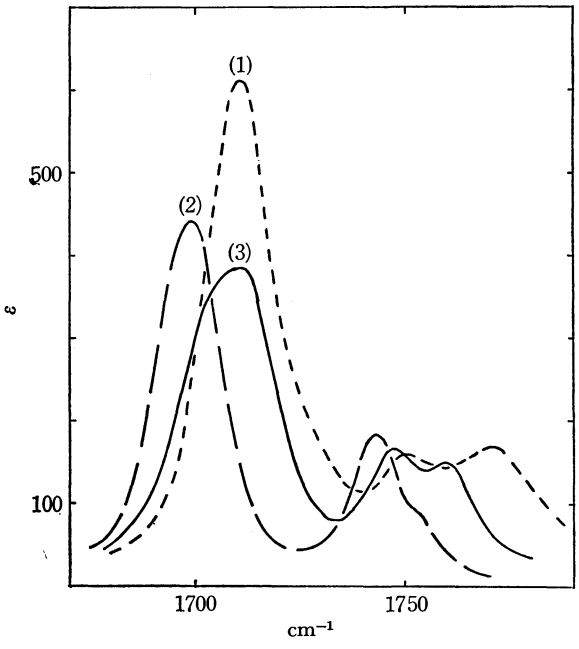

Fig. 6. The CO spectra of ethylthioacetic (1), α-ethylthiopropionic (2) and α-ethylthioisobutylic acid (3) in carbon tetrachloride.

Table 4. Apparent spectral data of α- and β-ethylthioalkanoic acids in CCl_4

Compound	Monomer				Dimer	
	ν_{OH}, cm^{-1}	ε	ν_{CO}, cm^{-1}	ε	ν_{CO}, cm^{-1}	ε
$CH_2(SEt)COOH$	3526	75	1771	169	1711	610
			1751	160		
$CH_3CH(SEt)COOH$	3528	55	1761	147	1709	400
			1747	164		
$(CH_3)_2C(SEt)COOH$	3529	56	1754	85	1699	440
			1743	183		
$CH_2(SEt)CH_2COOH$	3527	72	1762	200	1713	480

Thiosalicylic acid and its *S*-methylated compound show, in carbon tetrachloride, only single OH bands of the *cis*-carboxyl structure in the monomer region; hence, they form no hydrogen bond between the sulfur atom and the carboxyl group, although such a bonding occurs in *o*-alkoxybenzoic acids.[26] The two monomeric CO bands and the two SH bands of the former acid can probably be assigned much like those of its ester, because the spectral data of the two compounds are almost the same.

Ethyl *S*-methyl thiosalicylate shows, in carbon tetrachloride, two overlapped CO bands. In acetonitrile, the higher-frequency band is much weaker, with the frequency remaining almost unchanged, while the lower-frequency band shifts towards the lower-frequency side (Fig. 9B). This band-splitting is probably attributable to the Fermi resonance, but not to rotational isomerism or other absorptions, for the following reasons: (1) a band-splitting ascribed to the Fermi resonance is generally subject to a similar solvent effect,[27] while that ascribed to rotational isomerism

22) For example, M. Ōki and M. Hirota, This Bulletin, **33**, 119 (1960); **34**, 374 (1961).
23) N. Mori, Y. Takahashi, and Y. Tsuzuki, *ibid.*, **40**, 2720 (1967).
24) The *S*-methyl ether of this compound shows no significant absorption near 2560cm^{-1}.
25) N. Mori, unpublished data.
26) For example, M. Ōki, and M. Hirota, *ibid.*, **34**, 378 (1961); **36**, 290 (1962), and Ref. 28.
27) C. L. Angell, P. J. Krueger, R. Lauzon, L. C. Leitch, N. Noack, R. J. D. Smith, and R. L. Jones, *Spectrochim. Acta*, **11**, 926 (1959); R. N. Jones, C. L. Angell, T. Ito, and R. J. D. Smith, *Can. J. Chem.*, **37**, 2007 (1959).

TABLE 5. APPARENT SPECTRAL DATA OF THIOSALICYLIC ACID AND RELATED COMPOUNDS[a,b]

Compound	in CCl_4						in CH_3CN	
	ν_{SH}, cm^{-1}	ε	ν_{OH}, cm^{-1}		ν_{CO}, cm^{-1}	ε	ν_{CO}, cm^{-1}	ε
	2585	3						
	2585	3						
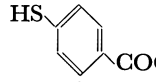	2586	8			1719[c]	700	1720sh 1714	 710
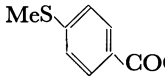					1719[c]	700	1720sh 1713	 800
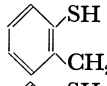	2560	20						
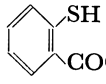	2556 2523	8[e] 32			1720sh 1714 1698	 360 320	1720sh 1707 1699	 600 180[e]
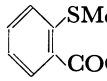					1722 1715	400 500	1720sh 1708	100[e] 620
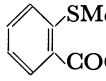			3531	(0.14)	1735 1691[d]	(0.11) (0.15)	1720sh 1718	 620
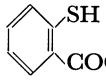	2558 2530	(0.41) (0.34)	3528	(0.35)	1733 1717 1687[d]	(0.18) (0.21) (0.49)	1720 1702sh	520 200[e]
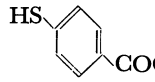	2586				1742 1693[d]	(0.17) (0.44)		

a) The value in parentheses is an optical density instead of ε.
b) sh: shoulder.
c) Relatively broadened on the higher-frequency side.
d) Dimer absorption.
e) Obtained by band-reflection.[9]

shows a reverse trend of solvent effect,[28] and (2) even in the other *p*-substituted benzoates where rotational isomers are not expected, a similar band appears near 1720 cm^{-1}.

It is further interesting that, in acetonitrile, thiosalicylic acid and its ethyl ester show, apart from the band ascribed to the Fermi resonance, two carbonyl bands; the relative intensities of the lower-frequency bands are much lower than those in carbon tetrachloride. There are at least two possibilities for the band-splitting: (1) absorptions due to groups other than the carbonyl or due to rotational isomers, and (2) intramolecular hydrogen bonding. The first one can probably be rejected since the other aromatic compounds, even those *o*-substituted, show no splitting. The second possibility should thus be considered. The basicity of acetonitrile is so strong as to allow benzoic acid to be practically monomeric even in a concentration of 1 mol/*l*.[28] Further, it has now been found that acetonitrile is a base so strong that the aliphatic and aromatic carboxylic acids examined in the present work show negligible dimer absorptions at 0.01 mol/*l* in carbon

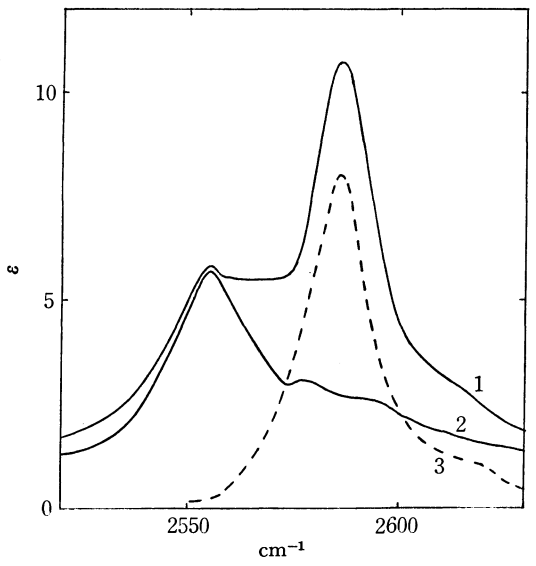

Fig. 7. The spectra of ethyl *p*-mercaptobenzoate (1) and its *S*-methylated compound (2); curve (3) is curve (2) subtrated from curve (1).

28) C. J. W. Brooks, G. Eglinton, and J. F. Morman, *J. Chem Soc.*, **1961**, 106.

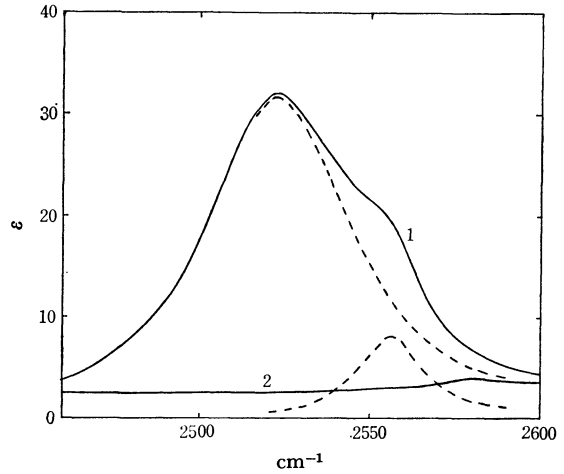

Fig. 8. The spectra of ethyl thiosalicylate (1) and its *S*-methylated compound (2); the dotted curves are the components graphically separated from curve (1).

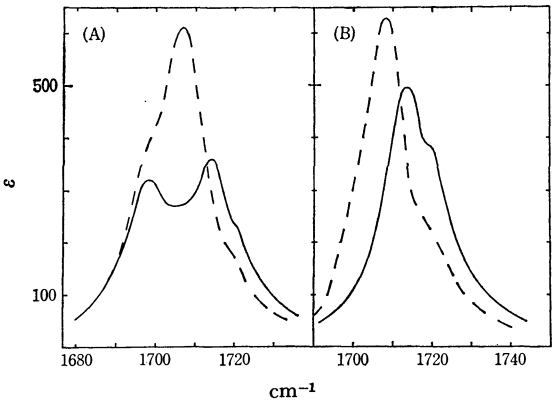

Fig. 9. The CO spectra of ethyl thiosalicylate (A) and its *S*-methyl compound (B) in CCl_4 (——) and CH_3CN (— —).

tetrachloride containing 20% by volume of acetonitrile. Nevertheless, the intramolecular hydrogen bond between the OH and CO groups in salicylic acid and also in its methyl ester can not be broken at all in acetonitrile, while the dimer formation of the acid through intermolecular hydrogen bonding is practically completely prevented.[29] Accordingly, the intramolecular hydrogen bonding in thiosalicylic acid and its ester is probably possible to some extent even in acetonitrile; however, this is not expected at all because of the very poor hydrogen-donating property of the mercapto group.

29) N. Mori, unpublished results: for salicylic acid, $\nu_{CO}=1695$ (monomer) and 1662 cm^{-1} (dimer) in CCl_4 and 1682 cm^{-1} in CH_3CN; for the methyl ester, $\nu_{CO}=1680$ cm^{-1} in both solvents. On the other hand, ethyl glycolate is internally bonded in CCl_4, but not in CH_3CN.

BULLETIN OF THE CHEMICAL SOCIETY OF JAPAN, VOL. 44, 1864—1868 (1971)

The Preparation and Properties of Mesoionic 5-Iminothiazole Derivatives

Toshie SHIBA and Hiroshi KATO[1)]

Department of Chemistry, Faculty of Science, Shinshu University, Asahi, Matsumoto 390

(Received October 28, 1970)

Mesoionic 5-iminothiazoles were prepared by the cyclization of *N*-thiobenzoyl-methylaminoacetonitriles with hydrogen chloride or acyl chlorides. The reaction between a 5-aminothiazolium chloride and acyl chlorides, isocyanate, sulfonyl chloride, and nitrous acid gave the corresponding *N*-substituted mesoionic 5-iminothiazole derivatives. The spectral data of these compounds as well as the ready bromination of the ring support the view that this ring system is aromatic.

Although the chemistry of mesoionic thiazole derivatives in general has been widely investigated,[2)] only a single derivative of mesoionic 5-iminothiazole (3,5-dihydro-5-iminothiazole or anhydro 3-substituted 5-aminothiazolium hydroxide) has been described in the literature.[3)] That paper concerns the formation of mesoionic 3-methyl-2,4-diphenyl-5-phenyliminothiazole by the proton-catalyzed rearrangement of mesoionic 1-methyl-2,3,5-triphenylimidazole-4-thione. This rearrangement has been found to be difficult to reproduce and no properties of the mesoionic 5-iminothiazole have been described. Unsuccessful attempts to prepare this ring system by the action of amines on 5-methylmercaptothiazolium salts have been reported earlier.[4)]

The preparation of some 3-substituted 5-aminothiazolium salts by the alkylation of the corresponding 5-aminothiazoles has been described earlier.[5,6)] In one case, even treatment with methyl iodide of 5-acetamido-2-thio-3-isopropylthiazoline in aqueus sodium hydroxide has been studied.[6)] It is reported, however, that this treatment, instead of affording the corresponding mesoionic compound or inner salt, gave the corresponding thiazolium hydroxide.

We wish to report here a more reliable method of

1) To whom inquiries should be addressed.

2) M. Ohta and H. Kato, "Nonbenzenoid Aromatics," ed. by J. P. Snyder, Academic Press, New York (1969), p. 117.

3) R. Huisgen, E. Funke, F. C. Schaeffer, H. Gotthardt, and E. Brunn, *Tetrahedron Lett.*, **1967**, 1809.

4) T. Shiba and H. Kato, This Bulletin, **43**, 3941 (1970).

5) A. H. Cook, I. M. Heilbron, and A. L. Levy, *J. Chem. Soc.*, **1947**, 1594; E. D. Sych and L. P. Umanskaya, *Zh. Obshch. Khim.*, **34**, 2068 (1964); *Chem. Abstr.*, **61**, 10805 (1964).

6) A. H. Cook and S. F. Cox, *J. Chem. Soc.*, **1949**, 2337.

synthesizing mesoionic 5-iminothiazoles, a method promising a wider synthetic applicability, and also some properties of the ring system thus prepared.

Results and Discussion

Preparation and Recations. The thiobenzoylation of two acetonitriles, Ia and Ib, gave *N*-thiobenzoylmethylaminoacetonitriles (IIa and IIb). The two nitriles, IIa and IIb, showed only a very weak absorption of a cyano group in the infrared region, suggesting the possibility that II may partly tautomerized to cyclic mesoionic iminothiazoles, II'. However, the lack of any infrared bands assignable to an NH group, and the fact that II did not react with acetic anhydride, eliminate such a possibility.

The treatment of thiobenzoylaminoacetonitriles, IIa and IIb, with hydrogen chloride in aprotic solvents gave 5-aminothiazolium hydrochlorides, IIIa and IIIb, as hygroscopic compounds. The hydrochlorides were characterized by conversion to the corresponding perchlorates and picrates. The structures of these salts were determined by elemental analyses, spectroscopic data, and the reactions to be described below. On heating the hydrochlorides, IIIa and IIIb, with acetyl and benzoyl chloride, the corresponding *N*-acetyl- and *N*-benzoyl-aminothiazolium chlorides, IVa—d,HCl, were formed. Alternatively, the same *N*-acylaminothiazolium chlorides, IVa—d,HCl, were prepared by the reaction of thiobenzoylaminoacetonitriles, IIa and IIb, with acetyl and benzoyl chloride in benzene. The mode of the formation of these compounds is analogous to that of sydnone imines.[7]

The treatment of the salts, IVa—d,HCl, with alkali afforded mesoionic 5-acyliminothiazoles, IVa—d. In a similar manner, the corresponding phenylcarbamoyl- and phenylthiocarbamoyl-iminothiazole, Va and Vb, were prepared by the treatment of 5-amino-3-methyl-2,3,4-diphenylthiazolium chloride (IIIa) with phenyl isocyanate and phenyl isothiocyanate respectively. Thiazolium chloride, IIIa, reacted with benzenesulfonyl chloride in the presence of a base to afford mesoionic 5-benzenesulfonyliminothiazole, VI. By the action of sodium nitrite on IIIa, *N*-nitroso-iminothiazole VII was formed slowly. It was anticipated that the elimination of a molecule of nitrogen from VII, in a fashion analogous to that with *N*-nitroso-sydnone imines,[8] would give the corresponding mesoionic 5-oxothiazole.[2,9] However, both the pyrolysis and photolysis of the *N*-nitroso derivative, VII, in aprotic solvents resulted in a polymer formation, and no nitrogen evolution was observed.

In order to obtain chemical support concerning the aromatic nature of the mesoionic 5-iminothiazole ring, the bromination of IVd was carried out. Bromination took place readily at the 4-position of IVd to afford 4-bromo-5-benzoylimino-3-methyl-2-phenylthiazole VIII. The structure of the bromide was assigned on the basis of elemental analyses, the lack of an NMR signal around τ 2.7, and the lack of an infrared band at 3080 cm^{-1} (*vide infra*).

The hydrochlorides III and acyliminothiazoles IV

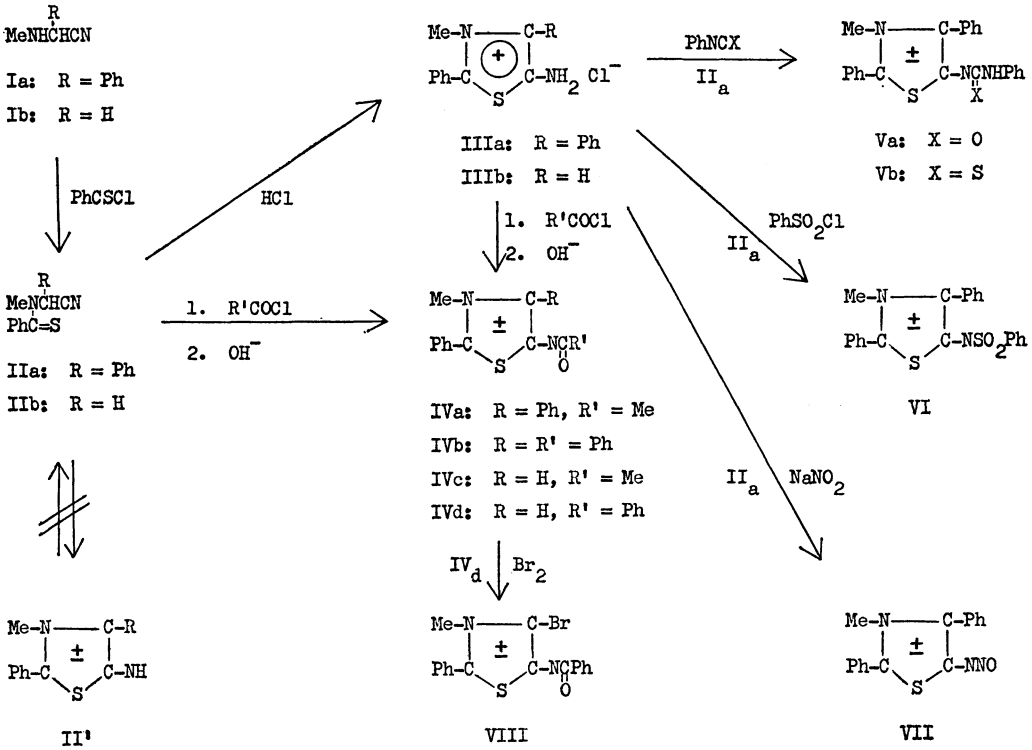

Scheme 1. Preparation and Reactions of 5-iminothiazoles

7) H. Kato, M. Hashimoto, and M. Ohta, *Nippon Kagaku Zasshi*, **78**, 707 (1957).

8) L. E. Kholodov and V. G. Yashunskii, *Byul. Izobret Tovarnykh Znakov, No.* **16**, 37 (1965); *Chem. Abstr.*, **64**, 3557 (1966); S. A. Zotova and V. G. Yashunski, *Zh. Organ. Khim.*, **3**, 1889 (1967).

9) A. Lawson and C. E. Searle, *J. Chem. Soc.*, **1957**, 1556; G. C. Barrett and A. R. Khokhar, *J. Chem. Soc., C*, **1969**, 1117.

are quite stable to acid, and were recovered unchanged after having been heated with 10% hydrochloric acid for one hour. It appears that the iminothiazoles have a considerable basicity because the hydrochloride IIIa was unchanged by treatment with aqueous sodium hydrogen carbonate. Even the *N*-acyl derivatives IV readily form hydrochlorides and picrates.

Spectral Properties (Cf. Tables 1 and 2). The large hypsochromic shifts of the ultraviolet absorption maxima of IV at the longest wave length with an increase in the solvent polarity show that they are n→π transitions; they may also suggest that there is a considerable charge separation between the heterocyclic ring and the exocyclic acylimido group.[10]

The infrared spectra of 5-iminothiazoles unsubstituted at the 4-position show a medium intensity peak at 3100 cm^{-1} (hydrochlorides) or 3080 cm^{-1} (free bases) which may be assigned as the C–H stretching band of the 4-position. None of the free bases of *N*-acyl (IVa—d) and *N*-carbamoyl (Va) derivatives shows an infrared absorption band of the carbonyl group in a region normally expected for an amide group. The infrared spectra of the corresponding salts (IVa—d, HCl, Va,HCl) show an absorption at 1630—1680 cm^{-1}, but this absorption is weaker than that expected for a normal amide carbonyl band. Moreover, they usually show both the absorption bands assignable to a hydroxyl and an ammonium (and/or amino) group.

The NMR signal of the 3-methyl group of mesoionic iminothiazoles, IV, appears at τ 6.05—6.25, a position which is higher by *ca.* 0.2 ppm than that of the corresponding aminothiazolium chlorides, IV,HCl. The signal of the proton at the 4-position of IVc and IVd appears at *ca.* τ 2.7, whereas that of thiazolium hydrochloride, IVc,HCl, is shifted considerably to a lower magnetic field and appears at τ 1.15. This shift of the proton signal with the hydrochloride may partly be due to a solvent effect, because this spectrum had to be taken in a mixture of deuteriochloroform and deuteriodimethyl sulfoxide. In fact, the position of the proton signal of the 4-position of IVb is fairly much dependent upon the solvent employed (Table 2). This shift is probably due to the formation of a hydrogen bond with the solvent.[11] The chemical shift values of the

TABLE 1. ULTRAVIOLET AND INFRARED SPECTRA OF 5-IMINOTHIAZOLE DERIVATIVES

Compound	λ_{max}^{EtOH} (nm) (log ε)	IR (KBr, cm^{-1})[a]
IIIa[b]	250 (4.004)	3420, 3230, 3100, 1670, 1565, 1475, 1360, 1320
	320 (4.021)	
IIIb[c]	350 (4.032)	3210, 3110, 1580, 1515, 1315
IVa,HCl	250 (4.039)	3640, 3240, 2930, 3680—2160, 1660, 1580, 1515, 1480, 1360, 1270
	320 (4.076)	
IVb,HCl	230 (4.356)	3600—2200,1630, 1580, 1480, 1280
	325 (4.170)	
IVc,HCl	240 (3.908)	3660—3200, 3100, 2900—2500, 2790, 2750, 2710, 2610, 1660, 1580, 1530, 1355, 1285
	318 (4.083)	
IVd,HCl	230 (4.233)	3650—2500, 2930, 1750,1650, 1580, 1520, 1304
	320 (4.164)	
Va,HCl		3660—2500, 1680,1580, 1550, 1485, 1300, 1215

	λ_{max}^{EtOH}	Pyridine	Tetrahydrofuran	Cyclohexane[d]	IR (KBr, cm^{-1})[a]
IVa	240 (4.078)			255	1550, 1520, 1450, 1380
	304 (3.868)	325 (3.951)	325 (4.017)	330	
	374 (3.992)	405 (4.067)	410 (4.071)	420	
IVb	228 (4.385)				1580, 1500, 1450, 1430, 1370
	328 (4.051)	340 (4.072)			
	390 (4.232)	435 (4.176)			
IVc	250 (3.987)			257	3080, 1560, 1490, 1470, 1380, 1220
	360 (4.028)	388 (4.102)	394 (4.051)	400	
IVd	287 (3.856)				3080, 1580, 1560, 1490, 1470, 1385, 1340
	372 (4.257)	397 (4.267)			
Va					3260, 1590, 1560, 1450, 1375, 1300

a) Only medium to strong bands between 4000—1200 cm^{-1} are listed. Underlined wave-numbers indicate the strongest bands.
b) UV spectrum was taken on perchlorate.
c) Perchlorate
d) Due to the low solubility in this solvent, extinction coefficients could not be determined.

10) A. E. Gillam and E. S. Stern, "An Introduction to Electronic Absorption Spectroscopy in Organic Chemistry," Edward Arnold, London (1955), P. 260; W. A. Lees and A. Buraway, *Tetrahedron*, **19**, 419 (1963).

11) J. W. Emsley, J. Feeney, and L. H. Sutcliffe, "High Resolution Nuclear Magnetic Resonance Spectroscopy," Vol. II, Pergamon Press, Oxford (1966), p. 855; R. F. Smith, J. L. Deutsch, P. A. Almeter, D. S. Johnson, S. M. Roblyer, and T. C. Rosenthal, *J. Heterocycl. Chem.*, **7**, 671 (1970).

Table 2. NMR spectra of 5-iminothiazole derivatives

Compound	2-Ph	3-Me	4-Ph	4-H	5-Substituent
IIIa	2.40—2.60	6.15	2.15—2.40 2.40—2.60	—	4.60—5.10
IIIb[a,b]	2.33	6.01	—	2.68	—
IVa,HCl	2.15—2.40	6.07	1.82—1.93 2.55—2.70	—	7.70
IVb,HCl	1.98—2.62	6.07	1.98—2.62	—	1.98—2.62
IVc,HCl[a]	2.30	5.88	—	1.15	7.68
IVa	2.42	6.25	2.30—2.62	—	7.81
IVb[a]	2.15—2.80	6.12	2.15—2.80	—	2.15—2.80
IVc	2.46	6.05	—	2.68[c]	7.74
IVd	2.46	6.09	—	2.72	1.65—1.78 2.50—2.65
VIII	2.43	5.98	—	—	1.55—1.73 2.50—2.64

a) Measured as a solution in $CDCl_3$-DMSO-d_6 (1:1)
b) Perchlorate
c) Chemical shifts in other solvents: DMF: 705, dioxane: 731, acetonitrile: 739, acetone: 743, $CDCl_3$-DMSO-d_6 (1:1): 753 Hz downfield from internal TMS.

3-methyl group and the 4-hydrogen atom are those usually encountered with common aromatic azoles[12] and many other mesoionic ring systems.[2]

From the properties of IV described above, one may infer that this ring system shows a certain degree of aromaticity, that there is a considerable charge separation between the ring and the exocyclic acylimido group, and that the acyl group is considerably polarized.

Experimental[13]

The Attempted Proton-catalyzed Isomerization of 1-Methyl-2,3,5-triphenylimidazole-4-thione.[3] *a*) A solution of 1 g of 1-methyl-2,3,5-triphenylimidazole-4-thione (imidazolethione) in 50 m*l* of chloroform was saturated with dry hydrogen chloride with cooling. After stirring for four hours at 20°C, the solvent was distilled off and the colorless residue of the hydrochloride (mp 195—197°) was collected. On treatment with aqueous sodium bicarbonate or even with water, 0.8 g of imidazolethione was recovered.

Imidazolethione was recovered in 75—100% yields, after treatment with bicarbonate or with water, when the chloroform solution was treated with: *b*) a slow stream of hydrogen chloride for fifteen hours at 20—30°C, *c*) with an equivalent amount of hydrogen chloride for five hours or overnight, or *d*) with conc. hydrochloric acid for two hours, or *e*) when a solution of imidazolethione in tetrahydrofuran was treated as has been described in procedure *a*). In every case, the crude hydrochloride or the recovered crude imidazolethione showed no infrared absorption at 1670 cm^{-1}.

1,3-Dimethyl-2,5-diphenylimidazole-4-thione[4] was also recovered unchanged when it was treated by methods similar to those described above.

N-Thiobenzoyl-α-phenyl-methylaminoacetonitrile (IIa) Into a solution of 3 g (0.019 mol) of thiobenzoyl chloride in 20 m*l* of triethylamine, there was dropwise added with stirring at 0°C, 2.8 g (0.019 mol) of α-phenyl-methylaminoacetonitrile. After thirty minutes' stirring, the solvent was removed under reduced pressure and the residue was extracted with benzene. The benzene extract was washed with water and dried over sodium sulfate. After the solvent had been distilled off, an oily residue remained; this solidified upon the addition of isopropanol, Recrystallization from isopropanol gave 2 g (54% yield) of yellow prisms melting at 79—81°C. IR: 2230 (CN), 1380, 1068 (C=S); NMR: 7.05 (3H, s, Me), 2.30—2.80 (10H ,m, Ph), 1.55 (1H, s, CH).

Found: C, 71.93; H, 5.32; N, 10.54%. Calcd for $C_{16}H_{14}N_2S$: C, 72.16; H, 5.30; N, 10.52%.

N-Thiobenzoyl-methylaminoacetonitrile (IIb). This was prepared in a 50% yield, by a method similar to that described above, from 2 g (0.028 mol) of methylaminoacetonitrile and 4.4 g (0.028 mol) of thiobenzoyl chloride. Colorless needles (from isopropanol); mp 123—124°C. IR: 2240 (CN), 1375, 1084 (C=S); NMR 6.70 (3H, s, Me), 4.92 (2H, s, CH_2), 2.60 (5H, s, Ph).

Found: C, 62.87; H, 5.43; N, 14.53%. Calcd for $C_{10}H_{10}N_2S$: C, 63.15; H, 5.30; N, 14.73%.

5-Amino-3-methyl-2,4-diphenylthiazolium Chloride (IIIa). Hydrogen chloride was saturated to a solution of 1 g of IIa in 40 m*l* of anhydrous ether. The white powder which slowly separated out was recrystallized from ethanol-acetone (2:5) to give 1 g (91% yield) of colorless prisms melting at 206—207°C.

Found: C, 63.32; H, 5.12; N, 9.52%. Calcd for $C_{16}H_{15}N_2SCl$: C, 63.57; H, 4.97; N, 9.27%.

Perchlorate. Colorless prisms [from ethanol-acetone (1:4)]: mp 302—303°C.

Found: C, 52.77; H, 4.05; N, 7.24%. Calcd for $C_{16}H_{16}N_2O_4SCl$; C, 52.48; H, 4.38; N, 7.61%.

Picrate. Yellow needles (from ethanol): mp 200—201.5°C. Found: C, 53.63; H, 3.26; N, 13.81%. Calcd for $C_{22}H_{17}N_5O_7S$: C, 53.33; H, 3.45; N, 14.13%.

5-Amino-3-methyl-2-phenylthiazolium Chloride (IIIb). This was prepared by the saturation of hydrogen chloride in a

12) *Cf. e.g.*, "NMR Spectra Catalog," Vol. I and II, Varian Associates, Palo Alto, Calif, (1962, 1963); H. A. Szymanski and R. E. Yelin, "NMR Band Handbook," IFI/Plenum, New York (1968).

13) The melting points were determined on a micro hot stage, and are not corrected. The ultraviolet spectra were recorded on a Hitachi model ESP-2U spectrophotometer and the infrared spectra were recorded as KBr disks on a Hitachi model EPI-SII spectrophotometer. The NMR spectra were measured using a JEOLCO JNM-4H-100 (100 MHz) spectrometer in deuteriochloroform solutions containing tetramethylsilane as internal standard, and the chemical shifts are given in τ values. The mass spectra were measured at 75 eV using a direct inlet technique.

benzene solution of IIb. Since it was very hygroscopic, it was characterized by converting it to the corresponding perchlorate and picrate. The yields were in the range of 80—95%.

Perchlorate. White prisms; mp 132—133°C. Found: C, 41.52; H, 3.58; N, 9.48%. Calcd for $C_{10}H_{11}N_2O_4SCl$: C, 41.38; H, 3.79; N, 9.65%.

Picrate. Yellow needles (from ethanol); mp 125—126°C. Found: C, 45.98; H, 3,37; N, 16.89%. Calcd for $C_{16}H_{13}N_5O_7S$: C, 45.83; H, 3,13; N, 16.70%.

5-Acetylamino-3-methyl-2,4-diphenylthiazolium Chloride (IVa, HCl). (*a*) A solution of 5 g (0.02 mol) of nitrile IIa and 3.1 g(0.04 mol) of acetyl chloride in 50 m*l* of benzene was allowed to stand for two days at room temperature. The white precipitate was recrystallized from acetone-isopropanol (4:1) to give 4.8 g (70% yield) of fine, colorless needles melting at 207—208°C (dec.).

Found: C, 62.43; H, 5.10; N, 7.72%. Calcd for $C_{18}H_{17}N_2OSCl$: C, 62.69; H, 4.97; N, 8.12%.

(*b*) A mixture of 0.22 g of thiazolium chloride, IIIa, and 3 m*l* of acetyl chloride was heated under reflux on a water bath for two hours. After cooling, the solid precipitate was collected, washed with ether, and recrystallized from acetone-isopropanol (4:1) to give the same product, IVa,HCl, in a 84% yield.

Picrate of IVa. Yellow needles (from ethanol); mp 166—167°C. Found: C, 58.19; H, 3.73; N, 11.42%. Calcd for $C_{29}H_{21}N_5O_8S$: C, 58.09; H, 3.51; N, 11.68%.

5-Acetylimino-3-methyl-2,4-diphenylthiazole (IVa). An aqueous solution of IVa,HCl was made alkaline with sodium hydrogen carbonate and was then extracted with benzene. The benzene extract was dried over sodium sulfate, the solvent was distilled off, and the residue was recrystallized from acetone to give yellow prisms; mp 229—230°C. Mass *m/e* (rel. intensity): 308(33,P), 293 (65, P—Me), 265 (1, P—Ac), 121 (100, PhC=S), 118 (37, PhC=MMe), 77 (43, Ph), 43 (27, Ac).

Found: C, 69.83; H, 5.12; N, 8.80%. Calcd for $C_{18}H_{16}N_2OS$: C, 70.10; H, 5.22; N, 9.08%.

By procedures similar to those described above, the following compounds were prepared.

5-Benzoylamino-3-methyl-2,4-diphenylthiazolium Chloride (IVb, HCl). Colorless prisms [from acetone-ethanol (4:1)]; mp 187—188°C, yield 74%.

Found: C, 67.60; H, 4.68; N, 6.68%. Calcd for $C_{23}H_{19}N_2OSCl$: C, 67.90; H, 4.71; N, 6.89%.

Picrate of IVb. Yellow needles (from ethanol); mp 166—167°C.

Found: C, 58.19; H, 3.73; N, 11.42%. Calcd for $C_{29}H_{21}N_5O_8S$: C, 58.09; H, 3.51; N, 11.68%.

5-Benzoylimino-3-methyl-2,4-diphenylthiazole (IVb). Yellow prisms (from acetone); mp 259—260°C; yield, 82%.

Found: C, 74.79; H, 4.87; N, 7.25%. Calcd for $C_{23}H_{18}N_2OS$: C, 74.58; H, 4.90; N, 7.56%.

5-Acetylamino-3-methyl-2-phenylthiazolium Chloride (IVc,HCl). Colorless prisms (from isopropanol); mp 243—244°C (dec); yield, 87%.

Found: C, 53.36; H, 5.02; N, 10.16%. Calcd for $C_{12}H_{13}N_2OSCl$: C, 53.63; H, 4.88; N, 10.42%.

5-Acetylimino-3-methyl-2-phenylthiazole (IVc). Colorless needles (from acetone); mp 219—220°C; yield, 75%. Mass *m/e* (rel. intensity): 232 (35, P), 217 (100, P—Me), 189 (1, P—Ac), 121 (74, PhC=S), 118 (28, PhC=NMe), 77 (very intense, Ph), 43 (very intense, Ac).

Found: C, 61.92: H, 5.29; N, 12.24%. Calcd for $C_{12}H_{12}N_2OS$: C, 62.06; H, 5.21; N, 12.06%.

5-Benzoylamino-3-methyl-2-phenylthiazolium Chloride (IVd,HCl). Colorless prisms (from isopropanol); mp 237—238°C; yield, 91%.

Found: C, 61.40; H, 4.56; N, 8.24%. Calcd for $C_{17}H_{15}N_2OSCl$: C, 61.72; H, 4.57; N, 8.46%.

5-Benzoylimino-3-methyl-2-phenylthiazole (IVd). Yellow leaflets (from acetone-ethanol); mp 261—262°C; yield, 90%.

Found: C, 69.18; H, 4.74; N, 9.73%. Calcd for $C_{17}H_{14}N_2OS$: C, 69.37; H, 4.80; N, 9.52%.

5-Phenylcarbamoylimino-3-methyl-2,4-diphenylthiazole (Va). This was prepared from IIa and phenyl isocyanate by heating them on a water bath for 2 hr, and then treating them with sodium hydrogen carbonate. Yellow prisms (from acetone-ethanol); mp 245—246°C; yield, 75%.

Found: C, 72.10; H, 4.75; N, 11.17%. Calcd for $C_{23}H_{19}N_3OS$: C, 71.67; H, 4.97; N, 10.90%.

Hydrochloride of Va. White prisms (from acetone); mp 230—231°C (dec.).

Found: C, 65.07; H, 4.52; N, 9.63%. Calcd for $C_{23}H_{20}N_3OSCl$: C, 65.47; H, 4.77; N, 9.95%.

5-Phenylthiocarbamoylimino-3-methyl-2,4-diphenylthiazole (Vb). Yellow leaflets (from aceton-ethanol); mp 241—242°C; yield, 82%.

Found: C, 68.50: H, 4.54; N, 10.10%. Calcd for $C_{23}H_{19}N_3S_2$: C, 68.82; H, 4.77; N, 10.47%.

5-Benzenesulfonylimino-3-methyl-2,4-diphenylthiazole (VI) To a solution of 0.5 g of IIIa in 5 m*l* of water, 0.3 g of benzenesulfonyl chloride and then two molar equivalents of aqueous potassium hydroxide were slowly added with cooling and stirring. The precipitate was recrystallized from ethanol to give 0.25 g (37% yield) of yellow prisms melting at 242—243°C. IR: 1130 (SO_2).

Found: C, 64.76; H, 4.23; N, 6.77%. Calcd for $C_{22}H_{18}N_2O_2S_2$: C, 65.02; H, 4.46; N, 6.89%.

5-Nitrosoimino-3-methyl-2,4-diphenylthiazole (VII). To a cooled solution of 1.0 g of IIIa in 6 m*l* of water, a solution of 0.3 g of sodium nitrite in 4 m*l* of water was added, after which the mixture was allowed to stand for two days at room temperature. The yellow precipitate which slowly separated out was recrystallized from ethanol to give 0.5 g (51% yield) of yellow prisms melting at 187—188°C (dec.). IR: 1110, 1190 (N-O-?).

Found: C, 64.85; H, 4.51; N, 13.99%. Calcd for $C_{16}H_{13}N_3OS$: C, 65.08; H, 4.44; N, 14.23%.

5-Benzoylamino-4-bromo-3-methyl-2-phenylthiazolium Bromide (VIII,HBr). To a suspension of 0.5 g of IVd in 20 m*l* of ether, 0.1 m*l* of bromine was added with stirring and cooling. After twenty minutes, the newly-formed precipitate was recrystallized from ethanol to give 0.5 g (80% yield) of white prisms melting at 184—185°C (dec.). IR: 3340, 1660, 1570, 1455, 1305, 1270.

Found: C, 44.60; H, 2.94; N, 5.96%. Calcd for $C_{17}H_{14}N_2OSBr_2$: C, 44.96; H, 3.11; N, 6.17%.

The Free Base VIII was formed by the treatment of the hydrobromide with aqueous sodium hydrogen carbonate. Yellow prisms (from ethanol); mp 235—236°C. IR: 1460, 1380.

Found: C, 54.84; H, 3.31; N, 7.22%. Calcd for $C_{17}H_{13}N_2OSBr$: C, 54.71; H, 3.51; N, 7.51%.

We wish to thank Professor Masaki Ohta of Tokyo Institute of Technology and Professor Kameji Yamane of this Department for discussions and encouragement. We are also indebted to Kyorin Chemical Laboratories for performing the elemental analyses and the mass-spectral determination.

Isolation and Characterization of Pteridines from *Pseudomonas ovalis*

Akira SUZUKI and Miki GOTO

Department of Chemistry, Gakushuin University, Toshima-ku, Tokyo

(Received October 29, 1970)

Four ribityllumazine compounds were isolated from the cultured medium of *Pseudomonas ovalis*. Three of them were characterized as 6-methyl-8-(1-D-ribityl)-2,4,7-trioxohexahydropteridine, 6-(3-indolyl)-8-(1-D-ribityl)-2,4,7-trioxohexahydropteridine and 6-(*p*-hydroxyphenyl)-8-(1-D-ribityl)-2,4,7-trioxohexahydropteridine by comparison with synthetic samples. The fourth compound, named *putidolumazine*, was supposed to be a new compound (2-carboxyethyl)-8-(1-D-ribityl)-2,4,7-trioxohexahydropteridine from its chemical and spectroscopic properties. This was confirmed from the identity of both natural and synthetic products.

6,7-Dimethyl-8-(1-D-ribityl)-2,4-dioxohexahydropteridine (Compound G)[1] and 6-methyl-8-(1-D-ribityl)-2,4,7-trioxohexahydropteridine (Compound V) (IV)[2] were isolated from *Eremothecium ashbyii* as a green and a purple fluorescent materials, respectively. Recently, two new ribityllumazines were isolated from *Achromobacter petrophilum* by Takeda and Hayakawa.[3] One of them was identified as 6-(3-indolyl)-8-(1-D-ribityl)-2,4,7-trioxohexahydropteridine (III)[4] and the other was supposed to be 6-(*p*-hydroxyphenyl)-8-(1-D-ribityl)-2,4,7-trioxohexahydropteridine (II), the structure being proposed on the basis of biosynthesis.[5]

The function of ribityllumazines was recently clarified; *i.e.* Compound G is an intermediate of riboflavin and Compound V functions as an inhibitor.[6] Tyrosine and tryptophan have been found to be effectively incorporated into II and III.[5]

This paper describes the isolation of four ribityllumazine compounds from cultures of *Pseudomonas ovalis*. Three of them have been identified as compounds II, III, and IV. The last compound (*Putidolumadine*) is assumed to be a new ribityllumadine compound, 6-(2-carboxyethyl)-8-(1-D-ribityl)-2,4,7-trioxohexahydropteridine (I), from spectroscopic and chemical data. This was confirmed by the synthesis from 2,6-dihydroxy-5-nitro-4-D-ribitylaminopyrimidine and α-ketoglutaric acid.

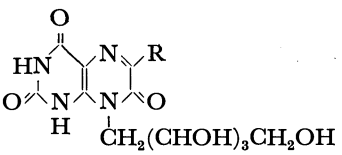

(I) R: $-CH_2CH_2COOH$

(II) R: 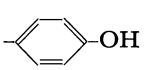

(III) R: 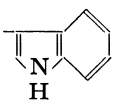

(IV) R: $-CH_3$

1) T. Masuda, *Pharm. Bull. Jap.*, **5**, 375 (1958).
2) T. Masuda, T. Kishi, and M. Asai, *ibid.*, **6**, 291 (1958).
3) I. Takeda and S. Hayakawa, *Agr. Biol. Chem.*, **32**, 873 (1968).
4) W. S. McNutt and I. Takeda, *Biochemistry*, **8**, 1370 (1969).
5) I. Takeda, *Hakko Kyokaishi*, **27**, 305 (1969).
6) G. W. E. Plaut, *J. Bio. Chem.*, **238**, 2225 (1963).

Experimental

Isolation of Ribityllumazines. *Pseudomonas ovalis* (IAM 1506) was cultivated for 10 days in a fermentation jar (capacity: 20 *l*) at 32°C with aeration. The medium used was 0.75% casein enzymatic hydrolysate (10 *l*); the solution was adjusted to pH 7.0 with ammonia. After centrifugation the culture was concentrated to about 100 m*l* *in vacuo* below 40°C. Ribityllumazines were separated by conventional chromatographic methods using a cellulose column (7×25 cm) and isopropyl alcohol-1% ammonia (2:1) as a solvent. The fluorescent compounds were separated into two bands, *i.e.* a band containing green, purple and blue fluorescent compounds (Fraction 1), and a band containing a greenish-blue fluorescent compound (Fraction 2). The two fluorescent bands were eluted and the eluates were evaporated to dryness *in vacuo* at below 40°C. The residues were again purified chromatographically using a cellulose column (5×12 cm; solvent: water) for Fraction 2 and a DEAE-cellulose column (5×22 cm; solvent: 1 *l* of water, followed by 0.003 N hydrochloric acid) for Fraction 1. The greenish-blue fluorescent compound from Fraction 2 was eluted and eluate was evaporated to dryness *in vacuo*. The residue was dissolved in a small amount of water, and acetone was added. The precipitate was washed with cold water and dried over P_2O_5; yield, 3 mg (UV: $\lambda_{max}^{0.1N\ NaOH}$ mμ, 260, 307, 403; $\lambda_{max}^{H_2O}$ mμ, 215, 299, 377; $\lambda_{max}^{0.1N\ HCl}$ mμ, 240, 295, 365). This compound was identified as 6-(*p*-hydroxyphenyl)-8-(1-D-ribityl)-2,4,7-trioxohexahydropteridine (II) by comparison with synthetic material (see blow) and also with Compound GB, which was isolated from *Achromobacter petrophilum*[3].

Table 1. Paper chromatography and electrophoresis of pteridines

Substance	Solvents[a] A	B	C	D	Electrophoresis[b]
Greenish-blue fluorescent compound	0.23	0.19	0.11	0.10	7
After KIO_4 oxidation and $NaBH_4$ reduction	0.37	0.26	0.09	0.22	6
Compound GB	0.23	0.19	0.11	0.10	7
II	0.23	0.19	0.11	0.10	7
VI	0.37	0.26	0.09	0.22	6

a) Solvents: A. isopropyl alcohol: 2% ammonium acetate (1:1)
B. isopropyl alcohol: 1% ammonia (2:1)
C. 3% aqueous ammonium chloride
D. *n*-butyl alcohol: acetic acid: water (4:1:1)
b) Distance (in mm) to anode after paper electrophoresis at pH 4.65 (sodium acetate buffer) for 60 min at 18V/cm.

The compound thus obtained (*ca.* 1 mg) was dissolved in 0.2 m*l* of water and 4 mg of potassium periodate was added. After one hour the product was purified by paper chromatography using water as a solvent. The oxidation product was then reduced with a small amount of sodium borohydride in 0.1 m*l* of 1% ammonia. The solution was kept standing at room temperature for 30 min, then adjusted to pH 1 with hydrochloric acid. The product was again purified by paper chromatography using water as a solvent. The final product was identified as 6-(*p*-hydroxyphenyl)-8-(2-hydroxyethyl)-2,4,7-trioxohexahydropteridine (VI) by comparison with synthetic material (see Table 1).

The material from Fraction 1 was separated into two purple fluorescent and one greenish-yellow fluorescent bands on a DEAE-cellulose column. The greenish-yellow compound was further purified by column chromatography using a cellulose column (7×25 cm) and isopropyl alcohol-1% ammonia (2:1) as solvent; yield, *ca.* 30 mg. The material was recrystallized twice from 50% acetic acid to give yellow crystals; yield, 15.3 mg, mp 285—286°C (decomp.) (UV: $\lambda_{max}^{0.1N\ NaOH}$ mμ, 271, 308, 401; $\lambda_{max}^{H_2O}$ mμ, 213, 312, 398; $\lambda_{max}^{0.1N\ HCl}$ mμ, 216, 317, 390).

Found: C, 50.40; H, 4.39; N, 14.50%. Calcd for $C_{19}H_{19}O_7N_5 \cdot H_2O$: C, 51.00; H, 4.73; N, 15.65%.

The compound was identified as 6-(3-indolyl)-8-(1-D-ribityl)-2,4,7-trioxohexahydropteridine (III) by comparison with synthetic material (see below) and also with Compound GY, which was isolated from *Achromobacter petrophilum* by McNutt and Takeda[4] (Table 2). The purple fluorescent compound was identified as 6-methyl-8-(1-D-ribityl)-2,4,7-trioxohexahydropteridine (IV) by comparison with Compound V of Masuda[2] (Table 2). The yield was *ca.* 2 mg.

Table 2. Paper chromatography and electrophoresis of pteridines

Substance	Solvents[a] A	B	C	D	Electrophoresis[b]
Greenish-yellow fluorescent compound	0.13	0.13	0.02	0.11	2
Purple fluorescent Compound	0.57	0.35	0.62	0.14	23
Compound GY	0.13	0.13	0.02	0.11	2
III	0.13	0.13	0.02	0.11	2
Compound V	0.57	0.35	0.62	0.14	23

a) and b): See the footnote in Table 1.

Another purple fluorescent compound (putidolumazine) was further purified by conventional chromatographic methods using the following column and solvent: 1. a cellulose column (7×25 cm); developer: isopropyl alcohol-1% ammonia (2:1), and 2. a Sephadex G-25 column (5.5×25 cm); developer: water. The crude product (30 mg) from 30 *l* of the cultured medium was recrystallized twice from water to give colorless needles; yield, 8 mg; mp >265°C (decomp.).

Found: C, 42.27; H, 4.44; N, 14.08%. Calcd for $C_{14}H_{18}O_9N_4 \cdot H_2O$: C, 41.58; H, 4.95; N, 13.86%, The compound contained neither S nor P. The sample was dried over P_2O_5 for 10 hr at 100—110°C and 3 Torr. *Rf*-values and UV-spectra of putidolumazine are given in Table 3 and Fig. 1.

Reaction of Putidolumazine. Esterification. Putidolumazine (15 mg, recovered from mother liquid) dissolved when it was suspended in absolute ethanol and saturated with dry HCl gas. The reaction mixture was concentrated *in vacuo* below 40°C and purified by chromatography using a cellulose column (5×25 cm; developer: 50% isopropyl alcohol). The eluate was evaporated to dryness *in vacuo* below 40°C, and pale brown precipitate was obtained by recrystallization from a ethanol - ether; yield, 12.4 mg. Recrystallization of the product from ethanol gave a faint yellow product; yield, 5.4 mg, mp 117—120°C; additional crops (*ca.* 5 mg) were also obtained from the mother liquid.

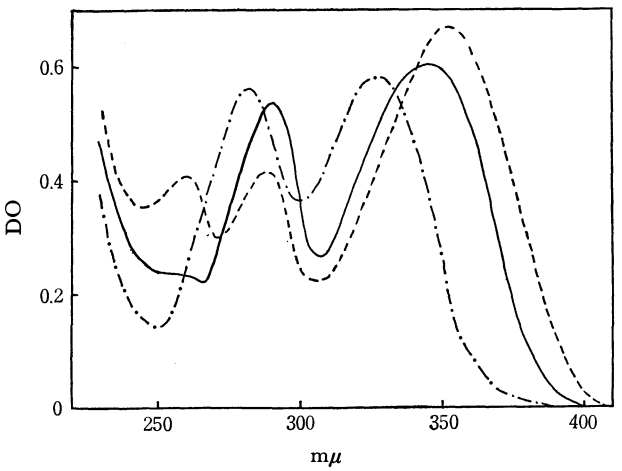

Fig. 1. Ultraviolet absorption spectrum of putidolumazine.
------: In 0.1N NaOH
——: In water
– · –: In 0.1N HCl

Found: N, 14.06%. Calcd for $C_{16}H_{22}O_9N_4$: N, 13.52%.

Acetylation of the Esterified Product: To a mixture of 1 m*l* of pyridine and 1 m*l* of acetic anhydride, 10 mg of the esterified product was added, and the whole was left standing at room temperature. After 2 days the reaction mixture was concentrated to dryness *in vacuo* below 40°C. Pale brown material was obtained by recrystallization from ethyl acetate-ether; yield, 6 mg. Mass spectrum of this compound is shown in Fig. 2.

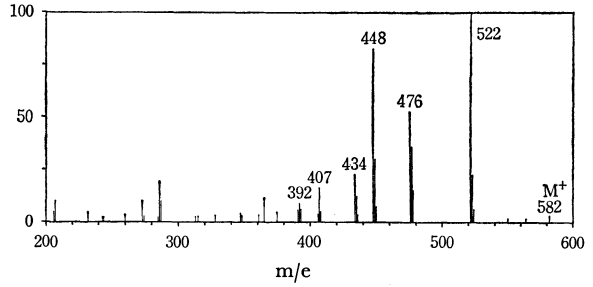

Fig. 2. Mass spectrum of acetylated putidolumazine-ester.

Periodate Oxidation: One milliliter of aqueous solution of putidolumazine (3.85×10^{-5} M) was treated with 2 m*l* of aqueous potassium metaperiodate solution (12.9×10^{-5} M, pH 4.2) at room temperature. At intervals the amount of understroyed periodate was estimated from UV-absorption (223 mμ) by the method of Dixon and Lipkin.[7] The compound (M, 386) consumed 4.70 mol of periodate per mole. For the sake of comparison, an authentic sample of Compound V of Masuda was subjected to periodate oxidation; it consumed 4.25 mol of periodate per mole.

$NaBH_4$ Reduction of the Periodate Oxidation Product: Putidolumazine (*ca.* 2 mg) was dissolved in 0.4 m*l* of water and 4 mg of KIO_4 was added. After 1 hr, the oxidation

7) J. S. Dixon and D. Lipkin, *Anal. Chem.*, **26**, 1092 (1954).

product was purified by paper chromatography using *n*-butyl alcohol-acetic acid-water (4:1:1) and isopropyl alcohol-water (2:1) as solvents. The periodate oxidation product was dissolved in 0.3 m*l* of warm water. The solution was cooled and a small amount of $NaBH_4$ was added. After standing at room temperature for 30 min, the solution was adjusted to pH 1 with hydrochloric acid and chromatographed on paper with a solvent of isopropyl alcohol-1% ammonia (2:1); the product was indistinguishable from synthetic 6-(2-carboxyethyl)-8-(2-hydroxyethyl)-2,4,7-trioxohexahydropteridine (V) (see below) (Table 3).

Photodecompositon: Putidolumazine (2.5 mg) was dissolved in 3 m*l* of 0.6 N NaOH. After addition of 0.3 m*l* of 30% H_2O_2, the solution was irradiated in a glass tube with an electric lamp of 100 W from a distance of 15 cm for 20 hr. The decomposition product was purified by paper chromatography using *n*-butyl alcohol-acetic acid-water (4:1:1) and isopropyl alcohol-1% ammonia (2:1) as solvents. The product was identified as 6-(2-carboxyethyl)-2,4,7-trioxohexahydropteridine (VII) by comparison with synthetic material (Table 3).

Table 3. Paper chromatography and electrophoresis of pteridines

Substance	Solvents[a]				Electrophoresis[b]
	A	B	C	D	
Putidolumazine	0:45	0.31	0.73	0.12	34
After KIO_4 oxidation and $NaBH_4$ reduction	0.55	0.37	0.68	0.23	39
After photoirradiation	0.36	0.28	0.47	0.21	32
After esterification	0.76	0.75	0.73	0.43	17
I	0.45	0.31	0.73	0.12	34
V	0.55	0.37	0.68	0.23	39
VII	0.36	0.28	0.47	0.21	32
Hydrolysis product of VIII—IX	0.39	0.21	0.61	0.04	68
Al-Hg reduction product of IX	0.52	0.60	0.65	0.12	38

a) and b): See the footnote in Table 1.

6-(2-Carboxyethyl)-8-(1-D-ribityl)-2,4,7-trioxohexahydropteridine (I). 2,6-Dihydroxy-5-nitro-4-D-ribitylaminopyrimidine[8] (0.4 g) in water (50 m*l*) was hydrogenated over a platinum oxide catalyst (0.2 g). After the theoretical amount of hydrogen was taken up, the catalyst was removed by filtration. The solution was acidified with acetic acid. (1 m*l*). α-Ketoglutaric acid (0.4 g) was added and the mixture was heated for 30 min on a steam bath. The solution was concentrated *in vacuo* to about 10 m*l* below 40°C, and acetone was added to the residue. The resulting pale yellow precipitate (280 mg) was purified by chromatography using a DEAE-cellulose column (3.5×18 cm; developer: 0.01 N HCl). A purple fluorescent band was eluted and the eluate was concentrated *in vacuo* below 40°C. The residue was recrystallized twice from water-ethanol to give colorless needless, yield, 130 mg (25.8%), mp >265°C (decomp.).

Found: C, 40.96; H, 4.73; N, 14.03%. Calcd for $C_{14}H_{18}O_9N_4 \cdot H_2O$: C, 41.58; H, 4.95; N, 13.86%.

6-(p-Hydroxyphenyl)-8-(1-D-ribityl)-2,4,7-trioxohexahydropteridine (II). 2,6-Dihydroxy-5-nitro-4-ribitylaminopyrimidine[8] (0.4 g) in water (50 mg) was hydrogenated over platinum oxide (0.2 g). After the theoretical amount of hydrogen was absorbed, the catalyst was removed. After acidification with acetic acid (1 m*l*), *p*-hydroxyphenylglyoxlic acid[9] (0.4 g) was added to the solution and the mixture was heated for 30 min on a steam bath. The solution was filtered and the filtrate was left standing overnight at 4°C. The yellow precipitate (250 mg) was recrystallized twice from water to give pale yellow crystals, yield, 140 mg (26.4%), mp 272—273°C (decomp.).

Found: C, 47.75; H, 4.77; N, 12.64%. Calcd for $C_{17}H_{18}O_8N_4 \cdot H_2O$: C, 48.11; 4.75; N, 13.20%.

6-(3-Indolyl)-8-(1-D-ribityl)-2,4,7-trioxohexahydropteridine (III). 2,6-Dihydroxy-5-nitro-4-D-ribitylaminopyrimidine[8] (0.2 g) in water (25 m*l*) was hydrogenated over platinum oxide (0.1 g). After the theoretical amount of hydrogen was taken up, the catalyst was removed. The solution was acidified with acetic acid (0.2 m*l*) and warmed. 3-Indolylglyoxylic acid[10] (0.12 g) in ethanol (3 m*l*) was added drop by drop, and the mixture was heated on a steam bath for 30 min. The solution was left standing overnight at 4°C. The brown product (96 mg) was recrystallized twice from 2 N HCl to give a pale yellow substance, yield, 60 mg (21.4%), mp 285—286°C (decom.).

Found: C, 50.77; H, 4.46; N, 15.61%. Calcd for $C_{19}H_{19}O_7N_5 \cdot H_2O$: C, 51.00; H, 4.73; N, 15.65%.

6-(2-Carboxyethyl)-8-(2-hydroxyethyl)-2,4,7-trioxohexahydropteridine (V). 5-Nitroso-6-(β-hydroxyethylamino)-2,4-dihydroxypyrimidine[11] (300 mg) was suspended in 5 m*l* of water, and sodium hydrosulfite (0.8 g) was added. When the solution became pale yellow, acetic acid (1 m*l*) and α-ketoglutaric acid (0.3 g) were added; the reaction mixture was heated on a steam bath for 1 hr. The solution was filtered and the filtrate was left standing overnight at 4°C. The needles (200 mg) thus obtained were further recrystallized from 50% acetic acid, yield, 125 mg (28.2%), mp 262—265°C.

Found: C, 45.07; H, 4.25; N, 19.17%. Calcd for $C_{11}H_{12}O_6N_4$: C, 44.60, H, 4.08; N, 18.91%.

6-(p-Hydroxyphenyl)-8-(2-hydroxyethyl)-2,4,7-trioxohexahydropteridine (VI). 5-Nitroso-6-(β-hydroxyethylamino)-2,4-dihydroxypyrimidine[10] (70 mg) was suspended in 1 m*l* of water and sodium hydrosulfite (150 mg) was added. When the solution became pale yellow, acetic acid (1 m*l*) and *p*-hydroxyphenylglyoxylic acid[9] (85 mg) were added and the solution was heated on a steam bath for 1 hr. The solution was filtered and the filtrate was left standing overnight at 4°C. The pale yellow product (79 mg) was recrystallized twice from 70% ethanol, yield, 32 mg (28.9%), mp>300°C.

Found: C, 50.74; H, 3.95; N, 16.54%. Calcd for $C_{14}H_{12}O_5N_4 \cdot H_2O$: C, 50.30; H, 4.22; N, 16.76%.

6-(2-Carboxyethyl)-2,4,7-trioxohexahydropteridine (VII). 4,5-Diaminouracil sulfate (250 mg) was dissolved in 20 m*l* of 1N NaOH by warming. α-Ketoglutaric acid (150 mg) was added and the mixture was heated on a steam bath for 1 hr. The solution was adjusted to pH 1 with concd. HCl and left standing at room temperature. The yellow precipitate (200 mg) was recrystallized from 1 N HCl to give pale yellow plates, yield, 50 mg (20.9%), mp 259—263°C (decomp.).

Found: C, 42.82; H, 2.68; N, 22.15%. Calcd for $C_9H_8O_5N_4$: C, 42.86; H, 3.20; N, 22.22%.

6-Ethoxycarbonyl-8-(1-D-ribityl)-2,4,7-trioxohexahydropteridine (VIII). Zinc powder (150 mg) was added to a suspension of

8) R. M. Cresswell and H. C. S. Wood, *J. Chem. Soc.*, **1960**, 4768.

9) M. Businelli, *Farm. Sci. e tec. (Paria)*, **5**, 522 (1950); *Chem. Abstr.*, **45**, 3819f (1951).

10) K. N. F. Shaw, A. McMillan, A. G. Gudmondson, and M. D. Armstrong, *J. Org. Chem.*, **23**, 1171 (1958).

11) W. S. McNutt, *J. Amer. Chem. Soc.*, **82**, 217 (1960).

4-ribitylamino-5-phenylazouracil[12] (150 mg) in water; the mixture was heated at 100°C for 10 min. Five N H_2SO_4 was added until the solution became clear. The solution was filtered once and adjusted to pH 1 with 4N NaOH. Diethyl mesoxalate (300 mg) was added and the solution was heated on a steam bath for 30 min. The solution was left standing at room temperature for 2 days. The pale yellow needles (52 mg, 32.8%) were recrystallized from ethanol to give faint yellow needles, mp 128—129°C.

Found: C, 43.74; H, 4.71; N, 15.30%. Calcd for $C_{14}H_{18}O_9N_4$: C, 43.52; H, 4.70; N, 14.50%.

Table 4. UV absorption maxima (mμ) of synthetic pteridines

Compound	max ($10^{-3}\varepsilon$ in parenthesis)	solvent
I	260(8.12), 288(8.31), 352(13.4)	0.1NNaOH
	289(10.7), 345(12.2)	H_2O
	282(11.2), 328(11.6)	0.1N HCl
II	260(12.7), 307(12.3), 403(22.1)	0.1NHaOH
	215(33.7), 299(12.0), 377(20.0)	H_2O
	240(14.4), 295(10.8), 365(19.7)	0.1N HCl
III	271(11.3), 308(10.3), 401(19.5)	0.1NNaOH
	213(39.1), 312(10.8), 398(18.6)	H_2O
	216(26.1), 317(8.38), 390(16.8)	0.1N HCl
V	258(6.00), 290(9.98), 350(13.9)	0.1NNaOH
	287(11.4), 341(12.8)	H_2O
	282(12.8), 328(13.1)	0.1N HCl
VI	259(12.9), 307(13.5), 401(21.4)	0.1NNaOH
	213(39.7), 298(13.4), 377(22.6)	H_2O
	239(14.6), 295(11.7), 364(20.0)	0.1N HCl
VII	279(9.55), 330(15.3)	0.1NNaOH
	278(10.3), 327(15.0)	H_2O
	278(11.1), 325(13.8)	0.1N HCl

Results and Discussion

Four pteridine compounds were isolated from the culture of *Pseudomonas ovalis*. Three of them were the pteridines already described, *i.e.* a purple fluorescent compound was identified as 6-methyl-8-(1-D-ribityl)-2,4,7-trioxohexahydropteridine[2] (Table 2), a greenish-yellow fluorescent compound as 6-(3-Indolyl)-8-(1-D-ribityl)-2,4,7-trioxohexahydropteridine[4] (Table 2) and a greenish-blue fluorescent compound as 6-(*p*-hydroxyphenyl)-8-(1-D-ribityl)-2,4,7-trioxohexahydropteridine[5] (Table 1) by comparison with natural and synthetic samples.

The fourth compound, designated as putidolumazine ($C_{14}H_{18}N_4O_9$), was supposed to be a new pteridine. UV-Spectra of this compound suggested that it was a 2,4,7-trioxohexahydropteridine with alkyl side chains at N-8 and C-6 positions (Fig. 1). Putidolumazine was stable against Al-Hg treatment[13] suggesting that it has $-CH_2-$ group at position 6. On photoirradiation in the presence of H_2O_2 it gave 6-(2-carboxyethyl)-2,4,7-trioxohexahydropteridine (VII); This compound was synthesized by condensation of 4,5-diaminouracil and α-ketoglutaric acid (Table 3). On oxidation with periodate followed by reduction with sodium borohydride, putidolumazine yielded 6-(2-carboxyethyl)-8-(2-hydroxyethyl)-2,4,7-trioxohexahydropteridine (V); this was identified by comparison with synthetic material (Table 3). Periodate consumption of putidolumazine suggests the presence of four neighboring hydroxy groups. Finally, acetylated putidolumazine ethyl ester gave a molecular peak of *m/e* 582 on mass spectrum.

From these results the structure of 6-(2-carboxyethyl)-8-(1-D-ribityl)-2,4,7-trioxohexahydropteridine (I) was postulated for putidolumazine. This compound was synthesized by condensation (reduction) of 2,6-dihydroxy-5-nitro-4-D-ribitylaminopyrimidine and α-ketoglutaric acid. Its identity with the natural product was confirmed (Table 3, 4; Fig. 1).

We thought that putidolumazine was produced by enzymic condensation with 4-ribitylamino-5-aminouracil and α-ketoglutaric acid produced from glutamic acid and the possible formation of putidolumazine has been implicated in the enzymic production of riboflavin.

We wish to thank Dr. T. Masuda and Dr. I. Takeda for the generous supply of natural compounds for comparison. Thanks are also due to Dr. T. Naito, Bristol-Banyu Research Institute, for microanalyses and Mr. T. Kinoshita, Sankyo Co., for obtaining mass spectrum.

12) W. Pfleiderer and G. Nübel, *Chem. Ber.*, **93**, 1406 (1960).

13) S. Matsuura, S. Nawa, M. Goto, and Y. Hirata, *J. Biochem.*, **42**, 413 (1955).

Studies on the Interaction of Isocyanides with Transition-metal Complexes. VII.[1] Insertion Reactions of Isocyanide into Alkyl-platinum Sigma Bonds[2]

Yasuhiro YAMAMOTO and Hiroshi YAMAZAKI

The Institute of Physical and Chemical Research, Wako-shi, Saitama

(Received October 29, 1970)

The reactions of *trans*-iodobis(phosphine)aklylplatinum(II) compounds with isocyanide were carried out. The reactions of isocyanide with the methyl and benzyl derivatives of platinum(II) with triphenylphosphine or dimethylphenylphosphine gave salt-like complexes [*trans*-$Pt(PR_3)_2(CNR')CH_3]I$ (**1**) ($PR_3=PPh_3$, $PPhMe_2$; $R'=C_6H_{11}$, $C(CH_3)_3$). When **1** was refluxed in benzene or toluene, an insertion of isocyanide took place, affording *trans*-iodobis(phosphine)(1-cyclohexylimino)alkylplatinum(II). Two P-CH_3 proton resonances were observed in the NMR spectrum of *trans*-$Pt(PPhMe_2)_2I[C(CH_3)=NC_6H_{11}]$, indicating that the two methyl groups on the same phosphorus atom are magnetically nonequivalent. It was deduced from this NMR behavior that all the iminoacyl complexes prepared have a five-coordinate structure.

We have reported that the reactions of cyclohexyl isocyanide with the metal alkyls, such as triphenylphosphine-π-cyclopentadienylnickel and tricarbonyl-π-cyclopentadienylbenzylmolybdenum, inserted isocyanide into a carbon-to-metal bond to give π-cyclopentadienyl(cyclohexyl isocyanide)(1-cyclohexylimino)ethylnickel[3] and tricarbonyl-π-cyclopentadienyl(1-cyclohexylimino)(2-phenyl)ethylmolybdenum.[4] Recently we also found that the reaction of isocyanide with *trans*-iodobis(phosphine)alkylpalladium(II) took place with successive insertions of isocyanide molecules, thus affording the iminoacyl complexes of palladium(II) with five-coordinate structures.[5,6]

In our extensive studies of the alkyl complexes of platinum(II), we found that isocyanides react with methyl and benzyl complexes of platinum(II) to produce five-coordinate iminoacyl complexes.

A recent note[7] on the reaction of methyl isocyanide with *trans*-halobis(triphenylphosphine)alkylplatinum(II) to give the iminoacyl complexes of platinum(II) has prompted us to report on other iminoacyl complexes obtained from isocyanides and alkyl complexes of platinum(II). We found that this type of iminoacyl complexes has a five-coordinate structure with a platinum atom bound to imino-nitrogen.

Results and Discussion

The treatment of cyclohexyl isocyanide with *trans*-iodobis(phosphine)methylplatinum(II) in a 1 : 1 molar ratio in benzene at room temperature gave colorless crystals formulated as a 1 : 1 adduct $Pt(PR_3)_2(CNC_6H_{11})(CH_3)I$ (**1**), based on its elemental analysis. The compounds (**1**) are soluble in methyl alcohol, methylene chloride, and chloroform, and are insoluble in nonpolar solvents such as benzene and hexane.

The IR spectrum of each compound showed a characteristic band in the range from 2178 to 2210 cm^{-1}, this spectrum was attributable to the coordinated isocyanide group. The value of the $\nu_{N\equiv C}$ bond of the coordinated isocyanide group was approximately 70 cm^{-1} higher than the corresponding value of the uncoordinated one. The formation of $[Pt(PPh_3)_2(CNC_6H_{11})(CH_3)]BPh_4$ from the reaction of **1a** with sodium tetraphenylborate in ethanol suggests an ionic nature for the (**1**) complexes.

In the NMR spectrum of **1a** measured in $CDCl_3$, the methyl resonance centered at 9.95 τ appears as a set of three triplets; it is interpreted to give $J_{P,H}=7.5$ Hz and $J^{195}_{Pt,H}=60$ Hz, the central one with an intensity approximately four times that of the outer triplets. The triplet resonance implies that the two phosphorus ligands are in mutually *trans*-positions.

It may be deduced from these results that the (**1**) complexes have an ionic square-planar structure.

When the **1a** complex in benzene was kept at 80°C for 2 hr, the migration of the methyl group to the isocyanide ligand took place, affording *trans*-iodobis(triphenylphosphine)(1-cyclohexylimino)ethylplatinum (II) (**2a**), *trans*-$Pt(PPh_3)_2I[C(CH_3)=NC_6H_{11}]$, characterized by the presence of an infrared band due to carbon-nitrogen double bond at 1604 cm^{-1}, as is seen in the IR spectrum. This structure was supported by the formation of *N*-cyclohexylacetoamide from the degradation of 2a with moist air.

$$\mathbf{2a} \longrightarrow CH_3CONHC_6H_{11}$$

An analogous complex, *trans*-$Pt(PPh_3)_2Cl[C(CH_2Ph)=NC_6H_{11}]$ (**2d**), was obtained from the reaction of *trans*-chlorobis(triphenylphosphine)benzylplatinum(II) with cyclohexyl isocyanide in a 1:1 molar ratio at 80°C. In this case, no attempts were made to isolate an intermediate ionic complex.

We had already reported that the insertion reaction of cyclohexyl isocyanide into the corresponding pal-

1) Part VI: Y. Yamamoto and H. Yamazaki, *J. Organometal. Chem.*, **24**, 717 (1970).

2) A part of this paper was presented at the Symposium of Organometallic Chemistry, Osaka, October 7, 1969. Preprints p. 172; The 23rd Annual Meeting of the Chemical Society of Japan, Tokyo, April 3, 1970. Preprints III, p. 1195.

3) Y. Yamamoto, H. Yamazaki, and N. Hagihara, This Bulletin, **41**, 532 (1968); *J. Organometal. Chem.*, 18, 189 (1969).

4) T. Yamamoto and H. Yamazaki, *ibid.*, **24**, 717 (1970).

5) Y. Yamamoto and H. Yamazaki, This Bulletin, **43**, 2653 (1970).

6) Y. Yamamoto and H. Yamazaki, *ibid.*, **43**, 3634 (1970).

7) P. M. Treichel and R. W. Hess, *J. Amer. Chem. Soc.*, **92**, 4731 (1970)

ladium(II) complex occurred at 0°C.[5,6] In the present reactions, the initial formation of a salt-like complex, accompanied by the insertion of isocyanide into a platinum-carbon sigma bond at an elevated to temperature, suggests that the reactivity of the Pt–CH_3 bond is lower than that of the Pd–CH_3 one.

When **1b** was handled in a way similar to that in the above-mentioned reaction (**1a**→**2a**), the unconverted starting materials were recovered without undergoing an insertion. On the refluxing of **1b** in toluene for 5 hr, the insertion of isocyanide proceeded, ultimately affording the iminoacyl complex (**2b**), *trans*-Pt $(PPhMe_2)_2I[C(CH_3)=NC_6H_{11}]$.

It was presumably the electronic effect of the phosphine ligands that the migration of the methyl group to the isocyanide ligand in the **1a** complex containing triphenylphosphine occurred more easily than that in **1b** containing dimethylphenylphosphine.

In the NMR spectrum of **2b** in $CDCl_3$, the C–CH_3 proton resonance showed a well-defined 1:4:1 triplet at 7.73 τ, arising from the coupling of ^{195}Pt–H ($^3J_{^{195}Pt,H}$ =33 Hz). The long-range coupling of $^4J_{P,H}$ was not observed, although it was noted in the analogous complexes of Pd(II).[5,6] The P–CH_3 proton resonances

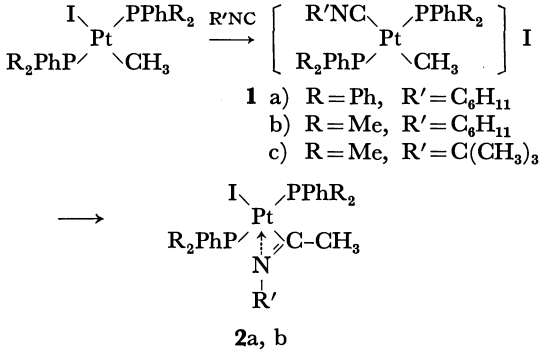

Scheme 1

Table 1. Products of reactions of *trans*-Pt $(PR_3)_2$ X(R) with isocyanides

Compound	Yield(%)	mp(°C)[a]	Analyses Found(Calcd) C	H	N	X	IR(cm^{-1})[b] N≡C	C=N
[*trans*-Pt$(PPh_3)_2$ $(CNC_6H_{11})CH_3$]I C_6H_6 (**1a**)	73	140—150	57.09 (57.26)	4.92 (4.81)	1.32 (1.34)	12.53 (12.10)	2203	
[*trans*-Pt$(PPhMe_2)_2$ $(CNC_6H_{11})CH_3$]I $1/2C_6H_6$ (**1b**)	93	55— 60	42.27 (42.58)	5.17 (5.16)	1.85 (1.84)	16.90 (16.66)	2183	
[*trans*-Pt$(PPhMe_2)_2$ $(CNC(CH_3)_3)$ CH_3]I $1/2C_6H_6$ (**1c**)	89	97— 99	40.56 (40.83)	5.04 (5.07)	1.90 (1.90)	17.59 (17.25)	2178	
[*trans*-Pt$(PPh_3)_2$ $(CNC_6H_{11})CH_3$]BPh_4 C_6H_6	100	170—180	71.65 (71.61)	5.89 (5.68)	1.12 (1.13)		2182	
trans-Pt$(PPh_3)_2$ I[$C(CH_3)=NC_6H_{11}$] (**2a**)	89	163—167	54.01 (54.44)	4.54 (4.57)	1.41 (1.44)	13.41 (13.07)		1604
trans-Pt$(PPhMe_2)_2$ I[$C(CH_3)=NC_6H_{11}$] (**2b**)	88	188—189	40.02 (39.95)	5.15 (5.03)	1.95 (1.91)	17.23 (17.59)		1611
trans-Pt$(PPh_3)_2$Cl[$C(CH_2Ph)=NC_6H_{11}$] (**2d**)	44	169—173	62.88 (62.86)	4.98 (5.06)	1.33 (1.47)	3.82 (3.71)		1590

a) All complexes decomposed with melting. b) KBr method.

Table 2. NMR Spectra of the isocyanide complexes in $CDCl_3$

Compound	τ
[*trans*-Pt$(PPh_3)_2(CNC_6H_{11})CH_3$]I C_6H_6 (**1a**)	9.95(t,[b] $J_{P,H}$=7.5Hz, $J_{^{195}Pt,H}$=60*Hz*, Pt–CH_3), 8.5–9.5(b, C_6H_{10}), 6.7–7.1 (b, C_6H^{c}), 2.45(b, P-C_6H_5), 2.70(s, C_6H_6[d])
[*trans*-Pt$(PPhMe_2)_2(CNC_6H_{11})CH_3$]I $1/2C_6H_6$ (**1b**)	9.75(t,[b] $J_{P,H}$=7.5Hz, $J_{^{195}Pt,H}$=60Hz, Pt–CH_3), 8.2–8.8(b, C_6H_{10}), 8.00(t,[b] $\lvert {}^2J_{P,H}+{}^4J_{P,H}\rvert$=7.5Hz, $J_{^{195}Pt,H}$=30Hz, P–CH_3) 5.85–6.4(b, C_6H^{c}), 2.0–2.6(b, P-C_6H_5), 2.65(s, C_6H_6)
[*trans*-Pt$(PPhMe_2)_2$ $(CNC(CH_3)_3)$ CH_3]I $1/2C_6H_6$ (**1c**)	9.70(t,[b] $J_{P,H}$= 7.5 Hz, $J_{^{195}Pt,H}$=60Hz, Pt–CH_3), 8.75(s,$C(CH_3)_3$), 7.98(t,[b] $\lvert {}^2J_{P,H}+{}^4J_{P,H}\rvert$=8Hz, $J_{^{195}Pt,H}$=60Hz, P-CH_3), 2.1–2.7(b, P-C_6H_5), 2.65 (s, C_6H_6)[d]
trans-Pt$(PPh_3)_2$I[$C(CH_3)=NC_6H_{11}$] (**2a**)	9.05(t, $J_{^{195}Pt,H}$=33Hz, C–CH_3), 8.0–9.5 (b, C_6H_{10}), 5.25–5.60(b, C_6H^{c}), 2.0–3.15(b, P-C_6H_5)
trans-Pt$(PPhMe_2)_2$I[$C(CH_3)=C_6H_{11}$][a] (**2b**)	8.2–9.3(b,C_6H_{10}), 8.01 and 8.07 (t,[b] $\lvert {}^2J_{P,H}+{}^4J_{P,H}\rvert$=8Hz, $J_{^{195}Pt,H}$=38Hz, P–CH_3), 7.73 (s, $J_{^{195}Pt,H}$=33Hz, C–CH_3) 5.95–6.3(b, C_6H^{c}), 1.9–2.7(b, P-C_6H_5)
trans-Pt$(PPh_3)_2$Cl[$C(CH_2Ph)=NC_6H_{11}$] (**2d**)	8.4–9.3(b, C_6H_{10}), 6.77(t, $J_{^{195}Pt,H}$=27Hz, C–CH), 6.0–6.4(b, C_6H^{c}), 3.10(s, C–C_6H_5), 2.2–2.9(b, P-C_6H_5)

a) Recorded by Varian HA-100B. Other samples were measured by JEOL C-60.
b) a set of three triplets.
c) α-proton of cyclohexyl group.
d) Benzene contained in the complexes.

appeared as two sets of three triplets centered at 8.01 and 8.07 τ respectively. The two P–CH_3 resonances are interpreted to arise from $J_{P,H}$[8]$=7$ Hz and $J_{^{195}Pt,H}=38$ Hz. The triplet resonance indicated that the two phosphorus ligands were coordinated to a metal in mutual *trans*-positions.[9] The presence of the two triplets also indicated that the two methyl groups on the same phosphorus atom were magnetically nonequivalent. If the **2b** complex has a square-planar structure, the magnetic nonequivalence will not be observed. Therefore, it seems reasonable to assume that the origin of nonequivalence is the absence of a plane of symmetry resulting from the coordination of lone-pair electrons of imino nitrogen to the platinum atom, thus giving the five-coordinate structure.

It may be concluded from the NMR spectrum of **2b** that these types of iminoacyl complexes of platinum (II), including those prepared in another recent paper,[5] have the five-coordinate structure.

Experimental

All the reactions were carried out under a nitrogen atmosphere. All the melting points are uncorrected; they were measured by a micro-melting-point apparatus, Yanagimoto Model MP-S2. The IR spectra were obtained by a Perkin-Elmer 521 spectrometer. The NMR spectra were recorded in $CDCl_3$ by means of JEOL C-60 and Varian HA-100B instruments, using tetramethylsilane as the internal standard. Isocyanides were prepared according to the procedures described in the literature.[10] *Trans*-iodobis(triphenylphosphine)methylplatinum(II) was prepared by Chatt and Shaw's method.[11] The elemental analyses, melting points, yields, and IR and NMR spectra of all the complexes prepared here are summarized in Tables 1 and 2.

Preparation of trans-*Pt(PPhMe$_2$)$_2$(CH$_3$)*. *Trans*-iodobis(dimethylphenylphosphine)methylplatinum was obtained by the reaction of *trans*-diiodobis(dimethylphenylphosphine)-platinum(II) with methylmagnesiumiodide.

Found: C, 33.17; H, 3.95; I, 20.12%. Calcd for $C_{17}H_{25}IP_2Pt$: C, 33.29; H, 4.11; I, 20.69%. Mp 146—150°C (decomp).

Preparation of trans-*Pt(PPh$_3$)$_2$Cl(CH$_2$Ph)*. A mixture of tetrakis (triphenylphosphine)platinum(II) (1 g, 0.98 mmol) and benzylchloride (10 ml) was kept at 75°C. After 5 hr, white crystals were observed. The evaporation of benzyl-chloride and recrystallization from benzene-hexane gave *trans*-chlorobis(triphenylphosphine)benzylplatinum(II) (0.6 g, 73%; mp 208—211°C (decomp.).)

Found: C, 61.03; H, 4.41; Cl, 4.18%. Calcd for $C_{43}H_{37}ClP_2Pt$: C, 61.41; H, 4.64; Cl, 14.29%. NMR ($CDCl_3$,τ): 7.69 (a set of three triplets, $J_{^{195}Pt,H}=99$Hz, $J_{P,H}=7.5$ Hz, CH_2), 2.1—3.5 (broad, P-Ph and Ph).

Preparation of [trans-*Pt(PPhMe$_2$)$_2$(CNC$_6$H$_{11}$)CH$_3$]I*. Cyclohexyl isocyanide (0.065 g, 0.6 mmol) in benzene (0.6 m*l*) was added, drop by drop to a solution of *trans*-Pt(PPhMe$_2$)$_2$I(CH$_3$) (0.36 g 0.59 mmol) in benzene (15 m*l*) at room temperature, and the solution was kept overnight. Colorless crystals (0.39 g, 93%) were filtered, washed by benzene-hexane, and identified as [*trans*-Pt-(PPhMe$_2$)$_2$(CNC$_6$H$_{11}$)-CH$_3$]I.

The other ionic complexes were obtained by the procedures described above.

Preparation of trans-*Pt(PPh$_3$)$_2$[C(CH$_3$)=NC$_6$H$_{11}$]*. [*trans*-Pt-(PPh$_3$)$_2$(CNC$_6$H$_{11}$)CH$_3$]I (0.2 g, 0.21 mmol) in benzene (25 m*l*) was kept at 80°C. After 2 hr, the reaction mixture was evaporated almost to dryness under a reduced pressure. Recrystallization from a benzene-hexane mixture gave colorless crystals, *trans*-iodobis(triphenylphosphine)(1-cyclohexylimino)ethylplatinum(II) (0.18 g, 90%).

Preparation of trans-*Pt(PPh$_3$)$_2$Cl[C(CH$_2$Ph)=NC$_6$H$_{11}$]*. Cyclohexyl isocyanide (0.05 g, 0.45 mmol) in benzene (0.45 m*l*) was added to a soluton of *trans*-chlorobis(triphenylphosphine)benzylplatinum(II) (0.38 g, 0.49 mmol). After the evaporation of the solvent almost to dryness, the viscous residue was kept at 80°C for 4 hr. Colorless crystals obtained were washed with benzene and identified as *trans*-chlorobis(triphenylphosphine)(1-cyclohexylimino)(2-phenyl)ethylplatinum (II).

Preparation of trans-*Pt(PPhMe$_2$)$_2$I[C(CH$_3$)=NC$_6$H$_{11}$]*. [*trans*-Pt(PPhMe$_2$)$_2$(CNC$_6$H$_{11}$)CH$_3$]I (0.22 g, 0.31 mmol) in toluene (3 m*l*) was refluxed for 5 hr. The reaction mixture was evaporated almost to dryness. Recrystallization from benzene-hexane gave colorless crystals, *trans*-iodobis(dimethylphenylphosphine)(1-cyclohexylimino)ethylplatinum(II) (0.19 g, 88%).

Preparation of trans-*Pt(PPhMe$_2$)$_2$I(CN)*. [*trans*-Pt(PPhMe$_2$)$_2$(CNC(CH$_3$)$_3$[CH$_3$]I (0.16 g, 0.24 mmol) in toluene (3 m*l*) was refluxed for 4 hr. The reaction mixture was evaporated almost to dryness. Recrystallization from benzene-hexane gave colorless crystals, iodo-cyanobis(dimethylphenylphosphine)platinum(II) (0.12 g, 82%; mp(decomp.) 150—153°C).

Found: C, 34.38; H, 3.68; N, 2.77; I, 21.89%. Calcd for $C_{17}G_{22}NP_2IPt$; C, 34.41; H, 3.74; N, 2.36; I, 21.39%. IR(KBr): 2122 cm^{-1} (N≡C). NMR($CDCl_3$, τ): 7.84 (a set of three triplets, $J_{^{195}Pt,H}=30$ Hz, $|^2J_{P,H}+{}^4J_{P,H}|=7.5$ Hz, P-CH_3), 2.1—2.7 (broad, C_6H_5).

8) Apparent coupling constant, $|^2J_{P,H}+{}^4J_{P,H}|$
9) J. M. Jenkins and B. L. Shaw, *Proc. Chem. Soc.*, **1963**, 291.
10) I. Ugi and R. Meyer, *Chem. Ber.*, **93**, 239 (1960).
11) J. Chatt and B. L. Shaw, *J. Chem. Soc.*, **1959**, 705.

Restricted Rotation Involving the Tetrahedral Carbon. I. Some Diels-Alder Adducts Derived from 9-Substituted Anthracenes

Michinori Ōki and Minoru Suda

Department of Chemistry, Faculty of Science, The University of Tokyo, Hongo, Tokyo

(Received November 10, 1970)

9-*t*-Butylanthracene was treated with dimethyl acetylenedicarboxylate and benzoquinone to give Diels-Alder adducts. The NMR spectra of these adducts suggest that the internal rotation about the C_1–C_{Bu} bond is not taking place on the NMR time scale. On the other hand, a Diels-Alder adduct prepared from 9-isopropylanthracene and dimethyl acetylenedicarboxylate shows the coalescence phenomenon of the NMR signals when the temperature is raised. The possibility of optical resolution due to hindered rotation about the sp^3–sp^3 carbon bond is pointed out.

There have been numerous examples of restricted rotations about the carbon-carbon single bonds. However, since the confirmation of the restricted rotation depends on the optical resolution, the identified examples have been limited to fairly stable isomers; in other words, a highly restricted rotation was necessary in order to note the hindered rotation. Optical resolutions of numerous biphenyl derivatives[1] and ansanoid compounds[2] are examples of this.

In recent years, it has become possible to study the internal rotation by means of NMR spectroscopy. This method has enabled us to study the exchange of protons as fast as 10^0—10^3 sec^{-1}. Prior resolution is not now necessary to study fairly fast internal rotation. Biphenyls[3], ketones[4] and ansanoids[5] have thus been studied by virtue of either the presence of dissymmetric protons of methylene, isopropyl, or other groups (*e.g.* **1**) or the different chemical shifts in the ring system (*e.g.* **2**).

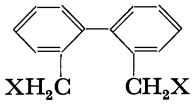

(1)

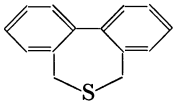

(2)

In the biphenyls and ketones, the pivot bond in question is the C_{sp^2}–C_{sp^2}, whereas in ansanoids the pivot bond is C_{sp^2}–C_{sp^3}. A very important point should be raised here. That is, in the tetrahedron theory of carbon, it is assumed that the rotation about the C–C single bond is free; otherwise, even a compound which has no asymmetric carbon could be resolved into optical isomers. Let us consider a molecule, C_{WXXY}, in which W is not spherically symmetric and is directed.[6] We can then write three stable conformations for the molecule, **3**, **4**, and **5**, where the arrow attached to W represents the direction of W. If the

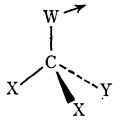

(3)

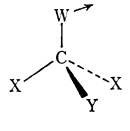

(4)

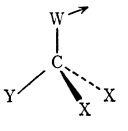

(5)

rotation about the W–C bond is free in the sense of classical organic chemistry, the molecule will not have any isomer, as the tetrahedron theory predicts. However, if the rotation about the W–C bond is slow, there will be three isomers for the C_{WXXY} molecule. The mirror image of **5** is identical with **5**, whereas **3** and **4** are mirror images of each other and are not identical. It will be proper to call **5** the *meso*-form, and **3** and **4** *dl*-form.

Since W can involve either sp^2- or sp^3-hybridized carbon in connecting with the C_{XXY} group, the restricted rotation in either the sp^2–sp^3 or the sp^3–sp^3 C–C bond could cause the isolation of the afore-mentioned isomers. There have been several papers concerning the above phenomena, but not much notice has been taken of the importance of the phenomenon.[7] As early as 1961, Brownstein[8] reported the NMR results of *meso*- and *dl*-forms of 2,5-dimethoxy-2,5-dimethyl-3,4-diphenylhexane (**6**) and pointed out the possibility of the presence of rotational isomers from the appearance of two sets of signals. However,

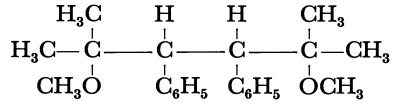

(6)

the close examination of the spectra of the pairs led the present authors to doubt the presence of the conformers. Rather, the spectra can best be interpreted by assuming the contamination by the other isomers, the *meso*- and *dl*-forms. Therefore, in our opinion, these data are not conclusive in establishing the restricted rotation about the central C_{sp^3}–C_{sp^3} bond.

There are, of course, many cyclic compounds, the

1) R. Adams and H. C. Yan, *Chem. Rev.*, **12**, 261 (1932).

2) A. Luttringhaus and G. Eyring, *Ann.*, **604**, 111 (1957); A. T. Blomquist, R. E. Stahl, and Y. C. Meinwald, *J. Org. Chem.*, **26**, 1687 (1961).

3) M. Ōki, H. Iwamura, and N. Hayakawa, This Bulletin, **36**, 1542 (1963); *ibid.*, **37**, 1855 (1964); R. J. Kurland, M. B. Rubin, and W. B. Wise, *J. Chem. Phys.*, **40**, 2426 (1964); W. L. Meyer and R. B. Meyer, *J. Amer. Chem. Soc.*, **85**, 2170 (1963).

4) M. Ōki and N. Nakamura, unpublished work.

5) M. Nakazaki, K. Yamamoto, and S. Okamoto, *Tetrahedron Lett.*, **1969**, 4597.

6) M. Ōki, "Rittaikagaku (Stereochemistry)" Tokyo Kagaku Dojin, Tokyo (1961), p. 5.

7) a) J. P. N. Brewer, H. Heaney, and B. A. Marples, *Chem. Commun.*, **1967**, 27; J. P. N. Brewer, I. F. Eckhard, H. Heaney, and B. A. Marples, *J. Chem. Soc., C.* **1968**, 664; G. P. Newsoroff and S. Sternhell, *Tetrahedron Lett.*, **1967**, 2539; c) E. A. Chandross and C. F. Sheley, Jr., *J. Amer. Chem. Soc.*, **90**, 4345 (1968); d) T. H. Siddall, III, and W. E. Stewart, *J. Org. Chem.*, **34**, 233 (1969); e) A. Riecker and H. Kessler, *Tetrahedron Lett.*, **1969**, 1227.

8) S. Brownstein, *Can. J. Chem.*, **39**, 1677 (1961).

conformations of which are frozen at the lower temperature, and even the equatorial isomer of chlorocyclohexane[9] has been isolated. However, these isomers are unstable at room temperature. *cis*-1,2-Di-*t*-butylcyclohexane has been reported by Kessler *et al.*[10] to have nonequivalent *t*-butyl groups in its NMR spectrum at room temperatur , and the two signals coalesce at 35°C. These results indicated that two *t*-butyl groups on the cyclohexane ring are not good enough to isolate the rotational isomers about the C_{sp^3}–C_{sp^3} bond, although the cyclohexane ring and the bulkiness of the *t*-butyl groups are considered to be favorable for freezing the conformations.

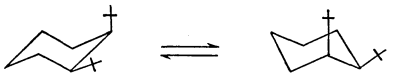

(or twisted boat conformations)

Recently Scheer *et al.* isolated a pair of isomers on treating the ethylene ketal (**7**) with methylmagnesium bromide.[11]

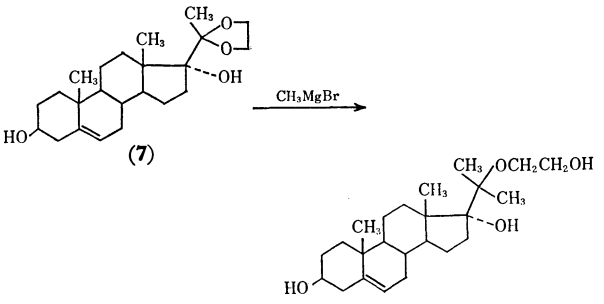

(**7**) (**8**)

They claim that these isomers (**8**) result from the restricted rotation about the C_{17}–C_{20} bond. The present authors have a feeling that this example is too complicated to demonstrate the presence of the isomers clearly and that simpler examples are needed.

We wish to report our findings about the restricted rotation in the Diels-Alder adducts of 9-substituted anthracene and point out the possibility of isolating the rotational isomers.

Results and Discussion

The treatment of 9-*t*-butylanthracene (**9**) with dimethyl acetylenedicarboxylate gave dimethyl 1-*t*-butyldibenzo[*b*,*e*]bicyclo[2.2.2]octatriene-7,8-dicarboxylate

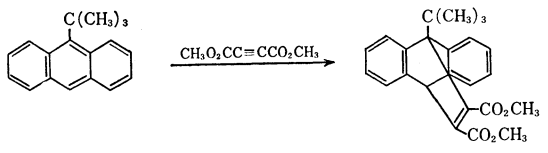

(**9**) (**10**)

(**10**). The NMR spectrum of **10** at room temperature is given in Fig. 1. As will be seen, the signal of the *t*-butyl group is split into two, the relative area being 1:2. This result can best be interpreted by assuming the restricted rotation about the C_1-C_{Bu} bond. Namely, the Newman projection (**11**) through the C_1-C_{Bu}

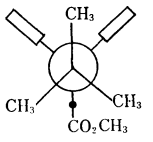

(**11**)

bond clearly explains why the *t*-butyl group should show two signals at the different chemical shift: the two methyls are equivalent, but the last methyl is located in a magnetically non-equivalent environment. Additional support for the above assignment can be obtained by looking at the NMR spectrum of 1-*t*-butyl-9,10:11,12-dibenzotricyclo[6.2.2.$0^{2,7}$]dodeca-4,9,11-triene-3,6-dione (**12**), which was prepared from **9** and *p*-benzoquinone. The Newman projection (**13**) of this compound shows that no pair of the three methyl groups are equivalent to each other; indeed, the NMR spectrum (Fig. 2) shows three methyl signals.

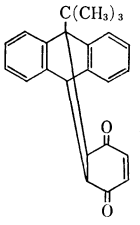

(**12**)

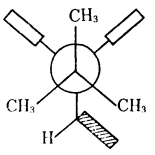

(**13**)

The shaded rectangle indicates the cyclohexenedione ring.

The two methyl signals of **10** are found not to coalesce even at 132°C. Thus, using the chemical-shift difference ($\Delta\nu_0$) and putting 405°K into Eq. (1), the free energy ($\Delta G^{\ddagger}$) of the activation for rotation is estimated to be not lower than 25 kcal/mol.

$$\Delta G^{\ddagger} = -RT\ln\frac{\pi h(\Delta\nu_0)}{\sqrt{2kT}} \qquad (1)$$

It will be possible to isolate isomers of this kind, since, if the free energy of activation is 20—30 kcal/mol, the isolation of isomers is possible at room temperature in biphenyl derivatives. Study along these lines is now in progress.

In an attempt at isolating the *meso*- and *dl*-forms of **3**—**5** type, the *t*-butyl group is now switched to the isopropyl goup: W, X, and Y are 2,3-dimethoxycarbonyl-5,6:7,8-dibenzobicyclo[2.2.2]octa-2,5,7-trien-1-yl, methyl, and hydrogen respectively. The isopropyl derivative (**14**) was prepared analogously with the other compounds.

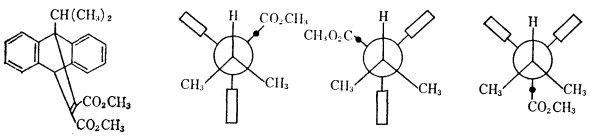

(**14**) (**15**) (**16**) (**17**)

The NMR spectrum (Fig. 3) of **14** at room temperature shows a pair of doublets for the methyl groups

9) F. R. Jensen and C. H. Bushweller, *J. Amer. Chem. Soc.*, **88**, 4279 (1966); *ibid.*, **91**, 3223 (1969).

10) H. Kessler, V. Husowski, and M. Hanack, *Tetrahedron Lett.*, **1968**, 4665.

11) F. Kohen, R. A. Mallory, and I. Scheer, *Chem. Commun.*, **1969**, 580.

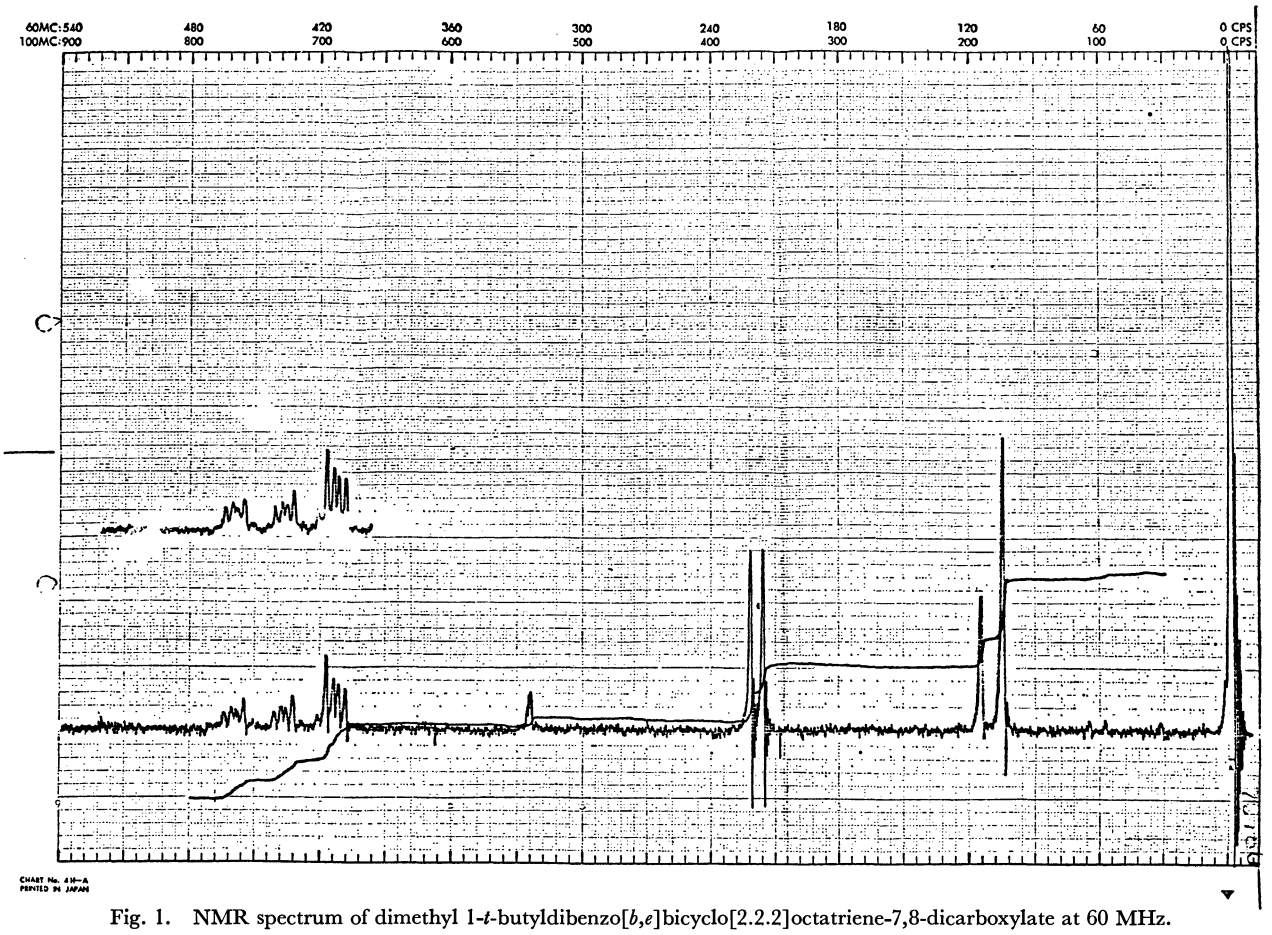

Fig. 1. NMR spectrum of dimethyl 1-*t*-butyldibenzo[*b*,*e*]bicyclo[2.2.2]octatriene-7,8-dicarboxylate at 60 MHz.

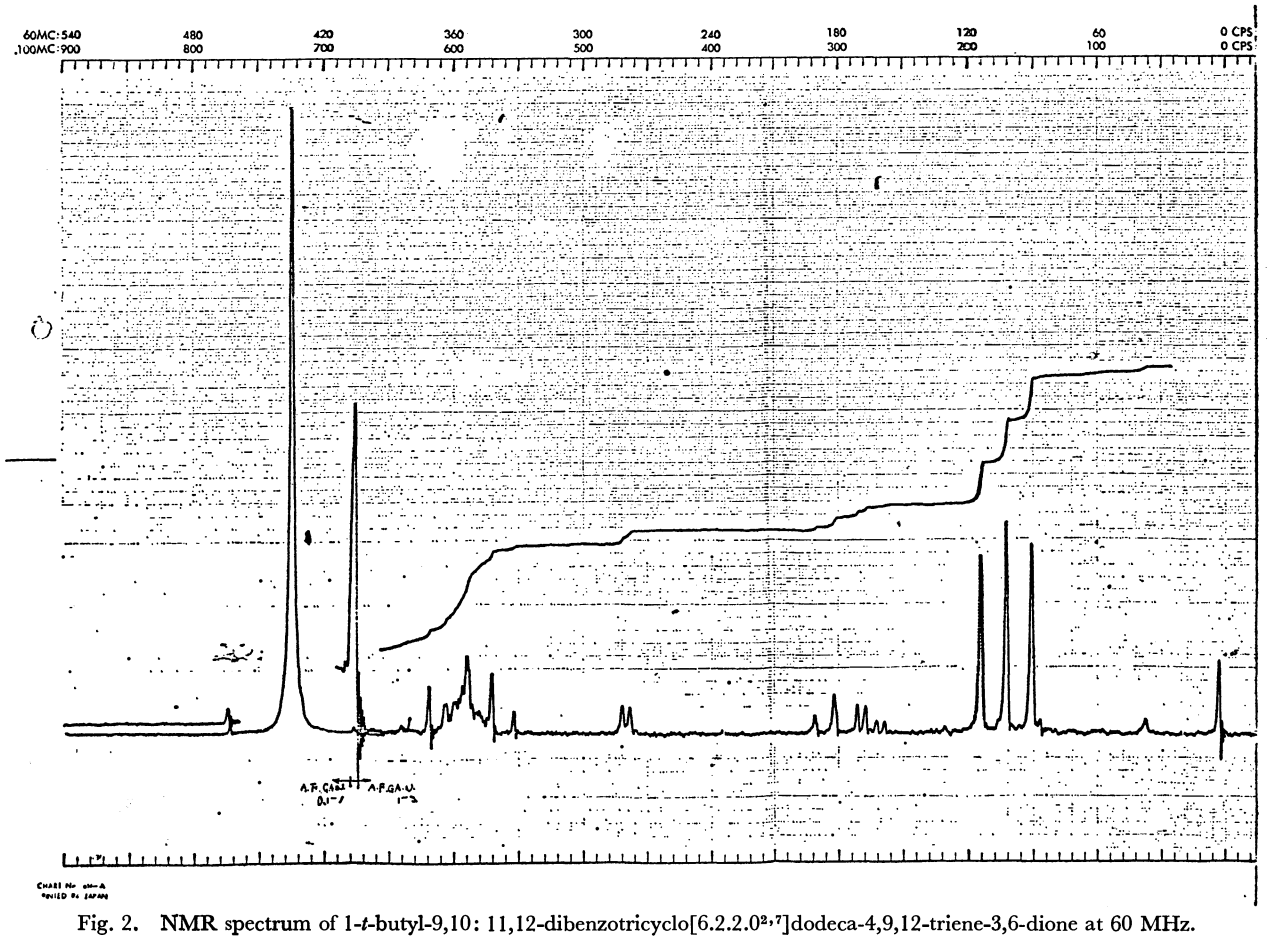

Fig. 2. NMR spectrum of 1-*t*-butyl-9,10: 11,12-dibenzotricyclo[6.2.2.0^{2,7}]dodeca-4,9,12-triene-3,6-dione at 60 MHz.

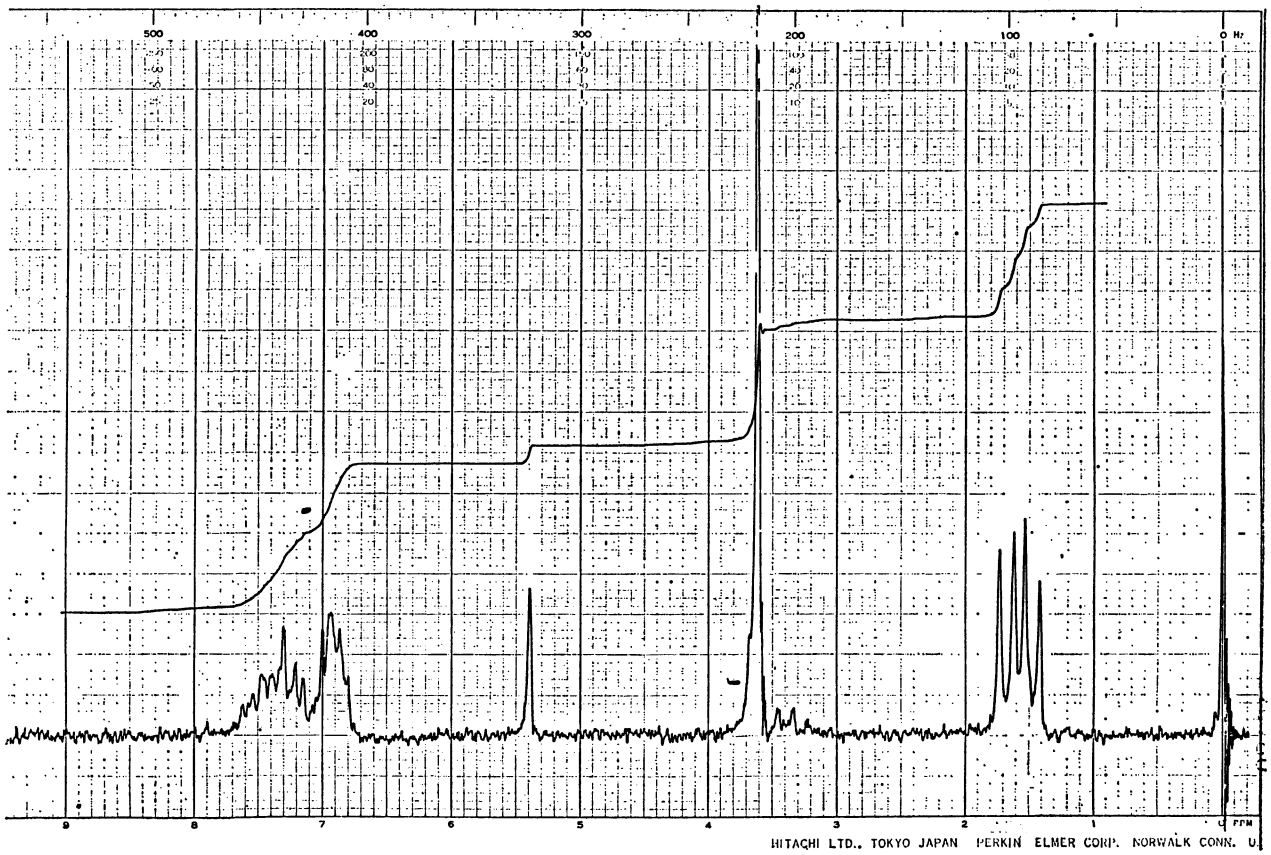

Fig. 3. NMR spectrum of dimethyl 1-isopropyldibenzo[*b*,*e*]bicyclo[2.2.2]octatriene-7,8-dicarboxylate at 60 MHz at room temperature.

in the isopropyl. The intensities are identical within the range of error. Since it may be assumed that methyl signals of the *meso*-form (**17**) are very close to one of the methyl groups in the *dl*-form (**15** and **16**), if the *meso*-form were present in a substantial amount, one of the methyl signals would have been stronger than the other. Thus, the absence of the other signals for the methyl groups of the isopropyl and the almost identical intensities of the pair of doublets indicate that the population of the *meso*-form will be very small, if present at all.

This can be interpreted by assuming that either the *meso*–form is thermodynamically less stable than the *dl*–form or the formation of the former is kinetically less favored than the latter. Either case is possible at the present stage, since the group carrying the methoxycarbonyl group is expected to be larger than the benzo group and the approach of the dimethyl acetylenedicarboxylate molecule from the side where two methyl groups are present will be disfavored relative to the side where a methyl and a hydrogen are present.

When the temperature is raised, the coalescence of the pair of doublets in the NMR spectra is observed. The T_c is 64°C in tetrachloroethane. The free energy of activation for the rotation about the C_{Pr}-C_1 bond is now obtained as 17.7 kcal/mol, using Eq. (1). From the temperature dependence of the half-band width of the signals the rate constants (k) can be obtained by Eq. (2):

$$k = \frac{\pi(\Delta\nu_0)^2}{2(W-W_0)} \tag{2}$$

where W_0 is the half-band width with an infinitely fast exchange rate and W, the half–band width at the observed temperature. The Arrhenius plot of $\log k$ *vs.* $1/T$ afforded E_a of 15.4±1.0 kcal/mol.

On the other hand, the free energy of activation ($\Delta G_c^{\ddagger}$) at the coalescence temperature is obtained by Eqs. (3) and (4):

$$k_c = \frac{\pi}{2}\Delta\nu_0 \tag{3}$$

$$\Delta G_c^{\ddagger} = -RT\ln\frac{hk_c}{k_BT} \tag{4}$$

where k_B is the Boltzmann constant.

It is, then, possible to derive $\Delta H_c^{\ddagger}$ and $\Delta S_c^{\ddagger}$ by putting these values into Eyring's equations, (5) and (6):

$$\Delta H_c^{\ddagger} = E_a - RT \tag{5}$$

$$\Delta S_c^{\ddagger} = \frac{1}{T}(\Delta H_c^{\ddagger} - \Delta G_c^{\ddagger}) \tag{6}$$

$\Delta H_c^{\ddagger}$=14.4±1.0 kcal/mol and $\Delta S_c^{\ddagger}$=−10±1 e. u. are thus obtained. These values suggest that, at 20°C, the rate constant is 0.78 sec^{-1} or the half-life time is 0.9 sec. Thus, in order to resolve this compound (**14**) into optically active isomers, the compound will have to be handled at the lower temperature.

The chemical shift of the methyl signal is 1.49 ppm from TMS at 130°C, whereas the average of the chemical shift of the methyl signals at room temperature is 1.55. This small change in the average chemical shifts may mean that the contribution of the conformation (**17**) is very little, even at 130°C. It could also

be deduced that the internal rotation occurring in **14** is not the full rotation, but the movement to and fro, in which the transition state is the eclipsing of the hydrogen of the isopropyl group and the methoxycarbonyl group. This assumption readily explains why the internal rotation in the *t*-butyl compound (**10**) is so much restricted, while that in the isopropyl compound (**14**) occurs with fair ease, for the methoxycarbonyl group is bulkier than the benzo group, as judged from the isomer distribution of **14**.

Experimental

Spectral Measurement. The NMR spectra were recorded on either a JEOL C-60H or Hitachi R-20A spectrometer. The temperature reading was calibrated by measuring the chemical shift difference between methylene and hydroxyl protons of ethylene glycol.

Dimethyl 1-t-Butyldibenzo[b, e]*bicyclo*[2.2.2]*octatriene-7,8-dicarboxylate (**10**).* An equimolar mixture of 9-*t*-butylanthracene[12] and dimethyl acetylenedicarboxylate was heated slowly until all the solid fused; the heating was then continued for several more minutes. The recrystallization of the product from either methanol or ethanol gave the desired product; mp 182—183°C.

Found: C, 76.65; H, 6.65%. Calcd for $C_{24}H_{24}O_4$: C, 76.57; H, 6.43%.

Dimethyl 1-Isopropyldibenzo [b, e] *bicyclo* [2.2.2] *octatriene-7,8-dicarboxylate* (***14***) was similarly prepared; mp 143.5—144.5°C

Found: C, 75.95; H, 6.20%. Calcd for for $C_{23}H_{22}O_4$: C, 76.22; H, 6.12%.

1-t-Butyl-9,10,11,12-dibenzotricyclo [6.2.2.$0^{2,7}$] *dodeca-4,9,12-triene-3,6-dione* (***12***). 9-*t*-Butylanthracene (4 g) and 3 g of benzoquinone in xylene were heated under reflux. The crystals obtained on cooling were recrystallized from ethanol; mp 161—166° (dec.).

Found: C, 83.93; H, 6.73%. Calcd for $C_{24}H_{22}O_2$; C, 84.17; H, 6.47%.

12) R. C. Parish and L. M. Stock, *J. Org. Chem.*, **31**, 4265 (1966).

BULLETIN OF THE CHEMICAL SOCIETY OF JAPAN, VOL. 44, 1880—1885 (1971)

Restricted Rotation Involving the Tetrahedral Carbon. II. 2-Substituted 4,6,8-Trimethylazulenes[1]

Michinori Ōki and Nobuo Nakamura

Department of Chemistry, Faculty of Science, The University of Tokyo, Hongo, Tokyo

(Received November 10, 1970)

1-(1-Hydroxyethyl)-4,6,8-trimethylazulene (**3**) was prepared by the lithium aluminum hydride reduction of 1-acetyl-4,6,8-trimethylazulene, and by the reaction of methylmagnesium iodide with 1-formyl-4,6,8-trimethylazulene. **3** showed various melting points according to its crystallization conditions and the reaction solvent. Their IR spectra both in solid states and in solutions, the NMR spectra at various temperatures, and the results of X-ray diffraction studies led to a conclusion that this phenomenon is attributable to polymorphism. From the temperature dependence of the NMR spectra of the *t*-butyl protons of 1-*t*-butyl-4,6,8-trimethylazulene, the internal rotation around the C_{Bu}–$C_{azulene}$ was concluded to be slow only at the lower temperature.

In the preceding paper,[2] the restricted rotation about the sp^3–sp^3 carbon-carbon bond was discussed and the possibility of isolating a pair of optical isomers and a *meso*-form of some triptycene-type compounds was mentioned. In the light of this consideration, the sp^2–sp^3 C–C bond should be able to supply another example of resolution into optical isomers provided that the rotation around the bond in question is really restricted and the group involving the very sp^2 carbon atom is directed in relation to the sp^3 part.

A search of the literature revealed that 3-(1-hydroxyethyl)-*s*-guaiazulene has been reported to show two different melting points and different dehydrative reactivities according to the methods of preparation: the lithium aluminum hydride reduction of 3-acetyl-*s*-guaiazulene and the Grignard reaction of methyl iodide with 3-formyl-*s*-guaiazulene.[3] These phenomena have been suggested to originate from "the isomerism caused by restricted rotation" around the azulene-to-3-substituent bond.

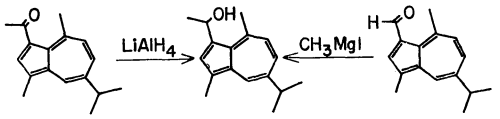

(1)

[70-71°], [72-73°]

If this were really the case, this should be a good example of restricted rotation around the sp^2–sp^3 carbon bond. Thus, we have undertaken an investigation of the isolation of three possible pairs of optical isomers of the afore-mentioned type of compound, which should exist as visualized by the following six models, where

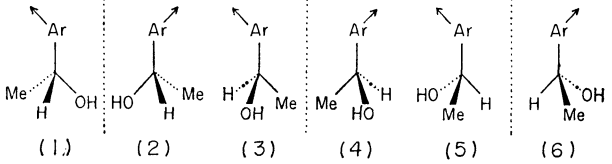

(1) (2) (3) (4) (5) (6)

1) A part of this article was presented at the 22nd annual meeting of the Chemical Society of Japan, Tokyo (1969).

2) M. Ōki and M. Suda, This Bulletin, **44**, 1876 (1971).

3) M. Miyazaki, M. Hashi, and T. Ukita, *Chem. Pharm. Bull.*, **8**, 140 (1960).

Ar is the azulene ring and where the arrow indicates the direction of the azulene group.

The purpose of this paper is to report the results of this investigation which indicate that the rotation around the bond in question is fast and that optical resolution is not possible.

Results and Discussion

4,6,8-Trimethylazulene derivatives were chosen as the model compounds, for the ring system is readily accessible[4] and has the same stereochemical environment as that studied by Ukita and his co-workers.

1-Acetyl-4,6,8-trimethylazulene (**1**) was obtained by the action of acetic anhydride and phosphorus pentoxide on 4,6,8-trimethylazulene and 1-formyl-4,6,8-trimethylazulene (**2**) by the action of the Vilsmeyer-Haak reagent.

Lithium aluminum hydride reduction of **1** in ether afforded blue needles of 1-(1-hydroxyethyl)-4,6,8-trimethylazulene (**3**-L), which melted at 93.5—95.0°C before recrystallization. When recrystallized from petroleum ether, two modifications of the alcohol showing different melting points were obtained according to the crystallization conditions. That is, when the hot solution was chilled quickly to about 0°C, blue granular **3**-L with a mp of 68—78°C was precipitated, while blue crystalline **3**-L with a mp of 81.0—81.1°C was formed when the hot solution was allowed to cool slowly to room temperature.

The reduction of **1** in 1:1 ether-tetrahydrofuran also yielded **3**-L as a dark blue crystalline mass, which changed to tiny violet needles after recrystallization; their melting points were 75.0°C and 87.5—88.5°C before and after recrystallization, respectively.

The reaction of **2** with the methyl Grignard reagent in 1:1 ether-tetrahydrofuran gave **3**-G as a dark blue crystalline mass melting at 80.5—81.5°C before recrystallization. However, the alcohol again changed to tiny violet needles melting at 87.5—88.5°C when the hot solution of the alcohol in petroleum ether was cooled slowly to room temperature.

These phenomena may be accounted for in two different ways. The first is, as has been suggested by Ukita *et al.*, the rotational isomerism, while the second is the polymorphism caused by the different packings in the crystal lattice. Since it is expected that the attacking reagent approaches the reaction site from the least-hindered side, the hydride reduction of **1** will yield **3**-L or its mirror image, as is shown schematically in Fig. 1. Similarly, **2** will afford **3**-Gb or its mirror image and in the case of **3**-Gb the rotation around the C_{α}–$C_{azulene}$ may be possible at room temperature because of the smaller barrier formed by the hydrogen atom; thus **3**-Gc will exist also.

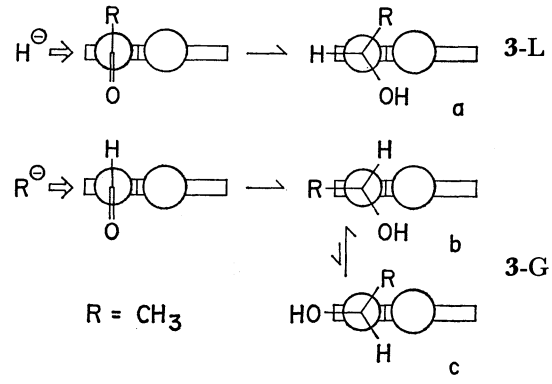

Fig. 1. Possible conformations of **3**-L and **3**-G (Newman type projection). C-1 carbon atom within 5-membered ring and C-8 methyl group attached to 7-membered ring are indicated by circles.

These considerations lead to the idea that, if the rotational isomer is the cause, there should be some differences in IR and NMR spectra among these modifications, because, for example, the force constants of C–O in **3**-Gb and **3**-Gc and the magnetic environments for the methyl protons are considered to be different. Thus, the following spectral studies have been undertaken.

The IR spectra of these compounds were recorded both with solid states and with carbon disulfide solutions, the former being shown in Figs. 2, 3, and 4, and the latter, in Fig. 5.

The correlations of their origins with the mp and IR spectra are summarized in Table 1.

A comparison of Figs. 2 and 4 reveals that, in solid states the difference between **3**-L and **3**-G appears in the spectral ranges of 1340—1260, 1080—1010, and 890—830 cm^{-1} if the reaction solvents differ from each other. When the same solvent is used for the reactions, the spectral difference, as judged by a comparison of

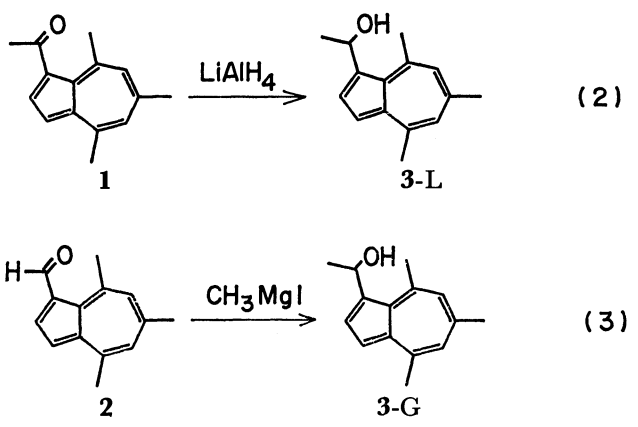

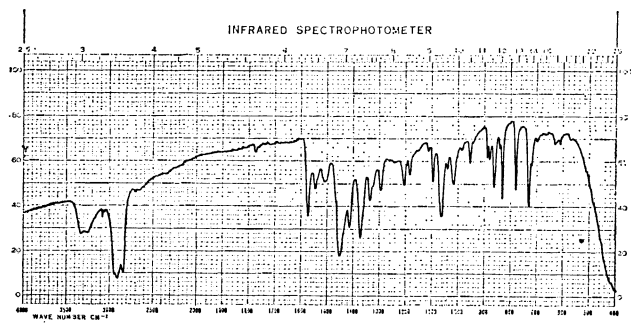

Fig. 2. IR spectrum of **3**-L (Nujol), mp 93.5—95.0°C.

4) K. Hafner and H. Kaiser, "Organic Synthesis," Vol. 44, p. 94 (1964).

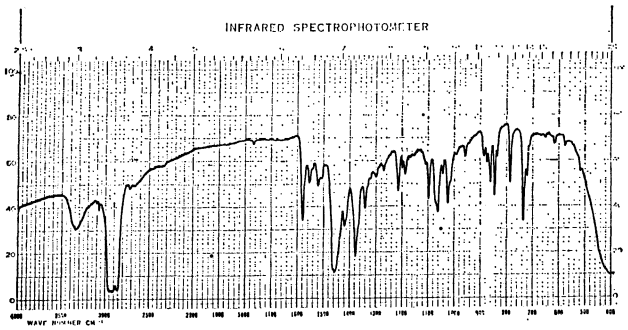

Fig. 3. IR spectrum of **3**-L (Nujol), mp 75.0°C.

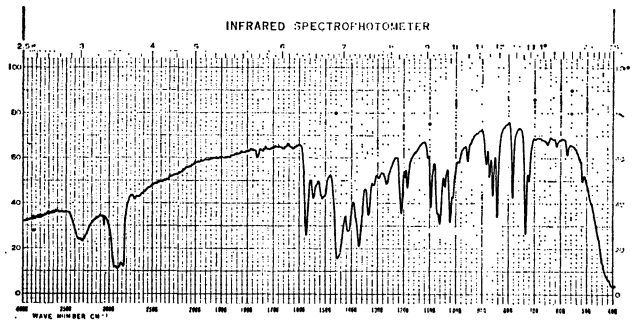

Fig. 4. IR spectrum of **3**-L (Nujol), mp 68—78, 81.0—81.1, 87.5—88.5°C, and **3**-G (Nujol), mp 80.5—81.5, 87.0—89.0°C.

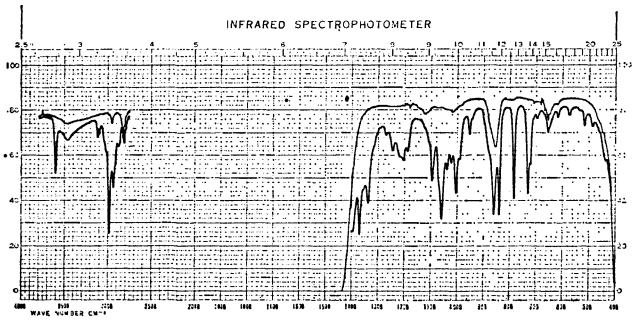

Fig. 5. IR spectrum of **3**-L and **3**-G (CS_2 soln, 0.109 mm KBr cell). The upper line is CS_2 and the lower the CS_2 soln.

Figs. 3 and 4, is confined to around 830 cm^{-1}. The IR spectra of the solution of **3**-L in carbon disulfide, however, were superimposable on those of **3**-G in every respect, one of them being illustrated in Fig. 5.

Some rotational behavior of these compounds is expected to be observable by recording the NMR spectra at various temperatures, since $R_{(a)}$ and $R_{(b)}$ ($R=CH_3$) are in different magnetic environments and a chemical shift difference between them is expected (Fig. 1). Though the NMR sampling was carried out according to Scheme 1, all the NMR spectra are superimposable upon each other; one of them is shown in Fig. 6 (a 1:1 **3**-L-**3**-G mixture in carbon disulfide).

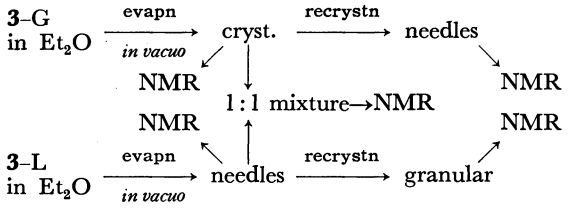

Scheme 1

These results, together with the IR results, may be interpreted by considering that a rapid exchange among the conformers, a, b, and c, is taking place at room temperature.

The NMR spectra of the alcohol, **3**, in carbon disulfide-pyridine was recorded at low temperatures. The methyl proton signal of CH_3-CH< appeared as a sharp doublet ($J=7$ Hz) at room temperature, but as the probe temperature was lowered, the signal decreased in height and increased in width. The changes in signal shape (as in Fig. 7) in the temperature range of −70——90°C apparently indicate that the internal rotation in question becomes sufficiently slow to be observed at these temperatures. Conversely, the internal rotation in question is very rapid, at least at room temperature.

Further evidence supporting the implication that the rotation around the C_α-to-azulene bond was slow at low temperature was obtained from variable-temper-

Table 1. Correlations of reactions with mp and IR

Reaction	Reaction solvent	Before recrystn		After recrystn	
		mp and cryst.	IR (Nujol)	mp and cryst.[a]	IR (Nujol)
$LiAlH_4$ redn	Et_2O	93.5—95.0°C blue needles	Fig. 2	68—78°C (cooled quickly) blue granular crystals 81.0—81.1°C (cooled slowly) blue crystals	Fig. 4
	Et_2O-THF (1:1)	75.0° dark blue crystalline mass	Fig. 3	87.5—88.5°C (cooled slowly) violet needles	Fig. 4
Grignard	Et_2O-THF (1:1)	80.5—81.5°C dark blue crystalline mass	Fig. 4	87.0—89.0°C (cooled slowly) violet needles	Fig. 4

a) The conditions of crystallization were given in parentheses.

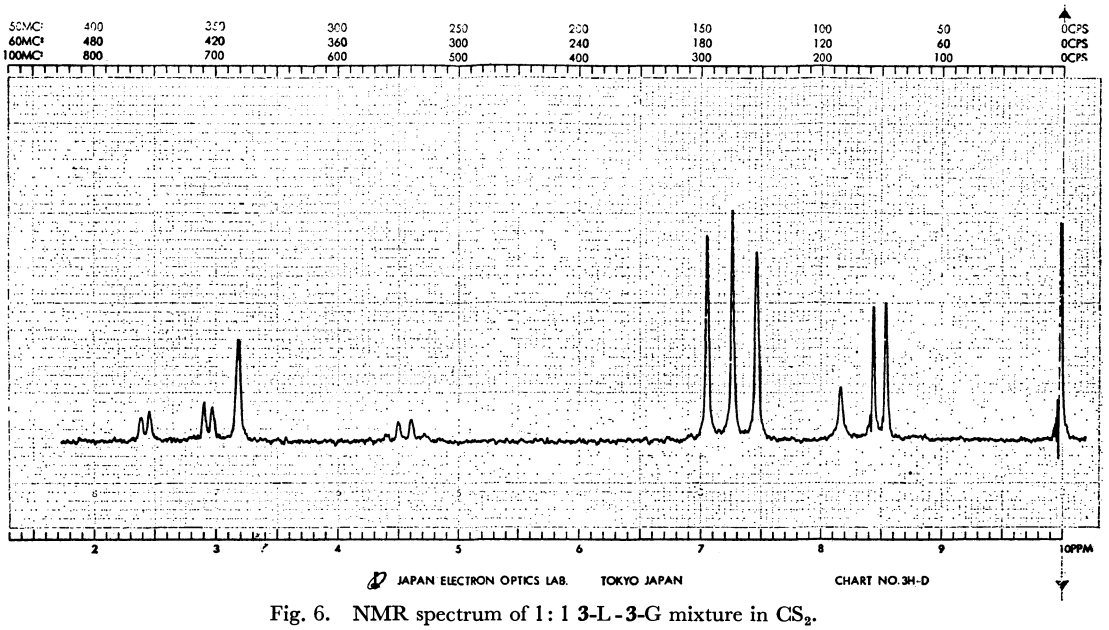

Fig. 6. NMR spectrum of 1:1 **3**-L-**3**-G mixture in CS_2.

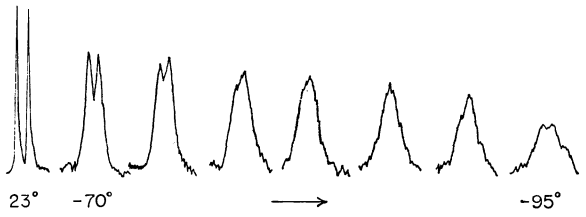

Fig. 7. Temperature dependence of β-methyl signal of 1-(1-hydroxyethyl)-4,6,8-trimethylazulene (1:1 wt/wt **3**-L-**3**-G in 1:1 v/v CS_2-C_5H_5N).

ature NMR studies of 1-*t*-butyl-4,6,8-trimethylazulene (**4**), which had been prepared by the reaction of 4,6,8-trimethylazulene with *t*-butyl alcohol in the presence of anhydrous tetrafluoroboric acid. The NMR spec-

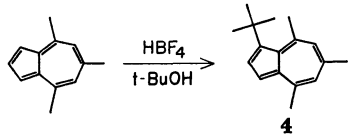

(4)

4

tral data of the *t*-butyl protons are shown in Table 2. Though the *t*-butyl signal was a sharp singlet at room temperature, it became somewhat broader as the temperature was lowered, and below 0°C apparent changes in both its height and half-width were observed. When the temperature reached −80°C, the relative height and the relative half-width were 2.4 and 1.4 respectively, with respect to the ring-methyl signal of the greatest height, and below −80°C there was little change in these figures.

Although no chemical-shift difference among the methyl groups of the *t*-butyl residue was observed in this experiment, those facts given above can be best accounted for by the theory that the internal rotation around the *t*-butyl-to-azulene bond is sufficiently slow only at −80°C on the NMR time scale and that it is too rapid at room temperature for the stable rotamers to be isolated.

Table 2. NMR spectral data of 1-*t*-butyl-4,6,8-trimethylazulene

Temp. °C	Rel. values of *t*-butyl signal[a]	
	height	half-width
23	3.8_4	0.56
−25	3.3_7	0.75
−80	2.3_6	1.3_6
−90	2.3_0	1.2_4

Spectrum was taken with CS_2 solution.
a) Relative values to the ring-methyl group of the greatest height

Thus, it is most probable to ascribe the many modifications of 1-(1-hydroxyethyl)-4,6,8-trimethylazulene to the polymorphism derived by the difference in the mode of crystal packing into the lattice. Indeed, the X-ray diffraction patterns (Fig. 8), whose angles and relative intensities have been obtained with good reproducibilities, show a difference supporting the conclusion.

Experimental[5]

The NMR spectra were taken with JEOL 3H-60 and C-60H spectrometer equipped with variable-temperature accessories, the IR spectra, with a HITACHI EPI-G2 grating infrared spectrophotometer, and the X-ray diffraction lines, with a diffractometer, Geigerflex, of the Rigaku Denki Co., Ltd.

The reduction and Grignard reaction were carried out under dry nitrogen, and the solvents were distilled over lithium aluminum hydride just before use.

1-Acetyl-4,6,8-trimethylazulene (1). From 11.3 g of 4,6,8-trimethylazulene,[4] 200 m*l* of acetic anhydride, and 5.3 g of phosphorus pentoxide, 7.0 g of 1-acetyl-4,6,8-trimethylazulene were formed; mp 72—73°C (reported mp 72—73°C[6]).

5) All the melting points are uncorrected.
6) K. Hafner, H. Pelster, and J. Schneider, *Ann. Chem.*, **650**, 74 (1961).

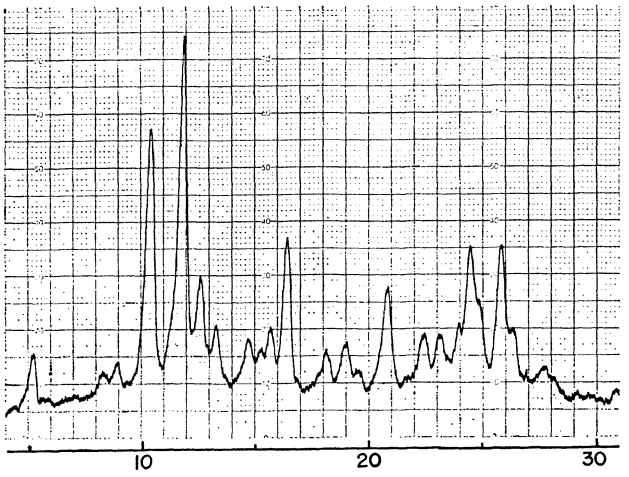

a) **3**-L, whose IR spectrum corresponds to Fig. 2

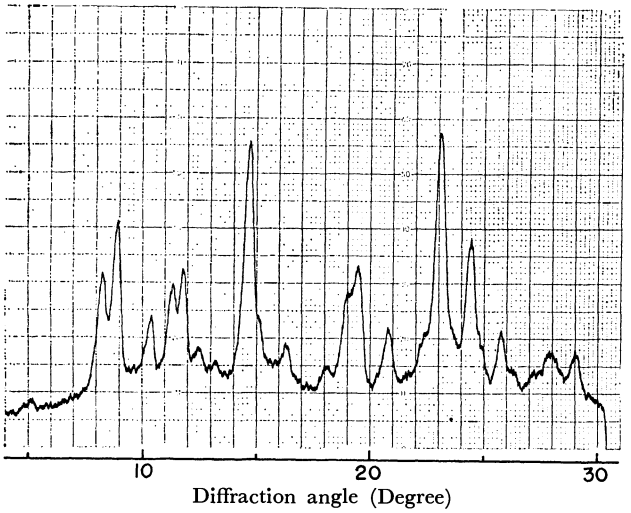

b) **3**-L, whose IR spectrum corresponds to Fig. 3

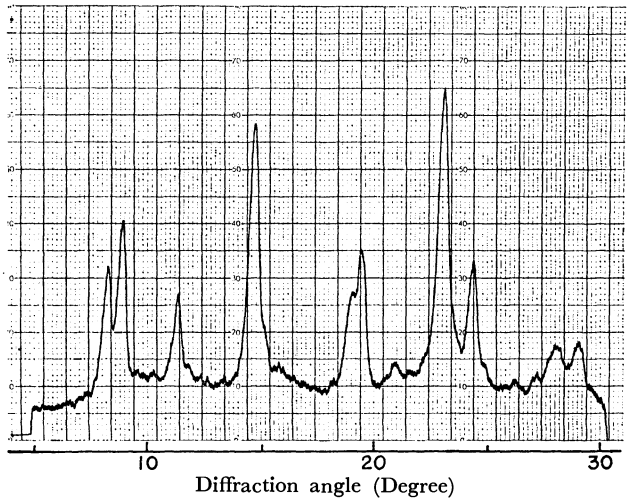

c) **3**-G, whose IR spectrum corresponds to Fig. 4

Fig. 8. X-ray diffraction patterns of **3**-L and **3**-G.

1-Formyl-4,6,8-trimethylazulene (2). 4,6,8-Trimethylazulene (17.0 g) was formylated with a Vilsmeyer-Haak reagent prepared from 45 m*l* of *N*,*N*-dimethylformamide and 17.0 g of phosphorus oxychloride to yield 13 g of 1-formyl-4,6,8-trimethylazulene; mp 105°C (reported mp 106—107°C[7]).

1-(1-Hydroxyethyl)-4,6,8-trimethylazulene (3-L): Reduction of 1 with Lithium Aluminum Hydride. a) Reduction in Ether: To a well-stirred suspension of 0.2 g of lithium aluminum hydride in 30 m*l* of anhydrous ether was added a solution of 1.5 g of **1** in 70 m*l* of anhydrous ether at 0°C; the reaction mixture was then stirred at this temperature for 30 min. At the end of this time, 10 m*l* of methanol and then 20 m*l* of water were added. The mixture was poured into a saturated sodium chloride solution and extracted with ether. The combined ether extracts were washed with water and dried over sodium sulfate. The solvent was evaporated *in vacuo* below 20°C. The blue needles so obtained melted at 93.5—95.0°C and had the IR absorption shown in Fig. 2 (Nujol). Found: C, 84.50; H, 8.81%; Calcd for $C_{15}H_{18}O$: C, 84.07; H, 8.47%.

3-L was recrystallized from petroleum ether (50—60°C fraction). When the hot solution was cooled quickly with ice water, blue granular solid was obtained; mp 68—78°C. However, when it was allowed to cool slowly to room temperature, a blue crystalline product was formed; mp 81.0—81.1°C. These **3**-L's showed identical IR spectra, as is shown in Fig. 4. NMR (δ from TMS in CS_2): 1.50 (3H, doublet, J=6.0 Hz), 1.82 (1H, singlet), 2.53 (3H, singlet), 2.73 (3H, singlet), 2.94 (3H, singlet), 5.44 (1H, quartet, J=6.0 Hz), 6.82 (2H, singlet), 7.05 (1H, doublet, J=4.0 Hz), 7.57 (1H, doublet, J=4.0 Hz).

b) Reduction in 1:1 Ether-Tetrahydrofuran: To a mixture of 0.2 g of lithium aluminum hydride and 30 m*l* of ether, was added a solution of 1.5 g of **1** in 20 m*l* of ether and 50 m*l* of tetrahydrofuran at 0°C. The reaction mixture was then treated as described in a). The blue product, mp 75°C before recrystallization, showed the IR spectrum given in Fig. 3 (Nujol). After recrystallization from petroleum ether, tiny violet needles, mp 87.5—88.5°C, were obtained. The IR spectrum (Nujol) is shown in Fig. 4.

Found: C, 84.36; H, 8.80%; Calcd for $C_{15}H_{18}O$: C, 84.07; H, 8.47%.

1-(1-Hydroxyethyl)-4,6,8-trimethylazulene (3-G): Reaction of 2 with Methylmagnesium Iodide. To an ethereal solution of methylmagnesium iodide prepared from 2.2 g of methyl iodide, 0.37 g of magnesium ribbon, and 30 m*l* of anhydrous ether, was added, drop by drop, a soluion of 1.98 g of **2** in 20 m*l* of anhydrous ether and 50 m*l* of anhydrous tetrahydrofuran at 0°C; the reaction mixture was stirred at this temperature for a further 30 min. The mixture was treated with 10 m*l* of methanol and then 20 m*l* of water, poured into a saturated sodium chloride solution, and extracted with ether. The combined extracts were washed with water and dried over sodium sulfate. The solvent was evaporated *in vacuo* below 20°C to yield a dark blue crystalline product, mp 80.5—81.5°C before recrystallization, whose IR spectrum (Nujol) is shown in Fig. 4.

After recrystallization from petroleum ether (50—60°C fraction), it was obtained as tiny violet needles; these needles melted at 87.0—89.0°C (reported mp 87—88°C[8]) and showed the IR spectrum illustrated in Fig. 4 (Nujol).

Found: C, 83.70; H, 8.93%; Calcd for $C_{15}H_{18}O$: C, 84.07; H, 8.47%.

1-t-Butyl-4,6,8-trimethylazulene (4). To a well-stirred mixture of 5.1 g of 4,6,8-trimethylazulene, 68 g of *t*-butyl alcohol, and 150 m*l* of anhydrous ether, 60 m*l* of a 54%

7) K. Hafner and C. Bernhard, *Ann. Chem.*, **625**, 116 (1959).
8) K. Hafner and C. Bernhard, *ibid.*, **625**, 122 (1959).

ethereal solution of anhydrous tetrafluoroboric acid[9] was added, drop by drop under nitrogen. The reaction mixture was allowed to stand at room temperature for 12 days and then poured onto crushed ice. The mixture was extracted three times with ether to recover the starting material. The aqueous layer was made alkaline with a 5% sodium hydroxide solution and extracted with ether. The extracts were washed with water and dried over sodium sulfate-potassium carbonate (2:1). The solvent was then evaporated *in vacuo*, and the residual dark blue oil was chromatographed on alumina to yield *ca.* 1 g of 1-*t*-butyl-4,6,8-trimethylazulene as a dark blue oil.

Found: C, 90.17; H, 9.99%; Calcd for $C_{17}H_{22}$: C, 90.20; H, 9.80%.

NMR (δ from TMS in CS_2): 1.54(9H, sharp singlet), 2.45 (3H, singlet), 2.69 (3H, singlet), 2.95 (3H, singlet), 6.72 (1H, broad singlet), 6.81 (1H, broad singlet), 7.00 (1H, doublet, J=5 Hz), 7.57 (1H, doublet, J=5 Hz). The two protons attached to the seven-membered ring of 1-*t*-butyl-4,6,8-trimethylazulene showed different positions of absorption from each other in their NMR spectra in carbon disulfide. This phenomenon was observed only in the case of **4**. In the case of the other 1-substituted 4,6,8-trimethylazulenes studied, including 1-benzoyl and 1-hydroxymethyl derivatives, the ring protons attached to the seven-membered ring appeared as a broad singlet in the 60 MHz MNR spectra in carbon disulfide.

9) K. Hafner, A. Stephan, and C. Bernhard, *Ann. Chem.*, **650**, 57 (1961).

We are deeply indebted to Dr. Yutaka Kawazoe and Dr. Mitsuhiro Tsuda, National Cancer Center Research Institute, Japan, for measuring the NMR spectra, and also to Dr. Isao Ikemoto, The University of Tokyo, for recording the X-ray diffraction lines.

BULLETIN OF THE CHEMICAL SOCIETY OF JAPAN, VOL. 44, 1885—1891 (1971)

Reactions of Tosylhydrazide Derivatives Having Olefinic Groups[1)]

Tadashi SATO and Itomi HOMMA*[1]

Department of Applied Chemistry, Waseda University, Shinjuku-ku, Tokyo

(Received December 7, 1970)

When α,β-unsaturated ketone tosylhydrazones (**5**) were heated in 85% aqueous acetic acid, a smooth decomposition was induced and β-tosylketones (**4**) were obtained in fair yields. Tosylhydrazones, devoid of an olefinic group in the specified position, failed to undergo the present reaction. When allyl halides (**17**) were reacted with the anion of tosylhydrazide in DMSO, substitution occurred on the N-1 of tosylhydrazide, unlike as in the case of the reaction of chlorides with tosylhydrazide in pyridine, which effected the substitution on N-2. On warming in acetic acid, these 1-allyltosylhydrazides (**18**) afforded olefins (**19**) in fair yields, with a complete allylic rearrangement. A concerted cyclic mechanism was proposed for the **5**→**4** and **18**→**19** reactions.

It has been remarked that compounds derived from tosylhydrazide undergo many interesting reactions, and many of these reactions have been used for synthetic purposes.[2)] The present paper will deal with two new types of reactions, one with α,β-unsaturated ketone tosylhydrazones, and the other with 1-allyltosylhydrazides.

a) α,β-Unsaturated Ketone Tosylhydrazone System. Since the article of Bamford and Stevens,[3)] the base-induced thermal reactions of ketone tosylhydrazones have been extensively studied, but the reactions under acidic conditions have not attracted so much interest. Henry and Moore[4)] thermolyzed several ketone tosylhydrazones in acetic acid, but the reaction proceeded in a complicated way and the product was a mixture of several compounds.

In connection with our studies of α,β-unsaturated ketone tosylhydrazones,[5)] we carried out the reactions of these tosylhydrazones under acidic conditions. It has previously been established that these hydrazones afford pyrazole derivatives on treatment with alkoxides,[5-7)] and conjugated dienes on treatment with alkyllithium.[8)]

Henry and Moore[4)] obtained β-tosylketone **4a** in a 29% yield by heating benzalacetophenone (**1**) and tosylhydrazide (**2**) in acetic acid. They proposed a mechanism of: (1) the decomposition of **2** into *p*-toluenesulfinic acid (**3**) and diimide, and (2) the 1,4-addition of **3** to benzalacetophenone to afford the product. The mechanism is reasonable because each step, both (1)[9)] and (2)[10)], is a known reaction. We thermolyzed benzalacetone tosylhydrazone (**5b**) in acetic acid and

1) The article has previously been reported in a preliminary form. T. Sato and I. Homma, Abstracts of papers presented at the 21st meeting of the Chemical Society of Japan, Osaka, April, 1968, Vol. III, p. 1814; T. Sato, I. Homma, and S. Nakamura, *Tetrahedron Lett.*, **1969**, 871.

*1 Present address: Kao Soap Co., Ltd., Tokyo.

2) L. F. Fieser and M. Fieser, "Reagents for Organic Synthesis," Vol. I, John Wiley & Sons, New York (1967), p. 1185; *ibid.*, Vol. II, (1969), p. 417.

3) W. R. Bamford and T. T. Stevens, *J. Chem. Soc.*, **1952**, 4735.

4) R. A. Henry and D. W. Moore, *J. Org. Chem.*, **32**, 4145 (1967).

5) T. Sato and S. Watanabe, This Bulletin, **41**, 3017 (1968).

6) R. K. Bartlett and T. S. Stevens, *J. Chem. Soc., C*, **1967**, 1964.

7) H. A. Staab and H-A. Kurmeir, *Chem. Ber.*, **101**, 2697 (1968).

8) W. G. Dauben, M. E. Lorber, N. D. Vietmeyer, R. H. Shapiro, J. H, Duncan, and K. Tomer, *J. Amer. Chem. Soc.*, **90**, 4762 (1968).

9) R. S. Dewey and E. E. vanTamelen, *ibid.*, **83**, 3729 (1961).

10) E. P. Kohler and M. Reimer, *Amer. Chem. J.*, **31**, 178 (1903).

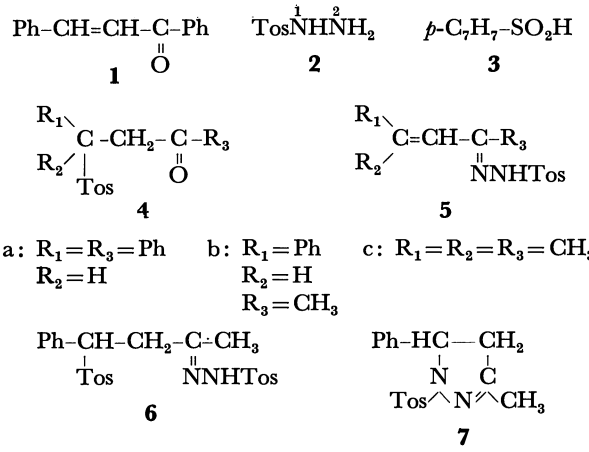

thus obtained Compounds **4b**, **6**, and **7** and the starting tosylhydrazone in 16%, 47% (stoichiometrically), 2.5%, and 5% yields, respectively. The formation of **6** is evidence that *p*-toluenesulfinic acid might intervene in the reaction.

We observed that a smooth decomposition was effected when the thermolysis was carried out in acetic acid *containing* 15% *of water*. The tosylhydrazones **5a**—**5c** afforded *β*-tosylketones **4a**—**4c** in yields of 76%, 68%, and 42%, respectively, no other products being isolated in the pure state. A concerted transfer of electrons in an intermediate **8** was presumed as the probable mechanism for the formation of **4** in view of the following observations. First, when **2** was heated under the present reaction conditions, a quantitative amount of 2-acetyltosylhydrazide (**9**) was obtained and no decomposition into diimide and *p*-toluenesulfinic acid was observed. 2-Acetyltosylhydrazide was a stable compound and was recovered unchanged on refluxing in an acetic acid-water mixture in the presence of benzalacetophenone. Second, when 3-methyl-2-cyclohexenone tosylhydrazone (**10**) was heated under the present reaction conditions, a quantitative amount of **9** was obtained. As 3-methyl-2-cyclohexenone and **3** afforded the *β*-tosylketone **11**, the failure of the **10**→**11** reaction could be ascribed to the incapability for **10** to take the cyclic configuration, as represented in **8**, which might be requisite for the tosyl migration. Acetophenone tosylhydrazone (**12**) also afforded **9** quantitatively under the same conditions. The formation of diimide in the reaction was evident because, when the reaction was carried out in the presence of

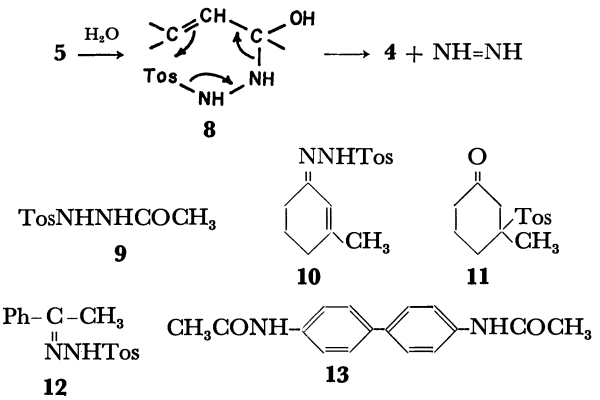

azobenzene, 27% (on the basis of **5b**) of diacetylbenzidine (**13**) was obtained. It has been established that azobenzene is reduced by diimide to hydrazobenzene,[11] which then affords **13** by the reaction sequence of benzidine rearrangement and acetylation in acetic acid.[12]

As a model for the intermediate **8**, a tosylhydrazide derivative, **14a**, was prepared from chloride **16** and **2** in pyridine. Although **14a** actually afforded **15a** on refluxing in ethanol, it was not possible, because of the symmetrical carbon skeleton of **14a**, to differentiate between the proposed cyclic mechanism (a) and the elimination-recombination mechanism on the same carbon atom (b). As an attempt to synthesize compound **14** with an unsymmetrical carbon skeleton, cinnamyl chloride (**17a**) and **2** were allowed to react under various reaction conditions, but the reaction mostly proceeded with nitrogen elimination, and cinnamyl *p*-tolyl sulfone resulted. In one case, when **17a** was treated with sodium salt of **2** in DMSO, nitrogen-elimination was avoided and a tosylhydrazide derivative was obtained. The product, however, proved not to be the expected **14b**, but an isomer, **18a**, as proved by

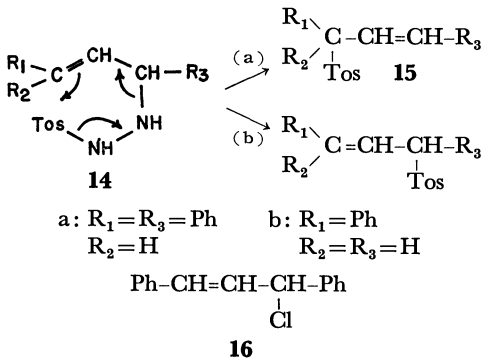

the following observations. The IR spectrum of the compound showed a sharp band at 3400 cm^{-1} for NH_2, and two strong bands, at 1340 and 1150 cm^{-1}, for the tosyl group. The NMR spectrum showed a singlet at δ 3.5 corresponding to two protons for NH_2. The structure was further confirmed by deriving it to the benzal derivative **20a** by treatment with benzaldehyde. It is conceivable that the substitution occurred on the N-1 of **2** because the hydrogen on this nitrogen would be the most acidic and would ionize first when treated with sodium hydride. The reaction presented a sharp contrast to that of **2** with chlorides in pyridine, in which case substitution occurred on the more basic N-2,as in the case of **16**→**14a**. Although our attempts to synthesize **14b** were thus unsuccessful, we observed instead that compound **18a** underwent an interesting fragmentation when treated with acetic acid.

b) 1-Allyltosylhydrazide System.[13] When **18a** was heated in acetic acid at 60°C, allylbenzene, **19a**, was unexpectedly obtained in a 66% yield. Allylbenzene was also obtained when **18a** was pyrolyzed at 110°C, but the yield was much lower in this case and

11) E. E. vanTamelen, R. S. Dewey, and R. J. Timmons, *J. Amer. Chem. Soc.*, **83**, 3725 (1961).
12) F. Sachs and C. M. Whittaker, *Ber.*, **35**, 1435 (1902).
13) The authors are indebted to Mr. Shohei Nakamura for his helpful assistance.

the product was contaminated with toluene and other minor unidentified compounds. As an extension of this type of reaction, some allyl halides, **17b—17e**, were reacted with **2** by the NaH/DMSO method. The resulting compounds (**18b—18e**) were shown to have primary amino group from the IR and NMR spectra and by deriving them to benzalamino derivatives **20b—20d**. Compounds **18b—18d**, when warmed at 30—60°C in acetic acid, afforded **19b—19d** in 55—70% yields.

Two features of the acid fragmentation of the tosylhydrazides are noteworthy: 1. The reaction proceeds so as to isolate double bond from conjugation with the phenyl group or to cause the endocyclic double bond to migrate to the thermodynamically more unfavorable exocyclic double bond. 2. The reaction proceeds with a complete allylic rearrangement, no other double-bond isomers being detected in any product on analysis by gas chromatography and by a study of the NMR spectrum.

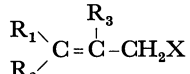

17

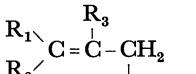

18

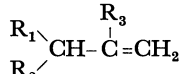

19

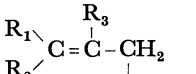

20

a: $R_1=Ph$, $R_2=R_3=H$, $X=Cl$
b: $R_1=R_2=Ph$, $R_3=H$, $X=Br$
c: $R_1=R_3=Ph$, $R_2=H$, $X=Br$
d: R_1, $R_3=-(CH_2)_4-$, $R_2=H$, $X=Cl$
e: $R_1=R_2=R_3=H$, $X=Cl$

The complete allylic rearrangement in the present reaction can be explained in terms of a concerted fragmentation of 1-allyltosylhydrazide **21**, or of the allyldiimide **22** formed *in situ* from **21**, by the elimination of *p*-toluenesulfinic acid.

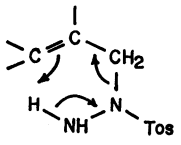

21

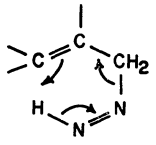

22

Similar types of double-bond migrations have been reported in the cases of: (1) the reaction of allylamines with difluoroamine,[14] (2) the unusual Wolff-Kishner reduction of α,β-unsaturated carbonyl compounds,[15] and (3) the reaction of allylmercuric derivatives with hydrogen chloride.[16] However, reactions (1) and (2) have limited general applicability because, in the former case, a special experimental technique is necessary for handling difluoroamine and, in the latter case, the reaction frequently gives the product as a mixture of double-bond isomers or proceeds in another directions.

The present reaction could be used for causing the double bond to migrate by the sequence of reactions shown in Scheme 1:

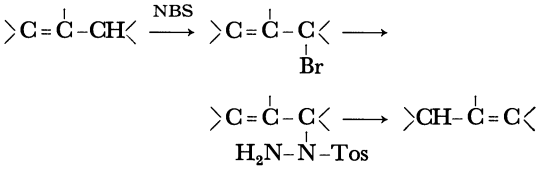

Scheme 1

Nickon and Hill[17] showed that the treatment of *N*-substituted sulfonamides, **23**, with an excess of hydroxylamine-*O*-sulfonic acid in the presence of aqueous alkali yielded the corresponding hydrocarbons, **25**, and proposed a scheme involving 1-substituted arylsulfonylhydrazides (**24**) as the possible pathway. As an example, they obtained toluene from *N*-benzyltosylamide, **23** (Ar=*p*-C_7H_7, R=$PhCH_2$), in a good yield. Similar types of reactions under alkaline conditions were

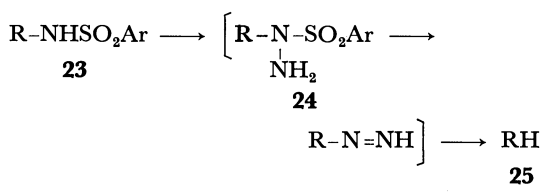

also reported by Cram.[18] With the intention of comparing the present reaction (in acetic acid) with the reaction under alkaline conditions, the base-induced decomposition of **18a** and **18b** was investigated. When **18a** was treated with sodium methoxide, allylbenzene and 1-phenylpropene were obtained in a ratio of 71:29, as determined from the relative area under each peak on the gas chromatogram. In the same way, **18b** gave a 55:45 mixture of 3,3-diphenylpropene (**19b**) and 1,1-diphenylpropene. As it was confirmed in a separate experiment that allylbenzene (**19a**) was isomerized to 1-phenylpropene to an extent of only 12.5% under the same conditions, it was evident that a portion of the 1-phenylpropene was formed directly from **18a**, instead of *via* allylbenzene (**19a**), under alkaline conditions. Presumably, fragmentations with and without the allylic rearrangement of **18a** occur competitively.

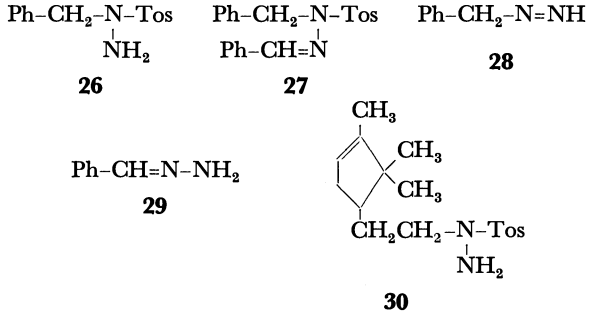

30

It is most probable that an olefinic group in the specified position is requisite for this type of fragmen-

14) C. L. Bumgardner and J. P. Freeman, *J. Amer. Chem. Soc.*, **86**, 2233 (1964).
15) I. Elphimoff-Felkin and M. Verrier, *Tetrahedron Lett.*, **1968**, 1515, and the references cited therein.
16) P. D. Sleezer, S. Winstein, and W. G. Young, *J. Amer. Chem. Soc.*, **85**, 1890 (1963).
17) A. Nickon and A. S. Hill, *ibid.*, **86**, 1152 (1964).
18) D. J. Cram and J. S. Bradshaw, *ibid.*, **85**, 1108 (1963).

tation to occur. When 1-benzyltosylhydrazide (**26**) was treated with acetic acid, a benzalamino derivative **27** was obtained in a 54% yield (calculated stoichiometrically). Obviously, the lack of an olefinic group in **26** forced the reaction to proceed in a way other than the one described above. A reasonable scheme for the formation of **27** would involve three steps: a) the elmination of *p*-toluenesulfinic acid from **26**, thus affording benzyldiimide (**28**), b) the tautomerization of the diimide into benzaldehyde hydrazone (**29**), and c) the reaction of the hydrazone, or the benzaldehyde formed therefrom, with the starting material, **26**. No smooth reaction proceeded with a compound in which the olefinic group was located in a position remote from the tosylhydrazide group, as in **30**. Under severer conditions, **30** afforded an unidentifiable mixture as the product.

Experimental

*Tosylhydrazones, **5a**, **5b**, **10**, and **12**.* The hydrazones were prepared by refluxing equivalent quantities of the ketones and tosylhydrazide (**2**) in methanol containing a trace amount of conc. hydrochloric acid for 1 hr. The details are summarized in Table 1.

*Mesityl Oxide Tosylhydrazone **5c**.* The compound was prepared according to the method reported by Closs.[19] Mp 118—122°C, Lit[19]: mp 105—110°C.

*Thermolysis of Tosylhydrazones **5a**, **5b**, **5c**, **10**, and **12** in Aqueous Acetic Acid.* A solution of 1g of hydrazone in 15 m*l* of 85% aqueous acetic acid was heated as specified in Table 2 for 3 hr. The subsequent evaporation of the solvent and the recrystallization of the residual solid afforded the product.

*β-Tosylketones **4a**, **4b**, **4c**, and **11**.* An aqueous solution of sodium *p*-toluenesulfinate was neutralized with dilute hydrochloric acid and shaken with ether. To the resulting ether solution was added an equivalent amount of ketone, and the separated solid was recrystallized. The details are summarized in Table 3.

*Thermolysis of Benzalacetone Tosylhydrazone (**5b**) in Acetic Acid.* A solution of 2g of benzalacetone tosylhydrazone (**5b**) in 25 m*l* of freshly-distilled acetic acid was refluxed for 3 hr. The solvent was removed *in vacuo*. The resulting oil solidified on treatment with a small amount of ether. The solid was washed with ether several times (ether-insoluble solid: named A). The ether washings were combined and the ether was removed. The residual solid (0.3 g) afforded crystals of mp 142°C when recrystallized from methanol. The compound was identified as **4b** by comparison with an authentic sample (IR spectrum, mp, and mixed mp). When

Table 1

Ketone	Product	Mp (Lit)	Crystn solvent		C(%)	H(%)	N(%)
Benzalaceto-	**5a**	146—148	Methanol	Found:	70.11	5.27	7.44
phenone	$C_{22}H_{20}N_2O_2S$	(156-157)[7]		Calcd :	70.20	5.36	7.44
Benzalacetone	**5b**	185—187	Dioxane-	Found:	64.80	5.65	8.89
	$C_{17}H_{18}N_2O_2S$	(195)[6]	water	Calcd :	64.95	5.77	8.91
3-Methyl-2-	**10**	134—135	Methanol-	Found:	60.72	6.69	10.33
cyclohexenone	$C_{14}H_{18}N_2O_2S$		water	Calcd :	60.42	6.52	10.07
Acetophenone	**12**	148	Ethanol	Found:	62.30	5.63	9.62
	$C_{15}H_{16}N_2O_2S$	(148)[3]		Calcd :	62.49	5.59	9.72

Table 2

Tosylhydrazone	Reaction condition	Product	Yield (%)	Crystn solvent
5a	Reflux	**4a**	76	Methanol
5b	Reflux	**4b**	68	Acetone-methanol-water
5c	95°C	**4c**	42	Methanol-water
5c	Reflux	**9**	92	Water
10	85°C	**9**	95	Water
12	Reflux	**9**	90	Water

Table 3

Tosylketone	Mp (°C)	(Lit)	Found C(%)	Found H(%)	Calcd C(%)	Calcd H(%)
4a	176—177	(169—170)[10]	72.71	5.32	72.51	5.53
$C_{22}H_{20}O_3S$		(170—171)[4]				
4b	143	(147—148)[10]	67.58	6.01	67.54	6.00
$C_{17}H_{18}O_3S$						
4c	88—89	(94)[20]	61.32	7.30	61.40	7.14
$C_{13}H_{18}O_3S$						
11[a]	90—91		63.24	6.97	63.14	6.81
$C_{14}H_{18}O_3S$						

a) This compound was also obtained by heating the starting components in 85% aqueous acetic acid.

19) G. L. Closs, L. E. Closs, and W. A. Böll, *J. Amer. Chem. Soc.*, **85**, 3796 (1963).

20) C. L. Arcus and J. Kenyon, *J. Chem. Soc.*, **1938**, 684.

the solid A was recrystallized from ethanol, 0.7 g of crystals with a mp of 140—142°C was obtained. The compound was identified as **6** by comparison with an authentic samle (IR spectrum, mp and mixed mp). From the mother liquor of the recrystallization process, 0.1 g of the starting tosylhydrazone, **5b**, and 0.05 g of crystals of **7** (mp 156—157°C) were obtained. On recrystallization from ethanol, the mp rose to 159—159.5°C (Lit[6]: mp 164—165°C).

Found: C, 64.72; H, 5.68; N, 8.89%. Calcd for $C_{17}H_{18}N_2O_2S$: C, 64.95; H, 5.77; N, 8.91%.

2-Acetyltosylhydrazide (9). An acetic-acid solution of tosylhydrazide (**2**) was refluxed for 2 hr. The solvent was then removed *in vacuo*, and the solid was recrystallized from water. Mp 146—147°C (Lit[21]: mp 151°C).

Found: C, 47.19; H, 5.01; N, 12.36%. Calcd for $C_9H_{12}N_2O_3S$: C, 47.37 ; H, 5.30; N, 12.28%.

4-Phenyl-4-tosyl-2-butanone Tosylhydrazone (6). a) An aqueous solution of 1 g of sodium *p*-toluenesulfinate was neutralized with dilute hydrochloric acid, and free *p*-toluenesulfinic acid was extracted with ether . To the resulting ether solution, we then added 1.6 g of benzalacetone tosylhydrazone (**5b**). The solid was filtered and recrystallized from ethanol. Mp 144—146°C. b) A methanol solution containing 1.5 g of **4b**, 1 g of tosylhydrazide (**2**), and a trace amount of conc. hydrochloric acid was refluxed for 2 hr. On cooling, a solid separated which was then recrystallized from ethanol. Mp 144—146°C. The compounds obtained from the two processes, a) and b), were identical.

Found: C, 61.41; H, 5.55; N, 6.01%. Calcd for $C_{24}H_{26}N_2O_4S_2$: C, 61.27; H, 5.57; N, 5.96%.

Thermolysis of Benzalacetone Tosylhydrazone (5b) in Aqueous Acetic Acid in the Presence of Azobenzene. A solution of 3g of benzalacetone tosylhydrazone (**5b**) and 1.7 g of azobenzene in 27 m*l* of acetic acid and 3 m*l* of water was refluxed for 5 hr. The solvent was evaporated *in vacuo*, and the residue was washed with petroleum ether (the petroleum ether-insoluble oil: named B). From the petroleum-ether washing, 0.7 g of azobenzene was recovered. The oil B partially crystallized when a small amount of chloroform was added. The solid was filtered (mother liquor: named C), and recrystallized from acetic acid. Crystals of diacetylbenzidine (**13**) (0.7 g) were thus obtained. Mp 328°C (Lit[12]: mp 330—331°C). Found: C, 71.62; H, 6.11; N, 10.21%. Calcd for $C_{16}H_{16}N_2O_2$: C, 71.62; H, 6.01; N, 10.44%. The work-up of the mother liquor of the recrystallization process of **13** afforded other crystals. Recrystallization from ethanol afforded a pure sample of 4-tosylazobenzene (0.3 g); mp 218—220°C. (Lit[22]: mp 224—225°C). Mixed mp with the authentic sample: 220°C. From the mother liquor, C, **4b** was obtained.

1,3-Diphenyl-2-propen-1-ol. To a solution of 20 g of benzalacetophenone in 50 m*l* of ethanol, we added, portion by portion, 1 g of sodium borohydride. The solution was stirred at room temperature for 3 hr, and then the ethanol was evaporated *in vacuo*. A small amount of acetic acid was added to decompose the excess borohydride, and water was added. The solution was shaken with ether and dried over sodium sulfate. The evaporation of the solvent afforded crystals which were recrystallized from ether-petroleum ether. Mp 56°C (Lit[23]: mp 58—59°C).

2-(1,3-Diphenyl-2-propen-1-yl)tosylhydrazide (14a). Thionyl chloride (7.5 m*l*) was added, drop by drop, to 18 g of 1,3-diphenyl-2-propen-1-ol with cooling by ice water, after which the resulting mixture was warmed at 80°C. After gas evolution had ceased, the excess thionyl chloride was removed *in vacuo*. The resulting oil (**16**) was added to a solution of 16 g of tosylhydrazide in 100 m*l* of pyridine with cooling by ice water, and the solution was stirred for 2 hr at room temperature. When the solution was poured into a cold hydrochloric acid (1:1), a solid separated. This was filtered, washed with ether, and recrystallized from ethanol. Prolonged heating in ethanol caused decomposition. Crystals of **14a** were obtained (8 g). Mp 132°C.

Found: C, 69.78; H, 5.84; N, 7.48%. Calcd for $C_{22}H_{22}N_2O_2S$: C, 69.82; H, 5.86; N, 7.40%.

Thermolysis of 14a. A small amount of **14a** was dissolved in ethanol and refluxed for 20 min. On cooling, a solid crystallized out; it was identified as **15a** by comparison with an authentic sample (IR spectrum, mp, and mixed mp).

1,3-Diphenyl-3-tosylpropene (15a). The crude chloride **16** obtained above and an equivalent quantity of *p*-toluenesulfinic acid was dissolved in benzene and refluxed for 2 days. The solvent was removed *in vacuo*, and the residual solid was recrystallized from ethanol. Mp 157—158°C.

Found: C, 75.87; H, 5.77%. Calcd for $C_{22}H_{20}O_2S$: C, 75.84; H, 5.79%.

The reaction of Cinnamyl Chloride with Tosylhydrazide. A solution of 2 g of tosylhydrazide and 0.5 g of cinnamyl chloride in 10 m*l* of pyridine was warmed to 70°C. The evolution of gas was observed. After the gas evolution had ceased, the solution was poured into a cold hydrochloric acid (1:1). The solid filtered and recrystallized from aqueous methanol (0.8 g). Mp 112—113°C. The compound was identified as cinnamyl *p*-tolyl sulfone by comparison with an authentic sample (IR spectrum, mp, and mixed mp).

Cinnamyl p-Tolyl Sulfone. Equivalent quantities of sodium *p*-toluenesulfinate and cinnamyl chloride in DMSO were kept at 80°C for 5 hr. Water was then added, and the mixture was shaken with ether. Thereafter ether was removed, and a mixture of benzene and ligroin was added. A solid separated on standing in a refrigerator; it was recrystallized from aqueous methanol. Mp 118—119°C (Lit[24]: mp 126—126.5°C).

Found: C, 70.03; H, 5.83%. Calcd for $C_{16}H_{16}O_2S$: C, 70.57; H, 5.92%.

1-Chloromethylcyclohexene (17d).[25] Into a solution of 5.2 g of 2-methylenecyclohexanol (bp 82—85°C/23 mmHg, prepared from ethyl 2-cyclohexanonecarboxylate[26]) in 100 m*l* of ether, we stirred 3.4 m*l* of thionyl chloride. When the solution was refluxed for 10 hr and poured into ice water, an ether layer was separated. The ether solution was washed with cold water and dried over calcium chloride. The ether was removed, and the residue was distilled. Bp 62—64°C/11 mmHg. The IR spectrum showed no band assignable to exo-methylene ($>C=CH_2$).

1-Allyltosylhydrazides 18a, 18b, 18c, 18d, and 18e, and 1 Benzyltosylhydrazide (26). To a solution of 1.86 g of tosylhydrazide (**2**) in 20 m*l* of DMSO, we added 0.5 g of sodium hydride (50%) with stirring and external cooling. After the gas evolution had subsided, an equivalent amount of halide was added, little by little, with cooling. The reaction mixture was then stirred for an additional 10 min and poured into ice water. The solid was filtered, washed with cold water several times, and recrystallized from benzene-

21) K. Freudenberg and F. Blünel, *Ann. Chem.*, **440**, 45 (1924).
22) W. Bradley and J. D. Hannon, *J. Chem. Soc.*, **1962**, 2713.
23) H. Meerwein and R. Schmidt, *Ann. Chem.*, **444**, 221 (1925).
24) V. Balish and Sp. Shanmuganathan, *J. Indian Chem. Soc.*, **35**. 31 (1958).
25) *cf.* M. Mousserson, R. Jacquier, and A. Fontaine, *Bull. Soc. Chim. Fr.*, **1956**, 1737.
26) A. S. Dreiding and J. A. Hartman, *J. Amer. Chem. Soc.*, **75**, 939 (1953).

TABLE 4

Halide	Product	Mp(°C)	Yield(%)		C (%)	H (%)	N (%)
17a	**18a**	105—107	80	Found:	63.74	5.96	9.52
	$C_{16}H_{18}N_2O_2S$			Calcd :	63.56	6.00	9.27
17b[27]	**18b**	109	65	Found:	69.95	5.80	7.46
	$C_{22}H_{22}N_2O_2S$			Calcd :	69.82	5.86	7.40
17c[28]	**18c**	109	87	Found:	69.93	6.11	7.29
	$C_{22}H_{22}N_2O_2S$			Calcd :	69.82	5.86	7.40
17d	**18d**[a]	92	75	Found:	60.14	7.43	10.10
	$C_{14}H_{20}N_2O_2S$			Calcd :	59.98	7.19	9.99
17e	**18e**	87—89	84	Found:	53.29	6.28	12.38
	$C_{10}H_{14}N_2O_2S$			Calcd :	53.09	6.24	12.38
$PhCH_2Cl$	**26**	120—121[b]	73	Found:	61.12	5.51	10.32
	$C_{14}H_{16}N_2O_2S$			Calcd :	60.86	5.84	10.14

a) Characteristic NMR signals: δ 5.64 (broad singlet, 1H) for =CH–; δ 3.58 (broad singlet, 2H) for $-CH_2-N$; δ 3.51 (sharp singlet, 2H) for $-NH_2$.
b) Lit[29]: mp 127.5—128.5°C.

TABLE 5

Benzal deriv.	Mp(°C)	Found			Calcd		
		C(%)	H(%)	N(%)	C(%)	H(%)	N(%)
20a $C_{23}H_{22}N_2O_2S$	128—129	70.87	5.61	7.22	70.75	5.68	7.18
20b $C_{29}H_{26}N_2O_2S$	147	74.47	5.55	6.12	74.66	5.62	6.01
20c $C_{29}H_{26}N_2O_2S$	166	74.38	5.42	5.87	74.66	5.62	6.01
20d $C_{21}H_{24}N_2O_2S$	109—110	68.07	6.58	8.18	68.46	6.57	7.60
27 $C_{21}H_{20}N_2O_2S$	108—109[a]	69.21	5.75	7.96	69.21	5.53	7.69

ligroin. The details are summarized in Table 4.

*Benzal Derivatives **20a**, **20b**, **20c**, **20d**, and **17**.* An ethanol solution of equivalent amounts of 1-substituted tosylhydrazide (**18a**—**18d**, and **26**) and benzaldehyde was kept at 70°C for 1 hr, and then at room temperature overnight. The crystals which thus separated were filtered and recrystallized from methanol. The details are summarized in Table 5.

*Thermolysis of 1-Allyltosylhydrazides **18a**, **18b**, **18c**, and **18d**, and 1-Benzyltosylhydrazide (**26**) in Acetic Acid.* Two grams of the hydrazide were dissolved in 15 m*l* of acetic acid, and the solution was heated. A gas evolution started at 30°C and became vigorous at 40—70°C. The solution was kept at the temperature specified in Table 6 until the gas evolution ceased. Excess water was then added, and the solution was shaken with ether. The ether layer was washed with an aqueous solution of sodium bicarbonate and dried over sodium sulfate. On the evaporation of the ether, an oil remained; it was then distilled. A gas-chromatographic investigation of the crude oil indicated that this oil was not contaminated with any of the isomers.

*Base-induced Decompositon of **18a**.* A solution of 0.8 g of **18a** and 2 g of sodium methoxide in 50 m*l* of ethanol was refluxed until no gas evolution was observed (40 min). Most of the ethanol was evaporated *in vacuo*, and water was added. The mixture was shaken with ether, and the ether solution was washed with water and dried over sodium sulfate. The oil which remained on the evaporation of ether was distilled under a vaccum (20 mmHg). All the materials which had distilled at the bath temperature of 70—80°C were collected and analyzed by gas chromatograpy. From the retention time and the relative area of each peak in the gas chromatogram, it was determined that the oil consisted of allylbenzene and 1-phenylpropene (71% and 29% respectively).

*Base-induced Decompositiom of **18b**.* A solution of 1 g of **18b** and 2 g of sodium methoxide in 50 m*l* of ethanol was refluxed for 5 hr. After the evaporation of the ethanol *in vacuo*, water was added and the mixture was shaken with ether. The ether layer was washed with water, and the ether was removed. The oil which remained was distilled under a vacuum (3 mmHg). All the materials which had been distilled before the bath temperature reached 170°C were collected and analyzed by gas chromatography. It was determined that the oil consisted of 3,3-diphenylpropene (**19b**) and 1,1-diphenyl-1-propene (55% and 45% respectively).

Base Treatment of Allylbenzene. A solution of allylbenzene (0.6 g), sodium *p*-toluenesulfonate (0.91 g), and sodium methoxide (4 g) in 100 m*l* of ethanol was refluxed for 40 min. A work-up of the reaction mixture in the way described above, and subsequent gas-chromatographic analysis, indicated that the reaction product consisted of two components (Fractions 1 and 2) (87.5% and 12.5% respectively). Each fraction was then collected. Fraction 1 was found to be allylbenzene by comparison with an authentic

27) K. Ziegler, A. Späth. E. Schaaf, W. Schumann, and E. Winkelmann, *Ann. Chem.*, **551**, 80 (1942).
28) A. Lütringhaus, H. B. König, and B. Böttchen, *ibid.*, **560**, 201 (1947).
29) C. S. Roony, E. J. Crago, Jr., C. C. Porter, and J. M. Sprague, *J. Med. Pharm. Chem.*, **5**, 155 (1962).

Table 6

Tosylhydrazide	Product	Yield (%)	Reaction condn(°C)	Identification
18a	**19a**	66	60	Identical with the authentic sample[30]
18b	**19b**	55	32—43	IR: 1630, 990, 910 cm^{-1} ($-CH=CH_2$); NMR: Identical with the reported one[31]
18c	**19c**	70	50—60	Identical with the authentic sample[32]
18d	**19d**	60	40	IR: Identical with the reported one[33]
26	**27**	54	70	Described above

sample (IR spectrum and retention time on gas chromatography). Fraction 2 was identified as 1-phenylpropene from its IR spectrum (955 cm^{-1} for the *trans* olefin).

*1-[2-(1,5,5-Trimethylcyclopenten-4-yl)ethyl]tosylhydrazide (**30**).* Into a DMSO solution of the tosylhydrazide anion, prepared in the way described above, we stirred an equivalent amount of 2-(1,5,5-trimethylcyclopenten-4-yl)ethyl tosylate[34] at room temperature. After 20 min, water was added and the mixture was shaken with ether. The evaporation of the ether afforded a solid which was then recrystallized from petroleum ether. Mp 83—84°C.

Found: C, 63.23; H, 8.05; N, 8.60%. Calcd for $C_{17}H_{26}N_2O_2S$: C, 63.33; H, 8.13; N, 8.69%.

Benzalamino derivative; mp 119—120°C. Found: C, 70.44; H, 7.52; N, 6.96%. Calcd for $C_{24}H_{30}N_2O_2S$: C, 70.22; H, 7.37; N, 6.82%.

30) E. E. Hershberg, *Helv. Chim. Acta*, **17**, 351 (1934).
31) C. Walling and L. Bollyky, *J. Org. Chem.*, **28**, 256 (1963).
32) K. T. Serijan and P. H. Wise, *J. Amer. Chem. Soc.*, **73**. 4766 (1951).
33) S. Pinchas, J. Shabtai, and E. Gil-Av, *Anal. Chem.*, **30**, 1863 (1958).
34) T. Sato and J. Higuchi, unpublished.

BULLETIN OF THE CHEMICAL SOCIETY OF JAPAN, VOL. 44, 1891—1895 (1971)

The Trialkylborane-initiated Graft Copolymerization of Methyl Methacrylate onto Hemoglobin[1)]

Koichi KOJIMA, Susumu IWABUCHI, and Kuniharu KOJIMA*,
Department of Applied Chemistry, Faculty of Engineering, Chiba University, Yayoi-cho, Chiba
and Niro TARUMI
Institute for Medical and Dental Engineering, Tokyo Medical and Dental University, Kanda-Surugadai, Chiyoda-ku, Tokyo

(Received December 14, 1970)

The graft copolymerization of methyl methacrylate by trialkylborane onto hemoglobin has been studied at 37°C. In aqueous media, graft copolymers were obtained in the form of a light brown powder or granules, while no grafting occurred in organic solvents, such as cyclohexanone, *n*-hexane, tetrahydrofuran, and toluene. The presence of water seems to be essential to the grafting. The hydrogen peroxide-decomposing property of hemoglobin was well preserved in the graft copolymers so obtained. The mechanism of the initiation is discussed.

Since the pioneering works by Furukawa *et al.*[2)] and by Kolesnikov and Klimentova,[3)] it has been shown that trialkylboranes can initiate the polymerization of various vinyl monomers in the presence of oxygen or oxygen-containing compounds.[4-9)] On the other hand, some reports on the preservation of blood by chemical treatment have appeared. Suzuki and Hachimori[10)] tried to protect blood by the reaction of aldehyde with hemoglobin in vain. Kondo[11)] disclosed that blood can be stabilized by enclosing or "wrapping" it with colloidal gelatin.

We have previously described the cocatalytic effects of pyridine and its derivatives on the polymerization of methyl methacrylate (MMA) by tri-*n*-butylborane (Bu_3B) in organic solvents.[12)] We have also studied the graft copolymerization of vinyl monomers

* To whom inquiries should be addressed.

1) Presented in part at the 23 rd Annual Meeting of the Chemical Society of Japan, Tokyo, April, 1970.

2) J. Furukawa, T. Tsuruta, and S. Inoue, *J. Polym. Sci.*, **26**, 234 (1957); *ibid.*, **28**, 227 (1958); *ibid.*, **40**, 237 (1959); *Makromol. Chem.*, **31**, 122 (1959).

3) G. S. Kolesnikov and N. V. Klimentova, *Izv. Akad. Nauk. USSR.*, **1957**, 652; *Chem. Abstr.*, **51**, 15458 (1957).

4) K. Fujii, T. Eguchi, J. Ukeda, and M. Matsumoto, *Kobunshi Kagaku*, **16**, 519 (1959).

5) C. H. E. Bawn, D. Margerison, and N. M. Richardson, *Proc. Chem. Soc.*, **1959**, 397.

6) G. Talamini and G. Vidotto, *Makromol. Chem.*, **50**, 129 (1961).

7) F. J. Welch, *J. Polym. Sci.*, **61**, 243 (1962).

8) F. S. Arimoto, *ibid.*, *Part A-1*, **4**, 275 (1966).

9) J. Grotewald, E. A. Lissi, and A. E. Villa, *Chem. Commun.*, **1965**, 21; *J. Polym. Sci., Part A-1*, **6**, 3157 (1968); *ibid.*, **7**, 3430 (1969).

10) S. Suzuki and Y. Hachimori, *Nippon Kagaku Zasshi*, **89**, 614 (1968).

11) A. Kondo, Japanese Patent 521609 (1967).

12) K. Kojima, Y. Iwata, M. Nagayama, and S. Iwabuchi, *J. Polym. Sci., Part B*, **8**, 541 (1970).

by trialkylborane initiators onto collagen,[13] proteins, and fibers.[14] In another previous paper,[15] we reported the graft copolymerization of MMA by Bu_3B in blood; MMA was found to be grafted onto blood components in the following order:

blood cells > hemoglobin > blood plasma.

In order to elucidate the MMA-grafting in blood, we tried to graft MMA by Bu_3B directly onto hemoglobin. This paper will report some interesting results on the subject.

Experimental

Materials. *Methyl Methacrylate*: One liter of commercial MMA was washed with three 100-m*l* portions of a saturated sodium hydrosulfite solution in a separatory funnel, and then with three 100-m*l* portions of a 20% sodium chloride solution. The MMA so washed was allowed to stand over silica gel overnight and then filtered and distilled in a nitrogen atmosphere under reduced pressure; bp 46°C/100 mmHg.[16]

Tri-n-butylborane (Bu_3B): Commercial Bu_3B (Callery Chemical Co., USA) was distilled under nitrogen just before use; bp 108—110°C/20 mmHg.[17]

Commercial *hemoglobin* and an isotonic sodium chloride solution were used without further treatment. All the *other materials used* were purified in the usual manner and were distilled just before use.

Graft Copolymerization. *Typical Procedure*: A mixture of 0.5 g of hemoglobin and 10 m*l* of an isotonic sodium chloride solution was placed in a stoppered glass tube (inner volume: *ca.* 60 m*l*). In another, smaller glass tube we added 0.10 m*l* of Bu_3B to 5.0 m*l* of MMA. This mixture was immediately poured into the first glass tube. Then, the glass tube was shaken in a thermostatted shaking apparatus at 37°C. The reaction was stopped by pouring the mixture into 200 m*l* of methanol. The precipitate was filtered, washed with methanol, and dried *in vacuo* to a constant weight. The dry precipitate was extracted with acetone in a Soxhlet extractor for 50—80 hr. The acetone-soluble extracts were reprecipitated with methanol to yield a homopolymer. Both the acetone-insoluble residue (graft copolymer) and the homopolymer were dried *in vacuo* to constant weights.

The infrared speatra were obtained with a Hitachi Model EPI-3T spectrophotometer.

Calculation

The total conversion, the percentage of grafting, and the efficiency of grafting were calculated as follows:

$$\text{total conversion} = \frac{\text{weights of poly (MMA) grafted and homopolymer}}{\text{weight of MMA charged}} = \frac{II+III}{I}$$

$$\text{percentage of grafting} = \frac{\text{weight of poly (MMA) grafted}}{\text{weight of MMA charged}} = \frac{II}{I}$$

$$\text{efficiency of grafting} = \frac{\text{weight of poly (MMA) grafted}}{\text{weights of poly (MMA) grafted and homopolymer}} = \frac{II}{II+III}$$

where

I: weight of MMA charged

II: (weight of the acetone-insoluble component) minus (weight of the backbone polymer)

III: weight of the acetone-soluble component (homopolymer)

The hydrogen Peroxide-decomposing Properties of hemoglobin and of the graft copolymer were determined as follows: To 50 m*l* of a 1% hydrogen peroxide solution were added 2 g of hemoglobin or the graft copolymer obtained from 2 g of hemoglobin. The mixture was well stirred. After 1/2, 1, 2, 3, and 5 hr, 1.0 m*l* portions of the hydrogen peroxide solution were taken up by means of a syringe and titrated with a 0.1 N potassium permanganate solution.

Results and Discussion

Effects of Solvents. The graft copolymerization of MMA by Bu_3B onto hemoglobin was carried out at 37°C in various solvents, both in aqueous and organic solvents. The results are listed in Table 1. The percentage of grafting was 7.8 in the isotonic sodium chloride solution and 12.1 in water, while no weight increase of the final product was observed in cyclohexa-

Table 1. Grafting of methyl methacrylate onto hemoglobin

Run No.	Hemoglobin (g)	Solvent	Bu_3B (m*l*)	Total yield (g)	Total conversion (%)	Weight of homopolymer (g)	Weight of graft copolymer (g)	Weight increase of hemoglobin (%)	Percentage of grafting (%)	Efficiency of grafting (%)
001	0.48	W	0.10	4.77	91.0	2.98	1.05	117	12.1	13.3
101	0.53	ISC	0.10	4.92	93.2	3.08	0.90	69	7.8	8.4
102	0.53	ISC	—	0.45	—	—	0.43	—	—	—
601	0.50	HX	0.10	2.90	51.0	2.41	0.47	—	—	—
602	0.50	CHN	0.10	1.51	21.5	1.03	0.47	—	—	—
603	0.50	THF	0.10	0.53	0.6	0.04	0.47	—	—	—
604	0.50	TOL	0.10	1.58	23.0	1.15	0.43	—	—	—

Grafting conditions: Methyl methacrylate: 5.0 m*l*; Solvent: 10 m*l*; 37°C; 2 hr W: water; ISC: isotonic sodium chloride solution; HX: *n*-hexane; CHN: cyclohexanone; THF: tetrahydrofuran; TOL: toluene.

13) E. Masuhara, K. Kojima, N. Tarumi, and Y. Higuchi, *Reports of Research Institute of Dental Materials*, **2**, 788 (1966).

14) K. Kojima, S. Iwabuchi, K. Kojima, and N. Tarumi, *J. Polym. Sci., Part B*, **9**, 25 (1971).

15) K. Kojima, S. Iwabuchi, K. Kojima, and N. Tarumi, a) *J. Polym. Sci., Part B*, in press; b) *ibid., Part A-1*, submitted.

16) S. Kambara *et al.*, "Tanryootai Gooseihoo (Monomer Synthesis)," Kyoritsu Shuppan, Tokyo (1957), p. 140.

17) E. Masuhara, K. Kojima, and T. Kimura, *Reports of Research Institute of Dental Materials*, **2**, 368 (1962).

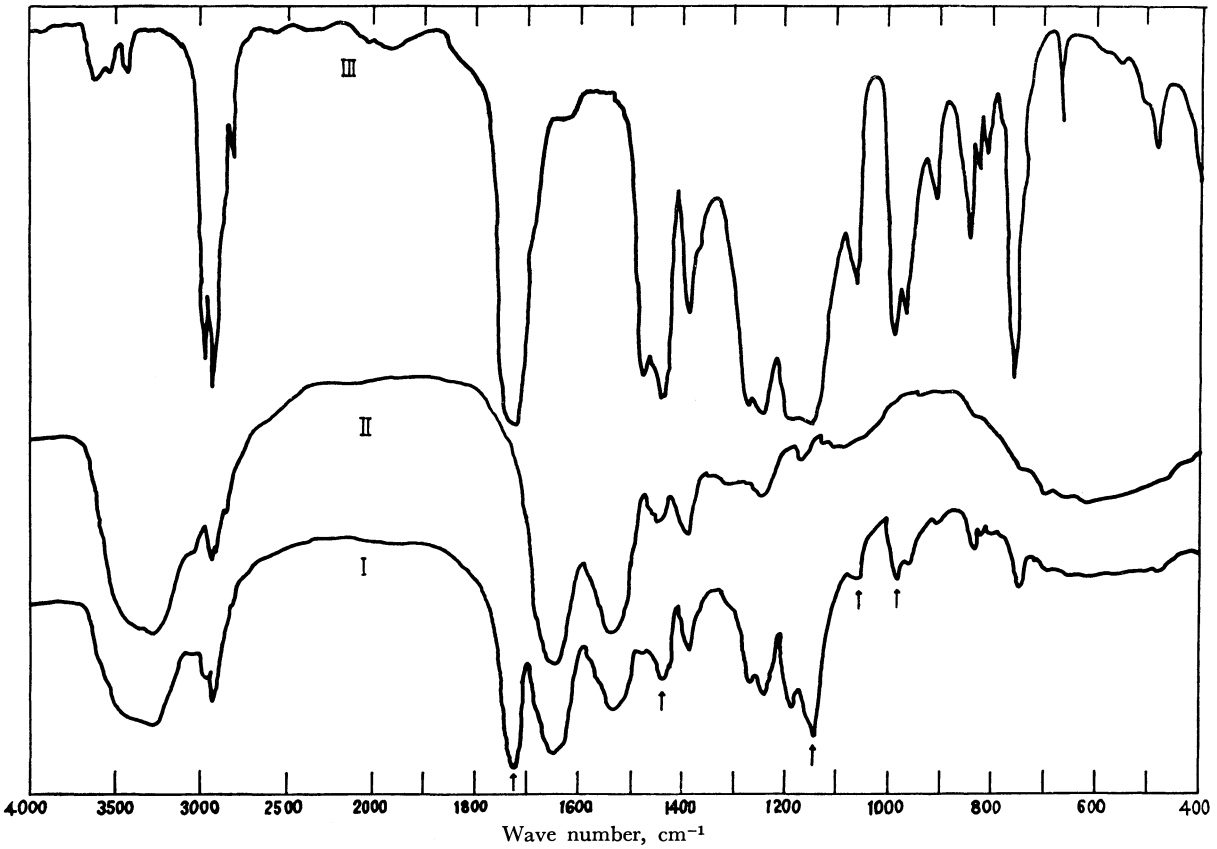

Fig. 1. Infrared spectra of graft copolymer, hemoglobin, and poly (MMA).
I: graft copolymer; II: hemoglobin; III: poly (MMA).

none, *n*-hexane, tetrahydrofuran (THF), and toluene. This means that, in the presence of water only, MMA was grafted by Bu_3B onto hemoglobin. Similar results were also obtained in the graft copolymerization of MMA by Bu_3B onto proteins, such as albumin and casein.[14]

When the graft copolymerization of MMA by Bu_3B onto hemoglobin was carried out in aqueous media, the acetone-soluble parts of the products were obtained in the form of a light brown powder or granules. The infrared spectra are given in Figure 1. The spectrum of the acetone-insoluble part (I in Fig. 1) showed characteristic absorption bands at 1730, 1450, 1150, and 990 cm^{-1}. Since none of these bands were seen in the spectrum of hemoglobin (II), while all of them were found in the spectrum of poly (MMA) (III), the bands may be assigned to the MMA-grafted hemoglobin. The acetone-insoluble parts may, therefore, be believed to be graft copolymers.

Figure 2 shows an electron micrograph of the acetone-insoluble part (graft copolymer).

For purposes of comparison, the same grafting procedure was done in the absence of Bu_3B. The spectra of the acetone-insoluble parts entirely agreed with that of hemoglobin (II), which means that no grafting occurred in the absence of Bu_3B.

Both di-*n*-butylzinc and the well-known benzoyl peroxide/dimethyl-*p*-toluidine system were incapable of initiating the graft copolymeriaztion of MMA onto hemoglobin under the same conditions. This would suggest that the graft copolymerization of MMA onto hemoglobin is specific for tri-*n*-butylborane under these conditions.

Fig. 2. An electron micrograph of the acetone-insoluble part (graft copolymer), ×500, (viewed in a JELCO JSM-U3 electron microscope).

Reaction Time. The effects of the reaction time on the grafting were also studied. Figure 3 indicates that the grafting proceeded very rapidly in the initial

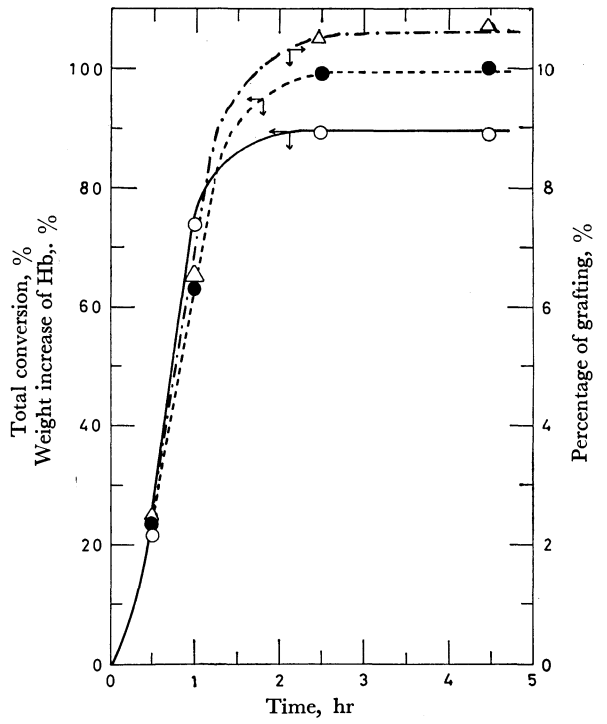

Fig. 3. Effects of reaction time on grafting.
(○): total conversion; (●): weight increase of hemoglobin; (△): percentage of grafting;
Hemoglobin: 0.5 g; MMA: 5.0 m*l*; Bu_3B: 0.10 m*l*; Solvent: 10 m*l*; 37°C.

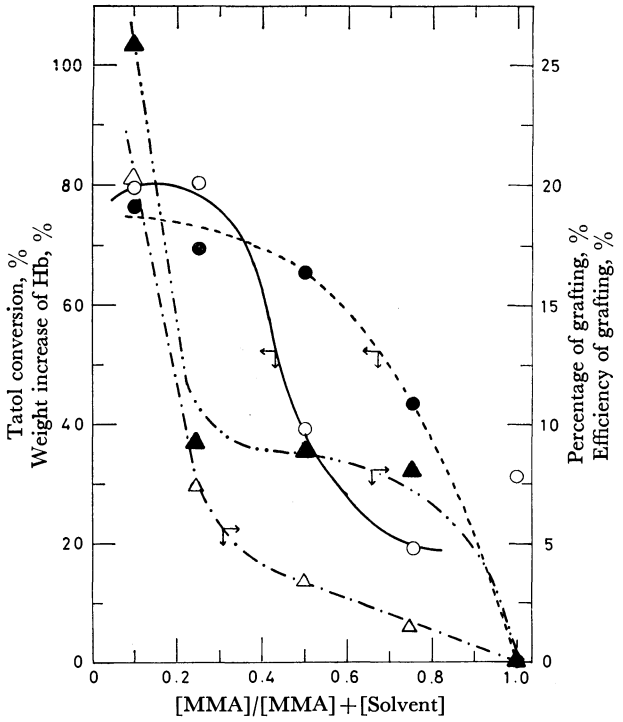

Fig. 4. Effects of monomer concentration.
(○): total conversion; (●): weight increase of hemoglobin; (△): percentage of grafting; (▲): efficiency of grafting.
Hemoglobin: 0.5 g; (MMA + solvent): 20 m*l*; Bu_3B: 0.10 m*l*; 37°C; 2 hr.

stage and then reached the saturation point in about an hour at 37°C.

Concentration of MMA. The concentration of MMA influenced the grafting (Figure 4). The total conversion was minimal when the concentration of MMA was 70—80%. The weight increase, the percentage of grafting, and the efficiency of grafting decreased with the increase in the concentration of MMA, so that at last no grafting was observed when the concentration of MMA was 100%, that is, in MMA itself and in the absence of water. This also shows that water is essential to the grafting.

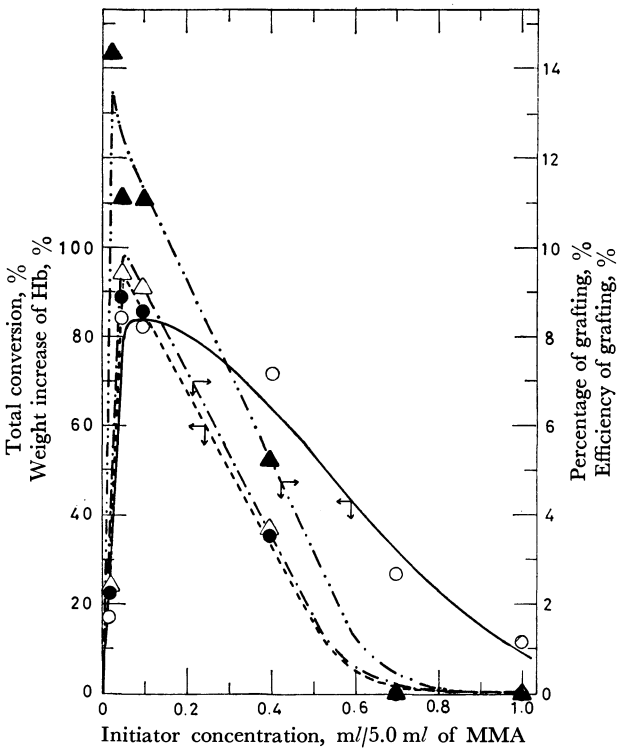

Fig. 5. Effects of initiator concentration.
Hemoglobin: 0.5 g; MMA: 5.0 m*l*; solvent: 10 m*l*; 37°C; 2 hr.

Concentration of Bu_3B. The dependence of the grafting on the concentration of Bu_3B is given in Fig. 5. There was an optimum concentration of 0.05—0.1 m*l* of Bu_3B/5.0 m*l* of MMA for the total conversion, the percentage of grafting, and the efficiency of grafting. All of these values decreased considerably when the concentration of Bu_3B increased much above the optimum concentration. A similar tendency was also observed in the system without hemoglobin.

Concentration of Hemoglobin. Figure 6 presents the relationship between the grafting and the concentration of hemoglobin. So long as the concentration was low, the total conversion was practically constant; when the former was higher than 0.4—0.5 g/5.0 m*l* of MMA, the latter decreased. Both the weight increase and the percentage of grafting had their optimum concentration of hemoglobin; especially, the weight increase gave relatively high values of 130—500% in the range of 0.05—0.30 g/5.0 m*l* of MMA. The higher the concentration of hemoglobin, the higher was efficiency of grafting.

On the Grafting Site. It is known that hemoglobin can accelerate the decomposition of hydrogen peroxide.

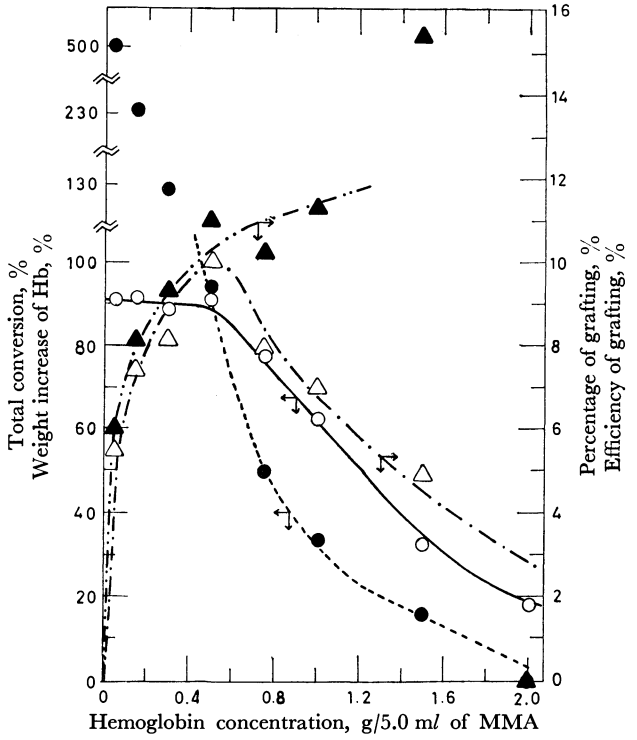

Fig. 6. Effects of homoglobin concentration.
(○): total conversion; (●): weight increase of homeglobin; (△): percentage of grafting; (▲): efficiency of grafting; MMA: 5.0 m*l*; Bu_3B: 0.10 m*l*; Solvent: 10 m*l*; 37°C; 2 hr.

This characteristic property remained practically unchanged after the graft copolymerization, as is shown in Fig. 7. This fact would suggest that MMA was not grafted onto the very part of the hemoglobin which possesses the hydrogen peroxide-decomposing ability. Fe^{2+} is known to be responsible for the decomposition of hydrogen peroxide. Therefore, Fe^{2+} may be supposed to be preserved without any change.

On the Reaction Mechanism. It is interesting to note again that the graft copolymerization of MMA by Bu_3B proceeded well only in aqueous media, although

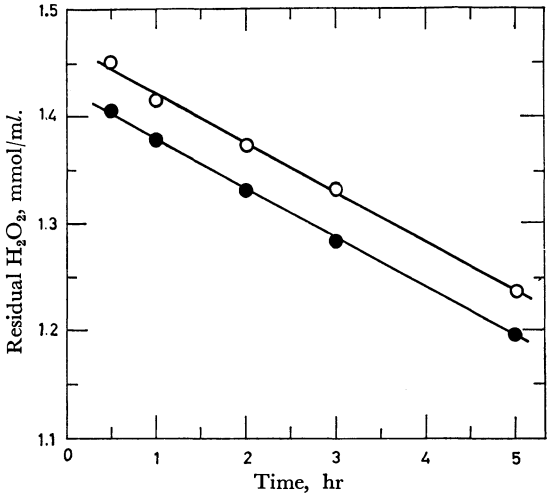

Fig. 7. Hydrogen peroxide-decomposing properties of hemoglobin and graft copolymer.
(○): hemoglobin; (●): graft copolymer. Initial concentration of H_2O_2: 1.46 mmol/m*l*; hemoglobin: 0.3 g; graft copolymer: 0.6 g.

water reacts with trialkylboranes to form hydroxy derivatives (*e.g.*, R_2BOH[18]) and, at last, inactive boric acid.[19] On the other hand, trialkylboranes can initiate the polymerization of MMA in ordinary organic solvents.[4-9] This dicrepancy could be explained by assuming the following three reaction steps:

Solvation:

$$Hb + n\cdot H_2O \longrightarrow (solv.\ Hb) \quad (1)$$

Formation of the complex:

$$(solv.\ Hb) + Bu_3B \longrightarrow complex \quad (2)$$

Formation of the active center:

$$complex \longrightarrow active\ center \quad (3)$$

to initiate the graft copolymerization

(Hb: hemoglobin)

Step 1 is supported by the fact that water is essential to the graft copolymerization and that no grafting occurred in the usual organic solvents. When proteins (such as albumin and casein) and fibers (such as wool, silk, and cotton) were treated similarly, the same phenomenon was also observed.[14]

We previously proposed the following reaction mechanism for the polymerization of MMA by the Bu_3B/pyridine system:[12]

$$pyridine + Bu_3B \longrightarrow complex \quad (4)$$

$$complex \longrightarrow radical \quad (5)$$

to initiate the polymerization

Steps 2 and 3 could be compared with Equations 4 and 5 respectively. The solvated hemoglobin seems to act as an electron donor in Step 2, just like pyridine in Eq. (4). All these backbone polymers contain hydrophilic groups such as amino and hydroxyl groups. The electron-donative property of the hydrophilic groups in hemoglobin is, therefore, believed to play an important role in the formation of the complex. Step 3 could be interpreted analogously in agreement with Eq. (5). In the Bu_3B/pyridine system, our ESR study suggested that the polymerization of MMA involves a free-radical mechanism.[12] Since (1) it is well known that the polymerization of vinyl monomers by trialkylboranes in the presence of oxygen or oxygen-containing compounds proceeds *via* a free-radical mechanism[6-8] and (2) radical polymerization is less sensitive to water than ionic polymerization, Step 3 may be supposed to involve a free-radical mechanism.

However, if an olefinic monomer is polymerizable by the free-radical mechanism, they can usually be polymerized with every other peroxide and azo initiator, too.[20] On the contrary, the benzoyl peroxide/dimethyl-*p*-toluidine system was ineffective on the graft copolymerization under the same conditions.

We thank Professor Eiichi Masuhara for his encouragement throughout this work. We are indebted to Mr. Akihiko Watanabe, Tokyo Medical and Dental University, for taking the electron micrograph.

18) B. M. Mikhailov, V. A. Vaver, and Y. N. Bubnov, *Dokl. Akad. Nauk SSSR*, **126**, 575 (1959); *Chem. Abstr.*. **54**, 26le(1960).
19) K. Kojima, unpublished data.
20) D. Braun, H. Cherdron, and W. Kern, "Praktikum der Makromolekularen Organischen Chemie," Alfred Hüthig, Heidelberg (1966), p. 100.

Studies of *N*-Sulfinyl Compounds. IV.[1] The Reactions of *N*-Sulfinylanilines and -phenylhydrazines with Styrene Oxide

Otohiko Tsuge and Shuntaro Mataka
Research Institute of Industrial Science, Kyushu University, Hakozaki, Fukuoka
(Received December 15, 1970)

The reaction of *p*-substituted *N*-sulfinylanilines with styrene oxide in the presence of tetraethylammonium bromide gave the corresponding 1,2,4,5- and 1,2,4,6-tetraarylpiperazines, whose configurations were established on the basis of the NMR spectral studies. On the other hand, while a similar reaction of *p*-substituted *N*-sulfinylphenylhydrazines with the oxide in benzene gave the corresponding diaryl disulfide, diaryl sulfide, and *p*-substituted biphenyl, the reaction in acetonitrile did not give the biphenyl. The pathways for these reactions are suggested.

It is known that *N*-sulfinylaniline reacts as a 1,3-dipolarophile with benzonitrile oxide[2] and diphenylnitrilimine.[3] Recently, Etlis *et al.*[4] found that the reaction of *N*-sulfinylaniline with 1,2-epoxides such as ethylene oxide, propylene oxide, and epichlorohydrin, in the presence of tetraethylammonium bromide (TEABr) gave the corresponding 1,2,3-oxathiazolidine-2-oxides.

In a previous paper,[5] we reported that *p*-substituted *N*-sulfinylanilines (I) reacted with ethylene carbonate in the presence of lithium bromide or TEABr, to afford the corresponding *N,N'*-diarylpiperazine. The pathway for the formation of the piperazine may be illustrated by the dimerization of the intermediate derived from the expected 1,2,3-oxathiazolidine-2-oxide with the elimination of sulfur dioxide, as is shown in Scheme 1.

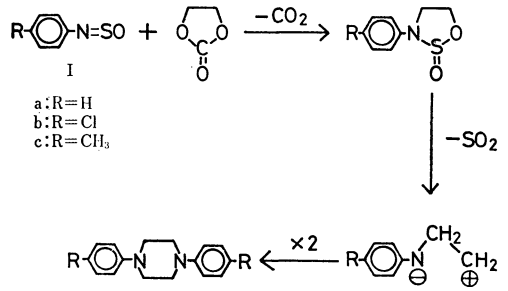

Scheme 1

On the basis of the above facts, the reaction of I with styrene oxide (II) which can behave like a 1,3-dipolar reagent, can be considered to result in the formation of either diaryl-1,2,3-oxathiazolidine-2-oxides or tetraarylpiperazines. However, little attention has been paid to the reaction of I with II.

When *N*-sulfinylaniline (Ia) and three molar amounts of II were heated with a small amount of TEABr in an atmosphere of nitrogen at 120°C for 7 hr, two crystalline compounds, IIIa (mp 204°C) and IVa (mp 219°C), were obtained. Both IIIa and IVa had molecular formula, of $C_{28}H_{26}N_2$ (M^+ *m/e* 390), which was equivalent to that of a dimer of an intermediate derived from an 1:1 adduct of Ia and II with the elimination of sulfur dioxide.

The IR spectra of IIIa and IVa did not show any bands due to the NH group, and the mass spectrum of IIIa was very similar to that of IVa. On the basis of the above observations and NMR spectra (Fig. 1), it may be deduced that IIIa and IVa are isomeric tetraphenylpiperazines.

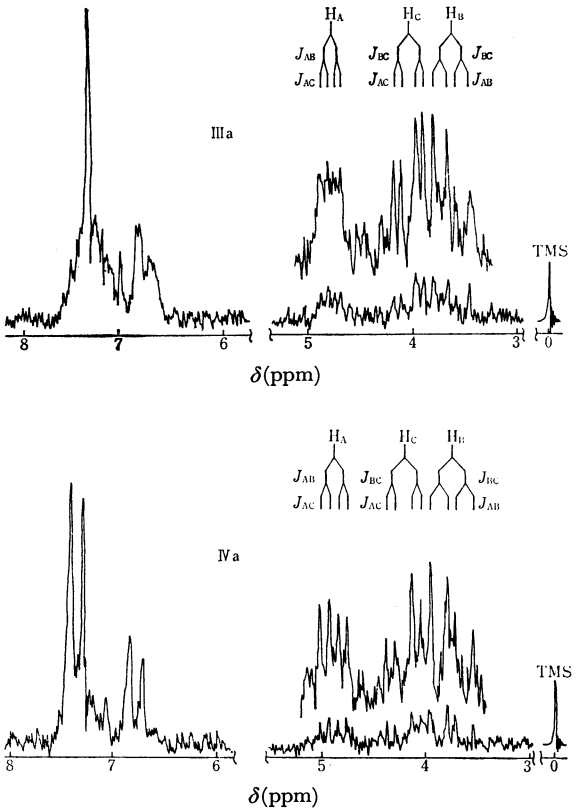

Fig. 1. NMR spectra of IIIa and IVa in $CDCl_3$

Recently, Hoberg[6] reported that the reaction of benzylidenaniline with diazomethane in the presence of diethylaluminum iodide gave 1,2,4,5- and 1,2,4,6-tetraphenylpiperazines, but their structural evidences were not given.

1) Part III: O. Tsuge and S. Mataka, *The Reports of the Research Institute of Industrial Science, Kyushu University*, **51**, 14 (1970).

2) P. Rajagopalan and B. G. Advani, *J. Org. Chem.*, **30**, 3369 (1965).

3) R. Huisgen, R. Grashey, M. Seidel, H. Knupfer, and R. Schmidt, *Ann. Chem.*, **658** 169 (1962).

4) V. S. Etlis, A. P. Sineokov, and M. E. Sergeeva, *Khim. Geterotskil. Soedin*, 682 (1966); *Chem. Abstr.*, **66**, 55150s (1967).

5) O. Tsuge, S. Mataka, M. Tashiro, and F. Mashiba, This Bulletin **40**, 2709 (1967).

6) H. Hoberg, *Ann. Chem.*, **707**, 147 (1967).

Table 1. Tetraarylpiperazines, III and IV

Compound	Yield (%)	Appearance (Recryst. Solvent)*	Mp (°C)	Formula	Analysis (%) Found (Calcd) C	H	N	MW (*m/e*)
IIIa	4	colorless prisms (L)	204	$C_{28}H_{26}N_2$	85.95 (86.11)	6.73 (6.71)	7.06 (7.17)	390
IVa	14	colorless needles (L)	219	$C_{28}H_{26}N_2$	85.80 (86.11)	6.68 (6.71)	7.13 (7.17)	390
IIIb	6	colorless prisms (PB)	228—229	$C_{28}H_{24}N_2Cl_2$	73.37 (73.23)	5.04 (5.23)	6.03 (6.10)	458
IVb	17	colorless needles (PB)	160—161	$C_{28}H_{24}N_2Cl_2$	73.42 (73.23)	5.50 (5.23)	6.02 (6.10)	458
IIIc	7	colorless needles (PB)	260—261	$C_{30}H_{30}N_2$	85.90 (86.08)	7.37 (7.22)	6.52 (6.69)	418
IVc	6	colorless needles (PB)	154—155	$C_{30}H_{30}N_2$	86.12 (86.08)	7.38 (7.22)	6.74 (6.69)	418

* L: ligroin (bp 80—110°C), PB: petroleum benzine (bp 40—65°C).

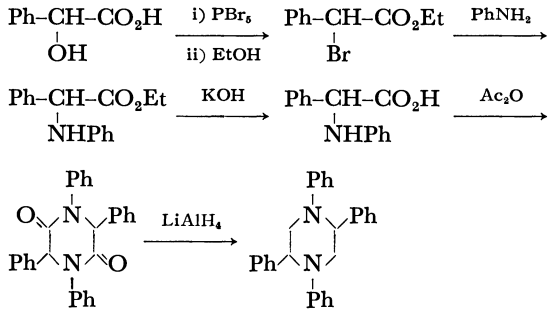

Scheme 2

1,2,4,5-Tetraphenylpiperazine was synthesized by the reduction of the tetraphenylpiperazine-3,6-dione[7] prepared unequivocally from mandelic acid, as is shown in Scheme 2. The melting points of 1,2,4,5- and 1,2,4,6-tetraphenylpiperazines reported by Hoberg[6] were 214 and 202°C respectively, but the 1,2,4,5-tetraphenylpiperazine prepared by the method shown in Scheme 2 melted at 204°C. Therefore, it is clear that tetraphenylpiperazines were erroneously identified by Hoberg;[6] it seems reasonable to assume that the compound melting at 202°C is 1,2,4,5-tetraphenylpiperazine and that melting at 214°C is 1,2,4,6-isomer.

The compound IIIa was proved, by the admixed melting point and by a study of its IR spectrum, to be identical with the authentic sample of 1,2,4,5-tetraphenylpiperazine prepared by the above method. In view of the reaction process (Scheme 3) and of the melting point reported by Hoberg,[6] the compound IVa was assumed to be 1,2,4,6-tetraphenylpiperazine.

A similar reaction of *N*-sulfinyl-*p*-chloro- (Ib) or -*p*-methylaniline (Ic) with II gave the corresponding tetraarylpiperazines, IIIb and IVb or IIIc and IVc. The yields, physical properties, results of elemental analyses, and NMR spectral data of III and IV are summarized in Tables 1 and 2 respectively.

The compounds IIIb—IIIc and IVb—IVc were assigned, by a comparison of their NMR and IR spectra (Fig. 2) with those of IIIa and IVa, to be the corresponding 1,2,4,5- and 1,2,4,6-tetraarylpiperazines respectively.

7) H. Henze, *Ber.*, **32**, 3058 (1899).

Table 2. NMR spectral data of tetraarylpiperazines

Compound	Chemical shift[a] δ (ppm) H_A	H_B	H_C	Coupling constant (Hz) J_{AB}	J_{AC}	J_{BC}
IIIa	4.77(d.d)	3.63(d.d)	4.02(d.d)	9	4	13
IIIb	4.73(d.d)	3.57(d.d)	4.01(d.d)	8	4	13
IIIc	4.63(d.d)	3.34(d.d)	3.83(d.d)	9	4	11.5
IVa	4.85(d.d)	3.75(d.d)	4.22(d.d)	11	5.5	14.5
IVb	4.81(d.d)	3.72(d.d)	4.10(d.d)	9.5	5.5	14.5
IVc	4.79(d.d)	3.67(d.d)	4.05(d.d)	9	5	15

a) d.d: double-doublet.

In connection with a previous paper,[5] the pathway for the formation of III and IV is illustrated in Scheme 3. That is, 3,5- (A) and 3,4-diaryl-1,2,3-oxathiazolidine-2-oxides (B) are formed by the (2+3) cycload-

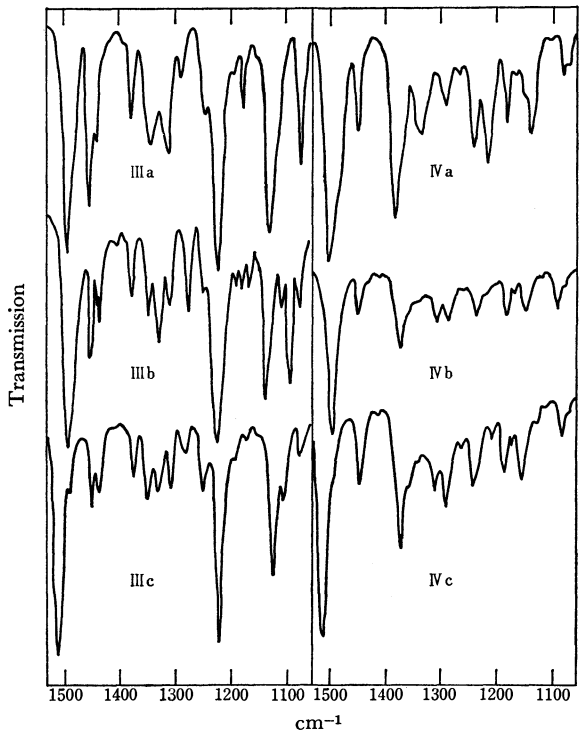

Fig. 2. IR spectra of III and IV (KBr).

dition of I to the 1,3-dipoles arising from the cleavage of *a* or *b* bond in II.

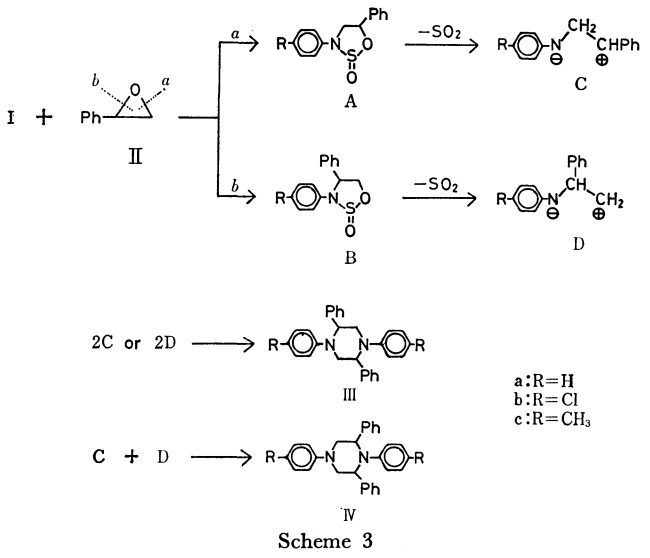

Scheme 3

The subsequent elimination of sulfur dioxide from A and B yields the 1,3-dipolar intermediates C and D respectively. The dimerization of C or D leads to the formation of III, while the (3+3) cycloaddition of C to D gives IV.

Three conformational isomers, III-1—III-3, and IV-1—IV-3, are possible for the respective structures of III and IV (Fig. 3).

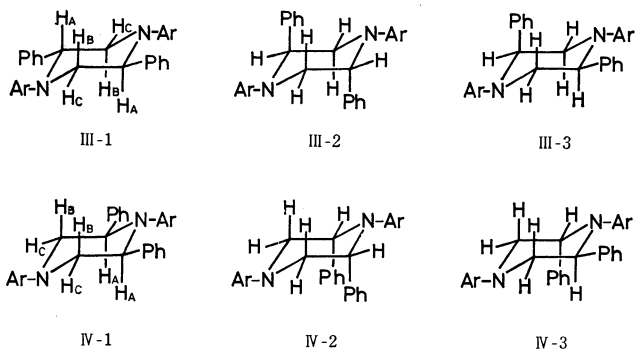

Fig. 3

As is shown in Fig. 1 and Table 2, the NMR spectra of all the III and IVisomers showed only one double-doublet (1H+1H) and two double-doublets (each 2H) in the methine and methylene regions respectively; these facts exclude the possibility of III-3 or IV-3 for the structure of III or IV. It is well known that, in cyclohexane derivatives, the values of the vicinal axial-axial ($J_{a,a}$) and axial-equatorial coupling constants ($J_{a,e}$) are 8—13 and 2—6 Hz, and that the value of the vicinal equatorial-equatorial coupling constant ($J_{e,e}$) is invariably and significantly smaller than that of $J_{e,e}$.[8]

Consequently, it may be deduced that the most reasonable structures for III and IV are the conformers, III-1 and IV-1, in which the two phenyl groups are in equatorial positions.

There has been no study of the reaction of *N*-sulfinylphenylhydrazines (V) with a 1,3-dipole, because V is less reactive than I. It appeared of interest to investigate the reaction of V with II.

When equimolar amounts of *N*-sulfinylphenylhydrazine (Va) and II were heated with a small amount of TEABr in refluxing benzene for 16 hr, diphenyl disulfide (VIa), diphenyl sulfide (VIIa), biphenyl (VIIIa), and colorless prisms (IX), mp 156—157°C, were obtained, accompanied with a large amount of tars.

A similar reaction of *N*-sulfinyl-*p*-tolylhydrazine (Vb) with II gave *p,p'*-ditolyl disulfide (VIb), *p,p'*-ditolyl sulfide (VIIb) and 4-methylbiphenyl (VIIIb), but no 4,4'-dimethylbiphenyl was formed.

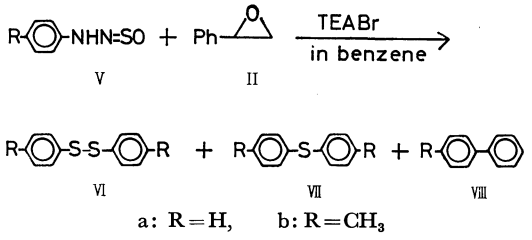

On the basis of these data, it is evident that the benzene used as the solvent participates in the formation of VIII.

When acetonitrile was used as the solvent in place of benzene, Vb reacted with II in the presence of TEABr to give only VIb and VIIb, but here the formation of VIIIb or 4,4'-dimethylbiphenyl was not observed. The products, VI, VII, and VIII, were isolated in pure forms by gas chromatography and were identified by comparison with authentic samples. Also, quantitative analyses were carried out on the basis of the areas of the individual peaks on the respective chromatograms.

The results are summarized in Table 3.

Table 3. Reactions of V with II in the presence of TEABr

V		II	TEABr	Solvent	Reaction time	Product: Total yield	Product: Composition (ratio)		
R	(g)	(g)	(mg)		(hr)	(mg)	VI	VII	VIII
H	1.0	0.78	70	benzene	16	200	14	4	1
CH_3	0.7	0.49	40	benzene	16	250	3	2	1
CH_3	1.0	0.68	60	CH_3CN	7	190	2	1	0

8) L. M. Jackman and S. Sternhell, "Applications of Nuclear Magnetic Resonance Spectroscopy in Organic Chemistry," 2nd Ed., Pergamon Press, Oxford, London, Edinburgh, New York, Toronto, Sydney, Paris, Braunshweig (1969), p. 286.

The reaction of Va with TEABr, or the reaction of Va with II in the absence of TEABr, did not take place, but Va was recovered quantitatively.

Many years ago, Michaelis and Ruhl[9] found that Va reacted with thionyl or acetyl chloride at a low temperature to give benzenediazonium chloride; they suggested the following reaction scheme:

$$\mathrm{PhNHN{=}SO} \longrightarrow \mathrm{PhN{=}N{-}SOH} \xrightarrow{\text{Y-Cl}} \mathrm{PhN{=}N{-}SO{-}Y} + \mathrm{HCl} \longrightarrow \mathrm{PhN_2^{\oplus}Cl^{\ominus}} + \mathrm{S} + \mathrm{YOH}\ (\mathrm{Y{=}SOCl\ or\ CH_3CO})$$

However, the formation of sulfur was not observed in the reaction of V with II. On the other hand, *N*-sulfinyl-α-methylphenylhydrazine, PhN(Me)N=SO, which does not show the tendency to isomerize to the azo compound, did not react with II under the influence of TEABr, but was recovered quantitatively; this suggests that the tautomerism of the *N*-sulfinyl compound (ArNHN=SO) to the azo compound (ArN=NSOH) plays an important role in the formation of products.

On the basis of the above facts and the formation of the symmetrical diaryl sulfide VII and asymmetrical biphenyl VIII, the reaction pathway for the formation of the products, VI—VIII, can tentatively be assumed to be that shown in Scheme 4.

$$\underset{\mathrm{V}}{\mathrm{ArNHN{=}SO}} \longrightarrow \underset{\mathrm{E}}{\mathrm{ArN{=}N{-}SOH}} \xrightarrow{\text{II+TEABr}} \underset{\mathrm{F}}{\mathrm{ArN{=}N{-}SO{-}Z}} + \mathrm{Et_4N^{\oplus}Br^{\ominus}}$$

$$\mathrm{F} \begin{cases} \longrightarrow \mathrm{Ar\cdot} + \mathrm{N_2} + \mathrm{\cdot SO{-}Z} \\ \longrightarrow \mathrm{ArS\cdot} + \mathrm{N_2} + \mathrm{ZO\cdot} \end{cases}$$

$$\mathrm{2ArS\cdot} \longrightarrow \underset{\mathrm{VI}}{\mathrm{ArS{-}SAr}}, \qquad \mathrm{Ar\cdot} + \mathrm{ArS\cdot} \longrightarrow \underset{\mathrm{VII}}{\mathrm{ArSAr}}$$

$$\mathrm{Ar\cdot} + \mathrm{PhH(solvent)} \longrightarrow \mathrm{ArPhH\cdot} \xrightarrow{\text{-H·}} \underset{\mathrm{VIII}}{\mathrm{Ar{-}Ph}}$$

$$(\mathrm{Z{=}PhCHCH_2OH\ or\ PhCH(OH)CH_2{-}})$$

Scheme 4

The intermediates (F) which are formed by the attack of 1,3-dipoles from II on the tautomer (E) of V are decomposed in two ways under these reaction conditions to yield aryl and arylthio radicals respectively. The formation of VI, VII, and VIII can be well understood in terms of the reactions shown in Scheme 4.

On the other hand, the molecular formula of compound IX (mp 156—157°C), which was obtained in a trace amount in the reaction of Va with II, was established from the molecular ion (M^+ *m/e* 262) in the mass spectrum and by elemental analysis, which showed the empirical formula to be $C_{14}H_{14}O_3S$. The IR spectrum of IX showed characteristic bands at 3480 (ν_{OH}) and at 1290 and 1140 cm^{-1} (ν_{SO_2}), while the NMR spectrum exhibited signals at 2.62 (1H, broad singlet, O*H*, exchanged with D_2O), 3.90—4.90 (3H, multiplet, >C*H* and -CH_2-), and 7.00—7.70 ppm (10H, multiplet, aromatic protons).

On the basis of the above observations, three isomers of benzenesulfonyl-phenylethanols, IX-1—IX-3, are possible for the structure of IX. However, it has been reported[10] that β-benzenesulfonyl-α-phenylethanol (IX-2) melts at 93—94°C, and the mass spectrum of IX seems to support the structure of IX-1; the fragment ion peaks appeared at *m/e* 244 (M^+-H_2O), 232 (M^+-CH_2O), 143 ($232^+-C_7H_5$), 121 (M^+-PhSO_2, base peak), 103 (121^+-H_2O, 87.7[11]), 91 ($C_7H_7^+$), and 77 (Ph^+) in the mass spectrum.

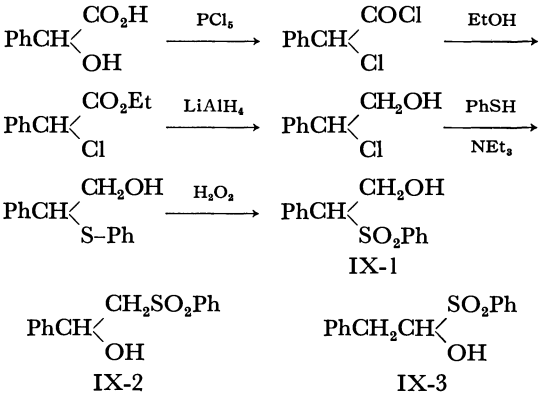

The compound IX was confirmed, by its admixed melting point and by a study of its IR spectrum, to be identical with β-benzenesulfonyl-β-phenylethanol (IX-1), mp 156—157°C, which was unequivocally prepared by the reaction of β-chloro-β-phenylethanol[12] with thiophenol and by subsequent oxidation with hydrogen peroxide.

However, the course of the formation of IX in the reaction of Va with II is not clear.

Experimental

All the melting and boiling points are uncorrected. The IR spectra were measured in KBr disks, and the NMR spectra were determined in deuteriochloroform at 60 MHz with a Hitachi R-20 NMR spectrometer, using TMS as the internal reference. The mass spectra were obtained on a Hitachi RMS-4 mass spectrometer, using a direct inlet and an ionization energy of 70eV.

Materials. The *N*-sulfinyl compounds were prepared by the reported methods[12-15] and were purified by fractional distillation or by recrystallization. *N*-sulfinylaniline (Ia), bp 80°C/12 mmHg (lit,[13] bp 80°C/12 mmHg); *N*-sulfinyl-*p*-chloroaniline (Ib), 101—102°C/5 mmHg (lit,[13]bp 237°C); *N*-sulfinyl-*p*-toluidine (Ic), bp 91.5—92°C/6 mmHg (lit,[13] bp 224°C); *N*-sulfinylphenylhydrazine (Va), mp 104.5—105.5°C (lit,[14] mp 105°C); *N*-sulfinyl-*p*-tolylhydrazine (Vb), mp 112—113°C (lit,[14] mp 112°C); *N*-sulfinyl-α-methylphenylhydrazine, mp 78°C (lit,[15] mp 77°C). The styrene oxide (II) was purified by distillation, bp 191°C.

The Reaction of Ia with II in the Presence of TEABr. After a mixture of 2.0 g of Ia and 5.2 g of II had been stirred

9) A. Michaelis and J. Ruhl, *Ann. Chem.*, **270**, 114 (1982).

10) L. Field, *J. Amer. Chem. Soc.*, **74**, 3919 (1952).

11) Observed metastable peak, *m/e*).

12) E. L. Eliel, C. Herrmann, and J. T. Traxler, *J. Amer. Chem. Soc.*, **78**, 1193 (1956).

13) A. Michaelis and R. Herz, *Ber.*, **23**, 3480 (1890).

14) A. Michaelis and J. Ruhl, *ibid.*, **23**, 474 (1890).

15) A. Michaelis, *ibid.*, **24**, 745 (1891).

with 0.45 g of TEABr under a slow stream of dry nitrogen at 120°C for 7 hr, the reaction mixture was allowed to stand overnight. A benzene solution of the mixture was then chromatographed on alumina, affording 0.75 g of colorless crystals and a large amount of resinous materials. Several fractional recrystallizations of the crystals from ligroin (bp 80—110°C) gave 0.12 g (4%) of 1,2,4,5-(IIIa), (mp 204°C) and 0.45 g (14%) of 1,2,4,6-tetraphenylpiperazines (IVa), mp 219°C.

Similar reactions of Ib and Ic with II in the presence of TEABr gave the corresponding 1,2,4,5- (IIIb and IIIc) and 1,2,4,6-tetraarylpiperazines (IVb and IVc) respectively. The yields, physical properties, and elemental analysis results are summarized in Tables 1 and 2.

The Preparation of 1,2,4,5-Tetraphenylpiperazine. *i)* Ethyl α-bromophenylacetate: A mixture of 20 g of mandelic acid and 100 g of phosphorus pentabromide was stirred at 100°C for 2 hr, and then the reaction mixture was cooled. After 20 m*l* of ethanol had been added to the mixture, it was refluxed for 10 min. The mixture was subjected to steam distillation, and then the distillate was extracted with 150 m*l* of chloroform. After the extract had been dried over anhydrous sodium sulfate, the solvent was distilled off to give a residue. The vacuum distillation of the residue gave 12 g (36%) of ethyl α-bromophenylacetate, bp 108—115°C/2 mmHg (lit,[16] bp 175°C/25 mmHg).

ii) Ethyl α-Anilinophenylacetate: After a mixture of 10.9 g of ethyl α-bromophenylacetate and 7.0 g of aniline had been stirred at 100°C for 4 hr, the reaction mixture was extracted with hot ligroin. The extract was concentrated *in vacuo* affording 9.4 g (83%) of ethyl α-anilinophenylacetate, mp 81—83°C (lit,[17] mp 83—84°C) as colorless needles.

iii) 1,2,4,5-Tetraphenylpiperazine-3,6-dione: A suspension of 8.4 g of ethyl α-anilinophenylacetate in 50 m*l* of 10% aqueous potassium hydroxide was refluxed for 3 hr, and then it was cooled. The resulting solution was neutralized with 1 N hydrochloric acid to afford a white precipitate. Filtration gave 5.6 g (75%) of crude α-anilinophenylacetic acid, mp 177—180°C (lit,[18] mp 181°C).

A mixture of 5.6 g of the acid and 2.8 g of acetic anhydride was stirred at 155°C (oil bath) for 2 hr, and then the mixture was filtered to give crystals. The crystals were washed with dilute aqueous ammonia and then diethyl ether, leaving 1.1 g (21%) of 1,2,4,5-tetraphenylpiperazine-3,6-dione, mp 258°C (decomp.) (lit,[7] mp 260°C (decomp.)).

iv) Reduction of 1,2,4,5-Tetraphenylpiperazine-3,6-dione: After a mixture of 0.1 g of 1,2,4,5-tetraphenylpiperazine-3,6-dione and 50 mg of lithium aluminum hydride in 30 m*l* of diethyl ether had been refluxed for 5 hr, the mixture was poured into water. The mixture was extracted with chloroform, and then the extract was evaporated *in vacuo*, leaving a yellowish-green, viscous oil. Purification by chromatography on alumina, using benzene as the eluent, followed by recrystallization from ligroin (bp 80—110°C), gave 10 mg (11%) of 1,2,4,5-tetraphenylpiperazine (IIIa), mp 204°C. This compound was proved, by the admixed melting point and by a study of its IR spectrum, to be identical with the compound (mp 204°C) obtained in the reaction of Ia with II.

The Reaction of Va with II in the Presence of TEABr. A solution of 1.0 g of Va and 0.78 g of II in 10 m*l* of benzene was refluxed with 70 mg of TEABr for 16 hr. The reaction mixture was then concentrated *in vacuo* to leave a red oil, which was chromatographed on alumina using benzene and then ethanol as eluents. The benzene-eluent gave 0.2 g of a pale green liquid, which was found, by gas chromatographic analysis, to be a mixture of diphenyl disulfide (VIa), diphenyl sulfide (VIIa), and biphenyl (VIIIa) (Table 3). The compounds, VIa—VIIIa, were isolated by gas chromatography, and were identified by a comparison of the IR spectra with those of respective authentic samples.

The ethanol-eluent was concentrated *in vacuo*, and the resulting residue was purified by chromatography on silica gel, using chloroform as the eluent, to give 30 mg of colorless crystals and intractable tars. The recrystallization of the crystals from benzene gave β-benzenesulfonyl-β-phenylethanol (IX), mp 156—157°C, as colorless prisms.

Found: C, 64.41; H, 5.36%. Calcd for $C_{14}H_{14}O_3S$: C, 64.11; H, 5.38%.

Similar reaction of Vb with II in benzene and acetonitrile were carried out; the results are given in Table 3. *p,p'*-Ditolyl disulfide (VIb), *p,p'*-ditolyl sulfide (VIIb), and 4-methylbiphenyl (VIIIb) formed in the reaction were isolated by gas chromatography, and were proved, by a comparison of the IR spectra, to be identical with the respective samples of VIb, VIIb, and VIIIb prepared by the reported methods.

The Preparation of β-Benzensulfonyl-β-phenylethanol. The reduction of ethyl α-chlorophenylacetate prepared by Walden's method[22] with lithium aluminum hydride in diethyl ether gave crude β-chloro-β-phenylethanol,[12] bp 164—166°C/4 mmHg.

A solution of 1.0 g of β-chloro-β-phenylethanol, 0.62 g of thiophenol, and 0.57 g of triethylamine in 10 m*l* of benzene was refluxed for 1.5 hr, and then the precipitated triethylamine hydrochloride was filtered off. The filtrate was concentrated *in vacuo* to leave 1.4 g of a yellow oil, which was used without further purification. A solution of 0.9 g of the oil and 2 m*l* of 30% hydrogen peroxide in 10 m*l* of acetic acid was stirred at room temperature for 4 days. After the reaction mixture had been poured into 50 ml of water, it was extracted twice with 50 m*l* of chloroform. The extracted was concentrated *in vacuo* to leave a viscous oil, which crystallized on standing at room temperature for a long while. Recrystallization from benzene gave 50 mg of β-benzenesulfonyl-β-phenylethanol, mp 156—157°C, as colorless prisms. This compound was proved, by the admixed melting point and by a study of its IR spectrum, to be identical with the compound (mp 156—157°C) obtained in the reaction of Va with II.

16) C. Hell and S. Weinzweig, *Ber.*, **28**, 2446 (1895).
17) C. A. Bischoff, *ibid.*, **30**, 2305 (1897).
18) H. Henze, *ibid.*, **32**, 3058 (1899).
19) H. Gilman, L. E. Smith, and H. H Parker, *J. Amer. Chem. Soc.*, **47**, 851 (1925).
20) E. Giesbrecht and H. Rheinboldt, *ibid.*, **69**, 2310 (1947).
21) M. Gomberg and J. C. Pernert, *ibid.*, **48**, 1372 (1926).
22) P. Walden, *Ber.*, **28**, 1295 (1895).

Kinetics and Equilibrium Positions of *cis-trans* Isomerization of 1,2-Bis(phenylthio)ethylene and Its Exchange with Benzenethiyl Radicals

Atsuyoshi OHNO, Tomo'o SAITO, Akio KUDO, and Gen-ichi TSUCHIHASHI
Sagami Chemical Research Center, Ohnuma, Sagamihara-shi, Kanagawa
(Received December 7, 1970)

Kinetics of the *cis-trans* isomerization of 1,2-bis(phenylthio)ethylene induced by benzenethiyl radicals and the exchange of phenylthio group have been studied by using thiophenol-*phenyl*-^{14}C. Pseudo-first order rate constants for the isomerization and the exchange are $2.08\pm0.22\times10^{-5}$ sec^{-1} and $2.03\pm0.26\times10^{-5}$ sec^{-1} at 50°C, respectively. The *cis/trans* ratio of this olefin is 55—58/45—42 at the completion of the reaction, which differs from the value obtained from the reaction induced by iodine (48—49/51—52). The difference has been interpreted with the idea that the isomer composition in the *cis-trans* isomerization is determined by kinetic factors when the reaction is initiated by thiyl radicals.

Many studies have been carried out on the *cis-trans* isomerization of olefins. We know that there are generally two types of equilibria, thermal and photochemical. The thermodynamically more stable isomer is favored by thermal or catalytic isomerization, while the unstable isomer is favored by photochemical isomerization. In the course of our studies on the photocycloaddition of thiobenzophenone to propenylbenzene, we have found that *cis-trans* isomerization of the olefin takes place during the reaction, but the equilibrium compositions of the isomers are completely different from those of thermal and photochemical ones. Thus thermal equilibrium of propenylbenzene forms (at 27°C) 21.8% of *cis*- and 78.2% of *trans*-isomers,[1] while direct photo-irradiation to this olefin produces an equilibrium mixture of about 60—68% *cis*- and 40—32% *trans*-isomers.[2] On the other hand, when thiobenzophenone is present in the photo-irradiated system, the *cis/trans* ratio changes to 3.1/96.9, which is the same as that when thiyl radicals are employed for the catalysts of the thermal isomerization of the olefin (*cis/trans*=4.1/95.9 at 52.3°C[2]). Since it is known that photo-irradiation to thiobenzophenone yields its n,π^* triplet state and this species behaves like a thiyl-radical,[3,4] there is no doubt that thiyl radicals play a different role form that of other radical catalysts in *cis-trans* isomerizations of olefins.

These findings prompted us to study the *cis-trans* isomerizations of 1,2-bis(phenylthio)ethylene induced by benzenethiyl radicals and iodine, and the exchange reaction of this olefin with isotopically labeled benzenethiyl radicals.

Results

All experiments were carried out in *p*-xylene at 50.0± 0.05°C. Isomerization of 1,2-bis(phenylthio)ethylene was initiated by benzenethiyl radicals derived from benzenethiol and azobisisobutyronitrile. The *cis-trans* ratios of the olefin at desired time intervals were determined by vpc and the equilibrium composition was found to be 55% and 45% for *cis*- and *trans*-olefins, respectively. Similar results were also obtained by isotope-labeling technique (*cis/trans*=57.6/42.4). Results are illustrated in Figs. 1 and 2. When 1,2-bis(phenylthio)ethylene was isomerized with the aid of iodine atoms, the composition of the olefin approached the asymptote of 48.5% *cis*- and 51.5% *trans*-isomers.

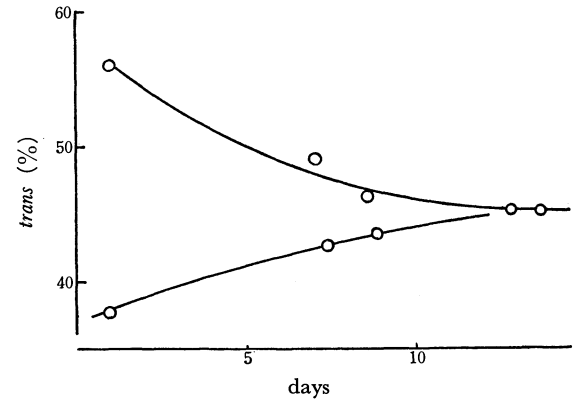

Fig. 1. Time-dependency of the isomer composition of 1,2-bis(phenylthio)ethylene catalyzed by benzenethiyl radicals and followed by vpc-method.

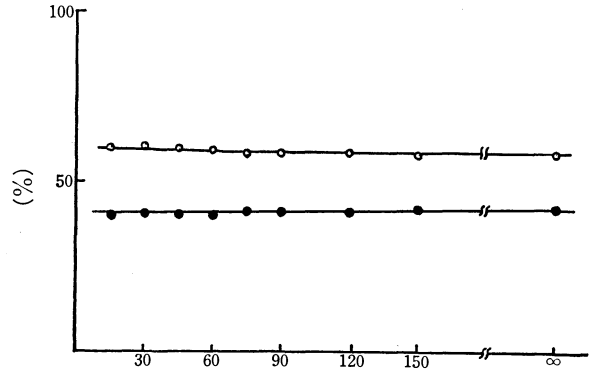

Fig. 2. Time-dependency of the labeled isomer composition of 1,2-bis(phenylthio)ethylene catalyzed by thiyl radicals and followed by isotope-labeling technique.
○: *cis*-isomer ●; *trans*-isomer

1) J. E. Kilpatrick, C. W. Beckett, E. J. Prosen, K. S. Pitzer, and F. D. Rossini, *J. Res. Natal. Bur. Stand.*, **42**, 225 (1949).
2) A. Ohno, Y. Ohnishi, and G. Tsuchihashi, *Tetrahedron Lett.*, 643 (1969).
3) A. Ohno, Y. Ohnishi, and G. Tsuchihashi, *J. Amer. Chem. Soc.*, **91**, 5038(1969).
4) E. S. Huyser and R. M. Kellogg, *J. Org. Chem.*, **30**, 2867 (1965).

Table 1. Kinetics of isomerization and exchange of 1,2-bis(phenylthio)ethylene

Starting isomer	*cis*	*trans*	*cis*	*trans*	*cis*
Olefin, g/50 m*l*	1.2286	1.2333	1.2286	1.2321	1.2327
AIBN, mg/50 m*l*	8.135	8.213	8.213	8.242	8.000
Thiophenol-^{14}C, mg/50 m*l*	311.45	311.70	311.70	310.90	310.90
No. of points plotted	8	8	8	10	9
Total activity,[a] 10^{-6} dpm/10 m*l*	1.982	2.017	1.971	2.010	1.988
	% Activity in olefin[b]				
Recovered isomer / Reaction time, min	*trans* *cis*	*trans* *cis*	*trans* *cis*	*trans* *cis*	*trans* *cis*
15	0.80 1.26	0.51 0.80	0.85 0.97	1.17 2.40	0.48 0.66
30	1.37 2.06	1.04 1.53	1.14 1.82	1.77 2.84	0.75 1.32
45	2.03 2.79	1.83 2.62	1.57 2.31	2.68 4.03	1.96 2.77
60	2.56 3.67	2.20 3.23	1.49 2.21	2.81 3.96	2.42 3.56
75	3.04 4.62	3.42 4.42	2.15 2.97	3.57 4.98	2.32 3.41
90	3.77 5.31	3.48 4.78	2.93 4.00	3.93 5.95	3.15 4.57
120	4.75 6.52	4.09 5.57	3.20 4.79	5.53 7.87	4.00 5.68
150	5.58 7.71	5.70 7.52	4.10 5.58	6.80 8.94	4.84 6.83
∞[c]	33.38 47.83	35.85 43.99	33.45 46.40	35.32 43.34	34.31 47.24
Composition, %	41.12 58.88	43.84 56.16	41.73 58.27	44.90 55.10	41.62 58.38
k_i or k_e,[d] 10^5 sec^{-1}	1.99 1.87	1.85 2.00	2.34 2.36	2.34 2.36	1.71 1.73

a) The total activity of the reaction mixture.
b) Percentage of the activity of an olefin to the total activity of the reaction mixture.
c) 15 days.
d) k_i for the recovered *trans*-olefin and k_e for the recovered *cis*-olefin, when the starting isomer is the *cis*-olefin, and *vice versa*.

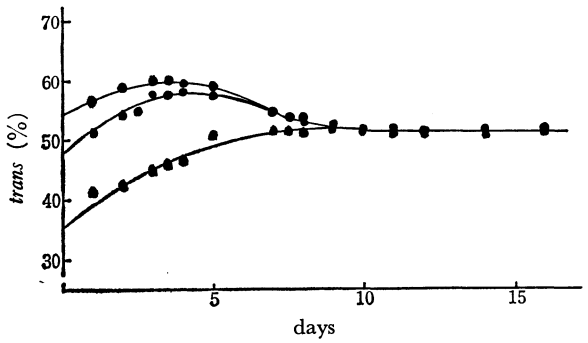

Fig. 3. Time-dependency of the isomer composition of 1,2-bis(phenylthio)ethylene catalyzed by iodine atoms and followed by vpc-method.

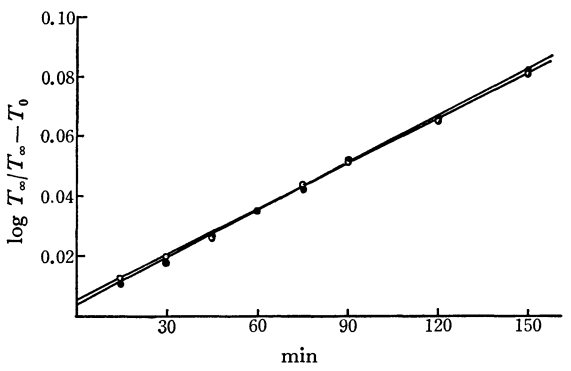

Fig. 4. The pseudo-first order rate plots for the isomerization and the exchange of 1,2-bis(phenylthio)ethylene (The first run of Table 1).
○: *cis*-isomer ●: *trans*-isomer

However, in this case, the composition does not change smoothly, and has a maximum point as shown in Fig. 3.

Pseudo-first order kinetics of the isomerization and exchange were followed by using benzenethiyl-*phenyl*-^{14}C radicals,[5] and rate constants k_i and k_e were found to be $2.08\pm0.22\times10^{-5}$ sec^{-1} and $2.03\pm0.26\times10^{-5}$ sec^{-1}, respectively.[6] The rate constants were calculated by the least-squares method using the data in Table 1. An example of the pseudo-first order rate plots is shown in Fig. 4.

Substantial amounts of diphenyl disulfide were formed during the reactions, but the yield was larger in the reaction with iodine than with benzenethiyl radicals. About 10% of 1,2-bis(phenylthio)ethane was also obtained from the reaction with iodine.

Discussion

As has been observed with propenylbenzene, benzenethiyl radical shifts the equilibrium composition of 1,2-bis(phenylthio)ethylene from that given by iodine. The latter constant is thought to be thermodynamically controlled.[7]

5) Since the rate of isomerization must be followed during the very early stage of the reaction in order to avoid complexity caused by the other isomer produced, the vpc-method is inadequate as it includes comparison of very small and very large peak areas which inevitably leads to large errors.

6) The *true* rate constants for the isomerization k'_i and the exchange k'_e should be calculated by $k'_i=\alpha k_1$ and $k'_e=\alpha k_0$ ($1\leq\alpha\leq2$). The value of α changes according to relative rates of the rotation of the central carbon-carbon bond in the intermediate radicals **3**, and the elimination of benzenethiyl radical from it. However, since both rate constants have the same factor, we will employ the observed rate constants k_i and k_e for discussions.

7) For example, E. L. Eliel, "Stereochemistry of Carbon Compounds," McGraw-Hill Book Co., New York, N. Y. (1962). pp. 337—346.

The kinetics of the *cis-trans* isomerization of diiodoethylene and its exchange with iodine have been studied extensively by Noyes and his co-workers.[8] The rate constants for the isomerization and the exchange with this system are, on an average, 1.5×10^{-3} sec^{-1} and 1.4×10^{-1} sec^{-1}, respectively, at 144°C. Thus, the exchange is one hundred times faster than the isomerization in this system. On the other hand, the kinetics with the system of 1,2-bis(phenylthio)ethylene and benzenethiyl radicals has revealed that the isomerization and the exchange proceed at the same rate. This is the main difference in the behavior of iodine and thiyl radicals.

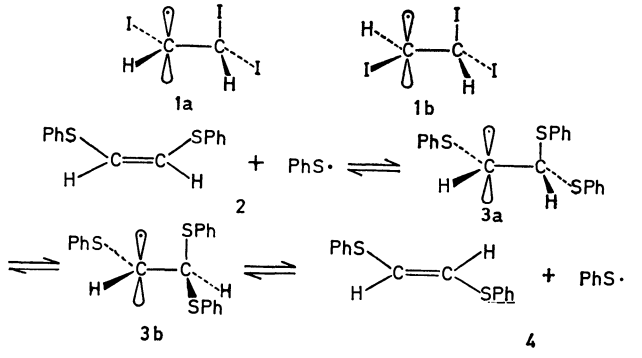

A greater exchange rate than that of isomerization in the case of diiodoethylene has been interpreted in terms of restricted rotation around the carbon-carbon bond[9] in the common intermediates, **1**.[7] If **3** had the life-time of the same order of magnitude as **1**, we should conclude that the energy barrier of the rotation in **3** must be lower than that in **1** in order to interpret the same rate of exchange and isomerization. This is, however, highly unlikely, since the volume of a phenylthio group is supposed to be large enough to form a barrier comparable to that of **1**. If one assumes the structure **5** only for the intermediate of the reaction

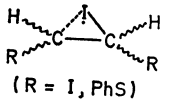

with iodine, the exchange should not be as fast as the isomerization considering the microscopic reversibility of the reaction. Consequently, we believe that the intermediates **3** have a life-time long enough to rotate the carbon-carbon bond freely, or that they are fairly stable and can be regarded as only one species instead of two distinct radicals. In other words, **3a** and **3b** are conformational but not configurational isomers. Thus, 1,2-bis(phenylthio)ethylene has a different equilibrium composition, when treated with benzenethiyl radicals, from that expected from thermodynamics, which can be seen from the reaction diagram schematically shown in Fig. 5. Since the intermediate **3** is energetically more stable than systems of **2** and **4**, thermodynamic stabilities of olefin isomers no longer

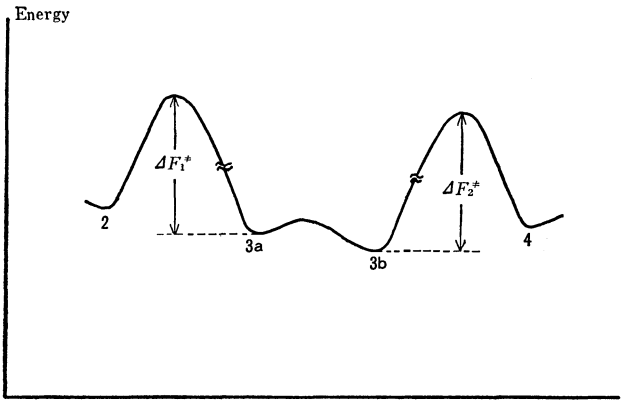

Fig. 5. Schematic energy diagram for reactions of 1,2-bis(phenylthio)ethylene with benzenethiyl radicals.

control the equilibrium composition, but free energies of activation of reactions **3**→**2** and **3**→**4** determine the amounts of isomers at the equilibrium state:

$$\frac{[2]}{[4]}=\frac{[cis\text{-olefin}]}{[trans\text{-olefin}]}=\exp\left(\frac{\Delta F_2^*-F_1^*}{RT}\right)$$

This explanation includes one ambiguous assumption that *cis-* and *trans*-olefins are produced only from conformations **3a** and **3b**, respectively. This possibility is discussed in terms of the angle of the rotation around the carbon-carbon bond at the transition state.[8]

The diagram in Fig. 5 can be explained by the fact that the addition of methanethiyl radical to ethylene is an exothermic reaction with $\Delta H=-14$ kcal/mol, while that of iodine atom to ethylene is an endothermic one with 7 kcal/mol.[10]

It should be noted that the third reaction, the formation of diphenyl disulfide by the combination of benzenethiyl radicals, takes place from **2** and **4** competitively during the isomerizations and exchanges, or leakage from the systems **2** and **4** occurs concurrently and the whole system is in dynamic equilibrium. In this connection, the term "equilibrium" composition may be inadequate, but it could be said that *the final compositions of isomers are determined by kinetic factors when the cis-trans isomerization of an olefin is catalyzed by thiyl radicals.*

It has been mentioned that the composition of isomers of 1,2-bis(phenylthio)ethylene does not approach the asymptote smoothly when the isomerization is catalyzed by iodine (Fig. 3). This indicates that the *true* or thermodynamic equilibrium composition should possess a larger proportion of the *trans*-isomer (smaller proportion of the *cis*-isomer) than that observed here. Since benzenethiyl radicals are produced, as can be seen by the formation of a large amount of diphenyl disulfide during the reaction, they also act as catalysts and the observed composition of isomers changes as the reaction proceeds. This may be an additional proof for the different catalytic behavior of a thiyl radical and an iodine atom in *cis-trans* isomerizations of olefins.

Further Comments on Propenyl Benzene. In our

8) R. M. Noyes, R. G. Dickinson, and V. Schomaker, *J. Amer. Chem. Soc.*, **67**, 1319 (1945).

9) A. Berthoud and C. Urech, *J. Chem. Phys.*, **27**, 291 (1930).

10) C. Walling, "Free Radicals in Solution." John Wiley & Sons, Inc., New York, N. Y. (1957), pp. 341 and 314.

proposal given above and previously,[2] we claim that the *cis-trans* isomerization of an olefin does not give a true or thermodynamically proposed equilibrium constant, when it includes a very stable intermediate and both isomers cannot equilibrate directly. Thus, it is reasonable to expect that such kind of phenomena could be observed from systems other than thiyl radical-catalyzed reactions.[11]

When allylbenzene is treated with potassium *tret*-butoxide in dimethylsulfoxide at 25°C, propenylbenzen with *trans/cis* ratio of 44.4 is formed.[12] However, if the reaction is

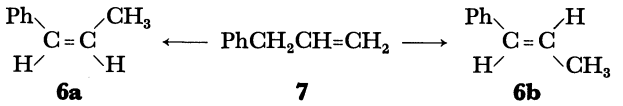

6a **7** **6b**

carried out starting form allylbenzene with potassium *tert*-butoxide in *tert*-butyl alcohol at 25°C, the *trans/cis* ratio in propenylbenzene changes to 12.9. Kinetically controlled equilibrium clearly exists in the latter case, since under the conditions the reactions **6a** to **7** and **6b** to **7** do not take place.

Another example can be seen in the isomerization of **7** to **6** catalyzed by palladium(II) chloride. Here again the reverse reactions are very slow and the final *trans/cis* ratio of 19.0 in **6** is controlled kinetically.[13]

These observations support our assumption that the isomer ratio in *cis-trans* isomerization of propenylbenzene induced by thiyl radicals are kinetically controlled.[2]

Experimental

Materials. The isomers of 1,2-bis(phenylthio)ethylenes were prepared after Parham and Herberling[14]; mp 31.5—32.0°C (lit,[14] 32.0—32.5°C) for the *cis*-isomer and 63.5—64°C (lit,[14] 64°C) for the *trans*-isomer. Azobisisobutyronitrile was purified by recrystallizations and used at the longest within 3 days. Thiophenol-*phenyl*-^{14}C was prepared from benzene-^{14}C and chlorosulfuric acid[15] followed by reduction with Zn-H_2SO_4[16] and purified as described previously[17]. The same procedure was employed for the purification of non-radioactive thiophenol. Iodine was purified by sublimations and used immediately. The solvent, *p*-xylene, was once distilled and carefully redistilled over sodium chips. All materials were stored at −18°C under an atomosphere of nitrogen and purities were confirmed by vpc prior to use.

Procedures. Reaction mixtures were prepared in a vacuum-dry box under an atomosphere of nitrogen or argon. An example for the experiment with vpc-method is as follows: 1 m*l* solutions of 0.10 M olefin, 0.056 M thiophenol, and 9.7×10^{-4} M of azobisisobutyronitrile each were combined and diluted to 5 m*l*. Aliquots of 50 μl were sealed in capillaries and immersed in a thermostat of 50.0±0.05°C. At desired intervals, compositions of aliquots were detected by vpc on a Hitachi K-53 (FID) with a column of XE-60 at 200°C. Peak areas of olefins were calculated by the half-height-width method and *cis/trans* ratios were calculated with the aid of a calibrating curve.

In experiments with thiophenol-*phenyl*-^{14}C, 22 m*l* solutions each prepared as described above were placed in ampuls and vacuum-sealed. After being immersed in the thermostat and picked up, two portions of 10 m*l* solutions were pipetted from the aliquot. To each solution, 700 mg of *cis*- and *trans*-1,2-bis(phenylthio)ethylene were added, respectively. The mixtures were washed immediately once with 20 m*l* of 10% aq-Na_2CO_3 and three times with 100 m*l* of water. After evaporation of the solvent, *cis*- and *trans*-olefins thus obtained were recrystallized from ethanol, vacuum dried, and subjected to activity-measurements on a Beckmann LS-250 Liquid Scintillation Counter. Activities were corrected with the aid of calibrating curves for each isomer. The total activity of the reaction mixture was obtained by pipetting 20 μl of solution from the aliquot after the reaction and subjecting to the activity countings.

The procedure for reactions with iodine was the same as described above except for the use of iodine in place of thiophenol.

11) We thank Dr. W. J. Muizebely of The Katholieke Universiteit, Netherlands for suggestions in his letter of August 25, 1969.

12) S. W. Ela and D. J. Cram, *J. Amer. Chem. Soc.*, **88**, 5791 (1966).

13) B. Cruikshank and N. R. Davies, *Aust. J. Chem.*, **19**, 815 (1966)

14) W. E. Parham and J. Herberling *J. Amer. Chem. Soc.*, **77**, 1175 (1955).

15) H. T. Clarke, G. S. Babcock, and T. F. Murray, "Organic Syntheses," Coll. Vol. I, pp. 85—86, 2 nd ed. (1965).

16) R. Adams and C. S. Marvel, *ibid.*, *Coll. Vol.* I, pp. 504—505.

17) T. Saito, A. Kudo, and N. Morikawa, *Radioisotopes*, in press, in Japanese.

The ESR Spectra of 2- and 6-Methoxyazulene Anion Radicals

Yusaku IKEGAMI and Shuichi SETO

Chemical Research Institute of Non-Aqueous Solutions, Tohoku University, Katahira-2-chome, Sendai

(Received December 21, 1970)

The electron spin resonance spectra of 2- and 6-methoxyazulene anion radicals have been examined. The radicals were generated from neutral species either by electrolytic reduction in *N,N*-dimethylformamide or by the reduction with alkali metals in ethereal solvents. The experimental splitting constants are explained satisfactorily in terms of the calculated spin densities by McLachlan's procedure.

The electron spin resonance (ESR) spectrum of azulene anion radical was first reported by Bernal *et al.*[1] The calculations of the π-electron spin density ρ_i for the anion radical were used with the experimental splitting constants a_i to make a comparison with the predicted bond angle variation of the parameters Q^{H}_{CH} in the McConnell relation, $a_i = Q^{H}_{CH}\rho_i$.[2] Among the relatively few studies on the anion radicals of azulene derivatives, a recent result on 2,2'-biazulenyl[3] has shown that the observed splitting constants are related to the calculated spin densities by rather larger Q^{H}_{CH} values (23—28 gauss) than that suggested by Bernal *et al.* Reddoch[4] has found the anomalous effects of temperature and concentration on the splitting constants for azulene anion radical. This is of interest in connection with the fact that azulene is a non-alternant hydrocarbon. Since only a few ESR works on azulene derivatives have been reported, more systematical studies are desired for elucidation of ESR spectroscopic properties of azulenes.

The present authors attempted to prepare the anion radicals of azulene derivatives. Two methoxy derivatives, 2- and 6-methoxyazulenes, were first chosen because the presence of the substituent at 2- or 6-position does not lower the structural symmetry of azulene, and also the affinity of methoxy substituent with ethereal solvents might favor the generation of relatively stable anion radicals. The ESR spectra of the radicals will be reported in this paper.

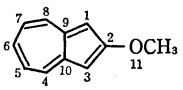

I

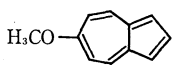

II

Experimental

Both of the materials, 2-methoxyazulene, mp 82—83°C[5], and 6-methoxyazulene, mp 112—113°C[6], were recrystallized from methanol and finally purified by sublimation in a vacuum. All solvents were degassed by at least five freezing-pumping cycles after being purified. 1,2-Dimethoxyethane (DME) and tetrahydrofuran (THF) were each preserved as solutions of sodium anthracenide in a flask connected with a high vacuum apparatus. *N,N*-Dimethylformamide (DMF) was distilled on to a molecular sieve (4A, small pellet) which had been flame dried in a vacuum. The solvent was moved usually by distillation into the reaction vessels connected with the sample tube for measurement.

The technique employed in the electrolytic generation of free radical is similar to that used by Hirayama.[7] A cell with platinum electrodes was designed so that electrolysis could be performed within the cavity for the preparation of radicals unstable at room temperature. Tetra-*n*-propylammonium perchlorate was used as the supporting electrolyte for the electrolysis in DMF. The alkali metal reduction was performed by the usual method, using lithium, sodium, and potassium metals as the reducing agents.

The ESR spectra were measured with a Hitachi X-band ESR spectrometer, Model MPU-3B or Model 771, using a field modulation of 100 kHz. Analysis of the spectra was confirmed by simulation for which a JEOL spectrum computer, JRA-5, was used.[8] Numerical calculations were carried out on the NEAC 2230 at the Computer Centre, Tohoku University.

Results and Discussion

2-Methoxyazulene Anion Radical. *a) Generation and Spectrum of the Radical*: Treatment of 2-methoxyazulene (I) solution with an alkali metal in degassed DME or THF at −5°C usually resulted in an immediate disappearance of its pink color. This is similar to the case of formation of azulene anion radical in which a deep

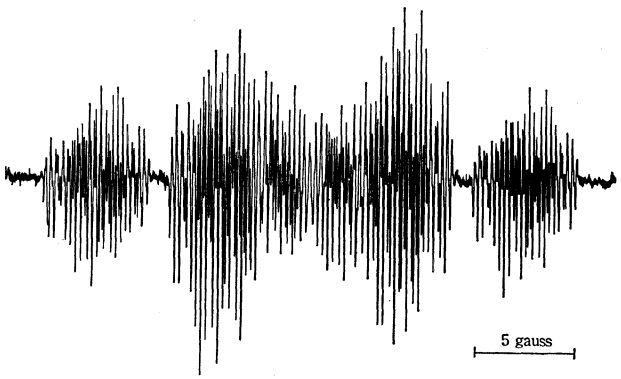

Fig. 1. ESR spectrum of the anion radical generated by the reduction of 2-methoxyazulene with sodium metal in THF (g=2.0032).

1) I. Bernal, P. H. Rieger, and G. K. Fraenkel, *J. Chem. Phys.*, **37**, 1489 (1962).

2) H. M. McConnell, *ibid.*, **24**, 632, 764 (1956); H. M. McConnell and H. H. Dearman, *ibid.*, **28**, 51 (1958); H. M. McConnell and D. S. Chesnut, *ibid.*, **28**, 107 (1958).

3) Y. Ikegami and S. Seto, *Mol. Phys.*, **16**, 101 (1969); This Bulletin, **43**, 2409 (1970).

4) A. H. Reddoch, *J. Chem. Phys.*, **41**, 444 (1964).

5) T. Nozoe, S. Seto, and S. Matsumura, This Bulletin, **35**, 1990 (1962).

6) K. Takase, T. Asao, Y. Takagi, and T. Nozoe, *Chem. Commun.*, **1968**, 368.

7) M. Hirayama, This Bulletin, **40**, 1822 (1967).

8) The authors express their thanks to the computer staff of JEOL, Co. Ltd.

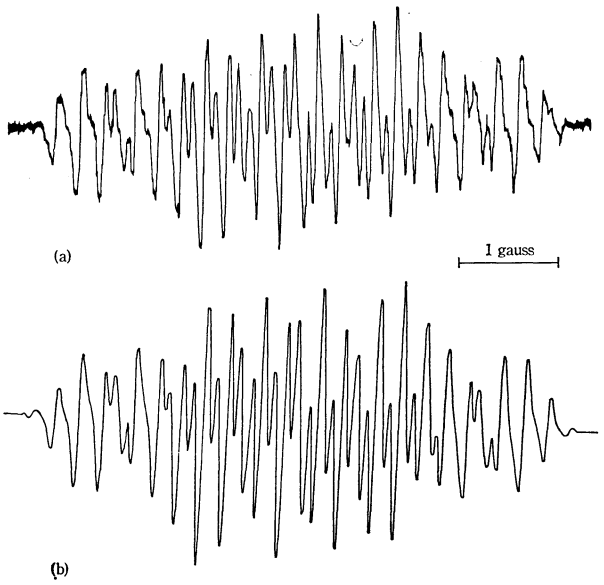

Fig. 2. (a) Enlarged spectrum for the lower 6 gauss of Fig. 1. (b) Simulated spectrum of the above ($\Delta H_{1/2}$=90 milligauss).

purple-blue color of the neutral species changed into a pale greenish yellow.[1] The colorless solution exhibited a strong ESR signal. Although the anion radical is stable for a long period at room temperature, careful procedure was required to obtain it, since a crystalline product was formed at times if the solution was kept in contact with the metal for a long period at room temperature.

Na—THF: The spectrum of the anion radical generated by the reduction of I with sodium metal in THF is shown in Fig. 1. Complicated hyperfine structure of the spectrum suggests the presence of splittings due to the coupling of the radical with a sodium cation. It is easy to read the two splitting constants, 8.598 and 6.133 gauss, from the spectrum, one of which represents the coupling with one hydrogen atom and the other that with two equivalent hydrogen atoms. The enlarged spectrum shown in Fig. 2a for the lower 6 gauss of Fig. 1 is analyzed with three splitting constants, 1.252 (2H), 0.237 (5H) and 0.567 gauss (1Na). A combination of these three constants with eight nuclear spins afforded the simulated spectrum shown in Fig. 2b, confirming the analysis.

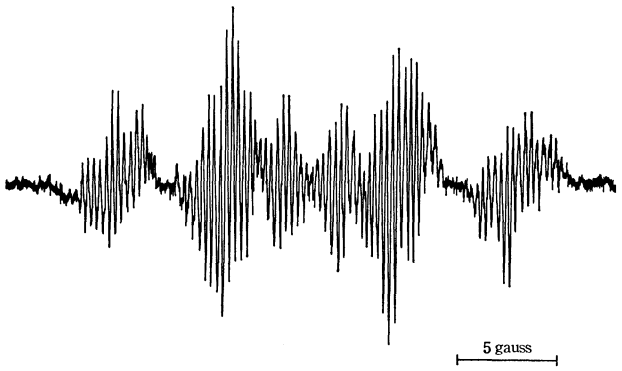

Fig. 3. ESR spectrum of the anion radical generated by the reduction of 2-methoxyazulene with sodium metal in DME (g=2.0030).

Na—DME: Figure 3 shows the spectrum of the anion radical formed by the reduction of I with sodium metal in DME. Hyperfine structure of the spectrum can be interpreted assuming that there are metal splittings with the coupling constant comparable to the least constant in the anion radical. Four splitting constants listed in Table 1 and rather large line-width ($\Delta H_{1/2}$, *ca.* 0.27 gauss) permit analysis of the hyperfine structure.

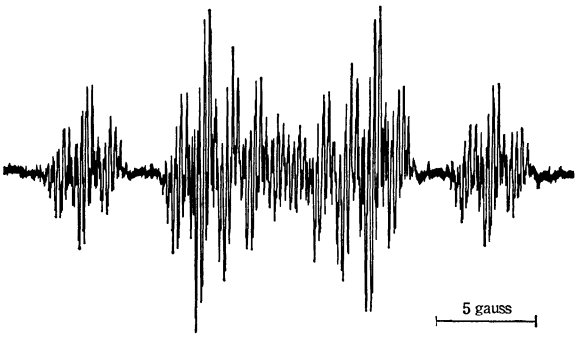

Fig. 4. ESR spectrum of the anion radical generated by the reduction of 2-methoxyazulene with potassium metal in THF (g=2.0017).

K—THF: Generation of the radical with potassium metal in THF afforded the spectrum shown in Fig. 4. It is easy to read three splitting constants, 8.359 (1H), 5.862 (2H) and 1.149 gauss (2H), from the spectrum. Final splittings are explained as those consisting of seven bands of relative intensities 1:4:7:8:7:4:1, each splits into three lines (a_i, *ca.* 0.1 gauss). Relative intensities of the seven bands should be due to the fact that the two constants for potassium metal and methoxy protons are close to each other.

K—DME, Li—THF and Li—DME: Hyperfine structures of the ESR spectra of the radical generated by these systems are simpler than those of Figs. 1 and 3, and the analysis of each spectrum revealed that the metal splitting constant is comparable to that of the least constant for the radical. The hyperfine lines are comparatively broad because of the large line-width close to the least splitting constant. The observed constants are included in Table 1.

Electrochemical Reduction: Electrolytic reduction of I in DMF at *ca.* 1.9V produced the anion radical, which exhibited the ESR spectrum shown in Fig. 5. Hy-

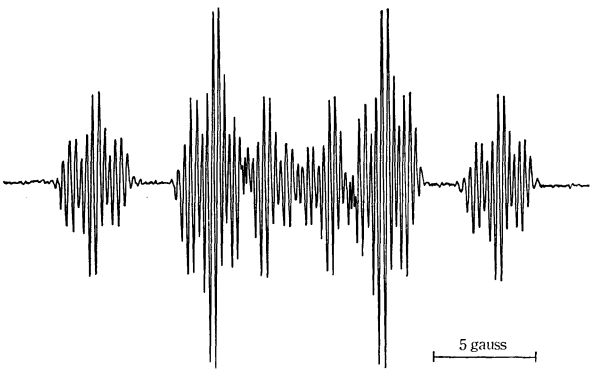

Fig. 5. ESR spectrum of 2-methoxyazulene anion radical generated by the electrolytic reduction in DMF (g=2.0038).

Table 1. Observed hyperfine splitting constants (a_i) for 2-methoxyazulene anion radical

Position	Electrolysis in DMF	a_i, gauss					
		K—THF	Na—DME	K—DME	Li—DME	Na—THF	Li—THF
1, 3 (2H)	0.26	0.1	0.29	0.24		0.23_7	0.23
4, 8 (2H)	5.804	5.862	5.670	5.96	6.02	6.133	6.21
5, 7 (2H)	1.097	1.149	1.163	1.17	1.21	1.252	1.31
6 (1H)	8.326	8.359	8.529	8.55	8.62	8.598	8.76
OCH_3(3H)	0.26	0.27	0.29	0.24	0.27	0.23_7	0.23
Metal		0.27	0.29	0.24	0.27	0.56_7	0.23

perfine structure of the spectrum can be readily analyzed with four splitting constants included in Table 1. The analysis was confirmed by spectral simulation.

The observed constants are summarized in Table 1. Assignments for the constants were given according to the type of splitting and by comparing them with the calculated spin densities.

b) Calculation of Spin Density. Calculations of unpaired spin densities (ρ_i) for the anion radical were carried out by employing the Hückel MO theory and the approximate configuration interaction treatment proposed by McLachlan.[9] The Coulomb and resonance integral parameters for C–OCH_3 group were chosen from the values suggested by Streitwieser.[10] The results are given in Table 2. As generally known for many aromatic anion radicals[9] including some azulene anion radicals,[1,3] the McLachlan's procedure gave much more satisfactory results than the Hückel MO calculations. The application of some other parameters for the 9,10-bond ($\beta_{9,10}$:1β) and the C–OCH_3 group (β_{C-O}: 0.6—1.0β, α_O: α+0.5—2.0β) did not alter the assignments for the observed constants shown in Table 2. The Q^H_{CH} values obtained by the McConnell relation are also shown in the table.

6-Methoxyazulene Anion Radical. a) Generation and Spectrum of the Radical: The anion radical of 6-methoxyazulene (II) is not so stable as that of 2-isomer. The solution of II in degassed DME or THF reacted readily with an alkali metal at room temperature losing its pink color, but no ESR signal has been observed.

Table 2. Calculated spin densities(ρ_i) for 2-methoxyazulene anion radical[a]

Position	ρ_i		$\lvert Q^H_{CH}\rvert$[b]
	Hückel	McLachlan	
1, 3	0.0009	−0.0161	16.2
2	0.1066	0.1048	
4, 8	0.2039	0.3032	19.1
5, 7	0.0125	−0.0753	14.6
6	0.2514	0.3819	21.8
9, 10	0.0980	0.0434	
11(OCH_3)	0.0114	0.0030	

a) Parameters for the calculation: $\alpha_{11}=\alpha+2\beta$, $\beta_{2,11}=0.8\beta$, $\beta_{9,10}=0.9\beta$ and $\lambda=1.2$.

b) Q^H_{CH} values in the relation of $a_i = Q^H_{CH}\rho_i$, in which the observed a_i in an electrolytic reduction and the McLachlan spin densities were used.

9) A.D. McLachlan, *Mol. Phys.*, **3**, 233 (1960).

10) A. Streitwieser, Jr., "Molecular Orbital Theory for Organic Chemists," John Wiley & Sons, New York (1962), p. 120.

The anion radical was identified when the pink solution came into contact with an alkali metal at −78°C and was measured at a temperature lower than −20°C. The radical generated with sodium metal in DME exhibited the ESR spectrum shown in Fig. 6, which was measured at −100°C. Three splitting constants, 6.63 (2H), 3.67 (1H) and 1.53 gauss (2H), are obtained from the hyperfine structure of the spectrum. The signal intensity decreases with increasing temperature and disappears completely at −10°C. Other systems, Li—THF, Na—THF and K—THF, also showed the ESR signals, each of which consists of broad hyperfine lines.

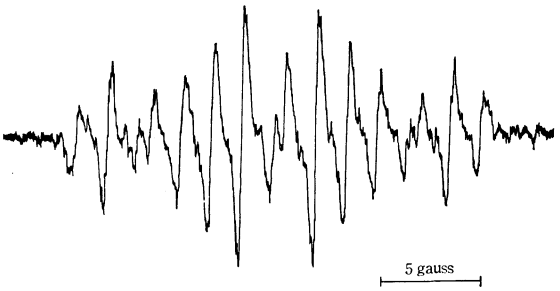

Fig. 6. ESR spectrum of the anion radical generated by the reduction of 6-methoxyazulene with sodium metal in THF, measured at −100°C.

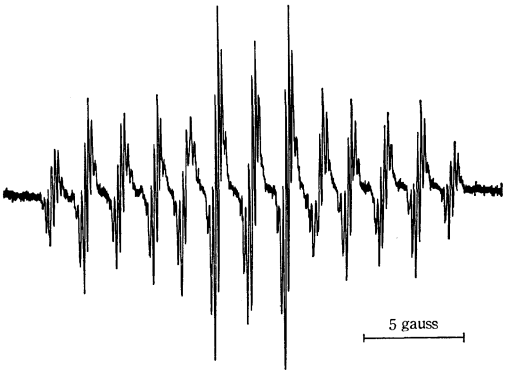

Fig. 7. ESR spectrum of 6-methoxyazulene anion radical generated by the electrolytic reduction in DMF at room temperature (g=2.0029).

In contrast to the above, electrolytic reduction of II produced the stable radical at room temperature. Electrolysis of the solution of II in DMF at *ca.* 1.9V resulted in a pale brown solution which exhibited an ESR spectrum shown in Fig. 7. No decay of the intensity of the spectrum is observed during the course of a few hours. Hyperfine structure of the spectrum is analyzed with four splitting constants listed in Table

3 and the assignments for the constants are reasonably made by comparing them with the calculated spin densities.

TABLE 3. OBSERVED HYPERFINE SPLITTING CONSTANTS (a_i) AND CALCULATED SPIN DENSITIES (ρ_i) FOR 6-METHOXYAZULENE ANION RADICAL

Position	a_i, gauss		ρ_i[a]		$\lvert Q_{CH}^{H}\rvert$[b]
	Na-DME	Electrolysis in DME	Hückel	McLachlan	
1, 3(2H)		0.16	0.0061	−0.0206	7.8
2 (1H)	3.67	3.542	0.1034	0.1113	31.8
4, 8(2H)	6.63	6.659	0.2216	0.3085	21.6
5, 7(2H)	1.53	1.701	0.0032	−0.0890	19.1
6			0.2480	0.3509	
9, 10			0.0806	0.0582	
OCH_3(3H)		0.16	0.0257	0.0236	

a) Parameters for the calculation: $\alpha_{11}=\alpha+2\beta$, $\beta_{6,11}=0.8\beta$, $\beta_{9,10}=0.9\beta$ and $\lambda=1.2$.
b) See footnote b in Table 2.

b) Calculation of Spin Density. Calculations of unpaired spin densities for the anion radical were carried out in a similar way as those for 2-isomer. The results are listed in Table 3 together with the Q_{CH}^{H} values obtained by the McConnell relation.

Discussion. Both 2- and 6-methoxyazulenes produced the stable anion radicals through their electrolytic reductions in DMF. The formation of radicals is consistent with the suggestion by polarographic study on azulene, which showed the first reversible reduction potential ($E_{1/2}$) at −1.10 V in DMF.[11] In the generation of 2-methoxyazulene anion radical by alkali metal reduction, the radical was identified as a rather unstable form sometimes producing solid precipitates. The instability might be due to the further reduction of the radical with alkali metal leading to the decomposition of 2-methoxyazulene structure in ethereal solvent. The solution did not reproduce the pink color of neutral species by exposure to air, while it is known that the complex of guaiazulene with sodium in ethereal solvent shows the immediate reappearance of the original blue color by exposure to air.[12]

The spectra of 2-methoxyazulene anion radical generated by the reduction with alkali metals all showed the coupling with the cation, indicating that the radical species exist mostly as ion pairs. For the radical solutions of Na—DME (Fig. 3), Li—DME and Li—THF systems, co-existence of the ion pairs and the solvent-separated ion pairs might be assumed to explain the asymmetric feature of the splittings observed within the outer 6 gauss of their spectra.

In Table 1, the splitting constants at 4(8)-, 5(7)- and 6-positions are smallest for a case of the generation of the radical by electrolytic reduction, and each of the constants increases for the reductions with alkali metals roughly in the order K—THF, Na—DME, K—DME, Li—DME, Na—THF and Li—THF systems. This is similar to the observation by Reddoch,[13] who pointed out the empirical correlation for proton coupling constants of azulene anion radical in various solvents with various cations. The variation of the constants can be ascribed to the electrostatic perturbation of the cation as stated by him.

The Q_{CH}^{H} values in Tables 2 and 3, which are given for the free radical in DMF, are reasonable if the variation of the value with bond angle in an aromatic ring is assumed as estimated by Bernal *et al.*[1] The value for each position is close to that at the same position for azulene anion radical.[1] However, the values on the carbon atoms in the seven-membered ring are clearly smaller than those for 2,2′-biazulenyl anion which is a very stable radical with deep blue color.[3]

We wish to express our appreciation to Profs. T. Toda and T. Asao for the supply of materials. We are also grateful to Prof. T. Isobe and Dr. H. Yokoi for their helpful discussions.

11) P. H. Given and M. E. Poever, *Coll. Czech. Chem. Comm.*, **25**, 3195 (1960).
12) J. Melville, *J. Amer. Chem. Soc.*, **55**, 3288 (1933); K. S. Birrell, *ibid.*, **57**, 893 (1935).
13) A. H. Reddoch, *J. Chem. Phys.*, **43**, 225 (1965).

Cyclic Acetylenes. XIII. The Syntheses and Properties of *p,p'*-Bridged Cyclic Diphenyldiacetylenes

Mutsuo KATAOKA, Takashi ANDO, and Masazumi NAKAGAWA
Department of Chemistry, Faculty of Science, Osaka University, Toyonaka, Osaka
(Received December 23, 1970)

Concerning the studies on the effect of ring strain on the electronic spectra of cylcic acetylenes, a series of polymethylene ether derivatives of *p,p'*-dihydroxydiphenyldiacetylene (VI_n, $n=13$, 14, 15, and 18) has been prepared by the oxidative coupling of *p*-hydroxyphenylacetylene polymethylene ethers (V_n, $n=13$, 14, 15, and 18) under a high dilution condition. A slight bathochromic shift accompanied by hypochromism was observed in the electronic spectra of VI_n resulting from the increase of the ring strain. The same trend has been observed in the *p,p'*-bridged cyclic tolans.[1] However, the bathochromic shift observed in the *p,p'*-series makes a contrast with the hypsochromic shift in the strained *o,o'*-bridged cyclic diphenyldiacetylene (I)[2] and *o,p'*-bridged cyclic tolans (II).[3] The NMR and IR spectra of VI_n were discussed.

As has been pointed out in previous papers, the increase of strain in the cyclic polymethylene ether derivatives of *o,o'*-dihydroxydiphenyldiacetylene (1)[2] and *o,p'*-dihydroxytolan (II)[3] brought about hypsochromic shift of their electronic spectra. In contrast, bathochromic shift was observed in the spectra of strained cyclic polymethylene ether derivatives of *p,p'*-dihydroxytolan.[1] We hoped to synthesize another series of *p,p'*-bridged cyclic acetylenes to get further insight into the effect of the ring strain on the electronic spectra of cyclic acetylenes. The present paper deals with the syntheses and the properties of *p,p'*-bridged cyclic diphenyldiacetylenes (VI_n).

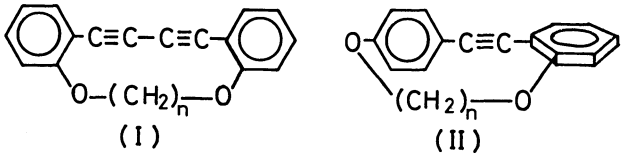

Syntheses. Alkylation of methyl 4-hydroxycinnamate with polymethylene dibromide gave the biscinnamic ester (III_n). Ester (III_n) was converted into bis-phenylpropiolic acid (IV_n) *via* bromination followed by dehydrobromination. Propiolic acid (IV_n) was decarboxylated without isolation to give *p*-hydroxyphenylacetylene polymethylene ether (V_n). α,ω-Diethynyl compounds (V_n) thus obtained was purified by means of chromatography on alumina. It is to be noted that a minor amount of hydration product, 1,14-bis(*p*-acetylphenoxy)tetradecane and 1-(*p*-ethynylphenoxy)-13-(*p*-acetylphenoxy)tridecane are obtained from the fractions eluted with benzene-ether in the case of $n=14$ and 13, respectively. The oxidative coupling of V_n according to the method of Eglinton under a high dilution condition using ether as an entraining agent afforded *p,p'*-bridged diphenyldiacetylene (VI_n) as colorless crystals. A solution of V_n in pyridine-ether (6:1) was added slowly into a refluxing solvent (pyridine-ether, 6:1) containing cupric acetate monohydrate. The temperature of the refluxing solvent was 83—84°C. The reaction conditions, the yields and the melting points of VI_n are summarized in Table 1. The monomeric nature of VI_n was confirmed by elemental analyses and molecular weight determination.

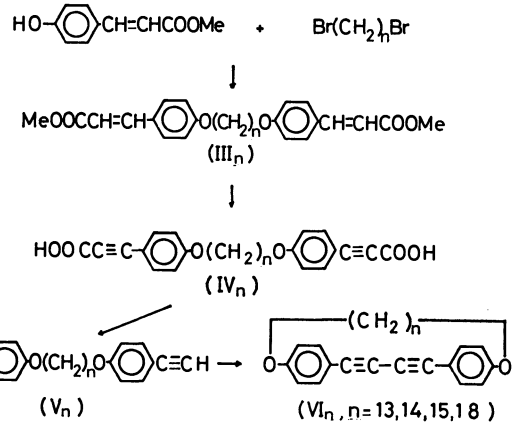

Table 1. The reaction conditions, yields and melting points of VI_n

n	Amount of V_n (mmol)	Amount of solvent (m*l*)	Period of addition of V_n (hr)	Yield of VI_n (%)	Mp of VI_n (°C)
18	1.52	280	7.5	60	138.8—140.0
15	1.70	350	7.5	53	168.8—169.2[a]
					174.7—176.0
14	1.19	210	6.0	37	167.2—169.2
13	1.72	400	5.5	0.8	151.2—153.0
	2.03	2500	8.0	2.0	

a) Dimorphism.

Preparation of VI_{14} by means of the alkylation of *p*-hydroxyphenylacetylene with 1,14-dibromotetradecane was found to be less satisfactory as compared with the above method presumably owing to the instability of the hydroxyacetylene.

Electronic Spectra. The electronic spectral data of *p,p'*-bridged diphenyldiacetylene (VI_n) measured in *n*-hexane and the absorption curves are recorded in Table 2 and Fig. 1 together with those of the open chain analog, *p,p'*-di-*n*-butoxydiphenyldiacetylene.

The absorption band at long-wavelength region consists of four distinct vibrational peaks (A~D) which are considered to arise from the stretching vibration of poly-yne linkage. All of these vibrational sub-

1) T. Ando and M. Nakagawa, This Bulletin, **44**, 172 (1971).
2) F. Toda and M. Nakagawa, *ibid.*, **34**, 862 (1961).
3) M. Kataoka, T. Ando, and M. Nakagawa, *ibid.*, **44**, 177 (1971).

TABLE 2. ELECTRONIC SPECTRA OF VI_n
λ_{max} in mμ ($\varepsilon \times 10^{-2}$)

n				A	B	C	D
18	203.5 (673)	240 (219)	268 (174)	283 (206)	300.5 (332)	320 (518)	342.5 (465)
15	204 (706)	240.5 (222)	269 (111)	284.5 (168)	301.5 (332)	321 (543)	343.5 (514)
14	204 (565)	241.5 (219)	269 (115)	285.5 (162)	302.5 (288)	321.5 (436)	344 (425)
13	204 (572)	241.5 (242)	269.5 (95)	287 (141)	303.5 (252)	323 (408)	345.5 (367)
n-Bu	203.5 (673)	238.5 (223)	267.5 (308)	281 (310)	298.5 (365)	318 (485)	340.5 (407)

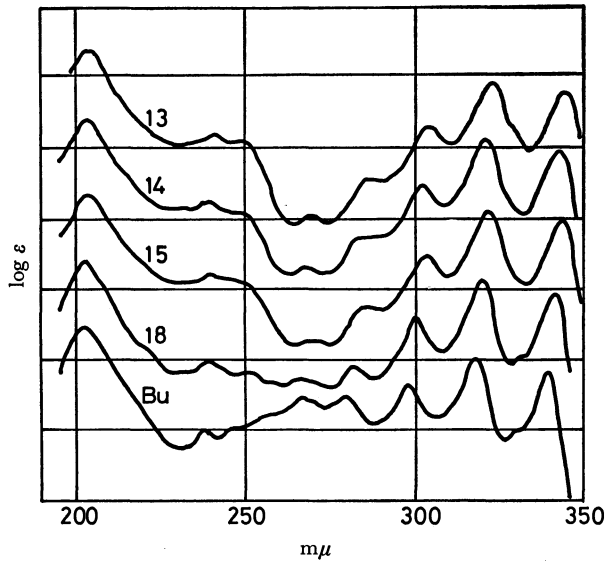

Fig. 1. The absorption curves of VI_n and p,p'-di-n-butoxydiphenyldiacetylene. The curves, with the exception of the di-butoxydiphenyldiacetylene at the bottom, are displaced upward on the ordinate axis by 1/3 log ε unit increments from the curve immediately below, and each horizontal line corresponds to log ε=4. (in n-hexane)

peaks exhibit bathochromic shift due to the decrease in the ring size making a sharp contrast with the hypsochromic shift observed in the strained o,o'-bridged diphenyldiacetylene (I)[1]

An inspection of molecular model of compound VI_n reveals that a chain of fifteen methylene groups is of the minimum length to link p,p'-position of dihydroxydiphenyldiacetylene without ring strain and the two phenyl groups are held almost in a coplanar fashion owing to the restricted rotation.

The absorption intensities of the four vibrational peaks exhibited an interesting change with that of the length of polymethylene bridge. As illustrated in Fig. 2, ε-values of the peaks A and B diminish monotonously with the decrease of the number of n. On the other hand, the absorption intensities of C and D attain maximum in the case of n=15, and then rapidly fall with the increase of ring strain. The nature of the transition corresponding to each of the vibrational peaks has not been clarified yet, and it is difficult to deduce a precise correlation between the ring strain and the above-mentioned intensity change. However, the spectral behavior of VI_n seems to be the result of the effects of coplanarity of the benzene rings (hyperchromism of C and D observed in VI_{15} and VI_{18}), the strain of the diacetylenic linkage caused by the short bridging chain (hypochromism of C and D observed in VI_{13} and VI_{14}) and the diminish of population of molecules in high vibrational sub-levels according to the decrease of the ring size (hypochromism of A and B according to the decrease of the number of n).

Nuclear Magnetic Resonance Spectra. As illustrated in Fig. 3, the protons on the benzene rings exhibit two AB pattern doublets at τ 2—3. The down field

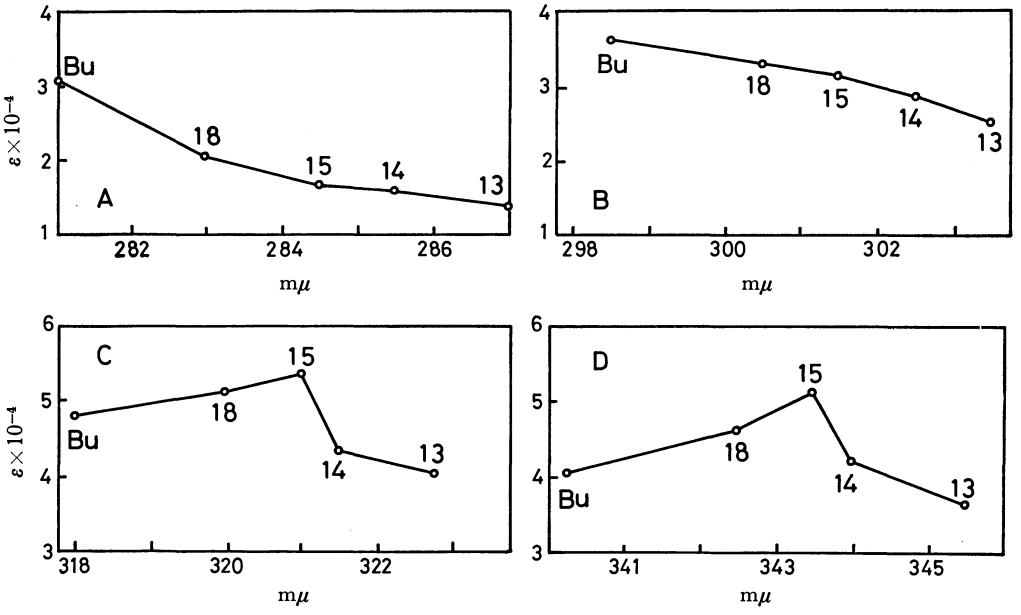

Fig. 2. Change in absorption intensities of the long-wavelength bands of VI_n.

Table 3. Assignment of NMR spectra of VI_n, 60 MHz in $CDCl_3$ (τ-value)

VI_n	Aromatic	α-Methylenes	β-Methylenes	Other methylenes
18	2.53 (4H), 3.08 (4H)	5.72 (4H)	8.37 (5H)[a]	8.84, 9.10 (27H)[a]
15	2.57 (4H), 3.06 (4H)	5.73 (4H)	8.42 (4H)	9.01 (22H)
13[b]	2.54 (4H), 3.04 (4H)	5.72 (4H)	8.47 (7H)[a]	9.04 (16H)
n-BuO	2.54 (4H), 3.14 (4H)	6.02 (4H)	8.0—8.3 (8H)	9.03 (6H)

a) Accurate intensity was not obtained owing to the poor resolution.
b) Measured on a 100 MHz spectrometer.

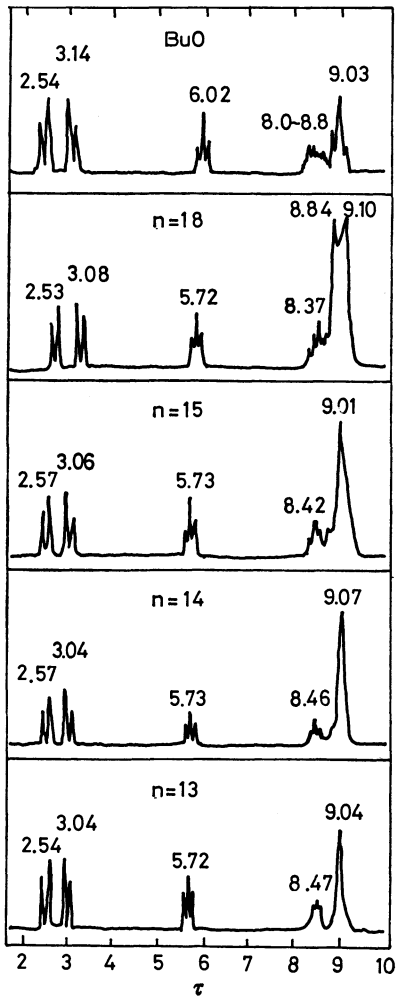

Fig. 3. NMR spectra of VI_n and *p,p'*-di-*n*-butoxydiphenyldiacetylene. The spectrum of VI_{13} was obtained on a 100 MHz spectrometer and the others were measured with a 60 MHz spectrometer (in $CDCl_3$).
(I_n) n=3,4,5,6 (III_n) n=13,14,15,16
(II_n) n=7,8,9,10,11,12 (IV_n) n=11,12,13,14,18

doublet was assigned to the ortho protons to the ethereal oxygen. The protons on the α-methylene groups adjacent to the ethereal oxygen exhibit distinct triplet at τ *ca.* 5.7. Another triplet was observed at around τ 8.4. A decoupling technique was applied for VI_{14} in which the centers of the two triplets were found at τ 5.73 and τ 8.46. The high field triplet was assigned to the methylene protons at the β-position to the ethereal oxygen, because the triplet at τ 5.73 was changed to a sharp singlet by the irradiation at τ 8.46. Therefore, the broad and intense peaks at τ *ca.* 9 should be assigned to the protons on other methylene groups. This indicates that an almost uniform magnetic environment is formed in the vicinity of the *p,p'*-bridged diphenyldiacetylene system as in the case of *p,p'*-bridged cyclic tolans.[1] The assignments are summarized in Table 3 together with that of *p,p'*-di-*n*-butoxydiphenyldiacetylene. The NMR spectroscopic feature of VI_n was found to be closely related to those of *p,p'*-bridged cyclic tolans, however, the slight down field shift of the τ-values of VI_n as compared with those of *p,p'*-bridged tolans seems to indicate that the diacetylenic unit in VI_n exerts more enhanced effect than the acetylenic linkage in the cyclic tolans.

Table 4. IR spectra of VI_n KBr-disk (cm^{-1})

VI_n	$\nu_{C=O}$	$\nu_{C=C}$ (arom.)	δ_{C-H} (arom.)
18	2120 (w)	1600 (s)	835 (s)
15	2120 (w)	1595 (s)	840 (m)
14	2130 (w)	1595 (s)	845 (m)
13	2120 (w), 2200 (w)	1600 (m)	835 (s)
n-BuO	2120 (w)	1959 (s)	830 (s)

(w): weak, (m): medium, (s): strong

Infrared Spectra. The characteristic peaks in the IR spectra of VI_n are tabulated in Table 4 with that of the open-chain analog, *p,p'*-di-*n*-butoxydiphenyldiacetylene. A decrease of intensity of the absorption band due to skeletal in-plane vibration of aromatic ring conjugated with the lone pair electrons in the substituent was observed in the spectra of VI_n as compared with that of the open-chain analog. The same trend has been observed in the IR spectra of *p,p'*-bridged tolans.[1] This seems to be attributable to a resonance inhibition of the oxygen with the benzene owing to a fixation of conformation by the spanning of the bridging chain. The splitting of $\gamma_{C\equiv C}$ band into two peaks (2120 and 2200 cm^{-1}) in the spectra of the strained VI_{13} may be pertinently attributed to some restriction of stretching vibration mode due to the ring strain. The same phenomenon has been observed in the spectrum of 2,4-hexadiynylene ether of 1,5-bishydroxymethylnaphthalene.[4]

Experimental

All melting points are uncorrected. The IR spectra were obtained with a Hitachi EPI-2 spectrophotometer by KBr-disk method, the electronic spectra with a Hitachi EPS-2 spectrophotometer and the NMR spectra with Varian A60 and Jeol JMN-4H-100 spectrophotometers. The molecular weights were measured on a Hitachi Perkin-Elmer 115 vapor osmometer.

Ethyl p-n-*butoxycinnamate.* To a refluxing mixture of methyl *p*-hydroxycinnamate (6.98 g, 39 mmol), *n*-butyl

4) T. Ando and M. Nakagawa, This Bulletin, **40**, 363 (1967).

bromide (11 g, 80 mmol), and anhydrous ethanol (120 ml) was added 56 ml of 0.70 M solution of potassium hydroxide in anhydrous ethanol over a period of 100 min. After further stirring for 2.5 hr, the reaction mixture was poured into water and extracted with ether. The extract was washed successively with a dilute sodium hydroxide and water, and dried. Evaporation of the solvent gave colorless crystals (7.48 g, 98%). This was recrystallized twice from *n*-hexane to give pure ethyl *p*-*n*-butoxycinnamate, mp 35.3—38.0°C.

Ethyl p-n-*butoxycinnamate dibromide.* Thirty six ml of 0.902 M solution of bromine in carbon tetrachloride was added under stirring over a period of 50 min to an ice-cooled solution of slightly crude ethyl *p*-*n*-butoxycinnamate (7.48 g, 31 mmol) in the same solvent (70 ml). Stirring was continued for 40 min at room temperature and then for 40 min at 50°C. The reaction mixture was washed with dilute sodium hydroxide and water successively and dried. The crystals (9.46 g, 74%) obtained by evaporation of the solvent were recrystallized twice from *n*-hexane to give pure dibromide, colorless prisms, mp 105.3—106.3°C. Found: C, 43.95; H, 4.94; Br, 39.47%. Calcd for $C_{15}H_{20}O_3Br_2$: C, 44.14; H, 4.94; Br, 39.16%.

p-n-*Butoxyphenylacetylene.* Anhydrous methanol (95 ml) was added to an ice-cooled intimate mixture of ethyl *p*-*n*-butoxycinnamate dibromide (5.44 g, 14 mmol) and powdered potassium hydroxide (21.4 g).[5] After a vigorous exothermic reaction had subsided, the mixture was refluxed for 4 hr. The reaction mixture was mixed with 6N hydrochloric acid (40 ml) and extracted with ether. The extract was washed with a saturated aqueous solution of sodium chloride and dried. The violet amorphous solid (2.84 g) obtained by the evaporation of the solvent was dissolved in anhydrous pyridine (28 ml). The pyridine solution was refluxed for 50 min in the presence of copper powder (280 mg). Petroleum benzine (100 ml) was added to the reaction mixture and washed thoroughly with 2N hydrochloric acid. After the usual washing and drying procedures, distillation of the solvent furnished a dark brown oily material (1.77 g). The IR spectrum of this substance indicates the presence of carbonyl function (1670 cm^{-1}) presumably owing to the formation of a minor amount of *p*-butoxyacetophenone. The crude material was chromatographed on alumina (15 g). The fractions eluted with petroleum benzine gave crude *p*-*n*-butoxyphenylacetylene (light brown liquid, 1.26 g, 53%) free from carbonyl compound. This was used without further purification for the following reaction.

p,p'-*Di*-n-*butoxydiphenyldiacetylene.* To a stirred mixture of cupric acetate monohydrate (1 g) and anhydrous pyridine (80 ml), was added a solution of *p*-*n*-butoxyphenylacetylene (2.26 g, 13 mmol) in pyridine (20 ml) over a period of 10 min at 50—55°C.[6] Stirring was continued for 4 hr at the same temperature. Benzene (100 ml) was added to the reaction mixture and washed thoroughly with 2N hydrochloric acid. The crude diacetylene (yellow crystals, 1.06 g, 47%), obtained by the usual washing, drying and evaporating procedures, was recrystallized twice from benzene to afford pure *p*,*p*'-di-*n*-butoxydiphenyldiacetylene, mp 154.7—155°C, colorless prisms. Found: C, 83.29; H, 7.64%. Calcd for $C_{14}H_{26}O_2$: C, 83.20; H, 7.56%.

1,13-Dibromotridecane, 1,14-Dibromotetradecane, and 1,18-Dibromooctadecane. The dibromoalkanes were prepared according to the method previously reported.[3]

1,15-Dibromopentadecane. To a stirred and refluxing solution of diethyl sodiomalonate in ethanol [from sodium (7.8 g, 0.34 g atom), diethyl malonate (53 ml, 0.35 mol) and anhydrous ethanol (170 ml)], was added 1,11-dibromoundecane (50 g, 0.16 mol)[3,7] over a period of 40 min. After stirring for further 2 hr, the solvent was removed under reduced pressure. The residue was mixed with ether, washed with water and dried. The crude reddish brown oily tetraethyl ester obtained by the evaporation of the solvent was added over 15 min-period to a stirred solution of potassium hydroxide (50 g) in water (100 ml). The mixture was refluxed for 13 hr under stirring. The reaction mixture was mixed with hot water (800 ml) and concentrated hydrochloric acid (200 ml). The oily material deposited crystallized on cooling under stirring. The tetracarboxylic acid thus obtained was heated to 160—180°C for 70 min to give 1,15-pentadecanedioic acid. The dioic acid in anhydrous methanol (160 ml) containing concentrated sulfuric acid (16 ml) was refluxed for 3 hr to give the dimethyl ester (bp 168—175°C/4 mmHg, 25.6 g, 53% based on dibromoundecane). The dimethyl ester was converted to 1,15-pentadecanediol by means of lithium aluminum hydride reduction.[3] 1,15-Dibromopentadecane (bp 147—150°C/10^{-3} mmHg, 71%) was obtained from the diol according to the method previously reported.[3]

α,ω-Bis-[p-(*2-methoxycarbonylvinyl*)*phenoxy*]*alkanes* (*III*n). As the alkylation of methyl *p*-hydroxycinnamate with α,ω-dibromoalkane was carried out under almost the same reaction conditions, the preparation of 1,15-bis[*p*-(2-methoxycarbonylvinyl)phenoxy]pentadecane (III_{15}) will be described as a representative example.

A solution of methyl *p*-hydroxycinnamate was mixed with a solution of sodium methoxide in methanol [prepared from sodium equivalent to the ester], and the solvent was removed under reduced pressure. The sodium salt of the ester (13.3 g, 67 mmol, yellow powder), thus obtained, was mixed with

TABLE 5. RESULTS OF THE PREPARATION OF III_n

III_n	Reaction time (hr)	Yield (%)	Mp (°C)	Solv. of recryst.	Elemental analysis (%)	C	H
18	19	39	130—134	B-M	Found	75.26	9.17
					Calcd	74.96	9.27
15	8	37	110—111	B	Found	74.40	8.54
					Calcd	74.43	8.57
14	4.5	21	134—137	B-H	Found	74.58	8.59
					Calcd	74.15	8.42
13	10	32	114—117	B	Found	73.47	8.24
					Calcd	73.85	8.26

B: benzene, M: methanol, H: *n*-hexane,

5) *Cf.* S. Misumi, This Bulletin, **34**, 1827 (1961).
6) G. Eglinton and A. G. Galbraith, *J. Chem. Soc.*, **1959**, 889.
7) *Cf.* R. Adams and R. M. Kamm, "Organic Syntheses," Coll. Vol. I, 2nd Ed., p. 250 (1948).

Table 6. Results of the preparation of V_n

V_n	Yield (%)	Mp (°C)	Crystal habit	Elemental analysis (%)	C	H	Solv. of recryst.
18	19	96.8—98.5	plates	Found	83.44	9.44	H
				Calcd	83.90	9.53	
15	16	72.2—73.0	prisms	Found	83.52	9.00	B-M
				Calcd	83.73	9.07	
14	25	93.0—94.2	leaflets	Found	83.66	8.84	H
				Calcd	83.67	8.90	
13	10	74.9—75.3	leaflets	Found	83.46	8.69	B-M
				Calcd	83.61	8.71	

H: *n*-hexane B: benzene, M: methanol

1,15-dibromopentadecane (11.6 g, 31 mmol). The mixture was heated on an oil-bath maintained at 165—170°C for 8 hr with occasional shaking. Benzene (100 m*l*) was then added to the reaction mixture and refluxed. The insoluble material was removed by filtration and filtrate was concentrated to *ca.* 50 m*l*. The yellow crystals deposited were recrystallized from benzene to afford pure III_{15} (6.71 g, 37%).

The results of the preparation of III_n are summarized in Table 5.

α,ω-Bis(p-*ethynylphenoxy*)*alkanes* (V_n). The bromination of III_n was carried out in chloroform at room temperature by the addition of a slight excess of 1N solution of bromine in the same solvent. Tetrabromides were obtained as viscous liquids and were subjected to the following reactions without purification. The procedures of dehydrobromination and decarboxylation used in the preparation of *p-n*-butoxyphenylacetylene were applied for the crude tetrabromides and the crude bis-phenylpropiolic acids (IV_n). After copper powder was removed by filtration, pyridine was distilled off under reduced pressure. The residue was mixed with ether and washed with dilute hydrochloric acid. The ether layer was dried over potassium carbonate. The crude material obtained by evaporation of the solvent was chromatographed on alumina. The fractions eluted with benzene afforded V_n as colorless crystals.

In the case of V_{14}, the fractions eluted with benzene-ether gave a minor amount of yellow crystals, mp 107—112°C (3% based on III_{14}). The substance was proved to be identical with bis(*p*-acetylphenoxy)tetradecane by comparison with an authentic sample which was prepared by the method described below. Also, in the case of $n=13$, a small amount of colorless solid (2% based on III_{13}, mp 86—92°C) was obtained from the fractions eluted with benzene-ether. This was recrystallized from *n*-hexane 5 times and from benzene-methanol 4 times to give colorless solid, mp 89—95°C. The structure of 1-*p*-ethynylphenoxy-13-*p*-acetylphenoxytridecane was assigned to this substance on the basis of NMR and IR spectroscopic evidences. Found: C, 80.34; H, 8.75%. Mol. wt. 438. Calcd for $C_{22}H_{38}O_3$: C, 80.14; H, 8.81%. Mol. wt. 435.

The results of the preparation of V_n are summarized in Table 6.

p,p'-*Dihydroxydiphenyldiacetylene Polymethylene Ether* (VI_n).

The preparation of VI_{14} is described as a typical example. A solution of the diethynyl compound (V_{14}, 515 mg, 1.2 mmol) in pyridine-ether (6:1, 60 m*l*) was slowly added over a period of 6 hr to a vigorously stirred refluxing solution of cupric acetate monohydrate (2 g) in pyridine-ether (6:1, 210 m*l*) employing a high dilution apparatus. The change of color of the reaction mixture from blue to greenish brown was observed. After the addition had been completed, the mixture was stirred for 30 min under reflux. The solvent was removed under reduced pressure and the residue was dissolved in ether. The ether layer was successively washed with dilute hydrochloric acid, dilute sodium hydroxide, and a saturated sodium chloride solution, and dried. The reddish brown solid obtained by evaporation of the solvent was subjected to a chromatography on alumina (20 g). Recrystallization of the yellow crystals obtained from the fractions eluted with benzene furnished the cyclic diacetylene, (187 mg, 37%). The reaction conditions, yields and the melting points are given in Table 1, the analytical data and molecular weights are summarized in Table 7.

Table 7. Elemental analysis and molecular weight of VI_n

VI_n	Elemental analysis (%)[a]	C	H	MW
18	Found	84.09	9.17	503[b]
	Calcd	84.25	9.15	485
15	Found	84.31	8.69	484[b]
	Calcd	84.12	8.65	443
14	Found	83.78	8.47	409
	Calcd	84.07	8.47	429
13	Found	83.90	8.29	411
	Calcd	84.01	8.27	415

a) Recrytallized from benzene –*n*-hexane.
b) Measured by the Rast method.

The crystals of VI_n are colorless needles and development of brown color was observed at the temperature around its melting point.

Another Preparation of 1,14-bis(p-*ethynylphenoxy*)*tetradecane* (V_{14}). p-*Hydroxyphenylacetylene.* A mixture of *p*-hydroxyacetophenone (5.0 g, 37 mmol), phosphorus pentachloride (8.5 g, 42 mmol) and benzene (7.5 m*l*) was stirred at 45°C for 10 min and then at 60°C for 20 min. Anhydrous ether (150 m*l*) was added to the reaction mixture. The ethereal solution was added over a period of 20 min to a solution of sodamide [from sodium 5.5 g, 0.24 g atom] in liquid ammonia (250 m*l*).[8] After stirring for 3.5 hr, ammonium chloride (17 g) was added to the reaction mixture, and the ammonia was allowed to evaporate. The residue was mixed with water and extracted with ether. The extract was washed with a saturated aqueous solution of sodium chloride and dried. The reddish brown extract was passed through a short column of alumina (20 g). The yield of *p*-hydroxyphenylacetylene was estimated to be *ca.* 1.5 g (35%), since an

8) I. L. Kotlyarevskii and M. I. Bardamova, *Izv. Akad. Nauk SSSR, Ser. Khim.*, **1964**, 2073.

aliquot (6 ml) of pale yellow filtrate (250 ml) gave 35 mg of a liquid which changed immediately to violet materials. Owing to the instability of *p*-hydroxyphenylacetylene, the ethereal solution was used for the subsequent reaction without isolation of acetylene.

Alkylation of p-*hydroxyphenylacetylene with 1,14-dibromotetradecane.* The aforementioned ethereal solution was evaporated *in vacuo* under the addition of anhydrous ethanol. The resulting ethanol solution of *p*-hydroxyphenylacetylene was mixed with 1,14-dibromotetradecane (1.20 g, 3.4 mmol). The mixture was refluxed, and to it was added over a period of 25 min, with stirring, 1N solution of potassium hydroxide in anhydrous ethanol (8.0 ml). After refluxing for further 2 hr, water was added to the reaction mixture and extraction was carried out with ether. The extract was successively washed with dilute sodium hydroxide and a saturated sodium chloride solution and dried. The deep brown solid (1.77 g) obtained by evaporation of the solvent was chromatographed on alumina (50 g). The fractions eluted with petroleum benzine gave 1,14-dibromotetradecane (283 mg, 24%). The substance (148 mg) obtained from petroleum benzine-benzene (1:4—1:1) fractions gave positive Beilstein's test. The substance was recrystallized from *n*-hexane to yield colorless prisms, mp 78.5—79.5°C. The structure of *p*-*ω*-bromotetradecanoxyphenylacetylene was assigned to this substance on the basis of IR spectroscopy and analytical data. Found: C, 67.22; H, 8.50; Br, 20.14%. Calcd for $C_{22}H_{33}OBr$: C, 67.16; H, 8.45; Br, 20.32%.

The fractions eluted with benzene afforded 40 mg (3%) of V_{14}. This was recrystallized from *n*-hexane to give pure V_{14}, mp 93.0—94.2°C, colorless leaflets.

*α,ω-Bis(*p-*acetylphenoxy)alkanes.* The reaction of 1,14-dibromotetradecane with *p*-hydroxyacetophenone according to the procedure for the preparation of α,ω-bis[*p*-(2-methoxycarbonylvinyl)phenoxy]alkanes (III_n) gave bis(*p*-acetylphenoxy)tetradecane in a yield of 57%, colorless prisms, mp 112.0—113.2°C (from benzene-ethanol). Found: C, 77.43; H, 9.18%. Calcd for $C_{30}H_{42}O_4$: C, 77.21; H, 9.07%.

Similarly, the reaction of *p*-hydroxyacetophenone with 1,18-dibromooctadecane gave bis(*p*-acetylphenoxy)octadecane in a yield of 1.3% colorless leaflets, mp 115.4—117.0°C (from benzene-ethanol). Found: C, 78.19; H, 9.76%. Calcd for $C_{34}H_{50}O_4$: C, 78.12; H, 9.64%.

Hydrogenation of V_{15} and V_{18}. The cyclic diacetylene, V_{15} (127 mg) in benzene was hydrogenated over palladium-carbon. A theoretical amount of hydrogen was absorbed over a 70 min period. The reduction product was chromatographed on alumina (5 g). The fractions eluted with *n*-hexane-benzene (4:1) gave 95 mg (75%) of colorless prisms, mp 59.8—60.3°C. Found: C, 82.89; H, 10.31%. Calcd for $C_{31}H_{46}O_2$: C, 82.61; H, 10.29%.

The hydrogenation of V_{18} gave colorless prisms, mp 102.3—102.7°C (from benzene-methanol). Found: C, 82.50; H, 10.62%. Calcd for $C_{34}H_{52}O_2$: C 82.87; H 10.64%.

BULLETIN OF THE CHEMICAL SOCIETY OF JAPAN, VOL. 44, 1914—1916 (1971)

Cyclic Acetylenes. XIV. The Effects of Ring Strain on the Electronic Spectra of Cyclic Tolans and Cyclic Diphenyldiacetylenes

Fumio TODA, Takashi ANDO, Mutsuo KATAOKA, and Masazumi NAKAGAWA

Department of Chemistry, Faculty of Science, Osaka University, Toyonaka, Osaka

(Received December 23, 1970)

Characteristic features of the electronic spectra of *o,o'*-bridged cyclic diphenyldiacetylenes (I_n), *o,p'*-bridged cyclic tolans (II_n), *p,p'*-bridged cyclic diphenyldiacetylenes (III_n) and *p,p'*-bridged cyclic tolans (IV_n) are compared. The hyperchromism observed in the longest-wavelength absorption maxima (λ_{max}) in the higher homologues of I_n, III_n, and IV_n as compared with the absorption intensities of the respective open-chain analogues is explained in terms of the coplanarity of the chromophore system, and the marked hypochromism observed in the lower homologues of these cyclic acetylenes is attributed to ring strain. The hypochromism observed in the series of II_n is ascribed to the superposition of the effects of ring strain and the twisting of phenyl groups. The bathochromic shifts of λ_{max} with the increase of ring strain in the *p,p'*-bridged series (III_n and IV_n) are explained by the pronounced increase of the energy of the ground state of the strained molecule of this series. On the other hand, the hypsochromic shifts of λ_{max} of *o,o'*-bridged series (I_n) are regarded as the result of the minor increase of energy of the ground state along with the increase of the ring strain.

In previous papers we reported the syntheses and properties of *o,o'*-bridged cyclic diphenyldiacetylenes (I_n),[1] *o,p'*-bridged cyclic tolans (II_n),[2] *p,p'*-bridged diphenyldiacetylenes (III_n)[3] and *p,p'*-bridged cyclic tolans (IV_n).[4] In the present paper, we wish to summarize the characteristic features of the electronic

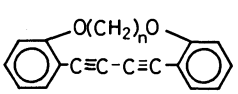

(I_n) n=3, 4, 5, 6

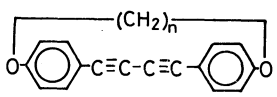

(III_n) n=13, 14, 15, 18

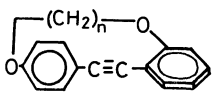

(II_n) n=7, 8, 9, 10, 11, 12

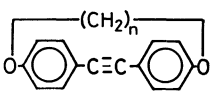

(IV_n) n=11, 12, 13, 14, 18

1) F. Toda and M. Nakagawa, This Bulletin, **34**, 862 (1961).
2) M. Kataoka, T. Ando, and M. Nakagawa, *ibid.*, **44**, 177 (1971).
3) M. Kataoka, T. Ando, and M. Nakagawa, *ibid.*, **44**, 1909 (1971).
4) T. Ando and M. Nakagawa, *ibid.*, **44**, 172 (1971).

spectra of these four series of cyclic acetylenes.

The locations of the longest-wavelength absorption maxima (λ_{max}) and their absorption intensities (ε) of I_n, III_n, and IV_n along with those of the open-chain reference substances are summarized in Tables 1, 3, and 4. A rough molecular geometry which is revealed by an examination of the molecular models of these compounds is also shown in the Tables. Since the longest-wavelength absorption maxima of *o,p'*-bridged cyclic tolans (II_n) disappear as the ring size decreases, the wavelength of the absorption peaks at *ca.* 300 nm along with the ε-values and the molecular geometry are recorded in Table 2.

Table 1. Molecular geometry and electronic spectral data of *o, o'*-bridged diphenyldiacetylenes (I_n)

n	Molecular geometry	λ_{max}	$\varepsilon \times 10^{-2}$
3	highly strained, rigid, planar	337 nm	159
4	strained, rigid, planar,	353	199
5	rigid, planar, strain free	353	365
6	slightly flexible, strain free	349	336
o, o'-Dimethoxy-diphenyl-diacetylene		349	286

Table 2. Molecular geometry and electronic spectral data of *o, p'*-bridged tolans (II_n)

n	Molecular geometry	λ_{max}	$\varepsilon \times 10^{-2}$
7	highly strained, rigid, twisted	302[a] nm	122
8	strained, rigid, twisted	301	120
9	strain free, slightly twisted	302	141
10	strain free,	302	151
11	strain free, slightly flexible	304	189
12	strain free, slightly flexible	305	208
o, p'-Dimethoxytolan		302.5	226

a) indicates the shoulder.

Table 3. Molecular geometry and electronic spectral data of *p, p'*-bridged diphenyldiacetylenes (III_n)

n	Molecular geometry	λ_{max}	$\varepsilon \times 10^{-2}$
13	highly strained, rigid, non-planar	345.5 nm	367
14	strained, rigid, non-planar	344	425
15	strain free, rigid, planar	343.5	514
18	strain free, planar	342.5	465
p, p'-Di-*n*-butoxy-diphenyl-diacetylene		340.5	407

Table 4. Molecular geometry and electronic spectral data of *p, p'*-bridged tolans (IV_n)

n	Molecular geometry	λ_{max}	$\varepsilon \times 10^{-2}$
11	highly strained, rigid, non-planar	318 nm	334
12	highly strained, rigid,	317	369
13	strain free, rigid, planar	317	443
14	strain free, rigid, planar	316	426
18	strain free, flexible	315	355
p, p'-Di-*n*-butoxytolan		313	319

The change of absorption intensities with that of the chain length is illustrated in Figs. 1 and 2. The hyperchromism of λ_{max} observed in the higher homologues of I_n, III_n, and IV_n as compared with the ε-values of the respective open-chain analogues can be reasonably ascribed to the enhanced coplanarity of the two phenyl groups as a result of the ring formation. The fact that the maximum ε-values are attained in I_5, III_{15}, and IV_{13} is consistent with the above-mentioned argument, because as indicated in Tables 1, 3, and 4, the molecular models indicate that these molecules are strain free and keep rigid and planar structures due to the presence of bridging chain of adequate length. However, the absorption intensities rapidly decrease with the decrease of chain length. The marked hypochromism of λ_{max} in the lower homologues of I_n, III_n, and IV_n should, therefore, be attributed to the increase of the ring strain.

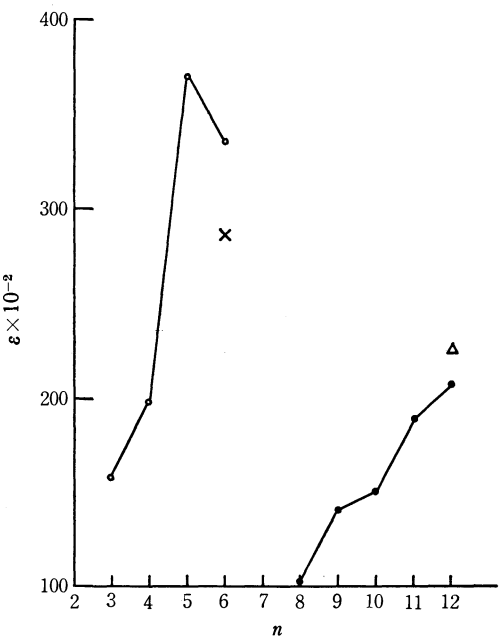

Fig. 1. The ε-values of *o,o'*-bridged diphenyldiacetylenes (I_n, ○——○), *o, p'*-bridged tolans (II_n, ●——●) and the the open-chain analogs (× = *o,o'*-dimethoxydiphenyldiacetylene; △ = *o,p'*-dimethoxytolan).

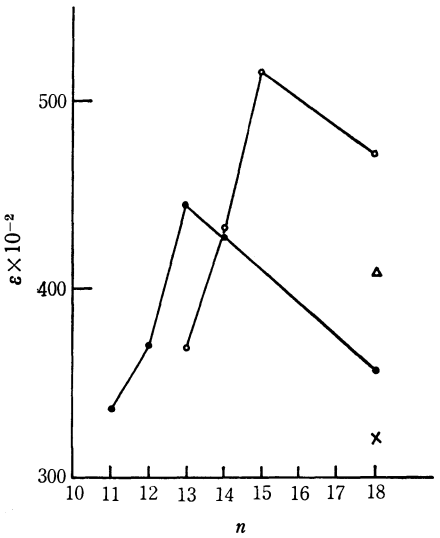

Fig. 2. The ε-values of *p,p'*-bridged diphenyldiacetylenes (III_n, ○——○), *p,p'*-bridged tolans (IV_n, ●——●) and the open-chain analogs (△ = *p,p'*-di-*n*-butoxydiphenyldiacetylene; × = *p,p'*-di-*n*-butoxytolan).

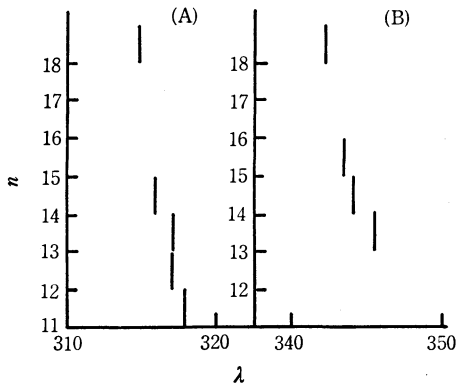

Fig. 3. The bathochromic shifts of the λ_{max} in the *p,p'*-bridged series. (A)=*p,p'*-bridged tolans (IV_n); (B)=*p,p'*-bridged diphenyldiacetylenes (III_n).

In the case of *o,p'*-bridged cyclic tolans (II_n), the decrease of chain length should increase the twisting of the two phenyl groups, *e.g.*, the molecular model of II_7 shows that the interplanar angle of the two phenyl groups should be almost rectangular. Therefore, the hypochromism observed in II_n should be regarded as the superposition of the effect of ring strain and the effect of twisting of the two phenyl groups.

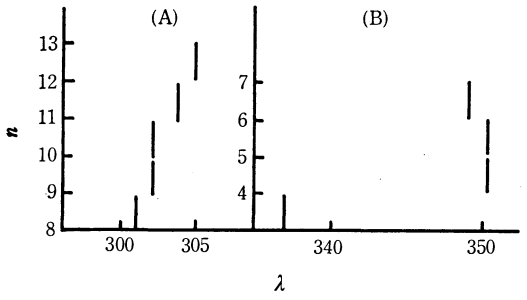

Fig. 4. The hypsochromic shifts of the λ_{max} in the *o,p'*- and *o,o'*-bridged series. (A)=*o,p'*-bridged tolans (II_n); (B)=*o,o'*-bridged diphenyldiacetylenes (I_n).

With regard to the effect of ring strain on the location of λ_{max}, the above-mentioned four series of cyclic acetylenes (I_n, II_n, III_n, and IV_n) exhibit striking contrast. As illustrated in Fig. 3, the increase of ring strain resulted in the bathochromic shifts of the λ_{max} of *p,p'*-bridged tolans (IV_n) and *p,p'*-bridged diphenyldiacetylenes (IV_n). On the contrary, as is shown in Fig. 4, the decrease of the ring size exerts hypsochromic effects on the λ_{max} of *o,o'*-bridged diphenyldiacetylenes

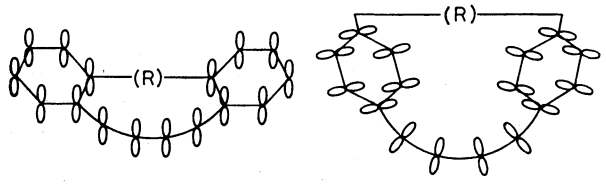

Strained *o,o'*-bridged series Strained *p,p'*-bridged series

Fig. 5. A schematic illustration of the *p*-orbitals of the strained *o,o'*- and the strained *p,p'*-bridged diphenyldiacetylenes.

(I_n) and that of *o,p'*-bridged tolans (II_n). The hypsochromism observed in the latter compounds (II_n) can not be ascribed only to the increase of ring strain, because the afore-mentioned twisting of the phenyl groups should also result in the increase of the transition energy of the long-wavelength bands of II_n. However, the difference in spectral behavior between the *o,o'*-series (I_n) and the *p,p'*-series (III_n and IV_n) seems to reflect the difference of the mode of ring strain in these two series of cyclic acetylenes.

The strained molecules of I_n are held in planar conformation regardless of the magnitude of the ring strain as illustrated in Fig. 5. The diacetylenic linkage in I_3 seems to be forced to bend due to the short bridging chain. However, the two phenyl nuclei should be held still in a coplanar position. Therefore, the *p*-orbitals which contribute to the conjugation of the entire chromophore system are also held in a parallel position independent of the magnitude of the ring strain.

In the *p,p'*-series (III_n and IV_n), as illustrated in Fig. 4, the two benzene nuclei should deviate from the coplanar position according to the increase of ring strain. Consequently, the *p*-orbitals which contribute to the conjugation of the entire chromophore should deviate from the parallel position in the strained members of III_n and IV_n.

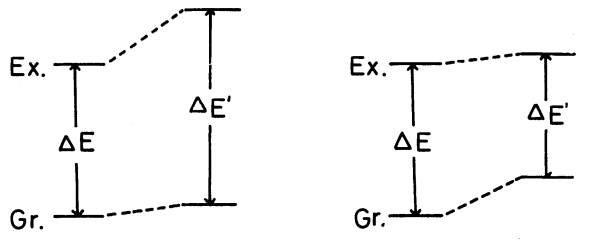

Fig. 6. The transition energies of the *o,o'*-bridged and the *p,p'*-bridged cyclic acetylenes.

Thus, it seems pertinent to assume that the increase of energy of the ground state of the strained molecule of *o,o'*-series (I_n) is smaller than that of the *p,p'*-series (III_n and IV_n), whereas, the increase of energy of its excited state is larger than or almost the same as that of *p,p'*-series (III_n and IV_n). This is illustrated schematically in Fig. 6. Thus, the transition energy $\Delta E'$ of the strained *o,o'*-bridged molecule (I_n) becomes larger than that of the strain free molecule ΔE. Consequently, in the case of *o,o'*-bridged series (I_n), the increase of ring strain produces a hypsochromic shift. Inversely, the transition energy $\Delta E'$ of the strained *p,p'*-bridged molecule (III_n and IV_n) becomes smaller than that of the strain free molecule ΔE, *i.e.*, the increase of ring strain in the series of *p,p'*-bridged cyclic acetylenes (III_n and IV_n) results in a bathochromic shift.

The Catalytic Dehydrogenation, Dehydroxylation, and Dehydroxymethylation of Benzyl Alcohol. III. The Effect of Metal Chlorides as Additives

Masayoshi ISHIGE,* Koji SAKAI, Masatoshi KAWAI, and Kazuo HATA

Department of Chemistry, Faculty of Science, Tokyo Metropolitan University, Setagaya-ku, Tokyo

(Received December 28, 1970)

This paper will describe the reaction of benzyl alcohol in the presence of various kinds of modified stabilized nickel catalysts, which had been prepared from the mother catalyst by treating it with solutions of appropriate metal chlorides. The catalytic activities of each modified catalyst for the formation of benzene, toluene, and benzaldehyde were compared in terms of the f_H, f_{CH_3}, and f_{CHO} values; the selectivities for the formation of benzene and toluene against that of benzaldehyde, S_H and S_{CH_3}, were also evaluated. In general, the formation of toluene and benzene was greatly affected both by the kind and by the amount of metal chlorides used as additives. The reaction was promoted by the addition of a proper quantity of alkali metal chloride. In the cases of the reactions by lowly-modified catalysts, the decreasing order of the f_H and f_{CH_3} values according to the kind of metal ion adsorbed on the catalyst was as follows: $Na^+ \geqq K^+ > Co^{2+} > Ca^{2+} > Cd^{2+} > Ba^{2+} > Hg^{2+} > Cu^{2+}$. On the other hand, in the higher degrees of modification, the corresponding order of the f_H and f_{CH_3} values was altered to be as follows: $K^+ > Na^+ > Co^{2+} > Cd^{2+} > Ba^{2+} \geqq Ca^{2+} > Cu^{2+} > Hg^{2+}$. With regard to the modified nickel catalysts treated with 0.08 N solutions, it was found that the sequence of the f_H and f_{CH_3} values due to the kind of metal ion was roughly correlated with that of the atomic numbers of the corresponding metals. The results are discussed in connection with the general concept of catalytic chemistry.

Preceding papers[1,2] have described the catalytic reactions of benzyl alcohol in the presence of various nickel catalysts and of modified stabilized nickel catalysts treated with solutions of sodium compounds. The reaction products mainly consisted of benzaldehyde, toluene, and benzene, sometimes accompanied by the formation of small quantities of certain hydrocarbons and carbon dioxide. The composition of the product was found to be variable under the influence of the chemical nature of the catalysts employed. Numerous papers on the hydrogenation of benzyl alcohol over various metal catalysts[3] have described the formation of toluene as a hydrogenolysis product of the alcohol. The palladium and nickel catalysts were proved to be especially preferable for the hydrogenolysis of benzyl alcohol to toluene. On the other hand, it has been shown that benzyl alcohol is converted to benzaldehyde, toluene, and benzene in the redox reaction of unsaturated organic compounds, with benzyl alcohol as the hydrogen donor and in the presence of nickel catalysts.[4]

In general, the behavior of benzyl alcohol adsorbed on the catalyst surface is so complex that this catalysis cannot be simply comprehended. Garbisch *et al.*[5] have discussed the mechanism of the hydrogenolysis of benzyl alcohols. Mitsui *et al.*[6] have reported that the hydrogenolysis of optically-active benzyl-type alcohols proceeds either with the retention or the inversion of the configuration through sterically-different adsorbed transition states of substrates, depending upon the kind of catalyst metal. On the other hand, Khan *et al.*[7] have offered another proposal regarding the configurational behavior in the catalytic hydrogenolysis of benzyl alcohols.

However, relation between the behavior of benzyl alcohol and the surface nature of the catalysts has not yet been explored clearly. In order to get further information on the operative factor of the catalytic reactions of benzyl alcohol, the present investigation was carried out into the reaction of benzyl alcohol catalyzed by modified nickel catalysts, which had been prepared by the treatment of the surface of a nickel catalyst with solutions of various metal chlorides.

Results

In all the experiments, we employed a stabilized nickel catalyst (hereafter abbreviated as S–Ni)(S 10),[8] from which various kinds of modified nickel catalysts were prepared by treating it with solutions of proper metal chlorides. By a procedure similar to that described in the preceding paper, the degree of modification for each modified S–Ni was controlled by using metal chloride solutions of varying concentrations.

When a given amount of the S–Ni catalyst was treated with aqueous NaCl, KCl, and $CaCl_2$ solu-

* Present address: Chemical Laboratory, Ochanomizu University, Otsuka, Bunkyo-ku, Tokyo.

1) Part II: M. Ishige, K. Sakai, M. Kawai, and K. Hata, This Bulletin, **44**, 1095 (1971).

2) M. Ishige, K. Sakai, M. Kawai, and K. Hata, *ibid.*, **43**, 2186 (1970).

3) H. Adkins and L. W. Covert, *J. Phys. Chem.*, **35**, 1684 (1931); N. S. Tikhomirova-Sidrova, *Zh. Obshch. Khim.*, **25**, 1504 (1955), *Chem. Abstr.*, **50**, 4825h (1956); J. H. Stocker, *J. Org. Chem.*, **27**, 2288 (1962); S. Nishimura and K. Mori, This Bulletin, **32**, 103 (1959); S. Nishimura, *ibid.*, **32**, 1158 (1959); **34**, 32 (1961); S. Nishimura and M. Hama, *ibid.*, **39**, 2467 (1966).

4) K. Sakai, T. Ito, and K. Watanabe, This Bulletin, **39**, 2230 (1966).

5) E. W. Garbisch, Jr., L. Schreader, J. J. Frankel, *J. Amer. Chem. Soc.*, **86**, 4233 (1967).

6) S. Mitsui, S. Imaizumi, and Y. Esashi, This Bulletin, **43**, 2143 (1970), and the references cited therein.

7) I. Jardine and F. J. McQuillin, *J. Chem. Soc., C*, **1966**, 458; D. A. Denton, F. J. McQuillin, and P. L. Simpson, *ibid.*, **1964**, 5535; A. M. Khan, F. J. McQuillin, and I. Jardine, *ibid., C*, **1967**, 136; *Tetrahedron Lett.*, **1966**, 2649.

8) *Cf.* a footnote of the preceding paper[1]; T. Yamanaka, *Kagaku Gijutsu*, **2**, 57 (1958).

tions of given concentrations, the amount of metal chlorides adsorbed on the catalyst surface was measured by the titration of the residual solution with a standard solution of silver nitrate. The amount of adsorbate determined in a 0.16N solution was found to be 0.15 meq per 1 g of the catalyst; this value was independent of the kind of metal chloride within about a 4% error: a linear relation between the amount of adsorbate and the initial concentrations of the metal chloride solutions was also observed.

The modified-nickel-catalyzed reaction of benzyl alcohol was practiced in a sealed tube by heating it at 162°C for 24 hr, then, the composition of the reaction mixture was evaluated by gas chromatography. It was previously found by kinetic observation[2] that the reaction proceeds as a first-order one, with the diminution of benzyl alcohol during the initial period of the reaction, but becomes complicated when more than 30% of benzyl alcohol is transformed. Thus, in order to avoid the difficulty of the kinetic analysis, the calculation of the rate was generally based upon the time required within the period before 30% of the alcohol reacted.

The f_H, f_{CH_3}, and f_{CHO} values, which had previously been defined as representing the catalytic activity for the formation of benzene, toluene, and benzaldehyde respectively, were calculated both from the observed rate constant of the alcohol, k_{alc}, and from the composition of the reaction products. The S_H and S_{CH_3} values, which indicate the selectivity factors for the formation of benzene and toluene with regard to that of benzaldehyde, were also estimated much as in the preceding report. The results obtained are summarized in Table 1. The plots of the f and S values *vs.* the degrees of the modification[9] for each modified S–Ni are also given in Figs. 1 and 2 respectively.

Table 1. Catalytic reactions of alcohol in sealed tubes in the presence of various modified S–Ni

Additive		Benzyl alcohol eacted (%)	Composition of products (mol %)			Rate constant $k_{alc}\times10^2$ (hr^{-1})	Activity			Selectivity	
Compound	Conc. of solution (N)		PhH	$PhCH_3$	PhCHO		f_H	f_{CH_3}	f_{CHO}	S_H	S_{CH_3}
None		30.9	39.8	37.9	22.3	1.44	57.3	54.6	32.1	25.2	23.1
NaCl	0.02	31.5	42.2	29.8	28.0	1.57	66.2	46.8	44.0	19.4	2.8
	0.04	28.9	38.7	31.0	30.3	1.42	55.0	44.1	43.0	10.6	1.0
	0.08	26.4	42.3	27.4	30.3	1.28	54.2	35.1	38.8	14.5	−4.3
	0.16	25.0	44.2	25.7	30.1	1.20	53.0	30.8	36.1	16.6	−6.8
KCl	0.02	30.9	42.9	35.8	21.3	1.44	61.8	51.6	30.7	30.6	22.6
	0.04	24.4	40.2	46.3	13.5	1.16	46.6	53.7	15.7	47.3	53.4
	0.08	26.0	39.2	40.8	20.0	1.25	49.0	51.0	25.0	29.3	31.0
	0.16	26.7	43.1	37.8	19.1	1.29	55.6	48.8	24.6	25.8	29.7
$CaCl_2$	0.02	21.8	22.6	46.6	30.8	1.02	23.1	47.5	31.4	−19.7	11.8
	0.04	22.0	21.9	43.4	34.7	1.04	22.8	45.1	36.1	−19.9	9.7
	0.08	24.5	19.6	42.0	38.4	1.08	21.2	45.4	41.5	−29.1	4.2
	0.16	21.6	17.6	44.0	38.4	1.01	17.8	44.4	38.8	−33.8	5.7
$BaCl_2$	0.02	21.5	22.3	43.3	34.4	1.01	22.5	43.7	34.8	−0.2	0.1
	0.04	20.5	22.4	44.9	32.7	0.96	21.5	43.1	31.4	−0.2	0.1
	0.08	20.7	19.8	46.4	33.8	0.97	19.2	45.0	32.8	−0.2	0.1
	0.16	21.8	18.8	44.5	36.7	1.03	19.4	45.8	37.8	−0.3	0.1
$CoCl_2$	0.02	24.7	28.2	41.9	29.9	1.17	33.0	49.0	35.0	−2.4	18.8
	0.04	26.4	29.1	44.0	26.9	1.28	37.2	56.3	34.4	3.4	21.5
	0.08	25.8	27.9	45.0	27.1	1.24	34.6	55.8	33.6	1.3	22.0
	0.16	28.9	31.0	35.1	33.9	1.42	44.0	49.8	48.1	−3.8	14.6
$CuCl_2$	0.02	18.6	18.9	43.5	37.6	0.85	16.1	37.0	32.0	−30.0	6.5
	0.04	20.8	22.7	41.3	36.0	0.97	22.0	40.1	34.9	−20.3	6.1
	0.08	19.4	19.1	41.7	39.2	0.89	18.0	39.2	36.9	−31.2	2.6
	0.16	18.5	23.2	38.4	38.4	0.85	19.6	32.4	32.4	−21.7	0.0
$CdCl_2$	0.02	22.2	25.3	45.0	29.7	1.04	26.3	46.8	30.9	−7.0	17.9
	0.04	20.1	24.5	44.2	31.3	0.93	22.8	41.1	29.1	−10.8	15.0
	0.08	16.8	14.8	46.0	39.2	0.76	11.2	34.9	29.8	−42.6	6.8
	0.16	23.5	24.2	46.5	29.3	1.11	26.9	51.6	32.5	−8.3	19.9
$HgCl_2$	0.02	20.3	21.6	43.9	34.5	0.94	20.3	41.3	32.4	−10.7	14.4
	0.04	22.4	25.5	43.3	31.2	1.06	27.1	45.9	33.1	−8.8	14.4
	0.08	15.5	11.9	14.5	74.0	0.69	8.0	10.0	51.1	−80.6	−71.0
	0.16	14.4	21.6	40.2	38.2	0.64	14.9	25.9	24.6	−24.8	2.2

9) The degrees of the modification are tentatively represented by the initial concentrations of the solution used on treatment.

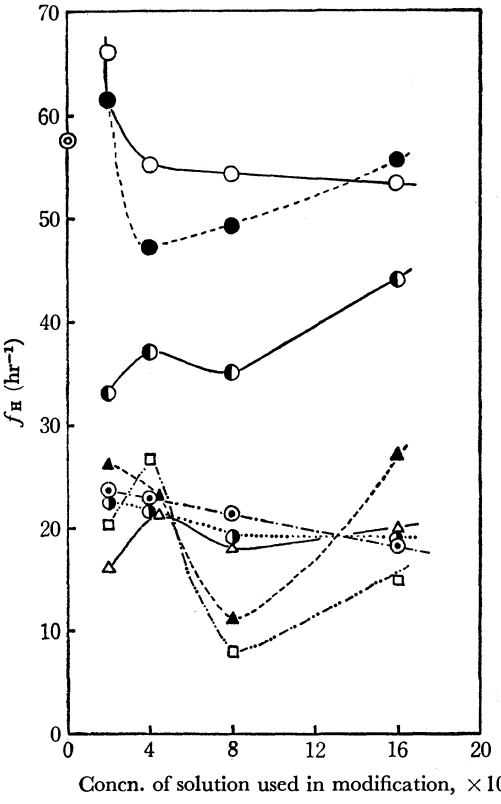

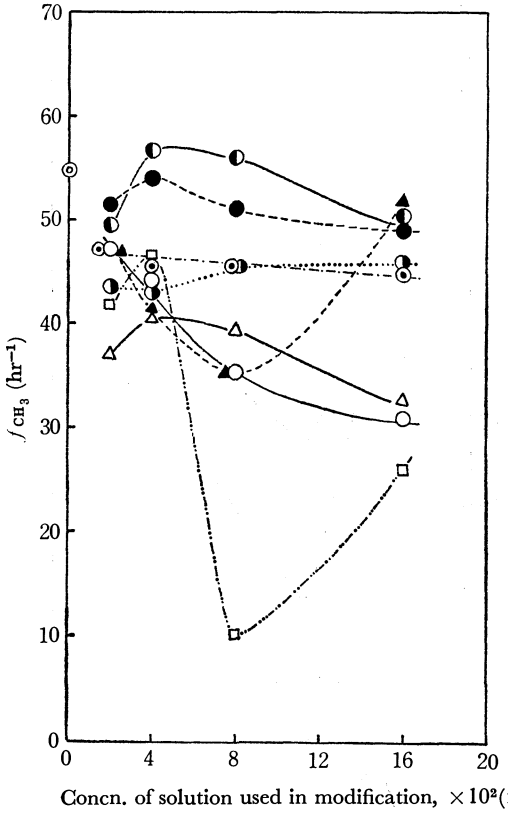

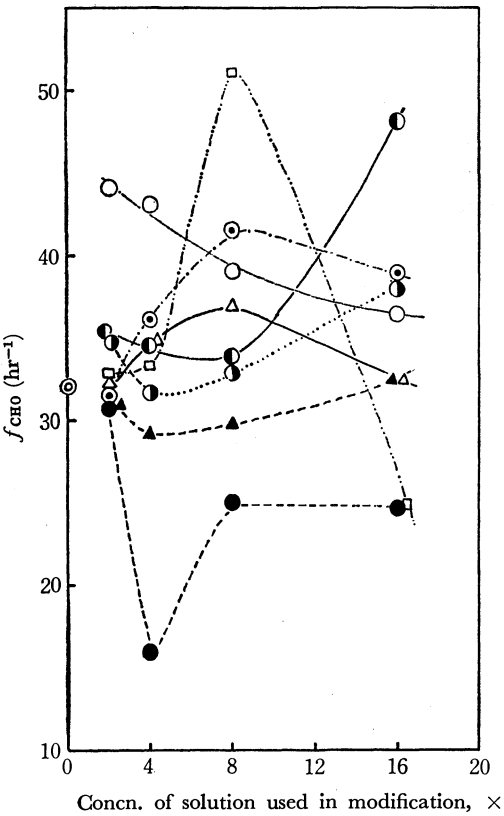

Fig. 1. The activities of modified catalysts for the formation of benzene, toluene, and benzaldehyde.
○ NaCl, ● KCl, ⊙ $CaCl_2$, ◑ $BaCl_2$, ◐ $CoCl_2$, △ $CuCl_2$, ▲ $CdCl_2$, □ $HgCl_2$, ◎ Control (unmodified S–Ni catalyst)

As may be seen in Fig. 1, the effects of metal chlorides as additives appear somewhat complicated; yet we can find some features of the additives in the catalysis: (1) A proper amount of alkali metal chloride acts as a promotor. (2) Alkaline earth metal chlorides are less influential than alkali metal chloride on the f value change with the increase in the amounts of the metals adsorbed on the catalyst. (3) The formation of toluene and benzene is largely influenced by both the kind and the amount of the adsorbate. (4) A remarkable change in the f values is observed when a varied amount of mercury(II) chloride is used as the additive.

On the basis of the f values for various modified S–Ni, it is noticeable that the effect of the additives is in a remarkably different order on lowly modified catalysts from that on more highly modified ones. In the reations with lowly modified catalysts, the f_H and f_{CH_3} values decrease generally according to the kind of metal cation used as additives in the following order: $Na^+ \geqq K^+ > Co^{2+} > Ca^{2+} > Cd^{2+} > Ba^{2+} > Hg^{2+} > Cu^{2+}$. This order is somewhat like the decreasing order of the heat of hydration of a metal complex.[10]

On the other hand, when modified catalysts with the same metal chlorides but in higher degrees were used, the f_H and f_{CH_3} values were observed to decrease in the following order on the average: $K^+ > Na^+ > Co^{2+} > Cd^{2+} > Ba^{2+} \geqq Ca^{2+} > Cu^{2+} > Hg^{2+}$. The correlation between the f values and the normal electrode potentials of corresponding metals was examined;

10) F. Basolo and R. G. Pearson, "Mechanisms of Inorganic Reactions," 2nd Ed. John Wiley & Sons, Inc. N. Y. (1967), p. 81; $-\Delta H$, (kcal): $K^+(79) > Na^+(100) > Ba^{2+}(316) > Ca^{2+}(382) > Cd^{2+}(437) > Hg^{2+}(441) > Co^{2+}(497) > Cu^{2+} \approx Ni^{2+}(507)$.

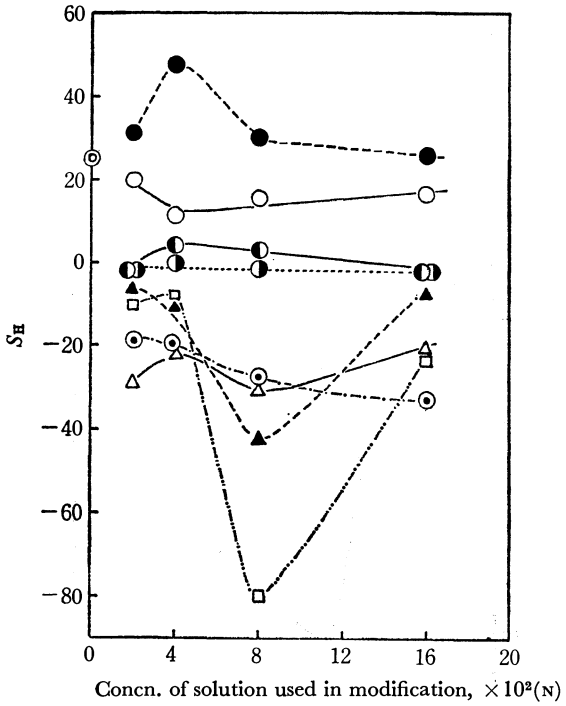

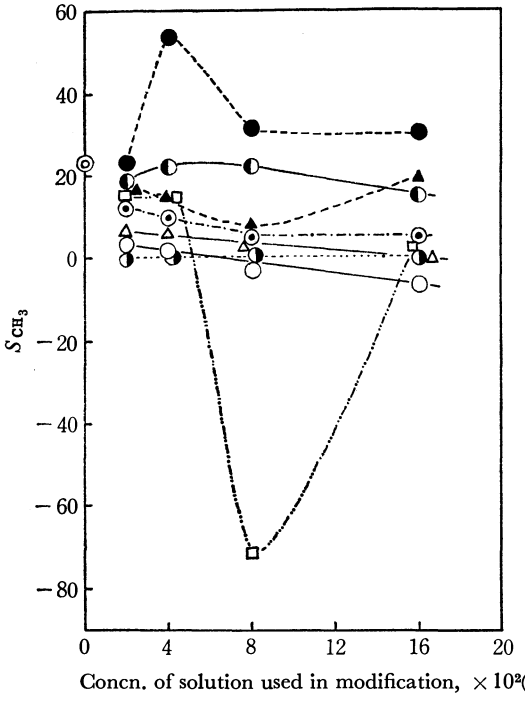

Fig. 2. The selectivities of modified catalysts for the formation of benzene and toluene against that of benzaldehyde. (The notations are the same as in Fig. 1).

the results are shown in Fig. 3. As may be seen in Fig. 3, the formation of benzene is assumed to be approximately correlated with the potential change in the catalyst surface caused by the addition of metal chlorides to the catalyst. However, it was found that the cobalt ion promotes the formation of benzene exceptionally, more than would be predicted from its electrode potential, whereas calcium and barium ions have the opposite effect on the reaction. The relation of the formation of toluene and benzaldehyde is not

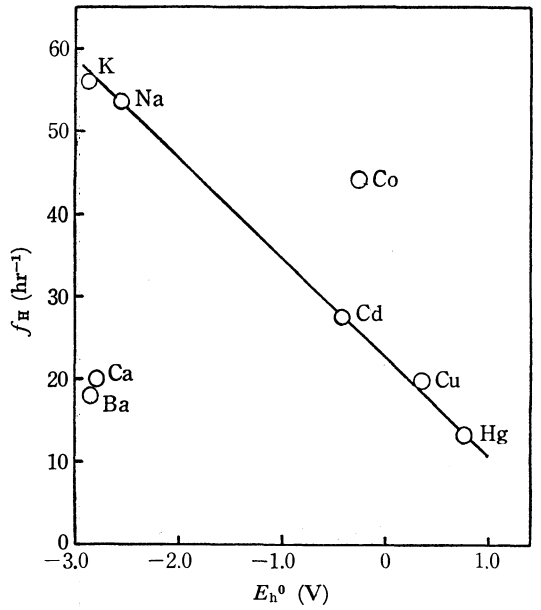

Fig. 3(a). The plots of f_H in the higher modification degree *vs.* the electrode potential of metal ($M^0 \rightleftarrows M^{n+} + ne^-$, 25°C).

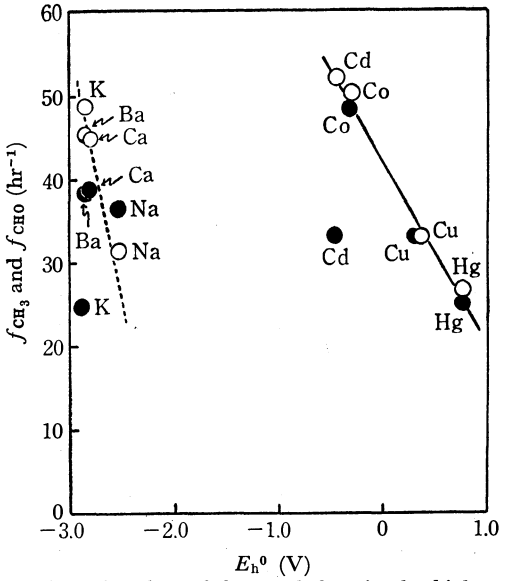

Fig. 3(b). The plots of f_{CH_3} and f_{CHO} in the higher modification degree *vs.* the electrode potential of metal ($M^0 \rightleftarrows M^{n+} + ne^-$, 25°C).
○ toluene, ● benzaldehyde

so clearly correlated with the electrode potential of metal as it is in the case of benzene. We can readily recognize that the relations between the f value and the electrode potential of the metal used as the additive may be roughly divided into two groups: the lower-electrode-potential group and the higher-electrode-potential group. The alkali and alkaline earth metals belong to the former group, whereas the transition metals belong to the latter one. Within each group, there is a tendency for the f values to vary in correlation with the electrode potential of the metals adsorbed on the catalyst.

With regard to the modified nickel catalysts treated with a 0.08N solution of each metal chloride, it is found that the decreasing sequence of the f_H and f_{CH_3}

values due to the kind of metal chloride is roughly associated with that of the atomic number of the corresponding metals. This finding leads to a consideration that the promoting and poisoning effects by metal chlorides may partially result from the polarizability of the metals as additives.

It is interesting that the general order of the decrease in the f_{CHO} values observed in the presence of the modified catalysts treated with 0.08N solutions of metal chlorides is roughly reversed for the formation of benzene and toluene (f_H and f_{CH_3} values). This observation implies that highly polarizable metal ions adsorbed on the catalyst are preferable to the dehydrogenation of benzyl alcohol.

The tendency of the changes is S_H and S_{CH_3} values brought about by the addition of metal chlorides is generally similar to that of the changes in f_H and f_{CH_3} values respectively. The general features of the change in selectivity caused by the adsorption of metal chlorides may be summarized as follows: (1) KCl can characteristically serve to increase the selectivity for the formation of benzene and toluene. (2) The S-value changes due to NaCl, $CaCl_2$, $BaCl_2$, and $CoCl_2$ are almost independent of their amounts. (3) A considerably large variation in S value is observed as a result of the addition of the mercury(II) ion.

Discussion

It is assumed that the change in selectivity for the formation of toluene and benzene in the presence of each modified S–Ni may come from the change in the catalytic activity for the formation of the corresponding products. Thus, with the purpose of examining the correlation between f and S values for the formation of toluene and benzene, log f was plotted against the S values. The results are shown in Fig. 4. In the case of the formation of benzene, the plots are distributed on nearly a straight line. For the production of toluene, the relation is not so clear as in the case for benzene, thought a faint linear relation is also observed.

A large amount of experimental evidence has already revealed the non-uniformity of the surface of the nickel catalyst.[11] A properly-devised poisoning experiment can often provide information on the possible presence of areas or centers on the catalyst surface possessing different degrees of catalytic activity. This consideration can be demonstrated when a suitable catalyst poison is selectively adsorbed first on the sites of greater activity and then upon less active sites. However, the reaction of benzyl alcohol catalyzed by modified S–Ni catalysts treated with metal chlorides cannot be explained simply by such a poisoning effect of the metal chlorides, because there is a promoting effect on the reaction from a proper kind and amount of metal chlorides,[12] and also because a regular variation in the catalytic activity is brought about on the modified S–Ni, depending on the property of the added metal cation. It is reasonable to conclude that the electrode

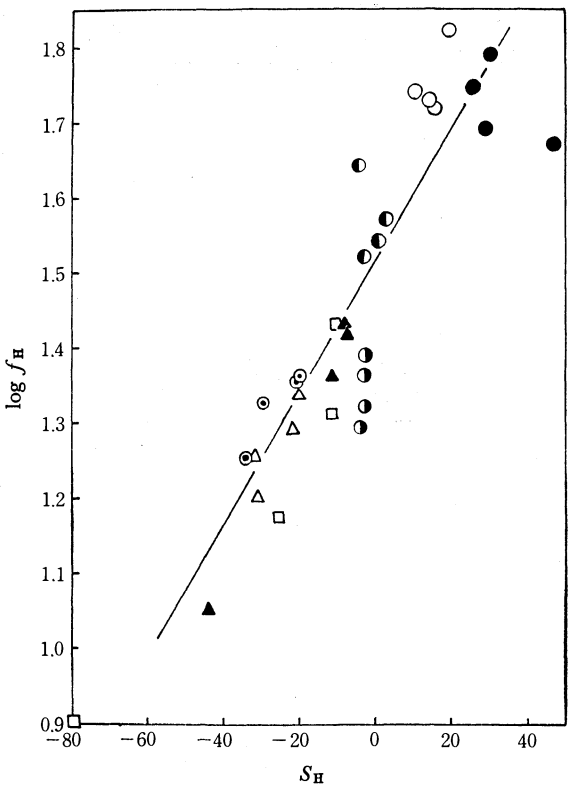

Fig. 4(a). The plots of log f_H *vs.* S_H. (The notations are the same as in Fig. 1).

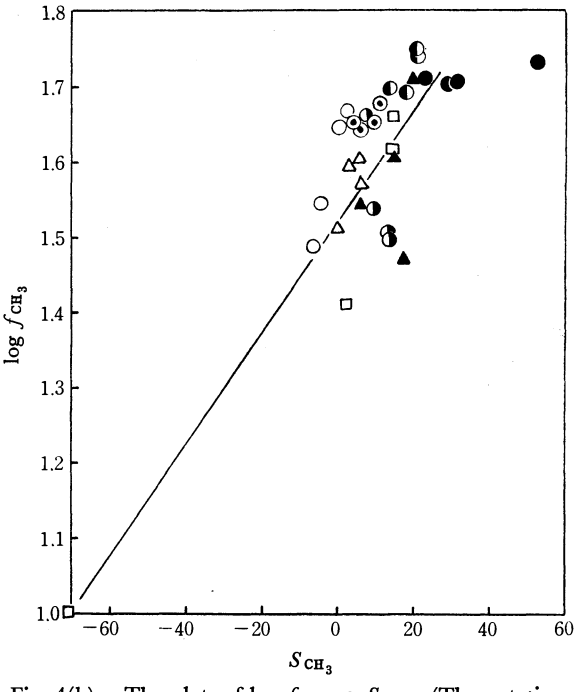

Fig. 4(b). The plots of log f_{CH_3} *vs.* S_{CH_3}. (The notations are the same as in Fig. 1).

11) W. W. Russell and W. V. Loebenstein, *J. Amer. Chem. Soc.*, **62**, 2573 (1940); A. T. Gwathmey and R. E. Cunningham, *Advan. Catal.*, **IX**, 25 (1957); **X**, 57 (1958); P. Emmett, *J. Phys. Chem.*, **63**, 1162 (1959); K. Hirota and S. Teratani, *Sci. Pap. Inst. Phys. Chem. Res.* (Tokyo), **57**, 206 (1963); I. Uhara, *Shokubai*, **9**, 127 (1967).

12) We have previously reported on the accelerating effect of NaCl on the reaction; *Cf.* Ref. 1; K. Sakai, M. Ishige, K. Watanabe, and K. Hata, This Bulletin, **43**, 1172 (1970).

potentials of the additive metals may play an important role in the promoting and retarding effects on the reaction, and that the polarizability of the metal ions adsorbed on the catalyst surface may be partially responsible for the change in f and S values. These observations suggest that this catalytic reaction of benzyl alcohol takes place in association with the acid and base functions of the catalyst surface.

It is known that the catalytic activity and selectivity are considerably correlated with the acid strength of heterogeneous metal catalysts,[13] and that the heterogeneous catalysis can be extensively elucidated by means of the acid-base concept.[14] In the formation of toluene and benzene from benzyl alcohol, it was found that the larger f values are mainly brought about by the addition of a hard metal ion, such as Na^+ and K^+, whereas the smaller f values are associated with the addition of a soft metal ion, *e.g.*, Hg^{2+}. Furthermore, the medium f values often result from the metals which belong on the borderline of the soft-hard classification. In the formation of benzaldehyde by dehydrogenation, the relation between the f_{CHO} values and the hardness of metal ions as additives tends to be opposed to that in the cases of the formation of toluene and benzene. Though a plausible explanation for this cannot yet be proposed, it seems that either the reaction path or the rate-determining step in the formation of benzaldehyde is different from that in the formation of toluene and benzene; that is, the more favorable formation of benzaldehyde is related to the change in the acid strength of the nickel catalyst by the addition of soft metal, whereas the formation of toluene and benzene is unfavorable under the same conditions.

Since the surface structure of the nickel catalyst is not sufficiently clear, it is very difficult to consider in what manner the substrate interacts with the active sites on the catalyst. However, according to the rule of the SHAB concept[13-15] that hard acids prefer hard bases and soft acids prefer solft bases, the hydroxyl group of the alcohol possessing a hard-base character will interact more strongly with the harder acid sites, and the phenyl group, as a soft base, will favorably coordinate to the softer acid sites. If the newly-formed coordination bond of each group to a metal is sufficiently strong, this should contribute to the cleavage of the C–O and C–C bonds of benzyl alcohol.

It can reasonably be inferred that the C–C bonds is more durable than the C–O bond in the catalytic fission, because the former bond is in a stable soft-soft combination, while the latter one is in a unstable hard-soft combination. This consideration is consistent with the finding of the present experiments that the f_{CH_3} values are generally larger than the f_H values.

Experimental

Material. *Benzyl Alcohol*: Benzyl alcohol used in all the experiments was purified by the previously-described procedure.[2] Its purity was confirmed by gas chromatography.

Catalyst: A commercial stabilized nickel (S 10) (supplied by the Nikko Shokai Co. Ltd.), containing 50% of kieselguhr, was used as a catalyst.

Preparation of Modified S–Ni. Various kinds of modified S–Ni catalysts were prepared by treating the S–Ni with aqueous solutions of various metal chlorides in the same manner as was described previously.[1] The degree of modification was controlled by adjusting the concentration of the aqueous solutions of each metal chloride to 0.02, 0.04, 0.08, and 0.16 N.

Reaction. Benzyl alcohol (2.00 m*l*) and a modified S–Ni catalyst (0.333 g) were heated at 162°C for 24 hr in a sealed tube. After the reaction was over, the tube was cooled with ice, then the reaction mixture was analyzed by gas chromatography.

The authors wish to express their hearty thanks to Dr. Ken-ichi Watanabe for his helpful encouragement.

13) *Cf.* M. Misono, *Shokubai*, **9**, 252 (1967), and the references cited therein.

14) R. G. Pearson, *J. Amer. Chem. Soc.*, **85**, 3533 (1963); *Science*, **151**, 172 (1966).

15) R. G. Pearson and J. Songstad, *J. Amer. Chem. Soc.*, **89**, 1827 (1967); *Chem. Eng. News*, **31**, 90 (1965).

Studies of the Synthesis of Furan Compounds. XXIV.[1] The Synthesis of 5-[2-(5-Nitro-2-furyl)-1-(4-nitrophenyl)vinyl]-1,3,4-oxadiazole and Its Related Compounds[2]

Ichiro HIRAO, Yasuhiko KATO, and Toshiyuki HIROTA

Laboratory of Organic Synthesis, Department of Chemical Engineering, Kyushu Institute of Technology, Tobata-ku, Kita-kyushu

(Received December 31, 1970)

5-[2-(5-Nitro-2-furyl)-1-(4-nitrophenyl)vinyl]-1,3,4-oxadiazoles and -1,3,4-thiadiazoles have been prepared from 3-(5-nitro-2-furyl)-2-(4-nitrophenyl)acrylic acid. All of these compounds exhibited strong antibacterial activities against *Staphylococcus aureus*.

A series of systematic investigations concerning the synthesis of 5-[2-(5-nitro-2-furyl)-1-substituted]vinyl-1,3,4-oxadiazole derivatives has been undertaken in order to obtain information on their chemical properties and on the relations between the chemical structures and the antibacterial activities. With the aim of establishing the influence of the β-substituents of the –C=C– chain upon the antibacterial activities in a continuation of a series of studies concerning the antibacterial properties of nitrofuran derivatives,[3–10] the present work has studied the introduction of a 4-nitrophenyl group into β-carbon, namely, 5-[2-(5-nitro-2-furyl)-1-(4-nitrophenyl)vinyl]-1,3,4-oxadiazole (III) and its related compounds.

Results and Discussion

3-(5-Nitro-2-furyl)-2-(4-nitrophenyl)acryloylhydrazine (I) was prepared from the chloride of 3-(5-nitro-2-furyl)-2-(4-nitrophenyl)acrylic acid[11] in the usual method.[3–10] The preparation of I using trichloroethylene or dioxane as a solvent was unsuccessful, but it was achieved by using methylene chloride as the solvent, although 1,2-bis[3-(5-nitro-2-furyl)-2-(4-nitrophenyl)acryloyl]hydrazine was not formed as the by-product.

5-[2-(5-Nitro-2-furyl)-1-(4-nitrophenyl)vinyl]-1,3,4-oxadiazolone (II) was obtained by the introduction of phosgene into a solution of I in dioxane-water (3:2,

TABLE 1. 1-[3-(5-NITRO-2-FURYL)-2-(4-NITROPHENYL)ACRYLOYL]-THIOSEMICARBAZIDES AND -*S*-METHYLISOTHIOSEMICARBAZIDES

No	R	Mp °C (decomp)	Yield %	Appearance[a]	Formula	Analysis % Found(Calcd) C	H	N
Thiosemicarbazides								
VI	H	177—179	78.1	Y Lf	$C_{14}H_{11}N_5O_6S$	44.37 (44.56)	2.89 (2.92)	18.63 (18.57)
VIa	CH_3	193	80.3	Y Pl	$C_{15}H_{13}N_5O_6S$	45.97 (46.04)	3.17 (3.32)	18.29 (17.90)
VIb	C_2H_5	180	85.1	Pa-Y Nd	$C_{16}H_{15}N_5O_6S$	47.72 (47.41)	3.65 (3.70)	17.65 (17.28)
VIc	C_6H_5	194	75.5	O Pm	$C_{20}H_{15}N_5O_6S$	52.82 (52.98)	3.04 (3.31)	15.27 (15.45)
S-*Methylisothiosemicarbazides*								
V	H	169	77.5	Y Gr	$C_{15}H_{13}N_5O_6S$	45.61 (46.04)	2.95 (3.32)	17.73 (17.90)
Va	CH_3	164	73.5	Y Gr	$C_{16}H_{15}N_5O_6S$	47.19 (47.41)	3.99 (3.70)	17.02 (17.28)
Vb	C_2H_5	173	74.2	Y Gr	$C_{17}H_{17}N_5O_6S$	48.99 (48.69)	4.54 (4.06)	16.32 (16.71)
Vc	C_6H_5	184	71.5	Y Gr	$C_{21}H_{17}N_5O_6S$	54.37 (53.96)	3.56 (3.64)	14.48 (14.99)

a) Abbreviations: Y Lf, yellow leaflets; Y Pl, yellow plates; Pa-Y Nd, pale yellow needles; O Pm, orange prisms; Y Gr, yellow granules.

1) Part XXIII of this series: I. Hirao, Y. Kato, T. Hayakawa, and H. Tateishi, This Bulletin, **44**, 780 (1971).
2) Presented at the 23rd Annual Meeting of The Chemical Society of Japan, Tokyo, April, 1970.
3) I. Hirao and Y. Kato, *Nippon Kagaku Zasshi*, **85**, 693 (1964).
4) I. Hirao and Y. Kato, *ibid.*, **86**, 633 (1965).
5) Y. Kato, Y. Hara, and I. Hirao, *ibid.*, **86**, 957 (1965).
6) Y. Kato and I. Hirao, *ibid.*, **87**, 1336 (1966).
7) I. Hirao, *ibid.*, **88**, 574 (1967).
8) Y. Kato, H. Nakajima, and I. Hirao, *ibid.*, **89**, 955 (1968).
9) I. Hirao, *ibid.*, **89**, 713 (1968).
10) Y. Kato, This Bulletin, **44**, 489 (1971).
11) I. Hirao and Y. Kitamura, *Bull. Kyushu Inst. Technol.*, No. **18**, 27 (1968).

TABLE 2. 5-[2-(5-NITRO-2-FURYL)-1-(4-NITROPHENYL)VINYL]-SUBSTITUTED 1,3,4-OXADIAZOLES AND 1,3,4-THIADIAZOLES

No	R	Mp (°C) (decomp)	Yield (%)	Recryst solvent[a)]	Appearance[a)]	Formula	Analysis (%) Found (Calcd) C	H	N
1,3,4-Oxadiazol-2-ones									
II	H	217—218	69.2	EOH	O-Y Lf	$C_{14}H_8N_4O_7$	48.73 (48.84)	2.00 (2.33)	15.85 (16.28)
IIa	$COCH_3$	190—191	89.6	Bz	Y Cb	$C_{16}H_{10}N_4O_8$	49.72 (49.75)	2.25 (2.59)	14.83 (14.51)
IIb	COC_2H_5	194—195	82.4	Bz	Ov-G Nd	$C_{17}H_{12}N_4O_8$	51.90 (51.00)	2.69 (3.00)	14.24 (14.00)
IIc	$COC_3H_7(n)$	131—133	75.8	MOH	Y Gr	$C_{18}H_{14}N_4O_8$	51.97 (52.20)	3.14 (3.38)	13.60 (13.53)
IId	$CH_2N(CH_3)C_6H_5$	180—181	57.1	Bz	O-Y Nd	$C_{22}H_{17}N_5O_7$	57.23 (57.01)	3.53 (3.67)	15.11 (15.12)
IIe	$CH_2N(C_2H_5)C_6H_5$	209—211	62.7	Bz	Re Nd	$C_{23}H_{19}N_5O_7$	57.43 (57.80)	3.63 (3.98)	14.32 (14.68)
IIf	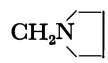	194—195	48.7	MOH-W (1:1)	Re Gr	$C_{19}H_{17}N_5O_7$	53.44 (53.38)	3.83 (3.98)	16.41 (16.40)
IIg	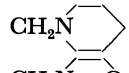	189—191	84.4	MOH	Bw Nd	$C_{20}H_{19}N_5O_7$	54.49 (54.42)	4.16 (4.31)	15.92 (15.88)
IIh	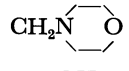	198—200	70.1	EOH	Y Fb	$C_{19}H_{17}N_5O_8$	51.47 (51.45)	3·67 (3.84)	15.44 (15.80)
IIi	CH_2OH	211—213	65.7	EOH	Y Lf	$C_{15}H_{10}N_4O_8$	47.52 (47.87)	2.34 (2.67)	14.89 (14.97)
2-Amino-1,3,4-oxadiazoles									
IV	H	246—247	71.5	EOH	Y Lf	$C_{14}H_9N_5O_6$	48.63 (48.99)	2.55 (2.62)	20.73 (20.41)
IVa	CH_3	227—228	73.8	MOH	O-Y Nd	$C_{15}H_{11}N_5O_6$	50.21 (50.40)	2.82 (3.08)	19.07 (19.21)
IVb	C_2H_5	221—222	50.1	MOH	O-Y Nd	$C_{16}H_{13}N_5O_6$	51.47 (51.75)	3.14 (3.50)	18.68 (18.88)
IVc	C_6H_5	241—242	78.5	MOH	O-Y Pm	$C_{20}H_{13}N_5O_6$	57.18 (57.30)	3.21 (3.10)	16.57 (16.70)
IVd	CH_2OH	231—232	67.2	DMF-W (1:1)	O-Y Pd	$C_{15}H_{11}N_5O_7$	51.51 (51.37)	2.64 (2.77)	17.54 (17.63)
IVe	$COCH_3$	235—237	81.5	MOH	Y Fb	$C_{16}H_{11}N_5O_7$	49.72 (49.87)	2.57 (2.86)	18.09 (18.18)
IVf	COC_2H_5	236—237	86.3	MOH	Y Lf	$C_{17}H_{13}N_5O_7$	51.06 (51.13)	3.52 (3.26)	17.36 (17.54)
IVg	$COC_3H_7(n)$	219—220	82.4	MOH	Y Lf	$C_{18}H_{15}N_5O_7$	52.12 (52.30)	3.51 (3.63)	16.87 (16.93)
2-Amino-1,3,4-thiadiazoles									
VII	H	238—240	42.1	MOH	Re Gr	$C_{14}H_9N_5O_5S$	46.82 (46.80)	2.60 (2.51)	19.09 (19.50)
VIIa	CH_3	214—215	78.5	MOH	Dp-Re Pm	$C_{15}H_{11}N_5O_5S$	48.51 (48.30)	2.71 (2.95)	18.53 (18.79)
VIIb	C_2H_5	226—227	45.1	MOH	O Fb	$C_{16}H_{13}N_5O_5S$	49.34 (49.61)	3.27 (3.36)	18.33 (18.06)
VIIc	C_6H_5	258—260	59.5	MOH	Re Gr	$C_{20}H_{13}N_5O_5S$	54.84 (55.17)	2.64 (2.99)	16.21 (16.09)
VIId	CH_2OH	256—257	48.3	Dx-W (3:2)	Y Gr	$C_{15}H_{11}N_5O_6S$	46.32 (46.27)	2.77 (2.83)	17.86 (17.99)
VIIe	$COCH_3$	294—295	80.6	DMF-W (3:1)	Y Pl	$C_{16}H_{11}N_5O_6S$	47.43 (47.88)	2.72 (2.74)	17.62 (17.46)
VIIf	COC_2H_5	286—287	69.2	DMF-W (4:1)	Y Gr	$C_{17}H_{13}N_5O_6S$	49.20 (49.16)	3.21 (3.13)	16.71 (16.87)
VIIg	$COC_3H_7(n)$	259—260	61.7	Dx	Y Gr	$C_{18}H_{15}N_5O_6S$	50.51 (50.35)	3.45 (3.50)	16.27 (16.32)

a) Abbreviations: EOH, ethanol; Bz, benzene; MOH, methanol; DMF, *N,N*-dimethylformamide; W, water; Dx, dioxane; O, orange; O-Y, orange yellow; Ov-G, olive green; Y, yellow; Re, red; Bw, brown; Dp-Re, deep red; Pa-Y, pale yellow; Lf, leaflets; Cb, cubes; Gr, granules;Nd, needles; Fb, fibers; Pm, prisms; Pd, powder; Pl, plates.

Table 3. Inhibitory activity of ten compounds on microorganisms

Compound	*Diplococcus pneumoniae* Dp-1	*Stereptococcus hemolyticus* Group A 089	*Staphylococcus aureus* 209P	*Bacillus subtilis* pcl 219	*Salmonella enteritidis* 1891	*Salmonella pullorum* Chuyu 114	*Escherichia coli* 0-55	*Klebsiella pneumoniae* ST-101	*Proteus vulgaris* HX 19	*Pseudomonus aeruginosa* 347
II	12.5	12.5	<0.4	3.2	>25	>25	>25	>25	>25	>25
IIa	12.5	12.5	0.8	6.2	>25	>25	>25	>25	>25	>25
IId	25	25	1.6	6.2	>25	>25	>25	>25	>25	>25
IIh	25	12.5	0.8	3.2	>25	>25	>25	>25	>25	>25
IIi	25	12.5	<0.4	6.2	>25	>25	>25	>25	>25	>25
III	6.2	12.5	3.1	25	>25	>25	>25	>25	>25	>25
IV	6.2	6.2	1.5	12.5	>25	>25	>25	>25	>25	>25
IVa	12.5	12.5	1.6	6.2	>25	>25	>25	>25	>25	>25
VII	6.2	6.2	1.5	6.2	>25	>25	>25	>25	>25	>25
VIIa	>25	>25	3.1	12.5	>25	>25	>25	>25	>25	>25
Contrast[a]	25	0.4	0.8	0.8	0.8	0.8	1.6	0.8	6.2	12.5

a) 3-(5-Nitro-2-furyl)-2-(2-furyl)acrylic amide was used in the test.

v/v) at 15—20°C. This compound was found, from the infrared absorptions[12] at 3360 cm^{-1} (N–H) and 1765 cm^{-1} (C=O), to take the keto structure, at least in the solid state. The treatment of II with a large excess of acid anhydrides or with 2—3 times as many moles of acid anhydrides in dioxane afforded the corresponding monoacyl derivatives, the 3-acetyl (IIa), 3-propionyl (IIb), and 3-butyryl (IIc) derivatives. These acyl derivatives commonly showed two C=O absorptions, near 1780 and 1740 cm^{-1}, but not the absorption at 3360 cm^{-1} characteristic of N–H in the mother compound, II.

As a N–H in an oxadiazolone ring is known to undergo the Mannich reaction to form an *N*-aminomethyl derivative, 3-aminomethyl derivatives (IId—h) were prepared by treating II with 37% formaldehyde and secondary amines (*N*-methylaniline, *N*-ethylaniline, pyrrolidine, pyperidine, and morpholine) in methanol or dioxane in the presence of *N,N*-dimethylformamide. The 3-hydroxymethyl derivative (IIi) was also obtained in a good yield from II and 37% formaldehyde.

When treated with refluxing ethyl orthoformate, I afforded 5-[2-(5-nitro-2-furyl)-1-(4-nitrophenyl)vinyl]-1,3,4-oxadiazole (III). 2-Amino-5-[2-(5-nitro-2-furyl)-1-(4-nitrophenyl)vinyl]-1,3,4-oxadiazole (IV) was prepared by the reaction of I with cyanogen bromide in refluxing methanol or by the cyclization of 1-[3-(5-nitro-2-furyl)-2-(4-nitrophenyl)acryloyl]-*S*-methylisothiosemicarbazide (V) in boiling ethanol, both in satisfactory yields. The similar treatment of 4-alkyl (or aryl)-1-[3-(5-nitro-2-furyl)-2-(4-nitrophenyl) acryloyl]-*S*-methylisothiosemicarbazides (Va—c) gave the 2-R-substituted amino-5-[2-(5-nitro-2-furyl)-1-(4-nitrophenyl)-vinyl]-1,3,4-oxadiazole, IVa, IVb, and IVc, in which R was methyl, ethyl, and phenyl. The treatment of IV with 37% formaldehyde afforded the 2-hydroxymethylamino derivative (IVd), and that with acid anhydrides gave the 2-acetylamino (IVe), 2-propionylamino (IVf), and 2-butyrylamino (IVg) derivatives. V and Va—Vc were each obtained by the reaction of methyl iodide with 1-[3-(5-nitro-2-furyl)-2-(4-nitrophenyl)acryloyl]thiosemicarbazide (VI) or its 4-substituted derivatives (VIa—c), which had been prepared from the acid chloride and thiosemicarbazide or from I and isothiocyanates.

When heated in phosphoryl chloride, VI was cyclized to 2-amino-5-[2-(5-nitro-2-furyl)-1-(4-nitrophenyl)-vinyl]-1,3,4-thiadiazole (VII). 2-Substituted amino derivatives were also obtained by the similar treatment of VIa—VIc in phosphoryl chloride and of VII with 37% formaldehyde or acid anhydrides. Thus, the 2-methylamino (VIIa), 2-ethylamino (VIIb), 2-anilino (VIIc), 2-hydroxymethylamino (VIId), 2-acetylamino (VIIe), 2-propionylamino (VIIf), and 2-butyrylamino (VIIg) derivatives were obtained. All of these compounds are listed in Tables 1 and 2.

Microbiological Assays.[13] The antibacterial activities of these compounds toward ten microorganisms were examined. The minimum amount of the compounds necessary for the complete inhibition of the growth was determined by the dilution method, using the usual bouillon agar medium (pH 7). Some of the results are shown in Table 3. The compounds of this group exhibited weak antibacterial activity against Gram-positive bacteria, but not against Gram-negative bacteria. In particular, all the compounds tested showed strong activity against *Staphylococcus aureus*. Ultimately, it was found that the introduction of a 4-nitrophenyl group instead of a 2-furyl group[10] into β-carbon lowered the activity greatly.

Experimental[14]

3-(5-Nitro-2-furyl)-2-(4-nitrophenyl)acryloyl chloride. A mixture of 3-(5-nitro-2-furyl)-2-(4-nitrophenyl)acrylic acid[11] (60.8 g, 0.2 mol), thionyl chloride (36 g, 0.2 mol), *N,N*-dimethylformamide (2 g), and 200 m*l* of monochlorobenzene was stirred at 65—70°C for 1 hr. The resulting solution was cooled with an ice-salt bath; the acid chloride was then separated as yellow crystals, filtered, washed with dry ether, and used in the next experiments without further purification.

12) The infrared absorption spectra in this experiments were obtained with a Shimadzu IR-27S spectrophotometer with KBr method.

13) The authors are indebted to Dr. R. Ueno and his staff of the Ueno Pharmaceutical Company, Ltd., for the assay.

14) All melting and decomposition points are uncorrected. Microanalyses were carried out with a Yanagimoto C. H. N. Corder MT-2 type.

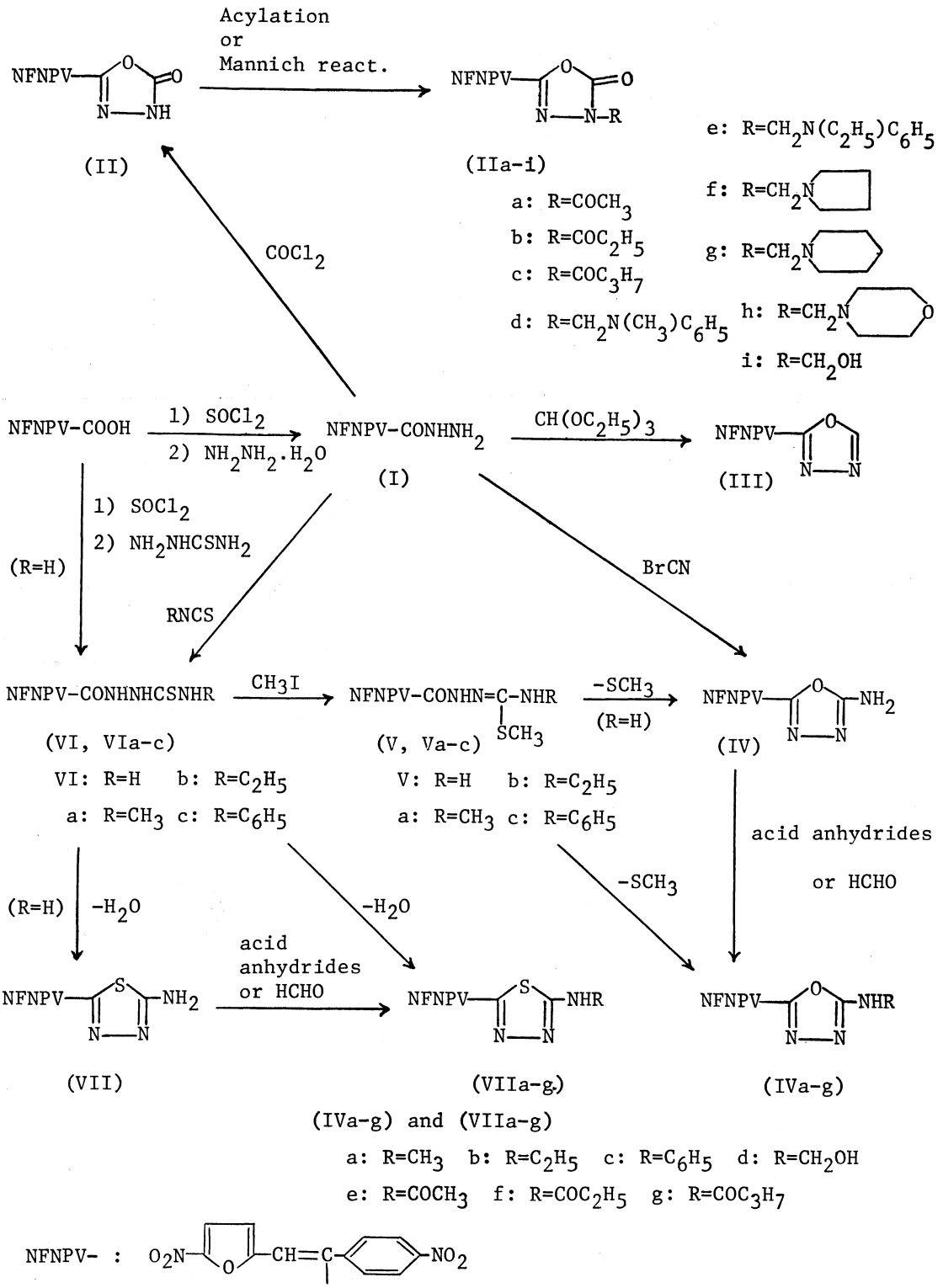

3-(5-Nitro-2-furyl)-2-(4-nitrophenyl)acryloylhydrazine (I). To a stirred, ice-salt, cooled (−5—0°C) mixture of 80% hydrazine hydrate (20.2 g, 0.4 mol), water (60 m*l*) and methylene chloride (140 m*l*), we added, drop by drop, a solution of the acid chloride (32.3 g, 0.1 mol) in 700 m*l* of methylene chloride during a period of 1.5 hr. After the addition had been completed over, the temperature was allowed to rise to room temperature and stirring was continued for an additional 2 hr. The resulting suspension was filtered, and the residue was washed with 50% aqueous methanol and then dried. This afforded 21.6 g (67.9%) of yellow crystals melting, with decomposition, at 165—168°C. Recrystallization from methanol gave ochreous prisms; mp 182—184°C dec. The yield was 20.4 g (64.2%).

Found: C, 49.16; H, 3.09; N, 17.79%. Calcd for $C_{13}H_{10}N_4O_6$: C, 49.06; H, 3.14; N, 17.62%.

1-[3-(5-Nitro-2-furyl)-2-(4-nitrophenyl)acryloyl]thiosemicarbazide (VI). A solution of the acid chloride (32.3 g, 0.1 mol) in dry dioxane (200 m*l*) was added slowly to a stirred suspension of thiosemicarbazide (18.2 g, 0.2 mol) and sodium bicarbonate (45 g, 0.54 mol) in 80 m*l* of dioxane. The suspension was stirred for 2 hr at room temperature and then

heated on a steam bath for 1 hr. After cooling, yellow precipitates were filtered out and poured into aqueous hydrochloric acid. The insoluble product was collected on a filter, washed with water, and then dried. In this way we obtained 29.4 g (78%) of a crude product melting at 143—148°C dec. Crystallization from methanol gave yellow leaflets.

4-Substituted 1-[3-(5-nitro-2-furyl)-2-(4-nitrophenyl)acryloyl]-thiosemicarbazides (VIa—c). A mixture of I (3.18 g, 10 mmol), alkylisothiocyanate (12 mmol), and methanol (140 m*l*) was refluxed for 2 hr. The resulting solution was cooled, and the precipitated product was collected by filtration. Recrystallization from methanol gave a pure product (Table 1).

1-[3-(5-Nitro-2-furyl)-2-(4-nitrophenyl) acryloyl]-S-methylisothiosemicarbazide (V) and Its 4-Substituted Derivatives (Va—c). To a stirred mixture of 5 mmol of VI (or VIa—c), methyl iodide (15 mmol), and ethanol (10—20 m*l*), we added, drop by drop, a solution of potassium hydroxide (5 mmol) in 20 m*l* of ethanol. After the addition, stirring was continued for 12 hr at room temperature. The resulting suspension was filtered, and the residue was washed with a small amount of ethanol and dried. If the product were heated in solvents, decomposition occurred and methyl mercaptane was evolved. Therefore, recrystallization from solvents could not be achieved, but these products were pure enough for elemental analyses.

5-[2-(5-Nitro-2-furyl)-1-(4-nitrophenyl)vinyl]-1,3,4-oxadiazol-2-one (II). To a stirred solution of I (7.9 g, 25 mmol) in 360 m*l* of dioxane-water (3:2, v/v), phosgene was introduced under cooling at 15—17°C. After 3 hr, the product was collected and washed with water to give 7 g (81.4%) of crude II, mp 161—163°C dec. Recrystallization from ethanol gave II, melting at 217—218°C dec and weighing 5.95 g (69.2%).

3-Acyl-5-[2-(5-nitro-2-furyl)-1-(4-nitrophenyl)vinyl]-1,3,4-oxadiazol-2-ones (IIa—c). A mixture of II (0.7 g, 2.30 mmol) and 13 m*l* of acid anhydride or 0.7 g of acid anhydride in 13 m*l* of dioxane was heated on a steam bath for 1—2 hr. The resulting solution was taken to dryness *in vacuo*, and the residue was washed with water, dried, and recrystallized. The yield and mps of products are given in Table 2.

3-Aminomethyl-5-[2-(5-nitro-2-furyl)-1-(4-nitrophenyl)vinyl]-1,3,4-oxadiazol-2-ones (IId—h). To a stirred solution of II (1.72 g, 5 mmol) in 40 m*l* of dioxane or 100 m*l* of methanol containing *N,N*-dimethylformamide (0.5 g), 37% formaldehyde (0.5 g, 6 mmol), and secondary amine (6 mmol) were added. The solution was stirred for 30 min at room temperature and warmed at 50—65°C for 1 hr. After cooling, the precipitate was filtered. When no precipitate appeared, water was added to the soltuion and the precipitated product was filtered. The yields and mps of the products are given in Table 2.

Hydroxymethylation of II, IV, and VII. A suspension of II, IV, or VII (each 3 mmol) in 37% formaldehyde (10 m*l*) was heated on a steam bath for 2—3 hr. After cooling, water (50—100 m*l*) was added, and the precipitated product was collected by filtration, washed with water, and dried. The product was purified by recrystallization.

5-[2-(5-Nitro-2-furyl)-1-(4-nitrophenyl)vinyl]-1,3,4-oxadiazole (III). A suspension of I (3.18 g, 10 mmol) in ethyl orthoformate (40 m*l*) was heated under reflux for 12 hr. The resulting solution was concentrated *in vacuo*, and the product was filtered and washed with cold ethanol. Recrystallization from ethanol gave III as yellow prisms; mp 218°C dec. The yield was 2.25 g (69%).

Found: C, 51.27; H, 2.12; N, 17.17%. Calcd for $C_{14}H_8N_4O_6$: C, 51.22; H, 2.44; N, 17.08%.

2-Amino-5-[2-(5-nitro-2-furyl)-1-(4-nitrophenyl)vinyl]-1,3,4-oxadiazole (IV). *Procedure A*: A mixture of I (2 g, 6.3 mmol), cyanogen bromide (1.05 g, 9.4 mmol), and 60 m*l* of methanol was heated under reflux for 1 hr. Cooling provided 2 g, (92.8%) of a yellow powder: mp 236—238°C dec. Crystallization was carried out from ethanol.

Procedure B: A suspension of V (1.6 g, 4.1 mmol) in ethanol (50 m*l*) was refluxed until the evolution of methyl mercaptane had ceased (*ca.* 3—4 hr). The resulting solution was taken to dryness *in vacuo*, and the residue was crystallized from ethanol to give 1 g (71.5%) of IV as yellow leaflets; mp 246—247°C dec, undepressed on admixture with a sample by *Procedure A* as above for IV.

2-Substituted amino-5-[2-(5-nitro-2-furyl)-1-(4-nitrophenyl)-vinyl]-1,3,4-oxadiazoles (IVa—c). These substances were prepared in the same way as IV above (*Procedure B*) using 5 mmol of 4-substituted *S*-methylisothiosemicarbazide derivatives (Va—Vc).

2-Amino-5-[2-(5-nitro-2-furyl)-1-(4-nitrophenyl)vinyl]-1,3,4-thiadiazole (VII) and 2-Substituted Amino Derivatives (VIIa—c). A mixture of 5 mmol of V (or Va—c) and phosphoryl chloride (10 m*l*) was heated under reflux for 2—3 hr. The solution was poured onto crushed ice, and the solidified product was filtered, washed with water, and dried. Two or three recrystallizations gave a pure product.

2-Acylamino Derivatives of IV and VII. Compound IV (or VII) (1.4 mmol) was covered with acid anhydride (5 m*l*) and heated on a steam bath for 2—3 hr. Water (30—40 m*l*) was added to the resulting solution to decompose the surplus acid anhydride. The product was filtered, washed with water, and dried. In this way the corresponding acyl products were obtained; recrystallizations were achieved from solvents or solvent pairs, as is shown in Table 2.

Electrochemical Reduction of Aza-heteroaromatic Compounds. IV.[1] Stabilities of Neutral Free Radicals Electrolytically Derived from 1-Methylcyanoquinolinium Perchlorates

Shozo KATO, Jun'ichi NAKAYA,* and Eiji IMOTO

Department of Applied Chemistry, Faculty of Engineering, University of Osaka Prefecture, Sakai-shi, Osaka
**Department of Chemistry, Faculty of Liberal Arts and Sciences, University of Osaka Prefecture, Sakai-shi, Osaka*

(Received December 28, 1970)

Three isomers of 1-methylcyanoquinolinium perchlorates were reduced by controlled potential electrolysis for one-electron transfer, and the reduction products were identified in order to clarify their reduction mechanisms and the effect of the cyano group on the stabilities of cyanoquinolinyl radicals. The 1-methyl-4-cyanoquinolinyl radical was stable enough to survive at room temperature under anaerobic conditions. The 1-methyl-2- and 1-methyl-3-cyanoquinolinyl radicals were short-lived and were subsequently dimerized to the 1,4-dihydrotype. The 1-methyl-4-cyanoquinolinyl radical was autoxidized to 1-methyl-4-cyanoquinolinium salts in an electrolyte solution and to 1-methyl-4-cyano-2-quinolone in an ethanol solution.

The mechanisms of the reduction of aromatic compounds containing cyano groups have been studied by many investigators, even if the discussion has been limited to the field of electrochemistry. For example, in acidic media 4-cyanopyridine is reduced to 4-aminomethylpyridine through a four-electron transfer;[2,3] in alkaline media, to pyridine through a two-electron transfer accompanied by decyanation reaction,[4] and in aprotic solvents, to the 4-cyanopyridinyl radical anion through a one-electron transfer.[5] As for phthalonitrile, a reductive decyanation reaction occurs.[6,7] Moreover, in benzonitrile derivatives which have substituents such as carbonyl groups, it is possible for two reduction pathways, the reduction of the cyano and carbonyl groups, to occur.[7,8]

A cyano group with a great resonating effect as well as a great electron-attracting effect would be expected to play an important role in stabilizing a pyridinyl radical. Actually, Schwartz, Kosower, and Shain[9] have detected a relatively stable 1-ethyl-4-cyanopyridinyl radical by means of cyclic voltammetry.

It may be easily suggested that the first polarographic reduction step of quaternary ammonium salts of aza-heteroaromatic compounds (R^+) is a one-electron transfer which does not involve protonation, even in aqueous solutions.

$$R^+ \xrightarrow{e} R\cdot \xrightarrow{e} (R^- \xrightarrow{H^+}) RH$$

The overall process thus contrasts to the case of free bases (R).

$$R \xrightarrow{e} (R^{\cdot-} \xrightarrow{H^+}) RH\cdot \xrightarrow{e} (RH^- \xrightarrow{H^+}) RH_2$$

A one-electron transfer to a quaternary ammonium salt should produce a neutral free radical, which may be able to avoid the disproportionation.

In the present paper, we will discuss the characteristics of the cyano group. We chose the following quinolinium compounds for study: 1-methyl-4-cyanoquinolinium perchlorate (Ia), 1-methyl-3-cyanoquinolinum perchlorate (IIa), and 1-methyl-2-cyanoquinolinium perchlorate (IIIa). These compounds are reduced by controlled potential electrolysis for one-electron transfer, and the structures of the reduction products are identified in order to clarify the mechanisms of electrochemical reduction, the effect of the cyano group on the stabilities of radicals or dimers produced by one-electron reduction, and the coupling sites of the dimers.

Results

Polarography. 1-Methyl-3-cyanoquinolinium perchlorate (IIa) and 1-methyl-2-cyanoquinolinium perchlorate (IIIa) give complicated polarograms in a buffered solution, while 1-methyl-4-cyanoquinolinium perchlorate (Ia) gives well-defined polarograms over a wide pH range of 2—10. The dependence of the half-wave potential ($E_{1/2}$) of Ia on pH clearly indicates that the first reduction does not involve a protonation step, in contrast with the second ($\Delta E_{1/2}/\Delta pH = -4$ mV for the first and -51 mV for the second).

The 1-methylcyanoquinolinium perchlorates are sensitive to nucleophiles. The height of the polarographic waves appreciably decreases with the passage of time. IIIa is the most sensitive of the three compounds; it is readily changed to 1-methyl-2-ethoxyquinolinium perchlorate by refluxing in aqueous ethanol for about 20 min. Such nucleophilic substitution reactions by solvents are known with respect to some heteroaromatic quaternary ammonium salts. The behavior of the hydrolysis is similar to that of 1-methyl-4-cyanopyridinium perchlorate reported by Kosower and Patton.[10]

In aprotic solutions, all the cyanoquinolinium salts give well-difined polarographic waves. Table 1 shows

1) For Part III in this series: see S. Kato, J. Nakaya, and E. Imoto, *Rev. of Polarogr.*, **17**, Nos. 2/3 (1971).
2) J. Volke, R. Kubicek, and F. Santavy, *Collect. Czech. Chem. Commun.*, **25**, 1510 (1960).
3) J. Volke and J. Holubek, *ibid.*, **28**, 1597 (1963).
4) J. Volke and A. M. Kardos, *ibid.*, **33**, 2560 (1968).
5) P. H. Rieger, I. Bernal, W. H. Reinmuth, and G. K. Fraenkel, *J. Amer. Chem. Soc.*, **85**, 683 (1963).
6) O. Manoušek, P. Zuman, and O. Exner, *Collect. Czech. Chem. Commun.*, **33**, 3979 (1968).
7) P. Zuman and O. Manoušek, *ibid.*, **34**, 1580 (1969).
8) P. Cársky and P. Zuman, *ibid.*, **34**, 498 (1969).
9) W. M. Schwarz, E. M. Kosower, and I. Shain, *J. Amer. Chem. Soc.*, **83**, 3164 (1961).
10) E. M. Kosower and J. W. Patton, *Tetrahedron*, **22**, 2081 (1966).

Table 1. Half wave potential and wave height of reduction- and oxidation-waves

Material	Solution	Before electrolysis $E_{1/2}$(V *vs.* SCE) (i_l(μA))		After electrolysis of controlled lst wave $E_{1/2}$(V *vs.* SCE) (i_l(μA))	
		R_1[a]	R_2	O[a]	R
Ia	pH 7	−0.56 (1.75)	−0.93 (1.70)	—	—
Ia	DMF	−0.57 (1.70)	−1.53 (1.25)	−0.56 (1.53)	−1.52 (1.53)
Ia	CH_3CN	−0.33 (2.65)	−1.31 (2.08)	−0.31 (2.23)	−1.30 (2.10)
IIa	pH 5	*ca.* −0.5 (2.03)	no	—	—[b]
IIa	DMF	−0.45 (1.70)	−1.70 (0.38)	—	—[c]
IIa	CH_3CN	−0.31 (2.73)	−1.66 (0.75)	+0.31 (2.73)	
IIIa	pH 5	*ca.* −0.4 (2.03)	no	—	—[b]
IIIa	DMF	−0.26 (1.25)	—[c]	−0.24 (0.70)	
IIIa	CH_3CN	−0.21 (2.90)	—[c]	−0.14 (2.15)	

a) R; reduction wave, O; oxidation wave.
b) The precipitates were formed after electrolysis.
c) indistinct wave.

Table 2. The electron numbers (n) required for the reduction

Material	Concn. (mM)	Solution	Controlled wave	Controlled potential (-E, V *vs*, SCE)	n
Ia	0.5	pH 7	1 st	0.70	1.02
Ia	5.0	pH 7	1 st	0.70	1.06
Ia	0.5	pH 7	2 nd	1.05	2.21
Ia	5.0	pH 7	2 nd	1.05	1.99
Ia	0.5	CH_3CN	1 st	0.50	1.05
Ia	0.5	DMF	2 nd	2.10	2.22
IIa	0.5	pH 5	1 st	0.80	1.00
IIa	7.5	pH 5	1 st	0.80	0.99
IIa	7.5	DMF	1 st	0.80	0.91
IIa	0.5	CH_3CN	1 st	0.60	0.93
IIIa	0.5	pH 2	1 st	0.70	1.13
IIIa	5.0	pH 5	1 st	0.70	1.10
IIIa	0.5	CH_3CN	1 st	0.40	1.03

the $E_{1/2}$ values of the quinolinium salts. It is clear that the cyano group has an effect on the positive shift of the reduction potential compared with quinolinium salts[1] by *ca.* 0.47 V.

General Electrolysis. The coulometric data (Table 2) suggest that Ia absorbs one electron per molecule by controlled potential electrolysis corresponding to the first wave, and two electrons per molecule, by the electrolysis corresponding to the second wave. As for IIa and IIIa, one-electron reduction also occurs by the electrolysis at the potential corresponding to the first wave.

One-electron reduction products formed by electrolysis precipitate in buffered solutions. A reduction wave is not observed when electrolysis is completed.

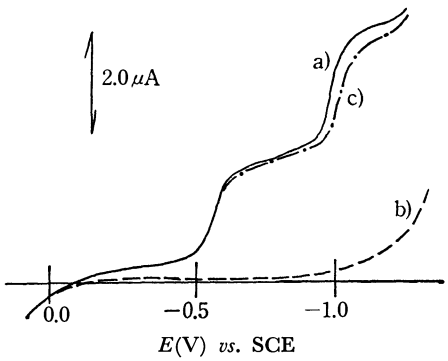

Fig. 1. Polarographic behavior of 1-methyl-4-cyanoquinolinium perchlorate (I_a), before and after one-electron electrolysis (pH 7).
a) before b) just after c) 15 min. after

Table 3. The recovery[a] of reduction products

Material	Reduction Product	pH	Time (min)	Yield (%)
Ia	1 e	7	3	90
Ia	2 e	7	15	trace
IIa	1 e	2	20	87
IIIa	1 e	2	20	29

a) The yields were measured polarographically after stirring at room temperature under aerobic condition.

However, it becomes observable at the original position after stirring at room temperature under aerobic conditions (Fig. 1). The recovery yield becomes larger in the order of IIIa<IIa<Ia (Table 3). On the contrary, the recovery yield of the two-electron reduction product of Ia is very slight; therefore, it may be concluded that the two-electron reduction product is not so sensitive to air as the one-electron reduction product.

When the quinolinium salts are subjected to one-electron electrochemical reduction in aprotic solvents under the same conditions as in the polarographic measurement, oxidation waves appear in all the cases (Table 1). In the case of Ia, an oxidation and a reduction wave are observed at the potentials identical with those of the first and the second waves of Ia respectively. Moreover, the heights of the oxidation and the reduction waves are almost identical with those of the first and the second waves of Ia (Fig. 2). On the other

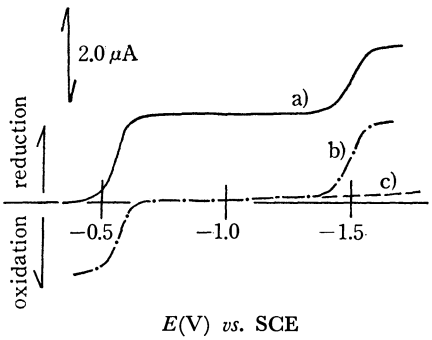

Fig. 2. Polarographic behavior of 1-methyl-4-cyanoquinolinium perchlorate (I_a), before and after electrolysis (in DMF).
a) before electrolysis
b) just after one-electron reduction
c) just after two-electron reduction

hand, both the solutions after the one-electron reduction of IIa and IIIa have oxidation waves at potentials less negative than those of the original reduction waves. The discordance in potential in those cases suggests the formation of the dimers. The two-electron reduction product of Ia shows no oxidation wave; this serves to confirm the lower oxidizability of two-electron reduction products.

Structure of the One-electron Reduction Product of 1-Methyl-4-cyanoquinolinium Perchlorate (Ia). Kosower and his co-worker[11] reported that 1-alkyl-4-cyanopyridinyl radicals are relatively stable, but that subsequent dimerizations cause decyanation reduction, thus forming alkylviologen radicals. As has been shown above, Ia shows an oxidation wave at the same potential as does the original reduction wave. Moreover, Ia is almost quantitatively recovered by the autoxidation, and the electron required for the reduction of one molecule of Ia is no more than unity. Moreover, the solution after the one-electron reduction of Ia shows a considerably different UV spectrum from the corresponding two-electron reduction product (Fig. 3). Hence, the one-electron reduction product of Ia seems to be a stable neutral radical which involves no decyanation reaction.

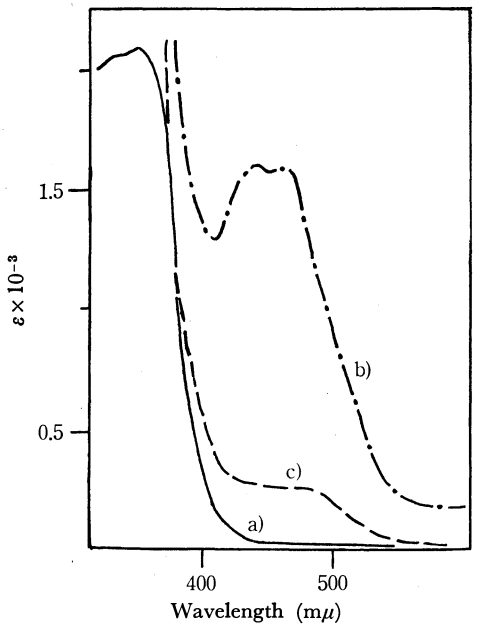

Fig. 3. Electronic spectra of 1-methyl-4-cyanoquinolinium perchlorate (I_a), before and after electrolysis (in DMF).
a) before electrolysis
b) just after one-electron reduction
c) just after two-electron reduction

During and after the electrolysis of an acetonitrile solution of Ia at the potential corresponding to the one-electron reduction (−0.9 V *vs.* $Ag/AgClO_4$), an ESR signal with a hyper-fine structure of $19 \times 5 = 95$ lines is observale (Fig. 4). The deep yellow crystalline precipitates obtained by the one-electron reduction of Ia also show an ESR signal in the solid state or in a

11) E. M. Kosower and J. L. Cotter, *J. Amer. Chem. Soc.*, **86**, 5524 (1964).

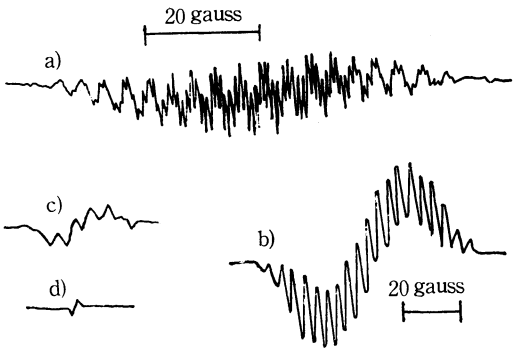

Fig. 4. ESR spectra of the one-electron reduction product of 1-methyl-cyanoquinolinium perchlorates in acetonitrile solution.
a) I_a, modulated width 1.5 gauss
b) I_a, modulated width 4.5 gauss
c) III_a, intermediate
d) II_a, intermediate

solution. The solution, after reduction with zinc powder, also shows the ESR spectrum. When the 5w/v-% acetonitrile solution of Ia is reduced by zinc dust, no signal is observed in its NMR spectrum (Fig. 5). The removal of zinc dust from the solution causes a quantitative recovery of the signals of Ia. Therefore, it is obvious that the one-electron electrochemical reduction product of Ia is a stable radical, one which is identical with the reduction product with zinc dust, and that the radical is stable even at high concentrations or in the solid state.

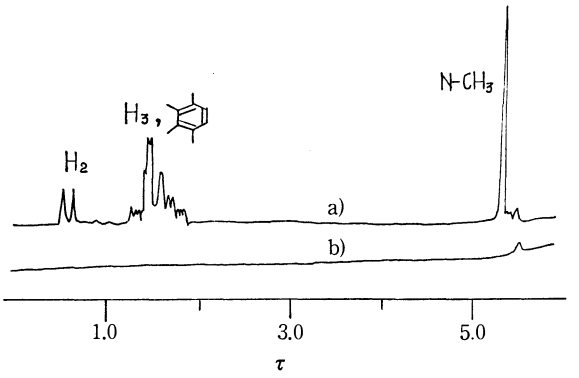

Fig. 5. NMR spectra of 1-methyl-4-cyanoquinolinium perchlorate (I_a), before and after Zn reduction (in CH_3CN).
a) before b) after

Autoxidation of 1-Methyl-4-cyanoquinolinyl Radical (Ib). When the solution after the electrolysis of Ia is exposed to air, Ib is autoxidized to Ia almost quantitatively. When Ib is refluxed in ethanol, 1-methyl-4-cyano-2-quinolone (IV) is isolated from the solution by means of recrystallization or sublimation. Accordingly, Ib seems to react with oxygen at the 2-position in the quinoline ring under aerobic conditions, forming a peroxide with a 1,2-dihydro structure which may decompose to IV. This spectrophotometric behavior further supports the idea that Ib intermediately produces the peroxide with the 1,2-dihydro structure. The ethanol solution of Ib shows the same UV maximum (360 mμ) as that of 1-methyl-4-cyano-1,2-dihydroquinoline (Ic), and Ib shows a strong band at

Table 4. UV-and IR-spectra of reduction products

Material	Reduction product	λ_{max}(mμ)	ν_{max}^{KBr}(cm^{-1})
Ia	1 e	447, 465 (DMF) 360 (EtOH)	2200, 2300 (C≡N) 1665 (C=C)
Ia	2 e	360 (EtOH) 361 (CH_3CN)	2230, 2300 (C≡N) 1645 (C=C)
IIa	1 e	330 (EtOH)	2200 (C≡N) 1645 (C=C)
IIIa	1 e	326 (EtOH) 344 (DMF)	2230 (C≡N) 1636 (C=C)

1665 cm^{-1} due to an absorption of cyclic amide and two bands due to the cyano group in its IR spectrum (Table 4).

Structure of the Two-electron Reduction Product of Ia. The two-electron reduction product of Ia has a UV maximum at about 360 mμ whether the solvent is protic or not; this indicates the formation of Ic. The fact that IV is obtained by the autoxidation of Ic also supports the 1,2-dihydro structure.

One-electron Reduction Products of 1-Methyl-3-cyanoquinolinium Perchlorate (IIa) and 1-Methyl-2-cyanoquinolinium Prechlorate (IIIa). The one-electron reduction products of IIa and IIIa show UV maxima at 330 and 326 mμ respectively, and IR maxima at 1648 and 1636 cm^{-1} due to ethylenic stretching vibration. These data support the idea that both products are the dimers of a 1,4-dihydro type structure. That they are dimers is proved by the results of elemental analysis and the molecular-weight determination. When the one-electron reduction of IIa or IIIa is performed in an ESR cavity, the ESR signal is detectable only by the *in situ* method (Fig. 4). Each signal intensity is extraordinarily small in comparison with that of Ia under identical conditions. Moreover, the intensity of the intermediary radical derived from IIa is smaller than that of IIIa. These results suggest that the rate of dimerization of the radical (IIb) is greater than that of the radical (IIIb). The fact that the one-electron electrochemical reduction product of IIa and the reduction product with zinc dust are the same dimer (IIb′), one which is oxidizable to IIa with silver perchlorate, is confirmed by UV and NMR spectroscopy.

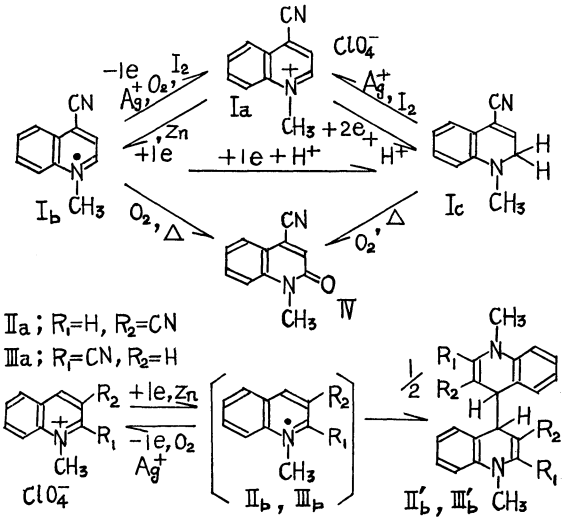

The reduction mechanisms of Ia—IIIa and the oxidation reaction of their reduction procucts are summarized in the following scheme.

Discussion

Stability of the Radical. As has been mentioned above, only Ia was able to stay as the radical in the solution. This is because the cyano group at the 4-position sufficiently resonates with the quinoline ring, and the unpaired electron can delocalize on each atom in the pyridine ring. On the other hand, IIb has a

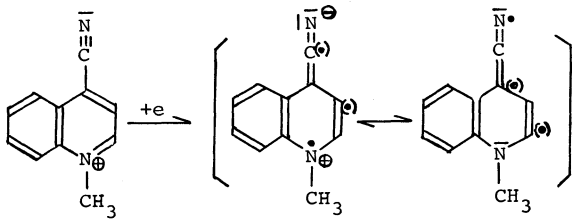

Ia Ib

cyano group at the position *meta* to ring nitrogen; as a result, the unpaired electron is difficult to delocalize. In the case of IIIb, the neighboring *N*-methyl group may sterically prevent it from keeping the co-planarity between the cyano group and the quinoline ring. Therefore, neither IIb nor IIIb is sufficiently stable, and so each radical dimerizes. The fact that the conjugated nitrile (>C=C<CN) of IIIb′ has a higher frequency than that of IIb′ in the IR spectrum (Table 4) suggests steric hindrance by the *N*-methyl group. However, the mighty radical-stabilizing effect of the cyano group is supported by the fact that even IIb or IIIb can be detected intermediately by ESR spectroscopy, though it is rather short-lived.

Elimination of the Cyano Group. Ib does not lead to a decyanation reaction in an aprotic or buffered solution. The stability of Ib is explanined in terms of the great conjugated system which causes the delocalization of the unpaired electron in comparison with the 1-ethyl-4-cyanopyridinyl radical.[11] The 1-methyl-2-cyanoquinolinyl radical, IIIb, does not lead to decyanation because it dimerizes at the 4-position, where the cyano group is not attached.

Oxidation of the One-electron Reduction Product. The fact that the recovery yield of the one-electron reduction product or the reactivity for oxygen decreases in the order of Ib>IIb′>IIIb′ is reasonable in view of the structures of the reduction products. Ib is somewhat resistant to dimerization, but since its unpaired electron is in the antibonding molecular orbital, it is very reactive to oxidizing agents. Though IIb′ and IIIb′ are dimers and the covalent bonds are formed by the reduction, the 4-4′ single bond of the dimers is not very resistant to oxidants because of the hindered resonance of the dihydroquinoline ring and the steric effect. The cyano group may sterically affect the stability of the bonding, and so IIb′ seems to be more reactive than IIIb′. The oxidative cleavage of such a single C–C bond has been reported for several dihydro-

quinoline derivatives, such as V,[12] VI,[13] and VII.[14]

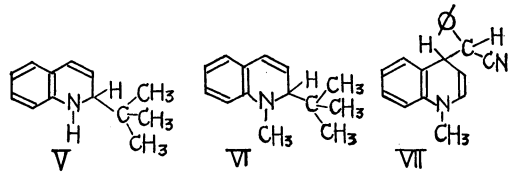

As has been described previously, Ib is autoxidized to the 1-methyl-4-cyanoquinolinium ion in electrolyte solution, while it is autoxidized to 1-methyl-4-cyano-2-quinolone in ethanol. Accordingly, the peroxide initially formed by air-oxidation is considered to have two ways of decomposition: the ionic way (in a buffered solution) and the radical one (in a solution which contains no electrolyte).

Experimental

The polarographic measurements (Yanagimoto Polarograph, Model P8-AP) and controlled potential electrolysis (Nichiakeiki Potentiostat Type NP-1A) for the coulometry were performed with a concentration of 5×10^{-4}M. In the case of the isolation of reduction products, the electrolysis were performed on solutions ranging in concentration from 5×10^{-3}M to 2×10^{-2}M. The IR spectra of the precipitates obtained from electrolyzed solutions were measured as KBr tablets or chloroform solutions. The molecular-weight was determined in benzene with an Hitachi Molecular-Weight Measuring Apparatus, Model 115.

The Nuclear Magnetic Resonance spectra were recorded with a Hitachi Perkin-Elmer R-20 High Resolution NMR Spectrometer at 60 MHz, using tetramethylsilane as the reference. The spectra of Ia were measured at a concentration of about 5w/v-% in acetonitrile, hydrogen oxide, deuterium oxide, and d_6-dimethyl sulfoxide (d_6-DMSO). After the first spectroscopic measurements, a sufficient amount of zinc powder or sodium dithionite was added to the solution, and the solution was warmed for a few minutes. Then the NMR spectra of the resulting deep red solution were again recorded.

The Electronic Spin Resonance spectra were recorded with a Hitachi ESR Spectrometer, Model MES-4001. Twenty ml of a 1-mM acetonitrile solution of a sample containing 0.1 M of TBAP was electrolyzed both *in situ* and in macroscale, using a platium cathode and a platium anode. The nitrogen used to degas the solution was previously passed over a hot copper gauze. The reference electrode used in in this experiment was an $Ag/AgClO_4$ electrode.

1-Methyl-4-cyanoquinolinium Perchlorate (Ia). In a 300-ml three-necked round-bottomed flask fitted with a dropping funnel and a reflux condenser, we placed 14.9 g of 4-cyanoquinoline (0.097 mol) and 80 ml of benzene, and then 12.3 g of dimethyl sulfate (0.098 mol) were added, drop by drop. The mixture was refluxed for about 12 hr on an oil bath. The precipitates thus formed were filtered, washed with benzene, and dried. The precipitates were added to an aqueous solution of 13.5 g (0.097 mol) of potassium perchlorate. The mixture was warmed on a water bath and then cooled. The resulting white precipitates (22.0 g, 0.082 mol, 85%) were recrystallized twice from 200 ml of 50 percent ethanol to give 19.7 g of Ia, mp 200—201°C.

Found: C, 48.96; H, 3.28; N, 9.86%. Calcd for $C_{11}H_9N_2O_4Cl$: C, 49.17; H, 3.38; N, 10.43%.

As will be described below, the conversion to the quinolinium perchlorate was possible by the used of hydrogen perchlorate instead of potassium perchlorate.

1-Methyl-3-cyanoquinolinium Perchlorate (IIa). 3-Cyanoquinoline (2.0 g, 0.013 mol) was dissolved in 50 ml of benzene, and then 1.8 g (0.014 mol) of dimethyl sulfate were added, drop by drop. The mixture was refluxed for 20 hr. The precipitates thus formed were filtered, washed with benzene, and dried to give 2.9 g (0.010 mol, 79%) of 1-methyl-3-cyanoquinolinium methylsulfate (IIa').

To a solution of 2.8 g (0.010 mol) of IIa' in 50 ml of water, we added 1.55 g (0.011 mol) of 70 percent hydrogen perchlorate. White precipitates were filtered out, washed with water and dried. The recrystallization of 2.2 g (0.008 mol, 82%) of the precipitates from 45 mol of 70% ethanol furnished 2.05 g of white needles of IIa, mp 200—202°C.

Found: C, 49.28; H, 3.31; N, 10.47%. Calcd for $C_{11}H_9N_2O_4Cl$: C, 49.17; H, 3.38; N, 10.43%.

1-Methyl-2-cyanoquinolinium Perchlorate (IIIa). 2-Cyanoquinoline (5.0 g, 0.0324 mol) was dissolved in 50 ml of benzene, and to the solution there were then added, drop by drop, 10.0 g (0.0794 mol) of dimethyl sulfate. The mixture was worked up as above. The aqueous solution (100 ml) of 7.0 g of 1-methyl-2-cyanoquinolinium methylsulfate was decolorized with Norit and then filtered. To the filtrate was added 4.5 g (0.027 mol) of 60 percent hydrogen perchlorate. The resulting white crystallines were filtered by suction, washed with water, and dried to give 4.25 g (0.016 mol, 63%) of IIIa, mp 204—205.5°C.

Found: C, 49.53; H, 3.36; N, 10.17%. Calcd for $C_{11}H_9N_2O_4Cl$: C, 49.17; H, 3.38; N, 10.43%.

1-Methyl-2-ethoxyquinolinium Perchlorate. A solution of 1.4 g (0.0052 mol) of IIIa in 32 ml of 90% ethanol was refluxed for a few hours and then cooled to give 0.66 g (0.0023 mol, 44%) of 1-methyl-2-ethoxyquinolinium perchlorate as white needles, mp 182—183°C.

Found: C, 49.74; H, 4.58; N, 4.82%. Calcd for $C_{12}H_{14}NO_5Cl$: C, 49.92; H, 4.90; N, 4.85%.

NMR spectrum (d_6-DMSO, τ): 0.86 (d,1, J=9.75Hz, H_4), 1.58—2.14 (m, 5, H_3 and aromatic H), 5.18 (q,2, J=5.94Hz, $-OC\underline{H}_2CH_3$), 5.81 (s,3, N-CH_3), 8.43 (t,3, J=5.94Hz, $-OCH_2C\underline{H}_3$).

One-electron Reduction of 1-Methyl-4-cyanoquinolium Perchlorate (Ia). In a 500-ml electrolytic cell were placed 2.00 g (0.0075 mol) of Ia, 3.80 g of sodium sulfate, 320 ml of Britton-Robinson buffered solution (pH 7), and 80 ml of distilled water. The solution was then deaerated by a stream of nitrogen while being continuously stirring with a magnetic stirrer. After complete deaeration, electrolysis was carried out at the cathodic potential of −0.70V *vs.* SCE with successive stirring under nitrogen. The electrolysis was stopped when almost no appreciable current passed through. The deep yellow precipitates thus produced were filtered by suction, washed with water, and dried. The precipitates were easily soluble in ether, ethanol, ethyl acetate, and benzene, but insoluble in water and ligroin. Immediately after the precitates were dissolved in solvents, the solutions assumed a dark yellow color; there after they turned light yellow.

Autoxidation of One-electron Reduction Product of Ia. The deep yellow precipitates obtained by the one-electron electrochemical reduction of 2.00 g of Ia were dissolved in ethanol, and the filtrate was evaporated to dryness. The light brown residue was recrystallized from 22 ml of ethanol to give 0.290 g

12) H. Staudinger, H. W. Klever, and P. Kober, *Ann. Chem.*, **374**, 1 (1910).
13) W. Bradley and S. Jeffrey, *J. Chem. Soc.*, **1954**, 2770.
14) J. Leonard and R. L. Foster, *J. Amer. Chem. Soc.*, **74**, 3671 (1952).

(0.0016 mol, 21%) of 1-methyl-4-cyano-2-quinolone. The melting point, the results of elemental analysis, and the UV, IR, and NMR spectra were in agreement with those of the authentic sample.

When the residue of the ethanol solution was sublimed under reduced pressure, 1-methyl-4-cyano-2-quinolone was also obtainable in a 34% yield.

Autoxidation of Two-electron Reduction Products of Ia. A buffered solution (pH 7) of 2.00 g of Ia was electrolyzed at the potential of −1.50V *vs.* SCE in the same way as in the one-electron reduction. The solution of resulting solid in ethanol was filtered, and the filtrate was evaporated to dryness. The residue was sublimed under reduced pressure to give 0.166 g (0.001 mol, 12%) of 1-methyl-4-cyano-2-quinolone.

Oxidation of the Two-electron Reduction Product of Ia with Iodine. Ia (2.00 g) was electrolyzed at −1.50V, and the resulting precipitates were dissolved in 30 m*l* of pyridine. A solution (40 m*l*) of 1.89 g (0.0075 mol) of iodine in methanol was added to this solution. The solvent was evaporated off, and the red-brown, oily material was extracted with water. The water was evaporated, and the residue was recrystallized twice from ethanol to give 0.057 g (3%) of 4-cyanoquinoline methiodide. The melting point, the results of elemental analysis, and the IR and UV spectrum were identical with those of the authentic sample.

One-electron Reduction of 1-Methyl-3-cyanoquinolinium Perchlorate (IIa). The solution of 0.806 g (0.003 mol) of IIa in 200 m*l* of a buffered solution (pH 5) was electrolyzed at −0.80V. The resulting precipitates were dissolved in 40 m*l* of methanol. The solution was poured into 500 m*l* of water after it had been filtered. The mixture was allowed to stand overnight, filtered, and dried to give 0.301 g (0.0009 mol, 59%) of a yellow dimer.

Found: C, 78.18; H, 5.42; N, 16.55%; mol wt, 342. Calcd for $C_{22}H_{18}N_4$: C, 78.07; H, 5.37, N, 16.56%; mol wt, 338.

The solution of 0.201 g (0.00075 mol) of IIa and 1.48 g of potassium perchlorate in 100 m*l* of DMF was electrolyzed at −0.80V. The resulting yellow solution was poured into water and allowed to stand overnight in a refrigerator to give 0.081 g (0.00024 mol, 64%) of the yellow dimer.

One-electron Reduction Product of 1-Methyl-2-cyanoquinolinium Perchlorate (IIIa). The solution of 0.537 g (0.002 mol of IIIa in 200 m*l* of a buffered solution (pH 5) was electrolyzed at −0.70V. The resulting gray reduction product was extracted with ether, and the extract was dried with sodium carbonate. The ether was evaporated to dryness at room temperature under reduced pressure to give an unidentified red-brown resin.

BULLETIN OF THE CHEMICAL SOCIETY OF JAPAN, VOL. 44, 1933—1938 (1971)

Iminodithiocarbonates. III.[1] Reactions with Some Electrophiles and the Structural Effect on Nucleophilic Reactivities and Basicities[2]

Yoshio UENO, Takeshi NAKAI, and Makoto OKAWARA

Research Laboratory of Resouces Utilization, Tokyo Institute of Technology, Ookayama, Meguro, Tokyo

(Received January 13, 1971)

With a view toward demonstrating the structural effect on the reactivity of iminodithiocarbonates, the reactions of some electrophilic reagents with the following four iminodithiocarbonates have been studied; 2-methylimino- (IVa) and 2-phenylimino-1,3-dithiolane (IVb) and *S,S'*-dimethyl-*N*-methyl-(Va) and *S,S'*-dimethyl-*N*-phenyl-iminodithiocarbonate (Vb). Cyclic IVa and its *N*-ethyl homologue reacted with an equimolar amount of phenyl isocyanate at room temperature giving 1:2 cycloadducts. However, the other imino compounds (IVb, Va, and Vb) did not react at all even at elevated temperature. All these imino compounds reacted with acid chlorides to afford the corresponding *N*-acyliminium salts which could, in some cases, be isolated; however the rate of formation of the salts varied significantly with the structure of the imino compound. Some reactions with alkyl halides and phenyl isothiocyanate were also attempted. From the present results and those previously obtained on their reactions with epoxides and with ketenes, it has been concluded that the nucleophilic reactivity of the imino compounds increases in the order Vb<Va<IVb<IVa. Furthermore, it was found that the basicity of the imino compounds increased in the order Vb<IVb<Va<IVa. The observed ring effect and *N*-substituent effect on the reactivity and basicity of the imino compounds are discussed in connection with similar effects on the stability of closely related tri(hetero)carbonium ions, *i.e.*, bis(alkylthio)-dialkylaminocarbonium ion (I).

In our previous paper on tri(hetero)-substituted carbonium ions,[3–5] we reported that the electrophilic reactivity of tri(hetero)substituted carbonium ions (I) depends upon their structural factors, *e.g.*, whether they are cyclic or open-chain. On the other hand, the reaction of iminodithiocarbonates (II) with an electrophile ($^+$E) should involve an initial formation of tri(hetero)-substituted carbonium ions (III). Thus it could be expected that the nucleophilic reactivity of

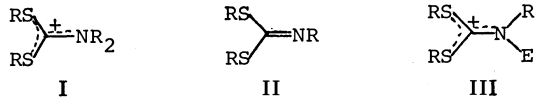

I II III

1) Part I: Y. Ueno, T. Nakai, and M. Okawara, This Bulletin, **43**, 162 (1970), Part II: Y. Ueno, T. Nakai, and M. Okawara, *ibid.*, **43**, 168 (1970).

2) Presented in part at the 22nd Annual Meeting of the Chemical Society of Japan, Tokyo, April, 1969.

3) T. Nakai, Y. Ueno, and M. Okawara, *Tetrahedron Lett.*, **1967**, 3831; This Bulletin, **43**, 156 (1970).

4) T. Nakai and M. Okawara, *Tetrahedron Lett.*, **1967**, 3835; This Bulletin, **43**, 1864 (1970).

5) T. Nakai, and M. Okawara, This Bulletin, **43**, 3528 (1970).

the imino compound (II) is closely related to the stability of the tri(hetero)carbonium ion formed (III).

However, little information has been available on the reaction of II with electrophilic reagents although there are a few papers reporting the reaction of II with epoxides[6] and with ketenes.[7] In order to obtain more elaborate information on the structural effect on the nucleophilic reactivity of iminodithiocarbonates (II), reactions of various types of II with some electrophilic reagents have been studied. Iminodithiocarbonates studied are: 2-methylimino-(IVa) and 2-phenylimino-1,3-dithiolane (IVb) and *S,S'*-dimethyl-*N*-methylimino-(Va) and *S,S'*-dimethyl-*N*-phenyliminodithiocarbonate (Vb). Furthermore, the basicity of these imino compounds has been measured. In this paper we will describe the results of the investigation and discuss the structural effect on nucleophilic reactivity and basicity.

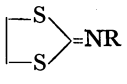

IVa, R=CH_3
b, R=C_6H_5

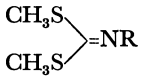

Va, R=CH_3
b, R=C_6H_5

Results

Thermal Isomerization. We reported that 2-methylimino-1,3-dithiolane (IVa) and *N*-ethyl homologue are ring-isomerized at 200°C to the corresponding thiazolidine-2-thione (VI), but 2-phenylimino compound (IVb) is not isomerized even under more drastic conditions.[6]

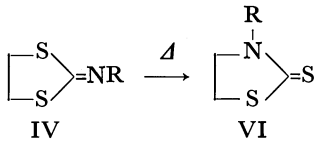

IV VI

R=CH_3, C_2H_5

Attempts to isomerize the open-chain compounds (Va and Vb) were made under various conditions. However, the two compounds were not isomerized to dithiocarbamates even at 250—270°C.

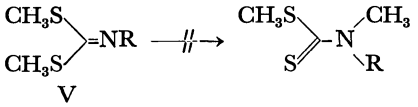

V

R=CH_3, C_6H_5

Harley-Mason has reported that *S,S'*-diphenyl-*N*-phenyliminodithiocarbonate remains unchanged on heating at 330°C.[8]

Reactions with Epoxides. We reported that the cyclic compounds (IVa and IVb) react with epoxides at 140—160°C to give the 2-oxazolidone derivatives (VII) in good yields and suggested that the initial process of this reaction is a cycloaddition of epoxides to the C=N bond of IV.[6,9]

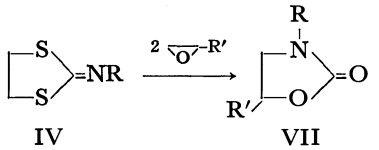

IV VII

R=CH_3, C_6H_5

The reactions of open-chain Va and Vb with propylene oxide were carried out under various conditions. It was found that neither Va nor Vb reacted with epoxide even at 170—180°C, but the starting materials were recovered.

Cycloaddition Reactions with Heterocumulenes. Metzger reported that *o*-chlorophenoxyketene or diphenylketene reacts with numerous iminodithiocarbonates including 2-propylimino-1,3-dithiolane and open-chain Va to afford the corresponding 1:1 cycloadduct (VIII),[7] *e.g.*

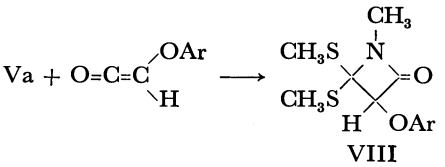

VIII

The reactions of the four iminodithiocarbonates with phenyl isocyanate were attempted. It was found that methylimino-dithiolane (IVa) reacted with an equimolar amount of phenyl isocyanate at room temperature to produce the 1:2 cycloadduct (IXa) in 65% yield. Similarly, ethylimino-dithiolane (IVa') and the isocyanate gave the 1:2 cycloadduct (IXa') in 16% yield in the presence of a small amount of lithium chloride; however, in the absence of the catalyst no reaction proceeded appreciably. In contrast to this observation, the other iminodithiocarbonates (IVb, Va, and Vb) did not react with the isocyanate even at elevated temperature and the starting materials were recovered almost quantitatively.

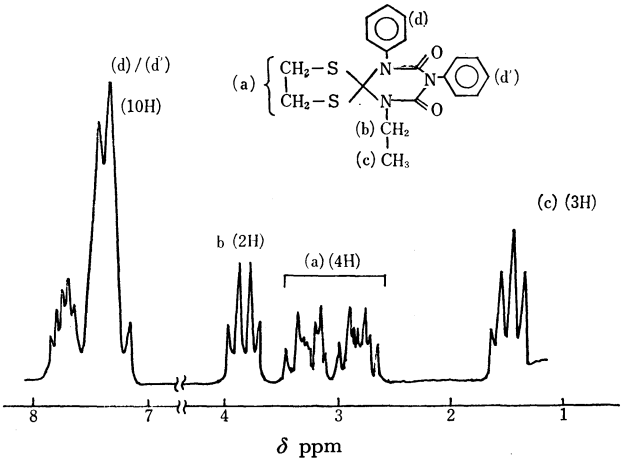

Fig. 1. The NMR spectrum of 1:2 cycloadduct IXa' in $CDCl_3$

Products IXa and IXa' were identified by means of elemental analyses and spectral data (IR and NMR). The IR spectra of IXa and IXa' showed two strong absorption bands at 1703 and 1668—1670 cm^{-1} indicating the presence of two kinds of carbonyl groups. The structure of IXa' was confirmed by the NMR spectrum (Fig. 1) which showed a triplet at δ 1.42

6) Y. Ueno, T. Nakai, and M. Okawara, *ibid.*, **43**, 162 (1970).
7) C. Metzger, *Chem. Ber.*, **101**, 1120 (1968).
8) J. Harley-Mason, *Nature*, **155**, 515 (1945).
9) Y. Ueno, T. Nakai, and M. Okawara, This Bulletin, **43**, 168 (1970).

($N-CH_2C\underline{H}_3$), a quartet at δ 3.83 ($N-\underline{C}H_2CH_3$), two multiplets centered at δ 3.28 and 2.28 ($S-\underline{C}H_2\underline{C}H_2-S$), and a multiplet centered at δ 7.45 (two phenyls). Unequivalence of the two ring-methylenes is noteworthy. It suggests that the phenyl nucleus would significantly deshield the methylene protons situated near the phenyl nucleus.

Product IXa is best explained as a result of an initial formation of the ionic 1:1 adduct (X) which then reacts with additional isocyanate, finally yielding the six-membered ring compound (IXa) instead of the formation of the more hindered four-membered 1:1 cycloadduct.

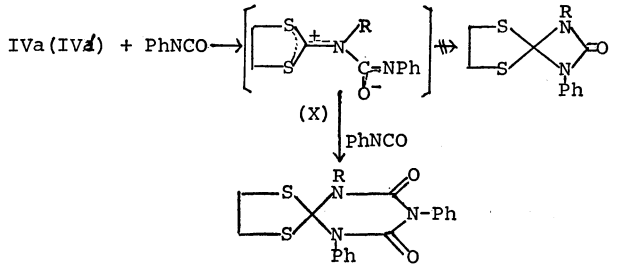

IXa, R=CH_3
a', R=CH_3CH_2

The formation of the 1:2 cycloadduct in equimolar condition is in direct contrast to the reaction of the isopropyl analog of IVa with ketenes described above, and to the reactions of mono-substituted azomethines with phenyl isocyanate only at elevated temperature giving six-membered 2:1 cycloadducts.[10]

Reactions of the four imino compounds with phenyl isothiocyanate were attempted; however, no significant reactions were observed.

Reactions with Acid Chlorides. The acylating reactions with acid chlorides have been carried out in the presence of tertiary amine. In these cases existance of acylammonium salts as reactive intermediates has been postulated. However, the acylammonium salts were so unstable that only a few salts have been successfully isolated. Acyliminium salts such as acylpyridinium salt are also too unstable to be isolated.

If the iminodithiocarbonates reacts with an acid chloride, the acyliminium salt formed would be greatly stabilized through delocalization of the positive charge by the two sulfur atoms as shown below.

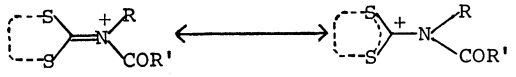

Reactions of imino-dithiolane IVa and IVb with acetyl chloride, benzoyl chloride, and methacryloyl chloride were carried out at room temperature in inert solvents such as ether or benzene. The reaction proceeded immediately to completion yielding crystalline adducts XI quantitatively. In the reaction of IVa with acetyl chloride it was necessary to cool the reaction mixture with dry ice-acetone bath because of violent heat evolution. On the other hand, in the reaction of IVb with benzoyl chloride, the reaction proceeded slowly. The acyliminium salts obtained were stable white solids in inert solvent, but they were hygroscopic in air. An exchange of the counter anion of Cl^- with $SbCl_6^-$ or $B(C_6H_5)_4^-$ was successful in the case of XIb and XIe. However, in other cases, the salts were easily hydrolyzed giving rise to the formation of HX salts of iminodithiocarbonates, XVI.

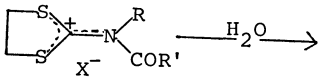

XIa,c,d.

XVI

TABLE 1. *N*-ACYLIMINIUM SALTS XI

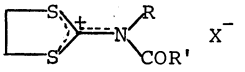

	R	R'	X	IR (KBr) ($\nu_{C=O}$) cm^{-1}	Mp (°C)
XIa	CH_3	CH_3	Cl	—	—
b	CH_3	C_6H_5	Cl	1700	126—129
b'	CH_3	C_6H_5	$SbCl_6$	1700	134—135
c	C_6H_5	CH_3	Cl	—	—
d	C_6H_5	C_6H_5	Cl	—	—
e	CH_3	$CH_2=C(CH_3)$	$B(C_6H_5)_4$	1740	110

Similarly, open-chain iminodithiocarbonates Va and Vb reacted with acetyl chloride to give very hygroscopic *N*-acethyliminium chlorides (XII) which were easily hydrolyzed with the moisture in air.

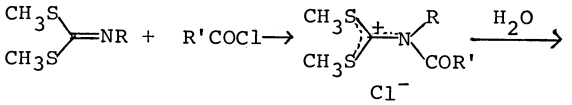

V XII

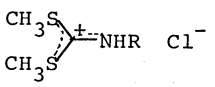

Stability of N-*Acyliminium Salts (XI, XII).* Cyclic iminium salts XI were more stable than open-chain analogs XII. This is in agreement with the fact that 2-dimethylamino-1,3-dithiolanium salt XIII in more stable than its open-chain analog XIV.[12]

XIII XIV

XIb and XIe in particular, were stable enough to be isolated and characterized by IR spectra and elemental analyses.

Thus, stabilization of XI is increased by the *N*-sub-

10) H. Ulrich, "Cycloaddition Reactions of Heterocummulenes," Academic Press, New York (1967), pp. 153—155.

stituent in the order $CH_3<C_6H_5<CH_2=\underset{\displaystyle CH_3}{\overset{|}{C}}-$.

This was rationalized by the following resonance effect, which caused the decrease in the positive charge on the nitrogen atom.

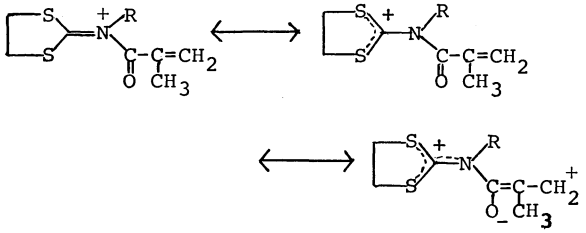

Acylation of Amine by N-*Acyliminium Salt XI.* The strong acylating ability of the *N*-acyliminium salt XI was demonstrated using the IVb acetyl chloride adduct, XIc. The solution of aniline in benzene was added to the suspension of XIc in the same solvent and the mixture was warmed in a water-bath for one minute to produce acetanilide in 52% yield.

Reactions with Alkyl Halides. Alkylation of imino-1,3-dithiolane IVa with active halides such as α-haloketone, α-haloester and benzyl halide easily took place, producing the *N,N*-dialkyliminium salts XV in acetonitrile or under neat conditions at room temperature. Thus, IVa reacted with phenacyl bromide, ethyl bromoacetate and *p*-nitrobenzyl bromide to give the iminium salts XVa, b, and c in 92, 93, and 92% yield, respectively.

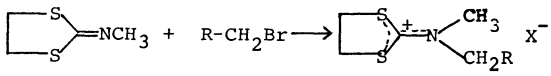

XVa, R=C_6H_5CO X=ClO_4
b, R=EtOCO X=ClO_4
c, R=p-$NO_2C_6H_4$ X=Br

In the case of XVa and XVb, the counter anion was exchanged into perchlorate anion by treating the salts with sodium perchlorate. Similarly, methylation of IVa with methyl iodide occurred to produce 2-dimethylamino-1,3-dithiolanium salt XIII in good yield.

On the other hand, 2-phenylimino-1,3-dithiolane (IVb) or *S,S'*-dimethyl-*N*-methyliminodithiocarbonate (Va) reacted with phenacyl bromide to give unidentified products and no simple alkylation products were obtained.

Determination of the Basicities of the Iminodithiocarbonates (IV and V) by Spectrophotometry. Basicities of IV and V were calculated using the following equation,[11]

$$pK_a = pK_{HAc} + \log (C_{Ac^-}/C_{HAc}) + \log (D - D_{B^-}/D_{HB} - D)$$

where D_{B^-}, D_{HB}, and D refer to the absorption coefficient of the iminodithiocarbonates measured in water

Table 2. Nucleophilic reactivities of iminodithiocarbonates

Reactants[g]	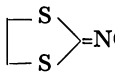	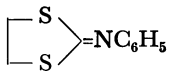	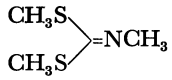	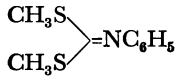
p*K*a	5.2	3.2	4.8	2.7
Thermal isomerization	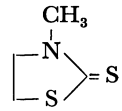	← N.R.[a] →		
Epoxide	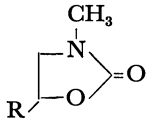	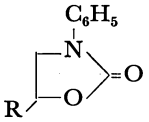	← N.R. →	
C_6H_5NCO	1:2 adduct[b]	← N.R. →		
C_6H_5NCS	← N.R. →			
RCOCl	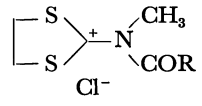	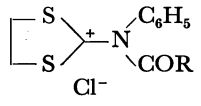	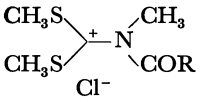	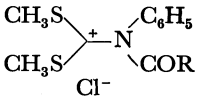
RCH_2X	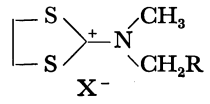	d)	d)	—
Ketene[c]	1:1 adduct[e]	—	1:1 adduct[f]	

a) no reaction b) 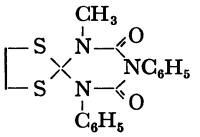 c) C. Metzger, *Chem. Ber.*, **101**, 1120 (1968).

d) unidentified products e) 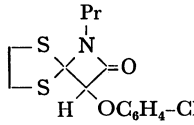 f) 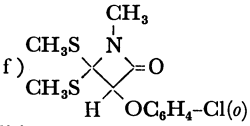

g) The respective reactions were carried out under similar conditions.

11) L. P. Hammet. L. A. Flexser, and A. Dingboll, *J. Amer. Chem. Soc.*, **57**, 2103 (1935).

(curve 1), in aqueous sulfuric acid (curve 2), and in acetic acid-sodium acetate buffer solution (curve 3), respectively. For the calculation, values of D_{B-}, D_{HB}, and D were taken from the curves 1, 2, and 3, respectively, at some wave lengths omitting than those in the neighborhood of the isobestic point. The value of pKa of acetic acid was taken as 4.76. Complete protonation of IVa was observed in over 18.2 wt% of aqueous sulfuric acid. The values of pKa of IVb, Va, and Vb were calculated in a similar manners. The pKa values are summarized in Table 2.

Correlation between Nucleophilic Reactivities and Structures of Iminodithiocarbonates. The nucleophilic reaction data of the iminodithiocarbonates including the previous results[6] are summarized in Table 2. We see that 1) nucleophilic reactivites of iminodithiocarbonates decrease in the order IVa>IVb>Va>Vb, and 2) this order is almost in agreement with that of basicities of the imino groups.

These observations indicate that the nucleophilic reactivities of iminodithiocarbonates may qualitatively be explained in terms of the basicities of the imino groups.

Ring Effect. The greater reactivities and basicities of cyclic IV than those of open-chain V show that the polarized structure (B) significantly contributes to the ground state of the former, and that the structure (B′) in the latter is less important.

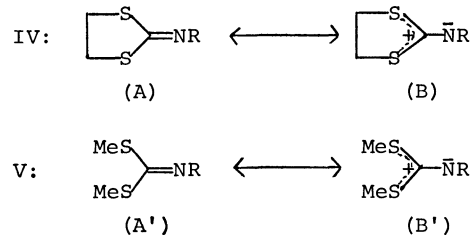

In other words, resonance stabilization of the polarized structure (B and B′) by the two sulfur atoms is greater in cyclic than open-chain analog.

A similar ring effect was observed in the greater basicities and reactivities toward epoxides of various cyclic thione compounds than in those of open-chain analog.[9]

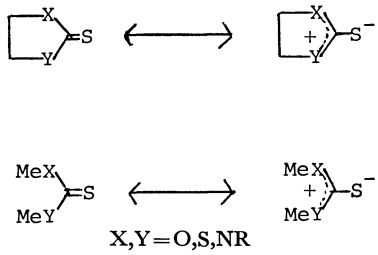

Moreover, the ring effect has also been observed in the stability of tri(hetero)substituted carbonium ion; thus cyclic cation XIII was more stable than open-chain analog XIV.[12] This is also true for the stability of N-acyliminium salts. In general, ring effects such as enhanced reactivity, basicity, and stability of the cyclic compounds might be recognized in the following compounds as compared with open-chain analogs.

(X, Y, Z=O, S, NR′)

The ring effect is probably attributed to a much greater overlap between the lone pairs of the heteroatoms and 2p orbital of sp^2 center carbon in the ring compounds than in the analogous open-chain compounds.

N-*Substituents.* In both cases of IV and V, the difference of pKa between the N-methyl and the N-phenyl derivatives is 2.0—2.1. This shows that a pair of electrons on the iminonitrogen of IV and V are delocalized over the phenyl nucleus to the same extent. Thus the smaller reactivities of N-phenyl derivatives can be explained by this electron delacalization. In summary, the nucleophilic reactivities of iminodithiocarbonates are explained in terms of the ring effect and the N-substituents.

Experimental

General. All melting and boiling points are uncorrected. IR and UV spectra were recorded with Hitachi EPI-S-2 and EPS-2 spectrometers, respectively. NMR spectra were obtained with a Japan Electron Optics JNL 4H-100 spectrometer. Chemical shifts are given in ppm from tetramethylsilane as an internal standard.

Materials. All iminodithiocarbonates were prepared by the methods previously reported: methylimino-1,3-dithiolane (IVa), bp 79—81°C/0.45 mmHg; ethylimino-1,3-dithiolane (IVa′), bp 85—87°C/0.30 mmHg; phenylimino-1,3-dithiolane (IVb), mp 47—48°C; N-methylimino-dithiocarbonate (Va), bp 110—112°C/70 mmHg; N-phenyliminodithiocarbonate (Vb), mp 34—35°C. Other reagents were either commercially available materials or prepared by a standard method.

Reaction of Methylimino-dithiolanes with Phenyl Isocyanate. Methylimino-dithiolane IVa (1.3 g, 0.01 mol) and phenyl isocyanate (1.2 g, 0.01 mol) were mixed at room temperature. A vigorous exothermic reaction occurred and crystals were immediately formed. After standing the reaction mixture at room temperature overnight, the precipitates were collected by filtration to give 1.2 g (65%) of the 1:2 cycloadduct (IXa). To remove the impurities (diphenylurea), the precipitates were washed several times with warm ether and recrystallized from acetonitrile: mp 231.5—232.5°C; IR (KBr) 1703 and 1670 cm^{-1} (C=O).

Found: C, 58.34; H, 4.39; N, 11.53%. Calcd for $C_{18}H_{17}N_3O_2S_2$: C, 58.22; H, 4.61; N, 11.32%.

The reaction of imino-dithiolane IVa′ with phenyl isocyanate was carried out under similar conditions in the presence of lithium chloride (0.10 g) to produce the cycloadduct IXa′ in 16% yield: mp 202—203°C (recrystallized from a mixture of ethanol and ether): IR (KBr) 1703 and 1668 cm^{-1} (C=O),

Found: C, 59.01; H, 5.00; N, 10.94%. Calcd for $C_{19}H_{19}N_3O_2S_2$: C, 59.21; H, 4.97; N, 10.90%.

The IR spectrum of IXa′ closely resembled that of IXa. The NMR spectrum of IXa′ is given in Fig. 1.

Reaction of Iminodithiocarbonates (IV or V) with Acid Chlorides. General Procedure: The iminodithiocarbonate was mixed with the acid chloride listed in Table 1 at room temperature in inert solvent (benzene, ether) or under neat conditions. Acyliminium salts were obtained as crystalline solids.

12) T. Nakai, Y. Ueno, and M. Okawara, This Bulletin, **43**, 3175 (1970).

Reaction of Imino-dithiolane IVa with Benzoyl Chloride. IVa (1.3 g, 0.01 mol) and benzoyl chloride (1.4 g, 0.01 mol) were mixed. A white crystalline precipitate XIb started to separate almost immediately. The acyliminium salt XIb was obtained in quantitative yield, mp 126—129°C (recrystallized from benzene); IR (KBr): 1700 cm^{-1} (C=O).

Found: N, 5.12%. Calcd for $C_{11}H_{12}NOS_2Cl$: N, 5.18%.

Conversion of the counter anion of the salt XIb into antimony hexachlorate anion by the addition of antimony pentachloride gave *N*-benzoyliminium antimony hexachlorate XIb′: mp 134—135°C; IR (KBr): 1700 cm^{-1} (C=O).

On the other hand, treatment of the reaction mixture with aqueous sodium tetraphenylborate gave only the hydrolyzed product, XVI (X=$B(C_6H_5)_4$: mp 157—158°C;

Found: C, 73.61; H, 6.29; N, 2.80%. Calcd for $C_{28}H_{28}BNS_2$: C, 74.16; H, 6.22; N, 3.09%.

Reaction of Imino-dithiolane IVa with Methacryloyl Chloride. The crystalline adduct was treated with aqueous sodium tetraphenylborate to give XIe in quantitative yield: mp 110°C (recrystallized from acetonitrile);

Found: N, 2.69%. Calcd for $C_{32}H_{32}NOS_2B$: N, 2.65%.

In other cases, the resulting adducts (XIa, c, and d) were difficult to isolate. They were solids stable only in inert solvents.

Acetylation of Aniline with Iminium Salt XI. To the suspension of XIc (prepared from 1.0 g of acetyl chloride and 1.0 g of IVb) in benzene, was added 0.48 g of aniline in benzene. After warming the reaction mixture for one minute on water-bath, the reaction mixture was poured into the cold water to give 0.35 g (52%) of acetanilide: mp 110—112°C (lit., 114°C) (recrystallized from water). The IR spectrum of this product was identical with that of authentic sample of acetanilide.

Reaction of Imino-dithiolane IVa with Alkyl Halides. General Procedure: 2-Methylimino-1,3-dithiolane IVa was mixed with the equimolar amount of alkyl halide in acetonitrile or under neat conditions at room temperature. The iminium salts were isolated as perchlorates by treating with aqueous sodium perchlorate.

Reaction of IVa with Phenacyl Bromide. The imino-dithiolane (11.2 g, 0.084 mol) IVa was mixed with phenacyl bromide (16.8 g, 0.084 mol) in acetonitrile (30 m*l*) at room temperature. Heat evolution took place with the addition of solid sodium perchlorate to the reaction mixture. After about 30 min, the reaction mixture was treated with excess aqueous sodium perchlorate to give the solid, which was washed with water and then with ether: (27 g, 92%); mp 194—195°C, IR (KBr); 1700 cm^{-1} (C=O), 1080 cm^{-1} (ClO_4^-); UV $\lambda_{max}^{H_2O}$ 257.5 mμ.

Found: C, 40.98; H, 4.00; N, 4.02%. Calcd for $C_{12}H_{14}NO_5S_2Cl$: C, 40.98; H. 4.01; N, 3.98%.

Reaction of IVa with Ethyl Bromoacetate. Similarly, IVa (1.3 g, 0.01 mol) was allowed to react with ethyl bromoacetate (1.7 g, 0.01 mol) under neat conditions to give salt (93%). The bromide anion was converted into perchlorate anion by treatment with aqueous sodium perchlorate to give XVb: mp 119.5—120.5°C (recrystallized from ethanol).

Found: C, 29.64; H, 4.31; N, 4.40%. Calcd for $C_8H_{14}NO_6S_2Cl$: C, 30.06; H, 4.41; N, 4.38%.

Reaction of IVa with p-*Nitrobenzyl Bromide.* IVa (6.5 g, 0.03 mol) and *p*-nitrobenzyl bromide (6.5 g, 0.03 mol) in acetonitrile (10 ml) were warmed on a water bath for 1 hr. Cooling the reaction mixture gave the iminium salt XVc containing one mole of water of crystallization. (10.1 g, 92%): mp 84—85°C (recrystallized from acetonitrile).

Found: C, 35.90; H, 4.02; N, 7.62%. Calcd for $C_{11}H_{13}N_2O_2S_2Br\cdot H_2O$: C, 35.98; H, 3.29; N, 7.63%.

Reaction of IVa with Methyl Iodide. A slight excess of methyl iodide was added to a solution of IVa in acetonitrile. Dithiolanium salt XIII was obtained in 90% yield: mp 184—186°C (recrystallized from acetonitrile).

Found: C, 22.08; H, 3.56; N, 5.30%. Calcd for $C_5H_{10}NS_2I$: C, 21.82; H, 3.66; N, 5.09%.

Determination of the pKa of Iminodithiocarbonates. The buffer solution was a mixture of acetic acid (0.35 mol/*l*) and sodium acetate (0.10 mol/*l*). As both IVb and Vb did not completely dissolve in water or in buffer solution, a small amount of ethanol (1—2%) was added to obtain in a clear solution. Concentration of the samples was approximately $1.0—1.7\times10^{-4}$ mol/*l*. The concentrations of sulfuric acid for complete protonation of iminodithiocarbonates were 18.2, 45.5, 57.5, and 57.5 wt % for IVa, IVb, Va, and Vb, respectively. The p*K*a values thus obtained are summarized in Table 3.

Table 3. pK_a of iminodithiocarbonates

	Wavelength (mμ)	Coefficient			pK_a
		D_B-(H_2O)	*D* (Buffer soln)	D_{HB} (H_2SO_4)	
IVa	235.0	7400	8200	8300	5.12
	240.0	6600	10100	10500	5.16
	244.5	5800	10700	11200	5.21
	Average				5.16
IVb	237	9800	9400	5700	3.55
	240	9700	9400	5500	3.10
	260	7000	7100	8300	3.14
	265	6400	6700	10200	3.15
	Average				3.24
Va	245	6900	11300	12700	4.71
	250	6100	12100	13500	4.85
	252	5700	12200	13800	4.82
	260	3900	9800	12000	4.61
	Average				4.75
Vb	260	5500	5800	15100	2.75
	265	4700	5000	16100	2.65
	270	4300	4600	14300	2.68
	275	4200	4400	12300	2.61
	Average				2.67

Solvolysis of Organic Phosphates. III[1] 3-Pyridyl and 8-Quinolyl Phosphates in Spontaneous Reaction[2]

Yukito MURAKAMI and Junzo SUNAMOTO

Department of Organic Synthesis, Faculty of Engineering, Kyushu University, Fukuoka

(Received January 13, 1971)

The spontaneous hydrolysis of 3-pyridyl and 8-quinolyl phosphates was investigated at 60, 70, and 80°C over the $-\log[H^+]$ range from 1 to 7 in aqueous media with an ionic strength of 0.10. The reactions followed apparent first-order kinetics with respect to the unreacted phosphate species, and the maximum rate was observed around $-\log[H^+]=2.5$. Reactive species of each phosphate in hydrolysis were the neutral zwitterion and the monoanion, the former being found to be more labile. In a moderately acidic region ($-\log[H^+]<2.0$), an apparent enhancement of the reaction rate was detected for both phosphates, which was attributed to the acid catalysis acting on the zwitterion species. The activation enthalpy for hydrolysis of the zwitterion and the monoanion falls near 30 kcal mol^{-1}. This is consistent with the reaction mechanism expected for hydrolysis of ordinary monoalkyl or monoaryl phosphate, in which the P–O bond cleavage takes place. The activation entropy data also provide an evidence for the unimolecular nature of the transition state. The kinetic solvent isotope effect k^{H_2O}/k^{D_2O} for the hydrolysis of both phosphates falls near unity. The isotope effect in this magnitude is consistent with the intramolecular proton-transfer mechanism. The results are, therefore, consistent with a mechanism for the hydrolysis of the zwitterion species of 8-quinolyl phosphate in which the quinolinium group donates a proton intramolecularly to the leaving ester oxygen atom in the transition state.

In an earlier study[3] dealing with the hydrolysis of pyridylmethyl phosphates in the presence and the absence of metal ions, we elucidated the correlation between reaction rate and structural specificity of the leaving alcohol group of the phosphates. As a result, the extent of participation of the pyridyl nitrogen in their reaction processes was discussed. The neutral zwitterion form of 2-pyridylmethyl phosphate **1** was

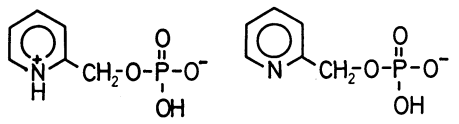

1 **2**

found to be more labile than the corresponding monoanion species **2**. The profound reactivity of the former was attributed to the unique intramolecular proton-transfer mechanism, in which the pyridinium group donates a proton to the leaving ester-oxygen in the transition state. In the hydrolysis reactions of 3- and 4-pyridylmethyl phosphates no such unique behavior was detected.

In the present work, the spontaneous hydrolysis of 3-pyridyl and 8-quinolyl phosphates has been investigated in conjunction with kinetic solvent isotope effect as well as activation entropy and enthalpy effects. The former phosphate has no pyridinium proton available for an intramolecular proton-transfer mechanism, while the latter has a structural analogy to 2-pyridylmethyl phosphate. It is expected that some aspects, such as an intramolecular proton-transfer mechanism, participation of a water molecule in the transition state, and the electronic effect of the hetero-aromatic nitrogen on reactivity may be clarified.

Experimental

Materials. Preparation and purification of 2-pyridylmethyl phosphate have been described previously.[4] 3-Pyridyl and 8-quinolyl phosphates were prepared by the reaction of 3-pyridinol and oxine respectively with phosphorous oxychloride, and purified by the column chromatographic technique with cation exchange resin. Detailed synthetic methods and purification procedures have been described elsewhere.[5] Heavy water was obtained from Mallinckrodt Chemical Works (99.8%, Deuter AR), and from E. Merck Ag. Darmstadt (99.75%, Uvasol^R) and used without furhter purification. Use of either of these reagents gave no noticeable difference in reaction kinetics. Sodium deuteroxide solution (0.1 N) was obtained by diluting 40% concentrated sodium deuteroxide (G.R.) purchased from Merck with deuterium oxide. Deuteroperchloric acid (0.1 N) was prepared by diluting 60% aqueous solution with deuterium oxide. Other solution in deuterium oxide were prepared directly by dissolving the anhydrous compounds. Other materials were of analytical grade and used without any particular purification.

Apparatus. The reaction vessel used for kinetic and potentiometric measurements was the same as that designed and use for the reactions of pyridylmethyl phosphates.[3] Electrodes used for pH measurements in kinetic runs were a set of glass electrode HG-6005 and reference electrode HC-605 of TOA Electronics, Ltd., Tokyo, or a set of Beckman glass electrode No. 39099 and Beckman reference electrode No. 39402. When the Beckman electrodes were adopted, a Beckman SS-2 pH meter was used in place of TOA HM-5A. Both of these pH meters were incorporated with TOA pH-stat HS-1B and TOA EPR-2T recorder in order to maintain pH-value constant during each run.

Kinetic Measurements. The reaction rate was determined by measuring the amount of inorganic orthophosphate liberated in the course of reaction. When an aqueous system was investigated, the experimental technique generally followed the procedure described previously.[2] When the

1) Contribution No. 211 from the Department of Organic Synthesis, Faculty of Engineering, Kyushu University.

2) Preliminary communication: Y. Murakami, J. Sunamoto, and H. Sadamori, *Chem. Commun.*, **1969**, 983.

3) Y. Murakami and M. Takagi, *J. Amer. Chem. Soc.*, **91**, 5130 (1969).

4) Y. Murakami, M. Takagi, and H. Nishi, This Bulletin, **39**, 1197 (1966).

5) Y. Murakami, J. Sunamoto, H. Sadamori, H. Kondo, and M. Takagi, *ibid.*, **43**, 2518 (1970).

reaction was carried out in deuterium oxide, the solution was made up initially to 35 m*l* in total volume and a 1.00-m*l* sample was drawn out from the vessel by a syringe at an appropriate time interval.

pD Measurements. The pH-meter was first calibrated with two standard aqueous buffer solutions, phthalate and phosphate buffers, and then potentiometric titration of deuteroperchloric acid with sodium deuteroxide of known concentration was carried out at a given temperature and a constant ionic strength. The difference (ΔpD) between the negative logarithm of a real concentration of deuterium ion, established by the titration of deuteroperchloric acid with sodium deuteroxide, and the apparent pH-meter reading is represented by the equation:

$$\Delta\text{pD} = -\log[\text{D}^+] - \text{"pH-meter reading"}$$

For example, at an ionic strength of 0.10 (KNO_3) and 70°C, ΔpD was determined to be 0.276. It was assumed that the ΔpD value was valid at the same temperature and ionic strength over the whole pD range studied. In this way, $-\log[\text{D}^+]$ values were established from pH-meter readings. Before determining ΔpD, the electrodes used were preequilibrated in deuterium oxide for 2 days or more. In each run, thereafter, the electrode system was conveniently checked with 0.05 M potassium biphthalate in deuterium oxide. The pH-meter reading of this reference solution corresponds to 4.21 in pD value at 70°C, 4.32 at 80°C, and 4.30 at 90°C.

Determination of Acid Dissociation Constants. The acid dissociation constants of 3-pyridyl and 8-quinolyl phosphates in aqueous solution at low temperature (25°C) were determined by titrating 2.0×10^{-3} M solution of the phosphates with a standard alkaline solution according to standard procedures. However, the acid dissociation constants obtained by this method at higher temperatures, especially the second one (K_{H_2A}), were suspected to involve a little uncertainty. The possible errors can be caused by trace hydrolysis of the phosphates during the course of measurements. Thus, under these circumstances as well as in the runs in heavy water at elevated temperatures, the kinetic (or dynamic) acid dissociation constants of each ionic species were evaluated by means of the equation:

$$k_0 = k_{H_2A}X_{H_2A} + k_{HA}X_{HA} + k_AX_A \qquad (1)$$

where k_0 is the over-all rate constant and ks stand for the specific rate constants of ionic species suffixed to them; H_2A, HA, and A refer to neutral, monoanionic, and dianionic species of the phosphate, respectively. Mole fraction X of each ionic species is related to the corresponding acid dissociation constant in terms of the following relationships:

$$T_E = [H_3A] + [H_2A] + [HA] + [A]$$

$$[H_3A] = \frac{[A]}{K_{H_2A}K_{H_2A}K_{HA}}[H^+]^3$$

$$[H_2A] = \frac{[A]}{K_{H_2A}K_{HA}}[H^+]^2$$

$$[HA] = \frac{[A]}{K_{HA}}[H^+]$$

Ks are acid dissociation constants of various ionic species suffixed to them, and T_E is the total phosphate concentration. In spite of the above general expression for reaction rate, the dianionic species of the present phosphates, as well as those of the pyridylmethyl phosphates,[3] were not reactive in the spontaneous hydrolysis. Thus, we could eliminate the last term in the right side of Eq. (1). The first approximation of the remaining four constants K_{H_2A}, K_{HA}, k_{H_2A}, and k_{HA} were carried out by solving the corresponding matrix of four rows and four columns, based on the data obtained in a pH range 3.0—6.0. The calculation was then iterated with the use of these evaluated four constants as a starting set until the best fit of the calculated values to the observed over-all rate constants was attained over the appropriate pH range studied ($-\log[H^+]=2.5$—7.0). All the calculation processes were programmed by means of Kyushu Daigaku Fortran and carried out on a FACOM 230-60 electronic computer of the Computer Center of Kyushu University.

Results

Acid Dissociation Constants. As mentioned in the experimental section, acid dissociation constants at elevated temperatures were evaluated by potentiometric method and/or by kinetic method. They are listed in Table 1, along with the values previously reported for 2-pyridylmethyl phosphate.[3]

Table 1. Acid dissociation constants of 8-quinolyl, 3-pyridyl, and 2-pyridylmethyl phosphates at various temperatures and $\mu=0.10$ (KNO_3)

Temp. °C	pK_{H_2A}	pK_{HA}
	8-Quinolyl phosphate	
25	4.17[a]	6.42[a]
80	4.16[a]	6.29[a]
80	4.09[b]	6.24[b]
80	4.05[c]	6.50[c]
	3-Pyridyl phosphate	
25	3.86[a]	5.64[a]
50	3.85[a]	5.62[a]
70	3.87[b]	5.76[b]
70	4.28[c]	5.71[c]
	2-Pyridylmethyl phosphate	
25	4.42[d]	6.29[d]
80	4.15[d]	6.54[d]
90	4.03[b]	6.46[b]
90	4.46[c]	6.46[c]

a) Determined by potentiometric titration.
b) Estimated by kinetic method using Eq. (1).
c) Estimated by kinetic method using Eq. (1) in deuterium oxide.
d) Reported previously[3] (determined by potentiometric titration).

Spontaneous Hydrolysis in Aqueous Media. 3-Pyridyl and 8-quinolyl phosphates were hydrolyzed at 60, 70, and 80°C in aqueous media for which an ionic strength was maintained at 0.10. The reactions followed apparent first-order kinetics with respect to the total concentration of the unreacted phosphate. The over-all rate constants, k_{obs}, thus obtained are listed in Table 2, together with the results in deuterium oxide as well as those for 2-pyridylmethyl phosphate in deuterium oxide.

The pH-rate profiles for 8-quinolyl, 3-pyridyl, and 2-pyridylmethyl phosphates are shown in Figs. 1, 2, and 3, respectively, along with the corresponding pD-rate profiles.

For the hydrolysis of 3-pyridyl phosphate, there is a narrow plateau on its experimental pH-rate profile

Table 2. Apparent first-order rate constants for the spontaneous hydrolysis of 8-quinolyl, 3-pyridyl, and 2-pyridylmethyl phosphates at $\mu=0.10$

$-\log [H^+]$[a]	Temp. °C	$k_{obs}\times 10^5$ sec^{-1}	Supporting electrolyte
	8-Quinolyl phosphate		
1.04	80	8.55	$HClO_4$
1.05	80	8.51	$HClO_4$
1.51	80	7.64	$HClO_4-NaClO_4$
1.52	80	7.07	$HClO_4-NaClO_4$
2.02	80	7.81	$HClO_4-NaClO_4$
2.04	80	7.52	$HClO_4-NaClO_4$
2.33	80	7.93	$HClO_4-NaClO_4$
2.97	80	7.53	$HClO_4-NaClO_4$
3.47	80	7.26	$NaClO_4$
3.53	80	7.18	$NaClO_4$
3.91	80	6.36	KNO_3
4.37	80	6.53	KNO_3
5.00	80	4.36	KNO_3
5.62	80	3.22	KNO_3
6.31	80	1.94	KNO_3
2.01	70	2.11	$HClO_4-NaClO_4$
4.31	70	1.42	KNO_3
2.00	60	0.717	$HClO_4-NaClO_4$
4.39	60	0.397	KNO_3
2.44[c]	80	7.36[d]	$DClO_4-KNO_3$
3.88[c]	80	7.71[d]	KNO_3
4.38[b,c]	80	6.34[d]	KNO_3
6.05[c]	80	3.61[d]	KNO_3
	3-Pyridyl phosphate		
1.02	70	9.00	$HClO_4$
1.03	70	8.83	$HClO_4$
1.42	70	7.75	$HClO_4-NaClO_4$
1.49	70	7.86	$HClO_4-NaClO_4$
2.00	70	7.72	$HClO_4-NaClO_4$
2.01	70	7.72	$HClO_4-NaClO_4$
2.37	70	7.39	$HClO_4-NaClO_4$
2.41	70	7.44	$HClO_4-NaClO_4$
3.06	70	6.97	$NaClO_4$
3.08	70	6.83	$NaClO_4$
3.31	70	6.44	$NaClO_4$
3.32	70	6.39	$NaClO_4$
3.82	70	4.92	KNO_3
3.83	70	4.67	$NaClO_4$
4.25	70	3.28	KNO_3
4.31	70	3.36	KNO_3
4.79	70	2.33	KNO_3
4.80	70	2.31	KNO_3
5.20	70	1.72	KNO_3
5.31	70	1.75	KNO_3
5.64	70	1.19	KNO_3
5.65	70	1.14	KNO_3
6.20	70	0.580	KNO_3
2.05	80	22.9	$HClO_4-NaClO_4$
4.52	80	8.58	$NaClO_4$
2.00	60	2.17	$HClO_4$
4.59	60	0.667	$NaClO_4$
2.08[c]	80	8.53[d]	$DClO_4$
3.66[c]	80	6.33[d]	KNO_3
4.31[c]	80	4.78[d]	KNO_3
5.33[c]	80	2.22[d]	KNO_3
6.63[c]	80	0.294[d]	KNO_3
	2-Pyridylmethyl phosphate		
2.23[c]	90	2.82[d]	$DClO_4-KNO_3$
3.80[c]	90	2.55[d]	KNO_3
4.36[c]	90	2.19[d]	KNO_3
6.95[c]	90	0.358[d]	KNO_3

a) Variation was maintained within ± 0.02 unless otherwise stated.
b) Variation was maintained within ± 0.04.
c) Value of $-\log [D^+]$ in deuterium oxide solution.
d) A reference electrode with calomel internal element which was placed in a bridge solution consisting of saturated potassium chloride solution was used.

in the pH region 2—3, where the major fraction of the phosphate is in the neutral zwitterion form. A similar observation was made for the hydrolysis of 8-quinolyl phosphate. Thus, we may propose that the neutral zwitterion and the monoanionic species of these phosphates are reactive as was confirmed to be the case for pyridylmethyl phosphates. To evaluate the specific rate constants for these reactive ionic species, fractional molar concentrations of various ionic species of each substrate were calculated by the aid of acid dissociation constsnts listed in Table 1. The following equation can be used for the calculation of the specific rate constants for these active species.

$$k_{obs} = k_{H_2A}X_{H_2A} + k_{HA}X_{HA}$$

where k_{obs} refers to the observed over-all rate constant. On the other hand, employment of Eq. (1) results in a simultaneous evaluation of rate constants and acid dissociation constants as mentioned in the previous section. The results are listed in Table 3.

In a moderately acidic region ($-\log[H^+]<2.0$), a good linear relationship between $k_{obs}-(k_{H_2A}X_{H_2A}+k_{HA}X_{HA})$ and the stoichiometric concentration of hydrogen ion exists for both phosphates. From the slope of the straight line, we tentatively estimated a specific rate constant for acid-catalyzed reaction, K_H^+: 8-quinolyl phosphate, $k_H^+=4.79\times 10^{-4}M^{-1}sec^{-1}$ at 80°C; 3-pyridyl phosphate, $k_H^+=5.00\times 10^{-4}M^{-1}sec^{-1}$ at 70°C.

Activation Parameters. Activation parameters for the hydrolysis of 8-quinolyl and 3-pyridyl phosphates are listed in Table 4. They were evaluated from the specific rate constants for the hydrolysis reactions of the neutral and monoanionic species (Table 3).

Discussion

In general, organic phosphates are polybasic acids and various ionic species with different degree of protonation exist in solution. The reactivity of these ionic species varies from one species to another, depending upon the structural property of the leaving alcohol group. In a series of solvolysis studies of

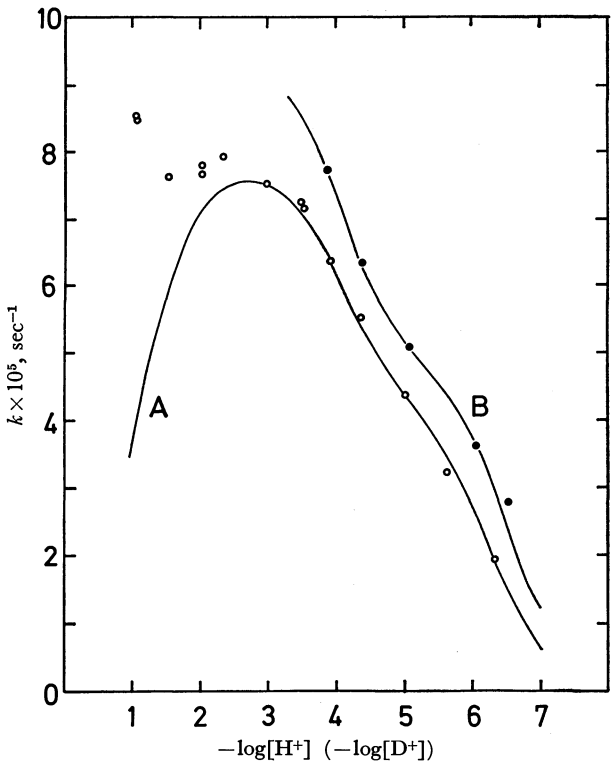

Fig. 1. Rate profiles for the spontaneous hydrolysis of 8-quinolyl phosphate in water (curve A) and in deuterium oxide (curve B) at 80°C and $\mu=0.10$.

The curves were calculated from the experimemtal data by means of Eq. (1) with the following constant: aqueous system, $pK_{H_3A}=1.0$, $pK_{H_2A}=4.09$, and $pK_{HA}=6.24$; $k_{H_3A}=0$ sec^{-1}, $k_{H_2A}=7.84\times10^{-5}$sec^{-1}, and $k_{HA}=4.19\times10^{-5}$sec^{-1}: deuterium oxide system, $pK_{H_2A}=4.05$ and $pK_{HA}=6.50$; $k_{H_2A}=9.65\times10^{-5}$sec^{-1} and $k_{HA}=4.83\times10^{-5}$sec^{-1}.

TABLE 3. FIRST-ORDER RATE CONSTANTS FOR THE HYDROLYSIS REACTIONS OF THE NEUTRAL AND THE MONOANIONIC SPECIES AT $\mu=0.10$[a]

Temp. °C	$k_{H_2A}\times10^5$ sec^{-1}	$k_{HA}\times10^5$ sec^{-1}
	8-Quinolyl phosphate	
80	7.97(7.84)	3.97 (4.19)
70	2.33	0.794
60	0.794	0.175
80	(9.65)[b]	(4.83)[b]
	3-Pyridyl phosphate	
80	25.0	5.75
70	7.69(7.63)	2.08 (1.92)
60	2.28	0.417
70	(7.21)[b]	(2.70)[b]
	2-Pyridylmethyl phosphate	
90	2.33(2.31)	0.414(0.458)
90	(2.78)[b]	(1.44)[b]

a) Numbers in parentheses are the values calculated by means of acid dissociation constants obtained from kinetic data.
b) In deuterium oxide.

phosphate esters containing pyridine moieties, the hydrolysis behavior of 3-pyridyl and 8-quinolyl phosphates has been investigated. Four kinds of ionic species have to be taken into consideration for each phosphate in the course of investigating hydrolysis mechanisms. 3-

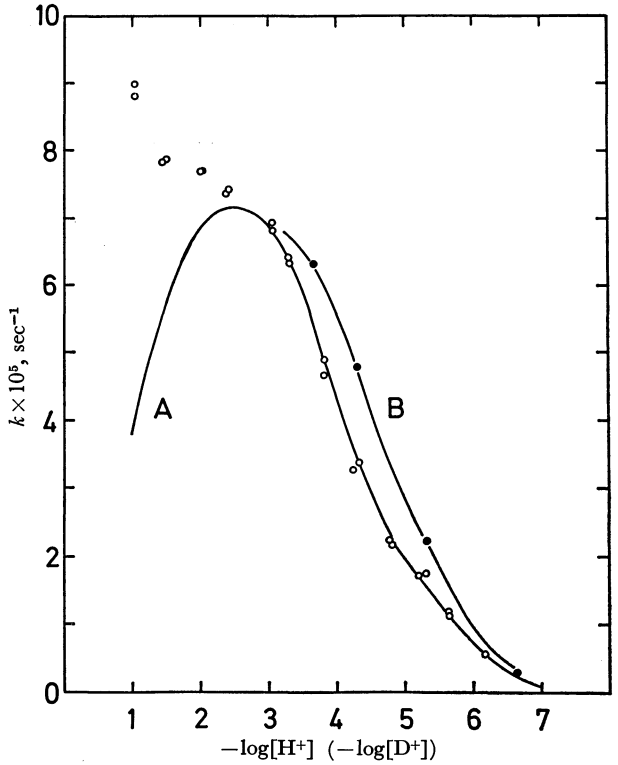

Fig. 2. Rate profiles for the spontaneous hydrolysis of 3-pyridyl phosphate in water (curve A) and in deuterium oxide (curve B) at 70°C and $\mu=0.10$.

The curves were calculated from the experimental data by the aid of Eq. (1) with the following constants: aqueous system, $pK_{H_3A}=1.0$, $pK_{H_2A}=3.87$, and $pK_{HA}=5.76$; $k_{H_3A}=0$ sec^{-1}, $k_{H_2A}=7.63\times10^{-5}$sec^{-1}, and $k_{HA}=1.92\times10^{-5}$sec^{-1}: deuterium oxide system, $pK_{H_2A}=4.28$ and $pK_{HA}=5.71$; $k_{H_2A}=7.21\times10^{-5}$sec^{-1} and $k_{HA}=2.70\times10^{-5}$sec^{-1}.

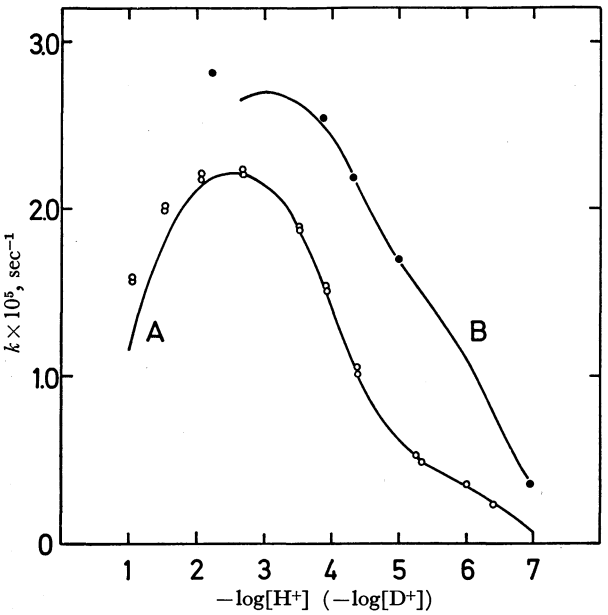

Fig. 3. Rate profiles for the spontaneous hydrolysis of 2-pyridylmethyl phosphate in water (curve A, experimental data were from our previous work[3]) and in deuterium oxide (curve B) at 90°C and $\mu=0.10$.

The curves were calculated from the data by means of Eq. (1) with the following constants: aqueous system; $pK_{H_3A}=1.0$, $pK_{H_2A}=4.03$, and $pK_{HA}=6.46$; $k_{H_3A}=0$ sec^{-1}, $k_{H_2A}=2.33\times10^{-5}$sec^{-1}, and $k_{HA}=0.458\times10^{-5}$sec^{-1}: deuterium oxide system, $pK_{H_2A}=4.46$ and $pK_{HA}=6.46$; $k_{H_2A}=2.78\times10^{-5}$sec^{-1} and $k_{HA}=1.45\times10^{-5}$sec^{-1}.

Table 4. Activation parameters for the spontaneous hydrolysis reactions of 8-quinolyl and 3-pyridyl phosphates

Phosphate	Neutral species			Monoanionic species		
	E kcal mol^{-1}	$\Delta H^{\neq}$ [a] kcal mol^{-1}	$\Delta S^{\neq}$ [a] e.u.	E kcal mol^{-1}	$\Delta H^{\neq}$ [a] kcal mol^{-1}	$\Delta S^{\neq}$ [a] e.u.
8-Quinolyl	27.0	26.3	+3	36.5	35.8	+22
3-Pyridyl	28.0	27.3	+2	30.7	30.0	+7

a) Value at 70°C.

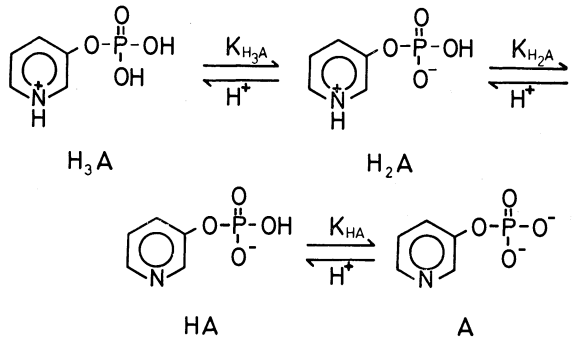

Scheme 1

Pyridyl phosphate affords, for example, four ionic species of different protonation degree due to the dissociation process shown in Scheme 1. Throughout this study we refer H_3A to the monocationic form, H_2A to the neutral zwitterion, and HA to the monoanionic form. Both H_2A and HA, however, involve the monoanionic phosphate group.

Hydrolysis of Neutral Zwitterion Species. In the kinetic and mechanistic studies of hydrolysis of the pyridylmethyl phosphates,[3] the species involving a monoanionic phosphate moiety, zwitterion form (H_2A) and monoanionic form (HA), were confirmed to be reactive toward hydrolysis, although the corresponding acidic hydrolysis did not proceed to any detectable extent in the pH range studied. In addition, irrespective of the phosphate species, the activation energies for the hydrolysis of zwitterion forms were approximately 30 kcal mol^{-1} and the corresponding Arrhenius' A values were in the same order of magnitude as other ordinary alkyl phosphates.[3] Thus, we proposed that the zwitterion species of the pyridylmethyl phosphates follow the same hydrolytic pathway, accompanied with the P–O bond cleavage, as expected for the monoanionic form of an ordinary alkyl phosphate. The reactivity of the zwitterion was much greater than that of the corresponding monoionic species. This trend was marked for 2-pyridylmethyl phosphate; 2.5 times as large as those for its 3- and 4-isomers in terms of the rate ratio k_{H_2A}/k_{HA} as listed in Table 3. This facile hydrolytic tendency of the zwitterion species of 2-pyridylmethyl phosphate was explained in terms of interamolecular proton-transfer mechanism.

The same mechanistic argument can be applied to the elucidation of the facile hydrolysis of H_2A species of 8-quinolyl phosphate in the light of its structural analogy to 2-pyridylmethyl phosphate, activation parameters, and kinetic solvent isotope effect. First, the zwitterion species of 8-quinolyl phosphate has a quinolinium proton at a suitable position for attacking the ester-oxygen atom. The phosphate moiety is constrained more effectively in the neighborhood of nitrogen due to the quinolyl ring structure than expected in 2-pyridylmethyl phosphate. The proton is, therefore, readily transferred in the transition state to the oxygen atom. The activation parameters listed in Table 4 may further qualify for this similarity of the hydrolytic pathway among the zwitterion species of 2-pyridylmethyl and 8-quinolyl phosphates. The activation energy for the H_2A species of 8-quinolyl phosphate is very close to that for the corresponding species of 2-pyridylmethyl phosphate; the former is 27.0 kcal mol^{-1} and the latter is 28.2 kcal mol^{-1}, respectively. This equality must be attributed to the similarity in their hydrolytic pathways. Also, the small and positive entropy of activation for the H_2A species of 8-quinolyl phosphate, +3, is consistent with the unimolecular nature of the transition state, and rules out the possibility of participation of a water molecule. Similar observation has been made in many hydrolysis reactions of the monoanionic phosphate species; *e.g.*, in the hydrolysis of glucose-6-,[6] isopropyl,[7] and nitrophenyl phosphates.[8]

Table 5. Kinetic solvent isotope effect in hydrolysis reactions of some organic phosphates containing an acidic group

Species	k^{H_2O}/k^{D_2O}	Reference
8-Quinolyl phosphate zwitterion	0.81	a)
8-Quinolyl phosphate monoanion	0.87	a)
3-Pyridyl phosphate zwitterion	1.06	a)
3-Pyridyl phosphate monoanion	0.71	a)
2-Pyridylmethyl phosphate zwitterion	0.84	a)
2-Pyridylmethyl phosphate monoanion	0.32	a)
Salicyl phosphate dianion	0.96	10
Methyl phosphate monoanion	0.87	b)

a) This work.
b) C.A. Bunton. D. R. Llewellyn, K. G. Oldham, and C. A. Vernon, *J. Chem. Soc.*, **1958**, 3574.

Further additional evidence for the intramolecular proton-transfer mechanism is provided for the neutral zwitterion species of both 8-quinolyl and 2-pyridylmethyl phosphates in terms of the kientic solvent isotope effect as listed in Table 5. As suggested by Westheimer[9] the deuterium oxide solvent isotope effect (k^H/k^D)

6) Ch. Degani and M. Halmann, *J. Amer. Chem. Soc.*, **88**, 4075 (1967).
7) L. Kugel and M. Halmann, *J. Org. Chem.*, **32**, 642 (1967).
8) C. A. Bunton, E. J. Fendler, E. Humeres, and K. Yang, *J. Org. Chem.*, **32**, 2806 (1967).
9) F. H. Westheimer, *Chem. Rev.*, **61**, 265 (1961).

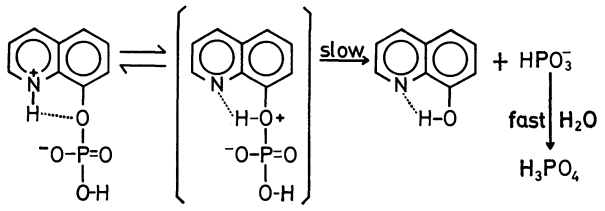

3 4

Scheme 2

reaches its maximum when the symmetric transition state is attained. On the other hand, if a transition state becomes asymmetric with respect to the position of a proton, without transfer or complete transfer of a proton to the ester oxygen (**3** or **4** in Scheme 2) in the transition state, the isotope effect (k^H/k^D) decreases markedly. A large deuterium oxide isotope effect was observed in none of the reactions including hydrolysis of salicyl phosphate dianion and methyl phosphate monoanion as shown in Table 5. Since the kinetic isotope effects for 8-quinolyl and 2-pyridylmethyl phosphates in their zwitterion forms are smaller than unity, a certain proton-transfer mechanism seems to be engaged in some analogy to A1 and A2 mechanisms. On the other hand, the small entropy of activation must eliminate the possibility of bimolecular process in the transition state. On the basis of the above arguments, the solvolysis mechanism for 8-quinolyl and 2-pyridylmethyl phosphates is closely related to A1 mechanism, even though the proton-transfer would not be as complete as expected in the A1 process. As a result, the most plausible reaction mechanism must involve the pre-equilibrium intramolecular proton-transfer (Scheme 2) in a manner similar to that suggested by Bender and Lawlor for the solvolysis of salicyl phosphate dianion.[10]

On the other hand, the value of deuterium kinetic solvent isotope effect for the zwitterion species of 3-pyridyl phosphate is approximately unity. As the molecular structure indicates, 3-pyridyl phosphate does not possess any proton suitably placed for an intramolecular hydrogen bonding. Such a kinetic isotope effect, therefore, must be attributed to another hydrolytic pathway. The data of activation parameters and of kinetic isotope effect are, however, consistent with the unimolecular and intramolecular proton-transfer mechanism. Thus, the zwitterion of 3-pyridyl phosphate seems to hydrolyze through the transition state similar to those for the monoanionic species as described below.

Hydrolysis of Monoanionic Species. 3-Pyridyl and 2-pyridylmethyl phosphates in their monoanionic forms seem to hydrolyze thourgh the same mechanistic path as proposed for the hydrolysis of methyl phosphate monoanion[11,12] in the light of the activation parameters and the kinetic solvent isotope effects.

The hydrolysis of 8-quinolyl phosphate monoanion provided relatively large activation parameters; a large positive entropy term in particular, $\Delta S^{\neq}=+22$. So far, such a large positive entropy term for solvolysis reactions does not seem to have been previously reported. We have not obtained any reliable activation parameters for the hydrolysis of 2-pyridylmethyl phosphate monoanion, which is analogous in structure to the 8-quinolyl phosphate monoanion. We are not ready to give a plausible explanation at present for the kinetic entropy effect. In any case, however, both kinetic deuterium oxide solvent isotope effect and activation entropy effect are in favor of unimolecular and intramolecular proton-transfer mechanism (Scheme 3).

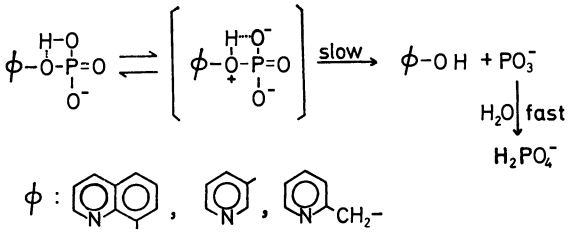

Scheme 3

Hydrolysis in Lower pH Region. The hydrolysis rates of 8-quinolyl and 3-pyridyl phosphates increase in the moderately acidic region ($-\log[H^+]=1.0$—2.0) in proportion to the stoichiometric concentration of acid. This rate enhancement is primarily due to the acid-catalyzed hydrolysis of the neutral zwitterion species. The increase of electron-withdrawing power of the alcohol moiety may cause the deficiency of charge density on the ester oxygen atom, and consequently the electrophilic attack by the hydronium ion would be less favored. Contrary to what would be expected, the zwitterion species of pyridylmethyl phosphates do not undergo acid-catalyzed hydrolysis to any detectable extent in a moderately acidic region. We believe, therefore, that the favorable acid catalysis for 3-pyridyl and 8-quinolyl phosphates is due to electron-withdrawing effect caused by the pyridinium proton, which results in the weakening of P–O bond. Resonance stabilization effect given to the yielded alcohol of phenolic nature may facilitate the hydrolysis reaction.

10) M. L. Bender and J. M. Lawlor, *J. Amer. Chem. Soc.*, **85**, 3010 (1963).

11) C. A. Vernon, *Chem. Soc. (London) Spec. Publ. No.* 8, 17 (1957); C. A. Bunton, D. R. Llewellyn, K. G. Oldham and C. A. Vernon, *J. Chem. Soc.*, **1958**, 3574.

12) T. C. Bruice and S. J. Benkovic, "Bioorganic Mechanisms," Vol. II, W. A. Benjamin, Inc., New York, N. Y. (1966), Chapter 5.

Relative Reactivities in the Addition of Free Trichloromethyl Radicals to Substituted Styrenes. An Attempt to Separate Polar and Resonance Effects[1]

Hideki SAKURAI, Shun-ichi HAYASHI, and Akira HOSOMI
Department of Chemistry, Faculty of Science, Tohoku University, Sendai
(Received January 20, 1971)

Relative reactivities in dibenzoyl peroxide-catalyzed addition of bromotrichloromethane to nine nuclear-substituted styrenes have been investigated with unsubstituted styrene. The effect of *meta* substituents upon the relative rates was correlated with the simple Hammett equation using either σ or σ^+ constants. The relative rates of *para*-substituted styrenes, however, did not obey the simple Hammett relation, with the results best explained on the basis of polar ($\rho\sigma^+$) and resonance (E_D) terms. All *para* substituents examined increase the reactivity.

$$\log (k/k_H) = \rho\sigma^+ + E_D$$

The E_D term shows a striking correlation with log$Q$ of the corresponding *para* styrene in Alfrey-Price's Q-e scheme of free-radical copolymerization. That the polar term originates in charge-transfer interactions between the olefin and the electrophilic trichloromethyl radical and can be expressed by $\rho\sigma^+$ is further supported by the evidence that charge-transfer energies of substituted styrenes showed good correlation with σ^+. Factors influencing the reactivity have been discussed.

There are few reactions of free-radical chemistry more extensively studied than addition to olefins, yet some of the basic problems of structure and reactivity remain unresolved. The substituent effects of styrenes, which should be studied as one of the most fundamental substrates, have not yet been investigated systematically in addition reactions except in copolymerization.[2]

Martin and Gleicher[3] have reported the addition of the trichloromethyl radical to substituted allylbenzenes, 3-butenylbenzenes and other 1-olefins where they observed linear correlations of the rate data by the Hammett-Taft equation.[4] More recently, Cadogan and Sadler[5] have reported the relative reactivities of addition of trichloromethyl and thiyl radicals to variously substituted olefins; in their report it was disclosed that the rate constant rations of substituted stilbenes and α-methylstyrenes toward these radicals obey the Hammett-Brown relation.[6]

$$\log (k/k_H) = \rho\sigma^+ \quad (1)$$

However, only three substituents were chosen, *i.e.* methoxy, methyl and bromo, all at the *para* position, no *meta* or other appropriate substituent being included to check the possibility that enhanced delocalization of the odd electron in the free radical was increasing the reactivity. They noted at the same time, however, that the reactivity of 4-nitro-*trans*-stilbene was greater than that predicted from the proposed relation (eq. (1)).

Numerous studies[7] of hydrogen abstraction from substituted toluenes and other alkylbenzenes have demonstrated that the relative reactivities are generally correlated by the Hammett equation, and sometimes better by the Hammett-Brown equation. We have also reported recently examples in which the importance of polar effects was demonstrated.[8] As part of a program directed toward the relations of structure and reactivity in the homolytic process, we have investigated the relative reactivities of substituted styrenes toward the trichloromethyl radical derived from bromotrichloromethane. Our special interest was to separate the factors influencing the reactivity: both resonance and the polar effects should be operating in homolytic addition to conjugated olefins.

Results

Competitive Reactions. Addition of bromotrichloromethane to olefins by a free-radical mechanism has been well established.[3,5,9-11] Kharasch, Reinmuth, and Urry reported in their chassical study that styrene afforded the 1:1 adduct in 78% yield at 70°C using 2.3 wt% diacetyl peroxide as an initiator. Formation of a 1:1 adduct of styrene and bromotrichloromethane in photochemically induced reactions[12] and even in an uncatalyzed thermal reaction[13] have also been reported.

1) Presented in part at the 21st Annual Meeting of the Chemical Society of Japan, Suita, Osaka, Japan (April 1, 1968), Abstracts, III, p. 2060.

2) a) C. Walling, E. R. Briggs, K. B. Wolfstein, and F. R. Mayo, *J. Amer. Chem. Soc.*, **70**, 1537 (1948), b) M. Imoto, M. Kinoshita, and M. Nishigaki, *Mackromol. Chem.*, **86**, 217 (1965), c) M. Imoto, M. Kinoshita, and M. Nishigaki, *ibid.*, **94**, 238 (1966).

3) M. M. Martin and G. J. Gleicher, *J. Amer. Chem. Soc.*, **86**, 233, 238 ,242 (1964).

4) R. W. Taft, Jr., "Steric Effects in Organic Chemistry," M. S. Newman, Ed., John Wiley & Sons, Inc., New York, N. Y. (1956), Chapter 13.

5) J. I. G. Cadogan and I. H. Sadler, *J. Chem. Soc., B*, **1966**, 1191.

6) H. C. Brown and Y. Okamoto, *J. Amer. Chem. Soc.*, **80**, 4979 (1958).

7) G. A. Russell and R. C. Williamson, Jr., *ibid.*, **86**, 2357 (1963), and references cited therein.

8) a) H. Sakurai and A. Hosomi, *J. Amer. Chem. Soc.*, **89**, 458 (1968). b) H. Sakurai and K. Tokumaru, "Chemistry of Free Radicals," H. Sakurai and K. Tokumaru eds., Nankodo, Tokyo, 1967, Chapt. 17.

9) M. S. Kharasch, O. Reinmuth, and W. H. Urry, *J. Amer. Chem. Soc.*, **69**, 1105 (1947).

10) J. I. G. Cadogan and D. H. Hey, *Quart. Rev.* (London), **8**, 308 (1954).

11) C. Walling, "Free Radicals in Solution," John Wiley & Sons, Inc., New York, N. Y. (1957), Chapt. 6.

12) M. S. Kharasch, E. Simon, and W. Nudenberg, *J. Org. Chem.*, **18**, 328 (1953).

13) W. A. Skinner, E. Bishop, D. Tieszen, and J. D. Johnson, *ibid.*, **23**, 1710 (1958).

Kinetic investigations of the photochemical telomerization of styrene[14,15] also showed that at sufficiently low molar ratios of styrene to bromotrichloromethane, only a 1:1 adduct was formed. In our hands, the high yields of a 1:1 adduct from styrene are also confirmed under the conditions employed in competitive reactions. Therefore, any error originating in the possible comsumption of styrenes by polymerization can be ignored.

Cadogan and Sadler[5] published a very elaborate analysis to establish a valid competitive method of measuring the relattve reactivities of olefins toward thiyl and trichloromethyl radicals. We empolyed a procedure essentially the same as theirs[3,5] (see Experimental).

A reactant ratio of bromotrichloromethane: X:Y of 4:1:1 was empolyed generally in the competitive addition of the trichloromethyl radical derived from bromotrichloromethane to styrenes. Effects of variation of both the bromotrichloromethane ratios and the degree of conversion of the styrene into adduct were examined in some detail for *p*-chlorostyrene-styrene system, as shown in Table 1.

The reactivity of *p*-chlorostyrene relative to styrene was found to be fairly constant, regardless of experimental conditions. The value for k_{Cl}/k_H of 1.06±0.03 is consistent with the value 1.0, by Kharasch *et al.*[12]

Table 1. Competitive experiment of styrene (A) with *p*-chlorostyrene (B) toward addition of bromotrichloromethane

Run	A mmol	B mmol	$BrCCl_3$ mmol	Reaction time (hr)	k_B/k_A
1	2.503	2.501	5.01	3.0	1.03
2	2.503	2.501	10.02	3.0	1.04
3	2.503	2.501	20.05	3.0	1.02
4	10.05	10.17	40.38	2.0	1.09
5	10.07	10.25	40.68	2.0	1.09
6	10.07	10.25	40.68	3.0	1.10
7	10.05	10.17	40.38	3.0	1.10
8	10.07	10.25	40.68	4.0	1.06
9	10.07	10.25	40.68	5.0	1.06
10	5.079	5.006	20.58	3.0	1.02
11	5.177	5.079	20.21	3.0	1.03
12	5.091	5.129	20.23	3.0	1.04

Table 2. Relative reactivities of substituted styrenes toward trichloromethyl radicals

Substituent	k/k_H[a]	
p-Methyl	1.74	±0.12
m-Methyl	1.08	±0.05
H	1.00	
m-Methoxy	1.05	±0.02
p-Chloro	1.06	±0.03
m-Chloro	0.767	±0.02
m-Trifluoromethyl	0.615	±0.00
p-Cyano	1.13	±0.04
m-Nitro	0.529	±0.02
p-Nitro	0.872	±0.07

a) Deviation listed for two to twelve runs.

Table 3. Charge-transfer energies and ionization potentials of substituted styrenes

Substituent	CT-Band (in CH_2Cl_2) mμ	CT-Band (in CH_2Cl_2) eV[a]	IP[b] eV
p-CH_3O	590 ± 5	2.10±0.02 (2.05)	7.9₉
p-CH_3	525 ± 3	2.36±0.02 (2.37)	8.2₅
m-CH_3O	520 ± 3	2.38±0.02	8.2₇
m-CH_3	485 ± 3	2.56±0.02	8.4₅
H	481 ± 3	2.58±0.02 (2.58)	8.4₇
p-Cl	481 ± 3	2.58±0.02 (2.57)	8.4₇
p-Br	481 ± 3	2.58±0.02	8.4₇
m-Cl	450 ± 5	2.75±0.03	8.6₄
m-CF_3	420 ± 3	2.95±0.02	8.8₄

a) Values in parenthesis were reported by M. Hatano, N. Tamura, and S. Kambara, *Kogyo Kagaku Zasshi*, **70**, 2012 (1967).

b) Calculated by Eq. (2).

In Table 2 are indicated the relative reactivities of nine nuclear-substituted styrenes toward the addition of the trichloromethyl radical.

Charge-transfer Spectra of Styrenes with Tetracyanoethylene. The charge-transfer spectra were taken in dichloromethane solution at an ambient temperature with tetracyanoethylene as an electron acceptor by the standard method.[16] The results are listed in Table 3. Ionization potentials (IP) were calculated from equation 2, and are also tabulated in the last column of the Table.

$$IP = (IP)_0 + (h\nu_{CT}) - (h\nu_{CT})_0 \quad (2)$$

The charge-transfer energies are plotted against σ^+ parameters as shown in Fig. 1. A reasonably good (r=0.98)linear relationship was obtained omitting the point for *m*-methoxystyrene.

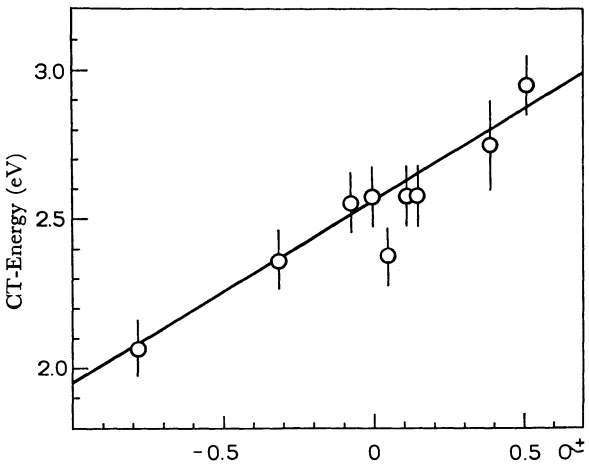

Fig. 1. Plots of charge-transfer energies of substituted styrenes-tetracyanoethylene complexes against σ^+ of the substituents.

Discussion

Figure 2 plots logarithm of the relative rates of additions against σ^+ constants. No very linear Ham-

14) J. C. Robb and D. Vofsi, *Trans. Faraday Soc.*, **55**, 558 (1959).
15) W. J. Kirkham and J. C. Robb, *ibid.*, **57**, 1757 (1961).
16) H. A. Benesi and T. H. Hildebrand, *J. Amer. Chem. Soc.*, **71**, 2703 (1949).

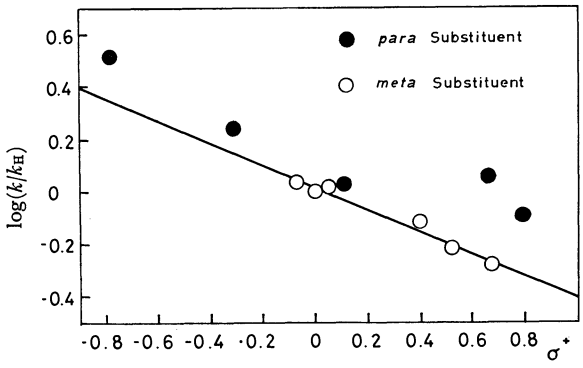

Fig. 2. Correlation of $\log(k/k_H)$ and σ^+ for addition of free trichloromethyl radicals to substituted styrenes in benzene at 80.0°.

mett correlation is found for the data as a whole, but clearly, the data for *meta*-substituted styrenes afford a nice linear relationship with σ or a somewhat better one with σ^+(*vide infra*).

$$\log (k_X/k_H) = -0.425\sigma + 0.019 \quad (r = 0.9689) \tag{3}$$

$$\log (k_X/k_H) = -0.418\sigma^+ + 0.018 \quad (r = 0.9847) \tag{4}$$

(r = correlation coefficient)

The ρ-values were calculated by the method of least squares, the negative ρ-value being consistent with the view that the trichloromethyl radical is of an electrophilic nature. In *meta*-substituted styrenes, the odd electron of the 1-phenyl-3,3,3-trichloropropyl radicals is conjugated not with the substituent but only with the π-electrons of the benzene ring. Thus further resonance stabilization of the resulting radicals due to the presence of the *meta*-substituent does not occur, and it is quite natural that the second-order substituent effect, seen in the relative rates, is polar for the *meta* series

The ρ-value obtained here is considerably lower than that of ionic reactions such as hydration of styrenes ($\rho = -3.42$ with σ^+ including *para* substituents).[17] This fact indicates that the polar effect in the addition of the trichloromethyl radicals is much smaller than in ionic reactions, although the polar effect is the crucial factor in determining the relative rates in *meta* styrenes.

The rate constant ratios of *para*-substituted styrenes, however, do not obey the Hammett relation. These data deviate considerably upward from the line of *meta* series. All *para* substituents examined increase the reactivity.

We have tried to get the relative rate for *p*-methoxystyrene, but the tendency of this monomer toward spontaneous polymerization was too high to obtain a reliable value. However, there is a close resemblance in the relative reactivity sequences of styrenes, α-methylstyrenes and *trans*-stilbene toward the trichloromethyl radical. Thus, the increase in reactivity toward the trichloromethyl radical due to the interaction of a given substituent group in the *para* position, as shown in Table 4, is the same within the limits of experimental error for these.[5] Therefore we

Table 4. Relative reactivities toward trichloromethyl radicals in olefins

X	X-C_6H_4-CH=CH_2 [a]	X-C_6H_4-CH=CH-C_6H_4-X [b] (*trans*)	X-C_6H_4-CMe=CH_2 [b]
4-MeO	——	3.4	3.2
4-Me	1.74	1.7	1.7
4-H	1.0	1.0	1.0
4-Br	——		0.7

a) Present study
b) Cadogan and Sadler[5]

may assume the relative rate for *p*-methoxystyrene to be around 3. 3.

It is an unlikely assumption that these *para*-substituent effects are due entirely to the stabilization of the somewhat electron-deficient free-radical in the transsition state by an inductive effect, since the reactivities of substrates containing a deactivating substituent group such as *p*-nitro- and *p*-cyanostyrene are far greater than those predicted on the basis of this polar effect alone. Therefore, the high observed relative rates for *para*-substituted styrenes are certainly due, at least in part, to the extra delocalization of the odd electron in the radicals.

Investigations of homolytic arylation by Simamura and co-workers[18] have shown that the influence of a substituent may be divided into resonance and inductive effects. Since in substitution at the *meta*-position of the substituted benzenes the conjugation of the odd electron dose not extend into the substituent group, as for *meta*-styrenes, the partial rate factors for arylations at the *meta* position are correlated only with the polar term; thus the Hammett relation holds. On the other hand, partial rate factors for *para* substitution are expressed by

$$\log (k_p/k) = \rho\sigma_p + \tau_p \tag{5}$$

where τ_p is a term for additional stabilization due to the conjgaution of the substituent group correlated with the difference of the extra resonance energy. That τ_p is a constant dependent only on the nature of the substituent group in the substrate is also demonstrated.

If it is assumed that the free-energy changes for the *para*-substituted styrense in free-radical addition can be also divided into polar and delocalization terms, with the former expressed by $\rho\sigma$ or $\rho\sigma^+$, the relative rates may be formulated as

$$\log (k_p/k_H) = \rho\sigma_p(\text{or } \rho\sigma_p^+) + E_D \tag{6}$$

where E_D is a term for additional stabilization due to extra delocailzation by the *para* substituent group.

Combining this equation with eqs. 3 and 4, numerical values of E_D are calculated with σ and σ^+ -parameters, respectively. The results are listed in Table 5.

Meanwhile, Alfrey and Price[19] proposed an empirical formula that expresses the monomer reactivity ratios, r, in free-radical copolymerization in terms of Q and e. Table 5 contains also log Q for the respective styrenes. There is a striking resemblance between the

17) W. M. Schubert, B. Lamm, and J. R. Reefe, *ibid.*, **86**, 4727 (1964).

18) R. Itô, T. Migita, N. Morikawa, and O. Simamura, *Tetrahedron*, **21**, 955 (1965).

19) T. Alfrey and C. C. Price, *J. Polym. Sci.*, **2**, 101 (1947).

TABLE 5. EXTRA-DELOCALIZATION TERMS FOR ADDITION OF TRICHLOROMETHYL RADICALS TO *para*-SUBSTITUTED STYRENES

X	E_D with σ	E_D with σ^+	log Q[a]
MeO[b]	0.40_4	0.19_2	0.13
Me	0.16_8	0.11_0	0.04
Cl	0.12_3	0.07_1	0.01
CN	0.33_4	0.32_9	0.27
NO_2	0.27_2	0.27_1	0.21

a) Taken from L. J. Young, *J. Polym. Sci.*, **54**, 411 (1961).
b) Estimated values.

values of log Q and E_D calculated with σ^+.

$$\log Q_p = 1.022E_{D(\sigma^+)} - 0.067 \quad (r=0.9995) \qquad (7)$$

The correlation of log Q with the value of E_D calculated with σ is less satisfactory (r=0.7090).

Therefore, if we assume that the E_D term in eq. 6 can be given by log Q log(k_m/k_H) of *meta* styrenes and log(k_p/k_H) —log Q of *para* derivatives should express the free-energy change of the reaction corrected for extra-resonance effect of the substituents. As shown in Fig. 3, these are plotted against σ^+ to give a nicely linear relation even with the hypothetical value of *p*-methoxystyrene.

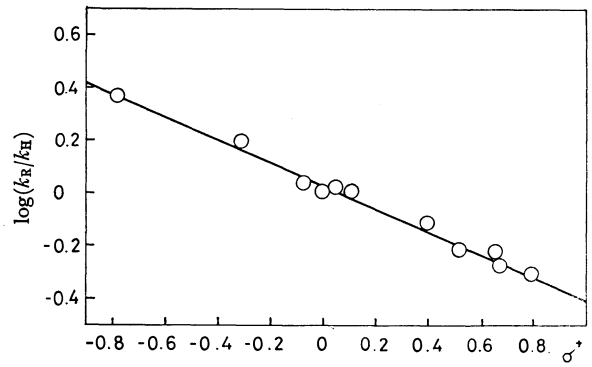

Fig. 3. Correlation of log(k_R/k_H) and σ^+ for addition of free trichloromethyl radicals to substituted styrenes in benzene at 80.0°. Reduced rates, k_R, are defined as k_m for *meta*-substituted styrenes, whereas k_p/Q for *para* series.

These findings now raise the question of why the polar term is given by $\rho\sigma^+$ instead of $\rho\sigma$ and/or why the resonance term should be log Q.

In the case of free-radical addition to olefins there is good indication that in the absence of any specific polar effects the rate of addition and the orientation are governed primarily by the localization energy of the substrate.[20] However, when an electrophilic radical such as the trichloromethyl radical is approaching to an olefinic double bond, the electrostatic interaction leads to a lowering of the potential energy of the system, and this should be an origin of the polar effect in addition reaction. It is not clear that electrophilic radicals can form a π-complex with olefin, but such interaction must originate in the charge-transfer interaction between the free radical and olefin. Therefore, the more developed the charge-transfer interaction at the transition state, the more the lowering of the potential energy of the system, and the relative extent of such a lowering effect of the free energy may be evaluated by ionization potential difference of olefins.

We have measured the charge-transfer frequencies of substituted styrene-tetracyanoethylene complex, and as seen in Fig. 1, there is a good correlation between the charge-transfer energy or ionization potential and σ^+ substituent constants. This correlation implies that the substituent effect in the charge-transfer interaction, *viz.*, the polar effect of the addition reaction, is governed by the $\rho\sigma^+$ relation.

It is established that in hydrogen abstraction reaction at non-benzylic position rates are correlated with σ, and that rates of abstraction of benyzlic and phenolic hydrogen by electron-seeking radicals follow generally the $\rho\sigma^+$ relation.[21] It should be emphasized that the latter $\rho\sigma^+$ relation is concerned with the polar effect of the substituent in stabilization of the benzylic carbonium ions and not with the extra stabilization of the benzylic radicals due to the delocalization of unpaired electron by the substituent. For addition reaction, the $\rho\sigma^+$ relation should be also recognized as a result of the charge-transfer interaction responsible for the polar effect.

The "Q and e" treatment must be regarded as empirical, but there is a good deal of evidence showing a satisfactory correlation of the localization energy with log Q of various types of vinyl monomers.[22] It is still a matter of question whether the E_D term observed in the present study can be equated to log Q. We might propose a new set of parameters equated directly to E_D. However, considering our basis for representing the polar effect as $\rho\sigma^+$, and the fact that the calculated E_D values based on the $\rho\sigma^+$ relation resemble nicely log Q, relative rates of addition of the trichloromethyl radical to substituted styrenes are best expressed by the following equation.

$$\log (k/k_H) = \rho\sigma^+ + \log Q_p \qquad (8)$$

Experimental

Materials. Bromotrichloromethane was of reagent grade purchased from Aldrich Chemical Co. and was used after distillation through a 35-cm column packed with glass helicoils. Styrene and *m*-nitrostyrene were commercial samples. *p*-Methoxy- and *m*-methoxystyrenes were prepared by decarboxylation of the corresponding cinnamic acids. *p*-Methyl-, *m*-methyl-, *p*-chloro, *m*-chloro-, *p*-bromo-, *p*-cyano-, and *m*-trifluoromethylstyrenes were obtained by dehydration of the corresponding secondary alcohols. *p*-Nitrostyrene was prepared by dehydrobromination of 2-(4′-nitrophenyl)ethyl bromide with triethanolamine. All samples were stored in a freezer and distilled under reduced pressure immediately before use. All physical constants and glpc analyses confirmed the purity of the materials used.

Procedure for Kinetic Runs. Samples of substituted

20) M. Szwarc and J. H. Binks, "Theoretical Organic Chemistry," Kekule Symposium, 1958, Butterworth Scientific Publications, London, (1959), p. 291.

21) H. Sakurai, A. Hosomi, and M. Kumada, *J. Org. Chem.*, **35**, 993 (1970).

22) a) G. S. Levinson, *J. Polym. Sci.*, **60**, 43 (1962), b) T. Fueno, T. Tsuruta, and J. Furukawa, *Nippon Kagaku Zasshi*, **78**, 1075 (1957).

styrene (X), styrene (Y, standard olefin), and an internal standard were accurately weighed into a flask, to which 5 m*l* of bromotrichloromethane and 10 m*l* of benzene containing dibenzoyl peroxide were added. A reactant ratio of bromotrichloromethane/styrene/substituted styrene/internal standard/dibenzoyl peroxide of 4:1:1:0.75:0.012 was employed. The reaction mixture was then placed in a glass tube and degassed by repeated freezing and melting in a vacuum. The tube was then sealed in a vacuum and immersed in a constant-temperature bath kept at 80° for 0.5—1 hr. The extent of total olefin consumption varied from 30—60%. The mixtures were analyzed by glpc on a column packed with polyethylene glycol 20 M or Apiezon L using helium as a carrier gas. In each run, the amount of chloroform was negligibly small, and hardly detectable, indicative of the absence of hydrogen abstraction by the trichloromethyl radical as a side reaction.

A survey of the literature and arguments above indicated that side reactions other than addition could be ignored and that the rate determining step should be the addition of the trichloromethyl radical to the olefins. The relative rates were thus followed by the disappearance of the styrenes. The ratio of rate constants for disappearance of the two styrenes was calculated from the usual expression

$$(k_X/k_Y) = \log([X_0])/[X_f])/\log([Y_0]/[Y_f]) \quad (6)$$

where $[X_0]$ and $[X_f]$ were the initial and final concentrations of styrene X-$C_6H_4CH=CH_2$(X), respectively, and $[Y_0]$ and $[Y_f]$ have a similar significance for Y-$C_6H_4CH=CH_2$(Y).

Charge-transfer Spectra. Charge-transfer spectra were run on a Shimadzu Model SV-50A automatic recording spectrophotometer using 10 mm quartz cell. Dichloromethane was used as the solvent throughout the experiment, concentrations of tetracyanoethylene and styrenes being kept at 10^{-4}—10^{-3} and 10^{-2}—10^{-1} mol/*l*, respectively. The solutions were made up and mixed immediately before measurements. These solutions decolorize fairly rapidly, but were stable enough to record the charge-transfer maxima two or three times.

A part of the work was done at the Department of Synthetic Chemistry, Kyoto University. We thank Professor M. Kumada for his help and encouragement.

BULLETIN OF THE CHEMICAL SOCIETY OF JAPAN, VOL. 44, 1949—1951 (1971)

The Preparation and Thermal Decomposition of Alkyl Acyl Dithiol- and Trithiocarbonates. A Convenient Method for the Synthesis of Thiolesters

Hiroshi YOSHIDA, Tsuyoshi OGATA, and Saburo INOKAWA

Department of Synthetic Chemistry, Faculty of Engineering, Shizuoka University, Hamamatsu

(Received January 21, 1971)

New alkyl acyl dithiol- and trithiocarbonates (**1** and **2**) were prepared from acid chlorides and tetramethylammonium alkyl dithiol- and trithiocarbonates (**3** and **4**). **1** and **2** decomposed at around 100°C to give the corresponding thiolesters in good yields. The kinetic studies of the decomposition of **1** and **2** showed that, in *o*-dichlorobenzene, the decomposition reaction was first order and that it proceeded *via* a four-membered intramolecular cyclic mechanism.

The decomposition of mixed carbonic carboxylic anhydrides (or alkyl acyl carbonates)[1] has been known to lead to two concurrent paths, A and B:

$$ROCO_2COAr \longrightarrow \begin{cases} ROCO_2R + (ArCO)_2O & (A) \\ ROCOAr + CO_2 & (B) \end{cases}$$

In contrast to these anhydrides, *p*-nitrobenzoic alkyl thiolcarbonic anhydrides (or *p*-nitrobenzoyl *S*-alkyl monothiocarbonates) (**5**) gave solely the corresponding thiolesters and carbon dioxide.[2]

$$O_2N\text{-}C_6H_4\text{-}CO_2COSR \longrightarrow O_2N\text{-}C_6H_4\text{-}COSR + CO_2$$

However, no other system of thiolcarbonates has been studied.

The present authors have found a convenient route for the preparation of *S*-alkyl *S*-acyl dithiol- and trithiocarbonates (**1** and **2**). In this report the thermal decompostion of **1** and **2** will be described.

Results and Discussion

In the course of the studies of the reaction of xanthates with tertiary amines, tetramethylammonium alkyl

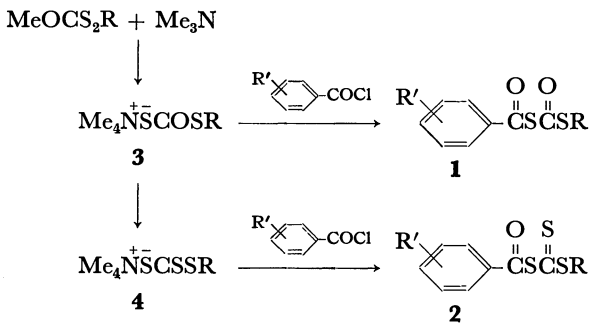

dithiol- and trithiocarbonate (**3** and **4**) were found to be prepared in good yields.[3] The action of acid chlorides on **3** and **4** at −10—0°C gave **1** and **2** (Table 1).

1) D. S. Tarbell and E. J. Longosz, *J. Org. Chem.*, **24**, 774 (1959).
2) L. Wei and D. S. Tarbell, *ibid.*, **33**, 1884 (1968).
3) H. Yoshida, *Nippon Kagaku Zasshi*, **89**, 883 (1968).

Table 1. *S*-alkyl *S*-acyl dithiol- and trithiocarbonates

Compound	R	R′	Mp(°C)	Anal. (%) Found (Calcd) C	H	NMR of *S*-methyl(δ) in o-$C_6H_4Cl_2$ 1 or 2	Decomposed thiolester
1a	Me	*p*-NO_2	72—73	42.00(42.02)	2.75(2.74)	2.33	2.38
1b	Me	*p*-Cl	72—75	44.49(43.81)	2.71(2.86)	2.32	2.37
1c	Me	H	20—23	50.77(50.92)	3.95(3.80)	2.29	2.36
1d	Me	*p*-Me	59.5—60	53.99(53.07)	4.73(4.45)	2.28	2.35
1e	Me	*p*-MeO	72—74	49.51(49.57)	4.23(4.16)	2.27	2.38
2a	Me	*p*-NO_2	130—133	39.81(39.55)	2.59(2.58)	2.58	2.38
2b	Me	*m*-NO_2	74—76.5	40.15(39.55)	2.69(2.58)	2.59	2.40
2c	Me	*p*-Cl	132—134	41.43(41.13)	2.61(2.68)	2.56	2.37
2d	Me	*m*-Cl	82.5—83.5	41.15(41.13)	2.99(2.68)	2.54	2.34
2e	Me	H	76—78	43.01(43.34)	3.59(3.53)	2.56	2.36
2f	Me	*p*-Me	88—90	49.83(49.55)	4.32(4.16)	2.58	2.38
2g	Me	*p*-MeO	62—63	46.80(46.49)	3.95(3.90)	2.56	2.35
2h	Et	H	41—43	49.17(49.55)	4.09(4.16)		

Compounds **1** and **2** decomposed gradually at temperatures above their melting points and vigorously at about 160°C, with the evolution of gases. The decomposition products were analyzed by vpc with known samples (Table 2). These results indicate that **1** and **2** decompose solely by sulfur-acyl bond fission to yield the corresponding thiolesters (path B).

Table 2. Thermal decomposition products of **1** and **2** without solvent

Material	Decomposition temp.(C°)	Product (Yield in %) R′-C$_6$H$_4$-COSR	RSCOSR	Gas
1b	80—90	92	8	COS
1c	80—90	94	5	COS
1d	95—100	88	6	COS
2e	110—120	91	3	CS_2
2h	110—120	87	4	CS_2

Table 3. First-order rate constants for the thermal decomposition of **1** and **2** in *o*-dichlorobenzene

Compound	Temp.(°C)	$k\times10^4$ sec^{-1}
1a	100.0	1.85
	96.0	1.25
	90.1	0.74
1b	100.0	1.35
1c	100.0	1.38
1d	100.0	1.06
1e	100.0	0.76
2a	105.8	2.38
	100.0	1.45
	96.0	1.02
2b	100.0	1.30
2c	100.0	1.05
2d	100.0	1.14
2e	105.8	2.23
	100.0	1.36
	94.7	0.83
2f	100.0	1.09
2g	100.0	0.887

The decomposition of the carbonates **1** and **2** in *o*-dichlorobenzene gave good first-order constants (k) up to 75% completion, as followed by NMR spectroscopy, and the constants were independent of the concentration of **1** and **2** at 0.5—3 weight% (Table 3). At these concentrations the crossed dialkyl dithiol- and trithiocarbonate were found to be produced in yields of less than 1%. Thus the decomposition of **1** and **2** seems to proceed practically *via* an intramolecular mechanism.

Compound **5** (R=*i*-Pr and *t*-Bu) has been suggested[2] to decompose *via* an intramolecular cyclic mechanism judging from activation parameters and the small solvent effect on the reaction. However the effect of the substituents of the acyl group has not yet been made clear.

Table 4. Activation parameters for the decomposition of **1** and **2** in *o*-dichlorobenzene

Compound	ΔE(kcal/mol)	ΔS(e. u.)
1a	24.0	−9.9
2a	23.8	−12.6
2e	24.5	−10.8
5(R=*t*-Bu)[a]	30.3	−5.1
5(R=*i*-Pr)[a]	30.6	−3.7

a) Taken from Ref. 2.

There are no marked difference in the activation parameters between **1** and **2**, as Table 4 shows, but the values considerably deviate from those of **5**.[2] This observation may be attributed to the nature of the bridge atoms, sulfur (**1** and **2**) and oxygen (**5**). The difference in the activation energies may come from the fact that, in bond energies, C–O>C–S. In going from the ground state to the transition state, a relatively larger loss in degree of freedom would occur in the **1** and **2** system than in the **5** system due to desolvation (bond length, C–S>C–O). This is consistent with the larger loss of entropy in the **1** and **2** system than in the **5** system. The samll negative values of the activation entropy seem to indicate that **1** and **2** decompose *via* a four-membered cyclic mechanism similarly to **5**.

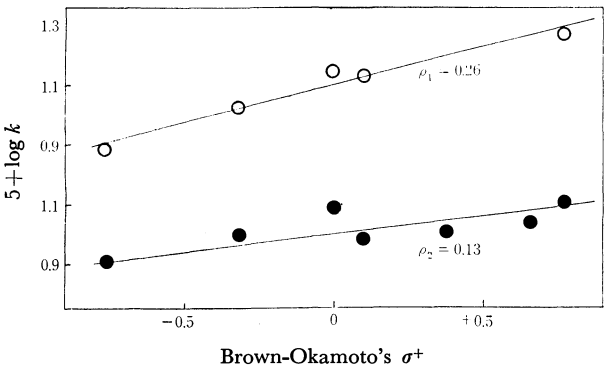

Fig. 1. Hamett relationship for the decomposition of **1** and **2** in *o*-dichlorobenzene at 100°C.
○ for **1**. ● for **2**.

Although an ordinary Hammett's plot of log*k* *vs* σ did not give a linear relationship, plots of log*k* *vs*. Brown-Okamoto's σ^+ gave relatively good straingh lines (Fig. 1). The small positive ρ values seem to indicate that, in the transition states of the decomposition of **1** and **2**, a partial charge on the reacting sites is not highly developed, and that the *S*-alkyl group, as a nucleophile, attacks the carbonyl carbon of the acyl group. The difference in ρ values, ρ_1 and ρ_2, may then, be attributed to the difference in nucleophilicity of *S*-alkyl groups of **1** and **2**, resulting from the difference in mesomeric effects of the carbonyl and the thiocarbonyl groups.

Thus the transition state may be pictured as in **6** with a partial negative charge on the sulfur, and a partial positive charge on the carbonyl carbon.

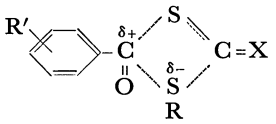

6 (X=O or S)

Experimental

Materials. Tetramethylammonium alkyl dithiol- and trithiocarbonate (**3** and **4**) were prepared according to the previously-described method.[3] To a dry ether suspension of **3** or **4**, we added, drop by drop at −10—0°C, an ether solution of acid chloride. After the removal of the tetramethyl ammonium chloride, the solution was concentrated *in vacuo*. The residual **1** or **2** was recrystalized from ligroin for **1** or from carbon tetrachloride for **2**. The physical constants of the products are collected in Table 1.

Thermal Decomposition of 1 and 2 without a Solvent. (*Table* 2). This reaction was carried out in a test tube at 100—160°C. At higher temperatures, a vigorous evolution of gas was observed. The decomposition products were analysed by vpc using known samples.

Kinetic Studies of the Decomposition of 1 and 2. Kinetic runs were carried out at a constant temperature in an oil bath. A solution of **1** or **2** in *o*-dichlorobenzene was sealed in an NMR sample tube. The rate was followed at suitable time intervals by analyzing the NMR spectra of *S*-methyl groups using a Hitachi Parkin-Elmer R-20 60 MHz spectrometer.

The authors wish to thank Mr. K. Adachi, K. Ishii, K. Unno, and S. Ishizuka for their assistance in the experiments.

BULLETIN OF THE CHEMICAL SOCIETY OF JAPAN, VOL. 44, 1951—1956 (1971)

Some Oxidation and Reduction Products of 4-Acetyltropolone and Its Methyl Ethers

Tetsuo NOZOE, Kahei TAKASE,* Kohei SHIMIZU, and Masafumi YASUNAMI

Department of Chemistry, Faculty of Science, Tohoku University, Katahira-2-chome, Sendai

(Received February 9, 1971)

The chemical properties of the acetyl side-chain of 4-acetyltropolone and its methyl ethers in relation to some oxidizing and reducing reagents were examined. The selenium-dioxide oxidation of one of the methyl ethers afforded a glyoxyloyl derivative in its hydrate form. The catalytic reduction of 4-acetyltropolone gave a mixture of 4-(1-hydroxyethyl)- and 4-ethyltropolones. The reduction of two isomeric methyl ethers with sodium borohydride gave 4-(1-hydroxyethyl)-2-methoxy- and 6-(1-hydroxyethyl)-2-methoxytropones respectively, from which two isomeric methyl ethers of 4-ethyltropolone were prepared in pure states.

Considering the reactivity of the acetyl group, 4-acetyltropolone (I), which has been obtained by the oxidation of 4-isopropenyltropolone (β-dolabrin),[1] should be expected to be one of the most important materials for the synthesis of troponoid compounds, since no acyltropolone except for formyltropolones[2] has yet been prepared by the direct acylation of tropolones because of the impossibility of the Friedel-Crafts

* Address correspondence to this author.

1) T. Nozoe, K. Takase, and M. Ogata, *Chem. & Ind.* (London), **1957**, 1070.

2) a) E. Sebe and S. Matsumoto, *Sci. Repts. Tohoku Univ., Ser. I.* **38**, 308 (1954); S. Matsumoto, *ibid.*, **42**, 209 (1958). b) R. D. Haworth and J. D. Hobson, *J. Chem. Soc.*, **1951**, 561; W. D. Crow, R. D. Haworth, and P. R. Jefferies, *ibid.*, **1952**, 3705. c) D. S. Tarbell, K. I. H. Williams, and E. J. Sehm, *J. Amer. Chem. Soc.*, **81**, 3443 (1959). d) J. W. Cook, R. A. Raphael, and A. I. Scott, *J. Chem. Soc.*, **1952**, 4416; S. Seto and K. Ogura, This Bulletin, **32**, 493 (1959).

reaction and the related acylation of tropolones.[3] The chemical properties of I, especially those of its acetyl side-chain have been investigated for some reactions — the condensation with arylaldehyde,[1] the Huang-Minlon reduction,[4] the Schmidt reaction,[5] and the ketal formation.[6] The present paper will describe the syntheses of some alkyl ethers of I and the results of the examination of the chemical properties of the acetyl side-chain of I and its methyl ethers in relation to some oxidizing and reducing reagents.

Results and Discussion

It is known that the tropolone nucleus is broken oxidatively by oxidizing reagents, such as potassium permanganate or chromic acid.[3] On the other hand, although selemium dioxide acts at the tropolone nucleus to give diselenide compounds,[7] this reagent is known to oxidize effectively the methyl side-chain of the methyl ethers of 4-methyltropolone, giving formyl derivatives.[2a] Now, some alkyl ethers of 4-acetyltropolone (I) have been synthesized for the first time and their oxidation with selenium dioxide has been examined.

Because of the highly mobile tautomerism in the tropolone nucleus,[3] tropolones which have substituents at the unsymmetric positions generally should give two kinds of isomeric ethers on *O*-alkylation. The same is true in the case of 4-acetyltropolone (I). Thus, the treatment of silver salt of I with methyl iodide gave a mixture of two isomeric methyl ethers, from which 4-acetyl-2-methoxy- (IIa) and 6-acetyl-2-methoxytropones (IIb) respectively were isolated in crystalline forms. The structures of these ethers were established from the infrared spectral data, showing the characteristic absorptions[8] due to the out-of-plane deformations at 834 and 785 cm^{-1} respectively. The chemical evidence to be presented later also supports these structures. The methylation of I with diazomethane was very complicated; the use of an excess amount of the reagent gave a resinous product, whereas the use of an equimolar amount of the reagent afforded a mixture of IIa and IIb. Two isomeric ethyl ethers, 4-acetyl-2-ethoxy- (IIIa) and 6-acetyl-2-ethoxytropones (IIIb), were also obtained by the treatment of silver salt of I with ethyl iodide. The infrared spectra of these ethers show the characteristic absorptions[8] at 817 and 784 cm^{-1} respectively. Furthermore, isopropyl ethers of I were obtained by the treatment of silver salt of I with isopropyl iodide, but only an isomer, 4-acetyl-2-isopropoxytropone (IVa), was isolated in a crystalline form. Its infrared spectrum shows the characteristic absorption[8] at 825 cm^{-1}. Another isomer, 6-acetyl-2-isopropoxytropone (IVb), was not isolated, but its existence was shown from an absorption at 790 cm^{-1}[8] in the infrared spectrum of the reaction mixture. In the case of the benzylation of I with benzyl chloride, a benzyl ether was isolated in a crystalline form, but its structure could not be determined because of the difficulty in assigning the characteristic absorption due to the out-of-plane deformation in the infrared spectrum.

The oxidation of IIa with selenium dioxide in aqueous dioxane gave a compound (V), $C_{10}H_{10}O_5$. The ultraviolet absorption spectrum of V is very similar to that of IIa. The infrared spectrum shows absorptions at 3360, 1096, 1057, and 1037 cm^{-1} associable with the hydroxyl group, in addition to an absorption at 1704 cm^{-1} corresponding to the carbonyl group. From these spectral data, as well as the results of the elementary analysis, V was assigned the structure of 4-(ω,ω-dihydroxyacetyl)-2-methoxytropone, a hydrate form of 4-glyoxyloyl-2-methoxytropone. The further oxidation of V with metaperiodic acid afforded 4-carboxy-2-methoxytropone (VI),[2c] which gave 4-carboxytropolone[2b,9] on hydrolysis with a sodium hydroxide solution. This finding shows that the acetyl side-chain of IIa was oxidized effectively with selenium dioxide. The hydrate, V, was so stable that it did not show any change upon heating at 110°C *in vacuo*. This stability of V is probably due to the inductive effect of the electron-withdrawing tropolone nucleus. In the case of the other isomeric ether, IIb, the treatment with selenium dioxide deposited selenium powder, but no identifiable product could be isolated.

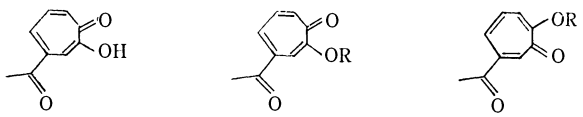

I

IIa: R=CH_3
IIIa: R=C_2H_5
IVa: R=i-C_3H_7

IIb: R=CH_3
IIIb: R=C_2H_5
IVb: R=i-C_3H_7

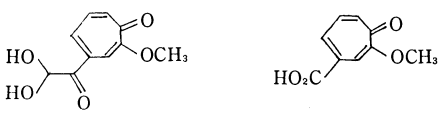

V

VI

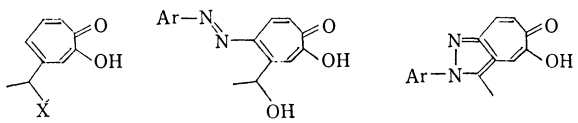

VII: X=OH
VIII: X=H
IX: X=Cl
Xa: X=OCH_3
Xb: X=OC_2H_5

XI: Ar=*p*-Tolyl

XII: Ar=*p*-Tolyl

3) a) P. L. Pauson, *Chem. Rev.*, **55**, 43 (1955). b) T. Nozoe, *Fortsch. Chem. Org. Naturstoffe*, **13**, 232 (1956).

4) T. Nozoe, K. Takase, and K. Umino, This Bulletin, **38**, 358 (1965).

5) K. Doi, *ibid.*, **34**, 501 (1961).

6) I. Murata, *ibid.*, **34**, 577 (1961).

7) E. Sebe and S. Matsumoto, *Sci. Repts. Tohoku Univ., Ser. I*, **38**, 297 (1954).

8) 2,4-Disubstituted tropones show the characteristic absorption due to the out-of-plane deformation in the 810—840 cm^{-1} range, and 2,6-disubstituted tropones show it in the 770—800 cm^{-1} range in the infrared spectra; T. Nozoe, K. Takase, and M. Yasunami, to be published.

9) a) T. Nozoe, Y. Kitahara, and S. Masamune, *Proc. Japan Acad.*, **29**, 17 (1953); T. Nozoe and Y. Kitahara, *ibid.*, **30**, 204 (1954); Y. Kitahara, *Sci. Repts. Tohoku Univ., Ser. I*, **40**, 74 (1956). b) J. R. Bartels-Keith, A. W. Johnson, and W. I. Taylor, *J. Chem. Soc.*, **1951**, 2352.

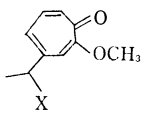

XIIIa: X=OH
XIVa: X=H
XVa: X=Cl

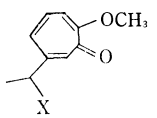

XIIIb: X=OH
XIVb: X=H
XVb: X=Cl

It is known that the tropolone nucleus generally resists catalytic hydrogenation with the palladium-carbon catalyst.[3] The same is true in the case of I. Thus, under similar conditions, the tropolone nucleus of I was not hydrogenated; only the acetyl group was hydrogenated, giving a mixture of 4-(1-hydroxyethyl)- (VII) and 4-ethyltropolone (VIII).[4] The ultraviolet spectrum of VII is similar to that of tropolone, and the infrared spectrum shows an absorption at 3370 cm^{-1} due to the hydroxyl group. The dehydroxylation of VII to VIII was performed effectively by treatment with iodine and red phosphorous in acetic acid. 4-(1-Chloroethyl)tropolone (IX) was derived from VII by treatment with thionyl chloride in the presence of pyridine. The chloro substituent in IX was very sensitive to nucleophilic attack; that is, the treatment of IX with potassium hydroxide in methanol or ethanol afforded 4-(1-methoxyethyl)-(Xa) and 4-(1-ethoxyethyl)-tropolones (Xb) respectively, whose structures were determined from their NMR spectral data. The azocoupling of VII with *p*-toluenediazonium chloride gave an azo compound (XI), which then afforded a 5-hydroxy-6(2*H*)-cyclohepta[*c*]pyrazolone derivative (XII)[10] by cyclization when heated over its melting point or when heated in an alcoholic solution in the presence of hydrochloric acid.

The reaction of I with sodium borohydride gave water-soluble products, but no identifiable compound was isolated from the reaction mixture; this may be a mixture of boron-complexes of the reduction products. On the other hand, the reduction of the methyl ethers, IIa and IIb, with sodium borohydride in aqueous methanol gave the corresponding alcohols, (XIIIa) and (XIIIb) respectively, in good yields. The infrared spectra show absorptions due to the hydroxyl groups at 3360 and 3380 cm^{-1} respectively, and no absorption corresponding to an acetyl carbonyl. On alkaline hydrolysis, both XIIIa and XIIIb gave the same compound, VII, in good yields. Consequently, in oredr to prepare VII conveniently from I, a mixture of the methyl ethers, IIa and IIb, without the separation of each component, could be treated with sodium borohydride and then hydrolyzed with alkali.

The methylation of 4-ethyltropolone (VIII) with diazomethane gave a mixture of two isomeric methyl ethers, 4-ethyl-2-methoxy-(XIVa) and 6-ethyl-2-methoxytropone (XIVb), but the separation of each component from this mixture could not be achieved effectively. However, XIVa and XIVb could be prepared in pure states from XIIIa and XIIIb respectively as follows. The treatment of XIIIa or XIIIb with thionyl chloride in the presence of pyridine gave 4-(1-chloroethyl)-2-methoxy- (XVa) or 6-(1-chloroethyl)-2-methoxytropones (XVb) respectively. Their reductive dechlorinations afforded XIVa and XIVb respectively in good yields.

The structures of two series of methyl ethers, IIa, XIIIa, XIVa, and XVa, and IIb, XIIIb, XIVb, and XVb, described above have been presumed only on the basis of a consideration of the infrared spectral data. Now, some chemical evidence for the structural proof of these ethers will be presented. It is known that the reaction of 2-methoxytropones and hydrazine proceeds in the mode of the normal substitution; for example, 2-methoxy-6-methyltropone (XVI) is known to react with hydrazine, giving 2-hydrazino-6-methyltropone (XVII).[11] Moreover, it has now been observed that 6-methyl-2-(*p*-tolylsulfonyloxy)tropone (XVIII)[12] also reacts with hydrazine in a similar manner, giving the same hydrazino compound, XVII.

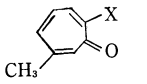

XVI: X=OCH_3
XVII: X=$NHNH_2$
XVIII: X=OTs

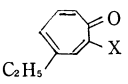

XIXa: X=OTs
XXa: X=$NHNH_2$

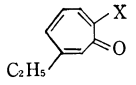

XIXb: X=OTs
XXb: X=$NHNH_2$

This close relation in the reaction mode between 2-methoxytropone, XVI, and 2-(*p*-tolylsulfonyloxy)-tropone, XVIII, could also be applicable to the structural correlation between the methyl ethers, XIVa and XIVb, and the *p*-tolylsulfonyl derivatives, (XIXa) and (XIXb), of 4-ethyltropolone (VIII) (the structures of the latter have been established).[13] Thus, on treatment with hydrazine, XIVa and XIXa gave the same hydrazino compound (XXa), whereas XIVb and XIXb gave another kind of the same hydrazino compound (XXb). From these facts, the structures of the methyl ethers, XIVa and XIVb, and, consequently, the structures of IIa and IIb were determined by chemical means.

Experimental

All the melting points are uncorrected. The ultraviolet absorption spectra were determined on a Beckman DU spectrophotometer, and the infrared spectra were recorded on a Shimadzu IR-27 infracord apparatus.

Silver Salt of 4-Acetyltropolone (I). Into a solution which had been prepared by the neutralization of I (5.0 g) in water (20 m*l*) with a 0.2 N potassium hydroxide solution (*ca.* 150 m*l*), a solution of silver nitrate (5.1 g) in water (20 m*l*) was stirred. A reddish-orange silver salt immediately precipitated; it was collected by filtration, washed with water, and dried *in vacuo*. Yield, 8.1 g.

Found: C, 38.27; H, 2.44%. Calcd for $C_9H_7O_3Ag$: C, 38.88; H, 2.60%.

4-Acetyl-2-methoxytropone (IIa) and 6-Acetyl-2-methoxytropone (IIb). a) To a suspension of silver salt (8.1 g) of I in dry benzene (150 m*l*), methyl iodide (10 g) was added, and then the mixture was refluxed for 1.5 hr. The silver

10) T. Nozoe, K. Takase, and K. Suzuki, This Bulletin, **38**, 362 (1965).

11) P. Akroyd, R. D. Haworth, and J. D. Hobson, *J. Chem. Soc.*, **1951**, 3427.

12) T. Sato, *Bull. Chem. Res. Inst. Non-Aqueous Solu., Tohoku Univ.*, **9**, 47 (1959).

13) T. Nozoe, K. Takase, and T. Sudo, to be published.

iodide thus formed was filtered off, and the benzene filtrate was washed with a 5% sodium hydrogen carbonate solution. After drying over anhydrous sodium sulfate, the evaporation of the solvent left crystals (2.5 g), mp 79—87°C. The sodium hydrogen carbonate solution was extracted with chloroform; the subsequent evaporation of the solvent gave further crops of crystals (2.8 g), mp 76—85°C. The fractional recrystallization of these crystals from ethyl acetate gave IIa as light brown micro-crystals, mp 122.5°C, and IIb as yellow needles, mp 107°C.

Found for IIa: C, 67.64; H, 5.33%. Found for IIb: C, 67.38; H, 5.39%. Calcd for $C_{10}H_{10}O_3$: C, 67.40; 5.66%. UV (MeOH) for IIa: λ_{max} nm (log ε); 250 (4.46), 309 (3.69), 322 (3.68), 369 (3.26). UV (MeOH) for IIb: λ_{max} nm (log ε); 245 (4.44), 310 (3.77), 372 (3.68).

b) To a stirred suspension of I (328 mg) in ether (5 m*l*), we added a slight excess of an ethereal solution of diazomethane at 0—5°C. The crystals thus formed were collected by filtration, affording a mixture (258 mg) of IIa and IIb.

4-Acetyl-2-ethoxytropone (IIIa) and 6-Acethyl-2-ethoxytropone (IIIb). Silver salt (1.36 g) of I was treated with ethyl iodide (1.56 g) in a manner similar to that described above; the crystals (901 mg), mp 55—62°C, thus obtained were fractionally recrystallized from ether, giving IIIa as yellow needles, mp 88.5—89°C and IIIb as yellow needles, mp 91—92°C.

Found for IIIa: C, 68.52; H, 6.01%. Found for IIIb: C, 68.69; H, 6.05%. Calcd for $C_{11}H_{12}O_3$: C, 68.73; H, 6.29%. UV (MeOH) for IIIa: λ_{max} nm (log ε); 250 (4.52), 310 (3.74), 370 (3.82). UV (MeOH) for IIIb: λ_{max} nm (log ε); 247 (4.49), 315 (3.87), 377 (3.74).

4-Acetyl-2-isopropoxytropone (IVa) and 6-Acetyl-2-isopropoxytropone (IVb). Silver salt (2.71 g) of I was treated with isopropyl iodide (2.2 g) in a manner similar to that described above, and the oily mixture (1.32 g) thus obtained was dissolved in ether, passed through an alumina column, and eluted with ether. The fractions crystallized were collected and recrystallized from petroleum ether, giving IVa as yellow prisms, mp 71—72°C.

Found: C, 69.91; H, 6.80%. Calcd for $C_{12}H_{14}O_3$: C, 69.88; H, 6.84%. UV (MeOH): λ_{max} nm (log ε); 252 (4.52), 310 (3.78), 325 (3.76), 370 (3.84).

The mother liquor of recrystallization did not crystallize, but its infrared spectrum shows an absorption at 790 cm^{-1}, corresponding to the characteristic absorption[8] for 6-acetyl-2-isopropoxytropone (IVb).

Benzyl Ether of I. Silver salt (820 mg) of I was treated with benzyl chloride (460 mg) in a manner similar to that described above; the crystals (230 mg) thus obtained were recrystallized from ethyl acetate, giving benzyl ether as orangish yellow prisms, mp 177°C.

Found: C, 75.85; H. 5.39%. Calcd for $C_{16}H_{14}O_3$: C, 75.57; H, 5.55%. UV (MeOH): λ_{max} nm (log ε); 237 (4.44), 320 (2.83).

4-(ω,ω-Dihydroxyacetyl)-2-methoxytropone (V). A mixture of IIa (712 mg) and selenium dioxide (490 mg) in dioxane (3 m*l*) containing a small amount of water (0.1 m*l*) was refluxed for 5 hr. The selenium thus deposited was filtered off, and the filtrate was allowed to stand at room temperature. The crystals thus formed were collected by filtration and recrystallized from dimethylformamide, giving V as fine, organish-yellow leaflets, mp 144—146°C.

Found: C, 56.93; H, 4.48%. Calcd for $C_{10}H_{10}O_5$: C, 57.14; H, 4.80%. UV (MeOH): λ_{max} nm (log ε); 248 (4.41), 322 (3.76), 350 (3.77).

4-Carboxy-2-methoxytropone (VI). To a suspension of V (105 mg) in a mixture of ethanol (4 m*l*) and water (0.5 m*l*), metaperiodic acid dihydrate (125 mg) was added. After being stirred for 3 hr at room temperature, the mixture was diluted with water and allowed to stand at room temperature. The crystals thereby formed were collected by filtration to give crude VI (19 mg). The extraction of the filtrate with ethyl acetate gave further crops of VI (77 mg). Recrystallization from 25% aqueous methanol afforded light brown micro-crystals, mp 245°C. The melting point reported[2c] is 254°C.

Found: C, 60.04; H, 4.57%. Calcd for $C_9H_8O_4$: C, 60.00; H, 4.48%. UV (MeOH): λ_{max} nm (log ε); 245 (4.45), 323 (3.82), 360 (3.83). The infrared spectrum shows sbsorptions at 2700—2500 and 1721 cm^{-1} (carboxyl).

The hydrolysis of VI by warming it with a dilute sodium hydroxide solution gave 4-carboxytropolone, mp 215°C. The melting point reported [2b] is 217°C.

Catalytic Reduction of 4-Acetyltropolone (I). A solution of I (3.0 g) in methanol (50 m*l*) was shaken, in the presence of 5% palladium-carbon, under a hydrogen atmosphere; 850 m*l* of hydrogen gas were consumed in a period of 15 hr at 18°C. The removal of the palladium catalyst and of the solvent left an oily material, to which a small amount of benzene was added; the mixture was then allowed to stand. The crude crystals (1.07 g), mp 85—89°C, thereby formed were collected by filtration. Recrystallization from ethyl acetate afforded 4-(1-hydroxyethyl)tropolone (VII) as pale yellow prisms, mp 97—98°C.

Found: C, 65.30; H, 6.21%. Calcd for $C_9H_{10}O_3$: C, 65.05; H, 6.07%. UV (MeOH): λ_{max} nm (log ε); 240 (4.45), 322 (3.86), 350 (3.77).

The filtrate was passed through a silica gel column and eluted with benzene. The removal of the solvent from the effluent gave an oily substance (600 mg). Distillation *in vacuo* and then recrystallization from petroleum ether gave 4-ethyltropolone (VIII) as colorless rhombic prisms, mp 42—43°C.

4-Ethyltropolone (VIII) from 4-(1-Hydroxyethyl)tropolone (VII). A mixture of VII (160 mg), iodine (50 mg), and red phosphorous (150 mg) in acetic acid (2 m*l*) containing a small amount of water (0.5 m*l*) was refluxed for 4 hr. A precipitate was filtered off, and the filtrate was diluted with water and then extracted with chloroform The removal of the solvent left an oily substance, which was distilled *in vacuo* and crystallized on being allowed to stand, giving VIII (130 mg). Recrystallization from petroleum ether gave colorless rhombic prisms, mp 42—43°C.

4-(1-Chloroethyl)tropolone (IX). To a solution of VII (340 mg) and pyridine (160 mg) in dry dioxane (3 m*l*), we added a solution of thionyl chloride (400 m*l*) in dry dioxane (2 m*l*); the mixture was then stirred for 5 hr at room temperature. After the removal of the solvent, the residue was recrystallized from petroleum ether, giving IX (260 mg) as yellow needles, mp 82—83°C.

Found: C, 58.53; H, 4.65%. Calcd for $C_9H_9O_2Cl$:C, 58.55; H, 4.91%. UV (MeOH): λ_{max} nm (log ε); 341 (4.48), 324 (3.85), 355 (3.75).

4-(1-Methoxyethyl)tropolone (Xa). A solution of IX (185 mg) in methanol (2 m*l*) containing a 6 N potassium hydroxide solution (1 m*l*) was refluxed for 2.5 hr. The reaction mixture was then diluted with water (20 m*l*), acidified with 6 N hydrochloric acid, extracted with benzene, and dried over anhydrous sodium sulfate. The evaporation of the solvent left crystals (185 mg) which were subsequently recrystallized from cyclohexane, giving Xa (150 mg) as colorless prisms, mp 65—66°C.

Found: C, 66.91; H, 6.41%. Calcd for $C_{10}H_{12}O_3$; C, 66.65; H, 6.71%. UV (MeOH): λ_{max} nm (log ε); 238 (4.46),

325 (4.17), 367 (3.98). NMR ($CDCl_3$): δ ppm; 1.42 (3H,d, J=6.5 Hz, $C\underline{H}_3$–CH), 3.27 (3H, s, CH_3O–), 4.20 (1H, q, J=6.5 Hz, CH_3–$C\underline{H}$–O), 6.93-7.46 (4H, m, ring protons).

4-(1-Ethoxyethyl)tropolone (Xb). To a solution of IX (550 mg) in ethanol (2 m*l*) we added a potassium hydroxide solution (6 m*l*) which had been prepared by dissolving potassium hydroxide (10 g) in a mixture of water (10 m*l*) and ethanol (40 m*l*), and then the mixture was refluxed for 2 hr. The reaction mixture was diluted with water (10 m*l*), acidified with 6 N hydrochloric acid, extracted with chloroform, and dried over anhydrous sodium sulfate. The evaporation of the solvent left a light brown, oily material (270 mg). This was dissolved in ether and chromatographed on a silica gel column. The first fraction, when eluted with ether, gave Xb (193 mg), mp 58—62°C. The second fraction gave the same compound (50 mg), mp 56—60°C. Recrystallization from cyclohexane afforded colorless prisms, mp 63—64°C.

Found: C, 68.00, H, 7.06%. Calcd for $C_{11}H_{14}O_3$, C, 68.02. H, 7.27%. UV (CH_3OH), λ_{max} nm (log ε); 238 (4.45), 325 (3.97), 365 (3.75). NMR ($CDCl_3$): δ ppm, 1.34 (3H, t, J=7.0 Hz, $C\underline{H}_3$–CH_2), 1.42 (3H, d, J=6.5 Hz, $C\underline{H}_3$–CH), 3.42 (2H, q, J=7.0 Hz, $CH_3C\underline{H}_2$–O–), 4.34 (1H, q, J=6.5 Hz, CH_3–$C\underline{H}$–O), 6.93—7.46 (4H, ring protons).

4-(1-Hydroxyethyl)-5-(p-tolylazo)tropolone (XI). To a solution of VII (160 mg) in pyridine (0.7 m*l*) we added a solution of *p*-toluenediazonium chloride which had been prepared by the diazotization of a solution of *p*-toluidine (120 mg) in water (1 m*l*) containing a 6N hydrochloric acid (0.5 m*l*) with a solution of sodium nitrite (80 mg) in water (0.5 m*l*), with stirring under cooling with ice-water. Water was added to the mixture, and the crystals thereby deposited were collected by filtration and recrystallized from benzene, giving XI (240 mg) as orange needles. These needles evolved gas at 123—126°C and melted at 202—204°C.

Found: C, 67.19; H, 5.34; N, 9.61%. Calcd for $C_{16}H_{16}O_3N_2$: C, 67.59; H, 5.67; N, 9.85%. UV (MeOH): λ_{max} nm (log ε); 232 (4.37), 300 (3.99), 397 (4.41).

5-Hydroxy-3-methyl-2-(p-tolyl)-6(2H)-cyclohepta[c]pyrazolone (XII). A mixture of XI (100 mg) in ethanol (10 m*l*) containing 6N hydrochloric acid (0.3 m*l*) was refluxed for 2 hr and then allowed to cool, giving XII (70 mg) as pale yellow needles, mp 203—204°C.[10]

4-(1-Hydroxyethyl)-2-methoxytropone (XIIIa). To a solution of IIa (160 mg) in 10% aqueous methanol (2 m*l*), sodium borohydride (40 mg) was added; the mixture was stirred for 1 hr at room temperature, and then diluted with water and extracted with ethyl methyl ketone. The extract was dried over anhydrous sodium sulfate; the subsequent evaporation of the solvent left crystals (150 mg), mp 118—120°C. Recrystallization from ethyl acetate gave XIIIa as colorless micro-needles, mp 121—122°C.

Found: C, 66.60; H, 6.42%. Calcd for $C_{10}H_{12}O_3$: C, 66.65; H, 6.71%. UV (MeOH): λ_{max} nm (log ε); 241 (4.46), 320 (3.88), 345 (3.92).

6-(1-Hydroxyethyl)-2-methoxytropone (XIIIb). The treatment of IIb (270 mg) in a manner similar to that described above gave XIIIb (180 mg) as colorless micro-needles, mp 139°C.

Found: C, 66.25; H, 6.43%. Calcd for $C_{10}H_{12}O_3$: C, 66.65; H, 6.71%. UV (MeOH): λ_{max} nm (log ε); 239 (4.43), 319 (3.70).

Hydrolysis of XIIIa and XIIIb. A solution of XIIIa (180 mg) in a 2N potassium hydroxide solution (2 m*l*) was refluxed for 1 hr; then it was diluted with water, acidified with 6N hydrochloric acid, and extracted with ethyl methyl ketone. The evaporation of the solvent gave VII (160 mg), mp 93—96°C. A similar treatment of XIIIb (180 mg) gave VII (160 mg), mp 95—97°C.

4-(1-Chloroethyl)-2-methoxytropone (XVa). To a solution of XIIIa (360 mg) in chloroform (3 m*l*) containing pyridine (180 mg), a solution of thionyl chloride (260 mg) in chloroform (1 m*l*) was added, drop by drop, at room temperature. After being stirred for 3 hr and then allowed to stand overnight, the mixture was washed with water and dried over anhydrous sodium sulfate. The evaporation of the solvent gave an oily XVa (311 mg). A sample for the elementary analysis was prepared by distillation *in vacuo*.

Found: C, 59.98; H, 5.36%. Calcd for $C_{10}H_{11}O_2Cl$: C, 60.46; H, 5.58%. UV (MeOH): λ_{max} nm (log ε); 243 (4.26), 330 (3.72).

6-(1-Chloroethyl)-2-methoxytropone (XVb). The treatment of XIIIb (180 mg) in a manner similar to that described above gave XVb (158 mg). Recrystallization from ethyl acetate gave colorless prisms, mp 85—86°C.

Found: C, 60.90; H, 5.39%. Calcd for $C_{10}H_{11}O_2Cl$: C, 60.46; H, 5.58%. UV (MeOH): λ_{max} nm (log ε); 242 (4.38), 325 (3.76).

4-Ethyl-2-methoxytropone (XIVa). A mixture of XVa (202 mg), 5% palladium-carbon (10 mg), and sodium acetate (90 mg) in methanol (6 m*l*) was subjected to hydrogenolysis at room temperature. The reaction was stopped when an equimolar amount of hydrogen gas had been uptaken. After the removal of the catalyst and of the solvent, the mixture was diluted with water and extracted with chloroform. The organic layer was dried over anhydrous sodium sulfate, and the solvent was evaporated, giving XIVa (168 mg) as a pale yellow oil. A sample for the elementary analysis was prepared by distillation *in vacuo*.

Found: C, 69.67; H, 7.10%. Calcd for $C_{10}H_{12}O_2 \cdot \frac{1}{2}H_2O$: C, 69.34; H, 7.57%. UV (MeOH): λ_{max} nm (log ε); 242 (4.38), 325 (3.76).

6-Ethyl-2-methoxytropone (XIVb). A mixture of XVb (90 mg), 5% palladium-carbon (20 mg), and sodium acetate (45 mg) in methanol (5 m*l*) was treated as has been described above, giving XIVb (73 mg). Recrystallization from petroleum ether afforded colorless needles, mp 53—55°C.

Found: C, 73.26; H, 7.10%. Calcd for $C_{10}H_{12}O_2$; C, 73.14; H, 7.37%. UV (MeOH): λ_{max} nm (log ε); 239 (4.44), 325 (3.86).

Picrate: Yellow crystals (from ethanol); mp 140—141°C.

Found: C, 48.70; H, 3.77; N, 10.80%. Calcd for $C_{16}H_{15}O_9N_3$: C, 48.86; H, 3.84; N, 10.68%.

2-Hydrazino-6-methyltropone (XVII). *a) From 2-Methoxy-6-methyltropone (XVI)*: A mixture of XVI (300 mg) and 80% hydrazine hydrate (250 mg) in water (0.5 m*l*) was heated for 5 min at 100°C, and then allowed to cool, giving XVII (250 mg) as yellow needles, mp 123—124°C. The melting point reported[11] is 134—135°C.

b) From 6-Methyl-2-(p-tolylsulfonyloxy)tropone (XVIII): A similar treatment of XVIII (290 mg) with 80% hydrazine hydrate (250 mg) in methanol gave yellow needles, mp 123—124°C, which were identical with XVII.

4-Ethyl-2-hydrazinotropone (XXa). *a) From 4-Ethyl-2-(p-tolylsulfonyloxy)tropone (XIXa)*: A mixture of XIXa (218 mg) and 80% hydrazine hydrate (1 m*l*) in methanol (1 m*l*) was heated for 10 min at 100°C. The mixture was diluted with water and extracted with ether, and then the ether solution was passed through an alumina column. The evaporation of the solvent from the effluent gave XXa (100 mg) as a reddish oil.

Found: C, 65.80; H, 7.25; N, 17.42%. Calcd for $C_9H_{12}ON_2$: C, 65.83, H, 7.37; N, 17.06%.

b) From 4-Ethyl-2-methoxytropone (XIVa): A similar treatment of XIVa (40 mg) with 80% hydrazine hydrate (0.5 m*l*) gave a reddish oily material (35 mg) which was identical with XXa.

6-Ethyl-2-hydrazinotropone (XXb). a) From 6-Ethyl-2-(p-tolylsulfonyloxy)tropone (XIXb): A mixture of XIXb (218 mg) and 80% hydrazine hydrate (1 m*l*) in methanol (1 m*l*) was treated as has been described above. The crystals (16 mg), mp 64—67°C, thus obtained were recrystallized from ether, giving XXb as orange needles, mp 71—72°C.

Found: C, 65.72; H, 7.18; N, 16.86%. Calcd for $C_9H_{12}O$-N_2: C, 65.83; H, 7.37; N, 16.06%.

b) From 6-Ethyl-2-methoxytropone (XIVb): A similar treatment of XIVb (20 mg) with 80% hydrazine hydrate gave yellow crystals (18 mg), mp 69—72°C. Recrystallization from ether gave yellow prisms, mp 71—72°C, which were identical with XXb.

The authors wish to thank the Takasago Perfumery Co., Ltd., for its assistance in the preparation of the β-dolabrin.

BULLETIN OF THE CHEMICAL SOCIETY OF JAPAN, VOL. 44, 1956—1961 (1971)

A Novel Cyclodimerization of Butadiene. A Synthetic Route to 2-Methylenevinylcyclopentane

Jitsuo KIJI, Kazuo MASUI,* and Junji FURUKAWA

Department of Synthetic Chemistry, Kyoto University, Sakyo-ku, Kyoto

(Received February 12, 1971)

In the presence of a controlled amount of alcohol, the dimerization of butadiene to produce 2-methylenevinylcyclopentane has been shown to occur by means of several nickel catalysts. The most effective nickel catalysts are: (1) $(Bu_3P)_2NiX_2$ (X=Cl and Br) and organolithium, (2) (*o*-tolyl)$NiX(PEt_3)_2$ (X=Cl, Br, and I), and (3) π-allylnickel bromide and tri-*n*-butylphosphine. A detailed study of the role of alcohol during the reaction by the arylnickels is presented. In the presence of butadiene, the aryl-nickel bond of (*o*-tolyl)$NiX(PEt_3)_2$ is reductively cleaved by methanol to give toluene, and then the dimerization of butadiene occurs. With CH_3OD as the reducing reagent, toluene is not deuterated, but with CD_3OD the aromatic ligand is deuterated on the carbon originally bonded to nickel to give monodeuterotoluene.

The dimerizations of butadiene in the presence of transition metals to cyclic or linear products have been extensively studied in the last decade by many workers.[1] The principal products are isomeric *n*-octatrienes, methylheptatrienes, 4-vinylcyclohexene, 1,5-cyclooctadiene, and 1,2-divinylcyclobutane. Until now, however, no effective catalysts have been reported to convert butadiene into a five-membered cyclic dimer, 2-methylenevinylcyclopentane (I) or 3-methylenevinylcyclopentane (II), except for the works of Müller[2] and Feldman,[3] who isolated the five-membered cyclic dimers of butadiene in low yields as a by-product.

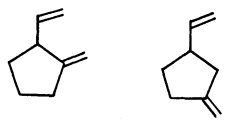

I II

The formation of intermediates which give several different products is expected when butadiene is allowed to react under the influence of transition-metal catalysts. Therefore, it is of considerable interest to compare the courses of the dimerization of butadiene by the different transition metals. The critical importance of appropriate auxiliary ligands to the catalytic effectiveness of Ziegler-Natta polymerization catalysts is well known. From our interest in the mechanism of transition-metal-catalyzing oligomerization and polymerization, we have examined the effects of appropriate ligands, using the reaction of butadiene by means of nickel catalysts as a model system. In the course of this work, we have confirmed the formation of 2 methylenevinylcyclopentane (MVCP) from the dimerization of butadiene by several nickel catalysts. A part of this study has already been reported in preliminary reports.[4,5] The new route to MVCP from butadiene is of interst in connection with certain synthetic problems and with the catalysis of transition metals.

In this paper we wish to report on the formation of MVCP and on some mechanistic studies of the cyclodimerization.

Results and Discussion

The following types of nickel catalysts in the presence of alcohol were effective for the cyclodimerization of butadiene to MVCP: (1) bis(trialkylphosphine)dihalo-

* Present address: Hitachi Chemical Company, Ltd., Hitachi.

1) C. W. Bird, "Transition Metal Intermediates in Organic Synthesis," Academic Press, New York (1967), p. 30.

2) H. Müller, D. Wittenberg, H. Seibt, and E. Scharf, *Angew. Chem., Int. Ed. Engl.*, **4**, 327 (1965).

3) J. Feldman, O. Frampton, B. Saffer, and M. Thomas, ACS Preprints, Division of Petroleum Chemistry, **9**, A55 (1964).

4) J. Kiji, K. Masui, and J. Furukawa, *Tetrahedron Lett.*, **1970**, 2561.

5) J. Kiji, K. Masui, and J. Furukawa, *Chem. Commun.*, **1970** 1310.

Table 1. Dimerization of butadiene by various nickel catalysts in the presence of protonic compounds[a]

Expt. No.	Ni Compd.	(mmol)	Organo-lithium[b]	(mmol)	Protonic compd.	(mmol)	Butadiene (mmol)	Produces[c] yield (%)
1	$(Bu_3P)_2NiCl_2$	(1.4)	*n*-BuLi	(0.72)	CH_3OH	(40)	80	MVCP (50)
2	$(Bu_3P)_2NiCl_2$	(1.3)	*n*-BuLi	(1.3)	CH_3OH	(40)	70	MVCP (70)
3	$(Bu_3P)_2NiCl_2$	(1.3)	*n*-BuLi	(2.6)	CH_3OH	(40)	70	MVCP (70)
4	$(Bu_3P)_2NiCl_2$	(1.3)	*n*-BuLi	(5.1)	CH_3OH	(40)	70	MVCP (50)
5	$(Bu_3P)_2NiBr_2$	(1.4)	*n*-BuLi	(1.4)	CH_3OH	(40)	120	MVCP (90)
6	$(Bu_3P)_2NiI_2$[d]	(0.58)	*n*-BuLi	(0.68)	CH_3OH	(25)	70	1,3,7-OT[e]
7	$(Bu_3P)_2Ni(NO_2)_2$	(1.1)	*n*-BuLi	(1.0)	CH_3OH	(25)	100	——
8	$(Bu_3P)_2Ni(SCN)_2$	(2.0)	*n*-BuLi	(2.0)	CH_3OH	(25)	100	——
9	$(Bu_3P)_2NiCl_2$	(1.5)	DMBALi	(1.5)	CH_3OH	(2.5)	80	VCH,[e] COD[e]
10	$(Bu_3P)_2NiCl_2$	(1.5)	DMBALi	(1.5)	CH_3OH	(25)	80	MVCP (70)
11	$(Bu_3P)_2NiCl_2$	(1.5)	DMBALi	(1.5)	CH_3OH	(75)	80	MVCP (45)
12	$(Bu_3P)_2NiCl_2$	(2)	DMBALi	(2)	C_6H_5OH	(10)	70	MVCP (20)
13	$(Bu_3P)_2NiCl_2$	(1.5)	DMBALi	(1.5)	$C_6H_5CH_2OH$	(5)	130	MVCP (5)
14	$(Bu_3P)_2NiCl_2$	(1.5)	DMBALi	(1.5)	$C_6H_5CH_2OH$	(20)	110	MVCP (70)
15	$(Bu_3P)_2NiCl_2$	(1.1)	*n*-BuLi	(1.1)		(17)	10	MVCP (10) VCH,[e] COD[e]
16	$(Et_2PhP)_2NiCl_2$	(1.1)	*n*-BuLi	(1.1)	CH_3OH	(25)	50	MVCP (60) VCH (5)
17	$(Cy_3P)_2NiCl_2$	(0.5)	*n*-BuLi	(0.5)	CH_3OH	(12)	30	1,3,7-OT (33) 1,3,6-OT (15)
18	$(Bu_3P)_2NiCl_2$	(1.3)	*n*-BuLi	(3.2)	H_2O	(28)	—	VCH (22) COD (28)
19	$(Bu_3P)_2NiCl_2$	(1.3)	*n*-BuLi	(1.3)	CH_3COOH	(17)	100	——
20	$(Bu_3P)_2NiCl_2$	(1.3)	*n*-BuLi	(1.3)	CF_3COOH	(10)	100	——

a) All reactions were carried out in benzene (1.8—5 ml) solution at 60—75°C for 40—50 hr.
b) *n*-BuLi, *n*-butyllithium; DMBALi, *o*-lithio-*N*,*N*'-dimethylbenzylamine.
c) MVCP, 2-methylenevinylcyclopentane; VCH, 4-vinyl-1-cyclohexene; COD, 1,5-cyclooctadiene; OT, octatriene.
d) Crystalline compound could not be obtaind.
e) In low yield.

nickel and organolithium, (2) *trans*-bis(triethylphosphine)halo-(*o*-tolyl)nickel, and (3) π-allylnickel bromide and tributylphosphine. The dimerization with these catalysts proceeded smoothly at 60—70°C, and MVCP free from significant by-products was easily obtained by distillation. No obvious dimerization was observed at room temperature. We have not tried to carry the reaction out above 100°C because the Diels-Alder reaction is expected to occur at higher temperatures. The most characteristic features of these catalysts are that they contain a halogen atom and should be used in the presence of a considerable and controlled amount of alcohol. Without alcohol, 4-vinylcyclohexene (VCH) and 1,5-cyclooctadiene (COD) were formed in low yields. The infrared spectrum of MVCP showed strong absorptions at 910 and 990 cm^{-1} due to a vinyl group and at 880 cm^{-1} due to a terminal methylene group. The absorption band at 1370 cm^{-1} for the methyl group was absent in the spectrum. The main product of hydrogenation over palladium-carbon was identical with *trans*-1-methyl-2-ethylcyclopentane.

Bis(tertiaryphosphine)dihalonickel Compounds and Organolithium. The results are summarized in Table 1. An inspection of Table 1 leads to the following conclusions concerning the factors which affect this cyclodimerization.

(a) It is essential to add alcohol in a 25—40 molar amount. In an experiment in which an amount of methanol equimolar to the nickel catalyst was added, no MVCP was formed except that vinylcyclohexene and cyclooctadiene were formed in low yields. On the other hand, the use of too large an amount of methanol resulted in the formation of higher-boiling products in addition to MVCP. Alcohols other than methanol can be used, but acids, phenols, and amines were less effective.

(b) The cyclodimerization proceeds satisfactorily in the presence of strong σ-donor phosphines without a bulky substituent. Strong electron donors, such as triethylphosphine and tri-*n*-butylphosphine, were effective as auxiliary ligands. On the contrary, bis(tricyclohexylphosphine)dichloronickel catalyzed not the cyclodimerization, but the linear dimerization, as is indicated by No. 17. Presumably, the marked difference in the behavior of $(Bu_3P)_2NiCl_2$ and $(Cy_3P)_2NiCl_2$ is a consequence of the difference in the bulkiness of the substituents on phosphorus, because the electron donor-acceptor properties of these two phosphines are similar; *i.e.*, no indication of any significant difference is provided by a comparison of the infrared CO stretching frequencies of $Ni(CO)_2(Phosphine)_2$ for tricyclohexylphosphine, 1973 cm^{-1}, with that for tri-*n*-butylphosphine, 1976 cm^{-1}.[6]

6) C. A. Tolman, *J. Amer. Chem. Soc.*, **92**, 2953 (1970).

TABLE 2. DIMERIZATION WITH (*o*-TOLYL)NiX(PEt_3)$_2$ IN THE PRESENCE OF PROTONIC COMPOUNDS[a]

Expt No.	Catalyst	(mmol)	Protonic compd.	(mmol)	Butadiene (mmol)	Dimer distribution (%) MVCP	VCH	COD	OT
1	IIIa X=Cl	(0.85)	CH_3OH	(20)	60	86	9	5	—
2	IIIb X=Br	(2.4)	CH_3OH	(40)	100	95	4	1	—
3	IIIc X=I	(0.5)	CH_3OH	(12)	50	92	5	3	—
4	IIId X=NO_2	(0.3)	CH_3OH	(12)	50	—	6	22	72
5	IIIe X=NCS	(1.1)	CH_3OH	(25)	70	—	14	16	70
6	IIIb X=Br	(1.4)		(17)	100	29	46	25	—
7[b]	IIIb X=Br	(0.4)	CH_3OD	(15)	15	—	—	—	—

a) All reactions except No. 7 were carried out in benzene (1—5 m*l*) solution at 70—75°C for 40 hr; yield of dimers, 50—70%.
b) Reaction at 70°C for 3 hr. Butadiene was recovered unchanged (not deuterated) and decomposition of the catalyst was not observed.

(c) The substituent, X, in $(R_3P)_2NiX_2$ is very important, although its behavior is obscure. It is essential for the nickel complex to contain a chlorine or bromine atom. No MVCP was formed, but linear dimers were formed in low yields when the substituents, the X's, were I, NO_2, CO, and SCN.

(d) *o*-Substituted aryllithium such as *o*-lithio-*N*,*N*′-dimethylbenzylamine[7] was effective, as was *n*-butyllithium. The other alkylation reagents, such as alkylaluminums, were ineffective.

Arylnickel Compounds. It is generally agreed that the first step in the reaction of transition metal halides and alkylmetals (*i.e.*, the first step in the preparation of Ziegler-Natta-type catalysts) is an alkylation. This mechanistic concept prompted us to examine the catalytic properties of the stable *o*-substituted arylnickels (III and IV) prepared by Chatt and Shaw,[8] because an arylnickel is presumed to be formed on the reaction of *o*-lithio-*N*,*N*′-dimethylbenzylamine with $(Bu_3P)_2NiCl_2$.

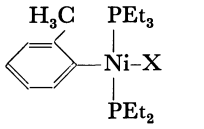

III

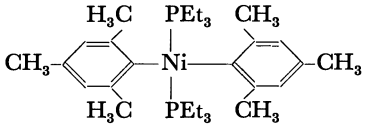

IV

a: X=Cl d: X=NO_3
b: X=Br e: X=NCS
c: X=I

These arylnickels (III and IV) are so stable that they can be handled in the open air. In spite of their chemical stability, they readily dimerized butadiene in the presence of alcohol.[5] The results are summarized in Table 2.

The iodine complex (IIIc) effected the cyclodimerization, while $(Bu_3P)_2NiI_2$ and organolithium catalyzed a linear dimerization. Interestingly, nitrironickel (IIId), isothiocyanatonickel (IIIe), and bis(triethylphosphine)-di(mesityl)nickel (IV) no longer brought about the cyclodimerization, but effected linear dimerization. Thus, in this catalytic system only halogen-bearing arylnickels were effective for the dimerization to the five-membered cycle (I). In the present study, however, the role of the halogen atom in the cyclodimerization has not been well understood so we cannot here discuss its behavior.

Bis(triethylphosphine)halo-(*o*-tolyl)nickels were recovered unchanged after heating the solution of methanol if butadiene was absent. Under the dimerization conditions in the presence of butadiene, the *o*-tolylnickels were decomposed to give toluene almost quantitatively, and were converted to a substance possessing the catalytic activity. In the working state of the catalysts, the aryl group originally attached to nickel is eliminated. Therefore, the presence of the aryl-nickel bond is not essential for the cyclodimerization, though the initiation of the dimerization may be affected by the aryl group. When the reaction with IIIb was stopped at an early stage (after three hours), toluene and the dimer, I, were not detected. Thus, the elimination of the aryl group and the cyclodimerization are associated with each other. This is consistent with the fact observed in the case of diethylbis(dipyridyl)iron, which catalyzes the dimerization of butadiene after the elimination of the ethyl group as butane, ethane, or ethylene.[9]

Of considerable importance is the observation that no deuterium was incorporated in toluene even if CH_3OD and CD_2=CH–CH=CD_2 were used instead of CH_3OH and CH_2=CH–CH=CH_2 respectively. The results are summarized in Table 3. This observation suggests that the cleavage of the arylnickel σ-bond in the presence of butadiene is not due to simple methanolysis. Since the use of CD_3OD resulted in the formation of monodeuterotoluene, it is clear that a hydrogen (deuterium) is transferred from a methoxide group to the coordinated *o*-tolyl group originally attached to nickel, thus liberating toluene. Accordingly, we began to consider the reductive cleavage of the aryl-nickel bond. Indeed, we have observed that the aryl-nickel bond of IIIb is cleaved by molecular hydrogen. Though the reaction was slow and a considerable amount of IIIb was recovered unchanged after the reaction, toluene was isolated in a 33% yield (based on the IIIb used); the complex under the influence of hydrogen showed a catalytic activity toward the dimerization of butadiene similar to that of IIIb combined with methanol.

7) A. Kasahara and T. Izumi, This Bulletin, **42**, 1765 (1969).
8) J. Chatt and B. L. Shaw, *J. Chem. Soc.*, **1960**, 1718.
9) A. Yamamoto, K. Morifuji, S. Ikeda, T. Saito, Y. Uchida, and A. Misono, *J. Amer. Chem. Soc.*, **90**, 1878 (1968).

Table 3. Reactions of (*o*-tolyl) $NiX(PEt_3)_2$ with reducing agents in the presence of butadiene[a]

III	(mmol)	Reductive cleavage of C-Ni bond				Catalytic dimerization		
		Reagent	(mmol)	Toluene[b] (%)	D % in toluene	Butadiene	(mmol)	MVCP[5] (%)
X=Br	0.4	——	——	0	——	C_4H_6	10	0
X=Cl	3.0	CH_3CD	40	67[c]	0	C_4H_6	15	25[c]
X=Br	1.0	CH_3OH	13	n.d[d]	0	$C_4H_2D_4$	6	55
X=Cl	1.5	CD_3OD	24	85[e]	*ca.* 95	C_4H_6	10	80
X=Br	0.4	H_2	30 (kg/cm²)	33[e]	0	C_4H_6	10	5

a) All reactions were carried out in benzene solution (1 m*l*) at 70—75°C for 24—48 hr.
b) Yield based on nickel complex used.
c) Isolated yield after distillation.
d) Not determined.
e) Gas chromatographic analysis using benzene as an internal standard.
f) Yield based on butadiene used.

While, in the cleavage of the aryl-nickel bond, no products other than toluene have been identified, the reaction evidently proceeds, by analogy to that of palladium,[10] through an oxidation of methanol, thus producing toluene and an active nickel catalyst which is effective for the dimerization to MVCP. The reduction of IIIb with molecular hydrogen also gives toluene and the active nickel catalyst. The dimerization using molecular hydrogen as the reducing agent is interesting in the point that a hydrogen migration during the dimerization is involved even in an aprotic solvent. In addition, dimers other than MVCP were not formed, though the formation of vinylcyclohexene and cyclooctadiene has been anticipated, because vinylcyclohexene and cyclooctadiene are the usual products of the dimerization of butadiene using nickel catalysts in an aprotic solvent.[1] In order to cyclodimerize butadiene to MVCP, the migration of one hydrogen must be involved. To our knowledge, for the dimerization of butadiene using nickel catalysts, protonic solvents such as alcohol,[2] phenol[3] and amine[11] must be always used for the formation of linear dimers. The experiment with molecular hydrogen suggests that alcohol is not necessary to the migration of hydrogen during the dimerization.

Bis(triethylphosphine)di(mesityl)nickel showed a different catalytic behavior from that of III (Table 4);

Table 4. Catalysis of $(mesityl)_2Ni(PEt_3)_2$[a]

Catalyst (mmol)	Reducing agent (mmol)	Butadiene (mmol)	Products (%)	
0.3	——	9	Vinylcyclohexene	50
			Cyclooctadiene	27
1.0	Methanol 25	100	1,3,6-*n*-Octatriene	14
			Higher boiling products[b]	
0.4	H_2 30 (kg/cm²)	10	Butane	*ca.* 30
			Ethylcyclohexane	33
			Cyclooctane	24

a) All reactions were carried out in benzene solution at 70—75°C for 24 hr.
b) The yields were not determined.

10) D. A. White and G. W. Parshall, *Inorg. Chem.*, **9**, 2358 (1970).
11) P. Heimbach, *Angew. Chem.*, **80**, 967 (1968).

even in the absence of the reducing agent, IV catalyzed the dimerization of butadiene to give 4-vinylcyclohexene and 1,5-cyclooctadiene in high yields.

Similarly, the aryl-nickel bond of bis(triethylphosphine)di(mesityl)nickel (IV) was cleaved by molecular hydrogen to form mesitylene. The mesityl complex, IV, was also an excellent catalyst precursor for the dimerization of butadiene described below, though the reaction catalyzed by IV differed from that by III. The catalytic behavior of IV would be consistent with the catalysis of $Fe(dipyl)_3$[9] or "naked nickel" combined with an electron-donating ligand[12] in the points that the distribution of the products is similar and IV is the precursor of an active catalyst containing no halogen atom.

On the other hand, if the mesityl complex, IV, was treated with hydrogen in the presence of butadiene, mesitylene was liberated and the reaction of butadiene was observed. In this case, however, instead of 4-vinylcyclohexene and 1,5-cyclooctadiene, only butane, ethylcyclohexane, and cyclooctane were formed as hydrogenated products. This is in marked contrast to the catalysis of III, which is inactive for hydrogenation.

π-Allylnickel Halide and Electron Donors. It is well known that π-allylic complexes are converted to dynamic σ-allylic ones.[13]

$$\pi\text{-Allyl}\cdot M\cdot X\cdot PR_3 + PR_3 \rightleftharpoons \sigma\text{-Allyl}\cdot M\cdot X\cdot (PR_3)_2$$

M: Ni and Pd. X: Halogen.

Thus, the π-allylnickel complex combined with strong electron donors was expected to show catalytic activities similar to those of the arylnickels described above. In fact, π-allylnickel bromide combined with tri-*n*-butylphosphine converted butadiene catalytically to MVCP. The results are summarized in Table 5. It is noteworthy that π-allylnickel iodide gave no MVCP but *trans*-1,4-polybutadiene. We examined the effect

12) W. Brenner, P. Heimbach, H. Hey, E. W. Müller, and G. Wilke, *Ann. Chem.*, **727**, 161 (1969).
13) G. E. Coates, M. L. H. Green, and K. Wade, "Organometallic Compounds," Vol. 2, Methuen, London (1968). p. 46.
14) R. G. Miller, R. D. Stauffer, D. R. Fahey, and D. R. Parnell, *J. Amer. Chem. Soc.*, **92**, 1511 (1970).
15) E. O. Fischer and G. Bürger, *Z. Naturforsch.*, **166**, 77 (1961).

Table 5. Dimerization by π-allylnickel bromide and electron donors[a)]

Expt No.	Catalyst (π-$C_3H_5NiBr)_2$ (mmol)	Donor	(mmol)	Products yield (%)
1	0.75	PBu_3	3	MVCP, 50
2	0.75	PPh_3	3	MVCP, 5; 1,3,6-OT,9
3	0.75	$P(OPh)_3$	3	——
4	0.75	NEt_3	3	——

a) All reactions were carried out in 5 ml of benzene at 70—75°C for 40 hr. 80 mmol of butadiene was used.

of some other electron donors. Phosphite and tertiary amine were ineffective.

Reaction Mechanism. The catalysts studied by us are different from the conventional nickel catalysts, which give linear dimers in protonic solvents.[1)] The essential features of our nickel catalysts giving the five-membered cycle (I) are that they contain a halogen atom and are to be used in the presence of a controlled amount of alcohol. The cyclodimerization involves a hydrogen migration caused by a protonic compound. This is confirmed by the reaction using deuteromethanol. The dimerization was duplicated using deuteromethanol (CH_3OD) in place of methanol (CH_3OH). A monodeuterated dimer was thus obtained. Fig. 1B shows a part of the NMR spectrum. The absorptions of 3.9 to 5.3 τ were unaffected by the deuteration. The signal centered at 7.6 τ is assigned to the hydrogens on the 3-carbon atom. The analysis of this dimer using mass spectrometry and the NMR technique demonstrated that it is about 50% deuterated in the 3 position.

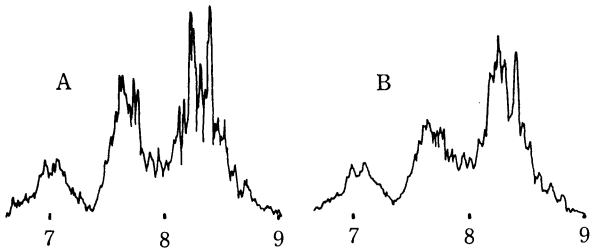

Fig. 1. NMR spectra of (A) normal- and (B) monodeuterated-MVCP.

Dimerization with nickel catalysts to cyclic or linear dimers is believed to proceed through a bis-π-allylic intermediate (V).[12)]

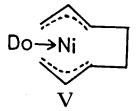

V

In our case, the internal insertion of a double bond into the nickel-carbon σ-bond to form a five-membered cycle has been proposed.[4)]

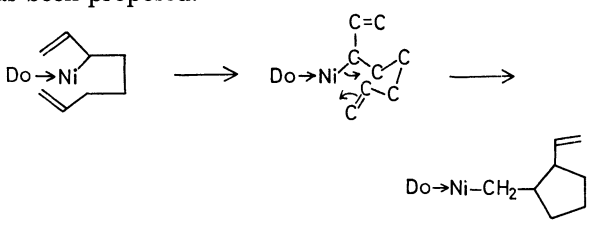

However, since halogen is essential to this catalyst, the structure of the intermediate of the dimerization may be more complicated.

Experimental

trans-Bis(tertiaryphosphine)dichloronickel and the bromo analog were prepared by adding the phosphine (2 mol) to a solution of the nickel halide (1 mol) in methanol. The derivatives of NO_2, SCN, and I were afforded by displacement reactions in which the appropriate metal salt was mixed with the dihalocomplex in acetone.[14)] Arylnickel complexes were prepared from a Grignard reagent according to the method of Chatt and Shaw.[8)] π-Allylnickel halides were prepared from the reaction of allyl halide with nickel carbonyl.[15)] Commercially-available *n*-butyllithium in hexane was used. *o*-Lithio-*N*,*N*′-dimethylbenzylamine was prepared from *N*,*N*′-dimethylbenzylamine and *n*-butyllithium in benzene.[7)] Commercially-available deuteromethanol was used without further purification. Tetradeuterobutadiene was prepared by H–D exchange between butadiene-β-sulfone and deuterium oxide.[9)] Commercially-available butadiene was used after drying with a 3 Å molecular sieve.

Gas-chromatographic analyses were carried out on a column, Silicon DC 550 on Celite, 1 m, at 100°C. The identification of vinylcyclohexene, cyclooctadiene, and *n*-octatrienes was done by comparing the retention time on the gas chromatogram and the infrared and NMR spectra with those of authentic samples. The identification of 2-methylenevinylcyclopentane was done by comparing the retention time and the infrared and NMR spectra of the hydrogenation product over palladium-carbon with those of *trans*-1-methyl-2-ethylcyclopentane.[16)]

*Dimerization by Bis(tri-*n*-butylphosphine)dichloronickel and* n*-Butyllithium.* Bis(tri-*n*-butylphosphine)dicloronickel, 0.67 g (1.3 mmol), was placed in a glass tube (20 mm in diameter). The tube was immediately fitted with a three-way stopcock through which solvent and reagents were introduced through a syringe. The system was placed under argon by evacuating it and filling it with argon several times. At room temperature, 5 ml of benzene and 1.3 mmol of *n*-butyllithium in 0.54 ml of *n*-hexane were added. The reaction mixture became warm and turned dark red. It was then stirred at room temperature for 30 min, and this was followed by the addition of 1.5 ml (40 mmol) of methanol. The solution was cooled to −78°C in a dry ice-acetone bath; then, 3.9 g (70 mmol) of liquefied butadiene was added and the tube was sealed with a flame. The reaction mixture was heated at 65—70°C for 40 hr. Distillation without separation of the catalyst gave 2.7 g (70%) of MVCP as a colorless liquid; bp 121—122°C, n_D^{24} 1.4553. (lit,[17)] n_D^{27} 1.4557)

General Procedure for Dimerization by Various Nickel Catalysts and Organolithium. The above procedure is illustrative. The amounts of reagents used and the reaction conditions are shown in Table 1. The reactions were carried out in the glass tube described above. The yields of the products were determined gas-chromatographically. The separation of the products, if necessary, was carried out by preparative gas chromatography, and the structure of the products was confirmed by comparing the NMR and infrared spectra of the products with those of authentic samples.

16) W. D. Huntsman, V. C. Solomon, and D. Eros, *J. Amer. Chem. Soc.*, **80**, 5455 (1958).

17) W. D. Huntsman and R. P. Hall, *J. Org. Chem.*, **27**, 1988 (1962).

Dimerization by trans-*Bis(triethylphosphine)chloro-(o-tolyl)-nickel.* In the glass tube, 0.36 g (0.85 mmol) of *trans*-bis(triethylphosphine)chloro-(*o*-tolyl)nickel was dissolved in 1.5 m*l* of benzene under an argon atmosphere; this was followed by the addition of 0.85 m*l* of methanol. The solution was cooled to −78°C in a dry ice-acetone bath, and then 3.5 g of liquefied butadiene were added. The sealed tube was heated at 70—75°C for 40 hr. Distillation gave 2.4 g of dimers. Gas-chromatographic analysis showed the presence of MVCP (86%), VCH (9%), and COD (5%).

The above procedure is illustrative. Reactions by other arylnickels are summarized in Table 2.

Reaction of Ia with CD_3OD and Dimerization of Butadiene. In a glass tube 0.61 g (1.5 mmol) of IIIa was placed. Under a nitrogen atmosphere 0.9 g of benzene and 1 m*l* of CD_3OD were added. The mixture was cooled in a dry ice-acetone bath to −78°C, and then 10 mmol of liquefied butadiene were added. The tube was heated at 70—75°C for 42 hr. Gas-chromatographic analysis (2 m Apiezon, 100°C), using benzene as an internal standard, showed the formation of 0.11 g (85% based on IIIa) of toluene and 0.48 g of MVCP. After the removal of the catalyst by distillation, toluene was separated by preparative gas chromatography. Mass spectroscopic analysis showed C_7H_7D of *ca.* 95% isotopic purity.

Reaction of IIIb with Hydrogen and Dimerization of Butadiene. In a 30-m*l*, stainless-steel pressure reactor, 0.21 g (0.41 mmol) of IIIb was dissolved in 2 m*l* of benzene. The reactor was cooled to −78°C, and then 10 mmol of liquefied butadiene was added under a nitrogen atmosphere. Hydrogen was charged up to 30 kg/cm² at that temperature. The mixture was heated at 70—75°C for 24 hr. Gas-chromatographic analysis showed the formation of toluene (33% yield on IIIb) and MVCP (5% yield on butadiene). From the reaction mixture, a yellow-brown solid was obtained. Recrystallization from methanol gave 0.03 g of the pure IIIb as yellow-brown needles, mp 102—103°C (lit,[8] mp 102—103°C).

Reaction of IV and Reaction of Butadiene Catalyzed by IV. All reactions using methanol (or without methanol) or hydrogen were carried out in ways similar to those described above in the glass tube or the stainless-steel pressure reactor respectively. The products were identified by comparing the infrared spectra and retention time with those of authentic samples. The formation of butane, ethylcyclohexane, and cyclooctane was confirmed by a study of the infrared and mass spectra.

Dimerization by π-Allylnickel Halide and an Electron Donor. The following procedure is a typical one. To 5 m*l* of benzene solution containing 0.75 mmol of π-allylnickel bromide, 0.61g (3 mmol) of tri-*n*-butylphosphine, 25 mmol of methanol and 80 mmol of liquefied butadiene were added, in this order. The glass tube was then sealed and heated at 70—75°C for 40 hr. Distillation gave MVCP in a 50% yield.

Dimerization by other π-allylnickel compounds were carried out in a similar way. The reaction conditions are summarized in Table 5.

BULLETIN OF THE CHEMICAL SOCIETY OF JAPAN, VOL. 44, 1961—1964 (1971)

Methylation of Phenol over Metallic Oxides

Takeshi KOTANIGAWA, Mitsuyoshi YAMAMOTO, Katsuyoshi SHIMOKAWA, and Yuji YOSHIDA

The Government Industrial Development Laboratory, Hokkaido, Higashi-Tsukisamu, Sapporo

(Received December 24, 1970)

Methylation took place only at *ortho* position of phenol under an atmospheric pressure at 350°C when the reaction was carried out over an MO–Fe_2O_3 catalyst containing Cu, Mg, Ca, Ba, Zn, Mn, Co, or Ni each as M. The aromatic fraction in liquid products was only *o*-cresol and 2,6-xylenol and products substituted at *para* and *meta* positions could not be obtained. However, gasification of methanol took place simultaneously as a side reaction. From the relation between methylation and gasification, the catalytic activity was found to be effective in the order Cu>Zn>Ba>Ca>Co>Mn>Mg>Ni. Deactivation of these catalysts was observed before the reaction reaches a steady state. The thermogravimetric curve of the used catalyst was measured. From thermal analysis the reduction of the catalyst seems to be a cause of deactivation in addition to deposition of carbonaceous materials onto the catalyst surface. The used catalysts were reclaimed through the process of Scheme 1.

The catalytic alkylation of phenols by vapor phase reaction with alcohols is well known and is used for preparation of alkyl phenols.[1-3] However, because of its low selectivity for a desired alkyl phenol, application of the reaction is limited.

Since poly(2,6-dimethyl)phenylene oxide, the so-called PPO resin, has been introduced as a new thermo-resistant polymer,[4-5] the synthesis of its monomer, 2,6-xylenol, has attracted special attention in industry. A large number of related patents and papers have appeared on synthetic methods using vapor phase or liquid phase reaction. It has been reported that the vapor phase reaction of phenol with methanol over magnesium oxide gives 2,6-xylenol in an exellent yield.[6] A vapor phase synthetic method using Ce_2O_3-MnO-MgO as a catalyst has also been reported.[7] This demonstrates that magnesium oxide is most favorable in the synthesis of 2,6-xylenol as compared

1) V. N. Ipatieff, J. Orlof, and G. Razoubaief, *Bull. Soc. Chim. Fr.*, **37**, 1576 (1925).
2) N. M. Cullinane and S. J. Chard, *J. Chem. Soc.*, **1945**, 821.
3) Y. Ogata and M. Itoh, *Kogyo Kagaku Zasshi*, **70**, 911 (1967).
4) A. S. Hay, G. F. Endres, and J. W. Eustance, *J. Amer. Chem. Soc.*, **81**, 6335 (1959).
5) A. S. Hay, *J. Polymer Sci.*, **58**, 581 (1962).
6) General Electric Company, U. S. 3446856 (1964).
7) S. Enomoto and M. Inoue, An abstract presented in the 23th Annual Meeting of the Catalysis Society of Japan, Sendai, 3, (1968).

with other catalysts which are used in the methylation of phenol.

We found that methylation occurs only at *ortho* position of phenol under an atmospheric pressure at 350°C when the reaction is carried out over an MO-Fe_2O_3 catalyst containing Cu, Mg, Ca, Ba, Zn, Co, Mn, or Ni each as M. This synthetic method of 2,6-xylenol using these types of catalysts is not found in literature. It is, therefore, of particular interest to selectively synthesize 2,6-xylenol without using magnesium oxide as the main component of catalyst. We wish to report on the methylation of phenol over a new type of catalyst.

Experimental

Materials. Phenol and methanol were of analytical reagent grade. They were free from any impurities as ascertained by gas chromatography. Cupric, magnesium, calcium, barium, zinc, manganese, nickel, cobalt, and ferric nitrate were also analytical reagent grade.

Preparation of Catalysts. The catalysts were prepared as follows: 1) After dissolution of 0.2 mol of ferric nitrate and 0.1 mol of magnesium, calcium, barium, or zinc nitrate in water, 14% aqueous ammonium solution was added to the solution until it gave a pH of 6.4 at room temperature. 2) After dissolution of 0.2 moles of ferric nitrate and 0.1 mol of cupric, manganeses, nickel or cobalt nitrate in water, 3N aqueous sodium hydroxide solution was added to the solution until it gave a pH of 9.6 at room temperature. The coprecipitate consisting of an individual metallic hydroxide and ferric hydroxide was washed several times with water and calcined in an electric furnace at 400°C for 3 hr with air pumped into the container. These catalysts were crushed and sieved to 12—14 mesh size particles.

Thermal Analysis of the Used Catalysts. A Rigaku Denki "Thermoflex 8002D" was employed in the differential thermogravimetric analysis.

Analysis of Products. Carbon dioxide in gaseous products was determined by means of the Hempel gas analytical method. Other gases were identified by comparing their respective retention time on the gas chromatogram against authentic samples, after which they were determined quantitatively by gas chromatography (Column: molecular sieve 13X, carrier gas: Ar gas). Liquid products were identified by gas chromatography and infrared spectrometry. Respective quantitative analysis was performed by gas chromatography (Column: Silicone DC 550 at 170°C and Porapak Q at 110°C, carrier gas: He gas).

Apparatus. A Pyrex glass tubular reactor (500 mm length, 20 mm o.d., 18 mm i.d.) was connected with a micro pump which feeds reactants, vertically supported and externally heated in an electric furnace. A vaporizer above the catalyst bed was surrounded by an electric heater and maintained at temperatures 250—280°C. The reactant vapors carried with nitrogen gas were led over the catalyst bed through the vaporizer. The reaction temperature was measured with an IC thermocouple placed in the middle of the catalyst bed. The product vapors were led through an air-cooled condenser and two dry ice traps, and non-condensable products were determined with a wet gas meter.

Results and Discussion

Phenol is methylated consecutively to 2,6-xylenol *via* *o*-cresol by the following processes.

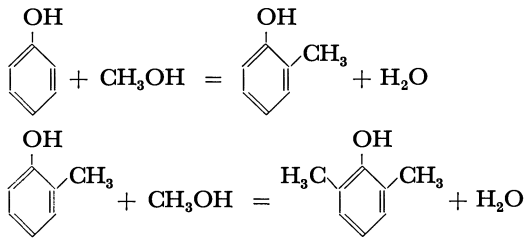

At a high temperature, however, it is decomposed to form benzene, toluene, and xylene. To avoid this, the optimal reaction condition was selected as follows. One mole of phenol is reacted with 10 moles of methanol at 350°C. Partial pressure of nitrogen gas carrier is 0.38 atom. The contact time is 1.6 sec at 350°C.

We see from Table 1a that phenol is selectively methylated at *ortho* position. Even with a large

Table 1a. Reaction products over MO-Fe_2O_3 catalyst

M of MO-Fe_2O_3	Cu	Mg	Ca	Ba	Zn	Mn	Co	Ni[a]
Phenol converted, mol %	95.3	8.8	68.7	82.5	88.4	24.0	63.9	67.5
Selectivity, %[b]								
o-Cresol	41.0	75.3	79.3	64.3	43.5	83.9	82.6	53.2
2,6-Xylenol	59.0	24.7	20.3	35.6	56.5	13.1	17.3	18.6
Methanol converted, mol %	42.3	5.1	23.1	28.7	66.5	2.2	23.8	98.3
Selectivity, %[c]								
Methylation	31.5	22.1	41.9	38.7	21.0	100	32.5	6.6
Gasification	68.5	77.9	58.0	61.3	79.0	—	67.5	93.3

a) Selectivity for benzene, toluene, xylene, and carbonization are 12.4, 5.0, 1.0, and 9.8, respectively.
b) Given by (moles of *o*-cresol or 2,6-xylenol per moles of phenol converted).
c) Given by (moles of methyl group in products or gaseous products per moles of methanol converted).

Table 1b. Compositions of gaseous products over MO-Fe_2O_3 catalysts

M of MO-Fe_2O_3	Cu	Mg	Ca	Ba	Zn	Mn	Co	Ni
Carbon dioxide, mol %	17.5	17.6	16.1	17.3	18.2	—	16.9	17.8
Hydrogen, mol %	53.5	49.1	37.4	39.0	64.2	—	51.7	64.4
Methane, mol %	21.7	27.0	37.0	35.3	7.9	—	21.4	12.6
Carbon monoxide, mol %	7.3	6.3	9.5	8.4	9.7	—	10.1	5.2

Table 2. Surface area of fresh and used catalysts

M of $MO-Fe_2O_3$	Cu	Mg	Ca	Ba	Zn	Mn	Co	Ni
Fresh catalyst, m^2/g	74.7	4.4	25.3	20.9	24.2	38.0	74.3	113.4
Used catalyst, m^2/g	22.1	5.2	21.8	18.5	17.0	25.1	42.4	76.9

excess of methanol, the aromatic fraction in liquid products is only *o*-cresol and 2,6-xylenol except for the case in which $NiO-Fe_2O_3$ catalyst is used. In contrast, methanol reacts through two simultaneous pathways, the methylation of phenol and the gasification of methanol itself. Using gaseous components in Table 1b, the gasification of methanol can be demonstrated by

$$CH_3OH = CO + 2H_2 \quad (1)$$

$$CO + 3H_2 = CH_4 + H_2O \quad (2)$$

$$CO + H_2O = CO_2 + H_2 \quad (3)$$

These pathways can be expected from the fact that the Fe_2O_3 catalyst promotes reactions (2) and (3). Thus, this type of catalyst promotes the selective methylation at *ortho* position of phenol and simultaneously the gasification of methanol. Effectiveness of these catalysts should be discussed from the relation between the main reaction and the undesired side reaction. Figure 1 shows the relation between the methylation and gasification. The upper-right region in Fig. 1 denotes where the methylation only takes place and lower-left region denotes where the gasification only takes place. Thus, it can be said that these catalysts are effective in the order Cu>Zn>Ba>Ca>Co>Mn>Mg>Ni.

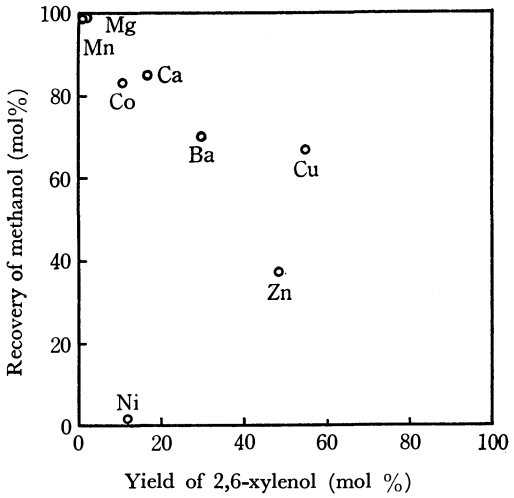

Fig. 1. Relation between methylation and gasification.

Tables 1a and 1b show the data which were obtained around six or seven hours after the commencement of the reaction. However, deactivation of the catalysts is observed before the reaction reaches a steady state. Figure 2 shows the course of deactivation.

The surface area and the differential thermogravimetric curve of the used catalysts were determined in order to estimate the degree of deactivation of catalyst which is said to depend on decrease of surface area caused by sintering of catalyst and also on the contamination of active sites by carbon deposition. The

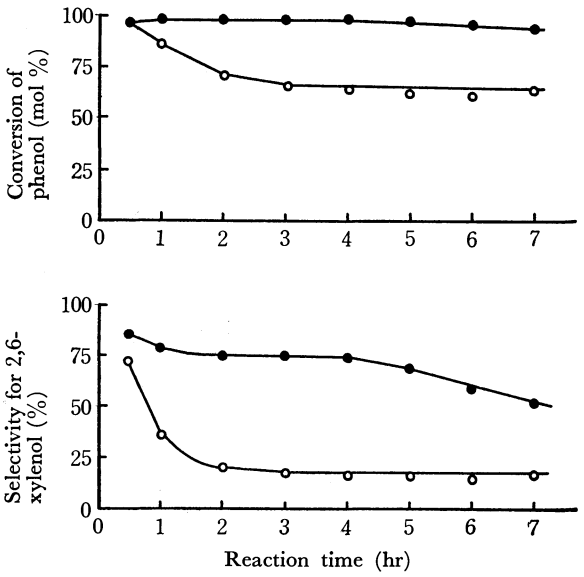

Fig. 2. Activity *vs.* reaction time.
—●— $CuO-Fe_2O_3$, —○— $CoO-Fe_2O_3$

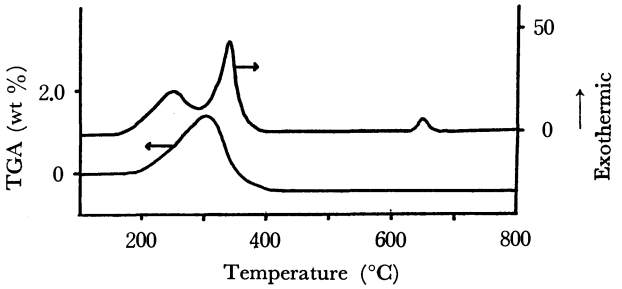

Fig. 3. A typical differential thermogravimetric curve.
Conditions: Heating rate 10°C/min, TGA sens. 5 mg DTA sens., ±100 μV, Atmosphere, air.

Table 3a. Free energies of formation[8]

Oxide	ΔG^0_f (kcal/mol)	Oxide	ΔG^0_f (kcal/mol)
CuO	−30.4	MnO	−86.8
MgO	−136.13	CoO	−51.0
CaO	−144.4	NiO	−51.7
BaO	−126.3	Fe_2O_3	−177.1
ZnO	−76.05	Fe_3O_4	−242.4

Table 3b. Molar enthalpies of formation at 970° K

Process	ΔH_{970} kcal/mol	Ref.
$CuO + Fe_2O_3 = CuFe_2O_4$ (I)	+5.05	(9)
$MgO + Fe_2O_3 = MgFe_2O_4$ (0.9 I)	−4.43	(9)
$ZnO+Fe_2O_3=ZnFe_2O_4$ (N)	−2.67	(9)
$MnO+Fe_2O_3=MnFe_2O_4$ (0.2 I)	−5.0	(10)
$CoO+Fe_2O_3=CoFe_2O_4$ (I)	−5.89	(9)
$NiO+Fe_2O_3=NiFe_2O_4$ (I)	−1.22	(9)

N—normal spinel M $(Fe_2)O_4$
I—inverse spinel Fe $(MFe)O_4$

TABLE 4. RESULTS OF DIFFERENTIAL THERMOGRAVIMETRIC ANALYSIS OF THE USED CATALYST

M of MO-Fe_2O_3	Cu	Mg	Ca	Ba	Zn	Mn	Co	Ni
Wt. increased, wt %	6.11	0.67	1.93	0.83	0.95	1.70	0.41	2.27
DTA(I), °C	233	237	217	222	222	240	232	334
Wt. decreased, wt %	2.00	trace	1.81	0.47	1.18	2.98	0.85	16.25
DTA (II), °C	334	270	326	310	326	375	276	395
DTA (III), °C	—	477	495	484	645	560	665[a)]	530[a)]

a) Measured from coprecipitates of hydroxides.

surface area of the fresh and the used catalysts is shown in Table 2 and a typical differential thermogravimetric curve is shown in Fig. 3.

Figure 3 is divided into three parts, (I) exothermic with a weight increase, (II) exothermic with a weight decrease, and (III) exothermic without a weight change. (I) is due to the oxidation of the used catalyst which has been reduced during the reaction. As would be expected from molar free energies in Table 3a,[8] hematite in the fresh catalyst is reduced to magnetite. This was confirmed through the thermal analysis of the mixture of MO and Fe_3O_4. (II) is due to the combustion of carbonaceous materials which deposited during the course of reaction. (III) is due to the following solid reaction.

$$MO + Fe_2O_3 = M(Fe_2)O_4$$
$$MO + Fe_2O_3 = Fe(MFe)O_4$$

It is expected from molar enthalpies of formation in Table 3b that (III) is exothermic except for CuO-Fe_2O_3.[9-10] The solid reaction was confirmed by means of X-ray diffractometry before and after the exothermic peak. Behaviors of the used catalyst in differential thermogravimetric analysis can be summerized as follows.

The result of thermal analysis is shown in Table 4.

Here, the degree of reduction in the case all catalysts except CuO–Fe_2O_3 does not exceed the calculated value which is given by the following expression.

$$[1 - (3MO, 2Fe_3O_4/3MO\text{-}Fe_2O_3)] \times 100$$

However, in the case of CuO-Fe_2O_3, it exceeds the calculated value (2.24%) because the reduction takes place not only in hematite, but also in cupric oxide. Thus, the reduction of the catalyst would give rise to the deactivation of the catalyst besides the decrease of the surface area and deposition of carbonaceous materials onto the catalyst surface. Thermal analysis was carried out in order to discuss deactivation of the catalyst, and Scheme 1 can be regarded as a process for the reclamation of the used catalyst.

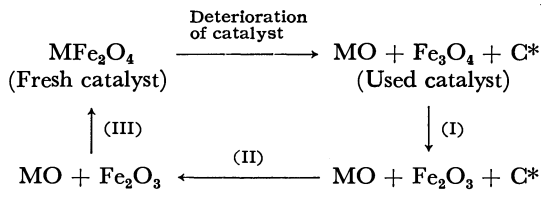

Scheme 1

C* shows carbonaceous materials.

A large number of studies, by the reaction of phenol with methanol over magnesium oxide or modified magnesium oxides, are mainly concerned with the ring substitutive reaction of phenol. However, this paper deals with not only the ring substitutive reaction, but also the thermal analysis of the used catalyst.

Thus, we may conclude that the present catalyst gives an excellent catalytic activity for selective methylation at *ortho* position of phenol and its activity is effective in the order Cu>Zn>Ba>Ca>Co>Mn>Mg>Ni, and the used catalyst is reclaimed through the process of Scheme 1.

8) "Kagaku Benran", Chemical Society of Japan, Maruzen, Tokyo (1966), p. 820.

9) A. Navrotsky and O. J. Kleppa, *J. Inorg. Nucl. Chem.*, **30**, 479 (1968).

10) L. A. Renznitskii, *Vest. Moskgos. Univ. Ser.*, **215**, 24 (1960).

NOTES

BULLETIN OF THE CHEMICAL SOCIETY OF JAPAN, VOL. 44, 1965—1966 (1971)

Mass Spectra of Phenyl *p*-Toluates and Toluanilides Substituent Effect in Fragmentation. II

Seizi KOZUKA, Hideo TAKAHASHI, and Shigeru OAE

Department of Applied Chemistry, Faculty of Engineering, Osaka City University, Sumiyoshi-ku, Osaka

(Received December 5, 1970)

The effect of substituent on mass spectra has been investigated considerably in recent years. In our previous work,[1] the Hammett correlation was observed in the three steps of fragmentation of *p*-substituted phenyl-*p*-toluenesulfonates; a positive ρ-value for the initial step and negative ρ-values for the succeeding two steps. We have extended our study to two classes of compounds, phenyl-*p*-toluates and toluanilides, since the fragmentation is considered to be similar to that of the sulfonates.

As expected, their mass spectra show the following similar three fragmentation steps.

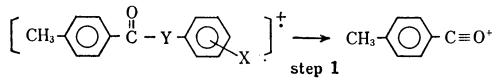

step 1

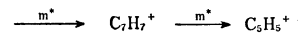

step 2 step 3

Y=O X: *p*-NO_2 *m*-NO_2, *p*-Cl, H, *m*-CH_3, *p*-CH_3, *p*-OCH_3, *p*-CN

Y=NH X: *p*-NO_2, *m*-NO_2, *p*-Cl, H, *m*-CH_3, *p*-CH_3, *p*-OCH_3

The relative peak heights (Z-value) of the fragmentation of these compounds are nicely correlated with the Hammett constants as shown in Figs. 1 and 2.

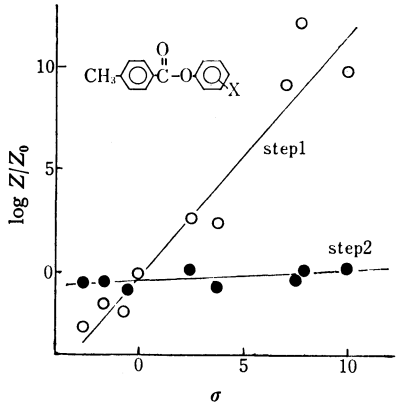

Fig. 1. Hammett plot of the relative peak height obtained in the fragmentation of phenyl *p*-toluates.

The positive ρ-values of the first steps of fragmentation are reasonable. However, no noticeable effect of substituent was found in the second and third steps unlike the case of sulfonates where negative ρ-values were obtained in the suceeding steps.

A possible rationale is that the internal energies

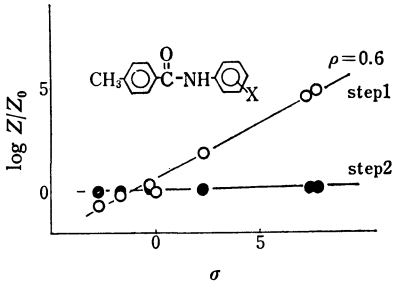

Fig. 2. Hammett plot of the relative peak height obtained in the fragmentation of *p*-toluanilide.

resulting from various activation energies of the decompositions of these compounds with different substituents were retained not in the fragment ions but in the leaving groups that depart from the molecular ions, and all acylinium ions resulting from different molecular ions would retain nearly identical internal energies and give rise to no substituent effect in the succeeding steps.

Another possibility is derived from the assumption that the parent and acylinium ions are formed from a common intermediate (super-excited state) as accepted in the usual treatment of fragmentation in terms of molecular orbital theory.[2] If this is the case, the observed substituent effect at the initial step could derived from the two competing reactions, leading to the parent ion and acylinium ion. At present, we have no definite evidence to make a choice between the two possibilities.

It is worthy to note that the acylinium ion formed

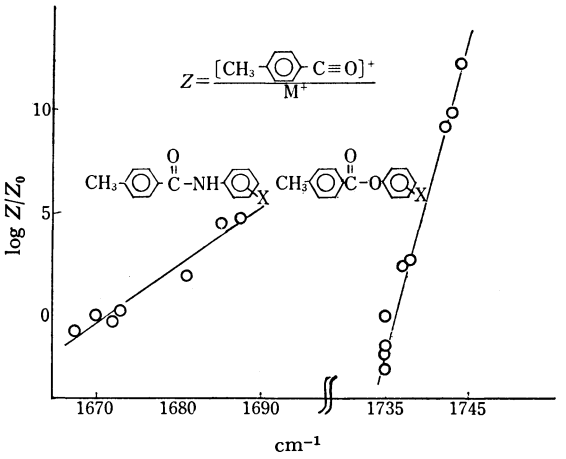

Fig. 3. The plot of the *Z*-values of the initial fragmentations of those compounds against carbonyl streching frequency.

1) Paper I of this series, S. Kozuka, H. Takahashi, S. Tamagaki, and S. Oae, This Bulletin, **43**, 1408 (1970).

2) K. Hirota, *Nippon Kagaku Zasshi*, **89**, 327 (1968).

Table 1. Relative abundance of major peaks of phenyl *p*-toluates and toluanilides

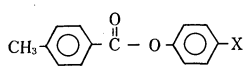

X	M^+	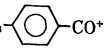	$C_7H_7^+$	$C_5H_5^+$
p-No_2	0.3	100	36.4	16.7
m-No_2	0.5	100	34.6	14.7
m-Cl	2.4	100	35.7	17.4
p-Cl	2.2	100	37.8	19.2
H	4.1	100	36.3	18.1
m-CH_3	6.5	100	32.0	15.7
p-CH_3	5.8	100	30.4	13.8
p-oCH_3	7.5	100	31.5	14.1
p-CN	0.4	100	38.9	19.8

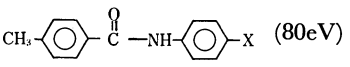

(80eV)

X	M^+	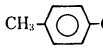	$C_7H_7^+$	$C_5H_5^+$
p-No_2	8.5	100	30.0	10.0
m-No_2	9.2	100	29.0	9.2
p-Cl	16.4	100	29.9	10.4
H	25.6	100	28.5	11.3
m-CH_3	24.4	100	28.2	10.3
p-CH_3	27.1	100	28.4	9.5
p-oCH_3	30.1	100	28.6	8.6

from the ester undergoes more facile decomposition than that derived from the anilide (Table 1). This suggests that the acylinium ions derived from different molecules would retain different internal energies even in the individual fragmentation of those compounds which show no noticeable effect of substituent in the succeeding steps.

The difference of ρ-values observed for the esters and anilides can be ascribed to the difference of bond strengths. As shown in Fig. 3, the deviation of the carboxyl stretching frequency with various substituents is apparently smaller with the esters than with the anilides. This suggests that the effect of substituent is more enhanced in the strength of C–O bond of the ester than that in the C–N bond of the anilide. A similar effect has also been observed in the usual reactions such as alkaline hydrolyses.[3,4]

Experimental

Mass spectra were recorded with a Hitachi RMU-6E single forcus spectrometer. The spectra are shown in Table 1. Infrared spectra were obtained in chloroform solution with 1 mm NaCl cell using JASCO IR-G.

3) M. L. Bender and R. J. Thomas, *J. Amer. Chem. Soc.*, **83**, 4183 (1961).
4) E. Tommila and C. N. Hinihelwood, *J. Chem. Soc.*, **1938**, 1801.

BULLETIN OF THE CHEMICAL SOCIETY OF JAPAN, VOL. 44, 1966—1967 (1971)

Oligomerization of Isoprene by the Catalyst Systems Consisting of Tetraallylzirconium and Aluminum Compounds

Yasuzo UCHIDA, Ken-ichi FURUHATA, and Shohei YOSHIDA

Department of Industrial Chemistry, Faculty of Engineering, The University of Tokyo, Hongo, Bunkyo-ku, Tokyo

(Received December 5, 1970)

Recently, we have reported on the oligomerization of isoprene by zirconium bases catalysts.[1] In this paper, we report on the oligomerization of isoprene by the catalyst systems consisting of tetraallylzirconium and aluminum compounds.

Tetraallylzirconium itself was not a good catalyst for the oligomerization of isoprene and 12% of isoprene was converted into 2,6-dimethyl-1, *trans*-3,6-octatriene (selectivity, 36%) in the reaction at 100°C for 2 hr. Ethylaluminium sesquichloride was found to be a particularly good co-catalyst and 66% of isoprene was converted into the dimer (selectivity, 78%; Al/Zr molar ratio, 2) under the same conditions.

Results and Discussion

We examined five aluminum compounds, triethylaluminum, diethylaluminum chloride, ethylaluminum sesquichloride, ethylaluminum dichloride, and aluminum trichloride as co-catalyst.

Effect of Et_3Al. When triethylauminum was used as a co-catalyst, the dimer yield was less than 3% in the region of the Al/Zr molar ratio between 1 and 11. The conversion of isoprene decreased at lower molar ratios and reached a minimum at 4.2. The conversion increased at Al/Zr molar ratios higher than 4.2.

Effect of Et_2AlCl. The effect of diethylaluminum chloride on the oligomerization of isoprene by tetraallylzirconium has been reported.[1] The dimer yield was about 40% in the region of the Al/Zr molar ratio between 4.5 and 10. The yield of trimers was less than 10%.

Effect of $Et_{1.5}AlCl_{1.5}$. The effect of the molar ratio of ethylaluminum sesquichloride on the oligomerization of isoprene is shown in Fig. 1. The maximum yield of the dimer was attained at the Al/Zr molar ratio

1) A. Misono, Y. Uchida, K. Furuhata, and S. Yoshida, This Bulletin, **42** 2330 (1969).

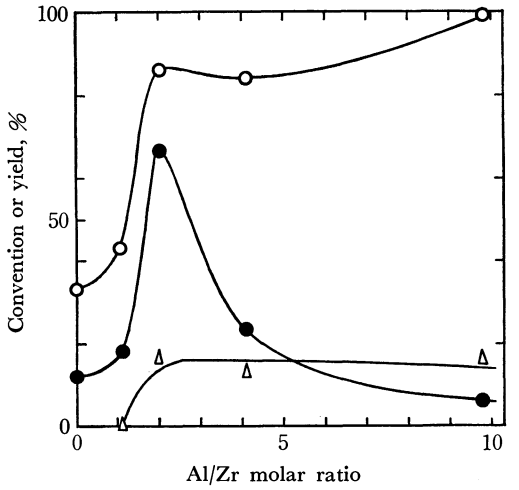

Fig. 1. Effect of $Et_{1.5}AlCl_{1.5}/Zr(C_3H_5)_4$ molar ratio.
—○—: Conversion of isoprene, %
—●—: Yield of the dimer, %
—△—: Yield of trimers, %
100°C, 2 hr, isoprene/$Zr(C_3H_5)_4$=100

of 2.

Effect of $EtAlCl_2$. Ethylaluminum dichloride showed a similar effect to that of ethyaluminum sesquichloride on the oligomerization of isoprene and the maximum yield of the dimer was attained at the Al/Zr molar ratio of 1. The conversion of isoprene was 66% and the dimer yield was 51% at this molar ratio. In contrast, isoprene was cyclopolymerized at room temperature by the catalyst system consisting of zirconium (IV) *n*-butoxide and ethylaluminum dichloride.[1]

Effect of $AlCl_3$. The conversion of isoprene and the dimer yield increased by the addition of aluminum trichloride to tetraallylzirconium. The maximum yield was observed at the Al/Zr molar ratio of 0.46 but both the conversion and the yield decreased at higher molar ratios. The maximum conversion was 48% and the maximum yield was 17%.

The results are summarized in Table 1. The acidity of aluminum compounds increases in the order $Et_3Al < Et_2AlCl < EtAlCl_2$.[2]

Absorption peaks of tetraallylzirconium in the nuclear magnetic resonance spectrum were shifted to lower field in the presence of diethylaluminum chloride. The difference of chemical shifts between methyl and methylene protons of diethylaluminum chloride in the mixed system was −1.0 ppm, while that of free diethylaluminum chloride was −0.9 ppm. This suggests that diethylaluminum chloride receives electrons from tetraallylzirconium.[3]

Table 1. Dimerization of isoprene by $Zr(C_3H_5)_4$ and aluminum compounds

Aluminum compound	Best Al/Zr[a] mol. ratio	Best yield of the dimer
Et_3Al[b]	×	×
Et_2AlCl	4.5—10	40%
$Et_{1.5}AlCl_{1.5}$	2	66%
$EtAlCl_2$	1	51%
$AlCl_3$	0.46	17%
none	—	12%

a) Al/Zr molar ratio where the yield of the dimer reached a miximum.
b) Yield of the dimer was less than 3%.
Reaction conditions: 100°C, 2 hr; Isoprene/$Zr(C_3H_5)_4$ molar ratio, 100.

The presence of a second component with adequate acidity seems to be necessary for the dimerization of isoprene by tetraallylzirconium.

Experimental

Reagents. Isoprene was dried over anhydrous sodium sulfate, distilled and deoxygenated by the freeze-thaw method with pumping.

Tetraallylzirconium was synthesized according to the reported method[4] and was stored at −78°C as an isoprene solution (3.29 wt% or 1.0 mole%). Isoprene hardly reacted at all under this condition.

Alkylaluminum compounds were diluted in dry benzene before use.

Aluminum trichloride was purified by sublimation.

Reaction Procedure. In a typical reaction, to a glass ampule filled with dry nitrogen, 2.36 g of benzene, 0.66 mmol of tetraalllylzirconium, 66 mmol of isoprene and 2.91 mmol of diethylaluminum choride (19.9 wt% benzene solution) were charged with syringes under a nitrogen stream. The ampule was then sealed and kept at 100°C for 2 hr.

Analysis. The dimer was determined to be 2,6-dimethyl-1,*trans*-3,6-octatriene by comparing its infrared spectrum with that of the authentic sample.[1]

Gas chromatography was used for calculating the conversion percentage of isoprene and the quantitative analysis of products. A 2 m stainless steel column, 4 mm in diameter and packed with poly(diethylene glycol succinate) on Shimalite was used. Operation conditions: column temperature, 112°C and 180°C for dimers and trimers, respectively; flash evaporator temperature, 300°C; carrier gas (helium) speed, 30 m*l*/min. Benzene was used as the internal standard.

Nuclear magnetic resonance spectra were recorded on a Nihon Denshi Model C-60.

2) H. Lehmkuhl, *Angew. Chem.*, **75**, 1090 (1963).
3) R. T. Narashimhan and M. T. Rogers, *J. Amer. Chem. Soc.*, **82**, 5983 (1960).
4) G. Wilke, B. Bogdanovic, P. Hardt, P. Heimbach, W. Keim, M. Kröner, W. Oberkirch, K. Tanaka, E. Steinrücke, D. Walter, and H. Zimmermann, *Angew. Chem.*, **78**, 157 (1966).

BULLETIN OF THE CHEMICAL SOCIETY OF JAPAN, VOL. 44, 1968—1969 (1971)

Dispersion State of Platinum on Zeolite and Hydrogenation of Ethylene

Toshihiko KUBO, Hiromichi ARAI, Hiroo TOMINAGA, and Taiseki KUNUGI

Department of Synthetic Chemistry, Faculty of Engineering, The University of Tokyo, Hongo, Bunkyo-ku, Tokyo

(Received December 8, 1970)

Some metal cations loaded on a zeolite by ion exchange are readily reduced by heating in a hydrogen stream. The reduced metals are highly disperesed in the cavities of the zeolite and show high catalytic activity for hydrogenation of unsaturated compounds. Strel'nikova and Lebedev[1] proposed a hypothesis that the catalytic hydrogenation is carried out on a "mixed ensemble" consisting of a metallic atom and an active center of the carrier. However, this is not in line with the findings that the reduction of cations in the cavities of zeolite gives tiny crystallites with diameters ranging 5—30 Å.[2]

A number of papers[3,4] have reported that catalytic behaviors of supported metal are dependent on the crystallite size or the degree of dispersion. Rabo[5] showed that zeolite catalyst loaded with platinum by ion exchange was less affected by sulfur compounds than similar catalysts prepared by impregnation.

We studied the behavior catalysis of the zeolite catalyst loaded with metals in a given dispersion state. Zeolite(NaY)-supported platinum catalysts were prepared either by ion exchange or impregnation method. After reduction with hydrogen, the platinum subjected to ion exchange was supposed to exist mainly in the cavity. While the impregnation method gave rather large platinum crystallites exclusively on the outer surface of zeolite. The two different catalysts were compared for their activities for the hydrogenation of ethylene.

Experimental

Two types of catalysts, (A) and (B), were prepared from zeolite–NaY with Si/Al ratio of 2.5. (A) was prepared by ion exchange with $Pt(NH_3)_4^{2+}$ aqueous solution, followed by drying at 100—110°C in the air and reduction with hydrogen at 200°C for 3 hr. (B) was prepared by impregnation with ($PtCl_6^{2-}$) aqueous solution, followed by drying and reduction under the same conditions as for (A).

Platinum content was 0.2 or 0.5 wt%. The catalytic activities were tested for hydrogenation of ethylene by use of pulse-technique. In the reactor, 0.1 g of catalyst was placed, and 0.15 m*l* of ethylene gas was injected into a large excess of hydrogen stream continuously flowing down the reactor. The product stream was analyzed by gas chromatography. Hydrogen was supplied from a commercial cylinder after purification over Deoxo catalyst and silica gel. The flow rate was 30 m*l*/min, and the pressure 300 mmHg (gauge).

Results and Discussion

Figure 1 shows that the activity of (A) at reaction temperature 35°C or 45°C rapidly decreases in the first ten injections of ethylene gas with 10 min intervals, and then reaches a constant level.

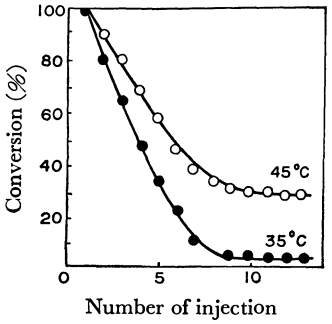

Fig. 1. Change of activity *vs.* number of injection.
0.5 wt% Ion exchanged catalyst (A)

The activity was completely recovered by heating the catalyst at 100°C for 30 min. This seems to be due to an adverse effect of water vapor in the hydrogen stream on the activity of (A). The activity of (B), however, is not affected by water vapor in the hydrogen stream as shown in Fig. 2.

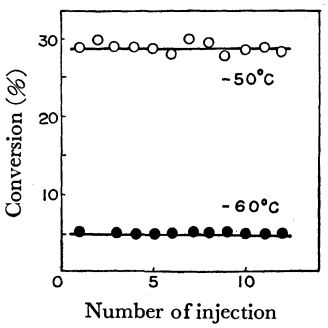

Fig. 2. Change of activity *vs.* number of injection.
0.5 wt% Impregnated catalyst (B)

Over 0.1 g of (A) kept at room temperature, hydrogen stream was introduced at a given flow rate. After 1 hr of hydrogen flow, without ethylene pulse injection, the catalyst lost its activity for ethylene hydrogenation at room temperature, *ca.* 20°C. This experiment suggests that the deactivation of the catalyst (A) is due to some impurity in the hydrogen. The hydrogen was analyzed for water content giving approximately 1—2 mg/*l*. When the hydrogen stream completely dried by refrigeration with liquefied nitrogen was used, (A)

1) Zh. V. Strel'nikova and V. P. Lebedev, *Intern. Chem. Eng.*, **7**, 199 (1967).
2) C. S. Brooks and G. L. M. Christopher, *J. Catalysis*, **10**, 211 (1968).
3) M. Boudart, A. W. Aldag, L. P. Ptak, and J. E. Benson, *ibid.*, **11**, 35 (1968).
4) G. C. Bond, The IV Intern. Congress on Catalysis No. 67 (1968) (Moscow)
5) J. A. Rabo, V. Schomaker and P. E. Pickert, The III Intern. Congress on Catalysis Sect. 2, No. 4 (1964) (Amsterdam)

was found to give 100% conversion of ethylene to ethane even at the reaction temperature −60°C. In this experiments, a pronounced tailing of gas chromatographic peak of ethane was observed. This could be attributed to the largely prolonged contact time due to strong adsorptive affinity of ethylene on zeolite surface. The catalytic activity never decreased in the presence of completely dried hydrogen.

Observation by electron microscope of (A) revealed that no platinum crystal with diameters larger than 10 Å, the limit of resolution of the electron microscope employed, existed. This means that the reduced platinum presumably exists as atoms and/or as tiny crystallites with diameters less than 10 Å in the cavities of zeolite. Therefore, the decrease in catalytic activity shown in Fig. 1 may be interpreted by the adsorption of water vapor sealing off the cavity mouth of the zeolite to prevent the access of the reactant to platinum site. After the water adsorption equilibrium which depends on temperature is attained, the activity of (A) becomes constant.

On the other hand, electron micrographs of (B) showed that platinum crystallite diameters were 30—100 Å. Platinum crystallites of these dimensions cannot exist in a cavity whose maximum diameter is 13 Å. The adsorption of water vapor on platinum crystallites, if any, might be negligibly small compared with that on zeolite. Consequently, the activity of (B) is constant as shown in Fig. 2.

Table 1. Influence of H_2O in H_2 gas on activation energy

	Catalyst	H_2 Reduction	H_2O/H_2 (mg/l)	Activation Energy (kcal/mol)
1)	0.5 wt%[a)]	200°C, 3 hr	2.3	34 (30— 50°C)
2)	0.5 wt%[b)]	200°C, 3 hr	2.3	10 (−60——30°C)
3)	0.2 wt%[a)]	200°C, 3 hr	1.1	10 (−15— 19°C)
4)	0.2 wt%[b)]	200°C, 3 hr	1.1	12 (−15— 18°C)

a) Ion exchanged. b) Impregnated.

After the activity of catalyst attained a constant level by repeated ethylene pulse injection, a logarithmic plot of $(1-x)^{-1}$ (x=conversion of ethylene, mole fraction) against T^{-1} (T=reaction temperature, °K^{-1}) was made, giving rise to an Arrhenius straight line. Since an excess of hydrogen was supplied, the hydrogenation rate was assumed to obey the pseudo-first-order kinetics for ethylene. Apparent activation energies from the above plots are shown in Table 1. These results indicate that apparent activation energy over the ion exchanged catalysts (A) is remarkably affected by the water content in a hydrogen stream, but not over the impregnated catalysts. The activation energy for hydrogenation of ethylene previously reported is 8.4 kcal/mol over Pt–SiO_2 catalyst[6], 9.9 kcal/mol over Pt–Al_2O_3,[7] and 10 kcal/mol over platinium plate.[8] These results are in fairly good agreement with those of 2), 3), and 4) in Table 1.

Another catalyst (C) was prepared by ion exchange followed by calcination at 350°C in the air for 3 hr and reduction at 200°C for 3 hr. The slope of the line below 0°C corresponds to an activation energy of 10 kcal/mol. Electron micrographs of (C) show the presence of platinum crystallites with diameters 20—70 Å. This means that platinum was partly aggregated on the surface and possibly exists in part in the cavity. Activity of the catalyst was tested for hydrogenation of ethylene in a hydrogen stream containing 2.3 mg/l of water. A logarithmic plot of $(1-x)^{-1}$ against T^{-1} gave two straight lines with different slopes intersecting at *ca.* 0°C. These results suggest that, below 0°C, ethylene reacts with hydrogen on platinum crystallites outside the cavity. The platinum in the cavity does not seem to be available at this temperature range because adsorbed water is frozen in the cavity to plug it. This is supported by the agreement of activation energy below 0°C for (C) with that for (B). Above 0°C, adsorbed water is released from cavity with the rise in reaction temperature, and the active site in the cavity is allowed to participate in hydrogenation. Thus, the apparent activation energy is larger than that below 0°C by *ca.* 20 kcal/mol, and agrees with that of catalyst (A), In this connection, it might be interesting to note that Dzhigit *et al.*[9] reported the heat of adsorption of water on Na-Faujasite to be 20—13.5 kcal/mol.

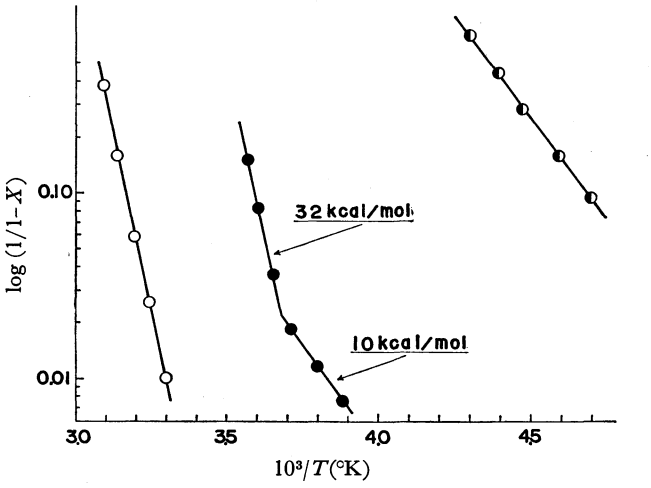

Fig. 3. Plot of $\log(1/1-x)$ *vs.* $1/T$(°K^{-1}).
Catalyst weight 0.100 g, sample size 6.7×10^{-6} mol, H_2 pressure 303—304 mmHg, H_2 flow rate 33 ml/min, H_2O content 2.3 mg/l.
—○— Catalyst (A) —◐— Catalyst (B)
—●— Catalyst (C)

6) C. A. Shuit and L. L. Von Reijen, *Adv. Catalysis*, **10**, 242 (1958).

7) G. C. Bond, *Trans. Faraday Soc.*, **52**, 1235 (1956).

8) A. Farkas and L. Farkas, *J. Amer. Chem. Soc.*, **60**, 22 (1938).

9) O M. Dzhigit, A. V. Kiselev, K. N. Mikos, and G. G. Muttik, *Zh. Fiz Khim.*, **38**, (7), 1791 (1964).

BULLETIN OF THE CHEMICAL SOCIETY OF JAPAN, VOL. 44, 1970—1972 (1971)

The Photolysis of 1-Phenylbicyclo[*n*.1.0]alkanes in Acidic Media

Shinsaku FUJITA, Yoshihito HAYASHI, and Hitosi NOZAKI

Department of Industrial Chemistry, Kyoto University, Yosida, Sakyô-ku, Kyôto

(Received December 21, 1970)

In continuation of our studies of the photochemical polar addition of acetic acid to 1-phenylcycloalkenes,[1] we have been interested in the title reaction of phenylcyclopropanes (**1a**, **1b**). This has been disclosed to involve proton addition to the cyclopropane ring and to give products, **2**—**6**, as a result of the expansion of the original $n+2$ rings to $n+3$ rings, where $n=3$ or 4. Such a photoinduced heterolysis is rare[2] and forms a sharp contrast to the previously recorded formation of carbenes in this kind of photolysis.[3]

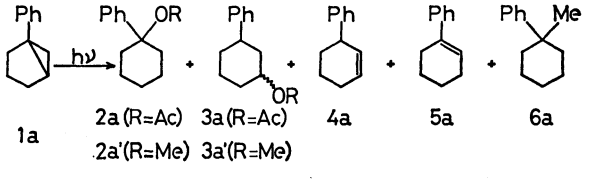

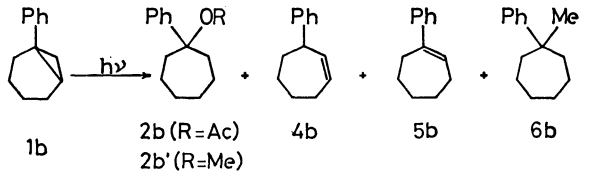

The irradiation of 1-phenylbicyclo[3.1.0]hexane (**1a**) was performed in acetic acid, and the resulting photoproducts were separated by preparative-scale thin layer (TLC) and gas chromatography (GC). The acetate fraction of TLC consisted of 5 components, among which 1-acetoxy-phenylcyclohexane (**2a**) and *cis* and *trans* isomers of 3-acetoxy-1-phenylcyclohexane (**3a**) were identified. The three hydrocarbons isolated were 1-(**5a**) and 3-phenylcyclohexene (**4a**) and 1-methyl-1-phenylcyclohexane (**6a**). The photolysis of 1-phenylbicyclo[4.1.0]heptane (**1b**) in acetic acid proceeded in a similar way to afford the corresponding acetate (**2b**), two isomerization products (**4b** and **5b**), and 1-methyl-1-phenylcycloheptane (**6b**). Methanol also added to the cyclopropane ring of **1a** or **1b** on UV irradiation in the presence of sulfuric acid. On the other hand, the photolysis of **1a** and **1b** under neutral conditions gave no ionic photoadducts, but only isomerization products in rather low yields.

The formation of acetates and ethers is ionic in nature, and protonated cyclopropanes[4] are plausible intermediates, as the attack of solvent molecules occurred on the both sides of cyclopropane rings. However, the possibility of the intermediary of **5a** and **5b** in the polar addition can not be excluded.[1] It should be emphasized that the C_1–C_{n+2} bonds of 1-phenylbicyclo[*n*.1.0]alkanes (**1**) were cloven exclusively. The alkylation products (**6a** and **6b**) can be explained as secondary photoprodncts arising from **2a** and **2b** respectively.[1]

Experimental

The mass spectra were determined on a Hitachi RMU-6L spectrometer, and the NMR data, on a JEOL C-60-H spectrometer in carbon tetrachloride at 60 MHz. Prepara-

TABLE 1. PHOTOLYSIS OF 1-PHENYLBICYCLO[*n*.1.0]ALKANES[a]

Substrate	Solvent	1%	Acetate or Ether			Hydrocarbons		
			R	2%	3%	4%	5%	6%
1a	AcOH	4	Ac	28	3[b]	15	7	4
	MeOH(H+)[c]	4	Me	35	3[b]	4	2	d
	MeOH	78	Me	d	d	e	11	d
1b	AcOH	40	Ac	24	d	10	2	1
	MeOH(H+)[c]	18	Me	47	d	10	4	d
	MeOH	75	Me	d	d	4	2	d

a) Direct irradiation was effected on 0.05 M solutions placed in quartz tubes with an external 200 w high pressure mercury arc under nitrogen atomosphere at room temperature during 5 hr. The reaction did not proceed in the dark at room temperature.
b) This is a mixture of *cis* and *trans* isomers.
c) Methanol contains 0.3% sulfuric acid.
d) Not detected.
e) The presence of a trace amount was detected.

1) S. Fujita, T. Nômi and H. Nozaki, *Tetrahedron Lett.*, **1969**, 3557; S. Fujita, Y. Hayashi, T. Nômi, and H. Nozaki, *Tetrahedron*, **27**, 1607 (1971).

2) C. S. Irving, R. C. Petterson, I. Sarkar, H. Kristinsson, C. S. Aaron, G. W. Griffin, and G. J. Boudreaux, *J. Amer. Chem. Soc.*, **88**, 5675 (1966).

3) D. B. Richardson, L. R. Durrett, J. M. Martin, Jr., W. E. Putnam, S. C. Slaymaker, and I. Dvoretzky, *J. Amer. Chem. Soc.*, **87**, 2763 (1965); M. Jones, Jr., W. H. Sachs, A. Kulczycki, Jr., and F. J. Waller, *ibid.*, **88**, 3167 (1966); H. Kristinsson, K. N. Mehrotra, G. W. Griffin, R. C. Petterson, and C, S. Irving, *Chem. Ind.* (London), **1966**, 1562.

4) C. J. Collins, *Chem. Rev.*, **69**, 543 (1969).

tive TLC was performed on silica-gel G (20×20×0.3 cm), using benzene as the solvent and as an eluant. Preparative GC was carried out using High Vacuum Silicone Grease 20% on Celite 545 (2 m, 180°C, helium as the carrier gas). The hydrocarbon contents were determined by GC.

*1-Phenylbicyclo[3.1.0]hexane (**1a**).* A solution of bromoform (135 g, 0.53 mol) in *n*-hexane (200 m*l*) was added, under 5°C, to a mixture of 1-phenylcyclopentene (40 g, 0.28 mol), potassium *t*-butoxide (59 g), and *n*-hexane (400 m*l*). The mixture was allowed to stand overnight at room temperature, poured into water, extracted with ether, and dried over sodium sulfate. After concentration, the unchanged olefin was recovered by distillation. The resulting residue (60 g) was subjected to reduction without further purification.

The crude dibromide was added to a solution of sodium metal (30 g) in liquid ammonia (*ca.* 500 m*l*) under −40°C for 2 hr. After stirring for an additional 2 hr, solid ammonium chloride was added and the solvent was allowed to evaporate at room temperature. The residue was diluted with water, extracted with ether, and dried over sodium sulfate. Subsequent concentration and fractional distillation gave **1a** (22 g, 50%) as a colorless liquid; bp. 69°C/1 mmHg. IR (neat): 3035, 3007, 2940, 2920, 2850, 1604, 1498, 1476, 1452, 1101, 1072, 1024, 935, 868, 799, 756 and 698 cm^{-1}. NMR (CCl_4): δ 7.12 (5H, s), 2.25—1.40 (7H, m) and 0.80—0.57 (2H, m). MS *m/e* (relative abundance): 158 (100), 143 (65), 130 (91), 129 (99), 128 (48), 117 (63), 115 (79), 104 (55), 91 (63), 77 (35), 51 (34), 39 (35).

Found: C, 91.1; H, 8.8%. Calcd for $C_{12}H_{14}$: C, 91.1; H, 8.9%.

1-Phenylbicyclo[4.1.0]heptane (**1b**)[5] was similarly prepared from 1-phenylcyclohexane.

*Direct Irradiation of **1a** and **2b** in Acetic Acid.* A 0.05M solution (200 m*l*) of 1-phenylbicyclo[*n*.1.0]alkane (**1**) in acetic acid was placed in eight quartz tubes (1.5ϕ×19 cm) and irradiated with a high-pressure mercury are under a nitrogen atmosphere for 5 hr. The combined photolysates were then neutralized with aqueous sodium hydrogen carbonate, extracted with ether, and dried over sodium sulfate. Concentration *in vacuo* and subsequent preparative TLC gave a mixture of hydrocarbons (**1**, **4**, **5** and **6**) and the corresponding esters (**2** and **3**). These two separated fractions were weighed and subjected directly to GC analyses. The results are summarized in Table 1. The preparative GC of the hydrocarbon fraction gave the starting material (**1**), 1- (**5**) and 3-phenylcycloalkene (**4**)[6] and 1-methyl-1-phenylcycloalkane (**6**).[1] All the hydrocarbons were identified by comparison with known samples. The esters (**2**) were distilled and subjected to spectrometric analyses. The *cis* and *trans* isomers of **3a** were isolated by preparative GC and compared with the authentic specimens to be described below.

*Direct Irradiation of **1a** and **1b** in Methanol Containing Sulfuric Acid.* A 0.05 M solution (200 m*l*) of **1** in methanol containing 0.3% sulfuric acid was irradiated as has been described above. The photolysate was analyzed by GC (Table 1). The ethers (**2a′** and **2b′**) were identical with the authentic samples.[1] The *cis* and *trans* isomers of **3a′** isolated by preparative GC were identical with the authentic samples described below.

*Direct Irradiation of **1a** and **1b** in Methanol.* A 0.05 M solution (200 m*l*) of **1** in methanol was irradiated. A usual work-up gave a mixture of hydrocarbons (**1**, **4**, and **5**) which was then analyzed by GC. The results are summarized in Table 1.

cis-*3-Acetoxy-1-phenylcyclohexane (*cis-**3a**). The reduction of 3-phenylcyclohexanone with lithium aluminum hydride gave a *cis*-rich mixture of 3-phenylcyclohexanol, from which the *cis* isomer was isolated by recrystallization from *n*-hexane. mp 78—79°C (lit,[7] 79—80°C).

A mixture of *cis*-3-phenylcyclohexanol (0.15 g, 0.85 mmol), acetic anhydride (5 m*l*), and pyridine (10 m*l*) was heated at 90—100°C for 2 hr. A work-up gave *cis*-**3a** (0.16 g, 86%), bp 75—80°C (bath temperature)/0.04 mmHg, which was contaminated with 1.6% of *trans* isomer. An authentic specimen of *cis*-**3a** was purified by preparative GC. IR (neat): 3030, 3010, 2900, 2840, 1737, 1603, 1497, 1451, 1367, 1242, 1200, 1029, 967, 756, and 699 cm^{-1}. NMR (CCl_4): δ 7.17 (5H, s), 4.97—4.48 (1H, m), 2.87—0.80 (12H, m+s (δ 1.97, 3H)). MS *m/e* (relative abundance): 218 (7), 158 (100), 143 (37), 130 (52), 129 (35), 117 (31), 104 (54), 91 (49).

Found: C, 77.2: H, 8.1%. Calcd for $C_{14}H_{18}O_2$: C, 77.0; H, 8.3%.

trans-*3-Acetoxy-1-phenylcyclohexane (*trans-**3a**). The Meerwein-Ponndorf reduction of 3-phenylcyclohexanone (4.2 g, 24 mmol) gave a mixture (3.4 g, 81%) of *cis*- and *trans*-3-phenylcyclohexanol (*cis* : *trans*=2.5 : 1),[7] from which the *cis* isomer was then removed by recrystallization.

A *cis-trans* mixture of 3-phenylcyclohexanol (0.034 g, 0.19 mmol, *cis*:*trans*=1:3), acetic anhydride (5 m*l*), and pyridine (10 m*l*) was refluxed. Distillation gave a mixture (0.035 g, 81%) of *cis*- and *trans*-**3a** (*cis*:*trans*=5:4). The analytical sample of *trans*-**3a** was purified by preparative GC. IR (neat): 3030, 3010, 2900, 2845, 1739, 1604, 1496, 1440, 1376, 1249, 1232, 1115, 1018, 958, 753, and 698 cm^{-1}. NMR (CCl_4): δ 7.16 (5H, s), 5.30—5.00 (1H, m), 2.95—0.90 (12H, m+s (δ 2.06, 3H)). MS *m/e* (relative abundance): 218 (3), 158 (100), 143 (38), 130 (39), 129 (32), 117 (16), 104 (28), 91 (32).

Found: C, 77.3; H, 8.5%. Calcd for $C_{14}H_{18}O_2$: C, 77.0; H, 8.3%.

cis- *and* trans-*3-Methoxyl-1-phenylcylohexane (**3a′**).* To a solution of 3-phenylcyclohexanol (1.0 g, 5.7 mmol, *cis*: *trans* =2.5: 1) in ether (50 m*l*), boron trifluoride etherate (5 m*l*) was added, drop by drop; then, a solution of diazomethane (from 20 g of *N*-methyl-*N*-nitrosourea) in ether (50 m*l*) was added. Subsequent concentration and distillation gave a mixture (0.80 g, 74%) of *cis*- and *trans*-**3a′** (*cis*:*trans*=7:1). The analytical samples of both the isomers were obtained by preparative GC.

The pure *cis* isomer **3a′** showed the following spectra. IR (neat): 3027, 3010, 2920, 2860, 2820, 1602, 1498, 1450, 1371, 1139, 1128, 1098, 756, and 702 cm^{-1}. NMR (CCl_4): δ 7.13 (5H, s), 3.35—0.80 (13H, m+s (δ 3.27, 3H)). MS *m/e* (relative abundance): 190 (66), 158 (75), 147 (100), 143 (67), 130 (41), 129 (37), 117 (62), 115 (41), 105 (29), 104 (98), 91 (87), 77 (28), 71 (43), 58 (46).

Found: C, 82.1; H, 9.6%. Calcd for $C_{13}H_{18}O$: C, 82.1; H, 9.5%.

The pure *trans*-**3a′** showed the following spectra. IR (neat): 3027, 3010, 2910, 2860, 2810, 1602, 1498, 1450, 1362, 1140, 1115, 1088, 756, 704 cm^{-1}. NMR (CCl_4): δ 7.13 (5H, s), 3.65—3.45 (1H, m), 3.30 (3H, s), 3.00—1.00 (9H, m).

5) O. M. Nefedov, N. N. Novitskaya, and A. D. Petrov, *Dokl. Akad. Nauk SSSR*, **152**, 629 (1963).

6) a) C. C. Price and J. V. Karbinos, *J. Amer. Chem. Soc.*, **62**, 1159 (1940).
b) A. C. Cope and S. S. Hecht, *ibid.*, **89**, 6920 (1967).

7) M. Balasubramanian and A. D'Souza, *Tetrahedron Lett.*, **1963** 1891.

MS *m/e* (relative abundance): 190 (2), 158 (100), 143 (37), (37), 130 (45), 129 (30), 117 (22), 115 (22), 104 (36), 91 77 (15), 71 (12), 58 (17).

Found: C, 81.9; H, 9.6%. Calcd for $C_{13}H_{18}O$: C, 82.1; H, 9.5%.

The authors are indebted to Professor Keiiti Sisido for his generous help. Financial support from the Ministry of Education, Japanese Government, and from Toray Science Foundation is acknowledged with pleasure.

BULLETIN OF THE CHEMICAL SOCIETY OF JAPAN, VOL. 44, 1972—1973 (1971)

The Catalytic Effect of Metal Ions on the Hydrolysis of Disodium Pyrophosphite

Shiro UEDA and Yoshinori SASAKI

Department of Synthetic Chemistry, Faculty of Engineering, Chiba University, Yayoi-cho, Chiba

(Received December 21, 1970)

It is well known that hydrolytic scissions of polyphosphate, the splitting of the $\overset{5}{P}$–O–$\overset{5}{P}$ linkage, and those of pyrophosphite, the splitting of the $\overset{3}{P}$–O–$\overset{3}{P}$ linkage, are strongly catalyzed by the hydrogen ion. Recently, Mesmer and Carroll[1] have studied in detail the kinetics and mechanism of the hydrolysis of pyrophosphite over an extensive pH range. The effect of metal ions on the acid hydrolysis of pyrophosphate has also been studied.[2] The present paper will deal with the effects of various metal ions on the rate of the hydrolysis of disodium pyrophosphite at pH 4.6.

The disodium pyrophosphite used in this work was prepared by heating purified monosodium orthophosphite under reduced pressure, and the product contained as much as 68% of disodium pyrophosphite when determined by iodine titration. This analysis is based upon the fact that the reaction of iodine with phosphite in a neutral solution occurs very rapidly, whereas the reaction with pyrophosphite is very slow under the same conditions.

The pH of a 0.03M disodium pyrophosphite solution containing the metal ion added as the chloride was quickly adjusted to 4.6 with hydrochloric acid at 60°C. The flasks, each containing 20 m*l* of this solution, were transferred to a bath regulated at 60±0.1°C. After selected periods of time, these flasks were rapidly cooled to 0°C, and the solutions were neutralized with sodium hydrogen carbonate. An appropriate amount of the disodium salt of ethylenediaminetetraacetic acid to mask the metal ions was added to the solutions, and then 30 m*l* of a standardized iodine solution (0.1 N) were added. The flasks were subsequently allowed to stand for 15 min in the dark. These solutions were titrated with a standardized sodium thiosulfate solution (0.1N) to the starch end point after being acidified with an acetic acid solution. The pH of the solutions could be maintained approximately at a constant value of 4.6 throughout each run, inasmuch as monosodium orthophosphite gives the pH value of 4.6.

Plots of the logarithm of the pyrophosphite concentration against the time are shown in Fig. 1, in which the linear relation indicates that the hydrolysis is to be regarded as of the first order. The addition of the copper (II) ion resulted especially in an increase in the rate constant, and the magnitude of this effect increased with an increase in the concentration.

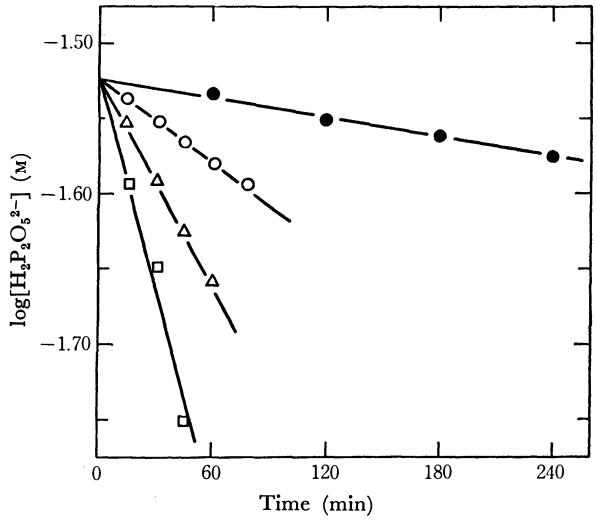

Fig. 1. Effect of concentration of copper(II) ion at pH 4.6 and 60°C. ● None added; ○ 0.5×10^{-3}M; △ 1.0×10^{-3}M; □ 2.0×10^{-3}M

The first-order rate constants, K, obtained with various metal ions are summarized in Table 1. The rates of hydrolysis in the presence of all the metal ions except the copper(II) ion were approximately equal to that in the absence of any metal ion, and were nearly independent of the metal-ion concentration.

Since the cleavage of the P–O–P linkage has generally been considered to be accelerated by the attack of hydrogen ion on the bridging oxygen atom, metal ions are also presumed to behave similarly. In this work, metal ions seem to act on the $\overset{3}{P}$–O–$\overset{3}{P}$ linkage in competition with the hydrogen ion and the sodium ion of disodium pyrophosphite. The behavior of the $\overset{3}{P}$–O–$\overset{3}{P}$ linkage towards the metal ion differs distinctly

1) R. E. Mesmer and R. L. Carroll, *J. Amer. Chem. Soc.*, **88**, 1381 (1966).

2) J. M. Rainey, M. M. Jones, and W. L. Lockhart, *J. Inorg. Nucl. Chem.*, **26**, 1415 (1964).

Table 1. First-order rate constants of hydrolysis in the presence of metal ions at pH of 4.6

Metal ions	Concn. (10^{-3}M)	$K \times 10^4$ (min^{-1})	Metal ions	Concn. (10^{-3}M)	$K \times 10^4$ (min^{-1})
Li^+	2	7.8	Cd^{2+}	2	7.3
K^+	2	6.5	Cd^{2+}	4	9.2
Ba^{2+}	2	7.6	Co^{2+}	2	6.8
Sr^{2+}	2	7.2	Co^{2+}	4	6.8
Ca^{2+}	2	7.7	Ni^{2+}	2	8.6
Na^+	20	7.0	Ni^{2+}	4	8.5
Mg^{2+}	2	7.0	Cu^{2+}	0.5	22
Mg^{2+}	4	6.9	Cu^{2+}	1	55
Mn^{2+}	2	6.5	Cu^{2+}	2	110
Mn^{2+}	8	9.4	None added (pH 5.9)		2.2
Zn^{2+}	2	12	None added (pH 4.6)		7.4
Zn^{2+}	4	17	None added (pH 4.3)		11

Initial concentration of $Na_2H_2P_2O_5$: 3×10^{-2}M.

from that of the $\overset{5}{P}$–O–$\overset{5}{P}$ linkage because of the lower oxidation states of phosphorus. Unlike pyrophosphate, pyrophosphite has hardly ever been reported to form metal-ion complexes.[3] Complex-ion formation causes the half-wave potential of a metal to shift to a more negative value in a polarographic study. A polarographic experiment was attempted for these reaction systems under the following conditions: mole ratio of pyrophosphite/metal ion, 3.6; metal-ion concentration, 0.001 mol/l; tetramethylammonium-bromide concentration, 0.1 mol/l; pH, 4.6; temperature, 30°C. However, the shifts of the half-wave potentials were hardly observed in any case.

The strength of the affinity between the pyrophosphite ion and the metal ions is assumed to depend upon their electrode potentials. Since all the experiments with regard to the metal-ion effects were carried out at pH 4.6, the copper(II) ion, which is more noble than the hydrogen ion, appears to have promoted the hydrolysis. On the other hand, the other metal ions, less noble than the hydrogen ion, have negligibly affected the rate. Although a silver ion or mercury(II) ion, being more noble than copper(II) ion, seems to promote strongly the rate of hydrolysis, the rate constants cannot be obtained because of the oxidation reduction between these ions and pyrophosphite.

3) D. Grant and D.S. Payne, *J. Inorg. Nucl. Chem.*, **26**, 1985 (1964).

BULLETIN OF THE CHEMICAL SOCIETY OF JAPAN, VOL. 44, 1973—1975 (1971)

The Chlorination of Cyclooctadiene with Cupric Chloride in Acetonitrile Containing Lithium Chloride

Sakae UEMURA, Akira TABATA, Yoshihiro KIMURA,* and Katsuhiko ICHIKAWA*

Institute for Chemical Research, Kyoto University, Uji, Kyoto

**Department of Hydrocarbon Chemistry, Faculty of Engineering, Kyoto University, Yoshida, Kyoto*

(Received December 22, 1970)

In previous papers, it was demonstrated that olefins can be chlorinated to form dichloroparaffins with cupric chloride under rather mild conditions.[1] The reaction of butadiene in acetic acid containing sodium acetate, however, gave 3,4-diacetoxy-1-butene and 1,4-diacetoxy-

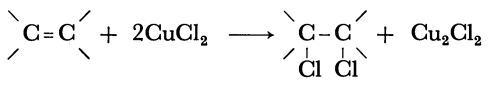

2-butene in place of the expected dichlorobutenes.[2] In this paper, the results of applying the method to cyclooctadienes and acrylonitrile and *trans*-crotyl chloride as reference substrates will be reported, and the results will be compared with those obtained by conventional chlorine gas-chlorination. In the presence of lithium chloride, anhydrous cupric chloride dissolves into acetonitrile to make a clear solution. In this solution, *cis*, *cis*-1,3-, and 1,5-cyclooctadienes were chlorinated (Table 1). In the cases of both 1,3- and 1,5-dienes, dichlorocyclooctenes were the main products, along with a high-boiling resinous residue. Only a small amount of tetrachlorocyclooctane (bp 164°C/10 mmHg; NMR, τ5.2—6.0, 4H, τ7.2—8.3, 8H) was obtained, even when more than four moles of cupric chloride were used for one mole of diene.

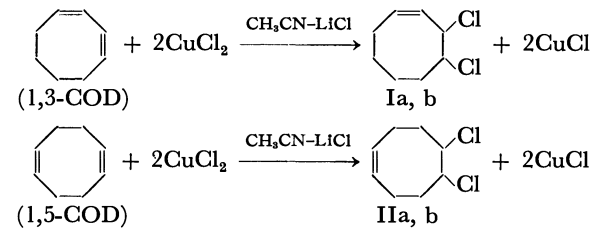

(a: *trans*, b: *cis*)

This is not due to the formation of an inactive complex which might be formed between dichlorocyclooctene and the resulting cuprous chloride, but to the low reactivity of the chloroolefin, since the further reaction of dichlorocyclooctene (isolated and purified)

1) K. Ichikawa, S. Uemura, T. Hiramoto, and Y. Takagaki, *Kogyo Kagaku Zasshi*, **71**, 1657 (1968); S. Uemura, T. Hiramoto, Y. Takagaki, and K. Ichikawa, *ibid.*, **72**, 2390 (1969); S, Uemura, Y. Takagaki, and K. Ichikawa, *ibid.*, **72**, 2577 (1969); K. Ichikawa, S. Uemura, Y. Takagaki, and T. Hiramoto, *Bull. Japan Petrol. Inst.* **12**, 77 (1970).

2) S. Uemura, T. Hiramoto, and K. Ichikawa, *Kogyo Kagaku Zasshi*, **72**, 1096 (1969).

Table 1. Chlorination of cyclooctadienes and related compounds with cupric chloride[a)]

Olefin	mol	Solv. CH_3CN ml	$CuCl_2$ mol	Time hr	Product	Yield[b)] %	*trans*:*cis*	Residue g
Cyclooctene	0.05	100	0.1	4	1,2-dichlorocyclooctane	9	53:47	—
Acrylonitrile	0.3	200	0.3	22	2,3-dichloropropionitrile	42		—
trans-Crotylchloride	0.05	100	0.1	22	1,2,3-trichlorobutane	trace		0.1
1,3-COD	0.05	100	0.1	4	I	44		0.6
1,3-COD	0.05	200	0.3	22	I	58	71:29	1.9
1,3-COD	0.15	200	0.3	22	I	58	69:31	1.8
1,5-COD	0.05	100	0.1	4	II	26		1.0
1,5-COD	0.05	200	0.3	22	II	65	38:62	1.2
					1,2,5,6-tetrachlorocyclo-octane	6		
1,5-COD	0.15	200	0.3	22	II	46	38:62	1.5
I	0.05	100	0.1	22	—			0.7
II	0.05	100	0.1	22	1,2,5,6-tetrachlorocyclooctane	8		0.1
In HOAc (200 ml) containing NaOAc (0.3 mol) at 82°C								
1,3-COD	0.15		0.3	3	I	1	80:20	
1,5-COD	0.15		0.3	3	II	trace		

a) Equimolar amounts of lithium chloride were added to cupric chloride, and the reaction was carried out under refluxing (at about 82°C).
b) Based on $CuCl_2$ used.

proceeded only slowly in the absence of cuprous chloride. The cyclic structure of the substrate cannot be the reason for the low reactivity, since *trans*-crotyl chloride also resisted the same reaction. Chlorine at the allylic position appers to decrease the reactivity of the double bond towards cupric chloride.

The reaction was slow in acetic acid containing sodium acetate, which is a convenient reaction medium for the chlorination of simple monoolefins with cupric chloride.[1)]

The structures of the dichlorocyclooctenes were inferred to be 3,4-dichloro- (I, from 1,3-COD) and 5,6-dichlorocyclooctene (II, from 1,5-COD) on the basis of the analytical data and the IR spectra. The results obtained so far show that only addition occurs and that no isomerization nor substitution proceeds in the liquid-phase chlorination of an isolated double bond with cupric chloride. Since 1,5-diene is not a conjugated one, the normal addition product, II, can be expected unless a transannular reaction occurs to form saturated bicyclic products. Although gas-chromatographical analysis gave two peaks with retention times close to one another, the results do not appear to show the presence of positional isomers, but only that of geometrical isomers resulting from *cis* and *trans* addition. Since the retention times of *trans* isomers of dichlorocycloparaffins are shorter than those of *cis* isomers in the gas chromatogram using Apz-L or PEG columns, the data in Table 1 were calculated on this assumption. Each of two isomers was separated by preparative gas chromatography. Their NMR spectra can be explained in term of these structures.

1,3-Cyclooctadiene is not a usual conjugated diene because of its cyclic structure. The two peaks with retention times close to each other on the gas chromatogram of the chlorinated product appear to show also the presence of *cis* and *trans* isomers, as in the case of 1,5-diene. The NMR spectrum of I is also consistent with these structures.

The *cis* and *trans* ratios in the chlorinated products of cyclooctene and cyclooctadienes, especially in the case of 1,5-diene, are much larger than that of cyclohexene, where the *cis* content was only 2% under the same reaction conditions.

Several attempts to hydrogenate the dichlorocyclooctenes by palladium and platium catalysts in order to confirm the structure further were unsuccessful. These compounds resisted hydroboration by Brown's method,[3)] also. The reason for the low reactivities is not yet clear.

A conventional chlorination of both diene with chlorine gas was carried out in acetonitrile (at 6–11°C) and in acetic acid (at 16–26°C). With 1,5-diene, the products were so complicated (16 or 17 peaks in gas chromatograms) that no definite compounds could de isolated, probably because of facile substitution at the allylic positions and transannular reaction.[4)] Although the products with 1,3-diene were also complicated (12 peaks in gas chromatograms), I(*trans*: *cis*=95:5) and 5-chlorocycloocta-1,3-diene (bp 75–79.5°C/11 mmHg; NMR τ 3.9—4.6, 4H, τ 5.05—5.45, 1H, τ 7.4—8.9, 6H: IR $\nu_{C=C}$ 1620 cm^{-1}) could be isolated in an almost pure form in this case.

Experimental

Materials. The organic materials were commercial products of the purest grade and were distilled and checked by gas chromatography. The 1,3-cyclooctadiene, bp 142—144°C, and 1,5-cyclooctadiene, bp 150—152°C, (distilled in the presence of *t*-butylcatechol) were both *cis*, *cis*- diene, since

3) H.C. Brown and K. Murray, *J. Amer. Chem. Soc.*, **81**, 4108 (1959).
4) see, for example, S. Moon, and C. R. Ganz, *J. Org. Chem.*, **35**, 1241 (1970).

the IR spectra of both diene showed absorptions at 1660 and 1410 cm^{-1} due to a *cis* double bond, but not at 1675 and 965 cm^{-1} due to a *trans* double bond. The inorganic materials were also commercial materials of an analytical grade and were used without purification. The chlorine gas was prepared by the conventional oxidation of hydrogen chloride with potassium permanganate; it was washed with water and then conc. H_2SO_4 before being introducing into the reaction mixture.

Analytical Instruments. The IR and NMR spectra were determined by the use of a HITACHI EPI-S2 apparatus and a JEOL JNM MH-60 or a Varian A-60 apparatus respectively. Gas chromatographies were carried out by the use of HITACHI K53 (PEG-20M 1 m or Apiezon-L 1 m columns) and SHIMADZU 5APTF (PEG 600 25%-Chromosorb-W 3 m column) apparatuses.

Procedure. Olefinic substrates were added to mixtures of solvents, cupric chloride (anhyd.) and lithium chloride at a reaction temperature. At proper intervals, small portions of the mixture were withdrawn and the decreases in the cupric chloride concentration were determined by iodometry. The reaction mixtures were worked up by the following successive treatments; filtration from the resulting inorganic materials, the evaporation of the solvents, dilution with water, extraction with benzene, and then distillation. Each fraction was analyzed by gas chromatography. The yields of the chlorinated products were calculated on the basis of the weights of the distillates and the g.l.c. analysis data.

trans *and* cis-*1,2-Dichlorocyclooctane.* Bp 103—109°C/11 mmHg, NMR ($CDCl_3$) τ 5.35—5.80 (m, 2H), 7.40—8.10 (m, 4H) and 8.0—8.80 (m, 8H).

1,2-Dichloropropionitrile. Bp 59—60°C/11 mmHg (lit[5]), bp 58°C/10 mmHg). IR 2950 (s), 2240 (m), 1440 (s), 1210 (s), 760 (s), 730 (s), and 660 (s),cm^{-1}. NMR ($CDCl_3$) τ 6.15 (d, J=5.5 Hz, 2H) and 5.3 (t, J=5.5 Hz, 1H).

Found: C, 29.08; H, 2.68; N, 11.40; Cl, 57.19%. Calcd for $C_3H_3NCl_2$: C, 29.07; H, 2.44; N, 11.30; Cl, 57.40%.

trans *and* cis-*3,4-Dichlorocyclooctene (Ia,b).* Bp 101°C/10 mmHg and 62—69°C/3 mmHg. NMR [τ 3.9—4.6, 2H (vinyl proton), 4.85—6.0, 2H (C<u>H</u>Cl) and 7.5—9.0, 8H (C<u>H</u>$_2$)].

Found: C, 53.86; H, 6.73; Cl, 39.05%. Calcd for $C_8H_{12}Cl_2$: C, 53.65; H, 6.75; Cl, 39.60%.

trans *and* cis-*5,6-Dichlorocyclooctene (IIa,b).* Bp 119°C/15 mmHg and 88—92°C/6 mmHg. NMR [τ 4.0—4.7, 2H (vinyl proton), 5.35—5.7, 2H (C<u>H</u>Cl) and 7.0—8.5, 8H (C<u>H</u>$_2$)].

Found; C, 53.66; H, 6.81; Cl, 39.50%. Calcd for $C_8H_{12}Cl_2$: C, 53.65; H, 6.75; Cl, 39.60%. IIa and IIb were separated into pure components by preparative gas chromatography (PEG 6000 25%-Chromosorb-W, 1.5 m column; carrier gas, He 120 ml/min at 150°C).

trans-*5,6-Dichlorocyclooctene (IIa).* Bp 74.5—75°C/6 mmHg. NMR [τ 4.2—4.5, 2H (vinyl proton), 5.35—5.6, 2H (C<u>H</u>Cl) and 7.0—8.5, 8H (C<u>H</u>$_2$)].

Found; C, 54.32; H, 6.88%. Calcd for $C_8H_{12}Cl_2$: C, 53.66; H, 6.71%.

cis-*5,6-Dichlorocyclooctene (IIb).* Bp 75—79°C/5 mmHg. NMR [τ 4.0—4.7, 2H (vinyl proton), 5.4—5.7, 2H(C<u>H</u>Cl) and 7.0—8.5, 8H, (C<u>H</u>$_2$)].

Found; C, 54.09, H, 6.86%. Calcd for $C_8H_{12}Cl_2$: C, 53.66, H, 6.71%.

5) N. B. Lorette, *J. Org. Chem.*, **26,** 2324 (1961).

BULLETIN OF THE CHEMICAL SOCIETY OF JAPAN, VOL. 44, 1975—1977 (1971)

The Absolute Configurations of 2-Phenylaziridine and Its Derivatives

Shinsaku FUJITA, Kazuo IMAMURA, and Hitosi NOZAKI

Department of Industrial Chemistry, Kyoto University, Yosida, Sakyo-ku, Kyoto

(Received December 31, 1970)

As the optical resolution of aziridines is rarely feasible because of their acid-sensitivity, optically-active aziridines have been obtained by the stereospecific ring-closure of suitable precursors, mainly of natural origin.[1] The present report will describe a novel synthesis of optically active 2-phenylaziridine (I) and its derivatives, and the determination of their absolute configulations.

The addition of iodine isocyanate[2] to styrene and subsequent treatment with (−)-menthol gave a mixture of the diastereomers of α-(iodomethyl)benzylcarbamic acid (−)-methyl ester (II), which was fractionally recrystallized from methanol. The less soluble diastereomer ($[\alpha]_D$ −73.0°) was treated with methanolic sodium hydroxide, and the resulting aziridine was separated from (−)-menthol by preparative thin-layer chromatography. The optically-active 2-phenylaziridine ((−)-I) thus obtained had an optical rotation of $[\alpha]_D$ −45.5° (75% optically pure, *vide infra*). Similarly, the ring-closure of the more soluble one (IIb) gave another enantiomer (+)-I. which was obtained only in a lower optical purity.

The absolute configuration of I was correlated to that of known α-methylbenzylamine, with the results illustrated in Schemes 1 and 2. The reduction of IIa ($[\alpha]_D$ −70.5°)and IIb with lithium aluminum hydride afforded (−)-N-methyl-α-methyl-benzylamine ((−)-III $[\alpha]_D$ −58.2°) and (+)-enantiomer respectively. On the other hand, the reaction of (R)-(+)-α-methylbenzylamine with ethyl chloroformate yielded (R)-(+)-ethyl α-methylbenzylcarbamate (VII), which in turn afforded (R)-(+)-III on LAH reduction. Therefore, the absolute configuratoins of enantiomers of I were

1) a) S. J. Brois and G. P. Geardsley, *Tetrahedron Lett.*, **1966**, **5113**. b) T. Taguchi and M. Kojima, *Chem. Pharm. Bull. Japan*, **7**, 103 (1959). c) P. G. Gassman and A. Fentiman, *J. Org. Chem.*, **32**, 2388 (1967). c) P. G. Gassman and A. Fentiman, *J. Org. Chem.*, **32**, 2388 (1967). d) P. G. Kostyanovsky, Z. E. Samojlova, and I. I. Tchervin, *Tetrahedron Lett.*, **1969**, 719. e) Y. Sugi and S. Mitsui, This Bulletin, **43**, 564 (1790).

2) a) S. Fujita, T. Hiyama, and H. Nozaki, *Tetahedron*, **26**, 4347 (1979). b) H. Nozaki, Y. Okuyama, and S. Fujita, *Can. J. Chem.*, **46**, 3333 (1968)

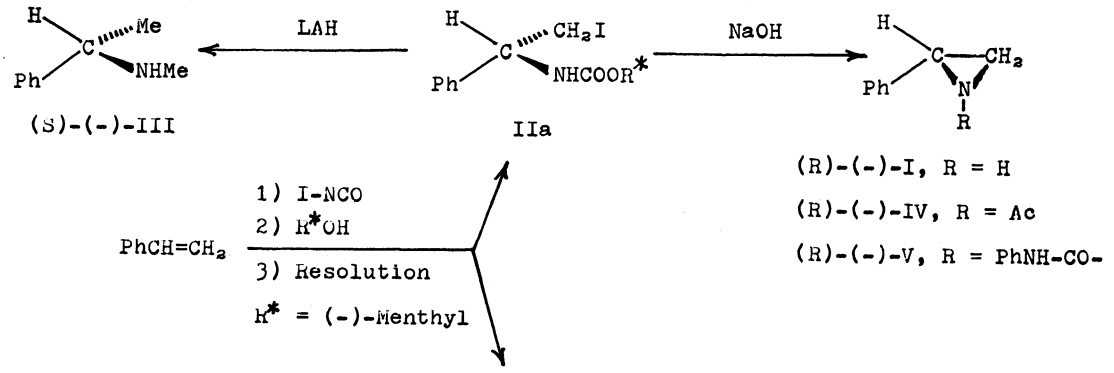

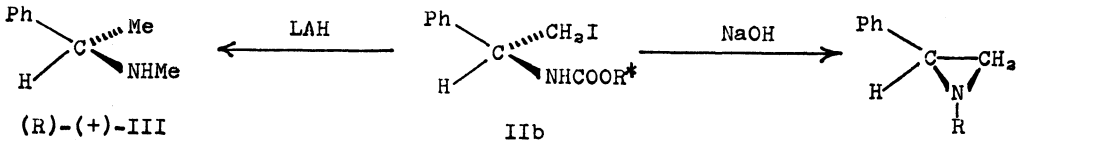

Scheme 1

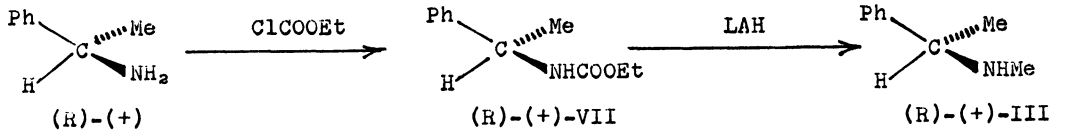

Scheme 2

concluded to be (R)-(−) and (S)-(+).

The following derivatives of (R)-(−)-I were prepared: (R)-(−)-1-acetyl-2-phenylaziridine (IV) and (R)-(−)-1-phenylcarbamoyl-2-phenylaziridine (V). (S)-(+)-1-Methyl-2-phenylaziridine (VI) was also prepared from (S)-(+)-I.

Experimental

All the melting points are uncorrected. Unless otherwise stated, each optical rotation was determined in chloroform at room temperature. The optically-active aziridines were identified by comparing the spectral data with those of racemic samples.

Addition of Iodine Isocyanate to Styrene. Iodine (50.8 g, 0.20 mol) was added in one portion to a cooled mixture of silver isocyanate (40.0 g, 0.26 mol), styrene (20.8 g, 0.20 mol), and dry ether (400 m*l*). Stirring was continued for 1 hr over an ice-salt bath and then for 4 more hr at room temperature. The silver salt then precipitated was filtered off. (−)-Menthol (31.3 g, 0.20 mol) was added to the filtrate, and the solution was allowed to stand in the dark for 4 days. The mixture was poured into ice water (700 m*l*) containing 20 g sodium sulfite and extracted with ether. The combined extracts were dried over sodium sulfate. Concentration gave a mixture of IIa and IIb (81.0 g, 94%). Fractional recrystallization (4 times) of the mixture from methanol yielded a IIa-rich mixture as white crystals (4.53 g); mp 149°C; $[\alpha]_D$ −73.0° (c=1.21 g/100 m*l*).

Found: C, 53.4; H, 6.5; I, 29.9; N, 3.2%. Calcd for $C_{19}H_{28}INO_2$: C, 53.1; H, 6.6; I, 29.6; N, 3.3%.

A IIb-rich mixture was obtained from the mother liquor. Mp 115°C; $[\alpha]_D$ −12.9° (c=0.64 g/100 m*l*).

(R)-(−)-2-Phenylaziridine (I). A mixture of IIa (8.95 g, 20.9 mmol, $[\alpha]_D$ −73.0°) and methanolic sodium hydroxide (10 N, 50 m*l*) was heated at reflux for 1.5 hr under a nitrogen atmosphere. After the evaporation of the solvent, the residue was extracted with ether and dried over sodium sulfate. Concentration and distillation gave a mixture of (R)-(−)-I, menthol, and acetophenone. Preparative-scale TLC (silica-gel G, using ether as a solvent and chloroform as a eluent) and subsequent distillation afforded pure (R)-(−)-I (0.64 g, 27%); bp 56°C/2.5 mmHg; $[\alpha]_D$ −45.5° (c=1.72 g/100 m*l*). Calculation indicated that the optically-pure sample has the optical rotation of $[\alpha]_D$ −60.3°.

(S)-(+)-2-Phenylaziridine (I). ($[\alpha]_D$ +29.4°, c=1,53 g/100 m*l*) was obtained similarly from IIb ($[\alpha]_D$ −12.9°).

(S)-(−)-N-Methyl-α-methylbenzylamine (III) from IIa. A solution of IIa (2.00 g, 4.7 mmol, $[\alpha]_D$ −73.0°) in ether was added, drop by drop at room temperature, to a suspension of lithium aluminum hydride (1.5 g) in ether (30 m*l*). The mixture was then heated at 50°C for 20 hr. The excess hydride was quenched with water and extracted with ether. Then combined ethereal solutions were then extracted with 15% hydrochloric acid. The aqueous layer was neutralized with 25 N aqueous sodium hydroxide, extracted with ether, and dried over sodium sulfate. Distillation afforded (S)-(−)-III (0.044 g, 6%, $[\alpha]_D$ −58.2°, c=0.88 g/100 m*l*). The optical purity was calculated to be 75.4%.

(R)-(+)-N-Methyl-α-methylbenzylamine (III). ($[\alpha]_D$ +45.8°, c=0.57 g/100 m*l*) was obtained from IIb ($[\alpha]_D$ −8.05°).

(R)-(+)-ethyl α-methylbenzylcarbamate (VII). A solution of ethyl chloroformate (0.56 g, 5.2 mmol) in ether (30 m*l*) was added at 0°C to a mixture of (R)-(+)-α-methylbenzylamine (1.24 g, 10 mmol, $[\alpha]_D$ +36.4° (neat), 91.7% optically pure), ether (20 m*l*), and water (30 m*l*). Then another solution of ethyl chloroformate (0.56 g, 5.2 mmol) and aqueous sodium hydroxide (NaOH 0.48 g in water 10 m*l*) were

added to the reaction mixture at the same time. Work-up gave (R)-(+)-VII (1.70 g, 88%); $[\alpha]_D$+64.4° (c=1.99 g/100 ml); bp 97—101°C/1 mmHg.

Found: C, 68.6; H, 7.9; N, 7.2%. Calcd for $C_{11}H_{15}NO_2$: C, 68.4; H, 7.8; N, 7.3%.

*(R)-(+)*N-*Methyl-α-methylbenzylamine (III).* The reduction of (R)-(+)-VII (0.58 g, 3.0 mmol, $[\alpha]_D$+64.4°, 91.7% optically pure) with lithium aluminum hydride gave (R)-(+)-III (0.34 g, 85%); bp 74°C/14 mmHg; $[\alpha]_D$+70.8° (c=1.92 g/100 m*l*). The optical rotation of pure (R)-(+)-III was calculated to be $[\alpha]_D$+77.2°.

(R)-(−)-1-Acetyl-2-Phenylaziridine (IV). A solution of acetyl chloride (0.10 g, 1.3 mmol) in ether (5 m*l*) was added at 0°C to a solution of (R)-(−)-I (0.23 g, 1.5 mmol, $[\alpha]_D$ −45.5°, optical purity 75.4%) and triethylamine (0.18 g) in ether (10 m*l*). The reaction mixture was stirred for 1 hr. The triethylamine hydrochloride thus precipitated was filtered off and washed well with ether. After the evaporation of the solvent, the oily residue was distilled to give (R)-(−)-IV (0.10 g, 31%); bp 56°C/0.2 mmHg; $[\alpha]_D$ −106° (c=1.28 g/100 m*l*). The optically pure sample was calculated to have the rotation of $[\alpha]_D$ −141°.

(R)-(−)-1-phenylcarbamoyl-2-phenylaziridine (V). Phenyl isocyanate (0.090 g) was added to a solution of (R)-(−)-I (0.090 g, $[\alpha]_D$ −45.5°, 75.4% optically pure) in ether (10 m*l*). After it had been stirred for 1.5 hr, the ether was evaporated *in vacuo* to give (R)-(−)-V (0.17 g, 94%); mp 97—99°C (lit. mp for racemic sample[3] 96.5—97.5°C); $[\alpha]_D$ −262° (c=1.56 g/100 m*l*). The optical rotation of pure (R)-(−)-V was calculated to be $[\alpha]_D$ −348°.

(S)-(+)-1-Methyl-2-phenylaziridine (VI). A 1.30 M solution (1.0 m*l*) of *n*-butyllithium in *n*-hexane was added, drop by drop under a nitrogen atmosphere, to a solution of (S)-(+)-I (0.15 g, 1.3 mmol, $[\alpha]_D$ +8.08°, 13.4% optically pure) in tetrahydrofuran (20 m*l*), and the mixture was stirred for 30 min at room temperature. To the reaction mixture we then added drop by drop methyl iodide (0.18 g); the mixture was stirred for 1 hr, poured into saturated aqueous ammonium chloride (20 m*l*), and extracted with ether. The combined etheral extracts were dried over sodium sulfate and concentrated *in vacuo*. The distillation of the oily residue afforded (S)-(+)-VI (0.076 g, 45%); bp 39°C/1 mmHg; $[\alpha]_D$ +32.1° (c=1.51 g/100m*l*). The optical rotation of pure (S)-(+)-VI was calculated to be $[\alpha]_D$ +241°.

The authors are grateful to Professor Keiiti Sisido for his generous help. Financial support from the Ministry of Education, the Japanese Government, and from the Toray Science Foundation is acknowledged with pleasure.

3) K. Kotera, S. Miyazaki, H. Takahashi, T. Okada, and K. Kitahonoki, *Tetrahedron*, **24**, 3681 (1968).

BULLETIN OF THE CHEMICAL SOCIETY OF JAPAN, VOL. 44, 1977—1979 (1971)

Effect of Hole Scavengers on the Radiolysis of Water

Takeshi SAWAI

Tokyo Metropolitan Isotope Research Center, Fukazawa, Setagaya-ku, Tokyo

(Received January 9, 1971)

Recently, a model for the radiolysis of water at low LET was proposed by Hamill.[1] According to the model, some charge recombination of the dry electron and the hole, which are produced early in the radiolysis of water, occurs before hydration and is responsible for the formation of molecular hydrogen and hydrogen peroxide, and these ion pairs can be scavenged by suitable solutes prior to hydration. This hypothesis has been supported by the quantitative correlation shown in recent studies[2,3] of aqueous solutions. The reaction of an electron with some solutes prior to hydration has been reported by the recent striking experiments of Hunt *et al.*[4] with pico second-pulsed radiolysis.

If the dry hole in water is trapped by a suitable solute (X^-), one can expect an increase in $G(e^-_{aq})$ by preventing the fast neutralization of the dry-charge pairs in water. The increase in $G(e^-_{aq})$ with an increase in the Cl^- concentration was shown in an earlier paper.[5] Moreover, the increase of $G(e^-_{solv})$ by Cl^- in the radiolysis of ethanol was recently reported by Khorana and Hamill.[6] The change in $G(e^-_{solv})$ is considered to be due to hole trapping by Cl^-.

The negative ions, SO_4^{2-}, ClO_4^-, or F^-, will also trap the hole[7]:

$$H_2O^+(H_3O^+) + X^- \longrightarrow X(HX) + H_2O \qquad (1)$$

The purpose of this work is to provide evidence for the hole trapping by halogen ions and SO_4^{2-}, and to examine the effect of the solutes on the yield of molecular products.

Experimental

Samples (10 m*l*) of aqueous neutral solutions containing 10^{-2}M KNO_3 and 5×10^{-2}M isopropanol (*i*-PrOH) for the testing of $G(e^-_{aq})$, $G(H_2)$, $G(H_2O_2)$, and 2×10^{-2}M KNO_3 aqueous solutions for G_{H_2} were used. These samples in the irradiation vessel with a break seal were purged with nitrogen gas, degassed by repeated freeze-pump-thaw cycles, and then irradiated with ^{60}Co γ-rays. Oxygenated 5 m*l* samples of

1) W. H. Hamill, *J. Phys. Chem.*, **73**, 1341 (1969).
2) P. L. T. Bevan and W. H. Hamill, *Trans. Faraday Soc.*, **66**, 2533 (1970).
3) T. Sawai and W. H. Hamill, *J. Phys. Chem.*, **74**, 3915 (1970).
4) R. K. Wolff, M. J. Bronskill, and J. W. Hunt, *J. Chem. Phys.*, **53**, 4211 (1970).
5) T. Sawai and W. H. Hamill, *ibid.*, **52**, 3843 (1970).
6) S. Khorana and W.H. Hamill, *J. Phys. Chem.*, **74**, 2885 (1970).
7) P. N. Moorthy and J. J. Weiss, "Solvated Electrons," Advances Chemistry Series **50**, ed. by R.F. Gould, American Chemical Society Publications, Washington, D.C. (1960), p. 180.

10^{-2}M KNO_3-*i*-PrOH solutions were used for the $G(OH)$ measurements. The dose rate, determined by means of a ferrous sulfate dosimeter, was 9.31×10^{18} eV/g hr. The methods of the measurement of H_2, acetone, H_2O_2, and NO_2^- are described elsewhere.[8] These yields were calculated from the slope of the linear portions of the product-dose curves. The energy absorbed in the samples was corrected by the use of the electron fraction of each sample.

Results and Discussion

In the deaerated *i*-PrOH-KNO_3 solutions, NO_3^- reacts with e^-_{aq} to form NO_2^-:

$$NO_3^- + e^-_{aq} \longrightarrow NO_2^- \quad (2)$$

H and OH radicals react with *i*-PrOH to form isopropanol radicals:

$$(CH_3)_2CHOH + H \longrightarrow (CH_3)_2COH + H_2 \quad (3)$$

$$(CH_3)_2CHOH + OH \longrightarrow (CH_3)_2COH + H_2O \quad (4)$$

In oxygenated solutions, $(CH_3)_2COH$ will react with O_2 to produce acetone and HO_2[9]:

$$(CH_3)_2COH + O_2 \longrightarrow (CH_3)_2CO + HO_2 \quad (5)$$

Almost all the H reacts with O_2 to form H_2O_2, because $k(H+O_2)[O_2]/k_3[i\text{-PrOH}]$ is about 50. The effect of hole scavengers on the yields of NO_2^-, H_2O_2, H_2, and acetone was measured under each set of conditions. These results are shown in Figs. 1 and 2. $G(NO_2^-)$ increases with an increase in the concentration of F^- and SO_4^{2-}. G(acetone) decreases with an increase in the Cl^- concentration, while in F^- or SO_4^{2-} solutions the yield is independent of the concentration of F^- and SO_4^{2-}. There is no dependence of G_{H_2}, G_H, and $G_{H_2O_2}$ on the solute concentration except for the cases of Br^- and I^-.

In a F^- solution, the reaction of H with F^- is very slow[10] ($k\approx10^4$M^{-1} sec^{-1}) and the reaction of OH with

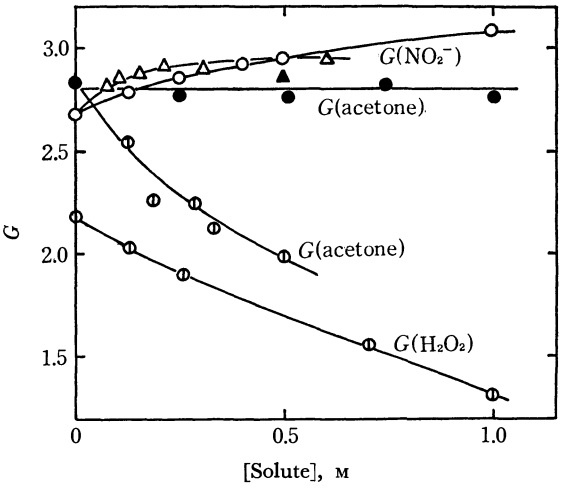

Fig. 1. Effects of solute concentration on $G(NO_2^-)$, $G(H_2O_2)$, and G(acetone) in 10^{-2}M KNO_3-isopropanol solutions.
●, ▲, ⏀: Yields in oxygenated solutions
○, △: Yields in deaerated solutions
○, ●: KF
△, ▲: Na_2SO_4
⏀: NaCl

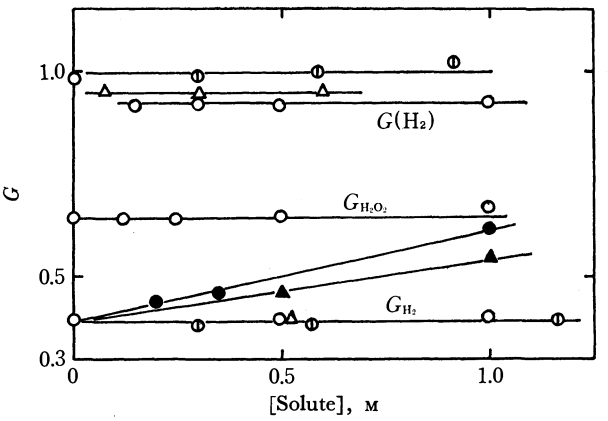

Fig. 2. Effects of solute concentration on G_{H_2}, $G(H_2)$, and $G_{H_2O_2}$ in deaerated solutions.
$G(H_2)$, $G_{H_2O_2}$: H_2 and H_2O_2 yields in 10^{-2}M KNO_3-isopropanol solutions
G_{H_2}: H_2 yield in 2×10^{-2}M KNO_2 solutions
○: KF, ⏀: $NaClO_4$, △: Na_2SO_4, ●: KI, ▲: KBr

F^- should not occur. In Fig. 1, $G(e^-_{aq})$ increases and G(acetone) dose not depend on the F^- concentration. The hole trapping by F^- will be:

$$H_2O^+ + F^- + H_2O \longrightarrow HF + OH + H_2O$$

$$\text{or } H_3O^+ + F^- \longrightarrow HF + H_2O,$$

since F_2^- has not been found even in aqueous F^- solutions at 77°K.[11] The increase in $G(e^-_{aq})$ seems to be due to the prevention of the geminate recombination of dry-charge pairs by the hole trapping. By the same expression used previously for the hole trapping,[5] $1/G_2^0$ can be obtained from the intercept of the plot of $\Delta 1/G(NO_2^-)$ *vs.* $1/[F^-]$. G_2^0 is 0.9 from Fig. 3, and $G(e^-_{aq})$ is 2.7 at $[F^-]=0$ in Fig. 1; therefore, $\sum G(\text{electrons})=3.6$ is obtained.

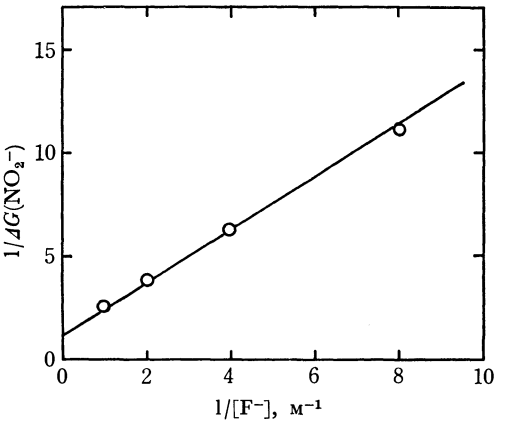

Fig. 3. $G(NO_2^-)$ as a function of the concentration of KF.

In SO_4^{2-} solutions, $G(e^-_{aq})$ increases with an increase in the concentration, and 0.5M SO_4^{2-} has no effect on G(acetone). The reaction of SO_4^{2-} with hole will be:

$$H_2O^+(H_3O^+) + SO_4^{2-} \longrightarrow SO_4^-(HSO_4^-) + H_2O.$$

The reaction of SO_4^- with NO_3^- can be ignored, since $k(SO_4^- + i\text{-PrOH})/k(SO_4^- + NO_3^-)$ is about 100,[12] and SO_4^-, a stronger oxidizing species than

8) T. Sawai, This Bulletin, **39**, 955 (1966).
9) E. Hayon, "Radiation Chemistry of Aqueous Systems," ed by G. Stein, John Wiley & Sons, Inc., N. Y. (1968), p. 157.
10) M. Anber and P. Neta, *Int. J. App. Radiation and Isotopes*, **18**, 439 (1967).
11) B. L. Bales and L. Kevan, *J. Phys. Chem.*, **74**, 1098 (1970).
12) I. Kraljic, *Int. J. Rad. Phys. Chem.*, **2**, 59 (1970).

Cl_2^-[13] reacts with *i*-PrOH probably to form an isopropanol radical, as in the case of OH. Therefore, $G(e^-_{aq})$ increases upon the hole trapping, while, G(acetone) is constant.

$G(e^-_{aq})$ increased and $G_{H_2O_2}$ decreased with an increase in the Cl^- concentration. We have reported before that these changes might be due to the hole trapping by Cl^-.[5] The Cl radical formed by the hole trapping reacts with Cl^- to produce Cl_2^-. It has been shown that Cl_2^- reacts with NO_3^- and *i*-PrOH:[13]

$$Cl_2^- + NO_3^- \longrightarrow 2Cl^- + NO_3 \quad (6)$$

$$Cl_2^- + (CH_3)_2CHOH \longrightarrow \text{Products} \quad (7)$$

Reaction (6) can be ignored because k_7 is much larger than k_6 ($k_6=1.4\times10^6$ and $k_7=6.1\times10^7$ M^{-1} sec^{-1}[1]). Therefore, the increase of $G(e^-_{aq})$ is probably due to the hole trapping. G(acetone) goes down with the Cl^- concentration, as is shown in Fig. 1. If the change in G(acetone) is due to the hole trapping by Cl^-, ΔG(acetone) should be $\leq \Delta G(e^-_{aq})$. However, at 1 M NaCl, for example, $\Delta G(e^-_{aq})$ is only $\sim$0.3 and ΔG(acetone) is $\sim$1.0. Some other reaction which reduces G(acetone) seems to occur. The reaction of Cl^- with OH is very slow in a neutral solution ($k=10^4 M^{-1}sec^{-1}$), but the reaction is relatively fast in an acid solution.

$$OH + Cl^- + H_3O^+_{aq} \longrightarrow Cl + 2H_2O \quad (8)$$

The acetone yield may be decreased by the reaction (8) in the spur, and the decrease in $G_{H_2O_2}$ with the Cl^- concentration[5] may not be due to hole trapping, but to the reaction (8).

According to the model of the radiolysis of water proposed by Hamill,[1] molecular hydrogen and hydrogen peroxide yields should decrease in the presence of hole scavengers, which prevent the reaction of the hole with dry electrons. As is shown in Fig. 2, however, F^- has no effect on $G_{H_2O_2}$, and G_{H_2} is almost independent of the solute concentrations except in the cases of Br^- and I^-. It has also been found that NO_3^-, which is a good scavenger for dry and solvated electrons, diminished G_{H_2} most effectively, while $G_{H_2O_2}$ was not affected at all.[14] These facts suggest that the molecular products in the radiolysis of water are not formed by the reaction of the hole with dry electrons.

13) M. E. Langmuir and E. Hayon, *J. Phys. Chem.*, **71**, 3808 (1967).

14) M. Anbar, "Fundamental Processes in Radiation Chemisty," ed. by P. Ausloos, John Wiley & Sons, Inc., N. Y. (1968), p. 651.

BULLETIN OF THE CHEMICAL SOCIETY OF JAPAN, VOL. 44, 1979—1980 (1971)

Hydration of the Cobalt(III) Complexes. II

Fumio KAWAIZUMI and Yutaka MIYAHARA

Department of Chemical Engineering, Faculty of Engineering, Nagoya University, Chikusa-ku, Nagoya

(Received January 12, 1971)

In our previous papers,[1-4] we reported the determination of hydration number of complexes by measurement of ultrasonic velocity. The complexes were those of cobalt and hexacyanoferate, and the effect of such lignads as en, pn, dien, and edta on the degree of hydration was also studied.

The present study deals with the determination of the degree of hydration of such complexes as $NH_4[Co(NO_2)_4(NH_3)_2]$, $NH_4[Co(C_2O_4)_2(NH_3)_2]\cdot H_2O$, $K[Co(NO_2)_4(NH_3)_2]$, $K[Co(NO_2)_2C_2O_4(NH_3)_2]\cdot H_2O$, $[Co(NO_2)(H_2O)_3(NH_3)_2]\cdot H_2O$, $[Co(H_2O)_3(NH_3)_3](NO_3)_3$, $[CoH_2O(NH_3)_5]Cl_3$, KNO_2, $KHC_2O_4\cdot H_2O$, and $K_2C_2O_4\cdot \frac{1}{2}H_2O$

The hydrated water around an ion can be conventionally divided into two layers,[5] a primary hydration layer in an extreme vicinity of the ion and a secondary outer layer. The water molecules in the former have no freedom of translational motion, and they move with the movement of the ion itself. The hydrated water molecules in the latter have some freedom of motion but they are also subjected to the electrostatic force of the ion. These hydrated water molecules play an important role in phenomena such as salt-in and salt-out effects.

The amount of hydrated water in the incompressible region around the ion is determined by the compressibility method. In order to obtain the relationship between the hydration numbers in the incompressible and primary layers, the complexes having H_2O in the inner sphere such as $[Co(H_2O)_3(NH_3)_3](NO_3)_3$ and $[CoH_2O(NH_3)_5]Cl_3$ were chosen. The salts such as $KHC_2O_4\cdot H_2O$ and $K_2C_2O_4\cdot \frac{1}{2}H_2O$ were taken to examine the effect of COO^- radical on the hydration.

The degree of hydration was determined from the adiabatic compressibilities of aqueous solutions obtained by the measurements of ultrasonic velocity by an ultrasonic interferometer. Measurements were carried out at 25°C. Details of experimental procedures and methods of determining the hydration number are the same as before.[1] The complexes were prepared by the methods in literature, and purified by recrystallization from their aqueous solutions. Since it is highly probable that in aqueous solutions the ligands NO_3 in $[Co(NO_3)_3(NH_3)_3]$ are completely relpaced by H_2O as

1) F. Kawaizumi, H, Nomura, and Y. Miyahara, *Nippon Kagaku Zashi*, **87**, 939 (1966).
2) F. Kawaizumi and Y. Miyahara, *ibid*, **88**, 937 (1967).
3) F. Kawaizumi and Y. Miyahara, *ibid.*, **89**, 655 (1968).
4) F. Kawaizymi and Y. Miyahara, *ibid*, **91**, 333 (1970).
5) J. O'M. Bockris, *Quart. Rev.*, **3**, 173 (1949).

Table 1. Results for the complexes

Sample	κ_1	K_{mo} (ml/mol)	h (mol/mol)
$NH_4[Co(NO_2)_4(NH_3)_2]$	44.74	64.9	3.6
$NH_4[Co(C_2O_4)_2(NH_3)_2]$	44.79	116	6.4
$K[Co(NO_2)_4(NH_3)_2]$	44.76	90.9	5.1
$K[Co(NO_2)_2C_2O_4(NH_3)_2]$	44.75	158	8.8
$[Co(H_2O)_3(NH_3)_3](NO_3)_3$	44.74	126	7.0
$[CoH_2O(NH_3)_5]Cl_3$	44.74	198	11.0
$[Co(NH_3)_6](NO_3)_3$	—	135[1]	7.5[1]
KNO_2	44.72	67.7	3.8

Table 2. Results for the oxalates

	κ_1	K_{mo}(ml/mol)	h(mol/mol)
$H_2C_2O_4$	—	8[6]	0.4[6]
KHC_2O_4	44.72	120	6.6
$K_2C_2O_4$	44.77	250	13.9

$$[Co(NO_3)_3(NH_3)_3] \xrightarrow{\text{in water}} [Co(H_2O)_3(NH_3)](NO_3)_3$$

we used an aqueous solution of $[Co(NO_3)_3(NH_3)_3]$ for the sample of $[Co(H_2O)_3(NH_3)_3](NO_3)_3$.

For all solutions, the ultrasonic velocity changed linearly with concentration.

The results are summarized in Tables 1 and 2, where κ_1 is the compressibility of solvent, K_{mo} the molar hydration volume, and h the hydration numbdr (mol/mol).

A hydration number was assigned for each single ion. The results are given in Tables 3 and 4. We see from Table 2 that the hydration number of oxalate increases linearly with the number of potassium atoms in a molecule, and the hydration number of potassium ion can be estimated from the slope. The hydration number 7 obtained is, however, much larger than that in Table 3.

The hydration number of $[Co(NO_2)_4(NH_3)_2]^-$ calculated from its ammonium salt and potassium salts are 1.6 and 1.9 respectively, confirming the additivity rule of hydration number.

It is interesting to note that by the replacement of one of NO_2 in $[Co(NO_2)_4(NH_3)_2]^-$ with C_2O_4 the hydration number increased remarkably. This suggests that C_2O_4 shows hydration when it is contained in the complex as a ligand, while –COOH as the single species shows hardly any hydration effect (Table 2). A similar effect of COO^- in $[Co\ edta]^-$ has been reported.[3,4]

Table 3. Hydration numbers of ionic species

Ionic species	h(mol/mol)
NH_4^+	2[2]
K^+	3.2[7]
NO_3^-	1.1[7]
NO_2^-	0.6
$[Co(NO_2)_4(NH_3)_2]^-$	1.6[a]—1.9[b]
$[Co(NO_2)_2C_2O_4(NH_3)_2]^-$	5.6
$[Co(C_2O_4)_2(NH_3)_2]^-$	4.4

a) from ammonium salt
b) from potassium salt

Table 4. Hydration numbers of cobalt complexes

Ionic species	h(mol/mol)
$[Co(H_2O)_3(NH_3)]^{3+}$	3.7
$[Co\ H_2O(NH_3)_5]^{3+}$	5.3
$[Co(NH_3)_6]^{3+}$	3.7—4.4[1]

Table 4 shows the change of hydration with the increase of the number of H_2O contained as a ligand. Here, water molecules contained as ligand are not counted as hydration water. Since the change is not so remarkable, it can be concluded that the water molecules contained as ligand correspond to the primary hyration layer, Frank and Wen's region A and those hydrated outside the ligand to the secondary layer, their region B.

The authors wish to express their thanks to the Ministry of Education and the Asahi Glass Science Foundation for the financial support granted for this research.

6) Y. Miyahara, This Bulletin, **25**, 326 (1952).
7) S. Sasaki and T. Yasunaga, *Nippon Kagaku Zasshi*, **72**, 366 (1951).
8) H. S. Frand and Wen-Yang Wen, *Discuss. Farady Soc.*, **24**, 133 (1957).

BULLETIN OF THE CHEMICAL SOCIETY OF JAPAN, VOL. 44, 1980—1981 (1971)

Proton Transfer through Hydrogen Bond in Solid Pyridine-Chloroacetic Acid Complexes as Evidenced by ^{35}Cl Nuclear Quadrupole Resonance

Hideaki CHIHARA and Nobuo NAKAMURA

Department of Chemistry, Faculty of Science, Osaka University, Toyonaka, Osaka

(Received January 13, 1971)

Hydrogen bond formation between dissimilar molecules is a prototype of acid-base interaction. Interesting examples are solid hydrates of acids, *e.g.* $HNO_3 \cdot H_2O$ and $(COOH)_2 \cdot 2H_2O$, in which protons are given up to the water of crystallization by the acid molecule if it is sufficiently strong or retained by the acid if it is weak. In solids, the electrostatic field generally built up in the lattice as a result of the proton transfer can further facilitate such a transfer; thus glycine exists in the form of zwitterions in the α crystal, while it assumes a molecular conformation in an isolated state.[1)]

The purpose of the present communication is to

1) S. Takagi, H. Chihara, and S. Seki, This Bulletin, **32**, 84 (1959); see also Y. Grenie, J. C. Lassegues, and C. Garrigou-Lagrange, *J. Chem. Phys.*, **53**, 2980 (1970).

present an experimantal evidence that protons have been transferred from chloroacetic acids to pyridine in the solid 1:1 complexes formed between them. The complexes are known in solution state to be in tautomeric equilibrium between the two forms, simple hydrogen bonded pair or ion-pair, as revealed by infrared[2] and the ultraviolet[3] spectral studies. Dielectric study[4] also suggested such possibilities.

Table 1. Chlorine quadrupole resonance frequencies at 77°K(MHz)

$(CCl_3COO)(C_5H_5NH)$ (1:1)	37.8396, 37.9275, 38.0166, 38.0722, 38.3075, 38.4915, 38.5118, 38.5932, 38.6002, 38.6365, 38.7205, 38.7598
$(CHCl_2COO)(C_5H_5NH)$ (1:1)	36.3882, 36.6843

We have measured the ^{35}Cl nuclear quadrupole resonance frequencies of pyridine complexes with di- and tri-chloroacetic acids in polycrystalline form. Frequencies measured at 77°K are given in Table 1. The trichloroacetic acid complex gives twelve resonance lines differing at most by 0.9 MHz, whereas the dichloroacetic acid complex gives only two; this suggests a relatively simpler crystal structure for the latter. Since the solid state effects are generally small[5] and we are interested in the state of the valence electrons of the chlorine atoms on which the effect of proton transfer is considered to appear, we take mean value ν_m of the observed resonance frequencies for each complex and compare them with those for pure acids and ammonium salts. Such a comparison is shown in Table 2.

We see that (a) in the series of pure acids, ν_m changes monotonously with the number of chlorine atoms contained in them (*i.e.* with the acid strength) and (b) in the series of ammonium salts of mono- and dichloroacetic acids, ν_m decreases with the number of acidic hydrogen atoms.

It is to be noted that pyridine-dichloroacetic acid has the ν_m value very close to that of $CHCl_2COONH_4$. If pyridine is linked to dichloroacetic acid through the O–H···N hydrogen bond and the proton is moving sufficiently rapidly between the two potential minima along the hydrogen bond, *i.e.* if there is a dynamic equilibrium between the covalent and the ionic forms, O–H···N and $O^-\cdots H\text{–}N^+$, the observed resonance frequency ν_m may be given by $\nu_m = P_i\nu_i + (1-P_i)\,\nu_c$ where P_i is the fractional importance of the ionic form and ν_i and ν_c are the frequencies characteristic of either form. Upon substitution of appropriate figures, ν_m= 36.54 MHz, ν_i=36.46 MHz, and ν_c=38.39 MHz, one obtains P_i=0.95 as compared with P_i=0.71 in a non-dissociative solvent at room temperature.[2] This would mean that in solid pyridine-dichloroacetic acid, the pyridine molecule deprives the acid of its carboxyl hydrogen almost completely, forming an ionic crystal lattice in which cations and anions are bonded by $N^+\text{–}H\cdots O^-$ hydrogen bonds. This is a situation locally analogous to that of glycine or other amino acid crystals. Comparison of the ν_m's for the pyridine complexes with di- and tri-chloroacetic acids also indicates that the same would hold for $CCl_3COO\cdot C_5H_5NH$.

Table 2. Comparison of mean ^{35}Cl resonance frequencies between pure chloroacetic acids and their salts and the shift of the frequency from those of the pure acids (MHz)

Substance	Mean Freq. (ν_m)	Shift ($\Delta\nu$)
CCl_3COOH	40.12[a]	—
$(CCl_3COO)_2HNH_4$	39.49[b]	0.63
$CCl_3COOH\cdot C_5H_5N$	38.37	1.75
$CHCl_2COOH$	38.39[a]	—
$(CHCl_2COO)_2HNH_4$	37.63[d]	0.76
$CHCl_2COONH_4$	36.46[d]	1.93
$CHCl_2COOH\cdot C_5H_5N$	36.54	1.85
$CH_2ClCOOH$	35.25[c]	—
$(CH_2ClCOO)_2HNH_4$	33.73[e]	1.52
$CH_2ClCOONH_4$	33.23[e]	2.02

a) H. Allen, *J. Phys. Chem.*, **57**, 501 (1953).
b) See Ref. 5.
c) H. Negita, *J. Chem. Phys.*, **23**, 214 (1955)
d) H. Chihara and N. Nakamura, unpublished results.
e) T. Yamamoto, N. Nakamura, and H. Chihara, unpublished results (room temperature values).

Attempts have been made to measure the quadrupole resonances in pyridine-monochloroacetic acid and ammonium trichloroacetate. However, no resonance could be detected for unknown reasons although several specimens prepared by different methods were examined. The dichloroacetic acid complex used in the present study was precipitated from cold pyridine solution of the acid, and the trichloroacetic acid complex was crystallised from an ethyl acetate solution containing an excess of pyridine. Both products were washed with ether and dried.

2) G. M. Barrow, *J. Amer. Chem. Soc.*, **78**, 5802 (1956).
3) J. Nasielski and E. V. Donckt, *Spectrochim. Acta*, **19**, 1989 (1963).
4) M. Davies and L. Sobczyk, *J. Chem. Soc.*, **1962**, 3000; S. R. Gough and A. H. Price, *J. Phys. Chem.*, **73**, 459 (1969).
5) D. Biedenkapp and A. Weiss, *Ber. Bunsenges. Phys. Chem.*, **70**, 788 (1966).

BULLETIN OF THE CHEMICAL SOCIETY OF JAPAN, VOL. 44, 1982—1983 (1971)

Ene Reaction of Azulenes with Some Dienophiles

Shô Itô,* Hitoshi Takeshita, and Tetsuya Makino
Department of Chemistry, Tohoku University, Sendai

(Received January 18, 1971)

The thermal reaction of azulenes with maleic anhydride and *p*-benzoquinone was reported by Treibs.[1)]

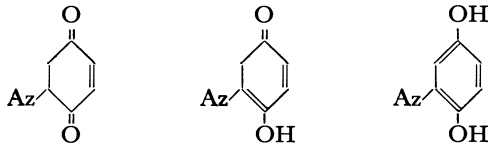

Ia Ib Ic

Az = 1-azulyl or 4-guaiazulyl

However, the structures of the products, especially Ia—Ic, said to be isolated after the reaction of azulenes and benzoquinone, seemed somewhat unconvincing. A reexamination conducted as a part of cycloaddition reactions of non-benzenoid aromatic compounds revealed that the reaction conditions are not appropriate, each reaction yielding a single product, and that the structures of the products must be revised. Our results are described herewith.

Guaiazulene (II) and maleic anhydride (III) react in chloroform or benzene even at room temperature to give 1-azulyl succinic anhydride (IV) as the single product. The structure of IV was confirmed from its mass spectrum (m.w. 294), IR spectrum ($\nu_{c=o}$ 1862, 1785 cm^{-1}) and NMR spectrum [δ 1.32 (6H, d, J= 6 Hz, isopropyl group), 2.63 (3H, s, methyl group at C_1), 2.97 (3H, s, methyl group at C_4), 2.98 (3H, m, C_β–H and methine proton of isopropyl group), 5.40 (1H, t, J=9 Hz, C_α–H), 6.90 (1H, d,d, J=11, 2 Hz, C_6–H), 7.50 (1H, d, J=11 Hz, C_5–H), 7.51 (1H, s, C_2–H), and 8.15 (1H, d, J=2 Hz, C_8–H)].

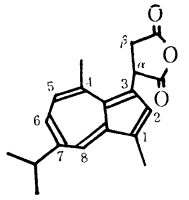

IV

The alternative structure in which succinic anhydride moiety is attached to 2-position of guaiazulene, was excluded when guaiazulene-3-d_1 yielded deuterium free IV (NMR and MS). Attempts to hydrolyze IV resulted only in the formation of a complex acidic mixture. Azulene (V) failed to react (complete recovery) with III even at elevated temperatures. The reaction in the presence of a catalytic amount of aluminum chloride resulted only in reddish brown resinous material.

Although guaiazulene reacted with *p*-benzoquinone (VI) rapidly to give only a mixture of green resinous

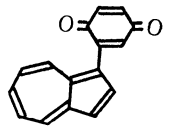

VII

products, azulene and VI at room temperature afforded the single product, 1-azulyl-*p*-benzoquinone (VII), as dark violet crystals. Structure elucidation was made on MS (1:1 adduct), IR ($\nu_{c=o}$ 1650 cm^{-1}) and NMR spectra [δ 6.87 (3H, overlapping, quinone hydrogens), 7.00—7.80 (4H, m, C_3, C_5, C_6, C_7–H), 8.11 (1H, d, J=4 Hz, C_2–H)], 8.48 (1H, d, J=11 Hz, C_4–H), 8.60 (1H, d, J=11 Hz, C_8–H)]. The ene-dione, the initial ene-reaction product, should have been dehydrogenated to VII by excess VI present. The difference in the reactivity of azulenes II and V can be explained by the inductive effect or hyperconjugation of alkyl groups which increase the electron density at C_1 position in II.

Experimental

Reaction of Guaiazulene (II) and Maleic Anhydride (III). II(540 mg) and III(530 mg) were dissolved in anhydrous benzene and kept at room temperature under stirring for 12 hours. After removal of benzene, the mixture was washed with petroleum ether to remove unreacted II(130 mg) and sublimed (steam bath) at reduced pressure (25 mmHg). The residue was recrystallized from petroleum ether to yield blue scaly crystals (IV), mp 127—128°C (450 mg, 56% yield).

Found: C, 77.41; H, 6.94%. Calcd for $C_{19}H_{20}O_3$: C, 77.00; H, 6.80%. λ_{max}^{MeOH} (ε) 248 nm (6600), 291 nm (8200), 306 nm (5200).

Reaction of Guaiazulene-3-d_1 (II-d_1) and Maleic Anhydride (III). II-d_1 (120 mg) and III (450 mg) were allowed to react under the conditions described above. The isolated adduct (35 mg) was identical with (IV) (mixed mp, MS, NMR).

Attempted Hydrolysis of IV. IV (35 mg) was kept at room temperature in aqueous methanol (30%). Silica gel thin layer chromatogram showed the development of complex green or dark brown spots with no definite shape. Attempts to isolate hydrolysate from the mixture failed.

Attempted Reaction of Azulene (V) and Maleic Anhydride (III). *i*) V (128 mg) and III (196 mg) were autoclaved at 250°C in anhydrous benzene for an hour. Silica gel thin layer chromatogram indicated the absence of spots other than starting material. *ii*) A catalytic amount of aluminum chloride was added to V (55 mg) and III (100 mg) in anhydrous benzene. The solution soon became red and resinous matter was separated out. No crystalline product was obtained.

Attempted Reaction of Guaiazulene (II) and p-Benzoquinone (VI). Benzene solution of II (198 mg) and VI (216 mg) was kept at room temperature for 24 hr in the dark. Silica

*To whom correspondence should be addressed.

1) W. Treibs, *Naturwissenschaften*, **43**, 156 (1960); **48**, 452 (1965).

gel column chromatography of the mixture first eluted a small amount of recovered II. No indication of the formation of adducts was obtained from silica gel thin layer chromatogram of the subsequent elutes.

The Reaction of Azulene (V) and p-*Benzoquinone (VI).* V (128 mg) and VI (216 mg) were kept in benzene at room temperature for 12 hours in the dark. The reaction mixture was chromatographed on a silica gel column to give 80 mg of recovered V and subsequently the adduct VII, blue black crystals, mp 111.5—112.5°C, 56 mg (24%).

Found: C, 82.07; H, 4.24%. Calcd for $C_{16}H_{10}O_2$: C, 82.04; H, 4.30%. $\lambda_{max}^{MeOH}(\varepsilon)$ 237 nm (4300), 292 nm (4100), 522 nm (broad).

BULLETIN OF THE CHEMICAL SOCIETY OF JAPAN, VOL. 44, 1983—1984 (1971)

Photochemical Oxidations of 4,5,9,10-Tetrahydropyrenes

Haruo SHIZUKA, Kenji SORIMACHI, Toshifumi MORITA, Kozaburo NISHIYAMA,[1] and Takeo SATO[1]

Department of Chemistry, Gunma University, Kiryu, Gunma

(Received January 22, 1971)

It is known that the photocyclizations of [2.2]-metacyclophanes in the presence of iodine yield 4,5,9,10-tetrahydropyrenes (Eq. (1)).[2-4] The further photochemical dehydrogenation of 4,5,9,10-tetrahydropyrene (II), induced by iodine, has been suggested;[5] the dehydrogenation products were 4,5-dihydropyrene (III) and pyrene (IV), as is shown in Eq. (2), where CH denotes cyclohexane.

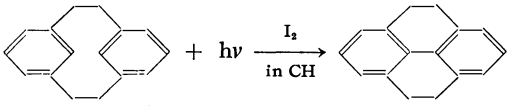

(I) (II) (1)

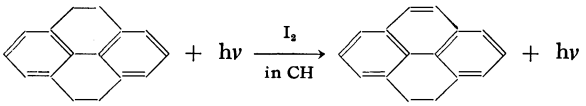

(II) (III)

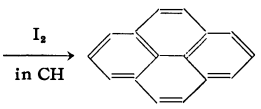

(IV) (2)

In the present work, the photolyses of II and 2,7-dimethyl-4,5,9,10-tetrahydropyrene (V) in aerated and degassed cyclohexane solutions have been carried out.

Experimental

The experimental procedure was almost the same as that previously described.[6] The II and V used in this work were prepared by the photocyclization of [2.2]metacyclophanes[2-4] and were purified by column chromatography (Al_2O_3) and by repeated recrystallizations. The photoproducts were separated by thin-layer chromatography and column chromatography (Al_2O_3 and *n*-hexane were used), and were purified by recrystallization.

The identifications were performed by means of NMR, UV, mp, and elemental analyses. A low-pressure marcury lamp, equipped with a Vycor glass filter, was used as the 2537Å radiation source. Actionometry was carried out using a ferric oxalate solution.[7] The solution was thoroughly degassed on a high-vacuum line by the freeze-pump-thaw technique.

Results and Discussion

It was found that the photoproduct of 2,7-dimethyl-4,5,9,10-tetrahydropyrene (V) in aerated cyclohexane was a different type from that of 4,5,9,10-tetrahydropyrene (II); the photooxidation of V gave a new type of product, 2-methyl-4,5,9,10-tetrahydropyrene-7-carbaldehyde (VI, mp 137—140°C), which resulted from the oxidation of the methyl group substituted at the 7 position of V by the UV irradiation (Eq. (3)), and in the case of II, 4,5-dihydropyrene (III) and pyrene (IV) were obtained as the photoproducts (Eq. (4)).

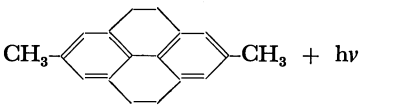

(V)

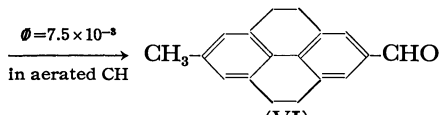

(VI) (3)

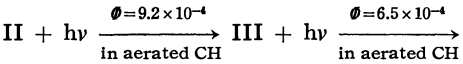

(4)

A 2,7-dimethyl substituent had a very large effect on the photochemical oxidation of 4,5,9,10-tetrahydropyrenes. In addition to the main product, VI, traces of 2,7-dimethyl-4,5-dihydropyrene and 2,7-dimethyl-

1) Department of Chemistry, Tokyo Metropolitan University, Setagaya-ku, Tokyo.

2) T. Sato, E. Yamada, Y. Okamura, T. Amada, and K. Hata, This Bulletin, **38**, 1225 (1965).

3) T. Sato, S. Akabori, S. Muto, and K. Hata, *Tetrahedron*, **24**, 5557 (1968).

4) T. Sato, M. Wakabayashi, S. Hayashi, and K. Hata, This Bulletin, **42**, 773 (1969).

5) T. Sato, K. Nishiyama, S. Shimada, and K. Hata, Paper presented at the Symposium on Organic Free-Radical Reactions, Oct., 1969 (Osaka).

6) *E. g.*, H. Shizuka and I. Tanaka, This Bulletin, **41**, 2343 (1968); H. Shizuka, Y. Takayama, I. Tanaka, and T. Morita, *J. Amer. Chem Soc.*, **92**, 7270 (1970).

7) C. G. Hatchard and C. A. Parker, *Proc. Roy. Soc.* (London), **A. 235**, 518 (1956).

Table 1. The assignments of the NMR spectra of 5,13-dimethyl[2.2]metacyclophane-related compounds dissolved in CCl_4

No.	Substance	Assignment δ
A	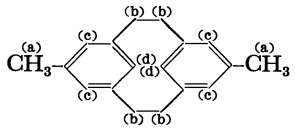	a, 2.33 (6H) b, 1.95, 2.08, 2.89, 3.02 (8H) c, 6.75 (4H) d, 4.05 (2H)
B	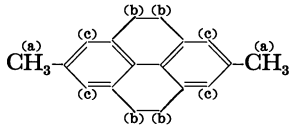 (V)	a, 2.24 (6H) b, 2.73 (8H) c, 6.74 (4H)
C	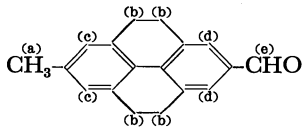 (VI)	a, 2.32 (3H) b, 2.88 (8H) c, 6.84 (2H) d, 7.50 (2H) e, 9.89 (1H)

pyrene were also detected by column chromatography. None of the products described above were obtained in the degassed system.

The NMR spectral data of 5,13-dimethyl [2.2]-metacyclophane-related compounds are listed in Table 1; they are similar to those of I and II reported by Sato *et al.*[8,9] The IR spectrum of the photoproduct (VI) showed the characteristic absorption band (at 1685 cm^{-1}) of the carbonyl group. Furthermore, the results of elemental analyses of the product supported these assignments.

The UV spectrum of the aerated cyclohexane solution of V changed upon irradiation with a 2537 Å light. The absorption band (286 nm, $\varepsilon=2.18\times10^4$) of V decreased, and new maxima of VI appeared at 321 ($\varepsilon=2.95\times10^4$) and 337 nm ($\varepsilon=2.98\times10^4$), with two isosbestic points at 260 and 303 nm. The UV spectral change showed that V was transformed into VI by the photochemical oxidation in the presence of oxygen. The quantum yield ($\phi=7.5\times10^{-3}$) for the VI formation from V was larger than that ($\phi=9.2\times10^{-4}$) of II, as is shown in Eqs. (3) and (4).

Finally, it can be said that the hydrogens of the methyl group in V are more reactive to photooxidation than those of the ethylene group in the molecule. A mechanistic study concerning the photochemistry of [2.2]-metacyclophanes and their derivatives is in progress.

8) T. Sato, S. Akabori, M. Kainosho, and K. Hata, This Bulletin, **41**, 218 (1968).

9) M. Fujimoto, T. Sato, and K. Hata, *ibid.*, **40**, 600 (1967).

BULLETIN OF THE CHEMICAL SOCIETY OF JAPAN, VOL. 44, 1984—1986 (1971)

A Polarographic Study of Amino Acids in Aqueous Solution

Shizuo FUJIWARA, Yoshio UMEZAWA, and Hidehiro ISHIZUKA

Department of Chemistry, Faculty of Science, The University of Tokyo, Bunkyoku, Tokyo

(Received January 25, 1971)

Only a few investigations have been made on the polarography of typical amino acids. Brdička[1] studied sulfur-containing amino acids and proteins using *Brdička's solutions*. Okazaki[2] reported a polarographic study of several α- and β-amino acids in a dioxane-water medium. He showed that there is a linear relation between the half-wave potentials and the pK_a for the amino acids, and suggested that the polarographic current observed in this system is due to the non-ionized form of the amino acids, *i.e.*, RNH_2COOH. In the present study a pH dependence of polarographic currents was analyzed in detail for several amino acids in water solutions with pH 2—4. A possible mechanism for reduction process is proposed, and a result which appears to be inherent in the polarography of amino acids is reported.

All chemicals are of reagent grade, and dissolved in water which has been deionized and distilled. Amino acids examined are L-alanine, β-alanine, γ-aminobutyric acid, L-arginine and L-lysine. Each sample solution contains 5 mM of amino acid and 1 M of LiCl. The pH values of the solutions were adjusted by adding HCl or LiOH. All measurements were performed at 23.0± 0.5°C using a Yanagimoto DC and AC polarograph Model PA-102. The flow rate of the dropping mercury electrode was 0.866 mg/sec, and the drop time was 8.16 sec in distilled water at a mercury column height of 55.0 cm with an open circuit.

All sample solutions give a polarographic wave at −1.55——1.65 V *vs.* mercury pool anode. This wave will be referred to hereafter as the main wave. A sub-wave accompanying a maximum of the first kind is observed over the shoulder of the main wave. This maximum increases in intensity with the lowering of the pH of the solution. AC polarograms for the present systems show two peaks A and B, which correspond to the main wave and the sub-wave in the DC polarograms, respectively. Peak B increases in intensity with the lowering of the pH of the solution (Figs. 1a and b). The limiting currents for the main wave (peak A) and the sub-wave (peak B) are proportional to the square root of the mercury column

1) R. Brdička, *Collection.*, **5**, 148, (1933); *Nature*, **139**, 330 (1937).
2) Y. Okazaki and T. Otsuki, *Rev. Polarog.* (Japan), **14**, 307 (1967).

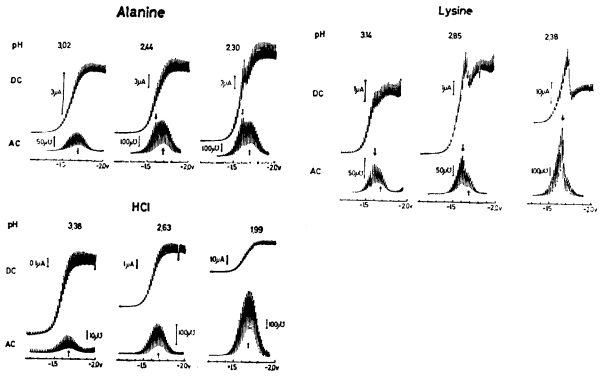

Fig. 1 a.

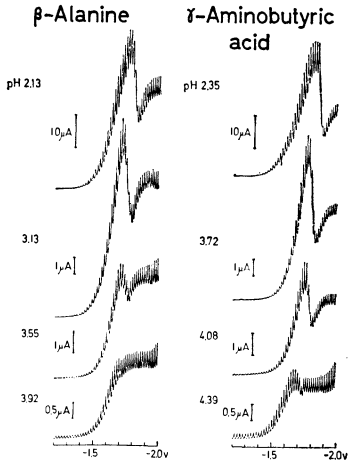

Fig. 1 b.

Fig. 1. DC and AC polarograms of typical amino acids.
a: DC and AC polarograms of some α-amino acids and HCl.
b: DC polarograms of β- and γ-amino acids.

height. This indicates that the main wave and sub-wave are both diffusion controlled.

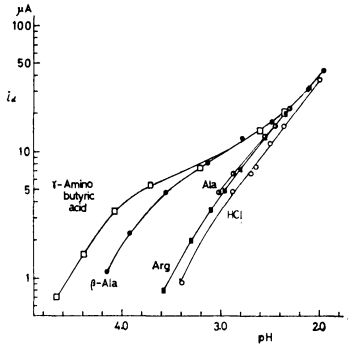

Fig. 2 a.

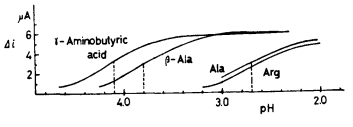

Fig. 2 b.

Fig. 2. pH dependence of the current intensities of some amino acids.
a: pH dependence of the sum of the current intensities of the main and the sub-wave.
b: pH dependence of the difference (Δi) in current intensity between HCl and the amino acids.

For the sake of comparison, the sum of the current intensities of the main and the sub-wave is plotted as a function of pH in Fig. 2a, where the values of the current intensity observed for HCl are also given. The difference Δi in current intensity between HCl and the amino acids in Fig. 2a is plotted in Fig. 2b. In the present systems it is sufficient to consider the equilibrium.

$$R(NH_3^+)COOH \rightleftarrows R(NH_3^+)COO^- + H^+ \quad (1)$$

The following relation holds at a given pH value.

$$pH = pK_a + \log \frac{[R(NH_3^+)COO^-]}{[R(NH_3^+)COOH]} \quad (2)$$

Equation (2) is used along with the data given in Fig. 2b to estimate the pK_a values for the amino acids. The values are given in Table 1, and are in fairly good agreement with pK_a values determined by standard methods.[3]

Table 1. pK_a values for amino acids

	This work	Standard methods (A)[a]	Standard methods (B)[b]
L-alanine	2.7±0.2	2.34	2.348
L-arginine	2.7±0.2	2.18	—
β-alanine	3.8±0.1	3.60	3.551
γ-aminobutyric acid	4.1±0.1	—	4.031

a) determined on cells with liquid junction.
b) determined on cells without liquid junction.

From the results, it can be concluded that the main wave is due to the free H^+ ion, and that the sub-wave (peak B) accompanying the first kind of maxima corresponds to the electrode reaction.[4]

$$R(NH_3^+)COOH \xrightarrow{e^-} R(NH_3^+)COO^- + \frac{1}{2}H_2 \quad (3)$$

The maxima of the first kind are observed over the sub-waves (peak B). They increase in intensity with the lowering of the pH of the solution, and differ in

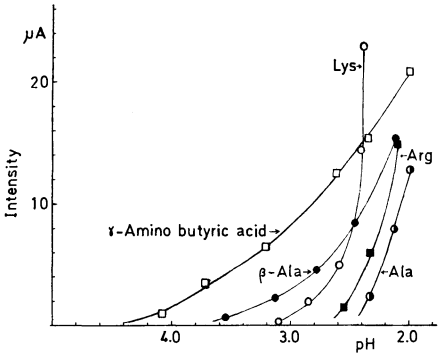

Fig. 3. pH dependence of the curreent intensities of the maxima.
Intensity: difference between the current intensity with the maximum and that without the maximum at the maximum potential.

3) J. P. Greenstein and M. Winitz, "Chemistry of the Amino Acids," Vol. 1., John Wiley and Sons, New York (1961), p. 486.
4) Possibility of the following reaction cannot be excluded.

$$R(NH_3^+)COOH \xrightarrow[2H^+]{e^-} R(NH_3^+)CHO + H_2O$$

However, the reactant is definitely $R(NH_3^+)COOH$.

shape for different amino acids and pH values. As seen in Fig. 3, the maxima disappear at pH values nearly equal to the pK_a values for the amino acids, and the slopes for L-lysine and L-arginine are much greater than those for the remaining monoamino-monocarboxylic acids. It should be noted in Fig. 1b that the widths of the maxima increase in the order α-, β-, γ-amino acids, and that in the cases of β-alanine and γ-aminobutyric acid the widths of the maxima increase with decreasing pH value.

Further investigation of the maxima would be useful for the polarographic study of amino acids.

BULLETIN OF THE CHEMICAL SOCIETY OF JAPAN, VOL. 44, 1986—1987 (1971)

Preparation of 1,7-Bis(*p*-hydroxyphenyl)heptane

Ichiro KAWASAKI, Kazuhiro MATSUDA, and Takeo KANEKO
Department of Chemistry, Faculty of Science, Osaka University, Toyonaka, Osaka

(Received January 29, 1971)

We prepared 1,7-bis(*p*-hydroxyphenyl)heptane in order to study the intramolecular oxidative coupling of phenolic compounds.

Treatment of 4-(*p*-methoxyphenyl)butyronitrile[1] with lithium methylanilide afforded an iminonitrile I. Hydrolysis of I with boiling sulfuric acid gave 1,7-bis(*p*-methoxyphenyl)-heptanone-4 (IIa). In addition to IIa a compound having no carbonyl group was isolated as a by-product by silica gel chromatography. The structure of this compound was assigned as 7,7'-dimethoxy-1,1'-spirobitetralin (IIIa) by NMR and MS spectra. The same compound was obtained easily by boiling IIa with hydrobromic acid to produce a phenolic compound IIIb followed by methylation with dimethyl sulfate. Huang Minlon reduction of IIa gave 1,7-bis(*p*-methoxyphenyl)heptane (IVa), and a phenolic compound IVb was also obtained by demethylation of IVa.

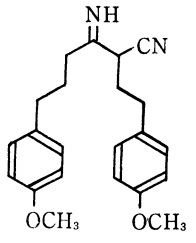

I

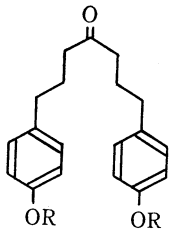

II a, R=CH_3
b, R=H

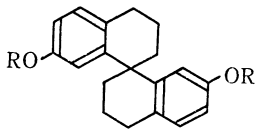

III a, R=CH_3
b, R=H

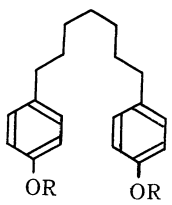

IV a, R=CH_3
b, R=H

Experimental

*3-Cyano-1,7-bis(*p*-methoxyphenyl)-4-iminoheptane (I).* Phenyllithium was prepared by adding bromobenzene (4.7 g) to lithium (0.4 g) in ether (40 m*l*) under nitrogen atmosphere. To this solution was added methylaniline (6.4 g) dissolved in ether (20 m*l*). After refluxing for 1 hr, 4-(*p*-methoxyphenyl)-butyronitrile (5.2 g) in ether (30 m*l*) was added dropwise to the above solution at room temperature. The solution was refluxed for 1 hr, then quenched with water. The organic layer was washed with water, dried and evaporated. The product (3.7 g, 74%) was obtained by distillation, bp 240—245°C/0.02 mmHg. IR: ν^{neat} 3480, 3380, 3250, 2300 cm^{-1}.

Hydrolysis of the Iminonitrile (I). I (9.3 g) was dissolved in 1:1 sulfuric acid (300 m*l*). The solution was heated at 60°C for 30 min and then under reflux for 30 min. The solution was diluted with water and extracted with ether. The ethereal extract was washed with water, dried and evaporated. Chromatography of the crude product on silica gel (elution with benzene) resulted in the separation of two compounds. Evaporation of the first fraction gave IIIa (0.7 g, 8.3%), mp 88 —89°C. IR: ν^{Nujol} 1615, 1575, 1275, 1235, 1040, 880, 845, 810 cm^{-1}. NMR: δ (CCl_4) 1.6—2.2 (8H, m), 2.6—3.0 (4H, m), 3.6 (6H, s), 6.25 (2H, d, J=3 Hz), 6.6 (2H, d-d, J=8—3 Hz), 6.95 ppm (2H, d, J=8 Hz). MS: *m/e* 308 (100), 280 (15.7), 279 (61.3), 249 (18.8), 248 (18.7), 221 (10.4), 174 (46.5), 159 (14.2), 147 (23.6), 134 (25.2), 121 (24.7%).

Found: C, 82.05; H, 7.85%. Calcd for $C_{21}H_{24}O_2$: C, 81.78; H, 7.84%.

The second fraction gave IIa (4.3 g, 50%), mp 31—33°C. IR: ν^{Nujol} 1705, 1615, 1585, 1305, 1240, 1030, 835, 815 cm^{-1}. NMR: δ(CCl_4) 1.9 (4H, q, J=6 Hz), 2.4 (4H, t, J=6 Hz), 3.8 (6H, s), 6.8 (4H, d, J=9 Hz), 7.1 ppm (4H, d, J=9 Hz).

Found: C, 77.39; H, 7.94%. Calcd for $C_{21}H_{26}O_3$: C, 77.27; H, 8.03%.

IIa (300 mg) was dissolved in 48% hydrobromic acid (50 m*l*) and heated for 1 hr under reflux. The reaction mixture was evaporated to dryness and extracted with ether. The ethereal extract was washed with sodium carbonate solution and water, dried and evaporated. The residue was recrystallized from chloroform to give IIIb (120 mg, 40%), mp 157—159°C. IR: ν^{Nujol} 3340, 3180, 1620, 1585, 1290, 1230, 1035, 860, 845 cm^{-1}. NMR: δ ($CDCl_3$), 1.6—2.3 (8H, m), 2.6—3.0 (4H, m), 4.2 (2H, broad s), 6.2 (2H, d, J=3 Hz), 6.6 (2H, d-d, J=3—8 Hz), 7.0 ppm (2H, d, J=8 Hz). MS: *m/e* 280 (91.4), 252(25.3), 251(100), 224 (17.3), 223(28.9), 160(38.3), 145(17.9), 133(19.8), 120(16.7), 107(25.3%).

Found: C, 81.09; H, 7.18%. Calcd for $C_{19}H_{20}O_2$: C, 81.39; H, 7.19%.

This compound was converted by treatment with dimethyl

1) Ki-U Kim, *J. Pharm. Soc. Japan*, **63**, 376 (1943).

sulfate into a dimethyl ether, which was identical with IIIa in IR spectra.

*1,7-Bis(*p*-hydroxyphenyl)heptanone-4 (IIb).* Ethylmagnesium bromide was prepared by adding ethyl bromide (21.8 g) to magnesium (4.8 g) in ether. To this solution was added diethylamine (14.6 g) and heated for 30 min under reflux. IIa (3.3 g) in ether was added to the solution. The reaction was carried out for 2 hr under reflux. The solvent was removed and the residue was heated to 179—190°C for 45 min. The reaction mixture was cooled, diluted with water and extracted with ether. The ethereal extract was washed with sodium carbonate solution and water. The ethereal layer was extracted with dilute potassium hydroxide solution and the aqueous layer was acidified with 6N hydrochloric acid and extracted with ether and dried. On evaporation of the solvent, the product solidified, (2.6 g, 80%). Recrystallization from ether-petroleum ether gave IIb, mp 115—117°C. IR: ν^{Nujol} 3320, 1685, 1610, 1590, 1510, 1220, 830 cm^{-1}. NMR: δ (CD_3OD), 1.8 (4H, q), 2.4 (4H, t), 2.5 (4H, t), 6.7(4H, d, J=8 Hz), 7.0 ppm (4H, d, J=8 Hz).

Found: C, 76.24; H, 7.41%. Calcd for $C_{19}H_{22}O_3$: C, 76.48; H, 7.43%.

*1,7-Bis(*p*-methoxyphenyl)heptane (IVa).* A mixture of IIa (3.3 g) potassium hydroxide (10 g), 80% hydrazine hydrate (40 m*l*) and triethylene glycol (10 m*l*) was heated for 2 hr at 140—160°C and then for 3 hr at 190—210°C. Water (300 m*l*) and 6N hydrochloric acid (30 m*l*) were added to the cooled solution. The product was extracted with chloroform and the chloroform extract was washed with water, dried and evaporated. Distillation of the residual oil gave IVa (2.2 g, 70%), bp 180—190°C/0.01 mmHg. IR ν^{neat} 1610, 1585, 1455, 1295, 1240, 1170, 1035, 820 cm^{-1}. NMR: δ(CCl_4), 1.2—1.6 (10H, m), 2.5 (4H, t, J=7 Hz), 4.75 (6H, s), 6.7 (4H, d, J=8 Hz), 7.0 ppm (4H, d, J=8 Hz).

Found: C, 80.89; H, 9.01%. Calcd for $C_{21}H_{28}O_2$: C, 80.73; H, 9.03%.

*1,7-Bis(*p*-hydroxyphenyl)heptane (IVb).* IVa (3.0 g) was dissolved in acetic acid (100 m*l*) and 48% hydrobromic acid (100 m*l*) and then heated under reflux for 30 min. The solution was evaporated *in vacuo*, and ether was added to the residue. The ethereal solution was washed with sodium carbonate solution and water, and then extracted with potassium hydroxide solution. The aqueous extract was acidified with 6N hydrochloric acid and reextracted with ether. On evaporation of the solvent, the product solidified (2.6 g, 85%). Recrystallization from benzene gave IVb, mp 98—99°C. NMR: δ ($CDCl_3$), 1.3—2.0 (10H, m), 2.7 (4H, t, J=7 Hz), 4.2 (2H, m), 6.95 (4H, d, J=8 Hz), 7.25 ppm (4H, d, J=8 Hz). MS: *m/e* 284(20), 107(100%).

Found: C, 80.06; H, 8.45%. Calcd for $C_{19}H_{24}O_2$; C, 80.24; H, 8.51%.

BULLETIN OF THE CHEMICAL SOCIETY OF JAPAN, VOL. 44, 1987—1989 (1971)

The Photoreduction of Benzophenone by Thioethers

Wataru ANDO, Junji SUZUKI, and Toshihiko MIGITA
Department of Chemistry, Gunma University, Kiryu, Gunma

(Received February 4, 1971)

Ultraviolet irradiation of benzophenone in 2-propanol leads to generation of radicals $Ph_2\dot{C}OH$, (A) and $Me_2\dot{C}OH$, (B), and then to formation of pinacol and acetone.

$$Ph_2C{=}O^* + Me_2CHOH \longrightarrow Ph_2\dot{C}OH + Me_2\dot{C}OH$$

The photoexcited ketone may also abstract α-hydrogen from other hydrogen donors, *e.g.*, amines and ethers.[1-4] In these systems the derived radicals may give the three possible radical recombination products. The reaction is, however, retarded and inhibited by the presence of mercaptan or disulfide in low concentration, as rapid reactions are introduced which convert the radicals A and B into the starting materials.[5,6]

$$Ph_2\dot{C}OH + RS\cdot\ (RSSR) \longrightarrow Ph_2C{=}O + RSH\ (RSH + RS\cdot)$$

$$Me_2\dot{C}OH + RSH \longrightarrow Me_2CHOH + RS\cdot$$

On the other hand, the presence of a relatively high concentration of phenyl sulfide or other thioethers which would not readily give the thiyl radical had no effect on photoreduction of benzophenone, indicating that organic sulfur was not a quencher or desensitizer in the reaction. Thus, among aliphatic sulfides, those bearing α-hydrogen atoms are expected to reduce benzophenone photochemically, since α-hydrogen atom was found to be reactive toward abstraction by radicals. On the other hand, sulfides bearing β-hydrogen but no α-hydrogen atoms are not expected to be effective reducing agents, because such sulfides like *t*-butyl sulfide have been known to generate thiyl radicals when the β-hydrogen atom was abstracted by radicals.[7]

Thus, the photoinduced reactions of benzophenone in various aliphatic sulfides were investigated, and the above expection was found to be correct.

Results and Discussion

Irradiation of 2 mmol benzophenone in 16 mmol dimethyl sulfide with high pressure mercury lamp for 48 hr gave benzopinacol, I, in 35% yield by decanting the unreacted dimethyl sulfide and washing the

1) S. G. Cohen and R. J. Baumgarten, *J. Amer. Chem. Soc.*, **89**, 3471 (1967).
2) E. Bergman and J. Fujise, *Ann.*, **483**, 65 (1930).
3) G. Ciamician and P. Silber, *Ber.*, **44**, 1554 (1911).
4) S. G. Cohen and S. Atkipis, *J. Amer. Chem. Soc.*, **88**, 3587 (1966).
5) S. G. Cohen, S. Orman, and D. A. Laufer, *ibid.*, **84**, 3905 (1962).
6) S. G. Cohen, D. A. Laufer, and W. V. Sherman, *ibid.*, **86**, 3060 (1964).
7) J. A. Kampmeier, R. P, Geer, A. J. Meskin, and Rose Marie D'Silva, *ibid.*, **88**, 1257 (1966).

remaining solid with petroleum ether (b.p., 30—60°C). Analysis of the unreacted dimethyl sulfide solution by vapor phase chromatography (Carbowax 20M, 10% on Celite 22) indicated the formation of di(methylthio)methane, II (1.5%), 1,2-di(methylthio)ethane, III (11%), and a mixture (36%) of three diphenyl substituted products, IV, V, and VI.[8]

$$Ph_2C{=}O^* + CH_3SCH_3 \longrightarrow \underset{\text{I}}{Ph_2C(OH)C(OH)Ph_2}$$

$$+ \underset{\text{II}}{MeSCH_2SMe} + \underset{\text{III}}{MeSCH_2CH_2Me}$$

$$+ \underset{\text{IV}}{Ph_2C(OH)CH_2SMe} + \underset{\text{V}}{Ph_2C{=}CH_2} + \underset{\text{VI}}{Ph_2C{=}CHSMe}$$

Structures of the reaction products are determined by independent syntheses and spectra analyses. Olefins, V and VI, may be produced from β-hydroxy sulfide, and IV by elimination of the components of RSOH and H_2O under vpc conditions. With regard to the mechanism of the formation of olefins from β-hydroxy sulfide, we might suppose that the elimination occurs *via* transitions C and D.

A similar olefin formation has been reported for the thermolysis of β-hydroxy sulfinamides.[9]

Photoreductions of benzophenone in diethyl sulfide and diisopropyl sulfide gave similar results. Irradiation of 2 mmol benzophenone in diethyl sulfide for 48 hr led to the consumption of 70% benzophenone and the formation of 40% pinacol I. Analysis of seaction mixture by vpc after removal of the pinacol rhowed the presence of diethyl disulfide (1.3%), 2,3-di(ethylthio)butane (20%), and a mixture (29%) of $Ph_2C(OH)CH(CH_3)SEt$ and $Ph_2C{=}CHMe$. In the reaction of benzophenone in diisopropyl sulfide, about 80% of benzophenone was consumed, and diisopropyl disulfide (3.3%), 2,3-di(isopropylthio)-2,3-dimethylbutane (13%), 1,3-di(isopropylthio) propane (9%), and a mixture (19%) of $Ph_2C{=}CMe_2$ and $Ph_2C(OH)CMe_2$-S(*i*-Pr) were obtained together with benzopinacol (45%). Photoreaction in di-*t*-butyl sulfide led to only 8% consumption of benzophenone, and the formation of *t*-butyl mercaptan (7.2%) and a trace of di-*t*-butyl disulfide on 48 hr irradiation.

Our results can be explained by the following reaction steps analogous to those for photoreaction in alcohol.

$$Ph_2C{=}O^* + RSCH_2R' \longrightarrow Ph_2\dot{C}OH + RS\dot{C}HR'$$

$$2\ RS\dot{C}HR' \longrightarrow RSCH(R')CH(R')SR$$

$$2\ Ph_2\dot{C}OH \longrightarrow Ph_2C(OH)C(OH)Ph_2$$

$$Ph_2\dot{C}OH + RS\dot{C}HR' \longrightarrow$$

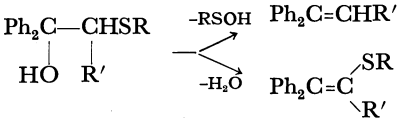

In the thioethers, α-C–H seems more susceptible than the β-C–H bond toward hydrogen abstraction by triplet ketone. The polar resonanced factor may contribute to stabilization of the transition state.

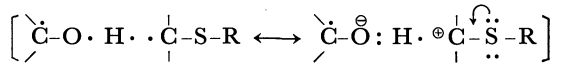

Low consumption of benzophenone in di-*t*-butyl sulfide is reasonably explained by the inhibiting effect of thiyl radical formed during the early stage of reaction.

$$Ph_2C{=}O^* + Me_3CSCMe_3 \longrightarrow Ph_2\dot{C}OH + CH_2{=}CMe_2 + Me_3CS\cdot$$

$$Me_3CS\cdot + Ph_2\dot{C}OH \longrightarrow Ph_2C{=}O + Me_3CSH$$

Distribution of the olefins formed by reactions in unsymmetrical thioethers is shown in Table 1.

Table 1. The formation of diphenyl olefins in photoreduction of benzophenone in thioethers

Thioether	Product A	Product B	Ratio A/B
n-PrSEt	$Ph_2C{=}CHEt$	$Ph_2C{=}CHMe$	1.5
i-PrSEt	$Ph_2C{=}CHMe$	$Ph_2C{=}CMe_2$	4.0
i-PrSMe	$Ph_2C{=}CMe_2$	$Ph_2C{=}CH_2$	3.7

Experimental

Photolysis of Benzophenone in Dimethyl Sulfide. 0.30 g of benzophenone was dissolved in 1 m*l* dimethyl sulfide. Irradiation in a Pyrex tube for 48 hr provided six products, I—VI. The course of photolysis was monitored by gas chromatography. After 40 hr the unreacted benzophenone in dimethyl sulfide was negligible. Benzopinacol was isolated by the addition of petroleum ether to the concentrated reaction mixture, and identified by comparison with authentic samples. Other products, II, III, IV, V, and VI were isolated by preparative gas chromatography. Structures of II, III, and V were identified by comparison with authentic samples. Compound IV shows NMR spectrum at 1.92 (s, 3-H), 3.30 (s, 2-H), 3.45 (s, 1-H), and 7.28 ppm (m, 10-H). VI shows NMR spectrum at 2.28 (s, 3-H), 6.40 (s, 1-H), 7.14 (s, 5-H) and 7.27 ppm (s, 5-H).

Found: C, 79.63; H, 6.12%. Calcd for $C_{15}H_{14}S$: C, 79.60; H, 6.24%.

Formation of Diphenyl Olefins, V and VI, from IV. Isolated compound IV by gas chromatography was reinjected into the gas chromatograph of 10% Carbowax 20M, 2 m×0.5 cm stainless column at 220°C. Two products, V and VI, were collected in the ratio 4:1, depending on the conditions of gas chromatograph. On heating the reaction mixture obtained from the photolysis of benzophenone and dimethyl sulfide at 220°C for 1 hr, IV could not be isolated by thin layer chromatography, and V and VI were found to be formed in the ratio of 1:2.5 from the analysis of gas chromatography. However, on heating IV in a Pyrex tube under the same conditions, and by direct analysis of NMR, it was found that IV was not consumed, and V and VI were not obtained.

8) Yields based on the consumed benzophenone.

9) E. J. Corey and T. Durst, *J. Amer. Chem. Soc.*, **88**, 5656 (1966).

Photolysis of Benzophenone in Thioethers. As a typical run, a solution of 295 mg of benzophenone in 1 m*l* thioether in Pyrex tubes was irradiated with the high pressure mercury lamp for 48 hr. Precipitated benzopinacol was removed by adding the petroleum ether and washing the solid. The solvent of the reaction mixture was evaporated off *in vacuo* and the residue was analyzed directly by gas chromatography. Products isolated by gas chromatography were characterized by comparison with authentic samples.

BULLETIN OF THE CHEMICAL SOCIETY OF JAPAN, VOL. 44, 1989—1990 (1971)

The Bulk Photoconductivity of Violanthrene Single Crystals

Mitsuyuki SOMA

Department of Chemistry, Faculty of Science, The University of Tokyo, Hongo, Tokyo

(Received February 10, 1971)

The bulk photoconductivity of single crystals of aromatic hydrocarbons in contact with the electrolyte electrode has been the subject of serveral reports.[1] This arrangement of electrodes has proved to have some advantages in distinguishing whether the charge carriers are produced in the bulk of the crystal or on the interface between the crystal and the electrodes.[2] So far, however, these works have been confined to the crystals of relatively small aromatic molecules and have not been extended to include crystals of large aromatic molecules, which are expected to have different electronic properties. In this note some peculiar features of the bulk photoconductivity in the single crystals of violanthrene, which has nine condensed aromatic rings, in contact with the liquid electrodes will be reported.

The violanthrene (violanthrene A, 1,2,9,10-dibenzoperopyrene) single crystals were prepared as follows. Powdered crystals of violanthrene which had been purified by repeated sublimation in a vacuum were sealed off in a glass tube with several cmHg of nitrogen gas. The tube was then placed in an electric furnace which was designed to attain an appropriate temperature gradient, after which the bottom of the tube was heated to a temperature slightly below the melting point of violanthrene (478°C) in order to sublime it. The single crystals grew on the upper wall of the tube at lower temperatures. Thus, single crystals with an area of approximately 0.1 cm^2 and a thickness below few hundred microns were easily obtained.

Measuring procedures were similar to the method described previously.[3] A violanthrene crystal was mounted between the two polystyrene half cells which were the modified types of Kallmann and Pope's cell.[4] Each half cell was filled with liquid which acted as an elctrode for the crystal. The crystal was illuminated by a 750 W tungsten lamp with metal interference filters through the electrode. The half width of the light transmitted through the filters ranged from 110 to 160 Å.

The dc photocurrent[5] was more than fifty times as large as the dark current at 5990 Å, intensity of incident light being 2.7×10^{15} photons/cm^2·sec. The photocurrent-voltage characteristics were similar for the wavelength range studied (4000 to 7000 Å). The photocurrent was proportional to the applied voltage in the lower-voltage region (ohmic region) up to the applied voltage of 10^4 V/cm; it began to deviate from Ohm's law to be dependent on the voltage superlinearly in the higher-voltage region (non-ohmic region). The photocurrent depended little on the direction of the applied field. This was especially true in the ohmic region. Moreover, in the ohmic region, the photocurrent was insensitive to the electrode conditions, such as the electrode material or the addition of chemicals. For example, when the aqueous electrode was replaced by alcoholic electrodes, such as methanol or ethanol, the photocurrent was almost unchanged; nor did the addition of ceric ion, iodine, or o-chloranil, which are ready to act as electron acceptor or hole injector to the crystal, affect the photocurrent in the ohmic region.

Figure 1 shows the spectral dependence of the photocurrent at the constant light intensity of 2.9×10^{14} photons/cm^2·sec. The absorption sepctra of a thin single crystal and of a solution[6] of violantherne are shown for comparison. The spectral response was dependent on the thickness of the crystal. When the thinner crystals were used, the maximum in the spectral response shifted towards a shorter wavelength, and for the crystals thicker than 20 μ (up to 150μ) the maximum at 5990 Å was emphasized. The current changed sublinearly with the intensity of the incident light. The slope of the photocurrent-intensity curve decreased with an increase in the intensity. The sublinear dependence of the photocurrent on the incident light intensity suggests that the bimolecular decay of the charge carriers plays an important role.

All the above findings suggest that the charge carriers produced in the bulk of the violanthrene crystal predominate at least in the ohmic region. This is in con-

1) H. Kallmann and M. Pope, *J. Chem. Phys.*, **32**, 300 (1960); P. Mark and W. Helfrich, *J. Appl. Phys.*, **33**, 205 (1962); J. W. Steketee and J. de Jonge, *Phillips Res. Reports*, **17**, 363 (1962); W. Mehl and J. M. Hale, *Discuss. Faraday Soc.*, **45**, 30 (1967).

2) N. Geacintov and M. Pope, *J. Chem. Phys.*, **45**, 3884 (1965); N. Geacintov and M. Pope, *ibid.*, **50**, 814 (1969).

3) M. Soma, *J. Amer. Chem. Soc.*, **92**, 3289 (1970).

4) H. Kallmann and M. Pope, *Rev. Sci. Instr.*, **30**, 44 (1959).

5) When the term "photocurrent" is used, the dark current is always subtracted.

6) E. Clar, "Aromatische Kohlenwasserstoffe," Springer Verlag, Berlin (1952).

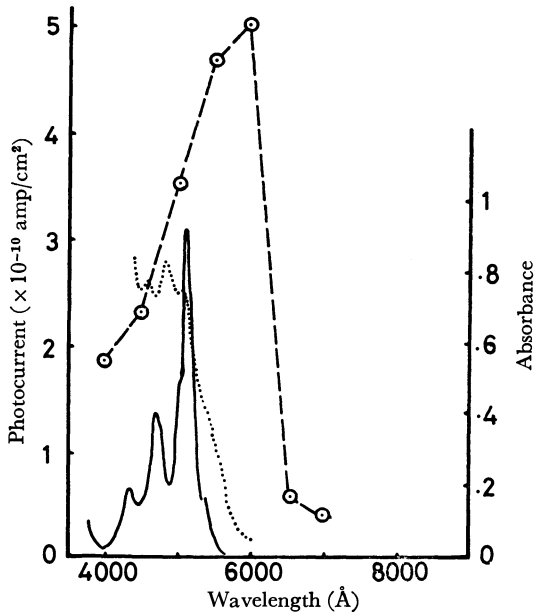

Fig. 1. Spectral dependence of the photocurrent in violanthrene crystal. Intensity of incident light, 2.9×10^{14} photons/cm·sec. Crystal thickness, 20 μ. Applied voltage, 6 V (in ohmic region). Dotted line shows the absorption spectrum of violanthrene single crystal of 2 μ thick in units of 10^4 cm^{-1}. Full line is the absorption spectrum of violanthrene in benzene (longer wavelength part, in 1-methylnaphthalene) in units of 10^5 l/mol·cm.[6]

trast with the cases of anthracene crystals in similar electrode arrangements. In that case, in the wavelength region corresponding to the first singlet excited state of anthracene the charge injection from the electrode always predominates.[1,3]

The bimolecular decay of carriers offers a qualitative explanation of the spectral response of the photocurrent. If we simply assume that the carriers are produced *via* one exciton mechanism in the bulk of the crystal and that they decay bimolecularly, the steady-state approximation for the carrier concentration gives, neglecting the diffusion of both the exciton and the carries;

$$\frac{dn(x)}{dt} = \alpha I_0 e^{-\epsilon x} - Rn(x)^2 = 0 \qquad (1)$$

where $n(x)$ is the carrier concentration at a certain distance, x, from the surface of the crystal $dn(x)/dt$ its time derivative, ϵ the absorption coefficient of the crystal, I_0 the incident light intensity, α the constant relating to the carrier production, and R is the bimolecular rate constant. The total number of carriers, N_c, in the crystal with a thickness of L and a unit area is expressed as follows:

$$N_c = \int_0^L n(x)dx \qquad (2)$$

From (1) and (2), we get:

$$N_c = 2\sqrt{\frac{\alpha I_0}{R}}[1-e^{-1/2\epsilon L}] \qquad (3)$$

N_0 has a maximum between $\epsilon=2/L$ and $\epsilon=3/L$. For the crystal 20 μ thick, these optical densities in the decadic unit are 4.3×10^2 and 6.4×10^2 cm^{-1} respectively. The corresponding value for the violanthrene crystal appears around the abosrption threshold above 5500 Å; this is in accordance with the observed spectral dependence of the photocurrent.

Whether the carrier generation process is an intrinsic one or an extrinsic one involving some impurities or defects is obscure at present. In this connection, it should be noted, however, that the fall-off in the photocurrent at 6000 Å for the thicker crystals corresponds in its energy (2.1 eV) roughly to the energy gap determined from the temperature dependecne of the dark conductivity (1.95 eV).[7]

The author wishes to express his gratitude to Professor Hiroo Inokuchi for his valuable discussions.

7) Y. Hori, Y. Maruyama, and H. Inokuchi, presented at Symposium on Molecular Structure, Fukuoka (1969).

BULLETIN OF THE CHEMICAL SOCIETY OF JAPAN, VOL. 44, 1990—1992 (1971)

The Synthesis of Poly[N^{ε}-(*l*)-menthyloxycarbonyl-L-lysine] and Its Secondary Structure

Hiroyuki YAMAMOTO and Tadao HAYAKAWA

Institute of High Polymer Research, Faculty of Textile Science and Technology, Shinshu University, Ueda

(Received February 12, 1971)

In a previous paper,[1,2] poly-γ-(*l*)-menthyl glutamate and poly-β-(*l*)-menthyl aspartate were synthesized and the secondary structures of these polymers were studied in order to investigate the effect of the side-chain with optically-active protect-group contributions to the polypeptide structure.

The syntheses of poly-L-lysine derivatives have been achieved in the preparation of the starting N^{ε}-benzyloxycarbonyl[3–5] and N^{ε}-trifluoroacetyl-L-lysine[6] as a monomer, and their chemical, physical, and biological

1) H. Yamamoto, Y. Kondo, and T. Hayakawa, *Biopolymers*, **9**, 41 (1970).

2) H. Yamamoto and T. Hayakawa, *ibid.*, **10**, 309 (1971).

3) E. Katchalski, J. Crossfeld, and M. Frankel, *J. Amer. Chem. Soc.*, **70**, 2094 (1948).

4) R. R. Becker and M. A. Stahmann, *ibid.*, **74**, 38 (1954).

5) T. Hayakawa, Y. Onchi, and J. Noguchi, *Nippon Kagaku Zasshi*, **80**, 81 (1959).

6) M. Sela, R. Arnon, and I. Jacobson, *Biopolymers*, **1**, 517 (1963).

properties have been studied extensively.[7-10] In the present study, poly-N^{ε}-(*l*)-menthyloxycarbonyl-L-lysine was synthesized, and the secondary structure of the polymer was studied by means of the optical rotatory dispersion (ORD), the circular dichroism (CD), and infrared spectroscopy (IR) techniques. The route of synthesis is as follows:

$$\text{lys} \xrightarrow{CuCl_2} \text{lys}\cdot 1/2\text{Cu} \xrightarrow[(2)\ \text{EDTA}\cdot 2\text{Na}]{(1)\ (l)\text{-Menthyl chloroformate}} N^{\varepsilon}\text{-}(l)\text{-Menthyloxycarbonyl lys} \xrightarrow{COCl_2} N^{\varepsilon}\text{-}(l)\text{-Menthyloxycarbonyl lys NCA} \xrightarrow{TEA} \text{Poly-}N^{\varepsilon}\text{-}(l)\text{-menthyloxycarbonyl lys}$$

Since the menthyl chloroformate decomposes almost instantly on contact with water, the N^{ε}-menthyloxycarbonylation of lysine is unsuccessful when the Schotten-Baumann method is used in an aqueous solution. The copper complex was prepared by the reaction of lysine with cupric chloride in methanol. The complex was reacted with menthyl chloroformate to give N^{ε}-(*l*)-menthyloxycarbonyl lysine. Poly-N^{ε}-(*l*)-menthyloxycarbonyl-L-lysine was prepared *via* N^{ε}-(*l*)-menthyloxycarbonyl-N^{α}-carboxy-L-lysine anhydride (NCA). The resulting polymer was obtained in a high yield and had a high molecular weight, as Table 1 shows. It was soluble in ethyl ether, tetrahydrofuran (THF), chloroform, dimethylformamide (DMF), trifluoroacetic acid (TFA), and dichloroacetic acid (DCA), and was insoluble in methanol.

Table 1. Molecular weight of poly[N^{ε}-(*l*)-menthyloxycarbonyl-L-lysine]

Solvent	Monomer NCA (mg)	Yield mg (%)	Molecular weight (DP)[a]	$[\eta]$[b] dl/g
Dioxane	460	354(88)	12300(40)	0.158
DMF	460	331(82)	10100(33)	0.156

a) By titration of the amino endgroup with 0.02N perchloric acid.
b) In DCA at 25°C.

Experimental

(l)-Menthyl Chloroformate. *(l)*-Menthyl chloroformate was prepared from (*l*)-menthol, quinoline, and phosgene as has been described by Westley and Halpern.[11]

N$^{\varepsilon}$-*(l)-Menthyloxycarbonyl-L-lysine.* To a suspension of L-lysine hydrochloride (3.66 g, 0.02 mol) in 3 m*l* of methanol, 0.46 g of sodium in 10 m*l* of methanol and 1.70 g (0.01 mol) of cupric chloride in 10 m*l* of methanol were added.[12] After 30 min, the mixture was cooled to 0°C and 2.80 m*l* of triethylamine (TEA) were added. Then 0.024 mol of *(l)*-menthyl chloroformate in 30 m*l* of toluene and 3.34 m*l* of TEA were added. This solution was allowed to stand at 0°C for 2 hr and then at room temperature for 2 hr. The reaction mixture was filtered and dried; yield, 6.0 g. A suspension of the copper complex of N^{ε}-menthyloxycarbonyl-L-lysine in an aqueous ethylenediamine-tetraacetic acid 2Na (EDTA 2Na) was treated by the method described by Kuwata and Watanabe;[13] yield, 1.20 g (30%). The product was recrystallized from 20% acetic acid. 1.05 g (26%), mp 228°C. $[\alpha]_D^{22} = -40.9$ (*c* 1.0, acetic acid).

Found: C, 62.25; H, 9.97; N, 8.34%. Calcd for $C_{17}H_{32}N_2O_4$: C, 62.16; H, 9.82; N, 8.53%.

N$^{\varepsilon}$-*(l)-Menthyloxycarbonyl-L-lysine NCA.* Dry phosgene was passed through a suspension of N^{ε}-*(l)*-menthyloxycarbonyl-L-lysine (1.1 g) in 25 m*l* of dry dioxane for 1 hr at 50°C. Nitrogen was then passed through the reaction mixture for 30 min. The solvent was removed at 40°C under reduced pressure. The residual oily product was crystallized by treating it with *n*-hexane; yield, 1.0 g. This was recrystallized from ethyl acetate and *n*-hexane; yield, 0.97 g (82%). Mp 106—107°C.

Found: C, 61.04; H, 8.32; N, 7.81%. Calcd for $C_{18}H_{30}N_2O_5$: C, 60.99; H, 8.53; N, 7.90%.

*Poly-*N$^{\varepsilon}$*-(l)-menthyloxycarbonyl-L-lysine.* N^{ε}-*(l)*-Menthyloxycarbonyl-L-lysine NCA was dissolved in dioxane and DMF at the concentration of 10%. Triethylamine was added to each solution at NCA/initiator ratios of 100/1. The mixture was polymerized in a sealed tube at 15°C for 3 days, at 40°C for a day, and at 100°C for 3 hr. The results are summarized in Table 1.

Found: C, 65.14; H, 9.66; N, 8.86%. Calcd for $C_{17}H_{30}N_2O_3$: C, 65.78; H, 9.73; N, 9.03%.

Methods. The ORD, CD, and IR measurements were made on the respective ORD/UV 5 instruments, both made by the Japan Spectroscopic Co., Ltd. The optical rotations are expressed as a reduced molar residue rotation. As for CD, the measured values of $\varepsilon_L - \varepsilon_R$ were converted to the molar ellipticity.

Results and Discussion

The IR spectrum of the polymer showed absorptions at 1663 cm^{-1} for amide I and at 1530 cm^{-1} for amide II, suggesting the existence of the α-helical conformation.

The ORD and CD curves of the polymer in ethyl ether are shown in Fig. 1. The polymer exhibits a trough at 233 mμ with $[m']_{233} = -12100$ deg-cm²/dm. Moreover, two negative dichroism bands near 222 mμ and 206 mμ, with $[\theta]_{222} = -20000$ and $[\theta]_{206} = -26600$, are observed. This behavior is essentially identical with that of the right-handed α-helical form of the other polyamino acids. The polymer gave similar α-helical curves in THF ($[m']_{233} = -10000$) and in chloroform ($[m']_{233} = -9500$), and exhibited the ORD behavior of a random coil in TFA. The lower $[m']_{233}$ and $[\theta]_{222}$ values can be considered to result from the fact that this phenomenon arose from the interaction of the solvent and the bulky menthyloxycarbonyl chromophore.[1]

The helix→random coil transition for poly-N^{ε}-benzyloxycarbonyl-L-lysine (PCLL) occurs at 40% DCA in a DCA-$CHCl_3$ mixed solvent.[14] Plots of the $[\alpha]_{546}$ values *versus* the solvent composition of poly-N^{ε}-*(l)*-menthyl-

7) E. Katchalski and M. Sela, *Advan. Protein Chem.*, **13**, 243 (1958).
8) M. Sela and E. Katchalski. *ibid.*, **14**, 391 (1959).
9) J. Applequist and P. Doty, "Polyamino acids, Polypeptides and Proteins," ed by M. Stahmann, Univ. Wisconsin Press, Madison, Wisc. (1962), p. 161.
10) E. Daniel and E. Katchalski, *ibid.*, p. 183.
11) J. W. Westley and B. Halpern, *J. Org. Chem.*, **33**, 3978 (1968).
12) R. W. Hay and L. J. Porter, *Aust. J. Chem.*, **20**, 675 (1967).
13) S. Kuwata and H. Watanabe, This Bulletin, **38**, 676 (1965).
14) G. D. Fasman, "Polyamino acids, Polypeptides and Proteins," ed. by M. Stahmann, Univ. Wisconsin Press, Madison, Wisc. (1962), p. 221.

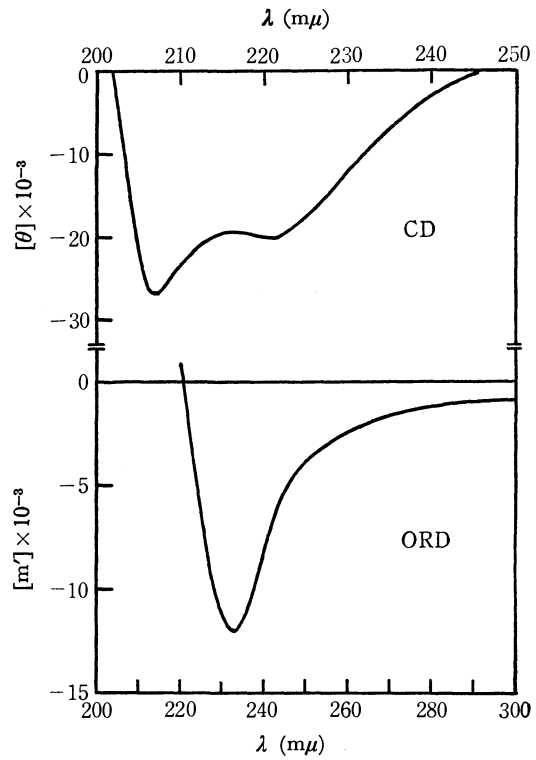

Fig. 1. ORD and CD of poly[N^{ε}-(*l*)-menthyloxycarbonyl-L-lysine] at 22°C in ethyl ether.

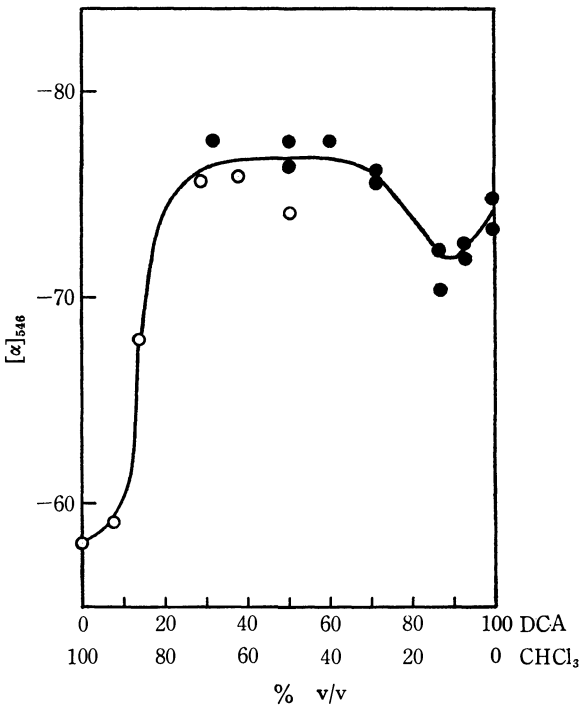

Fig. 2. Specific rotation $[\alpha]_{546}$ values of poly[N^{ε}-(*l*)-menthyloxycarbonyl-L-lysine] of varying solvent composition: (○), polymer dissolved in chloroform (solution diluted with DCA); (●), polymer dissolved in DCA (solution diluted with chloroform); at 22°C.

oxycarbonyl-L-lysine are shown in Fig. 2. This polymer causes a sharp transition at about 15% DCA. In comparison with PCLL, the helical structure of poly-N^{ε}-(*l*)-menthyloxycarbonyl-L-lysine is made rather unstable by the introduction of the N^{ε}-(*l*)-menthyloxycarbonyl group.

BULLETIN OF THE CHEMICAL SOCIETY OF JAPAN, VOL. 44, 1992—1994 (1971)

Aminocyclitols. XXV. Synthetic Studies on Streptamine and Its Analogs

Tetsuo SUAMI, Seiichiro OGAWA, Hiroshi SANO, and Naoyuki KATO

Department of Applied Chemistry, Faculty of Engineering, Keio University, Koganei-shi, Tokyo

(Received February 15, 1971)

In connection with the previous papers of this series,[1] streptamine[2] and its analogs were synthesized from *myo*-inosadiamine-1,3 dihydrochloride (**1**),[3] which was prepared by hydrazinolysis of 2,4,5,6-tetra-*O*-acetyl-1,3-di-*O*-*p*-toluenesulfonyl-*myo*-inositol,[4] followed by a catalytic hydrogenation.

Since an axial hydroxyl group on C-2 was expected to be the least reactive toward an acetylation among four hydroxyl groups in **1**, a selective acetylation seemed to be possible. That is, when **1** was acetylated with acetic anhydride in anhydrous pyridine at 5—10°C for 7 days, di-*N*,*N'*-acetyl-4,5,6-tri-*O*-acetyl-*myo*-inosadiamine-1,3 (**2**) was obtained in 59% yield. Its proton magnetic resonance (PMR) spectrum in dimethyl sulfoxide-d_6 (DMSO-d_6) reveals the acetyl methyl protons as two sharp signals at τ 8 region:[5] τ 8.20 (6) and 8.11 (9), which were attributed to two equatorial acetamido and three equatorial acetoxy groups, respectively. Therefore the absence of a signal at a region of an axial acetoxy group (τ 7.80—7.91)[5] supported the proposed structure of **2**.[6] Then **2** was treated with methanesulfonyl chloride at 0—5°C for 2 days and

1) T. Suami, S. Ogawa, and M. Uchida, This Bulletin, **43**, 3577 (1970).

2) M. L. Wolfrom, S. M. Olin, and W. J. Polglase, *J. Amer. Chem. Soc.*, **72**, 1724 (1950); K. Heyns and H. Paulsen, *Chem. Ber.*, **89**, 1152 (1956); T. Suami and S. Ogawa, This Bulletin, **38**, 2026 (1965); S. Ogawa, T. Abe, H. Sano, K. Kotera, and T. Suami, *ibid.*, **40**, 2405 (1967); N. Kurihara, T. Kurokawa, and M. Nakajima, *Agr. Biol. Chem.*, **31**, 1166 (1967); F. W. Lichtenthaler, H, Leinert, and T. Suami, *Chem. Ber.*, **100**, 2383 (1967).

3) T. Suami and S. Ogawa, This Bulletin, **40**, 1295 (1967).

4) T. Suami, F. W. Lichtenthaler, and S. Ogawa, *ibid.*, **40**, 1488 (1967).

5) F. W. Lichtenthaler and P. Emig, *Carbohyd. Res.*, **7**, 121 (1968).

6) The PMR spectrum of hexaacetyl *myo*-inosadiamine-1,3[3] in DMSO-d_6 shows four peaks: τ 8.21 (6), 8.06 (3), 8.03 (6) and 7.82 (3).

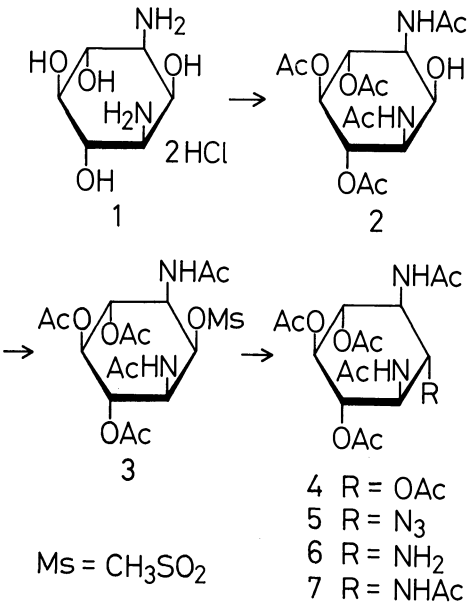

subsequently settled at room temperature for 2 days to give di-*N,N'*-acetyl-4,5,6-tri-*O*-acetyl-2-*O*-methanesulfonyl-*myo*-inosadiamine-1,3 (**3**) in 56% yield.

When **3** was treated with anhydrous sodium acetate in boiling 2-methoxyethanol, a Walden inversion occurred at C-2 to afford streptamine in 56% yield as its hexaacetyl derivative (**4**), which was identified with an authentic sample.[7] This result confirmed as well the assignment of structure of **2**.

While, on treatment with sodium azide in boiling 2-methoxyethanol, **3** gave di-*N,N'*-acetyl-4,5,6-tri-*O*-acetyl-2-azido-2-deoxy-*scyllo*-inosadiamine-1,3 (**5**) in 57% yield. A catalytic hydrogenation of **5** afforded di-*N,N'*-acetyl-4,5,6-tri-*O*-acetyl-2-amino-2-deoxy-*scyllo*-inosadiamine-1,3 (**6**)[8] in 88% yield, which, on acetylation, gave known hexaacetyl *scyllo*-inosatriamine-1,2,3 (**7**)[8,9] in 53% yield.

Experimental

The melting points were determined on a Mitamura Riken micro hot stage and are uncorrected. The PMR spectra were determined with a Varian A-60D spectrometer at the frequency of 60 MHz in DMSO-d_6 with tetramethylsilane as an internal standard. The infrared spectra were recorded in potassium bromide pellets.

Di-N,N'-*acetyl-4,5,6-tri*-O-*acetyl*-myo-*inosadiamine-1,3 (2).* Throughly dried *myo*-inosadiamine-1,3 dihydrochloride (**1**)[3] (0.40 g) was dissolved in hot anhydrous pyridine (18 m*l*) and cooled to 0—5°C by ice and water. To the solution was added acetic anhydride (1.1 m*l*, 5.5 molar equivalents) dropwise during 10 min under stirring. After keeping at 5—10°C for 7 days, the reaction mixture was filtered to remove an insoluble material and the filtrate was evaporated to dryness. The crystalline residue was recrystallized from ethanol to afford colorless needles (0.32 g, 59%) of **2**, mp 307—308.5°C. IR: 3460 (OH), 1750 (ester), 1670, 1615, and 1553 cm^{-1} (amide).

Found: C, 49.63; H, 6.29; N, 7.03%. Calcd for $C_{16}H_{24}N_2O_9$: C, 49.48; H, 6.23; N, 7.21%.

Di-N,N'-*acetyl-4,5,6-tri*-O-*acetyl-2*-O-*methanesulfonyl*-myo-*inosadiamine-1,3 (3).* Throughly dried **2** (120 mg) was dissolved in boiling anhydrous pyridine (6 m*l*) and cooled to 0—5°C by ice and water. Methanesulfonyl chloride (0.1 m*l*) was added dropwise under stirring and the reaction mixture was stored below 10°C for 4 days. An insoluble material was filtered off and the filtrate was evaporated to yield a crystalline residue which was triturated with ethanol, and the crystals were collected by filtration. The crude crystals of **3** weighed 81 mg (56%), mp 229—231°C. Further recrystallization from ethanol gave an analytical sample (52 mg), mp 231—231.5°C. IR: 1750 (ester), 1645, 1560 (amide), and 1180 cm^{-1} (OSO_2CH_3).

Found: C, 44.56; H, 5.84; N, 5.92; S, 6.51%. Calcd for $C_{17}H_{26}N_2O_{11}S$: C, 43.77; H, 5.62; N, 6.00; S, 6.87%.

Hexaacetyl Streptamine (4). A mixture of **3** (150 mg), anhydrous sodium acetate (150 mg) and 2-methoxyethanol (20 m*l*) was refluxed for 22 hr. The reaction mixture was evaporated to dryness and the resulting residue was treated with a mixture of acetic anhydride (15 m*l*) and pyridine (15 m*l*) at room temperature overnight. After filtering off an insoluble material, the mixture was evaporated to dryness and the residue was triturated with ethanol to give colorless crystals (78 mg, 56%) of **4**, mp 300°C (showing a transition at 237—238°C). This compound was identified with an authentic sample of **4** derived from antibiotic streptomycin[6] by comparing with IR spectra and the melting behaviors.

Di-N,N'-*acetyl-4,5,6-tri*-O-*acetyl-2-azido-2-deoxy*-scyllo-*inosadiamine-1,3 (5).* A mixture of **3** (200 mg), sodium azide (91 mg) and 2-methoxyethanol (10 m*l*) was refluxed for 20 hr. The reaction mixture was then worked up similarly as described under the preparation of **4**. The crude crystals of **5** so obtained was recrystallized from ethanol to give colorless needles (100 mg, 57%), mp 263—264°C (decomp.). Recrystallization from ethanol afforded an analytical sample, whose melting point did not change. IR: 2150 (N_3), 1750 (ester), 1655 and 1670 cm^{-1} (amide).

Found: C, 46.75; H, 5.63; N, 16.60%. Calcd for $C_{16}H_{23}N_5O_8$: C, 46.49; H, 5.61; N, 16.94%.

Di-N,N'-*acetyl-3,4,5-tri*-O-*acetyl-2-amino-2-deoxy*-scyllo-*inosadiamine-1,3 (6).* A solution of **5** (94 mg) in 90% aqueous dimethylformamide (10 m*l*) was hydrogenated in the presence of Raney nickel T-4[10] in a Parr shaker type apparatus under the initial hydrogen pressure of 4.5 kg/cm^2. After 14 hr, the catalyst was filtered off and the filtrate was evaporated to give a white powder (78 mg, 88%) of **6**. Recrystallization from ethanol gave colorless needles which showed a transition at 191—193°C. IR: 3400 (NH_2), 1750 (ester), 1640 and 1560 cm^{-1} (amide).

Found: N, 10.85%. Calcd for $C_{16}H_{25}N_3O_8$: N, 10.67%.

Hexaacetyl scyllo-*Inosatriamine-1,2,3 (7).* A 40 mg portion of **6** was treated with acetic anhydride (1 m*l*) and pyridine (1 m*l*) at room temperature overnight. The crude product was recrystallized from ethanol and ether to give colorless needles (23 mg, 53%) of **7**, mp 298—303°C (decomp.) This compound was identified with an authentic sample by comparing with the IR spectra.[8]

The authors wish to thank Professor Sumio Umezawa for his helpful advice, Professor F. W. Lichtenthaler

7) R. L. Peck, R. P. Graber, A. Walti, E. W. Peel, C. E. Hoffhine, Jr., and K. Folker *J. Amer. Chem. Soc.*, **68**, 29 (1946).

8) F. W. Lichtenthaler, P. Voss, and N. Majer, *Angew. Chem.* **81**, 221 (1969).

9) The authors thank Professor F. W. Lichtenthaler for identifying **7** with an authentic sample.[8]

10) S. Nishimura, This Bulletin, **32**, 61 (1959).

for his identification of compound **7** with an authentic specimen, Mr. Saburo Nakada for his elementary analyses and Mr. Hiroshi Itoda for his assistance in the preparative experiment. This research has been financially supported by a grant of the Japanese Ministry of Education.

BULLETIN OF THE CHEMICAL SOCIETY OF JAPAN, VOL. 44, 1994—1995 (1971)

The Dehalogenation of Organic Halides by Means of Iron(II) Chloride in Dimethyl Sulfoxide

Tamio SHIRAFUJI, Yasusi YAMAMOTO, and Hitosi NOZAKI

Department of Industrial Chemistry, Kyoto University, Yoshida, Sakyo-ku, Kyoto

(Received February 16, 1971)

A recent publication[1] recorded a Wurtz-type condensation effected by iron(II) chloride-diamine complexes in ethanol. This has prompted us to publish our independent findings on the title reaction,[2] which has been examined in continuation of a previous investigation of the reactions of organic halides with copper(I) chloride in dimethyl sulfoxide (DMSO).[3] The observed results summarized in Table 1 are partly parallel to those of diamine complex,[1] but we wish to point out that the present reaction does furnish a practical, simple method for preparing tetraphenylethylene and *trans*-stilbene.

Iron(II) chloride tetrahydrate dissolves in DMSO to give a reddish-brown clear solution upon stirring in a nitrogen atmosphere for several minutes.[4] Benzylic and allylic halides were allowed to react in this 1M solution of the iron(II) salt. Dichlorodiphenylmethane, under the controlled conditions shown in Table 1, gave 1,2-dichloro-1,1,2,2-tetraphenylethane as the sole condensation product; this product was then further dehalogenated to tetraphenylethylene. In contrast, the dehalogenation by means of copper(I) chloride in DMSO gave tetraphenylethylene exclusively.[3] No 1,2-dichloro-1,1,2,2-tetraphenylethane was isolated in the latter reaction under any of the conditions examined.

Such step-by-step reduction was also observed in the case of benzotrichloride, which afforded α,α,α',α'-tetrachlorobibenzyl or a mixture of *cis*- and *trans*-α,α'-dichlorostilbene, under the controlled conditions. Benzal bromide gave a good yield of *trans*-stilbene, whereas benzal chloride did not give any condensation products, but benzaldehyde only. Benzyl chloride also failed to give even a trace of bibenzyl. The sole product isolated was found to be benzyl alcohol. When the reaction was performed in a mixture of DMSO-ethanol, the resulting product was benzyl ethyl ether. These products may be explained by assuming the following schemes:

$$R\text{-}X + Fe^{II}L_m(SH)_n \longrightarrow R\text{-}XFe^{II}L_{m'}(SH)_{n'}$$

$$HX + R\text{-}S + Fe^{II}L_m(SH)_n \qquad R\cdot + Fe^{III}XL_{m-1}(SH)_n$$

L: DMSO, H_2O, halide ion
SH: protic solvent (EtOH)

TABLE 1. WURTZ-TYPE CONDENSATION INDUCED BY 1 M $Fe(II)Cl_2 \cdot 4H_2O$/DMSO SOLUTION[a]

Substrate	Reaction temp (°C)	time (hr)	Product yield in %[b]
Ph_2CCl_2 (Fe/X=2.5)	90	27	$Ph_2C{=}CPh_2$ (82)[c]
(Fe/X=0.5)	20—30	16	$Ph_2CClCClPh_2$ (65)[c]
$PhCCl_3$ (Fe/X=0.4)	60	27	$PhCCl_2CCl_2Ph$ (85)
$PhCCl_2CCl_2Ph$	90	17	$PhCCl{=}CClPh$ (*cis* 76, *trans* 18)
$PhCHBr_2$	80	21	$PhCH{=}CHPh$ (*trans* 83)[d]
PhCHBrCHBrPh (*meso*)	80	24	$PhCH{=}CHPh$ (*trans* 95)
PhCOCHBrCHBrPh	r.t.	24	$PhCOCH{=}CHPh$ (90)
$PhCHCl_2$	80	20	PhCHO (90)
$PhCH_2Cl$	80—90	20	$PhCH_2OH$ (69)
$PhCH{=}CHCH_2Cl$ (*trans*)	70—80	20	$PhCH{=}CHCH_2CH_2CH{=}CHPh$ (*trans* 34)
			$PhCH{=}CHCH_2OH$ (*trans* 33)

a) Unless otherwise stated the ratio of organic halides and iron(II) chloride was taken so as the atomic ratio of Fe: halogen to be 2.5:1.
b) Recovery was not considered in calculation of yields.
c) Benzophenone was obtained as solvolysis product.
d) Benzaldehyde was a minor product.

1) K. Onuma, J. Yamashita and H. Hashimoto, This Bulletin, **43**, 836 (1970). See also R. S. Wade, R. Havlin and C. E. Castro, *J. Amer. Chem. Soc.*, **91**, 7530 (1969).

2) A part of this work was presented at the 23rd Annual Meeting of Chemical Society of Japan, Tokyo, April 3, 1970 (No. 16332) and the 160th National Meeting of ACS, Chicago, Ill., Sept 17, 1970 (No. ORGN 139).

3) H. Nozaki, T. Shirafuji, and Y. Yamamoto, *Tetrahedron*, **25**, 3461 (1969).

4) The iron(II) iodide-DMSO complex was isolated and characterized.[5] Attempts at isolating iron(II) chloride-DMSO complex similarly did not succeed.

5) F. A. Cotton, R. Francis, and W. D. Horrocks, *J. Phys. Chem.*, **64**, 1534 (1960).

Cinnamyl chloride gave the Wurtz product in addition to the hydrolysate, cinnamyl alcohol. All these observations may tentatively be explained as follows. The halide-iron salt complex undergoes a one-electron transfer, thus affording the R· radicals, whose recombination gives the coupling products, R–R. The driving force toward this direction is probably the susceptibility of C–X bond cleavage and the stability of R·. The alternative path is the S_N reaction in the coordination sphere of the iron(II) ion. The ligand-ligand reaction gives the observed solvolysis products, such as benzaldehyde, benzyl alcohol, and cinnamyl alcohol.

Finally, it should be added that the present reagent is effective in inducing vicinal dehalogenation; this is exemplified by the reaction of stilbene dihalides as well as by that of benzalacetophenone dibromide.

Experimental

All the melting points are uncorrected. The mass spectra were determined on a Hitachi RMU-6L spectrometer, and the NMR spectra, on a JEOL C-60-H spectrometer, in $CDCl_3$ or CCl_4 solution at 60 MHz. The microanalyses were performed at the Elemental Analyses Center of Kyoto University.

General Procedure of Reactions of Organic Halides with Iron(II) Chloride Tetrahydrate in DMSO. Iron(II) chloride was dissolved in freshly-distilled (over CaH_2) DMSO under a nitrogen atmosphere so as to give a *ca.* 1 M solution upon heating with stirring at 60—70°C for 30 min; then the solution was maintained at an appropriate reaction temperature (20—80°C). A solution (*ca.* 0.4 M) of an organic halide in DMSO was then added to this drop by drop. The atomic ratio of halogen: Fe(II) was taken to be 1:2.5 unless otherwise stated. Heating and stirring were continued until TLC indicated the absence of the halide. The mixture was then treated with water and extracted with ether or benzene. The extract was washed with water, dried (Na_2SO_4), and concentrated *in vacuo*. The products were separated and identified as usual. The following description refers to cases which cannot be covered sufficiently by Table 1.

Dechlorination of Dichlorodiphenylmethane. Dichlorodiphenylmethane (1.18 g, 0.005 mol) was treated with a solution of iron(II) chloride (1.00 g, 0.005 mol) in DMSO (30 m*l*) at 20—30°C for 16 hr. The reaction products were washed with MeOH. The recrystallization of the resulting crystalline product from benzene-EtOH (1:1) gave 1,2-dichloro-1,1,2,2-tetraphenylethane (0.65 g, 65%), mp (decomp.) 175—178°C (lit,[6] 184—186°C), which was identified by elemental analyses and by comparison with an authentic sample (IR, MS). The further dehalogenation of the dichloride with iron(II) chloride in DMSO yielded tetraphenylethylene. The concentration of the filtrate gave benzophenone (0.20 g, 22%). In another run, dichlorodiphenylmethane (2.50 g, 0.011 mol) was treated with a solution of iron(II) chloride (10.6 g, 0.053 mol) in DMSO (50 m*l*). The crude product was washed with MeOH and recrystallized from benzene-EtOH (1:1) to afford tetraphenylethylene (1.43 g, 82%), mp 220—222°C (lit,[7] 222—224°C).

Dechlorination of Benzotrichloride. Benzotrichloride (2.00 g, 0.010 mol) was treated with a solution of iron(II) chloride (2.48 g, 0.012 mol) in DMSO (20 m*l*) at 60°C for 27 hr. A work-up gave α,α,α′,α′-tetrachlorobibenzyl (1.40 g, 85%), mp and mixed mp 159—160°C (EtOH) (lit,[8] 160—161°C), which was identified by means of its IR spectra. Tetrachlorobibenzyl (1.50 g, 0.005 mol) was treated with a solution of iron(II) chloride (10.0 g, 0.050 mol) in DMSO (50 m*l*) at 90°C for 17 hr. Chromatography on a short alumina column, followed by recrystallization (EtOH), afforded a mixture (1.17 g, 94%) of *cis*- and *trans*-α,α′-dichlorostilbene. Hand-sorting and recrystallizations gave pure constituents, the *cis* isomer as prisms, mp and mixed mp 60—62°C (lit,[9] 62—63°C), and the *trans* isomer as powdery microcrystals, mp and mixed mp 137—138°C (lit,[9] 142°C). The yields (*cis* 76%, *trans* 18%) were calculated on the basis of the product ratio determined by GLC (Apiezon L 30%).

Hydrolysis of Benzyl Chloride. Benzyl chloride (1.27 g, 0.010 mol) was treated with a solution of iron(II) chloride (4.98 g, 0.025 mol) in DMSO (30 m*l*) at 80—90°C for 20 hr, when TLC indicated the absence of benzyl chloride. The work-up of the mixture gave benzyl alcohol (0.75 g, 69%). However, the treatment of benzyl chloride (1.27 g, 0.010 mol) with EtOH (6 m*l*) and iron(II) chloride (1.99 g, 0.010 mol) in DMSO (30 m*l*) at 80—90°C, followed by a further usual work-up, gave benzyl ethyl ether (0.96 g, 70%). The treatment of benzyl chloride at 20°C gave no products but the starting material.

The authors are grateful to Professor Keiiti Sisido for his generous help. Financial support from the Minitstry of Education, Japanese Government, and from Toray Science Foundation is acknowledged with pleasure.

6) M. S. Kharasch and H. C. Brown, *J. Amer. Chem. Soc.*, **61**, 3432 (1939).
7) "Org. Syntheses," Coll. Vol. 4. p. 914. (1963).
8) D. C. Sayles and M. S. Kharasch, *J. Org. Chem.*, **26**, 4210 (1961).
9) H. Staudinger, *Ber.*, **49**, 1969 (1916).

BULLETIN OF THE CHEMICAL SOCIETY OF JAPAN, VOL. 44, 1996—1997 (1971)

Hydrogen Bonding in Sodium Tetrachloroaurate(III) Dihydrate and Sodium Tetrachloroiodate(III) Dihydrate

Kakuko ICHIDA, Yoko KURODA, Daiyu NAKAMURA, and Masaji KUBO
Department of Chemistry, Nagoya University, Chikusa, Nagoya

(Received February 24, 1971)

We have discussed the formation of O–H···Cl hydrogen bonds in the crystals of sodium tetrachloroaurate(III) dihydrate in connection to the positive temperature coefficient of nuclear quadrupole resonance frequency of chlorine in this compound.[1,2] An X-ray crystal analysis carried out by Bonamico *et al.*[3] has shown that one of the four chlorine atoms in an $AuCl_4^-$ ion is separated from two oxygen atoms by the shortest O···Cl distance of 3.36 Å and from two other oxygen atoms by the second shortest distance equal to 3.42 Å. Chlorine atoms of this type are responsible for the unusual temperature dependence of quadrupole resonance.[1] Although hydrogen atoms have not been located, it is conceivable that the chlorine atoms in question is involved in weak hydrogen bonds with four water molecules. In fact this is the key point for explaining the positive temperature coefficient mentioned above.

However, the O···Cl distance is appreciably longer than the sum of van der Waals radii, 3.2 Å. This presents a debatable problem in view of the accepted belief that a hydrogen bond, X–H···Y, is surely formed when the X···Y distance is shorter than the sum of van der Waals radii.[4]

The frequency shift of X–H stretching vibration presents another criterion for the formation of hydrogen bonds. Therefore, we have observed the infrared absorption of this compound at room and liquid-nitrogen temperatures. Samples were run as Nujol or hexachlorobutadiene mulls. Measurements were performed in the frequency range from 4000 to 700 cm^{-1}, using a JASCO DS-402G spectrophotometer.

At room temperature, three bands were observed at 3575, 3516, and 1618 cm^{-1}. Undoubtedly they are due to the intramolecular vibrations of water molecules because they show normal frequency shifts on deuteration. At liquid-nitrogen temperature, the frequencies and band shapes were practically unaltered in agreement with the results of our NQR study indicating that no phase transition takes place in the temperature range investigated. Although there are eight water molecules in a unit cell, vibrational coupling among them seems to be inappreciable, because no bands were split even at liquid-nitrogen temperature. Therefore the three bands were assigned to the antisymmetric stretching γ_3, symmetric stretching γ_1, and bending γ_2 of a water molecule, respectively.

Heavily but incompletely deuterated samples yielded a single band at 3545 cm^{-1} in place of the bands, γ_3 and γ_1 of undeuterated samples. The band is attributable to the γ_3 mode of HDO molecules diluted in D_2O molecules. The frequency is very close to the mean value of γ_3 and γ_1 of undeuterated water molecules. Since the vibration is almost free from coupling, the vibrational frequency is used for the following discussion on the O–H stretching frequencies of water molecules in various compounds.

The observed O–H stretching frequency, 3545 cm^{-1}, is significantly higher than those of water molecules, 3275 cm^{-1} in ice[5] and 3450 cm^{-1} in calcium sulfate dihydrate,[6] but is still lower than 3707.5 cm^{-1} of water vapor[7] and 3624 cm^{-1} of water molecules very loosely bound in the crystals of beryl.[8] A frequency shift of about 160 cm^{-1} from the frequency of water vapor provides an evidence in support of the formation of weak hydrogen bonds in the crystals of sodium tetrachloroaurate(III) dihydrate.

Attempts have been made to correlate the frequency shift $\Delta\gamma=\gamma^0_{XH}-\gamma_{XH}$ with the distance R between heavy atoms in hydrogen-bonded systems, X–H···Y. Here γ^0_{XH} refers to X–H stretching free from hydrogen bonding and γ_{XH} stands for the X–H frequency in the hydrogen-bonded systems. Lippincott and Schroeder[9] first succeeded in reproducing an asymptotic approach of $\Delta\gamma$ toward zero for large R by use of a semiempirical potential function proposed by themselves.

$$\frac{\gamma_{XH}}{\gamma^0_{XH}} = \left\{ r_0 e^{-\alpha}\left[r_0^2 - \frac{\alpha}{2}(r+r_0)^2\right]/r^3 + r_0^* \frac{D_0^* n^*}{D_0 n} e^{-\beta}\left[r_0^{*2} - \frac{\beta}{2}(r^*+r_0^*)^2\right]/r^{*3} \right\}^{1/2} \quad (1)$$

$$\alpha = n(r-r_0)^2/2r$$

$$\beta = n^*(r^*-r_0^*)/2r^*$$

where r is the X–H distance in a hydrogen-bonded system, r_0 is the corresponding values in an X–H system free from hydrogen bonding, D_0 is the dis-

1) A. Sasane, T. Matuo, D. Nakamura, and M. Kubo, This Bulletin, **43**, 1908 (1970); *J. Magn. Resonance*, **4**, 257 (1971).
2) C. W. Fryer and J. A. S. Smith, *J. Chem. Soc., A*, 1029 (1970).
3) M. Bonamico, G. Dessy, and A. Vaciago, *Atti Accad. Nazl. Lincei, Rend., Classe Sci. Fis., Mat. Nat.*, **39**, 504 (1965).
4) G. C. Pimentel and A. L. McClellan, "The Hydrogen Bond," W. H. Freeman, San Francisco (1960); W. C. Hamilton and J. A. Ibers, "Hydrogen Bonding in Solids," Benjamin, New York (1968).
5) D. F. Hornig, H. F. White, and F. P. Reding, *Spectrochim. Acta*, **12**, 338 (1958); C. Haas and D. F. Hornig, *J. Chem. Phys.*, **32**, 1763 (1960).
6) V. Seidl, O. Knop, and M. Falk, *Can. J. Chem.*, **47**, 1361 (1961).
7) W. S. Benedict, N. Gailar, and E. K. Plyler, *J. Chem. Phys.*, **24**, 1139 (1956).
8) D. L. Wood and K. Nassau, *ibid.*, **47**, 2220 (1967).
9) E. R. Lippincott and R. Schroeder, *ibid.*, **23**, 1099 (1955); R. Schroeder and E. R. Lippincott, *J. Phys. Chem.*, **61**, 921 (1957).

sociation energy of the X–H bond, and n is a semi-empirical parameter. Asterisks refer to the H···Y bond. Since the value of r is given as a function of R,[9] the dependence of the frequency shift on R can be obtained.

Recently, Bellamy and Owen[10] proposed a simple empirical relationship between $\Delta\gamma$ and R on the basis of the Lennard-Jones 6-12 potential function.

$$\Delta\gamma\ (\mathrm{cm^{-1}}) = 50[(d/R)^{12} - (d/R)^{6}] \qquad (2)$$

where d is the distance at which the potential energy curve intersects the abscissa.

The validity of Eqs. (1) and (2) has been checked especially for O–H···O systems, for which a large number of available data cover a wide range of R. For O–H···Cl systems, only hydroxylamine hydrochloride (R=2.99 Å) and chloral hydrate (3.15 Å) are cited in the original papers.[9,10] No evidence has been obtained for confirming that these equations are valid also for hydrogen bonding in inorganic chloride hydrates having a relatively large value of R.

Figure 1 shows the O–H stretching frequencies of

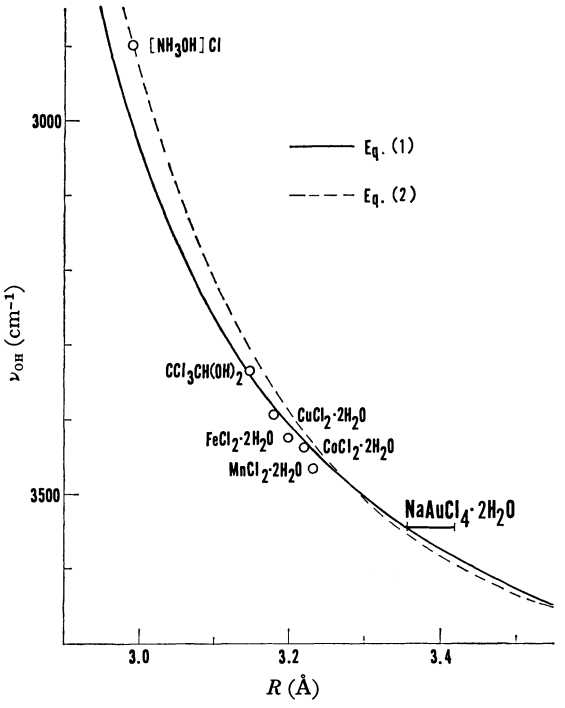

Fig. 1. O–H stretching frequency of hydrogen-bonded water molecules in various inorganic chloride hydrates plotted against the O···Cl hydrogen-bonded distance.

$CuCl_2\cdot 2H_2O$,[11] $CoCl_2\cdot 2H_2O$, $FeCl_2\cdot 2H_2O$, and $MnCl_2\cdot 2H_2O$[12] as observed for HDO species plotted against the O···Cl distance.[13,14] These crystals are particularly suitable to the present purpose, because each of them contains only one kind of water molecules and also beacuse they are isomorphous with one another except for the copper compound. Figure 1 shows two theoretical curves for the O–H···Cl systems quoted from the original papers also.[9,10] Both curves are drawn with γ^0_{OH} equal to 3700 $\mathrm{cm^{-1}}$. Agreement between theoretical and experimental data is excellent, indicating that relations (1) and (2) can be used for discussing hydrogen bonding in inorganic chloride hydrates having a relatively large value of R.

The O–H stretching frequency of sodium tetrachloroaurate(III) dihydrate is shown by a horizontal line in the figure in order to take into account two observed O···Cl distances possibly involved in hydrogen bonding. Since its deviation from the theoretical curves is rather trivial, it is concluded that although the hydrogen bonding is weak, the nature of the hydrogen bonds is essentially the same as those in other compounds mentioned above. The O···Cl distances are longer than the sum of van der Waals radii, but are considerably shorter than d (=3.85 Å) defined by Bellamy and Owen, which is very close to the sum of collision radii, 3.81 Å, of gas molecules. This implies that water molecules are bonded to $AuCl_4^-$ ions in this compound mainly by electrostatic and van der Waals forces.

Sodium tetrachloroiodate(III) dihydrate has been known to form crystals isomorphous with sodium tetrachloroaurate(III) dihydrate.[1] However, the crystal structure has not been determined in detail as yet. We have recorded the infrared spectra of this compound at liquid-nitrogen temperature, and observed bands at 3577, 3515, and 1611 $\mathrm{cm^{-1}}$ attributable to γ_3, γ_1, and γ_2 of water molecules, respectively. These values agree almost perfectly with those of water in sodium tetrachloroaurate(III) dihydrate. This fact indicates that weak O–H···Cl hydrogen bonds are formed in the crystals as in the case of sodium tetrachloroaurate(III) dihydrate and that the O···Cl distances are practically the same in these two compounds.

10) L. J. Bellamy and A. J. Owen, *Spectrochim. Acta*, **25A** 329 (1969).

11) R. A. Fifer and J. Schiffer, *J. Chem. Phys.*, **50**, 21 (1969).

12) R. A. Fifer and J. Schiffer, *ibid.*, **52**, 2664 (1970).

13) D. Harker, *Z. Krist.*, **93**, 136 (1936); S. W. Peterson and H. A. Levy, *J. Chem. Phys.*, **26**, 220 (1957).

14) B. Morosin and E. J. Graeber, *J. Chem. Phys.*, **42**, 898 (1965); B. Morosin, *ibid.*, **44**, 252 (1966).

SHORT COMMUNICATIONS

The Rearrangement of 2-Hydroxy-3,4-bis(diphenylmethylene)-cyclobutanone to the Enolizable Cyclobutenedione, 3,4-Bis(diphenylmethyl)-3-cyclobutene-1,2-dione *via* Methylenecyclobutenone Intermediate

Fumio Toda, Nobuhiro Ooi, Yoshikazu Takehira, and Katsuhiko Akagi
Department of Chemistry, Faculty of Engineering, Ehime University, Matsuyama
(Received March 3, 1971)

In the course of our studies of the reactions of 2,3-dimethylenecyclobutanones with a base, we have found that the title cyclobutanone (I)[1] dissolves in aqueous KOH easily and that the acidification of the solution affords the title cyclobutenedione (III) as colorless prisms in a 62% yield, mp 130—131°C. The structure of III was determined by means of the spectral data: λ_{max} (CH_3CN) 258 sh (8200), 265 sh (6600) and 271 sh nm (ε, 5300); ν_{max} (Nujol) 1790 and 1770 (unsplit doublet, CO) and 1580 cm^{-1} (C=C); NMR ($CDCl_3$) 2.5—3.0 (m, Ph, 20H), and 4.73 τ (s, CH, 2H). The oxidation of III with neutral H_2O_2 afforded the corresponding anhydride, bis(diphenylmethyl)maleic anhydride (IV), in a 71% yield, mp 171—172°C. It is well established that cyclobutenediones undergo a Bayer-Villiger-type oxidation with neutral H_2O_2 to give the corresponding maleic anhydrides.[2]

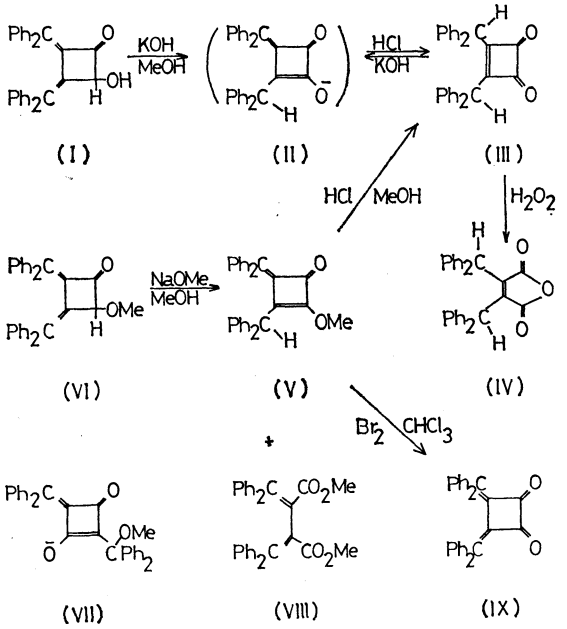

The dione III also dissolved in aqueous KOH and even in aqueous $NaHCO_3$, from which III was recovered quantitatively by acidification. Since the electronic spectrum of an alkaline solution of III (or of I) showed an absorption band at 330 nm (ε, 21700) which is comparable to that of the analogous anion VII obtained by dissolving 2,4-bis(diphenylmethylene)-cyclobutanedione in MeOH-KOH, 324 nm (ε, 24600),[3] the structure in the alkaline media may be said to be II. The acidification of a solution of III (or of I) in KOD-D_2O-MeOD (prepared by the addition of D_2O to MeONa in MeOD) with DCl-D_2O afforded III-d_2, which showed no methine proton signal in the NMR spectrum. Under neutral conditions, however, neither I nor III exchanged its methine hydrogen with deuterium by recrystallization from MeOD.

The rearrangement of I into II is likely, since the treatment of VI[4] with NaOMe in MeOH at room temperature afforded the rearranged product, V, as colorless prisms in a 30% yield, mp 126—127°C, in addition to the diester, VIII, as yellow needles in a 43% yield, mp 233—234°C. The structure of V was identified by means of the spectral data: λ_{max} (EtOH) 293 nm (ε, 17600); ν_{max} (Nujol) 1760 (CO), 1650 (*exo* C=C), and 1590 cm^{-1} (*endo* C=C); NMR ($CDCl_3$) 2.6—3.2 (m, Ph, 20H), 5.53 (s, CH, 1H), and 5.95 τ (s, OMe, 3H). The structure of V was further identified by the following reactions. The treatment of V in $CHCl_3$ with bromine afforded IX[5] in a 30% yield. The treatment of V in MeOH with hydrogen chloride afforded III in a 64% yield.

The cyclobutenediones which have been reported to date are all sensitive to the base and all undergo ring-cleavage.[2] The enolization of III in alkaline media without decomposition differs widely from these facts.

When the reaction of VI with NaOMe in MeOH was carried out under a nitrogen atmosphere, the major product was V (65%), and the minor one was VIII (1%). On the other hand, the treatment of V with NaOMe under an oxygen atmosphere afforded VIII in a 40% yield. On the basis of these results and the observation that 1,2-bis(diphenylmethylene)cyclobutene reacts with oxygen to afford 2,3-bis(diphenylmethylene)-butanedial quantitatively,[6] a possible reaction path leading to VIII is as follows:

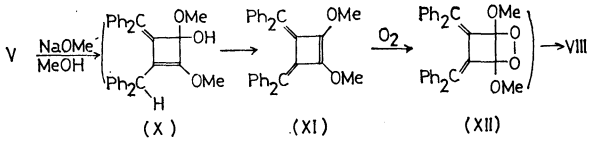

1) F. Toda, N. Ooi, and K. Akagi, unpublished data.
2) M. P. Cava and M. J. Mitchell, "Cyclobutadiene and Related Compounds," Academic Press, New York and London (1967), pp. 128—156.
3) G. A. Taylor, *J. Chem. Soc., C*, **1969**, 1755.
4) F. Toda and K. Akagi, *Tetrahedron*, in press.
5) F. Toda, H. Ishihara, and K. Akagi, *Tetrahedron Lett.*, **1969**, 2531.
6) F. Toda, M. Higashi, and K. Akagi, *Chem. Commun.*, **1969**, 1219.

Ambident Ion. IV. *C*-Alkylation of Enolate Anion Accompanying Retention of Configuration

Masakazu SUAMA, Toshio SUGITA, and Katsuhiko ICHIKAWA

Department of Hydrocarbon Chemistry, Faculty of Engineering, Kyoto University, Yoshida, Sakyo-ku, Kyoto

(Received March 22, 1971)

Recent report by Sommer and Korte[1] showed that charge-delocalized organolithium reagent coupled with optically active secondary halides with nearly complete inversion of configuration. According to Hart,[2] *C*-alkylation of phenoxide ion also proceeds with inversion of configuration. We wish to report our findings which are in sharp contrast to these results. Reaction of *sec*-butyl bromide with alkali metal salts of methyl acetoacetate and acetylacetone gives *C*- and *O*-alkylated products.[3]

$$(CH_3COCHCOR)^-M^+ + \textit{sec}\text{-BuBr} \longrightarrow \underset{\text{(I)}}{CH_3COCH(Bu^s)COR} + \underset{\text{(II)}}{CH_3C(OBu^s)=CHCOR} + MBr$$

a:R=OMe b:R=Me

Results with the optically active bromide in DMSO are given in Tables 1 and 2. Absolute configurations of optically active I and II, which are not known so far, have been determined in correlation with III and IV through the following reaction sequences:

$$(+)\ \underset{\text{MeC*HEt (Ia)}}{CH_3COCHCO_2CH_3} \xrightarrow[\text{2) H}^+]{\text{1) 5\% NaOH, 25°C}} (-)\ CH_3COCH_2C^*HMeEt\ \text{(III)}$$

$$(+)\ \underset{\text{MeC*HEt (Ib)}}{CH_3COCHCOCH_3} \xrightarrow{\text{20\% KOH, 40°C}} (-)\text{-III}$$

$$(+)\ \underset{\text{OC*HMeEt}}{CH_3C{=}CHCOR} \xrightarrow[\text{2) H}_2O]{\text{1) O}_3\text{ in CHCl}_3} \underset{\text{(II)}}{} (+)\ CH_3CO_2C^*HMeEt\ \text{(IV)}$$

It has been established that Ia and Ib have (−) R and IIa and IIb have (+) S structures.[4] The results show that *C*-alkylation proceeds with retention of configuration. The extents of the retention should be much higher (25—50%) than the observed values (Table 2), since control experiments showed that the starting active butyl bromide racemizes in the presence of metal halides which are formed by the reaction. This indicates that *C*-alkylation is not a simple S_N2 reaction by free carbanion species, and that some front-side attack to asymmetric center must have occurred. On the other hand, in the *O*-alkylation of sodium salts, taking the rate of racemization of the bromide into consideration, the results show almost complete inversion of configuration which suggests a typical S_N2 reaction of enolate anion (Table 2).

These stereochemical results show that *C*- and *O*-*sec*-butylations are not simple competitive reactions through a common transition state.[6] For a more detailed discussion, precise stereochemical and kinetical investigations are necessary.

TABLE 1. *sec*-BUTYLATION OF SODIUM AND LITHIUM ENOLATES BY OPTICALLY ACTIVE BROMIDE IN DMSO (50 g)

Exp.	Enolate	mmol	*sec*-Bu*Br mmol	Temp. °C	Time hr	Alkylates % I	Alkylates % II	Total Yield%
1	$(CH_3COCHCO_2CH_3)^-Na^+$	20	19	60°	41	48	52	65
2	$(CH_3COCHCO_2CH_3)^-Na^+$	31	31	50—55°	51	46	54	51
3	$(CH_3COCHCOCH_3)^-Na^+$	20	19	60°	42	26	74	54
4	$(CH_3COCHCO_2C_2H_5)^-Li^+$	32	33	50—55°	87	59	41	31

TABLE 2. STEREOCHEMICAL RESULTS OF *C*- AND *O*-ALKYLATION

Exp.	(−)R-*sec*-BuBr		(+)R-*C*-Alkylate			(+)S-*O*-Alkylate		
	α_D^{25},a)	Opt. Pur.c)	$[\alpha]_D^{25}$,b)	Opt. Pur.d)	Retention	$[\alpha]_D^{25}$,b)	Opt. Pur.e)	Inversion
1	12.52°	29.2%	+0.97°	3.2%	11%	+4.3°	19%	66%
2	11.72°	27.3%	——	2.7%	10%	+4.9°	23%	66%
3	12.52°	29.2%	+1.4°	4.5%	15%	+5.1°	18%	62%
4	11.72°	27.3%	+4.5°	6.0%	20%	+2.4°	10%	23%

a) Neat, l=1 dm. *b*) Solvent $CHCl_3$, c=5∼15. *c*) Based on a calculated maximum value of α_D −42.92°.[5] *d*) Calculated by the measured $[\alpha]_D$ of III and $[\alpha]_{D\,max}$ 9.9°.[4] *e*) Calculated by $[\alpha]_D$ of IV and $[\alpha]_{Dmax}$ 25.07°.[4]

1) L. H. Sommer and W. D. Korte, *J. Org. Chem.*, **35**, 22 (1970).

2) H. Hart and H. S. Eleuterio, *J. Amer. Chem. Soc.*, **76**, 516 (1954), reported *O*-alkylation 100% inversion and *C*-alkylation 56—82% inversion of configuration.

3) M. Suama and K. Ichikawa, *Nippon Kagaku Zasshi*, **92**, 252 (1971).

4) F. Nerdel and E. Henkel, *Chem. Ber.*, **86**, 1002 (1953). (+)S-4-methyl-2-hexanone, $[\alpha]_{D\,max}^{20}$+9.9° (neat, d 0.820). R. H. Pickard and J. Kenyon, *J. Chem. Soc.*, **105**, 830 (1914). (+)S-*sec*-butyl acetate, $[\alpha]_D^{20}$ 25.43° (neat, *d* 0.873), 25.07° ($CHCl_3$, *c* 5), 25.87° (EtOH, *c* 5).

5) D. G. Goodwin and H. R. Hudson, *J. Chem. Soc., B*, **1968**, 1333.

6) N. Kornblum, R. A. Smiley, R. K. Blackwood, and D. C. Iffland, *J. Amer. Chem. Soc.*, **77**, 6269 (1955).

The Reaction of Photo-excited Phenanthraquinone with Hydrogen Donors.[1] The Behaviors of the Resulting 1,2-Photo-adducts Studied by the CIDNP Technique

Kazuhiro MARUYAMA, Tetsuo OTSUKI, Heisaburo SHINDO,* and Tetsuo MARUYAMA*

Department of Chemistry, College of Liberal Arts and Science, Kyoto University, Kyoto

* *JEOL(USA) Inc., 235 Birchwood Avenue, Cranford, N.J. 07016, USA*

(Received March 24, 1971)

Strongly-enhanced PMR absorption signals due to the underlined proton of the 1,2-photo-adduct have been observed in the photochemical reaction of phenanthraquinone with alkyl aromatics *via* a radical in the electronic triplet state (Eq. (1)).[2]

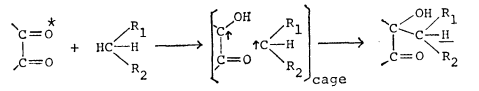

(1)

(I): $R_1=R_2=C_6H_5$, (II): $R_1,R_2=$ C_6H_4–C_6H_4

(III): $R_1,R_2=$ C_6H_4–O–C_6H_4

On the contrary, when 1,2-photo-adducts, especially those produced from the reaction of phenanthraquinone with diphenylmethane (I), fluorene (II), and xanthene (III), were heated in an NMR probe at a suitable temperature, we observed a strong, enhanced PMR emission signal at exactly the same position as was observed in the process described in Eq. (1). The optimal temperature to observe the strongest emission signal was at 150°C, 175°C, and 110°C respectively for I, II, and III (Fig. 1). Accompanying such a phenomenon, the 1,2-photo-adduct promptly decomposed to give phenanthraquinhydrone as black purple crystals and the dimer of the alkyl aromatic moiety.[4]

These exciting phenomena appear to be caused by the process described in Eq. (2); that is, the 1,2-photo-adduct is thermally activated to give the radical pair in the electronic singlet state in a solvent cage (the rate of k_1). The radical pair produced will be stabilized by the two competitive routes; the reverse reaction to the adduct, and the decomposition reaction out of the solvent cage (the rates of k_{-1} and k_2 respectively). Thus, the methine proton (underlined) of the reproduced adduct will be polarized with inversely-populated

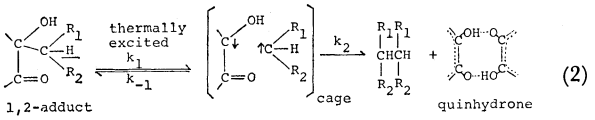

(2)

When $k_1 \simeq 0$ and/or $k_2 \gg k_{-1}$, we were not able to observe such a strong enhanced emission signal. Although the spin states to those in the process described in Eq. (1). enhanced absorption or emission PMR spectra observed here are compatible with those predicted by the CKO theory,[5] no such typical representation as in our experiments has ever been reported.

Furthermore, when the 1,2-photo-adduct was irradiated with and without a yellow filter (Kenko L40C UV cut filter) with a 500 W high-pressure Hg lamp at a suitable temperature just before thermal decomposition takes place, for example, at 125°C for I in neat diphenylmethane, it was found that an enhanced PMR absorption signal of the same methine proton (about 10 times the normal signal intensity) can be observed. At this temperature, the signal intensity of normal signal does not change between before and after irradiation. This phenomenon seems to be explainable by taking into account the process described in Eq. (3)

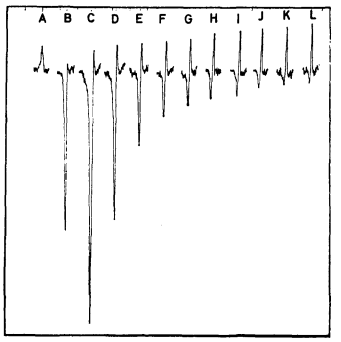

Fig. 1 Enhanced PMR emission signals (247 Hz down-field from TMS) observed in the course of thermal decomposition of 1,2-photo-adduct obtained from phenanthraquinone and xanthene (solvent:*o*-dichlorobenzene, 110°C). Signals (from **A** to **L**) were measured for every 10 sec. **A**: normal signal immediately after sample was inserted into an NMR probe. **B,C,D**……: enhanced PMR emission signal after thermal decomposition started, and the other signal due to proton of decomposition product begins to appear at a slightly upper field.

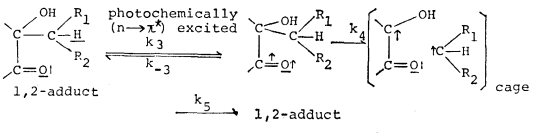

(3)

1) This work has been done at the Department of Chemistry, College of Liberal Arts and Science, Kyoto University.

2) K. Maruyama, H. Shindo, and T. Maruyama, This Bulletin, **44**, 585 (1971); K. Maruyama, H. Shindo, T. Otsuki, and T. Maruyama, *ibid.*, submitted for publication.

3) In the photo-excited triplet state.

4) This was confirmed both chemically and spectroscopically.

5) G. L. Colss and A. D. Trifunac, *J. Amer. Chem. Soc.*, **91**, 4554 (1969); **92**, 2183, 2186 (1970); G. L. Closs, C. E. Doubleday, and R. D. Paulson, *ibid.*, **92**, 2185 (1970); R. Kaptein and L. J. Oosterhoff, *Chem. Phys. Lett.*, **4**, 195, 214 (1969).

The Carbonylation of Alkyl Halide with Carbon Monoxide in the $SbCl_5$-Liquid Sulfur Dioxide System

Masatomo NOJIMA, Koichi TATSUMI, and Niichiro TOKURA

Department of Applied Chemistry, Faculty of Engineering, Osaka University, Suita, Osaka

(Recieved March 24, 1971)

The synthesis of several carboxylic acids or esters from olefins and alkyl halides with carbon monoxide, and water or alcohol catalyzed by acid catalysts has been studied by many investigators.[1a] Simon and Warner have reported the reaction in hydrogen fluoride with water, which gave isobutyric acid from isopropyl chloride.[1b]

Considerable success in this synthesis has been won by Koch and Haaf using formic acid as the source of carbon monoxide and sulfuric acid as the catalyst.[2] In spite of the applicability of the Koch method to a great variety of compounds, this reaction is accompanied by the considerable isomerization of the double bond and the carbon skeleton, which diminishes the utility of this method from the point of view of preparation.

To carry out the carbonylation under milder conditions, the present authors attempted the carbonylation of alkyl halides in the $SbCl_5$-liquid SO_2 system at $-70°C$ under atmospheric pressure. The selectivity of the reaction and the skeletal rearrangement of the substrate are also examined using mono- and dihalogeno-substituted cyclohexane derivatives. The reaction scheme is as follows:

$$RX + CO + ROH \xrightarrow[SbCl_5+SO_2]{1\,atm\ -70°} RCOOR + HX \quad (1)$$

A typical procedure is as follows. To a mixture of 20 g (0.07 mol) of $SbCl_5$ and 50 m*l* (about 0.5 mol) of liquid SO_2, a solution of 4.6 g (0.05 mol) of *t*-butyl chloride and 3.7 g (0.08 mol) of ethanol, dissolved in 20 m*l* of dichloromethane, was dropped at $-70°C$ over a thirty-minute period while a current of carbon monoxide gas was bubbled into the flask at a velocity of 70 m*l* per minute, after which the reaction was continued for thirty additional minutes. The reaction mixture was treated following the ordinary method; subsequent analysis by vpc showed the existence of only one product, the pivalic acid ethyl ester (4.2 g (66%)). All the products obtained were characterized by NMR, infrared, and mass spectroscopy.

The results obtained are summarized in Table 1. When a tertiary alkyl halide was used as the substrate the ester corresponding to the starting material was obtained in a fair yield without the isomerization of the carbon skeleton. A control experiment without liquid SO_2 gave no carbonylated product. The secondary halide reacted upon isomerization, and the yield of the corresponding ester was depressed as a result of the skeletal transformation. Moreover, the following facts are worth noting.

Table I. Reactions of alkyl halide with carbon monoxide

Halide	Product, (Yield %) [a]
$(CH_3)_3CCl$	$(CH_3)_3CCO_2C_2H_5$ (66)
$(CH_3)_2\underset{Br}{C}H\underset{O}{\overset{\|}{C}}CH_3$	$(CH_3)_2\underset{CO_2C_2H_5}{C}H\underset{O}{\overset{Cl}{\overset{\|}{C}}}CH_3$ (63)
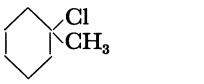	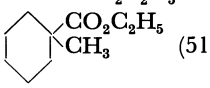 (51)
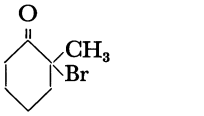	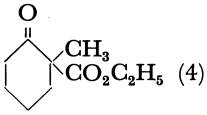 (4) 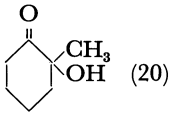 (20)
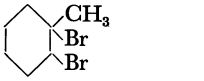	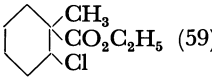 (59)
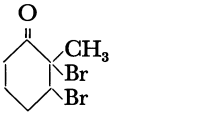	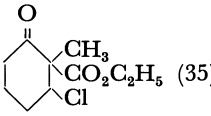 (35)
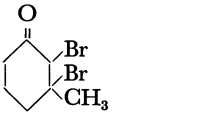	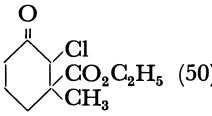 (50)
	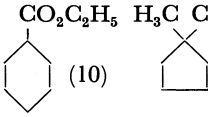 (10) 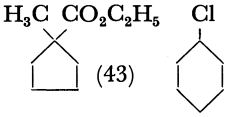 (43) 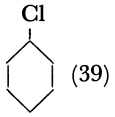 (39)
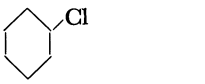	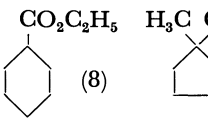 (8) 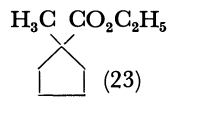 (23)
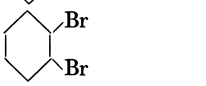	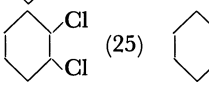 (25) 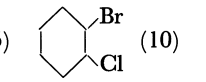 (10)
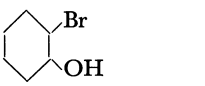	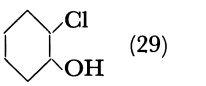 (29)
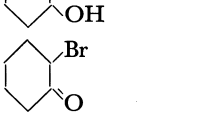	No Reaction

a) The products were analyzed by gas-liquid partition chromatography and characterized by NMR, IR, and mass spectra.

(1): The compound with vicinal dibromo substituents, one a tertiary, and the other, a secondary, bromide, reacts only with the tertiary bromide to yield the corresponding ester, while the secondary bromide exchanges its bromine with the chlorine atom by the reaction with antimony chloride.

(2): The reactivity of the tertiary and the secondary bromides in the neighborhood of a substituent such as a carbonyl group is greatly diminished in the carbonylation reaction.

1) a) G. A. Olah, "Friedel Crafts and Related Reactions," Vol. III, Part II, ed. by G. A. Olah, Interscience Publishers, New York (1964), p. 1257; b) J. H. Simons and A. C. Werner, *J. Amer. Chem. Soc.*, **64**, 1356 (1942).

2) H. Koch and W. Haaf, *Ann. Chem.*, **618**, 251 (1958).

Dimerization of C_2D_4 Catalyzed by Bis(triphenylphosphine)-σ-1-naphthyl Nickel (II) Bromide

Ken-ichi MARUYAMA, Tetsufumi KUROKI, Tsutomu MIZOROKI, and Atsumu OZAKI

Research Laboratory of Resources Utilization,
Tokyo Institute of Technology, Ookayama, Meguro-ku, Tokyo

(Received April 3, 1971)

It has been reported that bis(triphenylphosphine)σ-arylnickel (II) bromide catalyzes the selective dimerization of ethylene in the presence of boron trifluoride etherate in dry methylene chloride or benzene solution.[1] This catalyst system contains no substance such as alkylaluminum[2] or alkyllithium which is likely to provide a nickel hydride. We must clarify whether ethylene dimerization is catalyzed by a nickel hydride formed during the reaction and what substance supplies the hydrogen to the nickel complex if the nickel hydride is formed. For this purpose we studied the isotopic exchange between C_2H_4 and C_2D_4 and between C_2D_4 and other chemical species involved in the reaction system of the dimerization.

The isotopic exchange of C_2H_4–C_2D_4 (1:1) was carried out at 0°C for 5 or 10 min, using bis(triphenylphosphine)σ-1-naphthyl nickel (II) bromide (0.20 mmol) in the presence of boron trifluoride etherate (0.29 or 0.72 mmol) in dry methylene chloride (10 m*l*). Concurrent dimerization of ethylene was observed as follows.

$BF_3(Et_2O)$	Reaction time	Conversion	1-C_4'	*trans*-2-C_4'	*cis*-2-C_4'
0.29 mmol	10 min	46.5%	56	30	14
0.72 mmol	5 min	55.8%	29	50	21

In either case the isotopic distribution in the residual ethylene was C_2H_4 7%, C_2H_3D 26%, $C_2H_2D_2$ 37%, C_2HD_3 24% C_2D_4 6%, which was in good agreement with equilibrium distribution. This result shows that the rate of isotopic exchange is strikingly faster than the ethylene dimerization, and that one hydrogen atom is exchanged in one act of the exchange. Thus it is concluded that there must be an active hydrogen atom which catalyzes the exchange reaction. In this case, the active hydrogen atom is very likely provided as a nickel hydride.

The source of the active hydrogen was examined by the reaction of C_2D_4 (atomic fraction of hydrogen f_H= 0.020). The reaction condition was the same as in the above reaction. The results are shown in Table 1.

TABLE 1. ATOMIC FRACTION OF HYDROGEN (f_H) IN ETHYLENE OR BUTENE AFTER THE REACTION OF C_2D_4

No.	Ni complex (mmol)	BF_3OEt_2 (mmol)	CH_2Cl_2 (m*l*)	C_2D_4 introduced	React. time	f_H
1	0.20	0.79	10	1.16	3 hr	0.022[a]
2	0.20	0.72	10	1.00	10 hr	0.024[a]
3	0.20	0.72	10	1.13	150 hr	0.023[a]
4	0.20	0.72	30	1.10	5 min	0.020[b]
5	1.0	0.72	30	1.09	5 min	0.020[b]
6	2.0	0.72	30	1.07	5 min	0.021[b]
7	1.0	3.6	30	1.06	5 min	0.020[a] 0.020[b]
8	2.0	7.2	30	1.11	5 min	0.022[b]

a) Calculated from the butene formed.
b) Calculated from the residual ethylene.

If the active hydrogen comes from the solvent or the ligand, the atomic fraction of hydrogen in ethylene or butene formed should be higher than that in the starting material (f_H=0.020). However, no appreciable increase in f_H is observed as shown in Table 1, independent of the reaction time, the amount of catalyst, and the amount of solvent, while the amount of C_2D_4 is approximately fixed. This means that no hydrogen is supplied to the nickel complex from the solvent, triphenylphosphine, 1-naphthyl ligand or diethyl ether

It is concluded that the isotopic exchange and the dimerization of ethylene is catalyzed by a nickel hydride complex which is formed by the reaction of ethylene with the nickel complex.

1) K. Maruya, T. Mizoroki, and A. Ozaki, This Bulletin, **43**, 3630 (1970).
2) M. Uchino, Y. Chauvin, and G. Lefebvre, *C. R. Acad. Sci., Paris, Ser.* **265**, 103 (1967).

Kinetics of Chelate Formation between Lanthanum(III) and 4-(2-Pyridylazo)-resorcinol

Tamio ONODERA* and Masatoshi FUJIMOTO

Department of Chemistry, Faculty of Science, Hokkaido University, Sapporo

(Received April 16, 1971)

In connection with the slowest liberation of the proton in aqueous solutions from the heavily blocked internal hydrogen bond in a series of *o*-hydroxyazo dyes as reported by Eigen *et al.*,[1,2] we report here some interesting kinetic effects of the fast formation of metal chelate ring on the rate of subsequent protolytic dissociation of an inert hydrogen bond in a ligand molecule of similar structure.

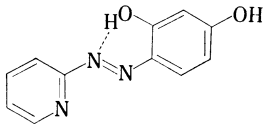

PAR

4-(2-Pyridylazo)-resorcinol (PAR)[3,4] was chosen as a typical ligand of this type requiring a prior rupture of the internal hydrogen bridge between the *o*-hydroxyl and the azo-group to form a final metal chelate of terdentate structure.[5] With the metal ions, for which the very fast substitution of the coordination water would be expected, the overall rate of chelate formation of such terdentate ligands as PAR would thus be determined by the slow rupture of the hydrogen bond. The reaction scheme is shown as follows:

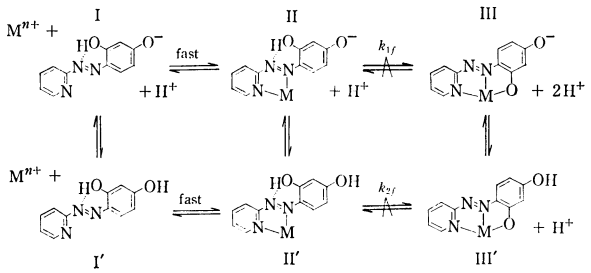

The present communication deals with the reaction of PAR with lanthanum(III) ion, the first member of the terpositive lanthanoids, which show quite regular change in ionic radii and substitute very rapidly their coordination water.[6,7] The continuous variation method showed a 1:1 complex formation. The apparent stability constant was spectrophotometrically determined to be $K=[\mathrm{LaPAR}][\mathrm{H}]/[\mathrm{La}][\mathrm{HPAR}]=10^{-3}$—$10^{-2}$ at about pH 5.9.

The rate constants for the dissociation and the recombination of the internal hydrogen bond of the ligand PAR were determined by the temperature-jump method to be $k_D=6.4\times10^5$ M^{-1}sec^{-1} and $k_R=6.2\times10^3$ sec^{-1}, respectively, at 25°C and ionic strength 0.1 ($NaClO_4$). Values of activation energy for k_D and k_R were 2.5 and 5.9 kcal·mol^{-1}, respectively.

The rate of formation of the La(III)-PAR complex was measured by the stopped-flow method in the pH range 4.2—6.2 buffered with hexamine and at 505 nm, the λ_{max} of the complex III. The rate was found to be dependent on the hydrogen ion concentrations and independent of the metal ion concentrations for the excess of lanthanum(III), suggesting the overall reaction rates determined by the slow rupture of the hydrogen bond in the steps II⇌III and II′⇌III′.

The rate constants $k_{1f}=38$ sec^{-1} and $k_{2f}=430$ sec^{-1} were obtained on the assumption that the hydrogen-bridged species II and II′ are inert as compared with the fully-chelated metal complexes III and III′. Lanthanum(III) reacts with the ligand PAR *ca.* 10^{-6} times as slow as with any ligands containing no internal hydrogen bond. The slowness in rupture of the internal hydrogen bond in the metal complex formation as compared with that in the protolysis of the free ligand can be attributed to the increased inertness of the hydrogen bond in the partly-chelated intermediates II and II′ containing two fused chelate rings.

Activation energy of the complex formation strongly suggests that the intermediates II and II′ retain the hydrogen-bonded structure of the ligand molecules and the rupture of this bond in turn constitutes the rate-determining step to form the final products III and III′. From a comparison of the rate constants of the hydrogen-bond dissociation in the ligand PAR with those of the metal complex formation, the activation energy was calculated to be 8.3 kcal·mol^{-1}, and experimentally found to be 8.1 kcal·mol^{-1}. Both values are in good agreement. Therefore, it would be reasonable to assume the given two-step mechanism involving the very fast metal chelate ring formation on the heterocyclic nitrogen atom and one of the azo-nitrogen atoms, and the subsequent slow chelate ring formation on the *o*-hydroxyl oxygen and other azo-nitrogen atoms to form the final terdentate structure with fused metal chelate rings.

The hydrogen-bonded ligand structure of PAR seriously affects the formation rate and the stability of the metal complexes.[8] The series of rare earth metal ions may reveal the influences of size and coordination requirements of the metal ions on the reaction mechanisms.

* Present address: Teijin, Ltd., Tokuyama, Yamaguchi.

1) M. Eigen and W. Kruse, *Z. Naturforsch.*, **186**, 857 (1963).

2) M. Eigen *et al.*, "Progress in Reaction Kinetics," Vol. 2, p. 285 (1964).

3) T. Iwamoto, This Bulletin, **34**, 605 (1961).

4) M. Hniličková and L. Sommer, *Collect. Czech. Chem. Commun.*, **26**, 2189 (1961).

5) A terdentate structure of the chelate is also predicted for PAR as demonstrated by the X-ray analysis of the Cu(II) complex of a similar ligand PAN [1-(2-pyridylazo)-2-naphthol]; *cf.* S. Ooi, D. Garter, and Q. Fernando, *Chem. Commun.*, **1967**, 1301.

6) G. Geier, *Ber. Bunsenges. Physik. Chem.*, **69**, 617 (1965).

7) N. Purdie and C. A. Vincent, *Trans. Faraday Soc.*, **63**, 2745 (1967).

8) Slow complex formation was also observed by the present authors between PAR and Cu(II), a d^9 element.

The Measurement of Water and Other Oxygen-containing Products in the Radiolysis of Cyclohexane Solutions of Nitrous Oxide

Ken-ichi TAKEUCHI, Kyoji SHINSAKA, Satoshi TAKAO, Yoshihiko HATANO, and Shoji SHIDA

Laboratory of Physical Chemistry, Tokyo Institute of Technology, Meguro-ku, Tokyo

(Received May 4, 1971)

Nitrous oxide has received more attention than any other solute among electron scavengers, but there is still considerable uncertainty as to the over-all mechanism of N_2 formation despite the large number of studies.[1] The difficulty in interpreting the results arises from the facts that the observed yield of N_2 is considerably greater than the expected yield of electron and that no quantitative analysis of all the oxygen-containing products formed after the decomposition of N_2O has yet been accomplished. As the oxygen-containing products, thus far, $C_6H_{11}OH$[2-4] and H_2O[5] have been reported to be formed in the cyclohexane-N_2O system.[6] The yield of $C_6H_{11}OH$, which accounted for only a small percentage of the expected yield of oxygen-containing products, was measured quantitatively. The previous measurements of H_2O, however, were quite inaccurate.[5,7,8] In the present study, the measurement of H_2O and other oxygen-containing products in the radiolysis of cyclohexane solutions of N_2O has been accurately carried out.

Cyclohexane was completely dehydrated before irradiation by using a liquid Na–K alloy. The samples, 2-m*l* portions of the cyclohexane with various N_2O concentrations, were irradiated by ^{60}Co-γ rays to a total dose of 9.2×10^{19}eV/g at room temperature. The total yields of H_2O and alcohols, denoted by ROH, were calculated stoichiometrically on the basis of H_2 yield produced by the reaction with the Na–K alloy after the removal of N_2O and radiolytic products of H_2 and N_2. The alloy, rather than either sodium or potassium alone, is preferable because the liquid alloy maintains a fresh active surface. The complete evolution of H_2 can be accomplished only if the alloy is free from its oxide, since the oxide reacts with H_2O without the liberation of H_2. The alloy was, therefore, carefully prepared in order to avoid the oxide. The accuracy of the method used for determining the total amounts of ROH was tested with several authentic samples in which a known amount of H_2O or $C_6H_{11}OH$ has been added to the completely dehydrated cyclohexane. The amount of H_2O or $C_6H_{11}OH$ added to the cyclohexane almost agreed with that computed from the yield of H_2. Especially great caution was used in the analysis of ROH containing the main product, H_2O, since the quantitative analysis of H_2O is known to be very difficult. In this experiment, good reproducibility and accuracy have been attained.[9] Furthermore, H_2O was not detected in the dehydrated cyclohexane either before or after irradiation. Oxygen-containing products other than H_2O were analyzed gas-chromatographically on a polyethyleneglycol-600 column at 100°C.

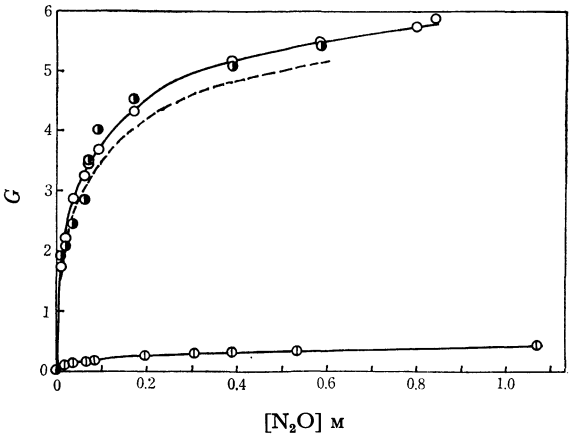

Fig. 1 Yields of N_2 (○), ROH (◑), $C_6H_{11}OH$ (⏀) and H_2O (---) from the cyclohexane-N_2O system.
The yield of H_2O is estimated by the difference between the yield of ROH and that of $C_6H_{11}OH$.

The yields of H_2 and N_2 at various N_2O concentrations approximately agree with those reported in earlier papars.[1] The yields of total ROH, $C_6H_{11}OH$ and H_2O obtained by the above method are shown in Figure 1. The yield of $C_6H_{11}OH$ approximately agrees with that previously reported.[3] The yield of total ROH surprisingly agrees with the yield of N_2 at all concentrations of N_2O. Figure 1 also shows that ROH consists of H_2O plus a small quantity of $C_6H_{11}OH$. No other oxygen-containing products, such as O_2, NO, aldehydes, ketones and ethers, were detected.

The above facts show that the decomposition of N_2O leads finally to the formation of N_2 and ROH in the ratio of one to one; this finding seems to be helpful in understanding the decomposition mechanism of N_2O in hydrocarbon solutions. Further study is now in progress.

1) J. M. Warman, K.-D. Asmus, and R. H. Schuler, *Advan. Chem. Ser.*, **82**, 52 (1968), and the references cited in.
2) R. Blackburn and A. Charlesby, *Nature*, **210**, 1036 (1966).
3) N. H. Sagert and A. S. Blair, *Can. J. Chem.*, **45**, 1351 (1967).
4) R. A. Holroyd, *Advan. Chem. Ser.*, **82**, 488 (1968).
5) S. Sato, R. Yugeta, K. Shinsaka, and T. Terao, This Bulletin, **39**, 156 (1966).
6) In other hydrocarbon-N_2O systems than cyclohexane[7,8] the formation of H_2O and alcohols were also detected.
7) A. Menger and T. Gäumann, *Helv. Chim. Acta*, **52**, 2477 (1969).
8) R. C. Koch, J. P. Houtman, and W. A. Cramer, *J. Amer, Chem. Soc.*, **90**, 3326 (1968).
9) Very recently in our laboratory the quantitative analysis of H_2O in the gas-phase radiolysis of N_2O-hydrocarbon mixtures has also been carried out gas-chromatographically.[10]
10) S. Takao, Y. Hatano, and S. Shida, This Bulletin, **44**, 873 (1971).

The Polarography of the Tricyano Cobalt(III) Complexes

Nobufumi MAKI and Kuwako OHKAWA*

Department of Chemistry, Faculty of Engineering, Shizuoka University, Johoku, Hamamatsu

(Received May 10, 1971)

Previously, several dicyano complexes of the $[Co(CN)_2N_4]$ type have been found to undergo the step-by-step reduction of Co(III)→Co(II)→Co(I)→Co(0) in DMSO (dimethyl sulfoxide) at the dropping mercury electrode (DME), where N_4 represents four nitrogen donors, which may come from two ligands, en, dip, and phen, or from four ammonia ligands.[1] However, it is not yet clear how the tricyano cobalt(III) complexes behave in DMSO. The present communication is concerned with the behavior of the *fac*- and *mer*-tricyano-diethylenetriaminecobalt(III) complexes[2] in DMSO.

These complexes were prepared by treating the $[Co(S_2O_3)_3dien]^{3-}$ ion with KCN. That is, an aqueous solution (20 m*l*) containing 8 g of KCN was stirred, drop by drop, into a mixture of $[CoCl_3dien]$ (10g) and $Na_2S_2O_3\cdot 5H_2O$ (29.6 g) dissolved in water (70 m*l*). The reaction below 5°C yielded the *mer*-complex, while that at 70—80°C produced the corresponding *fac*-complex. The former was purified by concentrating the solution of the complex *in vacuo* at room temperatures, and the latter, by crystallizing it from hot water (80°C). The purity was ascertained by elementary analyses and by studying the absorption spectra.

One would expect that the tricyano cobalt(I) complex would be present upon reduction in DMSO. Indeed, we did find that the *fac*- and *mer*-$[Co^{III}(CN)_2dien]$ complexes give rise to two well-defined waves at DME in DMSO (100%) containing 0.1 M tetraethylammonium perchlorate; the steps, each corresponding to a gain of one electron, represent the reduction of Co(III)→Co(II) and that of Co(II)→Co(I), while no further reduction to the metal takes place over the potential range between 0 and −2.7 V (*vs.* SCE). A linear-dependence of the current upon the concentration of the complex was confirmed over the range between $5\cdot10^{-4}$ and 10^{-2} M for the *fac*-isomer, and over the range between $5\cdot10^{-4}$ and $3.5\cdot10^{-3}$ M for the *mer*-isomer, since the solubility of the latter in DMSO is much smaller than the former. The current of each step was proportional to the square root of the mercury pressure on DME; the values of $i_l/\sqrt{h_{corr.}}$ were constant, irrespective of the mercury pressure, suggesting a diffusion-controlled feature.

Figure 1 illustrates the current-potential curves of the tricyano and dicyano complexes measured under the same experimental conditions. Thus, the wave-height is roughly proportional to the number of electrons participating in the electrode processes, the half-wave

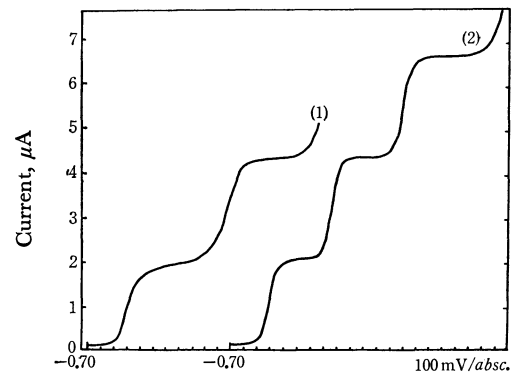

Fig. 1. Current-potential curves obtained at 10^{-3} M in DMSO containing 0.5M $[(C_2H_5)_4N]ClO_4$(25°C): (1) *mer*-$[Co(CN)_3dien]$; (2) *trans*-$[Co(CN)_2\,en_2]NO_3$.

TABLE 1. HALF-WAVE POTENTIALS OF MIXED CYANO COBALT(III) COMPLEXES IN DMSO CONTAINING 0.1M $[(C_2H_5)_4N]ClO_4$ (25°C)

Compound	1st Wave $Co^{III}\rightarrow Co^{II}$	2nd Wave $Co^{II}\rightarrow Co^{I}$	3rd Wave $Co^{I}\rightarrow Co^{0}$
fac-$[Co(CN)_3dien]\cdot H_2O$	−1.37	−1.83	no reduction
mer-$[Co(CN)_3dien]\cdot 3H_2O$	−1.09	−1.74	no reduction
cis-$[Co(CN)_2en_2]NO_3$	−0.95	−1.48	−1.99
trans-$[Co(CN)_2en_2]NO_3$	−0.97	−1.52	−1.99
cis-$Na[Co(CN)_4en]\cdot 7/2H_2O$	−1.59	−1.78	no reduction

V *vs.* SCE

potentials of which are summarized in Table 1. Here, it is of interest to note that a great difference was found to exist in the half-wave potentials of both waves between the *fac*- and *mer*-isomers. The values for the first and the second steps of the *fac*-isomer lie at potentials more negative than those for the *mer*-isomer by 280 and 90 mV respectively, indicating that the *fac*-cobalt(III) and cobalt(II) species are more stable towards the electrochemical reduction than are the *mer* ones. Such a large difference in reduction potentials has never yet been reported for steric isomers. Inversely, this result can be invoked to emphasize the larger stability of the resulting tricyano cobalt(I) complex with a mer form. The three cyanides located on coplanar coordination sites (mer form) may contribute much more to the stability of the univalent cobalt than those on a non-planar configuration do, as can be inferred from a comparison of *cis*- and *trans*-complexes with cyanides.[3]

The net processes of the electrode reaction can be fully interpreted in terms of the "*inert-inert*"-type reduction without any structural changes as follows:

$$[Co^{III}(CN)_3dien] \xrightarrow{e} [Co^{II}(CN)_3dien]^- \xrightarrow{e} [Co^{I}(CN)_3dien]^{2-}.$$

* Present address: Department of Chemistry, Faculty of Engineering, Tokushima University, Tokushima.

1) N. Maki, This Bulletin, **42**, 3617 (1969).

2) The *mer*-$[Co(CN)_3dien]$ complex was reported by Konya *et al*, while the *fac*-isomer was first prepared by Yoneda; H. Nishikawa and M. Shibata, *Inorg. Chem.*, **7**, 1165 (1968); H. Yoneda, Proc. 14th Symposium on Coord. Chem. Japan, (1963), p. 33.

3) N. Maki and K. Yamamoto, This Bulletin, **43**, 2450 (1970).

Prominent Catalysis of Sodium 2- or 4-Pyridinolate in the Aminolysis of Esters[1]

Nobuhiro NAKAMIZO

Tokyo Research Laboratory, Kyowa Hakko Kogyo Co., Ltd., Asahi-machi, Machida-shi, Tokyo

(Received May 18, 1971)

The bifunctional catalysis of 2-(1H)-pyridone (2-pyridinol) in the aminolysis of esters is a well-established phenomenon.[2-4] However, no report has been published concerning the catalytic activity of salts of pyridinols. During the course of the investigation of the catalysis in peptide synthesis,[4,5] the present author found that anhydrous sodium salts of the 2- or 4-pyridinol have a pronounced catalytic activity in the aminolysis of active esters. A preliminary kinetic study showed that the catalytic rate constant of the sodium 2-pyridinolate (I) in the reaction of *p*-nitrophenyl benzyloxycarbonyl-L-phenylalaninate (Z-L-Phe-ONp) with *t*-butyl glycinate (H-Gly-OBu^t) in anhydrous dioxane is about 20,000 (l^2/mol^2·min), whereas that of 2-pyridinol is 41 (l^2/mol^2·min).[4] Table 1 shows the results of some typical reactions.

I exhibited the catalytic activity not only for the aminolysis of "active" esters, but also for that of ordinary esters. When benzylamine (2 mmol) and methyl acetate (10 mmol) were heated for 5 hr at 78°C in dimethylacetamide (3 m*l*) in the presence of I (1 mmol), *N*-benzylacetamide (mp 60.5—62°C) was obtained in a 62% yield. In the absence of I, though, *N*-benzylacetamide could not be isolated. Moreover, when ethyl cyanoacetate (5 mmol) and thiourea (5 mmol) were refluxed for 5 hr in anhydrous methanol (3 m*l*) in the presence of I (10 mmol), 4-amino-6-hydroxy-2-mercaptopyrimidine was obtained in an 82% yield. No pyrimidine was produced in the absence of I. When triethylamine, which is similar to I in basicity, was used in place of I, only a trace amount of the pyrimidine was detected in the reaction mixture.[6] This fact suggests that the catalytic activity of I does not depend only on the basicity of the catalyst. During the course of the reaction of Z-L-Phe-ONp with *p*-nitroaniline in the presence of I, the transient formation of a compound which seems to be an active intermediate was observed on the thin-layer chromatogram.

From these facts, it may be considered that the present reactions proceed *via* a nucleophilic catalysis in which *O*-acyl pyridinol (II) or *N*-acyl pyridone (III) is formed as an active intermediate; that is, this catalysis is due to the high nucleophilicity of the pyridinolate anions and the high acylating activity of II[7] or III. Of course, the possibility that general-base catalysis is also a factor can not be disregarded. Whether the intermediate is II or III[8] is not clear at the present time.

Studies of the racemization in the presence of the catalysts are now in progress.

TABLE 1. CATALYSIS OF SODIUM 2- OR 4-PYRIDINOLATE IN THE AMINOLYSIS OF ARYL ESTERS

Acylating agent (mmol)	Amine (mmol)	2- or 4-Pyridinolate (mmol)	Solvent (m*l*)	Reaction temperarture °C	Half-life period, min	
					no catalyst	catalyst
Z-L-Val-ONp (1.0)	Benzylamine (1.0)	2 (1.0)	CH_2Cl_2 (20)	23	1440	<10
Z-L-Val-ONp (1.0)	H-L-Val-OMe (1.0)	2 (1.0)	AcOEt (5)	18	4200	<10
Z-L-Phe-ONp (2.0)	*p*-nitroaniline (2.0)	2 (2.0)	DMA[a] (5)	20	∞	50
Z-Gly-OPh (10.0)	piperidine (10.0)	2 (1.0)	AcOEt (10)	25	20	<2
Z-L-Phe-ONp (2.0)	*p*-nitroaniline (2.0)	4 (2.0)	DMA (5)	18	∞	50

a) dimethylacetamide

1) Catalysis in Peptide Synthesis with Active Esters. III.
2) H. C. Beyerman and W. Maassen van den Brink, *Proc. Chem. Soc.*, **1963**, 266.
3) H. T. Openshaw and N. Whittaker, *J. Chem. Soc., C*, **1969**, 89.
4) N. Nakamizo, This Bulletin, **42**, 1071 (1969).
5) N. Nakamizo, *ibid.*, **42**, 1078 (1969).
6) Triethylamine also has little catalytic effect on the aminolysis of Z-L-Phe-ONp.[4]
7) Y. Ueno, T. Takaya, and E. Imoto, This Bulletin, **37**, 864 (1964); Y. Ueno, S. Asakawa, and E. Imoto, *Nippon Kagaku Zasshi*, **89**, 101 (1968).
8) A.McKillop and M. J. Zelesko, *Tetrahedron Lett.*, **1968**, 4945.

Adsorption of Benzoic Acid on Gold in Perchlorate Solutions

Koichi KATOH* and G. M. SCHMID

Department of Chemistry, University of Florida, Gainesville, Fla. 32601 U.S.A.

(Received September 9, 1970)

The adsorption of benzoic acid from solutions of 10^{-2} to 10^{-5} M on gold electrode surface in perchlorate solutions of pH 1—4 was studied from differential capacity data obtained by a single pulse method. Strong adsorption is observed in the more acidic solutions. This points to predominant adsorption of benzoic acid molecule, rather than benzoate anions, possibly due to the π-electron interaction. At pH 1, benzoic acid replaces four water molecules. This interprets the flat adsorption of benzoic acid molecule on the gold electrode and the π-electron interaction with free electron of the metal surface. The standard free energy of adsorption $\Delta\bar{G}^{\circ}$ is -10.4 kcal/mol.

The adsorption of organic substances at metal-solution interface and the influence of surface coverage on kinetics of electrochemical reactions are important aspects of the study of heterogeneous processes.[1] Classically, on an electrode that is liquid and ideally polarizable, such as mercury, the surface excess of an organic substance can be measured as a function of potential and concentration with interfacial tension data using Gibbs' adsorption equation.[2] On solid electrodes, however, the interfacial tension is not accessible with the required precision and adsorption measurements have to be made by other means. Radioactive tracer techniques,[3] determination of concentration changes in solution,[4] and differential capacity measurements are being used for this purpose.[5]

In the adsorption of organic substances, the π-electron interaction between the adsorbing molecule and the metal substrate plays a dominant role.[7] However, the electrostatic attraction force between organic ions and an oppositely charged metal surface should also be important, especially for large molecules, where the solvation energy may be small. To investigate the relative importance of the π-electron interaction and electrostatic attraction, the adsorption of benzoic acid from aqueous solution was studied as a function of both pH and potential. Concentration ratio of benzoic acid to benzoate anions is controlled by pH with the dissociation constant of benzoic acid in aqueous solution. This allows the π-electron interaction with the substrate to remain relatively constant though the concentration of benzoate ions is changed by several orders of magnitude. Differential capacity measurements were made to evaluate the adsorption coverage. Gold was chosen as a substrate. There seems to be no hydrogen adsorption region[7] and gold approaches closer to the ideal polarizable electrode than, *e.g.* in the case of platinum.

Little is known about the electrochemical behavior of benzoic acid, which can be reduced on metals with high hydrogen overvoltage, *e.g.* lead, to benzyl alcohol.[8-11] Apparently, it can not be oxidized electrochemically in aqueous solution.[12] Both the acid and the free anions are used as corrosion inhibitors,[13] *e.g.* for steel, and are electrochemically stable under corrosion conditions.

Experimental

The gold electrodes were made from polycrystalline fine gold metal (Engelhard Industries, Newark, N.J. USA) and inserted in Teflon rod (cf. Fig. 3). They were polished before each run with 600 mesh polishing powder, washed in hot cleaning solution and thoroughly rinsed with triply distilled water. The exposed apparent surface area of the gold electrode was 0.071 cm^2.

An all Pyrex glass cell contained, in addition to the gold working electrode, a cylindrical bright platinum wire gauze counter electrode, a platinum flag polarizing electrode and a saturated calomel electrode (SCE). The polarizing electrode and the SCE were in side compartments separated from the main cell through two glass frits (platinum flag side) and a closed stopcock (SCE side).

Solutions of pH 1, 3, and 4 were made up from triply recrystallized sodium perchlorate, 70% reagent grade perchloric acid, and water distilled once from alkaline permanganate then twice in a quartz still. Reagent grade benzoic acid was used to prepare the solutions of 10^{-2} to 10^{-5} M. All solutions were deoxygenated with helium before and during the run.

The working electrode was polarized by a potentiostat according to Harrar.[14] Currents were measured as a voltage drop across a 1 or 10 kΩ precision resistor and potentials of the working electrode were measured against SCE. A Keithley 610B electrometer was used for the voltage measurements.

* Present address: Department of Applied Chemistry, Faculty of Engineering, Niigata University, Nagaoka 940, Niigata, Japan.

1) P. Delahay, "Double Layer and Electrode Kinetics," Interscience, New York (1965), pp. 197 ff.
2) D. C. Graham, *Chem. Rev.*, **41**, 441 (1947).
3) E. A. Blomgren and J. O'M. Bockris, *Nature*, **186**, 305 (1960). J. O'M. Bockris, M. Green, and D. A. J. Swinkels, *J. Electrochem. Soc.*, **111**, 743 (1964).
4) B. E. Conway, R. Barradas, and T. Zawidzki, *J. Phys. Chem.*, **62**, 676 (1958).
5) T. Murakawa, S. Nagaura, and N. Hackerman, *Corrosion Science*, **7**, 79 (1967).
6) A. N. Frumkin and B. B. Damaskin, "Modern Aspects of Electrochemistry", J. O'M. Bockris and B. E. Conway, eds., Vol. 3, p. 149 ff., Butterworth, Washington (1964).
7) G. M. Schmid, *Electrochim. Acta*, **12**, 449 (1967).
8) Fr. Fichter and I. Stein, *Helv. Chim. Acta*, **12**, 821 (1929).
9) S. Swann, Jr., and G. D. Lucker, *Trans. Electrochem. Soc.*, **75**, 411 (1939).
10) A. M. Shams El Din and G. Truempler, *Helv. Chim. Acta*, **44**, 48 (1961).
11) K. Natarajan, K. S. Udupa, G. S. Subramanian, and H. V. K. Udupa, *Electrochem. Tech.*, **2**, 151 (1964).
12) Fr. Fichter and E. Uhl, *Helv. Chim. Acta*, **3**, 22 (1920).
13) H. S. Venkataraman and B. Dandapain, *J. Proc. Inst. Chemists* (India), **37**, 71, 82 (1965).
14) J. E. Harrar, F. B. Stephens, and R. E. Pechacek, *Anal. Chem.*, **34**, 1036 (1962).

Differential capacity measurements were made with a rapid single pulse technique.[15] The differential capacities were measured from the slope of the potential-time curve of a fast rise rectangular current pulse on the working electrode at the start (t=0). The potential-time curves were displayed on the screen of a Tektronix 549 storage oscilloscope. Sometimes, the curves were bent near the start point, and the slope was measured at 25 μsec and 50 μsec. The curves were measured by the storage oscilloscope with a differential preamplifier. Voltage and time scales were 10 mV/cm and 5 μsec/cm. The pulses were taken from the gate of the oscilloscope and passed between the working and the counter electrode through a 33 kΩ resistance. This gave a current of 0.76 mA. Potential range was between 0.0 V and 1.40 V *vs.* SCE.

The reproducibility of the differential capacity measurements was usually $\pm$15%. This was attributed to differences of the surface condition of electrodes caused by unavoidable differences in pretreatment. In this experiment, the data were normalized to 17.9 μF/cm^2 at 1.40 V, the value was found for 10^{-2} M benzoic acid solution of pH 1. The reproducibility was then $\pm$5%.

Results and Discussion

Study of adsorption coverage on solid electrodes using differential capacity measurements is hampered by the fact that the measurements are sensitive to impurities in solution, faradaic processes occurring at the interface, the crystal structure exposed, and the roughness of the electrode surface. The capacity-potential curves measured on gold electrode in acidic solutions by different workers are similar, although some difference is evident.[16-20] Recent work on single crystal surface of gold electrodes indicates that small discrepancies in the capacities might be due to the nature of the crystal surface exposed.[19-20] It seems that on polycrystalline electrodes the broad maximum at 0—0.2 V and the anodic maximum at 1.2 V are of about equal height (~20 μF/cm^2),[18] whereas on (100) and (110) faces at gold electrode surfaces the anodic maximum is considerably large (~30 μF/cm^2).[17,19,20] On the (100) face electrodes, the broad maximum at 0—0.2 V splits into two peaks of about equal height, the one at the (110) face electrode into one peak and a small shoulder.[17] Small differences in the capacity curves on gold electrode may therefore simply be a matter of the structure of the crystal surface exposed. Thus, differential capacity measurements should be reliable for measuring the adsorption of organic substances on gold electrodes in acidic solutions.

Differential capacity *vs.* potential data obtained in 0.1 M perchloric acid and from 10^{-2} to 10^{-5} M benzoic acid are shown in Fig. 1. A significant depression

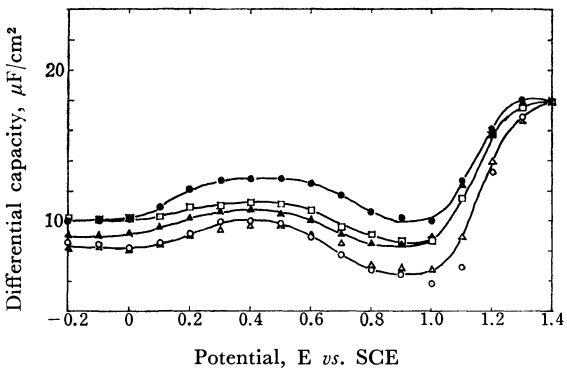

Fig. 1. Differential capacity *vs.* potential, Au in 0.1 M $HClO_4$ and 0, 10^{-5}, 10^{-4}, 10^{-3}, and 10^{-2} M benzoic acid. Capacities normalized at 1.4 V.
●: 0, □: 10^{-5}, ▲: 10^{-4}, △: 10^{-3}, ○: 10^{-2}

in the capacity due to the adsorption of benzoic acid was evident in 10^{-5} M solutions in the range 0—1.0 V. An additional significant depression occurred for 10^{-2} and 10^{-4} M benzoic acid at 0.8—1.2 V.

Coverage-potential curves were calculated from the data shown in Fig. 1 and Frumkin's equation[21] in the differentiated form:

$$C = C_0(1-\theta) + C_1\theta + (q_1-q_0)d\theta/dE \quad (1)$$

where C_0 and q_0 are capacity and charge of the uncovered surface, C_1 and q_1 those of the fully covered surface, and θ is the coverage with an organic substance. As seen in Fig. 1, no characteristic peaks of adsorption-desorption were present in this case. In our high speed capacity measurements these peaks are expected to be much smaller than those in data taken with alternating current at 1 kHz.[22] This may indicate that the adsorption-desorption region lies outside the potential range investigated, or alternatively, that the dependence of adsorption on potential in the range is small.

In general, the surface tension between a metal electrode surface and a solution becomes small on account of the adsorption of an organic substance on the electrode, and the correlation among differential capacity, charge, and surface tension is as follows:

$$C = (\delta q/\delta E)_\mu \qquad q = -(\delta\gamma/\delta E)_\mu$$

where C, q, E, γ, and μ is differential capacity, charge, potential, surface tension, and chemical potential, respectively. We can deduce that the differential capacity becomes small with the adsorption of an organic substance. From Fig. 1, we see that the coverage of adsorption in 10^{-3} and 10^{-2} M benzoic acid solutions showed almost fully coverage in this potential range, but not for 10^{-4} and 10^{-5} M solutions. In any case, if $d\theta/dE \approx 0$, we have

$$C = C_0(1-\theta) + C_1\theta \quad (2)$$

The coverage-potential curves are shown in Fig. 2 for 10^{-4} and 10^{-5} M benzoic acid. Differential capacities of 10^{-3} M benzoic acid solution were taken as C_1 because both data in 10^{-3} and 10^{-2} M solutions were almost the same.

15) J. S. Riney, G. M. Schmid, and N. Hackerman, *Rev. Sci. Instr.*, **32**, 588 (1961).
16) H. A. Laitinen and M. S. Chao, *J. Electrochem. Soc.*, **108**, 726 (1961).
17) G. M. Schmid and N. Hackerman, *ibid.*, **109**, 243 (1962).
18) G. M. Schmid and N. Hackerman, *ibid.*, **110**, 440 (1963).
19) J. Clavelier, A. Hamelin, and G. Valette, *Compt. rend.*, C **265**, 221 (1967).
20) A. Hamelin, J. Clavelier, and G. Valette, *ibid.*, C **266**, 435 (1968).
21) A. N. Frumkin, *Z. Physik*, **35**, 792 (1926).
22) W. Lorenz, *Z. Physik. Chem.*, (NF), **26**, 424 (1960).

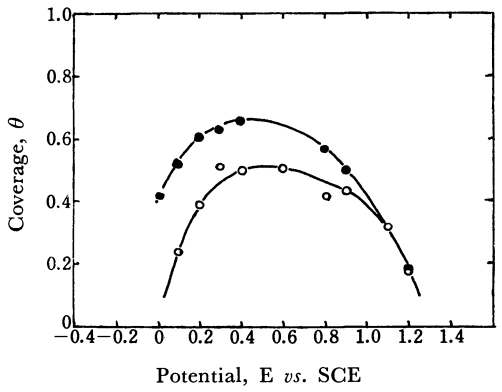

Fig. 2. Covereage *vs.* potential, Au in 0.1 M $HClO_4$ and 10^{-4} M, 10^{-5} M benzoic acid.
—●—: 10^{-4} M, —○—: 10^{-5} M

The coverage in higher potential range in Fig. 2 was unknown and could not be determined by going to higher potentials because of imminent oxygen evolution and electrode surface oxidation. It is known that adsorption of "oxygen" in acidic solution starts at approximately 1.0 V *vs.* SCE[23] and this is substantiated by the capacity curves shown in Fig. 1. Taking into account the fact that the electrode is covered with adsorbed oxygen, it is reasonable to assume that the amount adsorbed of benzoic acid becomes zero, and that the calculated θ values represent the actual fractional coverage with benzoic acid.

The change in the adsorption coverage with pH at constant concentration of benzoic acid can be assessed from the relative change of differential capacity. Values of this relative change are shown in Table 1 for 10^{-3} M benzoic acid and pH 1 and 4. It is seen

Table 1. Relative change in capacity, $(C_0-C)/C_0$, *vs.* potential and pH for 10^{-3} M benzoic acid

E *vs.* SCE	pH=1	pH=4
+0.1	0.229	0.072
+0.5	0.250	0.015
+0.6	0.280	0.075
+0.7	0.274	0.139

that an increase in pH remarkably reduces the amount of benzoic acid adsorbed. This leads to the conclusion that the adsorbing species is the benzoic acid molecule, rather than the benzoate anions and that in this case electrostatic attractive force between the anions and the positively charged electrode is not important.

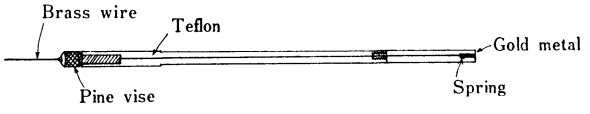

Fig. 3. Schematic diagram of a gold electrode.

23) R. A. Bonewitz and G. M. Schmid, *J. Electrochem. Soc.*, in press.

Adsorption of a solute molecule from solution onto an electrode surface must be considered as a competitive adsorption of the solute molecule and the solvent one. The competitive adsorption of two species from a liquid phase has been treated by numerous authors by means of the Langmuir isotherm.[24-26] Recently, a Temkin isotherm was applied to the adsorption of neutral molecules on electrodes.[27] The competitive adsorption of species of different sizes on electrode was treated by Dahms and Green.[28]

For competitive adsorption, equilibrium is assumed to be established between solvent, adsorbed solvent, solute species, and adsorbed solute species as Eq. (3). Thus, in aqueous solution:

$$n\,\mathrm{Water_{ads}} + \mathrm{Org_{sol}} \rightleftarrows n\,\mathrm{Water_{sol}} + \mathrm{Org_{ads}} \qquad (3)$$

where n is the number of molecules of water which occupies the same surface area as one molecule of the organic compound, $n=\Gamma_{\mathrm{max.w}}/\Gamma_{\mathrm{max.org}}$, with Γ_{max} (in mol/cm^2) the amount forming a monolayer of water or of organic species, respectively.

Under ideal conditions, one can write for equilibrium according to Eq. (3):

$$\bar{\mu}_{\mathrm{org.sol}} + n\,\bar{\mu}_{\mathrm{w.ads}} = \bar{\mu}_{\mathrm{org.ads}} + n\,\bar{\mu}_{\mathrm{w.sol}} \qquad (4)$$

where $\bar{\mu}_i$ is the electrochemical potential of species i. This gives the isotherm

$$\frac{X_{\mathrm{w.sol}}}{(1-\theta)^n \times X_{\mathrm{org.sol}}} = \exp\left(-\Delta\bar{G}^\circ/\boldsymbol{RT}\right) \qquad (5)$$

Here X_i represents the mole fraction of species i and

$$\Delta\bar{G}^\circ = \bar{\mu}^\circ_{\mathrm{org.ads}} - \bar{\mu}^\circ_{\mathrm{org.sol}} - n(\bar{\mu}^\circ_{\mathrm{w.ads}} - \bar{\mu}^\circ_{\mathrm{w.sol}}) \qquad (6)$$

In dilute solutions of the organic species the mole fraction $X_{\mathrm{w.sol}} \approx 1$ and the isotherm can be written as follows.

$$\frac{\theta}{(1-\theta)^n} = X_{\mathrm{org.sol}} \times \exp(-\Delta\bar{G}^\circ/\boldsymbol{RT}) = K_{\mathrm{ads}} \times X_{\mathrm{org.sol}} \qquad (7)$$

The equation differs from the Langmuir equation only by the power factor n.

By means of this equation, n was calculated to be 4 for benzoic acid in 10^{-1} M perchloric acid, and K_{ads} 4.5×10^7 at potentials 0.1 to 0.9 V. Replacement of 4 water molecules with one benzoic acid molecule is very reasonable (Stuart-Briegleb Models) and K_{ads} yields a $\Delta\bar{G}^\circ$ of -10.4 kcal/mol which is consistent with the weak adsorption of benzoic acid on gold electrode.

The authors are grateful for the financial support given to this work by the National Science Foundation, Grant No. NSF-GP-7742.

24) A. N. Frumkin, *Z. Physik. Chem.*, **116**, 466 (1925).
25) E. Blomgren and J. O'M. Bockris, *J. Phys. Chem.*, **63**, 1425 (1959).
26) R. G. Barradas and B. E. Conway, *Electrochim. Acta*, **5**, 349 (1961).
27) P. Delahay and D. M. Mohilner, *J. Amer. Chem. Soc.*, **84**, 4247 (1962).
28) H. Dahms and M. Green, *J. Electrochem. Soc.*, **110**, 1075 (1963).

Anisotropy of the Indirect Nuclear Spin-Spin Coupling Constants. III. Problems in the Structure Determination of the Molecule Dissolved in a Nematic Solvent

Hiroshi NAKATSUJI, Isao MORISHIMA, Hiroshi KATO,* and Teijiro YONEZAWA
Department of Hydrocarbon Chemistry, Faculty of Engineering, Kyoto University, Kyoto
(Received September 26, 1970)

Anisotropy of the indirect nuclear spin-spin coupling constant was studied theoretically. All the contributions to the coupling tensors were calculated for various molecules by using the INDO molecular orbitals. As shown in part I of this series, the calculated ^{13}C–H coupling anisotropy of $^{13}CH_3F$ is too small to be compared with the value obtained experimentally by Krugh and Bernheim. Thus we examined the substituent effect on the anisotropy in the $^{13}CH_3X$ series. It is concluded that the experimentally estimated value of the ^{13}C–H coupling anisotropy in $^{13}CH_3F$ as large as 1890 Hz is erroneous and that it contains some other effects which are more important than electronic effect. We believe that the change in molecular geometry from gas state to the solute state in a nematic solvent is the most probable origin for the differences between theories and experiments. For the directly bonded C–X couplings (X is C, N or F), their anisotropies are in the same order of magnitude as their isotropic couplings. For the non-bonded C–X nuclei, they seem negligible in magnitude. For the F–F couplings, their anisotropies are exceptionally large and the orbital term is a very important source of anisotropy. Furthermore, even for the isotropic F–F couplings, the orbital and spin dipolar terms are very important and sometimes make decisive contributions exceeding the Fermi contact term.

Since the experiment of Saupe and Englert,[1,2] extensive investigations of the molecules dissolved in liquid-crystal solvents have been carried out by means of nuclear magnetic resonance (NMR) technique.[3-5] Chemically fundamental data such as molecular motion and molecular geometry in liquid-crystal phase have accumulated, in addition to a more detailed knowledge of NMR parameters than those available by the usual NMR measurements in isotropic liquid phase. However, some difficulties exist in the determination of molecular geometry. In order to calculate molecular geometry (strictly speaking, ratios of the geometrical parameters) from spectral splittings, one needs the value of the anisotropy of the indirect nuclear spin-spin coupling constant (J).[3,6] The most frequent assumption is a disregard of the anisotropy of the indirect coupling constant. However, the molecular geometries obtained under this assumption sometimes differ slightly from those obtained by other measurements in gas phase (*e.g.* electron diffraction method, microwave method *etc*).[6,7] On the other hand, if one assumes that the geometry obtained by other measurements in gas phase can be used without any correction, one may calculate the anisotropy of the indirect coupling constant from spectral splittings. This treatment, however, has sometimes given extremely large anisotropy.[8]

For a solution of this situation, the following points must be clarified. (1) Can the anisotropy of the indirect coupling constant be assumed to be nearly zero ? (2) If so, why does the geometry obtained by means of NMR in liquid crystal solvent differ from that given by other measurements in gas phase ?

The main purpose of this series of investigation is to solve these problems theoretically. Possible origins of the coupling anisotropy were studied by both sum-over-state[9] and finite perturbation[10] methods on the basis of molecular orbital (MO) theory. The Fermi-spin dipolar cross term is important. For doubly and triply bonded nuclei, the orbital term is also important. However, for the ^{13}C–H coupling in CH_3F, the calculated anisotropy was too small to be compared with 1890 Hz obtained by assuming microwave geometry.[8a] Similar results were also obtained by Barfield[11] by valence-bond method, and by Buckingham and Love[12] with a similar MO treatment.

* Presest address: Department of General Education, Nagoya University, Chikusa-ku, Nagoya, Japan.

1) A. Saupe ans G. Englert, *Phys. Rev. Lett.*, **11**, 462 (1963).
2) G. Englert and A. Saupe, *Z. Naturforsch.*, **19a**, 172 (1964).
3) A. D. Buckingham and K. A. McLauchlan, "Progress in nuclear magnetic resonance spectroscopy," vol. 2, ed. J. W. Emsley, J. Feeney and L. H. Sutcliffe, Pergamon Press, New York (1967).
4) G. R. Luckhurst, *Quart. Rev.*, **22**, 179 (1968).
5) A. Saupe, *Angew. Chem. internat. Edition*, **7**, 107 (1968).
6) L. C. Snyder, *J. Chem. Phys.*, **43**, 4041 (1965).
7) a) G. Englert and A. Saupe, *Mol. Cryst.*, **8**, 233 (1969). b) E. Sackmann, *J. Chem. Phys.*, **51**, 2984 (1969). c) A. Saupe, G. Englert, and A. Povh, *Advan. Chem. Ser.*, **63**, 51 (1967). d) A. D. Buckingham, E. E. Burnell, C. A. de Lange, and A. J. Rest, *Mol. Phys.*, **14**, 105 (1968). e) L. C. Snyder and S. Meiboom, *J. Chem. Phys.*, **47**, 1480 (1967). f) D. N. Silverman and B. P. Dailey, *ibid.*, **51**, 655 (1969). g) G. Englert, A. Saupe and J. P. Weber, *Z. Naturforsch.*, **23a**, 152 (1968). h) G. Englert and A. Saupe, *Mol. Cryst.*, **1**, 503 (1966). i) P. Diehl, C. L. Khetrapal, and U. Lienhard, *Can. J. Chem.*, **46**, 2645 (1968). j) A. D. Buckingham, E. E. Burnell, and C. A. de Lange, *Mol. Phys.*, **16**, 521 (1969); **17**, 205 (1969).
8) a) T. R. Krugh and R. A. Bernheim, *J. Amer. Chem. Soc.*, **91**, 2385 (1969); *J. Chem. Phys.*, **52**, 4942 (1970). b) J. Bulthis, J. Gerritsen, C. W. Hilbers, and C. MacLean, *Rec. Trav. Chim.*, **87**, 417 (1968). c) W. Bovée, C. W. Hilbers, and C. MacLean, *Mol. Phys.*, **17**, 75 (1969). d) L. C. Snyder and E. W. Anderson, *J. Chem. Phys.*, **42**, 3336 (1965); *J. Amer. Chem. Soc.*, **86**, 5023 (1964). e) C. S. Yannoni, *J. Chem. Phys.*, **52**, 2005 (1970). f) A. D. Buckingham, E. E. Burnell, and C. A. de Lange, *Mol. Phys.*, **16**, 299 (1969). g) Private communication from Prof. H. Spiesecke.
9) H. Nakatsuji, H. Kato, I. Morishima, and T. Yonezawa, *Chem. Phys. Lett.*, **4**, 607 (1970). Part I.
10) H. Nakatsuji, K. Hirao, H. Kato, and T. Yonezawa, *ibid.*, **6**, 541 (1970). Part II.
11) M. Barfield, *ibid.*, **4**, 518; **5**, 316 (1970).
12) A. D. Buckingham and I. Love, *J. Magnetic Resonance*, **2**,338 (1970).

Theory of coupling anisotropy is described in the next section. It is applied to various molecules by using the INDO MO's of Pople *et al.*[13] The substituent effect in the $^{13}CH_3X$ series[14] will be discussed for the directly bonded ^{13}C–H coupling anisotropy in paticular. Another important aspect is the coupling anisotropy between F–F nuclei. For Problem (2), the possible factors are twofold; the vibrational effect and the effect due to the structural change from gas state to the solute state in a nematic solvent. Their relative importance is examined in the last section.

Theoretical Background

The essential part of the theory of the anisotropy of the indirect nuclear spin-spin coupling constant were given by us[9,10] and by Buckingham and Love.[12]

Anisotropy of the indirect coupling constant originates from three mechanisms: Fermi-spin dipolar cross (FSD) term, spin dipolar (SD) term and orbital (OB) term.[9,15] The Fermi-contact (FC) term is isotropic. These contributions can be developed in terms of molecular orbital theory, along lines similar to the treatment of Pople and Santry.[16] We introduce a reduced coupling constant $\boldsymbol{K}_{AB}$ defined by

$$\boldsymbol{K}_{AB} = (2\pi/\hbar\gamma_A\gamma_B)\boldsymbol{J}_{AB} \tag{1}$$

First we set the following three approximations (*Level A* approximation). (1) Use of the sum-over-state perturbation method, taking single Slater determinant built up from SCF MO's as zeroth order wavefunction. An improvement over this treatment may be achieved by using the finite perturbation[17] (or coupled Hartree-Fock[18]) method.[10] (2) LCAO-MO approximation. Actually the INDO SCF MO's expanded by all the valence AO's will be used. (3) One-center integral approximation. This approximation may be crude especially for the coupling tensor between directly bonded nuclei. However, since all the Hamiltonians considered (Eqs. (1)—(4)[9]) lay stress on the electronic structure in the vicinity of nuclei, and we use the INDO MO's based on the zero-differential overlap approximation (theoretically based on the orthogonalized AO's[19]), this approximation may be approved. It should be noted that under this approximation, the anisotropy of the H–H coupling constant becomes zero, which may be justified by the study of Barfield.[11]

As an example, the elements of coupling tensor obtained under Level A approximation are given for the FSD term as follows.

$$(\boldsymbol{K}_{AB}^{(2,3)})_{\alpha\alpha} = -(64\pi\beta^2/15)s_A(0)\langle r^{-3}\rangle_B \sum_i^{occ}\sum_j^{vac}({}^3\Delta E_{i\to j})^{-1} C_{is_A}C_{js_A}(2C_{ip_\alpha B}C_{jp_\alpha B} - \sum_{\delta(\neq\alpha)}' C_{ip_\delta B}C_{jp_\delta B}) + [\text{interchange term of A and B}] \tag{2-a}$$

$$(\boldsymbol{K}_{AB}^{(2,3)})_{\substack{\alpha\neq\beta}} = -(32\pi\beta^2/5)s_A(0)\langle r^{-3}\rangle_B \sum_i^{occ}\sum_j^{vac}({}^3\Delta E_{i\to j})^{-1} C_{is_A}C_{js_A}(C_{ip_\alpha B}C_{jp_\beta B} + C_{ip_\beta B}C_{jp_\alpha B}) + [\text{interchange term of A and B}] \tag{2-b}$$

The other contributions are summarized in Appendix. In Eq. (2), $s_A(0) = (s_A|\delta(\boldsymbol{r})|s_A)$, s_A and $p_{\alpha A}$ are the s-type AO and $2p_\alpha$AO (α is x, y or z) centered on atom A. $\sum_{\delta(\neq\alpha)}'$ means the summation over the directions x, y, and z except α. The other notations are the same as those used by Pople and Santry.[16]

Although we use Level A approximation in actual calculations, it is sometimes convenient to introduce further approximations: (4) Average excitation energy (ΔE) approximation.[20] (5) zero-differential overlap (ZDO) approximation. Hereafter we call this level of approximation Level B approximation, where the elements of coupling tensor are given for the FSD term by

$$(\boldsymbol{K}_{AB}^{(2,3)})_{\alpha\alpha} = (16\pi\beta^2/15)s_A(0)\langle r^{-3}\rangle_B({}^3\Delta E)^{-1} \times (2P_{s_A p_\alpha B}^2 - \sum_{\delta(\neq\alpha)}' P_{s_A p_\delta B}^2) + [\text{interchange term of A and B}] \tag{3-a}$$

$$(\boldsymbol{K}_{AB}^{(2,3)})_{\substack{\alpha\neq\beta}} = (16\pi\beta^2/15)s_A(0)\langle r^{-3}\rangle_B({}^3\Delta E)^{-1} \times (P_{s_A p_\alpha B}P_{s_A p_\beta B}) + [\text{interchange term of A and B}] \tag{3-b}$$

The other contributions are summarized in Appendix. In Eq. (3), $P_{s_A p_\alpha B}$ denotes the bond order between s_A and $2p_{\alpha B}$ AO's.

$$P_{s_A p_\alpha B} = \sum_i 2C_{is_A}C_{ip_\alpha B} \tag{4}$$

When localized AO's are introduced, the chemical picture of the coupling mechanisms becomes clear. Namely, each contribution to the $\sigma\sigma$-element of the coupling tensor, $(J_{AB})_{\sigma\sigma}$ becomes as follows.

$$[\text{FC term}] \propto P_{ss'}^2$$

$$[\text{FSD term}] \propto P_{s\sigma'}^2 + [\text{interchange term}]$$

$$[\text{SD term}] \propto 8P_{\sigma\sigma'}^2 + 2(P_{\pi\pi'}^2 + P_{\pi\bar{\pi}'}^2) + 9P_{\sigma\sigma'}(P_{\pi\pi'} + P_{\bar{\pi}\bar{\pi}'})$$

$$[\text{OB term}] \propto P_{\pi\pi'}P_{\bar{\pi}\bar{\pi}'}$$

These equations may be considered as showing the "paths" and "width" along which two nuclear moments interact. However, it should be noted that although this chemical picture is very intuitive, it sometimes leads to erroneous results, especially for the coupling constants between nuclei in polar bonds.[16] Thus, in the following applications, we use Level A approximation. The values of the one-center

13) J. A. Pople, D. L. Beveridge, and P. A. Dobosh, *J. Chem. Phys.*, **47**, 2026 (1967).
14) I. Morishima, A. Mizuno, H. Nakatsuji, and T. Yonezawa, *Chem. Phys. Lett.*, to be published.
15) N. F. Ramsey, *Phys. Rev.*, **91**, 303 (1953).
16) J. A. Pople and D. P. Santry, *Mol. Phys.*, **8**, 1 (1964).
17) J. A. Pople, J. W. McIver, Jr., and N. S. Ostlund, *J. Chem. Phys.*, **49**. 2960, 2965 (1968). See also, G. E. Maciel, J. W. McIver, Jr., N. S. Ostlund, and J. A. Pople, *J. Amer. Chem. Soc.*, **92**, 1, 11 (1970).
18) H. D. Cohen and C. C. J. Roothaan, *J. Chem. Phys.*, **43**, 534 (1965); R. E. Watson and A. J. Freeman, *Phys. Rev.*, **131**, 250 (1963).
19) P. -O. Löwdin, *J. Chem. Phys.*, **18**, 365 (1950).
20) M. Barfield, *ibid.*, **44**, 1836 (1966); **49**, 2145 (1968). See also, M. Karplus, *Rev. Mod. Phys.*, **32**, 455 (1960); H. M. McConnell, *J. Chem. Phys.*, **24**, 460 (1956).

integrals, $s_A(0)$ and $\langle r^{-3}\rangle_A$ are quoted from those summarized by Morton[21] except for $s_H(0)=0.550$ (a.u.).

Results and Discussion

General Features. In Tables 1—4, the coupling constants calculated in Level A approximation are summarized for various nuclear pairs. First, the relative importance of the coupling mechanisms is examined. As is well-known, the most important mechanism for the *isotropic* coupling constants is the FC term, the SD and OB mechanisms giving only small contributions. However, exceptions are found for the F–F couplings (Tables 3 and 4), where the OB and SD terms are very important and sometimes give predominant contributions exceeding the FC term. For the *anisotropies*, the FSD term is important (Tables 1–4). The OB term is important for the multiply bonded nuclear pairs (Tables 1 and 4) and for the F–F couplings (Tables 3 and 4). The SD term is less important.

Secondly, the anisotropies between non-bonded nuclear pairs are calculated to be very small as compared with those between directly bonded ones (Tables 1 and 2), except for the F–F coupling anisotropies (Tables 3 and 4).

Thirdly, for isotropic couplings, the calculated values are smaller than experimental ones. The disagreement may be due to the too large excitation energies calculated by the INDO method and/or the neglect of the self-consistency requirement[22] in the present perturbation treatment. An improvement can be achieved in the finite perturbation method.[10] However, the defect is not very serious for semi-quantitative discussions.

X–H Couplings. As seen from Eqs. (6), (A-1)—(A-4), the sources of the isotropic and anisotropic couplings between X and H nuclei are only the FC and FSD terms, respectively.

The calculated isotropic C–H coupling constants of methane, ethylene, and acetylene are 64.6, 80.1, and 141.9 Hz and the experimental values are 125.0, 156.2, and 249.0 Hz, respectively. Their calculated anisotropies, defined by $J_{xx}-1/2(J_{yy}+J_{zz})$, are 33.0, 24.5, and 18.0 Hz, respectively, where the x-axis of the coupling tensor is taken to be parallel to the C–H bonds. This sequence of change reflects that expected from changes in hybridization for the FC and FSD terms.

The calculated coupling constants between X–H nuclei in CH_3Y (Y=H, CH_3, CN, OH, NC, F, and I) are summarized in Table 1. The ^{13}C–H coupling anisotropy of CH_3F is also too small to be compared with the experimentally estimated value.[8a] Similar results were also obtained by Barfield,[11] and Buckingham and Love.[12] The difference between theories

Table 1. X–H couplings in the methyl derivatives

Molecule	Nuclei[a]	$(J_{XH})_{iso}$		$(J_{XH})_{aniso}$		S_{zz}
		Exptl	Calcd	Exptl	Calcd	
CH_4	^{13}C–H	125.0[b]	64.6	—	−9.9	—
C_2H_6	^{13}C–H	124.9[b]	57.8	—	−8.7	—
	(^{13}C–H)		0.3	—	0.3	
CH_3CN	^{13}C–H	136.0[c]	58.9	−50[d]	−8.7	0.1009[d]
	(^{15}N–H)	−1.75[c]	−0.2	—	2.1	
	(^{13}C–H)	−10.0[c]	1.4	—	1.1	
CH_3OH	^{13}C–H	141.0[b]	68.9	—	−10.7[e]	0.0050[d]
CH_3NC	^{13}C–H	145.2[f]	64.7	−108[g]	−9.8	0.0997[g]
	(^{13}C–H)		−0.1	—	−1.8	
	(^{15}N–H)	3.8[f]	−0.6	$\begin{pmatrix}-401\\ \pm 142\end{pmatrix}$[h]	−0.5	
CH_3F	^{13}C–H	148.8[i]	75.2	1890[i] ±130	−11.0	0.0166[i]
	(^{19}F–H)	46.3[i]	7.3	−18[i] ±54	−9.0	
CH_3I	^{13}C–H	151.4[j]	—	555[k]	—	0.0323[k]

a) The nuclei in parentheses are non-bonding.
b) N. Muller and D. E. Pritchard, *J. Chem. Phys.*, **31**, 768, 1471 (1959).
c) W. McFarlane, *Mol. Phys.*, **10**, 603 (1966): G. Englert and A. Saupe, *Mol. Cryst.*, **8**, 233 (1969).
d) A. Saupe, G. Englert, and A. Povh, *Adv. Chem. Ser.*, **63**, 51 (1967).
e) Free rotation about the C–O bond is assumed.
f) W. McFarlane, *J. Chem. Soc.*, **1967**, 1660.
g) H. Spiesecke, *Z. Naturforsch.*, **23a**, 467 (1968).
h) C. S. Yannoni, *J. Chem. Phys.*, **52**, 2005 (1970).
i) T. R. Krugh and R. A. Bernheim, *J. Amer. Chem. Soc.*, **91**, 2385 (1969).
j) S. L. Miller, L. C. Aamodt, G. Dousmanis, C. H. Townes, and J. Kraitchman, *J. Chem. Phys.*, **20**, 1112 (1952).
k) I. Morishima, A. Mizuno, H. Nakatsuji, and T. Yonezawa, *Chem. Phys. Lett.*, to be published.
l) $J_{aniso}=J_{\parallel}-J_{\perp}$, where $\parallel$ and $\perp$ mean parallel and prependicular with the molecular symmetry axis, respectively.

21) J. R. Morton, *Chem. Revs.*, **64**, 453 (1964).

22) P. W. Langhoff, M. Karplus, and R. P. Hurst, *J. Chem. Phys.*, **44**, 505 (1966).

TABLE 2. C-X COUPLING CONSTANTS (Hz)

Molecule	C-X	Isotropic, $(J_{XX'})_{iso}$ Calcd Fermi	Spin dipolar	Orbital	Total	Exptl	Anisotropic, $(J_{CX})_{aniso}$ Calcd Fermi-spin dipolar	Spin dipolar	Orbital	Total	Exptl
C_2H_6	^{13}C-^{13}C	6.6	0.4	−0.7	6.2	34.6[a]	12.7	0.7	1.5	14.8	—
C_2H_4	^{13}C-^{13}C	20.8	1.4	−5.4	16.8	67.6[a]	14.4	−2.2	8.9	22.7	—
C_2H_2	^{13}C-^{13}C	56.1	4.2	6.1	66.5	171.5[a]	14.2	−6.2	43.2	51.1	—
CH_3F	^{13}C-^{19}F	−99.2	9.4	−6.3	−96.0	−161.9[b]	93.5	−16.2	4.6	114.2	700± 130[b]
CH_3CN	$^{13}C\equiv^{15}N$	1.8	−1.9	−0.2	−0.3	−17.5[c]	−11.0	3.7	−27.7	−35.1	—
	^{13}C-^{13}C	15.3	0.3	−0.5	15.2	57.3[d]	16.7	0.1	1.9	18.7	—
	(^{13}C-^{15}N)[e]	0.0	−0.2	0.0	−0.2	—	−0.6	−0.2	0.8	0.0	—
CH_3NC	$^{15}N\equiv^{13}C$	10.5	−1.7	−0.3	8.5	±5.8[f]	−10.5	3.4	−25.5	−32.6	—
	^{13}C-^{15}N	−2.3	−0.3	0.4	−2.2	−10.7[g]	−9.2	−0.3	−1.0	−10.5	—
	(^{13}C-^{13}C)	1.2	0.0	0.1	1.3	—	1.1	0.3	1.1	2.5	—

a) R. M. Lynden-Bell and N. Sheppard, *Proc. Roy. Soc.*, **A269**, 385 (1962).
b) T. R. Krugh and R. A. Bernheim, *J. Amer. Chem. Soc.*, **91**, 2385 (1969).
c) W. McFarlane, *Mol. Phys.*, **10**, 603 (1966).
d) K. Frei and H. J. Bernstein, *J. Chem. Phys.*, **38**, 1216 (1963).
e) The nuclei in parenthesis are non-bonding.
f) I. Morishima, T. Yonezawa, and K. Goto, to be published.
g) W. McFarlane, *J. Chem. Soc. A*, **1967**, 1660.
h) $J_{^{13}C^{14}N} = -0.713 J_{^{13}C^{15}N}$
i) $(J_{CX})_{aniso} = J_{xx} - 1/2(J_{yy} + J_{zz})$, where x-axis is taken to be parallel with the C-X bond.

and experiments seem to be far beyond the accuracy of the theories.

Recently, the substituent effect on the directly bonded ^{13}C–H coupling anisotropies $(J_{CH})_{aniso}$ in methyl derivatives are obtained by analyzing the NMR spectra in the same way as for CH_3F.[14] They are also given in Table 1. First, we examine the isotropic ^{13}C–H couplings $(J_{CH})_{iso}$. From the experimental values, we can estimate the order of magnitude of the change in the electron distribution near the C–H bond induced by substitution. It is 2—6 %. The change of the same order is also reproduced by the INDO MO's. On the other hand, the substituent effect on the coupling anisotropy $(J_{CH})_{aniso}$ estimated from the experimental analyses is unusually large. In fact, in order to explain this substituent effect, a very large change must be assumed in the electronic structure in the vicinity of C–H bond. However, this contradicts the substituent effect seen for $(J_{CH})_{iso}$, while the calculated effect on $(J_{CH})_{aniso}$ is the same order as that on $(J_{CH})_{iso}$.

Thus, it is concluded that the experimentally estimated values of $(J_{CH})_{aniso}$ given in Table 1 still contain some other effects which are more important than the electronic effect. Then, a value of $(J_{CH})_{aniso}$ of CH_3F as large as 1890 Hz[8a] is erronious. We see in Table 1 that there is an approximate parallelism between the experimentally estimated values of $(J_{CH})_{aniso}$ and the orientation parameters S_{zz} in nematic solvent.

C–X Couplings. The calculated values of the C–X coupling constants of ethane, ethylene, acetylene, and methyl derivatives are summarized in Table 2, from which we see: 1) compared with C–H couplings, the magnitude of the C–X coupling anisotropies are comparable to those of the isotropic coupling constants. 2) the calculated value of ^{13}C–F coupling anisotropy is still small compared with the experimental value,[8a] although the value 207 Hz is obtained by finite perturbation method,[10] and 3) for the anisotropies of the ^{13}C-^{15}N couplings in CH_3CN and CH_3NC, the OB term contributes to a great extent, due to the triple bond character of these bonds. The sign of the isotropic $^{15}C\equiv^{13}N$ coupling constant of CH_3NC is expected to be positive and is the reverse of that of the same nuclear pair in CH_3CN.

Coupling Tensors of the Molecules Including Fluorine Nuclei. So far, we have seen that the coupling anisotropies between non-bonded nuclei are very small in magnitude compared with those between directly bonded nuclei. However, this is not always the case for the F–F couplings. Experimentally, Snyder and Anderson[8d] pointed out that the anisotropy of the F–F coupling in hexafluorobenzene might be considerably large. Similar suggestions were also given for symm-tetrafluorobenzene,[8b] 1,3,5-trifluorobenzene,[8b] 1,1-difluoroethylene,[8f] and tetrafluoroethylene.[8g]

The calculated coupling tensors of the molecules including fluorine nuclei are summarized in Tables 3 and 4. The following points are remarkable: 1) For the *isotropic* F–F couplings,[23] the OB and SD contributions are very important.[24] In the geminal F–F

23) J. N. Murrell, P. E. Stevenson, and G. T. Jones, *Mol. Phys.*, **12**, 265 (1967).
24) Importance of the orbital term in the isotropic F–F coupling constants has been stressed independently by Blizzard and Santry. (A. C. Blizzard and D. P. Santry, *Chem. Communications*, **1970**, 87).

TABLE 3. CALCULATED COUPLING TENSORS (Hz) OF THE FLUOROMETHANES AND DIFLUOROETHYLENES[a]

Molecule	Nuclei	Fermi	Fermi-spin dipolar	Spin dipolar	Orbital	Total	J_{iso} Exptl.
CH_3F	C-F[b]	−99.1	62.3 0 0 / 0 −31.1 0 / 0 0 −31.1	20.3 0 0 / 0 4.1 0 / 0 0 4.1	−3.2 0 0 / 0 −7.7 0 / 0 0 −7.7	−19.8 0 0 / 0 −133.9 0 / 0 0 −133.9	−161.9[c]
			0.0 (93.5)	9.5 (16.2)	−6.2 (4.6)	−95.8 (114.2)	
CH_2F_2	C_1-F_2	−95.3	67.1 11.8 0 / 11.8 −32.2 0 / 0 0 −34.2	12.5 −1.1 0 / 0.4 1.1 0 / 0 0 2.8	−0.4 −2.6 0 / −0.7 −1.4 0 / 0 0 −39.9	−16.1 8.1 0 / 11.4 −127.7 0 / 0 0 −167.4	−234.8[d]
			0.0 (100.3)	5.4 (10.6)	−13.9 (20.3)	−103.7 (131.5)	
F_2–C_1(H)(F_3)–H	F_2-F_3	−103.9	32.3 −0.7 0 / −0.7 32.3 0 / 0 0 −65.1	53.9 3.6 0 / 18.6 46.0 0 / 0 0 9.2	−24.4 11.6 0 / 7.1 −31.0 0 / 0 0 286.1	−42.1 14.5 0 / 24.9 −56.6 0 / 0 0 126.4	(+150)[e]
			0.0 (48.7)	36.4 (26.3)	76.9 (−152.0)	9.2 (−77.0)	
1,1-$C_2H_2F_2$	C=C	31.8	10.7 0 0 / 0 −5.4 0 / 0 0 −5.4	0 0 0 / 0 1.0 0 / 0 0 2.5	2.0 0 0 / 0 −10.7 0 / 0 0 −1.2	44.6 0 0 / 0 16.7 0 / 0 0 27.7	—
			0.0 (16.1)	1.2 (−1.8)	−3.3 (8.0)	29.7 (22.4)	
H, F, C_2=C_1, H, F	C_1-F_3	−59.2	−16.4 42.4 0 / 42.2 53.7 0 / 0 0 −37.3	3.0 4.8 0 / 1.9 4.7 0 / 0 0 −1.3	−15.1 12.2 0 / 12.4 −11.8 0 / 0 0 −25.6	−87.7 59.1 0 / 56.5 −12.6 0 / 0 0 −123.3	−287.0[d]
			0.0 (−24.6)	2.1 (1.3)	−17.4 (3.6)	−74.6 (−19.8)	
y, x, z	F_3-F_4	−24.3	−19.0 0 0 / 0 78.4 0 / 0 0 −59.3	29.4 −2.0 0 / 2.0 51.0 0 / 0 0 −3.4	−79.0 0.1 0 / −0.1 −36.3 0 / 0 0 174.0	−92.9 −2.0 0 / 2.0 68.7 0 / 0 0 87.0	+36.4[f]
			0.0 (−28.6)	25.7 (5.6)	19.6 (−147.9)	20.9 (−170.8)	
trans-$C_2H_2F_2$	C_1=C_2	35.5	9.4 −1.8 0 / −1.8 −4.6 0 / 0 0 −4.8	0 0.1 0 / 0.1 1.0 0 / 0 0 2.4	0.9 −1.5 0 / −1.5 −11.7 0 / 0 0 −1.0	45.8 −3.6 0 / −3.2 20.1 0 / 0 0 32.1	—
			0.0 (14.1)	1.1 (−1.7)	−3.9 (7.3)	32.7 (19.7)	
H, F_3, C_2=C_1, F_4, H	C_1-F_3	−65.4	−5.4 56.6 0 / 56.6 47.0 0 / 0 0 −41.7	4.2 6.2 0 / 3.8 7.5 0 / 0 0 −1.9	−11.4 0.1 0 / −1.0 −10.4 0 / 0 0 −7.5	−78.0 62.9 0 / 59.4 −21.3 0 / 0 0 −116.4	—
			0.0 (−8.1)	−3.3 (1.4)	−9.8 (−2.5)	−71.9 (−9.2)	
	F_3-F_4	13.4	12.1 35.5 0 / 35.5 11.8 0 / 0 0 −23.8	9.2 −3.4 0 / −0.8 7.7 0 / 0 0 −4.2	−92.7 95.6 0 / 95.6 −118.2 0 / 0 0 −7.7	−58.1 127.8 0 / 130.3 −85.3 0 / 0 0 −22.3	−124.8[g]
			0.0 (18.1)	4.2 (7.5)	−72.9 (−29.8)	−55.2 (−4.3)	
cis-$C_2H_2F_2$	C_1=C_2	30.6	10.2 0 0 / 0 −5.0 0 / 0 0 −5.2	0 −0.1 0 / 0.1 1.0 0 / 0 0 2.6	1.7 −2.1 0 / 2.1 −10.7 0 / 0 0 −0.8	42.5 −2.2 0 / 2.2 15.9 0 / 0 0 27.2	—
			0.0 (15.3)	1.2 (−1.8)	−3.3 (7.5)	28.5 (21.0)	
F_4, F_3, C_2=C_1, H, H	C_1-F_3	−70.7	−5.9 48.6 0 / 48.6 41.9 0 / 0 0 −36.0	5.0 7.1 0 / 3.6 7.9 0 / 0 0 −1.8	−12.6 1.0 0 / 0.6 −10.9 0 / 0 0 −7.5	−84.2 56.6 0 / 52.7 −31.8 0 / 0 0 −115.9	—
			0.0 (−8.9)	3.7 (2.0)	−10.3 (−3.4)	−77.3 (−10.4)	
	F_3-F_4	49.0	−27.9 0 0 / 0 46.4 0 / 0 0 −18.5	−1.0 −3.7 0 / 3.7 −6.5 0 / 0 0 11.2	−54.2 −42.1 0 / 42.1 11.9 0 / 0 0 39.7	−34.0 −45.8 0 / 45.8 100.8 0 / 0 0 81.4	±18.7[g]
			0.0 (−41.9)	1.2 (−3.4)	−2.6 (−80.0)	47.6 (−125.1)	

a) The notation of the tensor elements is as follows.

$$J_{AB}=\begin{bmatrix}(J_{AB})_{xx} & (J_{AB})_{xy} & (J_{AB})_{xz}\\ (J_{AB})_{yx} & (J_{AB})_{yy} & (J_{AB})_{yz}\\ (J_{AB})_{zx} & (J_{AB})_{zy} & (J_{AB})_{zz}\end{bmatrix}$$

The value given under each tensor is the contribution to the isotropic coupling constant, and the value given in parenthesis is the contribution to the coupling anisotropy defined by $J_{xx}-1/2(J_{yy}+J_{zz})$.

b) The C-F axis is parallel to the x-coordinate axis.

c) T. R. Krugh and R. A. Bernheim, *J. Amer. Chem. Soc.*, **91**, 2385 (1969).

d) N. Muller and D. T. Carr, *J. Phys. Chem.*, **67**, 112 (1963).

e) Assumed from the observed coupling constants of the substituted ethanes: J. W. Emsley, J. Feeney, and L. H. Sutcliffe, "High Resolution Nuclear Magnetic Resonance," Pergamon Press, p. 886 (1966).

f) G. W. Flynn and J. D. Baldeschwieler, *J. Chem. Phys.*, **38**, 226 (1963).

g) G. W. Flynn, M. Matsushima, and J. D. Baldeschwieler, *J. Chem. Phys.*, **38**, 2295 (1963); Y. Kanazawa, J. D. Baldeschwieler, and N. C. Craig, *J. Mol. Spect.*, **16**, 325 (1965) (this reports a negative sign for the isotropic F-F coupling constant in *cis*-$C_2H_2F_2$); M. Fukuyama, *Reports Govt. Chem. Ind. Res. Inst. Tokyo*, **61**, 129 (1966) (this reports a positive sign for the above coupling constant).

TABLE 4. CALCULATED COUPLING TENSORS[a](Hz) OF THE MONO- AND DI-FLUOROACETYLENE

Molecule	Nuclei[b]	Fermi	Fermi-spin dipolar		Spin dipolar		Orbital		Total		J_{iso}	J_{aniso}
			xx	yy[c]	xx	yy[c]	xx	yy[c]	xx	yy[c]		
C_2HF	C-C	71.4	9.7	−4.8	0.4	5.6	30.3	−5.5	111.7	66.6	81.7	45.1
	C-F	−64.8	127.5	−63.8	9.1	−1.6	−16.1	−12.5	55.8	−142.6	−76.5	198.4
	C-H	153.7	10.7	−5.3	0.0	0.0	0.0	0.0	164.4	148.4	153.7	16.0
	(C-F)	−18.1	6.0	−3.0	−1.2	8·4	50.0	−22.1	36.7	−34.8	−10.9	71.5
C_2F_2	C-C	101.3	8.1	−4.0	0.6	5.5	29.3	−4.0	139.2	98.8	112.3	34.4
	C-F	−69.9	146.8	−73.4	9.6	−1.3	−17.3	−6.6	69.2	−151.2	−77.7	220.3
	(C-F)	−21.2	15.2	−7.6	0.2	7.9	43.6	−11.3	37.8	−32.3	−8.9	70.1
	(F-F)	17.7	−1.3	0.6	−30.6	−4.1	76.6	−173.6	62.5	−159.3	−85.4	221.8

a) The molecular axis is parallel with the x-coordinate.
b) The nuclei in parenthesis are non-bonding.
c) $J_{zz}=J_{yy}$.

couplings (CH_2F_2 and 1,1-$C_2H_2F_2$), their signs cannot be explained unless *both* of the SD and OB contributions are included. In *trans*-$C_2H_2F_2$ (Table 3) and C_2F_2 (Table 4), the OB term is predominant and negative in sign. In *cis*-$C_2H_2F_2$, the contributions due to the SD and OB terms are very small and almost cancel each other, giving the positive coupling constant due chiefly to the FC term. Although both signs are reported (Ref. g in Table 3), the present calculation favours the positive sign. 2) For the F–F coupling anisotropies, the OB term is most important, although the FSD term is also important. The SD term seems less important. 3) For the C–F couplings, the anisotropy becomes large (in absolute magnitude) by fluorine substitution from CH_3F to CH_2F_2 chiefly due to an increase in the OB contribution. The change in the isotropic C–F coupling constants from CH_3F to CH_2F_2 cannot be explained without OB contributions.

Meaning of the Difference in Theoretical and Experimental Values

It has been made clear that the experimentally estimated ^{13}C–H coupling anisotropies of the methyl derivatives still contain some other effects more important than electronic one.

The experimental value of the coupling anisotropy is calculated from the NMR spectral splitting $(\Delta\nu)_{CH}$ obtained in a nematic solvent by means of the following formula for the C_{3v}-symmetry molecules.[3]

$$(J_{CH})_{aniso} = \{(\Delta\nu)_{CH} - (J_{CH})_{iso} - D_{CH}\}/(2/3)S_{zz}, \quad (5)$$

where S_{zz} is the orientation parameters of the molecular symmetry axis (z-axis) with respect to applied magnetic field and D_{CH} the anisotropy due to direct coupling. In Table 1, S_{zz} is obtained by assuming that the anisotropies of the indirect H–H couplings are zero.[6,7] This is justified by Barfield.[11] Krugh and Bernheim[8a] examined the effects on the isotropic coupling constant $(J_{CH})_{iso}$ due to the solvent change and the solvent phase change from nematic to isotropic phases, and concluded that they would not be major factors influencing the results. Thus, the most important factor should be the effect on D_{CH}, by which the value of the ^{13}C–H coupling anisotropy sensitively changes through Eq. (5).[8a,14] In order to obtain the values of $(J_{CH})_{aniso}$ given in Table 1, D_{CH} values were calculated from the r_0-structure determined by means of microwave technique in gas phase. However, since the NMR measurements of these molecules were carried out in their solute states in nematic solvents, the D_{CH} values in Eq. (5) should correspond to this state and method of measurement. If we designate this correction by Δ_M (M indicates a special molecule), it is given by

$$\Delta_M = [\text{NMR geometry in the solute state in nematic solvent}] - [\text{Microwave geometry in gas phase}] \quad (6)$$

The apparent substituent effect on $(J_{CH})_{aniso}$ given in Table 1 is reconsidered as representing the substituent effect essentially on Δ_M.

There are two possible origins of the effect on Δ_M. (a) Molecular (harmonic and anharmonic) vibrations.[7d,8a] The measured value is approximately $\ll 1/r^3 \gg$ in NMR and approximately $\ll 1/r^2 \gg$ in microwave spectroscopy.[25a] r is the internuclear distance and $\ll \gg$ denotes the statistical average.[26] (b) The change in molecular geometry from gas state to solute state in the nematic solvent.[7a,7c]

First, the effect (a) is examined. If we assume that the orientation parameter S_{zz} is independent of internal molecular vibration,[6] and that the anisotropy of the indirect H–H coupling constant is negligible, we obtain the following equation from Eq. (5).[27]

$$(T_{CH})_{zz} = \frac{(\gamma_C\gamma_H\hbar/2\pi)(\langle r_{HH}^2/r_{CH}^5\rangle - 2\langle 1/r_{CH}^3\rangle) + 2/3(J_{CH})_{aniso}}{(\gamma_H^2\hbar/2\pi)\langle 1/r_{HH}^3\rangle} \times (T_{HH})_{zz} \quad (7)$$

25) a) J. A. Ibers and D. P. Stevenson, *J. Chem. Phys.*, **28**, 929 (1958). b) S. J. Cyvin, "Molecular Vibrations and Mean Square Amplitudes," Elsevier Pub. Co. N. Y. (1968).

26) $\ll \gg$ denotes the statistical average in the solute state in a nematic solvent. However, if the molecular potential function in this state does not differ much from that in gas state, we can, to first approximation, use the vibrational average in gas state $< >$ in spite of $\ll \gg$.

27) The dependence of the "true" value of $(J_{CH})_{aniso}$ on the molecular vibration is negligible.

where $(T_{CH})_{zz}$ and $(T_{HH})_{zz}$ are the observed total anisotropic couplings.

Let us introduce the notation[25a]

$$r_n = \langle r^n \rangle^{1/n}.$$

As a special case, r_{-2} corresponds approximately to the microwave r_0 structure, if we neglect the Coriolis and other terms. Ibers and Stevenson[25a] gave the expansion of r_n as follows.

$$r_{\pm n} = r_e\left(1+\frac{\langle x\rangle}{r_e}-\frac{(1\mp n)}{2r_e^2}\langle x^2\rangle+\cdots\right), \tag{8}$$

where r_e is the equilibrium distance and x the displacement coordinate ($x=r-r_e$). From Eq. (8), we obtain

$$r_{-3} = r_{-2} - \frac{1}{2}\langle x^2\rangle/r_e+\cdots$$

$$\simeq r_0(\text{m.w.}) - \frac{1}{2}\langle x^2\rangle/r_e+\cdots, \tag{9}$$

which shows that if we use the microwave r_0 structure in Eq. (7), the main correction due to molecular vibration comes only from the harmonic one. It should be noted that the value of r_{-3} is always smaller than that of r_{-2}. For polyatomic molecules the displacement coordinate x_i is given by a linear combination of the normal coordinates Q_k:

$$x_i = \sum_k L_{ik}Q_k,$$

By virtue of the separability of normal coordinates in the harmonic oscillator treatment, the mean-square amplitude $\langle x_i^2\rangle$ is given by[25b]

$$\langle x_i^2\rangle = \sum_k L_{ik}^2\langle Q_k^2\rangle \tag{10}$$

where $\langle Q_k\rangle^2$ is given by

$$\langle Q_k^2\rangle = \frac{h}{8\pi^2 c\nu_k}\coth\frac{hc\nu_k}{2\kappa T} \tag{11}$$

$$\rightarrow \frac{h}{8\pi^2 c\nu_k}\ (T\rightarrow 0;\ \text{zero-point vibration}),$$

where ν_k is the wave number given in cm^{-1}, and T the absolute temperature. The values of L_{ik} and ν_k of methyl halides were summarized by Reichman and Overend, and Russel *et al.*[28]

We consider the effects of harmonic C–H stretching and H–C–H bending vibrations. By substituting the correction term of Eq. (9) into Eq. (7), the value of the first term (D_{CH} part) in the numerator becames smaller and that of the denominator larger (both these terms are positive). These corrections make the resulting value of $(J_{CH})_{aniso}$ larger than the uncorrected one.[29] Thus, for CH_3F and CH_3I, the effect of harmonic vibration can not explain the difference between theory and experiment. Moreover, it cannot explain the substituent effect on $(J_{CH})_{aniso}$ shown in Table 1. In fact, since $\nu_{HCH}(\nu_2)$ is more sensitive to substitution than $\nu_{CH}(\nu_1)$, it suffices to consider the correction term to $1/r_{HH}^3$ in the denominator of Eq. (7). From the observed wave numbers, the correction term is larger in CH_3I than in CH_3F. This is contrary to the substituent effect shown in Table 1.

The effect of anharmonicity is not so clear as that of harmonic vibration for lack of experimental constants. However, we could eliminate this effect approximately in the above treatment. Since the apparent anisotropies given in Table 1 are most sensitive to the H–C–H valence angle,[8a,14] this effect and especially the substituent effect, is not large enough to explain the large change. Thus, we believe that the effect (a) cannot interpret the difference between theory and experiment.

Next, the effect (b) is examined. It should be noted that important chemical and/or physical solvent-solute interactions must exist in the solute state in a nematic solvent. The orientation parameter S_{zz} indicates essentially the strength of interaction. We find an approximate parallelism between the apparent anisotropy (essentially proportional to Δ_M above) and S_{zz} (Table 1).[14] Although experiments showing this kind of parallelism are still few[29] and we cannot stress this finding, it gives a support to the effect (b).

There are further supports: Snyder and Meiboom[30] found a distortion of molecular geometry in a nematic solvent for neopentane and tetramethylsilane. A similar result was also found for tetramethyltin.[31] There are X-ray diffraction studies[32a] showing the geometrical change in condensed phase: Harris and Clayton[32b] reported a slightly larger C–F bond length of CF_4 in liquid state than in gas state. There are some experiments showing the geometrical change from gas phase to molecular crystal phase: The I–As–I valence angle in AsI_3 is 100.2°± 0.4° (electron diffraction)[33a] in gas phase and 102.0°± 0.1° (X-ray)[33b] in crystal phase. Similar differences are also found for $AsBr_3$,[34] $SbCl_3$[35] and SbI_3.[36] Thus, we believe that the effect (b) is the most important origin of Δ_M.

For methyl derivatives, the most probable change in molecular geometry from gas state to the solute state in nematic solvents may be a change in the H–C–H

28) The values of $\nu_1(a_1)$ and $\nu_2(a_1)$ are respectively 2995 and 1493 cm^{-1} for CH_3F, and 3048 and 1279 cm^{-1} for CH_3I. (S. Reichman and J. Overend, *J. Chem. Phys.*, **48**, 3095 (1968).) Since the matrix $\{L_{ik}^2\}$ is almost diagonal for the totally symmetric a_1 vibrations, ν_1 and ν_2 represent approximately the C–H stretching and H–C–H angular displacement frequencies, respectively. The values of L_{11}^2 and L_{22}^2 are respectively 1.0167 and 1.9251 for CH_3F. (J. W. Russell, C. D. Needham, and J. Overend, *J. Chem. Phys.*, **45**, 3383 (1966).)

29) Buckingham, *et al.* studied the structure of 3,3,3-trifluoropropylene dissolved in different nematic solvents at various temperatures (Ref. 7d). Their results show a parallelism between S_{zz} and the molecular structures calculated by neglecting the anisotropies of the indirect F–F couplings.

30) L. C. Snyder and S. Meiboom, *J. Chem. Phys.*, **44**, 4057 (1966).

31) K. Hayamizu and O. Yamamoto, *Symposium on Nuclear Magnetic Resonance*, **8**, 88 (1969) (in Japanese).

32) a) R. F. Kruh, *Chem. Revs.*, **62**, 319 (1962); K. Furukawa, *Rept. Progr. Phys.*, **25**, 395 (1962). b) R. W. Harris and G. T. Clayton, *J. Chem. Phys.*, **45**, 2681 (1966).

33) a) Y. Morino, T. Ukaji, and T. Ito, This Bulletin, **39**, 71 (1966). b) J. Trotter, *Z. Kristallogr.*, **121**, 81 (1965).

34) a) Gas phase; K. Hedberg, *Trans. Am. Cryst. Assocn.*, **2**, 79 (1966). b) Crystal phase; J. Trotter, *Z. Kristallogr.*, **122**, 230 (1966).

35) a) Gas phase; P. Kisliuk, *J. Chem. Phys.*, **22**, 86 (1954). b) Crystal phase; I. Lindqvist and A. Niggli, *J. Inorg. Nucl. Chem.*, **2**, 345 (1956).

36) a) Gas phase; S. M. Swingle, quoted by P. W. Allen and L. E. Sutton, *Acta Crystallogr.*, **3**, 46 (1950). b) Crystal phase; J. Trotter and T. Zobel, *Z. Kristallogr.*, **123**, 67 (1966).

valnece angle,[14] since it is most sensitive[37] to the value of the apparent anisotropy shown in Table 1, and the energy necessary for the change of this order will easily be compensated[37] by van der Waals forces and other interaction energies.[38]

A fuller examination of the origins of the effect (b) will help us to clarify the relationship between the molecular geometry in a solvent and the nature of solvent-solute interaction.[38]

The authors wish to thank Professor K. Machida, Kyoto University, for critical discussion about the last section. They also thank Professor K. Kuchitsu, the University of Tokyo and Professor K. Osaki, Kyoto University for valuable discussion, and Mrs. A. Mizuno and K. Hirao for active collaboration.

Appendix

Hereafter we abbreviate $2p_{\alpha A}$ AO as α_A ($\alpha=x$, y, or z), since only the 2p AO's appear in the following equations.

(i) SD term

(a) Level A approximation

$$(\boldsymbol{K}_{AB}^{(2)})_{\alpha\alpha} = -(4\beta^2/25)\langle r^{-3}\rangle_A\langle r^{-3}\rangle_B \sum_i^{occ}\sum_j^{vac} ({}^3\Delta E_{i\to j})^{-1} \times [4(2C_{i\alpha A}C_{j\alpha A} - \sum'_{\delta(\neq\alpha)} C_{i\delta A}C_{j\delta A})(2C_{i\alpha B}C_{j\alpha B} - \sum'_{\delta(\neq\alpha)} C_{i\delta B}C_{j\delta B}) + 9\sum'_{\delta(\neq\alpha)}(C_{i\alpha A}C_{j\delta A}+C_{i\delta A}C_{j\alpha A}) \times (C_{i\delta B}C_{j\alpha B}+C_{i\alpha B}C_{j\delta B})] \quad (A\cdot1\text{-a})$$

$$(\boldsymbol{K}_{AB}^{(2)})_{\substack{\alpha\\(\alpha\neq\beta)}\beta} = -(12\beta^2/25)\langle r^{-3}\rangle_A\langle r^{-3}\rangle_B \sum_i^{occ}\sum_j^{vac} ({}^3\Delta E_{i\to j})^{-1} \times [(4C_{i\alpha A}C_{j\alpha A} - 2\sum'_{\delta(\neq\alpha)} C_{i\delta A}C_{j\delta A})(C_{i\alpha B}C_{j\beta B}+C_{i\beta B}C_{j\alpha B}) + (C_{i\alpha A}C_{j\beta A}+C_{i\beta A}C_{j\alpha A})(4C_{i\beta B}C_{j\beta B} - 2\sum'_{\delta(\neq\beta)} C_{i\delta B}C_{j\delta B}) + 3(C_{i\alpha A}C_{j\gamma A}+C_{i\gamma A}C_{j\alpha A})(C_{i\beta B}C_{j\gamma B}+C_{i\gamma B}C_{i\beta B})] \quad (A\cdot1\text{-b})$$

(b) Level B approximation

$$(\boldsymbol{K}_{AB}^{(2)})_{\alpha\alpha} = (2\beta^2/25)\langle r^{-3}\rangle_A\langle r^{-3}\rangle_B({}^3\Delta E)^{-1} \times [2(4P^2_{\alpha A\alpha B}+P^2_{\beta A\beta B}+P^2_{\gamma A\gamma B}) + 9P_{\alpha A\beta B}(P_{\beta A\beta B}+P_{\gamma A\gamma B}) - 2(2P^2_{\alpha A\beta B}+2P^2_{\alpha A\gamma B} + 2P^2_{\beta A\alpha B}+2P^2_{\gamma A\alpha B}-P^2_{\beta A\gamma B}-P^2_{\gamma A\beta B}) + 9(P_{\alpha A\beta B}P_{\beta A\alpha B}+P_{\alpha A\gamma B}P_{\gamma A\alpha B})] \quad (A\cdot2\text{-a})$$

$$(\boldsymbol{K}_{\substack{AB\\(\alpha\neq\beta)}}^{(2)})_{\alpha\beta} = (6\beta^2/25)\langle r^{-3}\rangle_A\langle r^{-3}\rangle_B({}^3\Delta E)^{-1} \times [4(P_{\alpha A\alpha B}P_{\alpha A\beta B}+P_{\beta A\beta B}P_{\alpha A\beta B} + 3(P_{\alpha A\beta B}P_{\gamma A\gamma B}+P_{\alpha A\gamma B}P_{\gamma A\beta B}) - 2(P_{\alpha A\alpha B}P_{\beta A\alpha B}+P_{\beta A\beta B}P_{\beta A\alpha B} + P_{\alpha A\gamma B}P_{\beta A\gamma B}+P_{\gamma A\alpha B}P_{\gamma A\beta B})] \quad (A\cdot2\text{-b})$$

(ii) OB term

Under the one-center integral approximation, the contribution coming from $\mathscr{H}_1^{(a)}$ becomes zero, and we have only to consider the contribution coming from $\mathscr{H}_1^{(b)}$ (*cf.* Eqs. (1) and (2)).[9]

(a) Level A approximation

$$(\boldsymbol{K}_{AB}^{(1b)})_{\alpha\alpha} = 16\beta^2\langle r^{-3}\rangle_A\langle r^{-3}\rangle_B \sum_i^{occ}\sum_j^{vac} ({}^1\Delta E_{i\to j})^{-1} \times (C_{i\gamma A}C_{j\beta A}-C_{i\beta A}C_{j\gamma A}) \times (C_{i\beta B}C_{j\gamma B}-C_{i\gamma B}C_{j\beta B}) \quad (A\cdot3\text{-a})$$

$$(\boldsymbol{K}_{AB}^{(1b)})_{\alpha\beta} = 16\beta^2\langle r^{-3}\rangle_A\langle r^{-3}\rangle_B \sum_l^{occ}\sum_j^{vac} ({}^1\Delta E_{i\to j})^{-1} \times (C_{i\gamma A}C_{j\beta A}-C_{i\beta A}C_{j\gamma A})(C_{i\gamma B}C_{j\alpha B}-C_{i\alpha B}C_{j\gamma B}) \quad (A\cdot3\text{-b})$$

(b) Level B approximation

$$(\boldsymbol{K}_{AB}^{(1b)})_{\alpha\alpha} = 8\beta^2\langle r^{-3}\rangle_A\langle r^{-3}\rangle_B({}^1\Delta E)^{-1}(P_{\beta A\beta B}P_{\gamma A\gamma B} - P_{\beta A\gamma B}P_{\gamma A\beta B}) \quad (A\cdot4\text{-a})$$

$$(\boldsymbol{K}_{AB}^{(1b)})_{\alpha\beta} = 8\beta^2\langle r^{-3}\rangle_A\langle r^{-3}\rangle_B({}^1\Delta E)^{-1}(P_{\beta A\gamma B}P_{\gamma A\alpha B} - P_{\beta A\alpha B}P_{\beta A\gamma B}) \quad (A\cdot4\text{-b})$$

Note that, although the tensor due to the FSD term is symmetric, those due to the SD and OB terms are not necessarily symmetric. For the FC contribution, its tensor is diagonal and given by Pople and Santry[16] for both approximations.

37) For CH_3F, the increase in the H–C–H angle about 1° is necessary in order to explain the difference between theoretical and experimental values. For CH_3I, it is about 20′. For the molecules for which the values of the $(J_{CH})_{aniso}$ in Table 1 are negative, the decrease in the H–C–H angle is necessary (Ref. 14). The energy necessary for the change of this order in the H–C–H angle is less than 20~30 calories.

38) Saupe, Englert, and Povh (Ref. 7a, 7c, 7h) studied the molecular geometry of CH_3CN dissolved in three nematic solvents and observed slight differences in H–C–H angle. They interpreted these differences as due to those of the protonating abilities of these solvents. Englert and Saupe (Ref. 7a) obtained the C–N bond length considerably shorter than its microwave geometry, and they suggested that the change is caused by the solvent-solute interaction such as the interaction of the polar C–N bond with the electric reaction field induced by nematic solvent molecules.

Steric Effects in Azo Compounds. The Electric Dipole Moments and the Absorption Spectra of Azobenzene Derivatives

Shunzo YAMAMOTO, Norio NISHIMURA, and Shigeo HASEGAWA

Department of Chemistry, Faculty of Science, Okayama University, Tsushima, Okayama

(Received October 12, 1970)

The electric dipole moments of *trans*-4-*N*,*N*-dimethylaminoazobenzene and its derivatives, and the absorption spectra of azobenzene derivatives and their conjugate acids have been measured. The dipole moment and the intensity of the π–π^* band are clearly reduced by introduction of methyl groups into ortho positions to azo group. The twisting angle of the benzene rings with respect to the azo group has been estimated for 2,2′-disubstituted azobenzenes and their conjugate acids by means of the Braude equation. From the spectral intensity and transition energy, it was concluded that the conjugate acids are generally more susceptible than the bases to the steric effect.

It is well known that steric hindrance affects certain physical and chemical properties of organic compounds.[1] The twist of molecule about a *single* bond in a conjugated system is of particular interest, the physical properties being susceptible to the twist.[2–4] This makes experimental approach possible.

Minkin *et al.*[5] showed that aromatic azomethines have a nonplanar conformation in which the dihedral angle between the amino nucleus and the rest of the molecule plane is 40—60°. Acoplanarity of the molecule is supported by the following: low intensity of π–π^* conjugation band and absence of fluorescence in contrast to the isoelectronic analogues—stilbenes and azobenzenes; low basicity, nonisolation of *cis*-isomers.

The dipole moments of aromatic amines[6] and nitro compounds[7,8] are greatly reduced by ortho substitution. A similar effect has been reported for biphenyls,[9] stilbenes,[10] and other aromatic compounds.[11] The reduction in dipole moment by ortho substitution is interpreted as due to the reduced conjugation which arises from the twisting of molecule about a single bond in a conjugated system.[2]

It has been recognized that when the molecule is sufficiently crowded to render coplanarity of the conjugated atoms difficult or impossible, the electronic spectra differ from those expected for a planar model.

In a conjugated system X–Y, change in steric conformation about the single bond can give rise to three types of spectral effects[12]: (A) Slight twisting about the single bond, the spectroscopic result being hypochromic effect only. (B) moderate twisting resulting in both a hypochromic effect and a hypsochromic shift. (C) Severe twisting resulting in complete steric inhibition of resonance, and giving rise to the cumulative spectra of the two isolated chromophores X and Y.

Good example of type (A) are provided by alkylated benzaldehydes, acetophenones, cyclic aromatic ketones, and related compounds.[2] The angle of twist θ can be calculated according to the Braude equation,[2] by which Finar[13] evaluated the angle of twist for some sterically hindered pyrazoles. Jaffé and Orchin[12] attempted an unified explanation for the spectra of (A) and (B); the observed hypochromic effect exhibited by both slightly hindered and moderately hindered stilbenes could be explained by their interpretation.

Azobenzene and its meta- and para-substituted derivatives have planar structure which is due to the energy stabilization by extended π-electron conjugation.[14] However, if substituents are introduced into one or both benzene rings on the ortho positions to the azo group, a steric hindrance between the substituents and the lone-pair electrons on the N-atoms will make the molecule twist around the –N=N– bonds,[15,16] the extent of twist being determined by a compromise of the mesomeric stabilization with the steric factor.

The spectra of substituted azobenzenes have been reported by many workers,[17,18] and systematic studies of the effects of substituents on the spectra have been carried out. Gore and Wheeler[15] measured the

1) M. S. Newman, "Steric Effects in Organic Chemistry," ed. by M. S. Newman, John Wiley, New York (1956), pp. 164, 479.
2) E. A. Braude and F. Sondheimer, *J. Chem. Soc.*, **1955**, 3754.
3) H. Suzuki, This Bulletin, **32**, 1340 (1959).
4) H. H. Jaffé and M. Orchin, "Theory and Applications of Ultraviolet Spectroscopy," John Wiley, New York (1962). pp. 384—449.
5) V. I. Minkin, Yu. A. Zhdanov, E. A. Medyantzeva, and Yu. A. Ostroumov, *Tetrahedron*, **23**, 3651 (1967).
6) R. H. Birtles and G. C. Hampson, *J. Chem. Soc.*, **1937**, 10; C. E. Ingham and G. C. Hampson, *ibid.*, **1939**, 981.
7) H. Koford, L. E. Sutton, P. E. Verkade, and B. M. Wepster, *Rec. trav. chim.*, **78**, 790 (1959).
8) R. Nakashima, *Nippon Kagaku Zasshi*, **83**, 672 (1962).
9) K. B. Everard, L. Kumar, and L. E. Sutton, *J. Chem. Soc.*, **1951**, 2807.
10) K. B. Everard and L. E. Sutton, *ibid.*, **1951**, 2816.
11) J. W. Baker and W. T. Tweed, *ibid.*, **1941**, 796.
12) H. H. Jaffé and M. Orchin, *ibid.*, **1960**, 1078.
13) I. L. Finar, *ibid.*, **1968**. 725.
14) J. M. Robertson, *ibid.*, **1939**, 232.
15) P. E. Gore and O. H. Wheeler, *J. Org. Chem.*, **26**, 3295 (1961).
16) D. Gegiou, K. A. Muszkat, and E. Fischer, *J. Amer. Chem. Soc.*, **90**, 3907 (1968).
17) a) W. R. Brode, *ibid.*, **48**, 1984 (1926); *Ber.* **61**, 1722 (1928). b) A. H. Cook, D. G. Jones, and J. B. Polya, *J. Roy. Chem. Soc.*, **1939**, 1315; D. G. Jones, *J. Roy. Coll. Sci.*, **10**, 52 (1940). c) W. R. Brode, J. H. Gould, and G. M. Wyman, *J. Amer. Chem. Soc.*, **74**, 4641 (1952). d) G. M. Badger and R. G. Buttery, *J. Chem. Soc.*, **1953**, 2156.
18) a) L. Skulski, *Bull. Acad. Polon. Sci., ser. Sci. Chim.*, **12**, 719 (1956). b) P. P. Birnbaum, J. H. Linford, and D. W. G. Style, *Trans. Faraday Soc.*, **49**, 735 (1953).

spectra of some of 2,2′-disubstituted azobenzenes and calculated the angle of distortion from coplanarity by means of the Braude equation. However, no wide spectral investigation seems to have been made on these substances in relation to the steric effect. Only a few studies were made on how the steric effect causes the change in their dipole moments. This paper presents the dipole moment and the spectral data of azobenzene derivatives. The spectral data of their conjugate acids are also given, from which the molecular conformation is discussed.

Experimental

Compounds. Symmetrically substituted azobenzenes were prepared by the following procedures.[19]

4,4′-*Dimethylazobenzene*: A solution of 13.8 g of sodium nitrite in 200 m*l* of water was added dropwise with stirring to a solution of 20 g of *p*-toluidine in 136 m*l* of 13% hydrochloric acid, the temperature of the solution being kept below 5°C with ice bath. The diazonium solution was added to a stirred solution containing 70 g of cupric sulfate, 30 g of hydroxylamine hydrochloride, 48 m*l* of 50% solution of potassium hydroxide and 100 m*l* of 33% aqueous solution of ammonia. The product was dissolved in benzene, and the solution was passed through an alumina column, and then crystallized from benzene.

Azobenzene: mp 68°C (lit, 68°C)

2,2′-Dimethylazobenzene: mp 55°C (lit, 55°C)

3,3′-Dimethylazobenzene: mp 53°C (lit, 54—55°C)

4,4′-Dimethylazobenzene: mp 144°C (lit, 144°C)

2,2′-Dichloroazobenzene: mp 137°C (lit, 137°C)

3,3′-Dichloroazobenzene: mp 103.5°C (lit, 102—103.5°C)

4,4′-Dichloroazobenzene: mp 185°C (lit, 183—184°C)

2,2′-Dimethoxyazobenzene: mp 154°C (lit, 154—155°C)

4,4′-Dimethoxyazobenzene: mp 163.5°C (lit, 160.5—162.5°C)

2,3,2′,3′-Tetramethylazobenzene: mp 110—110.5°C (lit, 110—111°C)

2,4,2′,4′-Tetramethylazobenzene: mp 128—128.5°C (lit, 125—126°C)

2,5,2′,5′-Tetramethylazobenzene: mp 119—119.5°C (lit, 119°C)

3,4,3′,4′-Tetramethylazobenzene; mp 157°C (Found: C, 80.50; H, 7.86; N, 11.89%. Calcd: C, 80.63; H, 7.61; N, 11.76%).

2,2′-Dimethyl-3,3′-dichloroazobenzene: mp 154°C (lit, 153—154°C)

2,2′-Dimethyl-4,4′-dichloroazobenzene: mp 164—165°C (Found: C, 60.19; H, 4.59; N, 10.12%. Calcd: C, 60.23; H, 4.33; N, 10.04%).

The derivatives of 4-*N*,*N*-dimethylaminoazobenzene were prepared and purified by the following procedure.

4-N,N-*Dimethylaminoazobenzene*[20]: 4-*N*,*N*-Dimethylaminoazobenzene was prepared by diazotizing aniline and coupling the resulting diazonium salt with dimethylaniline in an acetate buffer. Other compounds of Types II and II′ were prepared in a similar way. The products were dissolved in benzene, and the solutions were passed through an alumina column, and then crystallized from benzene.

4-*N*,*N*-Dimethylaminoazobenzene: mp 118—119°C (lit, 119—120°C)

4-Methyl-4′-*N*,*N*-dimethylaminoazobenzene: mp 170—171°C (lit, 169.5—170°C)

4-Chloro-4′-*N*,*N*-dimethylaminoazobenzene: mp 158—158.5°C (lit, 158—158.5°C)

3-Nitro-4′-*N*,*N*-dimethylaminoazobenzene: mp 157—157.5°C (lit, 157—158°C)

4-Nitro-4′-*N*,*N*-dimethylaminoazobenzene: mp 228°C (lit, 230—231°C)

2,2′-Dimethyl-4-*N*,*N*-dimethylaminoazobenzene: mp 79—80°C (Found: C, 75.62; H, 7.97; N, 16.60%. Calcd: C, 75.85; H, 7.56; N, 16.59%).

2,4,2′-Trimethyl-4′-*N*,*N*-dimethylaminoazobenzene: mp 120—121°C (Found: C, 76.15; H, 7.94; N, 15.93%. Calcd: C, 77.37; H, 7.92; N, 15.72%).

2,2′-Dimethyl-4-chloro-4′-*N*,*N*-dimethylaminoazobenzene: mp 115—116°C (Found: C, 66.98; H, 6.56; N, 14.55%. Calcd: C, 66.77; H, 6.30; N, 14.60%).

2,2′-Dimethyl-5-nitro-4′-*N*,*N*-dimethylaminoazobenzene: mp 148—148.5°C (Found: C, 64.20; H, 6.23; N, 18.97%. Calcd: C, 64.41; H, 6.08; N, 18.78%).

2,2′-Dimethyl-4-nitro-4′-*N*,*N*-dimethylaminoazobenzene: mp 147—148°C (Found: C, 64.58; H, 6.38; N, 18.95%. Calcd: C, 64.41; H, 6.08; N, 18.78%).

Benzene: Benzene was purified successively by shaking with concentrated sulfuric acid and water, drying over sodium wire, and distillation.

Cyclohexane: Cyclohexane was washed several times with a mixture of concentrated nitric and sulfuric acids. After repeated washing with distilled water it was distilled over sodium.

Ethyl Alcohol: Ethyl alcohol was of reagent grade and was used without further purification.

Sulfuric Acid: Sulfuric acid of commercial special grade was used without purification.

Measurement of Dielectric Constant and Density. Six solutions of each compound with weight fractions between 0 and 0.015 were used. The solutions were allowed to stand in the dark for a few hours in order to avoid contamination with *cis*-isomers.

The dielectric constants were determined with a Dielectric Analyzer, Type FAM-3A, manufactured by Yamato Scientific Instrument Co. The oscillator, controlled by a quartz crystal, was operated at frequency of 2MHz. The accuracy of the precision variable condenser, taken from the average of several readings, was about one part in 10000 for the cell filled with air.

The densities of the same solutions were measured in an Ostwald type pycnometer of about 5 m*l*. All the measurements were carried out in a thermostat regulated at 25±0.01°C.

Further, to insure that the instruments were properly calibrated and that the method of calculation was appropriate, the dipole moments of *p*-chloroaniline and chlorobenzene were determined. The results were 2.99 D for *p*-chloroaniline, and 1.58 D for chlorobenzene, and were in good agreement with literature values (2.99 D for *p*-chloroaniline and 1.55 D and 1.58 D for chlorobenzene) which were obtained under similar condition.

Measurement of Absorption Spectra. Absorption spectra were measured with a Hitachi double beam spectrophotometer, Model 124. The absorption spectra of the bases were measured in cyclohexane solutions. The measurements for the conjugate acids were made in a mixture of ethyl alcohol and sulfuric acid. The solutions were kept to stand in the dark until the absorbance became constant. All the measurements were made at room temperature.

19) F. Meyer and E. Trampedach, *Ann.*, **320**, 125 (1902).
20) M. Isaks and H. H. Jaffé, *J. Amer. Chem. Soc.*, **86**, 2209 (1964).

Results

Azobenzene derivatives and their conjugate acids of the following types were used.

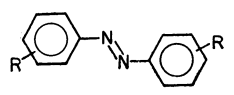

I

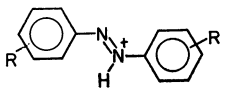

Ia

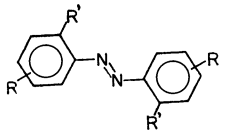

I'

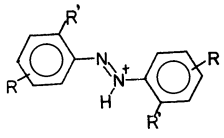

Ia'

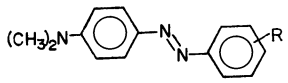

II

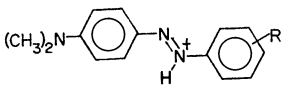

IIa

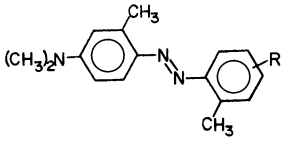

II'

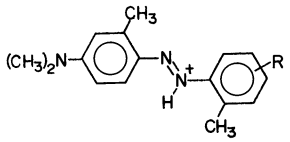

IIa'

Dipole Moment. It is generally recognized that both dielectric constant ε and density d of a solution are linearly related to the weight fraction w of the solute for dilute solutions. If these relationships hold, as was the case in this experiment, the molar polarization P can be calculated by means of the following Halverstadt-Kumler equation.[21]

$$P = \frac{(\varepsilon_0-1)}{(\varepsilon_0+2)} \cdot \frac{M}{d_0}\left\{1 + \frac{3a}{(\varepsilon_0+1)(\varepsilon_0+2)} - \frac{b}{d_0}\right\} \qquad (1)$$

where d_0 and ε_0 are the density and the dielectric constant of the solvent, respectively, and the constants a and b are the slopes of the linear plots of ε, and d against w, respectively.

The electric dipole moment of a solute is related to the molar polarization by the following well-known equation.

$$\mu^2 = (9\boldsymbol{k}T/4\pi N)(P-P_E-P_A) \qquad (2)$$

where P_E and P_A are the electronic and atomic polarizations, respectively. It is generally accepted that the sum (P_E+P_A) can be put equal to $1.05\,R_M$ in good approximation,[22] where R_M is the molar refractivity estimated from bond refractivities.[23,25]

The dipole moments of various substituted azobenzenes have been obtained on the basis of Eqs. (1) and (2), and are listed in Table 1 with relevant data. The calculated dipole moments $(\mu_0+\mu_g)$, where μ_0 is the dipole moment of a reference compound (R=H for Types II and II'), and μ_g denotes the group moment of the substituent R, are listed in the last column. We see that the choice of reference compound gives the relationship $\mu_{obsd} \approx (\mu_0+\mu_g)$. For *p*-nitro compound, however, the agreement is poor. This may arise from the large contribution of the type

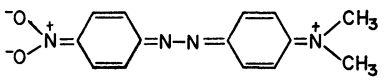

Table 1. Dipole moments of 4-*N*,*N*-dimethylamino-azobenzene derivatives with relevant data

Substituent R	*a*	*b*	R_M cc	*P* cc	μ_{obsd} D	$\mu_0+\mu_g$[a,b] D
Type II						
H	5.27	0.19	75.5	281.6	3.17	3.17
4'-CH_3	3.50	0.15	76.5	225.2	2.66	2.77
4'-Cl	9.20	0.22	76.7	516.3	4.61	4.71
3'-NO_2	16.80	0.24	78.3	922.5	6.41	6.19
4'-NO_2	25.50	0.28	78.3	1361.7	7.91	7.13
Type II'						
H	3.60	0.20	85.3	237.6	2.73	2.73
4'-CH_3	2.80	0.34	85.9	196.8	2.28	2.33
4'-Cl	7.60	0.29	86.0	467.3	4.29	4.27
5'-NO_2	14.40	0.24	87.6	883.0	6.22	5.83
4'-NO_2	21.60	0.24	87.6	1284.3	7.63	6.69

a) Vector combination
b) μ_g=0.40D for CH_3, 1.54D for Cl, and 3.96D for NO_2

Absorption Spectra. Azobenzene derivatives have two distinct absorption bands in the near ultraviolet and visible regions. The band at 320—360 mμ is relatively intense (ε, 10000—30000), whereas the band at 430—460 mμ is considerably weaker (ε, 400—1000). The former is known to be the π–π^* band (conjugation band) and the latter n–π^* band.[26] The absorption maxima and the molar extinction coefficients for Types I and I' are collected in Table 2.

It can be seen that both the position and intensity of the conjugation band are considerably affected by substitution. As far as these data are concerned, the substitution in azobenzene always produces a bathochromic shift as compared with the spectrum of azobenzene. For 3,3'-dimethyl- and 3,3'-dichloroazobenzenes, however, the shift is very small, since the mesomeric effect is inoperative in meta positions. In addition, the molar extinction coefficients of these substances do not differ much from the parent compound. Similar findings have been reported by Gore and Wheeler for azoxybenzene derivatives.[27]

Discussion

Braude and Sondheimer[2] proposed the following equation, which relates the interplanar angle θ between the aryl and the carbonyl chromophores of benzalde-

21) W. D. Kumler and I. F. Halverstadt, *J. Amer. Chem. Soc.*, **64**, 1941 (1942).
22) L. G. Groves and S. Sugden, *J. Chem. Soc.*, **1935**, 971.
23) For nitro group, the group refractivity of 8.5 cc was used.[24]
24) T. Shimozawa and U. Morino, *Nippon Kagaku Zasshi*, **81**, 20 (1960).
25) A. I. Vogel, W. T. Cresswell, G. H. Jeffery, and J. Leicester, *J. Chem. Soc.*, **1952**, 514.
26) H. H. Jaffé, Si-Jung Yeh, and R. M. Gardner, *J. Mol. Spectrosc.*, **2**, 120 (1958).
27) P. H. Gore and O. H. Wheeler, *J. Amer. Chem. Soc.*, **78**, 2160 (1956).

TABLE 2. ABSORPTION SPECTRA OF AZOBENZENES AND THEIR CONJUGATE ACIDS

No.	Base		Conjugate Acid		
	π-π^* band	n-π^* band	π-π^* band		
	λ_{max} (mμ) (ε)	λ_{max} (mμ) (ε)	λ_{max} (mμ)		(ε)
			45% H_2SO_4	90% H_2SO_4	
1	317 (22,100)	447 (450)	417	426	(26,400)
2	331 (18,900)	464 (550)	435	447	(24,900)
3	323 (20,900)	447 (470)	428	437	(26,400)
4	330 (27,000)	444 (630)	446	458	(36,400)
5	328 (15,000)	467 (450)	435	443	(20,500)
6	318 (19,300)	449 (430)	412	423	(22,400)
7	331 (26,400)	444 (640)	443	457	(34,700)
8	366 (10,300) [a]	454 (470)	492	491	(29,900)
8	310 (7,400) [a]				
9	353 (24,700)	418 [b]	501	493	(37,000)
10	332 (19,400)	458 (610)	437	453	(26,700)
11	346 (22,800)	458 (810)	464	476	(34,200)
12	336 (16,900)	463 (660)	447	467	(20,700)
13	333 (24,700)	441 (650)	460	470	(36,400)
14	329 (19,500)	461 (560)	428	441	(24,000)
15	346 (25,200)	461 (870)	461	476	(35,700)

a) Apparent molar extinction coefficient b) Shoulder

No.	Substituent	No.	Substituent	No.	Substituent
1	——	6	3,3'-dichloro	11	2,4,2',4'-tetramethyl
2	2,2'-dimethyl	7	4,4'-dichloro	12	2,5,2',5'-tetramethyl
3	3,3'-dimethyl	8	2,2'-dimethoxy	13	3,4,3',4'-tetramethyl
4	4,4'-dimethyl	9	4,4'-dimethoxy	14	2,2'-dimethyl-3,3'-dichloro
5	2,2'-dichloro	10	2,3,2',3'-tetramethyl	15	2,2'-dimethyl-4,4'dichloro

hyde and acetophenone derivatives to the dipole moment.

$$\cos^2\theta = (\mu_{obsd} - \mu_{90°})/(\mu_{0°} - \mu_{90°}) \quad (3)$$

where $\mu_{90°}$ is the moment for completely deconjugated system in which the phenyl and carbonyl planes are at right angle. This equation may hold for any system in which a change in dipole moment arises from a twist by which conjugation is broken.

For 2,2'-disubstituted *trans*-azobenzene derivatives, the situation becomes more complicated. For example, if the molecular frame takes a coplanar structure, conformations of the following types are possible.

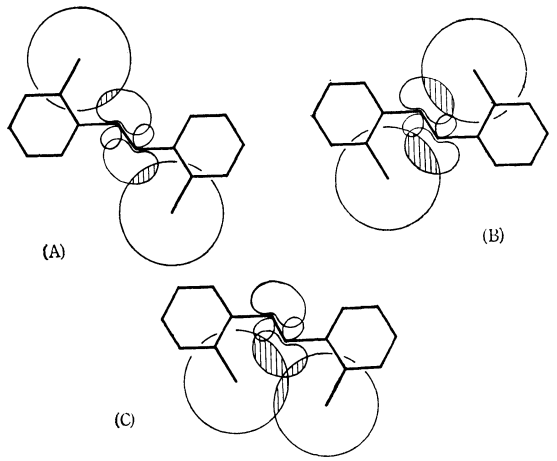

Fig. 1. Conformations of 2,2'-dimethylazobenzene.

In the above conformations, each mushroom-shaped region represents the sp^2-density function (ψ^2=0.01). The probability of finding the lone pair electrons within this region is *ca.* 0.95. The van der Waals radius for methyl group is assumed to be 2.0 Å.[28] The interaction energy between the methyl group and the n-electrons cannot be estimated in a simple manner. However, the steric hindrance will become severer in the order A<B<C. In conformation C, the van der Waals radii of the methyl groups also overlap. Thus, comformation A is the most likely, and conformation C is the least likely. In this case, the molecule will be twisted to some extent relative to conformation A, owing to the steric hindrance. It is noted that if the repulsion between the methyl group and the nitrogen atom is considered using van der Waals radii, there would arise no advantage by twisting. Actually, two types of twist may be possible as indicated:

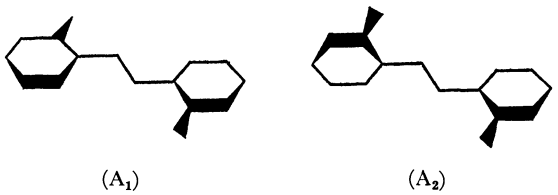

If one neglects both the long-range force between

28) L. Pauling, "The Nature of the Chemical Bond," 3rd ed., Cornell Univ. Press, New York, (1959), p. 260.

methyl groups and the resonance and overlap integrals between non-adjacent atoms, an equal number of isomer molecules of the above types will exist, and the observed dipole moment μ_{obsd} may be given by

$$\mu^2_{obsd} = (\mu^2_1+\mu^2_2)/2 \quad (4)$$

where μ_1 and μ_2 are the dipole moments of the isomers A_1 and A_2, respectively. In conformation A_1, the moments due to the two methyl groups, μ_{CH_3}, cancel each other. In conformation A_2, these moments do not cancel. If this is taken into account, Eq. (4) can be modified as

$$\mu^2_{obsd} = \mu^2_1 + 2\mu^2_{CH_3}\sin^2\theta \quad (5)$$

The group moment of methyl group is 0.40D.[29] If the angle of twist θ is small, as will be indicated later, the contribution of the second term can be neglected.[30]

We might conclude that ortho disubstituted azobenzenes are twisted in a way to take either one or both conformations of A_1 and A_2. It is generally accepted that the value of σ-moment is not affected considerably by twisting.[31] Hence, it is the π-moment that is affected by the twisting, and this will make the estimation of twisting angle possible by means of Eq. (3). However, in 2,2′-disubstituted azobenzenes, there are two bands around which the molecules are twisted. In order to examine the validity of the use of Eq. (3), in such cases, the π-moments of 4-*N*,*N*-dimethylaminoazobenzene and its derivatives were calculated as a function of θ, by means of the equation

$$\mu_\pi = e\sum Q_r r_r \quad (6)$$

where e is the electronic charge, and Q_r and r_r are the net charge and the position vector of rth atom, respectively. In calculating r_r, the following values for bond length were used: C–C=1.39 Å, C–N=1.45 Å, N=N=1.23 Å, C–Cl=1.70 Å, C–CH_3=1.53 Å; all the bond angles being assumed to be 120°. The net charge Q_r was estimated by means of the simple LCAO MO method. The displacement of the lone-pair electrons on the azo-nitrogens has been neglected, since these electrons would flow into both benzene rings symmetrically and would not change the dipole moment considerably.

In Table 3, the variation of the π-moments are shown as a function of the assumed twisting angle. Using $\mu(\theta)$-values, the twisting angle was calculated by means of Eq. (3). We see that the assumed and calculated twisting angles agree very well, showing that the Braude equation is applicable in the present case.

As Table 1 shows the dipole moment is clearly reduced by 0.19—0.44 D by the introduction of two methyl groups into ortho positions to azo-group. Thus the twisting angles were estimated by means of Eq. (3). They are listed in Table 4 which shows that θ is about 10° smaller for nitro compounds than for other compounds. For a 4-nitro compound, this might be ascribed to the large contribution of canonical resonance forms. However, it is difficult to express such a contribution for a 3 (or 5)-nitro compound. From Table 1 we see that observed values of μ are always larger than the expected values for nitro compounds, irrespective of the position of the substituent, suggesting the existence of a kind of combined contribution of the nitro group and the dimethylamino group. As Table 6 shows, the large red shift of the π–π^* band ($\Delta\lambda$=20 mμ for 3-nitro and 46 mμ for 4-nitro) with respect to the parent 4-*N*,*N*-dimethylaminoazobenzene may support this view.

From Table 2 we see that 2,2′-disubstituted azobenzenes have absorption maxima of the π–π^* band in a similar position but with lower intensities, as compared with the corresponding 4,4′-disubstituted ones.

TABLE 3. MESOMERIC DIPOLE MOMENTS OF 4-*N*,*N*-DIMETHYLAMINOAZOBENZENES AS A FUNCTION OF THE ANGLE OF TWIST

R	$\theta_{assumed}$ degree	$\mu(\theta)$	θ_{calcd} degree
H	0	6.78	0
	15	6.60	13
	30	5.79	31
	45	4.88	46
	60	3.78	64
	75	3.19	78
	90	3.05	90
4′-CH_3	0	4.51	0
	15	4.38	15
	30	3.89	32
	90	2.29	90
4′-NO_2	0	14.69	0
	15	13.89	20
	30	13.21	28
	90	7.91	90

Parameters used here are:[38]

X	*h*	*k*	*l*
N(azo)	0.5	$\cos\theta$	0
CH_3[13]	1.8	0.54	0
Cl[37]	1.8	0.8	0.18
$N(CH_3)_2$	0.8	1.0	0
		(1.2)[a]	

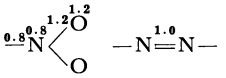

where *h*, *k*, and *l* are the coefficients of the following integrals:
$\alpha_x=\alpha+h\beta$, $\beta_{c-x}=k\beta$, $\alpha_{adj}=\alpha+l\beta$
a) In the nitrodimethylaminoazobenzenes

TABLE 4. ANGLE OF TWIST OF 2,2′-DIMETHYL-4-*N*,*N*-DIMETHYLAMINOAZOBENZENE AND ITS DERIVATIVES

R	$\mu_0°$(D)	μ_θ(D)	$\mu_{90°}$(D)	θ(°)
H	3.17	2.73	1.55	27
4′-CH_3	2.66	2.28	1.15	30
4′-Cl	4.61	4.29	3.09	27
4′-NO_2	7.91	7.63	5.51	20
5′-NO_2	6.41	6.22	4.92	21

29) C. P. Smyth and S. O. Morgan, *J. Amer. Chem. Soc.*, **49**, 1030 (1927).
30) Very recently, we found by means of X-ray analysis that 2,2′-dichloroazobenzene is symmetrically twisted about 12° relative to conformation A.
31) E. G. McRae and L. Goodman, *J. Chem. Phys.*, **29**, 334 (1958).

When four substituents are introduced into azobenzene, the situation becomes complicated. However, an ortho effect on the intensity of the π–π^* band is clearly seen in the table.

Gegiou *et al.*[16], studied sterically hindered azobenzenes (2,4,6- and 2,4,6,2′,4′,6′-methylsubstituted azobenzenes) and found that ortho methylation causes shifts of the n–π^* band to longer wavelengths and higher intensities. They suggested that the increase in intensity is due to the increase in the conjugation between phenyl ring and the lone pair electrons of a nitrogen atom. In the present case, a clear red shift by ortho substitution has been observed, but the increase in intensity is obscure. Introduction of substituent generally causes an increases in intensity of absorption band, even if the steric effect is absent (Table 2). Gegiou *et al.* compared the intensity for 2,4,6- and 2,4,6,2′,4′,6′-methylsubstituted azobenzenes with that for azobenzene. However, the comparison should have been made between sterically hindered azobenzenes and the corresponding unhindered ones. Hence, their suggestion is questionable.

A simple method for evaluating the ortho effect of the substituent at the 2 and 2′ positions from the intensity of the conjugation bands is to use the Braude equation $\varepsilon/\varepsilon_0=\cos^2\theta$ where ε_0 is the value of the extinction coefficient of a reference, unhindered parent compound and θ is the angle of twist to be calculated.[32] The values of θ, calculated according to the Braude equation for a number of azobenzene derivatives of the Type I′ are given in Table 5.

Table 5. Angle of twist of benzene rings in 2,2′-disubstituted azobenzenes and their conjugate acids[a]

No.	Base		Conjugate acid	
	$\varepsilon/\varepsilon_0$	θ	$\varepsilon/\varepsilon_0$	θ
2	0.698	33°	0.684	34°
10	0.787	27°	0.734	31°
12	0.684	34°	0.569	41°
5	0.567	41°	0.590	40°
8	0.417	50°	0.808	26°

a) The parent compounds are corresponding 4,4′disubstituted azobenzenes.

Gore and Wheeler[15] have used this equation to calculate the angle of twist for some 2,2′-disubstituted azobenzene. The values they estimated for 2,2′-dimethyl-, 2,2′-dichloro-, and 2,2′-dimethoxyazobenzenes are 23°, 35°, and 18°, respectively. It can be seen that for 2,2′-dimethoxyazobenzene, the twisting angle is considerably different from that of Gore *et al.* We have examined the possible causes of this disagreement and concluded that their ε-value (13100) for 4,4′-dimethoxyazobenzene was too small (compare ε-values for other compounds in the corresponding table).

32) S. Tabak, I. I. Grandberg, and A. N. Kost, *Tetrahedron*, **22**, 2703 (1966).

33) G. Gabor and K. H. Bar-Eli, *J. Phys. Chem.*, **72**, 153 (1968).

Table 6. Absorption spectra of 4-*N*,*N*-dimethylaminoazobenzenes and their conjugate acids

No.	Base		Conjugate acid	
	λ_{max}(mμ)	ε	λ_{max}(mμ)	λ_{max}(mμ)
16	400	30400	315	516
17	400	28800	329	510
18	400	31800	326	528
19	399	29900	341	520
20	410	34100	323	520
21	411	31000	338	510
22	420	31600	306	503
23	425	29800	319	492
24	446	33500	328	510
25	452	32000	335	504

No.	Substituent	No.	Substituent
16	——	21	2,2′-dimethyl-4′chloro
17	2,2′-dimethyl	22	3′-nitro
18	4′-methyl	23	2,2′-dimethyl-5′-nitro
19	2,2′,4′-trimethyl	24	4′-nitro
20	4′-chloro	25	2,2′-dimethyl-4′-nitro

Table 7. Angle of twist of benzene rings in 2,2′-dimethyl-4-*N*,*N*-dimethylaminoazobenzenes[a]

No.	$\varepsilon/\varepsilon_0$	θ	θ[b]
17	0.945	13°	27°
19	0.940	14°	30°
21	0.909	17°	27°
23	0.942	14°	20°
25	0.957	12°	21°

a) The parent compounds are corresponding ones which have no methyl groups in ortho positions.
b) Estimated from dipole moment.

According to Gabor and Bar-Eli,[33] there are two conformational trans isomers for 2,2′-dimethoxyazobenzene which have peaks at 370 and 310 mμ. In our case the twisting angle of 50°C for this compound was estimated using the apparent molar extinction coefficient at 370 mμ. Hence, the value must have been overestimated.

The absorption maxima and the molar extinction coefficients for molecules of Types II and II′ are shown in Table 6. The values of θ calculated by means of the Braude equation are given in Table 7. It should be noted that the values are about 10° smaller than those estimated from the dipole moments of these molecules. In both cases, the twisting angles of the species of Type II′ were calculated with the species of Type II as references. The group moments of the two methyl groups in ortho positions act so as to cancel each other. Introduction of methyl groups gives rise to an extra hyperchromic effect. The spectroscopic θ-values have not been taken into account for this effect, and this might be the cause for the discrepancy.

The twisting angles of the molecules of Type I′ are 10—20° larger than those of Type II′, as seen in Tables 5 and 7. Since the hyperchromic effect in Types I and I′ is almost the same in the absence of the steric effect, the values in Table 7 must have been underestimated.

The conjugate acids of azobenzenes (Types I_a and I_a') show a very strong band in the visible region. Its absorption maxima and extinction coefficients are collected in Table 2. The band has been attributed to the conjugation band. The substitution effect on it is larger for the acids than for the original bases. Further, the absorption spectra of the conjugate acids of azobenzenes are markedly affected by solvents. As the concentration of sulfuric acid in ethanol-sulfuric acid mixture increases, the conjugation band shifts to a longer wave-length. Thus the transition energy should be extrapolated to zero concentration of sulfuric acid for the discussion of steric effect. Actually, however, the comparison of the transition energies of the species of Type I_a with those of species of Type I_a' was made in a ethanol-sulfuric acid mixture (45 : 55 in volume), since the solvent effect is almost the same for these compounds.

All these compounds are protonated almost completely in 90 vol% sulfuric acid.[34] ε-Values in this condition are listed in Table 2. The angle of twist of these acids were calculated according to the Braude equation and are listed in Table 5. We see that the values are appreciably larger than those for free bases, indicating that the conjugate acids are more susceptible to the steric effect than the original bases. This is supported by the effect of substituents on the transition energies.

The influence of substituents on the transition energy was examined on the basis of the data in Table 2. The relationship between the transition energies of the conjugation band of the bases and those of the conjugate acid is shown in Fig. 2. The points for compounds of Types I and I_a give a straight line with a slope larger than unity. This indicates that the change in the transition energy of the base upon introduction of substituents is proportional to that for the acids and that this change is larger for the acid than for the base. The points for compounds of Types I′ and I_a', however, deviate upward from the line. The transition energies of compounds of Type I′ are similar to those of Type I. The deviation, therefore, arises from the fact that the effect of substituents on the transition energy for compounds of Type I_a' is smaller than that for compounds of Type I_a. This suggests that the steric effect on the transition energy for the base is negligible, but not for the acid.

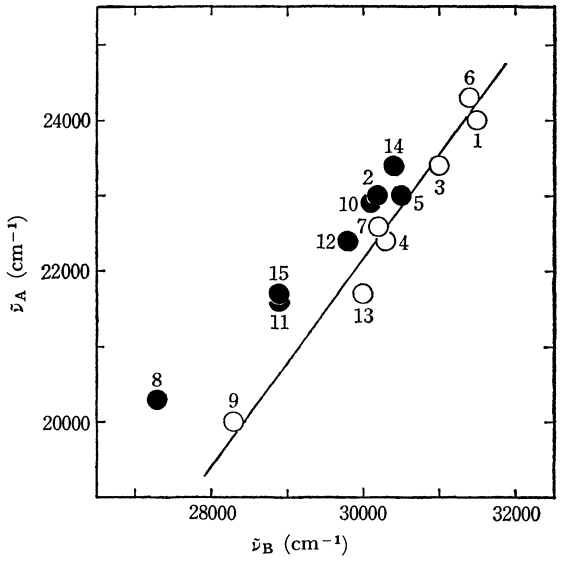

Fig. 2. The relationship between the transition energy of the conjugation band of the base ($\tilde{\nu}_B$) and that of the conjugate acid ($\tilde{\nu}_A$).
(○) Types I and I_a (●) Types I′ and I_a'

From the analysis of the spectral data, it has been clarified[35] that following two types of the conjugate acids for 4-*N*,*N*-dimethylaminoazobenzenes coexist in an acidic solution:

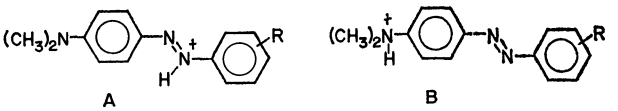

Absorption bands near 500 mμ and 320 mμ have been assigned to the conjugation bands of A and B, respectively (Table 6). As the former band is isolated, its position can be determined precisely. The latter band appearing in a ultraviolet region is rather obscure both in position and intensity. The equilibrium constant between A and B has been discussed, but no precise value has been obtained.[35] Hence the molar extinction coefficients of A and B could not be determined.

Although the twisting angles for the species of Type II_a' could not be estimated, the conjugate acids are

Table 8. Influence of methyl groups on transition energies

No	Substituent in 3′- or 4′-position	Two substituents in 2,2′-positions	$\tilde{\nu}_{max}$(cm^{-1})	$\Delta\tilde{\nu}$(cm^{-1})
a) 4-*N*,*N*-Dimethylaminoazobenzene Derivatives				
16	H	H	25000	0
17	H	CH_3	25000	
18	4′-methyl	H	25000	+100
19	4′-methyl	CH_3	25100	
20	4′-chloro	H	24400	−100
21	4′-chloro	CH_3	24300	
22	3′-nitro	H	23800	−300
23	5′-nitro	CH_3	23500	
24	4′-nitro	H	22400	−300
25	4′-nitro	CH_3	22100	
b) Conjugate Acids				
16	H	H	19400	+200
17	H	CH_3	19600	
18	4′-methyl	H	18900	+400
19	4′-methyl	CH_3	19300	
20	4′-chloro	H	19300	+300
21	4′-chloro	CH_3	19600	
22	3′-nitro	H	19900	+400
23	5′-nitro	CH_3	20300	
24	4′-nitro	H	19600	+200
25	4′-nitro	CH_3	19800	

34) Si-Jung Yeh and H. H. Jaffé, *J. Amer. Chem. Soc.*, **81**, 3274 (1959).

35) a) Si-Jung Yeh and H. H. Jaffé, *ibid.*, **81**, 3283 (1959).
b) F. Gerson and E. Heilbronner, *Helv. Chim. Acta*, **45**, 42 (1962).

susceptible to the steric effect than the bases are, in this case too (Table 8), since the introduction of methyl groups into 2 and 2′ positions increases the transition energy in the case of the conjugate acids, while it decreases in the case of the bases. Thus, the steric effect of the conjugate acids on the transition energy is similar to that of stilbene[12] which has no *n*-electron.

Possible explanations for the above findings are as follows:

a) The delocalization of the lone pair electrons of azo nitrogens into the phenyl rings is partly suppressed by the protonation to a nitrogen atom.

b) The repulsion energy between an ortho methyl group and the proton is larger than that between a methyl group and the lone pair electrons.[36]

c) For the conjugate acids the contribution of the following resonance forms is large in the excited state when the molecule is planar.

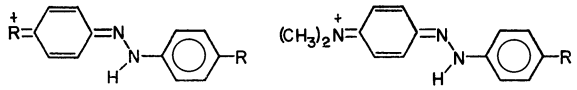

For the bases, however, such contribution may be smaller. As Beale and Roe have pointed out,[37] hindrance to planarity, in the absence of other effects, should increase the energy of the excited state more than that of the ground state, with a shift of the corresponding absorption to higher frequencies.

The authors are deeply grateful to Miss Hiromi Ohtani for elemental analysis.

36) N. L. Allinger and J. C. Tai, *J. Amer. Chem. Soc.*, **87**, 1227 (1965).

37) R. N. Beale and E. M. F. Roe, *ibid.*, **74**, 2302 (1952).

38) J. Kroner and H. Bock, *Chem. Ber.*, **101**, 1922 (1968).

39) H. H. Jaffé, *J. Chem. Phys.*, **20**, 279 (1952).

BULLETIN OF THE CHEMICAL SOCIETY OF JAPAN, VOL. 44, 2025—2030 (1971)

A Theoretical Study of the Electronic Structures of Several Methyl Compounds of Group I, II, and III Elements

Katsutoshi OHKUBO, Hidetoshi SHIMADA, and Masahide OKADA
Faculty of Engineering, Kumamoto University, Kurokami-machi, Kumamoto

(Received November 1, 1970)

The electronic states of the group I, II, and III methyl compounds were investigated using the extended Hückel method, with particular reference to the nature of the bond of metal-carbon. First, the monomers of the group I methyl compounds indicated remarkable electron-localizations on the carbon atom in CH_3. $(CH_3Li)_4$ was found to be a possible tetramer, its total energy being lower by 0.34 eV per CH_3Li unit than that of the CH_3-Li-monomer in spite of the unstability of $(CH_3Li)_2$. Second, $(CH_3)_4Be_2$ was more stable than $(CH_3)_2Be$ by *ca.* 4.04 eV per $(CH_3)_2Be$ unit. Third, the stability of $(CH_3)_3B$ in the form of a monomer was understood well by the fact that its π-bond nature is so much in comparison with that of $(CH_3)_3Al$. Finally, the reactivities in a series of the groups were discussed briefly in connection with the electronic states.

The reactivities of organometallic compounds, in particular those of compounds containing group I, II, and III elements have hitherto attracted many authors' attention.[1-13] An interesting proposal suggested by Gilman[1] and Rocho[2]: the reactivities have a direct relationship with the electronegativities of the metals. However, some obscurities still remain as a result of the lack of information concerning the molecular structures of the compounds.

Recently, the molecular structures of organometallic compounds have been observed in connection with the bridge-type polymerization of the compounds.[14,15] Many X-ray and spectrophotometric studies have been performed in making experimental analyses of the dimer- or polymer-structures of C_2H_5Li,[16,17] n-C_4H_9Li,[18] $(CH_3)_2Be$,[19,20] $(C_2H_5)_2Mg$,[20] $(CH_3)_3Al$,[21,22] and a characteristic monomer of (C-

1) H. Gilman, "Organic Chemistry," 2nd ed., Vol. 1, John Wiley & Sons, New York (1957), p. 520.
2) E. G. Rocho, D. T. Hurd, and R. N. Lewis, "The Chemistry of Organometallic Compounds," John Wiley & Sons, New York (1957).
3) M. Schlosser, *Angew. Chem.*, **76**, 124, 258 (1964).
4) G. E. Coates, "Organo-Metallic Compounds," 2nd ed., Chap. 1, Methuen, London (1960).
5) H. Gilman and J. W. Morton, "Organic Reactions," Vol. VI, Chap. 7; Vol. VIII, Chap. 6 (1951).
6) P. D. Bartlett, S. Fridman, and M. Stiles, *J. Amer. Chem. Soc.*, **75**, 1771 (1953).
7) R. Waack and P. West, *ibid.*, **86**, 4494 (1964).
8) G. E. Coates and F. Glockling, *J. Chem. Soc.*, **1954**, 22.
9) M. S. Kharasch and O. Reinmuth, "Grignard Reactions of Non-Metallic Substances," Constable & Co., London (1954).
10) S. T. Kharasch and O. Reinmuth, "Grignard Reactions of Organic Compounds," 3 Vols., Pergamon Press, London (1957).
11) G. Bahr and K. H. Thiele, *Chem. Ber.*, **90**, 1578 (1957).
12) R. L. Gerteis, R. E. Dickerson, and T. L. Brown, *Inorg. Chem.*, **3**, 872 (1964).
13) R. M. Salinger, "The Structure of the Grignard Reagents and the Mechanism of Its Reactions," in Survey of Progress in Chemistry, Vol. 1, ed. A. F. Scott, Academic Press, New York (1963).
14) F. A. Cotton and G. Wilkinson, "Advanced Inorganic Chemistry," 2nd. ed., Interscience Publishers, New York, Chaps. 8, 11, and 18 (1966).
15) G. Allegra, G. Pergo, and A. Immirzi, *Makromol. Chem.*, **61**, 69 (1963).
16) H. Dietrich, *Acta Cryst.*, **16**, 681 (1963).

$H_3)_3B$.[23,24] These studies suggested the striking features of the compounds mentioned above, namely, the so-called "*five-coordinate carbon*" or "*electron-deficient bridged bond*" of such compounds as the methyllithium tetramer,[25] the dimethylberyllium polymer,[19] and the trimethylaluminum dimer.[21,22] More recently, as to the molecular structures of the electron-deficient compounds, some molecular orbital calculations[26-29] have been performed with particular reference to the natures of the bond, such as the metal-carbon and metal-metal bonds, in $(CH_3Li)_4$,[26] $(CH_3)_6B_2$,[26] and $(CH_3)_6Al_2$.[26] In regard to the contributions of the π-type bonding (hyperconjugation) of alkyls to the formation of the bridged bond mentioned above, these calculations have provided the interesting information that the π-type bonding of the above polymer appears to be approximately the same as that of its monomer and less than 10% of the metal-carbon σ-bond in the compounds.

In the present paper, an extended Hückel molecular orbital calculation will be carried out for the methyl compounds of group I (Li, Na, K, Rb), group II (Be, Mg, Ca), and group III elements (B, Al). The main purpose of this study is to make an extensive consideration of the electronic states of the compounds in connection with their reactivities.[1,2]

Method of Calculations

The extended Hückel method proposed by Hoffmann[30] was used to make calculations for several methyl compounds of group I, II, and III elements: CH_3Li, $(CH_3Li)_2$, $(CH_3Li)_4$, CH_3Na, CH_3K, CH_3Rb, $(CH_3)_2Be$, $(CH_3)_4Be_2$, $(CH_3)_2Mg$, $(CH_3)_2Ca$, $(CH_3)_3B$, $(CH_3)_3Al$, and $(CH_3)_6Al_2$. The values of the orbital exponents of the elements were taken from those evaluated by Clementi,[31] while the following valence-state ionization potentials (vsip)[32,33] were employed for the diagonal H-matrix elements: H_{ii}(eV)$=-13.6$ (H 1s), -5.39 (Li 2s), -3.54 (Li 2p), -5.14 (Na 3s), -3.04 (Na 3p), -4.34 (K 4s), -2.17 (K 4p), -4.18 (Rb 5s), -2.60 (Rb 5p), -9.92 (Be 2s), -5.96 (Be 2p), -8.95 (Mg 3s), -4.52 (Mg 3p), -7.09 (Ca 4s), -3.96 (Ca 4p), -14.91 (B 2s), -8.42 (B 2p), -12.27 (Al 3s), -6.47 (Al 3p), -21.01 (C 2s), and -11.27 (C 2p). The Wolfsberg-Helmholtz approximation[34] was employed for the off-diagonal matrix elements (H_{ij}) as:

$$H_{ij} = K(H_{ii} + H_{jj})S_{ij}/2$$

where the value of the parameter, K, was taken to be 1.75.[30] The bond lengths of the group I methyl compounds were taken to be Li–C=2.19 Å,[35] Na–C=2.70 Å, K–C=3.10 Å, and Rb–C=3.29 Å. The atomic coordinates of $(CH_3Li)_2$ and $(CH_3Li)_4$ were calculated from the pertinent bond distances and bond angles.[14] The bond angles of carbon-metal-carbon for the group II methyl compounds were taken to be linear, assuming the $D_{\infty h}$-structures, and the following bond lengths were used: Be–C=1.98 Å, Mg–C=2.45 Å, and Ca–C=2.82 Å. The molecular structures of the group III methyl compounds were assumed to be D_{3h},[36] and the bond lengths of B–C and Al–C were set as 1.80 Å[37] and 2.28 Å[38] respectively. For the calculations of the dimer structures of $(CH_3)_4Be_2$ and $(CH_3)_6Al_2$, the bond lengths of Be–C,[39] Al–C_b,[40] and Al–C_t[41] were taken to be 1.93 Å,[42] 2.24 Å,[14] and 2.00 Å[14] respectively. In all the calculations, the bond distance of C–H was taken to be 1.09 Å for the sake of simplicity.

Results and Discussion

The Electronic States of the Group I Methyl Compounds. Among organometallic compounds of group I elements, lithium compounds can be distinguised by their associations[4] in such organic solvents as ether and tetrahydrofuran. From their experimental works, Brown *et al.*[42] and others[43-45] emphasized the hexamer structures of alkyllithiums, while

17) Z. K. Cheema, G. W. Gibson, and J. F. Eastman, *J. Amer. Chem. Soc.*, **81**, 3517 (1963).
18) F. A. Settle, M. Haggerty, and J. F. Eastman, *ibid.*, **86**, 2076 (1964).
19) A. I. Snow and R. E. Rundle, *Acta Cryst.*, **4**, 348 (1941).
20) E. Weiss, *J. Organometal. Chem.*, **4**, 101 (1965).
21) P. H. Lewis and R. E. Rundle, *J. Chem. Phys.*, **21**, 986 (1953).
22) R. G. Vranka and E. L. Amma, *J. Amer. Chem. Soc.*, **89**, 3121 (1967).
23) L. S. Bartell and B. L. Caroll, *J. Chem. Phys.*, **42**, 3076 (1965).
24) H. A. Levy and L. O. Brockway, *J. Amer. Chem. Soc.*, **59**, 2085 (1937).
25) E. Wiss and E. A. C. Lucken, *J. Organometal. Chem.*, **2**, 197 (1964).
26) H. Kato, K. Yamaguchi, T. Yonezawa, and K. Fukui, This Bulletin, **38**, 2144 (1965).
27) H. Kato, K. Yamaguchi, and T. Yonezawa, *ibid.*, **39**, 1377 (1966).
28) I. B. Golovanov and A. K. Piskunov, *Zh. Struct. Khim.*, **5**, 923 (1964).
29) A. H. Cowley and W. D. White, *J. Amer. Chem. Soc.*, **91**, 34 (1969).
30) R. H. Hoffmann, *J. Chem. Phys.*, **39**, 1397 (1963); **40**, 2474 (1964).
31) K. Clementi and D. Raimondi, *ibid.*, **38**, 2686 (1963).
32) J. Hinze and H. H. Jaffé, *J. Amer. Chem. Soc.*, **84**, 540 (1962).
33) J. Hinze and H. H. Jaffé, *J. Phys. Chem.*, **38**, 2686 (1963).
34) M. Wolfsberg and L. Helmholtz, *J. Chem. Phys.*, **20**, 837 (1952).
35) This length was derived from that of $(CH_3Li)_4$ reported in Ref. 14.
36) The angle of CBC in $(CH_3)_3B$ was reported as 119.4°± 0.3° by Ref. 23.
37) In Ref. 23, the mean bond length of B–C was reported to be 1.5783±0.0011 Å. We modified this value slightly.
38) The bond lengths of Al–C in $(CH_3)_6Al_2$ were determined to be 2.24 Å[21] (2.14±0.01 Å[22]) for the bridged distance and 1.99 Å[21] (1.97±0.01 Å[22]) for the exterior distance. We used approximate values as estimated from Ref. 21.
39) The same interatomic distance of Be–C was applied to those of the Be-terminal C and the Be- bridged C.
40) The C_b and C_t notations denote a bridged carbon and a terminal one respectively.
41) This length was an assumed one (see Ref. 14).
42) T. L. Brawn, D. W. Dickerhood, and D. A. Bafus, *J. Amer. Chem. Soc.*, **84**, 1371 (1962).
43) D. Margerison and J. P. Newport, *Trans. Faraday Soc.*, **59**, 2058 (1963).
44) T. L. Brawn, R. L. Gerteis, D. A. Bafus, and J. A. Ladt, *J. Amer. Chem. Soc.*, **86**, 2135 (1964).
45) A. G. Evans and D. B. Geoge, *J. Chem. Soc.*, **1961**, 4653.

Table 1. Electronic states of group I methyl compounds

Compound	Bond[a] length (Å)	P(M-C)[d] S(M-C)[b]	P(M-C)[c]	s(M)-s(C)	s(M)-p(C)	N(M-C)[e]	M(M-C)[f]	Energy (eV) HO[g]	LV[h]	Total
CH_3Li	2.19	0.191	0.232	−0.190	0.384	0.064	−0.152	−11.90	−4.77	−133.98
LiCl[i]	3.31	0.278	0.086	−0.034	0.140		0.032	−13.39	−5.09	−128.41
CH_3Na	2.70	0.121	0.294	−0.140	0.416	0.0424	−0.122	−11.66	−4.70	−133.11
NaCl[i]	3.65	0.160	0.052	−0.018	0.082		0.008	−13.39	−5.02	−128.39
CH_3K	3.10	0.057	0.142	−0.146	0.272	0.0248	−0.190	−11.60	−4.07	−132.37
KCl[i]	4.05	0.113	0.022	−0.008	0.034		0.002	−13.39	−4.27	−128.38
CH_3Rb	3.29	0.026	0.096	−0.094	0.224	0.0154	−0.054	−11.61	−3.84	−132.20
RbCl[i]	4.25	0.056	0.014	−0.004	0.018		0.0006	−13.39	−4.16	−128.38

a) Atomic distance of metal—carbon or metal—chlorine.
b) Total orbital overlap between metal (M) and carbon (C).
c) Bond order density between M and C.
d) Bond order density of M-C. s(M)-s(C) and s(M)-p(C) mean the bond order density between s-M orbital and s-C one and that between s-M orbital and p-C one in $sp\sigma$-bond of M-C, respectively.
e) AO bond population between the orbitals of M and C presented in d).
f) Total bond population between M and C.
g) This HO level is depended on the p-C orbital presended in d), while for the chlorides, it is depended on the p-lone pair orbital of Cl.
h) This level indicates the energy of the lowest vacant s-M orbital.
i) They are listed for the comparison's sake.

Weiner and his co-workers[46] supported the tetramer structures. The association of the lithium compounds may be attributed to very small contributions of orbital overlaps (including "*hyperconjugation*") between the lithium atom and carbon to the formation of their stable molecules. As to the other metal compounds, however, there is little information about their electronic states except that there is a tendency[47,48] for their slight covalent natures to increase with a decrease in their atomic numbers. These characteristics should be reflected in the total orbital overlap (S(M–C)) defined by the sum of orbital overlaps, the bond order density (P(M–C)), and the total bond population (M(M–C)). These values and, in addition, the energy levels (HO and LV) are shown in Table 1, while the atomic- and bond-populations are given in Fig. 1. As may be seen in Table 1, S(M–C) supports the previous idea as to the tendency[47,48] of the bond nature; moreover, P(M–C) suggests that the σ-bond of M–C is formed by the bonding orbital of s(M)–p(C) and the anti-bonding orbital of s(M)–s(C). The electrons of the M–C bond localize remarkably on the carbon atom, which is over the unit charge (see Fig. 1). In this case, the contribution of "*hyperconjugation*" can hardly be expected because of the negative π-bond character of the compounds. It is of interest here to pay attention to the bond nature of the metal halides for the sake of comparison. Notwithstanding the fact that the interatomic distances of M–Cl are larger than those of M–C, the halides indicate a more covalent nature of the bond than do the methyl derivatives. This reflects a negative contribution of the hyperconjugation of CH_3 group such as has been described above; a striking covalency of the lithium compounds is also seen, a covalency which may be attributed to the small radius of the Li ion and the larger effective nuclear charge of Li caused by the scanty shielding effect of the electrons on Li.

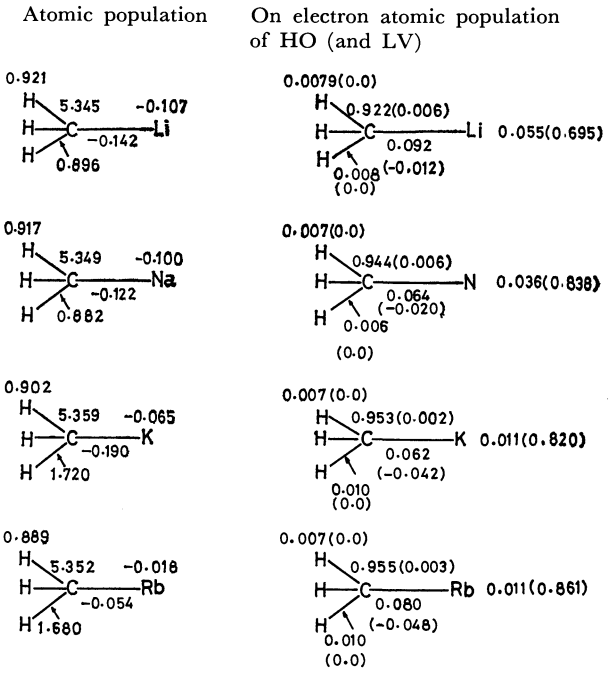

Fig. 1. Atomic population of the group I methyl compounds. (Values in parentheses are those of S-M orbitals.)

In regard to the associated polymer of alkyllithium, the present calculations give the interesting information that $(CH_3Li)_2$ is less stable than CH_3Li by *ca.* 0.25 eV per CH_3Li unit, while $(CH_3Li)_4$ is more stable by 0.34 eV per CH_3Li unit, neglecting core repulsions and electron-electron interactions (see Table 2). From this point of view, from their detailed calculations of the total energy, Cowley and White[29] have demonstrated the stability of $(CH_3Li)_4$ in comparison with

46) M. Weiner, G. Vogel, and R. West, *Inorg. Chem.*, **1**, 654 (1962).
47) L. Pauling, "The Nature of the Chemical Bond," Cornell Univ. Press, Chap. 3 (1960).
48) F. A. Cotton and G. Wilkinson, "Advanced Inorganic Chemistry," 2nd. ed., Interscience Publishers, New York, Chap. 16 (1966).

Table 2. Atomic and overlap populations for the methyllithium monomer, dimer, and tetramer

Compound	Atom	EHMO	Bond	EHMO	Total energy (eV) EHMO	Total energy (eV) SCF[a]
CH_3Li	Li	−0.107	Li-C	−0.152	−133.98	−282.32
	C	5.345	C-H	0.896		
	H	0.921				
$(CH_3Li)_2$	Li	−0.156	Li-Li	0.122	−267.45	—
	C	5.330	Li-C	−0.128		
	H	0.942	Li-C′	−0.102		
			C-H	0.902		
$(CH_3Li)_4$	Li	−0.282	Li-Li	−0.092	−537.26	−1241.75
	C	5.388	Li-C	−0.092		
	H	0.996	Li-C′	−0.054		
			C-H	0.964		

a) These data were cited from Ref. 29 for comparison.

Table 3. Overlap populations and energy states of group II methyl compounds

Compound	Bond	M(X-Y)[a]	Energy (eV) HO[b]	Energy (eV) LV[c]	Energy (eV) Total
$(CH_3)_2Be$	Be-C	0.106	−11.83	−4.32	−266.88
	C-H	0.886			
$(CH_3)_2Be_2$	$Be-C_b$	0.282	−12.31	−11.25	−541.84
	$Be-C_t$	0.346			
	Be-Be	0.274			
	C_b-H	0.718			
	C_t-H	0.728			
$(CH_3)_2Mg$	Mg-C	0.174	−11.80	−4.49	−266.30
	C-H	0.856			
CH_3MgBr[d]	Mg-C	0.308	−12.22	−6.78	−256.17
	Mg-Br	0.118			
	C-H	0.820			
$(CH_3)_2Ca$	Ca-C	0.104	−11.68	−5.19	−264.61
	C-H	0.836			

a) Total bond population of X-Y.
b) HO-orbital except that of Be-derivative is mainly depended on p-C orbital in $sp\sigma$-bond of M-C.
c) LV-level indicates that of the lowest vacant s-M orbital except Be-derivatives.
d) This was listed for the comparison's sake (Geometry is shown in Fig. 2).

that of CH_3Li (28.12 eV per CH_3Li unit). On the other hand, the electron population on the lowest vacant s-metal orbital[49] and that on the bond of metal-carbon at the highest occupied level[50] (see Fig. 1) may support a trend of the reactivities[1,2] such as RLi<RNa<RK<RRb<RCs for the addition reactions with carbonyl groups, because the larger value of the former may reflect the reactivity of the metal cation to the nucleophiles, while that of the latter may suggest a measure of the resistance to the cleavage of the M–C bond.

The Electronic States of Group II Methyl Compounds. Before speaking about the electronic states of the compounds, it may be mentioned that beryllium compounds usually have striking covalent natures which can be attributed to the small size of the metal (its metallic radius, 0.89 Å, is much smaller than Li's 1.22 Å), and have a far less electropositive character than Li in all aspects of their chemical behavior, while compounds of Ca, Ba, Sr, and Ra are all essentially ionic, though some Mg compounds show a covalent nature. Generally, the polymer structures of beryllium compounds such as the bridged $(BeCl_2)_n$ are well accepted; Mg compounds also have a polymer chain similar to that of Be compounds.[20] However, it can hardly be expected that a polymer chain exists in other group II metal compounds because of the striking ionic nature of the compounds. The energetic states and the overlap population (M(X–Y)) of the group II methyl compounds are summarized in Table 3. As Table 3 shows, M(X–Y) does not indicate reliable information about the polymeric character of Be and Mg derivatives. However, the characteristic covalency of Be compounds is reflected in the relatively large S(Be–C) value of 0.254 as compared with those of S(Mg–C) and S(Ca–C) (0.030 and 0.034 respectively), considering that S(Be–C) relates directly to (Be–C), which is immediately influenced by the selected ionization potentials (vsip) of Be and C. On the other hand, the total energies of $(CH_3)_2Be$ and $(CH_3)_4Be_2$ suggest, interestingly, that $(CH_3)_4Be_2$ is more stable than $(CH_3)_2Be$; the stabilized energy is about 4.04 eV per $(CH_3)_2Be$ unit. Moreover, the AO populations of the p_z-Be orbitals of both $(CH_3)_2Be$ and $(CH_3)_4$-

49) The value of this population indicates the electron-vacancy of the orbitals.
50) The highest occupied orbital is the $2p$-carbon one used for the formation of the σ-bond of M–C.

Table 4. Electronic states of group III methyl compounds

Compound	Bond	M(M-C)[a]	N_M(S)[b]	N_M(X)[b]	N_M(Y)[b]	N_M(Z)[b]	Energy (eV) HO	Energy (eV) LV[c]	Energy (eV) Total
$(CH_3)_3B$	B-C	0.536	0.710	0.241	0.241	0.209	−11.99	−4.62	−404.33
	C-H	0.828	(0.812)	(0.522)	(0.522)	(0.410)	(−12.30)	(−6.23)	
$(CH_3)_3Al$	Al-C	0.402	0.819	0.239	0.239	0.018	−12.01	−5.89	−402.16
	C-H	0.834	(0.603)	(0.165)	(0.165)	(0.052)	(−12.14)	(−5.01)	
$(CH_3)_6Al_2$	Al-C_b	0.322							
		(0.313)							
	Al-C_t	0.246							
		(0.704)							
	Al-Al	0.422	0.813	0.680	0.500	0.735	−11.32	−11.17	−799.81
		(0.468)							
	C_b-H	0.728							
		(0.790)							
	C_t-H	0.740							
		(0.800)							

a) Overlap population of metal-carbon.
b) AO population of the metal. D_3-ligand plane of the compound is on X-Y cross section, and the notations, X, Y, and Z, denote the p_x, p_y, and p_z-orbitals of metal, respectively.
c) This level corresponds to that of p_z-metal orbital.
Data in parentheses are those in Refs. 26 and 29 for dimethyl-boron or aluminum and dimethyl aluminum dimer, respectively.

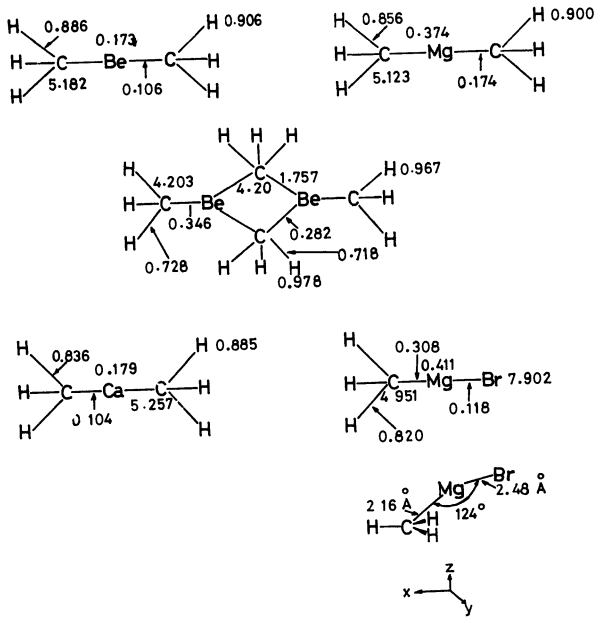

Fig. 2. Atomic populations of group II methyl compounds.

Be_2 (0.043 and 0.047 respectively) also predict the stability of the dimer, because the electrons on the p_z-orbital contribute to the stabilization of the dimer through the π-bond of Be–C. Under these circumstances, the relatively strong bond of Be–Be is enough to compensate for the weak bond of Be–C_b (see Fig. 2). However, the π-bond of Be–Be contributes little to this bond formation (less than 1.0%[51] of the total overlap). The above considerations may be understood from the data listed in Table 5. Furthermore, another striking feature of the dimer is also reflected in the atomic charge of the metal; that is, the bridged Be-atom (+0.24) is less positive than the Be in the monomer (+0.83). The charges of the metals (Be=+0.83, Mg=+0.63, and Ca=+0.82, as estimated from the atomic populations in Fig. 2) are, however, not in good agreement with such a trend of the reactivities[1,2] as RBe<RMg<RCa in the carbonyl group-addition reaction, probably because the behavior of RM (M=metal) in the reaction system can hardly be evidenced only from the electronic states of RM-monomers; that is, the interaction between the carbonyl groups and the monomer or dimer of RM was not taken into consideration at the molecular level. In connection with the stabilized dimer of $(CH_3)_4Be_2$, the energy state of the dimeric methyl beryllium is illustrated in Fig. 3.

Electronic States of the Group III Methyl Compounds. The most characteristic feature of the compounds of this series is the dimerization of the lower trialkyls of Al in spite of the stable monomers of trialkyls of B, Ga, In, and Tl in vapor and in solution.[52] Therefore, it is of interest to investigate the difference in the electronic states between trialkyl boron and trialkyl aluminum. The data as to these compounds are listed in Table 4. The smaller metal-carbon overlap population of $(CH_3)_3Al$ than that of $(CH_3)_3B$ first indicates less stability in $(CH_3)_3Al$. The most remarkable feature of $(CH_3)_3Al$ appears in the small AO population of the p_z-Al orbital (used for the π-bond of Al–C) as compared with $(CH_3)_3B$. This indicates the weak π-bond of Al–C. Considering the large contribution of the π-bond to the stabilization of the molecule, the remarkably small π-bond nature of Al–C (see Table 5) suggests the improbable existence of the trialkyl aluminum monomer. These circumstances are reflected in the slight different atomic populations of $(CH_3)_3B$ and $(CH_3)_3Al$, as is indicated in Fig. 4. However, the total energy of $(CH_3)_6Al_2$ failed to suggest its stability, as is indicated in Table 4. It is plausible here to focus on the lowest vacant p_z-

51) The π-bond character formed by the p_z-orbitals of the two Be atoms was 0.23% of the total overlap, neglecting the contribution of p_x-orbitals.
52) N. Muller and A. L. Otermat, *Inorg. Chem.*, **4**, 296 (1965).

$(CH_3)_2Be$		$(CH_3)_4Be_2$
		6.306 eV $0.84(X_{Be_1}-X_{Be_2})+0.64(X_{C_{15}}-X_{C_{10}})$[a]
		0.652 $1.00(Z_{Be_2}-Z_{Be_1})$
$1.22S_{Be_9}-0.40(Y_{C_1}-Y_{C_5})-0.37(S_{C_1}+S_{C_5})$	−0.015	−1.068 $0.63(S_{Be_2}-S_{Be_1})$
		−4.253 $-0.58(S_{Be_1}+S_{Be_2})+0.35(Y_{C_3}-Y_{C_4})$
$1.04X_{Be_9}-0.34(X_{C_1}+X_{C_5})$ $1.04Z_{Be_9}-0.34(Z_{C_1}+Z_{C_5})$	−4.423	−4.621 $-0.63(Z_{Be_1}+Z_{Be_2})+0.37(Z_{C_3}+Z_{C_4})$
		−10.807 $0.44(X_{C_3}+X_{C_4})+0.41(Y_{C_3}+Y_{C_4})+0.33(Y_{C_{11}}+Y_{C_1})$
		−11.085 $0.51(Y_{C_{11}}+Y_{C_{15}})+0.37(X_{C_3}+X_{C_4})$
		−11.253 $-0.49(Y_{C_{11}}-Y_{C_{15}})-0.35(X_{C_3}-X_{C_4})$
$0.64(Y_{C_1}+Y_{C_5})-0.20Y_{Be_9}+0.11(S_{C_1}+S_{C_5})$	−11.834	−12.315 $0.37(Y_{C_{11}}-Y_{C_{15}})+0.37(X_{C_3}-X_{C_4})+0.33(Y_{C_3}-Y_{C_4})$
		−12.850 $0.34(Y_{Be_1}+Y_{Be_2})+0.30(Y_{C_{11}}+Y_{C_{15}})+0.24(S_{C_{11}}-S_{C_{15}})$
		−12.983 $0.34(Y_{Be_2}-Y_{Be_1})$

a) The notations, X_{Be_1} and X_{Be_2}, denote the the p_x-Be orbitals of Be_1 and Be_2, respectively, and so on. Small coefficients below 10^{-1} and the values of H were neglected for the sake of simplicity.

Fig. 3 Energy diagrams of $(CH_3)_2Be$ and $(CH_3)_4Be_2$.

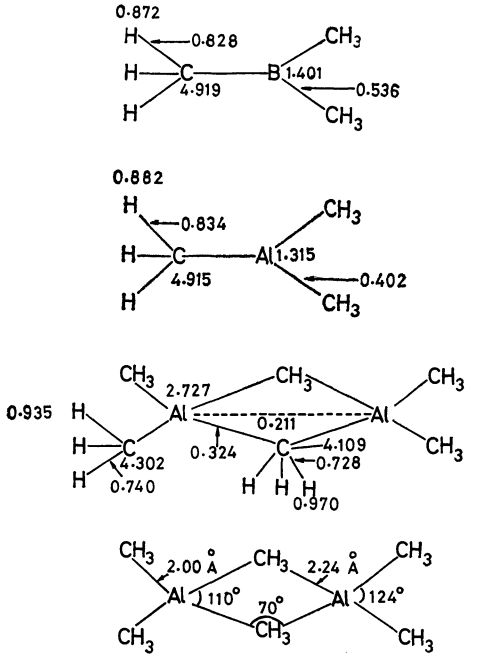

Fig. 4. Atomic and bond populations of $(CH_3)_3B$, $(CH_3)_3Al$ and $(CH_3)_6Al_2$.

Table 5. Overlap populations of σ- and π-bonds

Compound	N(M-C)[a] σ	π	Total
CH_3Li	−0.136	−0.016	−0.152
CH_3Na	−0.112	−0.010	−0.122
CH_3K	−0.038	−0.004	−0.042
CH_3Rb			
$(CH_3)_2Be$	0.070	0.036	0.106
$(CH_3)_4Be_2$	—[b]	0.012[c]	0.282(Be-C_b)
	—[b]	0.018[c]	0.346(Be-C_t)
	—[b]	0.0006[c]	0.274(Be-Be)
$(CH_3)_2Mg$	0.176	−0.002	0.174
$(CH_3)_2Ca$	0.106	−0.002	0.104
$(CH_3)_3B$	0.482	0.054	0.536
$(CH_3)_3Al$	0.398	0.006	0.402

a) Total bond population of metal-carbon.
b) Separation of the bond character into σ and π is not possible.
c) π-Bond overlap of p_z-orbitals on M and C (see Fig. 3).

metal orbital in connection with the reactivity of the compounds, because the electron-vacancy of the boron- or aluminum-orbital (M_B(LV) or M_{Al} (LV) respectively) may play an important role in the reaction with nucleophiles. M_B(LV) and M_{Al}(LV) are 0.880 and 0.991 respectively. Therefore, the appreciable vacancies of the orbitals on both metals may suggest the effectiveness of the orbitals for the attack of nucleophiles. In this point of view, Gilman[1] has reported the order of the reactivity for the attack of nucleophiles as RB<RAl. Finally, the π- and σ-overlap population of M–C in a series of the group I, II, and III methyl compounds are recorded in Table 5 for the sake of comparison.

The results obtained from the present study may be summarized as follows:

a) The striking nature of the covalency of lithium compounds appeared in the large total orbital-overlap. In all Group I methyl compounds, the electron-localization occurred on the C-atom in CH_3 over the C-unit charge. As to the stabilization of the alkyllithium polymer, $(CH_3Li)_4$ was more stable than CH_3Li in the order of *ca.* 0.34 eV per unit, although $(CH_3Li)_2$ was less stable than CH_3Li (*ca.* 0.25 eV per CH_3Li unit).

b) The dimer structure of $(CH_3)_4Be_2$ was stabilized in the energy of 4.04 eV per $(CH_3)_3Be$ unit, and the contribution of the σ-type Be–Be bond to the stabilization was relatively large, while that of the π-type bond was very small.

c) The π-bond character of the monomer of $(CH_3)_3Al$ was about 1/9 that of $(CH_3)_3B$; this would well explain the stability of trialkyl boron monomers.

The present calculations were carried out on the FACOM 230.60 computer at the Computer Center of the University of Kyushu.

Vibrational Analysis of the 2400—2800 Å Bands of 1,2,3- and 1,3,5-Trimethylbenzenes in Vapour Phase

V.N. VERMA, K.P.R. NAIR, and D.K. RAI

Department of Spectroscopy, Faculty of Science, Banaras Hindu University, Varanasi-5, India

(Received October 13, 1970)

The near ultraviolet absorption spectra of 1,2,3- and 1,3,5-trimethylbenzenes have been photographed in vapour phase at different vapour pressures on a Q-24 Zeiss Medium Quartz Spectrograph. Assuming C_{2v} symmetry for the 1,2,3- and D_{3h} symmetry for the 1,3,5-isomer, tentative assignments of the observed bands have been made in terms of various ground state and excited state fundamentals. The respective vibrational modes have also been suggested.

The electronic spectrum of mono-methylbenzene (toluene) has been studied by many workers.[1-5] Price *et al.*[6] reported the vacuum ultraviolet absorption spectra of the three isomeric dimethylbenzene(xylenes) in vapour phase. Complete analysis of the electronic spectra in the near ultraviolet region for the three xylenes has been made by Cooper *et al.*[7,8] and also by Singh.[9-11] For trimethylbenzenes, however, the work done is very limited and further work is clearly needed.

The Raman spectrum of 1,3,5-trimethyl benzene has been studied[12,13] and the polarization measurements are reported. The infrared spectrum of this molecule has been studied[14] in the range 600—3100 cm^{-1} in vapour, liquid and in solutions. Sponer[15] and Sponer and Stallcup[16] photographed the ultraviolet absorption spectrum of 1,3,5-trimethylbenzene in vapour phase and located the forbidden (0,0) band and assigned some of the other bands. Sen[17] studied the electronic absorption spectrum of this molecule in the liquid and solid states and discussed the shift in the (0,0) band on change of phase. Sreeramamurty[18] studied the absorption spectrum of 1,2,4-trimethylbenzene in vapour phase and discussed the substituent effect of CH_3 group. The vibrational analysis of the electronic spectra of 1,2,3-trimethylbenzene has not yet been reported, though Kohlrausch and Pongratz[13] have reported its Raman spectrum. An investigation of the absorption spectra of 1,2,3- and 1,3,5-trimethylbenzenes has been undertaken here and a complete analysis of the observed bands is being proposed.

Experimental

Pure samples of 1,2,3- and 1,3,5-trimethylbenzenes have been obtained from Koch-Light Laboratories and were used after redistillation under reduced pressure. The vapour absorption spectra were photographed on Q-24 Zeiss Medium Quartz Spectrograph. Absorption cells of various lengths were used. The temperature of the bulb attached to the middle of the tube and which acted as reservoir of experimental liquid was varied from -10 to 30°C. The source for continuous radiation from a Beckman hydrogen lamp was used. The bands were best developed with a cell of 75 cm and a bulb temperature at 25°C in the case of 1,2,3-isomer and with a cell of 70 cm and a bulb temperature of 30°C for the other isomer. They were recorded on Ilford N-40 plates with a slit width of 20 μ. Typical spectrograms are shown in Figs. 1 and 2. The spectra lie in the region 2400—2800 Å for both the isomers and the dispersion of the spectrograph in this region is about 9 Å/mm. The bands were measured on a Hilger L-76 comparator having a least count of 0.001 mm. The accuracy of measurement for the sharp bands is ± 5 cm^{-1} and for the diffuse bands is ± 10 cm^{-1}.

Results and Discussion

Nearly 56 bands for 1,2,3-isomer and 66 bands for 1,3,5-isomer have been observed. The bands are degraded towards the longer wavelength side. The frequencies of the observed bands along with their relative intensities and proposed assignments are given in Tables 1 and 2. The correlation of the observed fundamentals in the ultraviolet absorption spectra of 1,2,3- and 1,3,5-trimethylbenzenes with the corresponding Raman frequencies is given in Table 3. The prominent vibrational transitions are shown in Figs. 3 and 4 for 1,2,3- and 1,3,5-trimethylbenzenes respectively.

Under the usual approximation, *i.e.*, considering the CH_3 group as a mass-point, the six fold symmetry, D_{6h}, of benzene drops to C_{2v} for 1,2,3-isomer. The forbidden $A_{1g} \rightarrow B_{2u}$ transition of benzene therefore reduces to an allowed $A_1 \rightarrow B_2$ transition. On the other hand for 1,3,5-isomer remains as D_{3h} and the electronic transition is A'_1—A'_2. The transition therefore is still forbidden.

1) K. Masaki, This Bulletin, **11**, 346 (1936).
2) J. Savard, *Ann. de. Chim.*, **11**, 287 (1929).
3) N. Ginsberg, W. W. Robertson, and F. A. Matsen, *J. Chem. Phys.*, **14**, 511 (1946).
4) M. R. Padhye, *Indian J. Phys.*, **23**, 331 (1949).
5) H. Sponer, *J. Chem. Phys.*, **10**, 672 (1942).
6) W. C. Price, V. J. Hammond, J. P. Teegan, and A. D. Walsh, *Discuss. Faraday Soc.*, **9**, 53 (1950).
7) C. D. Cooper and H. Sponer, *J. Chem. Phys.*, **20**, 1248 (1952).
8) C. D. Cooper and M. L. N. Sastri, *ibid.*, **20**, 607 (1952).
9) I. S. Singh, *J. Sci. Res. Banaras Hindu University*, **7(2)**, 171 (1956—1957).
10) I. S. Singh, *ibid.*, **8(1)**, 19 (1957—1958).
11) I. S. Singh, *ibid.*, **8(1)**, 32 (1957—1958).
12) S. Venkateshwaran, *Phil. Mag.*, 17th Series **15**, 263 (1933).
13) K. W. F. Kohlrausch and A. Pongratz, *Monatsh.*, **65**, 13 (1934).
14) S. B. Banerjee and K. C. Medhi, *Indian J. Phys.*, **34**, 1 (1960).
15) H. Sponer, *Chem. Rev.*, **41**, 281 (1947).
16) H. Sponer and M. J. Stallcup, Contribution al'Elude de la Structure Moleculaire, Victor Henri Memorial Volume (Deseor, liege) (1948), p. 222.
17) S. K. Sen, *Indian J. Phys.*, **33**, 41 (1959).
18) K. Sreeramamurty, *Proc. Natl. Inst. of Sci., India*, **17**, 385 (1951).

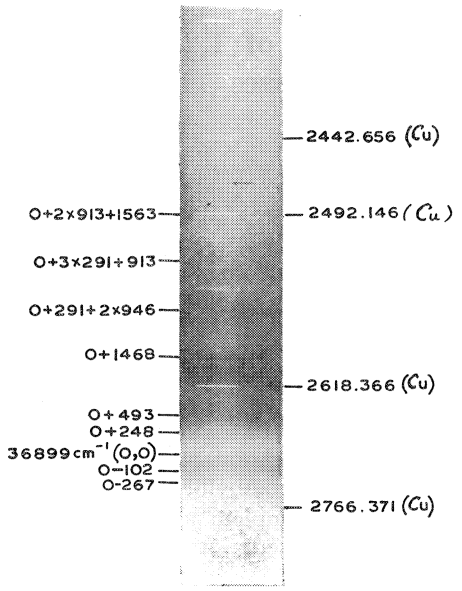

Fig. 1. Electronic absorption spectrum of 1,2,3-trimethylbenzene in vapour phase.

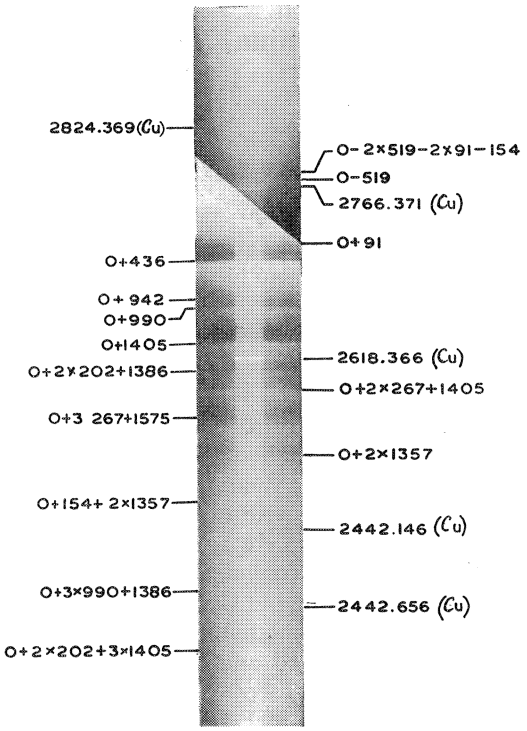

Fig. 2. Electronic absorption spectrum of 1,3,5-trimethylbenzene in vapour phase.

According to the Franck-Condon principle, if the internuclear distances in the ground and excited electronic states of the molecule are nearly the same, the (0,0) band of an allowed transition should either be most intense or one of the intense bands of the system. The strongest band at 36899 cm^{-1} appearing even at the lowest vapour pressure is assigned as the (0,0) band for 1,2,3-trimethylbenzene. The entire spectrum is analysed in terms of one ground state frequency of

Table 1. Vibrational analysis of the observed bands in the ultraviolet absorption spectrum of 1,2,3-trimethylbenzene in vapour phase

Wave number (cm^{-1})	Intensity	Separation from (0,0) band	Assignment	Wave number (cm^{-1})	Intensity	Separation from (0,0) band	Assignment
36632	ew	267	0−267	38249	m	1350	0+1350
36686	ew	213	0−2×52−102	38272	m	1373	0+453+913
36726	w	173	0−69−102	38317	m	1418	0+2×248+913
36742	w	157	0−52−102	38367	s	1468	0+1468
36797	m	102	0−102	38408	m	1509	0+2×493+523
36830	s	669	0−69	38462	m	1563	0+1563
36847	vs	52	0−52	38500	m	1601	0+523+1530−267
36865	vs	34	0−34	38542	w	1643	0+2×913−34−2×69
36899	vvs	0	(0,0)	38581	w	1682	0+2×913−2×69
37147	w	248	0+248	38790	w	1891	0+2×946
37190	m	291	0+291	38861	w	1962	0+2×523+913
37233	m	334	0+453−52−69	38897	m	1998	0+913+1350−267
37285	m	386	0+453−69	38920	m	2021	0+453+3×523
37318	ms	419	0+453−34	38961	m	2062	0+2×248+2×523
37352	s	453	0+453	38998	m	2099	0+3×248+1350
37392	s	493	0+493	39038	m	2139	0+248+2×946
37422	m	523	0+523	39082	m	2183	0+291+2×946
37588	w	689	0+946−267	39184	w	2285	0+453+2×931
37645	m	746	0+746	39252	w	2353	0+523+2×913
37695	w	796	0+2×248+291	39531	w	2632	0+3×248+2×946
37733	m	834	0+834	39556	w	2657	0+3×248+453+1468
37777	m	878		39589	m	2690	0+3×291+913
37812	s	913	0+913; 0+2×453	39647	m	2748	0+3×291+523+1350
37845	m	946	0+946	39682	m	2783	0+2×913+946
37895	w	996	0+2×493	39779	m	2880	0+2×493+2×946
37944	w	1045	0+291+3×248	40136	w	3237	0+248+291+2×1350
38143	w	1244	0+291+946	40190	w	3291	0+2×913+1468
38200	w	1301	0+1563−267	40289	ew	3390	0+2×913+1563

TABLE 2. VIBRATIONAL ANALYSIS OF THE OBSERVED BANDS IN THE ULTRAVIOLET ABSORPTION SPECTRUM OF 1,3,5-TRIMETHYLBENZENE IN VAPOUR PHASE

Wave number (cm^{-1})	Intensity	Separation from (0,0) band	Assignment	Wave number (cm^{-1})	Intensity	Separation from (0,0) band	Assignment
35853	w	709	$0-2\times519+2\times91+154$	38698	w	2136	$0+2\times436+1252$
35902	w	660	$0-2\times519+390$	38810	m	2248	$0+2\times436+1386$
35935	w	627	$0-519-583+202+267$	38868	s	2306	$0+942+1357$
35979	w	583	$0-583$	38931	vs	2369	$0+3\times267+1575$
36043	ew	519	$0-519$	39034	m	2472	$0+154+436+2\times942$
36562	(Calculated)	0	(0,0)	39100	m	2538	$0+2\times814+1386-519$
36653	w	91	$0+91$	39172	s	2610	$0+91+3\times841$
36716	m	154	$0+154$	39221	s	2659	$0+91+154+841+1575$
36764	m	202	$0+202$	39263	s	2701	$0+2\times1357$
36829	ms	267	$0+267$	39524	w	2962	$0+1386+1575$
36901	ms	339	$0+2\times91+154$	39584	w	3022	$0+202+3\times942$
36952	vs	390	$0+390$	39654	m	3092	$0+2\times841+1405$
36998	vvs	436	$0+436$	39691	m	3129	$0+2\times942+1252$
37287	w	725	$0+725$	39753	s	3191	$0+91+154+436+2\times1252$
37367	m	805	$0+91+267+436$	39802	m	3240	$0+267+3\times990$
37403	m	841	$0+841$	39868	m	3306	$0+154+1357$
37459	s	897	$0+990+436-519$	39942	w	3380	$0+2\times990+1405$
37504	s	942	$0+942$	40048	w	3486	$0+990+3\times1252$
37552	vs	990	$0+990$	40129	m	3567	$0+841+2\times1357$
37779	w	1217	$0+267+942$	40154	m	3592	$0+436+2\times1575$
37814	m	1252	$0+1252$	40196	w	3634	$0+2\times435+2\times1386$
37856	m	1294	$0+2\times91+267+841$	40245	w	3683	$0+2\times267+2\times1575$
37892	m	1330	$0+267+1575-519$	40289	m	3727	$0+2\times91+841+2\times1357$
37919	s	1357	$0+1357$	40346	m	3784	$0+3\times841+1252$
37948	s	1386	$0+1386$	40576	w	4014	$0+2\times436+1575$
37967	vs	1405	$0+1405$	40612	w	4050	$0+1252+2\times1405$
38137	m	1575	$0+1575$	40655	m	4093	$0+3\times841+1575$
38284	m	1722	$0+2\times154+1405$	40926	w	4364	$0+3\times990+1386$
38293	s	1731	$0+3\times391+202+1252$	40991	ew	4429	$0+942+3\times1357-583$
38351	s	1789	$0+2\times202+1386$	41039	ew	4477	$0+2\times154+3\times1386$
38392	m	1830	$0+436+1386$	41077	ew	4515	$0+436+3\times1357$
38443	s	1881	$0+2\times942$	41138	ew	4576	$0+436+990+2\times1575$
38498	vs	1936	$0+2\times267+1405$	41185	ew	4623	$0+2\times202+3\times1405$

N.B.; vvs=very very strong; vs=very strong; s=strong; ms=mediumstrong; m=medium; w=weak, and ew=extremely weak.

magnitude 267 cm^{-1} and 12 excited state frequencies of the magnitudes 248, 291, 453, 493, 523, 746, 834, 913, 946, 1350, 1468, and 1563 cm^{-1}. Difference bands at the separation of 34, 52, 69, and 102 cm^{-1} are observed on the longer wavelength side of the (0,0) band.

In the spectrum of the 1,3,5-isomer, because of the forbidden nature of the transition, the (0,0) band is not observed in the vapour phase. The (0,0) band appears with moderate intensity in the liquid and solid phase[17] at 36265 and 36326 cm^{-1} respectively, however, because of the expected shift in its position due to the intermolecular interactions, this by itself does not help in the location of the (0,0) band. A similar situation arises in the corresponding transition of benzene. It has been suggested that in benzene the transition becomes allowed due to interaction of a vibration of e_{1g} symmetry. In such a case bands would be observed on either side of the (0,0) band whose mutual separation would be the sum of the ground and excited state magnitudes of this vibration. A similar method can be used for the location of the (0,0) band in 1,3,5-trimethylbenzene also. We observed a strong band at 36998 cm^{-1} and a weak band at 36043 cm^{-1} and have taken these to correspond to $0\rightarrow1$ and $1\rightarrow0$ transitions involving this particular frequency making the transition allowed. In the Raman spectrum of 1,3,5-trimethylbenzene a depolarized line has been observed at 519 cm^{-1} and has been correlated to the 606 $cm^{-1}(e_{1g})$ in benzene. Taking this to be the frequency responsible for the appearance of the transition we can locate the missing (0,0) band at 36562 cm^{-1} (36043+519). A similar discussion by Sponer and Stallcup[16] leads to the estimated location of the (0,0) band at 36557 cm^{-1}. The entire spectrum is analysed in terms of two ground state frequencies of magnitudes 519 and 583 cm^{-1} and 12 excited state frequencies of magnitudes 267, 390, 436, 725, 841, 942, 990, 1252, 1357, 1386, 1405, and 1575 cm^{-1}. Bands are also observed at separation of 91, 154, and 202 cm^{-1} in the lower wavelength side of the main band and are assigned as due to $v'-v''$ transition.

In *o*-, *m*-, and *p*-xylenes the frequencies 720, 724, and 740 cm^{-1} respectively are assigned to the C–CH_3 stretch-

Table 3. Correlation of the fundamentals of 1,2,3- and 1,3,5-trimethylbenzenes observed in the ultraviolet absorption spectrum with their Raman fundamentals

1,2,3-Trimethylbenzene UV Absorption			1,3,5-Trimethylbenzene UV Absorption		
Raman[13]	Ground	Excited	Raman[12]	Ground	Excited
228			233		
269	267	269	275		267
318			519	519	
484		453	578	583	
509		493	847		841
536		523	976		942
654			998		990
744		746	1036		
810			1255		1255
888		834	1301		
990		946	1380		1357
1163					
1240			1611		1575
1377		1350			
1468		1468			
1589		1553			

ing vibration in the ground state.[19] Sreeramamurty[18] assigned this mode at 711 cm^{-1} in 1,2,4-trimethylbenzene. In the present study this mode is assigned at 746 cm^{-1} and 725 cm^{-1} for 1,2,3- and 1,3,5-isomers respectively.

There is a great controversy in the assignment of ring breathing mode arising from 992 cm^{-1} (a_{1g}) mode of benzene for the substituted benzenes. It is observed in many cases that the value of this mode usually decreases as the number of substituents increases. The frequencies of magnitude 834 and 841 cm^{-1} observed in the observed bands at 37733 cm^{-1} and at 37403 cm^{-1} for 1,2,3- and 1,3,5-isomers respectively have been assigned to this mode.

There is a band observed at 37422 cm^{-1} with medium intensity for the 1,2,3-isomer involving a separation of 523 cm^{-1} from (0,0) band. This is taken as an excited state fundamental. The Raman data show a band at 536 cm^{-1}. The corresponding frequency in 1,3,5-trimethylbenzene is observed at 36043 cm^{-1}. This mode of vibration has been identified as one of the components of the 606 cm^{-1} (e_{1g}) mode of benzene.

The band at 37814 cm^{-1} having separation of 1252 cm^{-1} from the (0,0) band is observed with medium intensity and can be correlated with the strong and polarized Raman line observed at 1255 cm^{-1} for 1,3,5-trimethylbenzene. In analogy with toluene,[3] this mode is identified as the a_1 part of the degenerate (e_{1g}) benzene vibration 3047 cm^{-1}. No such band is observed for 1,2,3-trimethylbenzene.

The medium strong band observed at 38249 cm^{-1} at a separation of 1350 cm^{-1} can be correlated with a band observed at 1377 cm^{-1} in the Raman spectrum of 1,2,3-isomer. Similarly a strong band at 37919 cm^{-1} at a separation of 1357 cm^{-1} can be correlated with 1380 cm^{-1} in Raman spectrum of 1,3,5-trimethylbenzene. In methyl substituted benzenes a strong Raman line always appears at about 1375 cm^{-1} which has been assigned to the C–H in-plane bending vibration in methyl groups. Similarly, the bands at 38367 cm^{-1} *i.e.* at the separation of 1468 cm^{-1} from the zero band for 1,2,3-isomer and at 37967 cm^{-1} *i.e.* at the separation of 1405 cm^{-1} for 1,3,5-trimethylbenzene are assigned to C–H out-of-plane (asymmetric) bending mode in the methyl group.

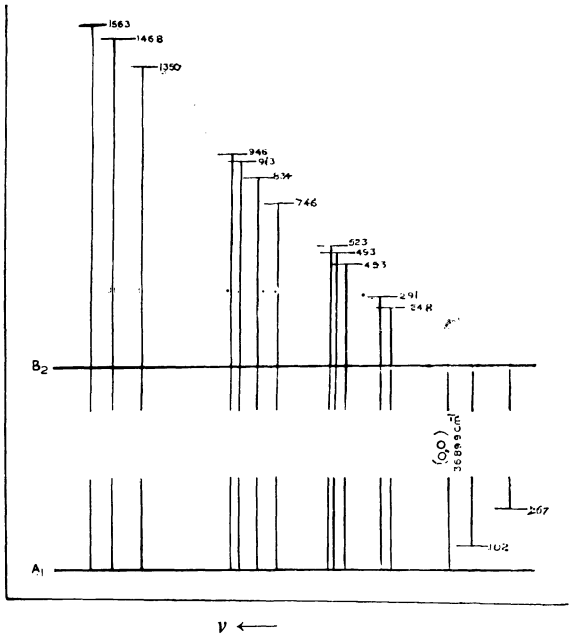

Fig. 3. Prominent vibrational transitions in the UV absorption spectrum of 1,2,3-trimethylbenzene in vapour phase.

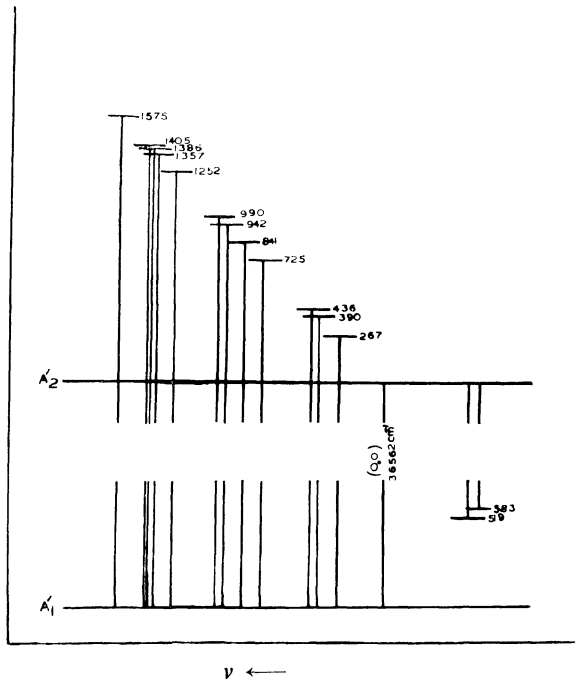

Fig. 4. Prominent vibrational transitions in the UV absorption spectrum of 1,3,5-trimethylbenzene in vapour phase.

19) K. S. Pitzer and D. W. Scott, *J. Amer. Chem. Soc.*, **65**, 803 (1943).

The medium strong band observed at 38462 cm^{-1} at a separation of 1563 cm^{-1} from the zero band for 1,2, 3-trimethylbenzene on the lower wavelength side can be correlated with 1589 cm^{-1} reported in Raman spectrum. Another medium strong band at 38137 cm^{-1} at a separation of 1575 cm^{-1} from the zero band can be correlated with 1611 cm^{-1} in Raman spectrum of 1,3, 5-trimethylbenzene. These Raman bands are polarized. This totally symmetric frequency may be assigned to the a_1 part of 1600 cm^{-1} (e_{1g}) benzene vibration.

The authors are thankful to Professor N. L. Singh for valuable discussions. Two of them (Verma and Nair) are grateful to C.S.I.R. New Delhi, India, for financial assistance.

BULLETIN OF THE CHEMICAL SOCIETY OF JAPAN, VOL. 44, 2035—2038 (1971)

Solid Complex Formation of Aminomalonic Acid with Glycine[1]

Toshio KINUGASA, Juziro NISHIJO,* Genzo HASHIZUME,** and Isamu IMANISHI*

Department of Chemistry, Faculty of Science, Kobe University, Nada-ku, Kobe

(Received November 13, 1970)

It was found by X-ray analysis that aminomalonic acid forms a solid complex with glycine in a molar ratio of 1 : 1 on crystallization from an aqueous solution. DTA-TGA of the solid complex at a heating rate of 1.0°C/min in air showed that the solid complex decarboxylates at higher temperature, but more slowly than aminomalonic acid and that both endothermic and following exothermic peaks which were distinctly observed in the region of decarboxylation of aminomalonic acid at temperatures 108—140°C are only slightly observed at 168—175°C. Activation energies in the thermal decomposition of aminomalonic acid and the solid complex, caluculated from themogravimetric curves, were 69.4 kcal/mol and 21.3 kcal/mol, respectively. The results indicate that aminomalonic acid is thermally more stabilized than the acid itself by forming the solid complex with glycine.

The authors reported[2] the results of differential thermal analysis of aminomalonic acid. Crystals were obtained by distilling off the solvent from a saturated aqueous solution of aminomalonic acid on a water bath at 25°C under a pressure of 10 mmHg. When the concentration process for each mother liquid was repeated seven or eight times, no further crystallization occurred easily with concentration, and a viscous residue remained, which turned into crystalline powder on being allowed to stand in air. Results of elementary analysis were: H, 5.60; C, 31.21%. Calculated values for aminomalonic acid and glycine are: H, 4.20; C, 30.26% and H, 6.67; C, 32.00%, respectively. Thus, it seems that a fair amount of glycine was contained in these crystals. On heating of aminomalonic acid with micro melting point apparatus,[3] decomposition took place accompanied with bubbling but no such phenomenon was observed for the crystalline powder. It seems that aminomalonic acid can form a solid complex with glycine on crystallization from an aqueous solution. The present study was carried out to confirm this supposition.

Experimental

Materials. Aminomalonic acid purified by recrystallization and glycine (Merck Co.) were dissolved in water with the molar ratio of 1 : 1 and the solvent was distilled off on a water bath at 25°C under a reduced pressure of 3—5 mmHg to leave a viscous residue. When this was allowed to stand in air, crystalline powder was obtained. These crystalline powder was obtained. These crystals are designated as AM_1–G_1 hereafter (AM: aminomalonic acid, G: glycine, the subscripts refer to the molar ratio). They were dried at 50°C for 5 hr., pulverized thoroughly in an agate mortar, and used for further experiments. Samples of different molar ratios were also prepared according to the same procedure.

Analysis. X-ray analysis was carried out with an X-ray diffractometer, Rigaku Denki Geigerflex, using Ni filtered CuK_α radiation. IR spectra were measured with a Nihon Bunko Grating Infrared Spectrometer, type DS-402G, by means of the KBr-pellet method. DTA-TGA was carried out by using the same apparatus as reported.[2] Samples of 200—500 meshes were used for measurements.

Determination of the contents of aminomalonic acid and γ-glycine. Aminomalonic acid was mixed with AM_1–G_1 to obtain samples with various weight ratios of aminomalonic acid to AM_1–G_1. The intensity [(half width) × (height)] of diffraction peaks due to aminomalonic acid at 24.1° (2θ) in these samples was measured to obtain a calibration curve used for the determination of aminomalonic acid content. Conditions of measurements were: 40 kV-1.5 mA, full-scale 400 count/sec, scanning speed 0.5°(2θ)/min, chart speed 20 mm/min. γ-Glycine was added to obtain the samples with various weight ratios of γ-glycine to AM_1–G_1. A calibration curve obtained with these samples, employing the height of diffraction peak due to γ-glycine at 21.8 (2θ) as peak intensity, was used for the determination of γ-glycine content. The conditions were the same as in the case of aminomalonic acid except for 40 kV-1.0 mA and 40 mm/min of chart speed.

Results and Discussion

The Complex Formation. X-ray diffraction patterns of aminomalonic acid, α-, β-, γ-glycine are

1) Presented at the 90th Annual Meeting of Pharmaceutical Society of Japan, Aug. 1970.

* Present address: Kobe Women's College of Pharmacy, Higashinada-ku, Kobe.

** Present address: Industrial Research Institute of Hyogo Prefecture, Suma-ku, Kobe.

2) T. Kinugasa, J. Nishijo, and G. Hashizume, *Nippon Kagaku Zasshi*, **90**, 584 (1969).

3) Yanagimoto melting point apparatus.

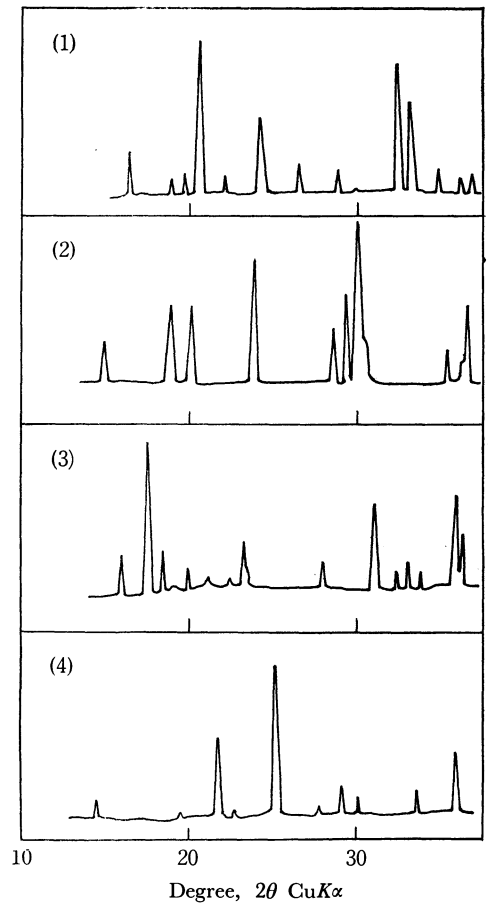

Fig. 1. X-ray diffraction patterns.
(1) Aminomalonic acid (2) α-glycine (3) β-glycine
(4) γ-glycine

shown in Fig. 1. The samples having ratios of aminomalonic acid to glycine 1 : 1, 1 : 2, 2 : 1, prepared according to method described in the experimental section, are shown in Fig. 2.

AM_1–G_1 gave a new diffraction pattern differing from each component, *viz.*, aminomalonic acid and glycine (α-, β-, γ-). AM_2–G_1 gave diffraction patterns of AM_1–G_1 and aminomalonic acid, whereas AM_1–G_2 gave those of AM_1–G_1 and γ-glycine. AM_4–G_3 and AM_5–G_4 also gave diffraction patterns of AM_1–G_1 and aminomalonic acid, while AM_3–G_4 and AM_4–G_5 gave those of AM_1–G_1 and γ-glycine.

TABLE 1. QUANTITATIVE DETERMINATION OF AMINOMALONIC ACID (IN AM_2–G_1, AM_4–G_3, AND AM_5–G_4) AND γ-GLYCINE (IN AM_1–G_2, AM_3–G_4, AND AM_4–G_5) BY X-RAY ANALYSIS

	Calcd %		Found %	
	AM	γ-Gly	AM	γ-Gly
AM_2–G_1	38.0		39.5	
AM_4–G_5	17.0		17.4	
AM_5–G_4	13.3		11.8	
AM_1–G_2		27.9		28.0
AM_3–G_4		11.6		11.5
AM_4–G_5		8.8		7.5

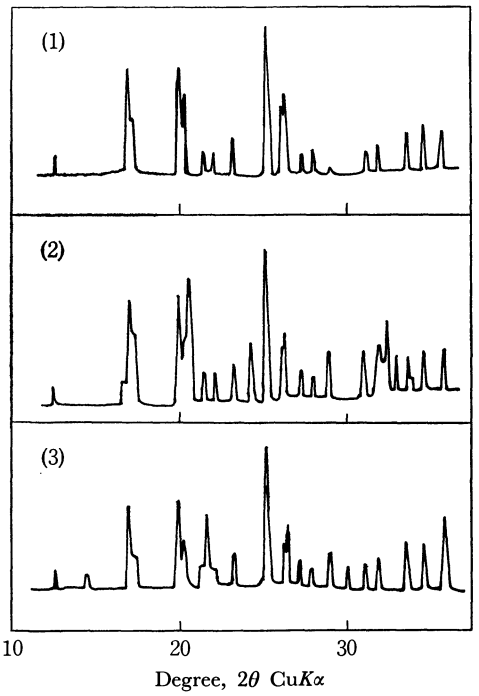

Fig. 2. X-ray diffraction patterns of AM_1–G_1 (1), AM_2–G_1 (2), and AM_1–G_2 (3).

The amount of aminomalonic acid was determined by means of calibration curves for AM_2–G_1, AM_4–G_3, and AM_5–G_4, and that of γ-glycine for AM_1–G_2, AM_3–G_4, and AM_4–G_5. The weight percentages of excess aminomalonic acid and γ-glycine, calculated by assuming that the crystals showing diffraction patterns of AM_1–G_1 are formed by the equimolar mixture of aminomalonic acid and glycine, agreed with the experimental values. The results are shown Table 1. Accordingly, it was confirmed that aminomalonic acid can form a solid complex with glycine in a molar ratio of 1 : 1 and the solid complex shows the diffraction patterns of AM_1–G_1. The diffraction angles and relative intensities are given in Table 2.

The infrared absorption spectra of the equimolar mechanical mixture of aminomalonic acid and γ-glycine (I), and AM_1–G_1(II) are shown in Fig. 3. Each absorption band in (I) could be assigned to those of aminomalonic acid and γ-glycine, whereas the absorption bands observed in (II) were different from

TABLE 2. X-RAY DIFFRACTION DATA OF AM_1–G_1

2θ(°)	$H/H°$	2θ(°)	$H/H°$
12.65	7	26.58	28
16.90	54	27.51	5
17.27	15	28.22	11
19.95	50	29.03	4
20.34	17	30.90	8
21.57	5	31.92	13
22.22	5	33.70	27
23.41	23	34.80	21
25.32	100	35.88	25
26.38	32	39.58	6

θ=Bragg angles. $H/H°$=relative height of diffraction peak.

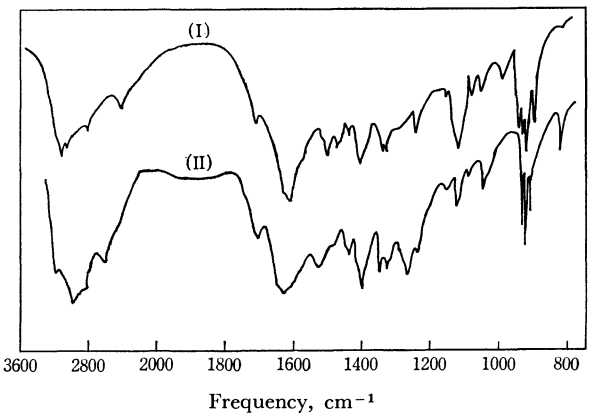

Fig. 3. Infrared spectra of equimolar mechanical mixture of aminomalonic acid and γ-glycine (I), and AM_1–G_1 (II).

those in (I). This indicates that there is an interaction between the molecules of aminomalonic acid and glycine.

Differential Thermal Analysis and Thermogravimetric Analysis. The solid line in Fig. 4 shows DTA–TGA curves of AM_1–G_1 in air. The amount of sample was 81.5 mg and the heating rate was 1.0°/min. For comparison, DTA–TGA curves of aminomalonic acid are shown by dotted lines. Conditions of measurements were the same as in AM_1–G_1 except for the sample amount, which was 50 mg in the present case. From the TGA curve of AM_1–G_1, the decarboxylation started at 115°C, the amount of carbon dioxide liberated did not reach the theoretical value until 170°C. In the DTA curve, endothermic and the succeeding exothermic peaks observed in the region of decarboxylation of aminomalonic acid, were slightly observed at temperatures 168°—175°C. An endothermic peak was also observed in the neighborhood of 185°C, which is supposed to be due to the transition of γ-glycine to α-glycine.

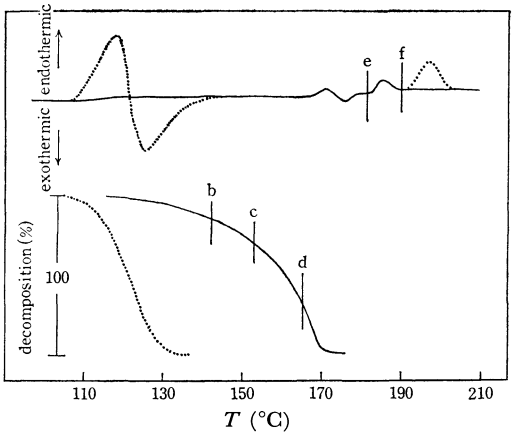

Fig. 4. DTA-TGA curves of AM_1–G_1 (solid lines) aminomalonic acid (dotted lines), in air.
Heating rate: 1.0°C/min. Sensivility: ±50 μV.
Reference: silica powder.

In order to examine the decarboxylation products of AM_1–G_1, samples were collected at the stages of b, c, d, e, and f in the DTA–TGA curves in Fig. 4 and X-ray analysis was carried out. The results are shown in Fig. 5. At stage b, the diffraction patterns of γ-glycine and several unknown diffraction peaks were observed along with those of AM_1–G_1. At stage c, γ-glycine, unknown material and α-glycine were observed in addition to the initials material, AM_1–G_1. The intensities of unknown diffraction peaks increased at c, but at stage d they disappeared and the diffraction peaks due to γ- and α-glycine were observed for AM_1–G_1. At e, diffraction peaks due to γ- and α-glycine were observed, and at f merely those due to α-glycine. Accordingly, the endothermic peak at about 185°C was due to the heat of transition from γ- to α-glycine. It shifted to the lower temperature side by 13°C as compared with that of aminomalonic acid. The unknown intermediate of decarboxylation is under investigation.

Activation Energies of Decarboxylation of AM_1–G_1 and Aminomalonic Acid. Coats and Redfern[4] derived

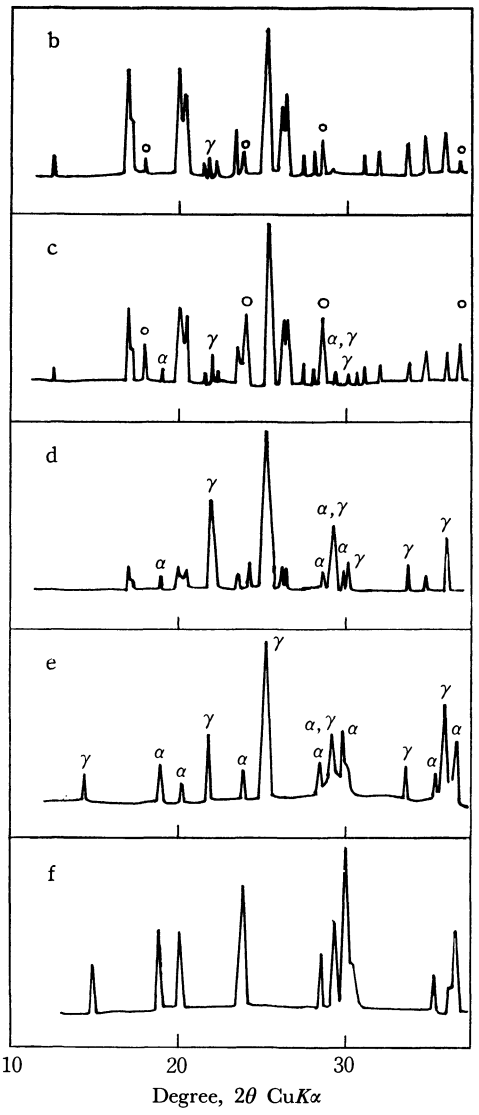

Fig. 5. X-ray diffraction patterns of decarboxylation products.
b, c, d, e, and f represent the places where the samples were collected in DTA–TGA curves of Fig. 6.
○: unknown material γ : γ-glycine α : α-glycine

4) A. W. Coats and J. P. Redfern, *Nature*, **201**, 68 (1964).

the following equations for the determination of activation energy of solid state reaction accompanied by weight decrease.

If $n \neq 1$,

$$\log_{10}\left\{\frac{1-(1-\alpha)^{1-n}}{T^2(1-n)}\right\} = \log_{10}\frac{AR}{aE}\left[1-\frac{2RT}{E}\right]-\frac{E}{2.3RT} \quad (1)$$

If $n=1$,

$$\log_{10}\left\{\frac{-\log(1-\alpha)}{T^2}\right\} = \log_{10}\frac{AR}{aE}\left[1-\frac{2RT}{E}\right]-\frac{E}{2.3RT} \quad (2)$$

where α=fraction of decomposition, n=order of reaction, E=activation energy, A=frequency factor, $a=\mathrm{d}T/\mathrm{d}t$, T=absolute temperature,

Using equation (1) or (2), the activation energy of decarboxylation reaction of AM_1–G_1 and aminomalonic acid was obtained from the TGA curves (Fig. 4). Assuming that $n=0$, 1/2, 2/3, or 1 in the decomposition range of 17 to 65% for AM_1–G_1 and 12 to 60% for aminomalonic acid,

$\log_{10}\{1-(1-\alpha)^{1-n}/T^2(1-n)\}$ or $\log_{10}\{-\log(1-\alpha)/T^2\}$ was plotted against $1/T$. The linear relation was obtained at $n=0$ for AM_1–G_1 and at $n=1$ for aminomalonic acid (Figs. 6 and 7). The value of activation energy obtained was 21.3 kcal/mol for AM_1–G_1 and 69.4 kcal/mol for aminomalonic acid. Although AM_1–G_1 has a smaller activation energy than aminomalonic acid and is advantageous from the viewpoint of reaction rate, AM_1–G_1 reacts more slowly even at a higher temperature.

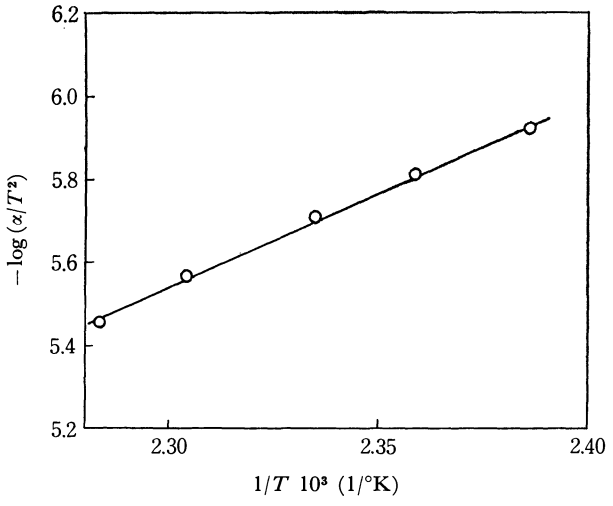

Fig. 6. Decarboxylation of AM_1-G_1. $n=0$

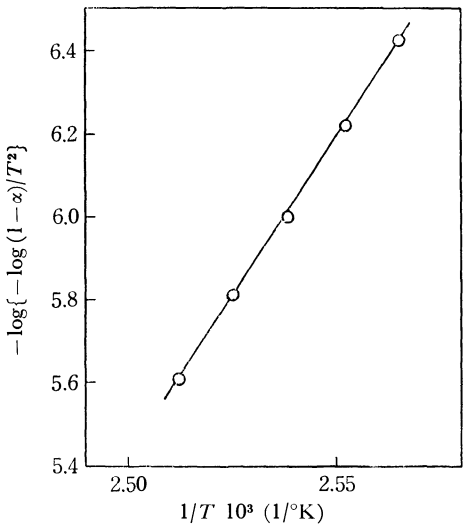

Fig. 7. Decarboxylation of aminomalonic acid. $n=1$

This indicates that the entropy term is effective in the depression of this reaction. This is attributed to the fact that, since the solid complex formed by the interaction of aminomalonic acid with glycine is thermally more stable than the crystals of aminomalonic acid alone, molecular motion is more restricted and the increase of entropy at the activated state was smaller in the solid complex than in the crystal of aminomalonic acid.

Conclusion

Aminomalonic acid can form an equimolar solid complex with glycine. In its crystalline state, aminomalonic acid is thermally stabilized due to its stronger interaction with glycine compared with the molecular interaction between aminomalonic acid molecules alone.

Photomicroscopic Observation of Dispersion State of Droplets in Flowing Emulsion[1)]

Kazushige SUZUKI and Takehiko WATANABE

Research Laboratory, Club Cosmetics, Co., Ltd., Naniwa-ku, Osaka

* *Laboratory of Biophysical Chemistry, College of Agriculture, University of Osaka Prefecture, Sakai, Osaka*

(Received December 11, 1970)

The viscosity of dilute emulsion with disperse phase of volume fraction $\phi=0.005$—0.06 was measured, and the dispersion state of emulsion droplets under shear was observed with a photomicroscope. Oil components used were aromatic hydrocarbons, *i.e.*, benzene, *o*-xylene, and toluene, and saturated hydrocarbons, *i.e.*, cyclohexane, decaline, *n*-hexane, *etc.* As emulsifier, Arlacel 60 or Arlacel 83 was used for W/O type emulsion and Tween 20 for O/W type one. For the W/O type emulsions of aromatic hydrocarbon of low emulsifier concentration (0.2%), Einstein's equation could be applied to the viscosity at a high rate of shear in the range of ϕ below 0.02, in spite of the presence of aggregates of droplets in the flowing emulsion. When ϕ becomes 0.04—0.06, the deviation from Einstein's equation was large. In the case of higher emulsifier concentration (1%), the deviation from Einstein's equation was noticeable even for $\phi=0.01$, when Arlacel 60 was used as stabilizer. The results may be brought about by the increase of effective volume fraction of disperse phase owing to the inclusion of continuous phase liquid in aggregates. In the case of W/O type emulsions of saturated hydrocarbon and O/W type ones, irrespective of the kind of oil phase liquid, the aggregates were completely redispersed into primary droplets at a high rate of shear, and Einstein's equation could be applied.

In our previous studies on non-Newtonian flow of W/O type emulsions,[2)] we found that water-in-benzene emulsion (volume fraction of disperse phase, 0.1—0.6) showed the most noticeable dependence of viscosity on the rate of shear and that the dispersed droplets in the system formed large aggregates at a low rate of shear as compared with other emulsions prepared with hydrocarbons other than benzene *i.e.*, cyclohexane, liquid paraffin, *etc.* In order to study the characteristics of non-Newtonian flow of emulsions, photomicroscopic observation of the dispersion state of droplets under shear was made with dilute emulsions (volume fraction, 0.005—0.06),[3)] and it was found that in water-in-benzene emulsion, the aggregates formed in the emulsion could not be redispersed into primary droplets even at higher rates of shear than 2000 sec^{-1}.

In this paper, photomicroscopic observations are described on the dispersion state of droplets in the flowing emulsions under shear, where the emulsions show Newtonian flow characteristics and their viscosities can be represented by Einstein's equation.

Experimental

Sample. W/O type emulsions were prepared by using either sorbitan monostearate (Arlacel 60) or sorbitan sesquioleate (Arlacel 83) as stabilizer, and O/W type emulsions by polyoxyethylene sorbitan monolaurate (Tween 20). The oil phase liquids such as benzene, toluene, *o*-xylene, cyclohexane, decaline, kerosene, liquid paraffin, *etc.* were mixed with carbon tetrachloride to adjust their density to that of water. The volume fraction of disperse phase ϕ was 0.005, 0.01, 0.02, 0.04, and 0.06. The emulsions were prepared from water and oil phase liquid containing the emulsifier by shaking by hand or by mixing together with a high-speed mixer.

Measurements. As shown in Fig. 1, a light source and a photomicroscope were placed perpendicular to the axis of the capillary of Maron-Belner type viscometer[4)] (capillary: 0.064 cm in diameter and 25.4 cm in length) at an appropriate position where a part of thick glass of the capillary was flatened by polishing. In order to photograph the droplet image moving at a high rate of shear, a Xe-flash system having flash duration time less than 100 μ sec was used as the light source. The circuit of the flash system is shown in Fig. 2. The flashing tube is fed at 3 kV under generation of 15 kV trigger voltage in the starting electrode. Duration time is mainly determined by the capacity of the condenser connected in series with the flashing tube. The system used was provided with a 5 μF condenser.

Aggregates of droplets at various rates of shear were photo-

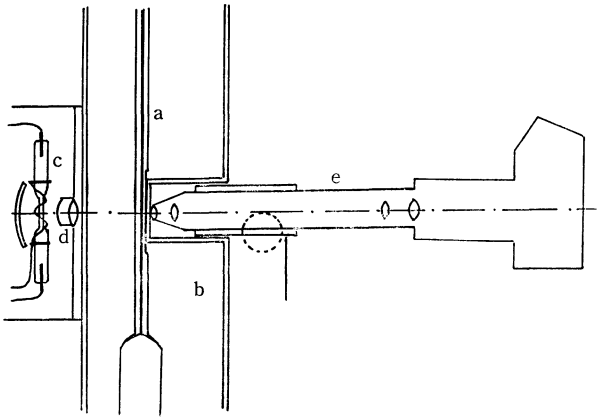

Fig. 1. Vertical section of apparatus.
a. Capillary portion of viscometer
b. Water bath
c. Xe flash tube
d. Condenser
e. Photomicroscope

1) Presented at the 21st Symposium of Colloid Chemistry, Kyoto, Nov. 3, 1968.

2) K. Suzuki, S. Matsumoto, T. Watanabe, and S. Ono, This Bulletin **42**, 2773 (1969).

3) K. Suzuki, T. Watanabe, and S. Ono, Proc. 5th Intern. Congr. Rheology, Vol. 2, 339 (1970).

4) S. H. Maron and R. J. Belner, *J. Appl. Phys.*, **26**, 1457 (1955).

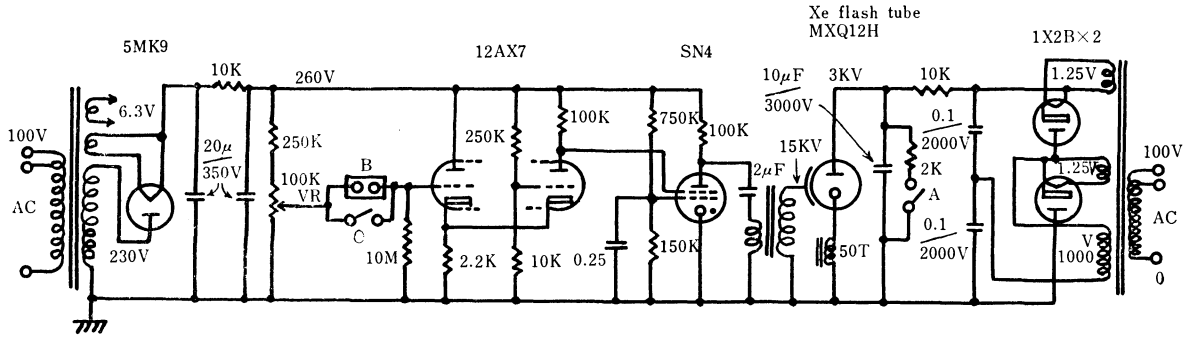

Fig. 2. The circuit of the flash system.
A : Discharge Button B : to Camera Synchro-plug C : Flash Button

graphed and at the same time the viscosity of the emulsion was measured. Measurements were carried out at 32°C in a constant-temperature bath. Viscosity was expressed in terms of relative viscosity η_{rel} defined by

$$\eta_{rel} = \frac{\text{Viscosity of emulsion}}{\text{Viscosity of continuous phase containing emulsifier}}$$

Results and Discussion

With the exception of W/O type emulsions of aromatic hydrocarbon having volume fraction $\phi=0.04$—0.06, all emulsions showed Newtonian flow characteristics at high rates of shear over 100 sec^{-1}. Relative viscosity (η_{rel}) of the emulsions under a shear stress at the capillary wall, 17 dyne/cm^2, at which the rates of shear exceed 2000 sec^{-1}, are plotted against ϕ (Figs. 3, 4, and 5). The solid lines are drawn according to Einstein's equation.

As shown in Fig. 3, with the emulsion stabilized with 0.2% Arlacel 60, Einstein's equation could be applied to represent η_{rel} of the benzene emulsions with ϕ below 0.02. Figure 6 shows microscopic photographs obtained with the benzene emulsion with $\phi=0.01$. We see that the size of aggregates decreases with the increase of rates of shear. However, the droplets in the flowing emulsion are not dispersed as primary droplets even at high rates of shear of 500—3000 sec^{-1}. When ϕ of benzene emulsions increased to 0.04—0.06, the discrepancy between the observed value of η_{rel} and that calculated by Einstein's equation became large, and the viscosity could be represented by an

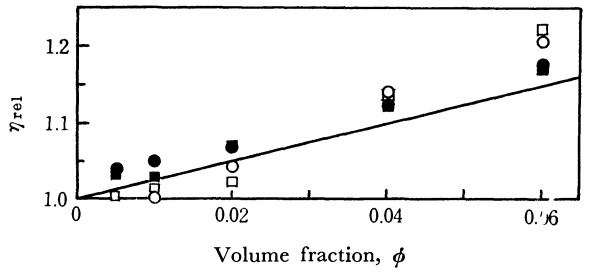

Fig. 3. Plots of relative viscosity *vs.* volume fraction for W/O emulsions stabilized by 0.2% Arlacel 60 at 32°C.
Solid line, calculated by Einstein's equation.
Medium: ○ Benzene (+CCl_4), □ Benzene (+CCl_4) prepared by Mixer, ● Cyclohexane (+CCl_4), ■ Cyclohexane (+CCl_4) prepared by Mixer

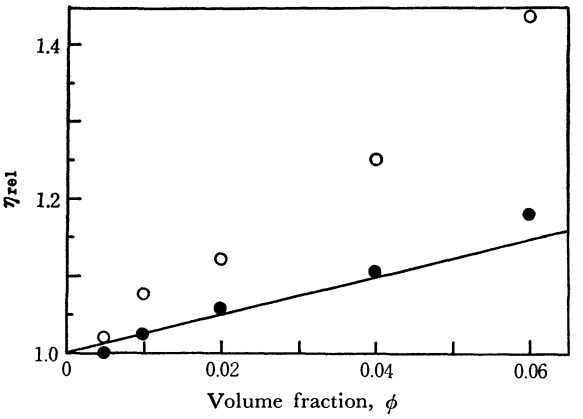

Fig. 4. Plots of relative viscosity *vs.* volume fraction for W/O emulsions stabilized by 1.0% Arlacel 60 at 32°C.
Solid line, calculated by Einstein's equation.
Medium: ○ Benzene (+CCl_4), ● Cyclohexane (+CCl_4)

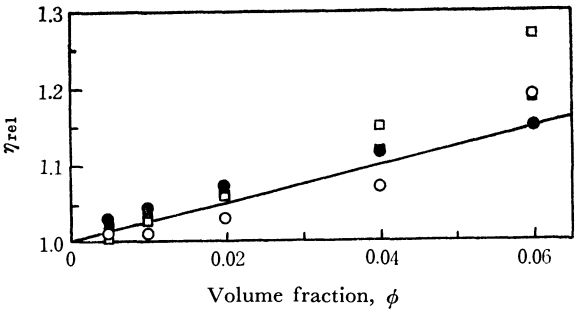

Fig. 5. Plots of relative viscosity *vs.* volume fraction for W/O emulsions stabilized by Arlacel 83 at 32°C.
Solid line, calculated by Einstein's equation.
Medium:
○ 0.2% Arlacel 83-Benzene (+CCl_4)
● 0.2% Arlacel 83-Cyclohexane (+CCl_4)
□ 1.0% Arlacel 83-Benzene (+CCl_4)
■ 1.0% Arlacel 83-Cyclohexane (+CCl_4)

equation consisting of series of power of ϕ as follows.

$$\eta_{rel} = 1 + 2.5\phi + 14\phi^2 + 50\phi^3$$

In cyclohexane emulsions shown in Fig. 3, the droplets were completely dispersed as primary ones at high rates of shear of 500—3000 sec^{-1} irrespective of the values of ϕ. The results obtained with toluene and *o*-xylene emulsions were similar to those obtained with benzene system, and the results with the systems using such saturated hydrocarbones as decaline, *n*-

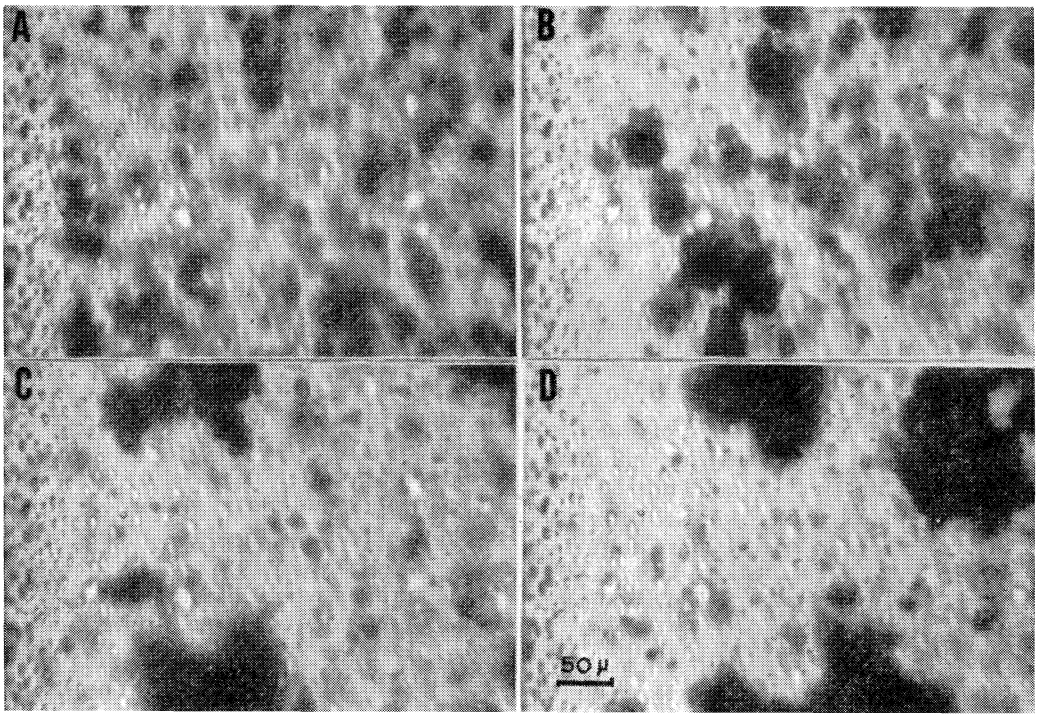

Fig. 6. Water in benzene ($+CCl_4$) emulsions ($\phi=0.01$) stabilized by 0.2% Arlacel 60 prepared by mixer.
shear stress, rate of shear
A; 17.2 dyn/cm², 2740 sec⁻¹
B; 7.65 dyn/cm², 1218 sec⁻¹
C; 3.48 dyn/cm², 555 sec⁻¹
D; 1.43 dyn/cm², 228 sec⁻¹

hexane, *etc.* as the suspending fluids were similar to those obtained with cyclohexane systems.

As shown in Fig. 4, in the benzene emulsions stabilized with 1% Arlacel 60, there were marked discrepancies between the value of η_{rel} and that calculated by Einstein's equation even with the emulsion of $\phi=0.01$. Even with the emulsion of $\phi=0.005$ showing Newtonian flow characteristics at a high rate of shear, the droplets in flowing emulsions were not dispersed as primary droplets. The size of aggregate was smaller in the case of emulsion stabilized with 1% Arlacel 60 (Fig. 7) than that with 0.2% Arlacel 60 (Fig. 6B). Thus, the higher values of η_{rel} of the former emulsion than the latter seems to be due to the increase of effective volume fraction of the disperse phase resulting from the formation of aggregate occluding the continuous phase liquid in the cluster of droplets.

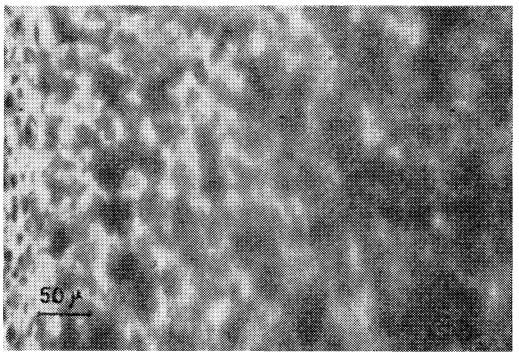

Fig. 7. Water in benzene ($+CCl_4$) emulsion ($\phi=0.01$) stabilized by 1.0% Arlacel 60 prepared by shaking by hand observed at shear stress, 8.34 dyn/cm², and rate of shear, 1230 sec⁻¹.

As shown in Fig. 5, in the benzene emulsions stabilized with Arlacel 83, discrepancies between the value of η_{rel} and that calculated by Einstein's equation was more marked with emulsions of high emulsifier concentration than those of lower concentration in the range of higher values of ϕ. However, the size of aggregate observed at a high rate of shear was smaller with emulsions of high emulsifier concentration. The increase in η_{rel} with the increase of emulsifier concentration is brought about by the increase of effective volume fraction of disperse phase owing to the formation of aggregate occluding the continuous phase liquid and/or owing to the increased solvation of droplets surface with the perfection of the emulsifier layer

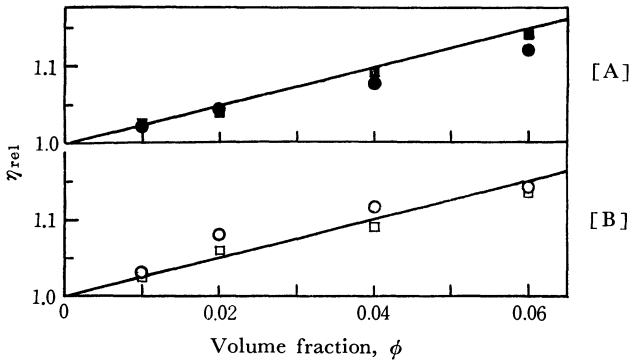

Fig. 8. [A] and [B], plots of relative viscosity *vs.* volume fraction for O/W emulsions stabilized by 0.01% Tween 20 at 32°C.
Solid line, calculated by Einstein's equation.
Disperse phase: ○ Benzene ($+CCl_4$), □ Benezene ($+CCl_4$) prepared by Mixer, ● Cyclohexane ($+CCl_4$), ■ Cyclohexane ($+CCl_4$) prepared by mixer

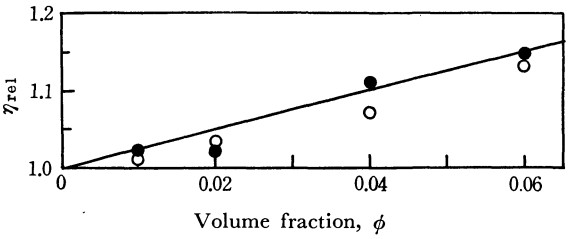

Fig. 8. [C], plots of relative viscosity *vs.* volume fraction for O/W emulsions stabilized by 0.1% Tween 20 at 32°C. Solid line, calculated by Einstein's equation.
Disperse phase: ○ Benzene (+CCl_4), ● Cyclohexane (+CCl_4)

around the droplets.

The above results show that in the case of water in benzene emulsion, droplets in the flowing emulsion at rates of shear below 3000 sec^{-1}, could not be dispersed as primary droplets. Albers and Overbeek[5] estimated the effective van der Waal's constant A between the water droplets in water in benzene emulsion from the minimum rate of shear to reach Newtonian region *i.e.*, to cause complete redispersion, and found a rather low value of $A=0.4\times10^{-14}$ erg based on the experimental value of the minimum rate of shear of $<100\ sec^{-1}$ for the emulsion stabilized by 1% Span 85 (sorbitan trioleate) of $\phi=0.14$ and $200\ sec^{-1}$ for the one stabilized by 1% Span 60 (sorbitan monostearate) of $\phi=0.175$. It should be mentioned that such a low value of A obtained by Albers and Overbeek was due to incomplete confirmation of the complete dispersion of droplets in the system.

In the case of O/W type emulsions irrespective of the kind of oil phase liquid, the aggregates formed in the emulsion were completely redispersed into primary droplets at a high rate of shear and Einstein's equation could be applied to represent the observed values of η_{rel} with the emulsions of values of ϕ as high as 0.06 as shown in Fig. 8.

The authors would like to express their gratitude to Professor Sôzaburo Ono for his discussions.

5) W. Albers and J. Th. G. Overbeek, *J. Colloid Sci.*, **15**, 489 (1960).

BULLETIN OF THE CHEMICAL SOCIETY OF JAPAN, VOL. 44, 2042—2045 (1971)

Proton Spin-Lattice Relaxation Studies of Intermolecular Interactions in Acetic Acid Solution

Kazuo SATO and Atsuo NISHIOKA

Department of Polymer Engineering, Tokyo Institute of Technology, Ookayama, Meguro-ku, Tokyo

(Received December 11, 1970)

Proton spin-lattice relaxation measurements were carried out by the rapid-passage method on the hydroxyl and methyl protons of acetic acid in carbon tetrachloride, benzene-d_6, and chloroform-d in order to investigate the effect of the self-association of acetic acid on the spin-lattice relaxation. It was found that there exists a maximum of the relaxation rate in carbon tetrachloride, and two maxima in benzene-d_6 and chloroform-d, on dilution with a solvent. This relaxation behavior was attributed to the change in the self-association mechanism of acetic acid. We tried to keep the proton-density constant in all solution in order to avoid any ambiguity arising from the change in density by using the analogous deuterated compounds.

Previously we have studied the effect of the intermolecular interaction on the proton spin-lattice relaxation time, T_1, of chloroform, benzene, and acetone in solution.[1] We found that T_1's are sensitive to the intermolecular interaction or the molecular association, even if its lifetime is very short. In this paper, we will study the spin-lattice relaxation of the hydroxyl and methyl protons of acetic acid in carbon tetrachloride, chloroform-d, and benzene-d_6 respectively.

Hydrogen bonding in carboxylic acids has been investigated by a number of workers using nuclear magentic resonance and infrared spectroscopy.[2-4] Reeves and Schneider[5] have investigated the dilution curves of the chemical shift of the hydroxyl proton of acetic acid in a series of non-interacting solvents, such as carbon tetrachloride and cyclohexane, and found that, on dilution, the resonance moves first to a low field, but on further dilution moves to a higher field compared with its position in pure acetic acid. They have interpreted these results in terms of a polymer-dimer equilibrium in a concentrated acid solution and a dimer-monomer equilibrium in more dilute solutions. Reeves[6] has studied the changes in the chemical shift of the hydroxyl proton in some carboxylic acids on dilution in several solvents, and given evidence for the existence of chain-like hydrogen-bonded polymers in solutions and for the formation of weak acid-solvent complexes in dichloro-

1) K. Sato and A. Nishioka, This Bulletin, **44**, 1506 (1971).
2) G. C. Pimentel and A. L. McClellan, "The Hydrogen Bond," W. H. Freeman and Company, San Francisco, California (1960).
3) J. C. Davis, Jr., and K. K. Deb, *Adv. Magnetic Resonance*, **4**, chap. 4 (1970).
4) R. Foster and C. A. Fybe, *Progr. NMR Spectry*, **4**, chap. I (1969).
5) L. W. Reeves and W. G. Schneider, *Trans. Faraday Soc.*, **54**, 314 (1958).
6) L. W. Reeves, *Can. J. Chem.*, **39**, 1711 (1961).

methane and 1,2-dichloroethane. Many other chemical shift studies have been made of acetic acid and some carboxylic acids in solutions, and valuable information has been obtained.

Relaxation measurements of carboxylic acids have also been made by several authers. Tatsumoto[7] has studied ultrasonic absorption in propionic acid and discussed the disociation mechanism and the solvent effect on relaxation. Goldammer and Zeidler[8] have measured the proton and deuteron spin-lattice relaxation time of methyl and the self-diffusion coefficient in a binary mixture of water and acetic acid.

It is the purpose of the present study to investigate the effect of the self-association, the change in the association mechanism of acetic acid, and the intermolecular interaction with a solvent on the spin-lattice relaxation, and to discuss the microdynamic behavior of acetic acid in solution. We believe that the information on the microdynamic behavior together with that on the equilibrium properties will aid us in understanding in detail the nature of acetic acid in solution.

Experimental

Materials. The acetic acid was a super-special-grade sample purchased from the Wako Pure Chem. Co., Ltd., and the carbon tetrachloride was a spectroscopic-grade sample purchased from the Tokyo Kasei Co., Ltd. The acetic acid-d_4, benzene-d_6, and chloroform-d were provided by E, Merck AG, Darmstadt, and were used without further purification. All the materials were stored in a water-free atmosphere. The proton-density of all the solutions was kept constant by using analogous deuterated compounds in order to avoid any ambiguity in the spin-lattice relaxation arising from its change. In the NMR spectrum at a high gain, no signals due to impurities were observed. The atmospheric oxygen dissolved in the samples was removed carefully by several free-pump-thaw cycles in a NMR sample tube, and then under a vacuum the tube was sealed. After sealing, the NMR measurements were carried out immediately.

NMR Measurements. The NMR spectrometer used in this study was a JNM-C-60H spectrometer of Japan Electron Optics. Lab. operated at 60 MHz. The measurements of T_1 were carried out at 25±1°C by the adiabatic rapid-passage method with sampling. The experimental errors were found to be within ±3%. The corrections for the macroscopic solution viscosity were not carried out.[1]

Results and Discussion

Carbon Tetrachloride Solution. In Fig. 1, the spin-lattice relaxation rate T_1^{-1}, of the methyl and hydroxyl proton of acetic acid *versus* the mole fraction of acid is shown. The proton density is constant at all compositions and equals to 41.65×10^{20} per unit of volume. It is clear that, on dilution with carbon tetrachloride, the T_1^{-1} of the hydroxyl proton gradually increases up to a value larger than that in pure acid

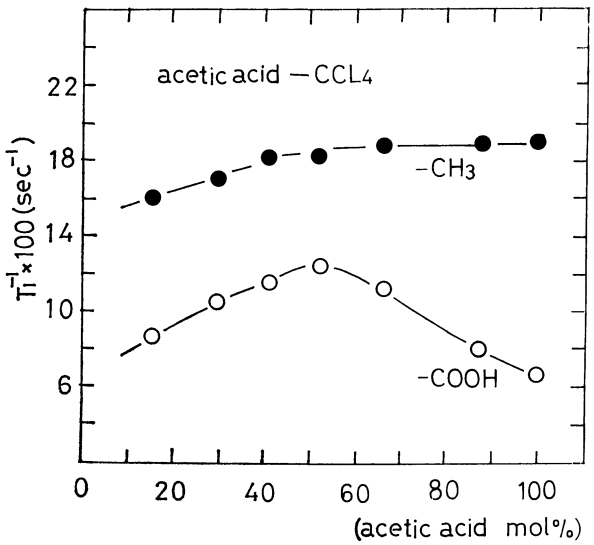

Fig. 1. Plots of $1/T_1$'s of the hydroxyl (○) and methyl (●) protons of acetic acid in carbon tetrachloride *vs.* apparent mole fraction of acetic acid.
The number of protons per unit volume is constant; $N=41.65\times10^{20}$.
Apparent mole fraction of acetic acid was varied by addition of acetic acid-d_4.

by a factor of 2 and that a broad maximum exists at 50 mol% of acid. No distinct maximum is observed in the plot of the T_1^{-1} of the methyl *versus* mole fraction of acid, but on dilution beyond 50 mol% the T_1^{-1} decreases distinctly.

Goldammer and Zeidler have shown that the maximum of the relaxation rate of the methyl protons and deuterons exists at 50 mol% of acid in a water-acetic acid system, and that at this concentration the self-diffusion coefficient exhibits the minimum. The disagreement regarding the relaxation behavior of the methyl between their results and those in the present study is considered to reflect the difference in the association mechanism and in the acid-solvent interaction in aqueous and non-polar environments. If the self-diffusion coefficient is determined for a carbon tetrachloride solution, a detailed discussion will be possible.

Over the experimental range of the acid concentration studied, the polymers of acids may be predominant over the cyclic dimer.[9] The minimum of the hydroxyl proton chemical shift has been observed at a lower concentration than 5 mol% of acid in carbon tetrachloride,[5] at which point the dimer should be predominant. Therefore, we will discuss the results of the spin-lattice relaxation studied in this experiment in terms of changes in the length of the polymer chains. On dilution, the length of the chains is considered to increase gradually, probably because of the decrease in the dielectric constant of the solution; the polymer must become more stable and rigid to compensate for the entropy decrease of the solution. As the microdynamic molecular motions of the stable and rigid polymer chains should be reduced extensively compared with those of the weak chains, the spin-lattice relax-

7) N. Tatsumoto, *J. Chem. Phys.*, **47**, 4561 (1967).
8) E. V. Goldammer and M. D. Zeidler, *Ber. Bunsenges. Phys. Chem.*, **73**, 4 (1969).
9) G. Mavel, *J. Phys. et. Radium*, **21**, 38 (1960).

ation rate must increase by a factor of 2 in the present study. On the other hand, in a solution more dilute than 50 mol% of acid, the polymer chains shorten. Moreover, in this concentration region, the polymer-dimer equilibrium may become appreciable, and the fraction of the dimer increases gradually.

Our interpretation does not conflict with the results of the chemical shift studies. The increase in the chain length on dilution is considered to result in the low field shift of the hydroxyl proton, because the fraction of the terminal acetic acid molecules, whose hydroxyl proton resonates at a higher field than that of the acid participating in the hydrogen bonding, decreases.[6] The observed chemical shift is the average of those of the protons in two different sets of circumstances because of the rapid averaging of the shielding effects. Contrary to the shortening of the chain length, the fraction of the dimer may increase in the lower concentration region. The hydroxyl proton of the dimer is considered to resonate at a lower field than that of acid participating in the internal hydrogen bonding of the chains, because the anisotropy of the susceptibility of the carbonyl group contributes more effectively to the hydroxyl proton of the dimer as a result of the cyclic structure of the dimer.[10] Thus, the average proton resonance may be concluded to move to the low field on dilution.

It may be supposed that, if experimental measurements were made on a solution more dilute than a 5—10 mol% acid solution, spin-lattice relaxation behavior due to the predominant dimer structure might be observed. The experimental results that the T_1^{-1} of the methyl, except in a dilute solution, does not follow the changes in the length of the polymer chains described above probably reflects the relatively free rotation of methyl about the C_3 axis. Indeed, Goldammer and Zeidler have shown that the correlation time of the internal rotation of the methyl is very short compared with that of the rotational motion of the whole molecule.

Benzene and Chloroform Solution. In Fig. 2, the plot of the T_1^{-1} of acetic acid in benzene-d_6 *versus* the acid concentration is shown. Contrary to the results on a carbon tetrachloride solution, two distinct maxima are observed in the relaxation behavior of the hydroxyl proton, but that of the methyl decreases linearly on dilution. We attribute the maximum in the high-concentration region to the changes in the polymer length described in the previous section, and that in the low-concentration region, to the relaxation behavior of the dimer and the dimer—monomer equilibrium which is not observed in carbon tetrachloride.

Shimizu[11] has investigated the change in the chemical shift of acetic acid in benzene, and found that the acid concentration at which the minimum of the hydroxyl proton chemical shift occurs is 30—40 mol%, higher than that in carbon tetrachloride. He has interpreted the results in terms of acid-benzene interaction, in which the acid monomer becomes stable and

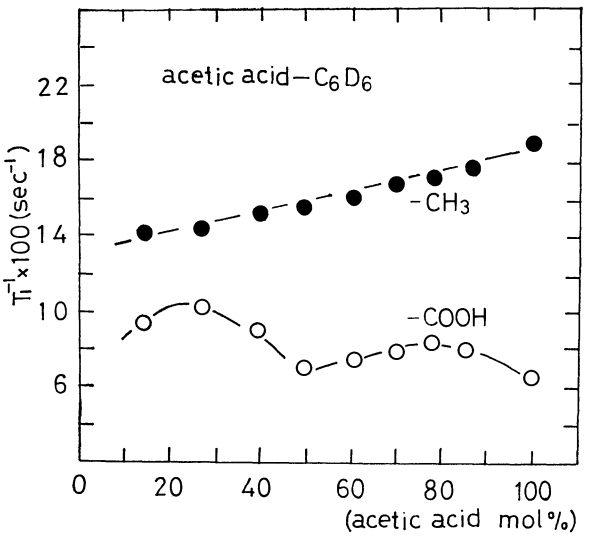

Fig. 2. Plots of $1/T_1$'s of the hydroxyl (○) and methyl (●) protons of acetic acid in benzene-d_6 *vs.* apparent mole fraction of acetic acid.
The number density of protons is constant; $N=41.65\times10^{20}$.
Apparent mole fraction of acetic acid was varied by addition of acetic acid-d_4.

the monomer fraction is appreciable even in the high-concentration region of acid where, in carbon tetrachloride, the monomer scarcely exists at all. The dimer fraction is considered to be predominant at the acid concentration of 30—40 mol%. At almost the same acid concentration, the maximum of the relaxation rate of the hydroxyl proton is observed. Therefore, our consideration described above is considered probably to be true. Davis and Pitzer[12] have also shown evidence for the interaction between benzene and acetic acid by their chemical shift measurements. In

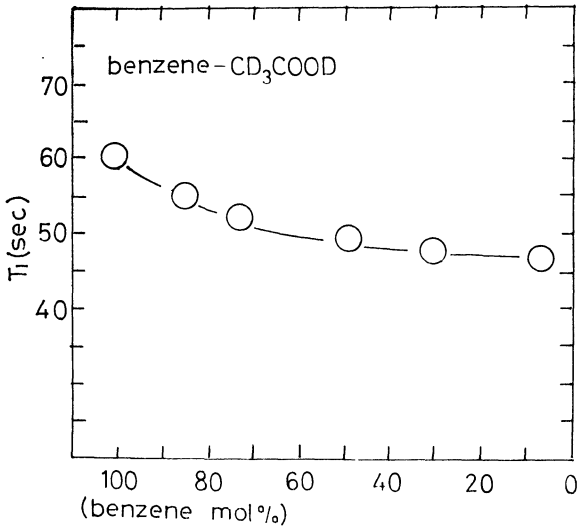

Fig. 3. Plot of $1/T_1$'s of benzene in acetic acid-d_4 *vs.* apparent mole fraction of benzene.
The number density of protons is constant; $N=40.5\times10^{20}$.
Apparent mole fraction of benzene was varied by addition of benzene-d_6.

10) N. Nakagawa, *Kagaku no Ryoiki*, **15**, 665 (1961).
11) H. Shimizu, *Nippon Kagaku Zasshi*, **81**, 1025 (1960).
12) J. C. Davis, Jr., and K. S. Pitzer, *J. Phys. Chem.*, **64**, 886 (1960).

Fig. 3, the T_1's of benzene in acetic acid-d_6 are shown *versus* the mole fraction of benzene. It is clear that the spin-lattice relaxation of benzene is affected by the presence of acetic acid. This implies that the interaction between benzene and acetic acid exists and influences the microdynamic molecular motion to the degree of changing the spin-lattice relaxation behavior.

It has been well known that the dimer form of acetic acid is considerably stable. For example, Reeves and Schneider[5] have shown that, even in the gaseous state, the acetic acid dimer exists. Therefore, we consider that the decrease in the microdynamic molecular mobility and the relaxation rate of the dimer should be greater than those of the monomer and the less stable polymers. This expectation can be clearly verified from Fig. 2. Recently, Rothschild[13] has studied the translational molecular motion of neat acetic acid and discussed the possibility that the dimeric form is stable and can perform the translational jumps as a unit. The relaxation rates of the polymers in benzene are smaller than those in carbon tetrachloride, and the position of the maximum in the former deviates to a higher acid-concentration region than that in the latter. It is suggested that the polymer chains become less stable and weak through the acid-benzene interaction and show a tendency to shorten in the higher-acid-concentration region.

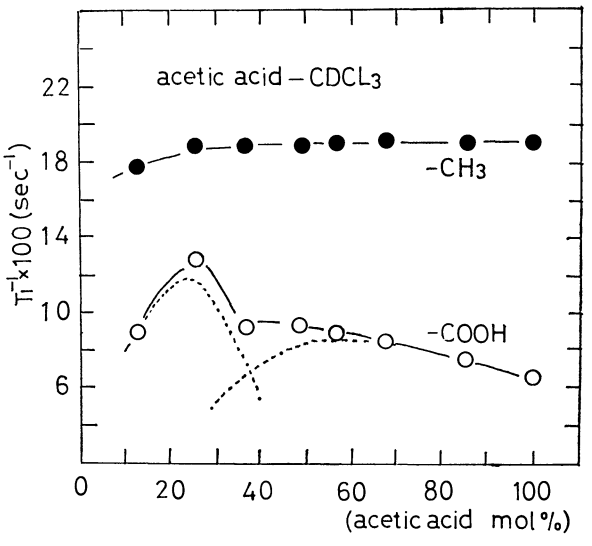

Fig. 4. Plots of $1/T_1$'s of the hydroxyl (○) and methyl (●) protons of acetic acid in chloroform-*d* *vs.* apparent mole fraction of acetic acid.
The number density of protons is constant; $N=41.65\times10^{20}$. Apparent mole fraction of acetic acid was varied by addition of acetic acid-d_4.

13) W. Rothschild, *J. Chem. Phys.*, **53**, 3265 (1970).

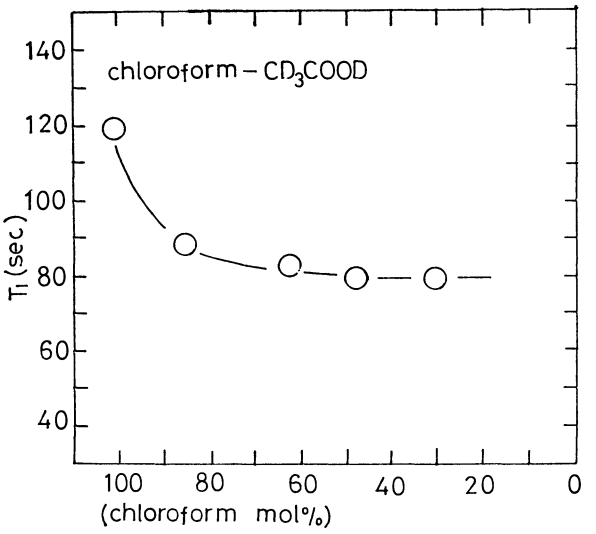

Fig. 5. Plot of $1/T_1$'s of chloroform in acetic acid-d_4 *vs.* apparent mole fraction of chloroform.
The number density of protons is constant; $N=29.8\times10^{20}$. Apparent mole fraction of chloroform was varied by addition of chloroform-*d*.

In Fig. 4, the plot of T_1^{-1} of acetic acid in chloroform-*d* is shown *versus* the acid concentration. It seems reasonable to decompose the curve thus obtained into two relaxation curves. In chloroform, there exist two maxima, just as in benzene. The one appearing at the low acid concentration is considered to reflect the relaxation behavior of the predominant dimer, while the other, at the high concentration, may be due to the relaxation of the polymers. Except for the position of the maximum at the high concentration, the other relaxation behavior, such as the relaxation rate and the position of the maximum at the low concentration, is almost identical with that in benzene. The small difference between the two cases may arise from the difference in the acid-solvent interactions. Chloroform interacts with acetic acid, and the spin-lattice relaxation is affected by the chloroform-acid interaction, as is shown in Fig. 5.

It was found that the self-association of acetic acid exerts a pronounced effect on the spin-lattice relaxation of the hydroxyl proton, and that the relaxation behavior largely depends upon the concentration of acid and the kind of solvents. The spin-lattice relaxation study may provide useful information about the microdynamic molecular motion of acid and may, together with the chemical shift and infrared measurements, allow us to infer the mechanism and the nature of the self-association of acetic acid.

The Protonation of Aromatic Hydrocarbon Radical Anions. II. Interpretations of the Rate Constants in Terms of HMO Calculations

Shigeo HAYANO and Masamichi FUJIHIRA

Institute of Industrial Science, The University of Tokyo, Roppongi, Minato-ku, Tokyo

(Received December 14, 1970)

The rates of the protonation of aromatic hydrocarbon radical anions with water in dimethylformamide (DMF)-water mixtures were measured by means of the decay of the visible absorption maxima of radical anions with time. The rates were found to be greatly accelerated by the increasing water content in DMF-water mixtures. This behavior suggests that the negative charge is much more localized in the transition state than in the original radical anion. The rate constants in DMF could be obtained by extrapolation. The correlation of these rate constants to the molecular structure of radical anions was discussed on the basis of the results of HMO calculations. This correlation and the solvent effect could be interpreted by means of the charge-transfer mechanism.

In a previous paper[1] a study of the mechanism of the protonation of the aromatic hydrocarbon radical anions in DMF-water mixtures was reported; there the radical anions of biphenyl, naphthalene, phenanthrene, anthracene, 1,2-benzanthracene, and pyrene were found to decay by a first-order reaction:

$$\frac{d[R^-]}{dt} = -2k[H_2O][R^-] = -k_{app}[R^-] \quad (1)$$

through the following sequence:

$$R^- + H_2O \xrightarrow{k} RH\cdot + OH^- \quad (2)$$

$$RH\cdot + R^- \rightleftharpoons RH^- + R \quad (3)$$

$$RH^- + H_2O \xrightarrow{k'} RH_2 + OH^- \quad (4)$$

The same results were obtained for anthracene by the use of the ESR technique by Umemoto.[2]

The present paper will deal with the rate of the protonation reaction of Eq. (2) in DMF-water mixtures obtained by measuring the change in the visible absorption maximum with the time,[1] with the effect of the solvent on the rate, and with the correlation of the observed rate constants with the molecular structures of the reagents.

Experimental

All the materials and apparatus were the same as in the previous paper.[1] As the supporting electrolyte, tetraethylammonium bromide (TEAB) was used. The measurements of the absorbance against the time were carried out at the λ_{max} of the radical anions: biphenyl, 407 mμ; naphthalene, 368 mμ; phenanthrene, 421 mμ; anthracene, 725 mμ; 1,2-benzanthracene, 415 or 758 mμ, and pyrene, 742 mμ. All the measurements were carried out at 20°C.

Results and Discussion

The Solvent Effects on the Rate of Protonation. The apparent rate constants, k_{app}, which are equal to $2k[H_2O]$ are given in Table 1, while the effect of the water content on the rate constant, $k(M^{-1}sec^{-1})$, as calculated from k_{app}, is shown in Fig. 1.

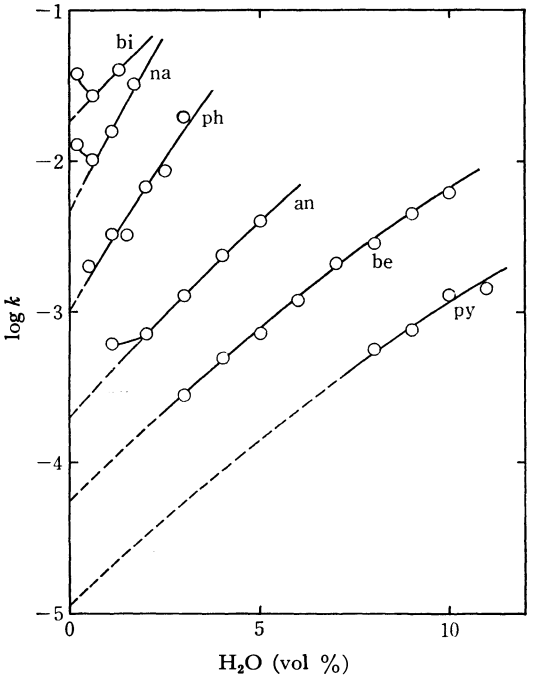

Fig. 1. The effect of water content on the rate constant k: bi, biphenylide; na, naphthalenide; ph, phenanthrenide; an, anthracenide; be, 1,2-benzanthracenide; py, pyrenide radical anion.

It is well known[3] that a bimolecular reaction such as that between anions and polar molecules shown in Eq. (5) is very much faster in dipolar aprotic solvents than in protic solvents:

$$Y^- + R_3CX \rightarrow \left[\begin{array}{c} R \quad R \\ \diagdown \quad \diagup \\ Y\cdots C\cdots X \\ | \\ R \end{array} \right]^- \rightarrow YCR_3 + X^- \quad (5)$$

where protic solvents, such as water, methanol, and formamide, are hydrogen-bond donors, while dipolar aprotic solvents, such as DMF, dimethylsulfoxide (DMSO), and acetonitrile, are not hydrogen-bond donors but are highly polar molecules. This behavior can be explained qualitatively as follows: a small anion, Y^-, in the original system where the negative

1) S. Hayano and M. Fujihira, This Bulletin, **44**, 1496 (1971).
2) K. Umemoto, *ibid.*, **40**, 1058 (1967).
3) A. J. Parker, "Advances in Physical Organic Chemistry," Vol. 5, ed. by V. Gold, Academic Press, New York, N. Y. (1967), p. 173.

TABLE 1. OBSERVED RATE CONSTANTS k_{app}

(a) Biphenyl

H_2O, %	k_{app}, sec^{-1}
0.2	8.6×10^{-3}
0.6	1.9×10^{-2}
1.3	5.9×10^{-2}

(b) Naphthalene

H_2O, %	k_{app}, sec^{-1}
0.2	2.9×10^{-3}
0.6	7.0×10^{-3}
1.1	2.0×10^{-2}
1.7	6.2×10^{-2}

(c) Phenanthrene

H_2O, %	k_{app}, sec^{-1}
0.5	1.1×10^{-3}
1.1	4.0×10^{-3}
1.5	5.3×10^{-3}
2.0	1.5×10^{-2}
2.5	2.4×10^{-2}
3.0	6.6×10^{-2}

(d) Anthracene

H_2O, %	k_{app}, sec^{-1}
1.1	7.6×10^{-4}
2.0	1.6×10^{-3}
3.0	4.4×10^{-3}
4.0	1.1×10^{-2}
5.0	2.2×10^{-2}

(e) 1,2-Benzanthracene

H_2O, %	k_{app}, sec^{-1}
3.0	9.4×10^{-4}
4.0	2.2×10^{-3}
5.0	4.0×10^{-3}
6.0	8.2×10^{-3}
7.0	1.6×10^{-2}
8.0	2.5×10^{-2}
9.0	4.5×10^{-2}
10.0	6.9×10^{-2}

(f) Pyrene

H_2O, %	k_{app}, sec^{-1}
8.0	5.1×10^{-3}
9.0	7.6×10^{-3}
10.0	1.4×10^{-2}
11.0	1.7×10^{-2}

charge is concentrated is greatly stabilized by the hydrogen-bonding interaction with protic solvents as compared with the activated complex in the transition state, where the charge is more dispersed, while such a specific solvation does not occur in aprotic solvents. Consequently, the activation free energy of the reaction in Eq. (5) in aprotic solvents is smaller than that in protic solvents.

As is shown in Fig. 1, however, such is not the case for the protonation reaction of aromatic hydrocarbon radical anions with water, where the reaction is faster in more protic media. The reason for this behavior seems to be as follows: the negative charge is more localized on a certain atom in the activated complex than in the original radical anion, and, therefore, the activated complex is more stabilized than is the radical anion by changing the solvent from aprotic to protic.[4]

The effect of increasing of water content on the rate constants depends upon the molecular structures of the aromatic hydrocarbons. That the rate constants of naphthalenide and phenanthrenide are more influenced by the water content than is biphenylide radical anion predicts that the rate of the protonation of biphenylide will be slower than those of naphthalenide and phenanthrenide in the case of higher-water-content media. In fact, the rates of the protonation of aromatic hydrocarbon radical anions in 2-propanol were measured by Dorfman *et al.*[5,6] to be in this order: naphthalenide>phenanthrenide>biphenylide.

As has been described above, the rates of the reactions of anions with polar molecules are greatly influenced by the hydrogen-bonding interaction of the anions with protic solvents. Therefore, for the rate constants obtained in aprotic solvents, the effect of the molecular structure on the rate can be interpreted in terms of MO calculations, without taking the hydrogen-bonding effect into account. In the present system, the rate constants in DMF free from water can be obtained by extrapolation. Increases in k were found at low concentrations of water (Fig. 1). These may be due to additional decay through other reactions, *e.g.*, protonation with DMF[7,8] or with impurities. These reactions can be practically eliminated from competition with the protonation with water if enough water is added.

Interpretations of the Rate Constants of the Protonation in Terms of HMO Calculations. Because of the succeeding rapid electron-transfer reaction (Eq. (3)), no products of the protonation reaction (Eq. (2)) could be observed in the present system. However, the structures of the products may be similar to that of the so-called σ-complex[9] in the aromatic substitution reaction, as is shown below, where naphthalene is taken as an example:

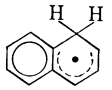

(6)

These structures were ascertained experimentally for the analogous reactions in low-temperature alcohols.[10,11]

4) S. Hayano and M. Fujihira, This Bulletin, **44**, 2051 (1971).
5) S. Arai, E. L. Tremba, J. R. Brandon, and L. M. Dorfman, *Can. J. Chem.*, **45**, 1119 (1967).
6) L. M. Dorfman, *Accounts Chem. Res.*, **3**, 224 (1970).
7) D. L. Maricle, *Anal. Chem.*, **35**, 683 (1963).
8) S. Wawzonek, R. Berkey, E. W. Blaha, and M. E. Runner, *J. Electrochem. Soc.*, **102**, 235 (1955).
9) G. W. Wheland, *J. Amer. Chem. Soc.*, **64**, 900 (1942).
10) J. A. Leone and W. S. Koski, *ibid.*, **88**, 224 (1966); J. A. Leone and W. S. Koski, *ibid.*, **88**, 656 (1966).
11) T. Shida and W. H. Hamill, *ibid.*, **88**, 3689 (1966).

In order to interpret the course of the reduction process, Hoijtink[12] assumed that the logarithm of the rate constant of protonation is linearly proportional to the charge density at a particular carbon atom. Then, the rate constant was expressed by:

$$k = \kappa \exp(C\rho_s/kT) = \kappa \exp(\gamma\rho_s) \quad (7)$$

where κ, C, and γ are constants and where the charge (or spin) density, ρ_s, at a carbon atom, s, is given by the square of the coefficient in the HMO for the first antibonding level. By this equation, the position in the hydrocarbon molecule at which proton addition occurs was explained, but the relative rates among different species could not be explained.

The rate constants of analogous reactions in alcohol

$$R^{\cdot-} + ROH \xrightarrow{k_a} RH\cdot + RO^- \quad (8)$$

were obtained by the technique of pulse radiolysis by Dorfman *et al.* They found that the rate constants for Reaction (8) depend upon the properties of the alcohol[6,13] and the nature of the aromatic radical anions.[5,6] They showed a fairly good correlation between the values for k_a and the acidity of the alcohol. They attempted to interpret the dependence of k_a on the nature of the aromatic radical anions in terms

TABLE 2. SPIN DENSITIES, LOCALIZATION ENERGIES AND COEFFICIENTS OF THE ENERGY OF THE LOWEST VACANT MO CALCULATED WITH SOME AROMATIC HYDROCARBONS

Molecule	$-m_{m+1}$[b]	Position	ρ_s	L_s^-	L	$2m_{m+1}+L$	k, $M^{-1}\,sec^{-1}$
Benzene	1.000	—	0.167[b]	1.536	2.536[a]	0.536	
Naphthalene	0.618	α	0.181[b]	1.681	2.299[b]	1.063	4.6×10^{-3}
		β	0.069	1.862	2.480		
Biphenyl	0.705	1	0.123				1.8×10^{-2}
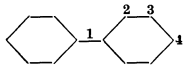		2	0.090	1.695	2.400[b]	0.990	
		3	0.020	1.839	2.544		
		4	0.158	1.742	2.447	1.037	
Anthracene	0.414	1	0.096[b]	1.84	2.25[a,b]		2.0×10^{-4}
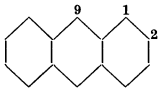		2	0.047	1.99	2.40		
		9	0.192	1.599	2.013	1.185	
Phenanthrene	0.605	1	0.116	1.713	2.318		1.0×10^{-3}
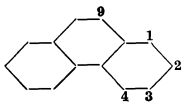		2	0.002	1.893	2.498		
		3	0.099	1.849	2.454		
		4	0.054	1.761	2.366		
		9	0.172	1.694	2.299	1.089	
1,2-Benzanthracene	0.452	1	0.000				5.5×10^{-5}
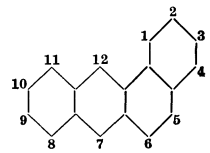		2	0.041				
		3	0.009				
		4	0.026				
		5	0.083				
		6	0.089				
		7	0.198	1.597	2.049	1.145	
		8	0.105				
		9	0.038				
		10	0.056				
		11	0.090				
		12	0.155	1.648	2.100	1.196	
Pyrene	0.445	1	0.136[b]	1.745	2.190[b]	1.300	1.2×10^{-5}
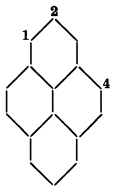		2	0.000	2.10	2.55		
		4	0.087	1.83	2.28		

a) Ref. 14. b) Ref. 15.

12) G. J. Hoijtink, *Rec. Trav. Chim.*, **76**, 885 (1957); G. J. Hoijtink, "Advances in Electrochemistry and Electrochemical Engineering," Vol. 7, ed. by P. Delahay and C. W. Tobias, Interscience Publishers, New York, N. Y. (1970), p. 221.

13) S. Arai and L. M. Dorfman, *J. Chem. Phys.*, **41**, 2190 (1964).

of the delocalization energy, but did not succeed. This failure was partly because the k_a values obtained in protic solvents were used for comparison.

The spin density, ρ_s, and the localization energy, L_s^-, of radical anions, and the coefficient, m_{m+1}, of the energy of the lowest vacant MO of the aromatic hydrocarbons studied in the present work, are given in Table 2, in which some of the values have been calculated by the present authors and others cited from the literature.[14,15] For comparison, the values of benzene are also given. The localization energy, L_s^-, is given by:

$$L_s^- = M^- - M_s \tag{9}$$

where the π-energy of the radical anion is $(n+1)\alpha+M^-\beta$ and that of protonated radical is $(n-1)\alpha+M_s\beta$, where s denotes the position of the carbon atom, and n, the number of π-electrons of the parent molecule. It is reasonable to assume that the protonation will occur at the position at which the localization energy is the smallest. Therefore, Hoijtink's assumption may be superseded by this localization method as far as the problem is the position at which the protonation occurs predominantly. The predictions by Hoijtink accord with those by the localization method except in the case of biphenyl. The experimental results[15] in the reduction of hydrocarbons with alkali metals agree with these predictions. The spin density of the biphenylide radical anion is the highest at position 4, but the localization energy is the smallest at position 2, and the reduction products have been reported to be 2,5-dihydrobiphenyl[16] or 1,4-dihydrobiphenyl.[17] The following discussion will be based on the assumption that the protonation occurs at the position with the smallest localization energy except in the cases of biphenylide and 1,2-benzanthracenide. For biphenylide, position 4 is also considered. The reduction product of 1,2-benzanthracenide has been reported to be the 7,12-dihydro-derivative.[18] The positions 7 and 12 are taken into consideration, for the two positions are not equivalent to each other.

For the common proton donor, the standard free energy of the protonation reaction (2) should have a linear relation with the value of the smallest localization energy, L^-, if the σ-bond energy changes caused by proton addition and the free energy changes of solvation are practically constant for these hydrocarbons:

$$\Delta G^\circ = L^- + \text{const.} \tag{10}$$

From the linear free-energy relationship, the logarithms of the observed rate constants can be expected to be linear in relation to the localization energy.

The ionization potential, I, of the radical anion

$$R^- \rightarrow R + e \tag{11}$$

is equal to the electron affinity of the parent molecule and is correlated with m_{m+1} by the following equation:

$$I = -(\alpha + m_{m+1}\beta) \tag{12}$$

These ionization potentials are known to be linear in relation to the polarographic half-wave potentials (or the reduction potentials) in aprotic solvents,[19] and a correlation between the reduction potentials and the rates of the analogous reactions has been reported.[20]

In Table 2, the rates of the protonation of aromatic hydrocarbon radical anions with water in DMF are also given. Neither the highest spin density, ρ_s, the smallest localization energy, L^-, nor m_{m+1} (or ionization potential I) is, however, found to have a linear relation to the observed rate constants.

In the preceding discussion, the reactivity has been attributed to only either the electronic structures of the aromatic substrate or those of reagents, and these treatments cannot make the reaction completely clear. We undertook to interpret this reaction by means of the charge-transfer mechanism proposed by Nagakura.[21] By this concept, it would be possible not only to explain the orientation rule, but also to predict the electronic structures of the activated complexes. Furthermore, the dependence of the protonation rates on the acidity of proton donors will be explained more feasibly.

According to Nagakura's mechanism, the reaction can be interpreted as a transfer process between the no-bond and charge-transfer structures (abbreviated hereafter to CT structure) and the reaction process can be represented by the potential energy curve shown in Fig. 2, where the protonation of naphthalenide is

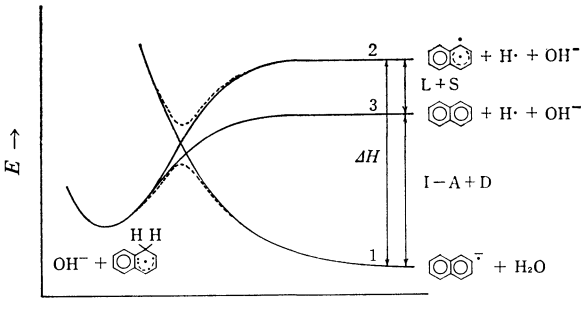

Fig. 2. Potential energy curve for the protonation of naphthalenide radical anion with water.

taken as an example. Curves 1 and 2 are associated with the no-bond and CT structures respectively. Curve 1 shows a repulsive feature, while Curve 2 resembles the Morse curve. The reaction proceeds along the dotted line which is formed by the resonance between the no-bond and CT structures. Further

14) F. H. Burkitt, C. A. Coulson, and H. C. Longuet-Higgins, *Trans. Faraday Soc.*, **47**, 553 (1951).
15) A. Streitwieser, Jr., "Molecular Orbital Theory for Organic Chemists," John Wiley & Sons, New York (1961), pp. 160, 178, 428.
16) I. P. Egorov, E. P. Kåplan, Z. I. Letina, V. A. Shiapochnikov, and A. D. Petrov, *J. Gen. Chem. U. S. S. R.*, **28**, 3284 (1958).
17) W. Hückel and R. Schwen, *Ber.*, **89**, 150 (1956).
18) W. E. Bachmann, *J. Org. Chem.*, **1**, 347 (1936).
19) A. Maccoll, *Nature*, **163**, 178 (1949).
20) M. Ichikawa, M. Soma, T. Onishi, and K. Tamaru, *J. Amer. Chem. Soc.*, **91**, 6505 (1969).
21) S. Nagakura, *Tetrahedron*, **19**, Suppl. 2, 361 (1963).

detailed discussion about the physical meaning of this diagram can be referred to Ref. 21. As is shown in Fig. 2, the energy difference, ΔH, between the no-bond and CT structures at an infinite distance is given as follows:

$$\Delta H = I - A + D + L + S \tag{13}$$

where I is the ionization potential of a radical anion, A is the electron affinity of the OH· radical, D is the dissociation energy of an O–H bond of the proton donor, L is the localization energy of aromatic hydrocarbon for the following process:

(14)

and S is the energy required for the change in the hybridization from the sp^2 to the sp^3 of the ring carbon atom attacked by the reagent.

Nagakura also assumed that the activation energy, ΔE^*, is approximately proportional to the energy difference, ΔH:

$$\Delta E^* = a\Delta H \tag{15}$$

where a may be regarded as a constant for at least a fixed combination of the aromatic substrate and a reagent. Hereafter, a will be assumed to be constant in the present systems. A, D, and S can be considered as constants for the series; consequently, the logarithms of the rate constants should show a linear relation to the sum of $I+L$. However, no such linear relation was found, as has been noted before, for L_s^- in Table 2 is equal to $L+m_{m+1}$, which has a linear relation to $L+I$. The position at which protonation occurs can, however, be explained in terms of the localization energy.

The reason why the relative reaction rates cannot be interpreted adequately by Eqs. (13) and (15), is as follows: the contribution of the $L+S$ terms to the activation energy probably does not parallel that of the $I-A+D$ terms, since any localization of electrons and hybridization from sp^2 to sp^3 occurs only in response to the approach of the reagent and at an infinite separation these terms are completely eliminated.[22] Therefore, the potential curve 2 of the CT structure in Fig. 2 should be written as Curve 3.

As a result, the contribution of $L+S$ to the activation energy is found to be less than that of $I-A+D$; the activation energy should be written as follows:

$$\Delta E^* = a(I-A+D) + b(L+S) \tag{16}$$

$$a > b \tag{17}$$

The position attacked by a proton is still interpreted by the L term.

For the present system, a plot of the logarithms of the observed rate constants against $2I+L$ (or $2m_{m+1}+L$) gives a linear correlation, as is shown in Fig. 3, where a is taken temporarily to be double b. For the present, the ratio of a to b is arbitrary to some extent. In Table 2, the values of $2m_{m+1}+L$ are given instead of $2I+L$. If much more data for the rate constants of the reactions were obtained for the series where only the ionization potentials are greatly different and the localization energies are almost constant, or for the series where only the localization energies are different, the values of a and b in Eq. (16) could be determined experimentally. The benzene radical anion is known to be protonated much more rapidly than the biphenyl radical anion.[11] This is reflected by the small value of $2m_{m+1}+L$ shown in Table 2.

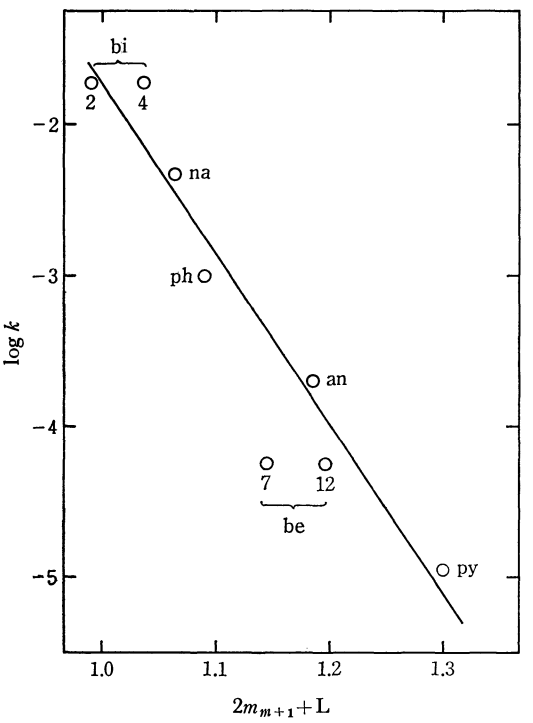

Fig. 3. Correlation of $\log k$ for protonation *versus* $2m_{m+1}+L$. For biphenylide and 1,2-benzanthracenide, the values for the positions 2,4 and 7,12, respectively, are shown. The abbreviations are the same as in Fig. 1.

In Eq. (14), the $-A$ and D terms represent the properties of the reagents, and the dependence of the rate constants on the properties of such proton donors as alcohols, water, and phenols can be interpreted by these terms. The activation energies are found from Eq. (16) to be smaller, as the reagents are more acidic, *i.e.*, as the dissociation energy, D, of the O–H bond is smaller and the electron affinity, A, of OH· or OR· is larger.

In addition, the solvent effect on the rate of protonation can be interpreted by this mechanism. The activated complex is a charge-transfer complex in which the no-bond and CT structures contribute to the resonance in almost equal proportions.[21] Therefore, the magnitude of the electron transfer between the radical anion and water is very close to 50% at the transition point: *i.e.*, about half a negative charge is localized on the oxygen atom of water in the activated complex. The solvent effect on the rates described above must be due to such a localized negative charge in the activated complex.[4]

The authors wish to thank Dr. M. Senō and Dr. M. Sukigara for their helpful discussions.

22) See comment by R. D. Brown in Ref. 21, p. 376.

The Effect of Water on the Reduction Potentials of Some Aromatic Compounds in the DMF-Water System

Shigeo HAYANO and Masamichi FUJIHIRA

Institute of Industrial Science, The University of Tokyo, Roppongi, Minato-ku, Tokyo

(Received December 15, 1970)

From the viewpoint of the interaction between the oxidized or the reduced form of a depolarizer and solvents, the solvent effect on the half-wave potentials was studied. Another factor affecting the $E_{1/2}$, *i.e.*, pH or ion-pair formation, was also examined. The correction for the liquid junction potential was carried out by the use of the ferrocene standard. The reduction products, radical anions or dianions, were found to be stabilized by the hydrogen-bonding with water where the hydrogen-bond interaction of the dianion was stronger than that of the monoanion. Aromatic hydrocarbon radical anions, whose charges are dispersed over the molecule, were less susceptible to this solvent transfer than were the anthraquinone radical anion and the dianion, whose charges are strongly localized.

In a previous paper,[1] a study of the rate of the protonation reaction of aromatic hydrocarbon radical anions with water has been reported; the rates were found to be greatly accelerated by the increase in the water content in DMF-water mixtures. This behavior was interpreted in terms of the hydrogen-bond interaction of radical anions or transition states with water.

The present work will deal with the interaction of the radical anions of several aromatic compounds with solvents.

Experimental

Materials. All the organic reagents except *p*-dinitrobenzene were obtained commercially. E.P.-grade anthraquinone was purified by recrystallization from ethanol, and E.P.-grade *p*-benzoquinone, by sublimation. G.R.-grade ferrocene, methylviologen, azulene, and fluoranthene were used without further purification. *p*-Dinitrobenzene was prepared and purified according to the method of Starkey[2] (mp. 173°C). The tetraethylammonium perchlorate (TEAP) and tetraethylammonium bromide (TEAB) were the same as have been described previously.[3] G.R.-grade lithium perchlorate was trihydrate and was dehydrated by heating it to a constant weight before preparing the DMF solution. G.R.-grade lithium hydroxide and a tetraethylammonium hydroxide aqueous solution were used without further purification. The solvents used were purified in the usual manner. The dimethylformamide (DMF) was the same as has been described previously.[3] The acetonitrile was dried over phosphorus pentoxide and then fractionally distilled; its water content was below 0.01%. G.R.-grade ethanol and acetone were used without further purification; their water contents were 0.3% and 0.2% respectively. These water contents were measured by Karl Fischer titration.

Polarography. A saturated calomel electrode was connected to the cell by a 1 N KNO_3-agar bridge,[3,4] which outlet was positioned just above the dropping mercury electrode. The use of a conventional aqueous potassium chloride agar salt bridge for precise work in non-aqueous solvents has been criticised.[5] Therefore, the use of the 1 N KNO_3 aqueous agar bridge must be checked; the effect of the dipping or aging time of the bridge was studied by the following experiments.

One end of the bridge was dipped in DMF-water solutions containing the same quantities of methylviologen and TEAP as the solution for polarographic measurements, while the other end was dipped in a 1 N KNO_3 aqueous solution. From one half-wave potential measurement with the bridge to another, the aging solution was renewed, because the dissolution of the bridge components contaminates the aging solution.

In the studies of other reducible substances, the 1 N KNO_3 agar bridges were aged in depolarizer free basic solutions. Each solution was deaerated by bubbling pure nitrogen[3] for 15—20 min. In the case of the solution which contained a small amount of water, the water content was determined by Karl Fisher titration just after recording a polarogram.

The pH-dependence of the half-wave potential was studied in Britton-Robinson buffer solutions. The polarographs used were Yokogawa Denki models POL-11 and POL-21 for recording the D.C. and A.C. polarograms respectively. The pH of the solution was measured with a Toa Denpa PM-5A pH meter. All the measurements were carried out at 25°C.

Results and Discussion

The Reference Electrode. The half-wave potentials of methylviologen in the DMF-water system are presented in Table 1. It is evident that the half-wave potentials are reproducible within ±10 mV independently of the aging time. However, at least 10—15 min are required for the practical setting of bridges. Therefore, the potential drift caused within 10—15 min is not presented. The drift of the potential may be much less with the 1 N KNO_3 aqueous agar bridge in a DMF-water system than with an aqueous agar KCl bridge in acetonitrile.[5] As the water contents in a DMF-water system are comparatively ineffective on the half-wave potentials and the summit potentials of methylviologen (Table 1 and Fig. 8), the existence of water extracted from the aqueous agar salt bridge has practically no influence on the half-wave potentials. In other experiments, however, it is desirable

1) S. Hayano and M. Fujihira, This Bulletin, **44**, 2046 (1971).
2) E. B. Starkey, "Organic Synthesis," Coll. Vol. II, (1950) p. 225.
3) S. Hayano and M. Fujihira, This Bulletin, **44**, 1496 (1971)
4) M. E. Peover and J. D. Davies, *J. Electroanal. Chem.*, **6**, 46 (1963).
5) J. F. Coetzee and G. R. Padmanabhan, *J. Phys. Chem.*, **66**, 1708 (1962).

Table 1. Effect of aging-time of 1 N KNO_3 agar bridges on the half-wave potentials of methylviologen in DMF-water system

H_2O	0%		20%		40%		60%		80%		100%	
day \ $-E_{1/2}$	I	II	I	II	I	II	I	II	I	II	I	II
0	0.48	0.87	0.53	0.91	0.56	0.94	0.59	0.97	0.62	1.00	0.67	1.03
1	0.48	0.87	0.53	0.92	0.56	0.94	0.58	0.97	0.62	1.00	0.68	1.03
3	0.47	0.86	0.52	0.92	0.56	0.94	0.58	0.98	0.62	1.00	0.68	1.03
10	0.48	0.87	0.52	0.90	0.56	0.94	0.58	0.98	0.61	1.00	0.67	1.03
20	0.48	0.87	0.51	0.92	0.57	0.94	0.59	0.98	0.62	1.00	0.67	1.03
30	0.48	0.87	0.51	0.91	0.56	0.95	0.58	0.98	0.62	1.00	0.67	1.03
70	0.48	0.88	0.51	0.91	0.57	0.95	0.59	0.98	0.62	1.01	0.67	1.03
120	0.49	0.90	0.52	0.92	0.55	0.94	0.59	0.98	0.62	1.00	0.66	1.03

I and II are $-E_{1/2}$ of the first and the second waves in V *vs.* SCE.

to use the aged bridge to prevent the accidental introduction of water into the solution, because the increase of water may remarkably affect the half-wave potentials or the summit potentials, as in the case of anthraquinone reduction (Fig. 5). The aging time of a week is adopted since such a bridge gives only a small potassium wave in a polarogram.

pH-Dependence of the Half-Wave Potentials. The $E_{1/2}$-pH plot for anthraquinone in water is shown in Fig. 1. The breaks in the curve (or the intersection of extrapolated linear parts) indicate the pK_a-values for the individual degrees of dissociation[6] in such a reversible system. The pK_a-values of anthrahydroquinone are found to be $pK_{a1}=10.9$ and $pK_{a2}=11.8$ from the plot in Fig. 1. Therefore, in the pH-region where the $E_{1/2}$ is pH-independent, the electrode process is a reversible two-electron transfer and the reduction product is the dianion.

The pH-dependence of the electrode process of *p*-dinitrobenzene has been studied by polarography[7] or by cyclic voltammetry.[8,9] The $E_{1/2}$-pH plot is similar to that of anthraquinone, and in an alkaline solution the reversible two-electron reduction to the dianion proceeds.

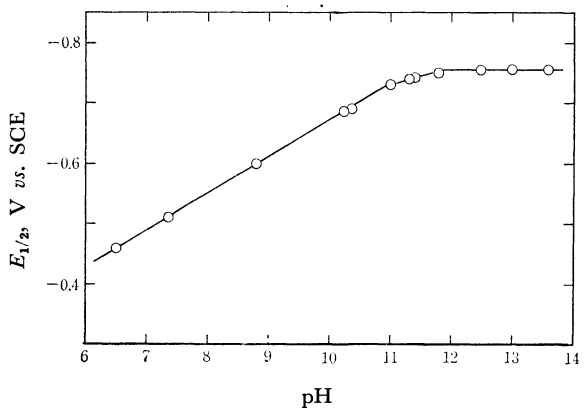

Fig. 1. $E_{1/2}$−pH plot of anthraquinone in water.

When the solvent effect on $E_{1/2}$ is discussed from the viewpoint of the solvation-energy difference between oxidized and reduced species before and after electron transfer, these pH-independent half-wave potentials to the dianion should be compared with those in other solvents in which also only the electron transfer occurs.

Ion-pair Formation. Ion-pair formation is another factor which exerts an influence on the value of the half-wave potential. In order to discuss the solvent effect on the half-wave potential, this factor must be eliminated as much as possible.

The formation of complexes between the radical anions or dianions and the cations of the supporting electrolyte in solvents with moderate dielectric constants, such as dimethylformamide and acetonitrile, has been studied,[4,10] and it has been found that the half-wave potentials for the production of dianions are shifted to the positive side of the potential to a much greater extent than those for the monoanions, and that this positive shift tendency is in the order of $Li^+ > Na^+ > K^+ > NEt_4^+ > NBu_4^+$ in respect to the cation. The difference between NEt_4^+ and NBu_4^+ is small. In the present study, tetraethylammonium salts were used in order to eliminate the effects of ion-pair formation on the half-wave potential.

The effect of increasing the lithium-ion concentration on the half-wave potentials of *p*-dinitrobenzene in DMF, while the total salt concentration is kept constant with tetraethylammonium perchlorate, is shown in Fig. 2. The shifts are greater for the dianion than for the monoanion, and the behavior is similar to that of anthraquinone.[4] One *p*-dinitrobenzene dianion is associated with two lithium cations above a 1.2×10^{-2} M lithium cation concentration. As the concentration of the lithium cation should be much higher than that of *p*-dinitrobenzene,[6] the dependence of $E_{1/2}$ on the lithium concentration could not be measured in the low-concentration range of lithium. As the $E_{1/2}$ values with TEAP are known, the intersections of the left-hand side of the straight line with the linear part, which is independent of the lithium-ion

6) J. Heyrovsky and J. Kuta, "Principle of Polarography," Academic Press, New York, N.Y. (1966), pp. 147, 161, and 181.
7) L. Holleck and H. J. Exner, *Z. Elektrochem.*, **56**, 677 (1952); L. Holleck and H. Schmidt, *ibid.*, **59**, 56 (1955).
8) W. Kemula, Z. Kublik, and R. Cyranski, *Roczniki Chem.*, **36**, 1349 (1962).
9) S. Hayano and M. Fujihira, presented at the 14th Symposium of Polarography, Hiroshima, Oct., 1968.
10) L. Holleck and D. Becher, *J. Electroanal. Chem.*, **4**, 321 (1962).

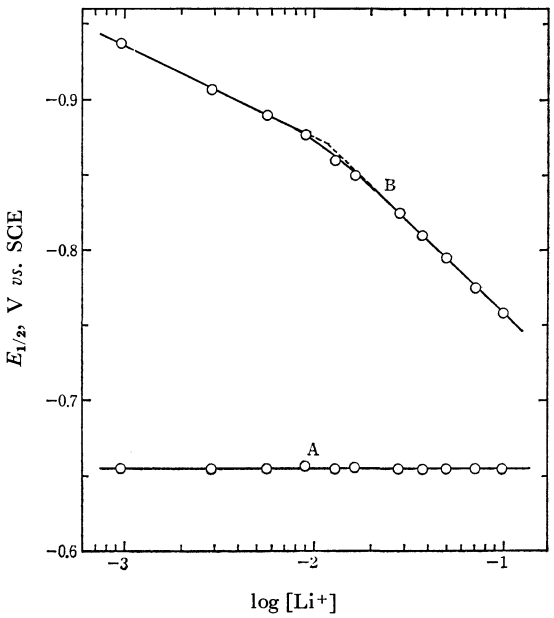

Fig. 2. Dependence of $E_{1/2}$ of *p*-dinitrobenzene on lithium ion concentration in DMF, A, *p*-DNB + e ⇄ *p*-DNB^-; B, *p*-DNB^- + e ⇄ *p*-DNB^{2-}.

concentration, may be estimated to be about 6×10^{-4} M. Therefore, a *p*-dinitrobenzene dianion forms a 1 : 1 complex with a lithium cation in the lithium concentration range of 6×10^{-4}—1.2×10^{-2} M. On the other hand, monoanions are not associated with lithium in the lithium-concentration range measured.

The Half-wave Potential of Some Organic Compounds in a Mixed Solvent System. The present work is intended to consider the effects of solvents on the reduction potential of organic compounds. Quinones and *p*-dinitrobenzene are reduced reversibly to the dianions in alkaline aqueous solutions, as has been described above. On the other hand, these compounds give two one-electron reversible waves in aprotic solvents.[11-13]

Then, the changes of half-wave potentials in the DMF-alkaline water system were measured.[15] The results with *p*-dinitrobenzene are shown in Fig. 3. The logarithms of the volume percent of water are used as the abscissa, because it is desirable to know in detail the change in the region which contains small amounts of water. The half-wave potentials of some organic compounds in DMF can be found in the literature, but usually the water contents, which are essentially more or less involved in the solvents, have not been described. As is shown in Fig. 3, however, the half-wave potentials were found to be constant in the region of water content below 0.1%. These values can be practically regarded as the half-wave potentials in DMF.

When the lithium salt is used as the supporting electrolyte in DMF, the $E_{1/2}$ values of the second wave are affected and shift to more positive potentials, as has been described above. This tendency continues until the water contents reach 20—30% (Fig. 3); that is, the dianion is stabilized by water without breaking the ion-pair with the lithium cation when small amounts of water are added.

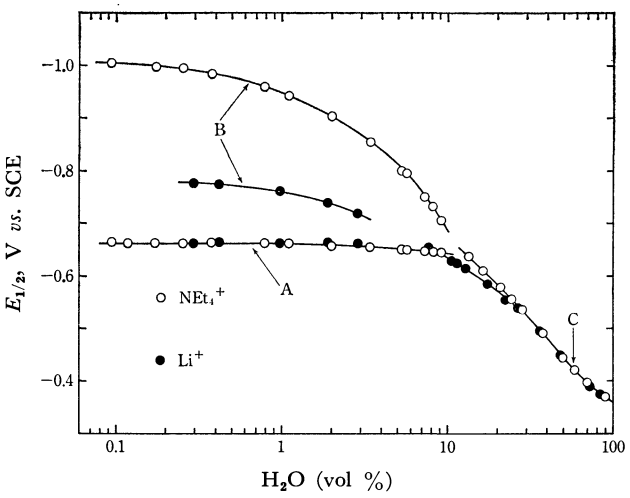

Fig. 3. Dependence of $E_{1/2}$ of *p*-dinitrobenzene on the alkaline water content in DMF-alkaline water system,[15] A, neutral → monoanion; B, monoanion → dianion; C, neutral → dianion.

In Figs. 4—8 can be seen the variation in the A.C. summit potentials of *p*-dinitrobenzene, anthraquinone, and some other organic compounds with the composition of the solvent medium, where no correction for the liquid junction potential is taken into account. As the half-wave potential reading of the very close waves is difficult, the A.C. summit potentials are shown instead of the half-wave potentials.[16] The variation in anthraquinone is similar to that in *p*-dinitrobenzene. In DMF, the difference in the summit potentials of anthraquinone is larger than that in *p*-dinitrobenzene; thus, the variations in the summit potentials of the first and the second waves of anthraquinone could be obtained over a wide range of composition in the DMF-alkaline water system. These compounds showed similar behavior in DMF-ethanol systems (Figs. 4, 5, and 7). On the other hand, anthraquinone showed little change in the summit potentials in DMF-ace-

11) M. E. Peover, *J. Chem. Soc.*, **1962**, 4540.
12) M. E. Peover, *Trans. Faraday Soc.*, **60**, 479 (1964).
13) Strictly speaking, the semiquinone formation constants

$$K = \frac{[S]^2}{[Ox][Red]}$$

of these compounds are small[14] in alkaline water and are large in aprotic solvents. The semiquinone formation constant is obtained by[6,14]

$$E_1 - E_m = E_m - E_2 = \frac{RT}{2F}\ln K$$

where E_1 is the reduction potential of the oxidized form to the semiquinone, E_2 is the reduction potential of the semiquinone to the reduced form, and E_m is the mid point potential.
14) R. Gill and H. I. Stonehill, *J. Chem. Soc.*, **1952**, 1845.
15) Below 10 percent of water in DMF, hydroxide anion reacts with *p*-dinitrobenzene to give nitrophenol, therefore 0.1 N perchlorate salt aqueous solutions were used instead of 0.1 N hydroxide aqueous solutions below 10 percent of water.
16) As the A. C. summit potentials agreed with the D. C. half-wave potentials within at most 20 mV for the present systems, these potentials may be looked as the same. Methylviologen, however, gave tensammetric peaks in addition to the faradaic peaks in the A. C. polarogram in water.

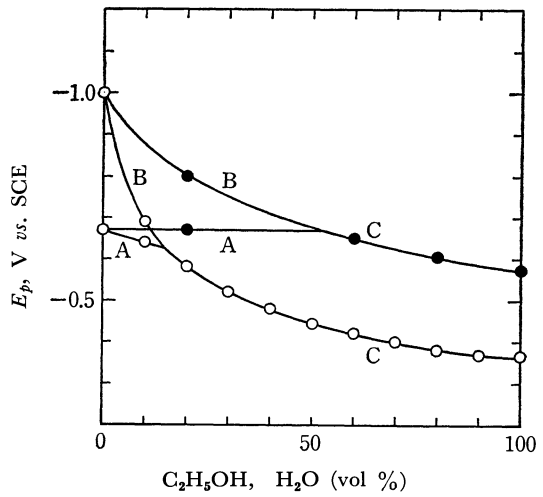

Fig. 4. E_p of *p*-dinitrobenzene in DMF-alkaline water[15] and in DMF-ethanol system, ○, DMF-alkaline water; ●, DMF-ethanol.

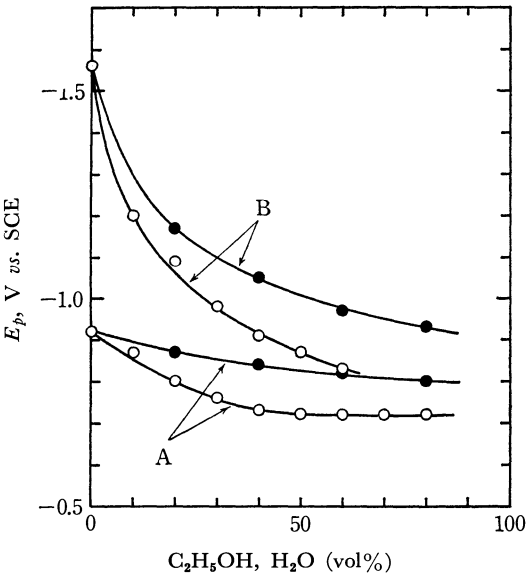

Fig. 5. E_p of anthraquinone in DMF-alkaline water and in DMF-ethanol system, ○, DMF-alkaline water; ●, DMF-ethanol.

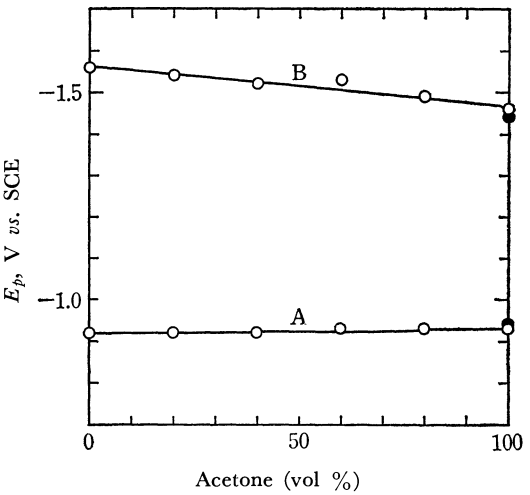

Fig. 6. E_p of anthraquinone in DMF-acetone and in acetonitrile, ○, DMF-acetone; ●, in acetonitrile.

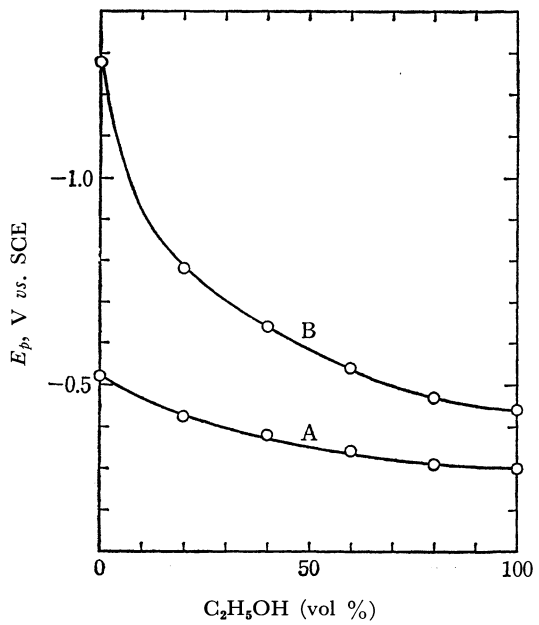

Fig. 7. E_p of *p*-benzoquinone in DMF-ethanol system.

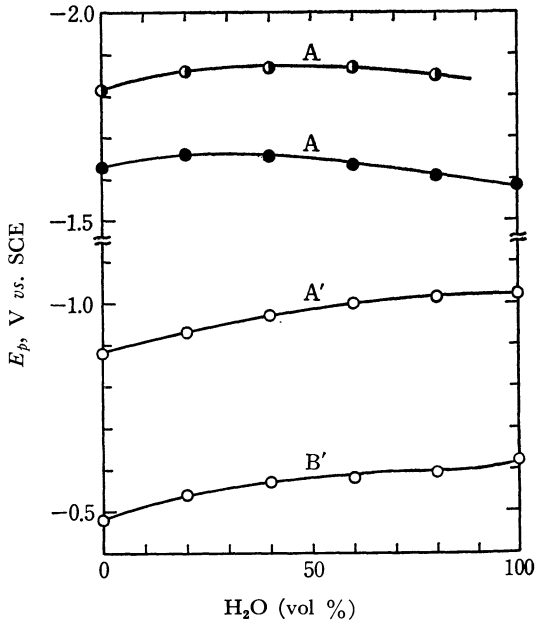

Fig. 8. E_p of methylviologen in DMF-water and E_p of azulene and fluoranthene in DMF-alkaline water system, ○, methylviologen; ●, azulene; ◑, fluoranthene. A′, monocation → neutral; B′, dication → monocation.

tone[17] and may similarly show little change in DMF-acetonitrile (Fig. 6).

The dielectric constants of the solvents used are given in Table 2. A comparison of the values of ε with the variation in the summit potentials described above leads to the conclusion that the solvent effect on the half-wave potentials cannot be explained by the Born equation only:

$$-\Delta G_{el}^{\circ} = \frac{Nz^2e^2}{2r}\left(1-\frac{1}{\varepsilon}\right)$$

17) As the supporting electrolyte, tetra-*n*-propylammonium perchlorate (Nakarai Chemicals reagent for polarography) was used, because of low solubilities of tetraethylammonium salts in acetone.

where e is the electronic charge, ε is the dielectric constant of the medium, N is Avogadro's number, and r is the radius of the ion. The Born equation predicts that the reduction potential of the neutral molecule to the anion shifts to a more positive potential in the solvent with the higher dielectric constant. In view of this, the remarkable positive shift of the half-wave potentials (or summit potentials) with an increase in the ethanol content in the DMF-ethanol system cannot be interpreted. The positive shift of the half-wave potentials with an increase in the water or alcohol content can be interpreted preferably by the hydrogen-bond interaction[11] of the produced anions with water or alcohol. As is shown in Figs. 4, 5, and 7, the summit potentials of the second waves, which correspond to the reductions from the monoanion to the dianion, shifted remarkably to a positive potential with an increase in the water or alcohol content. This may be due to the stronger hydrogen-bond interaction of the dianion than that of the monoanion. In the case of methylviologen, it is predicted that such a positive shift will not be observed, because two one-electron waves of methylviologen correspond to the reductions from the dication to the monocation and from the monocation to the neutral molecule, and generally the cation and the neutral molecule are much poorer acceptors of a hydrogen bond than the anion is. In fact, the behavior (Table 1 or Fig. 8) is different from that of *p*-dinitrobenzene or anthraquinone. The half-wave potentials show a rather negative shift with an increase in the amount of water. These shifts are not caused by the change in solvation, but by the liquid junction potential, for the half-wave potentials of ferrocene, which were assumed to give the same potentials in various solvents, also showed a negative shift in the DMF-water system as the water content increased. The half-wave potentials of ferrocene, measured by cyclic voltammetry with the Pt anode, are shown in Table 3. According to the assumption that ferrocene-ferricinium couple has the same potential in various solvents, the variation of $E_{1/2}$ in Table 3 is equal to the change in the liquid junction potential with the composition of the DMF-water system.

Table 2. Dielectric constants of solvents at 25°C

H_2O	DMF	CH_3CN	Ethanol	Acetone
78.5	36.7	36.7	24.3	20.7

Table 3. $E_{1/2}$ of ferrocene

DMF %	100	90	80	70	60
$E_{1/2}$	0.421	0.370	0.331	0.296	0.265
DMF %	50	40	30	20	10	0
$E_{1/2}$	0.242	0.221	0.206	0.193	0.175	0.160

18) L. H. Chopard-dit-Jean and E. Heilbronner, *Helv. Chim. Acta*, **36**, 144 (1953).

In Fig. 9, the variations in $E_{1/2}$ (or E_p) *versus* the $E_{1/2}$ of the ferrocene with the composition of the DMF-water (or DMF-alkaline water) systems for several organic compounds are shown. As has been described above, methylviologen shows almost constant half-wave potentials in the DMF-water system. On the other hand, anthraquinone shows a much grater positive shift of the summit potentials by the correction for the liquid junction potentials in the DMF-alkaline water system (*cf.* Fig. 5).

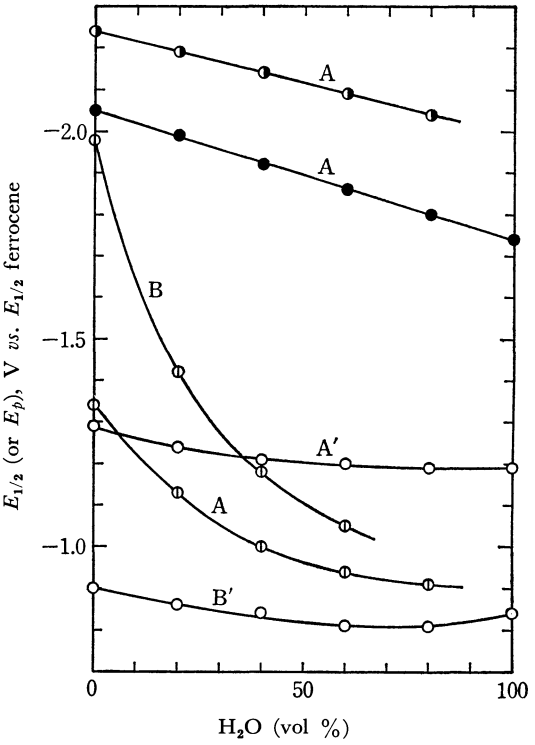

Fig. 9. $E_{1/2}$ of methylviologen, azulene, and fluoranthene, and E_p of anthraquinone *versus* $E_{1/2}$ of ferrocene, ○, methylviologen; ●, azulene; ◑, fluoranthene; ⓘ, anthraquinone.

In the case of aromatic hydrocarbons, protonations occur even in the DMF-alkaline water system and affect the half-wave potentials. However, azulene and fluoranthene are known to show a reversible one-electron reduction even in protic media.[18] The variations in their half-wave potentials in the DMF-alkaline water system are also shown in Fig. 9. The positive shift of the potentials with an increase in the water content in the DMF-alkaline water system is much less in the reduction of hydrocarbons than in the reduction of anthraquinone. In the case of aromatic hydrocarbons, the reduction products, radical anions, are known from ESR measurements to have a delocalized negative charge. On the other hand, anthraquinone anions have localized negative charges on the oxygen atoms. Therefore, the hydrogen-bond interaction of anions with water in the DMF-alkaline water system is much less in aromatic hydrocarbon anions than in anthraquinone or *p*-dinitrobenzene anions.

The Interpretation of the EPR Spectra of the Amorphous State of Group VIB Hydride Radicals by Means of the Gas-phase Data

Yashige KOTAKE, Mitsuo ONO, and Keiji KUWATA

Department of Chemistry, Faculty of Science, Osaka University, Toyonaka, Osaka

(Received December 17, 1970)

A new procedure for the interpretation of the amorphous EPR spectra of the group VIB hydride radicals, *i.e.*, OH, SH, SeH, and TeH, is proposed. The point of this method is to combine the observed hyperfine structure of these radicals in the gas phase and the calculation of the anisotropic hyperfine coupling constant. For this purpose, the Slater orbital and analytical Hartree-Fock orbitals were examined as unpaired electron orbitals by the comparative calculation of the hfs constants. The accuracy of this method was evaluated successfully by applying it to the OH radical. Moreover, in the case of the SH radical the newly-observed spectra in the amorphous state could be assigned to the SH radical.

The hyperfine (hf) interaction in diatomic hydride radicals is an important factor in clarifying the mechanism of the hf splitting of the proton. It also gives much information about the hf interaction in the hydride fragment of polyatomic radicals. The C–H fragment in organic radicals has been the subject of many theoretical and experimental works,[1] while the others have scarcely been investigated at all.

The EPR study of radicals trapped in a single crystal has given the most definite information about the hf interaction but simple radicals such as diatomic hydrides present experimental difficulties in the single crystal study, for they are too small to be stabilized easily; moreover, sometimes the presence of more than one orientation of radicals in the mother crystal makes the analysis difficult, as may be illustrated in the study of the hydroxy radical.[2] Moreover, as far as these solid phase data are concerned, they are under the influence of a matrix effect of a crystalline field.

About Group VIB hydride radicals, *i.e.*, OH, SH, SeH, and TeH, though solid-phase EPR data are poor except for the OH radical, their electric dipole transitions have been observed in the gaseous flow system.[3-7] The hyperfine structure (hfs) of the gas-phase spectra gives information about both the isotropic and anisotropic terms.

In this study we will propose a new procedure to evaluate the principal values of the hf-tensor by the analysis of the hfs of the gas-phase spectra with the aid of the theoretical calculation. The point of this method is to utilize the calculation of dipolar terms and to evaluate indirectly the Fermi contact term.

The usefulness of the method was confirmed for the OH radical, which has been intensively studied in the solid phase.

Moreover, the application to the SH radical gave a correct identification of the radical trapped in the solid phase. The complex spectra obtained by Gunning *et al.*[8] for SH were disproved by this application and on the basis of the consideration of the g-tensor. The hf parameters estimated by this method fit well to those of the newly-observed spectra. On the SeH and TeH radicals, some information about hfs could be obtained.

In the calculation of the anisotropic terms, the characteristics of the Slater orbital and the analytical Hartree-Fock SCF atomic orbital of the Group VIB atom were also discussed.

Theoretical

Because of the large rotational constants of Group VIB hydrides, they are not pure Hund's case (a) or (b) molecules. An intermediate coupling case between Hund's cases, (a) and (b), is treated in terms of Hund's (a) case. A small mixing of Hund's (b) case to a $^2\Pi$ molecule can be expressed as a $^2\Pi$ level slightly perturbed by a $^2\Sigma$ level. The wavefunction is written as a linear combination of two $^2\Pi$'s and a $^2\Sigma$ and the expansion coefficients are determined by the variation method using Van Vleck's matrix elements.[9] In the case of Group VIB hydrides (ground state $^2\Pi_{3/2}$, $J=3/2$ in the case (a), this wavefunction gives first-order expectation values, $W_{\rm hfs}^+$ and $W_{\rm hfs}^-$, or Frosh-Foley's strong field hf hamiltonian[10] for each of the lambda-type doublets as follows:[11]

$$W_{\rm hfs}^+ = (A_1+A_2)M_J M_I\,, \tag{1}$$

$$W_{\rm hfs}^- = (A_1-A_2)M_J M_I\,, \tag{2}$$

$$A_1 = [2a(2X+2-\lambda) + b(X+16-2\lambda) + c(X+4-2\lambda)]/15X\,, \tag{3}$$

$$A_2 = 2d(X-2+\lambda)/15X\,, \tag{4}$$

where:

$$X = [16-\lambda(\lambda-4)]^{1/2}\,, \tag{5}$$

Here λ is the ratio of the LS coupling constant to the rotational constant and:

$$a = 2g_I\beta\beta_N\langle 1/r^3\rangle_{\rm av}\,, \tag{6}$$

$$b = -g_I\beta\beta_N\langle(3\cos^2\theta-1)/r^3\rangle_{\rm av} + \frac{16\pi}{3}g_I\beta\beta_N\Psi^2(0)\,, \tag{7}$$

1) For example, H. M. McConnell and D. B. Chesnut, *J. Chem. Phys.*, **27**, 984 (1957).
2) T. E. Gunter, *ibid.*, **46**, 3818 (1967).
3) H. E. Radford, *Phys. Rev.*, **122**, 114 (1961).
4) H. E. Radford, *ibid.*, **126**, 1035 (1962).
5) C. C. McDonald, *J. Chem. Phys.*, **39**, 2587 (1963).
6) H. E. Radford and M. Linzer, *Phys. Rev. Lett.*, **10**, 443 (1968).
7) H. E. Radford, *J. Chem. Phys.*, **40**, 2732 (1964).
8) D. A. Stiles, W. J. R. Tyerman, O. P. Strausz, and H. E. Gunning, *Can. J. Chem.*, **44**, 2149 (1966).
9) J. H. Van Vleck, *Phys. Rev.*, **33**, 467 (1929).
10) R. A. Frosh and H. M. Foley, *ibid.*, **88**, 1337 (1952).
11) Eqs. (12a) and (12b) of Ref. 3.

$$c = 3g_l\beta\beta_N\langle(3\cos^2\theta-1)/r^3\rangle_{av}\,, \quad (8)$$

$$d = 3g_l\beta\beta_N\langle\sin^2\theta/r^3\rangle_{av}\,. \quad (9)$$

The coordinate used in these equations is shown in Fig. 1. These equations successfully explaine the hfs of the OH[3,4] and NO[12] radicals.

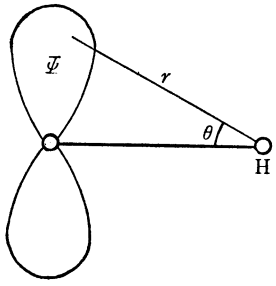

Fig. 1. Coordinate for Eqs. (6)—(9).

In Eq. (3) if a, the first term of b and c, can be calculated with sufficient accuracy, the Fermi contact term can be derived by putting the experimental values into A_1 and X.

The molecular integrals such as $<(3\cos^2\theta-1)/r^3>_{av}$ or $<1/r^3>_{av}$ can be calculated if an unpaired electron orbital and the interatomic distance are determined. If we adopt the LCAO-MO approximation in those hydrides, the unpaired electron orbital will be the np_x or np_y atomic orbital of the Group VIB atom, both orbitals are perpendicular to the molecular axis (z-axis). These atomic orbitals are frequently Slater orbitals or analytical Hartree-Fock (AHF) orbitals, the latter of which consist of a linear combination of Slater-type orbitals (STO).

An assumption of STO as an unpaired electron orbital made it possible to calculate these integrals analytically by the method of Barnett-Coulson.[13] The method of McConnell and Strathdee[14] is also applicable to the OH radical. Except for the STO of oxygen, however, it is, in fact, impossible to integrate analytically. For example, in the case of SeH, when we adopt the AHF orbital of selenium, 45 integrals must be calculated. Therefore, they are numerically integrated using Barnett-Coulson's formulation by means of an NEAC 2200—500 electronic computer. The upper limit of the numerical integration by Sympson's law was chosen so as to be five times larger than the equilibrium interatomic distance, for the contribution from the integration beyond this limit was smaller than five decimals places in the atomic unit.

From the Fermi contact term and the dipolar term, the principal values of the hf tensor, A_x, A_y, and A_z, can be determined on the basis of the following assumption of axial symmetry:

$$A_x = A_y = b\,, \quad (10)$$

$$A_z = b + c\,. \quad (11)$$

These principal values are, however, essentially those for the free molecule; thus, there should be a kind of limit in the comparison of the gas-phase hfs with the solid-phase one.

The dipolar term and other anisotropic terms reflect sharply the shape of the unpaired electron orbital of the radical; the calculation of their change with the interatomic distance is useful in examining this orbital. For example, the deviation of the value calculated by the Slater atomic orbital from the Hartree-Fock value will be a measure of its accuracy.

Experimental

The method of observing gas-phase EPR spectra has been developed by Carrington and his colleagues.[15] They designed new types of EPR cavities and pillboxes and observed several kind of new radicals. Among these radicals, the observation of OH, SH, and SeH is comparatively easy. The OH radical is produced by the microwave discharge of water, while the SH and the SeH radicals are produced by the reaction of the hydrogen atom with sulfur and selenium respectively. These spectra are electric dipole transitions between the lambda-type doublet, so the microwave must have an electrical component perpendicular to the external field. To create this condition, a TE_{012} cylindrical cavity with a quartz pillbox was used. A rapid-gas-flow system consists of a ULVAC-300 rotary pump which evacuates 300 l per min, a liquid nitrogen trap 60 mm in diameter, a pilani-gauge, and an accurate needle valve. The linear velocity of the gas flow was supposed to be *ca.* 10 m/sec.

In a preliminary experiment, the gas-phase EPR spectra of OH, SH, and SeH were obtained with sufficient intensities. As for the TeH radical, the spectrum could not be obtained with a good SN ratio. The spectrometer used was operated in the X band with 455 kHz-field modulation and a 30 cm JEOL electromagnet.

In order to observe the solid-phase spectrum of the hydrides, under the same conditions as were used in the gas-phase experiment, the reactants were trapped at the point of the cavity in the gas-phase experiment on a coldfinger which was cooled at the temperature of liquid nitrogen. The outline of this apparatus is shown in Fig. 2. Except

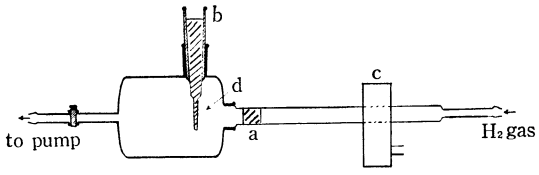

Fig. 2. Apparatus for trapping the radical in gas phase: a; evaporated film of S, Se, and Te, b; liq. N_2 Dewar vessel, c; cavity for discharge, d; coldfinger.

for OH, evaporated films of sulfur, selenium, and tellurium were made at the point of (a) in Fig. 2 and were attacked by the hydrogen atom which was generated in the microwave discharge of hydrogen gas. The microwave excitor was operated at 2450 MHz with a rectangular discharge cavity; its maximum output was 250 watt. The distance between the discharge (c) and the coldfinger (d) (*cf.* Fig. 2) was adjusted to get the best yield. The EPR measurement was done by transfering the coldfinger into a liquid-nitrogen Dewar vessel.

12) R. L. Brown and H. E. Radford, *Phys. Rev.*, **147**, 6 (1966).
13) M. P. Barnett and C. A. Coulson, *Phil. Trans. Roy. Soc.*, **243**, 221 (1951).
14) H. M. McConnell and J. Strathdee, *Mol. Phys.*, **2**, 129 (1959).
15) For exapmle, A. Carrington, and D. H. Levy, *J. Phys. Chem.*, **71**, 2 (1967).

To identify the solid-phase spectra, dihydrides and dideuterides of sulfur, selenium, and tellurium which had been diluted in H_2O and D_2O matrices were irradiated by a UV light of a 1-kW high-pressure mercury arc at 77°K; the EPR spectra were also observed at the same temperature. H_2Se and H_2Te were formed by the hydrolysis of Al_2Se_3 and Al_2Te_3 respectively; the latter substances were synthesized by the ignition of Se and Te with Al.

Results and Discussion

The lambda-type doubling frequencies, g values, A_1 and A_2 of OH, SH, SeH, and TeH and of their deuterides are tabulated in Table 1. The tendencies of the g value and the lambda-type doubling frequency, plus the molecular structure, can easily be explained by the theoretical expression of these constants.[16]

In Table 2 the experimental values and the calculated values of hfs constants are listed.

OH Radical. As for the former data of the hfs constants determined by Radford,[4] each experimental value could be compared to the calculated one. As can be seen in Table 2, the best accordance was obtained when the Slater orbital was adopted as an unpaired electron orbital. It may be noted that the unpaired electron orbital in the OH radical deviates from the pure $2p$ orbital of oxygen upon the repulsion of the O–H bond and by the spin polarization of the inner shell. The Slater orbital, although it is a simple AO, may be supposed accidentally to include these effects.

In the MO calculation, the molecular integrals, such as overlap and Coulomb integrals, have been cal-

TABLE 1. g-FACTORS, LAMBDA-TYPE DOUBLING, AND hfs OF GROUP VIB HYDRIDE RADICALS ($J=3/2$)

	g $((g_J^+ + g_J^-)/2)$[a]	Lambda type doubling (MHz)	hfs constant A_1(MHz)	hfs constant A_2(MHz)	Ref.
OH	0.9556	1666.3	27.1	0.5	3
OD	0.8895	310.1	4.8	—	3
SH	0.8379	111.4	5.6	—	6
SD	0.8344	34.3	1.0	—	this work
SeH	0.8080	14.4	1.9	—	7
SeD	0.8061	1.9	—	—	17
TeH	0.8037	6.6	1.8	—	7

a) g_J^+ and g_J^- denote the observed g-factors of each lambda type doublet.

TABLE 2. Hfs CONSTANTS OF GROUP VIB HYDRIDE RADICALS

		$2g_I\beta\beta_N\langle 1/r^3\rangle_{av.}$ (MHz)	$g_I\beta\beta_N\langle(3\cos^2\theta-1)/r^3\rangle_{av.}$ (MHz)	$16/3\pi\, g_I\beta\beta_N\Psi^2(0)$ (MHz)	Parameters used for calculation
OH	Obsd gas	86.0	44.4	−74.8	*Re*: UV[d]
	Obsd solid	—	—	−75	λ: Microwave[e]
	Calcd (Slater)	84.0	46.0	−73.4	
	Calcd (AHF)[a]	80.1	40.8	−62.2	
SH	Calcd (Slater)	29.9	10.9	−23.2	*Re*: UV[f] λ: UV[f]
	Calcd (AHF)[b]	24.2	3.9	−5.9	
SeH	Calcd $n=3.5$ (Slater)	24.3	9.2	−64.2	*Re*: EPR[g] λ: EPR[g]
	$n=4.0$	42.9	7.3	−102.6	
	Calcd (AHF)[c]	38.3	19.0	−114.9	
TeH	Calcd (Slater)	29.1	12.4	−98.1	*Re*: EPR[h] λ: EPR[h]

a) E. Clementi, C. C. J. Roothaan, and M. Yoshimine, *Phys. Rev.*, **127**, 1618 (1962).
b) R. E. Watson and A. J. Freeman, *ibid.*, **123**, 521 (1961).
c) E. Clementi, *J. Chem. Phys.*, **41**, 303 (1962).
d) G. Herzberg, "Molecular Spectra and Molecular Structure I. Spectra of Diatomic Molecules," D. Van Nostrand, New York, N. Y. (1950), p. 560.
e) Ref. 16.
f) D. A. Ramsay, *J. Chem. Phys.*, **20**, 1920 (1952).
g) Ref. 17.
h) Ref. 7.

16) G. C. Dousmanis, T. M. Sanders, Jr., and C. H. Townes, *Phys. Rev.*, **100**, 1735 (1955).

17) A. Carrington, G. N. Currie, and N. J. D. Lucas, *Proc. Roy. Soc.*, **A315**, 355 (1970).

culated by using the Slater orbitals. These integrals in the long internuclear distance differ from the AHF values. This property of the Slater orbital in the longer range appears less strongly for the dipolar term, which depends on r^{-3}, because it sharply decreases with r. As is well known, $<1/r^3>_{av}$ is a constant which shows the interaction between the hydrogen nucleus and the magnetic field generated by the orbital motion of an unpaired electron in a p orbital, so the inner shell spin density, which is induced by the spin polarization, has no effect on this constant. On the other hand, as the other anisotropic terms are originated by the interactions between the magnetic dipole of an unpaired electron and a hydrogen nucleus, the unpaired electron density in s orbital also has a small value. When a pure $2p$ atomic orbital is adopted as the unpaired electron orbital it is reliably established that the calculated value of the anisotropic terms except $<1/r^3>_{av}$ deviate a little from the experimental value.

Concerning the Fermi contact term, the good agreement of the experimental value with the estimated one in anisotropic terms results in a good correspondence between the experimental and estimated values. The MO calculation of this term was done by Kayama.[18] Introducing ten excited configurations to Freeman's LCAO-SCF-MO, he derived the value of -67.9 MHz. It was a very good agreement considering the accuracy of ordinary MO calculations. According to his result, the absolute value of the Fermi contact term increases with the interatomic distance; at 2.2 a.u., it gives -99.4 MHz. Even if we recognize the lack of monotony of the dependence of the σ–π interaction on the interatomic distance, however, his value at 2.2 a.u. is too large.[19]

The principal values of the hf-tensor of the OH radical, as determined by several investigators and as calculated by the method explained in the theoretical section, are listed in Table 3. Though the values obtained from the analysis of the solid-phase EPR spectra of the OH radical did not agree very well, the calculated results agreed fairly well.

By considering the accuracy of the above calculation of the anisotropic terms, the method of deriving the principal values of the hf-tensor can be said to be applicable when the appropriate atomic orbital for the unpaired electron orbital can be found.

18) K. Kayama, *J. Chem. Phys.*, **39**, 1507 (1963).

19) We calculated the Fermi term of OH by Pople's INDO (Intermediate Neglect of Diffential Overlap) method. By the approximate estimation of the one-center exchange integral of the oxygen and other integrals calculated from Pople's proposal, the SCF process repeated about forty times gave the final spin density as $\rho_{2p_{x,y}}=1.000$ or 0, $\rho_{2p_z}=0.094$, $\rho_{2s}=-0.065$, and $\rho_{1sH}=-0.029=-41.3$ MHz. Moreover, the dependence of the spin density of the H atom on the interatomic distance was:

	1.8342 a.u.	2.0 a.u.	2.2 a.u.
SCF-CI	−0.048	−0.056	−0.070
INDO	−0.029	−0.021	−0.013

At the equilibrium distance, the error of the value was bigger than Kayama's result, but the absolute value decreases with an increase in the interatomic distance.

Table 3. Hf-tensor of OH radical

	A_x(gauss)	A_y	A_z	Ref.
Calcd				
Slater	−42.6	−42.6	6.4	
AHF	−36.7	−36.7	6.9	
Obsd				
gas	−42.6	−42.6	5.0	4
ice	−26±4	−44±2	0±6	a
ice	−26±3	−43.7±0.05	±5±5	b
$CaSO_4\cdot 2H_2O$	−32.5	−43	3.3	2

a) J. A. Brivati, M. C. R. Symons, D. J. A. Tinling, H. W. Wardale, and D. O. Williams, *Chem. Commun.*, **1965**, 402.

c) G. H. Dibdin, *Trans. Faraday Soc.*, **63**, 2098 (1967).

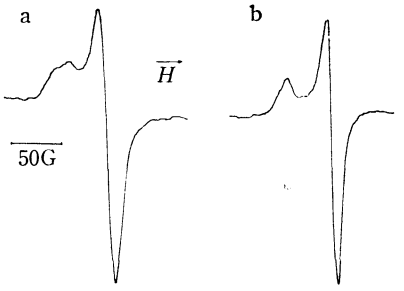

Fig. 3. EPR spectra of discharged product of a, H_2O and b, D_2O.

Figure 3 shows the EPR spectrum of the radical which is generated by the gas-phase microwave discharge of water and trapped at the temperature of liquid nitrogen. This spectrum shows no characteristic doublet of the OH radical, which was observed by the γ-ray[20] or tritium β-ray[21] irradiation of polycrystalline ice; it coincides with that from UV-irradiated H_2O_2 of a 20% aqueous solution.

From deuterium substitution, this spectrum is found to consist of two radical species; by a detailed analysis of the far-ultra violet photolysis of water and other related compounds these two species were identified as the HO_2 and HO_3 radicals.[22] The OH radical, which gives a strong EPR spectrum in the gas-phase, could not observed in the trapped phase. This phenomenon corresponds to the fact that the UV photolysis of the dilute solution of hydrogen peroxide (less than 3 wt%) gives the OH radical, while a more concentrated solution never gives it. This proves that, in the solid phase, the OH radicals may recombine easily; those in the gas-phase covert into HO_2 or other radicals as soon as they are trapped in the solid phase.

SH Radical. At the equilibrium interatomic distance, the calculated values from the Slater and AHF orbitals are rather different from each other. About the $3p$ orbital, though the true atomic orbital has three nodal planes, the Slater p AO's are always

20) For example, P. N. Moorthy, and J. J. Weiss, *Phil. Mag.* **10**, 659 (1964).

21) J. Kroh, B. C. Green, and J. W. T Spinks, *J Amer. Chem. Soc.*, **83**, 2201 (1961).

22) K. Kuwata, Y. Kotake, K. Inada, and M. Ono, to be published.

nodeless except for the origin, and generally the p Slater orbitals of different shell are nonorthogonal. The AHF atomic orbital for $3p$ of sulfur has two nodes other than the origin and is orthogonal to the p orbitals of the other shell. As anisotropic terms depend strongly on the shape of the orbitals, these properties of the Slater orbital are fatal in calculating the integrals.

For these reasons even if the influence of S–H bonding is considered, the AHF atomic orbital is much more reliable than the Slater one as an unpaired electron orbital. Sometimes the d orbital of a sulfur atom contributes to the sulfur and other atom bonding, but in the case of SH, the *ab initio* calculation of the electronic structure by Cade and Huo[23] showed that the contribution of the sulfur d-type orbital to the unpaired orbital is extremely small.

According to the hfs constants from the AHF wavefunction, the anisotropic term is much smaller than that of the OH radical; the estimated Fermi contact term also has a small negative value. The negative value of the Fermi term suggests that the mechanism of generating the isotropic hf interaction is the exchange interaction between the $3p_x$ or $3p_y$ orbital of a sulfur atom with the σ bond of SH.

The EPR spectra of the reactants under the same conditions as in the gas-phase experiment of SH are shown in Fig. 4. These spectra consist of the superposition of three peaks which show a deuterium substitution effect and the one broad singlet line. The

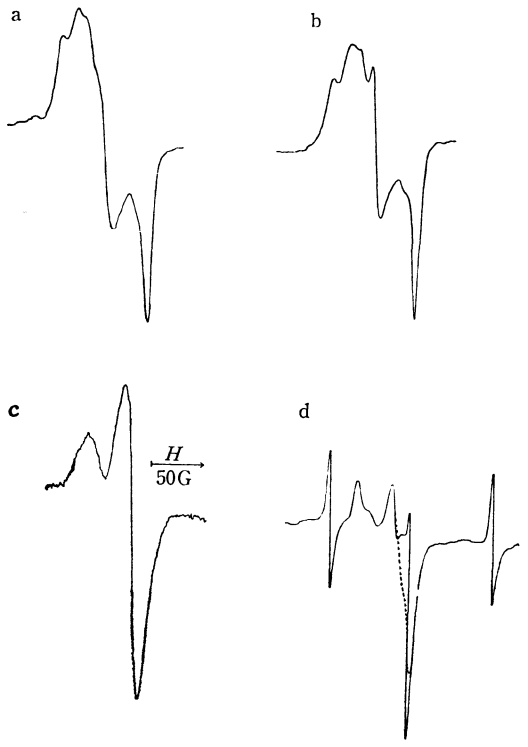

Fig. 4. EPR spectra of radicals formed by the reaction of sulfur with H atom (a), and D atom (b), and of UV photolyzed product of H_2S-H_2O system (c), and D_2S-D_2O system (d), broken line shows the substraction of D atom spectrum from central part.

23) P. E. Cade and W. H. Huo, *J. Chem. Phys.*, **47**, 649 (1967).

UV photolysis of the dilute solution of H_2S and D_2S gives a spectrum which corresponds to these three peaks.

By the decomposition of water and hydrogen peroxide, OH, HO_2, and other oxygen radicals can be obtained. On analogy with these radicals, SH, HS_2, and $(S)_n$ are proposed. Gunning *et al.*[8] obtained several spectra by the prolonged UV irradiation of pure H_2S and H_2S_2 and their deuterides at the temperature of liquid nitrogen. They obtained very complex spectra; their identification was seemingly difficult. In their analysis, the spectrum of SH indicates a large g anisotropy and does not have an axial symmetry. As for hfs, Gunning *et al.* directly compared the gas-phase hfs with that of the solid phase; however, this is incorrect, as may be seen in Eqs.(1) and (2) of the Theoretical section.

From the electronic structure of the SH radical, the $3p_x$ and $3p_y$ orbitals of the sulfur atom, which are perpendicular to the molecular axis, are seem to be nearly degenerate. The principal g_{ii} values $(i=x,y,z)$ of the g-tensor can be written as;

$$g_{ii} = g_e - \sum_{n \neq p} 2\zeta |\langle p|L_i|n\rangle|^2/(E_p - E_n) \qquad (12)$$

where E is the energy of the unpaired electron orbital p, where E_n is that of the nth orbital, and where ζ is the LS coupling constant. Assuming as the unpaired electron orbital the $3p_x$ or $3p_y$ orbital of a sulfur atom, and the SH bond as the nth orbital, g_{xx} and g_{yy} will give about the same value from Eq. (12) because of the near degeneracy. Eq. (12) indicates that an electronic structure like that of the SH radical will have an axial symmetric g-tensor. In our experiment, Fig. 4c shows almost axial symmetric spectra and a remarkable deuterium substitution effect; because they are radicals formed from a dilute solution of H_2S the radicals with more than two sulfur atoms may scarcely be formed. On the basis of these findings, this radical was identified with the SH radical. The superposed singlet spectrum of Fig. 4 showed no deuterium substitution effect. The trapped intermediate in the microwave discharge of sulfur vapor also gives a strong singlet line.[24] Therefore, this line may be attributed to the $(S)_n$ radical.

This identification was also supported by the calculation. By the use of the g-tensor of the SD spectrum, which was determined by the spectrum simulation assuming that the hfs of deuterium was so small to neglect, the SH spectrum could be reproduced from the calculated hf tensor, *i.e.*, $A_x=-3.5$, $A_y=-3.5$, and $A_z=0$ gauss. The simulated spectrum for SH is shown in Fig. 5 superposed on the observed spectrum.

In the case of the OH radical, the g- and hf-tensors were slightly different for each investigator. As for the SH radical, the influence of the trapped state may also change the spectral features; the discrepancy between the calculated and experimental results does not make the calculated results doubtful.

Recently Uehara and Morino[25] observed rotation-

24) Unpublished result.

25) H. Uehara and Y. Morino, *J. Mol. Spectrosc.*, **36**, 158 (1970).

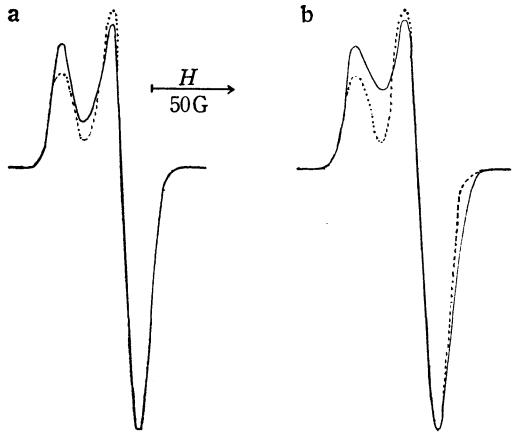

Fig. 5. Simulated spectra of SH ($g_x=2.0023$, $g_y=2.0100$, $g_z=2.035$).
a, using hf-tensor from AHF orbital ($A_x=A_y=12.2$, $A_z=0.5$ gauss)
b, using hf-tensor from the Slater orbital ($A_x=A_y=3.5$, $A_z=0.0$ gauss)
broken line shows the observed spectra of SH.

ally-excited SH ($J=5/2$) in the C-band. Though they could not resolve its hfs because of the large line-width, the accuracy of the calculation will be examined in the near future by gas-phase EPR or by microwave spectroscopy.

Comparison of the Slater Orbital with the AHF Orbital on the Calculation of Anisotropic Terms. In Fig. 6 the dependence of the values of $<(3\cos^2\theta-1)/r^3>_{av}$ on the interatomic distance between O and H and between S and H are shown for the Slater orbital and the AHF atomic orbital. The good agreement in the oxygen $2p$ orbital shows that the shape of the oxygen $2p$ Slater orbital fairly well resembles that of the AHF one. This may give support for the usefulness of the Slater orbital in MO calculation.

In SH, in spite of the large discrepancies from the AHF values, the value calculated using the Slater orbital as an unpaired electron orbital runs parallel with it. When we consider the nodeless property and the nonorthogonality of the Slater orbital, this parallelism is worth appreciating. Especially, the integrals calculated from $3p$ orbital have a maximum value for both the Slater and AHF orbitals. This is characteristic not only of the $3p$ orbital but also of the Slater $4p$ orbital. The fact that the anisotorpic dipolar interaction does not always decrease monotonously suggests that the hf interaction between indirectly-bonded atoms is sometimes important.

Figure 7 also shows the dependence of $<(3\cos^2\theta-1)/r^3>_{av}$ on the interatomic distance using the Slater orbitals of O, S, Se, and Te.

SeH and TeH Radicals. For the SeH radical, the unpaired electron orbital is assumed to be the $4p$ Slater orbital or the AHF orbital, which consists of a linear combination of nine STO's of the selenium atom. For TeH, the $5p$ Slater orbital of the tellurium atom is adopted. In this case, the assumption of the unpaired electron orbital as a pure p orbital is doubtful because, in the shell of the large-principal quantum number, the energy difference among the orbitals is

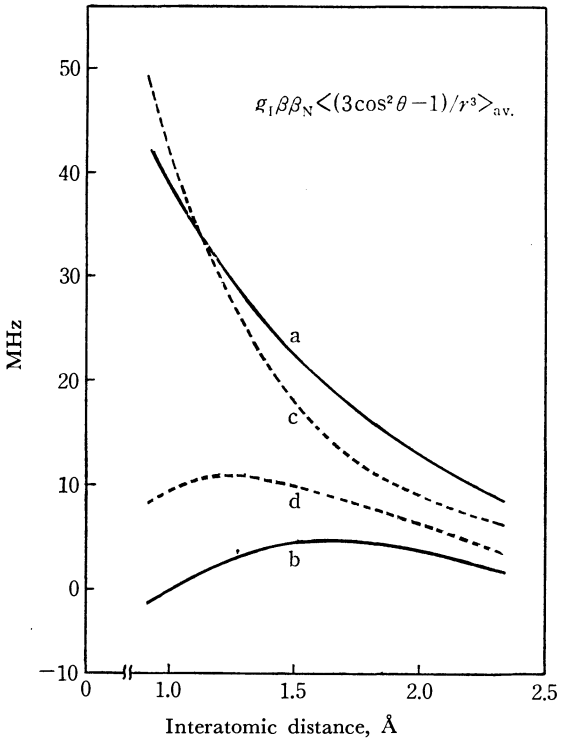

Fig. 6. Dependence of $g_I\beta\beta_N\langle(3\cos^2\theta-1)/r^3\rangle_{av}$ on the interatomic distance.
a, AHF orbital of O
b, AHF orbital of S
broken line shows the value of the Slater orbital of O (c) and S (d).

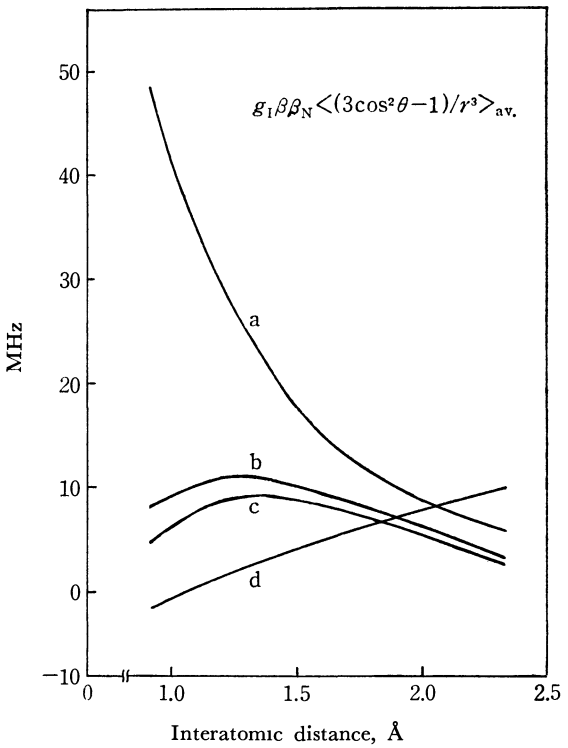

Fig. 7. Dependence of $g_I\beta\beta_N\langle3\cos^2\theta-1)/r^3\rangle_{av}$ of the Slater orbitals on the interatomic distance.
a, Oxygen b, Sulfur c, Selenium ($n=3.5$)
d, Selenium ($n=4$) and Tellurium

small enough for them to be hybridized easily. The calculated anisotropic terms are somewhat large compared to those in OH and SH.

The trapped products formed by the reaction of the hydrogen atom with the evaporated films of metallic selenium and tellurium gave no EPR signal. Their metallic colors proved that the SeH and TeH radicals are primarily formed and then decomposed into metals and the hydrogen atom immediately after trapping. Because the products are trapped in a highly concentrated state, the hydrogen atom formed from the decomposition of SeH and TeH could not be detected.

By the UV photolysis of dilute aqueous solutions of H_2Se and H_2Te and their deuterides, the EPR signal of the hydrogen atom or the deuterium atom were always detected. In this case, the SeH and the TeH radical are also unstable at the temperature of liquid nitrogen, and they decomposed into hydrogen atom and metals. The H_2Se–H_2O and the H_2Te–H_2O systems after the photolysis showed the color of red selenium and metallic tellurium. The hydrogen atom in this sample is less labile because of the surroundings, are mainly the water molecule, and the chance of the recombination is very small. The fact that the samples were always kept at the temperature of liquid nitrogen also stabilized the hydrogen atom. SeH and TeH are much unstable than OH and SH in both the gaseous and solid phases. Their stability is seemingly correlative with the strength of the reductivity of dihydrides.

BULLETIN OF THE CHEMICAL SOCIETY OF JAPAN, VOL. 44, 2062—2066 (1971)

The Electronic Structures of *trans* and *cis* Isomers of Some Halogenoethylenes

Hiroshi KATO, Kimihiko HIRAO,* Hideyuki KONISHI,* and Teijiro YONEZAWA*

Department of General Education, Nagoya University, Chikusa-ku, Nagoya

* *Department of Hydrocarbon Chemistry, Faculty of Engineering, Kyoto University, Sakyo-ku, Kyoto*

(Received December 31, 1970)

By using the closed-shell SCF MO method with the zero-differential overlap approximation for all valence electron systems previously presented by us, the electronic structures of *trans*- and *cis*- substituted ethylenes (treated substituent = CH_3, Cl, Br, and I) are studied. The calculated values of the π and valence electron charges, and the total energies of these isomers are presented. The natures of the higher occupied MO's, especially the lone-pair MO's, of chlorinated ethylenes are discussed in connection with the photoelectron observation. The calculated lowest π–π^* singlet transition energies accord well with the observed values. As to the rotational energy changes, the calculated results show that, at the perpendicular configurations, the triplet states for all the treated compounds are lowest, while the intermediate states for the *cis-trans* isomerizations of these compounds may be common to both the isomers.

Many theoretical and experimental studies have been carried out on the electronic structures of *trans*- and *cis*- isomers of substituted ethylenes.[1] On theoretical grounds, semi-quantitative discussions of this problem, however, need to consider explicitly not only the π-electronic structures but also the σ-electronic ones. For example, differences in the electronic structures of these isomers are in some case, mainly dependent on the interactions between the lone pairs of the substituted atoms, and the rotation about the ethylenic CC double bond causes the σ-π mixing. We have already given a semiempirical SCF MO method for all valence electron systems,[2,3] and the electronic structures of *trans*- and *cis*-isomers of butadiene, acrolein, and glyoxal have been calculated in satisfactory agreement with the observed results.[3]

In this paper, the method with an approximation of the zero-differential overlap[4] is used to study the electronic structures of the *trans*- and *cis*-halogenated ethylenes and related compounds, and also those of the twisted configurations caused by the *cis-trans* isomerizations of these compounds. The compounds treated in this paper are as follows: *cis*- and *trans*-butene-2, dichloro-, dibromo-, and diiodoethylenes, and some related chlorinated ethylenes.

Method and Parameters Used

The method employed in this paper is the semi-empirical SCF MO method for the closed shell of all valence electron systems, with approximations of the zero-differential overlap and empirical estimation of integral values. In this section, only the used parameters will be described, since the details have been given in previous papers.[4]

The one center exchange integral values and the valence-state ionization potential and electron affinity for the related atoms are estimated from those in Hinze and Jaffe's paper.[5] The values of the orbital exponent are those obtained by Clementi and Raimond.[6] The overlap integrals including the bromine atom

1) *E. g.*, P. G. Wilkinson and R. S. Mulliken, *J. Chem. Phys.*, **23**, 1895 (1955); G. M. Wyman, *Chem. Revs.*, **55**, 625 (1955).

2) T. Yonezawa, K. Yamaguchi, and H. Kato, This Buttetin, **40**, 536 (1967).

3) H. Kato, H. Konishi, H. Yamabe, and T. Yonezawa, *ibid.*, **40**, 2761 (1967).

4) T. Yonezawa, H. Konishi, and H. Kato, *ibid.*, **42**, 933 (1969); **41**, 1031 (1968).

5) J. Hiaze and H. H. Jaffe, *J. Chem. Phys.*, **38**, 1834 (1963).

6) E. Clementi and D. L. Raimond, *ibid.*, **38**, 2686 (1963).

(the principal quantum number, $n=4$) are calculated by the expansion formulas for $n=5$. The value of the parameter, K, for the estimation of core resonance integrals is taken to be 0.8 for the halogenated ethylenes and for 2-butene.[7] It is estimated so as to reproduce the good accordance between the calculated and observed lowest π-π^* singlet energies in vinyl chloride ($K=0.8$) in stead of in ethylene ($K=0.9$).

The molecular coordinates are adopted from the Sutton's Tables[8] and are summarized in Table 1,

Table 1. The molecular configurations used[a]

Substituent X	Bond distance (Å) C-C	Bond distance (Å) C-X	Bond angle (degree) ∠CCX
$-CH_3$	1.34	1.54	120
-Cl	1.34	1.72	123
-Br	1.34	1.85	121
-I	1.34	2.05	122

a) CH=1.07Å, ∠CCH=120° for all the compounds.

where the coordinates of the *cis*-forms are assumed to be the same as in the related *trans*-compounds, except for the relations between the terminal groups.[9]

Results and Discussions

Charge and Energy. The calculated π net charges and π bond orders are presented in Table 2, together with the net charges and E_{AB} values[4,11-13] for all valence electrons. The table indicates that the π delocalization is slightly stronger in *cis*-form than in its *trans* isomer, but the σ charges concentrate a little more on the halogen atoms of the *cis*-form than in the *trans*-forms. It is recognized that the E_{AB} values reflect the substituent effect, that is, the CC and CH bonds in substituted ethylenes are weakened compared with those in ethylene, but different tendencies between the results in Table 2 and the ones predicted by electronegativity for halogen atoms are indicated. These points will be discussed by more refined calculations.

Table 2. The charges and bond orders of 1,2-dihalogenated ethylenes

(a) π Net charge and π bond order

Compounds		π net charge C	π net charge X	π bond order C-X	π bond order C-C
Cl[a]	*t*	−0.039	+0.039	0.193	0.961
	c	−0.042	+0.042	0.199	0.958
Br[a]	*t*	−0.045	+0.045	0.208	0.955
	c	−0.049	+0.049	0.216	0.951
I[a]	*t*	−0.044	+0.044	0.204	0.956
	c	−0.046	+0.046	0.208	0.954

(b) Net charge and E_{AB} value (eV) for the valence shell

Compound		Net charge C	Net charge X	Net charge H	E_{AB} (eV) C-C	E_{AB} (eV) C-X	E_{AB} (eV) C-H
Ethylene		−0.016		+0.008	36.46		22.94
Cl	*t*	+0.197	−0.217	+0.020	32.45	18.01	20.98
	c	+0.197	−0.221	+0.025	32.51	17.98	21.01
Br	*t*	+0.055	−0.121	+0.066	33.13	16.48	21.49
	c	+0.065	−0.130	+0.065	33.23	16.39	21.37
I	*t*	+0.037	−0.055	+0.018	32.89	15.16	21.28
	c	+0.046	−0.059	+0.013	32.80	15.23	21.27

a) The notations, Cl, Br, and I to the dichloro-, dibromo- and diiodoethylenes, *t* and *c* are *trans*- and *cis*-compounds, respectively.

Table 3. The U_P values for atoms in chloroethylenes

Compound	AO electron density π	AO electron density $\bar{\pi}$	AO electron density σ	U_P values[a] Calcd	U_P values[a] Obsd
1-Cl	1.958	1.973	1.439	0.527	0.611
1,1-DiCl	1.956	1.956	1.447	0.508	0.717
1,2-DiCl-*t*	1.961	1.974	1.404	0.563	0.649
1,2-DiCl-*c*	1.958	1.974	1.411	0.550	0.638

a) $U_P = \left(\frac{\pi+\bar{\pi}}{2}\right) - \sigma$

b) See Ref. 14.

Different shifts in the *cis*- and *trans*-dichloroethylenes are observed by the PQR measurement;[14] that is, the nuclear quadrupole coupling constants of the Cl^{35} in the *cis*-form are smaller than these in the *trans*-isomer. The values of the PQR U_p values (the number of unbalances electrons) of Cl atoms in various chlorinated ethylenes are estimated by the approximation derived by Townes and Dailey.[15] The results obtained are listed in Table 3, together with the π, $\bar{\pi}$, and σ AO charges. (The $\bar{\pi}$ AO is perpendicular to the C-Cl bond and is on the molecular plane.) The calculated difference in U_p values in the *cis*- and *trans*-forms is in good agreement with the observed value,

7) As for 2-butene, the results with $K=0.9$ are in better accordance with the observed values.

8) "Tables of Interatomic Distances and Configurations in Molecules and Ions," ed. by L. E. Sutton, The Chem. Soc., London (1956, 1965).

9) As to the *cis*-dichloroethylene, it is suggested in Refs, 10 and 15 that this form may be staggered, that is, the two C-Cl bonds deviate out of the molecular plane. But this staggered form is calculated to be more unstable than its planar form, 0.02 eV at 5° and 0.13 eV at 15°. Thus, we do not consider this form, hereafter.

10) S. Saito, This Bulletin, **35**, 1483 (1962).

11) J. A. Pople, D. P. Santry, and G. A. Segal, *J. Chem. Phys.*, **43**, S129 (1965).

12) H. Konishi, H. Kato, and T. Yonezawa, This Bulletin, **43**, 1676 (1970).

13) E_{AB} is defined as follows: $E_{AB}=\sum_{r}^{\text{on A}}\sum_{s}^{\text{on B}} P_{rs}(H_{rs}^{c}+F_{rs})$, where the AO's r and s are belonging to the atom A and B, respectively.

P_{rs} is the bond order of r-s pair, and H_{rs}^{c} and F_{rs} are the off-diagonal r-s elements of core resonance integral and Fock operator, respectively. See Refs. 4 and 11.

14) *E.g.*, "Constants of Organic Compounds," ed. by M. Kotake, Asakura (1963), p. 491.

15) C. H. Townes and B. P. Dailey, *J. Chem. Phys.*, **17**, 782 (1949).

Table 4. Orbital energies of some chloroethylenes (eV)

Vinyl Chloride				1,1-Dichloroethylene			
Calcd		Obsd[a]		Calcd		Obsd[a]	
$11\pi^*$	+0.56	—	—	$14b_2\sigma^*$	+0.22	—	—
$10\sigma^*$	+0.49	—	—	$13b_1\pi^*$	+0.18	—	—
9π	−11.86	$a''\pi$	−10.18	$12b_1\pi$	−11.98	π	−10.00
$8n$	−13.31	$a'n$	−11.72	$11a_1n$	−13.74	n	−11.67
7π	−14.68	$na''\pi$	−11.87	$10b_2n$	−14.12	n	−12.17
6σ	−14.88	$a'\sigma$	−13.14	$9a_2\pi$	−14.21	$b_1\pi$	−12.51
				$8b_2\sigma$	−15.47	σ	−13.7
				$7b_1\pi$	−15.90	σ	−14.24

trans-Dichloroethylene				*cis*-Dichloroethylene			
Calcd		Obsd[a]		Calcd		Obsd[a]	
$14b_g\pi^*$	+1.03	—	—	$14a_2\pi^*$	+0.06	—	—
$13b_u\sigma^*$	−1.01	—	—	$13a_1\sigma^*$	−0.56	—	—
$12a_u\pi$	−11.63	π	−9.81	$12b_1\pi$	−11.57	π	−9.83
$11a_gn$	−13.34	b_un	−11.86	$11a_1n$	−13.18	b_2n	−11.71
$10b_un$	−14.14	$b_g\pi$	−11.93	$10b_2n$	−13.87	$a_2\pi$	−11.85
$9b_g\pi$	−14.97	a_gn	−12.06	$9a_2\pi$	−14.14	a_1n	−12.09
$8a_g\sigma$	−14.97	$a_u\pi$	−12.61	$8b_2\sigma$	−15.06	π	−12.51
$7a_u\pi$	−15.45	σ	−13.85	$7b_1n$	−15.33	σ	−13.72

a) Ref. 16.

but the errors in absolute values between the calculated and observed are over 20% in magnitude. As to these discrepancies, the table suggests that they are mainly due to the large AO charges on the Pσ AO's on the chlorine atoms. Further, the disorder in 1,1-dichloroethylene may be partially caused by the neglect of the Cl–Cl interaction.

Recently, the photoionization spectra of several chlorinated ethylenes were presented, and the symmetry assignments of some MO's were made; the highest occupied MO's in these compounds are of the π type, while the second lower group MO's are lone-pair MO's localized on the chlorine atoms.[16] In Table 4, the observed and calculated MO energies are summarized. The calculated energy values are about 2 eV lower than the observed values, but the orbitals sequences almost coincide. The symmetry assignments partially disagree with each other, especially for the lone-pair-type MO's. In order to reexamine this point, the calculated partial atom charges of the related MO's are collected in Table 5, together with the chlorine AO densities. Our results show that the 10 and 11 MO's are both of the lone-pair type in dichloroethylenes. The latter MO has the a_g symmetry in *trans* and the a_1 symmetry in *cis*-dichloroethylene, and C–Cl anti-bonding and Cl–Cl bonding; on the other hand, the formes MO is b_u in *trans*- and b_2 in *cis*-, and is C–Cl bonding and Cl–Cl anti-bonding. For 1,1-dichloroethylene, the same tendency is obtained as may be seen in the table, in spite of the stronger Cl–Cl interaction. Accordingly, it may be said that the stabilization of these two types

Table 5. The partial atomic charge densities in lone-pair-type MO's in dichloroethylenes

		Partial atomic charges			$\bar{\pi}$AO charge
		H	C	Cl	Cl(π)
trans-	$11a_gn$	0.10	0.12	0.78	(0.77)
	$10b_un$	0.02	0.01	0.97	(0.95)
	$8a_g\sigma$	0.16	0.17	0.76	(0.01)
cis-	$11a_1n$	0.07	0.10	0.83	(0.81)
	$10b_2n$	0.03	0.02	0.95	(0.90)
	$8a_1\sigma$	0.09	0.16	0.75	(0.01)
1,1-	$11a_1n$	0.02	0.14	0.84	(0.64)
	$10b_2n$	0	0.01	0.99	(0.84)
	$8b_2\sigma$	0.10	0.15	0.75	(0.03)

Table 6. The energy diferences between the *cis*- and *trans*-isomers

Substituent	ΔE (kcal/mol)[a]	
	Calcd	Obsd
-CH_3	−0.1	−1.0
-Cl	+2.3	+0.5[b]
-Br	+3.9	—
-I	+0.2	−0.6

a) $\Delta E = E(trans) - E(ci)$
b) Ref. 10, 18.
c) Ref. 19.

16) R. F. Lake, and H. Thompson, *Proc. Roy. Soc. London*, **A 315**, 323 (1970).

Table 7. Some lower electronic transition energies (eV) and moments (Å, in parentheses) of chlorinated ethylenes

		CH_2CHCl	CH_2CCl_2	*t*-CHClCHCl	*c*-CHClCHCl	$CHClCCl_2$	CCl_2CCl_2
π-σ	S [a]	5.23(0.138)	5.15(0.0)	4.04(0.0)	4.35(0.180)	4.38(0.071)	3.82(0.0)
	T	4.85	4.91	3.63	4.00	4.04	3.56
π-π^*	S	6.68(0.961)	6.44(0.980)	6.21(1.038)	6.13(1.001)	6.31(1.075)	6.46(1.074)
	T	4.17	3.95	3.81	3.82	3.99	4.38
π-π^*	S	7.63(0.017)	7.64(0.010)	7.19(0.0)	7.10(0.0)	7.64(0.015)	8.05(0.0)
	T	7.54	7.53	7.09	7.01	7.55	7.97
n-σ^*	S	7.06(0.271)	7.43(0.018)	6.38(0.356)	6.70(0.399)	7.28(0.564)	7.17(0.837)
	T	6.61	7.04	6.00	6.30	6.78	6.48
π-π^*	S	9.24(0.355)	8.13(0.658)	8.88(0.0)	8.66(0.0)	8.96(0.479)	9.23(0.575)
	T	8.26	7.46	8.50	8.23	8.63	8.04

a) The notations S and T refer to the singlet and triplet transition.

of lone-pair MO's depends mainly on the C–Cl bonding character and not on the Cl–Cl character, as was pointed out in our previous paper.[3] It is hoped that this discrepancy will be reinvestigated both theoretically and experimentally. Further, it is noticed that the lower vacant MO's are of the σ^* type and the strongly C–Cl antibonding. This result may be correlated to the ease of the C–Cl bond clevage by the polarographic reduction, as was shown by our previous results obtained by simple LCAO MO treatment.[17]

The energy differesces between the *cis*- and *trans*-isomers are listed in Table 6, together with the observed values,[10,18] where E is $E=E(trans)-E(cis)$; that is, the negative value of E indicated that the *trans*-isomer is more stable than the *cis*-form. The results calculated for 2-butene and dichloroethylenes accord with the observed values, but in the diiodo-compounds the results contradict each other.[19]

Electronic Transition Energy. In Table 7, the calculated lower electronic transition energies and moments for the chlorinated ethylenes are summarized. As to the lowest π–π^* singlet transition energies, the agreements between the calculated and observed values[18,20] are excellent: CH_2CHCl: 6.68 (6.70), CH_2CCl_2: 6.44 (6.45), *t*-CHClCHCl: 6.21 (6.36), *c*-CHClCHCl: 6.13 (6.53), $CHClCCl_2$: 6.31 (6.32), CCl_2CCl_2: 6.46 (6.29), where the numbers in parenthes are the observed values.[18,20] The other types of transitions have not yet been assigned by means of observations, but it is interesting that the lowest transitions obtained are π-σ^* transitions, as was suggested in our previous paper.[17]

The lowest π–π^* transition energies and oscillator strength values (Å) for various *cis*- and *trans*-isomers are collected in Table 8. The calculated values for the π–π^* transition energy in *cis*-isomers are considerably smaller than the observed values, and the order of magnitude for *cis*- and *trans*-isomers does not agree with the observations. As to the transition moments, the calculations show that values in the *trans*-isomers are larger than in *cis*-isomers. This tendency is to be expected from the symmetry consideration for these isomers; that is, the lowest π–π^* transitions belong to the b_u irreducible representation in the *trans*-isomer (C_{2h}) and to the b_2 in the *cis*-isomer (C_{2v}). Thus the components of the transition moment are x and y in b_u, and y in b_2 (the direction of y is parallel to the central CC bond and x is perpendicular to this bond), and the moment values (y) are nearly equal for the two isomers. Therefore, the differences between the *cis*- and *trans*-isomers are dependent on the x component values.

Table 8. The lowest π-π^* transition energies of some *cis*- and *trans*-isomers

Compound [a]	Calcd: Transition energy Singlet	Calcd: Transition energy Triplet	Calcd: Transition moments (Å)	Obsd: Transition energy Singlet(Tripler)
t-CH_3	6.33 (6.90) [d]	3.80 (4.37)	0.984 (0.988)	6.97(4.07) [b]
c-CH_3	6.30 (6.87)	3.78 (4.35)	0.948 (0.961)	7.10 [b]
t-Cl	6.21	3.81	1.038	6.36 [c]
c-Cl	6.13	3.82	1.001	6.53 [c]
t-Br	5.66	4.19	1.002	—
c-Br	5.49	4.11	0.923	—
t-I	5.38	4.34	0.984	—
c-I	5.27	4.26	0.876	—

a) The notations *t*- and *c*-, indicate *trans*- and *cis*-substituted ethylene, respectively.
b) M. Itoh, R. S. Mulliken, *J. Phys. Chem.*, **73**, 4332 (1969); A. J. Merer, R. S. Mulliken, *Chem. Rev.*, **69**, 639 (1969).
c) Refs. 18, 20.
d) In 2-Butene, the values in parentheses are obtained by $K=0.9$.

The Rotational Barrier. It is well known that the *cis-trans*-isomerization of ethylenic compounds occurs through the perpendicular configuration, in which the

17) K. Fukui, K. Morokuma, H. Kato, and T. Yonezawa, This Bulletin, **36**, 217 (1963).
18) J. P. Teegan and A. D. Walsh, *Discuss. Faraday Soc.*, **47**, 1 (1951).
19) H. Steinmetz and R. M. Noyes, *J. Amer. Chem. Soc.*, 4141 (1952).
20) A. D. Walsh, *Discuss. Faraday Soc.*, **41**, 35 (1945); A. D. Walsh and P. A. Warsop, *Trans. Faraday Soc.*, **64**, 1418 (1968); A. D. Walsh, P. A. Warsop, and J. A. B. Whiteside. *ibid.*, **64**, 1432 (1968).

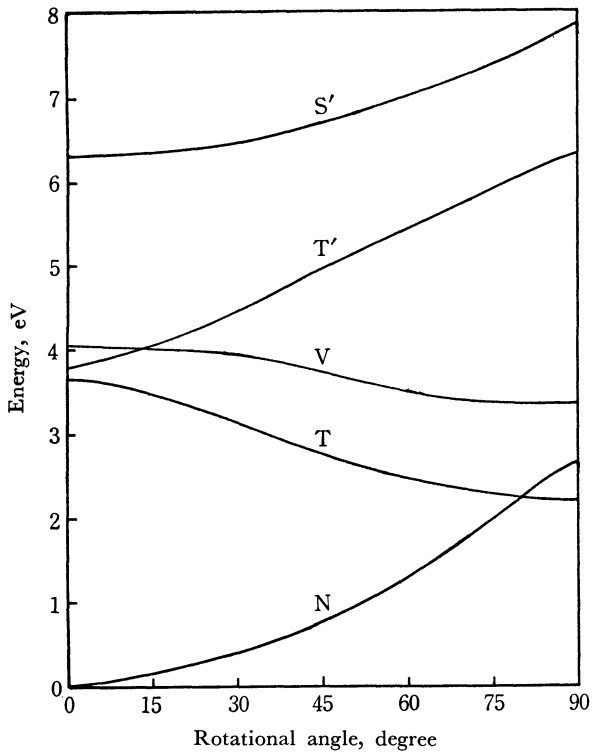

Fig. 1. Rotational energy barrier of *trans*-1,2-dichloroethylene.

triplet state is most stable.[1,21,22] In this section, we will present the potential energy changes caused by the rotation around the central CC double bond, where the rotational configurations are assumed to be unchanged, as in the planar *trans*-form, except for the rotational angles.[23] In Fig. 1, the energy changes for various rotational angles in the *trans*-dichloroethylene are plotted, the N, T, and V notations are the ground state and the lowest triplet and singlet states respectively. It may be noticed that the T and V states, in the twisted configurations are constructed mainly by the lowest π–π^* and π–σ^* excited states in the planar form.

By utilizing the obtained potential curves, the estimations of the force constant for the twisting vibration around a CC bond are made. The results obtained are presented in Table 9. Considering the approximations used, the agreements between them are fairly good, but the values in halogenated compounds are somewhat smaller.

At the twist angle of 90°, the above-mentioned states are labelled by the suffix m, N_m, T_m, and V_m; these energy values are listed in Table 10, together with the the angle, θ_1, at which the N and T states cross. In Fig. 2, the outlines of these state energy curves are given. From the table it is clear that the singlet and triplet energies decrease to minima at the perpendicular configuration, and that, in this state, the T_m states are the lowest. Further, the calculations show that the shapes of the potential energy curves of *cis*- and *trans*-isomers are not very different, and that the crossing of T and N states occurs near 90°. Thus, it may be said that the intermediate triplet states through the *cis-trans*-isomerization are common to both isomers. This result accords with the experimental conclusions for the *cis-trans*-isomerization in dichloroethylene.[22] It may, however, be noticed that since the R_m and V_m states converge to the degenerate state in ethylene, more knowledge of the configuration interaction will be necessary before we can discuss these states more quantitatively.

TABLE 9. THE FORCE CONSTANTS FOR TWISTING VIBRATIONS IN *cis*- AND *trans*-SUBSTITUTED ETHYLENE (mdyn Å/rad)

	Calcd	Obsd[a]
Ethylene	0.128	0.136
t-CH_3	0.158	0.162
c-CH_3	0.130	—
t-Cl	0.095	0.168
c-Cl	0.092	0.161
t-Br	0.098	—
c-Br	0.099	—
t-I	0.090	—
c-I	0.089	—

a) K. S. Pitzer and J. L. Hollenberg, *J. Amer. Chem. Soc.*, **76**, 1493 (1954).

TABLE 10. THE POTENTIAL ENERGIES (eV) IN PERPENDICULAR CONFIGURATIONS[a]

		T_m	N_m	V_m	θ_1
	t-CH_3	2.60	3.24	4.03	82°
	t-Cl	2.41	2.96	3.64	79°
	t-Br	2.33	2.51	3.25	82°
	t-I	2.47	2.68	3.32	85°
Ethylene	Calcd[b]	3.24	3.60	9.72	79°
	Obsd[c]	2.8	4.13	5.68	—

a) The reference energy of these states is chosen as that of the planar *trans*-form.
b) U. Kaldor and I. Shavitt, *J. Chem. Phys.*, **48**, 191 (1968).
c) R. McDiarmid and E. Charney, *ibid.*, **47**, 1517 (1967).

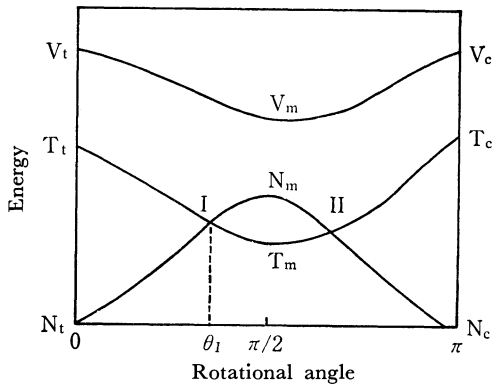

Fig. 2. A sketch of potential energy diagram.

The calculations have been carried out on the FACOM 230—60 Computer of Kyoto University.

21) A. J. Merer and R. S. Mulliken, *Chen. Revs.*, **69**, 639 (1969).
22) Z. R. Grabowski and A. Bylina, *Trans. Faraday Soc.*, **60**, 1131 (1964).
23) In the perpendicular configurations of these compounds, the molecular coordinates may change from the planar ones, but no accurate observed values have yet been presented.

Measurements of Total Cross Sections for the Scattering of Potassium Atoms by Rare Gases

Isao KUSUNOKI

Department of Chemistry, Faculty of Science, Kyoto University, Sakyo-ku, Kyoto

(Received January 21, 1971)

Total cross sections for the scattering of potassium by He, Ne, Ar, Kr, and Xe have been measured in the thermal energy range. The velocity of potassium beam is selected by a velocity selector of a slotted disk type. To obtain accurate total cross sections, the pumping effect of a McLeod gauge for the pressure measurements, the fringe effect of the scattering chamber, corrections for angular resolution and for thermal motion of the target gases are taken into consideration. A new type of scattering chamber with a variable length is used to eliminate the error of the effective scattering path length. Velocity dependence of total cross sections has been obtained and glory undulations are observed for potassium-xenon systems. For argon, krypton, and xenon the van der Waals constants are calculated from the absolute total cross sections. The values of C_{K-Ar}, C_{K-Kr}, and C_{K-Xe} are 237, 354, and 535×10^{-60} erg·cm^6, respectively, and are in good agreement with the theoretical ones of Dalgarno and Davison. For neon the velocity dependence of the total cross section can not be explained by the van der Waals potential, $-C/r^s$, where $s=6$. For helium the correction factors for thermal motion of the scattering gas are large and the value of s for attractive potential can not be determined unambiguously.

It is well known that total collision cross sections measured by the scattering of molecular beams can afford an excellent means to study interatomic forces. In the thermal energy range the total cross sections are mainly governed by the long range van der Waals attraction, and the van der Waals constants can be determined by the measurements of the total cross sections.

In the molecular beam study, the total cross sections for scattering of potassium atoms by rare gases have been measured by many investigators[1] since the pioneering work of Rosin and Rabi.[2] The reason for this choice may be that potassium is the easiest to handle and detect as the beam material, and rare gases are also easy to handle as target gases experimentally and theoretically. Thus, the total cross section for scattering of potassium atoms by argon atoms has been regarded as a standard in this kind of experiment.

However, there are several sources of errors in the method of determination of the absolute total cross section, and the values published by different investigators did not always coincide. On the other hand, the method of data analysis has improved in the last decade, and many experimental results in the past have been become obsolete. The main reasons are as follows.

(1) The treatment of Berkling *et al.*[3] for correction of the velocity distributions of the beam and target gases is superior to that of Rosin and Rabi,[2] because the former takes into account the velocity dependence of the total cross sections. It is also evident that monochromatic beams used in recent studies are superior to thermal beams.

(2) In measuring the pressures of scattering gases with a McLead gauge, mercury drag effect must be taken into consideration.[4]

(3) The concept for angular resolution was improved by Kusch[5] and Busch,[6] and it has been recognized that the correction can not be ignored for beams of rectangular cross sections.

(4) To estimate the van der Waals constant from the total cross section, the Schiff and Landau-Lifshitz approximation formula[7] is superior to the Massey-Mohr formula.[8,9]

(5) There are few papers in which the effective scattering lengths are determined experimentally and unambiguously.

In a previous paper, the author took into consideration the above-mentioned items (1), (2), and (4).[10] In the present work, the absolute total cross sections for the scattering of potassium atoms by rare gases have been measured with the velocity selected beams, and the van der Waals constants have been estimated by the Schiff and Landau-Lifshitz approximation. Moreover, the effective scattering lengths have been determined experimentally, and other possible sources of error have also been taken into account.

Theoretical

For the measurement of the total collision cross section of gas molecules by means of the molecular beams, Beer's law is applicable for attenuation of the beam intensity, thus

$$I = I_0 \exp(-nQL), \quad (1)$$

where I_0 and I are the intensities of primary and at-

1) *Cf. e.g.*, a review by R. B. Bernstein and J. T. Muckerman, in "Intermolecular Forces" (Advances in Chemical Physics, Vol. 12), J. O. Hirschfelder, Ed., Interscience, New York (1967), Chap. 8.

2) S. Rosin and I. I. Rabi, *Phys. Rev.*, **48**, 373 (1935).

3) K. Berkling, R. Helbing, K. Kramer, H. Pauly, Ch. Schilier, and P. Toschek, *Z. Physik*, **166**, 406 (1962).

4) H. Ishii and K. Nakayama, *Trans. 8th Vacuum Symp. and 2nd Intern. Congress* (Pergamon Press, 1961) p. 519.

5) P. Kusch, *J. Chem. Phys.*, **40**, 1 (1964).

6) F. Busch, *Z. Physik*, **193**, 412 (1966).

7) L. I. Schiff, *Phys. Rev.*, **103**, 443 (1956); L. D. Landau and E. M. Lifshitz, "Quantum Mechanics", Pergamon Press, London (1959) p. 416.

8) H. S. W. Massey and C. B. O. Mohr, *Proc. Roy. Soc.*, **A144**, 188 (1934).

9) R. B. Bernstein and K. H. Kramer, *J. Chem. Phys.*, **38**, 2507 (1963).

10) I. Kusunoki, This Bulletin, **40**, 69 (1967).

tenuated beams, respectively. Q is the total cross section, L is the scattering path length, and n is the density of the target gas in the scattering chamber. Equation (1) is only correct for the ideal case in which a monochromatic molecular beam passes through a static target gas. However, as the target gas atoms are always moving, it is necessary to replace Eq. (1) by the equation

$$I = I_0 \exp(-nQ_{eff}L), \tag{2}$$

where Q_{eff} is an average total cross section over the whole relative velocity range. According to Berkling *et al.*,[3] the effective total cross section $Q_{eff}(v_i)$ at a beam velocity v_i, is related to the absolute total cross section $Q_i(v_i)$ as follows,

$$Q_0(v_i) = Q_{eff}(v_i)/Fa_0(s, x), \tag{3}$$

where $Fa_0(s,x)$ is a correction factor. Numerical values of $Fa_0(s,x)$ for $s=4$, 5, 6, and 7 have been calculated by a computer.[11] The values for $s=6$ coincide with those tabulated in Ref. 3.

All the apparatuses always have finite angular resolutions for detection of the scattering event. Thus, the scattering inside the resolving angle should be corrected. In the present experiment the beam and the detector have rectangular cross sections perpendicular to the direction of the beam, and their heights are larger than their widths. The angular resolution is not uniform, and depends on the position in the plane of the detector and the point in the scattering region. However, for a narrow rectangular beam it is expected to be uniform along its height.

Consider a particle scattered in the scattering chamber from a point at a distance l from the plane of the detector, and at a distance z from the vertical central line of the beam (Fig. 1). If the trajectories of the unscattered atoms are sufficiently parallel to each other, a part of the beam scattered through an angle Θ and falls on the detector is given by

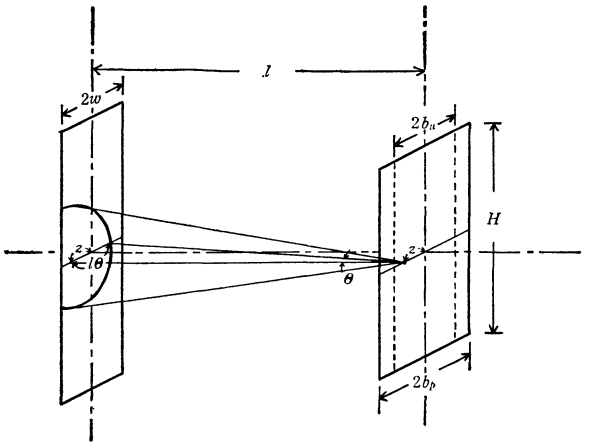

Fig. 1. Geometrical parameters for the correction of angular resolution.

$$2\pi n i(z) R(z, l, \Theta)\sigma(\Theta)\sin\Theta \mathrm{d}\Theta, \tag{4}$$

where n is the density of the scattering gas, $i(z)$ is the beam intensity at the scattering point, $R(z,l,\Theta)$ is the portion of the circumference of the circular cone of the scattered beam intercepted by the detector, and $\sigma(\Theta)$ is the differential cross section in the laboratory system.[12]

In the first approximation the correction term for angular resolution is obtained in the case of $z=0$ and $l=$constant, thus

$$\Delta Q(v_i) = 2\pi \int_0^{\pi} R(l, \Theta)\sigma(v_i, \Theta)\sin\Theta \mathrm{d}\Theta \tag{5}$$

A formula representing a more perfect correction for the angular resolution is

$$\Delta Q(v_i) = \frac{2\pi \int_{l_{cd}-L}^{l_{cd}} \int_{-b_p}^{b_p} \int_0^{\pi} i_0(z) \mathrm{e}^{-nQ(l_{cd}-l)} R(z, l, \Theta)\sigma(v_i, \Theta) \sin\Theta \mathrm{d}\Theta \mathrm{d}z \mathrm{d}l}{\int_{l_{cd}-L}^{l_{cd}} \int_{-b_p}^{b_p} i_0(z) \mathrm{e}^{-nQ(l_{cd}-l)} \mathrm{d}z \mathrm{d}l}, \tag{6}$$

where l_{cd} is the distance from the entrance slit of the scattering chamber to the detector, b_p is the half width of penumbra of the beam profile at the scattering plane, and L is the effective length of the scattering chamber.

We previously assumed a beam of infinite height, but in this experiment a beam of finite height is used. Thus the R-function has to be modified to a function of h, and Eq. (6) becomes

$$\Delta Q(v_i) = \frac{2\pi \int_{-H}^{H} \int_{l_{ed}-L}^{l_{cd}} \int_{-b_p}^{b_p} \int_0^{\pi} i_0(z) \mathrm{e}^{-nQ(l_{cd}-l)} R(h, z, l, \Theta)\sigma(v_i, \Theta) \sin\Theta \mathrm{d}\Theta \mathrm{d}z \mathrm{d}l \mathrm{d}h}{2H \int_{l_{cd}-L}^{l_{cd}} \int_{-b_p}^{b_p} i_0(z) \mathrm{e}^{-nQ(l_{cd}-l)} \mathrm{d}z \mathrm{d}l}, \tag{7}$$

where $2H$ is the height of the beam. However, in the experiment h is much larger than b_p (*i.e.* $H \sim 100\, b_p$), and the R-function is nearly independent of h over the whole region of h. Therefore, the final correction term can be given by Eq. (6). Unfortunately, n and Q are included in Eq. (6), and a calculation of the equation is intractable. If the distance l_{cd} is much larger than L, the correction term may be simplified to

$$\Delta Q(v_i) = \frac{2\pi \int_{-b_p}^{b_p} \int_0^{\pi} i_0(z) R(z, \Theta)\sigma(v_i, \Theta) \sin\Theta \mathrm{d}\Theta \mathrm{d}z}{\int_{-b_p}^{b_p} i_0(z) \mathrm{d}z}. \tag{8}$$

However, if b_p is larger than the half width of the detector w, there are some parts of the beam which do not contribute to I_0, but some atoms scattered from these parts fall on the detector. In such a case, the integral region of z in the denominators of Eqs. (6—8) should be from $-w$ to w.

The correction values can be calculated by a computer, but the calculation is troublesome. In the present case, Busch's method[6] seems to be satisfactory

11) These values will be published elsewhere.

12) The procedure to obtain $\sigma(\Theta)$ from $\sigma(\theta)$ in the center-of-mass system will be given elsewhere.

and will be used.

Experimental

Figure 2 shows a schematic drawing of the apparatus, which consists of an oven chamber, a velocity selector chamber, and a measuring chamber. A scattering chamber and a beam detector are placed in the measuring chamber. In each chamber a liquid-nitrogen cooled plate to remove the surplus beam atoms is equipped. The chambers are pumped by 4-inch oil diffusion pumps with cold traps, typical operating pressures in these chambers being about 2×10^{-7} Torr. The pressures are kept constant during an experimental run.

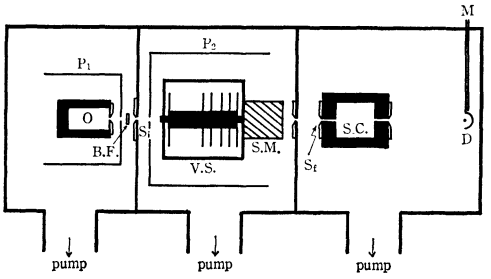

Fig. 2. Diagram of the beam apparatus. Drawing is not to scale. The labeled parts are: O, oven; B.F., beam flag; S_i, the first collimating slit; S_f, the final collimating slit; S.C., scattering chamber; D, detector; M, manipulator; $P_{1,2}$, liquid nitrogen cooled shields; V.S., velocity selector; S.M., synchronous motor.

Source. The oven is single chamber type and beam atoms effuse from a slit of 0.19 mm width. It is made of stainless steel and supported by three tungsten pins on a movable plate with dove-tails. The heater current of the oven is supplied by a DC power stabilizer. The temperature of the oven is measured by a chromel-alumel thermocouple, and the beam intensity is monitored by a surface ionization gauge in front of the source.

Velocity Selector. The velocity selector[13] is a slotted disk type. The number of disks is six and its total length L is 12.02 cm. The phase angle φ_0 is 0.2097 rad. and the velocity of the selected beams is given by

$$v = \frac{\omega L}{\varphi_0} = 360f \text{ (cm/sec)}, \tag{9}$$

where ω is the angular velocity of the rotating disks and f is the number of revolutions per second. The thickness of the disks is 3 mm, which is thicker than those used by the others.[14] However, the slits are cut obliquely along the beam path and its transmission is 47.6%. The width of the slits is 0.50 mm and the mean width of each tooth is 0.505 mm. The number of these slits or teeth is 360 per disk of diameter 12.5 cm. The length of slits in the radial direction is 5 mm. The resolution of the selector ($\Delta v/v$) is 3.96%. The selector is driven by a synchronous motor (Electronic Specialty Co. EF17H71). Power is supplied to the motor from a two-phase oscillator (NF circuit design block Co.). The number of revolutions of the selector is monitored by reflected light pulses from the disk surface painted with black stripes by a photomultiplier and a frequency counter.

13) K. Kodera and I. Kusunoki, *Oyobutsuri* (in Japanese), **38**, 20 (1969).

14) H. U. Hostettler and R. B. Bernstein, *Rev. Sci. Instrum.*, **31**, 872 (1960); S. M. Trujillo, P. K. Rol, and E. W. Rothe. *ibid.*, **33**, 841 (1962).

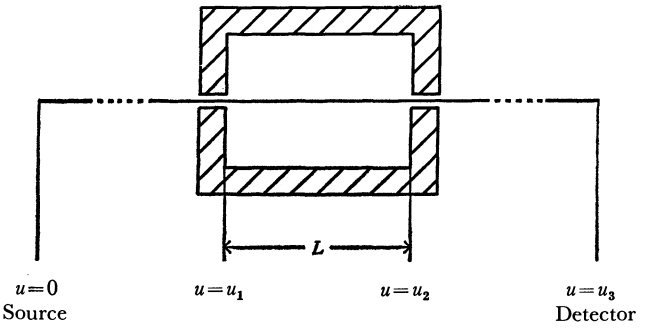

Fig. 3. Conventional scattering chamber.

Scattering Chamber. A conventional scattering chamber is shown in Fig. 3. Scattering gas in the chamber effuses out along the beam path. Thus, the effective path length L_{eff} for the beam attenuation can be given by

$$n_0 L_{eff} = \int_0^{u_1} n(u)\mathrm{d}u + n_0 L + \int_{u_2}^{u_3} n(u)\mathrm{d}u, \tag{10}$$

where n_0 is the number density of gas molecules inside the chamber, L is the inside length, and $n(u)$ is the density along the beam path. Rothe *et al.*[15] have driven an approximate formula for the estimation of L_{eff}, but a reliable estimation of $n(u)$ is not easy.

To avoid uncertainty of estimation by an approximate formula and obtain an exact value of n_0L, a chamber with a variable length, as shown in Fig. 4, is used. The chamber

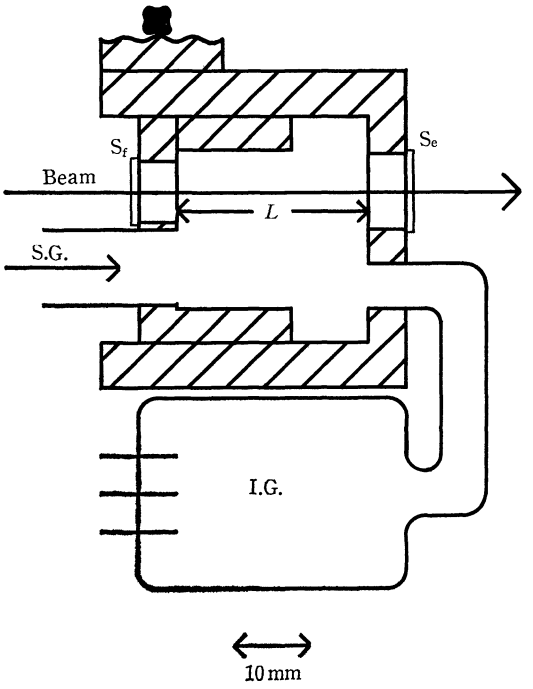

Fig. 4. Vertical cross section of the scattering chamber. S_f, entrance slit; S_e, exit slit; S.G., scattering gas; I. G., ionization gauge.

consists of two cylinders; one slides inside the other and the length of the chamber can be changed from 15 mm to 30 mm. Operation can be performed from outside the vacuum vessel. The dimensions of entrance and exit channels and slits are: channels:

15) E. W. Rothe, L. L. Marino, R. H. Neynaber, P. K. Rol, and S. M. Trujillo, *Phys. Rev.*, **126**, 598 (1962).

widths, 1.0 mm
heights, entrance 8 mm, exit 10 mm
lengths, 5.0 mm
slits:
widths, entrance 0.06 mm, exit 0.35 mm
heights, entrance 8 mm, exit 10 mm.
The entrance slit functions as a collimating slit in this beam system.

The scattering chamber is evacuated by a Hickman oil diffusion pump, and the scattering gases are introduced into the chamber from a gas reservoir through a glass capillary.

Detector. In order to detect the potassium beam, a Langumuir-Taylor surface ionization detector is used. The filament is biased by +90 V relative to the ion collector. Ion current is measured with a vibrating-reed electrometer and recorded by a two-pen recorder along with the pressure in the scattering chamber.

Angular Resolution. The distance from the source slit to the collimating slit l_{sc} is about 70 cm, and the distance from the collimating slit to the detector l_{cd} is 10.5 cm. The angle subtended by the collimating slit at the position of the source slit is 8.6×10^{-5} rad. Thus, trajectories of the atoms in the beam are almost parallel to each other. The angle subtanded by the collimating slit at the detector is 5.7×10^{-4} rad. The angle subtended by the detector at the scattering center, previously taken as a geometrical resolution, is 4.1×10^{-4} rad. The geometrical half width of the umbra of unscattered beam profile b_u is 0.02 mm, and that of the penumbra b_p is 0.049 mm. According to Kusch's criterion[5] the angular resolution determined by the beam profile is 4.0×10^{-4} rad.

Pressure Measurement. To determine the absolute cross section, the most important and the most difficult problem is to measure the absolute pressure of target gases. In the present experiment a large McLeod gauge calibrated in our laboratory by mercury weighing, is used as a standard pressure gauge. The McLeod gauge is similar to that of Rosenberg[16] and the gauge constant is 3.32×10^{-7} (*i.e.* $P=3.32\times h^2\times10^{-7}$ Torr, h in mm). With this large volume gauge the absolute pressures of the rare gases in the range of 5×10^{-5} to 5×10^{-4} Torr can easily be measured. However, it is not suitable to measure the pressure in the scattering chamber directly by the McLeod gauge, because the connecting tube between the chamber and the gauge becomes so long that a pressure gradient may arise between them, and furthermore, it can not measure the pressure continuously.

To measure the pressure of the rare gases in the scattering chamber an ionization gauge (Mitsubishi K-30) is connected directly to the scattering chamber with a short glass tube and placed in the measuring chamber. The tube is bent in order to prevent the gas from passing through it without collisions with the wall. This caution is necessary, because the temperature of the scattering gas should be equal to that of the wall anywhere in the chamber.

The sensitivities of the ionization gauge for rare gases are calibrated by the McLeod gauge described above. For calibration of the sensitivities the mercury drag effect has to be considered, because the mercury vapor stream from the McLeod gauge to the cold trap inserted between the ionization gauge and the McLeod gauge brings about an error in the absolute pressure measurement. The magnitude of the effect depends on the ambient temperature, the tubing diameter and length, the gas pressure, and the diffusion constant of the gas in mercury vapor. According to Takaishi,[17] the effect is estimated by the expression

$$\frac{P''-P'}{P'}=\frac{P_{Hg}}{P'}\left\{1-\frac{1}{B}\ln\left(\frac{P''}{P'}\right)\right\},$$

$$B=3\alpha^2\sigma^2\{m_g/(m_g+m_{Hg})\}^{1/2}rP_{Hg}/4kT \qquad (11)$$

where P' and P'' are the pressure of the gas in a McLeod gauge and that of the gas to be calibrated, respectively. P_{Hg} is a pressure of the mercury vapor at the temperature of T. $\pi\sigma^2$ is a collisional cross section between the mercury atom and a gas atom; m_g and m_{Hg} are the molecular weights of the gas and mercury, r is a radius of the connecting tube ($r=$ 0.4 cm), and α is a constant about 1.[18] To eliminate the effect completely, the cut-off position of the McLeod gauge is cooled with dry ice in order to remove the mercury vapor stream as described by Ishii and Nakayama.[4]

The sensitivities of the ionization gauge measured for rare gases are given in Table 1. The relative sensitivities are compared with the values of other authors. The present values determined by cooling the cut-off position are close to those of Rothe,[19] obtained by placing the McLeod gauge in a refrigerator to get rid of the mercury drag effect. On

Table 1. Sensitivities of ionization gauge for rare gases and relative sensitivities to argon

	X				
	He	Ne	Ar	Kr	Xe
Sensitivity, *SA*	2.87±0.06	4.80±0.07	23.6±0.5	34.1±0.8	48.5±0.4
SA_X/SA_{Ar}	0.122	0.204	1.00	1.45	2.06
Sensitivity, *SB*	2.91	5.00	26.0	40.0	59.0
SB_X/SB_{Ar}	0.112	0.192	1.00	1.54	2.27
SB_X/SA_X-1	0.01	0.04	0.10	0.17	0.22
B (at $T=295$°K)	0.023	0.055	0.097	0.145	0.190
$P''/P'-1$ (at $P'<1\times10^{-4}$ Torr)	0.02	0.05	0.10	0.16	0.21
Relative sensitivities to argon in other papers.					
Duschman and Young[19]	0.13	0.20	1.00	1.56	2.29
Rothe[20]	0.128	0.221	1.00	1.40	2.02

SA: Sensitivity calibrated by the McLeod gauge whose cut-off position is cooled with Dry Ice.
SB: Sensitivity calibrated by the McLeod gauge without consideration of the mercury drag effect.

16) P. Rosenberg, *Rev. Sci. Instrum.*, **10**, 131 (1939).
17) T. Takaishi, *Trans. Faraday Soc.*, **61**, 840 (1965).
18) Y. Sensui, private communication.
19) E. W. Rothe, *J. Vac. Sci. Technol.*, **1**, 66 (1964).

Table 2. Total cross sections at v_k = 720 m/sec

	He			Ne		Ar	Kr	Xe
Q_{eff}(Å²)	359±9			282±20		500±18	576±23	672±23
s	5	6	7	4	6	6	6	6
$Fa_0(s,x)$	1.27	1.47	1.54	1.056	1.117	1.059	1.027	1.018
Q_0	260	242	231	267	252	473±17	561±22	661±28
Q_w						505±18	602±24	714±30

the other hand, the values obtained without cooling are close to those of Dushman and Young,[20] in which no precaution against the effect has been taken. The magnitude of the effect is expressed by a factor $SB/SA-1$. As shown in Table 1, the values are in good agreement with those calculated with Takaishi's theory.

Results

The effective total cross section Q_{eff} is usually obtained by

$$I = I_0 \exp(-n_0 L_{eff} Q_{eff}) \tag{12}$$

where $n_0 L_{eff}$ is a value given by Eq. (10). If the beam attenuation is measured at different scattering lengths, the fringe effective represented by the first and third terms of Eq. (10) may be compensated, and the effective total cross section can be estimated by the equation

$$Q_{eff} = \frac{1}{L_1 - L_2}\left\{\left[\frac{\ln(I_0/I)}{n}\right]_1 - \left[\frac{\ln(I_0/I)}{n}\right]_2\right\} \tag{13}$$

where suffixes 1 and 2 refer to the values of different lengths of the scattering chamber, and L_1 and L_2 represent the inside lengths of the chamber without the channel region. During the measurement it is very difficult to change the length keeping the pressure constant, because the outgas from the wall by changing the length disturbs the pressure of the scattering chamber. A typical result is shown in Fig. 5 for the scattering of the velocity selected potassium beam (720 m/sec) by xenon with L=20, 25, and 30 mm. Using Eq. (13), Q_{eff} is estimated from the slopes of the lines as

$$Q_{eff}(720\ \text{m/sec}) = 672\ \text{Å}^2.$$

Results for all the rare gases are shown in Table 2.

The effective scattering length L_{eff} is also estimated from Fig. 5 by the equation

$$(L_i)_{eff} = \frac{1}{Q_{eff}}\left[\frac{\ln(I_0/I)}{n}\right]_i, \tag{14}$$

where Q_{eff} is a value obtained by Eq. (13). The effective scattering length obtained for various scattering gases are plotted in Fig. 6 against the geometrical length of the scattering chamber. The effective length L_{eff} is calculated for L_1=30 mm. Open circles are the values measured with the thermal beams, and solid circles are those measured with the velocity selected beams (720 m/sec). All the values fall within the range of 40.0±0.7 mm which is nearly equal to the length of the scattering chamber including channels at both ends. The value calculated by the equation

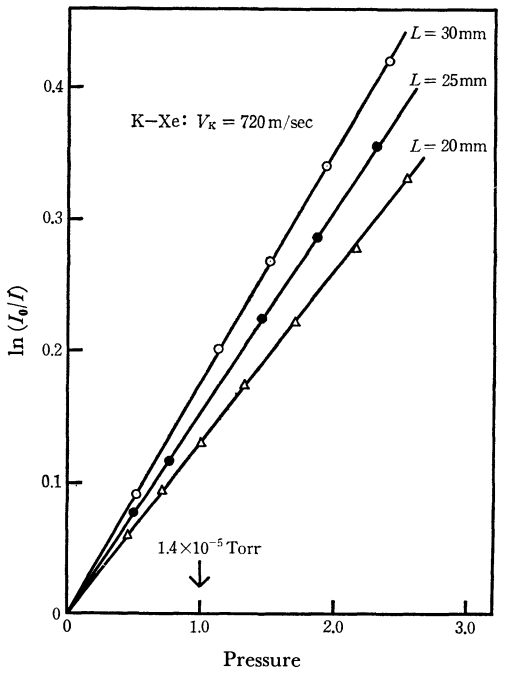

Fig. 5. Attenuation of potassium beam *vs.* pressure of xenon gas. L is the length inside the scattering chamber.

derived by Rothe *et al.*, shown by an arrow $\bar{A}$, is 38.4 mm, while $\bar{B}$ is the value calculated by the following equation derived by the author.

$$(L_i)_{eff} = \frac{l}{2}\left[1 + \frac{8Ka^2b}{8Ka^2b + 3(a+b)lc}\right] + L_i + \frac{l'}{2}\left[1 + \frac{8K'a'^2b'}{8K'a'^2b' + 3(a'+b')l'c'}\right], \tag{15}$$

where a, b, and l are the width, height, and length of the entrance channel, respectively, K its Clausing factor and c the width of the entrance slit; a', b', l', and K' are the corresponding quantities for the exit channel, and c' of the exit slit. In this case, the value of $(L_1)_{eff}$ amounts to 39.0 mm. Both of the calculated values are smaller than the experimental values, which are independent of the gaseous species and the beam velocity. Therefore, L_{eff}=40.0 mm is used in Eq. (12) to estimate Q_{eff}.

The absolute total cross section, $Q_0(v_i)$, may be obtained from $Q_{eff}(v_i)$ by means of Eq. (3). However, to estimate an accurate absolute total cross section, a correction for angular resolution has to be considered. Calculations of the correction described in the theoretical section are complicated and troublesome. In the present analysis, the Busch approximation for argon, krypton, and xenon is used because the discrepancy

20) S. Dushman, "Scientific Foundations of Vacuum Technique," John Wiley, & Sons, Inc., New York, London (1962), p. 324.

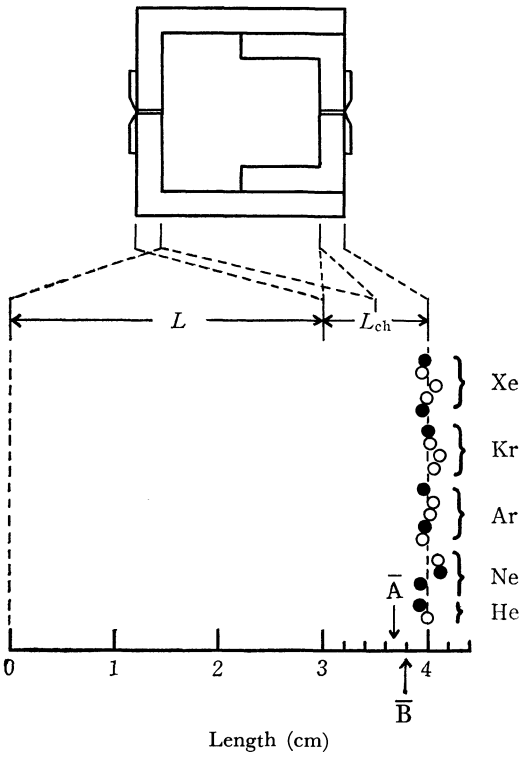

Fig. 6. Effective scattering lengths measured by rare gases. L_{ch}, length of channel region; ○, measured by thermal beam; ●, measured by the velocity selected beam.

from the exact calculation should be small. The correction factor[21] is given by

$$\frac{dQ}{Q} = 0.0765\sqrt{Q_0 k_i^2}\gamma\left(1 + \frac{0.368}{x^2}\right), \qquad (16)$$

$$\gamma = \frac{b_u + b_p}{l} \quad \text{for } w \leq b_p.$$

Then, the corrected absolute total cross section Q_w is calculated by

$$Q_w = \frac{Q_0}{(1 - dQ/Q)}. \qquad (17)$$

The correction amounts to 5-10%. In Table 2 the corrected total cross sections Q_0 and Q_w are listed for the beam velocity of 720 m/sec, which corresponds approximately to the most probable beam velocity and is obtained from 200 rps of the velocity selector. Figure 7 shows the variations in the total cross section Q_w for K–Ar, K–Kr, and K–Xe systems against the velocity of the potassium beam in a logarithmic scale. The straight lines with slopes of $-2/5$ correspond to $s=6$. For argon an agreement with $s=6$ is fairly good. The slopes of these curves for krypton and xenon are slightly steeper than $-2/5$. This means that s is smaller than 6, and between 5 and 6. This may be due to the glory effect or some unknown systematic experimental error. As the temperature of the scattering chamber is relatively high (*i.e.* room temperature), no undulation of the total cross section

21) F. Busch, H. J. Strunck, and Ch. Schlier, *Z. Physik*, **199**, 518 (1967).

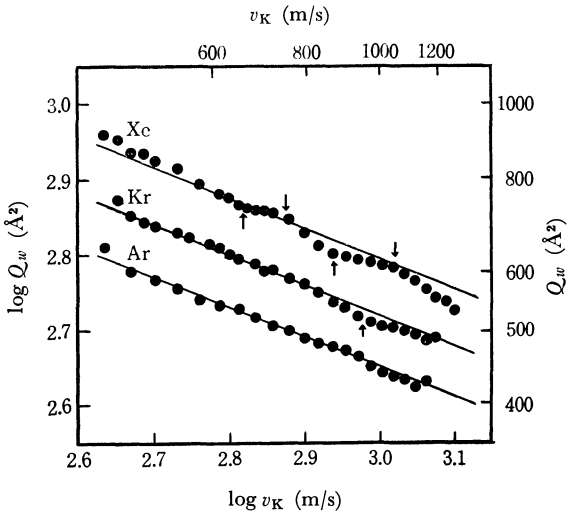

Fig. 7. log Q_w *vs.* log v_K plots for K-Ar, K-Kr, and K-Xe systems. Arrows show the positions of extrema.

is obtained for argon. However, a trace of undulation can be observed for krypton, and a more definite undulation for xenon.

For neon and helium similar treatments are not feasible, because it is not clear whether the interatomic potential can be approximated by a simple attraction with $s=6$ in the measured velocity range. For neon log Q_{eff} *vs.* log v_K plots are in Fig. 8. In this case, even after the correction with $Fa_0(6, x)$ a large discrepancy remains between the theoretical and the experimental curves. However, the values corrected with $Fa_0(4, x)$ are in fair agreement with the slope of $s=4$. The correction for angular resolution will give a less steep slope than that of the plotted values and results in a better agreement. For helium, log Q_{eff} *vs.* log v_K plot and the corrected values with $Fa_0(5, x)$, $Fa_0(6, x)$, and $Fa_0(7, x)$ are shown in Fig. 9. In this correction, factors of Fa_0 are very large, and it is not clear which correction is the best.

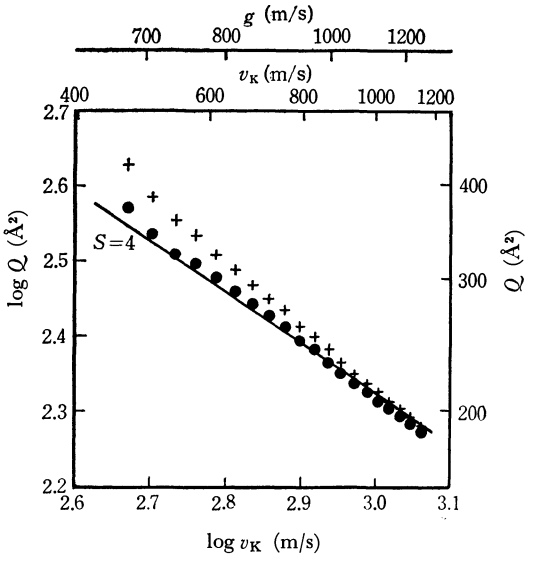

Fig. 8. log Q_{eff} and log Q_0 *vs.* log v_K plots for K-Ne system. +, data of Q_{eff}; ●, data of Q_0 corrected with $Fa_0(4, x)$.

Discussion

The relation between the total cross section and the van der Waals constant is given by

$$Q(v) = p\left[\frac{C}{\hbar v}\right]^{2/5}, \qquad (18)$$

where p is a dimensionless constant. It is 8.083 according to the SLL aproximation.

The van der Waals constants calculated from the total cross sections are listed in Table 3. C is a mean value over the measured velocities. The values of the present work are smaller than the experimental values of other authors. However, the values for argon, krypton, and xenon are in good agreement with recent theoretical values, being slightly smaller. For the K–Ar system, the discrepancies of our value with the theoretical one of Dalgarno and Davison[28] and with that of Mahan[29] are within 10%, which is within experimental uncertainty. The relative values of C for argon C_X/C_{Ar} are in good agreement with those of Dalgarno and Davison. For neon and helium, the van der Waals constants can not be derived from the experimental values of total cross sections, because in these cases interatomic interactions may not purely be those of a van der Waals nature.

From the glory undulation of the velocity dependence of the total cross section, the value of εr_m can be estimated. According to Bernstein and O'Brien,[30] the extremum condition can be given by

$$N - \frac{3}{8} = \frac{2\varepsilon r_m a_1}{\pi\hbar v_N}\left[1 - \frac{A_1\varepsilon}{a_1 E_N} + \frac{A_2\varepsilon^2}{a_1 E_N{}^2}\right], \qquad (19)$$

where $A_1=0.1625$, $A_2=0.0801$, a_1 is a known function of κ which is the curvature at the potential minimum, N is the index number of the extremum, and E_N is

Table 3. Van der Waals constants (10^{-60} erg·cm^6)

	K-Ar	K-Kr	K-Xe
Exporimental			
Florin[22]	280		740
Helbing-Pauly[23]	410		1070
Lulla *et al.*[24]	572		
Rothe-Neynaber[25]	300	500	
Brooks[26]	294		
Kusunoki[10],a)	250	340	530
present work	237	354	535
(C_{K-X}/C_{K-Ar})	(1.00)	(1.49)	(2.26)
Theoretical			
Dalgarno-Kingston[27]	267	400	648
Dalgarno-Davison[28]	260	380	600
	(1.00)	(1.46)	(2.30)
Mahan[29]	254	377	610

a) Previous values are reestimated from the total cross sections corrected with the angular resolution.

Table 4. Potential parameters obtained by various investigators

	potential	K-Kr			K-Xe			method
		εr_m 10^{-22} erg·cm	ε 10^{-14} erg	r_m Å	εr_m 10^{-22} erg·cm	ε 10^{-14} erg	r_m Å	
Beck[31]	Exp-6, for $\alpha=12$		1.24	6.0				r
Rothe *et al.*[32]	L-J (8,6)	6.88	1.30	5.29				u
Hundhausen-Pauly[33]	L-J (12,6)					1.52	9.4	r
	L-J (8,6)					1.81	7.3	
Beck-Loesch[34]	L-J (12,6)	7.62	1.3	5.85	11.9	2.5	4.75	u
	L-J (8,6)	6.83	1.5	4.55	10.7	3.0	3.6	
Busch *et al.*[21]	L-J (8,6)	6.84			10.6			u
Hollstein-Pauly[35]	L-J (12,6)	7.8			12.1			u
	L-J (8,6)	7.0			10.8			
Buck-Pauly[36]	(11,44 ; 84,6)		1.42	5.24		2.20	5.25	s. c.
Düren *et* al.[37]	9-parameters		1.45	4.84				s. c.
present work	L-J (12,6)	(8.0)	(1.7)	(4.67)	11.0	2.3	4.76	u
	L-J (8,6)	(7.2)	(1.7)	(4.13)	9.9	2.5	4.0	

r, rainbow effect, u, undulation of total cross section, s. c., semiempirical calculation.

22) H. Florin, Diplom Thesis, University of Bonn, (1964).
23) R. Helbing and H. Pauly, *Z. Physik*, **179**, 16 (1964).
24) K. Lulla, H. H. Brown, and B. Bederson, *Phys. Rev.*, **136**, A1233, (1964).
25) E. W. Rothe and R. H. Neynaber, *J. Chem. Phys.*, **42**, 3306, 4178 (1965).
26) P. R. Brooks, *Bull. Am. Phys. Soc.*, **10**, 382 (1965).
27) A. Dalgarno and A. E. Kingston, *Proc. Roy. Soc.* (London), **73**, 455 (1959).
28) A. Dalgarno and W. D. Davison, *Advan. At. Mol. Phys.*, **2**, 1 (1966).
29) G. D. Mahan, *J. Chem. Phys.*, **48**, 950 (1968).
30) R. B. Bernstein and T. J. P. O'Brien, *ibid.*, **46**, 1208 (1967).
31) D. Beck, *ibid.*, **37**, 2884 (1962).
32) E. W. Rothe, R. H. Neynaber, B. W. Scott, S. M. Trujillo, and P. K. Rol, *ibid.*, **39**, 493 (1963).
33) E. Hundhausen and H. Pauly, *Z. Physik*, **187**, 305 (1965).
34) D. Beck and H. J. Loesch, *ibid.*, **195**, 444 (1966).
35) M. Hollstein and H. Pauly, *ibid.*, **201**, 10 (1967).
36) U. Buck and H. Pauly, *ibid.*, **208**, 390 (1968).
37) R. Düren, G. P. Raabe, and Ch. Schlier, *ibid.*, **214**, 410 (1968).

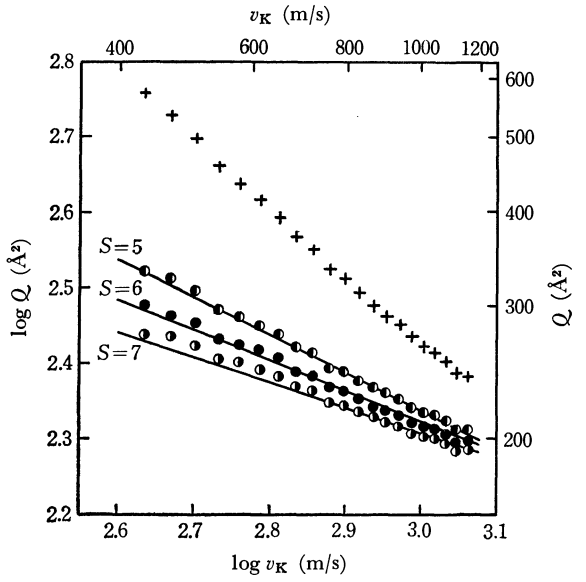

Fig. 9. $\log Q_{eff}$ and $\log Q_0$ *vs.* $\log v_K$ plots for K–He system.
◐, corrected with $Fa_0(5, x)$; ●, corrected with $Fa_0(6, x)$; ◑, corrected with $Fa_0(7, x)$; +, data of Q_{eff}.

$1/2\,\mu v_N^2$. In the present work, the velocities of a maximum and a minimum for K–Xe system are around 1040 m/sec and 870 m/sec, respectively. According to Beck and Loesch,[34] these values correspond to v_N for $N=3$ and 3.5. Thus, for the L-J(12, 6) potential the value $\varepsilon r_m = 11.0\times10^{-22}$ erg·cm is obtained. Similarly, the value $\varepsilon r_m = 8.0\times10^{-22}$ erg·cm is obtained for K–Kr system. If the L–J(8, 6) potential is assumed instead of the L–J(12,6) potential, the values εr_m are smaller than those for L–J(12, 6) potential, as shown in Table 4. However, these values may contain errors of about 10%, because the undulation is obscured by the thermal motion of target gases.

For the L–J(12, 6) potential, the van der Waals constant C is equal to $2\,\varepsilon r_m^6$. Then, if the values of εr_m are combined with the experimental values of C, ε, and r_m can be estimated separately. These values are listed in Table 4.

For the K–Ne or K–He system, the values of εr_m are unknown, but they may be smaller than 4.5×10^{-22} erg·cm for K–Ar system.[34] If the value of $\varepsilon r_m/\hbar g$ is less than 3—5, there is no extremum given by Eq. (19), and the velocity dependence of the total cross section is not represented adequately by Eq. (18).[38] In the present study, the values of $\hbar g$ for these systems are larger than 0.7×10^{-22} erg·cm. Therefore, if the value εr_m is smaller than 2.5×10^{-22} erg·cm, the above condition may be satisfied, and the velocity range will correspond to the transition range from the predominantly attractive $s=6$ to the predominantly repulsive $s=12$ ranges.

The present work was partly supported by the Toray Science Foundation. The author would like to thank Professor Kumasaburo Kodera for his valuable advice and guidance. The assistance of Mr. Atsuhiro Sakiyama during the course of the experiment is also acknowledged.

38) *Cf. e.g.*, a review by R. B. Bernstein, in "Molecular Beams" (Advances in Chemical Physics, Vol. 10), J. Ross, Ed., Interscience, New York (1966), Chap. 3.

Tritium Fractionation on the Crystal Growth of Sodium Sulfate Decahydrate from Its Tritiated Aqueous Solution

Haruhiko TANAKA* and Hisao NEGITA

Department of Chemistry, Faculty of Science, Hiroshima University, Higashi-sendamachi, Hiroshima

(Received January 25, 1971)

The fractionation of tritiated water (HTO) was examined during the crystallization of sodium sulfate decahydrate, $Na_2SO_4 \cdot 10H_2O$, from a slightly supersaturated solution which contained a trace amount of tritium. No appreciable fractionation of HTO was found to occur in the crystallization under both stirred and unstirred conditions. The factors which may influence the degree of the fractionation were generally considered in connection with the studies by deuterated water. It was suggested that virtually all of the water of crystallization in sodium sulfate decahydrate should come from free water in its aqueous solution, and should integrate into the crystal in accordance with the volume-diffusion model. This model was supported also by the energetical consideration of the sodium ion in the crystallization.

The fractionation of deuterated water in inorganic salt hydrates has previously been examined, but the results are conflict as to the phase into which deuterated water is enriched.[1-3] It seems from these studies that the enrichment of the isotope in a liquid phase occurs in some salts, while there is the reverse or no fractionation in the other salts.

Recently, it has been reported by the present authors that tritiated water (HTO) is diluted in some inorganic salt hydrates during the crystallization from their aqueous solutions.[4] In this study, it has been proposed, on the basis of the crystal growth theory and an ionic process in a solution, that HTO is diluted in any salt hydrate, or else no fractionation of the isotope occurs.

It has been reported, however, that deuterated water is slightly enriched in the crystal of sodium sulfate decahydrate, $Na_2SO_4 \cdot 10H_2O$.[1,3] In this connection, it seems interesting to examine the fractionation of HTO during the crystallization of the hydrated salt from a tritiated aqueous solution, since the results on the fractionation of HTO in copper sulfate pentahydrate and alum are parallel to that of deuterated water. In other words, HTO can be expected, according to the studies with deuterated water, to be enriched to some appreciable degree.

On the contrary, if HTO is diluted or not fractionated, the result can be explained in the same way as in our previous treatment,[4] assuming the mechanism of the crystallization of $Na_2SO_4 \cdot 10H_2O$ from its aqueous solution as well as the behavior of water molecules during the crystallization.

Experimental

The sodium sulfate decahydrate was obtained from a commercial source and was purified by filtration with fiber-free-filter papers and by recrystallization. The solvent was twice-distilled water which contained a trace amount of tritiated water. The single crystal of $Na_2SO_4 \cdot 10H_2O$ was grown from a slightly supersaturated tritiated aqueous solution at 29.65± 0.02°C by evaporating the solvent. The rate of solvent evaporation was adjusted in such a way that the relative supersaturation of the solution could be kept below *ca.* 2×10^{-3} during the crystallization.

The single crystals were thus obtained from both stirred and unstirred solutions under identical conditions unless otherwise stated. The crystal from a stirred solution was obtained by growing a seed attached to a copper wire which was rotated to give sufficient agitation.

Water from both the mother liquid and the hydrated single crystal was recovered by heating them until no further dehydration was observed under identical conditions. The tritium content in the water of crystallization was then compared with that in the corresponding mother liquid by analyzing the activity of tritium, as was described in a previous paper.[4]

Results and Discussion

The separation factor, S, of HTO for the equilibrium between solid and liquid phases has been given in a previous paper as follows:[4]

$$S = N_s/N_l, \quad (1)$$

where N_s and N_l are the mole fractions of HTO in the solid and liquid phases respectively. Table 1 gives the separation factor, S, together with the net counts per minute (cpm) coming from tritium; these counts are in proportion to N_s and N_l respectively.

TABLE 1. SEPARATION FACTOR, S, OF HTO DURING THE CRYSTALLIZATION OF $Na_2SO_4 \cdot 10H_2O$ FROM A SOLUTION AT 29.65±0.02°C

The condition of mother liq.	Net cpm of tritiated water[a]		Separation factor (S)[b]
	Mother liq. (N_l)	Crystal (N_s)	
Unstirred	31535±146	31615±132	1.003±0.005
Stirred	33260±127	33273± 87	1.000±0.004

a) Each sample water was 0.1 g, and its cpm was measured using a counter of 35% efficiency.
b) The accuracy of the value of S is indicated in terms of the probable error.

It may be seen from Table 1 that no practical fractionation of HTO occurs during the crystallization of $Na_2SO_4 \cdot 10H_2O$ from either the stirred or the unstirred solution.

Relation between the Present Data and Those of Other Workers. The data so far determined on the frac-

* Present address: Shinonome Branch School, Faculty of Education, Hiroshima University, Shinonome, Hiroshima.

1) M. Johansson and K. E. Holmberg, *Acta Chem. Scand.*, **23**, 765 (1969).
2) R. M. Barrer and A. F. Denny, *J. Chem. Soc.*, **1964**, 4677.
3) E. Uusitalo, *Suomen Kemistilehti*, **B31**, 362 (1958).
4) H. Tanaka and H. Negita, This Bulletin, **43**, 3079 (1970).

tionation of heavy water in $Na_2SO_4 \cdot 10H_2O$ are reproduced in Table 2.

Table 2. Fractionation of heavy water on crystallization of $Na_2SO_4 \cdot 10H_2O$ from a solution

Heavy water (mol%)	Temp. of crystn. (°C)	Rate of crystn.	Separation factor (S)
D_2O (10)	26.5—25.5	Rapid	1.014[a]
D_2O (0.1, 1.0)	4, 25	Slow	1.001, 1.002[b]
HTO ($\sim 10^{-7}$)	29.65	Very slow	1.000, 1.003

a), b) Taken from Refs. 1 and 3 respectively.

Our results are in good agreement with those of Uusitalo,[3] but are discordant with the results of Johansson and Holmberg.[1] In the study of Johansson and Holmberg, however, a large amount of the crystal was grown from a 200-m*l* solution by cooling the solution at a rather rapid rate. Moreover, as the mother liquid a solution containing about 10 mole% of D_2O was used. These experimental conditions may allow an increasing ambiguity in the results or give results discordant with ours, as may be expected from the following considerations:

(1) It seems in general that the separation factor should be sensitive to the temperature of crystallization.[5]

(2) There is an increasing inclusion of the mother liquid into the growing crystal in the case of crystallization from a highly supersaturated solution.

(3) In the case of the fractionation of the isotope in the crystal, the mother liquid is subject to a reverse isotope effect.[6]

(4) When the mother liquid contains as much as 10 mole% of D_2O of heavy water, its behavior should be different from that of the liquid which is not enriched in D_2O. This situation will in turn complicate the problem.

Accordingly, it seems that each result listed in Table 2 is correct under the corresponding experimental conditions, although there may be some ambiguity unless the experimental conditions are strictly controlled. It will be worthwhile to use the present data of the fractionation of HTO in understanding the process of the crystal growth of $Na_2SO_4 \cdot 10H_2O$.

Estimation of the Fraction of Free Water Molecules in the Solution. A number of studies have been made of the determination of the hydration numbers of the Na^+ ion; the results so far reported vary depending upon the methods of determination. It is assumed in the present case that the Na^+ ion is surrounded, on the average, by four water molecules.[7]

The lifetime of the hydrated species has been found to be extremely short at room temperature, *i.e.*, *ca.* 10^{-9} sec, as evidenced by the relaxation technique.[8] Neglecting the hydration of the sulfate ion in the concentrated aqueous solution of Na_2SO_4,[9] it can be assumed that Na^+ and SO_4^{2-} ions enter the crystal practically independently of the water as well as of its isotopic concentration. The relaxation time of the Na^+ ion for entering into the crystal, τ, is expressed as follows:

$$\tau = (\boldsymbol{h}/\boldsymbol{k}T) \exp(E/\boldsymbol{k}T), \quad (1)$$

where

$\boldsymbol{h}$=Planck's constant,
$\boldsymbol{k}$=the Boltzmann constant,
T=the absolute temperature, and
E=the activation energy of the cation for entering into the crystal from a solution, the minimum value of which has been assessed by Bennema to be *ca.* 10 kcal/mol.[10]

Accordingly, τ is estimated to be larger than *ca.* $10^{-5.5}$ sec at around room temperature. It follows that any water molecule in the vicinity of the Na^+ ion can reside in its hydration sphere only for an instant when the cation is fixed into the crystal.

Although intimate ion pairs may result at a high concentration of the Na_2SO_4 aqueous solution,[11] the lifetime of the species is also found to be very short, making it possible to treat it as separated ions. Moreover, it has been suggested by Samoilov that the Na^+ ion should migrate in the solution with almost no relation to the water in the vicinity.[9] It follows from the preceding argument that the water of crystallization in $Na_2SO_4 \cdot 10H_2O$ should practically result from free water molecules in the solution; that is, the species of the growth unit should be Na^+, SO_4^{2-}, and H_2O.

Calculation of Separation Factor in the Case of the Crystal Growth by a Surface-diffusion Mechanism. It has been reported in a previous paper that the separation factor, S, can be calculated on the basis of the ionic process in a solution and on the basis of the crystal-growth theory from a solution.[4] In the case of the crystal growth by a surface-diffusion mechanism, the rate of integration of a free water molecule into the crystal has been given by:

$$R = \alpha \Omega N_0 (\boldsymbol{k}T/2\pi m)^{1/2} (\sigma^2/\sigma_1) \tanh(\sigma_1/\sigma) \quad (2)$$

where

α=the correction factor,
Ω=the volume of a growth unit in the crystal,
N_0=the equilibrium concentration of growth units per cm^3 in the solution,
m=the mass of a growth unit,
σ=the relative supersaturation, and
σ_1=the parameter.

In exactly the same manner as before, the R_{HTO}/R_{H_2O} ratio is obtained in the case of the crystal growth with an essential process of a surface diffusion of growth

5) Very recently it has been found by the present authors that the separation factor is considerably influenced by the temperature in the case of the crystallization of alum from a solution. This finding will be presented in detail elsewhere.

6) In the present crystaplization, only *ca.* 1.5—2 g of the salt hydrate were obtained from a large amount of the mother liquid (*ca.* 800 g); thus, it may be possible to disregard this effect.

7) H. G. Hertz, *Angew. Chem. Int. Ed. Engl.*, **9**, 124 (1970).

8) F. Basalo and R. G. Pearson, "Mechanisms of Inorganic Reactions," John Wiley & Sons, Inc., New York (1967), Chap. 3.

9) O. Ya. Samoilov, "Structure of Aqueous Electrolyte Solutions and the Hydration of Ions," Consultants Bureau Enterprises, Inc., New York (1965), Chap. 5.

10) P. Bennema, Thesis, The Technical University of Delft (1965).

11) D. R. Rosseinsky, *J. Chem. Soc.*, **1962**, 785.

units as follows:

$$R_{HTO}/R_{H_2O} = 0.949, \quad (3)$$

where R_{HTO}/R_{H_2O} is the ratio of the integration of HTO into the crystal to that of H_2O molecules. Accordingly, the separation factor, S, in $Na_2SO_4 \cdot 10H_2O$ in the case of the surface-diffusion model can be simply calculated to be 0.949, since all of the water molecules of crystallization in $Na_2SO_4 \cdot 10H_2O$ can reasonably be assumed to result from free water in the solution, as has been described above. The preceding argument thus allows us to expect a considerable dilution of HTO in the crystal if the crystal grows by the surface-diffusion mechanism.

Calculation of Separation Factor on the Basis of a Volume-diffusion Mechanism of the Crystal Growth. If we adopt a volume-diffusion model for the growth from a solution in which a growth unit is directly transported from the solution to the kink without any surface diffusion,[10,12] the rate of the crystal growth is given by:

$$R = \{2\pi\lambda\varepsilon\beta D N_0 \Omega \boldsymbol{k}T/19\gamma a x_0)\}\sigma^2, \quad (4)$$

where

λ=the mean distance between one equilibrium position and a neighboring one in the solution,
ε=the measure of the interacting spirals,
β=the retarding factor,
D=the volume-diffusion constant,
γ=the edge free energy of a step with the length of a,
a=the shortest distance between growth units, and
x_0=the mean distance between the kinks.

It follows from Eq. (4) that the R_{HTO}/R_{H_2O} ratio is equal to the D_{HTO}/D_{H_2O} ratio, where D_{HTO}/D_{H_2O} is the ratio of the diffusion constants of HTO to H_2O molecules in a solution. When the crystal is grown from a well-stirred solution, the D_{HTO}/D_{H_2O} ratio becomes unity, giving no fractionation of HTO during the crystallization of $Na_2SO_4 \cdot 10H_2O$. In the case of the crystallization from an unstirred solution, the R_{HTO}/R_{H_2O} ratio can also be given by unity, since the value of D seems to be practically independent of the hydrogen isotope of the water molecules.[9]

Accordingly, it follows that no practical fractionation of HTO can be expected to occur during the crystallization of $Na_2SO_4 \cdot 10H_2O$ from either a stirred or an unstirred solution. It should be noted here that the calculation of the value of S on the basis of the volume-diffusion model leads to a satisfactory agreement with the present experimental results. That is, this argument implies that the crystal of $Na_2SO_4 \cdot 10H_2O$ grows by the volume-diffusion mechanism. This implication seems quite interesting in that the volume-diffusion mechanism has been proved for the first time to play an essential role in the crystallization of $Na_2SO_4 \cdot 10H_2O$, although the mechanism was proposed a long time ago and has been discussed generally from a theoretical point of view.[12-14]

The Relation between the Possible Volume-diffusion Mechanism and the Treatment by Bennema. According to Bennema,[12] the mean displacement of a growth unit on the crystal surface, x_s, is given by:

$$x_s = a \exp\{(E_{deads} - E_{sdiff})/2\boldsymbol{k}T\} \quad (5)$$

where a is the shortest distance between neighboring growth units in the crystal, where E_{deads} is the activation free energy for leaving the surface, and where E_{sdiff} is the activation free energy for making a diffusion jump from one equilibrium position to a neighboring one on the surface. The volume-diffusion mechanism can be assumed to play an essential role in the growth of ionic crystals when $a \gtrsim x_s$, *i.e.*, $E_{sdiff} \gtrsim E_{deads}$, since growth units come practically to enter the crystal without any surface diffusion in this case.

The $E_{sdiff} \gtrsim E_{deads}$ condition can be met if the concept of Samoilov as to the hydration of the Na^+ ion is adopted.[9] That is, the transfer of the ion practically without any hydration water in a solution leads to a considerable decrease in the dehydration activation free energy for entering into the surface, E_{deh}, and thus to much smaller values of E_{deads}. It is reasonable to assume, in this case, that E_{deh} should be replaced by the activation free energy of the ion for a diffusion jump in a solution, E_a.

It can be estimated that E_{deads} is equal to 4.2 kcal/mol or somewhat greater, and that E_{sdiff} ranges between 5 and 10 kcal/mol.[10] Accordingly, the possible energy diagram of the growth unit (Na^+ ion) can be given as in Fig. 1.

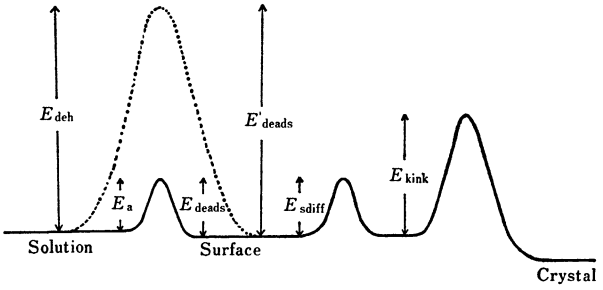

Fig. 1. The proposed energy diagram of Na^+ ion for entering into the crystal of $Na_2SO_4 \cdot 10H_2O$ from its aqueous solution.

In Fig. 1, E'_{deads} is the activation free energy for the Na^+ ion to leave the surface, which is needed if the ion must be dehydrated before entering into the surface (the curve is shown by a dotted line). This model has been adopted by Bennema in discussing the growth of some ionic crystals from their aqueous solutions.[10] Although the energetical consideration is rather ambiguous at this state, it can at least be stressed that the value of E_{deh} is as large as 10—30 kcal/mol, while the value of E_a is only *ca.* 4.2 kcal/mol.[10]

It can be concluded from the preceding discussion that the crystal growth of $Na_2SO_4 \cdot 10H_2O$ from its aqueous solution probably occurs by the volume-diffusion mechanism.

The authors wish to express their thanks to Dr. O. Yamamoto for his help in measuring the activity of tritium.

12) P. Bennema, *J. Cryst. Growth*, **5**, 29 (1969).
13) W. K. Burton, N. Cabrera, and F. C. Frank, *Phil. Trans. Roy. Soc.*, **A243**, 299 (1951).
14) A. A. Chernov, *Soviet Phys. Usp.*, **4**, 116 (1961).

Studies on the Interaction between Long Chain Alcohols and Alkyl Sulfates. I. Molecular Association between Long Chain Alcohols and Corresponding Alkyl Sulfates

Yoshikiyo Moroi, Kinshi Motomura, and Ryohei Matuura
Department of Chemistry, Faculty of Science, Kyushu University, Fukuoka

(Received January 28, 1971)

Molecular interaction between long chain alcohols and corresponding alkyl sulfates, such as dodecyl alcohol-sodium dodecyl sulfate, tetradecyl alcohol-sodium tetradecyl sulfate and hexadecyl alcohol-sodium hexadecyl sulfate, was studied by measurement of heat of complex formation, differential thermal analysis and infrared spectroscopy. It was found that there were two kinds of complexes, I and II, differing in the composition of alcohols and corresponding sulfates. The former is stable at temperatures below the melting point of alcohol, the molar ratio of alcohol to sulfate being 0.53—0.63. The latter is stable at temperatures above the melting point of alcohol, its molar ratio being 1.0. The heat of formation of II is 7—8 kcal/mol, which suggests that the complex is formed by a force similar to hydrogen bonding between alcohols and sulfates. The peak temperature in the DTA curve due to decomposition of the complex is about 10°C lower in I than in II and the characteristic absorption bands in IR spectrum are 3480 cm^{-1} and 3520 cm^{-1} in I and II, respectively, which correspond to hydrogen bond between two components.

The properties of solutions of the alkyl sulfates have been investigated in detail, but not those of their solids. The interaction of the pure substance with other compounds has been investigated only scantily.

It is well known that a detergent such as alkyl sulfate is used as a stabilizer of the water-in-oil emulsion and its stabilizing power is increased in the presence of polar long chain compounds such as alcohol, cholesterol, *etc.* Schulman and Rideal, and Goddard and Schulman reported on the molecular interaction between polar long chain compounds studied from the monomolecular films of long chain alcohols. They concluded that the film stabilization is caused by a phenomenon called "penetration."[1,2] Maruta *et al.* and Maruta and Tokiwa investigated the adducts separated from the dilute solution of dodecyl alcohol-sodium dodecyl sulfate in the presence of polyelectrolyte and showed that the molar ratio of such adduct is 2 in terms of the ratio of alcohol to sulfate.[3-6] Kung and Goddard investigated the interaction between a long chain alcohol and an alkyl sulfate in a bulk phase and recognized the molecular complex between them, molar ratio of which is 0.5.[7-10] Epstein *et al.* made the same studies with systems, dodecyl or tetradecyl alcohol-dodecyl or tetradecyl sulfate-water and recognized two kinds of adducts whose molar ratios are 0.5 and 1 in terms of the ratio of alcohol to sulfate.[11,12]

We found the results of these studies to be unconvincing and leading to no definite conclusion. In order to obtain improved results we investigated the molecular interaction between alcohols and sulfates by thermal, spectroscopic, and statistical thermodynamical methods.

The following abbreviations are used.

DOH, TOH, HOH: Dodecyl, Tetradecyl, and Hexadecyl alcohol, respectively

SDS, STS, SHS: Sodium Dodecyl, Sodium Tetradecyl, and Sodium Hexadecyl Sulfate, respectively

DTA: Differential Thermal Analysis

IR: Infrared Spectroscopy

Experimental

Materials. DOH, TOH, and HOH were purified by fractional distillation at reduced pressure. Purity was checked by melting point measurement and DTA curves which were identical with those in literature.

SDS, STS, and SHS were prepared from the corresponding alcohols and chlorosulfonic acid and by esterification with subsequent neutralization with sodium hydroxide. They were purified by repeated crystallization from ethanol and water, and then by elimination of a small amount of alcohols by heating at about 100°C under reduced pressure for more than ten hours. The purified SDS, STS, and SHS showed only one endothermic peak at 104, 118, and 124°C on DTA curves, respectively, without any endothermic peak of the melting of alcohol. The CMC values were 8.13×10^{-3} mol/l at 25°C, 2.5×10^{-3} mol/l at 40°C, and 6.2×10^{-4} mol/l at 40°C for SDS, STS, and SHS, respectively.

The specimens of mixtures of alcohols and sulfates used for DTA and IR measurements were prepared by the following two methods. a) Melt method. Weighed amounts of alcohols and sulfates were ground in a mortar and then kept at about 30, 45, and 55°C for dodecyl, tetradecyl, and hexadecyl compounds, respectively. b) Crystallization method. Weighed amounts of alcohols and sulfates were dissolved in ethanol and the solvent was eliminated by vaporization at temperatures 0—5°C. In both methods, the speci-

1) J. H. Schulamn and E. K. Rideal, *Proc. Roy. Soc.* (London), **B122**, 29 (1937).
2) E. D. Goddard and J. H. Schulman, *J. Colloid Sci.*, **8**, 309, 329 (1953).
3) I. Maruta, T. Sakai, F. Tokiwa, and T. Saito, *Nippon Kagaku Zasshi*, **82**, 1512 (1961).
4) I. Maruta and F. Tokiwa, *ibid.*, **82**, 1658 (1961).
5) I. Maruta and F. Tokiwa, *ibid.*, **82**, 1660 (1961).
6) I. Maruta and F. Tokiwa, *ibid.*, **83**, 732 (1962).
7) H. C. Kung and E. D. Goddard, *J. Phys. Chem.*, **67**, 1965 (1963).
8) H. C. Kung and E. D. Goddard, *ibid.*, **68**, 3465 (1964).
9) H. C. Kung and E. D. Goddard, *Proc. IVth Intern. Congr. Surface Active Substances, Brussels*, 751 (1964).
10) H. C. Kung and E. D. Goddard, *J. Colloid Sci.*, **20**, 766 (1965).
11) M. B. Epstein, A. Wilson, C. W. Jakob, L. E. Conroy, and J. Ross, *J. Phys. Chem.*, **58**, 860 (1954).
12) M. B. Epstein, A. Wilson, J. Gershman, and J. Ross, *ibid.*, **60**, 1051 (1956).

mens were kept above or below the melting points of alcohols.

Methods. The apparatus for the measurement of the heat of complex formation is shown in Fig. 1. Weighed amounts of ground sulfates were dropped into alcohols in a Dewer bottle which was inserted in a thermally controlled water bath at 35, 45, and 55°C for SDS, STS, and SHS, respectively. The heat evolved was estimated from the temperature rise of the system due to mixing, using a thermocouple. Each measurement was performed at least three times.

The DTA apparatus is characterized by a copper block and two pen recorders, one indicating the temperature of the specimen and the other the temperature difference between specimen and reference substance (Al_2O_3). The heating rate was about 3°C/min. The sample weight was about 25 mg. The specimen was cooled to 0, 12, and 25°C for SDS, STS, and SHS, respectively, before heating.

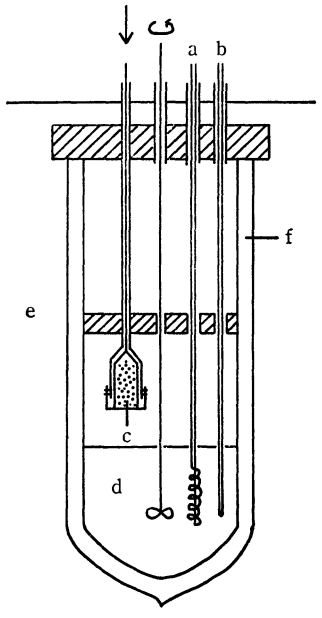

Fig. 1. Apparatus used for measurement of heat of complex formation.
(a) heater, (b) thermocouple, (c) sulfate,
(d) alcohol, (e) water bath, (f) Dewar bottle

The ratio of alcohol to sulfate in the complex was determined as follows. Since the thermal conductivity and packing of a specimen had a large effect on the DTA curve, a definite condition was necessary to calculate the amount of alcohol and complex from the peak area of the DTA curve. Only a specimen with a 1.5 ratio of alcohol to sulfate was used for determining the composition of the complex. The specific area of the alcohol of the above system was determined by subtracting the peak area of a weighed amount of specimen from the peak area of a weighed amount of specimen containing some extra alcohol, and then dividing the area difference by the amount of the added alcohol. The sulfate in the specimen should be completely changed to a complex on account of the large amount of peak area of excess alcohol. Under these conditions, the ratio of alcohol to sulfate in a complex could be determined.

The IR apparatus used was a 225-Hitachi grating infrared spectrophotometer. The specimens for IR were the same as those for DTA and were dispersed as a mull in chlorohexabutadiene. When IR measurements were carried out below melting point of alcohols, the cell holder was cooled by dry ice to a temperature just above dew point.

Results and Discussion

Heat of Complex Formation. The heat of complex formation is shown in Table 1. For comparison, ΔH of $C_{10}H_{21}OH$-SDS was measured and it was found to be nearly equal to 0, which indicates that the heat of mixing of alcohol and sulfate is negligible. Hence it can be said that ΔH's for the other three systems are heat of reaction. We assume that alcohols and sulfates make a complex in a solid state and that lattice sites in a complex are occupied by molecules of alcohol and sulfate.

Table 1. Heat of complex formation

System	Temp. (°C)	ΔH (kcal/mol-sulfate)
DOH-SDS	35.0	−7.35±0.3
TOH-STS	45.0	−7.83±0.4
HOH-SHS	55.0	−8.23±0.4
$C_{10}H_{21}OH$-SDS	35.0	0

DTA and IR. Many kinds of specimens were investigated by DTA and IR technique. Typical examples are shown in Figs. 2—4. The difference between results obtained by the melt and crystallization methods is almost negligible. DTA curves are composed of four endothermic peaks, which can be as-

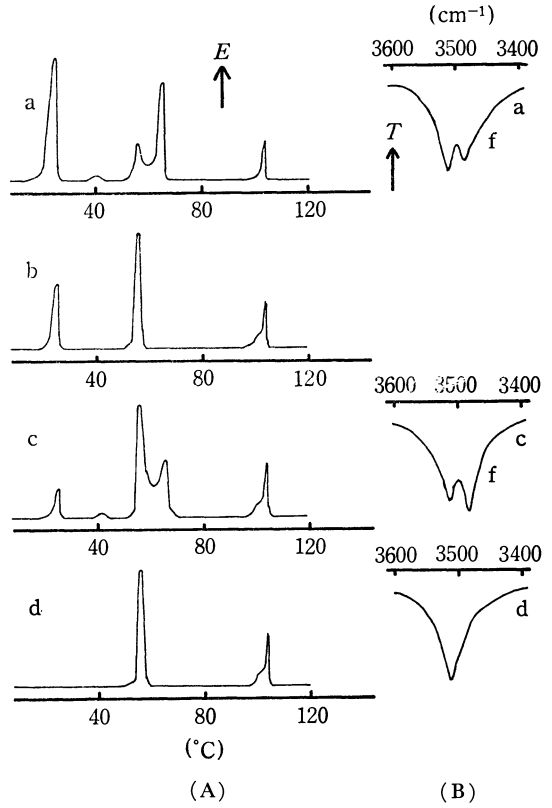

Fig. 2. DTA curves (A) and infrared spectra (B) of DOH-SDS system. Molar ratio of DOH to SDS:
(a), 1.5; (b), 1.0: (c), 0.67; (d), 0.5.
E: endothermic
T: transmittance
f: below melting point of DOH

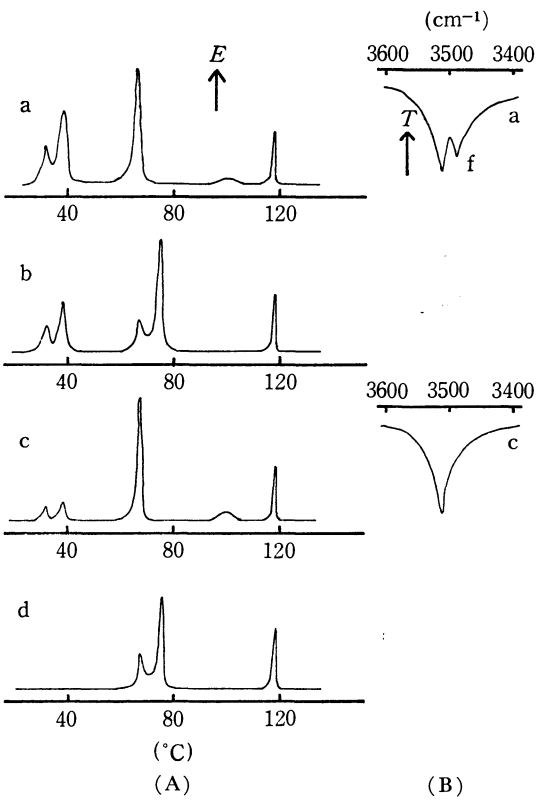

Fig. 3. DTA curves (A) and infrared spectra (B) of TOH-STS system. Molar ratio of TOH to STS: (a), 1.5; (b), 1.0; (c), 0.67; (d), 0.5.
E: endothermic
T: transmittance
f: below melting point of TOH

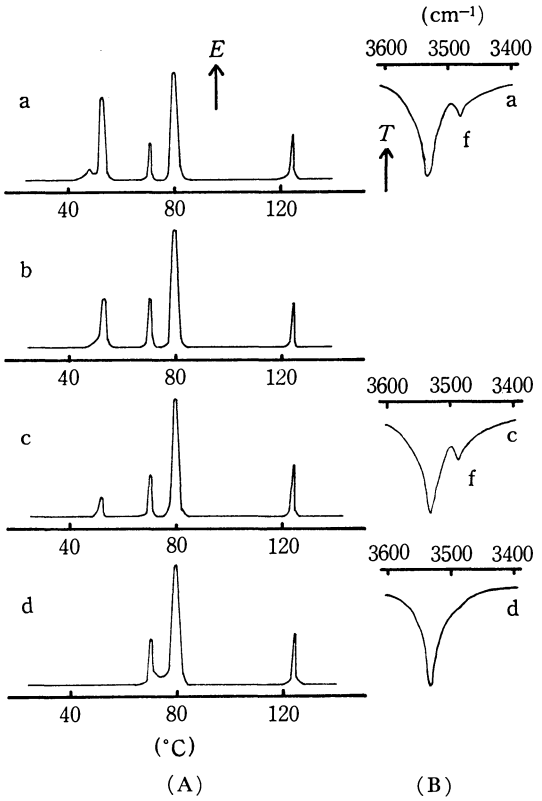

Fig. 4. DTA curves (A) and infrared spectra (B) of HOH-SHS system. Molar ratio of HOH to SHS: (a), 1.5; (b), 1.0; (c), 0.67; (d), 0.5.
E: endothermic
T: transmittance
f: below melting point of HOH

signed to melting of alcohol, decomposition of complex I, decomposition of complex II, and transformation of sulfate from a low temperature to a high temperature type. An endothermic peak due to the melting of alcohol decreases with the decrease of the ratio of alcohol to sulfate. There are two kinds of endothermic peaks due to the decomposition of the complex. One is due to the decomposition of complex I which is obtained by keeping specimens below melting point of alcohol for more than ten days. The other is due to the decomposition of complex II which is obtained by keeping the specimens above melting point of alcohol. There should be an endothermic peak due to transition of complex I to complex II in a DTA curve, but no such peak appeared. This can be attributed to the very long time required for the transition. Specimens often show two endothermic peaks, which indicates that II has not completely been transformed into I. The molar peak area of alcohol on decomposition is a little larger in I than in II. This means that alcohol is more strongly bonded to sulfate in I than in II.

The ratio of alcohol to sulfate were 0.53—0.63 and 1.0 for I and II, respectively, according to the method of composition determination mentioned above. Kung and Goddard determined the composition of this complex from the ratio at which the endothermic peak of alcohol disappeared.[7,8] This seems to be wrong, since a part of II whose molar ratio of alcohol to sulfate is 1.0 releases alcohol to turn into I whose molar ratio is 0.53—0.63, when II is cooled below the melting point of alcohol, as is shown by DTA measurement. Details of differential thermograms of three kinds of systems are summarized in Table 2.

Table 2. Results of DTA and IR

System	Complex	Decomposition temp. (°C)	Absorption band (cm^{-1})	Molar ratio of alcohol to sulfate
DOH-SDS	I	56—57	3479—3485	0.53—0.63
	II	65—66	3510—3515	1
TOH-STS	I	66—67	3479—3485	0.53—0.63
	II	74—75	3515—3520	1
HOH-SHS	I	69—70	3479—3485	0.53—0.63
	II	79—80	3530—3533	1

Spectra in the hydroxyl band stretching region are shown in Figs. 2—4. There are two kinds of absorption bands which belong to I and II, namely the bands near 3480 and 3520 cm^{-1} due to I and II, respectively. However, when the specimen is not cooled to a temperature below melting point of alcohol, only one absorption band near 3520 cm^{-1} appears. This indicates that I is completely transformed into II by the heat of IR ray. On the other hand, specimens kept below melting point of alcohol showed two kinds of absorption bands. In the case of system HOH-SHS

whose complex II can not be easily transformed into complex I due to high melting point of alcohol, the band of I appeared only as a shoulder in a absorption band of II. Goddard *et al.* could find only one absorption band near 3520 cm^{-1} due to II and insisted on the presence of only one kind of complex.[8] Details of infrared spectra of three systems of alcohol and sulfate are shown in Table 2.

Statistical Thermodynamical Consideration. It is enlightening to consider complex formation from the viewpoint of statistical thermodynamics. The main object of this consideration is to show why the molar ratio of alcohol to sulfate in a complex below melting point of alcohol is 0.53—0.63 and that above melting point of alcohol is 1.0. We denote alcohol and sulfate by A and B, respectively, and consider a binary mixture containing Nr molecules of alcohol and N molecules of sulfate on a lattice of $N(1+r)$ sites with a coordination number Z. Since each molecule has Z closest neighbours, there are in all $NZ(1+r)/2$ pairs of closest neighbours, the pairs being three kinds such as A–A, B–B, and A–B. We denote the energy per pair by $-2X/Z$ and assume complete randomness in placing the molecules on sites. It is also assumed that alcohol and sulfate are so similar in size and shape that they are interchangeable on a lattice. Then we can construct Table 3 for the number of pairs and related

Table 3. Number of pairs and certain related quantities

Kind of pair	Number of pairs	Energy per pair	Energy of all such pairs
A-A	$NZ\frac{r^2}{2(1+r)}$	$-2X'_{A-A}/Z$	$-NX'_{A-A}\frac{r^2}{1+r}$
A-B	$NZ\frac{r}{1+r}$	$-2X'_{A-B}/Z$	$-NX'_{A-B}\frac{2r}{1+r}$
B-B	$NZ\frac{1}{2(1+r)}$	$-2X'_{B-B}/Z$	$-NX'_{B-B}\frac{1}{1+r}$
All	$NZ\frac{1+r}{2}$		$-\frac{N}{1+r}(r^2X'_{A-A}+2rX'_{A-B}+X'_{B-B})=E_c$

quantities. The prime in Table 3 refers to the newly obtained complex, E_c being the configurational energy. According to definition, the configurational partition function Ω is given by

$$\Omega = \sum \exp(-E_c/\boldsymbol{k}T), \tag{1}$$

where the summation extends over the $\{N(1+r)\}!/N!(Nr)!$ distinguishable configurations. Thus we have

$$\Omega = \frac{\{N(1+r)\}!}{N!(Nr)!}\exp(-E_c/\boldsymbol{k}T). \tag{2}$$

Hence the configurational free energy F_c is given by

$$\begin{aligned} F_c &= -\boldsymbol{k}T\ln\Omega \\ &= -\frac{N}{1+r}(r^2X'_{A-A}+2rX'_{A-B}+X'_{B-B}) \\ &\quad + N\boldsymbol{k}T\{r\ln r-(1+r)\ln(1+r)\}. \end{aligned} \tag{3}$$

As configurational free energies of pure substances containing the same number of molecules are $-Nr$-X_{A-A} and $-XN_{B-B}$, the molar free energy of mixing of sulfate is given by

$$\begin{aligned} \Delta F_m &= -\frac{\boldsymbol{N}}{1+r}(r^2X'_{A-A}+2rX'_{A-B}+X'_{B-B}) + \boldsymbol{N}r\boldsymbol{X}_{A-A} \\ &\quad + \boldsymbol{N}X_{B-B} + \boldsymbol{R}T\{r\ln r-(1+r)\ln(1+r)\}, \end{aligned} \tag{4}$$

where $\boldsymbol{N}$ is Avogadro's number.

Concerning liquid or solid phase, we can, without serious error, replace internal energy and Helmholtz free energy by enthalpy and Gibbs free energy, respectively. Consequently the molar enthalpy of mixing of sulfate is given by

$$\begin{aligned} \Delta H_m &= -\frac{\boldsymbol{N}}{1+r}(r^2X'_{A-A}+2rX'_{A-B}+X'_{B-B}) \\ &\quad + \boldsymbol{N}r\boldsymbol{X}_{A-A} + \boldsymbol{N}X_{B-B}, \end{aligned} \tag{5}$$

where we assume that the temperature changes of X'_{A-A}, X'_{A-B}, X'_{B-B}, and X_{B-B} are negligible, which is permissible over the temperature range 20—60°C, *i.e.*, our experimental temperature range.

First, when $r=0$, we obtain the equation

$$\Delta H_m = -\boldsymbol{N}X'_{B-B} + \boldsymbol{N}X_{B-B} \equiv \Delta H_0. \tag{6}$$

The new parameter ΔH_0 is hypothetically equivalent to the transition enthalpy evolved when a sulfate is transformed into complex whose lattice sites are all occupied by sulfate molecules.

Second, when $r=1$, ΔH is given by

$$\begin{aligned} \Delta H &= -\frac{\boldsymbol{N}}{2}(X'_{A-A}+2X'_{A-B}+X'_{B-B}) \\ &\quad + \boldsymbol{N}X^1_{A-A} + \boldsymbol{N}X_{B-B} \end{aligned} \tag{7}$$

where X^1_{A-A} is the X_{A-A} of liquid alcohol and ΔH is equal to the heat of complex formation measured above melting point of alcohol, because the molar ratio of alcohol to sulfate in the complex is 1.0.

Substituting Eqs. (6) and (7) into Eq. (4) we obtain for the temperature below melting point of alcohol

$$\begin{aligned} \Delta G_m &= \frac{r-r^2}{1+r}\boldsymbol{N}X'_{A-A} + \frac{1-r}{1+r}\Delta H_0 \\ &\quad + (2\Delta H-2\boldsymbol{N}X^1_{A-A})\frac{r}{1+r} + \boldsymbol{N}r\boldsymbol{X}_{A-A} \\ &\quad + \boldsymbol{R}T\{r\ln r-(1+r)\ln(1+r)\}, \end{aligned} \tag{8}$$

and for the temperature above melting point of alcohol

$$\begin{aligned} \Delta G^1_m &= \frac{r-r^2}{1+r}\boldsymbol{N}X'_{A-A} + \frac{1-r}{1+r}\Delta H_0 \\ &\quad + (2\Delta H-2\boldsymbol{N}X^1_{A-A})\frac{r}{1+r} + \boldsymbol{N}rX^1_{A-A} \\ &\quad + \boldsymbol{R}T\{r\ln r-(1+r)\ln(1+r)\}. \end{aligned} \tag{9}$$

It is reasonable for $\boldsymbol{N}X^1_{A-A}$ to be replaced by molar heat of vaporization, since X is the energy for a molecule to part from the lattice site to an infinite separation. Similarly we can calculate $\boldsymbol{N}X_{A-A}$, using the specific heat capacity of alcohol equal to 0.36 cal/g measured for three kinds of alcohols and assuming that alcohol gas is ideal.

Thus, we get Table 4 for the three kinds of systems.

We calculated the minimum values of ΔG_m and r which made ΔG_m minimum, substituting seven values of -1, 0, 1, 2, 3, 4, 5 kcal/mol and 12, 13, 14, 15, 16,

Table 4. Values of NX_{A-A} and $NX^1{}_{A-A}$

System	Temp. (°C)	NX_{A-A} (kcal/mol)	$NX^1{}_{A-A}$ (kcal/mol)
DOH-SDS	20	22.8	
	35		15.1
TOH-STS	30	22.8	
	45		14.9
HOH-SHS	40	22.2	
	55		14.7

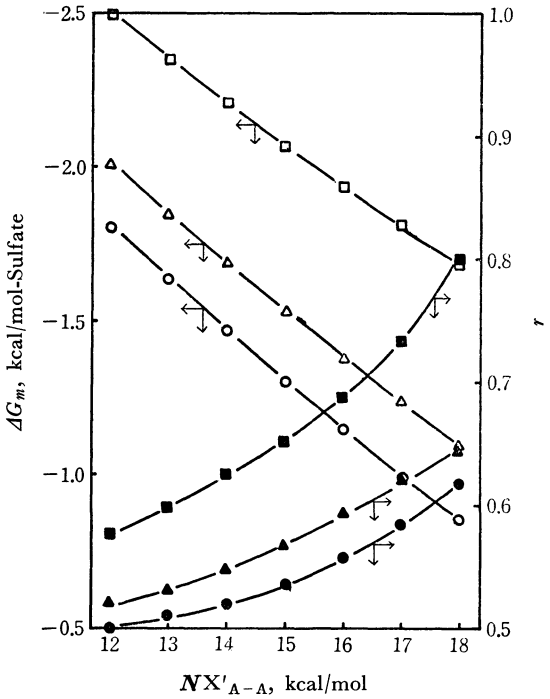

Fig. 5. Minimum of ΔG_m and r against X'_{A-A} at ΔH_0 equal to 1.0.
● ○: DOH-SDS
▲ △: TOH-STS
■ □: HOH-STS

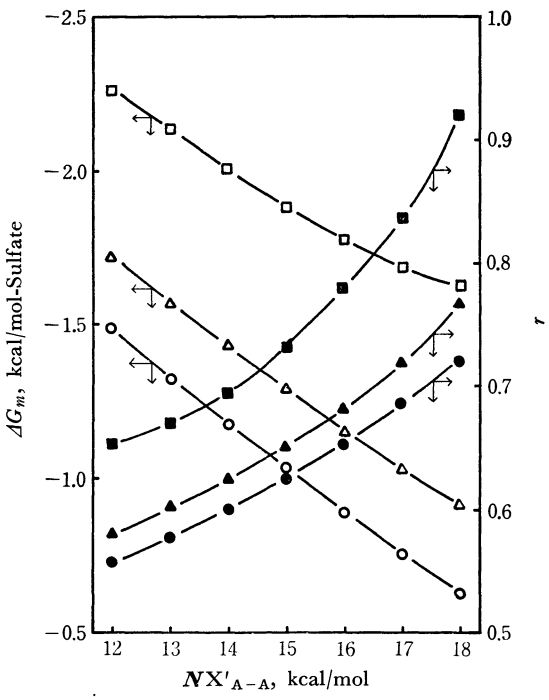

Fig. 6. Minimum of ΔG_m and r against X'_{A-A} at ΔH_0 equal to 2.0.
● ○: DOH-SDS
▲ △: TOH-STS
■ □: HOH-SHS

17, 18 kcal/mol into ΔH_0 and NX'_{A-A}, respectively. As a result we could obtain, as the values consistent with experimental results, only two values of ΔH_0 equal to 1 and 2 kcal/mol which we can accept as a reasonable values for a transition enthalpy of long chain compounds. The calculated results are shown in Figs. 5 and 6 for complex I only. The results of complex II always showed that the molar ratio of alcohol to sulfate equal to 1.0 made $\Delta G^1{}_m$ minimum. From Figs. 5 and 6, we see that the values of NX'_{A-A} 14—16, 13—15, and 12—13 kcal/mol for DOH-SDS, TOH-STS and HOH-SHS, are consistent with experimental results.

^{81}Br Nuclear Quadrupole Resonance of Modifications of Titanium Tetrabromide

Tsutomu OKUDA, Yoshihiro FURUKAWA, and Hisao NEGITA

Department of Chemistry, Faculty of Science, Hiroshima University, Hiroshima

(Received January 28, 1971)

^{81}Br NQR of titanium tetrabromide has been observed at temperatures between −196°C and 35.5°C, and its Zeeman effect has been measured at room temperature. The cubic form of titanium tetrabromide shows two resonance lines, as has been reported previously; their temperature coefficients change from positive to negative when the temperature is raised. The bond angles, ∠Br–Ti–Br, are in the range of 108.7° to 110.3°. The asymmetry parameters are 2.0 and 2.5%. On the other hand, the monoclinic form shows four resonance lines; 39.175, 39.184, 39.454, and 39.800 MHz at 11°C. The temperature coefficient of the lowest line is positive at the lower temperature, whereas those of the remainder are negative. The bond angles, ∠Br–Ti–Br, are found in the range of 108.8° to 110.1°. The asymmetry parameters are 1.2, 4.6, 2.1, and 3.5% for the bromine atoms in the order of increasing resonance frequencies. The ionic and double-bond characteristics of the Ti–Br bond in both forms are about 60 and 16%. These findings suggest that, in titanium tetrabromide, the crystal field has little effect on the molecular shape, the bond character, and the asymmetry parameter.

It had been known for a long time that titanium tetrabromide has several modifications and that one of them is a cubic form isomorphous with stannic tetraiodide.[1] Later, the presence of at least three modifications (Form 1, Form 2, and Form 3) was reported by Sackman *et al.*[2] They found that Form 1, which is a cubic form and which is usually obtained by the solidification of the melt, is transformed into Form 2 over a period of several days at room temperature, and that Form 3, which is prepared on cooling the molten substance rapidly, is transformed into Form 1 at −5°C. Recently, the crystal structure of Form 2 has been determined by means of the X-ray analysis by Brand and Schmidt.[3] They found that it is monoclinic and isomorphous with α-stannic tetrabromide. The crystal structure of the remainder has not yet been established. The NQR of Form 1 has been reported by Barnes and Engardt.[4] They found two resonance lines and the positive coefficient of the temperature dependence for the stronger resonance line, while the Zeeman effect on NQR has not yet been observed. In the present experiment, the reasonance frequencies of Form 2 were determined for the first time, and the temperature dependence and the Zeeman effect in both modifications were observed, in order to discuss the nature of the Ti–Br bonds and the molecular structures.

Experimental

Form 1 was obtained on the distillation of commercial titanium tetrabromide (Wako Pure Chem. Ind., Ltd.), while Form 2 was obtained by cooling Form 1 melted at a temperature above 100°C. The single crystals of these substances were prepared by the Bridgeman-Stockbarger method. The spectrometer used in the present experiment was a super-regenerative oscillator, and the absorption lines were observed on an oscilloscope. The magnetic field used for the Zeeman study was provided by the Helmholtz coil[5] with a field strength of about 200 gauss.

Results

The resonance frequencies of ^{81}Br in Form 1 were measured between −196°C and 35.5°C. Only two resonance lines (designated as ν_1 and ν_2) were observed in the whole temperature range studied. The temperature dependence of ν_2 was in good agreement with finding by Barnes and Engardt.[4] The resonance frequencies observed at room temperature are listed in Table 1, and the temperature dependence is shown in Fig. 1. The resonance frequencies of both ν_1 and ν_2 increase and then decrease through

Table 1. ^{81}Br NUCLEAR QUADRUPOLE RESONANCE FREQUENCIES IN TITANIUM TETRABROMIDE

Compound		Resonance frequency, MHz	
		20°C	−196°C
Form 1	ν_1	38.701	38.685
	ν_2	39.370	39.366
Form 2	ν_1'	39.162	39.209
	ν_2'	39.162	39.322
	ν_3'	39.428	39.641
	ν_4'	39.770	40.094

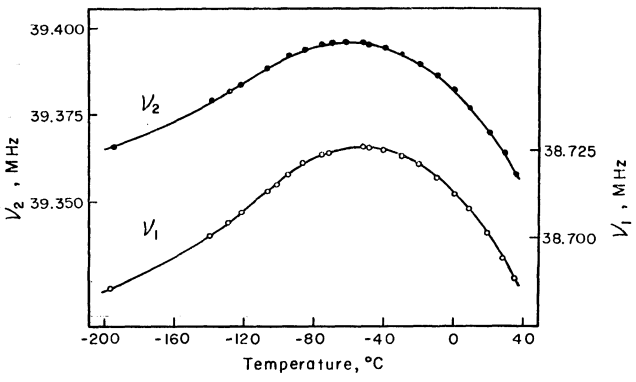

Fig. 1. Temperature dependence of ^{81}Br nuclear quadrupole resonance frequencies in Form 1.

1) O. Hassel and H. Kringstad, *Z. Physik. Chem.*, **B15**, 274 (1932).
2) H. Sackman, D. Demus, and D. Pankow, *Z. anorg. allg. Chem.*, **318**, 257 (1962).
3) P. Brand and J. Schmidt, *ibid.*, **348**, 257 (1966).
4) R. G. Barnes and R. D. Engardt, *J. Chem. Phys.*, **29**, 248 (1958).
5) K. Shimomura, *J. Phys. Soc. Jap.*, **12**, 657 (1957).

Table 2. The bond angles ∠Br-Ti-Br in Form 2

	∠Br_1-Ti-Br_2[a)]	∠Br_1-Ti-Br_3	∠Br_1-Ti-Br_4	∠Br_2-Ti-Br_3	∠Br_2-Ti-Br_4	∠Br_3-Ti-Br_4
NQR	110.09°	109.26°	1.9.53°	109.95°	108.75°	109.74°
X-ray	110.57°	109.45°	109.27°	109.32°	111.97°	106.13°

a) The bromine atoms contributing to ν_1', ν_2', ν_3', and ν_4' are labelled as Br_1, Br_2, Br_3, and Br_4.

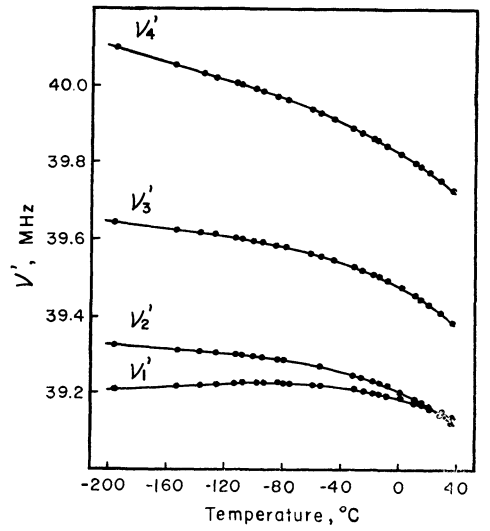

Fig. 2. Temperature dependence of ^{81}Br nuclear quadrupole resonance frequencies in Form 2.

peak at about −55°C, as the temperature rises from −196°C. The resonance frequencies of ^{81}Br in Form 2 were measured over the temperature range from −196°C to the melting point, as is shown in Fig. 2. Four resonance lines (designated as ν_1', ν_2', ν_3', and ν_4') were observed. When the temperature was lowered from room temperature to −196°C, no phase transition was observed. On the other hand, when the temperature was increased from −196°C, the resonance lines became broad around −20°C and disappeared at −15°C, while two lines with the same frequencies as those of Form 1 appeared. It is thus evident that the phase transition from Form 2 to Form 1 took place. The resonance frequencies are listed in Table 1, along with the results at the temperature of liquid nitrogen. The pattern of zerosplitting was obtained by measuring the Zeeman effect on each resonance line. Eight patterns were obtained for each of the two resonance lines, ν_1 and ν_2. Those

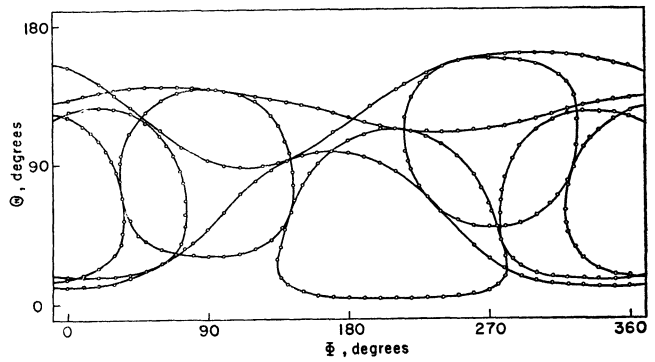

Fig. 3. Zerosplitting patterns of Zeeman lines of ν_1 in Form 1. Θ and Φ are polar and azimuthal angles, respectively, in the coordinate fixed to the sample.

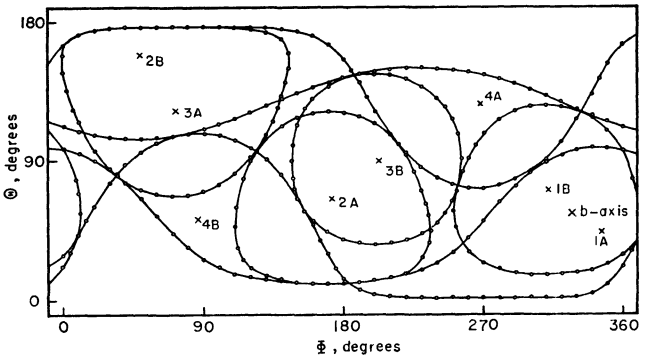

Fig. 4. Zerosplitting patterns of Zeeman lines of Form 2. Θ and Φ are polar and azimuthal angles, respectively, in the coordinate fixed to the sample.

for ν_1 are very similar to those for ν_2. The experimental results for ν_1 are shown in Fig. 3. In Form 2, two zerosplitting patterns were obtained for each of the two resonance lines, ν_3' and ν_4'. Since ν_1' and ν_2' cross each other at room temperature, it was difficult to identify four zerosplitting patterns. Accordingly, the assignment was done at 10°C, where each of the relevant lines was split into two.

The angles between any two Ti–Br bonds were calculated from the direction of the principal z axis of the field gradient. The bond angles, ∠Br–Ti–Br, in Form 1 are in the range of 108.8° to 110.3°; this indicates that the titanium tetrabromide molecule is nearly tetrahedral in the crystal. The results of Form 2 are listed in Table 2.

The values of the asymmetry parameter, η, were determined from the direction of the zerosplitting loci by means of the following relation:

$$\eta = 3(\sin^2\theta_{max} - \sin^2\theta_{min})/(\sin^2\theta_{max} + \sin^2\theta_{min}) \quad (1)$$

where θ_{max} and θ_{min} are the maximum and minimum zerosplitting angles. Consequently, the quadrupole coupling constants may be calculated by the following equation:

$$\nu = (eQq_{zz}/2)(1+\eta^2/3)^{1/2} \quad (2)$$

The values of η and eQq_{zz} derived in this way are listed in Table 3.

Table 3. Quadrupole coupling constants, asymmetry parameters and unbalanced p electrons of ^{81}Br in titanium tetrabromide at room temperature (20°C)

Compound	ν	eQq_{zz}, MHz	η, %	Up, %
Form 1	ν_1	77.397	2.0±1.5	12.0
	ν_2	78.732	2.5±1.5	12.2
Form 2	ν_1'	78.323	1.2±1.0	12.2
	ν_2'	78.297	4.6±0.6	12.2
	ν_3'	78.850	2.1±0.3	12.3
	ν_4'	79.524	3.5±0.6	12.4

Discussion

Temperature Dependence. In Form 1, the temperature dependence of ν_1 is similar to that of ν_2 as shown in Fig. 1. The maximum of the frequency-temperature curve appeared near −55°C. The temperature coefficient of ν_1 is slightly larger than that of ν_2 below −55°C, but it is almost the same in the range above −55°C. The temperature dependence is expressed by the sum of the Bayer term and the effect of the pressure dependence.[6] As will be described later, the $d\pi$–$p\pi$ bond may be involved in the Ti–Br bond of Form 1. As the thermal vibrations increase with an increase in the temperature, the π-bond character decreases. This, in turn, causes the resonance frequency to increase. This effect is combined with that of averaging the field gradient due to the vibration, and so the absolute value of the Bayer term becomes small. Since the temperature dependence is positive at low temperatures, the effect of the pressure dependence dominates the Bayer term. In stannic tetraiodide, the absolute value of the temperature coefficient of the higher resonance line is larger than that of the remainder.[7] It was proved experimentally that the resonance line with a larger temperature coefficient came from the resonant atom in the more symmetrical position. This is also the case for Form 1.

In Form 2, the absolute value of the temperature coefficient decreases in the order of the decreasing resonance frequency, and the temperature coefficient of ν'_1 is positive below the temperature of −80°C, as is shown in Fig. 2. In many halogenides, a lower resonance line has a smaller temperature dependence. This may be interpreted in terms of an intermolecular bond, such as the Sb–Cl binding in the crystal of antimony trichloride.[8] However, in titanium tetrabromide, the intermolecular interaction between Ti and Br atoms must be weak, because the Ti atom is surrounded tetrahedrally by Br atoms. The intermolecular interaction may be caused only by the neighboring Br atoms. Since the bond length has not been reported in the results of the X-ray analysis, we calculated the bond length on the basis of the atomic parameter which was used in the calculation of the structure parameter, $|F_o|$.[3] The results were 2.43, 2.35, 2.34, and 2.31 Å. The bond contributing to ν'_1 is the longest and is parallel to the b axis, whereas that for ν'_4 is perpendicular to the b axis, as Table 4 shows. It is of interest to note that the temperature coefficient of ν'_1 is the smallest.

Quadrupole Coupling Constant and Asymmetry Parameter. The results of the X-ray analysis[1] indicate that the crystal of Form 1 is isomorphous with that of stannic tetraiodide. According to the NQR study of stannic tetraiodide by Shimomura,[9] the lower resonance line is three times as strong as the higher. This relative intensity is reversed in Form 1 and α-stannic tetrabromide.[5] There is a pair of tetrahedral molecules in the crystal of both stannic tetraiodide and α-stannic tetrabromide; six atoms face each other in the former, but only two atoms in the latter. It was revealed recently that no such atoms exist in α-stannic tetrabromide, as had been presumed by Shimomura. Therefore, a crystal structure like that of stannic tetraiodide may show an NQR spectrum of Form 1. In order to clarify this point, we calculated the field gradient due to external atoms, using a point-charge model on the basis of the X-ray analysis.[1,7] The z axis was chosen along a metal-halogen bond, while the x and y axes were in an arbitrary direction perpendicular to the z axis. The charges on the metal and halogen atoms were assumed to be $4e_x$ and $-e_x$ respectively. The scanning radius was 30 Å. The results are shown below:

$TiBr_4$

Br_1—ν_1	Br_2—ν_2
$q_{xx}=-0.2959e_{Br}$ Å^{-3}	$q_{xx}=-0.2906e_{Br}$ Å^{-3}
$q_{yy}=-0.2959e_{Br}$ Å^{-3}	$q_{yy}=-0.3157e_{Br}$ Å^{-3}
$q_{zz}=0.5918e_{Br}$ Å^{-3}	$q_{zz}=0.6063e_{Br}$ Å^{-3}

SnI_4

I_1—ν_2	I_2—ν_1
$q_{xx}=-0.2377e_I$ Å^{-3}	$q_{xx}=-0.1172e_I$ Å^{-3}
$q_{yy}=-0.2397e_I$ Å^{-3}	$q_{yy}=-0.2946e_I$ Å^{-3}
$q_{zz}=0.4774e_I$ Å^{-3}	$q_{zz}=0.4119e_I$ Å^{-3}

It is evident that the results make possible a qualitative interpretation of the differences in the NQR spectra between Form 1 and stannic tetraiodide. Taking account of Sternheimer's antishielding effect,[10] the agreement between the calculation and observed values may be improved. One of the defects of the present calculation is the fact that the x and y axes are chosen arbitrarily. Accordingly, in calculating the field gradients for Form 1, we chose x and y axes in various directions perpendicular to the z axis. The value of the field gradients at the bromine atom contributing to ν_1 did not vary. On the other hand, at the atom contributing to the other line the values of q_{xx} and q_{yy} varied slightly, while q_{zz} remained as the same. The results of the X-ray analysis for stannic tetraiodide[11] show that the intramolecular distance, I–I, is slightly larger than the intermolecular distance. On the contrary, the intramolecular distance, Br–Br, in Form 1 is smaller than the intermolecular distance. The difference in the NQR spectra may be caused by this discrepancy.

Brand and Schmidt have reported that the crystal structure of Form 2 is isomorphous with that of α-stannic tetrabromide. In fact, Form 2 shows four resonance lines, in analogy with the spectrum of α-stannic tetrabromide. The lowest resonance line in α-stannic tetrabromide is lower by about 3 MHz than the other; this is ascribed to the presence of intermolecular interaction.[5] In Form 2, however, the spacing ν'_1 and ν'_4 was about 900 kHz. If Form 2

6) H. S. Gutowsky and G. A. Williams, *Phys. Rev.*, **105**, 464 (1957).
7) R. W. Ward, Thesis, Virginia Polytechnic Institute, (1968).
8) H. Chihara, N. Nakamura, and H. Okuma, *J. Phys. Soc. Jap.*, **24**, 306 (1968).
9) K. Shimomura, *J. Sci. Hiroshima Univ., Ser. A*, **17**, 383 (1954).
10) R. Sternheimer, *Phys. Rev.*, **80**, 102 (1950).
11) F. Meller and I. Fankushen, *Acta Crystallogr.*, **8**, 343 (1955).

has the same structure as α-stannic tetrabromide, the difference in the NQR spectrum may be caused by the contribution of the 3*d* orbital of the titanium atom to the Ti–Br bond. When the $d\pi$–$p\pi$ bond is formed, the resonance frequency becomes lower. Since the bromine-atom contribution to the ν'_1 is considered to take part in the interaction, as has been described above, the spacing of the highest and lowest resonance lines will be smaller.

As Table 3 shows, the values of the asymmetry parameters in Form 1 are small. This suggest that titanium tetrabromide is nearly tetrahedral in the solid state and that the Ti–Br bond is along the three-fold symmetry axis. The asymmetry parameter for ν_1 is similar to that for ν_2. It may be attributed to the fact that the angle of zerosplitting could not be determined definitely, since one resonance line gives rise to eight zero-splitting patterns and the lines of the Zeeman component are so weak. The asymmetry parameters in Form 2 are small because the molecule is tetrahedral, as is shown in Table 2. The difference between the asymmetry parameters of Form 1 and Form 2 is small. This suggests that the contribution to the field asymmetry from external ionic charges is so small that the molecular shape and the bond character of the Ti–Br in both crystal forms are almost unaffected.

Directions of the Ti–Br Bonds. The Zeeman measurements can determine the relative orientation of the Ti–Br bonds. Every angle between the Ti–Br bond and the crystal *b* axis in Form 1 is found to be equal to 54°44′; this value is in good agreement with that of the X-ray analysis. On the other hand, the results in Form 2 are listed in Table 4. The results of the X-ray analysis were calculated by using the atomic parameter of α-stannic tetrabromide, as has been described above. The agreement between the present results and those of the X-ray analysis is good. If the molecule in Form 2 will rotate around the axis perpendicular to the *b* axis in such a way that all the angles are the same with respect to the *b* axis, Form 2 will be transformed into Form 1. The bond angle, ∠Br–Ti–Br, is shown in Table 2. The results of the Zeeman analysis are in fairly good agreement with the results of the X-ray analysis, although the final decision should be made on the basis of a more accurate X-ray analysis.

Table 4. The angles between the crystal *b* axis and the principal *z* axis of the field gradient in Form 2

	$Ti\text{-}Br_1$	$Ti\text{-}Br_2$	$Ti\text{-}Br_3$	$Ti\text{-}Br_4$
NQR	19.54°	61.90°	61.63°	90.0°
X-Ray	19.40°	61.78°	61.17°	90.0°

Bond Character. Although the Ti–Br bond may be expected to be considerably ionic on the basis of the electronegativity difference between Ti and Br atoms, the observed resonance frequency is much lower than that estimated only in terms of the ionic character. Accordingly, the bond may involve a $d\pi$–$p\pi$ bond, by which the asymmetry parameter of the bromine atom is little affected. The number of unbalanced *p* electrons, *Up*, can be obtained using the following relation:[12]

$$Up = (1-s)(1-i-\pi) - \pi/2 \tag{3}$$

where *i* and π are the extents of the ionic and π-bond characters respectively, and where *s* is the *s* electron character, which is assumed to be 0.15.[13] The value of *Up* is evaluated from the observed quadrupole coupling constant:

$$Up = (eQq_{zz})_{obs}/(eQq_{zz})_{atom} \tag{4}$$

where $(eQq_{zz})_{atom}$ is 643.0 MHz.[14] In order to obtain the extent of the π-bond character, the value of the ionic character must be estimated first. Although a number of authors have reported procedures for estimating the degree of ionic character, we made use of Gordy's relation[15] and obtained an ionic character about 60% for both Form 1 and Form 2. Next, using this value of the ionic character, the value of the π-bond character was calculated to be about 16% by means of Eq. (3). Judging from these values of the bond character, the Ti–Br bond seems to be somewhat extraordinary among the various metal-bromine bonds.

12) R. Ikeda, D. Nakamura, and M. Kubo, *J. Phys. Chem.*, **69**, 2101 (1965).
13) B. P. Dailey and C. H. Townes, *J. Chem. Phys.*, **23**, 118 (1955).
14) V. Jaccarino and L. G. King, *Phys. Rev.*, **94**, 1610 (1954).
15) W. Gordy, W. V. Smith, and R. F. Trambarulo, "Microwave Spectroscopy," John Wiley & Sons, Inc., New York (1953), p. 284.

Interaction between TCNQ and Surfactant. III. The Effect of Light on the Spectra of TCNQ Solubilized in Surfactant Solutions

Shinya MUTO, Katsuhiko DEGUCHI, Yoshikazu SHIMAZAKI, Yoshiaki AONO, and Kenjiro MEGURO

Faculty of Science, Science University of Tokyo, Kagurazaka, Shinjuku-ku, Tokyo

(Received February 6, 1971)

The absorption spectra of 7,7,8,8-tetracyanoquinodimethane (TCNQ) solubilized in surfactant solutions were found to be influenced by day light (hereafter referred to as light). The formation of the monomer band of TCNQ anion radical in the aqueous solution of DPCl (dodecylpyridinium chloride), DPBr (dodecylpyridinium bromide) and $C_{12}E_8$ (homogeneous octaethylene glycol dodecylether) were enhanced by light. On the other hand, the spectra of TCNQ solubilized in surfactant micelle in the dark suggested that TCNQ exists as dimer anion radical form $(TCNQ)_2^-$. Thus, in solubilized state of TCNQ in micelle there is an equilibrium between monomer $TCNQ^-$ and dimer $(TCNQ)_2^-$, which seems to be easily influenced by light and surfactant. Appearance of a monomer radical band was remarkable in DPCl, DPBr, and $C_{12}E_8$ but only the dimer band was found in SDS even in the light.

In a previous paper,[1] we reported that when TCNQ was solubilized into surfactant solutions above critical micelle concentration (CMC), a remarkable coloration took place in the surfactant solutions, and charge transfer complex bands were found in the spectra. The bands were considered to be due to the formation of the charge transfer complex between solubilized TCNQ and surfactant molecule, where the electron donor is surfactant and the acceptor is TCNQ. This suggests a new phenomenon concerning the solubilization of TCNQ with a different mechanism of the color change at CMC.

In this paper, the results of the study of the effect of light irradiation on spectra of TCNQ solubilized in surfactant solution are given.

Experimental

Preparation of Reagents. TCNQ was synthesized by the usual method.[2] Purification of TCNQ was carried out by recrystallization 5 times in acetonitrile. The crystals obtained had a rust-colored flaky form. Its purity was confirmed by elementary analysis:

Found: C, 70.2; H, 1.99; N, 27.7%. Calcd for $C_{12}H_4N_4$: C, 70.6; H, 1.97; N, 27.4%. Melting point of the TCNQ was 293.5—296°C.

Dodecylpyridinium chloride (DPCl) was prepared as follows. A mixture of chlorododecane and dry pyridine was refluxed for about 15 hr at 115°C.[3] The product was recrystallized three times from acetone, then dissolved in warm methanol, mixed with charcoal, and filtered. The filtrate obtained was extracted with petroleum ether for about 100 hr. The product was recrystallized five times from acetone.

Dodecylpyridinium bromide (DPBr) was prepared in the same manner as DPCl, taking bromododecane and dry pyridine.

Sodium dodecyl sulfate (SDS) was prepared by the reaction of dodecanol with chlorosulphonic acid in gracial acetic acid and by neutralization of the resulting acid with sodium carbonate.[4] The product was extracted with petroleum ether for about 200 hr and recrystallized five times from water-isopropanol mixture.

Homogeneous octaethylene grycol dodecyl ether ($C_{12}E_8$), supplied from Nikko Chemical Co. Ltd., was used as nonionic surfactant. Homogenity of polyethylene chain length was confirmed by means of IR spectra, elementary analysis, NMR, thin layer chromatography, and gas-liquid chromatograpy.

The water used was purified by passing tap water through a mixed-bed of ion-exchange resin. It was then distilled from alkaline potassium permanganate in the presence of sodium hydroxide in a pyrex still. The specific conductance of the water was 1 to 1.9×10^{-6} ohm^{-1} cm^{-1} at 25°C.

Solubilization Measurement. Solubilization of TCNQ was carried out as follows. A small amount of TCNQ was added to 15 m*l* of surfactant solutions of different concentrations, and the mixture was shaken in a thermostat at 25°C for about 72 hr. The small amount of TCNQ used was due to the fact that TCNQ is almost insoluble in water. The period of shaking (72 hr) was determined from the study of equilibrium time of solubilization. Shaking was carried out in the daylight and in the dark.

The absorption spectra of TCNQ solubilized in surfactant solutions were measured with a Hitachi Spectrophotometer (Model EPS-2).

Results

When TCNQ was solubilized in surfactant solutions above CMC, a remarkable coloration characteristic of the surfactant was observed. In solubilization equilibrium, the color of TCNQ solubilized was green in DPCl solution, blueish green in DPBr solution, pink in SDS solution and pink to greenish yellow in $C_{12}E_8$ solution. The spectra of TCNQ solubilized in these surfactant solutions change their shapes by the action of light. The absorption spectra of TCNQ solubilized in DPCl are shown in Figs. 1 and 2. Figure 1 shows the spectra measured in daylight. The spectra obtained below CMC had a slight absorption from 550 to 900 mμ, and its intensities were very broad. The forms of absorption spectra change with the increase of surfactant concentration, and new

1) a) S. Muto, K. Deguchi, K. Kobayashi, E. Kaneko, and K. Meguro, *J. Coll. and Interface Sci.*, **33**, 475 (1970); b) S. Muto, K. Deguchi Y. Shimazaki, Y. Aono, and K. Meguro, *J. Coll. and Interface Sci.*, in press.

2) a) D. S. Acker and W. R. Hertler, *J. Amer. Chem. Soc.*, **84**, 3370 (1962); b) J. R. Vincent and L. I. Smith, *J. Org. Chem.*, **3**, 603 (1939).

3) W. P. J. Ford, R. H. Ottewill, and H. C. Parreira, *J. Coll. and Interface Sci.*, **21**, 522 (1966).

4) E. E. Dreger, G. I. Keim, G. A. Miles, L. Shedlovsky, and J. Ross, *Ind. Eng. Chem.*, **36**, 610 (1944).

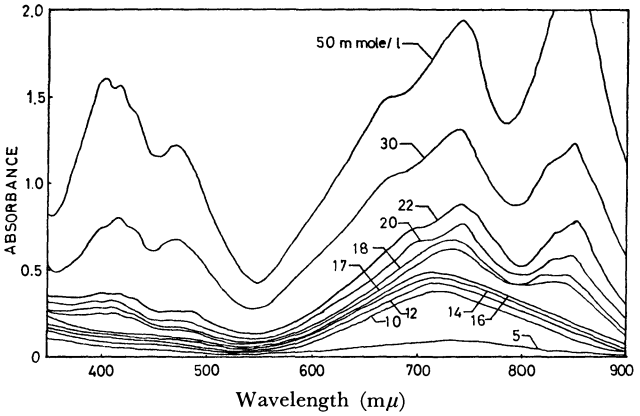

Fig. 1. Visible absorption spectra of TCNQ solubilized in DPCl solutions in the presence of the light.
Figures show concentration of surfactant solutions.

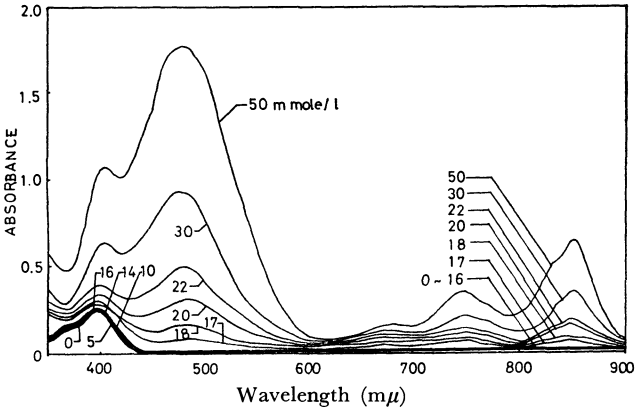

Fig. 2. Visible absorption spectra of TCNQ solubilized in DPCl solutions in the absence of the light. Figures show concentration of surfactant solutions.

TABLE 1. COMPARISON OF OPTICAL DENSITIES OF TCNQ SOLUBILIZED IN SURFACTANT SOLUTIONS AT DIFFERENT WAVELENGTH IN THE PRESENCE AND ABSENCE OF LIGHT AT 25°C

		Optical densities at different wavelength (mμ)			
		420	480	750	850
Concentration of DPCl solution is 30 mmol/*l* (above CMC)	Light condition	0.76	0.64	1.23	1.26
	Dark condition	0.63	0.94	0.20	0.35
Concentration of DPCl solution is 10 mmol/*l* (below CMC)	Light condition	0.22	0.12	0.34	0.22
	Dark condition	0.05	0.03	0.00	0.00

bands appeared at 420, 750, and 850 mμ (major) and 480 and 680 mμ (minor) above CMC.

Figure 2 shows the spectra obtained in the dark. In this case, a remarkable absorption cannot be found in the spectra below CMC, but new bands were observed at 420, 480, and 850 mμ (major) and 680 and 750 mμ (minor) above CMC. Comparison of optical densities of TCNQ solubilized in surfactant solutions at different wavelengths in the presence and absence of light is given in Table 1. As can be seen in Table 1, the ratio of the intensity at 420 mμ to that at 850 mμ in the presence of light was smaller than 1, but ratio was reversed in the absence of light.

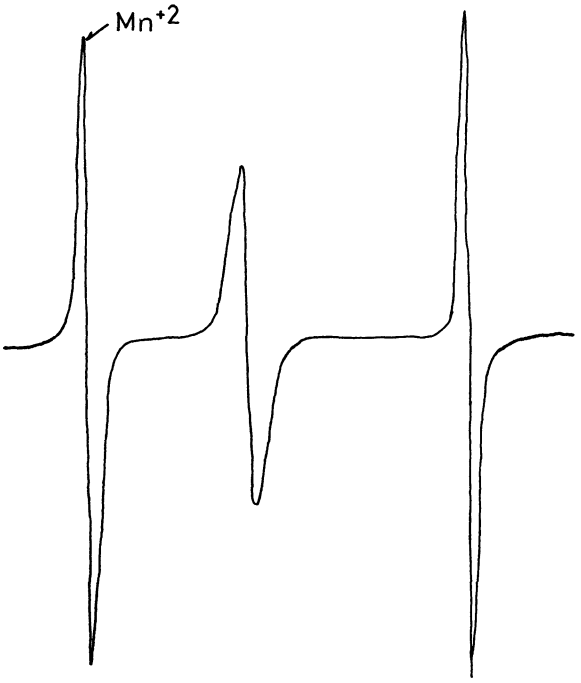

Fig. 3. Electron spin resonance spectra of TCNQ solubilized in 30 mmol/*l* DPCl solution in the presence of the light.

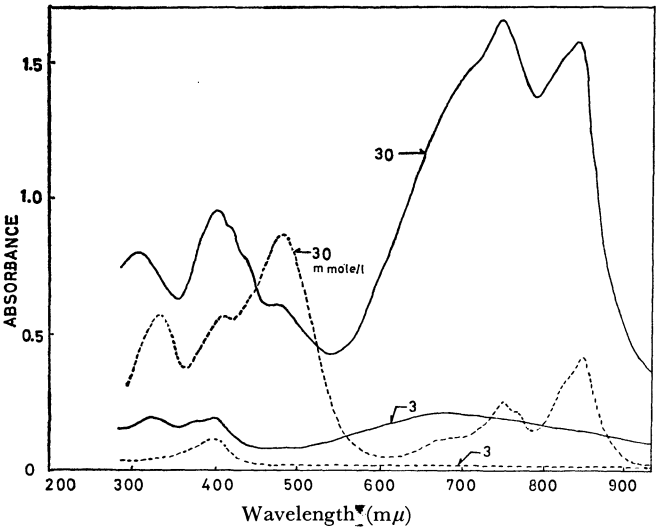

Fig. 4. Visible absorption spectra of TCNQ solubilized in DPBr solutions in the presence of the light and in the absence of the light. Figures show concentration of surfactant solutions.
The solid-line: in the presence of the light
The dashed portions: in the absence of the light

Figure 3 shows the ESR spectrum of TCNQ solubilized in DPCl solution above CMC. This is an evidence of the formation of charge transfer complex between TCNQ and surfactant.

Figure 4 shows the spectra of TCNQ solubilized in DPBr solution in the presence and absence of light. The results were almost the same as those obtained in DPCl solution.

The absorption spectra of TCNQ solubilized in anionic surfactant (SDS) are shown in Figs. 5 and 6. The shape of the absorption spectra of TCNQ solubilized in anionic surfactant solution was quite different. Figure 5 shows the spectra obtained in the presence of light, showing new bands at 400 and 600 mμ above, but no remarkable absorption below CMC. The spectra obtained in the dark are shown in Fig. 6, in which some change was found as compared with those obtained in the light, such as the increase at 400 mμ and decrease at 600 mμ with a slight shift of maximum absorption from 600 to 620 mμ.

Figure 7 shows the spectra of TCNQ solubilized in aqueous solution of homogeneous octaethyleneglycol dodecyl ether in the presence of light, giving the characteristic bands of charge transfer at 480, 750, and 850 mμ above CMC (the CMC value of $C_{12}E_8$ obtained by the surface tension method: 8.2×10^{-5} mol/l). Figure 8 shows the spectra measured in the dark. They are quite different from those in the light, with a decrease of intensities at 480, 750, and 850 mμ bands and the appearance of a new band at 400 mμ.

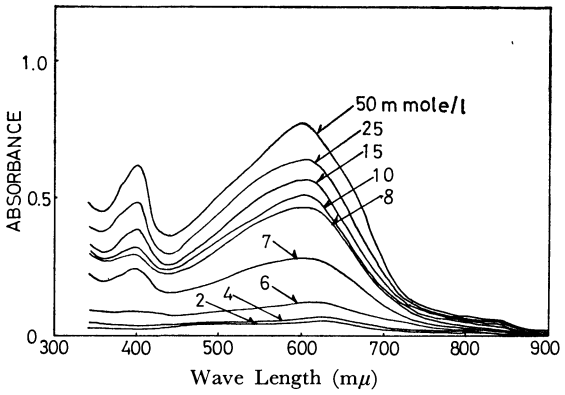

Fig. 5. Visible absorption spectra of TCNQ solubilized in SDS solutions (under light condition).

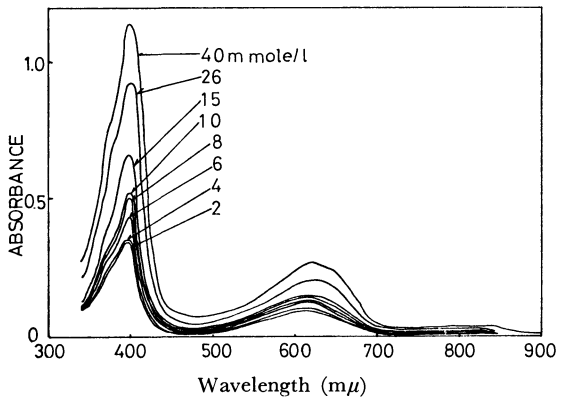

Fig. 6. Visible absorption spectra of TCNQ solubilized in SDS solutions (under dark condition).

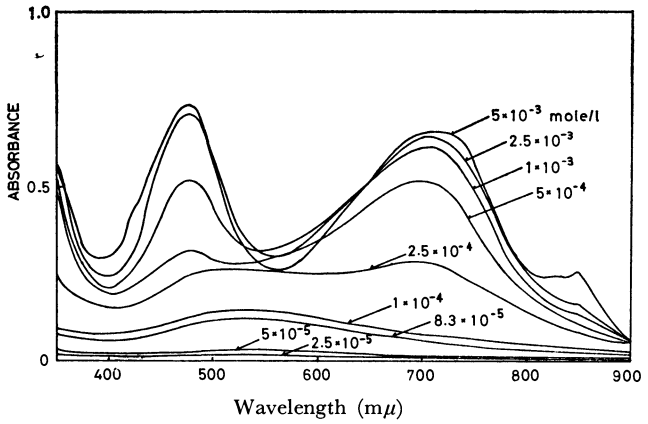

Fig. 7. Visible absorption spectra of TCNQ solubilized in octaethylene glycol dodecylether solutions in the presence of the light. Figures show concentration of surfactant solutions.

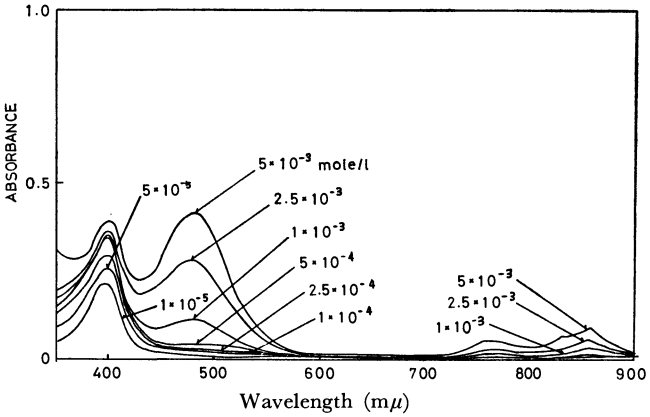

Fig. 8. Visible absorption spectra of TCNQ solubilized in octaethylene glycol dodecylether solutions in the absence of the light.
Figures show concentration of surfactant solutions.

Discussion

Scheibe[5] reported in his study of light effect on the color of acridine orange that the dimer of acridine orange dissociates into monomer by irradiation of the light. Boyd[6] studied the visible spectrum of aqueous Li^+TCNQ^- solution and found the existence of equilibrium between the dimer and monomer of the TCNQ anion radical, and concluded that the bands of about 380 mμ and 643 mμ are characterized with the dimer of TCNQ and 420, 750, and 850 mμ bands were caused by the monomer anion radical.

Melby and *et al.*[7] reported that charge transfer complex of TCNQ has characteristic absorption at 420, 750 and 850 mμ in acetonitrile. They suggested that these TCNQ complexes are represented by the general formula $D^+(TCNQ^-)$ where D is an electron donor molecule generally containing a nitrogen atom and an oxygen atom. The coloration accompanied by the solubilization of TCNQ in cationic surfactant solution was characterized by major maxima at 420 and 850 mμ in the light. The absorption seems to be due to the formation of charge transfer complex and formation of TCNQ monomer anion radical ion.

On the other hand, the spectra of TCNQ solubilized in cationic surfactant in the dark show a decrease of

5) G. Scheibe, *Z. Electrochem.*, **56**, 723 (1952).
6) R. H. Boyd and W. D. Phillips, *J. Chem. Phys.*, **43**, 2927 (1965).
7) S. R. Melby, R. J. Harder, W. R. Hertler, W. Mahler, R. E. Benson, and W. E. Mochel, *J. Amer. Chem. Soc.*, **84**, 3374 (1962).

the absorbance at 420, 750, and 850 mμ, but a 400 mμ band due to the dimer anion radical solubilized in micelle.

In the study of the spectra of TCNQ solubilized in anionic surfactant SDS solution, a typical dimer band of $(TCNQ)_2^-$ was found in the light. This does not differ with light irradiation, except for some increase of the absorbance at 620 mμ with no shift in wave length of the absorbed bands. The cause of the production of the anion radical dimer of TCNQ will be the interaction between the counter ion Na^+ ion and solubilized TCNQ in surfactant micelle.

In the light, the spectra of TCNQ solubilized in nonionic surfactant were characterized by major bands at 480, 750, and 850 mμ of monomer band of TCNQ anion radical. In the dark, the spectra of monomer bands at 480, 750, and 850 mμ decreased and a new band appeared at 400 mμ.

Solubilization can be classified into sandwich and palisade types. Non-polar substances are solubilized in the sandwich type, and polar substances in the palisade type. As TCNQ is a non-polar substance, we might expect that the solubilization of TCNQ is of the sandwich type. However, from our results, the solubilization of TCNQ seems to be closer to the palisade type. If the charge transfer band of TCNQ was due to charge transfer between TCNQ and the nitrogen of cationic surfactant, or the oxygen atom of ethyleneoxide or hydroxyl group in nonionic surfactant, its appearance could be explained by assuming a palisade type of solubilization of TCNQ, even though TCNQ molecule is non-polar. However, there still remain questions as to why TCNQ, a non-polar substance, solubilizes in a palisade type solubilization, and also as to the theoretical mechanism for the formation of charge transfer complex between TCNQ and quaternary ammonium salts, such as cationic surfactant in the dark.

BULLETIN OF THE CHEMICAL SOCIETY OF JAPAN, VOL. 44, 2090—2095 (1971)

The Gas-Phase Radiolysis of Cycloheptatriene

Katsuyoshi NAKAMURA, Setsuo TAKAMUKU, and Hiroshi SAKURAI

The Radiation Laboratory, The Institute of Scientific and Industrial Research, Osaka University, Suita, Osaka

(Received February 12, 1971)

The γ radiolysis of cycloheptatriene (CHT) in the gas phase has been investigated as a function of the pressure (2—14 mmHg) and in the presence of various additives (NO, O_2, NH_3, N_2O, and C_3H_8). The G values obtained at 10.5 mmHg and at a total dose of 1.1×10^{19} eV are as follows: hydrogen, 0.50; methane, 0.16; acetylene, 1.52; cyclopentadiene, 0.29; benzene, 0.65; toluene, 1.68; dimers, 2.99. The yields of toluene and cyclopentadiene decrease with the pressure and are not appreciably affected by these additives; this suggests a contribution of the excited CHT molecules formed by direct excitation to their formation. The formation of dimers and benzene is affected by a radical scavenger (O_2, NO), indicating the importance of the radical processes. The reaction products obtained *via* a $C_7H_7^+$ ion, which is well known to be produced by the irradiation of CHT, have not been observed, while in the radiolysis of CHT in the presence of benzene and a radical scavenger, biphenylmethane has been produced, presumably by a reaction of the $C_7H_7^+$ ion with benzene. Therefore, it was assumed that the $C_7H_7^+$ ion produced from CHT does not contribute to the dimer formation, but may initiate the ionic polymerization.

Recently, much attention has been paid to ion-molecule reactions in the gas-phase radiolysis. Mass spectrometric studies provide useful information with regard to the ions produced in the gas-phase radiolysis. In the mass spectrometry of alkylbenzenes,[1] the most abundant ion has been observed to be a $C_7H_7^+$ ion (m/e=91), which has a completely symmetrical tropylium structure rather than that of benzyl, in common with these alkylbenzenes. In a previous paper,[2] it was observed that the $C_7H_7^+$ ion produced by the γ irradiation of toluene, ethylbenzene, and *m*-xylene vapors adds to the respective aromatic-ring, finally forming benzylated products, predominantly at a *meta* position to the resident alkyl group. Furthermore, the reaction mechanism has been discussed on the basis of electrophilic aromatic substitution in the gas-phase[3] and compared with the analogous isopropylation of benzene and toluene.[4]

In conjunction with these problems, we have recently investigated the γ radiolysis of cycloheptatriene (CHT) vapor, which is known, from mass spectrometric studies, to produce a $C_7H_7^+$ ion similar to those obtained from alkylbenzenes.[5] The present paper will describe the product formation and the reaction mechanism of this gas-phase radiolysis of CHT, though clear information about the structure and the reactivity of the $C_7H_7^+$ ion has not been obtained.

Experimental

Materials. CHT was prepared by the pyrolysis of 7,7-dichloronorcarane, which has been produced from cyclo-

1) H. M. Grubb and S. Meyerson, "Mass Spectrometry of Organic Ions," F. W. Mclafferty, Ed., Academic Press, New York, 1963, p. 453.

2) Y. Yamamoto, S. Takamuku, and H. Sakurai, *J. Amer. Chem. Soc.*, **91**, 7192 (1969).

3) Y. Yamamoto, S. Takamuku, and H. Sakurai, *J. Phys. Chem.*, **74**, 3325 (1970).

4) S. Takamuku, K. Iseda, and H. Sakurai, *J. Amer. Chem. Soc.*, **93**, 2420 (1971).

5) S. Meyerson and P. N. Rylander, *J. Chem. Phys.*, **27**, 901 (1957); S. Meyerson, *J. Amer. Chem. Soc.*, **85**, 3340 (1963).

hexene;[6] it was distilled through a spinning-band column and then purified by preparative-scale gas chromatography using a 3-m PEG-6000 column at 65°C and, further, a 3-m DNP column at 65°C. Gas-chromatographic analysis on a 4.5-m PEG-6000 column showed the presence of toluene (0.024 mol%) and an unknown impurity (<0.07%). The purified CHT was degassed, dried over phosphorus pentoxide and a sodium mirror in a high-vacuum line, and then stored in a glass tube with a mercury cut-off at a low temperature.

Nitric oxide, nitrous oxide, and propane obtained from Takachiho Trading Co., and ammonia generated from 28% ammonia water were dried over a sodium mirror in a high-vacuum line and then purified by low-temperature distillations. The oxygen (minimum purity: 99.9%) was used without further purification.

Sample Preparation. The irradiation cells were Pyrex cylinders with a break-seal, approximately 105 m*l* in volume. Prior to the sample introduction, the cells were baked and evacuated overnight at a pressure of 10^{-6} mmHg. The pressure of the sample was measured by means of a mercury manometer; the pressure range was 2—14 mmHg. In the experiment with an additive, the amount of the additive was measured by a gas buret and transferred into the cell through a break-seal.

Irradiation and Dosimetry. Irradiation was carried out at room temperature with a 5000 Ci ^{60}Co source. Dosimetry was based on $G(C_2H_4 \rightarrow H_2) = 1.28$,[7] assuming that the energy distribution was proportional to the electron density. The dose rate in the present experiments was 3.82×10^{15} eV/hr·μmol (CHT). The G values in the runs with an additive were calculated on the basis of the energy absorbed by CHT alone. The total dose range was $(1.1—2.7) \times 10^{19}$ eV.

Analysis. The hydrogen yield in the product gas volatile at −196°C was determined from the volume difference measured with a standard Toepler pump and gas buret arrangement, before and after passage through a palladium thimble heated at ca. 300°C. The C_2—C_4 hydrocarbons volatile at −120°C were transferred into a capillary with a Toepler pump and analyzed gas-chromatographically using a 3-m silica gel column at 100°C. All the non-volatile products at −120°C except for dimers were identified by gas-chromatographic comparison with authentic samples using several columns (PEG-6000, DNP, and APL). The dimers were identified by means of a gas chromatograph-mass spectrometer combination, but the structures were not investigated except that of bitropyl. The yields of the gaseous and liquid products were determined by a comparison of the peak areas with those for known amounts of propane and benzene respectively, which were submitted to gas chromatography before each analysis.

Results

The product yields in the irradiated CHT at 10.5 mmHg are shown in Table 1, together with those of the radiolysis of toluene vapor.[3] The observed gaseous products were hydrogen, methane, and acetylene. The yields of ethylene and ethane were negligibly small. Cyclopentadiene, benzene, toluene, and several kinds of dimers were also formed as liquid products, though a part of the cyclopentadiene was observed in the dimeric form because of the instability of the monomer at room temperature. Several dimers whose carbon

Table 1. Yields in the γ radiolysis of cycloheptatriene vapor at room temperature and comparison with those of toluene vapor

	Cycloheptatriene[a]		Toluene[b]
	Pressure, mmHg		
	10.5	10.5	10.7
	Dose, 10^{19} eV		
	1.1	2.7	1.9
Products	G value		
H_2	0.50	c)	0.36
CH_4	0.16	c)	0.15
C_2H_2	1.52	1.49	0.41
C_2H_4	trace	trace	trace
C_2H_6	trace	trace	0.07
Cyclopentadiene	0.29	0.19	d)
Benzene	0.65	0.52	0.18
Toluene	1.68	1.50	—
Dimers	2.99	c)	0.47

a) This work, b) Ref. 4, c) Not determined, d) Not detected.

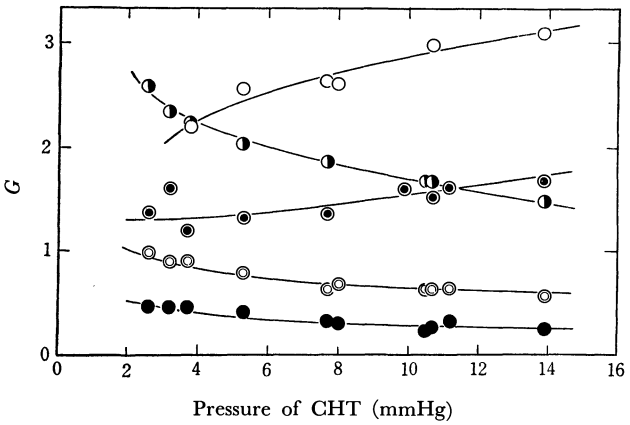

Fig. 1. The pressure dependence of the products yields in the radiolysis of cycloheptatriene vapor: ⊙, C_2H_2; ●, Cyclopentadiene; ◎, Benzene; ◑, Toluene; ○, Dimers.

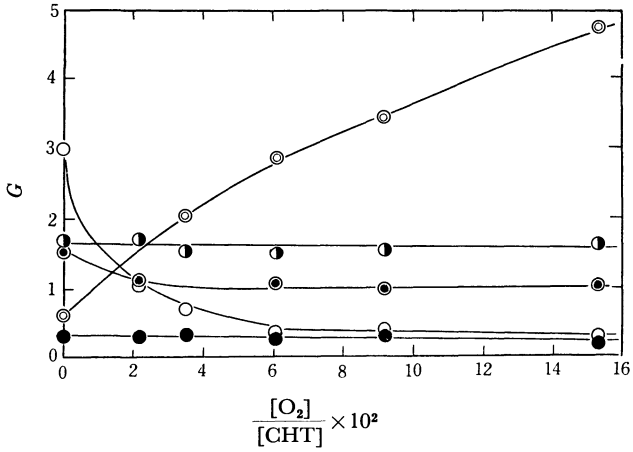

Fig. 2. The effect of an added O_2 in the radiolysis of cycloheptatriene vapor at 10.5 mm: ⊙, C_2H_2; ●, Cyclopentadiene; ⊙, Benzene; ◑, Toluene; ○, Dimers.

6) G. C. Robinson, *J. Org. Chem.*, **29**, 3433 (1964); H. E. Winberg, *ibid.*, **24**, 264 (1959).

7) R. A. Back, T. W. Woodward, and K. A. Mclauchan, *Can. J. Chem.*, **40**, 1380 (1962).

TABLE 2. THE EFFECTS OF ADDITIVES IN THE γ RADIOLYSIS OF CYCLOHEPTATRIENE VAPOR AT 10.5 mmHg

	None	NO		N_2O		NH_3		C_3H_8	
		Mol %							
		2.9	4.7	3.5	10.5	5.4	8.5	8.3	12.8
		G value[a]							
H_2	0.50	0.58	0.58	0.55	0.41	0.50	0.56	b)	b)
CH_4	0.16	b)	b)	b)	b)	0.12	0.05	b)	b)
C_2H_2	1.52	1.07	1.07	1.30	1.21	1.10	0.89	b)	b)
Cyclopentadiene	0.29	0.36	0.33	0.25	0.28	b)	0.31	0.24	0.24
Benzene	0.65	1.55	1.94	0.58	0.68	b)	0.57	0.65	0.65
Toluene	1.68	1.73	1.66	1.57	1.62	b)	1.64	1.58	1.68
Dimers	2.99	1.63	0.96	2.85	b)	3.25	2.85	b)	b)

a) The G values are calculated on the basis of energy absorbed by CHT alone. The total dose is 1.1×10^{19} eV.
b) Not determined.

number might be fourteen were detected gas-chromatographically, though the structure have not determined except for that of bitropyl.[8] The G value of the total dimers is calculated on the assumption that the sensitivity of the detection of dimers is equal to that of bitropyl.

The effect of the total dose was small except in the case of cyclopentadiene at a CHT pressure of 10.5 mmHg over the dose range from 1.1×10^{19} to 2.7×10^{19} eV, as is shown in Table 1. The product yields at a dose of 1.87×10^{17} eV/μmol (CHT) as a function of the CHT pressure are shown in Fig. 1. Though the results for hydrogen and methane are not shown in the figure, $G(H_2)$ and $G(CH_4)$ were essentially unaffected by the CHT pressure.

The experimental results obtained in the presence of an additive, *i.e.*, oxygen, nitric oxide, nitrous oxide, ammonia, or propane, are shown in Fig. 2 and Table 2. Of particular interest is the remarkable increase in the G value of benzene upon the addition of nitric oxide and oxygen. When iodine was added to CHT, the formation of benzene was also observed without γ irradiation, while in the case of oxygen no such behavior was observed. Another significant feature in the additive experiment is the notable decrease in the yield of the dimer upon the addition of a radical scavenger (NO or O_2).

The γ radiolysis of binary mixtures of CHT and benzene was carried out in the presence of nitric oxide (10 mol%). Biphenylmethane and biphenyl were produced with G values of 0.069 and 0.094 respectively, as determined on the basis of the energy absorbed by CHT at a [CHT]/[benzene] molar ratio of 0.466.

Discussion

In the gas-phase radiolysis of CHT, the observed products were hydrogen, methane, acetylene, cyclopentadiene, benzene, toluene, and dimers; Table 1 lists those products together with the results on toluene.[3] The yields of the radiolytic products from CHT were, in general, large compared with those from toluene, especially those of acetylene, benzene, and dimers. Furthermore, cyclopentadiene was a new product which was not observed in the radiolysis of toluene. In the mass-spectrometric studies[1] of these isomeric compounds (CHT and toluene), it is well known that the $C_7H_7^+$ ions are the most abundant in these compounds. However, the present observations seem to show that the common intermediate does not always produce the same final products in both the reaction systems, as will be discussed later. In the liquid-phase radiolysis of CHT, relatively low G values of gaseous products have been reported by Arai *et al.*,[9] and the main reaction was a polymer formation, though the yields of the liquid products were not measured.

Formation of Toluene. As for the radiolytic products from CHT vapor, a fairly large amount of isomerization to toluene was observed, as has been reported in the photolysis[9,10] and pyrolysis[11] of CHT. The toluene formation is essentially unaffected by the addition of appreciable amounts of various scavengers, *i.e.*, oxygen and nitric oxide for radicals, nitrous oxide for electron, ammonia for positive-ions, and propane as a hydride-transfer agent to a positive ion, as is shown in Fig. 2 and Table 2. Thus, it is most reasonable to assume that radicals and positive-ions may be excluded as precursors of toluene in the radiolysis of CHT vapor. On the other hand, an electronically- or vibrationally-excited CHT molecule has been shown to easily isomerize to toluene in photolytic investigations in the gas phase.[9,10] From these results, a direct excitation process such as this seems most reasonable:

$$\text{CHT} \rightsquigarrow \text{CHT}^* \quad (1)$$

$$\text{CHT}^* \longrightarrow \text{Toluene} \quad (2)$$

$$\text{CHT}^* + \text{CHT} \longrightarrow 2\,\text{CHT} \quad (3)$$

The isomerization to toluene (reaction (2)) is presumed to compete with the collisional deactivation (reaction (3)). The steady-state treatment of reactions (1), (2) and (3) gives Eq. (I):

$$1/G(\text{Toluene}) = 1/G^0(\text{Toluene})\{1+k_3/k_2[\text{CHT}]\} \quad (\text{I})$$

where G^0 (Toluene) is the G value of toluene at zero

8) Bitropyl was prepared by the method of Doering and Knox. (mp 61.8°C) W. von E. Doering and L. H. Knox, *J. Amer. Chem. Soc.*, **79**, 352 (1957).

9) S. Arai, M. Maemori, K. Yamaguchi, and S. Shida, This Bulletin, **36**, 590 (1963).
10) R. Srinivasan, *J. Amer. Chem. Soc.*, **84**, 3432 (1962).
11) W. G. Woods, *J. Org. Chem.*, **23**, 110 (1958).

pressure. According to Eq. (I), a plot of $1/G$(Toluene) *vs.* the CHT pressure should give a straight line with a slope of $1/G^0 \cdot k_3/k_2$. Such a plot is shown in Fig. 3, from which the ratio of the rate constant of the deactivation and that of the isomerization, k_3/k_2, as determined by the method of least squares, is found to be 0.051 $mmHg^{-1}$.

In the mercury-sensitized photolysis of CHT vapor by Arai *et al.*,[9] and in the direct photolysis by Srinivasan,[10] a similar kinetic treatment has been carried out. An interesting point is that the value of k_3/k_2 is greater in the photolysis than in the radiolysis; furthermore, it is greater at 3130 Å than at 2600 Å, or in the mercury-sensitized photolysis at 2537 Å, in which the value was 0.11 $mmHg^{-1}$. This means that the higher the energy provided to the CHT molecule, the shorter the lifetime of the active intermediate leading to the toluene formation and quenched poorly by collision, though the nature of the excited state is not clear in the present study. The G value of toluene extraporated to zero pressure is 2.6 in Fig. 3, indicating the G value of the excited CHT which isomerizes to toluene if it is not quenched by collisions.

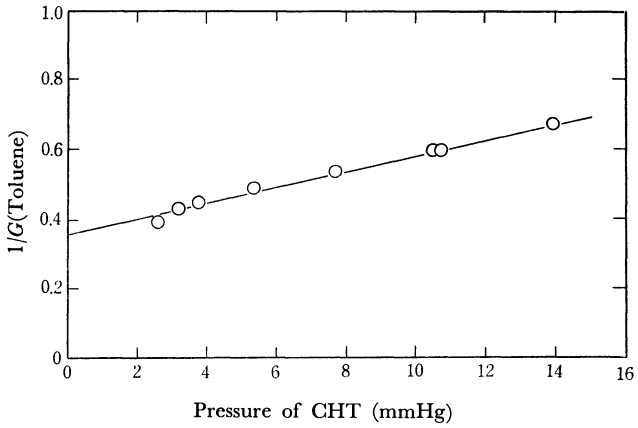

Fig. 3. Kinetic plots of $1/G$(Toluene) *vs.* pressure in the radiolysis of cycloheptatriene vapor.

Formation of Dimers. In the radiation chemistry of liquid hydrocarbon, a dimer which contains two hydrogen atoms less than the starting material has been observed as one of the typical products. For example, the bitropyl obtained from the radiolysis of liquid CHT has been observed to be formed *via* a symmetrical intermediate, the tropyl radical,[11] which has also been reported in the ESR study of the electron irradiated CHT at −196°C.[9] In the present study, bitropyl was not a predominant dimer, but many other dimers were produced to a similar extent, though their structures were not identified. The total dimer yields rapidly decreased upon the addition of oxygen and nitric oxide (Fig. 2 and Table 2), but the isomer distribution remained the same. It is generally assumed that the major effect of oxygen and nitric oxide on the product formation is due to the scavenging of free radicals, though it has been observed in some cases that nitric oxide acts as a charge-transfer agent,[12] since nitric oxide has an ionization potential (9.2 eV)[13] lower than those of many hydrocarbons. However, the decrease upon the addition of oxygen, which has a high ionization potential (12.1 eV),[13] strongly suggests a radical mechanism for the formation of dimers. On the other hand, CHT is also an efficient radical scavenger, so primarily-produced hydrogen atoms and hydrocarbon radicals may be almost all scavenged by CHT even in the absence of a radical scavenger:

$$\text{CHT} \rightsquigarrow \text{C}_7\text{H}_7\cdot + \text{H} \quad (4)$$

$$\text{H} + \text{CHT} \longrightarrow \text{C}_7\text{H}_9\cdot \quad (5)$$

$$\text{C}_7\text{H}_7\cdot + \text{CHT} \longrightarrow \text{C}_{14}\text{H}_{15}\cdot \quad (6)$$

$$\text{C}_7\text{H}_9\cdot + \text{CHT} \longrightarrow \text{C}_{14}\text{H}_{17}\cdot \quad (7)$$

$$\text{R}\cdot + \text{R}\cdot \longrightarrow \text{R-R} \quad (8)$$

$$\longrightarrow \text{RH} + \text{R(-H)} \quad (9)$$

where R is a monomeric or dimeric radical. It may be explained that many kinds of dimers are formed *via* these processes. These observations are obviously different from those for the dimer formation in the gas-phase radiolysis of toluene, in which the effect of nitric oxide is very small and in which ionic processes were predominant.[2,3]

Formation of Benzene. Benzene is a new product which was not reported in the photolysis of CHT vapor.[9,10] The G value of benzene decreased with an increase in the CHT pressure, though the pressure dependence is different from that of toluene. No significant effect on the yield was observed upon the addition of ammonia, propane, or nitrous oxide. Furthermore, it is an interesting fact that the addition of nitric oxide or oxygen remarkably increases the yield of benzene. These additional benzene yields are too large to be explained as the result of sensitization by nitric oxide or oxygen. It is assumed that the active species produced by the irradiation of CHT come to form benzene by means of the added nitric oxide or oxygen. Moreover, ionic species must be excluded, since the ultimate G value of the additional benzene which is obtained by the extrapolation of $1/\Delta G(\text{C}_6\text{H}_6)$ to the infinite concentration of oxygen as shown below is very large ($G_\infty(\text{C}_6\text{H}_6)=8.0$) compared to the G_e of CHT. Since nitric oxide and oxygen are both well known to act as radical scavengers, it seems to be most reasonable to expect the following radical process for the formation of the additional benzene:

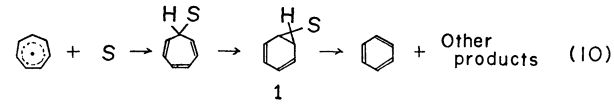

1

where S is a radical scavenger. The norcaradiene-type intermediate (1) was previously suggested in the formation of benzene.[14,15] When a radical scavenger

12) R. D. Doepker and P. Ausloos, *J. Chem. Phys.*, **43**, 3814 (1965).

13) K. Watanabe, *ibid.*, **26**, 542 (1957).

14) M. E. Volpin, D. N. Kurzanov, and V. G. Dulova, *Tetrahedron*, **8**, 33 (1960).

15) T. Mukai, T. Nakazawa, and K. Okayama, *Tetrahedron Lett.*, 1695 (1968).

is absent in the system, tropyl radicals such as those produced by reaction (4) may undergo an addition reaction with CHT, as is shown in reaction (6), thus leading to the dimer formation. The fact that a radical scavenger competes with CHT for tropyl radicals is shown when we plot the yields of benzene and dimers against the concentration of a radical scavenger (Fig. 2). The yields of benzene were increased by an increase in the concentration, while the yields of the dimers were decreased. However, the correlation between these changes in the yields was not satisfactory. This cannot be explained well, but it may be partly caused by the different efficiencies in the dimer formation and the benzene formation from tropyl radicals. Since the reaction of tropyl radicals with CHT (reaction (6)) produces not only dimers but also high-molecular products, the efficiency of the dimer formation becomes relatively low.

A quantitative treatment of the formation of benzene in the presence of a radical scavenger is given by Eq. (II):

$$\frac{1}{\Delta G(C_6H_6)} = \frac{1}{G_1}\left(1 + \frac{k_6}{k_{10}} \cdot \frac{[CHT]}{[S]}\right) \qquad (II)$$

where $\Delta G(C_6H_6)$ is the difference in the G value of benzene, with and without a scavenger, and where G_1 is the G value of the C_7H_7 radical produced by reaction (4). In Fig. 4, $1/\Delta G(C_6H_6)$ is plotted against [CHT]/[S]. From the extrapolation of the straight line to the intercept, the ultimate yield of a tropyl radical (G_1) is observed to be 8.0. The mechanism of the formation of benzene from pure CHT is not clear, but such a free radical process seems to play a part. In this case, instead of oxygen or nitric oxide other small fragment radicals may act as radicals scavengers.

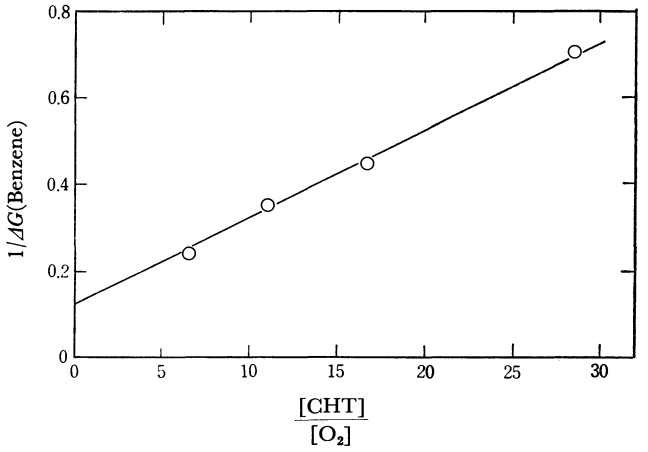

Fig. 4. Kinetic plots of $1/\Delta G$(Benzene) *vs.* [CHT]/[O_2] in the radiolysis of cycloheptatriene-O_2 mixtures.

Formation of Cyclopentadiene and Acetylene. In the mass spectrometry, a $C_5H_5^+$ ion, which could be a precursor of cyclopentadiene by a following hydride-transfer reaction, was reported to be produced by the secondary decomposition of a $C_7H_7^+$ ion:[1]

$$C_7H_7^+ \longrightarrow C_5H_5^+ + C_2H_2 \qquad (11)$$

However, under the radiolytic conditions, where the pressure is much higher compared than that of the mass-spectrometric conditions, a $C_7H_7^+$ ion is known to undergo a very fast ion-molecule reaction before its degradation to a $C_5H_5^+$ ion.[3] Moreover, the formation of cyclopentadiene is essentially unaffected by the addition of various scavengers (NO, O_2, N_2O, NH_3, or C_3H_8), much as in the case of toluene. These observations suggest a direct excitation process of the formation of cyclopentadiene and acetylene:

$$CHT \sim\!\!\wedge\!\!\wedge\!\!\rightarrow CHT^{**} \qquad (12)$$

$$CHT^{**} \longrightarrow \text{cyclopentadiene} + C_2H_2 \qquad (13)$$

$$CHT^{**} + CHT \longrightarrow 2\,CHT \qquad (14)$$

The effect of the CHT pressure on the yield of cyclopentadiene (Fig. 1) was consistent with the above mechanism. The nature of the excited CHT molecule that decomposes to cyclopentadiene and acetylene may be energetically higher than that of a precursor of toluene, since they are poorly quenched by collision and since the process (reaction (13)) was not observed in either the photolysis or the pyrolysis.

On the other hand, acetylene is not only formed by reaction (13) but also by some other processes, because the $G(C_2H_2)$ value is much larger than that of cyclopentadiene and the pressure dependence is different from that of cyclopentadiene. The effects of additives were also observed (Table 2), but the other processes have not yet been clarified.

The Fate of the Tropylium Ion. It was one of the principal purposes of this work to determine the fate of the $C_7H_7^+$ ion generated in the γ radiolysis of CHT vapor. Unfortunately, in the radiolysis of pure CHT vapor information about this has not been obtained from direct evidence, such as the identification of the reaction products *via* the $C_7H_7^+$ ion.

In the mass-spectrometric studies of simple alkylbenzenes,[1,5] it has been shown that the loss of an acetylene molecule (reaction (11)) is the only major decomposition process of the $C_7H_7^+$ ion at a low pressure. In the high-pressure mass spectrometry of toluene,[16,17] it has been reported that the $C_7H_7^+$ and $C_5H_5^+$ ions decay exponentially with the pressure, thus giving a new product ion, $C_{14}H_{15}^+$, However, the $C_{12}H_{13}^+$ product ion, which would be formed by a similar addition reaction of the $C_5H_5^+$ ion to toluene molecules, is absent among the ions in the spectra observed at high concentrations of toluene. It seems reasonable to assume that the addition reaction of the $C_7H_7^+$ ion to toluene and the reaction (11) are competitive and that, in the radiolysis in which the pressure is relatively high compared to that in the ionization chamber of the mass spectrometer, the $C_7H_7^+$ ion exclusively adds to toluene. Consistent with these observation, it has been shown that methyldiphenylmethanes, which are the main dimeric products in the gas-phase radiolysis of toluene, are formed by such an addition of the $C_7H_7^+$ ion to toluene, while the addition

16) S. Wexler and R. P. Clow, *J. Amer. Chem. Soc.*, **90**, 3940 (1968).
17) A. Giardini-Guidoni and F. Zocchi, *Trans. Faraday Soc.*, **64**, 2342 (1968).

products of the $C_5H_5^+$ ion are not present.[2,3] Moreover, it has been confirmed that the $C_7H_7^+$ ion adds also to benzene, which is added in the γ radiolysis of toluene, and thus produces diphenylmethane.[18] These observations suggest that aromatic compounds, such as benzene and toluene, are excellent reagents for the carbonium ion in the gas phase and that they produce relatively stable ions which finally change to the corresponding substituted alkylbenzenes. This technique might be useful for the investigation of the formation and the reactivity of the $C_7H_7^+$ ion in the radiolysis of CHT vapor. The preliminary results showed the formation of the expected biphenylmethane in the radiolysis of CHT vapor in the presence of benzene and a radical scavenger, though the G value was small (0.069). The low yield of diphenylmethane was supposed to be caused by the competitive reactions of the $C_7H_7^+$ ion with benzene and with CHT.

In the present investigation, though the precise reaction mechanism of the $C_7H_7^+$ ion is not yet clear, it is most reasonable to assume an ionic polymerization of CHT initiated by the $C_7H_7^+$ ion, for the dimeric products disappear upon the addition of a radical scavenger and CHT is expected to be subject to ionic polymerization, much as in the case of cyclopentadiene.[19] The mechanistic details of the reaction of the $C_7H_7^+$ ion are currently under investigation in these binary mixtures, CHT-benzene, CHT-toluene, and CHT-h_8-toluene-d_8.

We wish to thank Mr. Tamotsu Yamamoto and Mr. Tomikazu Sawai of the Radiation Laboratory for their assistance in the γ irradiations.

18) K. Nakamura, S. Takamuku, and H. Sakurai, to be published.

19) M. A. Bonin, W. R. Busler, and F. Williams, *J. Amer. Chem. Soc.*, **87**, 199 (1965).

BULLETIN OF THE CHEMICAL SOCIETY OF JAPAN, VOL. 44, 2095—2103 (1971)

The Crystal Structure of the 2 : 3 Complex of Zinc Phthalocyanine and *n*-Hexylamine[1]

Takashi KOBAYASHI, Tamaichi ASHIDA,* Natsu UYEDA, Eiji SUITO, and Masao KAKUDO*

Institute for Chemical Research, Kyoto University, Gokasho, Uji, Kyoto

* *Institute for Protein Research, Osaka University, Kitaku, Osaka*

(Received February 12, 1971)

Crystals of the 2 : 3 complex of zinc-phthalocyanine and normal hexylamine were studied. They are monoclinic, space group $P2_1/c$, with cell dimensions $a=12.40$, $b=15.76$, $c=20.05$, $\beta=93.2°$ and there are four phthalocyanine and six hexylamine molecules per cell. The phthalocyanine molecule is not planar and the central zinc ion is displaced from the plane by 0.48 Å toward the nitrogen atom of the amine. Zinc ion is of a square pyramidal five coordination. There are two bonding states for the amine in the complex crystal. One is weakly bonded and can be easily released from the lattice and the other is strongly bonded and coordinated directly to the zinc ion. None of the atomic parameters of these amines except those of the coordinating nitrogen were exactly determined.

Phthalocyanine and its metal derivatives have been regarded as important and being studied in many fields such as pigment industry, solid state physics of organic crystals, catalysis, colloid and coordination chemistry and X-ray crystallography. They assume a common molecular structure similar to porphin derivatives and are of interest also from a biological view point particularly when they form additive complexes with both aliphatic and aromatic amines with respect to Mn[2], Cr[3], Fe[4], and Zn[5] derivatives.

In the course of electron microscopy and X-ray diffraction study on the polymorphic transformation of powdery zinc phthalocyanine which usually takes place in various organic dispersion media, Kobayashi, Uyeda, and Suito[5] found that various additive complexes are produced as crystalline powders stoichiometrically taking up the molecules of amine in which the original powder was dispersed. By means of differential thermal analysis, the molecular ratio of amine molecules to the zinc phthalocyanine matrix was found to depend upon the species of amine itself, whereas the vibrational spectra of these compounds in both rock salt and far infrared regions strongly indicated[6] that the solvated amine molecules are, as strong n-donors, rigidly bound to the central zinc ion with the lone pair electrons of nitrogen atoms. In order to clarify the electronic configuration of the intermolecular bonding which has much to do with the physical properties of the complexes as the biological model or organic semiconductor, the three dimensional structure should be studied in more detail with respect

1) The main part of this work was carried out in the Institute for Protein Research, Osaka University.

2) J. A. Elvidge and A. B. P. Lever, *Proc. Chem. Soc.*, **1959**, 195.

3) J. A. Elvidge and A. B. P. Lever, *J. Chem. Soc.*, **1961**, 1257.

4) M. Whalley, *ibid.*, **1961**, 866.

5) T. Kobayashi, N. Uyeda, and E. Suito, *J. Phys. Chem.*, **72**, 2446 (1968).

6) T. Kobayashi, N. Uyeda, and E. Suito, *Bull. Inst. Chem. Res. Kyoto Univ.*, **47**, 401 (1969).

to the coordination number of the metal ion, the intermolecular bonding length, the mutual position of the phthalocyanine and solvated molecules. The crystal structure of pyridine complex of phthalocyanatomanganese was determined by Vogt *et al*[7]. to show that the pyridine molecules are perpendicularly conjugated with the nitrogen atoms to the central metal ions, a pair of which are further connected by an oxygen molecule to form a parallel double complex.

Although this result indirectly supported the idea about the molecular structure of the complexes of zinc-phthalocyanine as deduced from the vibrational spectra, no data about their crystal structures have been reported for those with aliphatic amines.

In view of this, three dimensional X-ray analysis has been undertaken with a well defined single crystal of *n*-hexylamine complex as the first example in a series of similar addition compounds of zinc phthalocyanine.

Experimental

Pure zinc phthalocyanine was prepared following the same procedure as described previously.[5] About 0.1 g of the powder zinc phthalocyanine was completely dissolved into 10 m*l* of specially prepared *n*-hexylamine. When the solvent was slowly evaporated at room temperature, purple hexahedral crystals were obtained in various sizes. After identifying the product as the expected complex with a rotation photograph, a crystal of about $0.2\times0.2\times0.5$ mm was chosen as a specimen for Weisenberg photographs with Ni-filtered Cu$K\alpha$ radiation. Intensity data were recarded on the Weisenberg photographs taken around the *a*-axis up to the ninth layer and around the *b*-axis up to the twelfth layer.

The number of independent reflections thus observed were about 3000 excluding the zero intensity reflections. Intensity data were derived from films prepared by the multiple-film equi-inclination technique. They were then converted to structure amplitudes after the usual Lorentz and polarization factors had been corrected. No correction for absorption was made.

The molecular ratio of *n*-hexylamine to zinc phthalocyanine was determined by thermal gravimetry,[5] and the density of the crystal was measured by the flotation method with an aqueous solution of potassium bromide.

Results

a) Crystal Data. The crystal of the *n*-hexylamine complex of zinc phthalocyanine belongs to the monoclinic system. The unit cell dimensions are

$$a = 12.40\,\text{Å} \pm 0.02$$
$$b = 15.76\,\text{Å} \pm 0.02$$
$$c = 20.05\,\text{Å} \pm 0.05$$
$$\beta = 93.2^\circ \pm 0.5$$
$$V = 3902.6\,\text{Å}^3$$

The systematic absences are recognized for reflections h0l and 0*k*0 with *l* and *k* odd, respectively, indicating that the space group is $p2_1/c$.

b) Number of n-*hexylamine Molecules in a Unit Cell.* The number of *n*-hexylamines relative to that of zinc phthalocyanine was determined by thermal gravimetry. When the complex is heated, decomposition takes place in two stages releasing *n*-hexylamine molecules stepwise at 140 and 180°C. At temperatures higher than 180°C, decomposition is completed leaving pure zinc phthalocyanine of the β polymorph. Thus, the total reaction can be described by the following equation, where *p* and *q* are the numbers of the component molecules in the complex and ZnPc and Am stand for zinc phthalocyanine and amine.

$$(\text{ZnPc})_p(\text{Amine})_q \rightarrow p\text{ZnPc} + q\text{Am}$$

The percentage weight loss W is related to *p* and *q* as follows.

$$W = \frac{q[\text{Am}]\times 100}{p[\text{ZnPc}] + q[\text{Am}]} = \frac{\text{Weight loss}\times 100}{\text{total weight of complex}}$$

where the brackets denote the molecular weights of components. The actual weight loss was determined to be 20.0%, which shows good agreement with the calculated value of 20.8% when $p : q$ is taken to be 2 : 3 (with $p : q = 1 : 1$, $W = 14.9\%$ and with $p : q = 1 : 2$, $W = 25.8\%$). Thus, the calculated density becomes 1.239 g/cm^3 if four phthalocyanine molecules are assumed to exist in the unit cell. Since the actual density was found to be 1.30 g/cm^3 by the floatation method, it seems reasonable to conclude that the unit cell has four zinc phthalocyanine and six *n*-hexylamine molecules.

c) Structure Determination. The coordinates of the zinc ion were derived from a three dimensional Patterson function as $x/a = 0.020$, $y/b = 0.028$, and $z/c = 0.182$. An electron density function was calculated with the phases due to the zinc ion. The Fourier maps showed all the non-hydrogen atoms of zinc phthalocyanine, and the nitrogen atom of a *n*-hexylamine 2.20 Å apart from the zinc ion lying almost in the center of the planar phthalocyanine molecule. The structure factors were calculated using these atomic positions shown in the maps and the atomic parameters were refined three times by successive cycles using the block-diagonal least-squares method. The discrepancy index R was 0.17 at this stage. Although the appearance of a nitrogen atom near the zinc ion indicated that only one *n*-hexylamine is coordinated to a phthalocyanine molecule, the positions of the carbon atoms of *n*-hexylamine could not be distinctly determined, since the electron density maps showed lower peaks at the positions of these atoms with only about one fifth of the peak heights of the carbon atoms in the phthalocyanine ring. With existence probabilities set as one half, the positions of the five carbon atoms of the *n*-hexylamine were added to those of the other well defined atoms. By use of this new set of positions, several cycles of structure factor calculations and least-squares refinements were performed to reach a discrepancy index of 0.15 in the final stage. No information concerning the other two amine molecules was obtained. The final atomic parameters and their thermal parameters are listed in Table 1, and the calculated and observed structure factors are compared in

7) L. H. Vogt, A. Zalkin, and D. H. Templeton, *Inorg. Chem.*, **6**, 1725 (1967).

Table 1. The positional parameters and isotropic thermal parameters

Atom	x	y	z	B	Atom	x	y	z	B
Zn	0.01962	0.02872	0.18170	*	C 12	0.50877	0.12408	0.08408	3.606
N 1	0.10521	−0.04846	0.24766	3.783	C 13	0.45632	0.15766	0.02716	3.664
N 2	0.16137	0.06436	0.14271	2.301	C 14	0.34198	0.15782	0.01901	3.187
N 3	−0.05425	0.05480	0.08941	2.184	C 15	0.28520	0.11969	0.07288	2.302
N 4	−0.10635	−0.05608	0.19602	2.395	C 16	0.16988	0.10414	0.08170	2.556
N 5	0.28715	0.00373	0.22868	2.952	C 17	−0.00722	0.10325	0.03831	2.717
N 6	0.09545	0.12683	0.03538	2.332	C 18	−0.09063	0.11998	−0.01443	1.823
N 7	−0.23224	−0.00763	0.10297	2.447	C 19	−0.09030	0.16462	−0.07564	2.884
N 8	−0.03627	−0.13280	0.29427	3.444	C 20	−0.18392	0.17164	−0.11725	3.682
N 9	−0.01453	0.14412	0.23692	5.166	C 21	−0.28283	0.13293	−0.09682	3.398
C 1	0.06365	−0.10772	0.29404	2.882	C 22	−0.28412	0.08595	−0.03626	2.540
C 2	0.15172	−0.13649	0.34291	3.272	C 23	−0.18578	0.07948	0.00645	2.588
C 3	0.15201	−0.19087	0.40053	4.965	C 24	−0.15921	0.03972	0.07096	2.372
C 4	0.25244	−0.20080	0.43515	5.279	C 25	−0.20204	−0.05155	0.16127	1.713
C 5	0.34347	−0.16660	0.41305	4.617	C 26	−0.28160	−0.10223	0.19443	3.426
C 6	0.34954	−0.10991	0.35705	4.501	C 27	−0.39357	−0.11560	0.18109	4.415
C 7	0.24789	−0.09446	0.32225	3.540	C 28	−0.44634	−0.16863	0.22930	7.114
C 8	0.21643	−0.04190	0.26417	3.349	C 29	−0.38543	−0.20911	0.28275	7.093
C 9	0.26108	0.04780	0.17321	2.404	C 30	−0.27565	−0.19173	0.30019	5.036
C 10	0.34414	0.08805	0.13040	2.284	C 31	−0.22428	−0.13906	0.25132	3.244
C 11	0.45630	0.08377	0.13603	3.397	C 32	−0.11389	−0.10909	0.25095	2.567

The estimated standard deviations for all atoms range from 0.003Å to 0.0365Å and average 0.023Å.

* The anisotropic temperature factor for zinc ion is defined by the expression

$$\exp\{-(h^2\beta_{11}+k^2\beta_{22}+l^2\beta_{33}+hk\beta_{12}+hl\beta_{13}+kl\beta_{23})$$

where $\beta_{11}=0.004467$ $\beta_{22}=0.002933$ $\beta_{33}=0.001438$ $\beta_{12}=-0.000322$ $\beta_{13}=0.000632$ $\beta_{23}=0.000740$

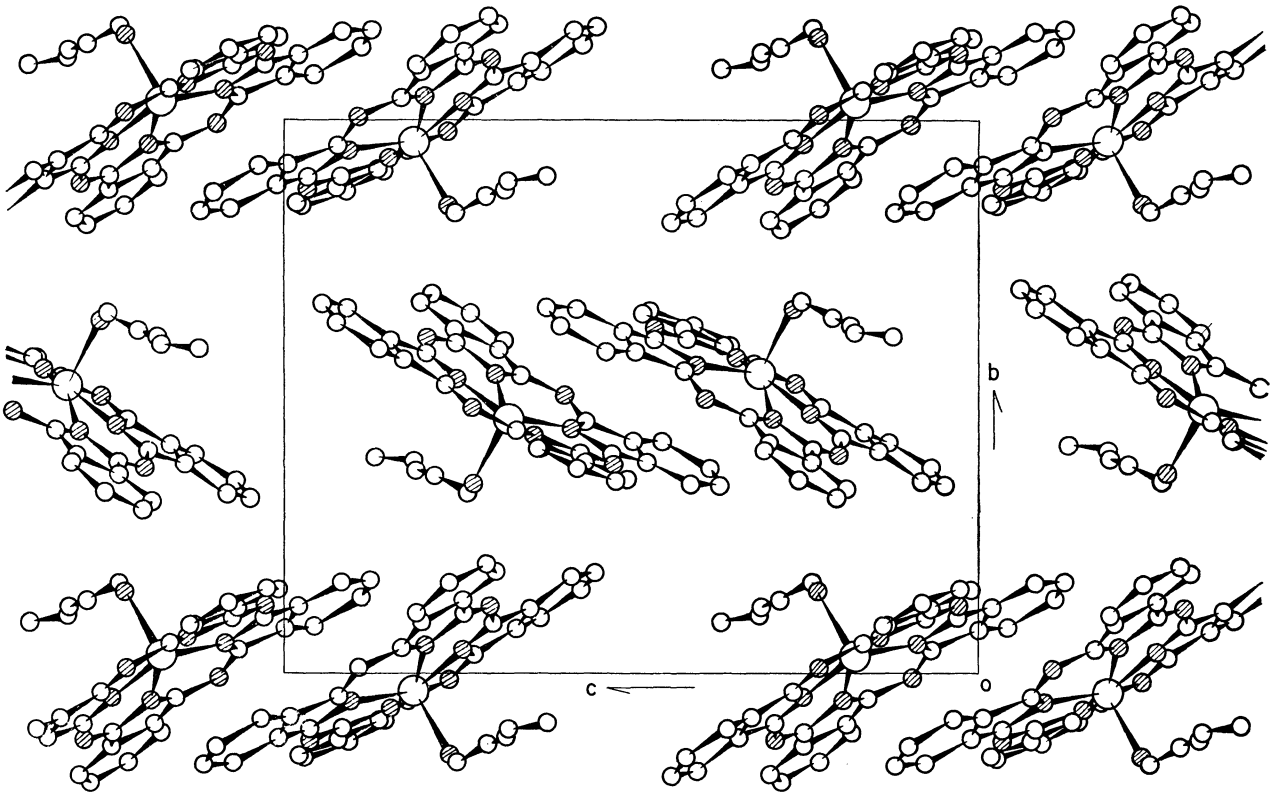

Fig. 1. The crystal structure viewed along the a axis.
◯ : Zn^{2+}, ◍ : N, ○ : C

TABLE 2. OBSERVED AND CALCULATED STRUCTURE FACTORS

K	FO	FC	K	FO	FC	K	FO	FC	K	FO	FC	K	FO	FC	K	FO	FC	K	FO	FC	K	FO	FC
H,L= 0 22			3	59	-51	H,L= 1 22			0	116	-108	5	16	8	H,L= 1-11			5	36	21	7	66	68	0	54	57	8	57	59
0	19	21	4	93	84	0	18	29	1	57	18	6	63	89	11	58	-12	4	46	48	10	27	23	1	26	9	9	59	11
2	25	32	5	23	-14	2	31	28	2	105	108	7	15	-14	12	17	-14	6	18	18	11	23	-13	2	98	-75	10	40	42
4	22	24	6	51	52	4	18	23	3	34	26	8	61	72	13	60	-8	H,L= 2 15			H,L= 2 4			4	76	-75	11	29	5
6	16	-1	7	22	16	H,L= 1 21			4	78	-77	9	25	-17	15	47	-51	2	49	54	0	36	41	5	30	-18	H,L= 2-14		
H,L= 0 21			8	56	49	1	26	45	6	25	-25	10	26	33	19	40	-12	3	34	30	1	52	47	6	35	17	0	50	-51
2	36	43	10	68	66	2	23	29	7	15	5	H,L= 1 -2			H,L= 1-12			4	32	29	3	22	45	7	35	-32	2	49	-43
3	17	16	11	38	34	4	20	18	8	37	30	0	73	-80	0	48	46	5	50	38	4	23	-26	9	48	-52	4	38	-46
4	20	30	13	28	43	H,L= 1 20			10	30	24	1	51	90	1	27	22	8	24	22	5	58	53	11	54	-58	6	33	-32
6	18	10	14	34	-10	3	19	22	H,L= 1 7			2	49	-88	2	19	17	9	25	-18	6	18	22	H,L= 2 -5			H,L= 2-15		
H,L= 0 20			H,L= 0 8			4	19	-20	1	28	-18	3	56	93	3	33	34	10	40	37	7	65	72	1	57	60	1	38	-30
2	20	-16	0	81	-81	5	20	14	2	56	-39	4	47	-62	4	21	24	H,L= 2 14			8	19	17	3	56	51	2	16	-16
3	25	30	2	62	-61	6	20	-22	3	23	-24	5	95	95	5	58	54	0	26	-31	9	69	71	4	67	-63	4	19	-22
4	21	-15	3	37	-26	H,L= 1 19			4	82	-85	6	64	-57	6	27	21	1	19	19	11	46	47	5	39	44	6	19	-32
5	20	20	4	46	-47	1	28	-42	5	27	-25	7	53	61	7	40	36	2	35	-37	H,L= 2 3			6	95	-93	8	34	-31
7	22	18	5	16	9	2	19	19	6	78	-73	8	20	-7	8	28	-24	3	52	32	1	39	-25	7	20	17	H,L= 2-16		
H,L= 0 19			6	15	-11	5	19	-24	8	51	-46	9	30	36	10	35	-33	4	24	-26	2	41	-24	8	53	-51	0	26	22
1	52	-58	9	28	-22	7	41	-23	9	24	19	10	36	39	11	34	31	9	22	19	3	55	-14	9	19	11	2	37	38
4	20	-11	12	34	49	H,L= 1 18			10	46	-50	11	44	50	H,L= 1-13			11	34	24	4	35	34	10	32	-23	4	35	35
6	19	-8	14	28	43	0	26	-28	H,L= 1 6			H,L= 1 -3			1	20	-28	H,L= 2 13			5	32	-28	11	17	-10	7	32	-29
7	20	-15	H,L= 0 7			1	24	23	1	86	-74	2	142	132	3	48	-47	1	47	-49	6	71	73	H,L= 2 -6			H,L= 2-17		
H,L= 0 18			1	16	-15	2	24	-20	2	67	65	4	276	269	4	46	51	2	25	-25	7	25	-28	0	64	56	1	36	31
0	43	-50	3	43	-41	5	45	-46	3	70	-83	5	161	-185	6	28	26	3	31	-59	8	62	65	1	26	24	3	34	39
2	24	-9	6	76	-75	7	50	-52	4	40	48	7	14	3	8	21	25	4	23	-21	10	24	21	2	70	58	9	25	7
3	18	-28	7	59	-53	9	41	-32	5	63	-58	8	62	-55	9	19	-19	8	30	-28	H,L= 2 2			3	68	62	H,L= 2-18		
4	39	37	8	102	-114	H,L= 1 17			6	20	-16	9	58	60	10	36	27	10	31	-30	0	25	-12	4	50	49	0	25	-10
5	45	-50	10	54	-57	1	26	28	7	87	-88	10	15	0	H,L= 1-14			H,L= 2 12			1	23	-19	5	82	-73	7	28	28
6	25	17	11	20	16	2	24	21	9	50	-44	11	29	33	0	60	-69	0	28	-16	2	15	7	6	66	75	H,L= 2-19		
7	36	-38	12	34	-33	6	38	-41	10	19	-11	H,L= 1 -4			2	51	-50	1	29	-27	3	11	-40	7	115	-96	1	47	-48
9	32	-26	H,L= 0 6			7	28	24	11	23	-19	0	121	92	4	43	-43	3	77	-28	5	31	-21	8	88	80	2	31	-36
H,L= 0 17			1	64	-61	8	24	-22	H,L= 1 5			1	121	-126	6	20	-18	4	35	31	6	40	-47	9	16	19	3	30	-31
1	31	28	2	103	94	H,L= 1 16			1	38	48	2	71	39	H,L= 1-15			5	29	-27	7	15	-17	10	28	21	H,L= 2-20		
3	18	24	3	15	12	0	31	29	2	55	-45	4	215	-231	2	22	-30	6	16	13	8	26	-21	11	37	30	0	25	-36
4	20	-21	4	32	29	1	18	15	3	68	71	5	116	143	3	21	-31	7	29	-33	9	54	-55	12	31	-30	2	20	-16
5	37	37	5	34	23	2	41	38	4	18	-15	6	112	-114	4	17	-21	8	41	-32	11	34	-41	H,L= 2 -7			3	23	-28
6	36	-26	6	64	-53	4	46	45	5	9	10	7	49	-60	6	29	12	9	27	-33	H,L= 2 1			1	25	18	4	19	-10
7	28	24	7	65	-58	6	20	26	6	61	45	9	80	79	7	20	16	11	51	-46	1	25	2	2	60	37	H,L= 2-21		
8	24	-17	8	20	-8	7	32	29	7	23	-18	9	83	-106	10	40	-37	H,L= 2 11			3	48	-6	3	19	-3	2	19	-26
H,L= 0 16			9	68	-71	H,L= 1 15			10	18	21	10	16	17	H,L= 1-16			1	51	57	4	58	-57	4	77	67	4	18	-23
0	29	32	11	42	-45	1	19	-23	11	25	-23	11	45	-48	0	45	50	3	21	74	5	8	-2	5	70	-69	H,L= 2-22		
2	47	39	H,L= 0 5			2	19	22	H,L= 1 4			H,L= 1 -5			1	32	-32	5	49	46	6	68	-81	6	47	44	0	23	25
4	35	27	1	51	52	3	31	26	0	86	43	1	37	60	2	32	24	6	18	-21	7	12	17	7	70	75	2	18	25
5	19	19	3	70	72	5	43	32	2	41	24	2	19	-23	3	28	-32	9	34	-27	8	39	-49	8	30	-25	4	16	18
7	22	24	4	68	59	6	25	30	3	85	113	4	69	-77	4	25	21	H,L= 2 10			10	58	-68	9	95	98	H,L= 3 22		
9	32	26	5	62	58	7	36	-30	4	24	30	5	58	62	5	19	13	0	61	53	11	6	-10	10	33	31	0	24	28
H,L= 0 15			6	120	110	8	72	65	5	68	87	6	35	-31	6	26	26	2	34	39	13	31	-6	12	53	70	2	16	18
1	29	-22	8	27	18	9	44	-35	6	19	-6	8	88	-90	9	32	-22	3	75	24	H,L= 2 0			H,L= 2 -8			H,L= 3 21		
5	10	-19	9	36	-31	10	40	45	7	57	52	9	24	22	H,L= 1-17			4	31	26	0	61	-49	0	61	-39	2	18	-8
6	30	32	H,L= 0 4			H,L= 1 14			9	56	64	10	51	-50	1	40	37	5	49	50	1	68	99	1	24	21	5	17	16
7	39	-33	0	39	33	0	56	-57	10	17	15	11	10	-16	3	25	24	6	14	7	2	29	24	2	61	-58	H,L= 3 20		
8	42	40	1	44	-24	2	51	-50	11	32	37	H,L= 1 -6			5	19	25	7	36	30	3	52	-15	3	15	15	0	26	-27
10	40	37	2	36	-37	4	31	-29	H,L= 1 3			0	69	57	6	18	15	9	20	25	4	9	12	4	41	-35	5	19	19
H,L= 0 14			4	42	-45	8	34	-30	1	144	-127	10	8	13	7	22	20	11	43	34	5	28	-37	5	50	50	H,L= 3 19		
0	64	-63	5	61	62	9	52	42	2	171	155	2	61	48	H,L= 1-18			H,L= 2 9			6	33	32	6	58	-65	1	32	-33
1	17	-15	6	29	25	11	24	26	3	133	124	4	69	72	5	19	25	1	62	-58	7	20	30	7	61	65	2	20	-15
2	56	-59	7	66	73	H,L= 1 13			4	93	76	5	54	-47	6	21	19	2	14	13	8	27	27	10	38	33	3	27	-35
4	37	-35	8	33	33	1	41	-32	5	46	-50	6	70	75	7	28	25	3	37	-63	9	14	-18	H,L= 2 -9			H,L= 3 18		
6	36	-32	9	51	58	2	18	-24	9	44	40	7	123	-112	9	26	19	4	40	41	10	20	-40	1	77	-71	0	39	-29
H,L= 0 13			10	16	-9	3	29	-26	11	22	16	8	70	61	H,L= 1-19			5	44	-42	11	15	-14	2	43	43	7	29	-23
1	26	-26	11	33	37	4	30	-26	H,L= 1 2			10	19	10	1	28	-29	6	62	67	12	25	-33	4	11	-9	H,L= 3 17		
3	28	-25	H,L= 0 3			5	33	-32	0	95	-114	11	61	63	3	25	-26	7	34	-28	13	26	5	5	26	-20	1	33	31
5	15	-16	1	82	-67	6	20	-25	1	30	51	14	25	-5	H,L= 1-21			8	49	48	H,L= 2 -1			6	87	-80	2	24	10
6	36	-38	2	130	-135	8	30	-24	2	70	-63	H,L= 1 -7			2	20	-28	11	27	20	1	68	28	7	49	-42	3	28	27
8	39	-41	3	218	-235	10	25	-16	3	83	-53	1	24	-9	4	23	-24	H,L= 2 8			2	207	166	8	33	-17	5	19	12
10	25	-24	4	146	-138	11	24	23	4	22	30	2	52	33	H,L= 1-20			0	99	-90	3	85	-58	9	59	-69	8	23	-24
H,L= 0 12			5	91	-113	H,L= 1 12			5	33	-33	4	65	72	2	20	-27	1	24	17	4	41	35	10	32	-25	H,L= 3 16		
0	70	70	6	37	31	0	43	43	6	37	-31	5	58	-44	4	19	-27	2	122	-112	5	69	65	11	60	-57	0	27	29
1	20	10	7	28	26	1	13	7	7	21	-22	6	39	35	7	21	-23	3	14	29	6	48	50	H,L= 2-10			2	43	41
2	51	49	8	51	50	2	53	59	8	13	-9	7	48	44	H,L= 1-22			4	91	-91	7	12	0	0	12	1	4	39	36
3	23	14	9	53	50	3	30	-33	9	72	-83	9	49	52	4	21	30	6	40	-34	8	74	75	1	51	47	H,L= 3 15		
4	21	18	10	21	-11	4	52	47	10	46	51	10	68	67	H,L= 2 22			8	17	-25	9	7	-5	2	39	39	1	35	-26
5	32	-26	11	26	23	5	46	-47	11	42	-46	13	47	0	0	25	29	9	19	10	10	29	24	4	19	14	2	51	49
6	27	24	H,L= 0 2			9	38	-32	H,L= 1 1			H,L= 1 -8			4	17	15	11	26	-17	11	15	-16	5	80	-78	3	32	21
7	61	-67	0	154	-191	11	45	-48	1	36	39	0	69	-66	H,L= 2 21			H,L= 2 7			12	30	32	6	14	-15	5	27	24
9	34	-31	1	92	-147	H,L= 1 11			2	50	-87	2	56	-60	1	19	25	1	39	-49	13	32	-36	7	78	-87	8	24	25
10	35	-31	2	71	-120	1	105	98	3	40	24	4	30	-42	3	19	10	3	74	10	14	32	35	9	76	-71	10	39	34
12	28	-26	3	83	-136	2	16	10	4	20	-4	5	38	38	4	19	23	4	39	-46	H,L= 2 -2			10	44	-46	H,L= 3 14		
H,L= 0 11			4	53	-65	3	87	93	5	10	8	6	32	-25	H,L= 2 20			5	12	-4	0	32	-62	11	23	-20	0	36	-49
1	83	84	5	72	-67	5	53	53	6	57	-65	7	23	17	4	21	-14	6	66	-72	1	12	8	12	42	-55	1	36	31
3	78	75	6	34	-24	6	15	-9	7	8	-6	8	37	-23	5	19	17	8	58	-57	2	59	-45	H,L= 2-11			2	53	-55
4	14	9	7	31	-37	H,L= 1 10			8	59	-65	9	25	22	6	19	-14	10	26	-26	3	83	105	1	46	51	3	48	43
5	34	29	9	25	-31	0	29	-25	10	50	-63	11	33	31	H,L= 2 19			11	21	14	4	53	-57	3	47	53	4	35	-27
8	19	-13	10	28	19	1	12	17	11	19	-23	H,L= 1 -9			1	46	-49	H,L= 2 6			5	46	50	5	48	42	11	37	31
11	50	-47	11	46	-51	2	33	37	12	33	-44	2	58	39	3	23	-15	0	82	74	6	5	5	H,L= 2-12			H,L= 3 13		
14	33	-8	12	38	38	3	43	48	H,L= 1 0			3	10	-13	H,L= 2 18			2	66	55	7	57	54	1	33	31	1	55	-60
H,L= 0 10			H,L= 0 1			4	44	39	0	235	240	4	43	-45	0	36	-35	3	37	-70	8	27	24	2	31	25	3	37	-38
0	58	46	2	36	117	5	53	48	2	153	175	5	40	-38	1	25	24	4	101	98	9	61	77	3	54	57	4	19	-17
1	15	-2	3	50	23	7	36	39	3	28	-20	6	85	-77	5	19	-21	5	85	-84	10	16	12	4	47	46	5	28	-25
3	30	23	4	106	-115	9	43	34	4	34	37	7	45	-38	7	45	-42	6	72	68	11	25	22	5	49	44	6	21	-23
4	19	21	5	72	-81	11	23	20	5	19	-30	8	56	-52	9	25	-21	7	59	-59	H,L= 2 -3			6	27	26	H,L= 3 12		
5	66	61	6	52	-63	H,L= 1 9			6	35	23	10	22	-16	H,L= 2 17			8	22	14	1	85	-96	7	60	58	0	50	-37
6	38	27	7	24	26	1	126	-115	8	13	8	H,L= 1-10			1	34	31	9	43	-42	2	90	79	8	29	20	1	25	20
7	62	58	8	75	-59	2	75	69	9	20	-18	0	88	86	2	24	22	11	20	-18	3	127	-113	11	24	24	2	20	-18
9	48	43	10	38	-36	3	82	-69	10	37	-47	1	14	2	3	23	8	H,L= 2 5			5	64	-62	H,L= 2-13			4	43	33
10	23	10	H,L= 0 0			4	60	61	11	13	-12	2	40	35	6	28	-28	1	98	103	6	44	44	1	20	-19	5	51	-53
11	48	49	2	240	250	5	20	-17	H,L= 1 -1			3	20	-20	8	30	-29	2	15	-17	7	43	32	2	61	65	6	14	12
13	28	20	4	278	-238	6	64	62	1	155	165	5	86	-85	H,L= 2 16			3	46	36	9	22	17	3	30	-31	7	43	-42
H,L= 0 9			6	46	23	8	45	39	2	49	-103	7	64	-64	0	31	26	4	20	3	9	31	24	4	46	41	8	42	-43
1	42	-43	8	40	26	10	35	33	3	87	98	9	45	-40	1	23	14	5	68	63	11	8	13	5	22	-24	9	27	-27
2	28	-27	14	35	-39	H,L= 1 8			1	20	-2	11	51	-48	2	46	47	6	36	-22	H,L= 2 -4			6	33	28	10	31	-29

TABLE 2. Continued

K	FO	FC	K	FO	FC	K	FO	FC	K	FO	FC	K	FO	FC	K	FO	FC	K	FO	FC	K	FO	FC
11	34	-34	7	47	-58	1	19	-13	H,L=	4	20	H,L=	4	6	1	20	18	0	46	44	2	22	20	H,L=	5	1	0	19	12
H,L=	3	11	8	37	-37	2	54	-54	0	24	-25	0	42	-42	2	17	-15	1	27	26	3	39	-38	1	10	-15	2	33	-28
1	27	26	9	26	-25	3	13	19	3	18	19	1	81	-77	3	55	48	2	47	43	5	45	-49	3	19	-15	3	28	34
2	40	39	10	31	-27	4	34	-61	5	26	29	2	34	25	5	72	62	3	44	45	6	17	-12	4	67	-69	4	51	-47
3	53	55	H,L=	3	1	5	43	44	H,L=	4	19	3	86	-80	6	18	-16	4	28	27	7	28	-26	5	19	17	5	50	47
4	15	7	1	24	8	6	25	-14	1	32	-36	4	67	64	7	60	63	5	35	31	9	36	-27	6	71	-76	6	21	-18
5	49	48	2	50	-47	7	25	18	3	33	-27	5	34	-29	9	62	56	7	30	33	11	29	-27	7	15	-12	7	38	31
6	48	-45	3	10	2	9	41	42	H,L=	4	18	6	23	-12	10	19	16	9	39	29	H,L=	5	11	8	37	-47	9	29	33
8	29	-21	4	43	-55	11	44	49	1	30	-27	7	54	-61	11	44	47	H,L=	4	-13	1	51	58	9	22	-20	11	33	34
9	44	-45	6	68	-67	H,L=	3	-9	3	31	-33	8	39	-33	H,L=	4	-3	2	51	53	2	18	-17	10	44	-40	H,L=	5	-9
11	34	-36	9	80	-93	2	38	21	5	19	-14	9	49	-46	1	92	-86	3	26	-29	3	50	61	11	21	20	1	74	-83
H,L=	3	10	9	15	13	3	48	-40	7	28	-21	11	22	-20	2	18	-11	4	51	45	4	56	-67	12	30	-41	2	13	5
0	51	44	10	35	-35	4	30	-38	H,L=	4	17	H,L=	4	5	3	88	-79	5	16	-12	5	58	57	H,L=	5	0	3	70	-68
2	38	34	H,L=	3	0	5	59	-59	2	27	-29	1	10	3	4	80	-40	6	43	51	6	21	-16	0	32	21	4	9	6
3	18	12	0	65	57	6	75	-74	3	35	35	2	20	-14	5	105	-92	7	24	19	10	27	-23	1	40	-31	5	38	-26
4	47	43	1	49	-30	7	26	-21	4	34	-35	3	120	120	6	39	-33	8	51	48	H,L=	5	10	2	50	50	6	22	-18
5	56	58	2	65	46	8	22	-12	5	18	20	4	64	-62	7	27	-30	10	31	30	0	58	50	3	9	-1	8	24	-27
6	36	35	3	10	-8	9	24	-20	6	19	-24	5	54	51	9	15	5	H,L=	4	-14	2	49	48	4	92	80	11	34	36
7	39	39	4	41	33	10	23	21	8	25	-26	7	26	-20	11	14	20	0	44	-42	3	14	7	5	14	10	H,L=	5	-10
10	24	-17	6	41	39	11	39	-35	H,L=	4	16	8	38	35	H,L=	4	-4	2	48	-51	4	39	49	6	36	28	0	47	-35
11	29	25	8	50	53	H,L=	3	-10	0	45	46	10	28	22	0	29	-28	4	35	-41	6	42	35	7	73	-70	2	14	-9
H,L=	3	9	10	14	17	0	74	58	2	36	35	1	10	3	1	31	-19	H,L=	4	-15	9	32	32	8	16	-13	5	37	-36
1	79	-63	11	10	-9	1	34	25	3	34	-9	2	20	-14	2	79	-61	1	60	-57	H,L=	5	9	9	61	-59	6	22	-23
2	46	-38	H,L=	3	-1	2	28	23	4	30	30	3	120	120	3	116	-112	2	36	-31	2	33	31	10	16	-17	7	66	-71
3	23	10	2	21	11	3	27	-20	6	20	11	4	64	-62	4	87	-82	3	34	-37	3	24	-21	11	26	-25	9	22	-24
4	52	63	3	28	48	4	26	-24	H,L=	4	15	5	54	51	5	108	-110	4	59	-60	4	27	23	H,L=	5	-1	10	35	32
5	37	28	4	57	51	5	82	-78	1	28	-19	7	26	-20	6	34	-32	5	25	-25	5	15	-17	1	23	28	11	29	-21
6	78	73	5	41	33	7	82	-83	3	26	22	8	38	35	7	74	-72	6	49	-49	6	67	65	2	66	69	H,L=	5	-11
8	45	41	6	98	106	9	60	-58	4	19	19	10	28	22	9	56	-51	8	26	-30	8	55	64	3	150	146	1	77	48
10	33	34	7	29	27	10	51	-47	6	45	36	H,L=	4	4	10	20	17	H,L=	4	-16	10	30	30	4	56	41	3	32	52
11	32	31	8	77	90	H,L=	3	-11	8	24	34	0	38	26	11	20	-20	1	18	-18	H,L=	5	8	5	63	62	4	23	-23
H,L=	3	8	9	9	14	1	62	63	10	22	22	1	34	27	H,L=	4	-5	2	28	-24	0	62	-63	7	37	-29	5	17	14
0	158	-170	10	47	46	3	41	33	H,L=	4	14	3	36	36	1	54	44	3	46	-50	2	76	-84	8	16	16	6	23	-22
1	20	19	H,L=	3	-2	5	38	35	0	74	-84	4	26	25	2	37	-26	5	51	-54	3	21	21	H,L=	5	-2	8	26	-23
2	66	-72	0	93	-56	6	13	-8	1	25	15	5	26	36	3	33	28	6	28	27	4	45	-45	0	40	-29	10	25	-17
4	13	0	1	37	18	7	22	13	2	55	-57	6	43	38	4	76	-74	7	36	-35	5	27	23	1	52	37	H,L=	5	-12
6	30	-21	2	25	-27	8	24	-23	4	20	-22	7	76	77	5	41	32	H,L=	4	-17	7	41	39	2	18	12	0	48	53
7	16	13	3	26	33	9	18	16	6	20	-15	8	23	-19	6	67	-71	1	36	32	8	31	-31	3	47	48	2	41	41
9	24	17	4	13	-7	10	30	-34	7	40	34	9	57	61	8	49	-46	3	25	28	9	52	43	4	37	29	4	36	38
H,L=	3	7	5	53	61	H,L=	3	-12	H,L=	4	13	11	33	39	9	22	-12	5	28	29	H,L=	5	7	5	44	42	5	16	16
1	60	-49	6	20	-15	1	34	30	1	50	-52	H,L=	4	3	10	47	-42	H,L=	4	-18	1	53	-52	7	57	58	H,L=	5	-13
2	37	-37	7	75	76	2	34	32	3	47	-48	1	80	-79	11	22	1	0	47	45	2	12	-8	8	16	-17	2	43	36
3	29	-21	8	23	-18	3	66	56	4	17	-8	3	30	-26	H,L=	4	-6	2	41	40	3	27	-30	9	49	52	4	30	29
4	48	-49	9	48	56	4	48	43	5	26	-28	4	63	65	0	113	114	3	19	18	4	25	-27	11	30	29	5	36	-41
6	44	-44	11	40	43	5	52	55	6	21	-16	5	43	-39	1	24	20	5	18	19	5	30	-26	H,L=	5	-3	7	28	-23
7	19	-11	H,L=	3	-3	6	57	62	9	32	11	6	63	64	2	92	86	7	23	23	6	43	-46	1	125	-123	8	34	31
8	41	-46	1	28	-39	7	72	74	H,L=	4	12	7	55	-63	3	40	40	9	39	35	8	33	-27	2	33	-25	10	31	34
10	47	-45	2	72	-46	8	41	34	2	15	11	8	25	23	4	79	71	H,L=	4	-19	H,L=	5	6	3	60	-60	H,L=	5	-14
11	16	12	3	80	-81	9	49	52	3	45	-37	9	17	-14	5	35	26	5	17	-13	0	53	43	4	26	17	0	48	-42
H,L=	3	6	4	55	-62	H,L=	3	-13	4	29	20	10	41	42	6	22	19	H,L=	4	-20	1	51	-34	5	47	-38	2	40	-42
0	74	74	5	22	-19	1	35	-39	5	69	-64	11	41	39	8	42	-45	0	20	-16	3	71	-75	6	34	34	3	19	-7
1	66	-55	6	19	5	2	80	80	7	19	-23	H,L=	4	2	10	22	-15	2	19	-25	5	77	-77	7	32	-23	4	34	-38
2	104	88	8	34	-26	3	23	-21	9	20	-22	0	132	-112	11	21	25	4	20	-26	7	41	-41	H,L=	5	-4	6	35	-32
3	83	-67	11	41	36	4	50	51	11	29	-30	1	18	-5	H,L=	4	-7	H,L=	4	-22	9	56	-33	0	109	-85	7	28	21
4	62	56	H,L=	3	-4	5	41	44	H,L=	4	11	2	71	-68	1	32	34	0	22	30	10	23	11	1	15	-6	H,L=	5	-15
5	31	-30	0	49	39	6	56	61	1	53	58	3	18	-14	3	47	33	2	20	25	11	37	-29	2	98	-91	1	43	-44
6	12	8	1	76	-64	7	47	43	2	14	10	4	37	-51	4	105	87	H,L=	5	22	H,L=	5	5	3	39	-39	3	20	-19
7	55	-55	2	90	-66	8	57	57	3	38	47	5	21	-23	6	61	61	0	15	23	1	14	25	4	85	-76	4	28	-28
9	46	-55	3	65	-65	10	40	41	4	28	-31	6	96	-108	7	40	-29	H,L=	5	20	2	74	-66	5	48	-46	6	28	-29
10	26	28	5	83	-79	H,L=	3	-14	5	70	64	7	21	-21	8	55	61	3	17	19	3	41	38	6	35	-34	8	24	-15
11	21	-16	6	64	52	0	53	-57	6	58	-57	8	35	-48	9	27	-23	5	24	35	4	55	-46	7	50	-41	H,L=	5	-16
H,L=	3	5	7	88	-84	2	58	-66	7	23	15	9	24	-19	10	65	64	H,L=	5	19	5	21	25	8	17	-12	3	16	-20
1	113	120	9	52	-60	4	27	-33	9	42	-36	10	31	30	H,L=	4	-8	1	27	-28	6	19	-13	9	51	-47	5	28	-34
2	36	-20	11	42	-45	5	19	-15	11	29	-32	12	25	33	0	82	-76	3	22	-21	7	23	21	H,L=	5	-5	6	20	23
3	109	92	H,L=	3	-5	H,L=	3	-15	H,L=	4	10	H,L=	4	1	2	45	-38	H,L=	5	18	8	26	19	1	36	33	7	21	-25
4	11	-3	1	63	52	1	62	-45	0	54	59	2	47	-33	3	20	14	2	28	-28	9	19	-11	2	29	-24	9	26	-28
5	54	59	2	29	-24	2	47	-36	2	44	50	3	25	-6	4	41	-38	3	22	-23	10	29	26	4	50	-40	H,L=	5	-17
6	9	4	3	42	30	3	33	-31	3	19	19	4	47	-46	5	47	45	4	34	-36	11	18	-17	6	57	-54	1	44	48
7	42	30	4	45	-25	4	68	-68	4	19	23	5	20	-17	6	24	-22	5	23	-29	H,L=	5	4	8	48	-45	3	21	18
9	24	19	5	20	19	5	19	-23	5	24	18	6	51	-60	7	46	37	7	22	-26	1	16	16	10	42	-40	5	19	18
10	20	19	6	85	-83	6	67	-60	6	22	22	7	13	-14	9	37	40	8	22	-6	3	16	18	H,L=	5	-6	H,L=	5	-18
H,L=	3	4	7	60	64	8	24	-26	8	20	15	8	56	-71	11	43	46	H,L=	5	17	4	31	25	0	114	112	0	46	42
0	48	20	8	60	-68	H,L=	3	-16	9	31	31	10	53	-63	H,L=	4	-9	2	52	-47	5	32	33	1	23	13	2	36	37
1	9	23	9	17	-12	0	19	23	10	21	-14	12	31	-36	1	42	-44	4	38	-40	7	48	53	2	124	114	5	18	13
2	22	27	10	37	-28	3	34	-30	11	29	36	H,L=	4	0	2	15	-8	6	46	-46	9	56	64	4	62	63	7	20	29
3	46	51	11	24	-19	5	48	-57	H,L=	4	9	0	112	102	3	66	-57	H,L=	5	16	10	17	-19	6	31	29	H,L=	5	-19
5	60	57	H,L=	3	-6	6	20	17	1	26	-26	1	29	11	4	22	-21	0	35	31	11	44	48	7	23	17	1	16	17
6	8	-15	0	101	98	7	29	-33	2	18	21	2	99	101	5	28	-23	2	31	30	H,L=	5	3	9	20	-16	H,L=	5	-20
7	51	52	2	30	24	H,L=	3	-17	3	22	-19	3	18	13	6	35	-38	3	18	-15	1	13	-17	10	32	-23	2	19	-16
9	41	42	3	32	-28	1	52	59	4	29	34	4	78	69	8	26	-25	4	20	18	2	26	24	11	18	-14	H,L=	6	21
11	49	55	4	11	19	3	25	20	5	42	31	5	29	-21	9	21	23	8	25	6	3	31	16	H,L=	5	-7	5	15	9
H,L=	3	3	6	54	48	5	23	14	6	64	58	6	47	48	10	24	20	H,L=	5	15	4	66	61	1	137	125	H,L=	6	20
1	70	-74	7	14	8	H,L=	3	-18	8	77	72	7	40	-34	11	33	27	1	36	30	5	36	-28	2	31	30	3	16	18
2	97	86	8	36	32	3	25	20	10	41	44	8	36	34	H,L=	4	-10	3	18	14	6	44	44	3	37	31	H,L=	6	19
3	76	-76	9	14	14	5	18	18	11	19	13	9	37	-34	0	21	11	4	42	31	7	48	-45	4	58	56	1	22	-28
4	42	54	11	29	25	7	24	27	H,L=	4	8	10	16	6	1	51	-52	6	46	35	8	34	38	5	25	21	3	17	-17
5	72	-76	12	42	-47	9	25	28	0	121	-115	11	36	-35	2	26	24	10	24	23	10	38	38	6	65	65	5	19	-12
6	25	21	H,L=	3	-7	H,L=	3	-19	1	21	15	H,L=	4	-1	3	65	-59	H,L=	5	14	11	38	35	8	26	26	H,L=	6	18
7	44	-71	2	45	-32	1	37	-40	2	71	-67	1	121	115	5	57	-60	0	39	-28	12	29	38	9	20	-18	0	20	-23
8	48	47	3	68	-62	3	44	-26	3	48	40	2	88	72	6	15	-9	5	48	40	H,L=	5	2	10	29	34	2	23	-23
9	19	-18	4	54	60	4	21	5	6	46	32	3	80	74	7	60	-52	6	46	-29	0	117	-110	1	137	125	3	18	-22
10	42	41	5	25	18	5	19	-20	9	46	40	4	68	54	8	23	23	7	50	44	1	41	28	2	31	30	8	20	2
H,L=	3	2	6	53	49	H,L=	3	-20	10	25	-5	5	56	45	H,L=	4	-11	H,L=	5	13	2	23	-1	3	37	31	H,L=	6	17
0	198	-97	7	58	51	0	21	-27	H,L=	4	7	6	50	48	1	49	51	1	44	-42	3	17	-8	4	58	56	2	31	-41
1	32	-24	8	51	56	2	24	-29	1	65	-58	7	59	59	2	42	-39	3	36	-32	4	29	20	5	25	21	4	30	-32
2	63	-60	9	14	13	H,L=	3	-22	3	30	-30	8	48	46	3	58	62	5	19	-24	5	43	-44	6	65	65	6	34	-25
3	11	-9	10	58	52	0	26	40	4	26	-26	9	31	30	4	29	-26	6	18	-12	6	72	-80	8	26	26	H,L=	6	16
4	70	-77	11	21	-16	2	27	38	6	46	-43	10	39	35	5	21	18	7	20	-22	8	43	-42	9	20	-18	0	21	14
5	21	-19	H,L=	3	-8	H,L=	4	22	8	56	-60	H,L=	4	-2	8	28	-28	H,L=	5	12	10	53	50	10	20	34	2	19	21
6	55	-47	0	57	-58	0	23	26	10	38	-32	0	21	-16	H,L=	4	-12	0	16	-6	12	34	54	H,L=	5	-8	3	18	-17

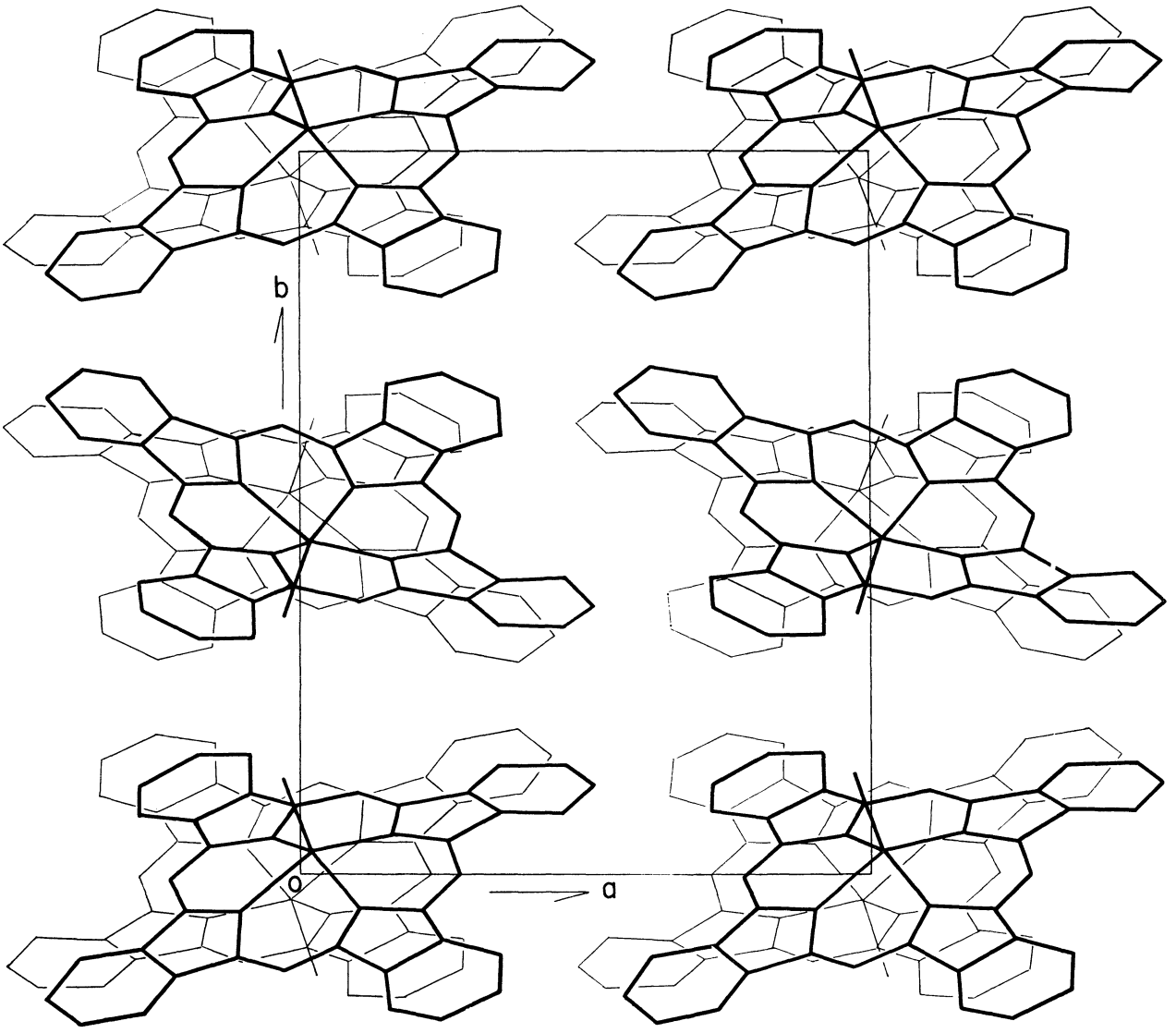

Fig. 2. The crystal structure viewed along the *c* axis.

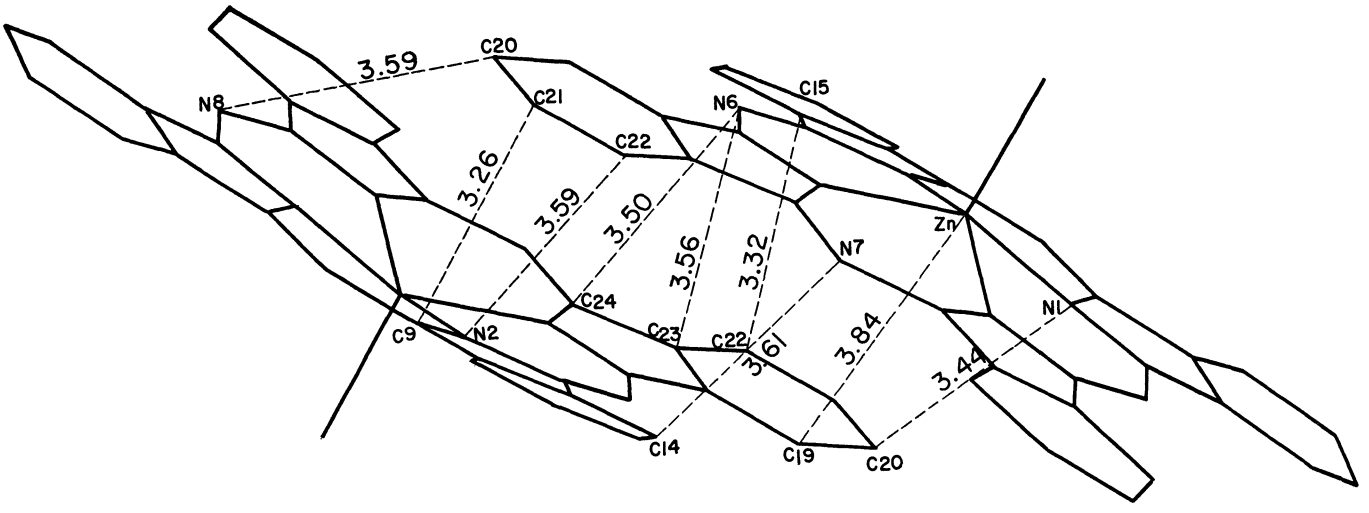

Fig. 3. Intermolecular distances between the paired molecules. The mean estimated standard deviation is about 0.023Å.

Table 2.[8] The atomic scattering factors for C, N, and Zn^{2+} were taken from International Tables for X-ray Crystallography, Vol. III (1962). Refinement was carried out on a HITAC 5020E of the University of Tokyo with the programs written by one of us (T.

8) The complete data of the F_o-F_c table are kept as Document No. 7110 in the office of the Bulletin of the Chemical Society of Japan. A copy may be secured by citing the document number and remitting ¥300 in advances for photoprints. (by check or money order payable to: Chemical Society of Japan).

A.). Figure 1 and 2 show the (100) and (001) projections of the structure. The zinc phthalocyanine molecules make a pair in the crystal and intermolecular distances between these paired molecules are also illustrated in Fig. 3.

Discussion

Bond distances and bond angles are given in Fig. 4-(a) and (b) only for a phthalocyanine molecule and the nitrogen atom of *n*-hexylamine bonded to it. The central zinc ion is coordinated to five nitrogen atoms, assuming a square pyramidal configuration as a whole. The four nitrogen atoms of pyrrole rings, N1 through N4, define a perfect plane with a shift of ±0.008 Å. The least-squares equation for this plane is

$$0.2671X - 0.7864Y - 0.5570Z = -1.8912$$

where X, Y, and Z are the coordinates (in Å) referring to the orthogonal axes a, b, and c, respectively. Shift of the zinc ion from this plane is significant, as is listed in Table 3 along with those of nine nitrogen atoms. It is obvious that the central zinc ion is displaced from the plane by nearly 0.5 Å presenting a pavilion roof shape, as shown in Fig. 5, which is an edge-on projection of the planar molecule viewed in a direction through two bridge nitrogen atoms, N6 and N8. Details of the coordinating feature around the zinc ion are given in Fig. 6. The Zn ion is displaced from the square nitrogen plane by 0.480 Å holding a bond length of 2.061 Å to the four pyrrole nitrogens on an average, and also that of 2.178 Å from the additive ligand nitrogen N9 toward which the Zn ion is shifted. The direction of the Zn–N9 bond is not perpendicular to the basal nitrogen plane, but slightly tilts towards the α carbon of *n*-hexylamine. Point C_t, the foot of a normal through Zn ion to the basal plane, is regarded as the center of the inner hole of phthalocyanine ring. The mean distance from C_t to the four pyrrole nitrogens is 2.005 Å on an average.

It seems worthwhile to compare the present data with those reported with regard to the five coordinated complexes of various metal derivatives of porphyrin which has the same central configuration as a phthalocyanine molecule. In Table 4, mean lengths and angles are listed for characteristic bonds which were reported concerning α-chlorohemin by Koenig[9] (1965), methoxyiron (III) mesoporphyrin-IX dimethyl ester (MeOFeMeso) by Hoard, Hamor, Hamor and Caughey[10] (1965), monochloroiron tetraphenylporphine (ClFe TPP) by Hoard, Cohen, and Glide[11] (1967) and monoaquozinc (II) tetraphenylporphine (H_2OZn TPP) by Glick, Cohen and Hoard[12] (1967). For comparison the list also includes the corresponding data for phthalocyanine formerly given by Robertson,[13] and its copper and platinum derivatives re-

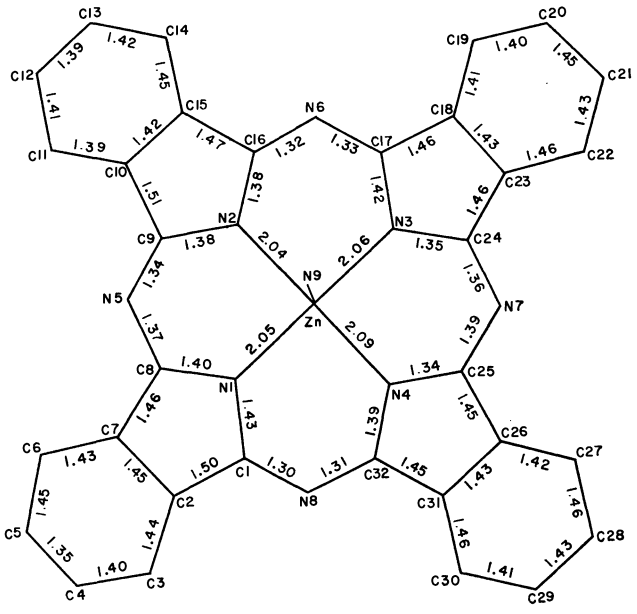

(a)

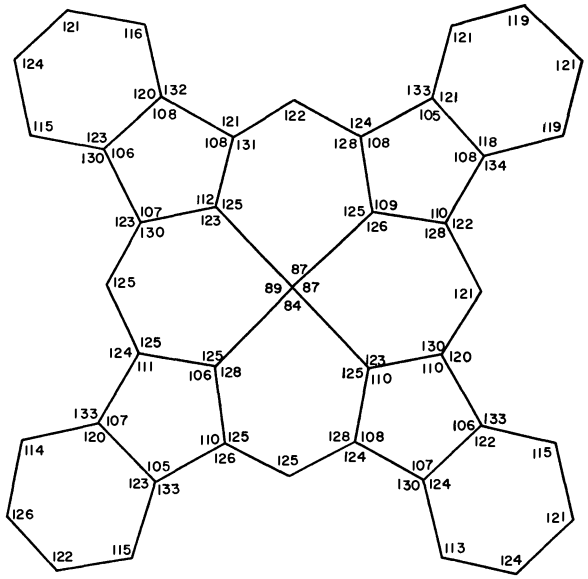

(b)

Fig. 4. Bond lengths (a) and inter-bond angles (b). The mean e.s.d. for lengths is about 0.023Å and for angles about 2.1°.

Table 3. Atomic displacements from the mean plane formed by four pyrrole nitrogen atoms

Atom	Shifts
N1	0.008
N2	−0.008
N3	0.008
N4	−0.008
Zn	−0.480
N5	0.181
N6	0.230
N7	0.037
N8	0.046
N9	−2.650

9) D. F. Koenig, *Acta Cryst.*, **18**, 663 (1965).
10) J. L. Hoard, M. J. Hamor, T. A. Hamor, and W. S. Caughey, *J. Amer. Chem. Soc.*, **87**, 2312 (1965).
11) J. L. Hoard, G. H. Cohen, and M. D. Glick, *ibid.*, **89**, 1992 (1967).
12) M. D. Glick, G. H. Cohen, and J. L. Hoard, *ibid.*, **89**, 1966 (1967).
13) J. M. Robertson, *J. Chem. Soc.*, **1936**, 1195. J. M. Robertson and I. Woodward, *ibid.*, **1937**, 219.

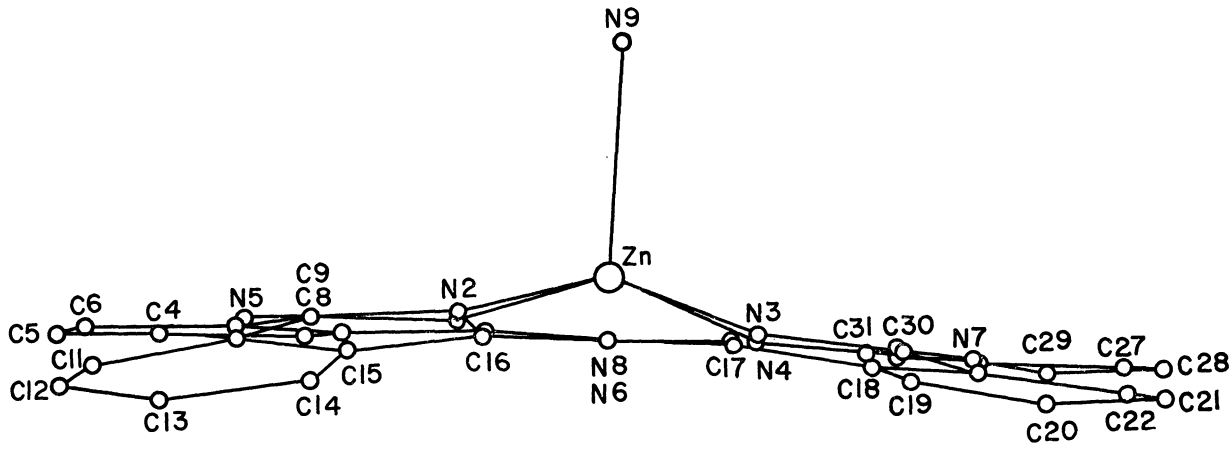

Fig. 5. Edge-on view of the molecule projected perpendicular to the direction through N6 and N8.

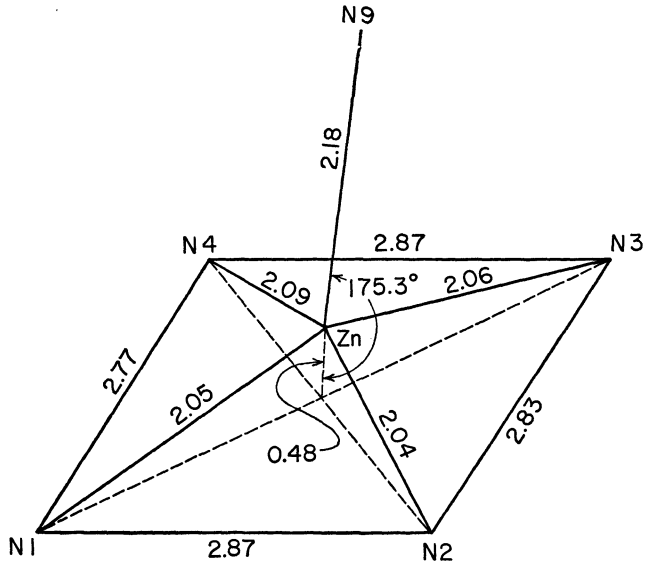

Fig. 6. The square-pyramidal coordinating feature around the zinc ion.

cently determined by Brown.[14,15]

The characteristic bonds are associated with the atoms which are the metal ion (M), the ligand nitrogen coordinated to the metal (N_p), the additive ligand atom (L), the α and β carbon of pyrrole rings (C_α, C_β) and the methin carbon (C_m) or the bridge nitrogen (N_b) both of which connect two adjacent pyrrole rings. Although it is obvious that the corresponding values do not differ much from one another, the zinc phthalocyanine complex shows a closer resemblance to α-chlorohemin than the aquo zinc TPP, particularly in the dimensions of such bonds as M–N_p, C_t–N_p, C_t–M and N_p–C_α, all being associated with the configuration of coordinate systems of the common convex type. A characteristic feature of the porphine skeleton in which the bond N_p–C_α is always longer than the C–C bonds in benzene ring in the case of phthalocyanines also holds in the present complex. The inner hole radius, C_t–N_p, is longer than that of any other phthalocyanine though it is closer to the radii of Pt derivatives of both modifications. It is likely that the complex formation does not affect the bond lengths around the bridge nitrogens. The molecule of phthalocyanine and its metal derivatives is well known as a flat molecule. As an example, the shifts of carbon atoms in copper phthalocyanine crystal from the mean plane were reported by Brown[14] to be within ±0.05 Å. Every divalent metal ion situated in the center of a phthalocyanine molecule takes a square planar four coordinate structure, where the metal ion bonds with four nitrogens through dsp^2 hybrid orbitals. These square planar configurations are possible for Mn, Fe, Ni, Pd, and the four coordinate square planar configurations are very stable especially for Co, Ni, Cu, Pt ions. The fact that the phthalocyanine derivatives of nickel or copper do not make an additive complex with amines, and manganese derivative reacts with molecules of amine to form a six coordinate complex, suggests that the reactivity of metal phthalocyanine with the various amines depends mostly on the electronic configurations in 3*d* orbitals of metal ion. In other words, manganous and ferrous ion can form six coordinate octahedral configurations with d^2sp^3 hybrid orbitals. The phthalocyanine derivatives of these two metal ions, therefore, can easily form molecular complexes with other ligands such as pyridine, aniline or other amines.

In contrast, divalent zinc ion whose 3*d* electron orbitals are filled with its own ten electrons is apt to take tetrahedral configuration by use of sp^3 hybrid orbitals. The zinc ion uses outer sp^2d hybrid orbitals in order to stay in phthalocyanine ring because the zinc ion is required to assume a square planar coordination which is not a stable configuration for the ion. Thus, zinc phthalocyanine shows a tendency to form a five or six coordinate complex when *n*-donor molecule exists. In the complex with *n*-hexylamine, the zinc ion takes a square pyramidal five coordination as shown in Fig. 6. In this case sp^2d^2 hybridized orbitals were used for the coordination. It is interesting to note that the phthalocyanine molecule which is usually considered to have a rigid planner configuration can be easily distorted by complex formation in the crystal.

14) C. J. Brown, *ibid.*, **1968**, 2488.
15) C. J. Brown, *ibid.*, **1968**, 2492.

TABLE 4. THE MEAN LENGTHS AND ANGLES OF CHARACTERISTIC BONDS IN VARIOUS PORPHYRINE DERIVATIVES

Metal Name	Fe α-Cl hemin	Fe Me-O-Fe mesoporph.	Fe Fe-TPP -Cl	Zn Aquo-Zn-TPP	Zn Zn-Phc *n*-hexyl.	Cu Cu-Phc	Ni Ni-Phc	Pt Pt-Phc (α)	Pt Pt-Phc (β)	Free H_2-Phc
C_t-M	0.475	0.455	0.383	0.19	0.48	0	0	0	0	0
C_t-N_p	2.007	2.002	2.012	2.04	2.00	1.935	1.83	1.98	1.98	1.92
M-N_p	2.062	2.073	2.049	2.05	2.06	1.935	1.83	1.98	1.98	1.92
M-L	2.218	1.842	2.129	2.20	2.17					
N_p-C_α	1.38	1.395	1.384	1.38	1.38	1.366	1.39	1.35	1.37	1.34
C_α-C_m (N_b)	1.38	1.377	1.399	1.42	1.34	1.328	1.34	1.33	1.33	1.34
C_α-C_β	1.45	1.446	1.446	1.43	1.47	1.453	1.46	1.49	1.43	1.49
C_β-C_β	1.33	1.368	1.380	1.37	1.43	1.400	1.38	1.37	1.46	1.39
$\angle C_\alpha N_p C_\alpha$	106.1	107	106	105.4	109.3	107.3	99.0	111	109	108.5
$\angle C_m(N_b)$	125.9	124.1		125.9	124.5	122.2	117	120	124	117
Ligand	Cl	O	Cl	O	N					
year	1965	1965	1967	1967	1971	1968	1937	1968	1968	1936
Ref.	8	9	10	11	this paper	13	12	14	14	12

Another example of five coordinate zinc ion can be seen in the molecule of aquozinc tetraphenyl porphine, where zinc ion takes a square-pyramidal structure although copper or palladium derivatives show a square-planar structure without any water molecule coordinated to them. In this case, bond distances of Zn–N and Zn–O are 2.05±0.01 Å and 2.20±0.06 Å, respectively, and in the case of zinc phthalocyanine-*n*-hexylamine complex the bond lengths of Zn–N and Zn–N (amine) are 2.06±0.02 Å and 2.18±0.02 Å. These similarities indicate that the zinc ions in both complexes take the same electronic configuration by sp^2d^2 orbitals for coordinations which seems more stable than the square planar structure of sp^2d orbitals. The paired molecules viewed in a direction perpendicular to the molecular plane shows that the intermolecular overlapping area is very small. In general, the packing manner in the crystals of the planar molecules like phthalocyanines is said to be stable when the overlap of π-electron is made as large as possible. Judging from these facts the small overlap of the pair of planar molecules may suggest the change of distributions of π-electron density in phthalocyanine molecules due to the charge transfer from amine to phthalocyanine ring.

The number of *n*-hexylamine molecules which exist in a unit cell of the complex was determined by means of differential thermal analysis (DTA) and thermal gravimetric analysis (TGA). There are three endothermic reactions at about 140, 155, and 180°C.

The first reaction detected at 140°C by DTA is related to the partial decomposition of the complex. When the amines have been released by decomposition, they are usually discharged instantly into the air. The endothermic reaction at 155°C is related to the evaporation of these discharged hexylamines at boiling point. Though the boiling point of *n*-hexylamine is 130°C, it is detected as a peak temperature at 155°C by DTA when the rate of temperature rise is 10°C/min. The last peak was attributed to the decomposition and evaporation of the *n*-hexylamine tightly bonded to zinc phthalocyanine. It should be emphasized that there are two bonding states for *n*-hexylamine in the complex crystal. One is weakly bonded and can be easily released from the lattice at a temperature lower than the boiling point of *n*-hexylamine. The other is strongly bonded and stable up to about 180°C. It is evident from TGA that the total number of *n*-hexylamine in a unit cell is six where as that of zinc-phthalocyanine is four. The electron density map obtained by Fourier synthesis gave only four *n*-hexylamine molecules coordinated directly to the zinc ion in a unit cell. The other two amine molecules did not appear in the course of the Fourier synthesis. These molecules are considered to be located at random in a space of crystal lattices and discharged out of the lattice even at low temperature. The coordinated *n*-hexylamine molecules are considered to be more stable so as to be decomposed at about 180°C. None of the atomic parameters of these coordinated amines except the nitrogen were exactly determined and the electron densities of five carbon atoms of the amine were only about 1/3-1/5 of the density of the carbons in phthalocyanine ring at the final stage of refinement. No terminal methyl carbon of the *n*-hexylamine was detected. The indistinctness of the atomic parameters was due to a molecular rotation or a static disorder of the paraffine chain of the amine. A preliminary structural study on a series of similar additive complexes shows that the crystals of such molecular complexes of zinc phthalocyanine with normal amine, whose carbon numbers are three, four, and five have an isomorphous structure with the complex reported here. It is observed that thermal stability decreases with the decrease of the carbon number of amine. In the case of the complex with propylamine (C=3) the weakly bonded amine in the crystal lattice easily escapes from the lattice even at room temperature leaving 1 : 1 complex behind. It may be possible to determine the position of all the atoms of amine in the crystal by means of low temperature Weisenberg camera because the quenching of the movement of amine molecule can be expected.

Rare-Gas-Sensitized Radiolysis of Toluene

Yukio YAMAMOTO, Setsuo TAKAMUKU, and Hiroshi SAKURAI

The Radiation Laboratory, The Institute of Scientific and Industrial Research, Osaka University, Suita, Osaka

(Received February 22, 1971)

The Ar-, Kr-, and Xe-sensitized radiolyses of toluene was studied at room temperature in the gas phase. The discussion was concentrated on the formation of three isomers of methyldiphenylmethane (MDPM), which, it had been suggested in a previous paper on the direct radiolysis of toluene, were formed by the ion-molecule reaction of $C_7H_7^+$ ions. The sensitization effect on the MDPM formation was extremely large in the case of Ar, and decreased in the order of Ar, Kr, and Xe. These results were explained in terms of charge transfer from these rare gases to toluene, resulting in the formation of the $C_7H_7^+$ ions. The isomer distribution of MDPM's in the rare-gas-sensitized radiolysis was considered on the basis of the reaction mechanism proposed previously. The sensitization effect on the formation of other products was also discussed briefly.

In the gas-phase radiolysis, ionic species formed by irradiation play significant roles in the product formation; therefore, mass spectrometric studies have provided valuable information about the primary process of the gas-phase radiolysis. In the case of simple alkylbenzenes, such as toluene, ethylbenzene, and xylenes, the most abundant ion in the mass spectra is the $C_7H_7^+$ ion,[1,2] and its reactions in the gas-phase radiolysis of these alkylbenzenes have been expected to be important. It was suggested, in previous papers on the gas-phase radiolysis of toluene, ethylbenzene, and *m*-xylene, that the $C_7H_7^+$ ions react with parent alkylbenzene molecules to form the corresponding benzylated alkylbenzenes, which are the major products of these radiolyses.[3-5] Furthermore, the mechanism of such an electrophilic substitution reaction of aromatic nuclei caused by the $C_7H_7^+$ ions was discussed on the basis of the isomer distribution and the pressure dependence of the yields of the products, methyldiphenylmethanes (MDPM's), in the gas-phase radiolysis of toluene.[4] The present investigation of the rare-gas-sensitized radiolysis of toluene has been carried out in order to obtain additional information about the mechanism of the formation of MDPM's in the radiolysis of toluene. In the rare-gas-sensitized radiolysis, the product distribution is often characteristic of the kinds of rare gases, and the investigations of such experiments using various rare gases are of value in connection with the study of the primary process of the radiolysis.

Experimental

The toluene was the same as that used in a previous study.[4] The rare gases were obtained from Takachiho Shoji Co. and were used without further purification. The stated purities were 99.999%, 99.9%, and 99.9% for Ar, Kr, and Xe respectively. The experimental procedures were almost identical with those reported previously.[4] The irradiation cells were Pyrex cylinders approximately 120 m*l* in volume, and irradiations were carried out at room temperature with a 5000 Ci cobalt-60 source. The dose rate at the dose for toluene were 3.1×10^{15} eV/hr·μmol and 7.4×10^{16} eV/μmol respectively. The irradiated samples were analyzed with a gas chromatograph using a flame-ionization detector after the gas fraction volatile at -120°C (rare gas and the product gases) had been removed; all the liquid products except dimers were analyzed with a 3-m Apiezon L column at 100°C, while for dimers a 6-m mixed nitrate column[6] was used with temperature programming from 60 to 120°C. The experimental details were presented in a previous paper.[4]

Results

As has previously been reported,[4] the products detected in the gas-phase radiolysis of toluene were hydrogen, methane, ethane, acetylene, benzene, ethylbenzene, xylenes, bibenzyl, and MDPM's, though in this study the gaseous products were not analyzed. The effect of the added rare gases, Ar, Kr, and Xe, on the product yields was studied at an almost constant pressure of toluene, 10.1 ± 0.3 mmHg; the results are presented in Table 1. Approximately linear relationships exist between the product yields and the pressure of the added rare gas, although some scattering was observed. From these results, the sensitization G values, G_s, indicating the increases in the G values of the products on the basis of the energy absorbed by the rare gas, were calculated; they are presented in Table 2.[7] As is shown in this table, G_s (MDPM's) is extremely large in the Ar-sensitized radiolysis, and also has a considerable value in the case of Kr. In both cases, the sensitization effect is largest on the formation of MDPM's. On the other hand, in the Xe-sensitized radiolysis, the G_s (MDPM's) value is very small and most of the MDPM's may be formed by the direct absorption of energy by toluene.

The isomer distribution of the MDPM's was approximately independent of the pressure of rare gas within

1) H. M. Grubb and S. Meyerson, "Mass Spectrometry of Organic Ions," ed. by F. W. McLafferty, Academic Press., New York (1963), p. 453.

2) Much attention has been paid to the structure and formation process of the $C_7H_7^+$ ions because of the isotope randomization observed in the mass spectra of labeled alkylbenzenes, and the $C_7H_7^+$ ions are believed to have a tropylium-ion structure (see Ref. 1).

3) Y. Yamamoto, S. Takamuku, and H. Sakurai, *J. Amer. Chem. Soc.*, **91**, 7192 (1969).

4) Y. Yamamoto, S. Takamuku, and H. Sakurai, *J. Phys. Chem.*, **74**, 3325 (1970).

5) Y. Yamamoto, S. Takamuku, and H. Sakurai, This Bulletin, **44**, 574 (1971).

6) W. W. Hanneman, C. F. Spencer, and J. F. Johnson, *Anal. Chem.*, **32**, 1386 (1960).

7) The dose rate for rare gases was determined by correcting for the electron densities of rare gases relative to toluene.

TABLE 1. THE EFFECT OF THE ADDED RARE GAS ON THE PRODUCT YIELDS IN THE GAS PHASE RADIOLYSIS OF TOLUENE

Added Rare Gas	Pressure, mmHg		G value				
	Rare gas	Toluene	Benzene	Ethylbenzene	Xylenes[a]	Bibenzyl	MDPMs[a]
—	—	10.2	0.17	0.05	0.06	0.03	0.43
Ar	29.3	10.2	0.43	0.10	0.14	n.d.[b]	3.0
	50.0	10.0	0.65	0.15	0.21	n.d.[b]	4.6
	79.4	9.9	0.83	0.17	0.25	n.d.[b]	6.2
	99.7	10.4	1.28	0.28	0.36	n.d.[b]	9.9
Kr	30.8	9.8	0.44	0.15	0.17	0.07	1.0
	52.8	10.3	0.62	0.22	0.25	0.09	1.1
	82.9	10.2	0.88	0.31	0.32	0.12	1.4
	100	9.8	0.91	0.34	0.30	0.13	1.5
Xe	31.9	10.4	0.63	0.31	0.23	0.17	0.55
	52.5	10.4	0.75	0.41	0.27	0.34	0.52
	82.4	10.2	1.3	0.76	0.39	0.50	0.58

a) Total yields of the three isomers. b) Not detectable.

TABLE 2. THE SENSITIZATION G VALUES IN THE RARE GAS SENSITIZED RADIOLYSIS OF TOLUENE
(toluene pressure, 10.1±0.3 mmHg)

Added rare gas	G_s[a]				
	Benzene	Ethyl-benzene	Xylenes	Bibenzyl	MDPMs
Ar	0.27	0.05	0.08	0	2.4
Kr	0.12	0.04	0.04	0.02	0.18
Xe	0.13	0.08	0.04	0.05	0.02

a) The increase of the product molecules per 100 eV energy absorbed by the added rare gas.

TABLE 3. THE ISOMER DISTRIBUTION OF MDPM

Added rare gas	Rare gas pressure mmHg	Isomer distribution, %		
		2-MDPM	3-MDPM	4-MDPM
—	—	12	76	12
Ar	50.0	12	74	14
Kr	52.8	8	85	7
Xe	52.5	13	75	11

the limits of experimental error; the percentages of the three isomers at a rare-gas pressure of about 50 mmHg are presented in Table 3, together with those obtained in the direct radiolysis of toluene. In all cases, a large portion of the MDPM's consists of 3-MDPM; it is formed by benzylation at the *meta* position of toluene. The dependence of the G_s values of the MDPM isomers on the toluene pressure was studied in the Ar- and Kr-sensitized radiolyses at constant rare gas pressures, 51.1 and 52.7 mmHg, of Ar and Kr respectively; the results are illustrated in Figs. 1 and 2. The pressure dependence of the G values of the MDPM isomers in the previous study of the radiolysis of pure toluene obtained is also shown with dotted lines in Fig. 2 for the sake of comparison. In both the Ar- and Kr-sensitized radiolyses, G_s(3-MDPM) decreased with an increase in the toluene pressure, while G_s(2-MDPM) and G_s(4-MDPM) were not appreciably affected by the toluene pressure. Such pressure dependencies of the G_s values of the MDPM isomers are similar to those of their G values in the direct radiolysis.

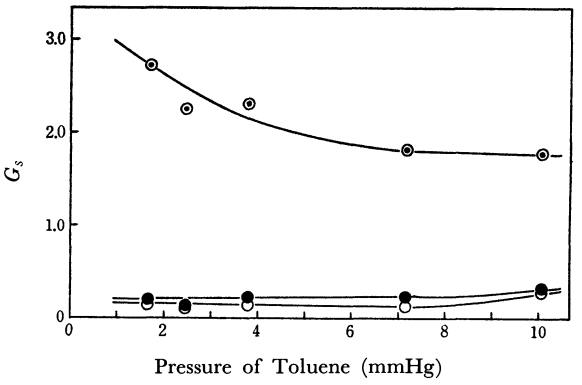

Fig. 1. The dependence of G_s(MDPM's) on toluene pressure in the Ar sensitized radiolysis at 51.1 mmHg of Ar pressure: ○, G_s(2-MDPM); ⊙, G_s(3-MDPM); ●, G_s(4-MDPM).

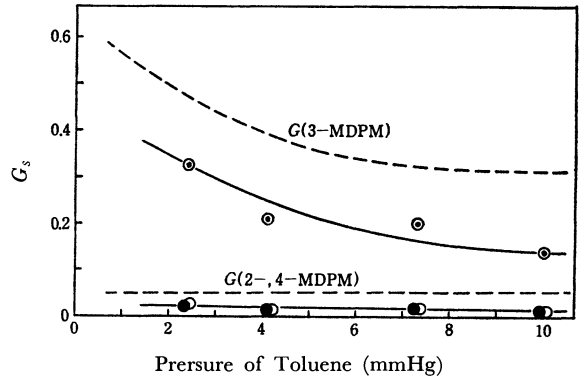

Fig. 2. The dependence of G_s(MDPM's) on toluene pressure in the Kr sensitized radiolysis at 52.7 mmHg of Kr pressure and that of G(MDPM's) in the radiolysis of pure toluene (dotted lines): ○, G_s(2-MDPM); ⊙, G_s(3-MDPM); ●, G_s(4-MDPM).

Discussion

The ionization potentials and the energy levels of the excited states of Ar, Kr, and Xe are shown in Table 4. Charge and excitation transfers from these states to toluene become the major modes of energy absorption by toluene molecules in the radiolysis of toluene in the presence of excess rare gas.

TABLE 4. IONIZATION POTENTIALS AND EXCITATION ENERGIES OF RARE GASES (in eV)[a)]

Rare gas	I.P.		Allowed state		Metastable state	
	$^2P_{3/2}$	$^2P_{1/2}$	$^3P_1$	$^1P_1$	$^3P_2$	$^3P_0$
Ar	15.75	15.93	11.62	11.82	11.56	11.72
Kr	14.00	14.66	10.03	10.64	9.91	10.56
Xe	12.13	13.43	8.43	9.57	8.31	9.44

a) B. Brocklehurst, *Radiation Res. Rev.*, **1**, 225 (1968).

The Sensitization on the Formation of MDPM's. In the previous paper on the gas-phase radiolysis of toluene, the following mechanism of the formation of MDPM's has been proposed on the basis of the pressure dependence of the yields of the three isomers.[4,8)]

$$C_6H_5CH_3 \rightsquigarrow C_6H_5CH_3^{+*} + e \quad (1)$$

$$C_6H_5CH_3^{+*} \longrightarrow C_7H_7^+ + H \quad (2)$$

$$C_7H_7^+ + C_6H_5CH_3 \longrightarrow \left(\text{C}_7\text{H}_8^+\text{-}\text{CH}_2\text{C}_6\text{H}_5\right)^* \quad (3)$$

I*

$$I^* + C_6H_5CH_3 \longrightarrow MDPM + C_7H_9^+ \text{ (minor)} \quad (4)$$

$$\longrightarrow I + C_6H_5CH_3 \text{ (major)} \quad (5)$$

$$I \longrightarrow \text{Im} \quad (6)$$

Im

$$Im + C_6H_5CH_3 \longrightarrow 3\text{-MDPM} + C_7H_9^+ \quad (7)$$

$$\longrightarrow \text{Adduct Ion} \quad (8)$$

where I* is an excited σ-complex producing three isomers of MDPM's, and where a less excited σ-complex, I, isomerizes to the most stable one, Im, which then produces 3-MDPM or a trimeric ion.

The G_s values of the MDPM's exhibit remarkable differences among the Ar-, Kr-, and Xe-sensitized radiolyses; they decreased in the order of Ar, Kr, and Xe, as is shown in Table 2. Such results can be explained as follows. The appearance potential of the $C_7H_7^+$ ion from toluene is 11.8 eV,[1)] and the possible mode of its formation by the rare-gas sensitization is considered to involve a charge-transfer process (see Table 4):[9)]

$$X \rightsquigarrow X^+ + e \quad (9)$$

$$X^+ + C_6H_5CH_3 \longrightarrow X + C_6H_5CH_3^{+*} \quad (10)$$

$$C_6H_5CH_3^{+*} \longrightarrow C_7H_7^+ + H \quad (11)$$

where X shows a rare gas such as Ar, Kr, and Xe. The excess energies available in the charge transfers from the $^2P_{3/2}(^2P_{1/2})$ states of Ar^+, Kr^+, and Xe^+ to toluene (Reaction (10)) are 6.93 (7.11), 5.18 (5.84) and 3.31 (4.61) eV respectively (the ionization potential of toluene is 8.82 eV[10)]), and end up as excess internal energies in the resulting toluene ion. Therefore, the probability of the fragmentation of the excited toluene ions to the $C_7H_7^+$ ions (Reaction (11)), *i.e.*, the sensitization effect on the formation of MDPM's, depends on the ionization potentials of rare gases and increases in the order of Xe, Kr, and Ar.

If the added rare gas contributed to the collisional stabilization of the excited σ-complex, I*, one might expect a more selective formation of 3-MDPM in these rare-gas-sensitized radiolyses than in the direct radiolysis of toluene. However, the isomer distribution of MDPM's was not affected by the addition of rare gas, except in the case of Kr (to be discussed below) (Table 3) and was approximately independent of the rare gas pressure, as has been discussed above. On this basis, it seemed reasonable to conclude that the collisional stabilization of I* with rare gas atoms can hardly compete with the reactions of I* with toluene molecules, Reactions (4) and (5). Two explanations may be offered for this observation. First, and less likely, it may be suggested that the collisional stabilization of I* with rare gas is less effective than that with toluene because the toluene molecule possesses a higher degree of freedom. A second, and perhaps more likely, explanation would be that Reaction (5) is not a simple collisional stabilization, but a certain rapid chemical reaction, involving addition and dissociation or the benzyl-cation transfer from I* to another toluene molecule[11)] analogous to the proton transfer (Reaction (4)).

As is shown in Figs. 1 and 2, the dependence of the G_s values of MDPM's on the toluene pressure in the Ar- and Kr-sensitized radiolyses is almost identical with the pressure dependence of the G values of MDPM's in the radiolysis of pure toluene. Such a result also indicates that the isomer distribution of MDPM's was altered only by the change in the toluene pressure and was not appreciably affected by the addition of the rare gas. Thus, the results obtained in this study suggest that the effect of the added rare gas on the formation of MDPM's is small, if present at all, except for the sensitization upon the primary formation of the $C_7H_7^+$ ions.

When the isomer distributions of MDPM's in the Ar- and Kr-sensitized radiolyses are compared, the percentage of 3-MDPM is found to be somewhat larger in the latter case than in the former case (Table 3).

8) An analogous mechanism was also proposed in the study of the reactions of $C_3H_7^+$ ions with aromatic hydrocarbons [S. Takamuku, K. Iseda, and H. Sakurai, *J. Amer. Chem. Soc.*, **93**, 2420 (1971).].

9) The excitation transfer from the $^1P_1$ state of Ar may also contribute to the sensitization upon the formation of the $C_7H_7^+$ ions.

10) S. C. Lind, "Radiation Chemistry of Gases," Reinhold, New York (1961), p. 270.

11) In such a reaction, I* might act as a less electrophilic reagent to another toluene molecule to form a less energetic complex, I, as has previously been proposed (see Ref. 8).

Such a discrepancy in the Ar- and Kr-sensitized radiolyses might be attributed to the difference in the internal energy of the $C_7H_7^+$ ions formed through the charge transfer from these rare gases to toluene; the internal energy of the $C_7H_7^+$ ions formed through the charge transfers from Kr is smaller than that from Ar because of the lower exothermicity of Reaction (10), and the addition of the less excited $C_7H_7^+$ ion to toluene results in the formation of a less excited complex, producing 3-MDPM with a higher probability. In the Xe-sensitized radiolysis, most of the MDPM's may be formed by direct energy absorption by toluene; the isomer distribution was similar to that in the direct radiolysis, as is shown in Table 3.

The Sensitization on the Formation of Other Products. As has been previously reported, in the gas-phase radiolysis of toluene the primary processes leading to the formation of benzene, ethylbenzene, xylenes, and bibenzyl are considered to be as follows:[4]

$$C_6H_5CH_3 \rightsquigarrow C_6H_5\cdot + CH_3\cdot \quad (12)$$

$$C_6H_5^+ + CH_3\cdot + e \quad (13)$$

$$\cdot C_6H_4CH_3 + H \quad (14)$$

$$C_6H_5CH_2\cdot + H \quad (15)$$

Thus, both the phenyl radicals and the phenyl cations have been considered to give rise to benzene, and the formation of ethylbenzene, xylenes, and bibenzyl has been attributed to combinations of the radicals, involving methyl, tolyl, and benzyl radicals. With regard to these products, the G_s values in the Ar-, Kr-, and Xe-sensitized radiolyses and the G values in the direct radiolysis do not differ significantly (Tables 1 and 2). However, from the results shown in Table 2 it may be considered that the sensitization effect on the formation of benzyl radicals, producing ethylbenzene and bibenzyl, increases in the order of Ar, Kr, and Xe; in the Xe-sensitized radiolysis, bibenzyl, the minor dimeric product in the direct radiolysis, was formed in a yield comparable to that of MDPM's at a higher pressure of Xe Table 1. As has previously been reported, in the mercury-photosensitized decomposition of toluene vapor at 2537 Å, the β C–H bond scission is a major primary process, as is the α C–C bond scission, and the only dimeric product detected is bibenzyl.[4] Thus, the distribution of the products formed by the Xe sensitization resembles that in the mercury-photosensitized decomposition rather than that in the direct radiolysis. Such a result may be attributed to the fact that the energy transferred from Xe to toluene in the sensitized radiolysis is smaller than those from Ar and Kr, and is also smaller than that directly absorbed by toluene.

We wish to thank Mr. Tamotsu Yamamoto and Mr. Tomikazu Sawai of the Radiation Laboratory for their assistance in the γ irradiations.

BULLETIN OF THE CHEMICAL SOCIETY OF JAPAN, VOL. 44, 2107—2109 (1971)

Heats of Immersion of Silica-alumina in Nonaqueous Solvents

Masaji MIURA, Toru IWAKI, Masayoshi KOMURO, Kusao TANAKA, and Kenji ITO

Department of Chemistry, Faculty of Science, Hiroshima University, Higashisenda-machi, Hiroshima

(Received March 1, 1971)

The heats of immersion of silica gel, alumina, and silica-aluminas in benzene, cyclohexane, and a solution of *n*-butylamine in benzene have been studied in connection with the acid properties of the surfaces. It was found that *n*-butylamine interacts more strongly with the surfaces of silica-aluminas than is the case in an aqueous system, which was previously investigated. Further, the interactions of benzene with the surfaces of silica-aluminas were discussed on the basis of the results of the adsorption isotherms of benzene on the surfaces.

Silica-alumina is one of the most important catalysts for various acid-catalyzed reactions.[1] These catalytic actions are considered to be connected with the acid sites on the surface of silica-alumina. In our previous study,[2] the surface properties of silica-aluminas with different contents of alumina were investigated by examining the relation between the property of the acid site and the heats of immersion in water and an aqueous solution of *n*-butylamine; it has been found that the molecule interacts preferentially with the strong acid sites and weakens the site strength. Therefore, it may be of interest to investigate the heats of immersion of silica-alumina in nonaqueous solvents. In this work, the heats of immersion of silica gel, alumina, and silica aluminas were measured in benzene, cyclohexane, and a solution of *n*-butylamine in benzene. Further, the interaction of benzene with the surfaces of the samples was discussed by examining the adsorption isotherms of benzene on the surfaces.

Experimental

Materials. Silica gel, alumina, and silica-aluminas with a content of 10% alumina, 10% SA, and that of 50% alumina, 50% SA, were prepared by the hydrolysis of ethyl ortho-silicate and/or aluminum isopropoxide by a procedure similar to that described in a previous paper.[2] The specific surface areas of the samples evacuated at 300°C for 3 hr were determined from the nitrogen adsorption by the BET

1) K. Tanabe and T. Takeshita, "Acid-Base Catalysis," Sangyo Tosho Pub. Co. Ltd., Tokyo (1965), p. 179.

2) M. Miura, Y. Kubota, T. Iwaki, K. Takimoto, and Y. Muraoka, This Bulletin, **42**, 1476 (1969).

method. The results are given in Table 1. The surface area of silica-alumina exhibits a low value at a content of 10% alumina; this is analogous to the previous finding.[2]

Benzene and cyclohexane were purified by distillation, with several pieces of metallic sodium added to remove any moisture.

Heat-of-immersion Measurement. Prior to the measurements, the samples were evacuated at 300°C for 3 hr in a vacuum of 10^{-5} mmHg. The heats of immersion of these samples in benzene, cyclohexane, and a solution of *n*-butylamine in benzene were measured at 25°C by using a calorimeter[3] which was improved so as to be able to hold four ampoules at a time. Since trace quantities of water dissolved in these liquids have a significant effect on the heat value, the water was removed by an activated molecular sieve in the following way. After each of these liquids had been placed in the calorimeter, a large quantity of the molecular sieve was added to the liquids. Next, after a thermal equilibrium in the system had been established, an ampoule containing the molecular sieve was broken in order to dehydrate the liquid completely just before another ampoule containing a sample was broken for the measurement of the immersional heat.

Adsorption Measurement. The adsorption isotherms of benzene on the samples were volumetrically determined at 25°C by using an adsorption apparatus equipped with greaseless Teflon cocks. The equilibrium pressure of benzene vapor was measured by means of a mercury manometer.

Results

The heats of immersion of the samples in benzene and cyclohexane are shown in Fig. 1 as a function of the alumina content. The heat value in benzene ranged from 82 to 110 erg/cm², and that in cyclohexane, from 48 to 77 erg/cm². The heat values of silica gel in benzene and cyclohexane were similar to those reported by Whalen.[4] In Fig. 2, the heats of immersion of these four samples in a 1 M solution of *n*-butylamine in benzene are shown as a function of the alumina content. In the figure, the heats of immersion in water and the aqueous solution of *n*-butylamine are also presented for comparison.[2] The adsorption isotherms of benzene on the surfaces of silica,

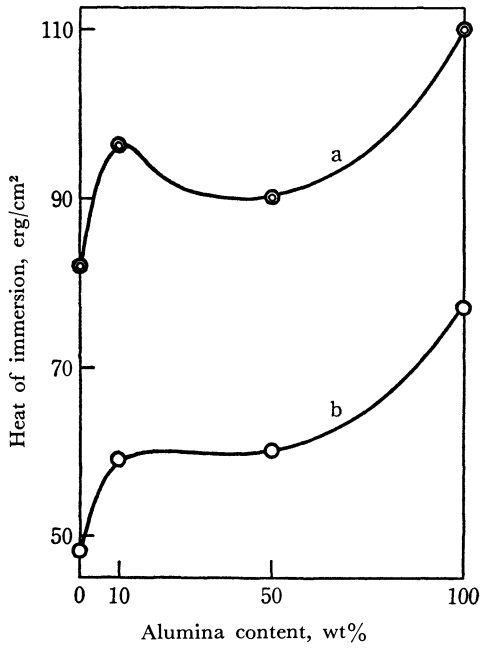

Fig. 1. Heats of immersion of silica-aluminas as a function of alumina content; (a) in benzene and (b) in cyclohexane.

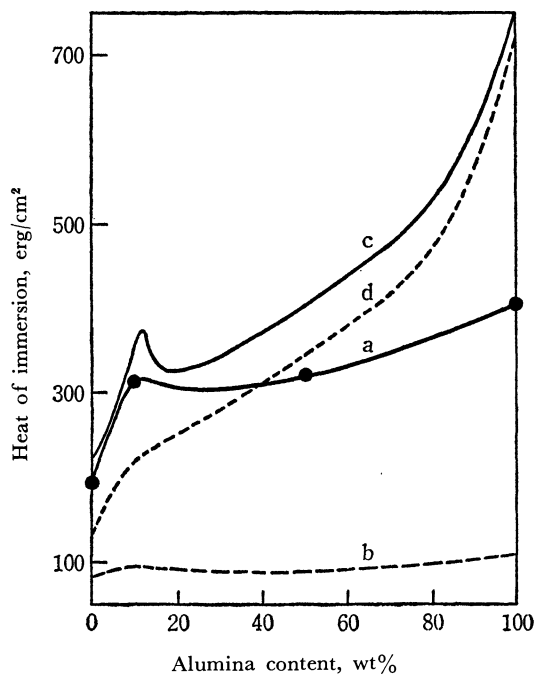

Fig. 2. Heats of immersion of silica-aluminas as a function of alumina content; (a) in the solution of *n*-butylamine in benzene, (b) in benzene, (c) in the aqueous solution of *n*-butylamine, and (d) in water.

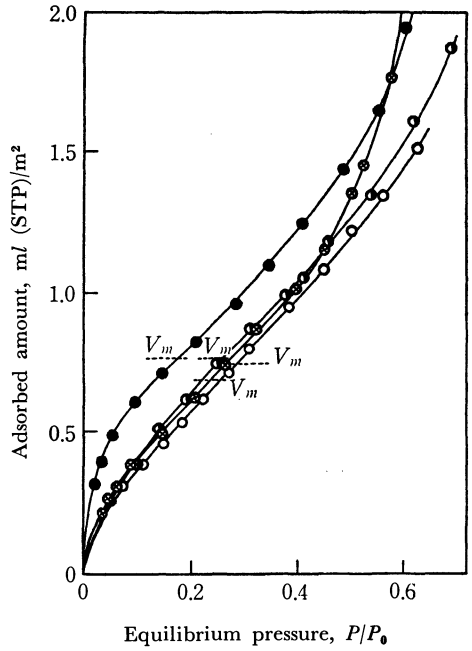

Fig. 3. Adsorption isotherms of benzene on the surfaces of the samples;
○: silica gel, ◑: 10% SA, ⊗: 50% SA, ●: alumina.

3) M. Miura, H. Naono, T. Iwaki, T. Kato, and M. Hayashi, *Kogyo Kagaku Zasshi*, **69**, 1623 (1966).

4) J. W. Whalen, *J. Phys. Chem.*, **66**, 511 (1962).

silica-aluminas, and alumina are shown in Fig. 3. The dotted line in the figure shows a monolayer volume, V_m, estimated from the BET plots.

Discussion

When the silica-alumina is evacuated at a high temperature, such as 300°C, some hydroxyl groups bound with the aluminum atoms of the surface of silica-alumina are removed, resulting in the formation of strong acid sites which consist of Brönsted- and Lewis-acid sites,[5] whereas the remaining aluminol groups may act as weak acid sites. As for the silica, there is no strong acid site in spite of the presence of silanol groups on the surface. The alumina surface has aluminol groups and Lewis-acid sites. In our previous study,[2] the acidity of silica-alumina was obtained as a function of the alumina content, and it was found that the number of acid sites was at a maximum at an alumina content of 10—20%.

As can be seen in Figs. 1 and 2, the immersional-heat values of silica-alumina in benzene and cyclohexane did not vary much with the alumina content; this is unlike the case in water, where the heat value increased appreciably with the alumina content. The factors responsible for the generation of the heat in water have been considered to be the property of the surface hydroxyl groups as well as the number and strength of the acid sites.[2] The heat values of 10% SA in benzene and cyclohexane were larger than, respectively, the values estimated from the sum of the contributions of silica and alumina. This phenomenon may be interpreted on the basis of the contribution of the large number of acids sites on 10% SA to the generation of the heat in a nonpolar solvent.

The difference between the heat values in benzene and the solution of *n*-butylamine in benzene is remarkably larger than that between those in water and an aqueous solution of *n*-butylamine, as may be seen in Fig. 2. In the absence of water, as expected, *n*-butylamine interacts strongly with these samples; it seems probable that the remarkably large heat arises from the strong interaction of *n*-butylamine with the strong acid site, especially with the Lewis-acid site on the surface of alumina.

On the basis of the adsorption isotherms of benzene on the samples in Fig. 3, let us examine the interaction of benzene with the surface. The monolayer volumes, V_m, resemble one another though the adsorption isotherm on alumina is located higher than the others. The monolayer volume was converted to the benzene surface area, S_B, by assuming the cross-sectional area of benzene molecule to be 40.3 Å^2.[6] The ratio of the benzene area to the nitrogen area, S_B/S_{N_2}, for each sample is listed in Table 1. The benzene molecules adsorbed do not cover all the nitrogen area, suggesting that particular sites for benzene molecules are present on the surface. The number of sites where the benzene molecule can be adsorbed is about 2 per 100 Å^2. This number of sites does not correspond to the number of acid sites. Benzene molecules may be adsorbed not only on the acid sites, but also on other sites, such as those of silanol groups.

The interaction of the benzene molecule with the polar surface of a solid is considered to originate from: (a) the van der Waals interaction, (b) the Coulomb interaction between the surface and π-electrons of benzene, and (c) the dipole-induced dipole interaction. The last interaction (c) may be negligibly small compared with the other interactions.[7] On the other hand, the interaction of the cyclohexane molecule with the surface may arise from only the van der Waals interaction.

The immersional-heat values of the samples in benzene in Fig. 1 are larger by 30—37 erg/cm^2 than those in cyclohexane. The difference between the heat values in benzene and cyclohexane, ΔH, is given in Table 1. If the difference between the surface enthalpy of benzene, 67.6 erg/cm^2, and that of cyclohexane, 57 erg/cm^2, is disregarded, and if the cyclohexane surface area is equal to the S_B, the ΔH value may be the contribution of the interaction of π-electrons of benzene with the surface, as a rough estimate. The interaction energy, q, which is obtained by dividing the ΔH value by the monolayer volume, V_m, is presented in the last column of Table 1. As for silica, this value is in good agreement with that given by Kiselev and Poshkus.[8] They obtained, from the heat of adsorption, a value of 2—3 kcal/mol for the energy of interaction between the π-electron of benzene and hydroxyl groups on the surface of silica. Since the π-electron acts as an electron donor in this interaction, the relatively large energy for 10% SA may be ascribed to the contribution of the large number of acid sites.

Table 1. Surface area, number of site for benzene, and difference between heat of immersion in benzene and that in cyclohexane

Material	S_{N_2}(m^2/g)	S_B/S_{N_2}	Site/100Å^2	ΔH(erg/cm^2)	q(kcal/mol)
SiO_2	352	0.81	2.0	34	2.4
10% SA	215	0.84	2.1	37	2.6
50% SA	362	0.75	1.9	30	2.3
Al_2O_3	179	0.84	2.1	33	2.3

5) M. R. Basila, T. R. Kanter, and K. H. Rhee, *ibid.*, **68**, 3197 (1964).

6) S. J. Gregg and K. S. W. Sing, "Adsorption, Surface Area and Porosity," Academic Press, London and New York (1967), p. 80.

7) N. Okuda, *Nippon Kagaku Zasshi*, **82**, 1118 (1961).

8) A. V. Kiselev and D. P. Poshkus, *Dokl. Akad. Nauk SSSR*, **120**, 834 (1958).

A Simple Relation among the Energy Differences between Conformers of XH_2C-CH_2Y, $C_6H_{11}X$, $C_6H_{11}Y$, and *trans*-1,2-$C_6H_{10}XY$

Etsuko FUJIMOTO, Kunio KOZIMA, and Yoshiko TAKEOKA*

Laboratory of Molecular Spectroscopy, Tokyo Institute of Technology, Ookayama, Meguro-ku, Tokyo

(Received March 4, 1971)

By measuring the infrared intensities, the energy differences between two conformers have been determined for bromocyclohexane, iodocyclohexane, *trans*-1-bromo-2-chlorocyclohexane, 1-bromo-2-chloroethane, ethylene bromohydrin, and ethylene iodohydrin in dilute solutions, and for cyclohexanol, *trans*-2-chlorocyclohexanol, ethylene chlorohydrin, and ethylene bromohydrin in vapors.

It was ascertained that the following relation holds for the energy differences:

$$E_t - E_g = (E_{aa} - E_{ee}) - (E_a - E_e) - (E_a' - E_e').$$

Here $E_t - E_g$ is the energy difference between the *trans* and the *gauche* isomer of XH_2C-CH_2Y, $E_{aa} - E_{ee}$ is that between the *aa*- and the *ee*-isomer of *trans*-1,2-$C_6H_{10}XY$, and $E_a - E_e$ and $E_a' - E_e'$ are those between the *a*- and the *e*-isomers of $C_6H_{11}X$ and $C_6H_{11}Y$ respectively, where X is a halogen and Y is a halogen or the O–H group.

The energy difference between the conformers may be considered to be the difference between the intramolecular potential energies, which are usually the sums of the potential energies for the various pairs of non-bonded atoms in each isomer. Furthermore, it is safe to assume, for similar molecules, that the potential energy between the same pair of non-bonded atoms does not differ from molecule to molecule, so long as the distance between non-bonded atoms remains almost the same. On the basis of these considerations, the following relation has been obtained:[1]

$$E_t - E_g = (E_{aa} - E_{ee}) - 2(E_a - E_e), \quad (1)$$

where E_t–E_g is the energy difference between the *trans* and the *gauche* isomer of 1,2-dihaloethane, XH_2C–CH_2X, E_{aa}–E_{ee} is that between the *aa*- and the *ee*-isomer of *trans*-1,2-dihalocyclohexane, $C_6H_{10}X_2$, and E_a–E_e is that between the *a*- and the *e*-isomer of halocyclohexane, $C_6H_{11}X$; this relation has been shown to be correct within the limit of experimental error when X is Cl.[1]

The relation can easily be extended to one for such compounds as XH_2C–CH_2Y, *trans*-1,2-$C_6H_{10}XY$, $C_6H_{11}X$, and $C_6H_{11}Y$, where X is a halogen and Y is a halogen or the O–H group. In an attempt to examine the extended relation, a study of the energy differences between two conformers has been carried out for bromocyclohexane, iodocyclohexane, *trans*-1-bromo-2-chlorocyclohexane, cyclohexanol, *trans*-2-chlorocyclohexanol, 1-bromo-2-chloroethane, ethylene chlorohydrin, ethylene bromohydrin, and ethylene iodohydrin by measuring the infrared intensities.

Experimental

Materials. The iodocyclohexane used in this research was prepared by adding cyclohexene to a solution of potassium iodide dissolved in 95% orthophosphoric acid.[2] The product was purified by fractional distillation; bp 48.5—49.0°C/4 mmHg.

The *trans*-1-bromo-2-chlorocyclohexane was prepared by adding a mixture of bromine and chlorine dissolved in chloroform to cyclohexene.[3] The product was purified by fractional distillation; bp 82.2—82.3°C/13 mmHg.

The ethylene iodohydrin was prepared by refluxing sodium iodide, absolute ethanol, and ethylene chlorohydrin.[4] The product was purified by fractional distillation; bp 47.6—47.8°C/3 mmHg.

The samples of bromocyclohexane, cyclohexanol, 1-bromo-2-chloroethane, ethylene chlorohydrin, and ethylene bromohydrin, which had been obtained from commercial sources, were purified by distillation.

The measurement of the infrared spectra and that of the integrated intensities of the infrared absorption bands were made by the method described in a previous paper.[5]

Results and Discussion

Existence of Conformers. By infrared studies of chlorocyclohexane[1] and bromocyclohexane,[6] it has been ascertained that two conformers, the *a*- and the *e*-isomer, exist in the liquid, while only the *e*-isomer exists in the solid.

Concerning iodocyclohexane, *trans*-1-bromo-2-chlorocyclohexane, and cyclohexanol, the infrared spectra were measured both in the liquid and in the solid. The results are shown in Tables 1-a, 1-b, and 1-c. Since several bands of the liquid-state spectra disappear on passing from the liquid to the solid, as can be seen from these tables, it is certain that the two conformers exist in the liquid, while only one of them remains in the solid.

Since the solid-state spectra of chloro-, bromo-, and iodocyclohexane show striking similarities, it is very probable that only the *e*-isomer exists in the solid of iodocyclohexane. Furthermore, additional evidence is obtained by the following consideration.

By comparing the liquid-state spectrum of iodo-

* Present address: Ohtsuma Women's University, Chiyoda-ku, Tokyo.

1) K. Kozima and K. Sakashita, This Bulletin, **31**, 796 (1958).

2) H. Stone and H. Shechtor, "Organic Syntheses," Vol. 31, p. 66 (1951).

3) R. E. Buckles, J. L. Forrester, R. L. Burham, and T. W. McGee, *J. Org. Chem.*, **25**, 24 (1960).

4) W. E. Noland and P. J. Hartman, *J. Amer. Chem. Soc.*, **76**, 3227 (1954).

5) E. Fujimoto, Y. Takeoka, and K. Kozima, This Bulletin, **43**, 991 (1970).

6) Yu. A. Pentin, Z. Sharipov, G. G. Kotova, A. V. Kamernitskii, and A. A. Akhrem, *J. Struct. Chem. USSR, English Transl.*, **4**, 174 (1963) (*Zh. Strukt. Khim.*, **4**, 194 (1963)).

Table 1-a. Infrared spectra of iodocyclohexane (cm^{-1})

Liquid	Solid	Liquid	Solid
436 (vw)	435 (vw)	1027 (w)	1022 (m)
446 (w)		1073 (w)	1073 (w)
	485 (s)	1095 (s)	1096 (s)
494 (m)	495 (m)	1164 (s)	
639 (m)		1173 (s)	1174 (s)
655 (vs)	652 (vs)	1244 (s)	
	788 (w)	1252 (s)	1254 (s)
801 (sh)		1294 (vw)	1294 (vw)
806 (s)	806 (s)	1332 (m)	1332 (s)
847 (m)	843 (w)	1346 (w)	
863 (m)		1447 (vs)	1446 (vs)
883 (s)	883 (s)	2604 (vw)	2600 (vw)
916 (w)	916 (w)	2668 (w)	2667 (w)
986 (s)	989 (s)	2854 (s)	2857 (s)
1004 (m)		2929 (vs)	2930 (vs)

w=weak, m=medium, s=strong, v=very, sh=shoulder

Table 1-b. Infrared spectra of *trans*-1-bromo-2-chlorocyclohexane (cm^{-1})

Liquid	Solid	Liquid	Solid
442 (w)	443 (m)	1048 (vw)	1048 (w)
484 (w)		1064 (vw)	
505 (m)	504 (s)	1098 (vw)	1097 (w)
540 (m)		1119 (m)	1119 (m)
584 (vs)		1132 (w)	
661 (m)			1163 (w)
692 (s)	690 (s)	1177 (s)	1179 (s)
735 (m)	732 (m)	1185 (s)	
745 (s)	742 (s)	1201 (m)	1203 (m)
	792 (vw)	1216 (m)	1218 (m)
815 (s)	815 (s)	1226 (w)	
818 (s)		1252 (w)	1254 (m)
842 (m)	843 (m)	1261 (w)	
863 (m)		1272 (m)	1274 (m)
869 (w)	869 (w)	1318 (w)	1319 (w)
905 (s)	907 (s)	1339 (m)	1336 (m)
938 (vw)	939 (vw)	1360 (w)	
956 (vw)	967 (vw)	1436 (s)	
976 (s)	978 (s)	1446 (s)	1447 (s)
999 (s)		2662 (vw)	2669 (vw)
1032 (w)	1032 (vw)	2852 (s)	2857 (s)
	1039 (w)	2920 (vs)	2927 (vs)

cyclohexane with those of the chloro- and the bromo-derivative, the 639- and the 655- cm^{-1} band of iodocyclohexane can safely be assigned to the C–I stretching vibration. For the bands assigned to the C-halogen stretching vibration of various halogen derivatives of cyclohexane, one of the present authors has previously pointed out the empirical rule[7] that the frequencies of the bands which are due to the halogen atoms attached to the *e*-positions of the ring are higher than those of the bands due to the same halogen atoms attached to the *a*-positions. According to this rule,

7) K. Kozima, *Bull. Tokyo Inst. Tech.*, **1952**, p. 49.

Table 1-c. Infrared spectra of cyclohexanol (cm^{-1})

Liquid	Solid
550—850 (bm) [a]	700—780 (bm) [a]
	780—870 (bm) [a]
	452 (vw)
	460 (w)
479 (bw)	480 (bw)
558 (m)	553 (s)
	560 (sh)
	783 (w)
789 (m)	787 (m)
835 (w)	
844 (m)	845 (m)
863 (w)	
889 (s)	888 (s)
925 (w)	922 (vw)
957 (sh)	
963 (vs)	963 (vs)
973 (vs)	973 (vs)
1024 (s)	1026 (s)
1033 (sh)	
	1049 (w)
1068 (vs)	1067 (vs)
	1077 (vs)
1139 (m)	1143 (w)
1172 (w)	1176 (w)
1237 (m)	1241 (w)
1254 (m)	1258 (w)
1296 (m)	1303 (w)
1324 (m)	
1346 (m)	
1363 (s)	1364 (s)
1450 (vs)	1447 (s)
	1461 (s)
	1494 (s)
2597 (vw)	2598 (vw)
2674 (w)	2672 (w)
2853 (s)	2862 (s)
2921 (vs)	2927 (vs)
3320 (vs)	3210 (vs)

b=broad

a) The broad bands may be due to the intermolecular hydrogen bond as is the case in *trans*-2-halocyclohexanols.[5]

the 639- and the 655- cm^{-1} band can be assigned to the *a*- and the *e*-isomer respectively. Therefore, the same conclusion can be drawn here, since the higher-frequency band persists in the solid.

In order to determine the stable isomer of *trans*-1-bromo-2-chlorocyclohexane in the solid, the relative intensities of two pairs of bands, the 815- and 818-cm^{-1} bands, and the 976- and 999-cm^{-1} bands, were measured both in the acetone solution and in the carbon disulfide solution. As can be seen in Fig. 1, the intensities of the lower-frequency bands increase when the solvent changes from carbon disulfide to acetone. As it is well known[8] that the more polar isomer stabilizes in polar solvents except in the case of benzene, it follows that the lower-frequency bands which per-

8) S. Mizushima, "Structure of Molecules and Internal Rotation," Acad. Press, New York (1954), p. 43; I. Watanabe, S. Mizushima, and Y. Masiko, *Sci. Papers Inst. Phys. Chem. Res. Tokyo*, **40**, 425 (1943).

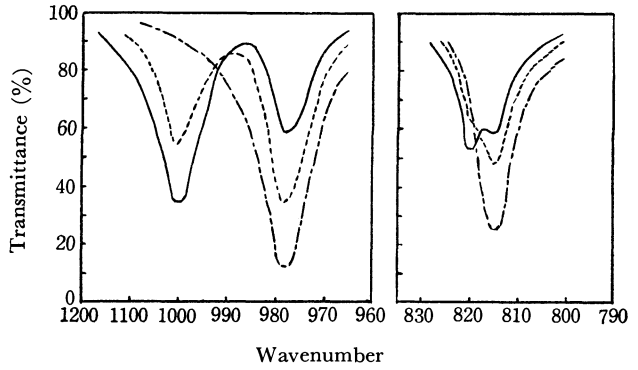

Fig. 1. Variation of infrared intensities of *trans*-1-bromo-2-chlorocyclohexane with changing medium.
—— in the carbon disulfide solution
---- in the acetone solution
·—· in the solid

sist in the solid are to be assigned to the *ee*-isomer, because the *ee*-isomer is more polar than the *aa*-isomer.

Concerning cyclohexanol, it is very probable, in view of the results on halocyclohexanes, that only the *e*-isomer exists in the solid. This is supported by the following consideration. Winstein and Holness[9] have pointed out that *cis*-4-*t*-butylcyclohexanol exists as the *a*-isomer, and that *trans*-4-*t*-butylcyclohexanol exists as the *e*-isomer, with regard to the C–O bond, because of the steric hindrance of the *t*-butyl group, and that the 955-cm^{-1} band is assigned to the C–O stretching vibration of the *cis* isomer, and the 1062-cm^{-1} band, to that of the *trans* isomer. According to these findings, the 1067-cm^{-1} band of cyclohexanol which persists in the solid may be assigned to the C–O stretching vibration of the *e*-isomer. In the spectra of the liquid and of the solution for cyclohexanol, the 957-cm^{-1} band may be assigned to the C–O stretching band of the *a*-isomer. At first glance it is not clear whether or not this band disappears in the solid, because this band is masked by two strong and broad bands. However, by assuming that these two bands are represented by Lorentz's curves, it can be seen that the 957-cm^{-1} band disappears in the solid.

It has been shown[10] that ethylene chlorohydrin possesses two conformers, namely, the *trans* and the *gauche* isomer, both in the vapor and in the liquid, while only the *gauche* isomer exists in the solid. The infrared spectra of the bromo- and the iodo-derivative in the liquid were also measured. In the frequency region of C–halogen stretching vibrations, there are two bands, namely, the 573 and 676 cm^{-1} bands for the bromo-derivative, and the 518 and 622 cm^{-1} bands for the iodo-derivative. Of the two pairs of bands, the intensities of the lower-frequency bands increase with a decrease in the temperature. This fact shows that for the cases of the bromo- and the iodo-derivative also the two conformers exist in the liquid.

Energy Differences between Conformers. For bromo-

9) S. Winstein and N. I. Holness, *J. Amer. Chem. Soc.*, **77**, 5562 (1955).
10) S. Mizushima, T. Shimanouchi, T. Miyazawa, K. Abe, and M. Yasumi, *J. Chem. Phys.*, **19**, 1477 (1951).

Table 2. Temperature dependence of relative integrated intensities and energy difference between isomers in the dilute solution

a) Bromocyclohexane
CS_2 solution: 0.15 mol/*l*
prism: KBr
spectral slit-width: 2.2 cm^{-1} at 658 cm^{-1}
2.8 cm^{-1} at 668 cm^{-1}

Temp. (°C)	Wave number	Isomer	$\log_e(T_0/T)_{max}$	$\Delta\nu_{1/2}$[a]	K	C_1a_1/C_2a_2
27	658	1 = *a*	0.490	5.7	1.50	0.25
	668	2 = *e*	1.61	6.7	1.57	
2	658	1 = *a*	0.518	5.1	1.51	0.23
	668	2 = *e*	1.75	6.4	1.57	

$E_a - E_e = 0.60$ kcal/mol

The symbols used in the table are the same as used in the previous article (5). The values of K were obtained from the table of Ramsay (*J. Amer. Chem. Soc.*, **74**, 72 (1952).)

b) Iodocyclohexane
CS_2 solution: 0.21 mol/*l*
prism: KBr
spectral slit-width: 4.2 cm^{-1} at 639 cm^{-1}
4.7 cm^{-1} at 655 cm^{-1}

34°	639	1 = *a*	0.455	6.0	1.38	0.17
	655	2 = *e*	1.84	7.1	1.64	
−6°	639	1 = *a*	0.437	5.4	1.38	0.14
	655	2 = *e*	1.87	7.0	1.64	

$E_a - E_e = 0.73$ kcal/mol

c) *trans*-1-Bromo-2-chlorocyclohexane
CS_2 solution: 0.18 mol/*l*
prism: NaCl
spectral slit-width: 4.4 cm^{-1} at 977 cm^{-1}
4.6 cm^{-1} at 1001 cm^{-1}

29°	1001	1=*aa*	1.07	7.5	1.51	2.1
	977	2=*ee*	0.546	7.5	1.46	
−27°	1001	1=*aa*	1.29	7.0	1.53	2.2
	977	2=*ee*	0.636	7.2	1.46	

$E_{aa} - E_{ee} = -0.12$ kcal/mol

d) 1-Bromo-2-chloroethane
CS_2 solution: 0.021 mol/*l*
prism: NaCl
spectral slit-width: 4.6 cm^{-1} at 1201 cm^{-1}
5.1 cm^{-1} at 1259 cm^{-1}

25°	1201	1 = *t*	2.03	6.2	1.68	2.3
	1259	2 = *g*	0.936	6.9	1.50	
−30°	1201	1 = *t*	2.23	6.3	1.68	3.1
	1259	2 = *g*	1.01	5.7	1.50	

$E_t - E_g = -0.95$ kcal/mol

e) Ethylene bromohydrin
C_6H_{12} solution: 0.035 mol/*l*
prism: KBr
spectral slit-width: 2.6 cm^{-1} at 573 cm^{-1}
3.5 cm^{-1} at 676 cm^{-1}

61°	676	1 = *t*	0.567	17.3	1.55	0.60
	573	2 = *g*	0.945	17.1	1.56	
11°	676	1 = *t*	0.658	14.6	1.55	0.52
	573	2 = *g*	1.51	12.3	1.56	

$E_t - E_g = 0.59$ kcal/mol

f) Ethylene iodohydrin
CS_2 solution: 0.022 mol/l
prism: KBr
spectral slit-width: 2.6 cm^{-1} at 518 cm^{-1}
3.2 cm^{-1} at 622 cm^{-1}

Temp. (°C)	Wave number	Isomer	$\log_e (T_0/T)_{max}$	$\Delta\nu_{1/2}{}^a$	K	C_1a_1/C_2a_2
31°	622	1 = t	0.392	15.1	1.55	2.1
	518	2 = g	0.263	10.5	1.55	
−19°	622	1 = t	0.516	12.3	1.55	1.6
	518	2 = g	0.415	9.6	1.54	

$E_t - E_g = 0.82$ kcal/mol

g) Ethylene iodohydrin
CS_2 solution: 0.015 mol/l
prism: LiF
spectral slit-width: 3.6 cm^{-1} at 3565 cm^{-1}
3.7 cm^{-1} at 3605 cm^{-1}

27°	3609	1 = f*	0.675	25.0	1.56	0.94
	3567	2 = h	0.696	25.9	1.56	
−21°	3609	1 = f	0.585	24.1	1.56	0.73
	3567	2 = h	0.728	26.7	1.56	

$E_f - E_h = 0.88$ kcal/mol

* The subscripts h and f refer to the hydrogen-bonded molecule and the non-bonded one, respectively.

cyclohexane, the values reported[11,12] do not agree with each other. Therefore, the relative integrated intensities of the 668- and the 658-cm^{-1} band of bromocyclohexane were measured as a function of temperature in the carbon disulfide in order to determine the energy difference. The results are shown in Table 2-a. From these data, the energy difference, E_a–E_e, is calculated to be 0.60 kcal/mol. The value thus obtained agrees with that of Jensen and Gale.[12]

For iodocyclohexane, the change in the relative integrated intensities of the 639- and the 655-cm^{-1} band with the temperature was measured. The results are shown in Table 2-b. From these data, the energy difference, E_a–E_e, is calculated to be 0.73 kcal/mol.

By comparing the values for bromo- and iodocyclohexane with the value of 0.33 kcal/mol for chlorocyclohexane,[1] it can be concluded that the stability of the *e*-isomer of halocyclohexane increases with an increase in the atomic radius of halogens.

For *trans*-1-bromo-2-chlorocyclohexane, the change in the relative integrated intensities of the 977- and the 1001-cm^{-1} band with the temperature was measured. The results are shown in Table 2-c. From these data, the energy difference, E_{ee}–E_{aa}, is calculated to be 0.12 kcal/mol.

Chiurdoglu *et al.*,[11] Masschelein,[13] and Neelakantan[14] have all estimated the energy difference of cyclohexanol in the liquid. Pickering and Price[15] have estimated it in the 0.3 mol/l carbon disulfide solution. However, these values cannot be taken to be the value of the energy difference, because the values are affected by the intermolecular hydrogen bond. The change in the relative integrated intensities of the 835-cm^{-1} band of the *a*-isomer and the 845-cm^{-1} band of the *e*-isomer with the temperature was measured in the vapor. The results are shown in Table 3-a. From these data, the energy difference of cyclohexanol is calculated to be 0.59 kcal/mol, the *e*-isomer being more stable.

Table 3. Temperature dependence of relative integrated intensities and energy difference between isomers in the vapor*

a) Cyclohexanol

Temp. (C)	Wave number	Isomer	C_1a_1/C_2a_2
183°	835	1 = a	1.1
	845	2 = e	
135°	835	1 = a	0.98
	845	2 = e	

$E_a - E_e = 0.59$ kcal/mol

b) *trans*-2-Chlorocyclohexanol

160°	705	1 = aa	0.18
	740	2 = ae	
60°	705	1 = aa	0.089
	740	2 = ee	

$E_{aa} - E_{ee} = 2.0$ kcal/mol

c) Ethylene chlorohydrin

160°	766	1 = t	0.55
	671	2 = g	
95°	766	1 = t	0.44
	671	2 = g	

$E_t - E_g = 1.1$ kcal/mol

d) Ethylene bromohydrin

128°	682	1 = t	0.63
	583	2 = g	
74°	682	1 = t	0.52
	583	2 = g	

$E_t - E_g = 0.98$kcal/mol

* The integrated intensities were measured by the same method as described in the reference of (21).

The energy difference of *trans*-2-halocyclohexanols in dilute solutions has been reported in a previous paper.[5] In order to determine the energy difference of *trans*-2-chlorocyclohexanol in a vapor, the relative integrated intensities of the C–Cl stretching bands were measured at 60°C by using a 1-m cell and at 160°C by using a 10-cm cell. The results are shown in Table 3-b. From these data, the energy difference can be calculated to be 2.0 kcal/mol, the *ee*-isomer being more stable. The energy differences in the vapor for the bromo- and the iodo-derivative could not be measured because of the low vapor pressure.

In order to determine the energy difference of 1-bromo-2-chloroethane, the relative integrated intensities of the 1201-cm^{-1} band of the *trans* isomer and the 1259-cm^{-1} band of the *gauche* isomer were measured in

11) G. Chiurdoglu, M. L. Kleiner, W. Masschelein, and J. Reisse, *Bull. Soc. Chem. Belges*, **69**, 143 (1960).
12) F. R. Jensen and L. H. Gale, *J. Org. Chem.*, **25**, 2075 (1960).
13) W. Masschelein, *J. Mol. Spectrosc.*, **10**, 161 (1963).
14) P. Neelakantan, *Proc. Indian Acad. Sci.*, **A57** (**2**), 94 (1963).
15) R. A. Pickering and C. C. Price, *J. Amer. Chem. Soc.*, **80**, 4931 (1958).

a solution. The assignments used were those reported by Kuratani *et al.*[16] The results are shown in Table 2-d. From these data, the energy difference, E_g–E_t, can be calculated to be 0.95 kcal/mol.

The energy difference in the vapor for ethylene chlorohydrin is calculated to be 1.1 kcal/mol from the data shown in Table 3-c, the *gauche* isomer being more stable. This value is nearly equal to that obtained by Mizushima *et al.*[10] It may be safe to consider that the 573- and the 676-cm^{-1} band of ethylene bromohydrin and the 518- and the 622-cm^{-1} band of ethylene iodohydrin are due to the C–halogen stretching vibrations. Of the pairs of bands for both compounds, the lower-frequency bands can be assigned to the *gauche* isomer, and the others, to the *trans* isomers, as is the case for ethylene chlorohydrin. The temperature dependence of the relative integrated intensities of these bands was also measured. The results for ethylene bromohydrin are shown in Tables 3-d and 2-e for the vapor and the dilute solution respectively. From these data, the energy differences, E_t–E_g, can be calculated to be 0.98 and 0.59 kcal/mol in the vapor and in the dilute solution respectively. The results for ethylene iodohydrin are shown in Table 2-f. From these data, the energy difference, E_t–E_g, can be calculated to be 0.82 kcal/mol.

There are two O–H stretching bands in the 3μ region of the infrared spectra of ethylene halohydrins, even in dilute carbon disulfide solutions, as in the cases of *trans*-2-halocyclohexanols.[5] The lower-frequency bands can be assigned to the O–H stretching vibration for the hydrogen-bonded molecules, and the others, to that of the non-bonded molecules. The lower-frequency bands can be safely assigned to the *gauche* isomer, because, in view of its molecular geometry, only the *gauche* isomer is able to form an intramolecular hydrogen bond. Of these pairs of bands, the intensities of the lower-frequency bands increase with a decrease in the temperature. Concerning ethylene iodohydrin, in the spectra of which the frequency difference between these bands is relatively large, the relative intensity of these bands was measured by changing the temperature. The results are shown in Table 2-g. From these data, the difference between the energy of the hydrogen-bonded molecule, E_h, and that of the non-bonded one, E_f, can be calculated to be 0.88 kcal/mol, the hydrogen-bonded molecule being more stable. When taking into account the experimental error usually introduced in the intensity measurements, this value can be said to agree with the energy difference between the conformers obtained by measuring the C–I stretching bands. This shows that the *gauche* isomer exists exclusively in the form with the intramolecular hydrogen bond in the dilute solution.

Relation of Energy Differences between Conformers. On the basis of the information presented above, the following relation can be obtained for such compounds as XH_2C–CH_2Y, *trans*-1,2-$C_6H_{10}XY$, $C_6H_{11}X$, and $C_6H_{11}Y$:

$$E_t - E_g = (E_{aa} - E_{ee}) - (E_a - E_e) - (E_a' - E_e'), \quad (2)$$

where E_t–E_g is the energy difference between the *trans* and the *gauche* isomer of XH_2C–CH_2Y, E_{aa}–E_{ee} is that between the *aa*- and the *ee*-isomer of $C_6H_{10}XY$, and E_a–E_e and E_a'–E_e' are those between the *a*- and the *e*-isomers of $C_6H_{11}X$ and $C_6H_{11}Y$ respectively.

TABLE 4. ENERGY DIFFERENCE BETWEEN ISOMERS (kcal/mol)

a) X=Cl, Y=Br (in the solution)

trans-1,2-$C_6H_{10}BrCl$ $E_{aa}-E_{ee}$	$C_6H_{11}Cl$ E_a-E_e	$C_6H_{11}Br$ $E_a'-E_e'$	ClH_2C-CH_2Br E_t-E_g	
			obsd.	calcd.
−0.12	0.33**	0.60	−0.95	−1.0

b) X=Cl, Y=OH (in the vapor)

trans-1,2-$C_6H_{10}ClOH$ $E_{aa}-E_{ee}$	$C_6H_{11}Cl$ E_a-E_e	$C_6H_{11}OH$ $E_a'-E_e'$	ClH_2C-CH_2OH E_t-E_g	
			obsd.	calcd.
2.0	0.34**	0.59	1.1	1.1

c) X=Cl, Y=OH (in the solution)

trans-1,2-$C_6H_{10}ClOH$ $E_{aa}-E_{ee}$	$C_6H_{11}Cl$ E_a-E_e	$C_6H_{11}OH$ $E_a'-E_e'$	ClH_2C-CH_2OH E_t-E_g	
			obsd.	calcd.
1.3*	0.33**	0.59	—	0.4

d) X=Br, Y=OH (in the solution)

trans-1,2-$C_6H_{10}BrOH$ $E_{aa}-E_{ee}$	$C_6H_{11}Br$ E_a-E_e	$C_6H_{11}OH$ $E_a'-E_e'$	BrH_2C-CH_2OH E_t-E_g	
			obsd.	calcd.
1.9*	0.60	0.59	0.59	0.7

e) X=I, Y=OH (in the solution)

trans-1,2-$C_6H_{10}IOH$ $E_{aa}-E_{ee}$	$C_6H_{11}I$ E_a-E_e	$C_6H_{11}OH$ $E_a'-E_e'$	IH_2C-CH_2OH E_t-E_g	
			obsd.	calcd.
2.2*	0.73	0.59	0.82	0.9

* The values reported in our previous article (5)
** The values reported in the reference of (1)

From Table 4-a it can be seen that Eq. (2) holds for the case in which X is Cl and Y is Br, since the agreement between the observed and the calculated value for the energy difference of ClH_2C–CH_2Br is satisfactory.

Potential functions for non-bonded hydrogen-hydrogen and for non-bonded carbon-hydrogen interaction energies have been given by Hendrickson.[17] According to these functions, the nuclear distances at the potential minima for hydrogen-hydrogen and carbon-hydrogen interactions are 2.5 and 2.8 Å respectively. Of these pairs of non-bonded atoms in these compounds, there are no pairs of shorter distances than those at the potential minima. Therefore, although the distances between the hydrogen

16) K. Kuratani, T. Miyazawa, and S. Mizushima, *J. Chem. Phys.*, **21**, 1411 (1953).

17) J. B. Hendrickson, *J. Amer. Chem. Soc.*, **83**, 4531 (1961).

atoms or between the hydrogen and the carbon atom may vary somewhat from molecule to molecule, it can be seen from the potential curves[17] that these changes do not affect the relation of Eq. (2) beyond the limit of experimental error. The pairs of non-bonded atoms which make an important contribution to the energy difference may be those of halogen-halogen, halogen-hydrogen, and halogen-carbon. However, these potential functions are not clearly known. From the fact that Eq. (2) holds for these compounds, it is, however, sure that, in the cases where the distances between the same pair of the non-bonded atoms are considered to be almost the same from the structural point of view, the potential energy between them is nearly the same from molecule to molecule at least for these compounds.

It seems that it would be interesting to consider the cases in which one of the substituents is an O–H group, and the other, a halogen. In these cases, one of the isomers forms an intramolecular hydrogen bond. The values of the frequency difference between the hydrogen-bonded O–H stretching band and the free one are shown in Table 5 for the *ee*-isomer of *trans*-2-halocyclohexanols and for the *gauche* isomer of ethylene halohydrins. From this table, it can be seen that the strength of the hydrogen bond of *trans*-2-chloro-, *trans*-2-bromo-, or *trans*-2-iodocyclohexanol is nearly equal to that of ethylene chloro-, ethylene bromo-, or ethylene iodohydrin respectively. Therefore, it seems probable that Eq. (2) holds for these cases. The results for the cases of the vapors of the chloro-derivatives are shown in Table 4-b. The agreement shown in this table is satisfactory. For the cases of the dilute solutions of the bromo- and the iodo-derivative the results are shown in Tables 4-d and 4-e respectively. In these tables, the value of the energy difference of cyclohexanol in the vapor is used, as the value in the dilute solution could not be measured because of the lack of an adequate solvent. Since, for this molecule, the dipole moment of the *e*-isomer is nearly equal to that of the *a*-isomer, the energy difference in the vapor seems not to be different from that in the dilute solution.[8] As Tables 4-d and 4-e show, the observed and the calculated values agree if account is taken of the experimental errors usually introduced in the intensity measurements. The energy difference of ethylene chlorohydrin in the dilute solution could not be measured because the bands of the usual non-polar solvents masked those of ethylene chlorohydrin. The value is, however, calculated by Eq. (2) to be 0.4 kcal/mol, as is shown in Table 4-c; this is lower by 0.7 kcal/mol than the value observed in the vapor. When taking into account the fact that the observed value of ethylene bromohydrin in the dilute solution is lower by 0.39 kcal/mol than that in the vapor, the estimated value of the chloro-derivative seems reasonable.

Table 5. Frequency difference between hydrogen-bonded O–H band and free one in the carbon disulfide solution (cm^{-1})

	trans-1,2-$C_6H_{10}XOH$	XH_2C-CH_2OH
X=Cl	25	28
X=Br	34	31
X=I	44	42

The dipole moment of the *trans* isomer of ethylene chlorohydrin, μ_t, is estimated to be 1.74 D by using the dipole moments of methanol[18] and methyl chloride[19] based upon the rule of the vector sum of bond moments. Since the dipole moment of the *gauche* isomer, μ_g, could not be estimated by using this rule because of the uncertainty of the moment due to the intramolecular hydrogen bond, it was calculated to be 1.79 D by the usual relation:

$$\mu^2 = (\mu_g^2+\mu_t^2\frac{1}{2}e^{-\Delta E/RT})/(1+\frac{1}{2}e^{-\Delta E/RT}),$$

where the value of ΔE used is the value of 1.1 kcal/mol obtained in the vapor and where μ is the dipole moment of 1.78 D observed in the vapor.[20] It can be seen from the results obtained above that the dipole moment of the *gauche* isomer is not very different from that of the *trans* isomer. Therefore, the finding that the *gauche* isomer is stabilized when the state changes from a dilute solution to a vapor violates the rule[8] that the more polar conformation is stabilized in a medium with a larger dielectric constant. The same violation can be seen in the cases of ethylene bromohydrin and *trans*-2-chlorocyclohexanol. However, this fact seems reasonable, because it is very probable the intramolecular hydrogen bond in the vapor is stronger than that in the dilute solution, as in the case with the intermolecular hydrogen bond between methanol and triethylamine.[21]

18) E. V. Ivash and D. M. Dennison, *J. Chem. Phys.*, **21**, 1804 (1953).
19) R. Karplus and A. H. Sharbaugh, *Phys. Rev.*,**75**,889 (1949).
20) C. T. Zahn, *Phys. Rev.*, **40**, 291 (1932).
21) E. Hirano and K. Kozima, This Bulletin, **39**, 1216 (1966).

The Coadsorption of Nitric Oxide, Nitrogen, and Oxygen on Rhenium

Teijiro TAMURA

Department of Chemistry, Faculty of Industrial Arts, Kyoto Technical University, Matsugasaki, Sakyo-ku, Kyoto

(Received March 8, 1971)

The coadsorption of nitric oxide, nitrogen, and oxygen on a polycrystalline rhenium filament was studied using flash desorption mass-spectroscopy. Substitutional desorption was not observed during the adsorption of nitric oxide, nitrogen, or oxygen on preadsorbed leayers. No oxygen or nitrogen adsorbs on rhenium saturated with nitric oxide. However, nitric oxide adsorbs on rhenium saturated with nitrogen or oxygen. The strength of the chemisorption bond between rhenium and adsorbed species becomes weaker in the order of: nitric oxide, oxygen, and nitrogen. When the same amount of nitric oxide molecules exist in various coadsorbed layers, the Tp of the nitrogen desorption spectrum from these layers is shifted to a lower temperature with an increase in the number of oxygen atoms in them, because the strength of the chemisorption bond of Re–N is weakened by the strongly-bonded Re–O. No desorption of the nitric oxide molecule from a coadsorbed layer of the "N_2+O_2" on rhenium was observed.

In the investigation of chemical reactions between metal and gas, studies of the chemisorption which precede these reactions will lead to a general understanding of the mechanism of chemical reactions. There has been much work done on the chemisorption of common gases, such as nitrogen,[1-6] oxygen,[7-11] hydrogen,[12,13] and carbon monoxide,[14-17] on metal surfaces.

The investigation of the chemisorption of nitric oxide, which possesses an odd number of electrons, is of interest. In a previous paper,[18] a study of the chemisorption of nitric oxide alone on rhenium has been reported.

In general, the temperature which gives the maximum rate of the desorption, Tp, and the peak height in the desorption spectrum from chemisorbed layers may be related to the desorption energy of the adsorbed species, so that different desorption spectra may be displayed by various adsorbed species with different surface coverages. Moreover, desorption spectra may be also changed by being affected by the coexistence of different adsorbed species. Thus, although the investigation of the coadsorption on metal surfaces is of interest, there have been only a few studies in this field.[8,19-22]

In the present investigation, the coadsorption of nitric oxide, nitrogen, and oxygen and the replacement of chemisorbed gases on a polycrystalline rhenium filament have been studied using flash desorption mass-spectroscopy.

Apparatus

The bakeable, ultra-high-vacuum apparatus used in this study was similar to that used in a previous work[18] except that it had two gas-supply system. It is shown in Fig. 1 schematically. The reaction systems, the volume of which was 0.8 l, contained a polycrystalline rhenium filament with a geometrical area of $A=0.6$ cm^2. The rhenium filament was analyzed spectroscopically. (Found: Si; 0.02%, Fe; 0.008%, Mg; 0.005%.) The ultimate pressure, read with a Bayard-Alpart gauge (B-A gauge), was 3×10^{-10} Torr in the system after a rigorous outgassing. The total pressure was measured by means of a Pirani gauge with a sensitivity of 7.2×10^{-8} Torr/μV for N_2 and NO, and 7.5×10^{-8} Torr/μV for O_2. An omegatron mass spectrometer was also used as a partial-pressure gauge; it had a sensitivity of 12 Torr^{-1} for N_2, 11.8 Torr^{-1} for NO, and 11 Torr^{-1} for O_2. The B-A gauge was used only in the ultimate-pressure measurement because the nitric oxide is dissociated by a hot filament of the gauge. The rhenium filament was heated to 2200°K using a transistor control circuit, as has been described previously.[18] The filament temperature was determined from a resistance-temperature relationship for rhenium;[23] above 1000°K, its temperature was measured with a micro optical pyro-

1) T. Oguri, *J. Phys. Soc. Jap.*, **18**, 1280 (1963).
2) J. T. Yates, Jr., and J. E. Madey, *J. Chem. Phys.*, **43**, 1055 (1965).
3) L. J. Rigby, *Can. J. Phys.*, **43**, 532 (1965).
4) T. E. Madey, and J. T. Yates, Jr., *J. Chem. Phys.*, **44**, 1675 (1966).
5) A. A. Parry, and J. A. Pryde, *Brit. J. Appl. Phys.*, **18**, 329 (1967).
6) M. D. Scheer, and J. D. McKinley, *Surface Sci.*, **5**, 332 (1966).
7) B. McCarroll, *J. Chem. Phys.*, **46**, 863 (1967).
8) J. H. Singleton, *ibid.*, **47**, 73 (1967).
9) W. Greaves, and R. E. Stickny, *Surface sci.*, **11**, 395 (1968).
10) R. P. H. Gasser, and C. J. Marsay, *ibid.*, **20**, 107 (1970).
11) T. Hamamura, and G. Tomita, This Bulletin, **40**, 1066 (1967).
12) P. W. Tamm, and L. D. Schmidt, *J. Chem. Phys.*, **52**, 1150 (1970).
13) K. F. Poulter, and J. A. Pryde, *Brit. J. Appl. Phys., Ser.* 2, **1**, 169 (1968).
14) P. A. Redhead, *Trans. Faraday Soc.*, **57**, 641 (1961).
15) T. E. Madey, J. T. Yates, Jr., and R. C. Stern, *J. Chem. Phys.*, **42**, 1372 (1965).
16) R. P. H. Gasser, R. Thwaites, and J. Wilkinson, *Trans. Faraday Soc.*, **63**, 195 (1967).
17) J. T. Yates, Jr., and T. E. Madey, *J. Chem. Phys.*, **51**, 334 (1969).
18) T. Tamura, This Bulletin, **44**, 590 (1971)
19) J. L. Robins, 1962 *Trans. 9th Nat. Vac. Symp.*, p. 510.
20) J. W. May, L. H. Germer, and C. C. Chang, *J. Chem. Phys.*, **45**, 2383 (1966).
21) P. J. Estrup, and J. Anderson, *ibid.*, **46**, 567 (1967).
22) R. P. H. Gasser, K. Roberts, and R. Thwaites, *Trans. Faraday Soc.*, **63**, 2765 (1967).
23) C. T. Sims, C. M. Craighead, R. I. Jaffee, D. N. Gideon, E. N. Wyler, F. C. Todd, D. M. Rosenbaum, E. M. Sherwood, and I. E. Campbell, "Investigations of Rhenium," Battle Memorial Institute, Wright Air Development Center Technical Report 54—371, June (1954), p. 47.

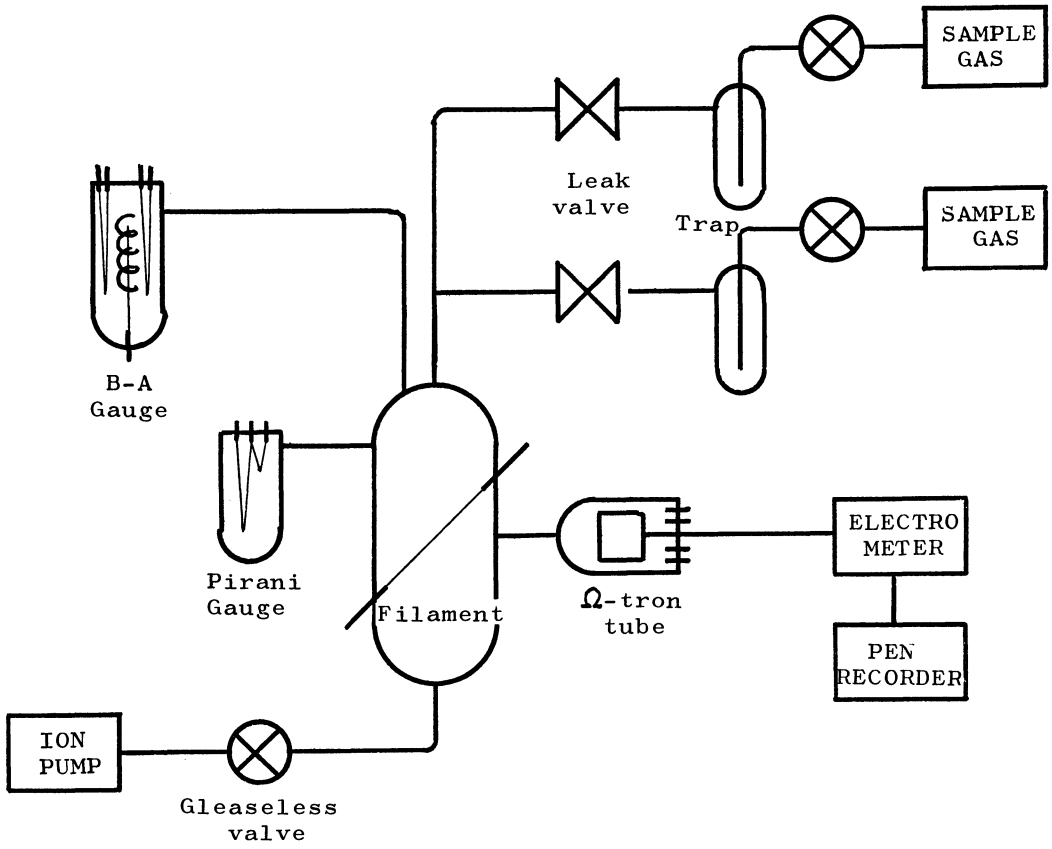

Fig. 1. Schematic drawing of Ultrahigh-vacuum apparatus for flash desorption mass spectroscopy.

meter.

The nitric oxide and nitrogen were prepared by the methods described in the previous paper. The oxygen was prepared by the thermal decomposition of high-purity potassium permanganate. The gas evolved was purified by liquid-nitrogen trap-to-trap distillation. No impurities up to mass 200 of any of the sample gases were detected by means of the omegatron mass spectrometer.

Procedure

Amount of Adsorption. The rhenium filament was purified by heating it at about 2000°K in oxygen of 1×10^{-6} Torr for several hours. The rhenium filament was then flashed to clean at 2200°K in a vacuum prior to the adsorption experiments, and then allowed to cool at room temperature. After nitric oxide had been passed through to obtain the saturation coverage, the system was evacuated; nitrogen or oxygen was then passed through to allow it to adsorb sufficiently. Such coadsorbed layers are expressed as "NO+N_2" or "NO+O_2". After the system had then been evacuated until the pressure dropped to 5×10^{-9} Torr, the rhenium filament was flashed at 2200°K in a closed system. The amount of molecules desorbed can be calculated from the pressure and the volume of the system. In the nitric-oxide adsorption, the number of molecules adsorbed is twice the number of molecules desorbed, because the desorbed gas is nitrogen.

Desorption Spectra. After the coadsorbed layer was formed, as has been described above, the slow flash desorption runs were initiated by using a transistor control circuit while the system was being evacuated. Ion currents of the omegatron mass spectrometer for each mass were recorded on the chart recorder.

Substitutional Desorption. For example, on the coadsorption of "NO+O_2", the ion current of the omegatron mass spectrometer corresponding to nitric oxide (preadsorbate) was measured during the adsorption of oxygen on rhenium saturated with nitric oxide. The substitutional desorption of nitric oxide could be detected from the change in this ion current

Results and Discussion

The amounts of nitrogen desorbed from various coadsorbed layers are shown in Table 1. The desorption spectra of nitrogen from the coadsorbed layers are shown in Fig. 2, while the temperatures of the desorption-peak maximum, Tp, are also shown in the second column of the table.

"*NO+N_2*". The substitutional desorption of nitric oxide was not observed during the adsorption of nitrogen on rhenium saturated with nitric oxide. Both the amount of nitrogen desorbed and the desorption spectrum of nitrogen from the "NO+N_2" layer were the same as those from a nitric oxide monolayer on rhenium. Therefore, nitrogen does not adsorb on the saturated nitric oxide layer on rhenium.

"*NO+O_2*". The substitutional desorption of nitric oxide was not observed in this case. Both the amount of nitrogen desorbed and the desorption spectrum of nitrogen from the "NO+O_2" layer were

TABLE 1. THE AMOUNT OF NITROGEN DESORBED AND THE Tp IN THE NITROGEN DESORPTION SPECTRUM FROM VARIOUS ADSORBED LAYERS ON RHENIUM

Layer	N_2 (desorbed) (molecules/cm^2)	Tp (°K)
NO	2.6×10^{14}	775
NO+N_2	2.6×10^{14}	775
NO+O_2	2.6×10^{14}	775
N_2+NO	3.4×10^{14}	775
O_2+NO	3.4×10^{13}	850
N_2	1.08×10^{14}	970
N_2+O_2	1.08×10^{14}	820
O_2+N_2	—	—

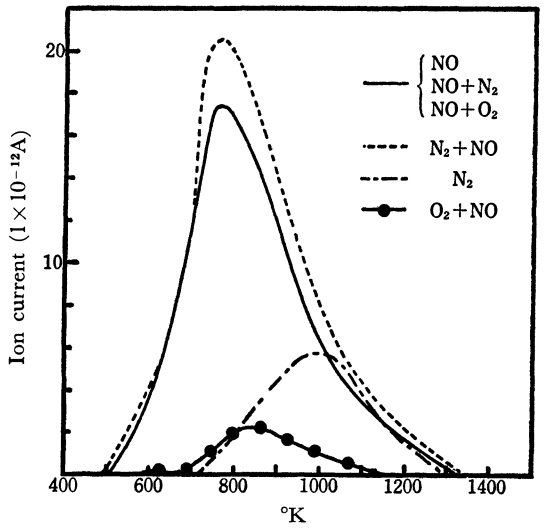

Fig. 2. Nitrogen desorption spectra from various coadsorbed layers on rhenium.

the same as those from a nitric oxide monolayer on rhenium. Although the oxygen desorption was observed at temperatures above 1500°K,[18] the majority of the oxygen evaporates as rhenium oxide at such a high temperature. Therefore, the detection of the amount of oxygen adsorbed is very difficult from the pressure burst in the flash-desorption experiment. Thus, it is impossible to know whether or not oxygen adsorbs on rhenium saturated with nitric oxide. If oxygen adsorbs on this surface, there may be some influence on the desorption spectrum of nitrogen. However, even the exposure of oxygen was changed in the coadsorption of "NO+O_2", the desorption spectrum of nitrogen from this layer being the same as that from a nitric oxide monolayer. From this fact, it may be considered that oxygen is not adsorbed on rhenium saturated with nitric oxide.

"*N_2+NO*". No substitutional desorption of nitrogen was detected during the adsorption of nitric oxide on the preadsorbed nitrogen layer. The Tp of the desorption spectrum of nitrogen from the "N_2+NO" layer was the same as that from a nitric-oxide monolayer, but the amount of nitrogen desorbed from this coadsorbed layer was 3.4×10^{14} molecules/cm^2, while the nitrogen desorbed from a nitric-oxide monolayer was 2.6×10^{14} molecules/cm^2. If the nitric-oxide molecule can be adsorbed on a site other than that occupied by preadsorbed nitrogen atoms, the nitric oxide of 3.04×10^{14} molecules/cm^2 will be adsorbed on rhenium saturated with nitrogen, as is shown in Fig. 3. (Nitrogen adsorbs dissociatively on rhenium.) From the amount of nitrogen desorbed, it is evident that an excess of 1.6×10^{14} molecules/cm^2 of nitrie oxide was adsorbed. The desorption spectra of nitric oxide from a nitric oxide monolayer and the "N_2+NO" layer on rhenium are shown in Fig. 4. The amount of desorbed nitric oxide as a molecule from the "N_2+NO" layer is more than that from a nitric-oxide monolayer. Furthermore, as is evident from Fig. 2, at an early stage the rate of nitrogen desorption from the "N_2+NO" layer in the nitrogen desorption spectrum is faster than that from a nitric-oxide monolayer. When nitric oxide was adsorbed on a preadsorbed nitrogen layer with a half coverage, "N_2(1/2)+NO", the amount of nitrogen desorbed from this layer was 3.0×10^{14} molecules/cm^2. By calculations similar to those in the case of "N_2(full)+NO", it can be concluded that an excess of 8×10^{13} molecules/cm^2 of nitric oxide is adsorbed. This is half the value of that from the "N_2(full)+NO" layer. The amount of the excess nitric oxide is proportional to the amount of preadsorbed nitrogen. From these facts, we can consider that some nitric oxide molecules were induced by the preadsorbed nitrogen atoms and were weakly held on it.

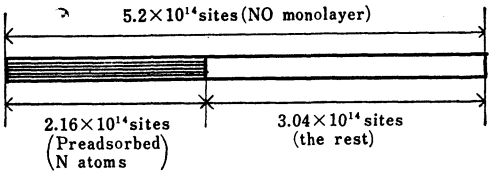

Fig. 3. The number of vacant and adsorbed sites in the nitrogen monolayer.

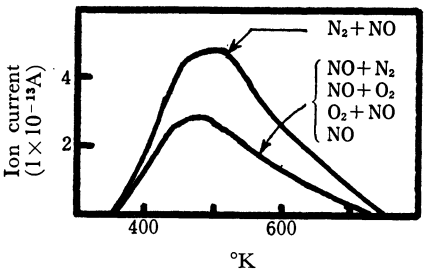

Fig. 4. Nitric oxide desorption spectra from various coadsorbed layers on rhenium.

"*O_2+NO*". No substitutional desorption of oxygen during the adsorption of nitric oxide was observed. Since the amount of nitrogen from the "O_2+NO" layer was 3.4×10^{13} molecules/cm^2, it shows that nitric oxide can adsorb on rhenium saturated with oxygen. The Tp of nitrogen desorption from this coadsorbed layer is 850°K.

This fact may suggest that the number of adsorptive sites for oxygen atoms is less than that for nitric oxide molecules. (Oxygen adsorbs dissociatively,[10] and nitric oxide adsorbs nondissociatively,[18] on rhenium.) If this is so, in the slow-flash desorption experiment of

nitric-oxide adsorption, the desorption of oxygen from the decomposition of nitric oxide must be observed in the temperature region of the nitrogen desorption. However, the desorption of neither molecular nor atomic oxygen was detected in this temperature region in these experiments.

If the oxygen atoms adsorbed are immobile, they will occupy two sites for oxygen adsorption, and some adsorptive sites will remain on the rhenium surface as vacant sites.[24] It is possible that nitric oxide adsorbs on these vacant sites. Oxygen adsorption was made on the rhenium surface while heating the rhenium filament to a high temperature at which adsorbed oxygen atoms were able to migrate over the surface;[25] the filament was afterward allowed to cool to room temperature. When this surface was exposed to nitric oxide, the amount of nitric oxide adsorbed on it was found to be about a half of that on the surface saturated with oxygen at room temperature. From the fact that, in the nitric-oxide adsorption, the desorption of neither molecular nor atomic oxygen is observed in the temperature region of nitrogen desorption, as has been mentioned above, nitric oxide can be said probably to adsorb on vacant sites formed with oxygen adsorption at room temperature, because the nitric oxide adsorbs nondissociatively.

On the other hand, although the desorption of nitric oxide molecules from the "O_2+NO" layer was observed by a slow-flash desorption experiment (Fig. 4), the nitric oxide desorption from a partial coverage of nitric oxide which desorbs the same amount of nitrogen as that from the "O_2+NO" layer was not observed. Moreover, the oxygen desorption from the "O_2+NO" layer was observed in the temperature region of the nitrogen desorption. We consider that some oxygen from the decomposition of nitric oxide in the "O_2+NO" layer was desorbed in this temperature region, for all the available sites for adsorption in first layer were occupied by oxygen atoms and nitric oxide molecules. It seems that a weakly-held adsorption of nitric oxide, such as could be seen in the coadsorption of the "N_2+NO", is also present in the "O_2+NO" layer. As has been mentioned above, it is considered that the nitric oxide adsorption in the "O_2+NO" layer has two types of binding states, that is, a gap-filling state and a weakly-bonded state on the immobile preadsorbed oxygen layer at room temperature. Although the Tp of nitrogen desorption from the "O_2+NO" layer was 850°K, the Tp of that from the partial coverage of nitric oxide which gave the same amount of nitrogen desorbed as that from the "O_2+NO" layer (the same amount of nitric oxide adsorbed) was 1000°K. There are more oxygen atoms in the "O_2+NO" layer than in the partial coverage of nitric oxide (the same amount of nitric oxide). This behavior may be interpreted as follows——the bonding strength of Re–N may be weakened by the oxygen adsorption, which binds strongly with rhenium in adjacent sites. We may thus consider that the nitrogen on the surface desorbs more easily and that the Tp of nitrogen desorption is shifted to a lower temperature (from 1000°K to 850°K).

"*N_2+O_2*". No substitutional desorption of nitrogen was also observed in this case, either. No desorption of nitric oxide molecule was observed from this layer during the slow-flash experiment. The amount of nitrogen desorbed from the "N_2+O_2" layer was the same as that from a nitrogen monolayer, but its Tp was 820°K and it was considerably shifted to a lower temperature. It is considered that the bonding strength of Re–N was also weakened as a result of the adsorption of oxygen atoms between the adsorbed nitrogen atoms, as has been described above. The Tp of nitrogen desorption from this coadsorbed layer is lower than that (870°K) from the partial coverage of nitric oxide giving the same amount of desorbed nitrogen. It is believed that the Tp might be shifted to a lower temperature, because there are more oxygen atoms in the "N_2+O_2" layer than in the partial coverage of nitric oxide (with the same amount of nitrogen atoms). Furthermore, the Tp of nitrogen desorption from the "N_2+O_2" layer is lower than that from the "O_2+NO" layer. It seems that the probability for the recombination of adsorbed nitrogen atoms is high, because the number of nitrogen atoms in the "N_2+O_2" layer is more than that in the "O_2+NO" layer.

"*O_2+N_2*". No desorption of either nitrogen or nitric oxide was observed by the slow-flash experiment. Therefore, nitrogen is not adsorbed on rhenium saturated with oxygen.

Conclusion

Since both the desorption spectra and the amounts of nitrogen desorbed from the "NO+N_2" and the "NO+O_2" layers were the same as those from the nitric oxide monolayer, it is considered that neither nitrogen nor oxygen is adsorbed on rhenium saturated with nitric oxide. Nitric oxide, however, adsorbs not only on vacant sites in the first layer, but on sites in the second layer on rhenium saturated with nitrogen or oxygen. Therefore, the bonding strength between rhenium and adsorbed species becomes weaker in the order of: nitric oxide, oxygen, and nitrogen.

When the more oxygen atoms exist in coadsorbed layers which include the same amount of nitrogen atoms, the Tp of the nitrogen desorption is shifted to a lower temperature.

No nitric oxide was detected in the desorption from a mixed nitrogen-oxygen layer. This indicates that nitric oxide was not produced in the adsorption and the desorption processes. Further, nitrogen does not adsorb on an oxygen-saturated rhenium surface, because the adsorption site for nitrogen is occupied by the oxygen atoms.

The author wishes to express his deep thanks to Professor Takuya Hamamura of this Institute, to Professor Kumasaburo Kodera and Dr. Masaru Onchi of Kyoto University for their kind discussions and encouragement, and to Dr. Minoru Ozasa of the Matsushita Electronics Corporation, who made the spectroscopic analysis of rhenium.

24) J. K. Roberts, *Proc. Roy. Soc., Ser. A*, **152**, 464 (1935).
25) K. Ishizuka, *J. Res. Inst. Catalysis, Hokkaido Univ.*, **15**, 95 (1967).

Magnetic Properties of Some Iminoxyl Polyradicals. II. TEMPOP Triradical and TEMPOS Tetraradical

Akira NAKAJIMA, Hiroaki OHYA-NISHIGUCHI, and Yasuo DEGUCHI*

Department of Chemistry, Faculty of Science, Kyoto University, Kyoto

** College of Liberal Arts and Science, Kyoto University, Kyoto*

(Received March 11, 1971)

The EPR spectra of the TEMPOP triradical and the TEMPOS tetraradical in solution showed seven and nine absorption lines respectively, which were interpreted as the hyperfine interaction between unpaired electron and ^{14}N nuclei in the case of $|J_{in}| \gg A$. The paramagnetic susceptibilities of TEMPOP and TEMPOS were measured. In the case of TEMPOP, no typical short-range ordering effect was found, but the $1/\chi_M - T$ curve deviated from the Curie-Weiss law at very low temperatures. In the case of TEMPOS, the $1/\chi_M - T$ curve was divided into four regions. In the first and third regions, the $1/\chi_M - T$ curves both obey the Curie-Weiss law. The second region is the intermediate region between the first and third regions. In the last region, $1/\chi_M - T$ shows a slight deviation from the Curie-Weiss law of the third region. In order to explain this behavior, some spin-cluster models with three and four spins were applied.

Recently, the magnetic properties of many organic stable free radicals have been investigated very actively.[1-5] It has been reported that many of these organic radicals exhibit some effects of the coupling of magnetic spins—for example, spin cluster or low-dimensional spin array—caused by an exchange interaction between unpaired electrons.

Among these, the iminoxyl radicals are the most interesting group, since they are very stable and many derivatives can be synthesized.[6,7]

Karimov and Rozantsev reported the EPR studies of some solid stable iminoxyl radicals and interpreted them in terms of the effect of the exchange interaction between unpaired electrons belonging to different radicals.[4b] Yamauchi *et al.*[5b] and Karimov[4c,4d] independently measured the paramagnetic susceptibility of 2,2,6,6-tetramethyl-4-hydroxypiperidine-1-oxyl (TANOL radical, Fig. 1a), characterized as a one-dimensional Heisenberg linear chain.

On the other hand, the present authors had an interest in the polyradicals of the iminoxyl group as spin

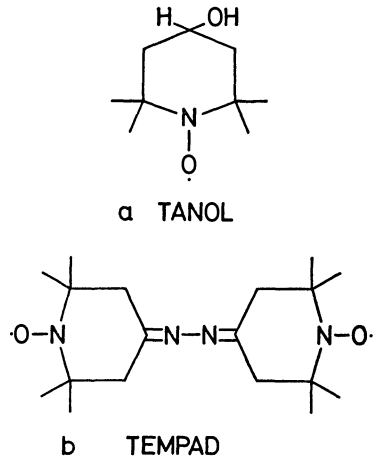

Fig. 1. Molecular structures of TANOL radical (a) and TEMPAD biradical (b).

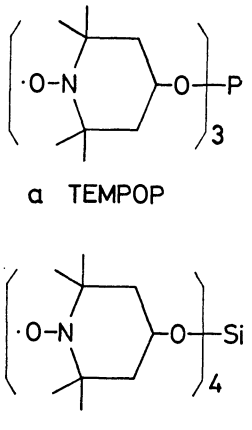

Fig. 2. Molecular structures of TEMPOP triradical (a) and TEMPOS tetraradical (b).

1) E. Müller and I. Müller-Rodloff, *Liebig Ann. Chem.*, **521**, 81 (1935); E. Müller, *Ztschr. Elektrochem.*, **51**, 23 (1945); J. Van den Handel, *Physica*, **18**, 921 (1952); H. Kainer and K. H. Hausser, *Ber.*, **86**, 1563 (1953); H. J. Gerritsen, R. Okkes, H. M. Gijsman, and J. Van den Handel, *Physica*, **20**, 13 (1954); K. H. Hausser and H. Kainer, *Z. Naturforsch.*, **9a**, 783 (1954); K. H. Hausser, *ibid.*, **11a**, 20 (1956).

2) A. S. Edelstein and M. Mandel, *J. Chem. Phys.*, **35**, 1130 (1961); R. S. Rhodes, J. H. Burgess, and A. S. Edelstein, *Phys. Rev. Letters*, **6**, 462 (1961); M. E. Anderson, R. S. Rhodes, and G. E. Pake, *J. Chem. Phys.*, **35**, 1527 (1961); J. H. Burgess, R. S. Rhodes, M. Mandel, and A. S. Edelstein, *J. Appl. Phys.*, **33s**, 1352 (1962); W. O. Hamilton and G. E. Pake, *J. Chem. Phys.*, **39**, 2694 (1963); A. S. Edelstein, *ibid.*, **40**, 488 (1964).

3) W. Duffy, Jr., *J. Chem. Phys.*, **36**, 490 (1962); W. Duffy, Jr. and D. L. Strandburg, *ibid.*, **46**, 456 (1967); W. Duffy, Jr., D. L. Strandburg, and J. F. Deck, *Phys. Rev.*, **183**, 567 (1969).

4) a) A. M. Prokhorov and V. B. Fedrov, *Sov. Phys. JETP*, **16**, 1489 (1962); A. M. Prokhorov and V. B. Fedrov, *ibid.*, **17**, 759 (1963). b) Yu. S. Karimov and E. G. Rozantsev, *Sov. Phys. Solid State*, **8**, 2255 (1967). c) Yu. S. Karimov, *Sov. Phys. JETP Letters*, **8**, 239 (1968). d) Yu. S. Karimov, *Sov. Phys. JETP*, **30**, 1062 (1969).

5) a) A. Nakajima, H. Nishiguchi, and Y. Deguchi, *J. Phys. Soc. Japan*, **24**, 1175 (1968). b) J. Yamauchi, T. Fujito, E. Ando, H. Nishiguchi, and Y. Deguchi, *ibid.*, **25**, 1558 (1968); J. Yamauchi, T. Fujito, H. Ohya-Nishiguchi, and Y. Deguchi, *Intern. Conf. L. T.*, 12, (1970). c) K. Mukai, This Bulletin, **42**, 40 (1969); T. Fujito, H. Nishiguchi, Y. Deguchi, and J. Yamauchi, *ibid.*, **42**, 3334 (1969).

6) O. L. Lebedev and S. N. Kazarnooskii, *Trudy Po. Khimii i Khim. Tekhno.*, **3**, 649 (1959).

7) There are many works concerned with this studies. For example, R. Briere, H. Lemaire, and A. Rassat, *Bull. Soc. Chim. Fr.*, **1965**, 3272.

clusters. In a previous work, we reported the paramagnetic susceptibility of bis(2,2,6,6-tetramethylpiperidine-4)azine-1,1′-dioxyl (TEMPAD biradical, Fig. 1b) and explained it as a pairing caused by an intra-molecular exchange interaction,[5a] but recent study has made it clear that the inter-molecular interaction is only the origin of the short-range ordering in the TEMPAD biradical.[8]

In this paper, we shall report the magnetic properties of two polyradicals, tris(2,2,6,6-tetramethylpiperidine-1-oxyl-4)phosphate (the TEMPOP triradical, Fig. 2a) and the tetrakis(2,2,6,6-tetramethylpiperidine-1-oxyl-4)silicate (the TEMPOS tetraradical, Fig. 2b), and will discuss them on the basis of some spin-cluster models.

Experimental

The TEMPOP triradical was prepared from the TANOL radical obtained by the oxidation of the corresponding amine by hydrogen peroxide, following the method of Neiman *et al.*[9] The TEMPOS tetraradical was also prepared from the same monoradical by the method of Rozantsev and Gulobev.[10] After purification by chromatography and recrystallization, the pure TEMPOP and TEMPOS (mps 143.5±0.5 and 160±1°C respectively) were obtained.

The electron paramagnetic resonance absorptions were measured using two 100 kHz modulated X-band spectrometers, JEOLCO's JES-3BX and JES-P-10.

The static magnetic susceptibility was measured with about 50—100 mg powder samples over the temperature range of 1.8—273°K and at a magnetic field strength of about 8—9 kOe, using a torsion balance described elsewhere.[11] All the data were corrected for the diamagnetic contribution calculated by the Pascal method (-3.57×10^{-4} emu/mol for the TEMPOP triradical and -4.82×10^{-4} emu/mol for the TEMPOS tetraradical).

Results and Discussion

TEMPOP Triradical. The EPR spectrum of the TEMPOP triradical in a tetrahydrofuran (THF) solution shows seven lines, all caused by the hyperfine interaction between three unpaired electrons and three ^{14}N nuclei, the splitting of which is 5.18 gauss and the g-value of which is 2.0060 (Fig. 3).[12] The spin Hamiltonian of this system is:

$$\mathcal{H} = -g\beta\mathrm{H}\cdot(\boldsymbol{S}_1+\boldsymbol{S}_2+\boldsymbol{S}_3) + A\sum_{i=1}^{3}\boldsymbol{I}_i\cdot\boldsymbol{S}_i + J_{\mathrm{in}}\sum_{\langle i,j\rangle}\boldsymbol{S}_i\cdot\boldsymbol{S}_i, \quad (1)$$

where A is the hyperfine interaction parameter and where J_{in} is the intra-molecular exchange interaction. When $|J_{\mathrm{in}}|\gg A$, the theoretical spectrum shows seven lines with an intensity ratio of 1 : 3 : 6 : 7 : 6 : 3 : 1. The experimental spectrum does not correspond accurately to this extreme case. We must pay attention to the fact that the line-widths of the inner three lines are fairly broad even in a very dilute solution. One may be able to explain them in terms of the dipole-dipole interaction between three unpaired electrons and/or some effects caused by the exchange interaction, which is not very large compared with the hyperfine interaction.[13] Taking account of this explanation, one can conclude that $A\lesssim|J|\ll kT$.

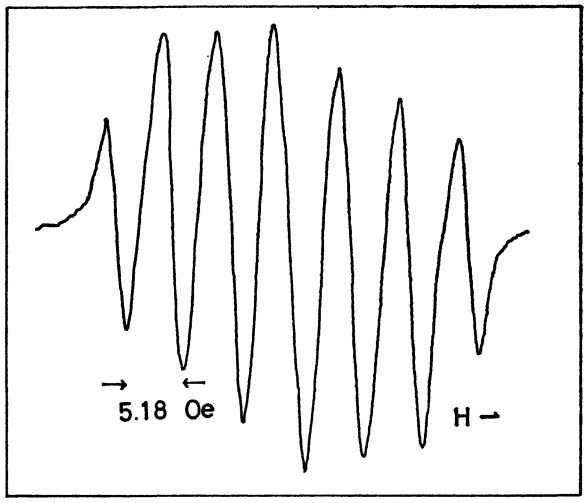

Fig. 3. The EPR spectrum of TEMPOP triradical in THF solution.

The inverse paramagnetic susceptibility of the powder TEMPOP triradical *versus* the temperature is shown in Fig. 4. The curve obeys the Curie-Weiss law except in the very low temperature region. The Curie constant, the effective Bohr magneton, and the Weiss constant, corresponding to a molecule with three unpaired electrons, are listed in Table 1. The devi-

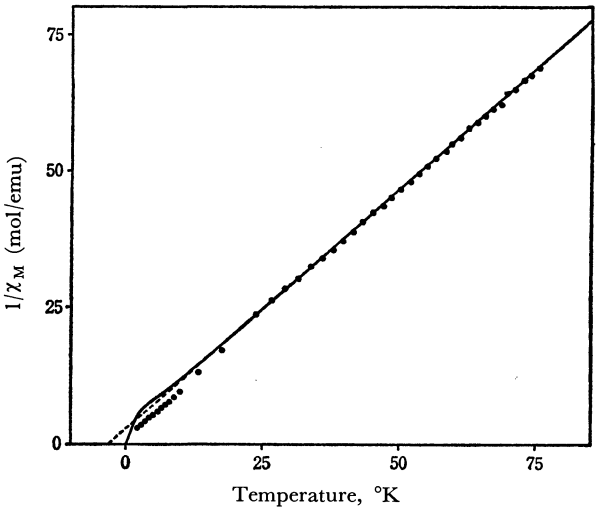

Fig. 4. The inverse paramagnetic susceptibility of powdered TEMPOP triradical *versus* temperature (truncated for clarity showing susceptibity between 1.8 and 77°K). The solid curve is that of the spin cluster with three spins of Eq. (3) as $J=-2.7$°K.

8) A. Nakajima, H. Ohya-Nishiguchi, and Y. Deguchi, to be published.

9) M. B. Neiman, E. G. Rozantsev, and V. A. Golubev, *Izv. A. N. SSSR, Ser. Chem.*, **1965**, 548.

10) E. G. Rozantsev and V. A. Golubev, *ibid.*, **1965**, 718.

11) M. Mekata, *J. Phys. Soc. Japan*, **17**, 796 (1962).

12) A. L. Buchachenko, V. A. Golubev, M. B. Neiman, and E. G. Rozantsev, *Dokl. A. N. SSSR*, **163**, 1416 (1965).

13) A. Hudson and G. R. Luckhurst, *Molecular Phys.*, **13**, 409 (1967).

TABLE 1. SOME MAGNETIC CONSTANTS OF TEMPOP TRIRADICAL AT THE HIGH TEMPERATURE RANGE COMPARED WITH THE CALCULATED VALUES OF THREE SPINS WITH $S=1/2$ AND $g=2.00$

Constant	Experimental	Calculation
C	1.14	1.141
μ_{eff}	3.01	3.000
θ	-3.5°K	—

C: the Curie constant
μ_{eff}: the effective Bohr magneton
θ: the Weiss constant

ation from the Curie-Weiss law in the very low temperature region probably suggests a short range ordering effect caused by the exchange interaction between spins belonging to different molecules.

The spin-cluster Hamiltonian with three spins, involving the exchange and Zeeman terms, is given by:

$$\mathscr{H} = -2(J_{12}\boldsymbol{S}_1\cdot\boldsymbol{S}_2+J_{23}\boldsymbol{S}_2\cdot\boldsymbol{S}_3+J_{31}\boldsymbol{S}_3\cdot\boldsymbol{S}_1) - g\beta\mathrm{H}\cdot(\boldsymbol{S}_1+\boldsymbol{S}_2+\boldsymbol{S}_3) \quad (2)$$

with the following eigen values:

a. Quartet State:

$$E_q = -(J_{12}+J_{23}+J_{31})/2 - g\beta\mathrm{H}m \qquad (m = 3/2,\ 1/2,\ -1/2,\ -3/2)$$

b. Doublet State:

$$E_{d\pm} = (J_{12}+J_{23}+J_{31}) - g\beta\mathrm{H}m \pm [2\{(J_{12}-J_{23})^2 + (J_{23}-J_{31})^2 + (J_{31}-J_{12})^2\}]^{1/2} \qquad (m = 1/2,\ -1/2)$$

The paramagnetic susceptibility is given from the Van Vleck formula,[24] and when $J_{12}=J_{23}=J_{31}=J$ (negative), the theoretical susceptibility is given by:

$$|J|\chi_M/N(g\beta)^2 = (x/4)(5+e^{3x})/(1+e^{3x}) \qquad (x = |J|/kT). \quad (3)$$

This curve is shown in Fig. 4 as $J=-2.7$°K.

As for the TEMPOP triradical one can conclude from Fig. 4 that the exchange interaction appearing in the static susceptibility is fairly weak compared with kT, and no typical short-range ordering effect can be found.

TEMPOS Tetraradical. The EPR spectrum of the TEMPOS tetraradical in the THF solution shows nine lines, all of them caused by the hyperfine interaction between four unpaired electrons and four ^{14}N nuclei, the splitting of which is 3.94 gauss and the g-value of which is 2.0058 (Fig. 5).[12] The spin Hamiltonian of this system is:

$$\mathscr{H} = -g\beta\mathrm{H}\cdot\sum_{i=1}^{4}\boldsymbol{S}_i + \mathrm{A}\sum_{i=1}^{4}\boldsymbol{I}_i\cdot\boldsymbol{S}_i + J_{\mathrm{in}}\sum_{\langle i,j\rangle}\boldsymbol{S}_i\cdot\boldsymbol{S}_j \quad (4)$$

When $|J_{\mathrm{in}}|\gg A$, $g\beta$H, the theoretical spectrum shows nine lines with the intensity ratio of 1 : 4 : 10 : 14 : 19 : 14 : 10 : 4 : 1; the experimental results just agree.

The inverse paramagnetic susceptibility of the powder TEMPOS tetraradical *versus* the temperature is shown in Fig. 6. It is appropriate to divide the curve into four regions (Region I: above 25°K, II: from 15 to 25°K, III: from 5 to 15°K, and IV: below 5°K). In the I and III regions, the $1/\chi_M$–T curve obeys the Curie-Weiss law. The magnetic constants of these two regions are listed in Table 2. The II region is the intermediate region between I and III. The temperature dependence of the χ_M in these three regions suggests the formation of a spin

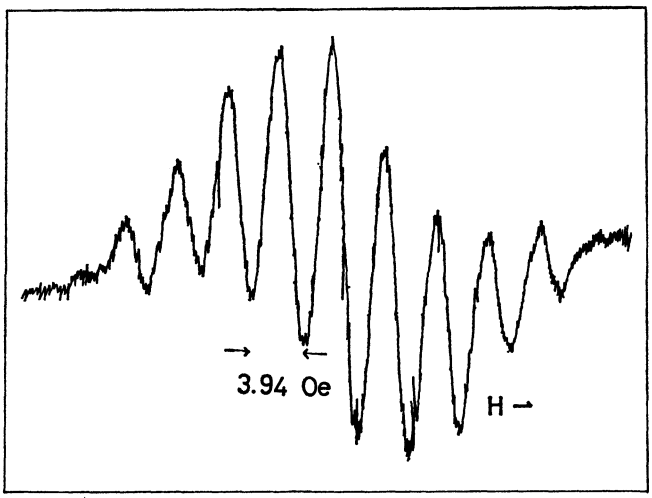

Fig. 5. The EPR spectrum of TEMPOS tetraradical in THF solution.

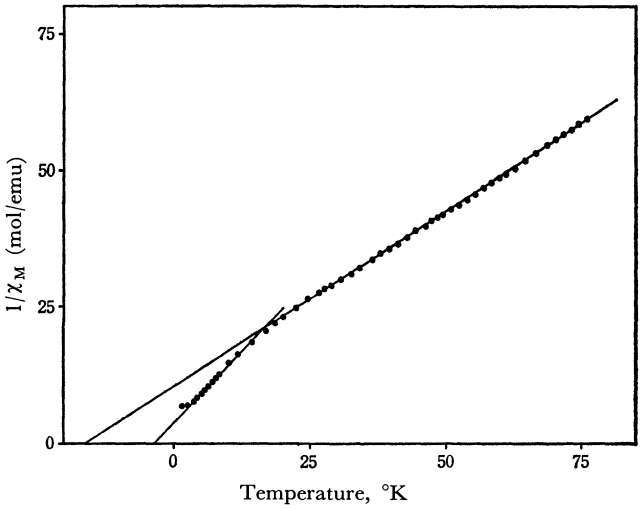

Fig. 6. Inverse paramagnetic susceptibility of TEMPOS tetraradical *versus* temperature (truncated for clarity showing susceptibility between 1.8 and 77°K).

TABLE 2. SOME MAGNETIC CONSTANTS OF TEMPOS TETRARADICAL

	C	μ_{eff}	θ
Experimental			
Region I	1.55	3.52	-3.5°K
Region III	0.98	2.80	-16°K
Calculation			
$S_{total}=1$	1.01	2.83	—
Four spins with $S=1/2$	1.51	3.46	—

14) K. Kambe, *J. Phys. Soc. Japan*, **5**, 48 (1949); J. H. Van Vleck, "The Theory of Electric and Magnetic Susceptibilities," Oxford (1932).

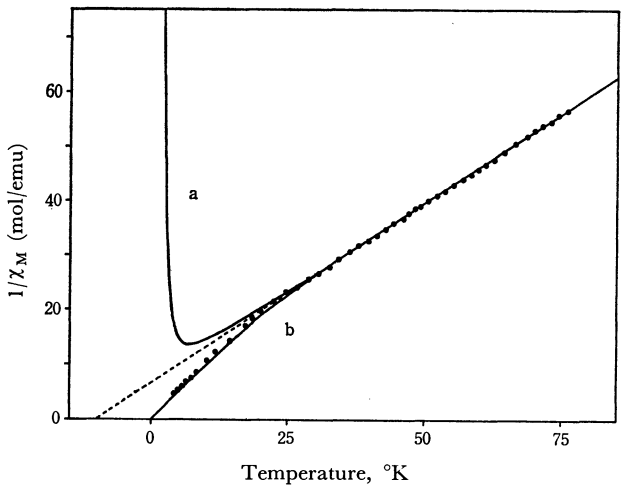

Fig. 7. Inverse paramagnetic susceptibility of TEMPOS tetraradical which was corrected for the inter-cluster interaction by multiplying $T/(T+3.5)$ with $1/\chi_M$. The solid curves are the theoretical $1/\chi_M - T$ of the spin cluster models with for spins: a) Tetrahedral model ($J=-5.55$°K), b) Trigonal model ($J=-15.9$°K).

cluster caused by the exchange interaction. In the IV region, the $1/\chi_M$–T shows a slight deviation from the Curie-Weiss law of the III region, with $\theta=-3.5$°K; this suggests the existence of an inter-cluster interaction, but in this paper, treating the exchange interaction in a cluster, we will not discuss the inter-cluster interaction further.

Now let us come back to our discussions of the I, II, and III regions. For the analysis of the results, two essential experimental parameters are taken into account. One is the μ_{eff} of the III region, which will give the total spin of the ground state; the other is the ratio of the Curie constants between the I and III regions ($\rho=C_I/C_{III}$), which indicates the relation of the spin states between the high- and low-temperature regions. In our case, $\mu_{eff}=2.80$—which corresponds to the total spin, S=1—and $\rho=1.58$.

As the TEMPOS tetraradical has four spins in a molecule, some spin-cluster models with four spins are applicable.[15] The spin Hamiltonian of the cluster models is:

$$\mathscr{H} = -2\{J_{12}\boldsymbol{S}_1\cdot\boldsymbol{S}_2 + J_{13}\boldsymbol{S}_1\boldsymbol{S}_3 + J_{14}\boldsymbol{S}_1\cdot\boldsymbol{S}_4 + J_{23}\boldsymbol{S}_2\cdot\boldsymbol{S}_3 + J_{24}\boldsymbol{S}_2\cdot\boldsymbol{S}_4 + J_{34}\boldsymbol{S}_3\cdot\boldsymbol{S}_4\} \quad (5)$$
$$(\text{all } \boldsymbol{S}_i = 1/2)$$

15) Of course we cannot say definitely that the exchange interaction occurs exclusively in a molecule, and the probability of the inter-molecular interaction will not be ommitted. Here we must understand that the above-mentioned models will be only practical ones.[8]

Table 3. Some spin cluster models with four spins

Model	$\lvert J\rvert\chi_M/N(g\beta)^2$	ρ	J
Tetrahedral	$\frac{2\times(5+e^{4x})}{5+9e^{4x}+2e^{6x}}$	—	−5.55°K
Rhombus	$\frac{2\times(5+e^{2x}+2e^{4x})}{5+3e^{2x}+7e^{4x}+e^{6x}}$	—	—
Trigonal	$\frac{2\times(5+e^{x}+2e^{4x})}{7+3e^{x}+6e^{4x}}$	1.50	−15.9°K

$S=1/2$ for all spins and $x=\lvert J\rvert/kT$. ρ is the ratio of the Curie constants between high and low temperature ranges. J was determined from the experimental Weiss constant, $\theta=-10$°K.

and the paramagnetic susceptibilities of each model, which is derived from the Van Vleck formula,[14] are listed in Table 3. The theoretical $1/\chi_M$–T curves of two typical models (tetrahedral and trigonal) are shown in Fig. 7 in comparison with the experimental result corrected for the inter-cluster interaction by multiplying $T(T+3.5)$ by $1/\chi_M$; the latter trigonal model ($\mu_{eff}=2.83$, $\rho=1.50$) agrees exactly with the experimental result, as $J=-15.9$°K. In our further discussions, we must proceed to a structural study of these polyradicals.

Summary

The paramagnetic susceptibilities of the TEMPOP triradical and the TEMPOS tetraradical have been measured; we have found some deviations from the Curie-Weiss law caused by an exchange interaction between electron spins. Though we could not make clear whether or not the exchange interaction occurs in a molecules, we adopted some spin-cluster models with three and four spins as one step to interpreting the experimental phenomena.

In TEMPOP triradical, we could find no suitable model, for this radical did not indicate any typical ordering phenomenon at any measuring temperature used so far. On the other hand, in the TEMPOS tetraradical, we found a short-range ordering effect and applied the spin-cluster models with four spins. The trigonal model best fit the experimental results.

The authors are very much obliged to Professor H. Takaki for his continuing guidance and encouragement through this work. The authors are also deeply indepted to Professor M. Mekata, Mr. J. Yamauchi and their collaborators for their helpful advice and discussions.

Spectrophotometric Determination of Anions by Solvent Extraction with Metal Chelate Cations. XIV[1] Determination of Iodide Ions with Tris(1,10-phenanthroline)iron(II)

Yuroku YAMAMOTO, Tsunehiko TARUMOTO, and Masahiro TSUBOUCHI

Department of Chemistry, Faculty of Science, Hiroshima University, Higashisenda-machi, Hiroshima

(Received October 2, 1970)

Iodide was extracted from the aqueous phase into nitrobenzene in a wide pH range of 3—9 by use of tris(1,10-phenanthroline)iron(II) chelate cations and then determined spectrophotometrically at 516 mμ. Beer's law was effective up to 8.0×10^{-5} M of iodide in the aqueous phase. Standard deviation of the determination was 1.1% at 15°C. The color intensity of the extracted species in nitrobenzene was constant for at least 3 hr. The distribution ratio was 1.02 at 15°C and 0.83 at 26°C. No serious interferences by foreign anions were observed except for perchlorate, chlorate, and thiocyanate. Cations did not essentially interfere with the determination.

Iodide can be determined colorimetrically through its catalytic action, by starch-iodide reaction or as a triiodo ion.[2] However, these procedures are tedious and delicate, and the reactions involved are not very well defined.

We have previously presented, as a short communication, a new method for the spectrophotometric determination of iodide which was based on the solvent extraction with tris(1,10-phenanthroline)iron(II) chelate cations.[3] At that time, acetate buffer solution was used, which showed a relatively high reagent blank in the pH range of 4 to 5. It was later found that the absorbance of the reagent blank is negligible when phosphate buffer solution is used instead. Here, an improved method is presented together with more detailed results.

Iodide ions are well extracted into nitrobenzene over a wide pH range of 3 to 9. Determination is carried out spectrophotometrically at 516 mμ. Beer's law is effective up to 8.0×10^{-5} M of iodide in the aqueous phase. A large amount of phosphate, sulfate, nitrate, or chloride does not interfere.

Experimental

Apparatus. Spectrophotometric measurements were made with a Hitachi 139 spectrophotometer with 10 mm glass cells. Shaking was done with an Iwaki Model KM shaker. pH measurements were done with a Hitachi-Horiba H-5 pH meter. Gamma ray counting of ^{131}I was done with an Aloka Model PSM 801 γ-ray spectrometer equipped with a NaI(Tl)crystal. An incubator, Taiyo Model M-1 with 200 times/min of shaking frequency was used as a temperature controlled shaker.

Reagent. Tris(1,10-phenanthroline)iron(II) sulfate solution. A solution of 4.0×10^{-3} M was prepared with ferrous ammonium sulfate and 1,10-phenanthroline.

Standard Iodide Solution: A standard iodide solution of 1.0×10^{-1} M was prepared with potassium iodide. Standardization was made by titration with silver nitrate solution.

Radioactive Iodide Solution: A radioactive iodide solution was prepared with NaI-^{131}I from Japan Radioisotope Association.

Buffer Solution: Phosphate buffer solution of 1.0 M was prepared with potassium dihydrogen phosphate and sodium monohydrogen phosphate. pH was adjusted to the desired values with sulfuric acid or sodium hydroxide.

Solvent: Nitrobenzene, purified by vacuum distillation at 20—30 mmHg, was used. It was equilibrated with distilled water before extraction. Other solvents were of analytical grade and were used without further purification.

Procedure. Calibration Curve: Take 5 ml of iodide solution of the concentration ranging from 8×10^{-5} to 4×10^{-4} M in a 100-ml separatory funnel. Add 5 ml of the tris(1,10-phenanthroline)iron(II) sulfate solution (4×10^{-3} M) and 5 ml of the phosphate buffer solution to adjust the pH of the mixture to 5.5. Dilute it to 25 ml with distilled water. Add 10 ml of nitrobenzene previously equilibrated with distilled water and shake the funnel for 2 min. About 30 min after the extraction, remove the organic layer and dehydrate it with 1 g of anhydrous sodium sulfate, allowing it to stand another 10 min. Measure its absorbance at 516 mμ with the reagent blank or nitrobenzene as a reference.

Distribution Ratio: a) By means of spectrophotometry. To 15 ml of aqueous solution of tris(1,10-phenanthroline)iron(II) iodide prepared from the synthesized salt (1×10^{-4} M) at pH 5.5 with phosphate buffer, add 15 ml of nitrobenzene and extract for 10 min at a constant temperature. After extraction, measure the absorbance of the aqueous and the organic phase at 510 mμ and 516 mμ, respectively. Use water or nitrobenzene as a reference.

b) By means of radioactivity measurement. To the same aqueous solution, add a trace amount of radioactive iodide solution. Proceed the extraction as above. After the extraction, measure the radioactivity of both phases.

Results and Discussion

Absorption Spectra. The absorption spectra of an extract and a reagent blank are shown in Fig. 1. The absorption maximum of the extract was identical with that of tris(1,10-phenanthroline)iron(II) iodide salt dissolved in nitrobenzene. The extracted species was confirmed to be $Fe(phen)_3\cdot I_2$ also by the continuous variation method, where phen represents 1,10-phenanthroline.

pH. This species shows a constant absorbance when extracted from aqueous phase with a wide pH range of 3 to 9 as shown in Fig. 2, indicating that the degree of extraction is maximum in this pH range. When acetate buffer solution was used instead of phos-

1) Part XIII of this series: S. Hayashi, K. Kotsuji, T. Sakurai K. Kimura, and Y. Yamamoto, This Bulletin, **38**, 1494 (1965).

2) F. Boltz, "Colorimetric Determination of Nonmetals," Interscience Publishers, New York, N. Y. (1958), p. 202.

3) Y. Yamamoto and S. Kinuwaki, This Bulletin, **37**, 434 (1964).

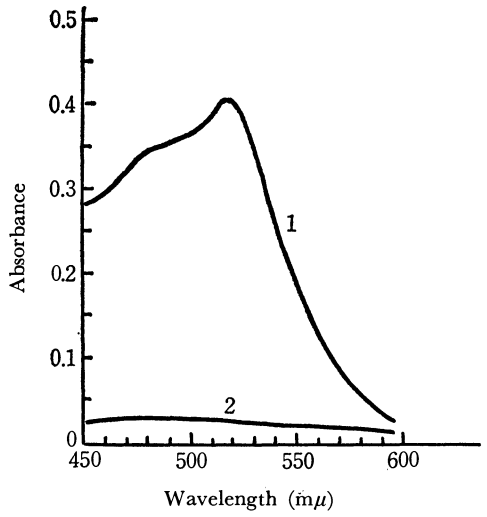

Fig. 1. Absorption spectra.
Reference: Nitrobenzene
Curve 1: Spectrum of tris(1,10-phenanthroline)iron(II) iodide in nitrobenzene extract.
[tris(1,10-phenanthroline)iron(II)] = 8.0×10^{-4} M
[iodide] = 4.0×10^{-5} M
Curve 2: Spectrum of the reagent blank.
Temperature: 15—16°C

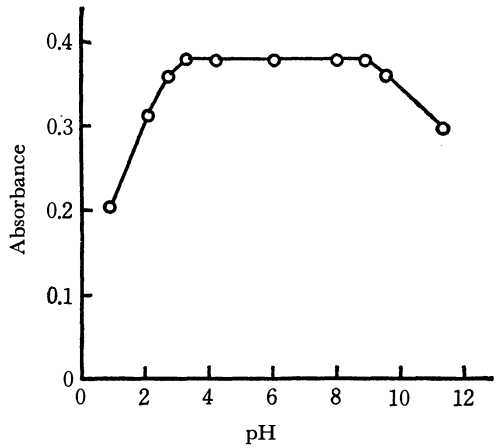

Fig. 2. Effect of pH.
[tris(1,10-phenanthroline)iron(II)] = 8.0×10^{-4} M
[iodide] = 4.0×10^{-5} M
Reference: Reagent blank
Temperature: 15—16°C

phate, the reagent blank showed a relatively high absorbance over a pH range of 4 to 6.[3,4] pH was adjusted to 5.5 throughout this experiment.

Concentration of Tris(1,10-phenanthroline)iron(II) sulfate. A constant amount of iodide (4.0×10^{-5} M) was extracted with varying amounts of the chelate. The result is shown in Fig. 3, from which it is seen that the maximum and constant extraction is attained at a mole ratio, the chelate : iodide=4 : 1. In this experiment the ratio was kept at about 10 : 1.

Shaking Time. Shaking time of the extraction was varied from 0.5 to 30 min. No difference was observed and therefore the shaking time was fixed to 2 min for convenience.

4) Y. Yamamoto, K. Kotsuji, S. Kinuwaki, and H. Sawamura, *Nippon Kagaku Zasshi*, **85**, 869 (1964).

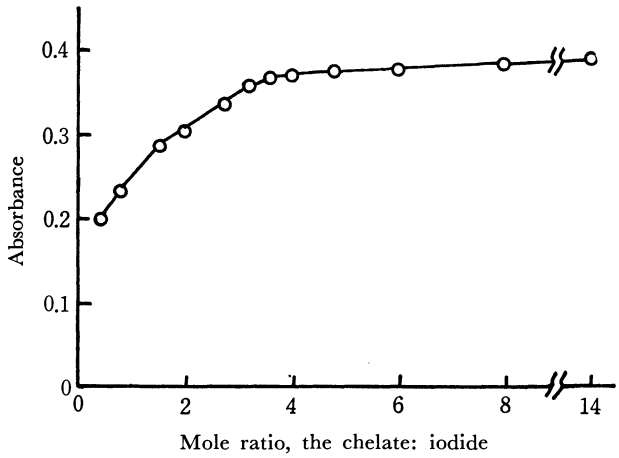

Fig. 3. Effect of the chelate concentration.
[iodide] = 4.0×10^{-5} M
Reference: Reagent blank
Temperature: 15—16°C

Stability of Color. Color intensity of the nitrobenzene phase was constant for 3 hr. A slight fading was observed after several hours (after 5 hr, 0.8%).

Frequency of Extraction. As shown in Table 1, the second and the third extracts still have appreciable absorbances. However, only the first extract was used in this experiment.

Table 1. Effect of frequency of extraction
(Iodide: 4×10^{-5} M, Reference: Nitrobenzene, Temp. 15—16°C.)

Number of extraction	Absorbance
1st	0.405
2nd	0.198
3rd	0.105
4th	0.053
5th	0.034
6th	0.024

Calibration Curve. The plot of absorbance of the nitrobenzene phase *versus* concentration of iodide in the aqueous phase gave a straight line up to 8.0×10^{-5} M. (*cf.* Fig. 4).

Precision. Six samples of iodide solution of 4.0×10^{-5} M were subjected to extraction. These samples gave a mean absorbance value of 0.380 against the reagent blank with a standard deviation of 0.004 or 1.1% at 15°C.

Distribution Ratio and Temperature Effect. Distribution ratio D by spectrophotometry will be expressed as:

$$D = \frac{[Fe(phen)_3I_2]_o + [Fe(phen)_3I^+]_o + [Fe(phen)_3^{2+}]_o}{[Fe(phen)_3I_2]_w + [Fe(phen)_3I^+]_w + [Fe(phen)_3^{2+}]_w}$$

because the synthesized salt of the formula, $Fe(phen)_3I_2$, is dissolved in the aqueous phase and therefore tris(1,10-phenanthroline)iron(II) cations exist in an equivalent amount to ioide. Results were as follows: at 15°C, 1.02 and at 26°C, 0.83, *i.e.*, the lower the temperature, the more effective is the extraction. This fact is also seen in Fig. 4 where calibration curves at various temperatures are shown. The distribution

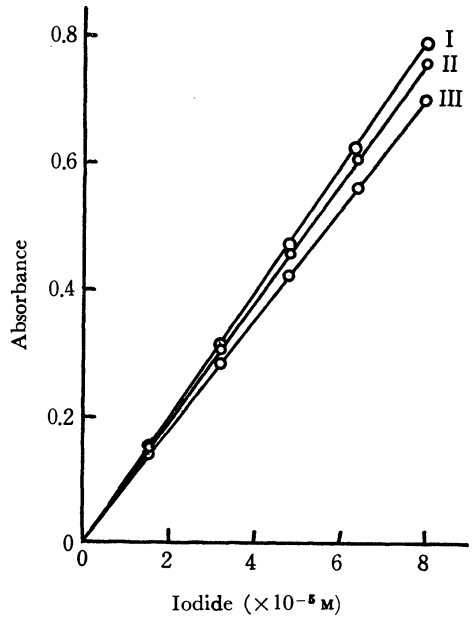

Fig. 4. Temperature effect on the calibration curve.
[tris(1,10-phenanthroline)iron(II)] = 8.0×10^{-4} M
Reference: Reagent blank
I : 11°C, II : 15°C, III : 22°C

TABLE 2. CHOICE OF ORGANIC SOLVENT
(Iodide: 4×10^{-5} M. Wavelength: 516 mμ.
Reference: pure solvent. Temp. 15—16°)

Solvent	Dielectric constant	Absorbance
Nitrobenzene	34.8	0.405
m-Nitrotoluene	23.8	0.134
o-Nitrotoluene	27.4	0.155
Benzene	2.3	~0
Benzonitrile	25.2	0.170
Toluene	2.4	~0
Chlorobenzene	5.6	~0
Chloroform	4.8	~0
Carbon tetrachloride	2.2	~0
Carbon disulfide	2.6	~0
Methyl-iso-butyl ketone	13.1	~0
2-Pentanone	15.4	~0
1,2-Dichloroethane	10.4	0.012
Isoamylalcohol	14.7	~0
Ethyl propionate	5.7	~0

ratio from radioactivity measurement with ^{131}I as a tracer agreed well with that from spectrophotometry. This means that *D* for iodide can be correctly estimated by measuring *D* for the chelate cations.

Choice of an Organic Solvent. Various organic solvents were tested. Of these, nitrobenzene was the most effective as shown in Table 2. Roughly saying, solvents with relatively high dielectric constants are able to extract the chelate ion pair.

Interference. Anions: Table 3 shows the effect of diverse anions on the recovery of iodide. Perchlorate, chlorate, and thiocyanate are easily extracted and therefore interfere with the determination even when they exist in an extremely low concentration. Bromide, cyanide, and bromate do not interfere with the determination if they are present in a concentration equal to or less than that of iodide, while as chloride can coexist several hundred times as much. Nitrate shows some effect while a large amount of sulfate and phosphate (used as buffer) shows none.

TABLE 3. EFFECT OF FOREIGN ANIONS
(Iodide taken: 4.0×10^{-5} M. Temp. 15—16°C)

Anion	Added as	Concentration (M)	Recovery of iodide (%)
Sulfate	Na_2SO_4	4×10^{-2}	100
Sulfate	Na_2SO_4	4×10^{-4}	100
Nitrate	$NaNO_3$	4×10^{-4}	105
Nitrate	$NaNO_3$	4×10^{-5}	100
Perchlorate	$KClO_4$	4×10^{-6}	110
Perchlorate	$KClO_4$	4×10^{-7}	100
Chloride	NaCl	4×10^{-2}	122
Chloride	NaCl	4×10^{-3}	103
Bromide	NaBr	4×10^{-3}	161
Bromide	NaBr	4×10^{-4}	100
Thiocyanate	KSCN	4×10^{-6}	108
Thiocyanate	KSCN	4×10^{-7}	100
Cyanide	KCN	4×10^{-3}	127
Cyanide	KCN	4×10^{-4}	100
Chlorate	$NaClO_3$	4×10^{-5}	113
Chlorate	$NaClO_3$	4×10^{-6}	100
Bromate	$KBrO_3$	4×10^{-3}	123
Bromate	$KBrO_3$	4×10^{-4}	100
Silicate	Na_2SiO_3	4×10^{-3}	100

TABLE 4. EFFECT OF FOREIGN CATIONS
(Iodide taken: 4.0×10^{-5} M, Temp. 15—16°C)

Cation	Added as	Concentration (M)	Recovery of iodide (%)
Magnesium	$MgSO_4$	4×10^{-3}	97.5
Calcium	$CaSO_4$	4×10^{-3}	97.0
Strontium	$SrCl_2$	4×10^{-3}	52.7
		4×10^{-3}	107[a]
Barium	$BaCl_2$	4×10^{-3}	106
Manganese(II)	$MnSO_4$	4×10^{-3}	100
Iron(III)	$Fe_2(SO_4)_3$	4×10^{-3}	80.4
		4×10^{-3}	93.5[a]
Cobalt(II)	$CoSO_4$	4×10^{-3}	97.5
Nickel	$NiSO_4$	4×10^{-3}	100
Copper(II)	$CuSO_4$	4×10^{-3}	97.5
		4×10^{-3}	100[a]
Zinc	$ZnSO_4$	4×10^{-3}	96.0
Cadmium	$CdSO_4$	4×10^{-3}	95.5
Mercury(II)	$HgSO_4$	4×10^{-5}	0
Aluminum	$KAl(SO_4)_2$	4×10^{-3}	97.5

a) 8×10^{-3} M EDTA added.

Cations: Table 4 shows the effect of diverse cations on the recovery of iodide. Almost any metals tested do not interfere. Mercury(II) that reacts with iodide interfere seriously. The interference of strontium seems inexplicable. Ferric ions form hydroxide at this pH. However, these interferences are easily eliminated by use of excess EDTA except for mercury(II).

Studies of 8-Mercaptoquinoline as Chelating Agents. I. Sodium Salt of 8-Mercaptoquinoline

Yoshiyuki MIDO and Eiichi SEKIDO
Department of Chemistry, Faculty of Science, Kobe University, Nada, Kobe
(Received December 4, 1970)

The infrared spectra of the sodium salt of 8-mercaptoquinoline and its related compounds have been measured in the region between 4000 and 400 cm^{-1}. Some substituent-sensitive bands have been investigated in order to find a clue to further infrared studies of its metal chelates. The thermal stabilities of the sodium salt have been examined by thermal gravimetric analysis and by differential thermal analysis. It has been shown that the sodium salt can be dried at temperatures between 100° and 200°C without any thermal change, and that, at *ca.* 210°C in air, the abrupt increase in weight of the sodium salt may be due to the absorption of oxygen. The effect of hydration on the sodium salt is discussed on the basis of results with regard to X-ray diffraction patterns, infrared spectra, and weights. The sodium salt is proposed to crystallize with two moles of water and to combine inequivalently with two waters of crystallization.

8-Hydroxyquinoline(oxine=HQ) is a convenient analytical reagent which reacts with various metal ions to form its metal chelates; the characteristics of the reagent and its metal chelates have been studied extensively.[1)]

Recently special attention has been paid to the 8-mercaptoquinoline(thiooxine=MQ) in which hydroxyl group of HQ is replaced by the thiol group and to the 8-selenoquinoline(selenooxine=SeQ) replaced by the selenol group.[2,3)] It may be of particular interest to compare the relationships between their dissociation constants and the stability constants of their metal chelates. Studies of MQ have been reported in the fields of analytical applications,[4–8)] absorption spectra,[4,9–11)] stability constants of metal complexes,[4,11)] and substituted compounds.[4,12–14)]

The central problem of this paper is to investigate the infrared spectra of the sodium salt of MQ for the purpose of finding a clue to further infrared studies of its metal chelates. Our interest lies particularly in the effect of the water of crystallization upon the infrared spectra because of its acceleration effect on the oxidation of the salt.

Experimental

Reagents. MQ, its disulfide, and its sodium salt were prepared and purified by the methods described in the literature.[8,11,15)] Hydrochloride of MQ was obtained from the Dojindo Pharmaceutical Co., Ltd. All the reagents were confirmed by a study of the absorption spectra.

Apparatus for Measurements. Thermal gravimetric analysis (TGA), differential thermal analysis (DTA), and studies by both X-ray diffractions and infrared spectra were carried out with a Chyo Thermobalance, a Rigaku-Denki Differential Thermal Analyser, a Rigaku-Denki Geigerflex D-3F X-Ray Analyser (Cu$K\alpha$ radiation) and a Hitachi EPI-2G Infrared Grating Spectrophotometer respectively. The weights of the salt were measured with a Mettler H-6 dig. Balance.

Results and Discussion

Infrared Spectra of MQ. The infrared spectra of MQ and its derivatives were obtained as Nujol and H.C.B. mulls. The infrared frequencies are summarized in Table 1. The spectra of MQ are essentially similar to those of HQ. In general, it has been suggested that a few bands in the 1600—1500 cm^{-1} region in quinoline derivatives are due to C=C and C=N vibrations.[16)] Furthermore, the bands in the 1200—1000 cm^{-1} region and those around 800 cm^{-1} are attributable to ring vibrations and C–H deformations influenced by chelation with a metal or by hydration respectively.[16)]

For the anhydride of MQ, which exists in a deep blue liquid, the effect of the substitution on the quinoline ring causes strong new bands at 2510, 990, and 654 cm^{-1}. The band at 2510 cm^{-1} is easily assigned to ν(SH), and the investigation of this vibration in a chloroform solution shows neither any possibility of hydrogen bonding nor any existence of the zwitter ionic from. The 990 cm^{-1} and the 654 cm^{-1} band rank as the highest and the second highest respectively of the substituent-sensitive bands affected

1) An example is; R. G. W. Hollingshead, "Oxine and its Derivatives," Butterworths Scientific Publications, London (1954).
2) E. Sekido, Q. Fernando, and H. Freiser, *Anal. Chem.*, **36**, 1768 (1964); **37**, 1556 (1965).
3) N. Nakamura and E. Sekido, *Talanta*, **17**, 515 (1970).
4) There are a number of publications which systematically studied by Bankovsky's group. For example some of the titles of them are "Study of 8-Mercaptoquinoline and its Derivatives," and "Analytical Application of 8-Mercaptoquinoline and its Derivatives."
5) V. I. Kuznetsov, Yu. A. Bankovsky, and A. F. Iyevinsh, *Zh. Anal. Khim.*, **13**, 267 (1958).
6) Yu. A. Bankovsky and A. F. Iyevinsh, *Zh. Anal. Khim.*, **13**, 507 (1958).
7) Yu. A. Bankovsky, J. Cirule, and A. Ievins, *Zh. Anal. Khim.*, **16**, 562 (1961); *Chem. Abstr.*, **56**, 7988i (1962).
8) J. A. W. Dalziel and D. Kealey, *Analyst*, **89**, 411 (1964).
9) Yu. A. Bankovsky, L. M. Chera, and A. F. Iyevinsh, *Zh. Anal. Khim.*, **18**, 688 (1963).
10) P. D. Anderson and D. M. Hercules, *Anal. Chem.*, **38**, 1702 (1966).
11) A. Corsini, Q. Fernando, and H. Freiser, *Anal. Chem.*, **35**, 1424 (1963).
12) G. Buehmann and R. Schmuek, *J. Prakt. Chem.*, **17**, 414 (1962).
13) D. Kealey and H. Freiser, *Anal. Chem.*, **38**, 1577 (1966).
14) A. Kawase and H. Freiser, *ibid.*, **39**, 22 (1967).
15) A. Edinger, *Ber.*, **41**, 937 (1908).
16) L. J. Bellamy, "The Infrared Spectra of Complex Molecules," John Wiley & Sons, Inc., New York (1958), p. 278.

Table 1. Observed frequencies (in cm^{-1}) of the 8-mercaptoquinolines and its disulfide

Sodium salt		Hydrochloride	8-Mercaptoquinoline	Disulfide
Salt	*Dry salt*			
3300 sb		3350 sb		
3055 m	3055 m		3050 m	3040 m
3015 m	3015 m		3015 m	3015 m
		2525 sb	2510 m	
1596 w	1598 w	1614 s	1600 s	1600 s
1583 w	1580 w	1592 s	1589 s	1588 s
1550 m	1550 m	1544 vs	1533 m	1552 w
1489 vs	1487 vs		1485 vs	1486 s
1446 s	1442 s	1440 w	1450 s	1448 s
1409 m	1406 m	1397 m	1412 m	1410 w
1366 w	1372 w	1378 m	1377) s 1364) s	1380) s 1368) s
1354 s	1356 s	1346 w	1352 s	1352 s
1294 s	1292 s	1280 s	1301 vs	1302 s
1231 w		1240 m		1238 w
1209 s	1212 s	1208 s	1216 m	1207 w
		1150 w	1144 w	1146 w
1189 w	1199 w	1141 w	1129 m	
		1129 w	1088 w	1130 w
1071 m	1067 m	1063 w	1064 m	1060 m
		1040 w	1028 w	1029 w
990 vs	990 vs	960 w	990 vs	974 s
835 w	837 w		(880 m)	833 w
817 s	808 m	820 vs	814 vs	819 s
800 w	800 w	800 w	798 vw	
785 s	772 s	768 s	782 vs	782 s
753) m 749)	730 s	750 s	752 s	766) sh 760) m
690 b				755 sh
660 s	661 m	659 m	654 s	655 s
629 w	627 w	610 w	626 s	634 w 626 w
553 m	545 m	537 m	540 m	553 w
530 b				536 w
524 m	527 m	520 w	520 w	529 w
		460 w	460 w	
436 m	437 m	423 w	429 s	437 m

by the mass of the substituent atom directly bonded to the ring (HQ; 1093[17] and 781 cm^{-1},[18], SeQ; 959 and 640 cm^{-1},[19]). Although a band near 9 μ assigned to the C–O vibration of metal oxinates[17] is clearly metal-sensitive, the 990 cm^{-1} and the 654 cm^{-1} bands also exhibit a similar character, as will be described in the succeeding paper.[20]

For the disulfide of MQ, the bands appear at 974 and 655 cm^{-1}. This is very important in the case of chelation between MQ and a metal because the oxidation of MQ can be checked by the presence of these bands.

The above facts suggest that these two bands with strong intensities usually have a considerable contribution by C–S bonding, though the lower band is more effective. Our consideration is supported also by the infrared studies of halogenobenzene[21] and benzenesulphonyl compounds.[22] Moreover, studies of this lower band of various metal chelates may be directly related to the analytical applications.[20]

For the sodium salt of MQ, a very strong and broad band around 3300 cm^{-1} assigned to bonded ν(OH) appears. On the other hand, with an increase in the degree of dryness, the sodium salt of MQ changes from light yellow to bright yellow (*dry salt*), and the physical state of the salt changes from rigid to bulky.

The thermal analysis and the X-ray diffraction measurement of the salt were carried out in order to confirm whether or not these phenomena resulted from the hydration on the salt.

Thermal Analysis of the Sodium Salt of MQ. Both TGA and DTA curves obtained in air and in nitrogen gas are shown in Fig. 1, where the scale of DTA is arbitrary. The dotted line and the solid line correspond to the curve of the sodium salt of MQ dried at room temperature (called *salt* hereinafter) and to that of the salt completely dried in a vacuum and at 150°C (called *dry salt*) respectively.

The weight loss of *salt* in the 100—200°C region is about 16% of the initial weight corresponding to *salt*

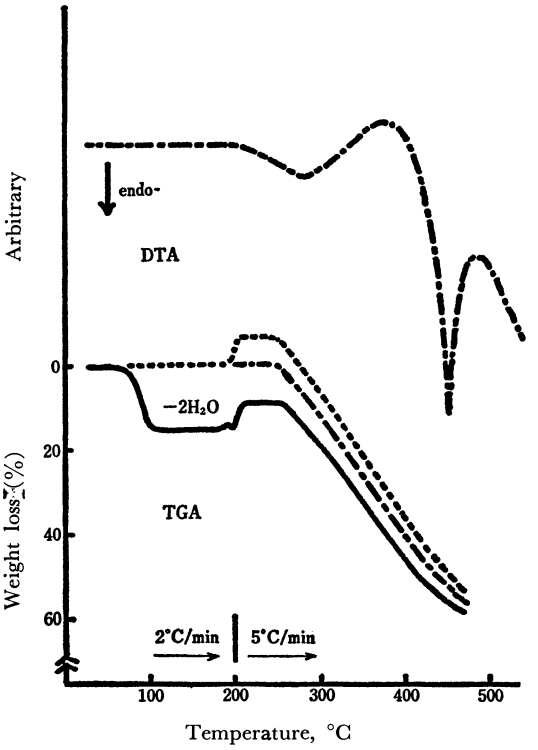

Fig. 1. DTA and TGA curves.
——: *salt* in air
----: *dry salt* in air
----: *dry salt* under nitrogen

17) R. G. Carles, H. Freiser, R. Freidel, L. E. Hilliard, and W. D. Johnston, *Spectrochim. Acta*, **8**, 1 (1956).
18) R. J. Magee and L. Gordon, *Talanta* **10**, 851 (1963).
19) Y. Mido, I. Fujiwara, and E. Sekido, to be published.
20) Y. Mido and E. Sekido, This Bulletin,**44** 2130 (1971).
21) D. H. Whiffen, *J. Chem. Soc.*, **1956**, 1350.
22) T. Uno, K. Machida, and K. Hanai, *Spectrochim. Acta*, **24A**, 1705 (1968).

with two moles of water of crystallization. At *ca.* 210°C, an abrupt increase in weight (about 7.5%) takes place in both *salt* and *dry salt*, and both salts turn brownish. There is a constant part of the weight in the 210—250°C region, and a weight loss due to decomposition occurs at higher temperatures.

The DTA curve of *dry salt* in nitrogen gas shows no thermal change[23,24] until 258°C, where thermal decomposition sets in.

The abrupt increase in weight in TGA may be attributable to the absorption of oxygen, as in suggested by the following facts: (1) The DTA curve of *dry salt* in nitrogen gas (the dot-dash line in Fig. 1) or in carbon dioxide did not show an abrupt increase. (2) The infrared spectra of the sample dried at 210°C in air exhibited a new strong band near 1100 cm^{-1} referrable to some rearrangement of atoms, though those of the sample dried at the same temperature in a vacuum did not show such a band. From the fact that the compounds containing sulfur tend to be oxidized in the process of thermal reaction, it may be concluded that the strong band is connected with a S–O vibration. (3) The DTA curve of *dry salt* in nitrogen gas showed no thermal change around 210°C.

X-Ray Diffraction Measurements. The X-ray diffraction patterns for *salt* and *dry salt* are shown in Fig. 2. These patterns indicate that the crystal structure of *dry salt* is different from that of *salt.* The X-ray pattern for a salt, containing *ca.* 10% of water,[25] seems to be made up of the superposition of the patterns of both *salt* and *dry salt.* The X-ray pattern for the other salt, containing more than 16% of water,[25] is obscure and weak.

Effect of Hydration on the Infrared Spectra. It should be noted that the sodium salt of MQ is strongly hygroscopic and that this property is closely connected with the oxidation of the salt. An increase in weight due to the absorbing water on *dry salt* was examined as a function of time at 25°C and at a relative humidity of 35% (Fig. 3). The result obtained from the increase in weight was in agreement with one of the results from TGA—the finding that the salt crystallizes with two moles of water.

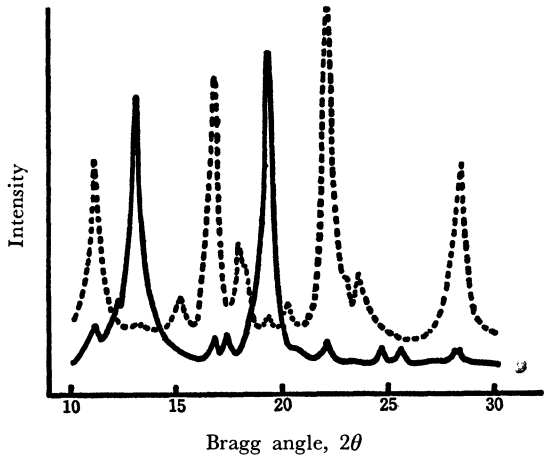

Fig. 2. X-Ray diffraction patterns of sodium salt of MQ.
——: *dry salt*, ----: *salt*

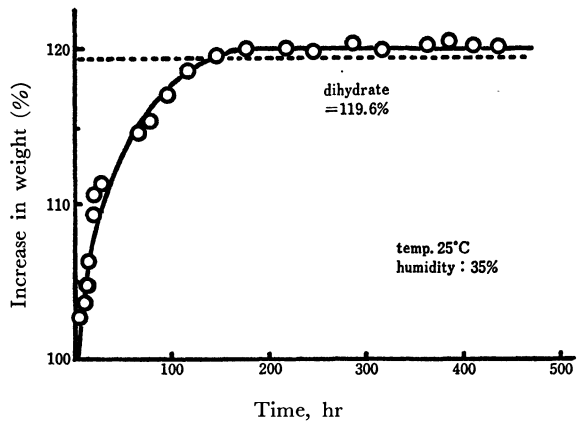

Fig. 3. Increase in weight due to the absorbing water on *dry salt* of MQ.

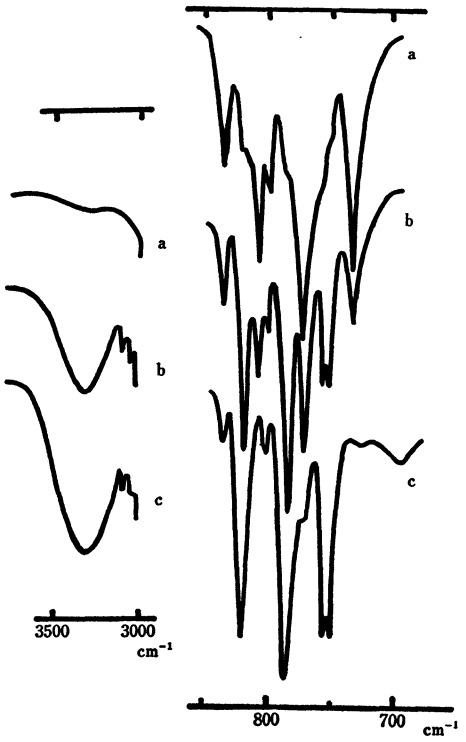

Fig. 4. O–H Stretching and C–H out-of-plane vibrations.
a) start, b) one day, c) one week

At the same time, the changes in the infrared spectra for the sodium salt of MQ were observed under the conditions specified above. The band at about 3300 cm^{-1} and the bands in the 850—700 cm^{-1} region exhibit remarkable changes in intensity and in frequency as is shown in Fig. 4. As the intensity of the 3300 cm^{-1} band(ν OH) becomes stronger and, simultaneously, those of these bands at 808, 772, and 730 cm^{-1} of *dry salt* diminish, two bands, at 817 and 785 cm^{-1}, and a doublet, at 753 and 749 cm^{-1}, appear and

23) W. W. Wendlandt and G. R. Horton, *Anal. Chem. Acta*, **23**, 332 (1960).
24) W. W. Wendlandt and G. R. Horton, *Anal. Chem.*, **34**, 1098 (1962).
25) This quantity of water determined by the weight loss of a salt.

gradually become stronger in their intensities.[26] This doublet is not observed in *dry salt*. Moreover, in *salt* there are two broader bands, at 690 and 530 cm^{-1}, which probably correspond to the librational modes of the water of crystallization (Table 1).[27] On the substitution of heavy water on *salt*, the 3300 cm^{-1} band shifted and split into two bands, at 2450 and 2370 cm^{-1}, the 690 cm^{-1} band was replaced by a band at 505 cm^{-1}, and the 530 cm^{-1} band was expected to shift to the region below 400 cm^{-1}. These results may provide strong evidence for the existence of an inequivalent bonding between two waters of crystallization and sodium salt, but it does not sufficiently account for the absence of a water molecule cyclically bound through a hydrogen bonding as proposed by Bankovsky.[9]

26) In the preliminary study for sodium salt of HQ and SeQ the same inclinations were also observed.

27) K. Nakamoto, "Infrared Spectra of Inorganic and Coordination Compounds," John Willey & Sons, Inc., New York London (1963), p. 156.

The authors wish to express their thanks to Mr. I. Fujiwara and Miss. T. Tohara for their assistance in the synthesis of salt and in the measurements, and to the Ministry of Education for a grant-in-aid.

BULLETIN OF THE CHEMICAL SOCIETY OF JAPAN, VOL. 44, 2130—2134 (1971)

Studies of 8-Mercaptoquinoline as Chelate Agents. II. Infrared Absorption Spectra of its Divalent Metal Chelates

Yoshiyuki MIDO and Eiichi SEKIDO

Department of Chemistry, Faculty of Science, Kobe University, Nada, Kobe

(Received December 4, 1970)

The infrared spectra of divalent metal thiooxinates have been measured in the region between 4000 and 400 cm^{-1}, and the relationships between these spectral bands and the characteristics of the metal-ligand bonding and the structures of the thiooxinates have been discussed. The plots of the frequencies of the metal-sensitive bands around 990 and 670 cm^{-1} against the atomic weight of the metal make it possible to classify these metal thiooxinates into two groups, one of which includes Cu-, Co-, Ni-, and Mn-thiooxinate, and the other, Cd-, Zn-, and Pb-thiooxinate. The deviation of the point for Zn-thiooxinate from the line belonging to thiooxinates with such metal atoms as have no available *d*-orbitals has been compared with the case of oxinates. Moreover, from the appearance of the 450 cm^{-1} band in the latter group, the structure of these thiooxinates may be tetrahedral. As for the frequencies of the two metal-sensitive bands mentioned above, those of Pd- and Pt-thiooxinate are the highest and that of Ag(I)-thiooxinate, examined for the sake of comparison, is the lowest. The possibility of the analytical application of the metal-sensitive band around 670 cm^{-1} has been discussed.

In the previous paper[1] describing infrared studies of 8-mercaptoquinoline, it was suggested that some substituent-sensitive bands are affected by the mass of the substituent atom directly bonded to the ring, and that these bands may be regarded as metal-sensitive bands (the 9μ band of metal oxinates,[2] for example, can be used for an analysis using infrared spectrometry).

Although several references concerning infrared studies of metal oxinates have been reported,[2-6] studies of the infrared spectra of the metal chelates of thiooxine with sulfur and nitrogen atoms as ligands have been limited in number.

From the investigations of the acid dissociation phenomena of oxine (HQ), thiooxine (MQ), and selenooxine (SeQ), HQ would be expected to yield a significantly more stable 1 : 1 metal chelate than MQ and SeQ, but this is not true. This has been interpreted as resulting from the greater covalent characteristic of the metal-ligand bond for thiooxinate and selenooxinate than in that for oxinate and from the possibility of π-bonding between the metal and ligand atoms for thiooxinate[7] or selenooxinate.[8]

In order to elucidate the relationships among some infrared bands, the character of the metal chelate-bonding, and the structure of thiooxinates, the infrared spectra of divalent metal chelates of MQ were studied.

Experimental

Reagents. The sodium salt of MQ was prepared by the method described in the previous paper.[1] The other reagents of an analytical grade were used without further purification.

Metal Thiooxinates. Divalent metal chelates of MQ were prepared under nitrogen gas and were purified by a technique developed from Dalziel-Kealey's method.[9] The

1) Y. Mido and E. Sekido, This Bulletin, **44**, 2127 (1971).
2) R. G. Charles, H. Freiser, R. Freidel, L. E. Hillard, and W. D. Johnston, *Spectrochim. Acta*, **8**, 1 (1956).
3) K. G. Stone, *J. Amer. Chem. Soc.*, **76**, 792 (1954).
4) J. E. Tachett and D. T. Sawyer, *Inorg. Chem.*, **5**, 692 (1964).
5) R. J. Magee and L. Gordon, *Talanta*, **10**, 851, 961 (1963), *ibid.*, **11**, 967 (1964), *ibid.*, **12**, 445 (1965).
6) J. C. Fanning and H. B. Jonassen, *J. Inorg. Nucl. Chem.*, **25**, 29 (1963).
7) A. Corsini, Q. Fernando, and H. Freiser, *Anal. Chem.*, **35**, 1424 (1963).
8) E. Sekido, Q. Fernando, and H. Freiser, *Anal. Chem.*, **36**, 1768 (1964); *ibid.*, **37**, 1556 (1965).
9) J. A. W. Dalziel and D. Kealey, *Analyst*, **89**, 411 (1964).

Table 1. Analytical data for various metal thiooxinates

Formula	Color	Analysis % Calcd C	Calcd H	Calcd N	Found C	Found H	Found N	pH for ppt.
$Mn(C_9H_6NS)_2$	yellow ochre	57.59	3.22	7.46	55.72	3.26	6.68	4.5
$Co(C_9H_6NS)_2$	brown	56.99	3.19	7.38	53.30	3.00	6.79	4.5
$Ni(C_9H_6NS)_2$	dark magenta	57.02	3.19	7.39	57.39	3.49	7.38	4.5
$Cu(C_9H_6NS)_2$	brown	56.31	3.15	7.29	56.17	3.35	7.40	4.5
$Zn(C_9H_6NS)_2$	bright yellow	56.04	3.14	7.26	56.12	3.16	7.42	4.5
$Cd(C_9H_6NS)_2$	chrome yellow	49.95	2.80	6.47	49.64	2.61	6.52	4.5
$Pb(C_9H_6NS)_2$	chrome yellow	40.98	2.29	5.31	41.29	2.51	5.60	5.5
$Pd(C_9H_6NS)_2$	brick reddish black	50.65	2.83	—	50.60	3.13	—	3.0
$Pt(C_9H_6NS)_2$	brown	41.94	2.35	—	41.59	2.86	—	10.0
$Ag(C_9H_6NS)$	chrome yellow	40.32	2.26	—	40.12	2.67	—	9.5

All of the metal thiooxinates were dryed at 120°C for several hours.

results of the elementary analysis of these metal chelates are summarized in Table 1. The results for Mn- and Co-thiooxinate are slightly different from those expected for each proposed formula.

Infrared Spectra. The infrared spectra were measured in the region between 4000 and 400 cm^{-1} with a Hitachi EPI-2G Infrared Grating Spectrophotometer. The spectrometer was calibrated with standard polystyrene film and water vapor. In the measurement, both the potassium bromide disc- and Nujol mulls-method were usually used, and both gave the same infrared spectra. To obtain a high resolution, the spectra in the special region where significant bands exist were repeatedly recorded at a slow speed and using a five-fold-scale expansion. The recorded spectra should be accurate to within ± 1 cm^{-1}.

Results and Discussion

The absorption frequencies of some divalent metal thiooxinates are summarized in Table 2. The spectra of the metal thiooxinates are all essentially similar to each other and to those of anhydride(liquid),[10] the disulfide and sodium salt of MQ which have been reported previously.[1]

Metal-Sensitive Bands and Structures of Metal Thiooxinates. Metal thiooxinates show a relatively strong absorption band in *the 1011—986 cm^{-1} region* and another strong band in *the 693—662 cm^{-1} region*, as shown in Table 2 and in Fig. 1. These bands have been assigned to substituent-sensitive bands.[1]

Although these thiooxinates show a few weak bands on the lower-frequency side of the metal-sensitive bands, it may be concluded, on the basis of an examination of the corresponding bands in each region of the disulfide of MQ (973 and 655 cm^{-1}), that all these thiooxinates are regular chelates except Mn-thiooxinate. For Mn-thiooxinate, as is shown in Fig. 1-(b), each metal-sensitive band appears as two bands, at 994 and 974 cm^{-1} (for *the 990 cm^{-1} band*) and at 674 and 655 cm^{-1} (for *the 670 cm^{-1} band*)

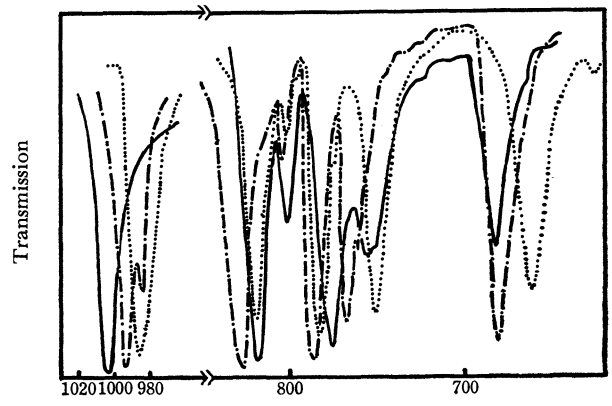

(a) ——: Cu-thiooxinate, ·—·: Zn-thiooxinate, ·····: Ag(I)-thiooxinate

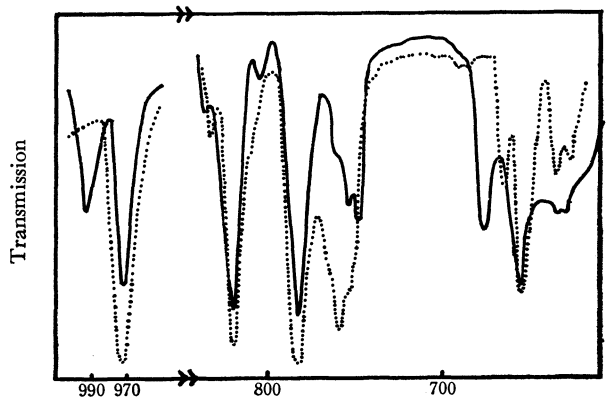

(b) ——: Mn-thiooxinate, ·····: Disulfide of MQ

Fig. 1. Infrared spectra of some metal thiooxinates.

respectively, and each latter band can be superimposed upon the corresponding bands of the disulfide of MQ. This suggests that these bands at 994 and 674 cm^{-1} may also be attributable to the metal-sensitive bands of a regular Mn-thiooxinate in a probable mixture with the disulfide of MQ and/or another chelate.

10) The absence of ν_{SH}(2515 cm^{-1}) in this spectrum may show the formation of metal chelate.

Table 2. Observed frequencies (in cm^{-1}) of divalent metal chelates of 8-mercaptoquinoline[a,b]

Mn	Co	Ni	Cu	Zn	Cd	Pb	Pd	Pt	Ag(I)
1600 m	1655 w			1595 w	1598 w	1594 w	1613 w	1597 w	1598 w
1590 m	1580 s	1587 m	1580 w	1585 w	1582 m	1584 w	1589 w	1583 w	1586 w
1555 vw	1553 m	1560 vw	1553 vw	1566 w	1553 vw	1554 w	1560 w	1558 m	1552 m
1489 s	1490 s	1491 s	1492 s	1489 s	1492 s	1494 s	1496 s	1498 s	1492 s
1449 m	1447 s	1448 m	1450 m	1449, 1443 s	1446 s	1448 s	1452 s	1453 s	1449 s
1415 vw	1411 w	1416 w		1413 w	1410 vw	1413 w	1417 w	1417 w	1416 w
1380 w	1372 m	1375 w	1376 m	1371 s	1377 m	1380, 1372 m	1384 m	1376 s	1377 s
1360 s	1360 s	1362 s	1360 s	1365 s	1360 s	1360 s	1363 s	1364 s	1356 s
1300 s	1299 s	1303 s	1300 s	1300 s	1300 s	1300 s	1303 m	1302 m	1297 s
1233 vw		1238 w	1235 vw	1235 m	1237 w	1234 m	1233 w		1232 w
1211 m	1211 s	1213 s	1209 s	1217 s	1212 s	1212 s	1215 m	1211 s	1211 s
1130 w	1134 w	1140 w	1130 vw	1129 w	1129 w	1134 w	1133 w	1136 w	1131 w
1060 m	1061 w	1072 w	1070 w	1069 w	1064 m	1070 w	1071 w	1081 w	1067 m
1028 vw	1044 w	1045 w	1043 vw	1045 w	1040 w	1040 w	1051 m	1065 m, 1054 w	1034 w
994 w	996 s	997 s	1002 s	994, 985 s[d] m	988 s	989 s	1008 s	1011 s	986 s
974 s[c]	974 s[c]	973 m	975 w		975 w			974 w	
	954 w	956 w	947 vw	954 vw	955 vw	940 vw	960 vw		950 vw
894 vw	880 vw	880 w	874 vw	886 vw	882 vw	880 vw	881 vw	870 vw	890 vw
852 vw	864 w	854 w		857 vw	848 w	844 vw	856 w		841 w
833 w, 820 s	824 s	818 s	817 s	826 s	819 s	819 s	813 s	811 s	819 s
805 w	803 w	806 w	807 w	805 w	805 w	803 w	801 w	803 w	803 w
782 s	777 s	778 s	776 s	786 s	778 s	781 s	764 s	761 s	782 s
760 w[c], 753 m, 748 m	748 s	748 s	744 s	767 s, 761 sh	746 s	754 m, 750 m	739 s	740 s	751 m
674 m	675 s	677 s	683 s	682 s	672 s	670 s	692 s	693 m	662 s
655 s[c]	655 m								
633, 626 m[c]	632 w	634 w	625 w	629 vw	630 w	625 w	613 w	610 w	624 w
	552 w	554 vw	554 vw	555 w	548 vw	547 vw	548 m	553 m	550 w
530 m	530 w	530 w	528 vw	534 w	527 vw	529 vw	530 w	524 w	526 w
	480	470 vw		470 vw					
	446 vw	456 vw	454 vw	454 s	443 m	440 m	444 vw	451 vw	444 vw
436 w	425 w	433 w			420 vw	420 vw	416 w	419 w	

a) Bands in the region between 4000 and 1700 cm^{-1}, where only a kind of fundamental bands ν(C–H) appear 2980 cm^{-1}, were not exhibited in this Table.
b) Abbreviation; w, weak; m, medium; s, strong; v, very strong.
c) *Cf.* Bands of its disulfide, 973(s), 833(w), 760(s), 755(sh), 655(s), 634(w), 626(w) see Fig. 1-(b).
d) A point of Zn* shown in Fig. 2. exhibits the average frequency of bands at 994 and 985 cm^{-1} for Zn-thiooxinate.

Because the results of the elementary analysis of Co-thiooxinate were also slightly different from the expected value for the proposed formula, the infrared spectrum of Co-thiooxinate was compared with that of Co(III)-thiooxinate prepared from the salt of Co (III). The comparison suggests that the Co-thiooxinate formed by a conventional method may be thiooxinate of the divalent cobalt and that the strong bands at 996 and 683 cm^{-1} may be assigned to the metal-sensitive bands for a regular divalent chelate. A more detailed discussion of Co-thiooxinate will be presented in the future.

Charles *et al.*[2] have examined the infrared spectra of a series of divalent metal oxinates. They described how, when the frequencies of the 9 μ peak associated with a C–O vibration are plotted against the mass of the corresponding metal, the points for the transition metal chelates nearly fall on a straight line (the frequencies increase remarkably as the mass of the metal increases), while the points for the remaining metal chelates fall near on another (the frequencies decrease slowly). They have suggested that this may indicate either the involvement of 3*d*-orbitals in the metal-ligand bonding for the transition metal oxinates or, alternatively, a difference in crystal structure for the two classes of chelates.

In this work, the plot of frequency of *the 990 cm^{-1} band* for thiooxinates is similar to that of the 9 μ band

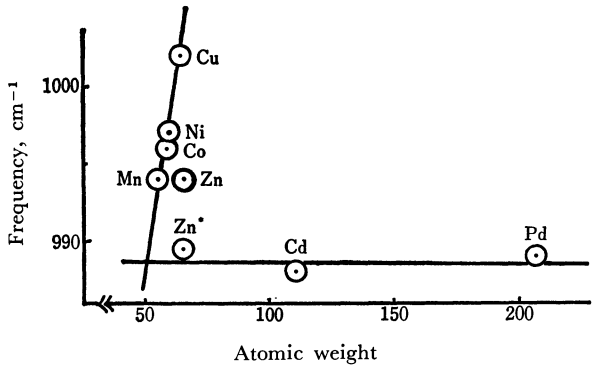

Fig. 2. Relationships between frequency of *the 990 cm^{-1} band* and atomic weight of central metal for divalent metal thiooxinate.
* A point of Zn* exhibits the average frequency of bands at 994 and 985 cm^{-1} for Zn-thiooxinate.

in oxinates, as is shown in Fig. 2. The character of this band may be not so simple as the diatomic vibration of oxinates, since the spectral shift is too little considering the large change in atomic weight upon the substitution of sulfur for oxygen as the coordinating atom. A similar plot of *the 670 cm^{-1} band* for thiooxinates is shown in Fig. 3. The similarity between these plots of *the 990 and 670 cm^{-1} bands* and the Charles plot supports their suggestion. Compared with the case of oxinates, the point for Zn-thiooxinate deviates considerably upwards from the lines belonging to thiooxinates with such metal atoms as have no available *d*-orbitals; the deviation from the line for the *670 cm^{-1} band* is larger than that for *the 990 cm^{-1} band.*

If the frequencies of *990 cm^{-1} bands* are arranged according to wave number, the order is as follows:

Cu->Ni->Co->Zn-=Mn->Pb->Cd-thiooxinate

This order is almost the same as that of the 9 μ band for metal oxinates[2] and also that of the 1250 cm^{-1} band for metal 2-(*o*-hydroxyphenyl)-benzoles,[11] which chelates through oxygen and nitrogen stoms. In the order of the frequencies for *the 670 cm^{-1} band* of thiooxinates, only the Zn-thiooxinate is located between Cu- and Ni-thiooxinate:

Cu->Zn->Ni->Co->Mn->Cd->Pb-thiooxinate

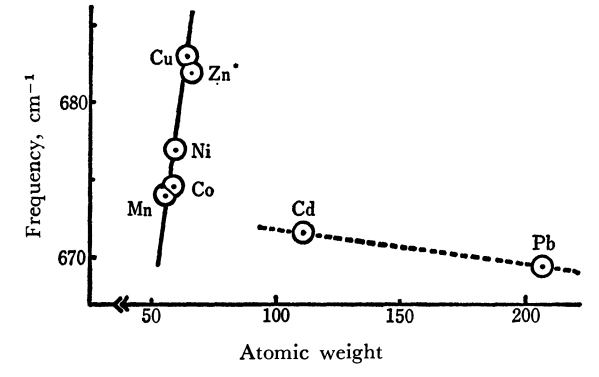

Fig. 3. Relationships between frequency of *the 670 cm^{-1} band* and atomic weight of central metal for divalent metal thiooxinate.

11) T. R. Harkins, J. L. Walter, O. E. Harris, and H. Freiser, *J. Amer. Chem. Soc.*, **78**, 260 (1956).

In metal selenooxinates, the bands around 975 and 660 cm^{-1} are metal-sensitive;[12] also the frequencies of both the bands are arranged in the same order as with *the 670 cm^{-1} band* for metal thiooxinates.

These facts may suggest that Zn-thiooxinate has a greater covalent character in metal-ligand bonding than does Zn-oxinate, and that the chemical affinity between the sulfur atom and the zinc ion is stronger than that between the oxygen atom and the cation.

A Peak near 450 cm^{-1} and the Structures of Metal Thiooxinates. A peak near 450 cm^{-1} appears in Zn-, Cd-, and Pb-thiooxinate, weakenning in relative strength in this order. In the transition-metal thiooxinates, this peak appears only slightly or not at all. Since the transition metal ions have *d*-orbitals available for dsp^2 bonding, it is reasonable to assume that they form square-planar complexes with MQ$_4$.

The method of group theory shows that the species of normal modes resulting from the D_{2h}-symmetry of the *trans* square-planar type include A_g, B_g, A_u, and B_u, of which the A_u and B_u species are active in the infrared. The 450 cm^{-1} band may be derived from one of the vibrations corresponding to A_g and B_g species from this type.

Therefore, it may be suggested that the degree of deviation from the square-planar structure is indicated by the effect on the strength of the 450 cm^{-1} band, and that Zn-thiooxinate, which has the largest strength, has a structure nearer to tetrahedral.

This consideration from the selection rule is conclusively supported by the X-ray diffraction studies confirming that Pb-thiooxinate is a distorted tetragonal pyramid[13] and suggesting that Zn-thiooxinate may be a tetrahedron.[14]

C–H Out-of-plane Bending Vibrations. All of the metal thiooxinates exhibit three strong bands assignable to C–H out-of-plane bending vibrations over the range between 820 and 740 cm^{-1}. Although the lowest band is most sensitive to metal, the relationship between its frequency and the atomic weight of the metal is not consistent. The lowest band for Zn- or Pb-thiooxinate splits into two bands; this may be additional evidence in favor of the structural consideration to be expected from the selection rule.

Pt-, Pd-, and Ag(I)-Thiooxinate. In general, the metal-ligand bonding in platinium or palladium chelates is strong covalent, and these chelates are both square planar.[15] The order of the frequencies of the metal-sensitive bands of both the thiooxinates precedes the order presented previously:

Pt->Pd->Cu-thiooxinate……

Also, the metal-sensitive bands of Ag(I)-thiooxinate, examined in order to compare them with divalent metal thiooxinate, appear at 986 and 662 cm^{-1}, and the frequencies of these bands are lower than those of

12) This will be discussed in a separate paper.
13) E. A. Shuga, V. M. Agre, J. A. Bankovskis, and E. Luksa, *Zn. Strukt. Khim.*, **8**, 171 (1967); *Chem. Abstr.*, **67**, 6480 m (1967).
14) J. A. Bankovskis, A. Ievins, A. Lokenbakh, and D. Zaruma, *Chem. Abstr.*, **54**, 1815li (1960).
15) K. Nakamoto, "Infrared Spectra of Inorganic and Coordination Compounds," John Wiley and Sons, Inc., New York (1963) p. 141.

divalent-metal thiooxinates.

Possibility of Analytical Applications. Although there is considerable similarity among the infrared spectra of metal thiooxinates, each spectrum exhibits a few characteristic bands, as has been mentioned above. Of these bands, *the 670 cm^{-1} band* has more analytical advantages: (1) There is enough apparent difference in the frequency to permit its use in the detection of two metal cations by means of a certain combination of metal cations. (2) There are no near bands affecting this band. (3) The relative intensity of this band is strong.

Pd-thiooxinate was selected as a reference on the basis of the following reasons; (1) the frequency of this band of Pd-thiooxinate is higher than that of any other metal thiooxinate, and (2) this chelate precipitates as a regular chelate over a wide range of pH.[16]

At the optimum pH for the formation of the other metal chelate, sodium salt of MQ reacts with a solution containing the palladium ion and the other metal ion to precipitate a mixture of the two metal chelates. In all these binary systems except the Pd–Pt system, the absorption bands of this mixture can be resolved into two components without any mutual interference; one is of Pd-thiooxinate, while the other is of the other metal thiooxinate.

The infrared spectra of both the Co–Ag and Cu–Ag systems indicated two distinguishable bands. The smallest difference in the frequency between two such bands observed in this binary systems was the 13 cm^{-1} obtained in the Co–Ag system. Therefore, if there is such a degree of difference at least, the metal cations can be identified by infrared study.

To obtain possible quantitative aspects, a typical calibration curve was drawn for Pd-thiooxinate employing the potassium bromide disc method.[5] As is shown in Fig. 4, Beer's law is followed in the 0.6—2.7 mg range of Pd-thiooxinate (0.15—1.11 mg of palladium) for the 300 mg disc.

As an example of a binary system, the Pd–Ni system is presented in Fig. 5. The nickel ion was undetectable in the precipitate from a mixture in which the gram-ionic ratio of the palladium ion to the nickel ion was 5 : 1, but when the ratio was reversed the palladium ion was detectable. This fact may explain why the molar extinction coefficient for this band of Pd-thiooxinate is larger than that of Ni-thiooxinate.

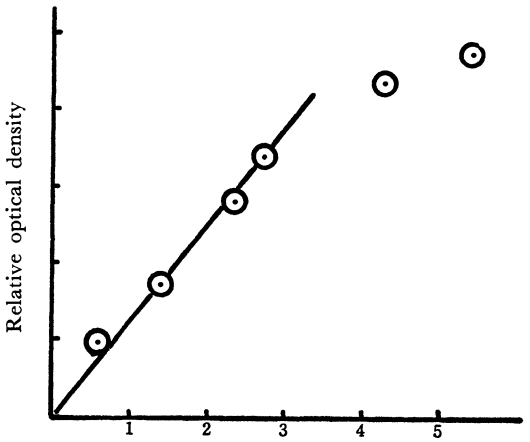

Concn. of Pd-thiooxinate in 300 mg KBr disc, (mg)

Fig. 4. Calibration curve.

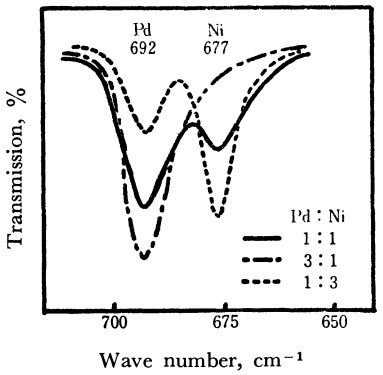

Wave number, cm^{-1}

Fig. 5. Infrared spectra of *the 670 cm^{-1} bands* in Pd-Ni system.

Analytical applications of infrared study to metal chelates may be expected to be very useful in the identification of metal thiooxinates, but the other advantage, in quantitative aspects, remains obscure. Some probable disadvantages may be the troublesome for potassium bromide disc preparation and the need for compensation between the relative opitical density and the weight of the dics.

The authors wish to express their thanks to Mr. I. Fujiwara for his assistance in synthesising and to the Ministry of Education for a grant-in-aid.

16) Yu. A. Bonkovsky, J. Cirule, and A. Ievins, *Zh. Anal. Khim.*, **13**, 507 (1958).

The Infrared Spectra and Normal Coordinate Treatments of L_3Sn-$Mn(CO)_5$ (L=Cl, Br, CH_3, and C_6H_5)

Satoru ONAKA[1)]

Department of Chemistry, Faculty of Science, The University of Tokyo, Bunkyo-ku, Tokyo

(Received January 7, 1971)

The infrared absorption spectra (2200—60 cm^{-1}) have been measured for four analogous compounds, Cl_3Sn–$Mn(CO)_5$, Br_3Sn–$Mn(CO)_5$, $(CH_3)_3Sn$–$Mn(CO)_5$, and Ph_3Sn–$Mn(CO)_5$. Normal coordinate analysis has been made for three molecules-Cl_3Sn–$Mn(CO)_5$, Br_3Sn–$Mn(CO)_5$, and $(CH_3)_3Sn$–$Mn(CO)_5$- on the basis of a modified Urey-Bradley force-field. The calculated frequencies attain close agreement with validly-assigned frequencies. The force constant, K(Sn–Mn), for each molecule varies with the substituent on the tin atom, and increases in the order of: K(Sn–Mn) of Cl_3Sn–$Mn(CO)_5$ > K(Sn–Mn) of Br_3Sn–$Mn(CO)_5$ > K(Sn–Mn) of $(CH_3)_3Sn$–$Mn(CO)_5$. The vibrational eigenvectors reveal that the Sn–Mn stretching vibrational modes are considerably coupled with other vibrational modes, especially with CMnC deformation and axial MnC stretching modes.

Recently, the nature of M–Co bonds (M=Si, Ge, and Sn) has been studied by means of NQR[2,3)] and the ^{119}Sn-Mössbauer effect,[4–6)] and it has been suggested that the stability of these compounds can be associated or correlated with M–Co π bonding.

The present author has also reported that the σ and π characteristics of the Sn–Mn bondings of a series of $R_{3-x}X_xSn$–$Mn(CO)_5$ compounds are extensively affected by the quantity of halogen on the tin atom; he reached this conclusion on the basis of ^{55}Mn- and ^{1}H-NMR and ^{119}Sn-Mössbauer-effect studies.[7,8)]

Although it is well recognized that the vibrational analysis is very profitable in determining the strengths of the bonds of interest as a total effect of σ and π interactions between atoms, especially in determining the strengths of the metal-metal bonds, such analysis has been successfully achieved in only a few cases[9–11)] because of the many difficulties which must be overcome. However, the diatomic or pseudo-diatomic models have been employed to obtain information about the strengths of the metal-metal bonds.[12,13)] According to Watters *et al.*,[10)] however, diatomic or pseudo-diatomic models may not be accurate for Cl_3-Si–$Co(CO)_4$ and Cl_3Ge–$Co(CO)_4$ because of the large extent of vibrational coupling with other modes.

The present author has now aimed to clarify the nature of the Sn–Mn bond further by making vibrational analyses of the series of L_3Sn–$Mn(CO)_5$ (L=Cl, Br and CH_3) compounds as a part of the study of the Sn–Mn bond. The present paper reports the infrared spectra of four molecules, Cl_3Sn–$Mn(CO)_5$, Br_3Sn–$Mn(CO)_5$, $(CH_3)_3Sn$–$Mn(CO)_5$, and Ph_3Sn–$Mn(CO)_5$, spectral assignments, their normal coordinate analyses, and the characterizations of the Sn–Mn bonds.

Experimental

The samples were prepared by the methods described in the literature.[14,15)] The purity of samples was determined by elemental analyses, by melting- or decomposing-point measurements, and by studying the infrared spectra (CO stretching region); the present values are in good agreement with previously published values.[15–17)]

The infrared spectra in the CO stretching region were measured with a Hitachi EPI-G2 spectrometer in a hexane solution with a KBr liquid cell. The Nujol mull samples were also examined with Hitachi EPI-G2, EPI-L spectrometers and a FIS-1 double-beam vacuum spectrophotometer in the region from 2200 to 60 cm^{-1}. The results are summarized in Table 1 and in Fig. 1.

Normal Coordinate Treatment

Spectral Assignment. The vibrational assignment for each molecule has been made by comparing the spectra of the four compounds with one another and by taking into consideration the calculated frequencies. The reported assignments of analogous compounds were also taken into account.[12,15–22)]

1) Present address: Department of Chemistry, Nagoya Institute of Technology, Showa-ku, Nagoya, Japan.

2) T. L. Brown, P. A. Edwards, C. B. Harris, and J. L. Kirsh, *Inorg. Chem.*, **8**, 763 (1969).

3) D. D. Spencer, J. L. Kirsch, and T. L. Brown, *ibid.*, **9**, 235 (1970).

4) D. E. Fenton and J. J. Zuckerman, *J. Amer. Chem. Soc.*, **90**, 6226 (1968).

5) D. E. Feonton and J. J. Zuckerman, *Inorg. Chem.*, **8**, 1771 (1969).

6) A.N. Karasyeov, N. E. Kolobova, L. S. Polak, V. S. Shpinel, and K. N. Anisimov, *Theor. Eksperim. Khim. Akad. Nauk. Ukr. SSR*, **2** (1966) 126. cited from V. I. Goldanskii, V. V. Khrapov, and and R. A. Stukan, *Organometallic Chemistry Reviews, A*, **4**, 225 (1969).

7) S. Onaka, Y. Sasaki, and H. Sano, This Bulletin, **44**, 726 (1971).

8) S. Onaka, T. Miyamoto, and Y. Sasaki, *ibid.*, **44**, 1851 (1971).

9) C. O. Quicksall and T. G. Spiro, *Inorg. Chem.*, **7**, 2365 (1968).

10) K. L. Watters, J. N. Brittain, and W. M. Risen, Jr., *ibid.*, **8**, 1347 (1969).

11) C. O. Quicksall and T. G. Spiro, *ibid.*, **8**, 2363 (1969).

12) N. A. D. Carey and H. C. Clark, *ibid.*, **7**, 94 (1968).

13) P. N. Brier, A. A. Chalmers, J. Lewis, and S. B. Wild, *J. Chem. Soc. A*, **1967**, 1889.

14) R. D. Gorsich, *J. Amer. Chem. Soc.*, **84**, 2486 (1962).

15) W. Jetz, P. B. Simons, J. A. J. Thompson, and W. A. G. Graham, *Inorg. Chem.*, **5**, 2217 (1966).

16) H. R. H. Patil and W. A. G. Graham, *ibid.*, **5**, 1401 (1966).

17) J. Dalton, I. Paul, J. G. Smith, and F. G. A. Stone, *J. Chem. Soc., A*, **1968**, 1195.

18) W. F. Edgell, J. W. Fisher, G. Sato, and W. M. Risen Jr., *Inorg. Chem.*, **8**, 1103 (1969).

19) R. C. Poller, *Spectrochim. Acta*, **22**, 935 (1966).

20) H. Kriegsmann and S. Pischtschan, *Z. anorg. allgem. Chem.*, **308**, 212 (1961).

21) D. A. Long, T. V. Spencer, D. N. Waters, and L. A. Woodward, *Proc. Roy. Soc.*, **A240**, 499 (1957).

22) M. A. Bennett and R. J. H. Clark, *J. Chem. Soc.*, **1964**, 5560

TABLE 1. OBSERVED INFRARED SPECTRA, VIBRATIONAL ASSIGNMENTS AND CALCULATED FREQUENCIES

Observed frequencies cm^{-1}	Intensity	Calculated frequencies cm^{-1}	Assignment	Approximate vibrational modes
$Cl_3Sn-Mn(CO)_5$				
2126	m	2125	S_5	CO str.
2046	vs	2048	S_{19}	CO str.
2040	s	2041	S_4	CO str.
650	vs	649	S_{13}	MnCO def.
642	vs	639	S_{27}	MnCO def.
~570	sh, vw	567	S_{28}	MnCO def.
548	vw			
535	vw	539	S_{16}	MnCO def.
497	vw			
451	s	447	S_{18}	MnC str.
406	w	407	S_1	MnC str.
394	vw	395	S_2	MnC str.
345	vs, br	354, 334	S_{20}, S_7	SnCl str.
240	w			
197	s	197	S_8	Sn-Mn str.
130	s	128	S_{21}	ClSnCl def.
		125	S_{23}	CMnC def.
112	vs	120	S_9	ClSnCl def.
		111	S_{24}	CMnC def.
85	w	82	S_9	ClSnCl def.
65	s	78	S_{25}	CMnSn def.
$Br_3Sn-Mn(CO)_5$				
2124	m	2124	S_5	CO str.
2045	vs	2047	S_{19}	CO str.
2038	s	2038	S_4	CO str.
645	vs	648	S_{13}	MnCO def.
630	vs	635	$S_{27}+S_{26}$	MnCO def.
~565	vw	563	$S_{27}+S_{28}$	MnCO def.
534	vw	539	S_{16}	MnCO def.
495	vw			
448	s	447	S_{18}	MnC str.
406	vw	404	S_1	MnC str.
392	w	395	S_2	MnC str.
240	vs	244, 216	S_{20}, S_7	SnBr str.
178	m	178	S_8	Sn-Mn str.
125	m	125	S_{23}	CMnC def.
108	m	112	S_{24}	CMnC def.
		106	S_{10}	CMnC, CMnSn-def.
90	s	85	S_{21}	BrSnBr def.
75	s, br	69	S_{21}	BrSnBr def.
		61	S_9	BrSnBr def.
$(CH_3)_3Sn-Mn(CO)_5$[a]				
2091	m	2091	S_5	CO str.
2027	w	2029	S_6	CO str.
2001	s	2001	S_4	CO str.
1995	vs	1996	S_{19}	CO str.
662	vs	663	S_{13}	MnCO def.
650	vs	654	S_{27}	MnCO def.
583	vw	578	$S_{27}+S_{28}$	MnCO def.
~555	vw, sh			
545	w	539	S_{16}	MnCO def.
518	s	514	S_{20}	Sn-CH_3 str.
502	s	503	S_7	Sn-CH_3 str.
482	s	481	S_{18}	MnC str.
~425	w, sh	420	S_2	MnC str.
413	m	413	S_1	MnC str.
179	s	179	S_8	Sn-Mn str.
164	m	163	S_{21}	CSnC def.
130	m	133	S_9	CSnC def.
		125	S_{25}	CMnC, CMnSn def.
108	m	113	S_{24}	CMnC, CMnSn def.
90	m	91	S_{10}	CMnC, CMnSn def.
		82	S_{22}	MnSnC def.
$Ph_3Sn-Mn(CO)_5$[b]				
2095	m		S_5	CO str.
2029	w		S_6	CO str.
2004	vs		S_4	CO str.
			S_{20}	CO str.
657	vs		S_{13}	MnCO def.
642	vs		S_{27}	MnCO def.
615	vw			
~590	vw, sh			
557	w			
545	w			
481	s		S_{18}	MnC str.
450	s		Absorption due to a mono-substituted C_6H_5 ring.	
428	vw			
420	vw			
413	w			
394	vw			
256	vs			
240	vs			
208	s			
204	s			
170	m		S_8	Sn-Mn str.
151	w			
120	w			
95	w			
85	w			

a) Absorptions due to a CH_3 group on tin atom which are observed at NaCl region are excluded from the Table.
b) Absorptions due to a C_6H_5 group on tin atom which are observed at NaCl region are excluded from the Table.

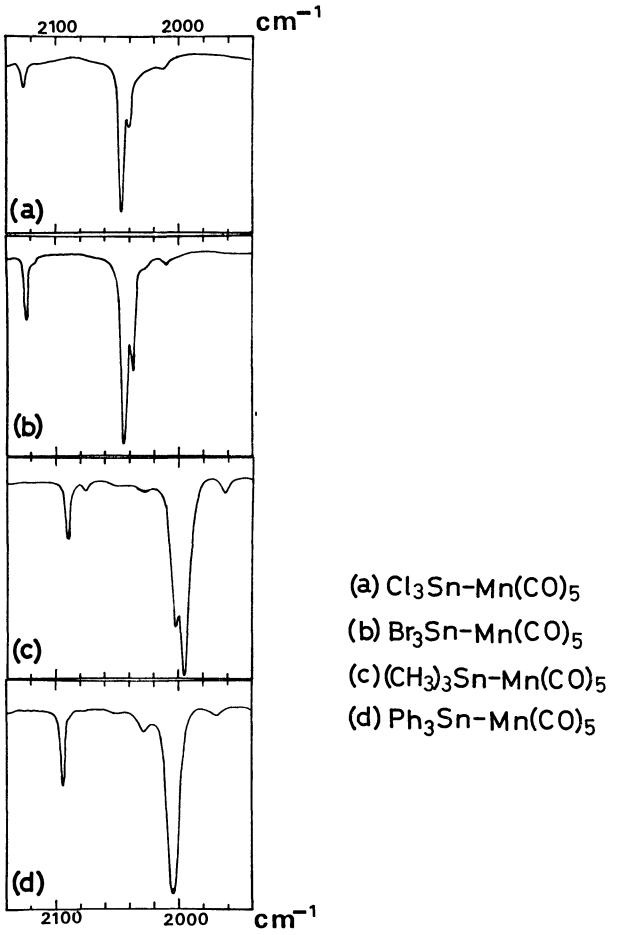

Fig. 1(a). Infrared spectra of L_3Sn-$Mn(CO)_5$.

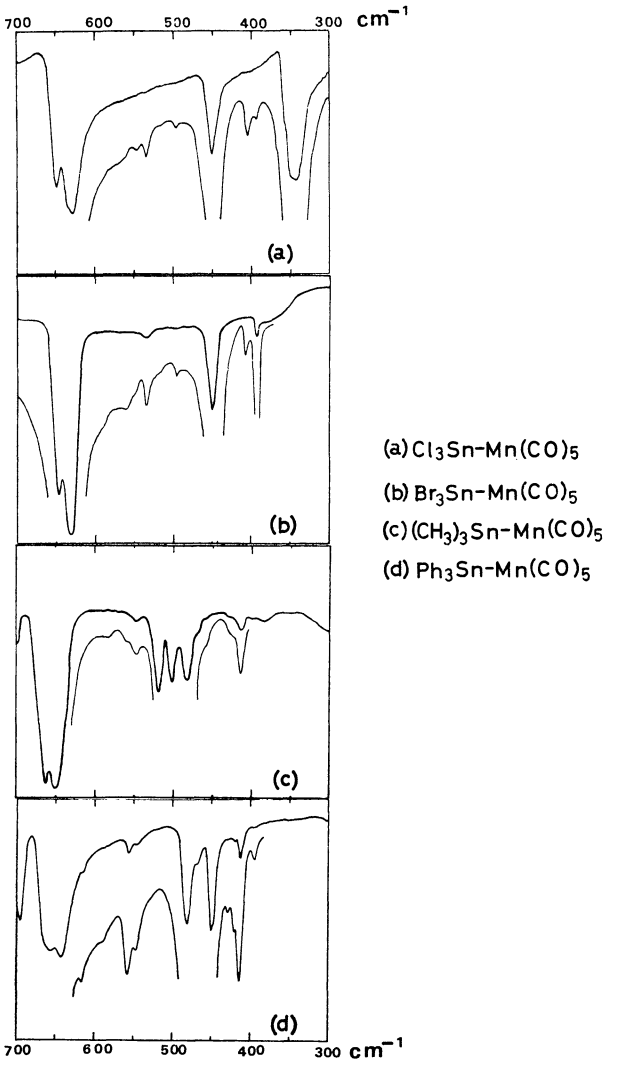

Fig. 1(b). Infrared spectra of L_3Sn-$Mn(CO)_5$.

The structure of $(CH_3)_3Sn$-$Mn(CO)_5$ is shown in Fig.2; it was determined by X-ray analysis.[23] In this molecule, the local symmetry around the tin atom is C_{3v}, and that of the manganese atom is C_4v.[24] In the vibrational analysis, this molecule can be regarded as a symmetry-top molecule, and the normal vibrations may be classified into 15 A_1, 2 A_2, and 11 E vibrations. It was assumed that the structure of X_3Sn-$Mn(CO)_5$ was the same as that of $(CH_3)_3Sn$-$Mn(CO)_5$. The close resemblance of their vibrational spectra supports this assumption.

The outline of the vibrational assignments is shown below.

The 2200—1900 cm^{-1} Region (CO Stretching Region): According to many reports on L-$Mn(CO)_5$-type compounds,[13,25-33] the highest-frequency absorption with a medium-to-weak intensity is assigned to the A_1 vibration; the most intense absorption is assigned to the E vibration due to the equatorial CO stretching mode, and the absorption with a medium-to-strong intensity to the A_1 vibration due to the axial CO stretching mode.

The 700—500 cm^{-1} Region: The highest-frequency absorption with a strong intensity is assigned to the A_1 vibration due to the equatorial MnCO bending mode, and the most intense absorption in this region is tentatively assigned to the E vibration due to the axial MnCO bending mode. The strong absorptions at 518 and 502 cm^{-1} for $(CH_3)_3Sn$-$Mn(CO)_5$ are assigned to the Sn-CH_3 stretching vibrations.[20]

The 500—350 cm^{-1} Region: The highest-frequency absorption with the strongest intensity in this region is assigned to the E vibration, and the weak absorptions around 400 cm^{-1} are assigned to the A_1 vibrations of the MnC stretching modes. The strong absorption at 450 cm^{-1} for Ph_3Sn-$Mn(CO)_5$ arises from the vibration of a mono-substituted benzene ring.[19]

The 350—200 cm^{-1} Region: The assignments of

23) R. F. Bryan, *J. Chem. Soc., A*, **1968**, 696.
24) The similar result has been reported for Ph_3Sn-$Mn(CO)_5$. Weber and R. F. Bryan, *Acta Cryst.*, **22**, 822 (1967).
25) L. E. Orgell, *Inorg. Chem.*, **1**, 25 (1962).
26) F. A. Cotton and C. S. Kraihanzel, *J. Amer. Chem. Soc.*, **84**, 4432 (1962).
27) T. L. Brown and D. J. Darensbourg, *Inorg. Chem.*, **4**, 1328 (1965).
28) F. A. Cotton and R. M. Wing, *ibid.*, **4**, 1328 (1965).
29) M. A. El-sayed and H. D. Kaesz, *J. Mol. Spect.*, **9**, 310 (1962).
30) H. D. Kaesz, R. Bau, D. Hendrickson, and J. M. Smith, *J. Amer. Chem. Soc.*, **89**, 2844 (1967).
31) R. M. Wing and D. C. Crocker, *Inorg. Chem.*, **6**, 289 (1967).
32) J. B. Wilford and F. G. A. Stone, *ibid.*, **4**, 389 (1965).
33) F. A. Cotton, A. Musco, and G. Yagupsky, *ibid.*, **6**, 1357 (1967).

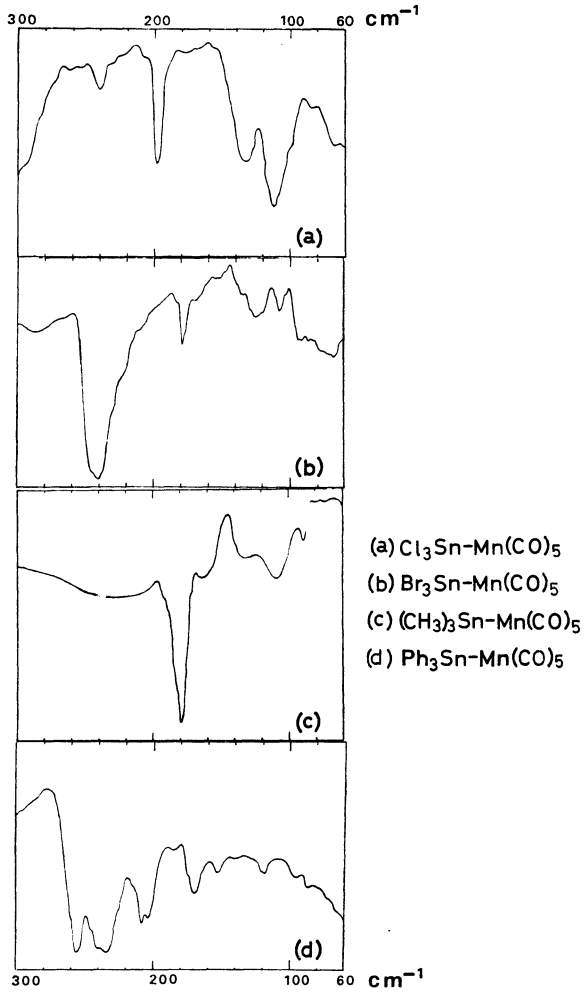

Fig. 1(c). Far-infrared spectra of L_3Sn-$Mn(CO)_5$.

the Sn–L stretching vibrations for each molecule are made on the basis of the assignments reported for SnX_4,[21] $Sn(CH_3)_3X$,[20] $SnPh_4$, and $SnPh_3X$.[19] The very strong and broad band at 345 cm^{-1} for Cl_3Sn–$Mn(CO)_5$ is assigned to the SnCl stretching vibration, and the similar band at 240 cm^{-1} for Br_3Sn–$Mn(CO)_5$, to the SnBr stretching vibrations.

The 200—170 cm^{-1} Region: The bands with strong to medium intensities observed at 197, 178, 179, and 170 cm^{-1} for Cl_3Sn–$Mn(CO)_5$, Br_3Sn–$Mn(CO)_5$, $(CH_3)_3Sn$–$Mn(CO)_5$, and Ph_3Sn–$Mn(CO)_5$ respectively are assigned to the Sn–Mn stretching vibrations.

The 170—60 cm^{-1} Region: For Cl_3Sn–$Mn(CO)_5$, the strong bands at 130 and 112 cm^{-1} are observed. These bands may be assigned to the deformation-vibrations of the $SnCl_3$ group. The bands observed at 125 and 108 cm^{-1} for Br_3Sn–$Mn(CO)_5$ may be assigned to the skeletal CMnC bending modes of the *E* species. The manganese carbonyl, $Mn_2(CO)_{10}$, also has two strong absorptions, at 120 and 110 cm^{-1}, which are due to the CMnC bending modes. The strong bands at 90—70 cm^{-1} for this molecule may be assigned to the $SnBr_3$ deformation-vibrations.[21] The bands at 160 and 130 cm^{-1} with medium intensities for $(CH_3)_3Sn$–$Mn(CO)_5$ may be assigned to the CSnC deformation-vibrations. The absorption

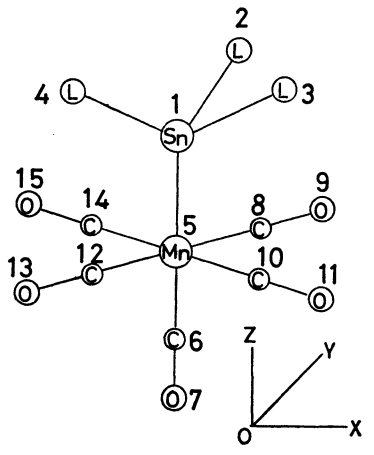

Fig. 2(a). The structure of L_3Sn–$Mn(CO)_5$.

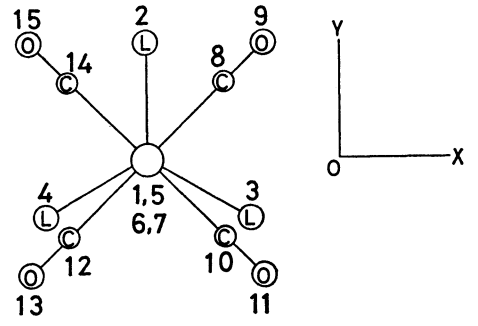

Fig. 2(b). The structure of L_3Sn–$Mn(CO)_5$.

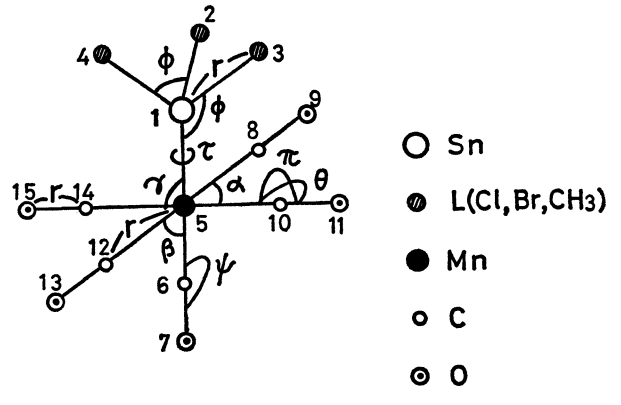

Fig. 3. Internal coordinates of L_3Sn–$Mn(CO)_5$.

at 110 cm^{-1} for the $(CH_3)_3Sn$–$Mn(CO)_5$ molecule may be assigned to the CMnC skeletal bending mode of the *E* species.

All the vibrational assignments are listed in Table 1.

The Procedure of Calculation. Frequency calculations were made for Cl_3Sn–$Mn(CO)_5$, Br_3Sn–$Mn(CO)_5$, and $(CH_3)_2Sn$–$Mn(CO)_5$ molecules on the basis of Wilson's GF matrix method,[34] in which CH_3 group was treated as one unit. The symmetry coordinates are constructed based on the C_{3v} symmetry group and C_{4v} for $Mn(CO)_5$ group respectively, which are listed

34) E. B. Wilson, *J. Chem. Phys.*, **9**, 76 (1941).

Table 2. Symmetry coordinates used in the calculation

Symmetry Species	Vibrational Modes	Symmetrys Coordinates*
A_1	MnC stretching	$S_1=\Delta r_1$
		$S_2=\Delta(r_2+r_3+r_4+r_5)$
		$S_3=\Delta(r_2-r_3+r_4-r_5)$
	CO stretching	$S_4=\Delta r_6$
		$S_5=\Delta(r_7+r_8+r_9+r_{10})$
		$S_6=\Delta(r_7-r_8+r_9-r_{10})$
	SnL stretching	$S_7=\Delta(r_{11}+r_{12}+r_{13})$
	SnMn stretching	$S_8=\Delta r_{14}$
	LSnL deformation	$S_9=\Delta(\phi_1+\phi_2+\phi_3-\phi_4-\phi_5-\phi_6)$
	CMnC, CMnSn deformation	$S_{10}=\Delta(\beta_1+\beta_2+\beta_3+\beta_4-\gamma_1-\gamma_2-\gamma_3-\gamma_4)$
		$S_{11}=\Delta(\beta_1-\beta_2+\beta_3-\beta_4-\gamma_1+\gamma_2-\gamma_3+\gamma_4)$
	CMnC deformation	$S_{12}=\Delta(\alpha_1-\alpha_2+\alpha_3-\alpha_4)$
	MnCO deformation	$S_{13}=\Delta(\pi_1+\pi_2+\pi_3+\pi_4)$
		$S_{14}=\Delta(\pi_1-\pi_2+\pi_3-\pi_4)$
		$S_{15}=\Delta(\theta_1-\theta_2+\theta_3-\theta_4)$
A_2	MnCO deformation	$S_{16}=\Delta(\theta_1+\theta_2+\theta_3+\theta_4)$
	Torsion	$S_{17}=\Delta\tau$
E	MnC stretching	$S_{18}=\Delta(r_2+r_3-r_4-r_5)$, $\Delta(r_2-r_3-r_4+r_5)$
	CO stretching	$S_{19}=\Delta(r_7+r_8-r_9-r_{10})$, $\Delta(r_7-r_8-r_9+r_{10})$
	SnL stretching	$S_{20}=\Delta(r_{12}-r_{13})$, $\Delta(2r_{11}-r_{12}-r_{13})$
	LSnL deformation	$S_{21}=\Delta(\phi_2-\phi_3)$, $(2\phi_1-\phi_2-\phi_3)$
	LSnMn deformation	$S_{22}=\Delta(\phi_5-\phi_6)$, $\Delta(2\phi_4-\phi_5-\phi_6)$
	CMnC deformation	$S_{23}=\Delta(\alpha_1-\alpha_3)$, $\Delta(\alpha_2-\alpha_4)$
	CMnC, CMnSn deformation	$S_{24}=\Delta(\beta_1+\beta_2-\beta_3-\beta_4-\gamma_1-\gamma_2+\gamma_3+\gamma_4)$, $\Delta(\beta_1-\beta_2-\beta_3+\beta_4-\gamma_1+\gamma_2+\gamma_3-\gamma_4)$
	CMnC, CMnSn deformation	$S_{25}=\Delta(\beta_1+\beta_2-\beta_3-\beta_4+\gamma_1+\gamma_2-\gamma_3-\gamma_4)$, $\Delta(-\beta_1+\beta_2+\beta_3-\beta_4-\gamma_1+\gamma_2+\gamma_3-\gamma_4)$
	MnCO deformation	$S_{26}=\Delta(\theta_1-\theta_2-\theta_3+\theta_4)$, $\Delta(\theta_1+\theta_2-\theta_3-\theta_4)$
	MnCO deformation	$S_{27}=\Delta\psi_1$, $\Delta\psi_2$
	MnCO deformation	$S_{28}=\Delta(-\pi_1-\pi_2+\pi_3+\pi_4)$, $\Delta(\pi_1-\pi_2-\pi_3+\pi_4)$

r_1—r_5 : Mn-C bonds
r_6—r_{10} : C-O bonds
r_{11}—r_{13} : Sn-L bonds
r_{14} : Sn-Mn bond
ϕ_1—ϕ_3 : L-Sn-L angles
ϕ_4—ϕ_6 : L-Sn-Mn angles
α_1—α_4 : C-Mn-C angles (in-plane)
β_1—β_4 : C-Mn-C angles
γ_1—γ_4 : C-Mn-Sn angles
π_1—π_4 : Mn-C-O angles (out-of-plane)
θ_1—θ_4 : Mn-C-O angles (in-plane)
ψ_1—ψ_2 : Mn-C-O angles (trans to Sn)
τ : Torsional angle around the Sn-Mn bond
* : Normalization constants are excluded.

in Table 2. The internal coordinates used are shown in Fig. 3. A normal coordinate analysis is made by solving a secular equation of 39th order. The values of the bond lengths, r(Sn–Mn), r(Mn–C), and r(C–O), listed in Table 3 are taken from the average values of $(CH_3)_3Sn$–$Mn(CO)_5$ and Ph_3Sn–$Mn(CO)_5$.[23,24] The bond lengths, r(Sn–Cl) and r(Sn–Br), are taken from the $(CH_3)SnCl_3$, and $(CH_3)SnBr_3$ values,[35] which were determined by electron-diffraction measurements. The L–Sn–L and L–Sn–Mn angles are assumed to be tetrahedral angles, and the C–Mn–C and Sn–Mn–C angles are assumed to be 90° on the basis of the crystal data.[23,24]

The modified Urey-Bradley force field is used for the calculation,[36] and twenty-four force constants are used for each molecule. The values of them are given in Table 4. The K, H, F, Y, and P symbols represent the stretching, deformation, repulsion, torsion and stretch-stretch interaction force constants respectively. The suffixes, a, e, i, o, t, and c, are explained in Table 4. The initial values of K_a(CO), K_e(CO), P_t(CO, CO), and P_c(CO, CO) of the Mn-$(CO)_5$ moiety are obtained by the Cotton-Kraihanzel method.[26] The other force constants for the Mn-$(CO)_5$ part are taken from the values for $Mo(CO)_6$

Table 3. The geometrical parameters used in calculation

r(Mn–C)=1.78$_2$Å[a]	∠L-Sn-L=tetrahedral angle[a]
r(C–O)=1.16$_6$Å[a]	∠L-Sn-Mn=tetrahedral angle[a]
r(Sn–Mn)=2.67$_4$Å[a]	∠C-Mn-C=90°[a]
r(Sn–CH_3)=2.13Å[a]	
r(Sn–Cl)=2.32Å[b]	
r(Sn–Br)=2.45Å[b]	

a) cited from the literature[23,24]
b) cited from the literature[35]

35) H. A. Skinner and L. E. Sutton, *Trans Faraday Soc.*, **40**, 164 (1944).
36) I. Nakagawa and T. Shimanouchi, *Spectrochim. Acta*, **22**, 759 (1966).

TABLE 4. FORCE CONSTANTS IN md/Å

	Cl_3Sn-Mn-$(CO)_5$	Br_3Sn-Mn-$(CO)_5$	$(CH_3)_3Sn$-Mn-$(CO)_5$
K_a(MnC)	1.8	1.8	1.9
K_e(MnC)	2.2	2.2	2.5_7
K_a(CO)	16.9	16.8_5	16.2_6
K_e(CO)	17.2_3	17.2_0	16.3_0
K(SnMn)	1.0	0.82	0.7
K(SnL)	1.8	1.3_9	1.9_5
H(LSnL)	0.06	0.04	0.05_5
H(MnSnL)	0.02	0.02	0.01
H_e(CMnC)	0.15	0.15	0.15
H_a(CMnC)	0.15	0.15	0.15
H(CMnSn)	0.10	0.10	0.10
H_i(MnCO)	0.8	0.8	0.8
H_o(MnCO)	0.85	0.85	0.9
H_a(MnCO)	0.86	0.83	0.9
F(L···L)	0.12	0.12	0.07
F(Mn···L)	0.05	0.05	0.05
F_a(C···C)	0.01	0.01	0.01
F_e(C···C)	0.01	0.01	0.01
F(C···Sn)	0.01	0.01	0.01
Y(Mn-Sn)[a]	0.005	0.005	0.005
P(MC, CO)	0.5	0.5	0.4
P(MC, MC)	0.4	0.4	0.4
P_t(CO, CO)	0.3	0.3	0.36
P_c(CO, CO)	0.17	0.17	0.22

a) md·Å
a: axial CO group
e) equatorial CO groups
i and *o*: in-plane and out-of plane MnCO bending modes of the square planar $Mn(CO)_4$ part.
t: *trans*
c: cis

calculated by Jones.[37] The initial set of force constants of the SnL_3 groups are aken from the SnL_3X and the SnL_4 molecules.[20,21] The initial values of K(SnMn) are estimated on the basis of the diatomic models from the IR frequencies. The values of the repulsion force constants, F(Mn···L) and F(C···Sn), are estimated from the Lennard-Jones potentials for inert gasses.[38-40] The initial value of H(MnSnL) is estimated considering the H(CMnC) and H(LSnL) values. The value of Y(Mn–Sn) is arbitrarily assumed to be 0.005 md·Å, taking into account the values of the ethane derivatives.[41]

The numerical calculation was carried out by using a HITAC 5020*E* of the Computation Center of the University of Tokyo and programs set up in the laboratory of Professor T. Shimanouchi.[42] First, the force constants of Br_3Sn–$Mn(CO)_5$ were determined. The values of the force constants were adjusted to get the best fit of the calculated frequencies with the observed ones, with reference made to the Jacobian matrix elements. Then, the frequencies of the other two molecules were calculated using the same values of the force constants as those of Br_3Sn–$Mn(CO)_5$, except those which had to be changed essentially.

Results

The final set of all the force constants are listed in Table 4. The frequencies calculated by means of these force constants are in good agreement with the observed values, as is shown in Table 1.

The eigenvectors here obtained show that the vibrational modes associated with the Sn–Mn stretching vibration are extensively coupled with the other vibrational modes, especially with the CMnC deformation and axial MnC stretching modes. The vibrational coupling in the ν(Sn–Mn) with other vibrations for Br_3Sn–$Mn(CO)_5$ is different from those of the other two molecules, and the SnBr stretching vibration is appreciably mixed. The purities of the vibrational modes assigned to the Sn–Mn stretching vibrations are evaluated from the potential energy distribution to the Sn–Mn stretching coordinate (PED), shown in Table 5.

TABLE 5. POTENTIAL ENERGY DISTRIBUTION MATRIX IN Sn–Mn STRETCHING VIBRATION

Approximate vibrational modes		$(PED)_{ij}$		
		Cl_3Sn-$Mn(CO)_5$	Br_3Sn-$Mn(CO)_5$	$(CH_3)_3Sn$-$Mn(CO)_5$
S_1	Mn-C str.	11	8	8
S_7	Sn-L str.		16	
S_8	Sn-Mn str.	68	46	64
S_9	L-Sn-L def.	5		6
S_{10}	C-Mn-C def.	14	22	24
S_{13}	Mn-C-O def.	4	5	5

$$(PED)_{ij}=\frac{(L_{ij})^2\cdot(F_S)_{ii}}{\lambda_j}\times 100$$

37) L. H. Jones, *J. Chem. Phys.*, **36**, 2375 (1962).
38) T. Shimanouchi, *Pure Appl. Chem.*, **7**, 131 (1963).
39) T. Shimanouchi, I. Nakagawa, J. Hiraishi, and M. Ishii, *J. Mol. Spectr.*, **19**, 78 (1966).
40) J. Hiraishi, I. Nakagawa, and T. Shimanouchi, *Spectrochim. Acta*, **20**, 819 (1964).
41) T. Miyazawa and K. Fukushima, *J. Mol. Spectroscopy*, **15**, 308 (1965).
42) Department of Chemistry, Faculty of Science, The University of Tokyo, Bunkyo-ku, Tokyo.

Discussion

For metal carbonyl compounds, it is well known that two types of electron donations act between the metal, M, and the ligand, CO, namely σ-electron donation from CO to M and π-electron back-donation from M to CO, and that the variation in the π-interaction between L and M in $LM(CO)_n$-type metal carbonyl compounds strongly affects the force constants, K(CO) and K(MC), in the following manner. The ligand, L, and the CO can both undergo π-bonding with the metal d orbitals. This π-interaction involves the back-donation of metal d orbitals to the vacant antibonding CO orbitals. If the ligand, L, can also accept metal d_π electrons into suitable π-type orbitals, it will compete with the CO for d electrons of the transition metal. The π-acceptor capability of L will also influence the force constants, K(CO) and K(MC). The grater the π-bonding to L, the less the electron density which will enter the antibonding orbitals of the CO, and the greater the CO stretching force constant, and the smaller the MC stretching force constant.[43-45]

The values of the force constants listed in Table 4 show that the strength of the Sn–Mn bond is strongly affected by the electronegativity of the L on the L_3Sn group; moreover, the smaller the values of K(MnC), the larger the values of K(CO) and K(SnMn) become. These facts suggest that not only the σ-electron donation but also the π-electron back-donation act on the Sn–Mn bond, and that the strength of the π-bond nature between Sn and Mn also varies with the substituent on the Sn atom. Therefore, it can be deduced that the π-bond strengths of the Sn–Mn bond increase in the order: $(CH_3)_3Sn–Mn(CO)_5 < Br_3Sn–Mn(CO)_5 < Cl_3Sn–Mn(CO)_5$, according to the above considerations and the force constants listed in Table 4. The difference in the π-bond strength between chloro- and bromo-complexes is, however, considered not to be large, because the K(MnC) and K(CO) force constants, which are a measure of the π-interaction between Sn and Mn, of the two compounds closely resemble each other. The values of the K-(SnMn) force constants, which are a direct measure of the total bond strength, $(\sigma+\pi)$, between Sn and Mn, are in the same order, but the difference in the K(SnMn) values of the two halogen complexes is much more enhanced.[46] One possible origin of this enhancement is due to the assumption of the same Sn–Mn bond length for these two compounds.

The author wishes to express his deep gratitude to Professor Takehiko Shimanouchi for his kind permission to use the programs set up in his laboratory for the calculations of the normal coordinate treatment analyses. Thanks are also due to Professor Yukiyoshi Sasaki for his encouraging advice and discussions.

43) A "spectrochemical series" for π bonding of ligands L (L= NO, PR_3, AsR_3, SbR_3, phen, dien and so on) have been obtained by making use of the IR data (ν(CO)): M. Bigorgne, *J. Organometal. Chem.*, **1**, 101 (1963); F. A. Cotton and C. S. Kraihanzel, *J. Amer. Chem. Soc.*, **84**, 4432 (1962), and *Inorg. Chem.*, **2**, 533 (1963); F. A. Cotton, *ibid.*, **3**, 702 (1964); G. R. Dobson, *ibid.*, **4**, 1673 (1965); W. D. Horrcks and R. C. Taylor, *ibid.*, **2**, 723 (1963).

44) W. A. G. Graham, *ibid.*, **7**, 315 (1968).

45) L. M. Haines and M. H. B. Stiddard, *Advan. Inorg. Chem. Radio-Chem.*, **11**, 53 (1969).

46) On the basis of ^{55}Mn–NMR data, the electronic nature around the Mn nucleus in the $Br_3Sn–Mn(CO)_5$ is in close resemblance to that of $Cl_3Sn–Mn(CO)_5$.

Studies on Cobaloxime Compounds. V. Oxidation of Formaldehyde with Cobaloximes and Aquocobalamin

Yorikatsu HOHOKABE and Noboru YAMAZAKI

Department of Polymer Science, Faculty of Engineering, Tokyo Institute of Technology, Ookayama, Meguro-ku, Tokyo

(Received January 20, 1971)

Catalytic activities of cobaloximes in the oxidation of formaldehyde were compared with each other and with the activity of aquocobalamin (vitamin B_{12a}). All the cobaloximes showed much less activities than B_{12a}. Chlorocobaloximes had the highest activities. Reaction order was found to be -0.18 with respect to the concentration of hydrogen ion, 0.71 to that of formaldehyde, and 0.49 to that of chloroaquocobaloxime. In anaerobic conditions, the reduced-state B_{12r} considered to be an intermediate in the air-oxidation reaction of aldehyde was detected spectrochemically, but not the reduced-state of cobaloxime. A much slower reaction of aldehyde with cobaloximes as compared with cobalamin was attributed to the higher reduction potentials of the former.

Concerning the vitamin B_{12}-dependent enzymatic system which converts diols to the corresponding aldehydes, further oxidation reaction of the aldehydes might occur with the aid of the B_{12} component. The vitamin B_{12}-formaldehyde complex was reported to be a one-carbon unit precursor in the biosynthesis of methionine.[1] The catalytic activity of aquocobalamin in the air-oxidation of some aldehydes was reported by Komai *et al.*[2]

In the present work, oxidation reaction of aldehydes was examined with cobalamin and cobaloximes in order to compare their chemical reactivity; the resemblance of cobaloxime compounds to cobalamin compounds in chemical behavior has been described elsewhere.[3,4]

Experimental

Materials. All the cobaloximes were prepared as reported previously.[5] Aquocobalamin was kindly supplied by Eisai Co. Commercial G. R. grade formalin (containing about 37% formaldehyde) was diluted with distilled water to suitable concentration. Acetaldehyde, propionaldehyde and benzaldehyde were commercial E. P. grade reagents. All other reagents were G. R. grade obtained commercially.

Procedures. *pH Measurement*: A pH Meter, Toa Electronics Ltd., model HM-5A, was used for pH determination.

pH Change during the Course of the Oxidation Reaction of Aldehyde: The reactions were carried out as follows. To a mixture of 6.0 m*l* of 5×10^{-4} M aqueous solution of a complex and 5.0 m*l* of 1.0 M formaldehyde was added first 35 m*l* of distilled water, followed by adjustment of pH of the solution to 7.00 with 5 mM NaOH, and by final addition of distilled water, whereby total volume was brought up to 50.0 m*l*. Thus, the final concentrations of formaldehyde and the complex were 0.10 M and 6.0×10^{-5} M, respectively. The reactions were conducted at 40°C with shaking in aerobic conditions. At appropriate intervals, the pH of the solution was measured and 2.0 m*l*-aliquot was taken for analysis of the remaining aldehyde. Aldehyde content was determined by titration: 4 m of 1 N NaOH and 5.0 m*l* of 0.1 N iodine solution were added to the aliquot. After 20 min, 2.0 m*l* of 3 N H_2SO_4 and a small amount of starch solution were added. Excess iodine was titrated with 0.1 N $Na_2S_2O_3$, from which the amount of the remaining aldehyde in the aliquot was calculated.

Dependence of the Rate upon the Concentrations of Hydrogen Ion, Formaldehyde, and Cobaloxime: The reactions were conducted in 0.5 M potassium phosphate buffer and the residual aldehyde content was determined. The dependence was examined in the pH range 5.8—7.8; the concentration of formaldehyde (2.35×10^{-2} M—2.03×10^{-1} M), and that of chloroaquocobaloxime (1.04×10^{-3} M—4.01×10^{-3} M).

Paper Chromatography: Formic acid formed in the reaction mixture was extracted with ether, and the ether layer was shaken with 1% NH_4OH aqueous solution. Ammonium formate solution thus obtained was used for paper chromatographic analysis in a mixed solvent of 95% ethanol and concd. NH_4OH (100 : 1, by vol.). Formate was detected by a blue spot at R_f 0.30 ($\pm$0.04) by spraying a bromophenol blue solution, whereas the authentic sample gave a spot at R_f 0.28 ($\pm$0.05).

Reduction of Cobaloxime by $NaBH_4$: Into 20 m*l* of 3.0×10^{-4} M solution of chloroaquocobaloxime was passed nitrogen gas and evacuated by a vacuum pump. After the N_2 passage-evacuation procedure was repeated five times, a small amount of solid $NaBH_4$ (*ca.* 1 mg) was added to the solution with stirring under a nitrogen atmosphere. Rapid color change in the solution from light yellowish brown to yellow took place, and the absorption maximum appeared at 463 mμ which is a characteristic band of cobaloxime(II), *i.e.*, $Co^{II}(DH)_2(H_2O)$ (DH: dimethylglyoximato monoanion). From the spectra for several concentrations of the cobaloxime, its molar extinction coefficient was determined to be $3.76\ (\pm0.17)\times10^3$.

Reduction of Cobaloxime and B_{12a} by Aldehydes: When formaldehyde was used instead of $NaBH_4$ at the final concentration 0.050 M, no reduction of chloroaquocobaloxime was observed even after 160 hr. However, this is ambiguous, since the hyperchromic shift of chloroaquocobaloxime occurs in aqueous solution. Therefore the reduction was examined for hydroxoaquocobaloxime (1.0×10^{-4} M) as well as aquocobalamin (3.0×10^{-5} M) with a large excess (hundreds times of the complex) of formaldehyde, acetaldehyde or benzaldehyde in 0.1 M potassium phosphate buffer (pH 7.1) at 40°C. Even after 120 hr no reduction was observed in the case of cobaloxime. On the contrary, B_{12a} was reduced by formaldehyde, acetaldehyde or benzaldehyde in 20 hr. This was demonstrated spectrochemically by the appearance of

1) B. W. Langer, Jr., and F. H. Kratzer, *Poultry Sci.*, **46**, 749 (1967); *Chem. Abstr.*, **67**, 9056*p* (1967).

2) T. Komai, S. Shimizu, R. Yamada, and S. Fukui, *Vitamins* (Japan), **35**, 395 (1967).

3) G. N. Schrauzer, *Accounts Chem. Res.*, **1**, 97 (1968); and the references cited therein.

4) Y. Hohokabe and N. Yamazaki, This Bulletin, **44**, 798 (1971).

5) N. Yamazaki and Y. Hohokabe, *ibid.*, **44**, 63 (1971).

the absorption maximum at 475 mμ in accord with the value reported in literature.[2]

Results and Discussion

It is expected that pH of the solution will decrease if oxidation of aldehyde takes place in the presence of a catalyst in aerobic conditions. The catalytic activities of several cobaloximes and aquocobalamin (B_{12a}) were examined in the oxidation of formaldehyde in the presence of air. Typical pH change during the course of the reaction is shown in Fig. 1. We see that

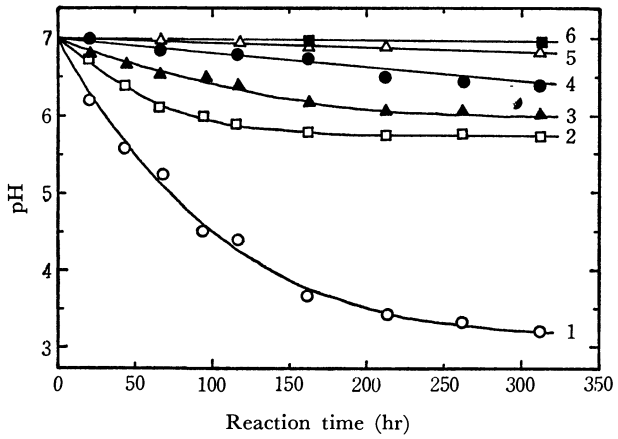

Fig. 1. pH change during the course of the oxidation reaction of formaldehyde.
[HCHO]=0.10 M, [Co]=6.0×10^{-5} M, at 40°C
1, B_{12a}; 2, $CoCl(DH)_2(H_2O)$; 3, $CoCl(DH)_2$(pyridine); 4, $CH_3Co(DH)_2(H_2O)$; 5, $Co(CN)(DH)_2(H_2O)$; 6, blank

B_{12a} acted as a much better catalyst than cobaloximes. After 300 hr the initial concentration of formaldehyde 0.10 M decreased to 0.082 M in the presence of B_{12a} with a concentration 6.0×10^{-5} M, which shows that the reaction proceeded catalytically. Of the cobaloximes, chlorocobaloximes exhibited the highest activity. The catalytic activity decreased in the order $B_{12a} \gg CoCl(DH)_2(H_2O) > CoCl(DH)_2$(pyridine) $> CoCl(DH)_2$(Copoly-AM-VPy) $> CH_3Co(DH)_2(H_2O) > Co(OH)(DH)_2(H_2O) \simeq Co(OH)(DH)_2$(Copoly-AM-VPy) $\simeq CH_3Co(DH)_2$(pyridine) $> Co(CN)(DH)_2(H_2O)$ as determined from the decrease of the pH of the reaction mixture, where DH denotes dimethylglyoximato monoanion and Copoly—AM-VPy a low molecular weight copolymer of acrylamide and 4-vinylpyridine.[6] The reason for the higher activity of chlorocobaloximes than hydroxo derivatives cannot be presented. Their higher activity than methyl or cyano derivatives might be due to weaker Co–Cl bond than Co–C bonds. Cyanocobalamin was reported to have no catalytic activity in the oxidation of aldehyde.[2] The oxidation of propionaldehyde was observed to take place much more slowly than that of formaldehyde in the presence of these catalysts.

Dependence of the reaction rates upon the concentrations of formaldehyde (2.35×10^{-2}—2.03×10^{-1} M), chloroaquocobaloxime (1.04×10^{-3}—4.01×10^{-3} M) and the acidity (pH 5.82—7.78) was examined.

6) N. Yamazaki and Y. Hohokabe, *Chem. Commun.*, **1968**, 829.

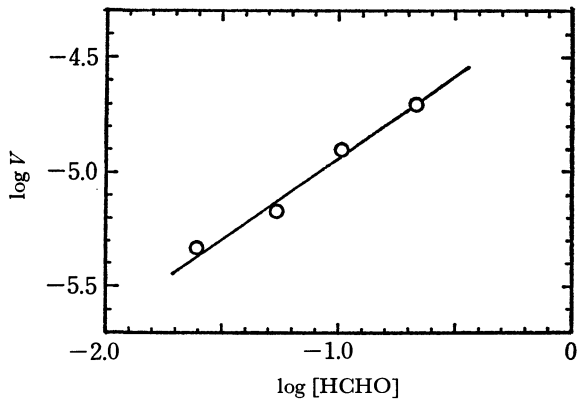

Fig. 2. Dependence of rate upon the concentration of formaldehyde.
[$CoCl(DH)_2(H_2O)$]=3.0×10^{-3} M, pH 7.0, at 40°C

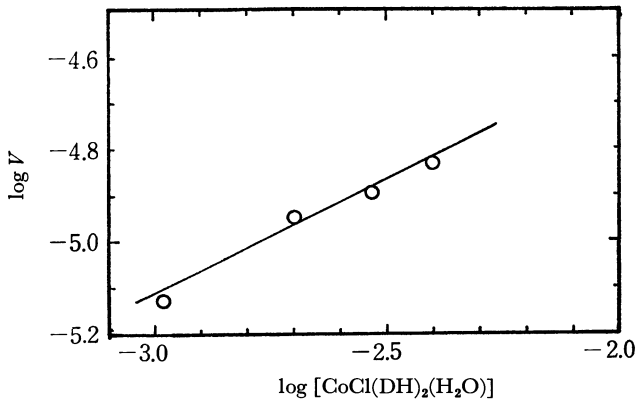

Fig. 3. Dependence of rate upon the concentration of chloroaquocobaloxime.
[HCHO]=0.10 M, pH 7.0, at 40°C

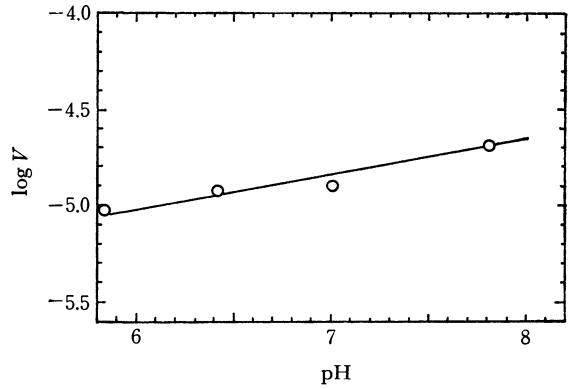

Fig. 4. Dependence of rate upon the pH.
[HCHO]=0.10 M, [$CoCl(DH)_2(H_2O)$]=3.0×10^{-3} M, at 40°C

The results are shown in Figs. 2, 3, and 4. The reaction rate increased with concentrations of aldehyde or cobaloxime, and slightly with pH. The reaction order was found to be −0.18 with respect to [H^+]; 0.71 to the concentration of aldehyde and 0.49 to that of cobaloxime.

The oxidation reaction of formaldehyde in the presence of chloroaquocobaloxime proceeded too slowly; only twice the number of moles of the aldehyde, as compared to the cobaloxime added, was oxidized after about 400 hr. Thus cobaloximes

had a quite low catalytic activity, though B_{12a} acted as a better catalyst as mentioned above. The formation of formic acid was confirmed by paper chromatagraphy. Authentic formic acid gave a spot at R_f 0.28 (±0.05) in 95% ethanol - *concd.* NH_4OH (100 : 1, by vol.), whereas the sample gave a spot at R_f 0.30 (±0.04).

A mechanism for the oxidation of aldehyde was proposed as follows.[2]

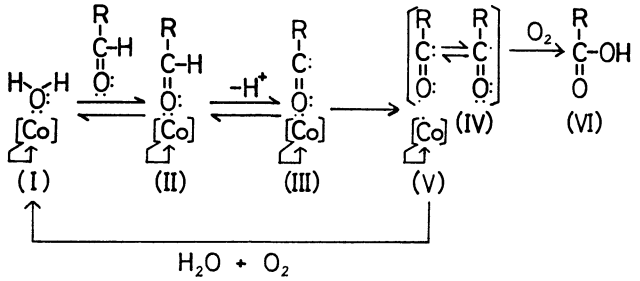

1) Aldehyde coordinates to the Co atom in exchange for H_2O of B_{12a}. 2) Proton leaves from the aldehyde-cobalamin complex. 3) The unstable intermediate thus formed splits to give an acyl radical and vitamin B_{12r}. 4) Under aerobic conditions, the acyl radical is attacked by oxygen molecule and converted to carboxylic acid. 5) B_{12r} is reoxidized to aquocobalamin (B_{12a}).

A similar mechanism could be applied to the reaction with cobaloximes. Much lower catalytic activity of cobaloximes as compared with aquocobalamin might be due to higher reduction potentials of the former. Thus, the difficulty of reduction of cobaloxime by aldehydes was demonstrated spectrophotometrically: Since chloroaquocobaloxime shows a hyperchromic shift in the visible region due to the aquation reaction, it is difficult to detect the formation of the reduced-state of cobaloxime spectro-chemically. Hence, the reaction of aldehydes with hydroxoaquocobaloxime was examined in an aerobic conditions, as well as with aquocobalamin. In the case of B_{12a}, with formaldehyde, acetaldehyde or benzaldehyde, the absorption maximum attributable to B_{12r} was observed at 475 mμ in 20 hr, which disappeared in contact with oxygen giving rise to the restoration of the spectrum of the original solution. On the other hand, in the case of cobaloxime, the absorption maximum at 463 mμ attributable to cobaloxime (II) could not be observed even after 120 hr under the same conditions.

Thus, it is concluded that the reduction of cobaloximes with aldehydes, if any, takes place much more slowly, than that of B_{12a}, and the low catalytic activity of the former can be attributed to their higher reduction potentials. This is supported by the observation that cobalamins are reduced at less negative potentials than the corresponding cobaloximes in the polarographic reduction,[7] and the reduction of cobaloximes by thiols is much slower than that of cobalamins.[8]

7) Y. Hohokabe and N. Yamazaki, This Bulletin, **44**, 1563 (1971).

8) G. N. Schrauzer and J. W. Sibert, *Arch. Biochem. Biophys.*, **130**, 257 (1969).

Studies on Cobaloxime Compounds. VI. Decomposition of Formic Acid with Cobaloximes and Cobalamins

Yorikatsu HOHOKABE and Noboru YAMAZAKI

Departmnt of Polymer Science, Faculty of Engineering, Tokyo Institute of Technology, Ookayama, Meguro-ku, Tokyo

(Received January 20, 1971)

Catalytic activities of cobaloximes in the decomposition reaction of formic acid were compared with each other and with those of cobalamins. In the cobalamin series, the activity decreased in the order aquocobalamin (vitamin B_{12a})>methylcobalamin>cyanocobalamin (vitamin B_{12}). In the cobaloxime series, the activity decreased in the order $Co(OH)(DH)_2(H_2O)>CoCl(DH)_2(H_2O)>Co(CN)(DH)_2(H_2O)>CH_3Co(DH)_2(H_2O)$. Cobalamins had much greater activities than the corresponding cobaloximes. The reaction proceeded with uptake of oxygen. No hydrogen gas was evolved in the reaction. The reaction rate slightly decreased with the increase of pH between 6.0 and 7.0. The reaction rate changes with 0.39 power of formic acid concentration less than 1×10^{-3} M (comparable to that of cobaloxime), and becomes independent of the concentration greater than 1×10^{-3} M. It changed with 0.89 power of the concentration of hydroxoaquocobaloxime. Aquocobalamin was reduced to B_{12r} in the presence of formic acid but not hydroxoaquocobaloxime in anaerobic conditions. The catalytic activities of cobaloximes lower than the corresponding cobalamins were attributed to the higher reduction potentials of the former.

So far, comparison between cobalamin and cobaloxime has been made in the reaction with CO,[1,2] O_2,[3] aldehyde,[4] electron transfer reaction,[5] photodecomposition reaction,[6,7] and other chemical and biochemical reactions.[8,9] Catalytic decomposition of formic acid by cobalamins was briefly described by Utsumi *et al.*[10]

In the present work, catalytic decomposition of formic acid by several cobaloximes and cobalamins was examined in order to compare their catalytic activities, and the results are given herewith.

Experimental

Materials. Preparation of the cobaloximes was described previously.[11] Cobalamins were kindly supplied by Eisai Co. All other reagents were commercial products of G. R. grade.

Procedures. *Decomposition Reaction*: The reactions were followed by means of the conventional Warburg manometric method.[12] A typical reaction mixture with a total volume of 4.0 m*l* contained 6×10^{-3} M of formic acid and 6×10^{-4} M of cobalamin or cobaloxime in 0.5 M phosphate buffer (pH 6.00). Two manometers were used for following a run, one with a chamber containing 0.2 m*l* of 20% KOH with a small filter paper to absorb CO_2 gas evolved in the reaction, and another without the alkali chamber. The pressure change resulting from the uptake of oxygen was followed with the former, and the total pressure change due to the difference between the uptake of oxygen and the evolution of CO_2 with the latter. Each reading was corrected by that of a thermobarometer. The reaction was carried out at 40°C with shaking at a rate of 100 rpm.

Reduction of Cobalamin or Cobaloxime with Formic Acid in Anaerobic Conditions: Reduction was examined for hydroxoaquocobaloxime (1.0×10^{-4} M) as well as aquocobalamin (3.0×10^{-5} M) in the presence of 5×10^{-3} M formic acid in 0.1 M phosphate buffer (pH 7.1) at 40°C under a nitrogen atmosphere, in the same way as reported previously.[4] B_{12a} was reduced in 20 hr which was demonstrated spectrochemically by the appearance of an absorption maximum at 475 mμ. No reduction was observed in the case of hydroxoaquocobaloxime even after 200 hr.

Gas Chromatography: The gases in the reaction mixture were examined by means of gas chromatography for hydrogen gas, which might be formed by non-oxidative decomposition of formic acid. For detection a Shimadzu Gas Chromatograph, model GC-4APT was used with nitrogen gas as carrier at the flow rate of 40 m*l*/min. Moelcular Sieves-13X (60—80 mesh) preheated at 500°C for 2 hr and cooled was packed in a steel column (3 mm×3 m). The detector temperature was 30°C, and the column temperature 20°C. Authentic hydrogen gas gave a retention time 89.4 sec. The gas phase of the reaction mixture with B_{12a} or chloroaquocobaloxime was thus examined and no hydrogen gas was detected.

Results and Discussion

Decomposition of formic acid with cobalamins or cabaloximes proceeded quantitatively with consumption of oxygen. The CO_2/O_2 ratios were 1.6—1.0. Initial rates for the decomposition of formic acid with some cobalamins and cobaloximes are summarized in Table 1. Aquocobalamin was found to be the most powerful catalyst among the cobalamins or cobaloximes examined. Methylcobalamin was the second. Cyanocobalamin showed the lowest activity among cobalamins, in good agreement with the results by Utsumi *et al.*[10] In the cobaloxime series, the catalytic activity decreased in the order hydroxo->chloro->cyano->methyl-aquocobaloxime.

Dependence of rate on the concentration of formic acid, hydroxoaquocobaloxime and pH was investigated. At a concentration comparable to that

1) L. P. Lee and G. N. Schrauzer, *J. Amer. Chem. Soc.*, **90**, 5274 (1968).
2) G. N. Schrauzer and L. P. Lee, *Arch. Biochem. Biophys.*, **138**, 16 (1970).
3) G. N. Schrauzer and L. P. Lee, *J. Amer. Chem. Soc.*, **92**, 1551 (1970).
4) Y. Hohokabe and N. Yamazaki, This Bulletin, **44**, 2142 (1971).
5) G. N. Schrauzer and J. W. Sibert, *Arch. Biochem. Biophys.*, **130**, 257 (1969).
6) Y. Hohokabe and N. Yamazaki, This Bulletin, **44** 2142 (1971).
7) G. N. Schrauzer, L. P. Lee, and J. W. Sibert, *J. Amer. Chem. Soc.*, **92**, 2997 (1970).
8) G. N. Schrauzer, *Accounts Chem. Res.*, **1**, 97 (1968).
9) Y. Hohokabe and N. Yamazaki, This Bulletin, **44**, 798 (1971).
10) I. Utsumi, K. Harada, and H. Miura, *Vitamins* (Japan), **38**, 472 (1968).
11) N. Yamazaki and Y. Hohokabe, This Bulletin, **44**, 63 (1971).
12) T. Sasagawa, "Zikken Kagaku Koza," Vol. **24**, Maruzen, Tokyo (1958), p. 85.

TABLE 1. INITIAL RATES FOR THE DECOMPOSISION OF FORMIC ACID WITH COBALAMINS AND COBALOXIMES[a)]

Material[b)]	Initial rate, M/min
Aquocobalamin	5.70×10^{-5}
Methylcobalamin	9.48×10^{-6}
Cyanocobalamin	1.29×10^{-6}
$Co(OH)(DH)_2(H_2O)$	1.92×10^{-6}
$CoCl(DH)_2(H_2O)$	3.31×10^{-7}
$Co(CN)(DH)_2(H_2O)$	2.64×10^{-7}
$CH_3Co(DH)_2(H_2O)$	1.92×10^{-7}

a) [HCOOH]=6.0×10^{-3} M, [Co]=6.0×10^{-4} M, in 0.5 M phosphate buffer (pH 6.00), at 40°C. (total volume: 4.0 m*l*). The estimated relative errors are not more than 5%.
b) DH denotes dimethylglyoximato monoanion.

of cobaloxime, the rate increased with the substrate concentration, the reaction order being about 0.4. However, at a higher concentration, the rate curves become flat as shown in Fig.1. The rate increased with the concentration of cobaloxime, the reaction order being 0.89 as shown in Fig 2. A slight decrease in rate with the increasing of pH was unexpected (Fig. 3), since the coordination of formate anion to the complex was considered to be easier than that of the protonated form of formic acid. No reason can be given at present.

Change of activity with the variation of the axial ligand in cobalamins and cobaloximes suggests that the formate coordinate to the cobalt atom in the sixth position as in acetate anion,[13] though the formation

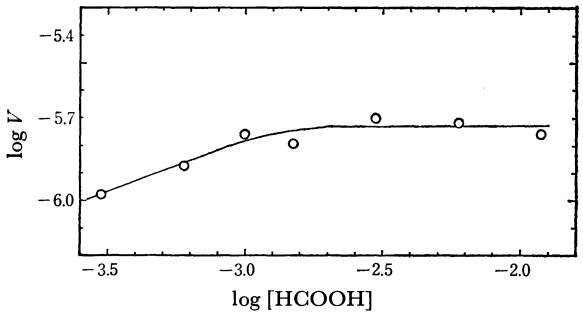

Fig. 1. Dependence of rate upon the concentration of formic acid.
[Co(OH)(DH)$_2$(H$_2$O)]=6.0×10^{-4} M, in 0.5 M phosphate buffer (pH 6.00), at 40°C

constant of acetate anion is very small. Thus two electrons are considered to be transferred from the formate anion coordinated to Co^{3+} in the complex to Co atom, producing CO_2 and H–Co^{1+}. The Co^{1+} species formed is quite unstable under these conditions and reoxidized to Co^{3+}. Otherwise, $HCO_2\cdot$ and Co^{2+} would be formed *via* one-electron transfer process, and oxidized by oxygen to CO_2+HO· and Co^{3+}, respectively. However, no detailed mechanism can be presented at present. The over-all decomposition reaction of formic acid in the presence of the cobalt catalyst in aerobic conditions may be written as

$$HCOOH + \tfrac{1}{2}\cdot O_2 + Co^{3+} \rightarrow CO_2 + H_2O + Co^{3+}.$$

Thus the CO_2/O_2 ratio should be 2.0 theoretically; the observed values were higher than unity, supporting the equation. Oxygen might be consumed by side reaction such as ligand oxidation of the complexes.[10] Much lower catalytic activities of cobaloximes as compared with cobalamins might be attributed to their higher reduction potentials, as in the oxidation of aldehyde.[4] An extremely slow reduction of cobaloximes by thiols in contrast to cobalamin has recently been demonstrated.[5] Reduction of B_{12a} with formic acid to B_{12a} was demonstrated spectrochemically by the appearance of the absorption maximum at 475 mμ in anaerobic conditions (pH 7.1). In contrast, reduction of hydroxoaquocobaloxime was not observed under similar conditions. Although B_{12s} might be expected to be formed in the reaction of B_{12a} and formic acid on the basis of the above mechanism, it was considered unstable under the conditions (pH 7.1) and converted to H·+ B_{12r} under a nitrogen atomosphere,[14] its presence being demonstrated in the visible spectrum. The hydrogen radical would attack the oxygen molecule in aerobic conditions and hence no hydrogen gas would be evolved, in agreement with the results we obtained.

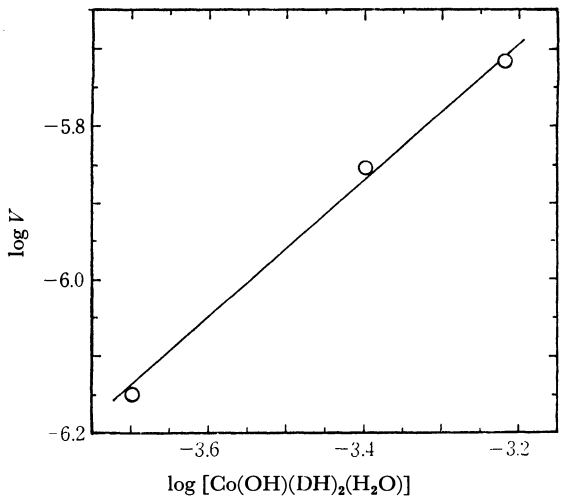

Fig. 2. Dependence of rate upon the concentration of hydroxoaquocobaloxime.
[HCOOH]=6.0×10^{-3} M, in 0.5 M phosphate buffer (pH 6.00), at 40°C

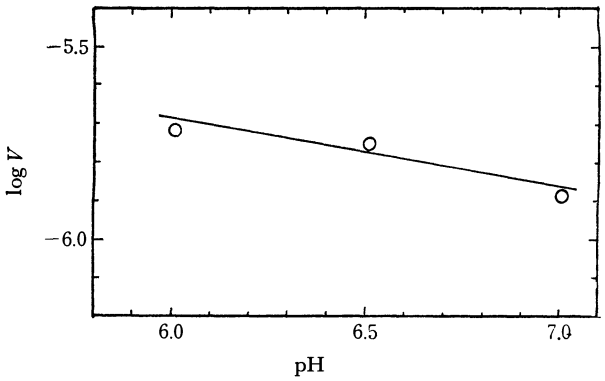

Fig. 3. pH Dependence of rate.
[HCOOH]=6.0×10^{-3} M, [Co(OH)(DH)$_2$(H$_2$O)]=6.0×10^{-4} M, in 0.5 M phosphate buffer, at 40°C

13) R. A. Firth, H. A. O. Hill, J. M. Pratt, R. G. Thorp, and R. J. P. Williams, *J. Chem. Soc., A*, **1969**, 381.
14) G. N. Schrauzer, E. Deutsch, and R. J. Windgassen, *J. Amer. Chem. Soc.*, **90**, 2441 (1968).

The Separation and Concentration of Acetylacetonato Chelates Using a Benzene Column

Kazuo MARUYAMA and Micho MASHIMA
Faculty of Engineering, Niigata University, Nagaoka
(Received February 4, 1971)

This paper is concerned with the application of the zone-melting technique to metal-chelate compounds. An organic solvent which is liquid at room temperature such as benzene, and several acetylacetonato and thenoyltrifluoroacetonato chelates as solutes were prepared. The effective distribution-coefficient k dependence on the molecular weight was revealed by the normal freezing technique. In the deployment process, the acetylacetonato chelates of Fe and Th were chosen as solutes because their k values were different. The experiment was carried out at 2 cm/hr, the rate of zone travel. When a 30-cm column was used, the "removal percentages" of Fe from Th were 41 and 85% for 3 and 5 zone passes respectively. However there was a 22% loss of Th in the latter case. Furthermore, a remarkable concentration was found, and it was shown that the concentration effect may be useful for micro-analysis. At this stage, a relatively large bubble of benzene was observed at the liquid and solid interface; therefore we can call this "three-phase zone-melting."

The zone-melting technique[1] has recently been adopted for various fields,[2-4] but there have been few reports an its application to metal-chelate compounds.[5-7] In our previous experiment,[8] as a first step of this application, aluminum was succesfully separated from iron with an organic solid solvent after these metals had been converted to complex compounds.

In this paper, as an enlargement of the application, an organic solvent which is liquid at room temperature, such as benzene,[9] was used. Several metal acetylacetonato and thenoyltrifluoroacetonato chelates were prepared as solutes. The effective distribution-coefficient (k) of the chelates was determined and discussed in connection with the variation in the center metal. Then, a deployment chromatogram was obtained by the combination of acetylacetonato chelates of iron and thorium. A remarkable concentration was found when a molten zone traveled downward along the charge of the benzene solution of the chelate; thus, this method seems to be useful for micro-analysis.

Experimental

Materials. The acetylacetone. 2-thenoyltrifluoroacetone, metal salts, and organic solvents such as benzene were all reagent-grade. The metal acetylacetonato chelates, $Fe(AcAc)_3$,[10] $Cr(AcAc)_3$,[11] $Co(AcAc)_3$,[12] $Al(AcAc)_3$,[13] $Th(AcAc)_4$,[14] $Zr(AcAc)_4$,[15] and $Be(AcAc)_2$,[16] and the 2-thenoyltrifluoroacetonato chelates, $Fe(TTA)_3$,[17] $Al(TTA)_3$,[18] and $Co(TTA)_2$,[19] were prepared by the standard procedure and were purified by recrystallization with a suitable solvent.

Apparatus and Procedure. As is shown in Fig. 1A, the zone apparatus used in this experiment consisted of five ring heaters composed of electrified nicrom wire, and a refrigerator to keep the benzene solution in the glass tube solid during the zone-melting. The refrigerator was made of a six-part aluminium box with a circulation of −20°C ethyleneglycohol. The rate of the molten zone could be varied at will, but 2- and 6-cm/hr rates were mainly adopted. The zone width was 0.8—1 cm. All the glass tubes were 5 mm in inner diameter and about 20 cm in length.

A tube for the deployment process was first charged with pure benzene and then frozen to 3 cm by dipping it in −20°C

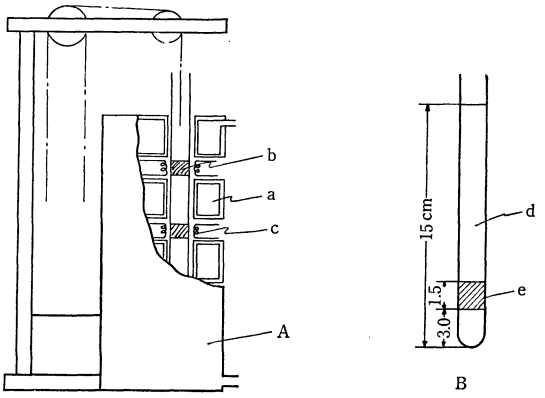

Fig. 1. Zone apparatus (A), and a column for deployment process (B).
a) cooler, b) molten zone, c) heater, d) solvent, e) chelates and solvent.

1) W. G. Pfann, *Trans. AIME*, **194**, 747 (1952).
2) W. R. Wilcox, *Chem. Rev.*, **64**, 187 (1964).
3) G. L. Pearson and M. Tanenbaum, *Phys. Rev.*, **90**, 153 (1953).
4) J. D. Loconti and J. W. Cahill, *J. Polym. Sci., Part A*, **1**, 3163 (1963).
5) H. Kobayashi and K. Ueno, *Bunseki Kagaku*, **15**, 1181 (1966).
6) K. Ueno, H. Kaneko, and N. Fujimoto, *Talanta*, **11**, 1371 (1964).
7) K. Ueno, H. Kaneko, and Y. Watanabe, *Microchem. J.*, **10**, 244 (1964).
8) M. Mashima and K. Z. Maruyama, This Bulletin, **44**, (1971), in press.
9) A. G. Anikin and G. M. Dugacheva, *Russ. J. Phys. Chem.*, **36**, 1115 (1962).
10) J. P. Mckaveny and H. Freiser, *Anal. Chem.*, **29**, 290 (1957).
11) J. P. Mckaveny and H. Freiser, *ibid.*, **30**, 1965 (1958).
12) R. G. Charles and M. A. Pawlikowski, *J. Phys. Chem.*, **62**, 440 (1958).
13) E. W. Berg and J. T. Truemper, *Anal. Chim. Acta*, **32**, 245 (1965).
14) R. W. Moshier and R. T. Sivers, "Gas Chromatography of Metal Chelates", Pergamon Press Ltd., Oxford, 1965.
15) W. B. Brown and J. F. Steinbach, *Anal. Chem.*, **31**, 1805 (1959).
16) J. A. Adams, E. Booth, and J. D. H. Strickland, *Anal. Chim. Acta*, **6**, 462 (1952).
17) R. A. Bolomey and L. Wish, *J. Amer. Chem. Soc.*, **72**, 4483 (1950).
18) H. C. Eshelman and J. A. Dean, *Anal. Chem.*, **31**, 183 (1959).
19) J. C. Reid and M. Calvin, *J. Amer. Chem. Soc.*, **72**, 2948 (1950).

ethyleneglycohol. The supercooling at the bottom can be defended against by this charging. The tube was then charged with a solution of a metal chelate in benzene on the frozen benzene layer and frozen to 1.5 cm. The remaining 10.5 cm was filled with pure benzene, which was also frozen, as is shown in Fig. 1B. Zone melting was started at the bottom of the tube. The tube for the normal freezing and concentration process was charged with a benzene solution of the chelate; only the tube for the latter purpose was frozen to 15 cm. In the concentration process, the zone was started from the top of the charge and a bubble of benzene was formed by increasing the heater temperature. The effective distribution - coefficient was measured by the normal freezing technique.[27-29]

Analysis. After the zone-melting procedure, the solidified charge was removed from the glass tube and cut into sections, and the metal concentrations in the various fractions were determined photometrically after the separation of the solvent. The analytical methods are summarized in Table 1.

TABLE 1. METHODS OF ANALYSIS

Zone melted charge → Metal ion solution.
{separated from the solvent
{by treating with 6 N HCl

		Refferences
Th^{4+}	Thorin method	20
Zr^{4+}	Alizarin S method	21
Cr^{3+}	Diphenylcarbazide method	22
Co^{3+}	Nitroso-R salt method	23
Al^{3+}	Oxine method	24
Fe^{3+}	*o*-Phenanthroline method	25
Be^{2+}	Aluminon method	26

Results and Discussion

The effective distribution - coefficient (k) may be important in the actual zone-melting procedure,[27-29] and so it is necessary to study the factors governing the k value. Seven metal acetylacetonate chelates were, therefore, subjected to normal freezing at the rate of 6 cm/hr, and the concentration of chelate along the charge was determined as the metal concentration. The initial concentration was 1.5%. These k values of seven metal acetylacetonato chelates were examined in relation to various characteristics of these chelates.

As a result of this examination, these k values, when plotted against the molecular weight as in Fig. 2, were found to reveal a molecular weight dependence and to show the greatest fractionation in the case of $Be(AcAc)_2$. Ideally, the size of the solute molecule is one of the most important factors in determining the k value.

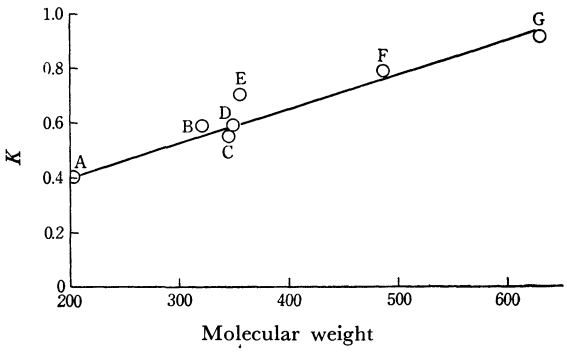

Fig. 2. Dependence of distribution-coefficient, k on molecular weight.
A) $Be(AcAc)_2$, B) $Al(AcAc)_3$, C) $Cr(AcAc)_3$, D) $Fe(AcAc)_3$, E) $Co(AcAc)_3$, F) $Zr(AcAc)_4$, G) $Th(AcAc)_4$.

From the point of view of mutual separation, a large difference in molecular weight may be desired. Therefore, $Fe(AcAc)_3$ (0.58) and $Th(AcAc)_4$ (0.90) were chosen as the solutes in the deployment process. In order to eliminate Fe from Th, the Fe must be greatly moved; therefore the effects of speed and zone passes on the movement of the Fe chelate were examined. The concentration effects of Fe were increased with a decrease in the zone speed and with an increase in the number of passes. For comparison, the k value of $Fe(AcAc)_3$ was 0.91 in benzoic acid, 0.95 in naphthalene, 0.96 in stearic acid, and 1.10 in ectyl alcohol.

Chromatograms after 3 and 5 zone passes using a 15-cm column at 2 cm/hr are shown in Fig. 3, using a mixture of Fe and Th chelates. Both Fe and Th weighed about 13 μg. The sample column was divided into five equal sections. The metal concentration was plotted *versus* a fractions of the charge. Judging from the k value, only $Fe(AcAc)_3$ was concentrated at the top of the charge; thus, a great difference in their distribution was observed. If the top section is removed, 39 and 55% of the total Fe may be eliminated from Th by 3 and 5 zone passes respectively.

Figure 4 shows the results in a 30-cm column. The zone speed, metal weight, and number of zone passes

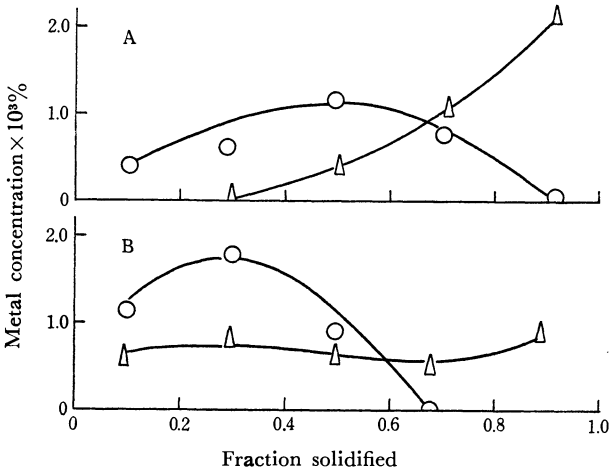

Fig. 3. Distribution of $Fe(AcAc)_3$ and $Th(AcAc)_4$ after 3 (B) and 5 (A) zone passes, using 15 cm-column, Fe; △ Th; ○.

20) V. I. Kuznetsov, *Rept. Acad. USSR*, **31**, 895 (1941).
21) D. E. Green, *Anal. Chem.*, **20**, 370 (1948).
22) R. T. Ptlaum and L. C. Howick, *J. Amer. Chem. Soc.*, **78**, 4862 (1956).
23) O. Hoffman, *Ber.* **18**, 46 (1885).
24) T. Dupuis and C. Duval, *Anal. Chim. Acta*, **6**, 394 (1949).
25) J. Hoste, *Anal. Chim. Acta*, **9**, 263 (1953).
26) C. L. Luke and M. E. Campbell, *Anal. Chem.*, **24**, 1056 (1952).
27) R. H. Mcfee, *J. Chem. Phys.*, **15**, 856 (1947).
28) J. A. Burton and W. P. Slichter, *ibid.*, **21**, 1987 (1953).
29) W. G. Pfann, *J. Appl. Phys.*, **35**, 258 (1964).

are the same as in the above experiment. The distribution of the solute in the 30-cm column was similar to that in the 15-cm column. In this case, if the top section is removed, 41% of the Fe may be eliminated by 3 zone passes, while and if the top two sections are removed, 85% of the total Fe may be eliminated by 5 zone passes, with a 22% loss of Th.

When the zone moved toward the bottom along with the uniform charge, a remarkable concentration was observed, as is shown in Fig. 5. With only 3 passes, the solute was fairly well concentrated at the bottom of the column. In this case, 56% of the Fe, 72% of the Co, and 41% of the Th of each metal were concentrated in the 3-cm region at the bottom. At this stage, there was a relatively large bubble of benzene between the liquid and solid phases; therefore, we can call this "three-phase zone-melting." This phenomenon may be attributed to the great difference in the vapor pressure of the chelate and solvent at this temperature.

The same experiments were also done quantitatively with thenoyltrifluoroacetonato chelates of Co, Al, and Fe. The distribution after 3 passes at 2 cm/hr is shown in Fig. 6. The relative concentration is there plotted *versus* the fraction solidified. The results reveal that the concentration effect was great in this order: Fe>Al>Co; this corresponds to the decrease in the vaper pressure at this temperature.[13]

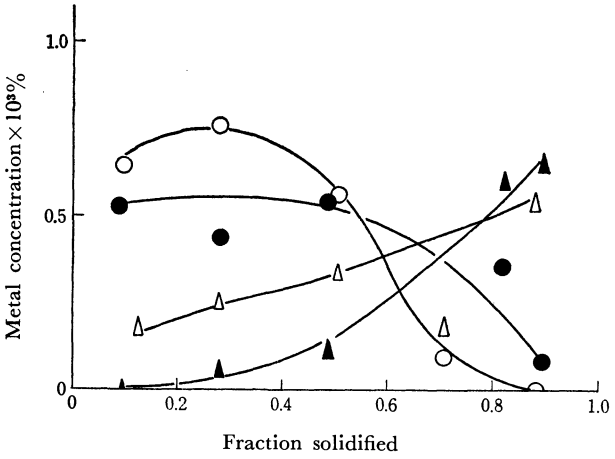

Fig. 4. Distribution of $Fe(AcAc)_3$ and $Th(AcAc)_4$ after 3 and 5 zone passes, using 30 cm-column, and about 13 μg, both of Fe and Th.
Fe; 3 passes △, 5 passes ▲, Th; 3 passes ○, 5 passes ●.

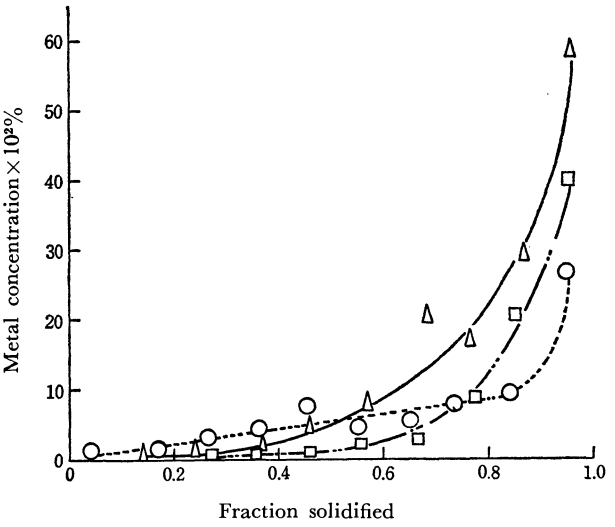

Fig. 5. Distribution of chelates in concentration process, $Fe(AcAc)_3$; △, $Co(AcAc)_3$; □, $Th(AcAc)_4$; ○.

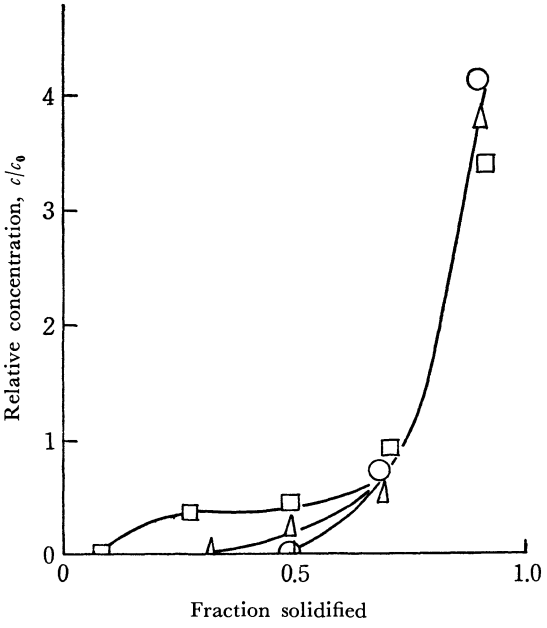

Fig. 6. Quantitative concentration of TTA chelates after 3 zone passes, using 5—6 μg as metal.
$Fe(TTA)_3$; ○, $Al(TTA)_3$; △, $Co(TTA)_2$; □.

Conclusion

As an application of the zone-melting technique for chelate-solvent systems, several metal acetylacetonato chelates in benzene were zone-melted. The molecular-weight dependence of the k value was revealed by the normal freezing technique. In the deployment process, the application was proved to be a promising method for the elimination of Fe from Th after they had been converted into metal chelates; the percentages of the removal of Fe were 39 and 55% for 3 and 5 zone passes respectively. When a 30-cm column was used, the percentages were 41 and 85% for 3 and 5 zone passes respectively. In the latter case, there was a 22% loss of Th.

A remarkable concentration was also found, and it was shown that this effect may be useful for microanalysis; 56% of the Fe, 72% of the Co, and 41% of the Th were concentrated in the 3-cm region of the bottom, with only 3 zone passes.

Furthermore, the possibility of the separation of one metal from another will increase when the concentration process is combined with the deployment process.

Syntheses of a New Series of Transition Metal Chelates of Diphenylphosphinothioylthiourea Anion

Iwao OJIMA, Takaharu ONISHI, Toschitake IWAMOTO, Naoki INAMOTO, and Kenzi TAMARU

Department of Chemistry, Faculty of Science, The University of Tokyo, Hongo, Tokyo

(Received February 16, 1971)

New thiourea derivatives, 3-diphenylphosphinothioyl-1-phenylthiourea (PTTU-A), 3-diphenylphosphinothioyl-1,1-diethylthiourea (PTTU-B), and 3-diphenylphosphinothioyl-1,1-dimethylthiourea (PTTU-C) were found to behave as bidentate ligands with transition metal ions such as Ni(II), Pd(II), Co(II), and Cu(II) to give a series of novel metal chelates. The structures of these complexes are discussed on the basis of magnetic susceptibilities, infrared spectra, electronic spectra, powder X-ray diffraction patterns and elemental analyses. Tentative assignments of two metal-sulfur stretching vibrations in the far infrared spectra were made for Ni-PTTU and Pd-PTTU, which have square-planar configurations. However, the structures of the Cu-PTTU complexes could not be determined by these methods because of the instability of the complexes. They were confirmed by electronic and ESR spectroscopies.

In recent years, chelate complexes with sulfur-donor ligands have been extensively studied as an interesting topic in the field of coordination chemistry and many reports have been published on the properties and reactivities of such complexes as the metal chelates of dithiocarbamates, dithioacetylacetonates, and dithiolates.[1] However, no chelate complexes which have a P=S→M structure have been synthesized so far except for metal dialkyldithiophosphinates.[2]

Thus, it is of considerable interest to synthesize chelate compounds possessing an enolizable P=S bond in the ligand. A part of this work has been described previously[3]

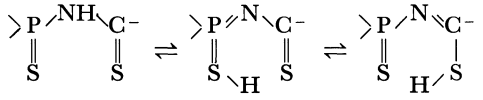

These new chelate rings are important as a unit of polynuclear complexes, and are interesting in connection with the model complexes of enzymatic system such as ferredoxin which is a metal complex with ligands containing sulfur as donor atoms.

The new thiourea derivatives, diphenylphosphinothioylthioureas, PTTU-A, PTTU-B, and PTTU-C, can act as sulfur-donor chelating reagents because their structures include both enolizable P=S and C=S bonds. In view of this the reactions of PTTU with transition metal halides such as nickel(II) chloride hexahydrate, palladium(II) chloride, cobalt(II) chloride hexahydrate, and copper(II) chloride dihydrate, were investigated.

Experimental

Syntheses of Ligands. Diphenylphosphinothioylthioureas were prepared by the reaction of diphenylphosphinothioyl isothiocyanate with amines. A typical procedure is described for the preparation of 3-diphenylphosphinothioyl-1,1-diethylthiourea (PTTU-B). A solution of diethylamine (0.51 g, 7.0 mmol) in 50 m*l* of ether was added to a solution of diphenylphosphinothioyl isothiocyanate (2.0 g, 7.3 mmol) in 50 m*l* of ether with stirring at room temperature. An exothermic reaction took place and white crystals of 3-diphenylphosphionothioyl-1,1-diethylthiourea (PTTU-B) were precipitated in quantitative yield. Mp 125—127°C, IR (KBr disk): 3120(ν NH), 1555(δ NH), and 1475(Amide II) cm^{-1}. Found: C, 58.75; H, 6.01; N, 7.83; S, 18.50%. Calcd: C, 58.60; H, 6.07; N, 8.04; S, 18.40%. 3-Diphenylphosphinothioyl-1-phenylthiourea (PTTU-A): White prisms, mp 143—145°C, IR(KBr disk): 3290, 3220, 3160, 3125(ν NH), 1620, and 1570(δ NH) cm^{-1}. Found: C, 61.85; H, 4.62; N, 7.38; S, 16.90%. Calcd: C, 61.94; H, 4.65; N, 7.60; S, 17.40%. Dimethylammonium salts of 3-diphenylphosphinothioyl-1,1-dimethylthiourea (PTTU-C): When a 40% aqueous solution of dimethylamine (1.30 g, 11.5 mmol) and diphenylphosphinothioyl isothiocyanate (1.35 g, 4.9 mmol) were mixed, an exothermic reaction took place. By a treatment similar to that described above, white crystals of a dimethylammonium salt of 3-diphenylphosphinothioyl-1,1-dimethylthiourea (PTTU-C) were obtained in almost quantitative yield. Mp 118—120°C (lit,[4] 119—121°C), IR (Nujol): 3290, 3240 (ν NH) and 1530 (δ NH) cm^{-1}.

Syntheses of Copmlexes.. A typical procedure is described for the preparation of bis[3-diphenylphosphinothioyl-1,1-diethylthioureato]nickel (Ni-PTTU-B): A solution of PTTU-B (1.4 g, 4.0 mmol) in 10 m*l* of dichloromethane was allowed to react with nickel(II) chloride hexahydrate (0.95 g, 2.0 mmol) in 40 m*l* of ethanol at room temperature with stirring for an hour. Dark green needles of Ni-PTTU-B precipitated, which were recrystallized from dichloromethane-ethanol. Ni-PTTU-B was accordingly obtained in a nearly quantitative yield. The Ni(II) and Pd(II) complexes of PTTU-A(Ni-PTTU-A and Pd-PTTU-A), Pd(II) and Co(II) complexes of PTTU-B (Pd-PTTU-B and Co-PTTU-B) and the Ni(II), Pd(II), and Co(II) complexes of PTTU-C (Ni-PTTU-C, Pd-PTTU-C and Co-PTTU-C) were prepared in a similar way.

Ni-PTTU-A: Dark green needles, mp 193°C (dec.). Found: C, 57.9; H, 4.4; N, 6.6; S. 16.0; Ni, 7.3%. Calcd: C, 57.7; H, 4.1; N, 7.1; S, 16.2; Ni; 7.4%.

Pd-PTTU-A: Orange-yellow prisms, mp 215°C (dec.). Found: C, 53.3; H, 3.6; N, 6.0; S, 14.5%. Calcd: C, 54.3; H, 3.8; N, 6.7; S, 15.2%.

Pd-PTTU-A: Reddish-brown prisms, mp 254°C (dec.).

1) G. N. Shrauzer, *Accounts. Chem. Res.*, **2**, 72 (1969); S. E. Livingstone, *Quart. Rev.*, **19**, 386 (1965); R. Mason, E. D. McKenzie, G. Robertson, and G. A. Rusholme, *Chem. Commun.*, **1968**, 1673; H. H. Wickmann and A. H. Trozzolo, *Inorg. Chem.*, **7**, 63 (1968); O. Siiman and J. Fresco, *ibid.*, **8**, 1846 (1969).

2) C. K. Jørgensen, *J. Inorg. Nucl. Chem.*, **24**, 1571 (1962).

3) I. Ojima, T. Iwamoto, T. Onishi, N. Inamoto, and K. Tamaru, *Chem. Commun.*, **1969**, 1501.

4) A. Schmidpeter and H. Groeger, *Chem. Ber.*, **100**, 3052 (1967).

Found: C, 47.8; H, 3.7; N, 3.9; S, 17.2%. Calcd: C, 47.4; H, 3.4; N, 4.3; S, 19.5%.

Ni-PTTU-B: Dark green needles, mp 200°C (dec.). Found: C, 49.0; H, 4.8; N, 6.7; S, 15.8%. Calcd: C, 51.0; H, 5.0; N, 7.0; S, 16.0%.

Co-PTTU-B: Bright green needles, mp 205—206°C. Found: C, 54.1; H, 5.2; N, 7.2; S, 16.8%. Calcd: C, 54.2; H, 5.4; N, 7.4; S, 17.0%.

Ni-PTTU-C: Dark green needles; mp 188—190°C (dec.). Found: C, 50.0; H, 4.7; N. 8.0; S, 18.2%. Calcd: C, 51.7; H, 4.6; N, 8.0; S, 18.4%.

Pd-PTTU-C: Orange-yellow prisms, mp 209—211°C (dec.). Found: C, 46.6; H, 3.8; N, 8.0; S, 16.8%. Calcd: C, 48.4; H, 4.3; N, 7.5; S, 17.2%.

Co-PTTU-C: Bright bluish-green needles, mp 194—195°C (dec.). Found: C, 49.8; H, 4.4; N, 7.8; S, 17.9%. Calcd: C, 51.6; H, 4.6; N, 8.0; S, 18.4%.

Measurements. The infrared spectra of these complexes in the region 4000—700 cm^{-1} were measured using KBr disks with a 402 *G* spectrophotometer (Japan Spectroscopic Co., Ltd). The far infrared spectra in the region 700—200 cm^{-1} were obtained with a Hitachi EPI-L spectrophotometer. Samples were mixed with paraffin or fused polyethylene or mulled in Nujol. Electronic spectra were recorded on a Hitachi EPS-S spectrophotometer. An ESR spectrometer JEOL Model JES-118 X band was used. Molecular weights were ebullioscopically determined with a Hitachi-Perkin-Elmer Model 115.

Results and Discussion

Syntheses of the Complexes and Their Magnetic Properties. First, PTTU-A was allowed to react with nickel(II) chloride hexahydrate in dichloromethane - ethanol solution under reflux for an hour to give dark green needles of Ni-PTTU-A in 60—70% yield. In the same manner, the reaction of PTTU-A with palladium(II) chloride was performed and reddish-brown prisms were obtained (Pb-PTTU'-A). The bis-phosphinothioylthioureato-metal structure of Ni-PTTU-A was confirmed on the basis of elemental analysis, UV spectrum, and magnetic susceptibility. However, for Pd-PTTU-A, elemental analysis and infrared spectra showed that the ligands have decomposed during the syntheses. In order to prevent thermal decomposition of the product, PTTU-A was allowed to react with palladium(II) chloride in dichlorometahne - ethanol at room temperature for 3 hr with stirring. Yellowish-orange prisms of Pd-PTTU-A were obtained in 90% yield. When Pd-PTTU-A was heated in dichloromethane ethanol under reflux for one hour, the reddish-brown prisms were obtained and on the basis of the melting point, infrared spectra, elemental analysis, and powder X-ray diffraction patterns were found to be identical with the Pd-PTTU'-A prepared as above.

The powder X-ray diffraction patterns of these complexes are shown in Fig. 1. By comparison of these spectra, it was found that Pd-PTTU'-A has a simpler structure than that of Ni-PTTU-A and Pd-PTTU-A. This suggests that in the Pd-PTTU'-A the six membered chelate rings remain intact, but the aniline group is lost. The structure of Pd-PTTU'-A, therefore, was suggested to be the one shown in Scheme 1.

An attempt to obtain crystalline Co-PTTU-A was unsuccessful, but its formation in solution was observed

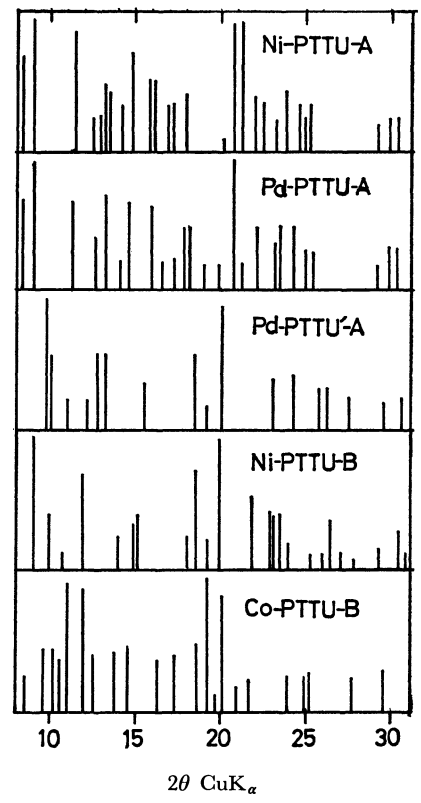

Fig. 1. The powder X-ray diffraction patterns of M-PTTU.

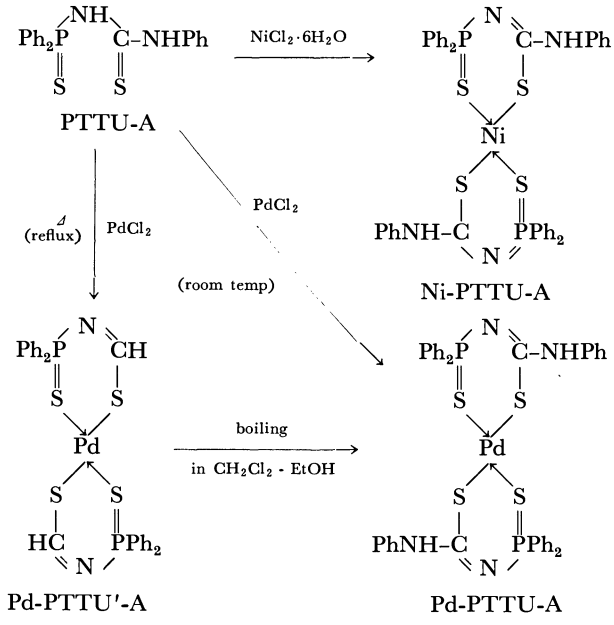

Scheme 1

by UV spectrum, as shown in Fig. 2. It is suggested that the central cobalt(II) (d^7) has a tetrahedral configuration.

Similarly, the nickel(II), palladium(II), and cobalt(II) complexes of PTTU-B and PTTU-C were obtained by the reaction of the corresponding PTTU with transition metal halides in dichloromethane-ethanol at room temperature with stirring for 1—2 hr as shown in Scheme 2. In contrast with Co-PTTU-A, Co-

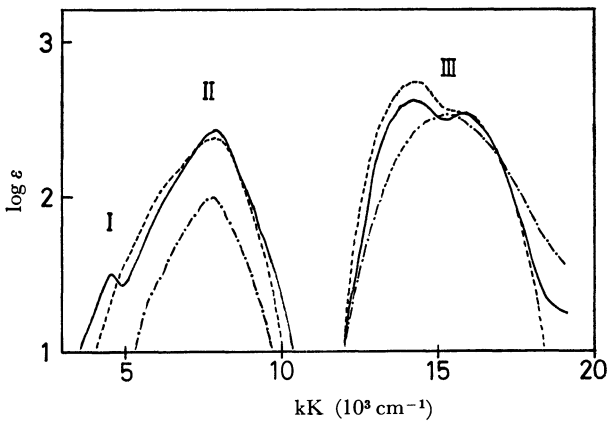

Fig. 2. The electronic spectra of Co-PTTU.

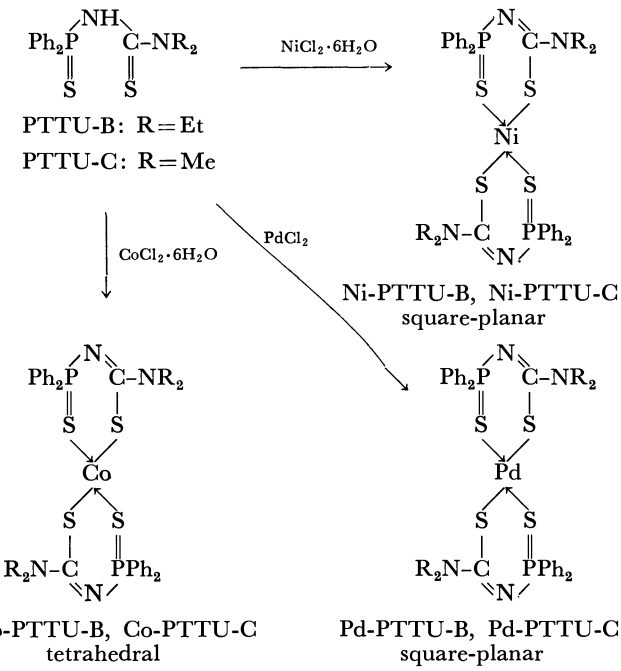

Scheme 2

PTTU-B and Co-PTTU-C were obtained as crystalline substances and a tetrahedral configuration was suggested on the basis of the magnetic susceptibility and electronic spectrum.

All these complexes have the same metal : ligand ratio (1 : 2). They are soluble in organic solvents such as benzene, chloroform, dichloromethane etc., but their solubilities in benzene were not high enough to determine their molecular weights except in the case of Co-PTTU. The molecular weights of Co-PTTU-B and Co-PTTU-C were ebullioscopically determined in benzene to be 751 and 678 (the calculated values for the monomers are 753 and 698), respectively. Except Co-PTTU, they are all diamagnetic at room temperature, which suggests that the complexes of Ni(II) and Pd(II) have square-planar configurations. Their crystal structures seem to be isomorphous according to the powder X-ray diffraction patterns as shown in Fig. 1. The effective magnetic moment of Co-PTTU-B, μ_{eff}=4.50 B.M. ($\chi_g=11.9\times10^{-6}$ cgsemu) at 297°K, and that of Co-PTTU-C, μ_{eff}=5.00 B.M. ($\chi_g=16.3\times10^{-6}$ cgsemu) at 297°K, correspond to the high spin state (S=2/3) of d^7 Co-(II) in a tetrahedral configuration. The powder X-ray diffraction pattern of Co-PTTU-B was quite different from those of Ni-and Pd-PTTU-B as shown in Fig. 1.

Electronic Spectra of Complexes. The electronic spectra of Ni-PTTU-A, Ni-PTTU-B and Ni-PTTU-C displayed an absorption band in the region of 17 kK and suggested a square-planar configuration of the central nickel(II) ions (d^8). The tetrahedral configurations for Co-PTTU-B and Co-PTTU-C. were suggested on the basis of the effective magnetic moment as described above. Moreover, the absorption bands appearing in the region 3-20 kK in the electronic spectra of Co-PTTU-A, Co-PTTU-B, and Co-PTTU-C can be assigned to Td symmetry. The absorption band III in the visible region and band II at 7.87 kK can be assigned to the transition from $^4A_2$ to $^4T_1$ (P) and from $^4A_2$ to $^4T_1$ (F), respectively. The values of $|Dq/B|$ and E/B were obtained by the use of the Tanabe-Sugano diagram according to the assignment mentioned above. Values of B and $10\,D_q$ were calculated to be 684 and 4790 cm^{-1}, respectively. It might be appropriate to assign the samll peak I, appearing in the spectrum of Co-PTTU-B at 4.65 kK, to the transition from $^4A_2$ to $^4T_2$ (the energy of this transition corresponds to $10\,Dq$). The value of Racah's electron repulsion parameter B corresponds to 60% of the free ions, thus reflecting the covalency of the cobalt-sulfur bonds. The value of Dq corresponds to 50% of that derived in the case of $[Co(H_2O)_6]^{2+}$ with O_h symmetry. This shows the adequacy of these assignments although the value of Dq(Td)/Dq(Oh) was slightly larger than 4/9. The values of B and Dq thus obtained are in reasonable agreement with those reported for several tetrahedral cobalt(II) complexes.[5] It is of interest that the cobalt(II) ion in Co-PTTU-A, Co-PTTU-B, and Co-PTTU-C has a tetrahedral configuration in contrast to the bis-dithioacetylacetonato-cobalt(II), which has a square-planar configuration.[6]

Infrared Spectra. The infrared spectra of the complexes were measured in the region 4000—200 cm^{-1}. In the far infrared spectra of the chelates with a square-planar structure, two metal-sulfur stretching vibrations were expected to appear in the region 500—200 cm^{-1},

Table 1. Characteristic bands in the infrared spectra of Ni-PTTU and Pd-PTTU (cm^{-1})

	νP=S	νM-S(ν_I)	νM-S(ν_{II})
Ni-PTTU-A	584	417	358
Pd-PTTU-A	582	412	336
Pd-PTTU-A	586	401	334
Ni-PTTU-B	580	391	340
Pd-PTTU-B	579	380	329
Ni-PTTU-C	579	404	344
Pd-PTTU-C	576	394	334

5) A. B. P. Lever, "Inorganic Electronic Spectroscopy," Elsevier Pub. Co., Amsterdam (1968), pp. 322—328.

6) R. Beckett and B. F. Hoskins, *Chem. Commun.*, **1967**, 909.

as previously reported.[7] The bands appearing in the region 420—320 cm^{-1} that are most sensitive to the metal ion are tentatively assigned in Table 1 to these vibrations because of the covalent nature of metal-sulfur bond and the mass effect. The assignment of P=S stretching bands is also given in Table 1.

The strong bands appearing in the region 650—590 cm^{-1} in the spectra of the ligands can be assined to P=S stretching vibrations (PTTU-A: 635, 607 cm^{-1}, PTTU-B: 594 cm^{-1}, PTTU-C: 650, 632 cm^{-1}). When the chelate rings were formed, these bands shifted to lower frequencies by 20—70 cm^{-1}, and appeared in the region 585—575 cm^{-1}. The bands assigned to the NH stretching vibrations of Ni-PTTU-A and Pd-PTTU-A appeared at 3260 and 3250 cm^{-1}, respectively. The medium-to-strong bands observed in the region 1200—1350 cm^{-1} may be due to the thiourea structure of the ligands, and considerable changes were observed, as shown in Fig. 3, when the complexes were formed. In the case of Pd-PTTU'-A in particular, large changes were observed in these bands (Fig. 3) together with the absence of a NH stretching band between 3500 and 3000 cm^{-1}. This suggests that the aniline group has been lost.

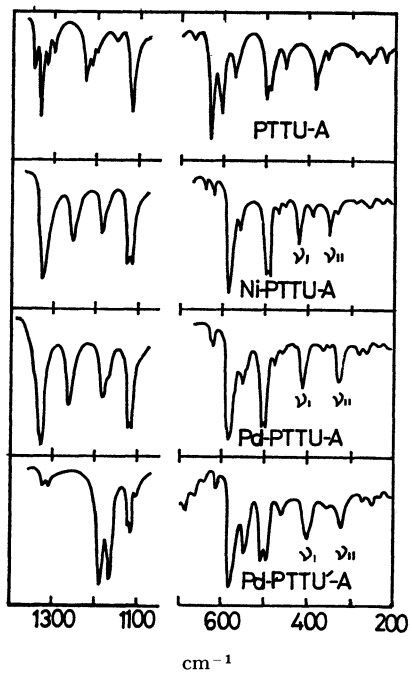

Fig. 3. The infrared and far infrared spectra of M-PTTU-A.

Synthesis of Cu-PTTU-B and Its ESR Spectra. When PTTU (2 eqiv.) and copper (II) chloride dihydrate (1 eqiv.) were reacted, a spontaneous reduction occurred and white grey prisms were precipitated. The structure was not clear, but the infrared spectrum suggests that the PTTU ligand remains although decomposition occurred in the other site. The copper contained in this complex was found on the basis of the magnetic susceptibility (diamagnetic) to be univalent.

7) I. Ojima, T. Onishi, T. Iwamoto, N. Inamoto, and K. Tamaru, *Inorg. Nucl. Chem. Lett.*, **6**, 65 (1970), and references therein.

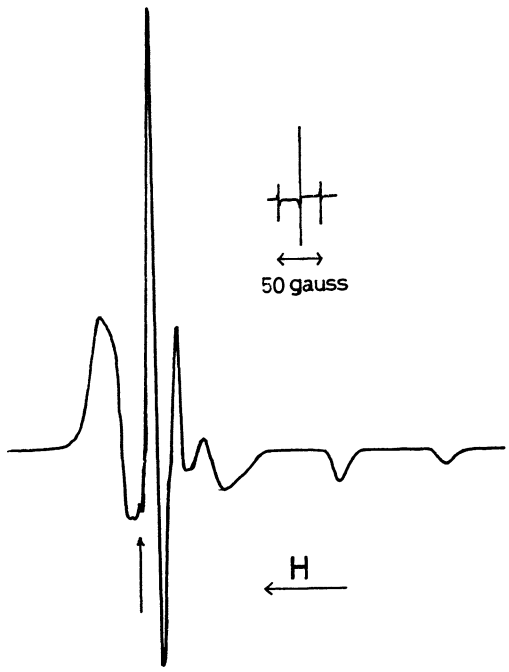

Fig. 4. ESR spectrum of Cu-PTTU-B in CH_2Cl_2-EtOH solution frozen at 77°K. The arrow indicates the resonance field for DPPH ($g=2.00354$).

Fig. 5. ESR spectrum of Cu-PTTU in CH_2Cl_2-EtOH solution at 15°C. The arrow indicates the resonance field for DPPH ($g=2.00354$).

The decomposition of Cu-PTTU-A and Cu-PTTU-C was so rapid that the initial formation of divalent complex could not be detected. In the case of PTTU-B, however, the formation of Cu-PTTU-B was observed in the presence of excess ligands (*ca.* 10 eqiv.) in CH_2Cl_2-EtOH solution by use of ESR spectroscopy, both at room temperature and in glassy state at 77°K. A broad absorption band was observed at 560 nm in the electronic spectrum. The observed ESR spectra of Cu-PTTU-B are shown in Figs. 4 and 5. The sample was prepared just before a measurement in a quartz tube by mixing PTTU-B in dichloromethane (10^{-1} mol/*l*) and copper (II) chloride dihydrate in ethanol

(10^{-2} mol/l). The deep violet color due to the formation of Cu-PTTU-B gradually disappeared at room temperature, but decomposition was completely suppressed at 77°K. The values of $g_{//}$, $g_{\perp}$, $|A_{//}|$ and $|A_{\perp}|$ obtained from the spectrum are 2.111, 2.026, 135×10^{-4} cm^{-1}, and 30×10^{-4} cm^{-1}, respectively. Similarly, the values of g_0 and $|A_0|$ are 2.060 and 60.1×10^{-4} cm^{-1}, respectively. Furthermore, the bonding parameter α^2 [8] was calculated to be 0.53 by the method proposed by Kivelson.[9] These values correspond precisely with those of CuS_4 type complexes, on the basis of the classification performed by Taminaga and Fujiwara,

Table 2. ESR parameters of copper(II) complexes

Ligand	Type	g_0[a]	$g_{//}$	$g_{\perp}$	$\lvert A_0\rvert$[a] ($\times10^4$ cm^{-1})	$\lvert A_{//}\rvert$ ($\times10^4$ cm^{-1})	$\lvert A_{\perp}\rvert$ ($\times10^4$ cm^{-1})
glycine	CuO_2N_2	2.129	2.252	2.068	69	196	5
L-alanine	CuO_2N_2	2.131	2.260	2.067	69	184	12
dith. dieth.	CuS_4	2.047	2.108	2.017	76	139	44
8-mercapt.	CuN_2S_2	2.075	2.158	2.034	63	114	38
PTTU-B	CuS_4	2.060	2.111	2.026	60	135	30

a) From solution at room temperature.

8) $\alpha^2=-A_{//}/P+(g_{//}-2.0023)+3/7(g_{\perp}-2.0023)+0.04$ with the orbital parameter $p=2\gamma\beta\beta_N\langle r^{-3}\rangle\sim0.36$ cm^{-1}

9) D. Kivelson and R. Neiman, *J. Chem. Phys.*, **35**, 149 (1961).

10) I. Taminaga and S. Fujiwara, *Spectroscopy Lett.*, **2**, 127 (1969).

Table 3. Bonding parameters, α^2, of copper(II) complexes

Type	Ligand	α^2	Type	Ligand	α^2
CuO_4	oxal.	0.84	CuN_2S_2	8-mercapt.	0.54
CuO_2N_2	L-alanine	0.84	CuS_4	dieth. dith.	0.55
CuN_4	dipyr.	0.80	CuS_4	PTTU-B	0.53

Abbreviation; oxal.: oxalic acid, dipyr.: 2,2′-dipyridyl, 8-mercapt.: 8-mercaptoquinoline, dieth.dith.: diethyldithiocarbamic acid, PTTU-B: 3-diphenylphosphinothioyl-1,1-diethylthiourea.

as shown in Tables 2 and 3.[10] An average of $g_{//}$ and $g_{\perp}$, 2.053 is in good agreement with g_0, 2.060, and an average of $|A_{//}|$ and $|A_{\perp}|$, 6.5×10^{-3} cm^{-1}, agrees with A_0, 6.0×10^{-3} cm^{-1}. These facts suggest that the species detected by ESR at room temperature is identical with the species existing at 77°K, and that the formation of a copper(II) complex by decomposition of the ligand did not occur.

The authors would like to thank Dr. I. Ikemoto and Mr. K. Ishii for the measurements of X-ray diffraction patterns and magnetic susceptibilities, and Prof. I. Nakagawa, Dr. T. Watanabe and Mr. T. Takeda for their helpful discussions. The authors are also indebted to Mr. S. Mohara of Sagami Chemical Research Center for the molecular weight determination.

BULLETIN OF THE CHEMICAL SOCIETY OF JAPAN, VOL. 44, 2154—2157 (1971)

Pd(II) Complexes with 2,2′-Diaminobiphenyl

Satoru ONAKA[1]

Department of Chemistry, Faculty of Science, The University of Tokyo, Bunkyo-ku, Tokyo

(Received February 18, 1971)

The new palladium(II) complexes with 2,2′-diaminobiphenyl (DABP) have been synthesized under various conditions. The hexa-coordinated palladium complex, $[Pd(DABP)_2Cl_2]$, has been prepared under a high pressure. The square planar diamagnetic complexes, $[Pd(DABP)_2]X_2$ (X=Cl, Br), have been synthesized under atmospheric pressure. As to the $[Pd(DABP)_2]Cl_2$ complexes, two isomers, the yellow complex and the yellow-green complex, are obtained according to the temperature at which the complexes are synthesized. Both the complexes, the yellow and the yellow-green complexes, are similar with respect to the powder X-ray diffraction pattern and the IR spectra in the region from 4000 cm^{-1} to 200 cm^{-1}, but are somewhat different with respect to the stability to air, the thermal stability, and the solubility in chloroform.

Stereochemical and preparative studies of the 2,2′-diaminobiphenyl (DABP)-metal complexes have been reported.[2,3] The compounds subjected to these studies were prepared under an atmospheric pressure. The present author has reported that the Ni(II), Co (II), and Cu(II) complexes with 2,2′-diaminobiphenyl synthesized under a high pressure differ from those complexes prepared under the atmospheric pressure with respect to the spectroscopic behavior and melting or decomposing points.[4] The present paper aims to throw light upon the effect that the preparative conditions may have on the coordination of the ligand to the central metal atom or the other properties in the case of Pd(II)-DABP complexes.

Experimental

Materials. 2,2′-diaminobiphenyl (DABP) was prepared as has been previously reported.[4] Commercially-available $PdCl_2$ and $PdBr_2$ were used.

Syntheses of Compounds. *$[Pd(DABP)_2]Cl_2$ (I) and (II):*

1) Present address: Department of Chemistry, Nagoya Institute of Technology, Showa-ku, Nagoya.

2) F. McCollough, Jr., and J. C. Bailar, Jr., *J. Amer. Chem. Soc.*, **78**, 714 (1956); T. Habu and J. C. Bailar, Jr., *ibid.*, **88**, 1128 (1966).

3) F. Hein and W. Jehn, *Z. Anorg. Allg. Chem.*, **341**, 244 (1965).

4) S. Onaka, T. Iwamoto, Y. Sasaki, and S. Fujiwara, This Bulletin, **40**, 1398 (1967).

Table 1. Analytical results

Compound	Elemental analysis Found/(Calcd) % C	H	N	Mdp[a] °C
$[Pd(DABP)_2]Cl_2$ (I) (yellow compound)	52.72	4.72	9.72	132—133
$C_{24}H_{24}N_4Cl_2Pd$	(52.81)	(4.43)	(10.27)	
$[Pd(DABP)_2]Cl_2$ (II) (yellow-green compound)	52.45	4.66	9.92	136.5—137
$C_{24}H_{24}N_4Cl_2Pd$	(52.81)	(4.43)	(10.27)	
$[Pd(DABP)_2]Br_2$ (III)	44.66	3.81	8.56	
$C_{24}H_{24}N_4Br_2Pd$	(45.42)	(3.81)	(8.83)	

a) Melting or decomposing point is uncorrected.

0.004 mol (0.74 g) of DABP was dissolved into 50 m*l* of ethanol. This solution was slowly dropped into a solution which contained 0.0014 mol (0.25 g) of $PdCl_2$ in 100 m*l* of ethanol below 50°C. The mixture was stirred for 2 hr under the same condition. The resulting yellow precipitates (I) were collected on a glass filter (4 *G*), washed with absolute ethanol, and then dried *in vacuo* for 24 hr at 80°C. (If the temperature is raised to 130°C in drying the precipitates, the compound turns grey-brown). Yield: 80%, based on $PdCl_2$. On the other hand, if the ethanol solution of DABP is dropped into the ethanol solution of $PdCl_2$ at a refluxing temperature, yellow-green precipitates (II) are obtained. (Yield: 80%, based on $PdCl_2$) The yellow-green product (II) is also obtainable by treating the yellow product (I) with an ethanol solution of DABP at a refluxing temperature for a few hours. This compound (II) is thermally more stable than the compound (I). The decomposing points for these compounds are shown in Table 1. Both the compounds are hygroscopic and turn grey-brown when left in air for a few hours. The yellow product is more stable than the yellow-green product in air. The solubility of the yellow-green product to chloroform is higher than that of the yellow product. The solubility of these compounds to methanol and water suggests the monomeric structure.[2,3]

$[Pd(DABP)_2]Br_2$ (III): Only a yellow product was obtained under the atmospheric pressure in the temperature region from 80°C to room temperature with the manner described above. Yield: 42%, based on $PdBr_2$.

$[Pd(DABP)_2Cl_2]$ (IV): In a steel autoclave, 0.01 mol (1.8 g) of palladium chloride, 0.02 mol (3.7 g) of DABP, 20 m*l* of ethanol, and 3 m*l* of concentrated hydrochloric acid were placed, and nitrogen gas was introduced at a pressure of 80 atm. Then the autoclave was heated at 120°C and shaken for 2 hr. A mixture of the yellow and grey powders was thus obtained. The yellow powder that was carefully separated from the grey powder was subjected to infrared measurement.

The results of the elemental analyses are shown in Table 1.

Magnetic Susceptibility.[5] The finely-powdered samples were measured with a Gouy balance at room temperature. The complexes prepared under the atmospheric pressure are diamagnetic.

Powder X-Ray Diffractometry. The powder X-ray diffraction data were obtained as has been previously described.[4] The results are shown in Table 2.

Table 2. The powder X-ray diffraction data

$[Pd(DABP)_2]Cl_2$ (I) (yellow product) 2θ, °	I/I_0	$[Pd(DABP)_2]Cl_2$ (II) (yellow-green product) 2θ, °	I/I_0
9.0	1.0	9.0	1.0
12.9	0.12	12.9	0.20
13.2	0.16	13.2	0.20
18.4	0.12	18.4	0.17
20.4	0.12	20.4	0.20
22.7	0.10	22.7	0.17
25.6	0.21	25.6	0.23
29.0	0.10	29.0	0.12

Relative intensities were calculated by comparing the height of the peaks. rad: $CuK\alpha_1$.
Less intensity lines are excluded.

Diffuse Reflection Spectra.[6] The reflection spectra in the ultraviolet and visible regions were measured with a Shimazu MP-S-50L apparatus equipped with a standard reflectance attachment. The reflectance rates were calculated by means of the Kubelka-Munk equation.[7]

Infrared Spectra. The infrared spectra were recorded with a Hitachi EPI-G2 spectrometer and a Hitachi EPI-L spectrometer for the samples in the Nujol mulls from 4000 cm^{-1} to 200 cm^{-1}. The results are shown in Fig. 1, in Fig. 3, and in Table 3.

Discussion

The magnetic measurements show that the complexes (I), (II), and (III) synthesized under atmospheric pressure are square planar. The coordination of the amino group to the palladium metal can be clearly explained on the basis of the infrared data. The absorption bands due to the amino group of the ligand amine are considerably shifted toward lower frequencies in its complexes. The far-infrared spectra of the compounds (I), (II), and (III) form additional evidence of the coordination of the amino group. It is expected that the participation of the halogen atoms in the coordination may cause remarkable shifts of the bands in the far-infrared region, depending on the halogen atoms.[8] As is shown in Fig. 1, the far-infrared spectrum of the compound (III) is almost the

5) The author's thanks are due to Professor Yukichi Yoshino, of the College of General Education of this University, for the use of the Gouy balance.

6) The author's thanks are due to Professor Sadao Yoshikawa, of Department of Applied Chemistry, Faculty of Engineering of this University, for the kind permission to use the reflectance spectrometer.

7) P. Kubelka and F. Munk, *Z. tech. Physik*, **12**, 593 (1931).

8) J. Hiraishi, I. Nakagawa, and T. Shimanouchi, *Spectrochim. Acta*, **24A**, 819 (1968).

Table 3. The characteristic infrared and the far-infrared bands of the DABP-complexes, cm^{-1}

DABP	$[Pd(DABP)_2]Cl_2$ (I)	$[Pd(DABP)_2]Cl_2$ (II)	$[Pd(DABP)_2]Br_2$ (III)	Assignment
3400, s	3360, s	3380, m	3380, s	NH_2 asym. str.
3380, s		3360, s		
3270, m				
3180, s	3150, m	3150, m	3140, s	NH_2 sym. str.
1635, vs	1615, s	1615, s	1610, vs	NH_2 bend.
	1585, vs	1575, s	1570, vs	
	1050, m	1050, s	1045, s	NH_2 wag.
486, vs				
452, w	458, w	456, w	455, w	
446, w	442, s	440, s	440, s	
433, w	432, m	429, s	427, m	
426, w				
	410, m	410, m	412, m	Pd–N str.
			405, w, sh	
321, sh	332, s	330, s	325, vs	
314, vs	314, s	313, s	310, vs	
277, m				
270, m				
204, s	225, m	235, m	230, m	

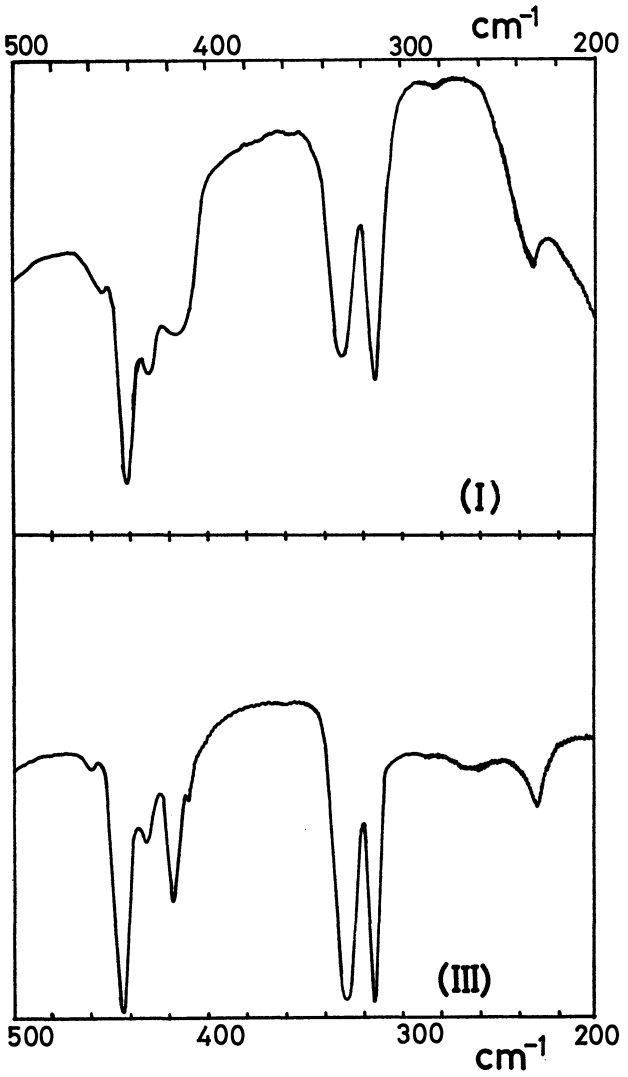

Fig. 1. The far-infrared spectra of DABP-Pd complexes. (I): $[Pd(DABP)_2]Cl_2$, (III): $[Pd(DABP)_2]Br_2$

same as that of compound (I) or (II), and bands which are assignable to a Pd–N stretching vibration with a reasonable intensity are observed at 410 cm^{-1} for compounds (I) and (II) and at 412 cm^{-1} for compound (III).[4,8,9] Therefore, the amine, DABP, acts as a bidentate ligand in these compounds.

Measurements of the powder X-ray diffraction analyses and the diffuse reflectance spectra of compounds (I) and (II) are made in order to clarify further the difference between the compounds (I) and (II). Compounds (I) and (II) give almost the same diffraction pattern, as is shown in Table 2. No serious differences are observed in the diffuse reflectance spectra of the compounds (I) and (II), as is shown in Fig. 2. Therefore, we may exclude the possibility that either the compound (I) or the compound (II) is a structural isomer, such as Vauquelin-type compounds or halogen-bridged compounds, as is shown below by (a),[10] or a diamine-bridged polynuclear complex, as is shown below by (b). Moreover, the

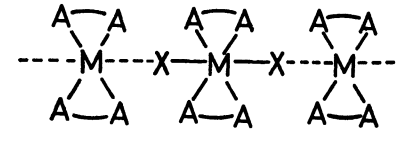

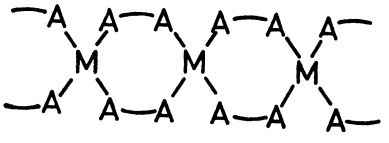

9) M. A. J. Jungbauer and C. Curran, *Spectrochem. Acta*, **21**, 641 (1965).

10) H. Reihlen and E. Flohr, *Chem. Ber.*, **67**, 2010 (1934).

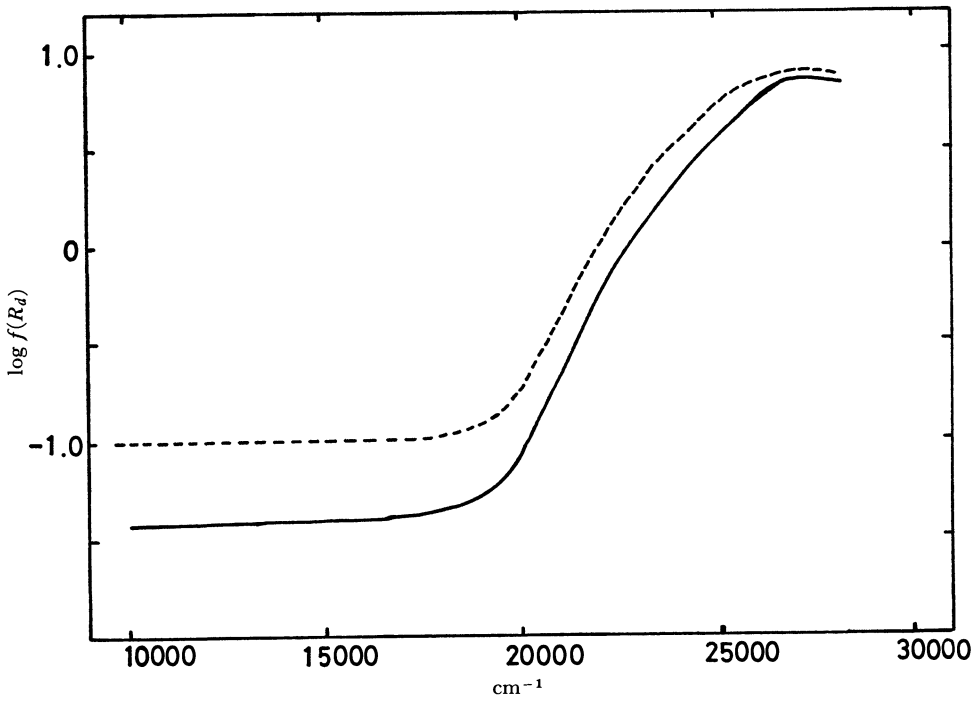

Fig. 2, The diffuse reflection spectra of the DABP-Pd complexes.
—— $[Pd(DABP)_2]Cl_2$ (I) ---- $[Pd(DABP)_2]Cl_2$ (II)

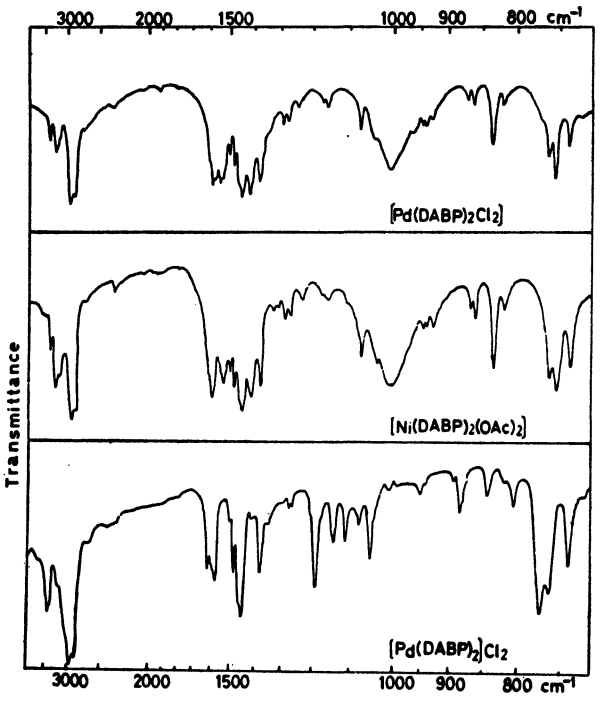

Fig. 3. IR spectra of Pd(II) complexes with DABP.

possibility that this isomerism is caused by the crystal dichroism[11] may be ruled out because of the size of the crystals: the fine precipitates (I) and (II) pass through a 3G-glass filter. It is well known that optically-active isomers are possible if the 2,2'-diaminobiphenyl is coordinated to a metal ion,[2-4] because the coordination with a metal ion prevents the rotation of the phenyl rings. As the compounds (I) and (II), however, show no optical activity, they may be racemic mixtures or of the meso form. A possible origin of this isomerism of these two compounds may be a conformational difference arising from the diamine which does not affect the optical activity.

The yellow compound (IV) synthesized under a high pressure gives a infrared spectrum which strikingly resembles that of $[Ni(DABP)_2(OAc)_2]$, as is shown in Fig. 3. Analytically-pure samples of the compound (IV) have not yet been obtained, though the infrared spectrum of Fig. 3 is clear evidence of the formation of a hexa-coordinated complex $[Pd(DABP)_2Cl_2]$.

It can be concluded that the preparative conditions have an important effect on the coordination of ligands to a metal atom, on the chemical behavior, and on the color of the compounds in the case of Pd-DABP complexes.

The author wishes to express his deep gratitude to Professor Yukiyoshi Sasaki for his encouraging advice and discussions.

11) S. Yamada, H. Yoneda, and R. Tsuchida, *Nippon Kagaku Zasshi*, **69**, 145 (1948).

Fourier Analysis of Alternating Current Polarography: Amplitude and Phase of Fundamental and Second Harmonic AC Polarographic Waves

Hiroyuki KOJIMA and Shizuo FUJIWARA

Department of Chemistry, Faculty of Science, The University of Tokyo, Hongo

(Received February 19, 1971)

The Fourier analysis of the instantaneous AC polarographic current was performed with a computer *on-lined* to a potentiostat. From the Fourier spectra, the amplitudes and phase angles of both the fundamental and the second harmonic AC polarographic waves were obtained. In the Cd(II) system, the current amplitude DC potential curves and phase angle-DC potential curves for the fundamental and the second harmonic AC polarographic waves were compared with the theoretical curves. The method is applicable to the accurate analysis of electrode reaction kinetics.

Alternating current (AC) polarography has been found to be useful in studying electrode reaction kinetics, and various instrumental and theoretical approaches have been attempted. The phase angle of the fundamental harmonic AC wave and the intensity of higher order harmonic AC waves were measured and analyzed theoretically by Smith and his coworkers,[1-7] who employed a potentiostat with a phase-sensitive detector and tuned amplifiers.

In the present work, it is shown that Fourier analysis of instantaneous AC polarographic waves gives the phase angle and amplitude of fundamental and second harmonic AC polarographic waves. In general, AC polarographic waves can be expressed in the following form.

$$I = I_1 \sin(\omega t + \varphi_1) + I_2 \sin(2\omega t + \varphi_2) + \cdots \quad (1)$$

where ω is the angular frequency of an applied AC potential, I is the total alternating current, I_1 (I_2) and φ_1 (φ_2) are the amplitude and phase angle of the fundamental (second) harmonic AC polarographic wave, respectively. The Fourier transforms of Eq. (1) are

$$I_k \cos\varphi_k = \frac{2}{T}\int_0^T I \sin k\omega t \, dt \quad (2)$$

$$I_k \sin\varphi_k = \frac{2}{T}\int_0^T I \cos k\omega t \, dt \quad (3)$$

$$k = 1, 2, \cdots,$$

where T is the period of original data. Equations (2) and (3) show that both the amplitude and phase angle of the fundamental and the second harmonic AC polarographic waves can be obtained by the Fourier transformation.

In this paper, an instrumentation for the Fourier transformation is presented and the feasibility of this method for the measurement of faradaic currents is discussed.

Experimental

Outline of the Procedure. Figure 1 shows a block-diagram of the apparatus, which is a modified version of a digital polarograph used to analyze fluctuations of *i-t* curves.[8] It is composed of a potentiostat, a computer,[9] a synchroscope[10] and their supporting equipments. A sinuisoidal alternating potential with small amplitude is superposed on the direct current potential which is applied to the electrode. Using the dropping mercury electrode, the polarographic current on which the AC wave is superposed is sampled during the single drop life, and is stored in the computer which is *on-lined* to the potentiostat. The Fourier transformation is performed after the DC component of the polarographic current is eliminated by shifting the zero level. Calculated Fourier spectra are recorded on a chart paper in bar-graph style.

Potentiostat. The potentiostat is constructed mainly from solid-state operational amplifiers. A three-electrode cell is used with the voltage follower circuit. The drop-synchronizer is functioned by the control of the computer. The alternating current potential which is superposed on the direct potential is 15 mV and its frequency is adjusted to 34.5 Hz.

Computer. The analog to digital converter samples the polarographic current in 8-bit digital data every 240 μ sec. At the start, the mercury drop is knocked off with a pulse provided by the computer. The computer waits 3.5 sec for the growth of the mercury drop and begins to sample the polarographic current. It samples 121 points during a period of the applied AC potential and continues to sample until 16 sets of digital data in total are obtained.

Synchroscope. The synchroscope controls the gate of the computer, *i.e.*, it sends a triggering pulse to the computer so that the computer can start sampling at the time when the phase angle of the applied AC potential becomes zero. At the end of the period of the applied AC potential, the computer stops sampling, waits for the next triggering pulse from the synchroscope and again begins to sample the polarographic current. Sampling by the computer is performed during every period of the applied AC potential with the aid of the control of the synchroscope. The AC voltage which is sent to the synchroscope as the triggering source has to be large enough to achieve stability of triggering level.

Measurements. A reversible system of Cd(II) ion in

1) D. E. Smith, *Anal. Chem.*, **35**, 602 (1963).
2) D. E. Smith, *ibid.*, **35**, 610 (1963).
3) T. G. McCord, E. R. Brown, and D. E. Smith, *ibid.*, **38**, 1615 (1966).
4) T. G. McCord and D. E. Smith, *ibid.*, **40**, 289 (1968).
5) T. G. McCord and D. E. Smith, *ibid.*, **41**, 1423 (1969).
6) T. G. McCord and D. E. Smith, *ibid.*, **42**, 2 (1970).
7) T. G. McCord and D. E. Smith, *ibid.*, **42**, 126 (1970).
8) T. Kugo, Y. Umezawa, and S. Fujiwara, *Chem. Instrument.*, **2(2)**, 189 (1969).
9) Model JRA-5 Spectrum Computer of Japan Electron Optics Laboratory Co.
10) Type 585 Cathode-Rey Oscilloscope of Tektronix, Inc.

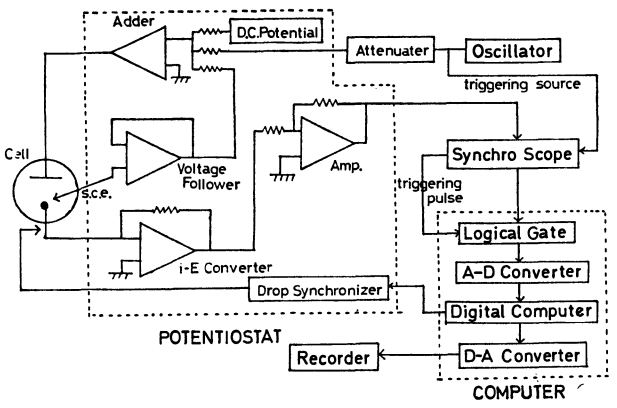

Fig. 1. Blockdiagram of the apparatus.

1.0 mol/l Na_2SO_4 was used. Before the measurements, the triggering level of the synchroscope is adjusted by inserting a standard resister (1.00 kΩ) in place of the cell. The standard resister is also employed in order to calibrate the frequency of the oscillator and the intensities of the Fourier spectra. Charging currents are measured with the use of a reference solution which does not contain a depolarizer. The cell resistance is measured to be 102 Ω at potentials where the faradaic current is negligible. All these measurements are carried out by the phase-selective detection involving the Fourier transformation. The flow rate of mercury is 1.44 mg/sec at mercury column height of 60 cm. The drop time is 5.8 sec at 0 V *vs.* SCE. All polarographic measurements are made at 22.5±0.5°C.

Results and Discussion

Fourier spectra of the Cd(II) System. Figure 2 shows Fourier spectra for the Cd(II) system at three potentials near the half-wave potential. The Fourier spectra are given at an interval of 2.15 Hz which is one sixteenth of the frequency of the applied AC potential. The 16th and the 32nd components correspond to the fundamental and the second harmonic AC polarographic waves, respectively. The sine part of the Fourier spectra corresponds to the component *in-phase* with the applied AC potential, whereas the cosine part represents the component which advances in phase by 90° relative to the AC potential.

Smith and Reinmuth[11] showed theoretically that in reversible electrode processes the phase angle of the fundamental harmonic AC polarographic wave is 45° at any DC potential, but the phase angle of the second harmonic AC wave[12] is 135° (−45°) at potentials more anodic (cathodic) than the half-wave potential. However, the Fourier spectra given in Fig. 2 are quite different in shape from this theoretical prediction. This result may be interpreted in terms of non-faradaic effects due to the double layer capacitance and the ohmic resistance of the system. The cosine part of the fundamental harmonic AC waves is larger in magnitude than the sine part (Figs. 2-a and 2-c). At −0.550 V or −0.651 V, the faradaic current is small, and the charging current becomes dominant. At −0.601 V which is approximately equal to the half-wave potential, the sine part of the fundamental harmonic AC wave is dominant (Fig. 2-b). In the vicinity of the half-wave potential, the faradaic current is large enough to result in a considerable amount of IR-drop.

The second harmonic-AC wave is inverted in phase angle across the half-wave potential, where the second harmonic AC wave disappears. The intensity of the second harmonic AC waves given in Fig. 2 is much

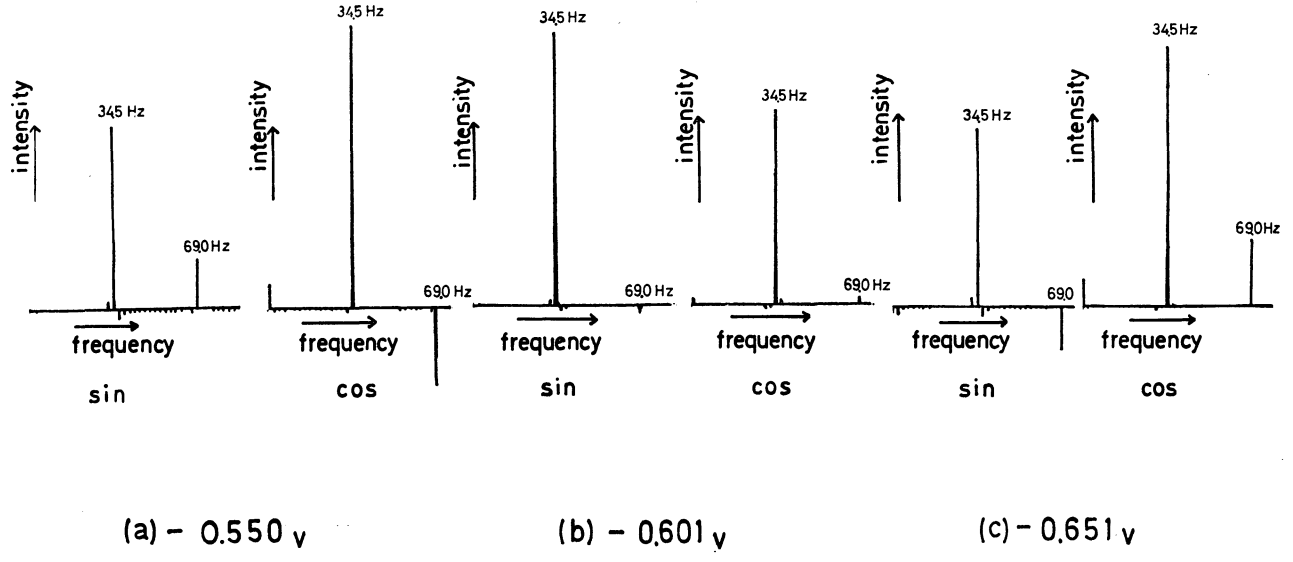

Fig. 2. Fourier spectra of Cd(II) system at (a) −0.550 V (b) −0.601 V and (c) −0.651 V.
System: 1.0 mM $CdCl_2$ in 1.0 M Na_2SO_4.
AC potential: 34.5 Hz, 30 mV peak-to-peak sine wave.
Measurement: instantaneous AC polarographic current during 3.5—5.0 sec of drop life.
Spectrum: each Fourier component is given at an interval of 2.15 Hz and the intensity is arbitrarily scaled.

11) D. E. Smith and W. H. Reinmuth, *Anal. Chem.*, **33**, 482 (1961).

12) The phase angle of the second harmonic AC wave is taken so that the sign of the amplitude can be positive.

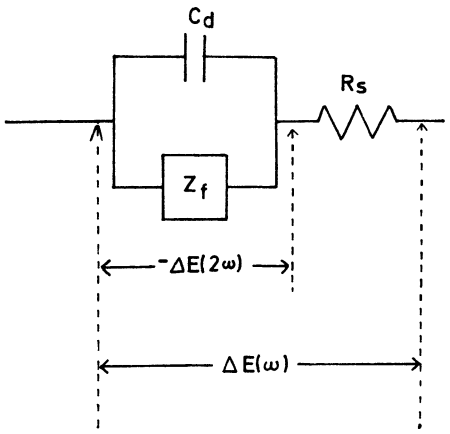

Fig. 3. Equivalent circuit to the cell.
$\Delta E(\omega)$ is the applied AC potential.
$\Delta E(2\omega)$ is the potential produced by the second harmonic alternating current.

smaller than what is predicted from the theory developed by Smith.[11] This discrepancy may be interpreted in terms of the IR-drop of the system as follows. The circuit which is equivalent to the cell is shown in Fig. 3, where Z_f, C_d, and R_s denote the faradaic impedance, the double layer capacitance and the cell resistance respectively. When an AC potential whose angular frequency is ω is applied to the electrade, and an additional AC potential with 2ω is also produced onto Z_f and C_d. This is because the second harmonic alternating current passes through R_s. The additional AC potential which is represented by $-\Delta E(2\omega)$ in Fig. 3 produces a fundamental harmonic AC wave with 2ω, which is opposite in phase to the second harmonic AC wave produced by the applied AC potential with ω. This leads to an appreciable decrease in the intensity of the second harmonic AC wave.[13]

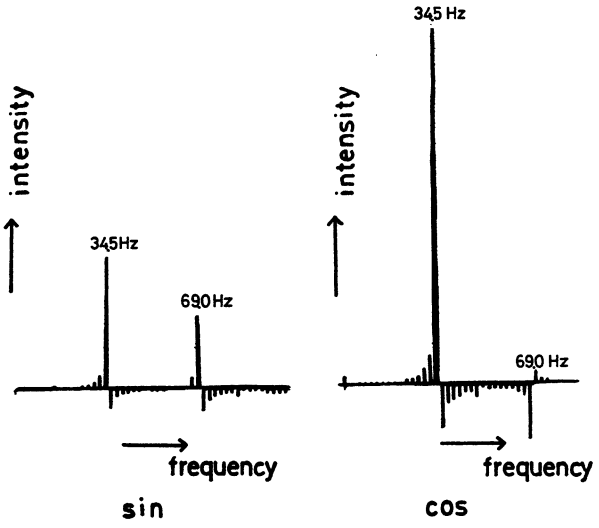

Fig. 4. Fourier spectrum of Cd(II) at −0.550 V.
The polarographic current is sampled consecutively during 16 periods of the applied AC potential without the aid of triggering pulses.

13) The double layer capacitance C_d also reduces the second harmonic AC wave a little.

In addition to the fundamental and the second harmonic AC waves mentioned above, a number of small peaks are observed in Fig. 2. Possible origins for these small peaks are the growth of the dropping mercury electrode and instability of the oscillater.

It can be shown that the growth of the mercury drop results in the additional small peaks, which become smaller in intensity as the frequencies of the small peaks are separated from those of the main components. It can also be shown that the drop growth makes only a minor contribution to the intensity of the main components. Details of the calculation are given in Appendix II.

Instability of the oscillator can effectively be compensated by the aid of a triggering pulse supplied by the synchroscope, which controls the start of sampling for every period of the applied AC potential. Sharp spectra such as shown in Fig. 2 can only be obtained under this control. Figure 4 shows an example obtained in the absence of the control of the synchroscope. We see that the intensity, and therefore the number of small peaks, is increased remarkably. Such spectra cannot be used to analyze faradaic components quantitatively.

Comparisons with the Calculated Curves. The current amplitude-DC potential curves are illustrated in Figs. 5 and 7 for the fundamental and the second harmonic AC polarographic waves, respectively.[14] The phase angle-DC potential curves are plotted in Figs. 6 and 8. In Figs. 5—8, solid lines show the

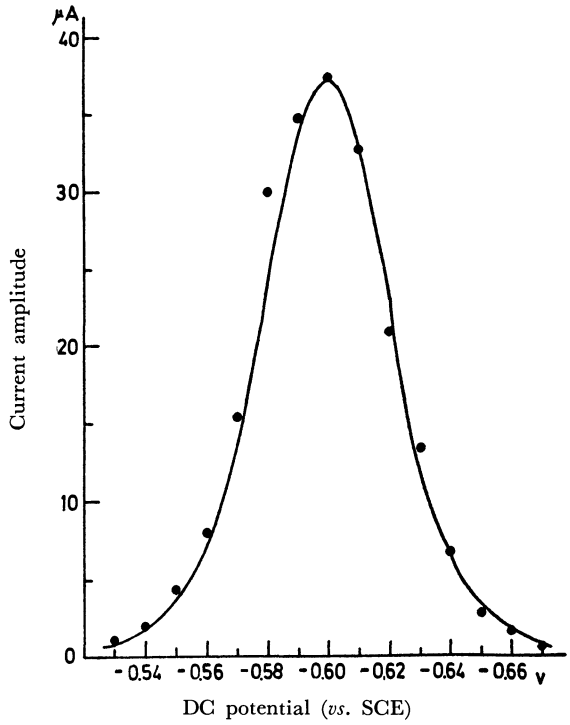

Fig. 5. Current amplitude-DC potential curve for the fundamental harmonic AC polarographic wave of the Cd(II) system.
(• • •): experimental, (——): calculated

14) Fourier spectra are measured every 10 mV in the range from −0.530 V to −0.660 V and the contribution from the non-faradaic effects is eliminated.

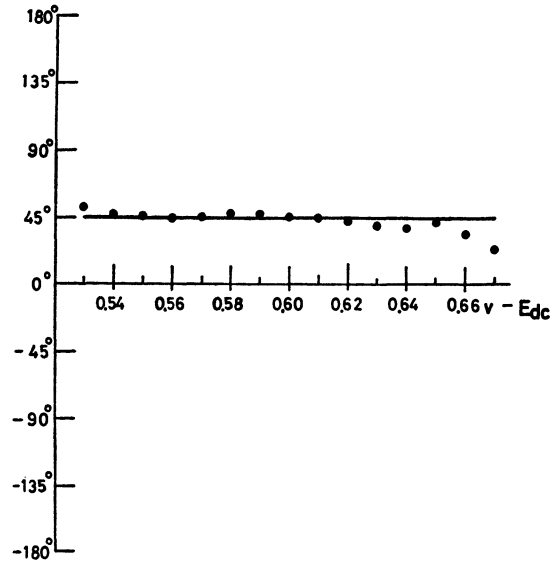

Fig. 6. Phase angle-DC potential curve for the fundamental harmonic AC polarographic wave of the Cd(II) system.
(• • •): experimental, (——): calculated

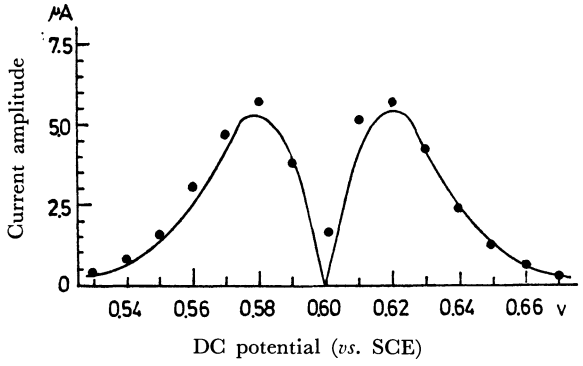

Fig. 7. Current amplitude-DC potential curve for the second harmonic AC polarographic wave of the Cd(II) system.
(• • •): experimental, (——): calculated

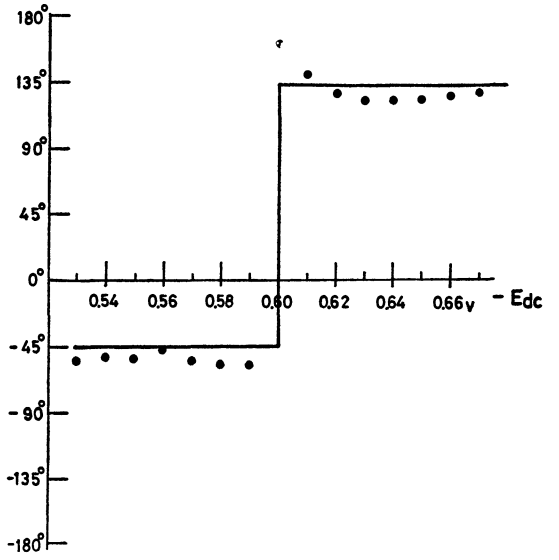

Fig. 8. Phase angle-DC potential curve for the second harmonic AC polarographic wave of the Cd(II) system.

theoretical curves obtained as in the following; the theoretical curves of the fundamental and the second harmonic-AC polarographic waves with the reversible process have been given by McCord and Smith[4] as

$$I(\omega t) = \frac{n^2F^2AC_0^*(\omega D_0)^{1/2}\Delta E}{4RT\cosh^2(j/2)}\sin(\omega t+\pi/4) \quad (4)$$

$$I(2\omega t) = \frac{n^3F^3AC_0^*(2\omega D_0)^{1/2}\Delta E^2\sinh(j/2)}{(4RT)^2\cosh^3(j/2)} \times \sin(2\omega t-\pi/4) \quad (5)$$

$$j = \frac{nF}{RT}(E_{dc}-E_{1/2}^r) \quad (6)$$

where $I(\omega t)$ and $I(2\omega t)$ represent the fundamental and the second harmonic AC waves, respectively. Other notations are defined in Appendix I. In calculating $I(\omega t)$ and $I(2\omega t)$, the value of $nFAC_0^*D_0^{1/2}$ was obtained using Eq. (7) along with the intensity of the diffusion-controlled DC polarographic wave,[15]

$$I_d(t) = \sqrt{\frac{7}{3}}nFAC_0^*D_0^{1/2}\frac{1}{\sqrt{\pi t}}. \quad (7)$$

As Figs. 5—7 show the experimental plots are in good agreement with the calculated curves. In Fig. 8 a considerable deviation is noticed in the case of the phase angle of the second harmonic AC wave. This is because Eq. (5) for the second harmonic AC wave is valid only for the ideally reversible process. The Cd(II) system which is not ideally reversible has a *quasi-reversibility* in the fundamental harmonic AC process. McCord and Smith have taken the effect of the *quasi-reversibility* into account, and given more precise equations.[4] The results given in Fig. 8 can satisfactorily be reproduced using these equations. As discussed by McCord and Smith, the phase angle of the second harmonic AC wave is influenced by the *quasi-reversibility* of the electrode reaction more sensitively than that of the fundamental harmonic AC wave.

General Characteristics of the Fourier Analysis. Figure 9 illustrates the charging current and its Fourier spectrum for a 1.0 mol/l Na_2SO_4 solution at −0.601 V. It should be noted that the charging current in-

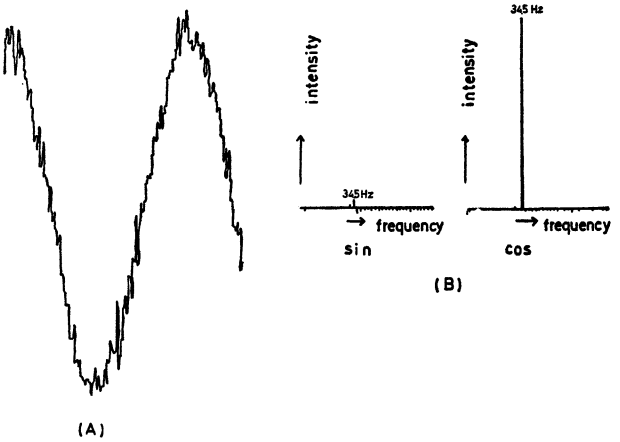

Fig. 9. Charging current and its Fourier spectrum of 1.0 M Na_2SO_4 solution at −0.601 V.

15) P. Delahay, "New Instrumental Methods in Electrochemistry," Interscience, New York (1954), p. 63.

volving much noise reproduces the Fourier spectrum satisfactorily. This is closely related to the process of numerical integration in the Fourier analysis; a possible contribution from noise is cancelled if the number of sampling points is large enough compared to the inverse of an average frequency of the noise. In this respect the results in Figs. 5—9 are not quite satisfactory. A computer with larger memory capacity and an analog to digital converter with higher resolution and speed would consolidate the advantage of the present method of Fourier analysis. *Accumulation* of signals would also serve for an improvement of the results.

In the analysis of electrode reactions, the second harmonic AC polarographic wave is more useful than the fundamental harmonic AC wave. In the first place, the former is not affected by the non-faradaic effects; the IR-drop of the system can be compensated properly by the application of the *positive feed back technique* in the potentiostat.[16-18] In contrast, when using the fundamental harmonic AC wave, it is difficult to eliminate accurately the effects of the double layer capacitance. Secondly, the line shape of the second harmonic AC wave responds more sensitively to the electrode reaction kinetics. As suggested by McCord and Smith,[4] the current amplitude-DC potential curve and the phase angle-DC potential curve are useful in analyzing the reaction scheme at the electrode.

In spite of these advantages, the second harmonic AC wave has seldom been used. This is because it is difficult to measure the second harmonic AC wave accurately for lack of sensitivity. The phase angle of the second harmonic AC wave in particular seems to have never been measured. In view of the above discussion, the method of the Fourier Transformation given here seems promising for an accurate analysis of the second harmonic AC wave.

The authors are indebted to Drs. Yoji Arata and Takeo Yamamoto for their valuable advice. They are also grateful to Mr. Teruhiko Kugo of Yanagimoto Manufacturing Co. for his helpful suggestions on measurements.

16) E. R. Brown, T. G. McCord, D. E. Smith, and D. D. Deford, *Anal. Chem.*, **38**, 1119 (1966).
17) E. R. Brown and D. E. Smith, *ibid.*, **40**, 1411 (1968).
18) E. R. Brown, H. L. Hung, T. G. McCord, D. E. Smith, G. L. Booman, *ibid.*, **40**, 1420 (1968).

Appendix

I. *Notations*

A = electrode area
C_0^* = initial concentration of oxidized form
E_{dc} = DC component of applied potential
ΔE = amplitude of applied alternating current potential
$E_{1/2}^r$ = reversible polarographic half-wave potential
F = Faraday's constant
R = gas constant
T = absolute temperature
n = number of electrons transferred in heterogeneous charge transfer step
$I_d(t)$ = instantaneous DC faradaic limiting current
$I\omega(t)$ = fundamental harmonic faradaic alternating current
$I(2\omega t)$ = second harmonic faradaic alternating current
ω = applied angular frequency
s = rate of increase in amplitude of polarographic alternating current
t = time

II. *Effect of the Drop Growth upon Fourier Spectra.* Equation (1) should be modified in order to take into account the effect of the drop growth. It is a good approximation that the amplitude of the AC polarographic current changes almost linearly. Using the rate s of the increase in the amplitude the AC polarographic wave can be represented by the equation

$$I = \sum_{k=1}^{\infty} (1+st) I_k \sin(k\omega t + \varphi_k), \tag{A1}$$

where k denotes the order of each harmonic AC component. Eq. (A1) is expanded into the Fourier series in the range $0 \leqq t \leqq T$,

$$\begin{aligned} I = \sum_{k=1}^{\infty} I_k \Bigg\{ & \cos\varphi_k \left(1 - \frac{s}{2\omega k}\right) \sin k\,\omega t \\ & + \sin\varphi_k \left(1 - \frac{s}{2\omega k}\right) \cos k\,\omega t \\ & + \frac{sT\cos\varphi_k}{2\pi} \sum_{\substack{n=0 \\ n \neq km}}^{\infty} \frac{-2km}{k^2m^2 - n^2} \cos n\frac{\omega}{m} t \\ & + \frac{sT\sin\varphi_k}{2\pi} \sum_{\substack{n=1 \\ n \neq km}}^{\infty} \frac{2n}{k^2m^2 - n^2} \sin n\frac{\omega}{m} t \Bigg\}, \end{aligned} \tag{A2}$$

where m represents $\omega T/(2\pi)$, *i.e.*, the number of periods of the fundamental harmonic AC components in T. Equation (A2) shows that the intensity of each main component of the Fourier spectra is reduced by $s/(2\omega k)$. Under the present experimental conditions, *viz.*, $\omega = 216.7$ and $s < 2$, the value of $s/(2\omega k)$ is less than 0.005 for each order harmonic AC component. Equation (A2) can also describe the behavior of small peaks beside each main component.

The Acylation of *bz*-Hydroxy- and *bz*-Methoxy-2,3-dimethylbenzofurans and the Synthesis of Furobenzopyranone Derivatives[1]

Yoshiyuki KAWASE, Seiji YAMAGUCHI, Nobuo OKI, and Fumiko OKUMURA

Department of Chemistry, Faculty of Literature and Science, Toyama University, Gofuku, Toyama

(Received July 6, 1970)

The action of acetic acid, phenylacetic acid, or β-phenylpropionic acid and polyphosphoric acid on 5-, 7-, and 6-hydroxy-2,3-dimethylbenzofurans afforded 6-acyl-5-hydroxy-, 6-acyl-7-hydroxy-, and 5-acyl-6-hydroxybenzofurans, some of which were also obtained by the Friedel-Crafts acylation of the corresponding methoxybenzofurans. The hydroxyketones thus obtained were converted to dimethylfuro derivatives of 4-hydroxycoumarins and isoflavones, and 3-benzyl-4-hydroxyfurocoumarins were also prepared by the thermal condensation of the hydroxybenzofurans and diethyl benzylmalonate.

The formylation and acetylation of *bz*-methoxy-2,3-dimethylbenzofurans have been reported by Royer *et al.*,[2] while the acetylation and phenylacetylation of 4- and 6-methoxy- and -hydroxybenzofurans have been reported by one of the present authors.[3] The acyl compounds obtained have been converted to dimethylfuro derivatives of coumarins, chromones, flavones, and isoflavones.[2-4]

In connection with this, the acetylation, phenylacetylation, and β-phenylpropionylation of 5-, 7-, and 6-hydroxy- (**3**, **9**, **15**) and -methoxy-2,3-dimethylbenzofurans (**2**, **8**, and **14**) were carried out in the present experiments; also, dimethylfuro derivatives of 4-hydroxycoumarins (**17**, **18**, and **19**) and of isoflavones (**20**, **21**, **22**, and **23**) were prepared from the acyl compounds in order to test the pharmacological activities.

The starting compounds, *bz*-methoxy-2,3-dimethylbenzofurans (**2**, **8**, and **14**), were prepared in good yields in the present experiments by the cyclodehydration of aryloxybutanones (**1**, **7**, and **12**) with polyphosphoric acid. The reagent seemed to be excellent in the case of 3-(*m*-methoxyphenoxy)-2-butanone[5] (**12**), as the 6-methoxybenzofuran (**14**) was obtained in the pure state.[6] For the preparation of the 6- or 4-hydroxybenzofuran, the cyclization of 3-(*m*-acetoxyphenoxy)-2-butanone (**13**) by sulfuric acid was attempted in order to obtain the 6-hydroxybenzofuran (**15**) in a low yield.

The action of acetic acid, phenylacetic acid, or β-phenylpropionic acid on the 5- and 7-hydroxy-2,3-dimethylbenzofurans[7] (**3** and **9**) in the presence of polyphosphoric acid afforded the corresponding 6-acyl compounds (**5a**, **5b**, **5c**, **11a**, **11b**, and **11c**), while the analogous β-phenylpropionylation of the 6-hydroxybenzofuran[8] (**15**) afforded the 5-(β-phenylpropionyl) compound (**16**) (Charts 1—3).

The 6-acyl-5-hydroxy compounds (**5a** and **5b**) were also obtained by the Friedel-Crafts acylation of the methoxybenzofuran (**2**) in carbon disulfide at the reflux temperature, while the β-phenylpropionylation under those conditions afforded the 6-acyl-5-methoxybenzofuran (**4c**), which was then dimethylated to **5c** by heating it with aluminum chloride in nitrobenzene (Chart 1). Royer *et al.*[2] have obtained the 6-acetyl-5-methoxybenzofuran (**4a**) by the Friedel-Crafts acetylation of the 5-methoxybenzofuran (**2**) at room temperature and then changed it to the hydroxyketone (**5a**) by demethylation. The Friedel-Crafts β-phenylpropionylation of the 7-methoxybenzofuran (**8**) afforded mainly the 4-acyl-7-methoxybenzofuran (**10c**), accompanied by a small amount of the 6-acyl-7-hydroxy compound (**11c**) (Chart 2) analogously

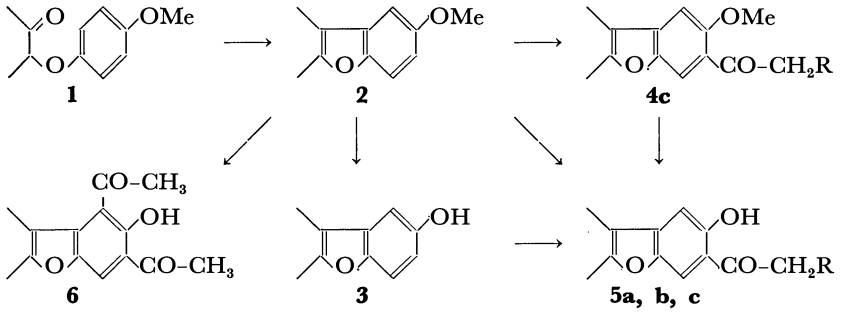

For all Chart: a) R=H, b) R=Ph, c) R=CH_2Ph

Chart 1

1) The major part of this work was presented at the 23rd Annual Meeting of the Chemical Society of Japan, Tokyo, April, 1970.

2) R. Royer, E. Bisagni, A.-M. Laval-Jeantet, and J.-P. Marquet, *Bull. Soc. Chem. Fr.*, **1965**, 2607.

3) Y. Kawase, M. Nanbu, and F. Miyoshi, This Bulletin, **41**, 2676 (1968).

4) Y. Kawase, M. Nanbu, F. Miyoshi, and H. Kawamura, *ibid.*, **41**, 2683 (1968).

5) Preliminary report: Y. Kawase, *Chem. Ind.* (London), **1970**, 687.

6) The reported cyclization by sulfuric acid or other reagents afforded a mixture of the 6- and 4-methoxybenzofurans (Ref. 7 and 8); their ratio was determined to be 97 : 3 in the case of sulfuric acid by estimating the areas of the peaks corresponding to each of the 3-methyl protons in the NMR spectrum (Ref. 5).

7) R. Royer, E. Bisagni, C. Hudry, A. Cheutin, and M.-L. Desvoye, *Bull. Soc. Chim. Fr.*, **1963**, 1003.

8) E. Bisagni and R. Royer, *ibid.*, **1962**, 925.

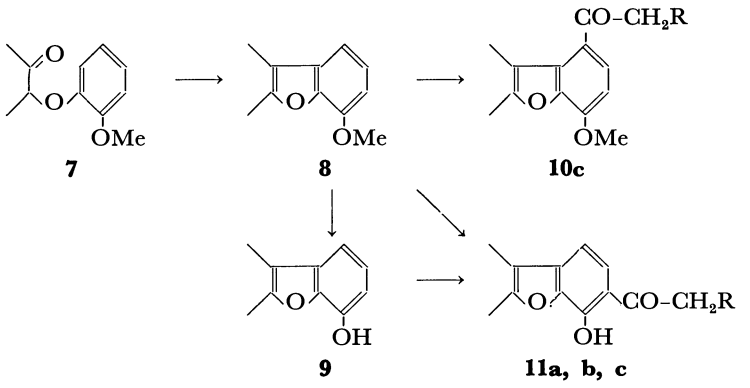

Chart 2

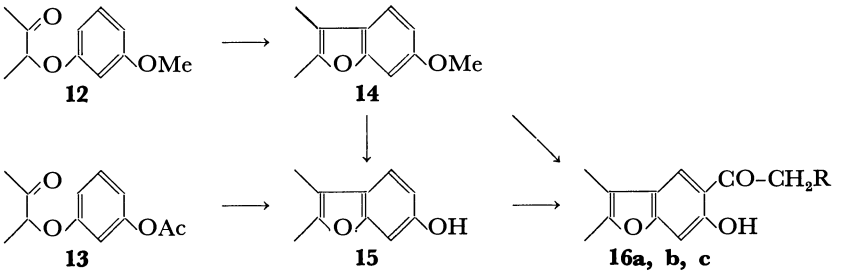

Chart 3

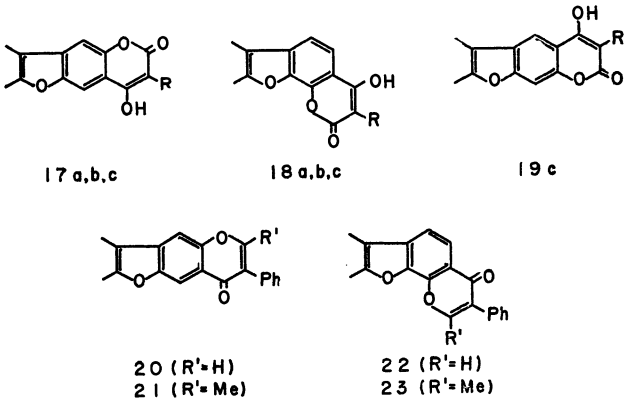

Chart 4

to what has been reported in the case of the acetylation.[2] The analogous β- phenylpropionylation of the 6-methoxybenzofuran (**14**) aforded also the 5-acyl-6-hydroxybenzofuran (**16c**), similarly as has been reported in the cases of the acetylation and phenylacetylation.[3] The Friedel-Crafts acetylation of **2** with a double amount of the reagents afforded the diacetyl compound (**6**), analogously to the cases of 5-methylbenzofuran[9] and 7-methoxybenzofuran.[2]

The positions of the acyl groups in the acylation product were determined by NMR spectroscopy; the methoxyketone (**4c**) and hydroxyketones (**5a**, **5b**, **5c**, and **16c**) have two singlets corresponding to two aromatic para protons, while the methoxyketone (**10c**) and hydroxyketones (**11a**, **11b**, and **11c**) have two doublets of J=8 Hz corresponding to two aromatic ortho protons (Table 3).

The hydroxyketones (**5a**, **5b**, **5c**, **11a**, **11b**, **11c**, and **16c**) thus obtained were converted to dimethylfuro derivatives of 4-hydroxycoumarins (**17a**, **17b**, **17c**, **18a**, **18b**, **18c**, and **19c**) by the action of diethyl carbonate and sodium,[4] and to dimethylfuro derivatives of isoflavones (**20**, **21**, **22**, and **23**) by the action of ethyl orthoformate and piperidine in pyridine or acetic anhydride and sodium acetate.[3] The furocoumarins (**17c**, **18c**, and **19c**) were also prepared by the thermal condensation of the hydroxybenzofurans (**3**, **9**, and **15**) with diethyl benzylmalonate, analogously as has been reported in the cases of 3-phenylfurocoumarins[10] (**17b**, **18b**, and **19b**) (Chart 4).

Experimental

All the melting points and boiling points are uncorrected. The IR spectra were measured as KBr disks on a Hitachi EPI-S spectrophotometer, the UV spectra were measured on a Hitachi 139 spectrophotometer, the NMR spectra were measured on a JEOL JNM-C-60H (60 MHz) spectrometer, and the mass spectra were measured on a JEOL JMS-OlS spectrometer. The detailed data are summarized in Tables 1—4.

The Preparation of Methoxybenzofurans. A mixture of 3-(*p*-methoxyphenoxy)-2-butanone[7] (**1**) (3 g) and polyphosphoric acid (n=2.5, 60 g) was heated at 100°C for 1 hr, after which the cooled mixture was poured into ice water. The mixture was extracted with ether, and the residual product from the ethereal solution was distilled to give methoxybenzofuran (**2**), bp 143—147°C/21 mmHg (lit,[7] bp 133—134°C/11 mmHg); 1.5 g (55%). Similarly, **8** and

9) R. Royer, Y. Kawase, M. Hubert-Habart, L. René, and A. Cheutin, *Bull. Soc. Chim. Fr.*, **1966**, 211.

10) J. -P. Lechartier, P. Demerseman, A. Cheutin, and R. Royer, *ibid.*, **1966**, 1716.

Table 1. Summarized data of reactions

Starting compd.	Reagent	Prod.	Mp °C(solv[a]) or bp °C/mmHg	Yield %
	Preparation of Aryloxybutanone			
b)	Cl-butanone	**13**	145—150/7	72.5
	Preparation of Methoxy- and Hydroxybenzofurans			
1	PPA[c]	**2**	143—147/21[d]	55
7	PPA	**8**	143—147/25[e]	59
12	PPA	**14**	141—144/21[f]	81
13	H_2SO_4	**15**	105—107 (Et)[g]	17
	Preparation of Methoxy- and Hydroxyketones			
2	$PhCH_2CH_2COCl - AlCl_3$	**4c**	105—108 (Et)	60
2	$AcCl - AlCl_3$	**5a**	140—141 (Et)[h]	81
3	AcOH - PPA	**5a**	140—141 (Et)[h]	39
2	$PhCH_2COCl - AlCl_3$	**5b**	134—135 (Et)	58
3	$PhCH_2CO_2H$ - PPA	**5b**	134—135 (Et)	15
3	$PhCH_2CH_2CO_2H$ - PPA	**5c**	139—140.5 (Et)	31.5
4c	$AlCl_3$	**5c**	139—140.5 (Et)	34
2	$AcCl - AlCl_3$	**6**	150.5—151 (Et)	67
8	$PhCH_2CH_2COCl - AlCl_3$	**10c**[i]	64—66 (Me)	42
		11c	98—98.5 (Me)	6
9	AcOH - PPA	**11a**	127—129.5 (Et)[j]	41
9	$PhCH_2CO_2H$ - PPA	**11b**	159.5—161.5 (Et)	48.5
9	$PhCH_2CH_2CO_2H$ - PPA	**11c**	98—98.5 (Et)	36
14	$PhCH_2CH_2COCl - AlCl_3$	**16c**[k]	100—101 (Et)	2
15	$PhCH_2CH_2CO_2H$ - PPA	**16c**	100—101 (Et)	8
	Preparation of Furocoumarins			
5a	$CO(OEt)_2$ - Na	**17a**	308 (Et)	67.5
5b	$CO(OEt)_2$ - Na	**17b**	284—285 (Et)[l]	72.5
3	$PhCH_2CH(CO_2Et)_2$	**17c**	285—286 (Et)	55
5c	$CO(OEt)_2$ - Na	**17c**	285—286 (Et)	30
11a	$CO(OEt)_2$ - Na	**18a**	310 (Et)	29.5
11b	$CO(OEt)_2$ - Na	**18b**	283—284 (Et)[m]	52
9	$PhCH_2CH(CO_2Et)_2$	**18c**	283.5—285 (Et)	42
11c	$CO(OEt)_2$ - Na	**18c**	283.5—285 (Et)	21
15	$PhCH_2CH(CO_2Et)_2$	**19c**	269—270 (Et)	8
16c	$CO(OEt)_2$ - Na	**19c**	269—270 (Et)	74
	Preparation of Furoisoflavones			
5a	$CH(OEt)_3$	**20**	233—234 (Et)	97
5a	Ac_2O - AcONa	**21**	150.5—151.5 (Et)	28
11a	$CH(OEt)_3$	**22**	216—217 (Et)	85
11a	Ac_2O - AcONa	**23**	198—201 (Et)	61

a) Et: ethanol, Me: methanol. b) *m*-Acetoxyphenol. c) Polyphosphoric acid. d) Lit. bp 133—134°C/11 mmHg (Ref. 7). e) Lit. bp 136°C/12 mmHg, mp 38.5°C (Ref. 7). f) Lit. bp 128—129°C/9 mmHg (Ref. 7). g) Lit. mp 107.5—108°C (Ref. 8). h) Lit. mp 141°C (Ref. 2). i) The crude product was crystallized from methanol to give **11c**, and **10c** was obtained from the mother solution. j) Lit. mp 130°C (Ref. 2). k) The crude product was distilled to give fraction a, bp 134—140°C/20 mmHg, and fraction b, bp 150—170°C/20 mmHg. The fraction b was crystallized to give **16c**, and the fraction a was purified by chromatography on silica gel, with cyclohexane and then benzene as the solvent, to give the recovery **14** (total 39%) and indanone (total 68%). l) Lit. mp 187°C (Ref. 10). m) Lit. mp 287°C (Ref. 10).

14 were also prepared by this procedure.

The Preparation of Hydroxybenzofurans. Hydroxybenzofurans (**3**, **9**, and **15**) were prepared by the demethylation of the methoxybenzofurans (**2**, **8**, and **14**) by following the methods of Refs. 7 and 8. Compound **15** was also prepared by the cyclization of **13** as follows:

*The Preparation of 3-(m-Acetoxyphenoxy)-2-butanone (**13**).* A mixture of *m*-acetoxyphenol (28 g), 3-chloro-2-butanone (20.5 g), acetone (150 ml), and anhydrous potassiun carbonate (70 g) was refluxed for 8 hr; the mixture was treated with water and then extracted with ether. The residual product from the ethereal solution was distilled to give **13**, bp 145—150°C/7 mmHg; 29.6 g (72.5%).

*The Cyclization of **13**.* Concentrated sulfuric acid (20 ml) was stirred into **13** (13.5 g) with cooling below 15°C, after which the mixture was kept at 15°C for 1 hr. The resulting mixture was poured into ice water and extracted with ether. The residual product from the ethereal solution was crystallized from cyclohexane to give **15**, mp 105—107°C (lit,[7] mp 107.5—108°C); 1.7 g (17%).

TABLE 2. THE IR SPECTRA AND ANALYSIS OF NEW COMPOUNDS

Compd.	ν_{CO}^{KBr}	Formula	Found		Calcd		$m/e(M^+)$
			C%	H%	C%	H%	
		Aryloxybutanone					
13	1775 1729	$C_{12}H_{14}O_4$	64.82	6.45	64.85	6.35	
		Methoxy- and Hydroxy-ketones					
4	1664	$C_{20}H_{20}O_3$	77.68	6.49	77.90	6.54	308
5b	1655	$C_{18}H_{16}O_3$	77.00	5.70	77.12	5.75	280
5c	1658	$C_{19}H_{18}O_3$	77.51	6.12	77.53	6.16	294
6	1671 1626	$C_{14}H_{14}O_4$	68.21	5.44	68.28	5.73	246
10c	1674	$C_{20}H_{20}O_3$	77.85	6.51	77.90	6.54	308
11b	1664	$C_{18}H_{16}O_3$	76.96	5.74	77.12	5.75	280
11c	1658	$C_{19}H_{18}O_3$	77.75	6.30	77.53	6.16	294
16c	1632	$C_{19}H_{18}O_3$	77.69	6.21	77.53	6.16	294
		Furocoumarins					
17a	1692	$C_{13}H_{10}O_4$	68.02	4.39	67.82	4.38	230
17c	1670	$C_{20}H_{16}O_4$	75.10	4.80	74.99	5.03	320
18a	1678	$C_{13}H_{10}O_4$	67.51	4.38	67.82	4.38	230
18c	1672	$C_{20}H_{16}O_4$	75.21	4.83	74.99	5.03	320
19c	1650	$C_{20}H_{16}O_4$	74.95	5.12	74.99	5.03	320
		Furoisoflavones					
20	1625	$C_{19}H_{14}O_3$	78.60	4.82	78.60	4.85	290
21	1637	$C_{20}H_{16}O_3$	78.79	5.19	78.93	5.30	304
22	1637	$C_{19}H_{14}O_3$	78.56	4.80	78.60	4.85	290
23	1635	$C_{20}H_{16}O_3$	78.73	5.35	78.93	5.30	304

TABLE 3. THE NMR SPECTRA[a)]

Compd.	Ph-H of benzofuran[b)]	Ph-H	2-Me	3-Me
	Methoxybenzofurans			
2			2.32	2.08
8			2.35	2.10
14			2.24	2.00
c)			2.24	2.24
	Methoxy- and Hydroxyketones			
4c	7H 7.60 4H 6.67	7.12	2.30	2.05
5a	7H 7.54 4H 6.76		2.36	2.08
5b	7H 7.61 4H 6.75	7.25	2.32	2.04
5c[d)]	7H 7.60 4H 6.85	7.26	2.34	2.06
6[d)]	7.70		2.37	1.97
10c	5H 7.31(d) 6H 6.48(d) J=8 Hz	7.14	2.35	2.10
11a[d)]	5H 7.49(d) 4H 6.88(d) J=8 Hz		2.41	2.12
11b	5H 7.52(d) 4H 6.73(d) J=8 Hz	7.24	2.43	2.12
11c	5H 7.39(d) 4H 6.70(d) J=8 Hz	7.17	2.38	2.08
16a	4H 7.40 7H 6.68		2.28	2.03
16b[d)]	4H 7.82 7H 6.91	7.34	2.33	2.11
16c	4H 7.48 7H 6.75	7.18	2.28	2.05

a) δ-Values in CCl_4 (about 5% solution), with TMS as the internal standard. b) d: Doublet. c) 2,3-Dimethyl-4-methoxybenzofuran. d) In $CDCl_3$.

The Acylation of the Hydroxybenzofuran with Carboxlyic Acid and Polyphosphoric Acid (PPA). A mixture of **3**[7] (2.4 g), acetic acid (1 g), and PPA (n=1.5, 45 g) was heated at 100°C for 1 hr. The cooled mixture was poured into ice water and then extracted with chloroform. The residual product from the chloroform solution was crystallized from ethanol to give **5a**, mp 140—141°C (lit,[2] mp 141°C); 1.3 g (39%). Similarly, the acetyl, phenylacetyl, and β-phenylpropionyl compounds (**11a**, **5b**, **11b**, **5c**, **11c**, and **16c**) were also prepared by this procedure.

The Friedel-Crafts Acylation of the Methoxybenzofurans. Powdered aluminum chloride (9.7 g) was added, with stirring and cooling, to a solution of **2**[7] (5 g) and acetyl chloride (2.5 g) in carbon disulfide (50 m*l*); the mixture was stirred

Table 4. The UV spectra

Compd.	λ_{max}^{EtOH} mμ[a] (log ε)
	Methoxybenzofurans
2	214(4.33), 255(4.02), 292.5(3.68), 301(3.62)
8	217(4.41), 251(4.09), 285(3.01)
14	217(4.24), 249(4.06), 256(4.06), 292(3.72)
b)	215.5(4.34), 258(4.08), 276[s](3.55), 287(3.45)
	Hydroxybenzofurans
3	216(5.36), 255(5.13), 295(4.73)
9	216(4.36), 250(4.12), 255.5(4.12), 286(3.16)
15	216(5.36), 248(5.09), 255(5.08), 293(4.76)
c)	218(5.35), 252(5.03), 281(4.44), 289(4.41)
	Hydroxyketones
5a	230(4.20), 316(4.30)
5b	213.5(4.18), 231(4.22), 318(4.33)
11a	239(4.33), 296(4.16), 336(3.96)
11b	211(4.38), 239(4.32), 301(4.17), 341(4.01)
16a	240(4.56), 267(3.97), 360(3.55)
16b	240(4.55), 360(3.57)
d)	243(4.49), 265.5(3.98), 280.5(3.82), 345(3.51)
e)	211.5(4.16), 244(4.50), 253(4.47), 283(3.95), 348(3.56)
	Furocoumarins
17a	214(4.50), 323(4.49), 338(4.28)
17b	216(4.55), 332(4.42), 342[s](4.40)
17c	216(4.52), 328.5(4.33), 340(4.25)
18a	212(4.40), 239.5(4.45), 245.5(4.44), 265[s](3.98), 285[s](3.92), 296(4.04), 323.5(4.06)
18b	215.5(4.45), 236.5(4.38), 250[s](4.33), 302[s](4.00), 332(4.22)
18c	217(4.49), 249(4.36), 300.5(4.03), 326(4.11)
19c	216(4.47), 246(4.46), 253(4.40), 301(4.14), 320(4.11), 331[s](4.08)
	Furoisoflavones
20	253(4.43), 315(4.25)
21	240(4.43), 312(4.28)
22	261(4.59), 311(4.03)
23	257(4.57), 309(4.08)

a) s: Shoulder. b) 2,3-Dimethyl-4-methoxybenzofuran. c) 2,3-Dimethyl-4-hydroxybenzofuran. d) 2,3-Dimethyl-4-hydroxy-5-benzofuranyl methyl ketone. e) 2,3-Dimethyl-4-hydroxy-5-benzofuranyl benzyl ketone.

at room temperature for 2 hr and then at the reflux temperature for 1 hr. The cooled mixture was poured into ice water containing hydrochloric acid and extracted with chloroform. The chloroform solution was washed with an aqueous sodium hydroxide solution, and the residual product from the chloroform solution was crystallized from ethanol to give **5a**, mp 140—141°C, identical with the sample described above. Yield, 4.7 g (81%). Similarly, **5b** was obtained by the action of phenylacetyl chloride, while the methoxyketone (**4c**) was obtained in the case of β-phenylpropionyl chloride. The β-phenylpropionylation of **8** afforded a small amount of **11c** and a fairly large amount of the methoxyketone (**10c**), while that of **14** afforded a small amount of **16c** and fairly large amounts of the recovered **14** and indanone. The diacetylation of **2** afforded the hydroxydiketone (**6**).

*The Demethylation of the Methoxyketone (**4c**).* A mixture of **4c** (1.4 g), nitrobenzene (40 ml), and powdered aluminum chloride (0.9 g) was heated at 100°C for 1 hr. The cooled mixture was poured into dilute hydrochloric acid, and the nitrobenzene was removed by steam distillation. The residual precipitates obtained were crystallized from ethanol to give **5c**, mp 139—140.5°C, identical with the sample described above. Yield, 0.46 g (34%).

The Preparation of Furocoumarins. *a) From the Hydroxyketones*: Small pieces of sodium (1.1 g) was added to a mixture of **5a** (1.1 g) and diethyl carbonate (40 ml), after which the mixture was heated at 110—120°C for 30 min. The cooled mixture was treated with a small amount of methanol and with water, and was then extracted with ether. The aqueous layer was acidified, and the crystalline precipitates thus formed were recrystallized from ethanol to give 6*H*-8-hydroxy-2,3-dimethylfuro[2,3-*g*][1]benzopyran-6-one (**17a**), mp 308°C (dec.); 0.8 g (67.5%). Similarly, 7-phenyl and 7-benzyl derivatives (**17b** and **17c**) of **17a**, 8*H*-6-hydroxy-2,3-dimethylfuro[3,2-*h*][1]benzopyran-8-one (**18a**) and its derivatives (**18b** and **18c**), and 7*H*-6-benzyl-5-hydroxy-2,3-dimethylfuro[3,2-*g*][1]benzopyran-7-one (**19c**) were also prepared by this procedure.

b) From the Hydroxybenzofurans: A mixture of **3** (0.5 g) and diethyl benzylmalonate (2.5 g) was refluxed for 8 hr. The cooled mixture was washed with ether, and the residual solid was crystallized from ethanol to give **17c**, mp 285—286°C, identical with the sample described above. Yield, 0.54 g (55%). Similarly, **18c** and **19c** were also prepared by this procedure.

The Preparation of Furoisoflavones. *a) By the Action of Ethyl Orthoformate*: A mixture of the hydroxyketone **5b** (0.4 g), ethyl orthoformate (4 g), piperidine (1 drop), and pyridine (16 ml) was refluxed for 8 hr, after which the cooled mixture was poured into dilute hydrochloric acid to form crystalline precipitates, which were then recrystallized from ethanol to give 8*H*-2,3-dimethyl-7-phenylfuro[2,3-*g*][1]benzopyran-8-one (**20**), mp 233—234°C; 0.4 g (97%). Similarly, 6*H*-2,3-dimethyl-7-phenylfuro[3,2-*h*][1]benzopyran-6-one (**22**) was also prepared by this procedure.

b) By the Action of Ac_2O-AcONa: A mixture of **5b** (0.5 g), anhydrous sodium acetate (2 g), and acetic anhydride (10 ml) was refluxed for 12 hr, the cooled mixture was then poured into water to form crystalline precipitates, which were recrystallized from ethanol to give the 6-methylderivative (**21**) of **20**, mp 150.5—151.5°C; 0.15 g (28%). Similarly, the 8-methyl derivative (**23**) of **22** was also prepared by this procedure.

The authors are grateful to the members of the Laboratory of Analysis, Faculty of Pharmacology of Toyama University, for the microanalyses and the NMR spectroscopy.

Some Displacement Reactions of Neopentyl Type Bromide Derived from Thujopsene[1]

Masaaki Ito, Kazuo Abe, Hitoshi Takeshita,* and Mitsuyoshi Yatagai*

Department of Industrial Chemistry, Kitami Institute of Technology, Kitami, Hokkaido

* *Department of Chemistry, Tohoku University, Sendai*

(Received December 26, 1970)

The reaction of thujopsene with gaseous hydrogen bromide at low temperature affords a 48% yield of neopentyl type bromide. The reactivity of the homoallyl bromide was inspected. First, the neopentyl type bromide was derived to a diethyl widdryl malonate in order to demonstrate the reaction which indicates the involvement of homoallylcyclopropylcarbinyl ion system. The malonate was converted to a carboxylic acid and then to isomeric lactone. To demonstrate the reaction which suggests the retention of carbon frame work in the reaction, the reaction of the neopentyl bromide was extended to Grignard reaction. The Grignard reagent reacted with cyclohexanone gave a tertiary alcohol, whereas a dimeric hydrocarbon was also obtained through the Wurtz type condensation. The tertiary alcohol was converted to a dehydrated hydrocarbon and then a glycol.

It is known that reactions of thujopsene I with several acids cause skeletal rearrangements to give a variety of types of compounds according to conditions. Treatment of I with oxalic acid in alcoholic solution gave widdrol II, widdryl ether III,[2] β-chamigrene IV, cuparene V, and hydrocarbons,[3] while, the reaction of I or II with mineral acid afforded the epimeric pair of the neopentyl type chlorides VI and VII by hydrochloric acid[4] and alcohols VIII and IX by sulfuric acid.[3] We thought it worthwhile to extend this reaction with hydrobromic acid to obtain more reactive bromo derivatives which could be employed in some displacement reactions. I was reacted with gaseous hydrogen bromide at low temperature giving a neopentyl type bromide, but no isomeric pair of this type. Evidence for this will be described.

Treatment of thujopsene obtained from Thujopsis dolabrata Sieb. et Zucc. with anhydrous hydrogen bromide yielded the bromide X in 48% after purification by fractional distillation. Among other products, "the hydrocarbon II" XI[3] was obtained as a second major product. The IR spectrum of X showed C–Br stretching frequency at 670 cm^{-1}. Gas-liquid chromatography revealed I to be a single compound, and the data of elemental analysis gives the molecular formula $C_{15}H_{25}Br$. NMR spectrum of X showed very similar features to that of VI, *i.e.*, four methyl singlets at 1.02 (3 Me) and 1.15 ppm, a vinyl hydrogen at 5.08 (singlet), and signal ascribed to a methylene hydrogens at 3.18 ppm (2H singlet) suggesting the structure shown.

The reactivity of the homoallyl bromide system of X was inspected. First, we examined the displacement with diethyl sodiomalonate, typical carbanion. Product XII isolated was not a diethyl malonate derivative expected from simple substitution, but skeletal rearrangement accompanying its formation. The gas-liquid chromatogram of XII showed it to be a single compound and saponification equivalent of XII showed it to be a diester $C_{15}H_{25}CH(COOC_2H_5)_2$. The NMR spectrum of XII showed, beside ethoxyl groups, (1.27 (6H) and 4.08 (4H)), 1.07 (3 Me, overlapping singlet), 1.00 (Me, singlet), 5.47 (1H, d, d, J=10.5, 6.0 Hz), and 3.20 (1H, s). Since the splitting pattern of the above olefinic proton signal accords with that of II,[5] XII must possess the widdryl skelton, and therefore its structure was deduced as diethyl widdryl malonate. Alkaline hydrolysis of XII gave a carboxylic acid XIII which, upon treatment with sulfuric acid in alcohol, afforded an isomeric lactone XIV in good yield. The carbonyl stretching frequency of XIV (1720 cm^{-1}), the lactonic ring, was free from a strain.

The rearrangement clearly indicates the involvement of homoallyl-cyclopropylcarbinyl ion system. Thus, the geometrical requirement for these interconversion leads to the α-orientation for the malonate moiety.

We extended the reaction of the neopentyl bromide X to Grignard reaction since the above mentioned homoallylcyclopropyl carbinyl ion should not be involved. The reaction with cyclohexanone was carried out in ether in the usual manner. The major product isolated by fractional distillation was found to be a tertiary alcohol XV. Its NMR spectrum revealed a sharp singlet at 5.30 ppm for an olefinic hydrogen, suggesting the retention of carbon frame work in the reaction. Four methyl signals at 0.99 (3H, s), 1.06 (3H, s), and 1.29 (6H, s) were in expected positions. When XV was passed through a silica gel column (Wako Gel Q-50), dehydrated hydrocarbon XVI was formed in nearly quantitative yield. Gas-liquid chromatogram of XVI proved it to be a single compound, whose NMR spectrum showed two singlets at 5.08 and 5.30 ppm. The singlet nature of the second olefinic hydrogen can not make the structure of XVI be regarded as XVIa, since various types of olefinic

1) This paper was read before 12th Symposium of Terpene, Essential Oil and Aromatics, Hamamatsu, Oct. 1968.

2) S. Nagahama, H. Kobayashi, and S. Akiyoshi, This Bulletin, **33**, 1467 (1960).

3) S. Ito and M. Yatagai, to be published. This part of work appared in the Abstract Papers of 14th Symposium on the Chemistry of Natural Products, p. 174, Fukuoka, Oct. 1970.

4) W. G. Dauben and L. E. Friedrich, *Tetrahedron Lett.*, **1967**, 1735.

5) S. Ito, K. Endo, H. Takeshita, T. Nozoe, and J. B. Stothers, *Chem. Ind.* (London), **1961**, 1618.

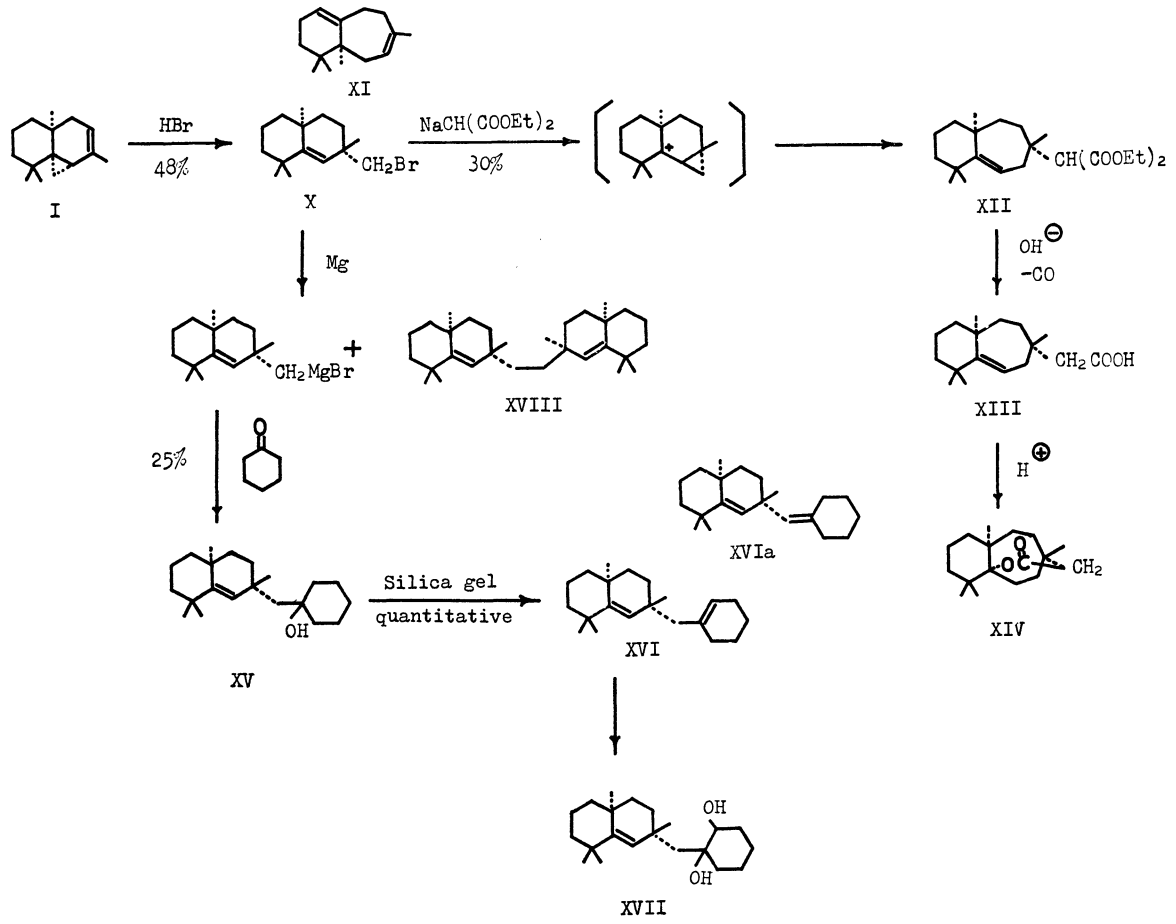

Scheme 1

hydrogen of cyclohexene often appeared without clear splittings. We carried out oxidation with osmium tetraoxide to afford the glycol XVII which clearly revealed a signal at 3.87 ppm due to a presence of a carbinyl proton with adjacent methylene group. Thus, the structure of XVI is as depicted.

The remaining crystalline mass on distillation of XV was recrystallized and gave a dimeric hydrocarbon XVIII in 14% yield. Its structure was deduced from elemental analysis, osmometric molecular weight determination, and mainly from the NMR spectrum which has a sharp singlet at 5.00 (2H), 0.91 (6H), 1.05 (6H), 1.09 (6H), and 1.13 (6H) ppm respectively, indicating a symmetric structure. We tried to obtain the same hydrocarbon on simple hydrolysis of the Grignard reagent and found the formation of XVIII in a fairly high yield through the Wurtz type condensation.

Experimental

All infrared absorption spectra were measured with a Shimadzu Model IR-27G grating spectrophotometer and the NMR spectra on a varian A-60A analytical spectrometer using tetramethylsilane as an internal standard. Gas-liquid chromatographic data were measured on a Shimadzu GC-1C gaschromatograph, using helium as a carrier gas. All melting points were obtained on a Büchi micro melting point apparatus and are uncorrected. Analyses performed on a Micro-Analyser, Shimadzu.

Thujopsene. This was isolated from Cedar H oil by repeated rectification: bp 119—120°C/10 mmHg, d_{20}^{20} 0.9362, n_D^{20} 1.5033, $[\alpha]_D^{20}$ −93.68.

Neopentyl-type Bromide of Thujopsene. Into freezing thujopsene in a round bottomed 200 m*l* flask was passed dry hydrogen bromide generated by dropping bromine into a mixture of red phosphorus and water and drying with calcium bromide, until absorption reached the calculated volume. The bromides were obtained in 48% yield at reaction temperature −20°C and in 40% at 0°C. The product was then dissolved in ether, washed with water, dried over calcium bromide and distilled, a fraction 149—151°C/10 mmHg, d_{20}^{20} 1.1592, $[\alpha]_D^{27}$ +83 (2% CCl_4) being collected. The gas-liquid chromatogram of the fraction exhibited two peaks, partly overlapping, due to compound X (*ca.* 70%, first eluted) and compound XI (*ca.* 30%, second eluted) which was identical with the authentic sample. The IR spectrum of X showed C–Br absorption at 15 μ.

Found: C, 63.82; H, 8.90%. Calcd for $C_{15}H_{25}Br$: C, 63.16; H, 8.83%.

No attempt was made to separate these two compounds on a preparative scale. The crude product was used directly in the following reactions.

Preparation of the Diethyl Malonate Derivative starting from the Neopentyl-type Bromide of Thujopsene. To an alcoholic solution of sodium ethylate containing 1.7 g metallic sodium (0.075 mol) and 40 m*l* absolute alcohol in an ice bath was added dropwise 12 g (0.075 mol) of diethyl malonate in a

100 ml flask equipped with a magnetic stirrer, and then 21.4 g (0.075 mol) of bromide X dropwise. The mixture was stirred for 0.5 hr after the addition was completed and then refluxed for 22 hr. The solvent was removed on a steam bath. The reaction mixture was poured into water and extracted with ether. The ether solution was dried and the solvent removed on the steam bath with a rotary evaporator. Analytically pure material XII bp 218—219°C/10 mmHg, d_{20}^{20} 1.0363, n_D^{20} 1.4891. $[\alpha]_D^{18}$ +87.4 (CCl_4), was obtained by further distillation. The yield was 30% theoretically. IR (carbon tetrachloride): $\nu_{C=O}$ 1752 cm^{-1} (S), 1726 cm^{-1} (S), λ_{max}^{MeOH} 215 mμ.

Found: C, 72.45; H, 9.83%. Calcd for $C_{22}H_{36}O_4$: C, 72.49; H, 9.95%.

Preparation of the Lactone XIV: Starting from the Diethyl Malonate XII. 814 mg (2.24 mmol) of XII was hydrolyzed in alcohol with 751 mg (13.4 mmol) of potassium hydroxide for 2 hr. After the usual work-up 762 mg of the dicarboxylic acid was obtained and then decarboxylated 2 hr at 150°C under a pressure of 20 mmHg. The resulting residue (160 mg) was dissolved in chloroform (7 ml) and the solution was added to a mixture of concentrated sulfuric acid (2 ml) and chloroform (2 ml) at −5°C. The mixture was swirled in an ice bath for 5 min and then poured on ice. The product was extracted with dichloroethane; the extract was washed with potassium bicarbonate solution and dried and the solvent was removed. Preparative tlc of the reaction mixture gave 16.5 mg of pure lactone XIV. The IR spectrum showed C=O absorption at 1720 cm^{-1}.

Grignard Reaction of Bromide X with Cyclohexanone. The Grignard reagent was prepared from 27.4 g (0.075 mol) of bromide X, 2.0 g (0.083 mol) of magnesium, and 10 ml of absolute ether in the usual way. It was cooled and 7.4 g (0.075 mol) of cyclohexanone in absolute ether was added dropwise with stirring for over 1 hr, cooled, and poured into a mixture of ice and an aqueous ammonium chloride solution. The ether layer was separated, and the aqueous layer was washed twice with ether. The combined ether extracts were washed with water, dried over anhydrous sodium sulfate, and evaporated to leave crude oil which upon distillation at 202—203°C/10 mmHg gave 5.7 g (25%) of XV as a colorless liquid. The thin-layer chromatogram (silica gel, *n*-heptane : ethylmethyl ketone=80 : 20) showed a spot at R_f 0.89. The gas-liquid chromatogram showed a single peak. The molecular weight was determined to be 298.5 (Calcd for 304.5). IR (carbon tetrachloride): ν_{OH} 3550 cm^{-1} (S).

Found: C, 82.48; H, 11.78%. Calcd for $C_{21}H_{36}O$: C, 82.83; H, 11.12%.

The distillation residue of the reaction mixture gave a crystalline compound XVIII after recrystallization from ethyl acetate. Analytically pure material melted at 88—89°C, $[\alpha]_D^{20}$ +69.4 (CCl_4), molecular weight: Found 408.4 (Calcd 410.7). IR (carbon tetrachloride: ν_{C-H} 2840, 2850, 2910, 2950, 3025 cm^{-1}.

Found: C, 88.02; H, 12.13%. Calcd for $C_{30}H_{50}$: C, 87.73; H, 12.27%.

The Grignard reagent prepared from 2.0 g (0.01 mol) of bromide X in the manner mentioned above was, hydrolyzed directly with a mixture of ice and an aqueous ammonium chloride solution. Crude crystalline XVIII weighed 2.4 g.

The melting point, mixed melting point and IR spectrum were identical with those of the by-product of the Grignard reaction mentioned above.

Dehydration of Tertiary Alcohol XV to Hydrocarbon XVI on a Silica-gel Column. Chromatagraphy of XV over a column of silica-gel (Wako-gel Q-50) using petroleum ether gave 2 g of XVI, n_D^{20} 1.5159, $[\alpha]_D^{20}$ +101.1 (CCl_4). The gas-liquid chromatogram showed a single peak. The molecular weight was determined to be 283 (calcd 286). IR (carbon tetrachloride): ν_{C-H} 2815, 2915, 3150 cm^{-1}. NMR (CCl_4), 5.09 (1H, singlet olefinic proton), 5.30 (1H, singlet olefinic proton) ppm.

Found: C, 87.64; H, 11.90%. Calcd for $C_{21}H_{34}$: C, 88.04; H, 11.96%.

Osmium Tetraoxide Oxidation of Hydrocarbon XVI. Five hundred milligrams of XVI was oxidized in chloroform and pyridine with 550 mg of osmium tetraoxide overnight. The reaction mixture was washed with water and the reagent was removed by passage of hydrogen sulfide into the solution and filtration. Pale yellow oil obtained by evaporation of the solvent was fractionated through the silica gel column to yield 50 mg of XVII. Colorless liquid.

Found: C, 78.55; H, 11.41%. Calcd for $C_{21}H_{31}O_2$: C, 78.69; H, 11.32%.

The authors wish to express their gratitude to Professor S. Ito for stimulating discussions, and to Takasago Perfumery Co., Ltd., for the donation of Cedar H.

Tetraaminoethylenes. I. The Preparation and Some Reactions of Tetrapiperidino- and Tetramorpholinoethylene[1]

Otohiko TSUGE, Kiyoshi YANAGI*, and Masako HORIE
Research Institute of Industrial Science, Kyushu University, Hakozaki, Fukuoka

(Received January 11, 1971)

The preparation of new tetraaminoethylenes was attempted by the reaction of chlorotrifluoroethylene (CTFE) with several amines. It has been found that CTFE reacted with piperidine and morpholine to give tetrapiperidino- (TPE) and tetramorpholinoethylene (TME) in moderate yields respectively, although no tetraaminoethylenes were formed in the reactions with diethylamine, pyrrolidine, aniline, *N*-alkylaniline, and diphenylamine. Also, it has been made clear that the compounds whose structures were previously assigned to the tetraaminoethylenes, obtained from 1,1-dimethoxytrimethylamine or ethyl orthoformate and secondary amines are the corresponding triaminomethanes. It has been found that TPE and TME reacted with halogens, halogen-, nitrocompounds, and aromatic carboxylic acids to form mainly the corresponding oxamidinium salts.

Tetraaminoethylenes, such as tetrakis(dimethylamino)ethylene (TDAE) and bi(1,3-diphenylimidazolidin-2-ylidene), are characterized both by their odor and by the versatility of their chemical reactivity.[2-6] Such current interest in unusually reactive tetraaminoethylenes prompted us to investigate the preparation of new tetraaminoethylenes and their chemistry.

In this paper, we wish to report the preparation of tetrapiperidino- (TPE) and tetramorpholinoethylene (TME), which are new tetraaminoethylenes, and their unusual reactions with halogens, halogen-, nitrocompounds, and aromatic carboxylic acids.

Results and Discussion

The Preparation of TPE and TME. An attempt was made to prepare new tetraaminoethylenes by the reactions of chlorotrifluoroethylene (CTFE) with aliphatic and aromatic amines according to Pruett's procedure.[7]

The reaction of CTFE with diethylamine gave only the compound assumed to be 1,2-bis(diethylamino)-1-chloro-2-fluoroethylene, while pyrroridine and aniline reacted with CTFE to give unidentified compounds, all in low yields. Also, no reactions of CTFE with *N*-alkylanilines and diphenylamine took place.

Although the preparation of new tetraaminoethylenes caused such difficulties, it has been found that similar reactions of CTFE with piperidine and morpholine afforded the expected tetraaminoethylenes, TPE (mp 151—152°C) and TME (mp 186—190°C), in moderate yields, accompanied by small amounts of the corresponding *N*-(diaminoacetyl)amines, whose structures were assumed on the basis of the elemental analyses and study of the IR spectra.

The structures of TPE and TME were confirmed by spectral studies as well as by elemental analyses; the molecular formulae of TPE and TME agreed with $C_{22}H_{40}N_4$ (M^+ *m/e* 360) and $C_{18}H_{32}O_4N_4$ (M^+ *m/e* 368) respectively.

After the completion of this work, we learned that two routes for the preparation of tetraaminoethylenes have been reported. Winberg *et al.*[8] described that tetraaminoethylenes, including TPE and TME, were obtained by the reactions of 1,1-dimethoxytrimethylamine with aliphatic secondary amines, and that TPE and TME melted at 59—61 and 170—171°C respectively. On the other hand, it has been reported by Hagedorn and Lichtel[9] that ethyl orthoformate reacted with *N*-alkylanilines to give the corresponding tetrakis(*N*-alkylanilino)ethylenes, which could not be obtained by Pruett's method, as has been mentioned above. However, it is surprising that the molecular weight (calculated value, 504.7) of tetrakis(*N*-ethylanilino)ethylene, mp 180—182°C (decomp.), was observed to be 312 or 336 by the vapor-pressure-osmometric determination.

In order to see whether or not the reported compounds are real tetraaminoethylenes, the reaction of 1,1-dimethoxytrimethylamine or ethyl orthoformate with amines was investigated. The reactions of 1,1-dimethoxytrimethylamine with piperidine and morpholine did not give any TPE and TME, but compounds which decomposed rapidly in air were obtained in low yields; these compounds were as-

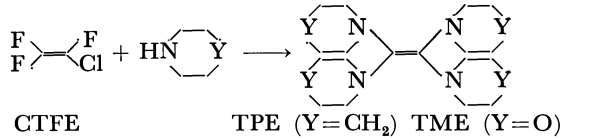

CTFE TPE (Y=CH_2) TME (Y=O)

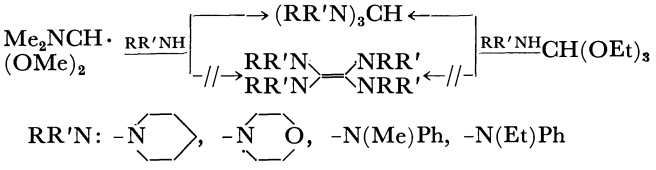

RR'N: -N⟨ ⟩, -N⟨ ⟩O, -N(Me)Ph, -N(Et)Ph

1) Presented at the 19th Annual Meeting (Yokohama, April, 1966) and the Kyushu Meeting (Fukuoka, October, 1966) of the Chemical Society of Japan.

* Present address: Department of Industrial Chemistry, The Second Engineering Faculty, Kinki University, Iizuka-shi, Fukuoka.

2) N. Wiberg and J. W. Buchler, *Chem. Ber.*, **96**, 3000 (1963).

3) N. Wiberg and J. W. Buchler, *ibid.*, **96**, 3223 (1963).

4) D. M. Lemal, R. A. Lovald, and K. I. Kawano, *J. Amer. Chem. Soc.*, **86**, 2518 (1964).

5) H. W. Wanzlick, B. Lachmann, and E. Schikora, *Chem. Ber.*, **98**, 3170 (1965).

6) H. E. Winberg and D. D. Coffman, *J. Amer. Chem. Soc.*, **87**, 2776 (1965.)

7) R. L. Pruett, J. T. Barr, K. E. Rapp, C. T. Bahner, J. D. Gibson, and R. H. Lafferty, *ibid.*, **72**, 3649 (1950).

8) H. E. Winberg, J. E. Carnahon, D. D. Coffman, and M. Brown, *ibid.*, **87**, 2055 (1965).

9) I. Hagedorn and K. E. Lichtel, *Chem. Ber.*, **99**, 524 (1966).

sumed, on the basis of the results of the elemental analyses, to be tripiperidino-, mp 52—56°C, and trimorpholinomethane, mp 142—147°C, respectively. Contrary to expectation, *N*-methyl- and *N*-ethylaniline reacted with ethyl orthoformate to afford tris(*N*-methylanilino)-, mp 268—269°C (decomp.), and tris(*N*-ethylanilino)methane, mp 181—185°C (decomp.), respectively. The structures of these compounds were established by the spectral studies as well as by the elemental analyses. Also, the reaction of ethyl orthoformate with morpholine or of 1,1-dimethoxytrimethylamine with *N*-ethylaniline gave the corresponding triaminomethanes.

It may be concluded from the above facts that TPE and TME obtained in this work are valid, and that the reported compounds were previously erroneously assigned to the tetraaminoethylenes.

The Reactions of TPE and TME with Halogens. Wiberg and Buchler[3] found that TDAE was oxidized easily with halogens, especially with bromine and iodine, to give the corresponding octamethyl-oxamidinium dihalides, $TDAEX_2$, and that several periodides, $TDAEI_n$ (n=4, 5, and 7), were also formed in the oxidation with iodine.

When chlorine gas was slowly passed through a benzene solution of TPE and TME at 0°C, the dichlorides $TPECl_2$, mp 240—241°C (decomp.) and $TMECl_2$, mp 265—266°C (decomp.), were obtained in good yields. Similarly, TPE and TME reacted with equimolar amounts of bromine and iodine to give the corresponding dihalides, $TPEBr_2$, mp 247°C (decomp.), $TPEI_2$, mp 282—284°C (decomp.), $TMEBr_2$, mp 300°C (decomp.), and $TMEI_2$, mp *ca.* 190°C (decomp.), respectively, accompanied by trace amounts of the hexahalides, $TPEBr_6$ and $TPEI_6$, in the reaction of TPE:

Table 1. Reactions of TPE and TME with halogens

TPE or TME	X_2	Reaction conditions: Solvent	Temp. (°C)	Time (min)	Products yields (%): $TPEX_2$ or $TMEX_2$	$TPEX_6$
TPE	Cl_2	benzene	0	15	100	
TME	Cl_2	benzene	0	15	80	
TPE	Br_2	*n*-hexane	0	10	70	+[a]
TME	Br_2	*n*-hexane	0	10	70	
TPE	I_2	benzene	0	10	88	+[a]
TME	I_2	benzene	0	10	24	

a) A plus sign, +, indicates a trace amount.

The above hexahalides were easily formed by the further reaction of $TPEBr_2$ or $TPEI_2$ with bromine or iodine, but the dihalides, $TPECl_2$, $TMECl_2$, $TMEBr_2$, and $TMEI_2$, did not give any perhalides under similar conditions.

The structures of dihalides were confirmed, by a study of the IR spectra as well as by the chemical transformations, to be the corresponding oxamidinium dihalides. The IR spectra of all the dihalides exhibited remarkably strong absorption bands which can be ascribed to the $[\rangle N{=}C{=}N\langle]^{\oplus}$ at 1620 and 1640 cm^{-1}. Also, the ion peak which corresponded to the molecular ion of TPE or TME appeared as the ion peak of the highest mass number in the respective mass spectra of dihalides.

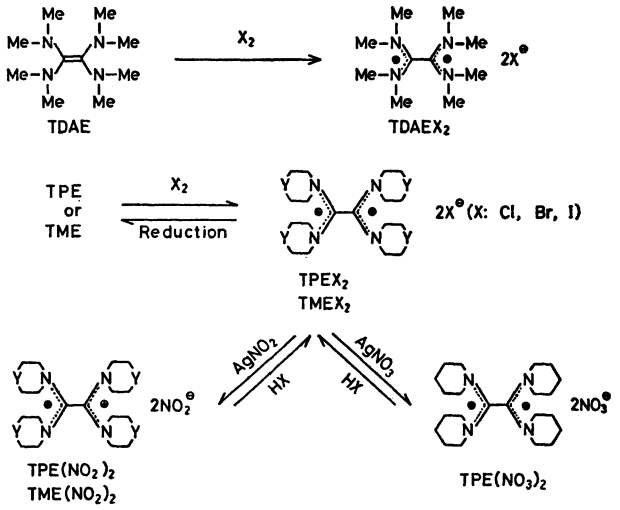

The dihalides in aqueous solutions were reduced with zinc dust to the original TPE or TME, although TME could not be isolated because of its instability in relation to water. Furthermore, when the dihalides were treated with silver nitrite or nitrate, the corresponding dinitrites $TPE(NO_2)_2$ and $TME(NO_2)_2$ or dinitrate $TPE(NO_3)_2$, whose IR spectra were similar to those of the corresponding dihalides, were obtained quantitatively.

Also, the dinitrites and dinitrate were easily transformed to the corresponding dihalides in the treatment with hydrogen halides. Incidentally, the hexahalides, $TPEX_6$, were reduced with zinc dust to give TPE.

The above observations indicate that the dihalides, dinitrites, and dinitrate are the corresponding oxamidinium salts. The results of the reactions of TPE or TME with halogens are shown in Table 1.

The Reactions of TPE and TME with Halogen-Compounds. It has been reported that TDAE reacted with cuprous chloride or carbon tetrachloride to give the dichloride, $TDAECl_2$, with the deposition of copper metal or decomposition of carbon tetrachloride.[3]

The reactions of TPE or TME with various organic halogen-compounds were also investigated. In all cases, the corresponding dihalides were obtained; the results are summarized in Table 2.

In particular, it is noteworthy that the compounds originated from the starting halogen-compounds were isolated in the reactions with benzal chloride, benzotrichloride, benzenesulfonyl chloride, phenacyl bromide, and 2,2-dichloroacenaphthenone: stilbene and 1,1,2,2-tetrachloro-1,2-diphenylethane (tolan tetrachloride), tolan tetrachloride, diphenyldisulfone, biphenacyl, and diacenaphthylidenedione were isolated respectively.

As is shown in Table 2, the yield of $TPECl_2$ in the reaction of TPE with benzyl chloride in the pres-

Table 2. Reactions of TPE and TME with halogen-compounds

TPE or TME	Halogen-compound	Reaction conditions			Products yields (%)[a]		
		Solvent	Temp. (°C)	Time (min)	$TPEX_2$ or $TMEX_2$		
TPE	$CHCl_3$	b)	reflux	180	40		
TME	$CHCl_3$	benzene	room temp.	30	+		
TPE	$CHBr_3$	benzene	room temp.	30	57		
TME	$CHBr_3$	benzene	room temp.	30	30		
TPE	CHI_3	benzene	room temp.	30	70		
TME	CHI_3	benzene	room temp.	30	47		
TPE	CCl_4	b)	0	30	66		
TME	CCl_4	b)	room temp.	120	40		
TPE	$PhCH_2Cl$	benzene	reflux	180	14		
TPE	$PhCH_2Cl$	benzene	reflux	60	9		
TPE	$PhCH_2Cl$	benzene	reflux	60	30[c]		
TPE	$PhCH_2Cl$	benzene	reflux	60	+[d]		
TME	$PhCH_2Cl$	benzene	reflux	180	10		
TPE	$PhCHCl_2$	benzene	reflux	30	83	$PhCCl_2CCl_2Ph$ $PhCH=CHPh$	10 +
TME	$PhCHCl_2$	benzene	reflux	30	40		
TPE	$PhCCl_3$	benzene	60	15	96	$PhCCl_2CCl_2Ph$	40
TME	$PhCCl_3$	benzene	60	15	51		
TPE	PhCOCl	benzene	40—50	120	86		
TME	PhCOCl	benzene	40	120	82		
TPE	$PhSO_2Cl$	benzene	room temp.	120	90	$PhSO_2SO_2Ph$	20
TME	$PhSO_2Cl$	benzene	room temp.	120	90	$PhSO_2SO_2Ph$	20
TPE	$PhCOCH_2Br$	benzene	60	30	70	$(PhCOCH_2)_2$	44
TPE	DCA[e]	benzene	room temp.	10	50	Diacenaphthylidenedione	27

a) A plus sign, +, indicates a trace amount.
b) The halogen-compound was used as the solvent respectively.
c) In the presence of benzoyl peroxide.
d) In the presence of *p*-benzoquione.
e) DCA: 2,2-Dichloroacenaphthenone.

ence of benzoyl peroxide is higher than in either the absence or presence of *p*-benzoquinone.

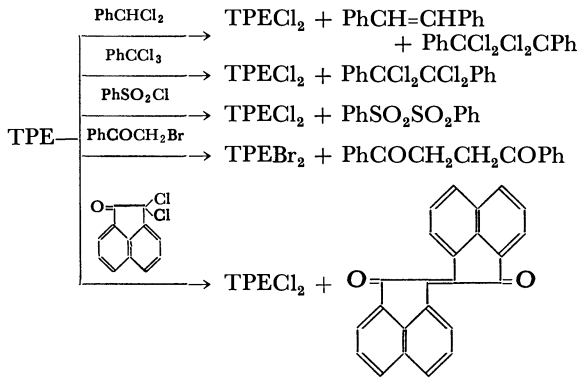

On the basis of the above facts, it seemed reasonable to assume that these reactions proceed through a free radical process.

The Reactions of TPE or TME with Nitro-Compounds. Previous investigations of the reactions of tetraaminoethylenes with nitro-compounds have not been extended beyond the reactions of TDAE with nitrobenzenes[10] and of bi(1,3-diphenylimidazolidin-2-ylidene) with nitromethane.[11]

The reactions of TPE or TME with several nitro-compounds were investigated.

It has been found that TPE and TME reacted with phenylnitromethane to give the respective dinitrites, $TPE(NO_2)_2$ and $TME(NO_2)_2$, which were identical with those obtained from the dihalides and silver nitrite. Surprisingly, TPE reacted with tetranitromethane to give a 1 : 2 addition product of TPE and tetranitromethane, accompanied by a small amount of the dinitrate, $TPE(NO_3)_2$. The nitrate was identified by a comparison of its IR spectrum with that obtained by the reaction of $TPEX_2$ with silver nitrate.

In the same way as in the case of TDAE,[10] TPE or TME formed charge-transfer complexes with nitrobenzene (NB), *m*-dinitro- (DNB), and 1,3,5-trinitrobenzene (TNB). Although purple-colored complexes with NB and DNB were not obtained as crystals, these complexes were established, by a spectroscopic estimation of the intensities of the absorption peaks at 514 mμ for TPE-NB, 450 mμ for TME-NB, 580 mμ for TPE-DNB, and 476.8 mμ for TME-DNB complex, to be TPE(NB), TME(NB), $TPE(DNB)_2$, and $TME(DNB)_2$ complexes respectively.

On the other hand, TPE reacted with TNB to form the charge-transfer complex $TPE(TNB)_2$, mp 122—124°C (decomp.), as a purple solid; it gradually decomposed in air.

10) N. Wiberg and J. W. Buchler, *Chem. Ber.*, **97**, 618 (1964).
11) H. -W. Wanzlick and E. Schikora, *ibid.*, **94**, 2389 (1961).

$$\text{TPE or TME} \xrightarrow{PhCH_2NO_2} \text{TPE}(NO_2)_2 \text{ or } \text{TME}(NO_2)_2$$

$$\text{TPE} \xrightarrow{C(NO_2)_4} \text{TPE}(NO_3)_2 + \text{TPE}[C(NO_2)_4]_2$$

$$\text{TPE or TME} \xrightarrow{NB} \text{TPE(NB) or TME(NB)}$$

$$\text{TPE or TME} \xrightarrow{DNB} \text{TPE}(DNB)_2 \text{ or } \text{TME(DNB)}$$

$$\text{TPE} \xrightarrow{TNB} \text{TPE}(TNB)_2$$

$$\text{TPE or TME} \xrightarrow{CH_3NO_2} \text{Y}\!\!<\!\!\text{N-CH=CH-NO}_2 \quad (\text{Y}=\text{CH}_2 \text{ or O})$$

Wanzlick and Schikora[11] found that bi(1,3-diphenylimidazolidin-2-ylidene) reacted with nitromethane to give 1,3-diphenyl-2-nitromethylimidazolidine upon the cleavage of the >C=C< bond in the ethylene.

When a benzene solution of TME or TPE was heated with nitromethane under an atmosphere of nitrogen, 1-nitro-2-piperidinoethylene, mp 94—95°C, or 2-morpholino-1-nitroethylene, mp 139—140°C, was obtained respectively.[12] The structures of the enamines were established by spectral studies as well as by elemental analyses.

The Reaction of TPE with Aromatic Carboxylic Acids. Little attention has been paid to the reactions of tetraaminoethylenes with carboxylic acids.

When a benzene solution of TPE was allowed to react with benzoic acid at room temperature, a compound, mp 104—105°C, was obtained as colorless needles. In the treatment with hydrobromic acid, the compound was easily transformed to $TPEBr_2$. The compounds was confirmed, by a study of its IR spectrum as well as by the elemental analysis, to the oxamidinium dibenzoate, $TPE(PhCO_2)_2$.

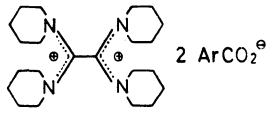

$TPE(ArCO_2)_2$ (Ar=Ph, p-MeC_6H_4, p-ClC_6H_4)

Similar reactions of TPE with *p*-methyl- and *p*-chlorobenzoic acid gave the corresponding oxamidinium salts, $TPE(p\text{-}MeC_6H_4CO_2)_2$, mp 101—103°C, and $TPE(p\text{-}ClC_6H_4CO_2)_2$, mp 109—111°C.

Experimental

All the melting and boiling points are uncorrected. The IR spectra were measured in KBr disks unless otherwise described, while the NMR spectra were determined at 60 MHz with a Hitachi R-20 spectrometer, using TMS as the internal reference. The mass spectra were obtained on a Hitachi RMS-4 spectrometer, using a direct inlet and an ionization energy of 70 eV.

The Reactions of CTFE with Amines. *i) With Piperidine*: In a 200 m*l*-autoclave cooled in a dry ice-methanol bath, 15 g (0.1 mol) of CTFE, which has been prepared from trichlorotrifluoroethane by the reported method,[13] and 110 g (1.92 mol) of piperidine were placed as rapidly as possible. The reaction mixture was stirred at room temperature for 3 hr and then at 80°C for 8 hr; during this time, the mixture gradually solidified and became difficult to stir. After the reaction mixture had been cooled, it was extracted with 500 m*l* of petroleum ether (bp 30—45°C), leaving a mixture of insoluble piperidinium chloride and fluoride. The extract was concentrated *in vacuo* under an atmosphere of nitrogen to yield 30 g (64%) of TPE; this, on recrystallization from ethyl acetate, afforded colorless needles, mp 151—152°C.

Found: C, 73.54; H, 11.30; N, 15.53%. Calcd for $C_{22}H_{40}N_4$: C, 73.38; H, 11.18; N, 15.55%. NMR spectrum in benzene: δ 0.86 (24H, multiplet) and 2.33 ppm (16H, multiplet). UV spectrum in *n*-hexane λ_{max} mμ (ε): 231.6 (15000), 258.4 (9900). Mass spectrum: *m/e* 360 (M^+), 275 ($M^+ -$ 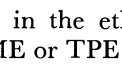), 193 ($275^+ -$ 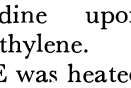), 110 ($193^+ -$ 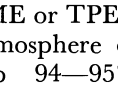), 84 (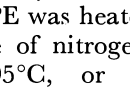).

Also, a trace amount of *N*-(dipiperidinoacetyl)piperidine, mp 93—94°C, was isolated from the mother liquor of recrystallization.

Found: C, 69.41; H, 10.76; N, 14.23%. Calcd for $C_{17}H_{31}ON_3$: C, 69.56; H, 10.65; N, 14.31%. IR spectrum (Nujol): 1635 cm^{-1} ($\nu_{C=O}$).

ii) With Morpholine: In the same manner as in the reaction with piperidine, a mixture of 15 g (0.1 mol) of CTFE and 110 g (1.26 mol) of morpholine was heated at 70°C for 6 hr. After the reaction mixture had then been extracted with 1 *l* of ethyl acetate, the extract was concentrated *in vacuo* under an atmosphere of nitrogen to give 22 g (47%) of crude TME. Recrystallization from ethyl acetate gave colorless prisms, mp 186—190°C.

Found: C, 58.60; H, 8.92; N, 15.19%. Calcd for $C_{18}H_{32}O_4N_4$: C, 58.67; H, 8.76; N, 15.21%. NMR spectrum in benzene: δ 2.72 (16H, multiplet) and 3.54 ppm (16H, multiplet). UV spectrum in *n*-hexane λ_{max} mμ (ε): 222.5 (15000), 275.5 (9900). Mass spectrum: *m/e* 368 (M^+).

From the mother liquor of recrystallization, *N*-(dimorpholinoacetyl)molpholine, mp 125—126°C, was obtained in a trace amount.

Found: C, 56.03; H, 8.63; N, 13.99%. Calcd for $C_{14}H_{25}O_4N_3$: C, 56.17; H, 8.42; N, 14.04%. IR spectrum: 1640 cm^{-1} ($\nu_{C=O}$).

iii) With Diethylamine: A similar reaction of 15 g (0.1 mol) of CTFE with 100 g (1.37 mol) of diethylamine at 80°C for 10 hr gave 28 g of diethylammonium halide and 25 g (89%) of a colorless liquid bp 46°C/0.5 mmHg, which was assumed to be 1,2-bis(diethylamino)-1-chloro-2-fluoroethylene.

Found: C, 53.93; H, 9.33; N, 12.23%. Calcd for $C_{10}H_{20}N_2FCl$: C, 53.92; H, 9.05; N, 12.58%.

A similar reaction of CTFE with pyrrolidine or aniline gave only a small amount of an unidentified compound as yellow crystals, mp 68.5—69.5°C (Found: C, 67.84; H, 6.69; N, 15.58%), or as red prisms, mp 209—210°C (Found: C, 80.97; H, 5.20; N, 13.61%), respectively. Also, no reactions of CTFE with *N*-alkylaniline and diphenylamine took place under similar conditions.

The Reaction of 1,1-Dimethoxytrimethylamine with Morpholine. After a mixture of 10 g of 1,1-dimethoxytrimethylamine[14]

12) We found that various compounds having an active methyl or methylene group reacted with TPE and TME in the same manner as in the case of nitromethane, affording the corresponding enamines. The results will be reported in the near future.

13) H. S. Booth, P. E. Burchfield, E. M. Bixby, and J. B. McKelvey, *J. Amer. Chem. Soc.*, **55**, 2231 (1933).

14) H. Eilingsfeld, M. Seefelder, and H. Weidinger, *Chem. Ber.*, **96**, 2671 (1963).

and 10 g of morpholine had been vigorously refluxed for 5 hr, the unreacted materials were distilled out *in vacuo* to leave colorless crystals. Recrystallization from ethyl acetate gave 3.1 g (10%) of trimorpholinomethane, mp 142—147°C, as colorless needles which easily decomposed in air.

Found: C, 57.24; H, 9.29; N, 15.10%. Calcd for $C_{13}H_{25}O_3N_3$: C, 57.61; H, 9.30; N, 15.51%.

A similar reaction of 1,1-dimethoxytrimethylamine with piperidine gave colorless crystals, mp 52—56°C, bp 147°C/3 mmHg. This compound was assumed to be tripiperidinomethane, but no elemental analysis could be carried out because of its instability.

The Reactions of Ethyl Orthoformate with N-*Alkylanilines. i) With* N-*Methylaniline*: A mixture of 7.4 g (0.05 mol) of ethyl orthoformate and 5.3 g (0.05 mol) of *N*-methylaniline was stirred with one drop of concentrated sulfuric acid at room temperature for 2 hr: during this time a suspended reaction mixture changed into a clear solution. The removal of the unreacted materials by distillation *in vacuo* gave 3 g of colorless crystals. The crystals were washed with methanol and then recrystallized from dimethylformamide to afford tris(*N*-methylanilino)methane, mp 268—269°C (decomp.), as colorless prisms.

Found: C, 79.86; H, 7.76; N, 12.74%. Calcd for $C_{22}H_{25}N_2$: C, 79.70; H, 7.60; N, 12.68%.

ii) With N-*Ethylaniline*: A mixture of 44.5 g (0.3 mol) of ethyl orthoformate and 36.4g (0.3 mol) of *N*-ethylaniline was gently refluxed for 20 hr. The reaction mixture was then concentrated *in vacuo*, leaving 0.6 g of colorless crystals. The crystals were washed with diethyl ether and then recrystallized from acetone to give tris(*N*-ethylanilino)methane, mp 181—185°C (decomp.), as colorless prisms.

Found: C, 80.76; H, 8.67; N, 11.19%. Calcd for $C_{25}H_{31}N_3$: C, 80.38; H, 8.37; N, 11.25%. NMR spectrum in deuterochloroform: δ 6.76 (15H, phenyl protons), 5.76 (1H, singlet, methine proton), 3.39 (6H, methylene protons) and 1.09 ppm (9H, methyl protons). UV spectrum in chloroform λ_{max} mμ (ε): 249.5 (28100), 295.5 (5140).

The Reactions of TPE and TME with Halogens. The reaction of TPE with bromine will be described as a representative reaction. When an equimolar amount of bromine was added to a solution of 0.5 g of TPE in 10 m*l* of *n*-hexane, an orange solid precipitated immediately. After 10 m*l* of *n*-hexane had then been added to the reaction mixture, filtration gave an orange solid. Several fractional recrystallizations from acetonitrile gave 0.54 g (70%) of $TPEBr_2 \cdot 2H_2O$, mp 247°C (decomp.), as pale yellow prisms and 0.2 g of $TPEBr_6$, mp 223°C (decomp.), as orange prisms.

The reaction conditions of TPE and TME with halogens, the yields, the physical properties, and the results of elemental analyses of the corresponding oxamidinium halides are shown in Tables 1 and 3.

The Reactions of TPE and TME with Halogen-Compounds. The reaction of TPE with benzal chloride is shown as a representative reaction. A solution of 3 g of TPE and 5.4 g of benzal chloride in 20 m*l* of benzene was refluxed for 1 hr. After the reaction mixture had been cooled, it was filtered to give 3 g (83%) of $TPECl_2 \cdot 2H_2O$. The filtrate was concentrated *in vacuo* to leave yellow crystals which, on recrystallization from a benzene-methanol mixture gave 0.5 g (19%) of 1,1,2,2-tetrachloro-1,2-diphenylethane, mp 163—164°C (lit,[15] mp 163°C), as yellow needles.

Found: C, 52.68; H, 3.13%. Calcd for $C_{14}H_{10}Cl_4$: C, 52.53; H, 3.15%.

Furthermore, a small amount of stilbene was isolated by the gas chromatography of the filtrate after the separation of tetrachlorodiphenylethane.

The reaction conditions of TPE and TME with other halogen-compounds and the yields of the products are summarized in Table 2.

In the reactions with benzenesulfonyl chloride, phenacyl bromide, and 2,2-dichloroacenaphthenone,[16] diphenylsulfone, biphenacyl, and diacenaphthylidenedione were obtained respectively besides the corresponding oxamidinium dihalide.

Diphenyldisulfone, mp 194—195°C (lit,[17] mp 193—194°C).

Found: C, 50.86; H, 3.53%. Calcd for $C_{12}H_{10}O_4S_2$:

Table 3. Physical properties and elemental analyses of oxamidinium halides

Compound	Appearance (Recryst. solvent)	Mp(°C)	λ_{max}^{EtOH} mμ(ε)	Analysis (%), Found (Calcd)		
				C	H	N
$TPECl_2 \cdot 2H_2O$	colorless prisms (MeCN-MeOH)	240—241 (decomp.)	213 (17400) 291.5 (12100)	56.52 (56.51)	9.57 (9.49)	11.94 (11.98)
$TMECl_2 \cdot 2H_2O$	light yellow prisms(MeCN-MeOH)	265—266 (decomp.)	214.5 (16100) a) 295 (11100)	45.47 (45.47)	7.77 (7.63)	11.60 (11.79)
$TPEBr_2 \cdot 2H_2O$	pale yellow prisms(MeCN)	247 (decomp.)	212 (19900) 291 (13400)	47.72 (47.48)	8.02 (7.97)	9.84 (10.07)
$TMEBr_2 \cdot H_2O$	pale yellow prisms(MeOH)	300 (decomp.)	210 (14500) a) 295 (9130)	39.49 (39.57)	6.24 (6.28)	9.95 (10.25)
$TPEI_2$	yellow prisms (MeOH)	282—284 (decomp.)	217 (45300) 291 (11100)	42.93 (43.00)	6.53 (6.57)	9.14 (9.12)
$TMEI_2$ c)	brown crystals b)	*ca.* 190 (decomp.)		33.18 (32.83)	5.18 (5.51)	8.46 (8.51)
$TPEBr_6$ c)	orange prisms (MeCN)	223 (decomp.)		31.53 (31.45)	4.98 (4.80)	6.50 (6.66)
$TPEI_6$ c)	brown crystals (MeOH)	232—234		23.55 (23.57)	3.59 (3.65)	4.99 (5.07)

a) The UV spectra were measured in water.
b) $TMEI_2$ was analyzed without further purification because of its insolubility.
c) The IR spectra of hexahalides as well as dihalides showed characteristic bands at 1620 and 1640 cm^{-1}.

15) C. Liebermann and J. Homeyer, *Ber.*, **12**, 1971 (1879).
16) O. Tsuge and M. Tashiro, This Bulletin, **26**, 970 (1963).
17) T. P. Hilditch, *J. Chem. Soc.*, **93**, 1526 (1908).

C, 51.06; H, 3.57%.

Biphenacyl was identified as 2,4-dinitrophenylhydrazone, mp 239—240°C (decomp.). Found: C, 56.32; H, 3.68; N, 18.79%. Calcd for $C_{28}H_{22}O_8N_8$: C, 56.18; H, 3.70; N, 18.72%.

Diacenaphthylidenedione, mp 294°C, was identified by comparison with an authentic sample prepared from acenaphthenone and acenaphthenequinone.

The Reaction of TPE with Phenylnitromethane. A solution of 1.5 g of TPE and 5 g of phenylnitromethane in 20 m*l* of xylene was stirred at 90°C for 15 min; during this time crystals precipitated gradually. After the solution had then been cooled, filtration gave 1.0 g (51%) of colorless crystals which, on recrystallization from acetonitrile afforded a dinitrile, $TPE(NO_2)_2 \cdot 2H_2O$, mp 188°C (decomp.), as pale pink prisms.

Found: C, 54.00; H, 9.19; N, 17.00%. Calcd for $C_{22}H_{40}O_4N_6 \cdot 2H_2O$: C, 54.07; H, 9.08; N, 17.20%. IR spectrum: 1620, 1640 cm^{-1}. UV spectrum in water λ_{max} mμ (ε): 216 (28000), 291.5 (13400).

This compound was also obtained by the reaction of dihalides, $TPEX_2$, with silver nitrite.

A similar reaction of TME with phenylnitromethane in benzene at 80°C gave a 30% yield of crude dinitrite, $TME(NO_2)_2$, which, on recrystallization from methanol, gave yellow prisms, mp 246—248°C (decomp.).

Found: C, 43.35; H, 7.05; N, 16.97%. Calcd for $C_{18}H_{38}O_8N_6 \cdot 2H_2O$: C, 43.54; H, 7.31; N, 16.93%. IR spectrum: 1620, 1640 cm^{-1}. UV spectrum in water λ_{max} mμ (ε): 210 (31600), 296 (14600).

This compound was also obtained by the reaction of dihalides, $TMEX_2$, with silver nitrite.

The Reaction of TPE with Tetranitromethane. When a solution of 0.7 g of TPE and 0.5 m*l* of tetranitromethane in 15 m*l* of diethyl ether was stirred at 0°C for 30 min, yellow crystals precipitated gradually. Filtration gave 1.1 g of yellow crystals which, on fractional recrystallization from acetone, afforded 0.9 g of a 1 : 2 adduct, $TPE[C(NO_2)_4]_2$, mp 112°C (decomp.), as yellow needles and a small amount of a dinitrate, $TPE(NO_3)_2$, mp 222—223°C (decomp.) as colorless crystals.

Found: C, 43.82; H, 6.10; N, 21.12%. Calcd for $C_{24}H_{40}O_{12}N_{10}$: C, 43.63; H, 6.10; N, 21.10%.

The dinitrate was easily obtained from the dihalides, $TPEX_2$, with silver nitrate.

Found: C, 50.93; H, 8.61; N, 15.85%. Calcd for $C_{22}H_{40}O_6N_6 \cdot 2H_2O$: C, 50.75; H, 8.52; N, 16.14%. IR spectrum: 1620, 1640 cm^{-1}.

The Reaction of TPE with 1,3,5-*Trinitrobenzene.* To a benzene solution of 0.5 g of TPE was added, drop by drop, a benzene solution of two equimolar amounts of 1,3,5-trinitrobenzene at room temperature, forming purple crystals. Filtration gave purple crystals, mp 122—124°C (decomp.), which easily decomposed in air. The compound was analyzed without further purification.

Found: C, 51.52; H, 6.43; N, 17.07%. Calcd for $C_{34}H_{46}O_{12}N_{10}$: C, 51.90; H, 5.90; N, 17.80%.

The Reaction of TPE with Nitromethane. After a solution of 0.8 g of TPE and 4 m*l* of nitromethane in 6 m*l* of benzene had been refluxed under an atmosphere of nitrogen for 1.5 hr, the reaction mixture was concentrated *in vacuo*. The residue was washed with petroleum ether (bp 30—45°C) to leave 0.4 g (58%) of orange crystals which, on recrystallization from carbon tetrachloride, gave 1-nitro-2-piperidinoethylene, mp 94—95°C (lit,[18] mp 95°C), as pale yellow scales.

Found: C, 53.60; H, 7.73; N, 18.07%. Calcd for $C_7H_{12}O_2N_2$: C, 53.82; H, 7.74; N, 17.94%. IR spectrum: 1635 cm^{-1} ($\nu_{C=C}$). NMR spectrum in deuterochloroform: δ 1.71 (6H, methylene protons), 3.40 (4H, methylene protons), 6.86 and 8.17 ppm (each 1H, doublet, olefinic proton). UV spectrum in ethanol λ_{max} mμ (ε): 216.9 (7250), 240 (3780), 357 (33400). Mass spectrum: *m/e* 156 (M^+).

From the washings, 0.2 g of TPE was recovered.

A similar reaction of TME with nitromethane gave a 46% yield of 2-morpholino-1-nitroethylene, mp 138—140°C (lit,[18] mp 140—141°C), as yellow prisms (from ethyl acetate).

Found: C, 45.46; H, 6.32; N, 17.78%. Calcd for $C_6H_{10}O_3N_2$: C, 45.56; H, 6.37; N, 17.71%. IR spectrum: 1630 cm^{-1} ($\nu_{C=C}$). UV spectrum in ethanol λ_{max} mμ (ε): 213 (8250), 238 (3630), 353.5 (23000). Mass spectrum: *m/e* 158 (M^+).

The Reaction of TPE with Benzoic Acid. A mixture of 0.7 g of TPE and two equimolar amounts of benzoic acid in 10 m*l* of benzene was stirred at room temperature for 4 hr. Filtration gave 0.65 g (70%) of a colorless solid which, on recrystallization from methanol - ethyl acetate, afforded the dibenzoate, $TPE(PhCO_2)_2 \cdot 2H_2O$, mp 104—105°C, as colorless needles.

Found: C, 67.43; H, 8.76; N, 8.58%. Calcd for $C_{36}H_{50}O_4N_4 \cdot 2H_2O$: C, 67.68; H, 8.52; N, 8.77%. IR spectrum: 1635, 1610, 1550 cm^{-1}.

Similar reactions of TPE with *p*-methyl- and *p*-chlorobenzoic acid gave the corresponding oxamidinium salts. $TPE(p\text{-}MeC_6H_4CO_2)_2 \cdot 2H_2O$: mp 101—103°C, colorless needles (from methanol - ethyl acetate). Yield, 52%.

Found: C, 68.13; H, 8.95; N, 8.53%. Calcd for $C_{38}H_{54}O_4N_4 \cdot 2H_2O$: C, 68.44; H, 8.77; N, 8.40%. IR spectrum: 1637, 1610, 1545 cm^{-1}.

$TPE(p\text{-}ClC_6H_4CO_2)_2 \cdot 2H_2O$: mp 109—111°C, colorless needles (from methanol - ethyl acetate). Yield, 75%.

Found: C, 60.82; H, 7.75; N, 7.77%. Calcd for $C_{36}H_{48}O_4N_4Cl_2 \cdot 2H_2O$: C, 61.09; H, 7.40; N, 7.91%. IR spectrum: 1640, 1610, 1595, 1540 cm^{-1}.

18) C. D. Hurd and L. T. Sherwood, Jr., *J. Org. Chem.*, **13**, 471 (1948).

Optical Activity of Bis-1,1′-spiroindanes. II. Absolute Configuration of Optically Active 5,5′- and 6,6′-Disubstituted-bis-1,1′-spiroindanes and Their Circular Dichroism Spectra

Sanji HAGISHITA, Kaoru KURIYAMA, Keiji SHINGU*, and Masazumi NAKAGAWA*

Shionogi Research Laboratory, Shionogi & Co., Ltd., Fukushima-ku, Osaka

* *Department of Chemistry, Faculty of Science, Osaka University, Toyonaka, Osaka*

(Received January 11, 1971)

An unequivocal determination of the absolute configuration of 5,5′- and 6,6′-disubstituted bis-1,1′-spiroindane and the behavior of the CD spectra of some 5,5′-disubstituted ones are described.

In the preceding paper,[1] the absolute configuration of (−)-6,6′-disubstituted-3,3,3′,3′-tetramethyl-bis-1,1′-spiroindanes was deduced to be (S)-configuration on the basis of the enantiomeric aspect of the CD spectra between (−)-6,6′-dihydroxy-3,3,3′,3′-tetramethyl-bis-1,1′-spiroindane, (−)-I and (+)-6,6′-dihydroxy-3,3,-5,3′,3′,5′-hexamethyl-bis-1,1′-spiroindane, (+)-II. The latter was determined to have (R)-configuration by an X-ray study of its 7,7′-dibromo derivative, (−)-III.[2] Also, the assignment of the absolute configuration was supported by the analysis of their CD spectra associated with the *p*-band transition by means of a coupled oscillator theory. However, there remains some ambiguity in the assignment of the absolute configuration, since a discrepancy is observed in the sign of the CD spectra of (−)-I and (+)-II associated with the *p*-band; also, the experimental CD spectrum in the α-band region is found to be inconsistent with the theoretical spectrum. Thus, it appeared to be important to establish the chemical correlation between the absolute configuration of (−)-I and that of (+)-II. Furthermore, as was pointed out in the previous paper, (+)-5,5′-dihydroxy-bis-1,1′-spiroindane, (+)-IX was considered to have (R)-configuration from the positively-signed Cotton effect associated with the α-band; this was done on the basis of an empirical observation that the sign of the CD spectra in the longest wavelength region was determined by the configuration of the spiro atom in bis-1,1′-spiroindanes. However, the empirical rule obtained previously could not be applied to (−)-III. Therefore, it is worthwhile to examine whether or not this rule can be applied to 5,5′-disubstituted derivatives.

In the present paper, an unequivocal determination of the absolute configuration of 5,5′- and 6,6′-disubstitutes bis-1,1′-spiroindane and the behavior of the CD spectra of some 5,5′-disubstituted ones will be described.

Chemical Correlation. 6,6′-Disubstituted bis-1,1′-spiroindane was easily prepared by the acid-catalysed cyclization of acetone with mono-substituted benzenes, such as phenols or toluene.[1,3] However, this method can not be applied to the preparation of 5,5′-disubstituted derivatives because of the orientation of the cyclization. As another route of preparing 5,5′-dimethoxy-bis-1,1′-spiroindane, we have adopted the cyclization of bis(3-methoxybenzyl)acetone with phosphorus oxychloride. However, the correlation of the absolute configurations of 6,6′-disubstituted derivatives with those of 5,5′-disubstituted derivatives has not yet been achieved by a chemical method.

The absolute configuration of (+)-6,6′-dihydroxy-3,3,5,3′,3′,5′-hexamethyl-bis-1,1′-spiroindane, (+)-II has already been established to be (R). Therefore, if the hydroxy group in (R)-(+)-II can be replaced by hydrogen, we can obtain the (R)-5,5′-dimethyl derivative VI. The conversion of the methyl groups of VI to other substituents or the replacement by hydrogen atoms will establish the configurational correlation among the 5,5′-, the 6,6′-disubstituted and the non-substituted spirobisindanes.

As is illustrated in the following scheme, the conversion has been realized. The treatment of the methanesulfonate of (R)-(+)-II with sodium in liquid ammonia afforded the desired deoxygenated product, the 5,5′-dimethyl derivative (R)-(+)-VI. (R)-(−)-3,3,3′,3′-Tetramethyl-bis-1,1′-spiroindane-5,5′-dicarboxylic acid (R)-(−)-VII was obtained by the chromium trioxide oxidation of (R)-(+)-VI. (R)-(−)-VII afforded (R)-(+)-5,5′-diamino-3,3,3′,3′-tetramethyl-bis-1,1′-spiroindane, (R)-(+)-VIII by the Schmidt reaction, as well as the nonsubstituted derivative (R)-(−)-V by the decarboxydation, according to the procedure[1] used for the 6,6′-dicarbohydroxy derivative (+)-IV.

As V obtained from (R)-(−)-VII had the same specific rotation at D-line and showed the same CD spectrum as that derived from (+)-IV, it is established, by the chemical correlation, that (S)-configuration must be assigned to (−)-6,6′-disubstituted bis-1,1′-spiroindanes; this assignment is in agreement with an inference based on the comparison of the CD spectra between (−)-I and (R)-(+)-II.

UV and CD Spectra. The UV and the CD spectra of these 5,5′-disubstituted derivatives are shown in Table 1 and in Figs. 1—4. The accessible UV and CD spectra of these compounds consist of three bands, which are termed α, *p*, and β from the longer wavelength, according to the classification by Clar. The analysis based upon the exciton theory was carried out for both the α- and the *p*-band systems of (R)-(+)-VI, (R)-(−)-VII, and (R)-(+)-VIII, the results are summarized in Table 2.

In dimeric systems with a C_2 symmetry axis, there are two coupling modes for each electronic transition

1) S. Hagishita, K. Kuriyama, M. Hayashi, Y. Nakano, K. Shingu, and M. Nakagawa, This Bulletin, **44**, 496 (1971).

2) To be published.

3) L. Taimr and J. Pospišil, *Chem. Ind.* (London), **1969**, 456, and the literature cited therein.

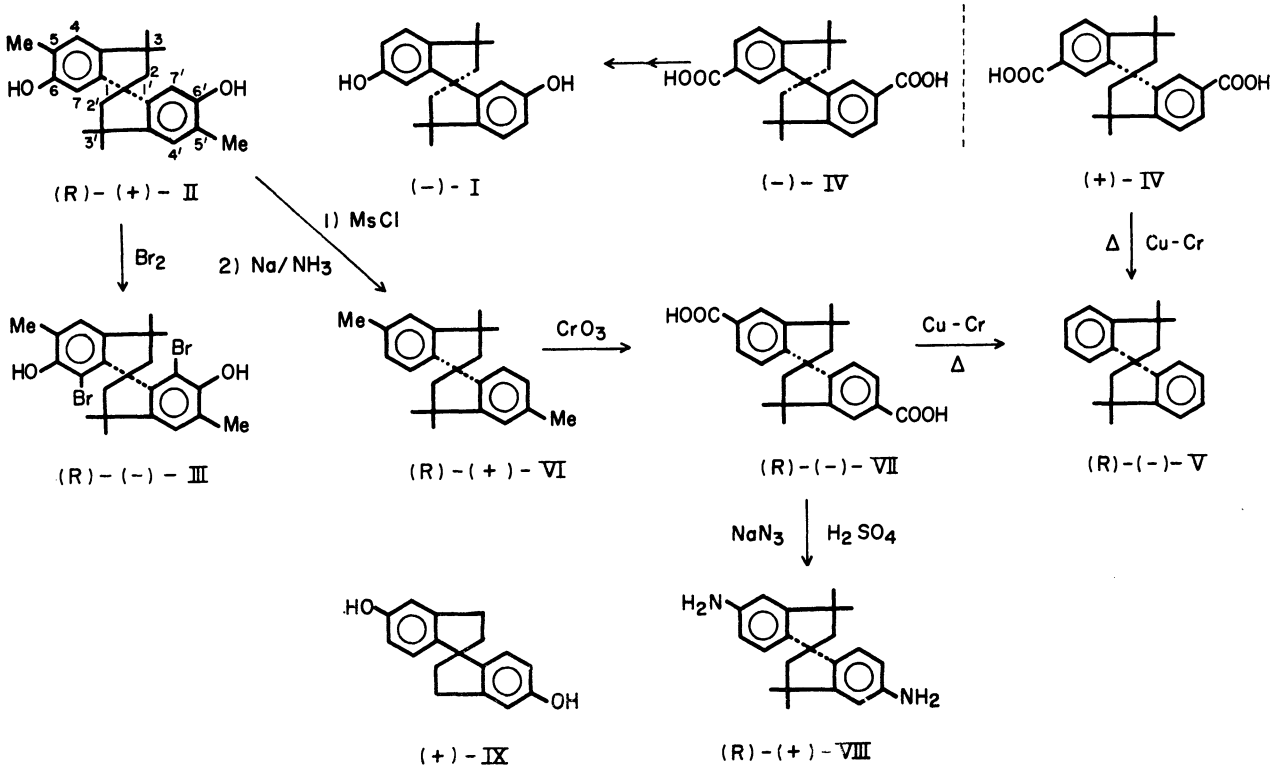

Scheme

TABLE 1. CD AND UV SPECTRA OF THE EXAMINED SPIRO COMPOUNDS

Compd	Solvent	UV $\lambda_{m\mu}^{max}$ ($\varepsilon \times 10^3$)			CD $\lambda_{m\mu}^{max}$ ($\Delta\varepsilon$)		
		α	p	β	α	p	β
(R)-V	Isooctane	272 (2.59)	223 (11.0)	213s (22.0)	273 (+5.54)	226a)(−0.94)	205! (+14.8)
		265 (2.24)	218s (18.2)		267 (+3.11)	221 (+10.2)	
		257 (1.43)			260 (+0.71)		
					253 (+0.40)		
(R)-VI	Isooctane	279 (3.04)	229 (14.5)	204! (60.1)	279 (+6.13)	231 (−4.02)	216 (+13.8)
		273 (2.22)	218 (20.0)		273 (+3.16)	223 (+7.11)	
		270 (2.27)			265 (+0.94)		
		265 (1.57)					
(R)-VII	MeOH	286 (4.74)	248 (24.7)	205 (68.5)	286 (−1.20)	250 (−10.0)	215 (+100.)
		278 (5.71)			278 (−1.39)	230s (+10.6)	205 (−114.)
(R)-VII	0.1 N-NaOH	284 (3.45)	247 (30.7)	205 (85.2)	284 (−0.98)	248 (−9.28)	213 (+51.6)
		276 (3.95)			276 (−0.59)	230s (+8.51)	
(R)-VIII	MeOH	288 (5.63)	243 (22.0)	203 (57.7)	297 (+4.73)	247 (−5.96)	213 (−20.8)
						230 (+2.76)	204 (+37.9)
(R)-VIII	HCl MeOH	290s (1.46)	225s (16.2)	200! (68.4)	285 (−0.16)	236 (+0.32)	200! (+56.8)
		275 (4.60)	215s (24.2)		275 (+2.71)	227 (−7.09)	
		267 (4.06)			268 (+2.05)		
		262s (3.79)			261 (+1.04)		

s: shoulder. !: lowest recorded values, not an extremum. a) As the result of re-examination, this weak CD band was found in (+)-(V) reported previously.

of the constituent monomer, one with *A*, and the other with *B* symmetry. The two coupling modes give rise to two CD bands with opposite signs, but the same in magnitude. Experimentally, the Cotton effects in the *p*-bands of these compounds are negative and then positive from the longer wavelength, and are almost identical in the magnitude of rotational strength, but in the α-band all the derivatives show mainly a single Cotton effect, as was observed in 6,6′-disubstituted derivatives.

In this method, we could obtain good results in the *p*-band region of the 6,6′-disubstituted derivatives, in

Table 2. Rotational strengths and frequency intervals of *R*-configuration

The values R and $\tilde{\nu}_A-\tilde{\nu}_B$ were calculated by the following equations:

$$R_A=-R_B=\pi\tilde{\nu}d\rho^2\cos v\cdot\cos t$$

$$\tilde{\nu}_A-\tilde{\nu}_B=2\rho^2(\cos^2 v-\cos^2 t+2\cos^2 r)/hcd^3$$

where d: the distance between the center of the two benzene rings; ρ: the transition dipole moment in the isolated chromophore; $\tilde{\nu}$: the wave number of the transition. The following value of the spectroscopic moment were used: COOH(−28), *t*-Butyl (2) and Methyl (7). The alkyl bridge which made up the spiro skeleton is regarded as a substituent except for (R)-(+)-VIII and the value of the *t*-Butyl was used. The angles r, t and v and d were calculated on the same geometry cited in the previous paper.[1]

Compd	Band	Found			Calculated				
		$\tilde{\nu}$ ($\times 10^2$ cm^{-1})	D (10^{-36} cgs)	R (10^{-40} cgs)	cos r	cos t	cos v	R (10^{-4} cgs)	$R\nu_A-\nu_B$ (cm^{-1})
(R)-(+)-VI	α A	363	2.34	+4.79	0.061	−0.811	0.582	−28.6	−39.1
	α B							+28.6	
	p B	444	1.40	−2.84	−0.890	0.233	−0.392	+ 4.01	+67.0
	p A			+4.54				− 4.01	
(R)-(−)-VII	α A	355	4.54	−1.90	−0.290	0.840	−0.458	−43.5	−80.1
	α B							+43.5	
	p B	403	24.3	−17.1	−0.842[a]	0.0[a]	0.540[a]	0.0	+1470.
	p A			+14.0				0.0	
(R)-(+)-VIII	α A	347	6.38	+9.07	−0.236	0.838	−0.491	−65.0	− 120.
	α B							+65.0	
	p B	412	22.9	−9.81	−0.859	0.056	0.508	−19.2	+2130.
	p A			+2.93				+19.2	

a) The values cos r, cos t and cos v amount to −0.866, 0.019 and 0.500, respectively, by the calculation on the envelope conformation described previously.[1] Employing them, the calculated sign of CD is consistent with that observed.

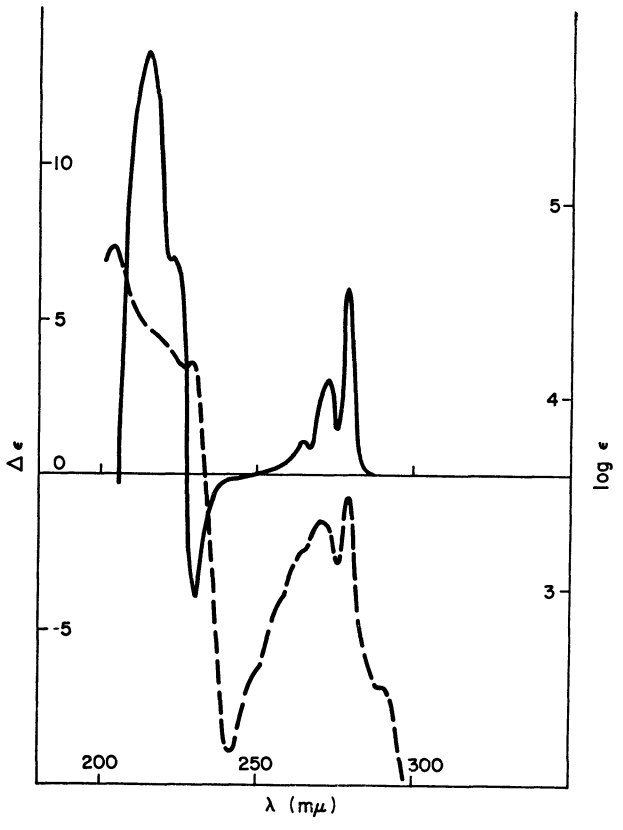

Fig. 1. CD (——) and UV (----) spectra of (R)-(+)-(VI) in isooctane.

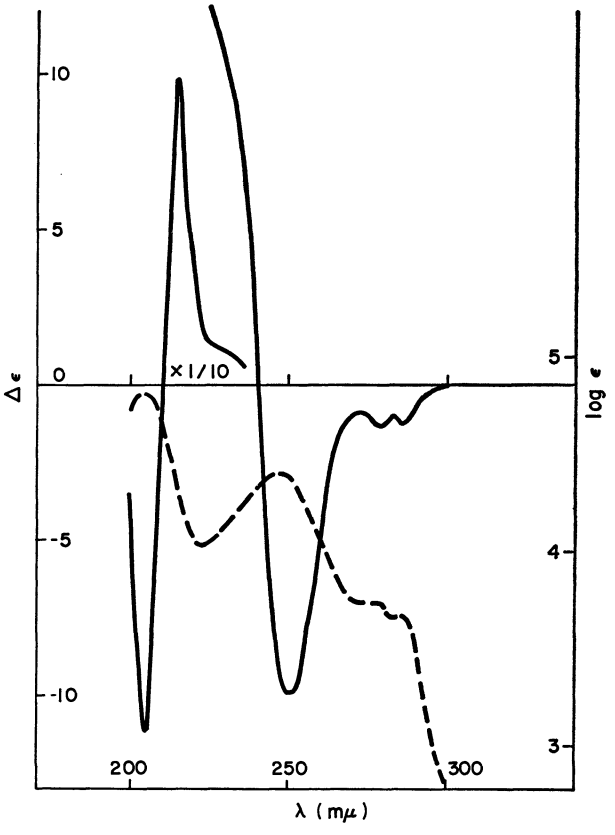

Fig. 2. CD (——) and UV (----) spectra of (R)-(−)-(VII) in methanol.

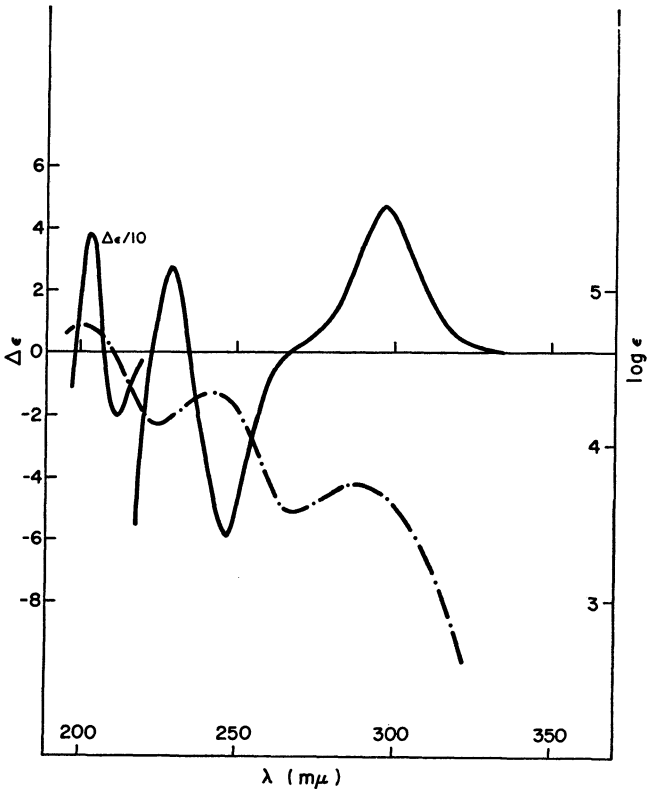

Fig. 3. CD (——) and UV (—·—·) spectra of (R)-(+)-(VIII) in methanol.

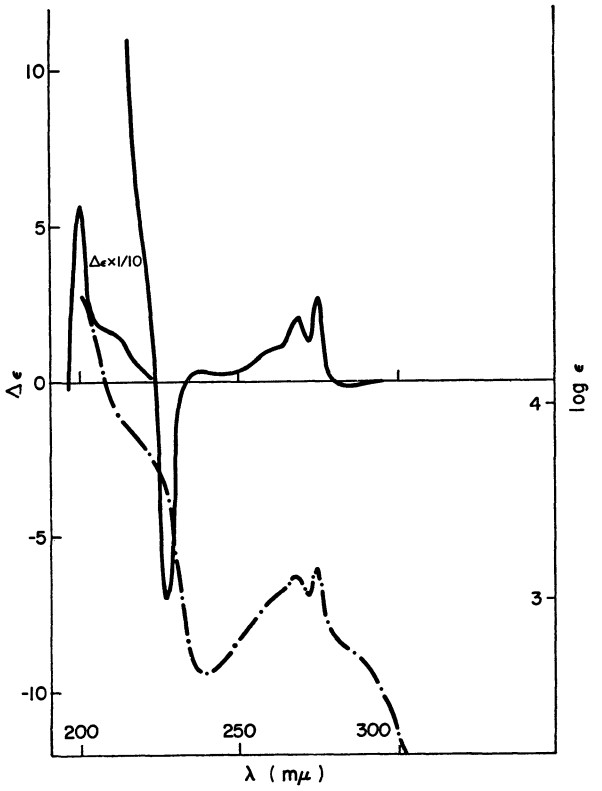

Fig. 4. CD (——) and UV (—·—·) spectra of (R)-(+)-(VIII)·HCl.

which substituents on benzene rings had a large value in the spectroscopic moment, as listed by Platt (Table 2). It can be said that the same results are observed in this series from the value in (R)-(+)-VIII, but the value of the cosine of the tangential angles, *t*, between the long-axis excitation dipole and the local Cartesian axis is small. Especially in (R)-(—)-VII, the excitation dipoles of the *p*-band of two chromophores are situated almost entirely on one plane. Therefore, the calculated value depends on the selection of the geometry of the molecule, the value of the spectroscopic moment for the alkyl bridge, and other factors. In such cases, extreme care must be taken in applying the coupled oscillator theory to the determination of the absolute configuration.

As is observed in 6,6′-disubstituted derivatives,[1] the values calculated by the coupled oscillator theory are not in accordance with those observed in the α-band region. The empirical rule obtained with 6,6′-disubstituted derivatives, that the spatial arrangement of the two benzene rings determines the sign of the CD in the longest-wavelength region, can be applied to (R)-(+)-VI and (R)-(+)-VIII, although the pattern of (R)-(—)-VII and (R)-(+)-VIII·HCl in the α-band does not agree with the above rule. The negative Cotton effect at the longest wavelength of (R)-(+)-VIII·HCl may not be correlated with the transition responsible for that of (R)-(+)-VIII. Therefore, the sign which corresponds to the same transition is positive in (R)-(+)-VIII·HCl (Figs. 1 and 4). The reason for the departure from the empirical rule of (R)-(—)-VII cannot, at present, be understood.

The CD of previously-prepared (+)-5,5′-dihydroxy-bis-1,1′-spiroindane, (+)-IX is similar to that of (R)-(+)-VIII in the pattern associated with the α- and *p*-bands. Since a hydroxy group has a large, positively-signed value in the spectroscopic moment, like an amino group, we can expect a similar CD pattern between VIII and IX with the same absolute configuration. Thus, we assign (R)-configuration to (+)-IX; this assignment is in agreement with that predicted previously.

Experimental

Melting points are uncorrected. Circular dichroism spectra were measured using a JASCO Model ORD/UV-6 apparatus. Optical rotations were measured on a Perkin-Elmer polarimeter Model 141 using a 1-dm quartz cell. Infrared spectra were taken with a JASCO Model 402G doublemonochromatic spectrophotometer. NMR spectra were measured in a solution of deuterio chloroform with a Varian A-60 spectrometer, using tetramethylsilane as the internal standard. Ultraviolet spectra were measured with a Hitachi Model EPS-3T spectrometer.

(R)-(+)-6,6′-Dihydroxy-3,3,5,5,3′,3′,5′-hexamethyl-bis-1,1′-spiroindanedimethanesulfonate. A solution of (R)-(+)-6,6′-dihydroxy-3,3,5,5,3′,3′,5′-hexamethyl-bis-1,1′-spiroindane ((R)-(+)-II, 2.2 g, $[\alpha]_D$ +18.9° (*c* 0.456, dioxane)),[1] and freshly-distilled methanesulfonyl chloride (2.2 m*l*) in pyridine (30 m*l*) was heated under reflux for one hour in a nitrogen atmosphere. A volatile material was then removed by distillation under reduced pressure. The residue was dissolved in ethyl acetate, after which the solution was washed with

water and dried over anhydrous sodium sulfate. After the evaporation of the ethylacetate under reduced pressure, the residue was crystallized from benzene-*n*-hexane to give prisms (2.14 g). mp 183—184°C, $[\alpha]_D$ +66.2° (*c* 0.998, chloroform). IR $\nu_{max}^{CHCl_3}$ 1368 cm^{-1}.

Found: C, 61.49; H, 6.56; S, 13.22%. Calcd for $C_{25}H_{32}O_6S_2$: C, 60.95; H, 6.55; S, 13.02%.

(R)-(+)-3,3,5,3',3',5'-Hexamethyl-bis-1,1'-spiroindane (R)-(+)-VI. A solution of the above obtained (+)-dimesyate (2.0 g) in dry tetrahydrofuran (10 m*l*) was added to liquid ammonia (150 m*l*). A small piece of sodium metal was then added under reflux with vigorous stirring. The end point of the reaction was shown by a persistent blue color of the reaction mixture. After stirring for 15 more min, ammonium chloride (0.5 g) was added and the ammonia was evaporated. Water (50 m*l*) was then added to the residue. The aqueous layer was extracted with ether and the combined organic layer was washed with water and dried on anhydrous sodium sulfate. The solvent was distilled under reduced pressure, and the residue was crystallized from methanolic water. Recrystallization from methanol gave prisms (811 mg, 65.6%). mp 76—78°C, $[\alpha]_D$ +1.8° (*c* 2.285, chloroform). NMR τ: 8.68 (6H, singlet), 8.63 (6H, singlet), 7.73 (4H, singlet), 7.67 (6H, singlet), 3.31 (2H, doublet, J=7.8 Hz), 2.9—3.2 (4H, multiplet).

Found: C, 90.56; H, 9.21%. Calcd for $C_{23}H_{28}$: C, 90.73; H, 9.27%.

(R)-(−)-3,3,3',3'-Bis-1,1'-spiroindane-5,5'-dicarboxylic Acid (R)-(−)-VII. Chromium trioxide (1.2 g) was added, in one portion, to a solution of (+)-VI (300 mg) in acetic acid (15 m*l*), water (9 m*l*), and concentrated sulfuric acid (1.5 m*l*). The mixture was heated under reflux for 7.5 hr and then poured into ice water (50 m*l*). After this mixture had been allowed to stand overnight, crystals were collected, washed with water, and then extracted with aqueous sodium hydroxide. The alkaline solution was acidified with dilute hydrochloric acid, and the resultant gel set aside overnight. The precipitated solid was dried and recrystallized from acetone-water (142 mg, 31.5%). mp>300°C, $[\alpha]_D$ −53.2° (*c* 0.468 dioxane). IR ν_{max}^{Nujol} 1690 cm^{-1}.

Found: C, 75.78; H, 6.64%. Calcd for $C_{23}H_{24}O_4$: C, 75.80; H, 6.68%.

(R)-(−)-3,3,3',3'-Tetramethyl-bis-1,1'-spiroindane (R)-(−)-V. A mixtur of (R)-(−)-VII (105 mg) and copper chromite (119 mg) in quinoline (3 m*l*, freshly distilled from copper chromite) was heated under reflux for 90 min. To the cooled reaction mixture, ether (20 m*l*) was added, after which an undissolved solid was removed by filtration. The solution was washed with 50% hydrochloric acid, aqueous sodium bicarbonate, and then water, and dried on anhydrous sodium sulfate. The ether was evaporated, and the residue was crystallized and recrystallized from ethanol to give colorless needles (42 mg, 52.7%). mp 124—125°C, $[\alpha]_D$ −30.4° (*c* 0.471, dioxane). The IR spectrum of this compound was identical with that of an authentic sample.[1)]

(R)-(+)-5,5'-Diamino-bis-1,1'-spiroindane (R)-(+)-VIII. Into a solution of (R)-(−)-VII (147 mg) in concentrated sulfuric acid (6.5 m*l*), sodium azide (215 mg) was added in small portions over a 50-min period at 40—45°C with stirring, Foaming occurred and stirring was continued at 50—55°C for 2 hr. The reaction mixture was allowed to stand overnight and then poured into ice water (50 m*l*). After this mixture had been made alkaline with 40% aqueous sodium hydroxide (35 m*l*) under cooling, yellow powders were collected, washed with water, and dried *in vacuo*. The crude powders were dissolved in benzene, and an amorphous solid was removed by filtration. After it had been concentrated to *ca.* 2 m*l* under reduced pressure, the solution was allowed to stand overnight; then the product was collected and dried *in vacuo* to give needles (64 mg). mp 208—210°C, $[\alpha]_D$ +8.3° (*c* 0.350, MeOH). IR ν_{max}^{Nujol} 3440, 3355 cm^{-1}.

Found: C, 82.55; H, 8.49; N, 9.41%. Calcd for $C_{21}H_{26}N_2$: C, 82.31; H, 8.55; N, 9.14%.

The Reaction of Nitriles with Phosgene. V[1]. Cyclization Reactions of *N*-(α-Chlorobenzylidene)carbamoyl Chloride

Shozo YANAGIDA, Masaaki YOKOE, Masataka OHOKA, and Saburo KOMORI

Department of Applied Chemistry, Faculty of Engineering, Osaka University, Yamadakami, Suita

(Received January 20, 1971)

N-(α-Chlorobenzylidene)carbamoyl chloride (**1**) reacts with hydrazine hydrate to give 3-phenyl-1,2,4-triazolone (**2**), with sodium azide in the presence of water to give 5-phenyltetrazole (**3**), and with aliphatic nitriles in the presence of hydrogen chloride to give 6-chloro-2-phenyl-5-substituted-4(3*H*)-pyrimidones (**5**) and 4,6-dichloro-2-phenyl-5-substituted pyrimidines (**6**). However, the reaction of **1** with trichloroacetonitrile or pivalonitrile in the presence of hydrogen chloride did not give the expected triazines.

N-(α-Chlorobenzylidene)carbamoyl chloride (**1**) was prepared first by the reaction of benzoyl isocyanate with phosphorous pentachloride.[2] However, in the course of our work on the reaction of nitriles with phosgene, the carbamoyl chloride (**1**) has been found to be easily obtainable by the reaction of benzonitrile with phosgene in the presence of hydrogen chloride.[3] The carbamoyl chloride (**1**) has two reactive chlorine atoms in the molecule and thus can be expected to be useful as a precursor for the synthesis of nitrogen heterocycles. The Netherland patent claims that the carbamoyl chloride (**1**) reacts with amidines to give 2-hydroxy-6-phenyl-4-substituted-*s*-triazines.[4] In this paper we will report some cyclization reactions of the carbamoyl chloride (**1**) with some nucleophiles.

The reaction of the carbamoyl chloride (**1**) with excess aniline or ammonia gave *N*-phenyl-*N'*-anilinoformyl benzamidine and *N*-carbamoyl benzamidine hydrochloride respectively. On the other hand, the treatment of the carbamoyl chloride (**1**) with hydrazine hydrate gave the compound formulated as $C_8H_7N_3O$, which was confirmed to be 3-phenyl-1,2,4-triazolone (**2**) on the basis of the IR, NMR, and mass spectra.

When the carbamoyl chloride (**1**) was allowed to react with sodium azide in aqueous acetone, 5-phenyltetrazole (**3**) was obtained, with the evolution of carbon dioxide. However, the reaction did not occur under anhydrous conditions, such as those in anhydrous THF.

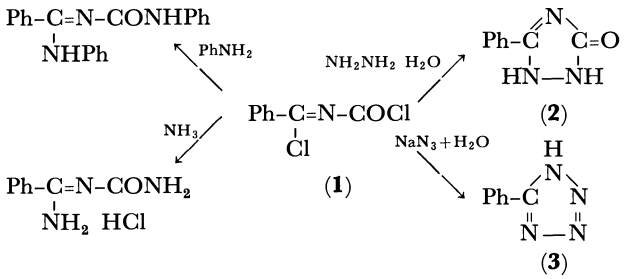

Scheme 1

Recently several reactions concerning the electrophilic attack on the α-methylene of the C=N group have been reported.[5-7] In our previous papers,[7,8] we reported the preparation of 6-chloro-2,5-disubstituted-4(3*H*)-pyrimidones (**7**) by the reaction of aliphatic nitriles with phosgene in the presence of hydrogen chloride, in which *N*-(chloroformyl)-*N'*-(α-chloroalkylidene)alkylamidine was proposed as an intermediate. We assumed that the presence of hydrogen chloride promotes the polarization of the C=N bond in the intermediate, thus making the α-methylene more nucleophilic.

In view of these speculations, the carbamoyl chloride (**1**) can be expected to react with aliphatic nitriles in the presence of hydrogen chloride to afford 6-chloro-2-phenyl-5-substituted-4(3*H*)-pyrimidones (**5**) through *N*-(chloroformyl)-*N'*-(α-chloroalkylidene)-benzamidine (**4**), as is snown in Scheme 2. As expected, we have found the cyclization reaction of the carbamoyl chloride (**1**) with aliphatic nitriles in the presence of hydrogen chloride.

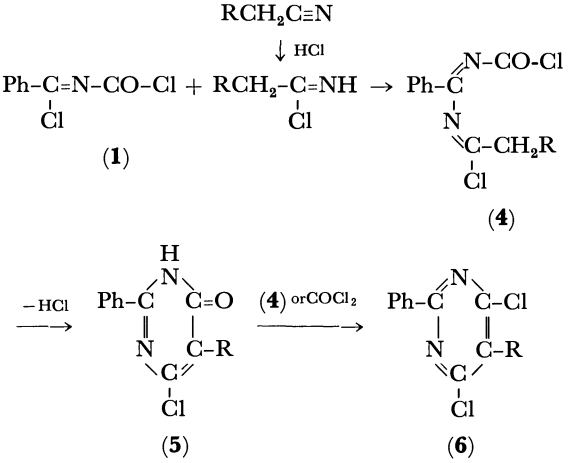

Scheme 2

When the carbamoyl chloride (**1**) was allowed to react with acetonitrile in the presence of hydrogen chloride (molar ratio 1 : 2 : 2) in a sealed glass tube at 60°C and the products were subjected to chromatographic separation, 6-chloro-2-phenyl-4(3*H*)-pyrimi-

1) Part IV, S. Yanagida, M. Ohoka, and S. Komori, *J. Org. Chem.*, **34**, 4127 (1969).

2) R. Neidlein and W. Haussmann, *Tetrahedron Lett.*, **1965**, 2423; *Chem. Ber.*, **99**, 239 (1966).

3) S. Yanagida, H. Hayama, M. Yokoe, and S. Komori, *J. Org. Chem.*, **34**, 4125 (1969).

4) Farbenfabriken Bayer A.-G., Neth. Appl. 301742 (1965). *Chem. Abstr.*, **64**, 8211 (1966).

5) A. J. Speziale and L. R. Smith, *J. Org. Chem.*, **27**, 4361 (1962).

6) H. Eilingsfeld, M. Seefelder, and H. Weidinger, *Chem. Ber.*, **96**, 2899 (1963).

7) S. Yanagida, M. Ohoka, M. Okahara, and S. Komori, *J. Org. Chem.*, **34**, 2972 (1969).

8) S. Yanagida, M. Ohoka, M. Okahara, and S. Komori, *Tetrahedron Lett.*, **1968**, 2351.

Table 1. The reaction of the carbamoyl chloride (**1**) with aliphatic nitriles

Run No.	R	Molar ratio 1 : RCN : HCl	Reaction time (hr) 30—35°C	60—65°C	Yield (%) 5	6	7
1	H	1 : 2 : 1.6	0	180	3.9	5.4	12
2	H	1 : 2 : 1.8	190	0	7.6	3.6	0
3	CH_3	1 : 2 : 1.7	0	220	8.2	trace	5.3
4	CH_3	1 : 2 : 2.0	170	290	1.8	23	trace
5	C_2H_5	1 : 2 : 2.0	170	240	15	9.4	0
6	C_3H_7	1 : 2 : 2.3	310[a]	300	19	9.4	trace
7	C_3H_7	1 : 2 : 2.3	190	0	13	trace	0
8	C_4H_9	1 : 2 : 2.2	160	260	24	5.0	trace

a) At room temperature.

done (**5a**), 4,6-dichloro-2-phenylpyrimidine (**6a**), 6-chloro-2-methyl-4(3*H*)-pyrimidone (**7a**), benzonitrile, and a tarry product were isolated. They were confirmed on the basis of the IR, NMR, and mass spectra, and by elemental analysis. It is known that the carbamoyl chloride (**1**) decomposes to benzonitrile and phosgene by heating.[3] Thus, the formation of **7a** is apparently due to the reaction of acetonitrile with the phosgene thus formed and hydrogen chloride.

The reaction of **1** with aliphatic nitriles was extended to propionitrile, butyronitrile, valeronitrile, and capronitrile, giving the corresponding pyrimidine derivatives, **5b-e**, **6b-e**, and **7b-e**. (Table 1)

The treatment of **1** with 3-chloropropionitrile under comparable conditions, however, resulted in the isolation of a polymeric product which was similar in both appearance and quality to that obtained by the reaction of 3-chloropropionitrile with phosgene in the presence of hydrogen chloride.[7]

In order to avoid the side reactions and to increase the yield of **5**, the reaction was carried out at 30—35°C and finally the reaction temperature was raised to 60—65°C, as is shown in Runs 4, 5, 6, and 8 in Table 1. The formation of **7** was indeed diminished, as expected, but the dichloropyrimidines (**6**) were still forme din considerable amounts. In all the experiments the total yields of **5** and **6** were independent of the chain length of nitriles, but did not exceed 30%. It is assumed that the low yields are partly due to the configurations of the intermediate *N*-chloroformyl-*N'*-(α-chloroalkylidene)benzamidine (**4**) and/or the protonated one (**4'**). The intermediates **4** and/or **4'**, may have the following four configurations:

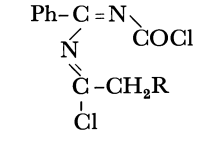

A

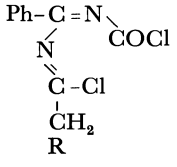

B

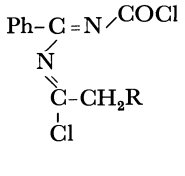

C

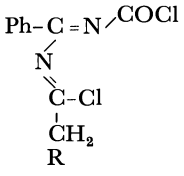

D

The protonation of **A**, **B**, **C**, and **D** would occur on a nitrogen bearing chloroalkylidene group.[7] It seems that **A** and protonated **A** are favorable configurations for the cyclization giving the **5** pyrimidones. However, judging from the facts that **6** did not produce under mild reaction conditions as is shown in Run 7 and that the pyrimidone **7** was formed only in traces in Runs 4, 6, and 8, non-cyclized intermediates which may exist in the **B**, **C**, and **D** and protanated **B**, **C**, and **D** forms may have a chlorinating ability and thus chlorinate **5** to give **6**, especially when the reaction temperature is raised. The chlorination by phosgene can not be neglected, either.

The treatment of the tarry residue obtained after column chromatographic separation with water gave a considerable amount of diacylamine (**9**) and a small amount of *N*,*N'*-diacylurea (**11**). The formation of **9** indicates the presence of *N*-(α-chloroalkylidene)-alkylamidine hydrochloride (**8**). As has been reported previously,[7] the pyrimidones **7** are formed by the reaction of **8** with phosgene. The isolation of **8** is now under investigation (Scheme 3).

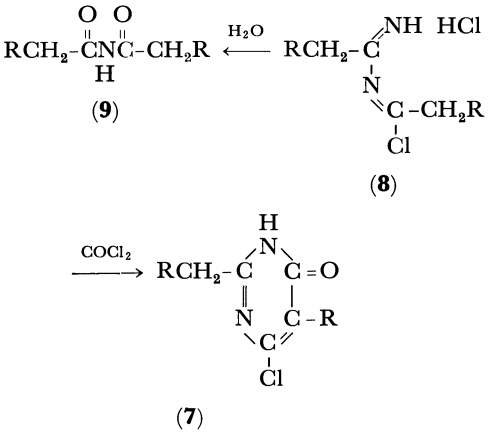

Scheme 3

The isolation of **11** suggests the formation of *N*-(α-chlorobenzylidene)-*N'*-(α-chloroalkylidene)urea (**10**), which appears to be formed by the attack of the carbonyl carbon of **1** on the nitrogen atom of the imidoyl chloride (Scheme 4). The pyrimidone **12**, which may be formed by the intramolecular cyclization of **10**, was not isolated.

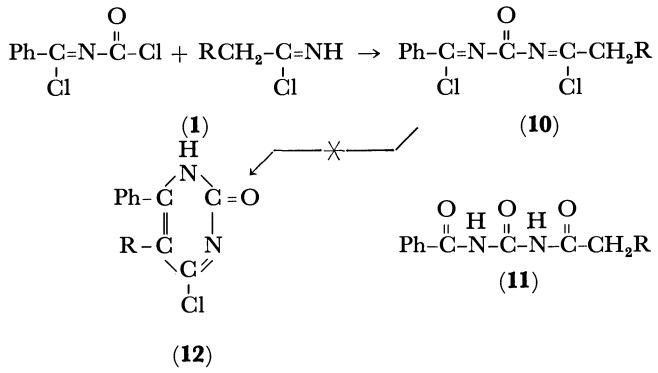

Scheme 4

In our preceding paper[3] we reported that the carbamoyl chloride (**1**) reacts with *p*-tolunitrile or benzonitrile in the presence of hydrogen chloride to give 2-chloro-4-phenyl-6-(*p*-tolyl)-*s*-triazine and 2-chloro-4,6-diphenyl-*s*-triazine respectively. Accordingly, it can be expected that **1** will react with aliphatic nitriles which have no α-hydrogen to give the corresponding triazines. However, the reaction of **1** with trichloroacetonitrile or pivalonitrile in the presence of hydrogen chloride gave only a small amount of 2-chloro-4,6-diphenyl-*s*-triazine, and the expected triazines were not obtained.

Experimental

All the melting points were determined on a Yanagimoto micromelting point apparatus and were corrected. The IR spectra were measured on a JASCO IR-E apparatus, the NMR spectra on a JEOL J.M. M-G-60 apparatus, and the mass spectra on a Hitachi RMU-6E apparatus.

N-(α-chlorobenzylidene)carbamoyl chloride was prepared from benzonitrile, phosgene, and hydrogen chloride according to our method.[3] The fraction with a bp of 85—90°C/1 mmHg was used.

Reaction of Aniline with ***1***. A solution of carbamoyl chloride **1** (1.0 g, 5 mmol) in 10 ml of benzene was added, drop by drop, to a solution of aniline (1.9 g, 20 mmol) in 15 *ml* of benzene under cooling in an ice-water bath. The precipitate thus formed was filtered and washed with cold water. After drying, they were recrystallized from aqueous acetone. The yield was almost quantitative (1.6 g, 100%), but the melting point was broad even after several recrystallizations. It began to melt around 159°C and melted completely below 172°C (lit,[9] 179—180°C) It was identified as *N*-phenyl-*N'*-anilinoformylbenzamidine on the basis of the following analytical results: IR(mull), 3200, 3070, 1695 and 1647 cm^{-1}; NMR(DMSO)(τ), 0.32(s, 1H), 0.55(s, 1H), 2.2—3.2(m, 15H); Mass(M^+) 315. Found: C, 76.30; H, 5.37; N, 13.42%. Calcd for $C_{20}H_{17}N_3O$, C, 76.17; H, 5.43; N, 13.33%,

Reaction of Ammonia with ***1***. The carbamoyl chloride **1** (1.8 g, 9.1 mmol) was stirred into an ethanol solution of ammonia under cooling. The precipitate thus formed was filtered, washed, dried, and recrystallized from a mixed solvent of methanol and isopropanol The yield was 49%. The melting point was also broad even after several recrystallizations. It began to melt around 167°C and melted completely below 185°C.(Lit,[10] 192—194°C). However, it was analyzed and identified as *N*-carbamoylbenzamidine hydrochloride on the basis of the following data: IR(mull), 3280, 3210, 1743 and 1671 cm^{-1}; Mass(M^+−HCl), 163. Found: C, 47.83; H, 5.05; N, 21.05; Cl, 18.09%. Cald for $C_8H_{10}N_3OCl$: C, 48.13; H, 5.05; N, 21.05; Cl, 18.09%.

Reaction of ***1*** *with Hydrazine Hydrate.* An acetone solution of hydrazine hydrate(0.25 g, 5 mmol) was mixed with the carbamoyl chloride **1** (0.5 g, 2.4 mmol) under cooling in an ice-water bath. The precipitate thus formed was treated as usual and recrystallized from acetone (58% yield). It was identified as 3-phenyl-1,2,4-triazolone (**2**) on the basis of the following data; mp 316.0—318.0°C (lit,[11] 321—322°C). Mass(M^+) 161, IR(KBr) *ca.* 3000, 1740 cm^{-1}, NMR (DMSO) (τ) *ca.* 2.25(m, 3H, *o*-H), −1.60(s, 1H, NH), −1.95(s, 1H, NH). Found: C, 59.50; H, 4.49; N, 26.29%. Calcd for $C_8H_7N_3O$: C, 59.62; H, 4.37; N, 26.07%.

Reaction of ***1*** *with Sodium Azide.* To a solution of sodium azide (0.16 g) in 1 m*l* of water we added a solution of the carbamoyl chloride **1** (0.5 g, 2.5 mmol) in 0.75 m*l* of acetone. The mixture was shaken in a water bath at 30°C. The precipitate thus formed was filtered, washed with acetone, and dried *in vacuo*. It was recrystallized from aqueous ethanol and identified as 5-phenyltetrazole (**3**) on the basis of the following analytical results: mp 217.0—219°C(dec)(lit,[12] 215°C(dec)). Mass(M^+) 146, IR(KBr) *ca.* 3000, 1560 cm^{-1}. Found: C, 58.00; H, 3.91; N, 38.53%. Calcd for $C_7H_6N_4$: C, 57.53; H, 4.14; N, 38.33%. Yield, 53%.

Reaction of ***1*** *with Aliphatic Nitriles in the Presence of Hydrogen Chlorides. General Procedure.* In a 20-m*l* glass tube we placed the carbamoyl chloride **1** (9.9 mmol), aliphatic nitrile (20 mmol), and chlorobenzene (2 g). Dry hydrogen chloride (16—17 mmol) was bubbled into the mixture under cooling. The tube was then stoppered, cooled in a dry ice-acetone mixture, sealed carefully, and allowed to stand at 30—35°C or heated to 60—65°C, as is shown in Table 1. After the end of the reaction, the reaction tube was chilled in dry ice-acetone mixture, and opened. The reaction mixture was concentrated under reduced pressure. In some cases, the removal of the hydrogen chloride gave the precipitate of the pyrimidone **5**. After the filtration of the precipitate, the mixture was concentrated as has been mentioned above. The resulting residue was chromatographed on silica gel. The dichloropyrimidines **6** were eluted with petroleum ether, the pyrimidones **5** with chloroform, and the pyrimidones **7** with a mixture of chloroform and ethanol. The pyrimidones **5** were purified by recrystallization from ethanol. The dichloropyrimidines **6** were purified by sublimation or recrystallization from aqueous ethanol. The analytical data are summarized in Tables 2 and 3.

The pyrimidones **7** were identified by comparison with authentic samples.

*Isolation of Diacylamines (****9****) and N-Benzoyl-N'-acylureas (****11****).* Oily products eluted with a mixture of chloroform and ethanol on the above-mentioned column chromatography were treated with aqueous acetone. The reaction mixture was then allowed to stand overnight. The resulting precipitates were filtered and sublimated under reduced pressure. Diacylamines **9** sublimed at 90°C under reduced pressure and *N*-benzoyl-*N'*-acylureas **11** at 140°C under the same conditions.

9) H. L. Wheeler, *J. Amer. Chem. Soc.*, **23**, 223 (1901).

10) K. R. Huffman and F. C. Schaefer, *J. Org. Chem.*, **28**, 1812 (1963).

11) G. Young and E. Witham, *J. Chem. Soc.*, **77**, 224 (1900).

12) A. Pinner, *Ann.*, **297**, 221 (1897).

Table 2. Analyses of 6-chloro-5-alkyl-2-phenyl-4(3*H*)-pyrimidones (**5**)

Pyrimidones (**5**)	mp (°C)	IR (KBr) (cm^{-1})	NMR (in CF_3COOH) (τ)	Mass (70 eV) (M^+)	Elemental analysis[a] C%	H%	N%
5a	228.0—231.0	1680, 1550[b] 1535	1.9—2.6 (m, 5H, ring) 3.13 (s, 1H, CH)	206	58.11 (58.13)	3.30 (3.41)	13.53 (13.56)
5b	272.0—274.0	1642, 1565 1541	1.8—2.4 (m, 5H, ring) 7.58 (s, 3H, CH_3)	220	59.97 (59.87)	3.93 (4.11)	12.81 (12.70)
5c	219.0—220.0	1640, 1573 1540	1.8—2.5 (m, 5H, ring) 7.17 (q, 2H, CH_2) 8.68 (t, 3H, CH_3)	234	61.70 (61.41)	5.00 (4.73)	11.85 (11.94)
5d	195.0—197.0	1648, 1548	1.78 (m, 2H, *o*-ring)[c] 2.53 (m, 3H, m, *p*-ring) 7.35 (t, 2H, CH_2) 8.35 (m, 2H, CH_2) 8.94 (t, 3H, CH_3)	248	62.87 (62.78)	5.18 (5.27)	11.22 (11.26)
5e	194.0—196.0	1650, 1546	1.9—2.5 (m, 5H, ring) 7.18 (c, 2H, CH_2) 8.33 (c, 4H, CH_2CH_2) 8.98 (c, 3H, CH_3)	262	63.87 (64.00)	5.84 (5.76)	10.67 (10.66)

a) Values in parenthesis are calculated ones. b) Nujol. c) In $CDCl_3$.

Table 3. Analyses of 4,6-dichloro-5-alkyl-2-phenylpyrimidines (**6**)

Pyrimidines (**6**)	mp (°C)	IR (KBr) (cm^{-1})	NMR (in CCl_4) (τ)	Mass (70 eV) (M^+)	Elemental analysis[a] C%	H%	N%
6a	97.0[b] 98.0	1545, 1514[c]	1.60 (m, 2H, *o*-ring) 2.56 (m, 3H, *m,p*-ring) 2.82 (s, 1H, CH)	224	53.58 (53.36)	2.57 (2.69)	12.36 (12.45)
6b	111.0—[d] 113.0	1550, 1501, 1405	1.68 (m, 2H, *o*-ring) 2.62 (m, 3H, *m,p*-ring) 7.56 (s, 3H, CH_3)	238	55.43 (55.25)	3.29 (3.37)	11.55 (11.72)
6c	74.0—75.0	1556, 1500, 1406	1.72 (m, 2H, *o*-ring) 2.65 (m, 3H, *m,p*-ring) 7.17 (q, 2H, CH_2) 8.76 (t, 3H, CH_3)	252	57.17 (56.94)	3.94 (3.98)	11.20 (11.07)
6d	67.0—70.0	1551, 1505 1405	1.65 (m, 2H, *o*-ring) 2.61 (m, 3H, *m,p*-ring) 7.17 (t, 2H, CH_2) 8.33 (m, 2H, CH_2) 8.92 (t, 3H, CH_3)	266	58.73 (58.44)	4.56 (4.53)	10.47 (10.49)
6e	62.0—63.0	1556, 1507 1400	1.68 (m, 2H, o-ring) 2.62 (m, 3H, m,p-ring) 7.16 (c, 2H, CH_2) 8.48 (c, 4H, CH_2CH_2) 9.00 (c, 3H, CH_3)	280	59.73 (59.80)	4.97 (5.02)	10.00 (9.96)

a) Values in parenthesis are calculated ones. b) Lit.[13] 96°C. c) Nujol. d) Lit[14] 110°C

N-Benzoyl-N'-acetylurea ***11a*** was confirmed by the following analytical results and by comparing its IR spectrum with that of the authentic sample prepared by the reaction of benzamide with acetyl isocyanate: mp 210—212°C (lit,[15] 187°C); IR(KBr disk) 3360, 3230, 1745 and 1690 cm^{-1}. NMR(CF_3COOH)(τ) 2.07(m, 2H), 2.37(m, 3H), 7.49(s, 3H). Mass(70 eV) *m/e* (rel. intensity) 147(40)-($C_6H_5CONCO^+$), 105(100)($C_6H_5CO^+$), 59(62)(CH_2=C-(OH)NH_2^+). Found: C, 58.43; H, 4.85; N, 13.61%. Calcd for $C_{10}H_{10}N_2O_3$: C, 58.24; H, 4.89; N, 13.59%.

The other ureas (**11**) and diacylamines (**9**) were confirmed on the basis of the IR and mass spectra as follows:

N-benzoyl-N'-valerylurea ***(11b)***: IR(mull) 3320, 3170, 1733, 1683, 1268, and 1190 cm^{-1}. Mass(70 eV) *m/e* (rel. intensity) 248(M^+), 147(30)($C_6H_5CONCO^+$), 105(85)-($C_6H_5CO^+$), 59(100)(CH_2=C(OH)NH_2^+).

N-Benzoyl-N'-caproylurea ***(11c)***: IR(mull) 3320, 3170, 1735, 1683, 1268, and 1187 cm^{-1}. Mass(70 eV) *m/e* (rel. intensity) 262(M^+), 147(7.5)($C_6H_5CONCO^+$), 105(100)-($C_6H_5CO^+$), 59(25)(CH_2=C(OH)NH_2^+).

Divalerylamine ***(9b)***: mp 96.0—99.0°C(lit,[16] 100°C). IR(mull) 3285, 3195, 1740, 1538, and 1506 cm^{-1}. Mass-(70 eV) *m/e* 185(M^+).

Dicaproylamine ***(9c)***. mp 91.0—93.0°C (lit,[17] 92.5°C). IR(mull) 3280, 3200, 1740, 1538, 1505, and 1170 cm^{-1}. Mass (70 eV) *m/e* 213(M^+).

This work has been supported in part by a grant-in-aid from Kokusan Gijutsu Shinkokai. We wish to express our thanks to the founder, the late Mr. Chikara Kurata.

13) J. A. Hendry and R. F. Homer, *J. Chem. Soc.*, **1952**, 328.
14) M. Robba and R. Moreau, *Bull. Soc. Chim. Fr.*, **1960**, 1648.
15) O. C. Billeter, *Ber.*, **36**, 3213 (1903).
16) M. J. Tarbouriech and M. A. Haller, *Compt. Rend.*, **137**, 128 (1903).
17) C. Norstedt and H. A. Wahlforss, *Chem. Ber.*, **25**, Ref., 637 (1892).

Photochemical Rearrangement of *N*-Substituted Benzylanilines[1]

Yoshiro OGATA and Katsuhiko TAKAGI

Department of Applied Chemistry, Faculty of Engineering, Nagoya University, Chikusa-ku, Nagoya

(Received January 26, 1971)

Photochemical migration of an alkyl group from nitrogen to ortho and para positions in *N*-substituted benzylanilines (I) has been studied. Quenching study suggests that the rearrangement proceeds *via* a triplet state. The rate of disappearance of *N*-(*p*-tolyl)-α-phenethylamine (III) in photolysis was found to be 3×10^7—3×10^8 sec^{-1}. Substituted benzylanilines (I) were synthesized to estimate their quantum yields of photorearrangement. A plot of the σ value for a substituent in the migrating benzyl group *vs.* logarithm of relative rate gives a positive ρ value with various quantum yields for intersystem crossing (0.1—1); the ρ value indicates that electron-withdrawing substituents in the benzyl group accelerate the rearrangement. A reaction scheme is presented.

In a previous paper,[2] it was reported that irradiation of *N*-alkylanilines with UV light gave rearranged products, *ortho*- and *para*-alkylanilines (5.5—42.5%), together with aniline (1.6—12.8%) and coupling product of alkyl radicals (0—3%). Intramolecularity of migration of the alkyl group from *N* to ortho and para positions is probable because (i) no cross-bred product was detectable, and (ii) appreciable optical activity was retained in both ortho- and para-rearranged products derived from optically active *N*-α-phenethylaniline.

Photochemical aromatic rearrangements involving the migration of a side-chain group to the ring carbon are known with some aromatic esters,[3] amides,[4] carbonates,[5] ethers,[6] and amines.[2] So far the mechanism of rearrangement has been studied in only a few cases. As an example, it has been suggested in the photo-Fries reaction (X : O, Y : COAr) by either a molecular pathway involving ion-separated intermediate,[7-9] or a radical-pair process in which acyl-O homolysis is followed by an attack of the resulting acyl radical on the ring of phenoxy radical in a solvent cage.[10]

$$C_6H_5\text{-}X\text{-}Y \xrightarrow{h\nu} \begin{matrix}[C_6H_5\text{-}X^- \ {}^+Y] \\ [C_6H_5\text{-}X\cdot \ \cdot Y]\end{matrix} \rightarrow o\text{- and } p\text{-}Y\text{-}C_6H_4\text{-}XH$$

The former molecular mechanism involving ion-separated species seems to be supported by (i) the substituent effect[8,10] with a positive ρ value for migrating benzoyl groups and a negative ρ value for aryloxy groups, (ii) acceleration by polar solvents,[9] and (iii) the quantum yield for *p*-tolyl acetate which is unaffected by a 100-fold change in solvent viscosity, in contrast with 20-fold enhancement of *p*-cresol formation.

N-Alkylanilines generally absorb 243—248 nm light to be excited to charge-separated species (IV),[2] hence electron-withdrawing groups in the migrating alkyl groups and electron-releasing groups on the anilino

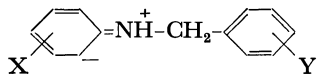

(IV)

group of *N*-alkylanilines may accelerate the rearrangement, if the reaction proceeds *via* a zwitterionic transition state (IV).

Since the mechanistic details of the photorearrangement of *N*-alkylanilines is unknown, we wish to report this mechanism, especially on the basis of substituent effect.

Results

Irradiation of *N*-phenylbenzylamine gave *ortho*- and *para*-benzylanilines (28.9 and 13.6%, respectively) together with aniline (5.8%) and bibenzyl (3.0%).

For elucidation of the reaction pathway, the para-position of the anilino group was shielded by a methyl group to yield ortho-rearranged product alone. A series of *N*-(*p*-tolyl)benzylamines with a substituent on the benzyl group (Ia—If) and phenylbenzylamines with a para substituent on the phenyl group (Ig—Ih) were prepared (Table 3).

The amines (Ia—If) were irradiated with ultraviolet light on a preparative scale as a solution of isopropanol–*t*-butanol (1 : 1 in vol.) (IPA–*t*-BuOH). The reaction products were separated by column chromatography, and identified and estimated by means of UV, IR, TLC and GLC techniques. The yields are summarized in Table 1. An attempt to crystallize the rearranged products failed.

In the case of the nitro compound (If), the rearranged product could not be obtained because of its slow rate of photorearrangement.

Measurement of Quantum Yields. Quantum yields for the disappearance of substrates were measured by the following method under UV light of 2537

1) Contribution No. 142.
2) Y. Ogata and K. Takagi, *J. Org. Chem.*, **35**, 1642 (1970).
3) For a review, see, for example, D. Bellus and P. Hrdlovic, *Chem. Rev.*, **67**, 599 (1967).
4) a) D. Elad, *Tetrahedron Lett.*, **1963** 873. b) H. Shizuka and I. Tanaka, This Bulletin, **41**, 2343 (1968); **42**, 52 (1969); **42**, 909 (1969).
5) a) C. Pac and S. Tsutsumi, *ibid.*, **37**, 1392 (1964). b) A. Davis and J. H. Golden, *J. Chem. Soc., B*, **1968**, 425.
6) a) D. P. Kelley, J. T. Pinhey, and R. D. G. Rigby, *Aust. J. Chem.*, **22**, 977 (1969). b) D. P. Kelley, J. T. Pinhey, and R. D. G. Rigby, *Tetrahedron Lett.*, **1966**, 5953. c) Y. Ogata, K. Takagi and I. Ishino, *Tetrahedron*, **26**, 2703 (1970).
7) M. R. Sandner and D. J. Trecker, *J. Amer. Chem. Soc.*, **89**, 5825 (1967).
8) G. M. Coppinger and E. R. Bell, *J. Phys. Chem.*, **70**, 3479 (1966).
9) D. A. Plank, *Tetrahedron Lett.*, **1968**, 5423.
10) H. Kobsa, *J. Org. Chem.*, **27**, 2293 (1962).

Table 1. Photochemical rearrangement of substituted *N*-benzylanilines[a]

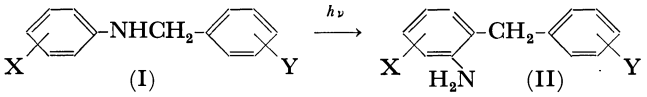

Photolysate	X	Y	Conv. (%)	Yield (%)[b]	Irrad. time (hr)
IIa	*p*-Me	*p*-Me	34.7	24.9	51
IIc	*p*-Me	H	56	24	40
IId	*p*-Me	*p*-Cl	76	12	31
IIe	*p*-Me	*p*-CN	56	31	51

a) In a IPA–*t*-BuOH (*ca.* 0.1 M). The mixtures were condensed by evaporation and chromatographed on a 300×20 mm column of SiO_2. Isomers were confirmed by IR ($-NH_2$), UV, TLC, and GLPC.
b) Based on the consumed substrates.

Å with a low pressure mercury lamp (Halos POL 30). Light intensities were measured with a potassium ferrioxalate solution. Disappearance of secondary amines was potentiometrically determined by Siggia's method.[11]

The reaction was interrupted when the conversion was less than *ca.* 20% to minimize the absorption of the UV light by photoproducts. The quantum yields of the *p*-toluidine formation were determined by GLC. The results are summarized in Table 2.

Table 2. Quantum yields for the disappearance of substituted *N*-benzylanilines and formation of *p*-toluidine

Substituted *N*-benzylaniline	X	Y	Quantum yield (ϕ)	
			Disappearance of starting material	Toluidine formation[b]
Ia	*p*-Me	*p*-Me	0.16±0.01	0.06±0.01
Ib	*p*-Me	*m*-Me	0.15±0.01	0.05±0.01
Ic	*p*-Me	H	0.20±0.02	0.08±0.03
Id	*p*-Me	*p*-Cl	0.23±0.03	—
Ie	*p*-Me	*p*-CN	0.27±0.03	trace
If	*p*-Me	*p*-NO_2	0.13±0.02	—
Ig	*p*-MeO	H	0.22±0.01	—[a]
Ih	*p*-Cl	H	—[a]	—[a]

a) Not determined.
b) Decomposition product.

In the case of amines with an electron-withdrawing group, especially in Ih with para-chloro group in the anilino group, a decrease of amine basicity made potentiometric determination of quantum yield difficult. Table 2 lists average quantum yields calculated from at least three observed values. The difference between these quantum yields is regarded as significant beyond experimental error. The potentiometry was checked to give reliable data of less than 10% error in comparison with GLC technique.

Reaction Multiplicity. In a preliminary experiment, a heavy atom effect was observed, *i.e.*, the photorearrangement of *N*-(*p*-methylbenzyl)aniline was accelerated in *n*-propyl chloride compared with that in *n*-hexane. The result seems to indicate the intermediacy of a triplet state.[12] The reaction multiplicity was further confirmed by quenching experiments. Solutions of 0.02—0.03 M *N*-(*p*-tolyl)-α-phenethylamine in IPA-*t*-BuOH containing a quencher, naphthalene, were irradiated on a merry-go-round apparatus with 2537 Å light. A plot of reciprocal of quantum yield *vs.* quencher concentration lies on a good straight line. The disappearance of substrate and the formation of the rearranged product were measured by GLC.

In quenching by naphthalene, self absorption by the quencher may affect the intensity of incident light. As an example, the ratio of the light quanta absorbed by naphthalene to those by Ia was calculated to be more than 20% in the presence of two equivalent amounts of naphthalene. A singlet state as well as a triplet state may be quenched. Quenching by piperylene was also examined. The Sterm-Volmer plots obtained with piperylene is shown in Fig. 1, in which a fairly good linearity is observed. Piperylene was confirmed to be transparent at least at a wavelength longer than 250 nm, although it exhibits an absorption maximum at 232 nm in methanol. In the measurement of fluorescence intensities of Ia with various amounts of piperylene, neither fluorescence intensity nor the maximum at 370 nm varies with the change of 0—4.5 equivalents amount of piperylene, which implies that piperylene does not quench the singlet of Ia at all, since the Stern-Volmer plot of Fig. 1 is obtained within a range of 3 equivalents amount of piperylene.

The results suggest that the rearrangement occurs *via* a triplet state. The energy transfer from the excited substrate to the quencher would be allowed, since the triplet energies of 61 kcal/mol (naphthalene) and 59 kcal/mol (piperylene) are probably lower than that of substrate, which is expected to be *ca.* 70 kcal/mol from those of aniline (77 kcal/mol), diphenylamine (72 kcal/mol) and triphenylamine (70 kcal/mol).

Measurement of the Rate of Photolysis of III. Aqueous monochloroacetic acid is easily hydrolyzed to give glycolic acid and chloride ion by irradiation of 2537 Å light. The quantum yield for the hydrolysis of the acid (0.5 M) has been determined to be 0.351 at 28°C.[13] The solution was employed as a chemical actinometer, as it is convenient to measure the light intensities of 2537 Å in diffused light. The amount of 0.02 M *N*-(*p*-tolyl)-α-phenethylamine(III) in IPA–*t*-BuOH containing an appropriate amount of piperylene was irradiated by 2537 Å light at 28°C with a merry-go-round apparatus.

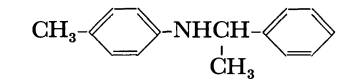

(III)

11) S. Siggia, J. G. Hanna, and I. R. Kervenski, *Anal. Chem.*, **20**, 1295 (1950).

12) S. P. McGlynn, M. J. Reynolds, G. W. Daigre, and N. D. Christobouleos, *J. Phys. Chem.*, **66**, 2499 (1962); S. P. McGlynn, F. J. Smith, and G. Cilento, *Photochem. Photobiol.*, **3**, 269 (1964).

13) a) R. N. Smith, P. A. Leighton, and W. G. Leighton, *J. Amer. Chem. Soc.*, **61**, 2299 (1939). b) L. B. Thomas, *ibid.*, **62**, 1879 (1940).

The conversion of substrate was determined by GLC using acenaphthene as an internal standard. The quantum yield for the disappearance of substrate was calculated to be 0.10 in the absence of a quencher. The Stern-Volmer plots (*cf.* Eq. (2)) obtained from reciprocals of the quantum yields ($1/\phi$) against the piperylene concentration ([Q]) gave a straight line, with a slope of 90 as shown in Fig. 1.

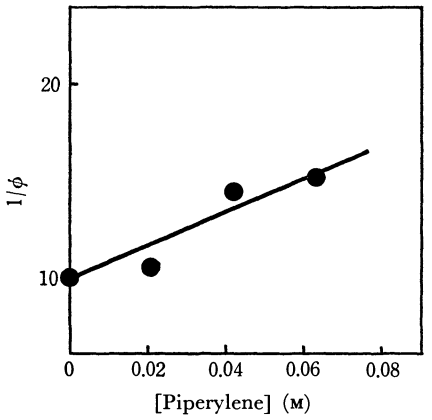

Fig. 1. Stern-Volmer plot of the disappearance of 0.02 M *N*-(*p*-toly)-α-phenethylamine (III).

The quenching rate was estimated by the following Debye equation.

$$k_q = 8RT/3000\eta \quad (1)$$

The rate constant k_q was 2.4×10^9 M$^{-1}\cdot$sec^{-1}, since the viscosity of IPA–*t*-BuOH, was found to be 0.0196 poise at 28°C. In the following Stern-Volmer equation, where k_d and k_r are rate constants for deactivation and reaction, respectively, [Q], the concentration of a quencher, and $f(=\phi_{isc})$, the quantum yield for intersystem crossing from excited singlet state to excited triplet state (Eq. (5)),

$$1/\phi = \{(k_d+k_r)/f\cdot k_r\} + \{k_q\cdot[Q]/f\cdot k_r\}, \quad (2)$$

the slope of the plot of $1/\phi$ *vs.* [Q] gave

$$k_q/f\cdot k_r = 90 \quad (3)$$

Assuming that the quenching rate is equal to the diffusion-controlled rate, we have $f\cdot k_r=2.7\times10^7$ sec^{-1}. The rate constant for the rearrangement was calculated to be 2.7×10^7—2.7×10^8 sec^{-1} because of $0.1<f<1$.

Discussion

The photochemical primary and secondary processes of the reaction can be expressed by means of Eqs. (4)—(10).

$$p\text{-}CH_3\text{-}C_6H_4\text{-}NHR \xrightarrow{h\nu} A^1 \quad (4)$$
$$(A^0)$$

$$A^1 \xrightarrow{k_{st}} A^3 \quad (5)$$

$$A^3 \xrightarrow{k_d} A^0 \quad (6)$$

$$A^3 \xrightarrow{k_r} [p\text{-}CH_3C_6H_4\text{-}NH\cdots\cdots R] \quad (7)$$
$$(I)$$

$$A^3 + Q \xrightarrow{k_q} A^0 + Q^3 \quad (8)$$

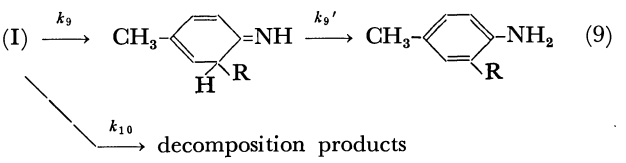

(9)

(10)

These equations give the quantum yield (ϕ) for the disappearance of substrate as

$$\phi = f\cdot k_r/(k_d + k_r + k_q[Q]) \quad (11)$$

From this equation, we obtain the following equation, since no quencher is added to the mixture, *i.e.*, [Q]=0.

$$\frac{1/\phi_H - 1/f_H}{1/\phi_X - 1/f_X} = \frac{f_X\cdot k_{rX}\cdot k_{dH}}{f_H\cdot k_{rH}\cdot k_{dX}} \quad (12)$$

Here, subscript X and H denote *N*-(*p*-tolyl)benzylamine substituted and unsubstituted in the benzyl ring, respectively; subscripts k_r and k_d denote the rate constants for Eqs. (6) and (7), respectively.

In general, the observed quantum yields for substituted *N*-(*p*-tolyl)benzylamines (I) decrease with the increase of electron-donative ability of the substituent, *e.g.*, from 0.27 in Ie (*p*-CN) to 0.16 in Ia (*p*-Me). The approximate linearity of the plot of log ϕ *vs.* Hammett σ was observed, in which a trend of an increase of the quantum yield with the increase of σ is obvious.

Since little information concerning f values is available at present, the following approximation was deduced to see a correlation between the σ value and the relative rate constant k_{rX}/k_{rH}, *i.e.* the approximate independence of f and k_d on substituents.

Firstly, as suggested by Lamola and Hammond,[14a] quantum yield f for intersystem crossing would depend little on substituent X, *i.e.*, $f_H\sim f_X\sim f$. They suggested that the same factors influence the rates of radiationless transitions ($S^1\rightarrow S^0$) and intersystem crossing ($S^1\rightarrow T^1$) in studying the substituent effect of substituted naphthalene on their quantum yields for f values. This means that a substituent hardly affects the efficiency of intersystem crossing.

Secondly, it can be assumed that the deactivation process (corresponding to k_{dX}) from a π–π^* excited state (as well as n–π^*) is hardly affected by substituent X. The approximate constancy of k_{dX}, but not k_{rX}, is often reported.[14b–f] Zimmerman[14c,d] estimated that the decay rate constant k_d remains nearly constant in the photorearrangement of 4,4'-diarylcyclohexanone, while k_r varies over *ca.* 100-fold. Mallory[14e] and Jungmann[14f] reported the substituent effect on the photocyclization of stilbenes to the corresponding phenanthrenes *via* a π–π^* excited state, in which a nice Hammett correlation with the correlation factor of 0.9996 between k_{rX}/k_{rH} and σ is observed assuming the decay

14) a) A. A. Lamola and G. S. Hammond, *J. Phys. Chem.*, **43**, 2129 (1965). b) N. C. Yang and R. L. Dusenbery, *J. Amer. Chem. Soc.*, **90**, 5899 (1968). c) H. E. Zimmerman and W. R. Elser, *ibid.*, **91**, 887 (1969). d) H. E. Zimmerman and N. Lewin, *ibid.*, **91**, 879 (1969). e) F. B. Mallory, J. T. Gorden, and C. S. Wood, *ibid.*, **85**, 828 (1963). f) H. Jungmann, H. Grünsten, and D. Schlte-Frohlinde, *Chem. Ber.*, **101**, 2690 (1968).

rate constant k_{dX} remains constant. The results seem to support the assumption that k_{dX} is approximately constant.

The substituents on the migrating benzyl group are expected to have less effect on the decay process of the excited energy on the aniline ring moiety of the substrate, if the excitation energy related to the 2537 Å light absorption at the latter moiety is localized on the aniline ring.[15]

From the above approximation, we have tentatively assumed that k_{dX} and f_X are independent of X for Ia—If studied. Hence, $(f_X/f_H)(k_{dH}/k_{dX})$ may be approximately constant, and Eq. (12) can be simplified to

$$\frac{1/\phi_H - 1/f}{1/\phi_X - 1/f} = \alpha\frac{k_{rX}}{k_{rH}} \tag{13}$$

where $\alpha = f_X \cdot k_{dH}/(f_H \cdot k_{dX})$. The Hammett equation is then applicable as in Eq. 14 which is shown in Fig. 2 based on the data on Table 2.

$$\log\left(\frac{1/\phi_H - 1/f}{1/\phi_X - 1/f}\right) = \sigma\rho + \text{const.} \tag{14}$$

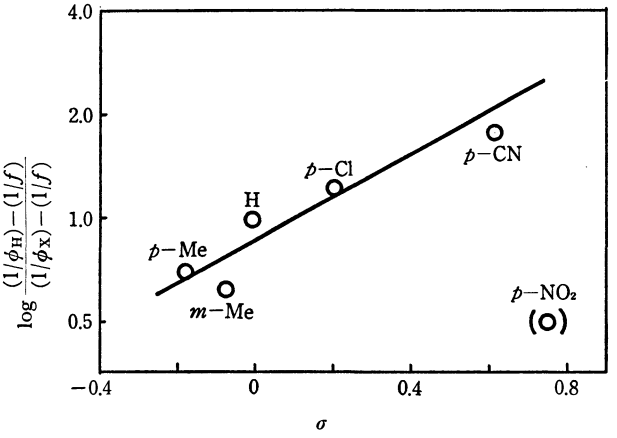

Fig. 2. Relationship between $\log\frac{(1/\phi_H)-(1/f)}{(1/\phi_X)-(1/f)}$ and σ with quantum yields for intersystem crossing (f) of 0.5.

The nitro compound was excluded, since its unusual behavior would be due to the deactivation of excited compound by the reduction of the nitro group to nitroso[16] and/or amino groups.[17]

The σ values used for the plot were quoted from Jaffe's review.[18] A positive ρ value was obtained from Fig. 2 with values of f 0.1—1. A plot of Eq. (14) gave a better correlation than that of log ϕ *vs.* σ value. This also supports the above approximation that k_{dX} is less affected by substituent. A linear Hammett plot has been presented in the photo-Fries reaction,[8,10] which seems to suggest the validity of the Hammett equation for some photoreactions.

The electron density on the anilino nitrogen atom is delocalized into the ring in an excited state of *N*-alkylaniline (*cf.* IV). In the case of ionic mechanism, the requirement for the rearrangement is the electron defficiency at benzyl carbon and the electron richness at ortho position of the anilino ring, thus a positive ρ value for the migrating group can be expected. This ionic scheme, however, cannot explain the by-product, bialkyl. It is natural that the rearrangement almost certainly proceeds *via* a radical process, although the possibility of an ionic rearrangement cannot completely be discarded.

Our previous view that the optical activity is retained in the photorearrangement of optically active *N*-α-phenethylaniline excludes the possibility of the intermediacy of free benzyl radical which should be nearly planar in the migrating transition state. Thus either a bridged intermediate (V), or a radical-pair resulting from the scission of nitrogen-benzyl bond, which can very rapidly recombine in a solvent cage,[10] is conceivable in the transition state.

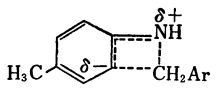

(V)

The positive ρ value can be explained by either reaction scheme. In the bridged scheme, the activated complex V should have more complete benzyl-ortho carbon bond and less complete benzyl-amino nitrogen bond, hence an electron-withdrawing group in the benzyl group can accelerate the rearrangement, because the rate seems to be determined by the electrophilic attack of the benzyl group but not by the benzyl-nitrogen bond fission.

In another mechanism of the homolytic scission in a solvent cage, the positive ρ value can be explained as follows. The rate-determining step for the homolytic rearrangement may be the coupling of benzyl radical with the anilino radical to give products, since the C–N fission step should be rapid in view of the analogous photo-rearrangement of *p*-substituted acetanilides which have high relative ratios ($\phi_B/\phi_F \sim 3$) of quantum yields for coupling of $CH_3CO\cdot$ and Ph-NH· to give starting materials (ϕ_B) compared to those of the forward reactions (ϕ_F).[4b] The observed ρ value suggests a higher contribution of substituent effect on the electrophilic nature of benzyl radical for an attack on the benzene ring. Although the substituent effect of benzyl radical attack is unavailable, reaction rates for phenylation of toluene by substituted phenyl radicals have been reported to vary with substituents in the order: *p*-NO_2>*p*-Cl>H>*p*-Me.[19] This means that the phenylation of toluene has a positive ρ value. Also the effect of substituent in the aryloxy ring in photo-Fries reaction is known to have a positive ρ value.[8,10]

On the other hand, the effect of substituent in anilino group on the present rearrangement is obscure on account of the small number of substituents and the difficulty in analysis. Further, the problem is complicated by the fact that a substituent para to the amino group is also meta to the attacking site. Observed

15) Suggested by the referee.
16) S. H. Hasting and F. A. Matsen, *J. Amer. Chem. Soc.*, **70**, 3514 (1948).
17) R. Hurley and A. C. Testa, *ibid.*, **88**, 4330 (1966).
18) H. H. Jaffe, *Chem. Rev.*, **53**, 191 (1953).
19) W. A. Pryor, "Free Radicals," McGraw-Hill Co., New York, N. Y. (1960), p. 262.

quantum yields are 0.20 (*p*-Me) and 0.22 (*p*-MeO), which are comparable to those observed with the substituents in benzyl groups.

Experimental

All mp and bp are uncorrected. IR spectra were measured by the method of liquid film using a Perkin-Elmer grating infrared spectrophotometer Model 337. UV spectra were measured with a Shimadzu UV spectrophotometer Model SV-50 A or a Hitachi spectrophotometer Model 124. GLC analysis was carried out by means of a Yanagimoto gas chromatograph with FID, Model GCG-550 F, employing a 1.7 m×2.5 mm column packed with PEG 20 M (2.5wt%) on Chamelite CS of 80—100 mesh using N_2 as a carrier gas at 160—250°C. Fluorescence spectra were measured at room temperature with a Hitachi fluorescence spectrophotometer, Model MPF-2A.

Preparation of Substituted Benzylanilines (I). Benzylanilines were prepared by the reaction of *p*-substituted anilines with substituted benzyl chlorides (or bromides) in an aqueous benzene solution containing $NaHCO_3$.[2] The products were purified by vacuum distillation, except for *p*-cyano (Ie) and *p*-nitro compounds (If) which solidified on distillation of starting materials and was purified by recrystallization from petroleum ether. The starting materials are listed in Table 3. All these amines were chromatographed for complete removal of unreacted toluidine before use.

Preparation of N-(p-Tolyl)-α-phenethylamine (III). *N*-(*p*-Tolyl)-α-phenethylamine(III) was prepared by the reaction of *p*-toluidine with α-chloroethylbenzene, mp 68.5—69°C (from petroleum ether), bp 130—133°C/2.5 mmHg, λ_{max}^{MeOH} (nm) (log ε), 248(4.10) and 302(3.27).

Isolation of Rearranged Products. On irradiation of *N*-substituted benzyl(*p*-tolyl)amines in a preparative scale, rearranged products were isolated.

All experiments were carried out in a cylindrical quartz vessel (20×150 mm) under N_2. A Halos high 300 W Hg lamp with a water cooling quartz jacket was used as a light source. Isolated products were identified and estimated by IR, UV, TLC, and GLC.

(2'-Amino-4'-methylphenyl)-4-methylphenylmethane (IIa). A solution of Ia (0.7 g) in *i*-PrOH-*t*-BuOH (30 ml) was irradiated in a quartz vessel for 51 hr. The condensed reaction mixture was chromatographed on a 15×300 mm column, slurry packed in benzene with 80—100 mesh silica gel, using benzene (600 g) and benzene- 3% acetone (100 g) as eluents. Fractions 4—9 was Ia (451 mg), fractions 21—41 was IIa (pale yellow oil, 63.4 mg, 24.9%), λ_{max}^{MeOH} (nm), 238, 292; ν_{max} (cm^{-1}), 3430, 3350, and fraction 85 was *p*-toluidine (62 mg).

(2'-Amino-4'-methylphenyl)phenylmethane (IIc). A solution of Ic (0.7 g) in *i*-PrOH-*t*-BuOH (30 ml) was irradiated for 40 hr. Column chromatography gave recovered starting material (Ic, 350 mg) and a rearranged solid product (IIc, 107 mg, 24%), λ_{max}^{MeOH} (nm), 237, 292; ν_{max} (cm^{-1}), 3430, 3350 (primary amine).

(2'-Amino-4'-methylphenyl)-4-chlorophenylmethane (IId). A solution of Id (0.7 g) in *i*-PrOH-*t*-BuOH (30 ml) was irradiated for 31 hr. In a similar manner, recovered Id (168 mg) and a rearranged liquid product (IId, 64 mg, 12%) were isolated, λ_{max}^{MeOH} (nm), 240 (sh), 294; ν_{max} (cm^{-1}), 3420, 3350 (primary amine), 1090 (C–Cl).

(2'-Amino-4'-methylphenyl)4-cyanophenylmethane (IIe). A solution of Ie (1.795 g) in ethanol (120 ml) in a quartz vessel (35×170 mm) was irradiated for 51 hr at room temperature. Rearranged product IIe (246 mg, 31%) was separated from the reaction mixture by column chromatography, λ_{max}^{MeOH} (nm), 235, 295; ν_{max} (cm^{-1}), 3430, 3350 (primary amine), 2200 (C–N). Rearranged products, except IIc, could not be crystallized even by keeping in an ice-box.

2-Phenethyl-4-methylaniline (IV). A solution of III (0.82 g) in methanol (30 ml) was irradiated in a quartz vessel for 25 hr. The condensed reaction mixture was similarly treated to yield the rearranged product (IV, 155 mg, 22%), ν_{max} (cm^{-1}), 3430 and 3350 (primary amine).

Measurement of Quantum Yield. Quantum yields were determined by method A or B. Method A affords the quantum yield for photolysis of *N*-benzylainlines, and method B

Table 3. Physical properties of substituted *N*-benzylanilines[a]

	X	Y	bp (°C/mmHg)	mp (°C)	λ_{max} (log ε) in MeOH	
Ia	*p*-Me	*p*-Me	130—137/0.5	54.5—55.0 (61—61)[19]	249 (4.18)	301 (3.26)
Ib[b]	*p*-Me	*m*-Me	137—140/1—2	liq.	246 (4.10)	302 (3.27)
Ic	*p*-Me	H	130—137/0.5 (312—313/760)[20]	liq.	249 (4.13)	302 (3.23)
Id	*p*-Me	*p*-Cl	140—147/0.5	46.5—47.0 (47—48)[20]	248 (4.19)	301 (3.31)
Ie[b]	*p*-Me	*p*-CN	—	90—92	241 (4.37)	300 (3.37)
If	*p*-Me	*p*-NO_2	—	68—70 (68)[21]	250 (4.26)	
Ig	*p*-MeO	H	160—170/1—2 (236—238/32)[22]	47—49 (52)[22]	249 (4.18)	312 (3.35)
Ih	*p*-Cl	H	138—150/1	42—43.5 (45)[23]	257 (4.30)	308 (3.34)

a) All materials were purified by column chromatography. b) New compound.

20) H. D. Low, *J. Chem. Soc.*, **101**, 154 (1912).
21) E. Lellmann and N. Mayer, *Ber.*, **25**, 3582 (1892).
22) E. Froelich and E. Wedekind, *ibid.*, **40**, 1010 (1907).
23) D. H. Peacock, *J. Chem. Soc.*, **125**, 1979 (1924).

was used for quenching studies to measure the rate of photolysis of *N*-(*p*-tolyl)-α-phenethylamine (III).

Method A. A spiral type low pressure Hg lamp (Halos POL 30) was employed as a light source of 2537 Å. The light intensity incident on the sample was measured by a potassium ferrioxalate solution as a chemical actinometer. The long-size quartz cell (50×24 mm) for UV spectrophotometer was used as a reaction vessel with flat faces perpendicular to light beams.

About 23 m*l* of a *ca.* 0.04 M amine solution in *i*-PrOH-*t*-BuOH was photolyzed until 20% conversion was attained.

After irradiation, the reaction mixture was diluted to 25.0 m*l* with isopropanol. The amount of photolyzed amine was determined by Siggia's method.[11]

An aliquot (10 m*l*) of the above product solution, after dilution with ethylene glycol (10 m*l*), was potentiometrically titrated with 0.1 N HCl in ethylene glycol-isopropanol.

Neutralization point was determined by plotting the apparent pH against volume of the acid solution to give the total amount of secondary plus primary amines.

Another aliquot (10 m*l*) of the solution was added with ethylene glycol (10 m*l*), and titrated similarly with acid to estimate the amount of the secondary amine after 30 min. mixing excess salicylaldehyde (*ca.* 0.3 m*l*). The amount of photolyzed amine was calculated as a difference (total amine)−(secondary amine), within ±10% experimental error. For example, an *i*-PrOH-*t*-BuOH solution of Ia (1.00×10^{-3} mol) was irradiated by 2537 Å for 10 hr, and then diluted to 25.0 m*l*. An aliquot (10 m*l*) of the diluted solution was potentiometrically analyzed for unreacted secondary amine to be 0.65×10^{-3} mol and the other aliquot (5 m*l*) for the unreacted amine to be 0.59×10^{-3} mol by the method of GLC analysis. Both analytical methods exhibit relative experimental errors below 10%.

Method B. A cylindrical low pressure Hg lamp (Halos HIL 30) was employed as a 2537 Å light source. Irradiation was carried out under diffused light on a turn table which rotates around the light source. Five cylindrical quartz vessels (200×8 mm) were used for the reaction. The incident light intensities were measured on the basis of the known quantum yield (0.351 at 28°C) for photochemical hydrolysis of 0.5 M aqueous monochloroacetic acid by 2537 Å irradiation.[13] The chloride ion produced from the acid was measured by means of back-titration of excess silver nitrate by standard ammonium thiocyanate. An aqueous solution of the acid was photolyzed for 3 hr to yield *ca.* 1.0×10^{-4} mol of chloride ion.

For the quenching studies, a solution of 0.02—0.03 M *N*-(*p*-tolyl)-α-phenethylamine in *i*-PrOH-*t*-BuOH (10 m*l*) containing an appropriate amount of the quencher (0—0.15 M in naphthalene, 0—0.06 M in piperylene) was used.

The authors wish to thank Dr. Y. Izawa for his advice and Sumitomo Chem. Ind. Co. for their gift of materials. Thanks are also due to Dr. K. Aoki for his aid in the fluorescence spectrophotometric analysis.

A Facile Desulfurization Reaction with a Combination of Two Kinds of Metals in Acidic Media. The Synthesis of Hypoxanthine

Nobuhiro NAKAMIZO*, Kazuo SHIOZAKI, Seiichi HIRAI, and Shiro KUDO

Sakai Factory, Kyowa Hakko Kogyo Co., Ltd., Sakai, Osaka

(Received February 15, 1971)

A facile desulfurization procedure has been presented for the method that synthesizes hypoxanthine in one step by heating 4,5-diamino-6-hydroxy-2-mercaptopyrimidine with a desulfurizing agent in formic acid. When Raney nickel prepared in the usual way was used as the desulfurizing agent, it was necessary for the ratio of nickel atoms to sulfur atoms (the Ni/S ratio) to be more than 2.6 : 1. On the contrary, when the Raney alloy *per se* was used, the amount of nickel could be diminished to a catalytic amount (Ni/S 0.2—0.3). The higher the content of aluminum in the alloy, the smaller the Ni/S ratio required for the desulfurization. In contrast with usual desulfurization reactions carried out in neutral media, most of the sulfur was released from the reaction mixture as hydrogen sulfide. Although aluminum or iron powder by itself had little desulfurizing activity, its addition to the Raney alloy was useful in diminishing the Ni/S ratio. Furthermore, combinations of nickel or cobalt salts and aluminum or iron powder were as effective as the Raney alloy as desulfurizing catalysts. In the case of a combination of nickel formate and aluminum powder, a large portion of the nickel ion was proved to be reduced to metallic nickel. The desulfurization reaction also proceeded smoothly in an aqueous solution of hydrochloric or sulfuric acid. On the basis of these facts, a mechanism was proposed with which the active nickel catalyst is regenerated by such auxiliary metals as aluminum or iron.

Since the study[1] by Bougault *et al.* in 1939, desulfurization reactions of sulfur-containing organic compounds by means of Raney nickel have been extensively used both for synthesis and for structure determination.[2-4] In general, the desulfurization reactions are conducted by heating a mixture of sulfur-containing substrates with "excess" Raney nickel (the ratio of Ni : substrate by weight being from about 1 : 1 to 10 : 1) in such a solvent as ethanol. The hydrogen required for the formation of a new C–H bond usually comes, not from external hydrogen, but from that retained by the catalyst during its preparation. Most of the original sulfur is converted to nickel sulfide during desulfurization.[5]

From such characteristics of the reaction, it can be said that it is undesirable for reductive desulfurization to use an amount of Raney nickel less than that required for the formation of nickel sulfide. In practice, much more of the catalyst than the theoretical amount must be used in order to obtain a good yield. From an industrial standpoint, however, not only Raney nickel is expensive, but also its preparation on a large scale is very troublesome. Consequently, in spite of the usefulness of this procedure in laboratory work, its industrial application has been highly limited.

In the synthesis of hypoxanthine (VI) from 4,5-diamino-6-hydroxy-2-mercaptopyrimidine (I) (Scheme 1), the present authors found that, when the desulfurization is carried out with the Raney nickel *alloy* itself or with a combination of a nickel salt and aluminum (or iron) powder in an acidic medium, it is possible to decrease the amount of nickel required to a great extent.

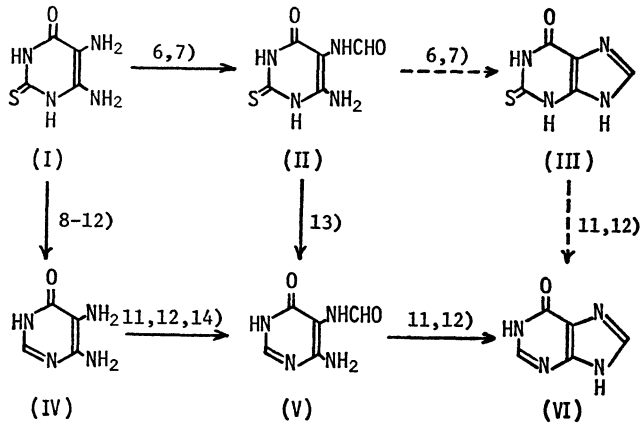

Scheme 1

Experimental

Materials. The formic acid, sodium dithionite, metallic salts, and metallic powder were all of commercial

* Present address: Tokyo Research Laboratory, Kyowa Hakko Kogyo Co., Ltd., Asahi-machi, Machida-shi, Tokyo.

1) J. Bougault, E. Cattelain, and P. Chabrier, *Compt. Rend.*, **208**, 657 (1939).
2) G. R. Pettit and E. E. van Tamelen, "Organic Reactions," Vol. 12, p. 356 (1962).
3) H. Hauptmann and W. F. Walter, *Chem. Rev.*, **62**, 347 (1962).
4) W. A. Bonner and R. A. Grimm, "The Chemistry of Organic Sulfur Compounds," ed. by N. Kharasch and C. Y. Meyers, Vol. 2, Pergamon Press, London (1966), p. 35.
5) L. Granarelli, *Anal. Chem.*, **31**, 434 (1959).
6) W. Traube, *Ann. Chem.*, **331**, 64 (1904).
7) G. B. Elion, W. H. Lange, and G. H. Hitchings, *J. Amer. Chem. Soc.*, **78**, 217 (1956).
8) R. O. Roblin, J. O. Lampen, J. P. English, Q. P. Cole, and J. R. Vaughan, *ibid.*, **67**, 290 (1945).
9) H. Getler, P. M. Roll, J. F. Tinker, and G. B. Brown, *J. Biol. Chem.*, **178**, 259 (1949).
10) A. Albert, D. J. Brown, and G. Cheeseman, *J. Chem. Soc.*, **1951**, 474.
11) G. B. Elion, E. Burgi, and G. H. Hitchings, *J. Amer. Chem. Soc.*, **74**, 411 (1952).
12) Y. Mizuno, T. Ueda, M. Kobayashi, Y. Shimizu and T. Murakami, *Yakugaku Zasshi*, **77**, 686 (1957).
13) G. B. Elion, *J. Org. Chem.*, **27**, 2478 (1962).
14) L. F. Cavalieri and A. Bendich, *J. Amer. Chem. Soc.*, **72**, 2587 (1950).

origin. The Raney nickel alloy was purchased from the Nikki Kagaku Co., Ltd.

4,5-Diamino-6-hydroxy-2-mercaptopyrimidine (I) was prepared by the procedure of Albert *et al.*[10] with some modifications. Into a suspension of 192 g of 4-amino-6-hydroxy-2-mercapto-5-nitrosopyrimidine[6] in 950 m*l* of water, 576 g of sodium dithionite was added with stirring. Within 3 min, the color of the reaction mixture disappeared, the temperature rose from 28°C to 50°C, and the pH dropped from 7 to 5.5. After cooling to 0°C, the product was separated by filtration, washed with water, and dried *in vacuo*. Yield, 99%. (Found: C, 30.69; H, 4.01; N, 35.27; S, 20.41%)

Desulfurization Procedure. In a 3-*l* three-necked flask fitted with a mechanical stirrer, a reflux condenser, and a thermometer, 50.0 g (0.316 mol) of I and 1900 g of formic acid of the concentration desired were placed. After an appropriate amount of the desulfurizing catalyst had then been added, the mixture was refluxed with stirring for eight hours. The gas evolved from the reaction mixture was passed into a 2.5 N solution (1 *l*) of sodium hydroxide in order to collect the hytrogen sulfide, and was finally led to a gas meter. Aliquots of the hydrogen sulfide solution were withdrawn at suitable intervals and analyzed by iodometry. After 8 hr, the waste catalyst was filtered off and washed with formic acid of a concentration equal to that used in the reaction. (Although an evolution of heat from the waste catalyst was sometimes observed during the filtration, there was no danger of ignition.) The filtrate and the washings were then combined and evaporated to dryness under a pressure of 100 mmHg on a water bath. To the residue was added 300 m*l* of water. The crude crystals of hypoxanthine thus obtained were thoroughly triturated, filtered, and washed with 100 m*l* of water.

Analytical Procedure. *Total sulfur* was analyzed by the method of Bethge.[15] *Sulfide-type sulfur* in the waste catalyst was transformed to hydrogen sulfide with hydrochloric acid and determined iodometrically. *Nickel or aluminum* was determined in the form of perchlorate by chelatometric titration. A mixture of an aliquot of the sample dissolved in perchloric acid and 50 m*l* of F/100 EDTA was heated to boiling, and then titrated with F/100 $Pb(NO_3)_2$ at pH 5, using xylenol orange as an indicator, in order to determine the total amounts of Ni and Al.

After this titration, 10 m*l* of a 5% NH_4F solution was added and the mixture was again boiled in order to decompose the Al-EDTA chelate. The EDTA liberated by this treatment was titrated with F/100 $Pb(NO_3)_2$ in order to estimate the amount of Al. From the difference between these two values, the amount of Ni was determined. For samples which contain so little amount Ni or Al that the chelatometric titration could not be used, spectrophotometric analysis[16,17] was applied. If pyrimidines and/or purines were present in the sample, they were decomposed with a nitric acid-perchloric acid mixture before analysing the metals. The amount of metallic nickel in the waste catalyst was determined by subtracting the sum of the amounts of the water-soluble and the sulfide-type nickel from that of the total nickel. Similarly, the amount of metallic aluminum was estimated from the difference between the amount of the water-soluble aluminum and the total aluminum.

15) P. L. Bethge, *Anal. Chem.*, **28**, 119 (1956).

16) H. Kitagawa and N. Shibata, *Bunseki Kagaku*, **7**, 284 (1958).

17) A. D. Horton and P. F. Thomason, *Anal. Chem.*, **28**, 1326 (1956).

Results and Discussion

The Raney-nickel desulfurization reaction is very useful for syntheses of organic compounds, in particular, that of heterocyclic compounds.[2,3] For example, hypoxanthine can be synthesized from 4,5-diamino-6-hydroxy-2-mercaptopyrimidine (I) *via* Raney-nickel desulfurization,[8-12] formylation,[14] and cyclization,[11,12] as is indicated in Scheme 1.

In the procedure to synthesize hypoxanthine in one step by heating the pyrimidine (I) with Raney nickel in 90% formic acid[18], when the ratio of nickel atoms to sulfur atoms (Ni/S ratio) was 6.6 : 1, crude hypoxanthine was obtained in an 87% yield (Table 1). The sulfur content of the product was 0.23%, indicating that the desulfurization was almost complete. The crude product gave pure hypoxanthine in an 83% yield after recrystallization. However, at a Ni/S ratio of less than 2.6 : 1, the reaction was incomplete and gave a deep yellow product which was difficult to purify. Thus, it was confirmed that, so long as Raney nickel is used as a desulfurizing agent, the use of an "excess" of nickel is essential.

Table 1. Desulfurization reactions of I with Raney Ni and Raney alloy in 90% formic acid

Desulfurizing agents	Ni/S	Crude VI yield, %	Sulfur[a] in crude VI %
Raney Ni	6.6	87	0.23
	2.6	79	2.37
	1.8	77	2.73
Ni-Al alloy	2.6	88	0.00
	1.8	78	0.01
	1.3	82	0.00
	1.2	83	0.10
	1.0	76	0.25
	0.8	74	0.08

a) S% for 2-mercapto-6-hydroxypyrimidine: 19.06%.

It is known that the results of the reductive desulfurization depend on the quantity of hydrogen available as well as on that of nickel, as Eqs. (1) and (2) show:

$$\mathrm{R\text{-}S\text{-}R' \xrightarrow{Ni} R\cdot + \cdot R' \begin{cases} \xrightarrow{\text{excess H}} \mathrm{RH + R'H} & (1) \\ \xrightarrow{\text{deficient H}} \mathrm{RR + RR' + R'R'} & (2) \end{cases}}$$

When a so-called "degassed" catalyst is used, dimeric products are mainly produced.[2,3] For the purpose of the hydrogenolytic desulfurization, as in the present work, the more hydrogen there is, the better will be the result. Papa *et al.*[19] found that nickel-aluminum alloy (Raney alloy) and aqueous alkali bring about a rupture of the carbon-sulfur linkage. In this case, the quantity of hydrogen available may be much more than that in the desulfurization with Raney nickel.

18) C.-E. Liau, K. Yamashita, and M. Matsui, *Agr. Biol. Chem.* (Tokyo), **26**, 624 (1962).

19) D. Papa, E. Schwenk, and H. F. Ginsberg, *J. Org. Chem.*, **14**, 723 (1949).

These facts and considerations prompted us to use Raney alloy *per se* in aqueous formic acid. Table 1 shows that, under conditions similar to those used with Raney nickel, the treatment with Raney alloy containing 50% Al by weight leads to an almost complete desulfurization, even when the Ni/S ratio is 0.8 : 1. In contrast with the usual desulfurization, which is carried out in a neutral medium, a large portion of the sulfur eliminated from the substrate during the reaction is transformed into hydrogen sulfide and is released from the reaction mixture. Only a small portion of the sulfur remains in the system as nickel sulfide. When the Ni/S ratio was 0.8 : 1, more than 90% of the sulfur in the starting material was recovered as hydrogen sulfide and nickel sulfide. It should be noted that the gram atoms of sulfur removed amount to more than the nickel used. Furthermore, the value of the Ni/S ratio can be greatly diminished by using a Raney alloy which contains more than 50% aluminum. The results are shown in Table 2. The higher the content of aluminum in the alloy, the smaller the Ni/S ratio required for the desulfurization. By using an alloy which is 70% aluminum, the desulfurization yield reached 90%, even when the Ni/S ratio was 0.2 : 1.

Table 2. Desulfurization reactions of I with Raney alloy in 80% formic acid

Ni-Al alloy	Ni/S	Yield of VI		Sulfur in crystal %	Desulfurization yield, %[a)]
		Crystal	Mother liquor		
Al 58%	0.50	77	9	0.08	94
	0.40	82	8	0.27	94
	0.30	66	10	0.47	91
	0.20	38	17	4.69	72
Al 70%	0.30	79	6	—	92
	0.25	77	5	—	91
	0.20	82	3	—	90

a) $\frac{H_2S(mol)\ evolved + S(atom)\ in\ NiS}{S(atom)\ in\ starting\ material} \times 100$

Figure 1 shows the dependence of the hydrogen sulfide evolution rate on the aluminum contents of the alloys used. If the Ni/S ratio is constant, the higher the content of aluminum, the more rapid the rate of the evolution of hydrogen sulfide.[20)]

Figure 2 shows the effect of the Ni/S ratio on the evolution rate of hydrogen sulfide in the reactions with the alloy containing 70% aluminum in 80% formic acid. The effect of the Ni/S ratio on the hypoxanthine formation rate is indicated in Fig. 3. It can be seen by a comparison of Fig. 3 with Fig. 2 that the rate of the formation of hypoxanthine is independent of the Ni/S ratio, unlike the rate of the evolution of hydrogen sulfide, and that the former is smaller than the latter. These facts suggest that if the requirements for the desulfurization are satisfied, the desulfurization rate can not be rate-determining. The rate-determining step is assumed to be the cyclization step of V to VI for the following reasons: 1) it is well known that the formylation reactions of I to II[6,7)] and of IV to V[14)] are very rapid in hot formic acid; 2) the cyclization reaction

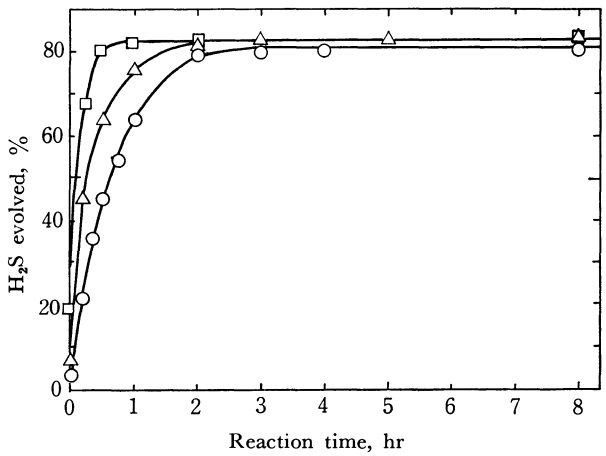

Fig. 1. Effect of Al content on the evolution rate of H_2S (Ni/S=0.30, in 80% HCOOH).
○ Al 58%; △ Al 65%; □ Al 70%

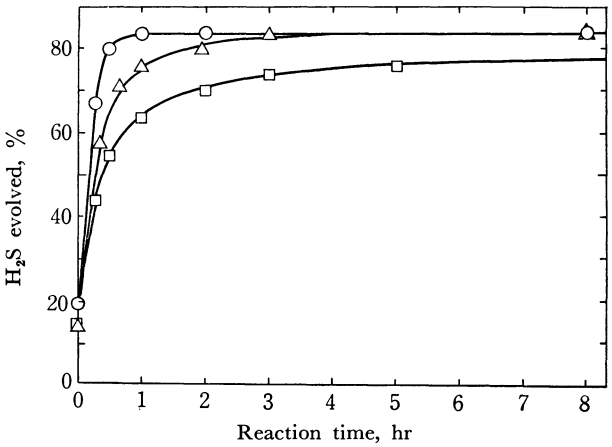

Fig. 2. Effect of the amounts of alloy on the evolution rate of H_2S (Al content of alloy: 70%, in 80% HCOOH).
○ Ni/S=0.30; △ Ni/S=0.25; □ Ni/S=0.20

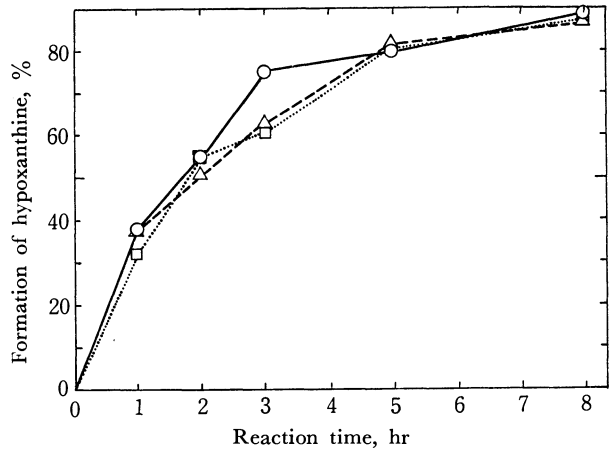

Fig. 3. Effect of the amounts of alloy on the formation rate of hypoxanthine (Al content of alloy: 70%, in 80% HCOOH).
○ Ni/S=0.30; △ Ni/S=0.25; □ Ni/S=0.20

20) It should be remembered that the rate of the evolution of hydrogen sulfide may not necessarily represent the rate of the C–S bond cleavage, because the former rate depends on the rate with which hydrogen carries hydrogen sulfide out of the reaction vessel. As expected, the rate of the evolution of hydrogen becomes more rapid as the quantity of aluminum increases.

of II to III is said to be more difficult than that of V to VI[21]; 3) the ultraviolet absorption spectrum of a spot (R_f 0.61, solvent system 5 N acetic acid : 1-butanol=1 : 2) which appeared on the paper-chromatogram of the reaction mixture was identical with that of V, and 4) V was recovered in a 5% yield from the mother liquor of hypoxanthine after 8 hours of reaction.

Figure 4 demonstrates the effect of the addition of aluminum or iron powder on the desulfurization reaction in which Raney alloy (Ni/S ratio=0.2 : 1) was used. These metallic powders clearly revealed an accelerating effect, though they were not so effective as aluminum in the Raney alloy. Thus, it was established that hydrogenolytic desulfurization in aqueous formic acid does not always require a stoichiometric amount or an "excess" of nickel, provided that a sufficient amount of metallic aluminum or iron is present.

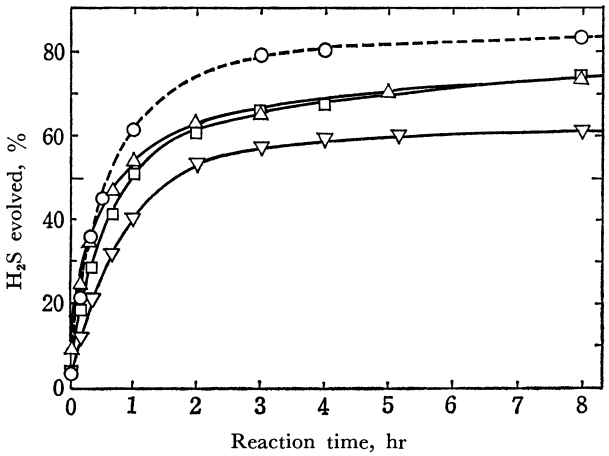

Fig. 4. Effect of addition of Al or Fe powder (Al content of alloy: 58%, in 80% HCOOH).

Ni/S	Additive	Total gram-eqs. of metals
○ 0.30	—	1.04
△ 0.20	Fe	1.04
□ 0.20	Al	1.04
▽ 0.20	—	0.70

As will be described later (see Table 3), metallic aluminum or iron by itself has little desulfurizing activity. Therefore, we propose the following mechanism for the desulfurization reaction with the Raney nickel alloy in acidic media (Eqs. (3) to (9)):

$$\text{-Ni-Al-} + H^+ \rightarrow \text{active Ni} + Al^+ + H \quad (3)$$

$$\text{-Ni-Ni-} + RSH \rightarrow \text{-Ni-R} + \text{-Ni-SH} \quad (4)$$

$$\text{-Ni-R} + H \rightarrow \text{-Ni-} + RH \quad (5)$$

$$\text{-Ni-SH} \rightarrow \text{Ni sulfide} + H \quad (6)$$

$$\text{-Ni-SH} + H^+ \rightarrow Ni^+ + H_2S \quad (7)$$

$$Ni^+ + Al \rightarrow Ni + Al^+ \quad (8)$$

$$\text{-Ni-SH} + H^+ \rightarrow Ni + H_2S + Al^+ \quad (9)$$
(-Al)

To simplify, let us consider the transfer of only one electron.

As is shown in Eq. (3), the Raney nickel alloy reacts with the acid to provide an active catalyst and hydrogen.

The substrate is adsorbed on the nickel surface to give an organic radical (Eq. (4)), which subsequently changes into the final product by combining with a hydrogen atom (Eq. (5)). On the other hand, the sulfur atom bonded to the nickel atom, depending upon the acidity of the medium, yields nickel sulfide (Eq. (6)) or gives a nickel ion and hydrogen sulfide (Eq. (7)). The nickel ion produced in the latter process is again reduced into metallic nickel by metals (these will hereafter be called "auxiliary metals") having a larger tendency of ionization, such as aluminum or iron.

Therefore, the auxiliary metals seem to play two roles, that of a hydrogen-atom supplier for the substrate (Eq. (3)) and that of a reducing agent for ionized nickel (Eq. (8)). Such a regenerating mechanism of metallic nickel with catalytic activity can be operative only when two requirements are satisfied—that metals having a larger tendency of ionization than nickel are present and that the reaction medium is acidic enough to liberate hydrogen sulfide from nickel sulfide. In the case of the Raney alloy, electron transfer from aluminum to nickel may occur within the crystal lattice of the alloy as at the local cells in the corrosion of metals (Eq. (9)). In brief, nickel is considered to be protected by the auxiliary metals against inactivation due to ionization.

If the regenerating mechanism of nickel described above is correct, it will not always be necessary to use nickel in the metallic state, that is, it will be possible to use, for the same purpose, many combinations of appropriate nickel *salts* and metals with oxidation-reduction potentials more negative than that of nickel. This expectation was realized, as is shown in Fig. 5

Table 3. Desulfurization reactions of I with desulfurizing agents other than Raney alloy in 80% formic acid

A	B[a]	A(atom)/S(atom)	H_2S evolved, %
$Ni(HCO_2)_2 \cdot 2H_2O$	Fe powder	0.5	80
$CoCl_2 \cdot 6H_2O$	Fe powder	0.5	80
$CuSO_4 \cdot 5H_2O$	Al powder	0.5	7[b]
$Pb(AcO)_2 \cdot 3H_2O$	Fe powder	0.5	0[b]
$Cd(AcO)_2 \cdot 2H_2O$	Fe powder	0.5	2[b]
$Ni(HCO_2)_2 \cdot 2H_2O$	Zn powder	0.5	7[b]
—	Al powder	—	6[b]
—	Fe powder	—	20
—	Zn powder	—	2[b]

a) 1.74 equivalents to the gram-atom of sulfur in the substrate
b) No hypoxanthine was detected in reaction mixture.

21) R. K. Robins, K. J. Dille, C. H. Willits, and B. E. Christensen, *J. Amer. Chem. Soc.*, **75**, 263 (1953).

Table 4. Fate of nickel and aluminum (in 80% formic acid)

			Ni-Al alloy (Al 58%)				$Ni(HCO_2)_2$+Al
Ni/S			0.50	0.40	0.30	0.20	0.50
Ni	Before the reaction		9.29g	7.41g	5.56g	3.71g	9.29g
	After the reaction	a	2.55	2.35	1.62	2.05	1.78
		b	1.74	1.38	1.29	0.51	0.90
		c	3.54	2.74	2.29	0.00	6.02
		d	0.17	0.14	0.33	1.01	0.03
		total	8.00	6.61	5.53	3.57	8.73
Al	Before the reaction		12.81	10.23	7.69	5.13	21.35
	After the reaction	a	7.69	6.49	5.82	4.05	14.33
		c	3.89	1.77	1.09	0.35	5.54
		d	0.07	0.08	0.12	0.21	0.05
		total	11.65	8.34	7.03	4.61	19.92

a) In soluble in the reaction mixture and water-soluble
b) In NiS
c) Metallic
d) Soluble in the reaction mixture

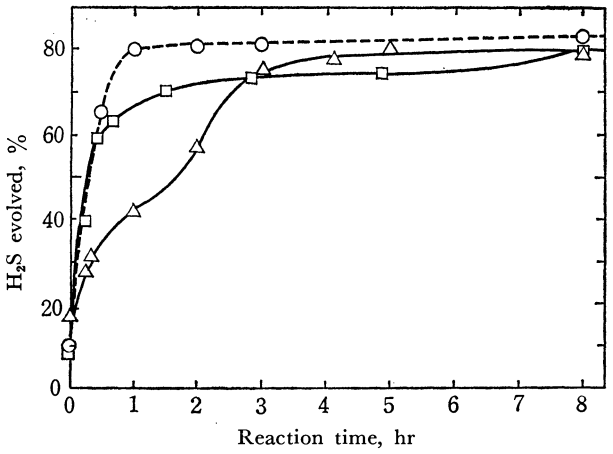

Fig. 5. Desulfurization with Ni or Co salt and Fe powder (in 80% HCOOH).
○ Ni-Al alloy (Ni/S=0.50);
△ $Ni(HCOO)_2 \cdot 2H_2O$ (Ni/S=0.50)+Fe;
□ $CoCl_2 \cdot 6H_2O$ (Co/S=0.50)+Fe

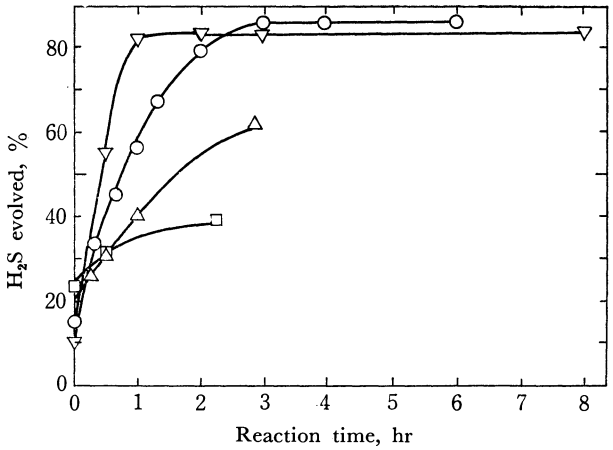

Fig. 6. Desulfurization in various acids.
(Al content of alloy: 58%, Ni/S=0.50)
▽ 80% HCOOH; ○ 1N H_2SO_4; △ 1N HCl; □ 2N HCl

and Table 3. The combination of nickel formate and iron powder caused about 80% of the theoretical yield of hydrogen sulfide to evolve. A similar result was also obtained when the combination of nickel formate and aluminum powder was used. Furthermore, even when a cobaltous chloride-iron powder system was used, a smooth desulfurization reaction was observed.[22]

Table 4 shows the fate of nickel and aluminum after the desulfurization reactions. It is clearly shown in the last column that a considerable portion of the nickel ions in the nickel formate was reduced to metallic nickel. When the desulfurization reaction was incomplete, as when the Ni/S ratio was 0.2 : 1 (see Table 2), little or no metallic nickel and aluminum remained after the reaction.

All of the desulfurization reactions described above were carried out in aqueous formic acid. Hence, there is a possibility that the formic acid might play a specific role in the reductive desulfurization. This is not the case, however. The desulfurization reaction was also successfully performed in some mineral acids, as is shown in Fig. 6. (In these cases, the product was not, of course, hypoxanthine, but 4,5-diamino-6-hydroxypyrimidine.) In particular, 1 N sulfuric acid was a good medium. Hydrochloric acid was inferior to sulfuric acid as a reaction medium. This disadvantage seems to be accounted for by the fact that hydrochloric acid allows a large portion of hydrogen to evolve before the reaction temperature required for desulfurization is reached. Therefore, the kinds and concentrations of acids must be selected so that the reaction of the auxiliary metals with acids does not proceed too violently below the temperature required for the desulfurization.

For the same reason, it is necessary to select the auxiliary metals, which should have a more negative oxidation-reduction potential than nickel (or cobalt), from such metals that the rate of the evolution of hy-

22) Since the presence of the auxiliary metals in the course of the desulfurization reaction is essential for the present purpose, the direct addition of the nickel or cobalt salt and the auxiliary metal to the reaction mixture is of greater advantage than the use of an Urushibara catalyst[23] prepared in the usual way.
23) Y. Urushibara, S. Nishimura, and H. Uehara, This Bulletin, **29**, 446 (1956).

drogen at a given acidity is not so fast as the rate of desulfurization. Zinc powder was, for example, unsuitable as an auxiliary metal, because it reacts with 80% formic acid so rapidly that the evolution of the theoretical amount of hydrogen was completed in the course of raising the temperature (below 60°C) (see Table 3).

Table 3 also reveals that the metallic salts other than nickel and cobalt salts, that is, cupric sulfate, lead diacetate, and cadmium diacetate, have little or no desulfurizing activity. Aluminum or zinc powder by itself shows little activity. As for iron powder, the desulfurization reaction was observed, but to a lesser extent.

Of great interest is the fact that the metals effective for the desulfurization in the present conditions are confined to the Group VIII metals in the periodic table. The question of why the Group VIII metals can dissociate the carbon-sulfur bond in the adsorbed compound into radicals is an important problem to be solved in the future.

In conclusion, the present procedure can be expected to provide a convenient technique for the desulfurization of acid-stable compounds not only in industry, but also in the laboratory.

BULLETIN OF THE CHEMICAL SOCIETY OF JAPAN, VOL. 44, 2197—2202 (1971)

Synthesis of Poly Substituted *cis*-Hydrindanes[1)]

Kagetoshi YAMAMOTO, Takashi SOHDA,* Ichiro KAWASAKI, and Takeo KANEKO**

Faculty of Science, Osaka University, Toyonaka, Osaka

(Received February 17, 1971)

cis-4-Carboxy-5-isopropyl-8-methylhydrindane-1,6-dione was synthesized from *cis*-1-hydroxy-8-methylhydrindanone-5 as a useful intermediate for the synthesis of picrotoxin and dendrobine.

cis-4-Carboxy-6-hydroxy-5-isopropyl-8-methylhydrindane lactone-4,6 (I) is a moiety of picrotoxinin, picrotin, tutin, coriamytrin, dendrobine and related alkaloids which are known as peculiar sesquiterpene and sesquiterpene alkaloid.[2)] *cis*-4-Carboxy-5-isopropyl-8-methylhydrindane-1,6-dione (II) may be regarded as a possible intermediate on the way to the synthesis of these compounds. We have studied the procedure to derive compound II from *cis*-1-hydroxy-8-methylhydrindanone-5 (III), which was prepared according to Boyce's method.[3)]

Formation of γ-lactone on six membered ring of *cis*-hydrindane was first studied. Sodium borohydride reduction of acetate IIIb gave an alcohol in good yield. Dehydration of alcohol IV gave a mixture of olefins V and VI, which could not be separated from each other by means of gas chromatography or TLC. Allylic oxidation of the mixture of olefins with *t*-butyl chromate afforded a mixture of α,β-unsaturated ketones VII (75%) and VIII (25%). Pure compound VII was isolated by chromatography on silica gel. Hydrocyanation of compound VII gave a cyanoketone and a pure epimeric isomer was separated (mp 105—107°C) by chromatography on silica gel. Their stereochemistry was determined by the fact that reduction with sodium borohydride and subsequent hydrolysis gave a γ-lactone (IR: 1760 cm^{-1}). An attempt to introduce an isopropyl group at C_5-position of compound VII was unsuccessful, but we were able to ascertain the procedure of the formation of lactone. We therefore dealt with 5-isopropyl-8-

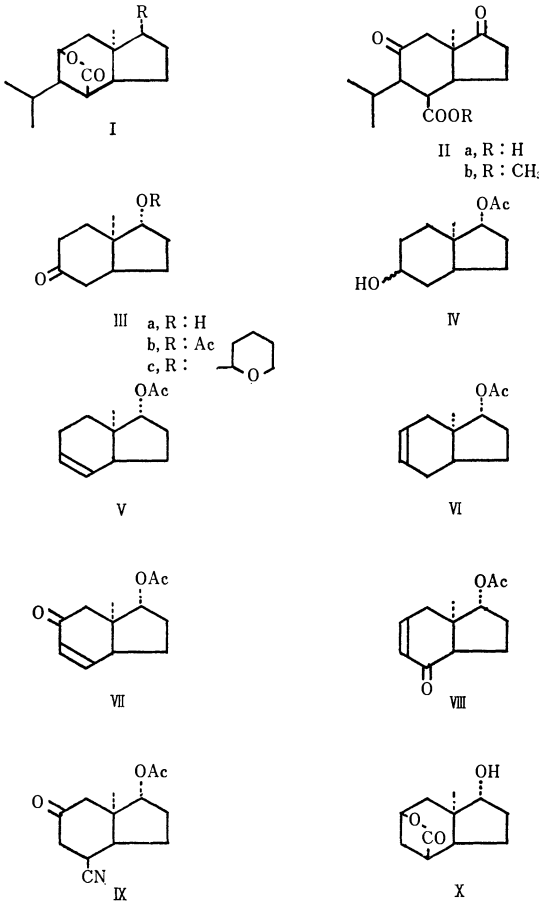

1) A part of this work was presented at the 22nd annual meeting the Chemical Society of Japan, Tokyo, April 3, 1969 and at the 14th symposium on the chemistry of natural products of the Chemical Society of Japan, Fukuoka, October 29, 1970.

* Present address: Chemical Research Laboratories, Takeda Chemical Ind., Ltd., Juso, Higashiyodogawa, Osaka.

** Present address: Research Laboratory of Shiseido Co. Ltd., Nippa-cho, Kohoku-ku, Yokohama.

2) L. A. Poter, *Chem. Rev.*, **67**, 441 (1967).

3) C. B. C. Boyce and J. S. Whitehurst, *J. Chem. Soc.*, **1960**, 4547.

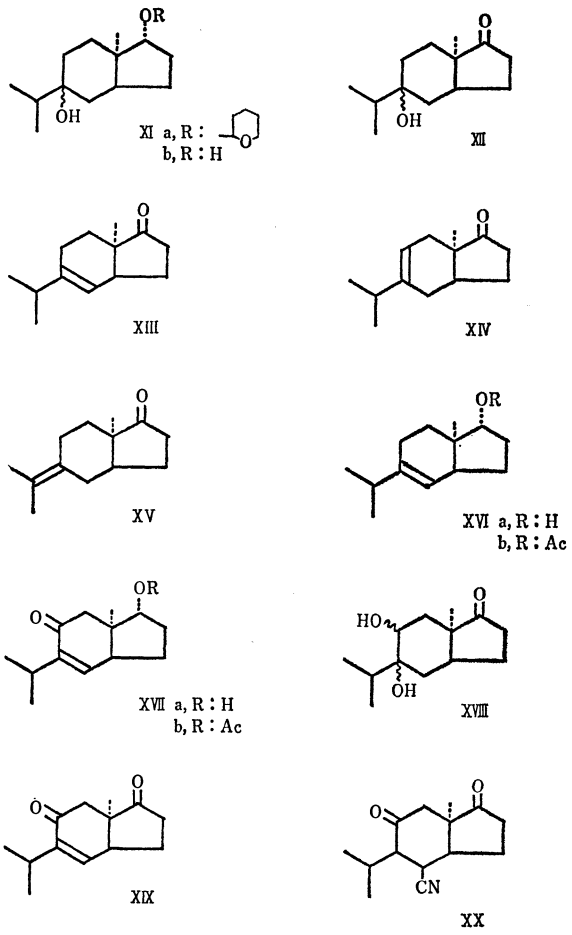

methylhydrindane derivatives in an analogous way.

To introduce the isopropyl group at C_5-position, compound III was treated with dihydropyran and a few drops of concentrated hydrochloric acid to give a pyranyl ether IIIc in good yield. Compound IIIc was treated repeatedly with isopropyllithium in petroleum ether to afford compound XIa in 52% yield. Dialcohol XIb, obtained from compound XIa by treatment with 2 N hydrochloric acid in tetrahydrofuran, was oxidized with chromium trioxide in a mixture of acetone and acetic acid to give a keto alcohol XII.

A Δ^4-olefinic compound will be obtained predominantly by dehydration of compound XII because a Δ^4-olefinic compound is more stable than a Δ^5-olefinic compound in *cis*-8-methylhydrindane system.[4]

A mixture of keto olefins was obtained from compound XII by heating at 200°C with potassium hydrogensulfate. VPC analysis of dehydration products showed three peaks with the ratio 7 : 3 : 1 (retention time: 2.7, 3.8, and 5.5 min, respectively). The main product was isolated by column chromatography using silica gel treated with silver nitrate.[5,6] The remaining isomers were separated by preparative gas chromatography. The structure of the main product XIII was confirmed by NMR spectra which showed olefinic proton at 5.32 ppm (d, 1H, J=2.5 Hz). The structures of the two other keto olefins were elucidated also by NMR spectra. Isomer XIV showed olefinic proton at 5.30 ppm (m, 1H), while isomer XV had no absorption of olefinic proton but olefinic methyl groups at 1.65 ppm (s, 6H).

Three other methods were investigated in order to increase the yield of XIII. Dehydration of XII by treatment with phosphorus oxychloride in pyridine gave XIII : XIV : XV=6 : 3 : 1. Dehydration by treatment with iodine-hydrochloric acid in benzene gave 6 : 3 : 1 and dehydration by heating on alumina which was treated with pyridine[7,8] gave 10 : 5 : 1. Evidently the most useful method was dehydration with potassium hydrogensulfate. Isomerization from XIV and XV to XIII did not occur under the conditions of sodium ethoxide or hydrochloric acid in ethanol.

For the preparation of compound XVII, allylic oxidation of compound XIII was studied. Direct oxidation of XIII with *t*-butyl chromate in benzene afforded an α,β-unsaturated ketone XIX in only 5% yield. On the other hand, reduction of XIII with lithium aluminum hydride in ether and successive acetylation gave compound XVIb in 90% yield. Oxidation of acetyl derivative XVIb with selenium oxide gave compound XVIIb in 19% yield and also gave a small amount of isomerized compound. Oxidation of XVIb with *t*-butyl chromate in benzene under reflux for 60 hr afforded a mixture, which was separated by silica gel chromatography to give compound XVIIb in 11% yield and recovered material XVIb in 50% yield. Therefore the latter route (XIII→XVIb→XVIIb) was useful for the preparation of the compound XVIIb.

Compound XVIIb was hydrolyzed with 2 N sodium hydroxide in methanol and then oxidized with Jones' reagent[9] to give compound XIX in good yield. Its structure was confirmed by the following synthetic route. Isomer XIV was treated with performic acid to afford diol XVIII in 30% yield. By subsequent oxidation with Jones' reagent and dehydration with iodine-hydrochloric acid in benzene under reflux, diol XVIII gave compound XIX in 60% yield. Hydrocyanation of diketo olefin XIX with potassium cyanide and ammonium chloride in dimethylformamide[10] afforded an isomeric mixture of cyanoketone, which showed three spot in TLC (R_f: 0.01, 0.41, and 0.38, ethyl acetate: benzene=3 : 10), in 85% yield. The main product (mp 117—118°C, R_f 0.38) separated by recrystallization, was recognized as an isomer XXi having an axial cyano group and an equatorial isopropyl group, since absorption of α-proton of cyano group appeared at 3.36 ppm (d-d) and their coupling constant was 3.5—1 Hz in NMR spectrum.[11] The conformation of the second isomer

4) L. Velluz, J. Valls, and G. Nonime, *Angew. Chem.*, **77**, 185 (1965).
5) B. de Vries, *Chem. Ind.* (London), **1962**, 1049.
6) A. S. Gupta and S. Dev, *J. Chromatog.*, **12**, 189 (1963).
7) E. J. Corey and A. G. Hortmann, *J. Amer. Chem. Soc.*, **87**, 5736 (1965).
8) E. von Rudolff, *Can. J. Chem.*, **39**, 1860 (1961).
9) A. Bowers, T. G. Halsall, E. R. H. Jones, and A. J. Lemin, *J. Chem. Soc.*, **1953**, 2548.
10) W. Nagata, S. Hirai, H. Itazaki, and K. Takeda, *J. Org. Chem.*, **26**, 2413 (1961).
11) G. J. Karabatos, G. C. Sonnichsen, N. Hsi, and D. J. Fenoglio, *J. Amer. Chem. Soc.*, **89**, 5067 (1967).

(mp 115—116°C, R_f 0.61) obtained by silica gel chromatography of the mother liquor, was suggested to be an isomer XXii by NMR spectrum which showed absorption of α-proton of cyano group at 2.8 ppm and methyl protons of isopropyl group at a lower field than that of XXi. The third isomer XXiii which was expected to have equatorial cyano and isopropyl groups could not be isolated in a pure state. Hydrolysis of the isomeric mixture of cyanoketone XX with 6N sulfuric acid in acetic acid under reflux for 100 hr afforded an isomeric mixture of carboxylic acid IIa. Separation of the isomeric mixture as its methyl ester IIb by chromatography on silica gel resulted in the isolation of an isomer (mp 93—94°C), which was identical with the isomer derived from XXi by TLC and gas chromatography in the same way.

Treatment of the isomer of IIb with methanolic sodium methoxide yielded an equilibrium mixture of IIb and diastereomer having epimeric configuration of carbomethoxyl group.

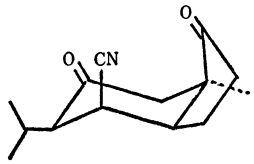

XX

i

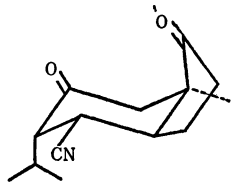

ii

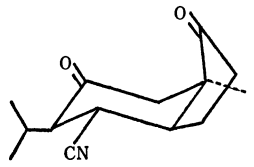

iii

Although the compound we aimed at was synthesized, it takes a long time to purify the intermediate and the method is troublesome. Studies of other methods to synthesize these compounds and the methods available for introduction of carbon chain at C_1-position are in progress.

Experimental

Preparation of 2-Methylcyclopentane-1,3-dione. 2-Methylcyclopentane-1,3-dione was prepared from diethyl oxalate *via* ester condensation according to Boyce's method.[12] Recently Grenda developed a convenient method for its preparation in a large amount from succinic anhydride and 2-buten-2-ol acetate.[13]

12) C. B. C. Boyce and J. S. Whitehurst, *J. Chem. Soc.*, **1959**, 2022.

13) V. J. Grenda, G. W. Lindberg, N. L. Wendler, and S. H. Pines, *J. Org. Chem.*, **32**, 1236 (1967).

cis-1-Hydroxy-8-methylhydrindanone-5 (IIIa). This was prepared by Boyce's method, mp 80—83°C.

cis-1-Acetoxy-8-methylhydrindanone-5 (IIIb). A mixture of IIIa (33.6 g), acetic anhydride (30.6 g), and pyridine (150 m*l*) was allowed to stand overnight, water was added and the separated organic layer was extracted with ether. The ethereal extract was washed and dried. The solvent was removed and the residual oil was distilled, bp 113—116°C/1 mmHg, 37 g (87%). IR: ν^{neat} 1740, 1710 cm^{-1}.

Found: C, 68.25; H, 8.64%. Calcd for $C_{12}H_{18}O_3$: C, 68.54; H, 8.63%.

cis-1-Acetoxy-8-methylhydrindan-5-ol (IV). To a solution of IIIb (36.8 g) in ethanol (100 m*l*) was added dropwise a solution of sodium borohydride (3 g) in ethanol (200 m*l*), and the reaction mixture was stirred for 10 hr at room temperature. Water and acetic acid were added to the reaction mixture which was then concentrated *in vacuo*. Water was added to the residue which was extracted with ether. The ethereal extract was washed and dried. The solvent was removed and the residual oil was distilled to give IV (32 g, 87%), bp 120—125°C/1 mmHg. IR: ν^{neat} 3400, 1740 cm^{-1}.

Found: C, 67.71; H, 9.47%. Calcd for $C_{12}H_{20}O_3$: C, 67.89; H, 9.50%.

cis-1-Acetoxy-8-methyl-6,7,8,9-tetrahydroindane (V and VI). To a solution of IV (21 g) in pyridine (100 m*l*) was added dropwise a mixture of phosphorus oxychloride (23 g) and pyridine (30 m*l*) under ice cooling. The reaction mixture was allowed to stand overnight at room temperature and then heated at 80°C for 4 hr. Ice was added to the cooled mixture and separated organic layer was extracted with ether. The ethereal extract was washed successively with 2N hydrochloric acid, sodium hydrogencarbonate solution and water and dried. The solvent was removed and the residual oil was distilled, bp 124°C/28 mmHg, 10.5 g (56%). IR: ν^{neat} 1740 cm^{-1}. NMR: $\delta(CCl_4)$ 5.62 (m, 2H), 2.0 ppm (s, 3H).

Found: C, 73.70; H, 9.27%. Calcd for $C_{18}H_{18}O_2$: C, 74.19; H, 9.34%.

This oil was a mixture of $\Delta^{4(5)}$- and $\Delta^{5(6)}$-olefin.

cis-1-Acetoxy-8-methyl-6,7,8,9-tetrahydroindanone-6 (VII). To a solution of a mixture of olefin (V and VI, 11.4 g) in benzene (100 m*l*) was added dropwise a solution of *t*-butyl chromate (prepared from 18.5 g of chromium trioxide) in acetic acid (4.5 g) and acetic anhydride (7.5 g) under reflux. After the reaction mixture was heated with stirring under reflux for 20 hr, water was added. Excess reagent was decomposed by addition of oxalic acid and separated organic layer was extracted with benzene. The benzene solution was washed with sodium hydrogencarbonate solution and water, and dried. On removing the solvent, the residual oil gave on distillation a mixture of VII and VIII, bp 124—128°C/3 mmHg, 4 g. The oil was chromatographed on silica gel and the fraction eluted with benzene gave pure VII. IR: ν^{neat} 1740, 1680 cm^{-1}. NMR: $\delta(CCl_4)$ 5.85 (d, 1H, J=10 Hz), 6.80 (d-d, 1H, J=10.5 Hz), 2.00 ppm (s, 3H).

Found: C, 69.47; H, 7.55%. Calcd for $C_{12}H_{16}O_3$: C, 69.21; H, 7.71%.

cis-1-Acetoxy-4-cyano-8-methylhydrindanone-6 (IX). To a solution of VII (1.27 g) in dimethylformamide (30 m*l*) and water (10 m*l*) was added a solution of potassium cyanide (0.54 g) and ammonium chloride (0.46 g) in water (15 m*l*). The reaction mixture was heated at 90°C for 20 hr and then the solvent was removed. To the residue was added water and it was extracted with chloroform. The chloroform solution was washed and dried. On evaporation of the solvent,

the residue was chromatographed on silica gel. The fraction eluted benzene-ether gave 350 mg of a crystalline substance, mp 105—107°C.

Found: C, 66.04; H, 7.19%. Calcd for $C_{13}H_{17}NO_3$: C, 66.36; H, 7.28%.

Reduction and Subsequent Hydrolysis of IX. Above cyanoketone IX (350 mg) was dissolved in ethanol and reduced with sodium borohydride in the usual way. The reaction mixture was evaporated *in vacuo*. Acetic acid and 6N sulfuric acid (3 : 1) were added to the residue and then it was heated under reflux for 30 hr. The hydrolyzate was extracted with ether and dried. On evaporation of the solvent, the residue showed IR absorption band at 1760 cm^{-1}.

cis-*8-Methyl-1-tetrahydropyranyloxyhydrindanone-5 (IIIc).* The ketol IIIa (17 g) was dissolved in 2,3-dihydropyran (50 m*l*) and then a few drops of concentrated hydrochloric acid were added. The reaction mixture was allowed to stand overnight at room temperature. Ether was added and the ether solution was washed with saturated sodium hydrogencarbonate solution and water, and dried. The solvent was removed and residual oil was distilled, 130—135°C/0.001 mmHg, 22 g (93%). IR; ν^{neat} 1720 cm^{-1} (cyclohexanone carbonyl).

Found: C, 71.15; H, 9.51%. Calcd for $C_{15}H_{24}O_3$: C, 71.39; H, 9.59%.

cis-*1-Tetrahydropyranyloxy-5-hydroxy-5-isopropyl-8-methylhydrindane (XIa).* To a solution of IIIc (25 g) in olefin free petroleum ether (50 m*l*), was added a solution of isopropyllithium (prepared from 2.1 g of lithium metal and 12 g of isopropyl chloride) in olefin free petroleum ether under nitrogen. After stirring for 3 hr under reflux, the reaction mixture was decomposed by the addition of 10% ammonium chloride solution (70 m*l*). The separated aqueous layer was extracted with ether. The combined organic layers were washed with saturated sodium chloride solution and dried. The solvent was removed and the remaining viscous yellow oil showed only 30% conversion to alcohol XIa in IR spectra. After three such treatments, the product was distilled, bp 140—145°C/0.001 mmHg, 15.4 g (total yield 52%). IR: ν^{neat} 3400 cm^{-1}. NMR: $\delta(CCl_4)$ 0.92 (d, 3H, J=7 Hz), 0.87 (d, 3H, J=7 Hz), 0.88 (s, 3H), 4.57 ppm (s, 1H).

Found: C, 72.36; H, 10.56%. Calcd for $C_{18}H_{32}O_3$: C, 72.93; H, 10.88%.

cis-*5-Hydroxy-5-isopropyl-8-methylhydrindanone-1 (XII).* To a solution of XIa (36.7 g) in tetrahydrofuran (120 m*l*), was added 2N hydrochloric acid (100 m*l*). After the solution was stirred for 5 hr at room temperature, 2N sodium hydroxide (100 m*l*) was added. The organic layer was separated and the aqueous layer was extracted with ether. The combined extracts were washed with water and dried. The solvent was removed and the residual oil was distilled to give a diol XIb (25 g), bp 135—138°C/0.001 mmHg. IR: ν^{neat} 3400 cm^{-1}. To a solution of XIb in acetone (50 m*l*) and acetic acid (100 m*l*), was added a solution of water (10 m*l*) and acetic acid (90 m*l*) containing chromium trioxide (13 g) under ice cooling. After stirring for 2 days at room temperature, ice (150 g) was added. The aqueous layer was extracted with ether. The ethereal extract was washed with saturated sodium hydrogencarbonate solution, and dried. The solvent was removed and the residual oil was distilled to give a ketol XII (20.5 g, 81%), bp 110—115°C/0.01 mmHg. IR: ν^{neat} 3450, 1740 cm^{-1} (cyclopentanone carbonyl). NMR: $\delta(CCl_4)$ 0.97 (s, 3H), 0.87 ppm (d, 6H, J=7 Hz).

Found: C, 74.24; H, 10.54%. Calcd for $C_{13}H_{22}O_2$: C, 74.11; H, 10.28%.

Dehydration of XII. i) XII (21 g) and potassium hydrogensulfate (2 g) were placed in a Claisen flask and then heated at 200°C for 30 min. After removal of the resulting water, the residue was subjected to distillation to give a mixture of olefins (16 g, 84%), bp 75—77°C/0.1 mmHg.

Found: C, 80.68; H, 10.40%. Calcd for $C_{13}H_{20}O$: C, 81.20; H, 10.48%.

The product showed no absorption of hydroxy group in IR spectra but three peaks by VPC analysis (P.E.G. 6000; their ratio was 7 : 3 : 1). The main product XIII (1.5 g) was isolated from the olefinic mixture (4.0 g) in a pure state by chromatography using silica gel pretreated with silver nitrate. IR: ν^{neat} 1740 cm^{-1}. NMR: $\delta(CCl_4)$ 0.96 (d, 6H, J=7 Hz), 0.94 (d, 3H), 5.32 ppm (d, 1H, J= 2.5 Hz). The second and the third isomer were obtained by preparative VPC (Carbowax-20M, at 170°C). $\Delta^{5(6)}$-Olefin XIV: NMR: δ (CCl_4) 0.94 (s, 3H), 1.02 (d, 6H, J=7 Hz), 5.30 ppm (m, 1H). Isopropylideneindanone XV: NMR: $\delta(CCl_4)$ 1.03 (s, 3H), 1.65 ppm (s, 6H).

ii) To a solution of XII (20 g) in pyridine (200 m*l*) was added phosphorus oxychloride (30.8 g) under ice cooling. The solution was warmed at 50°C for 3 hr. After cooling the solution was poured into ice-water (500 m*l*) and ex tracted with ether. The ethereal extract was washed with 5% hydrochloric acid, 10% sodium hydrogencarbonate solution and water, and dried. The solvent was removed and the residual oil was distilled to give a mixture of olefins (15 g, 84%). The ratio of XIII, XIV, and XV was 6 : 3 : 1 by VPC analysis.

iii) A mixture of XII (2.6 g) and alumina (8.0 g, Woelm grade I neutral, pretreated with 2% solution of pyridine) was evenly distributed on a glass "boat" consisting of a 20 cm glass tube. The glass boat was heated to 230°C by Corey's method under nitrogen. After 5 min, the product began to undergo distillation. The distillate was dissolved in ether and the ether solution was washed with water and dried. The solvent was removed and residual oil was distilled to give a mixture of XIII, XIV, and XV (2.1 g, 80%). Their ratio was 10 : 5 : 1 by VPC analysis.

cis-*1-Acetoxy-5-isopropyl-8-methyl-6,7,8,9-tetrahydroindane (XVIb).* A solution of XIII (13.5 g) in anhydrous ether (75 m*l*) was added to a stirred suspension of lithium aluminum hydride (1.4 g) in anhydrous ether (250 m*l*). The mixture was stirred for 4 hr at room temperature and then the required amount of ethyl acetate and water was added in order to decompose excess lithium aluminum hydride. The organic layer was separated and the aqueous layer was extracted with ether. The combined ethereal extracts were washed with water, and dried. The solvent was removed and the residual viscous oil was dissolved in pyridine (70 m*l*), and acetic anhydride (8 g) was then added under ice cooling with stirring. The reaction mixture was allowed to stand at room temperature overnight and then poured into ice-water. The organic material was extracted with ether and the ethereal extract was washed with water, and dried. The oil obtained by evaporating the solvent was distilled to give an acetate XVIb (14.8 g, 90%), bp 95—97°C/0.1 mmHg. IR: ν^{neat} 1745, 1380, 1240 cm^{-1}. NMR: $\delta(CCl_4)$ 0.97 (s, 3H), 1.0 (d, 6H, J=7 Hz), 2.0 (s, 3H), 4.8 (t, 1H), 5.37 ppm (d, 1H, J=2 Hz).

Found: C, 76.43; H, 10.22%. Calcd for $C_{15}H_{24}O_2$: C, 76.22; H, 10.24%.

cis-*1-Acetoxy-5-isopropyl-8-methyl-6,7,8,9-tetrahydroindanone-6 (XVIIb).* i) To a solution of XVIb (14.8 g) in anhydrous benzene (80 m*l*) was added a mixture of *t*-butyl chromate (prepared from 19 g of chromium trioxide, 13 g of acetic acid and 17.5 g of acetic anhydride) with stirring

at 70°C over 8 hr. After stirring for 40 hr at the same temperature, a solution of oxalic acid (20 g) in water (100 m*l*) was added to the cooled reaction mixture. The organic material was extracted with ether and the extract was washed successively with water, 5% sodium hydrogencarbonate solution and water. The residue obtained by evaporating the solvent was distilled to give 7.5 g of recovered starting material (bp 95°C/0.1 mmHg) and 6.1 g of XVIIb (bp 100—130°C/0.1 mmHg), which was purified by chromatography on silica gel (eluted by petroleum ether : ether= 9 : 1). XVIIb was obtained in a pure state, 1.6 g (11%). IR: ν^{neat} 1745, 1680, 1240 cm^{-1}. UV: λ_{max}^{EtOH} 240 mμ (ε 8600). NMR: $\delta(CCl_4)$ 0.98 (d, 6H, J=7 Hz), 1.08 (s, 3H), 1.82 (s, 3H), 4.75 (broad 1H), 6.24 ppm (d, 1H, J=3.5 Hz).

Found: C, 71.97; H, 8.86%. Calcd for $C_{15}H_{22}O_3$: C, 71.91; H, 8.76%.

ii) To a solution of XVIb (7.5 g) in benzene (60 m*l*) was quickly added selenium oxide (6 g), water (2.4 m*l*) and acetic acid (120 m*l*). The mixture was heated at 80°C for 1 hr. The reaction mixture was cooled to room temperature and added sodium acetate (24 g) and heated at 80°C for 5 min. After cooling, the deposited selenium was filtered off and the filtrate was poured into the saturated sodium chloride solution (240 m*l*). The aqueous layer was extracted with ether. The crude oil (8 g) obtained by evaporating the solvent was dissolved in a mixture of acetone (40 m*l*) and acetic acid (50 m*l*). To this solution was added a mixture of water (2 m*l*) and acetic acid (7 m*l*) containing chromium trioxide (2.5 g). After stirring for 12 hr at room temperature, the solution was poured into 100 g of ice and then extracted with ether. The ethereal extract was washed with saturated sodium hydrogencarbonate solution and water, and dried. The crude oil (5.5 g), obtained by removal of the solvent, gave an α,β-unsaturated ketone XVIIb (1.5 g, 19%) by purification of silica gel chromatography (eluted by petroleum ether : ether=10 : 1).

cis-*5-Isopropyl-8-methyl-6,7,8,9-tetrahydroindane-1,6-dione (XIX).* i) To a solution of XVIIb (1.4 g) in methanol (30 m*l*), was added 2N sodium hydroxide (30 m*l*). The solution was stirred for 4 hr at room temperature and then allowed to stand overnight. The solution was neutralized with acetic acid and evaporated. The residue was extracted with ether and the ethereal extract was washed with saturated sodium chloride solution, and dried. The residual oil obtained by evaporating the solvent was dissolved in acetone (30 m*l*). Jones' reagent (1.6 m*l*) was added to this solution with stirring under ice-cooling. After stirring for 20 min at room temperature, excess reagent was decomposed with methanol. The solvent was evaporated *in vacuo* and water was added to the residue which was extracted with ether. The ethereal extract was dried and evaporated. The residual oil was distilled to give a diketone XIX (1.2 g, 95%), bp 110°C/0.1 mmHg (bath temp.). IR: ν^{neat} 1740, 1680, 1630, 1410 cm^{-1}. NMR: $\delta(CCl_4)$ 0.98 (d, 3H, J=7 Hz), 1.02 (d, 3H, J=7 Hz), 1.10 (s, 3H), 6.47 ppm (d, 1H, J=3.5 Hz).

Found: C, 74.90; H, 8.70%. Calcd for $C_{13}H_{18}O_2$: C, 75.69; H, 8.80%.

ii) To a solution of XIII (5.3 g) in anhydrous benzene (30 m*l*) was added a solution of *t*-butyl chromate (prepared from 8 g of chromium trioxide, 5.3 g of acetic acid and 7 g of acetic anhydride) over 6 hr at 50—60°C with stirring. After stirring for an additional 30 hr at the same temperature, the solution was allowed to stand at room temperature overnight. A solution of oxalic acid (8 g) in water (50 m*l*) was added to the ice-cooled reaction mixture and the separated aqueous layer was extracted with ether. The combined extracts were washed with saturated sodium hydrogencarbonate solution and water, and dried. The residual oil obtained by removal of the solvent was purified by chromatography on silica gel (eluted by petroleum ether : ether=10 : 1) to yield a diketone XIX (250 mg, 4.5%).

iii) To a solution of XVIII (500 mg) in acetone (10 m*l*) was added 0.8 m*l* of Jones' reagent with stirring under ice-cooling. After stirring for 15 min at room temperature, excess reagent was decomposed with methanol (5 m*l*). Water was added and the solution was extracted with ether. The extract was washed with water and dried. The residual oil (450 mg) obtained by removal of the solvent was dissolved in benzene (10 m*l*) and to this solution was added iodine (10 mg) and a few drops of concentrated hydrochloric acid. The mixture was heated under reflux for 20 hr. After cooling, the organic layer was washed with saturated sodium thiosulfate solution and water, and dried. On distillation 300 mg of XIX (68%) was obtained.

cis-*5,6-Dihydroxy-5-isopropyl-8-methylhydrindanone-1 (XVIII).* To a mixture of formic acid (25 m*l*) and 30% hydrogen peroxide (3 m*l*) was added XIV (1.5 g) with stirring at 40°C. After stirring for an additional 4 hr at the same temperature, the reaction mixture was allowed to stand at room temperature overnight. After removal of excess formic acid, the remaining solution was added to a mixture of 10% sodium hydroxide solution (10 m*l*) and dioxane (40 m*l*) and then allowed to stand for one day at room temperature. The reaction mixture was concentrated *in vacuo* and the residue was extracted with ether. The ethereal extract was washed with water and dried. The crystals obtained by evaporating the solvent were recrystallized from ether to give XVIII (100 mg), mp 140—141°C. IR: ν^{nujol} 3450, 1735, 1415, 1380 cm^{-1}.

Found: C, 69.11; H, 9.75%. Calcd for $C_{13}H_{22}O_3$: C, 68.99; H, 9.80%. Concentration of the mother liquors gave an oily diol (450 mg).

cis-*4-Cyano-5-isopropyl-8-methylhydrindane-1,6-dione (XX).* A solution of XIX (1.5 g) in dimethylformamide (45 m*l*) was treated with a solution of potassium cyanide (0.94 g) and ammonium chloride (0.59 g) in water (15 m*l*). After stirring at 100°C for 20 hr, the solution was concentrated under reduced pressure and extracted with chloroform. The extract was washed with water and dried. The residue obtained by evaporating the solvent was crystallized from ether to give XXi (0.50 g), mp 117—118°C. IR: ν^{nujol} 2240, 1745, 1720, 1410, 1380 cm^{-1}. NMR: $\delta(CDCl_3)$ 1.0 (d, 6H, J=7 Hz), 1.26 (s, 3H), 3.36 ppm (d-d, 1H, J=3.5—1 Hz).

Found: C, 72.10; H, 8.20; N, 5.97%. Calcd for $C_{14}H_{19}O_2N$: C, 72.07; H, 8.21; N, 6.00%. Concentration of the mother liquor yielded 1.05 g of oil, from which an isomer XXii (20 mg) was separated by silica gel chromatography (eluted by petroleum ether : ether=10 : 1), mp 115—116°C. IR: ν^{nujol} 2250, 1740, 1715, 1410, 1380 cm^{-1}. NMR: δ ($CDCl_3$) 1.08 (d, 6H, J=7 Hz), 1.25 (s, 3H), 2.8 ppm (m, 1H).

cis-*4-Carboxy-5-isopropyl-8-methylhydrindane-1,6-dione (IIa).* A solution of the isomer XXi (400 mg) in a mixture of acetic acid (7 m*l*) and 6N sulfuric acid (20 m*l*) was heated under reflux for 100 hr. After cooling, the reaction mixture was extracted with chloroform. The extract was washed with water and dried. The crystals obtained by evaporating the solvent were recrystallized from ethyl acetate to give an acid IIa (300 mg, 65%), mp 162—163°C. IR: ν^{nujol} 3500—2500, 1740, 1720, 1690, 1410, 1380, 1185 cm^{-1}. NMR: $\delta(CDCl_3)$ 0.93 (d, 6H, J=7 Hz), 1.15 (s, 3H), 8.95 ppm

(s, 1H).

Found: C, 66.62; H, 7.95%. Calcd for $C_{14}H_{20}O_4$: C, 66.64; H, 7.99%. Its methyl ester had mp 93—94°C.

cis-*4-Carbomethoxy-5-isopropyl-8-methylhydrindane-1,6-dione (IIb)*. A stereoisomeric mixture of XX (750 mg) was hydrolyzed and followed by esterification with ethereal diazomethane. The methyl ester was obtained by distillation, bp 150°C (bath temp.)/0.1 mmHg, 650 mg (80%). The main isomer was isolated by silica gel chromatography (eluted by petroleum ether : ether=200 : 25), 450 mg, which was recrystallized from ether, mp 93—94°C. IR: ν^{nujol} 1750, 1740, 1710, 1405, 1380, 1170 cm^{-1}. NMR: $\delta(CDCl_3)$ 0.95 (d, 3H, J=7 Hz), 1.04 (d, 3H, J=7 Hz), 1.13 (s, 3H), 3.79 ppm (s, 3H).

Found: C, 67.64; H, 8.33%. Calcd for $C_{15}H_{22}O_4$: C, 67.99; H, 8.33%.

BULLETIN OF THE CHEMICAL SOCIETY OF JAPAN, VOL. 44, 2202—2206 (1971)

The Photochemistry of Heterocyclic Compounds. IV. The Mechanism of the Photodecomposition of Alloxan Monohydrate. The Effects of Solvents

Shigeo WAKE, Takeshi MAWATARI, Yoshio OTSUJI, and Eiji IMOTO

Department of Applied Chemistry, College of Engineering, University of Osaka Prefecture, Sakai-shi, Osaka

(Received February 22, 1971)

The photolyses of alloxan monohydrate (**1**) were carried out in water, 2-propanol, and dioxane. Irradiation in water produced alloxantin dihydrate (**2**), glyoxal (**5**), oxaluric acid (**6**), parabanic acid (**7**), and oxalyl diureide (**8**). However, when the photolyses were conducted in 2-propanol and dioxane, **2** and **5** were isolated as the main products. A detailed examination of the changes in the product distributions in the three solvents led to the conclusion that **2** and **5** are produced through the pathways involving the radical fission of the C–OH and C–CO bonds in **1**. On the other hand, **6**, **7**, and **8** were supposed to be produced by the pathways involving the photochemical hydrolysis of **1** to alloxanic acid (**13**).

In the previous papers of this series, we have reported the results of the photolyses of alloxan monohydrate (**1**) and its derivatives in aqueous solutions.[1,2] The irradiation of an aqueous solution of **1** with ultraviolet light afforded hydrogen, hydroxyl radical, alloxantin dihydrate (**2**), and other decomposition products. The processes for the formation of the former three products have been accommodated mechanistically by invoking the water-decomposition pathways illustrated in Scheme 1.

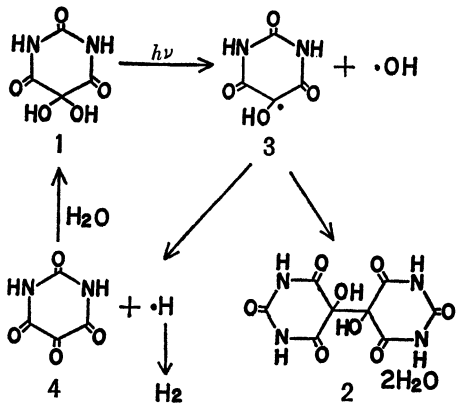

Scheme 1

This photochemical reaction was, therefore, of considerable interest in view of the fact that **1** might serve as a useful catalyst of the photochemical decomposition of water. However, the efficiency of **1** as a catalyst was low because of the participation of decomposition pathways other than those indicated in Scheme 1.

The present study was undertaken in order to obtain more information about the mechanism of the photolysis of **1**. Specifically, the solvent effect on the pathways of the photolysis was examined in detail in the hope of elucidating the nature of the excited state(s) involved. The retults will be presented in this paper.

Results

Photolyses of Alloxan Monohydrate (1). When a dilute solution (3.1×10^{-2} M) of **1** in water was irradiated with a low-pressure mercury lamp under nitrogen at room temperature,[3] **2**, glyoxal (**5**), oxaluric acid (**6**), parabanic acid (**7**), and oxalyl diureide (**8**) were isolated from the reaction mixture.[4] The relative yields of these products were dependent upon the irradiation time. The yield of **2** decreased, and that

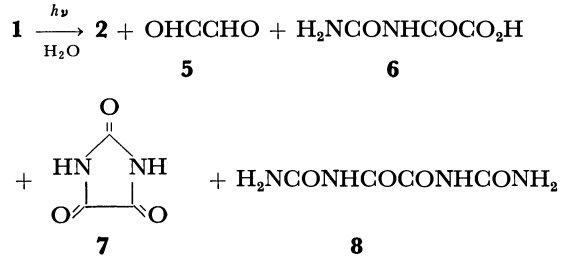

1) Y. Otsuji, S. Wake, and E. Imoto, *Tetrahedron*, **26**, 4139 (1970).

2) Y. Otsuji, S. Wake, and E. Imoto, *ibid.*, **26**, 4293 (1970).

3) Unless otherwise noted, all the irradiations were carried out with a 15-W low-pressure mercury lamp under a nitrogen atmosphere.

4) The evolution of a gas consisting of H_2, CO, and CO_2 was observed during the irradiation of **1**, as has previously been reported.[1] However, in this investigation no detailed analysis of the gas was attempted.

Table 1. The products obtained upon irradiation of alloxan monohydrate (**1**)[a]

Solvent	Irrad. time (hr)	Recovered starting material (%)	Alloxantin · $2H_2O$ (**2**)	Yield of products (%)[c]			
				Glyoxal (**5**)	Oxaluric Acid (**6**)	Parabanic acid (**7**)	Oxalyl diureide (**8**)
Water	3	61	8	0	2.4	—	0
	7	45	16	0.3	2.4	—	0
	20	18	8	1.0	0	47	0
	100[b]	0	0	—	0	28	3.8
2-PrOH	3	39	37	0.3	—	—	0
	7	15	40	0.8	—	—	0
	20	3	0	1.0	—	—	0
Dioxane	1.5	43	17	10	—	—	0
	3.5	26	17	30	—	—	0
	7	13	0	54	—	—	0

a) A 3.1×10^{-2} M solution of **1** was irradiated under N_2 atmosphere.
b) A 6.2×10^{-2} M solution of **1** was irradiated under N_2 atmosphere.
c) Based on total amount of the starting material.

of **5** increased, with an increase in the irradiation time. By 100 hr irradiation, only **7** (28%) and **8** (3.8%) were isolated. The results are summarized in Table 1.

The products were satisfactorily isolated by means of careful fractional crystallizations, as is presented in detail in the Experimental section. The unreacted starting material was separated from the reaction mixture as its semicarbazone (**9**). Glyoxal (**5**) was isolated as its 2,4-dinitrophenylhydrazone (**10**). It must be noticed here that **10** was obtained only when the reaction mixture was heated with an excess of a solution of 2,4-dinitrophenylhydrazine in 2 N hydrochloric acid on a boiling water bath for 3 hr or more. This result implies that **5** is produced by the acid hydrolysis of its precursor, which is presumably an acetal of **5** (**5** itself immediately forms **10** upon treatment with an acidic aqueous solution of 2,4-dinitrophenylhydrazine at room temperature).

The photolyses of **1** were also conducted in dioxane and 2-propanol under conditions similar to those employed for the photolyses in water. In these cases, **2** and **5** were isolated from the reaction mixture, the yields depending also on the irradiation time. The results are included in Table 1. The total yields of the isolated products for the photolyses of **1** in the organic solvents were better than those in water.

*Photolysis of **1** in the Presence of Urea.* We have recently found that, when the photolysis of an aqueous solution of **1** was carried out in the presence of urea, the evolution of H_2 completely ceased, although the evolution of CO and CO_2 was still observed. In order to shed light on the mechanism of this, an aqueous solution (6.2×10^{-2} M) of **1** in the presence of an equivalent of urea was irradiated for 7 hr. The subsequent fractional crystallization of the reaction mixture afforded **2** (0.2%), **8** (0.4%), uric acid glycol semihydrate (**11**, 9.1%), and some unidentified product (s) (**12**).

The compounds **11** and **12** thus obtained were also produced by the reaction of **1** with urea in the dark. A careful examination of this dark reaction revealed that the primary product was **11**, which was then gradually converted to **12**.

These results clearly suggest that a remarkable decrease in the photochemical reactivity of **1** in the presence of urea is due to the dark reaction between them, and that the **11** or **12** formed by this dark reaction would be photochemically unreactive.

Photolyses of Related Compounds. Since alloxanic acid (**13**) and **7** were supposed to be among the intermediates of the photolysis of **1** in water, their photochemistry was examined briefly.

The irradiation of a solution (6.2×10^{-2} M) of **13** in water for 7 hr under nitrogen afforded **6**(3%), **8**(1.3%), and a 1 : 1 adduct(or salt) (**14**, 35%) between **13** and urea, the starting material being recovered in a 49% yield. On the other hand, the irradiation of an aqueous solution of **13** in the presence of air for 7 hr gave **6**(1.8%), **7**(26%), **8**(0.4%), and a 1 : 1 adduct (or salt) (**15**, 3.7%) between **7** and urea along with complex unidentified product(s).

The photolysis of a 6.4×10^{-2} M solution of **7** in water for 3 hr under nitrogen produced **8** (1.4%) and complex unidentified product(s), the starting material being recovered in a 35% yield.

Finally, a solution of **2** in dioxane was photolyzed for 3.5 hr under nitrogen to give **5** in a 40% yield.

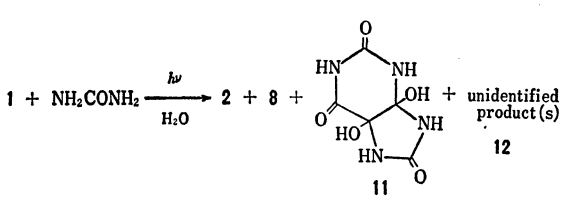

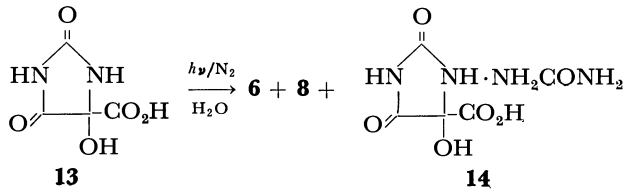

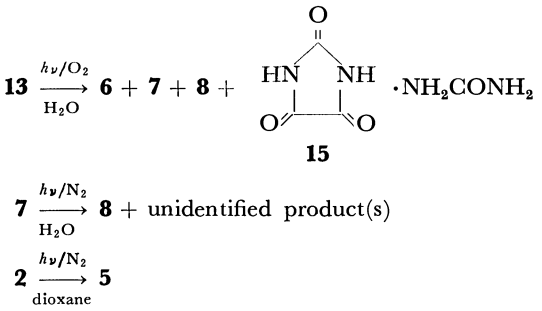

Discussion

A striking observation of this investigation concerns the effects of solvents on the product distributions in the photolyses of **1**. Experimental difficulties prevented us from making complete analyses of the products, specifically in the photolyses in hydroxylic solvents, and so no detailed discussion can be given at the present time; nevertheless, the following important conclusions can be drawn from the data in Table 1: (1) the products **2** and **5** are those derived from a radical intermediate, (2) the pathways leading to **2** and **5** are closely related to each other and **2** is converted to **5**, and (3) the products **6**, **7**, and **8** are those produced through the pathways involving ionic reactions of **1** or **2** with water.

Dioxane does not react to **1** in a manner characteristic of a nucleophilic reagent. Only the radical reactions are, therefore, expected to take place in this medium. Indeed, **6**, **7**, and **8** could not be isolated in detectable yields by the photolyses in dioxane. On the other hand, in water, which possesses a nucleophilic reactivity toward **1**, ionic products, **6**, **7**, and **8**, were formed, making the photochemical reaction a complex one.[5]

On the basis of these considerations as well as other experimental observations, we now propose a probable mechanism for the formation of **2** and **5** (Scheme 2).

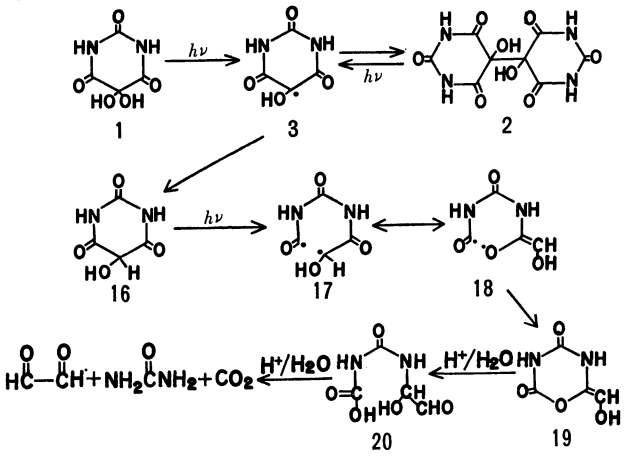

Scheme 2

5) In the experiments in 2-propanol, no attempt was made to isolate of ionic products. However, the tendency for the yields of the products **2** and **5** to vary with the irradiation time in 2-propanol was parallel to that in water, supporting the view that the ionic products are being also formed in 2-propanol.

Evidence that the process **1**→**3** really takes place probably through the $n\rightarrow\pi^*$ state of **1** has been presented in a previous paper.[1] The combination of two of the radical **3** gives **2**. The irradiation of **2** also produces **3**, as may be inferred from the fact that the photolysis of **2** in dioxane gave **5** in a high yield. The disproportionation of **3** or the abstraction of hydrogen atom from solvent by **3** affords dialuric acid (**16**). The cleavage of the C—C bond α to the carbonyl in **16** would produce the lactone **19** *via* **17** and **18**. The process **16**→**19** can be induced by the photoexcitation of **16**. That this kind of reaction really occurs has been established in the photochemistry of cyclic β-diketones. For example, 2-substituted 1,3-indanedione (**21**, R=alkyl or aryl) isomerizes to the phthalide **22** or **23** through the $n\rightarrow\pi^*$ state of **21**[6] upon irradiation with ultraviolet light.

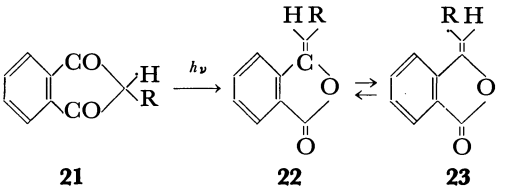

The acid hydrolysis of **19** affords **5**. The presence of the intermediate **19** in the reaction mixture, in which the aldehyde function of **5** is protected, accords with the experimental finding that heating with acid was neccessary to obtain **5**.

The solvent effects observed in this study are also consistent with the mechanism depicted in Scheme 2 if the reaction is initiated by the $n\rightarrow\pi^*$ excited states of **1**, **2**, and **16**. As is well established, the $n\rightarrow\pi^*$ excited state of a carbonyl group can be brought about in a higher probability in non-hydroxylic solvents such as dioxane than in hydroxylic solvents, such as water or 2-propanol. Indeed, our results (Table 1) indicate that **1** was photolyzed much more rapidly in dioxane than in water.

The mechanism of the formation of **6**, **7**, and **8** will now be only briefly discussed. A speculative mechanism which accommodates our results is shown in Scheme 3, although the real pathways must be much more complex.

The process **1**→**13** has been known to be achieved

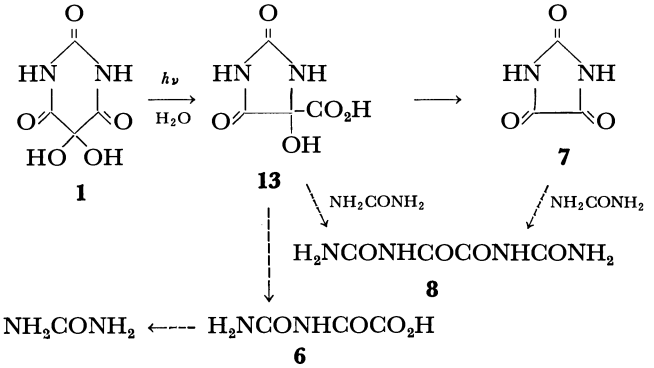

Scheme 3

6) J. Rigaudy and P. Derible, *Bull. Soc. Chim. Fr.*, **1965**, 3047, 3055, 3061.

by the action of alkali on **1**[7] in the dark, but **1** was stable under the conditions of our photochemical reactions. Hence, this process must be of photochemically-accelerated. Our previous work has shown the possibility of this sort of ionic photochemical reaction. Barbital (**24**) has been found to be hydrolyzed to diethylacetylurea by the attack of the hydroxide ion on the carbonyl carbon at the 4-position upon the irradiation of its aqueous solutions through the singlet excited state.[8] The close similarity between the structure of **1** and that of **24** suggests that the similar ionic reaction, which should lead to **13**, might be accelerated by the irradiation. Although the oxidation of **13** has been known to give **7**,[9] this oxidation must be carried out by the hydroxyl radical, which is generated by the irradiation of **1**, in our photochemical reaction. This view is further supported by the fact that the irradiation of **13** in the presence of oxygen caused a remarkable increase in the yield of **7** as compared with that in photolysis under a nitrogen atmosphere. That the other isolated products could, in fact, be produced from **7** and **13** was shown by the photolyses of their aqueous solutions.

Experimental

The melting points are uncorrected. The UV spectra were determined on a Hitachi EPU-2U recording spectrophotometer. The IR spectra were determined on a Hitachi-EPI-S2 infrared spectrophotometer. The microanalyses were performed with a Yanagimoto MT-1 CHN Corder. Irradiation was carried out with a 15 W Taika low-pressure immersion mercury lamp at room temperature.

Materials. Alloxan monohydrate (**1**), alloxantin dihydrate (**2**), and parabanic acid (**7**) were prepared by the methods described in a previous paper.[1] Alloxanic acid (**13**) was prepared from Barium alloxanate[10] by the method of Biltz and Kobel[11] and was purified by means of column chromatography using Amberlite CG-120 Type 1 as the adsorbent and ether as the eluent; mp 153—157°C (decomp.). (Found: C, 30.24; H, 2.71; N, 17.30%. Calcd for $C_4H_4N_2O_5$: C, 30.01; H, 2.52; N, 17.50%).

Preparation of Authentic Samples. Oxaluric acid (**6**) and alloxan-5-semicarbazone dihydrate (**9**) were prepared by the methods described in the previous paper.[1] Oxalyl diureide (**8**) was prepared by the method of Biltz and Topp;[12] mp 250°C (decomp.). (Found: C, 27.56; H, 3.54; N, 32.22%. Calcd for $C_4H_6N_4O_4$: C, 27.59; H, 3.47; N, 32.18%). Uric acid glycol semihydrate (**11**) was prepared by the method of Biltz and Heyn;[13] mp 164—165°C (decomp.). The 1 : 1 adduct (or salt) (**14**) between alloxanic acid (**13**) and urea was prepared by adding a solution of 0.8 g (5 mmol) of **13** in 1 m*l* of water to a solution of 0.3 g (5 mmol) of urea in 0.5 m*l* of water. The mixture was then allowed to stand at room temperature for 12 hr. The crystals thus deposited were collected by filtration to give 0.68 g (62%) of **14**; mp 149—150°C (decomp.). An analytical sample was prepared by recrystallization from water; mp 150—153°C (decomp.). (Found: C, 27.34; H, 3.71; N, 25.35%. Calcd for $C_5H_8N_4O_6$: C, 27.28; H, 3.66; N, 25.45%). The 1 : 1 adduct (or salt) (**15**) between parabanic acid (**7**) and urea was prepared by adding a solution of 2.3 g (20 mmol) of **7** in 40 m*l* of water to a solution of 1.2 g (20 mmol) of urea in 2 m*l* of water. The mixture was allowed to stand at 0°C for 12 hr. The crystals thus deposited were collected by filtration and recrystallized from water to give 2 g (27.5%) of **15**; mp 204—206°C (decomp.). (Found: C, 27.73; H, 3.57; N, 32.37%. Calcd for $C_4H_6N_4O_4$: C, 27.59; H, 3.47; N, 32.18%).

Unless otherwise noted, the structures of the photoproducts were identified by a mixed-melting-point test and by a comparison of the IR spectra of the products with those of the corresponding authentic samples.

*Photoreaction of Alloxan Monohydrate (**1**) in Water.* A solution of 1.5 g (9.4 mmol) of **1** in 300 m*l* of water was placed in a cylindrical reaction vessel, and then N_2 was bubbled for 30 min. Irradiation was then carried out under N_2 at room temperature. After irradiation for an appropriate period of time, the solvent was evaporated to dryness under reduced pressure, and the residue was washed thoroughly with water. The residue was identical with **2** in every respect. The aqueous filtrate was again evaporated to dryness under reduced pressure, and then a 10 m*l* portion of water was added to the residue. An insoluble precipitate, which was separated by filtration, was proved to be **6**. To the filtrate we added a solution of 1 g of semicarbazide hydrochloride and 1.5 g of NaOAc in 10 m*l* of water. The filtration of this mixture gave alloxan-5-semicarbazone dihydrate (**9**); mp 231—232°C (decomp.). Finally, an acid solution of 2,4-dinitrophenylhydrazine was added to the above filtrate, after which the mixture was heated for 3 hr on a water bath and allowed to stand overnight. Filtration gave 2,4-dinitrophenylhydrazone of glyoxal (**10**); mp 309—310°C (decomp.).

When a solution of 3 g (18.7 mmol) of **1** in 300 m*l* of water was irradiated for 100 hr, crystals were deposited on the bottom of the reaction vessel. The crystals were separated by filtration to give 0.06 g (3.8%) of **8**; mp 249°C (decomp.).

*Photoreaction of Alloxan Monohydrate (**1**) in Organic Solvents.* A solution of 1.5 g (9.4 mmol) of **1** in 300 m*l* of an organic solvent was irradiated as has been described above. After irradiation, the solvent was evaporated to dryness under reduced pressure, and the residue was washed with 20 m*l* of water. The aqueous filtrate was evaporated to dryness under reduced pressure, and the residue was washed again with 20 m*l* of water. These evaporation and washing operations were repeated three or four times until no more water-insoluble precipitate was obtained. All of the water-insoluble precipitate was proved to be **2**. The aqueous filtrate obtained by the final washing operation was treated with semicarbazide hydrochloride and then with 2,4-dinitrophenylhydrazine in a manner similar to that described above to give **9** and **10** respectively.

*Photoreaction of Alloxan Monohydrate (**1**) in the Presence of Urea.* A mixture of 3.0 g (18.7 mmol) of **1** and 1.1 g (18.3 mmol) of urea in 300 m*l* of water was irradiated for 7 hr under N_2. A precipitate deposited on the bottom of the reaction vessel was collected by filtration; it was proved to be 7 mg (0.4%) of **8**; mp 249°C (decomp.). The filtrate was evaporated to dryness under reduced pressure and the residue was washed with 20 m*l* of water. An insoluble precipitate, which was separated by filtration, was 7 mg (0.2%)

7) H. Biltz, M. Heyn, and M. Bergius, *Ann. Chem.*, **413**, 68 (1916).
8) Y. Otsuji, T. Kuroda, and E. Imoto, This Bulletin, **41**, 2713 (1968).
9) H. Kwart, R. W. Spayd, and C. J. Collins, *J. Amer. Chem. Soc.*, **83**, 2579 (1961).
10) F. Wöhler and J. V. Liebig, *Ann. Chem.*, **26**, 241 (1838).
11) H. Biltz and M. Kobel, *Ber.*, **54**, 1802 (1921),
12) H. Biltz and E. Topp, *ibid.*, **46**, 1404 (1913).
13) H. Biltz and M. Heyn, *ibid.*, **45**, 1677 (1912); *ibid.*, **47**, 459 (1914).

of **2**; mp 202—203°C (decomp.). The filtrate was evaporated to dryness under reduced pressure. The residue was triturated with 200 m*l* of ethyl acetate and then filtered.[14] The filtrate was evaporated to dryness, and the residue was washed with 10 m*l* of ethyl acetate. The residue was 0.36 g (9.1%) of **11**; mp 170—172°C (decomp.).

*Photoreaction of Alloxanic Acid (**13**).* A solution of 3 g (18.8 mmol) of **13** in 300 m*l* of water was irradiated under N_2 for 7 hr. The filtration of the deposited crystals gave 0.02 g (1.3%) of **8**; mp 218—225°C (decomp.). The filtrate was evaporated to dryness under reduced pressure. The residue was triturated with 200 m*l* of ethyl acetate and then filtered. The evaporation of the filtrate gave 1.47 g (49%) of the starting material. The insoluble solid obtained upon trituration with ethyl acetate was triturated with 5 m*l* of water, after which the water-insoluble crystals were separated by filtration to give 0.075 g (3%) of **6**, mp 172—173°C (decomp.). The evaporation of the aqueous filtrate gave 0.71 g (35%) of the 1 : 1 adduct (or salt) (**14**), which melted at 150.5—151.5°C after recrystallization from water.

*Photoreaction of Alloxanic Acid (**13**) in the Presence of Air.* A solution of 3 g (18.7 mmol) of **13** in 300 m*l* of water was irradiated with bubbling air for 7 hr. The filtration of the deposited crystals gave 6 mg (0.4%) of **8**; mp 224—229°C (decomp.). The filtrate was evaporated to dryness under reduced pressure. The residue was triturated with 80 m*l* of ethyl acetate and then filtered. The evaporation of the filtrate gave 0.56 g (26%) of **7**, which melted at 235—238°C (decomp.) after recrystallization from water. The insoluble solid obtained upon trituration with ethyl acetate was triturated with 5 m*l* of water and the insoluble crystals were separated by filtration. The evaporation of the filtrate gave 1 g of a mixture of complex unidentified products. The recrystallization of the water-insoluble crystals from water gave 45 mg (1.8%) of **6**, mp 193—195°C (decomp.). The mother liquor from the recrystallization was evaporated to dryness, and the residue was recrystallized from water to give crystals (0.06 g) which were identified as the 1 : 1 adduct (or salt), **15**.

*Photoreaction of Parabanic Acid (**7**) in Water.* A solution of 2.2 g (19 mmol) of **7** in 300 m*l* of water was irradiated under N_2 for 3 hr. The filtration of the deposited crystals gave 0.03 g (1.4%) of **8**, mp 238°C (decomp.). The filtrate was evaporated to dryness under reduced pressure, and the residue was washed with 20 m*l* of acetone. The filtration of the insoluble precipitate gave about 0.8 g of a mixture of complex unidentified products. The evaporation of the filtrate gave 0.77 g (35%) of **7**.

*Photoreaction of Alloxantin Dihydrate (**2**).* A solution of 0.5 g of **2** in 300 m*l* of dioxane was irradiated, and then the reaction mixture was treated in a manner similar to that employed for **1** in dioxane.

14) The structure of the residue, 1.3 g, mp 159—160°C (decomp.), remains unidentified. However, this residue showed the same IR spectrum as that of the unknown by-product obtained by the treatment of **1** with urea in the dark.

Studies on Stable Free Radicals. V[1]

Reactivity of a Stable Free Radical, 2,2,6,6-Tetramethyl-4-oxopiperidine-1-oxyl

Takao YOSHIOKA, Susumu HIGASHIDA, Syoji MORIMURA, and Keisuke MURAYAMA

Central Research Laboratories, Sankyo Co., Ltd., Shinagawa-ku, Tokyo

(Received February 22, 1971)

A stable *N*-oxyl radical, 2,2,6,6-tetramethyl-4-oxopiperidine-1-oxyl (I), afforded 1-hydroxy-2,2,6,6-tetramethyl-3-(2,2,6,6-tetramethyl-4-oxopiperidinoxy)-4-oxopiperidine (IX) by hydrogen-abstraction followed by the coupling reaction of the *N*-oxyl radical I with the *C* radical III derived from I. The product IX was characterized as the monoacetate (X), monobenzoate (XI), urethane (XII), semicarbazone (XIII), triol (XIV), triacetate (XV), and a new *N*-oxyl radical (XVI). It has been confirmed that i) the extremely stable *N*-oxyl radical abstracts the α-methylene-hydrogen of the ketone which affords a thermodynamically stable conjugated ketone, ii) radical I acts as a scavenger toward a *C*-radical intermediate and iii) the decomposition of radical I proceeds *via* the *C*-radical to give phorone (V).

Recently, the fact that 2,2,6,6-tetramethyl-4-oxopiperidine-1-oxyl (I) and its analogs are extremely stable free radicals[2] has been established by the elegant studies of Rozantzev and his co-workers.[2a] In spite of the stabilization of radical I, it was found that these radicals still have the ability to act as a hydrogen abstracting agent,[3] an oxdizing agent,[3f,4] and a radical scavenger.[3d-g] In addition, we found that the *N*-oxyl I decomposed to give the corresponding hydroxylamine II and phorone (V) by heating, but did not decompose by the action of light.[3g]. The probable mechanism for the decomposition of radical I is shown in Chart 1. The free radical intermediate III, which

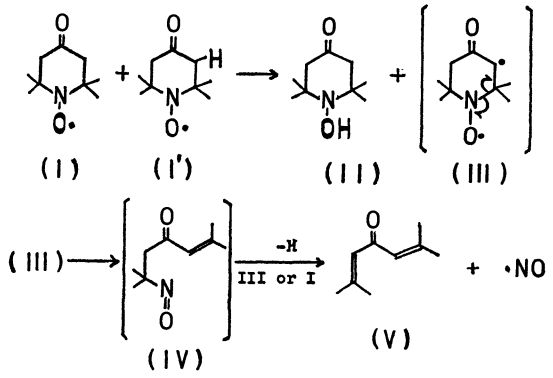

Chart 1

would be generated by the abstraction of an α-methylene ketone hydrogen by another radical I (=I'), was proposed.[3g] This mechanism was supported by the fact that the original radical I trapped intermediate III to give the coupling reaction product, 1-hydroxy-2,2,6,6-tetramethyl-3-(2,2,6,6-tetramethyl-4-oxopiperidinoxy)-4-oxopiperidine (IX) (Chart II).

Results and Discussion

When crystals of 2,2,6,6-tetramethyl-4-oxopiperidine-1-oxyl (I) were allowed to stand at room temperature for six months, the paramagnetic substance liquefied with subsequent formation of a grey precipitate (mp 139—140°C) which was shown to be diamagnetic by an ESR technique. Further, this product IX could be isolated as a by-product, when the *N*-oxyl I was prepared from the corresponding hindered amine[5] at temperatures 50—60°C. Elemental analysis, molecular weight determination and mass spectral data gave the formula $C_{18}H_{34}N_2O_4$ which corresponded to an O,O coupled dimer (VII) or an aldol condensation product (VIII). Structures VII and VIII were eliminated for the following reasons. In the IR spectrum, this product had a carbonyl band at 1720 cm^{-1} and a hydroxy band at 3360 cm^{-1}. In the NMR(τ)(100 Mc, in $CDCl_3$), it had a broad singlet at 5.25—5.60 (1H), a doublet at 5.74 (1H, J=1.5 Hz), a doublet at 7.12 (1H, J=12.0 Hz), a doublet of doublets at 7.61 (1H, J=12.0 Hz, 1.5 Hz), a broad apparent triplet due to an AA'BB' system (4H, J= *ca.* 15 Hz), and five singlets due to unequivalent methyl proton signals 8.65, 8.70, 8.72, 8.76 and 8.81 (24 H). From these spectral data, the structure of the product, $C_{18}H_{34}N_2O_4$, was assigned to be 1-hydroxy-2,2,6,6-tetramethyl-3-(2,2,6,6-tetramethyl-4-oxopiperidinoxy)-4-oxopiperidine (IX). The product IX was treated with acetic anhydride, benzoic anhydride, phenyl isocyanate, semicarbazide or sodium borohydride to give a monoacetate (X), a monobenzoate (XI), an urethane (XII), a disemicarbazone (XIII) or a triol (XIV),[6] respectively (Chart II). The derivatives X, XI and XII had no hydroxy band in the IR spectra. On exposure to air, triol XIV changed into 2,2,6,6-tetra-

1) Part IV. Ref. 3 g.

2) a) E. G. Rozantzev, "Free Nitroxyl Radicals," Plenum Press, New York, N. Y. (1970), p. 1. b) A. R. Forrester, J. M. Hay, and R. H. Thomson, "Organic Chemistry of Stable Free Radicals," Acad. Press, New York, N. Y. (1968), p. 180. c) K. Murayama, *Uki Gosei Kagaku Kyokai Shi*, **29**, 366 (1971).

3) a) M. S. Khloplyankina, A. L. Buchachenko, M. B. Neiman, and A. G. Vasil'eva, *Kinetika i Kataliz*, **6**, 394 (1965). b) A. L. Buchachenko, O. P. Sukhanova, L. A. Kalashnikova, and M. B. Neiman, *ibid.*, **6**, 601 (1965). c) V. V. Gur'yanova, B. M. Kovarskaya, L. A. Krinitskaya, M. B. Neiman, and E. G. Rozantzev, *Vysokomolekul Soedin*, **7**, 1515 (1965). d) E. G. Rozantzev and V. A. Golubev, *Izv. Akad. Nauk SSSR, Ser. Khim*, **1966**, 891. e) K. Murayama, S. Morimura, and T. Yoshioka, This Bulletin, **42**, 1640 (1969). f) K. Murayama and T. Yoshioka, *ibid.*, **42**, 1942 (1969). g) K. Murayama and T. Yoshioka, *ibid.*, **42**, 2307 (1969).

4) a) C. M. Poleos, N. M. Karayannis, and M. M. Labes, *Chem. Commun.*, **1970**, 195. b) K. Murayama, S. Morimura, and T. Yoshioka, Presented at the 90 th Annual Meeting of the Pharmaceutical Society of Japan, Sapporo, July, 1970, Preprints of the Meeting, No. II (1970), p. II—57.

5) a) F. Francis, *J. Chem. Soc.*, **1927**, 2897. b) D. Mackay and W. A. Waters, *ibid.*, *C*, **1966**, 813. c) K. Murayama, S. Morimura, O. Amakasu, T. Toda, and E. Yamao, *Nippon Kagaku Zasshi*, **90**, 296 (1969).

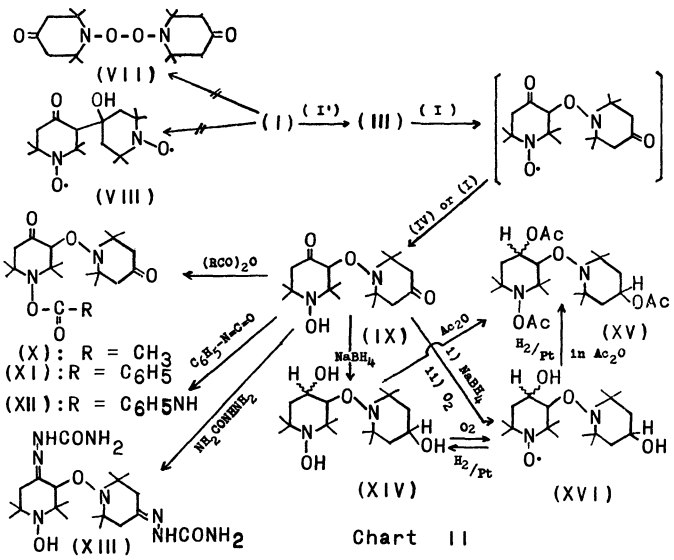

methyl-3-(2,2,6,6-tetramethyl-4-oxopiperidinoxy)-4-oxopiperidine-1-oxyl (XVI). When the new *N*-oxyl radical XVI was hydrogenated in the presence of the Adams catalyst in acetic anhydride solution, the corresponding triacetate (XV),[6] which was identical with triacetate derived from triol XIV, was obtained in good yield. These chemical reactivities corresponded to the properties of the assigned structure IX.

Thus we confirmed that i) the extremely stable *N*-oxyl radical I abstracted the α-methylene-hydrogen of the ketone which could give a thermodynamically stable conjugated ketone[3], ii) the radical I trapped a *C*-radical intermediate such as III, and iii) the decomposition of the radical I proceeded *via* the *C*-radical such as III to give phorone (V).

6) a) No antipode of triol XIV or triacetare XV was found. b) We were unable to establish the relative configuration of triol XIV and triacetate XV since the reductive cleavage of the C–N bond in XIV and XV to the corresponding 3,4-diol(triol XVII), which would be characterized as the acetonide, was unsuccessful using sodium borohydride or hydrogen in the presence of the Adams catalyst.

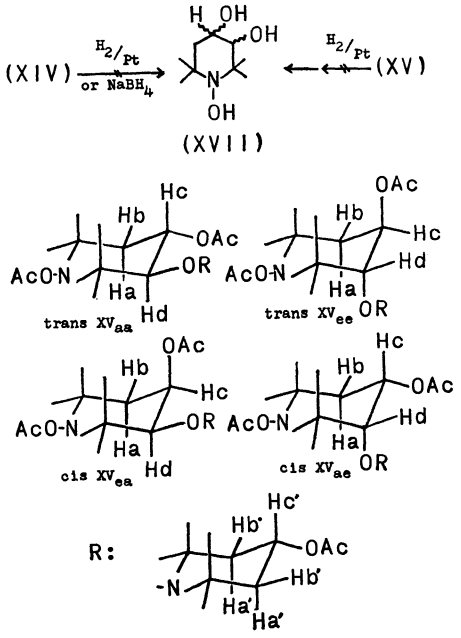

Further, the magnitude of the chemical shift and the coupling constant in the proton magnetic resonance was unreliable for configurational study because of the absence of the antipode of triol XIV and triacetate XV, and of the uncertainty in the conformation of the heterocyclic(piperidine) ring: the magnitude of the coupling constant (JHdHc=2.7 Hz) eliminated the *trans* XV_{aa}. However, the *trans* XV_{ee} and the *cis* XV_{ae} (or XV_{ea}) were undistinguishable by the coupling constant.

Experimental

All the melting points were uncorrected.

Unless otherwise stated, the IR spectra were determined by means of Nujol mull, and the molecular weight was determined by V. O. P. method. Mass spectra were obtained using a JEOL-JMS-OIS mass spectrometer.

1-Hydroxy-2,2,6,6-tetramethyl-3-(2,2,6,6-tetramethyl-4-oxopiperidinoxy)-4-oxopiperidine (IX). a) From the N-Oxyl I: When 1 kg of the crystals of 2,2,6,6-tetramethyl-4-oxopiperidine-1-oxyl (I)[3,5c] was allowed to stand for six months at room temperature, the crystals liquefied and then gave rise to *ca.* 100 g of a grey precipitate. The precipitate was filtered and washed with cold ether three times. The crude product was recrystallized from benzene to afford colorless prisms, mp 139—149°C (decomp.). The prisms were dried at 80°C for 3 hr under diminished pressure to give an analytically pure sample. Found: C, 63.43; H, 9.39; N, 8.33%; MW, 361.4 (in acetone). Calcd for $C_{18}H_{32}N_2O_4$: C, 63.50; H, 9.47; N, 8.23%; MW, 340.5. IR (cm^{-1}): ν_{O-H} 3360, $\nu_{C=O}$ 1720. NMR(τ)(in $CDCl_3$)(100 Mc): a broad singlet at 5.25—5.60 (1H), a doublet at 5.74 (1H, J=1.5 Hz), a doublet at 7.12 (1H, J=12.0 Hz), a doublet of doublets at 7.61 (1H, J=12.0 Hz, 1.5 Hz), a broad apparent triplet due to an AA'BB' system (4H, J=*ca.* 15 Hz) and five singlets due to unequivalent methyl proton signals at 8.65, 8.70, 8.72, 8.76 and 8.81 (24H).

b) From 2,2,6,6-Tetramethyl-4-oxopiperidine[5]: 2,2,6,6-Tetramethyl-4-oxopiperidine was oxidized with a 33% aqueous hydrogen peroxide solution at 50—60°C in the presence of EDTA and sodium tungstate. The reaction mixture was then saturated with potassium carbonate, and extracted with benzene. The benzene layer was washed with water saturated with sodium chloride and dried with potassium carbonate, and then the benzene solution was concentrated under

diminished pressure. The crude crystals, which separated from the reaction mixture, were filtered and washed with cold ether. The crude product was recrystallized from benzene to give an analytically pure sample, mp 139—140°C (decomp.), which was identical with the sample obtained by the above procedure *a*).

Monoacetate (X) of the Hydroxypiperidone IX. A solution of 0.5 g (1.47×10^{-3} mol) of IX in 1.5 m*l* of acetic anhydride was allowed to stand at room temperature for 18 hr. Evaporation of the solvent *in vacuo* gave an oily product. After the crude oil, dissolved with petroleum ether, was treated with active charcoal, pure crystals (0.4 g, 71.5%) were gradually obtained on concentration of the solution, and were recrystallized from petroleum ether three times to give an analytically pure sample, mp 89—90°C. Found: C, 62.90; H, 9.00; N, 7.33%; MW, 396.6 (in $CHCl_3$), 376 (in CCl_4). Calcd for $C_{20}H_{34}N_2O_5$: C, 62.83; H, 8.98; N, 7.35%; MW, 382.49. IR (cm^{-1}) (Grating): no ν_{O-H}; $\nu_{C=O}$ 1767,[7] 1745, 1722; (in CCl_4): 1785, 1745, 1725.

Monobenzoate (XI) of the Hydroxypiperidone IX. Into a mixture of 1.5 g (4.42×10^{-3} mol) of IX, 2.0 g (8.85×10^{-3} mol) of benzoic anhydride and 2.0 g (1.45×10^{-2} mol) of potassium carbonate in 4.0 m*l* of benzene was added slowly and dropwise 0.1 g of water with vigorous stirring at room temperature. Stirring was continued for 24 hr at room temperature after the evolution of carbon dioxide had ceased. The benzene layer was separated and washed with 5% aqueous solution of potassium carbonate and dried with potassium carbonate. The crude oil, obtained by evaporation of benzene *in vacuo*, solidified upon being scratched in a small amount of petroleum ether, (1.65 g, 84.5%). The crude crystals were dissolved in a small amount of benzene followed by addition of petroleum ether to give an analytically pure sample, mp 153.5-154.5°C. Found: C, 67.77; H, 8.15; N, 6.07%. Calcd for $C_{25}H_{36}N_2O_5$: C, 67.57; H, 8.16; N, 6.30%. IR (cm^{-1}): no ν_{O-H}; $\nu_{C=O}$ 1747, 1725.

Urethane (XII) of the Hydroxypiperidone IX. The ketone IX, 1.0 g (2.94×10^{-3} mol) exothermally dissolved at once in 0.6 g (5.04×10^{-3} mol) of pheny isocyanate, and the crude solid which separated was washed with petroleum ether, (1.3 g, 96.5%). An analytically pure sample was obtained by recrystallization from 95% ethanol, mp 147—148°C (decomp.). Found: C, 65.53; H, 8.18; N, 9.04%, MW, 488.5 (in acetone). Calcd for $C_{25}H_{37}N_3O_5$: C, 65.36; H, 8.13; N, 9.15%; MW, 459. IR(cm^{-1}): ν_{N-H} 3290; $\nu_{C=O}$ 1745, 1722.

Disemicarbazone (XIII) of the Hydroxypiperidone IX. Into a mixture of 0.34 g(1.00×10^{-3} mol) of IX and 0.3 g (3.66×10^{-3} mol) of sodium acetate in 4 m*l* of water was added gradually 0.3 g (2.70×10^{-3} mol) of semicarbazide hydrochloride with stirring for 3 hr at room temperature. The ketone IX dissolved and gave the crystals of the semicarbazone (0.35 g, 77.2%). An analytically pure sample was obtained by recrystallization from ethanol, mp 136°C (decomp.). Found: C, 52.79; H, 8.52; N, 24.39%. Calcd for $C_{20}H_{38}N_8O_4$: C, 52.84; H, 8.42; N, 24.65%. IR (cm^{-1}): ν_{O-H} 3460; ν_{N-H} 3350, 3270; $\nu_{C=O}$ 1678.

1,4-Dihydroxy-2,2,6,6-tetramethyl-3-(4-hydroxy-2,2,6,6-tetramethylpiperidinoxy)piperidine (=triol) (XIV). a) From the Hydroxypiperidone IX: Into a solution of 1.0 g (2.94×10^{-3} mol) of ketone IX in 20 m*l* of methanol was added ten 0.1 g portions (2.64×10^{-2} mol) of sodium borohydride under a nitrogen atmosphere for 5 hr at room temperature; then was added a solution of 0.5 g of ammonium chloride in 5 m*l* of water at 5°C. The solution was evaporated *in vacuo* to give a residue. The triol XIV was carefully extracted with absolute ethanol from the residue under nitrogen and obtained as an unstable crude product (0.75 g, 75%), which was recrystallized from methanol to give an analytically pure sample mp 168—171°C (decomp.).[6,8] Found: C, 63.07; H, 10.42; N, 8.27%. Calcd for $C_{18}H_{36}N_2O_4$: C, 62.77; H, 10.53; N, 8.13%. MS: M^+, *m/e* 343. IR (cm^{-1}): ν_{O-H} 3350; ν_{C-O} 1055.

b) From 2,2,6,6-tetramethyl-3-(2,2,6,6-tetramethyl-4-hydroxypiperidinoxy)-4-hydroxypiperidine-1-oxyl (=the diol-N-oxyl) (XVI): A solution of 0.1 g(2.94×10^{-4} mol) of the diol-*N*-oxyl XVI in 6 m*l* of methanol was shaken with hydrogen for 5 hr in the presence of the Adams catalyst until the yellow color disappeared. The catalyst was filtered off and the filtrate was evaporated under reduced pressure. After the residue was dissolved into a small amount of ether without exposure to air, the ethereal solution was diluted with petroleum ether. Gradually the unstable triol XIV crystallized, (84 mg, 84%), mp 167—171°C.[8]

1,4-Diacetoxy-2,2,6,6-tetramethyl-3-(4-acetoxy-2,2,6,6-tetramethylpiperidinoxy)piperidine (=triacetate) (XV). a) From the Diol-N-oxyl XVI: The diol-*N*-oxyl XVI, 2.0 g (5.82×10^{-3} mol), was dissolved in 60 m*l* of acetic anhydride and hydrogenated at room temperature for 5 hr in the presence of the Adams catalyst, until the yellow coloration of XVI disappeared. The catalyst was filtered off and 60 m*l* of pyridine was added into the filtrate. The reaction mixture was allowed to stand at room temperature for 24 hr. The solvent was then evaporated under reduced pressure. The crude oil obtained was dissolved in benzene, and the benzene layer was washed with a saturated aqueous solution of sodium bicarbonate. After the benzene was evaporated *in vacuo*, the residue solidified upon being scratched in a small amount of petroleum ether (2.2 g, 81.5%). The crude product obtained was recrystallized from petroleum benzine to afford an analytically pure sample, mp 173°C. Found: C, 61.50; H, 8.86; N, 5.96%. Calcd for $C_{24}H_{42}N_2O_7$: C, 61.25; H, 9.00; N, 5.95%. MS: M^+ *m/e* 470. IR (cm^{-1}): $\nu_{C=O}$ 1772, 1740. NMR(τ)(in C_5D_5N, 100 Mc)[6]: a doublet of doublets of doublets at 4.46 (1 Hc, J_{HcHb}=3.5 Hz, J_{HcHa}=3.0 Hz, and J_{HcHb}=2.7 Hz), a triplet of triplets at 4.90 (1 Hc′, $J_{Hc'Ha'}$=11.0 Hz, $J_{Hc'Hb'}$=5.0 Hz), a doublet at 5.93 (1 Hd, J_{HdHc}=2.7 Hz), doublets of doublets at 7.74 (1Hb, J_{HbHa}=15.5 Hz, J_{HbHc}=3.5 Hz) and at 8.19 (1 Ha, J_{HaHb}=15.5 Hz, J_{HaHc}=3.0 Hz), three singlets due to acetyl protons at 7.81 (3H), 7.97 (3H) and 8.01 (3H), and seven singlets due to methyl protons at 8.47 (3H), 8.52 (3H), 8.69 (3H), 8.77 (3H), 8.83 (6H), 8.87 (3H) and 8.92 (3H). Signals due to Ha′ and Hb′ overlapped with those due to the methyl protons and Ha at 8.5—8.1.

b) From the Triol XIV: A solution of 2.0 g (5.82×10^{-3} mol) of the triol XIV in 6 m*l* of acetic anhydride and 6 m*l* of pyridine was allowed to stand for 24 hr at room temperature. When the solvent was evaporated under reduced pressure, the crude product obtained was dissolved into benzene. The benzene layer was washed with a saturated aqueous solution of sodium bicarbonate. After the benzene was evaporated *in vacuo*, the residue solidified upon being scratched in a small amount of petroleum ether, (2.2 g, 81.8%), which was identical with the sample obtained by the above procedure *a*) (from XVI).

2,2,6,6-Tetramethyl-3-(2,2,6,6-tetramethyl-4-hydroxypiperidinoxy)-4-hydroxypiperidine-1-oxyl (=diol-N-oxyl) (XVI). a) From the Hydroxypiperidone IX: Into a solution of 0.6 g

7) O. Exner and B. Kanáč, *Collection Czech. Chem. Commun.*, **25**, 2530 (1960).

8) The crystals turned yellow on exposure to air.

(1.77×10^{-3} mol) of IX in 20 m*l* of methanol was added six 100 mg portions (1.58×10^{-2} mol) of sodium borohydride in the presence of oxygen (air) at room temperature. After additional stirring for 10 hr, a solution of 0.3 g of ammonium chloride in 5 m*l* of water was added into the mixture at 5°C. The solvents (methanol and water) were evaporated *in vacuo*. Extraction of *N*-oxyl XVI with absolute ethanol from the reaction mixture followed by evaporation *in vacuo* gave yellow paramagnetic crystals, (0.47 g, 78%), which was dissolved in a small amount of methanol and diluted with petroleum ether to give an analytically pure sample, mp 183—184°C (decomp.). Found: C, 63.07; H, 10.09; N, 8.21%; MW, 383.6 (in acetone). Calcd for $C_{18}H_{35}N_2O_4$: C, 62.91; H, 10.28; N, 8.17%; MW, 343. MS: M^+ *m/e* 343.258 (Calcd 343.259). IR (cm^{-1}): ν_{O-H} 3400; ν_{C-O} 1040.

b) From the triol XIV: When a solution of triol XIV in methanol was treated under an oxygen (air) atmosphere, the solution turned yellow. After the solution was allowed to stand at room temperature for two days, evaporation of methanol gave yellow crystals. The crude crystals were recrystallized from ether to give an analytically pure sample, mp 183—184°C (decomp.), which was identical with the sample obtained by the above procedure *a*) (from IX).

Thanks are due to Mr. H. Kuwano for 100 Mc-NMR, Mr. T. Kinoshita for mass spectrometry, Mr. H. Horiuchi and Mr. T. Kanai for their technical assistance.

BULLETIN OF THE CHEMICAL SOCIETY OF JAPAN, VOL. 44, 2210—2213 (1971)

The Synthesis of 1-Phenylazulene and 2-Phenylazulene from the Troponoid Compound

Tetsuo NOZOE, Kahei TAKASE* and Satoko FUKUDA

Department of Chemistry, Faculty of Science, Tohoku University, Katahira-2-chome, Sendai

(Received February 22, 1971)

1-Phenylazulene (I) and 2-phenylazulene (II) were synthesized from the troponoid compound. 3-Phenyl-(III) and 3-benzoyl-2*H*-cyclohepta[*b*]furan-2-ones (IV) were prepared by the reaction of 2-chlorotropone with ethyl phenylacetate and with ethyl benzoylacetate respectively. The reactions of III with malononitrile or ethyl cyanoacetate gave 1-phenylazulene derivatives, from which I was derived. On the other hand, the reactions of IV with ethyl cyanoacetate or diethyl malonate gave 2-phenylazulene derivatives, from which II was derived.

As has been described in previous papers,[1,2] it has been found that the reaction of 2*H*-cyclohepta[*b*]-furan-2-one derivatives with compound having a reactive methylene group, such as malononitrile, ethyl cyanoacetate, or diethyl malonate, gave azulene derivatives bearing the substituents at the 1-, 2-, and 3-positions. Moreover, the relationship between the kinds of substituents in the azulene derivatives formed and the structures of the starting 2*H*-cyclohepta[*b*]-furan-2-one derivatives or of the compounds with the reactive methylene group has also been revealed.[2] These findings suggest that this reaction can be used fruitfully in the synthesis of azulene derivatives bearing the desired substituents. As an application of this reaction, we have now studied the synthesis of 1-phenylazulene(I) and 2-phenylazulene(II) from the troponoid compound, though I has been synthesized by Plattner *et al.*[3] from bicyclo[5,3,0]decenone and by Hafner[4] through the condensation of the cyclopentadiene derivative and pyridinium salt, and II has also been synthesized by Plattner *et al.*[3] from phenylindane.

Considering the reaction mechanism[2] of the formation of azulene derivatives from 2*H*-cyclohepta-[*b*]furan-2-one derivatives, it is expected that 1-phenyl- and 2-phenylazulene derivatives should be formed from 3-phenyl- (III) and 3-benzoyl-2*H*-cyclohepta[*b*]furan-2-ones (IV) respectively by means of reactions analogous to those in the formations of the azulene-1-carboxylic esters (VIa) or 2-methylazulene derivatives (VIb) from 3-ethoxycarbonyl- (Va) or 3-acetyl-2*H*-cyclohepta[*b*]furan-2-ones (Vb)[2] respectively. Consequently, compounds III and IV

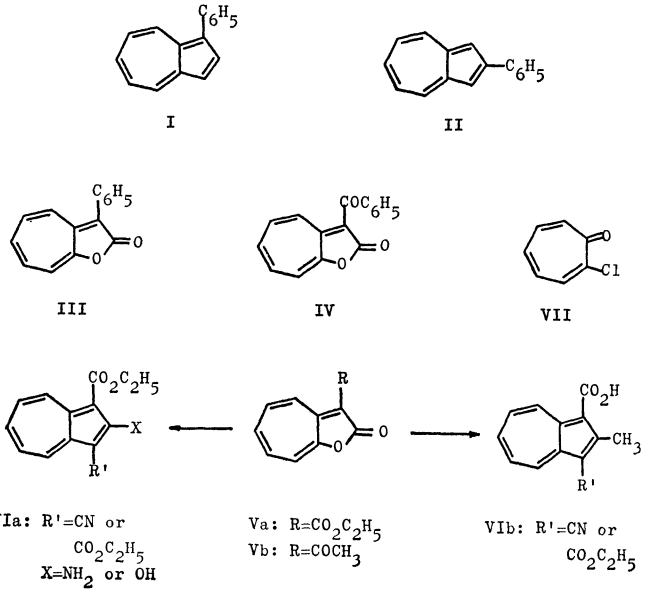

* Address correspondence to this author.

1) T. Nozoe, K. Takase, and N. Shimazaki, This Bulletin, **37**, 1644 (1964).

2) T. Nozoe, K. Takase, T. Nakazawa, and S. Fukuda, *Tetrahedron*, to be published.

3) Pl. A. Plattner, R. Sandrin, and J. Wyss, *Helv. Chim. Acta*, **29**, 1604 (1946); Pl. A. Plattner, A. Fürst, M. Gordon, and K. Zimmermann, *ibid.*, **33**, 1910 (1950).

4) K. Hafner, *Angew. Chem.*, **67**, 301 (1955).

should be important intermediates in the synthesis of 1-phenylazulene(I) and 2-phenylazulene(II) from the troponoid compound. Moreover, compounds III and IV are expected to be prepared from 2-chlorotropone(VII)[5] in a way analogous to the preparation of Va and Vb.[6]

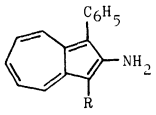

VIIIa: R=CN
VIIIb: R=$CO_2C_2H_5$

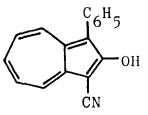

IX

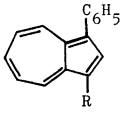

Xa: R=CN
Xb: R=$CO_2C_2H_5$

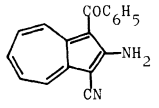

XI

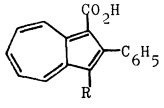

XIIa: R=CN
XIIb: R=$CO_2C_2H_5$

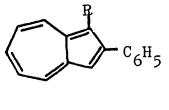

XIIIa: R=CN
XIIIb: R=$CO_2C_2H_5$
XIV: R=$CONH_2$

Results and Discussion

1-Phenylazulene. In order to prepare 3-phenyl-2*H*-cyclohepta[*b*]furan-2-one(III), the reaction of 2-chlorotropone(VII) with ethyl phenylacetate was examined. This reaction succeeded in the presence of sodium ethoxide, giving III in an 81% yield. The structure of III was revealed from the fact that its ultraviolet spectrum is similar to those of 2*H*-cyclohepta[*b*]furan-2-one derivatives,[6] while its infrared spectrum shows absorptions at 1736 and 1721 cm^{-1}, corresponding to those of the five-membered lactone.

Compound III easily reacted with malononitrile in the presence of sodium ethoxide to give an azulene derivative(VIIIa) in a good yield. The reaction of III with ethyl cyanoacetate also proceeded easily in the presence of sodium ethoxide to afford a mixture of a basic azulene derivative(VIIIb) and an acidic azulene derivative(IX). On the other hand, the reaction of III with diethyl malonate ended in the recovery of the original substance. The azulene derivatives obtained here, VIIIa, VIIIb, and IX, were assigned the structures of 2-amino-1-cyano-3-phenylazulene, ethyl 2-amino-3-phenylazulene-1-carboxylate and 1-cyano-2-hydroxy-3-phenylazulene respectively on the basis of a consideration of a reaction mechanism for their formation analogous to that for the formation of azulene derivatives from 2*H*-cyclohepta[*b*]furan-2-one derivatives,[2] as well as on the basis of the observations to be described below. The ultraviolet and visible absorption spectra revealed these compounds to be azulene derivatives. Their infrared spectra show the characteristic absorptions as shown in Table 1. Moreover, VIIIa gave a *N*-acetyl derivative, VIIIb gave a picrate, and IX gave a methyl ether with diazomethane.

Table 1. The infrared spectral data of the azulene derivatives

Compound	Absorptions, cm^{-1} (KBr)
VIIIa	3410, 3300, 3185 (NH_2); 2198 (CN)
IX	3135 (OH); 2222 (CN)
XI	3410, 3330, 3205 (NH_2); 2212 (CN); 1603 (CO)
XIIa	3330~2400, 1647, 931 (CO_2H); 2217 (CN)
Me ester of XIIa	2217 (CN), 1692 (CO)
XIIb	3165 (broad), 1647, 927 (CO_2H); 1698 (CO)
Me ester of XIIb	1678 (CO)

The treatment of VIIIa and of VIIIb with isoamyl nitrite in the presence of sulfuric acid in ethanol-dioxane gave deamination products, (Xa) and (Xb) respectively. Their infrared spectra show absorptions at 2208 and 1684 cm^{-1}, corresponding to those of the conjugated cyano and carbonyl groups respectively. The deamination of VIIIa was rather difficult; it produced a slightly soluble, black material, together with Xa. Upon heating in 100% phosphoric acid, both Xa and Xb gave the same blue hydrocarbon. Although its melting point, 61—62°C, was higher than that previously reported,[3] 54—55°C, its ultraviolet and visible absorption spectra and infrared spectrum were identical with those of 1-phenylazulene (I).[3] Moreover, the melting point of bistrinitrobenzolate was also identical with that of I.

2-Phenylazulene. 3-Benzoyl-2*H*-cyclohepta[*b*]furan-2-one (IV) was obtained in a 66% yield by the reaction of 2-chlorotropone (VII) with ethyl benzoylacetate in the presence of sodium ethoxide. The ultraviolet spectrum is similar to those of 2*H*-cyclohepta[*b*]-furan-2-one derivatives,[6] and the infrared spectrum shows an absorption at 1773 cm^{-1} corresponding to that of the five-membered lactone. These spectral data are consistent with the structure of IV.

Compound IV easily reacted with malononitrile in the presence of tert-butylamine to give a basic azulene derivative(XI). The reaction of IV with ethyl cyanoacetate and with diethyl malonate also proceeded easily in the presence of sodium ethoxide to give acidic azulene derivatives, XIIa and XIIb respectively. These azulene derivatives, XI, XIIa, and XIIb, were assigned the structures of 2-amino-1-benzoyl-3-cyanoazulene, 3-cyano-2-phenylazulene-1-carboxylic acid, and 3-ethoxycarbonyl-2-phenylazulene-1-carboxylic acid respectively on the basis of a consideration of the reaction mechanism for their formation analogous to that established for the formation of azulene derivatives from 2*H*-cyclohepta[*b*]furan-2-one derivatives,[2] as well as on the basis of the observations to be described below. The ultra-

5) T. Nozoe, S. Seto, H. Takeda, S. Morosawa, and K. Matsumoto, *Sci. Repts. Tohoku Univ., Ser. I*, **36**, 126 (1952); S. Seto, *ibid.*, **37**, 275 (1953); B. J. Abadir, J. W. Cook, J. D. Loudon, and D. D. V. Steel, *J. Chem. Soc.*, **1952**, 2350; W. von E. Doering and L. H. Knox, *J. Amer. Chem. Soc.*, **74**, 5683 (1952); W. von E. Doering and C. F. Hiskey, *ibid.*, **74**, 5688 (1952).

6) S. Seto, *Sci. Repts. Tohoku Univ., Ser. I*, **37**, 367 (1953).

violet and visible absorption spectra revealed these compounds to be azulene derivatives. Their infrared spectra show the characteristic absorptions shown in Table 1. Moreover, compound XI gave a *N*-acetyl derivative upon treatment with acetic anhydride, and gave 2-amino-1-cyanoazulene,[2] identified as the *N*-acetyl derivative, and benzoic acid upon heating in concentrated hydrobromic acid. On the other hand, compounds XIIa and XIIb, which were assumed to be carboxylic acids on the basis of their infrared spectra, were soluble in a sodium hydrogen carbonate solution and gave the corresponding methyl esters on methylation with diazomethane.

The derivation of 2-phenylazulene(II) from XIIa was achieved by a two-step procedure. Thus, XIIa gave 1-cyano-2-phenylazulene (XIIIa) or 1-carbamoyl-2-phenylazulene(XIV) upon heating in 100% phosphoric acid or in concentrated sulfuric acid respectively. The infrared spectra of XIIIa and XIV show the absorptions at 2208 cm^{-1} and at 3367, 3155, and 1631 cm^{-1}, corresponding to the conjugated cyano and carbamoyl groups respectively. The further treatment of XIV with 100% phosphoric acid gave a blue hydrocarbon in a good yield; it was identified with 2-phenylazulene (II)[3] on the basis of a comparison of the ultraviolet and visible absorption spectra and on the basis of the infrared spectra. On the contrary, the treatment of XIIIa in concentrated sulfuric acid gave mainly XIV, together with a small amount of II.

On the other hand, compound XIIb gave II directly and in a good yield upon heating in 100% phosphoric acid. However,when heated in concentrated hydrobromic acid, XIIb gave ethyl 2-phenylazulene-1-carboxylate (XIIIb) by decarboxylation, together with II. Compound XIIIb easily gave II in a good yield when heated in 100% phosphoric acid.

As has been described above, 1-phenylazulene(I) and 2-phenylazulene(II) were easily synthesized from troponoid compounds in good yields. Moreover, this synthetic procedure is thought to be desirable since all the steps proceeded under rather mild conditions; consequently, there is no trouble in the thermal isomerization between I and II at high temperatures.[3]

Experimental

All the melting points are uncorrected. The ultraviolet and visible absorption spectra were measured on a Hitachi EPS-3 spectrophotometer, while the infrared spectra were recorded on a Shimadzu IR-27 infracord apparatus.

*3-Phenyl-2*H*-cyclohepta*[b]*furan-2-one (III).* Into a solution of 2-chlorotropone(VII) (2.80 g) and ethyl phenylacetate (6.60 g) in anhydrous ethanol (15 m*l*), a sodium ethoxide solution prepared from sodium (920 mg) and anhydrous ethanol (20 m*l*) was stirred under cooling with ice water. After having been stirred for an additional 2 hr, the mixture was allowed to stand for 2 days in a refrigerator and then poured into water (300 m*l*). The crystals thereby formed were collected by filtration. Yield, 3.59 g; mp 135—140°C. Recrystallization from ethanol gave III as reddish-orange needles; mp 146—147°C.

Found: C, 81.27; H, 4.60%. Calcd for $C_{15}H_{10}O_2$: C, 81.06; H, 4.54%. UV (MeOH): λ_{max} nm (log ε); 226 (4.48), 265 (4.40), 400 (4.28).

2-Amino-1-cyano-3-phenylazulene (VIIIa). To a solution of III (380 mg) and malononitrile (200 mg) in anhydrous ethanol (5 m*l*), 1 M sodium ethoxide solution (3 m*l*) was added; the mixture was stirred for 2 hr and then allowed to stand for 2 days at room temperature. Water was added to this mixture, and the crystals thereby formed were collected by filtration to give VIIIa (390 mg); mp 190—193°C. Recrystallization from dioxane afforded red micro-needles; mp 195—196°C.

Found: C, 83.17; H, 4.63; N, 11.20%. Calcd for $C_{17}H_{12}N_2$: C, 83.58; H, 4.95; N, 11.47%. UV (MeOH): λ_{max} nm (log ε); 247 (4.44), 316 (4.76), 380 (4.02).

N-*Acetyl Derivative*: Violet prisms (from dimethylformamide); mp 225—226°C.

Found: C, 79.66; H, 5.05; N, 9.50%. Calcd for $C_{19}H_{14}ON_2$: C, 79.70; H, 4.93; N, 9.78%. UV (MeOH): λ_{max} nm (log ε); 246 (4.40), 314 (4.75), 357 (3.82), 545 (2.79).

Ethyl 2-Amino-3-phenylazulene-1-carboxylate (VIIIb) and 1-*Cyano-2-hydroxy-3-phenylazulene (IX).* To a solution of III (380 mg) and ethyl cyanoacetate (480 mg) in anhydrous ethanol (6 m*l*), a 1 M sodium ethoxide solution (8 m*l*) was added; the mixture was stirred for 2 hr and then allowed to stand for 2 days at room temperature. The reaction mixture was then poured into water and shaken with chloroform. The chloroform layer was dried over anhydrous sodium sulfate, after which the solvent was evaporated. The oily residue was solidified by the addition of ethanol, giving VIIIb (260 mg); mp 121—122°C. Recrystallization from ethanol gave red prisms; mp 124—125°C.

Found: C, 78.14; H, 5.79; N, 4.49%. Calcd for $C_{19}H_{17}O_2N$: C, 78.33; H, 5.88; N, 4.81%. UV (MeOH): λ_{max} nm (log ε); 255 (4.43), 320 (4.58).

Picrate: Violet needles (from ethanol); mp 137—138°C.

Found: C, 58.08; H, 3.86; N, 10.41%. Calcd for $C_{25}H_{20}O_9N_4$: C, 57.69; H, 3.87; N, 10.77%.

The aqueous layer was acidified with 6 N hydrochloric acid, and the crystals thereby formed were collected by filtration to give IX (130 mg); mp 213—216°C. Recrystallization from dioxane gave reddish brown micro-needles; mp 232—233°C.

Found: C, 80.71; H, 4.82; N, 5.35%. Calcd for $C_{17}H_{11}ON\text{-}1/2H_2O$: C, 80.30; H, 4.76; N, 5.51%. UV (MeOH): λ_{max} nm (log ε): 247 (4.50), 314 (4.70), 449 (2.77).

Methyl Ether: Reddish violet needles (from ethanol); mp 136—137°C.

Found: C, 83.19; H, 5.26; N, 5.15%. Calcd for $C_{18}H_{13}ON$: C, 83.37; H, 5.05; N, 5.40%. UV (MeOH): λ_{max} nm (log ε); 245 (4.37), 308 (4.66). 358 (3.61), 400 sh (3.11), 503 (2.57).

1-Cyano-3-phenylazulene (Xa). To a solution of VIIIa (470 mg) in a mixture of ethanol (6 m*l*) and dioxane (6 m*l*) containing concentrated sulfuric acid (0.4 m*l*), isoamyl nitrite (0.3 m*l*) was added; the mixture was then stirred for 5 hr at room temperature. The reaction mixture was then poured into water, extracted with chloroform, and dried over anhydous sodium sulfate. After the evaporation of the solvent, the residue was dissolved in benzene and passed through a short column of alumina. The evaporation of the solvent from the effluent left blue crystals (200 mg), mp 117—122°C, which were recrystallized from ethanol to give Xa as blue needles; mp 127—128°C.

Found: C, 89.37; H, 4.69; N, 5.94%. Calcd for C_{17}-

$H_{11}N$: C, 89.05; H, 4.84; N, 6.11%. UV (MeOH): λ_{max} nm (log ε); 241 (4.52), 300 (4.55), 375 (3.87), 570 (3.31).

Ethyl 3-Phenylazulene-1-carboxylate (Xb). To a solution of VIIIb (725 mg) in a mixture of ethanol (10 ml) and dioxane (6 ml) containing concentrated sulfuric acid (0.5 ml), isoamyl nitrite (0.4 ml) was added; when the mixture was then treated in a manner similar to that described above, it gave violet crystals (390 mg), mp 74—76°C. Recrystallization from ethanol gave Xb as violet scales; mp 82—83°C

Found: C, 82.87; H, 5.76%. Calcd for $C_{19}H_{16}O_2$: C, 82.58; H, 5.84%. UV (MeOH): λ_{max} nm (log ε); 243 (4.56), 285 (4.66), 303 (4.68), 382 (4.08), 560 (2.65).

1-Phenylazulene (I). *a) From Xa*: A mixture of Xa (100 mg) and 100% phosphoric acid (1 ml) was heated at about 120°C for 40 min, and then poured into water and extracted with chloroform. After drying over anhydrous sodium sulfate, the solvent was evaporated, and the oily residue was dissolved in benzene and chromatographed through an alumina column. The first effluent gave blue crystals (40 mg); mp 53—55°C. Recrystallization from ethanol gave I as blue scales; mp 61—62°C. The melting point previously reported was 54—55°C.[3]

Found: C, 93.97; H, 6.25%. Calcd for $C_{16}H_{12}$: C, 94.08; H, 5.92%. UV (MeOH): λ_{max} nm (log ε); 238 (450), 294 (4.62), 353 (3.83), 369 (3.84), 435 (2.08), 466 (2.13).

From the second effluent of the chromatography, Xa (37 mg) was recovered.

b) From Xb: A mixture of Xb (200 mg) and 100% phosphoric acid (2 ml) was heated at about 100°C for 1 hr, and then treated in a manner similar to that described above. The effluent of the chromatography gave blue crystals (142 mg), mp 57—59°C, which were recrystallized from ethanol to give I as blue scales, mp 61—62°C.

3-Benzoyl-2H-cyclohepta[b]furan-2-one (IV). Into a solution of 2-chlorotropone (VII) (3.5 g) and ethyl benzoylacetate (7.2 g) in anhydrous ethanol (10 ml), a 1 M sodium ethoxide solution was stirred under cooling with ice water. After stirring for an additional 2 hr, the mixture was allowed to stand overnight in a refrigerator and then poured into water (200 ml). The crystals thereby formed were collected by filtration and washed with a small amount of acetic acid, thus giving crude IV (4.1 g), mp 137—145°C. Recrystallization from glacial acetic acid afforded yellow prisms; mp 157—158°C.

Found: C, 76.81; H, 4.29%. Calcd for $C_{16}H_{10}O_3$: C, 76.79; H, 4.03%. UV (MeOH): λ_{max} nm (log ε); 227 (4.34), 257 (4.43), 427 (4.40).

2-Amino-1-benzoyl-3-cyanoazulene (XI). To a suspension of IV (500 mg) and malononitrile (200 mg) in anhydrous ethanol (5 ml), *t*-butylamine (15 drops) was added; the mixture was stirred for 5 hr at room temperature and then allowed to stand overnight. Water (30 ml) was added to this mixture, and the crystals thereby formed were collected by filtration, giving XI (520 mg); mp 214°C. Recrystallization from pyridine afforded orange micro-scales; mp 214—215°C.

Found: C, 79.26; H, 4.55; N, 9.98%. Calcd for $C_{18}H_{12}ON_2$: C, 79.39; H, 4.44; N, 10.29%. UV (MeOH): λ_{max} nm (log ε); 227 (4.37), 249 (4.24), 292 (4.47), 338 (4.48), 470 (3.43).

N-*Acetyl Derivative*: Orange needles (from dimethylformamide); mp 209—210°C.

Found: C, 76.39; H, 4.41; N, 9.01%. Calcd for $C_{20}H_{14}O_2N_2$: C, 76.42; H, 4.49; N, 8.91%. UV (MeOH): λ_{max} nm (log ε); 225 (4.36), 305 (4.62), 370 (3.91), 480 (2.79).

3-Cyano-2-phenylazulene-1-carboxylic Acid (XIIa). To a suspension of IV (250 mg) and ethyl cyanoacetate (230 mg) in anhydrous ethanol (3 ml), a 1 M sodium ethoxide solution (3 ml) was added; the mixture was stirred for 5 hr and then allowed to stand for 2 days at room temperature. The reaction mixture was dissolved in water (30 ml) and shaken with chloroform. The aqueous layer was acidified with 6 N hydrochloric acid, and the crystals thereby formed were collected by filtration, giving XIIa (250 mg); mp 228°C. Recrystallization from dioxane afforded red needles; mp 232—233°C.

Found: C, 78.88; H, 4.00; N, 4.90%. Calcd for $C_{18}H_{11}O_2N$: C, 79.11; H, 4.06; N, 5.13%. UV (MeOH): λ_{max} nm (log ε); 228 (4.40); 267 (4.32), 320 (4.69), 345 (3.91), 517 (2.74).

Methyl Ester. This ester was obtained by treatment of XIIa with diazomethane. Red micro-needles (from benzene); mp 173—174°C.

Found: C, 79.69; H. 4.57; N, 5.03%. Calcd for $C_{19}H_{13}O_2N$: C, 79.43; H, 4.56; N, 4.88%. UV (MeOH): λ_{max} nm (log ε); 230 (4.39), 269 (4.32), 320 (4.66), 525 (2.73).

3-Ethoxycarbonyl-2-phenylazulene-1-carboxylic Acid (XIIb). To a suspension of IV (500 mg) and diethyl malonate (0.65 ml) in anhydrous ethanol (8 ml), a 1 M sodium ethoxide solution (8 ml) was added; the mixture was then treated in a manner similar to that described above. The crude crystals (360 mg), mp 182°C (decomp.), obtained by the acidification of the aqueous layer were recrystallized from dioxane to give XIIb as red micro-needles; mp 190°C (decomp.).

Found: C, 71.39; H, 4.84%. Calcd for $C_{20}H_{16}O_4 \cdot H_2O$: C, 70.99; H, 5.36%. UV (MeOH): λ_{max} nm (log ε); 233 (4.34), 268 (4.24), 310 (4.60), 520 (2.70), 560 (2.69).

Methyl Ester. This ester was obtained by the treatment of XIIb with diazomethane. Red prisms (from methanol); mp 160—161°C.

Found: C, 75.45; H, 5.51%. Calcd for $C_{21}H_{18}O_4$: C, 75.43; H, 5.43%. UV (MeOH): λ_{max} nm (log ε); 233 (4.42), 273 (4.34), 305 (4.54), 515 (2.63).

Treatment of XI with Hydrobromic Acid. A mixture o XI (100 mg) and concentrated hydrobromic acid (1 ml) was heated at about 100°C for 2 hr, then diluted with water, made alkaline with 6 N potassium hydroxide solution, and extracted with chloroform. After drying over anhydrous sodium sulfate, the solvent was evaporated from the organic layer, the residue was heated with acetic anhydride (1 ml) for 15 min, and the crystals thereby formed were collected and recrystallized from ethyl acetate, thus giving 2-acetamido-1-cyanoazulene[2] (30 mg) as red needles; mp 225—226°C.

The alkaline aqueous layer was acidified with 6 N hydrochloric acid and extracted with chloroform. The solvent was evaporated, and the residue was sublimed under reduced pressure, thus giving benzoic acid (20 mg) as colorless crystals; mp 120—121°C.

1-Cyano-2-phenylazulene (XIIIa). A mixture of XIIa (100 mg) and 100% phosphoric acid (1 ml) was heated at about 100°C for 30 min, then diluted with water and extracted with benzene. The benzene solution was passed through a short column of alumina and the evaporation of the solvent from the effluent gave XIIIa (80 mg) as violet crystals; mp 110—111°C. Recrystallization from ethanol afforded violet plates; mp 115—116°C.

Found: C, 89.35; H, 4.80; N, 5.98%. Calcd for $C_{17}H_{11}N$: C, 89.05; H, 4.84; N, 6.11%. UV (MeOH): λ_{max} nm (log ε); 273 (4.22), 311 (4.24), 319 (4.78), 364

(3.93), 565 (2.78).

1-Carbamoyl-2-phenylazulene (XIV). A mixture of XIIa (100 mg) and concentrated sulfuric acid (1 m*l*) was heated at about 100°C for 40 min, and then diluted with water and extracted with chloroform. The chloroform solution was passed through a short column of alumina; the subsequent evaporation of the solvent from the effluent gave XIV (54 mg) as violet crystals, mp 186°C. Recrystallization from chloroform afforded violet plates; mp 189—190°C.

Found: C, 82.33; H, 5.16; N, 5.30%. Calcd for $C_{17}H_{13}ON$: C, 82.57; H, 5.30; N, 5.66%. UV (MeOH): λ_{max} nm (log ε); 243 (4.29), 303 (4.72), 310 (4.75), 364 (3.86), 383 sh (3.82), 565 (2.61).

2-*Phenylazulene (II).* *a) Treatment of XIV with Phosphoric Acid*: A mixture of XIV (35 mg) and 100% phosphoric acid (1 m*l*) was heated at about 100°C for 30 min, and then diluted with water and extracted with benzene. The benzene solution was passed through a short column of alumina; the subsequent evaporation of the solvent from the effluent gave II (20 mg) as blue crystals; mp 229°C. Recrystallization from benzene afforded blue plates; mp 231—232°C. The melting point previously reported[3] was 230°C.

Found: C, 94.08; H, 6.02%. Calcd for $C_{16}H_{12}$: C, 94.08; H, 5.92%. UV (isooctane): λ_{max} nm (log ε); 242 (4.11), 296 (4.79), 307 (4.81), 355 (3.73), 372 (4.05), 392 (4.19), 590 (2.46).

b) Treatment of XIIb with Phosphoric Acid: A mixture of XIIb (100 mg) and 100% phosphoric acid was heated at about 100°C for 30 min, and then treated in a manner similar to that described about to give II (57 mg) as blue plates; mp 231—232°C.

Treatment of XIIIa with Sulfuric Acid. A mixture of XIIIa (60 mg) and concentrated sulfuric acid (1 m*l*) was heated at about 100°C for 40 min, and then diluted with water and extracted with chloroform. The solvent was evaporated, and the residue was chromatographed on an alumina column. The first effluent, when eluted with benzene, gave II (12 mg) as blue plates; mp 231—232°C. The second effluent, when eluted with chloroform, gave XIV (35 mg) as violet plates; mp 189—190°C.

Treatment of XIIb with Hydrobromic Acid. A mixture of XIIb (100 mg) and concentrated hydrobromic acid was heated at about 100°C for 30 min, then diluted with water and extracted with chloroform. The solvent was evaporated, and the residue was chromatographed on an alumina column. The first effluent, when eluted with a 1 : 2 mixture of benzene and cyclohexane, gave II (27 mg) as blue plates; mp 231—232°C. The second effluent, when eluted with benzene-chloroform, gave ethyl 2-phenylazulene-1-carboxylate (XIIIb) (40 mg) as reddish-violet needles; mp 85—86°C.

Found: C, 82.84; G, 6.08%. Calcd for $C_{19}H_{16}O_2$: C, 82.58; H, 5.84%. UV (MeOH): λ_{max} nm (log ε): 226 (4.27), 308 (4.67), 356 (3.80), 366 (3.81), 550 (2.62).

Treatment of XIIIb with Phosphoric Acid. A mixture of XIIIb (17 mg) and 100% phosphoric acid (0.4 m*l*) was heated at about 100°C for 30 min. Subsequent dilution with water gave II (12 mg) as blue crystals; mp 231—232°C.

This research has been financially supported by grants of the Japanese Ministry of Education and of the Sankyo Co., Ltd.

The Synthesis of 7-Isopropyl-2,4-dimethylazulene (Se-Guaiazulene) from 4-Isopropyltropolone

Tetsuo NOZOE, Kahei TAKASE,* and Satoko FUKUDA

Department of Chemistry, Faculty of Science, Tohoku University, Katahira-2-chome, Sendai

(Received February 22, 1971)

7-Isopropyl-2,4-dimethylazulene (Se-guaiazulene) (I) was synthesized from 4-isopropyl-7-methyltropolone (II), which had itself been derived from 4-isopropyltropolone. The tropolone, II, was then converted to 3-acetyl-5-isopropyl-8-methyl-2*H*-cyclohepta[*b*]furan-2-one (VI) *via* the *p*-tolylsulfonyloxytropone derivative derived from II. The application of the azulene synthesis to VI gave 3-cyano-7-isopropyl-2,4-dimethylazulene-1-carboxylic acid (VII), from which I was obtained by the removal of the carboxyl and cyano groups.

Since the discovery of the method for synthesizing azulenoid compounds from troponoid compounds,[1] a number of 2-amino- and 2-hydroxyazulene derivatives have been synthesized directly from troponoid compounds.[2] Moreover, as has been described in one of our previous papers,[3] it has been found that the reaction of 4-acetyl-2*H*-cyclohepta[*b*]furan-2-one (3-acetyl-1-oxaazulan-2-one) with ethyl cyanoacetate or diethyl malonate gave 2-methylazulene derivatives. This finding suggests that 2-alkylazulene derivatives can be easily synthesized from troponoid compounds *via* 3-acyl-2*H*-cyclohepta[*b*]furan-2-ones. As an example of the application of this method to the synthesis of azulenoid compounds from troponoid compounds, we have now studied the synthesis of 7-isopropyl-2,4-dimethylazulene (Se-guaiazulene) (I), obtained from the natural sesquiterpenoid precursors, from the troponoid compound, though this azulene had already been synthesized by Sǒrm *et al.*[4] from an indanone derivative.

Results and Discussion

6-Isopropyl-3-methyltropolone(II)[5] was used as the starting material for the synthesis of 7-isopropyl-2,4-dimethylazulene (**I**). This tropolone has the methyl and isopropyl substituents at the positions favorable for the synthesis of I, and was prepared from 4-isopropyltropolone in an 85% yield by means of morphorinomethylation and subsequent reductive demorphorination.[6]

It is known that the reaction of 2-chloro- or 2-(*p*-tolylsulfonyloxy)tropones and ethyl sodioacetoacetate gives 3-acetyl-2*H*-cyclohepta[*b*]furan-2-one derivatives.[7,8] Accordingly, the derivation of 2-(*p*-tolylsulfonyloxy)- or 2-chlorotropone derivatives from II was first examined. The treatment of II with *p*-toluenesulfonyl chloride gave a kind of *p*-tolylsulfonyloxy derivative(III).[6] Because of the highly mobile tautomerism in tropolones,[2] two isomeric *p*-tolylsulfonyloxy derivatives would be expected to be formed from unsymmetrical tropolone derivatives, but, in this case, only an isomer was obtained in a good yield. A similar result has been observed in the case of 3-methyltropolone, which gave only one of the isomers, 7-methyl-2-(*p*-tolylsulfonyloxy)tropone,[8] this is thought to be due to the steric hindrance of the methyl group. Consequently, the (*p*-tolylsulfonyloxy)-tropone derivative, III, obtained here was assumed to have the structure of 4-isopropyl-7-methyl-2-(*p*-tolylsulfonyloxy)tropone. The 2-chlorotropone derivative (IV) was derived from III as follows. The treatment of III with hydrazine gave a hydrazinotropone derivative (V), which could be converted to IV by oxidative decomposition with copper sulfate in concentrated hydrochloric acid.[9]

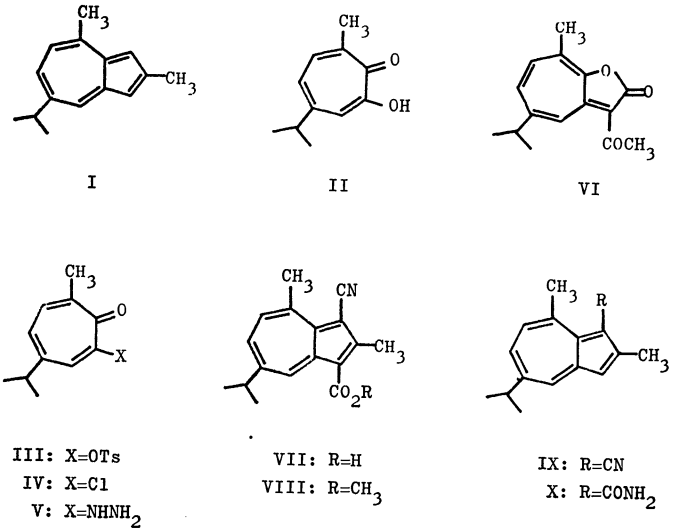

In order to obtain the 3-acetyl-2*H*-cyclohepta[*b*]-furan-2-one derivative(VI), the reaction of III or IV with ethyl acetoacetate was examined. This reaction took place upon the heating of a mixture of III or IV and ethyl sodioacetoacetate in benzene. When ethanol was used as the solvent in place of benzene, only a resinous substance was formed, even when

* Address correspondence to this author.

1) T. Nozoe, S. Matsumura, Y. Murase, and S. Seto, *Chem. and Ind.*, **1955**, 1257; T. Nozoe, S. Seto, S. Matsumura, and Y. Murase, This Bulletin, **35**, 1179 (1962).

2) T. Nozoe, K. Takase, H. Matsumura, and T. Asao, *Dai-Yuki-Kagaku (Comprehensive Organic Chemistry)*, **Vol. 13**, Chapters 7, 16, 19, and 20, Asakura Publishing Co., Tokyo (1960).

3) T. Nozoe, K. Takase, T. Nakazawa, and S. Fukuda, *Tetrahedron*, to be published.

4) F. Sǒrm, J. Kučera, and J. Gut, *Collect. Czech. Chem. Communs.*, **16**, 184 (1951).

5) T. Nozoe, T. Mukai, and K. Takase, *Sci. Repts. Tohoku Univ., Ser. I*, **36**, 40 (1952).

6) Y. Kitahara and T. Kato, This Bulletin, **37**, 859 (1964).

7) S. Seto, *Sci. Repts. Tohoku Univ., Ser. I*, **37**, 367 (1953).

8) T. Sato, *Nippon Kagaku Zasshi*, **80**, 1345 (1959).

9) S. Seto, *Sci. Repts. Tohoku Univ., Ser. I*, **36**, 275 (1953).

the mixture was cooled with ice water. The structure of VI was confirmed from the following evidence. Its ultraviolet absorption spectrum is similar to those of 2*H*-cyclohepta[*b*]furan-2-ones,[7] and its infrared spectrum shows absorptions at 1736 and 1639 cm^{-1}, corresponding to those of the five-membered lactone and the conjugated carbonyl group respectively. Moreover, it is known[8] that 2-(*p*-tolylsulfonyloxy)-tropones or 2-chlorotropones bearing the alkyl substituent at the 7-position gave such 2*H*-cyclohepta-[*b*]furan-2-one derivatives as are formed in a normal substitution reaction; that is, the carbanion attacked the 2-position of the tropone nucleus to give substitution products.

The derivation of the azulene derivative(VII) from VI took place when VI was treated with ethyl cyanoacetate in a way similar to that described in the formation of 2-methylazulene derivatives from 3-acetyl-2*H*-cyclohepta[*b*]furan-2-one.[3] The reaction of VI with diethyl malonate, however, ended in the recovery of the original substance. The structure of VII was established as 3-cyano-7-isopropyl-2,4-dimethylazulene-1-carboxylic acid on the basis of the consideration that the reaction mechanism was analogous to that of the formation of 2-methylazulene derivatives from 3-acetyl-2*H*-cyclohepta[*b*]furan-2-one,[3] as well as on the basis of the following evidence. This compound, VII, is an acidic substance and gave a methyl ester (VIII) upon methylation with diazomethane. The ultraviolet and visible absorption spectra of VIII are consistent with those of azulene derivatives. The infrared spectrum of VII shows absorptions at 3200—2500, at 1647 and 940, and at 2212 cm^{-1}, corresponding to those of the carboxyl and cyano groups respectively, and that of VIII shows absorptions at 1684 and 2217 cm^{-1}, corresponding to those of the conjugated ester and cyano groups respectively.

The decarboxylation of VII proceeded effectively when it was heated in phosphoric acid at about 100°C; this gave 3-cyano-7-isopropyl-2,4-dimethylazulene(IX). The infrared spectrum of IX shows the absorption at 2208 cm^{-1} corresponding to the cyano group. Upon further heating in concentrated sulfuric acid or 100% phosphoric acid at about 130°C for a long period of time, IX gave 7-isopropyl-2,4-dimethylazulene(I), which was identified with an authentic specimen[10] on the basis of a comparison of the ultraviolet and visible absorption spectra and the infrared spectra, and by an admixture of the trinitrobenzolates. On the other hand, when IX was heated in concentrated sulfuric acid at about 100°C, the cyano group could not be eliminated; rather, it was partially hydrolyzed to give a carbamoylazulene derivative (X), which also gave I upon heating in 100% phosphoric acid at about 130°C.

Since 4-isopropyltropolone has already been synthesized,[11] the results described above indicate the total synthesis of 7-isopropyl-2,4-dimethylazulene (Se-guaiazulene). The yield of I from 4-isopropyltropolone was 20%. In this case, there is no such trouble as in the thermal isomerization[4] between S-guaiazulene and Se-guaiazulene at high temperatures, since the reaction took place under rather mild reaction conditions.

10) Se-Guaiazulene prepared from guiene was supplied by Dr. Yoshiharu Matsubara of the Nippon Terpene Co., Ltd., for which we thank him.

11) T. Nozoe, S. Seto, K. Kikuchi, T. Mukai, S. Matsumoto, and M. Murase, *Proc. Japan Acad.*, **26** (7), 43 (1950); T. Nozoe, S. Seto, K. Kikuchi, and H. Takeda, *ibid.*, **27**, 146 (1951); J. W. Cook, R. A. Raphael, and A. I. Scott, *J. Chem. Soc.*, **1951**, 695.

Experimental

All the melting points are uncorrected. The ultraviolet and visible absorption spectra were measured on a Hitachi EPS-3 spectrophotometer, and the infrared spectra were recorded on a Shimadzu IR-27 infracord apparatus.

*4-Isopropyl-7-methyl-2-(*p*-tolylsulfonyloxy)tropone (III).* To a stirred solution of 6-isopropyl-3-methyltropolone(II) (4.07 g) in pyridine (8 m*l*), *p*-toluenesulfonyl chloride was added (6.5 g) under cooling with ice water. After it had been stirred for an additional 3 hr, the mixture was allowed to stand overnight in a refrigerator. Water was added to this mixture, and the crystals thereby formed were collected. Yield, 6.80 g; mp 76—78°C. Recrystallization from ethanol gave III (5.41 g) as colorless prisms; mp 85—86°C. The melting point previously reported was 86—87°C.[6]

2-Hydrazino-4-isopropyl-7-methyltropone (V). A mixture of III (1.65 g) and a 50% ethanolic hydrazine solution (10 m*l*) was refluxed for 3 hr. The solvent was evaporated, the residue was triturated with water, and the crystals thereby formed were collected by filtration. Recrystallization from ether gave V (450 mg) as yellow needles; mp 80—81°C.

Found: C, 68.57; H, 8.39; N, 14.40%. Calcd for $C_{11}H_{16}ON_2$: C, 68.72; H, 8.39; N, 14.57%.

2-Chloro-4-isopropyl-7-methyltropone (IV). To a solution of V (420 mg) in concentrated hydrochloric acid (10 m*l*) being heated at about 100°C, a 30% aqueous copper sulfate solution (10 m*l*) was added in one lot. After being heated for 5 min, the mixture was cooled to room temperature, diluted with water, and extracted with chloroform. The subsequent evaporation of the solvent left a brown, oily material which was then dissolved in benzene and passed through a short column of alumina. The evaporation of the solvent from the effluent gave IV (315 mg) as a pale yellow oil.

Found: C, 67.15; H, 6.62%. Calcd for $C_{11}H_{13}OCl$: C, 67.17; H, 6.66%.

*3-Acetyl-5-isopropyl-8-methyl-2*H*-cyclohepta*[b]*furan-2-one (VI).*
a) From III: Ethyl acetoacetate (4.20 g) was dissolved in a 1 M ethanolic sodium ethoxide solution (32 m*l*), and the solvent was evaporated to dryness, giving ethyl sodioacetoacetate. To this dry benzene (30 m*l*) and III (5.23 g) were added, and then the mixture was refluxed for 3 hr. The reaction mixture was shaken with water, and the organic layer was dried over anhydrous sodium sulfate. The evaporation of the solvent left a mixture of crystals and an oily material, from which VI (990 mg) was isolated, mp 141—143°C, by the addition of ether, followed by filtration. The ether-soluble part was chromatographed on an alumina column and eluted with ether to give further crops of VI (100 mg), mp 140—143°C. Recrystallization from ethanol afforded yellow needles; mp 144—145°C.

Found: C, 74.04; H, 6.63%. Calcd for $C_{15}H_{16}O_3$: C, 73.75; H, 6.60%. UV (MeOH): λ_{max} nm (log ε); 227 (4.42), 254 (4.12), 285 (4.41), 420 (4.40).

The aqueous layer was acidified with 6N hydrochloric acid and extracted with benzene. The benzene extract

was shaken with a 2 N sodium hydroxide solution (5 ml), to give the sodium salt of II (860 mg) as pale yellow scales.

b) From IV: To dried ethyl sodioacetoacetate prepared from ethyl acetoacetate (340 mg) and 1 M sodium ethoxide (2.6 ml), dry benzene (8 ml) and IV (350 mg) was added; the mixture was then treated as has been described above. The crude crystals (120 mg); mp 137—139°C, were recrystallized from ethanol to give VI as yellow needles (mp 144—145°C).

3-Cyano-7-isopropyl-2,4-dimethylazulene-1-carboxylic Acid (VII). To a solution of VI (450 mg) and ethyl cyanoacetate (450 mg) in anhydrous ethanol (5 ml), a 1 M sodium ethoxide solution (8 ml) was added; the mixture was stirred for 3 hr and then allowed to stand overnight at room temperature. The reaction mixture was dissolved in water and shaken with chloroform. The aqueous layer was acidified with 6 N hydrochloric acid, the product was extracted with chloroform, and the chloroform extract was shaken with a sodium hydrogen carbonate solution. The carbonate layer was acidified with 6 N hydrochloric acid to give VII (410 mg) as pale red crystals; mp 155°C (decomp.). Recrystallization from dioxane afforded pale red micro-needles; mp 157°C (decomp.).

Found: C, 76.71; H, 6.35; N, 5.38%. Calcd for $C_{17}H_{17}O_2N$: C, 76.38; H, 6.41; N, 5.24%.

Methyl 3-Cyano-7-isopropyl-2,4-dimethylazulene-1-carboxylate (VIII). To a suspension of VII (130 mg) in ethyl acetate (5 ml), an ethereal solution of diazomethane (2 ml) was added; the mixture was then stirred for 5 hr under cooling with ice water. The solvent was evaporated, the residue was dissolved in benzene, and the benzene solution was passed through a short column of alumina. The evaporation of the solvent from the effluent left red crystals (130 mg), mp 102—106°C, which were subsequently recrystallized from methanol to give VIII as reddish-violet micro-needles; mp 108-109°C.

Found: C, 76.93; H, 6.66; N, 4.74%. Calcd for $C_{18}H_{19}O_2N$: C, 76.84; H, 6.81; N, 4.98%. UV (MeOH): λ_{max} nm ($\log \varepsilon$); 243 (4.51), 270 (4.05), 296 (4.40), 308 (4.52), 344 (3.86), 373 (3.64), 500 (2.77).

3-Cyano-7-isopropyl-2,4-dimethylazulene (IX). A mixture of VII (270 mg) and 100% phosphoric acid (2 ml) was heated at about 100°C for 15 min, then diluted with water and extracted with chloroform. The solvent was evaporated, the residue was dissolved in benzene, and the benzene solution was passed through a short column of alumina. The subsequent evaporation of the solvent from the effluent gave crude IX (207 mg), mp 62—63°C. Recrystallization from ethanol afforded reddish-violet needles; mp 65—66°C.

Found: C, 86.07; H, 7.94; N, 6.06%. Calcd for $C_{16}H_{17}N$: C, 86.05; H, 7.67; N, 6.27%. UV (MeOH): λ_{max} nm ($\log \varepsilon$); 223 (4.20), 241 (4.30), 295 (4.66), 301 (4.73), 313 (4.40), 354 (4.03), 371 (3.98), 530 (2.75).

3-Carbamoyl-7-isopropyl-2,4-dimethylazulene (X). A mixture of IX (65 mg) and concentrated sulfuric acid (1 ml) was heated at 100°C for an hour, then diluted with water and extracted with chloroform. The chloroform solution was chromatographed on an alumina column and eluted with the same solvent. The subsequent evaporation of the solvent from the effluent left pale violet crystals (60 mg); mp 184—185°C. Recrystallization from chloroform gave X as violet plates; mp 186—187°C.

Found: C, 79.49; H, 7.87; N, 5.74%. Calcd for $C_{16}H_{19}ON$: C, 79.63; H, 7.94; N, 5.80%. UV (MeOH): λ_{max} nm ($\log \varepsilon$); 244 (4.37), 291 (4.70), 335 (3.64), 348 (3.77), 555 (2.66). IR (KBr); 3425, 3289, 3165, 1642 cm^{-1}.

7-Isopropyl-2,4-dimethylazulene (I). *a) From IX*: A mixture of IX (100 mg) and 100% phosphoric acid (1 ml) was heated at 120—130°C for 6 hr, then diluted with water and extracted with benzene. The benzene solution was passed through a short column of alumina; the subsequent evaporation of the solvent from the effluent left a blue-violet oil (80 mg).

Found: C, 90.62; H, 9.17%. Calcd for $C_{15}H_{18}$: C, 90.85; H, 9.15%. UV (MeOH): λ_{max} nm ($\log \varepsilon$); 245 (4.43), 280 (4.76), 290 (4.82), 308 (4.00), 334 (3.51), 348 (3.77), 362 (2.96), 565 (2.58), 580 (2.53), 606 sh (2.52), 665 sh (2.12).

The infrared spectrum and the ultraviolet and visible absorption spectra of this oil are identical with those of 7-isopropyl-2,4-dimethylazulene (I).[9]

Trinitrobenzolate: Violet micro-needles (from ethanol); mp 154—154.5°C. The melting point previously reported[4] was 152°C.

Found: C, 61.37; H, 5.36; N, 10.02%. Calcd for $C_{21}H_{21}O_6N_3$: C, 61.31; H, 5.15; N, 10.21%.

Picrate: Reddish violet micro-needles (from ethanol); mp 116—117°C. The melting point previously reported[4] was 110°C.

Found: C, 59.32; H, 4.95; N, 9.69%. Calcd for $C_{21}H_{21}O_7O_3$: C, 59.01; H, 4.95; N, 9.83%.

A similar treatment of IX (100 mg) in 75% sulfuric acid also gave I (70 mg).

b) From X. A mixture of X (50 mg) and 100% phosphoric acid (1 ml) was heated at 130—140°C for 2 hr and then treated in a manner similar to that described in a) to give I (37 mg).

This research has been financially supported by grants of the Japanese Ministry of Education and of the Sankyo Co., Ltd. The sample of 4-isopropyltropolone for this study was supplied by the Takasago Perfumary Co., Ltd.

The Bromination of 2-Methoxytropone and Its Bromo Derivatives

Tetsuo NOZOE, Kahei TAKASE*, and Masafumi YASUNAMI

Department of Chemistry, Faculty of Science, Tohoku University, Katahira-2-chome, Sendai

(Received February 25, 1971)

The reaction of 2-methoxytropone and its bromo derivatives with bromine was examined in various solvents. The treatment of 2-methoxytropone or 5-bromo-2-methoxytropone with bromine in methanol gave an addition product, 2,6-dibromo-7,7-dimethoxy- (II) or 2,4,6-tribromo-7,7-dimethoxy-2,4-cycloheptadien-1-one (XIV) respectively, together with the substitution products. On the contrary, the treatment of 2-methoxytropone with bromine in anhydrous ethanol, chloroform, or carbon tetrachloride gave a reddish complex compound. In aqueous ethanol or acetic acid, however, it gave 3,5,7-tribromotropolone. A possible reaction mechanism involving the nucleophilic attack of a methanol molecule on 2-methoxytropones at the 2-position is presented to account for the formation of the addition products.

It has been established that, on bromination with bromine, tropolone generally gives substitution products,[1-3] whereas tropone gives addition products which are only changed to substituted tropones upon heating in the presence of sodium acetate[4]; this fact is chemical evidence for the concept that the aromatic character of tropone is less than that of tropolone. On the other hand, in the case of 2-methoxytropone(I),[3,5,6] it is expected that its aromatic character is less than that of tropolone because of the localization of the double bonds, while its stability is larger than that of tropone because of the contribution of the mesomeric effect due to the methoxyl group; consequently, the behavior of I in regard to bromine is expected to be intermediate between that of tropolone and that of tropone. In order to find chemical evidence of this, the reaction of I and its bromo derivatives with bromine was examined.

Results and Discussion

The treatment of 2-methoxytropone(I) with bromine in methanol at 0—5°C gave an oily mixture, from which a dibromo compound(II), $C_9H_{10}O_3Br_2$, was subsequently isolated by crystallization. The chromatography of the mother liquor in an alumina column afforded a dibromo compound(III), $C_8H_6O_2Br_2$, together with 3,7-dibromo-2-methoxytropone (IV)[5] and 3,5,7-tribromo-2-methoxytropone(V).[5] The relative yields of these products varied in accordance with the molar ratio of bromine used, but II was always formed as the major product.

The infrared spectrum of II exhibits an absorption at 1692 cm^{-1} characteristic of the conjugated carbonyl group and absorptions at 1147, 1106, and 1070 cm^{-1} corresponding to the ether linkage. The NMR spectrum of II reveals two singlets, at 3.25 (3H) and 3.42 ppm (3H), corresponding to two methoxyl groups, and two doublets, at 4.75 (1H, J=7.5 Hz) and 7.25 (1H, J=9.0 Hz), and two double doublets, at 5.94 (1H, J=9.0, 12.0 Hz) and 6.37 ppm (1H, J=7.5, 12.0 Hz), corresponding to a partial structure, -ĊCHBr-CH=CH-CH=Ċ-. Moreover, II was easily changed to IV when its chloroform solution was passed through an alumina column. Judging from these facts, II must be assigned the structure of 2,6-dibromo-7,7-dimethoxy-2,4-cycloheptadien-1-one. The ultraviolet absorption spectrum is also consistent with this structure.

Compound II was stable under acidic treatment in spite of its ketal structure; that is, the treatment of II with concentrated hydrobromic acid resulted only in the recovery of the original compound, except for the formation of a small amount of IV. On the other hand, II was sensitive to alkaline treatment; that is, II was easily changed to IV by treatment with alumina, as has been described above. Moreover, the treatment of II with sodium methoxide easily gave methyl 2,6-dibromobenzoate(VI),[7] a rearrangement product, in a nearly quantitative yield, while treatment with sodium acetate in methanol gave IV and VI.

Compound III gave 3,5-dibromotropolone(VII)[1] upon hydrolysis with hydrobromic acid. Moreover, the treatment of III with hydrazine afforded hydrazinotropone(VIII), which in turn gave 2,4,7-tribromotropone(IX)[8] upon oxidative decomposition with copper sulfate in the presence of hydrobromic acid. From these facts, III was assigned the structure of 5,7-dibromo-2-methoxytropone. The ultraviolet absorption spectrum is also consistent with this structure.

When a solution of 2-methoxytropone(I) in anhydrous ethanol was treated with bromine, neither an addition product nor a substitution product was obtained; instead, a reddish compound (X) was formed. The same compound was also obtained on the treatment of I with bromine in chloroform or carbon tetrachloride. On the contrary, when I was treated with bromine in aqueous ethanol or acetic

* Address correspondence to this author.

1) T. Nozoe, S. Seto, Y. Kitahara, M. Kunori, and Y. Nakayama, *Proc. Japan Acad.*, **26 (7)**, 38 (1950); T. Nozoe, S. Seto, T. Mukai, K. Yamane, and A. Matsukuma, *ibid.*, **27**, 224 (1951).

2) J. W. Cook, A. R. Gibb, and R. A. Raphael, *J. Chem. Soc.*, **1951**, 2244.

3) W. von E. Doering and L. H. Knox, *J. Amer. Chem. Soc.*, **73**, 828 (1951).

4) T. Nozoe, T. Mukai, and K. Takase, *Sci. Repts. Tohoku Univ., Ser. I*, **39**, 164 (1956); T. Mukai, This Bulletin, **31**, 846 (1958).

5) T. Nozoe, S. Seto, T. Ikemi, and T. Arai, *Proc. Japan Acad.*, **27**, 102 (1951).

6) J. W. Cook, A. R. Gibb, R. A. Raphael, and A. R. Somerville, *J. Chem. Soc.*, **1951**, 503.

7) T. Nozoe, Y. Kitahara, and S. Masamune, *Proc. Japan Acad.*, **27**, 650 (1951).

8) T. Nozoe, Y. Kitahara, T. Ando. S. Masamune, and H. Abe, *Sci. Repts. Tohoku Univ., Ser. I*, **36**, 166 (1952).

acid, 3,5,7-tribromotropolone (XI)[1-3] was easily produced in a good yield. Compound X gave the addition compound, II, when dissolved in methanol, whereas it gave XI on treatment with water. On the other hand, the original compound, I, was reproduced when X was treated with water containing sodium hydrogen sulfite. These facts suggested that X must be a complex compound similar to that of tropone[4] or tropolone.[1,2]

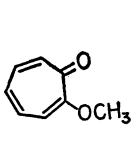

I

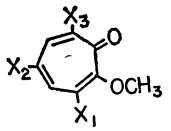

III: X_1=H, X_3=X_2=Br
IV: X_2=H, X_1=X_3=Br
V: X_1=X_2=X_3=Br
XII: X_2=X_3=H, X_1=Br
XIII: X_1=X_3=H, X_2=Br
XV: X_1=X_2=H, X_3=Br

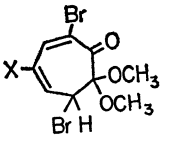

II: X=H
XIV: X=Br

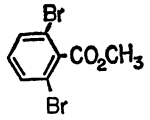

VI

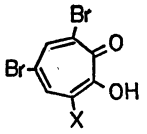

VII: X=H
XI: X=Br

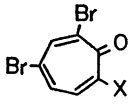

VIII: X=$NHNH_2$
IX: X=Br

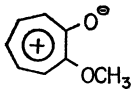

Ia

The reaction of bromo derivatives of 2-methoxytropone with bromine was also examined. The treatment of 3-bromo-2-methoxytropone(XII)[9] with bromine in methanol at 0—5°C afforded the substitution products, IV or V, by the use of one or two molar equivalents of the reagent respectively, but no addition product was isolated. On the other hand, a similar treatment of 5-bromo-2-methoxytropone(XIII)[5] with bromine gave an addition product (XIV), $C_9H_9O_3Br_3$, together with small amounts of IV and V. The infrared spectrum of XIV shows absorptions at 1706 cm^{-1} and at 1115 and 1071 cm^{-1}, corresponding to the conjugated carbonyl and the ether linkage respectively. The NMR spectrum reveals two singlets, at 3.25 (3H) and 3.40 ppm (3H), due to the methoxyl groups, and two doublets, at 4.71 (1H, J=4 Hz) and 7.53 (1H, J=2 Hz), and a double doublet, at 6.80 ppm (1H, J=9, 2 Hz), corresponding to a partial structure, –C(–)–CHBr–CH=CBr–CH=C(–)–. Moreover, it was easily changed quantitatively to V on being passed through an alumina column. From these facts, it is reasonable to assign the structure of 2,4,6-tribromo-7,7-dimethoxy-2,4-cycloheptadien-1-one to XIV.

The treatment of 7-bromo-2-methoxytropone(XV)[9] with bromine in methanol at 0—5°C resulted in the recovery of the original compound, but that at room temperature over a long period afforded IV. The dibromo compound, IV, and the tribromo compound, V, did not show any change when treated similarly.

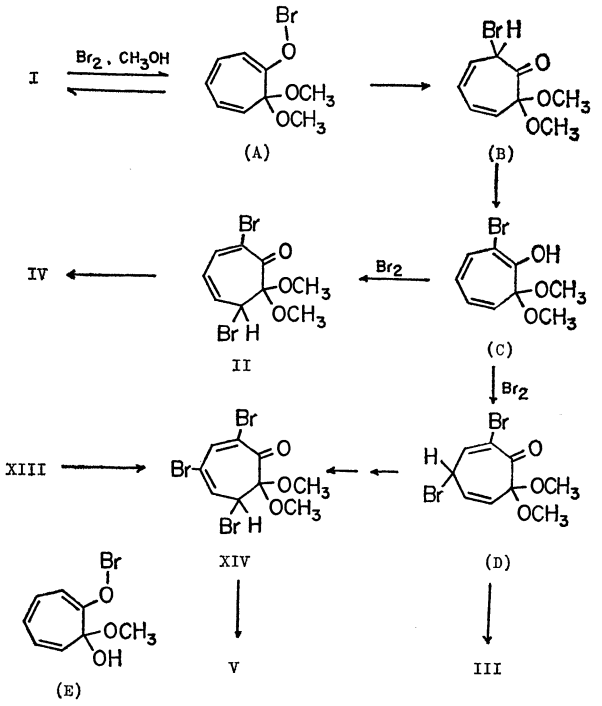

Chart 1. A possible mechanism for the reaction of 2-methoxytropone (I) with bromine in methanol.

From the findings described above, it is clear that the reaction of 2-methoxytropone(I) with bromine is markedly affected by the kind of the solvent used. It was also observed that the bromo substituents affected the reactivity of 2-methoxytropones toward bromine. Because of the rather large contribution of the polar structure(Ia),[5] the cationoid substitution can be expected to be difficult on I, for it is different from anisole. This is true when either anhydrous ethanol, chloroform, or carbon tetrachloride is used as the solvent, and I gave only a complex compound, X, as has been described previously. On the other hand, it was found that the treatment of I with bromine in methanol gave the addition compound, II, plus small amounts of the substitution products, IV and V. The formation of II is very interesting in the reaction mechanism. Although II has a structure corresponding to that consisting of the addition of a methanol molecule on IV, it is disproved that II is formed by the addition of methanol to IV, since IV did not show any change, at least under the present experimental conditions. Any possible mechanism for the formation of II would involve the nucleophilic attack of a methanol molecule on the 2-position of I, an attack which is facilitated by the coordination of the bromonium ion or its equivalent species on the carbonyl group, thus giving an intermediate (A), as is shown in Chart 1. The intermediate (A) changes immediately to a bromoketone-

9) T. Nozoe, Y. Kitahara, K. Yamane, and A. Yoshikoshi, *Proc. Japan Acad.*, **27**, 18 (1951).

type intermediate (B), which can then enolize to an enol-type intermediate (C). Although the two intermediates, (B) and (C), have structures consisting of the addition of a methanol molecule to 7-bromo-2-methoxytropone (XV), they are probably not produced through XV, since XV does not react with bromine under reaction conditions such as those under which I gave II. The reaction of bromine with the intermediate (C) affords the compound II. The substitution products, III, IV, and V, are assumed to be produced by the elimination of a methanol molecule from the corresponding addition compounds, (D), XIV and II respectively, which are formed through the intermediate (C). The addition compound XIV is also assumed to be formed from XIII through a similar reaction course.

In aqueous solvents, it is thought that a water molecule should attack the 2-position of I to give a hemiketal-type intermediate (E), which is similar to the intermediate (A). However, the intermediate (E) easily loses a methanol molecule, thus affording tropolone, which can then be easily brominated to give 3,5,7-tribromotropolone (XI).[1-3] On the other hand, in anhydrous ethanol it is presumed that an ethanol molecule can not attack the 2-position of I; consequently, probably no addition compound is formed. The reason for this has not yet been clear, but it seems to be due to the lesser nucleophilicity and/or to the greater sterical bulkiness of the ethanol molecule than that of the methanol molecule.

Experimental

All the melting points are uncorrected. The ultraviolet absorption spectra were taken on a Beckman DU spectrophotometer, and the infrared spectra, on a Shimadzu IR-27 infracord apparatus. The NMR spectra were determined with a Varian A-60 spectrometer on samples dissolved in deuteriochloroform and containing tetramethylsilane as an internal standard.

Bromination of 2-Methoxytropone(I) in Methanol. To a stirred solution of I (816 mg) in methanol (20 m*l*), a solution of bromine (1.0 g) in the same solvent (1 m*l*) was added under cooling at 0—5°C, after which the mixture was allowed to stand overnight in a refrigerator. The subsequent addition of water separated an oily material, which was then extracted with chloroform and dried over anhydrous sodium sulfate. The evaporation of the solvent left an oily residue (1.405 g), which was then crystallized by the addition of a small amount of methanol. The crystals (375 mg), mp 130—135°C, collected by filtration were recrystallized from benzene to give 2,6-dibromo-7,7-dimethoxy-2,4-cycloheptadien-1-one(II) as pale yellow prisms; mp 138—139°C.

Found: C, 33.32; H, 3.10%. Calcd for $C_9H_{10}O_3Br_2$: C, 33.47; H, 3.42%. UV (MeOH): λ_{max} nm (log ε); 330 (3.75).

All the filtrates were combined, and then the evaporation of the solvent left an oily material (870 mg) which was subsequently chromatographed on an alumina column. The fraction, when eluted with benzene, gave colorless crystals (130 mg). Recrystallization from methanol afforded 5,7-dibromo-2-methoxytropone(III) as colorless needles; mp 206—207°C.

Found: C, 32.72; H, 2.32%. Calcd for $C_8H_6O_2Br_2$: C, 32.01; H, 2.06%. UV (MeOH): λ_{max} nm (log ε); 275 (4.41), 320 (3.96), 335 (4.03), 373 (3.84).

Further elution with ether gave pale yellow crystals (85 mg). Recrystallization from ethyl acetate afforded 3,7-dibromo-2-methoxytropone(IV) as pale yellow needles, mp 134—135°C, which were identified with an authentic sample, mp 133—134°C,[5] by admixture and by a comparison of the infrared spectra.

A similar treatment of I (816 mg) with two or three molar equivalents of bromine gave II (839 mg), III (65 mg), IV (79 mg), and 3,5,7-tribromo-2-methoxytropone(V) (23 mg), mp 123—124°C,[5] and II (529 mg) and V (200 mg) respectively.

Treatment of II with Alumina. A solution of II (100 mg) in chloroform was passed through an alumina column. The subsequent evaporation of the solvent from the effluent gave IV (96 mg) as pale yellow needles; mp 134—135°C.

Treatment of II with Hydrobromic Acid. A solution of II (296 mg) in methanol (15 m*l*) containing concentrated hydrobromic acid (1 m*l*) was refluxed for 4 hr. The solution was concentrated to a small volume; the crystals thereby formed were then collected by filtration to give the original compound, II (265 mg), mp 138—139°C. The filtrate was diluted with water and extracted with chloroform. The subsequent evaporation of the solvent from the extract and the recrystallization of the residue from methanol gave IV (5 mg) as pale yellow needles; mp 134—135°C.

Treatment of II with Sodium Methoxide. A solution of II (592 mg) in methanol (20 m*l*) containing sodium methoxide (216 mg) was refluxed for 6 hr. The solvent was then evaporated, and the residue was dissolved in chloroform, washed with water, and dried over anhydrous sodium sulfate. The subsequent evaporation of the solvent left crystals (420 mg), mp 58—60°C, which were then recrystallized from petroleum ether to give methyl 2,6-dibromobenzoate(VI) as colorless needles; mp 63—64°C. This was identified with an authentic sample, mp 61—62°C[7] by admixture and by a comparison of the infrared spectra.

Treatment of II with Sodium Acetate. A mixture of II (1.48 g) and anhydrous sodium acetate (820 mg) in methanol (40 m*l*) was refluxed for 2.5 hr. The solution was then concentrated to a small volume, and to this was added water (30 m*l*). The precipitates thereby formed were collected by filtration and recrystallized from ethyl acetate to give IV (852 mg) as pale yellow needles; mp 134—135°C.

The subsequent evaporation of the solvent from the filtrate left an oily material (380 mg) which was then chromatographed on an alumina column and eluted with ether to give VI (354 mg) as colorless needles; mp 63—64°C.

3,5-Dibromotropolone (VII). A solution of III (60 mg) in methanol (30 m*l*) containing concentrated hydrobromic acid (4 m*l*) and water (4 m*l*) was refluxed for 3 hr. The subsequent evaporation of the solvent left crystals which were then recrystallized from methanol to afford VII (55 mg) as pale yellow needles; mp 152—153°C. VII was identified with an authentic sample, mp 152—153°C,[1] by admixture and by a comparison of the infrared spectra.

5,7-Dibromo-2-hydrazinotropone (VIII). To a suspension of III (294 mg) in ether (4 m*l*), 80% hydrazine hydrate (80 mg) was added under cooling at 0—5°C, after which the mixture was stirred for 9 hr. The orange crystals thereby formed were collected by filtration and recrystallized from ethyl acetate to give VIII (294 mg) as yellow needles; mp 155—156°C.

Found: C, 28.14; H, 2.56: N, 9.88%. Calcd for $C_7H_6ON_2Br_2$: C, 28.50; H, 2.05; N, 9.49%.

2,4,7-Tribromotropone (IX). Into a mixture of VIII

(260 mg) and concentrated hydrobromic acid (2 ml) being heated in a boiling water bath, a hot solution of 40% aqueous cupric sulfate solution was stirred; a vigorous evolution of nitrogen gas thus occurred. After the mixture had been heated for 5 min, it was allowed to cool to room temperature, diluted with water, and extracted with chloroform. After the chloroform solution had been dried over anhydrous sodium sulfate, the solvent was evaporated and the residue was dissolved in ether and passed through a short column of alumina. The subsequent evaporation of the solvent from the effluent, followed by the recrystallization of the residue from methanol, gave IX (60 mg) as pale yellow needles; mp 177—178°C. This was identified with an authentic sample, mp 177—178°C,[8] by admixture and by a comparison of the infrared spectra.

Reaction of I with Bromine in Anhydrous Ethanol. To a stirred solution of I (816 mg) in anhydrous ethanol (2 ml), a solution of bromine (1.0 g) in the same solvent (1 ml) was added under cooling at 0—5°C. A few minutes later, reddish orange precipitates were separated out. After being stirred for 5 min, the precipitates were collected by filtration to afford X (1.5 g) as a reddish powder.

Treatment of X with Methanol. A sample of X (500 mg) was dissolved in methanol (10 ml) and then allowed to stand overnight. The subsequent evaporation of the solvent left an oily material (384 mg) which was then crystallized by the addition of a few drops of methanol. The crystals (120 mg); mp 128—133°C, when collected by filtration, were recrystallized from ethyl acetate to give II (98 mg) as pale yellow prisms; mp 138—139°C.

All the filtrates were combined, the solvent was evaporated, and the oily residue (260 mg) was dissolved in ether and chromatographed on an alumina column. The fraction eluted with ether gave IV (83 mg) as pale yellow needles, mp 134—135°C, and V (56 mg) as yellow needles, mp 123-124°C.

Treatment of X with a Sodium Sulfite Solution. To a suspension of X (100 mg) in chloroform (2 ml), a 10% aqueous sodium hydrogen sulfite solution (9.5 ml) was added. After being stirred for 1 hr, the aqueous layer was separated and extracted with chloroform. All the chloroform layers were combined and dried over anhydrous sodium sulfate. The subsequent evaporation of the solvent left an oily material (43 mg) which was identified with 2-methoxytropone, I, by a comparison of the infrared spectra.

Treatment of X with Water. A suspension of X (200 mg) in water (5 ml) was stirred for 5 hr; the reddish color gradually disappeared, and pale yellow precipitates were formed. The product was collected by filtration and recrystallized from methanol to give 3,5,7-tribromotropolone (XI) (82 mg) as yellow needles, mp 121—122°C, which were identified with an authentic sample[1] by admixture and by a comparison of the infrared spectra.

Bromination of I in Ethanol. To a stirred solution of I (816 mg) in ethanol (10 ml) containing a small amount of water, a solution of bromine (3.10 g) in ethanol (10 ml) was added under cooling at 0—5°C. When a half of the bromine solution had been added, reddish precipitates were separated out; they gradually dissolved upon stirring for 1 hr. After being allowed to stand overnight, the reaction mixture was diluted with water (100 ml) and extracted with chloroform and the chloroform layer was dried over anhydrous sodium sulfate. The subsequent evaporation of the solvent left crystals (2.327 g) which were recrystallized from ethanol to afford XI (1.628 g) as yellow needles; mp 121—122°C.

Bromination of I in Acetic Acid. To a solution of I (816 mg) in acetic acid (10 ml), a solution of bromine (2.12 g) in the same solvent (5 ml) was added under cooling at 0—5°C. After being allowed to stand overnight, the reaction mixture was treated in a manner similar to that described above; this gave XI (1.10 g) as yellow needles; mp 121—122°C.

Bromination of 3-Bromo-2-methoxytropone (XII). To a solution of XII (215 mg) in methanol (2 ml), a solution of bromine (160 mg) in the same solvent (1 ml) was added under cooling at 0—5°C, after which the mixture was allowed to stand overnight at room temperature. The reaction mixture was diluted with water, and the precipitates thereby formed were collected by filtration and recrystallized from methanol to give IV (250 mg) as pale yellow needles; mp 134—135°C.

A similar treatment of XII (215 mg) with bromine (320 mg) gave V (205 mg) as yellow needles; mp 123—124°C.

Bromination of 5-Bromo-2-methoxytropone (XIII). To a solution of XIII (215 mg) in methanol (15 ml), a solution of bromine (350 mg) in the same solvent (2 ml) was added under cooling at 0—5°C. After being allowed to stand overnight, the reaction mixture was diluted with water and extracted with chloroform, and the organic layer was dried over anhydrous sodium sulfate. The subsequent evaporation of the solvent left an yellow oil (481 mg), which was crystallized by the addition of a small amount of methanol. Recrystallization from methanol gave 2,4,6-tribromo-7,7-dimethoxy-2,4-cycloheptadien-1-one (XIV) as pale yellow prisms; mp 107—108°C.

Found: C, 26.98; H, 2.38%. Calcd for $C_9H_9O_3Br_3$: C, 26.69; H, 2.24%. UV (MeOH): λ_{max} nm (log ε); 333 (3.73).

A solution of XIV (100 mg) in chloroform was passed through an alumina column. The subsequent evaporation of the solvent from the effluent gave V (76 mg) as yellow needles; mp 123—124°C.

Reaction of 7-Bromo-2-methoxytropone (VII) with Bromine. a) To a stirred solution of VII (107 mg) in methanol (8 ml), a solution of bromine (80 mg) in the same solvent (2 ml) was added under cooling at 0—5°C, after which the mixture was allowed to stand overnight in a refrigerator. The reaction mixture was diluted with water (50 ml) and extracted with chloroform. The subsequent evaporation of the solvent gave the original compound, VII (92 mg).

b) To a stirred solution of VII (214 mg) in methanol (15 ml), a solution of bromine (240 mg) in the same solvent (5 ml) was added under cooling at 0—5°C, after which the mixture was allowed to stand for 7 days in a refrigerator and then for a few days at room temperature. Then, the reaction mixture was diluted with water; the precipitates thereby formed were collected by filtration to afford pale yellow crystals (89 mg), which later gave IV (56 mg); mp 134—135°C, by recrystallization from methanol.

This research has been financially supported by grants from the Japanese Ministry of Education and the Sankyo Co., Ltd.

Aminocyclitols. XXVI. A Synthesis of Aminocyclopentanetetrols

Tetsuo SUAMI, Yukio SAKOTA, Kinnichi TADANO, and Shigeru NISHIYAMA

Department of Applied Chemistry, Faculty of Engineering, Keio University, Koganei-shi, Tokyo

(Received February 27, 1971)

Hydrogenation of 2,3-*O*-cyclohexylidene-5-nitro-1,2,3,4-cyclopentanetetrol, subsequently followed by hydrolysis and acetylation, afforded (1,4/2,3,5)- and DL-(1,2,3/4,5)-5-acetamido-1,2,3,4-tetra-*O*-acetyl-1,2,3,4-cyclopentanetetrol (**3** and **14**). Beginning with (1,4/2,3,5)-5-acetamido-1,4-di-*O*-acetyl-2,3-*O*-cyclohexylidene-1,2,3,4-cyclopentanetetrol (**2**), two hitherto unknown (1,2,3,4,5)- and DL-(1/2,3,4,5)-5-acetamido-1,2,3,4-tetra-*O*-acetyl-1,2,3,4-cyclopentanetetrol (**10** and **12**) were prepared. The structures were established by proton magnetic resonance spectra.

Six DL-pairs and four meso compounds are theoretically possible in aminocyclopentanetetrols and nowadays three DL-pairs and two meso compounds are known.[1,2]

A presence of five membered carbocyclic compounds in antibiotics aristeromycin[3,4] and pactamycin[5,6] has stimulated the authors to explore a synthesis of new aminocyclopentanetetrols. In 1965, Angyal and Gero[7] prepared 2,3-*O*-cyclohexylidene-5-nitro-1,2,3,4-cyclopentanetetrol (**1**) by cyclization of *cis*-3,4-cyclohexylidenedioxy-2,5-dihydroxytetrahydrofuran with nitromethane. Very recently, it has been described that two aminocyclopentanetetrols were obtained as their pentaacetyl-derivatives by catalytic hydrogenation of **1**.[2]

In the present article, the authors wish to report a preparation of four aminocyclopentanetetrols in which a DL-pair and a meso compound are hitherto unknown ones.

Catalytic hydrogenation of **1** in ethanol with Raney nickel T-4,[8] followed by acetylation afforded (1,4/2,3,5)-5-acetamido-1,4-di-*O*-acetyl-2,3-*O*-cyclohexylidene-1,2,3,4-cyclopentanetetrol (**2**)[2] in 40% yield. Hydrolysis of **2** in 80% aqueous acetic acid and subsequent acetylation of the hydrolyzate yielded (1,4/2,3,5)-5-acetamido-1,2,3,4-tetra-*O*-acetyl-1,2,3,4-cyclopentanetetrol (**3**)[1,2] of mp 147.5°C in 89% yield.

From the hydrogenation mixture, it was successfully attempted to isolate another isomer by a following procedure. The mother liquor from which the compound **2** had been obtained was settled in a refrigerator to give DL-(1,2,3/4,5)-5-acetamido-1,4-di-*O*-acetyl-2,3-*O*-cyclohexylidene-1,2,3,4-cyclopentanetetrol (**13**). Hydrolysis of **13** in 80% aqueous acetic acid, followed by acetylation, gave DL-(1,2,3/4,5)-5-acetamido-1,2,3,4-tetra-*O*-acetyl-1,2,3,4-cyclopentanetetrol (**14**).[1]

Beginning with the compound **2**, two unknown aminocyclopentanetetrols were prepared by the following reactions. When **2** was treated with ammonia in methanol, *O*-acetyl groups were selectively removed to give 5-acetamido-2,3-*O*-cyclohexylidene-1,2,3,4-cyclopentanetetrol (**8**) of mp 160.5°C in 61% yield. Methanesulfonylation of **8** with a large excess amount of methanesulfonyl chloride in pyridine afforded 1,4-di-*O*-methane sulfonyl derivative (**9**) in 69% yield. A treatment in boiling water and subsequent acetylation converted **9** to (1,2,3,4,5)-5-acetamido-1,2,3,4-tetra-*O*-acetyl-1,2,3,4-cyclopentanetetrol (**10**) of mp 173°C in a yield of 62%. The compound **10** showed a remarkable depression of the melting point, when it was mixed with (1,4,5/2,3)-5-acetamido-1,2,3,4-tetra-*O*-acetyl-1,2,3,4-cyclopentanetetrol of mp 176.5°C.[2]

A similar treatment of **8** with the smaller amount of methanesulfonyl chloride yielded a mixture of mono-*O*-methanesulfonyl derivative (**11**) and **9**. The mixture was heated in boiling water and subsequently acetylated to give a mixture of DL-(1/2,3,4,5)-5-acetamido-1,2,3,4-tetra-*O*-acetyl-1,2,3,4-cyclopentan-

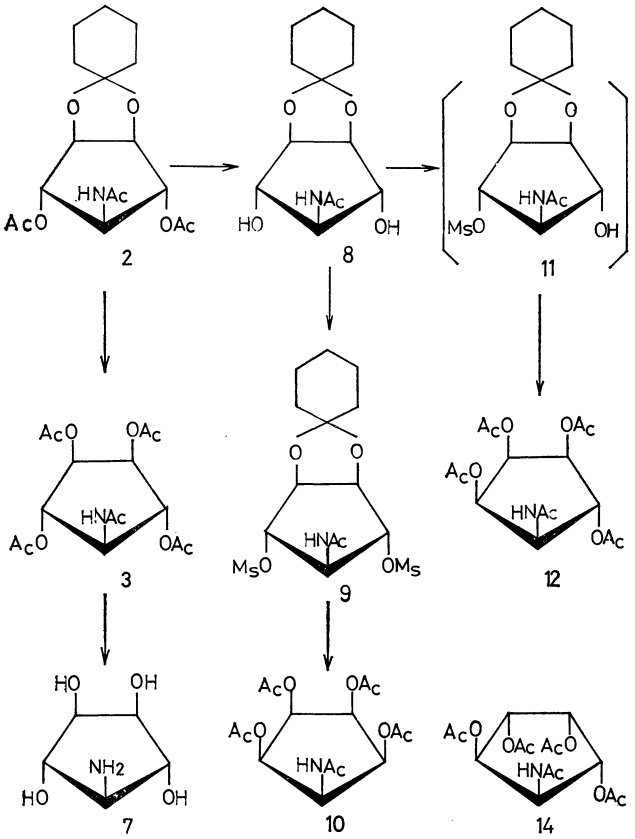

1) A. Hasegawa and H. Z. Sable, *J. Org. Chem.*, **31**, 4154 (1966).
2) R. Ahluwalia, S. J. Angyal, and B. M. Luttrell, *Aust. J. Chem.*, **23**, 1819 (1970).
3) T. Kishi, M. Muroi, T. Kusaka, M. Nishikawa, K. Kamiya, and K. Mizuno, *Chem. Commun.*, **1967**, 852.
4) T. Kusaka, H. Yamamoto, M. Shibata, M. Muroi, T. Kishi, and K. Mizuno, *J. Antibiotics (Tokyo), Ser. A*, **21**, 255 (1968).
5) A. D. Argoudelis, H. K. Jahnke, and J. A. Fox, *Antimicrobial Agents & Chemotherapy*, 191 (1961).
6) P. F. Wiley, H. K. Jahnke, F. McKellar, R. B. Kelly, and A. D. Argoudelis, *J. Org. Chem.*, **35**, 1420 (1970).
7) S. J. Angyal and S. D. Gero, *Aust. J. Chem.*, **18**, 1973 (1965).
8) S. Nishimura, This Bulletin, **32**, 61 (1959).

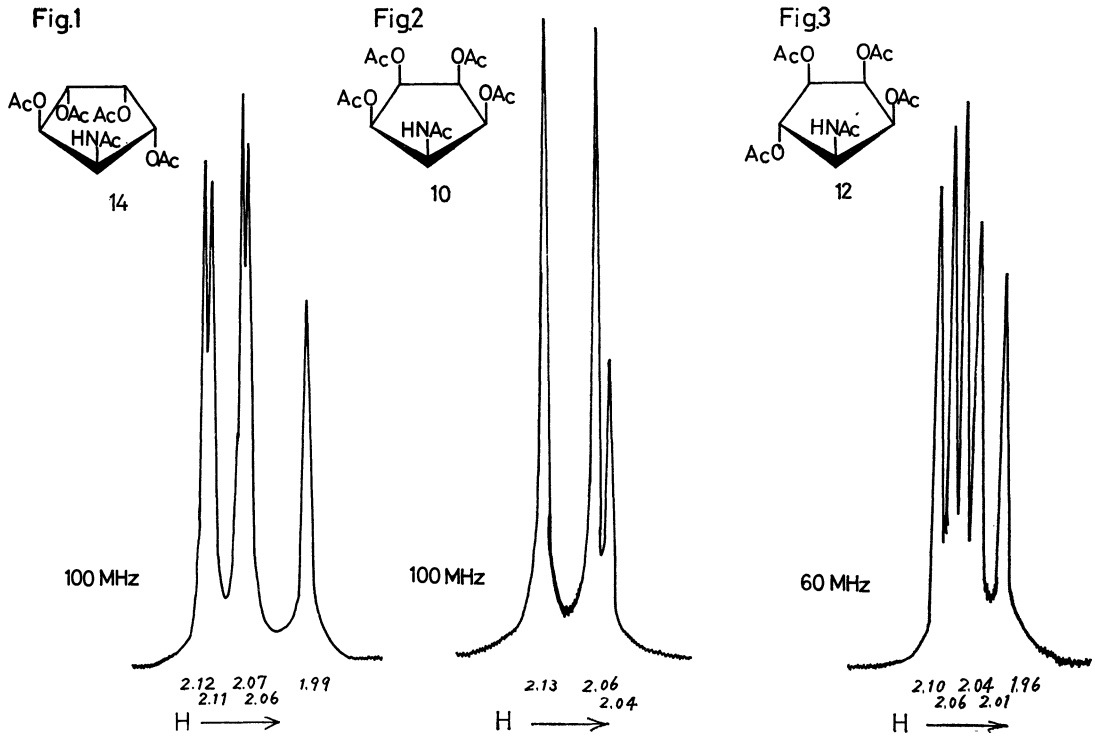

etetrol (**12**) of mp 116°C and the compound **10,** which were separated by a chromatographic fractionation.

The compound **3** (mp 147.5°C) was identical with the compound described by Hasegawa and Sable[1] and by Ahluwalia, Angyal, and Luttrell.[2] The proton magnetic resonance (PMR) spectrum of **3** revealed three sharp signals at δ 1.95, 2.05 and 2.08 (3 : 6 : 6 protons) which were attributed to an acetamido, two acetoxy (on C-2 and C-3) and two acetoxy groups (on C-1 and C-4) respectively.

The compound **13** showed three sharp signals in its PMR spectrum for an acetamido and two acetoxy groups at δ 1.96, 2.10 and 2.12 (3 : 3 : 3 protons), proving that the two acetoxy groups on C-1 and C-4 had different configurations for the acetamido group. And the compound **14** (mp 188.5°C) showed five sharp signals in its PMR spectrum at δ 1.99, 2.06, 2.07, 2.11 and 2.12 (3 : 3 : 3 : 3 : 3 protons) indicating that this compound was not symmetrical and identical with DL-(1,2,3/4,5)-5-acetamido-1,2,3,4-tetra-*O*-acetyl-1,2,3,4-cyclopentanetetrol described by Hasegawa and Sable.[1]

The compound **10** (mp 173°C) showed three sharp signals at δ 2.04, 2.06 and 2.13 (3 : 6 : 6 protons) in its spectrum, showing that **10** had a symmetrical molecular structure.

Among four theoretically possible meso compounds, two isomers of (1,2,3,4,5) and (1,2,3,4/5) have never been described and the compound **10** should be one of these two isomers.

The following reaction mechanism was proposed for the reaction from **9** to **10**. Removal of a methanesulfonyloxy group yields an oxazolinium ion with a participation of a neighboring *trans*-acetamido group and the cyclic carbonium ion is attacked by water to give *cis*-acetamido alcohol.[9,10] The same anchimeric reaction occurs again with another methanesulfonyloxy group to give the (1,2,3,4,5)-isomer.

The compound **12** (mp 116°C) exhibited five sharp signals in its spectrum at δ 1.96, 2.01, 2.04, 2.06 and 2.10 (3 : 3 : 3 : 3 : 3 protons) indicating that this compound was an unsymmetrical one. Therefore, it was reasonably established that **12** was DL-(1/2,3,4,5)-isomer. The above mentioned reaction mechanism is also proposed in this reaction.

Now seven isomers of aminocyclopentanetetrols have been described in their pentaacetyl derivatives and only three isomers remain unknown. An attempt to synthesize these isomers is still under way.

Experimental

A melting point was determined in a liquid bath and was uncorrected. PMR spectrum was recorded on a Varian A-60D spectrometer, unless otherwise noted, at a frequency of 60 MHz in deuteriochloroform with tetramethylsilane as an internal standard. The peak position was expressed in δ-value.

2,3-O-Cyclohexylidene-5-nitro-1,2,3,4-cyclopentanetetrol (***1***). A mixture of *cis*-3,4-cyclohexylidenedioxytetrahydrofuran-2,5-diol (10.4 g) and nitromethane (2.8 g) was treated with sodium methoxide by the method of Angyal and Gero[7] to give 8.1 g (65%) of **1** as an oily product. The product was used for a successive reaction without any purification.

(1,4/2,3,5)-5-Acetamido-1,4-di-O-acetyl-2,3-O-cyclohexylidene-1,2,3,4-cyclopentanetetrol (***2***). A 5.4 g portion of **1** was hydrogenated in ethanol (50 m*l*) with Raney nickel T-4

9) E. S. Gould, "Mechanism and Structure in Organic Chemistry," Holt, Rinehart and Winston, New York (1959), p. 566.
10) T. Suami and S. Ogawa, This Bulletin, **37**, 194 (1964).

catalyst[8] at 3.4 kg/cm² of hydrogen stream for 20 hr. After the catalyst was removed by filtration, the ethanol solution was evaporated under reduced pressure to give 4.7 g of a residual oil. The residue was acetylated in a mixture of acetic anhydride (20 m*l*) and pyridine (20 m*l*). The mixture was evaporated *in vacuo* and the residue was crystallized in benzene to give 3.2 g (45%) of needles, mp 137—139°C. Recrystallization from benzene gave 2.9 g (40%) of crystals, mp 140.5—141.5°C. PMR: δ 1.93 (3 protons, NAc) and 2.08 (6 protons, OAc×2). (Found: C, 57.33; H, 6.93; N, 3.77%).

*(1,4/2,3,5)-5-Acetamido-1,2,3,4-tetra-O-acetyl-1,2,3,4-cyclopentanetetrol (**3**).* A 1.33 g portion of **2** was heated under reflux for 4 hr in 80% aqueous acetic acid (20 m*l*) and the mixture was evaporated *in vacuo*. The residue was acetylated with acetic anhydride in pyridine to give 1.10 g (89%) of the crude product. Recrystallization from ether afforded needle crystals of mp 146.5—147.5°C. PMR: δ 1.95 (3 protons, NAc), 2.05 (6 protons, OAc×2, on C-2 and C-3), 2.08 (6 protons, OAc×2, on C-1 and C-4), 4.33(H), 5.21 (4H) and 6.44 (NH, J=8 Hz). (Found: C, 50.31; H, 5.80; N, 3.81%). Lit. mp 147°C[1] and 138.5—140°C.[2]

*(1,4/2,3,5)-5-Acetamido-1,2,3,4-tetra-O-trideuterioacetyl-1,2,3,4-cyclopentanetetrol (**4**).* A 0.12 g protion of **5** was treated with 0.7 m*l* of acetic anhydride-d_6 in 2.5 m*l* of pyridine to give 0.18 g (78%) of the product, mp 144—145°C. PMR: δ 1.95 (3 protons, NAc), 4.34 (H), 5.24 (4H) and 6.28 (NH).

*(1,4/2,3,5)-5-Acetamido-1,4-di-O-acetyl-2,3-di-O-trideuterioacetyl-1,2,3,4-cyclopentanetetrol (**16**).* A 50 mg sample of **15** was treated with 0.5 m*l* of acetic anhydride-d_6 in pyridine (1.0 m*l*) to give 20 mg of the product, mp 145°C. PMR: δ 1.95 (3 protons, NAc), 2.08 (6 protons, OAc×2, on C-1 and C-4), 4.33 (H), 5.25 (4H) and 6.08 (NH).

*(1,4/2,3,5)-5-Acetamido-1,2,3,4-cyclopentanetetrol (**5**).* A 0.5 g portion of **3** was selectively de-*O*-acetylated in methanol (50 m*l*) saturated with ammonia. The solution was evaporated under reduced pressure and the residue was washed with ethyl acetate to give a crude product. Recrystallization from ethanol afforded 0.14 g (53%) of the product, mp 169.5—171°C.

Found: C, 44.02; H, 6.71; N, 7.12%. Calcd for $C_7H_{13}NO_5$: C, 43.97; H, 6.85; N, 7.33%.

*(1,4/2,3,5)-5-Acetamido-1,4-di-O-acetyl-2,3-O-isopropylidene-1,2,3,4-cyclopentanetetrol (**6**).* A mixture of **5** (87 mg), anhydrous acetone (50 m*l*) and methanol (5 m*l*) was agitated for 48 hr in the presence of Drielite and a half drop of conc sulfuric acid. The reaction mixture was neutralized to pH 7 with Amberlite IR-4B and then evaporated under reduced pressure to give a crystalline residue. The residue was acetylated to give a crude product. Recrystallization from ethanol afforded 89 mg (63%) of needles, mp 177—178°C. PMR: δ 1.29 (3 protons, CH_3), 1.51 (3 protons, CH_3), 1.91 (3 protons, NAc), 2.05 (6 protons, OAc×2), 4.55 (3H), 5.04 (2H) and 6.37 (NH, J=8 Hz).

Foudd: C, 53.61; H, 6.77; N, 4.36%. Calcd for $C_{14}H_{21}NO_7$: C, 53.32; H, 6.71; N, 4.44%.

*(1,4/2,3,5)-5-Amino-1,2,3,4-cyclopentanetetrol (**7**).* A 1.05 g portion of **3** was heated under reflux in 6 N hydrochloric acid for 2 hr. The solution was evaporated *in vacuo* to give 0.61 g of a residue, The residue was dissolved in water and treated with Amberlite IRA-400(OH^-). The aqueous solution was evaporated and the residue was crystallized in absolute ethanol (10 m*l*) to give 0.39 g (89%) of the product, mp 159—161°C. The product showed a positive ninhydrin test.

Found: C, 40.59; H, 7.25; N, 9.58%. Calcd for $C_5H_{11}NO_4$: C, 40.26; H, 7.43; N, 9.39%.

*(1,4/2,3,5)-5-Acetamido-2,3-O-cyclohexylidene-1,2,3,4-cyclopentanetetrol (**8**).* A 3.55 g portion of **2** was dissolved in methanol (100 m*l*) previously saturated with ammonia and the solution was settled overnight at room temperature. Evaporation of the solution under reduced pressure yielded an oily residue, which was triturated in a mixture of ethyl acetate (9 m*l*) and ether (15 m*l*) to give 1.89 g (70%) of the crude product. Recrystallization from ethyl acetate afforded 1.65 g (61%) of the crystals, mp 159.5—160.5°C.

Found: C, 57.31; H, 7.80; N, 5.14%. Calcd for $C_{13}H_{21}NO_5$: C, 57.55; H, 7.81; N, 5.16%.

*(1,4/2,3,5)-5-Acetamido-2,3-O-cyclohexylidene-1,4-di-O-methanesulfonyl-1,2,3,4-cyclopentanetetrol (**9**).* To 1.00 g of **8** in dry pyridine (20 m*l*) was added 0.8 m*l* of methanesulfonyl chloride with a mechanical agitation under ice cooling. The mixture was settled overnight at room temperature and then it was poured into 50 m*l* of ice and water. The aqueous solution was stored in a refrigerator to give 0.95 g (62%) of crystals, mp 112—116°C. PMR: δ 1.64 (10 protons, cyclohexylidene group), 2.03 (3 protons, NAc), 3.14 (6 protons, OMs×2), 4.84 (5H) and 6.61 (NH, J=8 Hz).

Found: C, 41.70; H, 6.09; N, 3.26; S, 13.83%. Calcd for $C_{15}H_{15}NS_2O_9$: C, 42.14; H, 5.89; N, 3.28; S, 15.00%.

An alternative method was as followings. The aqueous solution was extracted with chloroform (50 m*l*×4) and the chloroform extracts were evaporated under reduced pressure and the residue was added to 30 m*l* of water to give 1.07 g (69%) of crystals, mp 111—114°C. Recrystallization from an organic solvent resulted in a partial decomposition of the product.

*(1,2,3,4,5)-5-Acetamido-1,2,3,4-tetra-O-acetyl-1,2,3,4-cyclopentanetetrol (**10**).* A mixture of **9** (200 mg) and water (20 m*l*) was heated under reflux for 40 min and then evaporated under reduced pressure. The residue was acetylated as usual and the product was recrystallized from ethanol to give 83 mg (62%) of needles, mp 172—173°C. Admixture of **10** with (1,4,5/2,3)-isomer which was prepared by the method of Ahluwalia *et al.*[2] showed a remarkable depression of the melting point.

PMR (100 MHz): δ 2.04 (3 protons, NAc), 2.06 (6 protons, OAc×2), 2.13 (6 protons, OAc×2), 4.85 (H), 5.37 (4H) and 5.86 (NH, J=9 Hz).

Found: C, 49.87; H, 6.08; N, 3.97%. Calcd for $C_{15}H_{21}NO_9$: C, 50.13; H, 5.89; N, 3.90%.

*DL-(1/2,3,4,5)-5-Acetamido-1,2,3,4-tetra-O-acetyl-1,2,3,4-cyclopentanetetrol (**12**).* To a solution of **8** (0.5 g) in pyridine (10 m*l*) was added methanesulfonyl chloride (0.4 m*l*) with an agitation under ice cooling. After 65 min the mixture was poured into ice cold water (15 m*l*) and the aqueous solution was extracted with chloroform (40 m*l*×3). The combined chloroform extracts were washed with 0.1 N hydrochloric acid and water. Evaporation of chloroform yielded an oily product. Tlc on silica gel with benzene-ethanol (5 : 1) showed **9** at R_f 0.7 and monomethanesulfonyl derivative (**11**) at R_f 0.6 as two major components.

The mixture of **9** and **11** was heated in water (40 m*l*) under reflux for 3 hr and evaporated under reduced pressure. The residue was hydrolyzed in 80% aqueous acetic acid and the hydrolyzate was acetylated to give an oily product. The crude product was chromatographed on a silica gel column (Wako gel C-200, 25 g, 400×18 mm) with benzene-ethanol (5 : 1) as an eluant and each fraction (2 m*l*) was tested by tlc. A substance with R_f 0.66 was found in the fractions from 9th to 17th, which were combined and evaporated to give 0.33 g of a residue. The residue was crystallized in ether and recrystallized from ether to give 89 mg (14%) of the compound **12** as fine needles, mp 116°C. PMR:

δ 1.96 (3 protons, NAc), 2.01, 2.04, 2.06, 2.10 (3 protons each, OAc), 4.52 (H), 5.33 (4H) and 6.16 (NH, J=8 Hz).

Found: C, 50.21; H, 5.84; N, 3.92%. Calcd for $C_{15}H_{21}NO_9$: C, 50.13; H, 5.89; N, 3.90%.

The fractions from 18th to 35th contained a product of R_f 0.52, which were combined and evaporated. The residue was recrystallized from ethanol to give 115 mg (17%) of the compound **10**, mp 172—173°C, which was identified by a comparison of IR spectrum and a mixed melting point determination with an authentic sample.

*DL-(1,2,3/4,5)-5-Acetamido-1,4-di-O-acetyl-2,3-O-cyclohexylidene-1,2,3,4-cyclopentanetetrol (**13**).* The crystalline nitro compound **1** (1.86 g, mp 102—108°C) which was prepared by the method of Ahluwalia *et al.*[2] was hydrogenated in ethanol with Raney nickel T-4[8] and subsequently acetylated as described in the preparation of **2**. After 0.70 g of **2** was obtained from the benzene solution, the mother liquor was settled in a refrigerator for three days to give 0.19 g of the crude product, mp 185—188°C. The product was recrystallized from benzene to give 0.13 g (5%) of **13**, mp 186—188°C. PMR: δ 1.50, 1.68 (10 protons, cyclohexylidene group), 1.96 (3 protons, NAc), 2.10 (3 protons, OAc) and 2.12 (3 protons, OAc).

Found: C, 57.99; H, 7.25; N, 3.85%. Calcd for $C_{17}H_{25}NO_3$: C, 57.45; H, 7.09; N, 3.94%.

*DL-(1,2,3/4,5)-5-Acetamido-1,2,3,4-tetra-O-acetyl-1,2,3,4-cyclopentanetetrol (**14**).* A 72 mg portion of **13** was hydrolyzed in 6 N hydrochloric acid (10 ml) for 1 hr under reflux. The solution was evaporated *in vacuo* and the residue was acetylated to give a crude product. Recrystallization from ether afforded 52 mg (72%) of **14** as needle crystals, mp 187—188°C. PMR (100 MHz): δ 1.99 (3 protons, NAc), 2.06, 2.07, 2.11, 2.12 (3 protons each, OAc), 4.85 (H), 5.40 (4H) and 6.12 (NH, J=8 Hz).

Found: C, 50.54; G, 5.51; N, 3.96%. Calcd for $C_{15}H_{21}NO_9$: C, 50.13; H, 5.89; N, 3.90%.

An alternative method was as followings. The benzene mother liquor from which **2** had been obtained in the preparation of **2** beginning with an oily nitro compound **1** was evaporated to give a dark residue (3.8 g). The residue was hydrolyzed in 80% aqueous acetic acid and the hydrolyzate was acetylated. The acetylated product was dissolved in chloroform and the solution was decolorized with activated alumina and evaporated. The residue was crystallized in chloroform-ether to give 0.21 g of needles. Recrystallization from chloroform-ether afforded 172 mg of crystals, mp 187—188.5°C. The product was identified to be **14** by a comparison of IR spectrum and a mixed melting point determination with an above mentioned product. The product showed a single spot in tlc with benzene-ethanol (5 : 1).

*(1,4/2,3,5)-5-Acetamido-1,4-di-O-acetyl-1,2,3,4-cyclopentanetetrol (**15**).* Hydrolysis of **2** (1.88 g) in boiling 80% aqueous acetic acid (40 ml) for 40 min afforded an oily product, which showed two major eomponents on tlc with benzene-ethanol (5 : 1) at R_f 0.3 and 0.5. The crude product was crystallized in ethanol giving 0.77 g of crystals, mp 161—164°C. Recrystallization from ethanol afforded 0.62 g (42%) of **15**, mp 167—168.5°C.

Found; C, 48.30; H, 6.34; N, 5.41%. Calcd for $C_{11}H_{17}NO_7$: C, 48.00; H, 6.22; N, 5.09%.

The authors are grateful to Professor Sumio Umezawa for his helpful advice and Mr. Saburo Nakada for his elementary analyses. This research was financially supported in part by a grant of the Japanese Ministry of Education.

Electronic Spectra of Square-Planar Bis(tertiary phosphine)dialkynyl Complexes of Nickel(II), Palladium(II), and Platinum(II)

Haruo MASAI, Kenkichi SONOGASHIRA, and Nobue HAGIHARA
The Institute of Scientific and Industrial Research, Osaka University, Suita, Osaka

(Received February 27, 1971)

Electronic spectra of *trans*-$[L_2M(C{\equiv}CR)_2]$, (L=tertiary phosphine or tertiary stibine, and M=Ni, Pd or Pt) have been studied in solution from 220 mμ to 360 mμ. Nickel and platinum complexes showed three intense absorption bands. The lowest energy band was particularly sensitive to substituents of alkynyl groups. This band was assigned empirically to the transition between the molecular orbitals involved in metal-alkynyl bonds. The possibility of π-interaction between the two alkynyl groups through central metal was discussed in relation to the influence of R.

We have been studying the properties of bis(tertiary phosphine)dialkynyl complexes, *trans*-$[L_2M(C{\equiv}CR)_2]$, where L is a tertiary phosphine or tertiary stibine, and M is nickel(II), palladium(II), and platinum (II). In a previous paper,[1] infrared spectra of the series of the complexes were discussed. From the influence of substituent R upon metal-carbon stretching frequencies, $d\pi$–$p\pi$ interaction (back-donation) was regarded as an important factor which reinforces the metal-alkynyl bond. The result threw light upon properties of the metal-carbon σ-bond which plays an important role in many reactions catalyzed by transition metal complexes.

For a discussion of the properties of this series of complexes, information on their electronic structure is necessary. However, only a few discussions on the electronic spectra of alkynyl complexes or of complexes having D_{2h} symmetry can be found.[2,3] Theoretical treatment of the spectra of these metals has been limited to the complexes in D_{4h} or T_d symmetry.

In this work, electronic spectra (220 mμ—360 mμ) of the series of alkynyl complexes in solution are reported and their general trends discussed in terms of π-interaction between metal and alkynyl groups.

Results and Discussion

General Features. Electronic spectra (UV) of *trans*-$[L_2M(C{\equiv}CR)_2]$, where M is Ni (II), Pd (II) or Pt (II), and L is a tertiary phosphine or stibine, were recorded in ether from 220 mμ to 360 mμ. Their absorption maxima (λ_{max}) and intensities (log ε) are listed in Table 1.

The intensities of absorption band are of the order of 4 in log ε scale. Thus, these bands are presumably due to the allowed transition within the molecule, *i.e.* intramolecular charge-transfer transition.[4] In our case, no band due to *d–d* transition was observed. It is probably obscured by intense charge-transfer bands.

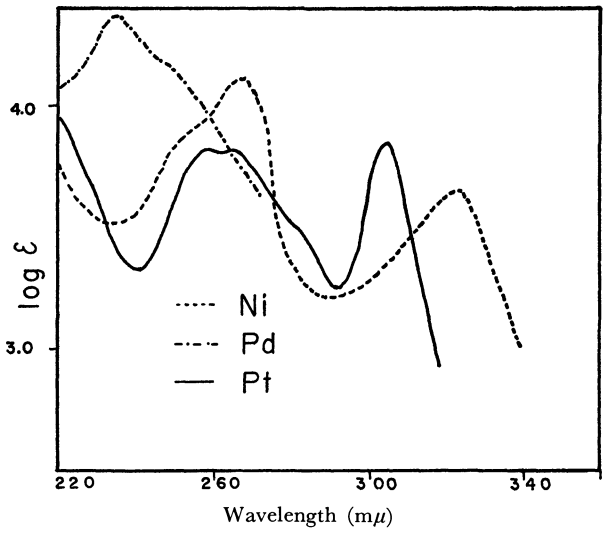

Fig. 1. Electronic spectra of *trans*-$[(Et_3P)_2M(C{\equiv}CH)_2]$ in ether.

The complexes show three intense absorption bands in this region expect for palladium complexes (Fig. 1 and Table 1), which exhibit unresolved bands at the shorter wavelength region than the others. Thus, we mainly discussed nickel and platinum complexes.

The characteristic feature of the palladium complexes has also been observed in UV spectra of teracyanide complexes of nickel(II), palladium(II) and platinum (II).[5,6]

Influence of Substituents of Alkynyl Groups. The change in substituents R's influences the wavelength of three absorption bands in different degrees (Fig. 2). The lowest energy band is most remarkably influenced as shown in Fig.2 and Table 1. Influence on the other bands was not clear, since in some cases they overlapped each other.

It is seen from Table 1 that the lowest energy band is subject to bathochromic effect of the substituents which increases in the following order.

$R=H<CH_3<CH_2F<CH_2{=}CH<HC{\equiv}C<Ph<CH_3C{\equiv}C$

for *trans*-$[(Et_3P)_2Ni(C{\equiv}CR)_2]$

1) H. Masai, K. Sonogashira, and N. Hagihara, *J. Organometal. Chem.*, **26**, 271 (1971).
2) P. J. Kim, H. Masai, K. Sonogashira, and N. Hagihara, *Inorg. Nucl. Chem. Lett.*, **6**, 181 (1970).
3) J. Chatt, G. A. Gamlen, and L. E. Orgel, *J. Chem. Soc.*, **1958**, 486.
4) B. N. Figgis, "Introduction to Ligand Fields," Interscience, New York (1966), Chapter 9.
5) a) H. B. Gray and C. J. Ballhausen, *J. Amer. Chem. Soc.*, **85**, 260 (1963). b) W. R. Mason, III, and H. B. Gray, *ibid.*, **90**, 5721 (1968).
6) A. J. McCaffery, P. N. Schatz, and P. J. Stephans, *ibid.*, **90**, 5730 (1968).

TABLE 1. ABSORPTION BANDS (mμ) AND INTENSITIES (log ε) OF *trans*-[$L_2M(C{\equiv}CR)_2$] IN ETHER

M	L	R	λ_{max} (log ε)		
Ni	Et_3P	H	322 (3.68)	266 (4.14)	254sh (3.93)
		CH_3	329 (3.68)	272 (3.87)	260sh (3.67)
		CH_2F	315br (3.74)	271 (4.16)	260sh (3.97)
		CH_2=CH	338 (3.15)	269 (3.51)	256sh (3.45)
		HC≡C[a]	341 (4.28)		
		Ph	343 (4.01)	275 (4.34)	
		$CH_3C{\equiv}C$[a]	343 (4.12)		
Pd	Et_3P	H	263sh (3.85)	245sh (4.16)	234 (4.37)
		CH_3	265sh (3.85)	251sh (4.09)	236 (4.32)
		Ph	300sh (4.46)	280sh (4.49)	245 (4.59)
Pt	Et_3P	H	304 (3.85)	267 (3.81)	258 (3.83)
		CH_3	313 (3.95)	276 (3.72)	258 (3.77)
		CH_2=CH	323 (4.24)	286 (4.01)	260 (4.38)
		HC≡C	321 (4.01)		
		$CH_3C{\equiv}C$[a]	324 (4.12)		
		Ph	328 (4.22)	288 (4.13)	264 (4.23)
		PhC≡C	349 (4.67)		
	Me_3P	H	302 (3.90)	265sh (3.90)	254 (3.93)
		CH_3	310 (4.21)	274sh (4.04)	255 (4.12)
		CH_2=CH	319 (4.35)	284 (4.13)	258 (4.47)
		Ph	325 (4.47)	285 (4.38)	261 (4.48)
	Et_3Sb	Ph	354 (4.37)	268 (4.77)	242 (4.62)
		PhC≡C	364 (4.59)		

a) see also Table 4. sh: shoulder

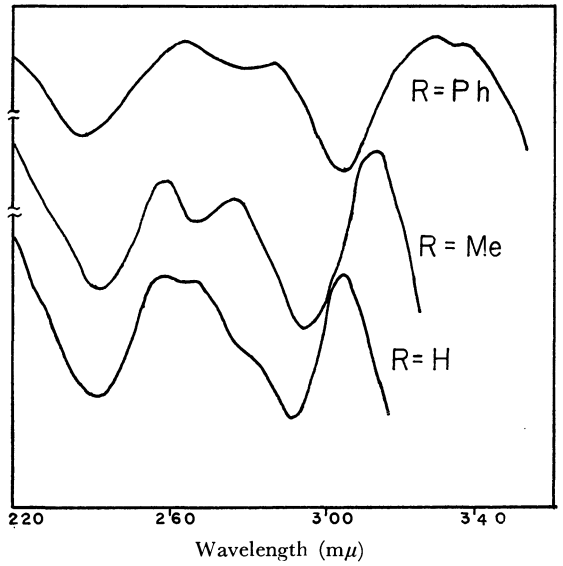

Fig. 2. Influence of R on spectra of *trans*-[$(Et_3P)_2Pt(C{\equiv}CR)_2$] in ether.

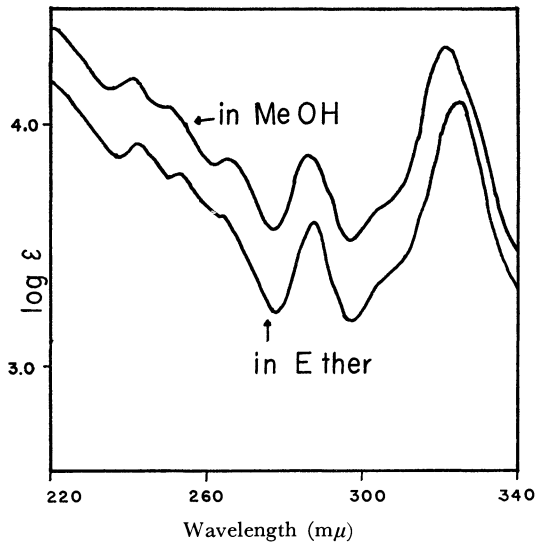

Fig. 3. Electronic spectra of *trans*-[$(Et_3P)_2Pt(C{\equiv}CC{\equiv}CCH_3)_2$] in ether and methanol.

$R=H<CH_3<HC{\equiv}C<CH_2{=}CH<CH_3C{\equiv}C<Ph<PhC{\equiv}C$

for *trans*-[$(Et_3P)_2Pt(C{\equiv}CR)_2$] and

$R=H<CH_3<CH_2{=}CH<Ph$

for *trans*-[$(Me_3P)_2Pt(C{\equiv}CR)_2$]

Complicated absorption bands of butadiynyl derivatives (Fig. 3)may be assigned by a solvent effect. Plots of the position of the lowest energy band against ionization potentials (IP) of free alkynes[7] showed a linear correlation (Table 2 and Fig. 4).

The lowest band is evidently due to the charge-transfer transition involved in metal-carbon bonds as deduced from the remarkable influence of alkynyl groups. The relative one-electron energy diagram for these complexes (D_{2h} symmetry) is shown in Fig.

7) V. I. Vedenyev, L. V. Gurvich, V. N. Kondrat'yev, V. A. Medvedev, and Ye. L. Frankevich, "Bond Energies, Ionization Potentials and Electron Affinities," Edward Arnold, London (1966), Table 8.

Table 2. Energy of lowest bands in eV scale (a), and IP's of free alkynes (b)

(a) *trans*-$[L_2M(C{\equiv}CR)_2]$

M	L	R=H	CH_3	CH_2=CH	HC≡C	Ph
Ni	Et_3P	3.84	3.76	3.66	3.63	3.60
Pt	Et_3P	4.07	3.96	3.83	3.86	3.77
	Me_3P	4.10	3.99	3.88		3.81

(b) IP's of RC≡CH (eV)

R=H	CH_3	CH_2=CH	HC≡C	Ph
11.40	10.36	9.9	10.2	9.15

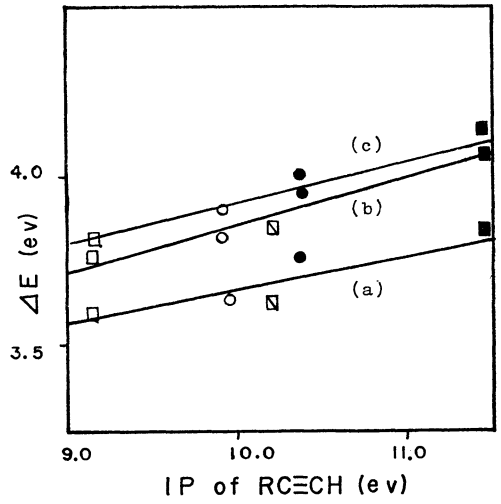

Fig. 4. Plots of transition energy of lowest bands (ΔE) against ionization potentials (IP) of RC≡CH; ■ R=H, ● R=CH_3, ▨ R=HC≡C, ○ R=CH_2=CH, □ R=Ph.
(a) *trans*-$[(Et_3P)_2Ni(C{\equiv}CR)_2]$ (b) *trans*-$[(Et_3P)_2Pt(C{\equiv}CR)_2]$
(c) *trans*-$[(Me_3P)_2Pt(C{\equiv}CR)_2]$

Table 3. Orbital transformation scheme for *trans*-$[L_2M(C{\equiv}CR)_2]$, (D_{2h})

Representation	Metal orbital	Ligand orbital	Remark
A_g	d_{z^2}, $d_{x^2-y^2}$	$\sqrt{1/2}(\sigma_1+\sigma_3)$	C≡CR
	s	$\sqrt{1/2}(\sigma_2+\sigma_4)$	L
B_{1g}	d_{xy}	$\sqrt{1/2}(\pi_{1h}+\pi_{3h})$	C≡CR
		$\sqrt{1/2}(\pi_{2h}+\pi_{4h})$	L
B_{2g}	d_{xz}	$\sqrt{1/2}(\pi_{2v}+\pi_{4v})$	L
B_{3g}	d_{yz}	$\sqrt{1/2}(\pi_{1v}+\pi_{3v})$	C≡CR
B_{1u}	p_z	$\sqrt{1/2}(\pi_{1v}-\pi_{2v})$	C≡CR
		$\sqrt{1/2}(\pi_{4v}-\pi_{2v})$	L
B_{2u}	p_y	$\sqrt{1/2}(\sigma_1-\sigma_3)$	C≡CR
		$\sqrt{1/2}(\pi_{4h}-\pi_{2h})$	L
B_{3u}	p_x	$\sqrt{1/2}(\sigma_2-\sigma_4)$	L
		$\sqrt{1/2}(\pi_{1h}-\pi_{3h})$	C≡CR

6, and the orbital transformation scheme in Table 3, derived from diagrams of tetracyanide complexes[5,6,8] and from our simple molecular orbital calculation.[9] The coordinate system is shown in Fig. 5.

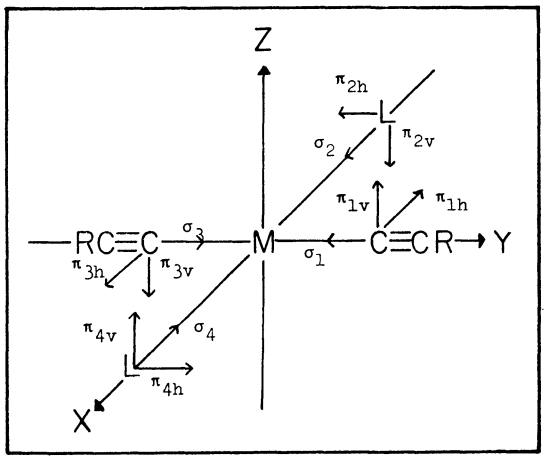

Fig. 5. Coordination system for the complex, *trans*-$[L_2M(C{\equiv}CR)_2]$.

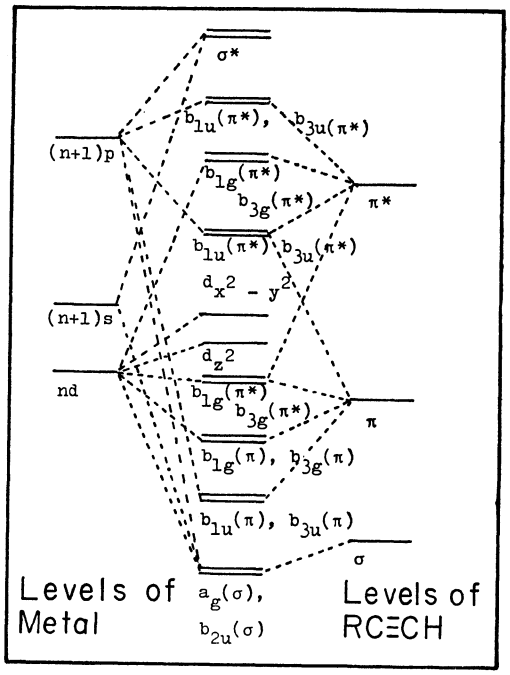

Fig. 6. Relative energy diagram of metal-carbon bond in *trans*-$[L_2M(C{\equiv}CR)_2]$.

The correlation shown in Fig. 4 suggests that the lowest band is presumably due to the transition from molecular orbitals consisting of bonding π-orbitals of alkynyl groups, *i.e.* $b_{1g}(\pi)$, or $b_{3g}(\pi)$, to $b_{3u}(\pi^*)$ or $b_{1u}(\pi^*)$ which contains the metal *p*-orbitals (Fig. 6 and Table 3).

The order of bathochromic shift of substituents is quite different from that of the square of metal-carbon stretching frequencies observed in the infrared spectra,[1] because the former concerns both ground and excited states and the latter only properties of the ground state.

The order of the bathochromic effect of R's is consistent with the increasing order of electronegativity

8) S. Kida, J. Fujita, K. Nakamoto, and R. Tsuchida, This Bulletin, **31**, 79 (1958).
9) N. Takeuchi, private communication.

of R's induced by the mesomeric effect, though some deviation was observed in nickel complexes.

As shown in Fig. 7, two alkynyl groups can mutually interact through metal d_{xy} and d_{yz} orbitals. Hence, a long conjugate system involving the metal *d*-orbitals is formed in the *trans* square-planar dialkynyl complexes, and b_{1g} (π) and b_{3g} (π) orbitals are used for the interaction. The bathochromic shift of the lowest band is regarded as evidence for existence of the conjugate system.

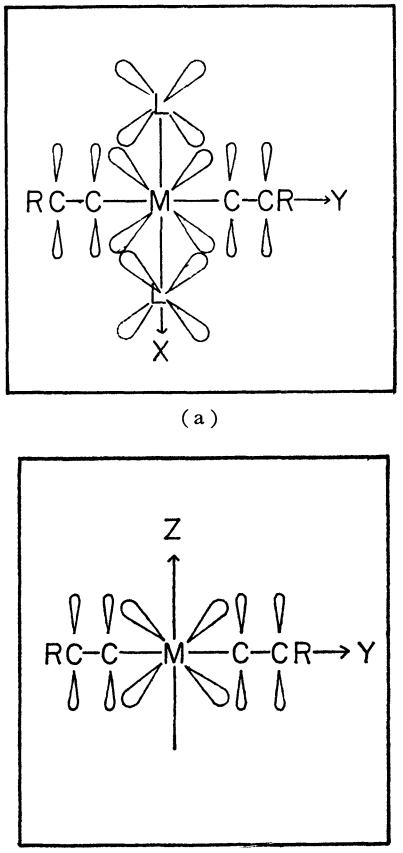

Fig. 7. Interaction between metal *d*-orbitals and alkynyl π-orbitals;
(a) *X*–*Y* plane (b) *Y*–*Z* plane

Influence of Solvents. Since the solution spectrum is inevitably influenced by solvents, we have studied the influence on the spectra of alkynyl complexes. There was no systematic influence on the intensities of absorption maxima. However, the lowest bands of the spectra showed a blue shift in alcohols (Fig. 8 and Table 4). No appreciable influence was observed in other solvents, such as *n*-hexane, cyclohexane, dichloromethane and acetonitrile, *i.e.* neither polar nor *n*-donor properties of solvents had influence upon the spectra.

The specific influence of alcohols is regarded as a consequence of some interaction between OH group and the alkynyl complexes. Formation of hydrogen bonding may be responsible for this effect. Here, proton acceptor orbitals are considered to be b_{3g} orbitals from the result of a study on electron donor-acceptor complexes.[10]

Table 4. Influence of solvents

(a) *trans*-[$(Et_3P)_2Ni(C{\equiv}CCH_3)_2$]

Solvent	Absorption band (mμ)		
n-hexane	329	272	260 sh
CH_2Cl_2	330	274	252 sh
CH_3CN	329	272	260 sh
C_6H_{12}	330	272	261 sh
MeOH	326	272	260 sh
EtOH	326	272	260 sh
i-PrOH	327	272	260 sh

sh; shoulder C_6H_{12}; cyclohexane

(b) *trans*-[$(Et_3P)_2Pt(C{\equiv}CCH_3)_2$]

Solvent	Absorption band (mμ)		
CH_2Cl_2	313	277	259
C_6H_{12}	314	277	258
ether	313	276	258
MeOH	308	274	257
i-PrOH	309	274	257

C_6H_{12}; cyclohexane

(c) *trans*-[$(Me_3P)_2Pt(C{\equiv}CH)_2$]

Solvent	Absorption band (mμ)		
C_6H_{12}	303	266	254
ether	302	265 sh	254
MeOH	299	265 sh	254
EtOH	299	262 sh	254
i-PrOH	300	262 sh	254

sh; shoulder C_6H_{12}; cyclohexane

(d) *trans*-[$(Et_3P_2)_2Ni(C{\equiv}CC{\equiv}CH)_2)_2$]

Solvent	Absorption band (mμ)			
ether	341	279 sh	268	252
MeOH	340	278 sh	268	252

sh; shoulder

(e) *trans*-[$(Et_3P)_2Ni(C{\equiv}CC{\equiv}CCH_3)_2$]

Solvent	Absorption band (mμ)			
ether	343	283	267	251
MeOH	342	282	267	251

(f) *trans*-[$(Et_3P)_2Pt(C{\equiv}CC{\equiv}CCH_3)_2$]

Solvent	Absorption band (mμ)					
ether	324	307 sh	287	266 sh	253	243
MeOH	322	305 sh	287	267	252	241

sh; shoulder

Butadiynyl derivatives, *trans*-[$(Et_3P)_2M(C{\equiv}CC{\equiv}CR)_2$], (M = Ni or Pt, R = H, CH_3 or Ph), gave very complicated spectra (Fig. 3). However, the lowest bands of these spectra displayed a similar behavior to those of the other alkynyl complexes in alcoholic solvents (Table 4 and Fig. 3). Thus, these bands may be regarded as the same as the lowest

10) H. Masai, K. Sonogashira, and N. Hagihara, *J. Organometal. Chem.*, in press.

Table 5. Novel alkynyl complexes, *trans*-[$L_2M(C{\equiv}CR)_2$]

M	L	R	Found		Calcd		mp (°C)
			C(%)	H(%)	C(%)	H(%)	
Ni	Et_3P	$CH_3C{\equiv}C$	63.00	8.81	62.74	8.62	121—122[a]
Pd	Et_3P	H	49.19	8.46	48.93	8.22	53— 56
		CH_3	51.21	8.44	51.37	8.62	85— 86
Pt	Et_3P	$CH_3C{\equiv}C$	47.59	6.70	47.39	6.51	156—157
	Me_3P	H	30.22	5.36	30.23	5.07	120[b]
		CH_3	34.04	6.16	33.88	5.69	105[b]

a) melted with decomposition
b) decomposed above this temperature

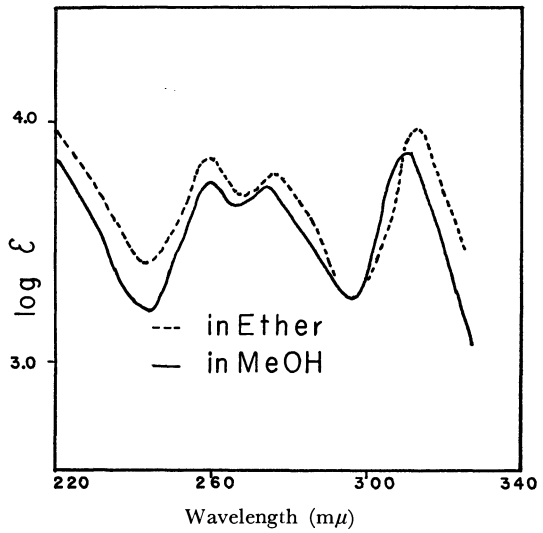

Fig. 8. Influence of solvents on spectra of *trans*-[$(Et_3P)_2$-$Pt(C{\equiv}CCH_3)_2$].

energy bands of the other alkynyl complexes.

Experimental

Electronic Spectra. Electronic spectra were recorded by a Hitachi EPS-3T recording spectrophotometer using 10 mm quartz cell.

Materials. *(a) Pentadiynyl Complexes,* trans-[*$(Et_3P)_2M(C{\equiv}CC{\equiv}CCH_3)_2$*], *(M=Ni or Pt)*: These complexes were prepared from the reaction of $[(Et_3P)_2MCl_2]$ with $CH_3C{\equiv}CC{\equiv}CNa$ in liquid ammonia which were prepared in situ from the reaction of $CH_3CCl_2CH_2CCl_2CH_3$ with 5 fold excess of sodium amide (Table 5).

(b) Other Complexes: Other complexes listed in Table 5 were prepared by the same procedure as described previously.[1]

The authors are grateful to Dr. Akira Nakamura, Osaka University, and Dr. Nozomu Takeuchi, Tokushima University, for their helpful discussions.

Linear Conjugated Systems Bearing Aromatic Terminal Groups. IV.[1] The Syntheses of Some Diarylacetylenes

Shuzo AKIYAMA, Kazuhiro NAKASUJI, and Masazumi NAKAGAWA
Department of Chemistry, Faculty of Science, Osaka University, Toyonaka, Osaka
(Received March 8, 1971)

The syntheses of 1,1′-, 9,9′-, and 1,9′-dianthryl-, 2,2′-, 3,3′-, and 9,9′-diphenanthryl-, 1,1′-and 2,2′-dipyrenyl-, and 6,6′-dichrysenylacetylenes according to the pyrolytic reactions of the corresponding β-ketoalkylidenetriphenylphosphorane derivatives (intramolecular Wittig reaction) were described.

In relation to studies on the electronic spectral properties of diarylpoly-ynes,[2] we tried to prepare 1,1′-dianthryl- and 9,9′-dianthrylacetylenes (I and II). However, all attempts to prepare dianthrylacetylenes according to the usual methods were unsucessful. The well-known mercuric oxide oxidation of *bis*-hydrazone of α-diketone was not feasible for the present case, because the condensation of anthraldehydes by means of potassium cyanide and the dimerization of anthracene carboxylic acids or their acid chlorides on treatment with magnesium-magnesium iodide could not be carried out. In the case of phenanthrene series, it was found that the reaction of 9,9′-diphenanthril with hydrazine gave only monohydrazone.[3] Bromine addition to di-(1-anthryl)-and di-(9-anthryl)-ethylenes[4] could not be performed owing to the poor solubility of the ethylenes in common organic solvents.

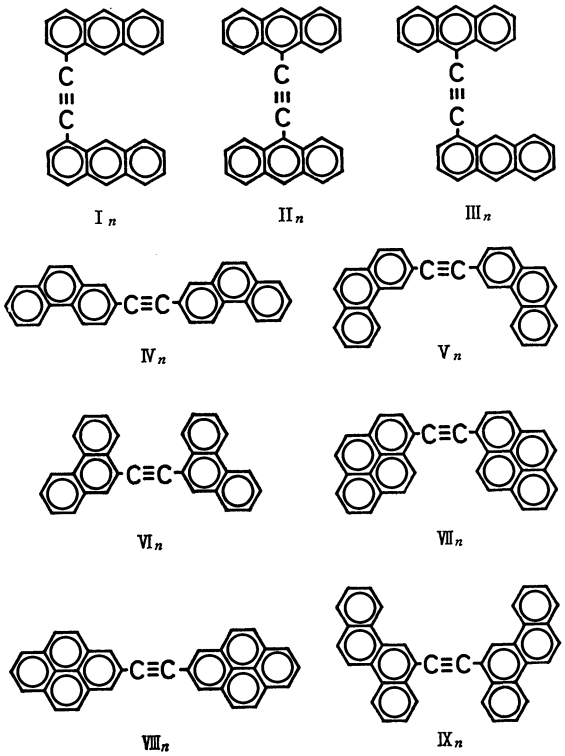

Gough and Trippett[5], and Märkl[6] proposed a new method of formation of acetylenic bond by a pyrolytic decomposition of β-ketoalkylidenetriphenylphosphorane. This method has been applied successfully to the preparation of dianthrylacetylenes I, II, and III, diphenanthrylacetylenes IV, V, and, VI, dipyrenylacetylenes VII and VIII and 6,6′-dichrysenylacetylene IX.

As summarized in the following scheme, the bromomethyl compounds (X_{a-h}) derived from corresponding aldehydes were converted to the phosphoranes XII_{a-h} *via* triphenyl phosphonium bromides XI_{a-h}.

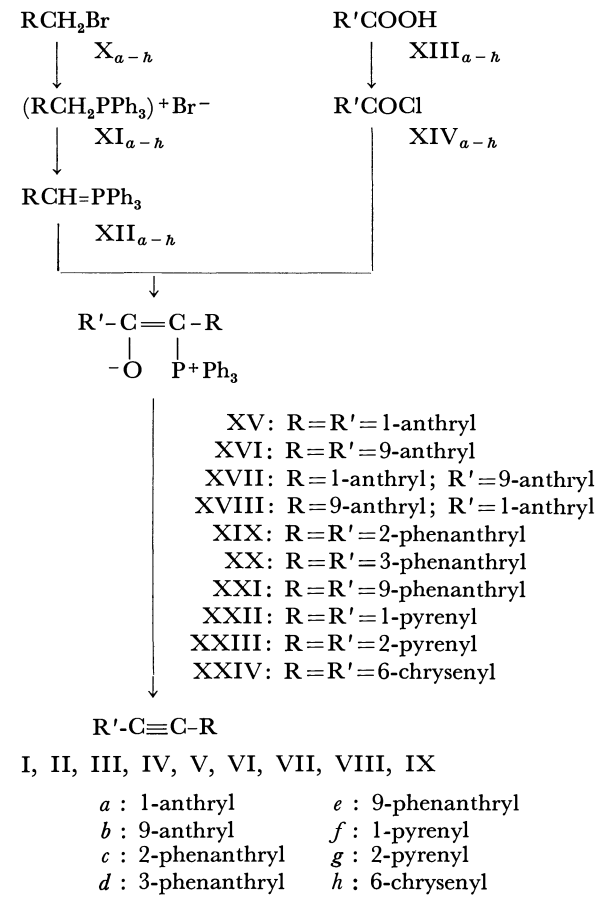

Scheme. Syntheses of the diarylacetylenes.

1) Part III: K. Nakasuji, S. Akiyama, K. Akashi, and M. Nakagawa, This Bulletin, **43**, 3567 (1970).
2) S. Akiyama and M. Nakagawa, *ibid.*, **40**, 340 (1967); K. Nishimoto, S. Akiyama, M. Nakagawa, and R. Fujishiro, *ibid.*, **39**, 2320 (1966); S. Akiyama and M. Nakagawa, *ibid.*, **43**, 3561 (1970).
3) Mp 255—258°C. Found: C, 84.61; H, 4.74; N, 6.53. Calcd for $C_{30}H_{20}N_2O$: C, 84.88; H, 4.75; N, 6.60%.
4) Unpublished.
5) S. T. D. Gough and S. Trippett, *Proc. Chem. Soc.*, **1961**, 302; *J. Chem. Soc.*, **1962**, 2333.
6) G. Märkl, *Chem. Ber.*, **94**, 3005 (1961).

The reaction of the phosphoranes XII_{a-h} with a half mole of the acid chlorides XIV_{a-h} in xylene, toluene or benzene afforded betaines XV-XXIV. All betaines thus obtained exhibit characteristic intense absorption due to $\nu_{C=O}$ of ylid carbonyl groups in 1500 cm^{-1} region.[7]

Pyrolyses of the betaines except for XV were performed at 200—300°C in the absence of solvent under reduced pressure resulting in the corresponding acetylenes I, III—IX in high yields. On the other hand, XV was found to decompose very easily in boiling xylene to yield II. 9,9′-Dianthrylacetylene II and 1,9′-dianthrylacetylene(III) were obtained directly when a 2 : 1 molar mixture of XII_b and XIV_b, and that of XII_b and XIV_a in xylene were heated under refulx. The same treatment of a mixture of XII_a and XIV_b gave a mixture of the betaine (XVII) and the acetylene(III). However, the same treatment of a mixture of XII_a and XIV_b gave XV containing a small amount of I. These facts observed in anthracene series seem to indicate the following sequence of thermal stability of the betaines: XVI<<XVIII XVII<<XV. The sequence of the thermal stability of the betaines clearly indicates that the steric hindrance facilitates the decomposition of betaine into acetylenes. The fact that the less hindered betaines (XIX—XXIV) of other series were obtained in good yields without decomposition is consistent with this inference.

Diarylacetylenes (I—IX) thus obtained were found to be fairly stable and scarcely soluble in common organic solvents. The electronic spectra of the dianthrylacetylenes are illustrated in Fig. 1. The sequence of the bathochromic shift was found to be I→III→II with an increasing loss of vibrational structures. The spectrum of II exhibits only a shoulder at the position corresponding to the longest-wavelength peak. The electronic spectral properties of 1,1′- dianthryl-and 9,9′-dianthrylacetylenes (I and II) have been discussed in relation to the spectral regularities of the dianthrylpoly-ynes.[2]

The electronic spectra of the diphenathryl-, the dipyrenyl- and 6,6′-dichrysenylacetylenes will be discussed in a forthcoming paper.

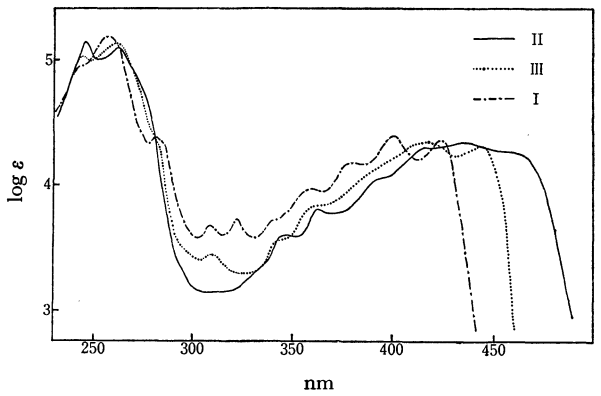

Fig.1 The electronic spectra of the dianthrylacetylenes (in tetrahydrofuran).

Experimental

All melting points are not corrected. The electronic spectra were obtained on a Hitachi EPS-3T spectrophotometer at room temperature. The IR spectra were measured with a Hitachi EPI-2 spectrophotometer by KBr-disk method.

1-Bromomethylanthracene (X_a). The bromide was prepared by the method reported previously.[8]

9-Bromomethylanthracene (X_b). Phosphorus tribromide (12.0 g, 0.044 mol) in chloroform (40 ml) was added over a period of 30 min to a mixture of 9-hydroxymethylanthracene (20.8 g, 0.1 mol), chloroform (350 ml) and pyridine (3.2 g, 0.044 mol) at −5°C. The mixture was allowed to gradually reach 20°C, after which it was stirred further for 1 hr. Cracked ice was added to the ice-cooled reaction mixture, and the organic layer separated was washed with water, sodium hydrogen carbonate solution and water, successively, and then dried. The yellow needles, mp 138—140°C, which were obtained in quantitative yield by the evaporation of the solvent *in vacuo* were recrystallized from petroleum benzine to give pure X_b as yellow needles, mp 139—140°C.

Found: C, 66.77; H, 4.19; Br, 29.54%. Calcd for $C_{15}H_{11}Br$: C, 66.44; H, 4.09; Br, 29.47%.

Anthrylmethyl-triphenylphosphonium Bromides (XI_a and XI_b). As the phosphonium bromides (XI_a and XI_b) were prepared according to a similar procedure, the preparation of XI_b will be described as an example. Triphenylphosphine (13.1 g, 0.05 mol) was added to a solution of X_b (11.1 g, 0.041 mol) in xylene (140 ml), and the mixture was refluxed for 17 hr. The crystals deposited were rinsed with a small amount of benzene, and then were recrystallized twice from water to give pure XI_b. Both of the salts were obtained in yields of over 90%. The physical properties and the analytical data are summarized in Table 1.

9,9′-Dianthrylacetylene (II). a) Pyrolysis of the Betaine (XVI_b) without Isolation. To a suspension of the phosphonium bromide (XI_b, 6.95 g, 0.013 mol) in xylene (70 ml), was added an ether solution of phenyllithium (1.18 N, 11.02 ml). The deep reddish-violet solution was stirred for 1 hr at 80°C, and then a hot solution of the acid chloride

Table 1. Physical properties and analytical data of XI_a and XI_b

	Mp (°C)	Crystal		Analytical data (%) C	H	Br
XI_a	275—280 (dec.)	pale yellow	Found:	73.91,	5.01,	14.62
XI_b	280 (dec.)	pale yellow	Found:	73.89,	4.91,	14.79
			Calcd for $C_{33}H_{26}BrP$:	74.30,	4.91,	14.98

7) *Cf.* A. J. Speciale and K. W. Ratts, *J. Amer. Chem. Soc.*, **85**, 2790 (1963).

8) S. Akiyama, S. Misumi, and M. Nakagawa, This Bulletin, **35**, 1826 (1962).

(XIV_b, 1.440 g, 6 mmol), prepared from 9-anthroic acid[9] and thionyl chloride in xylene (50 ml), was added. After the mixture had been stirred for 20 hr at 80°C, the mixture was refluxed for 2 hr. The hot solution was filtered to remove insoluble material which was digested with hot benzene three times (each 50 ml). The benzene extracts were combined with the filtrate, and the solvents were removed *in vacuo*. A small amount of benzene - petroleum benzine (1 : 1) was added to the residue, and the orange-yellow crystals deposited was collected by filtration (1.40 g, 62%). The crystals were re-dissolved in benzene, and the solution was percolated through a short column of alumina. The orange needles obtained by the concentration of the filtrate under reduced pressure were recrystallized from benzene to yield pure II, orange-red needles, which decomposed at *ca.* 310°C.

Found: C, 95.21; H, 4.77%; $M^+=378$. Calcd for $C_{30}H_{18}$: C, 95.21; H, 4.79%; Mol. wt. 378.

b) Pyrolysis of the Isolated Betaine (XVI_b). Using benzene as solvent, the same amounts of the reagents (XI_b, phenyllithium and XIV_b) used in the case of a) were treated in a similar manner. The mixture obtained was stirred for 20 hr at 15°C and then 4 hr at 35°C. The insoluble material was filtered, and repeatedly digested with benzene (total 500 ml) at 70°C. The extracts were combined with the filtrate. The yellow fine cubes, 2.150 g (55%) which was obtained by the evaporation of the solvent *in vacuo* were dissolved in hot benzene. The insoluble acetylene(II) was removed by filtration. Evaporation of the filtrate under reduced pressure gave betaine(XVI). The crude betaine was recrystallized twice from benzene to give pure XVI as yellow cubes. The yellow crystals turned to orange needles at 280°C, which decomposed at *ca.* 310°C (decomposition point of the acetylene, II).

Found: C, 88.51; H, 5.29%. Calcd for $C_{48}H_{33}OP$: C, 87.78; H, 5.07%. IR: 1496 (C=O) cm^{-1}.

Betaine (XVI, 0.131 g, 0.2 mmol) thus obtained was dissolved in xylene (20 ml), and the solution was refluxed for 3.5 hr to give a green fluorescent orange-yellow solution. Evaporation of the solvent afforded orange-red needles, 0.069 g (91%). Triphenylphosphine oxide (0.050 g, 89%) was obtained from the filtrate. The orange-red crystals were recrystallized from benzene to yield pure II.

1,1'-Dianthrylacetylene (I). Preparation of Betaine (XV). To a suspension of the phosphonium bromide (XI_a, 3.48 g, 6.5 mmol) in xylene (30 ml), was added at room temperature an ethereal solution of phenyllithium (0.87 N, 7.51 ml) under nitrogen atmosphere. After the mixture had been stirred for 1 hr at 80°C, a hot solution of the acid chloride of 1-anthroic acid[10] (XIV_a, 0.720 g, 3 mmol) in xylene (30 ml) was added, and stirred for 20 hr at 80°C. The insoluble material was filtered, and digested repeatedly with hot toluene (total 150 ml). The extracts were combined with filtrate, and the solvent was removed under reduced pressure. Benzene (3 ml) was added to the residue, and the yellow crystalline powder was collected by filtration, and washed with a small amount of benzene (0.570 g, 29%). The crystalline powder was recrystallized twice from toluene to give yellow cubes. The crystals fused at *ca.* 180—190°C under foaming. The melt solidified at 230°C to give needles, and re-melted at 267—270°C.

Found: C, 88.42; H, 5.38%. Calcd for $C_{48}H_{33}OP$: C, 87.78; H, 5.07%. IR: 1500 (C=O) cm^{-1}.

Pyrolysis of Betaine (XV). The betaine (XV, 0.100 g, 0.15 mmol) was heated under reduced pressure (18 mmHg) at 200°C for 30 min, Evolution of triphenylphosphine oxide was observed. The solid thus obtained was mixed with a a small amount of benzene, and was filtered to remove the oxide. The crude crystals thus obtained in an almost quantitative yield were dissolved in benzene, and the solution was passed through a short column of alumina. The crystals obtained by the evaporation of the filtrate were recrystallized twice from benzene to give pure I as bright yellow needles, mp 272—273°C.

The pyrolysis of betaine(XV) in boiling xylene was found to be very slow.

Found: C, 95.07; H, 4.80%. Calcd for $C_{30}H_{18}$: C, 95.21; H, 4.79%. UV in tetrahydrofuran: λ_{max} (log ε) 245* (4.96), 257(5.19), 281(4.39), 309(3.68), 322.5(3.72), 340*(3.70), 359(3.97), 380(4.18), 400(4.39), and 425(4.36) nm. (asterisks denote shoulders).

1,9'-Dianthrylacetylene (III). Preparation of Betaine (XVII). To a solution of phosphorane (XII_a), prepared according to the method used for betaine(XV), was added a xylene solution of the acid chloride of 9-anthroic acid, and the mixture was refluxed for 2 hr to complete the reaction. The yellow cubes, 0.745 g (38%), collected by filtration were recrystallized twice from benzene to give pure XVII as yellow cubes. The crystals melted at 230—250°C and turned to orange needles at 260°C. The crystals re-melted at 286—288°C.

Found: C, 88.22; H, 5.42%. Calcd for $C_{48}H_{33}OP$: C, 87.78; H, 5.07%. IR: 1497 (C=O) $cm.^{-1}$

Concentration of the filtrate gave a mixture (0.05 g) of XVII and orange-yellow needles. The mixture was recrystallized twice from benzene. The crystals thus obtained were dissolved in the same solvent, and the solution was passed through a short column of alumina. Pure III was obtained from the filtrate as orange-yellow needles, mp 286—288°C.

Pyrolysis of Betaine (XVII). Betaine(XVII) was treated according to the procedure used for the pyrolysis of XV, and the product was dissolved in benzene (40 ml). The filtrate which was obtained by the percolation of the benzene solution through a thin layer of alumina (2 g) was concentrated to afford acetylene(III), 0.036 g, 97%, mp 282—285°C. The material was recrystallized twice from benzene to yield pure III, orange-yellow needles, mp 286—288°C.

Found: C, 95.11; H, 4.79%. Calcd for $C_{30}H_{18}$: C, 95.21; H, 4.79%. UV in tetrahydrofuran: λ_{max} (log ε) 244(5.02), 261.5(5.14), 320(3.46), 344*(3.39), 362*(3.85), 419(4.36), and 444(4.32). (asterisks indicate shoulders).

Preparation of Betaine (XVIII). Betaine (XVIII) was obtained as tiny yellow cubes in a yield of 24% from XII_b and XIV_a according to the method used for XV. The crude betaine was recrystallized to afford pure XIII as tiny yellow cubes, which turned to orange at 230—240°C, and then solidified to give orange needles. The crystals re-melted at 286—288°C.

Found: C, 87.32; H, 5.00%. Calcd for $C_{48}H_{33}OP$: C, 87.78; H, 5.07%. IR: 1497 (C=O) $cm.^{-1}$

Pyrolysis of the Betaine(XVIII), a) Pyrolysis without Solvent. Pyrolysis of betaine(XVIII) was carried out according to the procedure used for XV. A benzene (40 ml) solution of the product was passed through a short column of alumina (3 g). The crude crystals, 0.055 g (95%), obtained by concentration of the filtrate were recrystallized twice from benzene to yield pure III as orange-yellow needles, mp 286—288°C.

Found: C, 95.01; H, 4.83%. Calcd for $C_{30}H_{18}$: C,

9) R. R. Burtner and J. W. Cusic, *J. Amer. Chem. Soc.*, **65**, 262 (1943).

10) J. W. Cook, *J. Chem. Soc.*, **1931**, 566.

Table 2. Physical properties and analytical data of XI_c, XI_d, and XI_e

	Mp (°C)	Yield (%)	Crystal	Analytical data (%)			
					C	H	Br
XI_c	292—293 (E)	82	needles	Found:	74.41	4.91	14.90
XI_d	291—292 (W)	90	cubes	Found:	74.35	4.86	14.95
XI_e	288—289 (E)	95	plates	Found:	74.11	4.96	14.82
				Calcd for $C_{33}H_{26}BrP$:	74.30	4.91	14.98

Solvents of recrystallization are given in parentheses. E=ethanol; W=water.

Table 3. Physical properties and analytical data of XIX, XX, and XXI

	Mp (°C)	Yield (%)	Crystal	Analytical data (%)			IR (cm^{-1})
					C	H	$\nu_{C=O}$
XIX	251—251.5 (B—E)	71	pale yellow cubes	Found:	87.43	5.02	1504
XX	240—242[a] (B)	77	pale yellow needles	Found:	87.55	5.08	1490
XXI	251—252[a] (B—C)	65	pale yellow cubes	Found:	88.01	5.24	1502
				Calcd for $C_{48}H_{30}OP$:	87.78	5.07	

a) Decomposition points. B=benzene; E=ethyl acetate; C=cyclohexane.

95.21; H, 4.79%.

b) Pyrolysis in Xylene. A solution of betaine(XVIII, 0.153 g) in xylene (20 ml) was refluxed for 8 hr. The residue obtained by the evaporation of the solvent *in vacuo* was dissolved in benzene, and was passed through a short column of alumina (3 g). III was obtained from the filtrate as orange-yellow needles, 0.047 g (54%), mp 286—288°C.

Formation of Acetylene(III) without Isolation of Betaine (XVIII). A xylene solution of betaine(XVIII) prepared by the above method was refluxed for 3 hr to give orange-yellow crystals, 0.314 g (38%). This was recrystallized twice from benzene to afford pure III, mp 286—288°C.

Found: C, 94.80; H, 4.75%. Calcd for $C_{30}H_{18}$: C, 95.21; H, 4.79%.

Bromomethylphenanthrenes (X_c, X_d, and X_e). According to a similar procedure used for the preparation of X_b, the hydroxymethylphenanthrenes were converted into bromomethyl derivatives. The melting points were found to be identical with reported values.[11]

Phenanthrylmethyl-triphenylphosphonium Bromides (XI_c, XI_d, and XI_e). Bromomethylphenanthrene (7.66 g, 0.028 mol) in toluene (70 ml) was mixed with triphenylphosphine (7.50 g, 0.029 mol), and the mixture was refluxed for 18 hr. The crystals deposited were washed with a small amount of benzene, and were recrystallized to give pure colorless salt. The results are summarized in Table 2.

Preparation of Betaines(XIX, XX, and XXI). Since the preparation of the betaines of phenanthrene series were performed under similar reaction conditions, that of 3-phenanthryl derivative(XX) will be described as an example. To a suspension of phosphonium bromide (XI_d, 4.700 g, 8.8 mmol) in toluene (55 ml), was added under nitrogen atmosphere a solution of phenyllithium in ether (0.64 N, 13.80 ml). After the orange-red mixture had been stirred for 30 min at 80°C, a hot solution of acid chloride (XIV_d, 0.960 g, 4 mmol) in toluene (30 ml) was added, and the mixture was stirred for 19 hr at 80°C. The insoluble material was filtered, and was digested with hot benzene (60 ml×2) and hot toluene (60 ml×2). The combined filtrate and extracts were concentrated under reduced pressure. The viscous oily residue was mixed with benzene - cyclohexane (1 : 1, 5 ml), and was warmed to give rise to crystallization. The pale yellow crystalline powder, 2.576 g (98%) was recrystallized from benzene to give pure XX. The physical properties and the analytical data are shown in Table 3.

Diphenanthrylacetylenes(IV, V, and VI). As the pyrolyses of betaines(XIX, XX and XXI) were carried out under the same conditions, the procedure employed for 3-phenanthryl derivative(XX) will be described as a typical example.

Betaine(XX, 0.329 g, 0.5 mmol) placed in an evacuated flask (18 mmHg) was gradually heated up to 250°C over a period of 15 min. Distillation of triphenylphosphine oxide was observed at 200°C. The cooled reaction mixture was digested with benzene (40 ml), and the resulting solution was passed through a short column of alumina (5 g). Concentration of the filtrate under reduced pressure afforded V

Table 4. Physical properties and analytical data of phenanthrylacetylenes (IV, V, and VI)

	Mp (°C)	Yield (%)	Crystal	Analytical data		
					C	H
IV	261—262 (E)	74	colorless fine needless	Found:	95.17	4.86
V	266—267 (T)	100	colorless cubes	Found:	94.90	4.85
VI	243—244 (B)	88	colorless columns	Found:	95.03	4.84
				Calcd for $C_{30}H_{18}$:	95.21	4.79

E=ethyl acetate; T=toluene; B=benzene.

11) E. Mosettig and J. van de Kamp, *J. Amer. Chem. Soc.*, **55**, 2995 (1933).

as almost colorless crystals in a quantitative yield. This was recrystallized to give pure V.

The physical properties and analytical data are summarized in Table 4.

Bromomethylpyrenes (X_f and X_g). To an ice-cooled suspension of 1-hydroxymethylpyrene (5.24 g, 0.023 mol) in chloroform (70 ml) containing pyridine (0.95 g, 0.012 mol), was added over a period of 20 min a solution of phosphorus tribromide (3.12 g, 0.012 mol) in chloroform (20 ml). The temperature was gradually raised to room temperature, and stirring was continued for 30 min. The reaction mixture was again chilled with an ice-bath, and cracked ice and chloroform (100 ml) were added. The organic layer was washed successively with water, aqueous sodium hydrogen carbonate and water, and then dried. Evaporation of the solvent under reduced pressure afforded pale yellow needles, mp 131—133°C, 6.45 g (96%). The crystals were recrystallized to give pure X_f. According to a similar procedure, X_g was obtained from 2-hydroxymethylpyrene.

The results are summarized in Table 5.

Pyrenylmethyl-triphenylphosphonium Bromides (XI_f and XI_g). A mixture of 1-bromomethylpyrene (X_f, 6.00 g, 0.020 mol), toluene (20 ml) and triphenylphosphine (6.55 g, 0.025 mol) was refluxed for 4 hr. The reaction mixture, upon cooling, gave phosphonium salt (XI_f) as colorless cubes in an almost quantitative yield. This was recrystallized twice from water to afforded pure XI_f. The 2-pyrenyl derivative (XI_g) was obtained under similar conditions from 2-bromomethylpyrene (X_g). The results are recorded in Table 6.

Table 5. Physical properties and analytical data of X_f and X_g

	Mp (°C)	Crystal	Analytical data (%)		
			C	H	Br
X_f	145—147[a] (B—C)	colorless cubes	Found: 69.24	3.78	27.21
X_g	160—161 (B—C)	colorless needles	Found: 69.30	3.76	26.69
			Calcd for $C_{17}H_{11}Br$: 69.17	3.76	27.07

a) Lit. value: mp 139—142°C.[12] B-C=benzene - cyclohexane

Preparation of Betaines (XXII and XXIII). An ethereal solution of phenyllithium (0.39 N, 10.0 ml) was added to a suspension of betaine (XI_f, 2.675 g, 3.9 mmol) in toluene (50 ml) in an atmosphere of nitrogen, and the mixture was stirred for 1 hr at 60°C. A hot solution of the acid chloride of pyrene-1-carboxylic acid (XIV_f, 0.476 g, 1.8 mmol) in toluene (40 ml) was then added to the mixture, and stirring was continued for 20 hr at 60°C. The insoluble material

Table 6. Physical properties and analytical data of XI_f and XI_g

	Mp (°C)	Crystal	Analytical data (%)			
XI_f	293—295 (dec.)[a] (W)	colorless cubes	Found:	75.12	4.64	14.32
XI_g	286—289 (dec.) (E)	colorless leaflets	Found:	75.37	4.70	14.59[b]
			Calcd for $C_{35}H_{26}BrP$:	75.41	4.70	14.33

a) Lit. value: mp265—268°C.[12]
b) The analytical specimen was dried *in vacuo* for 6 hr at 178—181°C.
W=water; E=ethanol.

Table 7. Physical properties and analytical data of XXII and XXIII

	Mp (°C)	Yield (%)	Crystal	Analytical data (%)		
					C	H
XXII	257—258 (B)	96	yellow cubes	Found:	88.55	4.72
XXIII	>300[a] (B)	88	yellow cubes	Found:	88.45	4.77
				Calcd for $C_{52}H_{33}OP$:	88.62	4.72

a) The crystals turned to colorless fine needles at *ca.* 180°C.

Table 8. Physical properties and analytical data of dipyrenylacetylenes (VII and VIII)

	Mp (°C)	Yield (%)	Crystal	Analytical data (%)		
					C	H
VII	266 (T)	93	yellow cubes	Found:	95.52	4.23
VIII	>360 (T)	88	faint yellow needles	Found:	95.93	4.29
				Calcd for $C_{34}H_{18}$:	95.75	4.25

T=toluene.

12) J. P. Greets and R. H. Martin, *Bull. Soc. Chim. Belges.*, **69**, 563 (1960).

was extracted under reflux repeatedly with toluene (total 200 ml) and then with benzene (total 300 ml). The extracts were combined with the filtrate, and the solvents were removed under reduced pressure. The crude crystals thus obtained were mixed with benzene - cyclohexane (1 : 1, 5 ml), and were filtered and washed with the same solvent. The crystals were recrystallized to give pure XXII. The 2-pyrenyl derivative(XXIII) was obtained according to the similar procedure.

The physical properties and analytical data are summarized in Table 7.

Dipyrenylacetylenes(VII and VIII). The thermal decomposition of betaines(XXII and XXIII) to give dipyrenylacetylenes (VII and VIII) was performed according to the procedure for the preparation of diphenanthrylacetylenes (IV, V and VI), and the results are summarized in Table 8.

6-Bromomethylchrysene (X_h). A solution of phosphorus tribromide (2.98 g, 0.011 mol) in tetrahydrofuran (10 ml) was added over a period of 20 min to an ice-cooled suspension of 6-hydroxymethylchrysene[13] (6.10 g, 0.024 mol) in tetrahydrofuran (140 ml) containing pyridine (0.8 g, 0.01 mol). After having been stirred for 1 hr at room temperature, the mixture was warmed to 30°C to give a homogeneous solution. Cracked ice was added to the ice-cooled solution, and the organic layer was separated. The organic layer was worked up in the usual manner to give colorless crystals in an almost quantitative yield. The crystals were recrystallized twice from dioxane to give pure X_h as colorless fine needles, mp 194—196°C.

Found: C, 70.92; H, 4.15; Br, 24.54%. Calcd for $C_{19}H_{13}Br$: C, 71.04; H, 4.08; Br, 24.88%. IR: 1500 (C=O) cm^{-1}.

6-Chrysenylmethyl-triphenylphosphonium Bromide(XI_h). The reaction of X_h with triphenylphosphine in toluene according to the usual conditions gave slightly crude XI_h. The crude material was recrystallized from methanol to give analytical specimen. The colorless plates thus obtained contained 1 mole of methanol of crystallization. The crystals cracked at *ca.* 200°C, and decomposed at 270—272°C.

Found: C, 74.09; H, 5.15; Br, 12.82%. Calcd for $C_{37}H_{28}BrP$–CH_3OH: C, 74.15; H, 5.24; Br, 12.98%.

Preparation of Betaine(XXIV). According to the procedure for the preparation of XXII and XXIII, the slightly crude XI_h was converted into betaine (XXIV) by the reaction with acid chloride(XIV_h).[14] The yellow cubes obtained in a yield of 89% was recrystallized twice from toluene to give pure material, yellow cubes, mp *ca.* 265°C (dec.).

Found: C, 88.70; H, 5.28%. Calcd for $C_{56}H_{37}OP$: C, 88.87; H, 4.93%.

6,6'-Dichrysenylacetylene(IX). The thermal decomposition of betaine(XXIV) under the conditions used in the preparation of diphenanthrylacetylenes(IV, V and VI) gave yellow crystals in an almost quantitative yield. The crystals were recrystallized from toluene to give pure IX as fine pale yellow needles. Acetylene(IX) was found to be highly stable, and neither fusion nor decomposition could be observed even at 330°C.

Found: C, 95.08; H, 4.63%. Calcd for $C_{38}H_{22}$: C, 95.37; H, 4.63%.

13) M. J. S. Dewar and R. J. Sampson, *J. Chem. Soc.*, **1957**, 2946.

14) K. Funke and E. Müller, *J. Prak. Chem.*, **144**, 242 (1936).

Linear Conjugated Systems Bearing Aromatic Terminal Groups. V. Syntheses and Electronic Spectra of 2,2′-, 3,3′-, and 9,9′-Diphenanthrylpoly-ynes

Shuzo Akiyama and Masazumi Nakagawa

Department of Chemistry, Faculty of Science, Osaka University, Toyonaka, Osaka

(Received March 8, 1971)

2,2′-, 3,3′-, and 9,9′-Diphenanthrylpoly-ynes (V_n, VI_n, and VII_n, $n=1$—6) were synthesized and their electronic spectra were measured. It was found that the longest-wavelength absorption maxima (λ_{max}) in the spectra of each series of the diphenanthrylpoly-ynes (V_n, VI_n and VII_n) shift linearly with the xth power of the number of acetylenic bond (n), [$\lambda_{max} \propto n^x$], being $x=1.3$ for V_n and $x=1.4$ for VI_n and VII_n.

In previous papers of this series,[1-4] it was shown that the shifts of the absorption maxima (λ_{max}) of the long-wavelength bands of diarylpoly-ynes, such as 1,1′-dianthryl-(I_n), 9,9′-dianthryl-(II_n), 1,1′-dinaphthyl-(III_n) and 2,2′-dinaphthylpoly-ynes (IV_n) with the increase of the number of acetylenic bonds (n) can be expressed by the empirical formula:

$$\lambda_{max} = An^x + B$$

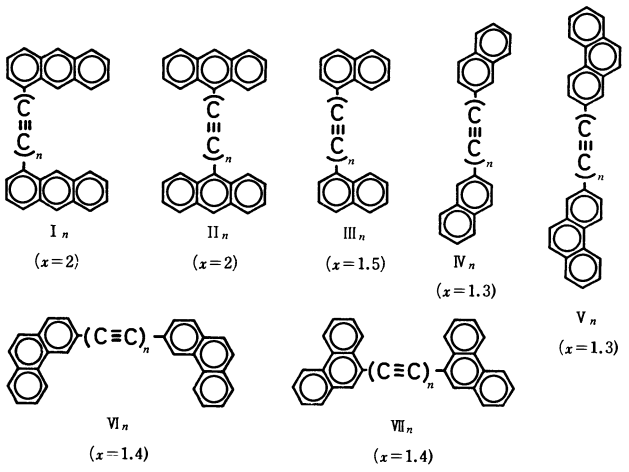

It is interesting that the values of x, given below the formulas, vary with the change of the nature of the terminal groups and the position of the linking of the polyacetylenic chain.

This paper deals with the syntheses and the electronic spectral characteristics of 2,2′-, 3,3′- and 9,9′-diphenanthrylpoly-ynes (V_n, VI_n, and VII_n, $n=1$—6).

Syntheses. Syntheses of diphenanthrylpoly-ynes (V_n, VI_n, and VII_n) were performed according to the analogous reaction sequence which had been employed in the syntheses of dianthryl-(I_n and II_n)[1,3] and dinaphthylpoly-ynes(III_n and IV_n).[4] Formyl and acetyl derivatives(VIII and IX) were used as starting materials. Preparation of diphenanthryl-acetylenes (V_1, VI_1, and VII_1) by means of an intramolecular Wittig reaction has been reported.[5]

Application of mild conditions to the conversion of the acetylenic hydroxy compounds to the corresponding chloro-derivatives was essential. Chloro-compounds(XI, XIV, XVI, XX, XXII, and XXVIII) were subjected to the following dehydrochlorination without isolation and purification owing to their intractable nature.

Elemental analyses of phenanthryldi-(XVII) and triacetylenes (XXIII) could not be performed due to their high instability. Diphenanthrylpoly-ynes (V_{1-5}, VI_{1-5}, and VII_{1-5}) were found to be fairly stable compounds. However, hexaacetylenes (V_6, VI_6 and VII_6) were unstable, and decomposed at room temperature in a few days. It was observed that the solubility of V_n, VI_n and VII_n in organic solvents remarkably decreased with the increase of the length of poly-yne chain. The color of crystals, melting points and IR absorption due to $\nu_{C\equiv C}$ are summarized in Table 1. The most intense peaks of the $\nu_{C\equiv C}$ bands of the diarylpoly-ynes (V_n, VI_n and VII_n) showed remarkable intensification and shift to lower wave number with the increase of the length of the poly-yne chain. The same trend has been observed in the IR spectra of the other series of diarylpoly-ynes.[1,3,4] The IR spectra of V_n are shown in Fig. 1 as a represen-

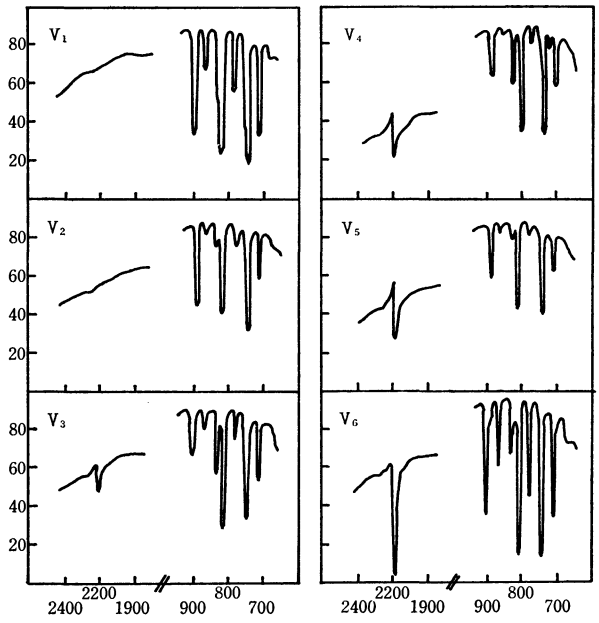

Fig. 1. Infrared spectra of 2,2′-diphenanthrylpoly-ynes (V_1—V_6) in the 1900—2400 cm^{-1} and 700—900 cm^{-1} region.

1) S. Akiyama and M. Nakagawa, This Bulletin, **40**, 340 (1967).
2) S. Akiyama, K. Nakasuji, K. Akashi, and M. Nakagawa, *Tetrahedron Lett.*, **1968**, 1121.
3) S. Akiyama and M. Nakagawa, This Bulletin, **43**, 3561 (1970).
4) K. Nakasuji, S. Akiyama, K. Akashi, and M. Nakagawa, *ibid.*, **43**, 3567 (1970).
5) S. Akiyama and M. Nakagawa, This Bulletin, **44**, 2231 (1971).

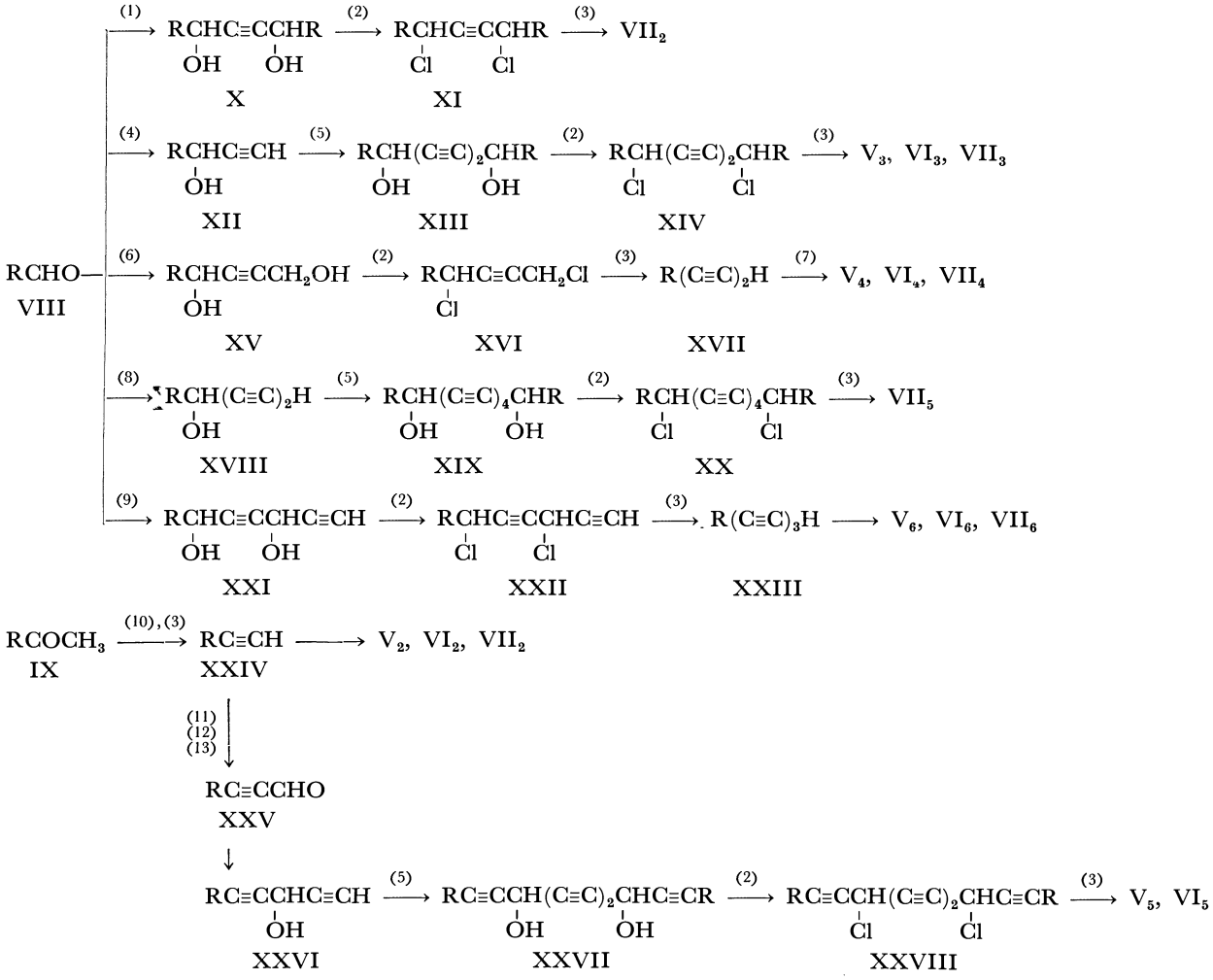

Scheme. Syntheses of diarypoly-ynes

R=2-, 3- or 9-phenanthryl

(1) $BrMgC{\equiv}CMgBr$ in benzene-tetrahydrofuran; (2) $SOCl_2$-pyridine in tetrahydrofuran; (3) $NaNH_2$ in liq. NH_3; (4) $LiC{\equiv}CH$ in liq. NH_3 or $BrMgC{\equiv}CH$ in tetrahydrofuran; (5) O_2-CuCl-NH_4Cl in methanol; (6) $BrMgC{\equiv}CCH_2OMgBr$ in tetrahydrofuran; (7) $Cu(OAc)_2H_2O$ in pyridine; (8) $Li(C{\equiv}C)_2H$ in liq. NH_3; (9) $BrMgC{\equiv}CCH(OMgBr)C{\equiv}CH$ in tetrahydrofuran; (10) PCl_5 in benzene; (11) C_2H_5MgBr in tetrahydrofuran; (12) *N*,*N*-dimethylformamide in tetrahydrofuran; (13) H_2SO_4.

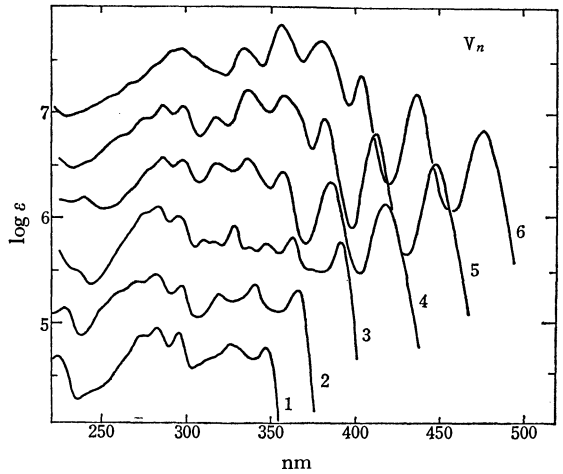

Fig. 2. Absorption curves of 2,2′-diphenanthrylpoly-ynes (V_1—V_6). Each curve, except for the lowest one, has been displaced upward by a 0.5 log ε unit increment from one immediately below it.

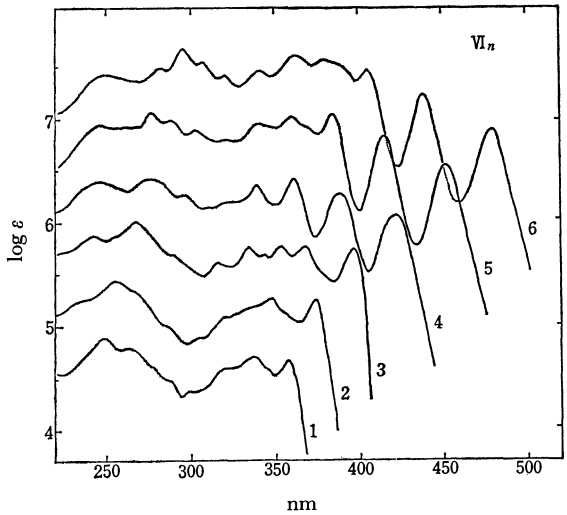

Fig. 3. Absorption curves of 3,3′-diphenanthrylpoly-ynes (VI_1—VI_6). Each curve, except for the lowest one, has been displaced upward by a 0.5 log ε unit increment from one immediately below it.

TABLE 1. PHYSICAL PROPERTIES OF DIPHENANTHRYLPOLY-YNES

n	V_n			VI_n			VII_n		
	color	Mp (°C)	$\nu_{C\equiv C}$	color	Mp (°C)	$\nu_{C\equiv C}$	color	Mp (°C)	$\nu_{C\equiv C}$
1	colorless	261—262		colorless	266—267		colorless	243—244	
2	colorless	243—244		pale yellow	280—282	2125 (vw)	pale yellow	256—257	2135 (vw) 2210 (vw)
3	pale yellow	*ca.* 270 (dec.)	2200 (s)	light yellow	*ca.* 260 (dec.)	2195 (s)	light yellow	285—286 (dec.)	2195 (s)
4	yellow	*ca.* 220 (dec.)	2195 (s)	yellow	*ca.* 200 (dec.)	2055 (w) 2110 (w) 2190 (s)	yellow	*ca.* 255 (dec.)	2060 (vw) 2115 (m) 2195 (s)
5	bright yellow	*ca.* 200 (dec.)	2175 (s)	orange yellow	*ca.* 190 (dec.)	2180 (s)	orange yellow	*ca.* 200 (dec.)	2070 (vw) 2130 (m) 2175 (s)
6	light orange	*ca.* 180 (dec.)	2025 (vw) 2145 (s)	light orange	*ca.* 100 (dec.)	2140 (s)	orange	*ca.* 130 (dec.)	2150 (s)

vw=very weak; m=medium; s=strong.

a) As hexaacetylene decomposed under pressure in the preparation of the KBr-disk, the spectrum was obtained by the Nujol mull method.

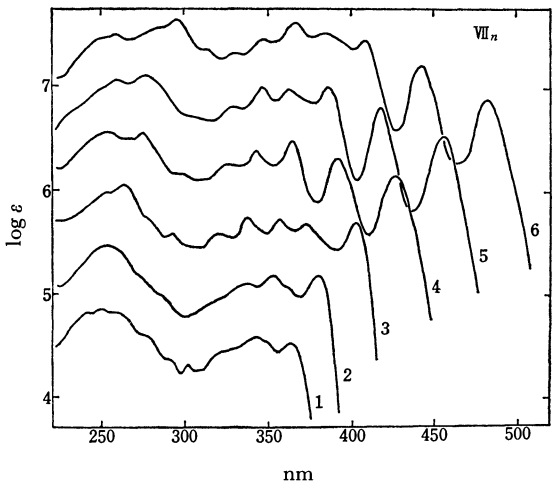

Fig. 4. Absorption curves of 9,9'-diphenanthrylpoly-ynes (VII_1—VII_6). Each curve, except for the lowest one, has been displaced upward by a 0.5 log ε unit increment from one immediately below it.

tative of the diphenanthrylpoly-ynes.

Electronic Spectra. The absorption curves and electronic spectral data of the three series of diphenanthrylpoly-ynes (V_n, VI_n and VII_n) are given in Figs. 2, 3, and 4, and Tables 2, 3, and 4.

Usually, the electronic spectra of the lower members of diarylpoly-ynes retain the characteristic of the spectra of the parent aromatic hydrocarbons corresponding to the respective terminal groups. However, in the case of the diphenanthryl derivatives (V_n, VI_n, and VII_n), the characteristic feature of the spectrum of phenanthrene can not be observed even in the spectra of diphenanthrylacetylenes (V_1, VI_1, and VII_1).

On the basis of free electron model (FEM),[6] the x-axis polarized transitions were assigned to ^1L_b and ^1C_b bands, and the y-axis polarized transitions were assigned to ^1L_a and ^1B_a bands for the electronic spectrum of phenanthrene (Fig. 5). The short-wavelength bands of diphenanthrylpoly-ynes (V_n, VI_n and VII_n) seem to be associated with the ^1C_b and the ^1B_a bands of phenanthrene.

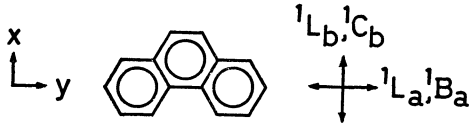

Fig. 5. Polarization diagram of phenanthrene.

The spectral feature of 3,3'-derivatives (VI_n) was found to be closely related to that of 9,9'-derivatives (VII_n). This indicates that the poly-yne chains extending in the same direction with regard to the molecular axis exert the same effect on the electronic spectra. On the other hand, 2,2'-derivatives (V_n) exhibit quite a different spectral feature as compared with 3,3'- and 9,9'-derivatives (VI_n and VII_n). The poly-yne chain attached to 2-position should exert a minor effect on the x-axis-polarized ^1C_b band, since the substituent at 2-position is parallel to the y-axis and can not contribute to the x-axis polarization. Consequently, the appearance of an absorption minimum at *ca.* 230—240 nm region in the spectrum of the lower member of 2,2'-derivative (V_n) might be ascribed to the separation of ^1C_b band and ^1B_a band due to the profound bathochromic shift of the y-axis-polarized ^1B_a band.

The long-wavelength bands of diphenanthrylpoly-ynes (V_n, VI_n, and VII_n) can be considered to arise from the interaction of poly-yne chromophore with ^1L_a band of the terminal group. ^1L_b band disappeared in the spectra of diphenanthrylpoly-ynes (V_n, VI_n, and VII_n) except for 2,2'-diphenanthrylacetylene(V_1), probably because of the large bathochromic shift of ^1L_a band. The remarkable enhancement of the vibrational fine structure and the regular bathochromic

6) H. B. Klevens and J. R. Platt, *J. Chem. Phys.*, **17**, 470 (1949); J. R. Platt, *ibid.*, **17**, 489 (1949); N. S. Ham and K. Ruedenberg, *ibid.*, **25**, 13 (1956).

Table 2. Spectral data of 2,2′-diphenanthrylpoly-ynes (V_1—V_6)

n	λ_{max} in nm and log ε (in parentheses) in tetrahydrofuran									
1	224 (4.67)	273 (4.88)	282.5 (4.95)	295.5 (4.90)	326 (4.80)	346.5 (4.68)	356 (3.32)			
2	227.5 (4.63)	271 (4.90)	282 (4.96)	296.5 (4.82)	318 (4.77)	340 (4.87)	366 (4.81)			
3	275.5[a] (5.08)	282.5 (5.12)	294.5 (5.02)	309 (4.80)	316 (4.77)	326.5 (4.93)	336.5 (4.72)	346 (4.77)	362 (4.83)	391 (4.78)
4	239.5 (4.69)	286 (5.09)	297 (5.07)	317 (5.02)	335 (5.08)	355.5 (4.95)	384 (4.85)	417 (4.65)		
5	264[a] (4.80)	275 (4.96)	288.5 (5.10)	297.5 (5.08)	316.5 (4.98)	335 (5.23)	357 (5.17)	381 (4.96)	411 (4.82)	447 (4.55)
6	297 (5.12)	333.5 (5.12)	355.5 (5.34)	378 (5.19)	403 (4.86)	436 (4.69)	476 (4.35)			

a) Shoulders.

Table 3. Spectral data of 3,3′-diphenanthrylpoly-ynes (VI_1—VI_6)

n	λ_{max} in nm and log ε (in parentheses) in tetrahydrofuran											
1	248.5 (4.88)	263.5 (4.78)	299 (4.38)	323 (4.59)	337 (4.69)	358 (4.67)						
2	256 (4.93)	285[a] (4.72)	306 (4.40)	321[a] (4.58)	348 (4.76)	374 (4.75)						
3	243.5 (4.87)	267.5 (5.00)	289.5 (4.68)	316 (4.60)	322[a] (4.57)	334 (4.76)	343 (4.67)	353 (4.77)	368 (4.77)	397 (4.74)		
4	245 (4.91)	275.5 (4.92)	296.5 (4.77)	321 (4.69)	339 (4.86)	361 (4.92)	388 (4.78)	422 (4.58)				
5	247 (4.95)	261 (4.92)	277 (5.06)	288.5 (4.98)	303 (4.88)	321.5 (4.79)	340 (4.94)	359 (5.02)	384 (5.03)	414 (4.83)	451 (4.55)	
6	249 (4.92)	270[a] (4.87)	282 (4.98)	296 (5.16)	307.5 (5.03)	321 (4.90)	341 (4.96)	363 (5.10)	379 (5.06)	405 (4.96)	438 (4.72)	479 (4.39)

a) Shoulders.

Table 4. Spectral data of 9,9′-diphenanthrylpoly-ynes (VII_1—VII_6)

n	λ_{max} in nm and log ε (in parentheses) in tetrahydrofuran										
1	240 (4.82)	250 (4.86)	257.5 (4.83)	277.5[a] (4.50)	290 (4.37)	302 (4.31)	341 (4.56)	363 (4.51)			
2	253 (4.97)	287[a] (4.46)	334 (4.58)	252 (4.69)	379 (4.67)						
3	250[a] (4.96)	263.5 (5.07)	291 (4.59)	303.5 (4.45)	319 (4.59)	337 (4.73)	357 (4.71)	372 (4.68)	402 (4.81)		
4	254 (5.04)	264 (4.98)	273.5 (5.06)	296.5 (4.66)	324.5 (4.74)	342 (4.89)	364 (4.97)	392 (4.79)	425 (4.59)		
5	258 (5.06)	275.5 (5.12)	327 (4.97)	345 (5.00)	363 (4.99)	387 (5.00)	416 (4.80)	453 (4.53)			
6	250[a] (4.94)	258 (4.98)	284.5 (5.04)	295 (5.13)	311[a] (4.84)	328 (4.81)	345 (4.95)	366 (5.11)	383 (5.00)	408 (4.93)	440 (4.68)	481 (4.35)

a) Shoulders.

shifts in the longest-wavelength bands with the increase of n are also observed in the three series of diphenanthrylpoly-ynes. The same trend has been observed in other series of diarylpoly-ynes.[1-4] The sequence of the bathochromic displacement of the longest-wavelength bands was found to be $V_n < VI_n < VII_n$ in apparent contradiction to what we expected from FEM. The same apparent discrepancy was also observed in the spectra of ethynyl- (XXIV), butadiynyl- (XVIII) and hexatriynylphenanthrenes. The apparent contradictions have been explained in terms of a configuration interaction.[7] As shown in Table 5, the spacings between the longest-wavelength vibrational sub-bands (λ_I) and the next longest-wavelength sub-bands (λ_{II}) are found to be 1900—2000 cm^{-1} except those of diphenanthrylacetylenes (V_1, VI_1, and VII_1). The spacings, as in the other diarylpoly-ynes, correspond to the stretching vibrations of acetylenic linkage in their IR spectra (*cf.* Table 1.)

The plots of the sub-peaks, λ_I and λ_{II} of the 2,2′-series (V_n) *versus* $n^{1.3}$ gave excellent straight lines as is shown in Fig. 6. (The plot of λ_{II} of V_1 is omitted.) In the cases of 3,3′- and 9,9′-diphenanthrylpoly-ynes (VI_n and VII_n), good linear correlations between λ_I, λ_{II} and $n^{1.4}$ were obtained (Figs. 7 and 8). It is interesting that the value x is dependent on the posi-

7) S. Akiyama, M. Nakagawa, and K. Nishimoto, This Bulletin, **44**, 1054 (1971).

Table 5. Spacings between the longest-wavelength maxima (λ_I) and the next longest-wavelength maxima (λ_{II}) (cm^{-1})

n	V_n	VI_n	VII_n
1	(1710)	(1740)	(1780)
2	2090	2000	2020
3	2040	1980	2000
4	1990	2070	1980
5	1960	1980	1960
6	1930	1910	1940

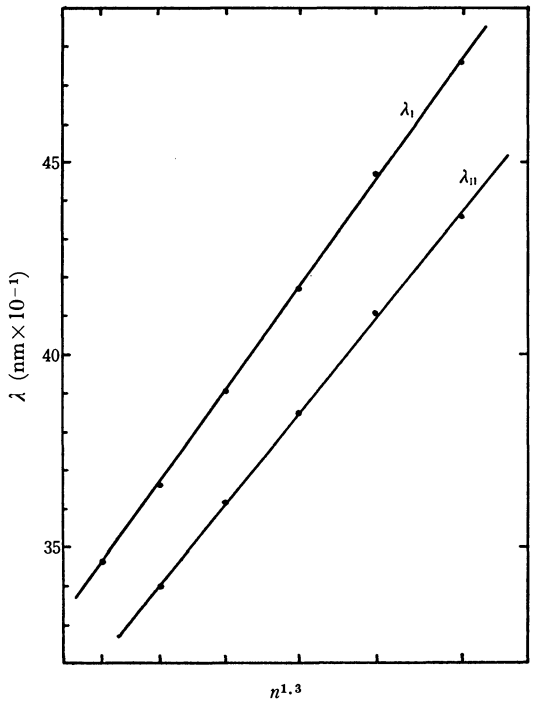

Fig. 6. Plot of λ_{max} *vs.* $n^{1.3}$ for 2,2′-diphenanthrylpoly-ynes (V_1—V_6).
λ_I: longest-wavelength maxima
λ_{II}: second-longest-wavelength maxima

tion of substitution as in the case of 1,1′- and 2,2′-dinaphthylpoly-ynes.[4]

The spectral reguralities are expressed by the following empirical formulas, and the agreement with the observed values is found to be excellent.

$$\lambda = An^x + B \text{ (in tetrahydrofuran)}$$

2,2′-series (V_n): $\lambda_I = 13.9\,n^{1.3} + 333$ nm
$\lambda_{II} = 12.3\,n^{1.3} + 310$

3,3′-series (VI_n): $\lambda_I = 10.8\,n^{1.4} + 347$
$\lambda_{II} = 9.4\,n^{1.4} + 324$

9,9′-series (VII_n): $\lambda_I = 10.5\,n^{1.4} + 352$
$\lambda_{II} = 9.0\,n^{1.4} + 329$

The spectral regularities in benzene and cyclohexane solution can be expressed by similar empirical formulas with about the same A and the same x as in the case of tetrahydrofuran solution, but with slightly modified B values.

The syntheses and electronic spectral properties of poly-ynes bearing other types of terminal groups will be reported in the near future.

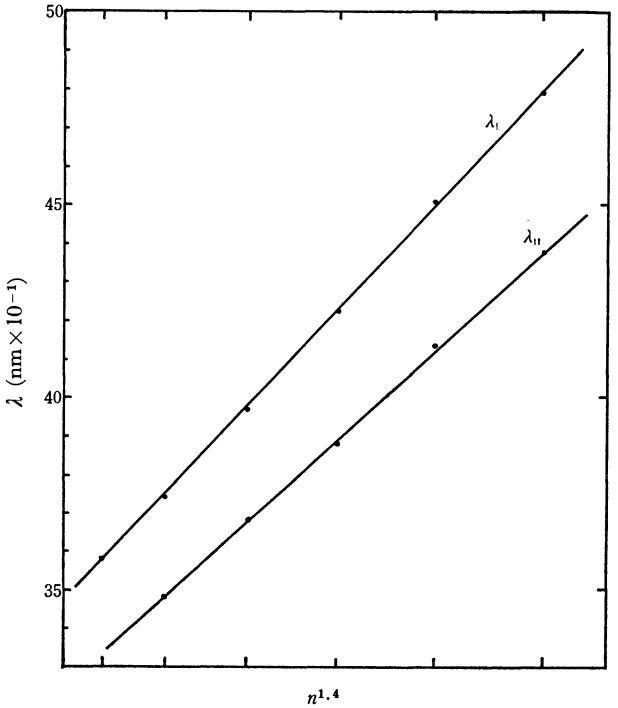

Fig. 7. Plot of λ_{max} *vs.* $n^{1.4}$ for 3,3′-diphenanthrylpoly-ynes (VI_1—VI_6).
λ_I: longest-wavelength maxima
λ_{II}: second-longest-wavelength maxima

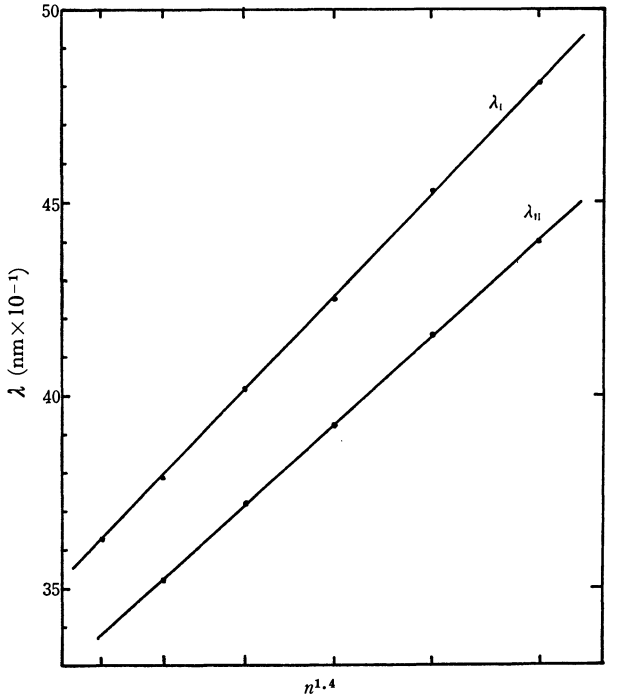

Fig. 8. Plot of λ_{max} *vs.* $n^{1.4}$ for 9,9′-diphenanthrylpoly-ynes (VII_1—VII_6).
λ_I: longest-wavelength maxima
λ_{II}: second-longest-wavelength maxima

Experimental

All the melting points are uncorrected. The electronic spectra were measured with a Hitachi EPS-3T spectrophotometer at room temperature employing a well-matched pair of 1-cm quartz cells. The IR spectra were obtained

on a Hitachi EPI-2 infrared spectrophotometer by KBr-disk method.

Acetylphenanthrenes (IX). 2- and 3-Acetylphenanthrenes. The acetylphenanthrenes were prepared according to the method of Mosettig and van de Kamp.[8]

9-Acetylphenanthrene. Diethyl ethoxymagnesiomalonate was prepared from magnesium (1.20 g, 0.05 g atom), diethyl malonate (8.0 g, 0.05 mol), anhydrous ethanol (5.05 g, 0.11 mol) and toluene (50 m*l*) and excess ethanol was removed. A solution of the acid chloride of 9-carboxyphenanthrene (6.03 g, 0.025 mol) in toluene (30 m*l*) was added to the toluene solution of ethoxymagnesiomalonate, and the mixture was heated for 2 hr at 80°C. 6 N Sulfuric acid was added to the ice-cooled reaction mixture. The organic layer was washed with water and a solution of sodium hydrogen carbonate, successively, and dried. The oily material obtained by the evaporation of the solvent under reduced pressure was mixed with acetic acid (40 m*l*) and 4 drops of concentrated sulfuric acid. The mixture was refluxed for 2.5 hr under evolution of carbon dioxide, then 4 N sulfuric acid (20 m*l*) was added to the reaction mixture. After having been refluxed for additional 3 hr, the reaction mixture was cooled. The solid deposited was collected and washed thoroughly with water and then dissolved in benzene (60 m*l*). The benzene solution was washed with sodium hydrogen carbonate solution and dried. The cubic crystals obtained by the evaporation of the solvent were re-dissolved in benzene and the solution was passed through a thin layer of alumina (6 g). The filtrate gave the acetyl compound, mp 73—74°C (lit. value, 74°C),[9] 5.14 g (94%). This material was recrystallized twice from ethanol to give an analytical specimen, mp 74°C, colorless needles.

Found: C, 87.43; H, 5.52%. Calcd for $C_{16}H_{12}O$: C, 87.24; H, 5.49%. IR: 1670 (C=O) cm^{-1}.

Formylphenanthrenes VIII. 2-Formylphenanthrene (2-VIII). 2-acetylphenanthrene was treated with alkaline sodium hypochlorite solution to give 2-carboxyphenanthrene. Lithium aluminum hydride reduction of the ester of the carboxyphenanthrene afforded 2-hydroxymethylphenanthrene. A solution of the hydroxymethyl compound (24.8 g, 0.12 mol) in pyridine (150 m*l*) was added to a chilled solution of chromium trioxide (36.0 g, 0.36 mol) in pyridine (500 m*l*).

The mixture was shaken in an ice-bath for 30 min, and then for 45 min at room temperature. The reaction mixture was poured into water (2.5 *l*) and was extracted with ether. The extract was washed successively with water, cold diluted hydrochloric acid, water, cold sodium hydroxide solution and water. The crude crystals (23.4 g, 97%) obtained on the evaporation of the solvent were converted into a sodium hydrogen sulfite adduct. Decomposition of the adduct gave 2-formylphenanthrene as colorless cubes, mp 55—58°C. The material was recrystallized twice from methanol-water to give pure specimen, mp 56—57°C. (lit. value, 59—59.5°C).[10]

Found: C, 87.48; H, 4.90%. Calcd for $C_{15}H_{10}O$: C, 87.35; H, 4.89%. IR: 2820, 2730 (CHO), 1695 (C=O) cm^{-1}.

3-Formylphenanthrene (3-VIII). According to the procedure for the preparation of the 2-formyl compound, the 3-hydroxymethyl compound was oxidized to give 3-formylphenanthrene in yield of 86%, colorless needles, mp 77—79°C (lit. value, 79.5—80°C).[10] The material was recrystallized twice from methanol to yield pure aldehyde, colorless needles, mp 79—80°C.

Found: C, 87.38; H, 4.89%. Calcd for $C_{15}H_{10}O$: C, 87.35; H, 4.89%. IR: 2835, 2740 (CHO), 1698 (C=O) cm^{-1}.

9-Formylphenanthrene (9-VIII). Dimethylformamide (4.4 g, 0.06 mol) was added dropwise to a stirred solution of 9-phenanthrylmagnesium bromide (prepared from 9-bromophenanthrene, 5.14 g, 0.02 mol and magnesium 0.504 g, 0.021 g atom)[11] in tetrahydrofuran under cooling in an ice-salt bath. After the addition had been completed, the cooling bath was removed and stirring was continued overnight. Diluted sulfuric acid was added to the reaction mixture, and then the mixture was extracted with benzene (50 m*l*). The extract was washed with a saturated solution of sodium chloride. A mixture of the extract and a saturated solution of sodium hydrogen sulfite was shaken overnight, and the deposited sulfite adduct was collected, washed with benzene, acetone, methanol, and water, successively. Treatment of the adduct with a saturated sodium hydrogen carbonate solution afforded 9-formylphenanthrene, mp 93—98°C, 2.46 g (62%). Recrystallization from benzene yielded pure 9-aldehyde, colorless fine needles, mp 100–102°C (lit. value. 100—101°C).[11]

Found: C, 87.28; H, 4.94%. Calcd for $C_{15}H_{10}O$: C, 87.35; H, 4.89%. IR: 2850, 2745 (CHO), 1690 (C=O) cm^{-1}.

1,4-Di(9-phenanthryl)-1,4-dihydroxy-2-butyne (X). To an ice-cooled solution of bis-Grignard derivative of acetylene (prepared from magnesium 1.75 g, 0.073 g atom and ethylbromide 9.70 g, 0.088 mol) in benzene-tetrahydrofuran (50 m*l*), was added a solution of 9-formylphenanthrene (6.18 g, 0.03 mol) in tetrahydrofuran (80 m*l*). After the mixture had been stirred at room temperature overnight, a saturated solution of ammonium chloride was added. The aqueous layer was removed, and was extracted with benzene. The organic layer was combined with the extract and dried (magnesium sulfate). It was concentrated under reduced pressure to yield colorless needles, mp 225—229°C, 5.41 g (83%), which was recrystallized from tetrahydrofuran-benzene, and then from tetrahydrofuran-toluene to afford pure butynediol, colorless needles, mp 230—235°C.

Found: C, 87.43; H, 4.97%. Calcd for $C_{32}H_{22}O_2$: C, 87.64; H, 5.06%. IR: 3430 (OH), 1070 (C–O) cm^{-1}.

Ethynylphenanthrenes (XXIV). 9-Ethynylphenanthrene (9-XXIV). A mixture of 9-acetylphenanthrene (2.20 g, 0.01 mol), phosphorus pentachloride (2.08 g, 0.01 mol) and benzene (25 m*l*) was refluxed for 1.5 hr. The viscous oily material obtained by the evaporation of the solvent *in vacuo* was kept in an evacuated desiccator containing potassium hydroxide for several hours. The crude chloride thus obtained was dissolved in tetrahydrofuran (10 m*l*), and the solution was added over a period of 10 min to a suspension of sodium amide (prepared from sodium 1.8 g, 0.08 g atom) in liquid ammonia (90 m*l*). After 1.5 hr, ammonia was allowed to evaporate, and ether (50 m*l*) and a saturated solution of ammonium chloride were added to the reaction mixture. The mixture was extracted with ether (200 m*l*). The residue obtained by evaporating the solvent was repeatedly digested with petroleum benzine (bp 60—80°C, 120 m*l*), and the benzine solution was passed through a short column of alumina (5 g). Concentration of the filtrate gave colorless cubes, mp 60—62°C, 1.71 g (85%). A solution of the crude crystals in petroleum ether (bp 40—60°C) was passed through a thin layer of alumina. The filtrate was concentrated to give pure material, color-

8) E. Mosettig and J. van de Kamp, *J. Amer. Chem. Soc.*, **52**, 3704 (1930).
9) E. Mosettig and J. van de Kamp, *ibid.*, **55**, 3445 (1933).
10) E. Mosettig and J. van de Kamp, *ibid.*, **55**, 2995 (1933).
11) C. A. Dornfeld and G. H. Coleman, "Organic Syntheses," Coll. Vol. III, p. 701 (1955).

less needless, mp 62.5—63°C. The ethynyl compound gave pale yellow silver and yellow cuprous acetylides.

Found: C, 94.98; H, 4.95%. Calcd for $C_{16}H_{10}$: C, 95.02; H, 4.98%. IR: 3295 (≡CH) cm^{-1}. UV (in *n*-hexane): λ_{max} (nm)(log ε): 213 (4.51), 234 (4.53), 256.5 (4.72), 260 (4.73), 237.5 (4.36), 287.5 (4.08), 259 (4.31), 312 (4.42), 331.5 (2.47), 339.5 (2.48), 347 (2.33), 355.5 (1.93).

2-Ethynylphenanthrene (2-XXIV). According to the procedure used in the preparation of 9-ethynyl compound, 2-acetylphenanthrene gave 2-ethynyl compound as colorless cubes in a yield of 72%, mp 72—76°C. A petroleum ether solution of this material was passed through a short column of alumina. Pure 2-ethynyl compound was obtained from the filtrate as colorless tiny cubes, mp 77—78°C. The 2-ethynyl derivative gave white silver and yellow cuprous acetylides.

Found: C, 95.00: H, 5.03%. Calcd for $C_{16}H_{10}$: C, C, 95.02; H, 4.98%. IR: 3295 (≡CH) cm^{-1}.
UV (in *n*-hexene): λ_{max} (nm) (log ε) 256 (4.78), 264 (5.00), 280 (4.38), 291 (4.50), 297.5 (4.09), 309 (2.36), 320 (2.30), 326 (2.48), 334 (2.50), 341.5 (2.71), 350.5 (2.51), 358.5 (2.78).

3-Ethynylphenanthrene(3-XXIV). The 3-ethynyl compound was prepared according to the above-stated procedure. Pale yellow needles, mp 100—106°C (62%) obtained were recrystallized three times from petroleum benzine to give pure material, colorless needles, mp 110—111°C. The ethynyl compound gave yellow silver and bright yellow cuprous acetylides.

Found: C, 94.69; H, 4.90%. Calcd for $C_{16}H_{10}$: C, 95.02; H, 4.98%. IR: 3290 (≡CH), 2090 (C≡C) cm^{-1}. UV (in *n*-hexane): λ_{max} (nm) (log ε) 219.5 (4.47), 237 (4.61), 251 (4.71), 258.5 (4.81), 274 (4.21), 278.5 (4.27), 296 (4.37), 309 (4.46), 330.5 (2.50), 338 (2.49), 346.5 (2.36), 355 (1.98).

2,2′-Diphenanthryldiacetylene (V_2). A solution of 2-ethynylphenanthrene (0.940 g, 4.7×10^{-3} mol) and cupric acetate monohydrate (10.0 g) in pyridine (50 m*l*) and methanol (5 m*l*) was stirred at 50°C for 3 hr.[12] The reaction mixture was cooled, and the insoluble material was collected by filtration, and washed with water, thus affording V_2 as colorless fine needles, mp 241—245°C, 0.794 g (84%). A second crop of V_2, 0.083 g (9%) was obtained by concentrating the filtrate. The combined crystals were dissolved in toluene, and the solution was passed through a short column of alumina to yield pure V_2, colorless needles, mp 243—244°C.

Found: C, 95.31; H, 4.48%. Calcd for $C_{32}H_{18}$: C, 95.49; H, 4.51%.

3,3′-Diphenanthryldiacetylene (VI_2). According to the procedure used in the preparation of V_2, 3-ethynylphenanthrene was converted into VI_2 as pale yellow needles in a yield of 86%. This material was recrystallized from toluene to give pure VI_2, pale yellow needles mp 280—282°C.

Found: C, 95.33; H, 4.53%. Calcd for $C_{32}H_{18}$: C, 95.49; H, 4.51%.

9,9′-Diphenanthryldiacetylene(VII_2). a) Oxidative Coupling of 9-Ethynylphenanthrene(9-XXIV). 9-Ethynylphenanthrene was oxidatively coupled according to the above procedure to give VII_2, pale yellow cubes, mp 256—257°C (97%). The crystals were recrystallized to yield pure VII_2, mp 256—257°C.

Found: C, 95.30; H, 4.57%. Calcd for $C_{32}H_{18}$: C, 95.49; H, 4.51%.

b) The Dehydrochlorination of 1,4-Bis-(9-phenanthryl)-1,4-dichloro-2-butyne(XI). A solution of thionyl chloride 0.43 g, 3.6 mmol) and pyridine (0.28 g, 3.6 mmol) in ether (5 m*l*) was added dropwise to a solution glycol (X, 0.562 g, 1.2 mmol) in tetrahydrofuran (15 m*l*) at −20°C over a period of 10 min. After being shaken for 1 hr at this temperature, the mixture was added to a stirred suspension of sodium amide (prepared from sodium 0.42 g, 18 mg atom) in liquid ammonia (60 m*l*). After 1 hr, ammonium chloride (2 g) was added to the mixture and the ammonia was allowed to evaporate. The solvent was then removed under reduced pressure. The residue was mixed with water, and the insoluble material was collected by filtration, washed with water and methanol, successively. The brown solid thus obtained was dissolved in toluene (150 m*l*) and the solution was passed through a short column of alumina (15 g). Concentration of the yellow filtrate gave VII_2 as yellow fine needles, mp 253—255°C, 0.394 g (81%). This material was recrystallized twice from toluene to give pure VII_2, mp 256—257°C.

Found: C, 95.47; H, 4.57%. Calcd for $C_{32}H_{18}$: C, 95.49; H, 4.51%. The hydrocarbons prepared by the two different methods gave identical electronic and IR spectra.

Phenanthryl-2-propyn-1-ols(XII). 9-Phenanthryl Derivative(9-XII). A solution of 9-phenanthaldehyde (8.00 g, 0.039 mol) in tetrahydrofuran (80 m*l*) was added over a period of 15 min to a suspension of lithium acetylide (prepared from lithium 0.83 g, 0.12 g atom) in liquid ammonia (200 m*l*) at −50—−55°C. After being stirred for 3 hr at this temperature, stirring was continued for further 3 hr at the temperature of the boiling point of ammonia. Then, ammonium chloride (3 g) was added to the reaction mixture, and the ammonia was allowed to evaporate. A saturated solution of ammonium chloride was added to the residue and the mixture was extracted with benzene. The extract was dried over magnesium sulfate. Evaporation of the solvent under reduced pressure gave an oily material. This material was mixed with benzene (20 m*l*) and was warmed to promote crystallization. The crystals were collected by filtration and were washed with a small amount of benzene to afford light brown tiny cubes, mp 129—133°C, 6.40 g (69%). Concentration of the filtrate gave the second crop, mp 119—124°C, 1.33 g (14%). The material was recrystallized from benzene 5 times to give pure sample, colorless needles, mp 134—135°C.

Found: C, 87.70; H, 5.20%. Calcd for $C_{17}H_{12}O$: C, 87.90; H, 5.21%. IR: 3380 (OH), 3300 (≡CH), 2100 (C≡C), 1067 (C–O) cm^{-1}.

2-Phenanthryl Derivative(2-XII). To an ice-cooled solution of ethynylmagnesium bromide (prepared from magnesium, 1.80 g, 0.075 g atom, ethylbromide, 8.20 g, 0.075 mol) in tetrahydrofuran (50 m*l*), was slowly added a solution of 2-formylphenanthrene (6.18 g, 0.03 mol) in the same solvent (60 m*l*). The cooling bath was removed then and the mixture was stirred overnight at room temperature. A saturated solution of ammonium chloride was added to the reaction mixture. The aqueous layer was extracted with benzene. The extract was combined with the organic layer, and dried. The oily material obtained by evaporation of the solvent under reduced pressure was mixed with benzene and was warmed to promote crystallization. The crystals thus obtained were washed with benzene-cyclohexane to give light brown fine crystals, 6.50 g (93%). A solution of the crystals in ethyl acetate was passed through a short column of alumina. The crystals obtained by concentrating the filtrate was recrystallized from benzene to afford pure 2-XII, pale yellow tiny cubes, mp 134.5—135°C.

Found: C, 87.92; H, 5.18%. Calcd for $C_{17}H_{12}O$: C,

12) *Cf.* G. Eglinton and A. R. Galbraith, *J. Chem. Soc.*, **1959**, 889.

87.90; H, 5.21%. IR: 3400 (OH). 3290 (≡CH), 2110 (C≡C), 1017 (C–O) cm^{-1}.

3-Phenanthryl Derivative(3-XII). According to the procedure for the preparation of 2-isomer, 3-formylphenanthrene gave 3-carbinol, light brown needles, mp 80—85°C in a yield of 82%. The crude material was recrystallized from benzene-cyclohexane to give pure material, pale yellow needles, mp 82—84°C.

Found: C, 87.37; H, 5.21%. Calcd for $C_{17}H_{12}O$: C, 87.90; H, 5.21%. IR: 3100—3600 (OH), 3295 (≡CH), 2100 (C≡C), 1056 (C–O) cm^{-1}.

1,6-Di(phenanthryl)-1,6-dihydroxy-2,4-hexadiynes(XIII).

9-Phenanthryl Derivative(9-XIII). Cuprous chloride (0.02 g, 2 mmol), ammonium chloride (0.14 g, 2 mmol) and 2 drops of concentrated hydrochloric acid were added to a solution of the 9-ethynyl carbinol (9-XII, 4.64 g, 0.02 mol) in methanol (80 ml). The mixture was vigorously stirred in oxygen atmosphere at a slightly elevated pressure. Deposition of pale yellow precipitate was observed after 1.5 hr. After being stirred overnight, the precipitate was collected by filtration. The precipitate was washed with methanol, diluted hydrochloric acid, and water, successively, and dried. The pale yellow powder, 3.51 g (76%), mp 210—215°C (dec.) thus obtained was recrystallized 5 times from tetrahydrofuran-benzene to give pure glycol (9-XIII) as colorless fine needles. mp 252—254°C (dec.).

Found: C, 87.99; H, 4.78%. Calcd for $C_{34}H_{22}O_2$: C, 88.29; H, 4.79%. IR: 3400 (OH), 1067 (C–O), 2140, 2250 (C≡C) cm^{-1}.

3-Phenanthryl Derivative(3-XIII). The Glaser oxidative coupling of 3-ethynyl carbinol(3-XII) under the reaction conditions used in the case of 9-isomer afforded 3-XIII as colorless powder in a yield of 66%. The material was recrystallized 3 times from acetone-benzene to yield pure 3-XIII, mp 208—210°C.

Found: C, 87.90; H, 4.78%. Calcd for $C_{31}H_{22}O_2$: C, 88.29; H, 4.79%. IR: 3600—3100 (OH), 2130 (C≡C), 1010 (C–O) cm^{-1}.

2-Phenanthryl Derivative(2-XIII). 2-ethynyl carbinol (2-XII) was converted to di-(2-phenanthryl)-diol(2-XIII) under the reaction conditions used in 3- and 2-isomers. Almost colorless powder (77%) thus obtained was recrystallized thrice from acetone-benzene to yield pure 2-XIII as colorless fine needles, mp 204—206°C (dec.).

Found: C, 88.36; H, 4.84%. Calcd for $C_{34}H_{22}O_2$: C, 88.29; H, 4.79%. IR: 3450—3100 (OH), 1000 (C–O) cm^{-1}.

9,9'-Diphenanthryltriacetylene(VIII$_3$). Formation of the Dichloride (9-XIV). A solution of thionyl chloride (0.36 g, 3 mmol) in pyridine (0.24 g, 3 mmol) was added to a solution of 9-glycol (9-XIII, 0.462 g, 1 mmol) in tetrahydrofuran (15 ml) over a period of 30 min at −20°C, and the mixture was shaken for 30 min.

Dehydrochlorination of 9-XIV. The above-mentioned reaction mixture was added to a suspension of sodium amide (prepared from sodium, 0.40 g, 0.017 g atom) in liquid ammonia (100 ml) under vigorous stirring at −70°C. After 30 min, ammonium chloride (2.0 g) was added to the reaction mixture, and the ammonia was allowed to evaporate. After the solvent had been removed under reduced pressure, a small amount of water was added to the residue. The insoluble material was successively washed with water, methanol, acetone, and benzene, and was dissolved in hot toluene (200 ml). The hot solution was passed through a thin layer of alumina (15 g). The light orange-yellow filtrate was concentrated under reduced pressure to yield VII$_3$ as yellow fine needles, 0.134 g (31%) mp 284—287°C (dec.). This substance was recrystallized from toluene to give pure VII$_3$, mp 285—286°C (dec.).

Found: C, 95.80; H, 4.24%. Calcd for $C_{34}H_{18}$: C, 95.75; H, 4.25%.

3,3'-Diphenanthryltriacetylene (VI$_3$). The procedure used for the preparation of VII$_3$ was applied to the 3-glycol (3-XIII) to give pale yellow fine needles in a yield of 39%, which decomposed at *ca.* 260°C. The material was recrystallized to afford pure VI$_3$, which decomposed at *ca.* 260°C without fusion.

Found: C, 95.71; H, 4.22%. Calcd for $C_{34}H_{18}$; C, 95.75; H, 4.25%.

2,2'-Diphenanthryltriacetylene (V$_3$) Chlorination of 2-glycol(2-XIII) followed by dehydrochlorination according to the reaction conditions used in the preparation of VII$_3$ and VI$_3$ gave pale yellow needles, dec. p *ca.* 270°C in a yield of 11%. This was recrystallized from toluene to give pure V$_3$, pale yellow needles, which decomposed, at *ca.* 270°C without fusion.

Found: C, 95.58; H, 4.22%. Calcd for $C_{34}H_{18}$: C, 95.75; H, 4.25%.

1-(Phenanthryl)-2-butyn-1,4-diol(XV). 9-Phenanthryl Derivative(9-XV). A solution of propargyl alcohol (5.04 g, 0.09 mol) in tetrahydrofuran (20 ml) was added dropwise in an ice-cooled solution of ethylmagnesium bromide in the same solvent (prepared from magnesium, 4.32 g, 0.18 g atom and ethyl bromide 20.0 g, 0.183 mol). After the mixture had been refluxed for 1 hr, it was cooled again with an ice-bath and a solution of 9-formylphenanthrene (9-VIII, 6.18 g, 0.03 mol) in tetrahydrofuran (90 ml) was added under stirring. The reaction mixture was stirred overnight at room temperature. A saturated solution of ammonium chloride was added to the mixture, and the organic layer was separated. The aqueous layer was extracted with benzene. The organic layer was combined with the extract and dried. After evaporation of the solvent, there remained an oily material which was mixed with a small amount of benzene. The crystals deposited on warming the mixture were washed with a small amount of benzene to yield light brown crystals, mp 133—135°C, 7.35 g (93%). The crystals were recrystallized three times from ethanol-cyclohexane to give pure diol, colorless needles, mp 138—139°C.

Found: C, 83.59; H, 5.70%. Calcd for $C_{18}H_{14}O_2$: C, 82.42; H, 5.38%. IR: 3350 (OH), 1017 (C–O) cm^{-1}. Recrystallization of the crude crystals three times from benzene afforded colorless needles, mp 104—106°C which contained half mole of benzene as a solvent of crystallization.

Found: C, 83.59; H, 5.70%. Calcd for $C_{18}H_{14}O_2$. 1/2 C_6H_6: C, 82.69; H, 5.69%.

3-Phenanthryl Derivative(3-XV). The above-mentioned procedure was adapted to 3-formylphenanthrene(3-VIII). The yield of crude crystals, light brown leaflets, mp 115—119°C was found to be 89%. The crude material was recrystallized four times from ethanol-benzene to give pure 3-XV, colorless leaflets, mp 122—124°C.

Found: C, 82.62; H, 5.40%. Calcd for $C_{18}H_{14}O_2$: C, 82.42; H, 5.38%. IR: 3600—3100 (OH), 1008 (C–O) cm^{-1}.

2-Phenanthryl Derivative(2-XV). According to the same procedure, a slightly impure 2-XV, mp 123—125°C was obtained from 2-formylphenanthrene(2-VIII). The crude material was recrystallized twice from acetone-benzene to afford pure 2-XV, colorless leaflets, mp 126—127°C.

Found: C, 82.37; H, 5.42%. Calcd for $C_{18}H_{14}O_2$: C, 82.42; H, 5.38%. IR: 3500—3100 (OH), 1000 (C–O) cm^{-1}.

9-Butadiynylphenanthrene(9-XVII). Formation of Dichloride (9-XVI). A solution of thionyl chloride (5.00 g, 0.042 mol) and pyridine (3.31 g, 0.042 mol) in ether (10 m*l*) was added over a period of 1 hr in a solution of 9-XV (4.200 g, 0.016 mol) in tetrahydrofuran (50 m*l*) under cooling with an ice-salt bath. After the mixture has been stirred for further 1 hr at room temperature, cracked ice was added, and the mixture was extracted with benzene. The extract was washed with water and an aqueous solution of sodium hydrogen carbonate, successively, and dried. The extract was concentrated to *ca.* 20 m*l* under reduced pressure, and the solution was subjected to the following reaction.

Dehydrochlorination of 9-XVI. The above-stated benzene solution of 9-XVI was added over a period of 15 min to a suspension of sodium amide (prepared from sodium 2.3 g, 0.1 g atom) in liquid ammonia (100 m*l*) at −70°C. After the mixture had been stirred for 30 min, ammonium chloride (10 g) was added, and the ammonia was allowed to evaporation. The residue obtained by evaporation of the solvent under reduced pressure was repeatedly digested with petroleum benzine (bp 60—80°C, total 500 m*l*). The benzine solution was percolated through a thin layer of alumina (5 g). Concentration of the colorless filtrate under reduced pressure afforded diacetylene (9-XVII) as colorless fine needles, mp *ca.* 110°C (dec.), 1.664 g (47%). Diacetylene (9-XVII) was found to be extremely unstable substance. The colorless crystals readily turned from blue to violet and then deep brown insoluble material. However, the solution of 9-XVII in benzine could be kept without decomposition in a refrigerator. Diacetylene (9-XVII) gave orange-yellow cuprous and yellow silver acetylides. UV (petroleum ether): λ_{max} (nm): 328.5 (L_a), 360 (L_b).

2-Butadiynylphenanthrene (2-XVII). Hexadiynediol (2-XV) was converted to diacetylene (2-XVII) according to the same reaction sequence under the conditions employed for the preparation of 9-XVII. Extremely unstable diacetylene (2-XVII) was obtained as colorless needles, mp *ca.* 110°C (dec.) in a yield of 50%. The substance gave yellow cuprous and light yellow silver acetylides. UV (petroleum ether): λ_{max} (nm): 314.5 (L_a), 365 (L_b).

3-Butadiynylphenanthrene(3-XVII). This substance was also prepared according to the method used for 9- and 2-isomer. The diacetylene(3-XVII) was obtained as colorless cubes in a yield of 15%. This substance was found to be highly unstable. It began to decompose at *ca.* 60°C and completely decomposed at 98—100°C. Diacetylene (3-XVII) gave orange cuprous and yellow silver acetylides. UV (petroleum ether): λ_{max} (nm): 326.5 (L_a), 362 (L_b).

9,9′-Diphenanthryltetraacetylene(VII$_4$). A mixture of the butadiynyl compound (9-XVII, 1.050 g, 4.65 mmol), cupric acetate monohydrate (10.0 g) and pyridine (50 m*l*) was stirred for 6 hr at 40°C.[12] The insoluble material was collected by filtration, and was washed thoroughly with water, then with a small amount of methanol and acetone. The yellow crystals, 1.018 g (97%). dec. p *ca.* 250°C were recrystallized four times from toluene to give pure tetraacetylene (VII$_4$), which decomposed at *ca.* 255°C without fusion.

Found: C, 95.69; H, 4.41%. Calcd for $C_{36}H_{18}$: C, 95.97; H, 4.03%.

3,3′-Diphenanthryltetraacetylene(VI$_4$). The oxidative coupling of 3-butadiynylphenanthrene(3-XVII) according to the above described procedure afforded yellow needles. dec. p *ca.* 190°C in a yield of 78%. The substance was recrystallized twice from toluene to give pure VI$_4$, yellow needles, which decomposed at *ca.* 200°C without fusion.

Found: C, 95.92; H, 4.02%. Calcd for $C_{36}H_{18}$: C, 95.97; H, 4.03%.

2,2′-Diphenanthryltetraacetylene(V$_4$). According to the procedure used in the cases of 3- and 9-isomers, diacetylene (2-XVII) was converted into tetrayne (V$_4$), yellow needles, 82%, dec. p *ca.* 220°C. The crude crystals in hot toluene were percolated through a thin layer of alumina. Pure V$_4$, yellow needles, which decomposed at *ca.* 220°C without fusion was obtained by concentration of the filtrate.

Found: C, 95.68; H, 3.95%. Calcd for $C_{36}H_{18}$; C, 95.97; H, 4.03%.

Phenanthrypropynals (XXV). 3-Phenanthrylpropynal (3-XXV). To a solution of ethylmagnesium bromide (prepared form magnesium, 2.30 g, 0.09 g atom, ethyl bromide, 13.0 g, 0.12 mol) in tetrahydrofuran (170 m*l*), was added over a period of 20 min a solution of 3-ethynylphenanthrene (3-XXIV, 12.25 g, 0.061 mol) in the same solvent (40 m*l*). After the mixture had been refluxed for 30 min, a solution of dimethylformamide (23.0 m*l*) in the same solvent (40 m*l*) was added under cooling with an ice-salt bath. The reaction mixture turned yellow, and then deposition of colorless crystals took place. The mixture was stirred for 2 hr at room temperature and then for 2.5 hr at 30°C. The mixture was poured into cold 5% sulfuric acid (600 m*l*) and benzene (150 m*l*). The mixture was stirred overnight, and extracted with ether. The extract was washed successively with water and sodium hydrogen carbonate solution, and dried. The oily material obtained by evaporation of the solvent, upon trituration with benzene-cyclohexane (1 : 1, 20 m*l*), gave yellow cubes, mp 130-133°C, 12.23 g (88%). The pure material was obtained by recrystallization of the crude crystals three times from benzene, and once from benzene-cyclohexane as yellow prisms, mp 132—134°C.

Found: C, 88.79; H, 4.43%. Calcd for $C_{17}H_{10}O$: C, 88.67; H, 4.38%. IR: 2840, 2740 (-CHO), 2210, 2180 (C≡C), 1658 (C=O) cm^{-1}.

2-Phenanthrylpropynal (2-XXV). The procedure described in the preparation of 3-aldehyde (3-XXV) was successfully adapted in the preparation of 2-aldehyde (2-XXV). The yellow fine needles, mp 104—108°C obtained in a yield of 62% were recrystallized four times from benzene-cyclohexane to give the pure material, yellow fine needles, mp 109—111°C.

Found: C, 88.62; H, 4.38%. Calcd for $C_{17}H_{10}O$: C, 88.67; H, 4.38%. IR: 2180 (C≡C), 1658 (C=O) cm^{-1}.

1-(Phenanthryl)-1,4-pentadiyn-3-ols (XXVI). 2-Phenanthryl Derivative (2-XXVI). To an ice-cooled solution of ethynylmagnesium bromide (prepared form magnesium, 1.44 g, 0.06 g atom and ethyl bromide, 7.20 g, 0.066 mol) in tetrahydrofuran (70 m*l*), was added a solution of 2-phenanthrylpropynal (2-XXV, 6.45 g, 0.028 mol) in tetrahydrofuran (60 m*l*). The temperature of the reaction mixture was gradually raised to room temperature and stirring was continued overnight. The mixture was hydrolyzed by the addition of a saturated ammonium chloride solution. The organic layer was then separated, and the aqueous layer was extracted with benzene. The extract was combined with the organic layer and was worked up in the usual manner to yield a dark-red oil. On being warmed with benzene (20 m*l*) it gave light brown needles, mp 120—122°C, 5.88 g (82%). The substance as recrystallized three times to give pure alcohol (2-XXVI), colorless needles, mp 121°C.

Found: C, 88.79; H, 4.71% Calcd for $C_{19}H_{12}O$: C, 89.04; H, 4.72%. IR: 3100—3450 (OH), 3295 (≡CH), 2330, 2110 (C≡C) cm^{-1}.

3-Phenanthryl Derivative (3-XXVI). The crude crys-

tals, mp 114—117°C (74%) which were obtained by the procedure described above were recrystallized three times from benzene and once from benzene - methanol to afford pure 3-XXVI as colorless tiny plates, mp 117—118°C.

Found: C, 88.87; H, 4.72%. Calcd for $C_{19}H_{12}O$; C, 89.04; H, 4.72%. IR: 3600—3100 (OH), 3280 (≡CH), 2210, 2110 (C≡C), 1012 (C–O) cm^{-1}.

1,10-Di(Phenanthryl)-1,4,6,9-decatetrayn-3,8-diols (XXVII). 2-Phenanthryl Derivative (2-XXVII). A mixture of 2-phenanthrylpentadiynol (2-XXVI, 2.80 g, 0.011 mol), cuprous chloride (0.35 g), ammonium chloride (0.30 g) and methanol (60 m*l*) was vigorously stirred under oxygen atmosphere at a slightly elevated pressure. After the mixture had been stirred for 48 hr, the solid deposited was collected by filtration. The solid was washed with a small amount of methanol, and then was dissolved in tetrahydrofuran-acetone (1 : 1;20 m*l*). The solution was passed through a short column of silica gel (5 g), and the filtrate was concentrated under reduced pressure to afford crude crystals, 2.40 g (84%), dec. p *ca.* 120°C. The substance was recrystallized from tetrahydrofuran-acetone to yield colorless needles, dec. p *ca.* 125°C. The unstable tetraacetylene glycol turned yellow in a short time.

Found: C, 89.21; H, 4.25%. Calcd for $C_{38}H_{22}O_2$: C, 89.39; H, 4.34%. IR: 3100—3400 (OH), 2235 (C≡C), 1008 (C–O) cm^{-1}.

3-Phenanthryl Derivative (3-XXVI). According to the above procedure, the 3-phenanthrylpentadiynol (3-XXVII) gave light brown crystals, dec. p *ca.* 110°C in a yield of 70%. Recrystallization of this material from acetone-ethanol and then from acetone-benzene afforded rather unstable colorless fine needles, dec. p *ca.* 140°C.

Found: C, 89.47; H, 4.34%. Calcd for $C_{38}H_{22}O_2$: C, 89.39; H, 4.34%. IR: 3600—3100 (OH), 2230 (C≡C), 1010 (C–O) cm^{-1}.

1,10-Di(9-Phenanthryl)-3,4,6,8-decatetrayn-1,10-diol (XIX). Formation of 1-(9-Phenanthryl)-2,4-pentadiyn-1-ol (XVIII). A solution of 1,4-dichloro-2-butyne(7.20 g, 0.059 mol) in ether (10 m*l*) was added over a period of 20 min to a suspension of lithium amide (prepared from lithium, 1.24 g, 0.179 atom) in liquid ammonia (250 m*l*) at −60°C. After having been stirred for 5 min, a solution of 9-formylphenanthrene (9.27 g, 0.045 mol) in tetrahydrofuran (150 m*l*) was added, and the mixture was stirred at −55°C for 1 hr, at −50°C for 1 hr and additional 1.5 hr at −40°C. Ammonium chloride (9 g) was then added to the reaction mixture at −60°C. After ammonia had been allowed to evaporate, water was added to the residue, and was extracted with benzene. Evaporation of the solvent from the dried extract gave a deep brown tarry material, which was re-dissolved in benzene, and then passed through a short column of alumina (7 g). However, no crystalline material could be obtained from the filtrate. The IR spectrum of the crude material indicated the presence of –C≡CH and OH groups. The absorption of C=O was found to be very weak. Owing to the unstable nature of diacetylene carbinol (XVIII), the crude material was subjected to the subsequent reaction.

Oxidative Coupling of Diacetylene Carbinol (XVIII). Cuprous chloride (0.30 g, 3 mmol) and ammonium chloride (0.20 g) were added to a solution of the above-mentioned crude carbinol (XVIII) in methanol (120 m*l*). The mixture was vigorously stirred under oxygen atmosphere at slightly elevated pressure. After having been stirred for 2 hr at room temperature, 2 drops of concentrated hydrochloric acid was added to the reaction mixture to dissolve the deposited cuprous acetylide. Stirring was continued overnight. The insoluble material deposited was washed with a small amount of methanol. The greenish-brown powder thus obtained was dissolved in tetrahydrofuran (60 m*l*) and the insoluble material was removed. The solution was percolated through a thin layer of alumina (10 g). The filtrate was concentrated under reduced pressure, and the tarry residue was mixed with a small amount of benzene. The mixture was warmed to promote crystallization. The crystals were dissolved in acetone and were precipitated by the addition of benzene to give fairly pure crystals, 2.25 g (20% based on 9-formylphenanthrene). The crystals decomposed at *ca.* 175°C without fusion. Owing to the instability of tetraacetylene glycol(XIX), the crude crystals were used in the following reaction.

IR: 3400 (OH), 2200, 2150, 2070 (C≡C), 1063 (C–O) cm^{-1}.

9,9'-Diphenanthrylpentaacetylene(VII_5). Formation of Dichloride(XX). A mixture of thionyl chloride (0.36 g; 3 mmol), pyridine (0.24 g, 3 mmol) and ether (5 m*l*) was added over a period of 20 min to a solution of the crude tetraacetylene glycol (XIX, 0.510 g, 1.0 mmol) in tetrahydrofuran (20 m*l*) at −20°C. The mixture was shaken for 30 min, and was immediately subjected to the following reaction.

Dehydrochlorination of Dichloride(XX). The mixture containing dichloride(XX) was added to a suspension of sodium amide (prepared from sodium, 0.40 g, 0.017 g atom) in liquid ammonia (100 m*l*) at −60°C under vigorous stirring. After 30 min, ammonium chloride (2 g) was added, and ammonia was allowed to evaporate. The residue obtained on removal of the solvent under reduced pressure was mixed with water. The insoluble material was washed successively with water, a small amount of acetone and benzene, and was dissolved in toluene (400 m*l*). The solution was passed through a short column of alumina (15 g). The yellow filtrate was concentrated under reduced pressure to yield orange-yellow needles, 0.213 g (45%). The substance was recrystallized twice from toluene to give pure VII_5, orange-yellow needles. The crystals decomposed at *ca.* at 200°C without fusion.

Found: C, 96.05; H, 3.85%. Calcd for $C_{38}H_{18}$; C, 96.18; H, 3.82%.

3,3'-Diphenanthrylpentaacetylene(VI_5). To a solution of di-(3-phenanthryl)-tetraacetylene glycol (3-XXVII; 0.510 g, 1 mmol) in tetrahydrofuran (15 m*l*), was added at −30°C a mixture of thionyl chloride (3.36 g, 3 mmol), pyridine (0.24 g, 3 mmol) and ether (5 m*l*) over a period of 15 min. The mixture was shaken for additional 5 min, and was added to a suspension of sodium amide (prepared from sodium, 0.40 g, 0.017 g atom) in liquid ammonia (90 m*l*) at −65°C. After having been stirred for 30 min, ammonium chloride (1 g) was added to the mixture, and ammonia was allowed to evaporate. The organic solvent was removed under reduced pressure, and the residue thus obtained was mixed with water. The insoluble material was washed successively with water, methanol, acetone and benzene, and was dissolved in hot toluene (400 m*l*). The hot solution was percolated through a thin layer of alumina (15 g). On cooling the yellow filtrate, orange-yellow needles, 0.276 g (58%) were obtained. The second crop of crystals, 0.029 g (6%) was obtained by the concentration of the mother liquor. The combined crystals were recrystallized from toluene to give pure VI_5, orange-yellow needles. It decomposed at *ca.* 190°C without fusion.

Found: C, 96.27; H, 3.74%. Calcd for $C_{38}H_{18}$: C, 96.18; H, 3.82%.

2,2'-Diphenanthrylpentaacetylene (V_5). According to

the procedure for the preparation of VI_5, the di-(2-phenanthryl)-tetraacetylene glycol(2-XXVII), were converted to V_5, silky yellow needles, in a yield of 22%. The crystals were recrystallized from toluene to afford pure V_5 as bright yellow fine needles. The crystals decomposed at *ca.* 200°C without fusion.

Found: C, 96.42: H, 3.78%. Calcd for $C_{38}H_{18}$: C, 96.18; H, 3.82%.

1-(Phenanthryl)-2,5-hexadiyn-1,4-diols (XXI). 9-Phenanthryl Derivative(9-XXI). A solution of 2,4-pentadiyn-3-ol[13] (3.08 g, 0.039 mol) in tetrahydrofuran (65 m*l*) was added over a period of 20 min to a stirred solution of ethylmagnesium bromide (prepared from magnesium, 2.05 g, 0.086 g atom and ethyl bromide, 10.4 g, 0.095 mol) in tetrahydrofuran (55 m*l*) at a temperature of 20—25°C. After 30 min, a solution of 9-phenanthraldehyde (VIII, R= 9-phenanthryl), (6.00 g, 0.029 mol) in tetrahydrofuran (60 m*l*) was added to the ice-cooled mixture, and the mixture was stirred at room temperature overnight. The reaction mixture was hydrolyzed by the addition of a saturated solution of ammonium chloride. The organic layer was combined with the benzene extract of the aqueous layer, and dried. Evaporation of the solvent gave a viscous oily material. The oily material was warmed with benzene (10 m*l*) to bring about crystallization. The light brown crystals, 6.10 g (74%) mp 135—140°C, obtained by washing with a small amount of cold benzene, were recrystallized three times from methanol-benzene. The colorless fine needles, mp 160—165°C, thus prepared, were re-dissolved in ethyl acetate, and the solution was passed through a short column of alumina to afford pure XXI (R=9-phenanthryl) as colorless fine needles, mp 169—171°C.

Found: C, 83.83; H, 4.90%. Calcd for $C_{20}H_{14}O_2$: C, 83.90; H, 4.93%. IR: 3500—3200 (OH), 3295 (≡CH), 2110 (C≡C), 1074, 1030 (C–O) cm^{-1}.

3-Phenanthryl Derivative (3-XXI). The light brown crystalline powder obtained from 3-phenanthraldehyde (3-VIII) according to the procedure used for the preparation of 9-isomer in a yield of 79% was recrystallized from methanol-benzene to yield light brown needles, mp 127—135°C. This material was recrystallized three times from acetone-benzene to give pure 3-phenanthryl diol (3-XXI) as colorless fine needles mp 141—143°C.

Found: C, 83.69; H, 4.96%. Calcd for $C_{20}H_{14}O_2$: C, 83.90; H, 4.93%. IR: 3600—3100 (OH), 3295 (≡CH), 2115 (C≡C), 1020 (C–O) cm^{-1}.

2-Phenanthryl Derivative (2-XXI). According to the procedure, 2-phenanthraldehyde (VIII, R=2-phenanthryl) was converted to slightly crude XXI (R=2-phenanthryl), light brown fine crystals, in a yield of 72%. The crystals were recrystallized three times from ethyl acetate-toluene to yield pure specimen as pale yellow leaflets, mp 151—153°C.

Found: C, 84.04; H, 4.92%. Calcd for $C_{20}H_{14}O_2$: C, 83.90; H, 4.93%. IR: 3500—3100 (OH), 3280 (≡CH), 2115 (C≡C), 1020 (C–O) cm^{-1}.

9-Hexatriynylphenanthrene(9-XXIII). Chlorination of Hexadiynediol(9-XXI). To a solution of diol (9-XXI, 1.716 g, 6 mmol) in tetrahydrofuran (16 m*l*) was added over 30 min a mixture of thionyl chloride (2.14 g, 18 mmol), pyridine (1.42 g, 18 mmol) and ether (7 m*l*) at −20°C. The mixture was allowed to reach room temperature, after which it was shaken for 30 min, and was subjected directly to the subsequent reaction.

Dehydrochlorination of Dichloride (9-XXII). The reaction mixture containing dichloride(9-XXII) was added to a vigorously stirred suspension of sodium amide (prepared from sodium, 1.00 g, 0.044 g atom) in liquid ammonia (100 m*l*) at −70°C. After the mixture had been stirred for 45 min, ammonium chloride (4 g) was added, and ammonia was allowed to evaporate. The organic solvent was distilled off under reduced pressure and the residue was digested repeatedly with petroleum ether (bp 60—80°C, total 300 m*l*). The solution was passed through a thin layer of alumina (6 g). A small portion of the pale yellow filtrate was concentrated under reduced pressure to result in the deposition of pale yellow fine needles. Rapid decomposition of the crystals to form black tarry material was observed. Triacetylene (9-XXI, UV (petroleum ether): λ_{max} 352 nm) gave yellow silver and orange cuprous acetylides. Owing to the unstable nature of 9-XXI, the petroleum ether solution was used in the following reaction.

3-Hexatriynylphenanthrene (3-XXIII). A colorless petroleum ether solution of triacetylene (3-XXIII) was obtained from the 3-phenanthryl glycol (3-XXI, 0.860 g, 3 mmol) under the same reaction conditions. Concentration of a small portion of the solution gave extremely unstable colorless cubes, which decomposed immediately to a brown material. Triacetylene (3-XXIII), UV (petroleum ether): λ_{max} 350 nm, gave orange cuprous and yellow silver acetylides. The petrolum ether solution was used directly for the subsequent reaction.

2-Hexatriynylphenanthrene (2-XXIII). 2-Phenanthryl diynediol (2-XXI, 2.00 g, 7 mmol) was converted to a petroleum ether solution of triacetylene (2-XXIII) according to the same procedure. Colorless fine needles obtained by the concentration of a small portion of the solution decomposed to blue insoluble material. Triacetylene (2-XXII, UV (petroleum ether): λ_{max} 342 (L_a), 370 (L_b nm) gave orange cuprous and yellow silver acetylides. The petroleum ether solution was subjected to the following reaction without isolation of 2-XXIII.

9,9′-Diphenanthrylhexaacetylene (VII_6). The petroleum ether solution of 9-hexatriynylphenanthrene (9-XXIII) was mixed with cupric acetate monohydrate (4.0 g) and pyridine (50 m*l*), and the mixture was concentrated to *ca.* 40 m*l* under reduced pressure. After the concentrated mixture had been stirred overnight at room temperature, the mixture was again concentrated to *ca.* 20 m*l* *in vacuo*. The insoluble material was washed with a small amount of methanol and then with water. The crude hexaacetylene, brown powder, 0.101 g (7% based on the diol, 9-XXI), thus obtained, was digested with hot toluene (100 m*l*), and the hot solution was passed through a short column of alumina (5 g). On cooling the orange filtrate, it gave orange fine needles. The crystals were recrystallized twice from toluene to give pure VII_6 as orange fine needles. This substance decomposed without fusion at *ca.* 130°C.

Found: C, 96.30; H, 3.67%. Calcd for $C_{40}H_{18}$: C, 96.36; H, 3.64%.

3,3′-Diphenanthrylhexaacetylene (VI_6). According to the same procedure, the petroleum ether solution of 3-hexatriynylphenanthrene (3-XXIII) gave crude VI_6, as yellow fine leaflets, 0.094 g (13% based on the glycol, 3-XXI). A benzene solution (350 m*l*) of the crude material was percolated through a thin layer of alumina (5 g). The orange yellow filtrate gave 0.056 g of pure VI_6 as orange yellow tiny plates, which decomposed at *ca.* 100°C without fusion.

Found: C, 96.41; H, 3.67%. Calcd for $C_{40}H_{18}$: C, 96.36; H, 3.64%.

2,2′-Diphenanthrylhexaacetylene (V_6). Brown crystalline powder, 0.380 g (22% based on the glycol, 2-XXI),

13) E. R. H. Jones, L. Skatteböl, and M. C. Whiting, *J. Chem. Soc.*, **1956**, 4765.

obtained under similar conditions from the above-mentioned petroleum ether solution of 2-XXIII was dissolved in benzene (300 m*l*). The benzene solution was passed through a short column of alumina (12 g). The deep yellow filtrate was concentrated to *ca.* 100 m*l* *in vacuo* to yield pure V_6 as light orange fine crystals, 0.102 g (6% based on the glycol, 2-XXI), which decomposed without fusion at *ca.* 185°C.

Found: C, 96.15; H, 3.62%. Calcd for $C_{40}H_{18}$; C, 96.36; H, 3.64%.

BULLETIN OF THE CHEMICAL SOCIETY OF JAPAN, VOL. 44, 2248—2253 (1971)

The Reaction of Dihalotetramethylbenzenes with Fuming Nitric Acid as a New Convenient Route to Some Dihalotrimethylbenzylic Compounds[1]

Hitomi SUZUKI, Kiyomi NAKAMURA, and Michiko TAKESHIMA

Department of Chemistry, Faculty of Science, Kyoto University, Sakyo-ku, Kyoto

(Received March 8, 1971)

Products obtained by the nitration of three isomeric dichloro and dibromotetramethylbenzenes with fuming nitric acid have been investigated. 3,6-Dihalo-1,2,4,5-tetramethylbenzene (dihalodurene) gave mainly 3,6-dihalo-2,4,5-trimethylbenzyl nitrate or 1,2-bis(nitrooxymethyl)-3,6-dihalo-4,5-dimethylbenzene, depending on the reaction temperature and the amount of nitrating agent. 4,6-Dihalo-1,2,3,5-tetramethylbenzene (dihaloisodurene) yielded a mixture of 3,5-dihalo-2,4,6-trimethylbenzyl nitrate and 2,6-dihalo-3,4,5-trimethylbenzyl nitrate, the latter in somewhat greater amount. 5,6-Dihalo-1,2,3,4-tetramethylbenzene (dihaloprehnitene) gave 5,6-dihalo-2,3,4-trimethylbenzyl nitrate as the sole nitrooxylation product. The reaction affords a new convenient route to precursors of various polysubstituted benzylic compounds hitherto not easily obtained by ordinary methods. Physical properties of some dihalotrimethylbenzylic compounds (chloride, nitrate, acetate, alcohol, and bisbenzyl ether) have been recorded.

On treatment with fuming nitric acid at low temperature, polyalkylbenzenes and their derivatives undergo side-chain nitrooxylation to give benzyl nitrates.[2-7] A noteworthy feature of this unusual reaction is that the product is usually composed of one isomer of specific orientation. Electron-withdrawing substituent brings about preferential side-chain nitrooxylation on the ortho methyl group, while the electron-releasing group is found to facilitate substitution on the meta methyl group. High positional selectivity, predominant substituent effect, and smooth occurrence of the reaction under mild conditions point to an ionic process.

From an interest in the anomalous nitration of polyalkylated aromatics, we investigated nitration of three isomeric dichloro and dibromotetramethylbenzenes with a view to obtaining further information on the general pattern of side-chain substitution in these systems, and clarifying the scope of synthetic utility of the reaction as a simple route to some polysubstituted benzylic compounds which are otherwise laborious to prepare.

Both dichlorotetramethylbenzenes and dibromotetramethylbenzenes react slowly with fuming nitric acid in dichloromethane at 0°C to give a pale yellow to light brown half-crystalline solid, mostly composed of dihalotrimethylbenzyl nitrates. The bromo compounds appear to be somewhat more reactive than the chloro compounds, and of the three isomeric dihalotetramethylbenzenes, 4,6-dihalo-1,2,3,5-tetramethylbenzene (dihaloisodurene) seems to be the most reactive.

1,2,4,5-Tetramethylbenzene (Durene) Series. 3,6-Dichloro-1,2,4,5-tetramethylbenzene (dichlorodurene) and 3,6-dibromo-1,2,4,5-tetramethylbenzene (dibromodurene) both reacted slowly with fuming nitric acid to give a crystalline solid, the major component of which was either dihalotrimethylbenzyl nitrate, or bis(nitrooxymethyl)dihalodimethylbenzene depending on the amount of nitric acid and the reaction temperature. With the use of three or four equivalent amounts of nitric acid at low temperature, the product was almost exclusively 3,6-dihalo-2,4,5-trimethylbenzyl nitrate. However, when dihalodurene was treated with a large excess of fuming nitric acid in an ice bath and the mixture was left standing for several hours, allowing the temperature of the system to gradually rise to room temperature, the product was a bis(nitrooxymethyl)dihalodimethylbenzene accompanied by some 5-nitro-3,6-dihalo-1,2,4-trimethylbenzene. If the reaction was allowed to proceed for a longer period, the latter compound constituted a significant portion of the product mixture. This product was no doubt derived from the initially formed benzyl nitrate through the replacement of the nitrooxymethyl group by the nitro group. Theoretically, three isomeric bis(nitrooxymethyl)dibromodimethyl-

1) The Reaction of Polysubstituted Aromatics. XXII. Part XXI: This Bulletin, **44**, 133 (1971).

2) L. I. Smith and S. A. Harris, *J. Amer. Chem. Soc.*, **57**, 1289 (1935); L. I. Smith and D. Tennenbaum, *ibid.*, **57**, 1293 (1935); L. I. Smith, F. L. Taylor, and I. M. Webster, *ibid.*, **59**, 1082 (1937); H. Suzuki and K. Nakamura, This Bulletin, **43**, 473 (1970).

3) L. I. Smith and J. W. Horner, *J. Amer. Chem. Soc.*, **62**, 1349 (1940); H. Suzuki, This Bulletin, **43**, 481 (1970).

4) H. Suzuki, This Bulletin., **43**, 879 (1970).

5) H. Suzuki, *Nippon Kagoku Zasshi*, **91**, 179 (1970).

6) K. Nakamura, This Bulletin., **44**, 133 (1971).

7) H. Suzuki and K. Nakamura, *ibid.*, **44**, 227 (1971).

benzenes can be derived from dibromodurene, and two of them, 1,3-bis(nitrooxymethyl)-2,5-dibromo-4,6-dimethylbenzene (I) and 1,4-bis(nitrooxymethyl)-2,5-dibromo-3,6-dimethylbenzene(II), were prepared from the corresponding bis(chloromethyl)benzenes by treatment with silver nitrate in hot acetonitrile. However, neither of these authentic specimens was found to be identical with the dinitrate obtained from dibromodurene. The bisnitrooxylated product is, therefore, most likely to be 1,2-bis(nitrooxymethyl)-3,6-dibromo-4,5-dimethylbenzene (III), although the authentic specimen is not available yet. This structural assignment is consistent with the observed directing effect of halogen atom and nitrooxymethyl group for the side-chain nitrooxylation of polymethylbenzene derivatives. The combined effect of the ortho/meta directing halogen[3] and the ortho directing nitrooxymethyl group[4] favors structure III over I and II.

Further nitrooxylation of bis(nitrooxymethyl)benzene could not be observed even by the action of a large excess of cold fuming nitric acid for a prolonged period. At somewhat higher temperature, the decomposition of the nitrate or the bis(nitrooxymethyl)-benzene into nitro or carbonyl compounds became prominent. No attempt has been made to identify them.

Chromatography of the crude nitration product on alumina requires some precaution since the active alumina converts the nitrate into bisbenzyl ether and benzyl alcohol during elution with benzene and ethanol. Dichlorotrimethylbenzyl nitrates were more readily decomposed than the bromo compounds. Light petroleum eluted unchanged material and benzyl nitrate, and the light petroleum - benzene mixture eluted bisbenzyl ether and nitro compound. Recovery of benzyl nitrates was usually unsatisfactory. Benzyl alcohol, bis(hydroxymethyl)benzene and unidentified carbonyl compounds were obtained from diethyl ether - ethanol eluates. The relative ratio of these products varied considerably depending on the activity of alumina and length of column.

1,2,3,5-Tetramethylbenzene (Isodurene) Series. 4,6-Dichloro-1,2,3,5-tetramethylbenzene (dichloroisodurene) and 4,6-dibromo-1,2,3,5-tetramethylbenzene (dibromoisodurene) reacted with fuming nitric acid more readily than durene analogs and gave a pale yellow pasty solid, PMR spectra of which showed two methylene peaks due to $-CH_2ONO_2$ at 4.24 and 4.48 τ with relative areas of 55 : 45 for chloro compound, and two peaks of relative intensity 66 : 34 at 4.12 and 4.43 τ for bromo derivative. These nitrates could be separated by fractional crystallization from ethanol. Direct comparison with the authentic specimens identified the benzyl nitrate with methylene proton absorption at higher field as 3,5-dihalo-2,4,6-trimethylbenzyl nitrate(IV), and another nitrate with lower field absorption as 2,6-dihalo-3,4,5-trimethylbenzyl nitrate(V). Attempted chromatographic separation of the product from dichloroisodurene on alumina resulted in nearly complete conversion of the nitrates to benzyl alcohol and bisbenzyl ether, but fairly selective decomposition occurred with the nitrates derived from dibromoisodurene. 2,6-dibromo-3,4,5-trimethylbenzylic product was adsorbed firmly on alumina and only a small portion was usually eluted as nitrate. 3,5-Dibromo-2,4,6-trimethylbenzylic compound was obtained mainly as bisbenzyl ether and alcohol. The structures of these bisbenzyl ethers were established by preparing authentic specimens from the corresponding alcohols. Under the conditions in which dihalodurenes were bisnitrooxylated, dihaloisodurenes were found to yield mononitrates together with a significant amount of nitro and carbonyl compounds.

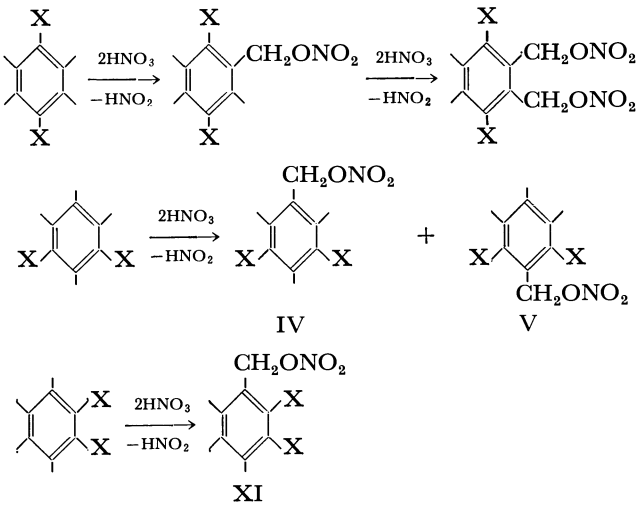

Fig. 1

Both nitrates IV and V derived from dihaloisodurene possess the methyl group at a position para to the nitrooxymethyl group (Fig. 1). The result is in line with the general observation that one of the main factors controlling the ease of side-chain nitrooxylation is the presence of the methyl group at a position para to the alkyl group to be nitrooxylated. This might indicate that the transition state of the anomalous substitution resembles a benzylic compound rather than a methylenecyclohexadiene, since the para methyl group is known to be more effective than halogen atom to delocalize the electron deficiency developed on the benzylic carbon atom during the reaction. The preferred formation of IV and V from dihaloisodurene may be explained as follows:

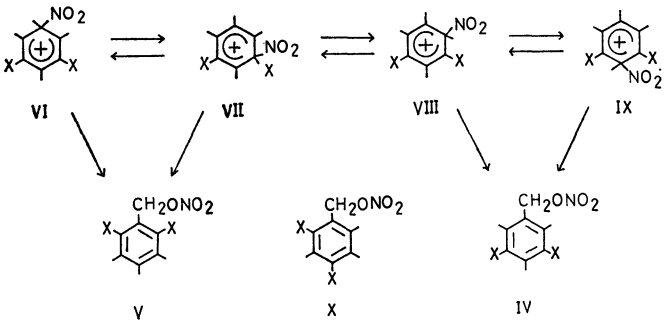

Fig. 2

Electrophilic attack of nitronium ion on dihaloisodurene would lead to an equilibrium mixture of four benzenonium ions VI—IX, in which VI and VII are supposed to predominate since three methyl groups can effectively contribute to the stabilization of these intermediates. Rearrangement of ions VI and VII according to the previously suggested mechanism,[6,7] which assumes migration of the nitro group from the attacking site to the α-carbon of the alkyl group from which the preferential proton removal takes place, will lead to V, because the proton release and subsequent migration of the nitro group would occur preferentially on the methyl group bonded to the more positively polarized ring carbon between two halogen atoms. Transformation of VI and VII into 4,6-dihalo-2,3,5-trimethylbenzyl nitrate(X) would be disfavored since the transition state can not be stabilized as effectively by the para halogen atom as by the para methyl group. On the other hand, less stable ions VIII and IX can be converted into IV more readily owing to the favorable orientation of substituent groups in the ring, the equilibrium being displaced in favor of these ions at the expence of the more stable ions VI and VII.

An alternative possibility may involve the ion-pair path; a proton is removed hyperconjugatively from the alkyl side-chain to form a sort of methylenecyclohexadiene or benzylic intermediate - nitrite ion pair, which will subsequently be converted into the nitrate. An increase in the formation of V relative to IV in going from chlorine to bromine is explained by the greater contribution of ions VI and VII in the equilibrium mixture as well as the easier migration of the nitro group due to the increased nuclear charge and bulkiness of bromine atom.

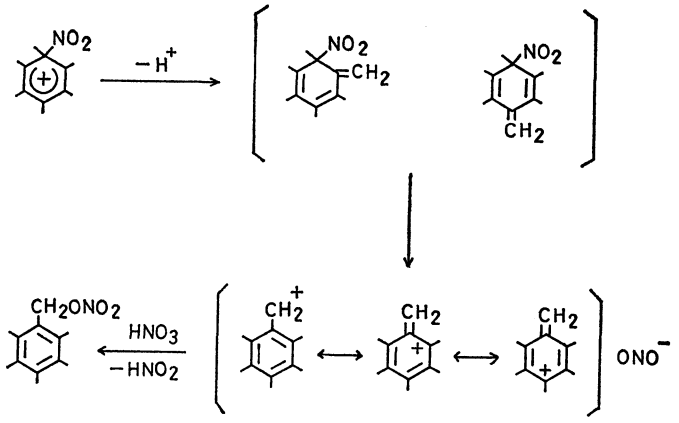

Fig. 3

1,2,3,4-Tetramethylbenzene (Prehnitene) Series. 5,6-Dihalo-1,2,3,4-tetramethylbenzene (dihaloprehnitene) was comparatively stable towards the action of cold nitrating agent, but slowly underwent side-chain nitrooxylation to give only one nitrate in good yield, which could be readily separated from the product mixture by fractional crystallization. The nitrate was identified as 5,6-dihalo-2,3,4-trimethylbenzyl nitrate(XI) by direct comparison with the authentic specimen prepared from 4,5-dihalo-1,2,3-trimethylbenzene through the ordinary sequence. Chromatographic behavior of the nitration product was similar to those obtained from dihaloisodurenes. Nitrate XI does not seem to undergo further nitrooxylation and is liable to suffer extensive decomposition by the action of a large excess of nitrating agent. The product mixture usually contains appreciable amounts of an unidentified crystalline solid which has absorption bands around 1610—1630 and 3400 cm^{-1}. Its structure has not been established yet. Formation of XI in preference to the isomeric 4,5-dihalo-2,3,6-trimethylbenzyl nitrate could be rationalized on the basis of a similar discussion as above.

The results indicate that the side-chain nitrooxylation of dihalotetramethylbenzenes with fuming nitric acid can provide a simple new method for the preparation of dihalotrimethylbenzylic compounds, some of which are laboriously obtained by the ordinary procedure.

Experimental

All melting points were determined with a hot-stage apparatus and are uncorrected. Infrared spectra were run as Nujol on a Jasco DS-402G spectrophotometer and only prominent peaks are recorded. PMR measurements were carried out on a Varian A-60A spectrometer and a JNM-3H spectrometer with carbon tetrachloride as solvent and tetramethylsilane as internal standard.

Dihalotetramethylbenzenes were prepared by halogenation of the corresponding hydrocarbons and purified through chromatography on alumina using light petroleum as eluant.

Authentic specimens of benzylic compounds were prepared essentially by the same sequence; chloride→nitrate, and chloride→acetate→alcohol→bisbenzyl ether. The general procedure is shown below with examples from the compounds of 3,5-dihalo-2,4,6-trimethylbenzylic series. Physical properties of some dihalotrimethylbenzylic compounds are summarized in Table 1.

3,5-Dibromo-2,4,6-trimethylbenzyl Chloride (XII). A crystal of iodine was added to a solution of 2,4,6-trimethylbenzyl chloride[8] (16.9 g) in carbon tetrachloride (50 ml), and bromine (*ca.* 33 g) was introduced dropwise at 0°C. The dibromobenzyl chloride soon began to separate from the mixture. The solvent was partly removed and the precipitate was recrystallized from light petroleum to give white needles (22.5 g, 69%), mp 125—127°C.

Found:C, 36.4; H, 3.3%. Calcd for $C_{10}H_{11}Br_2Cl$: C, 36.8; H, 3.4%.

Other dihalotrimethylbenzyl chlorides were similarly prepared by direct halogenation of the corresponding trimethylbenzyl chlorides. Yields varied from poor to moderate, depending on the structure of the chloride being halogenated. In some cases, a significant amount of unidentified higher halogenated products was formed as a by-product and its purification was tedious.

3,5-Dibromo-2,4,6-trimethylbenzyl Nitrate (XIII). A warm solution of silver nitrate (4.1 g) in acetonitrile (15 ml) was added all at once to a magnetically stirred solution of chloride XII (6.5 g) in acetonitrile (20 ml). The mixture was stirred for several hours, and silver chloride was filtered. After removal of the solvent in a vacuum, the residue was crystallized from light petroleum to give XIII (5.3 g), mp

8) R. C. Fuson and N. Rabjohn, "Organic Syntheses," Coll. Vol. III, 557 (1955).

Table 1. Physical properties of some dihalotrimethylbenzylic compounds

Compound		Mp (°C)	PMR spectra (τ) CH_2	PMR spectra (τ) CH_3	IR spectra[a] (cm^{-1})
3,6-Dihalo-2,4,5-trimethylbenzyl series					
Chloro	Alcohol	184—187	5.20	7.47 (1)[b] 7.57 (2)	717, 845, 998, 1041, 1187, 1208, 1270
	Chloride	94— 96	5.23	7.49 (1) 7.59 (2)	686, 723, 755, 843, 932, 1011, 1196, 1260
	Nitrate	80— 82	4.31	7.48 (1) 7.58 (2)	690, 752, 886, 975, 996, 1190, 1273* 1294, 1616, 1645*
	Bisbenzyl ether	222—223	5.24	7.59 (6)	718, 1002, 1073, 1089, 1191
Bromo	Alcohol	197—198	5.11	7.35 (1) 7.45 (2)	838, 992, 1041, 1175, 1282, 1314
	Chloride	118—119	5.16	7.38 (1) 7.48 (2)	676, 702, 747, 834, 923, 999, 1146, 1185, 1256
	Nitrate	97— 99	4.24	7.43 (1) 7.47 (2)	677, 756, 870, 963, 988, 1180, 1277, 1618, 1648*
	Bisbenzyl ether	240—241	5.39	7.32 (2) 7.54 (4)	724, 995, 1073, 1088, 1179
2,6-Dihalo-3,4,5-trimethylbenzyl series					
Chloro	Chloride	104—106	5.14	7.63 (2) 7.72 (1)	684, 704, 753, 905, 1019, 1172, 1260, 1299
	Nitrate	90— 91	4.27	7.62 (2) 7.68 (1)	703, 757, 867, 936, 969, 1271, 1629, 1643*
Bromo	Nitrate	111—112	4.13	7.56 (2) 7.63 (1)	699, 755, 867, 920, 973, 1273 1636
3,5-Dihalo-2,4,6-trimethylbenzyl series					
Chloro	Alcohol	193—194	5.24	7.43 (1) 7.48 (2)	817, 830, 992, 1027, 1168, 1208
	Acetate	102—103	4.89	7.52 (1) 7.61 (2) 8.00 ($COCH_3$)	707, 936, 956, 1023, 1175, 1215 1232, 1740
	Chloride	104—106	5.33	7.43 (2) 7.47 (1)	720, 796, 897, 978, 1012, 1176, 1255, 1302
	Nitrate	111—113	4.44	7.45 (1) 7.53 (2)	709, 755, 846, 893, 934, 966, 999, 1177, 1294, 1611
	Bisbenzyl ether	233—234	5.43	7.47 (2) 7.58 (4)	710, 942, 994, 1067, 1183, 1348
Bromo	Alcohol	205—206	5.17	7.28 (1) 7.44 (2)	805, 916, 978, 1005, 1024, 1159 1204
	Acetate	116—118	4.85	7.33 (1) 7.54 (2) 7.99 ($COCH_3$)	725, 920, 958, 1028, 1167, 1212 1233, 1742
	Chloride	125—127	5.39	7.35 (1) 7.50 (2)	678, 745, 888, 969, 987, 1019, 1163, 1255
	Nitrate	127—128	4.41	7.29 (1) 7.48 (2)	691, 755, 825, 885, 917, 964, 990, 1168, 1289, 1611
	Bisbenzyl ether	249—251	5.16	7.49 (6)	724, 929, 986, 1059, 1169, 1347
5,6-Dihalo-2,3,4-trimethylbenzyl series					
Chloro	Alcohol	193—194	5.18	7.57 (1) 7.62 (1) 7.74 (1)	916, 965, 1016, 1028, 1069, 1200
	Chloride	103—104	5.23	7.59 (1) 7.61 (1) 7.74 (1)	685, 753, 907, 942, 973, 1208 1260
	Nitrate	87— 90	4.32	7.58 (1) 7.67 (1) 7.75 (1)	699, 754, 890, 972, 1272*, 1298, 1612, 1645*
	Bisbenzyl ether	218—220	5.24	7.58 (2) 7.71 (2) 7.76 (2)	721, 917, 1009, 1061, 1088, 1206

Table 1. Continued

Compound		Mp (°C)	PMR spectra (τ) CH_2	PMR spectra (τ) CH_3	IR spectra[a] (cm^{-1})
5,6-Dihalo-2,3,4-trimethylbenzyl series					
Bromo	Alcohol	210—211	5.13	7.48 (1) 7.60 (1) 7.72 (1)	891, 951, 1019, 1028, 1065, 1192
	Chloride	127—128	5.15	7.49 (1) 7.62 (1) 7.73 (1)	748, 889, 925, 964, 1198, 1259
	Nitrate	98— 99	4.22	7.46 (1) 7.65 (1) 7.72 (1)	685, 755, 872, 963, 1278, 1634
	Bisbenzyl ether	263—264	5.12	7.49 (2) 7.68 (2) 7.74 (2)	722, 893, 1010, 1059, 1089, 1196

a) Principal peaks in the regions, 650—1350 and 1500—2000 cm^{-1}. Under certain conditions, benzyl nitrates show another asymmetric frequency band due to ONO_2 group in the 1640—1650 cm^{-1} region (indicated by asterisk). Appearance of this band is often accompanied by a small change in symmetric frequency in 1270—1290 cm^{-1} region.
b) Numerals in parentheses refer the number of methyl groups.

127—128°C.

Found: C, 33.9; H, 3.3%. Calcd for $C_{10}H_{11}Br_2NO_3$: C, 34.0; H, 3.1%.

Other dihalotrimethylbenzyl nitrates were prepared in a similar manner from the chlorides and recrystallized from light petroleum.

3,5-Dibromo-2,4,6-trimethylbenzyl Acetate (XIV). A mixture of chloride XII (9.8 g), silver acetate (5.2 g), and acetic acid (60 ml) was heated under gentle reflux for several hours. Silver chloride was filtered, and the reaction mixture was diluted with water to yield acetate as a white precipitate, which was recrystallized from light petroleum in the form of colorless needles (8.6 g), mp 116—118°C.

Found: C, 41.3; H, 3.9%. Calcd for $C_{12}H_{14}Br_2O_2$: C, 41.2; H, 4.0%.

A similar treatment of other dihalotrimethylbenzyl chlorides with silver acetate gave the corresponding acetates in high yields (75—89%).

3,5-Dibromo-2,4,6-trimethylbenzyl Alcohol (XV). Acetate XIV (3.5 g) was dissolved in a large volume of ethanol, to which was added an aqueous solution of sodium hydroxide (4 g). The mixture was gently refluxed for several hours and then poured into water to give XV (*ca.* 3 g), which was crystallized from boiling ethanol in the form of fine prisms, mp 205—206°C.

Other dihalotrimethylbenzyl alcohols were obtained similarly by analogous hydrolysis of the acetates using aqueous sodium hydroxide. Most dihalotrimethylbenzyl alcohols are only slightly soluble in light petroleum, carbon tetrachloride, benzene, and cold ethanol.

Attempt to prepare dibromotrimethylbenzyl alcohols by reducing dibromotrimethylbenzoic acids with lithium aluminum hydride in tetrahydrofuran proved unsatisfactory, since the bromine atom was partly or completely removed during the reduction.

Bis(3,5-dibromo-2,4,6-trimethylbenzyl) Ether (XVI). A mixture of XV and a catalytic amount of sulfamic acid was heated at 210—220°C in an oil bath. The alcohol melted to a pale yellow oil, and soon solidified to a white crystalline mass, which was taken up in a mixture of dichloromethane and ligroin and chromatographed on a short alumina column to remove any unchanged alcohol. Ether XVI crystallized from hot benzene as white needles and melted at 249—250°C. The yield was nearly quantitative.

Other bisbenzyl ethers were prepared in a similar way. The bromo alcohol needed somewhat higher temperature and longer heating than the chloro compound to complete the reaction.

2,6-Dimethyl-4-bromoaniline (XVII). 2,6-Dimethylaniline (12.1 g) was dissolved into a mixture of concentrated hydrochloric acid (30 ml) and water (220 ml), and the solution was cooled in an ice bath. A rapid stream of air saturated with bromine vapor was introduced with stirring until the solution assumed a distinctly yellow color. About 18—19 g of bromine was required. The bromoaniline hydrochloride came out of the solution as a white precipitate. The reaction mixture was made alkaline with aqueous sodium carbonate and the separated dark oil which soon solidified was filtered and recrystallized from ligroin to give large prisms (16.3 g, 82%), mp 50—51°C (lit,[9] 50—51°C). Acetanilide, mp 199—200°C (lit,[10] 198—200°C).

A similar treatment of 2,3-dimethylaniline gave 4,6-dibromo-2,3-dimethylaniline (mp 56—57°C) and unchanged starting material. The required monobromoaniline was obtained only in a small amount.

*2,5-Dibromo-*m*-xylene (XVIII).* A solution of XVII (20 g) in cold concentrated sulfuric acid (50 ml) was poured onto crushed ice (200 g) and diazotized with sodium nitrite (7.5 g). The resulting solution was filtered and the filtrate was added as rapidly as the foaming permitted to a boiling mixture of copper(I) bromide (7 g), cupper powder (*ca.* 1 g) and 47%-hydrobromic acid (80 ml). The separated black oil was removed by extraction with ether, washed with dilute aqueous sodium hydroxide and dried over anhydrous calcium chloride. The ethereal solution was distilled off to leave a dark oil, which on distillation under reduced pressure gave pale yellow oil (15 g, 57%), bp 120—121°C/15 mmHg (lit,[11] mp 28°C). Some 4-bromo-2,6-dimethylphenol (mp 79—80°C) was obtained as a by-product.

1,3-Bis(chloromethyl)-2,5-dibromo-4,6-dimethylbenzene (XIX).

9) E. Nölting, A. Braun, and G. Thesmar, *Ber.*, **34**, 2259 (1901).
10) E. G. Kleinschmidt and H. Braeuniger, *Pharmazie*, **1969**, 87.
11) J. J. Blanksma, *Rec. Trav. Chim. Pays-Bas*, **25**, 176 (1906).

A warm solution of XVIII (4 g) in chloromethyl methyl ether (*ca.* 5 g) was treated with 60%-fuming sulfuric acid (*ca.* 4—5 g) with vigorous stirring. The reaction proceeded with active liberation of heat and the mixture soon solidified into a black crystalline mass, which was washed with water, dissolved into a mixture of dichloromethane and ligroin, and freed from the polymeric substances through chromatography on a short alumina column. Removal of the solvent, followed by recrystallization of the product from carbon tetrachloride gave XIX (3.5 g, 64%) as long needles, mp 175—176°C.

Found: C, 33.0; H, 3.9%. Calcd for $C_{10}H_{10}Br_2Cl_2$: C, 33.3; H, 2.8%.

By a similar treatment, 2,5-dibromo-*p*-xylene gave *1,4-bis(chloromethyl)-2,5-dibromo-3,6-dimethylbenzene (XX)*, mp 213—215°C.

Found: C, 32.7; H, 2.8%. Calcd for $C_{10}H_{10}Br_2Cl_2$: C, 33.3; H, 2.8%.

1,3-Bis(nitrooxymethyl)-2,5-dibromo-4,6-dimethylbenzene(I). A warm solution of silver nitrate (2.1 g) in acetonitrile (10 m*l*) was added all at once with stirring to a hot solution of XIX (1.8 g) in acetonitrile (40 m*l*). The mixture was stirred with heating for several hours, and silver chloride was separated by filtration. Evaporation of the solvent *in vacuo*, followed by crystallization of the residue from hot ligroin gave white thin plates (2.5 g), mp 130—132°C. IR: 869, 971, 1179, 1278, 1620, and 1633 cm^{-1}, PMR: 7.36 (CH_3), and 4.25 τ (CH_2).

Found: C, 28.9; H, 2.5%. Calcd for $C_{10}H_{10}Br_2N_2O_6$: C, 29.0; H, 2.4%.

The above procedure applied to XX gave *1,4-bis(nitrooxymethyl)-2,5-dibromo-3,6-dimethylbenzene(II)*, mp 186—187°C, as white leaflets. IR: 876, 975, 1176, 1281, and 1628 cm^{-1}, PMR: 7.38 (CH_3) and 4.20 τ (CH_2).

Found: C, 29.0; H, 2.5%. Calcd for $C_{10}H_{10}Br_2N_2O_6$: C, 29.0; H, 2.4%.

General Procedure for Nitration of Dihalotetramethylbenzenes. A suspension of a dihalotetramethylbenzene (0.05 mol) in dichloromethane (50 m*l*) was vigorously stirred and fuming nitric acid (d=1.50) was added dropwise at 0°C over a period of 30 min. The solid part gradually dissolved giving a clear dark brown mixture, which was stirred for some hours and then quenched by being poured into ice water. The organic layer was throughly washed with aqueous sodium hydrogen carbonate and water. Evaporation of the solvent left a yellow to light brown pasty or half-crystalline solid, which was inspected by infrared, PMR, and thin-layer chromatography, and then subjected to chromatographic separation on alumina. Some nitrates were isolated by fractional crystallization of the product mixture from ethanol or ligroin.

Products were identified by elemental analyses, and by infrared and PMR spectra comparison or mixed melting as far as the authentic specimens were available. Typical examples of alumina chromatography are shown below for the nitration products from dibromotetramethylbenzenes.

i) A part (5 g) of light brown crystalline solid obtained from the nitration of dibromodurene (7.3 g) with fuming nitric acid (8 g) was placed on the top of alumina column and eluted with light petroleum to give unchanged starting material (1.2 g) and *3,6-dibromo-2,4,5-trimethylbenzyl nitrate* (0.5 g; Found: C, 33.9; H, 3.0; N, 4.0%. Calcd for $C_{10}H_{11}Br_2NO_3$: C, 34.0; H, 3.1; N, 4.0%). Elution with light petroleum-benzene gave *bis(3,6-dibromo-2,4,5-trimethylbenzyl) ether* (0.6 g; Found: C, 39.8; H, 3.3%. Calcd for $C_{20}H_{22}Br_4O$: C, 40.2; H, 3.7%); with ether-ethanol *3,6-dibromo-2,4,5-trimethylbenzyl alcohol* (1.3 g, Found: C, 39.1; H, 4.3%. Calcd for $C_{10}H_{14}Br_2O$: C, 38.7; H, 4.6%).

A similar treatment of the product (5 g) from the nitration with a large excess of fuming nitric acid at somewhat elevated temperature gave *3,6-dibromo-5-nitro-1,2,4-trimethylbenzene* (0.3 g, mp 198—200°C; Found: C, 33.9; H, 2.8%. Calcd for $C_9H_9Br_2NO_2$: C, 33.4; H, 2.8%) from light petroleum-benzene eluates; small amounts of bisbenzyl ether from benzene eluates; and finally *1,2-bis(hydroxymethyl)-3,6-dibromo-4,5-dimethylbenzene* (1.6 g, mp 225—226°C; Found: C, 37.1; H, 3.8%. Calcd for $C_{10}H_{12}Br_2O_2$: C, 37.0; H, 3.7%) from diethyl ether-ethanol eluates.

Direct crystallization of the latter nitration product from ethanol gave *1,2-bis(nitroxymethyl)-3,6-dibromo-4,5-dimethylbenzene* (mp 121—123°C) as white needles. IR: 847, 868, 940, 1180, 1274, 1280, 1629, and 1640 cm^{-1}, PMR: 7.41 (CH_3) and 4.23 τ (CH_2).

Found: C, 29.1; H, 2.7; N, 6.6%. Calcd for $C_{10}H_{10}Br_2N_2O_6$: C, 29.0; H, 2.4; N, 6.8%.

ii) A light yellow product (5 g) from the nitration of dibromoisodurene was chromatographed on alumina to give the recovered starting material (0.9 g) and *2,6-dibromo-3,4,5-trimethylbenzyl nitrate* (0.5 g, mp 111—112°C; Found: C, 34.3; H, 3.3%. Calcd for $C_{10}H_{11}Br_2NO_3$: C, 34.0; H, 3.1%) from light petroleum eluates. Light petroleum-benzene eluted a mixture of bisbenzyl ethers, most of which was composed of *bis(3,5-dibromo-2,4,6-trimethylbenzyl) ether* (0.3 g, Found: C, 40.6; H, 3.7%. Calcd for $C_{20}H_{22}Br_4O$: C, 40.2; H, 3.7%), and ether-ethanol eluted benzyl alcohol fraction, the major component of which was identified as *3,5-dibromo-2,4,6-trimethylbenzyl alcohol* (1.3 g, Found: C, 38.9; H, 4.2%. Calcd for $C_{10}H_{14}Br_2O$: C, 38.7; H, 4.6%). A greater part of 2,6-dibromo-3,4,5-trimethylbenzylic compounds was lost during elution.

iii) Chromatography of the nitration product from dibromoprehnitene (5 g) gave *5,6-dibromo-2,3,4-trimethylbenzyl nitrate* (0.7 g, Found: C, 34.0; H, 3.4; N, 3.9%. Calcd for $C_{10}H_{11}Br_2NO_3$: C, 34.0; H, 3.1; N, 4.0%) as colorless plates from light petroleum eluates; *bis(5,6-dibromo-2,3,4-trimethylbenzyl) ether* (0.2 g, Found: C, 39.7; H, 3.3%. Calcd for $C_{20}H_{22}Br_4O$: C, 40.2; H, 3.7%) from light petroleum-benzene eluates; an unidentified carbonyl compound from benzene-ether eluates (0.4 g, IR: 1625, 1735, and 3300—3400 cm^{-1}); and finally *5,6-dibromo-2,3,4-trimethylbenzyl alcohol* (1.2 g, Found: C, 39.0; H, 4.3%. Calcd for $C_{10}H_{14}Br_2O$: C, 38.7; H, 4.6%) from ethanol eluates.

By a similar treatment, the product (5 g) from dichloroprehnitene gave *5,6-dichloro*-2,3,4-*trimethylbenzyl nitrate* (0.5 g, Found: C, 45.2; H, 4.3%. Calcd for $C_{10}H_{11}Cl_2NO_3$: C, 45.5; H, 4.2%) and unchanged starting material (0.5 g) from light petroleum eluates. Light petroleum-benzene mixture eluted small amounts of nitro compound and *bis(5,6-dichloro*-2,3,4-*trimethylbenzyl) ether* (0.4 g, Found: C, 58.2; H, 5.5%. Calcd for $C_{20}H_{22}Cl_4O$: C, 57.2; H, 5.3%), and ether eluted an unidentified carbonyl compound (0.6 g, mp 178—179°C; Found: C, 60.8; H, 6.8%; IR: 3400, 1620, 1360, 1270, 1220, 1075, 1040, 1010, 900, 845, and 765 cm^{-1}). *5,6-Dichloro-2,3,4-trimethylbenzyl alcohol* (0.9 g, Found: C, 55.8; H, 5.8%. Calcd for $C_{10}H_{12}Cl_2O$: C, 54.8; H, 5.5%) was obtained as colorless plates from ethanol eluates.

NOTES

BULLETIN OF THE CHEMICAL SOCIETY OF JAPAN, VOL. 44, 2254—2255 (1971)

The Spectrophotometric Determination of Nickel(II) in a Solution Containing Cobalt(II), Utilizing EDTA and Bismuth as the Masking Reagent and the Demasking Reagent

Katsumi YAMAMOTO, Kousaburo OHASHI, and Ichiro HIRAKO
Department of Chemistry, Faculty of Science, Ibaraki University, Mito, Ibaraki
(Received May 11, 1970)

When hydrogen peroxide is added to a solution mixture of cobalt(II)-EDTA and nickel(II)-EDTA, the former chelate is easily oxidized to the cobalt(III)-EDTA chelate. This mixture in an acidic solution releases nickel(II) upon the addition of a bismuth(III) solution as the result of the nickel(II) in the EDTA chelate being replaced by bismuth(III), because, at pH 2.0, the apparent stability constants of nickel(II)-EDTA and bismuth(III)-EDTA $\log K'$ are 6.1 and 8.6 respectively.[1] Consequently, the exchange reaction between nickel(II)-EDTA and bismuth(III) should thermodynamically proceed almost quantitatively. The cobalt(III)-EDTA chelate does not participate in such an exchange reaction and is not replaced by bismuth(III). When the pH rises above 2.0, the difference in the apparent stability constants gradually decreases; consequently, the exchange is not quantitative. On the other hand, at a pH below 2.0, the formation of the bismuth(III)-EDTA chelate is not complete.

After the above exchange reaction had taken place, 4-(2-pyridylazo)-resorcinol(PAR) was added to the reaction mixture at pH 9.5, and the absorbance of the nickel(II)-PAR chelate was measured at 496 nm.

Bismuth(III) also reacts with PAR under these conditions, but the resulting bismuth(III)-PAR chelate is converted to the bismuth(III)-EDTA chelate by the addition of EDTA. On the other hand, the nickel(II)-PAR chelate, once formed, is stable upon the addition of EDTA.[2]

Thus, trace amounts of nickel(II) in a solution containing cobalt(II) can be determined sensitively by this method, although the procedure for determination is slightly complicated.

Experimental

Apparatus. All the spectrophotometric measurements were made with a Hitachi EPS-3-type recording spectrophotometer, using a 1-cm quartz cell. All the pH measurements were conducted with a Mitamura pH-mV meter.

Reagents. Cobalt and nickel metals with a purity of 99.99% were employed as the perchlorates. A bismuth(III) stock solution was prepared by dissolving GR-grade nitrate salt in a solution containing 1.0 N free nitric acid. Commercial PAR was used as the colorimetric reagent for nickel (II). All the other reagents were GR-grade materials.

Procedure. A series of nickel(II)-EDTA solutions of appropriate concentrations containing cobalt(II)-EDTA were placed in a 10-m*l* measuring flask; 0.5 m*l* of 30% hydrogen peroxide was then added. The pH was maintained at about 8.0 with a 0.2 N sodium hydroxide solution. To completely oxidize the cobalt(II)-EDTA chelate, the reaction mixture was allowed to stand for 15—20 min at 50°C. A 2-m*l* portion of a 5.86×10^{-4} M bismuth(III) was then added, and the pH was maintained at 2.0 with 0.2 N nitric acid and 0.2 N sodium hydroxide so that the exchange reaction proceeded in an acidic solution. The reaction mixture was warmed in a water bath at about 70°C for 40 min to complete the exchange reaction. To destroy the excess hydrogen peroxide, 1 m*l* of a 0.5 M sodium sulfite solution was added. After cooling with ice water to prevent the reversal of the reaction between bismuth(III)-EDTA and nickel(II), 1 m*l* of 0.047 M sodium borate and 1 m*l* of 2.00×10^{-3} M PAR were added. Any excess bismuth(III) present also reacts with PAR. Therefore, after the solution had stood for 5—10 min, a 2-m*l* portion of 2.2×10^{-2} M EDTA was added to convert the bismuth(III)-PAR chelate into the bismuth-(III)-EDTA chelate. Absorbance measurements were made at 496 nm against a solution containing the same concentration of PAR as a blank.

In the above procedure, if the addition of bismuth(III) is omitted and the PAR solution is added directly to the nickel(II)-EDTA complex solution, the nickel(II)-PAR chelate is not formed, for the apparent stability constant of the nickel(II)-EDTA chelate is larger than that of the nickel-(II)-PAR chelate.

Results

Absorption Spectra. The absorption curves of PAR and the nickel(II)-PAR chelate are shown in Fig. 1. PAR shows a maximum absorption at 415 nm, and the reddish nickel(II)-PAR chelate, at 496 nm.

Effect of the Heating Time on the Exchange Reaction. The exchange reaction between the nickel(II)-EDTA chelate and bismuth(III) is very slow at room temperature; it requires 40 min at pH 2.0 and 70°C to proceed quantitatively under the above experimental conditions.

Decomposition of Hydrogen Peroxide. The excess hydrogen peroxide, which destroys the nickel(II)-PAR chelate, must be decomposed before the addition of PAR to a reaction mixture. It was impossible to decompose the hydrogen peroxide completely by heating it for 40 min at 70°C. Thus, sodium sulfite was used to decompose the excess hydrogen peroxide.

1) A. Ringbom, "Complexation in Analytical Chemistry," Interscience Pub., New York (1963), p. 360.

2) Yoshio Shijo and Tsugio Takeuchi, *Bunseki Kagaku*, **14**, 511 (1965).

Table 1. Determination of nickel(II) in the presence of cobalt(II)

Amount taken Ni(II) (M)	Amount added Co(II) (M)	Molar ratio Co(II)/Ni(II)	Ni(II) found (M)	Error (%)
1.95×10^{-6}	5.04×10^{-6}	2.58	1.90×10^{-6}	−2.6
4.00×10^{-6}	2.00×10^{-5}	5.00	4.01×10^{-6}	+0.25
4.00×10^{-6}	3.90×10^{-5}	9.75	5.51×10^{-6}	+37.8
6.31×10^{-6}	1.59×10^{-5}	2.52	6.53×10^{-6}	+0.63
8.31×10^{-6}	8.10×10^{-6}	0.98	8.24×10^{-6}	−0.84
9.30×10^{-6}	2.38×10^{-5}	2.56	9.33×10^{-6}	+0.32
1.48×10^{-5}	4.12×10^{-5}	2.78	1.42×10^{-5}	−4.5

Table 2. Determination of nickel(II) in the presence of divers ions

Ion	Amount added (M)	Molar ratio M/Ni(II)	Ni(II) (M)		Error (%)
			Taken	Found	
Al(III)	4.20×10^{-5}	10.5	4.00×10^{-6}	4.02×10^{-6}	+0.50
Cd(II)	1.00×10^{-5}	2.5	4.00×10^{-6}	3.90×10^{-6}	−2.5
Cu(II)	5.00×10^{-6}	1.25	4.00×10^{-6}	4.01×10^{-6}	+0.25
Cu(II)	1.10×10^{-5}	2.75	4.00×10^{-6}	4.80×10^{-6}	+20.0
Hg(II)	5.00×10^{-5}	12.5	4.00×10^{-6}	4.01×10^{-6}	+0.25
Mn(II)	2.51×10^{-5}	6.28	4.00×10^{-6}	a)	
Pb(II)	1.00×10^{-5}	2.5	4.00×10^{-6}	4.01×10^{-6}	+0.25
Zn(II)	2.80×10^{-4}	70.0	4.00×10^{-6}	3.93×10^{-6}	−1.8

a) Very much interfere

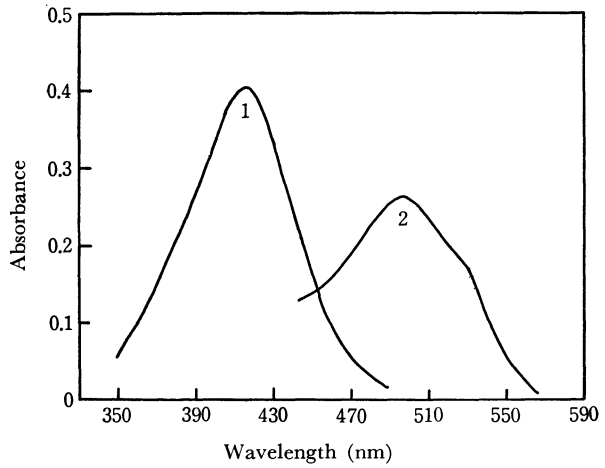

Fig. 1. Absorption spectra of PAR and Ni(II)-PAR chelate.
1. PAR 1.11×10^{-5} M
2. Ni(II)-PAR chelate 3.56×10^{-6} M
pH=9.5

With the addition of 1 ml of 0.5 M sodium sulfite to a reaction mixture, the change in the absorbance was not appreciable.

Concentration of EDTA. Bismuth(III) forms a reddish chelate with PAR, so a large excess of free bismuth(III) in a reaction mixture interferes seriously. Such an interference, however, can be avoided by using EDTA as a masking agent. EDTA displaces PAR easily from the bismuth(III)-PAR chelate. The addition of EDTA is also necessary for the masking of some foreign interfering elements, for example, cadmium(II), copper(II), and zinc(II). A 2-ml portion of 2.2×10^{-2} M EDTA was used as a masking agent.

Determination of Nickel(II). The nickel(II) was determined by the procedure described above. Beer's law was obeyed within the concentration range of 1.95×10^{-6} M to 1.48×10^{-5} M of nickel(II). The molar extinction coefficient was 7.3×10^{4}, and the sensitivity was very high. Table 1 shows the results of determinations in the presence of cobalt(II). When the concentration of the cobalt(II) becomes about ten times as much as the nickel(II), a large error was observed.

Effect of Diverse Ions. The effects of diverse ions on the colorimetric determination of nickel(II) utilizing the nickel(II)-PAR chelate were previously investigated by Shijo.[2] In the present experiments, the authors examined the effect of diverse ions which are highly sensitive in their reactions with PAR. These results are shown in Table 2. It was found that the interference of manganese(II) and copper(II) was very pronounced, but other metal ions did not interfere.

BULLETIN OF THE CHEMICAL SOCIETY OF JAPAN, VOL. 44, 2256 (1971)

The SCF MO Calculation of the g Value for the H_2NO Radical

Tetsuo MORIKAWA, Osamu KIKUCHI, and Kazuo SOMENO*

Department of Chemistry, Tokyo Kyoiku University, Otsuka, Tokyo

* *Government Chemical Industrial Reseaech Institute, Tokyo, Shibuya-ku, Tokyo*

(Received September 21, 1970)

In our previous papers,[1] an approximate open shell SCF MO method with the CNDO approximation[2] was proposed and applied to quantitative discussions of the electronic structure and ESR parameters of the aliphatic nitric oxide radicals. The results on the g tensor of the H_2NO radical showed that the value of g_{yy}, the principal value of g along the N–O bond, was somewhat unsatisfactory. The present note will show that improved results for the g_{yy} of the H_2NO radical can be obtained by a modification of the evaluation of electron repulsion integrals or bonding parameters.

The principal values of the g tensor for the H_2NO radical, as calculated by Stone's formula,[3] are listed in Table 1. The results are those obtained by the SCF MO CNDO or INDO[5] approximation, where the values of bonding parameters given in the original papers of Pople and Segal[2] were used.[6] A better agreement with the experimental data was obtained by both these calculation methods than the previous one. The value of g_{yy} could be especially improved by the INDO calculation. This is because of the increase in the excitation energy from the non-bonding orbital of the oxygen atom to the odd-orbital and the decrease in spin density on the oxygen atom.

TABLE 1. PRINCIPAL VALUES OF g TENSOR FOR H_2NO

	INDO[a]	CNDO/2[a]	CNDO/2[b]	Exp.[c]
g_{xx}	2.0045	2.0047	2.0050	2.0061
g_{yy}	2.0091	2.0104	2.0113	2.0089
g_{zz}	2.0023	2.0023	2.0023	2.0027
$g_{av.}$	2.0053	2.0058	2.0062	2.0059

a) Bonding parameters used are those in Ref. 2.
b) Results in Ref. 1.
c) Values for di-*t*-butyl nitric oxide in Ref. 4.

The dependence of the g tensor on the molecular geometry of the radical is a subject of importance in the present theoretical study. The g_{yy} of the H_2NO radical is very sensitive to the variation in the N–O bond length and the HNH bond angle, but the g_{yy} is not. The value of g_{yy} obtained by the INDO calculation, for example, changes from 2.0083(1.20 Å) to 2.0119(1.30 Å) at the fixed HNH angle of 120°. This comes from the fact that the oxygen lone-pair orbital, which makes a large contribution to g_{yy}, is very sensitive to these changes in molecular geometry. The theoretical estimation of g tensors must, therefore, be carried out on the basis of a careful examination of the molecular geometry of a radical. For the H_2NO radical, the CNDO or the INDO method gives the minimum energy near the assumed structure of this radical, shown in Fig. 1. As was pointed out by Segal,[7] the CNDO method leads to some success in the evaluation of the equilibrium bond length. Therefore, the present results on the g tensor for the radical assuming the structure are acceptable.

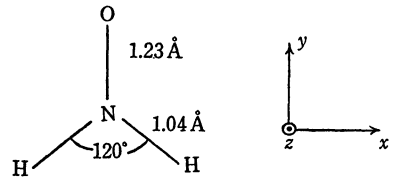

Fig. 1. Assumed stucture of H_2NO.

It may be concluded that the original CNDO/2 and INDO parametrizations give good theoretical results on the g value for the aliphatic nitric oxide radical. However, ambiguity still remains as to the applicability of these methods to other radicals. We have, though, applied the methods to several σ-type radicals and observed that the calculated principal values of the g-tensors of these σ-type radicals show good agreement with the experimental values.[8] Therefore, the theoretical investigation described here may be applicable to the estimation of g values of all other radicals.

1) O. Kikuchi, This Bulletin, **42**, 47, 1187 (1969).
2) J. A. Pople and G. A. Segal, *J. Chem. Phys.*, **43**, S129, S136 (1965).
3) A. J. Stone, *Proc. Roy. Soc., Ser. A*, **271**, 424 (1963).
4) O. H. Griffith, D. W. Cornell, and H. M. McConnell, *J. Chem. Phys.*, **43**, 2909 (1965).
5) J. A. Pople, D. L. Beveridge, and P. A. Dobosh, *ibid.*, **47**, 2026 (1967).
6) In our previous CNDO calculations, the values of the bonding parameters were adjusted empirically and were different from those of Pople and Segal.
7) G. A. Segal, *ibid.*, **47**, 1876 (1967).
8) T. Morikawa, O. Kikuchi, and K. Someno, to be published.

BULLETIN OF THE CHEMICAL SOCIETY OF JAPAN, VOL. 44, 2257—2258 (1971)

The Roles of Thiyl Radicals in the Radiolysis of a Mixed Aqueous Solution of Cysteine and Formate— Hydrogen Abstraction from Formate and the Formation of Carbon Dioxide

Makio MORITA, Katsuro SASAI, Makoto TAJIMA, and Masao FUJIMAKI
Department of Agricultural Chemistry, Faculty of Agriculture, The University of Tokyo, Hongo, Tokyo

(Received October 7, 1970)

Attempts were made to elucidate the role of thiyl radicals in the γ-radiolysis of aqueous solutions containing L-cysteine and formate, and the evidence was obtained for the abstraction of hydrogen and the acceleration of the CO_2 formation from formate by cysteine thiyl radicals.

Experimental

Triply-distilled water (pH 5.0) containing formic acid and cysteine was degassed in Pyrex ampoules and irradiated by a ^{60}CO γ-ray source (dose rate: 9×10^4 rads·h^{-1}, dose: 9×10^4 rads).[1] Amino acids were analyzed on an amino-acid analyzer. The gaseous products were analyzed as has been described.[2] The tritium liberated from ^3H-formate was measured as has been described.[3] The oxalic acid was estimated by measuring the permanganate reduction in acidic media (2 N sulfuric acid) at room temperature. The permanganate was colorimetrically determined at 525 nm. Before the analysis, the cysteine was removed with cation exchange resin.

Results and Discussion

In the radiolysis of aqueous solutions under deaerated and neutral conditions, formate reacts with hydroxyl radicals (OH) to yield carboxyl radicals ($\cdot CO_2^-$) (1), and $\cdot CO_2^-$ dimerized to oxalic acid[4,5] (2):

$$OH + HCO_2^- \xrightarrow{k_1} \cdot CO_2^- \quad (1)$$

$$2\cdot CO_2^- \longrightarrow HCO_2CO_2^- \quad (2)$$

Cystein (CySH) reacts with OH to yield cysteine thiyl radicals (CyS·) (3) and then reacts with e^-_{aq} to yield hydrogen sulfide and alanyl radicals (Cy·)(4). Cy· reacts with another molecule of cysteine to yield alanine (CyH) and CyS· (5). The CyS· produced through both the reactions dimerizes to cystine (CySSCy) (6).[6-8]

$$OH + CySH \xrightarrow{k_3} CyS\cdot \quad (3)$$

$$e_{aq}^- + CySH \longrightarrow Cy\cdot + H_2S \quad (4)$$

$$Cy\cdot + CySH \longrightarrow CyH + CyS\cdot \quad (5)$$

$$2CyS\cdot \longrightarrow CySSCy \quad (6)$$

The other reactions are considered to be less important than the reactions described above.[4-8]

In this investigation we have studied the radiolysis of a mixed solution of formate and cysteine. As is shown in Fig. 1, the yields of hydrogen sulfide and alanine were not affected by the formate. This is because, at pH 5.0, only 0.6—7% of formate exists in its acid form, and this form reacts efficiently with e_{aq}^-.

Hydroxyl radicals (OH) are competed for by the formate ion and cysteine ($k_1=2.9\times10^9$ M^{-1} sec,$^{-1}$[9] $k_3=3\times10^9$ M^{-1} sec^{-1} [10]). However, oxalic acid was not produced at all in the presence of 10^{-3} M cysteine at three concentrations of formate (10^{-3}, 10^{-2}, and 10^{-1} M), as is shown in Fig. 1. This indicates that, at 10^{-3} M, cysteine completely scavenges the $\cdot CO_2^-$ (7):

$$\cdot CO_2^- + CySH \xrightarrow{k_7} HCO_2^- + CyS\cdot \quad (7)$$

If the $\cdot CO_2^-$ is completely converted to CyS·, the OH radicals which have reacted with formate by reaction (1) will also produce CyS· and an unchanged yield of cystine may be anticipated, as is observed in the solution containing 10^{-3} and 10^{-2} M of formate (Fig. 1).

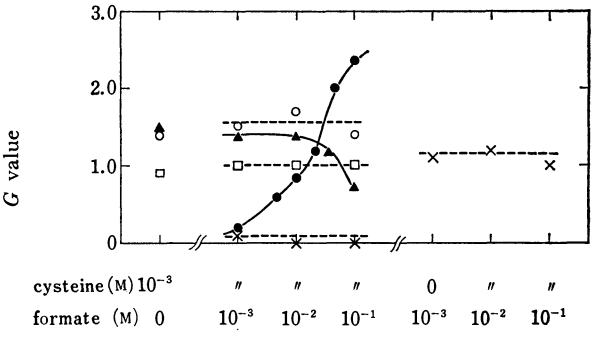

Fig. 1. Yields of the products from crysteine—formate solutions of various compositions.
×···×: oxalic acid, □···□: H_2S, ○···○: alanine, ●···●: CO_2, ▲···▲: cystine.
pH 5, dose: 9×10^4 rads.

It is well known that thiyl radicals abstract hydrogen from aldehydes.[11] In order to test whether or not

1) M. Fujimaki and M. Morita, *Agr. Biol. Chem.*, (Tokyo), **32**, 572, (1968).
2) M. Tajima, M. Morita, and M. Fujimaki, *ibid.*, **33**, 1277, (1969).
3) M. Morita and M. Fujimaki, This Bulletin, **41**, 1109, (1968).
4) W. M. Garrison, W. Bennett, and S. Cole, *Radiat. Res.*, **9**, 647, (1958).
5) T. J. Hardwick, *ibid.*, **12**, 5 (1960).
6) V. G. Wilkening, M. Lal, M. Arends, and A. Armstrong, *Can. J. Chem.*, **42**, 1209 (1967).
7) V. G. Wilkening, M. Lal, M. Arends, and A. Armstrong, *J. Phys. Chem.*, **72**, 185 (1968).
8) P. Markakis and A. L. Tappel, *J. Amer. Chem. Soc.*, **82**, 1613 (1960).
9) I. Kraljic and C. N. Trumbore, *ibid.*, **87**, 2547 (1965).
10) A. E. Samahy, H. L. White, and C. N. Trumbore, *ibid.*, **86**, 3177 (1964).
11) S. G. Cohen, J. D. Berman, and S. Orman, *Tetrahedron Lett.*, **1962**, 43.

Table 1. ^{3}H-liberation into water from ^{3}H-formate in the γ-radiolysis of its deaerated aqueous solution and addition effect of cysteine on it

Concn. of formate	cpm in 0.5 ml water distilled	
	Without cysteine	With 10^{-3} M cysteine
10^{-3} M	2210	1749
10^{-2} M	2372	13820
10^{-1} M	2699	136562

^{3}H-formate (50 μCi (nominal)/mmol) was used.
dose: 9×10^4 rads.

CyS· abstracts hydrogen of the formate, a tracer experiment using ^{3}H-formic acid was made. As is shown in Table 1, the liberation of tritium from formate to water was almost constant for the three concentrations of formate in the absence of cysteine, but it markedly increased with the concentration of formate in the presence of 10^{-3} M cysteine, the rate of the increase being approximately proportional to the formate concentration. This can be explained by the hydrogen abstraction by CyS· from the formate (8):

$$CyS\cdot + HCO_2^- \xrightarrow{k_8} CySH + \cdot CO_2^- \qquad (8)$$

The reaction is the reverse of (7), and CyS· and $\cdot CO_2^-$ will be mutually converted by (7) and (8). If k_8 is much smaller than k_7, $[\cdot CO_2^-]$ will be much smaller than [CyS·], yielding no oxalic acid. However, the rate of (8) and the rate of the liberation of hydrogen from formate will increase proportionally with the formate concentration, as is observed. As is shown in Fig. 1, the yield of cystine in the presence of 10^{-1} M formate was lowered, while that of carbon dioxide reciprocally increased. This result may be explained as follows: at high formate concentrations, reaction (6) may compete with a reaction of CyS· which produces CO_2. The species which reacts with CyS· to yield carbon dioxide may be the $\cdot CO_2^-$ or the $\cdot CO_2^-$-formate complex.[12]

12) N. Getoff, F. Guetlbauer, B. O. Schenck, and R. Wolgast, *Tetrahedron Lett.*, **1966**, 2725.

BULLETIN OF THE CHEMICAL SOCIETY OF JAPAN, VOL. 44, 2258—2259 (1971)

Electrooxidation of α-Methoxy-γ,γ-Dimethylaconic Acid

Sigeru Torii, Takuya Furuta, Teruo Miyaoka, Hidenori Sako, Hideo Tanaka, and Kenji Uneyama

Department of Industrial Chemistry, Okayama University, Okayama

(Received December 7, 1970)

Recently anodic alkoxylation of alkenes has been investigated extensively.[1] However, few studies have been made on the application of the reaction to cyclic olefins[1] or cyclic α,β-unsaturated carboxylic acids.[2] It is of interest that the acids have two reaction points (olefinic double bond and carboxy group) which may suffer anodic oxidation. Further one-electron oxidation of the acyloxy radical to an acyloxy cation can be possible since decarboxylation of the radical is not favorable.[3] Thus, we have examined the anodic oxidation of α-methoxy-γ,γ-dimethylaconic acid(I) in methanol as a model reaction of α,β-unsaturated cyclic carboxylic acids.

Experimental

Electrolysis of I. A stirred mixture containing 2.2 g of I[4] and 0.2 m*l* of sulfuric acid in 70 m*l* of commercial grade methanol was electrolyzed[5] using 3 cm^2 bright Pt electrodes for 3 hr at 20°C. Anode potential of electrolysis was 2.2±0.1 *vs.* SCE at current density of 0.1 A/cm^2. Under the electrolysis conditions, starting carboxylic acid I was almost completely consumed. The acidic portion (1.36 g) was recrystallized from benzene - ethanol to give 1.06 g of trimethoxy compound II and 0.30 g of IV.

The structural assignment of II was made by elemental analysis and IR and NMR spectra; mp 192.5—193°C, IR (Nujol) 1795 (lactone C=O) and 1760 (COOH) cm^{-1}, NMR (methyl ester) in $CDCl_3$, τ 8.53 (3H, s, CH_3), 8.42 (3H, s, CH_3), 6.50 (3H, s, CH_3O), 6.47 (3H, s, CH_3O), 6.37 (3H, s, CH_3O), 6.21 (3H, s, CO_2CH_3), M^+, *m/e* 262 (methyl ester).

Found: C, 47.99; H, 6.59%. Calcd for $C_{10}H_{16}O_7$: C, 48.39; H, 6.50%.

The structure of IV was assigned by mp, IR spectrum and vpc retention time of its methyl ester compared with authentic samples.[6]

The neutral portion (0.24 g) was fractionated by vpc using a SE-30 column at 150°C to give 0.20 g of carbonate III. The structure of III was established by spectral and elemental analyses; IR (neat) 1780, 1750 (C=O), 1210, 1170, 1130 cm^{-1}, NMR ($CDCl_3$) τ 8.35 (6H, s, gem. CH_3), 6.26 (3H, s, CH_3O), 6.10 (3H, s, CH_3O), M^+-60, *m/e* 172.

Found: C, 46.29; H, 5.43%. Calcd for $C_9H_{12}O_7$: C, 46.59; H, 5.21%.

Electrolysis of II. A mixture of 0.30 g of II and 0.08

1) N. L. Weinberg and H. R. Weinberg, *Chem. Revs.*, **68**, 449 (1968); H. Schafer, *Chem.-Ing-Techn.*, **41**, 179 (1969); *Angew. Chem.*, **81**, 940 (1969), and references cited therein.

2) No report on anodic oxidation of cyclic α,β-unsaturated carboxylic acids except for benzoic acid has been found in literature.

3) B. C. L. Weedon, "Advances in Organic Chemistry," Vol. 1, Interscience Publishers, Inc., N. Y. (1960).

4) S. Torii, S. Endo, H. Oka, Y. Kariya, and A. Takeda, This Bulletin, **41**, 2707 (1968).

5) Electrolyses were carried out by a procedure similar to that described in the paper: A. Takeda, S. Wada, S. Torii and Y. Matsui, This Bulletin, **42**, 1047 (1969).

6) A. Takeda and S. Torii, *Memoirs of School of Engineering, Okayama Univ.*, **1**, 44 (1966).

m*l* of sulfuric acid in 30 m*l* of commercial grade methanol was electrolyzed with a terminal voltage of 15 V at a current density of 0.1 A/cm² (anode cell voltage, 1.95±0.05 *vs.* SCE). After recovery of 0.20 g of unchanged II, 0.05 g of neutral materials obtained was subjected to preparative vpc (SE-30, 3 m, 150°C) to afford 0.03 g of III.

Results and Discussion

Products were α,α,β-trimethoxy-γ,γ-dimethylparaconic acid(II) (36%), terebic acid(IV) (16%), and γ,γ-dimethyl-α,β-carbonyldioxy-α,β-dimethoxybutyrolactone(III) (7.3%). Predominant formation of acidic compounds (II and IV) as compared with neutral compound III indicates that the olefinic double bond in I undergoes oxidation more readily than carboxy group. Trimethoxy compound II would result from two electron oxidation of I followed by methanolysis. Carbonate III would be produced from further oxidation of II, since electrolysis of II in a methanol-sulfuric acid mixture afforded III as the main neutral product.

Table 1. Products and their yields of the anodic oxidation of α-methoxy-γ,γ-dimethylaconic acid (I) in MeOH

Product	I[b]	II	III	IV
Yield[a] (%)	trace	36	7.3	16

a) Yield based on carboxylic acid I.
b) Recovered I.

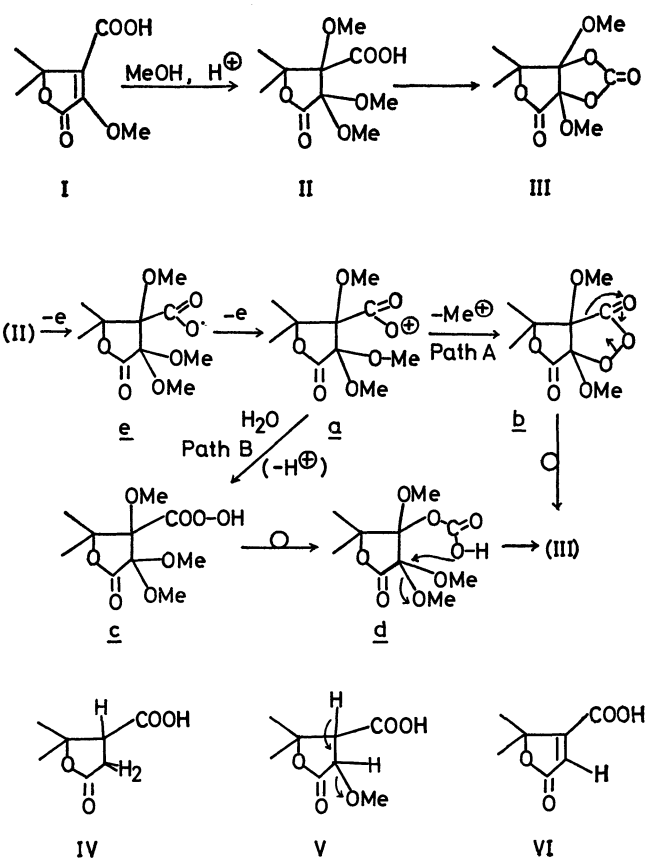

Scheme 1

A tentative mechanism for the formation of carbonate III is described in scheme 1. Assuming formation of acyloxonium ion **a**[7] in the carbonation reaction of II, one can rationalize the result by postulating the rearrangement of the peroxide intermediates (**b** or **c**), *viz.* (Path A) intramolecular peroxide rearrangement[8] of **b** to III and (Path B) peracid rearrangement of **c** and reclosure of **d** to III. The mechanism of the formation of terebic acid IV can involve the following processes: i) electrochemical reduction of I to V, ii) demethoxylation with the aid of acid, and iii) further reduction of VI.[9] We found that IV was not detected by vpc analysis when I was electrolyzed in an anode compartment separated by a glass filter and VI could be subjected to reduction for a very short period without separation of electrolysis compartments.

Further details of the carbonation mechanism can not be deduced from these preliminary results.

7) P. G. Gassman and F. V. Zalar, *J. Amer. Chem. Soc.*, **88**, 2252 (1966); T. Shono, I. Nishiguchi, S. Yamane, and R. Oda, *Tetrahedron Lett.*, **1969**, 1965.
8) D. B. Denney, *J. Amer. Chem. Soc.*, **78**, 590 (1956).
9) R. Fitting and B. Frost, *Ann. Chem.*, **226**, 370 (1884).

BULLETIN OF THE CHEMICAL SOCIETY OF JAPAN, VOL. 44, 2260—2261 (1971)

Bis(triphenylphosphine)-π-cyclopentadienyl-cobalt(I) and -rhodium(I)[1]

Hiroshi YAMAZAKI and Nobue HAGIHARA*

The Institute of Physical and Chemical Research, Wako-shi, Saitama 351

** The Institute of Scientific and Industrial Research, Osaka University, Yamada-Kami, Suita, Osaka*

(Received January 18, 1971)

Previously, we have reported the reaction of triphenylphosphine-π-cyclopentadienylcobalt diiodide with isopropylmagnesium bromide in the presence of diphenylacetylene; this afforded acetylene complexes with a π-$C_5H_5Co(PPh_3)$ moiety.[2] In our further study of this reaction, we have found that bis(triphenylphosphine)-π-cyclopentadienylcobalt(I) was the product when the reaction was carried out in the absence of diphenylacetylene.

A recent paper of Rinze *et al.*[3] describes the isolation of the same compound from the reaction of $H_3Co(PPh_3)_3$ or $HN_2Co(PPh_3)_3$ with cyclopentadiene. This report has prompted us to publish our results on the preparation and some reactions of bis(triphenylphosphine)-π-cyclopentadienylcobalt(I) and on the preparation of an analogous rhodium complex.

When triphenylphosphine-π-cyclopentadienylcobalt diiodide in benzene-ether was treated with isopropylmagnesium bromide, favorably in the presence of triphenylphosphine, a red solution resulted. Air-sensitive dark red crystals were isolated from the solution. They melted at 140—143°C with decomposition in a nitrogen-filled capillary tube. The proton NMR spectrum in C_6D_6 showed a singlet at τ 5.55 which was assigned to the five equivalent cyclopentadienyl protons, and complex bands at τ 2.1—3.2 which were assigned to the aromatic protons. On the basis of the elemental analysis, the compound was formulated as π-$C_5H_5Co(PPh_3)_2\cdot C_6H_6$ (**1**). The inclusion of a benzene molecule was confirmed by gas chromatography.

The similar treatment of triphenylphosphine-π-cyclopentadienylrhodium diiodide with isopropylmagnesium bromide in the presence of triphenylphosphine gave dark brown crystals. They are air stable in the solid state and melt at 190°C with decomposition. The infrared spectrum of the compound is almost identical with that of cobalt analogue. The proton NMR spectrum in C_6D_6 showed a singlet at τ 4.96 which was assigned to the five equivalent π-cyclopentadienyl protons and complex bands at τ 2.1—3.1 which were assigned to the aromatic protons. The detailed spectrum of the π-cyclopentadienyl protons consisted of a 1 : 3 : 3 : 1 quartet (J=0.6 Hz) showing the equivalence of ^{31}P and ^{103}Rh nuclei to couple with the protons. Elemental analysis suggested the compound to be π-$C_5H_5Rh(PPh_3)_2\cdot C_6H_6$ (**2**), analogous with the cobalt complex. Upon heating at 140°C for ten minutes under reduced pressure, the crystals turned pale brown and lost a benzene molecule to give an exact analysis for π-$C_5H_5Rh(PPh_3)_3$.

The compound (**1**) readily exchanges one triphenylphosphine with another ligand (L) and gives a complex of the type π-$C_5H_5Co(PPh_3)(L)$. When carbon monoxide was passed through the benzene solution of **1**, triphenylphosphine-carbonyl-π-cyclopentadienylcobalt (**3**)[4] was formed almost immediately; this was also described by Rinze *et al.*[3] The reactions with excess diphenylacetylene and with fumaronitrile afforded triphenylphosphine-π-cyclopentadienyl(tetraphenylcobaltacyclopentadiene) (**4**)[2] and triphenylphosphinefumaronitrile-π-cyclopentadienylcobalt (**5**)[2] respectively.

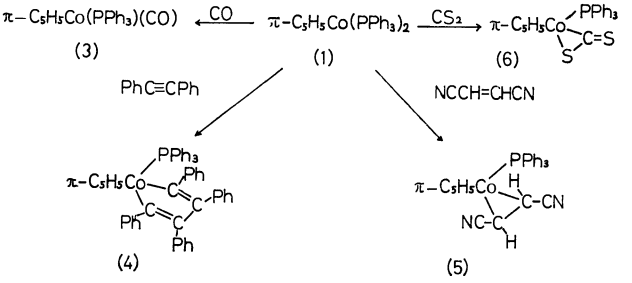

With carbon disulfide, air-stable dark red crystals with the empirical formula of π-$C_5H_5Co(PPh_3)(CS_2)$ were obtained. In the infrared spectrum of the compound, the ν(C=S) appeared at 1170 and 1155 cm^{-1}, suggesting a structure (**6**) which consists of the bonding of a type similar to that of known carbon disulfide complexes of transition metals.[5]

Studies of the reaction of rhodium compound, **2**, will be described separately.

Experimental

All the reactions were carried out in a nitrogen atmosphere. The melting points were determined on a Yanagimoto hot-stage apparatus unless otherwise stated. The proton NMR spectra were obtained on a Hitachi-Perkin Elmer R-20 spectrometer, with tetramethylsilane as the internal standard. The infrared spectra were obtained with a Jasco DS-402G spectrophotometer.

1) Presented at the 21st Annual Meeting of The Chemical Society of Japan, Suita, Osaka, April 3, 1968 (Preprints, III, p. 1972), and at the Symposium of Organometallic Compounds, Osaka, October 16, 1968 (Preprints, p. 123).

2) H. Yamazaki and N. Hagihara, *J. Organometal. Chem.*, **21**, 431 (1970).

3) P. V. Rinze, J. Lorberth, H. Nöth, and B. Stutte, *ibid.*, **19**, 399 (1969).

4) R. B. King, *Inorg. Chem.*, **5**, 82 (1966); H. G. Schuster-Wolden and F. Basolo, *J. Am. Chem. Soc.*, **88**, 1657 (1966).

5) M. C. Baird and G. Wilkinson, *J. Chem. Soc., A*, **1967**, 865; M. C. Baird, G. Hartwell, Jr., R. Mason, A. I. M. Rae, and G. Wilkinson, *Chem. Commun.*, **1967**, 92; T. Kashiwagi, N.Yasuoka, T. Ueki, N. Kasai, M. Kakudo, S. Takahashi, and N. Hagihara, This Bulletin, **41**, 296 (1968); A. J. Deeming and B. L. Shaw, *J. Chem. Soc., A*, **1969**, 1128.

The compounds π-$C_5H_5Co(PPh_3)I_2$[6] and π-$C_5H_5Rh(PPh_3)I_2$[7] were prepared according to the method described in the literature.

Bis(triphenylphosphine)-π-cyclopentadienylcobalt (1). A slurry of π-$C_5H_5Co(PPh_3)I_2$ (3.2 g) in ether (20 m*l*) and benzene (20 m*l*) was treated with isopropylmagnesium bromide (15 m*l* of a 1-mol ether solution) at room temperature. The resulting red solution was hydrolyzed with aqueous ammonium chloride, and the organic layer was dried with sodium sulfate. After filtration, the solution was concentrated and hexane was added. When the solution was kept in a refrigerator overnight, dark red crystals (1.1 g) were formed.

Found: C, 77.64; H, 5.74%. Calcd for $C_{47}H_{41}P_2Co$ (including a benzene molecule): C, 77.68; H, 5.69%.

In the presence of triphenylphosphine (1.3 g), **1** was obtained in a better yield (1.4 g) by the same procedure.

Bis(triphenylphosphine)-π-cyclopentadienylrhodium (2). According to a procedure similar to that described above, the title compound (1.3 g) was obtained from the reaction of π-$C_5H_5Rh(PPh_3)I_2$ (1.4 g) with isopropylmagnesium bromide (10 m*l* of a 1-mol ether solution) in the presence of triphenylphosphine (1.0 g) and in a mixture of benzene and tetrahydrofurane (1/1, 40 m*l*).

Found: C, 73.15; H, 5.30%. Calcd for $C_{47}H_{41}P_2Rh$ (including a benzene molecule): C, 73.24; H, 5.36%.

The crystals turned pale brown with the loss of the benzene when heated at 140°C under reduced pressure.

Found: C, 71.22; H, 5.15%. Calcd for $C_{41}H_{35}P_2Rh$: C, 71.10; H, 5.09%.

The Reaction of 1 with Carbon Monoxide. Carbon monoxide was passed through the solution of 1 (0.5 g) in benzene (15 m*l*) at room temperature. The red color immediately turned brown. The solution was chromatographed on alumina, with a benzene - hexane as the eluent. The red brown eluate was then concentrated to give red brown crystals of π-$C_5H_5Co(PPh_3)(CO)$ (**3**); mp 142—144°C (in a nitrogen-filled capillary tube (0.1 g). IR (Nujol): ν_{CO} 1915 cm^{-1}. NMR (τ in C_6H_6): 5.38 (singlet, π-C_5H_5).

Found: C, 69.91; H, 4.90%. Calcd for $C_{24}H_{20}OPCo$: C, 69.57; H, 4.87%.

The Reaction of 1 with Excess Diphenylacetylene. A mixture of **1** (1.0 g) and diphenylacetylene (0.9 g) in benzene (20 m*l*) was heated at 60°C for 10 min. The solution was chromatographed on alumina, with benzene as the eluent. The red eluate was then concentrated, and hexane was added to give red-brown crystals (0.9 g). The infrared spectrum of the crystals was identical with that of π-$C_5H_5Co(PPh_3)(PhC{\equiv}CPh)_2$(**4**).

The Reaction of 1 with Fumaronitrile. To a solution of **1** (0.4 g) in benzene (30 m*l*), fumaronitrile (0.1 g) was added at room temperature. After 10 min., the solution was concentrated and chromatographed on alumina, with a benzene - ethyl acetate mixture (**2/1**) as the eluent. After the evaporation of the solvent, the residue was recrystallized with benzene - hexane to give dark red crystals (0.19 g). The infrared spectrum of the crystals was identical with that of π-$C_5H_5Co(PPh_3)(NCCH{=}CHCN)$ (**5**).

The Reaction of 1 with Carbon Disulfide. To a solution of **1** (0.65 g) in benzene (10 m*l*), carbon disulfide (1 m*l*) was added. The resulting dark brown solution was concentrated and chromatographed on alumina, with benzene as the eluent. The chocolate-brown eluate was then concentrated, and hexane was added to give black crystals (0.18 g) of π-$C_5H_5Co(PPh_3)(CS_2)$ (**6**); mp 137—138°C (with decomp.).

Found: C, 62.33; H, 4.36; S, 13.87%. Calcd for $C_{24}H_{20}S_2PCo$: C, 62.55; H, 4.30; S, 13.63%. NMR (τ in $CDCl_3$): 5.50 (singlet, C_5H_5); 2—3 (complex bands, C_6H_5).

6) R. F. Heck, *Inorg. Chem.*, **4**, 855 (1965); R. B. King, *ibid.*, **5**, 82 (1966).

7) A. Kasahara, T. Izumi, and K. Tanaka, This Bulletin, **40**, 699 (1967).

BULLETIN OF THE CHEMICAL SOCIETY OF JAPAN, VOL. 44, 2261—2263 (1971)

Initiation Mechanism of Radiation-Induced Ionic Polymerization of Isobutene Studied by Ion Cyclotron Resonance

Masahiro IRIE, Katsuyuki AOYAGI, Koichiro HAYASHI, Junkichi SOHMA, and Teruo MIYAMAE*

Faculty of Engineering, Hokkaido University, Sapporo

** Japan Electron Optics Laboratory, Akishima, Tokyo*

(Received January 20, 1971)

Radiation induced polymerization of isobutene has been proved to proceed in cationic mechanism in liquid[1] and gas phases.[2] Investigation by high pressure mass spectrometer has been carried out to elucidate the initiation mechanism.[3] However, detailed processes of the ion-molecule reaction in isobutene, such as the role of fragment ions in the initiation, have not yet been made clear because of the difficulty to identity complex ion-molecule reactions by ordinary mass spectroscopy.

Recently, ion cyclotron resonance (ICR) technique has been successfully applied to analysis and interpretation of the complex ion-molecule reactions.[4] In this note we present the results obtained by the ICR study on isobutene and clarify the initiation mechanism of the radiation induced polymerization

1) J. J. Sparapany, *J. Amer. Chem. Soc.*, **88**, 1357 (1966).

2) H. Okamoto, K. Fueki, and Z. Kuri, *J. Phys. Chem.*, **71**, 3222 (1967).

3) V. Aquilanti, A. Galli, A. Giardini-Guidoni, and G. G. Volpy, *Trans. Faraday Soc.*, **63**, 926 (1967).

4) For examples, a) J. L. Beauchamp, L. R. Ander, and J. D. Baldeschwieler, *J. Amer. Chem. Soc.*, **89**, 4569 (1967). b) J. M. S. Henies, *ibid.*, **90**, 844 (1968). c) G. A. Gray, *ibid.*, **90**, 6002 (1968). d) M. T. Bowers, D. E. Elleman, and J. L. Beauchamp, *J. Phys. Chem.*, **72**, 3599 (1968). e) S. E. Burttrill, Jr., *J. Chem. Phys.*, **50**, 4125 (1969). f) M. T. Bowers, D. D. Ellman, and J. King, Jr., *ibid.*, **50**, 4787 (1969).

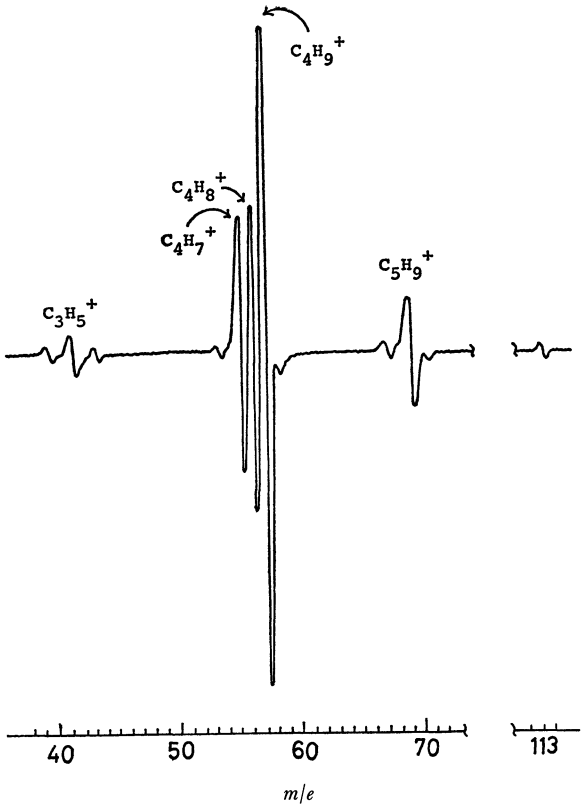

Fig. 1. Ion cycrotron single resonance spectrum of isobutene at 3×10^{-5} Torr.

in gas phase.

The ion cyclotron resonance spectrometer, which was constructed by the Japan Electron Optics Laboratory and utilized in this experiment, was a type similar to the conventional one.[4a] Isobutene was purified by passing it through a column of potassium hydroxide followed by drying with sodium-potassium alloy.

An ion cyclotron single resonance mass spectrum observed at 3×10^{-5} Torr is shown in Fig. 1. Peaks in the spectrum correspond to those obtained at 6×10^{-3} Torr by a high pressure mass spectrometer.[3] The relative intensity of the parent-plus-one ion ($m/e=57$) is about fifty percent of that of total ions at 3×10^{-5}. It should be mentioned that the dimer ion ($m/e=113$) is also observed at this pressure.
Such ICR data indicate that ion-molecule reactions take place at very low pressures.

It was found that abundance of ions depends upon pressure, and the dependence observed from ICR differs from that of high pressure mass spectroscopy.[3] The most remarkable contrast is that relative intensities of $C_4H_8^+$ and $C_4H_9^+$ show minimums at 6.5×10^{-5} and 9×10^{-5} Torr, respectively, though no minimum appears in mass spectroscopy. The intensity of $C_4H_9^+$ decreases with the increase of pressure from 3.0×10^{-5} to 9.0×10^{-5} Torr, but at higher pressures it increases with the increase of pressure. The pressure dependence of $C_3H_3^+$ also differs from that observed by the high pressure mass spectrometer. In contrast to $C_4H_9^+$, formation of $C_3H_3^+$ reaches a maximum at 9×10^{-5} Torr.

The ion-molecule reactions of these ions were studied

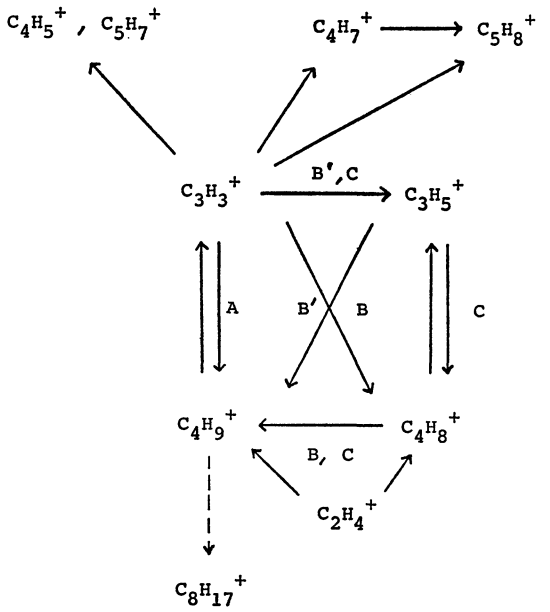

Fig. 2. Reaction scheme in isobutene observed by the ion cyclotron double resonance. Arrows show the ion-molecule reactions with isobutene. Solid arrows mean the reaction demonstrated by the ICR double resonance and broken arrow is a process deduced from the results.

by double resonance experiments. The over-all scheme is summarized in Fig. 2. $C_4H_9^+$ reacts with isobutene through two processes, the addition reaction to form dimer ion ($m/e=113$)[5] and the decomposition reaction to $C_3H_3^+$. The decomposition reaction is a sole process to produce secondary $C_3H_3^+$. Thus, the increase of the intensity of $C_3H_3^+$ with the increase of pressure implies that the decomposition of $C_4H_9^+$ by collision with isobutene into $C_3H_3^+$ is the dominant process at pressure below 9×10^{-5} Torr. Simultaneous appearance of the maximum of $C_3H_3^+$ with minimum of $C_4H_9^+$ at 9×10^{-5} Torr suggests additional paths besides the direct production of $C_4H_9^+$ from $C_3H_3^+$. The paths, including the direct production, are indicated as A, B, B', and C in Fig. 2. Each step of these paths has been confirmed by double resonance experiments. The indirect paths involve one or two intermediates and the reactions through these paths are higher orders, *viz.*, the second order for paths of either B or B', the third order for path C. Since the reactions of the higher orders become effective at higher pressures, contribution of the indirect paths to the production of $C_4H_9^+$ is more enhanced at higher pressures than at lower pressures. The maximum in pressure variation of the formation of $C_4H_9^+$ can be explained by assuming the competition among the reactions through the various paths described in Fig. 2.

$C_4H_9^+$ has been considered to be produced by a proton transfer from the parent ion.[1,2] Study of high pressure mass spectroscopy[3] suggested that a proton transfer from the other primary ions was also important to account for a large intensity of $C_4H_9^+$.

5) We could not confirm the process producing $C_8H_{17}^+$ by the double resonance experiment, because the abundance of $C_8H_{17}^+$ was very small.

The double resonance experiments clearly show that $C_4H_9^+$ is produced from $C_2H_4^+$, $C_3H_3^+$, $C_3H_5^+$, and $C_4H_8^+$. These fragment ions must play important roles in the initiation process of the polymerization induced by γ-irradiation in gas phase, because the ion-molecule chain which starts from *t*-butyl ion ($m/e=57$) is possibly the first step of polymerization.

BULLETIN OF THE CHEMICAL SOCIETY OF JAPAN, VOL. 44, 2263—2264 (1971)

Dipolar Interaction in TEMPAD Biradical

Jun YAMAUCHI, Teruaki FUJITO,* Akira NAKAJIMA,* Hiroaki O. NISHIGUCHI*, and Yasuo DEGUCHI*

The Institute for Chemical Research, Kyoto University, Uji

** Department of Chemistry, Faculty of Science, Kyoto University, Kyoto*

(Received February 6, 1971)

There have been a number of investigations regarding the magnetic properties of organic solids, especially those of stable free radicals. In addition to the measurement of the paramagnetic susceptibility, the electron spin resonance (ESR) has been used in the study of triplet states of aromatic molecules after the first successful experiments by Hutchison and Mangum[1] and by van der Waals and de Groot.[2] A molecule in a triplet state has degenerate Zeeman levels which are lifted even in the absence of an external magnetic field as a result of dipolar interaction between the unpaired electrons. This dipolar splitting can be obtained in rigid glassy solvents or in diamagnetic host crystals.

When one molecule with a single unpaired electron interacts with another, the problem can be reduced to a question of linear antiferromagnets. Soos adopted the pseudospin method to deal with a linear array of tightly bound electrons which are coupled to their neighbors.[3] In this case, the Hamiltonian can be described as follows:

$$H = \sum \{J(1+d)\boldsymbol{S}_{2i-1}\boldsymbol{S}_{2i} + J(1-d)\boldsymbol{S}_{2i}\boldsymbol{S}_{2i+1}\}, \qquad (1)$$

Where d is an alternation parameter, and J, an exchange integral. Because of the interpair exchange interaction, $J(1-d)$, the triplet states may propagate along the linear chains. These mobile triplet states are called "triplet excitons". The magnetic susceptibilities of $(\phi_3AsCH_3)^+(TCNQ)^-_2$ and $(\phi_3PCH_3)^+(TCNQ)^-_2$ can be well explained if one assumes $d\sim 1$ in Eq. (1).[4] Chesnut and Phillips first observed the ESR spectra of these molecules characterized by fine structure splittings.[5] The dipolar interaction was found by reducing the exchange interaction between triplet excitons at lower temperatures.

The TEMPAD biradical, shown in Fig. 1, has two unpaired electrons in a molecule and may be considered to have a dominant intramolecular spin interaction which forms the triplet state. The weak exchange interaction between the triplet entities may cause the triplet excitons to propagate in the crystal. These facts are confirmed, to some extent, by the magnetic susceptibility measurements.[6] The susceptibility of the TEMPAD biradical is not completely explained by the singlet-triplet model; a slight deviation from the model was observed. It was found that the triplet states in the radical are not actually localized in lattice sites, but are a little mobile because of the weak intertriplet interaction, which presumes the existence of the $J(1-d)$ interaction. However, it has not yet been clarified whether the exchange interaction which causes triplet states is the intra- or inter-molecular interaction. On the other hand, the fine structure arising from the dipole-dipole interaction between electron spins may be observed when the triplet entities are reduced by lowering the temperature. Therefore, we observed the ESR spectra of the TEMPAD biradical at a very low temperature in order to confirm the existence of triplet states and find a zero-field splitting.

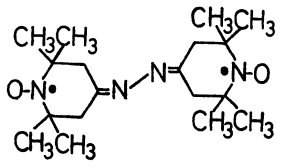

Fig. 1. Structural formula of TEMPAD biradical, bis-(2,2,6,6-tetramethylpiperidine-4-azine)-1,1'-dioxyl.

The sample was prepared from 2,2,6,6-tetramethyl-4-piperidone, following the same process as that of Rassat *et al.*[7] After recrystallization from ether, a pure sample, mp 182°C, was obtained.

The ESR absorption spectra were observed by the use of a JES-S10E type X-band spectrometer with an 80-Hz field modulation. The details of the experiments at very low temperatures will be described

1) C. A. Hutchison and B. W. Mangum, *J. Chem. Phys.*, **29**, 952 (1958).

2) J. H. van der Waals and M. S. de Groot, *Mol. Phys.*, **2**, 333 (1959).

3) Z. G. Soos, *J. Chem. Phys.*, **43**, 1121 (1965); W. Duffy, Jr. and K. P. Barr, *Phys. Rev.*, **165**, 647 (1968).

4) Z. G. Soos and R. C. Hughes, *J. Chem. Phys.*, **46**, 253 (1967).

5) D. B. Chesnut and W. D. Phillips, *ibid.*, **35**, 1002 (1961).

6) A. Nakajima, H. Nishiguchi, and Y. Deguchi, *J. Phys. Soc. Jap.*, **24**, 1175 (1968).

7) R. Briere, R. M. Dupeyre, H. Lemaire, C. Morat, A. Rassat, and P. Rey, *Bull. Soc. Chim. Fr.*, **1965**, 3290.

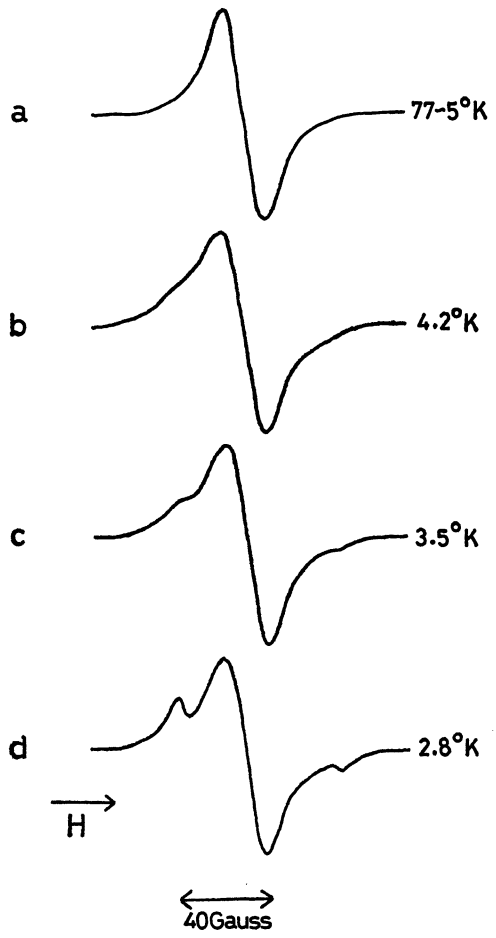

Fig. 2. Temperature dependence of the ESR absorption of a powder of TEMPAD biradical.

elsewhere.[8] The ESR measurements were carried out in powder samples. Fig. 2-a shows an exchange-narrowed Lorentz-type absorption in the higher-temperature region. When the temperature is lowered, the side peaks (Figs. 2-b, c, and d) appear. The newly-appeared doublet can be ascribed to the dipole-dipole interaction between the unpaired electrons. The spacing of the doublet resonances is evaluated as 76.6 gauss. If one assumes a localized spin density, the distance between the unpaired electrons can be calculated from the relation:

$$g\beta\langle 1/r^3\rangle = 38.3,$$

8) J. Yamauchi, This Bulletin, to be published.

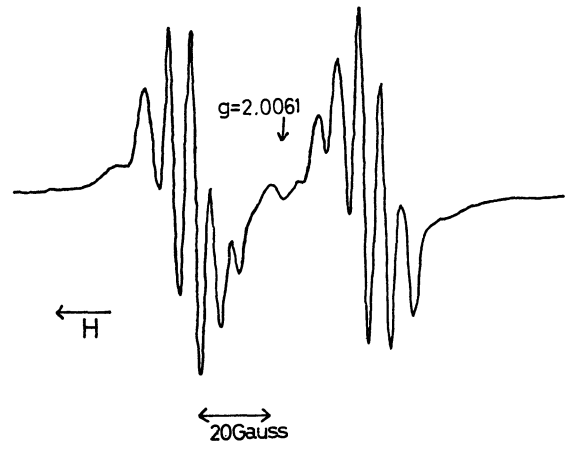

Fig. 3. ESR spectrum of a crystal of TEMPAD biradical diluted in the corresponding diamine for an arbitrary orientation.

where g is a g-factor, β, a Bohr's magneton, and $\langle 1/r^3\rangle$, an average distance between the unpaired electrons. $r\sim 8$ Å is quite well in accord with the distance between the unpaired electrons in a molecule, that is, $r\sim 9$ Å. On the other hand, the doublet splitting is also found at room temperature in the TEMPAD biradical diluted in the corresponding diamine. Although the spectrum, shown in Fig. 3, has not yet been completely analyzed, the dipole-dipole interaction is 40 gauss in order of magnitude; this corresponds to the intramolecular dipole-dipole interaction between the unpaired electrons. Hence, the doublet in Fig. 2 may be ascribed to the intramolecular dipole-dipole interaction.

The triplet-state population at the temperature where the doublet resonance starts to appear can be calculated to be 5% from this relation:

$$\rho = 1/[1+(1/3)\exp(\Delta/kT)],$$

where ρ is the density of the triplets, and $\Delta(\Delta/k = 26.4°K$[6]), the separation between lower singlet and upper triplet states. This phenomenon is similar to the cases of $(\phi_3AsCH_3)^+(TCNQ)_2^-$ and $(\phi_3PCH_3)^+$-$(TCNQ)_2^-$, which also exhibit dipole-dipole interaction at a triplet density of $\rho\sim 0.04$. Therefore, we may conclude that the dipole-dipole interaction can be observed by decreasing the exchange interactions between triplet entities in the solid state and that it can be ascribed to the intramolecular interaction between the unpaired electrons in a molecule.

BULLETIN OF THE CHEMICAL SOCIETY OF JAPAN, VOL. 44, 2265—2267 (1971)

Preparative and Structural Studies of Kostanecki's Compound

Yasusi YAMAMOTO, Kiyosi KUNO, and Hitosi NOZAKI

Department of Industrial Chemistry, Kyoto University, Yoshida, Kyoto

(Received February 22, 1971)

Kostanecki and Tambor[1] have reported that the reaction of α-phenoxyacetophenone with sodium in warm xylene gives an orange compound, $(C_8H_6O)_x$, mp 120°C. In 1956, Yates,[2] Wheeler,[3] and their coworkers studied the structure of Kostanecki's compound (**1**) and concluded that this compound was composed of 1,2,3-tribenzoylpropene in equilibrium with the corresponding enol form.

This paper will be concerned with a reaction leading to Kostanecki's compound (**1**) (Scheme 1) as well as with a structural investigation based on the NMR, mass, IR, and UV spectra.

When phenacyl bromide dissolved in dimethyl sulfoxide (DMSO) was treated with a solution of methylsulfinyl carbanion prepared from DMSO and sodium hydride[4] at room temperature, Kostanecki's compound (**1**) was obtained as orange crystals (10%), mp 120—123°C. Meanwhile, we found that a shorter reaction time (1 hr) at room temperature gave 1,2,3-tribenzoylcyclopropane (**2**) (3%) in addition to **1** (7%). The treatment of **2** with the same carbanion afforded **1** (12%), besides a 60% recovery of **2**. A better yield (50%) of **1** was obtained upon the reaction of **2** with the carbanion prepared from cyclopropyl phenyl sulfone and sodium hydride in hexamethylphosphoric triamide (HMPA).

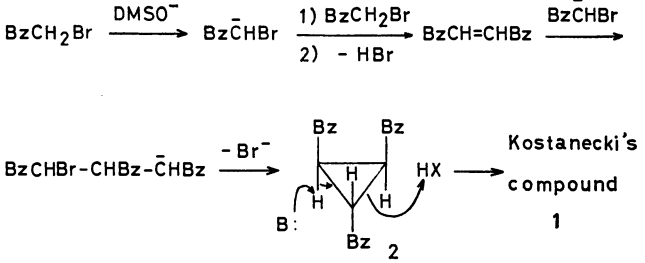

Scheme 1

On the basis of these results, we may explain the formation of **1** as is shown in Scheme 1. Initially, **2** is produced by the indicated route[5] and is then transformed to **1** by the basic ring opening.

The spectrometric properties of **1** have now made it impossible for us to believe in the previous conclusion that **1** is an equilibrium mixture of **1a** and **1b** (Scheme 2). It is proposed that the additional tautomeric isomers, **1c**—**1g**, are all in equilibrium and that the contribution of each structure depends on the phase in which the measurement is made. The **1c** isomer is a hemiacetal of **1b** and is isomerized to **1d** by the allyl-rearrangement of OH in **1c**. The **1e** ion pair is derived from **1c** or **1d** and is transformed to the **1f** salt by the substitution of $^-$OH into another anion, X^-. The innersalt formula **1g** may be proposed to explain the IR spectrum of Kostanecki's compound in the solid state (*vide infra*).

The mass spectra of **1** exhibited the fragment peaks due to the pyrylium ions shown in Scheme 3. The NMR of **1** in $CDCl_3$ (Fig. 1) consisted of a singlet at 4.73 ppm and a complex multiplet at 7.10—8.20 ppm in a ratio of *ca.* 1 : 11. This singlet disappeared upon the addition of MeOD. These results can not be explained by simply assuming **1a** and **1b**.

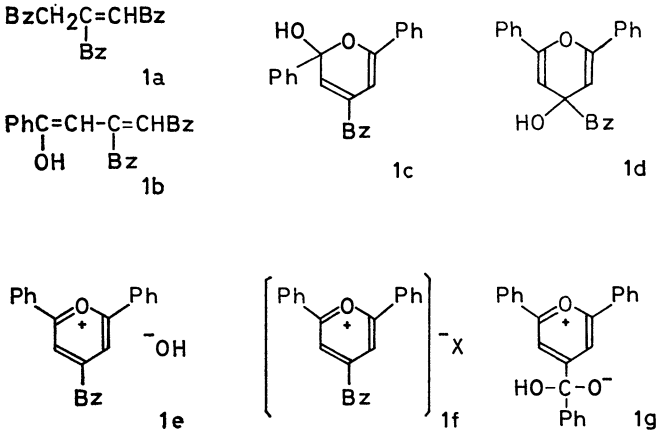

Scheme 2

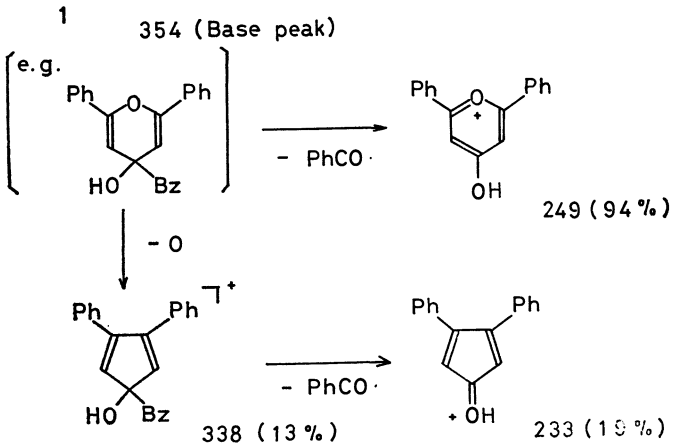

Scheme 3

1) St. v. Kostanecki and J. Tambor, *Ber.*, **35**, 1679 (1902).

2) P. Yates, D. G. Farnum, and G. H. Stout, *Chem. & Ind.* (London), **1956**, 821.

3) P. E. Devitt, E. M. Philbin, and T. S. Wheeler, *ibid.*, **1956**, 822; Idem., *J. Chem. Soc.*, **1958**, 510.

4) E. J. Corey and M. Chaykovsky, *J. Amer. Chem. Soc.*, **87**, 1345 (1965).

5) This route reminds us of the formation of **2** from sulfonium phenacylide and phenacyl bromide. See Ref 6.

Fig. 1. NMR spectrum of Kostanecki's compound (**1**) in deuterochloroform.

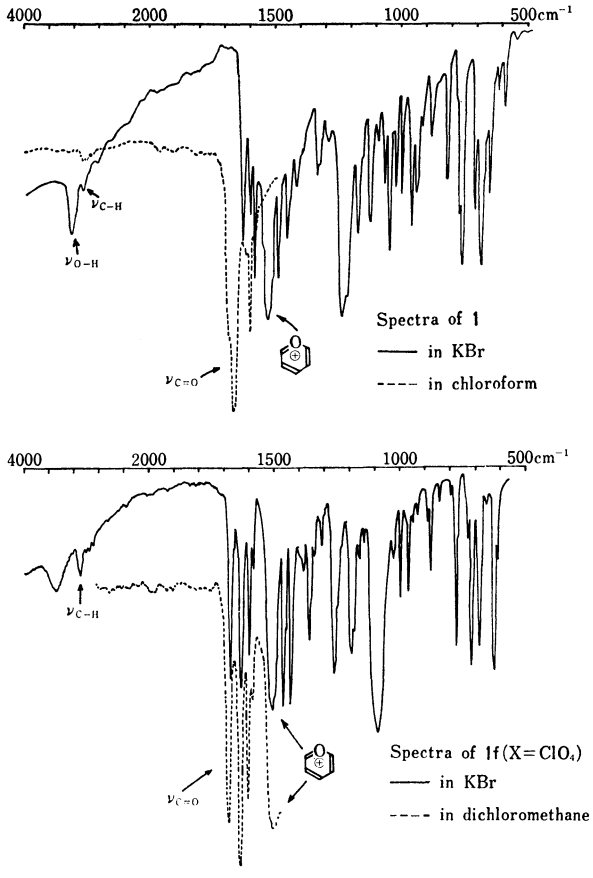

Fig. 2. Comparison of IR spectra of **1** and the pyrylium salt (**1f**) (X=ClO_4) in KBr and chloroform or dichloromethane.

Meanwhile, 2,6-diphenyl-4-benzoylpyrylium perchlorate (**1f**, X=ClO_4) (18%) was obtained as a crystalline solid, mp 233—235°C, upon the treatment of **1** with perchloric acid in chloroform at room temperature. The IR and UV spectra of **1** were compared with those of the **1f** perchlorate (X=ClO_4). The solid state IR of **1** was very analogous to that of the pyrylium perchlorate with the exception of the remarkable difference that the carbonyl band at 1665 cm^{-1} was missing in the IR spectrum of **1** (Fig. 2). As characteristic bands of pyrylium salt and of the hydroxy group were observed in the IR of **1** at 1530 and 3210 cm^{-1} respectively, **1g** can be said to be the best possibility of explaining the structure of **1** in the solid state.

The UV spectrum of **1** in ethanol was almost superimposable on that of the **1f** pyrylium salt (X=ClO_4), as is shown in Fig. 3.

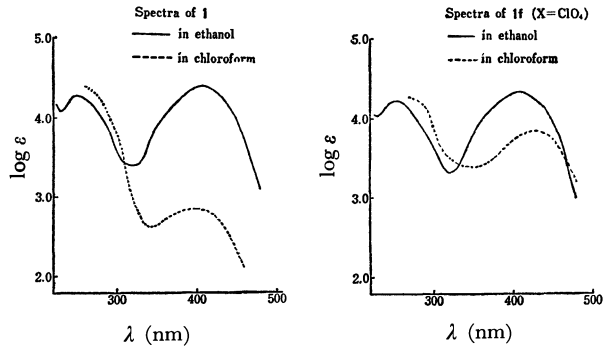

Fig. 3. Comparison of UV spectra of **1** and the pyrylium salt (**1f**) (X=ClO_4) in ethanol and chloroform.

This can be explained by assuming that the major contributing structures of **1** in ethanol are **1e** and/or **1f** (X=OEt); such an assumption is consistent with the disappearance of one proton singlet at 4.73 ppm upon CH_3OD treatment, as has been mentioned above. As is shown in Fig. 3, the absorptions of **1** in chloroform were completely different from those of **1f** (X=ClO_4) and the characteristic strong IR absorption of the pyrylium salt at 1530 cm^{-1} was absent in the spectrum of **1** in chloroform. The **1e**, **1f**, and **1g** structures could, therefore, be excluded in this state; the NMR spectrum (Fig. 1) was consistent with the **1b**, **1c**, and **1d** structures but not with **1a**.

Summarizing these results, we may conclude as follows: (1) The previous assumption of the **1a**⇄**1b** equilibrium is untenable. (2) The solid IR spectrum of **1** can be explained by means of **1g** in view of the absence of the carbonyl absorption. (3) The UV spectrum in ethanol supports the pyrylium salt formula **1e** and/or **1f** (X=OEt). (4) A chloroform solution of **1** gives spectra which are consistent with the **1b**, **1c**, and **1d** structures but not with **1a**, **1e**, **1f**, and **1g**. (5) The **1b**, **1c**, **1d**, **1e**, and **1g** structures are possibly in fast equilibrium, and the contribution of each specific one is controlled by the state in which the measurement is made.

Experimental

All the mps are uncorrected. The microanalyses were performed at the Elemental Analyses Center of Kyoto University. The NMR spectra were obtained in $CDCl_3$ on a 100 MHz instrument (Varian HA-100 spectrometer) by the courtesy of Toray Co. The mass spectra were obtained on a Hitachi RMU 6D spectrometer by the courtesy of Takeda Chemical Industries, Ltd.

Reaction of Phenacyl Bromide with Methylsulfinyl carbanion. A solution of sodium methylsulfinyl carbanion was prepared under N_2 from sodium hydride (0.72 g, 30 mmol) and dimethyl sulfoxide (DMSO) (40 m*l*). Into this we stirred a solution of phenacyl bromide (3.9 g, 20 mmol) in DMSO (10 m*l*) under ice-cooling over a period of 2 min. The reaction mixture was then stirred at room temperature for 3 hr, poured into water (300 m*l*), acidified with aqueous hydrochloric acid, and extracted with benzene. The evaporation

of the benzene gave a dark-brown oil, to which a small amount of benzene was added again, after which the mixture was allowed to stand overnight. Kostanecki's compound **(1)** was obtained as orange crystals; mp 120—123°C (lit,[1] 120°C) (0.25 g, 10%). Exact mass: 354.127 (base peak), 338.131 (13), 249.092 (94), and 233.099 (19). Calcd for $C_{24}H_{18}O_3$: 354.125, $C_{24}H_{18}O_2$: 338.130, $C_{17}H_{13}O_2$: 249.091, and $C_{17}H_{13}O$: 233.096.

A work-up of the reaction mixture after 1 hr at room temperature gave 1,2,3-tribenzoylcyclopropane **(2)**, mp 216°C (3%), besides **1** (7%). The product, **2**, was identical with an authentic sample.[6]

The Reaction of 1,2,3-Tribenzoylcyclopropane **(2)** *with Carbanion.* A solution of **2** (1.8 g, 5 mmol) in DMSO (20 m*l*) was added to a carbanion solution prepared from sodium hydride (0.14 g, 6 mmol) and DMSO (20 m*l*) under stirring at room temperature. After it had been stirred at room temperature for 3.5 hr, the reaction mixture was treated with water. The precipitating starting material (60%) was removed by filtration. The filtrate was acidified with aqueous hydrochloric acid and extracted with benzene. Concentration gave Kostanecki's compound **(1)** (0.21 g, 12%).[7]

Meanwhile, **2** (1.8 g, 5 mmol) in HMPA (20 m*l*) was treated with a carbanion solution prepared from cyclopropyl phenyl sulfone (4.1 g, 23 mmol) and sodium hydride (0.54 g, 23 mmol) in HMPA (20 m*l*) at 90°C for 24 hr to give **1** (0.89 g, 50%).

Preparation of 2,6-Diphenyl-4-benzoylpyrylium Perchlorate. Kostanecki's compound (0.067 g, 0.19 mmol) was dissolved in chloroform (50 m*l*). To this solution, aqueous perchloric acid (60%) (0.04 m*l*) was added, and the whole mixture was stirred at room temperature for 15 hr. The chloroform solution was dried over anhydrous sodium sulfate and evaporated to yield a yellow oil which solidified upon trituration with ether; mp 233—235°C (17 mg, 18%). The IR spectrum of this solid is shown in Fig 2.

Found: C, 66.1; H, 3.9%. Calcd for $C_{24}H_{17}ClO_6$: C, 66.0; H, 3.9%.

The authors are indebted to Professeor K. Sisido for his help and encouragement. This work was partially supported by the Scientific Research Fund of Ministry of Education, Japanese Government. Financial support from Toray Science Foundation is acknowledged with pleasure.

6) H. Nozaki, M. Takaku, and K. Kondo, *Tetrahedron*, **22**, 2145 (1965).

7) The yield is based on the substrates initially added.

BULLETIN OF THE CHEMICAL SOCIETY OF JAPAN, VOL. 44, 2267—2268 (1971)

Magnetic Susceptibilities of Ionic Electron-Donor-Acceptor Complexes

Minoru KINOSHITA, Takamaro MIZOGUCHI, and Hideo AKAMATU
Department of Chemistry, Faculty of Science, The University of Tokyo, Hongo, Tokyo

(Received February 24, 1971)

In previous papers, we discussed the magnetic properties of ionic electron-donor-acceptor complexes formed between aromatic diamines and tetracyano-*p*-quinodimethane[1,2] and benzoquinone derivatives.[3] Their magnetic susceptibilities showed large deviations from the Curie law and were explained by the linear chain model of the interacting unpaired electrons on radical ions. We report here the magnetic susceptibilities of the ionic complexes of tetracyanoethylene (TCNE) with *N,N,N',N'*-tetramethyl-*p*-phenylenediamine (TMPD) and *N,N'*-diphenyl-*p*-phenylenediamine (DPPD).

Tetracyanoethylene is known to be very reactive with aromatic amines.[4] Actually, of the seven amines tested, only the above two were found to give stable solid complexes. The complex of TMPD·TCNE (1 : 1) was precipitated as dark brown microcrystals by mixing cooled solutions (−10°C) of TMPD and TCNE in dichloromethane. The dark violet crystals of DPPD·TCNE (1 : 1) were prepared in a similar manner at −18°C. The complex of TMPD·TCNE turned reddish brown when it was kept in air for two days. The complex of DPPD·TCNE was found to be more stable.

The infrared absorption spectra of these solid complexes indicate that they are essentially of ionic type in their ground states. In the complex of DPPD·TCNE, for example, the C≡N stretching vibration was found at 2150 and 2110 cm^{-1}, while in neutral TCNE[5] it was reported to appear at 2270 and 2240 cm^{-1}. The C-C–C bending and wagging vibrations, observed respectively at 576 and 552 cm^{-1} in neutral TCNE,[5] were found at 510 and 480 cm^{-1} in the complex. These shifts observed upon complex formation are in line with those reported in the change from neutral TCNE to TCNE anion.[6]

The susceptibilities of these complexes were measured with freshly prepared samples by the Faraday method. Their observed molar magnetic susceptibilities are shown in Fig. 1 as a function of temperature. In the higher temperature region, the susceptibility decreased with decrease in temperature. The behavior is similar to that given previously,[1-3] and may be explained in terms of the singlet-triplet model or the linear Ising model. In the former model, the

1) M. Kinoshita and H. Akamatu, *Nature*, **207**, 291 (1965).
2) M. Ohmasa, M. Kinoshita, M. Sano, and H. Akamatu, This Bulletin, **41**, 1998 (1968).
3) Y. Sato, M. Kinoshita, M. Sano, and H. Akamatu, *ibid.*, **43**, 2370 (1970).
4) D. N. Dhar, *Chem. Revs.*, **67**, 611(1967).
5) T. Takenaka and S. Hayashi, This Bulletin, **37**, 1216 (1964).
6) J. Stankey, D. Smith, B. Letimer, and J. P. Devlin, *J. Phys. Chem.*, **70**, 2011 (1966).

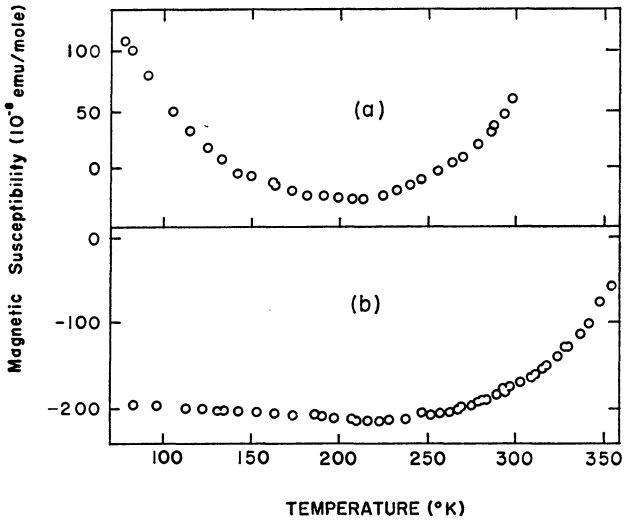

Fig. 1. Temperature dependence of the observed magnetic susceptibilities of (a) TMPD·TCNE and (b) DPPD·TCNE.

susceptibility is expressed by

$$\chi_p = (2Ng^2\beta^2/kT)[3+\exp(\delta/kT)]^{-1} \quad (1)$$

where δ is the singlet-triplet separation and N the Avogadro number, and in the latter by

$$\chi_p = (Ng^2\beta^2/2kT)\exp(-J/kT) \quad (2)$$

where J is the interaction energy of the unpaired electrons. If $\delta, J \gg kT$, these expressions are reduced to

$$\chi_p = C\exp(-E/kT)/T. \quad (3)$$

The intrinsic paramagnetic susceptibilities χ_p of these complexes were obtained after corrections had been made for the diamagnetic part ($\chi_d = -116\times 10^{-6}$ for TMPD·TCNE and $\chi_d = -214\times 10^{-6}$ for DPPD·TCNE) and for the impurity paramagnetism by the procedure described previously.[3] The plots of $\ln(\chi_p T)$ against $1/kT$ gave straight lines. The activation energy E was obtained to be 0.17 eV for TMPD·TCNE and 0.28 eV for DPPD·TCNE. However, the E values thus obtained do not explain the observed susceptibilities. In other words, they yield a very large value for N when substituted into parameter δ or J of the above equations together with χ_p obtained at a certain high temperature. Thus, it is very likely that the parameter δ or J decreases linearly with increase in temperature. On this assumption, the δ-values estimated at various temperatures from Eq. (1) with the obtained χ_p's and with $N=6\times 10^{23}$, were plotted against temperature in Fig. 2. The plots yielded straight lines of the form $\delta=\delta_0+\alpha T$. The values of δ_0 and α obtained from the analysis of Fig. 2 are given in Table 1, where the values for the complexes of chloranil and bromanil[3] are also shown for comparison.

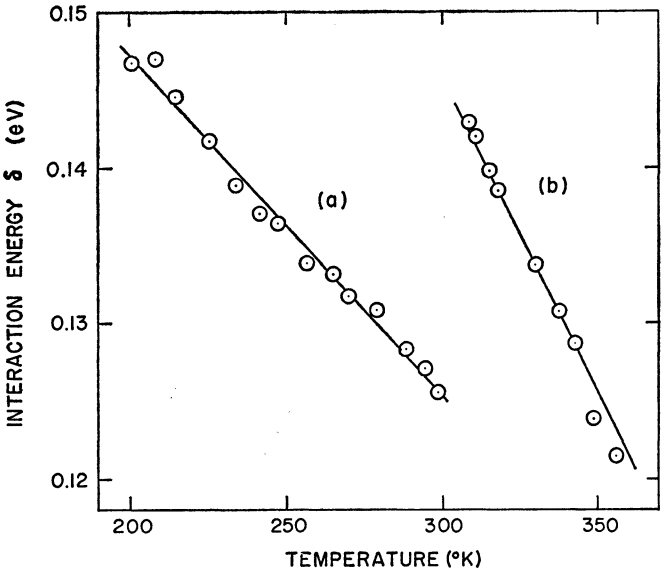

Fig. 2. Variations of the singlet-triplet energy separation δ with temperature for (a) TMPD·TCNE and (b) DPPD·TCNE.

Table 1. Temperature variation of interaction energy

	E (eV)	δ_0 (eV)	$\delta_{300°K}$ (eV)	α (eV/deg)
TMPD·TCNE	0.17	0.16	0.13	-1.9×10^{-4}
DPPD·TCNE	0.28	0.27	0.15	-4.0×10^{-4}
TMPD·*p*-CA	0.34	0.34	0.17	-6.0×10^{-4}
TMPD·*p*-BA	0.21	0.21	0.15	-1.8×10^{-4}
PD·*p*-CA	0.18	0.18	0.15	-0.8×10^{-4}
PD·*p*-BA	0.24	0.24	0.15	-4.4×10^{-4}

In the analysis, the value of δ_0 was expected to agree closely with E. The close agreement can be seen in Table 1. The negative value of α indicates that the interaction between unpaired electrons becomes weaker with the rise of temperature. The value of δ or J is determined by the combination of the exchange interaction of unpaired electrons and the charge-transfer resonance effect.[3] These effects are dependent directly upon the intermolecular spacings. Thus, it is not surprising that the value of $|\alpha|$ thus obtained coincides in order of magnitude with the expansion coefficients of the usual organic compouds. It should be noted that the unit cell dimension of anthracene:*s*-trinitrobenzene complex is known to change by about 2 percent between room temperature and -100°C in the direction of molecular stacking,[7] that is, the average linear expansion coefficient of the complex is also of the order of 10^{-4}.

7) D. S. Brown, S. C. Wallwork, and A. Wilson, *Acta Crystallogr.*, **17**, 168 (1964).

BULLETIN OF THE CHEMICAL SOCIETY OF JAPAN, VOL. 44, 2269—2270 (1971)

Magnetic Properties of Aromatic Hydrocarbon-Alkali Metal Salts. II. Anthracene-Alkali Metal Salts

Kimiko MASUDA*, Hiroaki OHYA-NISHIGUCHI, Yasuo DEGUCHI**, and Hideo TAKAKI
Department of Chemistry, Faculty of Science, Kyoto University, Kyoto

(Received March 2, 1971)

In a previous paper[1] we have reported that the magnetic susceptibility of the solvent-free biphenyl-potassium salt was paramagnetic and that it exhibited a broad maximum at 130±4°K. This susceptibility can be interpreted approximately by this expression:

$$\chi_M = \frac{2Ng^2\beta^2}{kT} \cdot \frac{1}{3+e^{\delta/kT}} \quad (1)$$

which implies the existence of singlet-triplet dimers. The biphenyl-rubidium and biphenyl-cesium systems also obey the above equation rather than Curie-Weiss law in the higher temperature range. The singlet-triplet separations of these salts are very small in comparison with that of the TCNQ radical salts. In order to investigate whether or not the susceptibilities of the aromatic hydrocarbon radical salts follow the singlet-triplet dimer model, we have measured the static magnetic susceptibilities and the EPR absorption of solid complexes composed of anthracene with sodium, potassium, rubidium, and cesium. In this paper we will discuss qualitatively the structures of the anthracene anion radical solids in comparison with those of the corresponding TCNQ radical salts.

Experimental

These powder salts were prepared in the same way in the previous paper.[1] Anthracene of the scintillation-counter grade was used without further purification. The anthracene was reduced with potassium or sodium in tetrahydrofuran, and with rubidium or cesium in dimethoxyethane, which could dissolve these ion pairs better than tetrahydrofuran. These solutions were then evacuated *in vacuo*, and powder crystals were precipitated. The anion radical salts were titrated with a standard oxalic acid solution, using phenolphtalein as the indicator. The ratios of alkali metal to anthracene were 0.9±0.1 for potassium, rubidium, and cesium. Three samples were obtained for sodium anthracene complexes: An–$Na_{0.7}$, An–$Na_{1.0}$, and An–$Na_{1.5}$. (These formulas represent the complexes in which the ratios of sodium to anthracene are 0.7, 1.0, and 1.5 respectively). Although Holmes-Walker and Ubbelohde[2] have reported their findings as to the magnetic susceptibility and conductivity of An–$Na_{2.02}$ synthesized in diethyl ether, we could obtain it in tetrahydrofuran. The solids were brown for An–Na and blue-black for the other alkali metal complexes.

Results and Discussion

Temperature Dependence of Magnetic Susceptibility. The measured paramagnetic susceptibilities of the radical salts on 1 mol of anthracene (χ_M) are shown in Fig. 1 as a function of the temperature. The diamagnetic contribution was calculated by Pascal's method ($\chi_M^{An-Na} = -1.37$, $\chi_M^{An-K} = -1.45$, $\chi_M^{An-Rb} = -1.53$, and $\chi_M^{An-Cs} = -1.65 \times 10^{-4}$ emu/mol). The magnetic susceptibility of An–K varies with the temperature and exhibits a broad maximum (T_c), as is shown in Fig. 1, which gradually shifts to a higher temperature as the solvent residual in the solid sample decreases. The T_c of An–K (IV), which was evacuated for about one day, is estimated to be 135±5°K. However, in the case of An–K(III) evacuated for about 2 days the susceptibility passes through its maximum at 165±5°K and the maximum susceptibility decreases in comparison with (IV). The shifts of the maximum point may be due partly to the mixing of the susceptibility of the monomer with that of the dimer and partly to the presence of a

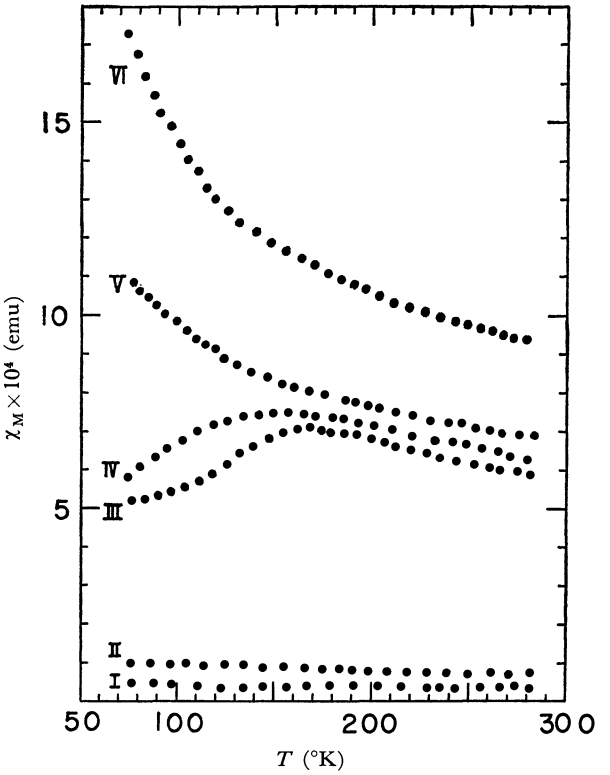

Fig. 1. Temperature dependence of the magnetic susceptibilities of anthracene-alkali metal salts.
I, An–$Na_{0.7}$; II, An–$Na_{1.5}$; III, An–K (solvent); IV, An–K; V, An–Rb; VI, An–Cs

* Present address: Department of Nuclear Engineering, Faculty of Engineering, Osaka University, Suita-shi, Osaka.
** Present address: College of Liberal Arts and Sciences, Kyoto University, Kyoto.

1) H. Nishiguchi, This Bulletin, **40**, 1587 (1967).
2) W. A. Holmes-Walker and A. R. Ubbelohde, *J. Chem. Soc.*, **1954**, 780.

residual solvent between anion radicals. Using the value for T_c=165°K determined from the experiment, we can estimate the singlet-triplet separation to be 0.0231 eV. The comparison of this result with the cases of biphenyl-K (0.0182 eV) and *meta*-terphenyl-K (0.0252 eV)[3] indicates that the singlet-triplet separations in the aromatic hydrocarbon anion(Ar)–K complexes do not vary in the order of magnitude. The singlet-triplet separation of the dimer may depend on the distance between the two constituent radicals; therefore, the small difference implies that the distance between the two anion radicals of these Ar–K complexes is of the same order of magnitude. It is instructive to compare the singlet-triplet separations of Ar–K and that of K(TCNQ) (0.2 eV),[4] since both salts are 1 : 1 complexes of the organic compounds and potassium. The large difference implies that the two anion radicals in Ar–K complexes are more separated from each other than in the case of K(TCNQ). As was suggested in the previous paper,[1] the difference in the singlet-triplet separations may indicate the existence of a potassium cation between the two radicals constituting the An–K complexes; the two spins interact indirectly, while the TCNQ anions in the K(TCNQ) complexes couple directly. The magnetic susceptibilities of the three samples of anthracene sodium complexes are very small and change little with the temperature or with various alkali metal concentrations. If one assumes the singlet-triplet dimer model, An–$Na_{1.0}$ and An–$Na_{0.7}$ could be attributed to the low-temperature range ($kT/\delta<1$). The small χ_M of An–$Na_{1.5}$ is probably due to its compositions containing dinegative ions and dimer clusters. The magnetic susceptibilities of An–Rb and An–Cs salts increase as the temperature decreases down to 77°K and do not show any maximum. They would be more suitable for the higher-temperature range ($kT/\delta>1$) of Eq. (1) than the same temperature range of the Curie-Weiss law on condition that $\delta_{An-Na}>\delta_{An-K}>\delta_{An-Rb}>\delta_{An-Cs}$.

Electron Paramagnetic Resonance Absorption. We have also observed the electron paramagnetic resonance of alkali metal complexes of anthracene. The EPR spectra of these salts changed with different alkali metals and with the temperature, as is shown in Fig. 2. The EPR spectrum of An–K salt which was evacuated for 2 days *in vacuo* exhibits an exchange-narrowed single line (1.8 G) broader than that (1.0 G) of the An–K which was evacuated for 2 hr, and the line width changed little with the temperature. The EPR spectra of An–Na exhibit an exchange-narrowed sharp single line comparatively broader than that of An–K, and the line width changed little with temperature. The EPR spectra of An–Cs salt exhibits a broad single line, and the line width increases with the temperature up to 28 gauss. These phenomena can also be seen in the cases of Bp–Cs and cupric acetate monohydrate.[5] The absorption of An–Rb varies from one sample to another. The EPR spectrum of An–Rb, which was evacuated for 1 hr, shows two lines at room temperature; one of them is sharp, and the other, comparatively broad. When the solvent was introduced to this sample, these two lines coalesced into a single sharp line. The EPR spectrum of An–Rb evacuated for 2 days shows a single lines at 77°K, one of them sharp, and the other, very broad. This broad line may correspond to the absorption of dimer clusters, and the other, to the single spin, as was seen in the cases of Bp–K and Bp–Rb.

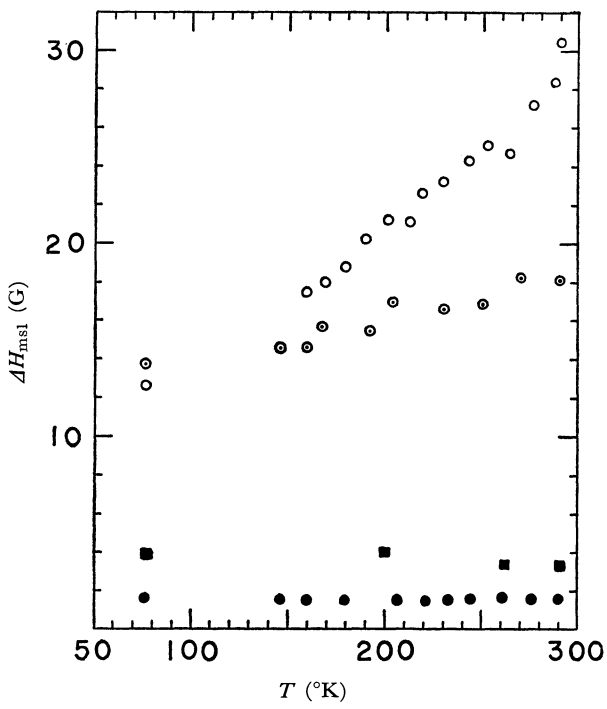

Fig. 2. Temperature dependence of the line width of the paramagnetic resonance absorption of the salts.
○, An–Cs; ⊙, An–Rb; ■, An–Na; ●, An–K.

3) Unpublished work.
4) R. G. Kepler, *J. Chem. Phys.*, **39**, 3528 (1963).
5) B. N. Figgis and R. L. Martin, *J. Chem. Soc.*, **1956** 3837.

BULLETIN OF THE CHEMICAL SOCIETY OF JAPAN, VOL. 44, 2271—2272 (1971)

Study on Scrambling in Decomposition of Labeled Acetyl Benzoyl Peroxide

Michio KOBAYASHI, Hiroshi MINATO, and Ryuki HISADA

Department of Chemistry, Tokyo Metropolitan University, Fukazawa, Setagaya-ku, Tokyo

(Received March 8, 1971)

Acetyl benzoyl peroxide [acetyl-^{18}O] and acetyl benzoyl peroxide [benzoyl-^{18}O] were decomposed in 0.1 M benzene solutions at 78° for 160 min (48% decomposition; its half life, determined by gas evolution, was 168 min.), and the undecomposed ABP-^{18}O was recovered and purified. The contents of oxygen-18 at the acetyl or benzoyl carbonyl were determined by converting the recovered ABP-^{18}O into acethydrazide or benzhydrazide. The results are shown in Table 1 and 2.

TABLE 1. OXYGEN-18 ANALYSIS OF ACETYL BENZOYL PEROXIDE [BENZOYL-^{18}O]

Sample	^{18}O excess atom %	
	Found	Calcd
$PhCON_2H_3$ derived from the starting ABP-^{18}O[a]	0.901[b]±0.007	(0.901)
$PhCON_2H_3$ derived from the recovered ABP-^{18}O	0.892[b]±0.016	0.901
Products of Decomposition		
$PhCO_2H$	0.466	0.451
$PhCO_2CH_3$	0.428	0.451
CO_2	0.196	—

a) When the starting ABP-^{18}O itself was directly subjected to pyrolysis, the ^{18}O excess atom % of the carbon dioxide formed was 0.252 %.
b) The average of the values obtained by two experiments.

TABLE 2. OXYGEN-18 ANALYSIS OF ACETYL BENZOYL PEROXIDE [ACETYL-^{18}O]

Sample	^{18}O excess atom %	
	Found	Calcd
$CH_3CONHN{=}CHPh$ derived from the starting ABP-^{18}O[a]	1.228	(1.228)
$CH_3CONHN{=}CHPh$ derived from the recovered ABP-^{18}O	1.169[b]+0.029	1.228
Generated CO_2 during decomposition	0.363[b]±0.003	—

a) When the starting ABP-^{18}O itself was directly subjected to pyrolysis, the ^{18}O excess atom % of the carbon dioxide formed was 0.365 %.
b) The average of the values obtained by two experiments.

Data in Table 1 and 2 indicate that scrambling of acetyl oxygen-18 appears to take place to small extent and that of benzoyl oxygen-18 was much less; these findings are in parallel with the results that scrambling of the labeled acetyl peroxide was extensive[1] whereas that of the labeled benzoyl peroxide was very small.[2,3]

Recently Goldstein and Judson[4] reported that oxygen scrambling of acetyl peroxide in isooctane was much more extensive than that in cumene. Therefore it is possible that scrambling of ABP is greater in solvents other than aromatic solvents. Further investigation is desirable in order to establish whether or not scrambling of the label of ABP is much affected by solvents.

Experimental

Benzaldehyde-^{18}O. A solution of 31 g of benzylideneaniline (0.17 mol) in 150 ml of ether was mixed with 11.0 g of ^{18}O-enriched water (1.3 atom % excess oxygen-18) and 19.7 g of concentrated sulfuric acid. After hydrolysis was complete, precipitates formed were filtered and the ether was evaporated under reduced pressure. The residue was distilled under reduced pressure, and 11.5 g of benzaldehyde-^{18}O was obtained at 61.0—63.5°C/14 mmHg.

Acetic anhydride-^{18}O. The method described by Oae, Kitao, and Kitaoka was used with some modification.[5] To a solution of 250 ml of anhydrous ethanol and 40 g of water enriched with 1.3 atom % excess oxygen-18, 23 g of sodium metal (1 mol) was added slowly with cooling. To this solution 41 g (1 mol) of acetonitrile was added, and the mixture was refluxed for 4 days. After hydrolysis was completed, the solvent was evaporated and the white crystals obtained was heated under reduced pressure until they melted. Sodium acetate formed amounted to 75.5 g (92%).

Then, 41 g (0.5 mol) of sodium acetate-^{18}O was treated with 89 g (0.75 mol) of thionyl chloride, and distillation yielded acetyl chloride-^{18}O (32.1 g; 82%). A mixture of 32.1 g (0.41 mol) of acetyl chloride-^{18}O and 34.5 g (0.42 mol) of sodium acetate-^{18}O was let to react at 140°C for 3 hr. Distillation of the mixture and the redistillation of the distillate yielded 24.5 g (57%) of acetic anhydride-^{18}O at 135—139°C.

Acetyl Benzoyl Peroxide [Acetyl-^{18}O] and Acetyl Benzoyl Peroxide [Benzoyl-^{18}O]. The method described by Juračka and Chromeček was used with some modification.[6] To a mixture of 10.6 g (0.1 mol) of benzaldehyde-^{18}O or benzaldehyde, 24.5 g (0.24 mol) of acetic anhydride or acetic anhydride-^{18}O and 6.3 g of magnesium carbonate, oxygen gas was bubbled for 7 hr at 40°C. After the reaction was over, 400

1) J. W. Taylor and J. C. Martin, *J. Amer. Chem. Soc.*, **89**, 6904 (1967).
2) M. Kobayashi, H. Minato, and Y. Ogi, This Bulletin, **41**, 2822 (1969).
3) J. C. Martin and J. H. Hargis, *J. Amer. Chem. Soc.*, **91**, 5399 (1969).
4) M. J. Goldstein and H. A. Judson, *ibid.*, **92**, 4119 (1970).
5) S. Oae, T. Kitao, and Y. Kitaoka, *ibid.*, **84**, 3359 (1962).
6) F. Juračka and R. Chromeček, *Chem. Prumysl.*, **6**, 27 (1956); A. Yamamoto, N. Inamoto, H. Morikawa, and O. Simamura, Abstracts of the 19th Anual Meeting of the Chemical Society of Japan, 3F202, 113 (1966).

m*l* of cold water was added and the mixture was extracted with 100 m*l* of ether. The ether extract was washed with a 5% sodium hydrogen carbonate solution and water, and then dried over anhydrous magnesium sulfate. Evaporation of the ether under reduced pressure yielded yellowish white crystal . After three recrystallization from *n*-hexane 11.8—12.5 g of white crystals was obtained (65—70%); mp 37.5—38.0°C.

Decomposition of ABP-^{18}O in benzene. A 0.1 mol/*l* solution of ABP-benzoyl-^{18}O or ABP-acetyl-^{18}O in benzene was degassed, and then decomposed for 160 min at 78°C. The carbon dioxide evolved was measured by a gas buret, and then collected in a liquid nitrogen trap and analyzed for excess oxygen-18.

About 40% of benzene was removed from the reaction mixture under reduced pressure. The benzene solution was washed with a 5% sodium hydrogen carbonate solution, which upon acidification yielded precipitates of benzoic acid. The benzene solution was washed further with water, dried over anhydrous magnesium sulfate, and evaporated under reduced pressure. When the residue was distilled *in vacuo* at room temperature, methyl benzoate was present in the distillate. The residue was recrystallized twice from *n*-hexane, and white crystals of undecomposed ABP were recovered.

Determination of Oxygen-18 Contents. (1) Oxygen-18 Content in Benzoyl Oxygen of ABP: To an ice-cooled solution of 1.5—2.0 g of anhydrous hydrazine and 15 m*l* of dry benzene a solution of 1.5—2.0 g of ^{18}O-enriched ABP in 15 m*l* of dry benzene was added drop by drop. Benzene and unreacted hydrazine were evaporated from the reaction mixture under reduced pressure, and other volatile compounds were removed under a reduced pressure of 8×10^{-4} mmHg at 70°C. The residue was recrystallized from benzene, and the crystals obtained were further purified by repeating recrystallizations three times from ether. The benzhydrazide-^{18}O obtained melted at 109—111°C (lit,[7] 112.5°C). This sample was converted by pyrolysis to carbon dioxide, which was subjected to mass spectrometric analysis for the determination of the oxygen-18 content in the benzoyl oxygen of ABP.

(2) Oxygen-18 Content in Acetyl Oxygen of ABP: In a way similar to that described above in (1) ^{18}O-enriched ABP was let to react with anhydrous hydrazine. After benzene and unreacted hydrazine were removed under reduced pressure, the residue was subjected to distillation at 40°C under a reduced pressure of 8×10^{-4} mmHg. The distillate was dissolved in dichloromethane, and freshly distilled benzaldehyde was added to this solution. The dichloromethane was removed under reduced pressure and the residue was recrystallized three times from ether. *N*-Benzylideneacethydrazide obtained melted at 134—135°C (lit,[8] 134°C). This sample was converted to carbon dioxide, which was analyzed for the determination of the oxygen-18 content in the acetyl oxygen of ABP.

(3) Mass-spectrometric Determination of Oxygen-18 Content. Samples of ABP, benzhydrazide, *N*-benzylideneacethydrazide, benzoic acid, and methyl benzoate were converted by the method of Rittenburg and Ponticorvo[9] to carbon dioxide, and the peak ratio 44/46 was determined by use of a Hitachi RMU-6E Type mass spectrometer.

7) R. Stollé, *J. Prakt. Chem.*, **69**, 145 (1904).
8) T. Curtius and H. Franzen, *Ber.*, **35**, 3234 (1902).
9) D. Rittenburg and L. Ponticorvo, *Int. J. Appl. Radiat. Isotopes*, **1**, 208 (1956).

BULLETIN OF THE CHEMICAL SOCIETY OF JAPAN, VOL. 44, 2272—2274 (1971)

On the Crystal Structure of Methane in Phase II

Masao HASHIMOTO, Michiko HASHIMOTO*, and Taro ISOBE
The Chemical Research Institute of Non-Aqueous Solutions, Tohoku University, Sendai

(Received March 12, 1971)

It is well known that there are two kinds of second-order phase transitions in solid methane, at 4.20°K and at 8°K. The most likely explanation of these transitions is that these are changes in the molecular orientation[1], but their exact mechanism and the structure of the each phase are still ambiguous.

X-Ray diffraction studies[2-4] show that the carbon atoms occupy *fcc* positions over the whole temperature range from 4.2 to 80°K. For the *fcc* carbon lattice, there are several possible structures, differing in the relative orientations of their molecules.

The IR and Raman spectra[5,6] of Phase II(20.4> T°K>8) were explained by postulating sites of either C_{2v} or D_2 structures.

Kimel *et al.*[7] have calculated the cohesive energy of crystalline methane for various possible structures using a potential function consisting of repulsive and attractive interactions between non-bonded atoms. They found that the tetragonal structures of the D_{3d} symmetry have the best paking.

In a previous work,[8] we found, for the C_2H_2 crystal, that the pair-potential calculation makes it possible to determine the space group when the crystal system and the lattice constants are already known.

In the present note, we will see, for the crystalline methane, that if the distance between the nearest two molecules is known, it is possible to determine not only the crystal system, but also the space group. This finding is very interesting, since the mechanism of

* Present address: Department of Pathology, Faculty of Medicine, Tohoku University, Sendai.

1) G. B. Savitsky and D. F. Hornig, *J. Chem. Phys.*, **36**, 2634 (1962).
2) S. C. Greer and L. Meyer, *Z. Angew. Phys.*, **27**, 198 (1969).
3) A. Schallamach, *Proc. Roy. Soc. Ser A*, **171**, 569 (1939),
4) W. Gissler and M. Stiller, *Naturwissenschaften*, **52**, 512 (1965).
5) A. Anderson and R. Savoie, *J. Chem. Phys.*, **43**, 3468 (1965).
6) C. Chapados and A. Cabana, *Chem. Phys. Lett.*, **7**, 191 (1970).
7) S. Kimel, A. Ron, and D. F. Hornig, *J. Chem. Phys.*, **40**. 3351 (1964).
8) M. Hashimoto, M. Hashimoto, and T. Isobe, This Bulletin, **44**, 649 (1971).

molecular condensation or crystallization can now be explained by means of pair-interaction potentials. All the computational work in this note were done at the Computer Center of Tohoku University using NEAC-2200-500 computer system.

Intermolecular Potential

Assuming the spherical symmetry of the component atoms of the methane molecule, the following equation was used to calculate the pair-potential energy:

$$v(r) = \sum_j (a_j \exp(-b_j r_j)/r_j d_j - c_j/r_j^6), \qquad (1)$$

where the summation, j, is extended to all the interatomic pairs of the two molecules. The a_j, b_j, c_j, and d_j parameters have been determined by several authors[9,10] so as to give the best agreement with the experimental results (see Table 1).

The relative orientation of the two interacting molecules is defined as is shown in Fig. 1.

Table 1. Set of parameters in Eq. (1)
set a: Ref. 9; set b: Ref. 10

atom-atom	set	a×10⁻³	b	c	d
C···C	a	237.0	4.32	298.0	0.0
	b	408.0	0.0	373.0	12.0
C···H	a	31.4	4.20	121.0	0.0
	b	205.0	0.0	133.0	12·0
H···H	a	6.60	4.08	49.2	0.0
	b	4930.0	0.0	51.5	12.0

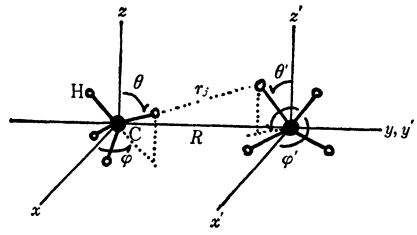

Fig. 1. The geometrical representation of two interacting methane molecules.

Calculation and Results

Figs. 2 and 3 indicate the $v(r)$ when $\varphi'=270°$ and $\theta'=0°$. Among the $v(r)$ values for various θ' and φ', those given in Figs. 2 and 3 have the deepest minimum. Since the methane molecule has a tetrahedral symmetry, there are twelve such minima about each methane molecule. Their centers of gravity form a face-centered cubic lattice. In each molecule three C–H bonds are placed nearly parallel to the a, b, and c cubic axes, and the remaining one, parallel to the direction of the body diagonals (see Fig. 4). This structure belongs to the T^4-$P2_13$ space group and is just the one suggested by Nagamiya[11].

Recently Savoie *et al.*[12] have proposed the T^4-$P2_13$ space group for the structure of Phase II on the basis of the far infrared data. This is also consistent with our results.

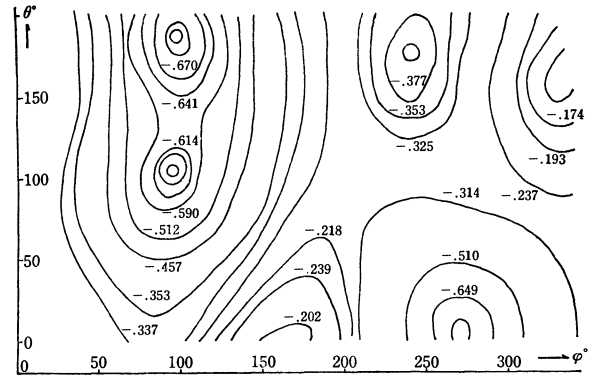

Fig. 2. θ-φ dependency of the pair potential using set b, in kcal/mol.

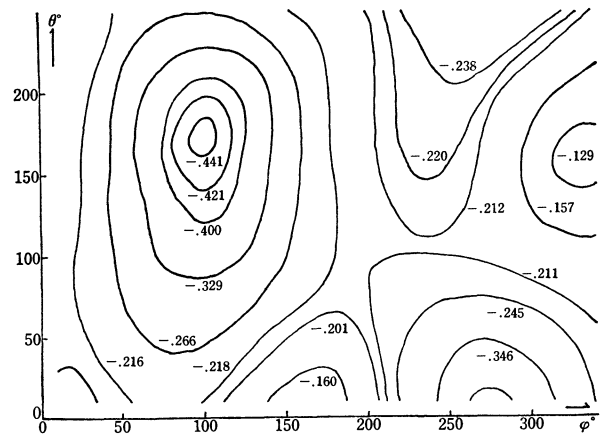

Fig. 3. θ-φ dependency of the pair potential using set a, in kcal/mol.

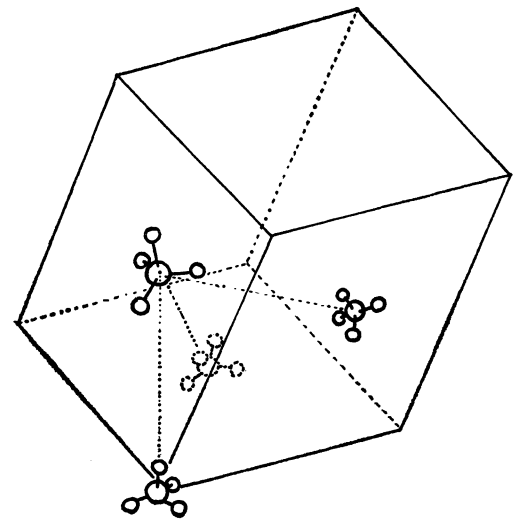

Fig. 4. The orientation of molecules that minimizes the pair potential when R=4.16 Å.

9) J. L. de Coen, G. Elefante, A. M. Liquori, and A. Damiani, *Nature*, **216**, 910 (1967).
10) N. G. Parsonage and R. C. Pemberton, *Trans. Faraday Soc.*, **63**, 311 (1967).
11) T. Nagamiya, *Progr. Theor. Phys.* (Kyoto), **6**, 702 (1951).
12) R. Savoie and R. P. Fourier, *Chem. Phys. Lett.*, **7**, 1 (1970).

The summation of $v(r)$ over the twelve nearest neighbours is 5.9 kcal/mol; this is roughly comparable with twice the sublimation energy of solid methane[13] at 0°K, 4.4 kcal/mol.

It may be suggested that the mechanism of the phase transition is a rotational one from the double minima in Fig. 2, but it is still ambiguous, for there are no such minima in Fig. 3. The validity of the parameters of Eq. (1) must be studied further.

13) J. H. Colwell, E. K. Gill, and J. M. Morrison, *J. Chem. Phys.*, **39**, 635 (1963).

BULLETIN OF THE CHEMICAL SOCIETY OF JAPAN, VOL. 44, 2274—2275 (1971)

The Radiolysis of Liquid Nitrogen Containing Hydrocarbons. III. Nitrile Formation from Solutions of Alkanes

Takefumi OKA, Tadashi SHINDO, and Shin SATO
Department of Applied Physics, Tokyo Institute of Technology, Ookayama, Meguro-ku, Tokyo
(Received March 15, 1971)

Recently, the radiolysis of liquid nitrogen containing simple olefins has been investigated in our laboratory in order to elucidate the mechanism of the reactions of nitrogen atoms with olefins.[1-3] In these studies, various nitrogenous compounds, such as hydrogen cyanide, acetonitrile, and propionitrile, were observed as products. The formation of these products was first attributed to the reactions of nitrogen atoms with olefins. However, a more detailed study showed that some of these products are formed by the reactions of alkyl radicals with nitrogen atoms.

In the study of the gas-phase reactions of active nitrogen with hydrocarbons, Safrany *et al.* showed that the reactions of nitrogen atoms with alkyl radicals do not produce nitriles, but hydrogen cyanide and ammonia.[4]

The present note will report the results of the radiolysis of liquid nitrogen containing simple alkanes and will discuss the mechanism of the formation of some of the nitrogenous products.

Experimental

Methane, ethane, and propane of a pure grade obtained from the Takachiho Trading Co. were used after bulb-to-bulb distillation. The samples were prepared and irradiated, and the products were analyzed as has been previously described.[2] Most of the samples were in ten-m*l* portions and were irradiated by ^{60}Co γ-rays for one hour at a dose rate of 0.9×10^{6} R/hr.

Results

Propane. The observed products were acetonitrile, a trace of propionitrile, ethane, ethylene, isobutane, *n*-butane, 2,3-dimethylbutane and/or 2-methylpentane, *n*-hexane, an unspecified basic compound and a non-volatile product. Hydragen cyanide and propylene were not observed. All the volatile products increased linearly with the irradiation time up to two hours, the initial concentrations of propane used being 1×10^{-4} and 6×10^{-4} in the mole fraction. The *G*-values of acetonitrile and hexanes are shown in Fig. 1 as a function of the concentration of propane. The *G*-value of acetonitrile (0.08) seems to be independent of the concentration of propane, while those of the hexanes are dependent on it. This feature is similar to those observed when ethylene and propylene are used as solutes.[2,3]

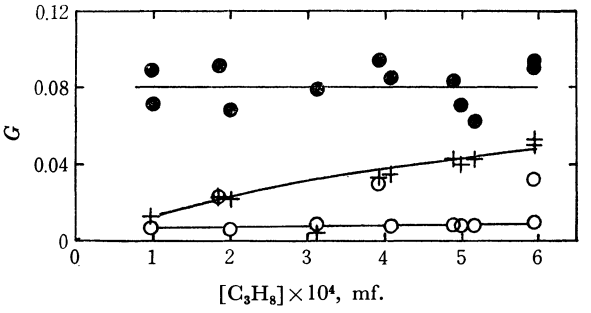

Fig. 1. *G*-values of acetonitrile (●), 2,3-dimethylbutane and/or 2-methylpentane (+) and *n*-hexane (○) as a function of the concentration of propane.

The presence of basic products was ascertained by the following method. After introducing hydrogen chloride onto a volatile product condensed at the temperature of liquid nitrogen, the system was warmed to room temperature. White particles were thus obtained. An aqueous solution of this solid was colored by the Nessler reagent. The non-volatile product was also soluble in water and was colored by the same reagent. The color observed for both solutions was similar to that when ammonium chloride was treated in the same manner. These three solutions showed similar absorption spectra in the region of 350 to 450 mμ. This result suggests that both volatile and non-volatile products contain basic nitrogenous compounds. However, they do not seem to be amines because ethyl and methyl amines have very weak absorptions in the wavelength region examined. Moreover, the volatile product is not simply ammonia, because the absorption at 430 mμ of the aqueous solu-

1) T. Oka and S. Sato, This Bulletin, **42**, 582 (1969).
2) T. Oka, Y. Suda, and S. Sato, *ibid.*, **42**, 3083 (1969).
3) T. Oka and S. Sato, *ibid.*, **43**, 3711 (1970).
4) D. R. Safrany and W. Jaster, *J. Phys. Chem.*, **72**, 518 (1968).

tion increased gradually with the elapsed time for 30 min after preparation. Such a behavior cannot be observed with the solution of ammonium chloride. Every effort we have made hitherto has failed to identify these basic products.

Ethane. The observed products were acetonitrile (G=0.025), hydrogen cyanide (G~0.001), propane (G~0.08), acetylene (G~0.01), and *n*-butane (G~0.04). The basic products were not examined.

Methane. The nitrogenous product observed was hydrogen cyanide (G=0.07). The other products were not analyzed.

Discussion

In a study of the reactions of active nitrogen with alkanes, it was reported that nitrogen atoms in its ground state do not react with methane and ethane at room temperature.[4] The nitrogenous compounds observed in the present study, therefore, may not result from the reactions of nitrogen atoms in its ground state with alkanes. The following processes can be considered for the formation of nitrogenous compounds:

a) The reactions of nitrogen atoms in its ground state with alkyl radicals, which are eventually formed by the reactions of excited nitrogen molecules or nitrogen molecule ions with alkanes:

$$RH + N_2^* \rightarrow R\cdot + H + N_2$$

b) The reactions of electronically-excited nitrogen atoms(^{2}D) with alkane molecules, and

c) The reactions of nitrogen atoms with olefins of impurities or products.

Case c) can, though, be ruled out on the basis of the following facts; 1) In the cases of ethane and propane, propylene is not a product; if formed, it gives rise to acetonitrile in the reaction with nitrogen atoms.[2] 2) The acetonitrile observed in the case of propane was a primary product. 3) The propane used contained no propylene as an impurity.

Case b) cannot be denied by the experimental facts. However, N(^{2}D) can be expected to form ammonia or amines rather than cyanides in reactions with alkanes, judging from the reactions of O(^{1}D),[5] S(^{1}D),[6] C(^{1}S),[7] and nitrene[8] with alkanes.

Case a), which is most likely, can explain the experimental results as follows; if the most abundant alkyl radicals are taken account of in each system, in the case of methane:

$$CH_3 + N \rightarrow HCN + 2H, \quad (1)$$

in the case of ethane:

$$C_2H_5 + N \rightarrow CH_3CN + 2H, \quad (2)$$

and in the case of propane:

$$iso\text{-}C_3H_7 + N \rightarrow CH_3CN + CH_3 + H. \quad (3)$$

These reactions have already been proposed to explain the formation of a part of the cyanides obtained in the radiolysis of liquid nitrogen containing olefins.[2-3] In the gas phase, it was suggested by Safrany and Jaster that these reactions produce HCN or NH.[4] This apparent disagreement may be due to the difference in deactivation.

The basic products observed might be imines, whose formation has been suggested in the thermolysis and photolysis of methylazide.[8] Obviously, further investigations are needed.

5) a) H. Yamazaki and R. J. Cvetanović, *J. Chem. Phys.*, **41**, 3703 (1964). b) W. B. DeMore, *J. Phys. Chem.*, **73**, 391 (1969).

6) a) A. R. Knight, O. P. Strausz, and H. E. Gunning, *J. Amer. Chem. Soc.*, **85**, 2349 (1963). b) K. Gollnick and E. Leppin, *ibid.*, **92**, 2217 (1970).

7) P. S. Skell and R. R. Engel, *ibid.*, **88**, 4883 (1966).

8) R. A. Abramovitch and B. A. Davis, *Chem. Rev.*, **64**, 149 (1964).

BULLETIN OF THE CHEMICAL SOCIETY OF JAPAN, VOL. 44, 2276—2277 (1971)

On Liquefaction Caused by the Trituration of Pairs of Solid Compounds

Tominosuke KATSURAI, Sadao MATSUO*, and Kozo SONE

Department of Chemistry, Faculty of Science, Ochanomizu University, Otsuka, Tokyo

** Department of Chemistry, Tokyo Kyoiku University, Otsuka, Tokyo*

(Received March 16, 1971)

Many pairs of solid compounds are known to give rise to liquefaction when they are brought into contact. Liquefaction is accelerated by trituration. The mode of liquefaction is of interest as an irreversible change which takes place in the contact area of two different phases. Features common to the liquefaction are twofold, *viz.*, either one or both of the solid compounds are hydrated, and the process is endothermic.[1-5]

This note deals with our search for new pairs for liquefaction and the results obtained. Since we had so far no guiding principle for selection of the pairs, we simplified the situation by choosing pairs consisting of (a) a hydrated inorganic salt and (b) an organic compound without water of crystallization (except oxalic acid). (a) is considered to supply the water necessary for liquefaction and (b) to make (a) liberate the water. Most of the salts (a) were sulfates because they are not hygroscopic but some chlorides were also tried. Chloral hydrate was taken up for the sake of comparison. For (b) we chose compounds which are able to form hydrogen bonds with water and seem to influence the structure of water. Simple amino-acids, urea,[6] acetamide which is structurally similar to urea and a series of organic acids were selected, in order to see if the change in structure might influence the mode of liquefaction.

Pairs of compounds consisting of one each from (a) and (b) were triturated in a porcelain mortar by hand for 10 min and the resulting changes were observed. Commercial products of the best grade were used. Roughly the same weights for each compound were taken. The molar ratio was made to be that of integers, *e.g.*, 5 g of $CuSO_4 \cdot 5H_2O$ and 4.8 g of urea make the ratio 1 : 4. The results are summarized in Table 1.

We see that there is no general, all-embracing rule for the occurrence of liquefaction. However, we note several interesting facts and rules. Of (a), $Na_2SO_4 \cdot 10H_2O$ undergoes liquefaction to the greatest extent, and $FeSO_4 \cdot (NH_4)_2SO_4 \cdot 6H_2O$ none.[7] On the other hand, $Fe_2(SO_4)_3 \cdot (NH_4)_2SO_4 \cdot 24H_2O$ undergoes liquefaction very easily with several organic compounds. Of (b), polar and highly water-soluble compounds favor liquefaction, *viz.*, urea, acetamide, malonic acid, malic acid, citric acid,[8] tartaric acid and chloral hydrate. Non-polar and water-insoluble compounds have no ability to give rise to liquefaction. This is exemplified by succinic acid and fumaric acid. Isomers differ in their behavior toward liquefaction as in the cases of α-alanine and β-alanine, and maleic acid and fumaric acid.

From the results so far obtained, we might prescribe the following not rigorous but practical tests to find new pairs for liquefaction. (1) Triturate a salt from (a) with urea. If liquefaction takes place, another compound belonging to (b) which gives rise to liquefaction on being triturated with (a) can be found. If liquefaction does not take place, no (b) can be found. (2) Triturate a compound from (b) separately with $Na_2SO_4 \cdot 10H_2O$ and $Fe_2(SO_4)_3 \cdot (NH_4)_2SO_4 \cdot 24H_2O$. If liquefaction takes place, another salt belonging to (a) which gives rise to liquefaction on being triturated with (b) can be found. If not, no (a) can be found.

In certain pairs, one compound of the pair can be liquefied without being kept in contact with the other. Equivalent amounts of $Na_2SO_4 \cdot 10H_2O$ and urea, each pulverized, were put into separate branches of a bifurcated glass tube. The tube was evacuated while they were being cooled with Dry Ice and then let to stand at room temperature. Urea liquefied in less than ten days. In the case of the pair $MgSO_4 \cdot 7H_2O$ and urea, the latter did not liquefy, although the pair liquefies on trituration. In the case of $FeCl_3 \cdot 6H_2O$ and acetamide, both became wet.

Sometimes we come across pairs which on trituration give rise to chemical changes. They are exemplified by the evolution of SO_2 in the pair $Na_2S_2O_3 \cdot 5H_2O$ and citric acid, and by that of HCl in the pair $AlCl_3 \cdot 6H_2O$ and citric acid or tartaric acid, as well as by the change of color to a deep bluish violet in the pair $CuSO_4 \cdot 5H_2O$ and glycine. We realize here the necessity of giving attention to possible solid-phase reactions such as ion exchange[9] and the formation of complex compounds.

1) Miss E. M. Walton, *Phil. Mag.*, **12**, 290 (1881).
2) T. Katsurai, *Kolloid-Z.*, **83**, 37 (1938).
3) T. Katsurai and K. Yamasaki, *ibid.*, **84**, 311 (1938).
4) T. Katsurai, *Sci. Pap. Inst. Phys. Chem. Res.* (Tokyo), **35**, 221 (1939).
5) T. Katsurai, *Bull. Inst. Phys. Chem. Res.* (Tokyo), **23**, 215 (1944).
6) D. V. Beauregard and R. E. Barrett, *J. Chem. Phys.*, **49**, 5241 (1968).
7) It is to be noticed, however, that this salt undergoes rapid liquefaction on being triturated with $FeCl_3 \cdot 6H_2O$, *cf.* (5).
8) J. W. Mullin and C. L. Leci, *Phil. Mag.*, **19**, 1075 (1969).
9) A. Clearfield and J. M. Troup, *J. Phys. Chem.*, **74**, 2578 (1970).

Table 1. Modes of liquefaction

Hydrated salt (a)	Organic compound (b)								
	H_2NCH_2COOH glycine	$CH_3CH(NH_2)$-COOH DL-α-alanine	$H_2NCH_2CH_2$-COOH β-alanine	o-$NH_2C_6H_4COOH$ anthranilic acid	$CO(NH_2)_2$ urea	CH_3CONH_2 acetamide	$(COOH)_2$ oxalic acid, anhydrous	$(COOH)_2 \cdot 2H_2O$ oxalic acid, hydrated	$HOOCCH_2$-COOH malonic acid
$Na_2SO_4 \cdot 10H_2O$	−	−	++	−	+++	++	++	+++	+++
$MgSO_4 \cdot 7H_2O$	−	−	−	−	+	−	−	−	−
$Al_2(SO_4)_3(NH_4)_2SO_4 \cdot 24H_2O$	−	−	+	−	+	−	−	−	−
$Al_2(SO_4)_3Na_2SO_4 \cdot 24H_2O$	+++	++	+++	−	+++	+++	−	+++	+
$Al_2(SO_4)_3K_2SO_4 \cdot 24H_2O$	−	−	++	−	+	−	−	−	−
$FeSO_4 \cdot 7H_2O$	−	−	+	−	++	−	−	−	−
$FeSO_4 \cdot (NH_4)_2SO_4 \cdot 6H_2O$	−	−	−	−	−	−	−	−	−
$Fe_2(SO_4)_3(NH_4)_2SO_4 \cdot 24H_2O$	+++	++	++	−	+++	−	++	+++	−
$CuSO_4 \cdot 5H_2O$	+	−	+	−	++	−	+	++	−
$ZnSO_4 \cdot 7H_2O$	++	−	++	−	+++	++	−	++	−
$AlCl_3 \cdot 6H_2O$	++	+	+++	−	+++	++	−	−	−
$FeCl_3 \cdot 6H_2O$	+++	+++	+++	+	+++	+++	+++	+++	−
$CCl_3CH(OH)_2$	−	−	−	−	+++	+++	−	−	−

Hydrated salt (a)	Organic compound (b)							
	$(CH_2COOH)_2$ succinic acid	$HOOCCH_2CH(OH)$-COOH malic acid	$C_3H_4(OH)(COOH)_3 \cdot H_2O$ citric acid	$C_2H_2(OH)_2$-$(COOH)_2$ tartaric acid	H—C—COOH ‖ H—C—COOH maleic acid	HC—COOH ‖ HOOC—CH fumaric acid	$CCl_3CH(OH)_2$ chloral hydrate	$C_6H_{12}O_6$ D-glucose
$Na_2SO_4 \cdot 10H_2O$	−	++	+++	+++	++	−	+++	++
$MgSO_4 \cdot 7H_2O$	−	−	−	−	−	−	−	−
$Al_2(SO_4)_3(NH_4)_2SO_4 \cdot 24H_2O$	−	−	−	−	−	−	−	−
$Al_2(SO_4)_3Na_2SO_4 \cdot 24H_2O$	−	−	+	++	−	−	++	−
$Al_2(SO_4)_3K_2SO_4 \cdot 24H_2O$	−	−	−	−	−	−	−	−
$FeSO_4 \cdot 7H_2O$	−	−	−	−	−	−	−	−
$FeSO_4 \cdot (NH_4)_2SO_4 \cdot 6H_2O$	−	−	−	−	−	−	−	−
$Fe_2(SO_4)_3(NH_4)_2SO_4 \cdot 24H_2O$	−	−	−	+	−	−	−	−
$CuSO_4 \cdot 5H_2O$	−	−	−	−	−	−	−	−
$ZnSO_4 \cdot 7H_2O$	−	−	−	+	−	−	+	−
$AlCl_3 \cdot 6H_2O$	−	−	−	−	−	−	−	−
$FeCl_3 \cdot 6H_2O$	−	−	+++	−	−	−	+	++
$CCl_3CH(OH)_2$	−	−	−	−	−	−	/	−

+++ denotes rapid and apparently complete, ++ medium, + slow and apparently partial, and — no liquefaction.

SHORT COMMUNICATIONS

Photodecomposition of Azidoformate in Alkyl Sulfides. I

Wataru ANDO, Nobukuni OGINO, and Toshihiko MIGITA
Department of Chemistry, Gunma University, Kiryu, Gunma
(Received March 1, 1971)

The reaction of azidoformate in alkyl sulfides under photolytical conditions has received little attention. We wish to describe the formation of a stable iminosulfurane by photoinduced reaction of methyl azidoformate with alkyl sulfides, and some properties of singlet and triplet carbomethoxynitrene in alkyl sulfides.

Irradiation of a solution of 1 mmol methyl azidoformate in 10 mmol of alkyl sulfide was carried out in quartz vessels under nitrogen atmosphere with a high pressure mercury lamp for one hour. *N*-Methoxycarbonylalkyliminosulfuranes (I—III) were obtained as pale yellow liquids in 40—60% yields by passing the reaction mixture through a silica gel column using ethyl ether, then methanol-ethyl ether (1 : 4) as eluting solvents. The structures of the sulfuranes are determined by comparison of their spectra with those of authentic samples.[1]

Product patterns resulting in photosensitized reaction of azidoformate with sulfides are quite different from those in direct photolysis.

$$N_3CO_2CH_3 + R_2S \xrightarrow{h\nu} R_2\overset{\oplus}{S}-\overset{\ominus}{N}CO_2CH_3 \quad 40—60\%\ \text{yields}$$

I, $R=CH_3$;
II, $R=C_2H_5$;
III, $R=i\text{-}C_3H_7$

A mixture of methyl azidoformate and alkyl sulfides (molar ratio 1 : 10) in Pyrex tubes was irradiated with a high pressure mercury lamp in the presence of acetophenone as triplet sensitizer.[2,3] Methyl carbamate was obtained as a major product (56% yield). Formation of alkyliminosulfuranes was not recognized from the NMR spectrum.

These results indicate that the triplet nitrene cannot be an intermediate of the formation of imonosulfuranes, analogous to the behaviors of carbene towards sulfur containing molecules.[4,5] This suggests a mechanism of iminosulfurane formation in which a singlet carbomethoxynitrene attacks an unshared electron pair on the sulfur atom of alkyl sulfides.

Table 1. Reaction of carbomethoxynitrene in a mixture of *cis*-4-methyl-2-pentene and dimethyl sulfide

Mole ratio Olefin/ Sulfide	Aziridines		Sulfurane (I)	Ratio
	Yields (%)	*trans* Isomer	Yield (%)	k_s/k_o
Olefin only	62.8	35.0	—	—
5	29.6	38.1	16.9	2.8
4	26.8	39.6	17.7	2.6
2	13.2	41.7	17.4	2.6
1	8.1	49.4	19.8	2.4
0.5	4.6	51.2	37.0	2.4
0.25	trace	*ca.* 70	44	—

Competitive reactions of dimethyl sulfide and *cis*-4-methyl-2-pentene towards the nitrene derived by the direct photolysis of methyl azidoformate were carried out. The results listed in Table 1 show the following tendencies in the relative rate between addition and iminosulfurane (I) formation, and in the stereochemistry of the addition to olefin. First, the relative rate constant of iminosulfurane (I) formation to addition k_s/k_o gradually decreased as the initial ratio of olefin and sulfide decreased. Secondly, although the yields of total aziridines decreased, the relative ratio of *trans* isomer increased as the initial concentration of sulfide increased. Even in the reaction with olefin alone, a considerable amount of *trans* aziridine was formed (*cis* : *trans*=2 : 1), that is to say, the addition is not strictly stereospecific. These tendencies can be best explained by assuming that the reaction of the singlet nitrene with solvent molecules competes with the intersystem crossing of the singlet to the triplet, and that the singlet adds to olefin stereospecifically and reacts with dimethyl sulfide giving iminosulfurane, while the triplet adds to olefin nonstereospecifically and reacts with the sulfide less easily without giving iminosulfurane. Increase in the initial concentration of sulfide will decrease the amount of aziridine derived from the singlet. This will diminish the probability of the intersystem crossing to give a less amount of the triplet nitrene and lower yields of the *trans* aziridine.

1) G. F. Whitfield, H. S. Beilan, D. Saika, and D. Swern, *Tetrahedron Lett.*, **1970**, 3543.
2) W. Lwolski and T. W. Mattingly, Jr., *J. Amer. Chem. Soc.*, **87**, 1947 (1965).
3) H. Nozaki, S. Fujita, H. Takaya, and R. Noyori, *Tetrahedron*, **23**, 45 (1967).
4) W. Ando, T. Yagihara, S. Tozune, and T. Migita, *J. Amer. Chem. Soc.*, **91**, 2786 (1969).
5) W. Ando, K. Nakayama, K. Ichibori, and T. Migita, *ibid.*, **91**, 5164 (1969).

3-*O*-Benzyl-5-deoxy-5-(ethylphosphinyl)-D-xylopyranose

Saburo INOKAWA, Yoshimi TSUCHIYA, Kuniaki SEO,* Hiroshi YOSHIDA, and Tsuyoshi OGATA

Department of Synthetic Chemistry, Faculty of Engineering, Shizuoka University, Johoku, Hamamatsu

* *Department of Applied Chemistry, Numazu Technical College, Ohoka, Numazu*

(Received March 18, 1971)

There has been a great deal of activity in recent years in connection with the syntheses of sugar analogs with nitrogen or sulfur in the hemiacetal ring.[1] Concerning sugar analogs with phosphorus in the ring, however, only one short report has been published, by Whistler and Wang,[2] who prepared 5-deoxy-3-*O*-methyl-5-(phosphinyl)-D-xylopyranose and 5-deoxy-3-*O*-methyl-5-(hydroxyphosphinyl)-D-xylopyranose in poor yields.

The present paper will report on the synthesis of 3-*O*-benzyl-5-deoxy-5-(ethylphosphinyl)-D-xylopyranose in 27% yield from **1**.

As a starting material, we used 3-*O*-benzyl-5-deoxy-5-iodo-1,2-*O*-isopropylidene-α-D-xylofuranose (**1**) (mp 76—76.5°C,[3] $[\alpha]_D^{14}$ −59.8° (*c* 4.5, acetone)), which has been prepared from 3-*O*-benzyl-1,2;5,6-di-*O*-isopropylidene-α-D-glucofuranose through the sequence of 3-*O*-benzyl-1,2-*O*-isopropylidene-α-D-glucofuranose, 3-*O*-benzyl-1,2-*O*-isopropylidene-α-D-xylofuranose, and 3-*O*-benzyl-5-*O*-tosyl-1,2-*O*-isopropylidene-α-D-xylofuranose. The Michaelis-Arbuzov reaction of **1** with diethyl ethylphosphonite gave, in an 87% yield, 3-*O*-benzyl-5-deoxy-5-(ethoxyethylphosphinyl)-1,2-*O*-isopropylidene-α-D-xylofuranose (**2**) (bp 105—110°C/10^{-2}—10^{-3} mmHg, syrup, $[\alpha]_D^{14}$ −15.3° (*c* 3.9, chloroform)). The reduction of **2** with lithium aluminum hydride, followed by oxidation with air, afforded, in an 85% yield, 3-*O*-benzyl-5-deoxy-5-(ethylphosphinyl)-1,2-*O*-isopropylidene-α-D-xylofuranose (**3**) (bp 120—130°C/10^{-2}—10^{-3} mmHg, syrup, $[\alpha]_D^{15}$ −34.5° (*c* 4.6, chloroform)). The structure of **3** was established by studies of the PMR and IR spectra. The PMR spectrum (chloroform-*d*) showed a characteristic J(P–H) value[4] of 462 Hz at τ 3.1 (one-proton multiplet, disappearing upon the addition of D_2O). The IR spectrum showed the absorption of a P–H group at 2350 cm^{-1} and that of a P=O group at 1260 and 1220 cm^{-1}. The methanolysis of **3** in a methanol solution containing hydrochloric acid did not afford a methyl glycoside with phosphorus in the ring, but methyl 3-*O*-benzyl-5-deoxy-5-(ethylphosphinyl)-D-xylofuranoside (syrup) (**4**) in an 82% yield. The PMR spectrum (chloroform-*d*) showed a J(P–H) value of 462 Hz at τ 3.1 (one-proton multiplet, disappearing upon the addition of D_2O), and the IR spectrum showed the absorption of a P–H group at 2350 cm^{-1}. The structure of **4** was then identified as a methyl furanoside. On the hydrolysis of **3** in 50% aqueous methanol containing sulfuric acid (2 N), two major spots (R_f 0.70 and 0.55) and one minor spot (R_f 0.15) could be observed on a thin-layer chromatogram (chloroform-methanol, 5 : 1 v/v). The constitution of the two major components was about 1 : 1. The component **5**, with R_f 0.70, was easily separated, in a 45% yield, from the mixture by extraction with chloroform. The PMR spectrum (chloroform-*d*) showed a J(P–H) value of 462 Hz at τ 3.1 (one-proton multiplet, disappearing upon the addition of D_2O), and the IR spectrum showed the absorption of a P–H group at 2350 cm^{-1}. The component **5** was then identified as 3-*O*-benzyl-5-deoxy-5-(ethylphosphinyl)-D-xylofuranose (syrup). The component **6**, with R_f 0.55, was separated, in a 37% yield, by alumina-column chromatography (chloroform-methanol, 5 : 1 v/v). In the PMR (dimethyl sulfoxide-d_6) and IR spectra of **6**, the absorption showing the presence of a P–H group completely disappeared and the absorption of a one-proton multiplet at τ about 5 assigned to H-1 appeared. Moreover, by the treatment of **5** with 2 N sulfuric acid, half of the **5** was led to **6**. Therefore, **6** was identified as 3-*O*-benzyl-5-deoxy-5-(ethylphosphinyl)-D-xylopyranose (syrup, $[\alpha]_D^{11}$ −7.0° (*c* 2.6, methanol)).

1) For example, H. Paulsen and K. Todt, *Advan. Carbohyd. Chem.*, **23**, 116 (1968).

2) R. L. Whistler and C.-C. Wang, *J. Org. Chem.*, **33**, 4455 (1968).

3) R. C. Young, P. W. Kent, and R. A. Dwek, *Tetrahedron*, **1970**, 3984.

4) H. R. Hays, *J. Org. Chem.*, **33**, 3690 (1968).

The Formation of $N_3P_3(NH_2)_6 \cdot H_2O$ and $N_3P_3(NH_2)_6 \cdot HCl$ from the Reaction Product between $(NPCl_2)_3$ and Ammonia

Etsuro KOBAYASHI

Government Chemical Industrial Research Institute, Tokyo, Honmachi, Shibuya-ku, Tokyo

(Received March 19, 1971)

In the course of the synthesis research into $N_3P_3(NH_2)_6 \cdot H_2O$ as a fireproof material, some experiments have been made on the reaction between $(NPCl_2)_3$ and liquid ammonia, a new adduct, $N_3P_3(NH_2)_6 \cdot HCl$, was found to be formed. The reaction conditions for the formation and the characteristics of the adduct have been investigated.

Previous studies have indicated that an ammonolysis of phosphonitrilic chlorides takes place very slowly.[1] Audrieht and Sowerby[2] have also reported that the complete replacement of the chlorine atoms in the phosphonitrilic chlorides could be achieved within 48 hr. However, in this study, the reaction between $(NPCl_2)_3$ and a large excess of liquid ammonia has been completed within several hours in an autoclave with an electro-magnetic stirrer, and the rate of reaction was accelerated by the addition of dioxane as the solvent to this reaction system. The reaction product is a mixture of $N_3P_3(NH_2)_6$ and NH_4Cl.

It has been reported that the addition of ethanol to an aqueous solution of the reaction product causes the precipitation of $N_3P_3(NH_2)_6 \cdot H_2O$.[3] However, the author found the following facts when he used this separation procedure.

After the ammonia involved in the reaction product was completely excluded under reduced pressure, the product was dissolved in water. The adduct, $N_3P_3(NH_2)_6 \cdot HCl$, was then precipitated by the addition of ethanol to the aqueous solution.

Found: P, 34.2; N, 46.5; Cl, 12.6%; P : N : Cl atomic ratio, 3.0 : 9.0 : 1.0. Calcd for $N_3P_3(NH_2)_6 \cdot HCl$: P, 34.73; N, 47.12; Cl, 13.25%.

The analyses of the typical products did not give the $N_3P_3Cl_{6-n}(NH_2)_n$ formula, but $N_3P_3(NH_2)_6 \cdot HCl$. Therefore, the formation reaction may be expressed by the following equation:

$$N_3P_3(NH_2)_6 + 6NH_4Cl \rightleftharpoons N_3P_3(NH_2)_6 \cdot HCl + 5NH_4Cl + NH_3$$

The equation was also confirmed by an examination of the reaction between $N_3P_3(NH_2)_6 \cdot H_2O$ and commercial ammonium chloride, and the heat of reaction was 1.24 kcal/mol (endothermic).

It is known[4] that the basicity of some aninophosphazens is comparable with that of parent amines, and adducts ($N_3P_3(NHR)_6 \cdot HCl$, where R is aliphatic amines) are formed with one molecule of hydrogen chloride even in the presence of ammonia. However, with the $N_3P_3(NH_2)_6 \cdot HCl$ adduct, it is considered that the molecule of hydrogen chloride can be removed with ammonia. In fact, $N_3P_3(NH_2)_6 \cdot H_2O$ was formed by the addition of ethanol to a reaction product solution that contained an excess amount of ammonia for the neutralization of hydrogen chloride in $N_3P_3(NH_2)_6 \cdot HCl$.

Found: P, 38.4; N, 51.7; Cl, 0.4%; P : N : Cl atomic ratio, 3.0 : 8.9 : 0.0. Calcd for $N_3P_3(NH_2)_6 \cdot H_2O$: P, 37.30; N, 50.61%.

Both compounds, $N_3P_3(NH_2)_6 \cdot H_2O$ and $N_3P_3(NH_2)_6 \cdot HCl$, are composed of a white crystalline powder, both dissolve in water (hydrate: the solubility at 25°C is 11.2 g anhydride/100 g soln; chloride: because of its high solubility, it could not be measured), but are insoluble in various organic solvents. The compounds showed their own characteristic IR absorption bands, as is shown in Fig. 1. Their DTA curves are distinguished from each other, and they were both converted by heating to phospham, which has an excellent flame resistance.

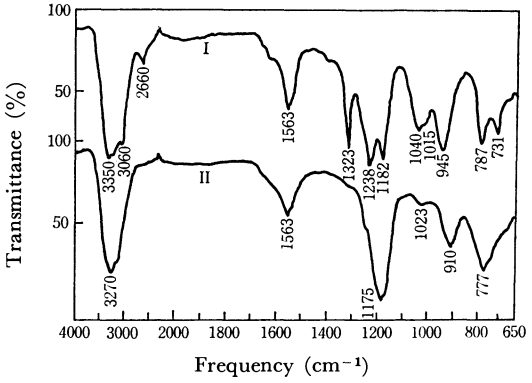

Fig. 1. Infrared spectra of trimeric phosphorus nitride diamides.
I: $N_3P_3(NH_2)_6 \cdot HCl$ II: $N_3P_3(NH_2)_6 \cdot H_2O$

1) A. M. de Ficquelmont, *Ann. Chim.*, **12**, 169 (1939).
2) L. F. Audrieth and D. B. Sowerby, *Chem. Ind.* (London), **1959**, 748.
3) H. Moureu and P. Rocquet, *Bull. Soc. Chim. Fr.*, [5] **3**, 821 (1936).
4) S. K. Ray and R. A. Shaw, *Chem. Ind.* (London), **1961**, 1173.

Nuclear Magnetic Resonance Spectra of Carbanions. VIII.[1] α-Picolyllithium

Kazuyori KONISHI, Kensuke TAKAHASHI,[2] and Ryuzo ASAMI

Department of Synthetic Chemistry, Nagoya Institute of Technology, Gokiso-cho, Showa-ku, Nagoya

(Received April 14, 1971)

The pmr spectra of the benzyl-type carbanions containing hetero atoms have not yet been reported as far as we know. We have recently observed the pmr spectra of α-picolyllithium in THF solutions. α-Picolyllithium was prepared from 6.35 mmol of α-picoline in contact with 6.05 mmol of phenyllithium in THF in a vacuum. A typical spectrum of α-picolyllithium is given in Fig. 1. One strong impurity signal is observed at 7.31 ppm; it is due to benzene. The other signals can be easily assigned by means of their intensities and structures except for some small impurity signals. The observed chemical shifts are given in Table 1, along with those of α-picoline and benzyllithium for comparison, taking the solvent peak at 1.79 ppm as a reference. The chemical shifts for the 0.22 and 0.58 mol/*l* solution of the carbanion were consistent within the limits of experimental error (±0.03 ppm). The coupling constants between the ring protons are $J_{34}=9.0$, $J_{35}=1.5$, $J_{36}=1.0$, $J_{45}=6.5$, $J_{46}=1.9$, and $J_{56}=5.5$ Hz, as evaluated from the first-order analysis for a 0.22 mol/*l* solution of the carbanion in THF. The data are compared with those of benzyllithium reported by Sandel and Freedman.[3] The ring protons of α-picolyllithium are more shielded than those of benzyllithium except for the 6-hydrogen, which is strongly affected by the nitrogen atom. The extra charge transferred from lithium to the pyridine ring in α-picolyllithium can be evaluated from the chemical shifts, using the procedures in a previous report.[4] The charges are -0.16_5, -0.15, -0.22, and -0.15 in units of the absolute value of the charge of an electron for the 3-, 4-, 5-, and 6-carbons respectively, taking picoline as the reference compound. There is a question of the magnitude of the proportional coefficient of the 10 ppm/electron, used for the charge estimation.[5] However, we can compare the extra charges transferred from lithium to the aromatic ring of the carbanions relatively. It is estimated that the more shielded the aromatic protons in the carbanions, the more stable the carbanions become. The extra charges are more transferred from lithium to the aromatic ring in α-picolyllithium than that in benzyllithium.[3] Therefore, the ionic nature of the metal-carbon bond in α-picolyllithium may be larger than that in benzyllithium, and α-picolyllithium may be more stable than benzyllithium. The methylene protons of α-picolyllithium are less shielded than the methyl protons of α-picoline. This tendency may be ascribed to the hybridization change in the α-carbon atom from sp^3 in α-picoline to near-sp^2 in α-picolyllithium, as was reported before in the α-methylstyrene dimer dianion.[4] The line width of the methylene proton signal is broader than the other ring proton signals in α-picolyllithium. Three reasons explaining this broadening may be considered. They are the nitrogen quadrupole relaxation effect, the coupling with ring protons, and the nonequivalency of the two methylene protons. The last reason seems to be most probable. Further studies are now in progress.

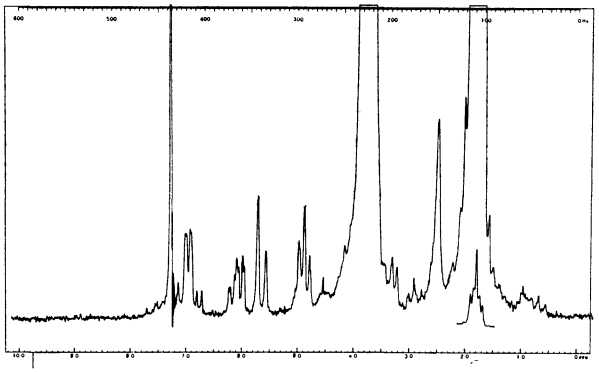

Fig. 1. A spectrum of a 0.58 mol/*l* α-picolyllithium in THF. Applied radio frequency increases from right to left near 60 MHz at a constant magnetic field.

TABLE 1. THE PROTON CHEMICAL SHIFTS OF α-PICOLYLLITHIUM AND THE RELATED COMPOUNDS IN THF AT 60 MHz IN ppm

Compound	Assignment				
	3-H	4-H	5-H	6-H	CH_2 or CH_3
α-Picolyllithium	5.68	6.08_5	4.87_5	6.92	2.53_5
Benzyllithium[a]	6.09	6.30	5.50	6.30	1.62[b]
α-Picoline	7.34_5	7.56	7.05_5	8.42	2.48_5

a) Ref. 3. b) Ref. 6.

1) Part VII in this series: M. Ushio, M. Takaki, K. Takahashi, and R. Asami, to be published in This Bulletin, **44**, No. 9 (1971).

2) To whom all correspondence should be addressed.

3) V. R. Sandel and H. H. Freedman, *J. Amer. Chem. Soc.*, **85**, 2328 (1963).

4) K. Takahashi, M. Takaki, and R. Asami, *J. Phys, Chem.* **75**, 1062 (1971).

5) R. V. Lawler and C. V. Ristagno, *J. Amer. Chem. Soc.*, **91**, 1534 (1969).

6) R. Waack, M. A. Doran, E. B. Baker, and G. A. Olah, *ibid.*, **88**, 1272 (1966).

Oxidation of Propylene over Cu(II)-Y Molecular Sieve under High Steam Concentration[1]

Isao Mochida, Shinji Hayata, Akio Kato, and Tetsuro Seiyama
Department of Applied Chemistry, Faculty of Engineering, Kyushu University, Fukuoka
(Received April 22, 1971)

In a previous paper,[2] it was reported that acrolein was formed from propylene over the Y molecular sieve ion-exchanged with cupric ion (Cu(II)-Y) in the presence of steam. As the molecular sieve is highly acidic, it is expected to play a bifunctional catalytic role for the synthesis of acetone from propylene through hydration and dehydrogenation under adequate conditions.

In the present study, reactions of propylene over this catalyst under high steam concentration was carried out using a flow reactor with a fixed catalyst bed. Feed and product compositions were analyzed by gas-chromatography. The procedures were similar to those reported by Ogasawara *et al.*[3]

The results obtained in the absence of oxygen (Fig. 1) indicate that isopropanol and acetone can be formed in place of another. This suggests that acetone is formed from propylene *via* hydration and dehydrogenation. The maximum yield of acetone was 1.3% at 315°C, where the yield is defined by (product moles)/(propylene fed).

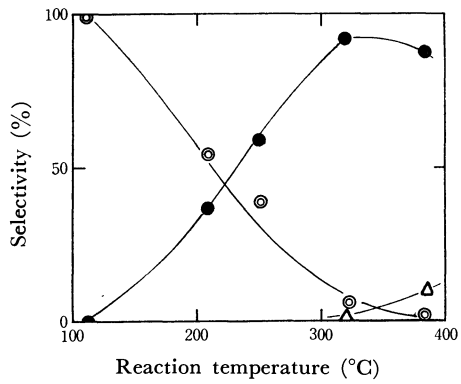

Fig. 1. Selectivity of products over Cu(II)-Y without oxygen.
Cu(II)-Y: 4 g. Reactant gas composition, C_3H_6:H_2O=1:20.
●: acetone, ◎: isopropanol, △: ethylene.

The results in the presence of oxygen are shown in Fig. 2. The main products other than carbon dioxide were isopropanol below 200°C, acetaldehyde at around 250°C and acetone above 450°C. It should be mentioned that acrolein was the main product under low steam concentration.[2] The maximum yields of acetaldehyde and acetone were 1.0 and 0.7%, respectively.

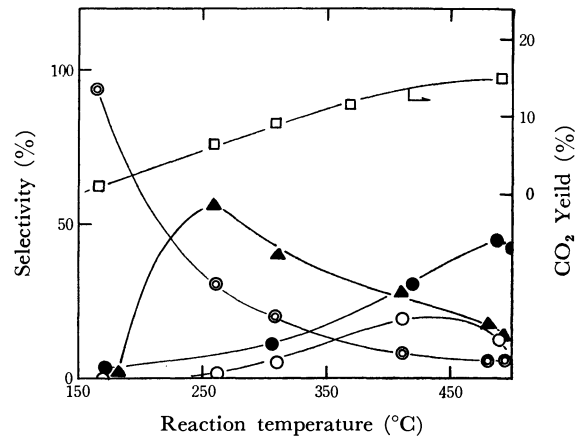

Fig. 2. Selectivity of propylene oxidation over Cu(II)-Y in the presence of oxygen (selectivity is based on products excluding carbon dioxide).
Cu(II)-Y: 2.7 g. Reactant gas composition, C_3H_6:O_2:H_2O =1:1:20.
□: CO_2 yield, ●: acetone, ◎: isopropanol, ▲: acetaldehyde, ○: acrolein.

Moro-oka *et al.*[4] and Ogasawara *et al.*[3] reported selective oxidation of propylene into acetone on molybdena catalysts. Backer and Carrick reported the oxidative cleavage of olefinic double bond on chromia catalyst.[5] From their results and ours, formation routes for acrolein, acetaldehyde, and acetone can be described as follows:

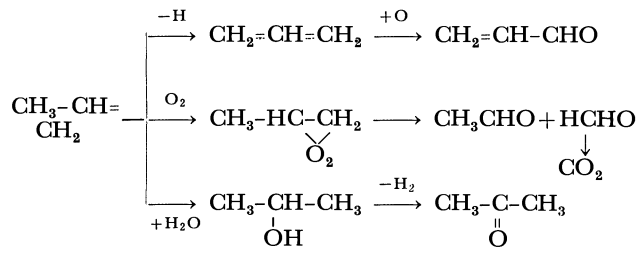

1) Catalytic Oxidation over Molecular Sieves ion-exchanged with Transition Metal Ion. V. Part IV, in press in This Bulletin.
2) I. Mochida, S. Hayata, A. Kato, and T. Seiyama, *J. Catalysis*, **19**, 405 (1970).
3) S. Ogasawara, S. Takahashi, A. Fukai, and Y. Nakada, *Kogyo Kagaku Zasshi*, **72**, 2244 (1969); S. Ogasawara, Y. Nakata, Y. Iwata, and H. Sato, *ibid.*, **73**, 509 (1970); S. Ogasawara, H. Sato, and Y. Iwata, *ibid.*, **73**, 509 (1970).
4) Y. Moro-oka, S. Tan, and A. Ozaki, *J. Catalysis*, **12**, 291 (1968); **17**, 125 (1970); S. Tan, Y. Moro-oka, and A. Ozaki, *ibid.*, **17**, 132 (1970).
5) L. M. Backer and W. L. Carrick, *J. Org. Chem.*, **33**, 616 (1968).

A Novel Bis(dimethylglyoximato)cobalt(III) Complex with a *cis*-Configuration

Nobufumi MAKI

Department of Chemistry, Faculty of Engineering, Shizuoka University, Johoku, Hamamatsu

(Received April 28, 1971)

Numerous cobalt(III) complexes of the *trans*-[CoX_2-$(dgH)_2$] type[1] have been reported, but the corresponding *cis*-isomers have not yet been synthesized. The steric condition arising from the extremely stable square-planar structure of the [$Co(dgH)_2$] type with a pair of hydrogen bonds is the reason why the formation of *cis*-isomers is so difficult. Nakahara,[2] however, has prepared the [$Co(dgH)_3$]·5/2 H_2O complex in a strongly basic solution for the rupture of the hydrogen bonds. The present communication will describe one of our attempts to prepare three new compounds of a cis-type involving an ethylenediamine, [$Co(dgH)(dgH_2)en$]Cl_2·$2H_2O$, [$Co(dgH)(dgH_2)en$]-Br_2·$2H_2O$, and [$Co(dgH)_2en$]ClO_4·1/3 H_2O.

Thirty grams of the [Co en_3]Cl_3·$3H_2O$ complex[3] were completely dissolved in 850 m*l* of water at 80°C. To this solution we then added 45.7 g of Na_2dg·$8H_2O$. The solution was directly heated to the boil (100°C) for 3 hr, and finally it was concentrated to 130 m*l*. On heating, the orange-yellow color of the solution soon turned dark brown, but no deposition of metallic cobalt was observed during the reaction. After the solution had been cooled in ice, sodium chloride precipitates formed and were filtered off. To the filtrate (130 m*l*), 36 m*l* of 35% HCl were added under ice-cooling. Then, brown crystals were deposited from the solution; these crystals were separated by filtration and washed with a small amount of cold water, ethanol, and ether. The yield was 34% of the theory. The purifications were carried out as follows: the crude complex (14 g) was dissolved in a requisite small amount of a 0.5 M NaOH solution (110 m*l*). After the filtration of the solution, the complex was precipitated again by stirring in 36 m*l* of HCl (25%), drop by drop, at 0°C. This procedure was repeated three times. The complex was then dried on $CaCl_2$ under 1 atmosphere. Found: Co, 18.72; C, 26.58; N, 18.83; H, 6.31; Cl, 15.74%. Calcd for [$Co(dgH)$-$(dgH_2)en$]Cl_2·$2H_2O$: Co, 18.89; C, 26.27; N, 18.38; H, 5.95; Cl, 15.51%.

The bromide and perchlorate of the complex were likewise precipitated by adding the corresponding acid (30—35%) instead of hydrochloric acid to the basic filtrate. The purification procedure was quite the same as above. Found: Co, 10.65; C, 21.53; N, 15.78; H, 5.11; Br, 29.15%. Calcd for [$Co(dgH)$-$(dgH_2)en$]Br_2·$2H_2O$: Co, 10.79; C, 21.99; N, 15.39; H, 4.98; Br, 29.26%. Found: Co, 12.78; C, 26.05; N, 18.71; H, 4.89; Cl, 8.03%. Calcd for [Co-$(dgH)_2en$]ClO_4·1/3 H_2O: Co, 12.96; C, 26.42; N, 18.48; H, 5.03; Cl, 7.80%.

The molar ratio of the halide ion to the complex cation was also examined by volumetric analyses; the results established an approximately 2 : 1 ratio for both the halide ions. The aqueous solutions of these compounds are strongly acidic with pH-values ranging from 0 to 1.2. Therefore, the DC polarograms of these compounds were almost in accord with the hydrogen waves in aqueous solutions. On the other hand, the results of examining them in DMSO revealed this complex to take a *cis*-configuration.[4]

Figure 1 shows the absorption spectra of *cis*-bis-(dimethylglyoximato)ethylenediaminecobalt(III) and its related complexes in the visible and ultraviolet regions. Although its first *d–d* band is partly overlapped with the charge-transfer band due to the oxime ligands, it seems likely that the first band shifts to a shorter wavelength in the following sequence of complexes: [Co en_3]$^{3+}$, [$Co(dgH)_2en$]$^+$, [$Co(dgH)_3$].

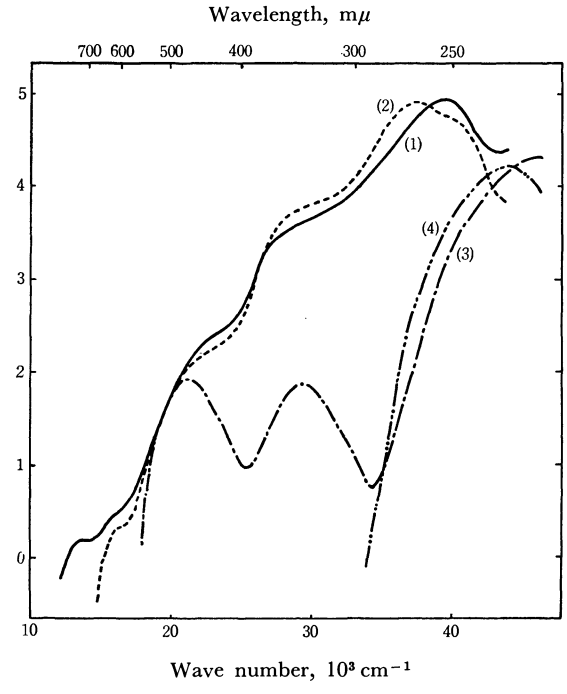

Fig. 1. Absorption spectra of *cis*-bis(dimethylglyoximato)-cobalt(III) and its related complexes: (1) —— *cis*-[$Co(dgH)_2$-en]ClO_4·1/3 H_2O in 0.1 N NaOH; (2) ---- *dl*-[$Co(dgH)_3$]·5/2 H_2O in 0.1 N NaOH; (3) ——— *dl*-[Co en_3]Cl_3 in H_2O; (4) ——— Na_2dg·$8H_2O$ in H_2O.

Since the pmr spectrum of the *cis*-[$Co(dgH)$-$(dgH_2)en$]Cl_2·$2H_2O$ complex in 99.7% D_2O shows that the broad band at 2.9 ppm downfield from DSS is in the same position as the single broad CH_2 band in the spectrum of [Co en_3]$^{3+}$, this band adjacent to the peak of CH_3-group may be assigned to the CH_2-group; this suggests the presence of an ethylenediamine bound to the cobalt.

1) Abbreviation used: dg=$CH_3C(NO)$·$C(NO)CH_3$.

2) A. Nakahara, This Bulletin, **27**, 560 (1954).

3) "Inorganic Syntheses," Vol. II, McGraw-Hill Book Co., New York, N. Y. (1946), p. 221.

4) N. Maki, This Bulletin, **44**, 1446 (1971).

Phosphorylation by Oxidation-Reduction Condensation.[1] Preparation of Active Phosphorylating Reagents

Teruaki MUKAIYAMA and Mitsunori HASHIMOTO

Laboratory of Organic Chemistry, Tokyo Institute of Technology, Ookayama, Meguro-ku, Tokyo

(Received April 30, 1971)

Active phosphorylating reagents such as imidazolylphosphonate,[2,3] 2-pyridyl ester of phosphoric acid,[4,5] and phosphoramidate,[6] especially phosphoromorpholidate,[7] are considered to be important intermediates in nucleotide synthesis. In the present experiment, the preparation of these active phosphorylating reagents such as imidazolylphosphonate, 2-pyridyl ester of phosphoric acid and phosphoromorpholidate by the oxidation-reduction condensation reaction[1] was studied.

First, the preparation of imidazolylphosphonate was attempted. In a typical reaction, triphenylphosphine (2 mmol) was added rapidly into a mixture of *p*-chlorophenyl dihydrogen phosphate (1 mmol), imidazole (5 mmol), triethylamine (1 mmol) and 2,2'-dipyridyl disulfide (2 mmol) in 5 m*l* of THF at room temperature. After stirring for 20 min, acetone solution of sodium iodide (1.5 mmol) was added to the reaction mixture and cooled down to 0°C. After being kept standing for 1 hr at 0°C, the precipitated white needle crystals were filtered off and washed with cold acetone. After removal of the solvent *in vacuo*, the sodium salt of *p*-chlorophenyl imidazolylphosphonate was obtained in a quantitative yield. UV: λ_{max} 270 mμ.

Found: C, 38.50; H, 2.51; N, 10.00%. Calcd for $C_9H_7O_3N_2PClNa$: C, 38.53; H, 2.52; N, 9.99%.

In the case of adenosine 5'-monophosphate, DMF was used in place of THF in the above experiment, and the corresponding adenosine 5'-imidazolylphosphonate was obtained in a quantitative yield without producing symmetrical pyrophosphate (AppA). *p*-Chlorophenyl-2-pyridyl phosphate was isolated as its cyclohexylammonium salt from *p*-chlorophenyl dihydrogen phosphate and 2-hydroxypyridine in high yield according to the following procedure. *p*-Chlorophenyl dihydrogen phosphate (1 mmol) was allowed to react with 2-hydroxypyridine (5 mmol), triphenylphosphine (2 mmol) and 2,2'-dipyridyl disulfide (2 mmol) in THF at room temperature for 3 hr. Cyclohexylamine (1.5 mmol) was then added to the reaction

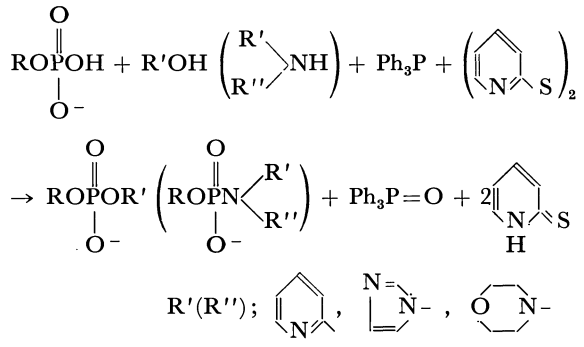

mixture cooled in an ice-bath and kept standing for 2 hr. The precipitated crystals were filtered off, washed with cold THF and dried *in vacuo*. The corresponding cyclohexylammonium salt of *p*-chlorophenyl-2-pyridyl phosphate, mp 164°C, was obtained in 80% yield. UV: λ_{max} 262 mμ.[8] Found: C, 52.95; H, 5.85; N, 7.40%. Calcd for $C_{17}H_{22}O_4N_2ClP$: C, 53.10; H, 5.76; N, 7.29%.

Next, it was found that adenosine 5'-phosphoromorpholidate, an important intermediate in the synthesis of pyrophosphates such as FAD (flavin Adenine dinucleotide), was obtained in a quantitative yield by this method. Triphenylphosphine (2 mmol) was added into the suspended DMF solution of adenosine monophosphate (1 mmol), morpholine (5 mmol), triethylamine (1 mmol) and 2,2'-dipyridyl disulfide (2 mmol) at room temperature. After the mixture was stirred for 1 hr, the suspended solution turned clear. By this time, paper chromatography and paper electrophoresis showed the presence of only one spot corresponding to adenosine 5'-phosphoromorpholidate. Determination by UV absorption after separation with paper chromatography showed that the adenosine 5'-phosphoromorpholidate was obtained in a quantitative yield. $\lambda_{max}^{pH\,7}$ 260 mμ (ε 1.59×10^4). R_f 0.41, isopropanol - concd. ammonium hydroxide - water (7 : 1 : 2).

In conclusion, it is noted that the present oxidation-reduction condensation produces active phosphorylating reagents such as imidazolylphosphonate, 2-pyridyl ester of phosphoric acid and phosphoromorpholidate in high yields in a short reaction time by simply mixing triphenylphosphine, 2,2'-dipyridyl disulfide and phosphate with imidazole, 2-hydroxypyridine or morpholine, respectively.

The authors wish to express their hearty thanks to Dr. Tsujiaki Hata for his advice.

1) T. Mukaiyama and M. Hashimoto, This Bulletin, **44**, 196 (1971).
2) R. Cramer, H. Schaller, and H. A. Staab, *Chem. Ber.*, **94**, 1612 (1961).
3) R. Cramer and H. Neunhoeffer, *ibid.*, **95**, 1664 (1962).
4) K. H. Scheit and W. Kampe, *ibid.*, **98**, 1045 (1965).
5) W. Kampe, *ibid.*, **99**, 593 (1966).
6) J. G. Moffatt and H. G. Khorana, *J. Amer. Chem. Soc.*, **80**, 3756 (1958).
7) J. G. Moffatt and H. G. Khorana, *ibid.*, **83**, 663 (1961).
8) W. Kampe, *Chem. Ber.*, **98**, 1031 (1965).

A Useful Method for Reductive Fission of Sulfides and Its Application to Carbon-Carbon Bond Formation

Teruaki MUKAIYAMA, Koichi NARASAKA, Kazuo MAEKAWA, and Masayasu FURUSATO
Laboratory of Organic Chemistry, Tokyo Institute of Technology, Ookayama, Meguro-ku, Tokyo
(Received June 11, 1971)

In connection with the activation of bivalent sulfur compounds with $CuCl_2$,[1] we report useful methods for both reductive fission of sulfides with $CuCl_2$-$LiAlH_4$ and carbon-carbon bond forming reaction with the use of allyl 2-pyridyl sulfide. The present work was investigated anticipating that the reductive fission of sulfides would proceed in the presence of $CuCl_2$ by an attack of a hydride generated from metal hydrides. As expected, the reduction proceeded effectively by the combined use[2] of $CuCl_2$ and $LiAlH_4$ as follows. First, 2 mol of $CuCl_2$ and 4 mol of $LiAlH_4$ were stirred for 1 hr in tetrahydrofuran under argon atmosphere (black precipitate appeared immediately), then diphenylmethyl phenyl sulfide(I) was added and the reaction mixture was refluxed for 3 hr. After successive hydrolysis, diphenylmethane was obtained in 73% yield. Similarly, benzophenone ethylenemercaptole (II) was reduced with 4 mol of $CuCl_2$ and 8 mol of $LiAlH_4$ under the same conditions to give diphenylmethane in 42% yield. The yield of diphenylmethane was increased to 84% when II was reduced with 4 mol of $CuCl_2$, 4 mol of $ZnCl_2$ and 16 mol of $LiAlH_4$ in the above experiment.

$$Ph_2CHSPh\ (I) \xrightarrow[3\text{ hr }94\%]{2CuCl_2+4LiAlH_4} Ph_2CH_2$$

$$p\text{-MeO-}C_6H_4CH(SEt)Ph \xrightarrow[3\text{ hr }73\%]{CuCl_2+2LiAlH_4} p\text{-MeO-}C_6H_4CH_2Ph$$

$$Ph_2C\begin{matrix}S\\S\end{matrix}\ (II) \xrightarrow[3\text{ hr }84\%]{4CuCl_2+4ZnCl_2+16LiAlH_4} Ph_2CH_2$$

For the reductive fission of sulfides, some methods have been noted.[3] However, unfavorable side reactions such as reduction of aromatic ring or carbon-carbon double bond generally accompany the desired reductive fission of carbon-sulfur bond. With the $CuCl_2$-$LiAlH_4$ method, the reductive fission of sulfides proceeded selectively with no such side reactions.

A new synthetic route for carbon-carbon bond formation involving the alkylation of allyl 2-pyridyl sulfide and a subsequent reductive fission of 2-thiopyridyl group from the alkylated products by the above mentioned reduction, was established. Selective alkylation of allyl 2-pyridyl sulfide was tried starting from the lithium salt. The alkylation of allylic phenylsulfides was reported by Biellmann and Ducep.[4] By introduction of 2-pyridyl group instead of phenyl group, it was expected that side reactions, such as a migration of double bond and a *cis-trans* isomerization, would be minimized by the effect of the stable five membered chelate ring formation of the carbanion. Actually, allyl 2-pyridyl sulfide (III) was easily converted into their carbanion with C_6H_5Li in tetrahydrofuran at −25——15°C. Subsequent alkylation with alkyl halides afforded the alkylated products in good yields after purification by silica gel column chromatography and distillation as shown in the Table. Analysis by vpc indicated that the products selectively contained α-alkylated products (IV) in 92—95% as shown in parentheses.

Reductive fission of 2-pyridyl group from the alkylated product (IV) proceeds successfully according to the following procedure with the use of $CuCl_2$-$LiAlH_4$; Treatment of IV with 4 mol of $CuCl_2$ and 8 mol of $LiAlH_4$ in tetrahydrofuran for 4 hr at room temperature, followed by distillation gave α-olefins (V), estimated to be 93% pure by vpc, in good yields.

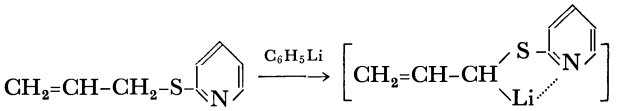

(III)

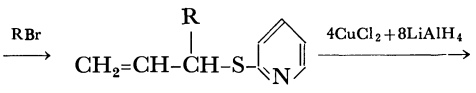

(IV)

$$CH_2=CH-CH_2-R$$
(V)

R	Yield %, (purity of IV or V %)			
	IV	bp(°C/mmHg)	V	bp(°C/mmHg)
Et	95 (93)	67—72/1.7		
$PhCH_2$	82 (92)	141—143/1.5	53 (93)	65/15
$PhCH_2CH_2$	82 (95)	144—148/0.27	80 (93)	91—92/20

1) T. Mukaiyama, K. Narasaka, and H. Hokonoki, *J. Amer. Chem. Soc.*, **91**, 4315 (1969); T. Mukaiyama, K. Narasaka, K. Maekawa, and H. Hokonoki, This Bulletin, **43**, 2549 (1970); T. Mukaiyama, K. Maekawa, and K. Narasaka, *Tetrahedron Lett.*, **1970**, 4669.

2) It is well known that the reductive fission of sulfides does not proceed with $LiAlH_4$ *etc.*; H. C. Brown, P. M. Weissman, and N. M. Yoon, *J. Amer. Chem. Soc.*, **88**, 1458, 1464 (1964).

3) A. R. Pinder and H. Smith, *J. Chem. Soc.*, **1954**, 113; N. S. Crossley and H. B. Henbest, *ibid.*, **1960**, 4413; R. Mazingo, D. E. Wolf, S. A. Harris, and K. Folkers, *J. Amer. Chem. Soc.*, **65**, 1013 (1943).

4) J. F. Biellman and J. B. Ducep, *Tetrahedron Lett.*, **1969**, 3707.

The Photoinduced Substitution Reaction of 2-Quinolinecarbonitrile

Norisuke HATA, Isao ONO, and Seiichi OGAWA

Department of Chemistry, College of Science and Engineering, Aoyama Gakuin University, Megurisawa-cho, Setagaya-ku, Tokyo

(Received May 6, 1971)

Recently, there has been considerable interest in photochemical alkylations of *N*-heterocyclic compounds.[1,2] However, photochemical hydroxyalkylations have been reported only in the case of quinoline by Stermitz *et al.*[2]; there, ultraviolet irradiations of the quinoline in ethanol solution gave the 2-(1-hydroxyethyl)quinoline in a 20% yield. In the present investigation, the authors found an interesting photochemical substitution reaction of 2-quinolinecarbonitrile in alcoholic solvents, affording 2-(1-hydroxyalkyl)-quinoline.

A solution of 0.8 g of 2-quinolinecarbonitrile in an alcoholic solvent (350 m*l* of ethanol, 1-propanol, or 2-propanol) in a Pyrex vessel was irradiated with a 250-W high-pressure mercury lamp for 18 hr while oxygen was bubbled in. After the removal of the solvent under reduced pressure, the residue was chromatographed on a silica-gel column by elution with a mixture of *n*-hexane and diethyl ether (1 : 1). The melting points and the yields of the main products thus obtained are given in Table 1. The UV spectra of these compounds were quite similar to that of quinaldine. The IR spectra of the products in KBr showed a peak at 3300 cm^{-1} (ν_{O-H}) and no absorption at 2230 cm^{-1} characteristic of the C≡N group. In addition to the UV and IR spectra, the structural determinations of the products were made on the basis of the NMR and mass spectra as well as by means of elemental analyses; the results are summarized in Table 1. It was concluded from these results that the quinolinecarbonitrile (I) changed photochemically in alcoholic solvents(II) to give 2-(1-hydroxyalkyl)-quinoline (III) as follows:

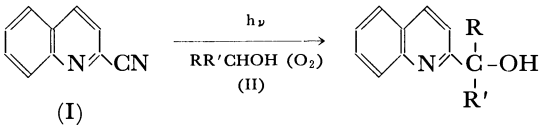

(I) (III)

IIa and IIIa: R=CH_3, R'=H
IIb and IIIb: R=C_2H_5, R'=H
IIc and IIIc: R=CH_3, R'=CH_3

When the irradiation was carried out where nitrogen was bubbled in instead of oxygen, the solution became reddish violet and two main products were separated: one was the product (III), while the other was unidentified. In the presence of piperylene as a triplet quencher,[3] however, no such coloration occurred and only the photoproduct (III) was obtained as a main product. These facts suggest that the lowest triplet state of 2-quinolinecarbonitrile is not responsible for the photochemical conversion (I)→(III).

Further studies are now in progress and will be reported soon.

TABLE 1. ANALYTICAL DATA FOR THE PHOTOPRODUCTS (III)

Solvent (II)	Product (III)	Mp (°C) Yield (%) Mass (M^+)	NMR[a]	Elemental analysis Found (%)	Calcd (%)
Ethanol (IIa)	(IIIa)	79—80 35 173	7.1—8.2 ppm (m, 6H, aromatic) 4.86 ppm (q, J=7 Hz, 1H, -C*H*(OH)-CH_3 4.50 ppm (s, 1H, -O*H*, deuterium exchangeable) 1.48 ppm (d, J=6.5 Hz, 3H, -CH(OH)-C*H*$_3$)	C 76.22 H 6.44 N 8.07	C 76.30 H 6.36 N 8.09 (for $C_{11}H_{11}NO$)
1-Propanol (IIb)	(IIIb)	68—69 45 187	7.0—8.1 ppm (m, 6H, aromatic) 4.77 ppm (s, 1H, -O*H*, deuterium exchangeable) 4.65 ppm (t, J=6 Hz, 1H, -C*H*(OH)-CH_2-CH_3) 1.4—2.1 ppm (m, 2H, -CH(OH)-C*H*$_2$-CH_3) 0.96 ppm (t, J=7 Hz, 3H, -CH(OH)-CH_2-C*H*$_3$)	C 76.57 H 6.49 N 7.83	C 77.01 H 6.95 N 7.49 (for $C_{12}H_{13}NO$)
2-Propanol (IIc)	(IIIc)	69—70 40 187	7.2—8.2 ppm (m, 6H, aromatic) 5.10 ppm (s, 1H, -O*H*, deuterium exchangeable) 1.53 ppm (s, 6H, -C(OH)-(C*H*$_3$)$_2$)	C 76.75 H 6.85 N 8.06	C 77.01 H 6.95 N 7.49 (for $C_{12}H_{13}NO$)

a) Measured in CCl_4 solution using TMS as an internal standard.

1) M. Ochiai and K. Morita, *Tetrahedron Lett.*, **1967**, 2349; M. Ochiai, E. Mizuta, Y. Asahi, and K. Morita, *Tetrahedron*, **24**, 5861 (1968); H. Nozaki, M. Kato, R. Noyori, and M. Kawanishi, *Tetrahedron Lett.*, **1967**, 4259; R. Noyori, M. Kato, M. Kawanishi, and H. Nozaki, *Tetrahedron*, **25**, 1125 (1969); F. R. Stermitz, R. P. Seiber, and D. E. Nicodem, *J. Org. Chem.*, **33**, 1136 (1968); E. F. Travecedo and V. I. Stenberg, *Chem. Commun.*, **1970**, 609.

2) F. R. Stermitz, C. C. Wei, and C. M. O'Donnell, *J. Amer. Chem. Soc.*, **92**, 2745 (1970).

3) It was estimated, from the first maximum of the phosphorescence spectrum (484 nm) in ethanol at 77°K, that the lowest triplet state of 2-quinolinecarbonitrile has an excitation energy of about 59 kcal·mol^{-1}.

A Stereospecific Racemization Catalyst for Amino Acid[1]

Kazuhiro HIROTA and Yoshiharu IZUMI

Division of Organic Chemistry, Institute for Protein Research, Osaka University, Kita-ku, Osaka

(Receied May 7, 1971)

It is known that pyridoxal, salicylaldehyde, *o*- or *p*-nitrosophenol, and aurintricarboxylic acid catalyze[2-6] non-enzymatically, in alkaline media, the racemization of optically-active amino acid in the presence of a metal ion. These reactions involve the formation of the chelate compounds of a Schiff base, which compounds promote the release of the proton at the α-carbon of the amino acid and the racemization of the amino acid. A possible chelate structure in *p*-nitrosophenol (*p*-quinoneoxime), as an example, is shown in I.

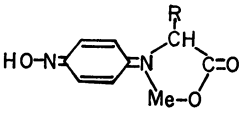

(I)

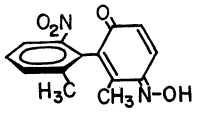

(II) (oxime type)

Therefore, when the optically-active asymmetric structure is introduced to the catalyst, it could bring about differences in the stabilities or in the rates of the formation of these chelates with a metal ion between L- and D-amino acids. Those differences could appear as differences in the racemization rates between L- and D-amino acids. Therefore, we wish to report here the first observation of the stereospecific racemization reaction for amino acid with the hindered biphenyl, (S)-2′-nitro-2-hydroxy-5-nitroso-6,6′-dimethylbiphenyl(II).[7] The racemization activities of the catalyst for L- and D-alanine respectively were studied in the presence of the cupric ion.

The procedure for the racemization reaction was as ollows; the reaction mixtures containing L- or D-alanine (0.5 mmol), cupric sulfate pentahydrate (0.05 mmol), and the catalyst (II) (0.0125 mmol) were adjusted to pH 10 with sodium hydroxide to make a total volume of 0.5 m*l* with water, and then the mixture was shaken in a sealed tube at 31° or 40°C. After the reaction, 6 N hydrochloric acid (0.5 m*l*) was added to stop the racemization reaction. The determination of the ratio of L- and D-alanines was performed as follows; the reaction mixtures were centrifuged to precipitate the used catalyst, and the supernatants were dried up. After the residues had been converted into l-menthyl D- and L-trifluoroacetylalaninates, the ratio of L- and D-alanines was determined by means of gas chromatography. Careful measurements, compared with the calibrated curve, led us to an estimated error of ±0.5%.

The catalytic activities for L- and D-alanines are compared in Table 1 in terms of the contents of the racemized D- and L-alanines and the difference between the two. Though the racemic catalyst, of course, showed no difference in the catalytic activities between L- and D-alanines, II possessed some stronger activities for L-alanine than for D-alanine. The difference in the catalytic activity lay in the range from 3.0 to 5.0% in the contents of L- and D-alanines racemized from the D- and L-alanines substrates respectively. Such a catalytic property may serve as a model for the high stereospecificities often observed in the interactions of metallo-enzymes and their substrates. A stereochemical relationship between the catalyst and substrate will be discussed in a presentation of a molecular model in This Bulletin in the near future.

TABLE 1. RACEMIZATION ACTIVITY OF THE CATALYST

Configuration of catalyst	Substrate	Exp. 1.		Exp. 2		Exp. 3	
		D- or L-ala. content (%)[b]	Difference[c]	D- or L-ala. content (%)	Difference	D- or L-ala. content (%)	Difference
Racemic	L-alanine	D : 20.4	0.6	D : 28.5	0.5	D : 34.0	0.5
	D-alanine	L : 19.8		L : 29.0		L : 34.5	
S	L-alanine	D : 20.1	3.2	D : 26.2	5.0	D : 29.5	3.0
	D-alanine	L : 16.9		L : 21.2		L : 26.5	

Reaction mixture (0.5 m*l*) containing 0.5 mmol alanine, 0.05 mmol $CuSO_4 \cdot 5H_2O$ and 0.0125 mmol catalyst (II) was shaken at pH 10.0.

a) Racemization conditions were as follows:
Exp. 1: at 31°C for 162 hr. Exp. 2: at 31°C for 168 hr. Exp. 3: at 40°C for 72 hr.

b) Content of D- or L-alanine after the racemization reaction.

c) Difference between contents of L- and D-alanines racemized from D- and L-alanines, respectively.

1) Presented at the 24th Annual Meeting of the Chemical Society of Japan, Osaka, April, 1971.

2) J. Olivard, D. E. Metzler, and E. E. Snell, *J. Biol. Chem.* **199**, 669 (1952).

3) K. Ohno, I. Sasaji, and M. Hara, Japan. Pat. 295110.

4) K. Toi, Y. Izumi, and S. Akabori, This Bulletin, **35**, 1422 (1962).

5) K. Hirota, and Y. Izumi, *ibid.*, **40**, 178 (1967).

6) K. Hirota, K. Miyamoto, and Y. Izumi, *ibid.*, **40**, 182 (1967).

7) II was derived from (S)-2′-nitro-2-amino-6,6′-dimethylbiphenyl; its diazonium salt was hydrolyzed to the phenol derivative, and then treated with sodium nitrite. The method will be reported in detail in the near future.

Hydrogen Abstraction of Excited Benzophenone in *N,N*-Dimethylaniline and 2-Methyltetrahydrofuran Solution at Low Temperature

Satoshi ARIMITSU* and Hiroshi TSUBOMURA

Department of Chemistry, Faculty of Engineering Science, Osaka University, Toyonaka, Osaka

(Received May 13, 1971)

Photochemical reactivities of aromatic ketones have been studied extensively,[1-5] Porter and his co-workers found that photoreduction of benzophenone in isopentane does not occur at temperatures 77°K—108°K, but proceeds above 108°K.[4] We wish to report that it occurs easily in a mixed glass of aromatic amine and ether at 77°K. Benzophenone (5×10^{-3} M) in a degassed mixture of *N,N*-dimethylaniline (DMA) and 2-methyltetrahydrofuran (2MTHF), about 1 : 3 by volume, at 77°K was photolysed in the region 350—400 nm through a glass filter with a high pressure mercury lamp for 10—30 sec. The results are shown in Fig. 1. The spectrum (appearing from 500 to 570 nm in curve d) is nearly in agreement with that of the ketyl radical at room temperature (curve e).[3,4] No ketyl radical was found by the photolysis of benzophenone in a 2MTHF matrix at 77°K.

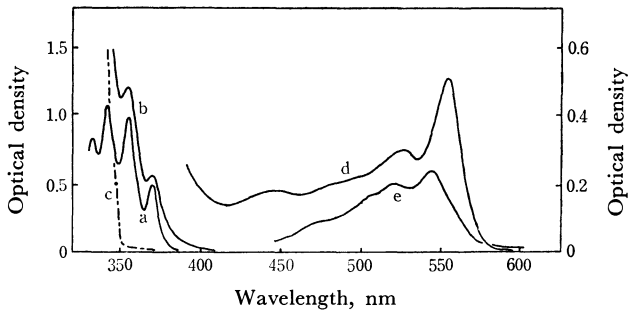

Fig. 1. a) Absorption spectrum of benzophenone in 2MTHF at 77°K. b) Absorption spectrum of benzophenone in DMA and 2MTHF at 77°K. c) Absorption of DMA and 2MTHF at 77°K. d) Absorption of sample used in b) after irradiation. e) Absorption of the ketyl radical obtained by flash illumination of a solution at room temperature.

The electronic spectrum of benzophenone in the DMA-2MTHF matrix shown by curve b suggests that an electron donor-acceptor complex is formed between benzophenone as an electron acceptor and DMA as a donor at 77°K. Therefore, it is suggested that the photochemical reactivity of benzophenone is activated significantly in the excited state of benzophenone-DMA complex. The ketyl radical appears also in a mixed matrix of DMA and trichlorotrifluoroethane, the latter having no hydrogen atom to abstract. This result definitely indicates that the ketyl is produced as a result of intermolecular hydrogen transfer from DMA to benzophenone. Thus, the absorption band at near 445 nm can be ascribed to DMA radical $\left(\phi\text{-N}\langle\begin{matrix}\dot{C}H_2\\CH_3\end{matrix}\right)$.[6]

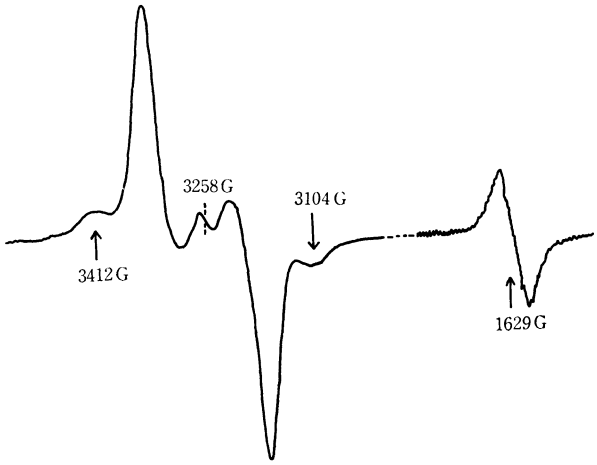

Fig. 2. ESR spectrum of benzophenone in DMA-2MTHF irradidiated at 77°K: (ν=9136 MHz.).

When benzophenone in a DMA-2MTHF matrix was irradiated at 77°K, an ESR spectrum was obtained as shown in Fig. 2. A weak absorption ascribable to the $\Delta m=2$ transition of a radical pair in a triplet state was found at 1629 gauss. A stronger spectrum which consists of two pairs of lines with a separation of 176 and 308 gauss appeared symmetrically with respect to the magnetic field strength of 3258 gauss. From the ESR spectrum we can immediately estimate the D value or the fine structure constant of the radical pair to be 154 gauss, and the average distance between the interacting radical 5.6_4 Å by using a point-spin-density approximation.[7] This result might be the first one indicating the presence of two photo-chemically formed unstable radicals which lie close to each other and form a combined triplet (S=1) state.

* Present address: Sagami Chemical Research Center, 3100 Ohnuma, Sagamihara, Kanagawa.

1) P. J. Wagner and G. S. Hammond, *Advance. Photochem.*, **5**, 99 (1961).

2) G. Porter and F. Wilkinson, *Trans. Faraday Soc.*, **57**, 1686 (1961); G. Porter and P. Suppan, *ibid.*, **61**, 1664 (1965).

3) H. Tsubomura, N. Yamamoto, and S. Tanaka, *Chem. Phys. Lett.*, **1**, 309 (1967).

4) T. S. Godfrey, J. W. Hilpern, and G. Porter, *ibid.*, **1**, 490 (1967).

5) N. C. Yang, R. L. Dusenbery, *J. Amer. Chem. Soc.*, **90**, 5899 (1968); P. J. Wagner, A. E. Kempainen, and H. N. Schott, *ibid.*, **92**, 5280 (1970).

6) S. Arimitsu, K. Kimura, and H. Tsubomura, This Bulletin, **42**, 1858 (1969).

7) Y. Kurita, *J. Chem. Phys.*, **41**, 3926 (1964).

The Production of New Carbonyl- and Thiocarbonyl-stabilized Phosphonium Ylids by the Reaction of the Triphenylphosphonium Methylid with *O*-Alkylxanthates

Hiroshi YOSHIDA, Hironori MATSUURA, Tsuyoshi OGATA, and Saburo INOKAWA

Department of Synthetic Chemistry, Faculty of Engineering, Shizuoka University, Hamamatsu

(Received May 17, 1971)

The reaction of phosphonium alkylids with *S*-alkyl thiolcarboxylates yields phosphonium acylalkylids in good yields.[1] However, no worker has reported on the reaction of dialkylcarbonates with phosphonium alkylids. In this communication, the reaction of triphenylphosphonium methylid (**1**) with *O*-alkylxanthates (**2**) to give new carbonyl- and thiocarbonyl-stabilized phosphonium ylids will be treated.

The reaction of **1** with a two fold amount of **2** was performed in toluene under a nitrogen atmosphere at various temperatures. The product was then purified by recrystallization from petroleum ether-ethyl acetate or by column chromatography. The structure of the product was confirmed by elemental analysis, NMR, IR and a Wittig reaction with benzaldehyde.

As Table 1 shows, the reaction at room temperature yields only thiocarboalkoxymethylene triphenylphosphorane (**3**); however, the reaction at 130°C yields **3** or **4**, or a mixture of the two. The alkyl groups attached to the ylids, **3** and **4**, are the *O*-alkyl groups of the starting xanthates, **2**.

TABLE 1. THE REACTION OF **1** WITH **2** IN TOLUENE

2		Reaction condition		Yield (%)	
R	R′	Temp. (°C)	hr	**3**(R)[a]	**4**(R)[a]
Me	Me	room temp.	24	38	—
		130	3.5	—	46
Me	Et	130	3	—	47
Et	Me	room temp.	24	41	—
		130	3	53[b]	
Et	Et	130	3	59[b]	
i-Pr	Me	130	3	56	—

a) The same group as the *O*-alkyl R of the xanthate **2**.
b) Nearly equimolar mixture of **3** and **4**.

Mps: **3** (R=Me) 164—165.5, **3** (R=Et) 137—139, **3** (R=*i*-Pr) 155—156.5, **4** (R=Me) 220—221, **4** (R=Et) 177—182°C.

The formation of **4** did not result from a intramolecular thion-thiol rearrangement of **3** similar to the Schönberg rearrangement,[2] since **3** (R=Me, Et, *i*-Pr) remained unchanged on heating at 130°C for a few hours. On the other hand, reaction **3** (R=Et) with **2** (R=R′=Me) gave, almost quantitatively, **4** (R=Me) and methyl ethyl dithiolcarbonate.

It is known that carboalkoxy ylids undergo alkylation with a variety of alkyl halides to afford normal alkylated ylids (alkylation on carbanion);[3] however, alkylation with triethyloxonium fluoroborate does not yield normal alkylation products (alkylation on carbonyl oxygen).[4] The alkylation of **3** with methyl and ethyl iodides yields exclusively an *S*-alkylated product.[5] Thus, the formation of **4** may be from the alkylation of **2** to the highly-polarized thiocarbonyl sulfur of **3**. The present authors have previously reported that **2** reacts with tertiary amines as an alkylating reagent and that the reactivity decreases in the order: Me≫Et>*n*-Pr≫*i*-Pr.[6] This order agrees well with that of the yield of **4** at 130°C (Table 1). Thus, the reaction of **1** with **2** to give **3** and/or **4** may be pictured as follows:

The physical and chemical properties of **3** and other analogs will be published later.

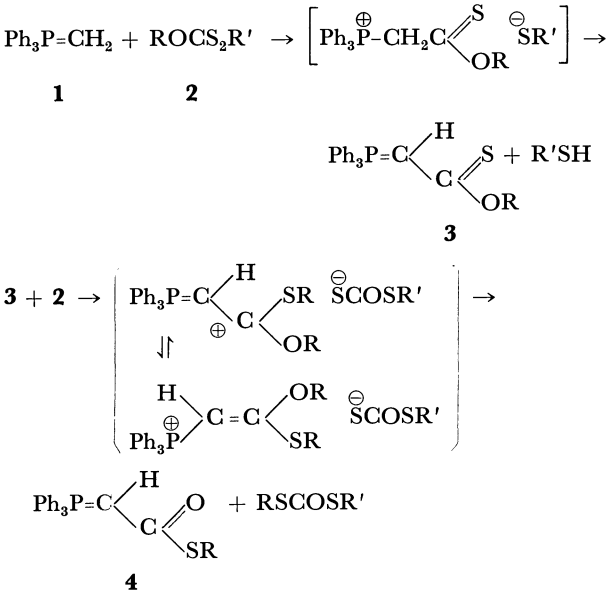

1) H. J. Bestmann and B. Anderson, *Chem. Ber.*, **95**, 1513 (1962).
2) A. Schönberg and L. Varga, *ibid.*, **63**, 178 (1930); H. R. Al-Kazimi, D. S. Tarbell, and D. Plant, *J. Amer. Chem. Soc.*, **77**, 2479 (1955); D. H. Powers and D. S. Tarbell, *ibid.*, **78**, 70 (1956).
3) H. J. Bestmann and H. Schulz, *Tetrahedron Lett.*, **1960**, 5; *Chem. Ber.*, **95**, 2921 (1962).
4) H. J. Bestmann, R. Saalfrank, J. P. Snyder, *Angew. Chem.*, **81**, 227 (1969).
5) H. Yoshida, unpublished results.
6) H. Yoshida, This Bulletin, **42**, 1948 (1969).

The Single-crystal Absorption Spectra of the Basic Rhodo Chromic Perchlorate

Akio URUSHIYAMA, Masayoshi NAKAHARA, and Yukio KONDO

Department of Chemistry, Faculty of Science, Rikkyo University, Nishi-ikebukuro, Toshima-ku, Tokyo

(Received May 27, 1971)

In several spectroscopic studies [1-5] concerned with the binuclear complexes of chromium(III), it has been found that the basic rhodo chromic complex, $[(NH_3)_5Cr\text{-}O\text{-}Cr(NH_3)_5]^{4+}$, shows some unfamiliar sharp absorption bands in the near-ultraviolet region. Previously, one of the present authors (Y. K.) has reported[6] that these sharp bands are strongly polarized. Recently, the crystal structure of the basic rhodo chromic chloride has been determined.[7,8] In the present communication, the polarized absorption spectra of the basic rhodo chromic complex salt related to the orientation of the dimeric unit will be reported.

The basic rhodo chromic complexes are situated on the centers of symmetry in the orthorhombic (space group *Pbca*) system of the chloride crystal, and the chromium atoms are located at $x=\pm0.62$, $y=\pm1.11$, and $z=\pm1.27$ (Å) if we take the point of origin as the symmetry center.[7] Unfortunately, the crystals, although they exhibit a dichroism (blue—through the light polarized parallel to the *a* axis, greenish blue—parallel to the *c* axis), are unsuitable for study by means of the microspectroscopic technique because of their shapes. However, a similar dichroism can be observed more distinctly on the thin plates of the perchlorate crystals, which *are* suitable for the microspectroscopic study. As the color of the chloride crystals has been related to the orientation of the complex, it seems reasonable to say that the absorption parallel to the four-fold rotation axis of the complex contributes greatly to the polarized absorption spectrum along the extinction direction of the perchlorate crystal, which shows greenish blue with the polarized light having the parallel electronic vector.

For the measurement of the absorption spectrum of the single crystal of microsize, an apparatus was constructed using a Hitachi EPS-3T spectrophotometer and a Nippon Kogaku POH polarizing microscope, together with two Olympus MO90 reflecting-type objectives (×90). The polarized absorption spectra of the basic rhodo chromic perchlorate are shown in Fig. 1.

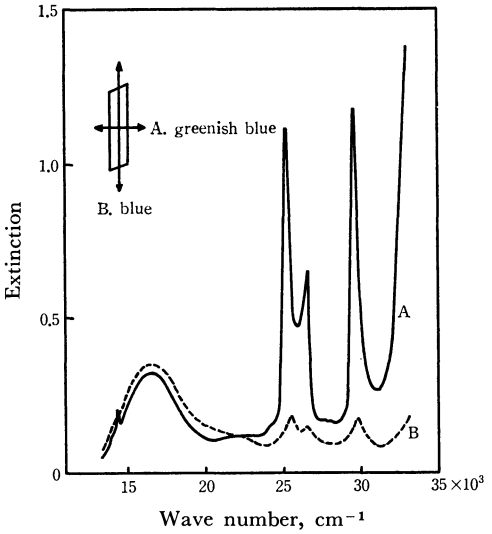

Fig. 1. Polarized absorption spectra of the basic rhodo chromic perchlorate.

It was found that: (i) the characteristic sharp absorption bands at 14320 cm^{-1} and in the near-ultraviolet region are all polarized along the four-fold rotation axis of the complex; (ii) the broad band in the 16600 cm^{-1} region seems to be slightly reduced in intensity along the four-fold rotation axis; (iii) the position of the absorption maxima of two broad bands, *i. e.*, 16600 cm^{-1} and 22000 cm^{-1}, seem to correspond to that of the so-called "first band" of the octahedrally-coordinated $Cr(III)O_6$ and $Cr(III)N_6$ types of complexes, respectively; (iv) the so-called "second band" of the *d–d* transition is obscure; and (v) as the total of the integrated intensities of the sharp bands in the near ultraviolet region is almost comparable to that of the band at 16600 cm^{-1}, the intensities of these bands are not so large as the ordinary charge-transfer absorption band shows. The characterization of the absorption bands of the basic rhodo chromic complex is very complicated. However, the assignment of the bands should be consistent with the results of the polarized spectroscopy. Further measurements at low temperatures are now in progress.

1) C. E. Schäffer, *J. Inorg. Nucl. Chem.*, **8**, 149 (1958).
2) M. Mori, S. Ueshiba, and H. Yamatera, This Bulletin, **32**, 88 (1959).
3) G. Schwarzenbach and B. Magyar, *Helv. Chim. Acta*, **45**, 1425 (1962).
4) L. Dubicki and R. L. Martin, *Aust. J. Chem.*, **23**, 215 (1970).
5) M. Morita and S. Shionoya, *J. Phys. Soc. Jap.*, **28**, 134 (1970).
6) 8th Symposium on Coordination Chemistry, Tokyo, November, 1958; Y. Kondo, "Coordination Bond" (in Japanese), ed. by R. Tsuchida and M. Kotani, Tokyo Kagakudozin, Tokyo (1961), p. 106.
7) A. Urushiyama, T. Nomura, and M. Nakahara, This Bulletin, **43**, 3971 (1970).
8) M. Yevitz and J. A. Stanko, *J. Amer. Chem. Soc.*, **93**, 1512 (1971).

1,1′-Dihydroxy-2,2′-azonaphthalene-4,4′-disulfonic Acid as a New Reagent for Magnesium

Yasuko NODA* and Haruo MIYATA

Department of Chemistry, Faculty of Science, Okayama University, Tsushima, Okayama

(Received May 31, 1971)

Eriochrome Black T (EBT) has been used exclusively as the metallochromic indicator in the chelatometric titration of magnesium with EDTA. Also, Patton and Reeder's dye (HSN, 2-hydroxy-1-(2-hydroxy-4-sulfo-1-naphthylazo)-3-naphthoic acid) has been used for calcium. The acid dissociation constants of these indicators are 6.3 and 11.6 for EBT,[1] and 9.2_6 and 13.6_7 for HSN[2] respectively, as pK_a values; the skeletal structures are as follows:

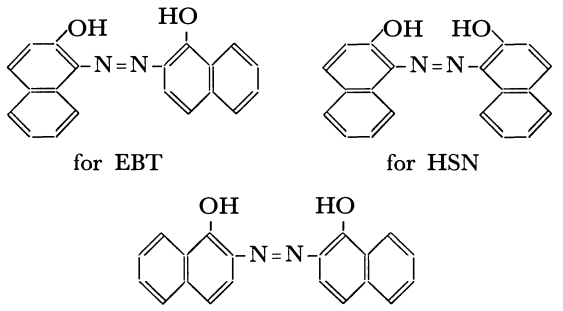

Structure 1

We expected that the pK_a values of the reagent with a skeletal structure such as Structure 1 would be lower than those of EBT or HSN, and that the conditional stability constant for its magnesium chelate would be higher. Therefore, 1,1′-dihydroxy-2,2′-azonaphthalene-4,4′-disulfonic acid[3] was synthesized as a reagent for magnesium from the diazotized 2-amino-1-naphthol-4-sulfonic acid, which was coupled with 1-naphthol-4-sulfonic acid. The pK_a values of this reagent are 5.0 and 11.1. A color change from blue to red upon treatment by this reagent with the magnesium ion is very sharp at pH 10. The absorption spectra of the reagent and its magnesium chelate are shown in Fig. 1. The absorption spectrum of calcium chelate at pH 7.7 is almost the same as that of the reagent itself at pH 6.46 (Curve 2) in Fig. 1. The existence of a 1-to-1 chelate was verified by the continuous-variation method, its conditional stability constant, K', and the stability constant, K, are listed in Table 1.

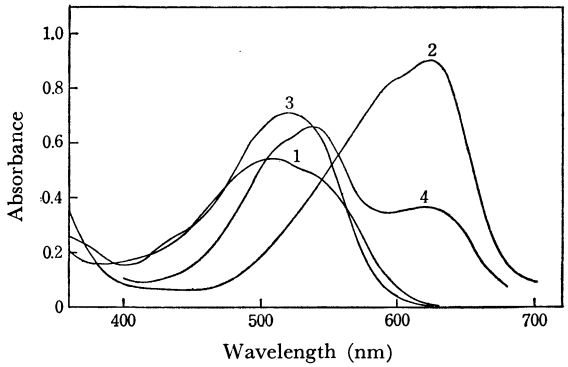

Fig. 1. Absorption spectra of the reagent and its magnesium chelate: 1 at pH 1.71; 2 at pH 6.46; 3 at pH 13; and 4 (magnesium chelate) at pH 7.69.
reagent concentration: 2.46×10^{-5} M
magnesium concentration, 2.46×10^{-3} M

By a comparison of these data, it was found that the reagent is a valuable indicator for the chelatometric titration of the magnesium ion at pH 10, and that also, it can be used in the colorimetric determination of magnesium in the presence of the calcium ion. Further details on the magnesium chelate will be reported elsewhere.

TABLE 1. ACID DISSOCIATION CONSTANTS OF THE REAGENTS, AND CONDITIONAL STABILITY CONSTANTS AND STABILITY CONSTANTS OF THESE CHELATES (t=25°C, μ=0.1)

Reagent	pK_{a1}	pK_{a2}	log K		log K' (at pH 10)	
			Mg	Ca	Mg	Ca
the reagent	5.0	11.1	7.0	4.7	5.9	3.6
EBT[1]	6.3	11.6	7.0	5.4	5.4	3.8
HSN[2]	9.2_6	13.6_7		5.8_5		
Calmagite[4]	8.14	12.35			5.69	3.68

* Present address: Yanagimoto Mfg. Co., Ltd., Kyoto.

1) G. Schwarzenbach and W. Biedermann, *Helv. Chim. Acta*, **31**, 678 (1948).

2) A. Itoh and K. Ueno, *Analyst*, (London), **95**, 586 (1970).

3) Found: C, 41.66; H, 3.50; N, 4.75%. Calcd for $C_{20}H_{12}O_8N_2S_2Na_2\cdot4H_2O$: C, 40.68; H, 3.41; N, 4.74%.

4) F. Lindstrom, *Anal. Chem.*, **32**, 1126 (1960).

The Magneto-Optical Rotatory Dispersion of Benzophenone in the $S_0 \rightarrow T$ (n-π^*) and the $S_0 \rightarrow S_1$ (n-π^*) Absorption Regions

Yoshiya TAKENOSHITA and Yoshiya KANDA

Department of Chemistry, Faculty of Science, Kyushu University, Fukuoka

(Received September 24, 1970)

The magneto-optical rotatory dispersion (MORD) of benzophenone has been measured in the spectral regions corresponding to its $S_0 \rightarrow S_1$ (n-π^*) and $S_0 \rightarrow T$ (n-π^*) absorption systems. The abnormal MORD in the $S_0 \rightarrow T$ absorption region has not always been observed, contrary to the results by Shashoua, only the normal MORD has always been observed. The MORD in the $S_0 \rightarrow S_1$ (n-π^*) absorption region changes its sign at about 340 mμ and is classified as a positive ($B+C/kT$) type, according to Stephens *et al.* It has been concluded that the MORD of the $S_0 \rightarrow S_1$ transition of benzophenone occurs as a result of the n,π^* state, S_1, being mixed with the B_{2u}-analogue state, S_3, and that then the S_1 state interacts magnetically with the S_3 under an external magnetic field.

Shashoua observed the MORD of benzophenone in 1960[1] and acetophenone in 1964[2] in the spectral regions corresponding to the absorption systems of these compounds. The electronic structure of benzophenone has been investigated in detail by analyses of its absorption and emission spectra.[3,4] It is well known that the lowest excited singlet state, S_1, and the lowest triplet state, T, are both of the n-π^* type.[5,6]

Some aspects of the magnetic field on the $S_0 \rightarrow T$ transition have been studied.[7,8] More recently, Eberhardt *et al.* studied the magnetic rotation spectra of the $S_0 \rightarrow T$ absorption of several small organic compounds.[9] Therefore, it seems that the MORD in the $S_0 \rightarrow T$ absorption region should be observed, and the experiments by Shashoua seem to support this idea. However, the f value of the $S_0 \rightarrow T$ absorption of benzophenone has been reported to be 0.6×10^{-7}, [10] and this region is overlapped by the tail of the strong $S_0 \rightarrow S_1$ absorption. Therefore, there remain some questions as to the reality of the observation of the MORD in the $S_0 \rightarrow T$ region of aromatic carbonyl compounds by Shashoua. Accordingly, we undertook an MORD experiment with benzophenone in the region of its $S_0 \rightarrow T$ absorption spectrum and also studied the rotatory dispersion in the spectral region of its $S_0 \rightarrow S_1$ absorption.

Experimental

A Shimadzu spectrophotometer, model QR-50, with an accessory for the observation of natural optical rotation was modified in order to observe the magnetic optical rotation. The light source was a 500-W Xe-lamp. The magnetic field was produced with an electric magnet, its field strength being 5080 gausses at 5.0 A d.c. The strength of the field was determined form Verdet's constant (min.gauss^{-1}.cm^{-1}) of water.[11]

When $\varepsilon(\nu)$ stands for the rotation of a light frequency, ν, of two quartz plates (0.20 cm in total width) and $V(\nu)$, for that of the quartz plates plus a sample with a total optical path of 1.20 cm, the rotation of a sample, $\theta(\nu)$, can be expressed as follows:

$$\theta(\nu) = V(\nu) - \varepsilon(\nu) + \delta(\nu) \quad (1)$$

where δ is the dispersion of air exchanged for the sample (it will be neglected in this experiment). The average experimental error was $\pm 0.005°$ degrees.

For the measurement of the MORD in the $S_0 \rightarrow T$ absorption region, two solutions, consisting of 3.08% and 3.14% of benzophenone in ethanol, and a solution of 1.88% in cyclohexane were used, while for the measurement of the MORD in the $S_0 \rightarrow S_1$ absorption region, a solution of 0.1916% benzophenone in ethanol was used at 10°C, its density being 0.799 g/cc.

Results and Discussion

The magnetic rotation angle (degree) of benzophenone has been measured in the spectral region between 340 and 480 mμ, which corresponds to its $S_0 \rightarrow S_1$ and $S_0 \rightarrow T$ absorption regions. The rotation angles of the samples in the latter region, which were calculated with Eq. (1) for each wavelength, are plotted against the wavelength in Fig. 1, in which, for the sake of comparison, Shashoua's data are also plotted.

It is necessary to use the specific magnetic rotation or the molar magnetic rotation in order to discuss the dispersion phenomenon in detail. The specific magnetic rotation, $[\theta]$, of a solution and the molar magnetic rotation, $[\alpha]_M$ of a solute are defined as follows:[12-14]

$$[\theta] = H\theta/\rho \quad (2)$$

$$[\alpha]_M = (10M/100k)([\theta] - k_s[\beta]) \quad (3)$$

where $[\alpha]_M$ is defined in the same way as the natural

1) V. E. Shashoua, *J. Amer. Chem. Soc.*, **82**, 5505 (1960).
2) V. E. Shashoua, *ibid.*, **86**, 2109 (1964).
3) D. S. McClure, *J. Chem. Phys.*, **17**, 665 (1949).
4) B. J. Mcclelland, *Trans. Faraday Soc.*, **57**, 2073 (1961).
5) R. Shimada and L. Goodman, *J. Chem. Phys.*, **43**, 2027 (1965).
6) C. Dijkgraaf and J. P. G. Roussean, *Spectrochim. Acta*, **23A**, 168 (1967).
7) R. W. Wood and G. Ribaud, *Phil. Mag.*, **27**, 1009 (1914).
8) R. Serber, *Phys. Rev.*, **41**, 489 (1932); T. Carroll, *ibid.*, **55**, 822 (1937).
9) W. H. Eberhardt, W. Cheng, and H. Renner, *J. Mol. Spectrosc.*, **3**, 664 (1959); W. H. Eberhardt and H. Renner, *ibid.*, **6**, 483 (1961).
10) Y. Kanda, H. Kaseda, and T. Matumura, *Sepectrochim. Acta*, **20**, 1387 (1964).
11) J. W. Redzer and W. Watson, *Phil. Trans.*, **A186**, 621 (1895); *Z. Phys. Chem. (Leipzig)*, **19**, 323 (1896).
12) W. Schütz, "Handbuch der Experimental Physik," XVI hrsg. von. W. Wien und F. Harms, Akademische Ver., Leipzig (1936), c.p. Magneto-Optik.
13) The addition low of Verdet-Schönrock; to refer to O. Schönrock, *Z. Phys.*, **46**, 314 (1928); *ibid.*, **79**, 707 (1932).
14) Y. I'Haya, "Bunshi Kagaku Kouza 10. Hikari to Bunshi I," ed. by K. Kanbe., Kyoritsu Co., Tokyo (1967), p. 107.

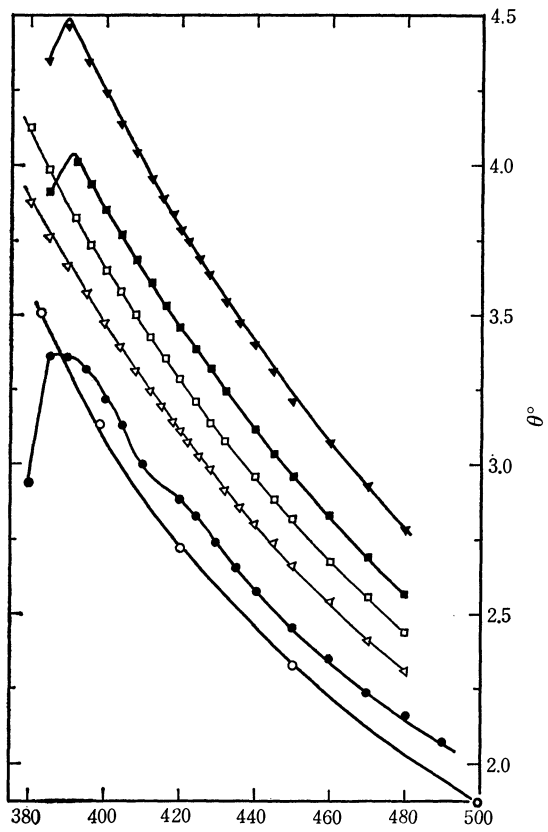

Fig. 1. The dispersion curves ($\theta°$) of benzophenone in alcohol; —○—, —●— alcohol and 2.5% benzophenone in a 5 cm cell at 30°C in 1.2×10^3 gauss by Shashoua; —□—, —■— alcohol and 3.14% benzophenone in a 5 cm cell at 11°C in 1.68×10^3 gauss; —△—, —▲— alcohol and 13.08% benzophenone 1 cm cell at 10°C in 8.06×10^3 gauss.

optical activity;[15] H is the strength of a magnetic field; ρ, the density of a solution; M, the molecular weight of the solute; k and k_s, the grams of the solute and the solvent respectively, and β, the specific rotation of the solvent. The MORD values in the region corresponding to the $S_0\rightarrow T$ and the $S_0\rightarrow S_1$ absorptions of benzophenone are shown in Fig. 2.

A. $S_0\rightarrow T$ Absorption Band. The 0–0 band of the phosphorescence spectrum of benzophenone was observed at 24,185 cm^{-1},[4] while the absorption maximum of its $S_0\rightarrow T$ transition was located at 24,300 cm^{-1}.[10] Shashoua observed an abnormal dispersion at 420 mμ[1] which he interpreted as due to the $S_0\rightarrow T$ absorption, since there is no other absorption in the region. As the interaction between a molecule in the triplet state and a magnetic field is proportional to the strength of the field, H, the MORD of benzophenone has been observed in the spectral region corresponding to the $S_0\rightarrow T$ absorption under a magnetic fields almost the same in strength and seven times as strong as that used by Shashoua. We observed no abnormal dispersion near 420 mμ in an alcoholic solution, even under 8000 gausses, nor did we do so in cyclohexane. That the rotation angles in a solution decrease in the three curves near 390 mμ to shorter wavelengths may be ascribed to experimental error, since the absorption coefficient of benzophenone increases abruptly in that region because of the presence of the $S_0\rightarrow S_1$ absorption and since the light that comes through the sample is naturally decreased in intensity. This makes the slit-width of the excitation monochromator wider and, accordingly, the measurement becomes less accurate. Therefore, it may be concluded no abnormal dispersion is observable in the $S_0\rightarrow T$ absorption region within the limits of our experiment. As is shown in Fig. 2, the molecular rotatory dispersion in the region from 390 to 430 mμ is too flat to be explained by either formula, $[\alpha]_M=A\nu^2/(\nu_0^2-\nu^2)^2$ or $[\alpha]_M=B\nu^2/(\nu_0^2-\nu^2)$.[8] Since the slope of the dispersion curve is small and the dispersion is constant at each wavelength in this region, the dispersion should be interpreted as a result of dispersions due to absorptions in the shorter wavelengths. Therefore, even if the rotation of the $S_0\rightarrow T$ transition were observable, it would be included within the limits of experimental error.

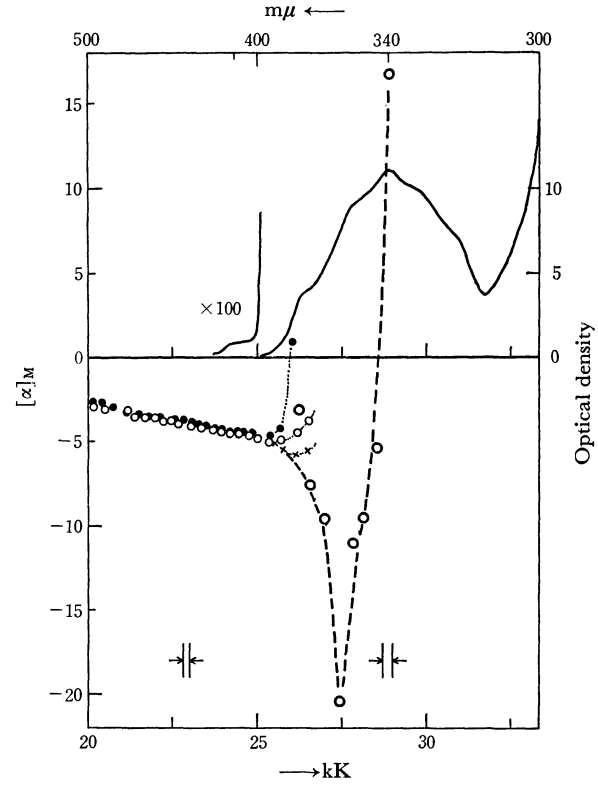

Fig. 2. The MORD and the absorption spectrum of benzophenone ○○○....., ●●●....., -⊙-⊙- in alcohol; ...×... ...×... in cyclohexane.

Theoretically speaking, the dispersion due to the $S_0\rightarrow T$ absorption could be classified as to the A-type.[16] It is, however, impossible to discuss quantitatively the order of the magnitude of the MORD of the $S_0\rightarrow T$ transition according to the results of this experiment. It should be noted that no abnormal MORD, but only a normal MORD, is observed in this region.

B. n–π^* ($S_0\rightarrow S_1$) Absorption Band. The absorption spectrum of benzophenone between 390 and 310 mμ is shown in Fig. 2. The MORD of the n–π^* absorption

15) C. Djirassi, "Optical Rotatory Dispersion," McGraw Hill Co., New York (1960).

16) M. Kimura, H. Kondo, and S. Hattori, *J. Phys. Soc. Jap.*, **20**, 1778 (1965).

region corresponding to the wavelength of the absorption maximum changes in sign at about 340 mμ, it may be interpreted as an I type, according to Shashoua,[2] or as a positive $(B+C/kT)$ type, according to Stephens *et al.*[17] As benzophenone is diamagnetic in the ground state, C is equal to zero.

Then, assuming a damped-oscillator model, according to Stephens *et al.*,[17,18] one obtains the following values:

$$[\alpha]_{M\,max} = 10 - 20\,\text{deg}\cdot l/\text{m.mol},\ \Gamma_{01} = 1.1 - 0.9\,\text{kK},$$

$\omega_{01}=28.7$ kK,

therefore, $B(S_0\rightarrow S_1)=1.8-1.5\times10^{-2}d^2\beta/\text{cm}^{-1}$ where Γ means a damping constant; ω_{01}, an energy difference in cm^{-1} between the S_0 and S_1 states, d, a dipole moment in Debye units, and β, a Bohr magneton.

According to theory of the Faraday effect, the B term has been given as follows:

$$B(S_0\rightarrow S_1) = \sum_{k\neq1} \boldsymbol{M}_{1k}\cdot(\boldsymbol{R}_{01}\times\boldsymbol{R}_{k0})/(\omega_k-\omega_1) + \sum_{k\neq0} \boldsymbol{M}_{k0}\cdot(\boldsymbol{R}_{01}\times\boldsymbol{R}_{1k})/\omega_k, \quad (4)$$

where the subscripts 0, 1, and k mean the ground, the n, π^* excited, and the kth excited states respectively, and where M and R stand for a magnetic and an electric dipole moment vector respectively.

It has recently been reported by Hoffman *et al.*[19] that the both phenyl rings of benzophenone are twisted out of the >C=O plane by 38° from the CNDO–MO calculations. Therefore, it is reasonable to discuss those states with C_2 symmetry. Therefore, the $S_0\rightarrow S_1$ transition is allowed in itself. Vala and Tanaka[20] pointed out, on the basis of their study of the polarized absorption spectra of the 4,4′-dichlorobenzophenone crystal, that there are four states in the 300—230 mμ region, that is, two CT states and two B_{2u}-analogue states, and that the transition moments from the ground state to the one of the former and to the one of the latter are parallel to the z or C=O axis. The order of these four states and the polarization data of these transitions would seem to be inconsistent with the polarization spectra reported by Shimada and Goodman.[5] However, if it is taken into account that these two sets of results are not essentially inconsistent with each other because of the difference in the experimental conditions, it may be concluded that the S_3 state corresponds to one of the B_{2u}-analogues and that the $S_0\rightarrow S_3$ involves two components parallel to the x and the z axes. (By the way, S_2 corresponds to one of the CT states.) Therefore, one obtains:

$$B(S_0\rightarrow S_1) = \sum^{B}\{M^y_{1k}R^z_{01}R^x_{k0}-M^x_{1k}R^z_{01}R^y_{k0}\}/(\omega_k-\omega_1) + \sum^{B}\{M^y_{k0}R^z_{01}R^x_{1k}-M^x_{k0}R^z_{01}R^y_{1k}\}/\omega_k. \quad (5)$$

The R^y_{k0} and R^y_{1k} matrix elements[21] are much smaller than R^x and R^z. As for the R^y_{1k} matrix element, although the S_k–S_1 transitions are not always negligible, the k states must be transformed like the x-coordinate. Therefore, the M^y_{k0} magnetic monents are nearly equal to zero. The main terms of $B(S_0\rightarrow S_1)$ are, then, as follow:

$$B(S_0\rightarrow S_1) = M^y_{13}R^z_{01}R^x_{30}/(\omega_3-\omega_1) + (\text{the similar terms for } k>3). \quad (6)$$

When $\omega_1=26.58$ kK, $\omega_3=39.00$ kK, $f_{10}=0.0029$, and $f_{30}=0.42$, assuming that $|R^z_{01}R^x_{30}|=(|R^z_{01}|^2\cdot|R^x_{30}|^2)^{1/2}=(f_{10}\cdot f_{30}/\omega_1\omega_3)^{1/2}$ and $|M^y_{13}|=10^{-1}-10^{-2}$, the order of the magnitude of the triple scalar products is $10^{-3}-10^{-4}$. It may be said that this order of magnitude is considerably close to our experimental value of $B(S_0\rightarrow S_1)$.

Finally, it can be concluded from the above discussions of the C_2 approximation that the MORD of the $S_0\rightarrow S_1$ transition (n–π^* absorption) of benzophenone occurs as a result of the perturbing state, S_3, being mixed into the S_1 state; then, the magnetic dipole transition is allowed through the magnetic dipole interactions between the S_3 and the S_1 states by the perturbation of the external magnetic field.

Although benzophenone is not a good example for discussing the properties of aromatic molecles by means of the MORD observation, it should be noted that some interesting characteristics of the MORD of benzophenone have been discussed. However, it is impossible to go further until more detailed data are accumulated.

The authour wish to thank Professors On Matumura and Yoshio Shibuya of the Department of Physics, Kyushu University, for providing them with the electric magnet.

17) P. J. Stephens, W. Süettaak, and F. N. Schatz, *J. Chem. Phys.*, **44**, 4592 (1966).
18) A. D. Buckingham and P. J. Stephens, *Ann. Rev. Phys. Chem.*, **17**, 399 (1966).
19) R. Hoffman and J. R. Swenson, *J. Phys. Chem.*, **74**, 415 (1970).
20) M. Vala and J. Tanaka, *J. Chem. Phys.*, **49**, 5222 (1968).
21) For instance, $R^y_{1k}=e<\phi_1|y|\phi_k>$.

Cleaning Effects of the Reactant in the Liquid-phase Isomerization of *m*-Xylene over a Silica-Alumina Catalyst under Pressure

Haruo TAKAYA, Naoyuki TODO, Tadasuke HOSOYA, Toshio MINEGISHI
Mikio YONEOKA,* and Hideki ŌSHIO**

The Government Chemical Industrial Research Institute, Tokyo, Mita, Meguro-ku, Tokyo
**Japan Gas-Chemical Company, Inc., Niigata Laboratory Enoki-cho, Niigata*
***The Research Laboratory, Central Glass Company, Ltd., Imafuku, Kawagoe-shi, Saitama*

(Received November 11, 1970)

The activity of silica-alumina catalyst in the isomerization of *m*-xylene was measured at the temperatures of 290°C, 320°C, 380°C, and 430°C in the liquid phase under a pressure of 300 kg/cm². The observed activities were considerably higher than those in vapor-phase reactions, moreover even after 20 days practically no decline in the activity was observed except for the measurements at 430°C. This superior ability of the catalyst in the liquid phase can be ascribed to the cleaning effect of the liquid reactant: in the liquid-phase reaction the high-boiling by-product, which, in vapor-phase reactions, diminishes the activity because of its strong adsorptivity on the surface sites, is successively dissolved in the reactant; therefore, more surface sites are constantly available for the isomerization. This interpretation was substantiated by the following results: 1) when the reaction was operated in the liquid phase, about eighteen times as much high-boiling by-product was obtained as in the vapor phase; 2) the activity in the liquid-phase reaction was much higher than that in the vapor phase; 3) the decreased activity caused by the interruption of the flow was regenerable when the flow was resumed; 4) the addition of the high-boiling by-product to the reactant *m*-xylene resulted in a considerable decrease in the activity. In addition, the identification of the components in the high-boiling by-products was carried out by means of mass and NMR spectroscopic studies.

In earlier papers, the present authors reported on the effect of pressure on the equilibrium composition of xylene isomers[1] as well as on the rate of the isomerization of *m*-xylene over a silica-alumina catalyst.[2] In these studies it was found that the silica-alumina catalyst revealed considerably higher activity in the liquid-phase reactions than in the vapor-phase reactions. Such an enhanced activity in the liquid-phase reactions can not be explained in terms of the increase in the coverage of xylenes on active sites, since the coverage is already high at atmospheric pressure.[3]

It was presumed from the charactersistic coloration of the products that the enhanced activity in the liquid-phase reaction is caused by the cleaning effect of the liquid reactant; in the liquid-phase reaction, the high-boiling by-product, which, in the vapor-phase reaction diminishes the catalyst activity because of its strong adsorptivity on the surface sites, is successively dissolved in reactant liquid xylenes; therefore, more surface sites are constantly available for the isomerization reaction. The purpose of this study is to confirm the above presumption.

Experimental

As is shown in Fig. 1, the equipment for carrying out continuous liqid-phase xylene isomerization under high pressure consisted of a pressure vessel, 3, containing a catalytic reactor, 4, and auxiliary equipment including pumps for xylene, 1 and 2, a pressure regulator, 5, and a product receiver, 6. All the equipment in contact with the process fluid was made of 18–8 stainless steel. The reactor placed on the lower flange, 7, of a pressure vessel, 1, had two porous sintered 18–8 stainless steel disks fixed by gland nuts, 10, serving to hold it steady as the catalyst bed. The pressure vessel was closely wound with nichrome resistance wire in three separate sections, 11, 12, and 13, to maintain isothermal conditions in the catalyst bed. The entire length of the reactor was covered with asbestos cloth for insulation, 15. The reaction temperature was measured with chromel-alumel theremocouples, 16 and 17, inserted in 18–8 stainless steel pipes, 18 and 19. In this way the temperature of the catalyst bed was controlled within 0.25°C of the desired temperature.

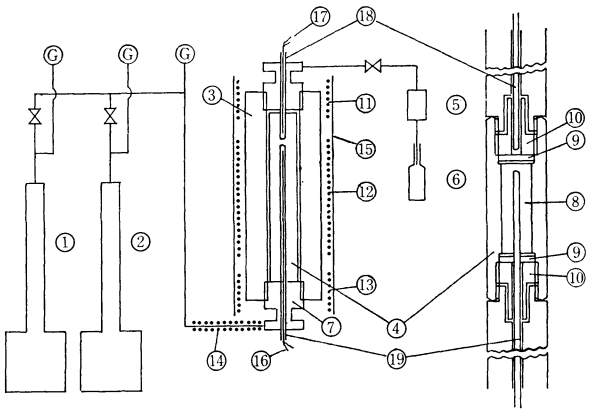

Fig. 1. The equipment.
1 and 2: Pumps for xylene. 3: Pressure vessel. 4: Reactor. 5: Pressure regulator. 6: Product receiver. 7: Lower flange. 8: Catalyst bed. 9: Porous sintered 18–8 stainless steel disk. 10: Gland nut. 11, 12, 13, and 14: Nichrome resistance wires. 15: Asbestos cloth. 16 and 17: Thermocouples. 18 and 19: 18–8 stainless steel pipes.

TABLE 1. THE COMPOSITION OF *m*-XYLENE USED AS A REACTANT

Benzene	Toluene	Ethyl-benzene	*p*-Xylene	*m*-Xylene	*o*-Xylene
trace	trace	trace	0.2	99.6	0.2

1) H. Takaya, N. Todo, T. Hosoya, T. Minegishi, and M. Yoneoka, This Bulletin, **43**, 2635 (1970).
2) H. Takaya, N. Todo, T. Hosoya, T. Minegishi, and M. Yoneoka, *Kogyo Kagaku Zasshi*, **73**, 1831 (1970).
3) K. L. Hanson and A. J. Engel, *A. I. Ch. E. Journal*, **13**, 260 (1967).

Table 2. Compositions of the products when powdered silica-alumina was used at a pressure of 300 kg/cm² (wt%)

Temperature	Toluene	*p*-Xylene	*m*-Xylene	*o*-Xylene	TMB[a)]	*W*/*F* g-cat·h/g
290°C	2.1	15.3	65.2	12.2	2.5	1.65
320°C	1.0	16.5	65.1	14.0	1.2	2.6×10^{-1}
380°C	0.2	12.6	76.8	10.0	t	7.0×10^{-3}
380°C	0.7	19.6	61.1	16.2	0.9	7.8×10^{-3}

a) TMB: Trimethylbenzene

In preparation for a series of runs, a weighed amount of catalyst was charged into the reactor in a dry box and moistened with *m*-xylene; then the reactor was placed in the pressure vessel. To make a run, *m*-xylene was passed through the reactor at a desired rate of 2 to 24 g/h under a pressure of 300 kg/cm², and then the reactor was heated to the desired temperature.

The catalyst was Nikki N633L silica-alumina crushed to a diameter of 1—1.4 mm or powdered Nikki N633L silica-alumina; both of these had been calcined at a temperature of 500°C for 20 hours. The purity of the *m*-xylene used as a reactant (produced by the Japan Gas-Chemical Co., Inc.) was 99.6 percent, as is shown in Table 1.

The product was analyzed by gas chromatography at 57°C. The column used for this measurement was 4 m in length and 1 mm in dia., and was packed with 5% bentone 34+ 5% DIDP on diasolid L (100—200 mesh).

In order to confirm the inhibiting effects of the high-boiling by-products on catalyst activity and to identify the components, the reaction products were fractionated under a pressure of 6—8 mm Hg and separated into several fractions. The components of the thus fractionated products were analyzed by means of a Hitachi double-beam mass spectrometer and a Varian-type NMR spectrometer. The mass spectra were obtained at ionization voltages as low as 15 V in order to allow only the parent peaks of the components to appear.

Results and Discussion

Activity of Powdered Silica-Alumina in the Liquid-phase Reaction. A heterogeneous catalytic reaction is considered to proceed in a series of mass transfer and kinetic steps. It has already been shown, however, that, in the liquid-phase isomerization of xylene, the kinetic steps are rate-determining up to the temperature of 380°C when powdered silica-alumina is used.

The results obtained at reaction temperatures of 290°C, 320°C, and 380°C under a pressure of 300 kg/cm² are shown in Table 2 and Fig. 2. It has been well recognized, in a study to follow the variation in the catalyst activity, that the variation is insensitive if the reaction has been equilibrated. Therefore, in this experiments the contact times, *W*/*F* (g-cat·h/g), were lowered with an increase in the reaction temperature so as to keep the *p*- and *o*-xylene contents in the products in the region of 0.12 to 0.15. In Fig. 2, the catalyst activities for isomerization and disproportionation are represented by the contents of *p*-xylene and toluene

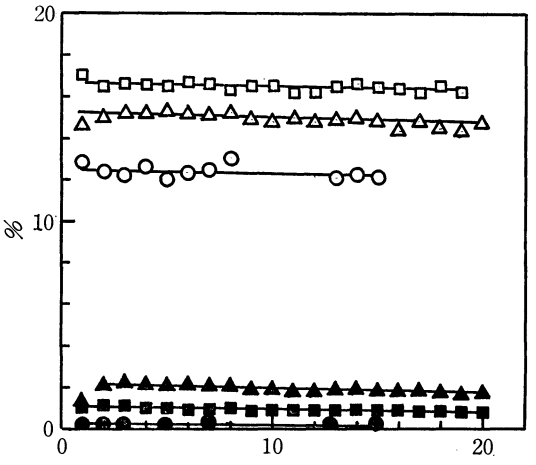

Fig. 2. Activity of powdered silica-alumina in the liquid-phase reaction at a pressure of 300 kg/cm².
△: *p*-Xylene, 290°C. ▲: Toluene, 290°C.
□: *p*-Xylene, 320°C. ■: Toluene, 320°C.
○: *p*-Xylene, 380°C. ●: Toluene, 380°C.

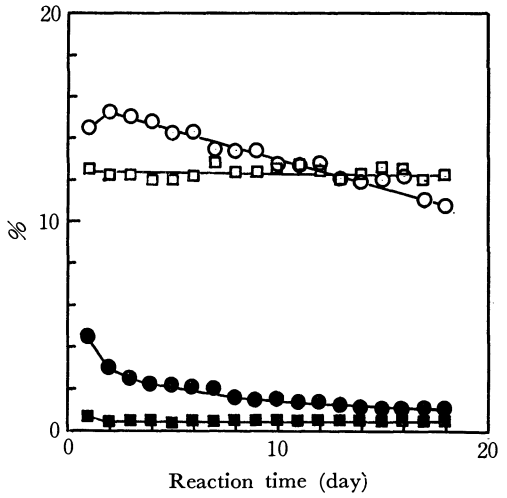

Fig. 3. Activity of granular silica-alumina in the liquid-phase reactions at a pressure of 300 kg/cm².
□: *p*-Xylene, 380°C. ■: Toluene, 380°C.
○: *p*-Xylene, 430°C. ●: Toluene, 430°C.

Table 3. Compositions of the products obtained by using granular silica-alumina (1—1.4 mm in dia.) under a pressure of 300 kg/cm². (wt%)

Temperature	Toluene	*p*-Xylene	*m*-Xylene	*o*-Xylene	TMB[a)]	*W*/*F* g-cat·h/g
320°C	1.6	11.5	71.5	9.3	1.8	2.4×10^{-1}
380°C	0.5	12.2	74.9	9.9	0.5	1.5×10^{-2}
430°C	4.5	14.5	62.4	12.9	5.3	7.4×10^{-3}

respectively, since these contents are nearly equal to those of *o*-xylene and trimethylbenzene respectively. It is clear from this figure that, in each of the three cases, but not at 430°C, practically no decline in the catalyst activity for the isomerization of *m*-xylene was observed, even after 20 days.

From Table 2 it can be seen that the ratio of the toluene content to the *p*-xylene content decreased with the reaction temperature. This result is consistent with the fact that the activation energy for the disproportionation over H–Y zeolite is smaller than that for the isomerization.[4]

Activity of Granular Silica-Alumina in the Liquid-phase Reaction. In Fig. 3 and Table 3, the results obtained by using a granular silica-alumina catalyst (1—1.4 mm in dia.) are shown. Figure 3 indicates that the activity decline did not occur at the temperature of 380°C. However, at the temperature of 430°C a gradual and comparatively large decline was observed; furthermore, the initial ratio of the toluene content to the *p*-xylene content increased considerably.

In an earlier paper[2] it was shown that the ratio of toluene to *p*-xylene increased with the contact time. Therefore, the remarkable increase in the disproportionation products at a higher temperature, such as 430°C, may be partially connected with the appearance of the contribution of the diffusion step to the reaction rate. Under such reaction conditions, the high-boiling by-product may accumulate, since its diffusion rate from the pores will be slower than the accelerated rate of the formation of the high-boiling by-product. This will be the cause of the decline in activity at 430°C.

Activity of Silica-Alumina in Vapor-phase Reactions at Atmospheric Pressure. In contrast with the results obtained in the liquid-phase reaction described above, it has been reported by many workers that, in the vapor-phase reaction, a steep decline in activity is unavoidable.[3,5] In order, therefore, to get information about the characteristic difference between the reaction in the liquid phase under high pressures and that in the vapor phase at atmospheric pressure, the following measurements were carried out. The reaction was operated at 292°C under a pressure of 300 kg/cm²; then the temperature was raised to 378°C at atmospheric pressure and kept at this temperature for 48 hr. After that, the reaction temperature was lowered again to 292°C and the pressure was increased to the initial pressure of 300 kg/cm². The activity indicated by the produced *p*-xylene is shown in Fig. 4. One of the most characteristic features in the vapor-phase isomerization is that the activity decreases steeply from 0.94 g/h g-cat. (B in Fig. 4) to 0.43 g/h·g-cat. (C in Fig. 4).

In addition, it must be noted that the observed activity in the vapor-phase reaction is much lower than that in the liquid-phase reaction. The vapor-phase reaction was carried out at a much higher temperature, at which a sufficient change in activity is observable, than that in the liquid phase. The comparison of the activities between the two reactions was made by the following procedure. As was reported in a preceding paper,[2] in the liquid-phase reaction under pressures the coverage of xylenes on surface sites is 1.0 and the observed activation energy for the isomerization from *m*-xylene to *o*-xylene is 37 kcal/mol, so long as the reaction temperatures are 380°C or less. Thus, the rate calculated for the isomerization from *m*- to *p*-xylene at 380°C by using this activation energy amounts to 76 times that at 292°C. On the other hand, the observed ratio of the rate for the vapor-phase reaction at 378°C to that for the liquid phase at 292°C is only 8.8. It is evident from the comparison that the activity of the silica-alumina catalyst in the liquid phase under a high pressure is much higher than that in the vapor phase.

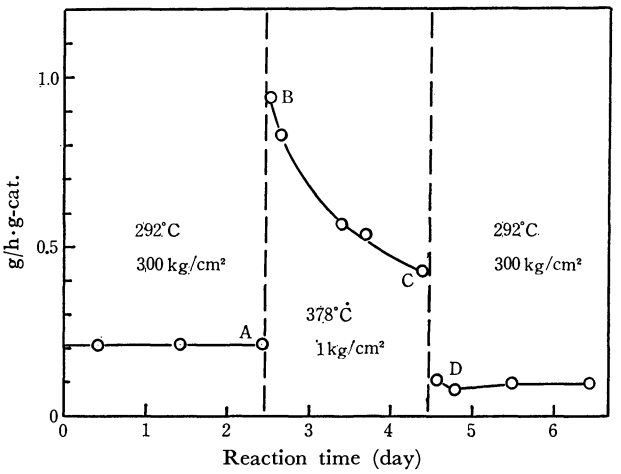

Fig. 4. Activity of silica-alumina in the vapor-phase reaction at atmospheric pressure.

Effect of the Interruption of the Flow on the Activity. As was described in the foregoing paragraph, an increase either in the contact time or in the reaction temperature tended to have the same effects on the

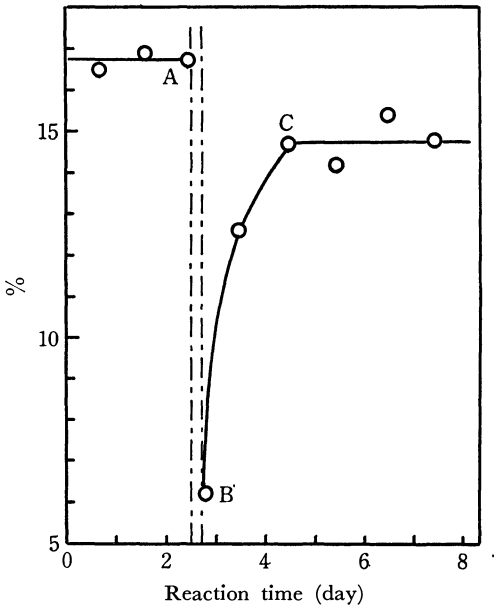

Fig. 5. Effect of the interruption of the flow on the activity.
○: *p*-Xylene.

4) H. Takaya, N. Todo, T. Hosoya, T. Minegishi, and M. Yoneoka, unpublished.

5) T. Iwasaki and R. Hatta, *Kogyo Kagaku Zasshi*, **63**, 1980, (1960).

Table 4. The compositions of the products at the representative points in Fig. 5 (Wt%)

Sample[a)]	Toluene	*p*-Xylene	*m*-Xylene	*o*-Xylene	TMB	TeMB[b)]	X[c)]
A	0.8	16.6	65.2	14.1	0.9		2.4
B_1	6.6	7.3	56.1	6.2	8.7	1.1	14.0
B_2	0.4	6.6	83.3	4.9			4.8
C	0.6	14.7	69.0	12.0	0.8		2.9

a) A: before the interruption of the flow. B_1 and B_2: 1.5 and 2.5 hr respectively after the resumption of the flow. C: 2 days after the resumption of the flow.
b) TeMB: Tetramethylbenzene.
c) X: Unidentified products.

product distribution and on the activity of the catalyst. In order, therefore, to get more detailed information about the effect of the product distribution on the decline in the activity, as an extreme case the flow of the feed was interrupted for 5 hr in the course of a stationary reaction at 320°C under 300 kg/cm²; the consequent variations in the activity and in the product distribution were followed. As is shown in Fig. 5, the *p*-xylene content decreased from a value of 16.6% before the interruption of the flow (A in Fig. 5) to 6.6% immediately after the resumption of the flow (B_2 in Fig. 5), and was then restored to an incomplete level of 14.7% after a two-day reaction. The compositions of the products at the representative points shown in Fig. 5 are tabulated in Table 4. From a comparison of the composition at 1.5 hr after the resumption of the flow (B_1) with those at A and C, it can be seen that the interruption of the flow results in an extraordinary increase in the disproportionation products and unidentified high-boiling by-products. On the basis of these results, it can be considered that the unidentified products, X, presumed to be responsible for retarding the isomerization, were accumulated on the surface sites of the catalyst during the interruption of the flow and were then eluted into the reactant solution after the resumption of the flow.

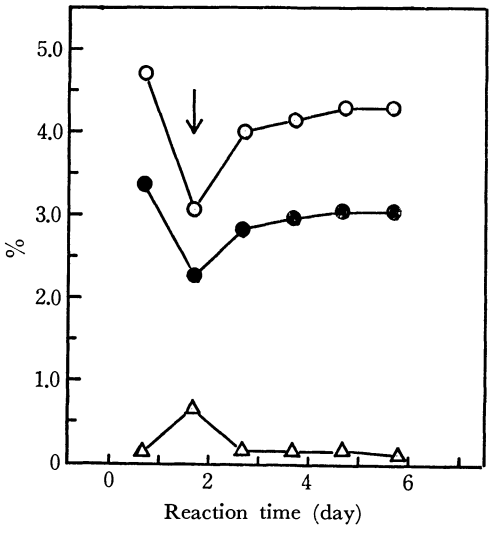

Fig. 6. Effect of the fraction 2 on the activity.
A downward arrow shows that a *m*-xylene solution containing 2 weight per cent fraction 2 was passed through the catalyst bed for 4 hr.
Reaction temperature: 280°C.
○: *p*-Xylene. ●: *o*-Xylene. △: Toluene.

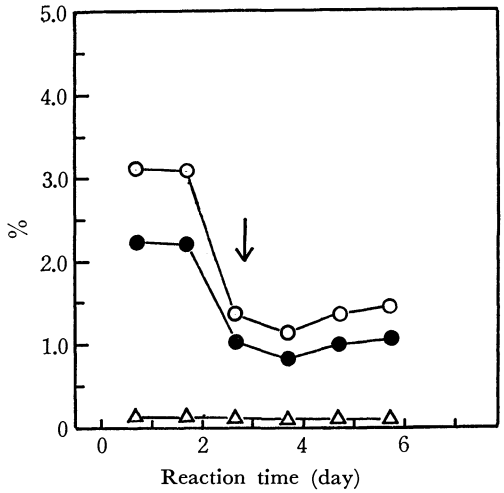

Fig. 7. Effect of the residue on the activity.
A downward arrow shows that a *m*-xylene solution containing 1 weight per cent residue was passed through the catalyst bed for 4 hr.
Reaction temperature: 280°C.
○: *p*-Xylene. ●: *o*-Xylene. △: Toluene.

The Effect of High-boiling By-products on the Activity. An experiment was carried out at 400°C under a pressure of 300 kg/cm², where the high boiling by-products could be produced in high yields. The total product after 9 days' operation, 1000 g, was distilled under a reduced pressure of 6—8 mmHg in the temperature ranges of 100—125°C (fraction 1), 125—150°C (fraction 2), and 150—200°C (fraction 3). The yields of these fractions and the residue are shown in Table 5.

Figures 6 and 7 show, respectively, the effects of the addition of fraction 2 and the residue on the activities; *m*-xylene solutions containing 2 weight percent of fraction 2 and 1 weight percent of the residue were passed through the catalyst bed for 4 hr in the course of a stationary reaction, using pure *m*-xylene as the reactant at 280°C under a pressure of 300 kg/cm². From Fig. 6 it is obvious that, by the addition of a minute quantity of the fraction 2, the *p*-xylene and *o*-xylene contents diminished and the toluene content increased. The varied contents were, however, restored to levels of about 90 percent of the initial values 4 days after the reactant was changed to pure *m*-xylene. As to the experiment with using a *m*-xylene solution containing 1 weight percent of the residue, the effect differed from that of fraction 2, as is shown in Fig. 7, the contents of *p*-xylene and *o*-xylene diminished to values less than half of the initial contents, whereas

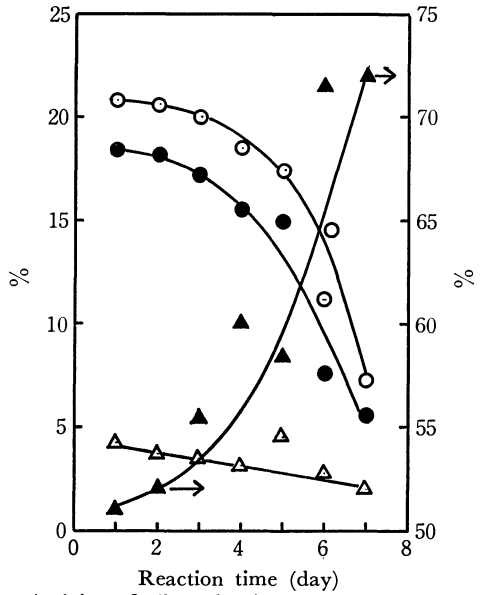

Fig. 8. Activity of silica-alumina at atmospheric pressure. W/F=0.5 h.

	1st day	2nd	3rd	4th	5th	6—7th
Reaction temperature(°C)	430	440	450	460	490	500

○: *p*-Xylene. ●: *o*-Xylene. ▲: *m*-Xylene. △: Toluene.

the toluene content was unaltered. Moreover, in this case, the reduced contents of *p*- and *o*-xylene were scarcely restored even 4 days after the reactant had been changed to pure *m*-xylene. The results clearly indicate that the high-boiling by-products have an inhibiting effect on the isomerization of *m*-xylene.

In contrast to the case of the liquid-phase isomerization under high pressure, only 1 g of high-boiling by-products could be separated from the product (800 g) obtained by 7 days reaction operated at a temperature above 430°C under atmospheric pressure. This result, when considered in connection with the remarkable decline in activity shown in Fig. 8, indicates that, in the vapor-phase isomerization high-boiling by-products are not easily desorbed from the catalyst surface, but are accumulated on the surface, this accumulation results in a large decline in the activity and in the low activity in the vapor-phase reaction.

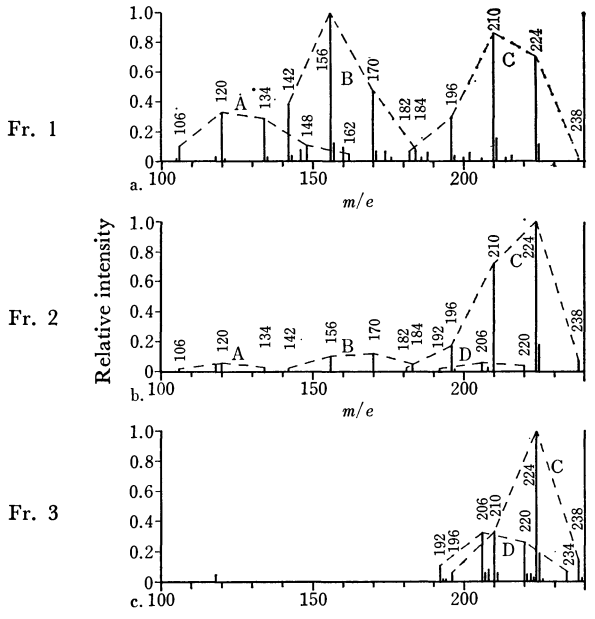

Fig. 9. Mass spectra of the fractions 1, 2 and 3.
A: Polymethylbenzene. B: Polymethylnaphthalene.
C: Polymethyldiphenylmethane. D: Polymethylanthracene or Polymethylphenanthrene.

Identification of High-boiling By-products. Figure 9 shows the mass spectra of the fractions 1, 2, and 3. It can be seen that all the spectra consist of several homologous series of the parent peaks: the successive peaks in a homologous series differ in mass number by 14, corresponding to the replacement of a hydrogen atom by a methyl group.

In the fractions 1 and 2, three series of polymethyl compounds were observed: A and B correspond to polymethylbenzene and polymethylnaphthalene respectively, while C corresponds to polymethyldiphenyl, polymethyldiphenylmethane, or polymethyldiphenylethane. The D series in the fractions 2 and 3 was identified as polymethylanthracene or polymethylphenanthrene.

Table 5. High-boiling by-products separated from the products (1000 g) of the reaction at 400°C under a pressure of 300 kg/cm². Distillation pressure: 6–8 mmHg

Fraction number	Temperature range (°C)	Yield (g)
1	100—125	3.2
2	125—150	14.7
3	150—200	3.0
Residue		1.4

As is shown in Table 5, the yield of fraction 2 amounts to 70 percent of total high-boiling by-products.

Therefore, the studies were concentrated upon the more accurate identification of the possible components of the main series, C. For this purpose, the fraction 2 was analyzed by means of NMR spectroscopy. The observed spectrum shows that all the polymethyl compounds have a methylene group in their structures. Moreover, the ratio of the number of the hydrogen atom in the methyl group to that in the methylene group was 6.5, and the ratio of the number of the hydrogen atom bound to the aromatic ring to that in the methylene group was 4.0. These findings imply

Table 6. Ratios of numbers of hydrogen atoms in the methyl group and bound with aromatic rings to that in methylene groups

	$-CH_2-$	$-CH_3-$	$-H$
The observed ratio for the fraction 2	1	6.5	4

The calculated ratios from the formulas

Mass number	Polymethyldiphenylmethane			Polymethyldiphenylethane		
	$-CH_2-$	$-CH_3$	$-H$	$-CH_2-$	$-CH_3$	$-H$
196	1	3	4	1	0.75	2.25
210	1	4.5	3.5	1	1.5	2
224	1	6	3	1	2.25	1.75

that the existence of polymethyldiphenyl should be excluded. Thus, the component must be either polymethyldiphenylmethane or polymethyldiphenlethane. The ratios calculated from the formulas of these compounds are also shown in Table 6. The agreement between the calculated and observed values is not satisfactory. However, it seems to be reasonable to say that the main component in the C series is polymethyldiphenylmethane rather than polymethyldiphenylethane, when one takes into account the fact that minute amounts of the compounds which have no methylene group, such as polymethylnaphthalene and polymethylanthracene, raise both the ratios.

We are very grateful to Dr. Yamamoto for his help in the measurements of the NMR spectra and to Dr. Fukuda for his help in the measurements of the mass spectra.

BULLETIN OF THE CHEMICAL SOCIETY OF JAPAN, VOL. 44, 2301—2308 (1971)

Linear Antiferromagnetic Interaction in Organic Free Radicals

Jun YAMAUCHI
The Institute for Chemical Research, Kyoto University, Uji
(Received December 26, 1970)

The static magnetic susceptibilities from 1.8°K to 300°K, and the ESR spectra from 1.5°K to 300°K, of several organic free radicals have been measured on powder samples. The broad maxima in the susceptibility which indicate the antiferromagnetic interaction and the broadening of the ESR absorption lines have been observed. The data are analysed on the basis of the linear Heisenberg model and shown to be consistent with the one-dimensional magnetic chain model of isotropic exchange interaction. Discussions are made of the grounds of susceptibility, the ESR, and the specific heat measurements. In addition to a short-range ordering of spins, the possibility of long-range ordering is also discussed in two radicals, BDPA-Bz and *p*-Cl-BDPA, on the basis of discontinuities in the slope of susceptibility, the rapid broadening of the ESR linewidth, and the disappearance of the ESR absorption.

Since the beginning of the history of free radical chemistry in 1900 when Gomberg published his discovery of the first stable radical, triphenylmethyl[1] a number of stable radicals have been prepared and investigated by means of modern techniques.[2] It is now possible to detect, and even to study, extremely unstable free radicals. As it is our purpose to examine the exchange interaction between unpaired electrons, the present study is confined to the stable radicals which can be obtained in a substantial concentration. A free radical is, as is well known, an atom, molecule or complex which contains one or more unpaired electrons. In the present paper we are concerned exclusively with organic free radicals which have one unpaired electron on each molecule.

The magnetic properties of the organic free radicals have attracted much interest in recent years. Although the radical molecules constituting the solid are quite complicated, the solid itself can be simply regarded as an array of molecules, each containing one unpaired electron in its highest filled orbital. At first sight it seems that the paramagnetic susceptibility can be described by the Curie law: $\chi_e = Ng^2\beta^2S(S+1)/3kT$, which can be applied to the radical solids with N spins of $S=1/2$. For all radicals measured above 77°K, however, this simple relation does not hold; the deviation apparently can be explained by the Curie-Weiss law with negative Weiss constants, which imply an antiferromagnetic exchange interaction between the unpaired electrons. Some of the ion-radical salts and charge-transfer complexes exhibit an anomalous paramagnetism which can be interpreted in terms of an exchange-coupled pair model.[3] This anomalous paramagnetism arises from strong exchange coupling between the unpaired electrons on adjacent molecules, each pair forming a lower singlet state and an upper triplet state. As the temperature is lowered, the singlet level becomes increasingly populated at the expense of the triplet level, so that the susceptibility decreases. The molar susceptibility for the singlet ground state dimers, each having a triplet state lying at an energy, Δ, above this ground state, is given as:

$$\chi = (Ng^2\beta^2S(S+1)/3kT)[1+(1/3)\exp(\Delta/kT)]^{-1}, \quad (1)$$

where $S=1$. In the ion-radical salts or charge-transfer complexes, the charged diamagnetic molecules may be considered to play an important role in forming dimers. For the sake of simplicity, we will limit ourselves to the radicals which are electrically neutral. The unpaired electron occupies a molecular orbital spreading over a whole molecular framework. According to the investigation of the hyperfine splittings of nitroxide radicals

1) M. Gomberg, *J. Amer. Chem. Soc.*, **22**, 757 (1900); *Ber.*, **33**, 3150 (1900).

2) See for example, D. J. E. Ingram, "Free Radicals as Studied by ESR" Butterworths, (London) (1958); A. R. Forrester, J. M. Hay, and R. H. Thomson, "Organic Chemistry of Stable Free Radicals" Academic Press, (London) (1968).

3) H. Nishiguchi, This Bulletin, **40**, 1587 (1967); Y. Sato, M. Kinoshita, M. Sano, and H. Akamatu, *ibid.*, **40**, 2539 (1967); **42**, 3051 (1969); D. B. Chesnut and W. D. Phillips, *J. Chem. Phys.*, **35**, 1002 (1961).

like TANOL,[4] the unpaired electron is exclusively localized on the N–O bond.[5] On the other hand, BDPA[6] has delocalized spin densities, even on the carbon atoms of biphenylene.[7,8] We studied the magnetic properties of two types of radicals in order to ascertain how the exchange interaction between the unpaired electrons would be affected by the delocalization of an unpaired electron. The stable radicals studied here are the following compounds.

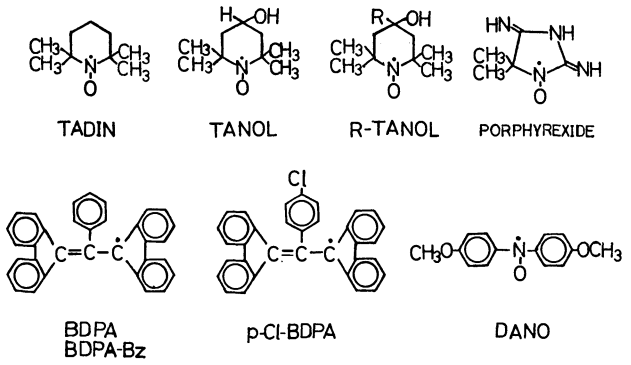

Fig. 1. Molecular structures of the radicals.

In many stable neutral radicals the susceptibility deviates from the Curie-Weiss law at low temperatures and shows a broad maximum. Rozantsev *et al.* have observed the temperature dependence of the intensities of the ESR spectra of TANOL and found a broad maximum in the intensities near 6°K.[9] The susceptibility had previously been measured by several investigators,[10,11] and a broad maximum at 6.5°K had been found. They suggested that this behavior of the paramagnet could be well described by the Heisenberg one-dimensional model with isotropic antiferromagnetic interaction. The magnetic susceptibility of BDPA-Bz has been measured above the temperature of liquid nitrogen by Duffy[12] and in the helium region by Edelstein *et al.* and by Pake *et al.*[13] Hamilton *et al.*[14] have used the proton Knight shift to measure the susceptibility and also measured the specific heat. They obtained the maximum susceptibility at 5.7°K and explained the phenomena tentatively. However, the accuracy of the measurements and the methods of analysis do not seem satisfactory.

Organic free radicals have plate-like structure of a low symmetry and condense into a crystalline solid with a small coordination number, as may be seen from the X-ray analysis of several radicals.[15–17] Therefore, the radicals may form a magnetic chain or plane different from that of the three-dimensionally interacting spin system. Since the distance between chains or planes is presumed to be much greater than the distance between nearest molecules in the chain or plane, the exchange coupling between nearest-neighbor electrons in different chains or planes is much weaker than that between nearest-neighbor electrons in the same chain or plane. The orbital occupied by the unpaired electrons is the $2P_z\pi$ - orbital, which has a uniaxial angular dependence. Therefore, we conjecture that organic free radicals are more likely to form a "magnetic chain" than a "magnetic plane."

From the theoretical point of view, the one-dimensional model of spin interaction is of considerable interest since it admits of an exact solution under certain simplifications which are actually possible in some cases. The magnetic behavior has several features different from that of usual three-dimensional spin systems.

The susceptibility and ESR measurements of several neutral stable radicals using a magnetic torsion balance and an ESR spectrometer at low temperatures were carried out in order to examine the exchange interaction and spin correlation in organic free radicals and in order to compare the observed values with the theoretically calculated ones. Later, more quantitative interpretations of the magnetic behavior will be made using the data published previously.

Experimental

The radical TANOL and its derivatives were prepared through the oxidation of the corresponding amine of 4-substituted 2,2,6,6-teramethylpiperidine following the process of Rozantsev.[18] They were purified a few times through recrystallization from ethereal alcohol. The details of the synthesis have been published elsewhere.[19] The samples of BDPA and its derivatives were prepared according to the procedures of Koelsch[20] and of Kuhn and Neugebauer.[8] After recrystallization from a benzene-benzine solutions, the melting points were found to agree well with the values in the literature. The results of the elementary analysis of carbon, hydrogen and nitrogen of each sample corresponded closely to the calculated values. As reported by Kuhn *et al.*, the radical solid BDPA complexes readily with such solvent molecules as benzene and acetone. BDPA with 1 mol of benzene will hereafter be abbreviated as BDPA-Bz, and BDPA containing no benzene molecule, as BDPA. BDPA-Bz was heated *in vacuo* at about 90°C for several hours; BDPA was thus obtained. BDPA, whose data have been published previously, is suspected to contain 1 mol of crystal benzene.

The susceptibility measurements were done, by means of a magnetic torsion balance described elsewhere,[21] on powder

4) 2,2,6,6-tetramethyl-4-piperidinol-1-oxyl.
5) R. Briere, H. Lemaire, and A. Rassat, *Bull. Soc. Chim. Fr.*, **1965** 3273; E. G. Rozantsev and M. B. Neiman, *Tetrahedron*, **20**, 131 (1964).
6) 1,3-bisdiphenylene-2-phenyl-allyl.
7) K. H. Hausser, *Z. Naturforsch.*, **14a**, 425 (1959).
8) R. Kuhn and F. A. Neugebauer, *Monatsh.*, **95**, 3 (1964).
9) Yu. S. Karimov and E. G. Rozantsev, *Soviet Physics-Solid State*, **8**, 2255 (1967).
10) J. Yamauchi, T. Fujito, E. Ando, H. Nishiguchi, and Y. Deguchi, *J. Phys. Soc. Japan*, **25**, 1558 (1968).
11) Yu. S. Karimov, *JETP Lett.*, **8**, 145 (1968).
12) W. Duffy, Jr., *J. Chem. Phys.*, **36**, 490 (1962).
13) J. H. Burgess, R. S. Rhodes, M. Mandel, and A. S. Edelstein, *J. Appl. Phys.*, **33**, 1352 (1962); M. E. Anderson, R. S. Rhodes, and G. E. Pake, *J. Chem. Phys.*, **35**, 1527 (1961).
14) W. O. Hamilton and G. E. Pake, *J. Chem. Phys.*, **39**, 2694 (1963).
15) A. W. Hanson, *Acta Cryst.*, **6**, 32 (1953).
16) J. Lajzerowicz-Bonneteau, *ibid.*, **B24**, 196 (1968).
17) P. Anderson and B. Klewe, *Acta Chem. Scand.*, **21**, 2599 (1967); D. E. William, *J. Amer. Chem. Soc.*, **91**, 1243 (1969).
18) E. G. Rozantsev, *Izv. Akad. Nauk SSSR, ser. khim.*, **12**, 2218 (1964).
19) K. Watanabe, J. Yamauchi, H. Takaki, H. Nishiguchi, and Y. Deguchi, *Bull. Inst. Chem. Res.* (Kyoto Univ.), **48**, 88 (1970).
20) C. F. Koelsch, *J. Amer. Chem. Soc.*, **79**, 4439 (1957).
21) M. Mekata, *J. Phys. Soc. Japan*, **17**, 796 (1962).

Table 1. Results from susceptibility measurements

	χ_d (10^{-4} emu/mol)	θ (°K)	T_m (°K)	χ_{max} (10^{-4} emu/mol)	$\chi_{T=0}$ (10^{-4}emu/mol)	$\chi_{max}/\chi_{T=0}$	J/k (°K)
TANOL	−1.1	−6	6.5	226	180±10	1.3	−5.0
TADIN	−1.1	−1	2.3	660	500±50	1.3	−1.8
cyclohexyl TANOL	−1.8	−2.5	(1.5)	—	—	—	(−1)
BDPA-Bz	−3.2	−8	5.6	199	150±10	1.3	−4.4
BDPA	−2.6	−8	10.9	153	90±10	1.7	−8.5
p-Cl-BDPA	−2.8	−6	5.6	196	150±10	1.3	−4.4
DANO[40]	−1.4	−3.4	4	287	200	1.4	−3.1

samples of about 100—50 mg in a field of 8.8 KOe. The measurements on all the samples were carried out in the temperature region attainable by pumping of liquid helium. No ferromagnetic impurities were found in any samples by checking the field dependence of magnetization up to 12 KOe at 4.2°K. The temperatures were measured with a carbon resister and an AuCo-Cu thermocouple calibrated by measuring the magnetic susceptibility of manganese Tutton salt and the vapor pressures of liquid helium, liquid hydrogen, and liquid nitrogen.

The ESR absorption spectra were observed between 1.5°K and 77°K using a JES-S1OE-type X-band spectrometer with an 80 Hz field modulation. The cavity with the TE_{102} mode was immersed in a liquid helium bath. The temperatures were measured with a carbon resister and an AuCo-Cu thermocouple attached to the cavity wall. An aqueous solution of peroxylamine disulfonate was used as a standard for the estimation of the *g*-value at room temperature. The magnetic field was calibrated from a hyperfine splitting of Mn^{2+} in MgO.

Results

Susceptibility. The data have been corrected for diamagnetism using Pascal's constants.[22] The calculated diamagnetic contribution is listed in Table 1. The absolute molar susceptibility, χ_M, corrected for diamagnetism, was compared with various theoretical calculations. All the radicals discussed here obey the Curie-Weiss law with a negative Weiss constant, θ, in a relatively high temperature region. The radical concentration of each sample, as determined from the susceptibility, was found to be nearly 100% within the limit of experimental accuracy. At lower temperatures, the molar susceptibility, however, deviates from the Curie-Weiss law and reaches a broad maximum at the T_m temperature. The values θ, T_m, and χ_{max} (the maximum susceptibility at T_m) of each sample are summarized in Table 1. When the temperature is decreased further, the susceptibility decreases comparatively slowly towards a finite susceptibility at $T=0$°K, $\chi_{T=0}$. The values $\chi_{T=0}$ in Table 1 are roughly estimated by the extrapolation of the χ_M-T curve. Figures 2—4 show the molar susceptibilities of the radicals.

ESR. ESR measurements were carried out in powder samples. The *g*-values were practically isotropic and were close to the free electron *g*-factor in all radicals; the latter factor is used in the theoretical

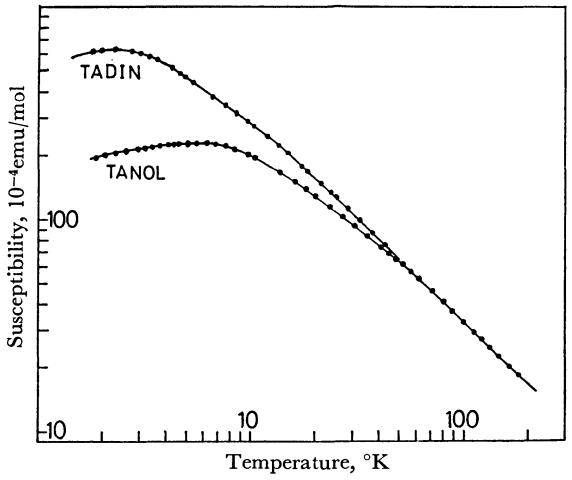

Fig. 2. Magnetic molar susceptibilities of TANOL and TADIN.

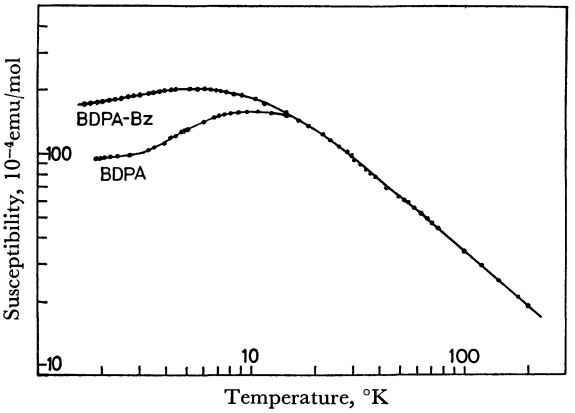

Fig. 3. Magnetic molar susceptibilities of BDPA-Bz and BDPA.

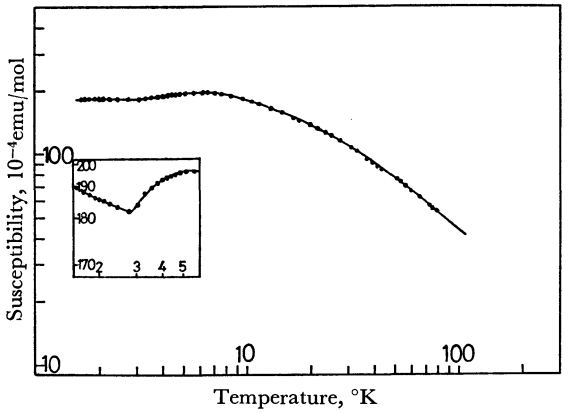

Fig. 4. Magnetic molar susceptibility of *p*-Cl-BDPA.

22) P. W. Selwood, "Magnetochemistry," Interscience Publisher, New York (1956).

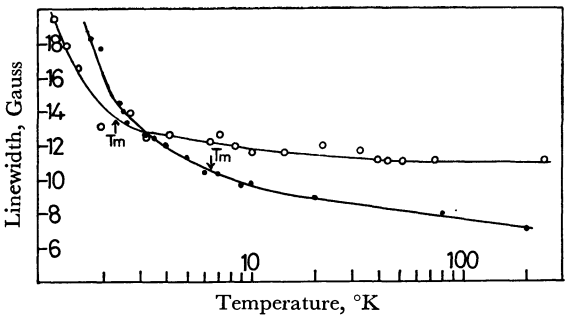

Fig. 5. Linewidths of TANOL (●) and TADIN (○).

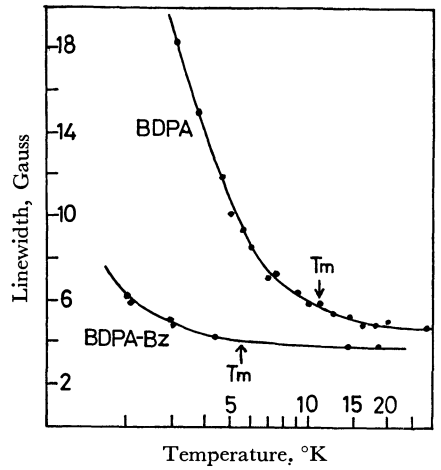

Fig. 6. Linewidth of BDPA-Bz and BDPA.

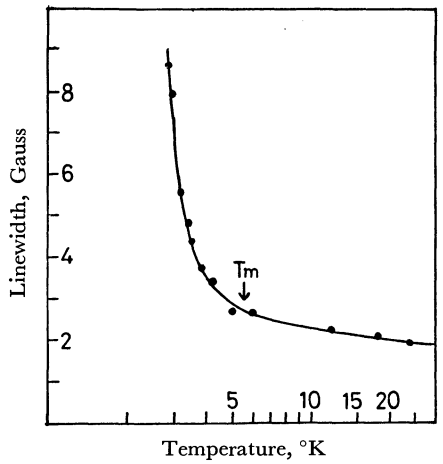

Fig. 7. Linewidth of *p*-Cl-BDPA.

calculation of susceptibility. The ESR absorption spectrum in each sample shows a single line which has an exchange-narrowed Lorentz shape. The linewidth, which was taken to be the peak-to-peak linewidth of the first derivative of the absorption spectrum, started to increase rapidly as the temperature was decreased below T_m, where the susceptibility went through a broad maximum. The ESR lines of all the radicals except *p*-Cl–BDPA[23] can be observed above the temperature of 1.8°K; the ESR line of *p*-Cl–BDPA broadens out and disappears as the temperature approaches 2.8°K from higher temperatures. Figures 5—7 show the temperature dependence of the linewidths of the radicals.

23) 1,3-bisdiphenylene-2-*p*-chlorophenyl-allyl.

Discussion

Susceptibility. It may be conjectured that the neutral organic free radicals, unlike ion-radical salts, have little tendency to form dimers. This fact is confirmed by a comparison of the experimentally-obtained susceptibility with that of the dimer model described by Eq. (1). If one enumerates the energy separation between singlet and triplet states, Δ, of Eq. (1) from the following relation;

$$\Delta/k = 1.60T_m, \tag{2}$$

Eq. (1) will reproduce qualitatively the experimental results of susceptibility, but the magnitude of the paramagnetic susceptibility differs from the observed value. The theory predicts a much larger value, χ_{max}, at T_m than the observed one; besides the deviation of the susceptibility becomes larger as the temperature is decreased below T_m. For instance, χ_{max} in TANOL is equal to 226×10^{-4} emu/mol; this is in contrast to the theoretical χ_{max} value of 298×10^{-4} emu/mol calculated from Eqs. (1) and (2) using T_m=6.5°K. Therefore, it may safely be said that no pairing of electron spins in the radicals and no dimerization of molecules occur.

Edelstein has successfully employed the linear Ising model for the qualitative interpretation of the susceptibilities of BDPA–Bz and PAC.[24] The Ising models are theories treating spatially-localized spins between which the exchange coupling is represented as $-2JS_{iz}S_{jz}$. Although Stout and Chisholm have treated the small interactions between Ising chains in $CuCl_2$ by introducing a molecular field,[25] organic free radicals have never been observed to have so large an anisotropic character. In fact, all organic free radicals have nearly isotropic *g*-values, so that the linear Ising model does not explain our results quantitatively. Therefore, we presume that it is not adequate to discuss the magnetic properties of organic free radicals on the basis of Ising models.

Soos *et al.* have analysed the temperature dependence of the magnetic susceptibility by treating the system as an alternating one-dimensional chain of Heisenberg spins;[26] the Hamiltonian is given by:

$$H = \sum_{i=1}^{N/2}\{J(1+d)S_{2i-1}S_{2i} + J(1-d)S_{2i}S_{2i+1}\}, \tag{3}$$

where $J(1+d)$ and $J(1-d)$ are the exchange constants between neighboring spins and where d is a parameter that represents the degree of alternation. Unfortunately, the theoretical susceptibility results do not agree with the more exact treatments for the limiting cases of d=1 and d=0. Recently Duffy and Barr obtained the exact eigenvalue spectrum and thermodynamic prop-

24) A. S. Edelstein, *J. Chem. Phys.*, **40**, 488 (1964).
25) J. W. Stout and R. C. Chisholm, *J. Chem. Phys.*, **36**, 979 (1962).
26) Z. G. Soos, *J. Chem. Phys.*, **43**, 1121 (1965); Z. G. Soos and H. M. McConnell, *ibid.*, **43**, 3780 (1965); Z. G. Soos, *ibid.*, **46**, 253 (1967); 4284 (1967).

erties of the same Hamiltonian as Eq. (3) and compared their results with the experimental results.[27] They fitted the susceptibility data with success in ion-radical salts, charge-transfer complexes, and only PAC and doubly-nitrated DPPH among neutral radicals. When $d \neq 0$, that is, in an intermediate alternation, there is an excited state with an energy gap from the ground state at $T=0$°K, so the susceptibility decreases exponentially as $T \to 0$°K. These schemes fail to explain a finite susceptibility at $T=0$°K unless $d=0$.

Previous to these investigations, theoretical calculations of the thermodynamic properties of one-dimensional long chains with isotropic and anisotropic interactions were made by Griffiths[28] and by Bonner and Fisher.[29] The corresponding spin Hamiltonian is given by:

$$\boldsymbol{H} = -2J\sum_{i=1}^{N}\{\boldsymbol{S}_{iz}\boldsymbol{S}_{i+1z}+\gamma(\boldsymbol{S}_{ix}\boldsymbol{S}_{i+1x}+\boldsymbol{S}_{iy}\boldsymbol{S}_{i+1y})\}, \quad (4)$$

which reduces to the Ising case when $\gamma=0$ and to the Heisenberg case when $\gamma=1$. Bonner and Fisher also estimated the behavior of susceptibility and specific heat for $N \to \infty$. The susceptibility for a pure antiferromagnetic Heisenberg chain displays a round maximum, and the corresponding specific heat exhibits an anomaly of the Schottky type. One of the crystalline solids which clearly exhibit antiferromagnetic linear chain behavior is $Cu(NH_3)_4SO_4 \cdot H_2O$, whose magnetic quantities can be explained qualitatively and also quantitatively in terms of this model, since each Cu^{2+} ion couples within a –O–Cu–O–Cu–O– chain and since interactions between chains are negligible.[30]

Organic free radicals have a plate-like structure of low symmetry with a small coordination number. Thus, the radicals may be expected to form magnetic chains, as has already been described in the introduction. Therefore, it is reasonable to analyse and discuss the results using the theory of the one–dimensional Heisenberg model based on Bonner and Fisher's calculations, which will be briefly summarized in the case of isotropic Heisenberg interaction with $\gamma=1$ and $N \to \infty$ in Eq. (4). The susceptibility displays a rounded maximum of height:

$$\chi_{max}/(g^2\beta^2/|J|) = 0.07346 \quad (5)$$

at

$$kT_m/|J| = 1.282. \quad (6)$$

The corresponding specific heat shows a Schottky-type anomaly associated with the broad susceptibility maximum and goes through the maximum of height:

$$C_{max}/Nk = 0.350 \quad (7)$$

at

$$kT_{mc}/|J| = 0.962. \quad (8)$$

It is worth remarking that χ_M can approach a finite nonzero value, $\chi_{T=0}$, at $T=0$°K, as there is no energy gap between the ground state and the first excited states when $\gamma=1$ and $N \to \infty$. $\chi_{T=0}$ is given by the following relation with the parameter J:

$$\chi_{T=0}/(g^2\beta^2/|J|) = 0.05066. \quad (9)$$

One can obtain the J parameter in Eq. (4) from several relations, (5), (6), (8), and (9). Assuming the J value from the T_m value experimentally obtained with the use of the (6) relation, we can evaluate the χ_M, χ_{max}, and $\chi_{T=0}$ values, which are dependent on the manner of evaluating J. On the other hand, the $\chi_{max}/\chi_{T=0}$ and T_m/T_{mc} ratios are independent of the J parameter and are equal to 1.45:1 and 1.33:1 respectively.

TANOL System: The temperature dependence of the magnetic susceptibilities of TANOL and TADIN[31] have been reported by several investigators.[10,11,32] In the case of TANOL, the exchange parameter was obtained as $|J|/k=5.0$°K; this agrees well with that obtained from the $\theta=2zJS(S+1)/3k$ relation with a nearest-neighbor parameter of $z=2$, with $S=1/2$, and with the Weiss constant $\theta=-6.0$°K. The χ_{max} value, 218×10^{-4} emu/mol, thus obtained from Eq. (5) is in good agreement with the experimental value, $\chi_{max}=226\times10^{-3}$ emu/mol. $\chi_{T=0}$ was then evaluated to be 180×10^{-4} emu/mol by extrapolation, while the same value can also be expected from Eq. (9). The Heisenberg linear chain for $N \to \infty$ and $\gamma=1$ predicts the theoretical ratio of $\chi_{max}/\chi_{T=0}=1.45$. On the other hand, the observed ratio, $\chi_{max}/\chi_{T=0}$, is equal to 1.3 (Table 1); this is in quite good accord with the theory. It may be said, therefore, that the spins in TANOL interact one-dimensionally with each other and that the interaction is isotropic in the sense of Heisenberg exchange interaction. A precise determination of the crystallographic structure of TANOL is monoclinic: $a=7.052\pm0.010$ Å, $b=14.081\pm0.018$ Å, $c=5.780\pm0.010$ Å, and $\beta=118°40'\pm10'$. The molecules are aggregated by the hydrogen bond and form chains parallel to the a-axis.[16] However, it is difficult to conclude whether the direction of linear exchange interaction is along the direction of hydrogen bonding or along the c-axis, where the lattice constant is the shortest. We are now engaged in clarifying this point.

The susceptibility of TADIN shows a broad maximum at $T_m=2.3$°K, after which χ_M decreases slowly towards a constant susceptibility. $J/k=-1.8$°K, which is obtained by following the same procedure as has been described above, reproduces well the experimental susceptibilities, χ_M, χ_{max}, and $\chi_{T=0}$. The $\chi_{max}/\chi_{T=0}$ ratio, 1.3:1, is also in good accord with the theory. Therefore, TADIN is considered to be a one-dimensional Heisenberg antiferromagnet.

The susceptibilities of TANOL derivatives (R= methyl, ethyl, phenyl, and cyclohexyl in Fig. 1) exhibit no broad maxima in the temperature range as low as 1.8°K, but deviate slightly from the Curie-Weiss law below about 4°K. The Weiss constants were found to be about 0°K (methyl and ethyl derivatives), −1°K (phenyl derivative), and −2.5°K(cyclohexyl derivative). The bulkier a substituent a radical has, the larger the Weiss constant becomes, but the exchange interactions are less than 1.5°K. The fact that TANOL has such a large exchange interaction as compared with those of TANOL derivatives may be ascribed either to the difference in the lattice distance of the crystal

27) W. Duffy, Jr., and K. P. Barr, *Phys. Rev.*, **165**, 647 (1968).
28) R. B. Griffiths, preprint, Stanford Univ. Carifornia
29) J. C. Bonner and M. E. Fisher, *Phys. Rev.*, **135**, A640 (1964).
30) R. B. Griffiths, *Phys. Rev.*, **135** A659 (1964); S. Saito, *J. Phys. Soc. Japan*, **26**, 1388 (1969).
31) 2,2,6,6-tetramethylpiperidine-1-oxyl.
32) J. Yamauchi, T. Fujito, H. Nishiguchi, and Y. Deguchi, Proceedings of 12th Inter. Conf. Low Temp. Phys., Kyoto (1970).

axis along which the magnetic chains are formed or to the difference in the strength of the hydrogen bond, which was found out by studying the infrared absorption spectra in Nujol. The details of this ascription will be published elsewhere.[33]

BDPA System: The molar susceptibility of BDPA-Bz, shown in Fig. 3, exhibits a broad maximum at $T_m=5.6$°K. χ_{max} and $\chi_{T=0}$ are obtained as 199 and 150×10^{-4} emu/mol respectively. Considering $\chi_{max}/\chi_{T=0}=1.3$ and the temperature dependence of the susceptibility in the especially low temperature region, the data can also be well explained in terms of the Hamiltonian ($N\to\infty$ and $\gamma=1$) described above. Thus, we obtain $J/k=-4.4$°K. If one excludes benzene molecules from BDPA-Bz by heating, the exchange interaction becomes larger, going from −4.4°K to −8.5°K. This radical, BDPA, also shows a susceptibility decreasing towards a finite susceptibility at $T=0$°K after $T_m=10.9$°K. However, the $\chi_{max}/\chi_{T=0}$ ratio, 1.7:1, is larger than the theoretical one, since $\chi_{max}=153\times10^{-4}$emu/mol is a little larger than the theoretical $\chi_{max}=130\times10^{-4}$ emu/mol. Thus, BDPA also has a one-dimensional Heisenberg interaction like BDPA-Bz. This fact can be understood by assuming that the removal of benzene molecules does not affect the spin structure in BDPA-Bz, but causes a stronger exchange interaction.

The data of *p*-Cl-BDPA are similar to those of BDPA-Bz, as is shown in Fig. 4 and summarized in Table 1. Therefore, the magnetic properties of *p*-Cl-BDPA are similar to those of BDPA-Bz. However, a discontinuity in the slope of susceptibility was found at about 2.8°K, after which the susceptibility rises again. This rise in the susceptibility has also been found in the neighborhood of 1.7°K in BDPA-Bz.[13] Such a discontinuity in *p*-Cl-BDPA indicates that there may be a phase transition into an antiferromagnetic state. This will be discussed below, together with the data of ESR measurements.

In the magnetic properties of BDPA-Bz and *p*-Cl-BDPA, there is a slight but significant difference between experiment and theory; that is, χ_{max} is lower than the theoretically-predicted value. At first sight, the radical concentration seems to become lower as the temperature is lowered. At T_m an assumed concentration decreases to 80% in both radicals. However, this is not due to a poor radical concentration, as one can understand from the facts that: 1)if the radical has a low concentration, the amount of the deviation of susceptibility is constant at all temperatures, 2) the radical concentrations of BDPA-Bz and *p*-Cl-BDPA are equal to above 100% if we estimate them from the susceptibility about 77°K, and 3) BDPA after the heat treatment of BDPA-Bz has about a 100% radical concentration in all temperature ranges. Although this effect is not completely accountable for at present, it may be associated with the electronic properties of allyl radicals, which behave as semiconductors,[34] as has been pointed out by Fedders and Kommandeur.[35]

ESR. The distinct character of linear magnetic chains is the development of short-range magnetic ordering without a definite transition to long-range ordering at low temperatures. The short-range magnetic ordering developed remarkably near T_m can be observed in the increase in the ESR linewidth below T_m. The data are illustrated in Figs. 5—7. The linewidth of each sample increases with the lowering of the temperature below T_m. Recently, the temperature dependence of the exchange-narrowed ESR linewidth of linear antiferromagnetic chains with the anisotropic exchange coupling was calculated by Kawasaki, using the double-time Green function method.[36] She found the following relation:

$$\Delta H/\Delta H_\infty = AT^{-1/4} \tag{10}$$

in the vicinity of 0°K, where ΔH_∞ is the linewidth at an infinite temperature and where A is a constant. The observed linewidth *versus* temperature below 77°K can be fitted to the following empirical relation:

$$\Delta H = \alpha \exp(\beta T_m/T) \tag{11}$$

where α and β are constant and where α may imply ΔH_∞. The α and β values of each sample are summarized in Table 2. We cannot fit the data with the relation (10) over a wide temperature region, even when the other exponents are applied. The broadening of the resonance may be attributed to an increase in the correlation time of the exchange motion because of magnetic ordering below the temperature of the susceptibility maximum. This pronounced increase in the linewidth of the paramagnetic resonance provides additional support for the present interpretation made from the susceptibility data.

Table 2. Parameters of temperature dependent linewidth: $\Delta H=\alpha\exp(\beta T_m/T)$

	T_m (°K)	α (Gauss)	β
TANOL	6.5	8.4	0.20
TADIN	2.3	8.2	0.48
BDPA-Bz	5.6	2.8	0.28
BDPA	10.9	3.5	0.49
p-Cl-BDPA	5.6	1.6	0.51

In *p*-Cl-BDPA the relation (11) holds above 4°K. The intensities of the ESR spectra decrease immediately below 4°K, and simultaneously the ESR linewidths broaden out. The disappearance and the broadening of the lines may be attributed to the coupling between neighboring chains, which induces a spontaneous magnetization. This phenomenon may imply the onset of long-range ordering, as it may be considered that the subsequent rapid increase in linewidth is the result of the critical fluctuation of electron spins in the neighborhood of the transition temperature.

In the case of BDPA-Bz, the ESR signal is so feeble that we cannot observe an absorption at about 1.6°K. This fact is probably related to the specific heat anomaly at 1.78°K[14]

33) to be published in this Bulletin.
34) D. D. Eley, K. W. Jones, J. G. F. Litter, and M. R. Willis, *Trans. Faraday Soc.*, **63**, 902 (1967).
35) P. A. Fedders and J. Kommandeur, *J. Chem. Phys.*, **51**, 1256 (1969); *ibid.*, **52**, 2014 (1970).
36) K. Kawasaki, *Prog. Theor. Phys.* (Kyoto), **42**, 174 (1969).

Specific Heat. According to the specific heat measurements of TANOL[37] and BDPA-Bz,[14] Schottky-type anomalies associated with the broad maximum susceptibility have been obtained at 4°K and 3°K respectively. The anomalies are predicted by the one-dimensional Heisenberg model. The maximum specific heat in TANOL is nearly what is expected from Heisenberg chains rather than from Ising chains, although in BDPA-Bz it is much smaller. This discrepancy in magnitude might be explained by assuming some type of electronic band structure.[35] The ratio of T_m to T_{mc} is unconnected with the exchange integral, J, and is equal to 1.3 for Heisenberg chains and to 2.4 for Ising chains. The observed T_m/T_{mc} ratios 1.6:1(TANOL) and 1.7:1(BDPA-Bz), deviate a little from the theoretically predicted ratio. The agreement with the theory is not so bad, however, if one takes into account of the accuracy of T_{mc}. Thus, the results of the specific heat measurements of TANOL and BDPA-Bz are not contradictory to the interpretation from the susceptibility measurements.

Other Radicals. The magnetic properties of other radicals will be discussed briefly below.

In porphyrexide the magnetic properties can be explained by the Ising model rather than by the linear Heisenberg model.[38] This is probably because the radical has a very small amount of anisotropy, which reduces the Heisenberg-type magnetic properties to Ising-type ones. The effect of this anisotropy was found in the temperature dependence of the ESR linewidth.[39]

The susceptibility data of DANO (di-*p*-anisylnitroxide) were shown by Duffy *et al*[40] to be consistent with the nearest-neighbor antiferromagnetic Heisenberg exchange of a quadratic layer lattice, because the radical is a magnetically layered crystal, as may be infered from the X-ray crystallographic study of Hanson.[15] However, as is shown in Table 1, $\chi_{max}/\chi_{T=0}$ and T_m/T_{mc} (T_{mc}=3°K) are in good agreement with the linear Heisenberg model. This radical presumably has a one-dimensional interaction, for it is possible that the radical forms a magnetic chain instead of a magnetic quadratic layer. This may be understood by taking into account the fact that the molecular orbitals of the unpaired electrons have a uniaxial angular dependence.

Exchange Interaction Mechanism. The exchange interaction originates from an overlap of the wave functions of the unpaired electrons. In compounds of transition ions, *d*-orbitals spread spatially in several directions so that magnetic planes can be formed. On the other hand, in organic free radicals the wave functions are described by $p_z\pi$-orbitals which have a uniaxial angular dependence. The exchange mechanism may be such that the interaction between unpaired electrons takes place through the overlap of the π-orbitals, as is shown in Fig. 8. Therefore, it may be understood that the neutral organic free radicals are one-dimensional antiferromagnets.

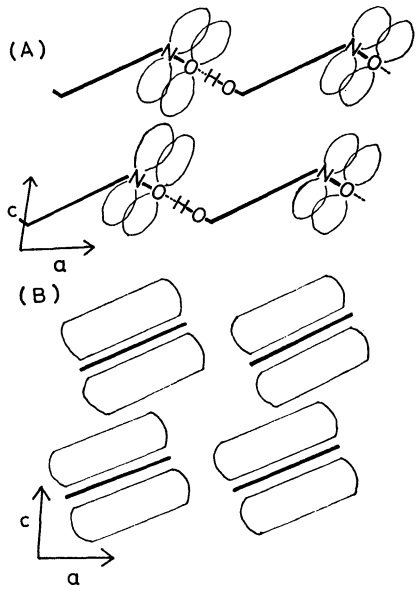

Fig. 8. Presumed exchange interaction mechanism between the unpaired electrons localized on N–O bonds (A) and between the delocalized unpaired electrons (B).
—: radical molecule, (⬭): π electron cloud.

Possible Existence of Long-range Ordering. It is well known theoretically[41] that the isolated magnetic linear chains do not have any magnetic phase transition but a broad maximum susceptibility, and that, in the presence of a small interaction between chains there occurs a magnetic transition from the short-range ordered state to the long-range ordered state in the lower temperature region. A sharp cooperative transition in organic free radicals has never been observed, although phase transitions associated with crystal deformation have been found.[42] There is a possibility for neutral organic free radicals to go into a long-range ordered state, since the interaction between chains cannot always be neglected. The data on BDPA-Bz and *p*-Cl-BDPA are considered to imply a long-range order at the Néel temperature of 1.78°K and 2.8°K respectively, because of: 1) the discontinuities of $d\chi_M/dT$ found at 1.7°K in BDPA-Bz[13] and 2.8°K in *p*-Cl-BDPA, 2) the rapid broadening and subsequent disappearance of the ESR absorption lines, and 3) the specific heat anomaly at 1.78°K in BDPA-Bz.[14] The long-range order in other radicals would be found if experiments were performed at lower temperatures.

Conclusion

The magnetic properties of neutral organic free radicals have been discussed qualitatively and quantitatively

37) H. Lemaire, P. Rey, A. Rassat, A. De. Combarieu, and J. Michel, *Mol. Phys.*, **14**, 201 (1968).
38) T. Fujito, H. Nishiguchi, Y. Deguchi, and J. Yamauchi, This Bulletin, **42**, 3334 (1969).
39) unpublished.
40) W. Duffy, Jr., D. L. Strandburg, and J. F. Deck, *Phys. Rev.*, **183**, 2218 (1969).
41) L. Onsager, *Phys. Rev.*, **65** 117 (1944); H. E. Stanley and T. A. Kaplan, *Phys. Rev. Letters*, **17**, 913 (1966).
42) W. Duffy, Jr., *J. Chem. Phys.*, **36** 490 (1962); D. D. Thomas, H. Keller, and H. M. McConnell, *ibid.*, **39**, 2321 (1963); C. T. Pott and J. Kommandeur, *ibid.*, **47**, 395 (1967); H. J. Monkrost, G. T. Pott, and J. Kommandeur, *ibid.*, **47**, 401, 408 (1967); K. Mukai, This Bulletin, **42**, 40 (1969); A. Kosaki, H. Suga, S. Seki, K. Mukai, and Y. Deguchi, *ibid.*, **42**, 1525 (1969).

on the basis of a linear Heisenberg model and on the basis of the following data: 1) the qualitative behavior of χ_M, 2) χ_{max} at T_m, 3) finite $\chi_{T=0}$, 4) $\chi_{max}/\chi_{T=0}$, 5) the Schottky-type anomaly of specific heat, 6) T_m/T_{mc}, and 7) the ESR linewidth. Although the interpretations may be tentative, except in the cases of TANOL and BDPA-Bz, for lack of data from crystal-structure and/or specific-heat measurements, the data on magnetic susceptibility, ESR linewidth, and specific heat are consistent with the linear Heisenberg antiferromagnetic exchange model in neutral organic free radicals. In comparison with a strong exchange interaction in a chain, the magnetic interaction between the chains is estimated to be very weak; thus, the neutral organic free radicals may be considered to be suitable crystals for studying the short-range order effect of the magnetic transition process.

The author is much obliged to Professor H. Takaki and Professor Y. Deguchi for a continuous encouragement throughout this work and also indebted to Dr. H. O. Nishiguchi, Dr. M. Mekata, and members of the laboratory for illuminating discussions. Thanks are also due to Mr. T. Fujito for a hearty cooperation in experiments.

BULLETIN OF THE CHEMICAL SOCIETY OF JAPAN, VOL. 44, 2308—2312 (1971)

An Acoustical Study of the Kinetics of Intermolecular Hydrogen Bonding and the Applicability of the Hammett Rule

Tatsuya YASUNAGA, Sadakatsu NISHIKAWA, and Nobuhide TATSUMOTO
Department of Chemistry, Fraculty of Science, Hiroshima University, Hiroshima

(Received January 23, 1971)

Rate and equilibrium constants for the hydrogen-bond dimerization of benzoic acid and meta- and para-substituted compounds in *N,N*-dimethylformamide have been determined by the measurement of the ultrasonic absorption in the 15—95MHz frequency range at 20°C, and the Hammett rule for the rapid monomer-dimer reaction has been examined. The forward and backward rate constants are 0.67×10^8 sec^{-1} and 2.8×10^7 sec^{-1} M^{-1} for para-toluic acid, 0.90×10^8 sec^{-1} and 1.9×10^7 sec^{-1} M^{-1} for meta-toluic acid, 1.6×10^8 sec^{-1} and 1.5×10^7 sec^{-1} M^{-1} for benzoic acid, 2.1×10^8 sec^{-1} and 2.4×10^7 $sec^{-1}M^{-1}$ for para-chlorobenzoic acid, and 3.3×10^8 sec^{-1} and 1.6×10^7 $sec^{-1}M^{-1}$ for metachlorobenzoic acid respectively. The forward and backward activation enthalpies for benzoic acid are 8.4 kcal/mol and 3.3 kcal/mol respectively. Using the substituent constants in Jaffe's table, the reaction constants in the Hammett rule are calculated to be 1.2 and −0.33 for the forward and backward reactions respectively.

There have been many reports[1] about the association of benzoic acid in nonassociated solvents. Maier and his coworker[2] found an excess absorption in carbon tetrachloride solutions of benzoic acid; they attributed this absorption to a perturbation of the equilibrium between the monomer and the hydrogen-bonding dimer of benzoic acid.

On the other hand, the Hammett rule, which is often used to account for the effect of substituents on aromatic compounds, has been used in studying the reaction of hydrolysis, acid dissociation, and so on.[3,4] The Hammett rule is characterized by a parameter which is independent of the reaction system, depending only on the substituents. It may be expected that the rule would hold true also for the rapid association and dissociation reactions for benzoic acid and meta- or para-substituted compounds. The ultrasonic absorption method, which provides a means of determining the rate constants for a reaction occurring in such a short time as shorter than 10^{-7} sec, seems to be very useful for examining the Hammett rule for this reaction.

Rassing and his coworkers[5] have already studied the Hammett rule for several para-substituted benzoic acids, but their measurements were limited to a few frequencies.

In this paper, we will present the ultrasonic absorption results for various meta- and para-substituted benzoic acid compounds and will evaluate the thermodynamic and kinetic values associated with the dimerization reaction.

Experimental

The ultrasonic absorption measurements were carried out in the frequency range from 15 to 95 MHz using the pulse technique which had been developed in our laboratory.[6] The cell was improved to prevent the dissolving of the binding materials into the solution by covering the transducer with a fused quartz plate 2 mm thick. The chemicals used were benzoic acid, meta-, para-toluic acids, meta-, para-chlorobenzoic acids, aniline, and methyl benzoate as solutes and *N,N*-dimethylformamide (DMF) as the solvent. These were all of the purest grade obtainable and were used without further purification. The measurements were made at various

1) G. C. Pimentel and A. L. McClellan, "The Hydrogen Bond," Reinhold Publishing Corp., New York, N. Y. (1960).
2) W. Maier and H. D. Rudolph, *Z. Phys. Chem.*, **10**, 83 (1957).
3) L. P. Hammett, *J. Amer. Chem. Soc.*, **59**, 96 (1937).
4) J. E. Leffler and E. Grunwald, "Rate and Equilibria of Organic Reaction," John Wiley & Sons, Inc. New York (1963).
5) J. Rassing, O. Østerberg, and T. A. Bax, *Acta Chem. Scand.*, **21**, 1443 (1967).
6) N. Tatsumoto, *J. Chem. Phys.*, **47**, 4561 (1967).

temperatures for benzoic acid and at 20°C for the other compounds.

Results and Discussion

Figures 1—5 show the ultrasonic absorption spectra in *N,N*-dimethylformamide solutions of benzoic acid, meta-, para-toluic acids, and meta- and para-chlorobenzoic acids at 20°C. These spectra can be represented by the following formula for a single relaxation:

$$\alpha/f^2 = \frac{A}{1 + (f/f_r)^2} + B \qquad (1)$$

where α is the absorption coefficient, f is the frequency, f_r is the relaxation frequency, and A and B are constants. Table 1 shows the ultrasonic parameters for these solutions.

As is shown in Fig. 6, the excess absorption was not observed in the pure solvent, *N,N*-dimethylformamide, or in the solutions of aniline or of methyl benzoate in the frequency range used in this experiment.

These results lead us to the conclusion that the

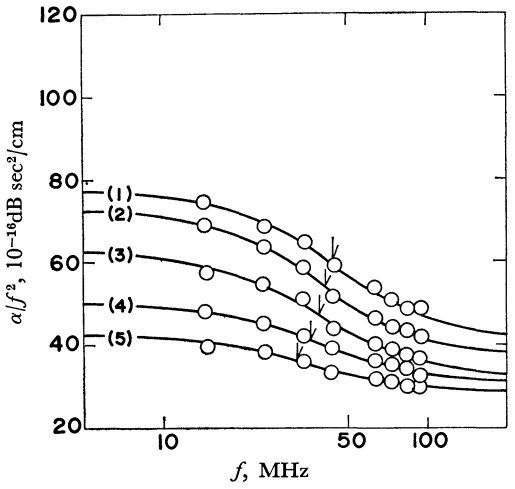

Fig. 1. Ultrasonic absorption spectra in DMF solution of benzoic acid at 20°C: (1) 3.0M; (2) 2.5M; (3) 2.0M; (4) 1.5M; (5) 1.0M.

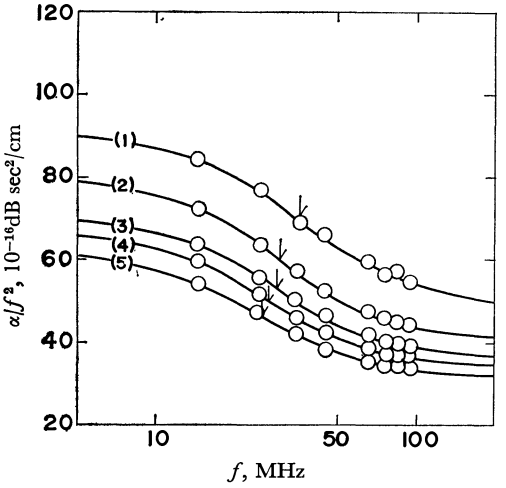

Fig. 2. Ultrasonic absorption spectra in DMF solution of *m*-toluic acid at 20°C: (1) 3.0M; (2) 2.4M; (3) 1.9M; (4) 1.5M; (5) 1.2M.

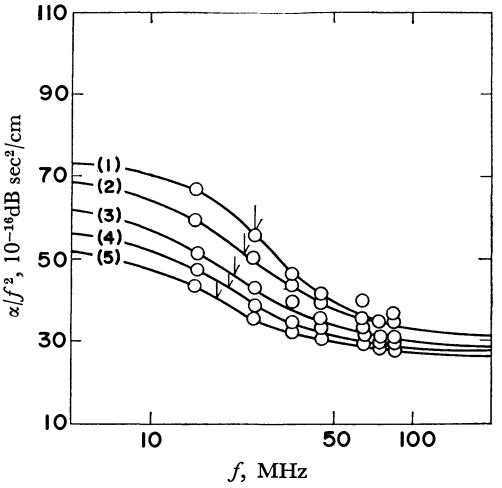

Fig. 3. Ultrasonic absorption spectra in DMF solution of *p*-toluic acid at 20°C: (1) 1.3M; (2) 1.1M; (3) 0.88M; (4) 0.71M; (5) 0.57M.

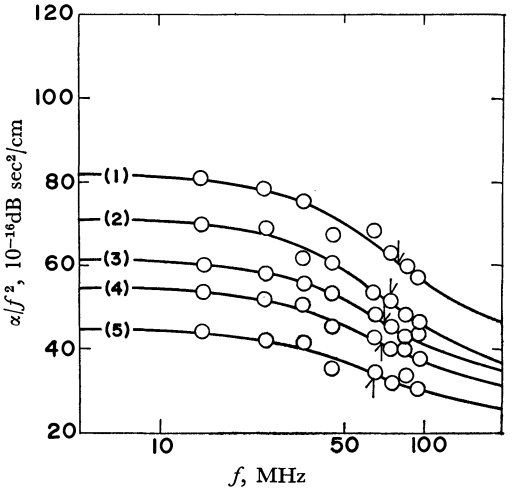

Fig. 4. Ultrasonic absorption spectra in DMF solution of *m*-chlorobenzoic acid at 20°C: (1) 3.0M; (2) 2.4M; (3) 1.9M; (4) 1.5M; (5) 0.9M.

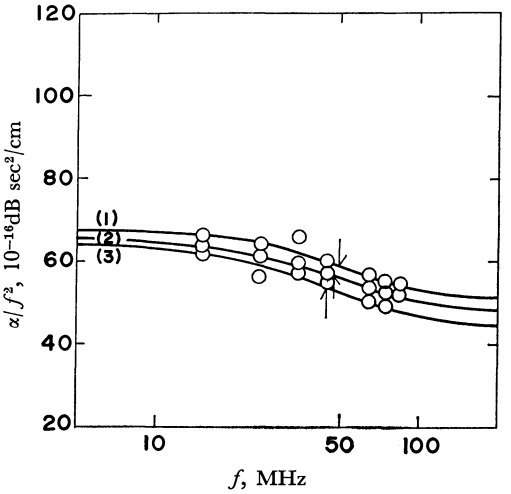

Fig. 5. Ultrasonic absorption spectra of DMF solution of *p*-chlorobenzoic acid at 20°C: (1) 1.4M; (2) 1.1M; (3) 0.87M.

TABLE 1. ULTRASONIC PARAMETERS FOR THE SOLUTION OF BENZOIC ACID, *m*-TOLUIC ACID, *p*-TOLUIC ACID, *m*-CHLOROBENZOIC ACID, AND *p*-CHLOROBENZOIC ACID AT 20°C

M	*A* 10^{-16} dB sec^2 cm^{-1}	*B*	f_r MHz
	Benzoic acid		
3.0	37	41	45
2.5	37.5	36.5	42
2.0	31.2	32.0	40
1.5	19.1	31.7	37
1.0	14.6	28.7	33
	m-Toluic acid		
3.0	41.0	49.2	35
2.4	40.8	39.0	30
1.9	34.0	36.4	29
1.5	32.5	34.2	27
1.2	30.2	32.2	25
	p-Toluic acid		
1.3	45.1	30.0	25
1.1	39.2	31.8	23
0.88	35.5	28.8	21
0.71	30.8	27.6	20
0.57	27.2	27.0	18
	m-Chlorobenzoic acid		
3.0	44.6	37.6	80
2.4	39.5	31.7	75
1.9	31.7	30.3	70
1.5	26.2	28.7	68
0.9	21.5	23.5	63
	p-Chlorobenzoic acid		
1.4	17.7	30.5	50
1.1	18.3	27.9	47
0.87	21.0	24.0	45

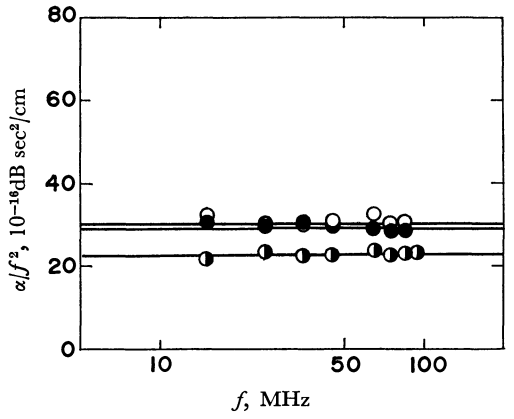

Fig. 6. Ultrasonic absorption spectra at 20°C: ◑, DMF; ○, DMF solution of methylbenzoate 30 vol%; ●, DMF solution of aniline 50 vol%.

excess absorption is associated with the reaction the site of which exists in the carboxyl group of benzoic acid and its substituted compounds. It has been reported[1] that the equilibrium between the monomer and the dimer formed by the intermolecular hydrogen bonding between the carboxylic proton and carbonyl oxygen exists in the solution of benzoic acid. Provided that the ultrasonic absorption is ascribed to the monomer-dimer reaction, the reaction scheme can be written as:

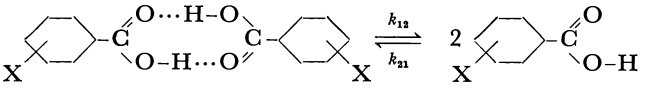

(2)

where k_{12} and $_{21}$ are the forward and backward reaction rate constants respectively and where X is meta- or para-substituent. Then, the rate equation can be represented by:

$$\frac{d[A_2]}{dt} = k_{21}[A_1]^2 - k_{12}[A_2] \quad (3)$$

where $[A_1]$ and $[A_2]$ are the concentrations of the monomer and the dimer respectively. The relation between the relaxation frequency, f_r, and the total concentration, $[C_0]$, is expressed by the following equation:

$$(2\pi f_r)^2 = (1/\tau)^2 = 8k_{12}k_{21}[C_0] + k_{12}^2 \quad (4)$$

where τ is the relaxation time.

Figure 7 shows the experimental plots of $(2\pi f_r)^2$ *vs.* $[C_0]$ for five compounds; the linearity of these plots confirms our assumption that the ultrasonic absorption is associated with the monomer-dimer reaction. The values of k_{12} and k_{21} were obtained from the intercept

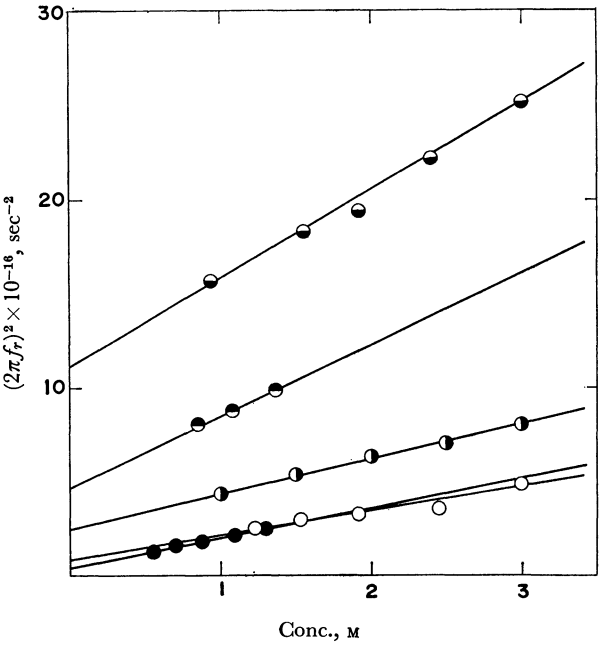

Fig. 7. The plots of $(2\pi f_r)^2$ *vs.* concentration at 20°C: ◑, benzoic acid; ●, *p*-toluic acid; ◓, *p*-chlorobenzoic acid; ◒, *m*-chlorobenzoic acid; ○, *m*-toluic aid.

TABLE 2. THE KINETIC VALUES OBTAINED FROM ULTRASONIC ABSORPTION SPECTRA AND SUBSTITUENT CONSTANTS

Compound	k_{12}, 10^8 sec^{-1}	k_{21}, 10^7 sec^{-1}M^{-1}	*K*, M	σ
p-Toluic acid	0.67	2.8	2.4	−0.170
m-Toluic acid	0.90	1.9	4.8	−0.067
Benzoic acid	1.6	1.5	10	0
p-Chlorobenzoic acid	2.1	2.4	9.3	0.227
m-Chlorobenzoic acid	3.3	1.6	20	0.373

and the slope of the curve in Fig. 7, while the equilibrium constant, K, was calculated by $K=k_{12}/k_{21}$. These values are listed in Table 2.

According to Eyring's rate theory, the rate constant can be written as:

$$k_i = \kappa\frac{kT}{h}\exp\left(-\frac{\Delta F_i^*}{RT}\right) = \kappa\frac{kT}{h}\exp\left(-\frac{\Delta H_i^*}{RT}+\frac{\Delta S_i^*}{R}\right) \quad (5)$$

where k_i is the rate constant, κ is the transmission coefficient, k is the Boltzmann constant, T is the absolute temperature, R is the gas constant, ΔF_i^* is the activation free energy, ΔH_i^* is the activation enthalpy, and ΔS_i^* is the activation entropy. Figure 8 shows the plots of $\ln k_i/T$ *vs.* $1/T$ for benzoic acid. Figure 9 shows the activation enthalpies which were calculated from the slopes in Fig. 8; it also shows the enthalpy change obtained through the difference between the activation enthalpies for the forward and backward reactions.

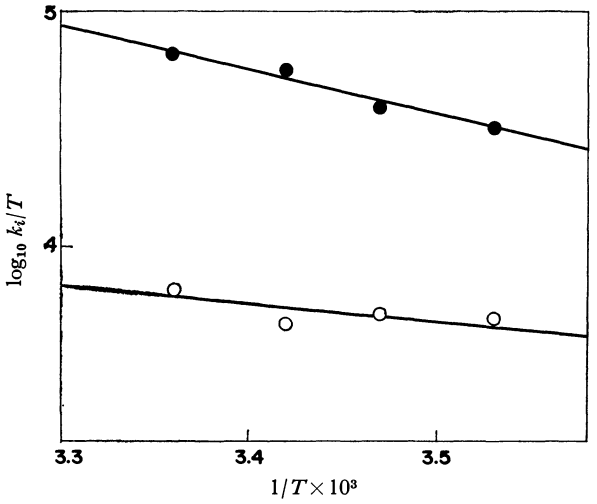

Fig. 8. Dependence of $\log k_i/T$ on $1/T$ for benzoic acid: ●, k_{12}; ○, k_{21}.

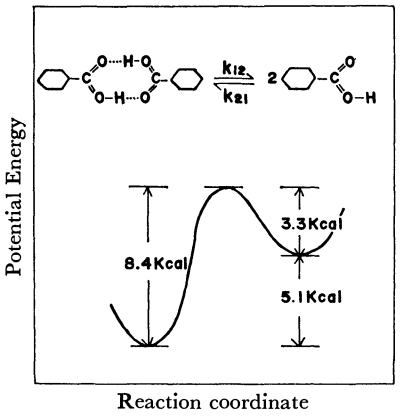

Fig. 9. Energy potential curve for monomer-dimer reaction in DMF solution of benzoic acid.

Now, provided that k_0 and k_j are the rate constants for the reaction in the unsubstituted compound and in a compound substituted in meta- or para-positions respectively relative to the carboxyl group, the following expression can be derived from Eq. (5):

$$\ln\frac{k_j}{k_o} = \frac{\Delta F_o^* - \Delta F_j^*}{RT} = \sigma\rho \quad (6)$$

where ΔF_o^* and ΔF_j^* are the activation free energies for benzoic acid and substituted compounds respectively. Equation (6) shows the well-known Hammett rule. σ is the substituent constant, which depends only on the nature and position of the substituent, X, and ρ is the reaction constant, which depends on the reaction, the condition under which it takes place, and the nature of the side chain.

In Fig. 10 the rate constants for the five compounds which were obtained in this experiment are plotted against the values of σ found in Jaffe's table.[7] The values of the reaction constants, ρ, obtained from the slope in Fig. 10 are 1.2 for the dissociation and −0.33 for the association in this reaction system.

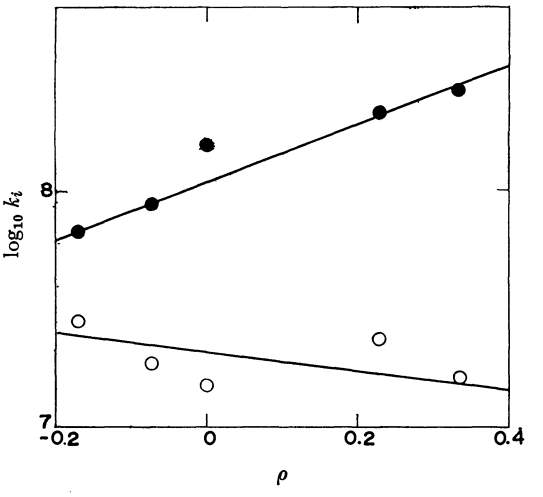

Fig. 10. The relation between the rate constant and the substituent constants: ●, k_{12}, ○, k_{21}.

As is shown in Fig. 7, the dependence of the relaxation frequency on the concentration shows that the excess absorption may be attributed to the perturbation of the equilibrium between the monomer and the dimer of benzoic acid or substituted compounds. The value of enthalpy change for benzoic acid, 5.1 kcal/mol, is small, as the breakage of the two hydrogen bonds in the dimer.[2,8] Borucki,[9] however, has reported that the enthalpy change in the monomer-dimer reaction for bonzoic acid in a polar solvent is smaller than that in a nonpolar solvent. The value, therefore, seems to be reasonable for the enthalpy change for the hydrogen bonding.

Figure 10 shows that the Hammett rule can be applied to the hydrogen-bonding reaction of meta- and para-substituted compounds of benzoic acid. According to previous theoretical studies of the Hammett rule,[3,10,11] σ can be correlated with the electron density.

7) H. H. Jaffe, *Chem. Rev.*, **53**, 191 (1953).
8) W. Maier, *Z. Elektrochem.*, **64**, 132 (1960).
9) L. Borucki, *Ber. Bunsenges. Physik. Chem.*, **71**, 504 (1967).
10) H. H. Jaffe, *J. Chem. Phys.*, **20**, 279 (1952).
11) H. H. Jaffe, *ibid.*, **21**, 415 (1953).

When the tendency of substituents to be electron donors increases and when the electron density at the reaction site becomes high, σ becomes more negative. As can be seen in Fig. 10, in the compound of which σ is great, *i.e.*, in which the electron density at the reaction site is low, the hydrogen bond in the dimer is weak and the rate of dissociation is fast, while in that of which σ is small, *i.e.*, in which the electron density is high, the bond is strong and the rate is slow. On the other hand, the reaction constant for the association is negative, and the activation enthalpy for the association is increased with σ. That is, the monomeric state is stabilized and the rate of association is decreased with an increase in σ. Consequently, the rates for the formation and breakage of hydrogen bonds in these compounds depend on the electron density at the reaction sites.

BULLETIN OF THE CHEMICAL SOCIETY OF JAPAN, VOL. 44, 2312—2321 (1971)

Electronic Structures of Tris(2,2′-bipyridyl) Complexes of Transition Metals in Lower Oxidation States

Ichiro HANAZAKI and Saburo NAGAKURA*

The Institute of Physical and Chemical Research, Yamato-machi, Saitama

** The Institute for Solid State Physics, The University of Tokyo, Roppongi, Minato-ku, Tokyo*

(Received January 26, 1971)

The electronic structures of various transition metal complexes with 2,2′-bipyridyl in low oxidation states are studied theoretically by the composite system method. The results show that the excess electrons are not localized on the metal ion but are transferred to some extent to the ligand antibonding π-molecular orbitals with the lower oxidation states of complex ions. The present theory can explain reasonably and systematically the observed magnetic moments and ESR spectra of the complexes, the simple one-electron treatment being inappropriate for a theoretical explanation of their magnetic properties. According to the present treatment, their electronic absorption spectra can be explained satisfactorily from a qualitative point of view as the overlapping of the π–π^* transition bands in the ligands with the metal-ligand charge-transfer transition bands.

A number of transition metal complexes in low oxidation states have been synthesized. In particular, the tris(2,2′-bipyridyl) complexes in various oxidation states have been synthesized for the iron-series transition metals and their magnetic properties have been investigated.[1–10] König studied their ESR spectra,[11] assuming that the excess electrons are localized completely on the metal ion. Hall and Reynolds explained the g value obtained by the ESR measurement for $[Fe(bip)_3]^0$ [12] on the same assumption. However, in view of the metal-ligand interaction, this assumption may not always be appropriate. In fact, their measurement of the electronic absorption spectrum[9,10] of $[Fe(bip)_3]^0$ indicates that most of the excess electrons delocalize to the bipyridyl π-electron systems, and their ESR and electronic absorption studies give different conclusions on the excess electron distribution of the same complex. This contradiction must be solved.

The present study has been undertaken to understand more extensively the electronic structures of tris(2,2′-dipyridyl) complexes in low oxidation states and to solve several problems on their magnetic and optical properties from the theoretical point of view. In particular, the distribution of "excess electrons" in the ground states of these complexes seems to be interesting in connection with their magnetic properties and with their oxidation-reduction abilities.

General Background of the Present Theoretical Consideration

The metal complexes in lower oxidation states treated in the present study are summarized in Table 1 together with those in ordinary oxidation states. We have adopted the two quantities to characterize the isoelectronic series;[13] namely, N_π, the total numbers of the metal $3d\pi$ electrons plus the π electrons in ligand

1) S. Herzog and R. Table, *Z. Anorg. Allg. Chem.*, **306**, 159 (1960); *Angew. Chem.*, **70**, 469 (1958); S. Herzog and H. Zuhlke, *Z. Chem.*, **6**, 434 (1966).

2) S. Herzog, *Naturwiss.*, **43**, 35 (1956); S. Herzog and U. Grimm, *Z. Chem.*, **6**, 380 (1966).

3) S. Herzog and M. Schmidt, *ibid.*, **3**, 392 (1963); **2**, 24 (1962).

4) a) S. Herzog, *Z. Anorg. Allg. Chem.*, **267**, 337 (1952); b) S. Herzog, U. Grimm, and W. Waicenbauer, *Z. Chem.*, **7**, 355 (1967).

5) S. Herzog. R. Klausch, and J. Lautos, *ibid.*, **4**, 150 (1964); G. M. Waind and B. Martin, *J. Inorg. Nucl. Chem.*, **8**, 551 (1958).

6) S. Herzog and H. Praekel, *Z. Chem.*, **5**, 469 (1965).

7) S. Herzog, *J. Inorg. Nucl. Chem.*, **8**, 557 (1958); *Z. Chem.*, **2**, 225, 208 (1962).

8) S. Herzog, G. Byhan, and P. Wulfert, *ibid.*, **1**, 370 (1961).

9) F. S. Hall and W. L. Reynolds, *Inorg. Chem.*, **5**, 931 (1966).

10) C. Mahon and W. L. Reynolds, *ibid.*, **6**, 1927 (1967).

11) E. König, *Z. Naturforsch.*, **19a**, 1139 (1964).

12) The tris-(2,2′-bipyridyl) complex is abbreviated to $[Me(bip)_3]^Q$, where Me=metal and Q is the charge on the complex.

13) The ligand-to-metal π-electron transfer is not taken into account in the present treatment. Therefore, N_π may be considered as the number of metal $3d\pi$ electrons when there is no π-electron transfer from the metal to ligands.

Table 1. $[Me(bip)_3]^Q$ Complexs in various oxidation states[a,b]

Q	N[c]						
	15	16	17	18	19	20	21
−2				Ti 0		Cr 2	
−1			Ti 1	V 0	Cr 1	Mn 3	Fe p
0	Sc 1	Ti 0	V 1	Cr 0	Mn 3	Fe p	Co 1
1		V 2	Cr 1			Co	
2	V 3	Cr 2	Mn 5	Fe 0	Co 4	Ni 2	
3	Cr 3	Mn	Fe 1	Co 0			

a) The synthesis and magnetic moment are described in Refs. 1—10.
b) The number in each site indicates the number of unpaired electrons deduced from the observed magnetic moment. The notation "p" denotes that the complex is paramagnetic but its magnetic moment has not been measured.
c) $N=N_\pi+N_\sigma$, where N_π is the total number of electrons in the $3d\pi$ and ligand antibonding π-orbitals and N_σ is the total number of electrons in the metal σ ($3d\sigma$, $4s$, $4p\sigma$) and ligand σ lone-pair orbitals

antibonding MO's, and Q, the charge of the complex as a whole.

The theoretical method is similar to that developed previously for the metal chelate compounds containing organic unsaturated molecules as ligands.[14-17] It is based on the composite-system method in which the π-electron system of the complex is divided into the metal and three ligand molecules. Thereafter, the interaction among the four components is considered by the configuration interaction among the ground, locally-excited and charge-transfer (CT) configurations. The π-electron wavefunctions and energy integrals for the ligand molecule were obtained previously by use of the SCFMO–CI method considering the effect of electrostatic potential field caused by the metal ion.[15] The metal-ligand resonance integral β necessary for the configuration interaction calculations is determined by the equation

$$\beta = -S_{MN}(I_M+I_N)/2 \qquad (1)$$

where I_M and I_N are the ionization potentials of the metal $3d\pi$ AO and the nitrogen $2p\pi$ AO, respectively, and S_{MN} is the overlap integral between these two AO's.

We assume that the complex has a D_3 symmetry as illustrated in Fig. 1. This geometrical configuration has been established for the ordinary tris-complexes[18,19]

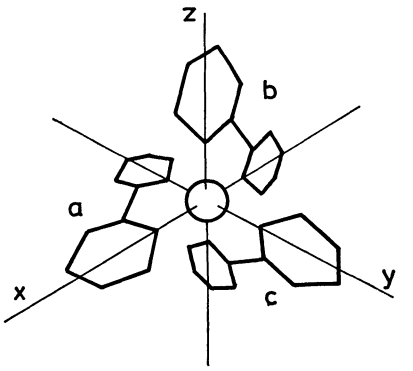

Fig. 1. The geometrical structure of tris-(2,2′-bipyridyl) complexes.

and also for some complexes in lower oxidation states.[20]

The π-Electron Distribution

First of all, we examine the magnetic properties of a series of complexes of $N_\pi=4$ on the assumption that the excess electrons are localized completely on the metal $3d\pi$ AO's. The calculation has been made by taking the ground configuration and the CT configurations in which a metal $3d\pi$ electron is moved to φ_7, the lowest vacant MO of a ligand, and by constructing spin-orbitals.[15] The result shows[21] that the lowest state is commonly ^3E for $[Cr(bip)_3]^{2+}$, $[V(bip)_3]^+$ and $[Ti(dip)_3]^0$. The result is independent of the metal-to-

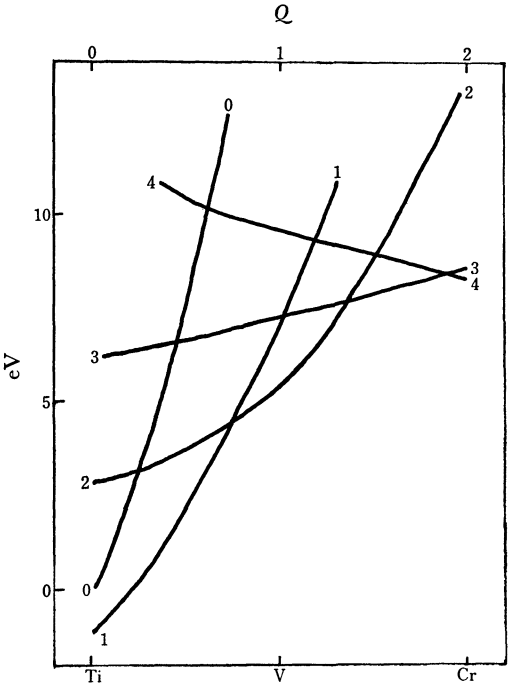

Fig. 2. Energies of the $N_\pi=4$ series of complexes with $N_{3d\sigma}=2$. The numbers in the figure represent the $N_{3d\pi}$ values.

14) I. Hanazaki, F. Hanazaki, and S. Nagakura, *J. Chem. Phys.*, **50**, 265, 276 (1969).
15) I. Hanazaki and S. Nagakura, *Inorg. Chem.*, **8**, 648, 654 (1969).
16) T. Itoh, N. Tanaka, I. Hanazaki, and S. Nagakura, This Bulletin, **41**, 365 (1968).
17) T. Itoh, N. Tanaka, I. Hanazaki, and S. Nagakura, *ibid.*, **42**, 702 (1969).
18) D. H. Templeton, A. Zalkin, and T. Ueki, *Acta Cryst.*, **21A**, 154 (Suppl.) (1966).
19) B. Morosin and J. R. Brathovde, *Acta Cryst.*, **17**, 705 (1964); b) B. Morosin, *ibid.*, **19**, 131 (1965); c) U. M. Padmanabhan, *Proc. Indian Acad. Sci.*, **47a**, 329 (1958); d) R. B. Roof, Jr., *Acta Cryst.*, **9**, 781 (1956).
20) G. Albrecht, *Z. Chem.*, **3**, 182 (1963).
21) The numerical calculation was performed by use of OKITAC 5090H and FACOM 270-30 electronic computers at the Institute of Physical and Chemical Research.

ligand CT energy which is taken as a parameter. Thus the theory can not explain the observed magnetic susceptibilities which indicate spin-triplet and -singlet states for the chromium and titanium complexes, respectively.[22]

Similarly, for the $N_\pi=3$ series, the theory predicts the $^4A_2$ ground state commonly for $[V(bip)_3]^{2+}$, $[Ti(bip)_3]^+$ and $[Sc(bip)_3]^0$, whereas the experimental results indicate quartet and doublet states for the ground states of the vanadium and scandium complexes, respectively[8,23] Hence, the assumption that the excess electrons are localized in the metal $3d\pi$ AO's seems inappropriate.

In connection with the above-mentioned discussion, we examine in detail the distribution of excess electrons for the isoelectronic series of $N_\pi=4,5$, and 8. Details of the calculation are summarized in the Appendix.

The calculated energies of various electron distributions for the $N_\pi=4$ series are shown in Fig. 2 for $N_{3d\sigma}=2$ as the function of Q[24]. Here $N_{3d\sigma}$ represents the number of electrons on the metal $3d\sigma$ AO's donated from $\chi_{N\sigma}$'s, the nitrogen lone pair AO's, through the σ-type dative bonds. Hence, each $\chi_{N\sigma}$ possesses $+N_{3d\sigma}/6$ positive hole. The figure does not show absolute values of energies, but relative ones taking the $N_{3d\pi}=4$ case as the standard. Here $N_{3d\pi}$ denotes the number electrons on the $3d\pi$ AO's; *i.e.*, $N_\pi-N_{3d\pi}$ electrons are on the ligand antibonding MO's. Although the estimated energy values are rough (probably with errors of a few eV's; see Appendix I for the detail), Fig. 2 clearly shows that most of the excess electrons are transferred to the ligand antibonding MO's for the lower Q values and that they are gradually concentrated to the metal $3d\pi$ AO's as Q increases. For instance, as shown in Fig. 2, three of the excess electrons in $[Ti(bip)_3]]^0$ are in the ligand antibonding MO's so that this substance may be thought to be the complex of bipyridyl anion radicals with $Ti^{3+}[(3d\pi)^1]$. The net charge on the metal is $+1$ since $N_{3d\sigma}=2$. On the other hand, the excess electrons in the chromium complex are almost completely localized in the metal $3d\pi$ AO's so that it seems to be an ordinary complex of neutral bipyridyl molecules with $Cr^{2+}[(3d\pi)^4]$ ion, the net charge on the metal being 0 since $N_{3d\sigma}=2$. Similarly, $[V(bip)_3]^+$ can be regarded as the metal complex with a neutral bipyridyl molecule and the two anion radicals.

Similar results are obtained for the isoelectronic series of $N_\pi=5$ and 8. The former is illustrated in Fig. 3. In contrast to the other complexes of the $N_\pi=5$ series,[1,2,4a,25] $[Mn(bip)_3]^{2+}$ has a high spin ground state with five

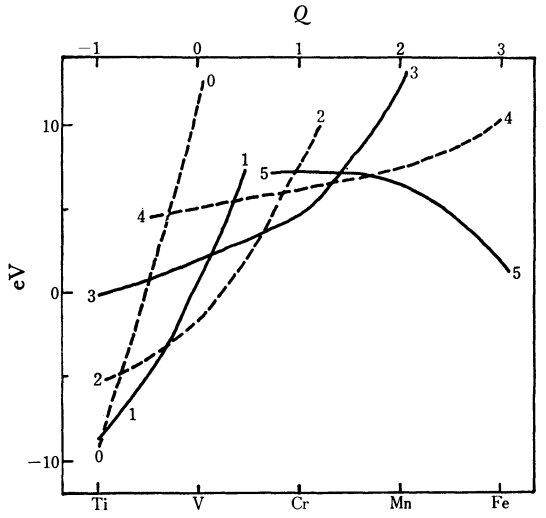

Fig. 3. Energies of the $N_\pi=5$ series of complexes with $N_{3d\sigma}=2$. The numbers in the figure represent the $N_{3d\pi}$ values.

unpaired electrons, two of them occupying probably the $3d\sigma$ orbitals.[26] As can be seen in Fig. 3, the lowest energy for the low spin configuration is relatively higher for this complex than for the others. Hence, stabilization through the exchange interaction may predominate, making the high spin state lower than the low spin state with $N_\pi=5$.

In the case of the isoelectronic series of $[Fe(bip)_3]^0$ corresponding to $N_\pi=8$, if the excess electrons are localized on the metal, two of them should occupy the $3d\sigma$ AO's since the $3d\pi$ AO's can receive at most six electrons (case I). On the other hand, if we put all 8 electrons in the π-electron system, at least two of them should occupy the ligand antibonding MO's (case II). In the former case, the $6-N_{3d\pi}$ electrons occupy the antibonding π MO's and $N_{3d\sigma}=2+n$, where n is the number of electrons transferred from $\chi_{N\sigma}$'s. In the latter case, the $8-N_{3d\pi}$ electrons are in the ligand antibonding MO's and $N_{3d\sigma}$ is just the electron number transferred from $\chi_{N\sigma}$'s. At the present stage, we can not conclude which case takes place actually for $[Fe(bip)_3]^0$ since we can not know the relative energies among the states with different $N_{3d\sigma}$ values. This problem is discussed later.

The Nature of the Ground State

Now we examine the nature of the ground states of the complexes in more detail on the basis of electron distribution. In the following calculation, the exchange interaction between $3d\pi$ AO's and the interaction with the lowest CT configurations are taken into account strictly.

$N_\pi=4$ Series. Assuming $N_{3d\sigma}=2$, the lowest enregy (ground) configuration of $[Ti(bip)_3]^0$ is that with $N_{3d\pi}=1$ as shown in Fig. 2. The second lowest is that with $N_{3d\pi}=0$. The configuration-interaction calculation is performed by considering eight triplet and six singlet ground configutations with $N_{3d\pi}=1$ and four triplet and three singlet CT configurations with

22) A. Earnshow, L. F. Larkworthy, K. C. Patel, K. S. Patel, R. C. Carlin, and E. G. Terezakis, *J. Chem. Soc.*, **A**, **1966**, 511.

23) N. Elliott, *J. Chem. Phys.*, **46**, 1006 (1967).

24) We do not treat explicitly the σ-electron system. However, the previous study[15] on $[Fe(bip)_3]^{2+}$ indicates that the $N_{3d\sigma}$ value of ~ 2 is appropriate for explaining the observed electronic absorption spectrum. For instance, the lowest configuration of $[Ti(bip)_3]^0$ is that with $N_{3d\pi}=2$ if we assume $N_{3d\sigma}=0$. This indicates that the net charge on the metal is $+2$. By an analogy with $[Fe(bip)_3]^{2+}$, at least two electrons should be transferred from $\chi_{N\sigma}$ to the $3d\sigma$ AO's. From this point of view, we adopt tentatively $N_{3d\sigma}=2$.

25) B. N. Figgis, J. Lewis, F. E. Mabbs, and G. A. Webb, *J. Chem. Soc.* **A**, **1966**, 422.

26) F. H. Burstull and R. S. Nyholm, *J. Chem. Soc.*, **1952**, 3570.

$N_{3d\pi}=0$. The energies of all the ground configurations which are equal to one another are taken as reference. The energies for all the CT configurations are commonly equal to E_{CT}, the CT energy from the $3d\pi$ AO to φ_7, and are taken as a parameter. All the off-diagonal matrix elements are determined by the quantity $B=C_{7N}\beta_{MN}$. The core resonance integral β_{MN} is given by the aid of Eq. (1) to be -1.87 eV by assuming the electron configuration of $[(3d\pi)^1(3d\sigma)^2]$ for Ti^+. C_{MN} is the coefficient of the $2p\pi$ AO of nitrogen in φ_7 and is determined to be -0.3886 by the previous calculation.[15,27]

The lowest state is shown in Fig. 4a for each spin and symmetry species of $[Ti(bip)_3]^0$. The ground state is $^1A_1$, being about 0.1 eV lower than the second lowest state, ^3E, within the reasonable range of E_{CT}. This result can explain the observed magnetic susceptibility.[1]

By taking three triplet and six singlet ground configurations with $N_{3d\pi}=4$ and twenty seven triplet and twenty four singlet CT configurations with $N_{3d\pi}=3$, a similar calculation has been made for $[Cr(bip)_3]^{2+}$.

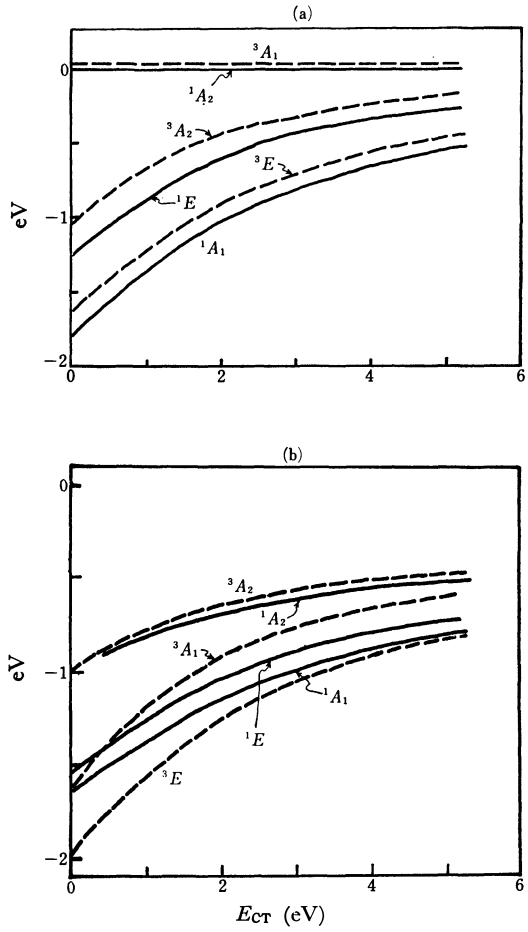

Fig. 4. Lower electronic states of the $N_\pi=4$ series of complexes. (a) $[Ti(bip)_3]^0$ and (b) $[V(bip)_3]^+$.

27) This is the value determined for the free bipyridyl molecule.[15] It varies with the change in the electron distribution, but the effect is not large: for instance, $C_{7N}=-0.3185$ if the potential field of the dipositive metal ion is taken into account.[15] The change in the β value is also not large because of the mutual cancellation of the changes in S_{MN} and I_{Me}; for instance, $\beta=-1.69$ eV if we assume $Ti^0[(3d\pi)^4]$.

The oxidation state of the metal is assumed to be $Cr^0[(3d\pi)^4(3d\sigma)^2]$ and β is estimated to be -1.26 eV. In addition, a new quantity K, the exchange integral between the two $3d\pi$ AO's, appears in the matrix elements[28] and is estimated to be 0.41 eV. The theoretical result predicts that the ground state ^3E is lower by $\sim$1 eV than the second lowest one. This is coincident with the observation.[22]

The ground state of $[V(bip)_3]^+$ is calculated by considering the fifty one ground and forty five CT configurations for $N_{3d\pi}=2$ and 3, respectively. Assuming the electron configuration of $[(3d\pi)^2(3d\sigma)^2]$ for V^+, we estimate β and K to be -1.63 and 0.513 eV, respectively. The lowest state is ^3E, as is shown in Fig. 4b. Perthel[29] obtained the effective magnetic moment of 2.80 Bohr magneton for $V(bip)_3I\cdot(1/2)py$, where py=pyridine. This value is close to that due to two unpaired electron spins, indicating the triplet ground state. On the other hand, König *et al.* could not observed the ESR signal of this substance in solution.[30,31] The reason why the ESR signal can not be observe at room temperature may probably be due to the fact that the orbitally degenerate ground state ^3E causes a large anisotropy in the g value and the hyperfine splitting, giving rise to a fairly short relaxation time.[32]

$N_\pi=5$ *Series.* A similar calculation has been made for $[Ti(bip)_3]^-$ by taking the ground and CT

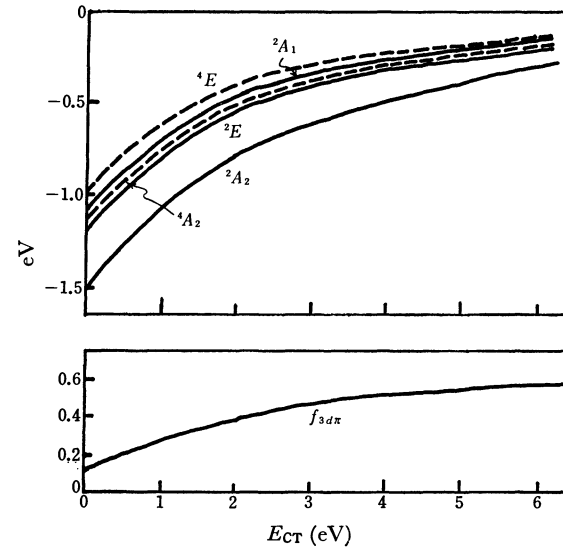

Fig. 5. Lower electronic states and spin densities on the $3d\pi$ AO's for $[V(bip)_3]^0$.

28) The E_{CT} value contains only the averaged spin interaction as is mentioned above. The $3d\pi$ exchange intergral K brings about the actual spin interaction in a rigorous manner.

29) R. Perthel, *Z. Phys. Chem.*, **211**, 74 (1959).

30) E. König, H. Fischer, and S. Herzog, *Z. Naturforsch.*, **18b**, 432 (1963).

31) S. Herzog, *Z. anorg. allg. Chem.*, **294**, 155 (1958).

32) König *et al.* suggested that the spin-orbit interaction gives a singlet ground state on the assumption that the excess electrons are localized on the metal. Hence, the ESR signal can not be observed if the substance is completely in the singlet ground state. This may hold as very low temperatures but not at room temperature. For, if the lowest state is singlet as they pointed out, a triplet state lies a little higher. The splitting is probably comparable to or smaller than the thermal energy at room temperature.

configurations with $N_{3d\pi}=0$ and 1, respectively. The result shows that the lowest state is $^2A_2$, being lower by about 0.3 eV than the second lowest one, ^2E. The $[V(bip)_3]^0$ complex is calculated to be also in the $^2A_2$ ground state by considering the ground and CT configurations with $N_{3d\pi}=2$ and 1, respectively. By assuming the electron configuration of $[(3d\pi)^2(3d\sigma)^2]$ for V^+, β and K are estimated to be -1.50 and 0.51 eV, respectively. The $[Cr(bip)_3]^+$ complex is shown to be in a $^2A_1$ ground state by the calculation taking into account the ground and CT configurations with $N_{3d\pi}=3$ and 4, respectively. The electron configuration of Cr^+ is assumed to be $[(3d\pi)^3(3d\sigma)^2]$ and the β and K values are evaluated to be -1.36 and 0.58 eV, respectively. All these results can explain the observed magnetic properties[1,2,4a] which indicate commonly the doublet ground state for the three substances. The lowest state for each spin and symmetry species is shown for the vanadium complex in Fig. 5.

Analysis of the ESR Data for the $N\pi=5$ Series

Let us examine the ESR data observed by König[11] on the basis of our theoretical results. The bonding and antibonding MO's constructed from the 4s AO (χ_{4s}) and the ligand σ AO's can be written as follows:[33]

$$\varphi = C_1\chi_{4s} + C_2\sum_l \tag{2}$$

$$\varphi^* = C_1'\chi_{4s} - C_2'\sum_l, \tag{3}$$

where $\sum_l$ is the symmetric linear combination of the nitrogen σ lone-pair AO's. The hyperfine coupling constant A_{Me} due to the metal nucleus can be represented approximately as

$$A_{Me} = A_{Me}^p + A_{4s}, \tag{4}$$

where

$$A_{Me}^p = [A_0^p + (\rho_{4s}^0/2)A_{4s}^p]f_{3d\pi} \tag{5}$$

and

$$A_{4s} = A_{4s}^0 f_{4s}. \tag{6}$$

Here A_0^p represents the hyperfine interaction due to the spin polarization of 1s, 2s, and 3s electrons produced by an unpaired electron on the 3$d\pi$ AO's. A_{4s}^p is a similar constant for a pair of 4s electrons. A_{4s}^0 represents the hyperfine interaction caused by an unpaired electron on χ_{4s}. The quantities $f_{3d\pi}$ and f_{4s} represent the spin densities on the 3$d\pi$ AO's and χ_{4s}, respectively. The latter represents only the electron spin transferred from the 3$d\pi$ AO's; that is, it does not include the 4s spin produced by exchange polarization.[34] The quantity ρ_{4s}^0 is written approximately as[35]

$$\rho_{4s}^0 = 2C_1^2 \tag{7}$$

Similarly, the hyperfine coupling constant due to the nitrogen nucleus can be written as

$$A_N = A_N^p + A_{2s} \tag{8}$$

where

$$A_N^p = A_{N0}^p f_{N\pi} \tag{9}$$

and

$$A_{2s} = A_{2s}^0 f_{2s}^N \tag{10}$$

A_{N0}^p represents the hyperfine coupling due to the spin polarization of nitrogen 1s and 2s electrons caused by an unpaired electron on the 2$p\pi$ AO. A_{2s}^0 represents the hyperfine coupling due to a spin on the 2s AO transferred from the metal 3$d\pi$ AO's. The quantities $f_{N\pi}$ and f_{2s}^N are the spin densities on the nitrogen 2$p\pi$ and 2s AO's respectively. The latter does not contain the electron spin induced through spin polarization.

By a combination of the above-mentioned relations with the expressions for spin densities given in Appendix II and with the observed coupling constants $|A_{Me}|=83.5$ and $|A_N|=2.3$ Gauss,[11] we can calculate the spin and electron densities in $[V(bip)_3]^0$ for a given value of E_{CT}.[36] The results are summarized in Table 2.

We can obtain solutions only for positive A_{Me} and A_N.

Table 2. Results of analysis of ESR data for $[V(bip)_3]^0$ and $[Cr(bip)_3]^+$ [a]

	$[V(bip)_3]^0$		$[Cr(bip)_3]^+$	
	$E_{CT}=$ 0(eV)	$E_{CT}=$ 5(eV)	$E_{CT}=$ 0(eV)	$E_{CT}=$ 1.3(eV)
f_{4s}	0.11	0.16	0.14	0.15
$f_{3d\pi}$	0.19	0.63	1.61	1.69
$f_{L\pi}$	0.85	0.41	−0.56	−0.64
f_{2s}^N	0.0057	0.0049	0.0046	0.0045
$f_{N\pi}$	0.033	0.016	−0.022	−0.025
$\rho_{3d\pi}$	1.49	1.93	3.51	3.29
ρ_{4s}^b	0.93	0.15	0.08	0.00
ρ_{4s}^a	0.086	0.99	0.23	0.17
$A_0^P f_{3d\pi}$	−20.2	−67.3	38.3	40.2
$A_{4s}^P(\rho_{4s}^0/2)f_{3d\pi}$	4.6	0.6	−0.1	0.0
A_{4s}	99.1	150.1	−60.3	−62.6
A_N^P	−0.8	−0.4	0.5	0.6
A_{2s}	3.1	2.7	2.5	2.5

a) The quantities in the first column are defined in the text and Appendix. The coupling constants are all given in the Gauss unit.

33) The following orthonormality conditions hold;

$$C_1^2 + C_2^2 + 2C_1C_2S = 1,$$
$$C_1'^2 + C_2'^2 - 2C_1'C_2'S = 1$$

and

$$C_1C_1' - C_2C_2' - (C_1C_2' - C_1'C_2)S = 0,$$

where S is the overlap integral between χ_{4s} and $\sum_l$, and is calculated to be 0.685 by use of the Slater AO for the nitrogen and four-terms function for χ_{4s}[J. W. Richardson, W. C. Nieuwpoort, R. R. Powell, and W. F. Edgell, *J. Chem. Phys.*, **36**, 1057 (1962)].

34) It is possible at least to a first-order approximation to divide the 4s spin density into f_{4s} and the spin density produced by the spin polarization effect.

35) The quantity ρ_{4s}^0 is the spin-paired electron density when we disregard the effect of the unpaired electrons of the 3$d\pi$ AO's. We ignore the contribution to ρ_{4s}^0 from the antibonding MO φ^*. It is also to be noted that this quantity differs in the definition from the density ρ_{4s}^0 defined in Eq. (11). The former is the net atomic population whereas the latter is the gross population.

36) The following values are adopted for the basic coupling constants (in Gauss);

$$A_0^p = -106.6, \quad A_{4s}^p = 91.57,$$
$$A_{4s}^0 = 923.1, \quad A_{N0}^p = -25,$$
$$A_{2s}^0 = 546.1$$

The A_{4s}^0, A_{N0}^p and A_{2s}^0 values are taken from Ref. 11. The others are newly estimated by extrapolations from the theoretical results of Watson and Freeman [*Phys. Rev.*, **123**, 2027 (1961)].

In this table, the 4*s* electron densities due to the electrons in φ and φ^* are defined as

$$\rho_{4s}^{b} = 2(C_1^2 + C_1C_2S) \quad (11)$$

and

$$\rho_{4s}^{a} = \gamma^2(C_1'^2 - C_1'C_2'S) \quad (12)$$

respectively, where γ is defined by Eq. (A9) in Appendix. The spin and electron densities thus determined seem to be reasonable for the E_{CT} values of 0 to 5 eV.

As can be seen from Table 2, A_{Me} is determined predominantly by the spin density on the 4*s* AO. Spin polarization causes only a minor effect. A_N is determined by the spin density on the 2*s* AO which transferred from the $3d\pi$ AO's through the trigonal field mixing. The spin polarization caused by the odd electron on the nitrogen $2p\pi$ AO also brings about a minor effect.

A similar analysis can be applied to $[Cr(bip)_3]^+$. By use of the value $S=0.736$ and of the observed coupling constants[11] $|A_{Me}|=21.8$ and $|A_N|=3.05$ Gauss, we can obtain the spin and electron distributions as functions of E_{CT}. The solution can be obtained only for $A_{Me}<0$ and $A_N>0$ and $E_{CT}\leq 1.3$ ev. The results of $[Cr(bip)_3]^+$ are also summarized in Table 2, and show some new aspects differing from those of the vanadium complex. The spin density on the $3d\pi$ AO's amounts to 1.6 in line with the fact that the spin density on the ligand π-electron systems is negative. This may be a little striking but is not an unexpected result. It can also be seen that the contribution of the 4*s* AO to the dative bonding is smaller than that of the vanadium complex.

$[Ti(bip)_3]^-$ gives no hyperfine structure.[11] This can be explained on the basis of the present theoretical result that the metal has almost no $3d\pi$ electron. The spin density f_{2s} also vanishes since $f_{3d\pi}\simeq 0$. A_N^p is non-vanishing but is probably very small as is observed for the vanadium and chromium complexes. In fact, it should not exceed 1/3 of the nitrogen hyperfine coupling constant of the bipyridyl anion radical,[37-39] since an unpaired electron is distributed on these ligand molecules. Therefore, it seems to be reasonable that the titanium complex exhibits no hyperfine structure.[40]

Electronic Absorption Spectra

Few experimental studies on electronic absorption spectra of metal complexes in lower oxidation state have been made, except for those $[Fe(bip)_3]^0$ and $[Fe(bip)_3]^-$ reported by Reynolds and co-workers.[9,10] Recently, however, Torii, Kobayashi, and their co-workers studied the electronic absorption spectra of a number of complexes in low oxidation states.[41,42] König and Herzog have also studied the electronic absorption spectra of the titanium, vanadium, and chromium complexes in various oxidation states.[43]

As was already mentioned, some ligands of the lower oxidation state complexes can be seen as the bipyridyl anion radicals or its dinegative ions. From this point of view, the π-electron structures of the anion radical and the dinegative ion of 2,2'-bipyridyl are examined theoretically in addition to that of the neutral bipyridyl studied previously.[15] The π-electron structure of the anion radical in the cis form was calculated by the SCFMO-CI method for the open shell system,[44] by taking a hundred singly and doubly excited configurations in the configuration interaction calculation.[45] The results are summarized in Table 3, showing a fairly good agreement with the observation for Na(bip) (sodium bipyridyl) in tetrahydrofuran.[10,39]

Table 3. Lower excited states of 2,2'-bipyridyl anion radical

	Calculated			Observed[a]	
	Transition energy (kK)	Oscillator strength	Symmetry[b]	Transition energy (kK)	Molar extinction coefficient
V_1	5.92	0.047	L	10.6 11.8 13.1	1300 1400 1100
V_2	8.20	0.002	S		
V_3	16.55	0.189	L	17.8 18.6	6600 6300
V_4	24.98	0.000	S		
V_5	26.70	0.085	L	24.2	shoulder
V_6	30.47	0.213	L	25.8	31600
V_7	33.36	0.022	S		
V_8	37.82	0.020	L		
V_9	37.88	0.023	S		
V_{10}	39.25	0.018	L		
V_{11}	39.93	0.060	S		
V_{12}	42.80	0.071	L	35	shoulder?
V_{13}	43.74	0.165	S	37.5	9400
V_{14}	47.43	0.027	S		
V_{15}	48.05	0.063	L		
V_{16}	48.86	0.001	S		
V_{17}	49.90	0.055	L		

a) Na(bip) in tetrahydrofuran.[39]
b) L and S denote the long- and short-axes polarized transitions, respectively.

The π-electron structure of the 2,2'-bipyridyl dinegative ion in the cis form was also calculated by the Pariser-Parr-Pople SCFMO-CI method, considering the electrostatic potential field caused by the metal charge (the metal charge was assumed to be +2).[14,15] The

37) E. König and H. Fischer, *Z. Naturforsch.*, **17a**, 1063 (1962).
38) J. dos Santos Veiga, W. L. Reynolds, and J. R. Bolton, *J. Chem. Phys.*, **44**, 2214 (1966).
39) Y. Torii, T. Yazaki, Y. Kaizu, S. Murasato, and H. Kobayashi, This Bulletin, **42**, 2264 (1969).
40) König attributed this to the smaller natural abundance of the titanium isotopes with nuclear spins. However, this seems to be unreasonable since the natural abundances do not differ so much between the titanium and chromium isotopes, the hyperfine structure due to the metal being observed for the latter. It is also not reasonable to attribute it to the short relaxation time since the ground state of $[Ti(bip)_3]^-$ is not degenerate and the separation from the lowest excited state is almost the same as that of $[V(bip)_3]^0$.
41) Y. Kaizu, T. Yazaki, Y. Torii, and H. Kobayashi, This Bulletin, **43**, 2068 (1970).
42) H. Kobayashi and Y. Torii, private communication.
43) E. König and S. Herzog, *J. Inorg. Nucl. Chem.*, **32**, 585, 601, 613 (1970).
44) H. C. Logguet-Higgins and J. A. Pople, *Proc. Phys. Soc.*, **A68**, 591 (1955).
45) This calculation has been performed by use of the program written by Dr. S. Iwata and Mr. H. Katsumata.

TABLE 4. LOWER EXCITED STATES OF 2,2′-BIPYRIDYL DINEGATIVE ION

Calculated[a]		Observed[b]
Transition energy (kK)	Oscillator strength	transition energy (kK)
17.40	0.115	15—17
20.72	0.531	
21.26	0.010	26.2
24.35	0.049	
33.79	0.546	
37.79	0.205	
43.42	0.008	
45.38	0.078	
48.67	0.010	
51.27	0.247	

a) The configuration interaction was considered among the 22 singly excited configurations for the cis form ion.

b) Li_2(bip) in tetrahydrofuran.[42] The absolute intensities are uncertain but the peak molar extinction coefficient of the first band, with a vibrational structure, is about 1/10 of that of the second band.

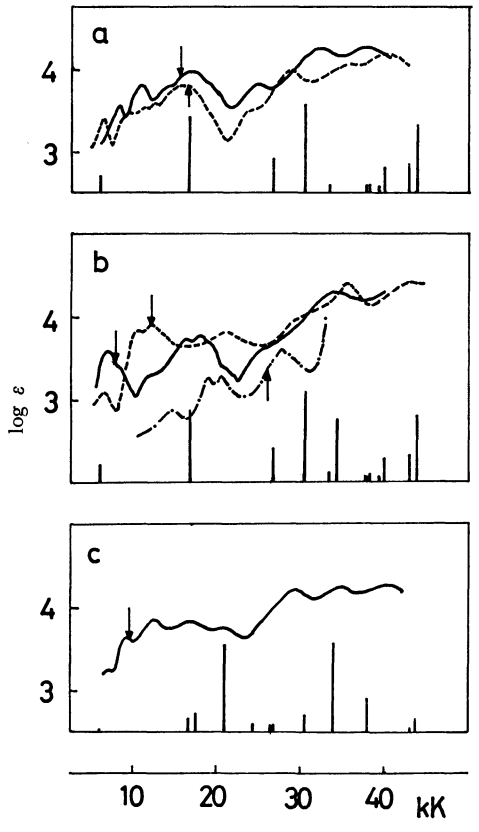

Fig. 6. The electronic absorption spectra of some complexes in lower oxidation states. The theoretical prediction is shown by the vertical lines. The length indicates the oscillator strength value in an arbitrary scale. The band position predicted for the CT transition is indicated by an arrow for each substance. (a) —$[V(bip)_3]^0$ and ---$[Ti(bip)_3]^0$. The theoretical result is that of bip^-. (b) —$[Cr(bip)_3]^+$, ---$[V(bip)_3]^+$ and ···$[Fe(bip)_3]^0$. The theoretical result is the weighted average of the calculations for bip^0 and bip^-. (c) $[Ti(bip)_3]^-$. The theoretical result is the 1:2 average of the calculations for bip^- and bip^{2-}.

result is shown in Table 4, together with the transition energies measured with Li_2(bip) (dilithium bipyridyl) in tetrahydrofuran[42]

The electronic absorption spectra[41,43] of $[V(bip)_3]^0$ and $[Ti(bip)_3]^0$, which can be considered as the metal complex with three bip^-, are shown in Fig. 6a together with the theoretical result for bip^-. The position of the lowest CT transition band predicted theoretically is indicated by an arrow. In the present theoretical study, we ignore the dipole interaction between the π–π^* transitions in different ligands and also the interaction of CT transition with the ligand π-π^* transition. This means that we disregard the splitting of each band due to the above-mentioned interactions. Therefore we confine ourselves to a qualitative comparison of the theoretical and observed results.

As is shown in Fig. 6a, the electronic absorption spectra of $[V(bip)_3]^0$ and $[Ti(bip)_3]^0$ are at least qualitatively explained by the overlapping of the π–π^* transition bands of bip^- and the metal-ligand π-electron transfer ones. The observed bands in the energy region lower than 10 kK are ascribed to the ligand π–π^* transitions (to V_1 and V_2 of Table 3). The bands in 10—20kK region can be due to the mixture of the CT transition and the ligand π–π^* transition to V_3. The 26 kK and 30 kK bands of titanium and vanadium complexes, respectively, are due to the ligand π–π^* transition to V_0 corresponding to the strong 26 kK band observed for Na(dip).[39]

In Fig. 6b are shown the electronic absorption spectra[30,41-43] of $[Cr(bip)_3]^+$, $[V(bip)_3]^+$,and $[Fe(bip)_3]^0$ which can approximately be considered to be the metal complex with a dip^0 and two dip^-. The corresponding theoretical prediction shown in Fig. 6b is the weighted average of the calculated band intensites for dip^0 and dip^-. The absorption bands of $[V(bip)_3]^+$ are well interpreted as the 1:2 mixture of the bip^0 and bip^- spectra except for the 10—12 kK band which can be ascribed to the metal-ligand CT transition on the basis of the present theoretical study. In the spectrum of $[Cr(bip)_3]^+$, the 6—8 kK band may be due to two transitions; the CT transition from φ_7 of bip^- to the $3d\pi$ AO's and the lowest π–π^* transition of bip^-. The other transitions can be well interpreted as the overlapping of the local excitations in bip^0 and bip^-.

Concerning $[Fe(bip)_3]^0$ there are two possibilities, cases I and II, as already mentioned. If we assume $N_{3d\sigma}=2$, both cases give the ground state in which two excess electrons are located on the ligands and the CT state about 3 eV about it. The CT directions differ for cases I and II; namely, from φ_7 to $3d\pi$ for the former and from $3d\pi$ to φ_7 for the latter. The absorption spectra of this complex and free bip^- are somewhat similar to each other, but differ significantly in their relative intensity ratios. This indicates a fairly strong perturbation affecting the bip^- electronic structure. In case II, the CT from $3d\pi$ to φ_7 can interact with the π–π^* transitions in bip^0 but not with those in bip^-. On the other hand, the CT transition predicted for case I can interact only with the π–π^* transitions of bip^-. Hence, the latter case seems to be more suitable to explain the relative intensities of the bands below 30 kK. It is difficult to determine the bip^-/bip^0 ratio in

the complex because of a strong disturbance by the absorption band of the dissociated free bip in the region above 30 kK. The absorption spectrum of the complex strongly perturbed by the CT interaction, however, may be explained by the overlapping of the absorption spectra of bip^- and bip^0 in a 2:1 ratio. This is because, according to a rough estimate of the ground state energy, the electron configuration in this ratio is most stable.

The absorption spectrum[42] of $[Ti(bip)_3]^-$ is shown in Fig. 6c, together with the theoretical prediction of the weighted average of the calculated intensities for bip^- and bip^{2-} in the 1:2 ratio. The correspondence seems to be fairly good if the 12 kK band is ascribed to the transition to the CT state which is predicted to lie about 1 eV above the ground state.

Discussion

The electron distribution of the ground state determined above indicates that excess electrons are localized on the metal for the complexes with a large Q value and are gradually transferred to the ligand π-electron systems as Q decreases. Hence, we can not distinguish the complexes in lower oxidation states clearly from those in normal oxidation states. Moreover, the term "oxidation state" should be considered as the charge on the complex as a whole and should not be directly related to the oxidation state of the metal ion only.

In this connection, it seems to be interesting to examine how many electrons move when an electron is added to the normal complex. For instance, adding an electron to the π-electron system of $[Cr(bip)_3]^{2+}$ in which four π electrons are localized on the metal, we find about two electrons in the ligand antibonding MO's; that is to say, the addition of an electron induces not only its delocalization to the ligands but also the transfer of another electron which is originally in the metal. A similar tendency can be found for the vanadium complex. Adding an electron to $[V(bip)_3]^{2+}$ in which three electrons are localized in the metal, we find two electrons in the $3d\pi$ AO's and the other two in the ligands. Adding another electron, we find two electrons in the metal and the other three in the ligands. This general tendency can be understood as follows; an electron in φ_7 repels the $3d\pi$ electron resulting in the reduction of the metal ionization potential whereas it lifts the orbital energies of the ligands to reduce their electron affinities. The former effect is fairly larger since the metal-ligand average distance is shorter than the interligand average distance. Hence, the addition of an electron makes the transfer of metal $3d\pi$ electron easier. For lower Q values, this tendency reaches a saturation since the metal ionization potential decreases rapidly with the decreasing net charge on the metal.

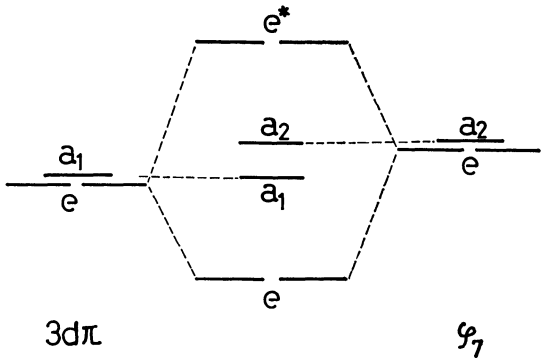

Fig. 7. The energy level diagram.

The magnetic behaviour of the ground state seems to be interpreted by the composite-system treatment adopted in the present work. The one-electron-orbital model adopted so far to the interpretation of the ESR result seems to be inappropriate for the low oxidation metal complexes under consideration. According to this model illustrated in Fig. 7, an unpaired electron of the $N_{3d\pi}=5$ complex should occupy the a_1 or a_2 orbital and should be localized completely on the metal or ligand, respectively. This is in serious disagreement with the present result which indicates an extensive delocalization of the unpaired electron both on the metal and ligands. The contradiction can be ascribed to the fact that the simple one-electron-orbital model completely ignores the strong exchange polarization of the e-orbital electrons due to the unpaired electron in the a_1 or a_2 orbital.

Tetrazakis and Carlin[46] explained the magnetism of $[Cr(bip)_3]^{2+}$ on the basis of the theory[47] presented by Figgis *et al.*, giving the trigonal splitting $\Delta\sim630$ cm^{-1} ($^3A_2$ is lower) and the orbital delocalization factor $k\sim0.6$. Although the k value seems to be consistent with the present result in which the metal-ligand CT configurations lie very close to the ground configurations, the Δ value is in serious disagreement with ours: $\Delta\sim-10^4$ cm^{-1} (^3E is lower). Since φ_7 is symmetric with respect to the bipyridyl molecule, it can not interact with the $3d\pi$ orbitals, whereas the e-symmetry orbital can interact with them. Hence, the result of Figgis *et al.* that Δ is positive (that is, the a_1 orbital is lower) is incorrect.

Next, we examine the magnetic property of $[Fe(bip)_3]^0$ qualitatively on the basis of Fig. 7. Although the one-electron-orbital model is inappropriate for quantitative treatment, it may be useful for the qualitative discussion of the spin state. By an analogy with the results for the $N_{3d\pi}=4$ and 5 series, the metal-ligand CT interaction is probably strong for this case with a low Q value. Hence the e^* orbital should lie far apart from the a_1 and a_2 orbitals, so that, in case II, the eight π electrons occupy the e, a_1, and a_2 orbitals, resulting in a spin singlet ground state. This is in contradiction to the observation. On the other hand, in case I, the six π electrons may occupy the e, a_1, and a_2 orbitals if the $3d\pi$ AO and ligand antibonding MO of the a_1 and a_2 symmetry, respectively, are close to each other. We have four unpaired electrons, two in the a_1 and a_2 orbitals and two in the σ orbitals of the e symmetry, with a spin quintet ground state. Thus examination of both the magnetism and the electronic absorption spectrum supports case I. Another supporting fact is that the substance readily decomposes to bipyridyl and iron on heating.[6] This can be understood as due to the weak σ-dative bonding caused by partial occupation of

46) E. G. Tetrazakis and R. L. Carlin, *Inorg. Chem.*, **6**, 2125 (1967).
47) B. N. Figgis, J. Lewis, F. E. Mabbs, and G. A. Webb, *J. Chem. Soc.*, **A**, **1966**, 1411.

the σ-antibonding MO's.

$[Mn(bip)_3]^-$ which is isoelectronic with $[Fe(bip)_3]^0$ shows a magnetic moment of 3.71 Bohr magneton.[3] This can not be explained on the basis of the even number of unpaired electrons. The substance should be considered as a mixture of the spin quintet and triplet species. The situation can be understood by the energy level scheme shown in Fig. 7. If the a_1 and a_2 orbitals are close to each other as for the iron complex, we have four unpaired electrons, and thus a spin quintet ground state. If a stronger metal-ligand interaction makes the a_1 and a_2 orbitals split, all the π electrons should be paired and we have the spin triplet ground state because of the unpaired electrons in the σ-antibonding orbitals. We have a mixture of the two species if the separation between the a_1 and a_2 orbitals is comparable with the exchange integral between the two $3d\pi$ AO's. The electron distribution in case II gives no reasonable explanation also for this complex.

$[Cr(bip)_3]^{2-}$ has two unpaired electrons.[4b] This is understood as predominance of the triplet state because of the large a_1–a_2 separation. Thus, for this isoelectronic series, the iron, manganese and chromium complexes, together with well-known $[Ni(bip)_3]^{2+}$, have two unpaired electrons in the σ-antibonding orbitals, in addition to those in the π-electron system.

The authors are deeply indebted to Prof. Hiroshi Kobayashi and Dr. Yasuo Torii of the Tokyo Institute of Technology for valuable discussion and for use of the spectral data before publication.

Appendix I

Here we will show the method calculating the energies for various π-electron distributions given in Figs. 2 and 3. Let us take $[Ti(bip)_3]^0$, $N_\pi=4$, as an example.

If we take the energy of the electron configuration $N_{3d\pi}=4$ and $N_{3d\sigma}=0$ as a reference, the energy of the configuration $N_{3d\pi}=3$ and $N_{3d\sigma}=0$ is just the CT energy to remove an $3d\pi$ electron to the lowest vacant MO φ_7 of one of the ligands (say, ligand a);

$$E(3,0) = I_{Me} - A_L - 3V_{MQ} + 2V_{OQ} - V_{MO} \quad \text{(A1)}$$

where the configurational energy is represented as $E(N_{3d\pi}, N_{3d\sigma})$. I_{Me} and A_L are the valence state ionization potentials corresponding to the ionization process $Ti^0[(3d\pi)^4]\rightarrow Ti^+[(3d\pi)^3]$ and the electron affinity of the ligand, respectively. V_{MQ}, V_{OQ}, and V_{MO} are, respectively, the electrostatic interaction energies between a $3d\pi$ electron and the formal charges due to π electrons on each ligand, between an electron in φ_7 of a ligand and the formal charges on one of the other ligands, and between $3d\pi$ electron and an electron in φ_7 of a ligand. I_{Me} is estimated to be 3.01 eV from the observed atomic term values by averaging all spin interactions. By the aid of SCF calculation for the free 2,2′-bipyridyl molecule, the following results are obtained: $A_L=0.02$,[48] $V_{MQ}=1.00$, $V_{OQ}=0.25$ and $V_{MO}=4.98$ (all in eV), and, therefore, $E(3,0)=-4.51$ eV. A_L is evaluated from the calculated φ_7 orbital energy ($\varepsilon_7=-1.72$ eV) of the ligand by the following equation;[48]

$$A_L = -\varepsilon_7 - 1.7 \quad \text{(A2)}$$

Next, we evaluate the energy of the configuration $N_{3d\pi}=2$ and $N_{3d\sigma}=0$. By considering the process to remove an electron from the ligand antibonding MO of the configurations $N_{3d\pi}=2$ to the $3d\pi$ AO, we have

$$E(3,0) = E(2,0) + I_L - A_{Me}^{\pi}(2,0) - V_{OO} + V_{MO} + 3V_{MQ} \quad \text{(A3)}$$

where I_L is the ionization potential necessary for removing a ligand antibonding-orbital electron, being equivalent to A_L defined above. In this case, A_L is evaluated to be 7.26 eV by Eq. (A2), since ε_7 is calculated to be −8.955 eV by the SCF MO calculation including the potential field caused by the metal charge (the net charge on the metal is +2 for $N_{3d\pi}=2$ and $N_{3d\sigma}=0$).[15] $A_{Me}^{\pi}(m,n)$ is the electron affinity of metal corresponding to the process $Ti^Q[(3d\pi)^m(3d\sigma)^n]\rightarrow Ti^{Q-1}[(3d\pi)^{m+1}(3d\pi\sigma)^n]$ where $Q=4-(m+n)$. $A_{Me}(m,n)$ is also defined in a similar manner. V_{OO} is the interaction between electrons in the lowest vacant MO's of different ligands and calculated to be 2.87 eV. V_{MO} and V_{MQ} have the same meanings as before and are calculated by use of the SCF MO's obtained by taking into account the potential field of the metal ion. Hence,[49]

$$E(2,0) = E(3,0) - 6.21 = -10.63\text{eV}. \quad \text{(A4)}$$

The configuration $N_{3d\sigma}=2$ and $N_{3d\sigma}=1$ can be produced from $N_{3d\pi}=2$ and $N_{3d\pi}=0$ by removing an electron from one of the MO's $\varphi_{N\sigma}$ constructed from the σ-lone pair AO's of nitrogens to the metal $3d\pi$ AO's.

$$E(2,1) = E(2,0) + I_\sigma - A_{Me}^{\sigma}(2.0) + V_{SQ} - 2V_{SO} + V_{MS} + 2V_{MO} - 3V_{MQ} \quad \text{(A5)}$$

where I_σ is the ionization potential to remove an electron from $\varphi_{N\sigma}$ and is taken to be 10.35 eV from the corresponding ionization potential of pyridine.[50] $A_{Me}^{\sigma}(2,0)$ is estimated to be 3.04 eV. V_{SQ}, V_{SO}, and V_{MS} are the interaction of an electron in $\varphi_{N\sigma}$ with the formal charge distributions in the π electron systems of three ligands with an electron in φ_7 and with a $3d\pi$ electron, respectively. They are estimated to be −8.35, 4.41, and 8.46 eV, respectively, by use of the SCF MO obtained by taking into account the potential field of the metal ion.[15] The interatomic interaction within a ligand molecule is calculated by use of the Slater AO's, whereas the interactions between different ligands and between the metal and ligand are calculated by use of the point-charge approximation. By use of these quantities, $E(2,1)$ is evaluated to be −2.17 eV.

The configuration with $N_{3d\pi}=2$ and $N_{3d\sigma}=2$ is produced from that with $N_{3d\pi}=2$ and $N_{3a\sigma}=1$ by removing another electron from $\varphi_{N\sigma}$ to $3d\sigma$ AO;

$$E(2,2) = E(2,1) + I_\sigma^+ + V_{SQ} - 2V_{SO} - A_{Me}^{\sigma}(2,1) - V_{MS} + 2V_{MO} - 3V_{MQ} \quad \text{(A6)}$$

where $I\sigma^+$ is the second ionization potential of $\varphi_{N\sigma}$ and estimated to be 15.87 eV correcting $I\sigma$ with respect to the electrostatic interaction between the nitrogen σ lone-pair AO's. The other quantities have the same meanings as before, and are calculated by use of the SCF MO's obtained putting a

48) We employ the correction of 1.7 eV.[16,17]

49) The energy $E(2,0)$ may be obtained by considering the process removing $3d\pi$ electron in the configuration $N_{3d\pi}=3$ to the ligand vacant MO. We employ here, however, the reverse CT process in order to utilize the previously obtained MO's for, ligand under the influence of dipositive metal ion.

50) M. I. Al-Jaboury and D. W. Turner, *J. Chem. Soc.*, **1964**, 4438; E. Clementi, *J. Chem. Phys.*, **46**, 4731, 4737 (1967); J. L. Whitten *et al.*, *ibid.*, **48**, 953 (1968); J. Del Benne and H. H. Jaffe, *ibid.*, **48**, 1811 (1968); M. A. El-bayoumi and O. S. Khalil, *ibid.*, **47**, 4863 (1967).

positive charge on the metal and $+1/6$ hole on each nitrogen σ AO. $E(2,2)$ is thus estimated to be 4.04 eV.

The estimated energy of each electron configuration should not be considered to be the energy of the actual state for the following reasons: (i) The energy change due to resonance interaction is not taken into account, (ii) the spin interaction is averaged out, and (iii) the stabilization due to electron rearrangement accompanied by electron transfer is not taken into account. Although the resonance and spin interactions are ignored in the estimation of electron distribution, they are taken into account in the calculation of the magnetic property of the ground state. Hence, we discuss here the third point. We evaluate the energy of the $N_{3d\pi}=3$ and $N_{3d\sigma}=0$ distribution to be 4.51 eV below the reference state with $N_{3d\pi}=4$. This is just the CT energy including no electron rearrangement effect. If we denote the stabilization due to the effect as Δ_1 (taken as positive), the absolute energy should be $-4.51-\Delta_1$ as illustrated in Fig. 8a. Similarly, the CT

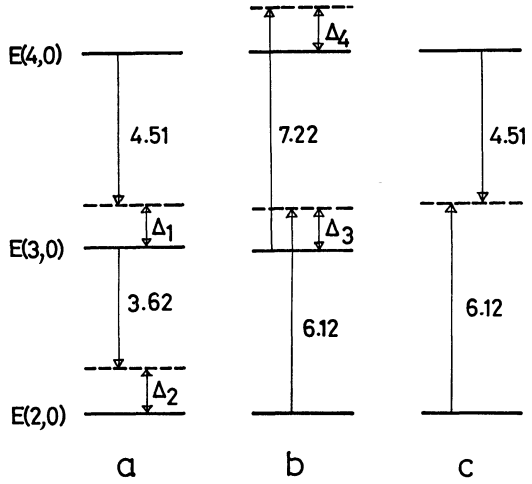

Fig. 8. The energy estimation for some electron distributions of $[Ti(bip)_3]^0$.

energy from the $N_{3d\pi}=3$ system to the $N_{3d\pi}=2$ system is calculated to be -3.62 eV on the basis of the electron distribution of the $N_{3d\pi}=3$ system. If we put the rearrangement energy of the $N_{3d\pi}=2$ system as Δ_2, the absolute energy of this system is $-(4.51+\Delta_1+3.62+\Delta_2)$. If we start from the $N_{3d\pi}=2$ system, we obtain the absolute energy of the $N_{3d\pi}=4$ system as $(6.12-\Delta_3+7.22-\Delta_4)$ above the former, as is illustrated in Fig. 8b. Since the relation

$$(4.51+\Delta_1+3.62+\Delta_2) = (6.12-\Delta_3+7.22-\Delta_4)$$

should hold, we obtain

$$\Delta_1 + \Delta_2 + \Delta_3 + \Delta_4 = 5.21 \text{ eV}.$$

Assuming $\Delta_1\simeq\Delta_2\simeq\Delta_3\simeq\Delta_4=\Delta$, the absolute value of the $N_{3d\pi}=2$ system is estimated to be $-4.51-3.62-2\Delta=-10.74$ eV. As illustrated in Fig. 8c, the corresponding energy can be evaluated by adding the energy of the $N_{3d\pi}=3$ distribution based on the $N_{3d\pi}=4$ to that based on the $N_{3d\pi}=2$. The sum $4.51+6.12=10.63$ eV, is very close to the estimated absolute energy given above. The energy of the $N_{3d\pi}=3$ system is obtained as -4.51 and -7.22 eV by calculations based on the distributions $N_{3d\pi}=4$ and 3, respectively. The absolute value can be estimated as $-4.51-\Delta=-5.8$ eV. Thus the electron rearrangement effect amounts to ± 1.3 eV for this state.

Appendix II

The ground state of $[V(bip)_3]^0$ is represented by the wavefunction

$$\Psi(^2A_2) = A_1\Psi_1 + A_2\Psi_2 + A_3\Psi_3 + B_1\Psi_1' + B_2\Psi_2' + B_3\Psi_3' \quad \text{(A7)}$$

where Ψ_1, Ψ_2, and Ψ_3 are the configurational wavefunctions with $N_{3d\pi}=2$ and Ψ_1^1, Ψ_2^1 and Ψ_3^1 are those of the CT configurations with $N_{3d\pi}=1$. The coefficients A_i's and B_i's have been determined by the calculation described in Appendix I.

Considering the mixing of the $3d\pi$ and $4s$ orbitals due to the trigonal field we have

$$\Psi'(^2A_2) = \Psi(^2A_2) - \gamma[A_1\sum\nolimits_2 + (3)^{-1/2}A_2(\sum\nolimits_1-(2)^{1/2}\sum\nolimits_4) - (2/3)^{1/2}A_3(\sum\nolimits_1-(2)^{1/2}\sum\nolimits_3) \quad \text{(A8)}$$

where $\sum_1$ to $\sum_4$ are the wavefunctions of the CT $(4s\rightarrow\varphi^*)$ configurations belonging to the $^2A_2$ symmetry.[51] The coefficient γ determines the extent of mixing and may be expressed as

$$\gamma = (C_1'/\Delta E)\langle\chi_{3d\pi}|\mathbf{V}_{tr}|\chi_{4s}\rangle \quad \text{(A9)}$$

where ΔE is the energy of electron transfer from $3d\pi$ to $4s$ and $\mathbf{V}_{tr}$ is the trigonal electrostatic field.

By use of this wavefunction, the spin densities can be expressed by their definitions as follows.

$$\begin{aligned}
f_{4s} &= (2/3)\gamma^2C_1'^2(A_2^2+2A_3^2)\\
f_{3d\pi} &= (2/3)A_2^2 + (14/27)A_3^2 - (1/3)B_1^2 + B_2^2 - (1/3)B_3^2 + (2/3)\gamma^2(A_2^2+2A_3^2)\\
f_{2s} &= (1/27)\gamma^2C_2'^2(A_2^2+2A_3^2) \quad \text{(A10)}\\
f_{L\pi} &= A_1^2 + (1/3)A_2^2 + (13/27)A_3^2 + (4/3)(B_1^2+B_3^2) + \gamma^2[A_1^2-(1/3)A_2^2-(2/3)A_3^2]\\
f_{N\pi} &= (1/3)(C_{7N})^2f_{L\pi}
\end{aligned}$$

where $f_{L\pi}$ represents the sum of the spin densities in the π-electron systems of three ligands.

The ground state wavefunction Ψ for $[Cr(bip)_3]^+$ can also be represented by Eq. (A7) except that the configurational wavefunctions Ψ_1 to Ψ_3 are those of $^2A_1$ with $N_{3d\pi}=3$ and Ψ_1' to Ψ_3' are those of $^2A_1$ with $N_{3d\pi}=4$. The interaction with the $4s$ AO can be written as

$$\Psi'(^2A_1) = \Psi(^2A_1) + (3)^{1/2}\gamma[A_1\sum\nolimits_1' + A_2\sum\nolimits_2' - A_3\sum\nolimits_3'] \quad \text{(A11)}$$

where $\sum_1'$ to $\sum_3'$ are the wavefunctions for the CT configurations corresponding to the electron transfer from the $3d\pi$ AO's to φ^*. The spin densities are expressed as

$$\begin{aligned}
f_{4s} &= (1/3)(A_1^2+A_2^2+5A_3^2)\gamma^2C_1'^2,\\
f_{3d\pi} &= (1/3)[A_1^2+A_2^2+5A_3^2+4(B_1^2+B_3^2)] + (2/3)\gamma^2[A_1^2+A_2^2+5A_3^2],\\
f_{2s} &= (1/54)(A_1^2+A_2^2+5A_3^2)\gamma^2C_2'^2, \quad \text{(A12)}\\
f_{L\pi} &= (1/3)[2(A_1^2+A_2^2-A_3^2)-(B_1^2-3B_2^2+B_3^2) + 2(A_1^2+A_2^2-A_3^2)\gamma^2],\\
f_{N\pi} &= (1/3)(C_{7N})^2f_{L\pi}
\end{aligned}$$

51) The electron transfers from φ to $3d\pi$ and to the vacant MO of ligand are ignored since their energies lie probably fairly higher than that of the electron transfer $3d\pi\rightarrow\varphi^*$.

Electron-transfer Phenomena in Some Three-dimensional Complex Thiocyanate Semiconductors

Masao HASHIMOTO,* Shichio KAWAI, and Ryôiti KIRIYAMA
Institute of Scientific and Industrial Research Osaka University, Suita-shi, Osaka
(Received February 3, 1971)

Measurements of the electrical conductivity, the photoconductivity, the electronic spectra, and the magnetic susceptibility were carried out with powder samples of $CuHg(SCN)_4$ and $(Cu_xZn_{1-x})Hg(SCN)_4$. The electrical conductivity (σ) of the compounds has been found to obey the usual exponential equation of electrical conduction, $\sigma=\sigma_0\exp(-E_t/KT)$. It was found that there was a close relation between the photocurrent spectra and the electron-transfer bands in both compounds. In terms of the band model, the nature of the semiconductivity and the photocurrent in their intrinsic region are discussed in connection with the electron-transfer phenomena.

The $M(II)Hg(SCN)_4$ series of compounds has been known for many years.[1] In $ZnHg(SCN)_4$ the zinc ion is surrounded by a slightly distorted tetrahedron of four nitrogen atoms,[2-4] while green $CuHg(SCN)_4$ has a quite different structure,[5] in which copper ions are surrounded octahedrally by four nitrogens and two sulfurs. However, their polymeric structure are similar. The structure of mixed crystals of $(Cu_xZn_{1-x})Hg(SCN)_4$ composition, with x smaller than 0.22, is also isomorphous with $ZnHg(SCN)_4$, and their color changes from pale pink to dark purple depending on the relative concentration of Zn^{2+} and Cu^{2+}.[6] The color of the mixed crystals is caused by the intense electron-transfer bands at about 330 and 550 mμ; green $CuHg(SCN)_4$ has also an electron-trasfer band at about 430 mμ.[6]

The present experiments were undertaken in order to elucidate the relation between the electron-trasfer phenomena and the semiconduction in inorganic complex salts with a three-dimensional framework. Braterman *et al.* have investigated the electrical conductivity of some complex cyanides and found no equality between the activation energy for the semiconduction and the optical absorption energy of the electron-transfer band.[7] Our present results, however, will show that the mechanism of intrinsic semiconduction in $CuHg(SCN)_4$ and $(Cu_xZn_{1-x})Hg(SCN)_4$ is closely related to the nature of their electron-transfer bands.

Experimental

Materials. The green compound, $CuHg(SCN)_4$, was prepared by mixing aqueous solutions of copper(II) sulfate and potassium mercury tetrathiocyanate. The precipitate was filtered off, washed with cold water, and dried at about 100°C in an air thermostat. The crystalline powder of $ZnHg(SCN)_4$ was obtained by a similar method of preparation. The purple mixed compounds $(Cu_xZn_{1-x})Hg(SCN)_4$ were prepared by adding mixed aqueous solutions of zinc and copper sulfate to aqueous solutions of potassium mercury tetrathiocyanate. The mole fractions of the copper ion in the products were assumed to be the same as those of the starting mixed solutions. All the materials thus obtained were identified by means of an X-ray diffractometer using Cu$K\alpha$ radiation.

Electrical Conductivity. The electrical conductivity measurements were carried out in a vacuum with pellets of the compounds. The electrode assembly used for our measurements is shown in Fig. 1. The electrical current at a constant field strength was measured with a Toa Dempa Model PM 18 microvolt-ammeter, capable of measuring currents down to 10^{-12} A. The field strengths were in the region between 100 to 450 V/cm. In order to prevent thermal decomposition under these experimental conditions, the measurements were carried out at temperatures below about 420°K.

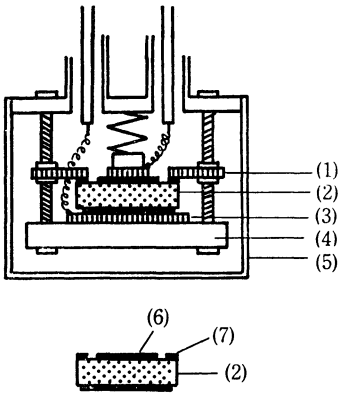

Fig. 1. Electrode assembly.
(1) Copper ring(guard electrode), (2) Specimen, (3) Copper plate, (4) Steatite, (5) Shield box, (6) Central electrode (evapolated gold), (7) Guard electrode(evapolated gold)

For the measurements of the photocurrent, a DC electric field was applied between the guard electrode and the central electrode of a pellet (Fig. 1). The surface between these two electrodes was then exposed to light. The photoconductivity was excited by a monochromatic light from a quartz prism monochrometer. A xenon-lamp was employed as the light source. The photocurrent was measured with the microvolt-ammeter mentioned above at field strengths ranging from 100 to 450 V/cm. The measurements were carried out at room temperature over the 380—1000 mμ spectral region. On the assumption that the photoconductivity is

* Present address: Department of Chemistry, Faculty of Science, Kobe University, Rokkodai-cho, Nada-ku, Kobe.

1) A. Rosenheim and Cohn, *Z. Anorg. Allg. Chem.*, **27**, 280 (1901).
2) W. Stahl and M. Staraumamis, *Z. Phys. Chem.* (Leipzig), **193**, 121 (1943—1944).
3) J. W. Jeffery, *Nature*, **159**, 610 (1947).
4) J. W. Jeffery and K. M. Rose, *Acta Cryst.*, **B24**, 653 (1968).
5) A. Korczyski, *Roczniki Chem.*, **36**, 1539 (1962).
6) D. Forster and D. M. L. Goodgame, *Inorg. Chem.*, **4**, 823 (1965).
7) P. S. Braterman, P. B. P. Phipps, and R. T. P. Williams, *J. Chem. Soc.*, **1965**, 6164.

linearly related to the intensity of the light, the spectral response of photocurrent was determined; that is, the measured values of the photocurrent were divided by the relative intensity of the light.

Electronic Spectra. The diffuse reflectance (R_d), *i.e.*, the ratio of the quantity of light reflected by a powdered sample to the quantity of light reflected by magnesium carbonate, was measured with a Shimadzu Spectrophotometer, with its integration attachment, in the visible region. In presenting the data of the reflectance measurements, it seems convenient to use Kubelka and Munk's expression,[8] $f(R_d)=(1-R_d)/2R_d$, for there is a certain parallel between this quantity and the extinction coefficient of the crystal.

Magnetic Susceptibility. The magnetic susceptibility of $ZnHg(SCN)_4$ and $(Cu_xZn_{1-x})Hg(SCN)_4$ were obtained by the Gouy method in the temperature range from 118 to 300°K. The Gouy tube was calibrated with a standard aqueous solution of nickel(II) chloride. The diamagnetic corrections were estimated from the observed magnetic susceptibility of $ZnHg(SCN)_4$.

Results

Electrical Conductivity. The electrical conductivity (σ) of the compounds was found to obey the usual exponential relation to the temperature:

$$\sigma = \sigma_0 \exp(-E_t/kT),$$

where σ_0 is a constant and where E_t is the thermal activation energy for the electrical conduction. The values of the specific conductivity at about 373°K (σ_{373}) are listed in Table 1, together with the thermal activation energy (E_t) as calculated from $\log\sigma$ *vs.* $1/T$ plots. It can be seen in Fig. 2 that the $\log\sigma$ *vs.* $1/T$ plots of $(Cu_xZn_{1-x})Hg(SCN)_4$ give two strainght lines, with a break around 393°K. The two notations, E_t^e and E_t^i, in Table 1 denote the activation energy for the lower (extrinsic) and the upper (intrinsic) part of the break respectively.

Table 1. Specific conductivity at 373°K (σ_{373}) and thermal activation energy measured with pellets of $(Cu_xZn_{1-x})Hg(SCN)_4$

x	σ_{373} $\mho$/cm	E_t^e eV	E_t^i eV
0.0	1.8×10^{-14}	1.2	1.6
0.03	3.3×10^{-13}	1.1	1.6
0.1	7.7×10^{-12}	0.9	1.5
0.2	9.3×10^{-11}	0.6	1.6
1.0	1×10^{-10}	—	2.2

It is noticeable that the conductivity of (Cu_xZn_{1-x})-$Hg(SCN)_4$ increases with an increase in the copper concentration. This shows that the increase in the copper concentration causes an increase in the number of charge carriers required for electrical conduction. Furthermore, the value of E_t^e gradually increases with a decrease in the copper concentration, while the value of E_t^i is almost constant, regardless of the relative concentrations of Cu^{2+} and Zn^{2+}. The lower activation energy (E_t^e) must result from the presence of lattice imperfections introduced by the doping of copper ions in the $ZnHg(SCN)_4$ lattice.

8) P. Kubelka and F. Munk, *Z. Tech. Phys.*, **12**, 593 (1931).

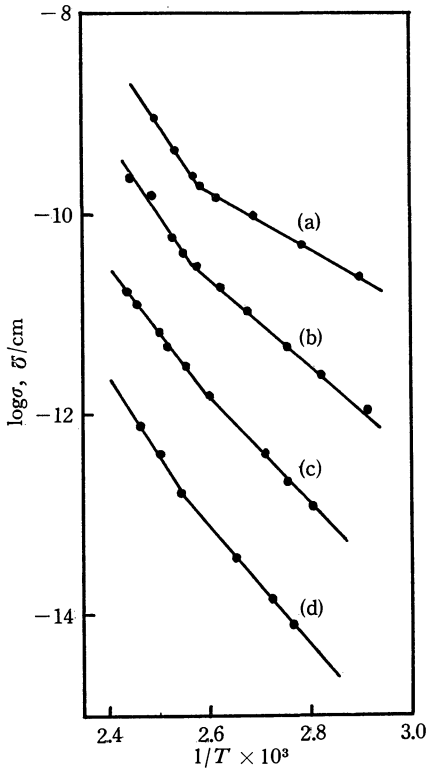

Fig. 2. Temperature dependence of specific conductivity (σ) of $(Cu_xZn_{1-x})Hg(SCN)_4$.
(a), x=0.2; (b), x=0.1; (c), x=0.03; (d), x=0

Electronic Spectra. In order to clarify the relation between the electrical conductivity and the depth of the characteristic color of $(Cu_xZn_{1-x})Hg(SCN)_4$, the electronic spectra of a series of the mixed crystals were measured in the visible region. Our results, obtained by diffuse reflectance (Fig. 3), are essentially in agreement with the spectrum of $(Cu_{0.14}Zn_{0.86})Hg(SCN)_4$ reported by Forster *et al.*[6] The band at 560 mμ has been identified as an electron-transfer band. It can be seen in Fig. 3 that the absorbance of the spectra

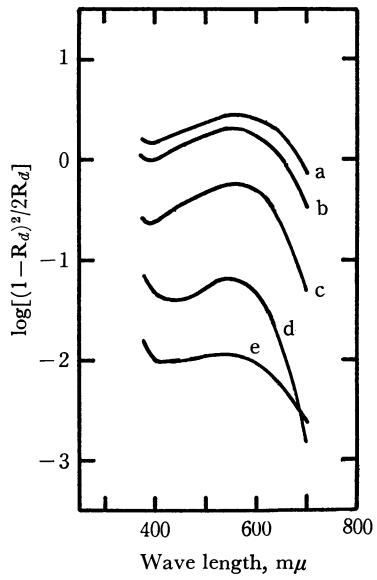

Fig. 3. Curves of $\log[(1-R_d)^2/2R_d]$ for $(Cu_xZn_{1-x})Hg(SCN)_4$
a), x=0.2; b), x=0.1; c), x=0.03; d), x=0.003; e), x=0.

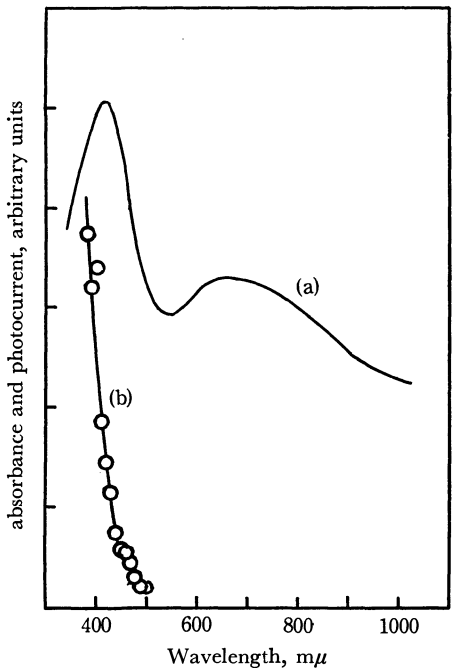

Fig. 4. Absorption and photocurrent spectra of $CuHg(SCN)_4$. (a), absorption spectrum(Ref. 6); (b), photocurrent spctrum.

increases with an increase in the copper concentration. This must be closely related to the fact that the electrical conductivity increases with an increase in the copper concentration.

Photocurrent Spectra. It seems to be of paticular interest that the inorganic complex salts, $CuHg(SCN)_4$ and $(Cu_xZn_{1-x})Hg(SCN)_4$, exhibit photoconductivity.

The photocurrent spectrum of $CuHg(SCN)_4$ is shown in Fig. 4, together with its electronic spectrum. The threshold energy of the photocurrent (E_o) is about 2.8 eV, slightly larger than the energy of the absorption edge of the electron-transfer band with its absorption peak at about 430 mμ. Although the threshold energy of the photocurrent (E_o) does not agree well with the energy of the absorption edge of the band at about 430 mμ, the photoconductivity response found for $CuHg(SCN)_4$ may be caused by the electronic transitions associated with the electron-transfer band at 430 mμ.

The photocurrent spectra of $(Cu_{0.03}Zn_{0.97})Hg(SCN)_4$, $(Cu_{0.1}Zn_{0.9})Hg(SCN)_4$, and $(Cu_{0.2}Zn_{0.8})Hg(SCN)_4$ are shown in Fig. 5, together with the electronic spectrum. What is evident on comparing the photocurrent and electronic spectra is that the photocurrent spectra are closely related to the electron-transfer band with its absorption edge at about 450 mμ. It is noticeable that the threshold values of the photocurrents are almost equal to about 450 mμ (E_o=2.8 eV) for all these three compounds. However, the tail of the photocurrent spectrum of $(Cu_xZn_{1-x})Hg(SCN)_4$ in the 450—600 mμ region seems to shift to the long-wavelength side, depending on the relative concentrations of Cu^{2+} and Zn^{2+}. As well as the thermal activation energy for electrical conduction in the extrinsic region (E_i^e), these tails are associated with the electronic levels of several sorts of lattice imperfections, which were probably introduced by the doping of Cu^{2+} in the $ZnHg(SCN)_4$ lattice.

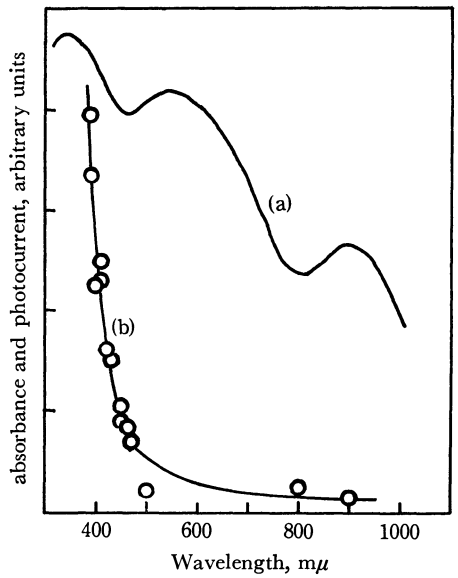

Fig. 5-a. Absorption and photocurrent spectra of $(Cu_xZn_{1-x})Hg(SCN)_4$. (a), absorption spectrum of $(Cu_{0.14}Zn_{0.86})Hg(SCN)_4$(Ref. 6); (b), photocurrent spectrum of $(Cu_{0.03}Zn_{0.97})Hg(SCN)_4$.

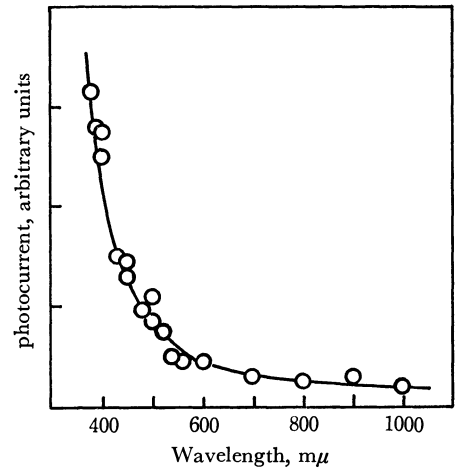

Fig. 5-b. Photocurrent spectrum of $(Cu_{0.1}Zn_{0.9})Hg(SCN)_4$.

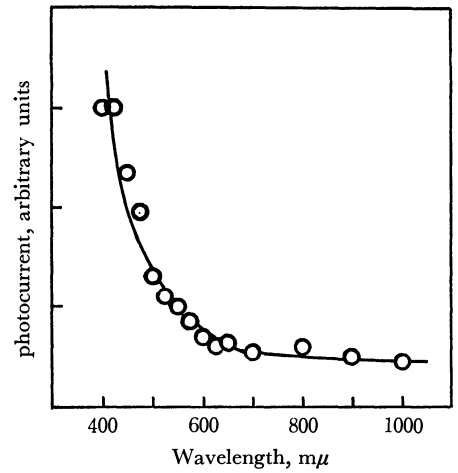

Fig. 5-c. Photocurrent spectrum of $(Cu_{0.2}Zn_{0.8})Hg(SCN)_4$.

Table 2. Effective magnetic moment (μ_{eff}) of Cu(II) in $(Cu_xZn_{1-x})Hg(SCN)_4$ lattice at room temperature

Compound	μ_{eff} B.M.
$(Cu_{0.1}Zn_{0.9})Hg(SCN)_4$	2.0
$(Cu_{0.2}Zn_{0.8})Hg(SNC)_4$	1.9

Magnetic Moments. The magnetic susceptibility of the mixed crystals, $(Cu_xZn_{1-x})Hg(SCN)_4$, obeys the Curier-Weiss law fairly well over the temperature range from 118 to 283°K, with quite a small Weiss constant. The values of the effective magnetic moments (μ_{eff}) of Cu(II) in $(Cu_xZn_{1-x})Hg(SCN)_4$ are listed in Table 2. Figgis has shown that Cu(II) in a perfectly regular tetrahedral environment should have an effective moment of about 2.2 B.M.[9] However, it is well established by measurements that the μ_{eff} of Cu(II) is 1.96—2.00 B.M. for Cs_2CuCl_4, 1.91 B.M. for $(Ph_3MeAs)_2CuCl_4$, and 1.96 B.M. for $(Ph_3MeAs)_2CuBr_4$.[10] In Cs_2CuCl_4, the values of the two Cl–Cu–Cl bond angles are 120° and 104°.[11] The value of μ_{eff} of Cu(II) in $(Cu_{0.1}Zn_{0.9})Hg(SCN)_4$ in this case is almost equal to that in Cs_2CuCl_4. Therefore, the degree of distortion of the CuN_4 tetrahedron in $(Cu_xZn_{1-x})Hg(SCN)_4$ may be expected to be almost identical with that of the $CuCl_4$ tetrahedron in Cs_2CuCl_4. In fact, $ZnHg(SCN)_4$ is isomorphous with $CoHg(SCN)_4$,[2] where the N–Co–N bond angles are 118° and 106°.[3,4] The degree of distortion in $(Cu_{0.2}Zn_{0.8})Hg(SCN)_4$ may larger than that in $(Cu_{0.1}Zn_{0.9})Hg(SCN)_4$, judging from the value of μ_{eff} found for $(Cu_{0.2}Zn_{0.8})Hg(SCN)_4$. Consequently, it follows that the mixed crystal with a higher copper concentration will include a greater amount of lattice imperfections caused by Cu^{2+} doping.

Discussion

Here, we will propose a qualitative discussion of the semiconducting nature of the three-dimensional complex salts studied. However, our discussion will be confined to the case of intrinsic semiconduction, because the experimental data are not sufficient to clarify the latttice imperfections which affect the extrinsic semiconduction in the lower-temperature range.

Measurements of the electrical conductivity and its temperature dependence showed that $CuHg(SCN)_4$ and the mixed crystal, (Cu, Zn)$Hg(SCN)_4$, were semiconductors with quite low conductivities. In the case of the mixed crystals, it may be concluded, from a comparison of their photocurrent spectra with their electronic spectra, that the charge carriers for the intrinsic semiconduction originate from electronic transitions associated with the electron-transfer band at about 330 mμ. It may be seen in Fig. 2 that the intrinsic conductivity of the mixed crystals increases with an increase in the copper concentration. This may be due to the increase in the number of charge carriers. In this case, the absorbance of the electron-transfer band at 330 mμ may be expected to increase. Unfortunately, our spectral data are restricted to the visible region; therefore, the compositional dependence of the absorbance of the band at 330 mμ is obscure.

In general, the electron-transfer processes are of two types: the transfer of an electron from an orbital mainly localized on the ligand(s) to an orbital mainly localized on the metal (abbreviated L→M), and the transfer of an electron in the opposite direction (abbreviated M→L).[12] Forster *et al.* have suggested that the electron-transfer bands of the mixed crystals are analogous to those found for $CuCl_4^{2-}$ and $CuBr_4^{2-}$.[6,13,14] This implies that the electron-transfer bands of the mixed crystals are of the L→M type. If it is possible to consider that the electron-transfer bands of the mixed crystals and $CuHg(SCN)_4$ are of the L→M type, a reasonable account for the intrinsic semiconduction of these compounds may be given on the assumptions that the charge carriers are positive holes originating from the electron transfer from thiocyanate to the copper ion and that the holes are conducted through a valence band formed by electronic levels of thiocyanate ions. This mechanism of semiconduction may well account for the fact that, in the case of the mixed crystals, only the higher-energy electron-transfer band is responsible for the photocurrent; that is, if the lower energy electron-transfer band arises from electronic transitions involving localized orbitals, such as nonbonding orbitals of the ligand, the positive holes in such orbitals are likely to be localized in the ligand, therefore making no contribution to the electrical conductivity. In fact, Ferguson has pointed out that the lowest-energy electron-transfer band of $CuCl_4^{2-}$ probably arises from transitions involving orbitals which are nonbonding in T_d symmetry.[13]

The thermal activation energy (E_t) is related to the optical energy (E_o) by the following expression:

$$E_o/E_t = \varepsilon_s/\varepsilon_o,$$

where ε_s and ε_o are the static and high-frequency dielectric constants respectively. If the interatomic bonding is ionic, E_t is smaller than E_o. For the complex salts studied, the values of E_t^i obtained from $\log\sigma$ *vs.* $1/T$ plots are smaller than the values of E_o obtained from the threshold values of the photocurrent and electronic spectra. This suggests that the chemical bonds between copper and thiocyanate ions are most likely to be electrostatic.[15] Furthermore, the extremely low conductivities of these complex salts may well be due to the strong ionic character of the chemical bonds.

9) B. N. Figgis, *Nature*, **182**, 1568 (1958).
10) D. M. N. Goodgame and F. A. Cotton, *J. Chem. Soc.*, **1961**, 2298.
11) L. Helmholz and R. F. Kruth, *J. Amer. Chem. Soc.*, **74**, 1176 (1952).
12) H. B. Gray, *J. Chem. Educ.*, **41**, 2 (1964).
13) J. Ferguson, *J. Chem. Phys.*, **40**, 3406 (1964).
14) P. S. Braterman, *Inorg. Chem.*, **2**, 448 (1963).
15) S. Yamada and R. Tsuchida, This Bulletin, **28**, 664 (1955).

Elimination Reaction on Solid Acid Catalysts. IV.* A δ_R LFER Study of the Esterification of Alcohols with Carboxylic Acids over Solid Acid Catalysts

Isao MOCHIDA, Yasuhide ANJU, Akio KATO, and Tetsuro SEIYAMA
Department of Applied Chemistry, Faculty of Engineering, Kyushu University, Fukuoka
(Received February 6, 1971)

The esterification between eight alcohols and seven carboxylic acids was studied over sodium-poisoned silica-alumina at 250°, using a microcatalytic gas chromatographic technique, in order to elucidate the mechanism of the esterification on a solid acid catalyst on the basis of a LFER (Linear Free-Energy Relationships) approach. Alcohols showed fairly close reactivities for the esterification with acetic acid, whereas, for the olefin formation by intramolecular dehydration and ethylether formation with ethanol, their reactivity varied very much according to the kind of alcohol. In contrast, the reactivities of carboxylic acids for the esterification varied with the structure and were correlated with E_s, Newman's steric-effect parameter, as was observed in the homogeneous acid catalysis, although the reactivity difference under the present conditions was small indeed. It is probably due to the elevated reaction temperature. No ethylacetate, but only thiolacetate, was found in the reaction of acetic acid with ethanethiol. From these facts, it may be concluded that the esterification over a solid acid catalyst may proceed through the attack of an oxonium ion from a carboxylic acid on an adsorbed alcohol, in the manner similar to that in the homogeneous acid-catalyzed esterification.

In a previous paper,[1] two possible mechanistic schemes for the esterification of ethanol with acetic acid were discussed:

Mechanism 1: $C_2H_5^+ + CH_3C(OH)_2^+ \longrightarrow CH_3C(O)OC_2H_5 + 2H^+$

Mechanism 2: $CH_3C(OH)_2^+ + C_2H_5OH_2^+ \longrightarrow CH_3C(O)OC_2H_5 + H_3O^+ + H^+$

One is the attack of the ethyl carbonium ion originating from ethanol on the oxygen atom of the adsorbed acetic acid (Mechanism 1), while the other is that of the oxonium ion from acetic acid on the adsorbed ethanol (Mechanism 2). The δ_C effect (the effect of the nature of the catalyst on the reaction rate),[2] poisoning effect, the kinetic study and a comparison with the dehydration of ethanol on the same catalyst[1,3] all indicate that Mechanism 2 is more probable in the heterogeneous esterification as well as in the homogeneous one.

A study of the dependence of the reactivity upon the reactant structure may give further information about the proposed reaction mechanism. Newman[4] argued the importance of the steric factors of carboxylic acids in homogeneous reactions on the basis of such an approach. In the present study, the mechanism of the esterification on the solid acid catalyst was considered on the basis of the δ_R (the effect of the nature of the reactants on the reaction rate) LFER,[2] using eight alcohols and seven carboxylic acids. A discussion from the same viewpoint was made of the comparisons between the esterifications and the dehydrations of these alcohls. The discrimination between the above two reaction mechanisms may be possible by determining the origin of the ethereal oxygen of the ester. For this purpose, the esterification of ethanethiol with acetic acid may be an adequate system if a common reaction mechanism can be assumed for both alcohols and thiols. An esterification of ethanethiol with acetic acid was, then, studied on the solid acid catalyst. Such a study was attempted in the homogeneous reactions, and the attack of the oxonium ion from benzoic acid was established.[5]

Experimental

Reagents. The alcohols in Table 1 were obtained from the Wako Junyaku Co. The carboxylic acids were obtained from the Tokyo Kasei Co. The ethanethiol was obtained from Nakarai Chemicals, Ltd. All of them were of a E.P. grade except for the ethanol, which was of a G.R. grade.

Catalysts. The catalysts in this work were silica-alumina (13% Al_2O_3) of Japan Cat., a cracking catalyst of the Shokubai Kasei Co. (abbreviated to SA), and the same catalyst impregnated with 0.4 meq Na/g(abbreviated to SA–Na). They were calcined at 550° for 8 hr in the atmosphere.

TABLE 1. THE RATES OF ACETATE FORMATION AND MIXED ETHER FORMATION WITH VARIOUS ALCOHOLS
Catalyst: SA-Na, 1-5 mg
Reaction temperature: 250°C.

No.	Alcohol (ROH)	Rate of acetate formation (mmol·ml/g·min)[a]	Rate of mixed ether formation (mmol·ml/g·min)[b]
1	Methanol	6.6	—
2	Ethanol	6.3	—
3	*n*-Propanol	8.0	0.12
4	*n*-Butanol	8.2	0.17
5	Isobutanol	7.8	0.19
6	Isopropanol	5.5	1.50
7	*s*-Butanol	8.3	1.56
8	*t*-Butanol	14.0	24.0

a) $ROH + CH_3COOH \longrightarrow CH_3COOR + H_2O$
b) $ROH + C_2H_5OH \longrightarrow C_2H_5OR + H_2O$

* Part III: I. Mochida, A. Kato, and T. Seiyama, *J. Catalysis*, in press.

1) I. Mochida, Y. Anju, A. Kato, and T. Seiyama, *J. Catalysis*, in press.
2) I. Mochida and Y. Yoneda, *ibid.*, **7**, 386, 393, **8**, 223 (1967).
3) I. Mochida, Y. Anju, A. Kato, and T. Seiyama, This Bulletin, **43**, 2245 (1970).
4) M. S. Newman, "Steric Effects in Organic Chemistry," ed. by M. S. Newman, Wiley (1956), p. 206.
5) L. S. Pratt and E. E. Reid, *J. Amer. Chem. Soc.*, **37**, 1932 (1915).

Apparatus and Procedures. For esterifications of alcohols with carboxylic acids and dehydrations of the mixed alcohols, the reaction temperature was 250°C. For the condensation reaction of ethanethiol with acetic acid, it was 300°C. The rates were calculated from the conversion measured by means of the microcatalytic gas-chromatographic technique.[1,3,6] Polyethylene glycol(PEG 1500) was used in an analytical column except in the esterifications of 2-ethyl-*n*-butyric acid and isovaleric acid with ethanol. In these cases, Tween 80+20% H_3PO_4 was used. A carboxylic acid and an alcohol were mixed in equimolar quantities. A fixed quantity (3.4×10^{-2} mmol) of the homogeneous mixture was injected in every run. The conversions of alcohols were kept below 10% except for *tert*-butanol. The same procedure was used for the reaction of mixed alcohols. The rate was expressed by the unit of mmol·ml/g·min. The details of the experiments were described in previous papers.[1,3]

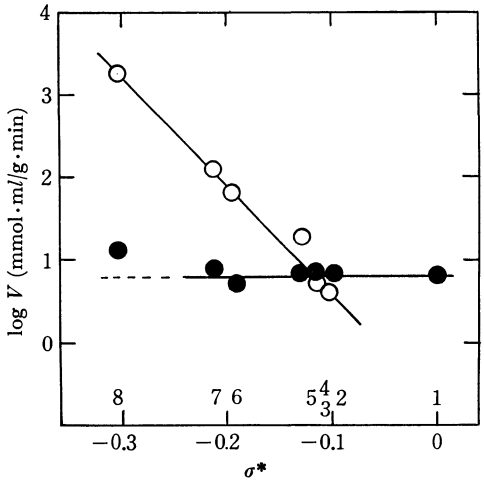

Fig. 1. Reactivities of alcohols as a function of σ^*.
Catalyst: SA–Na, 1—5 mg. Reaction temperature: 250°C. Flow rate: 90 ml/min. Numbers refer to the reagents designated in Table 1.
○, olefin formation; ●, esterification

Results and Discussion

δ_R *Effect as to Alcohols.* The mixture of an alcohol and an acetic acid gave an olefin and an ester without an ether on SA–Na at 250°C. The reactivities of eight alcohols, ROH, are compared in Fig. 1, where the rates of esterification and dehydration into olefin are plotted against Taft's σ^* for the R group. The σ^* values are defined as measures of the inductive electron-withdrawing power of an atom or group of atoms in a molecule. The values of σ^* were taken from the literature.[7] The reactivities of alcohols for the intramolecular dehydration to olefin varied very much amoung the alcohols, whereas those for esterification remained fairly constant. The large dependence of the dehydration rate upon σ^* may mean that the electron-releasing ability of the alkyl group is important in the intramolecular dehydration. Such results have also been reported in the absence of acetic acid.[8] The reactive alcohols tend to proceed into their intramolecular dehydration rather than into their intermolecular esterification, as has been observed in the metal sulfate supported by silica gel.[9] This fact may be understood if we remember that the intermediate from the alcohol with a high tendency to give the carbonium ion is too reactive to stay on the catalyst for the ester formation without being converted into olefin. The distinct difference in the reactivity tendencies suggests different rate-detarmining steps for these intra- and intermolecular reactions.

The ether formations through intermolecular reactions between ethanol and various alcohols were measured on SA–Na at 250°C. The rates are compared with those of acetate formations through the intermolecular reactions of alcohols with acetic acid in Table 1. For primary and secondary alcohols, the rates of the esterifications were much larger than those of the ethyl-ether formations.

The rates of ether formation with ethanol increase in this order of the ease of the formation of the corresponding carbonium ion from alcohols: primary <secondary<tertiary. This indicates a carbonium ion mechanism for the ether formation, in which ethanol is attacked by the carbonium ion from higher alcohol. If the esterification proceeds through a mechanism accompanying carbonium ions from alcohols, the ether formation will be faster than the esterification because more basic ethanol will have a larger susceptibility to the carbonium ion than that of acetic acid. The rates observed, however, do not agree with this expectation for primary and secondary alcohols. Therefore, the carbonium ion formation from alcohols

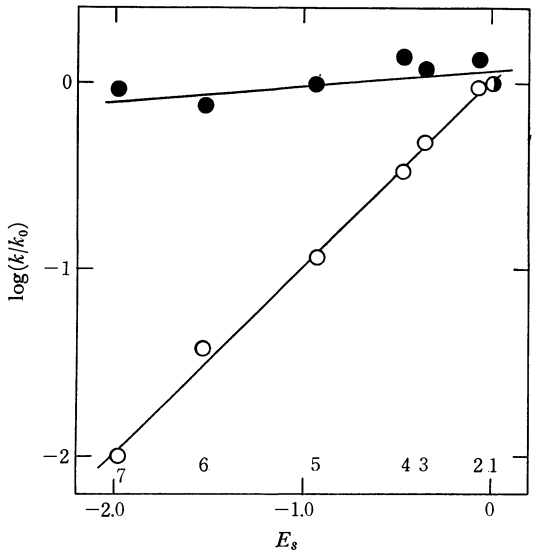

Fig. 2. Correlations between reactivities in esterification and E_s of carboxylic acids.
●, the rates in this work (Catalyst: SA–Na, 3—5 mg, Reaction temperature: 250°C. Flow rate: 90 ml/min)
○, rate constants in homogeneous acid-catalyzed reactions at 40°C. Data are taken from Newman (12). Numbers refer to the following reagents: 1, acetic acid, 2, propionic acid; 3, *n*-butyric acid; 4, isobutyric acid; 5, isovaleric acid; 6, pivalic acid; 7, 2-ethyl-*n*-butyric acid

6) R. J. Kokes, H. Tobin, and P. H. Emmett, *J. Amer. Chem. Soc.*, **77**, 5860 (1955).
7) R. W. Taft, Ref. 4, p. 619.
8) H. Adkins and P. P. Perkins, *J. Amer. Chem. Soc.*, **53**, 1520 (1931).
9) I. Mochida, A. Kato, and T. Seiyama, *J. Catalysis*, in press.

TABLE 2. DEPENDENCE OF THE ESTERIFICATION REACTIVITY ON THE STRUCTURE OF CARBOXYLIC ACID

Reaction temperature (°C)	s[a)]	Numbers of carboxylic acids used for analysis
20	1.03 ± 0.01	16
30	0.99 ± 0.01	17
40	0.93 ± 0.03	19

a) $\log(k/k_0)=s\,E_s$, where k and k_0 are the rate constants of esterification of ethanol with carboxylic acid and acetic acid, respectively.
Kinetic data were obtained from Ref. 12.

should be abandoned and Mechanism 2 seems more probable for the esterification.

For *tert*-butanol, the rate of mixed-ether formation was larger than that of esterification. A different mechanism should be supposed for the esterification of *tert*-butanol in the heterogeneous reaction as well as in the homogeneous reaction.[10)]

δ_R Effect as to Carboxylic Acids. The rates of the esterifications of ethanol with some carboxylic acids on SA–Na at 250°C are shown in Fig. 2 as a function of E_s,[11)] which is thought to represent the steric factor of the substituent. Newman[12)] proposed a sixtet rule for the reactivities of carboxylic acids in the homogeneous esterification, and stressed the importance of the steric factor in this reaction. The analysis of his data at 20, 30, and 40°C showed good correlations with the E_s of the carboxylic acid as is shown in Table 2 and Fig. 2. Large differences in the reactivities were observed. In the heterogeneous catalysis of the present study, a linear correlation was also found, as is shown in Fig. 2, although the kind of carboxylic acids has a smaller effect on the reactivity for esterification. The dependency of the esterification rate on the structure of carboxylic acids decrease with an increase in the reaction temperature in the homogeneous reaction, as may be seen in Table 2. Thus, the smaller reactivity differences among carboxylic acids in the present study may be explained by the reduction of the steric-effect at the higher reaction temperatures. It is interesting that the steric effect was small at the reaction of 250°C in spite of the expectation that the effect might be large on the solid catalyst surface. At any rate, such results do not conflict with Mechanism 2 and suggest, rather, the continuity of the reaction mechanism in homogeneous and heterogeneous acid-catalyzed reactions.

Reaction of Acetic Acid and Ethanethiol. It has been known that the thiol reacts with benzoic acid to produce thiol benzoate in an acidic medium.[5)] Whether or not the ester thus produced contains the sulfur atom may give information on the mechanism of esterifications. In the reaction of acetic acid with ethanethiol on SA at 300°C, no ethylacetate except thiol acetate was found by the use of the gas chromatograph.[13)] The further identification of thiol acetate was done by means of IR and MS analyses of the trapped sample. The existence of ethylthioacetate without ethylacetate in the product may support Mechanism 2; in this case, the carbon atom of the carbonyl group in the acetic acid, which is positively polarized, may attack the sulfur atom of thiol. The fact that the reactivity of thiol is lower than that of ethanol may be easily deduced by the above reaction mechanism because of the small basicity of the sulfur atom, as estimated from the value of electronegativity.[14)] In fact, the reactivity of thiol was only a tenth of that of ethanol.

All the above results suggest that the esterification over the solid acid catalyst may proceed through an attack of the oxonium ion from carboxylic acid on an adsorbed alcohol, in a manner similar to that in the homogeneous acid-catalyzed esterification.

Our thanks are due to Professor Yukio Yoneda of the University of Tokyo for generously providing us with a program of the least-square means. The electronic computaion was carried out on a FACOM 230–60 of the Computer Center of Kyushu University. We are also grateful to Mr. Hozumi Futada for his analysis by means of a Mass Spectrometer.

10) L. F. Fieser and M. Fieser, "Introduction to Organic Chemistry," Heath and Company (1957), p. 139.
11) R. W. Taft, Ref. 4, p. 598.
12) M. S. Newman, Ref. 4, p. 205.
13) Only thiol acetate and ethyldisulfide were detected. The latter might be produced from unreacted thiol by the catalytic action of the copper metal of the analytical column.
14) L. Pauling, "The Nature of the Chemical Bond," Corenl University Press, Ithaca, New York (1960), p. 90.

Mixed Monolayers of Poly(methyl acrylate) and Its Saponified Polymer

Seiichiro HIRONAKA,* Takashi KUBOTA, and Kenjiro MEGURO
Department of Chemistry, Faculty of Science, Science University of Tokyo, Kagurazaka, Shinjuku-ku, Tokyo
(Received February 20, 1971)

A film balance study of the mixed monolayers with various ratios of poly(methyl acrylate) and its saponified polymer or of the monolayers themselves was carried out on distilled water, and the mixed monolayers were compared with individual monolayers of the saponified polymers. These mixed monolayers expanded more than individual saponified polymers at the same degree of saponification, giving larger limiting areas. Their limiting areas deviated from the linearity between the limiting area and the degree of saponification, in contrast to the fact that the limiting areas of individual monolayers decreased linearly with an increase in the degree of saponification. This fact can be considered to be due to interactions between the side chains of the ploymers.

Recently, many studies of the mixed monolayers have been reported.[1-3] However, there have been few studies of the mixed monolayers of polymers.[4-6]

In general, when mixtures of two insoluble substances are spread on the water surface, it can be considered that they form either individual monolayers without two components' mixing or an ideal surface mixture by their complete mixing with one another. Mixtures of analogous compounds give the linear relation between the limiting area and the ratio of mixing and the existence of stoichiometric interaction, that is, the additivity of the film areas and the surface potentials. La Mer *et al.* have reported the ideal surface behavior of the mixed monolayers by studying the rate of the evaporation of water through the mixed monolayers.[1] Crisp has shown that the areas and the surface potentials of the mixed monolayers of poly(vinyl acetate) and poly(vinyl alcohol) were linear averages of the individual pure monolayers.[4] However, Labbauf has suggested that the areas obtained for the mixed monolayers of poly(ethyl acrylate) and poly(vinyl acetate) deviated largely, both positively and negatively, from the linear average values.[7]

In this investigation, we have studied the mixed monolayers of poly(methyl acrylate) and its saponified polymers, or the monolayers themselves, and discussed the two-dimensional behavior of polymers in terms of the deviation from the linearity of their limiting areas and the degrees of saponification.

Experimental

Monomer. Methyl acrylate (supplied by Toagosei Co., Ltd.) was used for radical polymerization. It was purified by distillation under reduced nitrogen atomosphere after its inhibitor had been removed by washing it with 5% sodium hydroxide aqueous solution and distilled water and after it had been dehydrated with silicon dioxide.

Polymerization. Poly(methyl acrylate) was prepared by radical polymerization, with α,α'-azobisisobutyronitrile as the initiator, in benzene at 50°C under a flow of nitrogen gas. The polymer thus obtained was purified by reprecipitation from its acetone solution into a large excess of methanol. The average molecular weight of this polymer, as determined by the measurement of the viscosity, was 659000.

Saponification. The saponifications of poly(methyl acrylate) were carried out in a homogeneous system of an acetone-water mixture (5:2 by volume), with sodium hydroxide as the catalyst, at 50°C until all the sodium hydroxide was consumed.[8] After the reaction, the saponified polymers were washed with a hydrochloric acid aqueous solution. They were purified by reprecipitation from an acetone solution into water, methanol, and ethyl ether. The saponification was confirmed by a study of the infrared spectra, while the degrees of saponification (mol%) of these polymers were determined by the elementary analyses to be 13.48, 24.16, and 48.34 mol%.

Surface-pressure Measurement. A modified Wilhelmy-type film balance was used to measure the surface pressure.[9] The film balance was enclosed in the chamber to allow thermostatic control at 20.0±0.2°C. The water in the trough was kept at 20.0±0.2°C by circulating water from a thermostat bath. The distilled water used as the substrate was in the range of pH 5.0—6.0. The trough was coated with highly pure, hard paraffin wax. The sensitivity of the torsion wire was about ±0.1 dyn/cm.

The monolayers were spread on the substrate from a mixed spreading solution of acetone-benzene (1:1 by volume) by means of an "Agla" microsyringe. Various organic liquids were examined as the spreading solvent, but the best was an acetone-benzene mixture (1:1 by volume).

Thirty minutes were allowed for the solvent to evaporate before compression was started. Every reading of the surface pressure was carried out after the films had been left for 5 min. after their compression. The rate of compression was 7.5 cm²/min.

Results and Discussion

The surface pressure measurements for all the polymers were repeated at least several times; their results were reproducible within the limits of experimental er-

* Present address: Faculty of Engineering, Tokyo Institute of Technology, Ookayama, Meguro-ku, Tokyo.

1) V. K. La Mer, L. A. G. Aylmore, and T. W. Healy, *J. Phys. Chem.*, **67**, 2793 (1963).
2) F. M. Fowkes, *J. Phys. Chem.*, **67**, 1982 (1963).
3) R. P. Quintana, A. Lasslo, and P. P. Bobbo, *J. Colloid and Interface Sci.*, **26**, 166 (1968).
4) D. J. Crisp, *Research (London) Suppl. Surface Chem.*, **17**, 23 (1947).
5) H. E. Ries, Jr., and D. C. Walker, *J. Colloid Sci.*, **16**, 361 (1961).
6) S. Wu and J. R. Huntsberger, *J. Colloid and Interface Sci.*, **29**, 138 (1969).
7) A. Labbauf, *J. Appl. Polymer Sci.*, **10**, 865 (1966).
8) I. Sakurada, Y. Sakaguchi, T. Iwagaki, and Y. Mikuzu, *Kobunshi Kagaku*, **21**, 426 (1964).
9) D. G. Dervichian, *J. Phys. Radium*, **6**, 221, 429 (1935).

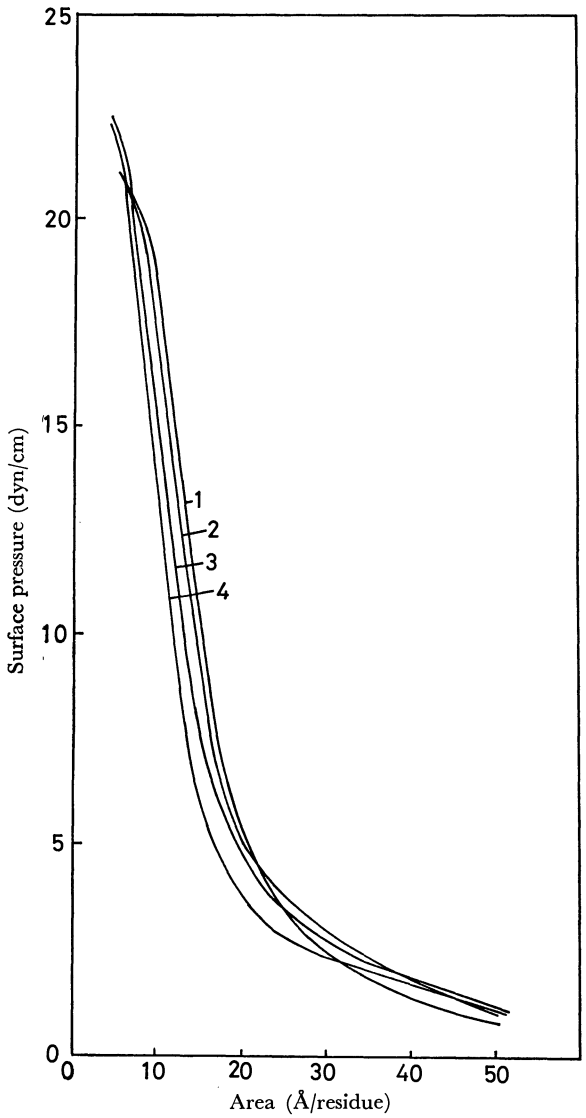

Fig. 1. The surface pressure-area isotherms of poly (methyl acrylate) and its saponified polymer on distilled water.
1– poly(methyl acrylate); 2– 13.93 mol% saponified polymer; 3– 24.16 mol% saponified polymer; 4– 48.34 mol% saponified polymer.

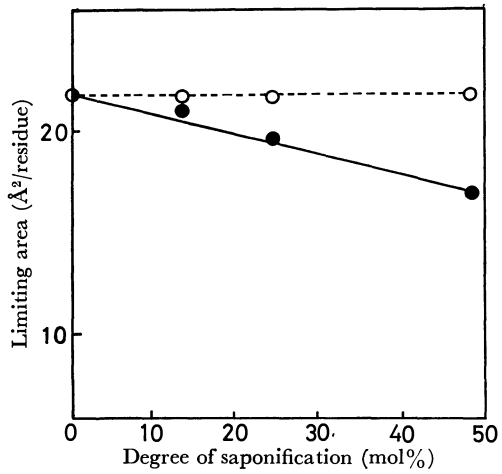

Fig. 2. The limiting areas of the saponified polymer *vs.* the the degree of saponification. ○: theoretical; ●: experimental; ◑: poly(methyl acrylate).

ror of the ±0.1 Å²/residue.

The surface pressure-area isotherms for poly(methyl acrylate) and its saponified polymers on distilled water are shown in Fig. 1. The limiting area obtained for poly(methyl acrylate) was 21.6 Å²/residue which corresponded well to 21.5 Å²/residue by Crisp.[10] This fact suggests that our sample is just the same as Crisp's. The limiting area for each saponified polymer was smaller than that of poly(methyl acrylate), and the theoretical values were calculated as follows. By using the limiting areas of 21.5 Å² per methyl acrylate residue and 22.0 Å² per acrylic acid residue reported by Crisp,[10] the theoretical value (A_t) of the saponified polymer when all the residues of the polymer were oriented on the water surface was calculated by this equation:

$$A_t = 21.5\left(1-\frac{X}{100}\right) + 22.0\frac{X}{100} \qquad (1)$$

where X is the degree of saponification (mol %).

Figure 2 shows the limiting area of the saponified polymer *vs.* the degree of saponification. The experimental and theoretical limiting areas for each saponified polymer are listed in Table 1. The limiting areas decreased linearly with an increase in the degree of saponification, but deviated from the ideal linearity of Eq. (1). It is considered that some of the hydrophilic residues of the polymer are submerged into the water phase by compressing the films,[11] and that the higher the degree of saponification, the larger the decrease in the limiting area.

Table 1. The limiting areas of poly(methyl acrylate) and its saponified polymer on distilled water

Sample	Limiting Area (Å²/residue)	
	Experimental	Theoraretical (by Crisp)
Poly(methyl acrylate)	21.6	21.5
13.93 mol% saponified polymer	21.0	21.65
24.16 mol% saponified polymer	19.5	21.69
48.34 mol% saponified polymer	16.8	21.79

The surface pressures of the mixed monolayers of poly(methyl acrylate) and the 48.34 mol% saponified polymer (mixed monolayers of the A series) and the 13.48 mol% and 48.34 mol% saponified polymers (mixed monolayers of the B series), mixed in various ratios, were measured under the same conditions as were used the individual monolayers. The surface pressure-area isotherms obtained for the mixed monolayer of the B series are shown in Fig. 3. The mixed monolayers expanded much more than the individual monolayers and gave larger limiting areas. Furthermore, these limiting areas were larger than those of the individual monolayers at almost the same degree of saponification. The mixed monolayers of the A series showed the same inclinations.

10) D. J. Crisp, *J. Colloid Sci.*, **1**, 49 (1946).
11) S. Hironaka and K. Meguro, *J. Colloid and Interface Sci.*, in press.

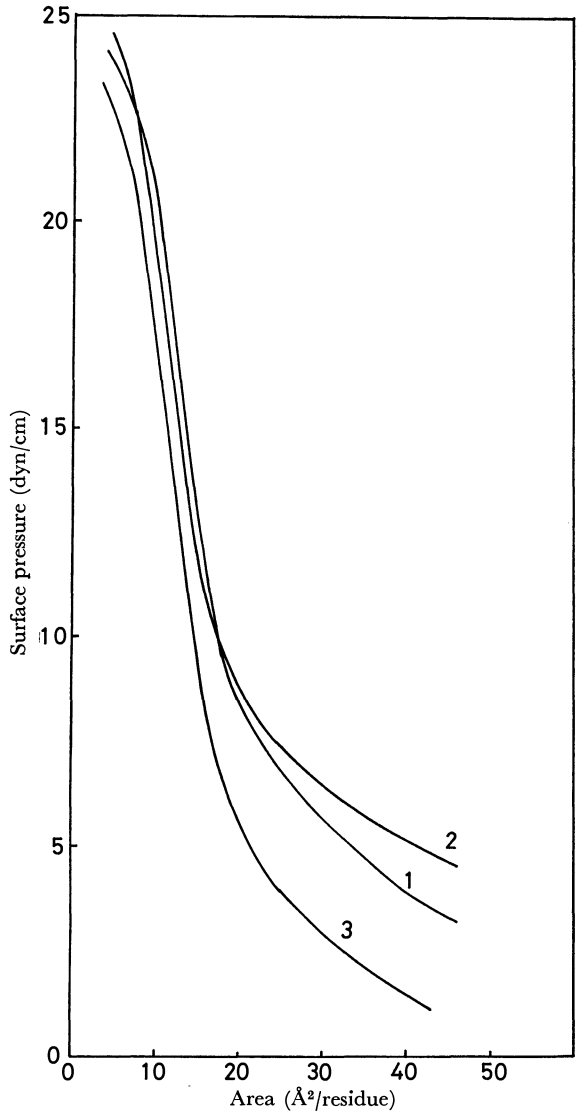

Fig. 3. The surface pressure-area isotherms of mixtures of 13.93 mol% saponified polymer and 48.34 mol% saponified polymer. 1– 19.95 mol% mixed polymer; 2– 29.97 mol% mixed polymer; 3– 39.95 mol% mixed polymer.

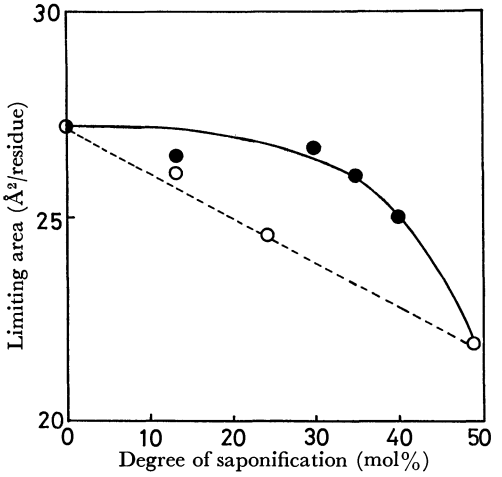

Fig. 4. The limiting areas of mixtures of poly(methyl acrylate) and 48.34 mol% saponified polymer *vs.* the degree of saponification by mixing. ○: pure saponified polymer; ●: mixed polymer; ◑: poly(methyl acrylate).

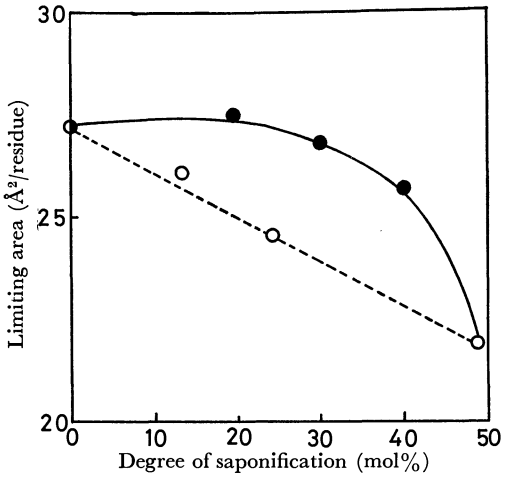

Fig. 5. The limiting areas of mixtures of 13.93 mol% saponified polymer and 48.34 mol% saponified polymer *vs.* the degree of saponification by mixing. ○: pure saponified polymer; ●: mixed polymer; ◑: poly(methyl acrylate).

The behavior of the ideal surface mixtures is generally exhibited by mixtures of close members of a homologous series.[1,4,12] The plots of the limiting areas of the mixed monolayers *vs.* the degrees of saponification by mixing are given in Figs. 4 and 5. If these mixed monolayers form the ideal surface solution, the plots should have the ideal mixing linearity, that is, the linearity between the limiting areas and the degrees of saponification obtained for the individual monolayers. However, the results of A and B series deviated largely and positively from the ideal mixing linearity and behaved like the nonideal surface solutions. This fact suggests that the behavior and orientations of the mixed monolayers are different from those of the individual monolayers. The individual monolayers have such orientations as some of their hydrophilic groups are submerged into the bulk, while one or two of them are hung with such hydrophobic anchors as methyl acrylate residues and so remain on the water surface. Therefore, they have limiting areas smaller than the theoretical values. On the other hand, with regard to the mixed monolayers, it is considered that the two component polymers have interactions between each other's sidechains, though they consist of binary mixtures of homologous polymers, and that the interactions exceed the decrease in the areas because of the submergence of some of the hydrophilic groups. Furthermore, it is conceivable that the dissociation of the hydrophilic groups facilitates this interaction between sidechains. As evidence for these suggestions, the mixed monolayers were more expanded and unstable than the individual monolayers at all surface pressures. Specially, at low surface pressures, the mixed monolayers were much more expanded than the individual monolayers. This suggests that the molecules of polymers have larger spaces for their free movements because of the interactions.

12) M. L. Robbins and V. K. La Mer, *J. Colloid Sci.*, **15**, 123 (1960).

Conclusion

Although the individual monolayers gave smaller limiting areas than the theoretical values because some of hydrophilic groups are submerged into the bulk, they exhibited a linearity between the limiting area and the degree of saponification. The mixed monolayers did not show the behavior of the ideal surface mixtures in spite of their consisting of close members of a homologous series, and their limiting areas deviated largely and positively from the ideal linearity upon mixing. These unexpected results suggest an interaction between sidechains of two component polymers which exceeds the decrease in the areas as a result of the submergence of some of the hydrophilic groups.

BULLETIN OF THE CHEMICAL SOCIETY OF JAPAN, VOL. 44, 2332—2339(1971)

Topological Index. A Newly Proposed Quantity Characterizing the Topological Nature of Structural Isomers of Saturated Hydrocarbons

Haruo Hosoya

Department of Chemistry, Ochanomizu University, Bunkyo-ku, Tokyo

(Received February 27, 1971)

A topological index Z is proposed for a connected graph G representing the carbon skeleton of a saturated hydrocarbon. The integer Z is the sum of a set of the numbers $p(G,k)$, which is the number of ways in which such k bonds are so chosen from G that no two of them are connected. For chain molecules Z is closely related to the characteristic polynomial derived from the topological matrix. It is found that Z is correlated well with the topological nature of the carbon skeleton, *i.e.*, the mode of branching and ring closure. Some interesting relations are found, such as a graphical representation of the Fibonacci numbers and a composition principle for counting Z. Correlation of Z with boiling points of saturated hydrocarbons is pointed out.

There are three conventional methods for distinguishing the carbon skeletons of the structural isomers of saturated hydrocarbons, which may or may not contain a ring or rings as illustrated in Fig. 1.

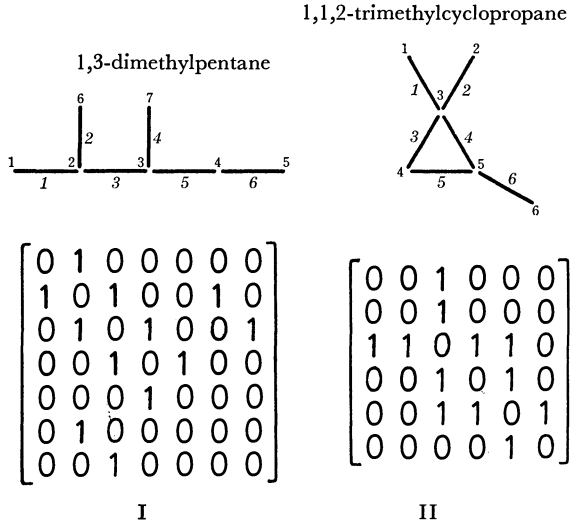

Fig. 1. Three conventional methods for characterizing the carbon skeletons of saturated hydrocarbons.

i) A systematic naming system in which the size of the ring and the sites of the branching are specified for the longest chain or largest ring.

ii) A graph in which each point corresponds to a carbon atom and the numbers of the attached hydrogen atoms are automatically determined so that each carbon atom satisfies the tetra-valency.

iii) A topological matrix in which the values of the off-diagonal elements 1 and 0 are respectively assinged to the bond and no-bond for the pairs of carbon atoms.

These three methods are equivalent to each other in the topological sense. Topology has contributed to the development of chemistry, *e.g.*, in predicting the numbers of the structural isomers,[1-4] by way of the so-called chemical inference using the structural formulae, through the electronic therories such as the Hückel molecular orbital, valence bond and free electron theories.[5] It has also been shown that some thermodynamic properties such as boiling point are correlated well with the topological nature of the compounds,[6,7] while sophisticated quantum mechanical calculations have been unsuccessful.

In this report a topological index Z is defined and proposed as a fourth candidate for classifying saturated hydrocarbons with respect to their topological nature. Although it does *not* necessarily give the structure of the isomer, it is roughly dependent on the topological

1) E. Cayley, *Ber.*, **8**, 1056 (1875).
2) H. Schiff, *ibid.*, **8**, 1542 (1875).
3) H. R. Henze and C. M. Blair, *J. Amer. Chem. Soc.*, **56**, 157 (1934).
4) G. Polya, *Acta Math.*, **68**, 145 (1938).
5) Extensive bibliography is given by J. R. Platt, "Encyclopedia of Physics," Vol. 37 (Molecule II), ed. by S. Flügge, Springer-Verlag, Berlin (1961), p. 173.
6) H. Wiener, *J. Amer. Chem. Soc.*, **69**, 17, 2636 (1947); H. Wiener, *J. Phys. Chem.*, **52**, 425, 1082 (1948).
7) J. R. Platt, *ibid.*, **56**, 328 (1952).

nature of a molecule, *i.e.*, the size and mode of branching and ring closure. It was also found to correlate well with the boiling point. This magic number Z is enumerated just from the carbon skeleton G of a given saturated hydrocarbon, and is of chemical and mathematical interest.

Theoretical

First, a brief summary of theoretical background is given as premises.[8,9] It seems that most of the formulations and algorithms developed in this paper have not yet been proposed in chemistry or in graph theory.[10]

Premises. A graph G consists of points (vertices or atoms) and lines (edges or bonds). We consider only connected non-directed graphs in which every point has at least one and at most four neighbors, and no loop (a line joining a point to itself) and no multiple lines (double or triple bonds) are involved. With these restrictions the graph is equivalent in a topological sense to the carbon skeleton of a saturated hydrocarbon or, in some cases, an unsaturated hydrocarbon. Distinction between σ- and π-electrons or between single and multiple bonds are meaningless for the moment.

Graphs are grouped into trees and non-trees depending upon whether they contain cycles (rings) or not. Chemically speaking, trees are chain hydrocarbons and non-trees cyclic ones.

An adjacency matrix $\boldsymbol{A}$ for graph G is defined in graph theory as a square matrix with the following elements:

$$a_{ij} = \begin{cases} 1 & \text{if the points } i \text{ and } j \text{ are neighbors,} \\ 0 & \text{otherwise.} \end{cases} \quad (1)$$

The order of $\boldsymbol{A}$ is the number of the points in G. Ham and Ruedenberg[11] called it a topological matrix. Since then a number of interesting relations have been derived.[5] It is obvious that the matrix characters of $\boldsymbol{A}$ are independent of the way of numbering the atoms.

The power series expansion, with respect to X, of the determinant $|X\boldsymbol{E}+\boldsymbol{A}|$ for graph G is called a characteristic polynomial, where $\boldsymbol{E}$ is a unit matrix of the same order N as $\boldsymbol{A}$.[12]

$$P_G(X) = \det|X\boldsymbol{E}+\boldsymbol{A}| = \sum_{i=0}^{N} f_i X^{N-i} \quad (2)$$

A secular determinant giving the Hückel molecular orbitals for the π-electrons of an unsaturated hydrocarbon is reduced to the same form as above. Besides the standard but iterative methods of Laplace, Newton, and Frame, useful graphical techniques of the expansion of $P_G(X)$ by use of recursion formulae were given by Heilbronner.[13]

Definition of Topological Index. Consider a graph or structure G with N carbon atoms. The topological index Z is defined stepwise as follows.

Definition 1 (*Non-adjacent number*): A non-adjacent number $p(G,k)$ is the number of ways in which k bonds are so chosen from G that no two of them are connected, $p(G,0)$ being unity and $p(G,1)$ the number of the bonds.

Definition 2 (*Z-counting polynomial*):

$$Q_G(Y) = \sum_{k=0}^{m} p(G,k) Y^k \quad (3)$$

Definition 3 (*Topological index*):

$$Z_G = \sum_{k=0}^{m} p(G,k) = Q_G(1) \quad (4)$$

where m is the maximum number of k for G.

Note that $p(G,m)$ is equal to the number of Kekulé structures for an unsaturated hydrocarbon in which each atom forming the carbon skeleton G supplies one electron to the π-system.[14] The Z-counting polynomial is introduced as a proof technique and is actually used in Appendix.[16] Unless confusion occurs the suffix G for Z, $P(X)$ and $Q(Y)$ may be omitted.

Let us take two compounds I(tree) and II(non-tree) in Fig. 1 as examples and enumerate these quantities. For convenience the bonds are numbered in italics. For both the compounds $p(G,0)=1$ and $p(G,1)=6$. The following pairs of bonds are the entries of $p(G,2)$:

I: *1-4*, *1-5*, *1-6*, *2-4*, *2-5*, *2-6*, *3-6*, and *4-6*,
II: *1-5*, *1-6*, *2-5*, *2-6*, and *3-6*.

Hence $p(I,2)=8$ and $p(II,2)=5$. For I there are two possible ways of choosing three bonds in which no two of them are connected, *i.e.*, *1-4-6* and *2-4-6*. However, for II one can not choose such combination. We have then $p(I,3)=2$ and $p(II,3)=0$. All other $p(G,k)$ values for $k>3$ are zero and we obtain

$$Q_I(Y) = 1 + 6Y + 8Y^2 + 2Y^3, \qquad Z_I = 17$$
$$Q_{II}(Y) = 1 + 6Y + 5Y^2, \qquad Z_{II} = 12.$$

Relation with Characteristic Polynomial. The characteristic polynomials of I and II are obtained as follows by decomposing the secular determinants.

$$P_I(X) = X^7 - 6X^5 + 8X^3 - 2X$$
$$P_{II}(X) = X^6 - 6X^4 + 2X^3 + 5X^2.$$

Note that for I, i) the power to X decreases by two and ii) the absolute values of the coefficents of $P(X)$ are identical to the set of numbers $p(G,k)$ or the coefficients of the Z-counting polynomial $Q(Y)$. For any tree these two characteristics are observed without exception.[17] i) is proved by the pairing theorem[18]

8) F. Harary, "Graph Theory," Addison-Wesley Publ. Co., Reading, Mass. (1969).
9) R. G. Busacker and T. C. Saaty, "Finite Graphs and Networks: An Introduction with Applications," McGraw-Hill Book Co., New York, N. Y. (1965).
10) A complete bibliography of graph theory is given by J. Turner, "Proof Techniques in Graph Theory," ed. by F. Harary, Academic Press, New York, N. Y. (1969), p. 189.
11) N. S. Ham and K. Ruedenberg, *J. Chem. Phys.*, **29**, 1199 (1958).
12) Alternatively, one may define $P(X)$ as $\det|X\boldsymbol{E}-\boldsymbol{A}|$.
13) E. Heilbronner, *Helv. Chim. Acta*, **36**, 170 (1953).
14) The numbers of Kekulé structures for unsaturated hydrocarbons were discussed by Ham[15] and others. See references cited in Ref. 5.
15) N. S. Ham, *J. Chem. Phys.*, **29**, 1229 (1958).
16) In the expansion of $Q_G(Y)$, Y has no significance except for a base symbol to which one can attach exponents.
17) These relations are approved by term-to-term inspection of the expansion of $\det|X\boldsymbol{E}+\boldsymbol{A}|$ into $P(X)$.
18) C. A. Coulson and G. S. Rushbrooke, *Proc. Cambridge Phil. Soc.*, **36**, 193 (1940).

for the Hückel molecular orbitals of alternant hydrocarbons, since a tree is alternant. Although ii) appears to be obvious, it seems to have never been stated explicitly. This relation is worthy of being restated as a theorem.

Theorem 1: The characteristic polynomial of a tree T is given by

$$P_T(X) = \sum_{k=0}^{m} (-1)^k p(T, k) X^{N-2k} \quad (5)$$

where m is the largest number of bonds disconnected to each other in T.

On the other hand, for non-tree graphs as II the above-mentioned relationship no longer holds, but is contaminated with the terms representing the size and branching mode of the rings.

Normal Paraffins. Denote a normal paraffin with N carbon atoms (n-N-ane) by $\bar{N}$. By induction it can be shown that

$$p(\bar{N}, k) = {}_{N-k}C_k = (N-k)(N-k-1)\cdots(N-2k+1)/k! \quad (k \neq 0) \quad (6)$$

$$P_{\bar{N}}(X) = \sum_{k=0}^{m} (-1)^k {}_{N-k}C_k X^{N-2k} \quad (7)^{19}$$

The interger m can be expressed as $m=[N/2]$, where a pair of square brackets are, after Gauss, the greatest integer not exceeding the real number in them.

As an example, for n-heptane one obtains $p(\bar{7},0)=1$, $p(\bar{7},1)=(7-1)/1=6$, $p(\bar{7},2)=(7-2)(7-3)/2\cdot1=10$, $p(\bar{7},3)=(7-3)(7-4)(7-5)/3\cdot2\cdot1=4$, and $p(7,k)=0$ for $k>3$, and $Z_7=1+6+10+4=21$, and

$$P_{\bar{7}}(X) = X^7 - 6X^5 + 10X^3 - 4X.$$

From the sets of $p(\bar{N},k)$ the following progression $\{Z_{\bar{N}}\}$ can be obtained.

N:	1	2	3	4	5	6	7	8	⋯
$Z_{\bar{N}}$:	1	2	3	5	8	13	21	34	⋯

The series $\{Z_{\bar{N}}\}$ recurs as

$$Z_{\bar{N}} = Z_{\bar{N-1}} + Z_{\bar{N-2}} \quad (N \geq 3) \quad (8)$$

This is just the Fibonacci series[20] and is given by the Binét formula[21]

$$Z_{\bar{N}} = \left\{ \left(\frac{1+\sqrt{5}}{2}\right)^{N+1} - \left(\frac{1-\sqrt{5}}{2}\right)^{N+1} \right\} \Big/ \sqrt{5} \quad (9)$$

Relation (8) can be proved from the definition of the topological index and the well-known recursion formula for $P_{\bar{N}}(X)$:[13]

$$P_{\bar{N}}(X) = X \cdot P_{\bar{N-1}}(X) - P_{\bar{N-2}}(X) \quad (N \geq 3) \quad (10)$$

Branched Paraffins. For branched paraffins $P(X)$ obtained from Eq. (5) without tedious effort of decomposing the determinant $|XE+A|$. The results for the lower members of normal and isomeric paraffins are given in Table 1 in the increasing order of the topological

Table 1. $p(G,k)$ values and topological index Z for the graphs corresponding to all the possible isomers of the lower members of saturated hydrocarbons

a. $N=1\sim6$

N	Graph (G)	$p(G,k)$[a] $k=0$	1	2	3	Z_G	bp(°C)[b]
1	·	1	0	0	0	1	-161.7
2	—	1	1	0	0	2	-88.6
3	— —	1	2	0	0	3	-42.2
4		1	3	0	0	4	-11.7
	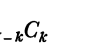	1	3	1	0	5	-0.5
5		1	4	0	0	5	9.5
		1	4	2	0	7	27.9
	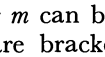	1	4	3	0	8	36.1
6		1	5	3	0	9	49.7
		1	5	4	0	10	57.9
		1	5	5	0	11	60.2
		1	5	5	1	12	63.5
	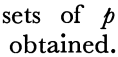	1	5	6	1	13	68.7

Table 1. b. $N=7$

Graph (G)	$p(G,k)$[a] $k=0$	1	2	3	Z_G	bp(°C)[b]
	1	6	6	0	13	80.9
	1	6	7	0	14	79.2
	1	6	8	0	15	80.5
	1	6	7	2	16	86.0
	1	6	8	2	17	89.7
	1	6	9	2	18	90.0
	1	6	9	3	19	91.9
	1	6	9	4	20	93.4
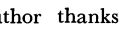	1	6	10	4	21	98.4

19) In other words we have

$$Q_{\bar{N}}(Y) = \sum_{k=0}^{m} {}_{N-k}C_k Y^k. \quad (7')$$

20) The author thanks Prof. E. Heilbronner, Basel, for his pointing out the Fibonacci series. The series $\{Z_{\bar{N}}\}$ rapidly converges to $\{(1+\sqrt{5})/2\}^{N+1}/\sqrt{5}$. For computer calculation one may use the expression with Gaussian brackets as

$$Z_{\bar{N}} = \left[\left(\frac{1+\sqrt{5}}{2}\right)^{N+1} \Big/ \sqrt{5} + 0.5 \right]. \quad (9')$$

21) N. N. Vorob'ev, "Fibonacci Numbers," Nauka Publ., Moscow (1964) (Japanese translation by T. Tsutsui, Tokyo Tosho Publ. Co., Tokyo (1966)).

TABLE 1. c. $N=8$

Graph (G)	$p(G,k)$[a] $k=0$	1	2	3	4	Z_G	bp(°C)[b]
	1	7	9	0	0	17	106.3
	1	7	11	0	0	19	99.3
	1	7	11	3	0	22	109.9
	1	7	11	4	0	23	114.8
	1	7	12	3	0	23	106.9
	1	7	12	4	0	24	113.5
	1	7	13	4	0	25	109.1
	1	7	12	5	0	25	112.0
	1	7	13	5	0	26	109.5
	1	7	13	6	0	27	115.6
	1	7	13	7	0	28	115.7
	1	7	12	7	1	28	118.3
	1	7	13	7	1	29	117.7
	1	7	14	7	0	29	117.7
	1	7	14	8	0	30	117.7
	1	7	14	8	1	31	119.0
	1	7	14	9	1	32	118.6
	1	7	15	10	1	34	125.7

a) The characteristic polynomial $P(X)$ and Z-counting polynomial $Q(Y)$ are respectively given by Eqs. (5) and (3).

b) American Petroleum Institute Research Project 44 at the National Bureau of Standards, "Selected Values of Physical and Thermodynamic Properties of Hydrocarbons Tables No. 1a, 2a, 3a, and 4a (1945).

index Z. Note the numbering character of Z. All the possible isomeric saturated hydrocarbons from methane to n-hexane are found to be "numbered" with Z except for neopentane which has the same Z value 5 as n-butane leaving the compound-6 blank. The Z value of 2,2,3-trimethylbutane, 13, is the same as that of n-hexane and the nine isomers of heptane are nicely "numbered" up to 21. For eighteen isomers of octane, numbering from 17 to 34 is a little disordered and redundancy increases very smoothly with N, since it is an outcome of a different way of partitioning a given interger Z into a set of $p(G,k)$'s.

Let us take a closer look at the $p(G,k)$ values. To all the isomers with the same number of carbon atoms the values of $p(G,0)$ and $p(G,1)$ are common by difinition. If one defines the decrement of the $p(G,k)$ value of an isomeric N-ane relative to the normal N-ane as

$$\delta p(N, k) = p(\bar{N}, k) - p(N, k), \tag{11}$$

we find additive contributions to the value of $\delta p(N,2)$ by the branching as

$$\delta p(N, 2) = (\text{Number of tertiary carbon atoms}) + 3(\text{Number of quarternary carbon atoms}). \tag{12}$$

Although higher members of $\delta p(N,k)$'s have similar additive relations, fairly complicated crowdness corrections are necessary, *e.g.*, terms which are functions of the number of adjacent pairs of tertiary and quarternary carbon atoms. Anyway a general trend of the lowering of the resultant Z value by the branching is thus evident.

Composition Principle for Z. In order to study the above problem quantitatively, the composition principle for enumerating the Z values of branched hydrocarbons is given as a theorem.

Theorem 2: The Z value of a given graph G is calculated as

Z_G = (Product of the Z values for the graphs G_1 and G_2 derived from G by cutting a bond b) + (Product of the Z values for all the graphs $G_{i1}, G_{i2}, \cdots$ $(i=1, 2)$ derived from G_1 and G_2 by cutting all the bonds incident to b in the *original* graph G).[22]

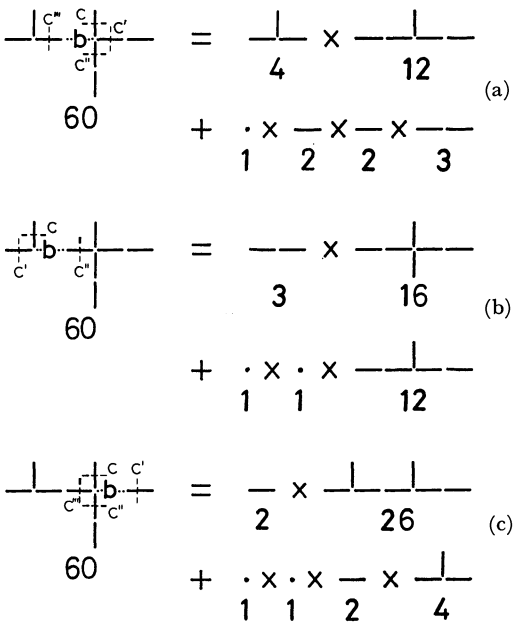

Fig. 2. Examples of the composition principle for the topological index Z. Bond b is cut first and then bonds c,c',.... Three different choices of b give the same Z value.

22) For ring compounds one can choose a bond whose deletion gives rise to one graph G_1 (=G-b) instead of generating two fragmental graphs. In this case read the first term in Theorem 2 as (The Z value of the graph G_1 derived from G by cutting a bond b).

See Fig. 2 for explanation. Graph G may be called 2,4-dimethyl-4-ethylhexane. Choose any one bond say bond b in Fig. 2a and cut it. The graph G is divided into isobutane and 3-methylpentane, whose Z values are, respectively, 4 and 12, giving the product 48. Then cut all the bonds c, c′, c″, and c‴ which *were* incident to bond b in the original graph G. The resultant graphs are one methane ($Z=1$), two ethanes ($Z=2\times2$) and one propane ($Z=3$), giving the product of Z's as 12. The Z value of the graph G is the sum of 48 and 12, namely 60. It should be confirmed that the Z value is uniquely obtained independent of the choice of bond b in the first step. This is actually the case as illustrated in Figs. 2b and 2c.

If one cuts the terminal bond of n-N-ane and applies Theorem 2, the recursion formula (8) is obtained, while if the jth bond is chosen the following equation is obtained.

$$Z_{\overline{N}} = Z_{\overline{j}} \cdot Z_{\overline{N-j}} + Z_{\overline{j-1}} \cdot Z_{\overline{N-j-1}} \qquad (13)^{23)}$$

A general proof of Theorem 2 is given in the Appendix. It is also shown that this composition principle can be applied to ring compounds (*vide infra*). If we neglect the second term of the right-hand side of Theorem 2, and if necessary apply Theorem 2 successively, we get the following theorem.

Theorem 3: If graph G is decomposed into a set of fragmental subgraphs G_1, G_2, ···by deleting a set of bonds b, c,···(G−b−c−···$=G_1+G_2+\cdots$, $G_1 \cap G_2=0$, ···), then

$$Z_G > Z_{G_1} Z_{G_2} \cdots.$$

Especially for a n-N-ane we get

$$\begin{aligned} Z_{\overline{N}} &> Z_{\overline{i}} \cdot Z_{\overline{N-i}} \\ Z_{\overline{N}} &> Z_{\overline{i}} \cdot Z_{\overline{j}} \cdot Z_{\overline{N-i-j}} \\ Z_{\overline{N}} &> Z_{\overline{i}} \cdot Z_{\overline{j}} \cdot Z_{\overline{k}} \cdot Z_{\overline{N-i-j-k}} \quad \text{and the like.} \end{aligned} \qquad (14)$$

The ralations are derived also from Eq. (13). By the aid of these composition principles let us study the regularities in the lowering of Z values by branching.

First consider a series of 2-methyl-($N-1$)-ane (Fig. 3a, $j=2$), in which a branch of a unit length is attached to the second atom counting from one end of a linear chain composed of ($N-1$) atoms. Application of Theorem 2 to this graph gives the general expression

$$Z_{2m-N} = Z_{\overline{N-1}} + Z_{\overline{N-3}} \quad (N \geq 3) \qquad (15)$$

where $2m$-N stands for the 2-methyl substituted isomer of N-ane. Generally for j-methyl substituted isomers we get

$$Z_{jm-N} = Z_{\overline{N-1}} + Z_{\overline{j-1}} \cdot Z_{\overline{N-j-1}} \quad (N-1 \geq j \geq 2) \qquad (16)^{24)}$$

Similarly for j,j-dimethyl-($N-2$)-ane ($N-2 \geq j \geq 2$,

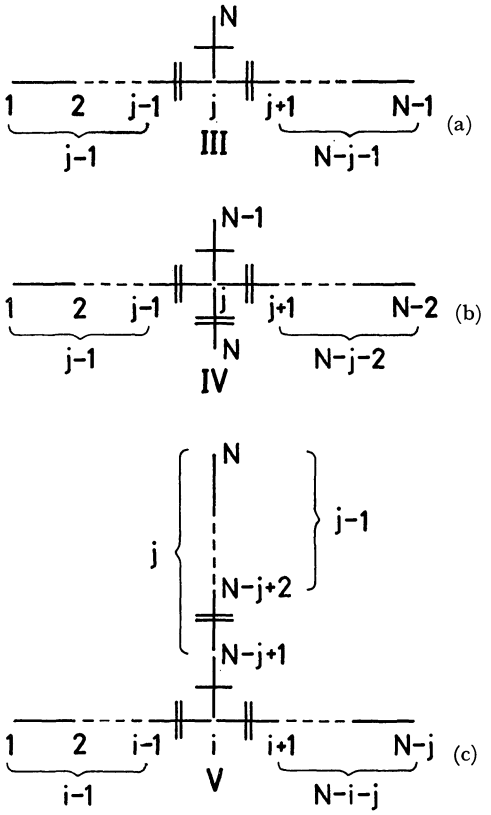

Fig. 3. Application of the composition principle to three different classes of branched hydrocarbons. A single line and two parallel lines dissecting bonds, represent the first and second cutting processes, respectively.

Table 2. Effect of branching on the $p(G,k)$ and Z values of decane isomers

Type[a]	j	Graph (G)	$p(G,k)$[b] $k=2$	3	4	5	Z_G
n-decane			28	35	15	1	89
III	2		27	30	9	0	76
	3		27	31	12	1	81
	4		27	31	11	0	79
	5		27	31	11	1	80
IV	2		25	22	3	0	60
	3		25	24	7	0	66
	4		25	24	5	0	64
V	1		27	31	11	0	79
	2		27	32	13	1	83
	3		27	32	12	0	81

a) See the corresponding structures in Fig. 3 with N=10 and $i=4$ (for V).
b) For all the graphs $p(G,0)=1$ and $p(G,1)=9$.

23) This is also proved by the known relation for $P(X)$,[13] *viz.*,
$$P_{\overline{N}}(X) = P_{\overline{j}}(X)P_{\overline{N-j}}(X) - P_{\overline{j-1}}(X)P_{\overline{N-j-1}}(X) \qquad (13')$$
or $$Q_{\overline{N}}(Y) = Q_{\overline{j}}(Y)Q_{\overline{N-j}}(Y) + Y \cdot Q_{\overline{j-1}}(Y)Q_{\overline{N-j-1}}(Y) \qquad (13'')$$

24) The corresponding expressions for the Z-counting and characteristic polynomials are as follows.
$$Q_{jm-N}(Y) = Q_{\overline{N-1}}(Y) + Y \cdot Q_{\overline{j-1}}(Y)Q_{\overline{N-j-1}}(Y) \qquad (16')$$
$$P_{jm-N}(X) = X \cdot P_{\overline{N-1}}(X) - P_{\overline{j-1}}(X)P_{\overline{N-j-1}}(X) \qquad (16'')$$
$$Q_{jjm-N}(Y) = Q_{\overline{N-2}}(Y) + 2Y \cdot Q_{\overline{j-1}}(Y)Q_{\overline{N-j-2}}(Y) \qquad (17')$$
$$P_{jjm-N}(X) = X \cdot P_{\overline{N-2}}(X) - 2 \cdot P_{\overline{j-1}}(X)P_{\overline{N-j-2}}(X) \qquad (17'')$$
$$Q_{ji-N}(Y) = Q_{\overline{i}}(Y)Q_{\overline{N-i}}(Y) + Y \cdot Q_{\overline{i-1}}(Y)Q_{\overline{j-1}}(Y)Q_{\overline{N-i-j}}(Y) \qquad (18')$$
$$P_{ji-N}(X) = X \cdot P_{\overline{i}}(X)P_{\overline{N-i}}(X) - P_{\overline{i-1}}(X)P_{\overline{j-1}}(X)P_{\overline{N-i-j}}(X) \qquad (18'')$$

denoted by *jjm-N*) series, we get (Fig. 3b)

$$Z_{jjm-N} = Z_{\overline{N-2}} + 2Z_{\overline{j-1}} \cdot Z_{\overline{N-j-2}} \quad (N-2 \geq j \geq 2) \quad (17)^{24)}$$

The result for the compound in which a chain of j atoms is attached to the ith position of n-$(N-j)$-ane is as follows.

$$Z_{ij-N} = Z_{\overline{j}} \cdot Z_{\overline{N-j}} + Z_{\overline{i-1}} \cdot Z_{\overline{j-1}} \cdot Z_{\overline{N-i-j}} \quad (N-j \geq i \geq 1) \quad (18)^{24)}$$

Examples of the calculated results are shown in Table 2 for decane isomers ($N=10$). Note the zig-zag variation of the Z values within a series of compounds and an interesting pattern of the $p(G,k)$ values. By successive applications of Eqs. (8), (13), and (14) to Eqs. (16)—(18), the following inequality is obtained.

$$Z_{\overline{N}} > Z_{jm-N}, Z_{jjm-N}, Z_{ji-N} \quad (19)$$

More generally this can be stated as a theorem.

Theorem 4: The value Z of the normal compound is the largest among the isomers with the same number of carbon atoms.

Table 3. Topological properties of cyclo-*N*-anes

N	$P(X)$	$Q(Y)$	Z
3	X^3-3X+2	$1+3Y$	4
4	X^4-4X^2	$1+4Y+2Y^2$	7
5	X^5-5X^3+5X+2	$1+5Y+5Y^2$	11
6	$X^6-6X^4+9X^2-4$	$1+6Y+9Y^2+2Y^3$	18
7	$X^7-7X^5+14X^3-7X+2$	$1+7Y+14Y^2+7Y^3$	29
8	$X^8-8X^6+20X^4-16X^2$	$1+8Y+20Y^2+16Y^3+2Y^4$	47

Cycloparaffins. For compounds with one or more rings, simple correlation between the $p(G,k)$'s and the coefficients of the characteristic polynomials is not always observed. $P(X)$, $Q(Y)$, and Z for the lower members of cyclo-*N*-ane (denoted by N^0) are given in Table 3. The coefficeints in $Q(Y)$ are systematically obtainable as

$$\begin{aligned} Q_{N^0} &= \sum_{k=0}^{m} ({}_{N-k}C_k \cdot N/(N-k))Y^k \\ &= 1 + NY + N(N-3)/2 \cdot Y^2 \\ &\quad + N(N-4)(N-5)/3! \cdot Y^3 \\ &\quad + N(N-5)(N-6)(N-7)/4! \cdot Y^4 + \cdots \end{aligned} \quad (20)$$

For ring compounds, however, no one-to-one correspondence between the coefficients of $P(X)$ and $Q(Y)$ exists.

For Z_{N^0} values the following two relations are found.

$$Z_{N^0} = Z_{\overline{N}} + Z_{\overline{N-2}} \quad (N \geq 3) \quad (21)$$

$$Z_{N^0} = Z_{N-1^0} + Z_{N-2^0} \quad (N \geq 5) \quad (22)$$

Note that Eq. (21) is a special case of Theorem 2 and the recursion formula (22) can be derived from Eq. (21). The series $\{Z_{N^0}\}$ form another family of the Fibonacci series, which can be expressed as

$$Z_{N^0} = \left(\frac{1+\sqrt{5}}{2}\right)^N + \left(\frac{1-\sqrt{5}}{2}\right)^N \quad (23)^{25)}$$

25) For computer calculation one can use the Gaussian expression.

$$Z_{N^0} = \left[\left(\frac{1+\sqrt{5}}{2}\right)^N + 0.5\right]. \quad (23')$$

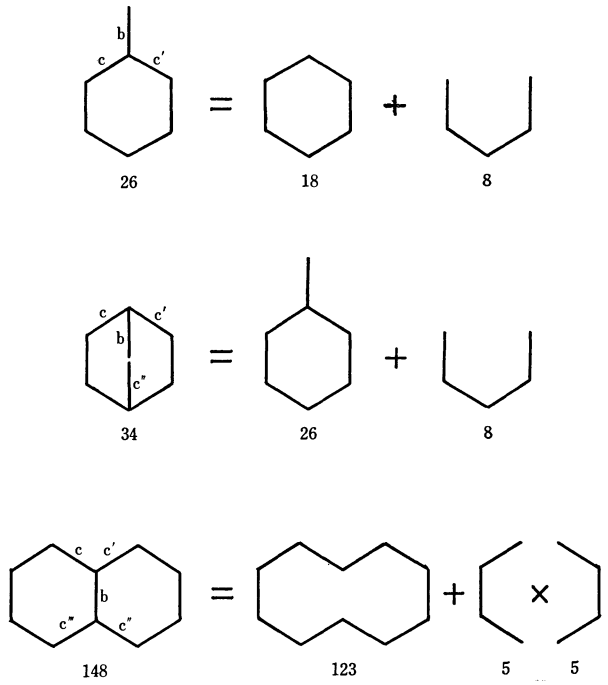

Fig. 4. Examples of application of the composition principle to ring compounds. The letters b, c,··· have the same meaning as in Fig. 2.

Table 4. Topological properties of the graphs corresponding to all the possible isomers of the lower members of monocyclic saturated hydrocarbons

N	Number[a)]	Z	n_i[b)] $i=4$	3	2	1	bp(°C)[c)]
3	1	4	0	0	3	0	−32.8
4	2	6	0	1	2	1	0.7
	3	7	0	0	4	0	12.5
5	4	8	1	0	2	2	20.6
	5	9	0	2	1	2	32.6
	6	10	0	1	3	1	35.9
	7	10	0	1	3	1	36.3
	8	11	0	0	5	0	49.3
6	9	12	1	1	1	3	52.4
	10	13	1	0	3	2	56
	11	14	1	0	3	2	56.8
	12	14	0	3	0	3	62.9
	13	14	0	2	2	2	58.3
	14	14	0	2	2	2	59
	15	15	0	2	2	2	62.8
	16	15	0	2	2	2	64
	17	16	0	1	4	1	69.2
	18	16	0	1	4	1	71.8
	19	17	0	1	4	1	70.6
	20	18	0	0	6	0	80.7

a) The numbers refer to the graphs in Chart 1.
b) The number of the carbon atoms with i neighboring carbon atoms. Namely, the numbers of quarternary, tertiary, secondary, and primary carbon atoms.
c) The data were taken from the reference in Table 1.

The composition principle (Theorem 2) can also be applied to complicated cycloparaffin derivatives as illustrated in Fig. 4. In Table 4 are given the topological indices of all the possible isomers of mono-

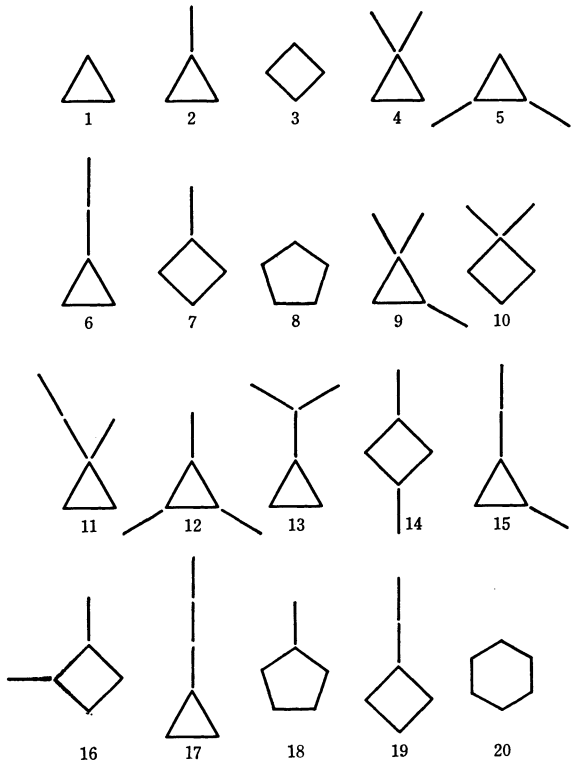

Chart 1

cyclic hydrocarbons with the carbon numbers from three to six.

The numbers of quarternary, tertiary, secondary, and primary carbon atoms for each graph are also shown. It is interesting to note that if one reads a set of the four integers for each graph as a four-digit integer it decreases as the Z value increases as long as the isomers of the same carbon number are compared. This suggests, though qualitatively, that the topological index for ring compounds also decreases with branching. This sort of calculation can be extended to higher members of the series and polycyclo compounds.[26]

Discussion

Comparison with Other Studies. Wiener proposed a path number w (Wiener number), which is the total number of bonds between all pairs of carbon atoms.[6] For example the w value of compound I in Fig. 1 is 46. This quantity turns out to be the half sum of the off-diagonal elements of a distance matrix **D** whose element d_{ij} is a number of bonds for the shortest path between atoms i and j.[27] Although it increases with carbon number and decreases with branching, no systematic relations such as recursion formula and composition principle, are found except for normal paraffins ($w=(n^3-n)/6$).

In ralation to the Wiener number, Altenburg proposed a polynomial $\sum_i n_i a_i$ for a carbon skeleton where n_i is the number of pairs of atoms whose distance is a_i or i C–C bonds.[28] The expression for compound I is $6a_1+7a_2+6a_3+2a_4$.[29]

Note that

$$w = \sum_i i \cdot n_i \tag{24}$$

For I we get $w=6\times1+7\times2+6\times3+2\times4=46$. As in the case of w, it is difficult to find useful relations for this polynomial expression.

Relation to Boiling Points. It was found that the boiling points of a number of saturated hydrocarbons are correlated fairly well with Z values. It is well known that for *non*-polar molecules the heavier the molecule the higher the boiling point becomes and the more the molecule is branched the lower the boiling point. The Z value has these characteristics. A number of empirical equations have been proposed to estimate the boiling points of a series of structural isomers by use of structural parameters and other physical quantities.[6,7,28,30,31] However, all of them require from three to six parameters and tedious calculations. In our case only one parameter is required. We can show that many empirical rules on the relation between boiling points of saturated hydrocarbons and structures of carbon skeleton are proved if we admit an empirical equation relating the Z value and boiling point. Of the physical and thermochemical quantities boiling point seems to have the best correlation with the topological index. It is also worth mentioning that of the quantities studied boiling point is the only quantity whose upper or lower limit for the isomeric compounds is the value of the normal compound.

It must be remembered that the topological index is defined for a topological graph which has nothing to do with distances, angles, steric strain, or hindrance. Therefore, without substantial modification, the value Z alone can not account for the difference in physical quantities of geometrical isomers such as *cis*- and *trans*-1,2-dimethylcyclopropane, nor for the overcrowded effect expected for compounds having vicinal quarternary carbon atoms. In this sense the proposed quantity Z is a kind of "index" for problems which are expected to be dependent on the topological nature of the skeleton of a system like a molecule.

Appendix

Proof of Theorem 2. Given three bonds a, b, and c and three graphs A, B, and C, a larger graph L is constructed as in Fig. 5a. It may be expressed as

$$\mathrm{L} = (\mathrm{A}+\mathrm{a}) + (\mathrm{B}+\mathrm{b}) + (\mathrm{C}+\mathrm{c}).$$

Similarly let us have

$$\mathrm{M} = (\mathrm{D}+\mathrm{d}) + (\mathrm{E}+\mathrm{e}) + (\mathrm{F}+\mathrm{f}).$$

26) K. Mizutani, K. Kawasaki, and H. Hosoya, *Natural Science Report of Ochanomizu Univ.*, Tokyo, **22**, 39 (1971).

27) Since Wiener did not treat ring compounds this is an extention of his definition.

28) K. Altenburg, *Kolloid-Z.*, **178**, 112 (1961).

29) Instead of a_i, a symbol a_i^2 is used in Ref. 28 meaning the root-mean-square value of the distance between all the atom pairs separated by i bonds. However, in the present paper we only consider topological distances.

30) K. Li, R. L. Arnett, M. B. Epstein, R. B. Ries, L. P. Bitler, J. M. Lynch, and F. D. Rossini, *J. Phys. Chem.*, **60**, 1400 (1956); J. B. Greenshields and F. D. Rossini, *ibid.*, **62**, 271 (1958).

31) K. Altenburg, *Brennstoff-Chem.*, **47**, 100, 331 (1966).

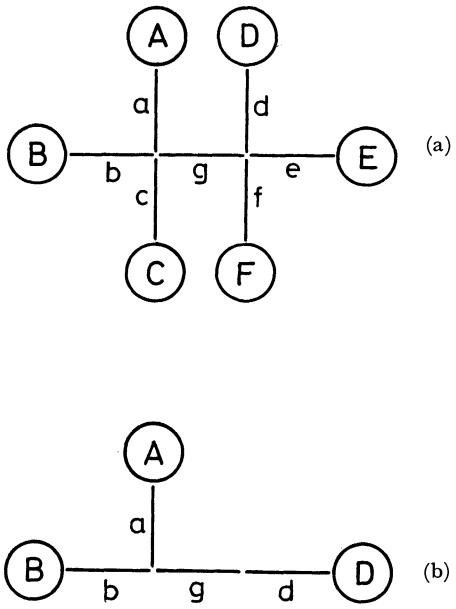

Fig. 5. Explanation for the proof of Theorem 2. The subgraphs A, B,···F are disconnected with each other.

By joining the graphs L and M with a bond g, a graph G can be constructed:

$$G = L + g + M$$

Now consider a number $p(G,k)$ for the graph G, the number of ways in which such k bonds are chosen from G that no two of them are connected. Each combination either includes or excludes the bond g. Since Z_G is the sum of $p(G,k)$'s, it is also divided into two parts, namely, g-including and g-excluding. It may be formulated as

$$Z_G = Z_G(+g) + Z_G(-g). \tag{A1}$$

Let us expand the following polynomial product,

$$\begin{aligned} Q_L(Y)Q_M(Y) &= \sum_{j=0}^{m_L}\sum_{k=0}^{m_M} p(L,j)p(M,k)Y^{j+k} \\ &= (0,0)+\{(0,1)+(1,0)\}Y \\ &\quad + \{(0,2)+(1,1)+(2,0)\}Y^2 + \cdots \\ &\quad + \{\cdots+(m_L, m-m_L)+\cdots \\ &\quad + (m-m_M, m_M)+\cdots\}Y^m \end{aligned} \tag{A2}$$

where the following abbreviated symbol is adopted:

$$(j,k) = p(L,j)p(M,k). \tag{A3}$$

The cofficient of Y^i in thr far right-hand side of Eq. (A2) is equal to the number of ways in which such i bonds are chosen from the graph G−g (or L+M) that no two of them are connceted. Hence

$$Z_G(-g) = Q_L(1)Q_M(1) = Z_L Z_M. \tag{A4}$$

On the other hand, the coefficients in the following product of the polynomials *multiplied* by Y are the contributions of the g-including combinations.

$$\begin{aligned} Q_{ABC}(Y)Q_{DEF}(Y)Y &= \sum_{j=0}^{m_{ABC}}\sum_{k=0}^{m_{DEF}} p(ABC,j)p(DEF,k)Y^{j+k+1} \\ &= (0,0)Y + \{(0,1)+(1,0)\}Y^2 \\ &\quad + \{(0,2)+(1,1)+(2,0)\}Y^3 \\ &\quad + \cdots + \{\cdots+(m_{ABC}, m-m_{ABC}-1)+\cdots\}Y^m, \end{aligned} \tag{A5}$$

where

$$\begin{aligned} ABC &= L - (a+b+c), \\ DEF &= M - (d+e+f), \end{aligned}$$

and

$$(j,k) = p(ABC,j)p(DEF,k). \tag{A6}$$

Thus we obtain

$$\begin{aligned} Z_G(+g) &= \{Q_{ABC}(Y)Q_{DEF}(Y)Y\}_{Y=1} \\ &= Q_{ABC}(1)Q_{DEF}(1). \end{aligned} \tag{A7}$$

Since the subgraphs A, B, and C in ABC are not connected to each other, the polynomial $Q_{ABC}(Y)$ is equal to the product of the constituent $Q(Y)$'s.

$$Q_{ABC}(Y) = Q_A(Y)Q_B(Y)Q_C(Y) \tag{A8}$$

Similarly we have

$$Q_{DEF}(Y) = Q_D(Y)Q_E(Y)Q_F(Y). \tag{A9}$$

Therefore we obtain

$$\begin{aligned} Z_G(+g) &= Q_A(1)Q_B(1)Q_C(1)Q_D(1)Q_E(1)Q_F(1) \\ &= Z_A Z_B Z_C Z_D Z_E Z_F \end{aligned} \tag{A10}$$

and

$$Z_G = Z_L Z_M + Z_A Z_B Z_C Z_D Z_E Z_F. \tag{A11}$$

Note that in the derivation no special restriction was imposed on the number of the subgraphs incident to the bond g. Thus for the system G′ as in Fig. 5b we obtain

$$Z_{G'} = Z_{L'}Z_{M'} + Z_A Z_B Z_D \tag{A12}$$

where

$$\begin{aligned} L' &= (A+a) + (B+b) \\ M' &= D + d \\ G' &= L' + g + M'. \end{aligned}$$

In this case, however, Eq. (A12) is already implied by Eq. (A11) if we consider graphs C, E, and F to be null and assume their Z values to be unity. This is consistent with the relation $Z_{\bar{0}}=1$ obtained from Eq. (9).

Extension of this theorem into ring compounds is approved if we note that a ring is formed by connecting any two of the subgraphs A, B,···F in the graph G.[22]

An Investigation of the Decomposition of the Intermediate Ions Produced by Electron Impact. I. $C_7H_7^+$ Ions from Several Substituted Toluenes

Susumu TAJIMA, Yoshio NIWA, Masahiko NAKAJIMA,* and Toshikazu TSUCHIYA

Government Chemical Industrial Research Institute, Tokyo, Honmachi, Shibuya-ku, Tokyo

**Mitsubishi Petrochemical Co., Ltd., Amicho, Inashiki-gun, Ibaragi*

(Received March 2, 1971)

The decomposition of the $C_7H_7^+$ ions produced by electron impact from toluene, *o*-, *m*-, *p*-xylene, *o*-, *m*-, *p*-chlorotoluene, *o*-, *m*-, *p*-methylbenzoic acid, *p*-nitrotoluene, and *p*-methylacetophenone has been investigated. By the determination of the relative abundances of normal and metastable ions, these $C_7H_7^+$ ions are shown to be identical in structure, except for the $C_7H_7^+$ ion from *p*-nitrotoluene. The relative rates of decomposition of these ions are compared in terms of the relative abundances of the ions $65^+/91^+$ ($=R$) and $46.5^*/91^+$ ($=R^*$) (where 46.5* is the abundance of the metastable ion for the $91^+ \rightarrow 65^+ + 26$ decomposition; 91^+ and 65^+ denote the abundance of ions at *m/e* 91 and 65 respectively). Further, using the internal energy, the relative rates are estimated by comparing their R and R^* values with the IRE curve (*i.e.*, R and R^* *versus* the bombarding electron energy) for *p*-methylacetophenone (PMAP), which was used as the standard compound.

By the quasi-equilibrium theory (QET),[1] the rate constant, k, for the decomposition of an ion produced by electron impact varies with the internal energy, E, according to Eq. (1):

$$k(E) = \nu(1-\varepsilon_0/E)^{n-1} \quad (1)$$

where ν is a frequency factor, where ε_0 is the activation energy for the decomposition, and where n is the number of effective harmonic oscillators of which the compound is assumed to be composed. Many authors have explained the influence of ν,[2] E,[3,4] and n[5] in the equation on the rate of the decomposition of the ions produced by electron impact. McLafferty *et al.*,[6] Cooks *et al.*,[7] and Jennings and Futrell[8] have studied the relative rates of the decomposition of a common intermediate ion, X^+, from different precursors. They investigated the following reaction:

$$M^+ \longrightarrow X^+ \xrightarrow{m^*} A^+ \quad (2)$$

where M^+ is a different precursor ion, where X^+ is a common intermediate ion, and where m* is the metastable ion for the $X^+ \rightarrow A^+$ decomposition. They investigated the relative rates of the decomposition of X^+ in terms of such ratios of abundances of ions as X^+/A^+, X^+/m^*, and/or m^*/A^+; then, using QET, they explained the relative rates qualitatively by the degrees of vibrational freedom in M^+ or the apparent heat of formation, which was assumed to be associated with the internal energy, E, for X^+.

In this paper, the rates of decomposition of $C_7H_7^+$ ions produced from certain toluene derivatives substituted by electron-withdrawing substituents are investigated. In the mass spectra of these toluene derivatives, the $C_7H_7^+$ ion is very prominent, and the ion decomposes successively through the $C_7H_7^+$ (*m/e* 91) $\xrightarrow{m^*(m/e\ 46.5)}$ $C_5H_5^+(m/e\ 65) + C_2H_2$ process, with the metastable peak at *m/e* 46.5. On the base of QET, we will examine the decomposition of the $C_7H_7^+$ ions as a function of the internal energy, E. The procedure is as follows: 1) the relative ion abundances ($65^+/91^+ = R$, $m^*/91^+ = R^*$) for the $C_7H_7^+$ ion produced by electron impact from *p*-methylacetophenone (PMAP) are measured; 2) the "ion abundance ratio efficiency curve" (IRE curve), which gives the relation of R and R^* to the electron accelerating voltage (V_e), is plotted; 3) the structure and the internal energy, E, of the $C_7H_7^+$ ions from substituted toluenes are estimated from these curves, *i.e.*, by comparing the R and R^* values obtained from each compound.

Experimental

The mass spectra were obtained by voltage scanning with a CEC 21-103C mass spectrometer. The V_e was measured with a potentiometer of Leeds & Northrup Co., Ltd. The electron-trap current was 10 μA. The temperatures of the ion source and the sample manifold were 250 and 125°C respectively.

With scanning, the voltage applied to the repeller electrodes varies in proportion to the ion-accelerating voltage. Because the bombarding electron energy is known to be affected by the repeller voltage,[9,10] it is desirable to measure the abundances of the *m/e* 91, *m/e* 65, and *m/e* 46.5 ions under the same ion-accelerating voltage, so that the effect of the repeller voltage on V_e can be nearly the same for all the ions studied. In this study, the optimum ion-accelerating voltage

1) H. M. Rosenstock and M. Krauss, "Mass Spectrometry of Organic Ions," ed. by F. W. McLafferty, Academic Press Inc., New York (1963), Chap. 1.

2) D. H. Williams and R. G. Cooks, *Chem. Commun.*, **1968**, 663.

3) W. A. Chupka and M. Kaminsky, *J. Chem. Phys.*, **35**, 1991 (1961).

4) M. Vestal, A. L. Wahrhaftig, and W. H. Johnston, *ibid.*, **37**, 1276 (1962).

5) W. A. Chupka, *ibid.*, **30**, 191 (1959).

6) F. W. McLafferty and W. T. Pike, *J. Amer. Chem. Soc.*, **89**, 5951 (1967); W. T. Pike and F. W. McLafferty, *ibid.*, **89**, 5954 (1967).

7) R. G. Cooks and D. H. Williams, *Chem. Commun.*, **1968**, 627; D. H. Williams, R. G. Cooks, and I. Howe, *J. Amer. Chem. Soc.*, **90**, 6759 (1968).

8) K. R. Jennings and J. H. Futrell, *J. Chem. Phys.*, **44**, 4315 (1966).

9) I. Omura, K. Higashi, and H. Baba, This Bulletin, **29**, 501 (1956).

10) L. Friedman, F. A. Long, and M. Wolfsberg, *J. Chem. Phys.*, **31**, 755 (1959).

for the most intense metastable peak was obtained first, and then all the ions were measured under this same accelerating voltage by adjusting the magnetic field.

The 180° mass spectrometer used does not have the field-free region in front of the magnetic analyser; however, it is known that the apparent mass (m*) of the metastable ion can be obtained by means of the same equation ($m^* = A^2/X$) as is used with other sector-type mass spectrometers.[11,12] The metastable ion-abundance measurements were based on the peak heights for the data.

All the samples studied were of a research grade, were obtained from Tokyo Kasei Co., Ltd., and were used without further purification upon checking the purity with the mass spectrometer. The ion abundances of the *m/e* 91, *m/e* 65, and *m/e* 46.5 of PMAP were measured at 1.0 eV intervals of the bombarding-electron energy. The abundances of these ions from the other compounds studied were measured at V_e= 20.0 eV. The probable error in the measurement of V_e is estimated to be less than ± 0.2 eV.

Results and Discussion

The "IRE curves" for PMAP are given in Fig. 1. The ordinates denote R and R^* ($\times 100$); hereafter, these curves will be termed the "R-standard curve" and the "R^*-standard curve" respectively. According to QET, the rate constant, k, for the decomposition of an ion is given by Eq. (1). An ion has its own distribution function of the internal energy, E, and an ion with a particular internal energy decomposes with a rate constant corresponding to the internal energy. For the decomposition of ions identical in structure, the rate constant, k, increases with an increase in the internal energy, E, of the ion, as can be seen from Eq. (1), since the frequency factor, ν, the activation energy, ε_0, and the number of harmonic oscillators, n, are the same for ions identical in structure.

For simplicity, it is assumed that all the X^+ ions are produced at the same time in the ionization chamber and that the A^+ ions do not decompose further. The latter assumption is reasonable when a low electron energy is used. Then, the intensities of the various ions in Eq. (2) are given by:[13]

$$I(X^+) = \int_0^{\varepsilon_0} P(E)\mathrm{d}E + \int_{\varepsilon_0}^{\infty} P(E)\exp\{-k(E)t_4\}\mathrm{d}E \quad (3)$$

$$I(A^+) = \int_{\varepsilon_0}^{\infty} P(E)[1-\exp\{-k(E)t_1\}]\mathrm{d}E \quad (4)$$

$$I(\mathrm{m}^*) = \int_{\varepsilon_0}^{\infty} P(E)[\exp\{-k(E)t_2\}-\exp\{-k(E)t_3\}]\mathrm{d}E \quad (5)$$

where $P(E)$ is the number of X^+ with the internal energy, E, (internal energy distribution function). In the above equation, we assumed further that the X^+ ions created at $t=0$ reach the exit slit in the ion source at time t_1, the field-free region at time t_2, the magnetic field at time t_3, and the end of the magnetic field at time t_4. R and R^* are given by:

$$R = I(A^+)/I(X^+) \quad (6)$$

$$R^* = I(\mathrm{m}^*)/I(X^+) \quad (7)$$

From Eqs. (1), (6), and (7), R and R^* can be treated as function of the internal energy, E.

Using, for simplicity, the expressions for $I(X^+)$, $I(A^+)$, and $I(m^*)$ given by Chupka[5] instead of Eqs. (3)—(5), the relations of R and R^* to the rate constant, k, calculated by a FACOM 270-30 computer are shown in Fig. 2. In this calculation, we used $t_1=t_2=2.5$ μsec, $t_3=3.3$ μsec, and $t_4=9.5$ μsec. These times were estimated from the dimensions of the mass spectrometer used in this study and from the conditions of measure-

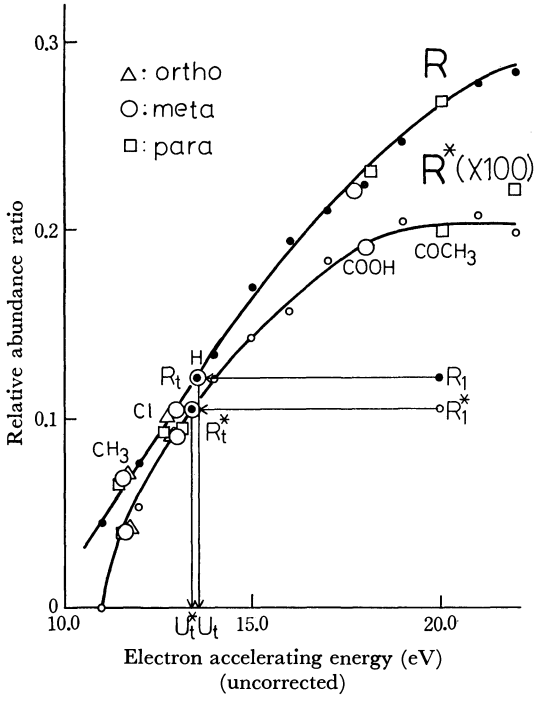

Fig. 1. IRE curves for *p*-methylacetophenone and relative abundance ratios of each compound at V_e=20.0 eV.

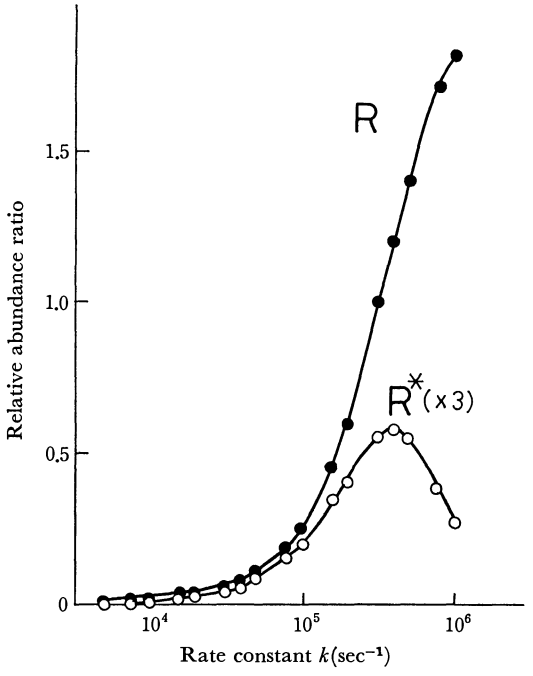

Fig. 2. Calculated relative abundance ratios $65^+/91^+$ and $m^*/91^+$ *vs.* rate constant k by using Chupka's equations.[5]

11) N. D. Coggeshall, *ibid.*, **37**, 2167 (1962).
12) A. S. Newton, *ibid.*, **44**, 4015 (1966).
13) I. Howe and D. H. Williams, *J. Amer. Chem. Soc.*, **91**, 7137 (1969).

ment. The internal energy of the parent ion, M^+, increases with an increase in V_e, so the internal energy, E, of X^+, produced by the decomposition of M^+, will also increase with an increase in V_e. Consequently, the greater the V_e value, the greater the average rate constant, $\bar{k}$. The behavior of R and R^* with V_e in Fig. 1 can be explained qualitatively when the curves in Fig. 1 are compared with those in Fig. 2, assuming k values lower than 5×10^5 sec^{-1}. The X^+ produced by the decomposition of M^+ from PMAP at a given V_e will have an internal energy corresponding to the V_e. The ion abundances related to the decomposition of X^+ give R and R^* values corresponding to the ordinates in Fig. 1. Thus, R and R^* can be taken as measures of the internal energy of X^+ in the sense mentioned above. The corresponding values on the abscissa show the internal energy of X^+ in this measure. When the average internal energy of X^+ is estimated in this measure, the R and R^* obtained for the X^+ must lie on a line perpendicular to the abscissa. In this study, we used the IRE curves for PMAP as a measure of the internal energy of the $C_7H_7^+$ ions from various compounds.

TABLE 1. RELATIVE ABUNDANCE RATIOS $65^+/91^+(R)$ AND $m^*/91^+(R^*)$ IN THE MASS SPECTRA OF EACH SUBSTITUTED TOLUENE AT $V_e=20.0$ eV

Substituent	R	$R^*(1\times00)$
H	0.122	0.105
o-CH_3	0.071	0.053
m-CH_3	0.068	0.048
p-CH_3	0.065	0.048
o-Cl	0.104	0.095
m-Cl	0.108	0.095
p-Cl	0.095	0.094
o-COOH	0.304	0.221
m-COOH	0.221	0.189
p-COOH	0.230	0.220
p-$COCH_3$	0.269	0.200
p-NO_2	0.460	0.491

In order to investigate the structure and the internal energy of the $C_7H_7^+$ ion from each substituted toluene, the R and R^* values for each compound in Table 1 have been compared with the standard curves. The data in Table 1 were measured at $V_e=20.0$ eV, because the abundance of the m/e 46.5 metastable ion peak was masked by other normal peaks (for example, by the m/e 47 peak) and the abundance of the metastable ion could not be determined exactly when V_e was higher.

The effective internal energy from every compound in Table 1 was estimated as follows. The R and R^* values were determined experimentally for each compound at $V_e=20.0$ eV. Two lines were drawn parallel to the abscissa from points on the ordinate corresponding to the R and R^* values. R_1 and R_1^* were determined where the lines intersected the R- and R^*-standard curves respectively. When perpendiculars passing through these points were drawn, the feet, U and U^*, were found to coincide within the limits of experimental error. The value of V_e corresponding to the feet was assumed to be a measure of the internal energy in the sense mentioned above. For example, in the case of toluene, the two feet are denoted as U_t and U_t^* in Fig. 1. U_t and U_t^* are found to be 13.6 and 13.4 eV respectively. This suggests that the structure and the internal energy distribution of the $C_7H_7^+$ ions from toluene at $V_e=20.0$ eV correspond to those of the $C_7H_7^+$ ions from PMAP at about $V_e=13.5$ eV. That is, if the structure and the internal energy distribution of the $C_7H_7^+$ ions from toluene at $V_e=20.0$ eV are identical with those of the $C_7H_7^+$ ions from PMAP at $V_e=13.5$ eV, ν, ε_0, and n in Eq. (1), and $P(E)$ in Eqs. (3)—(5) will be the same, respectively, for each of the $C_7H_7^+$ ions from the two compounds. Therefore, the relation between R_t and R_t^* in toluene is exactly the same as the relation between R and R^* in PMAP, and U_t will agree with U_t^*. If the $C_7H_7^+$ ions from toluene were not identical in structure and/or in internal energy with those from PMAP, ν, ε_0, and n in Eq. (1) would be different for these ions and $P(E)$ in Eqs. (3)—(5) would also be different. Therefore, the relation between R_t and R_t^* in toluene will differ from that in PMAP, and U_t will not generally coincide with U_t^*. The U and U^* values for other compounds in Table 1 coincide with each other within the limits of experimental error, as can be seen in Fig. 1. Therefore, the $C_7H_7^+$ ions produced from these compounds at $V_e=20.0$ eV have the same structure and internal energy distribution as the $C_7H_7^+$ ion produced from PMAP at each corresponding V_e. By using the isotope labelling technique, Meyerson *et al.*[14] have reported that the $C_7H_7^+$ ions from toluene, p-xylene, and p-chlorotoluene are "tropylium ions." Thus, the $C_7H_7^+$ ions produced from the compounds in Table 1 and PMAP in the V_e range of the present investigation can be inferred also to be tropylium ions which have various effective internal energies, as is indicated in Table 2.

TABLE 2. THE ELECTRON ACCELERATING VOLTAGE (U), AT WHICH THE INTERNAL ENERGY DISTRIBUTION OF THE $C_7H_7^+$ ION FROM PMAP IS EQUAL TO THAT OF THE $C_7H_7^+$ ION FROM EACH COMPOUND AT $V_e=20.0$ eV

Compound	U(eV)
Toluene	13.5
Xylene	11.8
Chlorotoluene	13.0
Methylbenzoic acid	~18.0

In the case of p-nitrotoluene, we could not plot the R and R^* in Fig. 1 because these values were too high in comparison with the values of the other compounds. When the IRE curves of p-nitrotoluene are regarded as the standard curves instead of that of PMAP, U does not agree with the U^* value in other compounds. These facts suggest that the structure of the $C_7H_7^+$ ion from p-nitrotoluene is not identical with that of the $C_7H_7^+$ ions from the other compounds studied here.

14) S. Meyerson and P. N. Rylander, *J. Chem. Phys.*, **27**, 901 (1957); H. M. Grubb and S. Meyerson, "Mass Spectrometry of Organic Ions," ed. by F. W. McLafferty, Academic Press Inc., New York (1963), Chap. 10.

Beynon *et al.*[15] have studied in detail the decomposition mechanism of nitrobenzene derivatives by electron impact. They have explained that the compounds decompose to fragment ions through some complicated intermediates. Recently, Westwood *et al.*[16] have reported the difference between the decomposition mechanism of *p*-nitrobenzene derivatives and that of *m*-isomers. One reason why the structure of the $C_7H_7^+$ ion from *p*-nitrotoluene is not identical with that of the $C_7H_7^+$ ions from other compounds may be these complicated decomposition processes.

From Table 1 it may be seen that while the *U* values for compounds with different substitutents differ from one another, the *U* values for the *o*-, *m*-, *p*-isomers containing the same set of substituents are nearly the same, except for methylbenzoic acid. This indicates that the internal energy distribution of the tropylium ion is affected by the species of substituents and not by the position of the substituents. The *U* values obtained for compounds in Table 1 are shown in Table 2. For example, in the case of toluene, the internal energy distribution of the $C_7H_7^+$ ion obtained at V_e=20.0 eV corresponds to that of the $C_7H_7^+$ ion from PMAP at about V_e=13.5 eV. One reason why the *U* values for *o*-, *m*-, *p*-methylbenzoic acid are distributed over a rather wide range compared to the case of the other compounds may be that the *R* and *R** values of methylbenzoic acid are in a relatively insensitive portion of the bombarding electron energy. In such a range, a slight error in measurement of ion abundances will result in a rather large spread in the corresponding electron energy. According to the results given in Table 2, the order of the internal energy of the $C_7H_7^+$ ions produced by the electron bombardment of the 20.0 eV energy is: methylacetophenone≃methylbenzoic acid> toluene>chlorotoluene>xylene. This order reveals an approximate tendency for the amount of the internal energy of the $C_7H_7^+$ ion from the compound to be larger as the electron-withdrawing property of the substituent is stronger.

Recently, Gross and McLafferty[17] have reported that substituted benzophenone, $Y\phi CO\phi$, with a weaker $Y\phi$-$CO\phi$ bond (ϕ and Y representing a benzol ring and a substituent respectively), yields the less energetic benzoyl ion when bombarded by electrons. On the contrary, Shapiro *et al.*[18] have indicated that substituted benzamide, described as $Y\phi NHCO\phi$, with a stronger $Y\phi NH$-$CO\phi$ bond, yields the less energetic benzoyl ion. Based on the information about the competing fragmentation of benzophenone, they have explained[18] the results of Gross and McLafferty.[17] It has been shown recently[19] that, when bombarded by electron, a disubstituted benzene, A-ϕ-Y (A being a common substituent for a series of compounds), gives a larger value of the summation of ions ($A\phi^+ + Y^+$) when the substituent Y has a stronger electron-withdrawing property. If this result is understood to indicate that the summation of the ions increases as the bond strength between the substituent, Y, and the aromatic moiety decreases, and if it is assumed that all of the molecular ions studied here have nearly the same internal energy distribution, the compound possessing a weak bond between the substituent, Y, and the aromatic moiety will leave a large internal energy to the $A\phi^+$ ion, *i.e.*, the tropylium ion in the present investigation. That is, as the energy spent to break the $(A\phi\text{-}Y)^+$ bond is smaller, a larger internal energy is left in the residual $A\phi^+$ ion. If this simple explanation is accepted, the relationship between the amount of internal energy of the $C_7H_7^+$ ions corresponding to $A\phi^+$ ions and the electron-withdrawing property of the substituents can be explained qualitatively in accordance with the conclusions of Shapiro *et al.*[18] Like the compounds studied by Shapiro *et al.*,[18] the molecular ions of the compounds in Table 1 do not undergo competing reactions to any appreciable extent, and they decompose almost exclusively into $C_7H_7^+$ ions at any ionizing energy.

In addition to the two parameters used in this study, the m^*/A^+ parameter is used by many authors to obtain the relative rate constant, *k*, for the decomposition. When the internal energy of X^+ for PMAP is smaller with a decrease in the V_e, this parameter is less reliable, since both the numerator, m*, and the denominator, A^+, are very small in this V_e region. Therefore, the m^*/A^+ parameter was not used in this study.

Conclusions

A procedure for investigating the identity of an ion produced by electron bombardment in mass spectrometry is proposed. "IRE curves" are first obtained for a standard compound, and the ion abundance ratio *R* and *R** from the comound to be studied is compared with the standard curve. By this procedure, the identity of the ion can be checked and the internal energy imparted to the ion can be estimated semiquantitatively.

The $C_7H_7^+$ ions from various toluene derivatives were investigated by this method. While the $C_7H_7^+$ ions from isomeric compounds possessing the same combination of substituents (Table 1) contain nearly equal amounts of internal energy, the $C_7H_7^+$ ions from compounds containing different sets of substituents contain quite different amounts of internal energy. The amount of internal energy contained by the ion from derivatives of toluene increases as the electron-withdrawing property of the substituent other than CH_3 increases.

The authors wish to thank Akio Hashizume and Nobuhide Wasada of this Institute for their valuable discussions.

15) J. H. Beynon, R. A. Saunders, and A. E. Williams, "The Mass Spectra of Organic Molecules," Elsevier Publishing Co., Amsterdam (1968), Chap. 5.

16) R. Westwood, D. H. Williams, and A. N. H. Yeo, *Org. Mass Spectrom.*, **3**, 1485 (1970).

17) M. L. Gross and F. W. McLafferty, *Chem. Commun.*, **1968**, 254.

18) R. H. Shapiro, J. Turk, and J. W. Serum, *Org. Mass Spectrom.*, **3**, 171 (1970).

19) S. Tajima, N. Wasada, and T. Tsuchiya, This Bulletin, in press.

Microwave Spectrum, Barrier Height to Internal Rotation of Methyl Group, and Dipole Moment of 3-Methylfuran

Teruhiko OGATA and Kunio KOZIMA

Laboratory of Molecular Spectroscopy, Tokyo Institute of Technology, Ookayama, Meguro-ku, Tokyo

(Received March 13, 1971)

The microwave spectrum of 3-methylfuran was measured in the frequency region from 8.2 to 30 GHz. By observing the *A-E* splittings due to the hindering rotation of the methyl group, the barrier height was determined to be 1.09 kcal/mol. The value is nearly the same as that of 2-methylfuran. The dipole moment was determined to be 1.03 D, which is a little larger than that of furan.

A few studies of the potential barrier to the internal rotation of the methyl group which is attached to a heterocyclic five-membered ring have recently been carried out by measuring the microwave spectra.[1-3] The barrier height to the rotation of the methyl group of 2-methylfuran was determined by Norris and Krisher[1] to be 1190 cal/mol.

Since the difference in the position of the methyl group which is attached to the furan ring may be expected to affect the value of the barrier height, it seemed that it would be interesting to determine the value for 3-methylfuran.

Experimental

The sample of 3-methylfuran was prepared and purified according to the method of Cornforth.[4] The infrared spectrum of 3-methylfuran thus obtained agreed with that previously reported.[5] The purity was checked with a vapor-phase chromatograph obtained by means of a 4-m column of dioctyl phthalate coated on celite. Runs at 120°C indicated only one component in the sample.

The microwave spectrum was investigated in the frequency region from 8.2 to 30 GHz by using a conventional 100-kHz Stark modulation spectrometer.[6] The measurements were made at about −20°C by using a 6-m absorption cell.

Results and Discussion

Microwave spectrum. In order to assign the absorption lines, the preliminary rotational constants were calculated by using the r_s-structure of furan obtained by Bak *et al.*[7] and the usual values of the bond lengths and the bond angles for the methyl group. By assuming a pseudo-rigid rotor approximation, the transition frequencies were calculated from the preliminary rotational constants. The lines of the *a*- and *b*-type transitions could be found quite close to their predicted frequencies and were assigned by their Stark patterns. The intensities of the *b*-type lines are weaker than those of the *a*-type lines. By considering the Stark patterns and the intensities, several pairs of the lines, which are separated by about few MHz, could be identified as doublets due to the transitions of the *A*- and the *E*-levels caused by the hindering rotation of the methyl group. The observed frequencies of the *a*- and *b*-type transitions of the *A*-levels for the vibrationally-ground state are shown in Table 1. The pseudo-rigid rotational constants for the *A*-levels were determined so as to get the best fit between the observed and the calculated frequencies by the use of the least-squares method. The constants thus obtained are shown in Table 2. By

Table 1. Observed and calculated frequencies of *A*-levels (MHz)[a]

Transition	ν_{obs}	$\nu_{obs}-\nu_{calc}$
a-type		
$1_{01}\rightarrow 2_{02}$	11593.80	−0.10
$1_{11}\rightarrow 2_{12}$	10804.93	0.06
$1_{10}\rightarrow 2_{11}$	12580.18	0.13
$2_{02}\rightarrow 3_{03}$	17152.28	0.03
$2_{12}\rightarrow 3_{13}$	16149.15	0.36
$2_{11}\rightarrow 3_{12}$	18804.80	0.13
$2_{21}\rightarrow 3_{22}$	17538.95	0.26
$2_{20}\rightarrow 3_{21}$	17925.17	0.03
$3_{03}\rightarrow 4_{04}$	22464.63	−0.08
$3_{22}\rightarrow 4_{23}$	23307.69	−0.34
$3_{31}\rightarrow 4_{32}$	23563.03	−0.01
$3_{30}\rightarrow 4_{31}$	23603.85	−0.21
b-type		
$0_{00}\rightarrow 1_{11}$	11372.40	−0.08
$1_{01}\rightarrow 2_{12}$	16331.29	0.17
$2_{12}\rightarrow 3_{03}$	12415.00	−0.03
$3_{12}\rightarrow 3_{21}$	15797.84	0.06
$3_{03}\rightarrow 3_{12}$	9052.39	−0.01
$4_{04}\rightarrow 4_{13}$	11528.80	0.13
$4_{13}\rightarrow 4_{22}$	15084.60	−0.06
$4_{14}\rightarrow 4_{23}$	22507.75	−0.07

a) Experimental uncertainty in the frequency measurements is ±0.1 MHz.

Table 2. Rotational constants and moments of inertia[a] of *A*-levels

A_A	8893.16±0.15 MHz
B_A	3366.91±0.05
C	2479.32±0.05
I_a^A	56.8276 amu·Å²
I_b^A	150.101
I_c	203.837

a) Conversion factor 5.05377×10^5 amu·Å²·MHz.

1) W. G. Norris and L. C. Krisher, *J. Chem. Phys.*, **51**, 403 (1969).
2) U. Andresen and H. Dreizler, *Z. Naturforsch.*, **25a**, 570 (1970).
3) E. Saegebarth, *J. Chem. Phys.*, **52**, 1476 (1970).
4) J. W. Cornforth, *J. Chem. Soc.*, **1958**, 1310.
5) M. Fetion, J. Gury, and M. P. Pascal, *Compt. rend.*, **247**, 1182 (1958).
6) T. Ogata and K. Kozima, This Bulletin, **42**, 1263 (1969).
7) B. Bak, D. Christensen, W. B. Dixon, L. Hansen-Nygaard, J. R. Andersen, and M. Schottländer, *J. Mol. Spectrosc.*, **9**, 124 (1962).

using these constants, the transition frequencies were calculated. The differences between the observed and calculated frequencies are listed in Table 1. The agreement is such that centrifugal distortion can be said not to be an important effect in the range studied.

Table 3. Molecular structure of 3-methylfuran

Assumed structural parameters	
$r(O-C_2)=1.362$ Å	$\angle C_5-O-C_2=106°33'$
$r(C_2-C_3)=1.361$ Å	$\angle O-C_2=C_3=110°41'$
$r(C_3-C_4)=1.431$ Å	$\angle C_2=C_3-C_4=106°03'$
$r(C-H)_{ring}=1.075$ Å	$\angle O-C_2-H=115°55'$
$r(C-H)_{methyl}=1.090$ Å	$\angle H-C-H=109°28'$
Fitted structural parameters	
$r(C_3-CH_3)=1.520$ Å	
$\angle C_4-C_3-(CH_3)=128°57'$	
Calculated rotational constants	
$A=8890.92$ MHz	
$B=3366.03$ MHz	
$C=2479.90$ MHz	

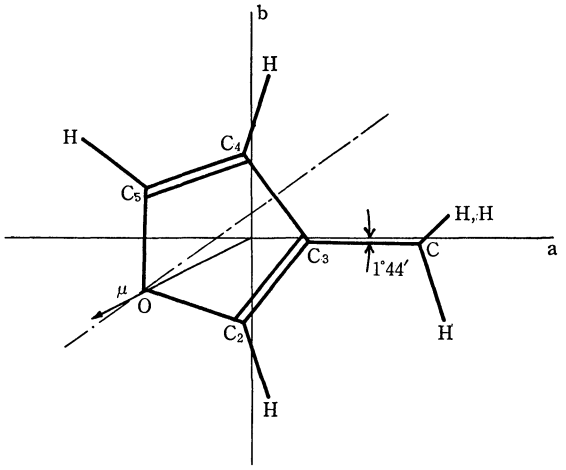

Fig. 1. Molecular structure and dipole moment of 3-methylfuran.

Molecular Structure and Internal Rotation. In order to determine the molecular structure, some of the molecular parameters were assumed by using the r_s-structure described above with the additional assumptions that all the C-H bond lengths and all the valency angles of the methyl group were 1.090 Å and 109°28′ respectively. These assumed values are listed in Table 3, in which the number attached to the symbol of each atom is shown in Fig. 1. By using these parameters, the angle of $\angle C_4C_3(CH_3)$ and the bond length of C_3–CH_3 were determined so as to get a good fit between the calculated rotational constants and the observed constants of A_A, B_A, and C. The results are shown in Table 3. Although it should be taken into account that the observed values of A_A and B_A are affected by the contribution of the hindering rotation of the methyl group, it is certain that the differences between these rotational constants and the unperturbed values of A and B are small enough to affect the molecular parameters determined above. From Table 3 it can be seen that the change in the structure of the furan ring caused by the substitution of the methyl group in the 3-position is negligible.

The potential energy function of the hindering rotation of the methyl group for this molecule may be expressed as usual by the following equation:

$$V(\alpha) = \frac{V_3}{2}(1-\cos 3\alpha) + \frac{V_6}{2}(1-\cos 6\alpha) + \cdots$$

where α is the relative angle of the internal rotation and where V_3 and V_6 are the potential constants. In this paper only the V_3 term is considered, for the V_6 term would introduce only a minor correction in the value of V_3.

The Hamiltonian can be written in the following manner:

$$H_A = A_A P_z^2 + B_A P_y^2 + C P_x^2$$

and

$$H_E = A_E P_z^2 + B_E P_y^2 + C P_x^2 + F W_{0E}^{(1)} \mathscr{P} + F W_{0E}^{(3)} \mathscr{P}^3$$

where

$$F = \hbar^2/2rI_a, \qquad r = 1 - \sum_{g=a,b} \lambda_g^2 I_a/I_g$$
$$\alpha = \lambda_a I_a/I_a, \qquad \beta = \lambda_b I_a/I_b$$
$$\mathscr{P} = \alpha P_z + \beta P_y$$
$$A_\sigma = A + F\alpha^2 W_{0\sigma}^{(2)}, \quad B_\sigma = B + F\beta^2 W_{0\sigma}^{(2)} \quad (\sigma = A \text{ or } E)$$

The notations have the same meanings as in Hershbach's paper.[8] The table of Hayashi and Pierce[9] was the source for the values of the perturbation coefficients, $W_{v\sigma}^{(n)}$. From the assigned transitions of the A- and E-levels, a rough estimate of the value of s, a parameter of the Mathieu equation, could be made. By using this value of s and the internal-rotation parameters shown in Table 4, the transition frequencies of the E-levels were calculated for the transitions which have large A-E splittings; the lines of the E-levels were found near the calculated frequencies and consequently assigned. Then, the accurate value of s was determined so as to give the best fit to the observed A-E splittings by means of the least-squares method, using a HITAC-5020 computer of the Computer Center of Tokyo University. The transition frequencies, ν_E, of the E-levels thus assigned and the A-E splittings, $(\nu_A-\nu_E)_{obs}$, are listed in Table 5, together with the calculated values of $(\nu_A-\nu_E)_{calc}$ which were obtained by using the cor-

Table 4. Barrier height to internal rotation of methyl group

Internal-rotation parameters	
$\alpha=0.056118$	$\beta=0.000134$
$F=1.678\times10^5$ MHz	$I_a=3.19$ amu·Å^2 [a]
Results	
$s=30.22\pm0.08$	
$A_A-A=2.33$ MHz	$B_A-B=0.00$ MHz
$V_3=1088\pm3$ cal/mol	

a) By using this assumed value the uncertainty of V_3 was estimated.

8) D. R. Hershbach, *J. Chem. Phys.*, **31**, 91 (1959).

9) See, J. E. Wollrab, "Rotational Spectra and Molecular Structure," Appendix 12, Academic Press, New York and London (1967). The authors are grateful to Dr. M. Hayashi for making a copy of the table.

TABLE 5. OBSERVED FREQUENCIES[a] OF E-LEVELS AND A-E SPLITTINGS (MHz)

Transition	ν_{obs}	$(\nu_A-\nu_E)_{obs}$	$(\nu_A-\nu_E)_{calc}$	Deviation
a-type				
$1_{01}\rightarrow 2_{02}$	11593.80	···	0.06	
$1_{11}\rightarrow 2_{12}$	10805.94	−1.01	−0.88	−0.13 (−0.14)
$1_{10}\rightarrow 2_{11}$	12579.35	0.83	0.88	−0.05 (−0.04)
$2_{02}\rightarrow 3_{03}$	17152.28	···	0.22	
$2_{12}\rightarrow 3_{13}$	16149.15	···	−0.18	
$2_{11}\rightarrow 3_{12}$	18804.80	···	0.27	
$2_{21}\rightarrow 3_{22}$	17564.48	−25.53	−25.48	−0.05 (−0.03)
$2_{20}\rightarrow 3_{21}$	17900.20	24.97	25.26	−0.29 (−0.31)
$3_{03}\rightarrow 4_{04}$	22464.07	0.56	0.47	0.09 (0.09)
$3_{22}\rightarrow 4_{23}$	23314.12	−6.43	−6.04	−0.39 (−0.39)
$3_{31}\rightarrow 4_{32}$	23581.14	−18.11	−18.15	0.04 (0.08)
$3_{30}\rightarrow 4_{31}$	23586.15	17.70	17.91	−0.21 (−0.25)
b-type				
$0_{00}\rightarrow 1_{11}$	11367.74	4.66	4.82	−0.16 (−0.14)
$1_{01}\rightarrow 2_{12}$	16327.27	4.02	3.94	0.08 (0.12)
$2_{12}\rightarrow 3_{03}$	12418.80	−3.80	−3.66	−0.14 (−0.17)
$3_{12}\rightarrow 3_{21}$	15796.63	1.21	1.17	0.04 (0.21)
$3_{03}\rightarrow 3_{12}$	9049.31	3.08	3.04	0.04 (0.07)
$4_{04}\rightarrow 4_{13}$	11525.90	2.90	2.79	0.11 (0.13)
$4_{13}\rightarrow 4_{22}$	15077.87	6.73	6.60	0.13 (0.20)
$4_{14}\rightarrow 4_{23}$	22494.02	13.73	13.37	0.36 (0.43)

a) Experimental uncertainty in the frequency measurements is ±0.1 MHz.

rected value of s. For the transitions in which the A-E splitting is less than 0.3 MHz, the splittings could not be measured; such transitions are shown by the dotted lines in the third column of Table 5. By using the Hamiltonian H_E mentioned above, the calculations were made by taking into account the terms of $FW_{oE}^{(1)}\mathscr{P}$ and $FW_{oE}^{(3)}\mathscr{P}^3$. The values shown in parentheses in the last column of Table 5 were tentatively calculated by neglecting the $FW_{oE}^{(3)}\mathscr{P}^3$ term. It can be seen that this neglect does not affect the result beyond the limits of experimental error. The determined value of s and the differences in A_A-A and B_A-B are shown in Table 4.

The value of V_3 calculated from the value of s is 1088±3 cal/mol. The uncertainty in the barrier arises primarily from the uncertainty in the assumed value of I_a. This assumed value, however, may be fairly reasonable, because the pseudo-inertial defect, $\Delta'=I_a-(I_a+I_b-I_c)$, is calculated to be 0.084 amu·Å^2, not very different from the value of 0.0458 amu·Å^2 [7] of the inertial defect of furan, where the unperturbed moments of inertia of 3-methylfuran, I_a, I_b, and I_c, are 56.8423 amu·Å^2, 150.101 amu·Å^2, and 203.837 amu·Å^2 respectively.

The barrier height of 3-methylfuran is not very different from that of 2-methylfuran, which is 1190 cal/mol.[1]

Dipole Moment. The dipole moment of 3-methylfuran for the ground vibrational state was determined from the second-order Stark effects of the $1_{01}\rightarrow 2_{02}$, $2_{02}\rightarrow 3_{03}$, $3_{03}\rightarrow 3_{12}$, and $4_{04}\rightarrow 4_{13}$ transitions of the A-level. The dipole moment and the observed and calculated Stark coefficients are given in Table 6.

TABLE 6. STARK EFFECT AND DIPOLE MOMENT OF 3-METHYLFURAN[a]

Transition		Stark coefficient (MHz(kV/cm)$^{-2}$) Observed	Calculated
$1_{01}\rightarrow 2_{02}$	$M=0$	−4.50±0.15	−4.47
	$M=1$	6.64±0.15	6.74
$2_{02}\rightarrow 3_{03}$	$M=0$	−1.12±0.12	−1.07
	$M=2$	3.47±0.13	3.50
$3_{03}\rightarrow 3_{12}$	$M=3$	5.94±0.13	5.85
$4_{04}\rightarrow 4_{13}$	$M=4$	2.92±0.10	2.87
	$\mu_a=0.91\pm0.01$ D		
	$\mu_b=0.48\pm0.03$ D		
	$\mu=1.03\pm0.02$ D		

a) The absorption cell was calibrated by using the $J=1\rightarrow 2$ transition of OCS, taking the dipole moment of OCS as 0.7152 D.[10]

The difference of 0.97 D between the dipole moment of tetrahydrofuran (1.63 D)[11] and that of furan (0.661 D)[12] is mainly due to the π-moment, μ_{mig}, caused by the migration of the π-electron of the oxygen atom in the furan ring. The μ_{mig} was calculated by Nagakura and Hosoya[13] to be 0.61 D and by Pujol and Julg[14] to be 0.89 D, pointing from a positive oxygen atom "up" the C(3)–C(4) bond. Therefore, it is certain that the direction of the total moment of furan is opposite to that of the μ_{mig}. Furthermore, it is known[15] that the moment, μ_b, along the b principal axis of the *trans* isomer of furfural is markedly smaller than that of the *cis* isomer. This fact is evidence in favor of this view. Based on the rule of vector addition for dipole moments, a relation among the dipole moment, μ, of 3-methylfuran, the μ_f value of the parent molecule, and the difference, μ_d, between the group moment of CH_3–C(sp^2) and the bond moment of H–C(sp^2) can be easily written as follow:

$$\frac{\sin(\theta+\varphi)}{\mu}=\frac{\sin\theta}{\mu_f}=\frac{\sin\varphi}{\mu_d}$$

where θ is the angle between μ and the C–CH_3 axis and φ, the angle between μ and the C_2 symmetry axis of the ring.

There are four possibilities for the direction of the experimentally-determined value of μ. However, by taking into account the fact that the value of μ_d is usually near 0.3 D,[16] only the direction shown in Fig. 1 is found to be possible. For this case, the θ and φ angles are 29±2° and 9±2° respectively. From the above relation we can calculate $\mu_f=0.80\pm0.06$ D and $\mu_d=0.27\pm0.04$ D, which points the negative end towards the C-atom of the ring. The values of μ_f and μ_d are resonable.

10) J. S. Muenter, *J. Chem. Phys.*, **48**, 4544 (1968).
11) W. L. G. Gent, *J. Chem. Soc.*, **1957**, 58.
12) M. H. Sirvetz, *J. Chem. Phys.*, **19**, 1609 (1951).
13) S. Nagakura and T. Hosoya, This Bulletin, **25**, 179 (1952).
14) L. Pujol and A. Julg, *Theoret. Chim. Acta*, **2**, 125 (1964).
15) F. Mönnig, H. Dreizler, and H. D. Rudolph, *Z. Naturforsch.*, **20a** 1323 (1965).
16) A. J. Petro, *J. Amer. Chem. Soc.*, **80**, 4230 (1958).

CNDO Calculations of Electronic Structures and Spectra of Nonalternant Conjugated Hydrocarbons

Akio TAJIRI,* Naoto OHMICHI, and Takeshi NAKAJIMA
Department of Chemistry, Tohoku University, Katahira, Sendai
(Received March 16, 1971)

The energetically most favorable geometrical structures with respect to C–C bond-length variation of fundamental nonalternant conjugated hydrocarbons have been examined using CNDO/2 approximation with its original parameterization. It was found that all the molecules examined should exhibit a marked bond alternation, accompanied with a molecular-symmetry reduction in the case of pentalene and heptalene. The predicted molecular dipole moments are in good agreement with the available experimental values. The electronic spectra have been calculated using a modified version of the CNDO/2 method proposed by Del Bene and Jaffe, with a new parameterization. The results are found to be in good agreement with experiment.

Bond distortions in the ground states of certain nonalternant conjugated hydrocarbons have drawn considerable theoretical attention in late years. It was noticed[1–3] that heptalene (IX, Fig. 1) shows no energy minimum for the D_{2h} symmetry suggested by the superposition of the two Kekule-type resonance structures, but has a lower energy if it takes an unsymmetrically-distorted nuclear arrangement that corresponds to either of the resonance structures and exhibits a strong bond alternation of a C_{2h} type in its periphery. The experimental information[4] agrees with this in indicating that π-electrons in this molecule are strongly localized in "double" bonds, rather than uniformly delocalized over the entire molecule.

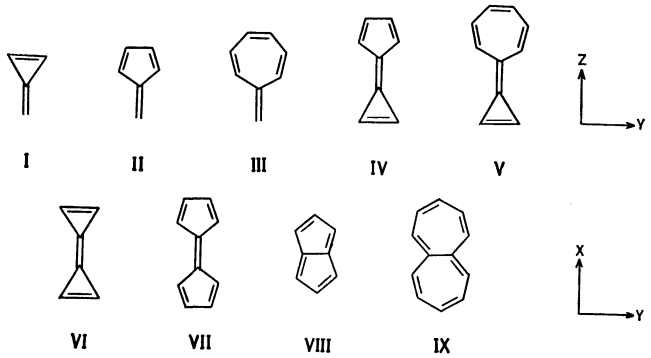

Fig. 1. Carbon skeletons and choice of axes for nonalternant hydrocarbons.

Theoretical justifications for such anomalous phenomena have been attempted by several authors.[1–3,5,6] Making allowance for the effects of σ-bond compression, they have succeeded in predicting that an unsymmetrical configuration resembling either of the two Kekule-type structures is actually energetically favored as compared with the fully symmetrical one. Binsch *et al.*[7–11] and Nakajima *et al.*[12,13] have recently developed a general theory of double-bond fixation in conjugated molecules and shown that bond alternations in certain nonalternant hydrocarbons are obtained theoretically as the energetically most favorable distortion rather than a presumed type of bond distortion.

In all the treatments so far made of the bond distortions in nonalternant hydrocarbons, however, complete σ-π separation has been assumed. That is, the total energy of a conjugated molecule is assumed to be the sum of the π-electron energy and the σ-core energy which may be regarded as the sum of the independent contributions from the C–C σ-bonds. The individual contributions of the σ-bonds have been approximated by a quadratic function of the bond-distance variation. The approximation used in computing the σ-core energy is not consistent with the molecular-orbital approximation used in calculating the π-electron energy.

It is the purpose of this paper to examine the ground-state geometries and electronic properties and the electronic spectra of certain fundamental nonalternant hydrocarbons by means of an all valence-electron molecular-orbital method, in which π-electrons and σ-electrons are treated with the same approximation.

Method of Calculation

The method used for predicting the energetically most favorable geometrical structures with respect to C–C bond-length variation is the semiempirical self-consistent all valence-electron molecular-orbital theory in the framework of the CNDO/2 approximation pro-

* Present address: Chemical Research Institute of Non-Aqueous Solutions. Tohoku University, Katahira, Sendai.

1) P. C. den Boer-Veenendaal, J. A. Vliegenthart, and D. H. W. den Boer, *Tetrahedron*, **18**, 1325 (1962).
2) L. C. Snyder, *J. Phys. Chem.*, **66**, 2299 (1962).
3) T. Nakajima and S. Katagiri, *Mol. Phys.*, **7**, 149 (1963).
4) H. J. Dauben, Jr., and D. J. Bertelli, *J. Amer. Chem. Soc.*, **83**, 4659 (1961).
5) P. C. den Boer-Veenendaal and D. H. W. den Boer, *Mol. Phys.*, **4**, 33 (1961).
6) T. Nakajima, T. Saijo, and H. Yamaguchi, *Tetrahedron*, **20**, 2119 (1964).
7) G. Binsch, E. Heilbronner, and J. N. Murrell, *Mol. Phys.*, **4**, 305 (1966).
8) G. Binsch and E. Heilbronner, "Structural Chemistry and Molecular Biology," ed. by A. Rich and N. Davidson, Freeman, San Francisco (1968), p. 815.
9) G. Binsch and E. Heilbronner, *Tetrahedron*, **24**, 1215 (1968).
10) G. Binsch, I. Tamir, and R. O. Hill, *J. Amer. Chem. Soc.*, **69**, 2446 (1969).
11) G. Binsch and I. Tamir, *ibid.*, **69**, 2350 (1969).
12) T. Nakajima and A. Toyota, *Chem. Phys. Lett.*, **3**, 272 (1969).
13) T. Nakajima, A. Toyota, and H. Yamaguchi, "Aromaticity, Pseudoaromaticity, Antiaromaticity. The 3rd Jerusalem Symposium," The Israel Academy of Sciences and Humanities, Jerusalem (1970), in press.

posed by Pople and his coworkers.[14-16]

Although it is known[16,17] that the CNDO/2 approximation successfully predicts geometrical structures, *viz.*, equilibrium bond angles and bond lengths of a variety of molecules, it is inadequate for the calculation of the energy quantities such as dissociation energy and excitation energy. For small molecules, the bonding energies calculated by use of the Pople-Segal bonding parameters are higher than the experimental by factors 3—8.[18]

A modification along this line of the Pople-Segal CNDO/2 theory has recently been made by Sichel and Whitehead.[18,19] Using the CNDO approximation, they have developed a semiempirical SCF MO method with atomic parameters derived from atomic valence-state energies, interatomic electron-repulsion integrals calculated by use of the semiempirical formulas and bonding parameters calibrated by use of the bonding energies of binary hydrides. Bonding energies calculated using these parameters for various small molecules were found to be in much better agreement with experiment than those calculated from the Pople-Segal CNDO/2 theory.

When used for the prediction of the energetically most favorable geometrical structures of conjugated molecules, however, the parameterization proposed by Sichel and Whitehead turns out to be less satisfactory and, in certain cases, completely inadequate. As an example, the equilibrium C–C bond length for ethylene predicted with their parameterization is smaller than 1.20 Å, and is considerably shorter than that (1.320 Å) predicted with the Pople-Segal CNDO/2 method and the experimental value (1.339 Å). For benzene, the SCF iterative procedure with the Sichel-Whitehead parameterization leads to the loss of the initially assumed D_{6h} symmetry for its ground state. This unexpected result arises mainly from the fact that because of the too small values of bonding parameters proposed by Sichel and Whitehead, the orbital-intermingling occurs between the initially chosen bonding and antibonding molecular orbitals in the course of the iterative procedure.

Recently, some modifications of the CNDO/2 procedure have been attempted by several authors[20-26] aiming at making it useful for predicting and interpreting spectroscopic data. Of these, the approximation proposed by Del Bene and Jaffé[21-24] is most noteworthy, the essential modification involving the use of reduced electron-repulsion integrals instead of theoretical ones and introduction of a new empirical parameter κ to differentiate resonance integrals between σ-type orbitals from those between π-type orbitals. The value of κ and bonding parameters have been adjusted so as to give the most consistent spectroscopic data for benzene, pyridine, and diazines.

However, Del Bene-Jaffé's approximation with the original parameterization does not work well for the prediction of electronic spectra of saturated molecules. For methane and ethane, it gives the lowest excitation energies higher by 3—4 eV than the experimental values. Of course, it is desirable to be able to treat conjugated molecules and saturated molecules at the same time using a single parameterization.

For the discussion of electronic spectra, we use the Del Bene-Jaffé-type modified CNDO/2 method with the values of κ and bonding parameters, β_C^0, β_H^0, readjusted, so that they may give the most consistent spectroscopic data in methane, ethylene and benzene.[27] The values chosen for β_C^0, β_H^0, and κ are -15.0 eV, -8.0 eV, and 0.75, respectively. One-center and two-center electron-repulsion integrals were evaluated with Sichel-Whitehead's formula and Mataga-Nishimoto's formula,[28] respectively, and the local core matrix elements with Sichel-Whitehead's formula.

It should be added that the Del Bene-Jaffé-type method with the present parameterization is inadequate for the prediction of the ground-state geometrical structures. If the internuclear potential energy, V_{AB}, is written as[18]

$$V_{AB} = Z_A Z_B \gamma_{AB}$$

where Z and γ are the atomic core charge and the atomic electron-repulsion integral, the equilibrium C–C bond length r_e for ethylene is predicted to be zero. On the other hand, the use of the point-charge approximation for V_{AB} gives to an infinitely large r_e for ethylene. Another formula available for V_{AB} is that recommended by Dewar and Klopmann:[29]

$$V_{AB} = \frac{Z_A Z_B}{r_{AB} + a}$$

However, the use of this formula with the value of a adjusted so as to reproduce the experimental r_e for ethylene unexpectedly results in the ground state of benzene being of D_{3h} symmetry.

We therefore used the CNDO/2 method with its original parameterization to predict the geometrical structures of nonalternant hydrocarbons, and the Del Bene-Jaffé-type modified CNDO/2 method with the new parameterization to discuss electronic spectra.

We made the following assumptions for prediction of the energetically most favorable ground-state geometry of each molecule.

(a) Only C–C bond distances were varied and the C–H bond distances were kept constant (1.00 Å), assuming the molecule to be planar.

14) J. A. Pople, D. P. Santry, and G. A. Segal, *J. Chem. Phys.*, **43**, S129 (1965).
15) J. A. Pople and G. A. Segal, *ibid.*, **43**, S136 (1965).
16) J. A. Pople and G. A. Segal, *ibid.*, **44**, 3289 (1966).
17) G. E. Segal, *ibid.*, **47**, 1876 (1967).
18) J. M. Sichel and M. A. Whitehead, *Theor. Chim. Acta*, **11**, 220 (1968).
19) J. M. Sichel and M. A. Whitehead, *ibid.*, **7**, 32 (1967).
20) H. W. Kroto and D. P. Santry, *J. Chem. Phys.*, **47**, 792 (1967).
21) J. Del Bene and H. H. Jaffé, *ibid.*, **48**, 1807 (1968).
22) J. Del Bene and H. H. Jaffé, *ibid.*, **48**, 4050 (1968).
23) J. Del Bene and H. H. Jaffé, *ibid.*, **49**, 1221 (1968).
24) J. Del Bene and H. H. Jaffé, *ibid.*, **50**, 1126 (1969).
25) C. Giessner-Pretre and A. Pullman, *Theor. Chim. Acta*, **13**, 265 (1969).
26) C. Giessner-Prettre and A. Pullman, *ibid.*, **18**, 14 (1970).
27) N. Ohmichi, A. Tajiri, and T. Nakajima, to be published.
28) N. Mataga and K. Nishimoto, *Z. Phys. Chem.*, **13**, 140 (1957).
29) M. J. S. Dewar and G. Klopmann, *J. Amer. Chem. Soc.*, **89**, 3089 (1967).

(b) The internuclear distances between nonneighboring atoms were all kept constant and estimated assuming all the rings to be regular polygons.

(c) Starting from the nuclear arrangement in which all the C–C bond lengths are assumed to be equal, the C–C bonds corresponding to the double bonds in the Kekule-type structure were shortened and, at the same time, all the remaining C–C bonds lengthened in the same amount.

In calculating electronic spectra, configuration mixing of the singly excited states is partially included; the number of the configuration interactions considered is 28 for I, II, and VI (Fig. 1) and 55 for other molecules.

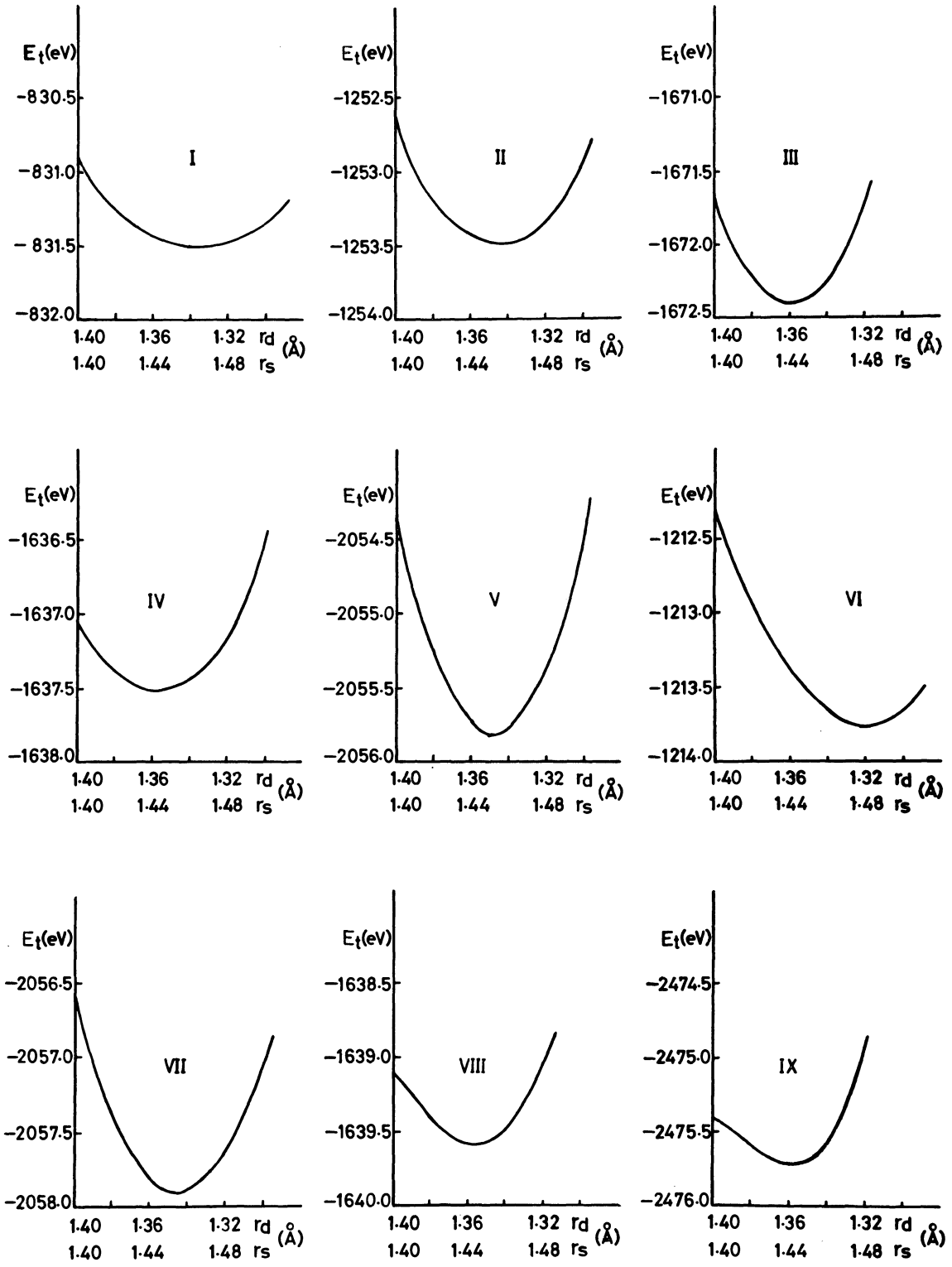

Fig. 2. Variations of total energies with C–C bond lengths. r_d and r_s mean the C–C bond lengths corresponding to the double bonds and single bonds, respectively, in the Kekulé-type structure.

Results and Discussion

Ground-State Properties. The nonalternant hydrocarbons examined are triafulvene (I), fulvene (II), heptafulvene (III), calicene (IV), triaheptafulvalene (V), triafulvalene (VI), fulvalene (VII), pentalene (VIII) and heptalene (IX) (Fig. 1). In Fig. 2, the total energies calculated for these molecules are plotted against the C–C bond-distance variation. All the curves exhibit an energy minimum at about 1.32—1.36 Å for the shorter bonds and 1.44—1.48 Å for the longer bonds, showing an agreement with the results of previous investigations[1–3,5,7,9,11,30] where in these nonalternant hydrocarbons a distorted structure in which a marked double-bond fixation exists is energetically favored as compared with the fully delocalized one. It should be noted that in pentalene (VIII) and heptalene (IX), such a bond distortion is accompanied with molecular-symmetry reduction from D_{2h} to C_{2h}. The stabilization energies which favor the C_{2h} structure for VIII and IX are calculated to be 11.04 and 6.90 kcal/mole, respectively.

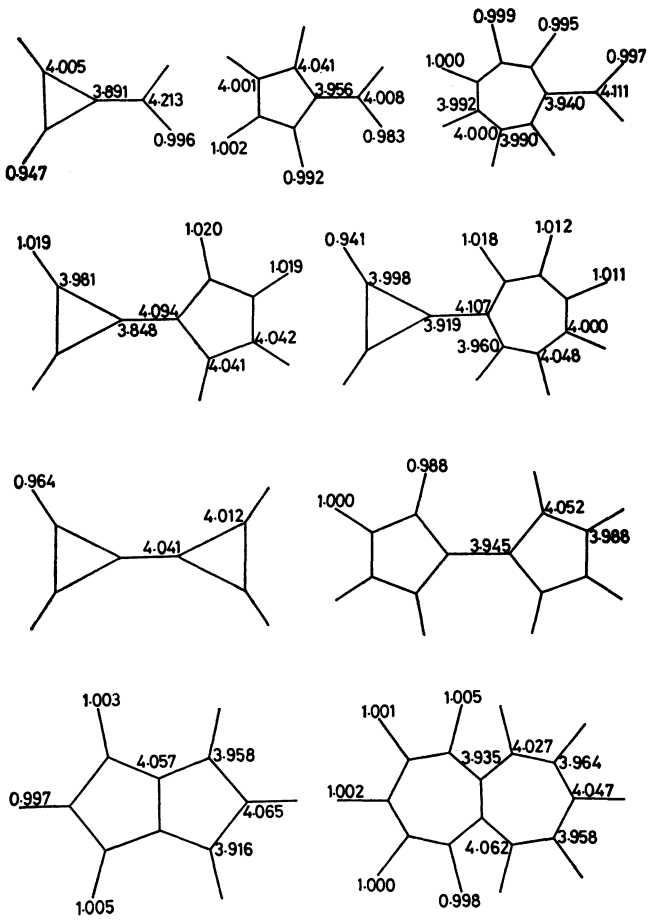

Fig. 3. Total atomic populations.

The total atomic populations calculated using the energetically most favorable set of C–C bond distances are shown in Fig. 3. The dipole moments calculated from these data for I, II, III, IV, and V are 2.12, 0.61, 0.98, 5.45, and 3.71 D, respectively. As for II, a dipole moment of 1.2 D[31] or 1.1 D[32] has, until recently, been adopted as the experimental value. Brown *et al.*[33] have measured the Stark effect of II and reported a dipole moment of 0.44 ± 0.02 D, which is considerably smaller than the experimental estimation. They have also calculated the dipole moment of II using the CNDO/2 procedure and obtained a theoretical value 0.89 D. The discrepancy between their value and ours seems to arise from the difference in the geometrical structures adopted. Our value obtained using the set of bond distances at which the total energy is minimized should in principle be more plausible and actually is reasonably near the new experimental value.

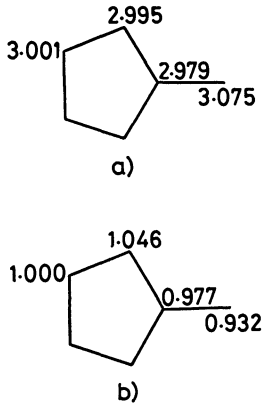

Fig. 4. Electron densities in fulvene: a) σ-electron densities; b) π-electron densities.

In Fig. 4, σ-electron and π-electron charge densities of II are shown separately. The π-electron distribution shows that the 5-membered ring is charged negatively, as is expected from the aromatic sextet rule. On the other hand, the σ-electron distribution reveals that the σ framework of the 5-membered ring is charged positively and the dipole moment due to σ charge has the direction opposite to that due to π charge. However, the dipole moment due to σ electrons (0.19 D) is completely masked by that due to π electrons (0.80 D), and the total dipole moment is such that the 5-membered ring is charged negatively. Such is the case with other polar molecules, I, III, IV, and V.

The theoretical dipole moments for III and IV are in good agreement with the experimental values 0.7 D[34] and 5.6—6.1 D,[30] respectively.

The dipole moment of I is predicted to be considerably larger than that of III, which means that the electron releasing power of the 3-membered ring is appreciably greater than that of the 7-membered ring. This fact is reflected in the appreciable dipole moment calculated for V; the dipolar structure of this molecule is such that the negative pole is directed towards the 7-

30) A. Julg, *J. Chim. Phys.*, **50**, 652 (1953).

31) G. W. Wheland and D. E. Mann, *J. Chem. Phys.*, **17**, 264 (1949).

32) J. Thiec and J. Wiemann, *Bull. Soc. Chim. Fr.*, **1956**, 177.

33) R. D. Brown, F. R. Burden, and J. E. Kent, *J. Chem. Phys.*, **49**, 5542 (1968).

34) Y. Kurita, S. Seto, T. Nozoe, and M. Kubo, This Bulletin, **26**, 272 (1953).

membered ring.

Electronic Spectra. The lower singlet transition energies and intensities calculated using the geometrical structures corresponding to the energy minimum are summarized and compared with the available experimental data in Table 1. Also included are the transition symmetries and types. It will be seen that the predicted transitions are in line with the observed absorption peaks and tails.

The transition energy for the longest wavelength transition of triafulvene (I) is predicted to be considerably smaller than predicted by Julg[30] (6.27 eV), Naka-

Table 1. Singlet transition energies (ΔE) and intensities (f)

Molecule	Transition Symmetry	Transition Type[a]	Theoretical ΔE (eV)	Theoretical f (cgs)	Experimental ΔE(eV)
I	B_2	$\pi\rightarrow\pi^*$ (0.89)	4.60	0.025	
	A_2	$\pi\rightarrow\sigma^*$	4.69	Forb.	
	B_1	$\sigma\rightarrow\pi^*$	4.95	0.000	
	A_2	$\sigma\rightarrow\pi^*$	5.55	Forb.	
	A_1	$\pi\rightarrow\pi^*$ (0.89)	6.01	0.32	
II	B_2	$\pi\rightarrow\pi^*$ (0.98)	3.76	0.031	3.32(f=0.012)[b], 3.42[c]
	A_2	$\sigma\rightarrow\pi^*$	4.75	Forb.	
	A_2	$\pi\rightarrow\sigma^*$	5.14	Forb.	
	A_1	$\pi\rightarrow\pi^*$ (0.92)	5.25	0.36	5.12[b,c] (0.32)[b]
III	B_2	$\pi\rightarrow\pi^*$ (0.98)	3.06	0.034	2.91(f=0.02)[d]
	A_1	$\pi\rightarrow\pi^*$ (0.91)	4.40	0.59	4.44(0.3)
	B_1	$\sigma\rightarrow\pi^*$	4.63	0.000	
	A_2	$\pi\rightarrow\sigma^*$	4.66	Forb.	
	A_2	$\sigma\rightarrow\pi^*$	4.97	Forb.	
	B_1	$\sigma\rightarrow\pi^*$	5.24	0.000	
IV	A_1	$\pi\rightarrow\pi^*$ (0.92)	4.46	0.061	
	B_2	$\pi\rightarrow\pi^*$ (0.95)	4.50	0.052	4.13(log ε =4.64), tail[e]
	B_2	$\pi\rightarrow\pi^*$ (0.94)	4.63	0.028	
	B_1	$\sigma\rightarrow\pi^*$	4.75	0.000	
	A_2	$\sigma\rightarrow\pi^*$	4.83	Forb.	
	A_2	$\sigma\rightarrow\pi^*$	4.84	Forb.	
	A_1	$\pi\rightarrow\pi^*$ (1.00)	5.21	0.000	
V	B_2	$\pi\rightarrow\pi^*$ (0.99)	2.09	0.006	
	B_1	$\pi\rightarrow\sigma^*$	3.13	0.000	
	B_2	$\pi\rightarrow\pi^*$ (0.98)	3.45	0.023	
	A_2	$\pi\rightarrow\sigma^*$	3.79	Forb.	
	A_1	$\pi\rightarrow\pi^*$ (0.96)	3.91	0.81	
	A_2	$\pi\rightarrow\sigma^*$	4.07	Forb.	
	B_1	$\pi\rightarrow\sigma^*$	4.42	0.000	
V	B_1	$\sigma\rightarrow\pi^*$	4.67	0.000	
	B_1	$\sigma\rightarrow\pi^*$	5.09	0.000	
VI	B_{2g}	$\pi\rightarrow\sigma^*$	2.42	Forb.	
	B_{2u}	$\pi\rightarrow\pi^*$ (0.86)	3.59	0.056	
	B_{3g}	$\pi\rightarrow\pi^*$ (0.97)	3.70	Forb.	
	B_{2g}	$\sigma\rightarrow\pi^*$	4.43	Forb.	
	B_{3u}	$\sigma\rightarrow\pi^*$	4.45	0.000	
	B_{2u}	$\sigma\rightarrow\sigma^*$ (0.20)	5.33	0.080	
VII	B_{2u}	$\pi\rightarrow\pi^*$ (0.98)	3.05	0.018	
	B_{3g}	$\pi\rightarrow\pi^*$ (0.97)	3.14	Forb.	2.98(log ε =2.41), tail[f]
	B_{1u}	$\pi\rightarrow\pi^*$ (0.93)	4.25	0.93	3.95(4.67)
	B_{3u}	$\pi\rightarrow\sigma^*$	5.29	0.000	
	A_u	$\pi\rightarrow\sigma^*$	5.31	0.000	
	B_{3u}	$\sigma\rightarrow\pi^*$	5.44	0.000	
VIII	A_g	$\pi\rightarrow\pi^*$ (0.99)	1.34	Forb.	1.72(log ε =1.95), tail[g]
	A_u	$\sigma\rightarrow\pi^*$	3.41	0.000	
	B_u	$\pi\rightarrow\pi^*$ (0.91)	4.06	0.28	3.27(3.99)
	A_u	$\pi\rightarrow\sigma^*$	4.41	0.000	
	B_u	$\pi\rightarrow\pi^*$ (0.93)	5.26	0.32	4.00 (4.52)
IX	A_g	$\pi\rightarrow\pi^*$ (0.99)	1.57	Forb.	Tail[h]
	B_u	$\pi\rightarrow\pi^*$ (0.92)	2.74	0.32	3.52(f=0.15)
	A_u	$\pi\rightarrow\sigma^*$	3.50	0.000	
	B_u	$\pi\rightarrow\pi^*$ (0.90)	3.95	0.26	4.84(?)
	A_u	$\sigma\rightarrow\pi^*$	4.15	0.000	
	A_u	$\pi\rightarrow\sigma^*$	4.32	0.000	
	A_u	$\sigma\rightarrow\pi^*$	4.59	0.000	
	A_u	$\sigma\rightarrow\pi^*$	5.34	0.000	
	B_u	$\pi\rightarrow\pi^*$ (0.86)	5.36	0.77	

a) The transition type indicated refers to the configuration with the largest weight. The weight of the $\pi\rightarrow\pi^*$ configuration in the state considered are indicated in parenthesis.

b) Reference. 30.

c) H. Schaltegger, M. Neuenschwander, and D. Meuche, *Helv. Chim. Acta*, **48**, 955 (1965).

d) W. von E. Doering and D. W. Wiley, *Tetrahedron*, **11**, 183 (1960).

e) Estimated from the spectrum of a tetrachlorodi-*n*-propyl derivative; Y. Kitahara, I. Murata, M. Ueno, K. Sato, and H. Watanabe, *Chem. Commun.*, **1966**, 180; A. S. Kende, P. T. Izzo, and P. T. MacGregor, *J. Amer. Chem. Soc.*, **88**, 3359 (1966).

f) W. von E. Doering, "Theoretical Organic Chemistry, Kekule Symposium." Butterworths, London (1959), p. 35 and personal communication to T. Nakajima.

g) The spectrum of hexaphenyl pentalene; E. Le Goff, *J. Amer. Chem. Soc.*, **84**, 3975 (1962).

h) Reference 4.

jima *et al.*[35] (5.61 eV), and Meyer[36] (5.08 eV) using the π-electron approximation, but in good agreement with the value (4.3 eV) calculated by Yamaguchi *et al.*[37] using the variable bond-length SCF CI π-MO method in which the effects of the bent bonds in the 3-membered ring are taken into account. Unfortunately, there are at present no experimental spectral data available for a direct comparison of theory and experiment.

In fulvene (II) and heptafulvene (III), the lowest $\pi \rightarrow \pi^*$ transition (B_2) polarized along the short axis and the next one (A_1) polarized along the long axis are well separated in energy. On the other hand, in calicene (IV) and fulvalene (VII), these two transitions are predicted to be very close in energy. This is in agreement with the experimental data.

In heptalene (IX), the agreement between theory and experiment is less satisfactory, the predicted transition energies being found to be fairly small as compared with the observed values. This may be attributed to a nonplanar conformation, possible in this molecule owing to the steric repulsion between the ortho hydrogen atoms.

35) T. Nakajima, S. Kohda, A. Tajiri, and S. Karasawa, *Tetrahedron*, **23**, 2189 (1967).
36) A. Y. Meyer, *Theor. Chim. Acta*, **8**, 178 (1967).
37) H. Yamaguchi, T. Nakajima, and T. L. Kunii, *Theor. Chim. Acta*, **12**, 349 (1968).

BULLETIN OF THE CHEMICAL SOCIETY OF JAPAN, VOL. 44, 2352—2355(1971)

Molecular Structure of Piperazine as Studied by Gas Electron Diffraction

Akimichi YOKOZEKI and Kozo KUCHITSU

Department of Chemistry, Faculty of Science, The University of Tokyo, Hongo, Tokyo

(Received March 24, 1971)

A study of piperazine by means of gas electron diffraction has given the following structural parameters (the r_g distances and the angles based on the r_α structure) with estimated limits of error: C–C=1.540±0.008 Å, C–N=1.467±0.004 Å, ∠C–C–N=110.4 ±0.8°, ∠C–N–C=109.0 ±0.8°, C–H=1.110±0.008 Å and ∠H–C–H=109.$_1$±5°; the molecule takes a chair conformation. The C–C distance is nearly equal to that in cyclohexane, and the C–N–C angle is slightly smaller than the C–C–N angle. These angles agree with those predicted by an SCF-CNDO/2 method.

In succession of the studies of triethylenediamine[1] and ethylenediamine,[2] the molecular structure of diethylenediamine (piperazine: Fig. 1) has now been

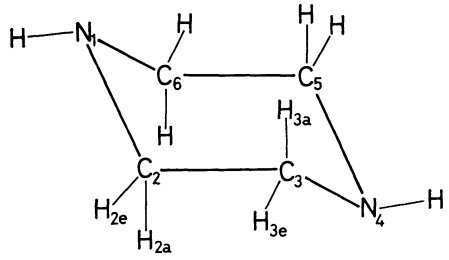

Fig. 1. The numbering of piperazine.

investigated by means of gas electron diffraction. Previous studies of this molecule (electron diffraction,[3] infrared,[4,5] and Raman[6]) showed that this molecule had a chair conformation (C_{2h} symmetry) analogous to cyclohexane. Davis and Hassel[3] reported that the C–N and C–C bond distances were 1.471 and 1.527 Å, respectively, the latter being claimed to be equal to that of cyclohexane, which they studied at the same time, 1.528 Å. However, their C–C distances are found to be about 0.013 Å shorter than that determined by a recent study of cyclohexane.[7] Furthermore, in comparison with the C–C distance in ethylenediamine,[2] 1.545±0.008 Å, their C–C distance seems to be questionably short. Their C–N distance and the C–C–N bond angle, on the other hand, seem to agree with those in ethylenediamine. The present paper reports on a reinvestigation of the piperazine structure and a comparison with those of analogous molecules.

Experimental

Anhydrous piperazine (Guaranteed Reagent, above 99% pure) was purchased from the Tokyo Chemical Industry Co., Ltd. Diffraction photographs were taken on Fuji Process Hard plates at 130°C using a high-temperature nozzle assembly[1] with an apparatus equipped with an r^3-sector.[8] The accelerating voltage (stabilized to within 0.01%) and the beam current were about 40 kV and 0.44 μA, respectively.

1) A. Yokozeki and K. Kuchitsu, This Bulletin, **44**, 72 (1971).
2) A. Yokozeki and K. Kuchitsu, *ibid.*, **43**, 2664 (1970); *ibid.*, in press.
3) M. Davis and O. Hassel, *Acta Chem. Scand.*, **17**, 1181 (1963).
4) P. J. Hendra and D. B. Powell, *J. Chem. Soc.*, **1960**, 5105.
5) P. J. Hendra and D. B. Powell, *Spectrochim. Acta*, **18**, 299 (1962).
6) L. Kahovek and K. W. F. Kohlrausch, *Z. Phys. Chem.*, **B35**, 29 (1937).
7) H. Kambara, K. Kuchitsu, and Y. Morino, This Bulletin, to be published.
8) Y. Murata, K. Kuchitsu, and M. Kimura, *Jap. J. Appl. Phys.*, **9**, 591 (1970).

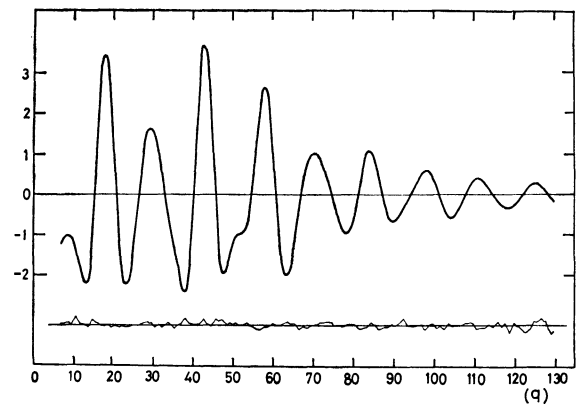

Fig. 2. Molecular intensity curve $qM(q)$ for piperazine. Upper curve: best-fit theoretical; lower curve: experimental minus theoretical.

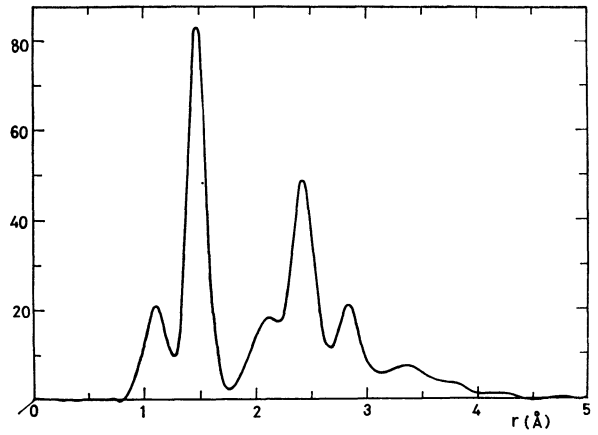

Fig. 3. Experimental radial distribution curve for piperazine with a damping factor of $\exp(-0.00014q^2)$.

The exposure times were about 150 and 60 sec for camera lengths of 113.69 and 249.06 mm. The vapor pressure of the sample at 130°C was estimated to be 70±30 Torr. The vacuum in the diffraction chamber was about 6×10^{-5} Torr during the exposure. In order to obtain correct scales of the diffraction patterns, photographs of reference gases (N_2 and CO_2 for the long and short camera lengths, respectively) were taken in experimental conditions similar to those for the sample, and the scale factors were calibrated to within 0.07% with reference to the r_a(C=O), 1.1646 Å,[8] and r_a(N-N), 1.1007 Å.[9] The photographic densities (0.19 to 0.57) of four plates for each camera length were measured at the intervals of integral q values with a digital microphotometer.[10] Experimental and theoretical molecular intensities and radial distribution function[11] are shown in Figs. 2 and 3, respectively.[12] Most of the calculations were performed by the use of a HITAC-5020E computer in the Computer Centre of the University of Tokyo.

Analysis

Mean Amplitudes of Vibration. The root-mean-square amplitudes and shrinkage corrections for thermal vibration[13] (at 130°C) were obtained from a normal-coordinate analysis by the use of the Urey-Bradley force constants estimated from those for cyclohexane[14]

Table 1. Estimated force constants for piperazine[a]

K(C-C)	2.3	H(C-C-N)	0.30	F(C-C-N)	0.70
K(K-N)	5.5	H(C-N-C)	0.35	F(C-N-C)	0.30
K(C-H)	4.3	H(C-C-H)	0.25	F(C-C-H)	0.47
K(N-H)	5.6	H(N-C-H)	0.28	F(N-C-H)	0.52
Y(C-C)	0.11	H(C-N-H)	0.32	F(C-N-H)	0.46
Y(C-N)	0.11	H(H-C-H)	0.42	F(H-C-H)	0.07

a) The Urey-Bradley force constants for piperazine estimated from those for cyclohexane[14] and several amides.[15] In md/Å units (except for Y in md·Å).

Table 2. Vibrational frequencies for piperazine (cm^{-1})

A_g		B_g		A_u		B_u	
Calcd[a]	Obsd[b]	Calcd	Obsd[b]	Calcd	Obsd[c]	Calcd	Obsd[c]
3298		2983		2976	2944	3298	3328
2977		2944		2929		2984	
2938		1542		1539		2944	2941
1441	1431	1484	1451	1445	1444	1506	1458
1318		1320		1309	1320	1336	1382
1297	1279	1277	1279	1293	1271	1307	1323
1190	1109	1261	1184	1231	1197	1079	1076
1086	1023	848	836	1011	1138	992	977
926		514	515	941	983	900	839
803				254		613	633
503	448					248	
390	404						

a) Calculated by the use of the Urey-Bradley force constants listed in Table 1.
b) Observed by Raman spectra (Ref. 6).
c) Observed by infrared spectra (Refs. 4 and 5).

9) K. Kuchitsu, This Bulletin, **40**, 498 (1967).
10) Y. Morino, K. Kuchitsu, and T. Fukuyama, *ibid.*, **40**, 423 (1967).
11) A. Yokozeki, K. Kuchitsu, and Y. Morino, *ibid.*, **43**, 2017 (1970).
12) Numerical experimental data of the leveled total intensity have been deposited with the Chemical Society of Japan (Document No. 7111). A copy may be secured by citing the document number and by remitting, in advance, ¥200 for photoprints. Payment by check or money order payable to: the Chemical Society of Japan, 5, 1-Chome, Kanda-Surugadai, Chiyodaku, Tokyo.
13) K. Kuchitsu and S. Konaka, *J. Chem. Phys.*, **45**, 4342 (1966).
14) H. Takahashi and T. Shimanouchi, *J. Mol. Spectrosc.*, **13**, 43 (1964).

Table 3. Calculated mean amplitudes and shrinkage corrections for piperazine[a)]

i—j	l_{ij}	d_{ij}	i—j	l_{ij}	d_{ij}
N_1—C_2	451	31	$N_1\cdots H_4$	1033	21
$N_1\cdots C_3$	657	4	C_2—H_2	787	120
C_2—C_3	520	23	$C_2\cdots H_1$	1021	74
$C_2\cdots C_6$	711	0	$C_2\cdots H_3$	1010	74
$C_3\cdots C_6$	715	−10	$C_2\cdots H_4$	988	43
$N_1\cdots N_4$	694	−9	$C_6\cdots H_{2a}$	1638	−22
N_1—H_1	738	148	$C_6\cdots H_{3a}$	1596	−35
$N_1\cdots H_2$	1057	78	$C_6\cdots H_{2e}$	1013	41
$N_1\cdots H_{3a}$	1561	−12	$C_6\cdots H_{3e}$	1080	17
$N_1\cdots H_{3e}$	1000	43			

a) Mean amplitudes (l_{ij}) and shrinkage corrections (d_{ij}) calculated for 130°C by the use of the force constants in Table 1. In 10^{-4} Å units. The hydrogen-hydrogen pairs are not listed.

and amides[15] (Table 1). The calculation was based on a C_{2h} structure with an equatorial N–H bond (see next subsection). The vibrational frequencies of piperazine calculated in this way are compared in Table 2 with observed infrared and Raman frequencies,[4,6] to which a tentative assignment, similar to that of Hendra and Powell,[5] was made. The mean amplitudes and vibrational corrections obtained here are listed in Table 3. The vibrational corrections and some of the mean amplitudes were used as fixed constants in the least-squares analysis.

Determination of Molecular Structure. The radial distribution curve has confirmed a chair (C_{2h}) conformation of the piperazine skeleton but has given no evidence as to the orientation of the N–H bonds (equatorial and/or axial). In this connection, Katritzky *et al.*[16,17] reported from the measurements of the dipole moments and the infrared NH-overtone spectra of piperidine that the N-hydrogen atom prefers the equatorial position in the gas phase and in non-interacting solvents with the ΔG^0 of 0.4—0.5 kcal/mol.

In order to determine the structural parameters, the following assumptions about the hydrogen positions were made for the r_a structure[18] of C_{2h} symmetry.

Table 5. Structural parameters for piperazine

	Present study[a)]	Davis & Hassel[b)]
C——C	1.540±0.008	1.527±0.005
C——N	1.467±0.004	1.471±0.005
∠C–C–N	110.4±0.8°	109.8±0.5°
∠C–N–C	109.0±0.8°	112.6±0.5°
C——H	1.110±0.008	1.11_2±0.01
∠H–C–H	$109._1$±5°	——
k	0.97±0.06	——

a) The r_g distances (Å) and the angles based on the r_a structure determined in the present study with estimated limits of error. The index of resolution k is dimensionless.
b) Ref. 3, where the physical significance of the parameters and their errors is not specified.

Table 6. Mean amplitudes for piperazine (in Å units)

Atom pair	Obsd[a)]	Calcd[b)]
N_1——C_2	0.048±0.005	0.045_1
$N_1\cdots\cdots C_3$	0.069±0.006	0.065_7
C_2——C_3	0.053±0.02$_2$	0.052_0
$C_2\cdots\cdots C_6$	0.065±0.02$_0$	0.071_1
$C_3\cdots\cdots C_6$	0.069±0.01$_7$	0.071_5
C_2——H_2	0.072±0.007	0.078_7
$C_2\cdots\cdots H_3$	0.110±0.07	0.101_0
$N_1\cdots\cdots H_2$	0.115±0.08	0.105_7

a) Determined by a least-squares analysis with estimated limits of error.
b) Calculated values in Table 3.

Table 4. Error matrix for piperazine[a)]

	X_1	X_2	X_3	X_4	X_5	X_6	l_1	l_2	l_3	l_4	l_5	l_6	l_7	l_8	k
X_1	32	−17	8	−36	2	44	12	−20	−45	−25	−17	− 5	82	−79	−63
X_2		16	− 2	16	− 8	13	− 8	12	29	16	10	6	−48	45	42
X_3			32	− 8	− 8	40	5	7	14	9	7	10	6	−12	40
X_4				56	−40	−108	4	8	13	−49	−44	− 8	25	24	16
X_5					59	67	4	20	−25	34	47	−14	−61	58	−51
X_6						331	−22	38	76	99	72	25	−216	183	134
l_1							21	− 6	−22	− 9	− 4	5	28	−26	−16
l_2								20	28	− 6	18	11	−60	55	51
l_3									75	40	28	24	−97	88	120
l_4										65	47	15	31	−41	72
l_5											56	13	−32	21	56
l_6												22	−16	4	59
l_7													275	242	−143
l_8														282	122
k															246

a) Error matrix for the independent parameters (X_i) and mean amplitudes (l_i): X_1=C–C, X_2=C–N, X_3=C–H, X_4=∠C–C–N, X_5=∠C–N–C, X_6=∠H–C–H, l_1=N_1–C_2, l_2=N_1–C_3, l_3=C_2–C_3, l_4=C_2–C_6, l_5=C_3–C_6, l_6=C_2–H_2, l_7=C_2–H_3, l_8=N_1–H_2. Units ($\times 10^{-4}$) for the distances are Å, those for the angles are rad., and the index of resolution k is dimensionless.

15) I. Suzuki, This Bulletin, **35**, 1279, 1449, 1456 (1962).
16) R. A. Y. Jones, A. R. Katritzky, A. C. Richards, R. J. Wyatt, R. J. Bishop, and L. E. Sutton, *J. Chem. Soc., B*, **1970**, 127.
17) R. W. Baldock and A. R. Katritzky, *Tetrahedron Lett.*, **1968**, 1159; *J. Chem. Soc., B*, **1968**, 1470.
18) K. Kuchitsu, T. Fukuyama, and Y. Morino, *J. Mol. Structure*, **1**, 463 (1968).

(1) The N–H bonds are equatorial, and the C–N–H angle is equal to that in dimethylamine, 108.8°.[19]

(2) The N–H bond distance is equal to that in ammonia, r_g (N–H) = 1.0302 Å.[20]

(3) The C–C–N plane is perpendicular to the H–C–H plane and bisects the H–C–H bond angle, and *vice versa*.

By taking into account the above geometrical constraints, the total number of the independent parameters was reduced to six: the C–N, C–C and C–H distances, and the C–C–N, C–N–C and H–C–H angles. They were determined, together with an index of resolution and several mean amplitudes, by a least-squares analysis on the molecular intensity curves. The error matrix[21] is listed in Table 4, and the most probable values of the structural parameters and the mean amplitudes are given in Tables 5 and 6 with estimated limits of error including random and systematic errors. The experimental systematic uncertainties in the scale factor and sector imperfection[18] were estimated to be 0.08% in total, while those due to the geometrical constraints mentioned above were estimated to be of the order of random standard errors, since moderate changes in the assumed values had no effect on the most probable values beyond their random standard deviations. The systematic errors in the mean amplitudes were estimated to be 5%,[18] within which the observed mean amplitudes agree with the calculated values. This justifies the above estimation of the force constants; in addition, the systematic errors caused by the use of constant parameters for some of the mean amplitudes seem to have little effect.

Discussion

The structural parameters determined in the present study are compared in Table 7 with those of related compounds studied by gas electron diffraction. The C–C distance, 1.540±0.008 Å, is significantly longer than that reported previously by Davis and Hassel,[3] 1.527±0.005 Å, and is essentially equal to that in cyclohexane,[7] 1.540 Å, and in ethylenediamine,[2] 1.545±0.008 Å, whereas that in triethylenediamine[1] is about 0.02 Å longer, as has been discussed in Ref. 2. The C–N distances in the three molecules are essentially equal to one another and are similar to that in methylamine, 1.467±0.002 Å.[22] In this connection, the C–N distance in dimethylamine is measured to be r_g = 1.455±0.002 Å,[23] r_s = 1.466±0.005 Å,[19] while that in trimethylamine is r_g = 1.454±0.002 Å,[23] r_s = 1.451±0.003 Å.[24] As for bond angles, piperazine, ethylenediamine and triethylenediamine have nearly equal C–C–N angles of about 110°. They are slightly smaller than the C–C–C angles observed in cyclohexane (111.4°)[7] and in normal alkanes (*e.g.*, butane, 112.2°).[25] The C–N–C bond angle, 109.0°±0.8°, supersedes that reported in Ref. 3, 112.6°±0.5°. The hydrogen parameters (C–H and ∠H–C–H) determined in the present study seem to be compatible with those in cyclohexane.[7]

Table 7. Structures of piperazine and related compounds

	DED[a]	TED[b]	EDA[c]
C——C	1.540±0.008	1.562±0.009	1.545±0.008
C——N	1.467±0.004	1.472±0.007	1.469±0.004
∠C–C–N	110.4±0.8°	110.2±0.4°	110.2±0.7°
∠C–N–C	109.0±0.8°	108.7±0.4°	——
C——H	1.110±0.008	1.11_0±0.01_2	1.109±0.008
∠H–C–H	$109._1$±5	$111._5$±$5._6$°	$112._7$±$8._5$°

DED: piperazine, TED: triethylenediamine, EDA: ethylenediamine. a—c): r_g distances (Å) and r_α angles with estimated limts of error.
a) Present study.
b) Ref. 1.
c) Ref. 2.

A conformational analysis[2] by the use of a CNDO/2 program[26] written by Segal[27] was made with the C–C–N and C–N–C angles varied from 100° to 120° in step of 0.5°. Other structural parameters were set equal to the values determined above. A set of ∠C–C–N = 110.5° and ∠C–N–C = 109.5° gave the minimum energy, and hence, the calculation is in agreement with the present experiment.

19) J. E. Wollrab and V. W. Laurie, *J. Chem. Phys.*, **48**, 5058 (1968).
20) K. Kuchitsu, J. P. Guillory, and L. S. Bartell, *ibid.*, **49**, 2488 (1968).
21) K. Hedberg and M. Iwasaki, *Acta Crystallogr.*, **17**, 529 (1964).
22) H. K. Higginbotham and L. S. Bartell, *J. Chem. Phys.*, **42**, 1131 (1965).
23) B. Beagley and T. G. Hewitt, *Trans. Faraday Soc.*, **64**, 2561 (1968).
24) J. E. Wollrab and V. W. Laurie, *J. Chem. Phys.*, **51**, 1580 (1969).
25) K. Kuchitsu, This Bulletin, **32**, 748 (1959); R. A. Bonham and L. S. Bartell, *J. Amer. Chem. Soc.*, **81**, 3491 (1959).
26) G. A. Segal, "Molecular Calculations with Complete Neglect of Differential Overap," Program 91, Quantum Chemistry Program Exchange, Indiana University, 1966. This program was rewritten at the Computer Centre of the University of Tokyo in FORTRAN-IV by Drs. Toshiyasu L. Kunii and Toshiaki Ohta, to whom the authors are indebted for allowing them to use the program.
27) J. A. Pople and G. A. Segal, *J. Chem. Phys.*, **44**, 3289 (1966).

Structures of Norbornane and Norbornadiene as Determined by Gas Electron Diffraction

Akimichi YOKOZEKI and KOZO KUCHITSU

Department of Chemistry, Faculty of Science, The University of Tokyo, Hongo, Tokyo

(Received March 30, 1971)

The structures of norbornane and norbornadiene in the gas phase have been investigated by electron diffraction. For the most probable models the r_g bond lengths and the bond angles (based on the r_a structure) with estimated limits of error are as follows: For norbornadiene: C_1–C_2=$1.535_4\pm0.007$ Å, C_2=C_3=$1.343_2\pm0.003$ Å, C_1–C_7=$1.57_3\pm0.01_4$ Å, $\angle C_1$–C_7–C_4=$94.{}_1\pm3.{}_0°$, and θ (the dihedral angle between the C_1–C_2–C_3–C_4 and C_4–C_5–C_6–C_1 planes)=$115.{}_6\pm2.{}_2°$; For norbornane: C–C(average)=$1.548_8\pm0.003$ Å, C_1–C_2=$1.53_9\pm0.01_2$ Å, C_2–C_3=$1.55_7\pm0.02_5$ Å, C_1–C_7=$1.56_0\pm0.02_4$ Å, $\angle C_1$–C_7–C_4=$93.{}_1\pm1.{}_7°$, and θ=$113.{}_1\pm1.{}_8°$. The frame structures of these molecules are similar to each other except for the C_2–C_3 bond distances. All the C–C–C valence angles are appreciably smaller than the tetrahedral angle ($\angle C_1$–C_7–C_4 in particular). The C_1–C_7 bridge bonds appear to be longer than the normal C–C single bond. The above structures are compared critically with those reported so far by other investigators. A method for estimation of systematic errors in the structural parameters derived from a least-squares analysis with fixed mean vibrational amplitudes is discussed.

Norbornane (bicyclo[2.2.1]heptane), norbornadiene (bicyclo[2.2.1]hepta-2,5-diene) (Fig. 1), and their

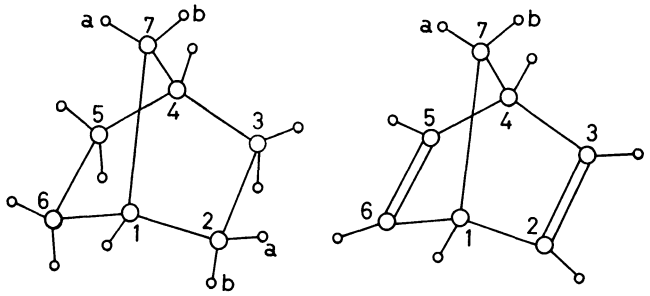

Fig. 1. The numbering of norbornane (left) and norbornadiene (right).

derivatives have been investigated in detail by physical and chemical methods with particular attention to the effect of intramolecular strain. Extensive studies by X-ray diffraction[1] have shown that the carbon bond angles in analogous molecules with camphane frameworks are less than the tetrahedral angle. Particularly striking is the value reported for the angle at the methylene bridge ($\angle C_1$–C_7–C_4: 93°—96°), so that the skeleton must be strained considerably. Theoretical calculations of the geometrical parameters and the conformational energy of norbornane also indicate the above trend.[2-6] The total strain energies in norbornane and norbornadiene, as measured by the heats of combustion and hydrogenation, are 18.4 and 29.0 kcal/mol, respectively.[7] Further support for this strain is given by NMR studies,[8] by which an unusual behavior of the rings toward the magnetic shielding and the proton coupling constants was observed and ascribed to the *p*-character of the C–C bonds in the strained rings. Chemical reactivities such as their high rates of solvolysis are also considered to be closely related to the above-mentioned characteristics.[9]

The present study was initiated to obtain as precise information as possible on the gas-phase structures of these molecules by electron diffraction so as to shed light on the strain effect. Several independent studies of electron diffraction,[10-13] including our preliminary report,[14] have recently been published. However, some of the internuclear distances and angles contained significant discrepancies with one another. In order to examine the origin of these discrepancies, a further analysis has here been carried out by making a critical comparison of the experimental data.[15] In addition, care has been taken in the estimation of uncertainties, particularly that of the systematic errors originated in the theoretical mean amplitudes of vibration used in the analysis.

Experimental

Diffraction photographs were taken on Fuji Process Hard plates at 20°C with an apparatus equipped with an r^3-sector.[16]

1) For example: D. A. Brueckner, Y. A. Hamor, J. M. Robertson, and G. A. Sim, *J. Chem. Soc.*, **1962**, 779; G. Ferguson, C. J. Fritcher, J. M. Robertson, and G. A. Sim, *ibid.*, **1961**, 1976; A. C. MacDonald and J. Trotter, *Acta Crystallogr.*, **18**, 243, **19**, 456 (1965); M. C. Baenziger, G. F. Richards, and J. R. Doyle, *ibid.*, **18**, 924 (1965); A. V. Frantini, K. Britts, and I. L. Karle, *J. Phys. Chem.*, **71**, 2482 (1967).

2) A.I. Kitaygorodsky, *Tetrahedron*, **9**, 183 (1960); **14**, 230 (1961).

3) C. F. Wilcox, *J. Amer. Chem. Soc.*, **82**, 414 (1960).

4) N. L. Allinger, J. A. Hirsch, M. A. Miller, I. Tyminski, and F. A. Van-Catledge, *ibid.*, **90**, 1199 (1968).

5) G. J. Gleicher and P. von R. Schleyer, *ibid.*, **89**, 582 (1967).

6) N. Bodor and M. J. S. Dewar, *ibid.*, **92**, 4270 (1970).

7) R. B. Turner, P. Goebel, B. J. Mallon, W. V. E. Doering, J. F. Coburn, Jr., and M. Pomerantz, *ibid.*, **90**, 4315 (1968).

8) For example, K. Tori, R. Muneyuki, and H. Tanida, *Can. J. Chem.*, **41**, 3142 (1963).

9) L. N. Ferguson, *J. Chem. Educ.*, **47**, 46 (1970).

10) W. C. Hamilton, thesis, California Institute of Technology (1954). V. Schomaker and W. C. Hamilton, unpublished research, cited in W. G. Woods, R. A. Carboni, and J. Roberts, *J. Amer. Chem. Soc.*, **78**, 5653 (1956).

11) T. W. Muecke and M. I. Davis, *Trans. Amer. Crystallogr. Ass.*, **2**, 173 (1966).

12) J. F. Chiang, C. F. Wilcox, Jr., and S. H. Bauer, *J. Amer. Chem. Soc.*, **90**, 3149 (1968).

13) a) G. Dallinga and L. H. Toneman, *Rec. Trav. Chim.*, **87**, 795 (1968). b) *ibid.*, **87**, 805 (1968).

14) Y. Morino, K. Kuchitsu, and A. Yokozeki, This Bulletin, **40**, 1552 (1967).

15) Professor S. H. Bauer and Dr. G. Dallinga have kindly supplied the authors with the experimental intensities obtained in their laboratories.

16) Y. Murata, K. Kuchitsu, and M. Kimura, *Jap. J. Appl. Phys.*, **9**, 591 (1970).

The vapor pressure of norbornane was about 20 Torr, and that of norbornadiene was about 40 Torr. Purified samples of norbornane and norbornadiene were kindly provided by Drs. Hiroshi Tanida and Kazuo Tori of Shionogi Research Laboratory. The vacuum was kept under 5×10^{-5} Torr while the sample gas was introduced into the chamber through a nozzle of 0.2 mm diameter. The beam current was about 0.21 μA. The accelerating voltage (about 40 kV) was stabilized within 0.01% during the experiment, and the electron wavelength was calibrated to within 0.07% with reference to the r_a(C=O) bond length of carbon dioxide, 1.1646 Å.[16] The camera lengths were measured to be 107.77 ± 0.01 and 243.22 ± 0.01 mm. The exposure times were about 210 and 60 sec for the shorter and longer camera lengths, respectively, for norbornane, and about 80 and 40 sec for norbornadiene. The photographs were developed at 20°C for 5 min with FD-131 developer diluted twice.

Four plates for each camera length were used for intensity measurements. The optical densities of the plates were measured at the intervals of integral q values (from 17 to 120 and 15 to 60 for the shorter and longer camera lengths, respectively) using an integrating digital microphotometer.[17] The optical densities thus obtained (0.09 to 0.52), were in the range where the densities were found to be proportional to the electron intensities. Most of the calculations were carried out on a HITAC-5020E computer in the Computer Centre of the University of Tokyo.

Analysis

The molecular intensities, $qM(q)$, were obtained from the observed total intensities by the usual procedure[18]; they are illustrated in Fig. 2.[19] Molecular intensites obtained from different photographic plates deviated from one another randomly by about 0.25.

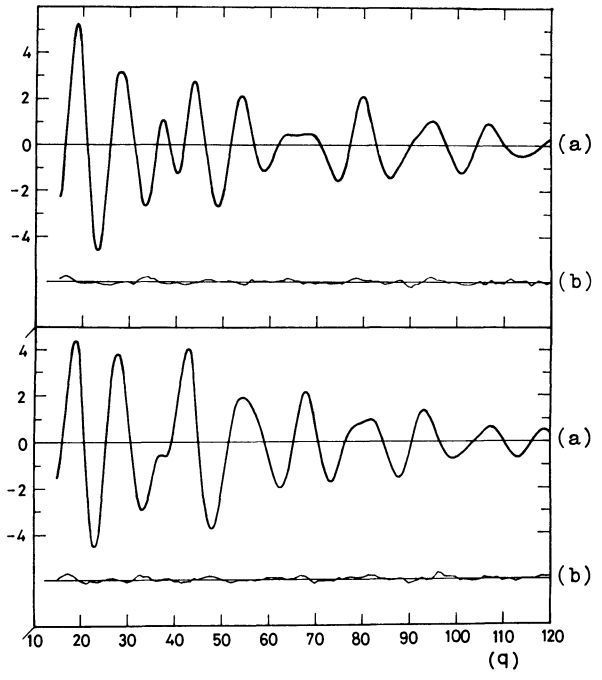

Fig. 2. Molecular intensity curves $qM(q)$ of norbornadiene (upper) and norbornane (lower). (a): best-fit theoretical; (b): experimental minus theoretical.

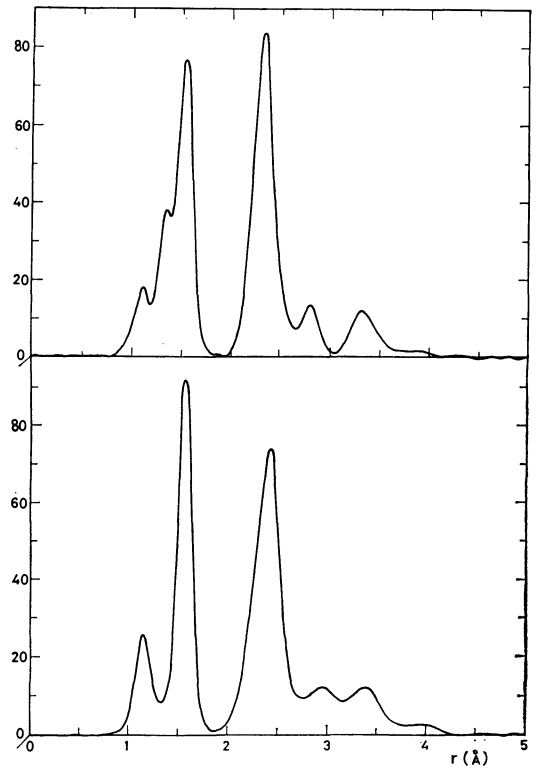

Fig. 3. Experimental radial distribution curves of norbornadiene (upper) and norbornane (lower) with a damping factor of $\exp(-0.00016q^2)$.

Radial Distribution Curves. Modified radial distribution (RD) curves obtained from the molecular intensity curves with a damping factor of $\exp(-0.00016q^2)$ are shown in Fig. 3.

Norbornadiene: Three peaks located in 1—2 Å correspond to the bonded pairs with their maximum positions for C–H at 1.11 Å, C=C at 1.33 Å, and C–C at 1.54 Å. The C–H and C–C peaks are composed of two nonequivalent atom pairs. The peaks in 2—3 Å contain all nonbonded C–C and some of the nonbonded C–H and H–H pairs. In spite of the considerable overlapping of peaks, the RD contour in this region was found to be sufficiently sensitive to determine the carbon skeleton structure. The lower peak at 2.8 Å is almost completely made of the C_2–C_5 and C_3–C_6 pairs, and hence, it affords a good measure of the dihedral angle θ between the C_1–C_2–C_3–C_4 and C_4–C_5–C_6–C_1 planes. A preliminary analysis of this peak showed that θ was about 116°, and from the 2.35 Å peak that $\angle C_1$–C_7–C_4 and $\angle C_1$–C_2–C_3 were about 91° and 107.5°, respectively. The peak in 3—4 Å is made of several nonbonded C···H and H···H pairs. The result of the above analysis was used as a starting model in a least-

17) Y. Morino, K. Kuchitsu, and T. Fukuyama, This Bulletin, **40**, 423 (1967).

18) A. Yokozeki, K. Kuchitsu, and Y. Morino, *ibid.*, **43**, 2017 (1970).

19) Numerical experimental data of the leveled total intensity have been deposited with the Chemical Society of Japan (Document No. 7112). A copy may be secured by citing the document number and by remitting, in advance, ¥200 for photoprints. Payment by check or money order payable to: the Chemical Society of Japan, 5, 1-Chome, Kanda-Surugadai, Chiyoda-ku, Tokyo.

squares refinement on molecular intensities.

Norbornane: The first peak of the RD curve corresponds to the bonded C–H distances, the average value of which is 1.11 Å. The second peak at 1.55 Å contains three closely-spaced nonequivalent C–C pairs. Being analogous to norbornadiene, the peaks in 2—3 Å correspond to nonbonded C···C, C···H, and H···H pairs. If the skeleton has C_{2v} symmetry, the longer distance of the C_2–C_5 and C_3–C_6 should correspond to the peak at 2.9 Å. Since all attempts to account for the RD peaks in terms of a C_2 structure were unsuccessful, a C_{2v} structure was favored.

TABLE 1. ESTIMATED FORCE CONSTANTS FOR NORBORNANE AND NORBORNADIENE[a]

K(C–C)	2.3	H(C–C–C)	0.32	F(C–C–C)	0.20
K(=C–C)	3.0	H(C–C=C)	0.25	F(C–C=C)	0.35
K(C=C)	7.4	H(C–C–H)	0.225	F(C–C–H)	0.41
K(C–H)	4.1	H(C=C–H)	0.21	F(C=C–H)	0.36
K(=C–H)	4.3	H(H–C–H)	0.40	F(H–C–H)	0.18
Y(=C–C)	0.16	Y(C=C)	0.50	Y_{cis}(C–C)	0.11
Y(C–C) *gauche*	0.15	W(C=C–H)	0.35		

a) Estimated force constants taken from those for cyclohexane[23] and several olefins (butene, pentene, *etc.*),[24] The torsional (Y) and wagging (W) force constants are in md·Å, and the others are in md/Å units.

TABLE 2. CALCULATED MEAN AMPLITUDES (l_{ij}) AND SHRINKAGE CORRECTIONS (d_{ij}) FOR NORBORNADIENE[a] (10^{-4} Å)

Atom pair	l_{ij}	d_{ij}	Atom pair	l_{ij}	d_{ij}
C_1——C_2	508	8	C_1·····H_7	1063	31
C_2——C_3	428	27	C_7·····H_1	1047	20
C_1——C_7	530	3	C_1·····H_2	982	49
C_1·····C_4	584	−4	C_2·····H_{7b}	1401	−14
C_1·····C_3	583	1	C_3·····H_1	972	18
C_2·····C_7	680	−4	C_4·····H_1	943	18
C_2·····C_6	714	−5	C_6·····H_2	1190	16
C_2·····C_5	769	−11	C_4·····H_2	955	35
C_2——H_2	784	109	C_7·····H_2	996	26
C_1——H_1	785	82	C_2·····H_{7a}	996	26
C_3·····H_2	984	62	C_5·····H_2	1173	12
C_2·····H_1	1028	25			

a) For 20°C. The H·····H pairs are not listed.

TABLE 3. CALCULATED MEAN AMPLITUDES (l_{ij}) AND SHRINKAGE CORRECTIONS (d_{ij}) FOR NORBORNANE[a] (10^{-4} Å)

Atom pair	l_{ij}	d_{ij}	Atom pair	l_{ij}	d_{ij}
C_1——C_2	530	11	C_7·····H_1	1058	21
C_2——C_3	526	23	C_2·····H_{7b}	1440	−17
C_1——C_7	530	5	C_6·····H_{2b}	1533	−14
C_1·····C_4	593	−3	C_7·····H_{2a}	1437	−7
C_2·····C_7	687	−2	C_4·····H_{2b}	1178	19
C_1·····C_3	617	0	C_5·····H_{2b}	1694	−40
C_2·····C_6	371	−1	C_7·····H_{2b}	1028	35
C_2·····C_5	821	−13	C_2·····H_{7a}	1006	28
C_1——H_1	785	84	C_6·····H_4	955	19
C_2——H_3	1072	63	C_2·····H_4	993	17
C_1·····H_2	1072	49	C_6·····H_{2a}	1059	34
C_1·····H_7	1063	34	C_5·····H_{2a}	1089	14
C_2·····H_1	1042	28			

a) For 20°C. The H·····H pairs are not listed.

Least-Squares Refinements on Intensity Curves. The intensity curve was fitted to the corresponding theoretical expression by a least-squares method with a preset weight function.[20] The mean amplitudes and shrinkage corrections of vibration[21] for all the internuclear distances were calculated on the basis of an estimated force model using the Urey-Bradley force field,[22] to which force constants for simple molecules with analogous geometrical arrangements (cyclohexane,[23] pentene, butene, *etc.*)[24] were transferred (listed in Table 1). A detailed procedure for the calculations is given elsewhere.[21] Numerical results are listed in Tables 2 and 3; they were used as fixed constants in the analysis. Systematic errors due to this constraint are examined in later sections. The asymmetry parameters κ for the bonded C–H were estimated to be 1.0×10^{-5} Å^3 and used as constants.[25]

Choice of Independent Parameters. Norbornadiene: This molecule is expected to have a C_{2v} structure. The RD analysis and a preliminary least-squares analysis on the intensity curves showed that the equilibrium structure of this molecule belongs to this symmetry. Thus the total number of independent parameters is twelve. In order to make the analysis easier, the following additional assum tions were taken into account.

1) The C–C–H angles are equal at the bridgehead, *i.e.*, $\angle$H–C_1–C_2=$\angle$H–C_1–C_6=$\angle$H–C_1–C_7.

2) All the C(sp^3)–H bond distances are equal.

3) The C(sp^2)–H bond distances are equal to that in ethylene, r_a=1.0896 Å.[26]

4) The vinylene group (C_1–CH=CH–C_4) is planar. These assumptions reduced the number of independent parameters to eight. Regarding the skeleton structure, three distances (C_1–C_2, C_2=C_3, and C_1–C_7) and two angles ($\angle C_1$–C_7–C_4 and θ defined above) were chosen. The parameters for hydrogen positions were $\angle$H–C_7–H, $\angle$C=C–H and the (weighted-average) C(sp^3)–H distance.

Norbornane: As mentioned in the preceding subsection, a C_{2v} structure was favored for this molecule, in which the structure are defined by fifteen independent parameters. Additional assumptions on the r_a structure[21,27] were as follows.

1) The H–C_2–H plane is perpendicular to the C_1–C_2–C_3 plane and bisects the C_1–C_2–C_3 angle, and *vice*

20) Y. Morino, K. Kuchitsu, and Y. Murata, *Acta Crystallogr.*, **18**, 549 (1965).

21) K. Kuchitsu and S. Konaka, *J. Chem. Phys.*, **45**, 4342 (1966).

22) The authors are grateful to Drs. Ichiro Nakagawa and Toyotoshi Ueda for allowing them to use programs "BGLZ" and "MV" and for their helpful advice on the force constants.

23) H. Takahashi and T. Shimanouchi, *J. Mol. Spectrosc.*, **13**, 43 (1964).

24) T. Shimanouchi, Y. Abe, and Y. Alaki, *Polymer J.* **2**, 199 (1971). The authors thank Professor Takehiko Shimanouchi and the other authors for giving their experimental results before publication.

25) K. Kuchitsu, This Bulletin, **40**, 498 (1967).

26) K. Kuchitsu, *J. Chem. Phys.*, **44**, 906 (1966).

27) G. Dallinga and L. H. Toneman, *J. Mol. Structure*, **1**, 11 (1967); K. Kuchitsu, T. Fukuyama, and Y. Morino, *ibid.*, **1**, 463 (1968).

versa.

2) The C–C–H angles are equal at the bridgehead, *i.e.*, $\angle H\text{–}C_1\text{–}C_2 = \angle H\text{–}C_1\text{–}C_6 = \angle H\text{–}C_1\text{–}C_7$.

3) All the C–H bond distances are equal.

4) All the H–C–H bond angles are equal.

Thus the number of independent parameters was reduced to seven. For the skeleton structure, three non-equivalent carbon-carbon distances, C_1–C_2, C_2–C_3, and C_1–C_7, and two angles, $\angle C_1\text{–}C_7\text{–}C_4$ and θ, were chosen as parameters. For hydrogen positions, a weighted-average C–H bond distance and the H–C–H angle were varied. In our earlier report,[14] the C_1–C_2 and C_2–C_3 distances were assumed to be equal, but this constraint has been released in the present analysis.

Results of the Analysis. The above analysis led to the most probable parameters with random standard

Table 4. Least-squares results for norbornadiene and norbornane[a]

Independent parameters	Norbornadiene I	Norbornadiene II	Norbornane
C_1——C_2	$1.533_2 \pm 0.001_4$	$1.532_9 \pm 0.001_3$	$1.536_2 \pm 0.002_9$
C_2——C_3	$1.338_7 \pm 0.001_2$	$1.338_3 \pm 0.001_1$	$1.552_7 \pm 0.008_7$
C_1——C_7	$1.571_1 \pm 0.003_1$	$1.571_2 \pm 0.003_0$	$1.557_9 \pm 0.008_6$
$\angle C_1\text{–}C_7\text{–}C_4$	$92.2 \pm 0.4°$	$96.0 \pm 0.2°$	$93.1 \pm 0.6°$
θ	$114.7 \pm 0.3°$	$116.4 \pm 0.4°$	$113.1 \pm 0.6°$
$\angle$C=C–H	$125._2 \pm 1._4°$	$122._3 \pm 1._3°$	——
$\angle$H–C–H	$114._7 \pm 3._0°$	$112._6 \pm 2._9°$	$109._9 \pm 1._5°$
C(sp^3)–H	$1.109_4 \pm 0.004_7$	$1.110_8 \pm 0.004_6$	$1.111_7 \pm 0.002_0$
k	$0.97_9 \pm 0.01_1$	$0.98_5 \pm 0.01_0$	0.986 ± 0.009

a) The r_a structures (in Å units for distances) with the random standard errors derived from least-squares analyses. The index of resolution k is dimensionless. For norbornadiene, two structures I and II significantly different from each other (particularly in the C_1–C_7–C_4 angle) have been obtained (see text).

Table 5. Error matrix for norbornadiene[a]

	C_1–C_2	C_2–C_3	C_1–C_7	C–H	$\angle C_1\text{–}C_7\text{–}C_4$	θ	$\angle$H–C–H	$\angle$C=C–H	k
C_1——C_2	14 13	7	−20	11	25	−22	38	42	−31
C_2——C_3	7	12 11	−12	10	13	−10	9	30	−17
C_1——C_7	−18	−11	31 30	−19	−39	35	−64	−50	47
C——H	8	9	−16	47 46	15	−19	77	54	−35
$\angle C_1\text{–}C_7\text{–}C_4$	12	6	−19	15	62 34	−38	103	43	−67
θ	−25	−13	39	−14	−21	53 63	−78	−72	55
$\angle$H–C–H	46	21	−72	65	−66	−120	461 501	197	−147
$\angle$C=C–H	40	28	−49	46	30	−76	201	258 226	−119
k	−30	−18	44	−29	6	69	−167	−120	107 105

a) Error matrix for the independent parameters. Units (10^{-4}) for the distances are Å, those for the angles are rad., and the index of resolution k is dimensionless. The upper and lower triangles represent the elements for the solutions I and II in Table 4, respectively (see text).

Table 6. Error matrix for norbornane[a]

	C_1–C_2	C_2–C_3	C_1–C_7	C–H	$\angle C_1\text{–}C_7\text{–}C_4$	θ	$\angle$H–C–H	k
C_1——C_2	29	−86	−21	−4	39	−57	−86	−22
C_2——C_3		87	−48	7	32	50	128	−48
C_1——C_7			86	−6	−65	66	−44	60
C——H				20	2	−5	46	6
$\angle C_1\text{–}C_7\text{–}C_4$					97	−84	105	−68
θ						99	−30	74
$\angle$H–C–H							313	38
k								92

a) Error matrix for the independent parameters. Units (10^{-4}) for the distances are Å, those for the angles are rad., and the index of resolution k is dimensionless.

errors shown in Table 4. The corresponding error matrices[28] are listed in Tables 5 and 6. Two alternative sets of solutions were obtained for norbornadiene. In particular, the C_1–C_7–C_4 angle converged to I 92.2°±0.4° and II 96.0°±0.2°, depending on the initial values of the analysis; any initial value smaller than 94° led to solution I, while any of those larger than that led to solution II. Changes in the other parameters due to correlation with the C_1–C_7–C_4 parameter were within about three times the corresponding random standard errors (see Table 4). These alternative solutions (I and II) were equally probable, since the variances $([V^*PV/(n-m)]^{1/2})$ for the solutions were 0.106 and 0.105, respectively. In this connection, the differences in the observed and the most probable theoretical intensities were similar to those among the observed intensities derived from different photographic plates. Accordingly, the variances derived from the above analysis did not provide a clearcut criterion on the resolution of this ambiguity. This problem is further investigated in the following section.

Estimation of Systematic Errors. For some of the parameters, systematic errors due to the uncertainties in the mean amplitudes fixed in the analysis are more important than the random standard errors. In other words, a unique determination of the structure depends critically on the correctness of the estimated amplitudes.[18] In order to investigate this problem, the following method has been considered.

Suppose a probability of finding a set of correct estimates of the mean amplitudes between l_1, l_2,···and $l_1+\mathrm{d}l_1$, $l_2+\mathrm{d}l_2$,··· is represented by $w(l)\mathrm{d}l \equiv w(l_1, l_2,\cdots)\cdot \mathrm{d}l_1\mathrm{d}l_2\cdots$. This function is not necessarily a Gaussian, nor may be symmetric about the most probable set. In principle, this function can be estimated if a probability of finding correct estimates of the force constants K, $w(K)\mathrm{d}K$, is known. In reality, an order-of-magnitude estimation of $w(l)$ is barely practicable, but it seems to be sufficient for the present purpose.

When a least-squares technique is applied to the molecular intensity with mean amplitudes fixed at l_1, l_2,···, the most probable estimates of the variable parameters, x_1, x_2,··· and their standard errors depend on l parametrically and constitute a probability distribution of the estimate, $W(x;l)\mathrm{d}x$; this function should conform, at least approximately, to a multidimensional Gaussian. The uncertainties in the mean amplitudes fixed in the analysis smear this error distribution in such a way that the total distribution, $P(x)\mathrm{d}x$, is a folding of the $W(x;l)$ and $w(l)$ functions,

$$P(x)\mathrm{d}x = \int W(x;\, l)w(l)\mathrm{d}l\mathrm{d}x, \qquad (1)$$

from which the systematic uncertainties from this origin in the x parameters may be estimated. The above equation can be integrated if analytical functions are assumed for $W(x;l)$ and $w(l)$; otherwise a numerical method may be used. Since a non-random problem is dealt with, the present analysis cannot have a full statistical significance. However, one may still apply the criterion of least squares to an automatic searching for a *plausible* set of parameters and their *possible uncertainties*.

In the present problem, the $w(l)$ function was estimated from our past experience: For simple molecules, errors in the experimental mean amplitudes are less than 10%, and those in the values calculated from assumed force fields are of a similar order. Usually, experimental and theoretical mean amplitudes for bonded atom pairs have smaller uncertainties than those for nonbonded atom pairs. Therefore, the uncertainties in the calculated mean amplitudes (Tables 2 and 3) were assumed to be 10 and 20% for bonded and nonbonded atom pairs, respectively.[29] The $w(l)$ function was assumed to be a product of individual probabilities, $w(l) = \prod_i w_i(l_i)$, where $w_i(l_i)$ were assumed to be independent of each other, constant in the ranges mentioned above and vanishing outside. Equation (1) was calculated by an approximate Monte-Carlo method. A set of the mean amplitudes l_i were prepared randomly by use of a function

$$l_i = l_{i0}\{1+2c_i(r-0.5)\}, \qquad (2)$$

where c_i is the estimated uncertainty in the theoretical amplitude l_i (10 or 20%), l_{i0} is given in Tables 2 and 3, and r is a set of uniform random numbers (0.0—1.0) generated by a program G5/TC/RUNI[30] in the program library of the Computer Centre of the University of Tokyo. Least-squares analyses were carried out with more than 20 sets of the fixed mean amplitudes sampled by Eq. (2) for either molecule. The resulting ranges Δ for the most-probable parameter values are listed in Table 7 together with their random standard errors

TABLE 7. ESTIMATION OF ERRORS

Independent parameters	Norbornadiene		Norbornane	
	σ_r[a]	$\Delta/2$[b]	σ_r	$\Delta/2$
(C——C)$_{av}$	···	···	0.001_0	0.001
C_1——C_2	0.001_4	0.004	0.002_9	0.010
C_2——C_3	0.001_1	0.001	0.008_7	0.021
C_1——C_7	0.003_0	0.009	0.008_6	0.021
∠C_1–C_7–C_4	0.2_1°	$2._8$°	0.6_5°	$1._5$°
θ	0.3_5°	$2._0$°	0.6_4°	$1._7$°
C(sp^3)–H	0.004_6	0.003	0.002_0	0.003
∠C=C–H	$1._3$°	$3._0$°	···	···
∠H–C–H	$3._0$°	$7._5$°	$1._5$°	$4._0$°

a) Random standard errors derived from least-squares analyses. Units for the distance parameters are Å.
b) One half the range Δ (difference between the upper and lower bounds of the most probable values) derived from the analyses with fixed mean amplitudes (see text).

σ_r, which characterize the widths of the $W(x;l)$ function; it turns out that the choice of the l sets does not influence σ_r significantly. In the total limits of error estimated from the table, the widths of $P(x)$ as represented by σ_r and Δ as well as other experimental systematic errors[27] (uncertainties in the scale factor (0.07%), sector imperfection (0.05%), *etc.*) were taken into ac-

28) K. Hedberg and M. Iwasaki, *Acta Crystallogr.*, **17**, 529 (1964).

29) A. Yokozeki and K. Kuchitsu, This Bulletin, **44**, 1783 (1971).

30) "Uniform Random Number Generator 1" programmed by M. Fushimi and K. Fujino, 1966.

TABLE 8. COMPARISON OF THE STRUCTURAL PARAMETERS IN NORBORNADIENE

Parameters	Present[a]	Ref. 14[b]	Ref. 13b[c]	Ref. 11[c]	Ref. 10[c]	Calcd[d]
C_1——C_2	$1.535_4\pm0.007$	1.535 ± 0.005	1.554 ± 0.002	1.549 ± 0.008	$1.522\pm0.01_1$	
C_2═══C_3	$1.343_2\pm0.003$	1.343 ± 0.005	1.341 ± 0.002	1.357 ± 0.005	1.333 ± 0.008	
C_1——C_7	$1.57_3\pm0.01_4$	$1.57_5\pm0.01_0$	1.514 ± 0.004	$1.56_8\pm0.01_5$	$1.55_8\pm0.01_6$	
$\angle C_1$–C_7–C_4	$94._1\pm3._0°$	$92.0\pm0.8°$	$99.5\pm0.6°$	$96.5°$ ……	$96._7\pm2._3°$	$92°$
θ	$115._6\pm2._2°$	$115.0\pm0.8°$	$111.4°$ ……	$115.4°$ ……	$110.8°$ ……	$113°$
C(sp^3)–H	$1.12_3\pm0.01_4$	$1.11_4\pm0.02_0$				
$\angle$C=C–H	$124\pm3°$	$123\pm4°$				
$\angle$H–C–H	$113\pm8°$	$(112°)$				

a) The r_g distances (Å) and the r_α angles determined in the present study with estimated limits of error (see text).
b) The r_g distances converted from the r_α distances given in Ref. 14.
c) Distances (r_g) are estimated by adding about 0.0015 Å to those reported in the references (probably r_α).
d) Calculated by a strain-relief scheme (see text).

TABLE 9. COMPARISON OF THE STRUCTURAL PARAMETERS IN NORBORNANE

Parameters	Present[a]	Ref. 14[b]	Ref. 13a[c]	Ref. 12[c]
$(C——C)_{av}$	$1.548_8\pm0.003$	1.549 ± 0.002	1.545 ……	1.555 ……
C_1——C_2	$1.53_9\pm0.01_2$	$1.54_2\pm0.01_5$	$1.53_4\pm0.01_4$	$1.55_6\pm0.01_2$
C_2——C_3	$1.55_7\pm0.02_5$	$1.54_3\pm0.02_5$	$1.57_8\pm0.01_8$	$1.55_1\pm0.01_5$
C_1——C_7	$1.56_0\pm0.02_4$	$1.57_0\pm0.01_6$	$1.53_5\pm0.03_5$	$1.55_9\pm0.01_5$
$\angle C_1$–C_7–C_4	$93._1\pm1._7°$	$93._2\pm1._5°$	$95._3\pm1._6°$	$96._0\pm1._0°$
θ	$113._1\pm1._8°$	$113._0\pm1._5°$	$111._3°$ ……	$108._0\pm1._5°$
$(C——H)_{av}$	$1.125_6\pm0.005$	$1.12_6\pm0.01_2$	1.11 ± 0.01	$1.11_5\pm0.01_5$
$\angle$H–C–H_{av}	$110\pm4°$	$110\pm3°$	$111\pm4°$	$108\pm1°$

a) The r_g distances (Å) and the r_α angles determined in the present study with limits of error (See text).
b) The r_g distances converted from the r_α distances given in Ref. 14.
c) Distances (r_g) are estimated by adding 0.0018 Å to the C–C distance and also 0.0055 Å to the C–H distances reported in the references (probably r_α).

count. They are listed in the first columns of Tables 8 and 9 accompanying the most probable parameters. For some of the parameters (*e.g.*, the C=C distance in norbornadiene), the P distributions seem to be essentially equal to the W distributions, whereas for other parameters (*e.g.*, the C_1–C_7–C_4 and θ angles) the W functions are broadened into the P functions so that the uncertainties in the parameter values originate entirely from the choice of the mean amplitudes.

For norbornadiene, the most-probable estimates of the C_1–C_7–C_4 parameter obtained in the above analyses scattered from 92° to 96°, whereas the values did not always depend on the starting parameters as mentioned in the preceding subsection. Since the error surface seems to have a broad minimum around 94° with respect to this parameter, a simple average over the estimated P distribution was taken as the final estimate of this parameter.

Despite the large uncertainties in the individual C–C bond distances mentioned above, their weighted-average values have been determined with much better accuracy. The C–C distance in norbornadiene has also been obtained uniquely without serious correlation with the mean amplitudes.

Comparison with Previous Results. The experimental values reported in the literature[10–14] are compared with the present results in Tables 8 and 9, where our preliminary results in the earlier communication[14] (r_α structures[21,27]) have been revised within their limits of error by taking into account the multiminimum solutions discussed above and the systematic errors due to the fixed mean amplitudes in the least-squares refinements.

Some of the parameters reported by other authors contradict one another beyond the quoted uncertainties. Possible sources of the discrepancies are considered to be (A) differences in the experimental intensity curves and (B) those in how the mean amplitudes are treated in the analysis.

Norbornadiene: The results obtained here are similar to those in Ref. 11 except for the scale. The double bond distance affords a good measure of the scale, since this distance can be determined with little ambiguity. The C=C distance determined here is in good agreement with that reported in Ref. 13b, whereas a scaling error of about 1% is involved in those of Refs. 10 and 11. On the other hand, the principal origin of the difference between the present structure and that of Ref. 13b is to be sought in source (B), since the experimental molecular intensity of Dallinga and Toneman[13b] agrees with ours to within the reproducibility of the observed intensity ($\Delta qM(q)\lesssim0.25$), and yet their results differ significantly from any of the others: (1) Their C_1–C_2 bond distance is longer than the C_1–C_7 distance, contrary to the results of all the other authors, and (2) their C_1–C_7–C_4 angle is much larger than those determined by the others.

The choice of the mean amplitudes seems to be responsible for the difference between Dallinga's results and ours. They adopted the mean amplitudes in cyclohexadiene, butadiene, *etc.* with no discrimination among the nonequivalent pairs and used them as fixed

constants: all the C–C amplitudes equal to 0.052 Å, all the nonbonded C···C amplitudes equal to 0.066 Å, all the nonbonded C···H amplitudes equal to 0.084 Å, and so forth. According to our estimates given in Table 2, however, significant differences exist among the amplitudes for nonequivalent pairs: For example, nonbonded C···C and C···H amplitudes range from 0.058 Å to 0.077 Å and from 0.094 Å to 0.140 Å, respectively. Judging from our finding discussed in the preceding subsection, their assumptions probably give rise to considerable systematic errors in their structural parameters. In fact, a theoretical molecular intensity curve based on their structural parameters and our theoretical mean amplitudes (Table 2), instead of their estimated amplitudes, deviates from our experimental curve beyond the uncertainties in the measurement. Furthermore, when some of the mean amplitudes were varied indiscriminately in the analysis of our intensity, a result similar to Dallinga's was obtained: C_1–C_2=1.558 Å, C_1–C_7=1.528 Å, $\angle C_1$–C_7–C_4=97° and θ=112°; however, the amplitudes obtained in this analysis seemed physically unrealistic: The C_1–C_2 (0.0600±0.0035 Å) and C_1–C_7 (0.0450±0.0028 Å) amplitudes are much too large and too small, respectively, and the $C_1\cdots C_3$ nonbonded amplitude (0.052±0.0022 Å) was similar to that of a bonded pair. After all, Dallinga's parameters seem to be one of the multisolutions resulting from a questionable choice of the mean amplitudes.

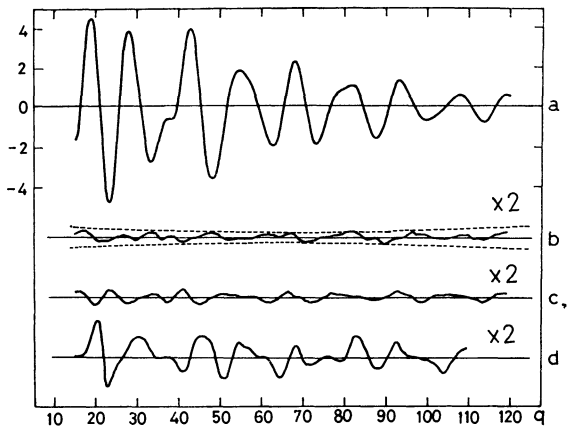

Fig. 4. Comparison of the experimental molecular intensity curves $qM(q)$ for norbornane. a: Present study; b: $[qM(q)_{exp}-qM(q)_{calc}]\times 2$ for the present measurement, where broken lines indicate the uncertainty level; c: [Curve a$-qM(q)$ measured by Dallinga and Toneman (Ref. 13a)]×2; d: [Curve a$-qM(q)$ measured by Chiang *et al.* (Ref. 12)]×2.

Norbornane: Our results are in good agreement with Dallinga's,[13a] except that the order of the C_2–C_3 and C_1–C_7 bond lengths is reversed, whereas Chiang's results[12] deviate from the others in the C–C weighted-average and θ; the C–C average is about 0.01 Å (see footnote c of Table 9) longer than the others, and the θ is about 4° smaller. The discrepancy in the C–C average seems to be a scaling error of about 0.5%. In this connection, experimental molecular intensity curves[12,13a,15] are compared in Fig. 4. Dallinga's curve agrees with ours to within the experimental uncertainties illustrated in Fig. 4 as broken lines, whereas Chiang's curve deviates significantly.[31] Therefore, the difference between Chiang's results and the others appears to be due to source (A), while that between Dallinga's results and ours is due to source (B). The differences between the individual C–C bond distances (C_1–C_2, C_2–C_3, and C_1–C_7) are within the estimated systematic errors due to the uncertainties in the mean amplitudes used in the analysis (see preceding section), so that it seems to be a hard problem at the present stage to discriminate the individual C–C bond distances unambiguously by electron diffraction alone. Additional information such as the rotational constants determinable from microwave spectroscopy may provide an effective solution of this problem.[27]

Discussion

Molecular Structure. The final results are listed in the first columns of Tables 8 and 9 with estimated limits of error including random and systematic errors.

The frame structure of norbornadiene is similar to that of norbornane, except that the C=C double bond distance seems to be slightly longer than that in ethylene (r_g=1.337 Å).[26] The C_1–C_2 bond distance is found to be about 0.03 Å longer than the C–C single bond adjacent to a C=C double bond (*e.g.*, 1.501 Å (r_s) in propylene[32]), and the C_1–C_7 bridge bond distance is about 0.03 Å longer than that in cyclohexane, 1.540 Å (r_g).[33] These lengthenings seem to indicate the effect of strong intramolecular strain, which also makes the C_1–C_7–C_4 angle decrease from the tetrahedral angle by more than 15°. Analogously, the C_1–C_2=C_3 angle is about 18° smaller than the C–C=C angle in *cis*-2-butene (*ca.* 125°),[34] whereas the C=C–H angle, 124°, seems to be normal.

For norbornane, the average value of the C–C bond distance, 1.548_8±0.003 Å, is about 0.01 Å longer than the normal single bond distance. Probably, this lengthening is due to the C_1–C_7 and C_2–C_3 bonds; they appear to be about 0.02 Å longer than the C_1–C_2 distance, though the differences are within their limits of error. The $C_1\cdots C_4$ distance, 2.26Å, is nearly equal to or a few hundredths of an angstrom shorter than that in norbornadience; the corresponding distances in the bicyclo-[2.2.2]-compounds (octane, octene, and octadiene) are about 0.3 Å longer.[29] All the C–C–C angles (the C_1–C_7–C_4 in particular), except for the C_2–C_1–C_6 angle (108.6°), are appreciably smaller than the tetra-

31) It is likely that the difference in the diffraction intensities obtained by Chiang *et al.*[12] from those obtained by Dallinga[13a] and in the present study (shown in Fig. 4) is due to the samples rather than to the apparatuses, since Chiang *et al.* found no essential difference between the intensity patterns taken at Cornell University and at the University of Oslo (by Bohn) by the use of portions of the same sample. (S. H. Bauer, private communication, April, 1971).

32) D. R. Lide, Jr., and D. Christensen, *J. Chem. Phys.*, **35**, 1374 (1961).

33) H. Kambara, K. Kuchitsu, and Y. Morino, This Bulletin, to be published.

34) T. N. Sarachman, *J. Chem. Phys.*, **49**, 3146 (1968); A. Almenningen, I. M. Anfinsen, and A. Haaland, *Acta Chem. Scand.*, **24**, 43 (1970); S. Kondo, Y. Sakurai, E. Hirota, and Y. Morino, *J. Mol. Spectrosc.*, **34**, 231 (1970).

TABLE 10. COMPARISON OF THE EXPERIMENTAL AND THEORETICAL STRUCTURES FOR NORBORNANE

Parameters	Obsd[a]	Calcd[b]					
		A	B	C	D	E	F
$(C—C)_{av}$	1.549	1.538	1.541	1.521			
$C_1—C_2$	1.53_9	1.534	1.543	1.520			
$C_2—C_3$	1.55_7	1.534	1.547	1.526			
$C_1—C_7$	1.56_0	1.551	1.531	1.513			
$\angle C_1$-C_7-C_4	$93._1°$	92.8°	93.9°	93.7°	92.0°	94—96°	93.0°
$\angle C_1$-C_2-C_3	$103._3°$	103.4°	102.9°	103.0°	103.0°	104°	103.0°
θ	$113._1°$	114.3°	110.1°	114.8°	113.9°	109°	113.0°

a) Observed structure determined in the present study (see Table 9). The C_1-C_2-C_3 angle was calculated from the independent parameters.

b) Theoretical structures calculated by a conformational analysis of the SCF-MINDO (A) or the strain-relief scheme (B—F). A: Ref. 6; B: Ref. 5; C: Ref. 4; D: Ref.2; E: Ref. 3; F: Present study (see text).

hedral angle. As discussed below, those anomalous values are consistent with the predictions based on the calculation of strain on bond angles and the interaction of the nonbonded C···C, C···H, and H···H atoms. X-ray observations[1] on similar angles in certain derivative molecules in the crystal phase are also in line with the above findings. Therefore, the angular distortions found in crystals should primarily be of intramolecular origin rather than of intermolecular origin.[18]

Intramolecular Strain. A calculation was made to account for the striking features in the skeletons of these molecules discussed above by means of a minimization of empirical strain energy.[29] A modified Urey-Bradley field similar to that developed by Jacob *et al.*[35] was employed with a "softer" set of nonbonded potential functions taken from Hendrickson's papers.[36] The force constants for the C–C–C and C–C=C angles were assumed to be equal to each other, 0.687 md·Å, and the equilibrium values for the former and the latter angles were chosen to be the tetrahedral and trigonal angles, respectively, while the torsional constant was taken from the height of the rotational barrier for ethane, 2.93 kcal/mol[37] for the carbon-carbon single bond. The analyses were made with bond lengths fixed to the values observed in the present work, and angular parameters for the skeleton were varied simultaneously in order to minimize the potential energy. The results, listed in the last column of Tables 8 and 10, account for the experimental values. Similar predictions made by other researchers[2-6] for norbornane, compared in Table 10, agree essentially with the present results in spite of the difference in the force fields and in the schemes, except that the dihedral angles θ in Refs. 3 and 5 are too small.

In order to account for the observed lengthening in the C–C bonds, bond lengths for the norbornane skeleton were varied in the above conformational analysis, where the stretching force constant and the equilibrium distance of the C–C bond were taken as 2.2 md/Å and 1.533 Å, respectively. The analysis resulted in all the C–C bond distances (C_1–C_2, C_2–C_3, and C_1–C_7) longer than 1.6 Å. This absurdity is no doubt due to the strong nonbonded repulsion assumed among the carbon atoms, since the mean next-to-bonded C···C distance of 2.412 Å is substantially shorter than the average value of 2.545Å in normal alkanes.[38] Gleicher and Schleyer[5] ignored those interactions of the 1–3 type in summing up all the nonbonded interactions, because they used a modified valence force field. The calculation made by Allinger *et al.*[4] is based on a similar scheme. However, neither prediction of the bond lengths, compared in Table 10, is in agreement with the observation. On the other hand, a conformational analysis made by Boder and Dewar[6] for norbornane by a semiempirical SCF-MO (MINDO/2) method predicted the C_1–C_7 distance to be longer than C_1–C_2 and C_2–C_3 distances, although their C–C weighted average was about 0.01 Å shorter than the observed value. According to another prediction of Dallinga and Ros[39] on the basis of an iterative extended Hückel method, the C_1–C_7 and C_1–C_2 distances for norbornane are practically equal and about 0.03 Å shorter than C_2–C_3. Therefore, a fully quantitative prediction of bond lengths in such bicyclic compounds seems to be beyond the reach of our control at the present stage.

The authors wish to thank Professor Emeritus Yonezo Morino for his continual encouragement and Drs. Hiroshi Tanida and Kazuo Tori of the Shionogi Research Laboratory for the samples used in this work. They are also indebted to Professor S. H. Bauer of Cornell University and Dr. G. Dallinga of Koninklijke/Shell-Laboratorium, Amsterdam for sending their experimental intensity curves and for their helpful discussions.

35) E. J. Jacob, H. B. Thompson, and L. S. Bartell, *J. Chem. Phys.*, **47**, 3736 (1967).
36) J. B. Hendrickson, *J. Amer. Chem. Soc.*, **83**, 4537 (1961).
37) S. Weiss and G. E. Leroi, *J. Chem. Phys.*, **48**, 962 (1968).
38) W. J. Adams, H. J. Geise, and L. S. Bartell, *J. Amer. Chem. Soc.*, **92**, 5013 (1970).
39) G. Dallinga and P. Ros, *Rec. Trav. Chim.*, **87**, 906 (1968).

Magnetic and Thermal Properties of Crystals Including Isolated Clusters. II. Heat Capacity of $Co_3(C_5H_5)_3S_2$ from 15 to 270 K and Mechanism of Phase Transition[1]

Michio SORAI, Akio KOSAKI, Hiroshi SUGA, Syûzô SEKI,
Toshikatsu YOSHIDA,* and Sei OTSUKA*

Department of Chemistry, Faculty of Science, Osaka University, Toyonaka, Osaka
**Department of Chemistry, Faculty of Engineering Science, Osaka University, Toyonaka, Osaka*

(Received March 31, 1971)

Heat capacity of $Co_3(C_5H_5)_3S_2$ was measured between 15 and 270 K. A phase transition was discovered at 192.5±0.1 K with the transition enthalpy and the entropy of 5253.4 J mol^{-1} and 28.894 J K^{-1} mol^{-1}, respectively. The transition entropy is well described as the sum of the configurational entropy of $R\ln 4$ due to cyclopentadienyl rings and the magnetic contribution of $R\ln 8$ due to cyclopentadienyl rings and the magnetic contribution of $R\ln 4$. The transition behavior is satisfactorily accounted for in the whole temperature region investigated in terms of the cooperative coupling between the orientational motion of the rings and the electronic states of a molecule on the basis of the Chesnut exciton model modified by the present authors. The model proposed here is to take both the temperature dependences of the energy parameters and the inversion of the spin state at higher temperatures into account. The measurements of infrared spectra and proton magnetic resonance were made as a function of temperature. These results are favorable to the present model. The electron spin resonance experiment also confirmed the present model.

In the course of our systematic magnetic and thermal investigations of isolated clusters, we reported, as series I,[2] the magnetic interaction of a trinuclear complex compound, $[Cr_3O(CH_3COO)_6(H_2O)_3]Cl\cdot 6H_2O$, which is one of the typical coordination compounds of the Werner-type with the spin quantum number of 3/2 per each Cr^{3+} ion. In this paper we will deal with magnetic and thermal properties of a trinuclear organometallic compound, $Co_3(C_5H_5)_3S_2$ [tris-(π-cyclopentadienylcobalt) disulfide].

Crystalline $Co_3(C_5H_5)_3S_2$, which was newly synthesized by two of the present authors (T.Y. and S.O.) and others,[3] consists of discrete molecules with the configuration shown in Fig. 1. The cobalt and sulfur atoms form a regular trigonal bipyramid with the cyclopentadienyl rings stereochemically disposed about the cobalt atoms such that lines passing from the center of the equilateral cobalt triangle through the cobalt atoms intersect the centroids of the cyclopentadienyl rings.[4] The magnetic susceptibility measured by two of the present authors (T.Y. and S.O.) and others[4] showed a maximum at 215 K. Above this temperature the susceptibility obeyed the Curie-Weiss law, but below 215 K it decreased rapidly reaching near zero at about 130 K. The effective magnetic moment μ_{eff} calculated from the susceptibility was found to be independent of temperature above 215 K and the average value of μ_{eff} was 2.53 B.M. Below this temperature, however, the μ_{eff} decreased gradually to zero at about 130 K. From the comparison of these values with the theoretical ones based on the orbital-quenched model and also from the simple molecular orbital treatment, it was proposed[4] that the magnetic property of the present compound may be explained by a ground singlet state at the low temperatures followed by a thermally accessible triplet state above 215 K.

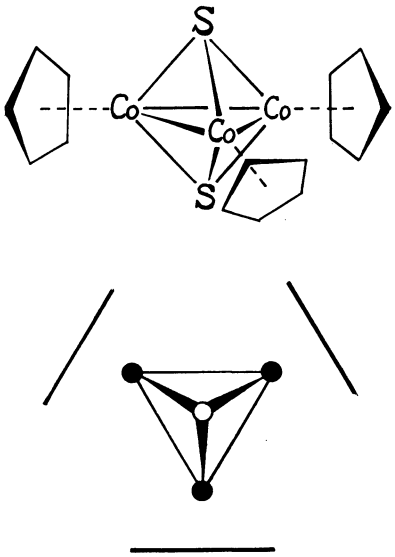

Fig. 1. Molecular configuration of $Co_3(C_5H_5)_3S_2$ (after Ref. 4).

The susceptibility maximum at about 215 K is suggestive of some cooperative effects in the present crystal. It should be, however, remarked here that unlike the preceding salt, $[Cr_3O(CH_3COO)_6(H_2O)_3]Cl\cdot 6H_2O$, the direct covalent bonds are formed among three metal atoms within a cluster and hence the cobalt atoms do not exist as ionic states in the present compound. The study of the magnetism accompanied by electronic excitation is somewhat difficult compared with that of the magnetism only due to spin states. The cooperative effects in such a system have not been fully investigated. One of the scare examples is the phenomenological theory for some dense magnetic excition systems by Chesnut,[5] who described successfully the gross aspects of the observed anomalous behaviors in some

1) A part of this paper was read at the 5th Japanese Calorimetry Conference, Osaka, (November, 1969), and at The Symposium on Magnetochemistry, Nagoya, (May, 1970).

2) M. Sorai, M. Tachiki, H. Suga, and S. Seki, *J. Phys. Soc. Jap.*, **30**, 750 (1971).

3) S. Otsuka, A. Nakamura, and T. Yoshida, *Liebig's Ann.*, **719**, 54 (1968).

4) S. Otsuka, T. Yoshida, and N. Kamijo, to be published.

5) D. B. Chesnut, *J. Chem. Phys.*, **40**, 405 (1964).

organic free-radical salts in terms of the relatively high exciton concentrations.

The purposes of the present paper are to measure the heat capacity and the related properties between 15 and 270 K and to clarify whether any cooperative phenomenon does exist or not in the present cluster system. As a result a heat capacity anomaly was discovered at 192.5 K with a large amount of the transition entropy unexpected solely from the magnetic contribution due to the old energy schemes.[4]

In order to get more insight into the mechanism of the phase transition we gave attention to the motional behavior of the cyclopentadienyl rings in a crystalline state. The physical properties of ferrocene, $Fe(C_5H_5)_2$, are favorably compared with those of the present crystal.

The transition behavior is satisfactorily accounted for in terms of the cooperative coupling between the orientational motion of the cyclopentadienyl rings and the electronic states on the basis of the Chesnut exciton model modified by the present authors.

Experimental and Results

Material. The present substance was prepared by the method[3] previously described and was recrystallized from a mixture of benzene and *n*-hexane to give dark prism crystals. The results of elementary analysis have been shown in the previous paper.

Heat Capacity. The heat capacity of $Co_3(C_5H_5)_3S_2$ crystal was measured by an adiabatic calorimeter[6] in the temperature range from 15 to 270 K. The

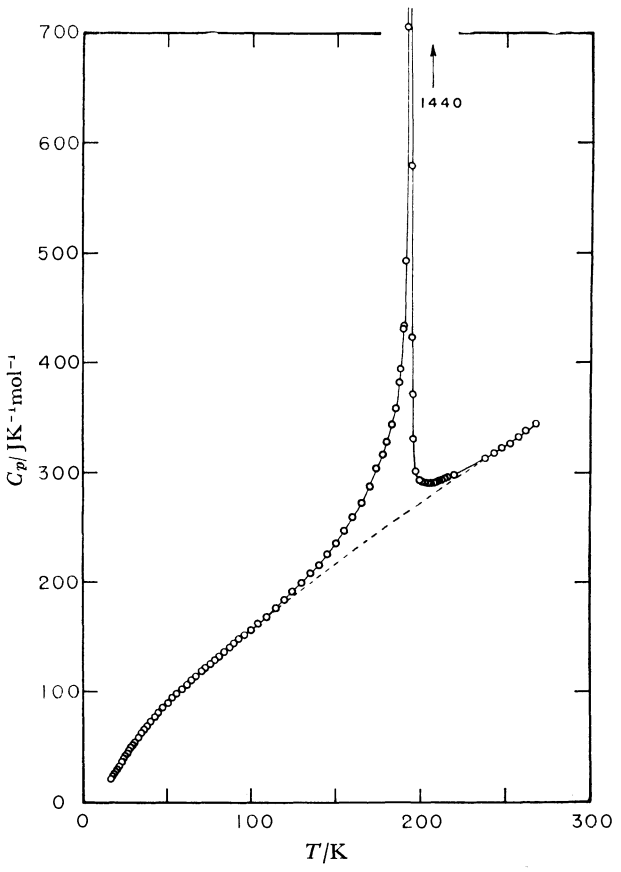

Fig. 2. The heat capacity of $Co_3(C_5H_5)_3S_2$ in the region from 15 to 270 K. Broken line indicates the "normal" heat capacity.

Table 1. The heat capacity of $Co_3(C_5H_5)_3S_2$ (Molecular weight 436.214).

T/K	C_p/JK^{-1} mol^{-1}	T/K	C_p/JK^{-1} mol^{-1}
Series I		160.296	259.865
213.544	293.606	165.370	273.152
215.951	294.697	169.764	287.221
219.856	297.436	174.051	303.801
		177.539	316.756
Series II		180.259	327.912
185.309	357.759	183.255	343.784
187.474	382.292		
189.897	431.324	Series V	
191.811	929.362	17.029	22.1788
193.338	848.175	17.657	24.0802
195.380	371.192	18.483	25.9588
197.666	301.046	19.452	28.4410
199.738	292.799	20.609	31.2609
201.820	291.226	21.878	34.4571
203.904	290.016	23.170	36.8831
205.987	289.981	24.342	40.0600
208.066	290.834	25.497	42.8414
210.140	291.676	26.651	44.8109
212.209	293.064	27.734	47.1279
		28.800	49.5101
Series III		29.927	51.9524
188.310	394.203	31.387	55.0027
190.162	435.352	33.104	58.7891
191.034	492.959	34.883	62.6953
191.641	705.223	36.644	65.9243
192.101	1216.80	38.404	69.1450
192.453	1437.31	40.381	72.9737
192.806	1207.14	42.545	76.6794
193.238	837.818	45.002	80.7959
193.788	578.937	47.733	84.9140
194.637	422.935	50.515	89.3507
195.992	331.177	53.268	93.6470
		56.038	97.7208
Series IV		58.900	102.198
81.181	133.192	61.701	106.352
83.568	136.611	64.509	110.780
86.451	140.529	67.334	114.760
89.497	144.640	70.155	118.413
92.645	148.511	72.981	121.545
95.945	151.914	75.896	124.630
99.755	157.117	78.539	128.206
104.368	163.035	81.149	131.951
109.281	169.431	83.321	138.521
114.313	176.733		
119.464	184.335	Series VI	
124.602	191.964	238.139	313.668
129.731	199.776	243.121	317.760
134.948	208.034	248.056	322.745
140.210	216.846	252.913	327.113
145.312	226.251	257.696	332.644
150.304	236.067	262.434	337.779
155.109	246.728	267.904	343.630

6) T. Matsuo, H. Suga, and S. Seki, *J. Phys. Soc. Jap.*, **30**, 785 (1971).

calorimeter cell contained 11.0344 g (=0.0252958 moles) of the sample and a small amount of helium gas to aid in heat transfer. As this substance is thermally stable but sensitive to air, all treatments were carried out in a dry-box under a stream of dried nitrogen gas.

The results of heat capacity measurements are summarized in Table 1 and plotted in Fig. 2. As can be seen from the figure at heat capacity anomaly was discovered reproducibly at 192.5 ± 0.1 K. This phase transition may be nonisothermal or of second-order because the time required for thermal equilibration after an energy input was not affected by the transition phenomenon. The heat capacity peak is very sharp in the vicinity of the transition point but the tail of excess heat capacity extends down to rather low-temperature side. It is therefore difficult to determine uniquely the enthalpy and the entropy of transition. A dashed line indicated at the base of the transition peak in Fig. 2 is a tentative but plausible curve which separates the excess heat capacities from the overall ones. The enthalpy and the entropy of transition calculated by use of this "normal" heat capacity were found to be 5253.4 $J\,mol^{-1}$ and $28.894\,JK^{-1}mol^{-1}$, respectively.

One of the most interesting features of this crystal that has come to light in the present thermal study is the large amount of transition entropy. The detailed discussions will be given in the next section where the entropy will be related to the mechanism of phase transition.

Infrared Absorption Spectra. The infrared absorption spectra of this substance were obtained by a Grating-type Infrared Spectrophotometer Model DS-402G (Japan Spectroscopic Co., Ltd.) in the range between 4000 and 400 cm^{-1} and by a Spectrophotometer No. FIS-001 (Hitachi Ltd.) in the range from 500 to 80 cm^{-1} at the temperatures of 295 and 120 K, respectively. For the sake of comparison the infrared spectra of ferrocene were also recorded on the same spectrophotometers. The nujol mull method was employed for the preparation of the samples.

In Figs. 3 and 4 the far-infrared spectra of $Co_3(C_5H_5)_3S_2$ and $Fe(C_5H_5)_2$ crystals are shown respectively in the range from 500 to 80 cm^{-1}. In both crystals many new absorption peaks were observed below each phase transition point.

Proton Magnetic Resonance. The proton magnetic resonance absorption spectra of the present substance

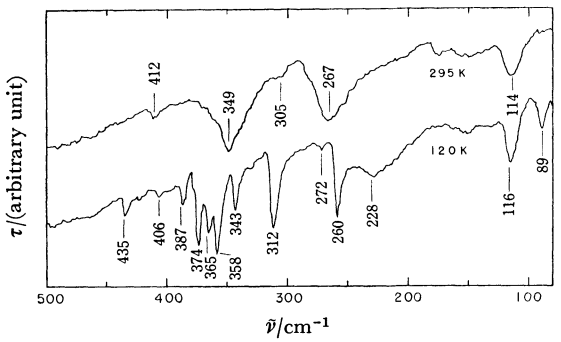

Fig. 3. The far-infrared spectra of $Co_3(C_5H_5)_3S_2$ in the region from 500 to 80 cm^{-1} at the temperatures of 295 and 120 K, respectively.

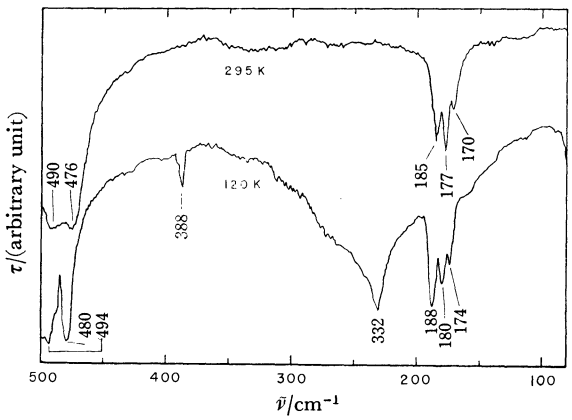

Fig. 4. The far-infrared spectra of $Fe(C_5H_5)_2$ in the region from 500 to 80 cm^{-1} at the temperatures of 295 and 120 K, respectively.

were obtained at a frequency of 21.4 MHz with a broad-line NMR Spectrometer Type BL-1 No. 2004 (Japan Electron Optics Laboratory Co., Ltd.) at 77 K and at room temperature.

The absorption peaks were symmetrical on both sides of the first derivative line. The line width changed from 3.1 gauss at 77 K to 2.6 gauss at room temperature. The second moments of the absorption curves obtained graphically were independent of temperature within the experimental errors between 77 K and room temperature. The average value of the second moment was 0.17 $gauss^2$. This value is not so accurate because the field modulasion amplitude employed here was rather large. It is, however, conceivable that the motional narrowing takes place already at a temperature as low as 77 K.

Phenomenological Nature of Phase Transition

The phase transition discovered at 192.5 K is obviously associated with some magnetic interactions, as revealed from the magnetic susceptibility measurement.[4] As was mentioned briefly in the preceding section, the entropy of transition has a large value of $28.894\,J\,K^{-1}mol^{-1}$ and cannot be explained solely by the magnetic contribution based on the thermal excitation of electrons in a molecule from a ground singlet state to an excited triplet state. In this energy scheme the magnetic entropy required for thorough excitation of electrons will be at most $R\ln 4$ ($=11.526\,J\,K^{-1}mol^{-1}$).

On the other hand, some insights into the nature of phase transition may be gained from a closer examination of the molecular and the crystal structures of the present substance. According to the results of X-ray diffraction analysis[4] the crystal belongs to the hexagonal system at room temperature. Its unit cell contains two chemical units and the space group is found to be $P6_3/m$ or $P6_3$. It is also indicated that the cyclopentadienyl ring is accurately coplanar. While there is no constraint imposed by crystal symmetry, the molecule itself has a point group symmetry of D_{3h}. This site symmetry may be accounted for by either a free rotation of or by a twofold orientational disorder

of each cyclopentadienyl ring.

It is, however, possible to exclude the case of free rotation in the present crystal as compared with the case of ferrocene crystal. In a gas phase a ferrocene molecule belongs to a symmetry of $D_{\infty h}$ indicating that no appreciable barrier to free or only slightly hindered rotation of the cyclopentadienyl rings exists.[7] According to Dunitz, Orgel, and Rich,[8] however, the D_{5d} configuration of ferrocene found in the solid state must arise from intermolecular interactions, where the repulsive interaction between hydrogen atoms belonging to adjacent molecules plays a dominant role. Edwards, Kington, and Mason[9] measured the heat capacity of ferrocene crystal, which is diamagnetic, and found a phase transition at 163.9 K with a secondary small C_p maximum at 169 K. On the assumption that each cyclopentadienyl ring can take up two orientations in the room temperature phase, one of which may be obtained by a rotation through 36° in the plane of the ring, they successfully accounted for the observed transition entropy of $R\ln 1.89$ as the twofold orientational disorder.

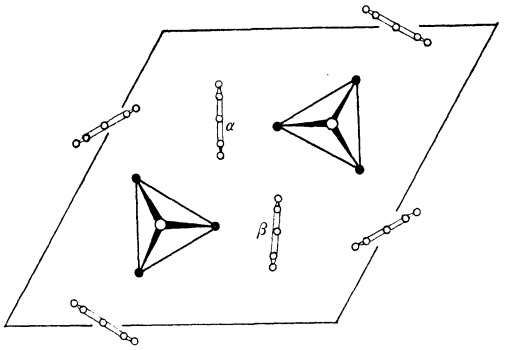

Fig. 5. A projection on the (001) plane of the crystal structure of $Co_3(C_5H_5)_3S_2$ (after Ref. 4).

Similar arguments may be applied to the present crystal, because the packing[4] of cyclopentadienyl rings belonging to different molecules, which are indicated for example as α and β in Fig. 5, has a close resemblance to that of ferrocene crystal along with the *c*-axis. As is the case of ferrocene we assumed that each cyclopentadienyl ring of $Co_3(C_5H_5)_3S_2$ can take up two orientations in the room temperature phase. But the difference from ferrocene is that the present compound has three cyclopentadienyl rings per one molecule. We further assumed that the interactions among three rings belonging to the same molecule would be negligible as each ring is separated far from the other two by a large core of cobalt and sulfur atoms. On these assumptions the number of energetically equivalent configurations attainable for one molecule may be eight ($=2^3$) and the configurational entropy due to the order-disorder phenomenon of the cyclopentadienyl rings amounts to $R\ln 8$. The observed transition entropy of 28.894 $JK^{-1}mol^{-1}$ is satisfactorily explained by the sum of this configurational entropy of $R\ln 8$ and the magnetic contribution of $R\ln 4$, which gives the value of 28.815 $JK^{-1}mol^{-1}$.

Strong evidences for the assumption that the ordering processes of cyclopentadienyl rings may be concerned in the phase transition can be obtained from the measurements of proton magnetic resonance and infrared spectra of this crystal as a function of temperature. As was mentioned in the previous section, the proton magnetic resonance of the present compound showed the motional narrowing already at a temperature as low as 77 K. And this fact is favorably compared with the case of ferrocene crystal[10] where the motional narrowing also takes place at 77 K and the activation energy for the reorientation is found to be as low as 2.3 kcal mol^{-1}. On the other hand, many new absorption peaks were observed in the infrared spectra of both the present substance and ferrocene below each phase transition point (see Figs. 3 and 4). Although we have not yet completed the assignments to these new peaks, it is likely that they are arising from fundamental and/or lattice bands due to some ordering processes of cyclopentadienyl rings below each phase transition point.

Modified Exciton Theory

In order to make more quantitative arguments about the mechanism of phase transition the phenomenological theory by Chesnut[5] based on the exciton model will be applied directly to the present system in the first half of this section, and in the latter half we will modify this exciton model to achieve the closest agreement between theory and experiment.

According to Chesnut[5] we imagine a system of N molecules, n of which are excited to a triplet state of energy $\varepsilon_0>0$. The mobile excited states will be referred to hereafter as "particles" and the system will be described as one with a particle (exciton) density $\rho=n/N$. The particle entropy of the system may be written as

$$\sigma/Nk = \rho\ln 3 - \rho\ln\rho - (1-\rho)\ln(1-\rho), \qquad (1)$$

and for the Helmholtz energy of the system Chesnut proposed the form as

$$A/N = \varepsilon_0\rho + \frac{1}{2}\varepsilon_1\rho^2 - kT[\rho\ln 3 - \rho\ln\rho - (1-\rho)\ln(1-\rho)], \qquad (2)$$

where $\varepsilon_0\rho$ represents the sum of the single-particle energies and the additional term quadratic in ρ may be attributable to an effective particle-particle interaction. The equilibrium value of ρ, which is obtained by minimizing A with respect to ρ, satisfies the following condition,

$$\rho = \left[\frac{1}{3}\exp(\varepsilon_0+\varepsilon_1\rho)/kT+1\right]^{-1}. \qquad (3)$$

The solution(s) of Eq. (3) must subject to another minimum condition,

$$\frac{1}{N}\frac{\partial^2 A}{\partial\rho^2} = \varepsilon_1 + \frac{kT}{\rho(1-\rho)} > 0. \qquad (4)$$

7) E. A. Seibold and L. E. Sutton, *J. Chem. Phys.*, **23**, 1967 (1955).

8) J. D. Dunitz, L. E. Orgel, and A. Rich, *Acta Crystallogr.*, **9**, 373 (1956).

9) J. W. Edwards, G. L. Kington, and R. Mason, *Trans. Faraday Soc.*, **56**, 660 (1960).

10) L. N. Mulay and A. Attalla, *J. Amer. Chem. Soc.*, **85**, 702 (1963).

On the other hand, the triplet excitation density ρ may be determined from the succeptibility measurement by using the following relation,

$$\chi = \frac{2Ng^2\mu_B^2}{3kT}\left[\frac{1}{3}\exp(\Delta E_{eff}/kT)+1\right]^{-1} \quad (5)$$

and

$$\rho = \left[\frac{1}{3}\exp(\Delta E_{eff}/kT)+1\right]^{-1}, \quad (6)$$

where ΔE_{eff} is the effective energy gap between the singlet and the triplet state, g the elctron g-factor and μ_B the Bohr magneton. The temperature dependence of ΔE_{eff} is obtainable from Eqs. (3) and (6);

$$\Delta E_{eff} = \varepsilon_0 + \varepsilon_1\rho. \quad (7)$$

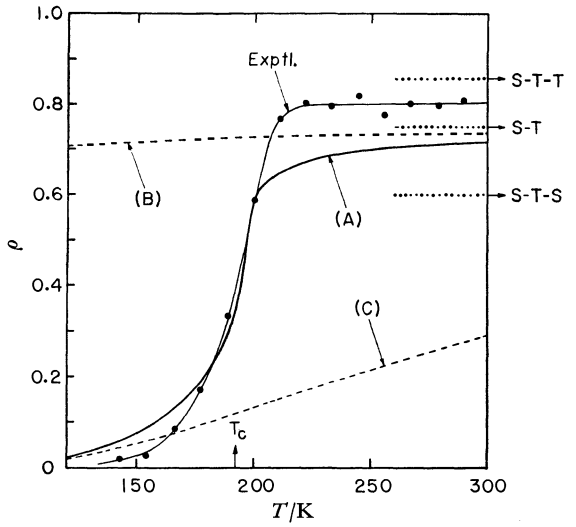

Fig. 6. Observed (curve drawn through black dots) and calculated values of the exciton density *versus* temperature for $Co_3(C_5H_5)_3S_2$. The values of energy parameters ε_1 and ε_0 used for the curves (A), (B), and (C) are indicated in the text.

The exciton density calculated from the succeptibility[4] of the present crystal is compared in Fig. 6 with the theoretical ones derived from Eq. (3). Curve (A) in this figure is corresponding to the best fit, the parameters of which were determined by trials and errors to be ε_0=0.05140eV and ε_1=−0.06559eV. Curves (B) and (C) are the ones in which the attractive interaction between particles is neglected; *i.e.*, ε_0=0.05140eV and ε_1=0 for curve (B) and ε_0=0.00221eV and ε_1=0 for curve (C). These two curves do not account for the experimental one at all. Three horizontal dotted lines indicated at the right-hand-side in Fig. 6 with the symbols *S*-*T*, *S*-*T*-*T* and *S*-*T*-*S* are respectively the limiting values of ρ in the case of $kT\to\infty$, where *S* means a singlet state, *T* a triplet state and a sequence of energy states are indicated as ground state - first excited state - second excited state.

In Fig. 7 the entropy of phase transition is compared with this model. The magnetic contribution estimated from Eq. (1) and the curve (A) in Fig. 6 exceeds the experimental entropy below about 165 K and hence the configurational entropy becomes negative below this temperature. We cannot accept such a feature from a physical reality.

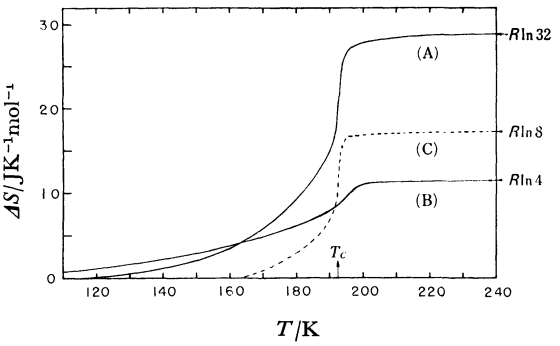

Fig. 7. The entropy of phase transition *versus* temperature for $Co_3(C_5H_5)_3S_2$. Curve (A) is the experimental value obtained from the heat capacity measurement. Curve (B) is the magnetic contribution calculated from Eq. (1) and the curve (A) in Fig. 6. Curve (C) is the configurational entropy determined by subtracting the value of curve (B) from that of curve (A) at respective temperature.

Apart from the details, however, this model is able to describe the gross aspects of the observed magnetic behavior. Then we attempt to modify this exciton model so that the closest agreement may be obtainable. As to the Chesnut model the energy parameters ε_1 and ε_0 are assumed to be independent of temperature. But this is not the case because a real system will be affected by thermal expansion. Moreover, the exciton density ρ determined from the experiment exceeds above near 208 K the limiting value of 0.75 based on the energy scheme of a ground singlet state followed by an excited triplet state (see Fig. 6). This feature may be interpreted either by considering a system with additional multi-degenerate state(s) above the first excited state such as *S*-*T*-*T* or by inverting the degeneracy of a ground and an excited state above 208 K. The latter model based on the inversion in the spin state seems to be more favorable to the present system as will be mentioned in the next section.

We modify the Chesnut exciton theory so as to take account of both a temperature dependence of the energy parameters and the inversion in the spin state above 208 K. In this model one of the energy parameters is eliminated by the condition: When ρ=3/4, $\Delta E_{eff}=\varepsilon_0(T)+\rho\varepsilon_1(T)=0$, then

$$\left.\begin{aligned}\varepsilon_0(T) &= -3\varepsilon_1(T)/4\\ \text{and}\qquad \Delta E_{eff} &= \varepsilon_1(T)\left(\rho-\frac{3}{4}\right).\end{aligned}\right\} \quad (8)$$

The temperature dependences of ε_1 and ε_0 were obtained by fitting Eqs. (3) and (8) to the experimental values of ρ. The results are shown in Fig. 8. Appreciable but different temperature dependences were found below and above the transition point. The following linear dependences were assumed:

$$\varepsilon_1/k = \begin{cases}184.0 - 6.471T & (T > T_c),\\ -1626 + 4.4T & (T < T_c).\end{cases} \quad (9)$$

On this assumption the temperature dependence of the exciton density except for the vicinity of the transition point is satisfactorily accounted for (see Fig. 9). As is shown in Fig. 10, the transition entropy obtained from

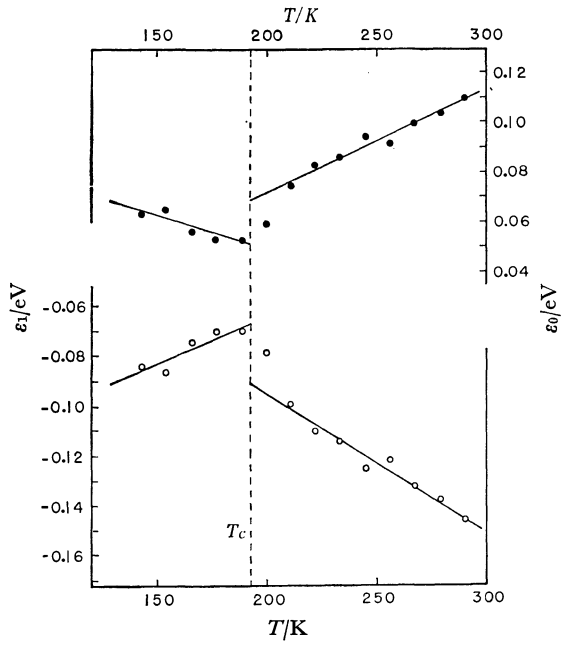

Fig. 8. The temperature dependences of the energy parameters ε_1 and ε_0 for $Co_3(C_5H_5)_3S_2$. Open and solid circles are the observed values. The straight lines are formulated in Eq. (9).

our heat capacity measurement is also well explained in the whole temperature region as the sum of the magnetic contribution derived from the present model and the configurational entropy due to the cyclopentadienyl rings. The effective energy gap ΔE_{eff} between a singlet and a triplet state is shown in Fig. 11 as a function of temperature. As can be seen from this figure, consideration of temperature dependence of the energy parameters well accounts for the actual behavior.

We have so far regarded the dominant origin of the temperature dependence of ε_1 and ε_0 as existing thermal expansion of real crystal but a remarkable difference in temperature dependence between both sides of the transition point will be a further problem.

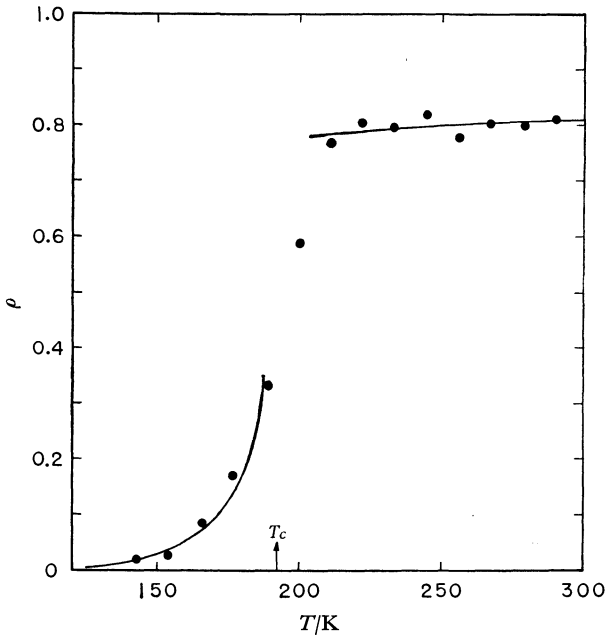

Fig. 9. Comparison of the exciton density between the observed (solid circle) and the calculated values (solid lines) based on the present model.

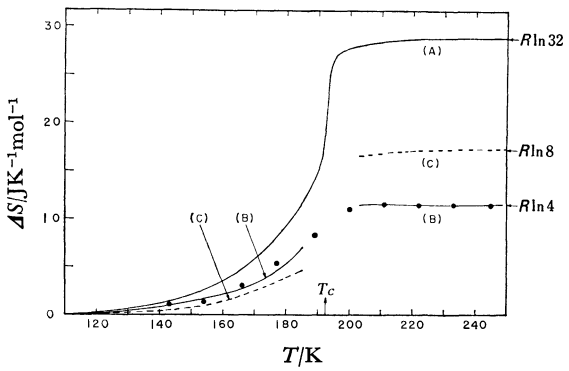

Fig. 10. The entropy of phase transition *versus* temperature for $Co_3(C_5H_5)_3S_2$. Curve (A), the experimental value determined from the heat capacity measurement; Curve (B), the magnetic contribution calculated based on the present model; Curve (C), the configurational entropy corresponding to the (A−B); Solid circle, the observed magnetic entropy determined from the magnetic susceptibility measurement.[4]

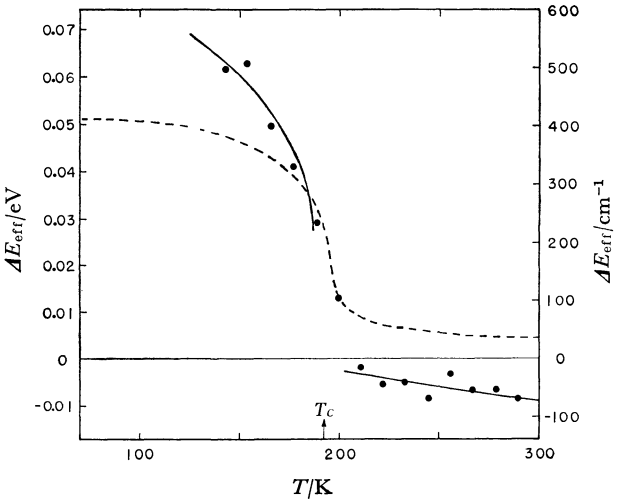

Fig. 11. Effective excitation energy ΔE_{eff} as a function of temperature for $Co_3(C_5H_5)_3S_2$. Solid circle, the observed value calculated from the susceptibility data;[4] Solid line, the theoretical value based on the present model; Broken line, the theoretical value based on the Chesnut exciton model.

Mechanism of Phase Transition

In this section we will present a physical picture for the temperature dependence of ΔE_{eff} and also for the inversion of spin state. In doing this, it is convenient to make arguments based on the electronic configuration of the present cluster molecule[4] and that of the nickel congener,[11] $Ni_3(C_5H_5)_3S_2$, derived from a simple molecular orbital scheme.

As we are interested in a relation between the electronic state and the spin state, our discussion will be

11) H. Vahrenkamp, V. A. Uchtman, and L. F. Dahl, *J. Amer. Chem. Soc.*, **90**, 3272 (1968).

confined to four truncated anti-bonding orbitals involved in the 3*d* orbitals of the cobalt atoms. According to Otsuka *et al.*,[4] the d_{z^2} orbitals of three cobalt atoms combine to give doubly degenerate anti-bonding orbitals $e'^*(d_{z^2})$, $(2\phi_1-\phi_2-\phi_3)/\sqrt{6}$ and $(\phi_2-\phi_3)/\sqrt{2}$. Here, ϕ_i is the d_{z^2} orbital of the *i*th cobalt atom and the coordinate axes at each cobalt atom are so chosen that the *z*-axis points to the centroid of the equilateral cobalt triangle, the *x*-axis lies in the triangle plane and the *y*-axis completes right-handed coordinate system. Similarly the $d_{x^2-y^2}$ orbitals give rise to two anti-bonding orbitals $e'^*(d_{x^2-y^2})$. The d_{xy} and the d_{zx} orbitals bring about non-degenerate anti-bonding orbital $a_1''^*(d_{xy})$ and $a_2'^*(d_{zx})$, respectively. Of all the valence electrons only eight electrons are accomodated in these anti-bonding orbitals. While it is not possible to settle the relative energy levels among these orbitals beyond the point of speculation, Otsuka *et al.* suggested that the configuration in the ground state will be $e'^*(d_{x^2-y^2})^4$, $e'^*(d_{z^2})^4$ leaving $a_1''^*(d_{xy})^0$ and $a_2'^*(d_{zx})^0$ vacant. Here, the superscript indicates the number of electrons accomodated in each anti-bonding orbital. Although their qualitative approach does not tell which orbital comes higher among the e'^* orbitals or among $a_1''^*$ and $a_2'^*$ orbitals, this energy scheme does not conflict with the gross aspect of magnetic behavior and with the bonding scheme[11] in the nickel congener.

It should be noticed here that the phase transition in the present crystal is satisfactorily accounted for by the sum of both configurational and magnetic contribution, the cooperative effect obviously arises from the gear-motion of cyclopentadienyl rings in the lattice. As was pointed out by Chesnut,[5] no cooperative phase transition may result in such a magnetic system as the present crystal where a discontinuity is not observed in the magnetic susceptibility curve. It is, however, possible to suppose that a cooperative coupling is still present between rotational motion of the cyclopentadienyl rings and the electronic state of a molecule. The existence of such a cooperative coupling is secured by the fact that the magnetic behavior can only be explained by varying the energy gap ΔE_{eff} with temperature and by introducing the inversion of spin state at higher temperatures.

We propose the following energy schemes as is shown in Fig. 12: (1) The energy levels of the $e'^*(d_{x^2-y^2})$ and the $a_1''^*(d_{xy})$ orbitals will not depend on temperature as the orbital overlap between these and the π-orbitals of each cyclopentadienyl ring is negligible. (2) The $e'^*(d_{z^2})$ level is also nearly independent of temperature. Although the small overlap exists, the reorientational motion of the ring will scarcely affect the energy state of this orbital because the overlapping is nearly symmetrical around each *z*-axis. (3) The $a_2'^*(d_{zx})$ will be sensitive to the motional behavior of the ring. Frequent reorientation of the ring would lead to almost complete smearing of the electron density around the circle formed by the rotating group. Hence the energy of this orbital will decrease with increasing reorientational motion of the ring. (4) The level-crossing is assumed to take place between the $a_2'^*(d_{zx})$ and the $e'^*(d_{z^2})$ at a certain temperature T^* and thus the inversion of spin state occures above T^*. In the present crystal the value of T^* is 208 K which is slightly higher than the phase transition point. Favorable evidence for the inversion of spin state is also obtained from the preliminary experiment of electron paramagnetic resonance by Kuwata,[12] who measured the absorption intensity and the line width as a function of temperature. (5) The physical meaning of ΔE_{eff} differs

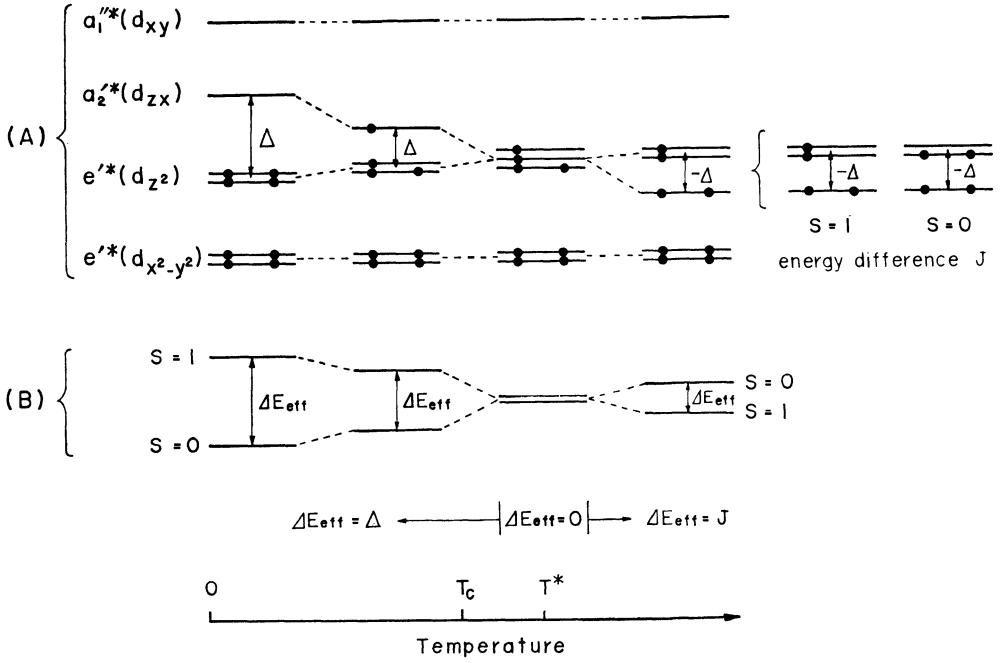

Fig. 12. Temperature dependence of (A) the electronic and (B) the spin states for $Co_3(C_5H_5)_3S_2$. The meanings of the molecular orbital symbols corresponding to each irreducible representations are indicated in the text.

12) K. Kuwata: private communicatoin (to be published).

from each other below and above T^*. ΔE_{eff} is equivalent to the level-spacing between the ground and the excited electronic states below T^*. Above T^*, on the other hand, ΔE_{eff} corresponds to the intra-J based on Hund's rule. The intra-J is in general almost independent of temperature. This fact really coincides with the present result as is shown in Fig. 11.

Conclusion

In the preceding sections of this paper we have shown the possibility of explaining the observed phase transition phenomenon of $Co_3(C_5H_5)_3S_2$ crystal based on the cooperative coupling between reorientational motion of the cyclopentadienyl rings in the lattice and the electronic state of a molecule. Magnetic behavior can be well described by introducing both the temperature dependences of the energy paramaters (ε_1 and ε_0) and the inversion of spin state at higher temperatures to the excition model derived by Chesnut.

Although the present model does not conflict with the existing experimental results, a possible model including the effects of higher excited states is still remaining. More rigorous calculation of molecular orbitals is necessary to gain more quantitative insight into the electronic state of the present crystal.

Heat capacity measurement of the nickel congener $Ni_3(C_5H_5)_3S_2$, will provide a useful information to judge the validity of the present arguments. Molecular and crystal structures of this compound are isomorphous with the present substance. This molecule, however, contains three more electrons compared with $Co_3(C_5H_5)_3S_2$ to give one unpaired electron in the ground electronic state.[11] So far as the energy scheme shown in Fig. 12 is adopted, anomalous magnetic behavior will not be expected for the nickel compound except for weak intercluster interactions. Even if a phase transition be observed in the nickel compound, such a phase transition would result solely from a configurational effect of cyclopentadienyl rings and the transition entropy would amount to only $R\ln 8$.

The authors would like to express their sincere thanks to Dr. Keiji Kuwata for informing the results of his ESR studies prior to publication and for his valuable discussions. Thanks are also extended to Mr. Shinichi Ishikawa for taking the infrared spectra.

BULLETIN OF THE CHEMICAL SOCIETY OF JAPAN, VOL. 44, 2371—2378(1971)

A General Matrix Method for Treating Elastic Constants of Molecular Crystals; Application to Orthorhombic Polyethylene

Yuji SHIRO and Tatsuo MIYAZAWA*

Faculty of Education, Hiroshima University, Shinonome, Hiroshima

**Institute for Protein Research, Osaka University, Kita-ku, Osaka*

(Received April 21, 1971)

A general method is developed for treating elastic constants of molecular crystals, with the ***B*** matrices as commonly used in normal-coordinate treatments. Equations are written in matrix forms, convenient for calculating elastic constants from intramolecular and intermolecular force field and are readily programed for electronic computations. Partial derivatives of elastic constants with respect to force constants are also derived, for least-square adjustments of force fields with reference to experimental elastic constants as well as vibrational frequencies. Matrix treatments of elastic constants are much simplified by the use of crystal symmetry, just as are treatments of normal vibrations. The matrix methods are explained for the example of orthorhombic polyethylene.

Normal coordinate treatments of molecular vibrations are useful for vibrational assignments of infrared and Raman spectra of polyatomic molecules. The ***GF*** matrix method derived by Wilson[1] is commonly used in treating molecular vibrations. Inverse-kinetic energy matrices (***G***) are constructed from ***B*** matrices, transformation matrices from Cartesian coordinates to intramolecular coordinates including bond-stretching, angle-bending[2] and internal-rotation coordinates.[3]

B matrices are also useful for treating normal vibrations of molecular crystals, where intermolecular coordinates are used together with intramolecular coordinates. In a previous paper,[4] applications of the ***GF*** matrix method were explained for factor-group vibrations of crystal lattices. Intermolecular and intramolecular force constants may be adjusted with reference to infrared and Raman frequencies observed for molecular crystals. However, too often, a unique set of force constants can not be obtained, because the number of observed frequencies is smaller than the number of force constants. In these cases, it is a common practice to assume certain type of potential functions.[2] Never-

1) E. B. Wilson, Jr., *J. Chem. Phys.*, **7**, 1047 (1939); **9**, 76 (1941).

2) T. Shimanouchi, *Nippon Kagaku Zasshi*, **86**, 261 (1965); "Physical Chemistry," Vol. 4, ed. by H. Eyring, Academic Press, New York, N. Y. (1970), p. 233.

3) T. Miyazawa and K. Fukushima, *J. Mol. Spectrosc.*, **15**, 308 (1965).

4) T. Shimanouchi, M. Tsuboi, and T. Miyazawa, *J. Chem. Phys.*, **35**, 1597 (1961).

theless, it is desirable to refer to additional experimental data that depend on force constants of crystals. For many inorganic crystals and some organic molecular crystals,[5] elastic constants have been measured and serve as useful data for studying force fields of crystals.

A general relation between force constants and elastic constants was discussed by Born and Huang.[6] However, in practical numerical treatments of elastic constants of molecular crystals together with their vibrational frequencies, it is important to formulate the transformation from the potential energy matrix ($\boldsymbol{F}$) to the elastic constant matrix ($\boldsymbol{C}$). This transformation may be derived with the $\boldsymbol{B}$ matrices as used in normal-coordinate treatments. Accordingly, in the present study, a general matrix method was developed for treating elastic constants from force fields of molecular crystals. Furthermore, partial derivatives of elastic constants with respect to force constants were derived and were formulated in matrix equations.

Energy Density due to Homogeneous Deformation

The potential energy (V) of a crystal lattice may be expressed in terms of an appropriate internal-coordinate vector ($\boldsymbol{R}$),

$$V = \frac{1}{2}\tilde{\boldsymbol{R}}\boldsymbol{F}_{\mathrm{R}}\boldsymbol{R} \tag{1}$$

where a tilde denotes transposed matrix or vector and $\boldsymbol{F}_{\mathrm{R}}$ is the potential energy matrix associated with the $\boldsymbol{R}$ vector.[1] For a crystal of N unit cells, the energy density (ε) is given as,

$$\varepsilon = \frac{1}{2}\tilde{\boldsymbol{R}}\boldsymbol{F}_{\mathrm{R}}\boldsymbol{R}/Nv \tag{2}$$

where v is the volume per unit cell.

A unit cell of a crystal lattice may be denoted with an index vector $\boldsymbol{L}$ with integral components (h,k,l), so that the internal-coordinate vector ($\boldsymbol{R}$) is expressed as

$$\boldsymbol{R} = \begin{bmatrix} \vdots \\ \boldsymbol{R}(\boldsymbol{L}) \\ \vdots \end{bmatrix} \tag{3}$$

where $\boldsymbol{R}(\boldsymbol{L})$ is the internal-coordinate subvector for the unit cell $\boldsymbol{L}$. If such a crystal is subjected to a homogeneous deformation, the resulting structure remains a perfect lattice and $\boldsymbol{R}(\boldsymbol{L})$ is actually independent of $\boldsymbol{L}$. Accordingly, the internal-coordinate vector ($\boldsymbol{R}$) may be transformed into the internal symmetry-coordinate vector ($\boldsymbol{R}^0$),

$$\boldsymbol{R}^0 = N^{-1}\sum_{\boldsymbol{L}}\boldsymbol{R}(\boldsymbol{L}) \tag{4}$$

The $\boldsymbol{R}^0$ coordinates are symmetric with respect to translational symmetry operations. A corresponding transformation need be carried out on the potential energy matrix ($\boldsymbol{F}_{\mathrm{R}}$), yielding

$$\boldsymbol{F}_{\mathrm{R}}{}^0 = \sum_{\boldsymbol{\lambda}}\boldsymbol{F}_{\mathrm{R}}(\boldsymbol{\lambda}) \tag{5}$$

where $\boldsymbol{F}_{\mathrm{R}}(\boldsymbol{\lambda})$ is the potential-energy submatrix, associated with the $\boldsymbol{R}(\boldsymbol{L})$ vector and the $\boldsymbol{R}(\boldsymbol{L}+\boldsymbol{\lambda})$ vector. Equation (2) is written as

$$\varepsilon = \frac{1}{2}\sum_{\boldsymbol{L}}\tilde{\boldsymbol{R}}^0\sum_{\boldsymbol{\lambda}}\boldsymbol{F}_{\mathrm{R}}(\boldsymbol{\lambda})\boldsymbol{R}^0/Nv = \frac{1}{2}[\tilde{\boldsymbol{R}}^0\boldsymbol{F}_{\mathrm{R}}{}^0\boldsymbol{R}^0]/v \tag{6}$$

and the energy density is now expressed with a finite number of internal symmetry-coordinates ($\boldsymbol{R}^0$). The $\boldsymbol{F}_{\mathrm{R}}{}^0$ matrix may also be used for treating infrared and Raman-active normal vibrations of molecular crystals.

Elastic Strain

In a homogeneous deformation of a crystal lattice, the displacement of the mth atom in the cell ($\boldsymbol{L}$) is given[7] as

$$\xi_\alpha(\boldsymbol{L}, m) = \sum_\beta U_{\alpha\beta}X_\beta(\boldsymbol{L}, m) + \rho_\alpha(m) \qquad (\alpha, \beta = x, y, \text{or } z) \tag{7}$$

where $U_{\alpha\beta}$ is external deformation parameter, $\boldsymbol{X}(\boldsymbol{L},m)$ is the position vector (column) of the mth atom of the cell ($\boldsymbol{L}$). The first term of the right side of Eq. (7) is due to the external deformation that is uniform throughout the crystal (even within a unit cell). The second term, $\boldsymbol{\rho}(m)$, is the internal strain vector of the mth atom that is common to every unit cell.

Now, for a crystal containing n atoms per unit cell, Eq. (7) may be reduced into a matrix form,

$$\tilde{\boldsymbol{\xi}}(\boldsymbol{L}) = \boldsymbol{P}(\boldsymbol{L})\boldsymbol{U} + \boldsymbol{\rho} \tag{8}$$

where

$$\tilde{\boldsymbol{\xi}}(\boldsymbol{L}) = [\xi_{\mathrm{x}}(\boldsymbol{L}, 1)\ \xi_{\mathrm{x}}(\boldsymbol{L}, 2)\ \cdots\ \xi_{\mathrm{x}}(\boldsymbol{L}, n)\ \xi_{\mathrm{y}}(\boldsymbol{L}, 1)\ \xi_{\mathrm{y}}(\boldsymbol{L}, 2)\ \cdots\ \xi_{\mathrm{y}}(\boldsymbol{L}, n)\ \xi_{\mathrm{z}}(\boldsymbol{L}, 1)\ \xi_{\mathrm{z}}(\boldsymbol{L}, 2)\ \cdots\ \xi_{\mathrm{z}}(\boldsymbol{L}, n)] \tag{9}$$

$$\tilde{\boldsymbol{P}}(\boldsymbol{L}) = \begin{bmatrix} \boldsymbol{X}(\boldsymbol{L}, 1) & \boldsymbol{X}(\boldsymbol{L}, 2) & \cdots & \boldsymbol{X}(\boldsymbol{L}, n) & 0 & 0 & \cdots & 0 & 0 & 0 & \cdots & 0 \\ 0 & 0 & \cdots & 0 & \boldsymbol{X}(\boldsymbol{L}, 1) & \boldsymbol{X}(\boldsymbol{L}, 2) & \cdots & \boldsymbol{X}(\boldsymbol{L}, n) & 0 & 0 & \cdots & 0 \\ 0 & 0 & \cdots & 0 & 0 & 0 & \cdots & 0 & \boldsymbol{X}(\boldsymbol{L}, 1) & \boldsymbol{X}(\boldsymbol{L}, 2) & \cdots & \boldsymbol{X}(\boldsymbol{L}, n) \end{bmatrix} \tag{10}$$

$$\tilde{\boldsymbol{U}} = [U_{\mathrm{xx}}\ U_{\mathrm{xy}}\ U_{\mathrm{xz}}\ U_{\mathrm{yx}}\ U_{\mathrm{yy}}\ U_{\mathrm{yz}}\ U_{\mathrm{zx}}\ U_{\mathrm{zy}}\ U_{\mathrm{zz}}] \tag{11}$$

$$\tilde{\boldsymbol{\rho}} = [\rho_{\mathrm{x}}(1)\ \rho_{\mathrm{x}}(2)\ \cdots\ \rho_{\mathrm{x}}(n)\ \rho_{\mathrm{y}}(1)\ \rho_{\mathrm{y}}(2)\ \cdots\ \rho_{\mathrm{y}}(n)\ \rho_{\mathrm{z}}(1)\ \rho_{\mathrm{z}}(2)\ \cdots\ \rho_{\mathrm{z}}(n)] \tag{12}$$

From the displacement vector ($\boldsymbol{\xi}$), the internal coordinate vector ($\boldsymbol{R}$) may be written as shown below, with the transformation matrix ($\boldsymbol{B}$)[1].

$$\boldsymbol{R} = \boldsymbol{B}\boldsymbol{\xi} \tag{13}$$

For a crystal under a homogeneous deformation, unit cells are all equivalent with one another and accordingly, the internal coordinate vector $\boldsymbol{R}(\boldsymbol{L})$ of the cell ($\boldsymbol{L}$) is given as

$$\boldsymbol{R}(\boldsymbol{L}) = \sum_{\boldsymbol{\lambda}}\boldsymbol{B}(\boldsymbol{\lambda})\boldsymbol{\xi}(\boldsymbol{L}+\boldsymbol{\lambda}) \tag{14}$$

5) K. H. Hellwedge, in Landolt-Boernstein Phys. Chem. Tables, new series, Group III-Vol. 1, Springer-Verlag, Berlin (1966), p. 1—39.

6) M. Born and K. Huang, "Dynamical Theory of Crystal Lattices," Oxford University Press, London (1954), Chapter III.

7) A. E. H. Love, "Mathematical Theory of Elasticity," Cambridge University Press, Cambridge (1934).

where $\boldsymbol{\lambda}$ is a difference-index vector and the $\boldsymbol{B}(\boldsymbol{\lambda})$ submatrix is independent of $\boldsymbol{L}$. On substituting Eq. (8) into Eq. (14), the $\boldsymbol{R}^0$ vector is now written as a sum of the terms due to external deformation ($\boldsymbol{U}$) and internal strain vector ($\boldsymbol{\rho}$),

$$\boldsymbol{R}^0 = \boldsymbol{R}(\boldsymbol{L}) = \boldsymbol{D}_U\boldsymbol{U} + \boldsymbol{B}_\rho\boldsymbol{\rho} \tag{15}$$

$$\boldsymbol{B}_\rho = \sum_{\boldsymbol{\lambda}}\boldsymbol{B}(\boldsymbol{\lambda}) \tag{16}$$

$$\boldsymbol{D}_U = \sum_{\boldsymbol{\lambda}}\boldsymbol{B}(\boldsymbol{\lambda})\boldsymbol{P}(\boldsymbol{L}+\boldsymbol{\lambda}) \tag{17}$$

It may be remarked that, under a homogeneous deformation, the transformation matrix ($\boldsymbol{D}_U$) for deformation parameters, is independent of the choice of cell ($\boldsymbol{L}$). A general method for calculating $\boldsymbol{D}_U$ matrix elements for bond-stretching, angle-bending and torsional coordinates is described in Appendix I.

Internal displacement coordinates, $\rho_\alpha(m)$, of Eq. (15) are not all independent, since the mass-weighted linear combinations, $\sum_m M(m)\rho_\alpha(m)/\sum_m M(m)$, give overall-translation coordinates ($\alpha=x$, y, and z) of the crystal. Accordingly, after an appropriate orthogonal transformation, the columns of the $\boldsymbol{B}_\rho$ matrix associated with these three redundant coordinates may be reduced to zero. In treating elastic constants, these redundant coordinates are deleted and remaining $3n$–3 internal displacements are used. However, the generality of the treatment of elastic constants may well be retained by deleting internal displacement coordinates [$\rho_x(m)$, $\rho_y(m)$, and $\rho_z(m)$] of any single atom (m), in place of the actual "overall-translation" coordinates.

Elastic Constant Matrix

The deformation parameters ($\boldsymbol{U}$) of Eq. (7) actually are not independent of "overall-rotation" modes of the crystal lattice. Accordingly, for deriving the elastic constant matrix ($\boldsymbol{C}$), it is necessary to introduce σ parameters as follows,

$$\begin{aligned}
\sigma_1 &= U_{xx} \quad \sigma_4 = U_{yz} + U_{zy} \quad \sigma_7 = U_{yz} - U_{zy} \\
\sigma_2 &= U_{yy} \quad \sigma_5 = U_{zx} + U_{xz} \quad \sigma_8 = U_{zx} - U_{xz} \\
\sigma_3 &= U_{zz} \quad \sigma_6 = U_{xy} + U_{yx} \quad \sigma_9 = U_{xy} - U_{yx}
\end{aligned} \tag{18}$$

For a homogeneous deformation, σ_1—σ_6 are external strain parameters whereas σ_7—σ_9 are "overall-rotation" parameters for the x, y, and z axes.[7]

The energy density (ε) may be expressed in terms of σ parameters, after the reverse transformation,

$$\boldsymbol{U} = \boldsymbol{T}_\sigma\boldsymbol{\sigma} \tag{19}$$

However, since the energy density (ε) is independent of "overall-rotation" parameters σ_7—σ_9, the last three columns of the transformation matrix ($\boldsymbol{T}_\sigma$) are redundant and accordingly σ_7—σ_9 will be left out of the external strain-parameter vector ($\boldsymbol{\sigma}$),

$$\tilde{\boldsymbol{\sigma}} = [\sigma_1\ \sigma_2\ \sigma_3\ \sigma_4\ \sigma_5\ \sigma_6] \tag{20}$$

$$\boldsymbol{T}_\sigma = \begin{pmatrix}
1 & 0 & 0 & 0 & 0 & 0 \\
0 & 0 & 0 & 0 & 0 & \frac{1}{2} \\
0 & 0 & 0 & 0 & \frac{1}{2} & 0 \\
0 & 0 & 0 & 0 & 0 & \frac{1}{2} \\
0 & 1 & 0 & 0 & 0 & 0 \\
0 & 0 & 0 & \frac{1}{2} & 0 & 0 \\
0 & 0 & 0 & 0 & \frac{1}{2} & 0 \\
0 & 0 & 0 & \frac{1}{2} & 0 & 0 \\
0 & 0 & 1 & 0 & 0 & 0
\end{pmatrix} \tag{21}$$

On substituting Eq. (19) into Eq. (15), the $\boldsymbol{R}^0$ vector is rewitten as,

$$\boldsymbol{R}^0 = \boldsymbol{D}_\sigma\boldsymbol{\sigma} + \boldsymbol{B}_\rho\boldsymbol{\rho} \tag{22}$$

where

$$\boldsymbol{D}_\sigma = \boldsymbol{D}_U\boldsymbol{T}_\sigma = [\sum_{\boldsymbol{\lambda}}\boldsymbol{B}(\boldsymbol{\lambda})\boldsymbol{P}(\boldsymbol{L}+\boldsymbol{\lambda})]\boldsymbol{T}_\sigma \tag{23}$$

From Eqs. (6) and (22), the energy density(ε) is derived as,

$$\varepsilon = \frac{1}{2}[\tilde{\boldsymbol{\sigma}}\tilde{\boldsymbol{D}}_\sigma + \tilde{\boldsymbol{\rho}}\tilde{\boldsymbol{B}}_\rho]\boldsymbol{F}_R{}^0[\boldsymbol{D}_\sigma\boldsymbol{\sigma} + \boldsymbol{B}_\rho\boldsymbol{\rho}]/v \tag{24}$$

However, the internal strain vector ($\boldsymbol{\rho}$) is related to the external strain parameters (σ),

$$\tilde{\boldsymbol{B}}_\rho\boldsymbol{F}_R{}^0\boldsymbol{B}_\rho\boldsymbol{\rho} + \tilde{\boldsymbol{B}}_\rho\boldsymbol{F}_R{}^0\boldsymbol{D}_\sigma\boldsymbol{\sigma} = 0 \tag{25}$$

so that the energy density (ε) is minimized with respect to internal strains ($\boldsymbol{\rho}$). Accordingly, the $\boldsymbol{\rho}$ vector given in Eq. (25) is put into Eq. (22) and the internal symmetry coordinates are now expressed in terms of the external strain parameters,

$$\boldsymbol{R}^0 = \boldsymbol{H}_\sigma\boldsymbol{\sigma} \tag{26}$$

where

$$\boldsymbol{H}_\sigma = \{\boldsymbol{E} - \boldsymbol{B}_\rho[\tilde{\boldsymbol{B}}_\rho\boldsymbol{F}_R{}^0\boldsymbol{B}_\rho]^{-1}\tilde{\boldsymbol{B}}_\rho\boldsymbol{F}_R{}^0\}\boldsymbol{D}_\sigma \tag{27}$$

The energy density is now derived as

$$\varepsilon = \frac{1}{2}\tilde{\boldsymbol{\sigma}}\tilde{\boldsymbol{H}}_\sigma\boldsymbol{F}_R{}^0\boldsymbol{H}_\sigma\boldsymbol{\sigma}/v = \frac{1}{2}\tilde{\boldsymbol{\sigma}}\boldsymbol{C}\boldsymbol{\sigma} \tag{28}$$

and the elastic constant matrix is thus derived as

$$\boldsymbol{C} = \tilde{\boldsymbol{H}}_\sigma\boldsymbol{F}_R{}^0\boldsymbol{H}_\sigma/v \tag{29}$$

On substituting Eq. (27) into Eq. (29), the elastic constant matrix is also written as,

$$\boldsymbol{C} = \{\tilde{\boldsymbol{D}}_\sigma\boldsymbol{F}_R{}^0\boldsymbol{D}_\sigma - \tilde{\boldsymbol{D}}_\sigma\boldsymbol{F}_R{}^0\boldsymbol{B}_\rho[\tilde{\boldsymbol{B}}_\rho\boldsymbol{F}_R{}^0\boldsymbol{B}_\rho]^{-1}\tilde{\boldsymbol{B}}_\rho\boldsymbol{F}_R{}^0\boldsymbol{D}_\sigma\}/v \tag{30}$$

The elastic stress vector ($\boldsymbol{S}_\sigma$) is now given as

$$\boldsymbol{S}_\sigma = \boldsymbol{C}_\sigma \tag{31}$$

and, therefore, when an elastic stress is applied to a crystalline lattice, the internal coordinate vector $\boldsymbol{R}^0$ is derived as

$$\boldsymbol{R}^0 = \boldsymbol{H}_\sigma\boldsymbol{\sigma} = \boldsymbol{H}_\sigma\boldsymbol{C}^{-1}\boldsymbol{S}_\sigma \tag{32}$$

Partial Derivatives of Elastic Constants

The potential energy submatrices, $\boldsymbol{F}_R(\boldsymbol{\lambda})$, have been shown to be useful for calculating elastic constants of molecular crystals. Accordingly, experimental elastic constants as well as vibrational frequencies may be referred to in adjusting force fields or force constants of

crystals. For least-square adjustments,[8] however, it is necessary to formulate partial derivatives of elastic constants with respect to force constants.

The potential-energy matrix ($\boldsymbol{F}_R^0$) may be expressed as a sum of matrices associated with force constants, $K(h)$,

$$\boldsymbol{F}_R^0 = \sum_h \boldsymbol{A}(h)K(h) \tag{33}$$

and accordingly

$$\Delta\boldsymbol{F}_R^0 = \sum_h \boldsymbol{A}(h)\Delta K(h) \tag{34}$$

Then, as proved in Appendix II, the derivatives of elastic constants with respect to force constants are expressed as,

$$\partial C_{ij}/\partial K(h) = [\tilde{\boldsymbol{H}}_\sigma \boldsymbol{A}(h)\boldsymbol{H}_\sigma]_{ij}/v \tag{35}$$

It may be seen that an elastic constant (C_{ij}) is expressed as a linear combination of partial derivatives $\partial C_{ij}/\partial K(h)$. Thus, from Eqs. (29), (33), and (35),

$$\begin{aligned} C_{ij} &= \{\tilde{\boldsymbol{H}}_\sigma \boldsymbol{F}_R^0 \boldsymbol{H}_\sigma/v\}_{ij} \\ &= \sum_h \{[\tilde{\boldsymbol{H}}_\sigma \boldsymbol{A}(h)\boldsymbol{H}_\sigma]_{ij}/v\}K(h) \\ &= \sum_h \{\partial C_{ij}/\partial K(h)\}K(h) \end{aligned} \tag{36}$$

This equation may be rewritten as

$$\sum_h [\partial C_{ij}/\partial K(h)]K(h)/C_{ij} = 1 \tag{37}$$

so that each term represents the fractional contribution of the hth potential term to the elastic constant (C_{ij}).

The equations for elastic constants, Eqs. (26), (28), (29), (35), (36), and (37), correspond closely with the equations for normal vibrations,[1,9]

$$\boldsymbol{R} = \boldsymbol{L}\boldsymbol{Q} \tag{38}$$

$$\boldsymbol{V} = \frac{1}{2}\tilde{\boldsymbol{Q}}\boldsymbol{\Lambda}\boldsymbol{Q} \tag{39}$$

$$\boldsymbol{\Lambda} = \tilde{\boldsymbol{L}}\boldsymbol{F}\boldsymbol{L} \tag{40}$$

$$\partial\lambda(a)/\partial K(h) = [\tilde{\boldsymbol{L}}\boldsymbol{A}(h)\boldsymbol{L}]_{aa} \tag{41}$$

$$\lambda(a) = \sum_h [\partial\lambda(a)/\partial K(h)]K(h) \tag{42}$$

$$\sum_h [\partial\lambda(a)/\partial K(h)]K(h)/\lambda(a) = 1 \tag{43}$$

where $\boldsymbol{L}$ is the eigenvector matrix, $\boldsymbol{Q}$ is normal-coordinate vector, $\boldsymbol{\Lambda}$ is diagonal frequency-parameter matrix, and $\lambda(a)$ is the ath frequency-parameter (squared angular frequency).

Partial derivatives of elastic constants [Eq. (35)] and frequency parameters [Eq. (41)] may now be used for least-square adjustments[8] of force constants of molecular crystals with reference to experimental elastic constants and vibrational frequencies.

Symmetry Treatments

Treatments of elastic constants may be simplified by the use of factor-group symmetry, just as are treatment of normal vibrations.[1] By an appropriate orthogonal transformation, new symmetry-coordinate vectors are set up,

$$\boldsymbol{R}_s^0 = \boldsymbol{T}_R \boldsymbol{R}^0 \tag{44}$$

$$\boldsymbol{\rho}_s = \boldsymbol{T}_\rho \boldsymbol{\rho} \tag{45}$$

and the potential-energy matrix ($\boldsymbol{F}_R^0$) is transformed accordingly,

$$\boldsymbol{F}_{Rs}^0 = \boldsymbol{T}_R \boldsymbol{F}_R^0 \tilde{\boldsymbol{T}}_R \tag{46}$$

$$\boldsymbol{A}_s(h) = \boldsymbol{T}_R \boldsymbol{A}(h) \tilde{\boldsymbol{T}}_R \tag{47}$$

From Eqs. (22), (44), and (45),

$$\boldsymbol{R}_s^0 = \boldsymbol{D}_{s\sigma}\boldsymbol{\sigma} + \boldsymbol{B}_{s\rho s}\boldsymbol{\rho}_s \tag{48}$$

where

$$\boldsymbol{D}_{s\sigma} = \boldsymbol{T}_R \boldsymbol{D}_\sigma \tag{49}$$

$$\boldsymbol{B}_{s\rho s} = \boldsymbol{T}_R \boldsymbol{B}_\rho \tilde{\boldsymbol{T}}_\rho \tag{50}$$

After defining

$$\begin{aligned} \boldsymbol{H}_{s\sigma} &= \boldsymbol{T}_R \boldsymbol{H}_\sigma \\ &= [\boldsymbol{E} - \boldsymbol{B}_{s\rho s}[\tilde{\boldsymbol{B}}_{s\rho s}\boldsymbol{F}_{Rs}^0 \boldsymbol{B}_{s\rho s}]^{-1}\tilde{\boldsymbol{B}}_{s\rho s}\boldsymbol{F}_{Rs}^0]\boldsymbol{D}_{s\sigma} \end{aligned} \tag{51}$$

the internal symmetry coordinate vector ($\boldsymbol{R}_s^0$) is expressed as,

$$\boldsymbol{R}_s^0 = \boldsymbol{H}_{s\sigma}\boldsymbol{\sigma} \tag{52}$$

$$= \boldsymbol{H}_{s\sigma}\boldsymbol{C}^{-1}\boldsymbol{S}_\sigma \tag{53}$$

and the elastic constant matrix ($\boldsymbol{C}$) is derived as

$$\boldsymbol{C} = \{\tilde{\boldsymbol{H}}_{s\sigma}\boldsymbol{F}_{Rs}^0 \boldsymbol{H}_{s\sigma}\}/v \tag{54}$$

$$\begin{aligned} &= \{\tilde{\boldsymbol{D}}_{s\sigma}\boldsymbol{F}_{Rs}^0 \boldsymbol{D}_{s\sigma} \\ &\quad - \tilde{\boldsymbol{D}}_{s\sigma}\boldsymbol{F}_{Rs}^0 \boldsymbol{B}_{s\rho s}[\tilde{\boldsymbol{B}}_{s\rho s}\boldsymbol{F}_{Rs}^0 \boldsymbol{B}_{s\rho s}]^{-1}\tilde{\boldsymbol{B}}_{s\rho s}\boldsymbol{F}_{Rs}^0 \boldsymbol{D}_{s\sigma}\}/v \end{aligned} \tag{55}$$

Partial derivatives of elastic constants with respect to a force constant are given as,

$$\partial C_{ij}/\partial K(h) = [\tilde{\boldsymbol{H}}_{s\sigma}\boldsymbol{A}_s(h)\boldsymbol{H}_{s\sigma}]_{ij}/v \tag{56}$$

The elastic constants of a symmetry species may be treated by the use only of relevant strain parameters (σ). For the example of orthorhombic crystals with the factor-group D_{2h}, strain parameters σ_1, σ_2, and σ_3 belong to the a_g species, and σ_4, σ_5, and σ_6 belong to the b_{1g}, b_{2g}, and b_{3g} species, respectively. $\boldsymbol{F}_{Rs}^0$, $\boldsymbol{A}_s(h)$ and $\boldsymbol{B}_{s\rho s}$ matrices are commonly used for treating normal vibrations and elastic constants belonging to the same symmetry species.

Finally it may be remarked that, before inverting the matrix of $[\tilde{\boldsymbol{B}}_{s\rho s}\boldsymbol{F}_R^0 \boldsymbol{B}_{s\rho s}]$ in Eqs. (51) and (55), the columns of the $\boldsymbol{B}_{s\rho s}$ matrices associated with "overall-translation" displacements, if any, need be deleted. Fortunately, however, for factor groups having the inversion operation, elastic strains belong to *gerade* species whereas "overall-translation" displacements belong to *ungerade* species. Accordingly, the $\boldsymbol{B}_{s\rho s}$ matrices associated with "overall-translation" displacements are separated, because of the inversion symmetry, from the $\boldsymbol{B}_{s\rho s}$ matrices as used for elastic properties.

Application to Polyethylene Crystal

The crystal structure of the orthorhombic polyethylene (Pnam-D_{2h}^{16}) was analysed by Bunn.[10] Two molecular chains pass through a unit cell along the c axis and there are four methylene groups per unit cell, with the lattice constants of $a_0=7.40$, $b_0=4.93$, and $c_0=2.54$ Å. The position vectors (Å) of four carbon atoms are

8) D. E. Mann, T. Shimanouchi, J. H. Meal, and L. Fano, *J. Chem. Phys.*, **27**, 43 (1957).

9) T. Miyazawa, *Nippon Kagaku Zasshi*, **76**, 1132 (1955).

10) C. W. Bunn, *Trans. Faraday Soc.*, **35**, 482 (1939).

$$\boldsymbol{X}(1) = \begin{bmatrix} -0.281 \\ -0.320 \\ -0.635 \end{bmatrix} \qquad \boldsymbol{X}(2) = \begin{bmatrix} 0.281 \\ 0.320 \\ 0.635 \end{bmatrix}$$

$$\boldsymbol{X}(3) = \begin{bmatrix} 3.419 \\ 2.785 \\ -0.635 \end{bmatrix} \qquad \boldsymbol{X}(4) = \begin{bmatrix} 3.981 \\ 2.145 \\ 0.635 \end{bmatrix}$$

In the previous study,[11] the frequency distribution and specific heat of the orthorhombic polyethylene crystal were treated with skeletal approximation; methylene groups were regarded as united atoms. The Urey-Bradley field[12] was used as the intramolecular force field, with the bond-stretching terms $[K_r(\Delta r)^2/2]$, angle-bending terms $[K_\phi(\Delta\phi)^2/2]$, repulsion terms $[K_q(\Delta q)^2/2]$ and internal-rotation terms $[K_t(\Delta t)^2/2]$ (see Fig. 1 for intramolecular coordinates). The intermolecular force field was expressed as a sum of three types of stretching terms, $P_1(\Delta p_1)^2/2$, $P_2(\Delta p_2)^2/2$, and $P_3(\Delta p_3)^2/2$, corresponding to intermethylene contacts of p_1=4.12, p_2=4.18, and p_3=4.57 Å, respectively. The intermethylene-stretching coordinates per unit cell are shown in Figs. 1 and 2 and are also listed below,

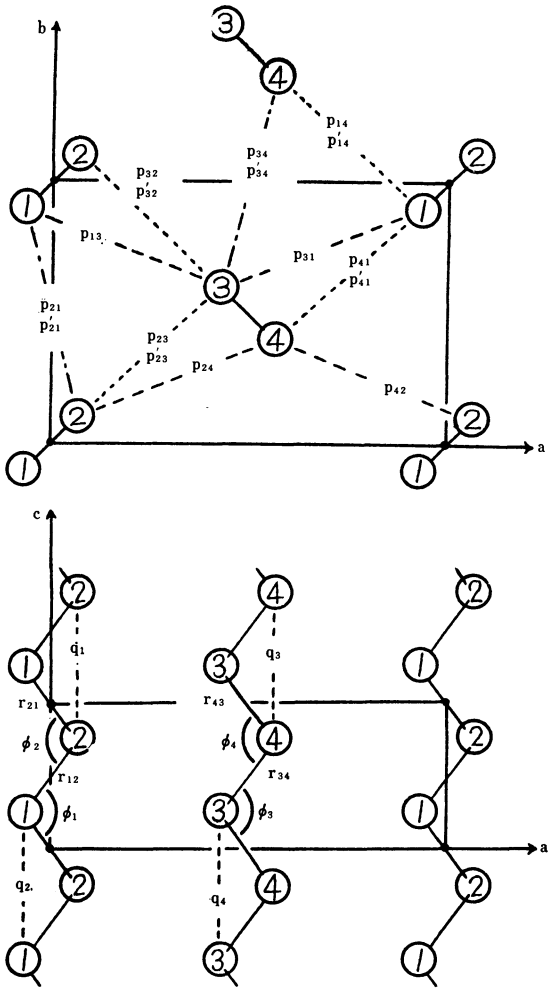

Fig. 1. Internal coordinates (*ab* and *ac* planes).

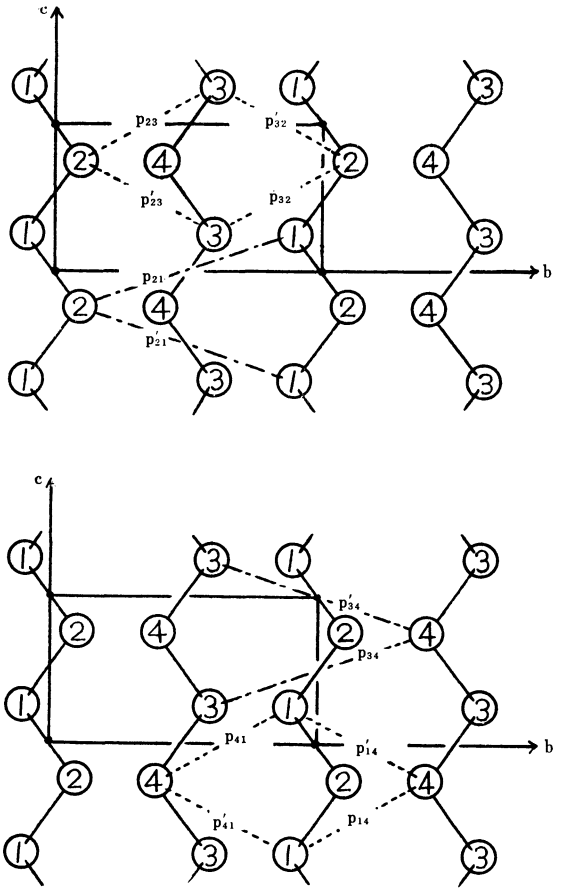

Fig. 2. Internal coordinates (*bc* plane).

Δp_1: Δp_{24}, Δp_{31}, Δp_{42}, and Δp_{13}
Δp_2: Δp_{23}, Δp_{41}, $\Delta p'_{23}$, $\Delta p'_{41}$, Δp_{32}, Δp_{14}, $\Delta p'_{32}$, and $\Delta p'_{14}$
Δp_3: Δp_{21}, $\Delta p'_{21}$, Δp_{34}, and $\Delta p'_{34}$

The intramolecular and intermolecular force constants were adjusted[11] as K_r=4.0 md/Å, K_ϕ=0.59 md Å/rad², K_q=0.35 md/Å, K_t=0.047 md Å/rad², $P_1=P_2$=0.025, and P_3=0.003 md/Å. These force constants were used in the present study of the elastic constants of polyethylene.

The internal coordinate vector ($\boldsymbol{R}$) of the crystal lattice was transformed, with translational operations, into the $\boldsymbol{R}^0$ vector with twenty-eight components,

$$\tilde{\boldsymbol{R}}^0 = [\Delta r_{12}{}^0, \Delta r_{21}{}^0, \Delta r_{43}{}^0, \Delta r_{34}{}^0, \Delta\phi_1{}^0, \Delta\phi_2{}^0, \Delta\phi_3{}^0, \Delta\phi_4{}^0, \Delta q_1{}^0, \Delta q_2{}^0, \Delta q_3{}^0, \Delta q_4{}^0, \Delta p_{24}{}^0, \Delta p_{31}{}^0, \Delta p_{42}{}^0, \Delta p_{13}{}^0, \Delta p_{23}{}^0, \Delta p_{41}{}^0, \Delta p'_{23}{}^0, \Delta p'_{41}{}^0, \Delta p_{32}{}^0, \Delta p_{14}{}^0, \Delta p'_{32}{}^0, \Delta p'_{14}{}^0, \Delta p_{21}{}^0, \Delta p'_{21}{}^0, \Delta p_{34}{}^0, \Delta p'_{34}{}^0]$$

Internal-rotation coordinates (Δt) were deleted because they are antisymmetric with respect to the inversion symmetry and are redundant in treating elastic constants which belong to *gerade* species.

According to the factor-group symmetry of D_{2h}, the $\boldsymbol{R}^0$ vector was then transformed into symmetry-coordinate vectors ($\boldsymbol{R}_s{}^0$) for the symmetry species of elastic constants;

$$\tilde{\boldsymbol{R}}_s{}^0(a_g) = [R_s{}^0(1), R_s{}^0(2), R_s{}^0(3), R_s{}^0(4), R_s{}^0(5), R_s{}^0(6)],$$
$$\tilde{\boldsymbol{R}}_s{}^0(b_{1g}) = [R_s{}^0(7), R_s{}^0(8), R_s{}^0(9)],$$
$$\tilde{\boldsymbol{R}}_s{}^0(b_{2g}) = [R_s{}^0(10), R_s{}^0(11), R_s{}^0(12)],$$
$$\tilde{\boldsymbol{R}}_s{}^0(b_{3g}) = [R_s{}^0(13), R_s{}^0(14), R_s{}^0(15), R_s{}^0(16), R_s{}^0(17)].$$

11) T. Kitagawa and T. Miyazawa, This Bulletin, **43**, 372 (1970).
12) T. Shimanouchi, *Pure Appl. Chem.*, **7**, 261 (1962).

The transformation matrix elements are shown below, for each of bond-stretching (Δr), angle-bending ($\Delta\phi$), repulsion (Δq), and intermethylene-stretching coordinates (Δp_1, Δp_2, and Δp_3).

$T_R(\Delta r)$	$R^0(1)$	$R^0(2)$	$R^0(3)$	$R^0(4)$
$R_s^0(1)$	$\frac{1}{2}$	$\frac{1}{2}$	$\frac{1}{2}$	$\frac{1}{2}$
$R_s^0(7)$	$\frac{1}{2}$	$-\frac{1}{2}$	$\frac{1}{2}$	$-\frac{1}{2}$
$R_s^0(10)$	$\frac{1}{2}$	$-\frac{1}{2}$	$-\frac{1}{2}$	$\frac{1}{2}$
$R_s^0(13)$	$\frac{1}{2}$	$\frac{1}{2}$	$-\frac{1}{2}$	$-\frac{1}{2}$

$T_R(\Delta\phi)$	$R^0(5)$	$R^0(6)$	$R^0(7)$	$R^0(8)$
$R_s^0(2)$	$\frac{1}{2}$	$\frac{1}{2}$	$\frac{1}{2}$	$\frac{1}{2}$
$R_s^0(14)$	$\frac{1}{2}$	$\frac{1}{2}$	$-\frac{1}{2}$	$-\frac{1}{2}$

$T_R(\Delta q)$	$R^0(9)$	$R^0(10)$	$R^0(11)$	$R^0(12)$
$R_s^0(3)$	$\frac{1}{2}$	$\frac{1}{2}$	$\frac{1}{2}$	$\frac{1}{2}$

$T_R(\Delta p_1)$	$R^0(13)$	$R^0(14)$	$R^0(15)$	$R^0(16)$
$R_s^0(4)$	$\frac{1}{2}$	$\frac{1}{2}$	$\frac{1}{2}$	$\frac{1}{2}$
$R_s^0(15)$	$\frac{1}{2}$	$\frac{1}{2}$	$-\frac{1}{2}$	$-\frac{1}{2}$

$T_R(\Delta p_2)$	$R^0(17)$	$R^0(18)$	$R^0(19)$	$R^0(20)$	$R^0(21)$	$R^0(22)$	$R^0(23)$	$R^0(24)$
$R_s^0(5)$	$8^{-1/2}$	$8^{-1/2}$	$8^{-1/2}$	$8^{-1/2}$	$8^{-1/2}$	$8^{-1/2}$	$8^{-1/2}$	$8^{-1/2}$
$R_s^0(8)$	$8^{-1/2}$	$8^{-1/2}$	$-8^{-1/2}$	$-8^{-1/2}$	$8^{-1/2}$	$8^{-1/2}$	$-8^{-1/2}$	$-8^{-1/2}$
$R_s^0(11)$	$8^{-1/2}$	$8^{-1/2}$	$-8^{-1/2}$	$-8^{-1/2}$	$-8^{-1/2}$	$-8^{-1/2}$	$8^{-1/2}$	$8^{-1/2}$
$R_s^0(16)$	$8^{-1/2}$	$8^{-1/2}$	$8^{-1/2}$	$8^{-1/2}$	$-8^{-1/2}$	$-8^{-1/2}$	$-8^{-1/2}$	$-8^{-1/2}$

$T_R(\Delta p_3)$	$R^0(25)$	$R^0(26)$	$R^0(27)$	$R^0(28)$
$R_s^0(6)$	$\frac{1}{2}$	$\frac{1}{2}$	$\frac{1}{2}$	$\frac{1}{2}$
$R_s^0(9)$	$\frac{1}{2}$	$-\frac{1}{2}$	$\frac{1}{2}$	$-\frac{1}{2}$
$R_s^0(12)$	$\frac{1}{2}$	$-\frac{1}{2}$	$-\frac{1}{2}$	$\frac{1}{2}$
$R_s^0(17)$	$\frac{1}{2}$	$\frac{1}{2}$	$-\frac{1}{2}$	$-\frac{1}{2}$

The potential-energy matrix ($\boldsymbol{F}$) was transformed accordingly as,

$$\boldsymbol{F}_{Rs}{}^0(a_g) = \begin{pmatrix} K_r & 0 & 0 & 0 & 0 & 0 \\ 0 & K_\phi & 0 & 0 & 0 & 0 \\ 0 & 0 & K_q & 0 & 0 & 0 \\ 0 & 0 & 0 & P_1 & 0 & 0 \\ 0 & 0 & 0 & 0 & P_2 & 0 \\ 0 & 0 & 0 & 0 & 0 & P_3 \end{pmatrix} \quad (57)$$

$$\boldsymbol{F}_{Rs}{}^0(b_{1g}) = \boldsymbol{F}_{Rs}{}^0(b_{2g}) = \begin{pmatrix} K_r & 0 & 0 \\ 0 & P_2 & 0 \\ 0 & 0 & P_3 \end{pmatrix} \quad (58)$$

$$\boldsymbol{F}_{Rs}{}^0(b_{3g}) = \begin{pmatrix} K_r & 0 & 0 & 0 & 0 \\ 0 & K_\phi & 0 & 0 & 0 \\ 0 & 0 & P_1 & 0 & 0 \\ 0 & 0 & 0 & P_2 & 0 \\ 0 & 0 & 0 & 0 & P_3 \end{pmatrix} \quad (59)$$

The internal strain vector $\boldsymbol{\rho}$ [Eq. (12)] of carbon atoms was also transformed into internal symmetry-strain vectors ($\boldsymbol{\rho}_s$) for the symmetry species of elastic constants,

$$a_g \text{ species}: \rho_s(1) = [\rho_x(1) - \rho_x(2) + \rho_x(3) - \rho_x(4)]/2$$
$$\rho_s(2) = [\rho_y(1) - \rho_y(2) - \rho_y(3) + \rho_y(4)]/2 \quad (60)$$
$$b_{1g} \text{ species}: \rho_s(3) = [\rho_z(1) - \rho_z(2) - \rho_z(3) + \rho_z(4)]/2 \quad (61)$$
$$b_{2g} \text{ species}: \rho_s(4) = [\rho_z(1) - \rho_z(2) + \rho_z(3) - \rho_z(4)]/2 \quad (62)$$
$$b_{3g} \text{ species}: \rho_s(5) = [\rho_x(1) - \rho_x(2) - \rho_x(3) + \rho_x(4)]/2 \quad (63)$$
$$\rho_s(6) = [\rho_y(1) - \rho_y(2) + \rho_y(3) - \rho_y(4)]/2 \quad (64)$$

The $\boldsymbol{B}_{s\rho s}$, $\boldsymbol{D}_{s\sigma}$, and $\boldsymbol{H}_{s\sigma}$ matrices were calculated, as shown in Tables 1—4, from $\boldsymbol{B}(\boldsymbol{\lambda})$ and $\boldsymbol{P}(\boldsymbol{L}+\boldsymbol{\lambda})$ submatrices, with Eqs. (16), (21), (23), (49), (50), and (51). Finally, with Eq. (54), the elastic constants were calculated as,

a_g species : $C_{11}=0.022_0$, $C_{22}=0.007_5$, $C_{33}=0.243$
$C_{23}=0.002_6$, $C_{31}=0.003_8$, $C_{12}=0.009_8$ md/Å^2

b_{1g} species: $C_{44}=0.001_5$ md/Å^2

b_{2g} species: $C_{55}=0.002_7$ md/Å^2

b_{3g} species: $C_{66}=0.012_6$ md/Å^2

Young's moduli of orthorhombic polyethylene were calculated as

$$E_a = 1/(C^{-1})_{11} = 0.009$$
$$E_b = 1/(C^{-1})_{22} = 0.003$$
$$E_c = 1/(C^{-1})_{33} = 0.243 \text{ md/Å}^2$$

In comparisn, Young's moduli measured at room temperature[13] are E_a=0.005, E_b=0.004, and E_c=0.235 md/Å^2. It may be remarked that the Young's modulus along the c axis (E_c) is due to the intramolecular force field and is much higher than the values of E_a or E_b which are due to intermolecular contacts. Finally, partial derivatives of elastic constants with respect to force constants were calculated with Eqs. (33), (47), and (56). The fractional distribution of potential terms is shown in Table 5.

The elastic constant along the c axis (C_{33}) is due to the intramolecular potential terms, K_r(22%), K_ϕ(38%), and K_q(40%), and the contributions of intermethylene terms (P_1, P_2, and P_3) are negligible. The elastic

13) I. Sakurada, T. Ito, and K. Nakamae, *J. Polym. Sci.*, Part C, **15**, 75 (1966); I. Sakurada, K. Kaji, K. Nakamae, and E. Shikata, Symposium on Macromolecules, 22F09, Matsuyama (1968).

TABLE 1. $D_{s\sigma}$, $B_{s\rho s}$, $H_{s\sigma}$, AND $H_{s\sigma}C^{-1}$ MATRICES OF THE a_g SPECIES

		$D_{s\sigma}$ (Å)			$B_{s\rho_s}$	
		σ_1	σ_2	σ_3	$\rho_s(1)$	$\rho_s(2)$
$R_s^0(1)$	$[r]$	0.414	0.537	2.109	−0.735	−0.838
$R_s^0(2)$[a]	$[\phi]$	−0.805	−1.046	1.851	1.432	1.632
$R_s^0(3)$	$[q]$	0	0	5.080	0	0
$R_s^0(4)$	$[p_1]$	6.637	1.613	0	0	0.884
$R_s^0(5)$	$[p_2]$	6.650	4.104	1.089	2.119	0
$R_s^0(6)$	$[p_3]$	0.140	8.161	0.716	−0.249	1.902

a) $D_{s\sigma}$ elements in rad and $B_{s\rho s}$ elements in rad/Å unit.

		$H_{s\sigma}$ (Å)			$H_{s\sigma}C^{-1}$ (Å³/md)		
		σ_1	σ_2	σ_3	$S_{\sigma 1}$	$S_{\sigma 2}$	$S_{\sigma 3}$
$R_s^0(1)$	$[r]$	0.04	0.02	1.11	0.01	0.01	0.05
$R_s^0(2)$[a]	$[\phi]$	−0.08	−0.05	3.80	−0.03	−0.09	0.17
$R_s^0(3)$	$[q]$	0	0	5.08	−0.01	−0.06	0.23
$R_s^0(4)$	$[p_1]$	8.21	2.84	1.17	5.32	−2.89	−0.00
$R_s^0(5)$	$[p_2]$	3.43	2.24	0.79	0.59	2.44	0.00
$R_s^0(6)$	$[p_3]$	3.91	11.02	3.27	−12.48	32.22	−0.00

a) $H_{s\sigma}$ elements in rad and $H_{s\sigma}C^{-1}$ elements in Å²rad/md unit.

TABLE 2. $D_{s\sigma}$, $B_{s\rho s}$, $H_{s\sigma}$, AND $H_{s\sigma}C^{-1}$ MATRICES[a] OF THE b_{1g} SPECIES

		$D_{s\sigma}$ σ_4	$B_{s\rho s}$ $\rho_s(3)$	$H_{s\sigma}$ σ_4	$H_{s\sigma}C^{-1}$ $S_{\sigma 4}$
$R_s^0(7)$	$[r]$	1.064	−1.660	0.00	0.01
$R_s^0(8)$	$[p_2]$	2.115	0	2.11	15.67
$R_s^0(9)$	$[p_3]$	2.416	0.563	2.78	20.58

a) Units are given in Table 1.

TABLE 3. $D_{s\sigma}$, $B_{s\rho s}$, $H_{s\sigma}$, AND $H_{s\sigma}C^{-1}$ MATRICES[a] OF THE b_{2g} SPECIES

		$D_{s\sigma}$ σ_5	$B_{s\rho s}$ $\rho_s(4)$	$H_{s\sigma}$ σ_5	$H_{s\sigma}C^{-1}$ $S_{\sigma 5}$
$R_s^0(10)$	$[r]$	0.934	−1.660	0.01	0.04
$R_s^0(11)$	$[p_2]$	2.692	0.858	3.17	12.60
$R_s^0(12)$	$[p_3]$	−0.317	0.563	−0.00	−0.01

a) Units are given in Table 1.

TABLE 4. $D_{s\sigma}$, $B_{s\rho s}$, $H_{s\sigma}$, AND $H_{s\sigma}C^{-1}$ MATRICES[a] OF THE b_{3g} SPECIES

		$D_{s\sigma}$ σ_6	$B_{s\rho_s}$ $\rho_s(5)$	$B_{s\rho_s}$ $\rho_s(6)$	$H_{s\sigma}$ σ_6	$H_{s\sigma}C^{-1}$ $S_{\sigma 6}$
$R_s^0(13)$	$[r]$	0.471	−0.735	−0.838	0.04	0.04
$R_s^0(14)$[b]	$[\phi]$	−0.918	1.432	1.632	−0.08	−0.07
$R_s^0(15)$	$[p_1]$	3.272	1.794	0	4.20	3.61
$R_s^0(16)$	$[p_2]$	5.224	0	1.665	5.32	4.58
$R_s^0(17)$	$[p_3]$	−1.070	−0.249	1.903	−1.08	−0.93

a) Units are given in Table 1.
b) See a) of Table 1.

TABLE 5. CONTRIBUTION (%) OF POTENTIAL TERMS

	K_r	K_ϕ	K_q	P_1	P_2	P_3
C_{11}	0	0	—	83	14	2
C_{22}	0	0	—	29	18	52
C_{33}	22	38	40	0	0	0
C_{23}	45	−44	—	35	18	46
C_{31}	50	−49	—	69	19	10
C_{12}	0	0	—	64	21	14
C_{44}	0	—	—	—	83	17
C_{55}	0	—	—	—	100	0
C_{66}	0	0	—	38	61	0

constant along the b axis (C_{22}) is largely due to the P_3 contacts (52%) which are nearly parallel to the b axis (see Figs. 1 and 2). The elastic constant along the a axis (C_{11}) is predominantly due to the P_1 contacts (83%) which are nearly parallel to the a axis (see Fig. 1). On the other hand, P_2 contacts are nearly parallel to body-diagonals of unit cells and, in fact, make greatest contributions to the elastic constants of C_{44}, C_{55}, and C_{66}.

Conclusion

In a previous paper by Walmsley,[14] a method for treating elastic constants of molecular crystals is presented, where molecules are regarded as rigid bodies and the potential energy is expressed as a sum of terms each due to the interaction of a different pair of molecules. However, a general method worked out in the present study for treating elastic constants is applicable to general force fields. For molecular crystals, molecules need not be regarded as rigid bodies and internal strains within molecules may also be taken into account.

14) S. H. Walmsley, *J. Chem. Phys.*, **48**, 1438 (1968).

The present equations for elastic constants are written in matrix form and are readily programed for electronic computation. Factor-group symmetry operations may be applied in refined treatments of elastic properties. Also, elastic constants and normal vibrations may be treated together, and derivatives for elastic constants and normal vibration frequencies may be used together for least-square adjustments of force constants with reference to experimental elastic constants and vibrational frequencies.

The authors wish to express their thanks to Prof. Hiromu Murata and Dr. Michiro Hayashi of Hiroshima University for their discussions and to Dr. Hiromu Sugeta and Dr. Teizo Kitagawa of Osaka University for part of numerical calculations and discussions.

Appendix I Transformation Matrix ($\boldsymbol{D}_U$)

For the elastic constants of molecular crystals, it is necessary to derive $\boldsymbol{D}_U$ matrix elements [Eq. (17)] associated with bond-stretching, angle-bending, and torsional coordinates. Explicit equations for each of these coordinates may be derived by the use of relevant $\boldsymbol{s}_i$ vectors[1] of the atoms (i) involved,

$$\boldsymbol{s}_i = [B_{xi}\ B_{yi}\ B_{zi}] \tag{A1}$$

After defining the position vector $X(i)$ of the ith atom,

$$X(i) = [X(i)\ Y(i)\ Z(i)] \tag{A2}$$

the row vector $\boldsymbol{D}_U$ for an internal coordinate may be derived from Eqs. (10) and (17),

$$\begin{aligned}\boldsymbol{D}_U &= \sum_i [B_{xi}X(i)\ B_{xi}Y(i)\ B_{xi}Z(i)\ B_{yi}X(i)\ B_{yi}Y(i)\\ &\qquad B_{yi}Z(i)\ B_{zi}X(i)\ B_{zi}Y(i)\ B_{zi}Z(i)]\\ &= \sum_i [\boldsymbol{s}_i \times \boldsymbol{X}(i)]\end{aligned} \tag{A3}$$

where $\times$ denotes a direct product.

For the stretching coordinate (Δr_{ij}) of the bond i—j, the $\boldsymbol{s}$ vectors are expressed by the unit vector from the atom j toward i,

$$\begin{aligned}\boldsymbol{s}_i &= \boldsymbol{e}_{ji}\\ \boldsymbol{s}_j &= -\boldsymbol{e}_{ji}\end{aligned} \tag{A4}$$

Accordingly, the $\boldsymbol{D}_U$ vector is derived as

$$\boldsymbol{D}_U(\Delta r_{ij}) = \boldsymbol{e}_{ji} \times \boldsymbol{X}(i) - \boldsymbol{e}_{ji} \times \boldsymbol{X}(j) = \boldsymbol{e}_{ji} \times \boldsymbol{r}_{ji} \tag{A5}$$

where $\boldsymbol{r}_{ji}$ is the vector from the atom j to i,

$$\boldsymbol{r}_{ji} = \boldsymbol{X}(i) - \boldsymbol{X}(j) \tag{A6}$$

For the bending coordinate ($\Delta\phi_{ijk}$) of the bond angle i–j–k, the $\boldsymbol{s}$ vectors may be expressed as,

$$\begin{aligned}\boldsymbol{s}_i &= \boldsymbol{p}_{ji}/r_{ji}\\ \boldsymbol{s}_j &= -\boldsymbol{s}_i - \boldsymbol{s}_k\\ \boldsymbol{s}_k &= \boldsymbol{p}_{jk}/r_{jk}\end{aligned} \tag{A7}$$

where the unit vectors $\boldsymbol{p}_{ji}$ and $\boldsymbol{p}_{jk}$ are perpendicular to $\boldsymbol{e}_{ji}$ and $\boldsymbol{e}_{jk}$, respectively, and point in the positive bending direction. Accordingly, the $\boldsymbol{D}_U$ vector is derived as

$$\begin{aligned}\boldsymbol{D}_U(\Delta\phi_{ijk}) &= \boldsymbol{s}_i \times r_{ji} + \boldsymbol{s}_k \times r_{jk}\\ &= \boldsymbol{p}_{ji} \times \boldsymbol{e}_{ji} + \boldsymbol{p}_{jk} \times \boldsymbol{e}_{jk}\end{aligned} \tag{A8}$$

For the torsional coordinate ($\Delta\tau_{ijkl}$) of the dihedral angle i–j–k–l, the $\boldsymbol{s}$ vectors may be expressed as

$$\begin{aligned}\boldsymbol{s}_i &= \boldsymbol{p}_{kji}/r_{ji} \sin\phi_{kji}\\ \boldsymbol{s}_j &= -\boldsymbol{s}_i + \boldsymbol{p}_{kji}\cos\phi_{kji}/r_{kj}\sin\phi_{kji} - \boldsymbol{p}_{jkl}\cos\phi_{jkl}/r_{jk}\sin\phi_{jkl}\\ \boldsymbol{s}_k &= -\boldsymbol{s}_l + \boldsymbol{p}_{jkl}\cos\phi_{jkl}/r_{jk}\sin\phi_{jkl} - \boldsymbol{p}_{kji}\cos\phi_{kji}/r_{kj}\sin\phi_{kji}\\ \boldsymbol{s}_l \boldsymbol{p} &= {}_{jkl}/r_{kl}\sin\phi_{jkl}\end{aligned} \tag{A9}$$

where the unit vectors $\boldsymbol{p}_{kji}$ and $\boldsymbol{p}_{jkl}$ are perpendicular to the planes of bond angles ϕ_{kji} and ϕ_{jkl}, respectively, and point in the positive torsional direction. Accordingly, the $\boldsymbol{D}_U$ vector is derived as

$$\begin{aligned}\boldsymbol{D}_U(\Delta\tau_{ijkl}) &= \boldsymbol{p}_{kji} \times (\boldsymbol{e}_{ji} + \boldsymbol{e}_{kj}\cos\phi_{kji})/\sin\phi_{kji}\\ &\quad + \boldsymbol{p}_{jkl} \times (\boldsymbol{e}_{kl} + \boldsymbol{e}_{jk}\cos\phi_{jkl})/\sin\phi_{jkl}\end{aligned} \tag{A10}$$

Appendix II Derivation of $\partial C_{ij}/\partial K(h)$

From Eqs. (29) and (34),

$$\Delta\boldsymbol{C} = [\tilde{\boldsymbol{H}}_\sigma \Delta \boldsymbol{F}_R{}^0 \boldsymbol{H}_\sigma + \Delta\tilde{\boldsymbol{H}}_\sigma \boldsymbol{F}_R{}^0 \boldsymbol{H}_\sigma + \tilde{\boldsymbol{H}}_\sigma \boldsymbol{F}_R{}^0 \Delta \boldsymbol{H}_\sigma]/v \tag{A11}$$

Also from Eq. (27)

$$\Delta \boldsymbol{H}_\sigma = -\boldsymbol{B}_\rho \Delta\{[\tilde{\boldsymbol{B}}_\rho \boldsymbol{F}_R{}^0 \boldsymbol{B}_\rho]^{-1} \tilde{\boldsymbol{B}}_\rho \boldsymbol{F}_R{}^0\} \boldsymbol{D}_\sigma \tag{A12}$$

and

$$\begin{aligned}\tilde{\boldsymbol{H}}_\sigma \boldsymbol{F}_R{}^0 \Delta \boldsymbol{H}_\sigma &= -\tilde{\boldsymbol{D}}_\sigma \{\boldsymbol{E} - \boldsymbol{F}_R{}^0 \boldsymbol{B}_\rho [\tilde{\boldsymbol{B}}_\rho \boldsymbol{F}_R{}^0 \boldsymbol{B}_\rho]^{-1} \tilde{\boldsymbol{B}}_\rho\} \boldsymbol{F}_R{}^0 \boldsymbol{B}_\rho\\ &\quad \times \Delta\{[\tilde{\boldsymbol{B}}_\rho \boldsymbol{F}_R{}^0 \boldsymbol{B}_\rho]^{-1} \tilde{\boldsymbol{B}}_\rho \boldsymbol{F}_R{}^0\} \boldsymbol{D}_\sigma\end{aligned} \tag{A13}$$

However, since

$$\{\boldsymbol{E} - \boldsymbol{F}_R{}^0 \boldsymbol{B}_\rho [\tilde{\boldsymbol{B}}_\rho \boldsymbol{F}_R{}^0 \boldsymbol{B}_\rho]^{-1} \tilde{\boldsymbol{B}}_\rho\} \boldsymbol{F}_R{}^0 \boldsymbol{B}_\rho = 0 \tag{A14}$$

the matrix $\tilde{\boldsymbol{H}}_\sigma \boldsymbol{F}_R{}^0 \Delta \boldsymbol{H}_\sigma$ and the transposed matrix $\Delta \tilde{\boldsymbol{H}}_\sigma \boldsymbol{F}_R{}^0 \boldsymbol{H}_\sigma$ in Eq. (A11) are both reduced to zero, leaving

$$\Delta\boldsymbol{C} = \{\sum_h [\tilde{\boldsymbol{H}}_\sigma \boldsymbol{A}(h) \boldsymbol{H}_\sigma] \Delta K(h)\}/v \tag{A15}$$

Accordingly, the partial derivative of the elastic constant (C_{ij}) with respect to the force constant $K(h)$ is given by Eq. (35) in the main text.

A Fermi Resonance with ν_6 of Acetonitrile

Hiroatsu MATSUURA

Institute for Protein Research, Osaka University, Kita-ku, Osaka

(Received April 30, 1971)

The rotation-vibration spectrum of ν_6 of acetonitrile measured by Nakagawa *et al.* has been reanalyzed by taking account of the Fermi resonance between the states $|v_6=1>$ and $|v_7=1, v_8=1>$. The previous assignment of Q branches by Amat *et al.* has been revised on the basis of the obtained values of band constants. The following band constants have been determined for the ν_6 band: $\nu_0=1447.9$ cm^{-1}, $\zeta=-0.305$ and $\alpha^A=0.046$ cm^{-1}. From the value of the resonance operator, the magnitude of the cubic force constant k_{678} has been estimated to be about 30 cm^{-1}.

Rotation-vibration spectra of acetonitrile CH_3CN have been studied by Parker, Nielsen, and Fletcher[1] and Nakagawa and Shimanouchi,[2] and anomalous rotational structures have been found in the ν_6 perpendicular band. Amat and Nielsen[3] interpreted the anomaly to be due to the Fermi resonance between the states $|v_6=1>$ and $|v_7=1, v_8=1>$ and made an assignment of observed Q branches. In the present study, the ν_6 band region in the spectra of Nakagawa and Shimanouchi[2] was reanalyzed and Amat's assignment was revised on the basis of the obtained values of band constants.

Spectral Analysis and Discussion

As shown in Fig. 1, the observed spectrum in the region 1300—1600 cm^{-1} consists of two series of Q branches (ν^+ and ν^-), higher- and lower-wave number components of the Fermi doublet. We have three possible vibrational states which can be coupled with and perturb the $|v_6=1, l_6=\pm1>$ state through Fermi-resonance operators; namely $|v_7=1, l_7=\mp1, v_8=1, l_8=\mp1>$, $|v_8=4, l_8=\mp2>$ and $|v_8=4, l_8=\pm4>$, which have rotation-vibration energies close to that of the $|v_6=1, l_6=\pm1>$ state. It has become evident, from the obtained values of the band constants, that the perturber is the $|v_7=1, l_7=\mp1, v_8=1, l_8=\mp1>$ state. In assigning observed Q branches, however, there are two possible K-numberings (Assignment I and Assignment II) as shown in Table 1; they differ in the assigned $K\Delta K$ numbers by one in the ν^- component. Assignment II corresponds to Amat's assignment.[3] Analyses of the band system were made according to the two assignments.

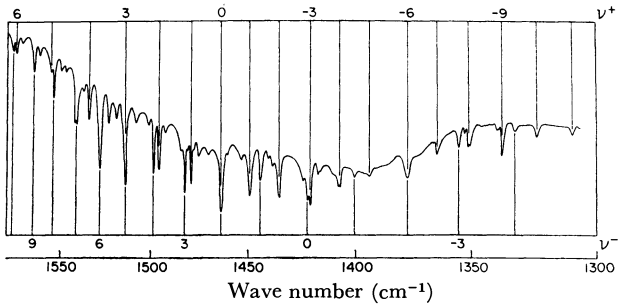

Fig. 1. Infrared spectrum of the ν_6 region of CH_3CN (Ref. 2). Numbers shown above and below the spectrum are $K\Delta K$ numbers for ν^+ and ν^- according to Assignment I.

In calculating the unperturbed band constants, the following matrix was set up for each K value

$$\begin{bmatrix} E^0(v_6=1, l_6=\pm1, K) & W \\ W & E^0(v_7=1, l_7=\mp1, v_8=1, l_8=\mp1, K) \end{bmatrix},$$

where E^0 denotes the unperturbed energy and W the matrix element of the Fermi-resonance operator. The unperturbed band constants and the resonance operator were determined by solving the above matrix and fitting observed wavenumbers to the wave number equation by the method of least squares. The results are given in Table 2. The values of ν_0, ζ, and α^A ($=A''-A'$) were calculated by assuming $B'=B''=0.3068$ cm^{-1} and $A''=5.280$ cm^{-1}.[4] From the ζ_7 value (0.422)[2] and the ζ value $[-(\zeta_7+\zeta_8)]$ of the $\nu_7+\nu_8$ band, we obtain $\zeta_8=0.863$ for Assignment I and $\zeta_8=0.764$ for Assignment II. Venkateswarlu *et al.*[5] have obtained $\zeta_8=0.88$ from microwave studies. The good agreement between the ζ_8 value for Assignment I and the microwave value is an evidence that favors Assignment I. From the ζ_6 and ζ_8 values of the present study and the ζ_5 and ζ_7 values previously determined,[2] we can check the ζ-sum rule ($\sum_t \zeta_t = 1+B/2A$); $\sum_t \zeta_t=1.042$ for Assignment I and $\sum_t \zeta_t=0.898$ for Assignment II, while $1+B/2A=1.029$. Agreement between the left- and right-hand sides is much better for Assignment I than for Assignment II.

Values of the rotation-vibration coupling constant α^A for localized vibrations, *e.g.* CH_3 stretching and CH_3 bending vibrations of CH_3X and CH_3CN, are expected to be similar for the same vibrational modes.[6,7] α^A values for the CH_3 rocking, and CH_3 asymmetric stretching vibrations of CH_3CN are, in fact, close to the corresponding values for CH_3Cl, CH_3Br and CH_3I. The α^A value for ν_6 of CH_3CN (CH_3 asymmetric deformation) was determined to be 0.046 cm^{-1} for Assignment I and 0.028 cm^{-1} for Assignment II. The former is much closer than the latter to the corre-

1) F. W. Parker, A. H. Nielsen, and W. H. Fletcher, *J. Mol. Spectrosc.*, **1**, 107 (1957).

2) I. Nakagawa and T. Shimanouchi, *Spectrochim. Acta*, **18**, 513 (1962).

3) G. Amat and H. H. Nielsen, "Molecular Orbitals in Chemistry, Physics and Biology," ed. by P.-O. Löwdin and B. Pullman, Academic Press, New York (1964), p. 293.

4) M. Kessler, H. Ring, R. Trambarulo, and W. Gordy, *Phys. Rev.*, **79**, 54 (1950).

5) P. Venkateswarlu, J. G. Baker, and W. Gordy, *J. Mol. Spectrosc.*, **6**, 215 (1961).

6) Y. Morino and J. Seto, Annual Meeting of the Chemical Society of Japan, Tokyo, 1958.

TABLE 1. Q-BRANCHES OF THE FERMI DIAD ν_6 AND $\nu_7+\nu_8$ OF CH_3CN

	Assignment I[a]				Assignment II			
	ν^+		ν^-		ν^+		ν^-	
	ν_{obs}[b]	$\Delta\nu$[c]	ν_{obs}[b]	$\Delta\nu$[c]	ν_{obs}[b]	$\Delta\nu$[c]	ν_{obs}[b]	$\Delta\nu$[c]
$^PQ_{11}$	1309.39	0.22			1309.39	0.42		
$^PQ_{10}$	1323.29	−0.02			1323.29	0.13		
$^PQ_9$	1337.01	−0.37			1337.01	−0.29		
$^PQ_8$	1350.63[d]	−0.76			1350.63[d]	−0.76		
$^PQ_7$	1364.39[d]	−0.95			1364.39[d]	−1.05		
$^PQ_6$	1377.60[d]	−1.64			1377.60[d]	−1.84		
$^PQ_5$	1393.33	0.22			1393.33	−0.07	1331.84	−0.41
$^PQ_4$	1407.06	0.09	1331.84	−0.04	1407.06	−0.27	1354.77	−0.18
$^PQ_3$	1420.88	0.01	1354.77	−0.03	1420.88	−0.36	1377.60	0.14
$^PQ_2$	1434.82	−0.03	1377.60	0.00	1434.82	−0.34	1400.36	0.60
$^PQ_1$	1449.14	0.10	1400.36	0.19	1449.14	−0.03	1422.30	0.51
$^RQ_0$	1463.34	−0.28	1422.30	−0.02	1463.34	−0.06	1443.88	0.48
$^RQ_1$	1478.81	−0.12	1443.88	0.16	1478.81	0.50	1463.34	−0.78
$^RQ_2$	1495.56	0.08	1463.34	−0.51	1495.56	0.52	1482.27	−0.57
$^RQ_3$	1513.85	0.06	1482.27	0.08	1513.85	−0.44	1498.66	−0.18
$^RQ_4$	1533.95	0.01	1498.66	−0.00	1533.95	−0.94	1513.85	0.56
$^RQ_5$	1555.53	0.02	1513.85	0.16	1555.53	−0.37	1527.81	0.68
$^RQ_6$	1577.98	−0.01	1527.81	0.04	1577.98	0.97	1541.38	0.69
$^RQ_7$			1541.38	0.12			1554.33	0.25
$^RQ_8$			1554.33	−0.01			1567.08	−0.28
$^RQ_9$			1567.08	−0.06			1579.67	−0.87
$^RQ_{10}$			1579.67	−0.05				

a) More likely assignment.
b) Observed wave number (cm^{-1}).
c) $\Delta\nu=\nu_{obs}-\nu_{calc}$.
d) Omitted from the least squares calculation.

sponding values[8,9] of 0.048 cm^{-1}, 0.048 cm^{-1} and 0.046 cm^{-1} determined for CH_3Cl, CH_3Br, and CH_3I, respectively. This is another basis for preferring Assignment I to Assignment II.

By comparing the results obtained for both assignments, it is now concluded that Assignment I is a more likely alternative; the results for Assignment I will therefore be used in subsequent parts of this paper. The better agreement between the observed and calculated wavenumbers for Assignment I than Assignment II (see Table 1) may also support this conclusion. In order to check the conclusion, approximate intensity ratios of the Q branches for the ν^+ and ν^- components with the same $K\Delta K$ numbers were calculated for the two assignments. However, a definite comparison could not be made due to overlapping of some of the Q branches and another kind of perturbation.

The unperturbed band origin of ν_6 was determined to be 1447.9 cm^{-1}. This wave number is about 6 cm^{-1} lower than the wave number[1,2] previously obtained without taking account of the Fermi resonance. From the wave number of the band origin for $\nu_7+\nu_8$ and those for ν_7 and ν_8,[2] the anharmonic term[10] $x_{78}+x_{l_7l_8}=-0.8$ cm^{-1} is obtained.

Assuming that the Fermi-resonance operator W is

TABLE 2. BAND CONSTANTS OF THE ν_6 AND $\nu_7+\nu_8$ BANDS OF CH_3CN IN cm^{-1}

Constant	Assignment I[a]		Assignment II	
	ν_6	$\nu_7+\nu_8$	ν_6	$\nu_7+\nu_8$
$\nu_0+A'(1-\zeta)^2-B'$	1456.54±0.07	1429.40±0.10	1461.34±0.21	1445.46±0.28
$2[A'(1-\zeta)-B']$	13.051±0.008	23.67±0.02	13.569±0.024	22.17±0.05
$(A'-B')-(A''-B'')$	−0.046±0.001	0.033±0.007	−0.028±0.004	−0.070±0.016
$\lvert W\rvert$	15.57±0.06		6.07$_5$±0.23	
ν_0[b]	1447.93	1401.97	1452.07	1420.86
ζ[b]	−0.305	−1.285	−0.350	−1.186
α^A[b]	0.046	−0.033	0.028	0.070

a) More likely assignment.
b) Calculated by assuming $B'=B''=0.3068$ cm^{-1} and $A''=5.280$ cm^{-1} (Ref. 4).

7) S. Reichman and J. Overend, *J. Chem. Phys.*, **48**, 3095 (1968).
8) Y. Morino and J. Nakamura, This Bulletin, **38**, 443 (1965).
9) H. Matsuura and J. Overend, *J. Chem. Phys.*, to be published.
10) H. H. Nielsen, "Handbuch der Physik," Vol. 37, ed. by S. Flügge, Springer-Verlag, Berlin (1959), p. 173.

determined by the following anharmonic term of the intramolecular potential

$$V = hck_{678}[q_{6a}(q_{7a}q_{8a}-q_{7b}q_{8b}) - q_{6b}(q_{7a}q_{8b}+q_{7b}q_{8a})],$$

we find the following non-zero matrix element

$$\langle v_6, l_6, v_7, l_7, v_8, l_8 | V/hc | v_6-1, l_6\pm1, v_7+1, l_7\pm1, v_8+1, l_8\pm1\rangle$$
$$= \pm(1/4\sqrt{2})k_{678}[(v_6\mp l_6)(v_7\pm l_7+2)(v_8\pm l_8+2)]^{1/2}.$$

Accordingly, from the $|W|$ value obtained in the present analysis, the magnitude of the cubic force constant k_{678} is estimated to be $|k_{678}|=2|W|=31$ cm^{-1}.

It has been found in the course of the analysis that there is another kind of perturbation, though much weaker than the one described above, for ${}^PQ_6-{}^PQ_8$ in the ν^+ component; the observed wave numbers deviate systematically from the calculated wave numbers (see Table 1). Amat and Nielsen[3] explained it as due to a Coriolis interaction between the states $|v_3=1\rangle$ and $|v_6=1\rangle$. The observed wavenumbers for these Q branches were omitted in determining the band constants given in Table 2.

The author wishes to thank Dr. Ichiro Nakagawa, the University of Tokyo, for providing the author with a copy of his original spectrum and for his valuable discussions. The author is also grateful to Professor Tatsuo Miyazawa, Osaka University, for his helpful discussions.

After this work was completed, the author has been informed by Professor. G. Amat that J. L. Duncan, D. Ellis, and I. J. Wright [*Mol. Phys.*, **20**, 673 (1971)] independently studied the same subject and obtained essentially the same results.

BULLETIN OF THE CHEMICAL SOCIETY OF JAPAN, VOL. 44, 2381—2386 (1971)

The Formation Constants and Composition of Tetraethylenepentaamineheptaacetato Nickel(II) Complexes measured by a Potentiometric Titration Method

Yoshitaka MASUDA, Yukiko HIRAI, and Eiichi SEKIDO

Department of Chemistry, Faculty of Science, Kobe University, Nada-ku, Kobe

(Received October 14, 1970)

Stability constants for nickel(II) complexes of tetraethylenepentaamineheptaacetic acid (TPHA: H_7L) were determined by the pH titration method. In an aqueous solution ($\mu=0.1$) three uninuclear complex species, NiH_2L, NiHL, and NiL, and a binuclear compound, Ni_2L seem to exist. The structures of uni- and bi-nuclear chelates are discussed with their visible absorption spectra. Formation of the hydroxo complex was not observed on the titration curves. In the present investigation no evidence was found for species of Ni_2HL either. The formation constants of the complexes stated above have been calculated as follows, (at 25 ± 0.1°C). $\log K_{ML}=16.18$, $\log K_{MHL}=10.00$, $\log K_{MH_2L}=6.16$, $\log K_{M_2L}=17.35$ and $\log K_{ML_2}=27.78$.

Ethylenediaminetetraacetic acid (EDTA) and many related polyaminopolycarboxylic acids form metal complexes which exist over a wide pH range, and have high stability constants. Among them, triethylenetetraminehexaacetic acid (TTHA, H_6L) has been shown as an interesting complexing agent by some workers. Přibil and co-workers[1] studied its analytical usefulness as a titrant for many metal ions. It is noteworthy that the equilibrium of complexation for mono- and diprotonated forms of uni-nuclear chelates have been investigated by Martell and Bohigian.[2] They also reported that there are some differences between the structure of the complex of alkaline-earth metals and that of transition metals. Further, Koryta and Kopanica[3] have undertaken the investigation of the polarographic behavior of cadmium(II)-TTHA complex. They reported that CdH_2L^{2-} species exists over a wide pH range and the logarithm of its formation constant is given as 10.36 at 25°C.

Recently, it has been found further that a new multi-dentate ligand,[4] TPHA (tetraethylenepentaamineheptaacetic acid H_7L) forms complexes with many transition metals. However, there are few equilibrium data for this new ligand in the literature. The acid dissociation constants of free TPHA have been first determined by Dyatrova[5] by a potentiometric titration method. Aihara, Kida, and Misumi[6] studied the reactions of the lanthanide(III) ion with TPHA. No stability constant data have been published for the transition metal chelates of this ligand. In this paper, are reported the stability constants of nickel(II)-TPHA complexes determined potentiometrically by a similar method to Bohigian and Martell's[2] and by deriving new equations for calculation.

1) R. Pribil and V. Vesely, *Talanta*, **10**, 939 (1962); R. Pribil and V. Vesely, *Talanta*, **11**, 319 (1964).

2) T. A. Bohigian, Jr., and A. E. Martell, *J. Amer. Chem. Soc.*, **89**, 832 (1967); T. A. Bohigian, Jr., and A. E. Martell, *Inorg. Chem.*, **4**, 1264 (1965).

3) G. Conradi, M. Kopanica, and J. Koryta, *Collect. Czechoslov. Chem. Commun.*, **30**, 2029 (1965).

4) I. Murase, T. A. Bohigian, and A. E. Martell, "Preparations of Complexes and Reaction Properties of ligands," ed. by S. Nakahara and M. Shibata, Nankodo, Kyoto (1970), p. 126.

5) N. M. Dyatrova, Yu. E. Belugin, and V. Ya. Temkima, *Chem. Abstr.*, **62**, 2288c (1965).

6) S. Misumi, S. Kida, and M. Aihara, *Coord. Chem. Rev.*, **3**, 189 (1968); S. Misumi *Nippon Kagaku Zasshi*, **89**, 723 (1968).

Experimental

Hitachi-Horiba model P pH meter fitted with extension glass and calomel electrode was calibrated with standard buffer solutions of pH 4.10 and 7.00. Actual hydrogen ion concentration was determined on the basis of the data tabulated by Harned and Owen.[7]

Reagent. The chemical formula of synthesized TPHA ligand[4] was given by $C_{33}H_{27}N_5O_{14}\cdot 4HCl\cdot 2H_2O$. The TPHA solution was standardized by the titration with a standard thorium nitrate solution. Standard carbonate-free potassium hydroxide solution was prepared as follows. G. R. potassium hydroxide (7.0 g) and G. R. barium chloride (2 g) were dissolved in demineralized water. The solution was set aside for a few days at ordinary temperature in a 1000 m*l* Erlenmyer flask. Excess of barium chloride in the solution was removed by passing the solution through a column of potassium-type cation exchange resion "Dowex 50-X12" (100—200 mesh). The resulting carbonate free potassium hydroxide solution was stored in a polyethylene bottle and protected from the atmosphere by a soda lime tube.

The potassium hydroxide solution was standardized by potentiometric titration with potassium phthalate solution. The solution of nickel nitrate was standardized titrimetrically by the EDTA procedure,[8] and was stored under pure nitrogen gas. Potassium nitrate was used to make the ionic strength to 0.1. Demineralized water free from carbonate was used in all the titrations.

Procedure. The experimental method consists of potentiometric titration of the hepta basic acid, TPHA, with potassium hydroxide solution in the absence and the presence of the nickel(II) ion at 1:1, 2:1, 1:2, and 3:1 molar ratios of metal ion to ligand. All titrations were carried out in a double walled glass titration cell of 200 m*l* capacity. The temperature was controlled to 25±0.1°C by circulating water through the double wall cell and the ionic strength of the solution were maintained constant at 0.10. Nitrogen free from carbon dioxide was continuously passed through the system in the titration cell. After each addition of aliquots of alkali titrant (0.05 m*l*), the solution was stirred with a magnetic stirrer and was allowed to stand for 3 min to attain equilibrium. The titrations were carried out from an initial pH 2.5 to 10.5.

Calculations

The values of the dissociation constants of TPHA (H_7L) obtained by Dyatrova[5] were used in this work, namely, pK_1, 9.95; pK_2, 8.85; pK_3, 5.56; pK_4, 3.82; pK_5, 2.79. The calculations were carried out in the range of a=3—6, where a is the equivalent base added per mole of ligand (above pH 2.9). The influence of pK_6 and pK_7 was not observed at all. The equations can be derived by modifying Martell's.[2] The following equilibria were considered for the calculation of stability constants for the ligand, H_7L and the metal ion, M^{2+}.

$$M + L \rightleftharpoons ML \qquad K_{ML} = [ML]/[M][L] \qquad (1)$$

$$M + HL \rightleftharpoons MHL \qquad K_{MHL} = [MHL]/[M][HL] \qquad (2)$$

$$MHL \rightleftharpoons ML + H \qquad K^{H}_{MHL} = [ML][H]/[MHL] \qquad (3)$$

$$M + H_2L \rightleftharpoons MH_2L \qquad K_{MH_2L} = [MH_2L]/[M][H_2L] \qquad (4)$$

$$MH_2L \rightleftharpoons MHL + H \qquad K^{H}_{MH_2L} = [MHL][H]/[MH_2L] \qquad (5)$$

$$M + H_3L \rightleftharpoons MH_3L \qquad K_{MH_3L} = [MH_3L]/[M][H_3L] \qquad (6)$$

$$MH_3L \rightleftharpoons MH_2L + H \qquad K^{H}_{MH_3L} = [MH_2L][H]/[MH_3L] \qquad (7)$$

Equations describing the total analytical concentration of metal ion (T_M), total ligand concentration (T_L), and electroneutrality can be written as follows.

$$T_L = \sum_{j=1}^{7}[H_jL] + [L] + [MHL] + [MH_2L] \qquad (8)$$

$$T_M = [M] + [MHL] + [MH_2L] \qquad (9)$$

$$T_H = (7-a)T_L = [H] - [OH] + \sum_{j=1}^{7} j[H_jL] + [MHL] + 2[MH_2L] \qquad (10)$$

From Eqs. (2), (3), (4), (5), (8), (9), and (10), Eqs. (11) and (12) are obtained.

$$[H_2L] = \frac{\{(6-a)T_L-[H]+[OH]\}K^{H}_{MH_2L}+\{(5-a)T_L-[H]+[OH]\}[H]}{(P-S)K^{H}_{MH_2L}+[H](P-2S)} \qquad (11)$$

$$K_{MH_2L} = \{(6-a)T_L-[H]+[OH]-[H_2L](P-S)\}/[H_2L]^2\cdot S \qquad (12)$$

where

$$P = 2 + K_2^{H}/[H] + \sum_{i=1}^{5}(i+2)[H]^i/\prod_{z=3}^{i+2}K_z^{H}$$

and

$$S = 1 + K_2^{H}/[H] + K_1^{H}K_2^{H}/[H]^2 + \sum_{i=1}^{5}[H]^i/\prod_{z=3}^{i+2}K_z^{H}$$

K_z^{H} may be defined as the zth acid dissociation constant of the TPHA ligand. $K_z^{H}=[H_{z-1}L][H]/[H_zL]$, $z=1, 2, \cdots, 7$.

The calculation of the stability constants of MHL and ML was made by a graphical method. A series of values for pK^{H}_{MHL} were assumed and corresponding values for K_{MHL} calculated from the following equations.

$$[HL] = \frac{[H]\{(6-a)T_L-[H]+[OH]\}+K^{H}_{MHL}\{(7-a)T_L-[H]+[OH]\}}{[H](Y-X)+Y\cdot K^{H}_{MHL}} \qquad (13)$$

$$K_{MHL} = \{(7-a)T_L-[H]+[OH]-[HL]\cdot Y\}/[HL]^2X \qquad (14)$$

where

$$X = 1 + K_1^{H}/[H] + \sum_{i=1}^{6}[H]^i/\prod_{z=2}^{i+1}K_z^{H}$$

and

$$Y = 1 + \sum_{i=1}^{6}(i+1)[H]^i/\prod_{z=2}^{i+1}K_z^{H}$$

When the resulting values of $\log K_{MHL}$ are plotted against the assumed values of pK^{H}_{MHL}, intersecting lines are obtained. The fact that all the lines obtained from different points on the titration curve intersect at one point indicates the existence of a set of unique values for $\log K_{MHL}$ and pK^{H}_{MHL}, which will satisfy the assumed reaction at any point along the titration curve in a certain range of a values. The values for $\log K_{ML}$ are calculated from Eq. (15).

$$K_{ML} = K^{H}_{MHL}\cdot K_{MHL}/K_1 \qquad (15)$$

where K_1 is the first acid dissociation constant of the

7) H. S. Harned and B. B. Owen, "The Physical Chemistry of Electrolytic Solution," Reinhold, New York (1958), pp. 634, 712.

8) K. Ueno, "Chelatometric Titration" (reprinted 12), Nankodo, Kyoto, (1967), p. 287.

ligand TPHA. The value of K_{MHL} is obtained in the same fashion on the process of the log K_{ML}. In a similar fashion, equations for the stability constant of the triprotonated TPHA complex can be obtained. The following equations for stability constant of the binuclear chelate compounds are derived.

$$[L] = \{(7-a)T_L - [H] + [OH]\}/Y' \quad (16)$$

$$K_{M_2L} = \{T_L - [L]X'\}/4[L]^3X'^2 \quad (17)$$

where

$$X' = 1 + \sum_{i=1}^{7}[H]^i/\prod_{z=1}^{i}K_z^H$$

and

$$Y' = \sum_{i=1}^{7}i[H]^i/\prod_{z=1}^{i}K_z^H$$

To calculate the formation constants of hydroxo complexes, the average number of hydroxide ions bound to the metal ion is described by

$$\bar{n}_{OH} = \frac{T_{OH} - [OH]}{T_M} = \frac{[M(OH)L] + 2[M(OH)_2L]}{[ML] + [M(OH)L] + [M(OH)_2L]} \quad (18)$$

T_{OH} represents concentration of the hydroxide ion added to any point along the titration curve. The relationship between $\bar{n}_{OH}$ and [OH] was equivalent to that between $\bar{n}_L$ and the free ligand concentration [L].[9] From a plot of $\bar{n}_{OH}$ *vs.* pOH, the formation constant of mono hydroxide complex was calculated as first approximation ($\bar{n}_{OH}=0.5$).

The extent of 1:2 chelate formation can be characterized by the complex formation function or the average co-ordination number introduced by Bjerrum.

$$\bar{n}_L = \frac{[ML] + 2[ML_2]}{[M] + [ML] + [ML_2]} = \frac{K_{ML}[L] + 2K_{ML_2}[L]^2}{1 + K_{ML}[L] + K_{ML_2}[L]^2} \quad (19)$$

[L] can be obtained by Eq. (16).

From some points along the titration curve, the values for $\bar{n}_L$ are plotted against [L]. $\log K_{ML}$ and $\log K_{ML_2}$ may be determined from values of pL at $\bar{n}_L$ values of 0.5 and 1.5 on the plot of $\bar{n}_L$ *vs.* pL.

Results and Discussion

Potentiometric pH Curves. The potentiometric titration curves of TPHA and of mixtures of nickel(II) and TPHA (1:2, 1:1, 2:1, and 3:1) are shown in Fig. 1. The titration curve of the acid (TPHA) points out two steps, that is, it appears as a well-defined inflextion at a between 4 and 5 involving the dissociation of the acid species, H_3L and H_2L and as a less distinction inflextion at a above 5 involving the dissociation of HL acid species. It is seen that this small inflextion is due to the least mutual electrostatic repulsion between the protonated amino groups. A 1:1 mixture of nickel(II) and acid (TPHA) exhibits a well-defined inflextion at $a=5.75$, whereas a 2:1 mixture shows one steep inflextion at $a=6.75$. In the case of a 1:1 mixture of nickel(II) and TPHA, inflextion is not seen exactly at $a=5$, $a=6$, and $a=7$. Although an explanation for this fact is not found, it may be suggested that sites of nickel(II) are not saturated for arrangement of TPHA ligand. The titration curve of 3:1 mixture of nickel(II) and TPHA is similar to the 2:1 curve up to $a=6.75$. This shows that metal ions more than two can't be bound to one TPHA molecule. Further addition of potassium hydroxide results in the formation of nickel hydroxide. The buffer region for $a>6.75$ is consistent with the pH region where the nickel(II) hydroxide is precipitated. This was checked by separate titrations of the corresponding nickel nitrate solutions in absence of TPHA.

The 1:1 curve indicates the formation of a protonated nickel chelate below $a=4.5$ and the formation of the hydroxo complex was not observed on those curves. These experiments indicate the presence of the complexes; MH_3L, MH_2L, MHL, ML, M_2L, and ML_2. From the knick of the titration curves at $a=4$, the following reaction is considered.

$$Ni^{2+} + H_7L + 4OH^- \rightleftharpoons NiH_3L + 4H_2O$$

At $a=5$ and $a=6$, the following reactions take place.

$$Ni^{2+} + H_7L + 5OH^- \rightleftharpoons NiH_2L + 5H_2O$$

$$Ni^{2+} + H_7L + 6OH^- \rightleftharpoons NiHL + 6H_2O$$

Above $a=6$, the following reaction takes place.

$$NiHL + OH^- \rightleftharpoons NiL + H_2O$$

In the 2:1 mixtures a binuclear complex is obviously predominant:

$$2Ni^{2+} + H_7L + 7OH^- \rightleftharpoons Ni_2L + 7H_2O$$

The Ionization of TPHA. Figure 2 shows the percentage of variously dissociated forms of the ligand, TPHA, at various pH's. The percentages have been calculated from Eq. (20) and by using Dyatrova's data of the dissociation constants[5] of TPHA. It has been assumed that pK_7 and pK_6 should be 2.0 and 2.5, respectively.

$$T_L = [H_7L] + [H_6L] + [H_5L] + [H_4L] + [H_3L] + [H_2L] + [HL] + [L] \quad (20)$$

For the sake of simplicity for calculation, a parameter D was introduced (Eq. (21)).

$$D = [H]^7/\alpha_7 + [H]^6/\alpha_6 + [H]^5/\alpha_5 + [H]^4/\alpha_4 + [H]^3/\alpha_3 + [H]^2/\alpha_2 + [H]/\alpha_1 + 1 \quad (21)$$

which α's indicate dissociation constants of TPHA ligand. Each of the distribution ratio may be represented by Eq. (22).

$$\begin{aligned} &[L]/T_L = 1/D & &[HL]/T_L = [H]/D\alpha_1 \\ &[H_2L]/T_L = [H]^2/D\alpha_2 & &[H_3L]/T_L = [H]^3/D\alpha_3 \\ &[H_4L]/T_L = [H]^4/D\alpha_4 & &[H_5L]/T_L = [H]^5/D\alpha_5 \\ &[H_6L]/T_L = [H]^6/D\alpha_6 & &[H_7L]/T_L = [H]^7/D\alpha_7 \end{aligned} \quad (22)$$

Below pH 3 three species, H_7L, H_6L, and H_5L are present in the solution in the absence of metal ions. In the range of pH 3.0 to 4.0, H_4L species is obviously predominant and in the range of pH 3.8 to 5.5, H_3L species is predominant. The percentage of H_2L species attained maximum value, 96% at the pH 7.0. The H_2L and HL species exist over the wide range from 4.5 to 9.8 and from 7.0 to 10.0 respectively. At pH$\geq$ 8.0, the percentage of the L species increased with increasing pH. In this range of pH, TPHA acts as a

9) J. Bjerrum, "Metal Ammine Formation in Aqueous Solution," E. Christensen, 2nd ed., P. Hasse and Son, Copenhagen (1957), p. 123.

diprotic acid. According to the diagram previously described, the species H_3L and H_2L, exist in a wide pH range. From infrared studies with respect to the structures of EDTA and DTPA,[10] the structures of the species, H_3L and H_2L will be inferred as follows.

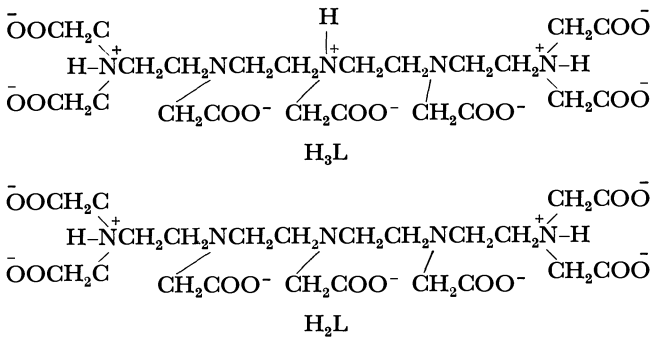

H_3L

H_2L

Graphical Solution for Stepwise Equilibrium Constants, K_{MHL} and pK^H_{MHL}, K_{MHL} and $pK^H_{MH_2L}$. The resulting values of log K_{MHL} were plotted against the assumed values of pK^H_{MHL} to give the intersecting curves shown in Fig. 3. (refer to Eqs. (13) and (14)). All curves obtained from the different points on one titration curve for the 1:1 Ni(II)–TPHA system intersect at one point, as shown in Fig. 3. This fact indicates the existence of a set of unique values for K_{MHL} and pK^H_{MHL}. The values for $\log K_{MHL}$ and pK^H_{MHL} are found to be 9.90_0 and 3.77_5, respectively.

In a similar fashion the value of log K_{MH_2L} was also determined (refer to Eqs. (11) and (12)). From the graphical determination of $pK^H_{MH_2L}$ and $\log K_{MH_2L}$, intersection of the resulting curves gives the values of

TABLE 1. STABILITY CONSTANTS OF NICKEL-TPHA COMPLEXES AT 25°C, $\mu=0.1$

Complex	Value	
ML	log K_{ML}	16.18
MHL	log K_{MHL}	10.00 (±0.03)
MH_2L	log K_{MH_2L}	6.16 (±0.10)
MH_3L	log K_{MH_3L}	5.26
M_2L	log K_{M_2L}	17.35
ML_2	log K_{ML_2}	27.78 (11.6)[a]

a) The second consecutive formation constant.

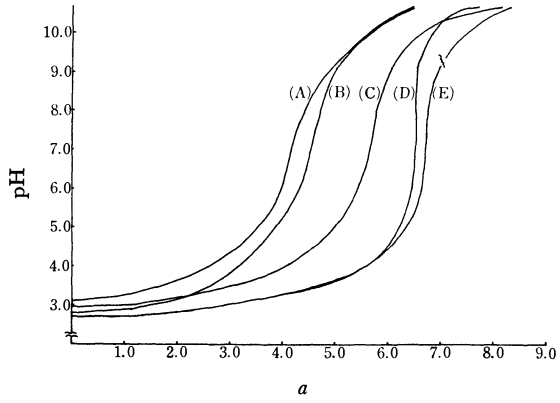

Fig. 1. Titration curves of 5×10^{-4}M TPHA(A) and 1:2(B) 1:1(C), 2:1(D), and 3:1(E) mixtures of Ni(II) and TPHA.

10) K. Nakamoto, Y. Morimoto, and A. E. Martell, *J. Amer. Chem. Soc.*, **85**, 309 (1963).

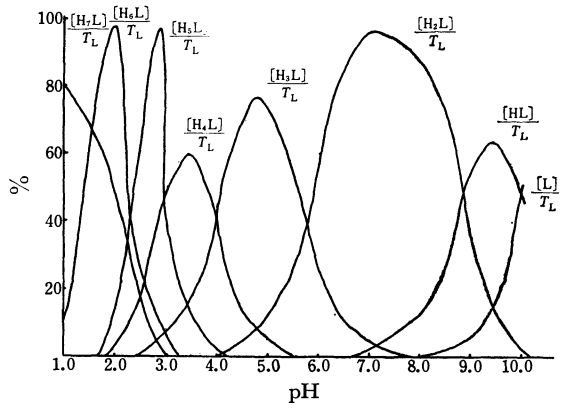

Fig. 2. Distribution diagram for the species of TPHA not containing metal.
The percentages are relation to total ligand.

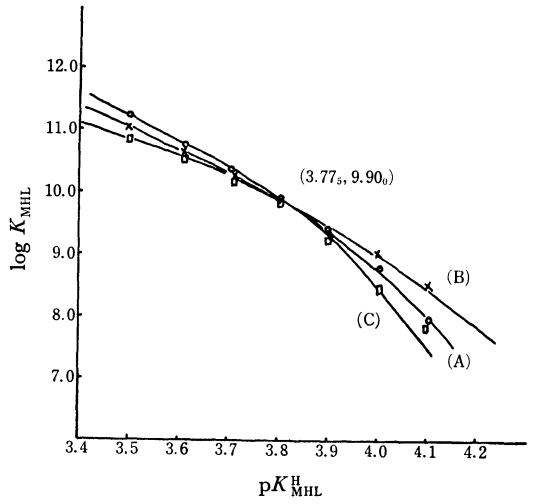

Fig. 3. Plots of log K_{MHL} *vs.* pK^H_{MHL} for 1:1 nickel chelates of TPHA.
a=3.7(A), a=3.9(B), a=4.1(C)

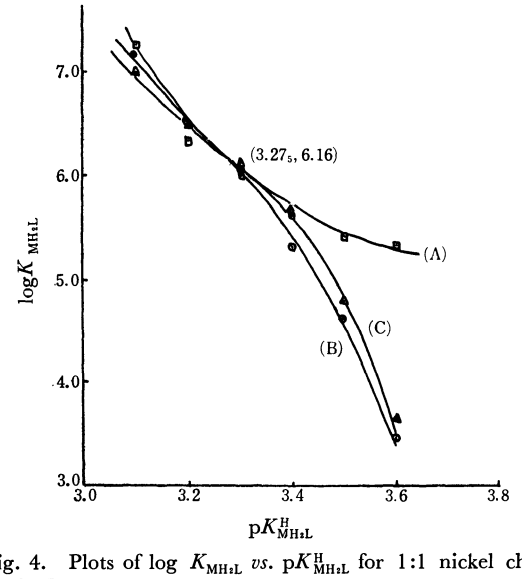

Fig. 4. Plots of log K_{MH_2L} *vs.* $pK^H_{MH_2L}$ for 1:1 nickel chelates of TPHA.
a=3.1(A), a=3.0(B), a=2.9(C)

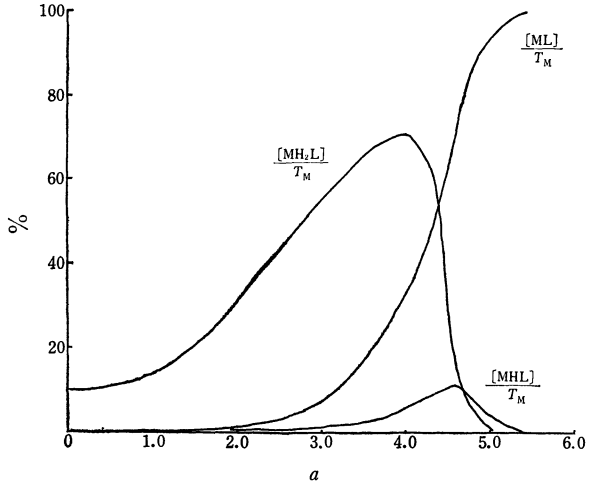

Fig 5. Distribution diagram of NiH_2L (1), NiHL (2), and NiL (3) drawn as a function of a for a 1:1 mixture of nickel(II) and TPHA (5×10^{-4} mol).
The percentages are relative to total metal.

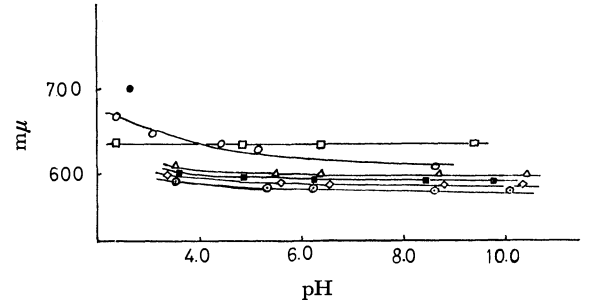

Fig. 6. Displacement of absorption maximum of nickel(II)-polyaminocarboxylic acid chelates (1:1) as a function of pH. polyaminocarboxylic acid; (□) NTA, (○) IDA, (△) EDTA, (■) TPHA, (◇) TTHA, (⊙) DTPA.
(●) nickel(II) perchlorate solution.

the equilibrium constants. For nickel(II), the values, $pK^{H}_{MH_2L}=3.275$ and $\log K_{MH_2L}=6.16$ were found (see Fig. 4). The value, $\log K_{MH_2L}=5.40$ calculated by using Eqs. (21) and (20) was less than the value of graphical solution. The disagreement between calculated and graphical solutions is due to the presence of species other than MH_2L and MHL complexes assumed for stepwise equilibrium constants. The value of $\log K_{MH_3L}$, 5.26 on the limiting range of pH measurement (3.0) was obtained.

Stability Constants of log K_{M_2L} and log K_{ML_2}. The stability constants of the complexes were calculated as described above (refer to Eqs. (16) to (17) and to Eq. (19)). The results are also given in Table 1.

The Percentages of the Species. Nickel(II) and TPHA form a normal and protonated complexes as described above. In Fig. 5. the percentages of the species, MH_2L, MHL, and ML in the solution of 1:1 mixtures of nickel(II) and the ligand, TPHA, are plotted as a function of a. Figure 5 clearly demonstrates the difference in the stabilities of MH_2L, MHL, and ML. It was shown that the MH_2L complex is present in the range between $a=1.0$ and $a=5.0$. The percentage of this species has a maximum value (70%) at $a=3.8$, while the MHL species is present from $a=2.0$ to $a=5.5$, although a maximum value at $a=4.6$ is only 11 pecent. However, the ML species predominated at $a\geq5.0$. An intersecting point of lines representing the species MH_2L and ML was observed at $a=4.4$. A similar behaviour is indicated for lines representing the species MHL, and MH_2L, too. Below $a=3$, the species other than MHL, MH_2L, and ML, such as triprotonated species, also exists. In the present investigation no evidence was found for species of M_2HL and ML(OH).

Stability Constants and the Structures of Nickel(II)-TPHA Complexes. The stability constants of the uninuclear nickel(II)-complexes with EDTA, DTPA, and TTHA were reported by several authors.[2,11,12] Table 1 shows the stability constants of nickel(II) complexes with TPHA. The stability constant of the 1:1 nickel(II)-TPHA normal complex is lower than the corresponding constants of the EDTA, DTPA, and TTHA chelates by 2—3 logarithmic units. The chelate effect of 1:1 nickel(II)-TPHA complex may be lowered by the following reasons: 1) the presence of a number of ligand atoms which do not bind to nickel(II), 2) the steric forces of some kinds, that is, steric strain, and 3) diminution of the degree of freedom in molecular rotation of the ligand molecules by chelation.

The stability constants of di- and mono-protonated complex are also calculated (refer to Table 1). As nickel(II) has the co-ordination number of six in spite of TPHA having twelve open positions for the co-ordination, polynuclear chelates may be formed. It is found that TPHA ligand does not bind to metals more than two and that binuclear hydrogen or hydroxo complex does not exist as the results of potentiometric titration under the given condition. The normal binuclear complex is more stable than uninuclear one. Possible structure of M_2L is indicated as follows. This fact may be explained in terms of binding of the functional donor groups in TPHA ligand inlayed with sites of two nickel(II) in the binuclear complex.

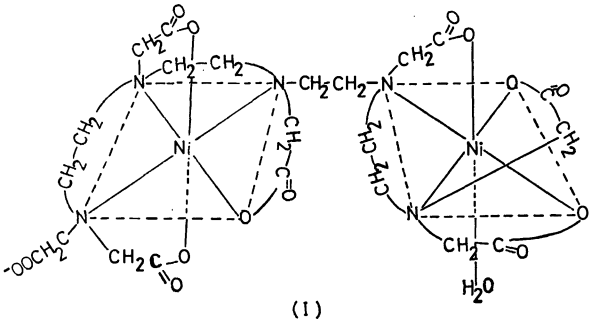

(I)

Six donor groups combined with nickel(II) are arranged in an octahedral configuration. Nickel(II)-TPHA complex can involve carboxylate and nitrogen donors combination, which satisfy co-ordination sites of nickel(II). In the extreme case, three different arrangements for the normal uninuclear complex are

11) G. Schwarzenbach, R. Gut, and G. Anderegg, *Helv. Chim. Acta*, **76**, 358 (1954).
12) S. Chaberek, A. E. Frost, M. A. Doran, and N. J. Bicknell, *J. Inorg. Nucl. Chem.*, **11**, 184 (1959).

considered as formulae II, III, and IV. In formula II, nickel(II) is co-ordinated with three nitrogen and three carboxylate donors, in formula III with five nitrogen donors and in formula IV with three nitrogen atoms and remote nitrogen donor having the high basicity.

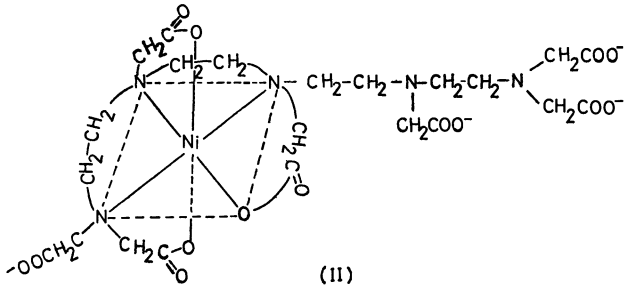

(II)

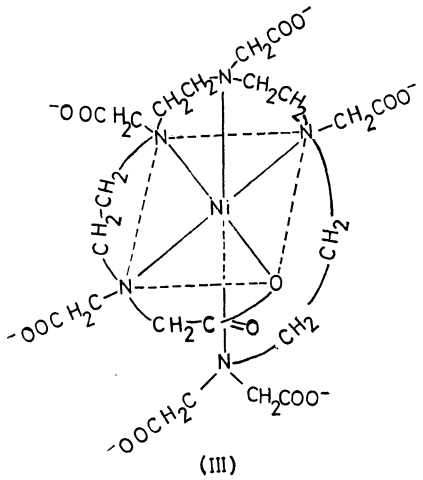

(III)

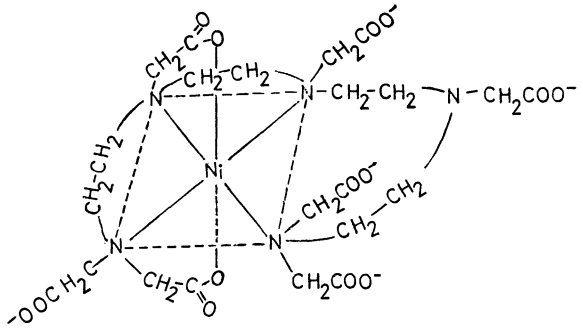

(IV)

A comparison of the visible absorption spectra of nickel(II)-polyaminocarboxylic acid complexes shows that the maxima are shifted to shorter wavelength as the number of co-ordinated nitrogen atoms increases. This fact suggests that the ligand field effect becomes powerful as the number of co-ordinated nitrogen atoms increases. However, for the nickel(II)-TPHA complex, the shift of the absorption maximum to shorter wavelength is smaller than for the DTPA complex with a rearrangment of donor groups involving three nitrogens and three caboxylate groups. It may be considered that the structure (II) is most probable one and is consistent with the reason mentioned before. On account of the ligand field strength and potential basicity of nitrogen atom of remote terminal amino group, the structure (IV) may be also present.

The following structures for mono- and diprotonated complexes may be suggested. More probable arrangements would involve co-ordination of metal ion by three nitrogen atoms and one carboxylate donor group, and un-co-ordinated groups exist in the structure as a terminal nitrogen atom remaining a proton and as carboxylate ion (refer to V and VI).

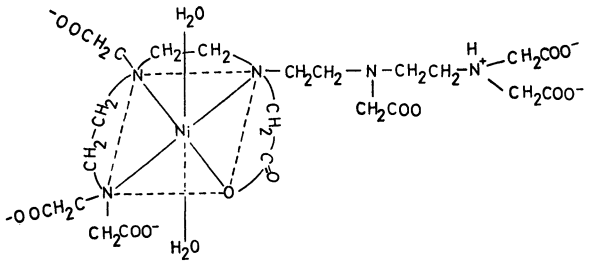

(V)

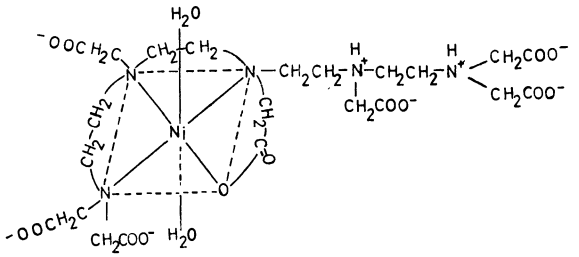

(VI)

Details concerning both the lack of a marked difference in behavior of the transition metal complexes and general validity of the Irving-William order will be reported in subsequent papers.

The authors wish to thank the Ministry of Education for the financial support granted for this research.

Polarographic Study of the Rates of the Dissociation Reactions of the Cobalt(II)-Acetylacetonate Complex and of the Nickel(II)-Acetylacetonate, -Glutamate, -Aspartate, and -Iminodiacetate Complexes

Mutsuo KODAMA, Hisao NUNOKAWA, and Noboru OYAMA*

Department of Chemistry, Ibaraki University, Bunkyo, Mito, Ibaraki

**Chemistry Department, Faculty of Engineering, Ibaraki University, Narisawa, Hitachi, Ibaraki*

(Received December 22, 1970)

The cobalt(II)-acetylacetonate complex and the nickel(II)-acetylacetonate, -glutamate, -aspartate and -iminodiacetate complexes were found to give kinetic waves due to the dissociation of these complexes at the electrode surface preceding the electron-transfer step. From the experimental examination of the nature of the kinetic current and a theoretical consideration, the mechanism and the rate constants of the dissociation of these complexes at the mercury-electrode surface were determined. The dissociation reactions were found to proceed through the following mechanism:

$$MX_2^{2-2m} \rightleftharpoons MX^{2-m} + X^{m-} \quad \text{rapid}$$

$$MX^{2-m} \underset{k_d}{\rightleftharpoons} M^{2+} + X^{m-} \quad \text{slow}$$

$$M^+ + 2e^- + Hg = M(Hg)$$

The rate constants, k_d's, for the dissociation reactions of cobalt(II)-acetylacetonate complex and of nickel(II)-acetylacetonate, -glutamate, -aspartate, and -iminodiacetate complexes at 25°C were estimated to be 9.3_0, 0.56, 0.69, $1.2_1 \times 10^{-2}$, and 2.5×10^{-4} sec^{-1} respectively. From a comparison of the rate constants, the dissociation of nickel(II)-aminopolycarboxylate complexes was concluded to proceed invariably through a reaction intermediate in which the leaving aminopolycarboxylate anions is bonded to the nickel(II) ion through one nitrogen and one oxygen atoms (Glycinate intermediate). In the formation reactions of cobalt(II)- and nickel(II)-acetylacetonate complexes in a 1:1 ratio, the dissociation of coordinated water from the metal(II) ion is rate-determining (water-loss mechanism).

Previously,[1,2] we reported that the cadmium(II)-EDTA complex in an acetate buffer solution and the zinc(II)-NTA complex in an ammonia buffer solution give kinetic waves due to the dissociation of these complexes preceding the electron-transfer step at the electrode surface; we then thoroughly investigated the nature of these kinetic waves from both theoretical and experimental viewpoints and determined the rates and the mechanism of the dissociation reactions of cadmium(II)-EDTA and zinc(II)-NTA complexes. Quite similar phenomena could also be observed in the polarography of the cobalt(II)-acetylacetonate (ACAC) complex and in that of the nickel(II)-ACAC, -glutamate (Glut), -aspartate (Asp) and -iminodiacetate (IDA) complexes. In this paper, we will study systematically the nature of the kinetic waves due to the dissociation of these complexes from both theoretical and experimental viewpoints, and will determine the mechanism and the rates. From a comparison of rate constants for the dissociation of the nickel(II)-aminopolycarboxylate complexes with those estimated on the basis of the proposed reaction intermediate, the structures of the reaction intermediates will be determined in detail. The mechanism of the formation reactions of 1:1 ratio cobalt(II)- and nickel(II)-ACAC complexes will also be discussed.

Experimental

Reagents. Standard nickel(II) and cobalt(II) nitrate solutions were prepared by dissolving known amounts of metallic nickel and cobalt (99.99% pure) in dilute nitric acid (1+1), and by then removing the excess nitric acid by distillation under reduced pressure. L-Glutamic acid (Glut), L-aspartic acid (Asp) and iminodiacetic acid (IDA) were recrystallized from their aqueous solutions by adding pure ethanol and hydrochloric acid. The acetylacetone used was purified twice by distillation under reduced pressure. The standard solutions of Glut, Asp, and IDA were prepared by dissolving known amounts of recrystallized Glut, Asp, and IDA in redistilled water. All the other chemicals used were of analytical-reagent grades and were used without further purification.

Apparatus and Experimental Procedures. All the DC current-voltage curves were measured by using a manual polarograph similar to that of Kolthoff and Lingane[3] or a Yanagimoto pen-recording polarograph PA-102. The characteristic feature of the dropping mercury electrode (DME) used in this study was described previously.[4] A saturated calomel electrode (SCE) with a large area was used as the reference electrode and was connected to the cell solution through a Hume and Harris-type salt bridge.[5] The pH value of the solution was measured with a glass electrode pH meter (a Hitachi-Horiba F-5). The dissolved oxygen in the solution was removed by bubbling pure nitrogen gas through the solution. The ionic strength of the solution was adjusted to 0.20 by adding an appropriate amount of pure sodium perchlorate or potassium nitrate. To keep the solution's pH constant, a sodium acetate-acetic acid mixture in the nickel-

1) N. Tanaka, R. Tamamushi, and M. Kodama, *Z. Phys. Chem., N. F.*, **14**, 141 (1958).

2) M. Kodama and M. Hashimoto, This Bulletin, **35**, 1802 (1962).

3) I. M. Kolthoff and J. J. Lingane, "Polarography," Vol. 1, Interscience Publishers, New York (1952), p. 297.

4) Y. Fujii, T. Ueda, and M. Kodama, This Bulletin, **43**, 409 (1970).

5) D. N. Hume and W. E. Harris, *Ind. Engng. Chem., Analyt. Edit.*, **15**, 465 (1943).

(II)-IDA system and a potassium dihydrogen phosphate-disodium hydrogen phosphate mixture in the nickel(II)-ACAC and -Asp systems were used. In the cases of the nickel(II)-Glut and cobalt(II)-ACAC systems, no buffer mixture was used, for the sample solution always contained a large excess of uncomplexed Glut or ACAC, and, hence, was considered to have a sufficient buffer capacity over the entire pH range covered ($7.80<pH<9.00$ in the cobalt(II)-ACAC system, $8.50<pH<9.30$ in the nickel(II)-Glut system).

Results and Discussion

Polarographic Behavior of Nickel(II) and Cobalt(II) Ions in Acetylacetonate Solutions. As is shown in Fig. 1, both nickel(II) and cobalt(II) ions in acetylacetonate solutions exhibited the polarographic steps at potentials where the aquo complexes of these metal(II) ions will give polarographic waves due to their reduction even under the experimental conditions where, from the thermodynamic point of view,[6] all the metal(II) ions may be considered to exist as acetylacetonate complex. The second wave of the nickel(II)-ACAC complex may correspond to its direct reduction. Its limiting current was proportional to the square root of the effective pressure of mercury. At lower solution pH's, the polarographic step corresponding to the direct reduction of cobalt(II)-ACAC complex could also be observed, but this step merges in the base current at higher pH's. The limiting current of the reduction wave of the cobalt(II)-ACAC complex and that of the first wave of the nickel(II)-ACAC complex were almost independent of the effective pressure of the mercury column within the limits of experimental error. Some typical data are given in Table 1. This fact clearly implies that both limiting currents are kinetic-controlled in nature. The polarogram of the cobalt(II)-ACAC complex and the first wave of the nickel(II)-ACAC complex gave linear log-plots ($\log(i/(i_1-i))$ *vs.* E_{dme}) with slopes of about 54 and 57 mV respectively, thus indicating an irreversible two-electron reduction. The results are not shown here. The reduction wave-height of the cobalt(II) ion in the ACAC solution was found to decrease with an increase in the solution's pH or with the concentration of uncomplexed ACAC. In the nickel(II)-ACAC system, although the total wave-height was almost constant under the present experimental conditions, the height of the first wave also decreased with an increase in the solution's pH or in the concentration of uncomplexed ACAC. Considering that the concentration of the deprotonated ACAC anion increases with an increase in the solutions' pH all the facts given above indicate that the first wave of the nickel(II)-ACAC complex and the polarographic step of the cobalt(II)-ACAC complex can be ascribed to the reduction of the uncomplexed metal(II) ion or a lower ACAC complex liberated by the dissociation of nickel(II) and cobalt(II) complexes of ACAC at the mercury electrode surface proceding the electron-transfer step.

Since all the systems studied in this paper contained a large excess of uncomplexed ACAC over the metal(II) ion, the dissociation of metal(II)-ACAC complexes can be treated as a psuedo-first-order reaction. Therefore, as both metal(II) ions form 1:1- and 1:2-ratio ACAC complexes under the present experimental conditions, the reaction mechanism can be written in a simpler form as (A) or (B):

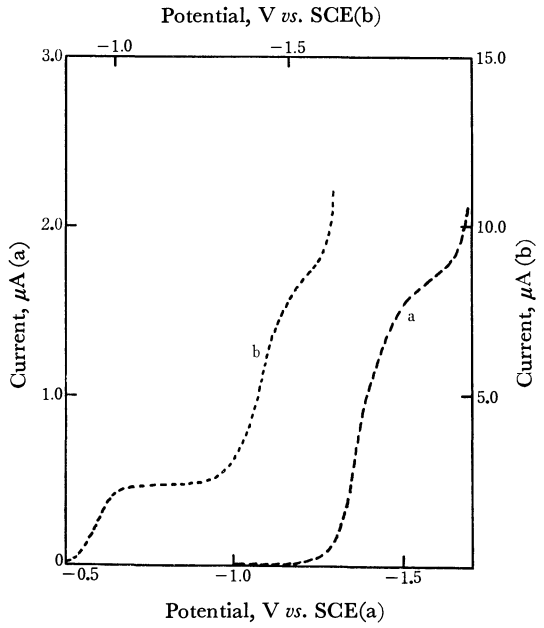

Fig. 1. Polarograms of metal(II)-ACAC complexes.
a) Co(II)-ACAC complex
The Co(II) concentration=1.0 mM
The concentration of uncomplexed ACAC=50.0 mM
pH=8.24, μ=0.20
b) Ni(II)-ACAC complex
The Ni(II) concentration=2.0 mM,
Total phosphate concentration=0.10 M
The concentration of uncomplexed ACAC=25 mM
pH=7.29, μ=0.20

TABLE 1. THE RELATION BETWEEN THE LIMITING CURRENT AND THE EFFECTIVE PRESSURE OF MERCURY

μ=0.20, 25°C

i) Co(II)-ACAC system
the concentration of cobalt(II) ion =2.0 mM,
pH=9.00
the concentration of uncomplexed ACAC =50.0 mM

H_c, cm	i_l, μA
55.0	0.480
65.0	0.480
75.0	0.485

ii) Ni(II)–ACAC system
the concentration of nickel(II) ion=2.0 mM,
pH=7.40
the concentration of uncomplexed ACAC=50.0 mM
the total concentration phosphate=0.10 M

H_c, cm	First wave-height i_l, μA	Second wave-height i_d, μA	$i_d/H_c^{1/2}$
55.0	1.64_0	5.71_0	0.771
65.0	1.65_1	6.22_1	0.773
75.0	1.67_3	6.69_3	0.775

$$(A)\quad \begin{cases} A \underset{}{\overset{K_{1a}}{\rightleftharpoons}} B & \text{rapid} \quad (1) \\ B \underset{k_{2a}}{\overset{\vec{k}_{2a}}{\rightleftharpoons}} O & \text{slow} \quad (2) \\ O + 2e^- \underset{\overleftarrow{k}}{\overset{\vec{k}}{\rightleftharpoons}} R & (3) \end{cases}$$

$$(B)\quad \begin{cases} A \underset{\overleftarrow{k}_{1b}}{\overset{\vec{k}_{1b}}{\rightleftharpoons}} O & \text{slow} \quad (4) \\ O + 2e^- \underset{\overleftarrow{k}}{\overset{\vec{k}}{\rightleftharpoons}} R & (3') \end{cases}$$

For the mechanims (A), where (3) is rapid in a polarographic sense, we previously[1] derived the general relations of the limiting current and the current-voltage curve by taking into consideration the diffusion processes of A and B from the bulk of the solution to the electrode surface and that of R from the mercury surface to the inside of mercury, and by assuming the conditions of the stationary state with respect to the concentrations of A, B, O, and R at the electrode surface. Equation (25) in Ref. 1 is applicable to the present systems, in which the (3) process is irreversible, without making any modification. That is, we can use the following relation to examine the nature of the limiting current:

$$\frac{1}{i_l} = \frac{1}{2AF \cdot K_{2a} \cdot D^{1/2} \cdot \vec{k}_{2a}^{1/2} \cdot C_B^0} + \frac{1}{2AF \cdot K^D \cdot C^0} \quad (5a)$$

where C^0 is equal to $C^0_A + C^0_B$ and where all the symbols used have the same meanings as in the previous paper.[1] As is clear from the log-plot slopes, the electron-transfer process (3) is assumed to be irreversible, *i.e.*, $\vec{k} \gg \overleftarrow{k}$, in the present systems. Therefore, Eq. (27) in Ref. 1 should be replaced by the (6_a) relation:

$$E = \text{constant} - \frac{0.0591}{2\alpha} \log \frac{i}{i_l - i} - \frac{0.0591}{4\alpha} \log \overleftarrow{k}_{2a} \quad (6a)$$

For the (B) mechanism, where (3′) is irreversible in nature, we had already derived the theoretical relations for the limiting current and for the current voltage curve.[2] The relations, (16) and (18) or (20), in Ref. 2 can be used without any modification. Thus, for the (B) reaction mechanism we can derive the following two relations:

$$\frac{1}{i_l} = \frac{1}{2AF \cdot K_{1b}^{1/2} \cdot D^{1/2} \cdot \vec{k}_{1b}^{1/2} \cdot C_A^0} + \frac{1}{2AF \cdot K^D \cdot C_A^0} \quad (5b)$$

$$E = \text{constant} - \frac{0.0591}{2\alpha} \log \frac{i}{i_l - i} - \frac{0.0591}{4\alpha} \log \overleftarrow{k}_{1b} \quad (6b)$$

Provided that the other experimental conditions are kept constant, both the polarographic wave of the cobalt(II)-ACAC complex and the first step of the nickel(II)-ACAC system gave excellent linear relations between $1/i_l$ and the $(1+K'_2[X]_f)[X]_f^{1/2}$ value or the $(1+K_2' \cdot [X]_f)/(\alpha_H)_X^{1/2}$ value. Typical results are shown in Figs. 2, 3, and 4. Here, $(\alpha_H)_X$ denotes the apparent (α_H) value of acetylacetone, defined as $1+5\cdot[H^+]/K_a$; K_a, the dissociation constant of the tautomeric enol acetylacetone; $[X]_f$, the concentration of uncomplexed acetylacetone, and K_2', the conditional second successive formation constant of the acetylacetonate complex. The aqueous equilibrium keto : enol ratio was assumed to be approximately four to one.[7] The keto: enol ratio 4:1 suggests that if the ketonization rate of the

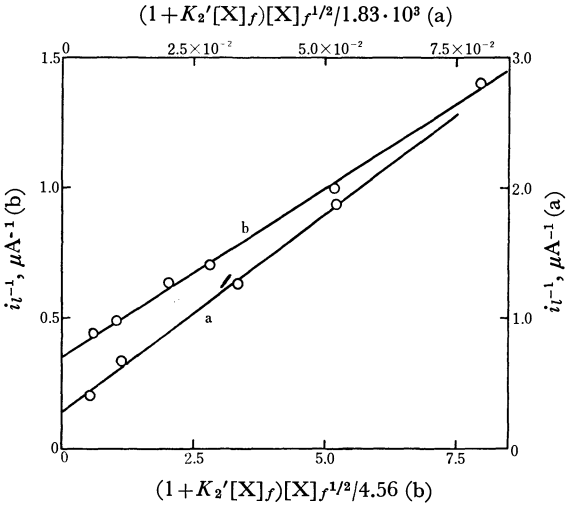

Fig. 2. The plot of $1/i_l$ against $(1+K_2'\cdot[X]_f)\cdot[X]_f^{1/2}$.
a) Co(II)-ACAC complex
The Co(II) concentration=1.0 mM
pH=8.24, μ=0.20, 25°C
The concentration of uncomplexed ACAC ranged from 30 to 150 mM
b) Ni(II)-ACAC complex
The Ni(II) concentration=2.0 mM
pH=7.40, μ=0.20, 25°C
The concentration of uncomplexed ACAC ranged from 15 to 100 mM
Total concentration of phosphate=0.10 M

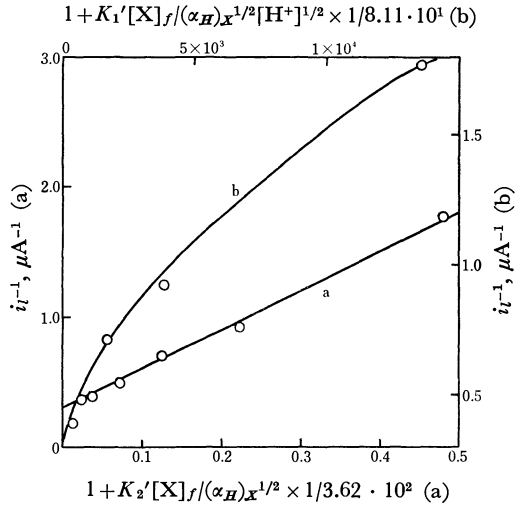

Fig. 3. The plot of $1/i_l$ against $(1+K_2'\cdot[X]_f)/(\alpha_H)_X^{1/2}$ or $(1+K_2'[X]_f)/(\alpha_H)_X^{1/2}[H^+]^{1/2}$.
The Co(II) concentration=2.0 mM
The concentration uncomplexed ACAC=50.0 mM
μ=0.20, 25°C
a) $1/i_l$ *vs.* $(1+K_2'[X]_f)/(\alpha_H)_X^{1/2}$ plot
b) $1/i_l$ *vs.* $(1+K_2'[X]_f)/(\alpha_H)_X^{1/2}\cdot[H^+]^{+1/2}$ plot

6) L. G. Sillen and A. E. Martell, "Stability Constants of Metal-Ion Complexes," 2nd Ed., The Chemical Society, London (1964). pp. 444—445.

7) F. C. Nachod, *Z. Physik. Chem.*, **A182**, 193 (1938).

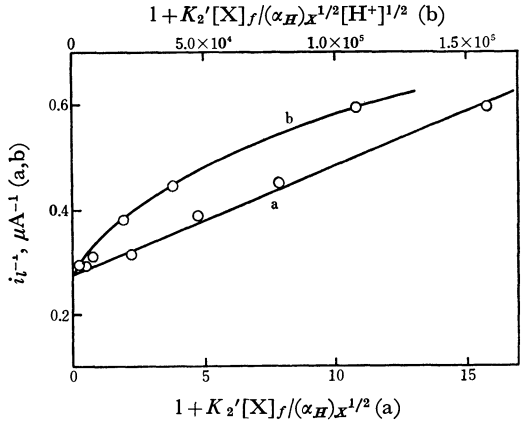

Fig. 4. The plot of $1/i_l$ against $(1+K_2'[X]_f)/(\alpha_H)_X^{1/2}$ or $(1+K_2'[X]_f)/(\alpha_H)_X^{1/2}\cdot[X]^{+1/2}$.
The Ni(II) concentration=2.0 mM
The concentration of uncomplexed ACAC=25.0 mM
Total concentration of phosphate=0.10 M
μ=0.20, 25°C
a) $1/i_l$ *vs.* $(1+K_2'[X]_f)/(\alpha_H)_X^{1/2}$·plot
b) $1/i_l$ *vs.* $(1+K_2'[X]_f)/(\alpha_H)_X^{1/2}\cdot[H^+]^{1/2}$ plot

enol ACAC, which is the initial product of the protonization of the ACAC anion, is slow, the ACAC anion concentration at the electrode surface will increase with an increase in the current, especially at lower ACAC concentrations. The rapid ketonization was confirmed by following the change in the absorbance at 270 mμ (the absorption maximum of the enol form). When perchloric acid was added to an ACAC solution of pH 10.5, the absorbance decreased so rapidly that we could not determine the ketonization rate exactly by using a conventional method. Since the $[X]_f/(\alpha_H)_X$ and $[M]_t/(1+K_2'\cdot[X]_f)$ values correspond to the concentration of uncomplexed ACAC anion and the bulk concentration of a 1:1 ratio metal(II)-ACAC complex, the above findings evidently show that the reaction mechanism for the first wave of the nickel(II)-ACAC complex can be expressed as:

$$I_a \begin{cases} MX_2^{2-2m} \overset{K_1}{\rightleftharpoons} MX^{2-m} + X^{m-} & \text{rapid} \quad (7) \\ MX^{2-m} \underset{k_f}{\overset{k_d}{\rightleftharpoons}} M^{2+} + X^{m-} & \text{slow} \quad (8a) \\ M^{2+} + 2e^- + Hg = M(Hg) & (9) \end{cases}$$

where X^{m-} means the ACAC anion. For the above reaction mechanism, Eqs. (5a) and (6a) can be rewritten as:

$$\frac{1}{i_l} = \frac{K_1^{1/2}\cdot(1+K_2'\cdot[X]_f)\cdot[X]_f^{1/2}}{2AF\cdot D^{1/2}\cdot k_d^{1/2}\cdot[M]_t\cdot(\alpha_H)_X^{1/2}} + \frac{1}{2AF\cdot K^D\cdot[M]_t} \quad (10a)$$

$$E_{1/2} = \text{constant} - \frac{0.0591}{4\alpha}\log\frac{[X]_f}{(\alpha_H)_X} \quad (10b)$$

As was discussed in the previous paper,[1] theoretically the $2AF\cdot D^{1/2}$ and $2AF\cdot K_d$ values in Eq. (10_a) are identical to $2.51\times10^5\cdot m^{2/3}\cdot t^{2/3}$ and $2\times6.07\times10^4\cdot m^{2/3}\cdot t^{1/6}\cdot D^{1/2}$ respectively. $[M]_t$ in Eq. (10a) signifies the total concentration of the metal(II)-ACAC complex and K_1, the formation constant of a 1:1 ratio metal(II)-ACAC

Table 2. The effects of pH and ACAC concentration on the half-wave potential
μ=0.20, 25°C

i) pH effect

System	pH	$E_{1/2}$ V *vs.* SCE	$\Delta E_{1/2}$, mV calcd	$\Delta E_{1/2}$, mV obsd	
Co(II)	7.81	−1.327	0	0	ACAC concentration=50.0 mM Cobalt(II) concentration=1.0 mM
	8.02	−1.332	−4.9	−5	
	8.24	−1.336	−9.3	−9	
	8.49	−1.338	−14.3	−11	
	8.90	−1.352	−20.2	−25	
Ni(II)	6.66	−0.954	0	0	ACAC concentration=25.0 mM Nickel(II) concentration=2.0 mM Total concentration of phosphate=0.10 M
	7.09	−0.964	−12.0	−10	
	7.29	−0.967	−17.7	−16	
	7.40	−0.974	−20.6	−20	
	7.68	−0.980	−28.0	−26	

ii) ACAC concentration effect

System	Concentration of uncomplexed ACAC mM	$E_{1/2}$ V *vs.* SCE	$\Delta E_{1/2}$, mV calcd	$\Delta E_{1/2}$, mV obsd	
Co(II)	30.0	−1.330	0	0	Cobalt concentration=1.0 mM, pH=8.24
	50.0	−1.336	−6.0	−6	
	100.0	−1.346	−12.0	−16	
Ni(II)	15.0	−0.966	0	0	Nickel(II) concentration=2.0 mM, pH=7.40 Total concentration of phosphate=0.10 M
	25.0	−0.974	−6.3	−7	
	40.0	−0.979	−11.9	−12	
	50.0	−0.982	−14.7	−16	
	75.0	−0.987	−19.6	−20	
	100.0	−0.991	−23.1	−24	

complex. Equation (10a) suggests that $\Delta E_{1/2}/\Delta\log [X]_f$ and $\Delta E_{1/2}/\Delta \log (\alpha_H)_X$ should be $-0.0591/4\alpha$ and $0.0591/4\alpha$ V respectively. These relations were also examined by using some typical data. The results are shown in Table 2. The agreement between the observed value and that calculated with the aid of Eq. (10b) can be regarded as satisfactory. On the other hand, if the reaction mechanism is written as:

$$I_b \begin{cases} MX_2^{2-2m} + H^+ \rightleftharpoons MX^{2-m} + HX^{1-m} & \text{rapid} \\ MX^{2-m} + H^+ \rightleftharpoons M^{2+} + HX^{1-m} & \text{slow} \\ M^{2+} + 2e^- + Hg = M(Hg) \end{cases}$$

the plot of $1/i_l$ agaist the $(1+K_2'\cdot[X]_f)/(\alpha_H)_X^{1/2}\cdot[H^+]^{1/2}$ value should yield a straight line at a constant $[X]_f$. The curves given in Figs. 3 and 4 completely eliminated the above reaction mechanism. By using the D value of 7.4×10^{-6}, the k_d values for the cobalt(II) and nickel(II)-ACAC complexes were estimated from the slopes of the linear relations shown in Figs. 2, 3, and 4 and listed in Table 3. In both systems, the k_d value determined from the slopes of the linear relation between $1/i_l$ and $(1+K_2'\cdot[X]_f)/(\alpha_H)_X^{1/2}$ agreed well with that determined from the slope of the linear relation between $1/i_l$ and $(1+K_2'\cdot[X]_f)\,[X]_f^{1/2}$. A phosphate buffer used in the nickel(II)-ACAC system to keep the solution pH constant had no effect on the rate of dissociation of the nickel(II)-ACAC complex. Although the K_3 value for the nickel(II)-ACAC complex has been reported by Izatt *et al.*,[8] the possibility of the formation of a 1:3 ratio nickel(II)-ACAC complex could be eliminated by the ion-exchanger test. Under the present experimental conditions, no nickel(II) ion was adsorbed at either the cation or anion exchanger.

Table 3. Rate constants

System	k_d, sec^{-1} 25°C	k_d, sec^{-1} 30°C	k_f, M^{-1} sec^{-1}
Co(II)-ACAC	9.3		6.4×10^5
Ni(II)-ACAC	0.56		1.7×10^5
Ni(II)-Gult	0.69	1.2_1	
Ni(II)-Asp	$1.2_1\times10^{-2}$		
Ni(II)-IDA	2.5×10^{-4}	3.6×10^{-4}	
	2.8×10^{-4} [10]		

Polarographic Behavior of Nickel(II) Ions in Glutamate, Aspartate, and Iminodiacetate Solutions. As in the cases of the metal(II)-ACAC complexes studied in this paper, the nickel(II) ions in glutamate, aspartate, and iminodiacetate solutions also gave kinetic waves as a result of their dissociation at the electrode surface. Some typical polarograms of the nickel(II)-Asp and -IDA complexes are shown in Fig. 5. Although the polarogram is not shown here, the nickel(II)-Glut complex also gave the two polarographic steps. The limiting currents of the first waves of the nickel(II)-Glut and -Asp complexes and the reduction step of the nickel(II)-IDA complex were almost independent of the effective pressure on the DME, indicating their kinetic nature

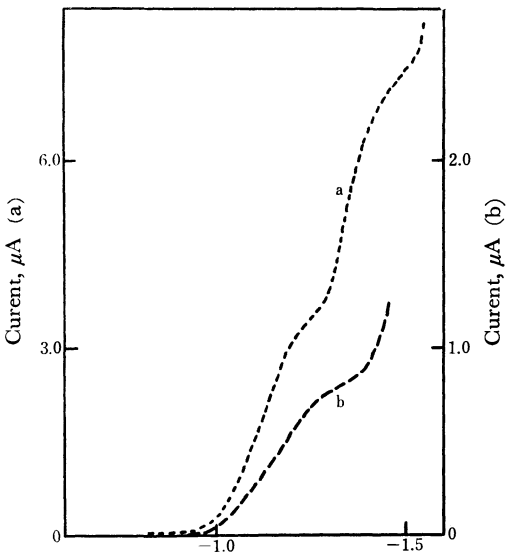

Fig. 5. Polarograms of nickel(II)-Asp and -IDA complexes.
a) Ni(II)-Asp complex
The Ni(II) concentration=2.0 mM
The concentration of uncomplexed Asp=20.0 mM
Total concentration of phosphate=0.10 M
pH=6.49, 25°C
b) Ni(II)-IDA complex
The Ni(II) concentration=2.0 mM
The concentration of uncomplexed IDA=40.0 mM
The acetate ion concentration=0.10 M
pH=5.50, 30°C

(the results are not shown). The second step observed in the nickel(II)-Glut and-Asp systems may be ascribed to the direct reduction of the nickel(II)-Glut and -Asp complexes. In both systems, the total wave-height was almost constant under the present experimental conditions and was exactly proportional to the square root of the effective pressure on the DME. In the case of the nickel(II)-IDA complex, however, the polarographic step corresponding to the direct reduction of the nickel(II)-IDA complex could not be observed (Fig. 5). This

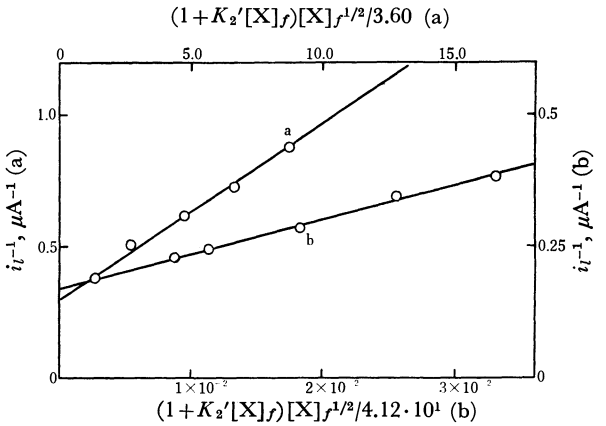

Fig. 6. The plot of $1/i_l$ against $(1+K_2'[X]_f)[X]_f^{1/2}$.
The Ni(II) concentration=2.0 mM
a) Ni(II)-Glut system
pH=8.50, 30°C
b) Ni(II)-Asp system
pH=6.25, 25°C
Total phosphate concentration=0.10 M

8) R. M. Izatt, W. C. Fernelius, C. G. Haas, Jr., and B. P. Block, *J. Phys. Chem.*, **59**, 170 (1955).

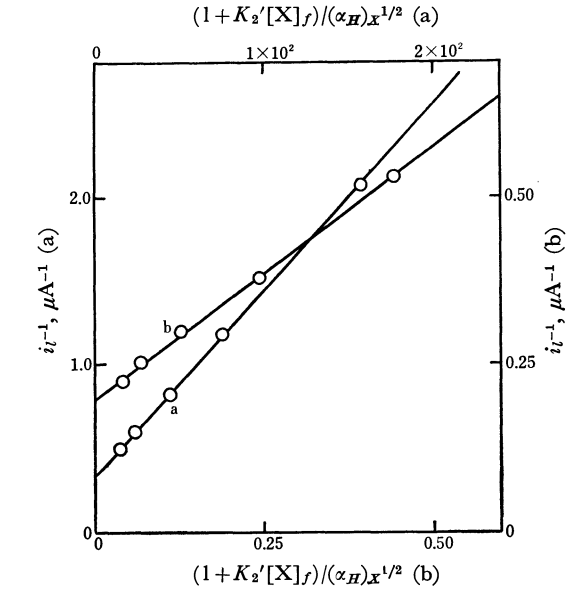

Fig. 7. The plot of $1/i_l$ against $(1+K_2'[X]_f)/(\alpha_H)_X^{1/2}$.
The Ni(II) concentration=2.0 mM
a) Ni(II)-Glut system
The concentration of uncomplexed Glut=30.0 mM, 30°C
b) Ni(II)-Asp system
The concentration of uncomplexed Asp=20.0 mM, 25°C
Total concentration of phosphate=0.10 M

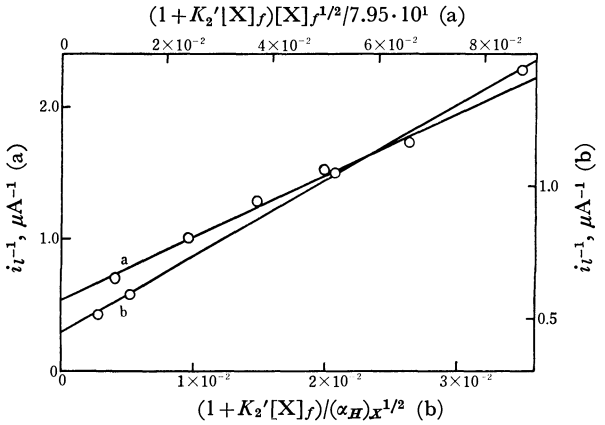

Fig. 8. The plot of $1/i_l$ against $(1+K_2'\cdot[X]_f)[X]_f^{1/2}$ or $(1+K_2'\cdot[X]_f)/(\alpha_H)_X^{1/2}$
The Ni(II) concentration=2.0 mM, 30°C
The concentration of acetate ion=0.10 M
a) $1/i_l$ *vs.* $(1+K_2'[X]_f)[X]_f^{1/2}$ plot
pH=5.50
b) $1/i_l$ *vs.* $(1+K_2'[X]_f)/(\alpha_H)_X^{1/2}$ plot
The concentration of uncomplexed IDA=20.0 mM

can be ascribed to the inertness of the nickel(II)-iminodiacetate complex. The first waves of the nickel(II)-Glut and -Asp complexes and the reduction wave of the nickel(II)-IDA complex gave linear log-plots with slopes falling in the range from 65 to 75 mV. As in the cases of the cobalt(II)- and nickel(II)-ACAC complexes, all three waves invariably gave linear relations between $1/i_l$ and $(1+K_2'\cdot[X]_f)\cdot[X]_f^{1/2}$ or $(1+K_2'\cdot[X]_f)/(\alpha_H)_X^{1/2}$, with intercepts corresponding to the reciprocal of the total wave-height. Here, K'_2 means the conditional second successive formation constant; $[X]_f$, the concentration of uncomplexed Glut, Asp, or IDA, and $(\alpha_H)_X$, the (α_H) value of Glut, Asp, or IDA. The results are shown in Figs. 6, 7, and 8. The linear relations found in the nickel(II)-Glut and -Asp systems evidently imply that the electrode reaction mechanism for the first waves of these complexes is also given by (I_a), and that the concentration dependence of the half-wave potential is also given by Eq. (10b). Some typical results obtained in the nickel(II)-Asp system are given in Table 4. The shifts of the half-wave potential, as

TABLE 4. THE EFFECTS OF pH AND THE CONCENTRATION OF UNCOMPLEXED ASPARTATE ON THE HALF-WAVE POTENTIAL

μ=0.20, 25°C, phosphate concentration=0.10 M

i) pH effect
The concentration of uncomplexed Asp=30.0 mM

pH	$E_{1/2}$ V *vs.* SCE	$\Delta E_{1/2}$, mV	
		calcd	obsd
6.05	−1.083	0	0
6.28	−1.093	−10.5	−10
6.46	−1.106	−18.9	−23
6.68	−1.115	−29.0	−32
6.87	−1.120	−37.7	−37

ii) Asp concentration effect
pH=6.28

Concentration of uncomplexed Asp (mM)	$E_{1/2}$ V *vs.* SCE	$\Delta E_{1/2}$, mV	
		calcd	obsd
15.0	−1.089	0	0
20.0	−1.096	−5.7	−7
30.0	−1.103	−15.7	−14
40.0	−1.113	−20.0	−24
50.0	−1.118	−24.1	−29

calculated with the acid of Eq. (10b) agreed well with those determined experimentally. As we observed in the acetylacetonate system, curves obtained by plotting the $1/i_l$ against the $(1+K_2'\cdot[X]_f)/(\alpha_H)^{1/2}\cdot[H^+]_X^{1/2}$ also eliminate the proton-assisted reaction mechanism. From the slopes of the linear relations shown in Fig. 6 and 7, the k_d values for the dissociation of the 1:1 ratio nickel(II)-Glut and -Asp complexes were determined to be 1.2_0 (30°C) and $1.2_1\times10^{-2}$ sec^{-1} (25°C) respectively.

As in the case of the nickel(II)-ACAC system, a phosphate buffer mixture had no effect on the wave-height of the nickel(II)-Asp complex. An acetate buffer, however, had a remarkable effect on the wave-height of the nickel(II)-IDA complex. The wave-height was increased remarkably by increasing the concentration of an acetate ion. This indicates that the acetate anion effectively assists the dissociation of the nickel(II)-IDA complex at the electrode surface. Judging from the magnitude of the formation constant of the nickel(II)-acetate complex,[9] an acetate anion can not participate in the formation of a mixed ligand complex of the nickel(II) ion involving an IDA anion under the present experimental conditions. Therefore, the ace-

9) N. Tanaka and K. Kato, This Bulletin, **32**, 516 (1959).

tate ion will help only the dissociation of a 1:1 nickel-(II)-IDA complex at the electrode surface. If the dissociation of a 1:1 nickel(II)-IDA complex proceeds through both the (8b) and (8a) reaction pathways, one can derive Eq. (11) for the limiting current:

$$NiX^0 + Ac^- \overset{(k_d)_{Ac}}{\rightleftharpoons} Ni(Ac)^+ + X^{2-} \quad (8b)$$

$$\frac{1}{i_l} = \frac{K_1^{1/2}\cdot(1+K_2'\cdot[X]_f)\cdot[X]_f^{1/2}}{2AF\cdot D^{1/2}\cdot(k_d^{1/2}+(k_d)_{Ac}^{1/2}\cdot K_{NiAc}^{1/2}\cdot[Ac^-])(\alpha_H)_X^{1/2}\cdot[Ni]_t} + \frac{1}{i_d} \quad (11)$$

where K_{NiAc} denotes the first formation constant of the nickel(II)-acetate complex; $[Ac^-]$, the concentration of the uncomplexed acetate ion, and $[Ni]_t$, the total concentration of the nickel(II)-IDA complex, and where i_d corresponds to the $2AF\cdot K^D\cdot[M]_t$ value in Eq. (10a). From Eq. (11), one can easily derive the following relation.

$$\frac{i_d i_l}{i_d - i}\times\frac{(1+K_2'\cdot[X]_f)\cdot[X]_f^{1/2}}{(\alpha_H)_X^{1/2}} = 2AF\cdot D^{1/2}\cdot[Ni]_t(k_d^{1/2}+(k_d)_{Ac}^{1/2}\cdot K_{NiAc}^{1/2}\cdot[Ac^-]) \quad (12)$$

This relation indicates that the plot of the left-hand side of Eq. (12) against $[Ac^-]$ will give a linear relation, the slope and intercept of which correspond to $2AF\cdot D^{1/2}\cdot[Ni]_t\cdot(k_d)_{Ac}^{1/2}\cdot K_{NiAc}^{1/2}$ and $2AF\cdot D^{1/2}\cdot[Ni]_t\cdot k_d^{1/2}$ respectively, if the dissociation of a 1:1 ratio nickel(II)-IDA complex at the electrode surface proceeds through the two reaction pathways, (8a) and (8b). The above relation was examined by using some typical experimental data. As is shown in Fig. 9, a fairly good linear relation could be obtained. From the slope and intercept of the linear relation in Fig. 9, the $(k_d)_{Ac}$ and k_d values at 30°C were determined to be 3.8×10^{-4} and $3._9\times10^{-4}$ respectively. In a similar way, the k_d value of the nickel(II)-Asp and Glut complexes at 15°C were also determined (Table 3). The k_d value for the nickel(II)-IDA complex determined in this study agrees well with that reported by Bydalek and Constant.[10] This agreement also supports the present author's explanation.

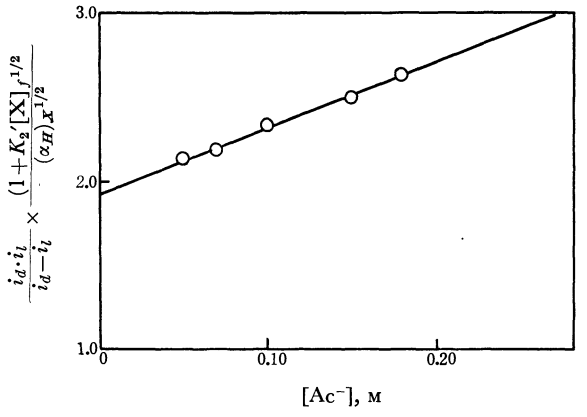

Fig. 9. The plot of $i_d\times i_l\ (1+K_2'[X]_f)[X]_f^{1/2}/(i_d-i_l)\cdot(\alpha_H)_X^{1/2}$ against the acetate ion concentration
The Ni(II) concentration=2.0 mM, 30°C, pH=5.40
The concentration of uncomplexed IDA=20.0 mM

From the $K_1=k_f/k_d$ relation, the formation rate constant, k_f, of the 1:1 ratio cobalt(II)-ACAC complex and that of the 1:1 ratio nickel(II)-ACAC complex were determined to be 6.4×10^5 and 1.7×10^5 $M^{-1}\cdot sec^{-1}$ respectively. These values are nearly identical with the characteristic water exchange rate constants of these metal(II) ions.[11] This fact indicates that, in the formation reaction of both cobalt(II)- and nickel(II)-ACAC complexes with a 1:1 ratio, the dissociation of water from the metal(II) aquo ion is the rate-determining step. The finding that, in the formation of the 1:1 cobalt(II)-ACAC complex, the dissociation of water from the cobalt(II) ion is the rate-determining step is contrary to the prediction of Pearson and Anderson[12] that the steric rearrangement of the ligand will provide the main activation energy barrier (sterically controlled substitution, SCS mechanism) in the formation of a six-membered chelate ring of the cobalt(II) complex. The k_f value for the 1:1 nickel(II)-ACAC complex is slightly larger than the characteristic water-exchange rate constant of the nickel(II) ion. However, this value can also be taken as evidence for the usual water exchange mechanism. Although Pearson and Moor[13] mentioned that the complexation reaction of neutral enol ACAC with the nickel(II) ion is very slow, and explained this slow reaction in terms of the SCS mechanism, there is, as yet, no satisfactory explanation for the distinct difference in the reaction rate between enol ACAC and its anion.

Generally, it is very hard to believe that, in the dissociation of nickel(II)-aminopolycarboxylate complexes, all three bond breakages are involved in the rate-determining step. Furthermore, as the nickel(II)-oxygen bond (carboxylate) breakage is much faster than

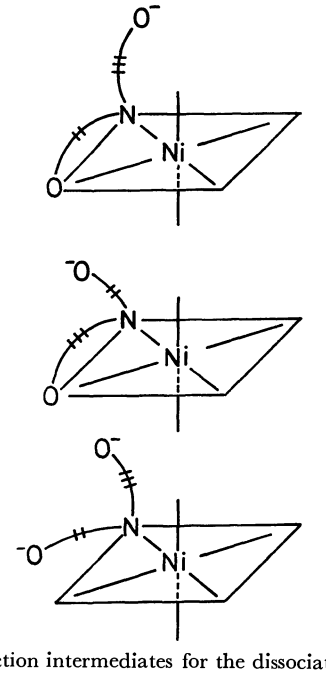

Fig. 10. Reaction intermediates for the dissociation of nickel-(II)-aspartate complex.

10) T. J. Bydalek and A. H. Constant, *Inorg. Chem.*, **4**, 833 (1965).

11) M. Eigen, *Ber. Bunsenges. Physik. Chem.*, **67**, 753 (1963).
12) R. G. Pearson and O. P. Anderson, *Inorg. Chem.*, **9**, 39 (1970).
13) R. G. Pearson and J. W. More, *ibid.*, **5**, 1523 (1966).

the nickel(II)-nitrogen bond (amine) breakage,[14] at least the nickel(II)-nitrogen bond breakage should be involved in the rate-determining step. Therefore, in the case of the nickel(II)-Asp complex, the dissociation can be expected to proceed through one of the following three reaction intermediates (Fig. 10). Here, one can eliminate the I_b reaction intermediate because the six-membered chelate ring is much more labile than the five-membered chelate ring in the substitution reaction of the nickel(II) ion complex. As was discussed by Rorabacher and Margerum,[15] the observed rate constant for the dissociation of the nickel(II)-aspartate complex can be related to the rate constant of the rate-determining step, k_{rds}, and the stability constant of the reaction intermediate prior to the rate-determining step, K_{int}, in the following manner:

$$k_d = \frac{k_{rds} \cdot K_{int}}{K_{MX}} \qquad (13)$$

Here, K_{MX} is the formation constant of the nickel(II)-Asp complex with a 1:1 ratio. With the aid of the above relation, we calculated the k_d values for two reaction intermediates, I_a and I_c. The k_d values calculated for these two reaction intermediates were $1.1_4 \times 10^{-2}$ and 4.5×10^{-3} sec^{-1} respectively. The k_d value estimated on the basis of I_a agrees better with the observed rate constant. In the calculation, the *N*-ethylglycinate and ammine complexes were used as models, and the electrostatic contribution was taken into consideration. The k_{rds} values[16] reported by Hammes and Steinfeld and by Margerum *et al.* were used.

Equation (13) also suggests that, if the dissociation of the nickel(II)-Glut and -IDA complexes proceeds through the glycinate reaction intermediate, as in the case of nickel(II)-Asp complex, the dissociation rate constant should be inversely proportional to the stability constant. The ratio of k_d was compared with that of the reciprocal of the stability constant, K_{MX}^{-1}. The results are shown in Table 5. In the case of the nickel-(II)-IDA system, the statistical factor was also taken into account. The agreement between the k_d ratio and the K_{MX}^{-1} ratio can be regraded as satisfactory. This agreement evidently implies that all three nickel(II)-aminopolycarboxylate complexes studied in this paper dissociate invariably through the reaction intermediate in which the leaving aminopolycarboxylate anion is bonded to the nickel(II) ion through the five-membered glycinate chelate ring, and that, in the dissociation of the nickel(II) ion complex, the six- and seven-membered chelate rings are much more labile than the corresponding five-membered chelate ring.

TABLE 5. RATIOS OF k_d AND K_{MX}^{-1}

System	k_d ratio	K_{MX}^{-1} ratio	log K_{MX} (μ=0.20)
Ni(II)-Glut	2.7×10^3	5.6×10^3	5.30
Ni(II)-Asp	4.8×10^1	1.4×10^1	6.91
Ni(II)-IDA	1.0	1.0	8.05

14) T. J. Bydalek and D. W. Margerum, *Inorg. Chem.*, **2**, 678 (1963).
15) D. B. Rorabacher and D. W. Margerum, *ibid.*, **3**, 382 (1964).
16) a) G. G. Hammes and J. I. Steinfeld, *J. Amer. Chem. Soc.*, **84**, 4639 (1962). b) D. W. Margerum, D. B. Rorabacher, and J. F. G. Clarke, Jr., *Inorg. Chem.*, **2**, 667 (1963).

Mixed-ligand Complexes of Copper(II). I. An ESR Study of Coordination Bonding[1]

Hiroshi YOKOI, Masaki OTAGIRI, and Taro ISOBE

Chemical Research Institute of Non-aqueous Solutions, Tohoku University, Katahira, Sendai

(Received January 13, 1971)

The sample solutions were prepared by mixing equal volumes of any two of the 1.00×10^{-2} mol/*l* solutions of the 1:2 complexes of copper(II) with ethylenediamine, *N,N*-dimethylethylenediamine, *N,N*-diethylethylenediamine, 1,3-diaminopropane, L-alanine, L-serine, *N,N*-diethylglycine, and *β*-alanine, where an equivolume mixture of water and methanol was used as the solvent. The X-band ESR measurements for these sample solutions were carried out at the temperature of liquid nitrogen. The observed ESR line shapes showed that only the mixed-ligand complexes are formed almost quantitatively in all the solutions except two: equivolume mixtures of the two complex solutions of ethylenediamine and *β*-alanine and those of ethylenediamine and *N,N*-dimethylglycine, in which the coexistence of two or more complex species was clearly demonstrated. The ESR line shapes and, furthermore, the intensities of the visible absorption indicated that the symmetry of the ligand field of the mixed-ligand complexes is as axial as that of the parent complexes. The ESR experimental results showed that the $g_{//}$ value of a mixed-ligand complex almost equals the mean of the $g_{//}$ values of its two parent complexes, but that there is not such a clear correlation between their $A_{//}$ values. It was interestingly concluded from the determined g values that the covalency of the metal-ligand bonds of a mixed-ligand complex are intermediate in degree between those of its two parent complexes.

Studies of mixed-ligand complexes from various angles have become very important in recent years, since mixed-ligand complexes occur during transition states of metal-ion-catalyzed reactions,[2] since they are important in analytical chemistry,[3] and since they can be regarded as models for metalloenzyme-substrate complexes.[4,5] Investigations of their stability in solutions, furthermore, are considered to be important in establishing a more advanced theory as to the stability of metal-ion complexes. Most studies of mixed-ligand complexes have so far been concerned with their stability.[6-10]

Recently, Farona *et al.* published a paper about the coordination bonding of mixed-ligand complexes, an investigation where various *β*-diketone chelate complexes of copper(II) were prepared and studied by the infrared, visible absorption, and ESR methods in connection with the parent complexes.[11] The ESR technique is effective in obtaining useful information about coordination, namely, about the strength and symmetry of the ligand field, in copper(II) complexes.[12] The purpose of this paper is to investigate more systematically the coordination of mixed-ligand complexes in connection with that of the parent complexes, using the ESR method, and using as the parent complexes the 1:2 chelate complexes of copper(II) with ethylenediamine, its alkyl derivatives, 1,3-diaminopropane, and various amino acids.

Experimental

Materials. The sample complexes, which were used as parent complexes in this study, were prepared according to the methods in the literature,[13,14] were recrystallized from water or methanol, and were identified by elemental analysis.[15-17] They are listed in Table 1. All of the reagents used were commercially available.

ESR and Optical Measurements. 1.00×10^{-2} mol/*l* solutions of the complexes listed in Table 1 were prepared by using an equivolume mixture of water and methanol as the solvent. These solutions were directly used as the samples of the parent complexes themselves, while equal volumes of any two of them were mixed and used as the samples of the mixed-ligand complexes. The ESR spectra of these samples were measured at the temperature of liquid nitrogen with a Hitachi X-band ESR spectrometer, Model MES-4001, equipped with a 100 kHz field modulation unit. The field was calibrated with an NMR probe and then with a benzene solution of vanadyl acetylacetonate. Some of the observed ESR spectra are shown in Figs. 1—4. The optical absorption spectra were measured at room temperature for the same sample solutions with a Hitachi spectrophotometer, Model

1) Preliminary report of this series: H. Yokoi, M. Otagiri, and T. Isobe, This Bulletin, **44**, 1445 (1971).
2) J. P. Collman and D. A. Buckingham, *J. Amer. Chem. Soc.*, **85**, 3039 (1963); D. A. Buckingham, J. P. Collman, D. A. R. Happer, and L. G. Marzilli, *ibid.*, **89**, 1082 (1967); A. Nakahara, K. Hamada, Y. Nakao, and T. Higashiyama, *Coordin. Chem. Rev.*, **3**, 207 (1968).
3) A. K. Babko, *Talanta*, **15**, 721 (1968); R. M. Dagnall, M. T. El-Ghamry, and T. S. West, *ibid.*, **15**, 1353 (1968); B. W. Bailey, J. E. Chester, R. M. Dagnall, and T. S. West, *ibid.*, **15**, 1359 (1968).
4) A. Goudot, "Mécanique Ondulatoire et Biologie Moléculaire," ed. by L. de Broglie, Revue Dóptique Téorique et Instrumentale, Paris (1961), p. 45.
5) A. S. Mildvan and M. Cohn, *J. Biol. Chem.*, **241**, 1178 (1966); E. J. Peck, Jr. and W. J. Ray, *ibid.*, **244**, 3754 (1969).
6) J. I. Watters and E. D. Longhram, *J. Amer. Chem. Soc.*, **75**, 4919 (1953); J. I. Watters, J. Mason, and A. Aaron, *ibid.*, **75**, 5212 (1953); R. Dewitt and J. I. Watters, *ibid.*, **76**, 3810 (1954).
7) S. Kida, This Bulletin, **29**, 805 (1956).
8) S. Kida, *ibid.*, **34**, 962 (1961).
9) H. Sigel, Proc. 3rd Symp. "Coordination Chemistry," Debrecen, Hungary, 1970, Vol. 1, ed. by M. T. Beck, Akádémiai Kiado, Budapest (1970), p. 191.
10) Y. Marcus and I. Eliezer, *Coordin. Chem. Rev.*, **4**, 273 (1969).
11) M. F. Farona, D. C. Perry, and H. A. Kuska, *Inorg. Chem.*, **7**, 2415 (1968).
12) B. R. McGarvey, "Transition Metal Chemistry," Vol. 3, ed. by R. L. Carlin, Marcel Dekker, New York (1967), p. 89.
13) P. Pfeiffer and H. Glasser, *J. Prakt. Chem.*, **151**, 134 (1938).
14) E. Abderhalden and E. Schnitzler, *Z. physiol. Chem.*, **163**, 94 (1927).
15) H. Yokoi and T. Isobe, This Bulletin, **41**, 2835 (1968).
16) H. Yokoi and T. Isobe, *ibid.*, **42**, 2187 (1969).
17) H. Yokio, M. Sai, T. Isobe, and S. Ohsawa, to be published.

Table 1. Parent complexes

Ligand	Abbr.	Copper(II) complex	No. of solution[a)]
Ethylenediamine	en	$[Cu(en)_2](ClO_4)_2$	I
N,N-Dimethylethylenediamine	dmen	$[Cu(dmen)_2](ClO_4)_2$	II
N,N-Diethylethylenediamine	deen	$[Cu(deen)_2](ClO_4)_2$	III
1,3-Diaminopropane	tn	$[Cu(tn)_2](ClO_4)_2$	IV
L-Alanine	L-Ala[b)]	$[Cu(L\text{-}Ala)_2]$	V
L-Serine	L-Ser[b)]	$[Cu(L\text{-}Ser)_2]$	VI
N,N-Dimethylglycine	dmg[b)]	$[Cu(dmg)_2]\cdot 3H_2O$	VII
β-Alanine	*β*-Ala[b)]	$[Cu(\beta\text{-}Ala)_2]\cdot 6H_2O$	VIII

a) 1.00×10^{-2} mol/*l*, Solvent: an equivolume mixture of water and methanol.
b) Those ligands represent the anions.

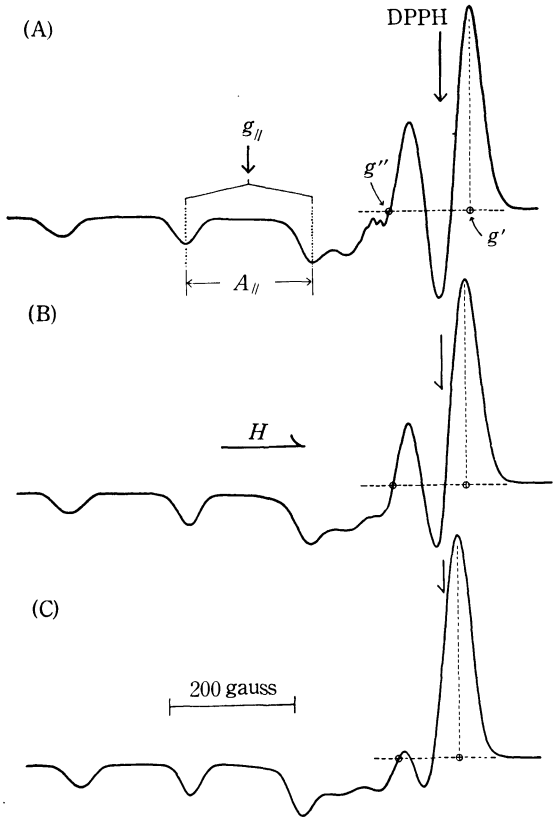

Fig. 1. The X-band ESR spectra of solution samples (measured at 77°K, Solvent: an equivolume mixture of water and methanol).
(A) the 1.00×10^{-2} mol/*l* solution of $[Cu(en)_2]^{2+}$
(B) the equivolume mixture of the (A) and (C) solutions
(C) the 1.00×10^{-2} mol/*l* solution of $[Cu(deen)_2]^{2+}$

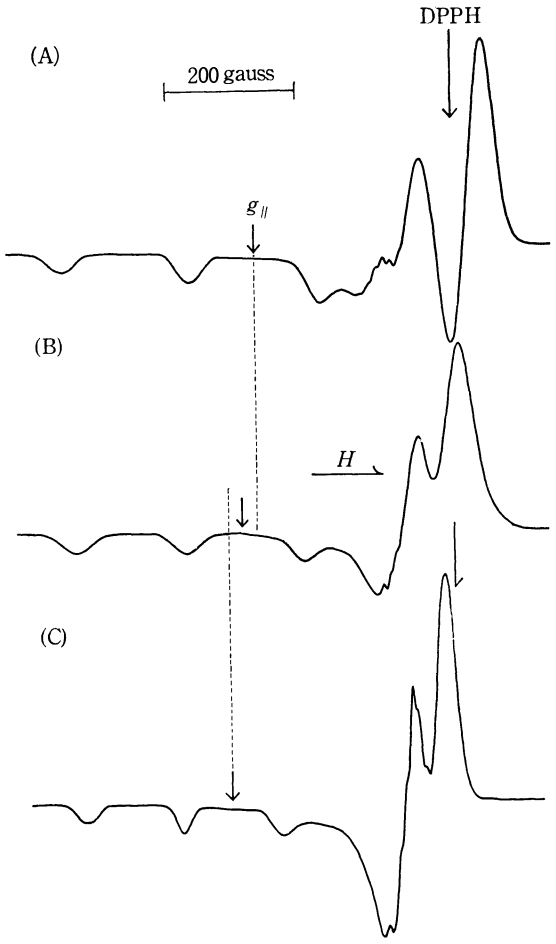

Fig. 2. The X-band ESR spectra of solution samples (measured at 77°K, Solvent: an equivolume mixture of water and methanol).
(A) the 1.00×10^{-2} mol/*l* solution of $[Cu(en)_2]^{2+}$
(B) the equivolume mixture of the (A) and (C) solutions
(C) the 1.00×10^{-2} mol/*l* solution of $[Cu(L\text{-}Ala)_2]$

EPS-3T. All the visible absorption spectra consisted of a single broad band; therefore, only the wavelengths of maximum absorption, λ_{max}, and the molecular extinction coefficients are listed in Tables 2 and 3.

Results and Discussion

Complex Species in Solution. When two kinds of copper(II) complexes with bidentate ligands are dissolved to make a solution, the following equilibrium is generally established in the solution:[6-8)]

$$CuA_2 + CuB_2 \rightleftharpoons 2CuAB \quad (1)$$

$$K = \frac{[CuAB]^2}{[CuA_2][CuB_2]} \quad (2)$$

where CuA_2 and CuB_2 represent parent complexes, and CuAB, a mixed-ligand complex. The relative amounts of the three complexes in the solution, therefore, vary according to the *K* value.

The ESR line shape of a single complex species of copper(II) complexes in the rigid solution has been

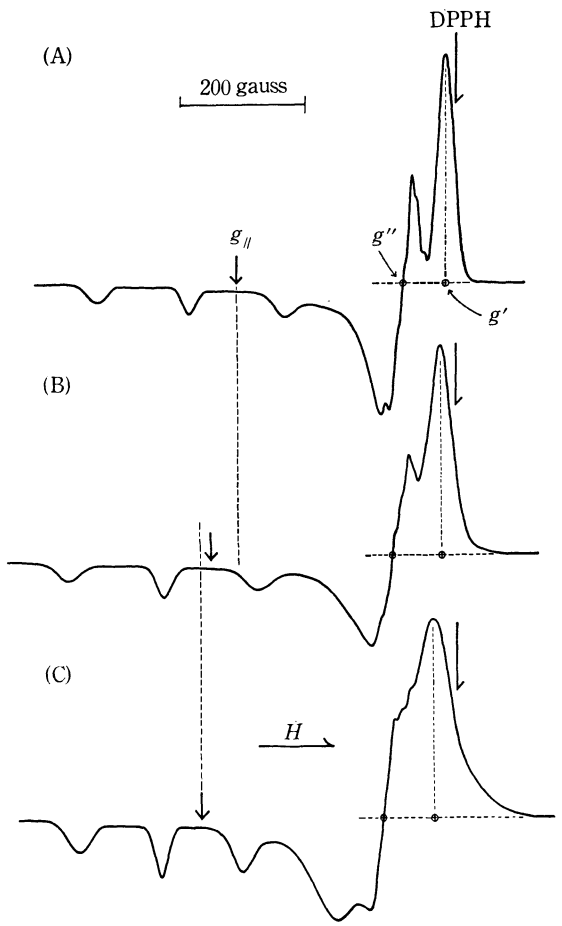

Fig. 3. The X-band ESR spectra of solution samples (measured at 77°K, Solvent: an equivolume mixture of water and methanol).
(A) the 1.00×10^{-2} mol/l solution of [Cu(L-Ala)$_2$]
(B) the equivolume mixture of the (A) and (C) solutions
(C) the 1.00×10^{-2} mol/l solution of [Cu(β-Ala)$_2$]

studied by several authors.[18,19] If two different complex species of copper(II) complexes coexist independently in the solution, the observed ESR spectrum will be made up of the superposition of their individual ESR spectra. Judging from the line shape, the ESR spectra of (B) in Figs. 1—3 can be said to be almost all due to a single complex species; furthermore, the absorption lines are different in position from those of the parent complexes. It can, therefore, be concluded that almost all the (B) spectra of Figs. 1—3 are due to mixed-ligand complexes; only mixed-ligand complexes are formed quantitatively in these systems. Such is the case with all the other sample solutions except two. The ESR spectra of these two exceptional solutions are shown in Fig. 4; the details in these cases will be discussed in the next paper of this series.[20] The line shapes in Fig. 4 clearly demonstrate that two or more complex species coexist in these solutions; this can, in short, be attributed to the comparatively small K values. However,

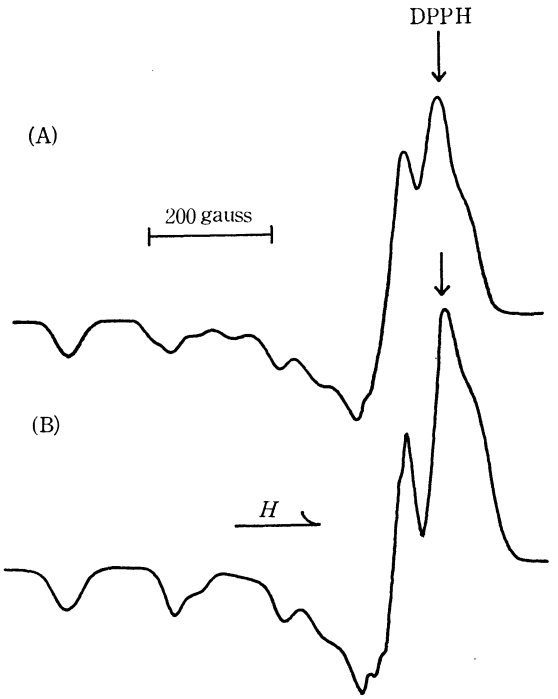

Fig. 4. The X-band ESR spectra of solution samples (measured at 77°K, Solvent: an equivolume mixture of water and methanol).
(A) the equivolume mixture of the 1.00×10^{-2} mol/l solutions of [Cu(en)$_2$]$^{2+}$ and [Cu(β-Ala)$_2$]
(B) the equivolume mixture of the 1.00×10^{-2} mol/l solutions of [Cu(en)$_2$]$^{2+}$ and [Cu(dmg)$_2$]

whether or not this ESR method is effective for the identification of two or more complex species in the solution depends upon the degree of separation between the absorption lines of different complex species, their line widths, and the value of K. If the K value is more than about 20, the identification of the parent complexes seems to be almost impossible for solutions with such broad line widths and such small line separations as those shown in Figs. 1—3.[20]

Symmetry of Ligand Field. When the three principal g values are designated in the order of increasing magnitude as g_1, g_2, and g_3, the axial symmetry of ligand field means that $g_1=g_2<g_3$. All the observed ESR spectra of mixed-ligand complexes were similar to each other in absorption line shape, as the several ESR spectra shown in Figs. 1—3 show; they all have an intense absorption line in the high-field part and three or four very weak absorption lines in the low-field part. It can be concluded from a theoretical consideration of the ESR line shape that the copper(II) complexes showing this type of line shape are of axial or near axial symmetry in the ligand field; all the mixed-ligand complexes dealt with in this study are approximately square-planar (tetragonal) complexes in a solution.[18,19]

When the g values at the positions of the two circles in Figs. 1 and 3 are designated as g' and g'', whose values are listed in Tables 2 and 3, these g values may be used as a measure in comparing the symmetry of the ligand field between the mixed-ligand complexes and the parent complexes, although this method of comparison is accompanied by somewhat complicated factors due to the hyperfine and extra-hyperfine structures.[17,18]

18) R. H. Sands, *Phys. Rev.*, **99**, 1222 (1955); T. Vänngard and R. Aasa, Proc. 1st Intern. Congr. "Paramagnetic Resonance," Jerusalem, 1962, Academic Press, New York (1963), p. 509.
19) R. Neiman and D. Kivelson, *J. Chem. Phys.*, **35**, 156 (1961).
20) H. Yokoi, M. Otagiri, and T. Isobe, this Bulletin, **44**, 2402 (1971).

Table 2. Experimental results of parent complexes

Sample solution[a)]	$g_{//}$	g'[b)]	g''[b)]	$-A_{//}$ $\times 10^4$ cm^{-1}	λ_{max} mμ	$\varepsilon_{\lambda max}$	$k_{//}^2$
I	2.206	1.975	2.071	209	554	66	0.56
II	2.208	1.984	2.057	194	570	146	0.55
III	2.213	1.996	2.045	185	594	192	0.54
IV	2.220	1.984	2.061	199	574	110	0.58
V	2.264	2.015	2.061	181	622	58	0.64
VI	2.267	2.020	2.063	180	628	52	0.64
VII	2.251	2.011	2.061	180	620	110	0.61
VIII	2.285	2.025	2.077	139	636	59	0.68

a) The numbers are the ones referred to in Table 1.
b) These g values correspond to the ones at the positions shown in Figs. 1 and 3.

Table 3. Experimental results of mixed-ligand complexes

Sample solution[a)]	No. of mixed-ligand complex	$g_{//}$	g'[b)]	g''[b)]	$-A_{//}$ $\times 10^4$ cm^{-1}	λ_{max}[c)] mμ	$\varepsilon_{\lambda max}$[c)]	$k_{//}^2$
I-II	1	2.210	1.980	2.056	204	561	94	0.57
I-III	2	2.210	1.984	2.050	202	576 (575)	121 (120)	0.55
I-IV	3	2.214	1.981	2.060	206	562	85	0.57
I-V	4	2.235	1.998	2.058	193	586 (590)	60 (64)	0.61
I-VI	5	2.233	1.996	2.055	194	587 (606)	58 (78)	0.60
I-VII[d)]	6							
I-VIII	7	2.242	2.006	2.061	184	598 (605)	62 (70)	0.61
II-III	8	2.211	1.990	2.051	188	586	173	0.54
II-IV	9	2.219	1.987	2.063	193	575	124	0.57
II-V	10	2.231	1.961	2.057	195	586	97	0.59
II-VI	11	2.235	1.996	2.058	195	587	89	0.60
II-VII	12	2.230	1.996	2.066	198	591	137	0.59
II-VIII	13	2.238	2.002	2.053	194	600 (607)	101 (105)	0.60
III-IV	14	2.218	1.990	2.057	190	586	134	0.56
III-V	15	2.226	1.996	2.050	199	590	116	0.58
III-VI	16	2.227	1.991	2.057	199	586 (580)	106 (90)	0.58
III-VII	17	2.229	1.993	2.062	195	592	176	0.58
III-VIII	18	2.237	2.022	2.061	194	610	135	0.59
IV-V	19	2.239	1.997	2.057	199	589	80	0.61
IV-VI	20	2.242	1.990	2.057	192	590	75	0.62
IV-VII	21	2.247	2.001	2.057	190	601	105	0.62
IV-VIII	22	2.244	2.004	2.058	187	597	83	0.62
V-VI	23	2.266	2.016	2.063	178	625	54	0.64
V-VII	24	2.256	2.012	2.059	181	620	79	0.62
V-VIII	25	2.272	2.016	2.050	158	634 (637)	60 (62)	0.65
VI-VII	26	2.262	2.013	2.061	182	622	73	0.64
VI-VIII	27	2.279	2.020	2.066	158	640	57	0.66
VII-VIII	28	2.262	2.017	2.064	193	633	81	0.62

a) The sample solution of two numbers hyphened together represents an equivolume mixture of the solutions of the numbers referred to in Table 1.
b) Those g values correspond to the ones at the positions shown in Figs. 1 and 3.
c) The numbers in parentheses represent the ones of pure mixed-ligand complexes determined by spectrophotometrical analysis, which will be described in our next paper of this series.[20)]
d) The ESR data could not be obtained for this mixed-ligand complex.

$\Delta g'$ and $\Delta g''$ are defined as follows:

$$\Delta g' = g'(\mathrm{M}) - g'(\mathrm{P_s})$$

$$\Delta g'' = g''(\mathrm{P_l}) - g''(\mathrm{M})$$

where $g'(\mathrm{M})$ and $g''(\mathrm{M})$ are the g' and g'' values respectively of a mixed-ligand complex, and where $g'(\mathrm{P_s})$ is the smaller value of the two g's of its parent complexes, and $g''(\mathrm{P_l})$, the larger value of the two g''s of the parent complexes. This, therefore, means that if $\Delta g' > 0$ and $\Delta g'' > 0$ for a mixed-ligand complex, the intense

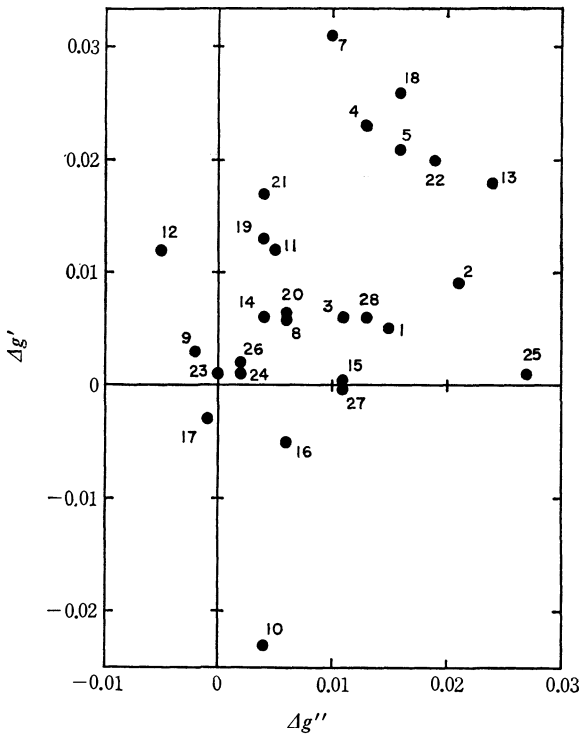

Fig. 5. A plot of $\Delta g'$ against $\Delta g''$ for mixed-ligand complexes (the description of $\Delta g'$ and $\Delta g''$ is given in the text, and the number of each point on the figure is the one referred to in Table 3).

absorption line in the high-field part of the complex appears at a position intermediate between those of its parent complexes. The experimental results are shown in Fig. 5, where most of the mixed-ligand complexes appear in the plus range of both $\Delta g'$ and $\Delta g''$. This fact indicates that the axial symmetry of the ligand field for the mixed-ligand complexes is kept at least in almost the same degree as for their parent complexes. This result is also supported by the intensity data of the visible absorption spectra. As may be seen in Tables 2 and 3, the $\varepsilon_{\lambda max}$ values of almost all the mixed-ligand complexes were intermediate between those of the corresponding two parent complexes, and none of the sample solutions had abnormal band widths; the dipole strengths of transition of the mixed-ligand complexes were intermediate between those of the parent complexes. The details will soon be published elsewhere. This spectral fact suggests that the mixed-ligand complexes are not much lower in the symmetry of their ligand fields than are the parent complexes, since it has generally been believed that the intensity of the visible absorption spectrum of a copper(II) complex always increases as the symmetry of the ligand

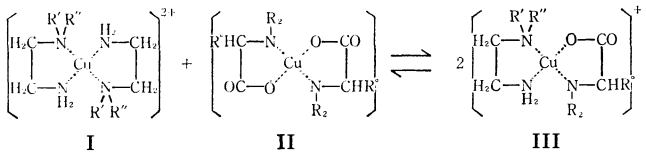

I II III

Fig. 6. A schematically represented example of the equilibrium of Eq. (1).

Table 4. Symmetry

Copper-(II) complex[a)]	Coordination groups	Assumed ligand field	Actual ligand field[b)]
I	D_{2h}	D_{2h}	near axial
II	D_{2h}	D_{2h}	near axial
III	no symmetry	no symmetry	near axial

a) The numbers of the copper(II) complexes are the ones referred to in Fig. 6.
b) Judged from the observed ESR line shapes.

field of the complex descends.[21,22]

When a typical representative example of Eq. (1) is schematically shown in Fig. 6, therefore, the symmetries of the coordinating groups and ligand field for each of the complexes in it can be expressed as is shown in Table 4. Accordingly, the symmetry of the ligand field does not coincide with the apparent symmetry of the coordinating groups, and the symmetry of the ligand field of the planar copper(II) complexes seems to be kept in a high degree, regardless of the different kinds of coordinating groups.

$g_{//}$ *and* $A_{//}$. According to the ligand field theory of a tetragonal copper(II) complex (D_{4h} symmetry assumed), the following antibonding molecular orbitals, in the order of increasing energy, can be formed for the "hole" configuration[23-25]:

$$\begin{aligned}
\varphi_{b_{1g}} &= \alpha d_{x^2-y^2} - \alpha' \phi_L(x^2-y^2) \\
\varphi_{b_{2g}} &= \beta_1 d_{xy} - \beta_1' \phi_L(xy) \\
\phi_{a_{1g}} &= \alpha_1 d_{z^2} - \alpha_1' \phi_L(z^2) \\
\varphi_{e_g} &= \begin{cases} \beta d_{xz} - \beta' \phi_L(xz) \\ \beta d_{yz} - \beta' \phi_L(yz) \end{cases}
\end{aligned} \tag{3}$$

In each of the wavefunctions, the ϕ_L in the second term on the right-hand side represents the ligand orbital which can be mixed with the copper d orbital expressed in the first term. The magnetic parameters can then be expressed approximately as follows:

$$\begin{aligned}
g_{//} &= 2 - \frac{8\lambda}{\Delta E_{xy}}(\alpha^2\beta_1^2 - f_1) \\
g_{\perp} &= 2 - \frac{2\lambda}{\Delta E_{xz}}(\alpha^2\beta^2 - f_2)
\end{aligned} \tag{4}$$

$$\begin{aligned}
A_{//} &= P\left[-\frac{4}{7}\alpha^2 - \kappa + (g_{//}-2) + \frac{3}{7}(g_{\perp}-2) + f_3\right] \\
A_{\perp} &= P\left[\frac{2}{7}\alpha^2 - \kappa + \frac{11}{14}(g_{\perp}-2) + f_4\right]
\end{aligned} \tag{5}$$

where $P=2\gamma\beta_0\beta_N\langle d_{x^2-y^2}|r^{-3}|d_{x^2-y^2}\rangle$, $\Delta E_{xy}=E_{xy}-E_{x^2-y^2}$, and $\Delta E_{xz}=E_{xz}-E_{x^2-y^2}$, and where f_1—f_4 are small and almost constant values for a variety of copper(II) complexes ($f_1, f_2 \leq 0.04$, $f_3 \leq 0.03$, and $f_4 \leq 0.005$).[15,24,25]

21) C. J. Ballhausen, *Progr. Inorg. Chem.*, **2**, 251 (1960); "Introduction to Ligand Field Theory," McGraw-Hill, New York (1962), p. 180.
22) R. L. Belford and W. A. Yeranos, *Mol. Phys.*, **6**, 121 (1963).
23) K. W. Stevens, *Proc. Roy. Soc.* (London), **A219**, 542 (1953); J. Owen, *ibid.*, **A227**, 183 (1955).
24) A. H. Maki and B. R. McGarvey, *J. Chem. Phys.*, **29**, 31, 35 (1958).
25) D. Kivelson and R. Neiman, *ibid.*, **35**, 149 (1961).

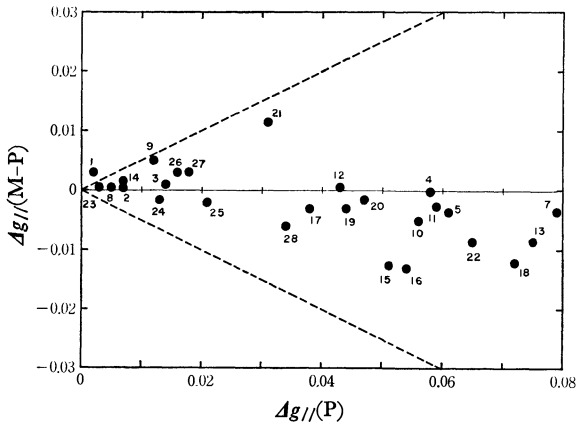

Fig. 7. A plot of $\Delta g_{//}$(M–P) against $\Delta g_{//}$(P) for mixed-ligand complexes.
$\Delta g_{//}(\mathrm{M-P}) = g_{//}(\mathrm{M}) - 1/2(g_{//}^{P_1} + g_{//}^{P_2})$
$\Delta g_{//}(\mathrm{P}) = |g_{//}^{P_1} - g_{//}^{P_2}|$
where $g_{//}$(M), $g_{//}^{P_1}$, and $g_{//}^{P_2}$ are the $g_{//}$ values of a mixed ligand complex, and its two parent complexes, P_1 and P_2, respectively. The numbers for the mixed-ligand complexes in Table 3 are employed on this figure.

The experimentally-determined $g_{//}$ and $A_{//}$ values are listed in Tables 2 and 3. The correlation between the $g_{//}$ values of the mixed-ligand complexes and those of the parent complexes is shown in Fig. 7, where, for a mixed-ligand complex, the absolute difference between the $g_{//}$ values of its two parent complexes, $g_{//}^{P_1}$ and $g_{//}^{P_2}$, is indicated on the abscissa ($\Delta g_{//}$(P)), and the difference between the $g_{//}$ value of the mixed-ligand complex, $g_{//}$(M), and the mean of $g_{//}^{P_1}$ and $g_{//}^{P_2}$, on the ordinate ($\Delta g_{//}$(M–P)). The dotted lines on this figure express the $g_{//}$ values of two parent complexes against any point of the abscissa. If $\Delta g_{//}$ (M–P)$=0$ for a mixed-ligand complex, accordingly, its $g_{//}$ value exactly equals the mean of the two $g_{//}$ values of its parent complexes. This figure clearly shows that the $g_{//}$ values of the mixed-ligand complexes dealt with here are almost equal to the average $g_{//}$ values of the parent complexes.

As to the $A_{//}$ value, a graph was prepared in a similar manner; it is shown in Fig. 8. This figure, however, shows that the points scatter over a considerably wide range, and such a regularity as is indicated for the $g_{//}$

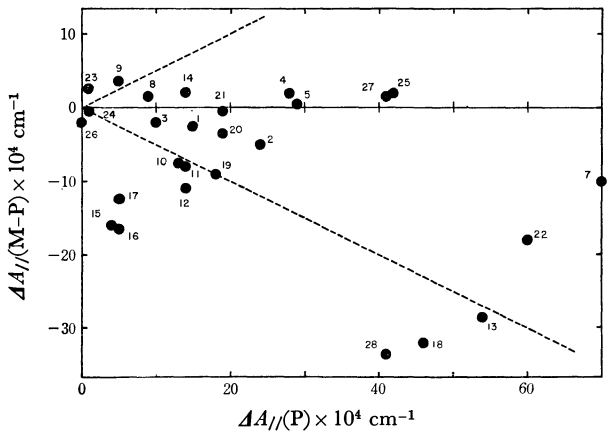

Fig. 8. A plot of $\Delta A_{//}$(M–P) against $\Delta A_{//}$(P) for mixed-ligand complexes ($\Delta A_{//}$(M–P) and $\Delta A_{//}$(P) are expressed in the similar equations to $\Delta g_{//}$(M–P) and $\Delta g_{//}$(P) respectively).

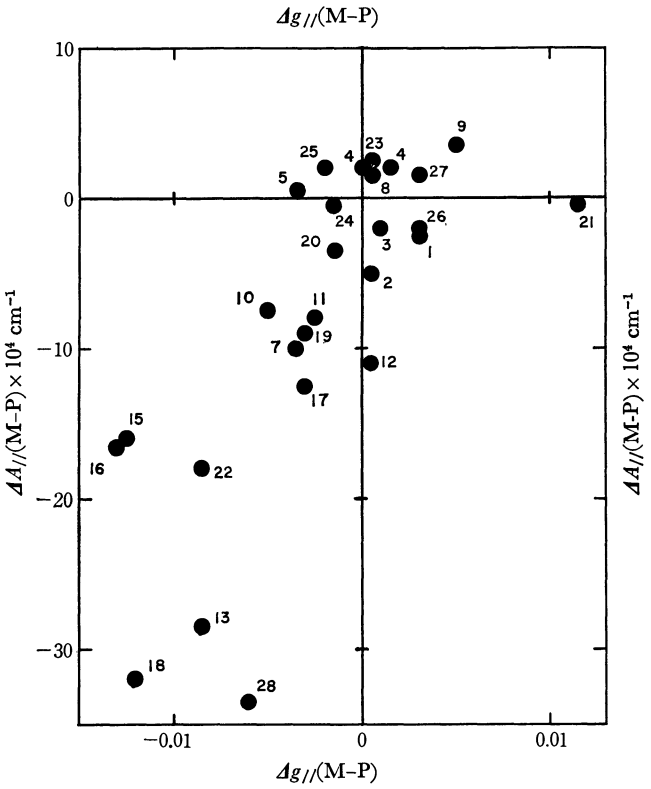

Fig. 9. A plot of $\Delta A_{//}$(M–P) against $\Delta g_{//}$(M–P) for mixed-ligand complexes.

value is difficult to find. As an experiment, $\Delta A_{//}$ (M–P) was plotted against $\Delta g_{//}$(M–P) (cf. Fig. 9). A rough tendency for $\Delta A_{//}$(M–P) to decrease with the decrease of $\Delta g_{//}$(M–P) seems to be found in this figure, but this tendency can not be understood only in terms of Eqs. (4) and (5) at the present stage.

Coordination Bonding. At present, the hyperfine parameters are less rigorously related to the structure than are the g values, since the hyperfine parameters depend in complicated ways upon the core spin polarization and, furthermore, upon the $4s$ orbital spin polarization and the p-electron admixture, and since a definite relation between these effects and the covalency of metal-ligand bonds has not yet been established.[26–32] It seems, accordingly, that much reliance can not be placed on Eq. (5). The degree of the covalency, therefore, is estimated only from the g values in this work.

Equation (4) is rewritten as follows:

$$g_{//} = 2 - \frac{8\lambda k_{//}^2}{\Delta E_{xy}} \qquad (6)$$

26) W. E. Blumberg, "The Biochemistry of Copper," ed. by J. Peisach, P. Aisen, and W. E. Blumberg, Academic Press, New York (1966), p. 49.
27) V. Heine, *Phys. Rev.*, **107**, 1002 (1957); J. H. Wood and G. W. Pratt, *ibid.*, **107**, 995 (1957).
28) B. Bleaney, "Hyperfine interaction," ed. by A. J. Freeman and R. B. Frankel, Academic Press, New York (1967), p. 1.
29) A. J. Freeman, *ibid.*, p. 53.
30) S. Koide, *Phil. Mag.*, **4**, 243 (1959); Y. Tanabe, *Progr. Theort. Phys.* (Kyoto), Suppl. **14**, 17 (1960); S. Sugano, *ibid.*, Suppl. **14**, 66 (1960).
31) H. Yokoi and T. Isobe, This Bulletin, **39**, 2054 (1966).
32) B. R. McGarvey, *J. Phys. Chem.*, **71**, 51 (1967).

where $k_{//}^2$ is the orbital reduction factor, relating to the bonding parameters, mainly α^2 and β_1^2. The ligand-field energy of ΔE_{xy} must, then, be estimated in order to determine the value of $k_{//}^2$ from Eq. (6). However, it is not easy to estimate this energy value exactly for the copper(II) complexes with a single broad absorption band in the visible region. Amines and amino acids are arranged in a near position in the spectrochemical series.[33] It seems, therefore, quite likely that all the complexes employed here are similar in the spacing of the energy levels of the *d*-orbitals. Accordingly, we assumed in this study that the ratio of the energy value of ΔE_{xy} to that of the wavelength of maximum absorption is almost constant for the complexes. The observed wavelengths of λ_{max} for all the 1—28 solutions listed in Table 3 except for the 6 and 7 solutions are considered to be nearly equal to those of mixed-ligand complexes themselves, as has been demonstrated in Table 3 by some examples, since the values of K are quite large for those mixed-ligand complexes, which we will discuss in the next paper in this series.[20] The above-mentioned assumption is the same as that the energy of λ_{max} may be directly used in comparing the complexes with each other in terms of the relative values of $k_{//}^2$. The $k_{//}^2$ values thus determined from Eq. (6) for all the mixed-ligand complexes are illustrated graphically in Fig. 10 in a manner similar to that in Figs. 7 and 8. The dotted lines on Fig. 10 also represent the two $k_{//}^2$ values of the parent complexes. It is clear in this figure that most of $k_{//}^2$ values of the mixed-ligand complexes are very close to the mean of the $k_{//}^2$ values of the corresponding parent complexes. It can, furthermore, easily be understood on a simple calculation that, even if the ligand-field energies of the mixed-ligand complexes vary widely from those of the parent complexes, most of the mixed-ligand complexes become intermediate in $k_{//}^2$ value between the parent complexes. Although $k_{//}^2$ is connected with the in-plane bondings, such may be the case with the out-of-plane bondings, judging from the results shown in Fig. 5.

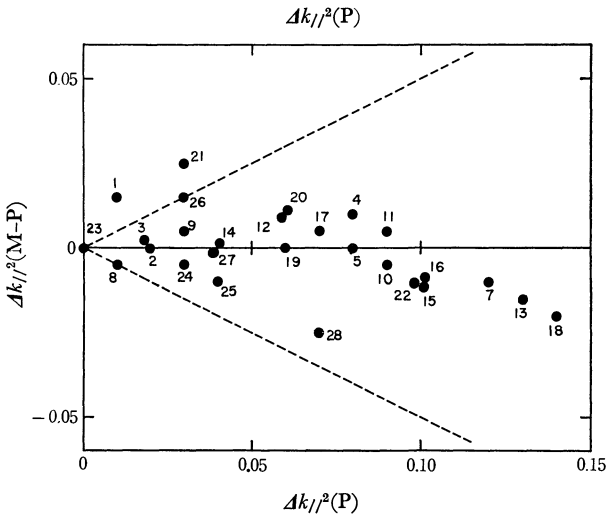

Fig. 10. A plot of $\Delta k_{//}^2$(M–P) against $\Delta k_{//}^2$(P) for mixed-ligand complexes ($\Delta k_{//}^2$(M–P) and $\Delta k_{//}^2$(P) are expressed in the similar equations to $\Delta g_{//}$(M–P) and $\Delta g_{//}$(P) respectively).

All the above facts suggest that, as to the metal-ligand bonds, the covalency of a mixed-ligand complex is close in degree to the mean of those of the parent complexes. It follows in Eq. (1) that, when the M–A bond is stronger than the M–B bond in the parent complexes, the M–A bond becomes weaker and the M–B bond stronger in the mixed-ligand complex than in the parent complexes; that is, the M–A and M–B bonds become close together in bond strength in a mixed-ligand complex.

33) K. Fajans, *Naturwissenschaften*, **11**, 165 (1923); R. Tsuchida, This Bulletin, **13**, 388, 436, 471 (1938).

Mixed-ligand Complexes of Copper(II). II. A Study of Dismutation Constants

Hiroshi Yokoi, Masaki Otagiri, and Taro Isobe

Chemical Research Institute of Non-aqueous Solutions, Tohoku University, Katahira, Sendai

(Received January 27, 1971)

The dismutation constants for mixed-ligand complexes of copper(II) involving, as bidentate ligands, ethylenediamine, L-alanine, β-alanine, and *N,N*-dimethylglycine were determined at two or three temperatures by both the spectrophotometric and ESR methods, and the thermodynamic constants were then derived from those data. It was found for these systems that the entropy change plays a main role in governing the equilibrium between a mixed-ligand complex and its parent complexes, and that the differences in the dismutation constants among the mixed-ligand complexes are due to the small but different values of the enthalpy term.

When two kinds of stable copper(II) complexes with bidentate ligand (A and B) are dissolved in a solvent, the following kind of equilibrium is generally established in the solution:

$$CuA_2 + CuB_2 \rightleftharpoons 2CuAB \quad (1)$$

$$K = \frac{[CuAB]^2}{[CuA_2][CuB_2]} \quad (2)$$

The reciprocal of K is designated by Watters *et al.* as the dismutation constant.[1] The studies of the equilibrium and of the coordinate bond for the mixed-ligand complexes seem to be important in coordination chemistry and in biochemistry, since these studies are concerned with extending such a fundamental concept as soft and hard acids and bases,[2] and since the mixed-ligand complexes are regarded as models for metalloenzyme-substrate complexes.[3,4] Furthermore, the complexes are important in analytical chemistry and in synthetic reactions catalyzed by metal ions.[5,6] Many studies of mixed-ligand complexes have been mainly concerned with their stability.[1,7-10]

In a previous paper,[11] we reported on an ESR study of the coordinate bond for mixed-ligand complexes with comparatively large K values, using, as bidentate ligands, ethylenediamine, its analogues, and amino acids. We pointed out that, for the two systems with ethylenediamine and β-alanine as A and B in Eq. (1) and with ethylenediamine and *N,N*-dimethylglycine, two or three complex species can clearly be identified from the ESR spectra in the solution, since the K values of these systems are comparatively small. The purpose of this paper is to investigate in full detail, by the use of both the spectrophotometric and ESR techniques, what factors govern the above-mentioned equilibrium, using as the parent complexes the 1:2 complexes of copper(II) with ethylenediamine, L-alanine, β-alanine, and *N,N*-dimethylglycine.

Experimental

The copper(II) complexes employed in this work, which had been prepared and purified in a previous work,[11] were $[Cu(en)_2](ClO_4)_2$, $[Cu(L\text{-}Ala)_2]$, $[Cu(\beta\text{-}Ala)_2]\cdot 6H_2O$, and $[Cu(dmg)_2]\cdot 3H_2O$, where en, L-Ala, β-Ala, and dmg are ethylenediamine and the anions of L-alanine, β-alanine, and *N,N*-dimethylglycine respectively. The sample solutions for the ESR and optical absorption measurements were 1.00×10^{-2} mol/l solutions of these four complexes and mixtures of any two of the solutions at various volume ratios, with an equivolume mixture of water and methanol being used as the solvent.

The ESR spectra of these sample solutions were measured at the temperature of liquid nitrogen with a Hitachi X-band ESR spectrometer, Model MES-4001, equipped with a 100 kHz field modulation unit. The field was calibrated with an NMR probe, and then with a benzene solution of vanadyl acetylacetonate. The optical absorption spectra were measured at temperatures of 20 and 50°C with a Hitachi spectrophotometer, Model EPS-3T, in the range from 340 to 700 mμ, using 10-mm quartz cells.

Results

The 1.00×10^{-2} mol/l solutions (solvent: an equivolume mixture of water and methanol) of $[Cu(en)_2](ClO_4)_2$, $[Cu(L\text{-}Ala)_2]$, $[Cu(\beta\text{-}Ala)_2]\cdot 6H_2O$, and $[Cu(dmg)_2]\cdot 3H_2O$ will hereafter be designated as Systems

1) R. Dewitt and J. Watters, *J. Amer. Chem. Soc.*, **76**, 3810 (1954); J. I. Watters, A. Aaron, and J. Mason, *ibid.*, **75**, 5212 (1953); J. I. Watters and E. D. Lougham, *ibid.*, **75**, 4819 (1953).

2) R. G. Pearson, *ibid.*, **85**, 3533 (1963); S. Ahrland, "Structure and Bonding," ed. by C. K. Jørgensen, J. B. Neilands, R. S. Nyholm, D. Reinen, and R. J. P. Williams, Springer-Verlag, Berlin (1968), p. 118.

3) A. Goudot, "Mécanique Ondulatoire et Biologie Moléculaire," ed. by L. de Broglie, Revue Dóptique Téorique et Instrumentale, Paris (1961), p. 45; F. P. Dwyer, "Chelating Agents and Metal Chelates," ed. by F. P. Dwyer and D. P. Mellor, Academic Press, New York (1964), p. 335; A. Schulman and F. P. Dwyer, *ibid.*, p. 383.

4) A.S. Mildvan and M. Cohn, *J. Biol. Chem.*, **241**, 1178 (1966); E. J. Peck, Jr., and W. J. Ray, *ibid.*, **244**, 3754 (1969).

5) A. K. Babko, *Talanta*, **15**, 721 (1968); R. M. Dagnall, M. T. El-Ghamry, and T. S. West, *ibid.*, **15**, 1353 (1968); B. W. Bailey, J. E. Chester, R. M. Dagnall, and T. S. West, *ibid.*, **15**, 1359 (1968).

6) J. P. Collman and D. A. Buckingham, *J. Amer. Chem. Soc.*, **85**, 3039 (1963); D. A. Buckingham, J. P. Collman, D. A. R. Happer, and L. G. Marzilli, *ibid.*, **89**, 1082 (1967); A. Nakahara, K. Hamada, Y. Nakao, and T. Higashiyama, *Coordin. Chem. Rev.*, **3**, 207 (1968).

7) S. Kida, This Bulletin, **29**, 805 (1956).

8) S. Kida, *ibid.*, **34**, 962 (1961).

9) H. Sigel, Proc. 3rd Symp. "Coordination Chemistry," Debrecen, Hungary, 1970, Vol. 1, ed. by M. T. Beck, Akádémiai Kiado, Budapest (1970), p. 191.

10) Y. Marcus and I. Eliezer, *Coordin. Chem. Rev.*, **4**, 273 (1969).

11) H. Yokoi, M. Otagiri, and T. Isobe, This Bulletin, **44**, 2395 (1971).

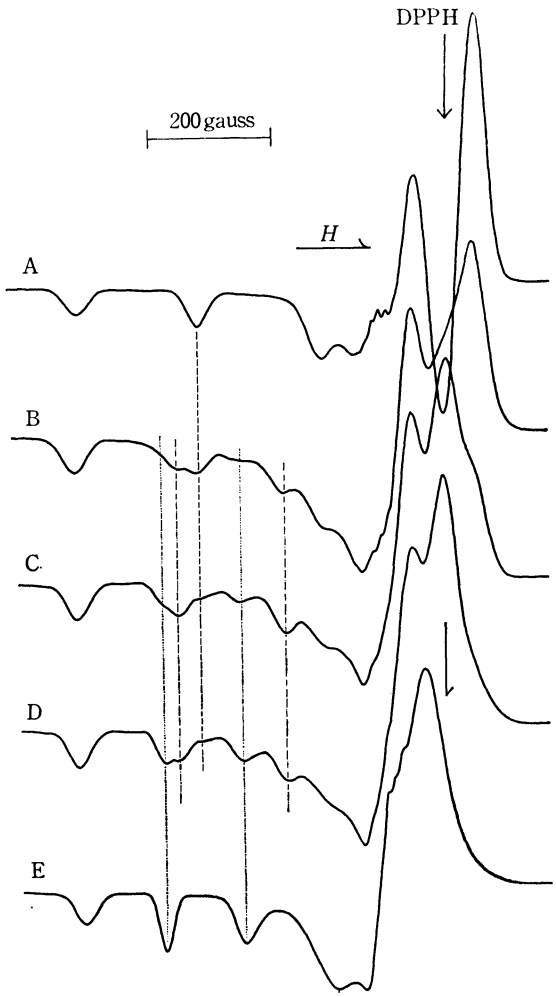

Fig. 1. The X-band ESR spectra (measured at 77°K, 1.00×10^{-2} mol/l per copper atom, Solvent: an equivolume mixture of water and methanol) of the mixed solutions of $[Cu(en)_2]^{2+}$ and $[Cu(\beta\text{-Ala})_2]$ at the following molar ratios: (A) 1 : 0, (B) 2 : 1, (C) 1 : 1, (D) 1 : 2, and (E) 0 : 1. Each of the vertical lines shown at the low field part locates an absorption line due to one of the three molecular species.

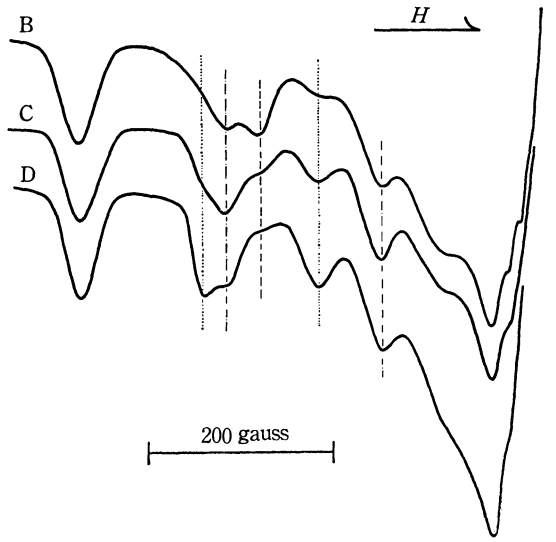

Fig. 2. Some of the enlarged ESR spectra of Fig. 1 at the low field part (the spectral names and the vertical lines are those referred to in Fig. 1).

I, II, III, and IV. The mixture of I and II, for example, is described as System I–II, and the volume ratio in the mixture is affixed to this expression in parentheses.

Determination of K by ESR. The ESR spectra of Systems I–II (1:1) and II–III (1:1), measured at the temperature of liquid nitrogen, which had already been presented in a previous paper,[11] indicated that the mixed-ligand complexes are almost quantitatively formed in the solution of these systems, and it was expected that the K values for these systems would be comparatively large. Attention must, however, be paid to the fact that the K values under discussion are determined at a certain temperature immediately before the sample solutions freeze in liquid nitrogen (sample glass tubes about 4 mm in diameter are directly immersed in liquid nitrogen in this study). Since the exact freezing temperature of these solutions on such rapid cooling is unknown, the temperature was assumed to be about −100°C in this work.[12] On the other hand, it was reported in a previous paper that the ESR spectra of Systems I–III (1:1) and I–IV (1:1) are not due to a single complex species, suggesting that the K values of these systems are remarkably small as compared with those of other systems.[11] In this study we made an attempt to determine the K values for these two systems from the ESR spectra, as will be described below.

The ESR spectra of System I–III at various volume ratios are shown in Fig. 1, while the enlarged spectra in the low-field part of Fig. 1 are shown in Fig. 2. These two figures clearly indicate that the ESR spectra are made up of the superposition of three different spectra; three complex species coexist in System I–III. It can easily be understood that the three complex species correspond to the two parent complexes and one mixed-ligand complex. If the molar ratio of these three complexes can be properly estimated from the ESR spectra, the K value can be calculated using Eq. (2). The hyperfine absorption lines of $I_z=-1/2$ for the three complexes appear near the base line in the low-field part, this fact being a factor in attaining greater accuracy in the following analysis, and the lines are superposed to a moderate extent upon each other, whereas the absorption lines of $I_z=-3/2$ overlap to too complete a degree to be analyzed. The most reasonable method for analyzing the ESR spectra with the aim of determining the molar ratio, therefore, seems to consist in resolving the spectral part of the overlapping absorption lines of $I_z=-1/2$ into the corresponding three components, and then in properly deriving the molar ratio from the resolved spectra.

It was assumed that the observed ESR line shape can

12) The freezing temperature of the equivolume mixture of water and methanol is −47°C ("The Merck Index," eighth edition ed. by P. G. Stecher, Merck & Co., Inc., New Jersey, U.S.A. (1968), p. 671). The freezing temperature of the sample solutions under discussion, however, is considered to be further lowered to a very large extent on such extremely rapid cooling as we adopted, since it has been reported that, when the cooling rate is increased, the freezing temperature of water is lowered owing to the phenomenon of supercooling (I. E. Kuhns and B. J. Mason, *Proc. Roy. Soc.* (London), **A302**, 437 (1968)).

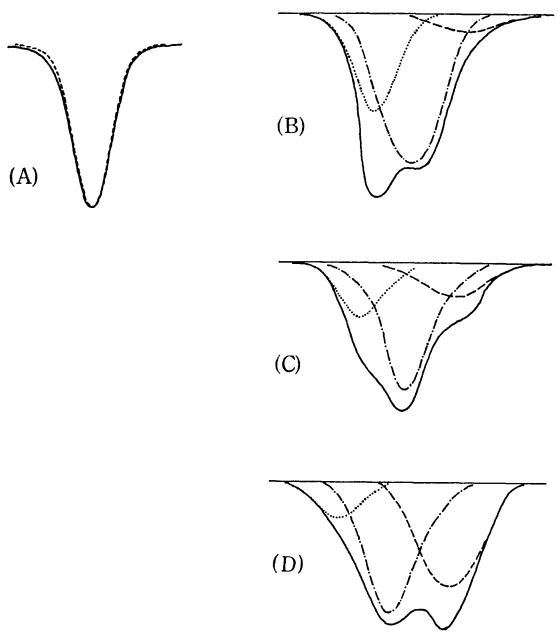

Fig. 3. The overlapping hyperfine absorption lines of $I_z=-1/2$ resolved into three components by the Gaussian analysis for the mixed solutions of $[Cu(en)_2]^{2+}$ and $[Cu(\beta\text{-Ala})_2]$ at the following molar ratios: (A) 0 : 1, (B) 1 : 2, (C) 1 : 1, and (D) 2:1.

be approximated by the following Gaussian curve:

$$S_i(H) = b\exp(-a^2(H_i^\circ - H)^2)$$
$$a = \sqrt{2}/\Delta H_i^{msl},$$
$$b = \sqrt{2/\pi}/\Delta H_i^{msl},\ \Delta H_i^{msl} = \Delta H_i/1.386$$

where ΔH_i is the half-width; ΔH_i^{msl}, the separation between the points of the maximum and minimum slopes, and H_i°, the magnetic field at the center of an absorption line, i. In order to check whether or not the Gaussian curve can simulate the observed absorption lines of $I_z=-1/2$ with a good approximation, the observed absorption line of System III was compared with a Gaussian curve; the results are shown in Fig. 3 (A). This figure suggests that the observed spectra can be analyzed by the Gaussian curves with a fairly good approximation.

The values of ΔH_i for the absorption lines of $I_z=-1/2$ of $[Cu(en)_2]^{2+}$ and $[Cu(\beta\text{-Ala})_2]$ were determined from their ESR spectra to be 17 and 12.5 gauss respectively. Some of the results obtained by this analysis are shown in Fig. 3, using 15 gauss as the ΔH_i value of the mixed-ligand complex. It is, furthermore, assumed that the molar ratio of the three complexes is approximately proportional to the ratio of the integrated intensities of the corresponding resolved Gaussian curves. This seems to be a reasonable assumption, since the three complexes are not extremely different from each other in their magnetic parameters. The ESR spectra of System I–IV, some of which are shown in Fig. 4, were analyzed in a similar way. The analysis for this system, however, was more difficult than for

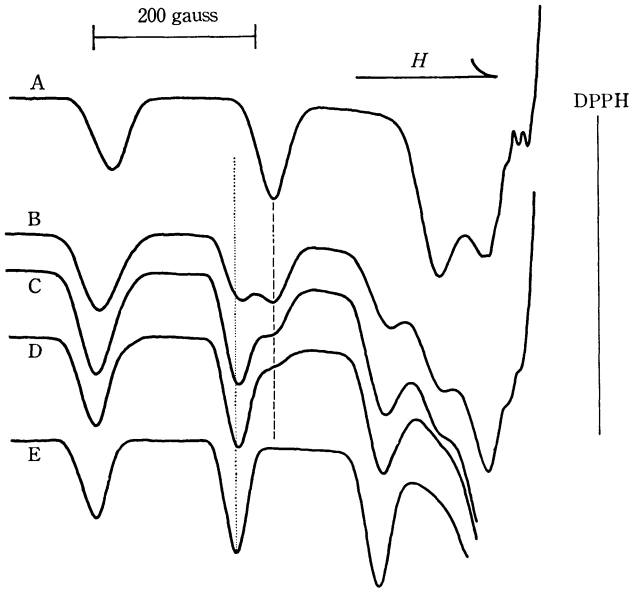

Fig. 4. The X-band ESR spectra (measured at 77°K, 1.00×10^{-2} mol/l per copper atom, Solvent: an equivolume mixture of water and methanol) of the mixed solutions of $[Cu(en)_2]^{2+}$ and $[Cu(dmg)_2]$ at the following ratios: (A) 1 : 0, (B) 2 : 1, (C) 1 : 1, (D) 1 : 2, and (E) 0 : 1. The absorption line of $I_z=-1/2$ of the mixed ligand complex, the location of which is not apparent in the line shape, appears between the two vertical dotted lines on the figure.

Table 1. Molar ratio determined from ESR spectra[a] by Gaussian analysis for the equilibrium

$$[Cu(en)_2]^{2+} + [Cu(\beta\text{-Ala})_2] \rightleftharpoons 2[Cu(en)(\beta\text{-Ala})]^+$$

$c_1\times10^2$ [b]	$c_2\times10^2$ [b]	$[Cu(en)_2]^{2+}$	$[Cu(\beta\text{-Ala})_2]$	$[Cu(en)(\beta\text{-Ala})]^+$	log K
2/3	1/3	0.43	0.11	0.46	0.65
7/11	4/11	0.36	0.13	0.51	0.74
3/5	2/5	0.33	0.16	0.51	0.71
5/9	4/9	0.25	0.20	0.55	0.78
1/2	1/2	0.18	0.21	0.61	0.99
3/7	4/7	0.16	0.27	0.57	0.88
1/3	2/3	0.14	0.34	0.52	0.75
				Mean value:	
					0.79±0.04

a) measured at 77°K, Solvent: an equivolume mixture of water and methanol.
b) c_1 and c_2 are the initial concentrations (mol/l) of $[Cu(en)_2]^{2+}$ and $[Cu(\beta\text{-Ala})_2]$ respectively.

Table 2. Molar ratio determined from ESR spectra[a] by Gaussian analysis for the equilibrium

$$[Cu(en)_2]^{2+} + [Cu(dmg)_2] \rightleftharpoons 2[Cu(en)(dmg)]^+$$

$c_1\times10^2$ [b]	$c_2\times10^2$ [b]	$[Cu(en)_2]^{2+}$	$[Cu(dmg)_2]$	$[Cu(en)(dmg)]^+$	log K
4/5	1/5	0.59	0.19	0.22	$\bar{1}$.64
2/3	1/3	0.48	0.32	0.20	$\bar{1}$.42
3/5	2/5	0.44	0.34	0.22	$\bar{1}$.51
1/2	1/2	0.32	0.44	0.24	$\bar{1}$.61
2/5	3/5	0.24	0.51	0.25	$\bar{1}$.71
1/3	2/3	0.17	0.64	0.19	$\bar{1}$.52
1/5	4/5	0.11	0.74	0.15	$\bar{1}$.44
				Mean value:	
					$\bar{1}$.55±0.04

a) measured at 77°K, solvent: an equivolume mixture of water and methanol.
b) c_1 and c_2 are the initial concentrations (mol/l) of $[Cu(en)_2]^{2+}$ and $[Cu(dmg)_2]$ respectively.

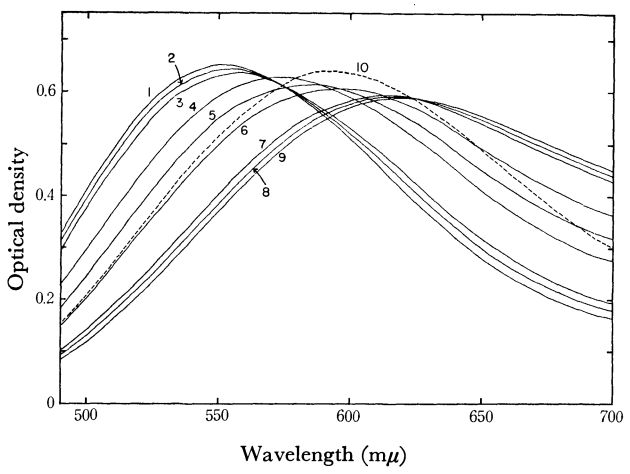

Fig. 5. The visible absorption spectra (measured at 20°C, solvent: an equivolume mixture of water and methanol) of the mixed solutions of $[Cu(en)_2]^{2+}$ and $[Cu(L\text{-}Ala)_2]$.

Curve	$c_1\times10^2$	$c_2\times10^2$
1	1	0
2	0.95	0.05
3	0.9	0.1
4	2/3	1/3
5	1/2	1/2
6	1/3	2/3
7	0.1	0.9
8	0.05	0.95
9	0	1
10	curve of $[Cu(en)(L\text{-}Ala)]^+$ (calcd)	

c_1: initial concentration (mol/l) of $[Cu(en)_2]^{2+}$
c_2: initial concentration (mol/l) of $[Cu(L\text{-}Ala)_2]$

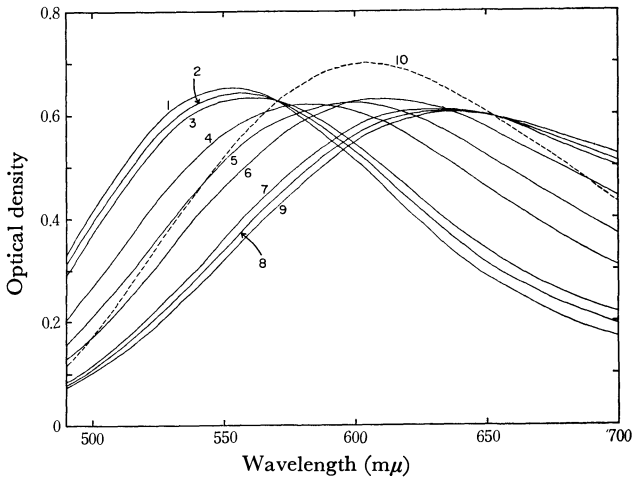

Fig. 6. The visible absorption spectra (measured at 20°C, solvent: an equivolume mixture of water and methanol) of the mixed solutions of $[Cu(en)_2]^{2+}$ and $[Cu(\beta\text{-}Ala)_2]$. The numbering for curves is the same as the one in Fig. 5.

System I–III, since the magnetic parameters of the three complexes for the former system were closer to each other and its K value was much smaller. It seems, therefore, that the error accompanying this analysis in System I–IV will inevitably become larger. All the results obtained are listed in Tables 1 and 2, together with the calculated values of $\log K$. It seems that much reliance can be placed on this ESR method, since the determined values of $\log K$ were held constant to a considerable extent for all the mixtures at various volume ratios.

Determination of K by Optical Absorption. The values of K were also determined at temperatures of 20 and 50°C by optical absorption measurements according to the Kida method.[7] Some of the observed spectra for Systems I–II and I–III are shown in Figs. 5 and 6 respectively. The spectral measurements for System II–III was carried out only at 20°C in a similar way; an especially careful experiment was required in order to obtain the exact isosbestic points, since the parent complexes are comparatively close to each other in the wavelength and the intensity of the maximum absorption. All the results obtained are listed in Tables 3—6, together with the calculated values of $\log K$.

Table 3. Results of the visible absorption measurements on the equilibrium
$[Cu(en)_2]^{2+} + [Cu(L\text{-}Ala)_2] \rightleftharpoons 2[Cu(en)(L\text{-}Ala)]^+$

Temperature (°C)	Wavelength (mμ)	$c_1\times10^2$	$c_2\times10^2$	D	ε_1	ε_2	ε_3	$\log K$
	574	2/3	1/3	0.614	62.0	48.3	ε_1	1.35
	574	1/2	1/2	0.603	62.0	48.3	ε_1	1.53
20	574	1/3	2/3	0.570	62.0	48.3	ε_1	1.46
	615	2/3	1/3	0.529	44.1	58.0	ε_2	1.51
	615	1/2	1/2	0.562	44.1	58.0	ε_2	1.42
	615	1/3	2/3	0.575	44.1	58.0	ε_2	1.39
							Mean value:	1.44±0.02
	576	2/3	1/3	0.613	63.8	48.3	ε_1	1.41
	576	1/2	1/2	0.614	63.3	48.3	ε_1	1.33
50	576	1/3	2/3	0.580	63.8	48.3	ε_1	1.41
	623	2/3	1/3	0.526	43.7	57.8	ε_2	1.44
	623	1/2	1/2	0.558	43.7	57.8	ε_2	1.38
	623	1/3	2/3	0.572	43.7	57.8	ε_2	1.30
							Mean value:	1.38±0.02

c_1, c_2: initial concentrations (mol/l) of $[Cu(en)_2]^{2+}$ and $[Cu(L\text{-}Ala)_2]$ respectively.
D: optical density of the solution.
ε_1, ε_2, ε_3: molar extinction coefficients of $[Cu(en)_2]^{2+}$, $[Cu(L\text{-}Ala)_2]$, and $[Cu(en)(L\text{-}Ala)]^+$ respectively.

Table 4. Results of the visible absorption measurements on the equilibrium
$[Cu(en)_2]^{2+} + [Cu(\beta\text{-Ala})_2] \rightleftharpoons 2[Cu(en)(\beta\text{-Ala})]^+$

Temperature (°C)	Wavelength (mμ)	$c_1\times10^2$	$c_2\times10^2$	D	ε_1	ε_2	ε_3	log K
	570	2/3	1/3	0.614	63.9	39.5	ε_1	0.67
	570	1/2	1/2	0.585	63.9	39.5	ε_1	0.78
	570	1/3	2/3	0.539	63.9	39.5	ε_1	0.93
20	654	2/3	1/3	0.434	27.3	56.0	ε_2	0.64
	654	1/2	1/2	0.495	27.3	56.0	ε_2	0.76
	654	1/3	2/3	0.536	27.3	56.0	ε_2	0.87
							Mean value:	0.78±0.04
	568	2/3	1/3	0.631	65.7	40.5	ε_1	0.67
	568	1/2	1/2	0.602	65.7	40.5	ε_1	0.83
50	568	1/3	2/3	0.553	65.7	40.5	ε_1	0.90
	656	2/3	1/3	0.451	28.7	57.5	ε_2	0.73
	656	1/2	1/2	0.511	28.7	57.5	ε_2	0.80
	656	1/3	2/3	0.551	28.7	57.5	ε_2	0.86
							Mean value:	0.80±0.03

c_1, c_2: initial concentrations (mol/l) of $[Cu(en)_2]^{2+}$ and $[Cu(\beta\text{-Ala})_2]$ respectively.
D: optical density of the solution.
ε_1, ε_2, ε_3: molar extinction coefficients of $[Cu(en)_2]^{+2}$, $[Cu(\beta\text{-Ala})_2]$, and $[Cu(en)(\beta\text{-Ala})]^+$ respectively.

Table 5. Results of the visible absorption measurements on the equilibrium
$[Cu(en)_2]^{2+} + [Cu(dmg)_2] \rightleftharpoons 2[Cu(en)(dmg)]^+$

Temperature (°C)	Wavelength (mμ)	$c_1\times10^2$	$c_2\times10^2$	D	ε_1	ε_2	ε_3	log K
	542	2/3	1/3	0.611	65.2	57.2	ε_2	0.09
	542	1/2	1/2	0.597	65.2	57.2	ε_2	0.16
20	542	1/3	2/3	0.585	65.2	57.2	ε_2	0.09
	554	2/3	1/3	0.668	65.9	71.0	ε_1	0.14
	554	1/2	1/2	0.676	65.9	71.0	ε_1	0.07
	554	1/3	2/3	0.684	65.9	71.0	ε_1	0.31
							Mean value:	0.14±0.03
	536	2/3	1/3	0.583	64.0	52.7	ε_2	0.21
	536	1/2	1/2	0.564	64.0	52.7	ε_2	0.03
50	536	1/3	2/3	0.544	64.0	52.7	ε_2	0.21
	558	2/3	1/3	0.684	66.8	76.5	ε_1	0.11
	558	1/2	1/2	0.699	66.8	76.5	ε_1	0.15
	558	1/3	2/3	0.714	66.8	76.5	ε_1	0.20
							Mean value:	0.15±0.03

c_1, c_2: initial concentrations (mol/l) of $[Cu(en)_2]^{2+}$ and $[Cu(dmg)_2]$ respectively.
D: optical density of the solution.
ε_1, ε_2, ε_3,: molar extinction coefficients of $[Cu(en)_2]^{2+}$, $[Cu(dmg)_2]$, and $[Cu(en)(dmg)]^+$ respectively.

Table 6. Results of the visible absorption measurements at 20°C on the equilibrium
$[Cu(\text{L-Ala})_2] + [Cu(\beta\text{-Ala})_2] \rightleftharpoons 2[Cu(\text{L-Ala})(\beta\text{-Ala})]$

Wavelength (mμ)	$c_1\times10^2$	$c_2\times10^2$	D	ε_1	ε_2	ε_3	log K
600	0.7	0.3	0.561	56.2	53.9	ε_1	1.20
600	0.5	0.5	0.559	56.2	53.9	ε_1	1.32
600	0.3	0.7	0.552	56.2	53.9	ε_1	1.20
						Mean value:	1.24±0.03

c_1, c_2,: initial concentrations (mol/l) of $[Cu(\text{L-Ala})_2]$ and $[Cu(\beta\text{-Ala})_2]$ respectively.
D: optical density of the solution.
ε_1, ε_2, ε_3,: molar extinction coefficients of $[Cu(\text{L-Ala})_2]$, $[Cu(\beta\text{-Ala})_2]$, and $[Cu(\text{L-Ala})(\beta\text{-Ala})]$ respectively.

Discussion

All the values of log K are summarized in Table 7; the values of K for Systems I–II, I–III, I–IV, and II–III are about 26, 6, 1, and 17 respectively. The K values of the second and third systems are comparatively smaller than those of the others. This is consistent with the following ESR result: the coexistence of three complex species for Systems I–III and I–IV was clearly established by a study of their ESR spectra. On the other hand, for Systems I–II and II–III the ESR absorption lines due to the parent complexes are very

Table 7. The value of log K

Temperature (°C)	System[a] I–II	I–III	I–IV	II–III
50	1.38±0.02	0.80±0.03	0.15±0.03	——
20	1.44±0.02	0.78±0.04	0.14±0.03	1.24±0.03
ca. −100[b]	——	0.79±0.10	−0.45±0.15	——

a) Systems I–II, I–III, I–IV, and II–III were designated as the mixed solutions of $[Cu(en)_2]^{2+}$ and $[Cu(L\text{-}Ala)_2]$, of $[Cu(en)_2]^{2+}$ and $[Cu(\beta\text{-}Ala)_2]$, of $[Cu(en)_2]^{2+}$ and $[Cu(dmg)_2]$, and of $[Cu(L\text{-}Ala)_2]$ and $[Cu(\beta\text{-}Ala)_2]$ respectively.
b) See the text.

difficult to detect in the spectra; only the mixed-ligand complexes are almost quantitatively formed for Systems I–II and II–III.[11] It is, furthermore, interestingly shown in the table that the values of log K determined by both the optical absorption and ESR methods are almost equal to each other for System I–III and are comparable in their order for System I–IV. These results suggest that the value of K does not depend largely upon the temperature and that this ESR method is an excellent one for determining the K values.

Kida definded log K_{stab} as follows:[7,8]

$$\log K_{stab} = \log K - \log K_{stat}$$

where K_{stat} is the value of K when the three complexes in Eq. (1) are distributed entirely statistically or randomly. Under these conditions, K_{stat} is equal to 4: accordingly, log K_{stat}=0.60. If log K_{stab} is positive for a system, the mixed-ligand complex is more stable than can be expected statistically. Kida pointed out that log $K_{stab}>0$ generally holds for such an equilibrium as is expressed in Eq. (1) by reason of the fact that both the electrostatic effect and the effect of the σ-covalency of the coordinate bond serve to promote the formation of a mixed-ligand complex.

The values of log K_{stab} are positive for all the systems except one, as may be seen in Table 7, but their values are quite different. It is important for us to investigate the reason for such different values, although it is not easy to do so at the present stage because of the insufficiency of data of this kind. The question whether or not the promotive formation of a mixed-ligand complex depends upon its stabilization in bond energy will, however, be answered by the experimental study of the temperature dependence of log K. log K is expressed as follows:[13]

$$\log K = \frac{1}{2.30R}\left(-\frac{\Delta H}{T} + \Delta S\right) \qquad (3)$$
$$\Delta S = \Delta S_r + \Delta S_s$$

where ΔS_s is the entropy term of log $K_{stat}=\Delta S_s/2.30R$ =0.60 concerning the statistical distribution among the three complexes in Eq. (1) and where ΔS_r is designated as the summation of all the other unknown entropy terms. The error inherent in the ESR method of determining the K values may be somewhat larger than in the optical absorption method, mainly because of the assumed proportionality between the molar ratio of the three complexes and the ratio of the integrated intensities of the corresponding resolved Gaussian curves and because of the troublesome nature of the Gaussian analysis itself. Accordingly, it seems reasonable that the errors, which are ±0.04 in Tables 1 and 2, were increased properly as much as about twofold for System I–III and about fourfold for System I–IV in Table 7. These increased errors, however, are, after all, counterbalanced from the point of view of the temperature dependence of log$K$ because of the very low temperature at which the K values are determined by the ESR method.

The thermodynamic constants were derived from the data in Table 7; they are listed in Table 8. The results in Table 8 indicate that the entropy change plays a main role in governing the equilibrium for all the systems. It is, furthermore, an interesting finding that the entropy values are almost constant for these systems, any one of which is concerned with ethylenediamine (as A in Eq. (1)) and amino acid (as B). On the other hand, the ΔG°_{293} values of the three systems are different from each other, and the enthalpy terms, whose values were different, are considered to be responsible for the differences in the value of ΔG°_{293}. Since the enthalpy term is related to the bond energies, the above-mentioned fact is consistent with Kida's proposal that the promotive formation of a mixed-ligand complex depends upon the electrostatic effect and also upon the effect of the σ-covalency of the coordinate bond. The enthalpy changes listed in Table 8 are comparatively small, especially for System I–III. This finding agrees with the ESR result already reported in a previous paper; the Cu–A and Cu–B bonds in Eq. (1) become close to each other in bond strength in the mixed-ligand complex, and there is an accompanying internal compensation for the bond energies.[11] A further study of the relations between these thermodynamic functions and the kinds of mixed-ligand complexes, or the other physico-chemical properties of the complexes, is now in progress. It is clear that all these data are fundamentally important for the structural estimation of the metalloenzyme-substrate complexes and for understanding their reaction mechanisms.

Table 8. Thermodynamic constants

		System[a] I–II	I–III	I–IV
ΔG^0_{293}	(kcal/mol)	−1.93±0.03	−1.05±0.06	−0.19±0.04
ΔH	(kcal/mol)	−0.86±0.58	0.01±0.20	1.20±0.31
ΔS	(e.u.)	3.65±0.21	3.62±0.09	4.12±1.20
ΔS_r	(e.u.)	0.89±0.21	0.86±0.09	1.36±1.20

a) The systems are the ones referred to in Table 7.

13) S. Bruckeinstein and L. D. Pettit, *J. Amer. Chem. Soc.*, **88**, 4790 (1966).

The Relation between the Volatilization Rates of Chlorine and Bromine Compounds from Volcanic Rocks on Heating

Kazuyoshi TAKAHASHI

Department of Chemistry, Faculty of Science, Tokyo Institute of Technology, Ookayama, Meguro-ku, Tokyo

(Received January 23, 1971)

Experiments on the volatilization rate of chlorine and bromine compounds from volcanic rocks were made at temperatures above 770°C in a stream of nitrogen, both in the presence of water vapor and without it. The rate of volatilization have been studied by following the change in the retained chlorine and bromine contents as a function of the heating time. Their contents retained in rocks during heating were estimated indirectly by determining their amounts evolved from rocks. The chlorine compounds are more volatile than those of bromine, regardless of the rock type. However, the difference in their volatility becomes quite small in the presence of water vapor. This fact suggests that there is little difference in the volatility between chlorine and bromine compounds in the presence of much water vapor, so the Br/Cl ratio in magma does not change very much during the crystallization process.

Sugiura[1] reported that the bromine and chlorine contents of volcanic rocks ranged widely, but that the Br/Cl ratios were to be found in a relatively narrow range, mostly from 1×10^{-3} to 6×10^{-3} by weight, regardless of the rock type. The present author and his co-workers determined the halogen contents of volcanic rocks.[2] Their Br/Cl ratios also fell in a narrow range, regardless of their contents in the rocks and of the rock type. These findings may show the close similarity between the volatilization rates of chlorine and bromine compounds, because the distribution of halogens in volcanic rocks is largely determined by their volatilization. Several studies of the volatilization of halogen compounds were carried out by heating volcanic rocks. Yoshida[3] and Yoshida *et al.*[4,5] studied the fractionation of halogen compounds through the process of volatilization and sublimation by determining their contents in the gases and sublimates obtained by heating rocks. Iwasaki and Katsura[6] carried out an experimental study of the volatilization rate of chlorine compounds from basaltic rock melts, neglecting the effect of water vapor. From the experimental results on the liberation of chlorine and fluorine compounds in the presence of water vapor, Sugiura[7] suggested that the distillation process of halogens with water vapor determines the distribution of halogens in volcanic rocks more than does the chemical and mineralogical nature of the rocks.

No attempt has, however, yet been made to study the rates of volatilization of bromine compounds from volcanic rocks on heating; this has been because of the lack of a suitable analytical method for the determination of bromine. The objective of the present paper is to make clear the relation between the rates of volatilization of chlorine and bromine compounds from volcanic rocks on heating. The experiments on the liberation of their compounds from volcanic rocks were made by heating rocks in a stream of nitrogen, both in the presence of water vapor and without it.

Experimental

Materials. The rock samples used in this study are listed in Table 1, together with their chlorine and bromine contents. The chlorine in rocks was determined by the method of Iwasaki *et al.*[8] with some improvements, while the bromine in the rocks was determined by the method of Takahashi *et al.*[9] Reagent-grade chemicals and redistilled water were used throughout this work.

Apparatus and Procedure. The apparatus used in this study is shown in Fig. 1. The method of generation of the water vapor was the same as that described by Sugiura.[7] The temperature of the furnace was kept constant within ±10°C and measured by a pyrometer with a platinum-platinum, 10% rhodium thermocouple. Two absorption vessels were connected to the three-way cock separately, each containing about 40 m*l* of water and 5 g of potassium hydrox-

TABLE 1. CHLORINE AND BROMINE CONTENTS OF THE ROCK SPECIMENS USED

No.	Sample	Cl ppm	Br ppm	Br/Cl $\times10^{-3}$ (weight ratio)
1	Basalt (lava of 1962 Miyake-jima Volcano, Tokyo Metr.)	600	1.66	2.8
2	Basalt (Takashima, Saga Pref.)	420	1.31	3.1
3	Andesite (lava of 1946 Sakura-jima Volcano, Kagoshima Pref.)	360	1.45	4.0
4	Liparite (Kozu-shima Volcano, Tokyo Metr.)	910	2.52	2.8
5	Obsidian (Shirataki, Hokkaido)	800	1.20	1.5

1) T. Sugiura, This Bulletin, **41**, 1133 (1968).
2) M. Yoshida, K. Takahashi, N. Yonehara, T. Ozawa, and I. Iwasaki, *ibid.*, **44**, 1844 (1971).
3) M. Yoshida, *ibid.*, **36**, 773 (1963).
4) M. Yoshida, I. Makino, N. Yonehara, and I. Iwasaki, *ibid.*, **38**, 1436 (1965).
5) I. Iwasaki, M. Yoshida, I. Makino, and N. Yonehara, *Bull. Volcanol. Sec. Japan*, **9**, 1 (1964).
6) B. Iwasaki and T. Katsura, This Bulletin, **40**, 1167 (1967).
7) T. Sugiura, *ibid.*, **41**, 1588 (1968).
8) I. Iwasaki, T. Katsura, and N. Sakato, *Nippon Kagaku Zasshi*, **76**, 1116 (1955).
9) K. Takahashi, M. Yoshida, T. Ozawa, and I. Iwasaki, This Bulletin, **43**, 3159 (1970).

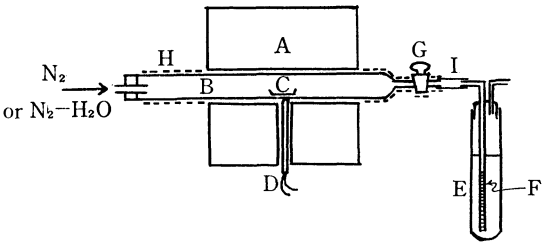

Fig. 1. Apparatus.

A	Electric furnace	B	Silica-glass tube
C	Platinum boat	D	Thermocouple
E	Absorption vessel	F	Silica-glass wool
G	Three-way cock	H	Glass heater
I	Silicone rubber tube		

ide. From 3 to 4 g of a finely-powdered sample, placed in a platinum boat, was inserted in the silica glass tube and then placed in the center of the furnace at a given temperature. Nitrogen gas freed of halogens by sodium hydroxide pellets was then allowed to flow through at a fixed flow rate of about 360 ml/min. The halogen compounds which were liberated from the sample were absorbed by the solution in the absorption vessel. After various periods of heating, the three-way cock was turned in order to trace the change in the amounts of chlorine and bromine evolved as a function of the heating time. After the solution in each absorption vessel has been adequately diluted, an aliquot of the solution was used for the determination of bromine. Another portion was used for the determination of chlorine after oxidizing the sulfide by heating the solution with a small amount of hydrogen peroxide. The chlorine was determined by the mercuric thiocyanate method[10] with some improvements, while the bromine was determined by a modification of the method reported in a previous paper.[9] The amounts of chlorine and bromine deposited on the inside surface of the silica-glass tube and the cock on the outgassing of the rocks were small enough to be neglected; the bromine was less than 5% of the total amount of bromine evolved from rocks, and the chlorine, less than 2% of the total amount of chlorine evolved.

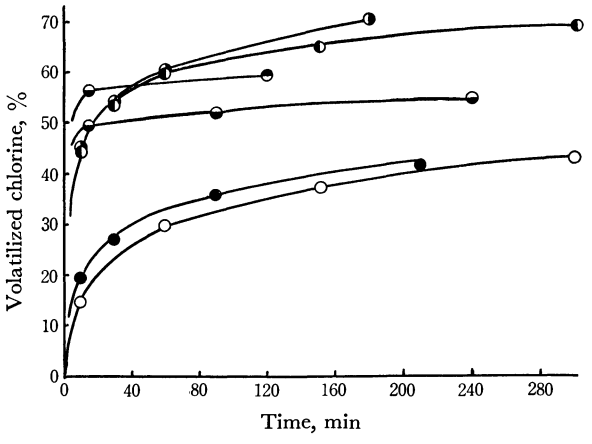

Fig. 2. Change in the percentage ratio of the volatilized chlorine content to the original chlorine content with heating time at different temperatures in N_2 and N_2-H_2O mixture.
Sample: Basalt from Miyake-jima, 4 g

○ 770°C	in N_2	● 770°C	in N_2-H_2O
◐ 950°C		◑ 950°C	
◒ 1170°C		◓ 1170°C	

10) T. Ozawa, *Bunseki Kagaku*, **17**, 395 (1968).

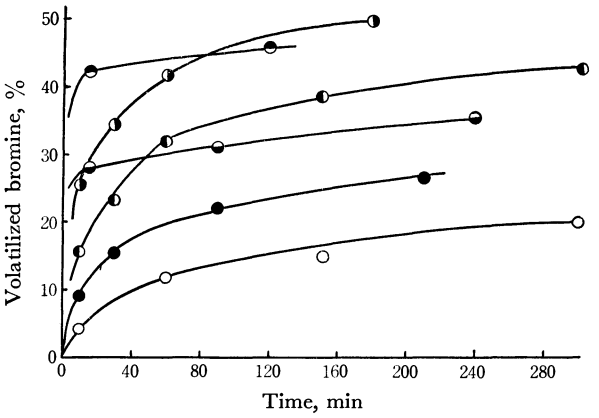

Fig. 3. Change in the percentage ratio of the volatilized bromine content to the original bromine content with heating time at different temperatures in N_2 and N_2-H_2O mixture.
Sample: Basalt from Miyake-jima, 4 g

○ 770°C	in N_2	● 770°C	in N_2-H_2O
◐ 950°C		◑ 950°C	
◒ 1170°C		◓ 1170°C	

Results and Discussion

The Rates of Volatilization of Chlorine and Bromine Compounds from Volcanic Rocks on Heating. The results of experiments conducted at different temperatures and at various heating times are shown in Figs. 2 and 3. In Figs. 2 and 3, only the results for basalt from Miyake-jima are presented, because the shapes of the curves for this basalt are very similar to those for all the other rocks used in this study. Figure 2 shows the change in the ratio (%) of the volatilized chlorine content to the original chlorine content with the heating time at different temperatures, both in the presence and absence of water vapor. Figure 3 shows the change in the ratio of the volatilized bromine content to the original bromine content, as in the case of chlorine. From the results shown in Figs. 2 and 3, it is evident that the rates of volatilization of chlorine and bromine compounds are remarkably fast in the initial heating

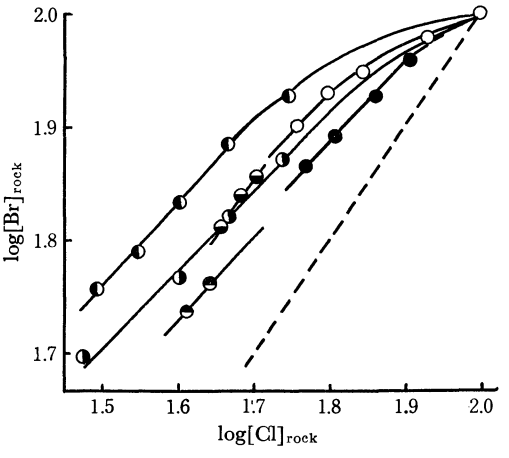

Fig. 4. The log-log relation between the percentage fractions of retained chlorine and bromine in rocks during heating.
Sample: Basalt, Miyake-jima, 4 g

○ 770°C	in N_2	● 770°C	in N_2-H_2O
◐ 950°C		◑ 950°C	
◒ 1170°C		◓ 1170°C	

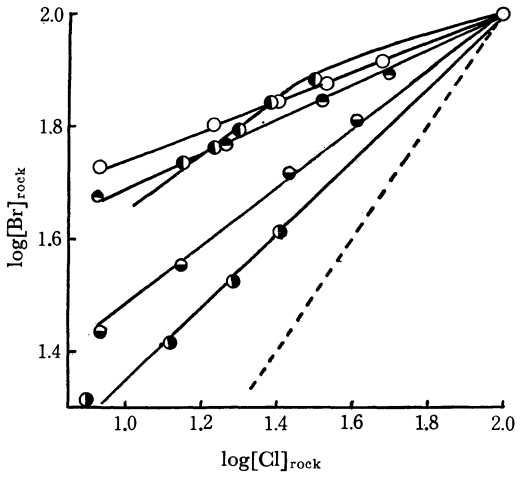

Fig. 5. The log-log relation between the percentage of retained chlorine and bromine in rocks during heating.
○ Andesite, Sakura-jima, 4 g: 950°C, N_2
◐ Basalt, Takashima, 4 g: 950°C, N_2
◑ Basalt, Takashima, 4 g: 950°C, N_2-H_2O
◔ Obsidian, Shirataki, 4 g: 950°C, N_2
◒ Obsidian, Shirataki, 4 g: 950°C, N_2-H_2O

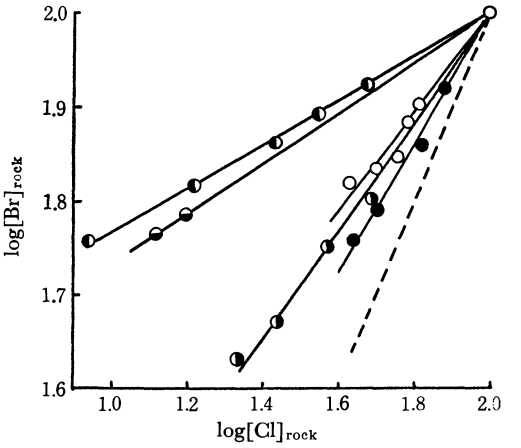

Fig. 6. The log-log relation between the percentage of retained chlorine and bromine in rocks during heating.
Sample: Liparite, Kozu-shima, 3 g
○ 770°C, ◐ 950°C, ◒ 1170°C } in N_2
● 770°C, ◑ 950°C } in N_2-H_2O

period, and that then the rates become slow. The liberation of their compounds from the rocks becomes remarkably difficult as soon as they begin to melt. The basaltic sample from Miyake-jima begins to melt after several minutes in the furnace at 1170°C. The chlorine and bromine compounds tend to volatilize more easily in the presence of water vapor than without it. There is an especially striking difference in the rate curves of the liberation of bromine compounds in nitrogen and in a N_2-H_2O mixture. Figure 3 shows that the bromine compounds are much more easily liberated in the N_2-H_2O mixture.

The kinetics of the volatilization of the chlorine and bromine compounds is very complex because a rock is a multicomponent and inhomogeneous system. According to Iwasaki *et al.*[11] and the results of the pH measurements, which are not listed in this paper, the chemical form of the chlorine evolved is mostly hydrogen chloride. This would be the case for bromine, also. For this reason, it is evident that water in rocks plays an important role in the kinetics of the volatilization of their compounds.

The Relation between the Rates of Volatilization of Chlorine and Bromine Compounds from Rocks on Heating.
Figures 4, 5, and 6 show the relation between the percentage fractions of retained chlorine and bromine in rocks during heating, both in the presence of water vapor and in its absence. $[Cl]_{rock}$ and $[Br]_{rock}$ represent the percentage of the retained chlorine and bromine contents respectively in relation to their original contents. The chlorine compounds are remarkably easier to release than those of bromine on heating in the absence of water vapor, regardless of the rock type. The plots of log $[Br]_{rock}$ *vs.* log $[Cl]_{rock}$ all yield approximately straight lines except for basalt. The ratio of the volatility of chlorine compounds to that of bromine compounds, k, was defined by the equation:

$$(-d[Cl]_{rock}/[Cl]_{rock}dt)/(-d[Br]_{rock}/[Br]_{rock}dt) = k.$$

From the slopes of the straight lines, the volatility ratios obtained for andesite from Sakura-jima, liparite from Kozu-shima, and obsidian from Imari on heating at 950°C in N_2 are 3.9, 4.3, and 3.4 respectively.

The Br/Cl ratio in rocks increases with an increase in the duration of heating because of the higher volatility of chlorine compounds. In other words, the lower the chlorine content retained in rocks on heating, the larger the $(Br/Cl)_{retained}$ ratio. It is interesting to note that these observations are similar to the relation between the Br/Cl ratio and the chlorine content of ordinary chondrites reported by Goles *et al.*[12] The Cl/Br ratio in ordinary chondrites increases rapidly with an increase in the chlorine content. The thermal history of meteorites seems to have a large influence on the abundance of chlorine and bromine in them.

On the other hand, the difference in volatility between chlorine and bromine compounds becomes remarkably small in the presence of water vapor. The effect becomes even stronger with an increase in the water-vapor pressure, and each curve in the log-log relation in Figs. 4, 5, and 6 gradually approaches the broken line which shows the case in which there is no difference in volatility between chlorine and bromine compounds.

The chlorine and bromine contents of magma are considered to decrease rapidly during cooling because of the volatilization of their compounds. Provided that the Br/Cl ratio in any magma is approximately constant and that chlorine and bromine do not enter into the rock-forming minerals in volcanic rocks, the ratio of the retained bromine to the retained chlorine in magmas can be determined by means of the difference in volatility between their compounds. If the chlorine compounds are more volatile than that of bromine under natural conditions, the Br/Cl ratio in rocks will increase as their contents decrease. As can be seen in Fig. 7, the Br/Cl ratios in volcanic rocks fall in a narrow range,

11) I. Iwasaki, T. Katsura, and N. Sakato, *Nippon Kagaku Zasshi*, **76**, 778 (1955).

12) G. G. Goles, L. P. Greenland, and D. Y. Jerome, *Geochim. Cosmochim. Acta*, **31**, 1771 (1967).

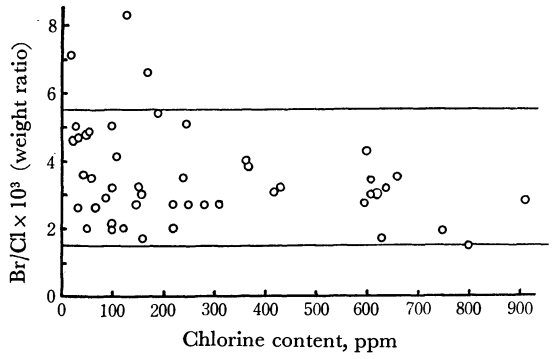

Fig. 7. Relationship between Br/Cl ratio and Cl content in volcanic rocks.

mostly from 1.5×10^{-3} to 5.5×10^{-3} by weight, regardless of the chlorine content and the rock type. This fact seems to result from the close similarity between the volatilities of chlorine and bromine compounds during the cooling process of magma under hydrous conditions.

In order to obtain information on the volatilities of chlorine and bromine compounds from magma, the data on the Br/Cl ratio in volcanic gases may be important. The data in high-temperature volcanic gases are especially required because the chlorine and bromine compounds in low temperature volcanic gases are fractionated by means of the process of sublimation and by other phenomena. For example, Mizutani[13] and Yoshida *et al.*[4] pointed out that bromine is strongly enriched in ammonium chloride as volcanic sublimate. From the results of heating experiments on the rocks, Yoshida *et al.*[4] showed also that bromine is deposited more easily than chlorine. The data on the chlorine and bromine contents in volcanic gases are insufficient. Sugiura *et al.*[14] and Honda[15] determined the Br/Cl ratios in volcanic gases from several active volcanoes in Japan. The Br/Cl ratios in gases with temperatures above 300°C are $(1—2)\times10^{-3}$ by weight. This value is a little smaller than that in volcanic rocks. According to Sugiura,[1] however, the Br/Cl ratios in the volcanic gases are nearly the same as those in volcanic rocks at each volcano studied. From these facts, it seems likely that there is little difference in volatility between chlorine and bromine compounds under magmatic conditions.

As has often been pointed out, water vapor which is believed to be ubiquitous in magma plays an important role in the volatilization of halogen compounds.[7,16,17] According to the very simple thermodynamic calculations of Kogarko and Ryabchikov,[17] reactions between water vapor and metal halides at high temperature yield volatile hydrogen halides. In the present study, the addition of water vapor slightly affected the volatilization of chlorine compounds, while it greatly affected that of bromine compounds. This suggests that water vapor formed in rocks on heating reacts with chlorine compounds more effectively than with bromine compounds through the process of the rapid escape of water vapor.

Conclusion

The chlorine compounds are more volatile than those of bromine on heating without water vapor, regardless of the rock type, so the lower the content of retained chlorine during heating, the larger the Br/Cl ratio in rocks. This relation is consistent with the correlation of the Br/Cl ratio with the chlorine content in ordinary chondrites. The difference in volatility between their compounds tend to become noticeably smaller in the presence of water vapor. This fact, and the close relation between the abundance of chlorine and that of bromine in volcanic rocks, show that the ratio of the volatilization loss of chlorine to that of bromine is nearly constant during the cooling process of hydrous magma.

The author wishes to express his hearty thanks to professor Iwaji Iwasaki of Tōhō University, and to Dr. Takejiro Ogawa, and Dr. Minoru Yoshida of the Tokyo Institute of Technology, for their many valuable discussions and suggestions during this study.

13) Y. Mizutani, *J. Earth Sci., Nagoya Univ.*, **10**, 149 (1962).
14) T. Sugiura, Y. Mizutani, and S. Oana, *ibid.*, **11**, 272 (1963).
15) F. Honda, *Geochem. J.*, **3** 187 (1970).
16) P. K. Kuroda and E. B. Sandell, *Bull. Geol. Soc. Am.*, **64**, 879 (1953).
17) L. N. Kogarko and I. D. Ryabchikov, *Geochemistry*, **1961**, 1192.

The Crystal Structure of Perchlorato-bis(2,2′-bipyridine)-copper(II) Perchlorate, $[Cu(ClO_4)(bipy)_2]ClO_4$

Hisayoshi NAKAI

Department of Chemistry, Faculty of Science, Osaka City University, Sugimoto-cho, Sumiyoshi-ku, Osaka

(Received January 25, 1971)

The structure of bis(2,2′-bipyridine)copper(II) perchlorate, $Cu(bipy)_2(ClO_4)_2$, has been determined from three-dimensional X-ray data collected by the photographic method. The compound forms triclinic crystals with $a=7.44(1)$, $b=14.93(1)$, $c=15.32(1)$ Å, $\alpha=136.3(0.1)$, $\beta=103.7(0.1)$, $\gamma=83.2(0.1)°$, and $Z=2$ in the space group $P\bar{1}$. The structure was solved by the usual Patterson and Fourier techniques and was refined by the least-squares method to an R value of 0.134. The crystal is composed of an infinite chain of $[Cu(ClO_4)(bipy)_2^+]_\infty$ and ClO_4^-; a perchlorate ion in the chain bridges two adjacent copper atoms through its two oxygen atoms. Roughly speaking, the coordination polyhedron around the copper atom is a tetragonally-distorted octahedron; the four nitrogen atoms of bipyridine molecules are arranged in a flattened tetrahedral manner (average Cu–N=1.99 Å), the least-squares plane of these atoms making an equatorial plane, while the polar positions are occupied by the two oxygen atoms of perchlorate anions, the Cu–O distances being 2.45 and 2.73 Å. The two pyridine rings are twisted slightly to each other in both of the bipyridine molecules; the dihedral angle between the pyridine planes is 13° in one bipyridine ligand and 4° in the other.

It is well known that the copper(II) ion can give numerous bis-bipyridine complexes with the general formula of $Cu(bipy)_2X_2\cdot nH_2O$.[1] In these complexes, however, two bipyridine molecules have to overcome a great difficulty; in case they take a completely coplanar arrangement around the Cu atom, there is severe steric interference between the hydrogen atoms on the 6- and 6′-carbon atoms of the two bipyridine molecules (Fig. 1). In fact, no such coplanar disposition of bipyridine molecules has been found for the bis-bipyridine metal complexes, including even the copper(II) complexes,[2-4] in which the bipyridine molecules are most likely to be on a plane.

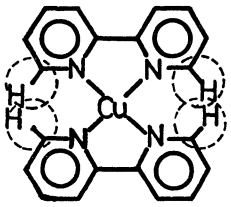

Fig. 1

The author has been very interested in the structure of bipyridine-copper(II) complexes, and has been attempting the crystal-structure analyses of a series of bis-bipyridine complexes in order to elucidate the disposition of the two bipyridine ligands around the copper(II) ion as well as the conformation of the bipyridine molecule in the complex. One of the results ($[Cu(NO_3)(bipy)_2]NO_3\cdot H_2O$) has already been reported briefly.[3] In this paper, the crystal structure of $Cu(bipy)_2(ClO_4)_2$ will be dealt with.

1) C. M. Harris, T. N. Locker, and H. Waterman, *Nature*, **192**, 424 (1961).

2) G. A. Barclay and C. H. L. Kennard, *ibid.*, **192**, 425 (1961); G. A. Barclay, B. F. Hoskins, and C. H. L. Kennard, *J. Chem. Soc., A*, **1963**, 5691.

3) H. Nakai, S. Ooi, and H. Kuroya, This Bulletin, **43**, 577 (1970).

4) I. M. Procter and F. S. Stephens, *J. Chem. Soc., A*, **1969**, 1248.

Experimental

The crystals of $Cu(bipy)_2(ClO_4)_2$ were prepared by Jaeger's method[5] and were recrystallized from a water-methanol mixture.

The lattice constants at room temperature were determined from $(h0l)$, $(0kl)$, and $(hk0)$ reflection data recorded on Weissenberg photographs on which the aluminum powder diffraction lines were superimposed for calibration. Cu$K\alpha$ radiation ($\lambda=1.5418$ Å) was used throughout the diffraction study. The density of the compound was determined by floatation in a benzene-bromoform mixture. Of the two possible triclinic space groups, $P\bar{1}$ and $P1$, the former was chosen initially; this choice was confirmed by the successful solution and refinement of the structure. The crystal data are listed in Table 1.

Table 1. Crystal data

$Cu(bipy)_2(ClO_4)_2$		
Triclinic		
$a=7.44\pm0.01$,	$b=14.93\pm0.01$,	$c=15.32\pm0.01$Å
$\alpha=136.3\pm0.1$,	$\beta=103.7\pm0.1$,	$\gamma=83.2\pm0.1°$
$Dm=1.68$ g/cm^3,	$Dc=1.69$ g/cm^3	
$Z=2$, Space group $P\bar{1}$		
Linear absorption coefficient for Cu$K\alpha$, $\mu=40.2$ cm^{-1}		

The intensity data of the $0kl$—$4kl$, $h0l$, and $hk0$ reflections were collected from crystals with dimensions of $0.15\times0.15\times1.0$ mm by the multiple-film equi-inclination techniques. The intensity scale was prepared from the same crystal and was used for the visual estimation of the 3064 independent reflcetions, but the intensities of 792 of them were too weak to be measured and so were assumed to be zero.

After the intensity data had been corrected for Lorentz-polarization effects and spot extension, the structure factors were placed on a common arbitrary scale by internal correlation. No absorption correction was made, for it was estimated that the maximum effect of absorption on the intensity was, at most, 15 per cent.

5) F. M. Jaeger and J. A. Dijk, *Z. Anorg. Chem.*, **227**, 273 (1936).

Structure Determination

The position of the copper atom was readily determined from the three-dimensional Patterson maps. A first Fourier synthesis, phased on the Cu atom, clearly gave the atomic positions of one bipyridine ligand and those of the coordinating ClO_4^- ion. The coordinates of the remaining non-hydrogen atoms were obtained from the subsequently-synthesized Fourier maps. In these diagrams, the electron-density distribution of the uncoordinating ClO_4^- ion was evidently indicative of its tetrahedral configuration, but was much more diffuse than that of the coordinating ClO_4^- anion. The crystal structure was refined by a block-diagonal least-squares method. Throughout the least-squares calculations, the following weighting scheme was employed:

$$w = 0.2, \text{ if } F_o \leq F_{\min} \ (= 0.5 = 0.01 \times F_{\max})$$

and

$$w = 1.0, \text{ if } F_{\min} < F_o.$$

The atomic scattering curves were taken from the International Tables for X-ray Crystallography, Vol. III,[6] the real part of the anomalous dispersion correction ($\Delta f' = -2.1$) being applied for the neutral copper atom. After three cycles of the refinements, the conventional R value was 0.17 for 2272 non-zero reflections. Three more cycles of the refinements with anisotropic thermal parameters for only the heavier atoms of Cu, Cl(1) and Cl(2) reduced the R value to 0.15. At this stage, the average isotropic temperature factor of the oxygen atoms of the uncoordinating ClO_4^- ion rose to 19 Å^2. In the further refinement, the anisotropic thermal parameters were introduced, in addition to the heavier atoms mentioned above, to the oxygen atoms of the uncoordinating ClO_4^- ion. The R value was improved to 0.134 by three cycles of the least-squares calculations. In the last cycle of the calculations, the maximum shift in any parameter was less than one-eighth of its estimated standard deviation. The final atomic coordinates and temperature factors are listed in Table 2.

Table 2 The atomic coordinates, thermal parameters, and their estimated standard deviations

ATOM	x	y	z	B(Å^2)
Cu	0.4174(4)	0.3636(2)	0.1304(2)	*
Cl(2)	0.175(1)	0.092(1)	0.369(1)	*
O(11)	0.183(6)	0.062(2)	0.436(2)	*
O(22)	0.083(5)	0.181(3)	0.388(3)	*
O(33)	0.353(3)	0.136(3)	0.412(3)	*
O(44)	0.173(3)	−0.025(2)	0.238(2)	*
Cl(1)	−0.0748(6)	0.3703(3)	0.1567(3)	*
O(1)	0.730(2)	0.321(1)	0.087(1)	7.4(3)
O(2)	0.934(2)	0.508(1)	0.267(1)	8.0(4)
O(3)	0.991(2)	0.314(1)	0.203(1)	6.9(3)
O(4′)	0.038(2)	0.336(1)	0.070(1)	5.8(3)
N(1)	0.356(2)	0.197(1)	0.069(1)	4.0(3)
C(1)	0.245(2)	0.097(2)	−0.043(2)	4.6(3)
C(2)	0.187(3)	−0.011(2)	−0.068(2)	5.9(4)
C(3)	0.251(3)	−0.010(2)	0.026(2)	6.1(4)
C(4)	0.370(3)	0.098(2)	0.142(2)	4.8(4)
C(5)	0.415(2)	0.201(2)	0.161(2)	4.5(3)
C(6)	0.539(2)	0.315(1)	0.278(1)	4.0(3)
C(7)	0.647(3)	0.320(1)	0.371(2)	4.9(4)
C(8)	0.759(3)	0.539(2)	0.496(2)	5.4(4)
C(9)	0.758(3)	0.435(2)	0.480(2)	5.7(4)
C(10)	0.651(2)	0.525(1)	0.396(1)	4.3(3)
N(2)	0.544(2)	0.416(1)	0.292(1)	3.8(3)
N(3)	0.345(2)	0.536(1)	0.196(1)	4.4(3)
C(11)	0.325(3)	0.638(2)	0.314(2)	5.8(4)
C(22)	0.245(3)	0.751(2)	0.350(2)	7.8(5)
C(33)	0.193(3)	0.743(2)	0.256(2)	8.8(6)
C(44)	0.205(3)	0.635(2)	0.128(2)	7.4(5)
C(55)	0.289(3)	0.524(2)	0.099(2)	5.4(4)
C(66)	0.312(3)	0.404(2)	−0.027(2)	5.5(4)
C(77)	0.271(3)	0.385(2)	−0.138(2)	7.6(5)
C(88)	0.305(3)	0.260(2)	−0.252(2)	8.5(6)
C(99)	0.381(3)	0.162(2)	−0.264(2)	7.5(5)
C(00)	0.415(3)	0.197(2)	−0.144(2)	6.5(5)
N(4)	0.377(2)	0.312(1)	−0.035(1)	5.0(3)

* Anisotropic thermal parameters ($\times 10^3$) with estimated standard deviations ($\times 10^3$) in parentheses. The expression of the anisotropic thermal parameters is $\exp[-(B_{11}\times h^2+B_{22}\times k^2+B_{33}\times l^2+B_{12}\times h\times k+B_{13}\times h\times l+B_{23}\times k\times l)]$.

Atom	B_{11}	B_{22}	B_{33}	B_{12}	B_{13}	B_{23}
Cu	27(1)	11(0.2)	9(0.2)	1(1)	2(1)	15(0.4)
Cl(2)	79(3)	14(1)	12(1)	−10(2)	−9(2)	18(1)
O(11)	267(24)	34(4)	27(4)	11(16)	68(15)	50(7)
O(22)	152(16)	29(5)	58(7)	60(14)	54(17)	62(10)
O(33)	65(9)	54(6)	53(6)	−21(11)	−42(11)	78(11)
O(44)	98(9)	16(2)	15(2)	−8(7)	−7(7)	17(4)
Cl(1)	17(2)	10(0.2)	9(0.1)	3(0.4)	4(0.1)	15(1)

Results and Discussion

The crystal structure of $Cu(bipy)_2(ClO_4)_2$ viewed down the a-axis is shown in Fig. 2, while the bond lengths and angles, together with their estimated standard deviations, are presented in Table 3. The crystal is composed of the perchlorate ion and an infinite chain of $[Cu(ClO_4)(bipy)_2^+]_\infty$ in which a ClO_4^- ion bridges two adjacent copper atoms. A schematic drawing of a part of the infinite chain is shown in Fig. 3.

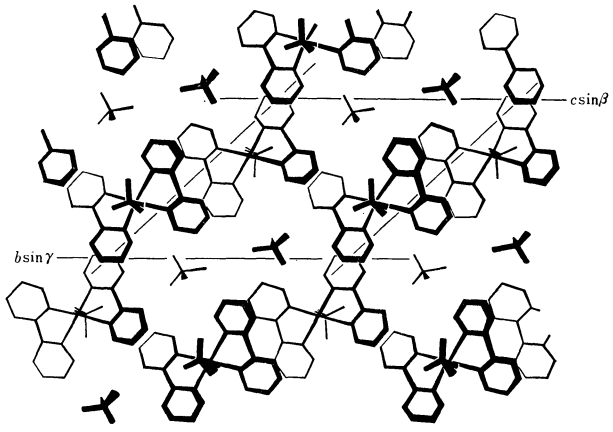

Fig. 2. a-axis projection of the crystal structure.

6) "International Tables for X-ray Crystallography," Vol. III, Kynoch Press, Birmingham (1962), p. 202.

TABLE 3. BOND LENGTHS (Å) AND ANGLES (DEG) WITH ESTIMATED STANDARD DEVIATION IN PARENTHESES

Cu–N(1)=1.98(2)	Cu–N(2)=1.97(2)
Cu–N(3)=2.02(2)	Cu–N(4)=1.99(2)
Cu–O(1)=2.45(2)	Cu–O(4′)=2.73(2)
N(1)–C(1)=1.33(3)	N(1)–C(5)=1.35(3)
C(1)–C(2)=1.45(4)	C(2)–C(3)=1.40(4)
C(3)–C(4)=1.41(4)	C(4)–C(5)=1.40(3)
C(5)–C(6)=1.46(3)	C(6)–C(7)=1.41(3)
C(7)–C(8)=1.40(3)	C(8)–C(9)=1.39(4)
C(9)–C(10)=1.42(3)	C(10)–N(2)=1.33(3)
C(6)–N(2)=1.37(3)	N(3)–C(11)=1.31(3)
N(3)–C(55)=1.34(3)	C(11)–C(22)=1.44(4)
C(22)–C(33)=1.32(5)	C(33)–C(44)=1.38(5)
C(44)–C(55)=1.46(4)	C(55)–C(66)=1.43(4)
C(66)–C(77)=1.47(4)	C(77)–C(88)=1.41(5)
C(88)–C(99)=1.39(5)	C(99)–C(00)=1.47(4)
C(00)–N(4)=1.34(3)	C(66)–N(4)=1.33(3)
Cl(1)–O(1)=1.48(2)	Cl(1)–O(2)=1.42(2)
Cl(1)–O(3)=1.42(2)	Cl(1)–O(4)=1.48(2)
Cl(2)–O(11)=1.37(4)	Cl(2)–O(22)=1.29(5)
Cl(2)–O(33)=1.33(4)	Cl(2)–O(44)=1.41(4)
N(1)–Cu–N(2)=83.8(0.7)	N(1)–Cu–N(3)=151.0(0.7)
N(1)–Cu–N(4)=102.0(0.8)	N(2)–Cu–N(3)=102.3(0.7)
N(2)-Cu–N(4)=161.1(0.8)	N(3)–Cu–N(4)=81.6(0.8)
O(1)–Cu–N(1)=98.0(0.7)	O(1)–Cu–N(2)=84.1(0.7)
O(1)–Cu–N(3)=110.7(0.7)	O(1)–Cu–N(4)=77.0(0.7)
O(4′)–Cu–N(1)=75.5(0.6)	O(4′)–Cu–N(2)=117.3(0.6)
O(4′)–Cu–N(3)=76.6(0.6)	O(4′)–Cu–N(4)=82.0(0.7)
O(1)–Cu–O(4′)=156.2(0.6)	Cu–N(1)–C(1)=127(2)
Cu–N(2)–C(10)=127(1)	Cu–N(1)–C(5)=113(1)
Cu–N(2)–C(6)=112(1)	Cu–N(3)–C(11)=124(2)
Cu–N(4)–C(00)=124(2)	Cu–N(3)–C(55)=111(2)
Cu–N(4)–C(66)=114(2)	Cu–O(4′)–Cl(1′)=124(1)
Cu–O(1)–Cl(1)=140(1)	N(1)–C(1)–C(2)=122(2)
C(1)–C(2)–C(3)=119(2)	C(2)–C(3)–C(4)=118(2)
C(3)–C(4)–C(5)=120(2)	C(4)–C(5)–C(6)=124(2)
C(4)–C(5)–N(1)=122(2)	N(1)–C(5)–C(6)=114(2)
C(5)–C(6)–C(7)=122(2)	C(5)–C(6)–N(2)=116(2)
N(2)–C(6)–C(7)=122(2)	C(6)–C(7)–C(8)=117(2)
C(7)–C(8)–C(9)=121(2)	C(8)–C(9)–C(10)=119(2)
C(9)–C(10)–N(2)=120(2)	C(10)–N(2)–C(6)=121(2)
N(3)–C(11)–C(22)=122(2)	C(11)–C(22)–C(33)=115(3)
C(22)–C(33)–C(44)=125(3)	C(33)–C(44)–C(55)=116(3)
C(44)–C(55)–C(66)=125(2)	C(44)–C(55)–N(3)=117(2)
C(55)–C(66)–N(4)=115(2)	N(3)–C(55)–C(66)=118(2)
C(55)–C(66)–C(77)=122(2)	C(66)–C(77)–C(88)=113(3)
C(77)–C(88)–C(99)=127(3)	C(77)–C(66)–N(4)=123(2)
C(88)–C(99)–C(00)=114(3)	C(99)–C(00)–N(4)=122(2)
C(00)–N(4)–C(66)=122(2)	O(1)–Cl(1)–O(2)=109(1)
O(1)–Cl(1)–O(3)=108(1)	O(1)–Cl(1)–O(4)=110(1)
O(2)–Cl(1)–O(3)=108(1)	O(3)–Cl(1)–O(4)=110(1)
O(2)–Cl(1)–O(4)=111(1)	O(11)–Cl(2)–O(22)=126(3)
O(11)–Cl(2)–O(33)=97(3)	O(11)–Cl(2)–O(44)=108(2)
O(22)–Cl(2)–O(33)=105(3)	O(22)–Cl(2)–O(44)=116(2)
O(33)–Cl(2)–O(44)=101(2)	

TABLE 4. THE DEVIATIONS OF THE ATOMS FROM THE LEAST-SQUARES PLANES

(X, Y, and Z are coordinates in Å unit referred to an orthagonal set of axis, where Y is parallel to b and X lies in the (ab) plane.)

Best planes through pyridine rings			
0.882 X−0.266 Y−0.389 Z=1.56			
N(1)	−0.01 Å	C(3)	0.00 Å
C(1)	−0.01	C(4)	−0.01
C(2)	0.01	C(5)	0.02
0.883 X−0.052 Y−0.467 Z=1.72			
N(2)	0.00 Å	C(8)	−0.01 Å
C(6)	0.01	C(9)	0.02
C(7)	−0.01	C(10)	−0.01
0.923 X+0.319 Y+0.217 Z=4.87			
N(3)	−0.01 Å	C(33)	−0.02 Å
C(11)	0.01	C(44)	0.01
C(22)	0.00	C(55)	0.00
0.933 X+0.257 Y+0.251 Z=4.46			
N(4)	0.02 Å	C(88)	0.03 Å
C(66)	0.00	C(99)	−0.01
C(77)	−0.02	C(00)	−0.01
Plane formed by Cu, N(1), and N(2)			
0.929 X−0.151 Y−0.339 Z=1.98			
Plane formed by Cu, N(3), and N(4)			
0.962 X+0.168 Y+0.216 Z=4.11			
Best planes through bipyridine ligands			
0.890 X−0.154 Y−0.430 Z=1.67			
N(1)	−0.13 Å	N(2)	0.12 Å
C(1)	−0.14	C(6)	0.01
C(2)	0.02	C(7)	−0.15
C(3)	0.16	C(8)	−0.14
C(4)	0.15	C(9)	0.02
C(5)	0.04	C(10)	0.12
0.932 X+0.285 Y+0.224 Z=4.66			
N(3)	−0.06 Å	N(4)	0.08 Å
C(11)	−0.03	C(66)	0.02
C(22)	0.01	C(77)	−0.05
C(33)	0.02	C(88)	−0.02
C(44)	0.05	C(99)	−0.03
C(55)	−0.01	C(00)	0.03
Plane formed by N(1), N(2), N(3), and N(4)			
0.994 X+0.108 Y−0.008 Z=3.64			
N(1)	0.68 Å	N(3)	0.24 Å
N(2)	−0.37	N(4)	−0.36
Distance from the above plane			
Cu	−0.03 Å		

In the complex cation the two Cu–O bond lengths are not equal; one is 2.73 Å, and the other, 2.45 Å. It is worthy of note that these values are within the range of 2.2—2.9 Å, the range[7] which is known as the axial Cu–O distance in the tetragonally-distorted octahedral geometry of Cu(II). Four nitrogen atoms of the bipyridine ligands are arranged around the copper atom in a flattened tetrahedral manner (Cu–N= 1.99 Å on the average); the copper atom lies almost on the least-squares plane defined by these nitrogen atoms, and the Cu–O bonds are approximately normal to this plane. This is attributable to the steric interference between the chelating ligands; since the $Cu(bipy)_2^{2+}$ moiety, as has been stated in the introduction, can not have a strictly coplanar structure, the two bipyridine molecules are forced to slant against one another, giving rise to the tetrahedral arrangement of their

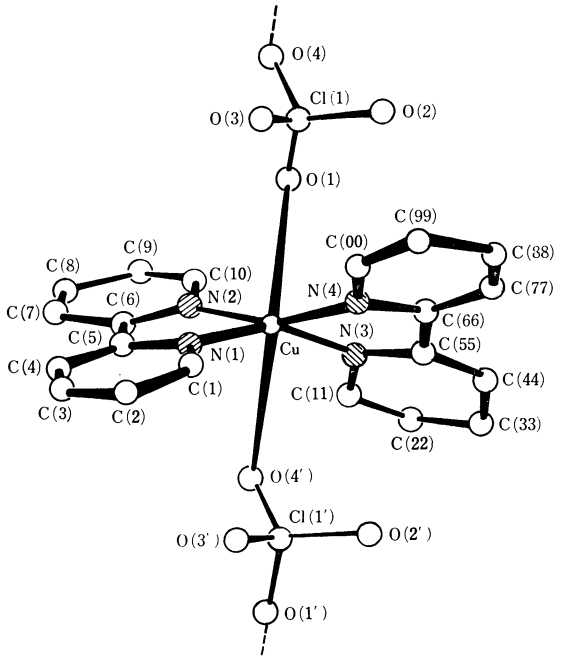

Fig. 3. A schematic drawing of a part of the infinite chain, $[Cu(ClO_4)(bipy)_2^+]_\infty$.

nitrogen atoms. The dihedral angle between the $Cu \begin{matrix} N(1) \\ N(2) \end{matrix}$ and $Cu \begin{matrix} N(3) \\ N(4) \end{matrix}$ planes is 37°.

As has been mentioned above, the axial Cu–O bonds are considerably longer than the Cu–N bonds; therefore, it is uncertain whether, in the strict sense, the oxygen atoms are in bonding with the copper atom or not. On the basis of the IR spectrum of $Cu(en)_2(ClO_4)_2$,[7] Hathaway and his coworkers inferred that the perchlorate anion is in "semi-coordination"[8] with the copper atom, irrespective of the Cu–O distance of 2.61 Å.[9] In the present compound, the distance of 2.45 Å between Cu and O(1) is significantly shorter than the Cu–O bond length in the ethylenediamine complex; hence, O(1) must be coordinated to Cu. Hathaway *et al.* investigated $Cu(bipy)_2(ClO_4)_2$, too. According to them, this compound gives a single broad reflectance band with a low intensity at 15.1×10^3 cm^{-1}, which is suggestive of a more tetragonally-distorted structure with an approximate center of symmetry, while it shows a single strong band at 1088 cm^{-1} and a weak band at 930 cm^{-1}, neigher of which is any evidence that ClO_4^- is coordinated or even semi-coordinated to Cu. Thus, they concluded that the compound should be formulated as $[Cu(bipy)_2](ClO_4)_2$ and that the complex cation has an essentially planar structure, although the two bipyridine ligands are twisted mutually by 10—30° towards a tetrahedral coordination This is not entirely in agreement with the result obtained in the present study regarding the aspect of the coordination of the ClO_4^- ion.

It should be remembered that the coexistence of the coordinating and uncoordinating ClO_4^- ions in the crystal would obscure the vibrational spectrum originating from the perchlorate anion and would make it difficult for them to establish the bonding feature of the anion. Considering such a situation as well as the presence of an approximate center of symmetry,[10] the present author should like to draw the following conclusion: having an appreciable influence on the chromophore $[CuN_4O(1)]$ with no center of symmetry, O(4') is possibly in "semi-coordination" with the copper atom, completing a distorted octahedron, though the Cu–O(4') distance is considerably longer than that of Cu–O(1). Thus, the complex could be regarded as hexa-coordinative.

The bipyridine ligands are not on a plane, but each individual pyridine ring is planar within the value of 0.03 Å. The pyridine rings of the bipyridine molecule are slightly twisted about the 2,2'-carbon bond by 13° and 4° for the molecules defined by N(1) and N(2) and by N(3) and N(4) respectively. Furthermore, the bond angle of α (123°) is larger than that of β by 7°, on the average. Although this value is not highly significant in view of its standard deviation, a similar difference in these bond angles (5—10°) is also observed in the crystal structures of the 2,2'-bipyridine molecule[11] and the bis-bipyridine complexes.[2-4,12]

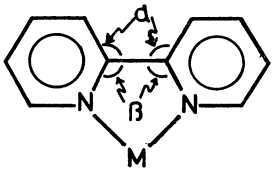

The average Cl–O bond length and O–Cl–O angle of the bridging ClO_4^- ion are 1.45 Å and 109.5° respectively, while those of the uncoordinating ClO_4^- anion are less accurate and can not be discussed in detail because of the distorted arrangement in the crystal lattice. The closest approach of the uncoordinating perchlorate ion to the bipyridine ligand is 3.25 Å between the O(11) and C(88) $[x, y, 1+z]$. This value is comparable with the O–C distance (3.24 Å) found in $[Cu(ONO)(bipy)_2]NO_3$.

The author wishes to thank Professor H. Kuroya, Dr. S. Ooi and Dr. Y. Kushi for their kind advices and encouragements throughout the present work. The author is also greatly indebted to Mr. K. Hirotsu, who adapted the HBLS-IV computer program[13] to the FACOM 270-30 computer at Osaka City University and granted me his kind permission of using it.

7) I. M. Procter, B. J. Hathaway, and P. Nicholls, *J. Chem. Soc., A*, **1968**, 1678.

8) D. S. Brown, J. D. Lee, B. G. A. Melson, B. J. Hathaway, I. M. Procter, and A. A. G. Tomlinson, *Chem. Commun.*, **1967**, 369.

9) A. Pajunen, *Suomen Kem.*, **40**, 32 (1967).

10) B. J. Hathaway, I. M. Procter, R. C. Slade, and A. A. G. Tomlinson, *J. Chem. Soc., A*, **1969**, 2219.

11) L. L. Merritt, Jr., and E. D. Schroeder, *Acta Crystallogr.*, **9**, 801 (1956).

12) M. Hinamoto, S. Ooi, and H. Kuroya, This Bulletin, **44** 586 (1971).

13) Y. Okaya and T. Ashida, HBLS-IV, "The Universal Crystallographic Computing System (I)," Japanese Crystallographic Association (1967), p. 65.

Stability Constants of Alkaline Earth Metals with *o*-Arsono-*o'*-hydroxy Azo Compounds

Kenyu KINA and Kyoji TÔEI

Department of Chemistry, Faculty of Science, Okayama University, Tsushima, Okayama

(Received February 25, 1971)

The acid dissociation constants of the *o*-arsono-*o'*-hydroxy azo compounds, and their chelate stability constants with alkaline earth metals, have been measured by the pH titration method at an ionic strength of 0.10 and at 25.0±0.1°C. These azo compounds were synthesized by the coupling reaction of diazotized *o*-aminophenylarsonic acid with naphthol sulfonates. As the coupling components, 1,8-dihydroxynaphthalene-3,6-disulfonic acid (chromotropic acid), 2-hydroxynaphthalene-3,6-disulfonic acid (R acid), and 1-hydroxynaphthalene-3,6-disulfonic acid were used. *o*-Arsonophenylazochromotropic acid (Neo-Thorin) formed the most stable chelates. It was concluded that the stabilization of the metal chelate ring of the Neo-Thorin was due to a quasi-aromaticity of the six-membered ring which was produced by the hydrogen bond between two naphtholic hydroxyl groups of chromotropic acid. The metal chelate stability order, Mg>Ca>Sr>Ba, is parallel to the reciprocal of the ionic radii of the metal ions.

According to Emi *et al.*,[1] the limit of the identification of the *o*-arsono-*o'*-hydroxy azo compounds depends of the coupling components rather than on the diazo components. Especially, the azo compounds of the chromotropic acid and the *R* acid, namely Neo-Thorin and thorin, are well-known as colorimetric reagents for Thorium. In general, the relation between the basicity of the coordinating site of the similar ligand and the metal chelate stability constants should present a good linearity from the standpoint of the Lewis acids and bases. The stability constants of the chelates which we have investigated, however, vary inversely with the basicity of the ligands. This result suggests the presence of a more significant factor than basicity. In this report, we will discuss these chelate systems from the electronic and structural points of view.

Experimental

Reagents. The azo compounds, 2-(2-arsonophenylazo)-1,8-dihydroxynapthalene-3,6-disulfonic acid disodium salt [Neo-Thorin], 1-(2-arsonophenylazo)-2-hydroxynaphthalene-3,6-disulfonic acid disodium salt [Thorin], and 2-(2-arsonophenylazo)-1-hydroxynapthalene-3,6-disulfonic acid disodium salt, were synthesized by the coupling reaction of diazotized *o*-aminophenylarsonic acid with the corresponding coupling components. These azo compounds were obtained as fine crystals.

In addition, a number of azo compounds for example, N.W. acid, and F acid, were obtained by the use of hydroxynaphthalene monosulfonic acid. These compounds, however, were not studied in this investigation because of their low solubility. A carbonate-free potassium hydroxide solution was prepared by the ion exchange method and was standardized titrimetrically against potassium hydrogen phthalate.

Reagent Solutions. The stock solutions of these ligands were standardized by potentiometric titration with standard 0.10 N potassium hydroxide. The stock solutions of magnesium, calcium, strontium, and barium were prepared by dissolving $Mg(NO_3)_2 \cdot 6H_2O$, $Ca(NO_3)_2 \cdot 4H_2O$, $Sr(NO_3)_2$, and $Ba(NO_3)_2$ of a guaranteed-reagent grade in distilled water. The concentration of the former two solutions was determined by chelatemetric titration,[2] while the concentration of the latter two was determined by the usual gravimetric method.

pH Titration Method. The measurements were carried out by the use of a micro-titration apparatus. The temperature was kept at 25.0±0.1°C throughout the titration by the circulation of water through a jacketed titration vessel with a capacity of 5 m*l*, and the ionic strength of the solutions was adjusted to 0.10 with potassium nitrate. Alkali was added from a calibrated 0.50 m*l* micrometer syringe to the solution in an atmosphere of nitrogen. The hydrogen-ion concentration was measured with an HRL-Model P pH meter (made by the Horiba Instruments Inc., Kyoto) equipped with a combined glass electrode (Metrohm, EA-125 U-type, Herisaw, Switzerland). The observed pH meter readings were converted into the actual hydrogen-ion concentrations by comparing them with the stoichiometric dissociation constant of acetic acid, which was obtained by titrating it before and after each measurement.[3] The pH ($-\log[H^+]$) region above 11.0 was calibrated by measurements of the KOH solution.[4]

Results and Discussion

Calculation of Acid Dissociation Constants and Chelate Stability Constants. The equilibria and the dissociation constants involved are:

$$H_3L \rightleftharpoons H_2L + H, \quad K_{a1} = [H][H_2L]/[H_3L],$$
$$H_2L \rightleftharpoons HL + H, \quad K_{a2} = [H][HL]/[H_2L],$$
$$HL \rightleftharpoons L + H, \quad K_{a3} = [H][L]/[HL],$$

where the ionic charge was neglected for the sake of convenience. The titration curve shows a well-defined inflection at $a=1$; therefore, the first dissociation step of this triprotic acid can be treated separately form the last two steps. The region before $a=1$ was treated as monoprotic acid, while after $a=1$ it was treated as diprotic acid. In general, the following relationship represents the step-by-step acid dissociation constant of the polyprotic acid:

1) K. Emi, K. Tôei, and K. Furukawa, *Nippon Kagaku Zasshi*, **79**, 681 (1957).

2) K. Ueno, "Chelatemetric Titration" (in Japanese), Nankodo, Tokyo (1967).

3) C. F. Richard, R. L. Gustafson, and A. E. Martell, *J. Amer. Chem. Soc.*, **81**, 1033 (1959).

4) H. S. Harned and B. B. Owen, "The Physical Chemistry of Electrolytic Solutions," 3rd. Ed., Reinhold Publ. Corp., N. Y. (1958), p. 752.

$$\sum_{i=1}^{n} \frac{iT_L - f}{f[H]^i} K_{a1} \cdot K_{a2} \cdot \cdots \cdot K_{ai} = 1,$$

$$f = (T_{OH} + [H] - [OH]),$$

where T_L represents the total concentration of ligand species and where T_{OH} represents the total concentration of the base added to the system. In all the calculations, the concentrations were corrected for the volume change resulting from the addition of the potassium hydroxide solution; the calculation formula of the monoprotic acid is as follows:

$$\frac{T_L - f}{f[H]} K_{a1} = 1,$$

while in the case of diprotic acid it is as follows:

$$\frac{2T_L - f}{f[H]^2} K_{a1}K_{a2} + \frac{T_L - f}{f[H]} K_{a1} = 1.$$

From the above equation, the dissociation constants, $K_{a1}K_{a2}$ and K_{a1}, were calculated by solving the simultaneous equation from two points on the ligand-only titration curve.

The chelate stability constants were calculated by means of the following equations:

$$K_{ML} = (T_L - F)/[L](F + T_M - T_L).$$

where

$$L = (3T_L - T_{OH} - [H] + [OH])/[H]/K_{a3} + 2[H]^2/K_{a3}K_{a2} + 3[H]^3/K_{a3}K_{a2}K_{a1},$$

$$F = [L]\{1 + [H]/K_{a3} + [H]^2/K_{a3}K_{a2} + [H]^3/K_{a3}K_{a2}K_{a1}\},$$

and where T_M represents the total concentration of the metal species. All the calculations were carried out by using an NEAC-2203 computer (The Nippon Electric Co., Ltd.) of the Electronic Computer Center of Okayama University. The *o*-arsono-*o'*-hydroxy azo compounds are numbered as follows:

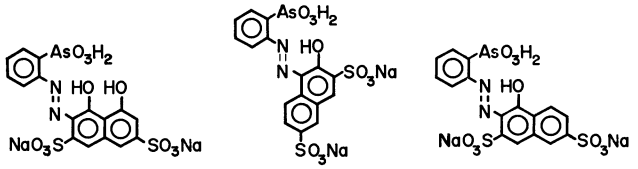

I II III

Titration Curves. The pH titration curves are illustrated in Figs. 1—3 for *o*-arsono-*o'*-hydroxy azo compounds, both on chelate systems and for each ligand alone. The dissociation constants, pK_{a1} and pK_{a2}, of phenylarsonic acid have been reported to be 3.39 and 8.25 respectively,[5] the clear inflections at $a=1$ and $a=2$, therefore, correspond to the dissociation of two arsonic protons. The pK_a value of an naphthlic proton is of an order of magnitude of 10, and this proton gives no inflection after $a=2$. The titration curve in the presence of a metal ion shows a lower pH value than in the presence of the ligand only. Such a depression of the titration curves indicates the formation of metal chelate species. The chelate stability order, Mg>Ca>Sr>Ba, can be readily

5) S. Nakashima, H. Miyata, and K. Tôei, This Bulletin, **41**, 2632 (1968).

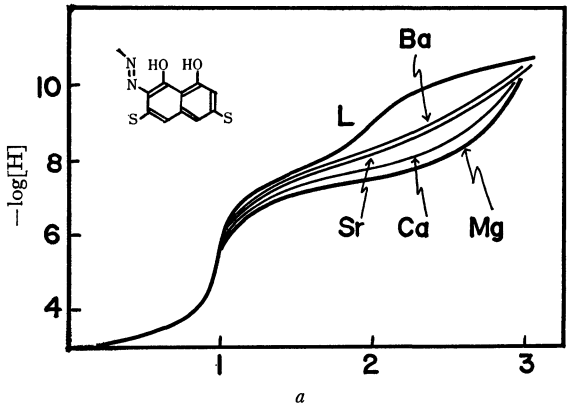

Fig. 1. Titration of 2-(2-arsonophenylazo)-1,8-dihydroxynaphthalene-3,6-disulfonic acid disodium salt and its chelate system at 25°C, $\mu=0.10$.
L, Ligand only; a=moles of base added per mole of ligand.
[Ligand]$=2.411\times10^{-3}$M, [Mg]$=2.216\times10^{-3}$M, [Ca]$=2.256\times10^{-3}$M, [Sr]$=2.078\times10^{-3}$M, [Ba]$=2.048\times10^{-3}$M.

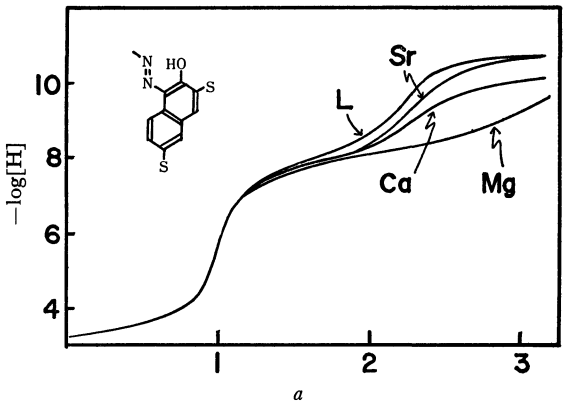

Fig. 2. Titration of 1-(2-arsonophenylazo)-2-hydroxynaphthalene-3,6-disulfonic and disodium salt and its chelate system at 25°C, $\mu=0.10$.
L, ligand only, [Ligand]$=1.734\times10^{-3}$M; a=moles of base added per mole of ligand.
The metal ions concentration are indentical to those described in Fig. 1.

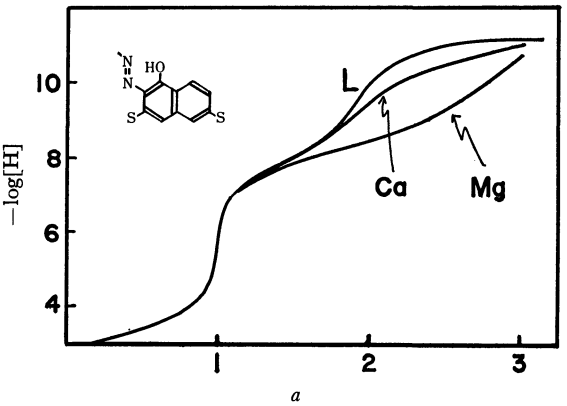

Fig. 3. Titration of 2-(2-arsonophenylazo)-1-hydroxynaphthalene-3,6-disulfonic acid disodium salt and its chelate system at 25°C, $\mu=0.10$.
L, Ligand only, [Ligand]$=2.452\times10^{-3}$M. The metal ions concentration are identical to those dercribed in Fig. 1.
a=moles of base added per mole of ligand.

TABLE 1. ACID DISSOCIATION CONSTANTS OF *o*-ARSONO-*o'*-HYDROXY AZO COMPOUNDS AND STABILITY CONSTANTS OF THEIR CHELATES
(t=25.0±0.10°C; μ=0.10 by KNO_3)

Ligand	Acid dissociation constants				Stability constants, log K_{ML}			
	pK_{a1}	pK_{a2}	pK_{a3}	pK_A	Mg	Ca	Sr	Ba
I	2.93	7.65	10.15	20.73	5.57	5.20	4.39	4.22
II	3.44	7.86	10.80	22.10	5.20	4.17	2.87	—
III	3.09	8.05	11.40	22.54	5.35	3.50	2.0	1.8

where $K_{a_1}=[H][H_2L]/[H_3L]$, $K_{a_2}=[H][HL]/[H_2L]$, $K_{a_3}=[H][L]/[HL]$, $K_{ML}=[ML]/[M][L]$.
— not measurable owing to precipitation

expected from the extent of the depression of pH. Evidently, Compound I formed a more stable chelate with Ca, Sr, and Ba than did the other two.

Acid Dissociation Constants. In Table 1, the pK_{a1} and the pK_{a2} values correspond to the dissociation of the arsonic group, while the pK_{a3} value corresponds to the dissociation of the naphtholic hydroxyl group. The overall acidity of the ligands is defined as the sum of the dissociation constants, $pK_A=(pK_{a1}+pK_{a2}+pK_{a3})$; therefore, the larger the pK_A value, the more basic the ligand. The basicity of the ligand increases as follows: Compound I<Compound II<Compound III. As Fig. 4 shows, there exists a strong hydrogen bond between the two oxygen atoms of the Compound I; this naphtholic hydroxyl group, therefore, does not dissociate under ordinary experimental conditions.[5] The pK_{a3} which corresponds to the dissociation of the first hydroxyl proton of Compound I is 10.15, a value lower than those of Compounds II and III. This higher acidity is also attributed to a strong intramolecular hydrogen bonding, which could stabilize the deprotonated anion. Actually, Compound II shows a higher basicity, because it can not form any hydrogen bond such as shown in Fig. 4.

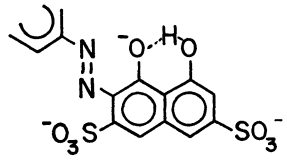

Fig. 4. Structure of hydrogen bonding.

Stability Constants. The chelate stability constants are also listed in Table 1. The stability constant of Compound II with the barium ion was not obtained because of precipitation. In general, the alkaline earth metals form an ionic coordination bond; the relation of the stability constants, $\log K_{ML}$, to the reciprocal of the ionic radii, $1/r$, of alkaline earth metals is given in Fig. 5. The stability constants increase with a decrease in the ionic radii; that is, the decrease in the order of the metal chelate stability is as follows: Mg>Ca>Sr>Ba. The stability order relation to the ligands, except the Mg chelates, is as follows: Compound I>Compound II>Compound III. According to the concept of Lewis acids and bases, the strong basic ligand would form the more stable chelate compound. However, the metal chelate stability constants of these compounds vary inversely with the basicities of the ligands.

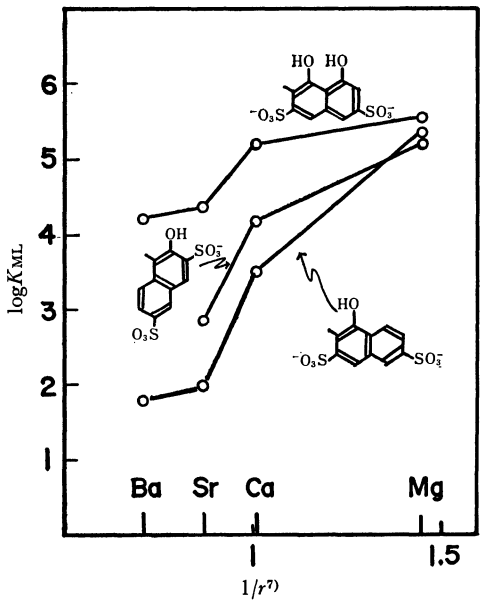

Fig. 5. Relation between $\log K_{ML}$ of the chelate of *o*-arsono-*o'*-hydroxy azo compounds and the reciprocal of the ionic radii.[7]

Such a difference depends largely on the nature of the naphtholic hydroxyl group. The chelate structure of Compound I may be as follows:

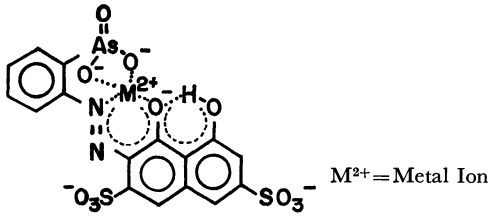

From the results of the measurement of the visible spectra of the free ligand, the λ_{max} values of Compounds I, II, and III are 505 mμ, 484 mμ, and 484 mμ, respectively; thus, Compound I indicates a bathochromic shift. This bathochromic effect of Compound I may be caused by the six-membered hydrogen bond ring acquiring a quasi-aromaticity which is similar to that of β-diketone derivatives.[6] As was shown in the above scheme, such a quasi-aromaticity is extremely advantageous for the stabilization of the six-membered chelate ring by means of the resonance effect.

6) K. Nakamoto, P. J. McCarthy, and A. E. Martell, *J. Amer. Chem. Soc.*, **83**, 1272 (1961).
7) W. M. Latimer, *J. Chem. Phys.*, **23**, 90 (1955).

TABLE 2. ACID DISSOCIATION CONSTANTS AND STABILITY CONSTANTS OF THE METAL CHELATES OF THE CATECHOL DERIVATIVES[8]

Ligand	pK_a	pK_a	Zn		Cu	
			$\log K_1$	$\log K_2$	$\log K_1$	$\log K_2$
Catechol	9.13	11.59	8.46	6.78	12.52	9.66
Catechol-4-sulfonate	8.26	12.16	9.40	7.20	13.29	10.23
Tiron	7.54	12.23	10.19	8.33	13.99	11.17

where $K_1=[ML]/[M][L]$, $K_2=[ML_2]/[L][ML]$

In the cases of Compounds II and III, they have lower $\log K_{ML}$ values than does Compound I because such an effect (the resonance effect) is absent. In the chelate system in which the resonance effect exerts a significant influence upon the chelate stability, the presence of a substituent group that increases the electron density of the donor atoms results in a decrease in the stability of the chelate ring. For example, the stability of the acetoacetic ester chelate is lower than that of the acetylacetone chelate. This has been explained on the basis of the electron-donating behavior of the ester group.[9] On the contrary, such a chelate system is stabilized by the presence of a electron-withdrawing group. A typical example of this can be seen in the Tiron. As Table 2 shows, the zinc or copper chelate of the Tiron is more stable than that of catechol or catechol-4-sulfonate, though the Tiron is less basic than the others. This phehomena shows that the localized electron on the oxygen atoms is dispersed by the sulfonate group; that is, such a stabilization may be due to the electron delocalization. From the structrural point of view, Compound II has a sulfonate group adjacent to the naphtholic hydroxyl group, as does the Tiron; therefore, Compound II forms a more stable chelate with Ca and Sr than does Compound III. This stabilization of the chelate ring may be the sulfonate group. As has been mentioned above, the main factor influencing the chelate stability is the nature of the naphtholic hydroxyl group with respect to calcium, strontium, and barium. On the other hand, the order of decrease in the stability constants of magnesium chelates is as follows: Compound I>Compound III>Compound II, although there is little difference among them. This order differs from the above-mentioned order. As is shown in Fig. 5, the magnesium ion has a much smaller ionic radius than those of calcium, strontium, and barium. Its chelating behavior, therefore, differs from that of the other alkaline earth metals. The stabilities of magnesium chelates are not greatly affected by the nature of the naphtholic hydroxyl group, but they are affected by its small ionic radius.

8) Y. Murakami, K. Nakamura, and M. Tokunaga, This Bulletin, **36**, 669 (1963).

9) A. E. Martell and M. Calvin, "Chemistry of the Metal Chelate Compounds," translated by M. Kobayashi, M. Fujimoto, and K. Mizumachi, lst. Ed., Kyoritsu Publ. Corp., Tokyo (1960), p. 136.

Analytical Study of the Lead Ion-selective Ceramic Membrane Electrode

Hiroshi HIRATA and Kenji HIGASHIYAMA

Wireless Research Laboratory, Matsushita Electric Industrial Co., Ltd., Kadoma, Osaka

(Received February 27, 1971)

The lead(II) ion-selective ceramic membrane electrode developed by sintering a mixture of lead, silver, and cuprous sulfides showed sensitivity, selectivity, and other response characteristics well suited to analytical utilization. The Nernstian slope was obtained over a concentration range from 10^{-1} to 10^{-6}M Pb^{2+} in activity, and the analytical range had a concentration of 10^{-1}—10^{-7}M when the membrane contained less than 30 wt% of cuprous sulfide and more than 1 wt% of lead sulfide. Among the common ions, silver, cupric, mercury(II), ferric, sulfide and iodide ions interfered seriously. About 10 times as many cadmium and bromide ions and more than 1000 times as many alkali metal, alkaline earth metal, zinc, aluminum, nickel, manganese(II), cobalt, and nitrate ions did not interfere with the lead ion, however. The electrode potentials did not change over a pH range from 2 to the pH at which the precipitation of lead hydroxide occurred. The electrode was safely used at temperatures from 0 to 95°C, and the potentials of the membrane satisfied the Nernstian equation within the limits of experimental error. The membrane electrode responded to activity changes very quickly: the rate of those changes was twice that in a lead sulfide-silver sulfide two-component ceramic electrode. A continuous potential measurement for 5 months promised long-term stability and accuracy. The rapid response rate and the long lifetime suggest that the continuous monitoring of some changing systems is feasible.

Ion-selective solid-state membrane electrodes can be classified conveniently into the following main groups: a single crystal membrane electrode, such as a fluoride ion-selective europium-doped lanthanum fluoride electrode:[1] a compacted polycrystalline electrode, where the membrane consists of a disc of a water-insoluble active material: a heterogeneous-membrane electrode, the so-called Pungor type, in which the active material is impregnated in an inert binder or matrix such as silicone rubber, and a glass electrode similar in principle and structure to a conventional glass pH electrode.[4]

For the lead ion-selective solid-state membrane electrode, a compacted polycrystalline electrode[5] has recently been developed by Orion Research, Inc.: here the membrane consists of lead sulfide incorporated with silver sulfide. A lead sulfide-impregnated silicone rubber membrane electrode[6] has since been prepared.

No electrode membrane has, however, yet been obtained by a sintering process, although a halide ion-sensitive electrode membrane was made by casting silver halide[7] and/or by hot-pressing a mixture of silver halide and a powdered thermoplastic polymer.

In our laboratory, a new type of cuprous sulfide ceramic membrane electrode which can be used for the measurement of cupric ion activity[9] has been prepared, and subsequently a lead sulfide ceramic electrode membrane incorporated with silver and cuprous sulfides has been developed.[10] The lead ion-selective electrode membrane obtained by a hot-pressing method permited lead-ion determination over a concentration range from 10^{-1} to 10^{-7} mol/*l*. In a previous paper, the relationship of the potential *vs.* the concentration curves and the compositions of the ceramic membranes was described. The present work was undertaken to provide some quantitative information regarding the analytical usefulness of a ceramic membrane electrode containing a mixture of lead, silver, and cuprous sulfides as the membrane for measuring the lead-ion concentration.

Experimental

Apparatus. An Orion model 801 digital pH meter was used for all the potentiometric measurements. The reference electrode was a Horiba Seisakusho model 2530-05T saturated calomel electrode to prevent contamination from a test solution.

The electric furnace for the preparation of the raw materials and the hot-pressing apparatus for making an electrode membrane were the same as previously reported.[10]

Chemicals. The lead, silver, copper, and sulfur were commercially-available materials, as pure as possible. The raw materials, PbS, Ag_2S, and Cu_2S, for preparing the membranes were obtained by the direct reaction of the corresponding metal with sulfur, as has previously been described.[10]

A stock solution of the 0.1M Pb^{2+} ion was prepared by direct weighing from Nakarai reagent-grade $Pb(NO_3)_2$ and was stored in polyethylene reagent bottles. A series of standard solutions of the lead ion was prepared by the suitable dilution of the stock solution, keeping the ionic strength of 0.1M by the addition of appropriate volumes of a 1M sodium nitrate solution. All the other chemicals were of Nakarai reagent grade and were used without further purification. The nitric acid and sodium hydroxide solutions were used to adjust the pH of the standard solutions. All the solutions were prepared from water which had been both deionized and distilled.

Preparation of the Ceramic Membrane. The ceramic membrane was obtained by the following two methods:

(1) A mixture of lead, silver, and cuprous sulfides was compressed and then sintered at 350—500°C for 3 hr in a hydrogen sulfide gas stream, and

(2) A mixture of lead, silver, and cuprous sulfides was

1) M. S. Frant and J. W. Ross, *Science*, **154**, 1553 (1966).
2) T. M. Haeu and G. A. Rechnitz, *Anal. Chem.*, **40**, 1058 (1968).
3) E. Pungor, *ibid.*, **39**, 28A (1967). H. Hirata and K. Date, *Talanta*, **17**, 883 (1970).
4) A. K. Convington, Current awareness, No. 15, 393, (1969).
5) J. W. Ross and M. S. Frant, *Anal. Chem.*, **41**, 967 (1969).
6) H. Hirata and K. Date, *ibid.*, **43**, 279 (1971).
7) I. M. Kolthoff and H. L. Sanders, *J. Amer. Chem. Soc.*, **59**, 416 (1937).
8) M. Mascini and A. Liberti, *Anal. Chim. Acta*, **47**, 339 (1969).
9) H. Hirata, K. Higashiyama, and K. Date, *ibid.*, **51**, 209 (1970).
10) H. Hirata and K. Higashiyama, *ibid.*, **54**, 415 (1971).

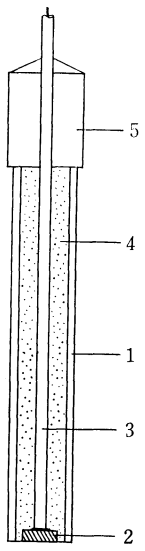

Fig. 1. Cross-section of lead ion selective ceramic membrane electrode.
1. stem 2. ceramic membrane 3. leading wire
4. insulator (epoxy resin) 5. cap

compressed and subsequently hot-pressed at 350—400°C for 2 hr under a pressure of 3—7 ton cm^{-2}.

Preparation of the Electrode. A cross-section of the lead(II) ion-selective ceramic membrane electrode is shown in Fig. 1. The ceramic membrane was fastened directly with a leading wire, and then mounted with epoxy resin adhesive in a stem of unbreakable epoxy resin, which is highly resistant to acids, bases, and organic solvents. The internal electrode and solution which are commonly used in usual selective electrodes, such as a glass pH electrode or a liquid ion-exchanger electrode, were eliminated in order to avoid any internal contamination of the membrane and in order to simplify the structure of the electrode. Then, the membrane surface was polished with diamond paste and washed with an ultrasonic wave cleaner.

Procedure. Potentiometric measurements for drawing the calibration curves were carried out in the conventional manner. The potentials developed by the membrane electrode were measured at 25.0 ± 0.1°C with a saturated calomel electrode as the reference electrode. Magnetic stirring was employed. The electrode potentials were attained rapidly, and in every case the equilibrium potentials were read within 2 min after the immersion of the electrodes into the standard solution. The reproducibility for different solutions with the same lead-ion concentration was within ± 0.5 mV if the electrode surface was kept clean and the stirring rate was constant.

Dynamic response curves were obtained after the rapid concentration or dilution of the standard solution by the addition of more concentrated lead nitrate or 0.1 M sodium nitrate solutions. In all cases, the resulting potentials *vs.* time curves were smooth and reproducible after the initial mixing period (the pH and ionic strength were kept constant).

Results and Discussion

Response of the Membrane Electrode to the Lead(II) Ion. In general, the mechanism of the response of solid-state electrodes is not so well understood as that of glass or liquid ion-exchanger membrane electrodes; by an analogical consideration of the glass membrane electrode, the ion-exchange theory[11] has been applied directly to the solid-state membrane electrode. Pungor[3] demonstrated with radiochemical methods that the rate of the iodide-ion exchange at the membrane-solution interface was very fast when a silver iodide-impregnated silicone rubber membrane was used. Buck[12] has presented such a theory assuming a rapid, reversible ion exchange at the membrane interfaces and mobile defects within the membrane crystal. While it is at least highly probable that these are necessary conditions for the operation of a solid-state ion-selective membrane electrode, experimental evidence supporting this theory has not been available for many solids now in use as membrane materials. It is especially very difficult to adapt this theory to a complicated mixed crystalline membrane electrode such as the present ceramic membrane electrode.

On the operation mechanism for an electrode such as a silver sulfide - cupric sulfide - compacted membrane electrode, Rechnitz *et al.*[13] suggested that this membrane was an ionic conductor which allowed the silver ion to pass and that this electrode transported the charge by the movement of silver ions, but the potential was determined indirectly by means of the availability of S^{2-}, which, in turn, was fixed by the activity of the divalent metal in contact with the membrane. Certainly, a pure lead sulfide ceramic membrane, in which no trace of silver could be detected by qualitative emission spectroscopy, as has previously been reported, proved non-responsive to the lead ion, but an impure lead sulfide ceramic membrane containing less than 0.01 wt% of silver was rather more sensitive than a pure one, and a membrane with 1% of silver sulfide added exhibited 27 mV for each ten-fold change in the lead-ion activity. Nevertheless, a very pure lead sulfide-impregnated silicone rubber membrane electrode was readily sensitive to lead ion activity without any trace of silver sulfide and showed sufficient selectivity among other cations or anions in spite of the fact that pure lead sulfide was not an ionic but an electronic semiconductor.

Recently, Brand and Rechnitz[14] have made impedance measurements of the electrode membranes. In the case of an electrode fabricated from a compacted disc containing a mixture of lead and silver sulfides, it was found that there was no net ion transport across the membrane cell, and that charges were built up at the membrane-solution interface, producing a capacitative effect. Such ion-blocking at the interface includes the absence of an ion-exchange reaction (ionic conduction within the membrane) or the absence of a charge-transfer reaction (electronic conduction within the membrane).

However, it is quite difficult, from the above point of view, to clarify the specific ion-selectivity and the effect of incorporation by silver sulfide.

Further investigations of the mechanism of the mixed crystalline membrane electrode were not, however,

11) G. Eisenman, *Anal. Chem.*, **40**, 310 (1968).
12) R. P. Buck, *ibid.*, **40**, 1432, 1439 (1968).
13) G. A. Rechnitz, *Instrumentation*, **41**, (12), 109 (1969).
14) M. J. D. Brand and G. A. Rechnitz, *Anal. Chem.*, **42**, 478 (1970).

carried out in the present study.

Calibration Curves. The experimental cell can be represented as:

$$\text{Lead ion-sensitive electrode} \left| \begin{matrix}\text{test solution} \\ \mu=0.1\ (NaNO_3)\end{matrix} \right\| 0.1\text{M } NaNO_3 \left| \text{SCE} \right.$$

The potential of this cell is given by:

$$E = \text{constant} + 2.303(RT/2F) \log a_{Pb^{2+}},$$

where the "constant" is the sum of the potentials at the leading wire-membrane contact interface, the saturated calomel electrode and the liquid-junction potential between a test solution and the reference electrode, and the potential across the membrane, when the silver-ion activity in the test solution is unity. Since the measurements were carried out at a constant ionic strength of 0.1 M, the junction potential was kept approximately constant.

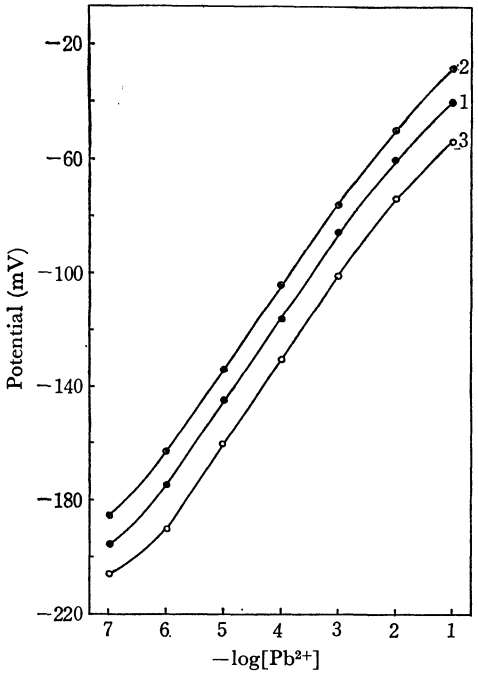

Fig. 2. Potential *vs.* concentration curves for the membranes prepared by hot-pressing method (at 370°C, for 2hr and under a pressure of 7 ton cm^{-2}).

1. PbS 30% Ag_2S 65% Cu_2S 5%
2. PbS 50% Ag_2S 40% Cu_2S 10%
3. PbS 80% Ag_2S 16% Cu_2S 4%

The actual potential of the ceramic membrane electrode *vs.* the saturated calomel electrode as a function of the lead-ion concentration is demonstrated in Fig 2. A straight line has been drawn, over a range of lead-ion activities from 10^{-1} to 10^{-6}M, with a slope of 29.5 mV per log [Pb^{2+}] unit. This value is in agreement with that predicted by the Nernst relationship. The experimental results suggest that the ceramic electrode membrane material used in the indicator electrode and the applied sintering process were very effective. Moreover, the analytical range of this electrode, as depicted in Fig. 2, was a concentration of 10^{-1}—10^{-7} mol/*l*.

Dynamic Response Characteristics. When an ion-selective membrane electrode is utilized for the concentration control of a reaction process or as an indicator electrode in the potentiometric titration, the dynamic-response characteristic is a very important factor. The response characteristics of the lead ion-sensitive membrane electrode were evaluated by exposing the electrode to a rapid change in lead-ion concentration (approximately twofold) and by recording the resulting e.m.f. *vs.* time function. The dynamic-response experiment was carried out with hot-pressed ceramic membranes containing 30, 50, and 80 wt% of lead sulfide. Some of the resulting response curves typical of the results obtained, are represented in Fig. 3.

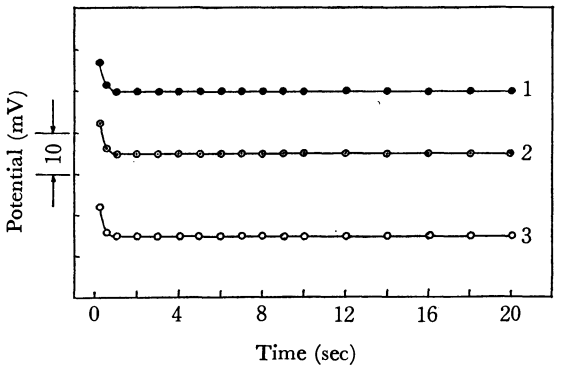

Fig. 3. Dynamic response curves.
Membranes for the curves 1, 2, and 3 are identical with those numbered in Fig. 2 in the compositions and preparation conditions respectively.

All the curves were smooth and of an identical shape; the expected (on the basis of calibration curves) e.m.f. value was attained in all cases. The response half-time $t_{1/2}$ of the electrode used depends on the stirring method, the efficiency of the solution mixing, and the cleanliness of the electrode surface, but it is independent of the initial lead-ion concentrations over the entire range studied. The response half-times obtained are of an order of less than one second for the present experimental conditions and are probably determined mainly by the mixing efficiency. Since the electrode used is an extremely low-solubility ceramic ionic semiconductor (the electrical resistance is less than 100 ohm-cm), the rapid response to changes in the lead-ion concentration is not unexpected. The high response rate of this electrode suggests that a continuous monitoring of lead-ion activities in aqueous solutions would be feasible.

Influence of pH. Figure 4 shows the influence of the pH on the lead ion-selective ceramic membrane electrodes in 10^{-2}, 10^{-4}, and 10^{-6}M Pb^{2+} solutions. The potentials did not change at pH values below 6.5. They did, however, decrease sharply when the pH increased above 6.5, for the precipitation of $Pb(OH)_2$ occurred. Of course, the pH at which the precipitation begins depends on the concentration of the lead ion. The resulting curves in Fig. 4 also show that the measurable pH range is independent of the lead-sulfide content in the membrane. However, the membrane containing much more than 50% of lead sulfide dissolved and the potential become unstable at a lead-ion concentration lower than 10^{-6} mol/*l*, when it was

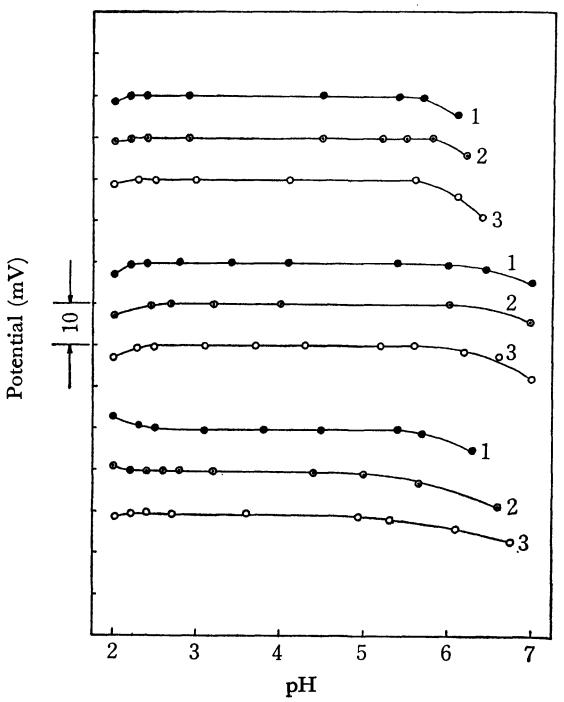

Fig. 4. Influence of the pH.
Membranes corresponding to the numbers of the curves are the same as those of Fig. 2 in their preparation conditions and compositions.

exposed in a solution with a pH below 2 for a long time.

Selectivity. No electrode is entirely selective towards a particular ion, and the presence of other ions may seriously impair electrode performance. It is, therefore, important to be aware of such interferences. An approximate selectivity constant can be derived experimentally from the ratio of ionic concentrations where the interfering ion causes deviation from the expected theoretical ($2.303\,RT/2F$) slope.[3]

Tests of the effects of several ions *e.g.* Ag^+, Cu^{2+}, Hg^+, S^{2-}, Fe^{3+}, I^-, Cd^{2+}, Br^-, alkali metal, alkaline earth metal, Zn^{2+}, Al^{3+}, Ni^{2+}, *etc.* on the lead ion-selective ceramic membrane prepared by the hot-pressing method were made in solutions containing 10^{-4}M of lead ions. The concentration ratios of common ions to lead ion were varied from 1 to 1000, Among the common ions, silver, cupric, mercury(I), ferric, sulfide, and iodide ions interfered seriously. About 10 times as many cadmium and bromide ions and more than 1000 times as much alkali metal, alkaline earth metal, zinc, aluminum, nickel, manganese(II), cobalt, and nitrate did not interfere with the lead ion. The lead-sulfide content in the ceramic membrane was independent of the selectivity in the present experimental range.

The numerical selectivity ratios of the electrode for the lead ion with respect to these common ions were not evaluated, but, in view of this finding, it is clear that this electrode is well suited for the selective analytical measurement of lead-ion activity in a wide variety of practical systems.

Effect of the Temperature. The electrode was safely used at temperatures from 0 to 95°C, and the potentials of the membrane satisfied the Nernstian equation within the limits of experimental error.

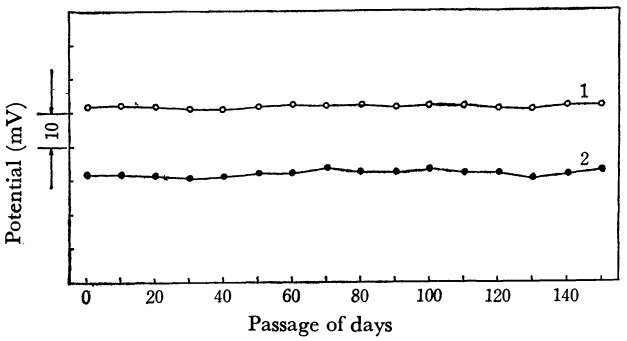

Fig. 5. Long term stability of the membranes hot-pressed at 370°C, for 2hr and under 7 ton cm^{-2}, containing
1. PbS 30% Ag_2S 65% Cu_2S 5%
2. PbS 50% Ag_2S 40% Cu_2S 10%

Lifetime. A continuous potential measurement was made using a hot-pressed ceramic membrane electrode in a specially-designed sample circulation cell. Figure 5 demonstrates that the ceramic membrane electrode had a very long lifetime and that the long-term stability and accuracy was well suited to the continuous monitoring of lead-ion activities in an aqueous solution in relation to the rapid response to changes in the lead-ion concentrations.

The authors thank Drs. S. Kisaka, K. Sugihara, and S. Hayakawa for their encouragement in this work. Thanks are also due to Messrs. T. Miyazawa and H. Yamao for X-ray analysis and microscopic photograph of the electrode membrane.

The Preparation and Absorption Spectra of the Geometrical Isomers of Carbonatoglycinatodiamminecobalt(III)[1]

Shuji KANAZAWA and Muraji SHIBATA

Department of Chemistry, Faculty of Science, Kanazawa University, Kanazawa

(Received March 1, 1971)

Three geometrical isomers of the $[CoCO_3(gly)(NH_3)_2]$ complex, the *mer*(*cis*-diammine)-, *mer*(*trans*-diammine)-, and *fac*-isomers, have been isolated from a reaction mixture of the *cis*-$[Co(CO_3)_2(NH_3)_2]^-$ ion with glycine by means of a study of the solubility difference and by means of ion-exchange chromatography. These isomers have been characterized by the absorption spectra, the PMR spectra, and the infrared spectra. The absorption spectrum of the *mer*(*trans*)-isomer is of special interest, and there is a clear shoulder in the second absorption band region which may be due to the splitting of the second band.

Recently there has been interest in the absolute configurations of the *tris*(α-amino-acid) complexes of cobalt(III)[2-5] and also their stereoselectivities.[4,6,7] In preparing such complexes, it has been recognized that the method using the tricarbonatocobaltate(III) anion as the starting material is of use in the preparation of possible isomers for a *tris*(α-amino-acid) complex.[3,4,7,8] In the present work we undertook to use the dicarbonatodiamminecobaltate(III) anion[9,10] in the preparation of the carbonatoglycinatodiamminecobalt(III) complex. This complex, like the *tris*(amino-acid) complexes, belongs to the general type of $[CoN_3O_3]$ and is expected to have three geometrical isomers, two of *mer* and one of *fac*. We succeeded in obtaining the three isomers from a reaction mixture of the starting material with glycine by studying the solubility difference and by ion-exchange chromatography. The isomers obtained were characterized mainly by the electronic absorption and proton magnetic resonance spectra. By the way, the corresponding ethylenediamine complexes of the [Cogly(chelate)en] type (the chelate represents CO_3^{2-}, $C_2O_4^{2-}$ or the malonate ion) have already been synthesized by Matsuoka *et al.*[11]

Experimental

Preparation. In a solution of 4 g (0.015 mol) of potassium *cis*-dicarbonatodiamminecobaltate(III)[9,10] in 10 m*l* of water, an equimolar amount (1.2 g) of glycine was dissolved. The mixture was then stirred at room temperature for 10—12 hr. During this reaction, a considerable amount of fine red crystals were precipitated. The crystals were collected by filtration and recrystallized from water containing a small amount of potassium bicarbonate. A portion of the filtrate was added to a cation-exchange column containing 100—200 mesh Dowex 50W×8 resin in the sodium form (diameter, 4.5 cm; resin height, 25 cm). When water was passed through the column at a rate of about 10 m*l*/min, four red-violet bands appeared. The first band consisted of negatively-charge complexes, such as $[Co(CO_3)_2(NH_3)_2]^-$ and $[CoCO_3(gly)_2]^-$. The other three bands were isomers of the desired complex; hence, they were collected in three fractions. The fractions were conveniently numbered Nos. 1—3 in the descending order of the bands. This chromatographic separation was repeated several times in order to treat all the reacted solution. Each fraction was then concentrated to a small volume under reduced pressure at about 40°C. When a small amount of ethanol was added to the concentrate and the whole was kept in a refrigerator for one day, the desired material was precipitated. Recrystallization was done from water containing a small amount of potassium bicarbonate. The compound which had precipitated during the process of reaction was identical with that obtained from the No. 2 fraction, and the former by far exceeded the latter in yield (1 g for the former, and 0.2 g for the latter). For the other compounds, the yields were 0.4 g from the No. 1 fraction and and 0.6 g from the No. 2 fraction.

Found for the complex from No. 1: C, 14.65; H, 4.82; N, 17.12. Calcd for $[CoCO_3(C_2H_4NO_2)(NH_3)_2]\cdot H_2O$: C, 14.70; H, 4.90; N, 17.15%.

Found for the complex from No. 2: C, 13.96; H, 4.94; N, 15.96. Calcd for $[CoCO_3(C_2H_4NO_2)(NH_3)_2]\cdot 2H_2O$: C, 13.70; H, 5.30; N, 15.97%.

Found for the complex from No. 3: C, 14.60; H, 4.51; N, 17.25. Calcd for $[CoCO_3(C_2H_4NO_2)(NH_3)_2]\cdot H_2O$: C, 14.70; H, 4.90; N, 17.15%.

Measurements. The absorption spectra were usually measured with a Hitachi EPU-2A spectrophotometer, but sometimes with a Cary-14 spectrophotometer by way of precaution. The infrared spectra were measured as KBr disks with a Jasco DS-301 spectrometer (4000—700 cm^{-1}) and also with a Hitachi EDI spectrometer (700—250 cm^{-1}). The proton magnetic resonance (PMR) spectra were recorded on a JEOL C-60H spectrometer operating at 60 Mc/sec. The spectra were measured in deuterated trifluoroacetic acid, using tetramethylsilane as the internal standard. The molar conductivity was measured with a Universal Bridge BV-Z-12A, using a 5×10^{-3}M aqueous solution. The absorption spectra of a single crystal were measured through the good offices of Professor Y. Kondo of Rikkyo University.

Results and Discussion

Although the chromatographic behavior described in the experimental section was evidence for the non-

1) Presented in part at the 23rd Annual Meeting of the Chemical Society of Japan, Tokyo, April, 1970.

2) B. E. Douglas and S. Yamada, *Inorg. Chem.*, **4**, 1561 (1965).
3) J. H. Dunlop and R. D. Gillard, *J. Chem. Soc.*, **1965**, 6531.
4) R. G. Denning and T. S. Piper, *Inorg. Chem.*, **5**, 1056 (1966).
5) M. Shibata, H. Nishikawa, and Y. Nishida, *ibid.*, **7**, 9 (1968).
6) R. D. Gillard and N. C. Payne, *J. Chem. Soc.*, *A*, **1969**, 1197.
7) K. Kawasaki, J. Yoshii, and M. Shibata, This Bulletin, **43**, 3812 (1970).
8) M. Shibata, H. Nishikawa, and K. Hosaka, *ibid.*, **41**, 130 (1968).
9) M. Mori, M. Shibata, E. Kyuno, and K. Hoshiyama, *ibid.*, **31**, 291 (1958).
10) M. Shibata, *Nippon Kagaku Zasshi*, **87**, 771 (1966).
11) N. Matsuoka, J. Hidaka, and Y. Shimura, This Bulletin, **39**, 1257 (1966).

charged species, the molar conductivities of the isomers gave additional proof of the fact. The molar conductivity values were 6 for the isomer from the No. 1 fraction, 8 for that from No. 2 fraction, and 10 mho cm^{-1} for that from the No. 3 fraction.

Three possible geometrical isomers for the present complex are shown in Fig. 1. The first one has two NH_3 groups in the *cis* position and three N (or O) atoms in the *cis-trans* positions (a); the second one has two NH_3 in the *trans* position and three N atoms in the *cis-trans* positions (b), and the third one has two NH_3 in the *cis* position and three N atoms in the *cis-cis* positions (c). Hereafter, these will be represented as the *mer*(*cis*)-, *mer*(*trans*)-, and *fac*-isomers respectively. Furthermore, the three isomers will also be represented as No. 1, No. 2, and No. 3 isomers according to the fraction number. In order to assign these possible structures to the isolated isomers, the data from the absorption, PMR, and IR spectra were used.

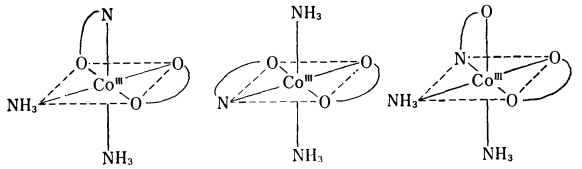

Fig. 1. Possible isomers.

Absorption Spectra. The absorption spectra of the three isomers in aqueous solutions containing potassium bicarbonate are shown in Fig. 2. The spectrum of the No. 3 isomer shows the first absorption band (ν_1) at 56.2×10^{13} sec^{-1} (log ε=2.04) and the second band (ν_2) at 80.1×10^{13} sec^{-1} (log ε=2.13). These values are very similar to those for the known *fac*(N)-[$CoCO_3$-(gly)en][11] (ν_1=56.6 (2.17), ν_2=80.4 (2.13)). This fact indicates that the No. 3 isomer can be assigned to the *fac*-form. When the spectrum of the No. 1 isomer is compared with that of the known *mer*(N)-[$CoCO_3$-(gly)en],[11] the ν_1 and ν_2 values for the former are, in some extent, smaller than those for the latter; for the present isomer, ν_1=54.2 (2.03) and ν_2=79.5 (2.25); for comparison, ν_1=56.6 (2.07) and ν_2=81.1 (2.17). However, the spectrum is very similar to that of the familiar *mer*-[Co(gly)$_3$] isomer[12,13] and exhibits a lower intensity in the first band (half width=*ca.* 12.5×10^{13} sec^{-1}) than in the second band.[14] From these facts, the structure of this No. 1 isomer can be regarded as either one of the two *mer*-forms.

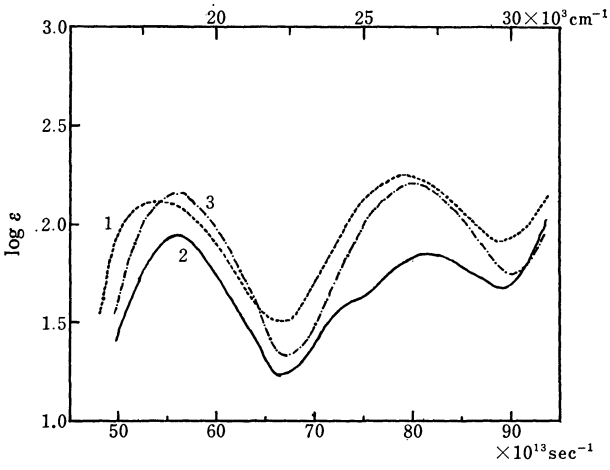

Fig. 2. Absorption spectra of the isomers in $KHCO_3$ aqueous solution.
1) *mer*(*cis*) ····· (No. 1)
2) *mer*(*trans*) —— (No. 2)
3) *fac*-isomer ·-·-· (No. 3)

The absorpsion spectrum of the No. 2 isomer shows a shoulder in the second absorption band region (ν_1= 56.0 (1.93), sh=74.8 (1.6), ν_2=81.8 (1.85)). Apart from this shoulder, the isomer is regarded as another *mer*-from on the basis of the broadened first absorption band (half width=*ca.* 11.2×10^{13} sec^{-1}).

It is a very interesting fact that such a shoulder appears in the second absorption band region. Splittings of the first absorption band are widely observed in *mer*-isomers of the *tris*(amino-acid) complexes and also in *trans*-isomers of dihalogenotetraammine-type complexes, and can be understood with the aid of a ligand field theory, such as Yamatera's prediction.[15] The splitting of the second band has, however, never been observed in the solution spectra of cobalt(III) complexes,[16] although such splitting has been observed in the crystal spectra for some complexes of cobalt-(III).[17]

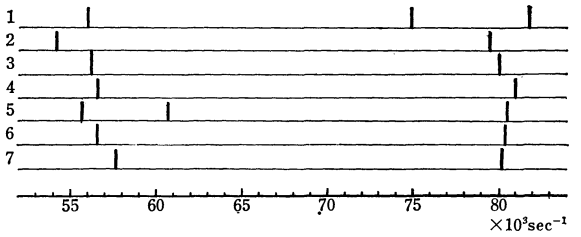

Fig. 3. Experimental band positions for [Co N_3O_3]-type complexes.
1. *mer*(*trans*)-[$CoCO_3$gly$(NH_3)_2$] (No. 2)
2. *mer*(*cis*)-[$CoCO_3$gly$(NH_3)_2$] (No. 1)
3. *fac*-[$CoCO_3$gly$(NH_3)_2$] (No. 3)
4. *mer*-[$CoCO_3$(gly)en][9]
5. *mer*-[Cogly$_3$][11]
6. *fac*-[$CoCO_3$glyen][9]
7. *fac*-[Cogly$_3$][11]

In Fig. 3 the experimental band positions for the present three and some related complexes are schematically represented. It seems to be unreasonable to regard the shoulder concerned as a component of the first band, because only a partial splitting or a braodened shape of the first band is observed in the other *mer*-isomers. When the second band maxima are compared among these isomers, it is noticed that the value (81.8) for the No. 2 isomer is considerably higher than those for the other isomers (80—81$\times10^{13}$ sec^{-1}).

12) Y. Shimura and R. Tsuchida, This Bulletin, **29**, 311 (1956).
13) M. Mori, M. Shibata, E. Kyuno, and M. Kanaya, *ibid.*, **34**, 1837 (1961).
14) N. Matsuoka, J. Hidaka, and Y. Shimura, *ibid.*, **40**, 1863 (1967).
15) H. Yamatera, *ibid.*, **31**, 95 (1958).
16) R. A. D. Wentworth and T. S. Piper, *Inorg. Chem.*, **4**, 709 (1965).
17) S. Yamada, *Coord. Chem. Rev.*, **2**, 83 (1967).

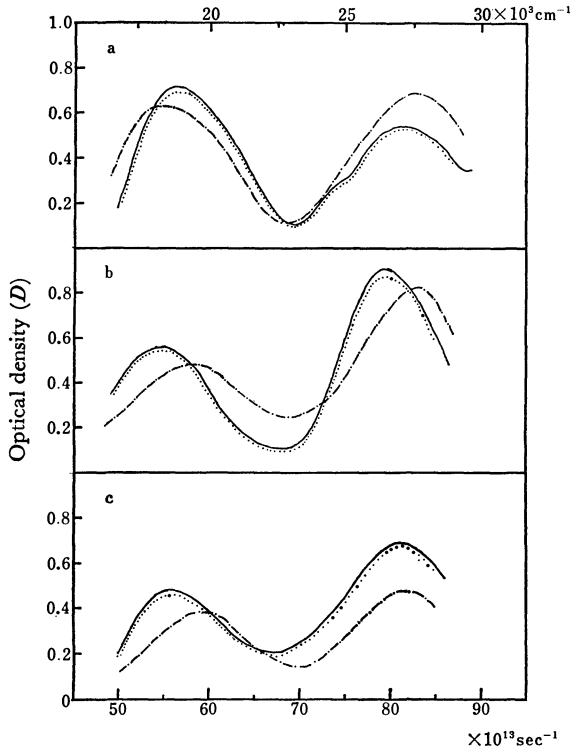

Fig. 4. Change of the spectra.
a) *mer(trans)*- b) *mer(cis)*- c) *fac*-isomer
Original soln. ——
Acidified soln. -·-·-
Alkalined soln. ·····

Furthermore, the intensity of the ν_2 band (ε=70.5) is considerably smaller than that of the ν_1 band (ε=95.8). From these facts, we can now assume the splitting of the second band for this isomer.

When the absorption spectrum of a solution of the No. 2 isomer acidified with perchloric acid was measured (Fig. 4(a)), the above-mentioned shoulder disappeared and the ν_1 band was observed at a considerably longer wavelength (at 54.7×10^{13} sec^{-1}), contrary to expectations of the positions of the CO_3^{2-} and H_2O ligands in the spectrochemical series. When the acidified solution was again alkalined with a large amount of potassium bicarbonate, the spectrum of the resulting solution was identical with that of the original solution. The spectra for the acidified solutions of the other two isomers showed some shifts of the ν_1 bands to the shorter-wavelength side (Fig. 4(b) and (c)). The spectra for the solutions again alkalined returned to the same spectra as in the original solutions. These facts suggest a configuration retention of these isomers in the process of acid hydrolysis.

The absorption spectra of a single crystal for the No. 2 isomer are shown in Fig. 5. The dichroism of this complex is clearly observed in the first absorption band region. Both of the polarized lights are strongly absorbed in the second band region, but the relative intensities of the two maxima differ for the two directions of the light.

PMR Spectra. Because of the limited solubility of the present compounds in water and because of the instability of their aqueous solutions, the samples for

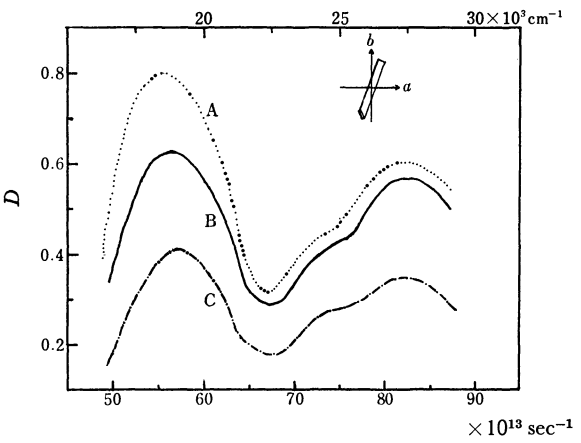

Fig. 5. Polarized single crystal spectra of *mer(trans)*-isomer.
A) along *a* axis ·····
B) along *b* axis ($b\perp a$) -·-·-
C) nonpolarized light ——

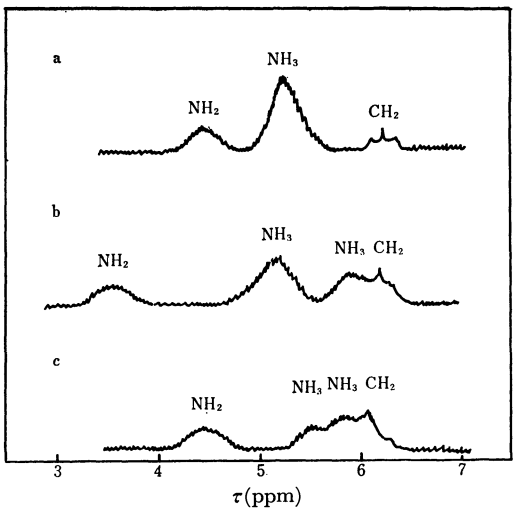

Fig. 6. PMR spectra on;
a) *mer(trans)*- b) *mer(cis)*- c) *fac*-isomer in CF_3COOD.

the measurement were dissolved in deuterated trifluoroacetic acid. On the assumption of the configuration retention in the process of acid hydrolysis, the PMR spectra, which are shown in Fig. 6, will now be discussed.

The spectrum on the No. 1 isomer shows two peaks due to the two NH_3 groups, at 5.1 and 5.8 ppm, and also a peak due to a NH_2 group of the chelated glycinate at 3.5 ppm (b). The integrated ratio of these three peaks is estimated to be 3:3:2, corresponding to the proton numbers concerned. This indicates the existence of two NH_3 groups in different environments; from this fact, this isomer can be identified as the *mer(cis)*-isomer. The spectrum on the No. 2 isomer shows two peaks, due to the NH_3 group and the NH_2 group, at 5.2 and 4.5 ppm respectively (a). From the area ratio of about 3:1, we can now judge this isomer to be the *mer(trans)* one. The spectrum of the No. 3 isomer exhibits one peak of the NH_2 protons at 4.6 ppm and one broad pattern at 5.7—6.4 ppm which may be resolved into three peaks due to the two different NH_3 groups and the one CH_2 group of the chelated glycinate

(c). These results would seem to support the previous conclusion that this isomer is of the *fac*-form.

Infrared Absorption Spectra. The spectra of the present three isomers are shown in Fig. 7. It is clear that the carbonate ion in each isomer coordinates to central cobalt atom as a bidentate ligand, because of the presence of the characteristic sym. ν(C–O), asym. ν(C–O), and sym. ν(C=O) bands at about 1020, 1280, and 1600 cm^{-1} respectively.[18] It is also clear that the glycinate ion coordinates as a bidentate ligand, because of the presence of the band near 1600 cm^{-1} as well as the absence of the deformation band of the $-NH_3^+$ group near 1500 cm^{-1}.[19]

When the spectra in the 700—1400 cm^{-1} region are compared among the three isomers, the spectrum of the *mer*(*trans*)-isomer reveals the simplest pattern and all of the bands are attributable to the CH_2 and NH_2 waggings (1350—1300 cm^{-1}), the CH_2 twisting (1200—1180 cm^{-1}), and the NH_2 and CO_3 out-of-plane rockings (850—800 cm^{-1}). The infrared spectrum of a lower symmetry complex, in general, exhibits a more complicated pattern than that of the related higher-symmetry complex.[20,21] From this point of view, it can be said that the No. 2 isomer has a *trans* configuration with respect to the coordinated NH_3 groups, whereas the No. 1 isomer has a *cis* configuration.

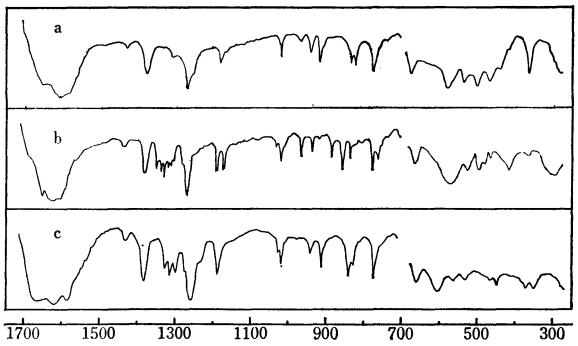

Fig. 7. Infrared spectra of;
a) *mer*(*trans*)- b) *mer*(*cis*)- c) *fac*-isomer.

18) K. Nakamoto, J. Fujita, S. Tanaka, and M. Kobayashi, *J. Amer. Chem. Soc.*, **79**, 4900 (1957).

19) J. Fujita, T. Yasui, and Y. Shimura, This Bulletin, **38**, 654 (1965).

20) R. A. Condrate and K. Nakamoto, *J. Chem. Phys.*, **42**, 2590 (1965).

21) K. Nakamoto, "Infrared Spectra of Inorganic Coordination Compounds," John Wiley & Sons, Inc., New York (1966), pp. 232—235.

BULLETIN OF THE CHEMICAL SOCIETY OF JAPAN, VOL. 44, 2427—2429 (1971)

Functional Group Analysis by Gas Chromatography. IV.[1] Pyrolytic Reaction of Carboxylic Acids in Sulfur Vapor

Tadashi HARA and Susumu ITO

Faculty of Engineering, Doshisha University, Kamikyo-ku, Kyoto

(Received March 8, 1971)

This paper deals with a quantitative gas chromatographic analysis of the product evolved by the pyrolytic reaction between carboxylic acid and sulfur vapor. About 10 mg of carboxylic acid was mixed with 2—3 g sulfur and made to react at 1000—1100°C for 10min. The gaseous product was taken in a gas sampler and subjected to gas chromatography. Carbon dioxide was produced from the carboxyl group, carbon disulfide from carbon, hydrogen sulfide from hydrogen and nitrogen molecule from nitrogen. The peak area ratios of carbon disulfide and hydrogen sulfide to carbon dioxide were found in the gas chromatogram with glycine as a standard substance, and the other carboxylic acids were analyzed on the basis of the relation between the peak area ratio and the chemical composition of glycine. Aliphatic and aromatic carboxylic acids gave satisfactory resuls by this method, but not pyridine carboxylic acid. Weighing a definite amount of sample is not needed in this method. Information concerning the chemical composition as well as the functional group of a carboxylic acid can be obtained.

Studies have been carried out synthetically and kinetically pertaining to the reaction between sulfur and organic compounds, especially aliphatic hydrocarbons in a gaseous phase.[2-7] However, none of them has been applied to the analysis of an organic compound.

In a conventional elementary analysis, the sample is subjected to combustion in an oxygen stream and converted into water and carbon dioxide, the water being determined gas-chromatographically with difficulty. Though the method is effective for knowing the chemical composition of the sample, it does not offer

1) Part III in this series, T. Hara and S. Ito, This Bulletin, **43**, 3320 (1970).

2) W. A. Bryce and Sir Cyril Hinshelwood, *J. Chem. Soc.*, **1949**, 3379.

3) W. J. Thomas and R. F. Strickland-Constable, *Trans. Faraday Soc.*, **53**, 972 (1957).

4) W. J. Thomas and B. John, *Trans. Inst. Chem. Eng.*, **45**, T119 (1967).

5) C. M. Thacker and E. Miller, *Ind. Eng. Chem.*, **36**, 182 (1944).

6) H. O. Folkins, E. Miller, and H. Henning, *ibid.*, **42**, 2202 (1950).

7) G. W. Nabor and J. M. Smith, *ibid.*, **45**, 1272 (1953).

any information about the functional group. We proposed a new method,[1] in which organic compounds were subjected to pyrolysis in sulfur vapor and the reaction products were analyzed gas-chromatographically. We could determine the chemical composition as well as the functional group.

We investigated the pyrolysis of carboxylic acids in sulfur vapor, in which the reaction products such as hydrogen sulfide, carbon dioxide and carbon disulfide are determined by means of gas chromatography. Since the carboxyl group is quantitatively converted into carbon dioxide, the reaction products other than carbon dioxide are represented on the basis of the amount of carbon dioxide.

Experimental

Reagents. Since commercial crystalline sulfur (analytical grade) contains carbon disulfide, it was dried at 90°C for 24 hr, pulverized and dried again. The other reagents were either of analytical grade, or purified. Helium was of commercial grade.

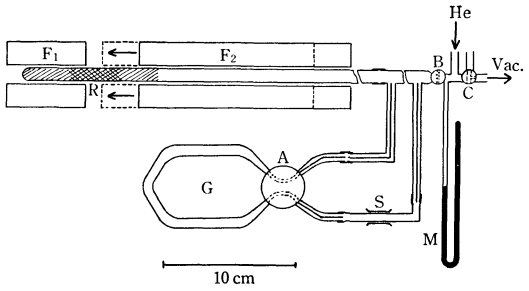

Fig. 1. Apparatus.
F_1,F_2: Electric furnace, G: Gas sampler,
S: Stroke pump, M: Manometer,
R: Reaction tube

Procedure. Two to three grams of powdered sulfur was divided into three portions, the first being charged into a 10 mm diam. × 400 mm quartz tube R with a closed end (Fig. 1). The second is mixed with about 10 mg of sample and charged into the tube, followed by the third portion. The tube was connected to the circulating system with rubber and evacuated through the cocks B and C, followed by replacement of air by helium.

The electric furnaces F_1 and F_2 were held at 750—800°C and 1000—1100°C, respectively. F_2 was placed at a certain position. After three minutes F_1 was placed at another position. F_2 is gradually moved. After completion of the reaction, cock A was closed and the gas sampler separated from the system, followed by gas chromatographic determination of the reaction products.

The reaction temperature was calibrated by a model experiment and maintained within a definite range.

The gas chromatogram was obtained with a Yanagimoto GCG-5DH gas chromatograph under the following conditions: A 2 m stainless steel column was charged with silica gel (60—80 mesh), and held at 100°C. Helium was flowed at the rate of 40 m*l* He/min, and the separated substances were detected with a thermal conductivity detector. The peak area in the gas chromatogram was approximated by the half-width method.

Results and Discussion

Effect of Reaction Temperature. In order to examine the effect of reaction temperature on the products, a dibasic aliphatic acid was treated at 800—850°C and 1000—1100°C, and the mole ratios of hydrogen sulfide or carbon disulfide to carbon dioxide were estimated. The results are shown in Fig. 2. The abscissa represents the theoretical mole ratios of hydrogen or carbon to the carbon dioxide based on the –COO– in the carboxylic acid, and the ordinate represents the experimental peak area ratios of hydrogen sulfide or carbon disulfide to carbon dioxide. The amount of carbon disulfide increased at higher temperature while that of hydrogen sulfide was independent of the reaction temperature. Though the amount of carbon disulfide was expected to increase with the rise of temperature, the reaction temperature was kept at 1000—1100°C since hydrogen sulfide had been reported to decompose at temperatures higher than 1000°C in accordance with the following reaction[8]:

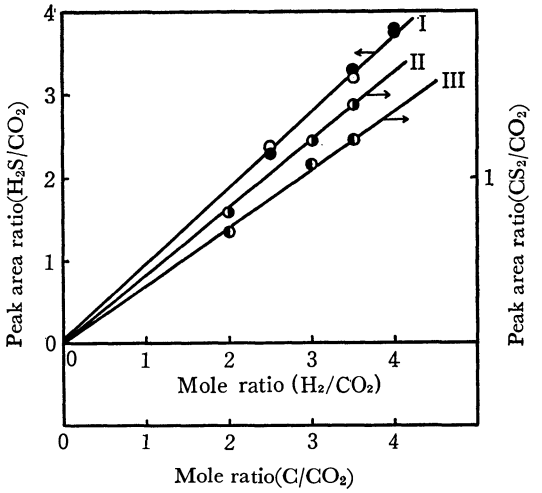

Fig. 2. Relationship between peak area ratios and mole ratios
I: H_2S, II, III: CS_2
○, ◐: 800—850°C, ●, ◑: 1000—1100°C

$$2H_2S \longrightarrow 2H_2 + S_2$$

Hydrogen sulfide was also produced by the reaction between hydrogen and sulfur at 1000—1100°C. Decomposition of hydrogen sulfide at the same temperature thus seems to be negligibly small in the presence of an excess sulfur. This is supported by the equilibrium constant for the reaction $H_2 + {}^1/_2\, S_2 \rightleftharpoons H_2S$, in which $K = P(H_2S)/P(H_2) \times P(S_2)^{1/2}$, and the values of log K are 1.305 at 1218°K and 0.964 at 1338°K.[9]

It is evident that the amount of hydrogen sulfide and carbon disulfide are proportional to the number of hydrogen and carbon atoms in the compounds such as adipic, suberic and azelaic acids.

Effect of Catalyst. Catalysts such as alumina,[5]

8) A. J. Owen, K. W. Sykes, and D. J. D. Thomas, *Trans. Faraday Soc.*, **49**, 1207 (1953).

9) "International Critical Tables," Vol. 7, ed. by E. D. Washburn, Mcgraw-Hill Book Co., Inc., New York and London (1930), p. 237.

silica gel,[5,6] and vanadium pentoxide[3,7] used for the reaction between hydrocarbon and sulfur, were applied to the present reaction. However, the amount of hydrogen sulfide and carbon disulfide evolved did not change so markedly and sulfur dioxide was produced by the reaction between the oxygen in the catalysts and sulfur vapor. These catalysts are not suitable for the determination of the compound containing sulfonic- and nitro-groups since they were converted into sulfur dioxide.[1]

Effect of Stainless Steel Column. The reaction between hydrogen sulfide and stainless steel tube was examined. However, no reaction was confirmed under the conditions in the present procedure.[10]

Determination of Factors by Glycine. The factors for determination of each components were calculated by the equation $E/CO_2=F(A(E)/A(CO_2))$, where E: mole number of a particular element in glycine, CO_2: mole number of carbon dioxide in glycine, $A(E)$: peak area of the compound containing a particular element in glycine, $A(CO_2)$: peak area of carbon dioxide in glycine, F: factor.

Assuming the factor of carbon dioxide $F(CO_2)=1$, the factors for nitrogen, hydrogen, and carbon are $F(N_2)=1.56$, $F(H_2)=1.04$ and $F(C)=2.97$. The chemical composition of nitrogen, hydrogen, carbon and carboxyl group as carbon dioxide is easily determined by multiplying $A(E)/A(CO_2)$ by F.

Analysis of Aliphatic Carboxylic Acids. The monobasic acids which boil at lower temperature were used as their sodium salts. No carbon dioxide was captured by sodium salt. *n*-Caproic and *n*-caprylic acids were charged in a glass capillary and analyzed. Table 1 shows the results obtained.

Analysis of Amino Acids. Though L-cysteine and L-cystine contain sulfur as components, the sulfur content cannot be estimated by the present method, which is one disadvantage. However, the sulfur content in a sulfonic group is determined as sulfur dioxide. Both L-cysteine and L-lysine were subjected to analysis as their hydrochlorides, but no effect of hydrochloride was found (Table 2).

Table 1. Analytical results of aliphatic carboxylic acids

Compound	Formula	
	Theoretical	Found
Sodium formate	HCO_2Na	$H_{1.0}CO_2$
Sodium acetate	CH_3CO_2Na	$C_{1.0}H_{3.3}CO_2$
Sodium propionate	$C_2H_5CO_2Na$	$C_{2.2}H_{5.3}CO_2$
Sodium butyrate	$C_3H_7CO_2Na$	$C_{2.9}H_{7.1}CO_2$
n-Caproic acid	$C_5H_{12}CO_2$	$C_{5.2}H_{12.3}CO_2$
n-Caprylic acid	$C_7H_{16}CO_2$	$C_{7.4}H_{16.9}CO_2$
Oxalic acid	$H_2(CO_2)_2(HCO_2)$	$C_{1.0}CO_2$
Adipic acid	$C_4H_{10}(CO_2)_2$ $(C_2H_5CO_2)$	$C_{1.8}H_{4.7}CO_2$
Pimelic acid	$C_5H_{12}(CO_2)_2$ $(C_{2.5}H_6CO_2)$	$C_{2.6}H_{5.7}CO_2$
Suberic acid	$C_6H_{14}(CO_2)_2$ $(C_3H_7CO_2)$	$C_{2.9}H_{6.8}CO_2$
Azelaic acid	$C_7H_{16}(CO_2)_2$ $(C_{3.5}H_8CO_2)$	$C_{3.4}H_{7.7}CO_2$
Fumaric acid	$C_2H_4(CO_2)_2$ (CH_2CO_2)	$C_{1.2}H_{2.1}CO_2$

Table 2. Analytical results of amino acids

Compound	Formula	
	Theoretical	Found
L-Alanine	$NC_2H_7CO_2$	$N_{0.8}C_{1.8}H_{6.9}CO_2$
L-Aspartic acid	$NC_2H_7(CO_2)_2$ $(N_{0.5}CH_{3.5}CO_2)$	$N_{0.6}C_{1.3}H_{3.5}CO_2$
L-Glutamic acid	$NC_3H_9(CO_2)_2$ $(N_{0.5}C_{1.5}H_{4.5}CO_2)$	$N_{0.5}C_{1.7}H_{4.6}CO_2$
L-Valine	$NC_4H_{11}CO_2$	$N_{1.2}C_{4.4}H_{11.4}CO_2$
L-Isoleucine	$NC_5H_{13}CO_2$	$N_{1.1}C_{5.4}H_{12.7}CO_2$
L-Cystine	$N_2C_4H_{12}S_2(CO_2)_2$ $(NC_2H_6SCO_2)$	$N_{0.9}C_{1.8}H_{6.3}CO_2$
L-Cysteine-HCl	$NC_2H_7SCO_2\cdot HCl$	$N_{1.0}C_{1.8}H_{6.9}CO_2$
L-Lysine-HCl	$N_2C_5H_{14}CO_2\cdot HCl$	$N_{1.8}C_{5.1}H_{14.3}CO_2$
L-Phenylalanine	$NC_8H_{11}CO_2$	$N_{0.8}C_{7.8}H_{10.9}CO_2$
L-Leucine	$NC_5H_{13}CO_2$	$N_{1.1}C_{5.3}H_{12.7}CO_2$

Analysis of Aromatic Carboxylic Acids. In the pyrolytic reaction of aromatic carboxylic acid at 800—850°C, the amount of carbon disulfide evolved was less than that in an aliphatic carboxylic acid. The same factors as for an aliphatic carboxylic acid could, however, be applied to the pyrolytic reaction of an aromatic carboxylic acid at 1000—1100°C (Table 3). This can be attributed to the fact that the carbon-carbon bond energy in a benzene ring is larger than that in an aliphatic compound. Pyridinecarboxylic acid alone did not give a satisfactory result, and no nitrogen being found in a gaseous product. It seems that the pyridine ring is still stable at the reaction temperature or converted into a nonvolatile substance, but this has not been confirmed. By this method we cannot estimate the absolute number of carboxylic group.

Table 3. Analytical results of aromatic carboxylic acids

Compound	Formula	
	Theroetical	Found
Benzoic acid	$C_6H_6CO_2$	$C_{6.3}H_{6.1}CO_2$
p-t-Butylbenzoic acid	$C_{10}H_{14}CO_2$	$C_{9.9}H_{14.3}CO_2$
o-Toluic acid	$C_7H_8CO_2$	$C_{6.9}H_{7.7}CO_2$
m-Toluic acid	$C_7H_8CO_2$	$C_{6.8}H_{8.2}CO_2$
p-Toluic acid	$C_7H_8CO_2$	$C_{7.1}H_{8.2}CO_2$
Terephthalic acid	$C_6H_6(CO_2)_2$ $(C_3H_3CO_2)$	$C_{2.9}H_{2.8}CO_2$

Information on the chemical composition as well as functional group of a compound is obtained by this method using an arbitrary amount of sample. The method can be applied to various compounds such as organic compounds or metal complexes.

10) S. Ito and T. Hara, *Nippon Kagaku Zasshi*, **90**, 1027 (1969).

The Synergic Solvent Extraction of Rare Earths. II. The Absorption Spectra of Neodymium-, Holmium-, and Erbium-TTA-TOPO Complexes with ClO_4^-, CNS^-, NO_3^-, and Cl^- Ions

Tomitsugu TAKETATSU and Nobuyo OHKURA
College of General Education, Kyushu University, Fukuoka

(Received March 20, 1971)

The synergic solvent extraction behavior of neodymium, holmium, and erbium in Ln^{3+}/X^-/HTTA/TOPO systems ($X^- = ClO_4^-$, CNS^-, NO_3^-, and Cl^-) have been investigated. When the rare earths are completely extracted into an organic layer, the following equation is assumed:

$$Ln(TTA)_3(TOPO)_{2(o)} + 3TOPO_{(o)} + H^+_{(a)} + X^-_{(a)} \rightleftharpoons (Ln(TTA)_2(TOPO)_5)^+X^-_{(o)} + HTTA_{(o)}$$

for which the mixed equilibrium constant is defined by $k_3 = [(Ln(TTA)_2(TOPO)_5)^+X^-]_{(o)}[HTTA]_{(o)}/[Ln(TTA)_3(TOPO)_2]_{(o)}[TOPO]^3_{(o)}[H^+]_{(a)}[X^-]_{(a)}$. The log k_3 value for the holmium/ClO_4^-, /CNS^-, /NO_3^-, and /Cl^- systems are about 8.3, 6.5, 5.3, and 3.6 respectively. An obvious difference between Ln^{3+}/SO_4^{2-}/HTTA/TOPO and Ln^{3+}/ClO_4^-/HTTA/TOPO systems is observed in the order of the distribution ratio on the extraction of a series of rare earths with an increase in the atomic number.

In the previous paper,[1] when holmium and erbium were completely extracted from aqueous perchlorate solutions into various organic solutions containing 2-thenoyltrifluoracetone (TTA) and tri-*n*-octyl phosphine oxide (TOPO), it was shown that the following equation held:

$$Ln(TTA)_3(TOPO)_{2(o)} + 3TOPO_{(o)} + H^+_{(a)} + ClO^-_{4(a)} \rightleftharpoons (Ln(TTA)_2(TOPO)_5)^+ClO^-_{4(o)} + HTTA_{(o)}$$

for which the mixed equilibrium constant was defined by $k_3 = [(Ln(TTA)_2(TOPO)_5)^+ClO_4^-]_{(o)}[HTTA]_{(o)}/[Ln(TTA)_3(TOPO)_2]_{(o)}[TOPO]^3_{(o)}[H^+]_{(a)}[ClO_4^-]_{(a)}$ and in which the k_3 linearly increased with an increase in the dielectric constant of the organic solvent used.

In the present paper, we will describe a spectrophotometric study of neodymium-, holmium-, and erbium-TTA-TOPO complexes extracted from aqueous solutions containing perchlorate, thiocyanate, nitrate, chloride, sulfate or acetate ions, also, we will discuss the formation of these metal TTA-TOPO complexes associated with various anions.

Experimental

The preparation of the reagents and all the experimental procedures were the same as in the previous paper.

Results and Discussion

(i) Absorption Spectra in Nd^{3+}/HTTA/TOPO/ClO_4^- System. The absorption spectra of a cyclohexane solution containing neodymium-TTA-TOPO complexes extracted from an acetate solution and of a 1,2-dichloroethane solution containing the complexes extracted from the perchlorate solution by the extraction procedure are given in Fig. 1. The patterns of these spectra are defined as α- and β-types respectively. The pattern of the α-type is identical with that of the $Nd(TTA)_3(TOPO)_2$ complexes in the literature.[2,3]

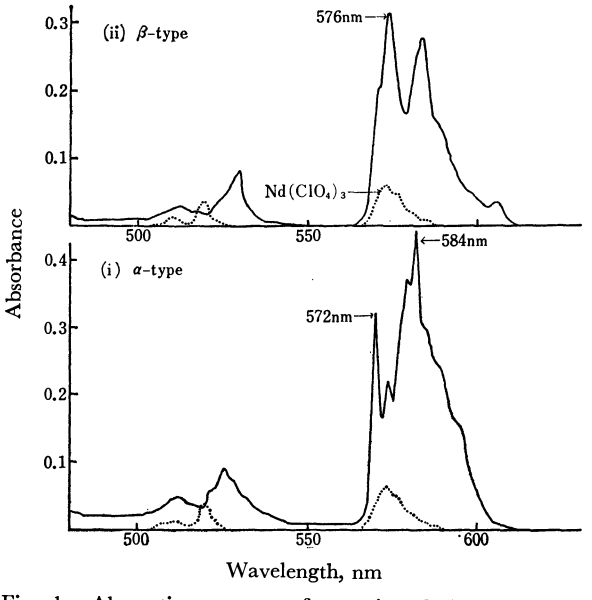

Fig. 1. Absorption spectra of organic solutions containing Nd-TTA-TOPO complexes.
(i) Aqueous layer: 0.00943M Nd^{3+}, 0.4M CH_3COO^-
Organic layer: 0.1M HTTA, 0.1M TOPO, cyclohexane
(ii) Aqueous layer: 0.00943M Nd^{3+}, 0.4M CH_3COO^-, 1.0M ClO_4^-
Organic layer: 0.1M HTTA, 0.1M TOPO, 1,2-dichloroethane

The absorption spectra of all the organic solutions containing the metal complexes extracted from the acetate solution gave an α-type spectrum. On the other hand, in the case of extraction from perchlorate solutions, the pattern of the spectra changed from the α- to the β-type with an increase in the dielectric constant of the organic solvent used, as was also observed in the cases of holmium and erbium.[1]

The variations in the absorption spectra of 1,2-dichloroethane solutions containing the neodymium-TTA-TOPO complex were studied as a function of the concentrations of perchlorate ions added to the acetate solution and of the hydrogen ions of the solutions containing a definite quantity of perchlorate ions.

1) T. Taketatsu and N. Toriumi, *J. Inorg. Nucl. Chem.*, **31**, 2235 (1969).
2) T. V. Hearly and J. R. Ferraro, *ibid.*, **24**, 1449 (1962).
3) T. Taketatsu and C. V. Banks, *Anal. Chem.*, **38**, 1524 (1966).

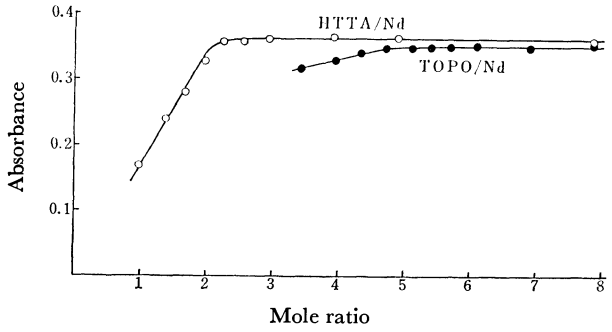

Fig. 2. Variation in absorbance with increasing of concentration of HTTA in the presence of excessive amount of TOPO and with that of TOPO in the presence of excessive amount of HTTA.
Aqueous layer: 0.0102M Nd^{3+}, 1.0M ClO_4^-, 0.5M CH_3COO^-.
Organic layer: varying HTTA, 0.1M TOPO or 0.1M HTTA, varying TOPO, 1,2-dichloroethane

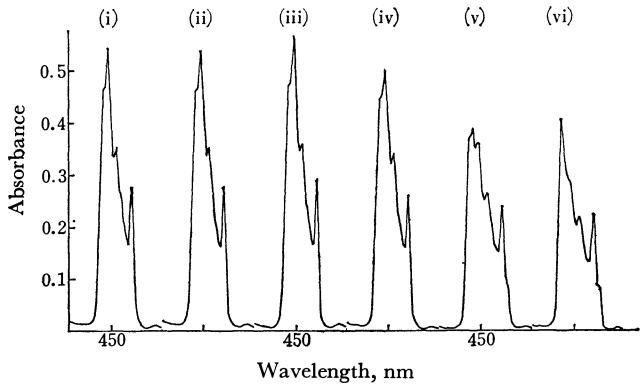

Fig. 3. Variation in absorption spectra with increasing of dielectric constant (ε) of organic solvents used in the Ho^{3+}/NO_3^-/HTTA/TOPO system.
Aqueous layer: 0.00541M Ho^{3+}, 1.20M NO_3^-.
Organic layer: (i) benzene (ε 2.28) (ii) trichloroethylene (ε 3.42) (iii) isopropyl ether (ε 3.88) (iv) chlorobenzene (ε 5.62) (v) dichloroethane (ε 9.08) (vi) 1,2-dichloroethane (ε 10.32), 0.2M HTTA, 0.2M TOPO.

The change in these absorption spectra from the α- to the β-type also progressed with an increase in the concentration of perchlorate or hydrogen ions.

The variations in the absorbance at 576 nm were studied as a function of the concentration of TTA *vs.* the neodymium added to the aqueous layer, using 1,2-dichloroethane solutions containing various amounts of TTA and a fixed, excessive amount of TOPO; we also studied them as a function of the concentration of TOPO *vs.* neodymium, using organic solutions containing a fixed, excessive amount of TTA and various amounts of TOPO. The results are given in Fig. 2. Breaks are observed at mole ratios of TTA: Nd=2:1 and TOPO: Nd=5:1 though the latter break is somewhat obscure.

It is supposed that the β-type complex has the chemical composition of $(Nd(TTA)_2(TOPO)_5)^+ClO_4^-$ for the

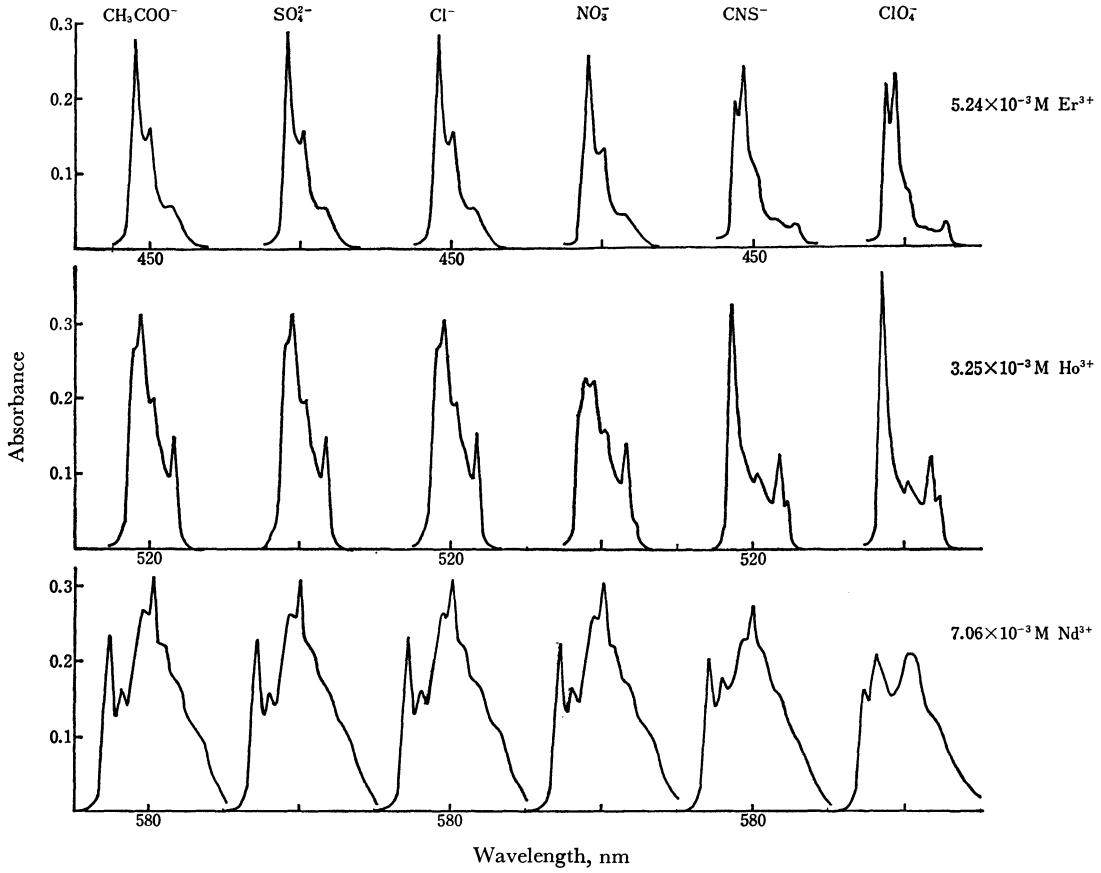

Fig. 4. Absorption spectra of 1,2-dichloroethane solutions in Er^{3+}, Ho^{3+}, and Nd^{3+}/CH_3COO^-/X^{n-}/HTTA/TOPO systems.
Aqueous layer: 0.1M SO_4^{2-}, Cl^-, NO_3^-, CNS^-, and ClO_4^-, 0.04M CH_3COO^-
Organic layer: 0.1M HTTA, 0.1M TOPO

electric conductivity of 1,2-dichloroethane solutions containing the neodymium complexes increases almost linearly with an increase in the absorbance at 576 nm, as was observed in the cases of holmium- and erbium-TTA-TOPO complexes.

Although the estimation of the k_3 value using the assumption described in the previous paper is not always accurate because the new band at 576 nm of the β-type spectrum appears in the middle of the bands at 572 and 584 nm of the α-type spectrum, it is assumed that the log k_3 value for neodymium using 1,2-dichloroethane is approximately 6 and that it is lower than that ($\log k_3 \fallingdotseq 8$) of holmium and erbium.

(ii) Absorption Spectra in Ln^{3+}/HTTA/TOPO/X^- Systems. The behavior of the absorption spectra of organic solutions containing rare earth-TTA-TOPO complexes extracted from an aqueous solution containing thiocyanate, nitrate, chloride, or sulfate ions in place of perchlorate ions was investigated. As an example, the absorption spectra of various organic solutions containing holmium extracted from acetate solutions containing a definite amount of nitrate ions are given in Fig. 3. It can be seen that the patterns of these spectra change from the α- to the β-type in accordance with an increase in the value of the dielectric constant, as was also observed in the case of the perchlorate ion. This phenomenon suggests that the nitrate ion associates with the TTA-TOPO complexes just as does the perchlorate ion.

The absorption spectra of 1,2-dichloroethane solutions containing neodymium, holmium, and erbium extracted from acetate solutions containing definite amounts of perchlorate, thiocyanate, nitrate, chloride, and sulfate ions are shown in Fig. 4. It can be seen that the extent of the change from the α- to the β-type is different according to the species of anions used and that the order of the effect is $ClO_4^- > CNS^- > NO_3^- > Cl^- > SO_4^{2-}$. It is considered that sulfate ions as well as acetate ions form scarcely any ion-associate complex because the α-type spectrum is not affected by the addition of a large amount of the ions.

From these results, it is assumed that the formula of the β-type complex can be represented as $(Ln(TTA)_2(TOPO)_5)^+X^-$: X^-=anions such as ClO_4^-, CNS^-, NO_3^-, and Cl^-. If the assumption for the Ln^{3+}/HTTA/TOPO/ClO_4^- system described in the previous paper can be generalized for the Ln^{3+}/HTTA/TOPO/X^- system, the following equation may be used:

$$Ln(TTA)_3(TOPO)_{2(0)} + 3TOPO_{(0)} + H^+_{(a)} + X^-_{(a)} \rightleftharpoons (Ln(TTA)_2(TOPO)_5)^+X^-_{(0)} + HTTA_{(0)}$$

for which:

$$k_3 = \frac{[(Ln(TTA)_2(TOPO)_5)^+X^-]_{(0)}[HTTA]_{(0)}}{[Ln(TTA)_3(TOPO)_2]_{(0)}[TOPO]^3_{(0)}[H^+]_{(a)}[X^-]_{(a)}}$$

Here, the k_3 value can be estimated spectrophotometrically from the degree of enhancement of a specific absorption band. The results for holmium-TTA-TOPO complexes using 1,2-dichloroethane solutions are given in Table 1. The average values of log k_3 for ClO_4^-, CNS^-, NO_3^-, and Cl^- systems are about 8.3, 6.5, 5.3, and 3.6 respectively.

In order to investigate the effect of the anion extracted into the organic layer on the equilibrium relation between α- and β-type complexes, the distribution ratio, D, of the X^- anion, $D=X^-_{(0)}/X^-_{(a)}$, where $X^-_{(0)}$ and $X^-_{(a)}$ are the total molar concentrations of the anion in a 1,2-dichloroethane soultion of 0.1M TOPO and an aqueous solution respectively, was measured using 0.05M sodium perchlorate, nitrate, and chloride solutions of about pH 3. The results obtained for ClO_4^-, NO_3^-, and Cl^- ions were 0.711, 0.082, and 0.011 respectively. In Fig. 5, it is shown that the plots of the log k_3 values for Ho^{+3}/HTTA/TOPO/ClO_4^-, /NO_3^-, and /Cl^- systems against the logarithm values of D for ClO_4^-, NO_3^- and Cl^- ions almost give a linearity.

Table 1. MIXED EQUILIBRIUM CONSTANT k_3 FOR Ho^{3+}/X^-/HTTA/TOPO/1,2-DICHLOROETHANE SYSTEMS

X^-	Concentration of X^- (M)	$[H^+]_{(a)}$ (M)	Absorbance at 445 nm	x[a]	log k_3
ClO_4^-	0.004	3.49×10^{-4}	0.387	1.58	8.33
ClO_4^-	0.006	3.16×10^{-4}	0.465	3.13	8.25
ClO_4^-	0.008	3.16×10^{-4}	0.502	4.82	8.18
SCN^-	0.2	3.89×10^{-4}	0.529	7.32	6.52
SCN^-	0.3	4.07×10^{-4}	0.542	9.40	6.44
SCN^-	0.5	3.98×10^{-4}	0.557	13.62	6.39
NO_3^-	0.2	6.76×10^{-4}	0.328	1.00	5.37
NO_3^-	0.3	6.76×10^{-4}	0.352	1.20	5.28
NO_3^-	0.4	6.76×10^{-4}	0.376	1.45	5.24
Cl^-	0.5	1.41×10^{-3}	0.124	0.137	3.74
Cl^-	1.0	1.59×10^{-3}	0.150	0.202	3.56
Cl^-	1.5	1.62×10^{-3}	0.160	0.232	3.44

0.2M HTTA and 0.2M TOPO in organic layer and 0.00541M Ho^{3+} in aqueous layer before shaking.

a) x represents the mole ratio of $(Ln(TTA)_2(TOPO)_5)^+X^-$ *vs.* $Ln(TTA)_3(TOPO)_2$

Calibration curves used:

absorbance at 445 nm	$(Ho(TTA)_2(TOPO)_5)^+ClO_4^-$	$Ho(TTA)_3(TOPO)_2$
0.590	0.00541 M	0.00 M
0.050	0.00	0.00541

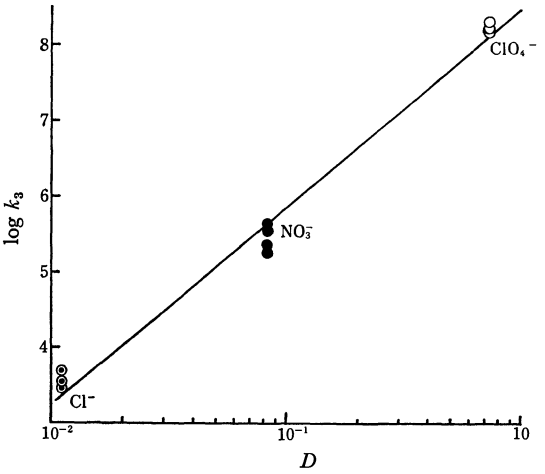

Fig. 5. Relationship between log k_3 for Ho^{3+} and distribution ratio D of ClO_4^-, NO_3^-, and Cl^-.

for log k_3: Aqueous layer: 0.00541M Ho^{3+}, varying ClO_4^-, NO_3^-, and Cl^-
Organic layer: 0.2M HTTA, 0.2M TOPO, 1,2-dichloroethane

for D: Aqueous layer: 0.05M ClO^-_4, NO^-_3, and Cl^-
Organic layer: 0.1M TOPO, 1,2-dichloroethane

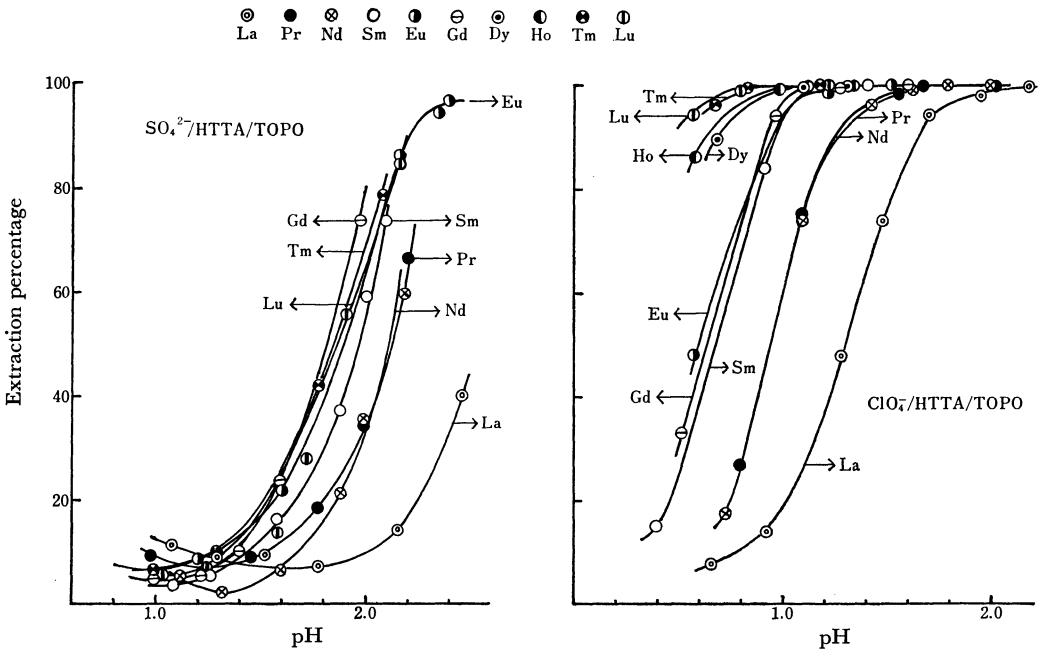

Fig. 6. Discrepancy of extracted amount of rare earths between ClO_4^-/HTTA/TOPO and SO_4^{2-}/HTTA/TOPO systems as a function of pH.
Aqueous layer: 0.1M SO_4^{2-} or ClO_4^-, rare earth acetates
Organic layer: 0.1M HTTA, 0.1M TOPO, 1,2-dichloroethane

Conocchioli, Tocher, and Diamond[4] reported that perchloric acid was extracted into a carbon tetrachloride solution of TOPO by the formation of the ion-associate complex $H_3O^+ \cdot n\text{TOPO} \cdot ClO_4^-$ ($n=1$ and 3). Therefore, it is assumed that the change from $Ln(TTA)_3(TOPO)_2$ to $(Ln(TTA)_2(TOPO)_5)^+X^-$ depends upon the molar concentration rather than on the kind of anion extracted with TOPO into the organic layer.

(iii) Extractability of Ln^{3+} in ClO_4^-/HTTA/TOPO and SO_4^{2-}/HTTA/TOPO Systems. An obvious discrepancy is observed in the order of extractability of a series of rare earths in relation to the formation of $Ln(TTA)_3(TOPO)_2$ and $(Ln(TTA)_2(TOPO)_5)^+ClO_4^-$ complexes. When the individual rare earth was extracted into a 1,2-dichloroethane solution containing TTA and TOPO from an aqueous acetate solution, the extractability of these elements was studied as a function of the pH value, which was adjusted with perchloric or sulfuric acid. The results are given in Fig. 6. For a perchloric acid system, the extractability of rare earths increases as the atomic number increases. On the other hand, for a sulfuric acid system, though the extractability of the lighter rare earth increases as the atomic number increases, that of heavier rare earths is the reverse with an increase in the atomic number.

4) T. J. Conocchioli, M. I. Tocher, and R. M. Diamond, *J. Phys. Chem.*, **69**, 1106 (1965).

The Chemical Behavior of Low Valence Sulfur Compounds. VII.[1] The Oxidation of Ammonium Sulfide and Ammonium Sulfite with Compressed Oxygen in Aqueous Ammonia Solution

Kunishige NAITO* and Taijiro OKABE

Department of Applied Chemistry, Faculty of Engineering, Tohoku University, Sendai

(Received March 20, 1971)

The oxidation of ammonium sulfide and ammonium sulfite with compressed oxygen in aqueous ammonia soultion was studied in order to confirm the formation of ammonium sulfamate. Ammonium sulfite is easily oxidized to ammonium thiosulfate through polysulfides with oxygen and further to ammonium sulfamate and ammonium sulfate. Suitable conditions for producing ammonium sulfamate were found to be: initial concentration of ammonium sulfide 2.0 mol/*l*, temperature 100°C, concentration of ammonia 12 mol/*l*, concentration of cupric ion 0.1 mol/*l* and oxygen pressure 50 kg/cm^2. Though ammonium sulfite is wholly oxidized to ammonium sulfate under the same conditions, it is partially oxidized to ammonium sulfamate besides sulfate in the presence of cupric ion under high concentration of ammonia. The mode of oxidation might differ from that of ammonium thiosulfate, ammonium sulfide and elemental sulfur because of no formation of polythionate as an intermediate.

In a previous study, the oxidation of ammonium thiosulfate was investigated for the purpose of production of ammonium sulfamate and it was found that the yield was improved by increasing the concentration of ammonia. Ammonium sulfide and ammonium sulfite can be easily obtained as industrial raw materials. If ammonium sulfamate could be produced by aqueous oxidation of these compounds, it would be of interest for industry. The aqueous oxidation of these compounds has been investigated and some results have been applied to the industrial production processes of ammonium sulfate.[2] However, no formation of ammonium sulfamate has been reported. We have studied the oxidation of ammonium sulfide and ammonium sulfite in concentrated aqueous ammonia solutions in order to obtain the suitable conditions for the industrial production of ammonium sulfamate.

Experimental

Apparatus and Procedure. The autoclave shown in a previous paper[3] was used.

An ammoniacal solution of ammonium sulfide was prepared from concentrated aqueous ammonia and hydrogen sulfide controlling the concentration of sulfide to be in the range 1.0—2.0 mol/*l*. A certain amount of cupric oxide as a catalyst, 400 m*l* of the above solution (or about 45 g of crystalline ammonium sulfite and 400 m*l* of concentrated aqueous ammonia) were put in the autoclave and kept in a heated glycerine bath. Temperature was regulated within 0.5°C. When the autoclave was heated to the desired temperature, oxygen was introduced, pressure being kept at a certain value. After the temperature and pressure became constant, about 15 m*l* of the reaction solution was withdrawn every few hours and was analyzed.

Analysis. Concentration of sulfide and free ammonia in the original solution were determined by iodometric and acidimetric titration.

Soluble sulfide, thiosulfate, sulfite, sulfamate, sulfate, and cupric ion were determined as follows.

Soluble Sulfide: Soluble sulfide appearing in the initial stage of the oxidation of ammonium sulfide was determined by iodometric differential titration.

Thiosulfate: In the presence of soluble sulfide, thiosulfate was determined by iodometry after removal of soluble sulfide as cadmium sulfide. In the presence of cupric ion, it was directly titrated with 0.05N standard solution of iodine after adding 0.01M EDTA solution for masking cupric ion, and adding 4N acetic acid until the sample solution became acidic with bromocresol purple.

Sulfite: After pouring the sample solution into 0.05N solution of iodine and then adding 0.01M EDTA solution as a masking reagent of cupric ion and 4N acetic acid, the excess iodine was titrated with 0.05N standard solution of sodium thiosulfate.

Sulfamate: In the oxidation of ammonium sulfide, sulfamate was determined by the same procedure described previously.[4] In the oxidation of ammonium sulfite, sulfamate was determined as follows: 0.1N potassium permanganate was added to the sample solution to oxidize sulfite to sulfate. After being kept standing for 10 min, the excess permanganate was decomposed by adding 2N solution of ammonium formate, and the precipitate formed was removed by filtration. Filtrate was acidified with 4N acetic acid and the barium sulfate precipitated was removed by filtration. After the filtrate was heated on a water bath and concentrated hydrochloric acid and 1M sodium nitrite were added, sulfamate was determined as barium sulfate by gravimetry.

Sulfate: In the oxidation of ammonium sulfide, sulfate was determined by the same procedure previously.[4] In the oxidation of ammonium sulfite, sulfate was determined as follows: After adding an aqueous solution formaldehyde into the sample solution and then acidifying it with 4N acetic acid, sulfate was precipitated as barium sulfate with the addition of 0.5M solution of barium chloride. Barium sulfate was determined by gravimetry.

* Present address: Dept. of Ind. Chem., Faculty of Engineering, Ibaraki University, Hitachi.

1) The preceding paper VI: M. C. Shieh, K. Katabe, and T. Okabe, This Bulletin, **43**, 3449 (1970).

2) Samuel B. Thomas, U. S. 2869844 (1959). Bergwerksverband zur Verwertung von Schutzrechten der Kohlentechnik G. m. b. H., Brit. 718675 (1954); Ger. 905243 (1954); Ger. 925408 (1955); S. Hori and S. Nakagawa, *Tokyo Kogyo Shikensho Hokoku* (Rept. Govt. Chem. Ind. Res. Inst., Tokyo), **37**, 1 (1942); S. Hori, *ibid.*, **46**, 297 (1952).

3) M. C. Shieh, H. Otsubo, and T. Okabe, This Bulletin, **38**, 1596 (1965).

4) K. Naito, M. C. Shieh, M. Yoshida, and T. Okabe, *ibid.*, **43**, 1365 (1970).

Results and Discussion

Oxidation of Ammonium Sulfide with Compressed Oxygen in Aqueous Ammonia Solution. Ammonium sulfide is rapidly oxidized with oxygen to thiosulfate through polysulfides. At the maximum concentration of thiosulfate, cupric ion once predipitated begins to dissolve in the solution and accelerate the oxidation of thiosulfate to form sulfamate and sulfate. A general view of the oxidation of ammonium sulfide is shown in Fig. 1. A small amount of imidodisulfonate and nitrite were also detected in the final solution.

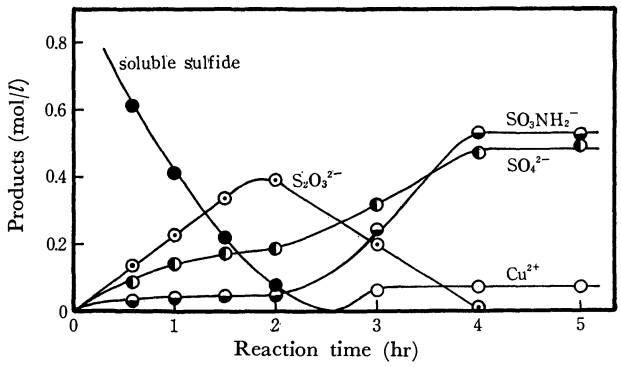

Fig. 1. General view of the whole reaction.
Temp.: 100°C, P_{O_2}: 25 kg/cm², NH_3 concn.: 12 mol/l, Cu^{2+} ion concn.: 0.05 mol/l, $(NH_4)_2S$ initial concn.: 1.0/mol/l

Effect of the Concentration of Cupric Ion: The effect of the concentration of cupric ion was examined in the range 0.05—0.3 mol/l. It was found that the proper concentration of cupric ion is 0.1 to 0.2 mol/l for the oxidation of ammonium thiosulfate.[4] The results are shown in Figs. 2, 3, and 4. The yield of sulfamate was not affected by the concentration of cupric ion.

Effect of Oxygen Pressure: The effect of oxygen pressure was examined in th range 25 to 75 kg/cm². Pressure is given in terms of total pressure, in which both the vapor pressure of water and ammonia are included in addition of that of oxygen. The yield of sulfamate decreases with the increase of oxygen pressure. It seems that there is an induction period at 25 kg/cm² due to the slow oxidation of thiosulfate under a low oxygen pressure.

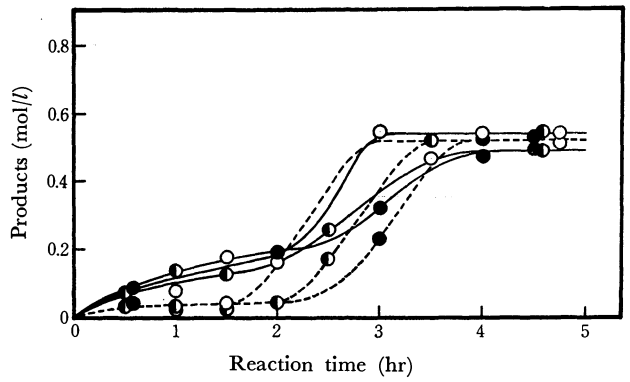

Fig. 2. Effect of the concentration of cupric ion (I).
Temp.: 100°C, P_{O_2}: 25 kg/cm², NH_3 concn,: 12 mol/l, $(NH_4)_2S$ initial concn.: 1.0 mol/l

Cu^{2+} ion concn.:	0.05 mol/l	0.1 mol/l	0.2 mol/l
SO_4^{2-}	—●—	—◐—	—○—
$SO_3NH_2^-$	--●--	--◐--	--○--

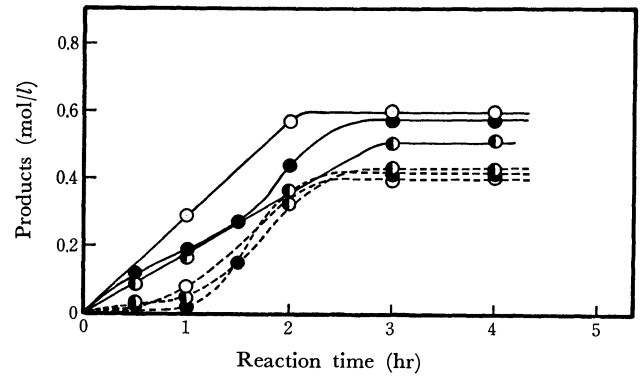

Fig. 3. Effect of the concentration of cupric ion (II).
Temp.: 100°C, P_{O_2}: 50 kg/cm², NH_3 concn.: 12 mol/l, $(NH_4)_2S$ initial concn.: 1.0 mol/l

Cu^{2+} ion concn.:	0.05 mol/l	0.1 mol/l	0.2 mol/l
SO_4^{2-}	—●—	—◐—	—○—
$SO_3NH_2^-$	--●--	--◐--	--○--

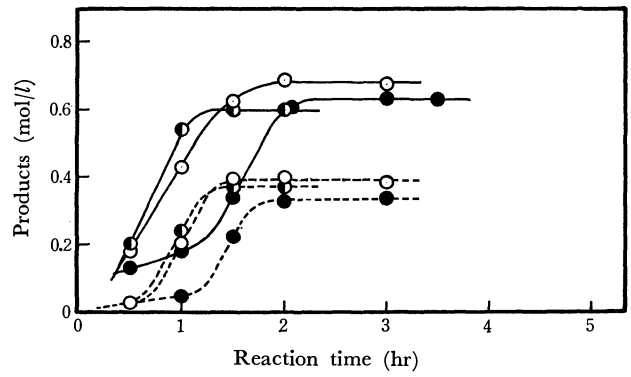

Fig. 4. Effect of the concentration of cupric ion (III).
Temp.: 100°C, P_{O_2}: 75 kg/cm², NH_3 concn.: 12 mol/l, $(NH_4)_2S$ initial concn.: 1.0 mol/l,

Cu^{2+} ion concn.:	0.05 mol/l	0.1 mol/l	0.2 mol/l
SO_4^{2-}	—●—	—◐—	—○—
$SO_3NH_2^-$	--●--	--◐--	--○--

Effect of the Initial Concentration of Ammonium Sulfide: The yield of sulfamate is affected largely by the concentration of thiosulfate formed as an intermediate. The effect was examined by varying the initial concentration of ammonium sulfide from 1.0 to 2.0 mol/l. The results are shown in Fig. 5. It was found that the yield of sulfamate increases with the increase of initial concentration of ammonium sulfide, but the reaction time is hardly affected.

From the results, it seems that ammonium sulfide is oxidized to thiosulfate through polysulfides, and thiosulfate is further oxidized to sulfamate and sulfate.

Suitable conditions for the preparation of ammonium sulfamate in the highest yield are: initial concentration on ammonium sulfide 2.0 mol/l, reaction temperature 100°C, concentration of ammonia 12 mol/l, concentration of cupric ion 0.1 mol/l and oxygen pressure 50 kg/cm².

Oxidation of Ammonium Sulfite with Compressed Oxygen in Aqueous Ammonia Solution. The oxidation of ammonium sulfite, whose initial concentration was 1.0 mol/

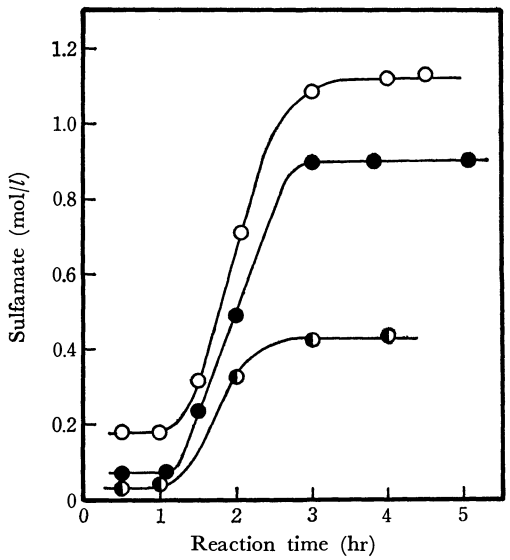

Fig. 5. Effect of the initial concentration of ammonium sulfide.
Temp.: 100°C, P_{O_2}: 50 kg/cm², NH_3 concn.: 12 mol/*l*, Cu^{2+} ion concn.: 0.1 mol/*l*
$(NH_4)_2S$ initial concn.:
○ 2.0 mol/*l*, ● 1.7 mol/*l*, ◐ 1.0 mol/*l*

l, was carried out in a concentrated aqueous solution of ammonia containing 0 to 0.2 mol/*l* of cupric ion at 60—120°C and under the pressure of 25 kg/cm². The results are shown in Figs. 6 and 7. The formation of ammonium sulfamate was observed in the oxidation of ammonium sulfite, and a small amount of dithionate was detected also in the final solution. Thiosulfate and polythionates which exist as intermediates in the oxidation of elemental sulfur, ammonium thiosulfate and ammonium sulfide were not detected during the course of oxidation. This suggests that the oxidation mechanism of ammonium sulfite differs from that of elemental sulfur, ammonium thiosulfate and ammonium sulfide.

The presence of cupric ion accelerates remarkably the oxidation, but makes the yield of sulfate decrease. The sulfite corresponding to the decrement of sulfate may be converted into dithionate, for a small amount of dithionate is detected in the final solution.

The elevation of temperature accelerates fairly the oxidation at temperature below 100°C, and improves the yield of sulfamate. This differs from that on the oxidation of ammonium thiosulfate and elemental sulfur. Though the formation of ammonium sulfamate has been achieved, its low yield makes the industrial application process still difficult.

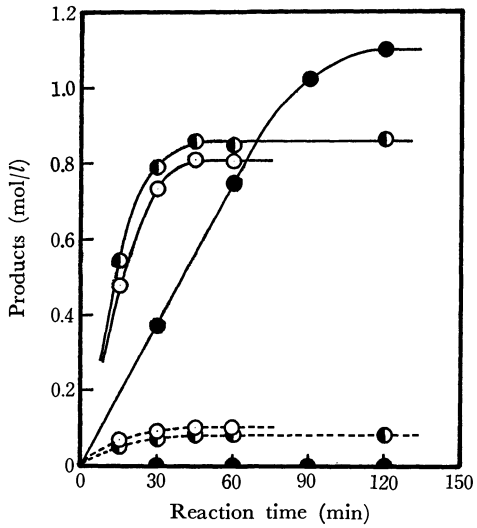

Fig. 6. Effect of the concentration of cupric ion.
Temp.: 100°C, P_{O_2}: 25 kg/cm², NH_3 concn.: 16 mol/*l*, $(NH_4)_2SO_3$ initial concn.: 1.0 mol/*l*

Cu^{2+} ion concn.:	0.2 mol/*l*	0.1 mol/*l*	0 mol/*l*
SO_4^{2-}	—○—	—◐—	—●—
$SO_3NH_2^-$	--○--	--◐--	--●--

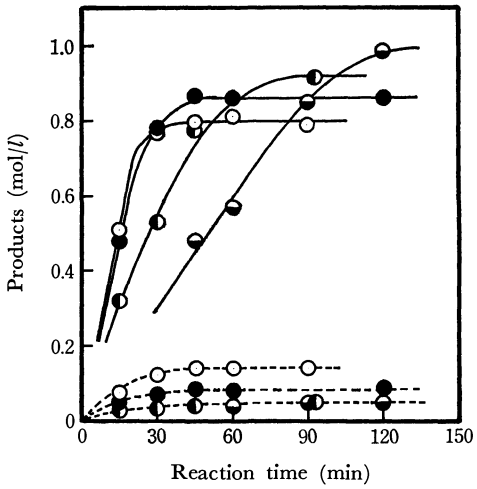

Fig. 7. Effect of temperature.
P_{O_2}: 25 kg/cm², NH_3 concn.: 16 mol/*l*, Cu^{2+} ion concn.: 0.1 mol/*l*, $(NH_4)_2SO_3$ initial concn.: 1.0 mol/*l*

Temp:	60°C	80°C	100°C	120°C
SO_4^{2-}:	—◒—	—◐—	—●—	—○—
$SO_3NH_2^-$	--◒--	--◐--	--●--	--○--

Rearrangement and Decomposition of Phosphoranyl Peroxides Produced *in situ* from Alkylidenephosphoranes and *t*-Alkylperoxy Anions

Koh-ichi YAMADA, Kin-ya AKIBA, and Naoki INAMOTO
Department of Chemistry, Faculty of Science, The University of Tokyo, Hongo, Tokyo
(Received November 13, 1970)

The reactions of alkylidenephosphoranes (I), produced *in situ* from the corresponding phosphonium salts and sodium ethoxide, with sodium salt of *t*-butyl hydroperoxide (II) were carried out in absolute ethanol. Carbanion (III) of phosphoranyl peroxide, formed by the reaction of I with II, underwent a rearrangement to produce *t*-butyl phenyl ether, alkyl *t*-butyl ether, and two kinds of phosphine oxides. Phosphoranyl peroxide (IV), formed by abstraction of proton from ethanol, decomposed in homolytic fashion to yield *t*-butyl alcohol and hydroxyphosphorane (V) as an intermediate, the decomposition of which gave benzene, hydrocarbon and corresponding phosphine oxides. Homolytic decomposition of IV was supported by the reaction of tetraphenylphosphonium bromide with II. The contribution of III was confirmed by the effect of base concentration on the amounts of rearrangement products. The reaction with cumylperoxy anion gave similar results. The mechanisms of these reactions were discussed.

There are a few reports on phosphorus peroxides such as diphenylphosphinyl peroxide[1] and *t*-butyl alkylperphosphonates,[2] but no report on the phosphoranyl peroxides.

We carried out the reactions of alkyltriphenylphosphonium bromides with sodium salt of *t*-butyl hydroperoxide in the presence of sodium ethoxide in ethanol in order to investigate the chemical behavior of *t*-butyl alkyltriphenylphosphoranyl peroxides.

Under the above conditions the following reactions would be expected to occur.

$$t\text{-BuOOH} + \text{EtO}^-\text{Na}^+ \rightleftarrows \underset{\text{II}}{t\text{-BuOO}^-\text{Na}^+} + \text{EtOH} \quad (1)$$

$$\text{Ph}_3\overset{+}{\text{P}}\text{CHRR}'\ \text{Br}^- \underset{\text{EtOH}}{\overset{\text{EtO}^-}{\rightleftarrows}} \text{Ph}_3\text{P=CRR}' \quad (2)$$

VIa: R=Ph, R′=H Ia: R=Ph, R′=H
VIb: R=R′=Ph Ib: R=R′=Ph
VIc: R=*n*-Pr, R′=H Ic: R=*n*-Pr, R′=H

$$\text{I} + \text{II} \longrightarrow \underset{\text{OO-}t\text{-Bu}}{\text{Ph}_3\text{P-}\overset{-}{\text{C}}\text{RR}'} \underset{\text{EtO}^-}{\overset{\text{EtOH}}{\rightleftarrows}} \underset{\text{III}}{}$$

$$\underset{\text{OO-}t\text{-Bu}}{\text{Ph}_3\text{P-CHRR}'} \longleftarrow \text{VI} + \text{II} \quad (3)$$

IV

This paper describes the difference in the decompositions of *t*-butyl alkyltriphenylphosphoranyl peroxides (IV) and the corresponding carbanions (III).

Results and Discussion

Sodium salt of *t*-butyl hydroperoxide (II) was produced *in situ* by addition of *t*-butyl hydroperoxide to absolute ethanol containing four times moles of sodium ethoxide. The position of the equilibrium (1) lies about 10^4 times to the side of II under the conditions given by Everett and Minkoff.[3]

To the solution was then added phosphonium bromide (VI) at room temperature under nitrogen to produce *in situ* alkylidenephosphorane (I), the formation of which was indicated by appearance of yellow color (in the case of Ia and Ic) or of reddish orange precipitate (in the case of Ib).

The reaction soon took place, the temperature of the mixture rose slightly, and the color of the solution gradually became pale. The reaction products were determined by vapor phase chromatography (vpc) and column chromatography. Peroxides (IV) could not be obtained under the reaction conditions.

Alkylphosphonium salts and alkylidenephosphoranes have been reported to react with sodium ethoxide in ethanol under reflux for several hours to give phosphine oxide and hydrocarbon:[4]

$$\text{Ph}_3\text{P=CRR}' \text{ or } \text{Ph}_3\overset{+}{\text{P}}\text{-CHRR}' \xrightarrow[\text{EtOH}]{\text{EtO}^-} \text{Ph}_3\text{P=O} + \text{RR}'\text{CH}_2 + \text{EtOEt} \quad (4)$$

This type of reaction occurred to a small extent in the case of Ia and appreciably in the case of Ib under the reaction conditions. The yields of products in Table 1 were roughly corrected for the contribution of the reaction (4), based on results of blank tests.

It is difficult to distinguish which of I and VI reacted with II, but we inferred that the reaction of I with II predominates in the present case, because the reaction rates was in the order Ib>Ia>Ic. This is also supported by the fact that II is a soft base whereas I is a softer acid than VI.[5]

The mechanisms for the formation of products are postulated as follows.

Carbanion (III) of pentacovalent phosphorus per-

1) R. L. Dannley and K. R. Kabre, *J. Amer. Chem. Soc.*, **87**, 4805 (1965).

2) a) A. Rieche, G. Hilgetag, and G. Schramm, *Chem. Ber.*, **95**, 381 (1962); b) T. I. Yurzhenko and B. J. Kaspruk, *Dokl. Akad. Nauk SSSR*, **168**, 113 (1966); *Chem. Abstr.*, **65**, 7210e (1966).

3) A. J. Everett and G. J. Minkoff, *Trans. Faraday Soc.*, **49**, 410 (1953). For pK_a value of ethanol, 17—18 was assumed.

4) M. Grayson and P. T. Keough, *J. Amer. Chem. Soc.*, **82**, 3919 (1960).

5) R. G. Pearson, *ibid.*, **85**, 3533 (1963); *Chem. Brit.*, **1967**, 103.

TABLE 1. YIELDS OF REACTION PRODUCTS (mol%, by vpc)

Phosphorane R / R′	Ia Ph / H		Ib Ph / Ph		Ic *n*-Pr / H		$Ph_4P^+ Br^-$ (VIII)			
$RR'CH_2$	65.0	63.8	90.2	83.9	0[a]	0[a]	0	0		
PhO-*t*-Bu	15.5	12.6	9.1	10.8	0	0	0	0		
RR′CHO-*t*-Bu	16.3	11.0	0	0	trace	trace	0	0		
RR′CHOEt	2.4	2.1	0	0	<2	<2	0	0		
PhH	7.6	7.4	trace	trace	80.2	78.5	81.8	72.1		
t-BuOH	64.9	68.4	84.2	78.5	70.2	98.0	100	98.4		
$Ph_3P{=}O$	61.2	62.0	81.3	80.7	16.9	20.0	68.8[b]	90.2	55.2[b]	
$Ph_2P(=O)CHRR'$	c)	c)	5.7	8.0	68.3	76.2	0	0		

a) Not detected as evolved gas.
b) Amount isolated by column chromatography.
c) Formation was detected, but the determination was unsuccessful due to insufficient resolution under various conditions.

oxide, first formed by the reaction of II with I, is in the equilibrium (3) with the corresponding phosphoranyl peroxide (IV). Carbanion (III) undergoes a rearrangement of the phenyl or alkyl group to β-oxygen of the peroxide bond to yield *t*-butyl phenyl ether, alkyl *t*-butyl ether and corresponding phosphine oxides as shown in course *a* in the following scheme.

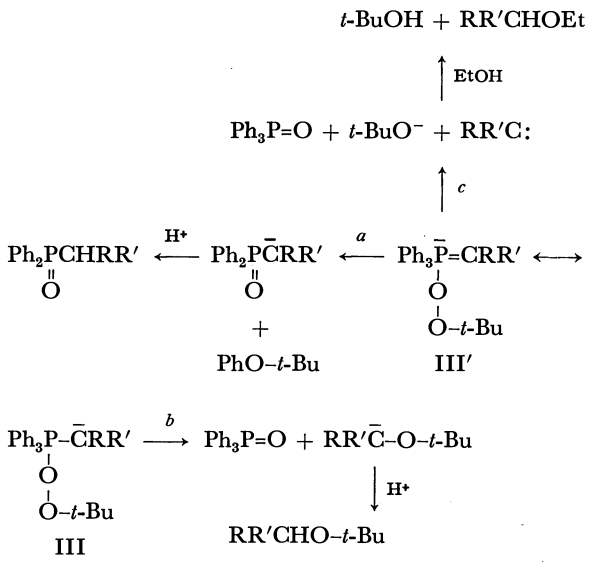

(5)

Rearrangement of the phenyl group may imply resonance contribution of III′, which may be supported by the existence of tris(biphenylene)phosphorane anion.[6] The diphenylmethyl group did not rearrange to the peroxide bond (course *b* in Scheme (5)) to form *t*-butyl ether, probably because of the steric hindrance or low nucleophilicity. The formation of alkyl ethyl ether may be ascribed to the intermediacy of carbene which reacts with solvent ethanol (course *c*).

On the other hand, it is considered that phosphoranyl peroxide (IV) undergoes a homolytic decomposition and the resulting radical (VII) abstracts hydrogen atom from ethanol to give hydroxyphosphorane (V), which decomposes to give benzene or hydrocarbons, and corresponding phosphine oxides:

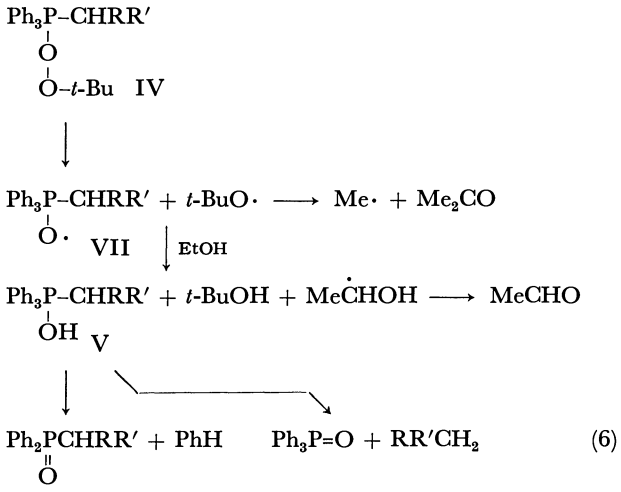

(6)

From the product ratio of hydrocarbon to benzene, the mobility of phenyl and alkyl groups fell in the order $Ph_2CH{>}PhCH_2{>}Ph{>}n$-Bu. This is in good agreement with that in the reaction of phosphonium halides with hydroxide ion,[7] which proceeds through hydroxyphosphoranes of type V. Detection of small amounts of acetone and acetaldehyde by vpc indicates the intermediacy of *t*-butoxy and α-hydroxyethyl radicals, respectively. Furthermore, in the case of Ib, a trace amount of tetraphenylethane was isolated by column chromatography, indicating the presence of diphenylmethyl radicals:

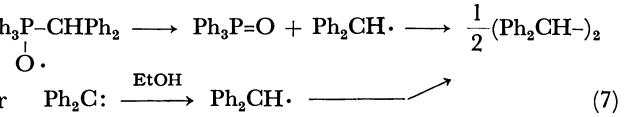

(7)

In order to clarify whether *t*-butyl tetraphenylphosphoranyl peroxide gives *t*-butyl phenyl ether and triphenylphosphine oxide by migration of the phenyl group, tetraphenylphosphonium bromide (VIII) was allowed to react with II under similar conditions. Benzene, *t*-butyl alcohol and triphenylphosphine oxide

6) D. Hellwinkel, *Chem. Ber.*, **98**, 576 (1965).

7) G. W. Fenton and C. K. Ingold, *J. Chem. Soc.*, **1929**, 2342; H. Hoffmann, *Ann. Chem.*, **634**, 1 (1960); G. Aksness and J. Songstad, *Acta Chem. Scand.*, **16**, 1426 (1962).

were obtained as the sole reaction product (Table 1) and no *t*-butyl phenyl ether was detected by vpc. The result supports the view that ethers are produced from the carbanion (III) and hydrocarbons from the neutral peroxide (IV), because in this case no carbanion can participate in the reaction.

When VIII and silver hydroxide were allowed to react in ethanol, benzene and triphenylphosphine oxide were obtained in nearly quantitative yields. These products should be formed from tetraphenylhydroxyphosphorane (IX) as an intermediate:

$$\underset{\text{VIII}}{Ph_4\overset{+}{P}\ Br^-} + AgOH \longrightarrow AgBr + \underset{\text{IX}}{Ph_4P\text{-}OH}$$

$$\longrightarrow Ph_3P{=}O + PhH \quad (8)$$

Thus the intermediacy of hydroxyphosphorane (V) was supported.

From the above mechanistic consideration, we can evaluate the ratio of participation of carbanion (III), the amount of which is equal to the sum of the amounts of ethers, and that of the phosphoranyl peroxide (IV), the amount of which is equal to the sum of the amounts of benzene and hydrocarbon, in the course of reaction. The results are shown in Table 2. However, it is not possible to discriminate the homolytic decomposition of III, if it take place at all, from that of IV.

Table 2. Relative ratio of participation of III and IV as intermediates

	III[a]		IV[b]		III+IV (≡100)	
Ia	34.2	25.7	72.6	71.2	106.8	96.9
Ib	9.1	10.8	~90.2	~83.9	99.3	94.7
Ic	~2	~2	80.2	78.5	82.2	80.5
			97.1[c]	98.5[c]	99.1[c]	100.5[c]

a) [PhO-*t*-Bu]+[RR'CHO-*t*-Bu]+[RR'CHOEt].
b) [PhH]+[RR'CH$_2$].
c) The amount of butane was assumed to be the same as that of triphenylphosphine oxide according to Scheme (6).

In order to make the participation of carbanion (III) conclusive, the effect of the concentration of sodium ethoxide on the yields of the rearrangement products (*t*-butyl ethers) was examined in the case of benzylidenetriphenylphosphorane (Ia). The results are shown in Table 3. The yields of *t*-butyl phenyl ether and benzyl *t*-butyl ether increased gradually with the concentration of sodium ethoxide. This reveals the existence of equilibrium between III and IV, and the formation of *t*-butyl ethers from carbanion (III).

Table 3. Effect of concentration of sodium ethoxide on yields of *t*-butyl ethers in ethanol (mol %)

([$Ph_3\overset{+}{P}CH_2Ph\ Br^-$] : [*t*-BuOOH] : [EtONa] = 1 : 1 : *x*)

x	1	2	4	10	20
PhO-*t*-Bu	8.2	10.3	10.1	10.1	15.3
PhCH$_2$O-*t*-Bu	9.3	12.2	13.4	17.8	24.7
Total	17.5	22.5	23.5	27.9	40.0

Similarly the reaction of sodium salt of cumyl hydroperoxide with Ia was carried out in ethanol under similar conditions and similar results were obtained (Table 4), though the yield of benzyl cumyl ether decreased probably because of the steric hindrance in the cumylperoxy group.

Table 4. Yields of reaction products of Ia with sodium salt of cumyl hydroperoxide in ethanol

Product	Yield (mol%)	
$PhCH_3$	63.8	61.0
$PhOCMe_2Ph$	13.6	15.2
$PhCH_2OCMe_2Ph$	<2	<2
$PhCH_2OEt$	trace	trace
PhH	4.5	3.0
$PhCMe_2OH$	75.1	79.6
$Ph_3P{=}O$	70.7	78.8

Experimental

Materials. Alkyltriphenylphosphonium bromides were prepared by the methods reported in literature: benzylthiphenylphosphonium bromide,[8] mp 271—274°C; *n*-butyltriphenylphosphonium bromide,[9] mp 232—234°C; benzhydryltriphenylphosphonium bromide,[10] mp 238—240°C; tetraphenylphosphonium bromide,[11] mp 281—284°C. Commercially available *t*-butyl and cumyl hydroperoxides were used after distillation under reduced pressure. *t*-Butyl phenyl ether was prepared from *t*-butyl peroxybenzoate and phenylmagnesium bromide,[12] bp 44—46°C/2 mmHg, n_D^{20} 1.4923. Benzyl *t*-butyl ether (bp 60—62°C/3.5 mmHg) and cumyl phenyl ether (mp 43—46°C) were prepared similarly. Benzyl ethyl ether (bp 183—185°C), benzhydryl ethyl ether (bp 158—161°C/18 mmHg), *n*-butyl ethyl ether (bp 90—91°C), benzhydryl *t*-butyl ether (mp 53—55°C), *n*-butyl *t*-butyl ether (bp 123—125°C) and benzyl cumyl ether which could not be distilled without decomposition but was confirmed to be almost pure by vpc, were prepared by the usual method. Benzyldiphenylphosphine oxide was prepared by the procedure of Hoffmann and Tesch,[13] mp 192—193°C. Benzhydryldiphenylphosphine oxide was prepared by the method described in literature,[14] mp 305—305.5°C.

Reactions of Alkylidenetriphenylphosphoranes with Sodium Salt of t-Butyl Hydroperoxide. Only typical examples are described.

a) Benzylidenetriphenylphosphorane (Ia): Sodium salt of *t*-butyl hydroperoxide (0.05 mol) was prepared in absolute ethanol by addition of *t*-butyl hydroperoxide (5.1 m*l*, 0.05 mol) in ethanol (300 m*l*) containing excess sodium ethoxide (0.20 mol) under nitrogen atmosphere. To this solution benzyltriphenylphosphonium bromide (21.6 g, 0.05 mol) was added with stirring in one portion, and yellow color appeared instantaneously showing the formation of benzylidenetriphenylphosphorane. The color of the solution faded to pale yellow after about 15 min and a white precipitate appeared. The mixture was stirred overnight at room temperature and the

8) K. Friedrich and H. G. Henning, *Chem. Ber.*, **92**, 2756 (1959).
9) R. Mechoulam and F. Sondheimer, *J. Amer. Chem. Soc.*, **80**, 4386 (1958).
10) L. Horner and E. Lingnaw, *Ann. Chem.*, **591**, 135 (1955).
11) J. Dodonow and H. Medox, *Ber.*, **61**, 907 (1928).
12) C. Friesell and S. O. Lawesson, *Org. Syn.*, **41**, 91 (1961).
13) A. K. Hoffmann and A. G. Tesch, *J. Amer. Chem. Soc.*, **81**, 5519 (1959).
14) H. Hoffmann, R. Grünewald, and L. Horner, *Chem. Ber.*, **93**, 861 (1960).

amount of remaining peroxide was pursued by iodometry at appropriate intervals. Finally the solution was heated at 60°C for 2 hr. About 5% of the initial hydroperoxide remained unchanged.

The precipitate (NaBr, 2.2 g) was filtered and liquid products were determined by vpc after neutralization with hydrogen chloride in ethanol. From the filtrate ethanol was distilled off and the residue was chromatographed on alumina. Triphenylphosphine oxide (8.6 g, 0.031 mol, 62.1%), mp 155—156°C, was obtained and determined by mixed mp with an authentic sample and the IR spectrum. Benzyldiphenylphosphine oxide was not determined precisely but identified by vpc, and isolated in a small amount by column chromatography.

b) *Diphenylmethylenetriphenylphosphorane (Ib)*: The reaction was carried out under the same conditions and in the same scale as those for a), but in this case the corresponding phosphorane precipitated immediately as an orange-red solid and gradually disappeared during the reaction. The reaction was faster than that of benzylidenetriphenylphosphorane and the temperature of the mixture rose to 40—50°C after 2 hr. The products were determined by vpc. Diphenylmethane was also isolated by distillation under reduced pressure and triphenylphosphine oxide (11.3 g, 81.3%) was obtained by column chromatography on alumina. Elution with ether gave 10 mg of tetraphenylethane, mp 204—208°C. The structure was determined based on spectral data and by mixed melting point with an authentic sample.

c) n-*Butylidenetriphenylphosphorane* (*Ic*): The reaction was performed under the same conditions and in the same scale as those for a), except that a gas burrette was equipped to the system in order to measure the volume of *n*-butane, which is expected to be evolved. The reaction was slower than that of benzylidenetriphenylphosphorane. No gas evolution was observed in this system, *n*-butane evolved being probably completely soluble in ethanol. *n*-Butyl ethyl ether, triphenylphosphine oxide and diphenyl-*n*-butylphosphine oxide were determined by vpc. The two oxides were also obtained by column chromatography and the melting points were 155°C and 87—93°C (lit,[15] mp 95°C), respectively.

d) *Tetraphenylphosphonium bromide* (*VIII*): This reaction was carried out in the same manner and scale as those for a). Benzene and *t*-butyl alcohol were determined by vpc and triphenylphosphine oxide (7.7 g, 55.2%) was obtained by column chromatography on alumina.

Reaction of Benzylidenetriphenylphosphorane with Sodium Salt of Cumyl Hydroperoxide. To sodium ethoxide (0.08 mol) in ethanol (150 m*l*) was added cumyl hydroperoxide (2.8 m*l*, 0.02 mol) and then 8.7 g (0.02 mol) of benzyltriphenylphosphonium bromide was added. The reaction was carried out by the same procedure as mentioned above. The products were determined by vpc.

Reaction of Tetraphenylphosphonium Bromide with Silver Hydroxide. Silver hydroxide (2.5 g, 0.02 mol) freshly prepared, was added to tetraphenylphosphonium bromide (8.4 g, 0.02 mol) in ethanol (150 m*l*) with stirring. Pale brown precipitate was simultaneously formed and stirring was continued for one hour. The precipitate (AgBr, 3.5 g, 93%) was then filtered off. From the filtrate, benzene (85.5%) was determined by vpc. After removal of ethanol, the residue was recrystallized from benzene, yielding triphenylphosphine oxide (14.8 g, 86.2%), mp 149—156°C.

15) W. Kuchen and H. Buchwald, *Chem. Ber.*, **92**, 227 (1959).

BULLETIN OF THE CHEMICAL SOCIETY OF JAPAN, VOL. 44, 2440—2443 (1971)

The Preparation of Geometrical Isomers of β-Nitrostyrene and Their Addition Reactions with Ethanol

Kimiaki YAMAMURA, Setsuo WATARAI, and Toshio KINUGASA*

Institute of Chemistry, College of General Education, Kobe University, Tsurukabuto, Nada, Kobe

**Department of Chemistry, Faculty of Science, Kobe University, Rokkodai, Nada, Kobe*

(Received December 1, 1970)

The preparation of the geometrical isomers of ethyl α-nitrocinnamate and α-nitrochalcone is described. Ethyl (*E*)-α-nitrocinnamate and (*Z*)-α-nitrochalcone were obtained by the thermal- or photoisomerization of the corresponding geometrical isomers, which were themselves produced predominantly through the Knoevenagel reaction. The facile addition of ethanol to the double bonds of β,β-dinitrostyrene, ethyl α-nitrocinnamates, and α-nitrochalcones without any catalyst at room temperature is also described.

The Knoevenagel condensation of benzaldehyde with primary nitroalkanes leads to the preferential formation of *trans*-β-nitrostyrenes, in which the nitro group and the phenyl group are on opposite sides of the carbon-carbon double bond.[1]

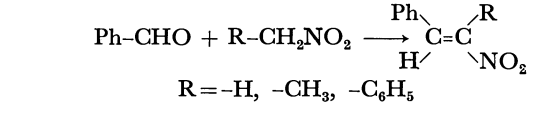

On the other hand, it is known that the base-catalyzed condensation reactions of benzaldehyde with ethyl phenylacetate and with desoxybenzoin afford predominantly ethyl (*E*)-α-phenylcinnamate with a *trans*-cinnamic ester moiety and (*E*)-α-phenylchalcone with a *trans*-chalcone moiety respectively.[2,3] Therefore, it seems to be worthwhile to examine the configurations of ethyl α-nitrocinnamate (β-carbethoxy-β-nitrostyrene) (I) and α-nitrochalcone (β-benzoyl-β-nitrostyrene) (II), obtained by the condensation of

1) a) E. A. Braude, E. R. H. Jones, and G. G. Rose, *J. Chem. Soc.*, **1947**, 1104; b) J. P. Freeman and T. E. Stevens, *J. Org. Chem.*, **23**, 136 (1958); c) G. Drefahl and G. Heublein, *Chem. Ber.*, **93**, 497 (1960).

2) I. Shahak, *J. Chem. Soc.*, **1961**, 3160.

3) A. Dornow and F. Boberg, *Ann.*, **578**, 101 (1952).

benzaldehyde with ethyl α-nitroacetate or ω-nitroacetophenone, since I and II can be regarded as β-nitrostyrene derivatives as well as α-nitrocinnamate and α-nitrochalcone respectively. The formation of a single geometrical isomer of I or II has been reported with no configurational assignment.[4]

The present paper will deal with the preparation of *cis*- and *trans*-isomers of I and II, and with the isomerization reaction of these compounds. The nucleophilic addition of ethanol to the carbon-carbon double bonds of these compounds under very mild conditions is also described.

The nitro valence vibrations and the ultraviolet spectra of these β-nitrostyrenes in correlation with their stereochemical configurations have been reported in a previous paper.[5]

Results and Discussion

Preparation. The condensations of *N*-benzal-*n*-butylamine with ethyl α-nitroacetate and with ω-nitroacetophenone according to the method reported by Dornow *et al.*[4] afforded ethyl α-nitrocinnamate (I) and α-nitrochalcone (II) in 88 and 82% yields respectively. The stereochemical configurations of the compounds were identified as ethyl (*Z*)-α-nitrocinnamate (Iz) with a *cis*-β-nitrostyrene moiety and (*E*)-α-nitrochalcone (IIE) with a *trans*-β-nitrostyrene moiety respectively, on the basis of their IR and UV spectroscopic behavior.[5] The formation of Iz is noteworthy,

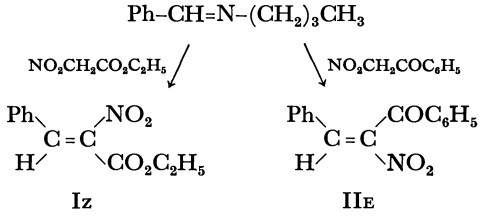

because the formation of the *cis*-β-nitrostyrene derivative as a main product of the condensation of benzaldehyde with an aliphatic nitro compounds has never been reported in the literature. The only compounds having a well-established *cis*-β-nitrostyrene configuration are α-nitrostilbene[6] and its derivatives.[7]

The geometrical isomers of Iz and IIE were obtained by the thermal isomerization and/or by the photoisomerization of each compound. Ethyl (*Z*)-α-nitrocinnamate (Iz), on heating at 175°C for 8 hr, gave a mixture from which an oily yellow material has been isolated. The structure of the oily material was identified as ethyl (*E*)-α-nitrocinnamate (IE). Both isomers, IE and Iz, gave the same equilibrium mixture when treated for 8 hr at this temperature, and the ratio of IE/Iz was found to be *ca.* 1:1. This ratio seemed inconsistent with the finding that IE was not formed in the Knoevenagel reaction. Since, however, the gradual conversion of IE into Iz was observed at room temperature in the dark, Iz appears to be thermodynamically the more stable isomer.

(*E*)-α-Nitrochalcone (IIE) was recovered unchanged when subjected to the same thermal treatment, while under much more drastic conditions it gave tarry substances, along with a trace of benzoic acid. On the other hand, the (*Z*)-α-nitrochalcone (IIz) obtained by the photoisomerization of IIE could isomerize very readily to give IIE in a 90% yield when treated for 3 hr at 170°C, thus indicating the greater stability of IIe.

All the geometrical isomers of I and II easily isomerized to their counterparts when the benzene solution was irradiated with a high-pressure mercury lamp. Starting from both isomers of I, photoequilibrium was established for 8 hr, the ratio IE/Iz was found to be *ca.* 1:1. In the case of II, photoequilibrium was established more rapidly under the same conditions, and the ratio IIe/IIz at equilibrium was found to be 2:3 (as is shown in Fig. 1).

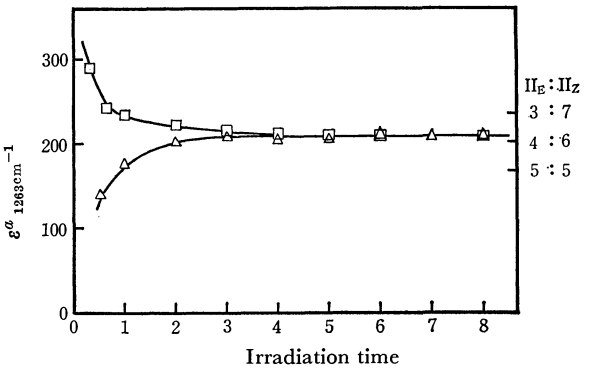

Fig. 1. Plots of the apparent molar absorbance of characteristic band of IIz(1263 cm^{-1}) *vs.* irradiation time in the photoisomerization of IIE and IIz.
-□—□- IIz → IIE
-△—△- IIE → IIz

The Addition of Ethanol. It was observed that the intensity at the absorption maxima in the region of $\pi \rightarrow \pi^*$ of ethyl α-nitrocinnamates, IE and Iz, and α-nitrochalcones, IIE and IIz, decreased considerably

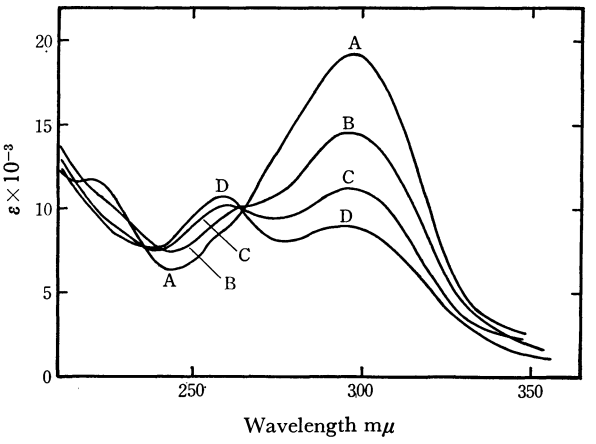

Fig. 2. Variations of UV spectra of (*Z*)-α-nitrochalcone (IIz) in ethanol at 20°C.
A: 0 hr, B: 1 hr, C: 2 hr, D: 3 hr

4) a) A. Dornow and H. Menzel, *Ann.*, **588**, 40 (1954); b) A. Dornow, A. Müller, and S. Lupfer, *ibid.*, **594**, 191 (1955).
5) S. Watarai, K. Yamamura, and T. Kinugasa, This Bulletin, **40**, 1448 (1967).
6) a) F. Heim, *Ber.*, **44**, 2013 (1911); b) B. Flurscheim and E. L. Holmes, *J. Chem. Soc.*, **1932**, 1463.
7) a) R. Reichert and W. Kuhn, *Ber.*, **74B**, 328 (1941); b) T. E. Stevens and W. D. Emmons, *J. Amer. Chem. Soc.*, **80**, 338 (1958).

with the time when the ethanolic solutions were left standing at room temperature, even in the dark (Fig. 2). Also, β-bromo-β-nitrostyrene (III) showed a slight but evident decrease in the intensity at the absorption maximum under the present conditions. These results can be explained by assuming the addition of ethanol to the carbon-carbon double bonds of these compounds.

Actually, colorless needles were isolated from the ethanolic solutions of each geometrical isomer of II after keeping the solutions in the dark at room temperature for 24 hr, they were found to be identical with authentic 1-ethoxy-1-phenyl-2-nitro-2-benzoylethane (IV).[8] When the ethanolic solution of IIE or IIz was refluxed, ω-nitroacetophenone was produced together with IV. It might be thought that ω-nitroacetophenone was formed *via* IV, because ω-nitroacetophenone was also obtained by refluxing the ethanolic solution of IV. Similarly, 1-ethoxy-1-phenyl-2-nitro-2-carbethoxyethane (V), an ethanol adduct of I, was obtained from either of the geometrical isomers. β-Bromo-β-nitrostyrene (III) was less reactive toward ethanol than was either I or II, and its ethanol adduct, 1-ethoxy-1-phenyl-2-nitro-2-bromoethane (VI), could be obtained by refluxing the ethanolic solution of III for 120 hr or by treating III with equimolar sodium ethoxide in THF. Upon the treatment of VI with sodium ethoxide, ω-nitroacetophenone was formed. Recently, Hata *et al.* reported that ω-nitroacetophenone and its diethyl acetal were obtained from III upon treatment with excess sodium ethoxide.[9]

On the other hand, in the cases of (*E*)- and (*Z*)-α-nitrostilbenes (VIIE and VIIz), β-methyl-β-nitrostyrene and β-nitrostyrene, the addition of ethanol did not occure when their ethanolic solutions were allowed to reflux for an extended period. Additionally, α-benzoylchalcone, ethyl α-benzoylcinnamate, and diethyl benzalmalonate were recovered unchanged from their ethanolic solutions.

Although the reaction of nucleophilic reagents at the carbon-carbon double bond conjugated with the electron-withdrawing groups is well known,[10] it is noteworthy that the β-nitrostyrenes, which hold the nitro group and other strong electron-withdrawing groups at the same carbon atom, readily undergo the addition of ethanol without any catalyst at room temperature. In particular, β,β-dinitrostyrene (VIII) is very reactive to ethanol. The addition of ethanol seemed to come to completion instantaneously when VIII was dissolved in ethanol, since the solution had no maximum in the $\pi\rightarrow\pi^*$ region, but showed a lower intensity absorption near 370 mμ. Its UV spectrum was identical with that of 1-ethoxy-1-phenyl-2,2-dinitroethane (IX), which was otherwise obtained from the ethanolic solution of VIII after it had stood at room temperature. The UV spectrum of VIII in *n*-hexane did not vary even when the mixture stood for a long

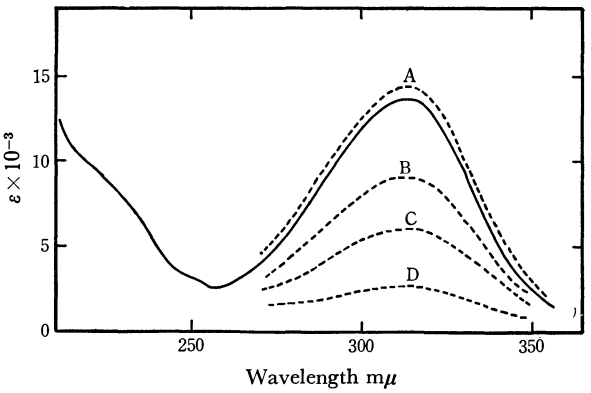

Fig. 3. UV spectra of β,β-dinitrostyrene (VIII).
—— in *n*-hexane
------ variations of UV spectra in ethanol-*n*-hexane (3:97) at 20°C; A: 0 hr, B: 0.5 hr, C: 1 hr, D: 2 hr

time, but in the *n*-hexane-ethanol mixture (97: 3) the absorption intensity at the maximum in the $\pi\rightarrow\pi^*$ region decreased very rapidly, as was expected (Fig. 3).

Thus, very significant differences in reactivities toward nucleophilic reagents, such as alcohol, were observed among various β-nitrostyrene derivatives, some rate coefficients (*k*), summarized in Table 1, for these ethanol-addition reactions were also measured.

TABLE 1. FIRST-ORDER RATE COEFFICIENTS AND ETHANOL ADDUCTS

$$C_6H_5\text{–}CH{=}C(X)(NO_2) + EtOH \longrightarrow C_6H_5\text{–}CH(OEt)\text{–}CH(X)(NO_2)$$

Substituent X	β-Nitrostyrenes	*k* × 10/hr (at 25°C)	Ethanol adducts: Compds. No.	Ethanol adducts: Mp (bp)°C
$CO\cdot OC_2H_5$	IE	1.05	V	39 — 40
	Iz	0.587		
$CO\cdot C_6H_5$	IIE	0.965	IV	118 —121
	IIz	3.41		
Br	III	0.07[a]	VI	(143/9 mmHg)
NO_2	VIII	very fast	IX	29 — 30
C_6H_5	VIIE & VIIz	—	b)	93.5— 94.0

a) Value at 30°C.
b) This compound was obtained by treating VIIE or VIIz with sodium ethoxide in the ethanolic solution.

Of the three pairs of *cis-trans* isomers of β-nitrostyrenes investigated, I, II, and VII, (*Z*)-α-nitrochalcone (IIz) gave the largest *k* value, six times the value of ethyl (*Z*)-α-nitrocinnamate (Iz). On the other hand, IIE, with a *cis*-chalcone moiety, showed almost the same degree of value as IE, with a *cis*-cinnamic ester moiety. These data indicate that the *trans*-chalcone conjugation, which is sterically little affected in IIz, contributes effectively to this addition reaction, although the extent of its contribution is far less than that of the *trans*-β-nitrostyrene conjugation in the case of VIII.

The *k* values of Iz and IIE, which were the major products of the Knoevenagel reaction, were evidently smaller than those of their counterparts, IE and IIz respectively.

8) H. Wieland, *Liebig's Ann. Chem.*, **328**, 154 (1903).
9) M. Shiga, M. Tsunashima, H. Kono, I. Motoyama, and K. Hata, This Bulletin, **43**, 841 (1970).
10) For a review, see S. Patai and Z. Rappoport, in S. Patai, "The Chemistry of Alkenes," Interscience Publishers, Inc., New York, N. Y. (1964), p. 469.

Further studies of the difference in the *cis*- and *trans*-compounds of this series are in progress.

Experimental

All the melting points and boiling points are uncorrected. The UV spectra were obtained with a Hitachi model EPS-3 spectrophotometer; the data of some β-nitrostyrenes in *n*-hexane are presented in Table 2. The measurements of the IR spectra were made in chloroform on a Nihon-Bunko model DS-402G grating infrared spectrophotometer.

Teble 2. UV spectra of *cis*- and *trans*-β-nitrostyrenes in *n*-hexane[a] (C_6H_5–CH=C(X)–NO_2)

Substituent	Compds. No.	λ_{max} mμ	ε
CO·OC_2H_5	IE	285	14200
	Iz	282	17200
CO·C_6H_5	IIE	301	16300
	IIz	298	17100
C_6H_5	VIIE	307	13300
	VIIz	282	21500
NO_2	VIII	313	13500

a) Data in the ethanolic solutions were presented in the previous paper.[5]

Materials. β-Nitrostyrene,[11] β-methyl-β-nitrostyrene,[12] β-bromo-β-nitrostyrene (III),[13] (*E*)- and (*Z*)-α-nitrostilbenes (VIIE and VIIz),[6a] β,β-dinitrostyrene (VIII),[14] α-benzoylchalcone,[15] ethyl α-benzoylcinnamate,[16] and diethyl benzalmalonate[17] were prepared as has been described in the literature. Ethyl (*Z*)-α-nitrocinnamate (Iz, mp 72.5—73.5°C, yield 88%) and (*E*)-α-nitrochalcone (IIE, 91.5—92.5°C, yield 82%) were prepared essentialy according to the procedures reported by Dornow *et al.*,[4] but each compound was obtained in a far better yield than that described in the literature (lit,[4] yield: Iz, 45%; IIE, 48%).

Thermal Isomerizations of IE and Iz. Iz (30 g) was heated at 175°C for 8 hr under reduced pressure (3 mmHg). Cooling for 24 hr below −10°C, followed by filtration, gave the recovery of Iz (15 g). The filtrate was chromatographed over Wako-gel Q-22 using a mixture of benzene-petroleum ether(1:2.5) as an eluent. The first fraction contained Iz, while the subsequent fractions gave a yellow oil, which, when purified by chromatography until the refractive index indicated a constant value, gave 15.0 g of ethyl (*E*)-α-nitrocinnamate (IE); n_D^{20} 1.5780; yield 50%.

Found: C, 59.88; H, 5.28; N, 6.24%. Calcd for $C_{11}H_{11}O_4N$: C, 59.72; H, 5.01; N, 6.33%.

Starting from IE, Iz was obtained in about a 50% yield under similar conditions.

Thermal Isomerization of IIz. IIz, obtained by the photoisomerization of IIE, was isomerized in a manner similar to that described above to give (*E*)-α-nitrochalcone (IIE) in a 90% yield.

Photoisomerizations of α-Nitrochalcones (IIE and IIz). A solution of IIE (20 g) in 1650 m*l* of benzene was irradiated for 3 hr, and then the solvent was evaporated *in vacuo*. Fractional crystallization from benzene-petroleum ether gave colorless flakes of IIz; mp 103—104°C.

Found: C, 71.04; H, 4.77; N, 5.35%. Calcd for $C_{15}H_{11}O_3N$: C, 70.88; H, 4.79; N, 5.68%.

In a similar manner, IIE was obtained from IIz.

Photoisomerization of IE and Iz. Under conditions similar to those described above, *cis*- and *trans*-isomers of ethyl α-nitrocinnamate isomerized each other without any difficulty.

Preparation of IV. IIE (1 g) was dissolved in 60 m*l* of ethanol, and this solution was kept in the dark for 24 hr. The solvent was then evaporated *in vacuo*. Fractional crystallization from benzene gave 0.3 g of an ethanol adduct, IV, as colorless needles; mp 118—121°C.

Found: C, 68.16; H, 5.97; N, 4.72%. Calcd for $C_{17}H_{17}O_4N$: C, 68.21; H, 5.73; N, 4.68%.

Preparation of V. In a manner similar to that described above, Iz gave the ethanol adduct (V) as colorless plates; mp 39—40°C.

Found: C, 58.20; H, 6.48; N, 5.23%. Calcd for $C_{13}H_{17}O_5N$: C, 58.42; H, 6.41; N, 5.24%.

Preparation of VI. III (1 g) was dissolved in 80 m*l* of ethanol and was heated under reflux for 72 hr, and then the solvent was evaporated *in vacuo*. The ethanol adduct, VI, was thus obtained almost quantitatively. Yellow oil; bp 143°C/9 mmHg.

Found: C, 43.75; H, 4.64; N, 5.07%. Calcd for $C_{10}H_{12}NO_3Br$: C, 43.78; H, 4.36; N, 5.11%.

This compound was also prepared as follows. To a solution of III (2.3 g, 0.01 mol) in THF (60 m*l*), sodium ethoxide (0.7 g, 0.01 mol) was added at room temperature. The mixture was stirred for 1 hr and then poured into 200 m*l* of ice water. Then, CO_2 gas was bubbled through the mixture for 1 hr. The aqueous mixture was extracted with three 300 m*l*-portions of benzene. After the removal of the benzene, the ethanol adduct, VI, was obtained by distillation under reduced pressure.

Preparation of IX. VIII (1 g) was dissolved in 50 m*l* of ethanol, and the mixture was kept at 30°C for 24 hr. After the ethanol had then been evaporated *in vacuo*, the residual pale yellow liquid was chromatographed on Wako-gel Q-22, using *n*-hexane as the eluent. The first fraction gave 0.9 g of pale yellow crystals of IX; mp 29—30°C; yield, 72.8% (lit,[14] 29—31°C).

Equilibrium Ratios in the Isomerizations. The equilibrium ratios in the thermal- and photoisomerizations were determined by comparison with the known ratio of isomers and the characteristic absorption bands of the isomerization mixtures, at appropriate time intervals, as is shown in Fig. 1.

Kinetic Measurements. The ethanolic solutions of the β-nitrostyrenes (about 10^{-5}M concentrations) were thermostated, and the UV spectra, at appropriate time intervals, were measured. The logarithm of molar absorbance at the wavelength in the $\pi \rightarrow \pi^*$ region against the time was linear. The first-order rate coefficients (*k*) were calculated by the usual method.

The authors are indebted to Miss Masuko Nishinaka for her IR measurements and elemental analyses.

11) D. E. Worrall, "Organic Syntheses," Coll. Vol. I, p. 413 (1948).
12) H. B. Hass, A. G. Susie, and R. L. Heider, *J. Org. Chem.*, **15**, 8 (1950).
13) W. E. Parham and J. L. Bleasdale, *J. Amer. Chem. Soc.*, **73**, 4664 (1951).
14) S. S. Novikov, V. M. Belikov, V. F. Dem'yanenko, and L. V. Lapshina, *Izv. Akad. Nauk SSSR, Otd. Khim. Nauk*, **1960**, 1295.
15) E. F. Pratt and E. Werble, *J. Amer. Chem. Soc.*, **72**, 4638 (1950).
16) G. S. Cruiskshanks, *J. prakt. Chem.* (2) **89**, 194 (1914).
17) F. H. Allen and F. W. Spangler, "Organic Syntheses," Coll. Vol. III, p. 377 (1955).

The Preparation of Amino-*s*-triazines with Amino- or Nitrophenyl Groups

Yasuo YUKI, Toshio KAKURAI,* and Tatsuya NOGUCHI*

Department of Fiber and Polymer, Nagoya Institute of Technology, Gokiso, Showa-ku, Nagoya

(Received December 1, 1970)

Amino-*s*-triazines with nitro groups were prepared by the reaction of biguanide derivatives with appropriate carboxylic acid derivatives (acyl chloride, anhydride, or ester) or by reaction between dicyanodiamide derivatives and nitrile. Amino-*s*-triazines with aminophenyl groups were prepared by the reduction of the corresponding nitro-compounds. Acylamino-*s*-triazines have been found to be formed when an excess of acyl chloride or anhydride is used.

The amino-*s*-triazines bearing extra amino groups attached to the side chain are interesting since these compounds can serve as possible intermediates for the synthesis of new triazine derivatives.

In this paper the preparation of amino-*s*-triazines bearing phenyl substituents with nitro or amino groups will be described.

In general,[1] amino-*s*-triazine derivatives have been prepared by the reaction of appropriate biguanide derivatives with acyl chloride, anhydride, or ester, or from appropriate dicyanodiamide derivatives with nitrile in the presence of strong alkali. These two methods were used in the present work.

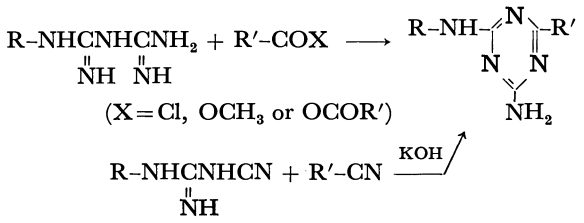

Results and Discussion

The synthetic results are summed up in Table 1. The reaction of biguanide derivatives with methyl formate proceeded rapidly, but the corresponding reaction with methyl acetate was slow and gave poor yields of the desired materials.[2] With methyl benzoate, the reaction was found to proceed even more slowly than in the cases of methyl acetate and methyl formate. Therefore, acyl chloride or acid anhydride was used to obtain *s*-triazine from biguanide derivatives. In the present work, when an excess of acetic anhydride or benzoyl chloride was used as the acylation reagent, it was found that acylated amino-*s*-triazines were obtained as the by-products. On the other hand, when excesses of biguanide derivatives were used, it was found that no acylamino-*s*-triazines were obtained.

UV Spectra. The UV spectra of *s*-triazines have been reported by several investigators.[3-7] *s*-Triazines without phenyl or anilino groups attached directly to the triazine ring have ε values of around 10^3.[3]

The UV spectral data of *s*-triazines described in Table 1 are summed up in Table 2. These triazines have ε values of about 10^4. It can be seen from Table 2 that, while it has been known that 2,4-diamino-6-phenyl-*s*-triazine and 2-amino-4-anilino-6-phenyl-*s*-triazine have their absorption maxima at 245 mμ[8] ($\varepsilon = 22.2\times10^3$) and at 260 m$\mu$[8] ($\varepsilon = 43.4\times10^3$), *s*-triazines with *p*-nitroanilino substituents and those with *p*-aminophenyl substituents were found to reveal their absorption maxima at 344—352 mμ and at 315—320 mμ respectively. The comparisons of the absorption maxima of 4- or 6-substituted-*s*-triazines are described in Table 3. That is, the introduction of a nitro group into the *para* position of a 4-anilino-substituent, or that of an amino group into the *para* position of a 6-phenyl-substituent, of the 2-amino-*s*-triazine ring results in a large bathochromic shift, as expected. This is due to the resonance interaction involving contributions from the following structures:

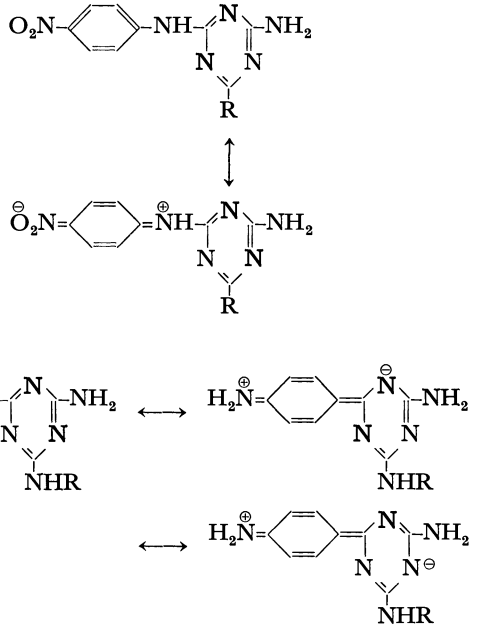

* Present address: Faculty of Engineering, Tokyo Institute, of Technology, Ookayama, Meguro-ku, Tokyo.

1) E. M. Smolin and L. Rapoport, "The Chemistry of Heterocyclic Compounds", Vol. 13, ed. by A. Weissberger, Wiley (Interscience), New York, N. Y. (1959), p. 217.

2) Y. Yuki, T. Kakurai, and T. Noguchi, This Bulletin, **43**, 2123 (1970).

3) C. G. Overberger and S. L. Shapiro, *J. Amer. Chem. Soc.*, **76**, 1855 (1954).

4) S. L. Shapiro, V. A. Parrino, and L. Freedman, *J. Org. Chem.*, **25**, 379 (1960).

5) S. L. Shapiro, V. A. Parrino, and L. Freedman, *ibid.*, **26**, 3331 (1961).

6) G. Takimoto, *Nippon Kagaku Zasshi*, **85**, 159 (1964).

7) G. Morimoto, *ibid.*, **87**, 785 (1966).

8) Y. Yuki, T. Kakurai, and T. Noguchi, *Yuki Gosei Kagaku Kyokai Shi*, **26**, 1119 (1968).

TABLE 1. *s*-TRIAZINE DERIVATIVES

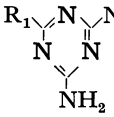

Compounds	R_1	R_2	Method[a]	Yield (%)	mp[b] (lit.) (°C)	Found (Calcd) C(%)	H(%)	N(%)	
1	$C_6H_4NO_2(p)$	H	A	89	322 (330—331[e])				
2	$C_6H_4NO_2(m)$	H	A	82	240—241 (243—245[d])				
3	H	$C_6H_4NO_2(p)$	B	48	335 (325[e], 347[f])	47.80 (46.55	3.23 3.47	37.08 36.19;	$C_9H_8N_6O_2$)
4	H	$C_6H_4NO_2(m)$	B	43	226—227	46.17 (46.55	3.43 3.47	35.66 36.19;	$C_9H_8N_6O_2$)
5	CH_3	$C_6H_4NO_2(p)$	C	90	269	49.07 (48.78	4.02 4.09	34.10 34.13;	$C_{10}H_{10}N_6O_2$)
6	CH_3	$C_6H_4NO_2(m)$	C	55	224—225	48.94 (48.78	3.80 4.09	34.62 34.13;	$C_{10}H_{10}N_6O_2$)
7	C_6H_5	$C_6H_4NO_2(p)$	C A	75 58	230—231	58.68 (58.44	3.66 3.92	26.39 27.26;	$C_{15}H_{12}N_6O_2$)
8	C_6H_5	$C_6H_4NO_2(m)$	C	90	213—215	59.33 (58.44	3.57 3.92	27.27 27.26;	$C_{15}H_{12}N_6O_2$)
9	$C_6H_4NO_2(p)$	C_6H_5	C	77	223—224	58.25 (58.44	4.13 3.92	27.43 27.26;	$C_{15}H_{12}N_6O_2$)
10	$C_6H_4NO_2(m)$	C_6H_5	C	93	205—206 (212—213[g])	57.99 (58.44	4.32 3.92	27.11 27.26;	$C_{15}H_{12}N_6O_2$)
11	$C_6H_4NO_2(p)$	$C_6H_4NO_2(p)$	C	98	364	50.72 (51.00	2.92 3.14	26.78 27.75;	$C_{15}H_{11}N_7O_4$)
12	$C_6H_4NO_2(p)$	$C_6H_4NO_2(m)$	C	69	266	51.83 (51.00	3.30 3.14	26.76 27.75;	$C_{15}H_{11}N_7O_4$)
13	$C_6H_4NO_2(m)$	$C_6H_4NO_2(p)$	C A	89 41	278	50.28 (51.00	3.87 3.14	26.86 27.75;	$C_{15}H_{11}N_7O_4$)
14	$C_6H_4NO_2(m)$	$C_6H_4NO_2(m)$	C	82	277	51.29 (51.00	3.08 3.14	26.92 27.75;	$C_{15}H_{11}N_7O_4$)
15	$C_6H_3(NO_2)_2$-3,5	C_6H_5	C	77	297	51.43 (51.00	3.43 3.14	27.21 27.75;	$C_{15}H_{11}N_7O_4$)
16	$C_6H_3(NO_2)_2$-3,5	H	C	90	361	39.52 (39.00	2.65 2.55	34.74 35.37;	$C_9H_7N_7O_4$)
17	$C_6H_4NH_2(p)$	H	A	56	196—197 (206[d])				
18	$C_6H_4NH_2(m)$	H	A	85	206—208 (212—213[d])				
19	$CH_2C_6H_4NH_2(p)$	H	A	56	255—256.5	55.84 (55.54	5.17 5.60	39.56 38.86;	$C_{10}H_{12}N_6$)
20	H	$C_6H_4NH_2(p)$	D	54	288	53.50 (53.46	4.80 4.98	42.28 41.56;	$C_9H_{10}N_6$)
21	H	$C_6H_4NH_2(m)$	D	78	215—216	54.24 (53.46	4.76 4.98	42.80 41.56;	$C_9H_{10}N_6$)
22	CH_3	$C_6H_4NH_2(p)$	D	90	246—247	55.14 (55.54	5.16 5.59	38.05 38.86;	$C_{10}H_{12}N_6$)
23	CH_3	$C_6H_4NH_2(m)$	D	90	176—177	55.89 (55.54	5.66 5.59	38.45 38.86;	$C_{10}H_{12}N_6$)
24	C_6H_5	$C_6H_4NH_2(p)$	D	84	195.5—196	65.37 (64.75	4.77 5.03	30.39 30.22;	$C_{15}H_{14}N_6$)
25	C_6H_5	$C_6H_4NH_2(m)$	D	69	190—191	64.99 (64.75	4.83 5.03	30.79 30.22;	$C_{15}H_{14}N_6$)
26	$C_6H_4NH_2(p)$	C_6H_5	D	78	203—204	64.91 (64.75	5.75 5.03	29.34 30.22;	$C_{15}H_{14}N_6$)
27	$C_6H_4NH_2(m)$	C_6H_5	D	67	162—163	65.08 (64.75	4.81 5.03	30.72 30.22;	$C_{15}H_{14}N_6$)

a) A, from dicyanodiamide and nitrile; B, from biguanide and ester; C, from biguanide and acyl chloride or anhydride; D, reduction of the corresponding nitro-*s*-triazine. b) The mp above 250°C was measured by DSC. c) V. A. Titkov and I. D. Pletnev, *Zh. Obshch. Khim.*, **33**, 1983 (1963); *Chem. Abstr.*, **59**, 15408f (1963). d) Ref. 1. e) J. T. Thurston and D. W. Kaiser, US 2493703 (1950); *Chem. Abstr.*, **44**, 2574d (1950) f) I. Groth, Brit. 794398 (1958); *Chem. Abstr.*, **53**, 420e (1959). g) Ref. 5.

TABLE 2. UV SPECTRA OF *s*-TRIAZINES

Compounds	$\lambda_{max}^{(m\mu)}$ ($\varepsilon \times 10^{-3}$)	solvent[a]
1	280 (19.5)	MCS
2	232 (22.8), 270s(7.7)	MCS
3	344 (19.1)	MCS
4	261 (21.4), 274 (21.6), 340s(1.4)	MCS
5	345 (15.4)	MCS
6	260s(25.1), 273 (27.0), 340 (1.6)	MCS
7	248 (28.9), 348 (23.8)	Et
8	261 (41.6)	Et
9	272 (33.0), 290s(29.6)	MCS
10	245s(27.7), 259 (34.4), 310s(6.6)	MCS[b]
11	279 (17.0), 352 (20.0)	MCS
12	268 (26.3), 275s(25.7)	MCS
13	245 (31.6), 350 (20.0)	MCS
14	245s(35.6), 258 (41.3)	MCS
15	245s(27.3), 257 (31.2)	MCS
16	243 (23.4), 300s(3.1)	MCS
17	315 (23.7)	Et
18	233 (32.7), 263s(12.0), 328 (2.4)	Et
19	242 (13.7), 290s(2.5)	Et
20	245s (9.6), 282 (14.3)	MCS
21	245 (20.0), 270s(13.9), 300s(7.6)	MCS
22	245s(9.5), 283 (16.3)	MCS
23	244 (19.4), 270s(13.7), 300s(6.7)	MCS
24	255 (26.9), 265s(26.5)	Et
25	227s(28.5), 247 (31.8), 258s(30.0) 300s(8.0)	Et
26	257 (16.7), 316 (25.4)	Et
27	233 (28.1), 258 (31.0), 310s(9.2)	Et
28[c]	316 (39.7)	MCS
29[c]	320 (39.7)	MCS
30[c]	237 (53.9), 256s(35.4), 306 (10.7)	MCS

a) Solvent: MCS, methyl cellosolve: Et, ethanol.
b) Shapiro has reported 255 mμ (ε, 39.7×10^3) in methanol (Ref. 5).
c) Reported previously (Y. Yuki, S. Sakurai, T. Kakurai, and T. Noguchi, This Bulletin, **43**, 2130 (1970)).
28: 2-amino-4-*p*-aminoanilino-6-*p*-aminophenyl-*s*-triazine,
29: 2-amino-4-*m*-aminoanilino-6-*p*-aminophenyl-*s*-triazine,
30: 2-amino-4-*m*-aminoanilino-6-*m*-aminophenyl-*s*-triazine.

TABLE 3. COMPARISONS OF THE ULTRAVIOLET ABSORPTION MAXIMA OF SUBSTITUTED *s*-TRIAZINES

4 or 6-Substituent	λ_{max}(mμ)	Compound
p-Nitroanilino	344—352	3,5,7,11, and 13
m-Nitroanilino	258—274	4,6,8,12, and 14
p-Nitrophenyl	275—290	1,9,11, and 12
m-Nitrophenyl	232—259	1,10,13, and 14
p-Aminoanilino	265—283	20,22, and 24
m-Aminoanilino	258—270	21,23, and 25
p-Aminophenyl	315—320	17,26,28, and 29
m-Aminophenyl	233—237 256—265	18,27, and 30

On the other hand, the introduction of a nitro or amino group into the *meta* position of a phenyl or anilino group attached to the 2-amino-*s*-triazine ring leads to little or no bathochromic effect, as is shown in Table 3.

Experimental

All the melting points were uncorrected, and mps above 250°C were measured by means of a Differential Scanning Calorimeter (DSC). MCS denotes methyl cellosolve.

*2-Amino-4-*m*-nitroanilino-*s*-triazine (4).* This product was predpared by the procedure detailed by Overberger and Shapiro.[9] When *m*-nitrophenylbiguanide (*m*-NPB) was treated with methyl formate in methanol, it gave **4** (43%). The removal of the solvent from the filtrate gave a residue which was then recrystallized from a methanol-ethanol mixture to afford formic acid salt of *m*-NPB, mp 186—187°C (decomp).

Found: C, 40.25; H, 4.31; N, 30.80%. Calcd for $C_9H_{12}N_6O_4$: C, 40.30; H, 4.51; N, 31.33%.

*2-Amino-4-*p*-nitroanilino-6-methyl-*s*-triazine (5).* Into a solution of 8.9 g (40 mmol) of *p*-nitrophenylbiguanide (*p*-NPB) in 100 m*l* of acetone, we slowly stirred 2.0 g (20 mmol) of acetic anhydride with ice-cooling. After 1 hr, the precipitate (8.73 g) was separated and washed with hot water to yield 3.0 g of the product, which was then treated with methanol-MCS mixture to give 0.2 g of insoluble, crude 2-acetamido-4-*p*-nitroanilino-6-methyl-*s*-triazine (**31**), mp 275°C. This was recrystallized from DMF, mp 286°C. The filtrates (acetone and methanol-MCS) were combined, and from this there were obtained 4.5 g (90%) of **5**, recrystallized from MCS, mp 269°C.

*2-Acetamido-4-*p*-nitroanilino-6-methyl-*s*-triazine (31).* To a solution of 1.23 g (5 mmol) of **5** suspended in 10 m*l* of dioxane, we added 3 m*l* of acetic anhydride, and then the solution was refluxed for 5 hr. We thus obtained 1.10 g (76%) of the product, which was subsequently recrystallized from DMF, mp 287°C.

Found: C, 50.03; H, 3.92; N, 28.84%. Calcd for $C_{12}H_{12}N_6O_3$: C, 50.00; H, 4.20; N, 29.15%. UV: λ_{max}^{MCS}mμ ($\varepsilon \times 10^{-4}$) 234(2.64) and 343(2.03).

*2-Amino-4-*m*-nitroanilino-6-methyl-*s*-triazine (6).* This compound was previously prepared by the reaction of *m*-NPB with methyl acetate.[2] In the present work the reaction of *m*-NPB with acetic anhydride was carried out as above. Acetic anhydride (1.02 g) and 4.44 g of *m*-NPB gave 1.34 g (55%) of **6**, mp 224—225°C, and 0.30 g of 2-acetamido-4-*m*-nitroanilino-6-methyl-*s*-triazine, recrystallized from DMF mp 259°C.

Found: C, 49.66; H, 4.04; N, 29.56%. Calcd for $C_{12}H_{12}N_6O_3$: C, 50.00; H, 4.20; N, 29.15%. UV: λ_{max}^{MCS}mμ ($\varepsilon \times 10^{-4}$), 231(2.13) and 271(3.00).

*2-Amino-4-*p*-nitroanilino-6-phenyl-*s*-triazine (7).* a) When *p*-NPB (6.66 g, 30 mmol) was treated with 4.20 g (30 mmol) of benzoyl chloride and 2.0 g (36 mmol) of sodium hydroxide, it gave 2.95 g (32%) of **7** and 1.45 g of 2-benzamido-4-*p*-nitroanilino-6-phenyl-*s*-triazine, which was recrystallized from DMF, mp 265°C.

Found: C, 63.20; H, 3.73; N, 20.64%. Calcd for $C_{22}H_{16}N_6O_3$: C, 64.07; H, 3.91; N, 20.38%. UV: λ_{max}^{MCS}mμ ($\varepsilon \times 10^{-4}$) 256(2.98) and 347(1.86).

b) *p*-NPB (4.70 g, 21 mmol) was treated with 1.40 g (10 mmol) of benzoyl chloride in acetone to give 2.30 g (75%) of the product, mp 228—229°C.

Found: C, 56.13; H, 3.94; N, 26.28%. Calcd for $C_{15}H_{12}N_6O_2 \cdot 1/2\ H_2O$: C, 56.78; H, 4.13; N, 26.49%.

c) *p*-Nitrophenyldicyanodiamide (*p*-NPD) (1.0 g, 5 mmol) was treated with 1 m*l* of benzonitrile and 0.1 g of sodium

9) C. G. Overberger and S. L. Shapiro, *J. Amer. Chem. Soc.*, **76**, 93 (1954).

hydroxide in MCS under reflux for 5 hr. There was thus obtained 0.89 g, (58%) of **7**, which was recrystallized from MCS-water, mp 230—231°C.

Found: C, 58.15; H, 3.63; N, 26.73%. Calcd for $C_{15}H_{12}N_6O_2$: C, 58.44; H, 3.92; N, 27.26%.

*2-Amino-4-*m*-nitroanilino-6-phenyl-*s*-triazine (8).* a) *m*-NPB (6.66 g, 30 mmol) was treated with 4.60 g (33 mmol) of benzoyl chloride and 2.0 g (36 mmol) of sodium hydroxide give to 5.02 g (54%) of **8** and 2.76 g of 2-benzamido-4-*m*-nitroanilino-6-phenyl-*s*-triazine, which was recrystallized from DMF, mp 266—267°C.

Found: C, 63.86; H, 3.66; N, 20.53%. Calcd for $C_{22}H_{16}N_6O_3$: C, 64.07; H, 3.91; N, 20.38%. UV: $\lambda_{max}^{MCS}m\mu$ ($\varepsilon\times10^{-4}$) 261(3.77).

b) Into 4.50 g (20.3 mmol) of *m*-NPB dissolved in 50 m*l* of acetone, we stirred, drop by drop, 1.27 g (9.1 mmol) of benzoyl chloride in 50 m*l* of acetone with ice-cooling over a half-hour period. As the precipitate, 2.03 g of hydrochloride of *m*-NPB were thus obtained. The filtrate was condensed and poured into water. A yellow product, 2.52 g (90%) of **8**, was obtained.

*2-Amino-4-anilino-6-*p*-nitrophenyl-*s*-triazine (9).* Phenylbiguanide (30 g, 0.17 mol) was treated with 25 g (0.13 mol) of *p*-nitrobenzoyl chloride. The precipitate was filtered to yield 27.5 g of the pure product.

Found: C, 57.72; H, 4.06; N, 27.09%. Calcd for $C_{15}H_{12}N_6O_2$: C, 58.44; H, 3.89; N, 27.27%.

From the filtrate we obtained 4.5 g of **9** and 4.0 g of *p*-nitrobenzoic acid. The total yield of the product was 32 g (77%), recrystallized from a water-MCS mixture, mp 223-224°C.

*2-Amino-4-*p*-nitroanilino-6-*m*-nitrophenyl-*s*-triazine (13).* a) *p*-NPB (15 g, 68 mmol) was treated with 9.3 g (50 mmol) of *m*-nitrobenzoyl chloride. We thus obtained 15.7 g (87%) of the product, mp 275°C.

b) The reaction of *p*-NPD (2.15 g 10.5 mmol) with *m*-nitrobenzonitrile (1.56 g, 11 mmol) was carried out using 0.2 g of potassium hydroxide in MCS under reflux for 5 hr; it gave 1.52 g (41%) of **13**, which was recrystallized from a DMF-MCS mixture, mp 278°C.

*2-Amino-4-*m*-aminoanilino-*s*-triazine (21).* Tin (0.6 g) and 0.55 g (2.36 mmol) of **4** were suspended in 10 m*l* of ethanol containing 3.0 m*l* of 12 N hydrochloric acid, after which the solution was refluxed for 1 hr. On cooling, the precipitate was filtered and dissolved in hot water. A further amount of sodium hydroxide was added. There was thus obtained 0.37 g of a product (78%) which was recrystallized from methanol, mp 215—216°C.

The authors wish to thank Mr. T. Saito of Tokyo Institute of Technology for his elementary analysis and Miss H. Asanuma for her help in the measurements of UV spectra.

BULLETIN OF THE CHEMICAL SOCIETY OF JAPAN, VOL. 44, 2447—2453 (1971)

Syntheses and Thermal Isomerizations of Bicyclo[3.2.2]-nona-2,6,8-triene and Its Benzo Analog[1,2]

Teruji TSUJI, Hiroyuki ISHITOBI, and Hiroshi TANIDA

Shionogi Research Laboratory, Shionogi & Co., Ltd., Fukushima-ku, Osaka

(Received December 31, 1970)

A convenient synthesis of bicyclo[3.2.2]nona-2,6,8-triene (**1**) was devised starting from the cycloheptatriene-maleic anhydride adduct. Benzo[*f*]bicyclo[3.2.2]nona-2,6,8-triene (**2**) was prepared starting from benzo[*f*] bicyclo[3.2.2]nona-3,6,8-trien-2-one. Heating **1** in *n*-hexane at 160—180°C gave almost quantitatively 3-vinyl-cycloheptatriene (**9**) besides a trace of 7-vinylcycloheptatriene (**10**). It was found however that **10** undergoes thermal isomerization into **9** under milder conditions. The result from **1** is thus rationalized by the existence of an equilibrium between **1** and **10** preceding the conversion of **10** into **9**. On the other hand, benzo analog **2** does not isomerize in a similar manner and instead, is transformed by heating at 270—290°C into benzobarbaralane (**14**) and hydrobenzindene (**15**). The contrast in behavior is discussed.

Despite the great interest involved, relatively little is known about bicyclo[3.2.2]nona-2,6,8-triene (**1**), a highly unsaturated polycyclic C_9H_{10} hydrocarbons, perhaps because of the difficulty in synthesizing it.[3]

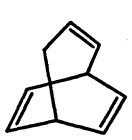

1

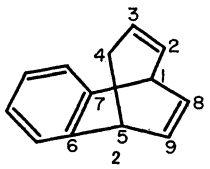

2

Synthesis of **1** has been achieved independently by three groups,[3a-c] through multi-step processes and/or by ones involving troublesome purification procedures. During the course of studies on the cycloaddition reactions of cycloheptatriene,[4] we found a simple syntheses of **1**. This paper deals with the synthesis and

1) Presented at the IUPAC Symposium of Nonbenzenoid Aromatic Compounds in Sendai, August, 1970.

2) The numbering used is shown in the charts. Compounds in which the substituent on the aliphatic ring is directed toward the benzene ring are difined as *endo*; those in which the substituent is directed away from the benzene ring are defined as *exo*.

3) a) M. Jones and S. D. Reich, *J. Amer. Chem. Soc.*, **89**, 3935 (1967); b) J. Daub and P. v. R. Schleyer, *Angew. Chem. Int. Ed. Engl.*, **7**, 468 (1968); c) J. B. Grutzner and S. Winstein, *J. Amer. Chem. Soc.*, **90**, 6562 (1968); d) S. W. Staley and D. W. Reichard, *ibid.*, **91**, 3998 (1969).

4) T. Tsuji, S. Teratake, and H. Tanida, This Bulletin, **42**, 2033 (1969).

thermal rearrangement of **1** and a benzo variant, benzo[*f*]bicyclo[3.2.2]nona-2,6,8-triene (2). The thermal behavior of unsaturated polycyclic hydrocarbons is typically a unimolecular reaction, and as such can frequently give important data for testing the theories of such processes.[5] In this connection and because of our interest in such reactions,[6] thermolyses of the present [3.2.2]triene systems were investigated.

Results and Discussion

Synthesis. The cycloaddition of cycloheptatriene to maleic anhydride was reported by Alder and Jacobs[7] to produce a single adduct, tricyclo[3.2.2.$0^{2,4}$]-non-6-ene-8,9-dicarboxylic anhydride (**3**). The photosensitized addition with the same materials has also been found by Schenk *et al.* to form mainly the same adduct, together with two other minor compounds.[8,9] Conversion of **3** into bicyclo[3.2.2]nona-2,6-diene-8,

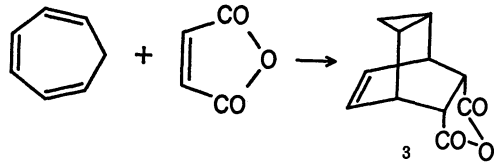

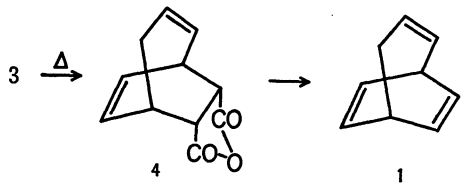

9-dicarboxylic anhydride (**4**) with opening of the cyclopropane ring was accomplished by heating **3** in chlorobenzene at 220°C. Such a relatively easy cleavage of cyclopropane was not observed with a similar treatment of the dihydro derivative of **3** (**5**).[10] Electrolytic bisdecarboxylation, principally by applying the reported procedure,[12] was carried out on **4** to obtain **1**, the physical properties of which were consistent in all respects with the reported data.[3a-c]

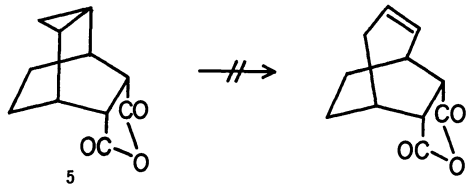

Essentially the same route reported for the preparation of bicyclo[3.2.1]octa-2,6-diene[13] and **1**[3c] was applied for the synthesis of **2**. Lithium aluminum hydride reduction of benzo[*f*]bicyclo[3.2.2]nona-3,6,8-trien-2-one (**6**) (prepared by the addition of benzyne to tropone)[14] gave a mixture of the *endo*- and *exo*-alcohols (**7**), which were methylated with dimethyl sulfate. *endo*- and *exo*-ethers (**8**) were treated with sodium-

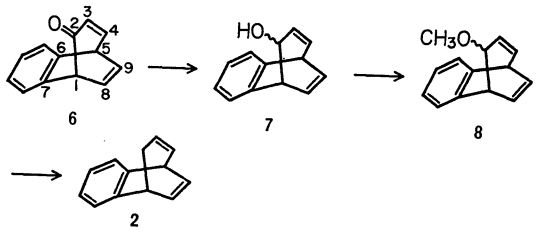

potassium alloy in dimethoxyethane and then quenched with methanol to yield **2** as crystals from **6** in 43% yield. The UV, IR, NMR, and mass spectral data are consistent with the indicated structure for **2** (see Experimental). The NMR pattern of the aliphatic moiety is very similar to that of **1**[3c] and shows the C_3 vinyl proton at an unusually high field τ 5.71. Since all the peaks reported for 2-methylnaphthalene,[15a] and benzobicyclo[2.2.2]octatriene[15b,c] but no other peaks were observed in the mass spectrum of **2**, it is considered that the fragmentation of **2** begins with the formation of the benzotropyrilium ion and the benzobicyclo[2.2.2]octatriene ion (*m/e* 154).

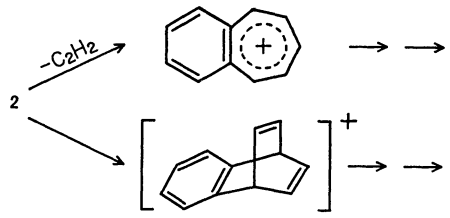

Thermal Isomerization of Bicyclo[3.2.2]nonatriene (**1**). When a solution of **1** in *n*-hexane was heated in a degassed sealed ampoule in the temperature range 160—180°C, the reaction mixture initially showed an almost quantitative formation of 3-vinylcycloheptatriene (**9**)[3b] besides a trace of 7-vinylcycloheptatriene (**10**).[16] Further heating of the mixture resulted in a

5) A review, H. M. Frey, "Advances in Physical Organic Chemistry," Vol. 4, V. Gold Ed., Academic Press, New York, N. Y. (1966), pp. 147—193.

6) H. Tanida and Y. Hata, *J. Amer. Chem. Soc.*, **91**, 6775 (1969).

7) K. Alder and G. Jacobs, *Chem. Ber.*, **86**, 1528 (1953).

8) G. O. Schenk, J. Kuhls, and C. H. Krauch, *Ann. Chem.*, **693**, 20 (1966).

9) Alder and Jacobs[7] originally assigned the *endo* configuration to the dicarboxylic anhydride group in **3**, while Schenk and his coworkers[8] suggested the *exo* configuration on the grounds that treatment of **3** with a basic iodine-potassium iodide solution did not cause iodolactonization. We re-examined the thermal cycloaddition reaction of cycloheptatriene with maleic anhydride and configuration of the adduct. From our preliminary results we prefer the *endo* configuration. Details of our re-examination will be reported soon.

10) A bond-breaking process in simple cyclopropanes requires an activation energy as high as ~63 kcal.[11] Therefore, the result from **5** would be more common.

11) B. S. Rabinowitch, E. W. Schlag, and K. Wiberg, *J. Chem. Phys.*, **28**, 504 (1958); B. S. Rabinowitch and E. W. Schlag, *J. Amer. Chem. Soc.*, **86**, 5996 (1960).

12) P. Radlick, R. Klem, S. Spurlock, J. J. Sims, E. E. van Tamelen, and T. Whitesides, *Tetrahedron Lett.*, **1968**, 5117; H. H. Westberg and H. J. Dauben, Jr., *ibid.*, **1968**, 5123.

13) J. M. Brown, *Chem. Commun.*, **1967**, 638.

14) J. Ciabattoni, J. E. Crowley, and A. S. Kende, *J. Amer. Chem. Soc.*, **89**, 2778 (1967).

15) a) "Catalog of Mass Spectral Data," American Petroleum Institute, Research Project 44, Carnegie Institute of Technology, Pittsburgh, Pennsylvania, Ref. 1, spectra Nos 855; b) R. G. Miller and M. Stiles, *J. Amer. Chem. Soc.*, **85**, 1798 (1963); c) T. Goto, A. Tatematsu, Y. Hata, R. Muneyuki, H. Tanida, and K. Tori, *Tetrahedron*, **22**, 2213 (1966).

16) R. B. King and F. G. A. Stone, *J. Amer. Chem. Soc.*, **83**, 3590 (1961).

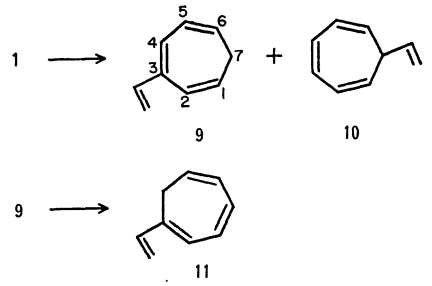

hydrogen shift transforming **9** into 1-vinylcycloheptatriene (**11**). The structure of **11** was determined principally by the NMR spectrum which shows a doublet at τ 7.46 (J=7.0 Hz) arising from two methylene protons at C_7.[17] The 7-vinyl isomer **10** was independently synthesized and subjected to thermal isomerization. It was observed that **10** isomerizes into a 1:9 mixture of **1** and **9** in the temperature range 120—140°C, and that the products are the same as those from the thermolysis of **1**, although the reaction proceeded at lower temperatures. No isomerization of **1** thus formed was confirmed under the present conditions. The results are therefore compatible with an equilibrium between **1** and **10** preceding the conversion of **10** into **9**. A further support of this view was

$$\mathbf{1} \underset{k_{-1}}{\overset{k_1}{\rightleftharpoons}} \mathbf{10} \xrightarrow{k_2} \mathbf{9}$$

provided by a trapping experiment. Thermolysis of **1** in the presence of maleic anhydride produced a tricyclic adduct bearing a vinylcyclopropane moiety (**12**), which was identical with the product obtained from the cycloaddition of **10** with maleic anhydride in boiling dioxane.

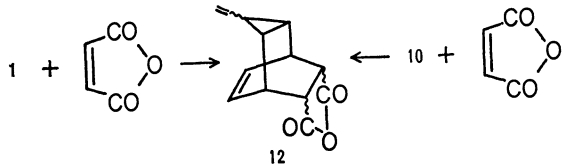

The rates of disappearance of **1** and **10** (k_t and k'_t, respectively) on thermolysis were determined by use of vpc. Good first-order kinetics was observed in all runs. The rate constants thus observed are listed in Table 1, with the kinetic parameters derived at 159.2°C. Since it was confirmed experimentally that the concentration of **10** did not exceed 1.4% of the total of reaction components through all the reaction period, it is not unreasonable to approximate a steady state on **10**. Thus we obtain

$$k_t = k_1k_2/(k_{-1}+k_2) \text{ and } k_t' = k_{-1} + k_2$$

where k_1 and k_{-1} are the interconversion rates between **1** and **10**, and k_2 is the rate of conversion of **10** into **9**. The constants, k_1, k_{-1}, and k_2, in Table 2 are thus calculated and the derived kinetic parameters produce a free energy diagram as shown in Fig. 1. The energy barrier $\Delta F^{\ddagger}$ for the interconversion between **1** and **10** at 159.2°C is 35.0 kcal/mol from **1** and 33.2 kcal/mol from **10**.

A mechanism which accommodates all the results is

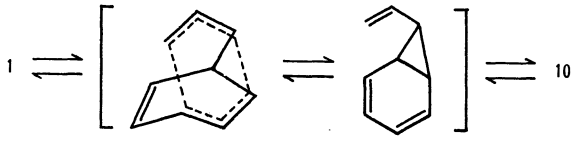

17) Cycloheptatrienes having no substituent at C_1 and C_6 show a triplet due to the protons at C_7. Refer to R. Roth, *Angew. Chem. Int. Ed. Engl.*, **2**, 688 (1963); A. P. ter Borg and H. Kloosterziel, *Rec. Trav. Chem., Pays-Bas*, **82**, 741 (1963).

Table 1. Rate constants of thermolysis[a]

Compound	Temp °C	k, sec^{-1}	$\Delta H^{\ddagger}$, kcal	$\Delta S^{\ddagger}$ cal/deg
	159.2	1.70×10^{-5}	34.3[b]	−1.8[b]
	180.2	1.13×10^{-4}		
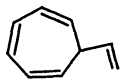	119.7	3.61×10^{-5}		
	140.0	2.49×10^{-4}		
	159.2	1.30×10^{-3}	29.8[b]	−3.5[b]
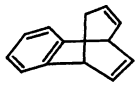	268.5	1.18×10^{-4}	46.8[d]	5.5[d]
	289.8	6.36×10^{-4}		

a) Carried out with 0.1N solution in *n*-hexane.
b) Calculated at 159.2°C.
c) Calculated by Arrhenius plots.
d) Calculated at 268.5°C.

Table 2. Analysis of observed rate constants[a]

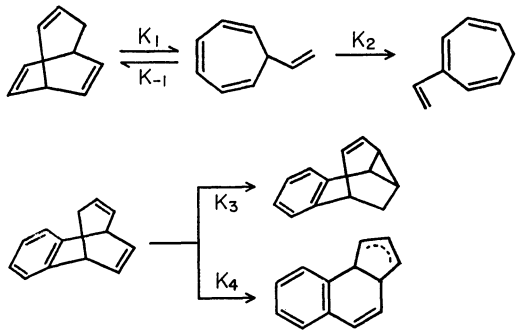

Process	Temp °C	k, sec^{-1}	$\Delta H^{\ddagger}$, kcal	$\Delta S^{\ddagger}$, cal/deg
k_1	159.2	1.94×10^{-5}	34.1[b]	−1.9[b]
	180.2	1.28×10^{-4}		
k_{-1}	119.7	2.89×10^{-6}		
	140.0	2.49×10^{-5}		
	159.2	1.58×10^{-4}[a]	33.4[b]	0.49[b]
k_2	119.7	3.32×10^{-5}		
	140.0	2.24×10^{-4}		
	159.2	1.15×10^{-3}[c]	29.5[b]	−4.5[b]
k_3	268.5	8.43×10^{-5}	48.3[d]	10.8[d]
	289.8	4.79×10^{-4}		
k_4	268.5	3.37×10^{-5}	43.8[d]	−1.4[d]
	289.8	1.57×10^{-4}		

a) For calculations of k_1, k_{-1}, and k_2, see Text.
b) Calculated at 159.2°C.
c) Calculated by Arrhenius plots.
d) Calculated at 268.5°C.

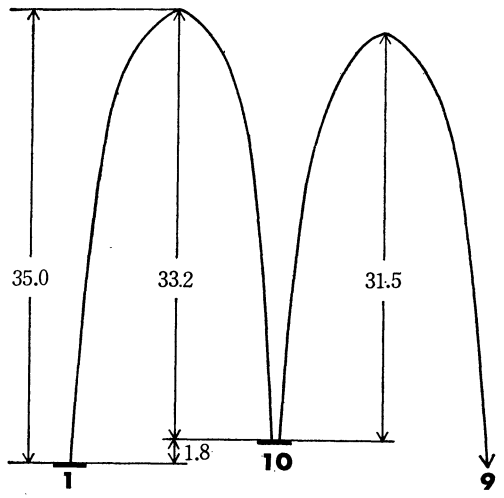

Fig. 1.

the Cope rearrangement (a [3,3]sigmatropic rearrangement) passing through *cis*-7-vinylnorcaradiene (**13**) as a transition state or an intermediate. The rearrangement of *cis*-6-vinylbicyclo[3.1.0]hex-2-ene to bicyclo[3.2.1]octa-2,6-diene[18] and the formation of bicyclo[3.2.2]nona-3,6,8-trien-2-one by treatment of cyclohepta-2,4,6-trienylacetyl chloride with triethylamine, presumably by a Cope rearrangement of the cyclohepta-2,4,6-trien-7-yl ketene intermediate,[19] are thought to be related precedents, although they are one-way reactions corresponding to the k_{-1} process and not interconversion as in the present case. The isomerization of **10** into **9** is an example of the familiar 1,5-hydrogen shift. It is noted that the kinetic parameters ($\Delta H^{\ddagger}=29.5$ kcal, $\Delta S^{\ddagger}=-4.5$ cal/deg at 159.2°C) are comparable with those reported for the thermal isomerization of 1,4-bis(7-cycloheptatrienyl)benzene into 1,4-bis(3-cycloheptatrienyl)benzene ($\Delta H^{\ddagger}=29.8$ kcal, $\Delta S^{\ddagger}=-3.9$ cal/deg at 140°C),[20] but not with those for the isomerization of 7-phenylcycloheptatriene into 3-phenylcycloheptatriene ($\Delta H^{\ddagger}=26.9$ kcal, $\Delta S^{\ddagger}=-11.7$ cal/deg: for which the specific temperature has not been reported).[21] The 7 substituents in these molecules have freedom of rotation around the C'_1–C_7 axis, but it is somewhat restricted after the hydrogen has shifted, because the π-electrons in the substituents now come to conjugation with the unsaturation in the ring. The observed entropy decrease is compatible with this decreasing freedom of motion in the molecules.

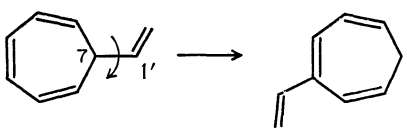

Thermolysis of Benzobicyclo[3.2.2]nonatriene (2). The thermal transformtion of **2** in *n*-hexane was monitored by vpc at two temperatures, 268.5°C and 289.8°C and found to give mainly benzo[3,4]barbaralane (**14**) and the hydrobenzindene (**15**) (in total, 95%), with a trace of an unidentified compound. The ratios of **14** and **15** were 2.5:1 at 268.5°C and 3.0:1 at 289.8°C.[22] Rates and kinetic parameters are summarized in Tables 1 and 2. The two major products, **14** and **15**, were isolated by vpc. The structure of **14** was assigned on the basis of spectral evidence. The presence of two vinyl protons and the absence of a double bond conjugated with benzene were indicated by NMR and UV, respectively. The 100 MHz NMR data obtained using double and triple resonance techniques are in line with the structure **14** (see Experimental). Also, the NMR demonstrated that **14** possess a fixed structure, and not a fluxional character like barbaralane.[23] Conceivable alternatives to structures **14**, **16**, **17**, and **18** were ruled out by NMR. The methylene protons appear as a triplet at a field higher than usually expected for allylic protons and show no coupling with the vinyl protons. These facts eliminate structure **16**. The

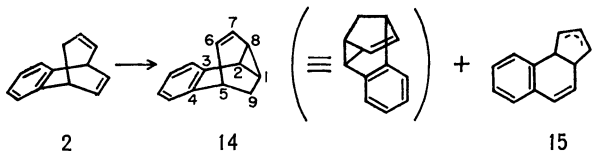

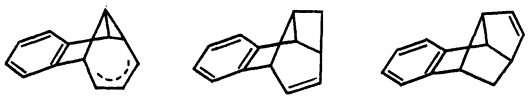

identical coupling constants ($J=7.6$ Hz) between H_1 and H_2, H_1 and H_8, and H_2 and H_8 support the existence of a three-membered ring, but not that of structure **17** or **18**. The UV maximum at 268 mμ (ε 8500) observed in product 15 indicates the presence of a double bond conjugated with a benzene ring. The NMR spectrum of **15** exhibits a doublet of doublets at τ 3.8 assignable to a vinyl proton adjacent to a benzene ring. Catalytic hydrogenation over palladium on carbon resulted in the uptake of 2 moles of hydrogen to yield the known 2,3,3aβ,4,5,9bβ-hexahydro-1*H*-benz[*e*]indene.[24] Consequently, the structure of **15** was determined to be either 3a,9b-dihydro-3*H*-benz[*e*]indene or its double-bond isomer, 3a,9b-dihydro-1*H*-benz[*e*]indene.

The formation of **14** can be explained by postulating an intramolecular ene reaction[25] through such a six-membered transition state as **19**, which involves one of the allylic hydrogens. Concerning the formation of

18) J. M. Brown, *Chem. Commun.*, **1965**, 226; C. Cupas, W. E. Wattes, and P. v. R. Schleyer, *Tetrahedron Lett.*, **1964**, 2503.

19) M. J. Goldstein and B. G. Odell, *J. Amer. Chem. Soc.*, **89**, 6356 (1967).

20) R. W. Murry and H. L. Kaplan, *ibid.*, **88**, 3527 (1966).

21) A. P. ter Borg and H. Kloosterziel, *Rec. Trav. Chem., Pays-Bas*, **82**, 741 (1963).

22) It was found that the reverse reaction from **14** to **2** takes place at a sufficiently slow rate compared with that of **2**→**14**, and is insignificant. Such a reverse reaction was not found for **15**, which decomposed very slowly on further heating.

23) U. Biethan, H. Klusacek, and H. Musso, *Angew. Chem. Int. Ed. Engl.*, **6**, 176 (1967); W. V. E. Doering, B. M. Ferrier, E. T. Fossel, J. H. Hartenstein, M. Jones, Jr., G. Klumpp, P. M. Rubin, and M. Saunders, *Tetrahedron*, **23**, 3943 (1967).

24) R. Muneyuki and H. Tanida, *J. Amer. Chem. Soc.*, **90**, 656 (1968).

25) As an excellent review, *cf.* H. M. R. Hoffmann, *Angew. Chem.*, **81**, 597 (1969).

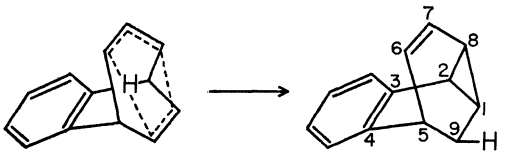

19 14

15, we have considered the Cope rearrangement leading to the *cis*-7-vinyl-2,3-benzonorcaradiene transition state or intermediate, followed by a vinylcyclopropane-

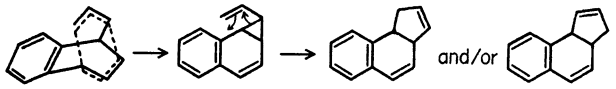

20

cyclopentene rearrangement. A pair of *exo*- and *endo*-2-methoxy derivatives of **2** (**8**) were prepared in order to get stereochemical information on the migrating C_4 site (inversion or retention). It was found however that epimerization of the methoxyl group takes place at a temperature (190°C) below that at which the thermo-

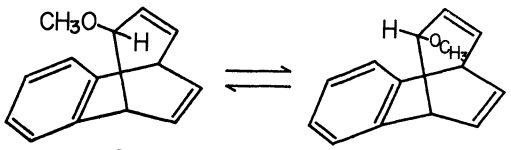

8

lysis occurs, and on thermolysis at ~230°C both epimers gave almost the same complex product mixtures. These findings can be understood by proposing an equilibrium between **2** and the norcaradiene intermediate (**20**)[26] preceding the product formation, which is analogous to the equilibrium between **1** and **10**. A rotation of the vinyl group in **20** followed by the return to **2** results in the epimerization. A resonable explanation for the present results is to assume the following reaction schema.

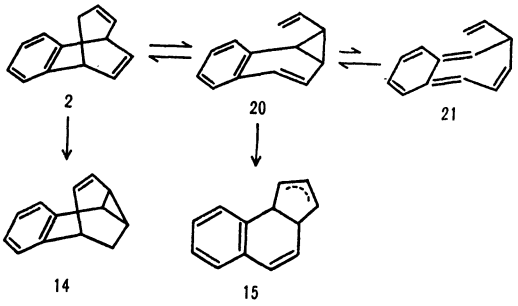

2 20 21 14 15

The question arises, why do the parent (**1**) and the benzo (**2**) compounds react differently? Transformation of **20** into the cycloheptatriene intermediate (**21**) must involve loss of aromaticity of the benzene ring which is thermodynamically unfavored. Such an unfavorable factor is not present in the reaction of **1**. As a result, the thermal isomerization of **2** must proceed by a different mechanism, requiring a temperature higher than that for **1**.

26) The vinyl-unsubstituted derivative of **20** has been found to be a stable compound. W. V. E. Doering and M. J. Goldstein, *Tetrahedron*, **5**, 53 (1959).

Experimental

All melting points were taken in sealed capillaries and are corrected. Infrared spectra were determined with a Nippon Bunko IR-S spectrometer, ultraviolet spectra with a Beckman DK-2A spectrometer, and NMR spectra with a Varian Associates A-60A and/or HA-100. Mass spectra were taken on a Hitachi RMU-6 mass spectrometer. Vpc analysis was carried out on a Hitachi-Perkin-Elmer gas chromatograph F-6D equipped with a hydrogen flame ionization detecter using one of the following columns: (A) 1 m×3mm, stainless steel column packed with 5% XE 60 on Chromosorb W; (B) 1 m×3 mm stainless steel column packed with 5% SE on the same support; (C) 2 m×3 mm stainless steel column packed with 5% diethylene glycol succinate polyester on the same support. Helium was used as a carrier gas. Preparative vpc was carried out with a Yanagimoto gas chromatograph GCG, equipped with 6 m×14 mm stainless steel column, packed with 20% Silicon 550 on the Chromosorb W.

Bicyclo[3.2.2]nona-2,6-dien-8,9-dicarboxylic Anhydride (4). A solution of 10 g of the cycloheptatriene-meleic anhydride adduct (**3**) in 70 m*l* of chlorobenzene was placed in a heavy-walled glass ampoule, cooled to −70°C and sealed. The ampoule was placed in a steel bomb and heated at 220°C for 17 hr. The reaction mixture was cooled, decolorized by treatment with charcoal, filtered, and concentrated under reduced pressure. The residue was extracted with warm carbon tetrachloride. The solution was decolorized again, filtered and cooled to separate 4.5 g crystalline **4**. Concentration of the mother liquor gave 1.0 g of **4** (in total, 55% yield), homogeneous on vpc. Recrystallizaton from carbon tetrachloride afforded a pure sample; mp 136—138°C (lit,[8] mp 138—139°C); IR (CCl_4): 3060 (C=C), 1868, 1780, and 1223 cm^{-1} (C=O); NMR ($CDCl_3$): τ 7.60 (m, 2H at C_4), 6.9 (broad m, 2H at C_1 and C_5), 6.52 (d-d, J=9.3 and 2Hz, 1H at C_8 or C_9), 6.23 (d-d, J=9,3 and 2 Hz, 1H at C_8 or C_9), 4.6 (d-t-d, J=10.2, 3.2, and 1 Hz, 1H at C_3), 4.1 (d-d-t, J=10.2, 8.0, and 2.3 Hz, 1H at C_2), 3.9 (d-d-d, J=8.8, 6.6 and 1.5 Hz, 1H at C_6), 3.57 (d-d-d, J=8.8, 6.7, and 1.5 Hz, 1H at C_7).

Found: C, 69.82; H, 5.27%. Calcd for $C_{11}H_{10}O_3$: C, 69.46; H, 5.30%.

Bicyclo[3.2.2]nona-2,6,8-triene (1). A solution of 3.0 g of **4** and 4 m*l* of triethylamine in 100 m*l* of 85% pyridine-water was placed under nitrogen atmosphere in an electrolysis apparatus equipped with two stationary electrodes made of platinum gauze, nitrogen inlet tube, and glass tube for cooling, and maintained below room temperature with strirring. Electrolysis was conducted for 300 min at 70 V. During the reaction, the current fell from 1.0 A to 0.20 A, and then remained constant. The dark reaction mixture was diluted with 300 m*l* of saturated sodium chloride solution and extracted three times with 200 m*l* of pentane. The combined pentane extract was washed twice with 20 m*l* of dilute hydrochloric acid, then 200 m*l* of water, and dried over sodium sulfate. Evaporation of the solvent and distillation of the residue at 61—62°C (45 mmHg) gave 367 mg of **1** (19.7%), which was homogeneous on vpc (column C) and had physical properties identical with the reported data.[3a-c]

Benzo[f]bicyclo[3.2.2]nona-2,6,8-triene (2). To a stirred suspention of 500 mg of lithium aluminum hydride in 50 ml of ether was added at −20°C a solution of 5.0 g of the ketone **6**[14] in 100 m*l* of ether. After the mixture had been stir-

red for 2.5 hr, the usual work-up gave 5.0 g of an alcohol mixture **7**. A solution of 5.0 g of **7** and 5.0 g of methyl iodide in 50 m*l* of dimethoxyethane was cooled to −15°C and stirred for 15 min during the additon of 750 mg of sodium hydride. The reaction proceeded with evolution of hydrogen gas. After further addition of 1.0 g of methyl iodide, the reaction mixture was warmed to room temperature, stirred for 3.0 hr, and then poured into water. After extraction with ether, evaporation of the solvent and distillation at 96—98°C (0.1 mmHg) gave 4.2 g of a crude ether. Further purification by elution chromatography over 100 g of Merck standard alumina using ether gave 3.6 g of **8**.

To a stirred solution of 3.6 g of **8** in 36 m*l* of dimethoxyethane, 3 m*l* of sodium-potassium alloy (1:5) was added at −10°C and the mixture was stirred for 4 hr. The reddish brown solution was poured into 50 m*l* of could methanol and diluted with water. After extraction with ether and washing with water, evaporation of the ether left 2.3 g of residue. Sublimation of the residue under reduced pressure afforded 2.0 g of **2**, mp 58—59°C. Total yield from **6** was 43%. IR (CS_2): 3026 and 1632 cm^{-1} (C=C); λ_{max}^{hexane} mμ (log ε): 265 (377) and 272 (397); NMR (CCl_4): τ 7.75 (m, 2H at C_4), 6.55 (m, 2H at C_1 and C_5), 5.1 (d-t-d, J=10.5, 3.8, and 1 Hz, 1H at C_3), 3.98 (d-d-t, J=10.5, 8, and 2 Hz, 1H at C_2), 3.77 (d-d-d, J=8,7, and 1.5 Hz, 1H at C_9), 3.37 (d-d-d, J=8,7 and 1.5 Hz, 1H at C_8), and 3.0 (aromatic 4H); mass spectrum (70 eV) *m/e* 168, 167, 165, 154, 153, 152, 141, 128, 115, 102, 89, 83, 76, 63, 51, 39.

Found: C, 92.80; H, 7.17%. Calcd for $C_{13}H_{12}$: C, 92.81; H, 7.19%.

Thermolysis of 1. A 0.1N solution of **1** in *n*-hexane was degassed, sealed in an ampoule and placed in a constant temperature bath controlled in the range 160—180°C. Analysis of the thermolysis products was carried out by vpc (column C at 50°C with a flow pressure of 1 kg/cm^2) and showed the formation of three products, whose retention times were 4 min, 8 min, and 8 min 30 sec, while that of **1** was 5 min 20 sec. The peak at 4 min was identical with that of independently synthesized **10**. The peak at 8 min was identified as **9**, which was obtained as the main product on thermolysis of **10** as reported by Daub and Schleyer.[3b] The peak at 8 min 30 sec did not appear at the initial stage of pyrolysis, but increased gradually as the reaction proceeded by further isomerization of the initially formed **9**. This isomerization product was assigned as 1-vinylcycloheptatriene (**11**) on the basis of its NMR spectra,[17] τ 7.46 (d, J=7.0 Hz, 2H at C_7).

Thermolysis was followed by vpc using dodecane as an interanl standard, and integration of the component peaks was carried out with a planimeter. After correction for the relative sensitivity of the detector, decreases in the concentration of **1** were determined by comparing the peak area of **1** with that of the standard. With this technique the yield of **9** was quantitative, at least for the half-life of the reaction. Vpc of the infinity ampoule (more than the 10 half-lives) showed complete disappearance of **1** and two peaks corresponding to **9** and **11** with areas of approximately 2:3. Thermolysis rates determined by following the decrease of **1** for two half-lives, were shown to be first-order.

Thermolysis of 10. The reaction was carried out at a temperature in the range 120—140°C and gave quantitatively a mixture of **1** and **9** in the ratio 1:9. Formation of **11** was not observed up to the three half-lives, and no rearrangement of **1** was observed under the present conditions. The rates of conversion of **10** into **1** and **9** were determined by the same technique employed for **1** and gave first-order constants.

3-Vinyltricyclo[3.2.2.0^{2,4}]nona-6-ene-8,9-dicarboxylic Anhydride (12). (a) A mixture of 100 mg of **1** and 100 mg of maleic anhydride in 10 m*l* of *n*-hexane was sealed in a degassed ampoule and heated at 160°C overnight. Vpc analysis of the reaction mixture on column A at 180°C with a flow pressure of 1.0 kg/cm^2 showed three peaks with retention times of 2 min 30 sec, 3 min 20 sec, and 3 min 40 sec with areas in the ratios 2:1:20. Evaporation of the solvent and recrystallization from ligroin gave 120 mg of **12**, mp 168—169°C, corresponding to the main peak with a retention time of 3 min 20 sec; IR ($CHCl_3$): 1865 and 1780 cm^{-1} (C=O), NMR ($CDCl_3$): τ 8.76 (m, 3H at C_2, C_3, and C_4), 6.76 (t, J=2 Hz, 2H at C_8 and C_9), 6.45 (m, 2H at C_1 and C_5), 4.2—5.2 (m, vinyl 3H), and 4.05 (d-d, J=5 and 3.5 Hz, 2H at C_6 and C_7).

Found: C, 71.99; H, 5.59%. Calcd for $C_{13}H_{12}O_3$: C, 72.21; H, 5.59%.

The minor peak, having a retention time of 3 min 20 sec, was identical with that of the product obtained from the reaction of **9** with maleic anhydride.

(b) A solution of 300 mg of **10** and 250 mg of maleic anhydride in 20 m*l* of dioxane was refluxed for 2 hr. After the usual work-up, recrystallization from carbon tetrachloride gave 450 mg of **12**, identical with the main product in procedure (a).

Thermolysis of 2. A solution of 900 mg of **2** in 40 m*l* of *n*-hexane was placed in an ampoule, cooled to −70°C, purged with nitrogen and sealed. The ampoule was heated at 230°C for 140 hr in the absence of light. After evaporation of the solvent, 900 mg of the residue was subjected to preparative vpc at a column temperature of 200°C with a flow rate of 300 m*l*/min of helium gas. The chromatogram showed three peaks with retention times of 50, 63, and 72 min with areas in the ratio 1:2:5. The fraction (63 mg) corresponding to the peak with a retention time of 50 min was identical with the starting material (**2**). Collection of the second peak, at 63 min, gave 130 mg of the hydrobenzindene (**15**): bp 80°C (0.3 mmHg), n_D^{25} 1.5987; λ_{max}^{hexane} mμ (ε): 260 (8080) and 268.5 (8500); NMR (CCl_4): τ 5.8—8.0 (complex signals due to aliphatic 4H), 4.3 (m, vinyl 3H), 3.8 (d-d, J=10 and 2 Hz, benzylic vinyl 1H) and 3.0 (m, aromatic 4H)].

Found: C, 92.80; H, 7.17%. Calcd for $C_{13}H_{12}$: C, 92.81; H, 7.19.

The third fraction, at 72 min, was collected to give 301 mg of benzobarbaralane (**14**), bp 76—78°C (0.25 mmHg), $n_D^{24.3}$ 1.6037; λ_{max}^{hexane} mμ (ε): 255 (692), 269.5 (550) and 276.5 (484); NMR ($CDCl_3$): τ 8.56 (t, J=2.3 Hz, 2H at C_9), 7.95 (t-d-d, J=7.6, 5.3, and 1.2 Hz, 1H at C_8), 7.82 (t-t, J=7.6 and 2.3 Hz, 1H at C_1), 7.45 (t, J=7.6 Hz, 1H at C_2), 6.78 (d-t-d, J=6.9, 2.3, and 1.4 Hz, 1H at C_5), 4.40 (d-d-d, J=9.6, 5.3, and 1.4 Hz, 1H at C_7), 4.20 (d-d-d, J=9.6, 6.9, and 1.2 Hz, 1H at C_6), and 3.0 (m, aromatic 4H); the mass spectrum was identical with that of **2**.

Found: C, 92.67; H, 7.24%. Calcd for $C_{13}H_{12}$: C, 92.81; H, 7.19%.

Kinetic measurements were carried out with a 0.1N solution of **2** in *n*-hexane using a vpc technique on column B at 100°C under a pressure of 1.0 kg/cm^2. Retention times of **2**, **15**, and **14** were 20, 34, and 41 min, respectively. Pentamethylbenzene, whose retention time was 8 min, was used as an internal standard. Extrapolation of the product compositions to zero time gave kinetically controlled ratios for **14** and **15**, of 2.5 at 268.5°C and 3.0 at 289.8°C, respectively. The decreasing rate of **2** was followed up to two half-lives and shown to be first-order.

2,3,3aβ,4,5,9bβ-Hexahydro-1H-benz[e]indene. A solution of 40 mg of **15** in 10 m*l* of methanol was hydrogenated at atmospheric pressure and room temperature over 5% palladium on carbon. Uptake ceased after absorption of 11 m*l*

of hydrogen. After the usual work-up, the hydrogenated product (37 mg), boiling at 80—82°C (1 mmHg), $n_D^{21.0}$ 1.5532, was found to be identical with the reported compound.[24]

Found: C, 90.40; H, 9.31%. Calcd for $C_{13}H_{16}$: C, 90.64; H, 9.36%.

Endo- *and* exo-*2-methoxybenzo*[f]*bicyclo*[*3.2.2*]*nona-3,6,8-triene.* A 7:3 mixture of the *endo*- and *exo*-2-methoxy compounds (**8**) was separated by preparative tlc using silica gel G (E. Merck Co.) as an adsorbent, and developing with ether-pentane (1:4). Collection and vacuum distillation of the more mobile fraction gave 580 mg of the *endo* compound, bp 115°C (0.25 mmHg), n_D^{25} 1.5758. Vpc (column C at 150°C with a flow pressure of 1 kg/cm^2) showed a single peak with a retention time of 8 min: IR (CCl_4): 1632 cm^{-1} (C=C) and 1100 cm^{-1} (C–O), NMR (CCl_4): τ 6.73 (s, 3H of CH_3O), 6.1—6.6 (m, 3H of C_1, C_2, and C_5), 5.1 (d–t, J= 10.2 and 2.5 Hz, 1H at C_3), 3.90 (d–d–d, J=10.2, 7.8, and 1 Hz, 1H at C_4), 3.70 (d–d–d, J=8.0, 6.4, and 1 Hz, 1H at C_8), 3.26 (d–d–d, J=8.0, 5.5, and 1 Hz, 1H at C_9) and 3.0 (m, aromatic 4H).

Found: C, 84.79; H, 7.05%. Calcd for $C_{14}H_{14}O$: C, 84.81; H, 7.12%.

The less mobile fraction gave 270 mg of the *exo* compound, bp 103°C (0.17 mmHg), n_D^{24} 1.5729. Vpc showed it to be homogeneous with a retention time of 6 min 30 sec: IR (CCl_4): 1631 (C=C) and 1100 cm^{-1} (C–O), NMR (CCl_4): τ 6.67 (s, 3H of CH_3O), 6.40 (m, 2H at C_1 and C_5), 6.10 (m, 1H at C_2), 5.03 (d–m, J=10.8 Hz, 1H at C_8), 3.86 (d–d–t, J=10.8, 5.0, and 1.0 Hz, 1H at C_4), 3.72 (d–d–d, J=9.0, 8.0, and 1.5 Hz, 1H at C_8), 3.30 (d–d–d, J=9.0, 6.0, and 1.5 Hz, 1H at C_9), and 3.0 (m, aromatic 4H).

Found: C, 84.43; H, 7.08%. Calcd for $C_{14}H_{14}O$: C, 84.81; H, 7.12%.

Thermolysis of 8. A 0.1N solution of the exo or endo methoxy compounds (two separate experiments) was degassed, sealed in an ampoule and heated at 190°C for 17 hr. Epimerization between the two alcohols was observed by vpc. Orientations of the methoxyl groups were determined by measurement of infrared hydroxyl bands in the corresponding saturated alcohols, which were obtained by hydrogenation of the two double bonds in **7**.

Benzo[*f*]bicyclo[3.2.2]nona-3,6,8-trien-2(*endo*)-ol had mp 91—91.5°C. Found: C, 84.65; H, 6.64%. Calcd for $C_{13}H_{12}O$: C, 84.75; H, 6.57%. The *exo* epimer had mp 109—109.5°C. Found: C, 84.91; H, 6.62%.

Benzo[*f*]bicyclo[3.2.2]non-6-en-2(*endo*)-ol had mp 52—53°C. Found: C, 83.09; H, 8.52%. Calcd for $C_{13}H_{16}O$: C, 82.93; H, 8.57%. IR (CCl_4): 3618 (free OH) and 3583 cm^{-1} (associated OH). The *exo* epimer had mp 95—96°C. Found: C, 82.90; H, 8.57%. IR (CCl_4): 3620 cm^{-1} (free OH).

BULLETIN OF THE CHEMICAL SOCIETY OF JAPAN, VOL. 44, 2453—2455 (1971)

The Reactions of β-Ketosulfonium Salts with Sulfenamide Derivatives

Teruaki MUKAIYAMA, Kazuo HOSOI, Shun INOKUMA, and Takanobu KUMAMOTO
Laboratory of Organic Chemistry, Tokyo Institute of Technology, Ookayama, Meguro-ku, Tokyo
(Received January 28, 1971)

2-Phenylthio-2-(dimethylsulfuranylidene)acetophenone was obtained in good yield by the reaction of dimethylphenacylsulfonium bromide with *N,N*-diethylbenzenesulfenamide. The reaction of dimethyl-α-methylphenacylsulfonium bromide with *N,N*-diethylbenzenesulfenamide gave α-phenylthioacrylophenone in good yield. The reactions of α-phenylthioacrylophenone thus obtained with various active methylene compounds were investigated.

Recently it was reported that sulfenamide derivatives reacted with active methylene compounds to give mono- or di-sulfenylated compounds in good yields. As an example, the reaction of *N,N*-diethylbenzenesulfenamide with acetylacetone in dichloromethane at room temperature gave 3-phenylthio-2,4-pentadione in 77% yield.[1)]

We studied the equimolar reactions of β-ketosulfonium salts with sulfenamide derivatives with the expectation that α-alkyl or arylthio-β-ketosulfonium salts and amines would be formed as a result of the introduction of sulfenyl group in place of the hydrogen atom attached to the α-carbon of the sulfonium salts. When *N,N*-diethylbenzenesulfenamide was treated with dimethylphenacylsulfonium bromide in dichloromethane at room temperature for an hour, 2-phenylthio-2-(dimethylsulfuranylidene)acetophenone and diethylammonium bromide were obtained in 70% and quantitative yields, respectively.

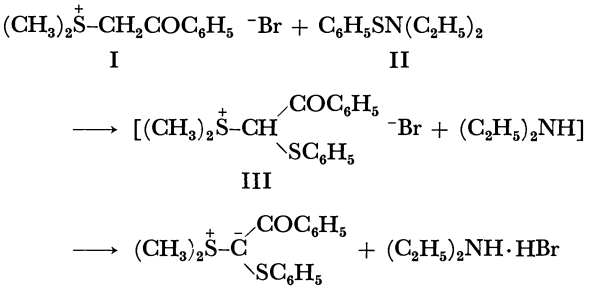

The result is explained as follows. Sulfonium salt (I) reacted with *N,N*-diethylbenzenesulfenamide (II) to form sulfenylated compound (III) and diethylamine as expected. The initially formed sulfonium salt was rapidly converted to 2-phenylthio-2-(dimethylsulfuranylidene)acetophenone by the influence of diethylamine.

The reactions of dimethyl-α-methylphenacylsulfonium bromide with *N,N*-diethylbenzenesulfenamide and

1) T. Mukaiyama, S. Kobayashi, and T. Kumamoto, *Tetrahedron Lett.*, **1970**, 5115.

active methylene compounds were investigated with the expectation that initially formed dimethyl-α-methyl-α-phenylthiophenacylsulfonium bromide would further react with active methylene compounds to produce condensation products. However, the reaction of dimethyl-α-methylphenacylsulfonium bromide with *N*, *N*-diethylbenzenesulfenamide in dichloromethane at room temperature for 4 hr and the subsequent addition of dibenzoylmethane in refluxing dichloromethane for 4 hr afforded 2-benzoyl-1,5-diphenyl-4-phenylthio-1,5-pentadione and diethylammonium bromide in 70% and quantitative yields, respectively. The unexpected formation of 2-benzoyl-1,5-diphenyl-4-phenylthio-1,5-pentadione may be explained by considering an initial formation of sulfonium salt (V) and diethylamine from equimolar amounts of dimethyl-α-methylphenacylsulfonium bromide (IV) and *N*,*N*-diethylbenzenesulfenamide (II). Salt (V) rapidly reacts with diethylamine formed at the same time to give α-phenylthioacrylophenone (VI). The Michael addition of VI and dibenzoylmethane results in the formation of 2-benzoyl-1,5-diphenyl-4-phenylthio-1,5-pentadione.

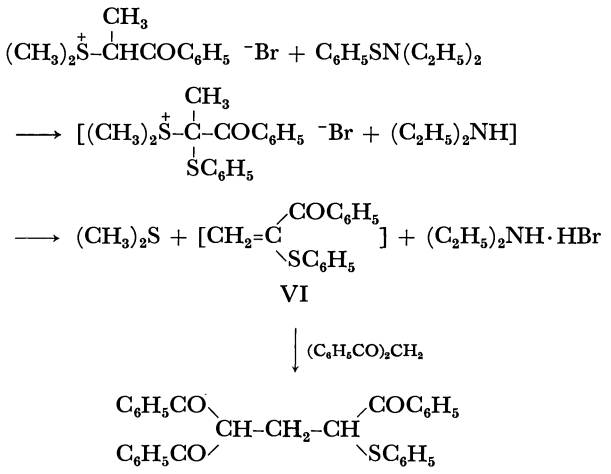

The presumed intermediate, α-phenylthioacrylophenone, was isolated in 98% yield by the reaction of dimethyl-α-methylphenacylsulfonium bromide with *N*, *N*-diethylbenzenesulfenamide, without the addition of dibenzoylmethane, in dichloromethane at room temperature for 4 hr.

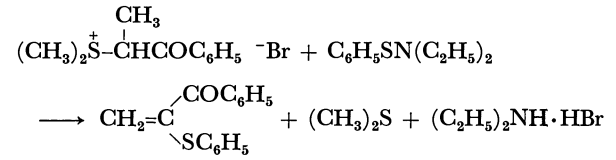

The α-phenylthioacrylophenone isolated by the above reaction did not react with dibenzoylmethane even when they were refluxed in dichloromethane for 4 hr. However, when the reaction was carried out in the presence of a catalytic amount of diethylamine and an equimolar amount of dimethyl sulfide, 2-benzoyl-1,5-diphenyl-4-phenylthio-1,5-pentadione was obtained in 70% yield.

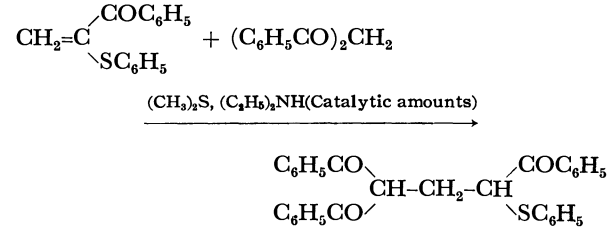

Similarly, it was established that reactions of dimethyl-α-methylphenacylsulfonium bromide with *N*,*N*-diethylbenzenesulfenamide and various active hydrogen compounds such as benzenethiol, ethanethiol, ethyl malonate, malononitrile, ethyl acetoacetate, without isolation of α-phenylthioacrylophenone, afforded 1:1 addition compounds or 1:2 addition compounds in good yields (Table 1).

TABLE 1. REACTIONS OF DIMETHYL-α-METHYLPHENACYLSULFONIUM BROMIDE WITH *N*,*N*-DIETHYLBENZENESULFENAMIDE AND ACTIVE HYDROGEN COMPOUNDS

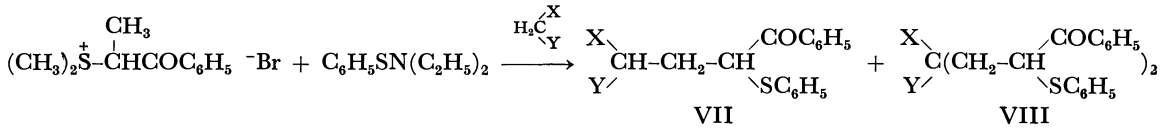

CH_2(X)(Y)	VII	VIII	Mp (°C)	Analyses Found (Calcd) (%) C	H	N	S
HSC_6H_5	93%		oil	72.28 (71.99)	5.25 (5.18)		17.24 (17.46)
HSC_2H_5	85%		130 —131[a]	53.31 (53.27)	5.93 (5.65)		22.63[a] (22.41)
$CH_2(COC_6H_5)_2$	70%		123.5—124	77.81 (77.57)	5.37 (5.21)		6.64 (6.89)
$CH_2(CO_2C_2H_5)_2$		63%	178.5—179.5	69.49 (69.36)	5.61 (5.66)		9.91 (9.99)
$CH_2(CN)_2$		75%	132.5—133.0	72.34 (72.51)	4.92 (4.86)	5.35 (5.13)	11.80 (11.71)
$CH_2(COCH_3)(CO_2C_2H_5)$	45%		175.5—176	68.32 (68.09)	6.27 (5.99)		8.89 (8.64)

a) This was identified by transformation into sulfonium methyl sulfate.

Experimental

Materials. *N,N*-Diethylbenzenesulfenamide (II) was prepared according to the method of Lecher and Holschneider,[2] bp 96—97°C/8 mmHg (lit, 90°C/3.5 mmHg). Dimethylphenacylsulfonium bromide (I) was prepared from dimethyl sulfide and phenacyl bromide in dry acetone. Similarly, dimethyl-α-methylphenacylsulfonium bromide (IV) was prepared from dimethyl sulfide and α-bromopropiophenone.[3]

Reaction of Dimethylphenacylsulfonium Bromide with N,N-*Diethylbenzenesulfenamide.* A mixture of dimethylphenacylsulfonium bromide (2.61 g, 0.01 mol) and *N,N*-diethylbenzenesufenamide (1.81 g, 0.01 mol) was stirred in dichloromethane (50 m*l*) for an hour at room temperature. The reaction mixture was poured into water to remove diethylammonium bromide and the dichloromethane layer was collected. After the dichloromethane layer was dried with sodium sulfate, the solvent was removed under reduced pressure giving white crystals. The recrystallization from benzene gave 2-phenylthio-2-(dimethylsulfuranylidene)acetophenone,[4] mp 136—136.5°C, 2.00 g, (70%). (lit, 136°C).

Reaction of Dimethyl-α-methylphenacylsulfonium Bromide with N, N-*Diethylbenzenesulfenamide and Dibenzoylmethane.* A mixture of dimethyl-α-methylphenacylsulfonium bromide (1.43 g, 0.005 mol) and *N,N*-diethylbenzenesulfenamide (0.91 g, 0.005 mol) was stirred in dichloromethane (50 m*l*) at room temperature. Evolution of dimethyl sulfide was recognized by its characteristic odor accompanied by disappearance of the crystals of sulfonium salt. After stirring for 4 hr, dibenzoylmethane (1.12 g, 0.005 mol) was added to the reaction mixture and the mixture was refluxed for 4 hr. The solvent was removed under reduced pressure giving oily residue. Fifty milliliters of water was added into the residue and resulting oil was extracted with ether (50 m*l*). Removal of ether gave white crystals. Recrystallization from ethanol gave 2-benzoyl-1,5-diphenyl-4-phenylthio-1,5-pentadione, 1.62 g (70%), mp 123—124°C.

Found: C, 77.81; H, 5.37; S, 6.64%. Calcd for $C_{30}H_{24}O_3S$: C, 77.57; H, 5.21; S, 6.89%. The NMR spectrum: τ= 1.7—2.8 (m, 20H), τ=4.43 (t, 1H), τ=5.12 (t, 1H), τ=7.27 (t, 2H).

Similarly, various addition products of active hydrogen compounds, such as benzenethiol, ethanethiol, ethyl malonate, malononitrile or ethyl acetoacetate, and α-phenylthioacrylophenone were obtained from dimethyl-α-methylphenacylsulfonium bromide, *N,N*-diethylbenzenesulfenamide and active hydrogen compounds. The results are listed in Table 1. The products were identified by elemental analyses, NMR spectra and IR spectra.

Reaction of Dimethyl-α-methylphenacylsulfonium Bromide with N, N-*Diethylbenzenesulfenamide.* A mixture of dimethyl-α-methylphenacylsulfonium bromide (1.43 g, 0.005 mol) and *N,N*-diethylbenzenesulfenamide (0.91 g, 0.005 mol) was stirred in dichloromethane (50 m*l*) for 4 hr at room temperature. The solvent was removed under reduced pressure giving a mixture of crystals and oil. Fifty milliliters of water was added into the mixture and resulting oil was extracted with ether (50 m*l*). After removal of the solvent, the oil was chromatographed on silica gel and elution with a mixture of petroleum ether (25—30°C) and benzene (1:1) gave α-phenylthioacrylophenone, 0.84 g (70%), mp 106—108°C.

Found: C, 74.82; H, 5.20; S, 13.21%. Calcd for $C_{15}H_{12}SO$: C, 74.99; H, 5.03; S, 13.32%. The NMR spectrum: τ= 1.8—2.8 (m, 10H), τ=7.55 (S, 1H), τ=7.65 (S, 1H).

Reaction of α-Phenylthioacrylophenone with Dibenzoylmethane. Into a solution of α-phenylthioacrylophenone (2.40 g, 0.01 mol) and dibenzoylmethane (2.24 g, 0.01 mol) in dichloromethane (50 m*l*), dimethyl sulfide (0.62 g, 0.01 mol) and a catalytic amount of diethylamine were added under stirring. The mixture was refluxed for 5 hr. After removal of the solvent, the residue was chromatographed on silica gel and elution with mixture of petroleum ether (25—35°C) and benzene (1:1) gave 2-benzoyl-1,5-diphenyl-4-phenylthio-1,5- pentadione, 3.00 g (70%), mp 123°C.

2) H. Lecher and F. Holschneider, *Ber.*, **57**, 757 (1924).

3) T. Mukaiyama, K. Hagio, H. Takei, and K. Saigo, This Bulletin, **44**, 161 (1971).

4) Y. Hayasi, M. Takaku, and H. Nozaki, *Tetrahedron Lett.*, **1969**, 3179.

Effect of Ring Size on the Acid-Catalyzed Reduction of Cyclic Sulfoxides by Iodide Ion[1]

Seizo TAMAGAKI, Masao MIZUNO, Hiroshi YOSHIDA,
Hiroo HIROTA, and Shigeru OAE
Department of Applied Chemistry, Faculty of Engineering, Osaka City University, Sumiyoshi-ku, Osaka
(Received February 1, 1971)

Acid-catalyzed reduction of various cyclic sulfoxides with iodide ion were kinetically investigated. The rates of reduction of thianthrene, phenoxathiin, dibenzothiophene oxides were found to be in a linear relation with their basicities, while those of alicyclic sulfoxides fall in the following sequence with a 700 fold range; 5-> 4->open>7->6- membered cyclic sulfoxides. This rate sequence seems to be correlated better by the steric effect than by basicity difference. For further information on the possible effect of steric hindrance, a few methyl alkyl sulfoxides were also subjected to the same reaction, but the results could not be explained by steric effect only.

The acid-catalyzed reduction of sulfoxide with iodide ion has been suggested to proceed by way of S_N2 type process on the sulfur atom.[2] Many similar S_N2 displacement reactions on the trivalent sulfur atom have been found. A distinct example[3] is oxygen exchange of diaryl sulfoxides with acetic anhydride or dilute sulfuric acid where the exchange leads to the inversion of configuration around the sulfur atom. Namely, the rate of oxygen exchange of diaryl sulfoxide is equal to that of racemization at a higher concentration (>80%) of sulfuric acid and the formation of radical cation intermediate was detected.[4] In the reactions at lower acid concentrations than 80% the mechanism changes from S_N1 (a) type to S_N2 (b) type displacement reaction shown below:

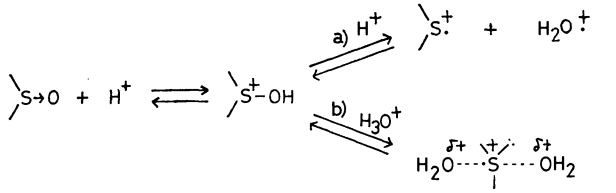

If the nucleophile in the above scheme, *i.e.*, H_2O, is replaced by such-reducing nucleophiles as iodide ion, the reaction does not lead to a reversible oxygen exchange but results in the predominant reduction illustrated below

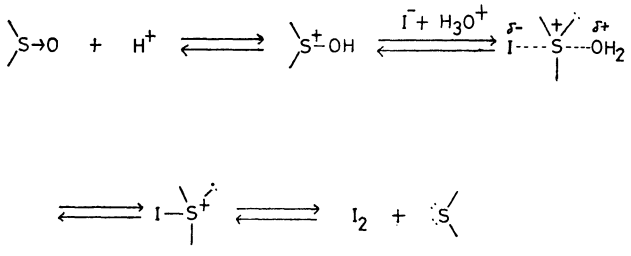

By means of this reduction, we have investigated the nucleophilic displacement reaction on the trivalent sulfur atom of both aliphatic acyclic and cyclic sulfoxides. Although the structural effect on the reactivity of carbocyclic compounds has been examined by many workers and explanations have been given,[5] there is practically no investigation concerning the relation between the reactivity and the structure of heterocyclic compounds. We have therefore conducted a thorough kinetic study on the reduction of some simple alicyclic sulfoxides in order to disclose the effect of ring-size on the rates of the nucleophilic displacement reaction at the trivalent sulfur atom.

Experimental

Materials and kinetics: The boiling points or melting points of sulfoxides used are listed in Table 1.[6] The characterizations of reduction products of the acyclic sulfoxides were described[2] and the reduction of alicyclic sulfoxides such as five-, six- and seven- membered sulfoxides gave the corresponding sulfides in good yields of more than 80% under the kinetic conditions. However, in the case of the reduction of trimethylene sulfoxide, trimethylene sulfide was susceptible to decomposition to afford a polymer as white precipitates by the action of perchloric acid, although the sulfoxide itself was very stable to the same concentration of the acid. Special commercial grade 70%-perchloric acid was used for kinetics. Concentration of the acid was determined to be 11.83 mol/*l* with a standard solution of potassium hydroxide prepared by titrating with 0.200 mol/*l* potassium hydrogen phthalate. Water was distilled under nitrogen atmosphere and stored in a large nitrogen-flushed bottle. The aqueous solution of sodium iodide containing 0.50 mol/*l* was prepared and stored under nitrogen atmosphere. The reactor bottle was immersed in a thermostatted bath. Rate measurements were carried out by introducing a constant nitrogen stream into the reaction vessel in order to eliminate autoxidation of iodide ion to iodine which causes kinetic errors. The reaction was quenched by pouring the reaction mixture into a

1) Paper XXXVII on Sulfoxides.
2) F. Montanari, *Chem. Commum.*, **1969**, 3; S. Allenmark, *Acta Chem. Scand.*, **17**, 2715 (1963); D. Landini and F. Montanari, *Tetrahedron Lett.*, **1964**, 2691; J. H. Kruger, *Inorg. Chem.*, **5**, 132 (1966); S. Allenmark and H. Johnson, *Acta Chem. Scand.*, **21**, 1672 (1967); R. A. Strecker and K. K. Andersen, *J. Org. Chem.*, **33**, 2234 (1968); D. Landini, G. Modena, F. Montanari, and G. Scorrano, *J. Amer. Chem. Soc.*, **71**, 7168 (1970).
3) S. Oae and N. Kunieda, This Bulletin, **41**, 696 (1968).
4) S. Oae and N. Kunieda, *ibid.*, **42**, 1324 (1969).
5) H. C. Brown and M. Borkowski, *J. Amer. Chem. Soc.*, **74**, 1894 (1952); H. C. Brown and G. Ham, *ibid.*, **78**, 2735 (1956).
6) D. S. Tarbell and C. Weaver, *ibid.*, **63**, 2939 (1941); W. V. Whitehead, R. D. Dean, and F. A. Fidle, *ibid.*, **73**, 3632 (1951); G. G. Bennett and A. L. Hoak, *J. Chem. Soc.*, **1927**, 2456; E. A. Fehnell, S. Goodyear, and J. Berbowitz, *J. Amer. Chem. Soc.*, **73**, 4578 (1951).

mixed solution containing 5% of sodium iodide and 4 mol/*l* of $AcONa \cdot 3H_2O$ in 50 m*l*. Rate constants listed in Table 1 are the average of several runs.

Table 1. Boiling or melting point of sulfoxides

Sulfide	Bp, °C/mmHg (Mp, °C)	Sulfoxide	Bp, °C/mmHg (Mp, °C)
CH_3SCH_3	38	CH_3SOCH_3	86/25
$CH_3SC_2H_5$	65— 66	$CH_3SOC_2H_5$	72— 74/11
CH_3S-i-C_3H_7	83— 84	CH_3SO-i-C_3H_7	82— 83/13
CH_3S-sec-C_4H_9	111—112	CH_3SO-sec-C_4H_9	93/10
CH_3S-tert-C_4H_9	95— 97	CH_3SO-tert-C_4H_9	79— 82/10
$C_2H_5SC_2H_5$	91	$C_2H_5SOC_2H_5$	84/12
	95— 96		91/14
	119—120		113—114/14
	141—142		124—125/14
	170—171	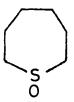	144—145/14
	(120—123)		(205—8)
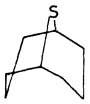	(170—171)	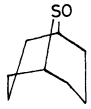	(140/5)[a]

a) sublimed temp.

Results and Discussion

Effect of Basicity on Rate. The acid-dependency of this reaction was studied and the rates were shown to be in linear relationships with the Hammett acidity-function (ho) in perchloric acid but the slope was found to vary from one sulfoxide to an other.[7] However, the effect of basicity on the overall rate of reduction of the sulfinyl group has not been examined. First we reexamined the basicities of several sulfoxides. Tamres and Seales[8] investigated the hydrogen-bonding ability of cyclic sulfoxides and concluded that the basicities of the cyclic sulfoxides fall in the following sequence assuming the parallelism[9] between the basicity and hydrogen-bonding ability with methanol.

6- $\geq$ 5- $>$ 4-membered ring sulfoxides

We measured the hydrogen-bonding abilities of sulfoxides with more acidic substrate, *i.e.*, phenol and found that the basicity sequence is not in complete agreement with that found in literature. The hydrogen-bonding abilities of several other acyclic and cyclic sulfoxides are listed in Table 2 and the plot of the rate constants against the differences of O–H stretching frequencies relative to the free phenol OH stretching frequency is shown in Fig. 1. Thus, the basicities newly determined fall in the following sequence:

5- $>$ Et–SO–Et $>$ 7- $>$ DMSO $>$ 6- $>$

(3.3.1) $>$ (2.2.1) $>$ 4-membered sulfoxides

The kinetic results of the reductions are also summarized

Table 2. $\Delta\nu_{OH}$[a] for various sulfoxides in CCl_4

Compound	$\Delta\nu_{OH}$	$\Delta\nu_{OH}$[8]
	295	—
	375	161
	349	155
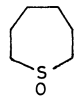	357	—
	340	—
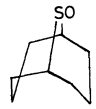	346	—
CH_3SOCH_3	350	158
EtSOEt	355	167
n-BuSOBu-*n*	370	—
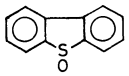	286	—
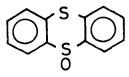	220	—
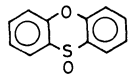	270	—
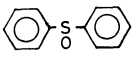	264	—

a) unit in cm^{-1}

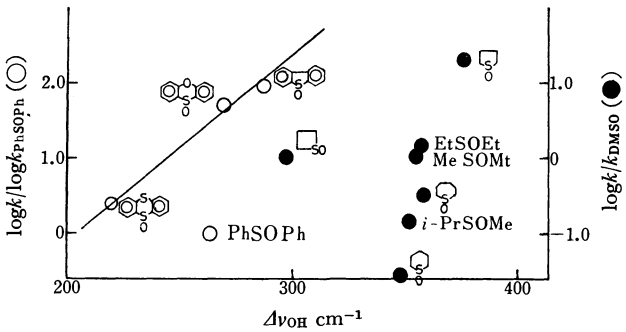

Fig. 1. Plot of log k_{rel} against $\Delta\nu_{OH}$

7) D. Landini, F. Montanari, H. Hogeveen, G. Maccagnani, *Tetrahedron Lett.*, **1964**, 2691; *ibid.*, **1966**, 3309; *Chem. Commum.*, **1968**, 86; J. H. Kruger, *Inorg. Chem.*, **5**, 132 (1966).

8) M. Tamres and S. Seales, Jr., *J. Amer. Chem. Soc.*, **81**, 2100 (1959).

9) D. Landini, G. Modena, G. Scorrano, and F. Taddei, *ibid.*, **91**, 6703 (1969).

TABLE 3. REACTION RATE OF DIBENZO DERIVATIVES AT 298°K

Compound	$HClO_4$, M	H_0	$k \times 10^{-5}$ sec^{-1}	25° k_{rel} (log k_{rel})
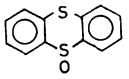	5.82	−2.71	9.11	2.4 (0.38)
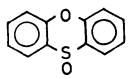 a)	5.82	−2.71	194	51.0 (1.71)
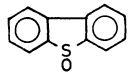	2.85 (5.82)	−1.17 (−2.71)	25.0 (725)	91.0 (1.96) b)
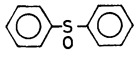	5.44 (5.82) 6.75	−2.49 (−2.71) −3.39	2.07 (3.78) 24.1	(1.0) b) (0.0)

a) Slope *vs* H_0: 0.95.
b) Numerals in parenthesis indicate the interpolated values.

in Tables 3 and 4.

We see that the sequence of the hydrogen-bonding abilities is not always identical with that for the reduction, although the five-membered sulfoxide reacts remarkably fast as expected from its hydrogen-bonding ability. Thus, we may conclude that the overall rate of reduction may not entirely be controlled by the basicity of the sulfinyl groups.

Another illustration for the effect of basicity can be made with the dibenzo derivatives of a few heterocyclic sulfoxides (Table 3). The plot of the rate constants against the hydrogen bonding abilities is shown in Fig. 1, which indicates an approximate linearity between the rate constants and the hydrogen-bonding abilities. While diphenyl sulfoxide deviates far below the line, this phenomenon is easily accounted for by the steric hindrance caused by the four ortho hydrogens on the two phenyl rings. However, there is no further information as to what extent the protonation step influences the over-all rate of the reduction of these sulfoxides.

Activation Parameters. We see from Table 4 that the range of rates from the lowest one for the six-membered sulfoxide to that of the highest for the five-membered ring sulfoxide is 700 fold and the relative rates of the sulfoxides fall in the following decreasing order: 5-> 4->DMSO>7->6- membered cyclic sulfoxides. The nucleophilic substitution reaction of carbocyclic compounds[10] involving the rehybridization of reaction

TABLE 4. REDUCTION OF ALIPHATIC SULFOXIDES

Compound	Temp, °C	Pseudo-lst-order rate const, sec^{-1}	Activation enthalpy (kcal/mol)	entropy (e.u.)	$k_{rel}^{25°}$
	15	$3.78+0.07 \times 10^{-4}$	20.0	−6.7	34.7
	20	$7.13+0.13 \times 10^{-4}$			
	25	$12.6+0.078 \times 10^{-4}$			
	15	$0.98+0.14 \times 10^{-2}$	15.7	−15.1	717
	20	$1.60+0.10 \times 10^{-2}$			
	25	$2.55+0.10 \times 10^{-2}$			
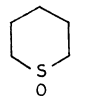	25	$3.55+0.16 \times 10^{-5}$	17.6	−21.6	1.00
	30	$6.16+0.07 \times 10^{-5}$			
	35	$9.65+0.25 \times 10^{-5}$			
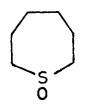	20	$2.16+0.11 \times 10^{-4}$	16.1	−22.2	9.9
	25	$3.51+0.10 \times 10^{-4}$			
	30	$5.57+0.05 \times 10^{-4}$			
DMSO	15	$4.56+0.09 \times 10^{-4}$	17.4	−15.2	32.6
	20	$7.57+0.09 \times 10^{-4}$			
	25	$13.1+0.3 \times 10^{-4}$			
CH_3SOEt	15	$5.07+0.09 \times 10^{-4}$	17.0	−16.5	4.00
	20	$8.04+0.13 \times 10^{-4}$			
	25	$14.22+0.66 \times 10^{-4}$			
EtSOEt	15	$6.38+0.22 \times 10^{-4}$	17.3	−15.1	51.2
	20	$10.28+0.22 \times 10^{-4}$			
	25	$18.2 +0.08 \times 10^{-4}$			
CH_3SO-iC_3H_7	20	$1.02+0.02 \times 10^{-4}$	18.1	−17.0	5.3
	25	$1.88+0.02 \times 10^{-4}$			
	30	$2.94+0.03 \times 10^{-4}$			
CH_3SO-t-Bu		too slow			
(3.3.1)[a]		too slow			
(2.2.1)[b]		too slow			

a) 9-thia-monoxybicyclo(3.3.1)octane
b) 7-thia-monoxybicyclo(2.2.1)heptane

10) P. J. C. Fierens and P. Verschelden, *Bull. Soc. Chim. Belges*, **61**, 427, 609 (1952); *ibid.*, **68**, 580 (1958).

center from sp^3 to sp^2 shows a similar tendency, namely, 5- > open > 7- > 6- > 4- membered ring sulfoxides except the four-membered ring compound which is known to undergo solvolysis through a different course.

The apparent parallelism in reaction sequence between the two series of reactions undergoing displacement reaction on the two different atoms may be made clear by assuming both reactions to proceed through similar transition states. That is, in the case of sulfoxides the formation of trigonal bipyramidal structure such as (A) might be involved as in the S_N2 process on the carbon atom (B).

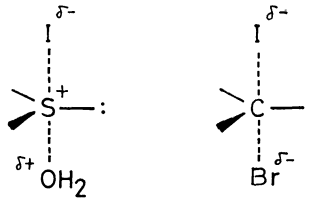

(A) (B)

Further evidence for the S_N2 like displacement at the sulfur atom may be the large negative activation entropy, −15 e.u., which is comparable to that of a typical S_N2 reaction on the carbon atom.

We have extended the study of this reduction to the series of methyl alkyl sulfoxides in order to re-examine the steric nature of this reaction. Strecker and Andersen[11] reported the importance of steric effect in a similar reduction of phenyl alkyl sulfoxides in which the rate constants decreased monotopically with increasing bulkiness of the alkyl group. However, there is a small rate acceleration by substitution of the ethyl group suggesting that in this series of methyl alkyl sulfoxides the ethyl group acts as an electron-donating group to facilitate the initial protonation step rather than as a steric hindrance group toward the incoming nucleophile at the second step. Likewise, the rate of reaction of diethyl sulfoxide is also about 30% faster than that of dimethyl sulfoxide. This seems to indicate that the steric inhibition is more important in the reaction of phenyl alkyl sulfoxides, perhaps due to the fact that the presence of a bulkier phenyl group makes the reaction center more sensitive to steric hindrance while in the series of methyl alkyl sulfoxides, the small methyl group can easily tolerate the steric inhibition of another primary alkyl group.

In view of thermodynamic parameters it is clear that the difference in reactivities of cyclic sulfoxides is mainly caused by the change in activation entropy. The activation entropy obviously decreases with increasing ring size and takes more negative value in the reaction of six- and seven- membered cyclic compounds and becomes less negative in reactions of four- and five-membered cyclic sulfoxides. The results can be best rationalized in terms of rigidity of the transition complex; namely, the less negative activation entropy for the five-membered cyclic sulfoxide indicates the transition state to have a similar rigidity to the ground state, and no reorganization of the molecular geometry along the reaction coordinate might be required. In other words, molecules which have already built-in ordered structure at the ground-state can reach the transition state without much loss of entropy to disturb the molecular motions. This gain of activation entropy would decrease the free energy of activation. For the enthalpy of activation, the five membered cyclic compound is so constrained already at the ground state that far less energy is required to reach the transition state, thus resulting in the lowest energy of activation among the aliphatic sulfoxides.

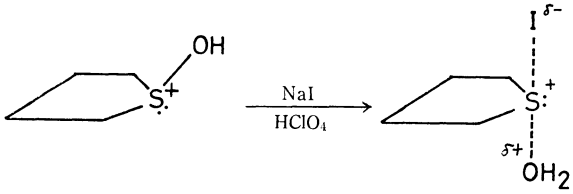

This is confirmed by an examination of the reaction of dibenzothiophene oxide which is very rigid due to the two benzo groups on both sides of thiophene molecule.

As anticipated, dibenzothiophene oxide has a less negative entropy of activation and a much lower enthalpy of activation, *i.e.*, $\Delta S^{\ddagger} = -10.4$ e.u. and $\Delta H^{\ddagger} = 18.5$ kcal/mol than $\Delta S^{\ddagger} = -15.1$ e.u. for tetramethylene sulfoxide and $\Delta H^{\ddagger} = 20.0$ kcal/mol for diphenyl sulfoxides.

Consideration of rigidity can be extended also to the four-membered sulfoxide system where the angle strain due to the smaller C–S–C angle and the molecular rigidity is evident. Thus, the four-membered cyclic sulfoxide is expected to have a large value of enthalpy and a less negative value of entropy of activation and hence to be highly reactive. This was the case for the highly strained four-membered cyclic sulfoxide. The observed large activation enthalpy amounting to 20 kcal/mol is in line with the relatively large energy required to overcome the accompanying unusual angle strain, while the less negative value of entropy of activation supports the view that the molecular shape is relatively unchanged in reaching the transition state.

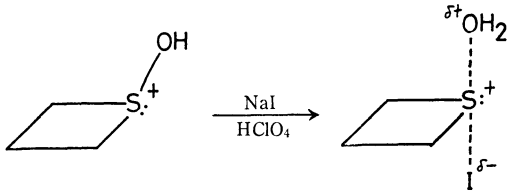

However, in this case, from the consideration of less negative entropy of activation of −6.7 e.u., there is a possibility that the direct nucleophilic attack of iodide ion on the sulfur or carbon atom provides the ring-opening product instead of the corresponding normal reduction product, *i.e.*, trimethylene sulfide. Because of the instability of trimethylene sulfide which decomposed to form a polymer in the highly acidic condition we chose for the kinetic study, we can give no plausible mechanism.

When the ring size becomes larger than five, the sulfoxides should display entirely different patterns in

11) R. A. Strecker and K. K. Andersen, *J. Org. Chem.*, **33**, 2234 (1968).

the thermodynamic parameters from those of tetramethylene sulfoxide, since the molecules are no longer rigid.

Entropies of activation for the reduction of pentamethylene and hexamethylene sylfoxides are smaller by 6 e.u. than that of tetramethylene sulfoxide. Although these reactions may not be of a simple elementary process, a possible structure for the transition state may be obtained from a consideration of the activation parameters.

If the reaction proceeds keeping the molecular shape unchanged all through the process, the attack of iodide ion at the sulfur atom should be hindered by the presence of the axial hydrogens on β-carbon atoms of pentamethylene sulfoxide and the rate depressed. However, since the molecule is not rigid it can avoid such a steric strain by distorting or twisting the ring into a half-chair form.[12] This idea of half-chair form at the transition state does not violate the microscopic reversibility principle and both the entering and leaving groups have to occupy equivalent positions.

The same idea may be applied to the reaction of the seven-membered cyclic compound. The extremely slow rate of reduction of the bicyclic (3.3.1)-9-sulfoxide also may serve to support the above mentioned argument. Such a rigid compound which has built-in two chair forms should be in a much more unfavorable

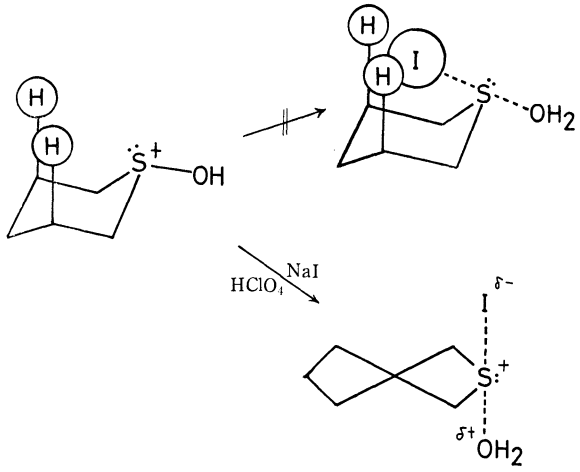

situation in the process of the relief of steric strain as compared with the case of the six-membered sulfoxide. The molecule is so rigid that it cannot bend the bonds to assume the energetically favorable conformation to allow an attack of nucleophile to come close to the reaction center.

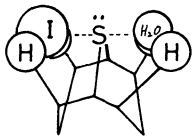

12) J. C. Martin and J. J. Uebel, *J. Amer. Chem. Soc.*, **86**, 2937 (1964).

BULLETIN OF THE CHEMICAL SOCIETY OF JAPAN, VOL. 44, 2460—2464 (1971)

The Bromination of 4-Acetyltropolone

Kahei TAKASE*, Kazuya SASAKI, Kohei SHIMIZU, and Tetsuo NOZOE
Department of Chemistry, Faculty of Science, Tohoku University, Katahira-2-chome, Sendai
(Received February 9, 1971)

The bromination of 4-acetyltropolone was examined, and two kinds of monobromo compounds, 4-acetyl-3-bromo- and 4-acetyl-7-bromotropolones, two kinds of dibromo compounds, 4-acetyl-3,7-dibromo- and 7-bromo-4-(ω-bromoacetyl)tropolones, a tribromo compound, 4-acetyl-3,5,7-tribromotropolone, and a tetrabromo compound, 3,5,7-tribromo-4-(ω-bromoacetyl)tropolone, were obtained. The third isomer of the monobromo compounds, 4-acetyl-5-bromotropolone, was synthesized from 4-acetyltropolone through 4-acetyl-5-aminotropolone. Moreover, an isomeric dibromo compound, 4-acetyl-5,7-dibromotropolone, was obtained by the debromination of the tribromo compound.

4-Acetyltropolone (I)[1] may be expected to be one of the most important materials for synthetical studies in troponoid chemistry, and in a previous paper[2] we reported on the properties of I and its methyl ethers in reaction to several oxidizing and reducing reagents. This paper will describe the results of our studies of bromination of I as one of a series of investigations of acetyltropolones.

The bromination of I is interesting in comparison with those of the other 4-substituted tropolones, such as 4-methyl-,[3] 4-ethyl-[4] and 4-isopropyltorpolones,[5] which

* Address correspondence to this author.

1) T. Nozoe, K. Takase, and M. Ogata, *Chem. Ind.*, **1957**, 1070.

2) T. Nozoe, K. Takase, K. Shimizu, and M. Yasunami, This Bulletin, **44**, 1951 (1971).

3) T. Nozoe, T. Mukai, and K. Matsui, *Proc. Japan Acad.*, **27**, 646 (1951); T. Nozoe, T. Mukai, M. Kunori, T. Muroi, and K. Matsui, *Sci. Repts. Tohoku Univ., Ser. I*, **35**, 242 (1952); R. D. Haworth and J. Hobson, *J. Chem. Soc.*, **1951**, 561.

4) T. Nozoe, K. Takase, and K. Umino, This Bulletin, **38**, 358 (1965).

5) T. Nozoe, T. Mukai, and K. Takase, *Proc. Japan Acad.*, **26**, 19 (1950); T. Nozoe, E. Sebe, S. Mayama, and S. Iwamoto, *Sci. Repts. Tohoku Univ., Ser. I*, **36**, 184 (1952); M. Yasunami, K. Takase, and T. Nozoe, *Tetrahedron Lett.*, **1970**, 4327.

have been studied well. Moreover, it seems to be important to prepare ω-bromoacetyl derivatives of I from the point of view of synthetical studies.

Results and Discussion

The bromination of 4-acetyltropolone was examined under the various reaction conditions listed in Table 1. In each experiment, the product was usually a complex mixture of several bromo compounds, and the separation into components was rather difficult. The major products and some minor products were eventually isolated by means of fractional recrystallization. The bromo compounds thus obtained were two kinds of monobromo (II) and (III), two kinds of dibromo (IV) and (V), and a tribromo compound (VI); their data are summarized in Table 1. The further bromination of the bromo compounds obtained here was also examined; some of these results are also listed in Table 1.

Table 1. Bromination of 4-acetyltropolone (I) and its monobromo derivatives (II) and (III)

Compound	Reaction conditions: Bromine mol. eq.	Reaction conditions: Medium	Bromination products: II	III	IV	V	VI
I	1—2	NaOAc-MeOH	++				
	1—2	MeOH	+			++	
	1	NaOAc-HOAc		++	+		+
	3	NaOAc-HOAc					++
	2	HOAc	+			++	
	1	$CHCl_3$	+			++	
	(NBS)	$CHCl_3$		+			
II	1	MeOH					++
	1—2	NaOAc-HOAc			+		++
III	1	NaOAc-MeOH			++		+
	1	MeOH				++	+
	1—2	NaOAc-HOAc					++

The bromination products isolated are shown by ++ for the major one, and + the minor one.

Table 2. The NMR spectra of the bromo derivatives of 4-acetyltropolone, δ ppm in $CDCl_3$ (intensity, signal pattern, coupling constant; Hz)

Compd.	Ring proton	Acetyl or bromoacetyl
II	6.70(1H, dd, J=7.8, 3.7) 7.38(1H, d, J=3.7) 7.42(1H, d, J=7.8)	2.59(3H, s)
III	7.47(1H, dd, J=10.4, 1.6) 7.92(1H, d, J=1.6) 8.37(1H, d, J=10.4)	2.68(3H, s)
V	7.47(1H, dd, J=10.3, 1.8) 7.89(1H, d, J=1.8) 8.41(1H, d, J=10.3)	4.43(2H, s)
VI	8.50(1H, s)	2.65(3H, s)
XII	6.97(1H, s) 7.10(1H, d, J=12.0) 7.77(1H, d, J=12.0)	2.57(3H, s)
XIII	8.52(1H, s)	4.49(2H, s)
XIV	6.99(1H, s) 7.25(1H, s)	2.58(3H, s)

a) s: singlet, d: doublet, dd: double doublet.

These bromo compounds showed the positive ferric chloride test characteristic of tropolones, and their ultraviolet absorption spectra indicated that all of them were tropolone derivatives. From the orientation in cationoid substitution at the tropolone nucleus[6] and from the reactivity of the acetyl group, it was expected that the bromo substituents of these bromo compounds should be present at the 3-, 5-, 7- and/or ω-positions. Moreover, it was assumed that the compound bearing the bromo substituents at the tropolone nucleus would be stable under a mild alkaline treatment, whereas ω-bromo compounds would be sensitive. On the basis of these considerations, as well as on that of the NMR data shown in Table 2 and the chemical evidence to be described below, the structures of the bromo compounds, II–VI, were determined as follows.

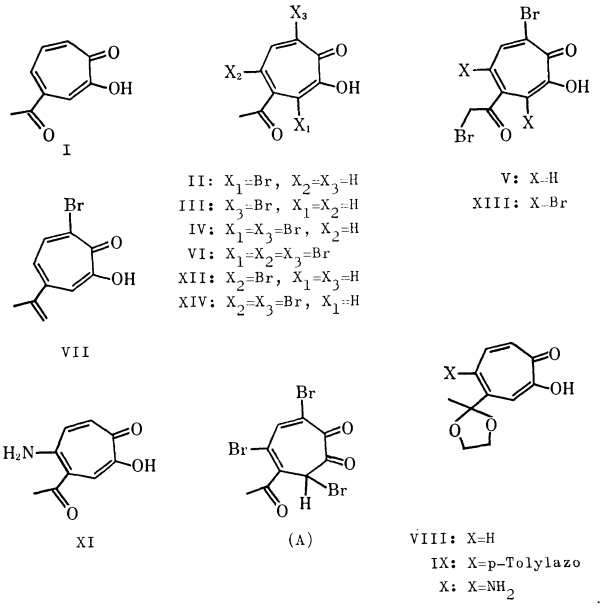

One of two monobromo compounds, II, was assigned the structure of 4-acetyl-3-bromotropolone on the basis of the NMR spectral data, which showed the presence of an acetyl group and three adjacent ring protons, as is shown in Table 2. The other monobromo compound, III, was identical to 4-acetyl-7-bromotropolone, which had been obtained from 7-bromo-4-isopropenyltropolone (VII)[7] by oxidation with hydrogen peroxide, followed by oxidation with metaperiodic acid, or by the Schmidt reaction. This structure was also revealed from the NMR spectral data shown in Table 2.

The dibromo compound, IV, was assigned the structure of 4-acetyl-3,7-dibromotropolone from the fact that IV was also obtained from both the monobromo compounds, II and III, on further bromination. The other dibromo compound, V, was assigned the structure of 7-bromo-4-(ω-bromoacetyl)tropolone, since it was also obtained from III by further bromination and gave

6) T. Nozoe, K. Takase, and H. Matsumura, "Dai Yuki Kagaku (Comprehensive Organic Chemistry)," Vol. 13, Chapter 5—9, Asakura-Shoten Tokyo (1960).

7) K. Takase, T. Kusunose, and T. Meguro, presented at the 12th Annual Meeting of the Chemical Society of Japan, Abstracts, (1959), p. 232.

a resinous material when treated with dilute alkali. This structure was also supported by the NMR spectral data, which showed the presence of the bromoacetyl group and three adjacent ring protons, as is shown in Table 2. The tribromo compound, VI, was assumed to be 4-acetyl-3,5,7-tribromotropolone, since it was obtained on the bromination of IV and gave a stable sodium salt when treated with a sodium hydroxide solution. The NMR spectral data shown in Table 2 also supported this assumption.

As a result of the structural determination of the bromination products described above, it became clear that, on the bromination of 4-acetyltropolone (I), the positions at which bromination occurred predominantly were remarkably affected by the reaction conditions, such as the presence or absence of sodium acetate and the kind of solvent used. Thus, as is shown in Table 1, in the presence of acetate, bromination occurred only on the tropolone nucleus at the 3- and/or 7-position, whereas, in the absence of acetate, it occurred on the acetyl group as well as on the tropolone nucleus. This behavior of I is thought to be due to the dissociation of I, in the presence of sodium acetate, to its anion, in which the 3-, 5-, and 7-positions of the tropolone nucleus are more reactive toward the cationoid reagents. A similar tendency was also observed on the bromination of the monobromo compound, III.

It is interesting to find that, on the bromination of I in the presence of sodium acetate, the use of acetic acid as the solvent gave a 7-bromo compound, III, whereas the use of methanol gave a 3-bromo compound, II, predominantly. Moreover, it is noteworthy that the sterically-hindered 3-position was predominantly attacked with the reagents in the medium of methanol–sodium acetate, while no 3-bromo derivative is known to be obtained on the bromination of 4-alkyltropolones, except for the finding that the bromination of 4-isopropyltropolone in ethanol at −15°C afforded a small amount of the 3-bromo derivative, together with the other bromo derivatives.[5] The reason for the predominant formation of II is not yet apparent.

The third isomer of the monobromo derivative of I, that is, 4-acetyl-5-bromotropolone could not be obtained by the bromination of I, but it was derived from I as follows. Since the azo-coupling of I gave a cyclohepta[*c*]pyrazolone derivative,[8] the ethylene ketal (VIII)[9] of I was coupled with *p*-toluenediazonium chloride to give an azo compound (IX). The catalytic hydrogenation of IX in methanol over palladium on carbon gave an amino-ketal (X), which was then hydrolyzed to an amino-ketone (XI). The application of the Sandmeyer reaction to X or XI gave a bromo compound (XII). It is reasonable to assign the structure of 4-acetyl-5-bromotropolone to XII, since it has been known that the *p*-tolylazo group generally enters at the 5-position of the tropolone nucleus.[6] This structure was also supported by the finding that the bromination of XII gave VI in a good yield, as well as by its NMR spectral data, shown in Table 2.

The dibromo compound, IV, gave the tribromo compound, VI, when treated with bromine in the presence of sodium acetate. On the other hand, the similar treatment of the dibromo compound, V, gave a tetrabromo compound (XIII). The structure of XIII was identified as 4,5,7-tribromo-4-(ω-bromoacetyl) tropolone from the findings that it was derived from V and that its NMR spectrum showed two singlets at 4.49 (2H) and 8.52 ppm (1H).

Although the tribromo compound, VI, was stable under a mild alkaline treatment, giving only sodium salt, it gave a dibromo compound (XIV) when heated with sodium iodide in ethanol. This dibromo compound, different from IV, was assigned the structure of 4-acetyl-5,7-dibromotropolones on the basis of the finding that it gave the tribromo compound, VI, on bromination, as well as on the basis of its NMR spectral data, shown in Table 2. This debromination reaction is thought to take place through a diketone-type intermediate (A).

Experimental

All the melting points are uncorrected. The ultraviolet absorption spectra were measured on a Beckman DU spectrophotometer, while the infrared spectra were recorded on a Shimadzu IR-27 infracord apparatus. The NMR spectra were determined with a Varian A-60 spectrometer on samples dissolved in deuteriochloroform, containing tetramethylsilane as the internal standard.

Bromination of 4-Acetyltropolone (I). *a) Bromination in Methanol in the Presence of Sodium Acetate*: Into a suspension of I (3.20 g) and sodium acetate (2.40 g) in methanol (100 m*l*), a solution of bromine (3.50 g) in glacial acetic acid (6 m*l*) was stirred under cooling with ice water; the mixture was then stirred for 2 hr. After the addition of water (150 m*l*), the mixture was allowed to stand overnight in a refrigerator; the crystals thereby formed were collected by filtration. Yield, 4.35 g; mp 170—185°C. Recrystallization from methanol gave 4-acetyl-3-bromotropolone (II) (2.75 g) as pale yellow scales; mp 193—194°C.

Found: C, 44.67; H, 3.09%. Calcd for $C_9H_7O_3Br$: C, 44.47; H, 2.90%. UV (MeOH): λ_{max} nm (log ε); 260 (4.42), 340 (3.94), 385 (3.76), 410 (3.74). IR (KBr disk); $\nu_{C=O}$, 1712 cm^{-1}.

A similar treatment of I (320 mg) with two molar equivalents of bromine also gave II (220 mg); mp 193—194°C.

b) Bromination in Methanol in the Absence of Acetate: Into a suspension of I (960 mg) in methanol (15 m*l*), a solution of bromine (1.92 g) in the same solvent (5 m*l*) was stirred under cooling with ice water, after which the mixture was stirred for 2 hr. The solvent was then evaporated, and the residue was fractionally recrystallized from methanol. The less soluble part gave II (10 mg) as pale yellow scales; mp 193—194°C. The readily-soluble part gave 7-bromo-4-(ω-bromoacetyl)tropolone (V) (1.20 g) as yellow needles; mp 147—149°C. The melting point rose to 149—151°C upon further recrystallization from methanol.

Found: C, 33.58; H, 1.93%. Calcd for $C_9H_6O_3Br_2$: C, 33.57; H, 1.88%. UV (MeOH): λ_{max} nm (log ε); 260 (4.43), 335 (3.79), 385 (3.71). IR (KBr disk); $\nu_{C=O}$, 1702 cm^{-1}.

A similar treatment of I (320 mg) with an equimolar amount of bromine gave V (50 mg), mp 149—151°C, together with an oily material.

8) T. Nozoe, K. Takase, and K. Suzuki, to be published.
9) I. Murata, This Bulletin, **34**, 577 (1961).

c) Bromination in Acetic Acid in the Presence of Sodium Acetate: Into a solution of I (1.60 g) and sodium acetate (1.20 g) in glacial acetic acid (30 m*l*), a solution of bromine (1.80 g) in the same solvent (2 m*l*) was stirred under cooling with ice water. After being stirred for 3 hr, the mixture was diluted with water and the crystals thereby formed were collected by filtration. Yield, 2.30 g; mp 90—98°C. Repeated recrystallizations from methanol gave 4-acetyl-7-bromotropolone (III) (920 mg) as yellow needles; mp 132—133°C.

Found: C, 44.73; H, 2.58%. Calcd for $C_9H_7O_3Br$: C, 44.47; H, 2.90%. UV (MeOH): λ_{max} nm (log ε); 227 (4.38), 345 (3.97), 446 (3.92). IR (KBr disk); $\nu_{C=O}$, 1686 cm^{-1}.

All the filtrates of the recrystallization were combined, the solvent was evaporated, and the residue was fractionally recrystallized from methanol. The slightly-soluble part gave 4-acetyl-3,5,7-tribromotropolone (VI) (350 mg) as yellow needles; mp 158—159°C.

Found: C, 27.12; H, 1.27%. Calcd for $C_9H_5O_3Br_3$: C, 26.96; H, 1.26%. UV (MeOH): λ_{max} nm (log ε); 272 (4.47), 355 (4.14), 442 (4.13). IR (KBr disk); $\nu_{C=O}$, 1712 cm^{-1}.

The readily-soluble part gave further crops of III (110 mg); mp 132—133°C.

The first aqueous filtrate was extracted with chloroform; the subsequent evaporation of the solvent left an oily material, which was then solidified by the addition of methanol. Recrystallization from methanol gave 4-acetyl-3,7-dibromotropolone (IV) (70 mg) as pale yellow scales; mp 151—152°C.

Found: C, 34.16; H, 2.12%. Calcd for $C_9H_6O_3Br_2$: C, 33.57; H, 1.88%. UV (MeOH): λ_{max} nm (log ε); 268 (4.41), 345 (3.95), 425 (4.06). IR (KBr disk); $\nu_{C=O}$, 1703 cm^{-1}.

d) Bromination in Acetic Acid in the Absence of Acetate: To a solution of I (320 mg) in glacial acetic acid (6 m*l*), a solution of bromine (650 mg) in the same solvent (0.5 m*l*) was added; the mixture was then stirred for 2 hr under cooling with ice water. Water was added to this mixture, the product was extracted with chloroform, and the solvent was evaporated, leaving crystals. Recrystallization from methanol gave V (310 mg) as yellow needles; mp 149—151°C.

e) Bromination in Chloroform: To a solution of I (320 mg) in chloroform (5 m*l*), a solution of bromine (320 mg) in the same solvent (1 m*l*) was added under cooling with ice water, after which the mixture was stirred for 3 hr. The crystals thereby formed were collected by filtration and recrystallized from methanol, giving II (50 mg) as pale yellow scales; mp 193—194°C.

All the filtrates were combined in a chloroform solution and washed with water. The evaporation of the solvent left an oily material, which was then crystallized by the addition of methanol, giving yellow crystals (250 mg); mp 144—146°C. Recrystallization from methanol gave V (80 mg) as yellow needles; mp 149—151°C.

f) Bromination with N-*Bromosuccinimide*: To a solution of I (800 mg) in chloroform, *N*-bromosuccinimide (800 mg) was added, after which the mixture was stirred for 5 hr at room temperature. The solvent was then evaporated, and the residue was recrystallized from methanol, giving III (240 mg) as yellow needles; mp 132—133°C.

Bromination of 4-Acetyl-3-bromotropolone (II). *a) Bromination in Methanol*: To a suspension of II (240 mg) in methanol (5 m*l*), a solution of bromine (160 mg) in the same solvent (1 m*l*) was added, after which the mixture was stirred for 2 hr under cooling with ice water. The subsequent evaporation of the solvent left crystals, which were then fractionally recrystallized from methanol to give VI (60 mg) as pale yellow needles; mp 158—159°C; II (50 mg) was also recovered.

b) Bromination in Acetic Acid in the Presence of Sodium Acetate: To a solution of II (240 mg) and sodium acetate (130 mg) in glacial acetic acid (8 m*l*) a solution of bromine (160 mg) in the same solvent (1 m*l*) was added, after which the mixture was stirred for 2 hr under cooling with ice water. Water was added to this mixture, and the crystals thereby formed were collected and fractionally recrystallized from methanol, thus giving VI (90 mg) as yellow needles, mp 158—159°C, and IV (40 mg) as pale yellow scales, mp 151—152°C.

A similar treatment of II (240 mg) with two molar equivalents of bromine gave VI (240 mg); mp 158—159°C.

Bromination of 4-Acetyl-7-bromotropolone (III). *a) Bromination in Methanol in the Presence of Sodium Acetate*: To a suspension of III (720 mg) and sodium acetate (300 mg) in methanol (15 m*l*), a solution of bromine (480 mg) in the same solvent (1 m*l*) was added, after which the mixture was stirred for 3 hr under cooling with ice water. The reaction mixture was diluted with water, and the product was extracted with chloroform. The evaporation of the solvent left an oily material, which was solidified by the addition of methanol. Fractional recrystallization from methanol gave IV (420 mg) as pale yellow scales, mp 151—152°C, and VI (50 mg) as yellow needles, mp 158—159°C.

b) Bromination in Methanol in the Absence of Acetate: To a suspension of III (240 mg) in methanol (5 m*l*), a solution of bromine (160 mg) in the same solvent (1 m*l*) was added, after which the mixture was stirred for 3 hr under cooling with ice water. The solvent was then evaporated, and the residue was fractionally recrystallized from methanol to give V (90 mg) as yellow needles mp 149—151°C, and VI (50 mg) as yellow needles, mp 158—159°C.

c) Bromination in Acetic Acid: To a suspension of III (240 mg) and sodium acetate (100 mg) in glacial acetic acid (8 m*l*), a solution of bromine (160 mg) in the same solvent (1 m*l*) was added, after which the mixture was stirred for 2 hr under cooling with ice water. Water was then added to the mixture, and the crystals thereby formed were collected and fractionally recrystallized from methanol to give VI (80 mg) as yellow needles, mp 158—159°C, III (80 mg) was also recovered.

A similar treatment of III (120 mg) with two molar equivalents of bromine gave VI (160 mg); mp 158—159°C.

4-Acetyl-7-bromotropolone (III) from 7-Bromo-4-isopropenyltropolone (VII).[7] a) To a solution of VII (960 mg) in formic acid (7 m*l*), a 30% hydrogen peroxide solution (0.5 m*l*) was dropped in at 40—55°C; the mixture was then kept at this temperature for 3 hr. The solvent was evaporated, and the oily residue was dissolved in an N sodium hydroxide solution (10 m*l*). This solution was warmed at 50—60°C for 5 hr, and then acidified with 2N sulfuric acid and shaken with chloroform. To the aqueous layer potassium periodate (460 mg) was added, after which the mixture was stirred for an hour at room temperature. The crystals thereby formed were collected and recrystallized from methanol to give III (250 mg) as yellow needles; mp 132—133°C.

b) A solution of VII (480 mg) in chloroform (1 m*l*) was stirred to a mixture of sodium azide (400 mg), chloroform (2 m*l*), and concentrated sulfuric acid (2 m*l*) at about 20°C. After being stirred for 3 hr, the mixture was allowed to stand overnight; then it was poured into ice water and extracted with chloroform. The solvent was evaporated, and the residue was recrystallized from methanol to give III (150 mg) as yellow needles; mp 132—133°C.

4-(1,1-Ethylenedioxyethyl)tropolone (VIII). A mixture of I (2.20 g), ethyleneglycol (4.10 g), and benzene (15 m*l*) was refluxed for 5 hr in the presence of *p*-toluenesulfonic acid (10 mg). The benzene-soluble part was collected by decantation; the subsequent evaporation of the solvent gave VIII (2.68 g), mp 90—93°C. Recrystallization from petroleum ether af-

forded colorless needles; mp 98—99°C. The melting point previously reported[9] was 97—98°C.

Found: C, 63.95; H, 5.44%. Calcd for $C_{11}H_{12}O_4$: C, 63.45; H, 5.81%. UV (MeOH): λ_{max} nm (log ε); 238 (4.45), 320 (3.89), 350 (3.78).

4-(1,1-Ethylenedioxyethyl)-5-(p-tolylazo)tropolone (IX). Into a solution of VIII (600 mg) in pyridine (2 ml), we stirred a solution of *p*-toluenediazonium chloride which had been prepared by the diazotization of a solution of *p*-toluidine (330 mg) in 2N hydrochloric acid with a solution of sodium nitrite (240 mg) in water (1.5 ml); we did this under cooling with ice water. After additional stirring for 2 hr, water was added to this mixture and the crystals thereby formed were collected and recrystallized from benzene to give IX (470 mg) as red micro-prisms; mp 176—178°C.

Found: C, 65.95; H, 5.38; N, 8.42%. Calcd for $C_{18}H_{18}O_4N_2$: C, 66.24; H, 5.56; N, 9.58%. UV (MeOH): λ_{max} nm (log ε); 230 (4.39), 293 (4.00), 385 (4.35).

5-Amino-4-(1,1-ethylenedioxyethyl)tropolone (X). A suspension of IX (660 mg) in methanol (12 ml) was shaken under a hydrogen atmosphere in the presence of 5% palladium-carbon (80 mg); 100 ml of hydrogen gas was consumed during a period of 7 hr. After the subsequent removal of the catalyst, the solution was concentrated to a small volume and allowed to cool, thus giving X (270 mg); mp 164—166°C. Recrystallization from methanol afforded yellow plates; mp 166—167°C.

Found: C, 59.04; H, 5.65; N, 6.30%. Calcd for $C_{11}H_{13}O_4N$: C, 59.18; H, 5.87; N, 6.28%. UV (MeOH): λ_{max} nm (log ε); 238 (4.38), 360 (4.12), 387 (4.08).

4-Acetyl-5-aminotropolone (XI). A solution of X (200 mg) in methanol (5 ml) containing N hydrochloric acid (0.5 ml) was refluxed for an hour. The subsequent concentration of the solution gave XI (150 mg) as reddish-orange needles; mp 180—181°C.

Found: C, 60.39; H, 4.76; N, 7.47%. Calcd for $C_9H_9O_3N$: C, 60.33; H, 5.06; N, 7.82%. UV (MeOH): λ_{max} nm (log ε); 247 (4.47), 365 (4.12), 465 (3.93).

4-Acetyl-5-bromotropolone (XII). Into a solution of X (220 mg) in 50% aqueous dioxane (2.5 ml) containing 6N sulfuric acid (0.9 ml), a solution of sodium nitrite (75 mg) in water (0.2 ml) was added at 0—5°C. After stirring for an additional 30 min, this mixture was added to a solution of cuprous bromide (350 mg) in concentrated hydrobromic acid (1.9 ml), after which the mixture was stirred for 3 hr under cooling with ice water. The mixture was diluted with water, and the copper chelate compound thus precipitated was collected by filtration. Through a suspension of this copper chelate in chloroform, hydrogen sulfide gas was passed, after which the copper sulfide thereby formed was filtered off. The subsequent evaporation of the solvent from the filtrate left some crystals (170 mg); mp 105—125°C. Recrystallization from methanol gave XII (90 mg) as pale yellow needles; mp 142—143°C.

Found: C, 44.09; H, 2.80%. Calcd for $C_9H_7O_3Br$: C, 44.47; H, 2.90%. UV (MeOH): λ_{max} nm (log ε); 235 (4.29), 248 (4.30), 335 (4.04), 4.10 (3.54). IR (KBr disk); $\nu_{C=O}$, 1709 cm^{-1}.

A similar treatment of XI (70 mg) gave XII (30 mg); mp 142—143°C.

Bromination of 4-Acetyl-5-bromotropolone (XII). To a solution of XII (50 mg) and sodium acetate (40 mg) in glacial acetic acid (1 ml), a solution of bromine (65 mg) in the same solvent (0.5 ml) was added, after which the mixture was stirred for 2 hr under cooling with ice water. Water was then added to this mixture, and the crystals thereby formed were collected and recrystallized from methanol to give VI (70 mg) as yellow needles; mp 158—159°C.

Bromination of 4-Acetyl-3,7-dibromotropolone (IV). To a solution of IV (110 mg) and sodium acetate (30 mg) in glacial acetic acid (2 ml), a solution of bromine (60 mg) in the same solvent (0.5 ml) was added, after which the mixture was stirred for 2 hr. Water was then added to this mixture, and the crystals thereby formed were collected and recrystallized from methanol to give VI (110 mg) as yellow needles; mp 158—159°C.

3,5,7-Tribromo-4-(ω-bromoacetyl)tropolone (XIII). To a solution of V (640 mg) and sodium acetate (200 mg) in glacial acetic acid (20 ml), a solution of bromine (320 mg) in the same solvent (1 ml) was added, after which the mixture was stirred for 2 hr under cooling with ice water. Water was then added to this mixture, and the crystals thereby formed were collected and recrystallized from methanol to give XIII (490 mg); mp 161—162°C. Further recrystallization from the same solvent afforded yellow needles; mp 164—165°C.

Found: C, 22.23; H, 1.09%. Calcd for $C_9H_4O_3Br_4$: C, 22.53; H, 0.84%. UV (MeOH): λ_{max} nm (log ε); 273 (4.48), 360 (4.14), 450 (4.18). IR (KBr disk); $\nu_{C=O}$, 1730 cm^{-1}.

4-Acetyl-5,7-dibromotropolone (XIV). A solution of VI (400 mg) and sodium iodide (300 mg) in ethanol (10 ml) was refluxed for 3 hr. To this solution we then added water (30 ml) containing a small amount of sodium hydrogen sulfite, and the mixture was stirred for 30 min. The crystals thereby formed were collected and recrystallized from methanol to give XIV (90 mg) as yellow, silky needles; mp 191—192°C.

Found: C, 33.73; H, 1.94%. Calcd for $C_9H_6O_3Br_2$: C, 33.57; H, 1.88%. UV (MeOH): λ_{max} nm (log ε); 265 (4.40), 353 (4.15), 430 (4.00). IR (KBr disk); $\nu_{C=O}$, 1700 cm^{-1}.

This research has been financially supported by grants from the Japanese Ministry of Education and the Sankyo Co., Ltd.

Synthesis and Properties of Two Annelated Annulenes

Katsusuke ENDO,* Yoshiteru SAKATA, and Soichi MISUMI

The Institute of Scientific and Industrial Research, Osaka University, Suita, Osaka

(Received February 15, 1971)

Two annelated tridehydro[18]annulenes, trinaphtho[1,9,8,7-*abc*: 1′,9′,8′,7′-*ghi*:1″,9″,8″,7″-*mno*]- and tribenzo [*a,g,m*]-5,11,17-tridehydro[18]annulenes (VI and VII), were synthesized by the Castro reaction of cuprous salts of 1-ethynyl-7-iodonaphthalene (IX) and 4-[*o*-iodophenyl]-3-buten-1-yne (XIV), respectively. The UV spectra of these annelated annulenes revealed an extended delocalization of π-electrons around the inner eighteen membered ring. However, from the chemical shifts of the inner protons (H_A and H_B) it is concluded that both VI and VII are non-aromatic compounds.

The molecular orbital theory of cyclic conjugated systems by Hückel predicted that systems containing $(4n+2)$ π-electrons would display an aromatic character. This rule has been substantially confirmed by many investigations of various nonbenzenoid conjugated systems, particularly by elegant works on annulenes and dehydroannulenes.[1] Thus it was thought to be of interest to prepare annelated annulenes in order to realize the effect of annelation on aromaticity of annulene and dehydroannulene. Recently some planar and non-planar annelated annulenes (I—V)[2] were synthesized, but no direct evidence for the presence of the aromatic character was found in the compounds except for an anion of dibenzocyclononatetraene (IV)[2d] and derivatives (V)[2e] of [18]annulene containing heterocycles.

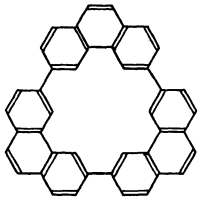

I

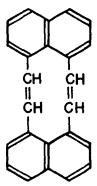

II

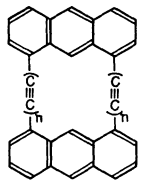

III, n=2,4

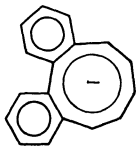

IV

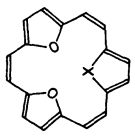

V, X=O,S

We have attempted to get better understanding of the effect of annelation on aromaticity. The present paper reports the results of a study of two planar annelated derivatives of aromatic 1,7,13-tridehydro[18]-annulene,[3] trinaphtho[1,9,8,7-*abc*: 1′,9′,8′,7′-*ghi*: 1″,9″, 8″,7″-*mno*]- and tribenzo[*a,g,m*]-5,11,17-tridehydro-[18]annulenes (VI and VII), to which Kekulé type structures of the inner eighteen membered ring systems can be assigned. The chemical shift of the inner protons (H_A and H_B) can provide significant information with regard to the diamagnetic ring current around the ring systems, *viz.*, the existence of aromatic character.

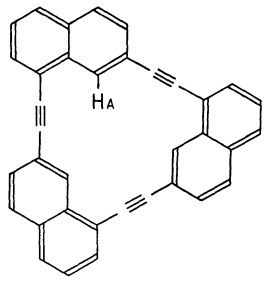

VI

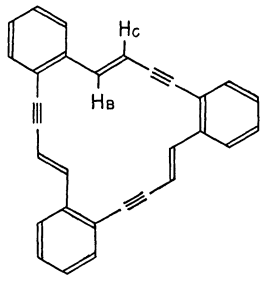

VII

Results and Discussion

Synthesis 1-Acetyl-7-iodonaphthalene (VIII) was obtained by the acetylation of β-iodonaphthalene according to the Harnik method[4] in 18.5% yield. Ketone VIII was treated with phosphorus pentachloride in phosphorus oxychloride, followed by dehydrochlorination of the resulting chloride mixture with alcoholic potassium hydroxide to give 49% yield of 1-ethynyl-7-iodonaphthalene (IX). The Castro reaction[5] of dry cuprous salt of IX in pyridine afforded a cyclic acetylene compound in 8.0% yield. This compound was found to be fairly stable and can be kept without any change for a long time. The structure of VI was assigned to it based on the following. The lack of absorption due to the terminal ethynyl group in the IR- and NMR-

* Present address: Fuji Photo Film Co., Minamiashigaramachi, Kanagawa.

1) F. Sondheimer, *Pure Appl. Chem.*, **7**, 363 (1963); *Proc. Roy. Soc., Ser.* A, **297**, 173 (1967); F. Sondheimer, I. C. Calder, J. A. Elix, Y. Gaoni, P. J. Garratt, K. Grohmann, G. di Maio, J. Mayer, M. V. Sargent, and R. Wolovsky, *Spec. Publs. Chem. Soc.*, No. 21 (1967), p. 75; E. Vogel, *Chimia*, **22**, 21 (1968).

2) a) H. A. Staab and H. Bräunling, *Tetrahedron Lett.*, **1965**, 45; H. A. Staab, H. Bräunling, and K. Schneider, *Chem. Ber.*, **101**, 879 (1968). b) R. H. Mitchell and F. Sondheimer, *J. Amer. Chem. Soc.*, **90**, 530 (1968). c) S. Akiyama, S. Misumi, and M. Nakagawa, This Bulletin, **33**, 1293 (1960), **35**, 1829 (1962). d) P. J. Garratt and K. A. Knapp, *Chem. Commun.*, **1970**, 1215. e) G. M. Badger, "Aromatic Character and Aromaticity," Cambridge University Press, London (1969); G. M. Badger, G. E. Lewis, and U. P. Singh, *Aust. J. Chem.*, **19**, 257, 1461 (1966); G. M. Badger, J. A. Elix, and G. E. Lewis, *ibid.*, **19**, 1221 (1966).

3) F. Sondheimer, Y. Amiel, and Y. Gaoni, *J. Amer. Chem. Soc.*, **81**, 1771 (1959), **84**, 270 (1962); L. M. Jackman, F. Sondheimer, Y. Amiel, D. A. Ben-Efraim, Y. Gaoni, R. Wolovsky, and A. A. Bothner-By, *ibid.*, **84**, 4307 (1962); I. C. Calder, P. J. Garratt, H. C. Longuet-Higgins, F. Sondheimer, and R. Wolovsky, *J. Chem. Soc., C*, **1967**, 1041.

4) M. Harnik and E. V. Jensen, *Israel J. Chem.*, **3**, 13 (1965).

5) R. D. Stephens and C. E. Castro, *J. Org. Chem.*, **28**, 3313 (1963); C. E. Castro, E. J. Gaughan, and D. C. Owsley, *ibid.*, **31**, 4071 (1966); C. E. Castro, R. Havlin, V. K. Honwad, A. Malte, and S. Mojé, *J. Amer. Chem. Soc.*, **91**, 6464 (1969).

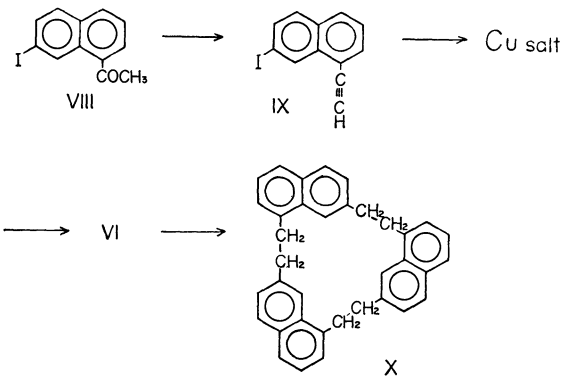

spectra suggests the cyclic structure of VI. Furthermore, the elemental analysis of VI and molecular weight determination of its hydrogenated product (X) which is satisfactorily soluble for vapour pressure osmometry established the formation of VI by trimolecular Castro reaction of IX.

An acetylenic alcohol (XII) was prepared by Reformatsky-type reaction of *o*-iodobenzaldehyde (XI)[6] with propargyl bromide using aluminum[7] in an excellent yield of around 80%. The normal Reformatsky reaction as well as the Grignard reaction afforded lower yields of XII. Chloride XIII, obtained by treatment of XII with phosphorus oxychloride, was dehydrochlorinated with methanolic potassium hydroxide. Chromatography of the reaction product on alumina gave *o*-iodophenylbutenyne (XIV) in an overall yield of 30% based on XII. The Castro reaction of cuprous salt of the butenyne XIV gave a cyclic trimer VII of fairly stable and bright yellow needles in 13.0% yield and a small amount of cyclic tetramer XV. Structures of trimer VII and tetramer XV were confirmed by elemental analysis, IR and NMR spectra and molecular weight determination.

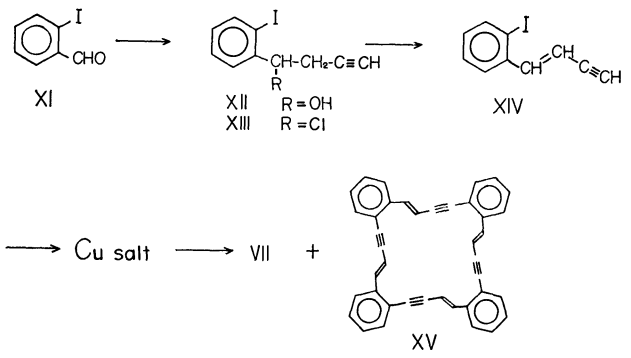

Electronic Spectra The electronic spectra of VI and VII as well as those of diphenylbutenyne (XVI) and 1,7,13-tridehydro[18]annulene (XVII)[3] as reference substances are shown in Fig. 1. The spectrum of a cyclic trimer (I) of phenanthrene shows the maxima at the same wavelengths as those of biphenanthryl and

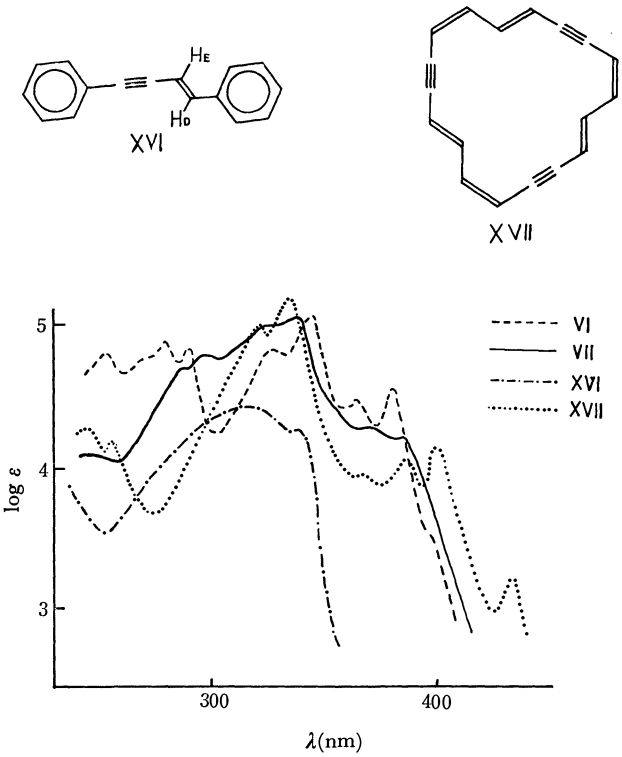

Fig. 1. The electronic spectra of VI, VII, XVI (in THF) and XVII (in isooctane).

terphenanthryl, whereas the maxima at the longest wavelength of VI and VII exhibit distinct red-shift as compared with those of tetramer XV and XVI. The absorption curve of VI is similar to that of XVII except for the lack of the maximum at near 430 nm, whereas VII shows broad and structureless absorption in contrast to VI and XVII. Thus, a comparison of these spectra suggests that both VI and VII are intermediates between I and XVII in respect of the delocalization of π-electrons. The fact that the by-product XV showed broad absorption curve and hypsochromic and hypochromic shifts of the maxima as compared with VII indicates a nonplanar structure of XV in agreement with a presumption from a skeletal molecular model.

Table 1. Chemical shifts (τ) and coupling constants (J) of inner protons of VI, VII, and XVII as well as those of olefinic protons of XV and XVI in $CDCl_3$

	VI	VII	XV	XVI	XVII[3]
τ 1.51[a]	3.36	3.51	3.69	2.44	
	2.87	2.56	3.04	8.26	
J	16.2	16.2	16.2	15.6 Hz	

a) in $AsCl_3$ solution

NMR Spectra. The NMR spectra of VI, VII, and XVI are given in Table 1. The spectrum of VI shows two peaks, a singlet at τ 1.51 and a multiplet at τ 1.85—2.55, with an area ratio 1:5 and no other peak at a higher field. The peak at τ 1.51 is assigned to the proton H_A of naphthalene nuclei on account of its being singlet and of its area ratio to the other aromatic protons at τ 1.85—2.55. The position of the proton H_A is at a

6) W. S. Rapson and R. G. Shuttleworth, *J. Chem. Soc.*, **1941**, 487.

7) P. Läuger, M. Prost, and R. Charlier, *Helv. Chim. Acta*, **42**, 2379 (1959); K. Eiter and H. Oediger, *Ann. Chem.*, **682**, 62 (1965); F. Sondheimer, Y. Amiel, and Y. Gaoni, *J. Amer. Chem. Soc.*, **84**, 270 (1962).

lower field than that of α-proton (τ 2.19)[8] of naphthalene.

Two plausible elucidations may be given. First, the effect of diamagnetically induced ring current around the inner eighteen membered ring system is considered. If the magnitude of the ring current were not large, it would be overcome by the magnetic anisotropy of the triple bonds and other two naphthalene nuclei. As a result, the proton H_A may be observed at a slightly lower field than α-proton of naphthalene. Secondly, such a small shift of the proton H_A to the lower field would be only caused by the magnetic anisotropy of the triple bonds and naphthalene nuclei. In order to solve this problem, the magnitude of the magnetic anisotropies should be estimated. An estimate of the extent to which the shift of the proton H_A of VI is affected by both π-electron systems was performed according to the following McConnell equation[9] by using the distances and angles shown in Fig. 2.

$$\Delta\sigma = \Delta\chi\sum_{i=1}^{n}\frac{1}{3R^3}(1-3\cos^2\theta) \qquad (1)$$

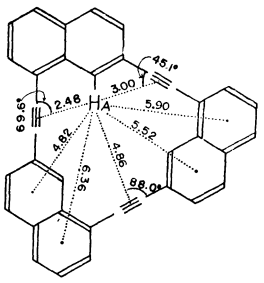

VI

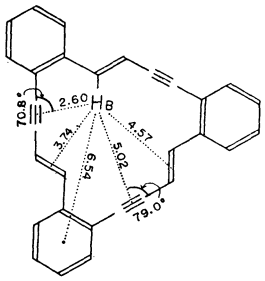

VII

For three triple bonds ($\Delta\chi = -11.8\times10^{-6}$ cm^3/mol),[10] the total shielding effect was calculated to be −0.20 ppm from equation (1). The shielding effect of two naphthalene nuclei, in which the shielding contribution of each naphthalene was approximated as a sum of ring currents of two benzene rings according to theoretical predictions,[11] was calculated to be −0.71 ppm by use of Johnson–Bovey table.[12] A total value −0.91 ppm due to both shielding effects was consequently found to be in good agreement with the observed shift, −0.68 ppm, from α-proton of naphthalene.[8] Similarly, the shift of proton H_B of VII from proton H_D of XVI was calculated as in VI, and the whole effect, −0.50 ppm, of double bonds, triple bonds, and benzene nuclei was found to be reasonable as compared with the observed shift −0.17 ppm. Table 1 also shows the equal coupling constant of olefinic protons in VII, XV, and XVI.

Consequently, a considerable delocalization of π-electrons in VI and VII was revealed in the electronic absorption spectra as aforementioned. However, it can be concluded that the results obtained from NMR spectra support the second elucidation stated above and provide no positive evidence for the presence of diamagnetically induced ring current in the eighteen membered ring systems of both VI and VII, and that both the annelated annulenes are non-aromatic.

Experimental

All melting points are uncorrected. The electronic spectra were taken on a Hitachi EPS-3T, the infrared spectra on a Jasco DS-402G, the NMR spectra on a Hitachi R-20, the mass spectra on a Hitachi RMU-7 and the molecular weight on a Knauer vapour pressure osmometer.

1-Ethynyl-7-iodonaphthalene (IX). A mixture of 1-acetyl-7-iodonaphthalene[4] (10.0 g, 33.8 mmol) and phosphorus pentachloride (10.4 g, 50 mmol) in phosphorus oxychloride (100 m*l*) was refluxed with stirring for 1 hr. After the reaction was over, phosphorus oxychloride was evaporated under reduced pressure and the residue was dried in a desiccator over potassium hydroxide overnight. To the crude chloride thus obtained was added 40 g of powdered potassium hydroxide and ethanol (100 m*l*). The mixture was stirred under gentle reflux for 30 min. The residual solid obtained by evaporation of ethanol in vacuum was triturated with benzene. The benzene extract was washed with water and dried over sodium sulfate. After the solvent was removed *in vacuo*, the residue (14.02 g) was chromatographed on alumina (300 g) with benzene-petroleum ether (1:9) to give yellow oil of IX, 4.60 g (49.0% yield). NMR ($CDCl_3$): τ 1.34 (s, proton at C_8), 2.1—2.9 (m, other arom. protons), 6.60 (s, ≡CH).

Mercuric Salt of IX: A solution of potassium mercuri-iodide[13] was obtained by adding 10% aq. sodium hydroxide (0.6 m*l*) to a mixture of mercuric chloride (0.275 g, 1.05 mmol) and potassium iodide (0.695 g, 4.2 mmol) in water (0.7 m*l*). To this was added a solution of IX (0.292 g, 1.05 mmol) in 6 m*l* of ethanol with stirring to yield white precipitate of mercuric salt. After it had been filtered immediately and washed with 50% aq. ethanol, the precipitate was recrystallized from benzene to afford 0.266 g (67.0%) of mercuric salt, colorless fine needles, mp 263.5—264.7°C (decomp.).

Found: C, 38.20; H, 1.63%. Calcd for $C_{24}H_{12}I_2Hg$: C, 38.19; H, 1.60%.

Trinaphtho[1,9,8,7-abc: 1′,9′,8′,7′-ghi: 1″,9″,8″,7″-mno]-5,11,17-tridehydro[18]annulene (VI). To a solution of Ilosvay's reagent[14] was added a solution of iodonaphthylacetylene (IX) (4.60 g, 16.5 mmol) in 80 m*l* of ethanol to give immediately yellow precipitate of cuprous salt. The cuprous salt obtained by filtration was washed with water, ethanol, and ether, successively, and dried *in vacuo* at 40°C, 3.52 g (62.5%).

The cuprous salt (1.73 g, 5.08 mmol) in dry pyridine (50 m*l*) was heated with stirring at 120°C under nitrogen for 8 hr. After cooling, the reaction mixture was poured into water (150 m*l*) and extracted with ether. The extract was washed with dil. hydrochloric acid, 5% aq. sodium bicarbonate, and water, successively, and dried over magnesium sulfate. After the solvent had been evaporated, the residue was chro-

8) F. A. Bovey, "NMR Data Table for Organic Compounds," Vol. 1, John Wiley & Sons, Inc., New York (1967), p. 265.
9) H. M. McConnell, *J. Chem. Phys.*, **27**, 226 (1957).
10) S. Castellano and J. Lorenc, *J. Phys. Chem.*, **69**, 3552 (1965); J. A. Pople and K. G. Untch, *J. Amer. Chem. Soc.*, **88**, 4813 (1966).
11) L. M. Jackman and S. Sternhell, "Application of Nuclear Magnetic Resonance Spectroscopy in Organic Chemistry," 2nd ed., Pergamon Press, London (1969), p. 96; N. Jonathan, S. Gordon, and B. P. Dailey, *J. Chem. Phys.*, **36**, 2443, (1962).
12) C. E. Johnson, Jr., and F. A. Bovey, *J. Chem. Phys.*, **29**, 1012 (1958).
13) J. R. Johnson and W. L. McEwen, *J. Amer. Chem. Soc.*, **48**, 469 (1926); B. B. Elsner and P. F. M. Paul, *J. Chem. Soc.*, **1951**, 893.
14) The reagent is obtained from cupric sulfate, aq. ammonia and hydroxylamine hydrochloride.

matographed on alumina with benzene. The residual solid (0.18 g) obtained from 4—6th fractions was recrystallized from benzene to afford 61 mg (8.0% yield) of VI, pale yellow needles, decomp. over 360°C.

Found: C, 95.72; H, 4.08%. Calcd for $C_{36}H_{18}$; C, 95.97; H, 4.03%. IR (KBr disk): 1610, 1585, 888, 831, 827 cm^{-1}. UV (in THF); λ_{max} (ε), 254 (59100), 266* (50200), 279 (78200), 290 (65600), 327 (69000), 342 (122000), 360 (25400), 365 (29000), 380 (33800), 396* nm (3410) (* inflection).

Reduction of VI. The acetylenic compound VI (40.3 mg, 9.0×10^{-2} mmol) and 10% palladium-on-charcoal (143 mg) in benzene (70 m*l*) were shaken with hydrogen at 50°C for 10 hr. After cease of hydrogen absorption, the catalyst was filtered and the solvent was evaporated under reduced pressure. The residue was recrystallized from petroleum ether to yield colorless needles of reduction product (X), mp 286—286.5°C, 38.8 mg (93.5%).

Found: C, 92.92; H, 6.54%. Calcd for $C_{36}H_{30}$: C, 93.46; H, 6.54%. Mol wt: Found; 477 (vapour pressure osmometry), 462 (mass spectrum). Calcd for $C_{36}H_{30}$; 462.6. IR (KBr disk): 830 (s), 748 (s) cm^{-1}. UV (in THF): λ_{max} (ε), 228 (193000), 278 (20600), 287 (22600), 316* (1580), 323 nm (1540) (* inflection).

o-Iodophenyl Propargyl Carbinol (XII). To aluminum metal plate (1.1 g, 40.7 mg atom), activated on heating with small pieces of mercuric chloride and iodine, was added a solution of propargyl bromide (7.2 g, 60 mmol) in dry tetrahydrofuran (10 m*l*) with stirring at room temperature. After consumption of aluminum metal, *o*-iodobenzaldehyde[5] (XI) (13.9 g, 60 mmol) in dry tetrahydrofuran (20 ml) was added dropwise to the solution at −60°C with stirring and the mixture was stirred at 0°C for 1 hr. After addition of saturated aqueous ammonium chloride (50 m*l*), the aqueous layer was separated and extracted twice with ether. The combined organic solution was washed, dried over magnesium sulfate and the solvent was removed under reduced pressure. A solution of the residue (15.64 g) in benzene-petroleum ether (1:1) was passed through a short column of alumina (30 g) and eluted with the same solvent. The effluent was concentrated to yield reddish brown oil of crude carbinol XII, 12.84 g (78.8%).

NMR ($CDCl_3$): τ 2.1—3.3 (m, 4H, arom.), 5.02 (quart., 1H, tert.), 6.96 (broad s, 1H, OH), 7.0—7.9 (m, 2H, $-CH_2-$), 7.95 (t, 1H, ≡CH).

4-[o-Iodophenyl]-3-buten-1-yne (XIV). To a cold solution of the carbinol XII (6.8 g, 25 mmol) in dry pyridine (30 m*l*) was added dropwise a mixture of dry pyridine (20 m*l*) and phosphorus oxychloride (20 m*l*) with stirring. The mixture was stirred below 5°C for 20 min, then carefully poured onto 300 g of ice and extracted with benzene. The extract was washed with water, dried and concentrated *in vacuo*. The oily residue was passed through a short column of alumina (15 g) with benzene-petroleum ether (1:1). The effluent was evaporated under reduced pressure to yield reddish brown oil of *o*-iodophenyl propargyl chloride (XIII), 3.26 g.

A mixture of the crude chloride XIII (3.26 g) and powdered potassium hydroxide (1.68 g, 30 mmol) in methanol (7 m*l*) was stirred at 50°C for 40 min. The reaction mixture was poured into 140 m*l* of water and extracted with benzene. The extract was washed with water, dried over magnesium sulfate and concentrated *in vacuo*. The residue (2.10 g) was dissolved in benzene-petroleum ether (3:17) and passed through a short column of alumina. The effluent was evaporated under reduced pressure to give unstable XIV as pale yellow oil, 1.77 g, 28.0% yield based on the carbinol XII (34.3% yield in the other run).

NMR ($CDCl_3$): τ 2.1—3.4 (m, 4H, arom.), 2.84 (d, 1H, olefin. H_1 at C_4), 4.10 (double d, 1H, olefin. H_2 at C_3), 6.94 (d, 1H, ≡CH), $J_{H_1,H_2}=15.6$ Hz.

Mercuric Salt of XIV: Mercuric salt of XIV was obtained according to the same method as IX and recrystallized from benzene, colorless needles, mp 227—232°C (decomp.).

Found: C, 34.06; H, 1.75%. Calcd for $C_{20}H_{12}I_2Hg$: C, 33.99; H, 1.71%.

Tribenzo[a,g,m]-5,11,17-tridehydro[18]annulene (VII). Well dried cuprous salt (10.0 g, 31.5 mmol) of XIV, obtained in a yield of 77% according to the same method as for IX, was heated in dry pyridine (350 m*l*) with stirring under nitrogen. The mixture was heated up to 120°C and the stirring at this temperature was continued for 8 hr. After cooling, the mixture was poured into 1.5 *l* of water and extracted with benzene. The extract was washed with dil. hydrochloric acid, 5% aq. sodium bicarbonate and water, successively, and dried over magnesium sulfate. The solvent was removed *in vacuo* to give 3.81 g of residue. The residue was chromatographed on alumina (250 g) with benzene-petroleum ether (1:1). The column was eluted with benzene-petroleum ether (the ratios 1:1 for 20 fractions and 7:3 for the successive 10 fractions of each 50 m*l*). The solid, obtained from 5—8th fractions, was recrystallized from benzene to give colorless prisms of the cyclic tetramer XV, 0.124 g (2.4% yield), decomp. over 260°C.

Found: C, 95.00; H, 4.93%. Calcd for $C_{40}H_{24}$: C, 95.21; H, 4.79%. Mol wt: Found; 509 (vapour pressure osmometry). Calcd for $C_{40}H_{24}$; 504.6. IR (KBr disk): 950 (s), 750 (s), 675 (s), 526 (m), 503 (m), 485 cm^{-1} (m). UV (in THF): λ_{max} (ε), 252 (36200), 292.5 (71700), 312.5 nm (70900).

The combined effluent of 14—30th fractions was evaporated *in vacuo* and the residue was recrystallized from benzene to afford yellow needles of the cyclic trimer VII, 0.527 g (13.0% yield), decomp. over 275°C.

Found: C, 95.37; H, 4.59%. Calcd for $C_{30}H_{18}$: C, 95.21; H, 4.79%. Mol wt: Found; 372 (vapour pressure osmometry). Calcd for $C_{30}H_{18}$; 378.5. IR (KBr disk): 950 (s), 750 (s), 745 (s), 515 (m), 498 cm^{-1} (m). UV in (THF): λ_{max} (ε), 241.5 (12300), 251* (12000), 287* (45500), 297.7 (58900), 325 (103000), 337 (114000), 366 (19800), 384 nm (15800) (* inflection).

1,4-Diphenylbutenyne (XVI). Butenyne XVI was prepared by the Castro reaction of the cuprous salt of 4-phenyl-3-buten-1-yne, obtained according to Eiter,[7] with iodobenzene, mp 96.7—97.8°C (lit,[15] mp 95°C).

15) V. Grignard and Tcheoufaki, *C. R. Acad. Sci., Paris*, **188**, 1533 (1929); *Rec. Trav. Chim. Pay-Bas*, **48**, 903 (1929).

Di- and Trimethylenebis(ethylphenacyl)sulfonium Ylides

Shinzi KATO, Hideharu ISHIHARA, Masateru MIZUTA, and Yoshio HIRABAYASHI
Faculty of Engineering, Gifu University, Kakamihara, Gifu

(Received February 22, 1971)

Bissulfonium phenacylides were obtained by the reactions of dimethylene and trimethylene bisethylphenacylsulfonium salts with sodium hydride. The chemical properties of these bis-ylides are similar to those of monosulfonium phenacylides. Biscarbamoylsulfonium phenacylides were obtained as stable crystals by the reactions of the above bis-ylides with phenyl isocyanate.

Recently, considerable information has accumlated concerning sulfur-stabilized ylides.[1-5] However, bissulfonium ylides have received little attention, except for the bissulfonium ylide of structure I.[6] In this paper, an attempt at the syntheses and reactions of bisylides of the II and III structures will be described.

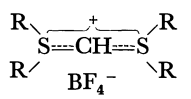

I

R: Methyl
Ethyl

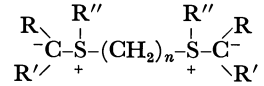

II

R : H
R′ : Benzyl
R″: Ethyl

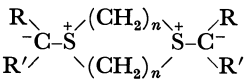

III

R: H
R′: Benzyl

By the use of open-chain sulfides (methylene, dimethylene, and trimethylene bisethylsulfide) and cyclic sulfides (1,3-dithiolane, 1,3-dithiane, 1,4-dithiane, and 1,3,5-trithiane) as the starting materials, an attempt has been made to synthesize phenacyl bissulfonium salts. Dimethylene and trimethylene sulfides among these sulfides gave bissulfonium salts by reactions with phenacylbromide. The subsequent treatment of these bissulfonium salts with sodium hydride gave bissulfonium phenacylide (Structure II). Several reactions of the above-mentioned bis-ylides were carried out (*cf.* Chart 1).

Results and Discussion

Bissulfonium Salts. Dimethylenebissulfonium

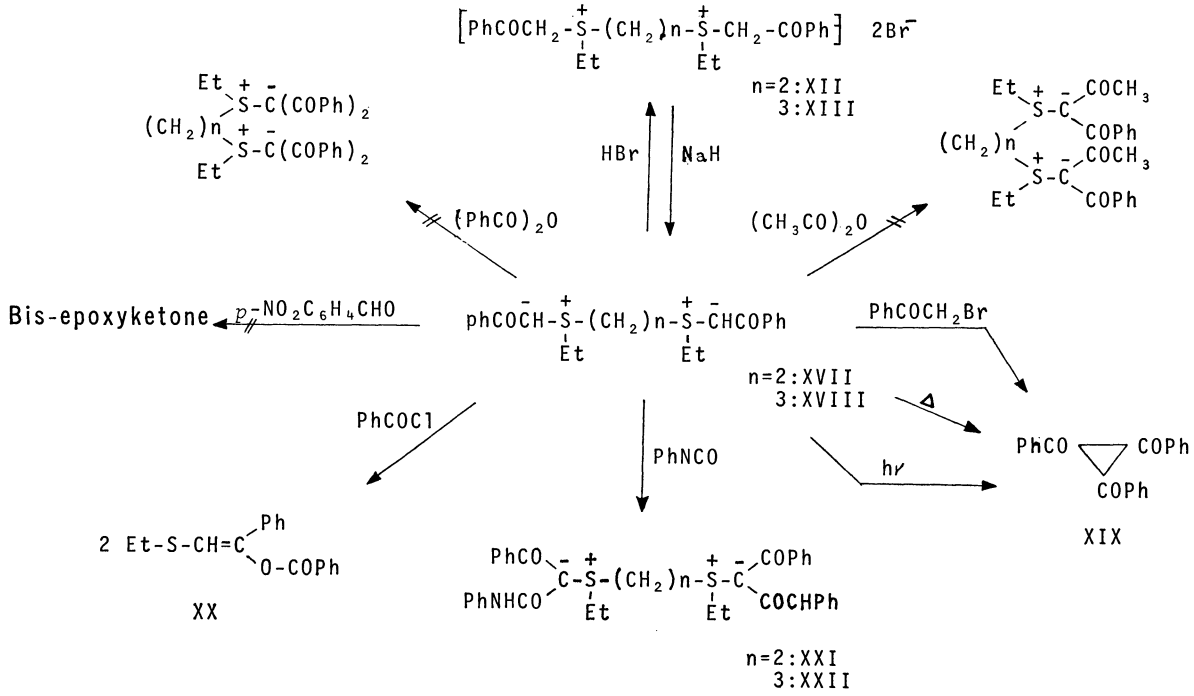

Chart 1. Reactions of Bissulfonium ylides

1) H. Nozaki, M. Takaku, D. Tsunemoto, Y. Yamamoto, and K. Kondo, *Nippon Kagaku Zasshi*, **81**, 1 (1967).
2) Y. Kishida, *Yuki Gosei Kagaku Kyokai Shi*, **26**, 1037 (1968).
3) Preparation a) H. Nozaki, D. Tsunemoto, Z. Morita, K. Nakamura, K. Watanabe, M. Takaku, and K. Kondo, *Tetrahedron*, **23**, 4279 (1967). b) A. F. Kook and S. G. Moffatt, *J. Amer. Chem. Soc.*, **90**, 740 (1968). c) W. Ando, T. Yagihara, S. Tozune, S. Nakado, and T. Migita, *Tetrahedron, Lett.*, **1969**, 1979.
4) Reaction. a) K. W. Ratts and A. Yao, *J. Org. Chem.*, **33**, 66 (1968). b) M. T. Hatch, *ibid.*, **34**, 2133 (1969). c) Y. Hayashi, and R. Oda, *Tetrahedron Lett.*, **1968**, 853. d) U. Schöllkopf, *ibid.*, **1969**, 2619. e) G. Schmidt, *ibid.*, **1969**, 2623. f) T. Mukaiyama, M. Higo, H. Takei, This Bulletin, **43**, 2566 (1970).
5) was prepared by the reaction of the corresponding diethylphenacylsulfonium bromide in THF with sodium hydride: mp 77—78°C; IR (KBr): $\nu_{C=O}$ 1505 cm.$^{-1}$)
6) C. P. Lillya and P. Millar, *J. Amer. Chem. Soc.*, **88**, 1560 (1966).

TABLE 1. MONO- AND BISSULFONIUM SALTS, AND BIS-YLIDES

Compound	Mp (°C)	Formula	Analysis (%) Found					Calcd				
			C	H	N	S	Br	C	H	N	S	Br
XI	oil	$C_{12}H_{19}OS_2Br$	46.1	5.5		19.1	23.5	46.58	5.67		19.08	33.82
XII	128—130	$C_{21}H_{28}O_2S_2Br$	48.3	5.1		16.2	29.2	48.00	5.09		16.36	29.09
XIII	136—138	$C_{22}H_{30}O_2S_2Br$	48.6	5.2		11.2	28.1	48.94	5.32		11.53	28.37
XIV	99—100	$C_{11}H_{13}OS_2Br$	43.0	4.2		20.5	26.0	43.28	4.26		20.98	26.33
XV	110—111	$C_{12}H_{15}OS_2Br$	45.1	4.6		20.3	25.1	45.14	4.70		20.06	25.08
XVI	130—131	$C_{12}H_{15}O_2S_2Br$	45.2	4.7		19.9	25.0	45.14	4.70		20.06	25.08
XVII	oil	$C_{21}H_{27}O_2S_2$	67.8	6.8		16.5		67.69	6.67		16.42	
XVIII	—	$C_{22}H_{29}O_2S_2$	68.5	6.9		12.7		68.32	6.93		12.62	
XXI	184—185	$C_{36}H_{36}N_2O_4S_2$	67.0	5.6	4.3	9.8		66.87	5.57	4.33	9.90	
XXII	194—195	$C_{37}H_{38}N_2O_4S_2$	67.2	6.0	4.2	9.6		67.27	6.06	4.24	9.69	

bromide (XII) was obtained as a white solid in a 40% yield by the reaction of dimethylene bisethylsulfide and phenacylbromide. The structure was confirmed by a study of its IR spectrum ($\nu_{C=O}$ 1662 cm^{-1}) and elemental analysis. A similar procedure for trimethylenebisethylsulfide gave trimethylene bisethylphenacylsulfonium bromide (XIII) as a white solid in a 55% yield. However, similar procedures for methylenebisethylsulfide and cyclic sulfides gave only monosulfonium salts in 30—90% yields, except for 1,3,5-trithiane.

The UV absorption curves of the bissulfonium salts (XII and XIII) do not obery Beer's law in cyclohexane solutions. Similar deviations from Beer's law by bissulfonium salts have been reported by Lillya[6] and Nicholson.[7]

Bissulfonium Phenacylides. The reaction of the bis-salt (XII) with sodium hydride in THF at 0——5°C gave a light yellow dimethylene bisethylsulfonium phenacylide (XVII). The structure of XVIII was confirmed by the results of elemental analysis and the spectroscopic data. This structure was further chemically confirmed by the formation of XII through the action of hydrogen bromide in an aqueous ethanol, and by the formation of XXI (as crystals in over a 50% yield) through the action of phenyl isocyanate in THF by an analogous treatment of XIII with sodium hydride, trimethylenebisethylsulfonium phenacylide (XVII) was obtained in a 72% yield (Table 1).

These bis-ylides (XVII and XVIII) were solids (although they could not be crystallized) and were fairly stable below 0°C. They decomposed on standing in the atmosphere or in a solution (ethanol and THF at room temperature), and the absorption due to ylide carbonyl in the 1520—1500 cm^{-1} range disappeared completely after two weeks. Furthermore, the addition of a few drops of water to XVII and XVIII accelerated their decomposition. They were also subject to thermal decomposition. The heating of the bis-ylide (XVII) in THF gave *trans*-1,2,3-tribenzoylpropane (XIX) in a 47% yield (based on the XVII used). The same products was obtained from XVII in 85% and 22% yields by treatment with phenacylbromide and by irradiation (UV) in THF at room temperature respectively.

It has been reported that the course of the acylation of the mono-ylides varied with the nature of the acylating agent and with the structure of the mono-ylides; dimethyl-oxy-sulfonium phenacylide[8] underwent a *C*-acylation with benzoylchloride, while methylphenylsulfonium phenacylide[9] and dimethylsulfonium phenacylide[10] underwent an *O*-acylation with benzoylchloride, but a *C*-acylation with benzoic anhydride.

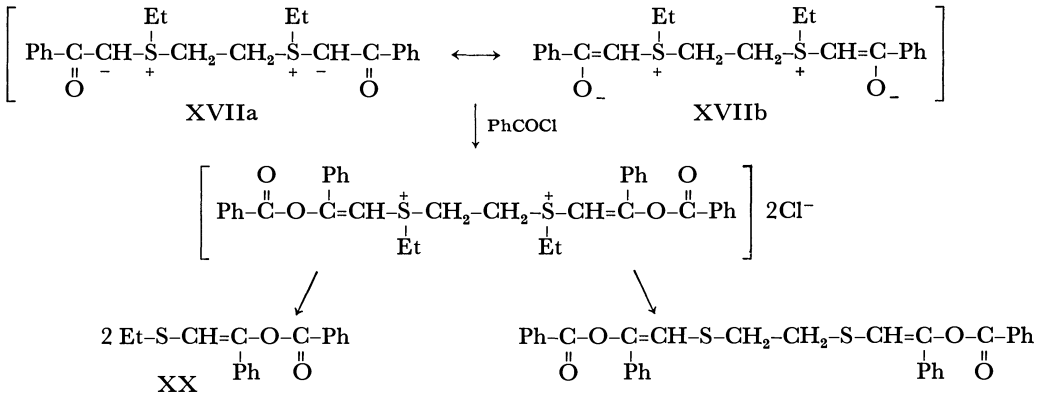

Scheme 1

7) D. C. Nicholson, E. Rothstein, R. W. Saville, and R. Whitly, *J. Chem. Soc.*, **1953**, 4019.

8) H. König and H. Metzger, *Chem. Ber.*, **98**, 3733 (1965).

9) H. Nozaki, K. Kondo, and M. Takaku, *Tetrahedron*, **22**, 2145 (1966).

10) A. W. Johnson and R. T. Amel, *J. Org. Chem.*, **34**, 1240 (1969).

The acylation of XVII and XVIII with benzoylchloride resulted in an *O*-acylation, affording the enol benzoate (XX) of ethylmercaptoacetophenon in 78 and 71% yields respectively (Scheme 1)

The IR spectrum and the results of the elemental analysis of XX were consistent with those of an authentic sample prepared by the reaction of diethylsulfonium phenacylide (XXIII)[5] with benzoylchloride. The results suggest that the contribution of the enol form in the bis-ylides (XVII and XVIII) was stronger than that in dimethyl-oxy-sulfonium phenacylide.

The reaction of XVII and XVIII with benzoic anhydride did not give a product corresponding to *C*- or *O*-acylation; from the reaction products, benzoic acid in a 60% yield (based on the benzoic anhydride used), together with traces of the cyclopropane (XIX) and of a product with a melting point over 300°C, were obtained on a column chromatographic separation (alumina).

The treatment of the bis-ylides (XVII and XVIII) with phenyl isocyanate in THF at 0——5°C afforded other bis-ylides (XXI and XXII)[11] as colorless crystals in 53 and 87% yields respectively.

Johnson and Amel[10] reported that dimethylsulfonium phenacylide (XXIII) reacted with *p*-nitrobenzaldehyde to give a epoxide in a 10% yield, while Nozaki *et al.*[8] reported that the reactions of methylphenylsulfonium phenacylide with benzaldehyde or *p*-nitrobenzaldehyde did not afford epoxyketones. We have not been able to obtain mono- or bis-epoxyketone by the reactions of bis-ylides (XVII and XVIII) with *p*-nitrobenzaldehyde.

Nozaki[9] and Johnson[10] reported that the irradiation of monosulfonium phenacylide gave the cyclopropane (XIX). Ratt[12] and Johnson[10] reported the trapping of the carbene intermediate from monosulfonium phenacylide and *p*-nitrophenacylide by the use of triphenylphosphine and dimethylbenzylamine. We carried out the irradiation of the bis-ylides (XVII and XVIII) in THF with a high-pressure mercury lamp (300 W) and thus obtained the cyclopropane (XIX in a 20% yield), along with unidentified oily substances. We failed, however, to trap the benzoylcarbene with the above trapping reagents.

Experimental

General. All the melting points are uncorrected. The IR spectra were recorded on a JASCO grating infrared spectrophotometer IR-G. The UV spectra were measured on a Hitachi 124 spectrophotometer. The photochemical reactions were effected by the use of a Eikosha high-pressure mercury apparatus.

α,ω-alkanedithiols were prepared by the reactions of α,ω-dibromoalkanes with thiourea and by the subsequent hydrolysis of the salts: 1,2-ethanedithiol,[13] bp 61—63°C/45 mmHg; 1,3-propanedithiol, bp 72°C/25 mmHg.

Open-chain Sulfides and Cyclic Sulfides were prepared according to the directions in the literature and were purifided by distillation or recrystallization: methylenebisethylsulfide (IV),[14] bp 95—97°C/39—40 mmHg; dimethylenebisethylsulfide (V),[15] bp 209—213°C/760 mmHg; trimethylenebisethylsulfide (VI),[16] bp 86.0—87.5°C/8—9 mmHg; 1,3-dithiolane (VII),[17] bp 56—68°C/8—10 mmHg; 1,3-dithiane (VIII),[18] mp 52—53°C; 1,4-dithiane (IX),[19] mp 111.0—111.5°C; 1,3,5-trithiane (X),[20] mp 212—213°C.

The data of elemental analyses for mono- and bissulfonium bromides and phenacylides given below are summarized in Table 1.

Methylene Bisethylmonophenacylsulfonium Bromide (XI).[21] A solution of phenacylbromide (8.0 g, 0.04 mol) and IV (2.7 g, 0.02 mol) in methanol (150 m*l*) was refluxed for 6 hr. After the subsequent removal of the methanol, we added ether (200 m*l*) to the residue; further extraction of the insoluble parts with several portions of ether afforded 2.7 g (24.5%) of a clear, brownish residue (XI): IR (neat): $\nu_{C=O}$ 1670 cm^{-1}.

Dimethylenebisethylphenacylsulfonium Bromide (XII) and Trimethylenebisethylphenacylsulfonium Bromide (XIII). A mixture of phenacylbromide (8.0 g, 0.04 mol) and V (3.0 g, 0.02 mol) was warmed for 15 min at 50—60°C and then allowed to stand for two days at room temperature. To the reaction mixture (a light yellow solid), we then added several portions of acetone. The insoluble parts were recrystallized from hot acetone-ether to give IX (4.6 g, 41.8%) as colorless, microfine crystals: mp 128—130°C; IR (KBr): $\nu_{C=O}$ 1662 cm^{-1}. Similarly, a reaction mixture (a dark brown solid) of phenacylbromide (8.0 g, 0.04 mol) and VI (3.2 g, 0.02 mol) gave XIII (5.8 g, 57.2%) as colorless, microfine crystals on recrystallization from hot acetone - water: mp 136—138°C; IR (KBr): $\nu_{C=O}$ 1662 cm^{-1}.

1,3-Dithiolane-1-phenacylsulfonium Bromide (XIV) and 1,3-Dithianephenacylsulfonium Bromide (XV). A mixture of phenacylbromide (8.0 g, 0.04 mol) and VII (2.2 g, 0.02 mol) was warmed for 5 min at 50—60°C and then allowed to stand for two days below 15°C. To the reaction mixture (a dark red solid) we then added several portions of acetone. The insoluble part (a white solid) was recrystallized from methanol - acetone (3:1) to give XIV (4.2 g, 67.1%) as colorless, microfine crystals: mp 99—100°C; IR (KBr): $\nu_{C=O}$ 1662 cm^{-1}. Similarly, a reaction mixture of phenacylbromide (8.0 g, 0.04 mol) and VIII (2.4 g, 0.02 mol) gave XV (4.4 g, 69.2%) as colorless crystals after recrystallization from hot acetone - water: mp 110—111°C; IR (KBr): $\nu_{C=O}$ 1662 cm^{-1}.

1,4-Dithiane-1-phenacylsulfonium Bromide (XVI). 1,4-dithiane (2.4 g, 0.02 mol) was dissolved in phenacylbromide (8.0 g, 0.04 mol) at 80—90°C, and then the mixture was kept for 5 min at 90—100°C. To the reaction mixture (a light yellow solid) we then added several portions of hot methanol to give XVI (6.4 g, 93.7%) as colorless, microfine crystals; mp 130—131°C; IR (KBr): $\nu_{C=O}$ 1668 cm^{-1}.

Reaction of 1,3,5-Trithiane (X) with Phenacylbromide. A

11) The structures of XXI and XXII were comfirmed by their IR spectra and elemental analyses. The crystalline bis-ylides (XXI and XXII) were readily soluble in THF, chloroform, methanol, and water, and were fairly stable on standing in atmosphere at room temperature and on refluxing in THF.

12) K. W. Ratts and A. N. Yao, *J. Org. Chem.*, **31**, 1185 (1966).

13) A. J. Speziale, "Organic Syntheses," Coll. Vol. IV, p. 401.

14) S. Oae, W. Tagaki, and A. Ohno, *Tetrahedron*, **20**, 427 (1964).

15) A. Fraling, *Rec. Trav. Chim.*, **81**, 1009 (1966).

16) A. W. Wedkind, *Ber.*, **58**, 2513 (1925).

17) A. Schönberg and N. Preafko, *Chem. Ber.*, **100**, 778 (1967).

18) D. T. Gibson, *J. Chem. Soc.*, **1930**, 12.

19) R. C. Fuson, R. D. Lipscomb, B. C. Mckusick, and L. J. Reed, *J. Org. Chem.*, **11**, 513 (1946).

20) R. W. Bost and E. W. Constable, "Organic Syntheses," Coll. Vol. II, p. 610.

21) In order to obtain methylenebisethylsulfonium salts, a mixture of IV and phenacylbromide in methylenechloride was treated with silvertetraflurorborate. The glistering colorless crystals (mp 153—154°C) was obtained, but this compound was unstable.

solution of X (1.4 g, 0.01 mol) and phenacylbromide (5.2 g, 0.03 mol) in benzene (200 m*l*) was refluxed for 10 days. After the removal of the benzene, methanol was added to the residue. By washing the insoluble part with several portions of methanol - acetone, trithiane (1.3 g) was then recovered.

Dimethylenebisethylsulfonium Phenacylide (XVII). To a suspension of XII (2.2 g, 0.04 mol) in 30 m*l* of anhydrous THF at 0——5°C, sodium hydride (0.008 mol) was added: the mixture was then vigorously stirred for 5 hr below 5°C. After the removal of the sodium bromide from the reaction mixture, the evaporation of the THF and treatment with petroleum-ether gave a pale yellow residue which solidified below 5°C, but which could not be crystallized. The chromatography of this residue on alumina gave XVII (62%) and a trace of *trans*-1,2,3-tribenzoylpropane (XIX); IR (neat): $\nu_{C=O}$ 1515 cm^{-1}; UV: λ_{max}^{EtOH} 229 mμ (ε 2.12×10^4), 308 mμ (ε 2.12×10^4). The IR spectrum of XIX was identical with that of an authentic sample prepared by the treatment of phenylmethylsulfonium phenacylide with phenacylbromide.

Trimethylenebisethylsulfonium Phenacylide (XVIII): Yield, 72%; IR (neat): $\nu_{C=O}$ 1510 cm^{-1}; UV: λ_{max}^{EtOH} 229 mμ (ε 2.61×10^4), 308 mμ (ε 2.50×10^4).

Acylation of the bis-ylides (XVIII). Enolbenzoate of Mercaptoacetophenone (XX): A solution of XVII (1.1 g, 0.0025 mol) and benzoylchloride (0.7 g, 0.005 mol) in anhydrous THF was stirred for 3 hr at room temperature. The white precipitates were then washed with THF - *n*-hexane (1:4) and dried over P_2O_5 to give XX (0.9 g, 64%): mp 107—108°C; IR (KBr): $\nu_{C=O}$ 1738 cm^{-1}; ν_{C-O-C} 1190 cm^{-1}, Found; C, 71.4; H, 5.6; S, 11.5%, (Calcd for $C_{17}H_{16}O_2S$: C, 71.83; H, 5.63; S, 11.27%). The melting point the results of elemental analysis, and the IR spectrum were identical with those of an authentic sample prepared by the reaction of diethylsulfonium phenacylide with benzoylchloride.

A similar treatment of XVIII (1.1 g, 0.0025 mol) with benzoylchloride (0.7 g, 0.0025 mol) gave XX (0.99 g, 71%).

Reaction of the bis-ylides (XVII and XVIII) with p-*Nitrobenzaldehyde.* A solution of XVII (1.1 g, 0.0025 mol) and *p*-nitrobenzaldehyde (0.75 g, 0.005 mol) in 30 m*l* of anhydrous THF was refluxed for 20 hr. After the subsequent evaporation of the THF, the chromatography of the residue on alumina gave *p*-nitrobenzylalcohol (0.8 g, 23%), together with a trace of the cyclopropane (XIX) and an intractable oil (1.0 g).

A similar treatment of XVIII (1.1 g, 0.0025 mol) with *p*-nitrobenzaldehyde gave *p*-nitrobenzylalcohol, the cyclopropane (XIX), and an intractable brown oil in a ratio analogous to that above.

*Reaction of the bis-ylide (XVII and XVIII) with Phenyl Isocyanate. Dimethylenebisethylsulfonium Benzoyl (*N-*phenylcarbamoyl) Methylide (XXI):* Phenyl isocyanate (0.6 g, 0.005 mol) and XVII (1.1 g, 0.0025 mol) were stirred in anhydrous THF (30 m*l*) for 5 hr at 0——5°C. After the subsequent evaporation of the THF, the recrystallization of the residue from AcOEt or chloroform - AcOEt gave XXI (0.85 g, 53%): mp 184—185°C; IR (KBr): $\nu_{C=O}$ 1640 and 1513 cm^{-1}; UV: λ_{max}^{EtOH} 243 mμ (ε 4.44×10^4), 284 mμ (ε 4.32×10^4).

Trimethylenebisethylsulfonium Benzoyl (N-*phenylcarbamoyl*) *Methylide (XXII):* A similar treatment of XVIII (1.1 g, 0.0025 mol) with phenyl isocyanate (0.6 g, 0.005 mol) gave XXII (1.0 g, 61%): mp 194—195°C; IR (KBr): $\nu_{C=O}$ 1635 cm^{-1}; UV: λ_{max}^{EtOH} 243 mμ (ε 4.28×10^4), 284 mμ (ε 4.11×10^4). trans-1,2,3-*Tribenzoylpropane (XIX). XVIII and Phenacylbromide:* An equimolar mixture of XVIII (1.1 g, 0.0025 mol) and phenacylbromide (0.5 g, 0.0025 mol) in THF was stirred at room temperature for 5 hr. The subsequent concentration of the solution and recrystallization of the residue from benzene gave the cyclopropane XIX (0.32 g, 48% based on the XVIII); mp 214—215°C.

Thermolysis of XVIII: A solution of XVIII (1.05 g, 0.0025 mol) in THF (20 m*l*) was heated under reflux for 24 hr. The subsequent evaporation of the solvent and the recrystallization of the residue from benzene gave a 47% yield (0.105 g, based on the XVII) of the XIX cyclopropane.

A similar treatment of XVIII (1.1 g, 0.0025 mol) gave a 40% yield (0.088 g, based on the XVIII) of the XIX cyclopropane.

Photolysis of XVIII: A solution of XVIII (1.1 g, 0.0025 mol) in THF (10 m*l*) was irradiated for 15 hr in a Pyrex tube. The subsequent concentration of the solution and recrystallization of the residue gave an 8% yield of XIX.

The Acid-catalyzed Reaction of Isocyanide with Oxetane

Takeo SAEGUSA, Naotake TAKA-ISHI, and Yoshihiko ITO

Department of Synthetic Chemistry, Faculty of Engineering, Kyoto University, Sakyo-ku, Kyoto

(Received February 23, 1971)

The reaction of isocyanide with oxetane in the presence of $BF_3 \cdot OEt_2$ was studied; in this reaction a 1:1 cyclic adduct, 2-iminotetrahydrofuran, was formed. From 2-methyloxetane, 2-imino-5-methyltetrahydrofuran was exclusively formed. These findings suggest an S_N2 mechanism for the cleavage of the oxetane ring. Oxetanes with electron-withdrawing substituents gave γ-alkoxybutyronitrile as the main product, along with 2-iminotetrahydrofuran. A reaction scheme involving an imidoyl cation was proposed to explain the formation of cyclic and linear products.

Several papers have been reported on the cycloaddition reaction of isocyanide.[1] We have reported the Lewis-acid-catalyzed cyclizations reaction of isocyanide with ketone, aldehyde, and a Schiff base.[2-4] In addition, we have presented a preliminary report[5] upon a new cycloaddition reaction of isocyanide with four-membered cyclic ethers (oxetanes) with a BF_3 catalyst, in which reaction 2-iminotetrahydrofuran was produced.

In this paper we wish to report on our further studies of the scope of the reaction of isocyanide with substituted oxetanes and some mechanistic studies.

Results and Discussion

In the reaction of oxetane (**1a**) with *t*-butyl isocyanide (**2a**) in the presence of $BF_3 \cdot OEt_2$ at room temperature, 2-*t*-butyliminotetrahydrofuran (**5a**) was produced, along with *t*-butyl cyanide (**3a**) and *N*-*t*-butylpivalimidoyl cyanide (**4a**). The two by-products, **3a** and **4a**, were found to be produced from **2a** with $BF_3 \cdot OEt_2$ in the absence of **1a** (Eq. (1)).

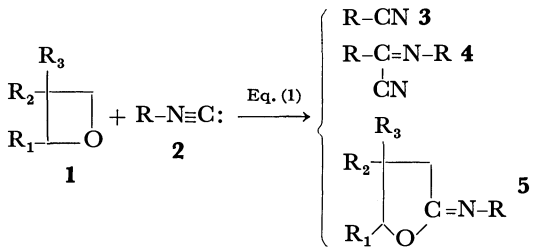

1a, $R_1=R_2=R_3=R_4=H$

2, 3, 4
- **a**, R = *t*-Bu-
- **b**, R = Me-C(Et)-
- **c**, R = *t*-Bu-CH_2-C(Et)(Me)-
- **d**, R = 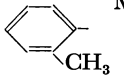

5a, $R_1=R_2=R_3=R_4=H$, R = *t*-Bu

Some results of the reaction of **1a** with **2a** are shown in Table 1. As the catalyst, an equimolar amount of $BF_3 \cdot Et_2O$ was required. A smaller amount of $BF_3 \cdot Et_2O$ gave a poorer result. The reaction proceeded rapidly at room temperature. At lower temperatures the conversion percent was low and the starting materials were recovered unchanged. As the reaction solvent, CH_2Cl_2 gave better results. Basic solvents like tetrahydrofuran and acetonitrile gave poor yields.

TABLE 1. REACTION OF *t*-BUTYL ISOCYANIDE (**2a**) WITH OXETANE (**1a**)[a]

t-BuNC (mmol)	 (mmol)	$BF_3 \cdot OEt_2$ (mmol)	Solvent (5 ml)	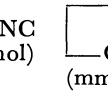 (**5a**) Yield (%)[b]
5	5	0.75	CH_2Cl_2	10
5	5	5	CH_2Cl_2	48
10	5	5	CH_2Cl_2	70
5	10	5	CH_2Cl_2	34
5	5	5	CH_2Cl_2	33[c]
5	5	5	CH_2Cl_2	14[d]
5	5	5	C_6H_6	32
5	5	5	n-C_7H_{16}	6
5	5	5	THF	9
5	5	5	CH_3CN	7
10	5	5	Et_2O	38

a) Reaction at room temperature for 2 hr.
b) Determined by glpc.
c) Reaction at 0°C.
d) Reaction at −78°C.

The structure of **5a** was established by elemental analysis and by a study of its IR and NMR spectra, as well as by the acid hydrolysis product. In the acid hydrolysis of **5a** with silicic acid, γ-butyrolactone (**6a**) was formed. The conversion of **5** to **6** has already been reported by Stirling.[6]

The same reaction was observed with other *t*-alkyl and phenyl isocyanides. The results are shown in Table 2. In the case of cyclohexyl isocyanide, the cationic polymerization of cyclohexyl isocyanide predominated and the iminotetrahydrofuran could not be isolated. However, the IR spectrum of the reaction mixture showed an absorption at 1715 cm^{-1} which was attributed to the cyclic imino group.

Then, the reaction of **2a** with various alkyl-substituted oxetanes was examined. The results are shown

1) B. Zeeh, *Synthesis*, **1969**, 65.
2) T. Saegusa, N. Taka-ishi, and H. Fujii, *Polym. Lett.*, **5**, 779 (1967).
3) T. Saegusa, N. Taka-ishi, and H. Fujii, *Tetrahedron*, **24**, 3795 (1968).
4) T. Saegusa, N. Taka-ishi, I. Tamura, and Fujii, *J. Org. Chem.*, **34**, 1145 (1969).
5) T. Saegusa, N. Taka-ishi, and Y. Ito, *Synthesis*, **1970**, 475.
6) C. J. M. Stirling, *J. Chem. Soc.*, **1960**, 255.

Table 2. Reaction of isocyanides with oxetane[a)]

	R–N≡C (mmol)		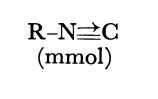 (mmol)	CH_2Cl_2 (ml)	Reaction time (hr)	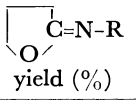 yield (%)
(**2b**)	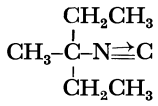	8	10	10	13	23 (**5b**)
(**2c**)	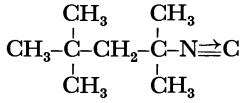	30	15	30	24	54 (**5c**)
	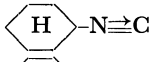	10	10	10	13	not isolated
(**2d**)	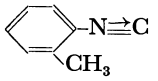	20	10	20	16	45[b)] (**5d**)

a) Reaction conditions: r.t., $BF_3 \cdot OEt_2$ (equimolar amount to oxetane).
b) Identified by the comparison of the glpc retention time and IR spectrum with the authentic sample.[7)]

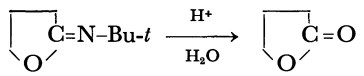

5a **6a**

in Table 3. 2-*t*-Butyliminotetrahydrofuran derivatives were obtained in relatively high yields. 2-Methyloxetane (**1e**), the unsymmetrical oxetane, gave 2-*t*-butylimino-5-methyltetrahydrofuran (**5e**) exclusively. The structure of **5e** was confirmed by its acid hydrolysis with silicic acid, where by γ-valerolactone was formed. The alternative possible product, 2-*t*-butylimino-3-methyltetrahydrofuran (**7**), could not be found in the reaction mixture.

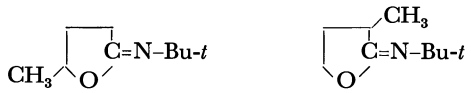

5e **7**

In the cases of oxetanes with two electron-withdrawing substituents at the 3-position, the linear product, γ-alkoxybutyronitrile derivative (**8**), was produced along with the cyclic adduct, **5** (Eq. (2)). The results are summarized in Table 4.

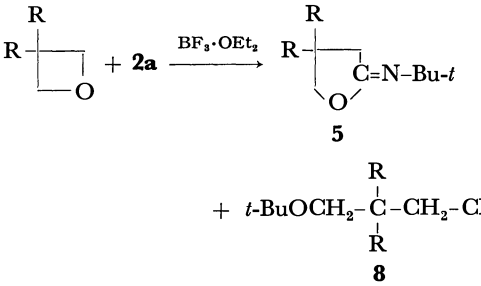

(2)

(R: $ClCH_2$–, ICH_2–, $EtOCH_2$–)

Reaction Scheme

Considering the cationic isomerization of **2**, which takes place along with the formation of **5**, a reaction scheme involving the *t*-alkyl cation and the imidoyl cation as the key intermediates may be presented as follows:

$$RNC + BF_3 \cdot OEt_2 \rightleftarrows (RNC \rightarrow BF_3) + Et_2O$$
$$(RNC \rightarrow BF_3) \longrightarrow R^+[BF_3 \cdot CN]^- \qquad (3)$$

Table 3. Reaction of *t*-butyl isocyanide with substituted oxetanes

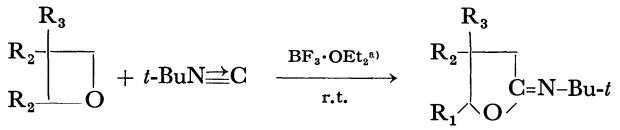

Compound	Oxetane (mmol) R_1	R_2	R_3		*t*-BuN≡C (mmol)	CH_2Cl_2 (ml)	Reaction time (hr)	Yield (%)[b)]
5e	CH_3	H	H	30	45	30	1	47
5f	H	$-(CH_2)_2-$		20	40	30	7	60
5g	H	CH_3	H	30	60	30	3	74
5h	H	CH_3	CH_3	20	40	20	3	80
5i	H	Et	Et	8.8	17.5	10	3	42
5j	H	$-(CH_2)_5-$		10	20	20	12	87

a) Equimolar amount to oxetane. b) Based on oxetane.

7) T. Mukaiyama and K. Sato, This Bulletin, **36**, 99 (1963).

TABLE 4. REACTION OF *t*-BUTYL ISOCYANIDE WITH OXETANES HAVING BY ELECTRON WITHDRAWING SUBSTITUENTS[a)]

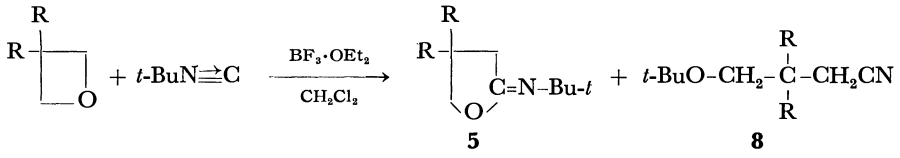

	Oxetane (mmol) R		*t*-BuN≡C (mmol)	$BF_3 \cdot OEt_2$ (mmol)	CH_2Cl_2 (ml)	Yield (%) 5	Yield (%) 8
1k	$ClCH_2$	30	30	11	30	17[b)]	7
1k	$ClCH_2$	12.5	11	10	10	6[b)]	22
1k	$ClCH_2$	1	2	1	1	—	32
1l	ICH_2	10	20	10	20	—	24
1m	$EtOCH_2$	20	40	20	20	69	6

a) Reaction time was 1 day. b) Isolated as a complex with catalyst.

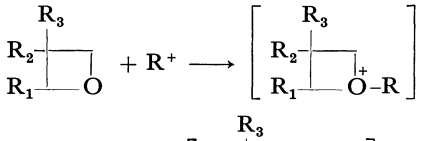

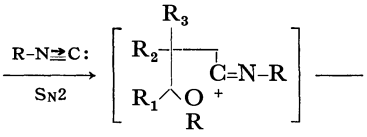

10

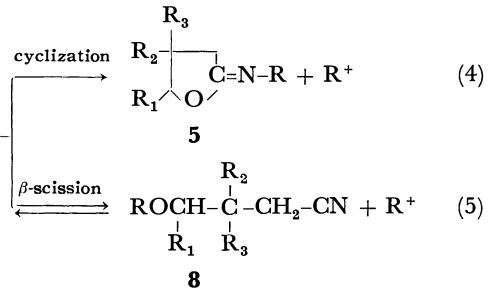

The initial generation of the *t*-butyl cation complex (Eq. (3)) has been shown in a previous paper.[8] As both 1-ethyl-1-methylpropyl isocyanide (**2b**) and 1,1,3,3-tetramethylbutyl isocyanide (**2c**) were isomerized by $BF_3 \cdot OEt_2$ to the corresponding nitriles, (**3b**) and (**3c**), the initiation reaction producing the *t*-alkyl carbonium ion is supported. The cyclic trialkyloxonium ion of oxetane (**9**) undergoes ring-cleavage as a result of the attack of isocyanide as a nucleophile.

An alternative scheme starting with the cyclic dialkyloxonium ion of oxetane (**11**) may also be assumed for the formation of the cyclic adduct (Eq. (6)). Especially, the second scheme of Eq. (6) can be taken to explain the reaction of *o*-tolyl isocyanide, where no isomerization of the isocyanide takes place. The water responsible for the protonic-acid complex may be ascribed to the incomplete dehydration of the reagents. The protonic-acid complex due to the water impurity has been assumed in the initiation of the BF_3-catalyzed polymerization of oxetane.[9,10]

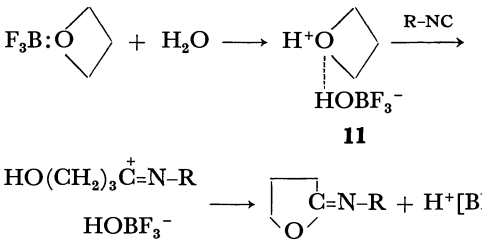

In the reaction of **1e** with **2a**, the formation of **5e** *via* the cleavage of the ether linkage at the less substituted carbon suggests an S_N2 mechanism for the ring cleavage. The S_N2 mechanism is also supported by the reaction of oxetane-3-spirocyclopropane (**1f**). When a mixture of **1f** and **2a** was treated with $BF_3 \cdot OEt_2$ at room temperature, only the oxetane ring was cleaved to form 2-*t*-butyliminotetrahydrofuran-4-spirocyclopropane (**5f**). If the cleave of the oxetane ring of **1f** proceeded *via* S_N1 mechanism, the isomerization of the cyclopropyl ring would have occurred, *i.e.*, the treatment of **1f** with aqueous hydrochloric acid has been reported, and in it the cleavage of the ether linkage and the enlargement of the carbocyclic ring occurred.[11]

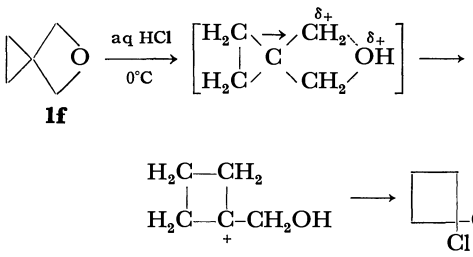

The re-cyclization of **10** to **5** (Eq. (4)) has been supported by a reference reaction in which 3,3-bis(chloromethyl)-4-*t*-butoxybutyronitrile (**8k**) was treated with triethyloxonium fluoroborate to give β,β-bis(chloromethyl)-γ-butyrolactone (**6k**) (Eq. (7)). The treatment of ω-benzyloxybutyronitrile (**13**) with triethyloxonium fluoroborate, followed by the hydrolysis of the reaction mixture, gave γ-butyrolactone in a yield of 31% (Eq. (8)).

8) T. Saegusa, N. Taka-ishi, and Y. Ito, *J. Org. Chem.*, **34**, 4040 (1969).

9) J. B. Rose, *J. Chem. Soc.*, **1956**, 546.

10) J. Furukawa and T. Saegusa, "Polymerization of Aldehydes and Oxides", Wiley (Interscience), New York (1963).

11) S. Searles and E. F. Lutz, *J. Amer. Chem. Soc.*, **81**, 3674 (1959).

Table 5. Characterizations of 2-iminotetrahydrofuran

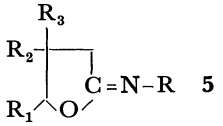

Compound 5	R_1	R_2	R_3	R	Bp, °C (mmHg)	NMR absorption, τ (Solvent: a) $CDCl_3$, b) CCl_4)
a	H	H	H	*t*-Bu	76 (22)	[a] 5.70 (2H, t, $-CH_2O-$) 7.50 (2H, m, $-CH_2-C=N$) 7.90 (2H, m, $-CH_2-CH_2-CH_2-$) 8.71 (9H, s, *t*-Bu)
b	H	H	H	$CH_3-\overset{Et}{\underset{Et}{C}}-$	87 (7)	[a] 5.80 (2H, t, $-CH_2O-$) 7.58 (2H, m, $-CH_2-C=N$) 7.90 (2H, m, $-CH_2-CH_2-CH_2-$) 8.52 (4H, m, $2CH_3CH_2-$) 8.92 (9H, s, *t*-Bu) 9.10 (3H, s, CH_3-C-Et) 9.21 (6H, t, $2CH_3CH_2-$)
c	H	H	H	$t\text{-Bu}-CH_2-\overset{CH_3}{\underset{CH_3}{C}}-$	90 (5)	[b] 5.77 (2H, t, $-CH_2O-$) 7.65 (2H, m, $-CH_2-C=N-$) 7.94 (2H, m, $-CH_2-CH_2-CH_2-$) 8.40 (2H, s, *t*-$BuCH_2-$) 8.76 (6H, s, $2CH_3$) 9.02 (9H, s, *t*-Bu–)
e	CH_3	H	H	*t*-Bu–	78 (20)	[b] 5.52 (1H, m, CH_3CHO-) 7.40—8.40 (4H, m, $-CH_2-CH_2-$) 8.66 (3H, d, CH_3CH-) 8.82 (9H, s, *t*-Bu)
f	H	$\{CH_2\}_2$		*t*-Bu	95 (19)	[b] 5.94 (2H, s, $-CH_2O-$) 7.57 (2H, s, $-CH_2-C=N$) 8.78 (9H, s, *t*-Bu) 9.20—9.50 (4H, m, $-CH_2-CH_2-$)
g	H	CH_3	H	*t*-Bu	75 (18)	[b] 6.00 (2H, m, $-CH_2O-$) 7.65 (3H, m, $CH_3CH-CH_2-C=N$) 8.79 (9H, s, *t*-Bu) 8.90 (3H, m, CH_3)
h	H	CH_3	CH_3	*t*-Bu	80 (19)	[b] 6.16 (2H, s, $-CH_2O-$) 7.77 (2H, s, $-CH_2-C=N$) 8.80 (9H, s, *t*-Bu) 8.85 (6H, s, $2CH_3$)
i	H	Et	Et	*t*-Bu	100 (11)	[b] 6.11 (2H, s, $-CH_2O-$) 7.77 (2H, s, $-CH_2-C=N$) 8.30—8.80 (4H, m, $2CH_3CH_2-$) 8.81 (9H, s, *t*-Bu) 9.09 (6H, t, $2CH_3CH_2-$)
j	H	$\{CH_2\}_5$		*t*-Bu	112 (8)	[a] 6.09 (2H, s, $-CH_2O-$) 7.66 (2H, s, $-CH_2-C=N$) 8.35—8.65 (10H, m, $\{CH_2\}_5$) 8.78 (9H, s, *t*-Bu)
m	H	$EtOCH_2-$	$EtOCH_2-$	*t*-Bu	107 (4)	[b] 5.98 (2H, s, $-CH_2O-$) 6.50 (4H, q, $2CH_3CH_2-$) 6.64 (4H, s, $2CH_3CH_2OCH_2-$) 7.68 (2H, s, $-CH_2-C=N$) 8.79 (6H, t, $2CH_3CH_2-$) 8.80 (9H, s, *t*-Bu)

Table 5. (Continued)

Compound 5	R_1	R_2	R_3	R	Bp, °C (mmHg)	NMR absorption, τ (Solvent: a) $CDCl_3$, b) CCl_4)
n	H	*t*-$BuOCH_2$–	*t*-$BuOCH_2$–	*t*-$BuCH_2$–C(–CH_3)(–CH_3)–	120 (2)	[a] 6.09 (2H, s, $-CH_2O-$) 6.75 (4H, s, 2*t*-$BuOCH_2$–) 7.75 (2H, s, $-CH_2-C=N-$) 8.45 (2H, s, *t*-$BuCH_2$–) 8.79 (6H, s, $2CH_3$) 8.84 (18H, s, 2*t*-BuO–) 9.05 (9H, s, *t*-$BuCH_2$–)

Table 6. Elemental analyses of lactones

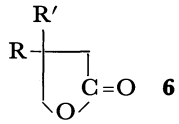

6

Compound	R	R′	Formula	Calcd, % C	Calcd, % H	Found, % C	Found, % H
6f	$-(CH_2)_2-$		$C_6H_8O_2$	64.27	7.19	64.24	7.37
6g	CH_3	H	$C_5H_8O_2$	59.98	8.05	60.81	8.34
6h	CH_3	CH_3	$C_6H_{10}O_2$	63.13	8.83	62.98	9.10
6i	Et	Et	$C_8H_{14}O_2$	67.57	9.93	67.79	9.98
6j	$-(CH_2)_5-$		$C_9H_{14}O_2$	70.10	9.15	70.34	9.12
6k	$ClCH_2$	$ClCH_2$–	$C_6H_8O_2Cl_2$	39.37	4.40	39.15	4.33
6m	$EtOCH_2$	$EtOCH_2$–	$C_{10}H_{18}O_4$	59.38	8.97	59.80	9.14
6n	*t*-$BuOCH_2$–	*t*-$BuOCH_2$–	$C_{14}H_{26}O_4$	65.08	10.14	64.79	10.17

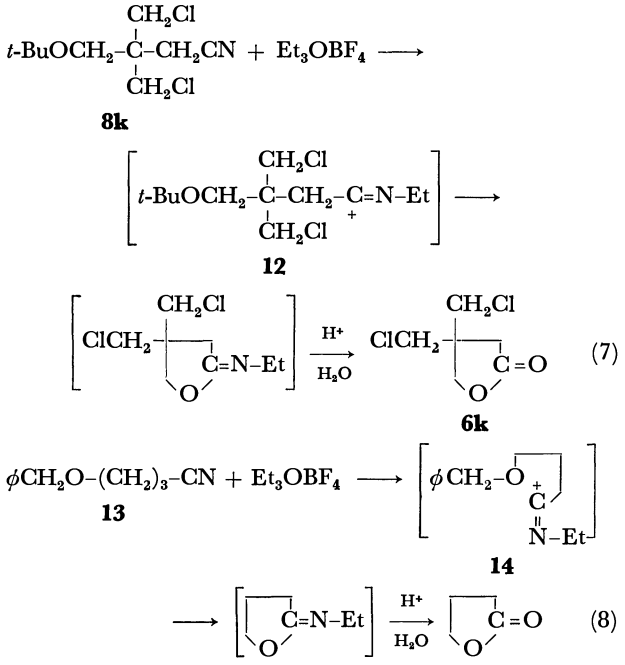

The imidoyl cations, **12** and **14**, are considered as the reaction intermediates in these reference reactions. Similar cyclization reactions to 2-iminotetrahydrofuran have been reported in the reaction of ω-hydroxy nitrile[12] and unsaturated nitrile.[13]

12) E. M. Schultz, C. M. Robb, and J. M. Sprague, *J. Amer. Chem. Soc.*, **69**, 2454 (1947).

13) R. F. Raffauf, *ibid.*, **74**, 4460 (1952).

The cyclization of the imidoyl cation intermediate to 2-iminotetrahydrofuran seems to proceed rapidly. Any amide which might be derived from the imidoyl cation, if any was present, was not detected in the hydrolysis mixture of the reaction system.

It is of interest that **8** is formed only when oxetane is substituted by electron-withdrawing groups. This observation is explained by the low nucleophilicity of the ether oxygen of the imidoyl cation, **10**. The cyclization of **10** to **5** may be slow in these oxetanes; consequently, the formation of **8** by the β-scission of **10** may be predominant. In oxetanes substituted by chloromethyl and iodomethyl groups which have large σ_m values, the ratio of **8** to **5** in the product is high in comparison with that in 3,3-bis(ethoxymethyl)oxetane (**1m**). It has been known that substituent groups exert an influence on the basic strength of the ether oxygen of 3,3-disubstituted oxetanes.[14] Therefore, it is not unreasonable to assume that the nucleophilicity of the ether oxygen of **10** is influenced by substituent groups. Interference by the steric effect of the substituent for re-cyclization is less probable, because **8** was not formed in the cases of 3,3-diethyloxetane (**1i**) and oxetane-3-spirocyclohexane (**1j**), where substituent groups are as bulky as these of **1k** and **1l**. The formation of **8** by the β-scission of **10** is analogous to the β-scission of the imidoyl cation observed in the cationic isomerization and dimerization reaction of *t*-alkyl isocyanide.

14) S. Iwatsuki, N. Takigawa, M. Okada, Y. Yamashita, and Y. Ishii, *Kogyo Kagaku Zasshi*, **67**, 1236 (1964).

Experimental

Reagents. *Oxetane*: Published procedures were utilized for the preparation of oxetane,[9] 2-methyloxetane,[15] oxetane-3-spirocyclopropane,[11] 3-methyloxetane,[15] 3,3-dimethyloxetane,[16] 3,3-diethyloxetane,[16] oxetane-3-spirocyclohexane,[17] 3,3-bis(iodomethyl)oxetane,[18] and 3,3-bis(ethoxymethyl)oxetane.[19] The 3,3-bis(chloromethyl)oxetane was a commercial sample which was purified by rectification under nitrogen prior to use. The 3,3-bis(*t*-butoxymethyl)oxetane was a new compound which was prepared, by a modification of Farthing's method,[19] in a yield of 12%; bp 94—95°C/7 mmHg. Found: C, 67.43; H, 11.98%. Calcd for $C_{13}H_{26}O_3$: C, 67.19; H, 12.15%. The structure was confirmed by a study of the NMR and IR spectra.

Isocyanide: Cyclohexyl isocyanide and *t*-butyl isocyanide were prepared according to Ugi's procedure.[20] 1-Ethyl-1-methylpropyl isocyanide was prepared according to Otsuka's method.[21] 1,1,3,3-Tetramethylbutyl isocyanide[21] was prepared by a modification of Ugi's method.[20] *o*-Tolyl isocyanide was prepared according to Ugi's procedure.[22] Triethyloxonium tetrafluoroborate ($Et_3O^+BF_4^-$) was prepared according to the method of Meerwein.[23] γ-Benzyloxybutyronitrile was prepared according to the method of Bennett *et al.*[24] $BF_3 \cdot Et_2O$ was a commercial reagent which was used without purification. The solvents were purified by the usual methods.

2-t-Butyliminotetrahydrofuran (5a). Into a solution of *t*-butyl isocyanide (**2a**) (0.83 g, 10 mmol) and oxetane (**1a**) (0.29 g, 5 mmol) in 5 m*l* of methylene chloride, $BF_3 \cdot Et_2O$ (0.71 g, 5 mmol) was added drop by drop with stirring at 0°C. After being allowed to stand at room temperature for 2 hr, the reaction mixture was poured into aqueous NaOH. The organic layer was then separated from the aqueous phase, and the aqueous phase was extracted twice with 5 m*l* portions of methylene chloride. The combined organic extracts were dried over magnesium sulfate and then subjected to distillation. From the volatile fraction, *t*-butyl cyanide (**3a**) and *N*-*t*-butylpivalimidoyl cyanide (**4a**) were obtained; they were identified by comparison with authentic samples. From the second fraction (bp 76°C/22 mmHg), **5a** was obtained in a yield of 70%. The IR spectrum of **5a** showed an absorption at 1712 cm^{-1} which was attributed to cyclic imidate. The NMR spectrum data are listed in Table 5. γ-Butyrolactone was obtained on the treatment of **5a** with silicic acid.

Found: C, 67.18; H, 10.57; N, 9.76%. Calcd for $C_8H_{15}NO$: C, 68.04; H, 10.71; N, 9.92%.

2-Iminotetrahydrofurans Other than 5a. Into a solution of an isocyanide and an oxetane (mol ratio, 2:1) in methylene chloride, an equimolar amount of $BF_3 \cdot Et_2O$ was added drop by drop with stirring at 0°C. The mixture was warmed to room temperature and then allowed to stand for the prescribed length of time shown in Table 2 and Table 3. The procedure employed for the isolation of **5** was almost the same as that used for **5a**. The NMR spectra data of **5** are given in Table 5. Elemental analysis was carried out upon the corresponding lactones, **6**, which were obtained by the treatment of **5** with silicic acid. The analytical data of **6** are shown in Table 6.

Reaction of 1a with 1,1,3,3-Tetramethylbutyl Isocyanide (2c). This reaction was carried out under the conditions given in Table 2. According to a procedure similar to that used in the isolation of **5a**, the methylene chloride layer was subjected to distillation. From the volatile fraction, 2,2,4,4-tetramethylpentanenitrile (**3c**) was obtained; bp 75°C/23 mmHg. The IR spectrum of **3c** showed an absorption at 2225 cm^{-1} ($\nu_{C\equiv N}$). The NMR spectrum of **3c** in $CDCl_3$ showed three singlets, at τ 8.47 (2H, $-CH_2-$), 8.60 (6H, $2CH_3$), and 8.90 (9H, *t*-Bu).

Found: C, 77.90; H, 12.12; N, 10.33%. Calcd for $C_9H_{17}N$: C, 77.63; H, 12.31; N, 10.06%. From the second fraction (bp 90°C/5 mmHg), 2-(1,1,3,3-tetramethylbutyl)iminotetrahydrofuran (**5c**) was obtained in a yield of 54%. The NMR spectrum data of **5c** are given in Table 5. **5c** was treated with silicic acid to give γ-butyrolactone.

Reaction of 3,3-Bis(chloromethyl)oxetane (1k) with 2a. Into a solution of **2a** (2.49 g, 30 mmol) and **1k** (4.65 g, 30 mmol) and 30 m*l* of methylene chloride, $BF_3 \cdot Et_2O$ (1.56 g, 11 mol) was added dropwise with stirring at 0°C. The reaction mixture was then left to stand at room temperature for 1 day. After the removal of needle crystals (mp 177—178°C), the reaction mixture was quenched with 10% aqueous NaOH. The methylene dichloride layer was distilled to give 3,3-bis(chloromethyl)-4-*t*-butoxybutyronitirle (**8k**), bp 100—120°C/5 mmHg, in a yield of 7%. The IR spectrum of **8k** showed an absorption at 2235 cm^{-1} ($\nu_{C\equiv N}$). The NMR spectrum of **8k** in CCl_4 showed signals at τ 6.35 (4H, s, $2ClCH_2-$), 6.58 (2H, s, *t*-BuOCH_2-), 7.43 (2H, s, $-CH_2-CN$), and 8.75 (9H, s, *t*-Bu).

Found: C, 51.21; H, 7.45; N, 5.97%. Calcd for $C_{10}H_{17}NOCl_2$: C, 50.43; H, 7.20; N, 5.88%. The needle crystals were washed twice with ethyl ether and, by analysis, were found to be the catalyst complex of 2-*t*-butylimino-4,4-bis(chloromethyl)tetrahydrofuran (**5k**). The IR spectrum of this complex showed an absorption at 1708 cm^{-1} which was attributed to cyclic imidate. The NMR spectrum in d_6-DMSO showed signals at τ 5.19 (2H, s, $-CH_2O-$), 6.10 (4H, s, $2ClCH_2-$), 6.80 (2H, s, $-CH_2CN$), and 8.65 (9H, s, *t*-Bu–).

Found: C, 36.96; H, 5.69; N, 4.53%. Calcd for $C_{10}H_{17}NOCl_2-BF_3$: C, 39.26; H, 5.60; N, 4.58%. β,β-Bis(chloromethyl)-γ-butyrolactone (**6k**) was obtained by the treatment of the catalyst complex of **5k** with aqueous NaOH; bp 100—120°C (5 mmHg). The IR spectrum of **6k** showed an absorption at 1770 cm^{-1} ($\nu_{C\equiv N}$). The NMR spectrum of **6k** in $CDCl_3$ showed signals at τ 5.75 (2H, s, $-CH_2O-$), 6.24 (4H, s, $2ClCH_2-$), and 7.33 (2H, s, $-CH_2-C=O$). The analytical data are shown in Table 6.

Reaction of 3,3-Bis(iodomethyl)oxetane (1l) with 2a. This reaction was carried out under the conditions shown in Table 5. According to a procedure similar to that used in the isolation of **5a**, the methylene chloride extract was concentrated and subjected to glpc analysis. 3,3-Bis(iodomethyl)-4-*t*-butoxybutyronitrile (**8l**) was isolated by preparative glpc in a yield of 24%. The IR spectrum of **8l** showed an absorption at 2240 cm^{-1} ($\nu_{C\equiv N}$). The NMR spectrum of **8l** in CCl_4 showed signals at τ 6.57 (4H, s, $2ICH_2-$), 6.60 (2H, s, $-CH_2O-$), 7.39 (2H, s, $-CH_2CN$), and 8.72 (9H, s, *t*-Bu).

Reaction of 3,3-Bis(ethoxymethyl)oxetane (1m) with 2a. This

15) S. Searles, K. A. Pollart, and F. Block, *J. Amer. Chem. Soc.*, **79**, 952 (1957).
16) S. Searles, D. G. Hummel, S. Nukina, and P. E. Throckmorton, *ibid.*, **82**, 2928 (1960).
17) T. W. Campbell and V. S. Foldi, *J. Org. Chem.*, **26**, 4654 (1961).
18) T. W. Campbell, *ibid.*, **22**, 1029 (1957).
19) A. C. Farthing, *J. Chem. Soc.*, **1955**, 3648.
20) I. Ugi and R. Meyr, *Chem. Ber.*, **93**, 239 (1960).
21) S. Otsuka, K. Mori, and K. Yamagami, *J. Org. Chem.*, **31**, 4170 (1966).
22) I. Ugi, U. Fetzer, U. Eholzer, H. Knupfer, and K. Offermann, *Angew. Chem.*, **77**, 492 (1965).
23) H. Meerwein, E. Battenberg, H. Gold, E. Pfeil, and G. Willfang, *J. Prakt. Chem.*, **154**, 83 (1940).
24) G. M. Bennett and A. L. Hock, *J. Chem. Soc.*, **1927**, 472.

reaction was carried out under the conditions shown in Table 4. According to a procedure similar to that used in the isolation of **5a**, the fraction boiling at 100—110°C (4 mmHg) was collected and then subjected to glpc analysis. By preparative glpc, 2-*t*-butylimino-4,4-bis(ethoxymethyl)tetrahydrofuran (**5m**) and 3,3-bis(ethoxymethyl)-4-*t*-butoxybutyronitrile (**8m**) were isolated separately in yields of 69% and 6% respectively. The IR spectrum of **4m** showed an absorption at 1715 cm^{-1} ($\nu_{C\equiv N}$). The NMR spectrum data of **5m** are given in Table 5. Elemental analysis was carried out upon the corresponding lactone (**6m**) (Table 6). The IR spectrum of **8m**, showed an absorption at 2235 cm^{-1} ($\nu_{C\equiv N}$). The NMR spectrum of **8m** in CCl_4 showed signals at τ 6.51 (4H, q, $2CH_3CH_2O$–), 6.60 (4H, s, $2CH_3CH_2OCH_2$–), 6.65 (2H, s, *t*-$BuOCH_2$–), 7.58 (2H, s, $-CH_2-CN$), 8.75 (9H, s, *t*-Bu), and 8.78 (6H, t, $2CH_3CH_2O$–).

Found: C, 65.96; H, 10.81; N, 5.43%. Calcd for $C_{14}H_{27}NO_3$: C, 65.33; H, 10.57; N, 5.44%.

*Reaction of 3,3-Bis(t-butoxymethyl)oxetane (**1n**) with **2c**.* Into a solution of **1n** (1.15 g, 5 mmol) and **2c** (1.39 g, 10 mmol) in 20 m*l* of methylene chloride, $BF_3 \cdot OEt_2$ (0.78 g, 5 mmol) was added dropwise with stirring at 0°C. The reaction mixture was then allowed to stand at room temperature for 3 days. According to a procedure similar to that used in the isolation of **5a**, 2-(1,1,3,3-tetramethylbutyl)imino-4,4-bis(*t*-butoxymethyl)tetrahydrofuran (**5n**) was obtained in a yield of 38%; bp 110—120°C/2 mmHg. The IR spectrum of **5n** showed an absorption at 1715 cm^{-1} ($\nu_{C\equiv N}$). The NMR spectrum data of **5n** are given in Table 5. Elemental analysis was carried out upon the corresponding lactone (**6n**) (Table 6).

Reaction of 8k with $Et_3O^+BF_4^-$. A solution of **8k** (0.43 g, 1.8 mmol) and $Et_3O^+BF_4^-$ (0.68 g, 4 mmol) in 10 m*l* of methylene chloride was allowed to stand at room temperature for 5 days. Then the reaction mixture was poured into aqueous NaOH, and the methylene chloride layer was treated with silicic acid. **6k** was thus obtained in a yield of 31%, as determined by glpc analysis.

*Reaction of β-Benzyloxybutyronitrile (**13**) with $Et_3O^+BF_4^-$.* A solution of **13** (0.88 g, 5 mmol) and $Et_3O^+BF_4^-$ (0.85 g, 5 mmol) in 5.5 m*l* of methylene chloride was allowed to stand at room temperature for 6 days. According to procedures similar to the above, γ-butyrolactone was thus obtained in a yield of 31% as determined by glpc analysis.

BULLETIN OF THE CHEMICAL SOCIETY OF JAPAN, VOL. 44, 2479—2483 (1971)

Decomposition of *m*-Nitrobenzenesulfonyl Peroxide in Several Solvents[1]

Yasukazu YOKOYAMA, Hiroko WADA, Michio KOBAYASHI,[2] and Hiroshi MINATO

Department of Chemistry, Faculty of Science, Tokyo Metropolitan University, Fukazawa, Setagaya, Tokyo

(Received March 8, 1971)

Rates of decomposition of *m*-nitrobenzenesulfonyl peroxide in chloroform, nitrobenzene, chlorobenzene, and benzene were determined, and activation parameters were calculated. Products of decomposition in nitrobenzene were *m*-nitrophenyl *m*-nitrobenzenesulfonate and *m*-nitrobenzenesulfonic acid, whereas those in chloroform were *m*-nitrobenzenesulfonic acid, hexachloroethane, and phosgene (when air is present). Activation parameters and reaction products indicate that the reaction in chloroform involves homolytic cleavage of the O–O bond, whereas that in nitrobenzene involves electrophilic attack of the peroxide on aromatic nuclei. When sulfonyl-^{18}O labeled *m*-nitrobenzenesulfonyl peroxide was decomposed in benzene, about 35—36% of the label was found in the phenolic oxygen of *m*-nitrophenyl *m*-nitrobenzenesulfonate. This finding could be accounted for by a mechanism which involves a loose π-complex prior to the formation of a σ-complex.

The published chemistry of the bis(arenesulfonyl) peroxides is still very limited. In 1966 and 1970 Dannley and his co-workers[3] reported that the thermal decomposition of *m*-nitrobenzenesulfonyl peroxide in benzene, chlorobenzene, or toluene produced *m*-nitrobenzenesulfonic acid and the corresponding aryl *m*-nitrobenzenesulfonate. On the basis of the relative yields and orientations of the esters obtained from mixtures of benzene or toluene with chlorobenzene, they calculated partial rate factors and concluded that these products arose from electrophilic attack of the peroxide on aromatic compounds.

So far no good ways for production of sulfonyloxy radicals have been reported yet, and it appeared of interest to investigate the possibility of the homolytic decomposition of arenesulfonyl peroxides to produce arenesulfonyloxy radicals. Therefore, the decomposition of *m*-nitrobenzenesulfonyl peroxide (NBSP) has been investigated in chloroform and nitrobenzene; these solvents were chosen because they appeared least likely to receive electrophilic attack of the peroxide. Then the rate of decomposition in nitrobenzene was compared with those in chlorobenzene, benzene, and toluene. The results will be described in this paper.

Results and Discussion

Decomposition of NBSP in chloroform was followed by iodometric titration. The rates were of first order, and the first-order rate constants were 1.25, 4.88, and 9.90×10^{-5} sec^{-1} at 25.0, 35.0, and 40.0°C, respectively. From these values, E_a and $\Delta S^{\neq}$ were calculated to be 24.5 kcal/mol and 4.6 e.u., respectively. The products of

1) Organic Sulfur Compounds Part XXIV.
2) To whom correspondence should be addressed.
3) R. L. Dannley and G. E. Corbett, *J. Org. Chem.*, **31**, 153 (1966); R. L. Dannley, J. E. Gagen, and O. J. Stewart, *ibid.*, **35**, 3076 (1970).

decomposition in chloroform were analyzed, and the results are shown in Table 1.

Table 1. Products of decomposition of NBSP in chloroform

Product	mol/mol of NBSP	
	Absence of O_2	Presence of O_2
m-$O_2NC_6H_4SO_3H$	1.79	2.06
C_2Cl_6	0.03	—
$COCl_2$	—	1.58

These results indicate that the decomposition of NBSP in chloroform involves homolytic cleavage of the O–O bond of NBSP, and the reaction steps are represented as follows.

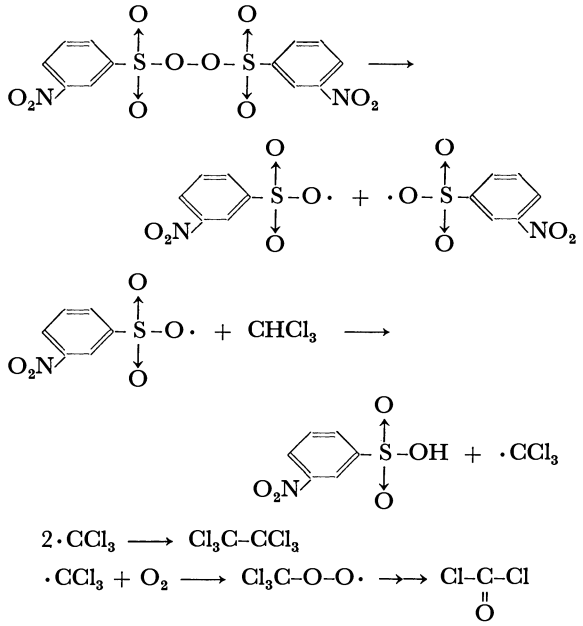

$$2\cdot CCl_3 \longrightarrow Cl_3C\text{-}CCl_3$$

$$\cdot CCl_3 + O_2 \longrightarrow Cl_3C\text{-}O\text{-}O\cdot \longrightarrow\!\!\rightarrow Cl\text{-}\overset{\overset{O}{\|}}{C}\text{-}Cl$$

Then the decomposition of NBSP in nitrobenzene was investigated. The rates of decomposition in this solvent were also of first order in NBSP, and the rate constants were 1.40, 3.80, and 32.0×10^{-5} sec^{-1} at 20.0, 30.0, and 60.0°C, respectively. From these values E_a and $\Delta S^{\neq}$ were calculated to be 16.7 kcal/mol and −24 e.u., respectively. The products of decomposition in nitrobenzene are shown in Table 2. The products of decomposition and activation parameters indicate that the decomposition of NBSP in nitrobenzene is ionic, and the reaction probably proceeds as shown below.

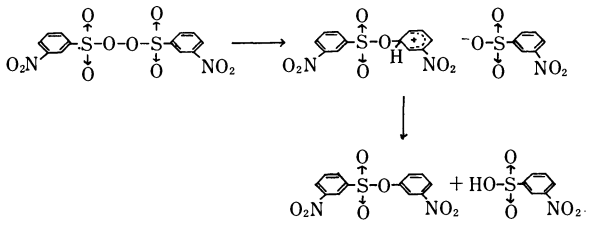

Dannley and his co-workers did not determine the rate constants of decomposition of NBSP. Therefore it appeared of interest to determine the rate constants in various aromatic compounds. Kinetic studies were performed in chlorobenzene and benzene, and the results are shown in Table 3. Activation parameters and relative magnitude of rate constants are consistent with a mechanism which involves a nucleophilic attack of an aromatic compound on the peroxidic oxygen.

Table 2. Products of decomposition of NBSP in nitrobenzene

Product	mol/mol of NBSP
m-$O_2NC_6H_4SO_3H$	0.90
m-$O_2NC_6H_4SO_3C_6H_4$-NO_2-m	0.72

Table 3. Rate constants of decomposition NBSP in various Solvents

Solvent	Temp. (°C)	10^5k_1 (sec^{-1})	E_a (kcal/mol)	$\Delta S^{\neq}$ (e.u.)
$CHCl_3$	20.0	1.25	24.5	4.58
	35.0	4.88		
	40.0	9.90		
$C_6H_5NO_2$	20.0	1.40	16.7	−26.2
	30.0	3.80		
	60.0	32.0		
C_6H_5Cl	5.0	12.6	18.4	−13.2
	10.0	23.7		
	20.0	75.0		
C_6H_6	5.0	24.6	18.4	−12.0
	10.0	44.6		
	15.0	69.3		

Table 4. Comparison of rate constants and partial rate factors

Solvent	$10^5k_{10^\circ}$ (sec^{-1})	k_X/k_H	Partial rate factor
$PhCH_3$	—	—	para, 73.8[b]
PhH	44.6	1.00	1.00
PhCl	23.7	0.53	para, 2.8
$PhNO_2$	0.500[a]	0.012	meta, 0.0336
$CHCl_3$	0.115[a]	—	—

a) Calculated by extrapolation of log k *vs.* $1/T$ plots.
b) Ref. 3.

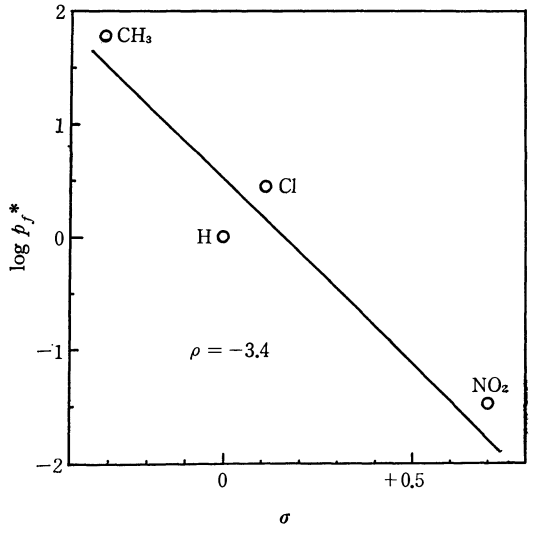

Fig. 1. Hammett plots for the decomposition of NBSP in aromatic solvents ($*f_f$=partial rate fatctor)

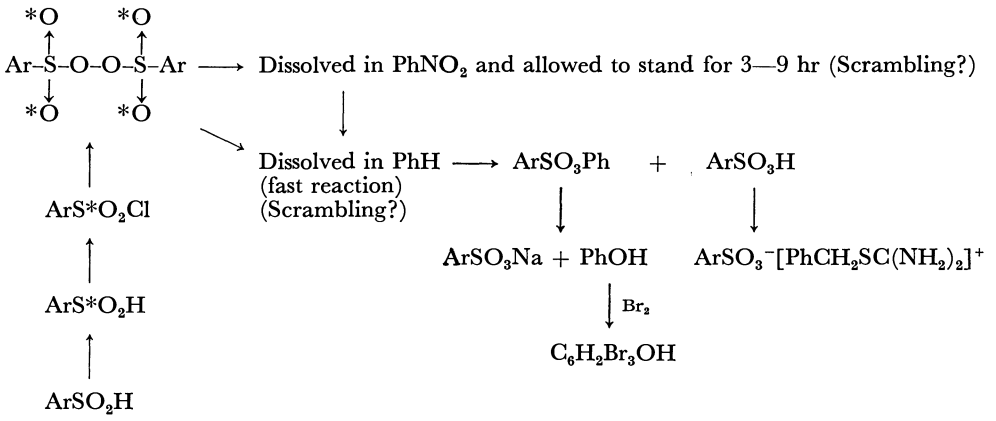

The rate constants at 10°C were compared and partial rate factors were calculated, which are shown in Table 4. Figure 1 is the Hammett plots of these partial rate factors against Hammett's σ values: ρ was found to be −3.4. The large negative ρ value indicates that the peroxidic oxygen is strongly electrophilic at the transition state, and the electron-releasing substituents on the aromatic solvents greatly facilitate the reaction.

In order to study the mechanism of the reaction between NBSP and aromatic compounds, sulfonyl-^{18}O labeled NBSP was prepared, and scrambling of the label was examined under various conditions. The experiments are summarized in the following scheme. The results are shown in Table 5.

The following three cases are possible as the mechanisms of the reaction between NBSP and benzene.

A) Specific attack on peroxidic oxygen

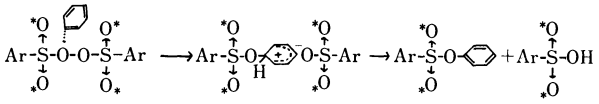

0% at phenolic oxygen

B) Specific attack on sulfonyl oxygen

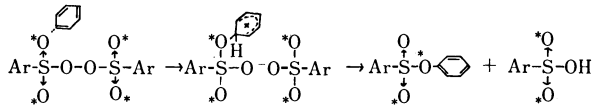

100% at phenolic oxygen

C) Scrambling during preparation or standing, and then the reaction with benzene

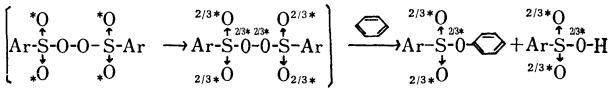

67% at phenolic oxygen

The possibility that the label was scrambled during the preparation of NBSP was excluded by use of the reaction of NBSP with triphenylphosphine. When the NBSP, prepared from *m*-nitrobenzenesulfonyl-^{18}O chloride with 1.08 excess ^{18}O atom %, was let to react with triphenylphosphine, the triphenylphosphine oxide produced was found to contain no excess oxygen-18.

Table 5. Excess oxygen-18 in the sulfonyl-labeled NBSP and the products of its reaction with benzene

Expt No.	NBSP used	Treatment	*m*-$O_2NC_6H_4SO_3C_6H_5$		*m*-$O_2NC_6H_4SO_3^-$ $[PhCH_2SC(NH_2)_2]^+$		C_6H_4BrOH	Y/X ×100
			Excess ^{18}O%	Excess ^{18}O% in SO_2	Excess ^{18}O%	Excess ^{18}O% in SO_2	Excess ^{18}O% (Y)	
1	A	$PhNO_2$ 6 hr; then PhH, 18°C	0.404	1.01	0.417	1.04	0.37	35
2	B	PhH, 16°C	0.415	1.04			0.40	36
3	B	$PhNO_2$ 3 hr; then PhH, 16°C	0.405	1.00			0.40	36
4	B	$PhNO_2$ 9 hr; then PhH, 16°C	0.408	1.01			0.39	36

NBSP No.	*m*-$O_2NC_6H_4S*O_2Cl$		(m-$O_2NC_6H_4S*O_2)_2O_2$	
	Excess ^{18}O%	Excess ^{18}O% in SO_2	Excess ^{18}O%	Excess ^{18}O% in SO_2 (X)
A	0.520	1.04	0.420	1.05
B	0.540	1.08	0.440	1.08

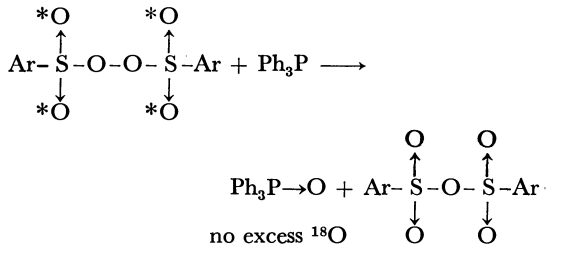

This finding establishes not only the non-occurrence of the scrambling of the label of NBSP during its synthesis but also the specific attack of triphenylphosphine upon the peroxidic oxygen of NBSP.

The data shown in Table 5 indicate that scrambling of the label does take place. When experiments 2, 3, and 4 are compared, it is clear that this scrambling does not take place during the long standing in nitrobenzene, but during the reaction with benzene. These findings indicate that Mechanism C) does not represent the reaction taking place.

The fact that the percentage of oxygen-18 excess found in the phenolic oxygen was neither 0% nor 100% shows that neither Mechanism A nor Mechanism B) alone can explain the reaction taking place. The figure 35—36% could be accounted for by an assumption that benzene molecules attack both peroxidic and sulfonyl oxygens. However, the possibility that the π-electrons of benzene nucleus attack negatively charged oxygen atoms of sulfonyl groups must be very small.

A more attractive mechanism for the reaction between NBSP and benzene is the following one.

D) Formation of a π-complex, and then a σ-complex.

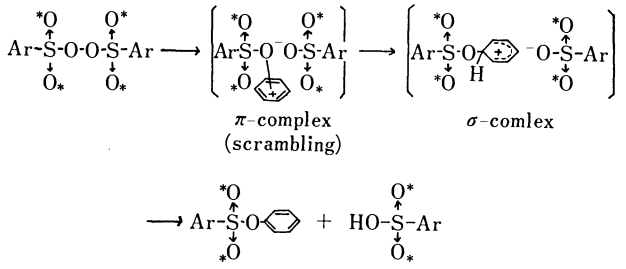

Experimental

Materials. Nitrobenzene, chlorobenzene, benzene, toluene, and chloroform were purified by conventional procedures, and were distilled before use. Chloroform was used immediately after distillation in order to avoid contamination due to autooxidation.

m-Nitorobenzenesulfonyl peroxide was prepared from *m*-nitrobenzenesulfonyl chloride and hydrogen peroxide according to the method of Dannley and Corbett.[3] Yield, 12%, mp 112°C (dec.) (lit,[3] 112°C). The purity of the peroxide was determined by iodometric titration[4] to be 97.2%.

Determination of Rates of Reaction in Various Solvents. Into 100 m*l* of nitrobenzene in a flask placed in a bath of constant temperature, 0.625 g of NBSP (1.50 mmol) was added, and the flask was quickly shaken. At suitable intervals, certain amounts of the solution were withdrawn, and added to a flask containing crystals of potassium iodide. Then 10 m*l* of water was added, and the iodine liberated was titrated by a sodium thiosulfate solution.

Rates of reaction in other solvents were determined in a similar manner. Rates of reaction in chloroform were determined in sealed ampoules.

Products of Decomposition in Chloroform. *a) In a Degassed Chloroform*: A solution containing 0.941 g (2.33 mmol) of NBSP and 150 m*l* of chloroform was degassed, and placed in a bath of 40.0°C for 14 hr. The brown-colored solution was shaken with water. Evaporation of the aqueous extracts yielded 0.846 g (4.17 mmol) of *m*-nitrobenzenesulfonic acid, which was determined by converting it into *S*-benzylisothiuronium sulfonate. The chloroform solution was dried and evaporated. An oil obtained was analyzed by gas chromatography and it was found to contain 0.070 mmol of hexachloroethane.

b) In Chloroform Containing Air: A solution containing 0.260 mmol NBSP in 20 m*l* of chloroform was placed in a bath of 30.0°C for 29 hr in the presence of air. The solid *m*-nitrobenzenesulfonic acid which precipitated was decanted off, and aniline was added to the solution. Crystalline *N*, *N'*-diphenylurea formed weighed 0.0846 g (0.41 mmol); mp 233—234°C (decomp.). The same experiment was repeated for analysis of *m*-nitrobenzenesulfonic acid. After the decomposition the chloroform solution was washed with water. When the aqueous extracts were evaporated, 0.535 mmol of *m*-nitrobenzenesulfonic acid was obtained.

Products of Reaction in Nitrobenzene. In 20 m*l* of nitrobenzene 0.540 g (1.34 mmol) of NBSP was dissolved. A flask containing the solution was placed in a bath at 30.0°C for 2 days. Then the solution was washed with water several times. When the aqueous extracts were evaporated, *m*-nitrobenzenesulfonic acid was found, which was converted to its benzylisothiuronium salt (1.22 mmol).

When the nitrobenzene solution was evaporated, brownish solids remained, which was recrystallized in hexane and found to be *m*-nitrophenyl *m*-nitrobenzenesulfonate, mp 98—103°C. The ester was refluxed in 10 m*l* of 0.3N sodium hydroxide solution for 5 days, and the nitrophenol produced was methylated by use of dimethyl sulfate. When the nitroanisole obtained was analyzed by gas chromatography, only one peak was observed which corresponded to that of *m*-nitroanisole.

Preparation of Sulfonyl-^{18}O labeled m-*Nitrobenzenesulfonyl Peroxide.* In 41.5 m*l* of $H_2{}^{18}O$ (1.53 excess-^{18}O atom %) 23.5 g of *m*-nitrobenzenesulfinic acid was dissolved and the solution was heated at 90°C for 45 min after which the exchange of oxygen was almost complete. The sulfinic acid was converted to its sodium salt, which was treated with chlorine for 25 min and converted to *m*-nitrobenzenesulfonyl chloride. Crude crystals obtained (20 g) were recrystallized in hexane; yield, 10 g, mp 61—63°C. Its excess oxygen-18% was analyzed by mass spectrometry, and the results are shown in Table 5.

By using sulfonyl-^{18}O labeled *m*-nitrobenzenesulfonyl chloride and 30% hydrogen peroxide, sulfonyl-^{18}O labeled NBSP was prepared according to the method of Dannley and Corbett.[3]

Reaction of Sulfonyl-^{18}O labeled NBSP with Aromatic Solvents. As a representative case the experimental procedure used for Experiment 2 in Table 5 will be described. In 140 m*l* of purified nitrobenzene 2.002 g of sulfonyl-^{18}O labeled NBSP was dissolved, and the solution was stirred for 6 hr under a nitrogen atmosphere at 18°C. Then 300 m*l* of purified benzene was added, and the mixture was allowed to stand for 48 hr under a nitrogen atmosphere.

The reaction mixture was extracted with water. The *m*-nitrobenzenesulfonic acid in the aqueous extracts were con-

4) R. N. Haszeldine, R. B. Heslop, and J. W. Lethbridge, *J. Chem. Soc.*, **1964**, 4902.

verted to its *S*-benzylisothiuronium salt, which amounted to 1.405 g (76.5%). Crude crystals were recrystallized in ethanol-water, and the purified crystals (0.10 g) melting at 140.0—142.3°C were subjected to the mass-spectrometric analysis.

The aromatic hydrocarbon layer was dried over anhydrous magnesium sulfate, and the solvents were distilled under reduced pressure. The residue was chromatographed by a column containing 50 g of Florisil, and 1.008 g of phenyl *m*-nitrobenzenesulfonate was obtained from fractions eluted by hexane-benzene; yield, 72.4%. Crude crystals were recrystallized in methanol, and the purified crystals melting at 91—91.5°C were subjected to the mass-spectrometric analysis.

In order to separate the phenolic oxygen from the sulfonyl oxygen the ester was hydrolyzed. In 5 m*l* of a 0.3N sodium hydroxide solution in 70% dioxane-30% water, 0.252 g of phenyl *m*-nitrobenzenesulfonate was added, and the mixture was heated at 60°C in an ampoule for 7 days. After the solution was acidified by hydrochloric acid, a Br_2-KBr solution was added and white precipitates formed were washed with a sodium hydrogen sulfite solution and then with water. After drying, crude crystals of 2,4,6-tribromophenol weighed 0.335 g. They were purified by sublimation at 140°C under reduced pressure, and the purified crystals weighed 0.227 g (75.7%); mp 88.5—91.0°C.

The possibility that the oxygens of phenyl *m*-nitrobenzenesulfonate are scrambled during its hydrolysis can be excluded on the basis of the findings of Bunton and Frei, who studied the alkaline hydrolysis of phenyl *p*-toluenesulfonate in dioxane-water.[5] They showed that no C–O bonds were cleaved during hydrolysis and the S–O bond fission took place exclusively.

Reaction of Sulfonyl-^{18}O labeled NBSP with Triphenylphosphine. A solution of 2.0 g of triphenylphosphine in 20 m*l* of dichloromethane was slowly added to a stirred solution of 0.70 g of sulfonyl-^{18}O labeled NBSP in 50 m*l* of dichloromethane at room temperature. The reaction mixture was extracted with water, and the aqueous extracts were evaporated. Crystals of *m*-nitrobenzenesulfonic acid obtained were converted to its *S*-benzylisothiuronium salt, which amounted to 0.683 g. The dichloromethane solution was evaporated and the residue was washed with ether. The ether-insoluble solids were dissolved in benzene, and the solution was filtered in order to remove benzene-insoluble solids. When the benzene filtrate was evaporated, 0.480 g of white solids of triphenylphosphine oxide were obtained. They were recrystallized from ether, and purified crystals were subjected to the mass-spectrometric analysis.

Oxygen-18 Analysis. The oxygen-18 analyses were carried out according to the method of Rittenberg and Ponticorvo.[6] Each sample was pyrolyzed in the presence of mercuric chloride and mercuric cyanide at 400°C for 4 hr, and the oxygen-18 atom% of the carbon dioxide produced was determined by use of a Hitachi RMU-6D type mass spectrometer.

Grateful acknowledgement is made to the donors of the Petroleum Research Fund, administered by the American Chemical Society, for support of this research.

5) C. A. Bunton and Y. F. Frei, *J. Chem. Soc.*, **1951**, 1872.

6) D. Rittenberg and L. Ponticorvo, *Int. J. Appl. Radiat. Isotopes*, **1**, 208 (1956).

A New Route to Polycondensed Aromatics: Photolytic Formation of Triphenylene and Dibenzo[*fg*, *op*]naphthacene Ring Systems[1]

Takeo SATO, Shigeru SHIMADA, and Kazuo HATA

Department of Chemistry, Faculty of Science, Tokyo Metropolitan University, Setagaya-ku, Tokyo

(Received March 12, 1971)

Application of photo-aryl coupling reactions for the syntheses of triphenylene and dibenzo[*fg*,*op*]naphthacene was explored. Three types of reactions were developed: Photocyclodehydrogenation of polyphenyl compounds, photolytic reactions of iodoarenes, and photocyclodehydrohalogenation of halogenopolyaryls. The effects of solvent, oxidant, and wavelength on the photocyclization of *o*-terphenyl and 2,2′-diphenylbiphenyl to the triphenylene and naphthacene, respectively. were examined. The conversion was best achieved by the reaction carried out in an aromatic solvent in the presence of an equimolar amount of iodine using a quartz or a Vycor vessel. Versatility of the processes was shown by the formation of naphthacene starting from either 2,2′-diphenylbiphenyl (57% yield), 2,2′-bis(2-chlorophenyl)biphenyl (67%), 1,2,3-triphenylbenzene (21%), or 2,6-diiodobiphenyl.

Difficulties in obtaining pure samples of polycondensed aromatic compounds are largely overcome by utilizing the intramolecular photo-aryl coupling reaction.[2] Versatility of the process was examined by applying it to the synthesis of phenanthrene,[3] triphenylene,[4,5] pyrene,[6,7,8] and dibenzo[*fg*, *op*]naphthacene (I) ring systems.[1]

In this paper we wish to describe three types of photochemical processes, namely, a cyclodehydrogenation reaction of polyphenyls, a photolytic reaction of iodoarenes, and a cyclodehydrohalogenation reaction of halogenopolyphenyls, all aiming at the development of a synthetic means for triphenylene and dibenzonaphthacene I.

Results and Discussion

Photolytic Cyclodehydrogenation of Polyphenyls. Triphenylene was obtained in nearly quantitative yield by the irradiation of a dilute benzene solution of *o*-terphenyl (*ca.* 1.7×10^{-2}M) containing an equimolar amount of iodine (Scheme 1).[4] Similarly photocyclodehydrogenation of 2,2′-diphenylbiphenyl and 1,2,3-triphenylbenzene produced dibenzonaphthacene I in yields of 57% and 21%, respectively, as reported in a preliminary paper (Scheme 1)[1].

Representative examples for the preparation of triphenylene and I are shown in Tables 1 and 2, respectively. For comparison some of the previous data[4] are also included in Table 1.

The following generalization was deduced from a series of experiments: The reaction can be carried out under a stream of nitrogen but the presence of oxygen does not impede cyclization. Oxygen alone, however, is not effective as an oxidant. An equimolar amount of iodine is required to facilitate the reaction. As for solvent, aromatic solvents such as benzene or chlorobenzene are more suitable than cyclohexane. Use of a

TABLE 1. THE PHOTOCYCLODEHYDROGENATION REACTION OF *o*-TERPHENYL TO TRIPHENYLENE[a]

o-Terphenyl mmol	Iodine mmol	Solvent	Lamp[c]	Filter	Atmosphere	Yield, %
1.04	none	C_6H_6 or C_6H_{12}	1000-H	quartz	air	0[d]
1.04	0.20	C_6H_{12}	1000-H	quartz	air	11.9
1.06	0.20	C_6H_{12}	1000-H	quartz	nitrogen	19.6
1.02	1.00	C_6H_{12}	1000-H	quartz	nitrogen	29.1
1.04	trace	C_6H_6	1000-H	quartz	nitrogen	26.2
1.00	1.01	C_6H_6–C_6H_{12}[b]	1000-H	quartz	nitrogen	45.4
1.02	1.01	C_6H_6	1000-H	quartz	nitrogen	87.9
1.01	1.01	C_6H_5Cl	1000-H	quartz	nitrogen	78
1.01	1.01	C_6H_6	100-L	Vycor	nitrogen	87
1.00	1.00	C_6H_6	1000-H	Pyrex	nitrogen	2
1.01	1.02	C_6H_6	1000-H	glass	nitrogen	0

a) Irradiation was carried out for 20 hr using 60-m*l* solutions.
b) A 1:1 solution was used.
c) 1000-H: a 1-kW high-pressure mercury lamp. 100-L: a 100-W low-pressure mercury lamp.
d) Irradiation was continued for 46 hr.

1) Photo-Aryl Coupling and Related Reactions. VII. Part VI: T. Sato, S. Shimada, and K. Hata, *Chem. Commun.*, **1970**, 766.
2) T. Sato, *Yuki Gosei Kagaku Kyokai Shi*, **27**, 715 (1969).
3) T. Sato, Y. Goto, T. Tohyama, S. Hayashi, and K. Hata, This Bulletin, **40**, 2975 (1967).
4) T. Sato, Y. Goto, and K. Hata, *ibid.*, **40**, 1997 (1967); see also N. Kharasch, T. G. Alston, H. B. Lewis, and W. Wolf, *Chem. Commun.*, **1965**, 242.
5) T. Sato, S. Shimada, and K. Hata, This Bulletin, **42**, 766 (1969).
6) T. Sato, E. Yamada, Y. Okamura, T. Amada, and K. Hata, *ibid.*, **38**, 1049 (1965).
7) T. Sato, M. Wakabayashi, S. Hayashi, and K. Hata, *ibid.*, **42**, 773 (1969).
8) S. Hayashi and T. Sato, to be submitted to this Bulletin.

Table 2. The photocyclodehydrogenation reaction of 2,2′-diphenylbiphenyl and 1,2,3- triphenylbenzene to dibenzo[*fg,op*]naphthacene (I)[a)]

Compound mmol	Iodine mmol	Benzene ml	Lamp	Filter	Yield, %
2,2′-Diphenylbiphenyl					
1.01	1.04	80	100-L	Vycor	57
1.02	1.04	60	1000-H	quartz	34
0.52	0.52	30	1000-H	Pyrex	1
1,2,3-Triphenylbenzene					
0.19	0.20	60	100-L	Vycor	21

a) Irradiation was carried out for 72 hr under nitrogen.

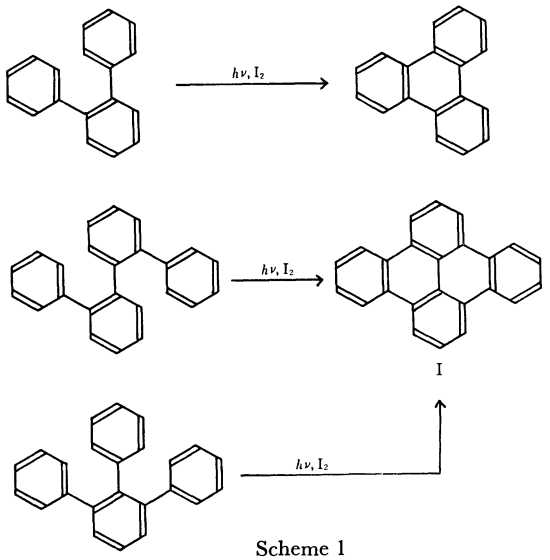

I

Scheme 1

benzene-cyclohexane mixture gave a medium result.

This is in a sharp contrast to the related photocyclization of *cis*-stilbene to phenanthrene, for which cyclohexane is a preferred solvent and both oxygen and iodine are equally effective.[9)] Only a catalytic amount of iodine is enough to effect cyclization.

Wavelength effects were studied by carrying out photolysis using various filters. Although the reaction proceeded satisfactorily either with a quartz or a Vycor filter, it was suppressed by a Pyrex filter. No reaction occurred when a glass filter was inserted.

A possible pathway of the reaction is shown in the following equation for the case of *o*-terphenyl as an example. *o*-Terphenyl shows a UV maximum at 235 nm in ethanol. By photoexcitation, the molecules give dihydrotriphenylene II via a concerted process. Dehydrogenation of II generates triphenylene.

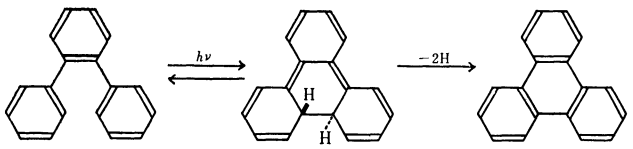

II

9) F. B. Mallory, C. S. Wood, and J. T. Gordon, *J. Amer. Chem. Soc.*, **86**, 3094 (1964); C. S. Wood and F. B. Mallory, *J. Org. Chem.*, **29**, 3373 (1964); F. R. Stermitz in O. L. Chapman ed. "Organic Photochemistry," Vol. 1, Marcel Dekker, New York (1967), p. 249; E. V. Blackburn and C. J. Timmons, *Quart. Revs.*, **23**, 482 (1969) and papers cited therein.

This sequence is formulated after the well-studied *cis*-stilbene - phenanthrene reaction,[9)] for which the structure of the intermediate, 4a,4b-dihydrophenanthrene (III), was determined beyond doubt either by chemical and spectroscopic methods[10)] or by direct trapping.[11)] A *trans* relationship of the tertiary hydrogens as shown in II and III is based on the conrotatory photocyclization of 1,3,5-hexatriene systems.[12)]

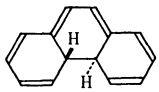

III

Spectral changes of a benzene solution of *o*-terphenyl during irradiation indicated the appearance of new bands at ~360, 375, and 400 nm, possibly due to II. Most peaks of triphenylene were masked by absorption due to the solvent. Detailed spectral and kinetic studies on the formation of II will be reported elsewhere.[13)]

With 2,2′-diphenylbiphenyl and 1,2,3-triphenylbenzene the structure of the intermediate can be written as IV and V. Although a stepwise cyclization *via* IV or V is favored to a simultaneous double cyclization

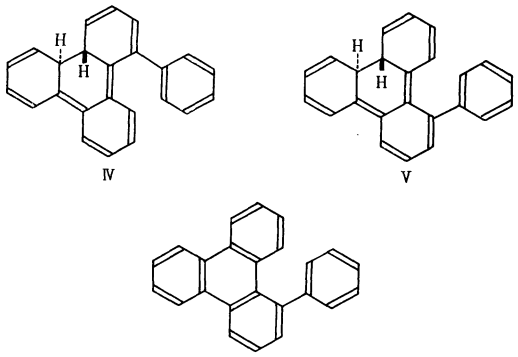

IV V

VI

reaction, no 1-phenyltriphenylene (VI) was isolated from the reaction mixture. Even when the conversion was incomplete, the rest of the material was found to be the starting compound. It is highly probable that VI, once formed, is rapidly cyclized to I since the molecular arrangement becomes favorable for further ring closure.[14)]

10) F. B. Mallory, C. S. Wood, J. T. Gordon, L. C. Lindquist, and M. L. Savitz, *J. Amer. Chem. Soc.*, **84**, 4362 (1962); W. M. Moore, D. D. Morgan, and F. R. Stermitz, *ibid.*, **85**, 829 (1963); M. V. Sargent and C. J. Timmons, *ibid.*, **85**, 2186 (1963); M. V. Sargent and C. J. Timmons, *J. Chem. Soc.*, **1964**, 5544; K.A. Muszkat and E. Fischer, *ibid., B*, **1967**, 663; E. V. Blackburn, C. E. Loader, and C. J. Timmons, *ibid., C*, **1970**, 163.

11) T. D. Doyle, N. Filipescu, W. R. Benson, and D. Banes, *J. Amer. Chem. Soc.*, **92**, 637 (1970).

12) R. B. Woodward and R. Hoffmann, "The Conservation of Orbital Symmetry," Verlag Chemie Gmbh (1970).

13) Upon irradiation benzene solutions of *o*-terphenyl exhibit spectral changes under both oxygen and deaerated conditions. On the other hand, no spectral changes occur in cyclohexane.

14) As a measure of photocyclization, the sum of the free valence numbers in the first excited state of atoms undergoing cyclization is calculated by the HMO method. The values found for 2,2′-diphenylbiphenyl, 1,2,3-triphenylbenzene, and 1-phenyltriphenylene VI are 0.962, 1.003, and 0.962, respectively. For details, see T. Sato and T. Morita, This Bulletin, in press.

Inability of oxygen to enter into a hydrogen abstraction step seems to reflect either an essential difference in the ability of hydrogen abstraction between oxygen and iodine or a factor concerning concentration. The latter possibility is indicated by experiments using a varying amount of iodine. Presumably tertiary hydrogens of II are less reactive than those of III, since rather higher concentration of II can be expected in the photoequilibrium when a favorable geometry for cyclization and extra conjugation extending over four rings are considered.

Incident light will be largely absorbed by solvent benzene. Enhancement of the reaction rate by the aromatic solvent indicates the possibility of sensitization. Action of iodine through complexation with the aromatic ring must also be considered.

The photocyclization of polyphenyl is proved to be an efficient synthetic method for certain polycondensed aromatics and may be further applied in various fields. Besides involving high yields and simple procedures the process has a simplified isolation technique. With triphenylene pure material was obtainable merely by concentrating the benzene solution after it was washed with sodium thiosulfate. It is more simple in the case of I, since the material separates out of the solution during the course of formation resulting from irradiation. Single recrystallization of the collected material from xylene gave pure I, mp 351—352°C.

Starting from substituted *o*-terpehnyls a number of triphenylene derivatives such as VII and VIII, were prepared.[5]

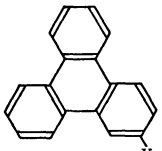

VII

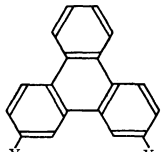

VIII

Substituents include CH_3, C_6H_5, Br, Cl, F, $COOC_2H_5$, and CN. The preparation of 2-cyanotriphenyelne, (VII/CN) and ethyl triphenylene-2-carboxylate (VII/$COOC_2H_5$) are described in Experimental. Most of the available synthetic methods known for triphenylene and its derivatives[15] can not be modified to allow introduction of such a variety of functional groups. Syntheses via trimerization are used to give some sym.-trisubstituted triphenylenes.[16] The electrophilic substitution reaction of triphenylene results in the formation of both 1- and 2-substituted compounds and it is difficult to control and direct the orientation.[17]

Only synthetic method reported for I is that of Sako,[18] who obtained I in 35—40% yield by decomposition of the bis-diazonium salt derived from 2,2′-diamino-6,6′-diphenylbiphenyl. There are several reports on the formation of I though not suitable for synthetic purposes.[19]

A possible alternative synthesis after Scheme 1 would be a thermal cyclodehydrogenation reaction over metal catalysts. The thermal conversion of *o*-terphenyl to triphenylene required high temperatures of 625°C with chromia-on-alumina (10% yield)[20] or 490°C with palladium-platinum-charcoal (63% yield).[21] Most substituents would not survive such severe reaction conditions. Attempted cyclodehydrogenation of 2,2′-diphenylbiphenyl using the metal catalyst produced a phenyl migration product, 2-phenyltriphenylene (VII/C_6H_5). Neither 1-phenyltriphenylene (VI) nor I was produced.

Concerning the limitations of the photocyclodehydrogenation reaction, no cyclization occurred with nitro-*o*-terphenyls.[5] Iodo-*o*-terphenyls underwent extensive C–I homolysis.[5] A similar limitation was also found for stilbenes, for which the effect of substituents on the quantum yields was studied.[22] No cyclization occurred with diphenylquaterphenyl (IX).

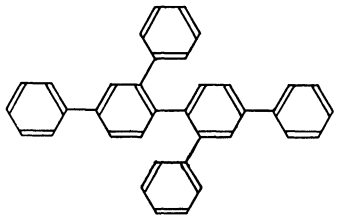

IX

Photolytic Reactions of Iodoarenes. Due to low bond dissociation energies (~55 kcal/mol) of the C–I bond, iodoarenes undergo a facile photolysis reaction to give aryl and iodo radicals.[23,24] Application to biaryl syntheses was described by Wolf *et al.*[25]

Polyphenylation is expected when polyiodoarenes are photolyzed in benzene. Several examples are shown in Table 3. Liberated iodine can effect photocyclization when an *o*-terphenyl structure is present. Such an example is illustrated in the accompanying equation.[5]

The photolysis reactions of polyiodoarenes are summarized in Table 4. The construction of highly con-

15) H. Heaney and I. T. Miller, *Org. Synth.*, **40**, 105 (1960) and references cited therein.

16) R. C. Hinton, F. G. Mann, and I. T. Miller, *J. Chem. Soc.*, **1958**, 4704; F. H. Marquardt, *ibid.*, **1965**, 1517; I. M. Matheson, O. C. Musgrave, and C. J. Webster, *Chem. Commun.*, **1965**, 278; P. Canonne and A. Regnault, *Tetrahedron Lett.*, **1969**, 243.

17) Ng. Ph. Buu-Hoi and P. Jaquignori, *J. Chem. Soc.*, **1953**, 941; C. C. Barker, R. G. Emmerson, and J. D. Periam, *ibid.*. **1955**, 4482; P. M. G. Bavin and M. J. S. Dewar, *ibid.*, **1955**, 4486, **1956**, 164; M. J. S. Dewar, T. Mole, and E. W. T. Warfard, *ibid.*, **1956**, 3581; M. J. S. Dewar and T. Mole, *ibid.*, **1957**, 342; R. Bolton and P. B. D. de la Mare, *ibid.*, *B*, **1969**, 170.

18) S. Sako, This Bulletin, **9**, 55 (1934).

19) G. Wittig and G. Lehmann, *Chem. Ber.*, **90**, 875 (1957); G. Wittig, E. Hahn, and W. Tochterman, *ibid.*, **95**, 439 (1962); I. B. Goldberg., R. F. Borch, and J. B. Bolton, *Chem. Commun.*, **1969**, 223.

20) C. H. Hansch and C. F. Geiger, *J. Org. Chem.*, **23**, 477 (1958).

21) P. G. Copeland, R. E. Dean, and D. McNeil, *J. Chem. Soc.*, **1960**, 1687.

22) H. Jungmann, H. Güsten, and D. Schulte-Frohlinde, *Chem. Ber.*, **101**, 2690 (1968).

23) J. M. Blair, D. Bryce-Smith, and B. W. Pengilly, *J. Chem. Soc.*, **1959**, 3174; A. Job and G. Emschwiller, *Compt, rend.*, **179**, 52 (1924).

24) R. K. Sharma and N. Kharasch, *Angew. Chem.*, **80**, 69 (1968).

25) W. Wolf. T. Erpelding, P. G. Naylor, and L. Tokes, *Chem. and Ind.*, **1962**, 1720; W. Wolf and N. Kharasch, *J. Org. Chem.*, **30**, 2493 (1965).

Table 3. The photolytic phenylation of polyiodoarenes[a)]

Compound	Irrad. time, hr	Product	Yield, %
p-Diiodobenzene	95	*p*-Terphenyl	52
4,4′-Diiodobiphenyl	71	1,1′:4′,1″:4″,1‴-Quaterphenyl	63
1,3,5-Triiodobenzene	147	1,3,5-Triiodobenzene	79

a) Benzene solutions (1.7×10^{-2}M) were irradiated using a 1-kW high-pressure lamp.

Table 4. Photoreactions of iodoarenes

Compound	mmol	Benzene m*l*	Irrad. time, hr	Product, %			
				Biphenyl	*o*-Iodobiphenyl	Triphenylene	I
o-Diiodobenzene[a)]	1.02	100	48	trace	28	2	
2-Iodobiphenyl[a)]	1.04	100	24	11	11	11	
2,6-Diiodobiphenyl[a,b)]	1.01	100	120	trace	2	42	trace
2,2′-Diiodobiphenyl[c,d)]	0.52	30	21		1	3	

a) 100-L lamp
b) 1000-H lamp
c) 1,2,3-Triphenylbenzene was formed in 24% yield.
d) Dibenziodolium iodide was formed in 21% yield. Recovery of the starting material was 23%.

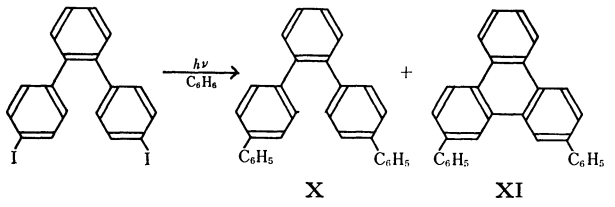

X XI

densed ring systems would become possible *via* polyphenylation-cyclization scheme.

The photolysis of *o*-diiodobenzene in benzene produced triphenylene in addition to 2-iodobiphenyl and *o*-terphenyl. Similar results have been reported[26)] and the formation of a benzyne intermediate was postulated.[26,27)] The yield of triphenylene was improved by starting from 2-iodobiphenyl.

The photolysis of 1,2,3-triiodobenzene gave *m*-terphenyl and triphenylene but no 1,2,3-triphenylbenzene and/or its cyclization products. 2,6-Diiodobiphenyl produced I in a low yield, but again an alternative route leading to triphenylene was the major one (Scheme 2).

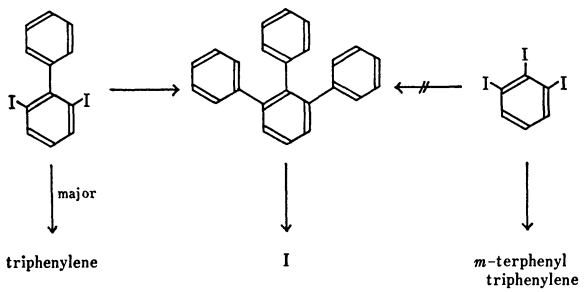

triphenylene I *m*-terphenyl triphenylene

Scheme 2

As a possible precursor to I, 2,2′-diiodobiphenyl was photolyzed in benzene. However, a solid material was produced which was identified as dibenziodolium iodide (XII), mp 213—214°C decomp.[28)] 2,2′-Diiodobiphenyl was regenerated from compound XII either by heating alone or by refluxing in xylene.[28)] Formation of XII is explained by assuming an intermediacy of iodobiphenylyl radical XIII. An intramolecular radical attack on iodine to give XIV is followed by a radical recombination step (Scheme 3). That an aryl

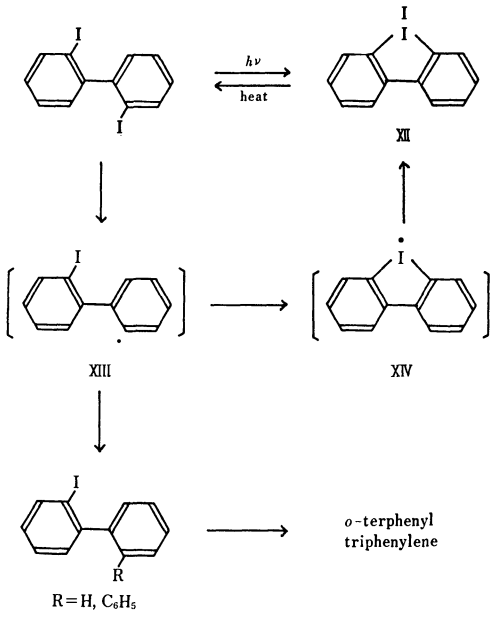

Scheme 3

radical has a very high affinity to iodine has been noticed earlier.[29)] Other products of the reaction include *o*-iodobiphenyl, *o*-terphenyl and triphenylene, the formation of which can also be explained by assuming XIII. *o*-Terphenyl radical XVII derived from 2-iodo-*o*-

26) J. A. Kampmeier and E. Hoffmeister, *J. Amer. Chem. Soc.*, **84**, 3787 (1962).
27) N. Kharasch and R. K. Sharma, *Chem. Commun.*, **1967**, 492.
28) H. Irving and R. W. Reid, *J. Chem. Soc.*, **1960**, 2078.
29) D. L. Brydon and J. I. G. Cadogan, *Chem. Commun.*, **1966**, 744; D. L. Brydon and J. I. G. Cadogan, *J. Chem. Soc., C*, **1968**, 819; J. F. Bunnett and C. C. Wamser, *J. Amer. Chem. Soc.*, **88**, 5534 (1966).

terphenyl undergoes an intramolecular arylation to give XVIII, from which triphenylene produced (Scheme 4, route a, X=Y=I).

Photolytic Cyclodehydrohalogenation of o-Halogenopolyphenyl. Photolytic reactions of iodoarenes were further examined using 2,2′-dihalogenobiphenyls (XV). Irradiation of 2-chloro- and 2-bromo-2′-iodobiphenyls (XV: X=Cl, Br; Y=I) for 79 hr using a 1-kW high-pressure lamp gave triphenylene in 37 and 25% yields respectively. The course of the reaction is illustrated in Scheme 4, route b. 2-Halogeno-*o*-terphenyl (XVI)

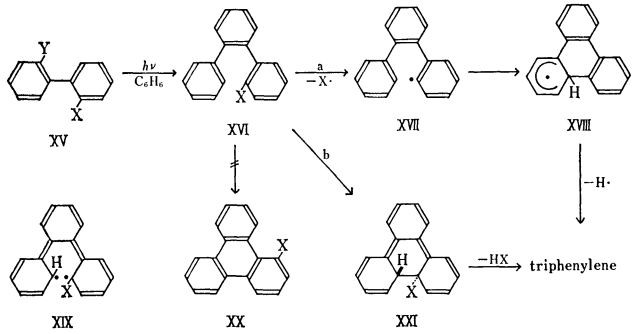

Scheme 4

formed by photolytic phenylation of XV will cyclize to XXI, dehydrohalogenation of which affords triphenylene. A higher electron density at the carbon atom carrying a halogen by its conjugation effect (*e.g.* XIX) is assumed to promote reaction coupled with ready extrusion of hydrogen halide. 2,2′-Dibromobiphenyl (XV, X=Y=Br) was recovered unchanged on irradiation with a high-pressure lamp but was converted to triphenylene (20%) by using a 100-W low-pressure lamp.

An alternative way of cyclization to give 1-halogenotriphenylenes (XX) was not observed although oxidative cyclization leading to them was possible. At least with the chloride it is not likely that triphenylene is formed by the homolysis of C–X bonds after route a. The photolysis proceeds with increasing difficulties as the strength of the C–X bond increases.[24] Under the conditions studied no C–Cl cleavage occurred through C–Br bonds were partially photolyzed particularly when a low-pressure lamp was used.[5] Under conditions where extensive cleavage of the C–Br bond occurs triphenylene formation is possible by both routes a and b.

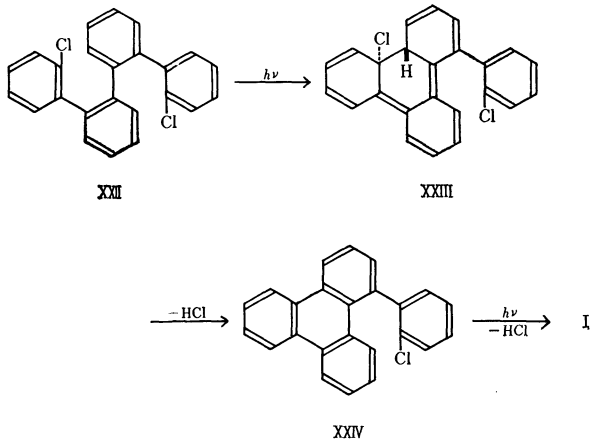

Scheme 5

In contrast to the oxidative cyclizations stated in the preceding sections, the cyclodehydrohalogenation reaction requires no added oxidant. When a benzene solution of 2,2′-bis(2-chlorophenyl)biphenyl (XXII) was irradiated for 20 hr under a stream of nitrogen I was obtained in 67% yield. The course of the reaction assuming an intermediacy of XXIII is shown in Scheme 5. No triphenylene derivative XXIV was detected. The reaction mechanism is in agreement with recent findings on the photolysis of certain *o*-halogenoarenes.[30]

Experimental

Starting Materials. Most compounds were purchased or prepared by the methods described in literature. Several new syntheses and modified procedures will be given below.

1,2,3- and 1,3,5-Triiodobenzene. By reductive deamination[31] of 3,4,5-triiodoaniline[31] 1,2,3- and 1,3,5-triiodobenzenes were produced, and then separated by column chromatography on alumina.

1,2,3-Triiodobenzene was recrystallized from ethanol as colorless plates, mp 110—113°C.[32]

Found: C, 16.07; H, 0.83%. Calcd for $C_6H_3I_3$: C, 15.81; H, 0.66%.

1,3,5-Triiodobenzene was recrystallized from ethanol as colorless needles, mp 177—179°C.[32] IR (KBr): 1735, 1700, 840 cm^{-1}.

Found: C, 16.02; H, 0.70%. Calcd for $C_6H_3I_3$: C, 15.81; H, 0.66%.

Dihalogenobiphenyls. They were prepared by the thermal decomposition of dibenziodolium halides[33] prepared from 2-iodosylbiphenyl by treatment with sulfuric acid followed by anion exchange.

Thermal reactions of dibenziodolium chloride, bromide, and iodide were carried out at 295, 290, and 210°C respectively.[34,35] From each reaction mixture the corresponding 2-halogeno-2′-iodobiphenyls were obtained as the major product. Each halide was purified by column chromatography on alumina: 2-chloro-2′-iodobiphenyl, mp 60—62°C; 2-bromo-2′-iodobiphenyl, mp 87.5—88°C; 2,2′-diiodobiphenyl, mp 108.5—110°C.

2,6-Diiodobiphenyl. 2,6-Diaminobiphenyl prepared by the reduction of 2,6-dinitrobiphenyl[36] was bis-diazotized and then decomposed with potassium iodide. After purification by column chromatography on alumina, it was recrystallized from *n*-hexane as prisms, mp 80—81°C. IR (KBr): 760, 720, 690, and 680 cm^{-1}.

Found: C, 35.62; H, 2.02%. Calcd for $C_{12}H_8I_2$: C, 35.49; H, 2.00%.

4′-Iodo-m-terphenyl. This was prepared from 4′-amino-*m*-terphenyl by diazotization followed by decomposition with potassium iodide, bp 183—187°C/0.2—0.3 mmHg. IR (KBr): 1000, 890, 820, 750, and 690 cm^{-1}.

Found: C, 60.72; H, 3.58%. Calcd for $C_{18}H_{13}I$: C, 60.70;

30) W. A. Henderson, Jr., and A. Zweig, *J. Amer. Chem. Soc.*, **89**, 6778 (1967)
31) H. Gilman, *Org. Synth.*, Coll. Vol. I, 133, 240 (1956).
32) W. J. Hickingbottom in E. H. Rodd, "Chemistry of Carbon Compounds" Vol. III, Elsevier Publishing Co., Amsterdam (1956).
33) J. Collette, D. McGreer, R. Clawford, F. Chubb, and R. B. Sandin, *J. Amer. Chem. Soc.*, **78**, 3819 (1956).
34) T. Sato, S. Shimada, K. Shimizu and K. Hata, This Bulletin, **43**, 1918 (1970).
35) H. Heaney and P. Lees, *Tetrahedron*, **24**, 3717 (1968).
36) C. Bjorklund, M. Nilson, *Acta Chem. Scand.*, **22**, 2338 (1968); C. Bjorklund and M. Nilson, *Tetrahedron Lett.*, **1966**, 675.

H, 3.68%.

4-Cyano-o-terphenyl. a) 4-Amino-*o*-terphenyl[5] was diazotized and treated with cuprous cyanide solution in the usual manner. Vacuum distillation at 158—160°C/1 mmHg produced colorless needles, mp 122.5—123.5°C, recrystallization from *n*-hexane. IR (KBr): 2220 cm^{-1}.

b) A mixture of 17 g (0.055 mol) of 4-bromo-*o*-terphenyl[5] 5.2 g (0.058 mol) of cuprous cyanide in 9 m*l* of pyridine was refluxed for 8 hr.[38] After washing with aqeous ammonia the mixture was extracted with benzene. Extraction with *n*-hexane gave 8.2 g of 4-cyano-*o*-terphenyl.

Found: C, 89.37; H, 5.20; N, 5.31%. Calcd for $C_{19}H_{13}N$: C, 89.38; H, 5.13; N, 5.49%.

Ethyl o-Terphenyl-4-carboxylate. A solution of 10 g (0.039 mol) of 4-cyano-*o*-terphenyl, 80 m*l* of ethanol and 28 m*l* of concentrated sulfuric acid was refluxed for 7 hr was obtained 3.8 g (32%) of the ethyl ester by chromatographical purification. IR (KBr): 1720 cm^{-1} as colorless needles, mp 81—81.5°C. IR (KBr): 1720 cm^{-1}.

Found: C, 83.69; H, 6.02%. Calcd for $C_{21}H_{18}O_2$: C, 83.42; H, 6.00%.

1,2,3-Triphenylbenzene. This was prepared by photolysis of 2,6-diiodobiphenyl in benzene in a 24% yield, mp 156—157°C. IR (KBr): 750, and 690 cm^{-1}.

Found: C, 93.75; H, 6.00%. Calcd for $C_{24}H_{18}$: C, 94.08; H, 5.92%.

2,2'-Bis(2-chlorophenyl)biphenyl (XXII). This was prepared from 2-chloro-2'-iodobiphenyl by the Ullmann reaction carried out at 250—260°C for 20 min, colorless plates from *n*-hexane, mp 129.5—130.5°C. IR (KBr): 760 and 735 cm^{-1}.

Found: C, 76.26; H, 4.30%. Calcd for $C_{24}H_{16}Cl_2$: C, 76.81; H, 4.30%.

3',2''-Diphenyl-1,1':4',1'':4'',1'''-quaterphenyl (X). This was prepared by the Ullmann reaction of 4'-iodo-*m*-terphenyl at 280—300°C, mp>350°C. IR (KBr): 890, 830, 755, and 690 cm^{-1}.

Found: C, 93.71; H, 5.64%. Calcd for $C_{36}H_{26}$; C, 94.28; H, 5.72%.

Photochemical Reactions. Either a 1-kW high-pressure lamp (Wako HBC-1000) or a 100-W low-pressure lamp (Ushio UL2-1HQ) was used as a light source for the external irradiation of sample solutions. For experiments using the high-pressure lamp the set-up was immersed in a bucket kept cool with running water. The spiral-shaped low-pressure lamp was used in combination with a quartz cooling unit into which a reaction vessel made of Vycor was inserted.

Photolyses were carried out under a nitrogen current unless otherwise stated using sample solutions with concentration of *ca.* 1.7×10^{-2}M in appropriate solvents.

The analysis of the reaction mixture was performed by column chromatography on alumina by eluting with *n*-hexane or benzene, or a mixture of the two. Materials were characterized by comparing their physical properties and spectral data with those of the authentic compounds. For a qualitative study gas chromatographical analysis was also employed using a Hitachi K-53 machine in combination with XE-60 silicone gum rubber on chromosorb W column.

Representative results are summarized in Tables 1—4. The preparation of triphenylene and I by the photolytic cyclodehydrogenation reaction of polyphenyl compounds are compiled in Tables 1 and 2. Application of photolytic phenylation reaction is summarized in Tables 3 and 4. Typical examples are given.

1,1':4',1'':4'',1'''-Quaterphenyl. The irradiation of a benzene solution (60 m*l*) containing 403 mg (0.99 mmol) of 4,4'-diiodobiphenyl for 71 hr produced the quaterphenyl in 63% yield, recrystallized from benzene, mp 304—305°C.[39] IR (KBr): 820, 750, and 680 cm^{-1}. UV ($CHCl_3$): 298 nm (log ε 4.75).

Found: C, 94.37; H, 6.08%. Calcd for $C_{24}H_{18}$: C, 94.08; H, 5.92%.

1,3,5-Triphenylbenzene. A solution of 481 mg (1.06 mmol) of 1,3,5-triiodobenzene in 60 m*l* of benzene was irradiated for 147 hr. 1,3,5-Triphenylbenzene was obtained in 79% yield, recrystallized from ethanol as colorless needles, mp 168—170°C.[32] IR (KBr): 870, 740, and 690 cm^{-1}.

Found: C, 93.91; H, 5.90%. Calcd for $C_{24}H_{18}$: C, 94.08, H, 5.92%.

Photolysis of 4'-Iodo-m-terphenyl. A benzene solution (60 m*l*) containing 362.7 mg (1.02 mmol) of 4'-iodo-*m*-terphenyl was irradiated for 48 hr. The product was separated by column chromatography on alumina to give *m*-terphenyl (29%), 2'-phenyl-*p*-terphenyl (5%) and 2-phenyl-triphenylene (28%), mp 180.5—181°C.[5] Recovery of the starting material was 25%.

2'-Phenyl-*p*-terphenyl was characterized by elemental analysis.

Found: C, 93.32; H, 5.88%. Calcd for $C_{24}H_{18}$: C, 94.08; H, 5.92%.

Photolysis of 2,2'-Diiodobiphenyl. Irradiation of 2,2'-diiodobiphenyl resulted in the formation of an insoluble matter which began to separate immediately after the reaction. It was identified as dibenziodolium iodide, mp 210°C dec.,[28] and was obtained in 21% yield.

Gas chromatography analysis of the benzene solution identified 2-iodobiphenyl (1%), *o*-terphenyl (1%), starting material (23%), and triphenylene (3%) in the order of the retention times (Table 4).

Triphenylene. *a) From o-Terphenyl.* Triphenylene was obtained in an almost 90% yield by the photolysis of *o*-terphenyl and iodine in benzene (Table 1). The experimental procedures are essentially the same as before.[4]

b) From 2-Chloro- and -bromo-2'-iodobiphenyls: A solution of 287 mg (0.91 mmol) of 2-chloro-2'-iodobiphenyl in 60 m*l* of benzene was irradiated with the high-pressure lamp for 79 hr. Triphenylene (37%) and the starting material (14%) were isolated.

From 2-bromo-2'-iodobiphenyl 25% of triphenylene was produced, 16% of the starting material being recovered.

Upon irradiation with the low-pressure lamp for 65 hr 2,2'-dibromobiphenyl afforded 20% yield of triphenylene.

2-Cyanotriphenylene (VII, R=CN). A benzene solution (60 m*l*) of 256 mg (1.0 mmol) of 4-cyano-*o*-terphenyl and 258 mg (1.01 mmol) of iodine was irradiated in a quartz vessel using the high-pressure lamp for 96 hr. By repeated recrystallizations from ethanol and chromatography on Florisil 28 mg of colorless needles was obtained, mp 220—221°C. IR (KBr): 2220 cm^{-1}.

Found: C, 89.14; H, 4.39%. Calcd for $C_{19}H_{11}N$: C,90.09; H, 4.38%.

Ethyl Triphenylene-2-carboxylate (VII, R=$COOC_2H_5$). A benzene solution (60 m*l*) of 305 mg (1.01 mmol) of ethyl *o*-terphenyl-4-carboxylate and 256 mg (1.01 mmol) of iodine was irradiated as above. Colorless needles were obtained, mp 129.5—130.5°C, from ethanol. IR (KBr): 1700 cm^{-1}.

Found: C, 83.70; H, 5.34%. Calcd for $C_{21}H_{16}O_2$: C,

37) H. France, I. M. Heilbron, and K. H. Hey, *J. Chem. Soc.*, **1939**, 1288.

38) K. Akanuma, H. Amemiya, T. Hayashi, K. Watanabe, and K. Hata, *Nippon Kagaku Zasshi*, **81**, 333 (1960).

39) W. E. Bachmann and H. T. Clarke, *J. Amer. Chem. Soc.*, **49**, 2094; (1927) S. T. Bowden, *J. Chem. Soc.*, **1931**, 1111.

83.98; H, 5.37%.

Dibenzo[fg,op]*naphthacene (I).* *a) From 2,2′-Diphenylbiphenyl*: A solution of 310 mg (1.0 mmol) of 2,2′-diphenylbiphenyl, mp 116—117°C,[39] λ_{max} 228 nm (log ε 4.54), and 265 mg (1.0 mmol) of iodine in 60 m*l* of benzene was irradiated with a low-pressure lamp through a Vycor vessel. After 72 hr, a crystalline deposit was collected and was recrystallized from xylene, pale yellow prisms, mp 351—352°C,[18] yield 57%. UV (C_6H_6): 373 (log ε 2.36), 363 (2.76), 354 (2.85), 328.5 (4.21), 315 (4.26) and 288 nm (4.73).

Found: C, 95.66; H, 4.71%. Calcd for $C_{24}H_{14}$: C, 95.33; H, 4.67%.

b) From 1,3,5-Triphenylbenzene: Compound I was obtained in 21% yield (Table 2).

c) From 2,2′-Bis(2-chlorophenyl)biphenyl (XXII): A solution of 366 mg (0.98 mmol) of XXII in 60 m*l* of benzene was irradiated with the low-pressure lamp for 20 hr to give 67% of I.

d) From 2,6-Diiodobiphenyl: Among other products compound I was obtained in a low yield (Table 4).

BULLETIN OF THE CHEMICAL SOCIETY OF JAPAN, VOL. 44, 2490—2495 (1971)

Aromatic Bromination by the Use of Organic and Inorganic Thallium Salts[1)]

Sakae UEMURA, Kazuhiro SOHMA, Masaya OKANO, and Katsuhiko ICHIKAWA*

Institute for Chemical Research, Kyoto University, Uji, Kyoto

**Department of Hydrocarbon Chemistry, Faculty of Engineering, Kyoto University, Yoshida, Kyoto*

(Received March 15, 1971)

Using organic and inorganic Tl salts, the following aromatic brominations were carried out in a CCl_4 or HOAc solvent and were found to occur very smoothly; (A) aromatic bromination with $TlBr_3 \cdot 4H_2O$, (B) aromatic bromination with Br_2 in the presence of Tl(III) and Tl(I) salts, and (C) the bromination of arylthallium(III) compounds. From a study of the relative rates and selectivities of benzene and toluene, it was deduced that an arylthallium(III) compound was not involved as an intermediate in the A and B reactions, that Tl(III) salts were more effective catalysts than Tl(I) salts for the B bromination, and that the A reaction was essentially identical with the B reaction with the $TlBr_3 \cdot 4H_2O$ catalyst. By considering the difference in the catalytic behavior of Tl(III) and Tl(I) salts in the B reaction, probable mechanisms are suggested.

Aromatic bromination with bromine in the presence of metallic iron or Lewis acid catalysts (*e.g.*, $FeCl_3$, $FeBr_3$, $AlCl_3$, $AlBr_3$, and $ZnCl_2$) is a well-known reaction.[2)] On the other hand, bromination with a certain metal halide itself, *e.g.*, $CuBr_2$, has also been reported.[3)] In view of the effectiveness of Tl(III) halides as Lewis-acid catalysts,[4-6)] it seems that it would be of interest to know their functions in the two types of bromination described above. Recently it was reported in a communication that, in the presence of Tl(III) acetate, bromine reacted with aromatics to give pure monobromocompounds.[7)] In addition, although it has been known that arylmercury(II) compounds react smoothly with bromine to give aryl bromide,[8)] there have been no reports about the analogous bromination of arylthallium(III) compounds. Hence, some characteristics of the following bromination reatcions were examined; (A) aromatic bromination with $TlBr_3 \cdot 4H_2O$, (B) aromatic bromination with bromine in the presence of Tl(III) and Tl(I) catalysts, and (C) the bromination of arylthallium(III) compounds with bromine. Some findings on the C reaction are of interest in connection with the problem of whether or not an arylthallium(III) compound is involved as an intermediate in the A and B reactions. Probable mechanisms for the Tl(III) and Tl(I) salt-catalyzed brominations were also considered on the basis of their selectivity data.

Results and Discussion

A. Aromatic Bromination with $TlBr_3 \cdot 4H_2O$. Aromatic compounds were added to a mixture of carbon tetrachloride (or acetic acid) and thallium(III) bromide tetrahydrate at the refluxing temperature. The reaction mixture was heterogeneous with molten Tl(III) salt in a CCl_4 solvent, while it was homogeneous in an acetic acid solvent. The red-brown color in the gas and liquid phases which was observed at the initial stage of the reaction because of the partial decomposition of $TlBr_3 \cdot 4H_2O$ [Eq.(1)] gradually disappeared as the reaction proceeded. Indeed, about a 9% conversion of $TlBr_3 \cdot 4H_2O$ to $TlBr \cdot TlBr_3$ in 1hr at 77°C was confirmed iodometrically by a blank experiment. Some

1) Presented at the 23rd Annual Meeting of the Chemical Society of Japan, Tokyo, April, 1970.

2) See for example, R. C. Fuson, "Reactions of Organic Compounds," John Wiley & Sons, New York, N. Y. (1962), p. 58.

3) P. Kovacic and K. E. Davis, *J. Amer. Chem. Soc.*, **86**, 427 (1964).

4) "Friedel-Crafts and Related Reactions," Vol. I, ed. by G.A. Olah, Interscience Publisher, New York, N. Y. (1965), p. 256.

5) L. I. Kashtanov, *J. Gen. Chem(U.S.S.R)*, **2**, 515 (1932); *Chem. Abstr.*, **27**, 975 (1933).

6) E. C. Taylor and A. McKillop, *Accounts of Chem. Res.*, **3**, 338 (1970).

7) A. McKillop, D. Bromley, and E. C. Taylor, *Tetrahedron Lett.*, **1969**, 1623.

8) H. C. Brown and C. W. McGary, Jr., *J. Amer. Chem. Soc.*, **77** 2300 (1955).

Table 1. Reactions of aromatics with $TlBr_3 \cdot 4H_2O$ in CCl_4[a]

Aromatics (100 mmol)	Products mmol (Yield[b] %) [I]	[II]	[III]	Tl^{3+} consumed[c] (%)
Benzene	1.9 (23)	0.4 (10)	0	35
Benzene[d]	1.9 (25)	—	0	32
Toluene	4.7[e] (59)	trace	trace	33
Toluene[d]	5.0[f] (47)	—	1.2 (12)	44
o-Xylene	8.3[g] (78)	0.3 (6)	1.4 (13)	44
p-Xylene	5.9 (60)	0.2 (5)	3.4 (33)	41
Ethylbenzene	4.9[h] (51)	0.7 (15)	0.5 (6)	40
Mesitylene[i]	3.9 (73)	0.4 (8)	—	29
Anisole	10.1[j] (65)	0.2 (3)	—	65
Bromobenzene	—	7.0[k] (77)	—	38

a) $TlBr_3 \cdot 4H_2O$ 24.2 mmol, CCl_4 80 m*l*, 77°C, 1 hr.
b) Calculated on the basis of the amount of consumed Tl^{3+} salt.
c) Determined by iodometry.
d) HOAc (80 m*l*) solvent.
e) $o/p=1.64$; trace of $C_6H_5CH_2Br$ is present.
f) $o/p=1.09$; traces of $C_6H_5CH_2Br$ and $C_6H_5CH_2OAc$ are present.
g) A mixture of approximately equal amounts of 3-bromo and 4-bromoderivatives.
h) $o/p=1.24$
i) 18.6 mmol of $TlBr_3 \cdot 4H_2O$ were used.
j) $o/p=0.049$
k) $o/p=0.33$

$$2TlBr_3 \cdot 4H_2O \longrightarrow Tl[TlBr_4] + Br_2 + 8H_2O \quad (1)$$

typical results are shown in Table 1. The products were monobromocompounds (major) and dibromocompounds (minor), and occasionally diarylmethanes were formed as by-products from alkylbenzenes. The yields of the products were calculated on the basis of the Tl(III) salt consumed according to Eqs. (2), (3), and (4). With less reactive aromatics, such as nitrobenzene,

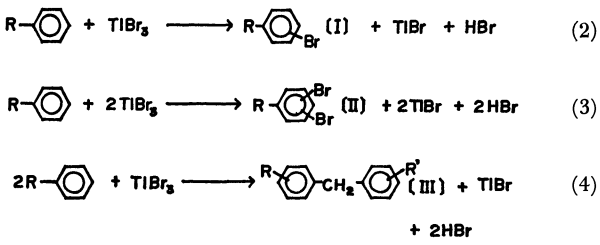

ethyl benzoate, and pyridine, no reaction occurred, even during a longer reaction time at the refluxing temperature. The reaction with benzene and toluene did not occur at 20°C, but with toluene it occurred slowly at 39°C, without any appreciable liberation of bromine. III, the yield of which changed greatly from run to run, could be formed *via* the corresponding benzyl bromides, which were formed by some route or other. A control experiment showed that benzyl bromide and toluene gave a 90% yield of phenyltolylmethane in the presence of $TlBr_3 \cdot 4H_2O$ (see Experimental section).

No evolution of hydrogen bromide was observed, probably because of the complexation with the $TlBr_3$ present [Eq.(5)] giving $HTlBr_4$ as with $HTlCl_4$.[9] This complex seems to suppress further bromination, because an elongation of the reaction time did not lead to an increase in the yields of bromocompounds. The same phenomenon had been observed in the $ZnCl_2$-catalyzed bromination of aromatics.[10]

$$TlBr_3 + HBr \longrightarrow H[TlBr_4] \quad (5)$$

As may be seen in the table, this bromination is rather slow and is apt to be accompanied by some side reactions, so the method is hopeless for preparative purposes.

B. Aromatic Bromination with Bromine in the Presence of Tl(III) and Tl(I) Catalysts. In the presence of small amounts of Tl(III) or Tl(I) salts, aromatics reacted with bromine smoothly in carbon tetrachloride at the refluxing temperature to give pure monobrominated compounds in good yields [Eq. (6)]. The mixtures were heterogeneous (under these experimental conditions only 29—33% of the Tl salts were dissolved in the solvent). In contrast to A reaction, the TlX_3-catalyzed reaction proceeded rather rapidly and a vigorous evolution of HBr gas was observed. Such a difference can be explained by assuming a stronger interaction of the Tl(III) salt with bromine than with

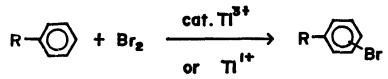

HBr. Some typical data are shown in Table 2. From toluene, a mixture of *o*- and *p*-bromotoluenes was rapidly obtained; in this mixture Tl(III) and Tl(I) catalysts favoured *o*-isomer formation and *p*-one formation respectively, while only traces of the *m*-isomer were

Table 2. Aromatic bromination by Tl catalyst[a]

Aromatics (100 mmol)	Catalyst (1.3mmol)	React. time (min)	Products [I] mmol (yield, %)
Benzene	$TlBr_3 \cdot 4H_2O$	5	22.2 (89)
Benzene	$Tl(OAc)_3$	5	20.7 (83)
Benzene	TlOAc	120	11.3 (45)
Benzene	TlBr	300	15.9 (64)
Benzene	$Hg(OAc)_2$	60	trace
Benzene	$Pb(OAc)_4$	60	trace
Benzene	—	60	—
Toluene	$Tl(OAc)_3$	5	24.2 (97)[b]
Toluene	$TlBr_3 \cdot 4H_2O$	5	23.0 (92)[c]
Toluene	TlBr	5	20.0 (80)[d]
Toluene	—	5	20.0 (80)[e]
Bromobenzene	$Tl(OAc)_3$	90	16.7 (67)

a) CCl_4 80 m*l*, Br_2 25 mmol, 77°C. b) $o/2p=0.67$ c) $o/2p=0.70$ d) $o/2p=0.24$ e) Only $C_6H_5CH_2Br$ was obtained.

9) R. J. Meyer, *Z. Anorg. Allg. Chem.*, **24**, 337 (1900).
10) L. J. Andrews and R. M. Keefer, *J. Amer. Chem. Soc.*, **78**, 4549 (1956).

Table 3. Bromination of arylthallium (III) compounds[a]

ArTlXY	(mmol)	Br_2 (mmol)	React. time (min)	Products mmol (%)[b] [I]	[II]
$C_6H_5Tl(OAc)(ClO_4\cdot H_2O)$	10	25	120	6.5 (65)	1.3 (13)
	2.5	4	20	2.2 (88)	—
p-$CH_3C_6H_4Tl(OAc)(ClO_4\cdot H_2O)$	10	25	120	—	8.0 (80)
	1.6	2.6	20	1.1 (69)	trace
p-$CH_3C_6H_4Tl(OAc)Br$	1.6	1.6	20	1.1 (69)	trace
$(C_6H_5)_2TlBr$	5.8	11.6	60	10.1 (87)	—
$C_6H_5Tl(OAc)(ClO_4\cdot H_2O)$	10 [c]	10	3	1.63 (16.3)	trace
p-$CH_3C_6H_4Tl(OAc)(ClO_4\cdot H_2O)$	10 [c]	10	3	2.22 (22.2)	0.15 (1.5)

a) CCl_4 80 m*l*, 77°C. b) Calculated on the basis of Br_2. c) Competitive reaction, $k_T/k_B=1.45$.

formed (detected by studying the NMR spectra). When enough water to dissolve the Tl(III) salt (more than 0.9 g in this case) was added to the reaction mixture, the major product from toluene became benzyl bromide rather than bromotoluenes. Under comparable reaction conditions without a Tl(III) or Tl(I) catalyst, benzene gave no brominated compounds, while toluene gave only benzyl bromide, even in the dark. In sharp contrast to Tl(III) acetate, mercury(II) and lead (IV) acetates, which have an isoelectronic structure with the Tl(III) salt and which exhibit similar behavior in many reactions,[11] showed no catalytic action in this bromination. Tl(III) salts are more effective than Tl(I) salts as catalysts; this is clearly reflected by the yields of bromobenzenes from benzene.

C. Bromination of Arylthallium(III) Compounds with Bromine. When bromine was added to a suspension of arylthallium(III) compounds (ArTlXY) in carbon tetrachloride at the refluxing temperature, the desired brominated products were readily obtained in good yields regardless of the kinds of X and Y [Eq.(7)]. However, the presence of excess bromine resulted in the formation of dibrominated compounds [Eq. (8)]. Some typical data are shown in Table 3.

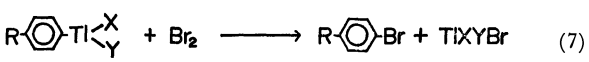

(7)

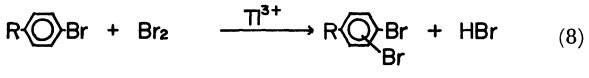

(8)

(R=H, CH_3; X,Y=OAc, ClO_4; OAc, Br; C_6H_5, Br)

From a competitive reaction of the phenylthallium(III) compound and the p-tolyl compound (X=OAc, Y=ClO_4) the relative rate ratio, k_T/k_B, was determined; its value was nearly 1.5 (in CCl_4 at 77°C). In the case of X=OAc and Y=Br, a similar value was obtained. Hence, it seems reasonable to assume that the k_T/k_B ratios for the bromination of $ArTlBr_2$ or $ArTl(OAc)_2$ are nearly 1 or 2. This means that the bromination of the phenylthallium(III) compounds and the p-tolyl compound proceeds at similar rates. These estimated k_T/k_B values differ from those values (7 and 24 for $TlBr_3\cdot 4H_2O$ and $Tl(OAc)_3$ respectively) obtained in the Tl(III) salt-catalyzed reaction B, to be described below. In the B reaction, if rate-determining aromatic thallation is involved, this disagreement can be understood. However, the reported k_T/k_B value (2.6) for aromatic thallation[12] also disagrees with the values for the B reaction. In addition, the following experimental fact must be noted. Although arylthallium (III) compounds reacted easily with KI to give aryliodides,[6] when a mixture of 10 mmol of $TlBr_3\cdot 4H_2O$ and 40 m*l* of HOAc was treated with 50 mmol of KI (H_2O: HOAc=1:1 solution) and 50 mmol of benzene at 100°C, no traces of iodobenzene and phenylacetate (the acetolysis product of iodobenzene) were formed. Aromatic thallation is rather slow and can usually occur in polar solvents and under acidic conditions when reactive aromatics or strong electrophilic Tl(III) salts such as $Tl(OCOCF_3)_3$ are used as substrates.[6,13] Therefore, in a nonpolar CCl_4 solvent the possibility of aromatic thallation seems very rare.[7] From all these facts, it can be deduced that the Tl(III)-catalyzed bromination does not proceed *via* an arylthallium (III) compound.

D. Relative Reactivities of Benzene and Toluene in the A and B Brominations. In order to ascertain the nature of the transition states of bromination using

11) See for example, W. Kitching, *Organometal. Chem. Rev.*, **3**, 35, 61 (1968).

12) P. M. Henry, *J. Org. Chem.*, **35**, 3083 (1970).

13) K. Ichikawa, S. Uemura, T. Nakano, and E. Uegaki, This Bulletin, **44**, 545 (1971).

Table 4. Competitive bromination of benzene and toluene[a)]

Tl salt (mmol)	Br_2 (mmol)	Solvent (80 ml)	React. temp. (°C)	React. time (min)	Bromotoluene[b)] k_T/k_B	Bromotoluene[b)] $o/2p$	Total[c)] yield (mmol)
$TlBr_3 \cdot 4H_2O$ (24.2)	—	CCl_4	77	5	15	0.80	4.7[d)]
$TlBr_3 \cdot 4H_2O$ (24.2)	—	CCl_4	39	120	6.5	0.84	6.9
$TlBr_3 \cdot 4H_2O$[e)] (24.2)	—	CCl_4	39	120	5.4	0.76	4.5
$TlBr_3 \cdot 4H_2O$ (24.2)	—	HOAc	114	5	44	0.59	4.7
$TlBr_3 \cdot 4H_2O$ (1.0)	25	CCl_4	77	5	7	0.67	17.5
$Tl(OAc)_3$ (1.3)	25	CCl_4	77	5	24	0.60	17.5
TlOAc[f)] (1.0)	10	CCl_4	77	5	293	0.30	8.0
TlBr[f)] (1.3)	10	CCl_4	77	5	705	0.22	7.6

a) Benzene (100 mmol), toluene (100 mmol). b) No or trace amounts of *m*-bromotoluene were formed. c) Sum of bromotoluene and bromobenzene; unless otherwise noted no dibromocompounds were found. d) Traces of dibromocompounds were found. e) Benzene (200 mmol), toluene (100 mmol). f) Benzene (100 mmol), toluene (10 mmol).

Table 5. Partial rate factors for bromination of toluene

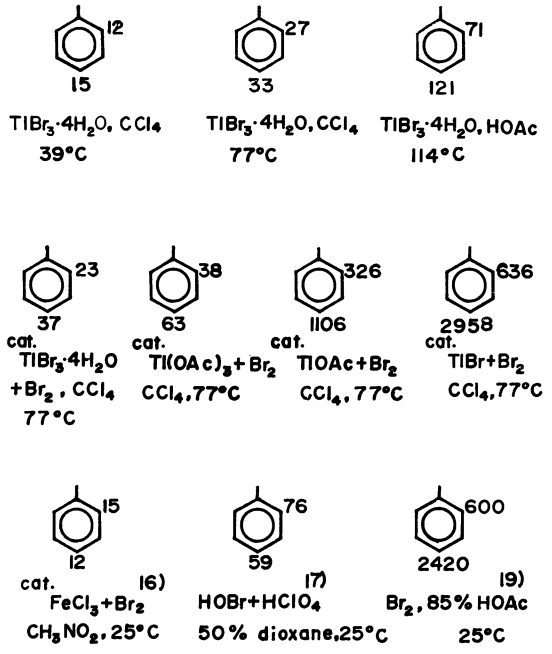

Tl salts, competitive reactions of benzene and toluene were carried out under various conditions. Some data on the relative rate ratio (k_T/k_B) and on the isomer ratio ($o/2p$) in the bromotoluenes formed are shown in Table 4. Neither the k_T/k_B ratio nor the $o/2p$ ratio changed significantly when the reaction time for a TlX_3-catalyzed reaction was varied from 5 to 60 min. On the basis of these data, partial rate factors were calculated; they are listed in Table 5, together with some previously reported values. Table 4 shows that the positional selectivity (reflected by the $o/2p$ ratio) increases with an increase in the substrate selectivity (k_T/k_B ratio). This is a general correlation which has been established in several electrophilic substitutions of aromatics.[14)] Our data on relative reactivities are rather limited and are not precise enough for us to undertake a detailed discussion; however, at least the following qualitative deductions are possible. First, there are no significant differences in either the k_T/k_B or $o/2p$ ratio for the two bromination reactions (A and B) using $TlBr_3 \cdot 4H_2O$. This suggests that the A and B brominations are essentially the same. Second, the remarkable differences in both the k_T/k_B ratio and the partial rate factor between TlX_3- and TlX-catalyzed brominations suggests two distinct attacking species for the two reactions. In the Tl(III)-catalyzed reaction, the observed k_T/k_B ratios were of the same order as those for the reaction with other metal chlorides catalysts (*e.g.*, 10—31 for $AlCl_3$ in $C_6H_5NO_2$ at 30°C, and 10—21 in CH_3NO_2,[15)] 3.6—32 for $FeCl_3$ in CH_3NO_2 at 25°C,[16)] and 148 for $ZnCl_2$ in HOAc at 25.4°C[10)]). The partial rate factors obtained were also comparable to those values for the $FeCl_3$-catalyzed bromination with bromine (in CH_3NO_2)[16)] and the perchloric acid-catalyzed bromination with hypobromous acid (in 50% dioxane).[17)] For the latter reaction, kinetic evidence for the attack of Br^+ or its hydrated form has also been given.[18)] On the other hand, in the Tl(I)-catalyzed reaction, both values (the k_T/k_B ratios and the partial rate factors) were quite large and were comparable to those for a bromination without a catalyst (in 85% HOAc),[19)] in which molecular bromine is considered to be the reactive species.[18)] Recently Olah[20)] cited a clear correlation between the electrophilicity of the reagent and the nature of the transition state. He reached the following conclusions. When the electrophilic species is sufficiently reactive, *i.e.*, in the case of a low k_T/k_B value and a high $o/2p$ ratio, the position of the transition state is represented by a much earlier state resembling the starting aromatics (oriented π-complex-like); on the other hand, in the reaction with a weak electrophile (a high k_T/k_B value and a low $o/2p$

14) See for example, R. O. C. Norman, and R. Taylor, "Electrophilic Substitution in Benzenoid Compounds," Elsevier Publishers, (1965), p. 56.

15) S.Y. Caille and R.J.P. Corrin, *Chem. Commun.*, **1967**, 1251.

16) G. A. Olah, S. J. Kuhn, S. H. Flood, and B. A. Hardie, *J. Amer. Chem. Soc.*, **86**, 1039 (1964).

17) P.B.D. de la Mare and J.T. Harvey, *J. Chem. Soc.*, **1956**, 36.

18) a) C. K. Ingold, "Structure and Mechanism in Organic Chemistry," 2nd ed., Cornell Univ. Press (1969),p. 345. b) Ref. 14 p. 122 and p. 130.

19) H.C. Brown and L.M. Stock, *J. Amer. Chem. Soc.*, **79**, 1421 (1957).

20) G. A. Olah, M. Tashiro, and S. Kobayashi, *ibid.*, **92**, 6369 (1970).

ratio), a late transition state resembling the intermediate (σ-complex-like) is involved. Taking account of this conclusion and the observed differences in selectivities, we propose the following reaction paths and transition states for these reactions. When the Tl (III) catalyst is used, the reaction may involve the initial formation of a polarized complex (probably an ion-pair containing Br^+) from Br_2 and TlX_3 and its subsequent attack on aromatics (oriented π-complex). The latter step would be rate-determining. In the case of the Tl (I) catalyst, the interaction between aromatics and Br_2 would be more important than that between Br_2 and TlX, for the Tl (I) salt is expected to be a rather weak Lewis acid because of two s-electrons in the outer shell. The transformation of the ArH·Br_2 (π-complex) to the ArH·Br^+ (σ-complex) would be essentially rate-determining, and Tl (I) salt may assist in breaking the Br-Br bond. The transition states for these reactions may be represented as follows:

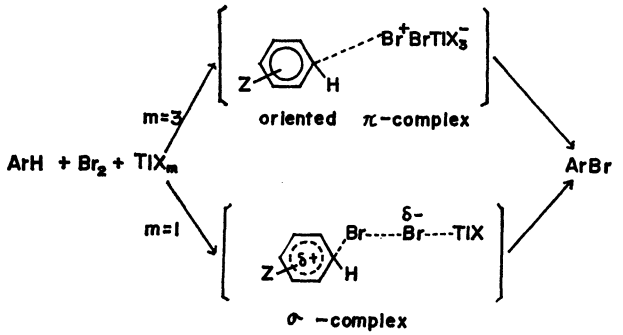

Experimental

Materials. All the starting materials were used after distillation. The $TlBr_3 \cdot 4H_2O$ (mp 40—42°C, lit, 40°C;[21] the purity as determined by iodometry was greater than 97%), TlBr and TlOAc were commercial products. The $Tl(OAc)_3$ was prepared by dissolving Tl_2O_3 into acetic acid at 60°C for 20 hr, collecting white crystals after cooling, and drying over CaO (the purity was greater than 98%). The arylthallium (III) compound ($C_6H_5TlOAc \cdot ClO_4 \cdot H_2O$ and p-$CH_3C_6H_4TlOAc \cdot ClO_4 \cdot H_2O$) were prepared by the reaction of benzene or toluene with $Tl(OAc)_3$ in the HOAc-$HClO_4$ solvent. The synthetic method of these compounds was described in detail in a separate paper.[13] p-$CH_3C_6H_4TlOAcBr$ was prepared by the addition of an aqueous KBr solution to the aqueous p-$CH_3C_6H_4TlOAc \cdot ClO_4 \cdot H_2O$ solution at room temperature. The white precipitates which were formed instantly were recrystallized from benzene; mp>300°C (Found: C, 24.42; H, 2.22%. Calcd for $C_9H_{10}O_2TlBr$: C, 24.89; H, 2.32%). The phenyl analogues were prepared similarly. The diphenylthallium(III) bromide was prepared from phenylboric acid and $TlBr_3 \cdot 4H_2O$ in boiling water according to the reported method;[22] mp>300°C (Found: C, 32.86; H, 2.18%. Calcd for $C_{12}H_{10}TlBr$: C, 32.87; H, 2.30%).

Reaction of Aromatics with $TlBr_3 \cdot 4H_2O$. An aromatic compound (100 mmol) was added to a suspension of molten $TlBr_3 \cdot 4H_2O$ (24.2 mmol) in 80 m*l* of CCl_4 at the refluxing temperature (77°C). The reaction mixture was kept at that temperature for 1 hr, during which period the red-brown color of bromine which was observed at the initial stage gradually disappeared. Yellowish-white precipitates were filtered off, and the filtrate was washed with water and a sodium bicarbonate solution, dried over Na_2SO_4, and distilled. All the products were analyzed by g.l.c. and by a study of the IR and NMR spectra. The $o/2p$ ratio of isomeric bromotoluenes (bp 72°C/20 mmHg), bromoethylbenzenes (bp 71°C/10 mmHg), and bromoanisoles (bp 77°C/7 mmHg) were also determined by g.l.c. and by a study of the NMR spectra (for example, methyl protons of o- and p-bromotoluenes were observed at τ 7.62 and 7.73 respectively).

Bromination of Benzene with Bromine in the Presence of the $TlBr_3 \cdot 4H_2O$ Catalyst. Benzene (100 mmol) was added to a mixture of CCl_4 (80 m*l*), Br_2 (25 mmol) and $TlBr_3 \cdot 4H_2O$ (1.3 mmol) at the refluxing temperature (77°C). After 5 min, the red-brown color of the solution completely disappeared. The reaction mixture was then cooled rapidly and treated as has been described above to give 22.2 mmol of bromobenzene; bp 50°C/20 mmHg (yield, 89%).

Reaction of p-*Tolylthallium(III) Acetate Perchlorate Monohydrate with Bromine.* Carbon tetrachloride (42 m*l*) containing 25 mmol of bromine was added to a mixture of the p-tolylthallium(III) compound (4.72 g, 10 mmol) and CCl_4 (38 m*l*) at 77°C. The red-brown color of bromine gradually disappeared, while the evolution of HBr gas was observed. After 2 hr, the reaction mixture was cooled and worked up as usual. The only products obtained were isomeric dibromotoluenes; no isomeric bromotoluenes was detected by g.l.c. Distillation gave a mixture of dibromotoluenes, which were shown by their IR spectra to be 1-methyl-2,4-dibromotoluene and 1-methyl-3,4-dibromotoluene. Yield, 2.0 g (80%); bp 100—130°C/3.5 mmHg.

Reaction of p-*Tolylthallium(III) Acetate Bromide with Bromine.* A CCl_4 (2.6 m*l*) containing 1.6 mmol of bromine was added to a mixture of p-tolylthallium(III) acetate bromide (1.6 mmol) and CCl_4 (27.4 m*l*) at 77°C. Within 1 min, the bromine disappeared; after 20 min, the reaction mixture was cooled rapidly and treated as has been described above. G.l.c. analysis with bromobenzene as the internal standard showed that 1.06 mmol (yield, 66%) of p-bromotoluene and a trace of dibromotoluene were the only products.

Competitive Bromination of Benzene and Toluene in the Presence of $TlBr_3 \cdot 4H_2O$ Catalyst. A mixture of benzene (100 mmol) and toluene (100 mmol) was added to a stirred mixture of CCl_4 (80 m*l*), Br_2 (25 mmol) and $TlBr_3 \cdot 4H_2O$ (1 mmol) at 77°C. After 5 min, the reaction mixture was cooled rapidly and worked up as usual. The amounts of bromobenzene and isomeric bromotoluenes and the $o/2p$ ratio of the latter compounds were determined by g.l.c. analysis. The total yield of both bromocompounds was 76%, and the k_T/k_B value was 7.

Competitive Bromination of the Phenylthallium(III) Compound and the p-*Tolyl Compound.* A CCl_4 (40 m*l*) solution of bromine (10 mmol) was stirred into a suspension of equimolar (each 10 mmol) amounts of $C_6H_5TlOAc \cdot ClO_4 \cdot H_2O$ and p-$CH_3C_6H_4TlOAc \cdot ClO_4 \cdot H_2O$ in CCl_4 (40 m*l*) at 77°C. After 3 min, the reaction was stopped. G.l.c. analysis showed that bromobenzene (1.63 mmol), bromotoluenes (2.22 mmol), and dibromotoluenes (0.15 mmol) were thus formed.

Authentic Samples for G.l.c. Analysis. The bromobenzene, o-, m-, and p-bromotoluenes, o-, m-, and p-bromoanisoles, o- and p-dibromobenzenes, were commercial products. The bromoxylenes, bromomesitylene and bromoethylbenzenes were each isolated and determined by studying their NMR and IR spectra. The dibromoalkylbenzenes were prepared from bromine and the corresponding monobromoalkylbenzenes.

21) V. Thomas, *Ann. Chim. Phys.*, **11**, 204 (1907).
22) F. Challenger and B. Parker, *J. Chem. Soc.*, **1931**, 1462.

The isomeric phenyltolylmethanes (*o*- and *p*-) were prepared by heating benzyl bromide (20 mmol) and toluene (100 mmol) in the presence of the $TlBr_3 \cdot 4H_2O$ (25 mmol) catalyst at 77°C for 1 hr; yield, 3.1 g (18 mmol, 90%); *o*/*p*= 1.38; bp 100—102°C/2 mmHg. The *p*-tolyl-*p*-xylyl-methane was prepared from *p*-xylene, $Tl(OAc)_3$, and $HClO_4$ by a method reported in a separate paper.[13] Diarylmethanes from *o*-xylene and ethylbenzene could not be isolated in the pure form, but their NMR spectra revealed the presence of a methylene proton at τ 6.0—6.20.

Spectral Measurements. The NMR spectra were determined by a Varian A-60 spectrometer, using TMS as the internal standard in $CDCl_3$. The IR spectra were obtained by means of HITACHI EPI-2 and EPS-3T. G.l.c. analysis was carried out on a SHIMADZU 5APTF apparatus, using PEG 6000 (25%)-Chromosorb-W 3-m and Apz-L (30%)-Celite 3-m columns and on a HITACHI F-6 apparatus using Apz-L 1-m columns.

BULLETIN OF THE CHEMICAL SOCIETY OF JAPAN, VOL. 44, 2495—2501 (1971)

A New Rearrangement Reaction of Azoxybenzene with Arenesulfonyl Chloride

Shigeru OAE, Tetsuya MAEDA, Seizi KOZUKA, and Mamoru NAKAI
Department of Applied Chemistry, Osaka City University, Sugimoto-cho Sumiyoshi-ku, Osaka
(Received March 15, 1971)

Azoxybenzene was found to react with arenesulfonyl chloride to afford *o*- or *p*-arenesulfonyloxyazobenzene. This new rearrangement reaction is found in various substituted azoxybenzenes and arenesulfonyl chlorides. By the use of the ^{18}O tracer technique, the *ortho* rearrangement was found to proceed *via* an intramolecular path, while the rearrangement to the *para* position was intermolecular. The yields of the rearranged products were determined by the isotopic dilution technique, while the migratory aptitude was also determined by the use of azoxybenzene-1-^{14}C. It was found that the ratio of the sulfonyloxy migration to the phenyl ring attached to the azoxy side to that of the azo side is 1 to 2 for the *ortho* rearrangement. On the bases of these observations, the mechanism of this new rearrangement reaction is discussed.

Azoxybenzene is known to undergo Wallach rearrangement in strong acidic media, such as sulfuric,[1] chlorosulfonic,[2] and fluorosulfonic acids,[3] to afford *p*-hydroxy azobenzene, and the reaction has been shown by an ^{18}O tracer experiment[4] to be an acid-catalyzed[5] intermolecular rearrangement. The following two mechanisms have been suggested:[6]

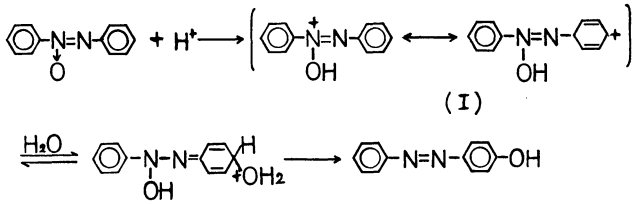

(I)

$+H_2O + H^+$ (I)

The former one is similar to that of the Bamberger reaction[7] and involves the initial formation of an intermediate (I), upon which subsequent nucleophilic attack by either water or a $-OSO_3H$ group takes place, while the other perhaps involves the symmetrical dication (II), in which both phenyl rings are liable to nucleophilic attack.

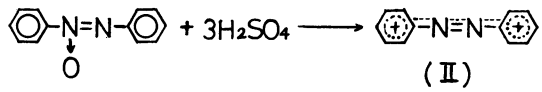

(II)

$+ H_3O^+ + 3HSO_4^-$ (2)

Meanwhile, the reactions of pyridine and isoquinoline *N*-oxides with arenesulfonyl chloride are known to give 3-pyridyl and 4-isoquinolyl arenesulfonates, apparently *via* the oxygen-bridged ion-pair path[8] (III):

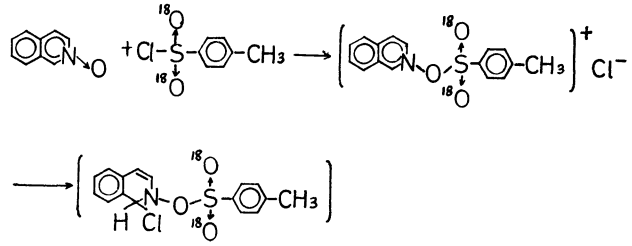

1) O. Wallach and L. Belli, *Ber*, **13**, 525 (1880).
2) V. O. Lukashevich and T. N. Kurdyumova, *Zh. Obshch, Khim.* **18**, 1963 (1948).
3) T. E. Stevens, *J. Org. Chem.*, **33**, 2667 (1968).
4) S. Oae, T. Fukumoto, and M. Yamagami, This Bulletin, **36**, 601 (1963).
5) M. M. Shemyakin, T. E. Agadzharyan, V. I. Maimind, and R. V. Kundryavtsen, *Izv. Akad. Nauk SSSR, Ser. Khim.*, **1963**, 1339.
6) H. J. Shine, "Aromatic Rearrangement," Elsevier Publ. Co., New York (1967), p. 275.
7) a) C. K. Ingold, "Structure and Mechanism in Organic Chemistry," 2nd. Ed., Cornell Univ. Press, The George Bunta Company, Inc. (1969), p. 907; b) M. Murakami and Y. Yukawa, "Name Reaction in Organic Chemistry," (Jinmei-Yuki-Hannoshu), Vol. II, Asakura Book Publ. Co., Tokyo (1954), p. 228.
8) S. Oae, K. Ogino, S. Tamagaki, and S. Kozuka, *Tetrahedron*, **25**, 5761 (1969).

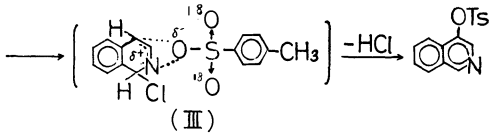

(III)

On the other hand, it has been suggested that the reaction of phenyl hydroxylamine with the same reagent to give *o*-hydroxy aniline proceeds through a concerted 6-membered cyclic process (IV).[9]

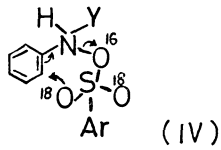

(IV)

In both cases, the initial step of the reaction is believed to be the sulfonylation of the *N*-oxide function. Therefore, it seemed that it would be interesting to use acylating agents, *e.g.*, acetic anhydride or arenesulfonyl chloride, for the study of the rearrangement of azoxybenzene, since, if the initial acylation proceeds successfully at the *N*-oxide function, then the subsequent rearrangement would proceed as in the similar rearrangement of a number of tertiary amine *N*-oxides with acylating agents. The Wallach reaction and the rearrangements of aromatic amine oxide with acylating agents have one common feature, *i.e.*, the generation of a cationic center in the course of the reaction. As in the Kuhara modification[10] of the Beckmann rearrangement of oximes the arenesulfonylation of the azoxy group may lead to an interesting modification of the Wallach rearrangement. Thus, we have investigated the title reaction and now wish to report a new rearrangement to afford *o*- and *p*-arenesulfonyloxyazobenzenes.

Results and Discussion

Unlike other aromatic and heteroaromatic oxides, the reaction of azoxybenzene with acetic anhydride[11] is sluggish and affords mainly reduced products, such as acetanilide and azobenzene. On the other hand, the reaction of azoxybenzene with arenesulfonyl chloride gave rearranged products, *i.e.*, *o*- and *p*-arenesulfonyloxyazobenzenes, along with arenesulfonic acid and hydrogen chloride. The reaction is also rather sluggish without a solvent, but proceeds smoothly in a polar solvent such as nitrobenzene. The results are summarized in Table 1. The yields of the products were determined by means of the isotopic dilution method using azoxybenzene-1-^{14}C.[12] The following five successive steps are conceivable for this rearrangement: (1) the sulfonylation of azoxy oxygen, (2) the nucleophilic attack of the chloride anion, (3) the

Table 1. The reaction of azoxybenzene-1-^{14}C with various sulfonyl chloride in nitrobenzene

Sulfonyl Chloride Reaction Conditions	Products Yield(%)	M.P. (°C)
O_2N-C$_6$H$_4$-SO_2Cl 110°C, 25hr	C$_6$H$_5$-N=N-C$_6$H$_4$-OSO_2-C$_6$H$_4$-NO_2 (59.7) C$_6$H$_5$-N=N-C$_6$H$_4$-OSO_2-C$_6$H$_4$-NO_2 (24.8)	144-6 170-1
Br-C$_6$H$_4$-SO_2Cl 110°C, 30hr	C$_6$H$_5$-N=N-C$_6$H$_4$-OSO_2-C$_6$H$_4$-Br (28.8) C$_6$H$_5$-N=N-C$_6$H$_4$-OSO_2-C$_6$H$_4$-Br (36.8)	100-1 175-6
CH_3-C$_6$H$_4$-SO_2Cl 110°C, 50hr	C$_6$H$_5$-N=N-C$_6$H$_4$-OSO_2-C$_6$H$_4$-CH_3 (0.6) C$_6$H$_5$-N=N-C$_6$H$_4$-OSO_2-C$_6$H$_4$-CH_3 (61.4)	85-6 159-60
CH_3SO_2Cl 110°C, 50hr	C$_6$H$_5$-N=N-C$_6$H$_4$-OSO_2CH_3 (63.8)	156-7

9) G. T. Tisue, M. Grassmann, and W. Lworuski, *ibid.*, **24**, 999 (1968).

10) M. Kuhara, K. Matsumiya, and N. Matsunami, *Mem. Coll. Sci. Univ. Kyoto*, **1**, 105 (1914); *Chem. Abstr.*, **9**, 1613 (1915).

11) S. Oae, T. Maeda, and S. Kozuka, This Bulletin, **44**, 442 (1971).

12) L. C. Behr and E. C. Hendley, *J. Org. Chem.* **31**, 2715 (1966).

cleavage of the N–O bond, (4) the nucleophilic attack of the sulfonate group at either the *o*- or the *p*-position of either phenyl ring, and (5) the elimination of hydrogen chloride.

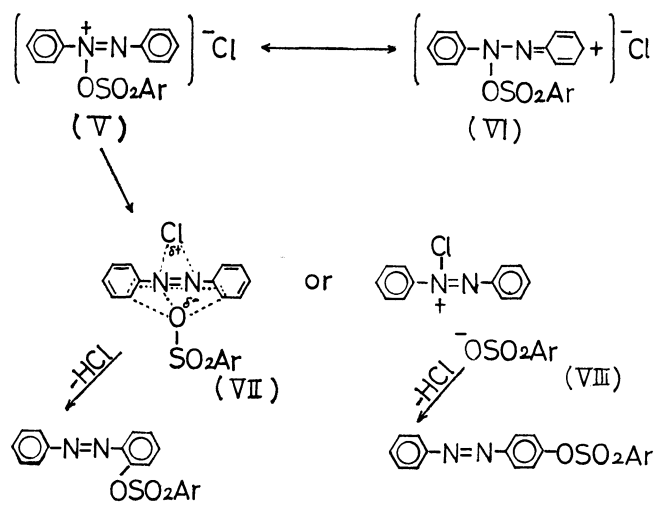

The formation of V is reasonable because, in the similar reaction of isoquinoline *N*-oxide with tosyl chloride, the formation of a similar *N*-tosyloxy salt was actually observed.[8] The nucleophilic attack of the chloride ion on the –N=N– group VII or VIII may be considered on the basis of the following evidence.

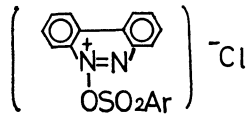

(IX)

i) In the reaction of sterically twisted benzocinnoline *N*-oxide with *p*-nitrobenzenesulfonyl chloride, no rearranged product was obtained because of the steric hindrance of the attack of the chloride ion on the azo group after the arenesulfonylation of the *N*-oxy function (IX).

ii) If chloride ion attacks the *para* position of azoxybenzene, which is considered to be the most active site for nucleophilic attack,[13] *p*-chloroazobenzene could be found in the reaction of azoxybenzene with *p*-nitrobenzenesulfonyl chloride as in the reaction of quinoline *N*-oxide with tosyl chloride to give 4-chloroquinoline.[14] However, the results of the isotopic dilution analysis showed no formation of *p*-chloroazobenzene.

iii) When both *para* positions are blocked by substituents, as in the case of *p,p'*-dimethylazoxybenzene, the rearrangement to the *ortho* position occurs as is shown below:

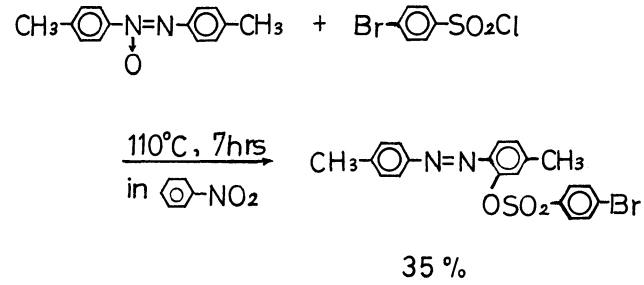

Therefore, the attack of the chloride anion on the *para* position of VI does not seem as a prerequisite step for this rearrangement. Apparently the rearrangement proceeds easily with a better leaving *p*-nitrobenzenesulfonyloxy group, as in many other rearrangements involving electron-deficient centers. The data in Table 1 show that the ratio of the *ortho* migration to the *para* migration changes with the change in the *para* substituent on benzenesulfonyl chloride. That is, the rearrangement to the *ortho* position is predominant when the substituent is the nitro group. On the other hand, the rearrangement occurs mainly to *para*, accompanied by only a minor *ortho* rearrangement, when an electron-releasing methyl group is substituted. When the chloride ion approaches the azo group of V, a better leaving group, such as *p*-nitrobenzenesulfonate, would cleave heterolytically and migrate to the *ortho* position intramolecularly *via* the formation of the transition complex VII. In the case of *p*-methylbenzenesulfonate, which is a poor leaving group in comparison with *p*-nitrobenzenesulfonate, the chloride ion is added before the cleavage and VIII is formed prior to the rearrangement to the *para* position, since the *para* position of II is a much more electron-deficient site than the *ortho* position from the calculation of the electron density using the ω technique.[13] Our usual ^{18}O tracer experiments were carried out with ^{18}O-labelled *p*-substituted arenesulfonyl chloride: the findings on the ^{18}O distributions of the sulfonates, hydrolyzed products, *etc.* are tabulated in Table 2.

An inspection of the data reveals that the whole pattern of migration is very similar to that of the Wallach rearrangement. That is, *o*-brosyloxyazobenzene retains the original oxygen atom of azoxybenzene, implying an intramolecular oxygen-bridged ion-pair process for the *ortho* migration. On the other hand, all the oxygen atoms of *p*-brosyloxyazobenzene are completely scrambled, suggesting a solvent-separated ion-pair process or an intermolecular nucleophilic process for the *para* migration.

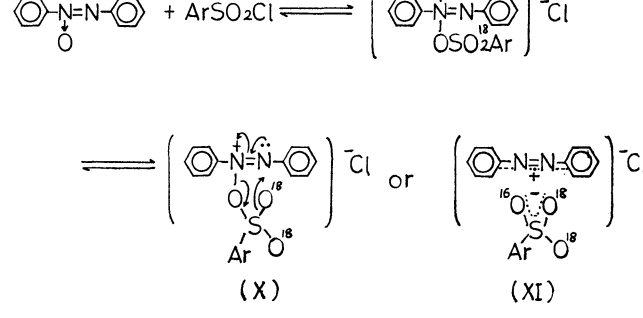

(X) (XI)

13) B. S. Thyagarajan, "Mechanism of Molecular Migrations," Vol. 1, John Wiley & Sons, Inc., New York (1968), p. 101.

14) M. Murakami and E. Matsumura, *Nippon Kagaku Zasshi*, **72**, 509 (1951).

TABLE 2. ^{18}O ANALYTICAL RESULTS OF THE REACTON OF AZOXYBENZENE WITH *p*-SUBSTITUTED ARENESULFONYL CHLORIDE

Compounds	Excess atom% ^{18}O(calc.)
Br-C$_6$H$_4$-SO$_2$Cl	1.18
C$_6$H$_5$-N=N-C$_6$H$_3$(OSO$_2$-C$_6$H$_4$-Br)-	0.77(0.79)
C$_6$H$_5$-N=N-C$_6$H$_3$(OH)-	0.17
C$_6$H$_5$-N=N-C$_6$H$_3$(OSO$_2$-C$_6$H$_4$-Br)-	o.79(o.79)
C$_6$H$_5$-N=N-C$_6$H$_3$(OH)-	0.79
Br-C$_6$H$_4$-SO$_3$H (as thiuronium salt)	o.82
C$_6$H$_5$-N(→O)=N-C$_6$H$_5$ (recovered)	o.14
O$_2$N-C$_6$H$_4$-SO$_2$Cl	o.68
C$_6$H$_5$-N=N-C$_6$H$_3$(OSO$_2$-C$_6$H$_4$-NO$_2$)-	o.52(o.54)
C$_6$H$_5$-N=N-C$_6$H$_3$(OH)-	0.28

TABLE 3. THE COUNTING DATA OF THE PHOTOLYSIS OF AZOXYBENZENE-1-^{14}C

Substance	Activity
C$_6$H$_5$-N(→O)=N-C$_6$H$_5$	3.08x10^{5}dpm/m mole
C$_6$H$_5$-NHCO-C$_6$H$_5$	3.84x10^4 "
C$_6$H$_5$-NH$_2$ (OH)	2.77x10^5 "

The small excess of ^{18}O found in the recovered azoxybenzene seems to suggest that there is a pre-equilibration of oxygen atoms between the azoxybenzene and arenesulfonyl groups prior to the rearrangement *via* either X or XI, though to a very minor extent; this is probably responsible for the small incorporation of ^{18}O in the *o*-hydroxyazobenzene obtained.

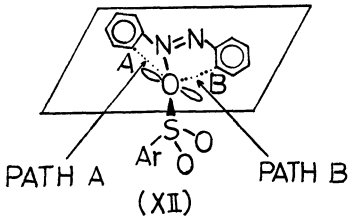

(XII)

Meanwhile, another interesting point of this rearrangement is that the sulfonyloxy group migrates to the two phenyl rings attached to the *N*-oxide group and the azo nitrogen, *i.e.*, in an intermediate XII for the *ortho* rearrangement. (Path A or Path B). The scheme involving the four-membered oxygen-bridged intermediate (Path A) resembles the intermediate of the isoquinoline rearrangement III. On the other hand, the photochemical rearrangement of azoxybenzene is known to proceed intramolecularly through a five-membered oxygen-bridged path, like Path B, as is be described below.

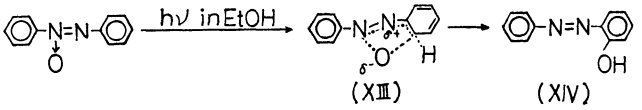

To shed further light on the mechanism, the reaction was carried out with azoxybenzene-1-^{14}C, and the location of the C-14 was determined by the reductive cleavage of *o*-hydroxyazobenzene XIV with sodium hydrosulfite to *o*-aminophenol and aniline. Aniline was converted to benzanilide, which was then subjected to the usual ^{14}C-activity measurements.

The data in Table 3 reveal that the photochemical rearrangement leads to no significant delocalization of the isotopic ^{14}C during the *ortho* rearrangement. However, there was a definite, though small, scrambling, and the ratio of Path A to Path B in an intermediate XII was found to be 13:87. This result shows that the main pathway for the photo rearrangement of azoxybenzene involves an intermediate XIII. Meanwhile, in the reaction of azoxybenzene-1-^{14}C with *p*-nitrobenzenesulfonyl chloride to afford *o*-(*p*-nitrobenzenesulfonyloxy)azobenzene, the ^{14}C distribution is somewhat different, as is shown in Table 4.

Incidentally, the synthesis of azoxybenzene-1-^{14}C and the degradation scheme are as is shown below:

TABLE 4. THE COUNTING DATA OF THE REACTION OF AZOXYBENZENE WITH *p*-NITROBENZENESULFONYL CHLORIDE FOR THE ORTHO REARRANGEMENT

Reaction condition	Activity of Compouns	
(1) 110°C, 30hrs	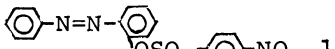	1.18×10^5 dpm/m mole
	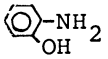	7.67×10^4 "
	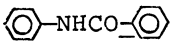	3.92×10^4 "
(2) 140°C, 20hrs	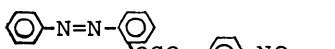	1.10×10^5 "
	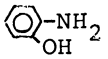	6.62×10^4 "
		3.62×10^4 "

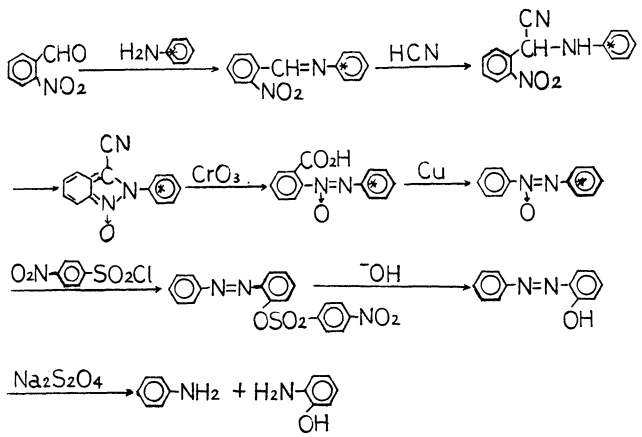

Earlier, Hahn and Jaffé[15] reported that the Wallach rearrangement of both α- and β-isomers of 4-methyl-azoxybenzene yields 2-hydroxy-4′-methylazobenzene as the sole rearrangement product. They suggested that

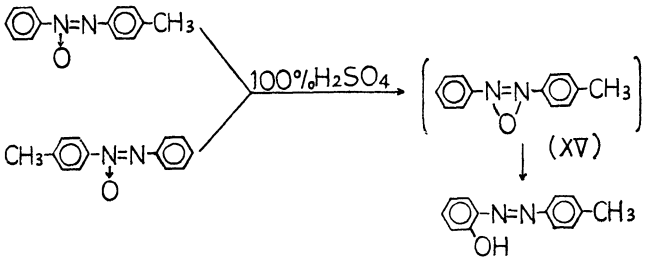

the initial step of this rearrangement is the formation of a common intermediate, probably 3-membered NNO ring XV. In this new rearrangement with arenesulfonyl chloride, the formation of a symmetrical 3-membered ring is quite unlikely since the migratory aptitude did not change with the variation of the reaction conditions, as is shown in Table 4. These data reveal that two-thirds of the migration of the sulfonyloxy group proceeds *via* Path B, while one third proceed A through Path A. The mode of the migration of the sulfonyloxy group in this reaction is similar to that in the photolysis of azoxybenzene.[16] A plausible model for the migration of the sulfonylation to azoxybenzene is illustrated by XII. The azoxybenzene molecule is plannar, and the sulfonyl group approaches the plane of azoxybenzene in a nearly perpendicular direction. Thus, one of the two *p* orbitals of the azoxy oxygen can lie parallel in the plane of azoxybenzene. To rearrange to the *ortho* position intramolecularly, it is necessary for the lone pair of azoxy oxygen to overlap with the *p*-orbitals of the *ortho* carbon atom in the phenyl ring. Therefore, the freedom of rotation around the C–N bond is necessary for the rearrangement to the *ortho* position. Meanwhile, the distance between the oxygen atom and the *ortho* carbon atom (A) in XII is longer than that between the oxygen atom and the other *ortho* carbon (B). Perhaps these factors are at least in part responsible for the facile rearrangement at the *ortho* position through Path B.

Although, a somewhat greater scrambling of ^{14}C was observed in the case of the *para* rearrangement of the sulfonyloxy group, there is a tendency similar to that of the *ortho* rearrangement, as is shown in Table 5. The data in Tables 4 and 5 reveal an unequal distribution of ^{14}C. These data imply that the presence of a symmetrical intermediate like dication II or a 3-membered NNO ring XV, as was seen in Wallach rearrangement, is unlikely in the course of sulfonyloxy migration for either the *ortho* or *para* position. On the basis of the ^{18}O and ^{14}C tracer experimental data, perhaps such intermediates XII and VIII are conceivable for the *ortho* and the *para* rearrangements respectively.

Experimental

Materials. *p*-Bromobenzenesulfonyl chloride (mp 75—76°C from ligroin) was obtained by the chlorosulfonylation of

15) C-S Hahn and H. H. Jaffé, *J. Amer. Chem. Soc.*, **84**, 946 (1962).

16) G. M. Badger and R. G. Buttery, *J. Chem. Soc.*, **1954**, 2243.

Table 5. The counting data of the reaction of azoxybenzene wite tosyl chloride for para rearrangement

Reaction Conditions	Activity of Compouns	
110°C, 50hrs	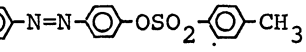	2.39×10^5 dpm/m mole
	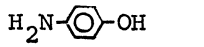	1.40×10^5 "
	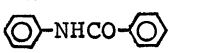	9.03×10^4 "

bromobenzene with chlorosulfonic acid. *p*-Nitrobenzenesulfonyl chloride (mp 76—77°C from ligroin) was prepared by the oxidative chlorination of *p,p'*-dinitrodiphenyldisulfide in nitric and hydrochloric acids through bubbling with Cl_2 at 65°C. Benzo[*c*]cinnoline-1-oxide (mp 137—138°C from aq. ethanol) was synthesized from 2-nitro-2-aminobiphenyl and 1N methanolic sodium hydroxide. 4,4'-Dimethylazoxybenzene (mp 69—71°C from ethanol) was synthesized by the reduction of *p*-nitrotoluene with methanolic sodium hydroxide. ^{18}O-Labeled *p*-bromobenzenesulfonyl chloride was synthesized from *p*-bromothiophenol and ^{18}O-labeled water in dry chloroform by bubbling Cl_2 through at 0°C. ^{18}O-Labeled *p*-nitrobenzenesulfonyl chloride was synthesized similarly.

Azoxybenzene-1-^{14}C was prepared by the condensation of *o*-nitrobenzaldehyde with aniline-1-^{14}C in four steps according to the process reported by Behr.[12] Aniline-1-^{14}C was synthesized, starting from barium carbonate-^{14}C, through seven steps. The synthetic method was described previously.[17]

The Reaction of Azoxybenzene with Arenesulfonyl Chloride. A typical run was carried out as follows. Azoxybenzene and an excess of *p*-nitrobenzenesulfonyl chloride were mixed in nitrobenzene as solvents. The mixture was then heated at 110°C for 25 hr. After the reaction was completed, the nitrobenzene was steam-distilled. The residue was dissolved in methylene chloride, washed with water, dried with sodium sulfate, and chromatographed through an active alumina column, using methylene chloride as the eluent. The *o*- and *p*-(*p*-nitrobenzenesulfonyloxy)azobenzene were separated by recrystallization. These compounds were identified by a comparison of their properties with those of the authentic samples which were synthesized by reacting *o*- or *p*-hydroxyazobenzene with *p*-nitrobenzenesulfonyl chloride in pyridine. The yield was determined by the isotopic dilution technique. The other reactions were carried out similarly.

Isotopic Dilution Method. A typical run was carried out as follows. A mixture of azoxybenzene-1-^{14}C (0.10720 g) and *p*-toluenesulfonyl chloride (0.5 g) in nitrobenzene (2.0 m*l*) was heated at 110°C for 50 hr. After the reaction was completed, authentic samples of *o*-(*p*-toluenesulfonyloxy)azobenzene (0.09190 g) and *p*-(*p*-toluenesulfonyloxy)azobenzene (0.05486 g) were added to the reaction mixture. After the nitrobenzene had been removed by steam distillation, the residue was chromatographed and recrystallized from ethanol. Thus, *o*-(*p*-toluenesulfonyloxy)azobenzene (1.50×10^5 dpm/mmol) and *p*-(*p*-toluenesulfonyloxy)azobenzene (1.76×10^4 dpm/mmol) were separated. The recrystallization was continued until the specific radioactivity was settled. The ratio of the products was determined by calculation with the following equation:

$$W_x = \frac{W_1}{\left(\frac{S_0}{S_2}-1\right)}$$

where W_x: the weight of the desired substance
W_1: the weight of the added authentic substance
S_0: specific activity of the desired substance
S_2: specific activity of the separated substance

The results are given in Table 1.

Measurement of ^{14}C Activity. All the compounds were counted with a liquid scintillation counter (TEN) in a toluene solution, using POPOP as the scintillator.

The Reaction of 4,4'-Dimethyl Azoxybenzene with p-*Bromobenzenesulfonyl Chloride.* A mixture of 4,4'-dimethylazoxybenzene (0.80 g) and *p*-bromobenzenesulfonyl chloride (1.0 g) was heated in nitrobenzene at 110°C for seven hours. 2-(*p*-Bromobenzenesulfonyloxy)-4,4'-dimethylazobenzene (mp 139—140°C from ethanol: 0.54 g) was obtained by the procedure described above. This compound was identified by comparison with the authentic sample synthesized by reacting 2-hydroxy 4,4'-dimethylazobenzene with *p*-bromobenzenesulfonyl chloride in pyridine.

^{18}O-Tracer Study. The reactions of azoxybenzene with ^{18}O-labeled *p*-bromobenzenesulfonyl and *p*-nitrobenzenesulfonyl chlorides were carried out and the ^{18}O analysis was carried out in the usual way.[18] A typical run was as follows. A mixture of azoxybenzene (3.0 g) and ^{18}O-labeled *p*-bromobenzenesulfonyl chloride (4.0 g) in nitrobenzene (30 m*l*) was heated at 110°C for 30 hr. 2-(*p*-Brosyloxy)azobenzene (mp 100—101°C, 1.0 g) and 4-(*p*-brosyloxy)azobenzene (mp 175—176°C, 1.5 g) were then obtained by usual work-up, and a 0.4 g portion of the azoxybenzene recovered was subjected to ^{18}O analysis. The hydrolysis of 4-(*p*-brosyloxy)azobenzene (1.2 g) was carried out under refluxing in 20 m*l* of 20% sodium hydroxide for 5 hr. Then the solution was acidified with 10% HCl and extracted with ether. After the removal of the solvent, recrystallization from benzene gave 4-hydroxyazobenzene (mp 152—154°C, 0.3 g). The aqueous layer was carefully neutralized with Na_2CO_3, using phenolphthalein as the indicator. Then, a 10% EtOH solution of *s*-benzylisothiuronium salt (0.4 g) was added to the neutral solution. The precipitate thus formed was collected and recrystallized from ethanol. This crystal (mp 174—176°C 0.3 g) were identified as the thiuronium salt of *p*-bromobenzenesulfonic acid by comparing it with the authentic sample. 2-(*p*-Brosyloxy)-azobenzene was hydrolyzed similarly. The ^{18}O-analytical results of these esters and the hydrolyzed compounds are listed in Table 2.

Degradation of o-(p-*Nitrobenzenesulfonyloxy)azobenzene*-x-^{14}C. A mixture of the title compound (1.0 g) in 10 m*l* of ethanol and 2 m*l* of water was subjected to alkaline hydrolysis with

17) S. Oae, N. Furukawa, M. Kise, and M. Kawanishi, This Bulletin, **39**, 1212 (1966).

18) S. Oae, T. Kitao, and Y. Kitaoka, *Tetrahedron*, **19**, 827 (1964).

5.0 g of sodium hydroxide under reflux for five hours. After the reaction has subsided, the reaction mixture was poured into ice cold water and filtered. The filtrate was acidified with 10% hydrochloric acid and extracted with ether. After the evaporation of the ether, crude *o*-hydroxyazobenzene was obtained and recrystallized from ethanol (mp 81—82°C): 0.3 g of the pure compound was thus obtained. Into a mixture of 0.205 g of *o*-hydroxyazobenzene (0.001 mol) and 0.53 g of sodium hydrosulfite (0.003 mol) in 2 m*l* of water, 0.24 g of sodium hydroxide (0.006 mol) was added. The solution was then heated at 80°C for eight hours until the red color of *o*-hydroxyazobenzene disappeared. After the reaction, two times as much water was added to the reaction mixture and the solution was extracted with ether. Then, 0.05 g of benzoyl chloride was added to the ether solution. After heating on a hot plate, the ether was evaporated and the residue was recrystallized from ethanol to obtain benzanilide (mp 161—163°C, 0.034 g) After acidification with 10% hydrochloric acid, the water layer was made weakly alkaline with sodium carbonate and extracted with ether. After the subsequent evaporation of the ether, crude *o*-aminophenol was recrystallized with ethanol (mp 172—174°C) to obtain 0.043 g of the pure sample. The degradation of *p*-(*p*-toluenesulfonyloxy)-azobenzene was carried out similarly.

Photochemical Rearrangement of Azoxybenzene-1-^{14}C. A mixture of 0.544 g of azoxybenzene-1-^{14}C in 200 m*l* of ethanol was irradiated for 48 hr using a high-pressure mercury arc lamp at 20—25°C. After the condensation of the reaction mixture, it was poured into an alkaline solution, *i.e.*, 3 g of sodium hydroxide in 200 m*l* of water, and filtered under reduced pressure. The filtrate was acidified with 10% hydrochloric acid and extracted with ether. After the evaporation of the ether, crude *o*-hydroxyazobenzene was recrystallized from ethanol. The degradation of the ^{14}C-labeled *o*-hydroxyazobenzene to aniline and *o*-aminophenol was done by the procedure used previously.

BULLETIN OF THE CHEMICAL SOCIETY OF JAPAN, VOL. 44, 2501—2505(1971)

Phenylazo *p*-Tolyl Sulfone as a Source of Phenyl Radical[1)]

Michio KOBAYASHI, Hiroshi MINATO, Minoru KOJIMA, and Nobumasa KAMIGATA

Department of Chemistry, Tokyo Metropolitan University, Fukazawa, Setagaya-ku, Tokyo

(Received March 16, 1971)

Mechanism of the decomposition of phenylazo *p*-tolyl sulfone(I) was investigated. Orientations and partial rate factors of substituted biphenyls produced by the decomposition of I in benzene-substituted benzene mixtures were used as the criteria for judging the nature of the decomposition. When CaO- or MgO-suspension was present, autocatalytic heterolysis of I was suppressed to some extent, but for complete suppression 20—40 w/v % CaO or MgO was necessary. Pyridine and quinoline were found to be effective for suppression of the autocatalysis. When sufficient amount of pyridine, quinoline, MgO or CaO were present, orientations and partial rate factors for phenylation of substituted benzene were similar to those obtained by phenyl radical produced by benzoyl peroxide on *N*-nitrosoacetanilide. The rate of decomposition of I was determined in PhC_2H_5, $PhOCH_3$, PhCl, $PhNO_2$, pyridine and DMF in the presence of pyridine. An isokinetic relationship was found to hold for activation parameters for the decomposition in these solvents, and the isokinetic temperature was 88.6°C. Values of activation enthalpy and entropy were rather large; $\Delta H^{\ddagger}=39.6$ kcal/mol and $\Delta S^{\ddagger}=34.4$ e.u./mol in DMF.

When trifluoroacetic acid is present in the medium, phenylazo *p*-tolyl sulfone decomposed heterolytically, yielding phenyl cation, nitrogen and *p*-toluenesulfinic acid.[2)] Bunnett and Happer reported that when sodium methoxide is present *o*-halophenylazo phenyl sulfone yielded *o*-halophenyl anion, nitrogen, formaldehyde and benzenesulfinic acid.[3)] Rosenthal and Overberger reported that in the presence of suspended calcium oxide phenylazo phenyl sulfone decomposed homolytically, yielding phenyl and benzenesulfonyl radicals.[4)] Kice and Gabrielsen reported that phenylazo methyl sulfone also decomposed homolytically when suspended calcium oxide was present.[5)]

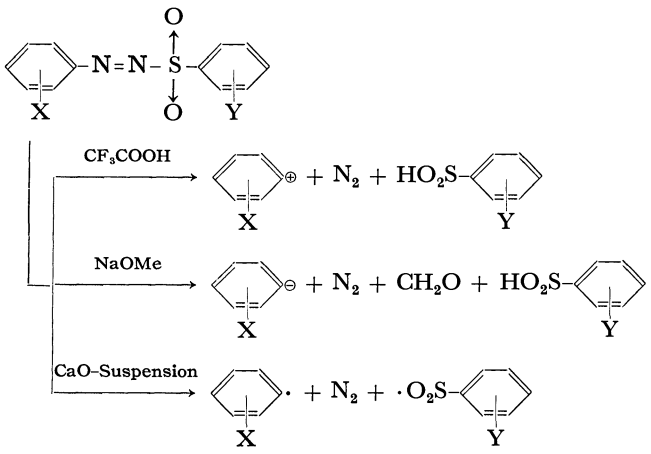

Azosulfones are interesting compounds as the source for aryl radicals and arenesulfonyl radicals, but it seems that the conditions which guarantee completely homolytic decomposition of azosulfones have not been established yet. It is not certain that to what extent the

1) Organic Sulfur Compounds, Part XXV.

2) M. Kobayashi, H. Minato, and N. Kobori, This Bulletin, **43**, 219 (1970).

3) J. F. Bunnett and D. A. R. Happer, *J. Org. Chem.*, **32**, 2701 (1967).

4) C. G. Overberger and A. J. Rosenthal, *J. Amer. Chem Soc.*, **82**, 108, 117 (1960).

5) J. L. Kice and R. S. Gabrielsen, *J. Org. Chem.*, **35**, 1004 (1970).

heterolytic decomposition of azosulfones is suppressed when suspended calcium oxide is present. Further detailed investigation of the mechanism of decomposition of azosulfones seemed desirable. Such investigation was carried out in our laboratories, and the effectiveness of added bases such as calcium oxide, magnesium oxide, pyridine, and quinoline was determined. In order to determine whether or not phenyl cation is being produced, orientations and partial rate factors for phenylation in aromatic solvents were measured. These results will be described in this paper.

Experimental

Materials. Aromatic solvents were purified according to conventional methods.[2]

Phenylazo *p*-tolyl sulfone was synthesized by the reaction between benzenediazonium chloride and sodium *p*-toluenesulfinate, and recrystallized from methanol; mp 90—91°C (decomp.).

Pyridine and quinoline were refluxed over potassium hydroxide and then distilled; pyridine, 114—115°C/760 mmHg, quinoline, 137°C/45 mmHg.

Calcium oxide was ground to fine powder and then used. Magnesium oxide which is available as fine powder was used as received.

Kinetic Measurements. A flask containing a mixture of 60 m*l* of a solvent and 8—13 mmol of pyridine was placed in a constant temperature bath. After the temperature of the mixture reached that of the bath, 3 mmol of I was dissolved (the concentration is about 0.05 mol/*l*). Amounts of nitrogen gas generated were measured by a gas buret.

Analysis of Phenylated Products. Three mmol of I was dissolved in aromatic solvents (a mixture of 0.12 mol of benzene and 0.12 mol of a substituted benzene) containing 3—20 mmol of pyridine or quinoline, and a flask containing the solution was placed in a constant temperature bath.

Since azobenzene is one of the products and it interferes the gas-chromatographic determination of biphenyls, it had to be removed by reduction. To the reaction mixtures containing anisole, chlorobenzene or ethylbenzene, zinc powder and methanolic hydrochloric acid were added and azobenzene was reduced; then the mixture was washed with water, dried over anhydrous magnesium sulfate, and concentrated under reduced pressure. The reaction mixtures containing benzonitrile or nitrobenzene were washed with a 5% sodium carbonate solution and water, dried over anhydrous magnesium sulfate, and then concentrated.

When calcium oxide or magnesium oxide was used in place of pyridine or quinoline, the reaction mixtures were filtered and then treated in a similar manner.

Biphenyls in the concentrated mixtures were determined by a Hitachi K-53 Gas Chromatograph.

Results and Discussion

Rosenthal and Overberger reported that when 0.13—0.33 w/v% calcium oxide was present the autocatalysis by acidic products (arenesulfinic acids and arenesulfonic acids) were prevented and the decomposition followed a first-order rate law.[4] We determined the orientations and partial rate factors for the phenylation of substituted benzenes (0.12 mol benzene +0.12 mol a substituted benzene) with I in the absence of CaO and in the presence of 0.5 g CaO (0.5 g CaO corresponds to 2.19 w/v% in the case of benzene-chlorobenzene). The results are shown in Table 1.

Partial rate factors in the presence of 0.5 g CaO are quite different from those in the absence of CaO, but they are still different from the partial rate factors for phenylation with phenyl radical produced from benzoyl peroxide[6] or *N*-nitrosoacetanilide.[7] This finding indicates that the autocatalytic heterolysis is not completely suppressed. Therefore, the amounts of calcium oxide suspension were increased. Since magnesium oxide is commercially available as powder much finer than calcium oxide, some experiments were carried out in the presence of magnesium oxide. The results of experiments with benzene-chlorobenzene are shown in Table 2.

When 5.0 g of MgO was present (21.9 w/v%), the orientations and partial rate factors are similar to those by phenyl radical, and no further change was observed when amounts of magnesium oxide were increased. Therefore, the orientations and partial rate factors for

Table 1. Orientations and partial rate factors for the phenylation of PhX with *p*-TsN_2Ph (a) in the absence of CaO and (b) in the presence of 0.5 g CaO[a]

X in PhX		Orientations(%)			Partial rate factors			Yield of total biphenyls (%)
		o-	*m*-	*p*-	k_o/k	k_m/k	k_p/k	
OCH_3	a)	57.8	14.8	27.4	2.37	0.61	2.26	
	b)	68.8	16.4	14.8	3.99	0.95	1.73	
C_2H_5	a)	49.5	24.5	26.0	1.41	0.70	1.48	14.0
	b)	51.3	30.2	18.5	2.08	1.23	1.49	13.0
Cl	a)	53.0	20.3	26.7	1.13	0.43	1.14	21.9
	b)	57.3	22.7	20.0	2.89	1.15	2.01	32.6
CN	a)	43.1	36.9	20.0	0.89	0.71	0.77	
	b)	51.8	22.0	26.2	2.68	1.16	2.75	
NO_2	a)	38.0	62.0	0	0.60	0.98	0	12.8
	b)	47.5	23.7	28.8	2.45	1.23	2.98	18.0

a) Each experiment was carried out with a mixture of 0.12 mol of benzene and 0.12 mol of a substituted benzene. Reaction temperature; 60.0°C

6) G. H. Williams, "Homolytic Aromatic Substitution," Pergamon press, Oxford (1960), pp. 68, 73,

7) R. Ito, T. Migita, N. Morikawa, and O. Simamura, *Tetrahedron*, **21**, 955 (1965).

TABLE 2. ORIENTATIONS AND PARTIAL RATE FACTORS FOR THE PHENYLATION OF PhCl WITH *p*-TsN_2Ph IN THE PRESENCE OF VARIED AMOUNTS OF CaO OR MgO[a]

Additive	Weight (g)	Orientations(%)			Partial rate factors		
		o-	*m*-	*p*-	k_o/k	k_m/k	k_p/k
CaO	0.5	57.3	22.7	20.0	2.89	1.15	2.01
	10.0	59.6	22.7	17.7	3.77	1.47	2.30
	20.0	60.0	22.1	17.9	3.91	1.44	2.34
MgO	1.0	60.0	22.0	19.0	2.73	0.96	1.73
	5.0	60.2	21.4	18.4	4.67	1.66	2.59
	10.0	61.5	22.0	16.4	4.37	1.57	2.35

a) Reaction temperature: 60.0°C

TABLE 3. ORIENTATIONS AND PARTIAL RATE FACTORS FOR THE PHENYLATION OF PhX WITH *p*-TsN_2Ph IN THE PRESENCE OF 5.0 g MgO[a]

X in PhX	Orientations (%)			Partial rate factors			Yield of total biphenyls (%)
	o-	*m*-	*p*-	k_o/k	k_m/k	k_p/k	
OCH_3	68.6	19.9	11.5	5.79	1.67	1.94	
C_2H_5	53.5	30.5	16.0	2.20	1.26	1.36	8.4
Cl	60.9	21.7	17.4	4.52	1.67	2.60	32.6
CN	57.4	14.3	28.3	6.15	1.53	6.06	
NO_2	64.6	8.6	27.1	13.33	1.81	11.25	39.0

a) Reaction temperature: 60.0°C

the phenylation of various substituted benzenes were determined in the presence of 5.0 g magnesium oxide. The results are shown in Table 3. These values are comparable to those reported for phenylation with phenyl radical.[6,7]

Since the systems containing calcium oxide and magnesium oxide are heterogeneous, variation of the size of particles and the rate of stirring influence on the results of experiments. Some organic compounds usable in place of calcium oxide are desirable for reproducibility and convenience in the experiments generating phenyl radicals from azosulfones. Experiments were carried out with pyridine and quinoline as organic weak bases, and the results are shown in Tables 4 and 5. Both orientations and partial rate factors are similar to those obtained with 5.0 g magnesium oxide, and these data show that both pyridine and quinoline are effective in preventing autocatalytic heterolysis of I.

Abramovitch and Saha[8] reported that in the presence of pyridine benzenediazonium salts decompose homolytically according to a scheme shown below.

TABLE 4. ORIENTATIONS AND PARTIAL RATE FACTORS FOR THE PHENYLATION OF PhX WITH *p*-TsN_2Ph IN THE PRESENCE OF PYRIDINE[a]

X in PhX	Orientations (%)			Partial rate factors			Yield of total biphenyls (%)
	o-	*m*-	*p*-	k_o/k	k_m/k	k_p/k	
OCH_3	65.0	22.5	12.5	4.91	1.69	1.89	
C_2H_5	49.1	32.6	18.3	2.00	1.33	1.49	12.6
Cl	58.3	23.0	18.8	3.32	1.31	2.16	48.7
NO_2	64.5	7.7	27.8	10.36	1.26	8.70	54.4

a) [pyridine]/[*p*-TsN_2Ph]=2—8 (mol ratio) Reaction temperature: 60.0°C

TABLE 5. ORIENTATIONS AND PARTIAL RATE FACTORS FOR THE PHENYLATION OF PhX WITH *p*-TsN_2Ph IN THE PRESENCE OF QUINOLINE[a]

X in PhX	Orientations (%)			Partial rate factors			Yield of total biphenyls (%)
	o-	*m*-	*p*-	k_o/k	k_m/k	k_p/k	
OCH_3	65.8	21.4	12.8	4.79	1.56	1.89	
C_2H_5	53.5	30.1	16.4	2.02	1.14	1.24	13.2
Cl	60.6	22.8	16.6	3.63	1.36	1.99	46.7
CN	49.4	15.6	35.0	5.20	1.66	7.38	
NO_2	65.7	8.3	26.0	11.07	1.42	8.78	47.8

a) [quinoline]/[*p*-TsN_2Ph]=1.6—10.0 (mol ratio) Reaction temperature: 60.0°C

8) R. A. Abramovitch and J. G. Saha, *Tetrahedron*, **21**, 3297 (1965).

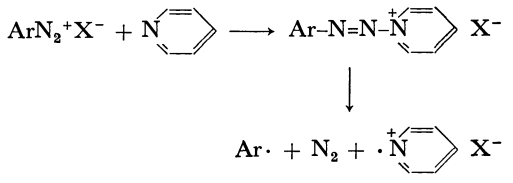

In the presence of pyridine, I could undergo a similar reaction.

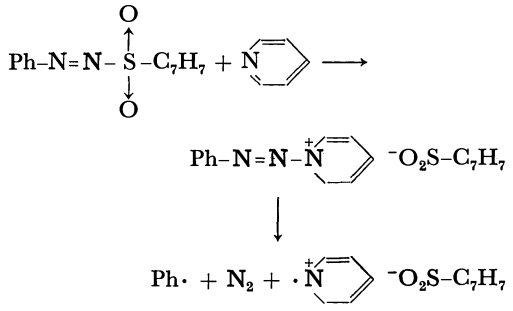

However, such possibility can be rejected on the basis of the following considerations; a) magnesium oxide and calcium oxide can be used in place of pyridine and similar results are obtained, b) the infrared spectrum of I in pyridine showed no absorptions at 2260—2280 cm^{-1} ascribable to a diazonium salt, c) rates of decomposition of I in the presence of pyridine are quite different from those of diazonium salts in the presence of pyridine, and d) orientations and partial rate factors obtained with I in the presence of pyridine are considerably different from those obtained with diazonium salts in the presence of pyridine.

Figure 1 shows the Hammett plots of *para* partial rate factors against Hammett σ values. The ρ values obtained from the right half line was 1.21 (at 60°C), which is comparable to the ρ value for phenylation with *N*-nitrosoacetanilide (1.27, at 20°C) or that with benzoyl peroxide (1.14, at 80°C), but somewhat different from that with phenylazotriphenylmethane (0.93, at 60°C).[9] These data show that the phenylation with phenyl radical is very little dependent on the temperature but considerable dependent on the source of phenyl radical.

The effect of temperature on the phenylation with phenyl radical has not been investigated in detail. Therefore it has not been established whether or not it is meaningful to compare the orientations and partial rate factors obtained at different temperatures with

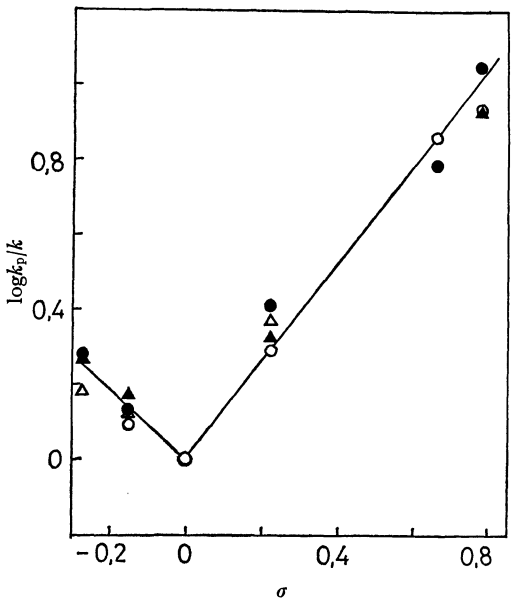

Fig. 1. Hammett plot for phenylation with *p*-TsN_2Ph in the presence of pyridine, quinoline, MgO, and CaO.
ρ=1.21 (at 60°C)
▲ Pyridine ● MgO
○ Quinoline △ CaO

different phenyl radical sources. In order to clarify this question, orientations of phenylation with I at various temperatures were measured, and the results are shown in Table 6. When the temperature was raised, phenylation at *ortho* position gradually decreased and phenylation at *meta* or *para* position gradually increased. Such tendency was greatest for the phenylation of chlorobenzene. However, the changes are not so significant even in the case of chlorobenzene. These findings indicate that activation energies for phenylation at *ortho*, *meta*, and *para* positions do not differ greatly. This finding supports the commonly accepted interpretation that the similarity in the data on the phenylations with benzoyl peroxide or *N*-nitrosoacetanilide at different temperatures must arise from the same intermediate, phenyl radical.

The rates of decomposition of I in various solvents were determined by measuring the nitrogen gas evolved. As shown in Fig. 2, autocatalysis is observed in the absence of calcium oxide or pyridine (curve b) where-

TABLE 6. ORIENTATIONS FOR THE PHENYLATION OF PhX WITH *p*-TsN_2Ph IN THE PRESENCE OF PYRIDINE AT VARIOUS TEMPERATURES[a]

Reaction Temp. (°C)	$PhOCH_3$			PhC_2H_5			PhCl			$PhNO_2$		
	o-	*m*-	*p*-	*o*-	*m*-	*p*-	*o*-	*m*-	*p*-	*o*-	*m*-	*p*-
60.0	65.0	22.5	12.5	49.1	32.6	18.3	58.3	23.0	18.8	64.5	7.7	27.8
80.0				50.2	32.7	17.1	51.5	28.7	19.8	60.6	11.2	28.2
85.4	63.7	20.8	15.5	48.2	34.8	17.0	50.2	29.1	20.7	59.9	12.3	27.8
90.6	64.3	20.8	14.9	45.8	36.0	18.2	52.2	28.5	19.3	60.8	12.0	27.2
93.1				48.0	33.7	18.3						
95.6							51.8	28.8	19.4	60.5	11.6	27.9
99.1	61.9	22.1	16.0									

a) [pyridine]/[*p*-TsN_2Ph]=2—4 (mol ratio)

9) M. Kobayashi, H. Minato, N. Watanabe, and N. Kobori, This Bulletin, **43** 258 (1970).

Table 7. First-order rate constants for the decomposition of *p*-TsN_2Ph in the presence of pyridine[a)]

Reaction Temp. (°C)	Solvent ε	PhC_2H_5 2.41	$PhOCH_3$ 4.30	PhCl 5.61	Pyridine 12.3	$PhNO_2$ 34.6	DMF 36.7
				$k\times10^4$ (sec^{-1})			
80.0		1.32		0.494	0.489	0.671	0.591
85.4		1.97	0.793	1.08	1.04	1.16	1.11
90.6		5.06	1.51	2.52	1.79	2.24	3.78
93.1		5.92					
95.6			2.94	5.38	3.42	5.15	5.33
99.1			4.82				

a) $[p\text{-}TsN_2Ph]_0=0.05$ mol/*l*, $[\text{pyridine}]_0/[p\text{-}TsN_2Ph]_0=2$—4 (mol ratio), except the decomposition in pyridine as the solvent.

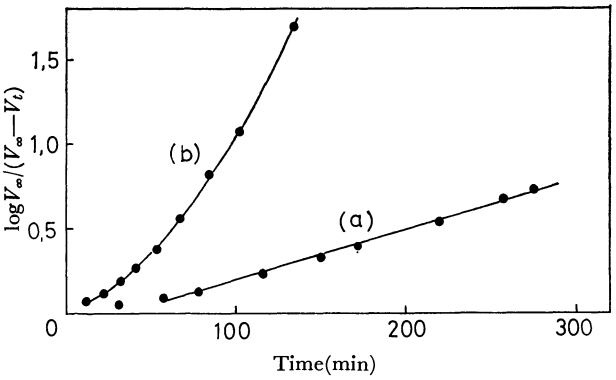

Fig. 2. Rate of decomposition of *p*-TsN_2Ph in PhCl at 85.4°C. *V*: volume of nitrogen evolved, $[p\text{-}TsN_2Ph]_0=0.05$ mol/*l* a) [pyridine]=0.135 mol/*l* b) [pyridine]=0

as the rates of decomposition followed a first-order rate equation when pyridine is present (line a). The molar ratio, [pyridine]/[I], was kept in the range of 2—4, and the rate constants, *k*, were not influenced by the concentration of pyridine. First-order rate constants for the decomposition of I in solvents of various dielectric constants were determined in the presence of pyridine, and the results are shown in Table 7.

Rate constants in Table 7 are not dependent on the dielectric constants of media, and this fact also supports the homolytic nature of the decomposition of I in the presence of pyridine. Activation parameters for the decompositions in these solvents were obtained, and shown in Table 8. An isokinetic relationship holds for these activation parameters, as shown in Fig. 3, and the isokinetic temperature, β, was 88.6°C.

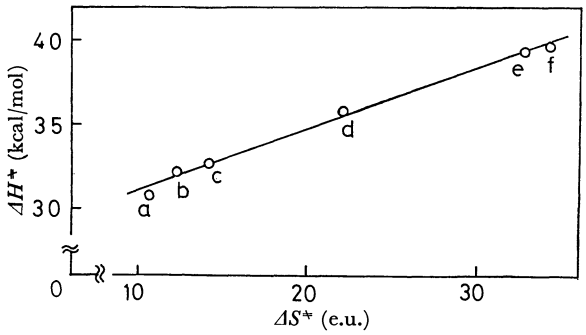

Fig. 3. Isokinetic relationship for the decomposition of *p*-TsN_2Ph in the presence of pyridine in various solvents. β=88.6°C; a, PhC_2H_5 b, C_5H_5N c, $PhNO_2$ d, $PhOCH_3$ e, PhCl f, DMF

Table 8. Activation parameters for the decomposition of *p*-TsN_2Ph in the presence of pyridine

Solvent	ΔH^*(kcal/mol)	ΔS^*(e.u.)
PhC_2H_5	30.8	10.7
pyridine	32.2	12.3
$PhNO_2$	32.6	14.1
$PhOCH_3$	35.9	22.2
PhCl	39.4	32.8
DMF	39.6	34.4

Variation in activation parameters in these solvents is fairly large, but cannot be rationalized easily. However, it is of interest to note that activation entropies for decomposition of this azosulfone are rather large compared with those of common radical initiators with similar activation enthalpies; this azosulfone, in chlorobenzene, $\Delta H^*=39.4$ kcal/mol, $\Delta S^*=32.8$ e.u., *t*-butyl peracetate,[10] in chlorobenzene, $\Delta H^*=38$ kcal/mol, $\Delta S^*=17$ e.u., di-*t*-butyl peroxide,[11] in *t*-butylbenzene, $\Delta H^*=37.8$ kcal/mol, $\Delta S^*=13.8$ e.u. Because of these rather large activation entropies, this azosulfone decomposes at temperatures lower than those used for di-*t*-butyl peroxide or *t*-butyl peracetate. Compounds decomposing with activation entropies comparable to those of this azosulfone are phenylazo phenyl sulfides; van Zwet and Kooyman reported that E_a and ΔS^* for the decomposition of *p*-tolylazo *p*-*t*-butylphenyl sulfide in benzene were 36 kcal/mol and 33 e.u., respectively.[12]

10) P. D. Bartlett and R. R. Hiatt, *J. Amer. Chem. Soc.*, **80**, 1398 (1958).

11) J. H. Raley, F. F. Rust, and W. E. Vaughan, *ibid.*, **70**, 1337 (1948).

12) H. van Zwet and E. C. Kooyman, *Rec. Trav. Chim., Pays-Bas*, **86**, 1143 (1967).

Studies of Azo Colors. VIII.[1] The Azo-coupling Reactions of Active Methylene Compounds

Yōji HASHIDA, Morio KOBAYASHI, and Kohji MATSUI

Department of Synthetic Chemistry, Faculty of Engineering, Gunma University, Tenjincho, Kiryu, Gunma

(Received March 17, 1971)

The kinetics of the azo-coupling reactions of various active methylene compounds with diazobenzene-4-sulfonic acid have been studied spectrophotometrically. In the reactions of all the active methylene compounds used, it was found that the reaction rate was proportional to both the concentration of the diazonium salt and the carbanion (or enolate ion) of the azo component. In the reactions of a series of β-dicarbonyl compounds, a plot of the logarithms of the rate constants against the pK_a values of active methylene compounds gave a straight line. However, the correlation between the reactivity and pK_a was found unsatisfactory in the case of active methylene compounds with such electron-withdrawing substituents as NO_2, CN, COR, SO_2R, and Cl. These results are discussed in terms of the nucleophilicity of these carbanions.

The reaction of aromatic diazo compounds with aromatic amines or phenols is well known to be a diazo-coupling reaction, and the kinetics of the reaction has been extensively studied in connection with the reaction mechanism and the effects of the substituents on the reactivity.[2]

On the other hand, aliphatic compounds containing an activated methylene or methyl group are known to react also with aromatic diazonium salts to form azo compounds or their tautomers. Although many active methylene compounds are known,[3,4] no systematic quantitative studies of their coupling reactions have yet been made. Therefore, little is known concerning the reaction mechanism and the relationship between the reactivity and the structure.

This paper will report the kinetics of the coupling reaction of various active methylene compounds with diazobenzene-4-sulfonic acid, and the structural effect of the active methylene compound on the reactivity.

Experimental

Materials. Bis(methylsulfonyl)methane and bis(ethylsulfonyl)methane were prepared by the method of Fromm.[5] Ethyl nitroacetate was prepared by the method of Arndt[6] from ethyl acetoacetate and nitric acid. *p*-Nitroacetoacetanilide was prepared according to the method of Fierz-David.[7] The other active methylene compounds and sulfanilic acid were of commercial origin and were used after purification by recrystallization or distillation. Their purities were confirmed by their physical constants and by thin-layer chromatography or gas chromatography.

pK_a *Measurement.* The pK_a value of the azo component was measured spectrophotometrically at a appropriate wavelength in water (ionic strength, μ; 0.25) at 20±0.1°C. In the case of ethyl cyanoacetate, due to the decomposition in an alkaline solution, the extinction of carbanion was taken as a function of the time and was extrapolated back to zero time. The decomposition of ethyl cyanoacetate, however, was negligibly small in the pH range where kinetic measurements were performed. The results are given in Table 2 and Table 3.

Kinetic Measurements. The general experimental techniques are quite similar to those used in an earlier experiment.[8] The kinetic measurements were carried out when the azo component was present in at least a twenty-five-fold excess as compared to the diazonium salt. The apparent rate constant (k') was calculated using Eq. (1) by measuring the concentration of the product spectrophotometrically in a buffered aqueous solution at 20±0.1°C:

$$k't = 2.303 \log \frac{a}{a-x} = 2.303 \log \frac{E_\infty}{E_\infty - E_t} \quad (1)$$

a: concentration of the dyestuff at an infinite time (a is proportional to the E_∞ extinction)

x: concentration of the dyestuff at time t (x is proportional to the E_∞ extinction)

The bimolecular rate constant (k_2) was obtained from Eq. (2):

$$k_2 = k'/[A^-] = k'[H^+]/K_a^{AH}[AH] \quad (2)$$

where $[A^-]$, $[AH]$, and K_a^{AH} represent the concentration of the carbanion, the undissociated form of the azo component, and the dissociation constant of AH respectively. The results are tabulated in Table 2 and Table 3. The initial concentration of the diazonium salt was 4×10^{-5} mol/l in all of the kinetic runs. The components of the buffer solutions used were as follows:

pH	Component			
2.0	0.066 mol	CH_3COONa	+0.084 mol	HCl/l
2.8	0.063 mol	CH_3COONa	+0.063 mol	HCl/l
3.7	0.066 mol	CH_3COONa	+0.059 mol	HCl/l
4.3	0.040 mol	CH_3COONa	+0.080 mol	CH_3COOH/l
4.7	0.063 mol	CH_3COONa	+0.047 mol	CH_3COOH/l
5.2	0.063 mol	CH_3COONa	+0.031 mol	CH_3COOH/l
5.8	0.040 mol	CH_3COONa	+0.003 mol	CH_3COOH/l
6.2	0.013 mol	Na_2HPO_4	+0.038 mol	KH_2PO_4/l
6.8	0.011 mol	Na_2HPO_4	+0.009 mol	KH_2PO_4/l
7.2	0.015 mol	Na_2HPO_4	+0.005 mol	KH_2PO_4/l

1) Part VII: Y. Hashida, S. Sekiguchi, and K. Matsui, *Kogyo Kagaku Zasshi*, **74**, 240 (1971).

2) H. Zollinger, "Azo and Diazo Chemistry," Interscience Publishers, New York, N. Y. (1961), p. 221.

3) S. M. Parmerter, "Organic Reaction," Vol. 10, ed. by R. Adams, John Wiley & Sons, Inc., New York, N. Y., (1959), p. 1.

4) E. Enders, "Methoden der Organischen Chemie (Houben-Weyl)," Band X/3 (Stickstoffverbindungen 1), George Thieme Verlag., Stuttgart (1965), p. 471.

5) E. Fromm, *Ann.*, **253**, 155 (1889).

6) F. Arndt and J. P. Rose, *J. Chem. Soc.*, **1935**, 1.

7) H. E. Fierz-David and F. Ziegler, *Helv. Chim. Acta*, **2**, 779 (1928).

8) Y. Hashida, K. Nakajima, S. Sekiguchi, and K. Matsui, *Kogyo Kagaku Zasshi*, **72**, 1132 (1969).

The ionic strength of the buffer solution was adjusted to 0.25, by the addition of potassium chloride.

Results and Discussion

Kinetic Equation. The mechanism expressed by the following equations is suggested as the most probable for the coupling of an active methylene compound:[9]

$$\mathrm{X}\diagdown \mathrm{CH_2} + \mathrm{B} \underset{k_{BH}}{\overset{k_B}{\rightleftharpoons}} \mathrm{X}\diagdown \overset{-}{\mathrm{C}}\mathrm{H} + \mathrm{BH^+} \quad (3)$$
$$\mathrm{Y}\diagup \qquad\qquad\qquad\quad \mathrm{Y}\diagup$$

$$\mathrm{X}\diagdown \overset{-}{\mathrm{C}}\mathrm{H} + \mathrm{Ar}\overset{+}{\mathrm{N}}_2 \xrightarrow{k_2}$$
$$\mathrm{Y}\diagup$$

$$\mathrm{X}\diagdown \mathrm{CH{-}N{=}N{-}Ar} \qquad \mathrm{X}\diagdown \mathrm{C{=}N{-}NH{-}Ar} \quad (4)$$
$$\mathrm{Y}\diagup \qquad\qquad\quad \mathrm{Y}\diagup$$

For instance, in the reactions of acetoacetanilide[10] and pyrazolones,[11,12] the ionization of the methylene group occurs first, followed by the rate-controlling step of the reaction; the rate of the coupling has been expressed by Eq. (5):

$$v = k_2[\mathrm{Ar}\overset{+}{\mathrm{N}}_2][\mathrm{X{-}}\overset{-}{\mathrm{C}}\mathrm{H{-}Y}] \quad (5)$$

The kinetic equation is similar to that for the coupling to phenols.[1]

On the other hand, in the case of nitroethane, the ionization of the C–H bond occurs slower than the second step, and a kinetic expression (6) has been presented:[13]

$$v = k_B[\mathrm{B}][\mathrm{X{-}CH_2{-}Y}] \quad (6)$$

Equation (6) is similar to the one that applies to the base catalyzed halogenation of aliphatic compounds containing an activated methylene group. Thus, at present, two types of kinetic equations are known for the coupling reactions of active methylene compounds. Therefore, the reactions of other aliphatic compounds with diazonium salts are of interest with respect to the kinetic equation. In this paper, the active methylene compounds shown in Table 2 and Table 3 have been examined from the above point of view.

As is shown in Table 1, the first-order dependence with the diazonium salt was confirmed in the reaction of malononitrile according to Eq. (1) by using an excess of the azo component; the reaction also shows a first-order dependence on the concentration of malononitrile, judging from the results using different concentrations at a constant pH.

The dependence of log k' on pH was linear, as is shown in Fig. 1, with a unit slope over the pH range where

Table 1. Coupling rate constant of diazobenzene-4-sulfonic acid with malononitrile (20°C, μ: 0.25)

pH	Concentration of malononitrile (mol/l) $\times 10^3$	k' (min^{-1})	k_2 (l/mol·min) $\times 10^{-8}$
4.37	1.00	0.0965	4.21
4.38	4.00	0.356	3.80
4.38	2.00	0.205	4.37
2.88	2.00	0.00623	4.19
3.74	2.00	0.0417	3.90
4.74	2.00	0.498	4.65

the concentration of the dissociated form of malononitrile is much lower than that of the undissociated form. This result is consistent with a presumption that the rate determining step is the reaction of a carbanion with a diazonium salt.[10–12,14] Therefore, a second-order rate constant (k_2) was determined from Eq. (2). The k_2 values thus obtained are independent of the acidity of the medium, as is shown in Table 1.

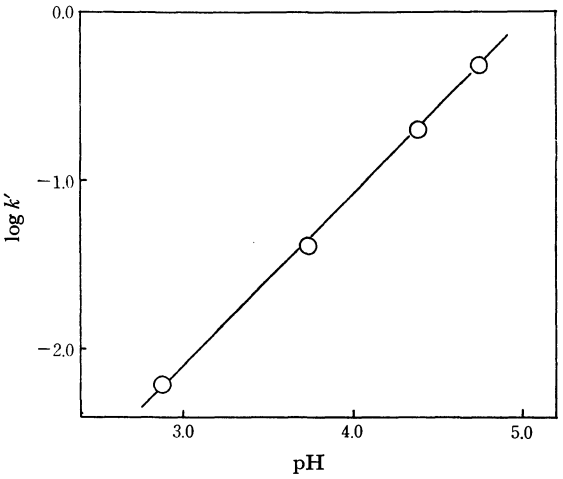

Fig. 1. Dependence of the rate constant (k') for the coupling reaction of diazobenzene-4-sulfonic acid with malononitrile on pH. (Concentration of malononitrile: 2×10^{-3} mol/l)

In all the active methylene compounds studied, it was found that the rate of coupling was expressed by Eq. (5) under the given set of conditions (Table 2 and Table 3) in a manner similar to that described above. Thus, in the present work we have found that the kinetic expression differs from that used for the reaction of nitroethane. It is assumed that a difference in the relative rates of the stages (3) and (4) is responsible for the difference in their kinetic expressions (5 and 6). In the active methylene compounds used, not only the reaction circumstances, such as the component of the buffer solution, which affect the velocity of stage (3) as a base, but also the magnitude of k_2, are not same as in the case of nitroethane. However, it is assumed that the slow ionization of nitroethane is at least partly responsible for the kinetic equation, Eq. (6), which differs from those of the other active methylene compounds. It is well known that the ionization of nitro-

9) Ref. 2, p. 199.
10) V. Macháček, J. Panchartek, V. Štěrba, and M. Večeřa, *Collect. Czech. Chem. Commun.*, **35**, 844 (1970).
11) I. Dobáš, V. Štěrba, and M. Večeřa, *ibid.*, **34**, 3905 (1969).
12) I. Dobáš, V. Štěrba, and M. Večeřa, *ibid.*, **34**, 3895 (1969).
13) V. Macháček, J. Panchartek, V. Štěrba, and M. Večeřa, *ibid.*, **33**, 3154 (1968).
14) C. Wittwer and H. Zollinger, *Helv. Chim. Acta*, **37**, 1954 (1954).

Table 2. Rate constants of the coupling reaction of diazobenzene-4-sulfonic acid with β-dicarbonyl compounds (20°C, μ: 0.25)

Exp. No.	β-Dicarbonyl compounds	pK_a	k_2 (l/mol·min)	pH[a]
1	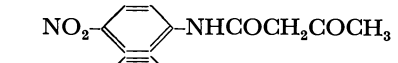	9.65	1.22×10^7	4.3—5.2
2	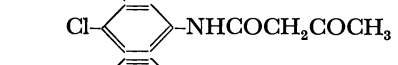	10.25	3.27×10^7	4.3—5.2
3	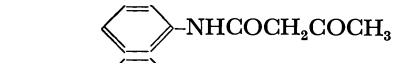	10.46	4.84×10^7	4.3—5.2
4	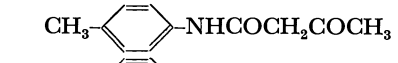	10.55	5.66×10^7	4.3—5.2
5	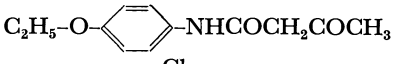	10.62	5.70×10^7	4.7—5.2
6		9.71	1.50×10^7	3.7—4.7
7		10.26	3.05×10^7	4.3—4.7
8	$CH_2(COOC_2H_5)_2$	13.3[b]	4.8×10^8	6.2—7.2
9	$CH_3COCH_2COOC_2H_5$	10.79[c]	3.10×10^7	4.7—5.8
10	$CH_3COCH_2COOCH_3$	10.57	1.34×10^7	4.7—5.8
11	$CH_3COCH_2COCH_3$	9.01[c]	1.92×10^6	3.7—4.7
12	$C_6H_5COCH_2COCH_3$	8.77[d]	1.20×10^6	3.7—4.7
13	$CH_3COCH_2COCF_3$	6.40 (6.3[e])	4.31×10^2	4.3—6.2
14		6.38[f]	6.67×10^2	4.3—6.2
15	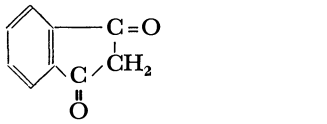	7.12	9.60×10^5	3.7—4.7
16	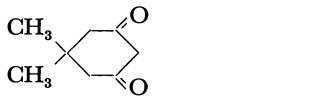	5.22[g]	1.99×10^4	2.0—2.8
17	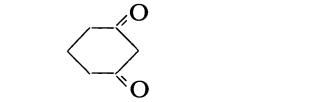	5.07	6.06×10^3	2.8—3.7

a) pH range in which the reaction rate was measured
b) R. G. Pearson and J. M. Mills, *J. Amer. Chem. Soc.*, **72**, 1692 (1950).
c) W. S Walisch and H. A. Ruppersberg. *Chem. Ber.*, **92**, 2622 (1959).
d) M. Laloi and M. Rubinstein, *Bull. Soc. Chim. Fr.*, **1965**, 310.
e) J. C. Reid and M. Calvin, *J. Amer. Chem. Soc.*, **72**, 2948 (1950).
f) E. H. Cook and R. F. Taft, Jr., *ibid.*, **74**, 6103 (1952).
g) R. P. Bell and R. R. Robinson, *Trans. Farady Soc.*, **57**, 965 (1961).

ethane occurs substantially more slowly than those of the other active methylene compounds of the same acid strength.[15]

Effect of the Structure of the Azo Component on the Reactivity. Although many investigations concerning carbanion have been reported in the literature, there have been only fragmentary reports about the structural effect of the carbanion on the reactivity. Therefore, it seemed that is would be of interest to compare the reactivities of various carbanions towards the diazonium salt.

It may be seen in Table 2 that the effects of substituents in the benzene ring, including *ortho*-substituents, on the reactivity are small in acetoacetanilide (No. 1—7), and that the reaction is accelerated by an electron-donating substituent (No. 4 and 5). This result may be

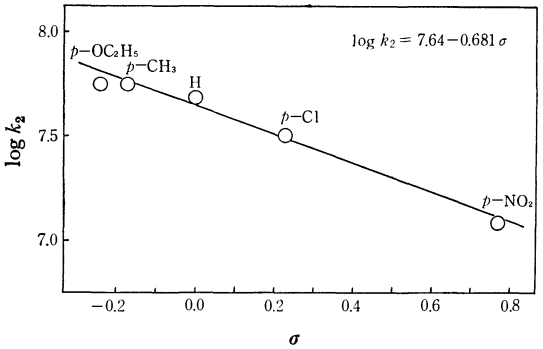

Fig. 2. Hammett plot for the reaction of diazobenzene-4-sulfonic acid with substituted acetoacetanilides.

15) R. G. Pearson and R. L. Dillon, *J. Amer. Chem. Soc.*, **75**, 2439 (1953).

interpreted on the basis of the increase in the nucleophilic character of the enolate ion, as will be described later. Figure 2 represents the linear dependence of log k_2 on the substituent constnat (σ). The small ρ value (0.681) can be explained in terms of the insulating effect of the NH–CO group for the transmission of the electronic effect of the substituent.

In β-dicarbonyl compounds (No. 1—17), the k_2 value varies considerably with the nature of the neighboring group. In Table 2, it may be seen that in general, the higher the pK_a value of a β-dicarbonyl compound, the more readily does the reaction occucr. The correlation between the reactivity and the pK_a value of an azo component is represented graphically in Fig. 3 by plotting the logarithms of the rate constants against the pK_a values.

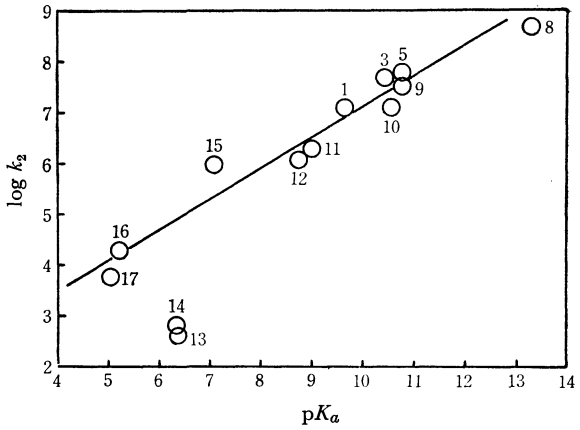

Fig. 3. Relation between pK_a values and rate constants (k_2) for the reaction of diazobenzene-4-sulfonic acid with β-dicar bonyl compounds. (The numbers refer to the β-dicarbonyl compounds as listed in Table 2.)

It is apparent from Fig. 3 that the plots of all the β-dicarbonyl compounds including alicyclic derivatives (No. 15—17), except for trifluoro-derivatives (No.13 and 14), are on a straight line. These results indicate that the reactivity of an enolate ion (7), that is, the nucleophilicity of an enolate ion towards the diazonium cation, is closely related to its pK_a value.

(7)

A similar relationship between the reactivity and the pK_a of phenols has been found in the coupling reaction (8) of *p*-substituted phenols with diazobenzene-4-sulfonic acid.[16]

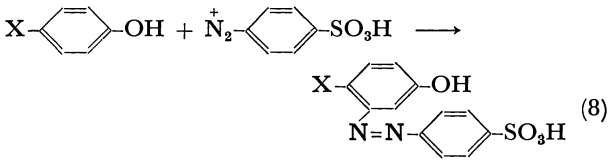

(8)

A similar parallelism between reactivity and pK_a has been observed for various active methylene compounds which include such activating substituents as CN, NO_2, COR, and Cl, as is shown in Table 3.

However, it is clear from Fig. 4 that, in contrast to the case of the β-dicarbonyl compound, a simple correlation was not observed. These results shown that the pK_a value is not a decisive measure of the nucleophilic reactivity of a carbanion in the coupling reaction.

Table 3. Rate constants of the coupling reaction of diazobenzene-4-sulfonic acid with various active methylene compounds (20°C, μ: 0.25)

Exp. No.	Active methylene compound	pK_a	k_2 (l/mol·min)	pH
18	$ClCH_2COCH_3$	13.57[a]	8.82×10^7	6.2—7.2
19	$CNCH_2CONH_2$	13.45	2.06×10^9	5.2—6.2
20	$ClCH_2COCH_2Cl$	12.88[a]	2.43×10^8	5.8—6.8
21	$CH_3SO_2CH_2SO_2CH_3$	12.32 (12.50[b])	3.10×10^7	6.2—7.2
22	$C_2H_5SO_2CH_2SO_2C_2H_5$	11.97	1.97×10^6	6.2—7.2
23	$CNCH_2COOC_2H_5$	11.4	1.6×10^8	4.3—5.2
24	$CNCH_2CN$	11.01 (11.16[a])	4.09×10^8	2.8—4.7
25	$NO_2CH_2COOC_2H_5$	5.62 (5.82[c])	1.29×10^3	3.7—4.7
26		7.15[d]	3.99×10^6	2.0—2.9
27	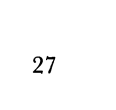	6.65[e]	1.15×10^6	2.0—2.9
28	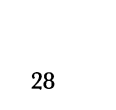	4.49	8.21×10^3	2.9—3.7

a) F. Hashimoto, G. Tanaka, and S. Nagakura, *J. Mol. Spectrosc.*, **10**, 401 (1963).
b) W. Walter and H. L. Wiedemann, *Ann. Chem.*, **685**, 29 (1965).
c) Ref. 15. d) Ref. 11. e) Ref. 12.

16) Y. Hashida, I. Shimoda, S. Sekiguchi, and K. Matsui, *Kogyo Kagaku Zasshi*, **74**, 73 (1971).

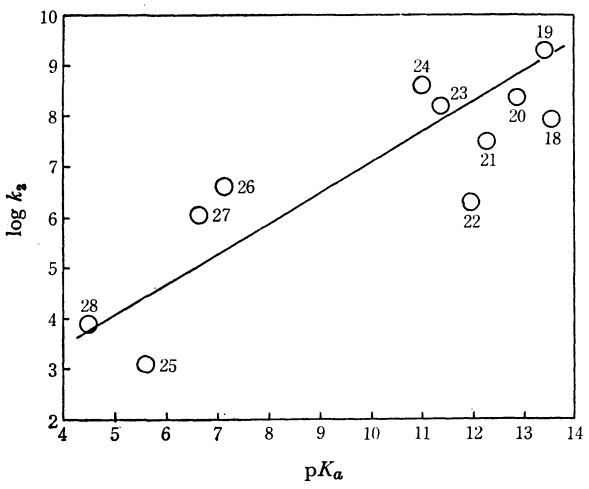

Fig. 4. Relation between pK_a values and rate constants (k_2) for the reaction of diazobenzene-4-sulfonic acid with various active methylene compounds. (The numbers refer to the compounds as listed in Table 3. The line here is drawn to same as that in Fig. 3.)

In general, there is no theoretical reason to expect a close parallelism between the nucleophilicity and the basicity,[17-9] since the nucleophilicity reflects a kinetic phenomenon, while the basicity is concerned with an equilibrium phenomenon. Nevertheless, it may be pointed out that the nucleophilicity is fairly well correlated with the basicity, and good correlations have been obtained by restricting nucleophilic reagents with a similar limited structure, such as substituted anilines or phenols.[2] However, with nucleophilic reagents with different structures, a close parallelism between basicity and nucleophilicity has not been found to hold;[21] the deviations from the line are usually explained by such factors as the polalizability, the steric effect, and the α-effect[22]

The above generalization fits our results. Within β-dicarbonyl compounds or *p*-substituted phenols, the reactivity was found to correlate well to the pK_a scale, whereas only an unsatisfactory linear relation has been observed over the wide range of active methylene compounds examined, as is shown in Table 3. These results can be explained by assuming that, in the former, the influencing factors on reactivity other than the pK_a value are the same, while in the latter cofactors exert different effects on the reaction rate. It is not easy to account for the deviation from the pK_a-log k_2 relationship. Unfortunately, there are not sufficient data available on the reactivities of a series of carbanions. Therefore, it is not apparent that the order of reactivity of carbanions illustrated in Figs. 3 and 4 is applicable to other reactions. This problem is now under investigation.

17) J. Miller, "Aromatic Nucleophilic Substitution," Elsevier Publishing Company, Amsterdam (1968), p. 180.

18) C. K. Ingold, "Structure and Mechanism in Organic Chemistry," Cornell University Press., Ithaca and London (1969), p. 448.

19) J. E. Leffler and E. Grunwald, "Rates and Equilibria of Organic Reaction," translated ed., by Y. Tsuno, M. Sawada, N. Shimizu, and T. Fujii, Hirokawa Shoten, Tokyo (1968), p. 227.

20) K. Okamoto, H. Kushiro, I. Nitta, and H. Shingu, This Bulletin, **40**, 1900 (1967).

21) R. G. Pearson, H. Sobel, and J. Songstad, *J. Amer. Chem. Soc.*, **90**, 319 (1968).

22) J. O. Edward and R. G. Pearson *ibid.*, **84**, 16 (1962).

Photocycloaddition of Thiocarbonyl Compounds to Multiple Bonds. VII. The Reaction of Thiobenzophenone with Acetylenic Compounds

Atsuyoshi OHNO, Tamotsu KOIZUMI, and Yutaka OHNISHI
Sagami Chemical Research Center, Ohnuma, Sagamihara-shi, Kanagawa

(Received March 22, 1971)

Photocycloaddition of thiobenzophenone to acetylenic compounds, R-C≡C-R′ (R=COOH, Ph, CH_2OH, and CN; R′=H: R=COOMe; R′=COOMe), affords 1-phenyl-2-thia-1,2-dihydronaphthalene derivatives. The key step to the product is an intra-molecular aromatic substitution of the composite vinylic biradical **13**. The difference in reactivity of acetylenic and olefinic compounds as well as that between thiobenzophenone and benzophenone are discussed. Ethoxyacetylene does not undergo the reaction. This is interpreted in terms of electronegativity of a radical center in **13**. It is found that cyanoacetylene reacts with butanethiyl radical in contrast to its olefin analog, acrylonitrile.

It has been reported that the photocycloaddition of thiobenzophenone to olefins leads to the formation of 1,4-dithiane derivatives or to thietane derivatives depending on the wavelength of light utilized and the structure of the olefin.[1,2] Similar reactions with ketones are well known and always result in the formation of oxetane derivative.[3,4]

The Paterno-Büchi reaction is also applicable to acetylenic compounds. However, the oxetene derivatives formed are too unstable to be isolated and the final products are α,β-unsaturated ketones.[5,6] It is

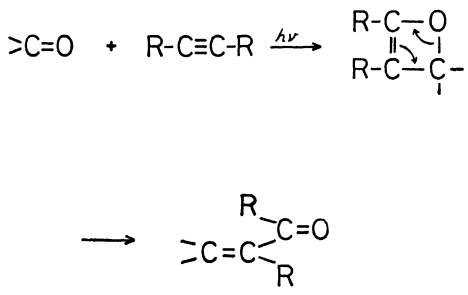

(1)

interesting to see whether the difference between ketones and thioketones observed in the reactions with olefins is also observed in the reactions with acetylenic compounds. Thus, we have studied the photocycloaddition of thiobenzophenone to several acetylene derivatives[7] and found that the reaction has completely different features from those involving olefins.

Results

The reactions of propiolic acid (**1**), phenylacetylene (**2**), propargyl alcohol (**3**), cyanoacetylene (**4**), and dimethyl acetylenedicarboxylate (**5**) yielded 1-pnenyl-2-thia-1,2-dihydro-4-naphthoic acid (**7**), 1,4-diphenyl-2-thia-1,2-dihydronaphthalene (**8**), 1-phenyl-2-thia-1,2-dihydro-4-hydroxymethylnaphthalene (**9**), 1-phenyl-2-thia-1,2-dihydro-4-cyanonaphthalene (**10**), and dimethyl 1-phenyl-2-thia-1,2-dihydronaphthalene-3,4-dicarboxylate (**11**), respectively, after irradiation with 5890 Å light from sodium lamps (480 W). The

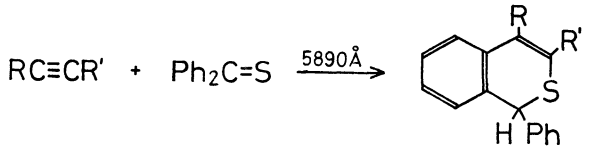

1—5

1; R=COOH, R′=H
2; R=Ph, R′=H
3; R=CH_2OH, R′=H
4; R=CN, R′=H
5; R=COOMe, R′=COOMe
6; R=OEt, R′=H

7—11

7; R=COOH, R′=H
8; R=Ph, R′=H
9; R=CH_2OH, R′=H
10; R=CN R′=H
11; R=COOMe, R′=COOMe

reaction with ethoxyacetylene (**6**) did not proceed under these conditions. Reaction conditions and yields of products are summarized in Table 1.

The structures of the products were identified by NMR, IR, Mass spectra, elemental analyses, and chemical reactions. When **8** was treated with Raney Ni (W-2), it afforded 1,3-diphenylindane in 73% yield by reductive desulfuration.[8,9] The compound **9** was synthesized independently in 89% yield by reduction of **7** with lithium aluminum hydride. The carboxylic acid was also converted into **10** in several steps (27%).

When **8** was titrated with bromine in carbon tetrachloride, one equivalent of bromine was consumed and, after recrystallizations from ethanol, 1,4-diphenyl-2-thia-1,2-dihydro-3-ethoxynaphthalene (**12**) was isolated.

1) a) A. Ohno, Y. Ohnishi, and G. Tsuchihashi, *J. Amer. Chem. Soc.*, **91**, 5038 (1969); b) A. Ohno, Y. Ohnishi, and G. Tsuchihashi, *Tetrahedron Lett.*, **1969** 283; c) A. Ohno, Y. Ohnishi, and G. Tsuchihashi, *ibid.*, **1969**, 161.

2) G. Tsuchihashi, M. Yamauchi, and M. Fukuyama, *ibid.*, 1971 (1967).

3) a) G. Büchi, C. G. Imman, and E. S. Lipinsky, *J. Amer. Chem. Soc.*, **76**, 4327 (1954); b) G. Buchi and N. C. Yang, *ibid.*, **79**, 2318 (1957).

4) For recent reviews, see a T. R. Evans, A, A. Lamola, P.A. Leermakers, and N. J. Turro, "Energy Transfer and Organic Photochemistry," Interscience Publishers, New York, N. Y. (1969), pp. 210—224; b) J. N. Pitts, Jr. and J. K. S. Wan, in "The Chemistry of the Carbonyl Group," ed. by S. Patai, Intersicence Publishers, New York, N. Y. (1966), Chapter 16.

5) G. Büchi, J. T. Kofron, E. Loller, and D. Rosenthal, *J. Amer. Chem. Soc.*, **78**, 876 (1956).

6) H. J. T. Bos and J. Boleiji, *Rec. Trav. Chim. Pays-Bas*, **88**, 465 (1969).

7) A. Ohno, T. Koizumi, Y. Ohnishi, and G. Tsuchihashi, *Tetrahedron Lett.*, **1970**, 2025.

8) W. A. Bonner and R. A. Grimm, in "The Chemistry of Organic Sulfur Compounds, "Vol. 2, ed. by N. Kharasch and C. Y. Meyers, Pergamon Press, New York, N. Y. (1966), pp. 35—71.

9) H. Hauptmann and W. F. Walter, *Chem. Rev.*, **62**, 347 (1962).

Table 1.[a] Reactions of thiobenzophenone with acetylenes

Acetylene	Thiobenzophenone/ Acetylene, g/g	Solvent, ml	Reaction time, hr	Product	Yield,[b] %
1	2.5/10.0	THF, 40	240	**7**	26
2	3.0/12.0	Cyclo-hexane, 40	70	**8**	56
3	3.0/12.0	Cyclo-hexane, 40	115	**9**	28
4	2.5/10.0	Ether, 40	36	**10**	20
5	3.0/12.0	THF, 40	20	**11**	28
6	2.5/10.0	Cyclo-hexane, 40	500	no reaction	

a) Reactions were carried out at the temperature of running water.
b) Based on thiobenzophenone.

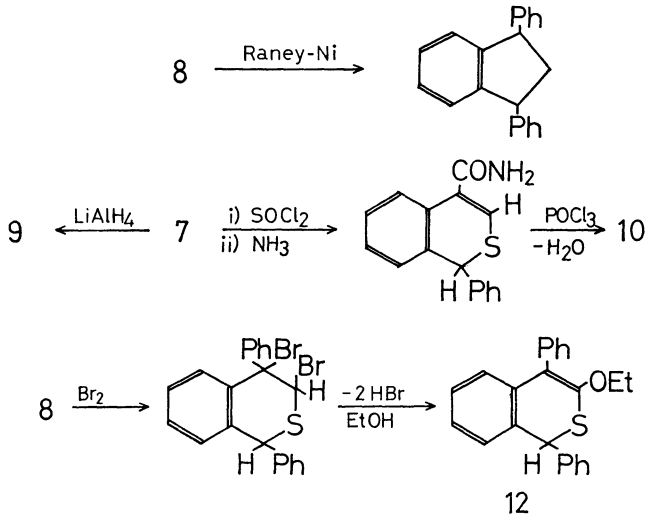

Discussion

As previously reported,[1a] it is evident that irradiation with 5890 Å light excites thiobenzophenone to its n,π^* singlet state, which is rapidly deactivated to n,π^* triplet state by intersystem crossing. Since the n,π^* triplet state of thiobenzophenone behaves similarly to a thiyl radical,[1a] the reaction is undoubtedly initiated by the attack of the n,π^* triplet state of thiobenzophenone to an unsaturated carbon atom[10] and the following is the most reasonable mechanism:

$$Ph_2C{=}S \xrightarrow{5890\text{Å}} {}^3(Ph_2C{=}S)_{n,\pi^*}$$

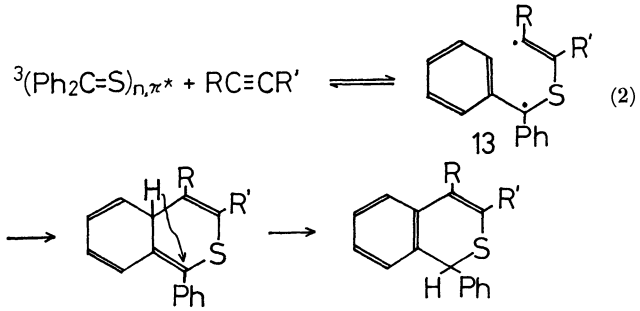

10) A. A. Oswald and K. Griesbaum, in "The Chemistry of Organic Sulfur Compounds," Vol. 2, ed. by N. Kharasch and C. Y. Meyers, Pergamon Press, New York, N. Y. (1966), pp. 246—254.

The last step of the reaction, intra-molecular hydrogen migration, has been proved by the aid of deuterium-labelling technique. Thus, no deuterium was incorporated in the product even when the reaction was carried out in perdeuterated isopropyl alcohol or in deuterated chloroform as a solvent. However, since this is thermally forbidden 1,3-sigmatropic migration,[11] the actural course might be more complicated.

The above results exemplify the difference in reactivity of σ- and π-radicals. When an olefin is employed as a substrate, the radical center at the end carbon in the intermediate biradical **14**, where an odd electron exists in a p-orbital (π-radical), either attacks another molecule of thiobenzophenone forming another composite biradical **15**, or combines with the radical center at the benzhydryl position forming a stable molecule **16**. The reaction course depends on the nature of the R groups. It is known that the thiocarbonyl-sulfur is preferentially attacked by such carbon radicals.[12]

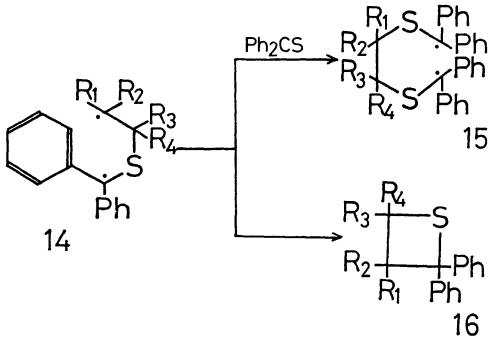

On the other hand, the corresponding radical center in **13** contains an odd electron in a sp^2 orbital (σ-radical) and can only attack the thiocarbonyl-sulfur with difficulty, which is in contrast to the facile attack on the aromatic ring.[13-15] Thus, the reactivity toward a phenyl ring and that toward a thiocarbonyl-sulfur are reversed in **13** and **14**. The fact that the reaction with **6** does not proceed, contrary to the expectation that the

11) J. B. Hendrickson, D. J. Cram, and G. S. Hammond, "Organic Chemistry," 3rd Ed., McGraw-Hill Book Co., New York, N. Y. N. Y. (1970), pp. 860—862.

12) G. Tsuchihashi, M. Yamauchi, and A. Ohno, This Bulletin, **43**, 968 (1970). The lower the ionization potential of a radical, the larger the tendency to attack thiobenzophenone.

addition of n,σ^* triplet state of thiobenzophenone to an electron-rich carbon-carbon triple bond might be fast,[1a, 16] supports the interpretation. That is, an α-oxygen increases the inoization potential of an odd electron by its inductive effect. This reduces the facility of a radical to attack the aromatic ring. Since the electronegativity of an orbital of σ-radical that has an α-oxygen is not as small as that of a π-radical, it cannot attack the thiocarbonyl-sulfur either. Consequently, the thiobenzophenone is regenerated from **13** by the reverse reaction. It should be noted that all these reactions are competitive.

Although no concrete evidence has yet been obtained for a discussion of factors that result in combination of two radical centers in carbonyl compounds (Eq. (1)) and aromatic substitution in thiocarbonyl compounds (Eq. (2)), one possible explanation is that a longer bond length and smaller bond angle in the C–S–C moiety than in the C–O–C leads **13** to favorable cyclization over its oxygen analog.[17] It should be noted that the attack to an aromatic ring must take place from the side of out-of-plane with the ring and the biradical should be helical.[18] An alternative possibility is the n,π^* singlet state being the active species in the reaction of carbonyl compounds, where a four-membered ring is formed in one-step.[19] We cannot expect a larger reactivity of the *ortho*-position in the thiobenzophenone moiety in **13** than that of its oxygen analog, because spin densities at *ortho*–positions in thiobenzophenone ketyl and in benzophenone ketyl are almost equivalent.[20]

Herein arises another important difference between olefinic and acetylenic compounds. The potocycloaddition of thiobenzophenone to acrylonitrile and methyl acrylate proceeds *via* an ionic mechanism. Thus, only irradiation with 3660 Å light is effective, because this wavelength excites thiobenzophenone to its π,π^* singlet state, which has the character of a thiolate anion.[1a,c] Irradiation with 5890 Å light, however, is ineffective in producing photocycloadducts with these olefins, because a thiyl radical-like species is produced in this process. In contrast, the corresponding acetylene analogs, **4** and **1**, undergo the reaction on irradiation with 5890 Å light. It is highly unlikely to expect the n,π^* singlet state of thiobenzophenone as reactive species in the reaction with acetylenes under the above conditions.[21] Thus, we should expect that these acetylenic compounds react with the n,π^* triplet state of thiobenzophenone or a thiyl radical.

This difference can be interpreted in terms of molecular orbital considerations. Since an acetylenic bond is composed of two orthogonal π-orbitals, even if electrons in one orbital are withdrawn by an electron-attracting group, others in the second orbital will be rearranged to compensate the charge-separation in the molecule. Consequently the electron-deficiency at the end carbon is not as great as that in the corresponding position in olefinic compounds and this is still susceptible to the electrophilic attack of a thiyl radical. The situation is visualized in Figure 1 with **4**, where two molecular orbitals of π-symmetry ($\chi\pi_1$ and $\chi\pi_2$) are calculated by McLean and Yoshimine with SCF-LCAO-MO method with Slater–type functions.[22]

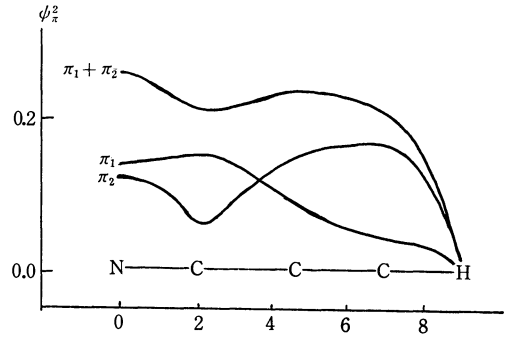

Fig. 1. A diagram for the π-electron densities in cyanoacetylene.

In order to test whether the above theoretical consideration is applicable to true thiyl radicals, we have studied radical additions of butanethiol to cyanoacetylene and found that cyanoacetylene *does* add the thiol, affording 2-(*n*-butylthio)acrylonitrile, under conditions where the reaction with acrylonitrile does not proceed,[23] indicating larger susceptibility of cyanoacetylene than acrylonitrile to the attack of thiyl radicals. We do not, of course, consider this to be the only reason for the difference between acetylenic and olefinic compounds.

Experimental

Material. Thiobenzophenone was prepared and puri-

12) a) E. L. Eliel, M. Eberhardt, O. Simamura, and S. Meyerson, *Tetrahedron Lett.*, **1692**, 749; b) J. F. Garst and R. S. Cole, *ibid.*, **1963**, 679.

14) a) A phenyl radical derived from phenylazotriphenylmethane cannot easily be captured by thiobenzophenone: G. Tsuchihashi and M. Yamauchi, personal communication, 1969; b) A styryl radical derived from cinnamoyl peroxide attacks a phenyl ring very easily, provided certain oxidizing agents are present: N. Wada, K. Tokumaru, and O. Simamura, personal communication, 1970; c) N. Wada, PhD Thesis, The Univ. of Tokyo, December 1970.

15) M. Levy and M. Szwarc, *J. Amer. Chem. Soc.*, **76**, 5981 (1954).

16) H. J. Alkema and J. F. Arens, *Rec. Trav. Chim. Pays-Bas*, **79**, 1257 (1960).

17) Investigations with Driding models reveal that the end vinylic carbon in **13** can position itself over the carbon of a phenyl ring with only slight strain in the C-S-C angle, while the corresponding carbon in the oxygen analog of **13** of located far from the phenyl ring.

18) G. H. Williams, "Homolytic Aromatic Substituion," Pergamon Press, New York, N. Y. (1960), p. 50.

19) a) N. J. Turro, P. Wriede, J, C. Dalton, D. Arnold, and A. Grick, *J. Amer. Chem. Soc.*, **89**, 3950 (1967); b) N, J. Turro and P. A. Wriede, *ibid.*, **90**, 6863 (1968); c) N. J. Turro and P. A. Wriede, *ibid.*, **92**, 320 (1970); d) J. C. Dalton, P. A. Wriede, and N. J. Turro, *ibid.*, **92**, 1318 (1970).

20) H. C. Heller, *ibid.*, **89**, 4288 (1967). Also see A. Hudson and K. D. J. Root, *J. Chem. Soc., B*, **1970**, 656 for $PhXCH_2$ (X=O,S) radicals.

21) G. N. Lewis and M. Kasha, *J. Amer. Chem. Soc.*, **67**, 994 (1945).

22) A. D. McLean and M. Yoshimine, "Tables of Linear Molecule Wave Functions," published as a supplement to IBM J. Res. Develop., IBM Co., San Jose, Calif, (1967), p. 223.

23) C. D. Hurd L. L. Gershbein, *J. Amer. Chem. Soc.*, **69**, 2328 (1947).

fied as previously described.[24,25] Commercial acetylenes were used except for cyanoacetylene.[26] They were purified by distillation prior to use.

Photocycloaddition. The reaction was carried out in tetrahydrofuran, ether, or cyclohexane as an inert solvent. Isopropyl alcohol-d_8 and chloroform-d_1 were also inert to the reaction. The apparatus and detailed procedure have been described.[18,25]

Characterization of 1-Phenyl-2-thia-1,2-dihydro-4-naphthoic Acid (7). After the reaction, the solvent was evaporated under reduced pressure. A mixture of ether and *n*-hexane was added to the residue, which was allowed to stand in a refrigerator until precipitation occurred. The crystals were filtered and the filtrate was subjected to silica gel column chromatography with *n*-hexane - chloroform (8:3) mixture as an eluent. Crystals thus obtained were combined to the former ones and recrystallized from aq-acetone giving 0.88 g (26% yield) of **7**: mp 164—166°C: NMR δ ($CDCl_3$, TMS); 5.13 (d, H, J=1.5 Hz), 7.90 (d, R′=H, J=1.5 Hz), 6.90—7.44 and 8.00—8.12 (m, H_{ar}), and 10.21 (s, CO_2H): IR; 3050, 3010, 1660, 1420, and 1260 cm^{-1}: MS *m/e* (species, %); 268 (M^+, 100), 250 (M^+-18, 10), 235 (M^+-SH, 14), 221 (M^+-HCO_2H, 24), 191 (M^+-Ph, 134), and 145 (PhC_2HCO_2, 13): MW; Calcd for $C_{16}H_{12}O_2S$: 268. Found: 265.

Found: C, 71.61; H, 4.56; S, 11.94%. Calcd for $C_{16}H_{12}O_2S$: C, 71.64; H, 4.48; S, 11.94%.

Characterization of 1,4-Diphenyl-2-thia-1,2-dihydronaphthalene (8). The solvent was evaporated from a reaction mixture under reduced pressure. The residue was chromatographed on silica gel with *n*-hexane — chloroform (8:3) mixture as an eluent yielding 2.55 g (56% yield) of a pale green glassy solid, **8**. All attempts, for further purification including separation on tlc, were unsuccessful.[27] However, the structure was confirmed by chemical reactions as well as the following spectral data: NMR δ (CCl_4, TMS); 4.96 (d, H, J=1.0 Hz), 6.19 (d, R′=H, J=1.0 Hz), and 6.85—7.20 (m, H_{ar}): IR; 3050, 3010, 1600, and 1450 cm^{-1}: MS *m/e* (species, %): 300 (M^+, 100), 267 (M^+-SH, 27), 223 (M^+-Ph, 103), and 178 (PhC_2HPh, 10): MW; Calcd for $C_{21}H_{16}S$: 300. Found; 275.

Characterization of 1-Phenyl-2-thia-1,2-dihydro-4-hydroxymethylnaphthalene (9). The residue obtained from the usual treatment was chromatographed on silica gel. The chromatogram was developed by 300 m*l* of *n*-hexane — chloroform (4:6) mixture and was then eluted by chloroform yielding 1.08 g (28% yield) of pale yellow oil, **9**. This compound is highly hygroscopic.[27] The structure was confirmed by chemical and spectral evidence: NMR δ ($CDCl_3$, TMS); 2.90 (broad s, OH), 4.51 (Broad s, CH_2), 5.05 (d, H, $J<0.5$ Hz), 6.36 (d, R′=H, $J<0.5$ Hz), and 6.90—7.54 (m, H_{ar}): IR 3500—3100, 3040—3000, 765, and 695 cm^{-1}: MS *m/e* (species, %); 254 (M^+, 100), 221 (M^+-SH, 20), 177 (M^+-Ph, 156), and 115 (PhC_3H_3, 34).

Characterization of 1-Phenyl-2-thia-1,2-dihydro-4-cyanonaphthalene (10). The residue obtained was chromatographed on silica gel with *n*-hexane — chloroform (9:1) mixture as an eluent. The solid thus obtained was recrystallized from aq-ethanol yielding 0.615 g (20% yield) of **10**: mp 70—72°C: NMR δ ($CDCl_3$, TMS); 5.21 (d, H, $J<0.5$ Hz), 7.10 (d, $J<0.5$ Hz),[28] and 6.80—7.85 (m, H_{ar}): IR; 3080—3000, 2217, 1580, 1540, and 1440 cm^{-1}: MS *m/e* (species, %); 249 (M^+, 100), 222 (M^+-HCN, 8), 216 (M^+-SH, 12), and 172 (M^+-Ph, 172).

Found: C, 76.85; H, 4.74; N, 5.53; S, 12.88%. Calcd for $C_{16}H_{11}NS$: C, 77.07; H, 4.45; N, 5.62; S, 12.86%.

Characterization of Dimethyl 1-Phenyl-2-thio-1,2-dihydronaphthalene-3,4-dicarboxylate (11). The residue obtained was chromatographed on silica gel with *n*-hexane - chloroform (8:3) as an eluent. Crystals thus obtained were recrystallized from *n*-hexane - benzene mixture, yiedling 1.45 g (28.3% yield) of **11**; mp 90—91°C: NMR δ (CCl_4, TMS); 3.66 (s, CH_3), 3.80 (s, CH_3), 5.05 (s, H), 6.78—6.94 and 7.02—7.50 (m, H_{ar}): IR; 1710—1745 cm^{-1} ($\nu_{C=O}$): MS *m/e* (species, %); 340 (M^+, 100), 309 (M^+-OCH_3, 22), 307 (M^+-SH, 9), 263 (M^+-Ph, 170), and 221 ($PhC_6H_4\cdot C_2S$, 98).

Found: C, 67.08; H, 4.96; S, 9.42%. Calcd for $C_{19}H_{16}O_4S$: C, 67.04; H, 4.74; S, 9.42%.

Reductive Desulfuration of 8. A mixture of 0.73 g of **8** and excess Raney Ni (W-2) in benzene was refluxed for 27hr. After the reaction, the mixture was filtered and the solvent was evaporated from the filtrate under reduced pressure. The remaining crystals were recrystallized from benzene-methanol (1:1) mixture giving 0.48 g (73% yield) of 1,3-diphenylindane: mp 157—159°C (lit,[29] 156—157°C). The spectral data also supported the structure.

Bromination of 8. An ice-cooled carbon tetrachloride (3 m*l*) solution of **8** (4.33×10^{-4} mol) was titrated with 6.25×10^{-2}N solution of bromine in carbon tetrachloride. The bromine was consumed when 7 m*l* of the solution (4.375×10^{-4} mol of Br_2) had been added. The mixture was stirred for additional 1 hr. A small amount of precipitate thus obtained was filtered and recrystallized from ethanol. The structure of the crystal was identified by NMR and mass spectra to **12**: NMR δ (DMSO-d_6, TMS); 1.12 (t, 3H), 3.43 (q, 2H), 6.78 (s, 1H), and 7.40 (m, 14H): MS *m/e* (species, %); 344 (M^+, 100), 300 (M^+-CH_3CHO, 422), 267 (M^+–Ph and/or 300–SH, 56), 223 (300–Ph, 81), and 165 ($PhC\cdot C_6H_4$, 69).

Reduction of 7 to 9.[30] Into a three-necked flask containing 47 mg of $LiAlH_4$ and 5 m*l* of dry ether, 263 mg of **7** in 20 m*l* of dry ether was added slowly with stirring. The mixture was stirred for 10 hr under refluxing. Ethanol, water, and 10% H_2SO_4 were then added successively to decompose excess $LiAlH_4$. The organic materials were extracted with ether and the ether layer was dried over Drierite. After the solvent was evaporated under reduced pressure, 0.221 g (89% yield) of pale yellow oil remained, whose NMR, IR, and mass spectra were identical with those of **9** obtained by photocycloaddition.

Conversion of 7 to 10.[31,32] A mixture of **7** (0.968 g) and $SOCl_2$ (1.0 g) was kept at 30—35°C for 3 hr. The mixture was cooled in an ice-bath and 30 m*l* of conc. NH_4OH was added dropwise. The organic materials were extracted with chloroform and the chloroform layer was dried over Drierite. Crude crystals of the amide (0.35 g) were obtained after evaporation of the solvent under reduced pressure: mp 145—149°C: NMR δ ($CDCl_3$, TMS); 5.15 (d, 1H, $J<0.5$ Hz), 5.94 (broad

24) B. F. Gofton and E. A. Braude, "Organic Syntheses," Coll. Vol. IV, p. 927 (1963)

25) A. Ohno, Y. Ohnishi, M. Fukuyama, and G. Tsuchihashi, *J. Amer. Chem. Soc.*, **90**, 7038 (1958).

26) We thank Dr. K. Morita of Takeda Chemical Industries, Ltd. for kindly supplying this compound.

27) Elemental analyses had a deviation of about 1% from the theoretical value for carbon, although satisfactory results were obtained for sulfur.

28) Identified by spin decoupling technique.

29) K. Ziegler, H. Grabbe, and F. Ulrich, *Chem. Ber.*, **57**, 1983 (1924).

30) H. H. Zeiss, C. E. Slimowicz, and V. Z. Pasternak, *J. Amer. Chem. Soc.*, **70**, 1981 (1948).

31) R. E. Kent and S. M. McElvain, "Organic Syntheses," Coll. Vol. III, p. 490 (1955).

32) A. R. Surrey, *ibid.*, Coll. Vol. III, p. 535 (1955).

s, 2H), and 7.10—7.50 (m, 10H): IR; 3990, 3190, 1640, 1613, 1485, and 1414 cm^{-1}.

To a mixture of the amide (0.35 g), NaCl (1.5 g), and CCl_4 (10 m*l*) ,0.3 g of $POCl_3$ was added with stirring, and the mixture was refluxed for 3 hr. The mixture was cooled to room temperature. The precipitate was filtered and the filtrate was dried over Drierite. After evaporation of the solvent under reduced pressure, 0.23 g (27% yield based on **7**) of **10** was obtained: mp 70—72°C. Spectral data were identical with those of **10** obtained by photocycloaddition.

Photoaddition of n-*Butanethiol to* ***4***. A mixture of *n*-butanethiol (1.76 g) and **4** (1.0 g) was prepared in a dry box under an atmosphere of CO_2. To a half portion of this mixture was added 50 mg of benzoylperoxide (BPO). The two half portions were placed in Vycor ampules. The ampules were vacuum-sealed and subjected to irradiation with light of 2537 Å from a 160 W low-pressure mercury lamp (Riko-Kagaku Sangyo) for 3 hr at room temperature. The oily products obtained after evaporating volatile materials were chromatographed on silica gel with *n*-hexane containing 10% benzene as an eluent. The products were identified to be *cis*-2-(*n*-butylthio)acrylonitrile, contaminated by a small amount of the *trans*-isomer, by the following evidence: NMR δ (CCl_4, TMS); 0.95 (m, 3H), 1.57 (m, 4H), 2.90 (t, 2H, J= 6.8 Hz), 5.22 (d, 1H, J=10.5 Hz), and 7.11 (d, 1H, J=10.5 Hz).

Yields were determined by vpc (Hitachi K-53 (FID) with a column of 20% SE-30 at 150°C) to be 13.7% (without BPO) and 27.0% (with BPO).

We thank Dr. G. Tsuchihashi of SCRC and Professor R. L. Schowen of the University of Kansas for their helpful discussions.

BULLETIN OF THE CHEMICAL SOCIETY OF JAPAN, VOL. 44, 2515—2520 (1971)

Selective Cleavage of Cysteine Peptides

Toshishige INUI

Institute of Chemistry, College of General Education, Osaka University, Toyonaka, Osaka

(Received March 25, 1971)

The cysteine peptides such as IV were cyclized to thiazolidone peptides through the corresponding *S*-chlorocarbonyl derivatives. In some peptides such as XXII, however, no cyclized products were isolated because of decomposition of the *S*-chlorocarbonyl intermediates. By the mild alkaline hydrolysis of the thiazolidone peptide the carboxylic acid from the *N*-terminal amino acid or peptide and 2-oxothiazolidine-4-carbonyl derivatives were isolated as a result of the selective cleavage of the peptide bond in which an amino group of cysteine residue participated. This cleavage reaction was applied to several cysteine peptides. The same results were observed whenever the corresponding thiazolidone peptides were formed.

In studying the sequence of amino acid residues in proteins, the selective cleavage of peptide bonds on the special amino acid residue by enzyme or by chemical modification is very valuable in the elucidation of their structure.[1] The use of cyanide ion on cystinyl peptides gives rise to cleavage at the peptide linkage involving the amino group of the cysteine residue.[2] Treatment with base on *S*-acylcysteinyl peptides also afforded a similar cleavage on peptide bond.[3] Modification of cysteinyl residues to *S*-2-aminoethylcysteinyl residues[4] and dehydroalanyl residues[5] can be used to cleave on its residue in proteins.

Protected serine and threonine peptides were cleft selectively by treatment with alkali on their corresponding oxazolidone peptides, which were obtained by the action of phosgene, to give *N*-protected amino acids or

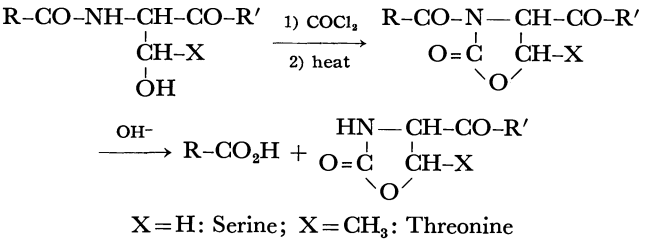

X=H: Serine; X=CH_3: Threonine

peptides and the corresponding oxazolidone derivatives.[6] Cysteine peptides may be expected to cause a similar cleavage because of the reactivity of thiol group. Actually ethyl *N*-benzoyl-L-cysteinate (I) was cyclized to the corresponding thiazolidone derivative (II) by

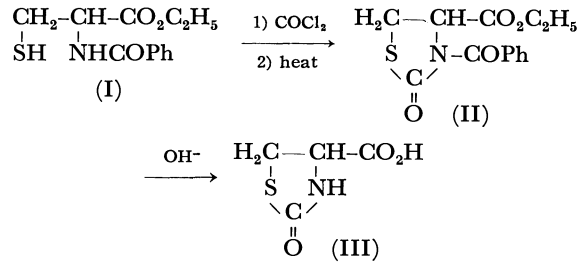

1) For reviews, *cf.* B. Witkop, *Advan. Protein Chem.*, **16**, 221 (1961); T. F. Spande, B. Witkop, Y. Degani, and A. Patchornik, *ibid.*, **24**, 97 (1970).

2) J. L. Wood and N. Catsimpoolas, *J. Biol. Chem.*, **238**, PC-2887 (1963).

3) Y. Degani, A. Patchornik, and J. A. Maclaren, *J. Amer. Chem. Soc.*, **88**, 3460 (1966).

4) H. Lindley, *Nature*, **178**, 647 (1956); M. A. Raftery and R. D. Cole, *Biochem. Biophys. Res. Commun.*, **10**, 467 (1963).

5) M. Sokolovsky, T. Sadeh, and A. Patchornik, *J. Amer. Chem. Soc.*, **86**, 1212 (1964).

6) T. Kaneko, I. Takeuchi, and T. Inui, This Bulletin, **41**, 974 (1968); T. Kaneko, S. Kusumoto, T. Inui, and T. Shiba, *ibid.*, **41**, 2155 (1968).

treatment with phosgene followed by refluxing in xylene. Hydrolysis of II with alkali in 70% ethanol provided L-2-oxothiazolidine-4-carboxylic acid (III) without any racemization.[7] If cysteine peptides are cyclized with phosgene to the corresponding thiazolidone peptides at their cysteine residue, the peptides thus obtained will selectively be cleft in two parts at the amino group of cysteine residue by alkaline hydrolysis.

First, *N*-benzyloxycarbonyl-L-phenylalanyl-L-cysteine methyl ester (IV) in which cysteine residue was located in the *C*-terminal position was studied as a model peptide for the cleavage reaction. Reduction of *N*, *N'*-bis(*N*-benzyloxycarbonyl-L-phenylalanyl)-L-cystine dimethyl ester with zinc and hydrochloric acid in methanol gave IV which was converted with phosgene into *S*-chlorocarbonyl compound (V) by using a method

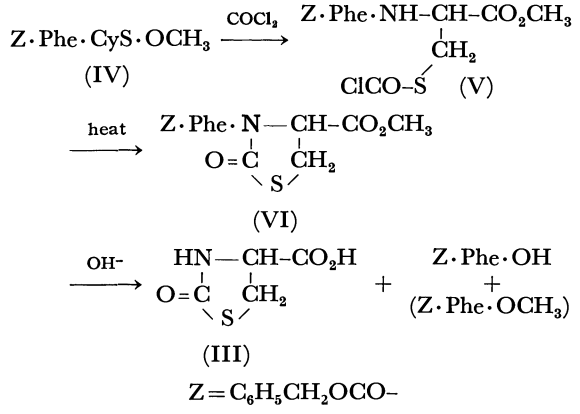

similar to that in previous papers.[6,7] The *S*-chlorocarbonyl compound V was heated in xylene under reflux to cyclize the thiazolidone peptide VI in good yield. The thiazolidone peptide VI was treated with a mixture of 1 N potassium hydroxide and methanol (1:2.5, v/v) at room temperature to give *N*-benzyloxycarbonyl-L-phenylalanine and L-2-oxothiazolidine-4-carboxylic acid (III, $[\alpha]_D$ −58°)[7] without any racemization in yields of 64 and 82%, respectively. The structures of the products isolated were confirmed by comparison of their properties such as melting point and optical rotation with those of the corresponding authentic specimens. On the other hand, the alkaline hydrolysis of VI with about 0.3N methanolic potassium hydroxide solution afforded *N*-benzyloxycarbonyl-L-phenylalanine and methyl *N*-benzyloxycarbonyl-L-phenylalaninate, which was characterized as *N*-benzyloxycarbonyl-L-phenylalanine hydrazide. Another component, however, 2-oxothiazolidine-4-carboxylic acid was obtained as a racemic form ($[\alpha]_D$ −3.9°). The same cleavage reactions also occurred on *N*-benzyloxycarbonyl-L-alanyl-L-cysteine methyl ester (VII) and *N*-benzyloxycarbonyl-L-phenylalanylglycyl-L-cysteine methyl ester (X), both giving the corresponding cleavage products as shown in Table 1. From the results, we see that the peptides are cleft selectively at the peptide linkage involving the amino group of the cysteine residue though the optical properties of the products vary with experimental conditions.

Next, *N*-benzoyl-L-cysteinyl-L-phenylalanine methyl ester (XV) was chosen as a model compound containing cysteine which was located in the middle of the peptide chain. In a similar way to that reported for the S→N acyl group migration of *S*-acylcysteine derivatives,[8,9] peptide XV was prepared from *S*-benzoyl-L-cysteinyl-L-phenylalanine methyl ester hydrochloride (XIV). The cyclized product, L-3-benzoyl-2-oxothiazolidine-4-carbonyl-L-phenylalanine methyl ester (XVII)

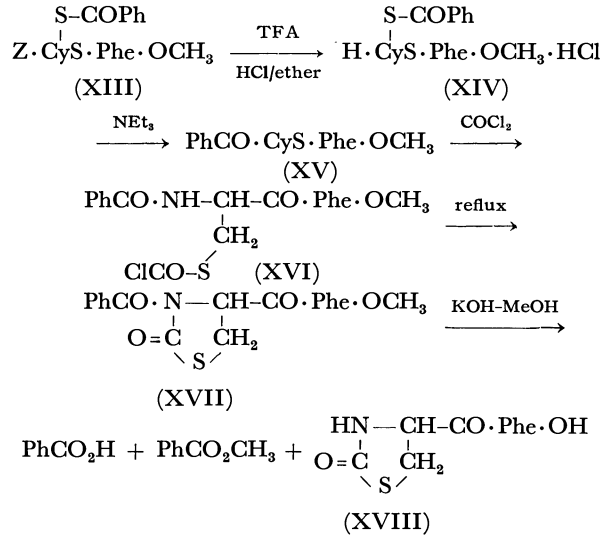

Table 1. Results of cleavage reaction of cysteine peptides

Peptide	Thiazolidone derivative	Condition[a]	Products isolated by cleavage reaction (yields)[b]	
IV	VI	KOH–MeOH	Z·Phe·OH (64%)	III (82%)
IV	VI	KOH/MeOH	Z·Phe·OH (27%) Z·Phe·OCH_3 (34%)	III (74%) (Racemized)
VII	IX	KOH–MeOH	Z·Ala·OH (54%)	III (39%)
X	XII	KOH–MeOH	Z·Phe·Gly·OH (70%)	III (80%)
X	XII	KOH/MeOH	Z·Phe·Gly·OH (32%) (Partially racemized)	III (67%) (Racemized)
XV	XVII	KOH–MeOH	$PhCO_2H$ (10%) $PhCO_2CH_3$ (28%)	XVIII (68%)

a) KOH-MeOH: mixture of 1N potassium hydroxide and methanol (1:2.5, v/v)and KOH/MeOH: 0.3N methanolic potassium hydroxide solution.
b) Unless otherwise stated, the amino acid residue has an L-configuration.

7) T. Kaneko, T. Shimokobe, Y. Ota, E. Toyokawa, T. Inui, and T. Shiba, *ibid.*, **37**, 242 (1964).
8) R. G. Hiskey, T. Mizoguchi, and T. Inui, *J. Org. Chem.*, **31**, 1192 (1966).
9) L. Zervas, I. Photaki, A. Cosmatos, and D. Borovas, *J. Amer. Chem. Soc.*, **87**, 4922 (1965).

was obtained from XV *via* the corresponding *S*-chlorocarbonyl intermediate XVI in a relatively poor yield. Similarly, hydrolysis of XVII with alkali afforded methyl benzoate, benzoic acid and L-2-oxothiazolidine-4-carbonyl-L-phenylalanine (XVIII) which was purified as its cyclohexylammonium salt (Table 1). Similar cyclizations on *N*-benzoyl-L-cysteinylglycine methyl ester (XIX) and *N*-benzyloxycarbonyl-L-phenylalanyl-L-cysteinylglycine methyl ester (XXII) to their thiazolidone derivatives through the corresponding *S*-chlorocarbonyl compounds (XX and XXIII) were studied. XX was cyclized to the thiazolidone derivative (XXI) in only a small yield, the alkaline hydrolysis of which could not be carried out, and was accompanied with formation of a cystine peptide. In the case of XXIII, no cyclized product was obtained since the corresponding *S*-chlorocarbonyl intermediate XXIII, was decomposed by heating in toluene with the evolution of bad smelling gas.

In conclusion, selective cleavage of cysteine peptide takes place at the amino group of cysteine residue in original peptide whenever its *S*-chlorocarbonyl derivative is cyclized to the corresponding thiazolidone derivative.

Experimental[10]

N,N'-Bis(N-benzyloxycarbonyl-L-phenylalanyl)-L-cystine Dimethyl Ester. To a suspension of dimethyl cystinate hydrochloride (8.5 g, 0.025 mol) in chloroform (150 m*l*) were added triethylamine (7.0 m*l*, 0.050 mol) and a solution of *N*-benzyloxycarbonyl-L-phenylalanine (15.0 g, 0.050 mol) in chloroform (70 m*l*). A solution of *N,N'*-dicyclohexylcarbodiimide (11.2 g, 0.054 mol) in chloroform (20 m*l*) was added and the reaction mixture was allowed to stand overnight at room temperature. *N,N'*-dicyclohexylurea thus precipitated was removed by filtration and the filtrate was successively washed with water, dilute hydrochloric acid and dilute aqueous sodium hydrogen carbonate solution. The dried solution was evaporated *in vacuo* to give white crystals which were recrystallized from ethanol. Yield, 15.1 g (72.6%), mp 137—139°C, $[\alpha]_D^{22}$ −88.9° (*c* 3.12, *N,N*-dimethylformamide).

Found: C, 60.98; H, 5.59; N, 6.88%. Calcd for $C_{42}H_{46}N_4O_{10}S_2$: C, 60.71; H, 5.58; N, 6.74%.

N-Benzyloxycarbonyl-L-phenylalanyl-L-cysteine Methyl Ester (IV). According to the method employed in the reduction of cystine derivatives to cysteine derivatives by Zervas,[11] a suspension of the above cystine peptide (15.1 g, 0.018 mol) in methanol (150 m*l*) containing concentrated hydrochloric acid (12.0 m*l*) was treated with zinc dust (6.0 g) in small portions at a time for 30 min at about 50°C. Undissolved zinc was then filtered off and the filtrate was diluted with water to separate IV as white crystals. Yield, 11.6 g (76.8%), mp 126—127°C after recrystallization from ethyl acetate-petroleum ether (50—90°C), $[\alpha]_D^{20}$ −14.4° (*c* 2.19, methanol), lit,[8] mp 125—127°C.

Found: C, 60.32; H, 5.80; N, 6.60; S, 7.48%. Calcd for $C_{21}H_{24}N_2O_5S$: C, 60.56; H, 5.81; N, 6.73; S, 7.70%.

N-Benzyloxycarbonyl-L-phenylalanyl-S-chlorocarbonyl-L-cysteine Methyl Ester (V). Phosgene was passed through a solution of IV (14.6 g, 0.035 mol) and *N,N*-dimethylaniline (4.3 g, 0.035 mol) in dioxane (140 m*l*) for 30 min at 10—12°C. The reaction mixture was stirred for 4 hr below 20°C and bubbled with a stream of carbon dioxide (or nitrogen) to remove excess phosgene. The separated *N,N*-dimethylaniline hydrochloride was filtered off and the crystals obtained by evaporation of the filtrate were washed with benzene and water. Yield, 10.7 g (64%), mp 154—155°C after recrystallization from benzene, $[\alpha]_D^{22}$ −5.6° (*c* 2.15, dioxane).

Found: C, 55.45; H, 5.20; N, 5.92%. Calcd for $C_{22}H_{23}N_2O_6SCl$: C, 55.17; H, 4.84; N, 5.85%.

Treatment of a solution of V in benzene with an etheral solution of aniline gave *N*-benzyloxycarbonyl-L-phenylalanyl-*S*-(*N*-phenylcarbamoyl)-L-cysteine methyl ester; mp 165.3—165.5°C, $[\alpha]_D^{22}$ −51.5° (*c* 2.10, *N,N*-dimethylformamide).

Found: C, 63.06; H, 5.46; N, 7.76; S, 5.52%. Calcd for $C_{28}H_{29}N_3O_6S$: C, 62.79; H, 5.46; N, 7.85; S, 5.99%.

Methyl L-3-(N-Benzyloxycarbonyl-L-phenylalanyl)-2-oxothiazolidine-4-carboxylate (VI). A solution of V (7.2 g, 0.015 mol) in xylene (140 m*l*) was heated under reflux for 5 hr. Evaporation of the solvent afforded an oil which was crystallized by seeding or by scratching on the wall of the vessel. Yield, 5.8 g (88%), mp 103—105°C. Recrystallization from ethyl acetate raised the melting point to 112.0—112.5°C, $[\alpha]_D^{20}$ −75.8° (*c* 1.47, methanol).

Found: C, 59.88; H, 5.07; N, 6.34; S, 7.12%. Calcd for $C_{22}H_{22}N_2O_6S$: C, 59.72; H, 5.01; N, 6.33; S, 7.25%.

Alkaline Hydrolysis of VI. a) With Potassium Hydroxide in Aqueous Methanol: To a suspension of VI (3.10 g, 7 mmol) in methanol (35.0 m*l*) was added 1N potassium hydroxide (14.0 m*l*, 14 mmol) and the reaction mixture was stirred for 1.5 hr at room temperature. After evaporation of the solvent *in vacuo*, the residue was diluted with water and the aqueous solution was acidified with 1N hydrochloric acid (8.0 m*l*) to pH 3. The separated oil was extracted twice with ethyl acetate. Evaporation of the dried solution *in vacuo* provided an oily *N*-benzyloxycarbonyl-L-phenylalanine which was crystallized by seeding. Yield, 1.35 g (64.3%), mp 82—89°C and 88—89°C after recrystallization from ethyl acetate-petroleum ether (50—90°C), lit,[12] mp 88—89°C. A mixed melting point with the authentic sample showed no depression.

It was also identified as its cyclohexylammonium salt,[13] mp 168—169°C, $[\alpha]_D^{19}$ +37.4° (*c* 1.69, ethanol).

An additional 1N hydrochloric acid (8.0 m*l*) was added to the remaining aqueous solution. The residue obtained by evaporation of the acidic solution was extracted three times with hot ethyl acetate. The extract was evaporated *in vacuo* to dryness leaving III as a crystalline residue. Yield, 0.85 g (82.5%), mp 157—164°C and 172—173°C after recrystallization from acetone-petroleum ether (50—90°C), $[\alpha]_D^{22}$ −57.9° (*c* 1.89, water), lit,[7] mp 171—172.5°C, $[\alpha]_D^{16}$ −57.3° (*c* 2.7, water).

Hydrolysis of this sample with 6N hydrochloric acid and subsequent oxidation with air by the usual procedure afforded L-cystine in a yield of 57%, $[\alpha]_D^{19}$ −211° (*c* 1.18, 1N hydrochloric acid), lit,[14] $[\alpha]_D^{25}$ −212° (*c* 1, 1N hydrochloric acid).

b) With Methanolic Potassium Hydroxide Solution: In a manner similar to that described above, a suspension of VI (3.10 g, 7 mmol) in methanol (35.0 m*l*) was treated with 1N methanolic potassium hydroxide solution (14.5 m*l*, 14.5 mmol). After evaporation of the solvent, the residue was diluted with water to give an oil which was extracted twice

10) All melting points are uncorrected.

11) L. Zervas and I. Photaki, *J. Amer. Chem. Soc.*, **84**, 3887 (1962).

12) W. Grassmann and E. Wünsch, *Chem. Ber.*, **91**, 462 (1958).

13) An authentic sample was prepared from *N*-benzyloxycarbonyl-L-phenylalanine by treatment with cyclohexylamine; mp 169.0—169.5°C, $[\alpha]_D^{22}$ +37.1° (*c* 2.06, ethanol). Found: C, 69.37; H, 7.81; N, 7.10%. Calcd for $C_{23}H_{30}N_2O_4$: C, 69.32; H, 7.59; N, 7.03%.

14) J. P. Greenstein and M. Vinitz, "Chemistry of the Amino Acids" Vol. 3, John Wiley & Sons, New York (1961) p. 1879.

with ethyl acetate. Evaporation of the dried extract provided methyl *N*-benzyloxycarbonyl-L-phenylalaninate as an oil (wt, 1.24 g). Infrared spectra of this sample were identical with those of an authentic sample which was prepared from methyl L-phenylalaninate and benzyloxycarbonyl chloride. Treatment of a solution of the oil in methanol with a solution of an excess of hydrazine hydrate (about 95%) in methanol gave *N*-benzyloxycarbonyl-L-phenylalanine hydrazide. Yield, 0.75 g (34.2%), mp 161—163°C and 170.5—171°C after recrystallization from ethanol, $[\alpha]_D^{24}$ −6.9° (*c* 1.24, *N*, *N*-dimethylformamide), lit, mp 167—168°C[15], mp 168°C.[16] A mixed melting point with the authentic sample [mp 171.0—171.5°C, $[\alpha]_D^{24}$ −7.0° (*c* 1.28, *N*,*N*-dimethylformamide)] showed no depression.

Found: C, 65.34; H, 6.02; N, 13.45%. Calcd for $C_{17}H_{19}N_3O_3$: C, 65.16; H, 6.11; N, 13.41%.

The aqueous solution was acidified to pH 3. From ethyl acetate extract, *N*-benzyloxycarbonyl-L-phenylalanine was isolated as its cyclohexylammonium salt. Yield, 0.74 g (26.6%), mp 160—162°C and 169.5—170.0°C after recrystallization from ethanol-ether, $[\alpha]_D^{21}$ +37.9° (*c* 2.28, ethanol). No melting point depression upon the authentic sample[13] was observed.

As the third product, III was obtained from the acidic solution. Yield, 0.76 g (74.5%), mp 151—153°C and 153.5—154.5°C after recrystallization from acetone-petroleum ether (50—90°C), $[\alpha]_D^{20}$ −3.9° (*c* 2.92, water).

Hydrolysis of this sample with 6N hydrochloric acid and subsequent oxidation gave cystine having $[\alpha]_D^{20}$ −24.8° (*c* 1.39, 1N hydrochloric acid).

N-Benzyloxycarbonyl-L-alanyl-L-cysteine Methyl Ester (VII). In a similar way to that described for the preparation of IV, *N,N'*-bis(*N*-benzyloxycarbonyl-L-alanyl)-L-cystine dimethyl ester[17] (10.2 g, 15 mmol) was reduced to thiol peptide VII with zinc (9.0 g) and concentrated hydrochloric acid (19.5 ml) in methanol (120 ml). Yield, 8.1 g(79.5%), mp 114—116°C and 116.5—118.0°C after recrystalization from ethyl acetate, $[\alpha]_D^{20}$ −26.5° (*c* 1.27, methanol), lit,[8] mp 114—116°C.

Found: C, 53.03; H, 5.99; N, 8.20%. Calcd for $C_{15}H_{20}N_2O_5S$: C, 52.93; H, 5.92; N, 8.23%.

N-Benzyloxycarbonyl-L-alanyl-S-chlorocarbonyl-L-cysteine Methyl Ester (VIII). In the same manner as has been described for the preparation of V, a solution of VII (10.2 g, 0.030 mol) in dioxane (120 ml) was treated with a gentle stream of phosgene in the presence of *N,N*-dimethylaniline (3.6 g,0.030 mol) at 9—11°C for 25 min. After removal of excess phosgene by passage of carbon dioxide, VIII was obtained as a syrup which was crystallized by seeding. Yield, 10.5 g(86.8%), mp 94.5—95.5°C after recrystallization from chloroform-petroleum ether (50—90°C).

Found: C, 48.12; H, 4.66; N, 7.09%. Calcd for $C_{16}H_{19}N_2O_6SCl$: C, 47.70; H, 4.75; N, 6.95%.

It was also identified as *N*-benzyloxycarbonyl-L-alanyl-*S*-(*N*-phenylcarbamoyl)-L-cysteine methyl ester by treating with aniline; mp 158.5—159.5°C after recrystallization from benzene, $[\alpha]_D^{22}$ −30.4° (*c* 1.90, *N*,*N*-dimethylformamide).

Found: C, 57.42; H, 5.22; N, 9.07%. Calcd for $C_{22}H_{25}N_3O_6S$: C, 57.50; H, 5.48; N, 9.14%.

Methyl-L-3-(N-Benzyloxycarbonyl-L-alanyl)-2-oxothiazolidine-4-carboxylaye(IX). Heating of VIII (6.1 g, 15 mmol) in xylene (120 ml) under reflux for 5 hr followed by evaporating *in vacuo* gave IX as a syrup, wt, 5.6 g (101%). It gave a negative Beilstein's test and exhibited a main spot, accompanied by three minor spots, upon thin-layer chromatography with silica gel G(tlc).

This was used for the following cleavage reaction without further purification.

Alkaline Hydrolysis of IX. Hydrolysis of IX (3.68 g,10 mmol) was carried out in methanol (49.0 ml) by adding 1N potassium hydroxide (21.0 ml, 21 mmol) and by keeping the solution at room temperature for 1.5 hr. After methanol had been evaporated *in vacuo*, the residue was diluted with water and acidified with 1N hydrochloric acid (11.0 ml) to pH 3. Extraction with ethyl acetate and subsequent evaporation of the solvent gave *N*-benzyloxycarbonyl-L-alanine as a syrup which was purified as its cyclohexylammonium salt.[18] Yield, 1.85 g (54.4 %), mp 86—87°C after recrystallization from acetone-ether, $[\alpha]_D^{24}$ −10.2° (*c* 3.14, water). A mixed melting point with the authentic sample showed on depression.

Found: C, 59.83; H, 8.41; N, 8.05%. Calcd for $C_{17}H_{26}N_2O_4\cdot H_2O$: C, 59.98; H, 8.29; N, 8.23%.

On the other hand, the aqueous layer separated from the ethyl acetate extract was further acidified with an additional 1 N hydrochloric acid (11.0 ml) and evaporated *in vacuo* to give a residue. From the residue, III was isolated by extracting with hot ethyl acetate. Yield, 0.57 g (39.3%), mp 169—170°C and 172—173°C after recrystallization from acetone-petroleum ether(50—90°C), $[\alpha]_D^{23}$ −58.0° (*c* 2.31, water).

Properties of this sample such as infrared spectra were identical with those of the authentic sample.[8]

N-Benzyloxycarbonyl-L-phenylalanylglycyl-L-cysteine Methyl Ester (X). A mixed solution of *N*-benzyloxycarbonyl-L-phenylalanylglycine[19] (8.9 g, 0.025 mol) and methyl L-cysteinate, prepared from its hydrochloride[11] (4.3 g, 0.025 mol) and triethylamine (3.5 ml, 0.025 mol), in chloroform (90 ml) was treated with a solution of *N,N'*-dicyclohexylcarbodiimide (5.3 g, 0.026 mol) in chloroform (15 ml) at room temperature for 4 hr. After *N,N'*-dicyclohexylurea had been removed by filtration, the filtrate was washed successively with water, dilute hydrochloric acid, dilute aqueous sodium hydrogen carbonate solution and water. Evaporation of the dried solution gave a solid which was dissolved into ethyl acetate. The ethyl acetate solution separated from another *N,N'*-dicyclohexylurea was concentrated *in vacuo* to give X as white crystals. Yield, 9.7 g (82.8%), mp 129—132°C and 135—136°C after recrystallization from ethyl acetate, $[\alpha]_D^{22}$ −25.2° (*c* 1.96, *N*,*N*-dimethylformamide).

Found: C, 58.23; H, 5.78; N, 8.88%. Calcd for $C_{23}H_{27}N_3O_6S$: C, 58.34; H, 5.75; N, 8.87%.

It was oxidized with 1/10 N iodine-potassium iodide solution to the disulfide, *N,N'*-bis(*N*-benzyloxycarbonyl-L-phenylalanylglycyl)-L-cystine dimethyl ester, mp 187—188°C, $[\alpha]_D^{22}$ −49.7° (*c* 1.83, *N*,*N*-dimethylformamide).

Found: C, 58.26; H, 5.39; N, 8.70%. Calcd for $C_{46}H_{52}N_6O_{12}S_2$: C, 58.46; H, 5.55; N, 8.89%.

15) G. W. Anderson and R. W. Young, *J. Amer. Chem. Soc.*, **74**, 5307 (1952).

16) J. I. Harris and J. S. Work, *Biochem. J.*, **46**, 196 (1950).

17) This peptide was synthesized by the carbodiimide method in a similar manner to that for *N,N'*-bis(*N-benzyloxycarbonyl*-L-phenylalanyl)-L-cystine dimethyl ester as shown above. Yield, 75—80%, mp 160—161°C after recrystallization from ethanol, $[\alpha]_D^{22}$ −67.0° (*c* 1.98, *N*,*N*-dimethylformamide). Found: C, 53.20; H, 5.58; N, 8.09%, Calcd for $C_{30}H_{38}N_4O_{10}S_2$: C, 53.08; H, 5.64; N, 8.25%.

18) The authentic sample was prepared as a hydrate from *N*-benzyloxycarbonyl-L-alanine by treatment with cyclohexylamine; mp 85.5—86.0°C, $[\alpha]_D^{23.5}$ −10.2° (*c* 2.78, water). Found: C, 59.79; H, 8.34; N, 8.18%. Calcd for $C_{17}H_{26}N_2O_4\cdot H_2O$: C, 59.98; H, 8.29; N, 8.23%.

19) D. W. Clyaton, J. A. Farrington, G. W. Kenner, and J.M. Turner, *J. Chem. Soc.*, **1957**, 1398.

It was also identified as an *S*-benzoyl derivative, *N*-benzyloxycarbonyl-L-phenylalanylglycyl-*S*-benzoyl-L-cysteine methyl ester, by treating with benzoyl chloride in pyridine; mp 152—153°C, $[\alpha]_D^{22}$ −36.2° (*c* 2.67, *N,N*-dimethylformamide).

Found: C, 62.40; H, 5.41; N, 7.27%. Calcd for $C_{30}H_{31}N_3O_7S$: C, 62.38; H, 5.41; N, 7.27%.

N-Benzyloxycarbonyl-L-phenylalanylglycyl-S-chlorocarbonyl-L-cysteine Methyl Ester (XI). In a way similar to that for the preparation of V phosgene was passed through a solution of X (4.73 g, 10 mmol) in dioxane (50 m*l*) in the presence of *N,N*-dimethylaniline (1.21 g, 10 mmol) at 15°C for 20 min. From the reaction mixture, XI was obtained as crystals. Yield, 3.61 g(67.4%), mp 144—145°C (decomp.).

Found: C, 54.33; H, 4.89; N, 7.71%. Calcd for $C_{24}H_{26}N_3O_7SCl$: C, 53.78; H, 4.89; N, 7.84%.

Methyl L-3-(N-Benzyloxycarbonyl-L-phenylalanylglycyl)-2-oxothiazolidine-4-carboxylate (XII). A solution of XI (5.85 g, 10.9 mmol) in xylene (120 m*l*) was heated for 3 hr under reflux. The reaction mixture was cooled to room temperature to deposit XII as crystals. Yield, 4.85 g(89.0%), mp 175.5—177.0°C and 177.5—178.5°C after recrystallization from ethanol, $[\alpha]_D^{22}$ −81.5° (*c* 1.43, *N,N*-dimethylformamide).

Found: C, 57.60; H, 5.00; N, 8.63%. Calcd for $C_{24}H_{25}N_3O_7S$: C, 57.71; H, 5.04; N, 8.41%.

Alkaline Hydrolysis of XII. a) With Potassium Hydroxide in Aqueous Methanol: XII (3.30 g, 6.6 mmol) was hydrolyzed with a mixture of 1 N potassium hydroxide (14.0 m*l*, 14.0 mmol) and methanol (35.0 m*l*). After evaporation of the solvent, the residue was diluted with water and acidified with 1 N hydrochloric acid to pH 3. From ethyl acetate extract, *N*-benzyloxycarbonyl-L-phenylalanylglycine was isolated; Yield, 1.65 g (70.2%), mp 151.5—153.0°C. Recrystallization from ethyl acetate raised the melting point to 153—154°C, $[\alpha]_D^{20}$ −9.1° (*c* 3.12, acetic acid), lit,[19] mp 154°C, $[\alpha]_D^{18}$ −10.2°C (*c* 4.3, acetic acid)

From the acidic solution separated from ethyl acetate extract, III was isolated as crystals. Yield, 0.78 g (80.4%), mp 164—166°C and 171.5—172.5°C after recrystallization from acetone-petroleum ether (50—90°C), $[\alpha]_D^{22}$ −58.0° (*c* 2.65, water).

b) With Methanolic Potassium Hydroxide Solution: XII (3.20 g, 6.4 mmol) was hydrolyzed with 0.3 N methanolic potassium hydroxide solution (45.0 m*l*, 13.5 mmol). After evaporation of the solvent, the residue was dilute with water and acidified with 1N hydrochloric acid to pH 3. From ethyl acetate extract, *N*-benzyloxycarbonylphenylalanylglycine was isolated; yield, 0.72 g (31.6%), mp 152—153°C, $[\alpha]_D^{24}$ −6.0° (*c* 1.93, acetic acid).

From the aqueous solution, III was isolated; yield, 0.63 g (67.0%), mp 153—154°C, $[\alpha]_D^{24}$ −2.4° (*c* 2.94, water).

N-Benzyloxycarbonyl-S-benzoyl-L-cysteinyl-L-phenylalanine Methyl Ester (XIII). To a mixed solution of *N*-benzyloxycarbonyl-*S*-benzoyl-L-cysteine[20] (36.0 g, 0.10 mol) and methyl L-phenylalaninate prepared from its hydrochloride (22.0 g, 0.10 mol) and triethylamine (14.0 m*l*, 0.10 mol) in chloroform (450 m*l*) a solution of *N,N'*-dicyclohexylcarbodiimide (22.0 g, 0.11 mol) in chloform (50 m*l*) was added, and the reaction mixture was allowed to stand overnight at room temperature. After filtration of *N,N'*-dicyclohexylurea, the filtrate was worked up in the usual way. Yield, 41.4 g (79.6 %), mp 136—137°C after recrystallization from ethanol, $[\alpha]_D^{20}$ −30.7° (*c* 1.01, ethanol).

Found: C, 64.38; H, 5.44; N, 5.39%. Calcd for $C_{28}H_{28}N_2O_6S$: C, 64.60; H, 5.42; N, 5.38%.

20) L. Zervas, I. Photaki, and N. Ghelis, *J. Amer. Chem. Soc.*, **85**, 1337 (1963).

S-Benzoyl-L-cysteinyl-L-phenylalanine Methyl Ester Hydrochloride (XIV). A solution of XIII (5.20 g, 10 mmol) and phenol (2.0 g) in trifluoroacetic acid (15 m*l*) was heated for 30 min under reflux. Evaporation of the solvent followed by addition of ether gave *S*-benzoyl-L-cysteinyl-L-phenylalanine methyl ester trifluoroacetate as crystals. Yield, 3.24 g (64.8%), mp 137°C.

To a solution of the trifluoroacetate (23.5 g, 0.047 mol) in methanol (40 m*l*) was added absolute ether (120 m*l*) saturated with hydrogen chloride. The reaction mixture was diluted with ether (400 m*l*) to separate XIV as crystals. Yield, 16.4 g (82.4%), mp 151—152°C (decomp.) and 153.5—154.0°C (decomp.) after recrystallization from methanol-ether, $[\alpha]_D^{24}$ +1.5° (*c* 2.61, ethanol); +3.1° (*c* 4.55, ethanol).

Found: C, 56.67; H, 5.39; N, 6.61%. Calcd for $C_{20}H_{22}N_2O_4S \cdot HCl$: C, 56.80; H, 5.48; N, 6.62%.

N-Benzoyl-L-cysteinyl-L-phenylalanine Methyl Ester (XV). A suspension of XIV (1.51 g, 3.57 mmol) in chloroform (20 m*l*) was treated with triethylamine (0.50 m*l*, 3.57 mmol) and the reaction mixture was stirred for 4 hr at 25—35°C. After evaporation of the solvent, the residue was dissolved into ethyl acetate and the ethyl acetate solution was washed successively with water, dilute hydrochloric acid, dilute aqueous sodium hydrogen carbonate solution and water. Evaporation of the dried solution provided XV as white crystals. Yield, 1.16 g (84.0%), mp 154—155°C after recrystallization from ethyl acetate, $[\alpha]_D^{20}$ −32.1° (*c* 1.32, ethanol).

Found: C, 62.31; H, 5.64; N, 7.48%. Calcd for $C_{20}H_{22}N_2O_4S$: C, 62.16; H, 5.74; N, 7.25%.

When the reaction was carried out below 25°C, pure XV was not isolated.

N-Benzoyl-S-chlorocarbonyl-L-cysteinyl-L-phenylalanine Methyl Ester (XVI). In a similar way to that for the preparation of V, phosgene was passed through a slution of XV (5.80 g, 15 mmol) in dioxane (60 m*l*) in the presence of *N,N*-diemthylaniline (1.82 g, 15 mmol) at 10—15°C for 20 min. From the reaction mixture, XV was isolated as crystals melted at 133—134°C (decomp.). Yield, 5.58 g (82.8%). Recrystallization from benzene raised the melting point to 137.0—137.5° C (decomp.), $[\alpha]_D^{25}$ −40.0° (*c* 2.06, dioxane).

Found: C, 56.36; H, 4.66; N, 5.72%. Calcd for $C_{21}H_{21}N_2O_5SCl$: C, 56.18; H, 4.72; N, 6.24%.

Methyl L-3-Benzoyl-2-oxothiazolidine-4-carbonyl-L-phenylalaninate (XVII). A solution of XVI (3.00 g, 6.68 mmol) in xylene (60 m*l*) was heated for 3.5 hr under reflux. The crude product XVII precipitated when the reaction mixture was cooled to room temperature. Yield, 1.06 g (38.5%), mp 213.5—214.5°C. It gave a negative Beilstein's test. Recrystallization from ethyl acetate raised the melting point to 216—217°C, $[\alpha]_D^{23.5}$ +34.2° (*c* 1.29, *N,N*-dimethylformamide).

Found: C, 61.45; H, 4.88; N, 6.59%. Calcd for $C_{21}H_{20}N_2O_5S$: C, 61.15; H, 4.89; N, 6.79%.

Alkaline Hydrolysis of XVII. A suspension of XVII (2.06 g, 5.0 mmol) in methanol (30 m*l*) was treated with 1 N potassium hydroxide (11.0 m*l*, 11.0 mmol) for 1.5 hr at room temperature with stirring. After evaporation of the solvent, the residue was diluted with water to separate an oil which was extracted with ethyl acetate. Methyl benzoate was isolated as a sweet-smelling oil from the extract; yield, 0.19 g (27.9%). Properties of this sample such as infrared spectra were identical with those of the authentic sample.

The aqueous solution separated from the ethyl acetate extract was acidified with 1 N hydrochloric acid to pH 1 to give an oily product which was extracted twice with ethyl acetate. Evaporation of the dried extract left a syrup (wt, 1.54 g) which was extracted three times with hot petroleum ether (50—90°C). The extract was evaporated *in vacuo* to

give crystals which were identified as benzoic acid by its infrared spectra; yield, 0.06 g (10.0%).

From the remaining syrup (wt, 1.50 g), XVIII was isolated as its cyclohexylammonium salt by treating with cyclohexylamine. Yield, 1.34 g (68.0%), mp 204.5—205.5°C (decomp.) and 207.5—208.0°C (decomp.) after recrystallization from ethanol-ether, $[\alpha]_D^{22}$ −6.0° (*c* 1.66, ethanol).

Found: C, 57.98; H, 7.02; N, 10.48%. Calcd for $C_{19}H_{27}N_3O_4S$: C, 57.99; H, 6.92; N, 10.68%.

N-Benzoyl-L-cysteinylglycine Methyl Ester (XIX). In a way similar to that described for the preparation of XV, a solution of *S*-benzoyl-L-cysteinylglycine methyl ester hydrochloride[20] (6.65 g, 20 mmol) and triethylamine (2.80 m*l*, 20 mmol) in chloroform (80 m*l*) was stirred for 4 hr at room temperature. From the reaction mixture, pure XIX was isolated. Yield, 4.49 g (75.7%), mp 114—115°C, $[\alpha]_D^{20}$ −32.3° (*c* 2.69, methanol).

Found: C, 52.64; H, 5.40; N, 9.35%. Calcd for $C_{13}H_{16}N_2O_4S$: C, 52.69; H, 5.44; N, 9.45%.

Oxidation of XIX by 1/10 N iodine-potassium iodide solution gave a disulfide, *N,N'*-bisbenzoyl-L-cystinyldiglycine dimethyl ester; mp 226—227°C, $[\alpha]_D^{20}$ −211° (*c* 1.65, *N,N*-dimethylformamide).

Found: C, 52.80; H, 4.68; N, 9.56%. Calcd for $C_{26}H_{30}N_4O_8S_2$: C, 52.87; H, 5.12; N, 9.49%.

N-Benzoyl-S-chlorocarbonyl-L-cysteinylglycine Methyl Ester (XX). In a manner similar to that for the preparation of V, XX was obtained from a solution of XIX (5.50 g, 18.6 mmol) in dioxane (75 m*l*) by treatment with an excess of phosgene in the presence of *N,N*-dimethylaniline (2.25 g, 18.6 mmol). Yield, 3.35 g(50.3%), mp 109—110°C (decomp.).

Methyl L-3-Benzoyl-2-oxothiazolidine-4-carbonylglycinate (XXI) and N,N'-Bisbenzoyl-L-cystinylglycine Dimethyl Ester. A solution of XX (2.51 g, 7.0 mmol) in xylene (50 m*l*) was heated for 2 hr under reflux and cooled to room temperature to separate out crystals (wt, 0.49 g, mp 189—192°C). It gave a negative Beilstein's test and exhibited two spots upon tlc.

The crude product was dissolved into ethanol (50 m*l*) and kept for a short time at room temperature to separate crystals. Yield, 0.14 g (6.8%), mp 205—208°C and 224°C after recrystallization from ethanol, $[\alpha]_D^{20}$ −206° (*c* 1.06, *N,N*-dimethylformamide). Its structure was confirmed to be *N,N'*-bisbenzoyl-L-cystinyldiglycine dimethyl ester by comparison of the properties with those of the oxidized product of XIX.

The mother liquor separated from crystals was allowed to stand overnight at room temperature. XXI was separated as the second product. Yield, 0.14 g (6.2%), mp 203—204°C. Recrystallization from ethanol changed the melting point to 202.5—203.0°C, $[\alpha]_D^{20}$ −36.7° (*c* 0.98, *N,N*-dimethylformamide).

Found: C, 52.08; H, 4.21; N, 8.45%. Calcd for $C_{14}H_{14}N_2O_5S$: C, 52.16; H, 4.38; N, 8.69%.

N-Benzyloxycarbonyl-L-phenylalanyl-S-trityl-L-cysteinylglycine Methyl Ester. A solution containing *N*-benzyloxycarbonyl-L-phenylalanine (7.93 g, 26.5 mmol), *S*-trityl-L-cysteinylglycine methyl ester hydrochloride[21] (12.50 g, 26.5 mmol), and triethylamine (3.70 m*l*, 26.5 mmol) in methylene chloride (100 m*l*) was treated with a solution of *N,N'*-dicyclohexylcarbodiimide (5.47 g, 26.5 mmol) in methylene chloride (10 m*l*). The crystalline peptide was obtained by the usual procedure; yield, 15.10 g (79.6%), mp 165—167°C. Recrystallization from ethanol raised the melting point to 176.0—176.5°C, $[\alpha]_D^{20}$ −12.6° (*c* 2.23, *N,N*-dimethylformamide).

Found: C, 70.40; H, 5.83; N, 6.11; S, 4.39%. Calcd for $C_{42}H_{41}N_3O_6S$: C, 70.47; H, 5.77; N, 5.87; S, 4.48%.

N-Benzyloxycarbonyl-L-phenylalanyl-L-cysteinylglycine Methyl Ester (XXII). A solution of the above *S*-trityl peptide (7.16 g, 10 mmol) in acetic acid (200 m*l*) was treated with a solution of mercuric chloride (5.43 g, 20 mmol) in methanol (20 m*l*) followed by a solution of crystalline sodium acetate (1.37 g, 10 mmol) in methanol (25 m*l*). After standing for 4 hr at room temperature, the precipitates were collected and washed with aqueous acetic acid, water, and ether. Yield, 5.85 g (82.6%).

A stream of hydrogen sulfide was passed through a solution of the above *S*-chloromercury compound in a mixture of *N,N*-dimethylformamide (40 m*l*) and methanol (20 m*l*) for 15 min, and the precipitated mercuric sulfide was filtered off. The filtrate was diluted with water (250 m*l*) to give a thiol peptide XXII as crystals. Yield, 2.43 g (75.7%), mp 164—165°C. After recrystallization from ethyl acetate, the melting point was raised to 171—172°C, $[\alpha]_D^{20}$ −15.9° (*c* 2.26, *N,N*-dimethylformamide).

Found: C, 58.36; H, 5.84; N, 8.61; S, 6.72%. Calcd for $C_{23}H_{27}N_3O_6S$: C, 58.34; H, 5.75; N, 8.87; S, 6.77%.

It was oxidized to *N,N'*-bis(*N*-benzyloxycarbonyl-L-phenylalanyl)-L-cystinyldiglycine dimethyl ester by the treatment with 1/10 N iodine-potassium iodide solution; mp 220—223°C, $[\alpha]_D^{20}$ −86.4° (*c* 2.20, *N,N*-dimethylformamide), lit,[20] mp 223—224°C, $[\alpha]_D^{25}$ −87° (*c* 1, *N,N*-dimethylformamide).

Found: C, 58.54; H, 5.52; N, 8.88%. Calcd for $C_{46}H_{52}N_6O_{12}S_2$: C, 58.46; H, 5.55; N, 8.89%.

N-Benzyloxycarbonyl-L-phenylalanyl-S-chlorocarbonyl-L-cysteinylglycine Methyl Ester (XXIII). In a way similar to that for the preparation of V, XXIII was obtained from a suspension of XXII (4.73 g, 10 mmol) in dioxane (50 m*l*) by treatment with excess phosgene in the presence of *N,N*-dimethylaniline (1.21 g, 10 mmol). Yield, 3.65 g (68.1%), mp 142—144°C (decomp.) and 153—154°C (decomp.) after recrystallization from benzene, $[\alpha]_D^{20}$ −33.4°C (*c* 2.87, dioxane).

Found: C, 53.95; H, 4.87; N, 7.86%. Calcd for $C_{24}H_{26}N_3O_7SCl$: C, 53.78; H, 4.89; N, 7.84%.

In order to obtain a cyclized product, a solution of XXIII (2.5 g, 4.7 mmol) in toluene (50 m*l*) was heated for 3 hr under reflux and then concentrated to dryness to give a brownish syrup, from which no detectable substance was isolated.

21) G. Amiard, R. Heymes, and L. Velluz, *Bull. Soc. Chim. Fr.*, **1956**, 698.

Studies on Aminosugars. XXVII. Synthesis of Several Glycosides Containing (6-Amino-6-deoxy-D-glucopyranosyl)-2-deoxystreptamine[1]

Yoshio NISHIMURA, Tsutomu TSUCHIYA, and Sumio UMEZAWA

Department of Applied Chemistry, Faculty of Engineering, Keio University, Koganei-shi, Tokyo

(Received April 7, 1971)

Racemic *O*-isopropylidene derivative of *N,N'*-diethoxycarbonyl-2-deoxystreptamine was glycosidized with 6-azido-2,3,4-tri-*O*-benzyl-6-deoxy-α-D-glucopyranosyl chloride to afford two kinds of positional isomers of α-glucoside, which led to 4-*O*-(6-amino-6-deoxy-α-D-glucopyranosyl)- and 6-*O*-(6-amino-6-deoxy-α-D-glucopyranosyl)-2-deoxystreptamine. In a similar manner, 4-*O*-(6-amino-6-deoxy-α and β-D-glucopyranosyl)-6-*O*-(α-D-glucopyranosyl)-2-deoxystreptamines and 4-*O*-(6-amino-6-deoxy-α and β-D-glucopyranosyl)-6-*O*-(6-amino-6-deoxy-α-D-glucopyranosyl)-2-deoxystreptamines were synthesized.

A number of chemotherapeutically useful compounds of 2-deoxystreptamine aminoglycosides have been obtained from the metabolites of microorganisms. The compounds include neomycins, kanamycins, paromomycins and gentamicins. In order to investigate the relationship between structure and antibiotic activity, the structural modification of either the aminocyclitol[2] or the sugar moiety[3,4] has been made. It appears so far that alterations have a profound effect on antibiotic activity and that the 2-deoxystreptamine moiety plays an important role in exhibiting activity. We have recently reported the total syntheses of kanamycin A,[5] B,[6] and C[7] as well as the syntheses of paromamine[8] and neamine.[4c] In relation to these syntheses, we were interested in altering the sugar moieties of kanamycin, and reported[9] the syntheses of the positional isomers of α-D-glucosyl-2-deoxystreptamines as a basic experiment of the syntheses of α-glycosides of 2-deoxystreptamine.

2-Deoxystreptamine has three hydroxyl groups at C-4,5, and 6, and there exist three kinds of 2-deoxystreptamine glycosides. As for the glycosyl components of 4-*O*-glycosyl-2-deoxystreptamines, 2-amino-2-deoxy-D-glucose (in kanamycin C, paromomycins, and gentamicin A), 6-amino-6-deoxy-D-glucose (in kanamycin A), 2,6-diamino-2,6-dideoxy-D-glucose (in kanamycin B, neomycins, and neamine), and partially substituted 2,6-diamino-2,3,4,6-tetradeoxy-D-glucose (in gentamicin C_1, C_2, and C_{1a}) are found. They are attached to the 2-deoxystreptamine with an α-glucosidic linkage. As for the glycosyl component of 6-*O*-glycosyl-2-deoxystreptamines, 3-amino-3-deoxysugars such as 3-amino-3-deoxy-D-glucose (in kanamycins), gentosamine[10] (in gentamicin A) and garosamine[11] (in gentamicin C) are found. They are also linked to the 2-deoxystreptamine with an α-linkage. As for the glycosyl component of 5-*O*-glycosyl-2-deoxystreptamines, only D-ribose is found, linked with β-linkage, in paromomycins, neomycins, and vistamycin.[12] On the other hand, 5-*O*-(2-amino-2-deoxy-α-D-glucopyranosyl)-2-deoxystreptamine[3,13] was synthesized and found to have antibacterial activity against mycobacteria.

This paper reports the synthesis of 4-*O*- and 6-*O*-(6-amino-6-deoxy-α-D-glucopyranosyl)-2-deoxystreptamine (**7a** and **7b**), 4,6-di-*O*-(6-amino-6-deoxy-α-D-glucopyranosyl)-2-deoxystreptamine (**20**) and 4-*O*-(6-amino-6-deoxy-α-D-glucopyranosyl)-6-*O*-(α-D-glucopyranosyl)-2-deoxystreptamine (**14**). In addition some derivatives containing β-glycosidic linkages are described. Since 4-*O*-(6-amino-6-deoxy-α-D-glucopyranosyl)-2-deoxystreptamine moiety[14] is considered to be the origin of the antibacterial activity of kanamycin A and 3-amino-3-deoxy-D-glucose moiety attached to C-6 of 2-deoxystreptamine is considered the enhacing factor of the activity, the latter moiety has been changed.

Synthesis of Glucosides. 6-Azido-2,3,4-tri-*O*-benzyl-

1) Part XL of "Studies on Antibiotics and Related Substances" by Sumio Umezawa. A part of this paper was read at the 23rd Annual Meeting of the Chemical Society of Japan, Tokyo, April, 1970. (See Abstracts of Papers of the Meeting Vol. III, p. 1902).

2) a) W. T. Shier, K. L. Rinehart, Jr., and D. Gottlib, *Proc. Nat. Acad. Sci.*, **63**, 198 (1969); b) T. Suami, S. Ogawa, T. Yoshizawa, and S. Umezawa, This Bulletin, **36**, 459 (1963); *ibid.*, **37**, 1538 (1964); c) S. Umezawa, T. Tsuchiya, S. Nakada, and K. Tatsuta, *ibid.*, **40**, 395 (1967).

3) T. Tsuchiya, H. Fujita, and S. Umezawa, *J. Antibiot.* (Tokyo), *Ser A*, **17**, 181 (1964).

4) a) T. Tsuchiya and S. Umezawa, This Bulletin, **38**, 1181 (1965); b) S. Umezawa, K. Tatsuta, T. Tsuchiya, and E. Yamamoto, *ibid.*, **40**, 1972 (1967); c) K. Tatsuta, E. Kitazawa, and S. Umezawa, *ibid.*, **40**, 2371 (1967); d) S. Inouye, *J. Antibiot.* (Tokyo), *Ser. A*, **20**, 6 (1967); *Chem. Pharm. Bull.*, **15**, 1888 (1967): *ibid.*, **16**, 573 (1968); e) T. Kobayashi, T. Tsuchiya, K. Tatsuta, and S. Umezawa, *J. Antibiot.* (Tokyo), **23**, 225 (1970).

5) S. Umezawa, K. Tatsuta, and S. Koto, This Bulletin, **42**, 533 (1969).

6) S. Umezawa, S. Koto, K. Tatsuta, H. Hineno, Y. Nishimura, and T. Tsumura, *ibid.*, **42**, 537 (1969).

7) S. Umezawa, S. Koto, K. Tatsuta, and T. Tsumura, *ibid.*, **42**, 529 (1969).

8) S. Umezawa and S. Koto, *ibid*, **39**, 2014 (1966).

9) Y. Nishimura, T. Tsuchiya, and S. Umezawa, *ibid.*, **43**, 2960 (1790).

10) H. Maehr and C. P. Schaffner, *J. Amer. Chem. Soc.*, **89**, 6787 (1967).

11) a) D. J. Cooper and M. D. Yudis, *Chem. Commun.*, **1967**, 821; b) W. M. zn Reckendorf and E. Bischof, *Tetrahedron Lett.*, **1790**, 2475.

12) E. Akita, T. Tsuruoka, N. Ezaki, and T. Niida, *J. Antibiot.* (Tokyo), **23**, 173 (1970).

13) S. Umezawa, T. Tsuchiya, and H. Fujita, *ibid.*, *Ser A*, **19**, 222 (1966).

14) S. Umezawa and T. Tsuchiya, *ibid.*, **15**, 51 (1962).

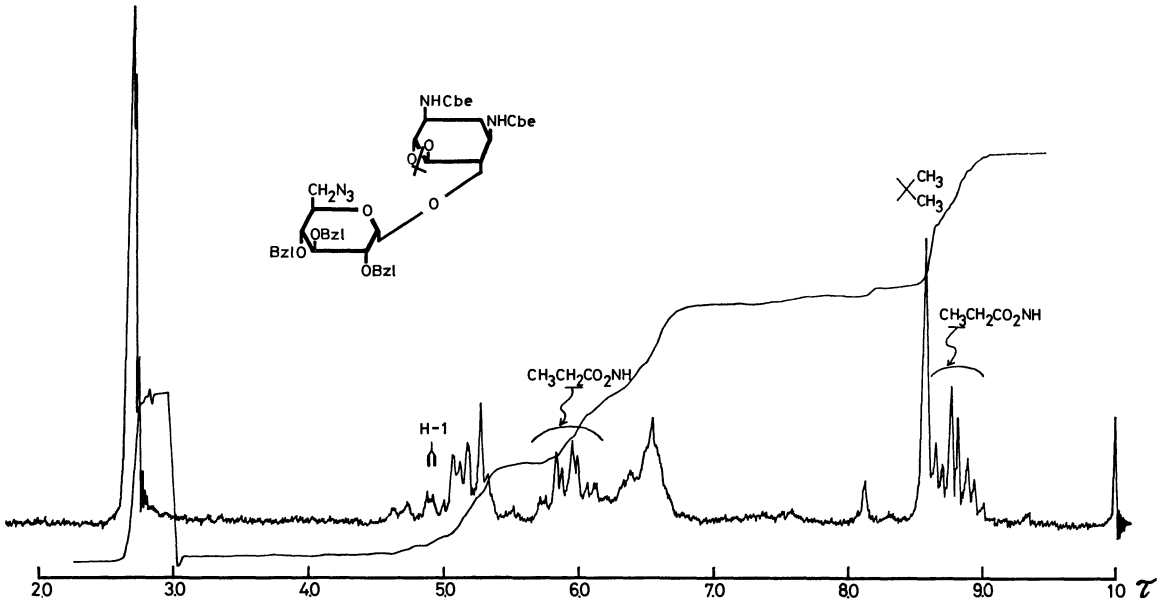

Fig 1. The NMR spectrum of **3b** in $CDCl_3$.

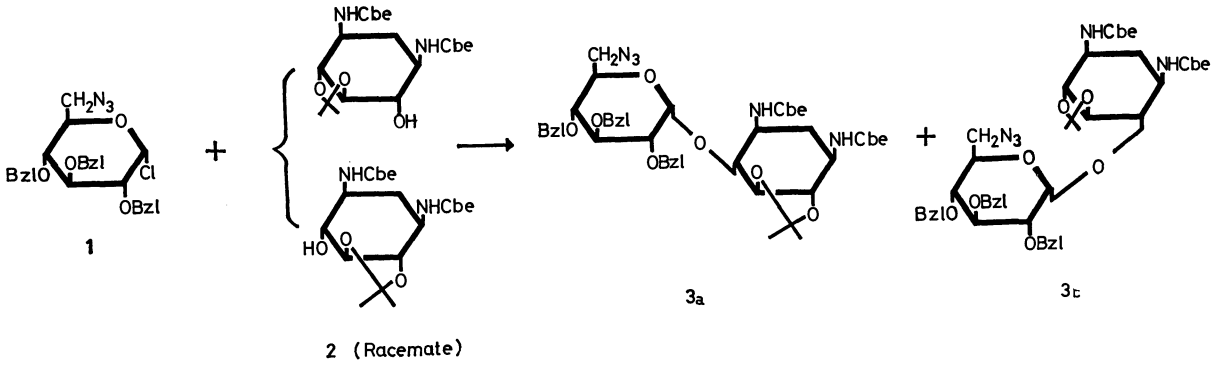

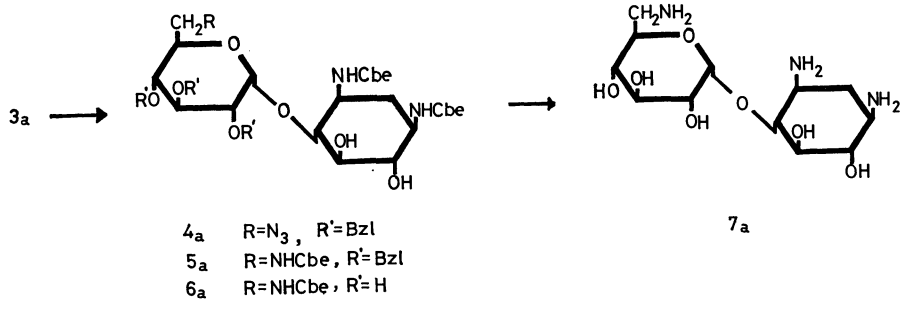

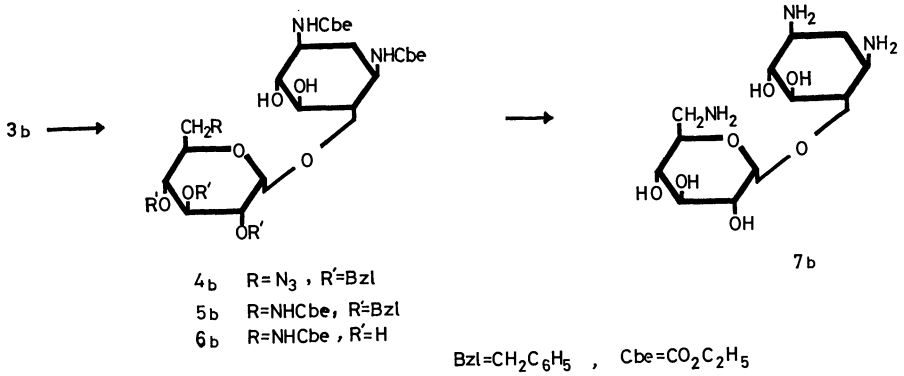

Bzl=$CH_2C_6H_5$, Cbe=$CO_2C_2H_5$

Chart 1.

6-deoxy-α-D-glucopyranosyl chloride (**1**)[15] was condensed with a racemic mixture (**2**) of *N,N'*-diethoxycarbonyl-4,5- and 5,6-*O*-isopropylidene-2-deoxystreptamine[9] in dry benzene-dioxane in the presence of mercuric cyanide and freshly prepared Drierite (Chart 1). The azide derivative of glycosyl chloride has been found to be more suitable for glycosidation than the acylamino or aryloxycarbonylamino derivatives of glycosyl halides, since the azide derivatives is more stable and easily hydrogenated into an amino derivative. Solvents, completely dried, were indispensable for the condensation. Benzene was dried over lithium aluminum hydride and dioxane was dried with sodium metal under reflux. The condensation products were purified by column chromatography. The main product (R_f 0.51) was still proved to be a mixture of two products. The major product in the mixture was isolated by recrystallization from ethanol-aqueous ammonia in a yield of 40%. The compound was proved to be 6-*O*-(6-azido-2,3,4-tri-*O*-benzyl-6-deoxy-α-D-glucopyranosyl)-*N,N'*-diethoxycarbonyl-4,5-*O*-isopropylidene-2-deoxystreptamine (**3b**) by its IR, NMR (Fig. 1) and elemental analysis and by the fact that it was led to 6-*O*-(6-amino-6-deoxy-α-D-glucopyranosyl)-2-deoxystreptamine.

The mother liquor of the recrystallization described above contained the 4-*O*-isomer, namely 4-*O*-(6-azide-2,3,4-tri-*O*-benzyl-6-deoxy-α-D-glucopyranosyl)-*N,N'*-diethoxycarbonyl-5,6-*O*-isopropylidene-2-deoxystreptamine (**3a**) accompanied by **3b**. Since the difficulty in separation of **3a** from **3b** remained, the isopropylidene groups were removed by acid and the deacetonated mixture (**4a** and **4b**) was chromatographed on silica gel to give **4a** and **4b** in yields of 12 and 48% (including that from **3b** obtained by recrystallization) based on **2**, respectively. It is noteworthy that we came across a low yield of 4-*O*-glucosides in the preparation of 4-*O*-(2,3,4,6-tetra-*O*-benzyl-α-D-glucopyranosyl)-*N,N'*-diethoxycarbonyl-5,6-*O*-isopropylidene-2-deoxystreptamine.[9] Since 4,6-di-*O*-glucosides (**9** and **16**) were prepared in good yields (60—70%) from mono-6-*O*-glucosides (**8** and **4b**) and **1**, the low yields of 4-*O*-glucosides may be not due to the intrinsic nature of C_4-OH, but to the presence of a 5,6-*O*-isopropylidene group.

Azide groups of **4a** and **4b** were reduced with Raney nickel and hydrogen to the amino groups, which were ethoxycarbonylated to give 4-*O*- and 6-*O*-(2,3,4-tri-*O*-benzyl-6-deoxy-6-ethoxycarbonylamido-α-D-glucopyranosyl)-*N,N'*-diethoxycarbonyl-2-deoxystreptamine (**5a** and **5b**), respectively. The subsequent debenzylation with palladium black and hydrogen gave 4-*O*- and 6-*O*-(6-deoxy-6-ethoxycarbonylamido-α-D-glucopyranosyl)-*N,N'*-diethoxycarbonyl-2-deoxystreptamine (**6a** and **6b**) respectively. When simultaneous reduction and debenzylation of **4a** or **4b** were performed by use of palladium black and hydrogen, several undeterminable products were obtained. The reaction was not pursued any further. However, Ainsworth's work suggests[16] that the amino groups liberated are damaged during the reaction. Treatment of **6a** and **6b** with hot 1N barium hydroxide gave 4-*O*- and 6-*O*-(6-amino-6-deoxy-α-D-glucopyranosyl)-2-deoxystreptamine (**7a** and **7b**), respectively, in good yields.

6-*O*-(2,3,4,6-Tetra-*O*-benzyl-α-D-glucopyranosyl)-*N,N'*-diethoxycarbonyl-2-deoxystreptamine[9] (**8**) and **1** were condensed to give 4-*O*-(6-azide-2,3,4-tri-*O*-benzyl-6-deoxy-α- and β-D-glucopyranosyl)-6-*O*-(2,3,4,6-tetra-*O*-benzyl-α-D-glucopyranosyl)-*N,N'*-diethoxycarbonyl-2-deoxystreptamine (**9** and **10**) in yields of 71 and 10%, respectively (Chart 2). In order to determine whether the newly formed glycosides **9** and **10** are a 4-*O*-glycoside or 5-*O*-glycoside, the end products (**14** and **15**) derived from them were oxidized with periodate and followed by acidic hydrolysis. Paper chromatography of

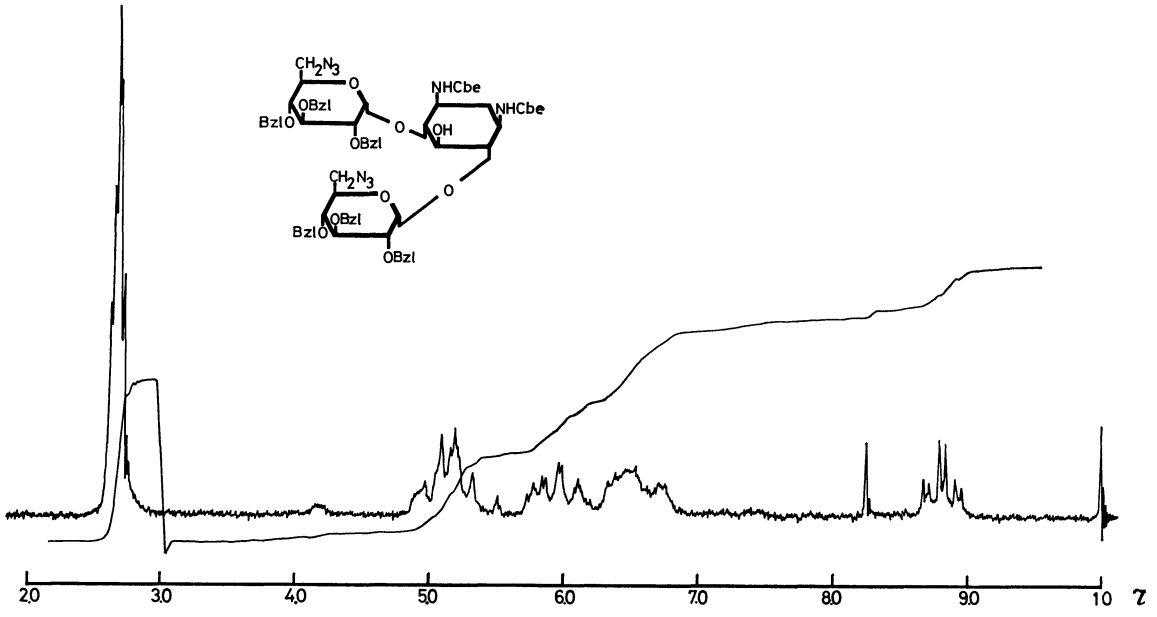

Fig 2. The NMR spectrum of **16** in $CDCl_3$.

15) S. Umezawa, Y. Takagi, and T. Tsuchiya, the details will be published elesewhere.

16) C. Ainsworth, *J. Amer. Chem. Soc.*, **78**, 1635 (1956).

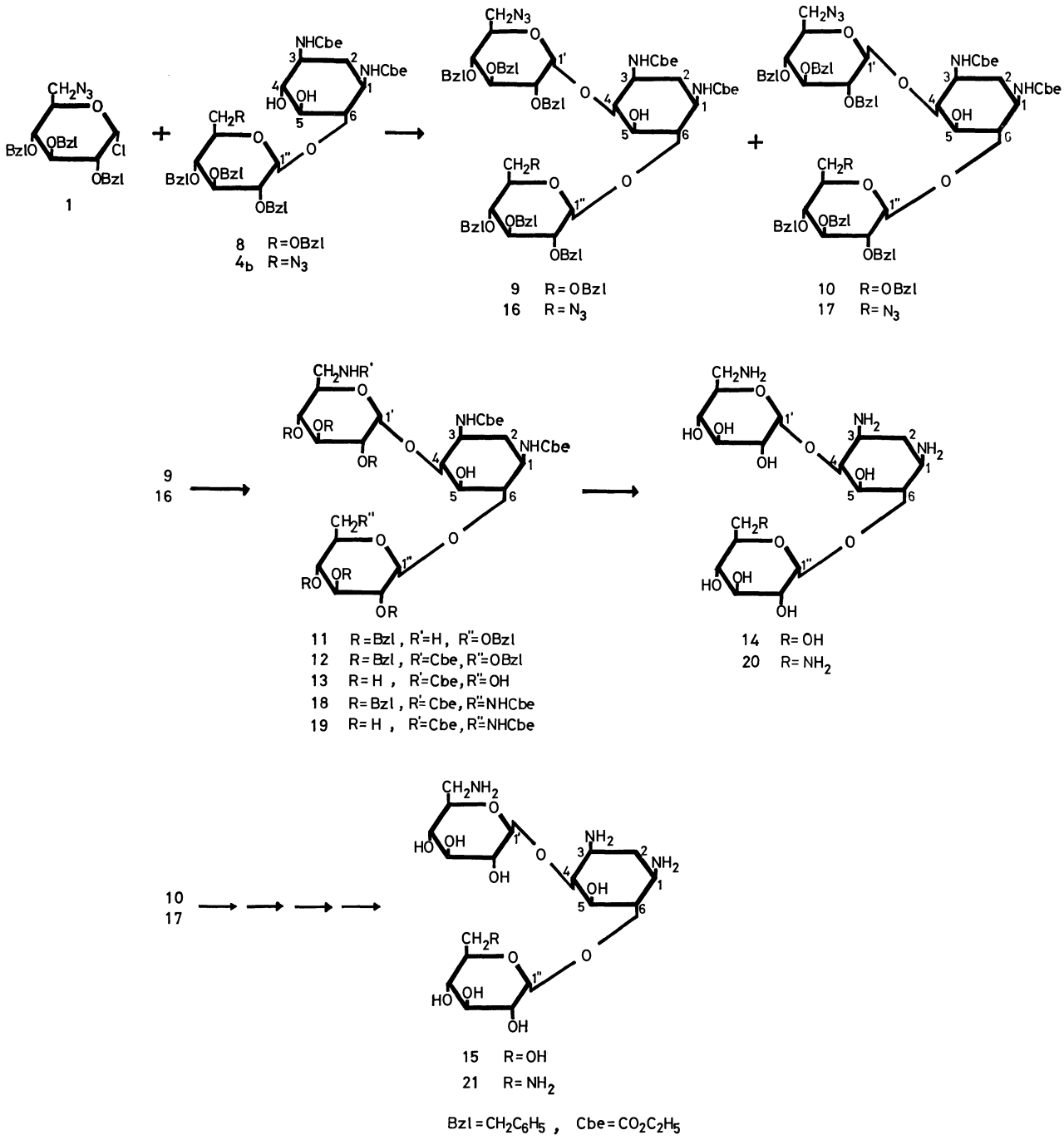

Chart 2.

the hydrolyzates showed the presence of 2-deoxystreptamine, indicating both **9** and **10** are 4,6-di-*O*-glycosides. The main product **9** was reduced with Raney nickel and hydrogen to give 4-*O*-(6-amino-2,3,4-tri-*O*-benzyl-6-deoxy-α-D-glucopyranosyl)-6-*O*-(2,3,4,6-tetra-*O*-benzyl-α-D-glucopyranosyl)-*N*,*N'*-diethoxycarbonyl-2-deoxystreptamine (**11**), which was then *N*-ethoxycarbonylated to give a tri-*N*-ethoxycarbonyl derivative (**12**). Subsequent debenzylation gave **13** and deethoxycarbonylation the final product, 4-*O*-(6-amino-6-deoxy-α-D-glucopyranosyl)-6-*O*-(α-D-glucopyranosyl)-2-deoxystreptamine (**14**). The corresponding β-isomer, 4-*O*-(6-amino-6-deoxy-β-D-glucopyranosyl)-6-*O*-(α-D-glucopyranosyl)-deoxystreptamine (**15**) was similarly prepared, starting from **10**.

A similar scheme was also carried out for the preparation of 4-*O*-(6-amino-6-deoxy-α and β-D-glucopyranosyl)-6-*O*-(6-amino-6-deoxy-α-D-glucopyranosyl)-2-deoxystreptamine (**20** and **21**) starting from **4b** and **1** (Chart 2). The NMR spectrum of a condensation product, 4,6-di-*O*-(6-azido-2,3,4-tri-*O*-benzyl-6-deoxy-D-glucopyranosyl)-*N*,*N'*-diethoxycarbonyl-2-deoxystreptamine (**16**) is shown in Fig 2.

The characteristic features of the above mentioned synthesis and that reported previously[9] are: 1) α-glucoside is the main product and the yield of β-isomer is very low, even though it is formed, 2) 4-O and 6-O positional isomers are successfully separated by recrys-

Table 1. Antibacterial spectra **7a**, **7b**, **14**, and **20**

Test organisms[a]	Minimal inhibitory concentration (mcg/ml)			
	7a	**7b**	**14**	**20**
Staphylococcus aureus FDA 209 F	50	>100	100	100
Staphylococcus auleus Smith	6.25	>100	12.5	6.25
Escherichia coli NIHJ	50	>100	100	100
Sarcina lutea PCI 1001	>100	>100	>100	>100
Salmonella typhosa T-63	25	>100	50	50
Proteus vulgaris OX19	25	>100	25	100
Bacillus subtilis NRRL B-558	12.5	>100	12.5	25
Pseudomonas aeruginosa A3	>100	>100	>100	>100
Mycobacterium smegmatis ATCC 607	25	>100	50	25

a) Nutrient agar, 37°C, 18 hr.

tallization or by column chromatography of either the condensed products or the deacetonation products.

Structural assignment. α-glucosidic structures of 4-*O*- and 6-*O*-(6-amino-6-deoxy-α-D-glucopyranosyl)-2-deoxystreptamine (**7a** and **7b**, respectively) were proved by their specific rotations ($[\alpha]_D^{20}+89°$ as **7a**·dihydrochloride and +82° as **7b**·dihydrochloride) and coupling constants (each ~3 Hz) of anomeric protons in their NMR spectra.

Assignment of 4-*O*- and 6-*O*-glycoside to **7a** and **7b**, respectively, were performed by the determination of the values of Δ[M] in tetramminecopper(II) sulfate solutions (**TACu**).[17] The Δ[M] values of **7a** and **7b** were +645° and −230° respectively. The former was in accord with that (+640°) of natural 4-*O*-(6-amino-6-deoxy-α-D-glucopyranosyl)-2-deoxystreptamine,[13] and the sign and the absolute value of the Δ[M] indicated that **TACu** formed a complex between C-1 NH_2 and C-6 OH in deoxystreptamine moiety. Since methyl 6-amino-6-deoxy-α-D-glucopyranoside shows Δ[M]+80°[17] indicating that the C-6 amino group gives almost no effect on the Δ[M] value, the above assignment for **7a** is substantiated. On the other hand, Δ[M]−230° of **7b** is anomalously low in absolute value. However, the deviation from the normal value (900—700°) will be interpreted by considering the steric state of **7b**. If 6-amino-6-deoxy-D-glucose and 2-deoxystreptamine moieties of **7a** and **7b** are situated as far as possible from each other as seen in kanamycin, which is indicated by X-ray crystallographic analysis,[18] the C-6 amino groups of **7a** and **7b**, can come near the C-3 NH_2 and C-5 OH groups, respectively, of 2-deoxystreptamine moiety. Thus the anomalous Δ[M] value of **7b**, can be explained by assuming the complexing between C-5 OH in 2-deoxystreptamine moiety and C-6 NH_2 group in sugar moiety occurs and the value of Δ[M] attributable to the complexing is fairly large and the sign is positive.

Antibiotic Activity. The antibacterial activities of synthetic compounds **7a**, **7b**, **14**, **15**, **20**, and **21** were tested. It is particularly noteworthy that the 4-*O*-isomer (**7a**), which was proved to be the same as the natural origin,[14] has antibacterial activity (Table 1), while the 6-*O*-isomer (**7b**) has no antibacterial activity. **7a**, **14**, and **20** which contain 4-*O*-(6-amino-6-deoxy-α-D-glucopyranosyl)-2-deoxystreptamine have antibacterial activity, even though it is low. This shows that 3-amino-3-deoxy-D-glucose moiety attached to C-6 OH of 2-deoxystreptamine especially enhances the activity of 4-*O*-(6-amino-6-deoxy-α-D-glucopyranosyl)-2-deoxystreptamine moiety. Since 6-*O*-(3-amino-3-deoxy-α-D-glucopyranosyl)-2-deoxystreptamine have no antibacterial activity, this conclusion may be substantiated.

It has been confirmed that **15** and **21** which contain 4-*O*-(6-amino-6-deoxy-β-D-glucopyranosyl)-2-deoxystreptamine show no antibacterial activities, indicating that the α-glucosidic linkage at C-4 of 2-deoxystreptamine is indispensable for exhibiting antibacterial activity.

Experimental

The NMR spectra were measured with a Varian A-60D spectrometer. Tetramethylsilane (τ 10.00; for the solutions other than deuterium oxide) and sodium 4,4-dimethyl-4-silapentane-1-sulfonate (τ 10.00; for the solutions of deuterium oxide) were used as internal standards. Thin-layer chromatography (tlc) was carried out on microscope slides coated with silica gel, and the spots were visualized with sulfuric acid. Paper chromatography (ppc) was carried out on Toyo Roshi No. 50 paper.

*6-O-(6-Azido-2,3,4-tri-O-benzyl-6-deoxy-α-D-glucopyranosyl)-N,N′-diethoxycarbonyl-4,5-O-isopropylidene-2-deoxystreptamine (**3b**,) and a Mixture of **3b** and 4-O-(6-Azido-2,3,4-tri-O-benzyl-6-deoxy-α-D-glucopyranosyl)-N,N′-diethoxycarbonyl-5,6-O-isopropylidene-2-deoxystreptamine (**3a**).* A mixture of **1** syrup, ($[\alpha]_D^{24}+119°$ (*c* 1, $CHCl_3$), 8.3 g, 17 mmol) and freshly prepared Drierite (7 g) in dry benzene-dioxane (4:1, 75 ml)[19] was heated at 60°C under stirring for 30 min, and **2** (racemic mixture, 3.76 g, 11 mmol) and well dried powder mercuric cyanide (9 g) were added to the mixture, which was refluxed for 26 hr under vigorous stirring. The reaction mixture was filtered and the residue was washed with chloroform. The filtrate and the washings combined were evaporated to

17) S. Umezawa, T. Tsuchiya, and K. Tatsuta, This Bulletin, **39**, 1235 (1966).

18) G. Koyama, Y. Iitaka, K. Maeda, and H. Umezawa, *Tetrahedron Lett.*, **1968**, 1875.

19) Benzene and dioxane were dried strictly as follows: benzene was distilled with a fractionating column and the main portion was dried over lithium aluminum hydride. After storage for several days, the upper layer was taken for use. Dioxane was distilled and the main portion was refluxed with sodium metal for several hours and used immediately.

give a syrup, which was dissolved in chloroform and the solution was washed with 2% sodium bicarbonate solution and water. The solution was dried over sodium sulfate and evaporated. The syrup (~14 g) was chromatographed on a column (45×410 mm) of alumina (E. Merck AG, 650 g) with benzene - acetone (5:1). The condensation product was eluted, after the chloride (**I**) remained eluted, giving a paleyellow syrup (~12 g). On tlc with chloroform - ethyl acetate (3:1), the syrup showed two spots of R_f 0.50 (major) and 0.37 (minor). One fourth of the syrup was chromatographed on a column (35×315 mm) of silica gel (Wako Gel, 130 g) with chloroform-ethyl acetate (3:1) and the portion (360—460 m*l*) containing the major product (R_f 0.50) was evaporated to give a syrup (1.58 g). The syrup, however, on tlc with benzene - acetone (5:1), showed still two spots of R_f 0.51 (major) and 0.60 (minor). Further chromatography on a column (28×530 mm) of silica gel (Wako Gel, 150 g) with benzene - acetone (5:1) gave a syrup (R_f 0.51, **3a**+**3b**, 1.4 g). Recrystallization from ethanol containing a small quantity of aqueous ammonia gave crystals of **3b**, 0.88 g (47%), mp 184.5—185.5°C, $[\alpha]_D^{16}$+48° (*c* 1, chloroform); IR (KBr): 2100 (N_3), 1695 (amide I), 1540 cm^{-1} (amide II); NMR ($CDCl_3$): τ 8.83 and 8.78 (3H, t. each, *J* 7 Hz, $CH_2C\underline{H}_3$), 8.58 (6H, s., isopropylidene), 2.67, 2.68, and 2.71 (5H s. each, $OCH_2C_6\underline{H}_5$).

Found: C, 63.07; H, 6.87; N, 8.50%. Calcd for $C_{42}H_{53}N_5O_{11}$: C, 62.75; H, 6.65; N, 8.71%.

Evaporation of the mother liquor gave a syrup (0.5 g) which was still a mixture of **3a** and **3b**.

*4-O-(6-Azido-2,3,4-tri-O-benzyl-6-deoxy-α-D-glucopyranosyl)-N,N′-diethoxycarbonyl-2-deoxystreptamine (**4a**) and 6-O-(6-Azido-2,3,4-tri-O-benzyl-6-deoxy-α-D-glucopyranosyl)-N,N′-diethoxycarbonyl-2-deoxystreptamine (**4b**).* *a) From the mixture of **3a** and **3b**:* A solution of the mixture (1.94 g) in 80% acetic acid (10 m*l*) was heated at 90°C for 20 min and poured into water. The resulting precipitate (1.78 g) was chromatographed on a column of silica gel (Mallinckrodt, 200 g) with benzene-methyl ethyl ketone (3:1). **4a** (R_f 0.17 on tlc with the same solvent system) was obtained from the early fractions, yield 1.08 g (12.3%, based on one-half of **2**). From the late fractions, **4b** (R_f 0.12) was obtained, yield 0.55 g. **4a** was recrystallized from acetone to give needles, but not **4b**.

*b) **4b** from **3b**:* The crystalline **3b** (3.2 g) was treated as above to give **4b** quantitatively, yield, 3.12 g. Total yield of **4b** by a) and b) was 48% based on one-half of **2**.

Compound **4a**: mp 218—219°C, $[\alpha]_D^{26}$+74.3° (*c* 1, chloroform); IR (KBr): 2100 (N_3), 1690, 1540 cm^{-1}; NMR (in $CDCl_3$ containing D_2O): τ 8.80 and 8.78 (3H t. each, *J* 7 Hz, $CH_2C\underline{H}_3$), 6.1—6.7 (11H, skeleton protons), 5.89 and 5.86 (2H q. each, *J* 7 Hz, $C\underline{H}_2CH_3$), 5.35 (1H, d., *J* 11 Hz) and 5.08 (1H d., *J* 11 Hz) forming an AB quartet ($OC\underline{H}_2C_6H_5$ at C-2(?)), 5.17 and 5.08 (2H s. each, $OC\underline{H}_2C_6H_5$ at C-3 and C-4), 5.00 (1H, d., *J* 3 Hz, H-1′[20]), 2.69 (5H s., $OC\underline{H}_2C_6H_5$), 2.65 (10H s., $OC\underline{H}_2C_6H_5$).

Found: C, 61.56; H, 6.43; N, 8.86%. Calcd for $C_{39}H_{49}N_5O_{11}$: C, 61.32; H, 6.47; N, 9.17%.

Compound **4b**: mp 178—179°C $[\alpha]_D^{22}$+38° (*c* 0.5, chloroform); IR: a similar pattern with that of **4a**; NMR (in $CDCl_3$ containing D_2O): τ 8.85 and 8.76 (3H t. each, *J* 7 Hz, $CH_2C\underline{H}_3$), 6.1—6.7 (11H, skeleton protons), 5.92 and 5.85 (2H q. each, *J* 7 Hz, $C\underline{H}_2CH_3$), 4.9—5.5 (~7 H m.), 2.67, 2.63 and 2.61 (each 5H s., $OCH_2C_6\underline{H}_5$).

Found: C, 61.18; H, 6.21; N, 8.87%. Calcd for $C_{39}H_{49}N_5O_{11}$: C, 61.32; H, 6.47; N, 9.17%.

*4-O-(2,3,4-Tri-O-benzyl-6-deoxy-6-ethoxycarbonylamido-α-D-glucopyranosyl)-N,N′-diethoxycarbonyl-2-deoxystreptamine (**5a**).* Compound **4a** (0.40 g) was dissolved in aqueous ethanol (1:16, 8.5 m*l*) by heating and the solution was hydrogenated with Raney nickel (T-4) and hydrogen under 50 lb/sq. inch pressure at 40—45°C for 12 hr. On tlc with benzene-methyl ethyl ketone (2:1), **4a** (R_f 0.3) disappeared and a product (R_f 0) appeared. Filtration and evaporation of the solution gave a solid (0.38 g), which was dissolved in acetone (5 m*l*), and water (5 m*l*) was added under vigorous stirring to the solution. To the resulting suspension, anhydrous sodium carbonate (0.42 g) was added and after agitation for a while, carboethoxy chloride (0.28 g) was added slowly. After agitation was continued for 30 min, a product (R_f 0.15) appeared on tlc. The solution was evaporated to give a residue, which was dissolved in chloroform and the solution was washed with water. Drying over sodium sulfate and evaporation gave a residue (0.41 g). Recrystallization from equeous ethanol gave a colorless solid, 0.36 g (86%), mp 198—199°C, $[\alpha]_D^{23}$+24° (*c* 0.7, chloroform); IR: no peak near ~2100 cm^{-1} (N_3) was observed; NMR (in pyridine-d_5 containing small amount of D_2O): τ 8.80 (9H t., *J* 7 Hz, $CH_2C\underline{H}_3$), 2.65 (15H s., $OCH_2C_6\underline{H}_5$).

Found: C, 62.32; H, 6.91; N, 5.06%. Calcd for $C_{42}H_{55}N_3O_{13}$: C, 62.28; H, 6.85; N, 5.19%.

*6-O-(2,3,4-Tri-O-benzyl-6-deoxy-6-ethoxycarbonylamido-α-D-glucopyranosyl)-N,N′-diethoxycarbonyl-2-deoxystreptamine (**5b**).* A solution of **4b** (0.23 g) in aqueous ethanol (1:20, 10.5 m*l*) was hydrogenated for 20 hr as in the procedure for **4a** and the reduction product (0.21 g, R_f 0 with benzene-acetone 2:1) was allowed to react with carboethoxy chloride to give **5b** (0.21 g). Recrystallized from aqueous ethanol; a colorless solid 0.18 g (74%), mp 243—244°C, $[\alpha]_D^{26}$ +24° (*c* 0.6, acetone); NMR (in pyridine-d_5 containing small amount of D_2O): τ 8.87 and 8.82 (6H and 3H t. respectively, $CH_2C\underline{H}_3$), 4.05 (1H d., *J* 3 Hz, H-1″), 2.4—2.6 (15H m., $OCH_2C_6\underline{H}_5$).

*4-O-(6-Deoxy-6-ethoxycarbonylamido-α-D-glucopyranosyl)-N,N′-diethoxycarbonyl-2-deoxystreptamine (**6a**).* Compound **5a** (0.31 g) was dissolved in a mixture of ethanol (11 m*l*) and water (4 m*l*) by heating. After addition of several drops of acetic acid, the solution was hydrogenated with freshly prepared palladium black and hydrogen under 50 lb/sq. inch pressure at 40—45°C for 12 hr. On tlc with benzene-methanol (4:1), **5a** (R_f 0.6) disappeared and a product (R_f 0.2) appeared. Filtration and evaporation of the solution gave a solid, which was treated with aqueous acetone (2:1) to give an amorphous solid, 0.20 g (97%), mp 266—267°C, $[\alpha]_D^{20}$+44° (*c* 0.7, aqueous ethanol 1:1); IR (KBr): 3200—3500, 1695, and 1545 cm^{-1}; NMR (in a mixture of D_2O and pyridine-d_5 of approximately 1:1): τ 8.90 (9H t., *J* 7 Hz, $CH_2C\underline{H}_3$), 6.8—6.3 (11H, skeleton protons), 6.01 (6H q., *J* 7 Hz, $C\underline{H}_2CH_3$), 4.82 (1H, d., *J* 3 Hz, H-1′). No benzyl protons were observed. Found: C, 46.44; H, 7.24; N, 7.55%. Calcd for $C_{21}H_{37}N_3O_{11}$: C, 46.75; H, 6.91; N, 7.79%.

*6-O-(6-Deoxy-6-ethoxycarbonylamido-α-D-glucopyranosyl)-N,N′-diethoxycarbonyl-2-deoxystreptamine (**6b**).* **6b** was prepared from **5b** likewise as described above and the product was reprecipitated from aqueous acetone (3:1), yield 97%. Mp 242.5—244°C, $[\alpha]_D^{20}$+67° (*c* 0.6, aqueous ethanol 1:1); NMR (in a mixture of D_2O and pyridine-d_5 of approximately 1:1): τ 8.90, 8.87, and 8.82 (3H t. each, *J* 7 Hz, $CH_2C\underline{H}_3$), 6.4—5.6 (~17 H), 4.43 (1H d., *J* 3 Hz, H-1″).

Found: C, 46.83; H, 6.91; N, 7.42%. Calcd for $C_{21}H_{37}N_3O_{13}$: C, 46.75; H, 6.91; N, 7.79%.

*4-O-(6-Amino-6-deoxy-α-D-glucopyranosyl)-2-deoxystreptamine (**7a**).* A solution of **6a** (0.14 g) in 1N barium hydroxide

20) The anomeric hydrogen of a glycoside moiety attached to C-4 and C-6 of 2-deoxystreptamine is designated as H-1′ and H-1″ respectively; See Ref. 4e.

(6 ml) was heated at 90°C for 5 hr and the resulting solution was neutralized with carbon dioxide. The suspension was boiled for a while, centrifuged, and the upper layer was filtered. The residue was washed with boiling water several times. The filtrate and washings combined were evaporated. The resulting residue was dissolved in water and the solution was filtered and the filtrate was evaporated. The procedure was repeated twice more. The residue was charged on a column (10×140 mm) of Amberlite IRC 50 (NH_4^+ form) and after washing with water developed with 0.1N ammonia. The portion (70—160 ml) containing **7a** was evaporated to give a colorless solid, 0.06 g (69%). An aqueous solution of the product was neutralized with hydrochloric acid to pH 3 and the solution was concentrated. Addition of acetone gave **7a**·dihydrochloride, $[\alpha]_D^{22}+89°$ (*c* 0.3, water), $[\alpha]_{436}^{22}+153°$ (*c* 0.3, water), $[\alpha]_{436TACu}^{22}+316°$ (*c* 0.3, TACu), $\Delta[M]_{TACu}^{22}$[16] $+645°$; $R_{f\,2\text{-deoxystreptamine}}$ 0.38 (ppc with *n*-butanol-pyridine-water-acetic acid 6:4:3:1) IR spectrum was quite the same as that obtained from the natural antibiotic.[14] NMR (in D_2O): τ 8.75 (1H q., $J\sim12$ Hz, H_{ax}-2), 7.97 (1H double triplets, $J\sim3$ and ~12 Hz, H_{eq}-2), 4.73 (1H d., $J\sim3$ Hz, H-1′)

Found: C, 36.34; H, 7.21; Cl, 17.51%. Calcd for $C_{12}H_{25}N_3O_7\cdot2HCl$: C, 36.37; H, 6.87; Cl, 17.89%.

The value of $\Delta[M]_{TACu}^{22}$ corresponded to that (+640°) of the natural product.

6-O-(6-Amino-6-deoxy-α-D-glucopyranosyl)-2-deoxystreptamine (7b). **6b** was treated similarly as in the procedure for **7a** yielding **7b**, yield 65%. Dihydrochloride, $[\alpha]_D^{22}+82°$ (*c* 0.3, water), $[\alpha]_{436}^{22}+150°$ (*c* 0.3, water), $[\alpha]_{436(TACu)}^{22}+92°$ (*c* 0.3, TACu), $\Delta[M]_{TACu}$ −230°; $R_{f\,2\text{-deoxysteptamine}}$ 0.45 (ppc with *n*-butanol-pyridine-water-acetic acid); The IR spectra of **7b** was the same as that of **7a**. NMR (in D_2O): τ 8.53 (1H q., $J\sim12$ Hz, H_{ax}-2), 7.83 (1H double triplet, $J\sim3$ and ~12 Hz, H_{eq}-2), 4.87 (1H, d., $J\sim3$ Hz, H-1″).

Found: C, 36.54; H, 7.03; Cl, 17.42%. Calcd for $C_{12}H_{25}N_3O_7\cdot2HCl$: C, 36.37; H, 6.87; Cl, 17.89%.

4-O-(6-Azido-2,3,4-tri-O-benzyl-6-deoxy-α- and β-D-glucopyranosyl)-6-O-(2,3,4,6-tetra-O-benzyl-α-D-glucopyranosyl)-N,N′-diethoxycarbonyl-2-deoxystreptamine (9 and 10, respectively). A mixture of **1** (1.21 g, 2.4 mmol) and freshly prepared Drierite (1.5 g) in anhydrous benzene-dioxane (3:1, 20 ml) was heated at 60°C under stirring for 30 min and **8**[9] (1.35 g, 1.6 mmol) and well dried mercuric cyanide (1.24 g) were added to the mixture, which was refluxed for 10 hr under vigorous striring. Mercuric cyanide (1.24 g) was again added and the reaction was further continued for 10 hr. The mixture was filtered and the residue was washed with chloroform. The filtrate and washings combined were evaporated to give a syrup which was dissolved in chloroform. The solution was washed with water, dried over sodium sulfate and evaporated to give a thick syrup (2.3 g). On tlc with benzene-acetone (10:1), the syrup showed four spots of R_f 0.43 (major), 0.33 (minor), 0.28 (minor), and 0.20 (minor). The syrup was chromatographed on a column (27×330 mm) of silica gel (Mallinckrodt, 120 g) with benzene-acetone (10:1), and the fractions of 200—300 ml and 360—450 ml containing the major (R_f 0.43) and minor (R_f 0.20) products were evaporated to give solids, respectively (**9**, 1.50 g, 71% based on **8**; **10**, 0.33 g, 16% based on **8**). **10** was recrystallized from ethanol, but not **9**. Compound **9**: mp 53—57°C, $[\alpha]_D^{20}+80°$ (*c* 0.8, acetone); IR (KBr): 2100 cm^{-1} (N_3); NMR (in $CDCl_3$): τ 8.86 and 8.83 (3H t. each $J\sim7$ Hz, $CH_2C\underline{H}_3$, overlapped with peaks of H_{ax}-2), 5.7—6.8 ($\sim$21H, skeleton protons and $C\underline{H}_2CH_3$), 4.8—5.7 ($\sim$17H; seven $OC\underline{H}_2C_6H_5$, two anomeric protons and one amide proton (?)), 4.0 (1H, amide proton), 2.55—2.75 (35H, five singlets, seven $OCH_2C_6\underline{H}_5$).

Found: C, 68.44; H, 6.43; N, 5.51%. Calcd for $C_{73}H_{83}N_5O_{16}$: C, 68.15; H, 6.50; N, 5.44%.

Compound **10**: mp 176—176.5°C, $[\alpha]_D^{20}+82°$ (*c* 0.7 acetone); IR (KBr): 2120 cm^{-1} (N_3); NMR (in $CDCl_3$): τ 8.86 and 8.84 (3H t. each), 5.7—6.8 ($\sim$21H), 4.95—5.7 ($\sim$16H), 4.80 (1H d., $J\sim3$ Hz), 3.7 (1H, amide proton), 2.6—2.75 (35H).

Found: C, 68.01; H, 6.64: N, 5.35%. Calcd for $C_{73}H_{83}N_5O_{16}$: C, 68.15; H, 6.50; N, 5.44%.

4-O-(6-Amino-2,3,4-tri-O-benzyl-6-deoxy-α-D-glucopyranosyl)-6-O-(2,3,4,6-tetra-O-benzyl-α-D-glucopyranosyl)-N,N′-diethoxycarbonyl-2-deoxystreptamine (11). Compound **9** (0.65 g) was dissolved in hot aqueous ethanol (16:1, 8.5 ml) and the solution was hydrogenated with Raney nickel (T-4) and hydrogen under a pressure of 50 lb/sq. inch at 40—45°C for 5 hr. On tlc with benzene-acetone (1:1), **9** (R_f 0.94) disappeared and a product (R_f 0.61) appeared. Filtration and evaporation of the solution gave a colorless solid (0.56 g), which was recrystallized from ethanol to give crystals of **11** (0.51 g, 80%), mp 130—131°C, $[\alpha]_D^{22}+59°$ (*c* 0.8, $CHCl_3$); IR (KBr): no peak near 2100 cm^{-1} (N_3). NMR (in $CDCl_3$): τ 8.83 and 8.80 (3H t. each, *J* 7 Hz, $CH_2C\underline{H}_3$ overlapped with H_{ax}-2 peaks), $\sim$7.9 (1H unresolved m. H_{eq}-2), 6.9—7.5 (3H m., NH_2 and OH), 5.7—6.9 (21H, skeleton protons and $C\underline{H}_2CH_3$), 5.0—5.65 (14H, seven $OC\underline{H}_2C_6H_5$), 4.95 (1H d., $J\sim3$ Hz, anomeric proton at 1″ (?)), 4.78 (1H d., $J\sim3$ Hz, anomeric proton at 1′ (?)), 4.28 and 3.96 (1H each, amide protons), 2.6—2.75 (35H four singlets, seven $OCH_2C_6\underline{H}_5$).

Found: C, 69.26; H, 6.71; N, 3.61%. Calcd for $C_{73}H_{85}N_3O_{16}$: C, 69.56; H, 6.80; N, 3.33%.

4-O-(2,3,4-Tri-O-benzyl-6-deoxy-6-ethoxycarbonylamido-α-D-glucopyranosyl)-6-O-(2,3,4,6-tetra-O-benzyl-α-D-glucopyranosyl)-N,N′-diethoxycarbonyl-2-deoxystreptamine (12). Water (5 ml) and sodium carbonate (0.22 g) were added to a solution of **11** (0.34 g) in acetone (5 ml), under vigorous stirring, and carboethoxy chloride (0.15 g) was added to the resulting suspension. The reaction was continued under stirring for 30 min at room temperature. On tlc with benzene-acetone (3:1), the starting material **11** (R_f 0.13) disappeared and a product (R_f 0.75) appeared. The solution was evaporated and the residue was dissolved in chloroform. The solution was washed with water, dried over sodium sulfate and evaporated to give a thick syrup of **12**; 0.37 g (97%), $[\alpha]_D^{20}+54°$C (*c* 1.2, acetone); NMR (in $CDCl_3$): τ 8.85, 8.82, and 8.77 (3H t. each $CH_2C\underline{H}_3$, overlapped with H_{ax}-2 peaks), $\sim$8.0 (1H m., H_{eq}-2), 5.65 $\sim$6.7 (23H), 4.7—5.6 (17H), 3.95 (1H), 2.55—2.7 (35H, seven $OC\underline{H}_2C_6\underline{H}_5$).

Found: C, 68.67; H, 6.76; N, 3.44%. Calcd for $C_{76}H_{89}N_3O_{18}$: C, 68.50; H, 6.73; N, 3.15%.

4-O-(6-Deoxy-6-ethoxycarbonylamido-α-D-glucopyranosyl)-6-O-(α-D-glucopyranosyl)-N,N′-diethoxycarbonyl-2-deoxystreptamine (13). A solution of **12** (0.33 g) in aqueous ethanol (1:7, 16 ml) containing several drops of acetic acid was hydrogenated with palladium black and hydrogen under 50 lb/sq. inch pressure at 40—45°C for 15 hr. Filtration and evaporation of the solution gave a residue. Recrystallization was accomplished by dissolving the residue in aqueous ethanol (1:1, 8 ml) with subsequent addition of acetone; 0.15 g (84%), mp 164.5—165.5°C, $[\alpha]_D^{20}+88°$ (*c* 0.5, aqueous ethanol 1:1); IR (KBr): 1690 (sharp), 1545 cm^{-1}; NMR (in pyridine-d_5 containing small amount of D_2O): τ 8.75, 8.72 and 8.69 (3H t. each, $CH_2C\underline{H}_3$), $\sim$7.7 (1H, H_{ex}-2), 5.35—6.3 ($\sim$23H), 4.2—4.7 (overlapped with DOH).

Found: C, 45.03; H, 6.82; N, 6.15%. Calcd for $C_{27}H_{47}N_3O_{18}\cdot H_2O$: C, 45.05; H, 6.86; N, 5.84%.

4-O-(6-Amino-6-deoxy-α-D-glucopyranosyl)-6-O-(α-D-gluco-

pyranosyl)-2-deoxystreptamine (14). A solution of **13** (0.14 g) in 1N barium hydroxide (6 m*l*) was heated at 90°C for 5 hr and then neutralized with carbon dioxide. A product ($R_{f\,2\text{-deoxystreptamine}}$ 0.32) appeared on paper chromatography with *n*-butanol – pyridine – water – acetic acid (6:4:3:1). By a similar procedure to that for **7a**, a crude product was obtained. The product was passed through a short column (11×40 mm) of Sephadex G 10 and the fraction containing the product was concentrated to a small volume which was again passed through a short column of Dowex 1×2 (OH form, 0.5 m*l*). The solution obtained was evaporated to give a colorless solid (88 mg), which was purified by dissolving in a mixture of water, methanol and ethanol with subsequent addition of acetone; a hygroscopic solid, 79 mg (82%), $[\alpha]_D^{22}$ +135° (*c* 0.5, water), NMR (in D_2O): τ 8.3—9.0 (1H unresolved m., H_{ax}-2), 7.85—8.2 (1H unresolved m., H_{eq}-2), 5.8—7.3 (~17H, skeleton protons), 4.87 (1H d., J~3 Hz, H-1″), 4.55 (1H d., J~3 Hz, H-1′).

Found: C, 44.35; H, 7.21; N, 8.36%. Calcd for $C_{18}H_{35}N_3O_{12}$: C, 44.53; H, 7.27; N, 8.66%.

4-O-(6-Amino-6-deoxy-β-D-glucopyranosyl)-6-O-(α-D-glucopyranosyl)-2-deoxystreptamine (15). Compound **10** (0.17 g) was reduced with Raney nickel and hydrogen and the amino derivative formed (0.15 g, R_f 0 on tlc with benzene - acetone (10:1) was acylated with carboethoxy chloride to give the corresponding hepta-*O*-benzyl-tri-*N*-ethoxycarbonyl derivative (R_f 0.24) accompanied by a by-product (R_f 0.1). The main product was isolated by column chromatography on silica gel with benzene-acetone (10:1). After being debenzylated with palladium black and hydrogen, the product was hydrolyzed with 1N barium hydroxide and the product was purified by a similar procedure as in the preparation of **14** to give the final product **15** (30 mg, 47%), $[\alpha]_D^{22}$ +63° (*c* 0.6, water): NMR spectrum (in D_2O) of **15** showed a similar pattern to that of **14** except for the peaks of one of anomeric protons: τ 5.37 (1H d., J~7 Hz, H_{ax}-1′), 4.87 (1H d., J~3 Hz, H_{eq}-1″)

Found: C, 44.64; H, 7.33%. Calcd for $C_{18}H_{35}N_3O_{12}$: C, 44.53; H, 7.27%.

4,6-Di-O-(6-azido-2,3,4-tri-O-benzyl-6-deoxy-α-D-glucopyranosyl)-N,N′-diethoxycarbonyl-2-deoxystreptamine (16) and 4-O-(6-Azido-2,3,4-tri-O-benzyl-6-deoxy-β-D-glucopyranosyl)-6-O-(6-azido-2,3,4-tri-O-benzyl-6-deoxy-α-D-glucopyranosyl)-N,N′-diethoxycarbonyl-2-deoxystreptamine (17). A mixture of **1** (1.7 g, 3.5 mmole) and freshly prepared Drierite (1.5 g) in dry benzene-dioxane (3:1, 20 m*l*) was heated at 60°C for 30 min under stirring, and **4b** (1.88 g, 2.5 mmol) and well dried powder mercuric cyanide (1.9 g) were added. The mixture was refluxed under stirring. The reaction was monitored by tlc with benzene - acetone (20:1). After 6 hr mercuric cyanide (1.9 g) was again added. After 10 hr mercuric cyanide (1.9 g) was further added and the reaction was continued for 10 hr (26 hr in total). The mixture was filtered and treatment was carried out as in the preparation of **3a** to give a syrup. On tlc with benzene - acetone (20:1) the syrup showed three spots of R_f 0.16 (**16**), 0.1 and 0.04 (**17**). The syrup was chromatographed on a column (35×330 mm) of silica gel (Mallinckrodt, 150 g) with benzene-acetone (20:1) and the fractions of 240—360 m*l* and 510—960 m*l* were evaporated to give a solid, 1.8 g (**16**, 60%) and 0.58 g (**17**, 19%), respectively. Both **16** and **17** were recrystallized from ethanol.

Compound **16**: mp 158—159°C $[\alpha]_D^{22}$ +91° (*c* 0.9, chloroform); IR (KBr): 2100 cm^{-1} (N_3); NMR (in $CDCl_3$): τ 8.85 and 8.81 (3H t. each, $CH_2C\underline{H}_3$), 5.6—6.8 (~21H), 4.8—5.5 (~15H), 4.15 (1H), 2.55—2.7 (30H, five singlets, six OCH_2-$C_6\underline{H}_5$).

Found: C, 64.70; H, 6.29; N, 9.50%. Calcd for $C_{66}H_{76}N_8O_{15}$: C, 64.90; H, 6.27; N, 9.18%.

Compound **17**: mp 185.5—186.5°C, $[\alpha]_D^{22}$ +62° (*c* 0.7, chloroform); IR (KBr): 2100 cm^{-1} (N_3).

Found: C, 65.13; H, 6.12; N, 8.94%. Calcd for $C_{66}H_{76}N_8O_{15}$: C, 64.90; H, 6.27; N, 9.18%.

4,6-Di-O-(6-ethoxycarbonylamido-2,3,4-tri-O-benzyl-6-deoxy-α-D-gluco-pyranosyl)-N,N′-diethoxycarbonyl-2-deoxystreptamine (18). Compound **16** (0.7 g) was dissolved in hot aqueous ethanol 1:11, 9 m*l*) and hydrogenated with Raney nickel and hydrogen under the pressure of 50 lb/sq. inch at 40—45°C for 14 hr. On tlc with benzene - acetone (20:1), the starting material (R_f 0.28) disappeared and a product (R_f 0) appeared. Filtration and evaporation of the solution gave a solid (0.64 g) which was treated with carboethoxy chloride (0.32 g) in a similar manner as described in the preparation of **5a** to give a crude solid (0.70 g). The product was passed through a column (25×65 mm) of silica gel (Mallinckrodt, 12 g) with the aid of benzene-acetone (5:1). From the fraction of 30—130 m*l*, the final product was obtained as a syrup (0.65 g, 86%) which crystallized on standing, mp 79—81°C, $[\alpha]_D^{23}$ + 36° (*c* 0.9, chloroform); NMR (in $CDCl_3$): τ 8.86, 8.82, 8.80, and 8.77 (3H t. each, $CH_2C\underline{H}_3$), 2.6—2.73 (30H, OCH_2-$C_6\underline{H}_5$).

Found: C, 66.05; H, 6.58; N, 4.25%. Calcd for $C_{72}H_{88}N_4O_{19}$: C, 65.84; H, 6.75; N, 4.27%.

4,6-Di-O-(6-ethoxycarbonylamido-6-deoxy-α-D-glucopyranosyl)-N,N′-diethoxycarbonyl-2-deoxystreptamine (19). Compound **18** (0.5 g) was dissolved in hot aqueous ethanol (3.5:10, 13.5 m*l*) and hydrogenated with palladium black and hydrogen. On tlc with benzene - methanol (4:1), **18** (R_f 0.78) disappeared and a product (R_f 0.2) appeared. Filtration and evaporation of the solution gave **19** which was recrystallized from aqueous ethanol (1:1), 0.25 g (97%); mp 282—283°C, $[\alpha]_D^{20}$+73° (*c* 0.8, aqueous ethanol 1:1); NMR (in pyridine-d_6 containing a little D_2O): τ 8.79, 8.77, 8.72, and 8.70 (3H t. each, J 7 Hz, $CH_3C\underline{H}_2$)

Found: C, 46.37; H, 6.90; N, 6.98%. Calcd for $C_{30}H_{52}N_4O_{19}$: C, 46.63; H, 6.78; N, 7.25%.

4,6-Di-O-(6-amino-6-deoxy-α-D-glucopyranosyl)-2-deoxystreptamine (20). Compound **19** was hydrolyzed in a smilar manner as in the preparation of **7a** and **20** was obtained in 75% yield; $[\alpha]_D^{23}$ +138° (*c* 0.5, water); NMR (in D_2O): τ 4.88 (1H d., J~3 Hz, H-1″), 4.58 (1H d., J~3 Hz, H-3′).

Found: C, 44.78; H, 7.33%. Calcd for $C_{18}H_{36}N_4O_{11}$: C, 44.62; H, 7.49%.

4-O-(6-Amino-6-deoxy-β-D-glucopyranosyl)-6-O-(6-amino-6-deoxy-α-D-glucopyranosyl)-2-deoxystreptamine (21). Compound **17** was hydrogenated with Raney nickel and the corresponding amino compound was *N*-ethoxycarbonylated. The product had R_f 0.44 on tlc with benzene - acetone (5:1). Debenzylation and deethoxycarbonylation were accomplished by similar procedures as in the preparation of **15** to give the final product **21** in 59% yield (based on **17**); $R_{f\,2\text{-deoxystreptamine}}$ 0.23 (ppc with *n*-butanol - pyridine - water - acetic acid 6:4:3:1), $[\alpha]_D^{22}$ +65° (*c* 0.7, water); NMR (in D_2O): τ 5.37 (1H d., J 7 Hz, H_{ax}-1′), 4.87 (1H d., J~3 Hz, H_{eq}-1″).

Found: C, 44.91; H, 7.39%. Calcd for $C_{18}H_{36}N_4O_{11}$: C, 44.62; H, 7.49%.

The authors wish to thank Dr. Masa Hamada and members of the Institute of Microbial Chemistry for bioassay and Mr. Saburo Nakada for the elemental analysis. The authors also wish to thank Messrs. Kazuo Goto, Toshio Sumida, and Ryujiro Namba for their technical assistance.

Studies on Aminosugars. XXVIII. Synthesis of β-L-Idopyranosides through the Corresponding 5-Enopyranosides[1]

Daishiro IKEDA, Tsutomu TSUCHIYA, and Sumio UMEZAWA

Department of Applied Chemistry, Faculty of Engineering, Keio University, Koganei-shi, Tokyo

(Received April 7, 1971)

Methyl 6-deoxy-β-L-idopyranoside (**7**), methyl 2-amino-2,6-dideoxy-β-L-idopyranoside (**13**) and methyl 3-amino-3,6-dideoxy-β-L-idopyranoside (**28**) have been prepared through the corresponding suitably protected 5-enopyranoside precursors in good yields.

As part of the investigation of the syntheses and reactions of aminosugars, the preparation and reaction of several 5-enoses were carried out. This paper reports the syntheses of 5-enoses starting from methyl α-D-glucopyranoside, methyl 2-amino-2-deoxy-α-D-glucopyranoside and methyl 3-amino-3-deoxy-α-D-glucopyranoside, and the behavior of these unsaturated sugars toward catalytic hydrogenation.

Helferich and Himmen described[2,3] the transformation of methyl 2,3,4-tri-*O*-acetyl-6-deoxy-6-iodo-α-D-glucopyranoside and methyl 2,3,4-tri-*O*-acetyl-6-deoxy-6-bromo-β-D-glucopyranoside to methyl 2,3,4-tri-*O*-acetyl-6-deoxy-α-D-*xylo*-hex-5-enopyranoside (**5**) and its β-D isomer, by reaction with silver fluoride in pyridine. We used the general method for the present purpose. Regarding C-6 halogeno compounds, the starting materials, Evans, Long, and Parrish[4] recently described a convenient synthesis of methyl 6-chloro-6-deoxy-α-D-glucopyranoside (**2**) by selective chlorination of the primary hydroxyl group of methyl α-D-glucopyranoside (**1**) by use of methanesulfonyl chloride in dimethylformamide (DMF). We accordingly tried the reaction of **2** with silver fluoride, but the chloro derivative hardly reacted at all with it. The corresponding bromo derivative, namely methyl 6-bromo-6-deoxy-α-D-glucopyranoside (**3**), was prepared analogously by the method of Evans *et al.* and the product was found to react with silver fluoride but not as expected. As shown by Hough and Otter[5] in the case of 5-deoxy-5-iodo-1,2-*O*-isopropylidene-α-D-xylofuranose, it seems that the presence of free hydroxyl groups in **3** prevents the formation of an enose. **3** was therefore acetylated to the tri-*O*-acetyl derivative (**4**) and treated with silver fluoride.

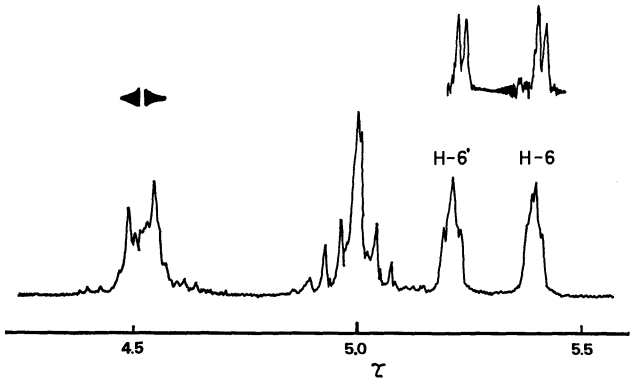

Fig. 1. The NMR Spectrum of **5** in $CDCl_3$.

By this reaction **5** was successfully prepared. The NMR spectrum (Fig. 1) of **5** showed narrow multiplets at τ 5.36 and 5.18. Irradiation at τ 4.53 resulted in the collapse of multiplets to a pair of resolved doublets (J 1.7 Hz). Small coupling is typical for terminal methylene protons supporting the structure **5**.

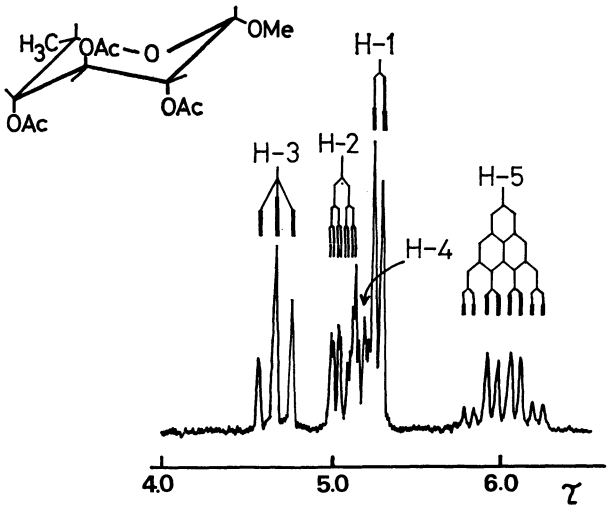

Fig 2. The NMR Spectrum of **6** in $CDCl_3$.

5-Enopyranoside (**5**) was then hydrogenated with palladium black and hydrogen to give methyl 2,3,4-tri-*O*-acetyl-β-L-idopyranoside (**6**) quantitatively. The NMR spectrum of **6** is shown in Fig. 2. The exclusive formation of β-L-idopyranoside is noteworthy in contrast with the hydrogenation of 1,2,3,4-tetra-*O*-acetyl-6-deoxy-β-D-*xylo*-hex-5-enopyranose. It has recently been reported that the latter was converted[6] into a mixture of 96% of the 6-deoxy-D-gluco and 4% of the 6-deoxy-L-ido isomer by hydrogenation with the same catalyst. Hydroboration[7] of methyl 6-deoxy-α-D-*xylo*-hex-5-enopyranoside has also been reported to afford a mixture of methyl α-D-gluco and β-L-ido isomer in the ratio 1:2.5. The anomeric α-*O*-methyl group in **5**, therefore, may be the dominating cause for exclusive formation of the β-L-ido derivative in the hydrogenation with palladium black and hydrogen.

The protecting groups of **6** were finally removed in a basic condition to give methyl 6-deoxy-β-L-idopyrano-

1) A part of this paper was read at the 23rd Annual Meeting of the Chemical Society of Japan, Tokyo, April, 1970. (See Abstract of Papers of the Meeting, Vol. III p. 1901).

2) B. Helferich and E. Himmen, *Ber.*, **61**, 1825 (1928).

3) B. Helferich and E. Himmen, *ibid.*, **62**, 2136 (1929).

4) M. E. Evans, L. Long, Jr., and F. W. Parrish, *J. Org. Chem.*, **33**, 1074 (1968).

5) L. Hough and B. Otter, *Chem. Commun.*, **1966**, 173.

6) L. Hough, R. Khan, and B. A. Otter, in "Deoxy Sugars" (Advances in Chemistry Series, No. 74), ed. by S. Hanessian, Amer. Chem. Soc., Washington (1968), p. 120.

7) J. Lehman, *Carbohyd. Res.*, **2**, 1 (1966).

side (**7**). As for 6 deoxy-L-idose, it was prepared by Meyer and Reichstein[8] and Wolfrom and Hanessian[9] from 1,2,*O*-isopropylidene-D-glucofuranose through multi-step procedures.

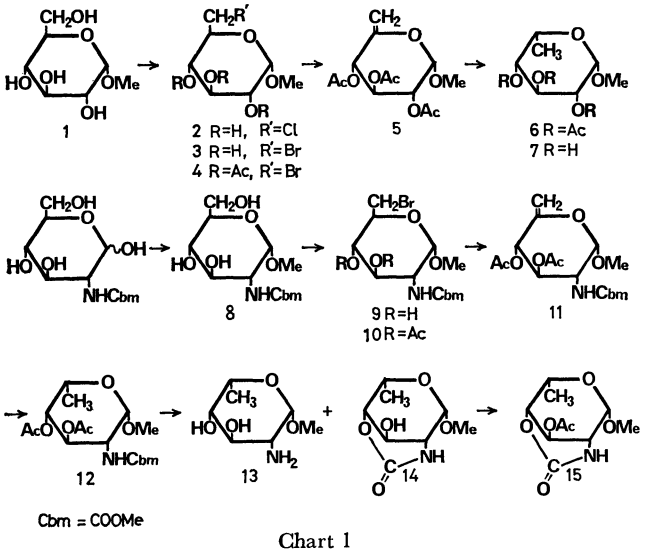

Chart 1

The above synthesis has been extended to amino-sugars, and methyl 2-amino-2,6-dideoxy-β-L-idopyranoside (**13**) has been prepared from methyl 2-deoxy-2-methoxycarbonylamino-α-D-glucopyranoside (**8**). 2-Amino-2-deoxy-D-glucose was *N*-methoxycarbonylated and then treated with hydrogen chloride in methanol to give **8** in 78% yield with no detectable formation of β-isomer. Glucoside (**8**) was brominated in a similar manner as in the preparation of **3**. The resulting 6-bromo derivative (**9**) was acetylated and then treated with silver fluoride in DMF. In this case the reaction to make 5,6-unsaturation was appreciably slower than that in the case of **5**, and methyl 3,4-di-*O*-acetyl-2,6-dideoxy-2-methoxycarbonylamido-α-D-*xylo*-hex-5-enopyranoside (**11**) was obtained in 30% yield, leaving much starting material (**10**) unchanged. In regard to the synthesis of an aminoglucoside having 5-eno structure, Kiss and Burkhardt[10] reported the preparation of methyl 4-*O*-acetyl-3-*O*-benzyl-2-benzyloxycarbonylamido-2,6-dideoxy-α-D-*xylo*-hex-5-enopyranoside from the corresponding 6-iodo precursor in a good yield.

Hydrogenation of the 5-eno derivative (**11**) gave β-L-idopyranoside (**12**) in 90% yield, and subsequent hydrolysis with 1N barium hydroxide gave methyl 2-amino-2,6-dideoxy-β-L-idopyranoside (**13**) in 56% yield. The NMR spectrum of **12** is shown in Fig. 3. In this hydrolysis, another product (**14**) was formed in 33% yield, which resisted further hydrolysis. Even after 3 hr heating at 100°C in 1N barium hydroxide solution, only half of the product was transformed to **13**. The structure of **14** was determined through the NMR spectrum (Fig. 4) of its acetyl derivative (**15**) as methyl

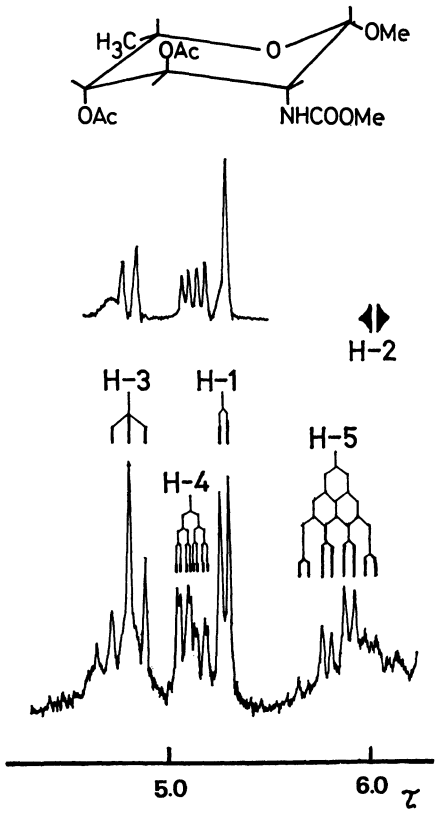

Fig. 3. The NMR spectrum of **12** in $CDCl_3$.

2-amino-2,6-dideoxy-β-L-idopyranoside 2,4-carbamate, but not 2,3-carbamate. In the NMR spectrum of **15**, H-2 resonated at τ 6.27 and appeared as double triplets (J 4.4 and 2 Hz). Double irradiation technique showed that the coupling constants relating to H-2 were $J_{2,3}$ 4 Hz, $J_{2,NH}$ 4 Hz, $J_{2,4}$ 2 Hz and $J_{2,1}$ 0 Hz. These coupling constants and others ($J_{3,4}$ 4 Hz, $J_{4,5}$ ~0 Hz) suggest that the preferred conformation of **15** is IC chair. Moreover, observation of a long-range coupling ($J_{2,4}$ 2 Hz) in **15** as well as the position of acetoxyl methyl resonance at τ 7.85, situated in the region of an axial acetoxyl methyl,[11] also support the IC conformation in which H-2 and H-4 are in di-equatorial orientation.

3-Amino-3-deoxy-D-glucose was led to the corresponding L-idopyranoside by a series of similar reactions. 3-Amino-3-deoxy-D-glucose prepared by the fermentation[12] of *Bacillus aminoglucosidicus* was *N*-methoxycarbonylated and glycosidated with hydrogen chloride - methanol to afford a mixture of α- (**16**) and β-anomer (**17**). Separation of the anomers was performed by resin column chromatography. The α-anomer was brominated in an analogous manner to those described above to give 6-bromo derivative (**18**) in 85% yield. After subsequent acetylation, the acetyl derivative (**19**) was treated with silver fluoride in pyridine. It was found that unsaturation does not

8) A. S. Meyer and T. Reichstein, *Helv. Chim. Acta*, **29**, 139 (1946); *ibid.*, **29**, 152 (1946).

9) M. L. Wolfrom and S. Hanessian, *J. Org. Chem.*, **27**, 1800 (1962).

10) J. Kiss and F. Burkhardt, *Helv. Chim. Acta*, **52**, 2622 (1969).

11) R. U. Lemieux, R. K. Kulling, H. J. Bernstein, and W. G. Schneider, *J. Amer. Chem. Soc.*, **80**, 6098 (1958); L. D. Hall, *Adv. Carbohyd. Chem.*, **19**, 51 (1964).

12) S. Umezawa, K. Umino, S. Shibahara, M. Hamada, and S. Omoto, *J. Antibiotics*, **20A**, 355 (1967).

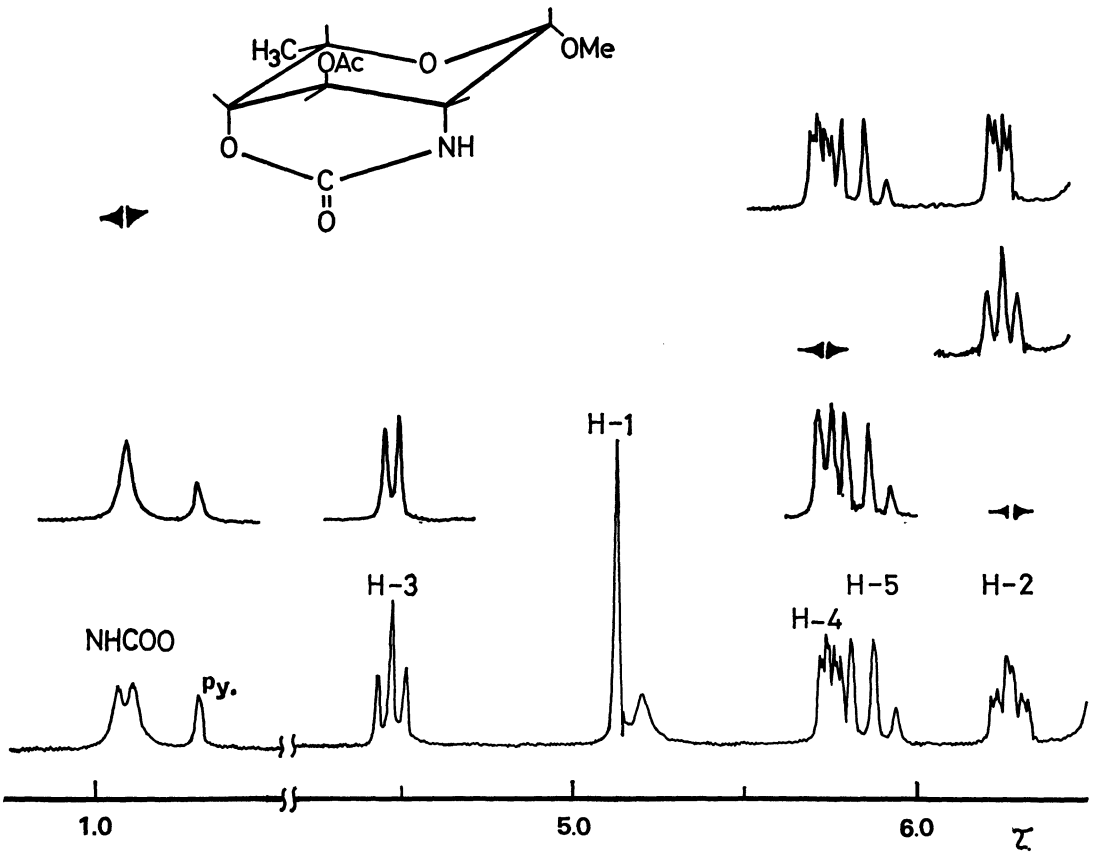

Fig. 4. The NMR spectrum of **15** in pyridine-d_5.

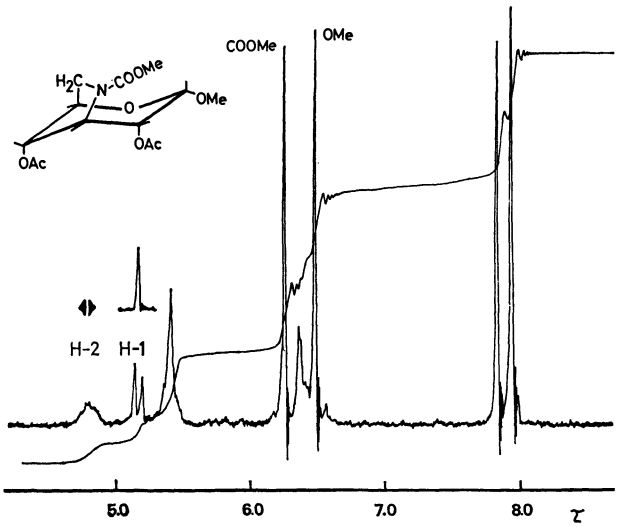

Fig. 5. The NMR spectrum of **20** in $CDCl_3$.

occur and a 3,6-imino derivative (**20**) was formed instead. No absorption ascribable to amide II was observed in its IR spectrum. The NMR spectrum indicated the presence of two axial acetyls, O–CH_3, $NCOOCH_3$, one anomeric proton and six other protons (Fig. 5). Irradiation at τ 4.80 caused the doublet of H-1 at τ 5.15 to collapse to a singlet. The broadened signal (τ 4.68—4.88) centered at τ 4.80 was therefore assigned to H-2; at the same time, the unresolved pattern and the narrow half-height width (~8 Hz) of H-2 suggested the presence of a long-range coupling between H-2 and H-4 as well as a small coupling between H-2 and H-3. These results and the presence of a narrow multiplet (τ 5.3—5.5) of H-3, 4, and 5 complex suggest the preferred conformation of **20** to be IC and, consequently, **20** has a 3,6-imino structure. Formation of structurally related 3,6-imino derivatives from suitably protected 6-*O*-mesyl or 6-*O*-tosyl precursors by the action of sodium acetate were recently

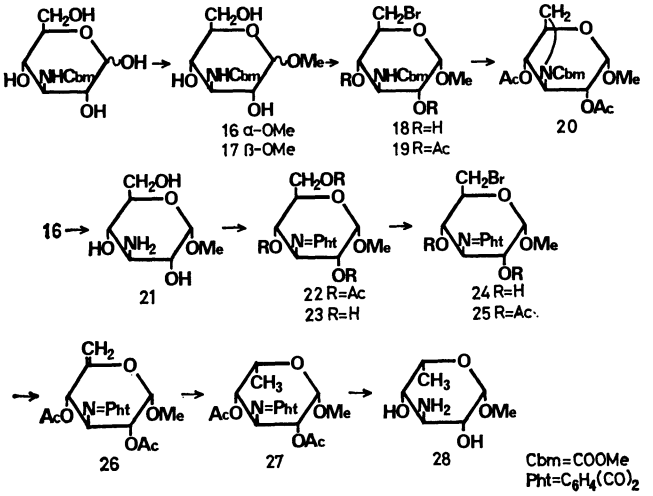

Chart 2

reported by Reckendorf *et al.*[13]

Failure of the formation of a 5,6-unsaturated compound from **19** was presumed to be due to the presence of an amino hydrogen in **19**. Accordingly, an attempt was made to use a 3-phthalimido derivative in place of **19**. Methyl 3-amino-3-deoxy-α-D-glucopyranoside (**21**) was prepared by alkaline hydrolysis of **16**, and then treated with phthalic anhydride and acetic anhydride to give an *O*-acetylated 3-phthalimido derivative (**22**). Subsequent deacetylation gave a 3-phthalimido derivative (**23**). Bromination of **23** in an analogous manner as described above gave a 6-bromo derivative (**24**), which was then acetylated. The reaction of the acetylated product (**25**) with silver fluoride proceeded smoothly, and afforded a 5,6-unsaturated compound (**26**) in 79% yield. The NMR spectrum of **26** is shown in Fig. 6. The catalytic hydrogenation of 5-enopyranoside gave β-L-ido derivative (**27**) in 87% yield. The NMR spectrum of **27** is shown in Fig. 7. The protecting groups of **27** were finally removed with *n*-butylamine to give methyl 3-amino-3,6-dideoxy-β-L-idopyranoside (**28**) in 77% yield.

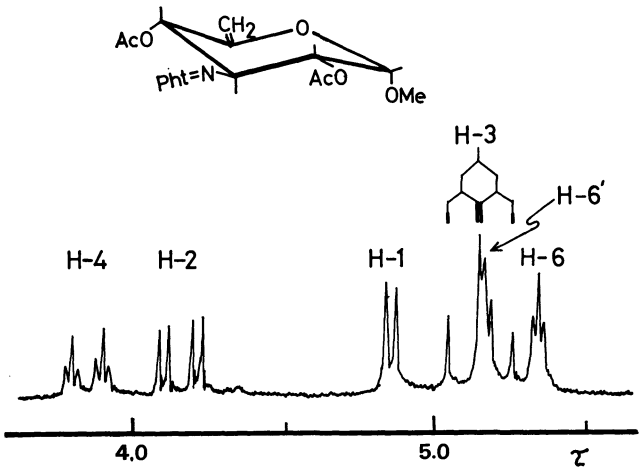

Fig. 6. The NMR Spectrum of **26** in $CDCl_3$.

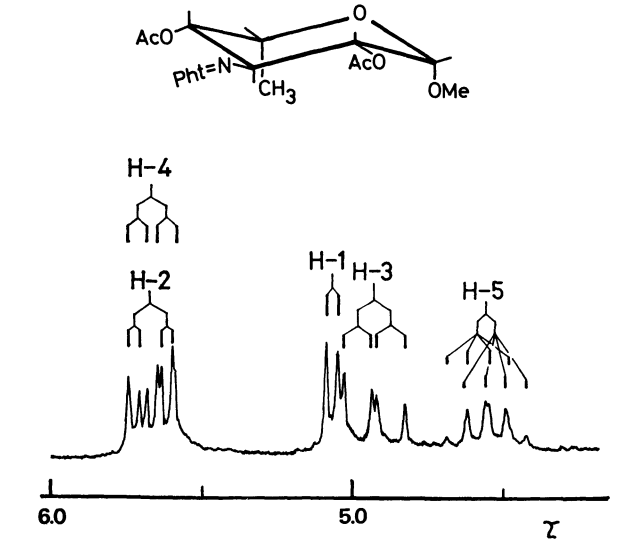

Fig 7. The NMR spectrum of **27** in $CDCl_3$.

Conformations of β-L-Ido Compounds. The NMR spectra of these final products **7**, **13**, and **28** were compared. Each proton having the same structural number of these compounds had almost the same splitting pattern and couplings. The shift-values of the corresponding protons also were in accord except for the shift-value of the proton bearing an amino group: the H-2 and H-3 protons in **13** and **28** resonated at 0.75 and 0.76 ppm higher field than that of the resonance of H-2 and H-3 of **7**, respectively. These findings show that **7**, **13**, and **28** have the same conformation. The values of the vicinal coupling constants of these compounds, $J_{1,2}$ 2, $J_{2,3}$ ~5, $J_{3,4}$ ~5 and $J_{4,5}$ 3 Hz suggested that the preferred conformation of **7**, **13**, and **28** is IC chair, but not CI. A twist-boat structure as shown by Coxon[14] was also considered, but the observation of a long-range coupling between H-2 and H-4 ($J_{2,4}$ ~1Hz) in **7** and **28** suggested that H-2 and H-4 are in diequatorial orientation and a twist-boat structure is improbable. The small $\Delta[M]_{TACu}$[15] value (+159°) of **13** also supports the view that 2-amino and 3-hydroxyl groups of **13** are not diequatorial. The results show that the structural change from α-D-gluco to β-L-ido form caused conformational change from CI to IC, and this may be responsible for the easy formation of 2,4-carbamate (**14**) from **12**. Compounds **6** and **12**, both having β-L-ido structure, also were presumed to have IC conformation. Comparison of their NMR spectra with the spectrum of methyl 2,3,4-tri-*O*-acetyl-6-deoxy-α-D-glucopyranoside (**6'**) support the above conclusion. On the other hand, compound **27** was presumed to have CI conformation. This is supported by a comparison of the τ-value of the C-methyl protons (τ 8.58) of **27** with the τ-values of the C-methyl protons of **6**, **7**, **12**, **13**, and **28** (τ ~8.70), suggesting that the C-methyl group of **27** is axial. The fact that only **27** of the β-L-ido derivatives has CI conformation may be interpreted by the presence of a bulky phthalimide group.

Experimental

The NMR spectra were measured with a Varian A-60D or a Varian HA-100 (at 100 MHz) spectrometer. Tetramethylsilane (τ10.00; for the solution other than deuterium oxide) and sodium 4,4-dimethyl-4-silapentane-1-sulfonate (τ 10.00; for the solution of deuterium oxide) were used as the internal standards. Thin-layer chromatography (TLC) was carried out on microscope slides coated with silica gel, and the spots were visualized with sulfonic acid. Paper chromatography (ppc) was carried out on Toyo Roshi No. 50 paper.

Methyl 6-Bromo-6-deoxy-α-D-glucopyranoside (3). To a stirred solution of methyl α-D-glucopyranoside (**1**) (1.0 g) in dry DMF (10 m*l*, dried over calcium hydride), mesyl bromide[16] (1.6 g) was added dropwise and the solution was

13) W. M. zu Reckendorf, *Ber.*, **97**, 1275 (1964); W. M. zu Reckendorf and N. Wassiliadou-Micheli, *ibid.*, **103**, 37 (1970); W. M. zu Reckendorf, *ibid.*, **103**, 995 (1970).

14) B. Coxon, *Carbohyd. Res.*, **1**, 357 (1966).

15) S. Umezawa, T. Tsuchiya, and K. Tatsuta, This Bulletin, **39**, 1235 (1966).

16) G. Sieber, *Ann.*, **631**, 180 (1960).

maintained at 65°C for 18 hr. On TLC with ethyl acetate-ethanol-water (45:5:3), the solution showed two spots of R_f 0.64 and 0.85 in approximately equal strength. The solution was evaporated and coevaporated with toluene to give a brown syrup which was dissolved in methanol and the solution was then neutralized with 2.4M sodium methoxide in methanol. On TLC, the spot of R_f 0.85, which was supposed to originate from an *O*-formyl by-product[4] disappeared, and a spot (R_f 0.17) corresponding to the starting material (**1**) appeared. The solution was evaporated and the residue was charged on a column of silica gel (100 g) and developed with the solvent mixture described above. The portion (180—300 ml) containing the substance of R_f 0.64 was evaporated to give a colorless solid which was recrystallized from ethyl acetate yielding 770 mg (58%), mp 136—137°C (lit,[17] 126—127°C), $[\alpha]_D^{20}$+126° (*c* 1, methanol) (lit,[17] +137°); IR spectrum (KBr): no peaks between 1500—2500 cm^{-1}, 940, 897, 887, 815(vw), 757, 750 (sh), and 694 cm^{-1}; NMR (in D_2O): τ 6.56 (3H s., OCH_3), 6.0—6.65 (6H), 5.18 (1H d., J 3 Hz, H-1).

Found: C, 33.00; H, 5.23; Br, 30.57%. Calcd for $C_7H_{13}O_5Br$: C, 32.70; H, 5.10; Br, 31.09%.

Methyl 2,3,4-Tri-O-acetyl-6-bromo-6-deoxy-α-D-glucopyranoside (4). To a solution of **3** (688 mg) in pyridine (12 ml), acetic anhydride (1.7 g) was added and the solution was allowed to stand overnight. A spot (R_f 0.44) appeared on TLC with benzene-ethyl acetate (6:1). After addition of a small amount of water (0.2 ml) followed by standing for 1 hr, the solution was evaporated and the residue was dissolved in chloroform. The solution was washed in turn, with saturated potassium hydrogensulfate solution, water, saturated sodium hydrogencarbonate solution and water, dried over sodium sulfate and evaporated to give a colorless solid. Recrystallization from ethanol yielding 956 mg (98%), mp 125—125.5° $[\alpha]_D^{20}$+121° (*c* 1, chloroform).

Found: C, 40.92; H, 5.33; Br, 20.41%. Calcd for $C_{13}H_{19}O_8Br$: C, 40.74; H, 5.00; Br, 20.86%.

IR spectrum (KBr): 1750; 931, 910(w) 880(w), 810, 752, and 682(w) cm^{-1}; NMR (in $CDCl_3$): τ 7.96, 7.92, and 7.89 (each 3H s., OAc), 6.48 (3H s., OCH_3), 5.94 (1H octet, J 3.6 and 9.7 Hz, H_{ax}-5), 4.48 (1H triplet with small splittings (~0.5 Hz), J 8.5 Hz, probably H_{ax}-3); $J_{4,5}$ 9.7 Hz, $J_{5,6}$ 3 Hz, $J_{5,6'}$ 6 Hz

Methyl 2,3,4-Tri-O-acetyl-6-deoxy-α-D-xylo-hex-5-enopyranoside (5). To a solution of **4** (1.01 g) in dry pyridine (12 ml, dried over calcium hydride), anhydrous silver fluoride (1.5 g) was added and the mixture was stirred at 50°C for 20 hr in the dark. A spot (R_f 0.72) and three weak spots (R_f 0.55, 0.50 and 0.35) appeared on TLC with benzne - ethyl acetate (3:1). The main spot showed fluorescence[18] by the sodium fluorescein-bromine test according to Stahl for double bond although it has an identical R_f-value with that of **4**. Addition of ether (50 ml) to the reaction mixture gave precipitates which were filtered and washed with ether. The ether layer and washings combined were evaporated and the residue was again dissolved in ether. The solution was washed successively with potassium hydrogensulfate solution, sodium hydrogencarbonate solution and water, dried over sodium sulfate and evaporated to give a solid (680 mg) which was negative to the Beilstein test for halogens. The solid was chromatogrqphed on a column of silica gel (60 g) with benzene - ethyl acetate (3:1) and the portion containing **5** was evaporated to give a residue, which was recrystallized from ethanol yielding 430 mg (54%), mp 93—94°C, $[\alpha]_D^{20}$+117° (*c* 1, chloroform) (lit,[2] +117°).

Found: C, 51.44; H, 6.15%. Calcd for $C_{13}H_{18}O_8$: C, 51.65; H, 6.00%.

IR spectrum (KBr): 1755 (s., ester), 1660 (alkene); 955 (m), 935, 907 (m), 897 (m), 872, 783, and 737 cm^{-1}; NMR (in $CDCl_3$): τ 7.95, 7.90 and 7.86 (each 3H s., OAc), 6.51 (3H s., OCH_3), 5.36 (1H m., half-height width was ~3 Hz, H-6), 5.18 (1H m., half-height width was ~4 Hz, H-6'), 4.65—5.1 (2H unresolved m.), 4.2—4.6 (2H unresolved m.). Irradiation at τ 4.53 caused the multiplets at τ 5.36 and 5.18 to collaspse to two clear-cut doublets (each has J 1.7 Hz) showing that the small coupling originated from geminal olefinic protons of H-6,6'.

Methyl 2,3,4-Tri-O-acetyl-6-deoxy-β-L-idopyranoside (6). A solution of **5** (100 mg) in dioxane (1.5 ml) was hydrogenated with palladium black and hydrogen under 50 lb/sq. inch pressure at 40°C overnight. A spot (R_f 0.45) appeared on TLC with benzene - ethyl acetate (3:1). After filtration the solution was evaporated to give a solid, which was recrystallized from ethanol yielding 98 mg (99%), mp 93.5—94°C, $[\alpha]_D^{20}$+46° (*c* 1, chloroform).

Found: C, 51.30; H, 6.31%. Calcd for $C_{13}H_{20}O_8$: C, 51.31; H, 6.63%.

IR spectrum (KBr): 1760, 1740; 972 (m), 952, 926 (m), 915, 876, 782, and 700 (m) cm^{-1}; NMR (in $CDCl_3$): τ 8.68 (3H d., J 6.7 Hz, C_5-CH_3), 7.87 (6H s., OAc), 7.86 (3H s., OAc), 6.43 (3H s., OCH_3), 5.82 (1H octet, J 6.7, 6.7, 6.7, and 3 Hz (=$J_{4,5}$), H_{eq}-5), 5.20 (1H d., $J_{1,2}$ 2.2 Hz, H-1), 5.08—5.23 (1H m., H-4), 5.02 (1H octet, J 2.2, 4.8, and ~0.8 Hz (=$J_{2,4}$), H-2), 4.69 (1H t., $J_{2,3}$=$J_{3,4}$ 4.8 Hz, H-3).

Small coupling constants of $J_{2,3}$, $J_{3,4}$ and $J_{4,5}$ and the occurrence of long-range coupling of $J_{2,4}$ suggested the preferred conformation of **6** to be IC chair. The conformtion was also substantiated by comparison of the NMR spectrum of **6** with that of methyl 2,3,4-tri-*O*-acetyl-6-deoxy-α-D-glucopyranoside (**6'**) prepared by hydrogenation of 6-bromo derivative (**4**).

Compound **6'**: mp 60—61°C (lit,[19] 77—78°), $[\alpha]_D^{20}$+152° (*c* 1, chloroform) (lit,[19]+153.6°, chloroform); IR spectrum (KBr): 1755; 930, 900, 893, 840 (w), and 753 cm^{-1}; NMR (in $CDCl_3$): τ 8.79 (3H d., J 6.5 Hz, C_5-CH_3), 8.00, 7.97, and 7.93 (each 3H s., OAc), 6.58 (3H, s. OCH_3), 6.05 (1H octet, J 6.5, 6.5, 6.5, and 10.0 Hz, H-5). The three equatorial acetoxy methyl protons of **6'** resonated at τ 7.93, 7.97, and 8.00, whereas those of **6** resonated at τ 7.86, 7.87, and 7.87 suggesting the presence of three axial acetoxyl groups in **6** in its preferred conformation.[12]

Methyl 6-Deoxy-β-L-idopyranoside (7). A solution of **6** (110 mg) in dry methanol (2 ml) was treated with sodium methoxide. After addition of a small amount of Amberlite IR-120 (H^+ form) pretreated with methanol, the solution was filtered, evaporated, and the residue was recrystallized from ethyl acetate to give a solid, 60 mg (98%), mp 81—81.5°C, $[\alpha]_D^{25}$+74° (*c* 1, water).

Found: C, 47.48; H, 7.92%. Calcd for $C_7H_{14}O_5$: C, 47.18; H, 7.92%.

IR spectrum (KBr): 1055, 1020, 1003, 970, 916, 808, and 761 cm^{-1}; NMR (in D_2O): τ 8.69 (3H d., J 6.7 Hz, C_5-CH_3), 6.45 (3H s., OCH_3), 6.35—6.52 (1H m., H-4), 6.28 (1H octet, J 5, 2, and 1 Hz, H-2), 5.97 (1H t., J 5 Hz, H-3), 5.84 (1H octet, J 6,7, 6.7, 6.7, and 3Hz, H-5), 5.20 (1H d., J 2 Hz, H-1); $J_{1,2}$ 2 Hz, $J_{2,3}$=$J_{3,4}$ 5 Hz, $J_{4,5}$ 3Hz, and $J_{2,4}$ ~1 Hz.

Methyl 2-Deoxy-2-methoxycarbonylamido-α-D-glucopyranoside (8). To a mixture of glucosamine hydrochloride (12 g) and anhyd-

17) S. Hanessian, *Carbohyd. Res.*, **2**, 86 (1966).

18) M. Ishikawa, S. Hara, T. Furuya, and Y. Nakazawa, "Thin-layer Chromatography," Nanzando Co., Japan (1963), p. 55

19) J. Compton, *J. Amer. Chem. Soc.*, **60**, 395 (1938).

rous sodium carbonate (7.75 g) in 50% aqueous acetone (200 ml), methoxycarbonyl chloride (9 ml) was added under stirring and the clear solution was allowed to stand at room temperature for 15 min. A spot (R_f 0.39) of *N*-methoxycarbonylglucosamine appeared on TLC with ethyl acetate-methanol (5:1). The solution was evaporated and the residue was dried *in vacuo*. The residue was suspended in 4% hydrogen chloride in methanol (200 ml) and the mixture was refluxed for 18 hr, whereupon a brown clear solution resulted. A new spot (R_f 0.48) appeared on TLC with the same solvent mixture as described above. The brown solution was neutralized with basic lead carbonate, centrifuged, and the supernatant layer was evaporated. The residue was then chromatographed on a column of silica gel (300 g) with ethyl acetate - methanol (5:1), and the portion containing the substance of R_f 0.48 was evaporated to give a colorless solid which was recrystallized from methanol-ether; 10.5 g (78%), mp 126—128°C $[\alpha]_D^{22}$ +135° (*c* 2, methanol).

Found: C, 42.94; H, 6.93; N, 5.75%. Calcd for $C_9H_{17}NO_7$: C, 43.01; H, 6.82; N, 5.57%.

IR spectrum (KBr): 1700, 1550; 950 (w), 940 (w), 925 (w), 900, 850, 785, 760, 720 (w), and 700 (w) cm^{-1}; NMR (in D_2O): τ 6.60 (3H s., OCH_3), 6.32 (3H s., $NHCOOC\underline{H}_3$), 6.1—6.6 (6H m., H-2,3,4,5,6,6'), 5.18 (1H d., J 2 Hz). No signal corresponding to H_{ax}-1 was observed indicating that the product was a pure α-isomer.

Methyl 6-Bromo-2,6-dideoxy-2-methoxycarbonylamido-α-D-glucopyranoside (9). Compound **8** (6.65 g) in DMF (60 ml) was treated with mesyl bromide (6.8 g) at 65°C for 15 hr. After evaporation, the residue was treated with sodium methoxide in methanol as usual, and the crude product obtained was chromatographed on a column of silica gel with benzene - methyl ethyl ketone (1:2) to separate the product (R_f 0.42) and **8** (R_f 0.22). The product was recrystallized from benzene - ethyl acetate (1:2) yielding 5.34 g (64%); mp 138—140°C, $[\alpha]_D^{25}$ +114° (*c* 0.5, methanol).

Found: C, 34.49; H, 5.03; N, 4.31; Br, 25.38%. Calcd for $C_9H_{16}NO_6Br$: C, 34.39; H, 5.14; N, 4.46; Br, 25.47%.

IR spectrum (KBr): 1730, 1530; 972, 945, 895, 772, and 717 (w) cm^{-1}; NMR (in D_2O): τ 6.56 (3H s., OCH_3), 6.30 (3H s., $NHCOOC\underline{H}_3$), 5.17 (1H d., J 2 Hz, H-1).

Methyl 3,4-Di-O-acetyl-6-bromo-2,6-dideoxy-2-methoxycarbonylamido-α-D-glucopyranoside (10). Prepared from **9** by the general procedure. Mp 104—105°C, $[\alpha]_D^{22}$ +111° (*c* 0.5, chloroform).

Found: C, 39.11; H, 4.99; N, 3.54; Br, 20.44%. Calcd for $C_{13}H_{20}NO_8Br$: C, 39.21; H, 5.06; N, 3.52; Br, 20.07%.

IR spectrum (KBr): 1760, 1730, 1535; 940, 925, 880, 780, 760, and 725 (w) cm^{-1}; NMR (in $CDCl_3$): τ 7.99 and 7.94 (each 3H s., OAc), 6.52 (3H s., OCH_3), 6.4—6.65 (2H m., H-6,6'), 6.32 (3H s., $NHCOOC\underline{H}_3$), 6.07 (1H q., J 3.5 and 10 Hz, H-2), 5.75—6.15 (1H m., H-5), 5.20 (1H d., J 3.5 Hz, H-1), τ 4.55—5.2: eight peaks which were analyzed as XABY(=$H_2H_3H_4H_5$) system: τ 5.00 (1H q., $J_{4,5}$ ~8 Hz, $J_{3,4}$ ~9.5 Hz, H-4), τ 4.77 (1H q., $J_{2,3}$ ~10 Hz, $J_{3,4}$ ~9.5 Hz, H-3).

Methyl 3,4-Di-O-acetyl-2,6-dideoxy-2-methoxycarbonylamido-α-D-xylo-hex-5-enopyranoside (11). To a solution of **10** (2.83 g) in dry pyridine (28 ml), anhydrous silver fluoride (3.3 g) was added and the mixture was stirred at 65°C for 18 hr in the dark. Two spots (R_f 0.68 and 0.62) appeard on TLC with benzene - ethyl acetate (5:2). The former spot was proved to originate from both **10** and **11** (they had the same R_f value) and the latter from a by-product, which increased with the prolongation of reaction. Ether was added to the reaction mixture and the resulting mixture was treated as in the preparation of **5**. The crude product obtained was then chromatographed on a column of silica gel (80 g) with benzene - ethyl acetate (5:2) and the portion containing **10** and **11** was evaporated to give a syrup (1.29 g) which was crystallized by addition of ethanol to give **11** (411 mg). Another crop (121 mg) was obtained from the mother liquor. Total yield was 30%. The mother liquor was proved to be constituted mainly from **10**. Attempted change in the reaction conditions could not raise the yield of **11**. Mp 85—88°C, $[\alpha]_D^{25}$ +89° (*c* 0.5, chloroform)

Found: C, 48.94; H, 6.10; N, 4.30%. Calcd for $C_{13}H_{19}NO_8$: C, 49.21; H, 6.04; N, 4.41%.

IR spectrum (KBr): 1760, 1740, 1670 (C=C), 1540; 945, 930 (w), 900 (w), 875, 852 (w), 790 (sh), 780, 748 (w), and 725 (w) cm^{-1}; NMR (in $CDCl_3$): τ 7.96 and 7.88 (each 3H s., OAc), 6.53 (3H s., OCH_3), 6.30 (3H s., $NHCOOC\underline{H}_3$), 5.85 (1H double triplets, J ~10, ~10, and 3.5 Hz, H-2), 5.38 (1H t., J ~1.8 Hz, H-6), 5.20 (1H t., J ~1.8 Hz, H-6'), 5.15 (1H d., J 3.5 Hz, H-1), ~5 (1H broad doublet, J ~10 Hz, $N\underline{H}COO$-), 4.77 (1H t., J 9.7 Hz, H-3), 4.48 (1H double triplets, J ~1.8, ~1.8, and ~10 Hz); $J_{1,2}$ 3.5 Hz, $J_{2,3}$ 9.7 Hz, $J_{3,4}$ 9.7 Hz, $J_{4,6}=J_{4,6'}=J_{6,6'}$ ~1.8 Hz.

Methyl 3,4-Di-O-acetyl-2,6-dideoxy-2-methoxycarbonylamido-β-L-idopyranoside (12). Compound **11** was hydrogenated in dioxane with palladium black and hydrogen on 90% yield in a similar manner as in the preparation of **6**. Syrup, $[\alpha]_D^{22}$ +45° (*c* 1, chloroform)

Found: C, 48.73; H, 6.75; N, 4.65%. Calcd for $C_{13}H_{21}NO_8$: C, 48.90; H, 6.63; N, 4.39%.

IR spectrum (KBr): 1760, 1730, 1525; 930, 890, 860, 805, 778, 760, and 723 (w) cm^{-1}; NMR (in $CDCl_3$ at 60 and 100 MHz): τ 8.74 (3H d., J 6.7 Hz, C_5-CH_3), 7.88 and 7.90 (each 3H s., OAc), 6.48 (3H s., OCH_3), 6.30 (3H s., $NHCOOC\underline{H}_3$), 6.03 (1H unresolved m., H-2), 5.85 (1H octet, J 6.7, 6.7, 6.7, and 3 Hz, H-5), 5.27 (1H d., J ~2.5 Hz, H-1), 5.10 (1H quartet with small splittings (~0.8 Hz) and the pair in the lower field being most intense; J 3, 4.8, and ~0.8 Hz, H-4), 4.82 (1H t., J 4.8 Hz, H-3), 4.6—4.9 (1H, $N\underline{H}COO$-?); $J_{1,2}$ ~2.5 Hz, $J_{2,3}$ 4.8 Hz, $J_{3,4}$ 4.8 Hz, $J_{4,5}$ 3 Hz, $J_{2,4}$ ~0.8 Hz.

Irradiation of H-2 caused the H-1 doublet to collapse to a singlet, the H-4 octet to a quartet (J 3 and 4.8 Hz), and the H-3 triplet to a doublet. Irradiation at τ 5.85 (H-5) caused the doublet at τ 8.74 (CH_3) to collapse to a singlet, the doublet at τ 5.27 (H-1) to an incomplete doublet, and the octet at τ 5.10 (H-4) to a doublet (J 4.8 Hz). Irradiation of H-4 caused the H-5 octet to collapse to a quartet (J 6.7 Hz) and the H-3 triplet to a doublet.

Methyl 2-Amino-2,6-dideoxy-β-L-idopyranosie (13) and Methyl 2-Amino-2,6-dideoxy-β-L-idopyranoside 2,4-Carbamate (14). Compound **12** (643 mg) in 1N barium hydroxide (25 ml) was heated in a boiling water bath for 1 hr. After carbon dioxide was introduced, the mixture was heated for a while, centrifuged, and the supernatant layer was evaporated. The residual precipitates were treated with hot water several times and the solution was evaporated. The combined residues were extracted with methanol and the solution was evaporated to give a solid (~840 mg). On TLC with ethyl acetate-methanol (5:1), the solid gave two spots of R_f 0.13 (**13**, major, ninhydrin positive) and R_f 0.79 (**14**, minor, ninhydrin negative), the latter differering from the spot of the starting material (**13**, R_f 0.94). An aqueous solution of the solid was chromatographed on a column of Amberlite IRC-50 (H^+ form, 30 ml) with water. The portion containing **14** was evaporated to give a solid, 136 mg (33%), mp 177—180°C $[\alpha]_D^{25}$ +64.5° (*c* 0.8, methanol). IR spectrum (KBr): 1695; 950, 905, 893, 845, 765, 750, and 705 cm^{-1}.

Found: C, 47.24; H, 6.68; N, 6.59%. Calcd for C_8H_{13}-

NO_5: C, 47.29; H, 6.45; N, 6.89%.

The resin column was then treated with 0.3N ammonia and the solution containing **13** was evaporated to give a syrup, 198 mg (56%), R_f 0.66 (ppc with *n*-butanol-pyridine-water-acetic acid 6:4:3:1), $[\alpha]_D^{20}$ +97.4° (*c* 1.4, methanol), $\Delta[M]_{TACu}$+159°. IR spectrum (KBr): 945, 895 (w), 865, 840 (w), 775, and 700 (w) cm^{-1}.

Found: C, 47.60; H, 8.72; N, 8.12%. Calcd for $C_7H_{15}NO_4$: C, 47.45; H, 8.53; N, 7.90%.

NMR spectrum of **13** (in D_2O):τ 8.70 (3H d., *J* 6.7 Hz, C_5-CH_3), 7.03 (1H octet, *J* 4.5, 2, and 1Hz, H-2), 6.45 (3H s., OCH_3), 6.35—6.55 (1H m., H-4), 6.02 (1H t., *J* 4.5 Hz, H-3), 5.88 (1H octet, *J* 6.7, 6.7, 6.7, and 3 Hz, H-5), 5.22 (1H d., *J* 2 Hz, H-1); $J_{1,2}$ ~2 Hz, $J_{2,3}=J_{3,4}$ 4.5 Hz, $J_{4,5}$ 3 Hz, $J_{2,4}$ ~1 Hz. These coupling constants showed the preferred conformation of **13** to be IC.

Methyl 3-O-Acetyl-2-amino-2,6-dideoxy-β-L-idopyranoside 2,4-Carbamate (15). To a solution of **14** (90 mg) in pyridine (1.8 ml), acetic anhydride (0.08 ml) was added and the solution was allowed to stand overnight. On TLC with ethyl acetate, a spot (R_f 0.54) appeared accompanied by two weak spots of R_f 0.21 (**14**) and R_f 0.36. The solution was evaporated and the residue was dissolved in chloroform. The solution was washed successively with saturated potassium hydrogensulfate solution, saturated hydrogencarbonate solution and saturated sodium chloride solution, dried over sodium sulfate and evaporated to give a residue. The residue was dissolved in chloroform and the solution was passed through a short column of silica gel (3 g) with the aid of ethyl acetate and the eluate containing **15** was evaporated to give a colorless solid, 84 mg (80%). Recrystallization from ethanol, mp 165—166°C $[\alpha]_D^{24}$+26° (*c* 1.7, chloroform).

Found: C, 48.62; H, 6.15; N, 5.53%. Calcd for $C_{10}H_{15}NO_6$: C, 48.98; H, 6.17; N, 5.71%.

IR spectrum (KBr): 1755, 1725, 1700; 950, 912, 900 (sh), 885, 838 (w), 795 (w), 765 (sh), 760, 750, and 697 cm^{-1}. No peak was observed between 1475—1650 cm^{-1}; NMR (in pyridine-d_5 at 100 MHz): τ 8.63 (3H, d., *J* 6.7 Hz, C_5-CH_3), 7.85 (3H s., OAc), 6.53 (3H s., OCH_3), 6.27 (1H double triplets, *J* 4, 4, and 2 Hz, H-2), 5.85 (1H q., *J* 6.7 Hz, H-5), 5.75 (1H quartet with small splittings (*J* ~0.5 Hz), *J* 4 and 2 Hz, H-4), 5.13 (1H s., H-1), 4.47 (1H t., *J* 4 Hz, H-3), 1.08 (1H d., *J* 4 Hz, NHCOO–); $J_{1,2}$ ~0 Hz, $J_{2,3}$ 4 Hz, $J_{3,4}$ 4 Hz, $J_{4,5}$ 0—0.5 Hz, $J_{5,6}$ 6.7 Hz, $J_{NH,2}$ 4 Hz, $J_{2,4}$ 2 Hz.

Irradiation at τ 1.08 (NH) caused H-2 double triplets to collapse to a quartet (*J* 4 and 2 Hz). Irradiation of H-3 caused the H-4 multiplet to collapse to a singlet (not a quite sharp singlet), H-2 double triplets to an incomplete doublet. Irradiation of H-4 caused H-2 double triplets to collapse to a triplet (*J* 4 Hz) and H-3 triplet to a doublet (*J* 4 Hz), Irradiation of H-5 caused methyl doublet (τ 8.63) to collapse to a singlet. Irradiation of H-2 caused the H-4 multiplet to collapse to a doublet (*J* 4 Hz) and doublet of NH to a singlet.

Methyl 3-Deoxy-3-methoxycarbonylamido-α and β-D-glucopyranoside (16 and 17). Crude 3-amino-3-deoxy-α-D-glucose (2 g) obtained by fermentation[13] was dissolved in 50% aqueous acetone (40 ml). Anhydrous sodium carbonate (1.5 g) and methoxycarbonyl chloride (1.9 ml) were added successively to the solution under stirring and the mixture was stirred for 1 hr at room temperature. A ninhydrin negative spot (R_f 0.46) appeared on TLC with methyl ethyl ketone-methanol (5:1). The solution was evaporated and the residue was extracted with methanol. Evaporation of the extract gave a brown powder, which was dissolved in 4% hydrogen chloride in methanol (40 ml) and the solution was refluxed for 20 hr. A new spot (R_f 0.54) appeared on TLC. The resulting solution was neutralized with basic lead carbonate, filtered, and evaporated. An aqueous solution of the residue was chromatographed on a column of Dowex 1×2 (OH form, 500 ml) with water. From the earlier eluate (600—750 ml), **16** was obtained as a colorless solid which was recrystallized from ethanol-ethyl acetate yielding 803 mg, mp 178—181°C $[\alpha]_D^{20}$+152° (*c* 1, methanol); NMR (in D_2O): τ 6.55 (3H s., OCH_3), 6.32 (3H s., $NHCOOCH_3$), 5.17 (1H d., $J_{1,2}$ 3 Hz, H-1).

Found: C, 43.25; H, 7.04; N, 5.63%. Calcd for $C_9H_{17}NO_7$: C, 43.01; H, 6.82; N, 5.57%.

From the late eluate (780~930 ml) **17** was obtained as a colorless solid which was recrystallized from ethanol-ethyl acetate yielding 209 mg, mp 146—148°C, $[\alpha]_D^{22}$+6° (*c* 1, methanol); NMR (in D_2O): τ 6.42 (3H s., OCH_3), 6.31 (3H s., $NHCOOCH_3$), 5.54 (1H d., $J_{1,2}$ 7.5 Hz, H-1).

Found: C, 43.12; H, 6.95; N, 5.60%.

Methyl 6-Bromo-3,6-dideoxy-3-methoxycarbonylamido-α-D-glucopyranoside (18). Compound **16** (443 mg) in DMF (4.8 ml) was treated with mesyl bromide (570 mg) at 65°C for 15 hr. A new spot (R_f 0.62) and a very weak spot (R_f 0.25) appeared on TLC with methyl ethyl ketone. Successive de-*O*-formylation[4] gave a slight amount of starting material (**16**, R_f 0.25) in contrast to the case of **3**. Crude product obtained was purified by column chromatography with silica gel (20 g) with methyl ethyl ketone - ethyl acetate yielding a solid of 478 mg (85%), mp 197—198°C, $[\alpha]_D^{20}$+128° (*c* 0.8, methanol).

Found: C, 34.80; H, 5.16; N, 4.67, Br. 24.90%. Calcd for $C_9H_{16}NO_6Br$: C, 34.39; H, 5.14; N, 4.46; Br. 25.45%.

Methyl 2,4-Di-O-acetyl-6-bromo-3,6-dideoxy-3-methoxycarbonylamido-α-D-glucopyranoside (19). Compound **18** was acetylated in a similar manner as in the case of **3** to give **19**, mp 205—210°C, $[\alpha]_D^{20}$+95° (*c* 1, chloroform).

Found: C, 39.48; H, 5.09; N, 3.36; Br, 19.76%. Calcd for $C_{13}H_{20}NO_8Br$: C, 39.21; H, 5.06; N, 3.52; Br, 20.07%.

IR spectrum (KBr): 1750, 1710, 1550; 981, 925, 800 (w), 773(m), 760, and 710 (w) cm^{-1}; NMR (in $CDCl_3$): τ 7.91 (6H s., OAc), 6.51 (3H s., OCH_3), 6.34 (3H s., $NHCOOCH_3$), 5.96 (1H octet, *J* 3, 6, and 9.7 Hz, H_{ax} -5); No peak in the field lower than τ 4.95 was observed (compare with the spectrum of **4**).

Methyl 2,6-Di-O-acetyl-3,6-dideoxy-3,6-imino-N-methoxycarbonyl-α-D-glucopyranoside (20). A mixture of **19** (256 mg) and silver fluoride (240 mg) in dry pyridine (1.8 ml) was stirred at 60°C overnight in the dark. On TLC with benzene-ethyl acetate (2:1), two spots (R_f 0.18 and 0.44 (minor)) appeared but the latter was proved to be that of the starting material (**19**). The reaction mixture was extracted with ether and the organic layer was treated in a similar manner as in the preparation of **5**. The crude mixture obtained was chromatographed on a column of silica gel with benzene - ethyl acetate (2:1) and the portion containing the substance showing R_f 0.18 was evaporated to give a colorless syrup, 165 mg (80%), $[\alpha]_D^{20}$+70° (*c* 1, chloroform).

Found: C, 49.41; H, 6.20; N, 4.61%. Calcd for $C_{13}H_{19}NO_8$: C, 49.21; H, 6.04; N, 4.41%.

IR spectrum (KBr): 1750, 1715, 1540 (w); 930, 910, 880 (m), 830, 770, 725 (w), and 685 cm^{-1}; NMR (in $CDCl_3$):τ 7.91 and 7.81 (each 3H s., OAc), 6.46 (3H s., OCH_3), 6.22 (3H s., $NHCOOCH_3$), 6.3—6.6 (2H m., H-6,6′), 5.3—5.5 (3H m., H-3,4,5), 5.15 (1H d., J 3.3 Hz, H-1), 4.68—4.88 (1H unresolved broad peak having half-height width of ~8Hz, H-2).

Methyl 3-Amino-3-deoxy-α-D-glucopyranoside (21). To an aqueous solution (40 ml) of **16** (800 mg), barium hydroxide octahydrate (1.8 g) was added and the mixture was heated at 95°C for 1.5 hr. After introducting carbon dioxide, the

mixture was heated for a while, centrifuged, and the supernatant layer was evaporated. The residue was extracted with methanol and the solution was evaporated to give a solid which was dissolved in a small amount of methanol. Ethyl acetate was added to the solution to give ninhydrin-positive crystals (546 mg, 92%), mp 175—176°C (lit,[20] 167—168°C), $[\alpha]_D^{23}$+165° (*c* 0.6, methanol) (lit,[20] +144.4° (water)).

Methyl 2,4,6-Tri-O-acetyl-3-deoxy-3-phthalimido-α-D-glucopyranoside (22). To a solution of **21** (459 mg) in dry pyridine (9 ml), phthalic anhydride (510 mg) was added and the solution was heated at 90°C for 30 min. A phthalimido derivative (R_f 0.54 with tailing on TLC with methyl ethyl ketone - methanol 4:1) was produced. To the resulting pale yellow solution, acetic anhydride (9 ml) was added and the solution was heated at 90°C for 1 hr. A spot (R_f 0.68) appeared on TLC with benzene - ethyl acetate (5:3). The solution was evaporated and the residue was dissolved in chloroform. The solution was washed successively with potassium hydrogensulfate solution, soldium hydrogencarbonate solution, and water, dried over sodium sulfate and evaporated to give a solid. The product was dissolved in a mixture of benzene - ethyl acetate (2:1) and passed through a short column of silica gel with the aid of the same solvent mixture. The eluate was evaporated and the residue was recrystallized from ethanol yielding pale yellow crystals, 914 mg (87%), mp 175—177°C, $[\alpha]_D^{22}$+75° (*c* 1, chloroform).

Found: C, 56.13; H, 5.06; N, 3.28%. Calcd for $C_{21}H_{23}NO_{10}$: C, 56.12; H, 5.16; N, 3.12%.

IR spectrum (KBr): 1755, 1725; 732, 724 cm^{-1}; NMR (in $CDCl_3$): τ 8.11, 8.06 and 7.89 (each 3H s., OAc). It is noteworthy that two acetyl methyl protons resonated at higher field than usual. The signal at τ 7.89 seems to originate from protons of 6-*O*-acetyl (compare with the spectrum of **25**). τ 6.51 (3H s., OCH_3), 5.4—6.1 (3H m., H-5,6,6'), 5.18 (1H q., *J* 10, 11 Hz, H-3), 4.88 (1H d., *J* 3.5 Hz, H-1), 4.31 (1H, t., *J* 9.8 Hz, H-4), 4.22 (1H q., *J* 3.5, 11 Hz, H-2), 1.9—2.35 (4H m.); $J_{1,2}$ 3.5 Hz $J_{2,3}$ 11 Hz, $J_{3,4}$ 10 Hz, $J_{4,5}$ ~9.8 Hz.

Methyl 3-Deoxy-3-phthalimido-α-D-glucopyranoside (23). A solution of **22** (802 mg) in methanol was treated with sodium methoxide. A spot (R_f 0.58) appeared on TLC with ethyl acetate. The product was recrystallized from acetone yielding 570 mg (98%), mp 194—197°C, $[\alpha]_D^{22}$+103° (*c* 1, methanol); IR spectrum (KBr): 1775 (w), 1710; 970 (w), 910, 873 (w), 847 (vw), 802 (w), 777 (w), and 730 cm^{-1}.

Found: C, 55.85; H, 5.49; N, 4.02%. Calcd for $C_{15}H_{17}NO_7$: C, 55.72; H, 5.30; N, 4.33%.

Methyl 6-Bromo-3,6-dideoxy-3-phthalimido-α-D-glucopyranoside (24). To a solution of **23** (499 mg) in dry DMF (5.5 ml), mesyl bromide (770 mg) was added and the solution was heated at 65°C overnight. On TLC with benzene - ethyl acetate (1:2), two spots of R_f 0.79 (**24**) and 0.70 (an *O*-formyl compound) appeared in approximately equal color strength. The solution was evaporated and the residue was neutralized with sodium methoxide in methanol. On TLC, the spot of R_f 0.70 disappeared and a spot (R_f 0.25, **23**) appeared. In contrast to the case of the preparation of **18**, the bromination of **23** turned out to compete with *O*-formylation. The bromination procedure was repeated to raise the yield of **24**. The above methanolic solution was evaporated and the residue was coevaporated with toluene. The residue was dissolved in DMF (4.5 ml) and treated with mesyl bromide (730 mg). After the de-*O*-formylation of the resulting product with sodium methoxide in methanol, the mixture was subjected to chromatography on a column of silica gel (13 g) with benzene - ethyl acetate (1:2). From the earlier eluate (37—70 ml), **24** was obtained as a solid, which was recrystallized from benzene - ethyl acetate (3:1) yielding 360 mg (61%); mp 178—178.5°C, $[\alpha]_D^{22}$+88° (*c* 0.5, methanol); IR spectrum (KBr): 1725, 1715; 928 (w), 905, 870 (w), 802 (w), 780 (w), 726, and 717 cm^{-1}.

Found: C, 46.43; H, 4.38; N, 3.88; Br, 20.33%. Calcd for $C_{15}H_{16}NO_6Br$: C, 46.65; H, 4.18; N, 3.63; Br, 20.69%.

From the late eluate, the starting material (**23**, 120 mg) was recovered.

Methyl 2,4-Di-O-acetyl-6-bromo-3,6-dideoxy-3-phthalimido-α-D-glucopyranoside (25). Prepared from **24** by the general procedure. The final product was a syrup, which was solidified by trituration with water, mp 76.5—79.5°C, $[\alpha]_D^{23}$+49.2° (*c* 0.8, chloroform).

Found: C, 48.87; H, 4.47; N, 3.08; Br, 16.52%. Calcd for $C_{19}H_{20}NO_8Br$: C, 48.53; H, 4.29; N, 2.98; Br, 16.99%.

IR spectrum (KBr): 1755, 1725, 927, 887, 868, 798, 772 (w) and 725 (s) cm^{-1}; NMR (in $CDCl_3$): τ 8.09 and 8.07 (each 3H s., OAc), 6.47 (3H s., OCH_3), 6.4—6.6 (2H m., H-6,6'), 5.85 (1H octet, *J* 4, 6, and 10 Hz, H-5), 5.17 (1H q., *J* 10 and 11 Hz, H-3), 4.85 (1H d., *J* 3.5 Hz, H-1), 4.33 (1H t., *J* 10 Hz, H-4), 4.26 (1H q., *J* 3.5, 11 Hz, H-2), 1.9—2.35 (4H m.); $J_{1,2}$ 3.5 Hz, $J_{2,3}$ 11 Hz, $J_{3,4}$ 10 Hz, $J_{4,5}$ 10 Hz, $J_{5,6}$ 6 Hz, $J_{5,6'}$ 4 Hz.

Methyl 2,4-Di-O-acetyl-3,6-dideoxy-3-phthalimido-α-D-xylo-hex-5-enopyranoside (26). Compound **26** was prepared from **25** in a similar manner as for the preparation of **5** from **4**. Recrystallization from ethanol gave pale yellow crystals (79%), mp 191—192°C, $[\alpha]_D^{20}$+50° (*c* 0.5, chloroform); R_f 0.52 (TLC with benzene - ethyl acetate 5:1).

Found: C, 58.68; H, 4.91; N, 3.69%. Calcd for $C_{19}H_{19}NO_8$: C, 58.61; H, 4.92; N, 3.60%.

IR spectrum (KBr): 1760, 1725, 1670 (C=C); 960, 932, 908 (w), 898, 878 (w), 845 (w), 800, and 725 (s) cm^{-1}; NMR (in $CDCl_3$ at 100 MHz): τ 8.07 and 8.03 (each 3H s., OAc), 6.50 (3H s., OCH_3), 5.35 (1H triplet with very small splittings (<0.3 Hz), *J* ~2 Hz, H-6), 5.18 (1H t., *J* ~2 Hz, H-6'), 5.16 (1H q., *J* 10 and 11 Hz, H-3), 4.85 (1H d., *J* 3 Hz, H-1), 4.16 (1H q., *J* 3 and 11 Hz, H-2), 3.85 (1H double triplets, *J* 2, 2 and 10 Hz, H-4), 1.95—2.35 (4H m.); $J_{1,2}$ 3 Hz, $J_{2,3}$ 11 Hz, $J_{3,4}$ 10 Hz, $J_{4,6}$=$J_{4,6'}$ ~2 Hz, $J_{6,6'}$ ~2 Hz.

Irradiation of H-4 resulted in collapse of the H-6 and H-6' triplets to two doublets (each *J* ~2 Hz), and of H-3 triplet to a doublet (*J* 11 Hz).

Methyl 2,4-Di-O-acetyl-3,6-dideoxy-3-phthalimido-β-L-idopyranoside (27). A solution of **26** (294 mg) in dioxane (3 ml) was hydrogenated with palladium black and hydrogen in a similar manner as for the preparation of **6**. A spot (R_f 0.58) appeared (the R_f of **26** was 0.62) on TLC with benzene-ethyl acetate (5:1). After filtration the solution was evaporated to give a solid which was passed through a short column of silica gel with the above solvent mixture. The eluate was evaporated to give a solid, 253 mg (87%), mp 66—69°C, $[\alpha]_D^{22}$+59° (*c* 0.9, chloroform).

Found: C, 58.17; H, 5.32; N, 3.69%. Calcd for $C_{19}H_{21}NO_8$: C, 58.31; H, 5.41; N, 3.58%.

IR spectrum (KBr): 1780, 1755, 1725; 935, 925 (sh), 907 (sh), 872 (m), 810, 800, and 725 (s) cm^{-1}: NMR (in $CDCl_3$ at 100 MHz): τ 8.58 (3H d., *J* 6.7 Hz, C_5-CH_3), 8.08 (6H s., OAc), 6.52 (3H s., OCH_3), 5.45 (1H double quartet, *J* 6.7, 6.7, 6.7 and 6 Hz, H-5), 5.06 (1H q., *J* 11 and 9 Hz, H-3), 4.93 (1H d., *J* 3.5 Hz, H-1), 4.35 (1H q., *J* 9 and 6 Hz, H-4), 4.33 (1H q., *J* 3.5 and 11 Hz, H-2); $J_{1,2}$ 3.5 Hz, $J_{2,3}$ 11 Hz $J_{3,4}$ 9 Hz, $J_{4,5}$ 6 Hz.

Irradiation at τ 4.38 caused the H-5 multiplet to collapse to a quartet, the H-3 quartet to a broad singlet and the H-1

20) S. Peat and L. F. Wiggins, *J. Chem. Soc.*, **1938**, 1810.

doublet to a singlet. Irradiation at τ 4.33 caused the above multiplet to collapse to a quartet, the H-3 quartet to a narrow multiplet and the H-1 doublet to a sharp singlet.

Methyl 3-Amino-3,6-dideoxy-β-L-idopyranoside (28). To a solution of **27** (163 mg) in dry methanol (1.6 ml), *n*-butylamine (0.38 g) was added and the solution was refluxed for 9 hr. Evaporation of the solution gave a residue, which was extracted with ether several times. The ether-insoluble mass was dissolved in methanol, and the solution was filtered. Ether was added to the solution to give crystals of **28**, 44 mg. As the ether-soluble part still contained **28**, it was charged on a column of Amberlite IRC-50 (H^+ form) and, after washing with water, developed with 0.3N ammonia. The portion containing **28** was evaporated to give another crop (21 mg). Total yield was 77%. R_f 0.53 (ppc with *n*-butanol-pyridine-water-acetic acid 6:4:3:1); mp 146—148°C $[\alpha]_D^{21}+93°$ (*c* 1, methanol); $\Delta[\dot{M}]_{FACu}-242°$.

Found: C, 47.70; H, 8.49; N, 8.13%. Calcd for $C_7H_{15}NO_4$: C, 47.45; H, 8.53; N, 7.90%.

IR spectrum (KBr): 923, 890, 808, and 760 cm^{-1}; NMR (in D_2O): Although the spectrum was not clear enough to permit detailed analysis, the pattern resembles that of methyl 6-deoxy-β-L-idopyranoside (**6**) except for the chemical shift of H-3 which resonated at 0.76 ppm higher field that than of H-3 of **6**: τ 8.67 (3H d., J 6.7 Hz, C_5-CH_3), 6.73 (1H t., J ~5 (?) Hz, H-3), 6.48 (3H s., OCH_3), 6.40—6.55 (1H m., H-4), 6.40 (1H m., H-2), 5.85 (1H octet, J 6.7, 6.7, 6.7, and 3 Hz, H-5), 5.23 (1H d., J ~2 Hz, H-1).

The authors wish to thank Dr. Hiroshi Naganawa of the Institute of Microbial Chemistry for carrying out decouplings in the NMR spectra and to Mr. Saburo Nakada for the elemental analysis. The authors also wish to thank Messers. Shuzo Kawabe and Takeo Miyazawa for their technical assistance.

BULLETIN OF THE CHEMICAL SOCIETY OF JAPAN, VOL. 44, 2537—2541(1971)

Intramolecular Fluorescence Quenching Effect by *p*-Nitrophenyl and *p*-Nitrophenoxy Groups

Kiyoshi MUTAI

Department of Chemistry, College of General Education, The University of Tokyo, Komaba, Meguro, Tokyo

(Received April 15, 1971)

The intramolecular fluorescence quenching efficiency of *p*-nitrophenyl and *p*-nitrophenoxy groups in homologous series of *p*-$O_2NC_6H_4(CH_2)_nNH$-1-Naphthyl (I, $n=1$—7) and *p*-$O_2NC_6H_4O(CH_2)_nNH$-1-Naphthyl (II, $n=2$—6), respectively, has been determined. The quenching effect is observed even in the highest homologs of both series. From the fact that the fluorescence intensity of $n=2$ homolog of I is higher than that of $n=1$, together with spectroscopic data it is concluded that the higher intensity of $n=2$ than $n=1$ of the across-space intramolecular charge-transfer band is due to the larger absorbance per interacting molecule of n=2, the origin of which might be attributed to the different interacting conformations of these homologs. The effect of the number of methylene groups (n) on the fluorescence spectral shape has also been found.

Although *intermolecular* charge-transfer (CT) interaction has been studied extensively, it is only recently that across-space *intramolecular* CT interaction has begun to draw the attention of chemists.[1] One of the characteristics of the latter type interaction is that the interaction under more or less restricted conditions can be observed, and accompanying CT spectral features may provide valuable data for a further understanding of the CT phenomenon. In this paper some conformational effects on the CT spectrum are shown by the aid of fluorescence spectroscopy.

The *p*-nitrophenyl, *p*-$O_2NC_6H_4$–, group can play the role of electron-acceptor in the across-space intramolecular CT interaction in a series of *p*-$O_2NC_6H_4$-$(CH_2)_n$-NHAr.[2] It has been found that the intensity of the CT band of $n=2$ homolog is higher than that of $n=1$ homolog regardless of the Ar group. For instance, the ratios of the apparent absorption coefficients, $\varepsilon(n=2)/\varepsilon(n=1)$, observed in carbon tetrachloride solution for the derivatives of Ar=phenyl, =*p*-methoxyphenyl, and =1-naphthyl are 3.0, 1.7, and 1.4, respectively. A similar phenomenon has been reported in other homologous series of compounds.[1a,1f] On the other hand, the position of the CT band of the $n=1$ homolog is a little longer in wavelength, that is, the transition energy is smaller in this homolog. These spectral characteristics could be attributed to the presence of intramolecular N—H$\cdots\pi$ interaction, but the same order of intensities observed in the *N*-alkylated derivatives of I[3] suggests that this explanation is incorrect. In connection with the CT interacting state there are

1) a) W. N. White, *J. Amer. Chem. Soc.*, **81**, 2912 (1959); b) S. Shifrin, *Biochem. Biophys. Acta*, **96**, 173 (1966); c) J. W. Verhoeven, I. P. Dirkx, and Th. J. de Boer, *Tetrahedron Lett.*, **1966**, 4399; d) A. J. de Gee, J. W. Verhoeven, I. P. Dirkx, and Th. J. de Boer, *Tetrahedron*, **25**, 3407 (1969); e) J. W. Verhoeven, I. P. Dirkx, and Th. J. de Boer, *ibid.*, **25**, 4037 (1969); f) H. A. H. Craenen, J. W. Verhoeven, and Th. J. de Boer, *Tetrahedron Lett.*, **1970**, 1167; g) R. Carruthers, F. M. Dean, L. E. Houghton, and A. Ledwith, *Chem. Commun.*, **1967**, 1206; h) M. Ōki and K. Mutai, *Tetrahedron Lett.*, **1968**, 2019; i) M. Itoh and E. M. Kosower, *J. Amer. Chem. Soc.*, **90**, 1843 (1968); j) J. P. Carrión, D. A. Deranleau, B. Donzel, K. Esko, P. Moser, and R. Schwyzer, *Helv. Chim. Acta*, **51**, 459 (1968); k) P. Moser, *ibid.*, **51**, 1831 (1968).

2) M. Ōki and K. Mutai, *Tetrahedron*, **26**, 1181 (1970).

3) K. Mutai, to be published.

two possibilities for the interpretation of the spectral features. (1) The CT interaction is favorable in $n=1$ as is noted in the transition energy, and the number of interacting molecules per mole is larger than that in $n=2$. This situation is probable from the viewpoint of entropy for the two interacting groups to meet, but the interacting conformation subject to the restrictions caused by the shorter methylene chain diminishes the CT intensity per interacting molecule. (2) The interaction in the higher homolog ($n=2$) is favored with regard to the interacting energy, since a scale model indicates that the π-electron clouds of the two group can overlap more sufficiently in this homolog, and its higher intensity reflects larger population of the interacting molecule than in $n=1$.

It would be easy to find a correct explanation if the absorption intensities per interacting molecule or the ratios of the interacting to non-interacting molecule for both homologs could be determined. Unfortunately, only a part of the molecules interact and there is no reliable way to determine their values. However, for the present purpose, it is not necessary to know the precise values. It is adequate only to determine in which of the two homologs the population is larger or, in other words, the interacting groups have a greater chance of access to each other.

The approach employed in the present study is fluorescence quenching effect,[4] since the phenomenon is known to be greatly dependent on the distance between a fluorescer and a quencher by whichever mechanism it takes place.[5,6] This characteristic is convenient for comparing the degree of proximity of the two groups in a homologous series of compounds, if one group is fluorescer and the other can quench it. In the present case the 1-naphthyl group is introduced to the amino nitrogen, thus producing a 1-naphthylamino group known as a strong fluorescent moiety. This group, of course, can work as an electron-donor in across-space intramolecular CT interaction with the *p*-nitrophenyl group.

Results

Fluorescence spectra due to the 1-naphthylamino moiety in *p*-$O_2NC_6H_4(CH_2)_nNH$-1-Naphthyl (I) are reproduced in Fig. 1 and data given in Table 1. Benzene-cyclohexane mixture (1:4) was used as a solvent because benzene increases the dissolving power of the solvent. A slight decrease in the fluorescence intensity was observed in this solvent as compared with cyclohexane which is a typical inert solvent with poor dissolving power, but no appreciable change in spectral shape was found. The order of fluorescence intensity is $n=1<2<3<5<4<6<7$. Obviously the quenching effect increases as n or chain length decreases with the exception of $n=4$. Even in the highest homolog studied ($n=7$) in which neither the CT interaction nor N–H$\cdots\pi$ interaction, hence no intramolecular force advantageous for the two groups to be close together, has been detected, the quenching effect by *p*-nitrophenyl group

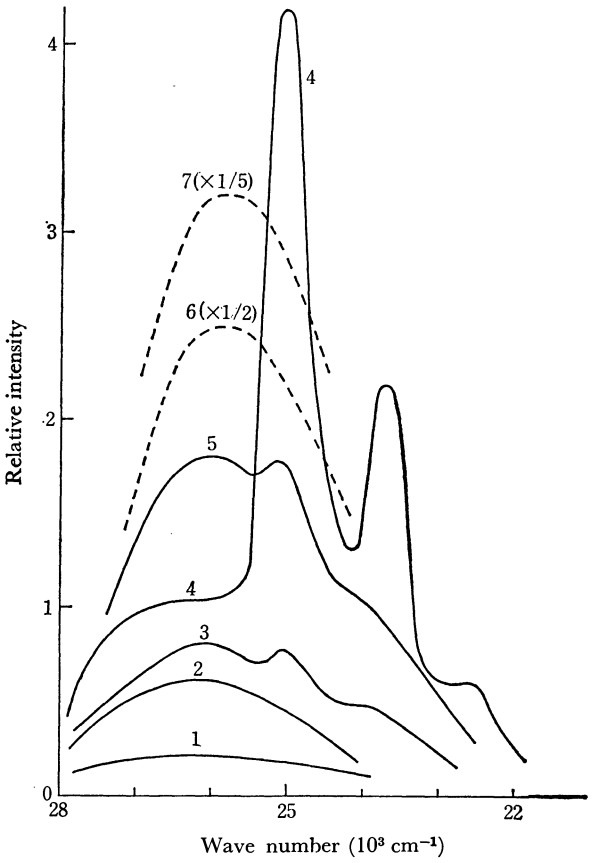

Fig. 1. Fluorescence spectra of *p*-$O_2NC_6H_4(CH_2)_nNH$-1-Naphthyl in benzene-cyclohexane (1:4) mixture. Figures attached to the curves denote n, the number of methylene groups. The scale of the curves of $n=6$ and $n=7$ is reduced to 1/2 and 1/5, respectively. The excitation wavelength was 313 nm.

Table 1. Relative integrated fluorescence intensity of $Ar(CH_2)_nNH$-1-Naphthyl

Ar=*p*-$O_2NC_6H_4$ (I)		Ar=*p*-$O_2NC_6H_4O$ (II)	
n	Rel. intensity[a]	n	Rel. intensity[a]
1	1.0		
2	2.8		
3	3.9	2	1.7
4	10	3	1.6
5	8.6	4	12
6	23	5	12
7	73	6	17

Compounds	Rel. intensity[a]
EtNH-1-Naphthyl	4.4×10^3
$PhCH_2NH$-1-Naphthyl	5.7×10^3
p-$ClC_6H_4CH_2NH$-1-Naphthyl	5.1×10^3

a) The integrated region is from 21×10^3—28×10^3 cm^{-1}, and the values in the Table are relative to that of *p*-$O_2NC_6H_4CH_2NH$-1-Naphthyl.

4) The author wishes to thank Dr. Jun-ichi Aihara, University of Hokkaido, for his suggestion of this effect.

5) T. Förster, *Discuss. Faraday Soc.*, **27**, 1 (1959).

6) For recent reviews, see a) N. J. Turro, "Molecular Photochemistry," W. A. Benjamin, Inc., New York, N. Y. (1965), p. 97; b) A. A. Lamola, "Technique of Organic Chemistry," Vol. XIV, ed. by P. A. Leermakers and A.Weissberger, Interescience Publishers, New York, N. Y. (1969), p. 17.

is obvious in comparison with *N*-ethyl-, *N*-benzyl-, or *N*-(*p*-chlorobenzyl)-1-naphthylamine (Table 1). The latter compounds can be regarded as model ones which exhibit fluorescence free of any quenching effect. For this purpose, the latter two which are solid at room temperature have an advantage with respect to easy handling and stability over liquid *N*-ethyl derivative which becomes wine-red on standing overnight in the dark after distillation.

In the spectra of $n=3$, 4, and 5, vibrational progressions were observed, especially well-developed in that of $n=4$. The separation between the peaks is approximately 1330—1350 cm^{-1}.

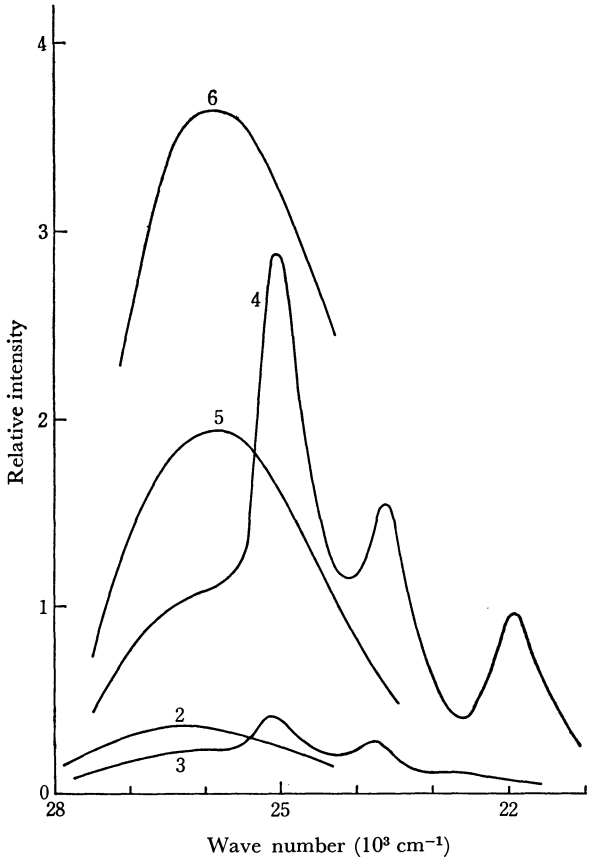

Fig. 2. Fluorescence spectra of *p*-$O_2NC_6H_4O(CH_2)_nNH$-1-Naphthyl in benzene-cyclohexane (1:4) mixture. The figures attached to the curves denote *n*. The excitation wavelength was 313 nm.

The *p*-Nitrophenoxy group in a homologous series of *p*-$O_2NC_6H_4O(CH_2)_nNH$-1-Naphthyl (II) also showed fluorescence quenching effect, the fluorescence spectra of which are reproduced in Fig. 2. The lowest homolog of this series used in the present study is $n=2$, since the $n=1$ homolog is too unstable. In this series the chain length (the number of atoms combining two groups) with *n* methylenes corresponds to that with $n+1$ methylenes in I, since an ether oxygen is inserted between *p*-$O_2NC_6H_4$- and CH_2 groups in II. Probably the different bond distance of C–O and C–C makes no significant effect on quenching efficiency. Thus it is noteworthy that vibrational structure also appeared in II only when $n=3$ and 4.

The relative intensities of I and II measured in a common medium are summarized in Table 1. Since the fluorescent moiety is common to both series, the values could be a measure of efficiency of the quenchers.

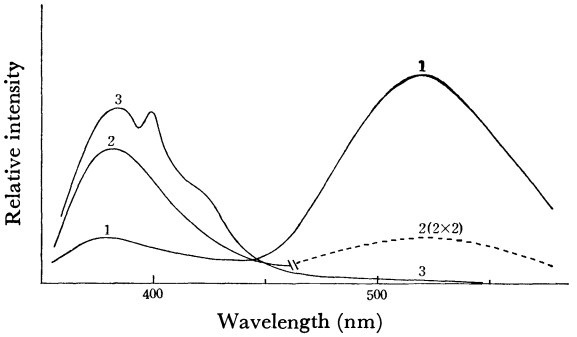

Fig. 3. Fluorescence spectra of *p*-$O_2NC_6H_4(CH_2)_nNH$-1-Naphthyl in benzene-cyclohexane (1:4) mixture. The scale of the curve of $n=2$ in longer wavelength region is doubled The excitation wavelength was 313 nm.

In the longer wavelength region than that of the fluorescence due to 1-naphthylamine moiety, a broad peak appears in the lower homologs of I (Fig. 3) and II. The origin of this peak has been assigned to the excited CT state on the basis of its intramolecular characteristics and excitation spectrum.[7,8]

Discussion

From the fluorescence intensities of I, we might conclude that naphthylamino and *p*-nitrophenyl groups have a greater chance of access in $n=1$ homolog than in $n=2$. However, the conclusion should be scrutinized from the viewpoint of quenching or energy transfer mechanism.

In the higher homologs ($n\geqq4$) in which the CT interaction of N–H$\cdots\pi$ interaction is scarcely observed, the quenching effect takes place undoubtedly beyond collisional diameters of the two aromatic groups. This long-range effect suggests that a resonance-energy transfer mechanism is predominating.

In the lower ones, exchange transfer mechanism as well as resonance mechanism is possible as suggested by the occurrence of the intramoledular CT interaction, because both exchange mechanism and the CT interaction require the overlap of the π-electron clouds of the aromatic rings. Examination of a scale molel shows that only partial overlap of the electron clouds is allowed for $n=1$ owing to the limitation of bond angles but sufficient overlap is possible for $n\geqq2$ in which two aromatic rings can assume a parallel face-to-face arrangement. In the study of the excimer, this latter conformation is regarded as an important, if not essential, condition for excimer formation on theoretical[9] and experimental[10] grounds. As an example, in a series of diphenyl end-substituted alkanes $Ph(CH_2)_nPh$, only

7) K. Mutai, *Chem. Commun*, **1970**, 1209.
8) K. Mutai, *Tetrahedron Lett.*, **1971**, in press.
9) a) G. J. Hoijtink, *Z. Elektrochem.*, **64**, 156 (1960); b) J. N. Murrell and J. Tanaka, *Mol. Phys.*, **7**, 363 (1963—1964); c) T. Azumi and S. P. McGlynn, *J. Chem. Phys.*, **41**, 3131 (1964); d) T. Azumi, A. T. Armstrong, and S. P. McGlynn, *ibid.*, **41**, 3839 (1964); e) T. Azumi and S. P. McGlynn, *ibid.*, **42**, 1675 (1965).

$n=3$ shows excimer emission[10a] which is not observed in $n=2$. Therefore, as far as exchange mechanism is concerned, the greater quenching efficiency and lower fluorescence intensity are expected for $n=2$ if the population of the CT interacting molecule is the same as or greater than $n=1$.

As for resonance mechanism, which does not require the overlap of the electron clouds, and is largely dependent on the distance between two groups, the intensity of $n=2$ should be lower if the population of $n=2$ is the same as or greater than $n=1$, since the flexibility of the longer chain of $n=2$ permits closer approach of the aromatic rings with each other. The above supposition may be cited as an evidence that in a series of alkanes substituted by 1-naphthyl on one end, $Ar(CH_2)_n$-1-Naphthyl, the intramolecular energy transfer efficiency is nearly the same in $n=2$ and $n=3$ when Ar is 9-anthryl (energy acceptor),[11] and $n=2<n=3$ when Ar is 4-benzoylphenyl[12] (here, $n=2$ and $n=3$ correspond to $n=1$ and $n=2$ homologs of I, respectively, in the number of chain atoms). The same order of interaction effects has also been reported in a series of 9,9′-polymethylene-bisadenines from a study of their hypochromism of absorption spectra and emission spectra.[13] This suggests that in I higher fluoroescence intensity or lower quenching effect should be observed in $n=1$.

In order to explain the results the presence of the intramolecular CT interaction should be taken into account. The overlap of the π-electron clouds is insufficient in $n=1$, but if the population of the CT, interacting molecule of $n=1$ exceeds that of $n=2$, then more quenching effect on lower fluorescence intensity is expected for $n=1$. As is seen in Fig. 3, the transition from the excited intramolecular CT state to the ground state in another radioactive process. In this sence, as far as the fluorescence of the amine moiety is concerned, the CT interaction is a quenching process, since the interacting molecules absorb a part of incident light to decrease the apparent quantum yield of the fluorescence process of the amine moiety. The order of intensities of the CT fluorescence bands ($n=1>n=2$) may be an evidence of the difference of population of the CT interacting molecules. Another evidence has been obtained from the infrared study of I. It has been shown that in the lower homologs there exists intramolecular N-H$\cdots\pi$ interaction which fixes molecular conformation to prohibit the overlap of the π-electron clouds of the aromatic rings, and the population of the free molecule from this interaction is abnormally large in $n=1$.[14] It has also been established that this "free" state is competitive with or more stable than the N-H$\cdots\pi$ interacting state,[15] indicating that the "free" state contains another interacting state, *viz.*, the CT interaction. This shows the population of the CT interacting molecule is larger in $n=1$ than in $n=2$. This conclusion, in turn, suggests the larger intensity of the CT absorption for an interacting molecule of $n=2$. The difference is probably due to the different interacting conformations of the compounds in which more sufficient orbital overlap is possible for $n=2$, resulting in larger value of the transition moment of the CT absorption of $n=2$.[16,17] If the explanation is correct, this may be an example of the conformational effects on the spectral features of the CT interaction.

The quenching effect of both *p*-nitrophenyl and *p*-nitrophenoxy groups is due to the overlap of their absorption spectra with the fluorescence spectrum of the naphthylamine moiety. The region of the overlap is larger in *p*-nitrophenoxy group. This is probably the reason why larger quenching efficiency is observed in II when the fluorescence intensities of the homologs of I and II with the same number of chain atoms are compared. Lack of the quenching effect in benzyl and *p*-chlorobenzyl groups can be attributed to the small overlap of their absorption spectra with the fluorescence.

It is interesting that the appearance of vibrational structure depends strongly on the number of methylene groups. The peak separation suggests its relation with C–N stretching vibtation. Perhaps certain numbers of methylenes make a contribution through a certain type of their vibrational mode to allow the transition to the upper vibrational levels of the ground state.[18] The structure is most remarkable in $n=4$ of I and II in which the fluorescence intensities are more than those expected from the values of their next lower and higher homologs. This suggests that the originally radiationless or forbidden transition becomes radiative due to the same cause as the appearance of the structure.

Experimental

Materials. The compounds used were purified through the known methods.

N-[ω-(*p*-Nitrophenyl)alkyl]-1-naphthylamines (I, $n=4$, 5, and 6). Syntheses of this series of compounds were performed as described previously.[2,14]

N-[ω-(*p*-Nitrophenoxy)alkyl]-1-naphthylamines (II, $n=2$—6). These compounds were prepared by the same procedure as has been reported.[20]

The mp's and results of elemental analyses of the products are given in Table 2.

Spectral Measurement. Fluorescence spectra were recorded on an Aminco-Bowman spectrophotofluorometer. In every series of measurements, the CT fluorescence band was used as a reference of intensity in order to determine a factor for adjusting photomultiplier sensitivity and fluctuation of the intensity of incident light. A Hanovia xenon mercury

10) a) F. Hirayama, *ibid.*, **42**, 3163 (1965); b) M. T. Vala, Jr., J. Haebig, and S. A. Rice, *ibid.*, **43**, 886 (1965); c) J. W. Longworth and F. A. Bovey, *Biopolymers*, **4**, 1115 (1966); d) E. A. Chandross and J. Ferguson, *J. Chem. Phys.*, **47**, 2557 (1967).

11) O. Schnepp and M. Levy, *J. Amer. Chem. Soc.*, **84**, 172 (1962).

12) A. A. Lamola, P. A. Leermakers, B. W. Byers, and G. S. Hammond, *ibid.*, **87**, 2322 (1965).

13) D. T. Browne, J. Eisinger, and N. J. Leonard, *ibid.*, **90**, 7302 (1968).

14) M. Ōki and K. Mutai, This Bulletin, **38**, 393 (1965).

15) M. Ōki and K. Mutai, *ibid.*, **39**, 809 (1966).

16) R. S. Mulliken and W. B. Person, "Molecular Complexes," Wiley-Interscience, New York, N. Y. (1969), p. 23.

17) J. N. Murrell, *J. Amer. Chem. Soc.*, **81**, 5037 (1959).

18) The overtones of the accordion like vibration of polymethylene chains may be responsible for this phenomenon.[19]

19) R. F. Schaufele and T. Shimanouchi, *J. Chem. Phys.*, **47**, 3605 (1967).

20) M. Ōki and K. Mutai, *Spectrochim. Acta*, **25A**, 1941 (1969).

TABLE 2. ELEMENTAL ANALYSES AND YIELDS OF NEW COMPOUNDS

n	Yield %	mp, °C	Molecular formula	Carbon, %		Hydrogen, %		Nitrogen, %	
				Calcd	Found	Calcd	Found	Calcd	Found
			p-$O_2NC_6H_4(CH_2)_nNH$-1-$C_{10}H_7$						
4	47	94—95	$C_{20}H_{20}N_2O_2$	74.97	74.80	6.29	6.21	8.74	8.93
5	38	109—110	$C_{21}H_{22}N_2O_2$	75.42	75.29	6.63	6.59	8.38	8.46
6	8	88—89	$C_{22}H_{24}N_2O_2$	75.83	75.99	6.94	6.76	8.04	7.94
			p-$O_2NC_6H_4O(CH_2)_nNH$-1-$C_{10}H_7$						
2	39	143—144	$C_{18}H_{16}N_2O_3$	70.11	70.28	5.23	5.09	9.09	9.17
3	28	110—111	$C_{19}H_{18}N_2O_3$	70.79	70.50	5.63	5.62	8.69	8.50
4	18	117—118	$C_{20}H_{20}N_2O_3$	71.41	71.54	5.99	6.08	8.33	8.14
5	35	93—94	$C_{21}H_{22}N_2O_3$	71.98	72.28	6.33	6.19	8.00	7.73
6	36	93—94	$C_{22}H_{24}N_2O_3$	72.50	72.67	6.64	6.60	7.69	7.50

lamp of 150 W was used as a light source. The photomultiplier used is 1P28. The emission curves shown in Figs. 1—3 were not corrected for the wavelength dependence of the sensitivity of the spectrometer and photomultiplier.

The author wishes to thank Dr. Akira Kuboyama, Government Chemical Industrial Research Institute, for permission to use the spectrophotofluorometer. He also wishes to express his gratitude to Prof. Michinori Ōki of the University of Tokyo for his interest and encouragement during this work. Thanks are also due to the Matsunaga Science Foundation for financial support.

BULLETIN OF THE CHEMICAL SOCIETY OF JAPAN, VOL. 44, 2541—2545 (1971)

Thermal Decomposition of Benzoyl *p*-Toluenesulfonyl Peroxide[1]

Ryuki HISADA, Hiroshi MINATO, and Michio KOBAYASHI
Department of Chemistry, Tokyo Metropolitan University, Fukazawa, Setagaya-ku, Tokyo

(Received April 24, 1971)

Benzoyl *p*-toluenesulfonyl peroxide (BTP) was synthesized by addition of barium hydroxide and water to a mixture of *p*-toluenesulfonyl chloride and peroxybenzoic acid in dichloromethane at −15°C. Rates of decomposition of BTP in inert solvents increased rapidly as the decomposition proceeded. This autocatalysis was prevented and the reaction followed a first-order rate equation when magnesium oxide suspension was present in the medium for removal of *p*-toluenesulfonic acid produced by the decomposition. The products of decomposition were analyzed. When magnesium oxide suspension was present, main products were those ascribable to homolysis (biphenyl, 44 mol%, in benzene; chlorobenzene, 44 mol%, hexachloroethane, 27 mol%, in carbon tetrachloride), but products ascribable to ionic reactions were also present (phenyl *p*-toluenesulfonyl carbonate, 22—26 mol%).

Investigations in our laboratories revealed that *m*-nitrobenzenesulfonyl peroxide decomposed homolytically in chloroform, whereas its O–O bond was cleaved heterolytically in aromatic solvents.[2] Razuvaev, Likhterov, and Etlis studied the decomposition of acetyl cyclohexanesulfonyl peroxide in several solvents, and their products indicated that both homolytic and heterolytic reactions were taking place.[3] They also studied the decomposition of benzoyl alkanesulfonyl peroxide in benzene and carbon tetrachloride, and they found no products ascribable to homolytic cleavage of the O–O bond.[4]

Aroyl arenesulfonyl peroxides have not been reported in the literature. As an example of these unknown peroxides, synthesis of benzoyl *p*-toluenesulfonyl peroxide has been attempted in order to determine its properties and the nature of its decomposition under various conditions.

Results and Discussion

A literature survey revealed a paper describing an unsuccessful attempt for synthesis of benzoyl benzenesulfonyl peroxide. Kirmse and Horner mixed benzenesulfonyl chloride and sodium perbenzoate in 1:1 water-dioxane at 0°C, and the products were benzoyl peroxide, benzoic acid and carbon dioxide.[5]

After numerous attempts, it was found that addition of barium hydroxide and water to a mixture of *p*-

1) Organic Sulfur Compounds. Part XXVI.

2) Y. Yokoyama, H. Wada, M. Kobayashi, and H. Minato, This Bulletin, **44**, 2479 (1971).

3) G. A. Razuvaev, V. R. Likhterov, and V. S. Etlis, *Zh. Obshch. Khim.*, **31**, 274 (1961); G. A. Razuvaev, L. M. Terman, V. R. Likhterov, and V. S. Etlis, *J. Polymer Soc.*, **52**, 123 (1961).

4) G. A. Razuvaev, V. R. Likhterov, and V. S. Etlis, *Zh. Obshch. Khim.*, **32**, 2033 (1962); *Tetrahedron Lett.*, **1961**, 527.

5) W. Kirmse and L. Horner, *Chem. Ber.*, **89**, 836 (1956).

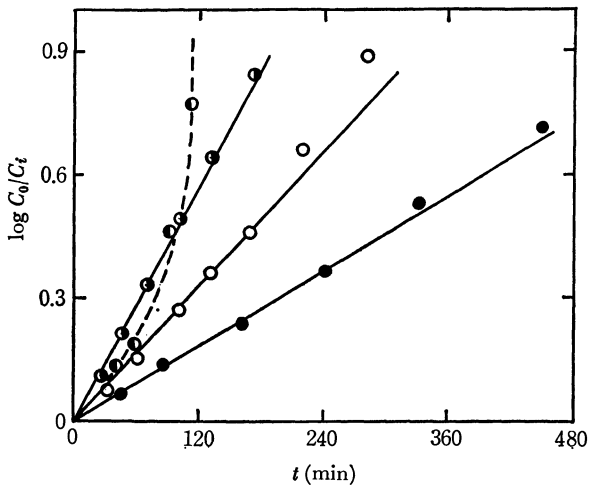

Fig. 1. Plots of $\log(C_0/C_t)$ *vs.* time for the decomposition of BTP in C_6H_6
● 40.0°C, ○ 45.0°C, ◑ 50.0°C, in the presence of MgO,
◐ 40.0°C, in the absence of MgO

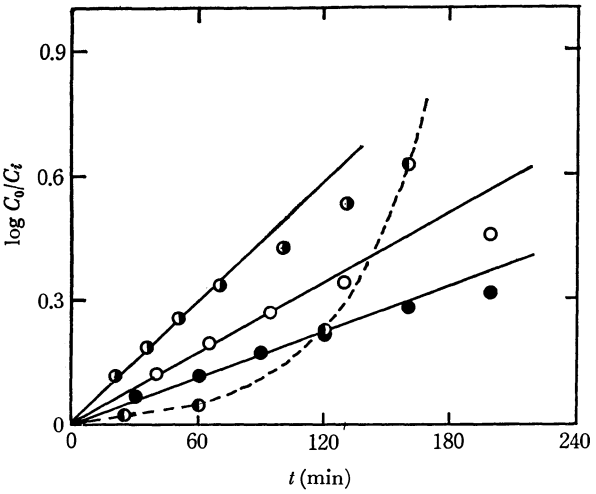

Fig. 2. Plots of $\log(C_0/C_t)$ *vs.* time for the decomposition of BTP in CCl_4
● 40.0°C, ○ 45.0°C, ◑ 50.0°C, in the presence of MgO,
◐ 40.0°C, in the absence of MgO

toluenesulfonyl chloride and peroxybenzoic acid in dichloromethane at −15°C resulted in the formation of benzoyl *p*-toluenesulfonyl peroxide (BTP).

When BTP was decomposed in benzene or carbon tetrachloride, the rate of decomposition increased rapidly with the progress of decomposition, as Figs. 1 and 2 show. When trifluoroacetic acid was added, the rate was very fast from the beginning, and the decomposition was complete in 3 hr at room temperature. These findings indicate that the decomposition of BTP is much accelerated by the *p*-toluenesulfonic acid produced by the decomposition. In order to investigate the possibility of the homolysis of BTP, such ionic autocatalysis must be prevented, and it was found that when powdery magnesium oxide was suspended in the medium the acceleration of rates was prevented and the decomposition followed a first-order rate equation till about two half-lives in benzene and one half-life in carbon tetrachloride. Rate constants and activation parameters

Table 1. First-order rate constants for the decomposition of BTP

Temp. (°C)	in C_6H_6+ suspended MgO $k_1\times10^5$ (sec^{-1})	in CCl_4+ suspended MgO $k_1\times10^5$ (sec^{-1})
40.0	5.79	6.78
45.0	10.82	11.00
50.0	19.02	18.30
E_a (kcal/mol)	23.91	19.94
$\Delta S^{\pm}$ (e.u.)	−3.65	−16.06

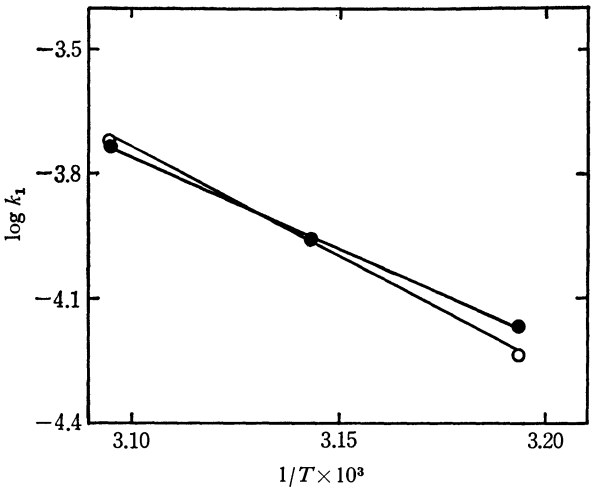

Fig. 3. Arrhenius plots for the decomposition of BTP
○ in C_6H_6+MgO, ● in CCl_4+MgO

are shown in Table 1 and Fig. 3.

The products of decomposition of BTP in benzene or carbon tetrachloride in the presence and absence of suspended magnesium oxide and in benzene in the presence of trifluoroacetic acid were analyzed, and the results are summarized in Table 2.

Table 2. Decomposition products of BTP[a)]

BTP (mmol)	5.0	5.0	5.0	5.0	5.0
Solvent (m*l*)	C_6H_6 50	C_6H_6 50	CCl_4 170	CCl_4 170	C_6H_6 75
Additives (mmol)	— 50	MgO 50	MgO 50	— 50	CF_3CO_2H 50
Products (mol/mol of BTP)					
Carbon dioxide		0.41	0.33	0.49	
Phenyl *p*-toluenesulfonyl carbonate	0.48	0.22	0.24	0.26	0.71
Biphenyl	0.01	0.44			0.005
Chlorobenzene			0.26	0.44	
Hexachloroethane			0.12	0.27	
Benzoic acid	0.23	0.10	0.33	0.09	0.15
p-Toluenesulfonic acid	0.33	0.57	0.57	0.33	0.10
Phenyl benzoate	0.04	0.08	0.01	0.02	0.01
p-Tolyl benzoate	trace	0.004	0.01	0.001	trace
Phenyl *p*-toluenesulfonate	trace	0.01	0.01	0.02	0.004
Chloride ion			0.05	>0.04	
Accounted for					
Phenyl (%)	76	84	86	85	88
p-Tolyl (%)	81	80	83	61	81

a) Temperature, 45°C; Reaction time, 15 hr.

In the absence of suspended magnesium oxide, one of the major products was phenyl *p*-toluenesulfonyl carbonate formed by carboxy inversion process.

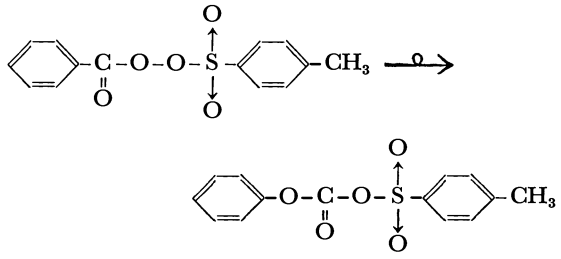

When trifluoroacetic acid was present, 71 mol% of BTP was converted to the mixed anhydride, and this finding shows that this rearrangement is accelerated by acid.

Even when suspended magnesium oxide was present in benzene or carbon tetrachloride to adsorb *p*-toluenesulfonic acid produced, about 22—26 mol% of BTP rearranged to the mixed anhydride. Therefore, the tendency for such rearrangement must be interpreted to be inherent in this peroxide rather than given by acid catalyst. The electron-withdrawing power of a *p*-toluenesulfonyloxy group is far greater than that of a benzoyloxy group, and even under the conditions which ensure the absence of acid in the medium the rearrangement proceeded at moderate rates at these temperatures.

However, when magnesium oxide was added, the yield of biphenyl increased from 1 to 44 mol% in benzene, and the yields of chlorobenzene and hexachloroethane in the carbon tetrachloride increased from 26 to 44 mol% and from 12 to 27 mol%, respectively. These data show that magnesium oxide is effective in reducing heterolysis and promoting homolysis.

When BTP was decomposed in carbon tetrachloride in the presence of magnesium oxide, the yield of chlorobenzene was 44 mol% whereas that of hexachloroethane was 27 mol%; the latter corresponds to 54 mol % of trichloromethyl radical. Thus about 10 mol% trichloromethyl radical must be produced by abstraction of chlorine atom from carbon tetrachloride by radicals other than phenyl radicals. Therefore, benzoyloxy radical and/or *p*-toluenesulfonyloxy radical must abstract chlorine atom from carbon tetrachloride.

Formation of *p*-tolyl benzoate can be accounted for by the following recombination of radicals in cage.

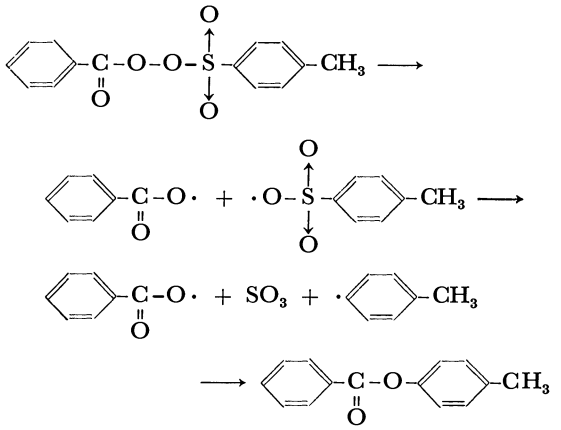

Formation of phenyl *p*-toluenesulfonate can be explained by addition of *p*-toluenesulfonyloxy radical to benzene and subsequent hydrogen abstraction from the cyclohexadienyl radical or by geminate cage recombination of *p*-toluenesulfonyloxy radical with phenyl radical produced by fragmentation of benzoyloxy radical.

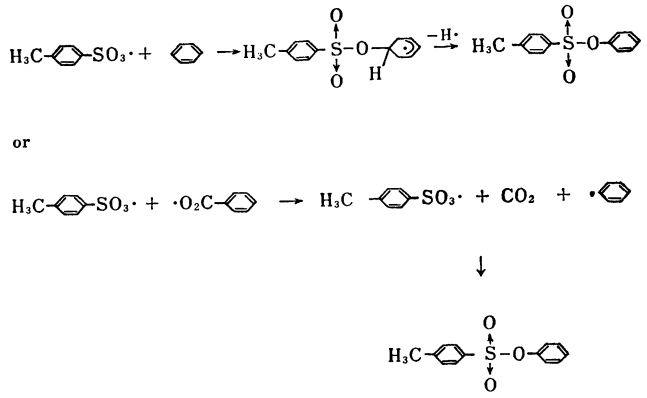

However, the fact that some sulfonate was formed even in the decomposition of BTP in the presence of trifluoroacetic acid indicates that at least part of the sulfonate arose from the mixed carbonate by an ionic path.

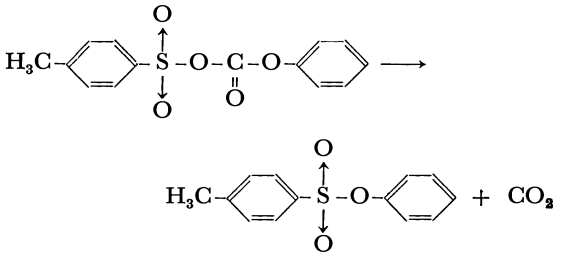

When *m*-nitrobenzenesulfonyl peroxide was decomposed in benzene, the main reaction products were *m*-nitrobenzenesulfonic acid and phenyl *m*-nitrobenzenesulfonate produced by electrophilic attack of a peroxidic oxygen atom on benzene.[6] If a similar reaction takes place with BTP, phenyl benzoate is the product expected in benzene. However, the yield of this ester in the absence of magnesium oxide was only 4 mol%, and this finding shows that positive character of the benzoyloxy oxygen of BTP is not large enough to accept nucleophilic attack of benzene readily.

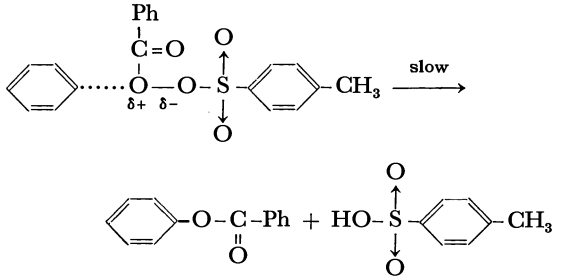

When magnesium oxide was added, the yield of phenyl benzoate was doubled (8%), but the majority of this amount probably arose from attack of benzoyloxy radical on benzene.

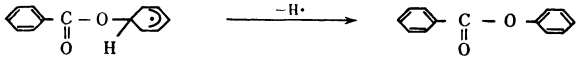

6) R. L. Dannley and G. E. Corbet, *J. Org. Chem.*, **31**, 153 (1966).

Razuvaev, Likhterov, and Etlis[4] studied the decomposition of benzoyl ethanesulfonyl peroxide. They found that in benzene phenyl ethanesulfonyl carbonate was produced in 83 mol% yield and no biphenyl was found, whereas in carbon tetrachloride neither chlorobenzene nor hexachloroethane was formed. Therefore, BTP has greater tendency to undergo homolytic cleavage of the O–O bond than benzoyl ethanesulfonyl peroxide.

Experimental

Materials. Benzene was washed with concentrated sulfuric acid and water successively, dried over anhydrous calcium chloride and distilled at 80.0°C. Carbon tetrachloride was washed with a 10% sodium carbonate aqueous solution and water, dried over anhydrous calcium chloride, and distilled over phosphorus pentoxide. Boiling point was 76.7°C. *p*-Toluenesulfonyl chloride was recrystallized from *n*-hexane; mp 69—70°C. Peroxybenzoic acid was prepared according to Braun's method.[7] Magnesium oxide was used after heating in a crucible for 2 hr.

Preparation of Benzoyl p-*Toluenesulfonyl Peroxide (BTP).* A solution of 19.1 g of *p*-toluenesulfonyl chloride (0.1 mol) in 160 m*l* of dichloromethane was cooled to −15°C in a 500 m*l* three-necked flask equipped with a mechanical stirrer, an addition funnel, and a thermometer. A solution of 17.9 g of peroxybenzoic acid (0.13 mol) in 150 m*l* of dichloromethane was slowly added into the cooled and stirred solution. After the temperature of the mixture became below −15°C, 5 m*l* of water was slowly added and then 41.0 g of barium hydroxide (0.13 mol) was added in portions in 15 min. The temperature of the mixture should be kept below −12°C during the addition. After the addition was completed, the mixture was stirred at −12°C for 1.5 hr, and then washed with 10 *l* of ice water. The dichloromethane solution was dried over anhydrous magnesium sulfate, and the solvent was removed under reduced pressure. A brownish residue obtained was recrystallized from ether at −20°C, and 16.1 g of light yellowish crystals was obtained; yield, 52.8%. Recrystallization was repeated for two more times, and the crystals melting at 59.5°C were used for experiments. Iodometric analyses indicated the purity of 99.80%. The main infrared absorptions appeared at 1790, 1400, 1225, 1195 and 1180 cm^{-1} (in CCl_4). BTP was stable at −20°C, and no appreciable decomposition was observed when it was stored at −20°C for one month.

Found: C, 57.77; H, 3.85; S, 11.05%. Calcd for $C_{14}H_{12}O_5S$: C, 57.53; H, 4.14; S, 10.97%.

Kinetic Measurements. All the measurements were carried out under nitrogen atmosphere. A solution of 1.91 g of BTP (6.5 mmol) in 190 m*l* of benzene or carbon tetrachloride was deaerated by bubbling nitrogen for 30 min at 10°C. The solution was placed in a constant temperature bath, and after suitable intervals 15.0 m*l* aliquots of the solution were withdrawn and subjected to the iodometric analysis using a 0.05N sodium thiosulfate solution.[8]

When the runs were carried out in the presence of 2.62 g (65 mmol) of magnesium oxide suspension, 20.0 m*l* aliquots were withdrawn, the magnesium oxide was removed by a centrifuge, and 15.0 m*l* of the solution was subjected to the iodometric analysis.

Products of Decomposition of BTP. *(1) In Benzene*: A 0.1M solution of BTP in benzene was decomposed at 45.0±0.1°C for 15 hr. The reddish brown solution obtained was washed with water and then with a 10% sodium bicarbonate solution. The *p*-toluenesulfonic acid which dissolved into the water washings was titrated with bromothymolblue as the indicator. The sodium bicarbonate extracts were acidified by addition of hydrochloric acid, and the benzoic acid obtained was extracted with ether. The amount of benzoic acid was determined gravimetrically after evaporation of ethereal extracts. The benzene layer was dried over anhydrous magnesium sulfate, and then divided to three portions. One portion was used for determination of biphenyl and phenyl benzoate by vapor phase chromatography (Column: Apiezon L, 2 m; internal standard, dibenzyl). Another portion was used for determination of *p*-tolyl benzoate and phenyl *p*-toluenesulfonate by vapor phase chromatography after refluxing the solution with added aniline for 30 min, washing with water and then drying (Colum: Apiezon L, 2 m; internal standard, phenyl *p*-chlorobenzoate). The other portion was used for determination of phenyl *p*-toluenesulfonyl carbonate by elution chromatography after removal of benzene under reduced pressure (Wako Gel Q22 200 mesh; eluant, 1:2 *n*-hexane - benzene). The identities of biphenyl, phenyl benzoate, *p*-tolyl benzoate, and phenyl *p*-toluenesulfonate were established by comparison of the infrared spectra of these products, obtained by elution chromatography, with those of the authentic samples.

(2) In Carbon Tetrachloride: A 0.029M solution of BTP in carbon tetrachloride was decomposed at 45.0±0.1°C for 15 hr under nitrogen atmosphere. The carbon dioxide generated was absorbed in a 0.1N sodium hydroxide solution, which was titrated with a 0.2N sulfuric acid solution.[9] Then this solution was titrated for chloride ion by a 0.1N silver nitrate solution with potassium chromate as an indicator. The carbon tetrachloride solution was washed with water and a 10% sodium hydrogen carbonate solution, and then dried over anhydrous magnesium sulfate. The aqueous extracts were titrated by a 0.1N sodium hydroxide solution for *p*-toluenesulfonic acid and hydrogen chloride, and then titrated for chloride ion by a 0.1N silver nitrate solution with potassium chromate as the indicator. The $NaHCO_3$-extracts were acidified, and the benzoic acid separated was extracted with ether and determined gravimetrically. The carbon tetrachloride solution was divided into three portions. One portion was used for determination of chlorobenzene and hexachloroethane by vapor phase chromatography (Column, Silicone oil SE30, 2 m; internal standard, *p*-dichlorobenzene). Another portion was used for determination of ester by vapor phase chromatography after the treatment of the solution with aniline and then with water. The other portion was used for determination of phenyl *p*-toluenesulfonyl carbonate by elution chromatography.

(3) In Benzene and Carbon Tetrachloride with Suspended Magnesium Oxide: A 0.05M solution of BTP in benzene or a 0.029M solution of BTP in carbon tetrachloride containing suspended magnesium oxide was stirred with a mechanical stirrer under nitrogen for 15 hr at 45.0°C. Then magnesium oxide was dissolved by addition of dilute sulfuric acid, and the mixture was refluxed for 5 min. Carbon dioxide and hydrogen chloride expelled were titrated by the methods described above. (Expulsion of hydrogen chloride from the water-containing mixtures must be incomplete, and hence the actual amounts of hydrogen chloride produced were probably

7) G. Braun, "Organic Syntheses," Coll. Vol. I, p. 431 (1961).

8) P. D. Bartlett and B. T. Storey, *J. Amer. Chem. Soc.*, **80**, 4954 (1958).

9) K. Uneyama, W. Tagaki, I. Minamida, and S. Oae, *Tetrahedron*, **24**, 5271 (1968).

greater than the values obtained by titration.)

The mixture was separated into aqueous and organic layers, and both layers were analyzed by the methods described above. Since the amount of *p*-toluenesulfonic acid cannot be determined by acid-base titration, it was determined gravimetrically by converting it into its *S*-benzylisothiuronium salt as follows. The aqueous layer was made alkaline, and evaporated under reduced pressure. The sodium *p*-toluenesulfonate in the residue was dissolved by hot methanol, and the methanolic solution was evaporated under reduced pressure. Some water and hydrochloric acid was added, and *p*-toluenesulfonic acid was converted to its *S*-benzylisothiuronium salt.

(4) In Benzene Containing Trifluoroacetic Acid: After a 0.1M solution of BTP in benzene and a benzene solution of trifluoroacetic acid were deaerated separately by nitrogen, they were mixed and stirred at room temperature. After 1 hr, the color of the solution was reddish brown. After 15 hr, the benzene solution was washed with water and then with a sodium hydrogen carbonate solution. The products of the reaction were analyzed according to the methods described above. The amount of *p*-toluenesulfonic acid was determined after it was converted into its *S*-benzylisothiuronium salt.

Synthesis of Phenyl p-*Toluenesulfonyl Carbonate.* To a solution of 11.8 g (0.04 mol) of anhydrous silver *p*-toluenesulfonate in 100 m*l* of acetonitrile, 6.4 g (0.04 mol) of phenyl chloroformate (94—95°C/41 mmHg) was added, and the mixture was refluxed for 18 hr. After the silver chloride was filtered, the acetonitrile was evaporated under reduced pressure. Recrystallization of the residue in 1:1 *n*-hexane-ether yielded 8.6 g of phenyl *p*-toluenesulfonyl carbonate (67%), mp 64—65°C.

Found: C, 57.83; H, 4.17; S, 10.97%. Calcd for $C_{14}H_{12}O_5S$; C, 57.53; H, 4.14; S, 10.97%. IR: 1795, 1395, 1230, 1180 cm^{-1} (KBr).

Grateful acknowledgement is made to the donors of the Petroleum Research Fund, administered by the American Chemical Society, for support of this research.

NOTES

BULLETIN OF THE CHEMICAL SOCIETY OF JAPAN, VOL. 44, 2546—2547 (1971)

Synthesis of Three New Azaparacyclophanes Containing Four Benzene Rings

Yoshikuni URUSHIGAWA,[1] Takahiko INAZU, and Tamotsu YOSHINO
Department of Chemistry, Faculty of Science, Kyushu University, Hakozaki, Fukuoka
(Received August 1, 1970)

As a part of studies of paracyclophane chemistry in our laboratory,[2] three new azaparacyclophanes containing four benzene rings connected with four bridges in the para-position, such as *N,N'*-dimethyl-2,18-dimethyl-2,18-diaza[3.1.3.1]paracyclophane (V), *N,N'*-dimethyl-2,19-diaza[3.2.3.2]paracyclophane (IX), and *N,N',N'',N'''*-tetramethyl-2,11,20,29-tetraaza[3.3.3.3]-paracyclophane (XIII), were synthesized.

The objects of this experiment were to synthesize the azaparacyclophanes with different lengths of bridges, to compare their spectral properties, and to determine whether or not they form an inclusion compound. The synthetic method and results will be described below.

For the synthesis of the above-mentioned compounds, we adopted an amide-formation method in the critical ring-closing step. The azaparacyclophanes, V, IX, and XIII, were prepared by the condensation of each diacid chloride and diamine and by subsequent reduction, while compound V was obtained by the further *N*-methylation of the corresponding cyclic secondary amine, IV.

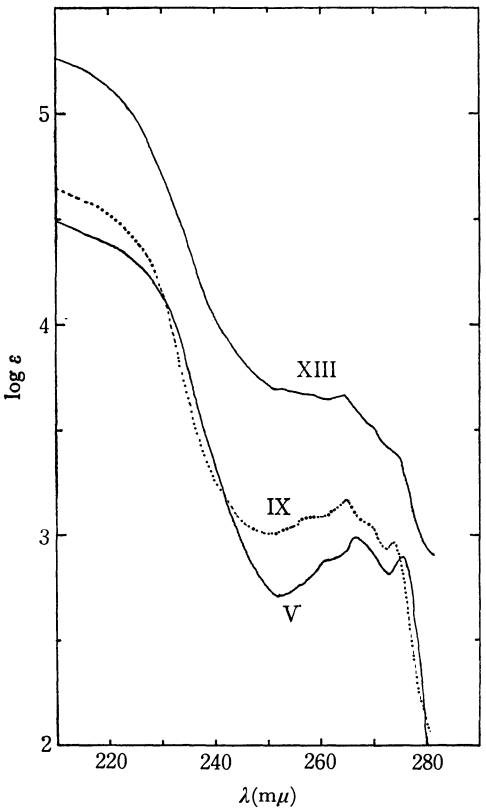

Fig. 1. UV spectra of azaparacyclophane V, IX, and XIII in ethanol.
V: λmax 266.5 mμ, log ε=2.99
IX: λmax 264.5 mμ, log ε=3.16
XIII: λmax 264.5 mμ, log ε=3.15
Curve XIII is displaced upward by 0.5 unit from the two curves below.

Figure 1 records the UV spectra of the azaparacyclophanes, which may be separated into two groups with respect to the length of the bridges. Compounds IX and XIII both contain bridges of more than one methylene unit and have almost equal intensities and wavelengths in λ max. On the other hand, compound V which contains one methylene unit, shows a shift to a slightly longer wavelength and a lower intensity compared to the others. The same effect has been pointed out by Cram[3] in a series of diphenylalkanes and related to the proximity of the benzene rings in the diphenylmethane moiety. The above facts may indicate the presence of a transannular electronic effect between benzene rings in V.

The crystallization of the compound XIII from benzene or dioxane gave crystals whose composition corresponded to that of a molecular compound consisting of one molecule of XIII and one molecule of benzene or dioxane. The presence of benzene or dioxane in the isolated substance mentioned above was concluded from the NMR spectra and the composition. In the case of the other paracyclophanes with methylene or ethylene as bridges, no such molecular compound has yet been isolated. It is now under investigation whether or not the benzene or dioxane molecules are included in the empty space of the paracyclophane ring.

Experimental

All melting points are uncorrected; they were measured in a sealed tube filled with nitrogen. The UV spectra were measured on a Hitachi EPI-3T spectrometer in ethanol. The NMR were measured with a Varian A-60 spectrometer in carbon tetrachloride. The molecular weights were measured by means of a Hitachi Perkin-Elmer 115 molecular-weight-determination apparatus, using benzene as the solvent.

2,18-Diaza[3.1.3.1]paracyclophane-3,17-dione (III). The diacid chloride I (3.22 g, 0.011 mol) in 500 m*l* of distilled benzene was subjected to cyclization with the diamine II (5 g, 0.022 mol) in 500 m*l* of distilled benzene over a 10 hr period, in a 5 *l* flask containing 2 *l* of benzene, under refluxing and stirring, according to the procedure of Stetter.[4] The still-hot reaction mixture was filtered, and then the solvent was

1) Present address: Water Pollution Control Division, Resources Research Institute, Ukima, Kita-ku, Tokyo.
2) See also T. Kawato, T. Inazu, and T. Yoshino, This Bulletin, **44**, 200 (1971).
3) D. J. Cram and M. F. Antar, *J. Amer. Chem. Soc.*, **80**, 3103 (1958).
4) H. Stetter and J. Marx, *Ann. Chem*, **607**, 59 (1957).

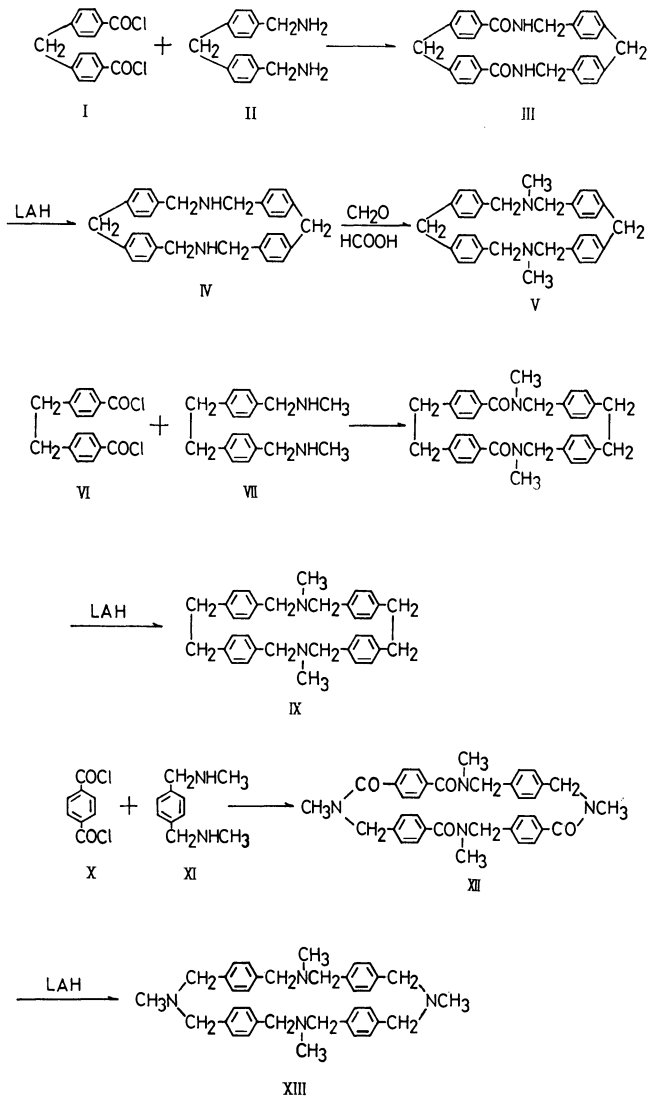

evaporated to give 1.2 g of a white precipitate. After crystallization from dioxane, 1 g (20%) of white crystals melting at 312—313°C was obtained. Found: C, 80.56; H, 5.82; N, 6.30%. Calcd for $C_{30}H_{26}N_2O_2$: C, 80.69; H, 5.87; N, 6.27%.

N,N′-Dimethyl-2,19-diaza[3.2.3.2]paracyclophane-3,18-dione (VIII). The diacid chloride VI (2.8 g, 0.009 mol), in 500 m*l* of distilled benzene was subjected to cyclization with the diamine VII (4.8 g, 0.018 mol) in 500 m*l* of distilled benzene over a 9 hr period, using the same procedure as was used for compound III. By treating the reaction mixture as above, 3.1 g (65%) of a crystalline product were obtained. A small portion of the product was crystallized from benzene to give white prisms melting at 239—240°C. Found: C, 81.06; H, 6.97; N, 5.26%. Calcd for $C_{34}H_{34}N_2O_2$: C, 81.24; H, 6.82; N, 5.57%.

N,N′,N″,N‴-Tetramethyl-2,11,20,29-tetraaza[3.3.3.3]paracyclophane-3,10,21,28-tetraone (XII.) The diacid chloride (1.5 g, 0.007 mol), in 500 m*l* of distilled benzene, was subjected to cyclization with the diamine XI (2.5 g, 0.015 mol) in 500 m*l* of distilled benzene over a 8 hr period, using the procedure described above. By treating the reaction mixture as above, we obtained 1.45 g (67%) of a white powder which gave white needles decomposing over 380°C by extraction with methanol using a Soxhlet-extractor. Found: C, 73.65; H, 6.29; N, 9.48%. Calcd for $C_{36}H_{36}N_4O_4$: C, 73.45; H, 6.16; N, 9.52%.

2,18-Diaza[3.1.3.1]paracyclophane (IV). A mixture of 1 g of compound III, 1 g of lithium aluminum hydride, and 150 m*l* of dioxane was refluxed for 64 hr under stirring. After the reaction mixture had then cooled, dilute hydrochloric acid was added to the mixture so that the inorganic substances were dissolved in solution, leaving the amine hydrochloride. After treatment with sodium hydroxide and crystallization from benzene, the hydrochloride gave 660 mg of white needles melting at 210.5—211.5°C (70%). Found: C, 86.49; H, 7.21; N, 6.43%. Calcd for $C_{30}H_{30}N_2$: C, 86.08; H, 7.22; N, 6.69%.

N,N′-Dimethyl-2,18-diaza[3.1.3.1]paracyclophane (V). A mixture of 40 m*l* of formic acid, 660 mg of compound IV, and 3 m*l* of 37% formalin was refluxed for 24 hr. After cooling, 10 m*l* of conc. hydrochloric acid were added, and the excess formalin and formic acid were removed by evaporation. The colorless residue was treated with a sodium hydroxide solution and extracted with benzene. After evaporation, 619 mg of white powder were obtained. White crystals melting at 254—256°C were obtained by crystallization from benzene (550 mg, 78.6%). Found: C, 86.09; H, 7.67; N, 6.00%; mol wt, 439. Calcd for $C_{34}H_{34}N_2$: C, 86.05; H, 7.67; N, 6.27%; mol wt, 446.6.

N,N′-Dimethyl-2,19-diaza[3.2.3.2]paracyclophane (IX). A mixture of 1.35 g of compound VIII, 1 g of lithium aluminum hydride, and 150 m*l* of dioxane was refluxed for 48 hr under stirring. The complex thus formed and the excess lithium aluminum hydride were decomposed by adding methanol and then a sodium sulfate solution. The reaction mixture was warmed and filtered, and the filtrate was concentrated to give white prisms melting at 236—238°C (763 mg, 61.4%). Found: C, 85.95; H, 8.10; N, 5.92%; mol wt 463. Calcd for $C_{34}H_{38}N_2$: C, 86.03; H, 8.07; N, 5.90%; mol wt, 474.6.

N,N′,N″,N‴-Tetramethyl-2,11,20,29-tetraaza[3.3.3.3]paracyclophane (XIII). A mixture of 377 mg of compound XII, 1 g of lithium aluminum hydride, and 100 m*l* of dioxane was refluxed for 72 hr under stirring. To the reaction mixture were added 1 m*l* of a 15% sodium hydroxide solution, and 3 m*l* of water. The mixture was warmed and filtered, and the filtrate was concentrated to give 148 mg (37%) of white needles, XIII-D, which contained dioxane. After heating at 90°C under reduced pressure, XIII-D gave pure XIII: mp 196—198.5°C; NMR (CCl_4) τ 7.68 (12H, singlet, N–CH_3), 6.71 (16H, singlet, PH–CH_2–N), 2.81 (16H, singlet, aromatic); mol wt, 534 (calcd. 532.7); Found: C, 81.28; H, 8.36; N, 10.44%. Calcd for $C_{36}H_{44}N_4$: C, 81.16; H, 8.33; N, 10.52%.

On the other hand, the data of XIII-D were as follows: mp 188—196°C; NMR (CCl_4) τ 6.41 (8H, singlet, dioxane) in addition to the bands of XIII; Found: C, 76.96; H, 8.40; N, 8.89%. Calcd for $C_{36}H_{44}N_4+C_4H_8O_2$: C, 77.38; H, 8.44; N, 9.02%. These results clearly show the presence of dioxane in a ratio of one to one. The crystallization of XIII from benzene also gave the same type of compound containing the benzene: mp 191—197°C; NMR (CCl_4) τ 2.73 (6H, singlet, benzene) in addition to the band of XIII; Found: C, 82.12; H, 8.47; N, 9.07%. Calcd for $C_{36}H_{44}N_4+C_6H_6$: C, 82.58; H, 8.25; N, 9.17%.

BULLETIN OF THE CHEMICAL SOCIETY OF JAPAN, VOL. 44, 2548—2550 (1971)

Reaction Rates in Binary Mixed Solvents. VI.[1] An Sn Ar Reaction in a Methanol-Acetonitrile Mixture

Yasuhiko KONDO, Kohei UOSAKI, and Niichiro TOKURA

Department of Applied Chemistry, Faculty of Engineering, Osaka University, Suita, Osaka

(Received August 3, 1970)

The present authors have previously developed a method of estimating the solvation patterns of the solute species involved in a reaction by analyzing the relation between the observed rate constants and the composition of the solvent.[1-3]

Since many data on rate constants and solvent activity coefficients were accumulated for **Sn Ar** reactions by Parker *et al.*,[4,5] the reaction is very appropriate for a discussion of the validity of our methods and the consistency between our method and Parker's parameters.

When an inorganic salt is involved as a reactant, one of the most important problems is how to evaluate the salt effects on reaction rates.[6] In some cases, these effects were ascribed to the incomplete dissociation of the inorganic salt in non-aqueous solvents;[7-10] in other cases, there are different reasons.[11-13]

In this report, first we will describe the quantitative treatment of the dependence of the observed rate constant on the initial concentration of potassium thiocyanate, a nucleophile; next, we will consider the solvation patterns of the species involved in the reaction based on the present authors' method and Parker's parameters.

Experimental

Materials. 2,4-Dinitroiodobenzene was prepared by refluxing 2,4-dinitrochlorobenzene and sodium iodide in dimethylformamide.[14] The crude product was recrystallized three or four times from a benzene-petroleum benzin mixture.

Potassium thiocyanate and sodium thiocyanate of a guaranteed-grade reagent were dried over silica gel.

The solvents used were purified by a method described elsewhere.[15,16]

Kinetic Procedure. The reaction rates were measured by two methods. In the first, a solution of 2,4-dinitroiodobenzene was added to a solution of potassium thiocyanate in a long-necked reaction vessel maintained at the reactions temperature. Aliquots of 5 m*l* were withdrawn at given intervals from the vessel. In the other method, the reaction were carried out in a high-pressure glass vessel with a volume of *ca.* 20 m*l* with a stainless steel screw stopper.

In either case the reactions were stopped by pouring the reaction mixture into a vessel containing water and light petroleum. After the extraction of inorganic salts from the organic layer, the concentration of the iodide ion produced was determined potentiometrically using a silver nitrate solution.

Results and Discussion

Salt Effects. The reaction followed the second-order kinetics for each run. The rate expression can then be written as follows:

$$\frac{dX}{dt} = k_{obs}\,(\text{2,4-dinitroiodobenzene})(\text{KSCN}) \qquad (1)$$

where X denotes the concentration of iodide ions formed in the reaction. The observed rate constant, k_{obs}, decreased as the initial concentration of potassium

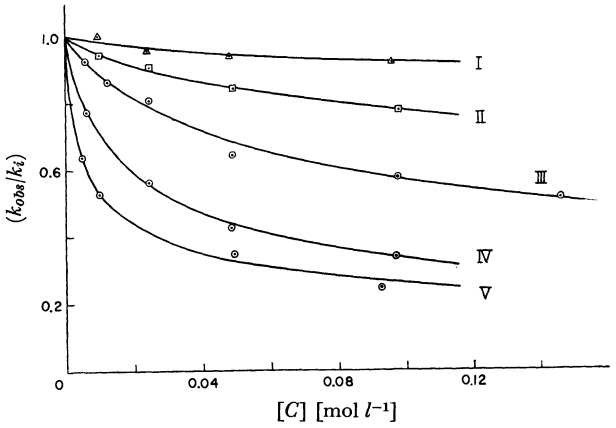

Fig. 1. The dependence of observed rate constants on the initial concentration of a nucleophile.
I, 2,4-dinitroiodobenzene+KSCN in pure methanol; II, 2,4-dinitroiodobenzene+KSCN in methanol (10 mol%)-acetonitrile (90 mol%) mixture; III, 2,4-dinitroiodobenzene +KSCN in pure acetonitrile; IV, 2,4-dinitroiodobenzene+ NaSCN in pure acetonitrile; V, 2,4-dinitroiodobenzene+ KSCN in pure acetone; ———, calculated values; △, ⊡, ⊙, observed values

1) Part V: Y. Kondo, Y. Kusaka, and N. Tokura, This Bulletin, **42**, 1708 (1969).
2) Y. Kondo and N. Tokura, *ibid.*, **40**, 1433 (1967).
3) Y. Kondo, Y. Honjo, and N. Tokura, *ibid.*, **41**, 987 (1968).
4) R. Alexander, E. C. F. Ko, A. J. Parker, and T. J. Broxton, *J. Amer. Chem. Soc.*, **90**, 5049 (1968).
5) A. J. Parker, *Chem. Rev.*, **69**, 1 (1969).
6) Farhat-Aziz and E. A. Moelwyn-Hughes, *J. Chem. Soc.*, **1959**, 2635.
7) L. J. LeRoux and S. Sugden, *ibid.*, **1939**, 1279.
8) W. Bruce, M. Kahn, and J. A. Leary, *J. Amer. Chem. Soc.*, **87**, 2800 (1965).
9) Y. Pocker and A. J. Parker, *J. Org. Chem.*, **31**, 1526 (1966).
10) N. N. Lichtin and K. N. Rao, *J. Amer. Chem. Soc.*, **83**, 2417 (1961).
11) C. A. Bunton and L. Robinson, *ibid.*, **90**, 5965 (1968).
12) S. D. Ross, M. Finkelstein, and R. C. Petersen, *ibid.*, **90**, 6411 (1968).
13) R. A. Sneen and F. R. Rolle, *ibid.*, **91**, 2140 (1969).
14) J. F. Bunnett and R. M. Conner, *J. Org. Chem.*, **23**, 305 (1958).
15) J. F. Coetzee, G. P. Cunningham, D. K. McGuire, and G. R. Padmanabhan, *Anal. Chem.*, **34**, 1139 (1962).
16) "Technique of Organic Chemistry, VII. Organic Solvents," ed. by A. Weissberger, Interscience, New York (1955).

thiocyanate increased. Typical examples are shown in Fig. 1. The experimental error of each rate constant was estimated to be less than ±2% from duplicate runs.

The method of analyzing the salt effects is based on the Acree hypothesis.[6-10,17] According to this hypothesis, the observed rate constants are expressed as sums of two components, *i.e.*, a rate constant for free ions, k_i, and a rate constant for ion pairs, k_{ip}, as follows:

$$k_{obs} = k_i\alpha + (1-\alpha)k_{ip} \quad (2)$$

where α stands for the degree of dissociation of potassium thiocyanate.

Since, for an ion pair, a thermodynamic dissociation constant, K_d, and a dissociation constant defined in terms of the concentration, K_c, are expressed by Eq. (3),[10] Eq. (2) can be rearranged to Eq. (4):

$$K_d = C\alpha^2 f_\pm^2/(1-\alpha) = K_c f_\pm^2 \quad (3)$$

$$k_{obs} = [\{-K_c+(K_c^2+4K_cC)^{1/2}\}/2C](k_i-k_{ip}) + k_{ip} \quad (4)$$

where $f_\pm$ and C stand for an activity coefficient and the stoichiometric concentration of potassium thiocyanate.

The experimental results were analyzed on the basis of Eq. (4) using a NEAC 2200—500 computer by the steepest descent method; the calculated values of k_i, k_{ip}, and K_c are listed in Table 1. The lines in Fig. 1 show the values calculated on the basis of these parameters.

Table 1. Calculated values of k_i, k_{ip}, and K_c at 40°C

Solvent	Nucleophile	$10^5\times k_i$	$10^5\times k_{ip}$	K_c
Acetonitrile	NaSCN	72.0	—	0.0165
Acetonitrile	KSCN	69.1	—	0.0635 (0.0380[19])
Acetonitrile Methanol (90:10 mol%)	KSCN	17.7	8.28	0.0827
Acetonitrile Methanol (70:30 mol%)	KSCN	5.04	4.34	0.0804
Acetonitrile Methanol (50:50 mol%)	KSCN	2.89	2.43	0.0819
Acetonitrile Methanol (25:75 mol%)	KSCN	2.03	1.79	0.0850
Methanol	KSCN	1.95	1.56	0.0909[a]
Acetone	KSCN	1125	96.6	0.0045 (0.0034[18])

Unit: k_i and k_{ip} : ($l\cdot mol^{-1}\cdot sec^{-1}$), K_c; ($mol\cdot l^{-1}$)

Values in parentheses show the dissociation constant determined by conductivity measurements.

a) The value from the reference[20] was used for the calculation.

Rate Constant in Binary Mixed Solvents. As a first approximation, assuming that the difference in k_i between methanol and acetonitrile results from the specific solvation of the thiocyanate ion by methanol and that all the other systems, *i.e.*, thiocyanate ion-acetonitrile, 2,4-dinitroiodobenzene-solvent mixtures and an activated complex-solvent mixture, form ideal solutions, by simplifying Eqs. (13) and (14) in Part IV[3] of this series the following equations are obtained:

$$(k_1/k_4) = (K_r+1) = 35.4 \quad (5)$$

$$\ln k_{mix} = x_1 \ln k_1 + x_4 \ln k_4 + x_4 \ln (K_r+1) - \ln (x_4K_r+1) \quad (6)$$

where methanol is indicated by the subscript 4 and where K_r refers to the equilibrium constant of the hypothetical reaction of methanol with the thiocyanate ion. The solid curve in Fig. 2 is the theoretical value calculated from these equations.

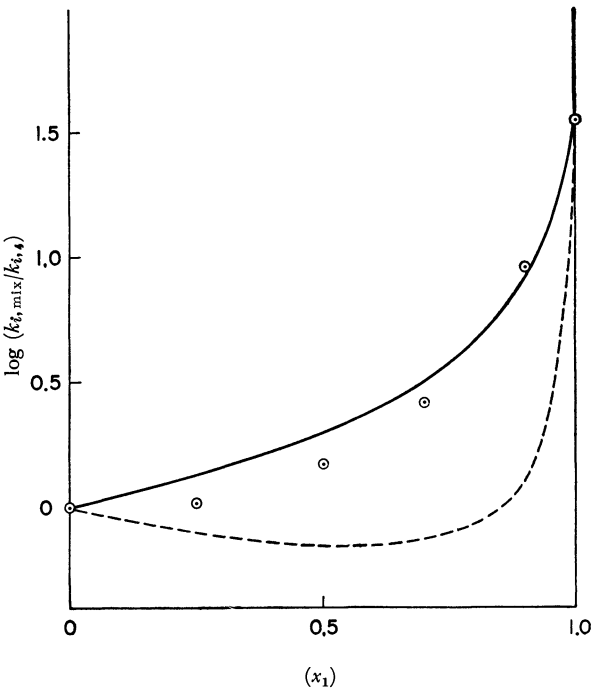

Fig. 2. Comparisons of calculated values with observed values. ———, calculated values by first model; ------, calculated values by the second model; ⊙, free ion rate constants

In the second approach, the concept of solvent activity coefficients[4] has been taken into account.

The relation between the solvent activity coefficient reported by Parker *et al.*,[4] γ, and the activity coefficient used by the present authors,[2] β_i, is given by Eq. (7), and the coefficient, ${}^4\gamma^1$, can be correlated to the equilibrium constant of the hypothetical reaction, K, on the basis of the definition of Ref. 2, when a solute is more stabilized in the solvent 1 than in the solvent 4.

$${}^4\gamma^1 = (\beta_1/\beta_4) = ({}^1\gamma^4)^{-1} = 1/(K+1) \quad (7)$$

Making use of the following solvent activity coefficients,[4] the relation,[2] Eq. (11), and several rules,[2] the final equation for rate constants in mixed solvents is obtained as follows:

$$\log {}^0\gamma^s_{SCN^-} = 2.6\ ^{4)} \quad (8)$$

$$\log {}^0\gamma^s_{RX} = -0.4\ ^{4)} \quad (9)$$

17) S. F. Acree and H. C. Robertson, *J. Amer. Chem. Soc.*, **39**, 1902 (1915).

18) P. G. Sears, E. D. Wilhoit, and L. R. Dawson, *J. Phys. Chem.*, **60**, 169 (1956).

19) H. L. Yeager and B. Kratochvil, *ibid.*, **74**, 963 (1970).

20) P. G. Sears, R. R. Holmes, and L. R. Dawson, *Trans. Electrochem. Soc.*, **102**, 145 (1955).

$$\log {}^{0}\gamma_{M}^{s}* = 0.65 \quad (10)$$ [21]

$$k_{mix} = k_0 \frac{(\beta_{SCN^-,mix}\beta_{RI,mix})}{\beta_{M^*,mix}} \quad (11)$$

$$\begin{aligned}\ln k_{mix} = {} & x_1 \ln k_1 + x_4 \ln k_4 \\ & + x_4 \ln (K_{SCN^-}+1) - \ln (x_4 K_{SCN^-}+1) \\ & + x_1 \ln (K_{RX}+1) - \ln (x_1 K_{RX}+1) \\ & - \{x_4 \ln (K_{M^*}+1) - \ln (x_4 K_{M^*}+1)\} \end{aligned} \quad (12)$$

where the subscript 1 refers to acetonitrile, and the subscript 4, to methanol, and where $K_{SCN^-}=3.97\times 10^2$, $K_{RX}=1.51$, and $K_{M^*}=3.47$.

The values calculated by means of Eq. (12) are shown by a dotted curve in Fig. 2.

21) $\log {}^{0}\gamma_{M}^{s}*$ was estimated by means of the relation[4]:
$\log {}^{0}\gamma_{M}^{s}* = \log {}^{0}\gamma_{SCN^-}^{s} + \log {}^{0}\gamma_{RX}^{s} - \log (k^s/k^0)$

Of the three solvent activity coefficients, that of the thiocyanate ion is the largest; this is equivalent to the idea that the rate of the reaction is controlled by the strong solvation of the thiocyanate ion by methanol. In the former treatments, this factor has been taken into account as the hypothetical reaction of thiocyanate ion with methanol. In the latter treatments, the solvent activity coefficients have been transformed into equilibrium constants in order to reproduce Parker's concept in our model.

Both models can explain the general behavior of the rate constant in a mixed solvent, and there is consistency between our model and the solvent activity coefficient reported by Parker *et al.* in that a strong solvation of the thiocyanate ion by methanol is the main factor making the rate in methanol slower than in acetonitrile.

BULLETIN OF THE CHEMICAL SOCIETY OF JAPAN, VOL. 44, 2550—2552 (1971)

Studies of Ethylenediamine-*N,N'*-diacetatocobalt(III) Complexes. II. The Preparation and Identification of Ethylenediamine-*N,N'*-diacetatocobalt(III) Complexes, with Some Anions as the Additional Ligand

Kashiro KURODA and Kiyokatsu WATANABE

Department of Chemistry, Faculty of Science, Ehime University, Matsuyama, Ehime

(Received December 9, 1970)

Several authors[1-8] have reported cobalt(III) complexes which contain the tetradentate ethylenediamine-*N,N'*-diacetate (EDDA). However, the number of such complexes is still small in comparison with those of such other series as the triethylenetetraminecobalt(III) series, and only a few anionic species have been isolated. The reason for this situation has been discussed in the preceding report.[1] It has also been discussed there how chloro(ethylenediamine-*N,N'*-diacetato)aquocobalt(III) or ethylenediamine-*N,N'*-diacetato(diaquo)cobalt(III) perchlorate has a character suitable as a starting material for the preparation of the series, and the preparations of some cationic species from these complexes have been illustrated. In this report, two new anionic species as well as the known oxalato complex, which have been derived from the chloroaquo or the diaquo complex, will be dealt with. The geometrical configuration of the complexes obtained was identified by means of their electronic absorption spectra and NMR spectra.

1) Part I of this series, K. Kuroda and K. Watanabe, This Bulletin, **44**, 1034 (1971).
2) M. Mori, M. Shibata, E. Kyuno, and F. Maruyama, *ibid.*, **35**, 75 (1962).
3) J. I. Legg and D. W. Cooke, *Inorg. Chem.*, **4**, 1576 (1965).
4) J. I. Legg, D. W. Cooke, and B. E. Douglas, *ibid.*, **6**, 700 (1967).
5) J. I. Legg and B. E. Douglas, *ibid.*, **7**, 1452 (1968).
6) C. W. Van Saun and B. E. Douglas, *ibid.*, **8**, 115 (1969).
7) P. J. Garnett, D. W. Watts, and J. I. Legg, *ibid.*, **8**, 2534 (1969).
8) P. F. Coleman, J. I. Legg, and J. Steele, *ibid.*, **9**, 937 (1970).

Experimental

Materials, Analysis, Apparatus, and Measurements. Ethylenediamine-*N,N'*-diacetic acid (Dotite Reagents), cesium chloride and acetate (Wako Pure Chemicals), and all the other reagent-grade chemicals were used without further purification. The apparatus used and the procedures for the analysis and the measurements have been described in the preceding report.[1]

Preparations. *(1) Cesium Dinitro(ethylenediamine-*N,N'*-diacetato)cobaltate(III) Monohydrate, $Cs[Co(EDDA)(NO_2)_2]\cdot H_2O$*: In 30 m*l* of water, 0.4 g of the chloroaquo complex $[Co(EDDA)(Cl)(H_2O)]\cdot H_2O$,[1] was suspended and heated until the complex dissolved completely. After the subsequent addition of 0.2 g of sodium nitrite, the mixture was evaporated to dryness at ~70°C; during the evaporation the color changed to a deep orange-red. The residue was extracted with ~2 m*l* of water, and after the addition of 0.4 g of cesium chloride to the extract, it was kept at 0°C for one day. The orange-red precipitate thus formed was recrystallized from a small amount of water by the addition of cesium chloride, and washed with ethanol and ether. Yield, 0.3 g.

Found: C, 14.87; H, 2.56; N, 11.61%. Calcd for $Cs[Co(EDDA)(NO_2)_2]\cdot H_2O = CoC_6H_{12}O_9N_4Cs$ (476.02): C, 15.14. H, 2.54; N, 11.77%.

*(2) Cesium Diazido(ethylenediamine-*N,N'*-diacetato)cobaltate(III), $Cs[Co(EDDA)(N_3)_2]$*: In 30 m*l* of water, 0.4 g of the chloroaquo complex was dissolved as in the case of (1). After the addition of 0.18 g of sodium azide, the solution was evaporated to dryness at ~70°C. The residue was dissolved in 2 m*l* of water, and then 0.2 g of cesium chloride was added;

A dark green precipitate appeared upon cooling. It was recrystallized from a small amount of water by the addition of cesium chloride, and then washed with methanol and ether. Yield, 0.3 g.

Found: Co, 12.92; C, 15.76; H, 2.36; N, 24.75%. Calcd for $Cs[Co(EDDA)(N_3)_2]=CoC_6H_{10}O_4N_8Cs$ (450.04): Co, 13.10; C, 16.01; H, 2.24; N, 24.90%.

(3) Cesium α-cis-*Oxalato(ethylenediamine*-N,N′-*diacetato)cobaltate(III) Dihydrate, α-cis-Cs[Co(EDDA)(ox)]·2H_2O*:

(4) Sodium β-cis-*Oxalato(ethylenediamine*-N,N′-*diacetato)cobaltate(III) Monohydrate, β-cis-Na[Co(EDDA)(ox)]·H_2O*: These two isomers were separated from a reaction product. The *β-cis* isomer was also prepared independently from the diaquo complex.

Into a mixture of cobalt(II) chloride hexahydrate (2.3 g), ethylenediamine-*N,N′*-diacetic acid (1.8 g), and sodium oxalate (2.7 g) in 50 m*l* of water, we bubbled air at ~55°C for 2 hr, during which time 10 m*l* of hydrogen peroxide (30%) was added drop by drop. The resulting mixture was kept at 0°C overnight, and then the undissolved excess sodium oxalate was filtered off. The red-violet filtrate was concentrated on a steam bath to ~15 m*l*, and 30 m*l* of methanol was added. The precipitate thus formed was collected on a glass filter; then it was fractionally extracted with 5 m*l* of cold water and with 10 m*l* portions of warm (~35°C) water twice. The first extract was discarded. Two-gram portions of cesium acetate were added to the second and the third extracts. In the second extract a large amount of a precipitate formed immediately, while in the third a small amount of a precipitate appeared after a while. The precipitate was recrystallized from warm water upon the addition of cesium acetate. The filtrate from the third fraction was placed in a refrigerator overnight; a large amount of a precipitate which was apparently different from the above one thus appeared. This precipitate was recrystallized from warm water with the addition of sodium perchlorate; the appearance of crystals was also slow. The color of the former was violet, while that of the latter was deep red-violet.

Found: C, 19.50; N, 5.69% for the violet isomer. Calcd for $Cs[Co(EDDA)(ox)]\cdot 2H_2O=CoC_8H_{14}O_{10}N_2Cs$ (490.05): C, 19.61; N, 5.72%. Found: C, 26.04; N, 7.68% for the red-violet isomer. Calcd for $Na[Co(EDDA)(ox)]\cdot H_2O=CoC_8H_{12}O_9N_2Na$ (362.12): C, 26.54; N, 7.74%.

By the evaporation of the second extract *in vacuo* without cesium acetate (the temperature depressed during the process), sodium salt of the violet isomer appeared as deep violet needles. This crystal dissolved in its own water of crystallization as the temperature was raised. This indicates that the sodium salt of the violet isomer is more soluble than that of the red-violet isomer.

The same product as the red-violet isomer was also obtained from $[Co(EDDA)(H_2O)_2]ClO_4$.[1] A mixture of the diaquo complex (0.37 g) and sodium oxalate (0.13 g) in 5 m*l* of water was heated on a water bath; deep red-violet crystals appeared as the evaporation proceeded. The yield was nearly quantitative (0.33 g).

Results and Discussion

Preparative Procedures. Most of the Co(III)-EDDA complexes in the literature were synthesized directly from a cobalt(II) salt, EDDA, and the necessary ligand. The method of preparation used in this study, in contrast, utilized the substitution reaction of the starting chloroaquo or diaquo complex with the various anions. One advantage of this method is that we can mix equivalent amounts of the reactants; therefore, we can reduce the number of components in the reaction mixture as much as possible. Hence, the crystallization of the product becomes easier. It was found that the cesium ion made a good precipitate in aqueous media with most of the anionic species studied.

The potassium salt of the α-*cis* isomer of the oxalato complex was first obtained by Van Saun and Douglas,[6] and the sodium salt of the β-*cis* isomer (dihydrate), by Coleman *et al*[8]. The violet and the red-violet isomer in this study showed absorption spectra identical with those of their respective complexes, although the analyses indicated that our β-*cis* isomer was the monohydrate. Coleman *et al.* separated the β-*cis* isomer by means of ion-exchange chromatography; hence, their method took a long time. The preparation has been simplified in two ways. First, the α-*cis* and the β-*cis* isomers were separated from a reaction mixture by the use of fractional extraction and fractional precipitation with the cesium ion; hence, no special or time-consuming technique was needed. Second, the sodium salt of the β-*cis* isomer was easily obtained by evaporating a solution of $[Co(EDDA)(H_2O)_2]ClO_4$ and sodium oxalate. Despite the α-*cis* configuration of the diaquo complex,[1] the deposit was exclusively the β-*cis* isomer; this means that the β-*cis* isomer is supplied by the shift of the equilibrium between the two isomers:

α-*cis* isomer ⇌ β-*cis* isomer

↓

deposit

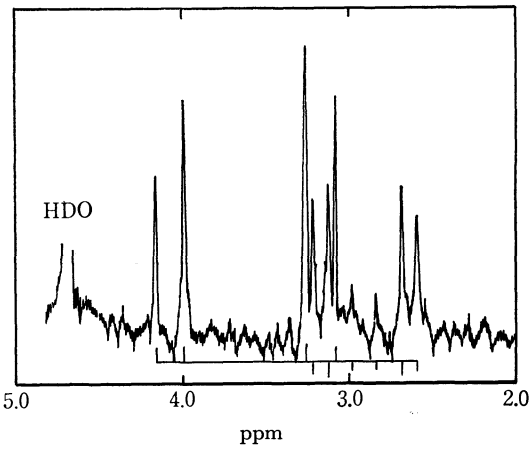

Fig. 1. PMR spectrum of $Cs[Co(EDDA)(N_3)_2]$ in D_2O.

Table 1. Resonance frequencies in the PMR spectra of $Cs[Co(EDDA)(X)_2]$ in D_2O (ppm downfield referred to TMS as zero)

X	Glycinate protons	Ethylene protons
N_3	3.08, 3.26, 3.98, 4.16	2.58, 2.68, 2.83
	J_{AB}=18 Hz	2.97, 3.12, 3.22
NO_2	3.13, 3.32, 4.18, 4.36	2.73, 2.82, 2.95
	J_{AB}=18 Hz	3.03, 3.16, 3.26

NMR Spectra. The pmr spectrum of the diazido complex is shown in Fig. 1. It has the characteristic feature of the α-*cis* isomer,[3,6] in which an AB quartet

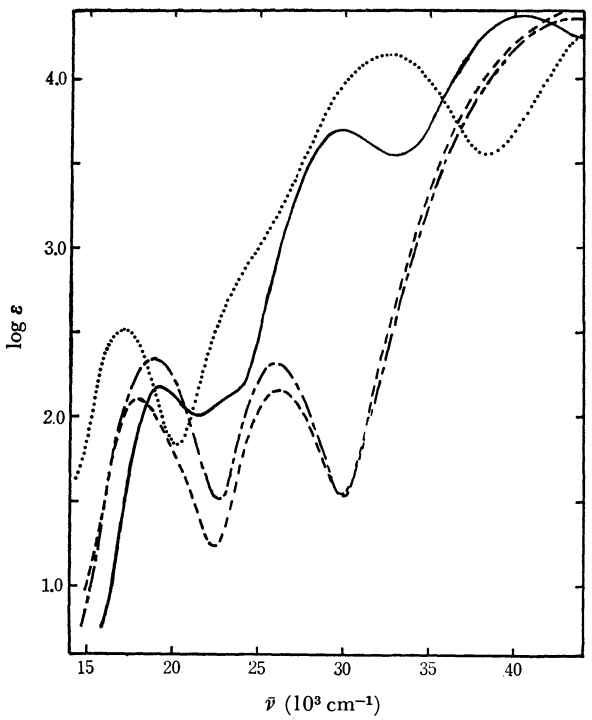

Fig. 2. Absorption spectra of some Co(III)-EDDA complexes.
———: Cs[Co(EDDA)$(NO_2)_2$]
·····: Cs[Co(EDDA)$(N_3)_2$]
– – –: α-*cis*-Cs[Co(EDDA)(ox)]
—·—·—: β-*cis*-Na[Co(EDDA)(ox)]

pattern originating from the two equivalent glycinate and symmetrical A_2B_2 absorptions from the ethylene protons are observable. The nitro and the violet oxalato complexes also showed analogous spectra. It is, therefore, certain that the nitro and the azido complexes are α-*cis* isomers. The numerical values are summarized in Table 1.

Electronic Absorption Spectra. The electronic absorption spectra are shown in Fig. 2, while the numerical values of the maxima are summarized in Table 2. In the spectrum of the nitro complex, it is clearly indicated that a band exists at $\sim 23 \times 10^3$ cm^{-1}. There is a slight but distinct shoulder around 24×10^3 cm^{-1} in that of the azido complex, too. The shoulder of the azido complex may be assigned to the second band covered by the strong ligand-specific band. On the other hand, the band of the nitro complex can not be the second band, since the position is in too low a wave-number region for the second band of this complex. As the nitro complex has the α-*cis* configuration (*trans* with respect to O), and hence belongs approximately to the *trans*-[CoA_4B_2]-type, a large split of the first band can be expected; such a split has been observed in the spectra of a large number of *trans*-[CoA_4B_2]-type complexes. Therefore, it is reasonable to assign the band to the Ib band; in other word, the presence of this band is further evidence that the complex is an α-*cis* isomer. Mori *et al*[2] previously reported the preparation and absorption spectrum of the nitro complex, but their spectrum differs considerably from that of our complex; especially, the band mentioned above can not be clearly observed. We considered that their complex was a different kind of nitro complex or that it included impurities because it was precipitated by ethanol.

Table 2. Absorption maxima of the electronic spectra of Co-EDDA complexes

	Ia $\bar{\nu}$(kK) (ε)	Ib $\bar{\nu}$(kK) (ε)	II $\bar{\nu}$(kK) (ε)	Sp $\bar{\nu}$(kK) (ε)
Cs[Co(EDDA)$(NO_2)_2$]	19.23 (150)	23 (100)		29.8 (5000)
Cs[Co(EDDA)$(N_3)_2$]	17.04 (323)		sh	32.6 (13800)
α-*cis*-Cs[Co(EDDA)(ox)]	17.83 (124)	sh	26.1 (143)	
β-*cis*-Na[Co(EDDA)(ox)]	18.85 (217)		25.9 (205)	

BULLETIN OF THE CHEMICAL SOCIETY OF JAPAN, VOL. 44, 2552—2553 (1971)

Über die Umsetzungen von Ammonium Tetracarbonyl Kobaltat mit Aromatischen Aldehyden

Ilsong RHEE, Membo RYANG, und Shigeru TSUTSUMI

Abteilung für Petroleum-Chemie, Fakultät der Ingenierwissenschaft, Osaka Universität, Suita, Osaka

(Eingegangen am 26. Dezember, 1970)

Vor kurzem haben wir berichtet, dass die *N*-unsubstituierten Imin Komplexe durch die Umsetzung von Aldehyden mit Kobalt-hexaammin-Komplexen erhalten wurden und eine neuartige Synthese von Nitrilen durch Oxidation von denselben Imin-Komplexen mit Brom gefunden wurde.[1] Weil das zu Kobalt koordinierende Ammoniak in Vergleich zum freien Ammoniak sehr unterschiedlich auf Aldehyde wirkt, haben wir die Reaktion von Aldehyden mit Ammonium Tetracarbonyl Kobaltat [$NH_4 \cdot Co(CO)_4$] eingehend untersucht.

Bei der Umsetzung von Hydrido Tetracarbonyl Kobaltat [$HCo(CO)_4$] mit Lewis-Basen (B) entstehen die Salze mit der Formel [$BHCo(CO)_4$].[2] Wir unter-

1) I. Rhee, M. Ryang, und S. Tsutsumi, *Tetrahedron Lett.*, **1970**, 3419.

2) R. F. Heck, *J. Amer. Chem. Soc.*, **86**, 2819 (1964).

suchten spektroskopisch die Bildung von $NH_4 \cdot Co(CO)_4$ bei der Umsetzung von $HCo(CO)_4$ mit Ammoniak und beobachteten weiter, dass $NH_4 \cdot Co(CO)_4$ mit aromatischen Aldehyden zu primären Amin Derivaten leicht reagierte.

Die aus $HCo(CO)_4$ und Ammoniak erhaltene ölige Substanz löst sich in polaren Lösungsmitteln und war stabil unter Stickstoff oder Kohlenmonoxid, war jedoch sehr luftempfindlich. Das IR Spektrum in Acetonitril wies auf Anwesenheit von ν_{NH} (3350 cm^{-1}) und ν_{CoCO} (1880—1960 cm^{-1}) hin. Die kurzwellige Verschiebung der ν_{CoCO} Bande in dem Kobalt Komplex deutet auf eine höhere Elektronendichte auf Kobalt als im Falle des $HCo(CO)_4$ (ν_{CoCO} 2049 und 2066 cm^{-1}). Das NMR Spectrum in Acetonitril wies auf ein Signal bei τ 6.78 hin, doch erschien das Proton-Signal von $HCo(CO)_4$ bei τ 20.0 und zeigte das Signal des freien Ammoniak in Acetonitril bei τ 9.36. Aus dem obigen Resultat wurde die Bildung des $NH_4 \cdot Co(CO)_4$ angenommen, obgleich das Molekulargewicht noch nicht bestimmt werden konnte.

$$HCo(CO)_4 + NH_3 \rightleftharpoons NH_4 \cdot Co(CO)_4$$

Liess man die Reaktion von dem obigen Öl, NH_4-$Co(CO)_4$, mit Benzaldehyd in Acetonitril unter dem Normaldruck des Kohlenmonoxids bei 45—55°C für 5 Stdn. laufen, so konnte man in 80.5%[3] Ausbeute Benzylbenzalamin isolieren. Die jeweilige Ausbeute in den verschiedenen Lösungsmitteln betrug 78.0 (in *n*-Pentan), 70.5 (in Ethanol) und 80.0% (in Pyridin). Analog verläuft die Reaktion mit *p*-Methoxybenzaldehyd zu dem entsprechenden primären Amin-Derivat (86.0%).

Aus der Reaktion von Benzaldehyd mit Ammoniak in Acetonitril bei 45—55°C entstand 1,3,5-Triphenyl-2,4-diazapentadien-(1,4) (83.3%), jedoch liess sich Benzylbenzalamin nicht erkennen.

Daher ershien es wahrscheinlich im Falle des NH_4-$Co(CO)_4$, dass das intermediär auftretende Imin durch Komplex-Formation mit Kobalt stabilisiert wurde.

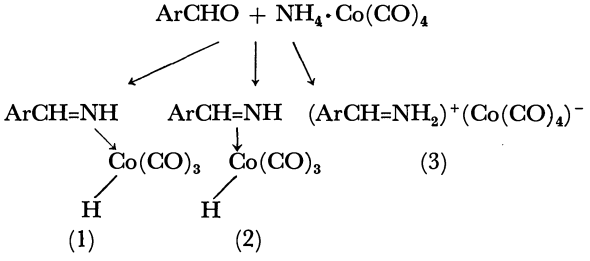

Obgleich die Information für das intermediäre Produkt infolge dessen Unhaltbarkeit noch nicht erhalten werden konnte, wurde angenommen, dass die *N*-substituierte Imin- oder Immonium-Gruppe intermediär mittels $HCo(CO)_4$ zu primärem Amin reduziert wurde und das Amin bei Reaktion mit Aldehyd Aldimin ergab.

$$\text{Intermediär} \xrightarrow{HCo(CO)_4} ArCH_2NH_2 \xrightarrow{ArCHO} ArCH_2N{=}CHAr$$

Experimenteller Teil

Umsetzung von $HCo(CO)_4$ mit Ammoniak. Nachdem eine trockene Gas-Mischung von Ammoniak (10 ccm) und Kohlenmonoxid (10 ccm/min) in die *n*-Pentanlösung (10 ccm) des $HCo(CO)_4$[4] (2 ccm) bei −50°C (2 Stdn.) eingeführt wurde, wurde das überschüssige Ammoniak durch Einführung des Kohlenmonoxids bei Raumtemperatur völlig abgejagt. Von der zurückbleibenden *n*-Pentanlösung trennt sich das gelbliche Öl, $NH_4 \cdot Co(CO)_4$, ab.

Reaktion von $NH_4 \cdot Co(CO)_4$ mit Aromatischen Aldehyden. In Lösung von $NH_4 \cdot Co(CO)_4$ (2.0 ccm, 15 mMol) in Acetonitril (20 ccm), dargestellt in einem 30 ccm Reaktionsrohr mit Tropftrichter und Rückflusskühler, wird Aldehyd (30 mMol) zugetropft. Die Badtemperatur hält man während der ganzen Reaktionszeit (4 Stdn.) bei 45—55°C. Das Reaktionsgemisch wurde mit Jod-Methanol (3 g/20 ccm) zersetzt und mit Äther extrahiert. Die vereinigten Ätherextrakte wurden je 3 mal mit 10 ccm 10 proz. $Na_2S_2O_3$-Lösung und 10 ccm Wasser gewaschen, über $MgSO_4$ getrocknet und i. Vak. eingedampft. Man destilliert den Rückstand.

Benzylbenzalamin: Sdp. 135—140°C/3 mmHg, 0.8 g. IR-Spektrum; $\nu_{C=N}$ 1650 cm^{-1}. NMR-Spektrum (CCl_4); τ 1.78 (1H, t, J=2.0 Hz), 2.55 (10H, m) und 5.30 (2H, d, J=2.0 Hz). Massenspektrum; Molmasse 195.

Gef.: C, 86.11; H, 6.71; N, 7.17%. Ber. für $C_{14}H_{13}N$ (195): C, 86.04; H, 6.62; N, 7.05%.

1,3,4,6-Tetraphenyl-2,5-diazahexadien-(1,4); Schmp. 171°C (aus Ethanol). IR-Spektrum; $\nu_{C=N}$ 1650 cm^{-1}. NMR-Spektrum ($CDCl_3$); τ 2.12 (2H, s), 2.62 (20H, m) und 5.28 (2H,s) Massenspektrum; M^+/e=388, m^+/e=194 ($Ph\overset{+}{C}H{=}CHPh$).

Gef.: C, 86.56; H, 6.23; N, 7.21%. Ber. für $C_{28}H_{24}N_2$ (388):C, 86.47; H, 6.05; N, 7.34%.

p-*Methoxybenzyl*-p-*methoxybenzalamin*: Sdp. 145—147°C/2 mmHg, 0.9 g. IR-Spektrum; $\nu_{C=N}$ 1650 cm^{-1}. NMR-Spektrum (CCl_4); τ 1.88 (1H, t, J=1.8 Hz), 2.80 (8H, m), 5.40 (2H, d, J=1.8 Hz), 6.24 (3H, s), und 6.30 (3H, s).

Reaktion von Ammoniak mit Benzaldehyd. In einer Lösung von Benzaldehyd (1 g) in Acetonitril (20 ccm) wurde bei 45—55°C (0.5 Stdn.) Ammoniak eingeführt. Aus dem Reaktionsgemisch wurde das Lösungsmittel abdestilliert.

1,3,5-Triphenyl-2,4-diazapentadien-(1,4): Schmp. 102°C (aus Äther), 0.75 g (83.3%). IR-Spektrum; $\nu_{C=N}$ 1633 cm^{-1}. NMR-Spektrum ($CDCl_3$); τ 1.47 (2H, s), 2.40 (15H, m) und 4.05 (1H, s). Massenspektrum; Molmasse 298.

Gef.: C, 84.53; H, 6.05; N, 9.39%. Ber. für $C_{21}H_{18}N_2$ (298): C, 84.70; H, 6.20; N, 9.34%.

3) Ausbeute anhand des $2HCo(CO)_4$. Weiter wurde 1,3,4,6-Tetraphenyl-2,5-diazahexadien-(1,4) nur wenig gebildet.

4) H. W. Sternberg, I. Wender, und M. Orchin, "Inorg. Syn.," Vol., 5, McGraw-Hill Book Company, New York, 1957, p. 192.

BULLETIN OF THE CHEMICAL SOCIETY OF JAPAN, VOL. 44, 2554—2555 (1971)

Synthesis of Carboxylic Acid Derivatives of Adenine and Theophylline

Koichi KONDO, Mikiji MIYATA, and Kiichi TAKEMOTO
Faculty of Engineering, Osaka University, Suita

(Received March 1, 1971)

Michael-type addition reaction of purine with ethyl acrylate gives the corresponding *N*-β-carboxyethyl derivatives,[1] which are also obtained by the reaction of purine with β-halopropionate under base-catalyzed conditions.[2]

In this communication, we report new syntheses of carboxylic acid derivatives of adenine and theophylline.

When sodium salt of adenine[3] was treated with diethyl bromomalonate in dimethylformamide (DMF), diethyl adenyl-9-malonate (I) was easily obtained. It was hydrolyzed in alkaline solution to give its carboxylic acid derivatives (II and III).

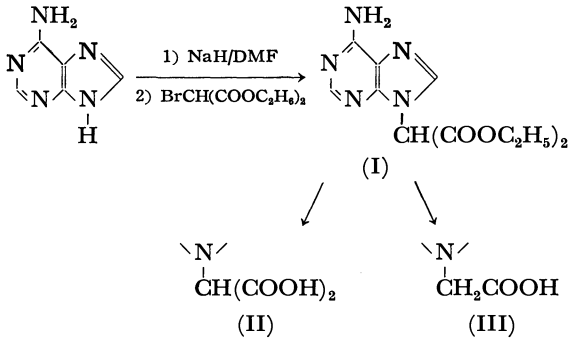

7-(β-carboxyethyl)theophylline (IV) was prepared when theophylline was allowed to react with β-propiolactone in DMF under base-catalyzed conditions. Its ethyl ester (V) was prepared from IV in ethanol in the presence of acetyl chloride.

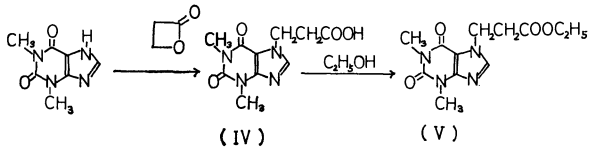

Adenine was also converted into 9-(β-carboxyethyl)-adenine (VI) under the same reaction conditions. A similar result concerning the reaction of adenine with γ-butyrolactone has also been reported.[4]

The reaction of VI with phosphorus pentachloride gave the hydrochloride salt of acid chloride derivative, which was treated with triethylamine in DMF to afford a substance assumed to be a polymer containing adenine nuclei in the main chain (VII). The infrared spectrum of VII showed a new C=O stretching band corresponding to amide structure at 1630 cm^{-1}. The molecular weight of VII was not determined because of its insolubility in common solvents.

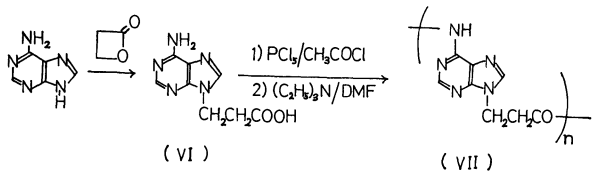

Ultraviolet spectra of I and VI showed λ_{max} near 260 nm, which suggests that the derivatives in question correspond to adenine substituted in 9-position. In the case of IV and V, λ_{max} appeared at 274 nm, which shows that the substituent was introduced into 7-position.

Carboxylic acid derivatives II and III as well as polymer VII thus obtained showed no melting points below 300°C, and were insoluble in common organic solvents.

Experimental

Diethyl-9-Adenylmalonate (I). A suspension of 1.35 g (10 mmol) of adenine and 0.52 g of 54% oily sodium hydride in 50 m*l* of DMF was stirred at ambient temperature for 1.5 hr. To the solution was added 3.5 g (14.7 mmol) of diethyl bromomalonate. After stirring for 6.5 hr, the reaction mixture was evaporated to dryness *in vacuo*. The residue was recrystallized from aqueous ethanol; yield 1.43 g (38%). Colorless needles, mp 172—173°C. IR (KBr): 3270, 3100 (ν_{N-H}), 1770, 1745 ($\nu_{C=O}$), 1670 ($\nu_{C=N}$), 1600 (δ_{N-H}), 1215 (ν_{C-O}), 2950 (ν_{C-H}), cm^{-1}. UV (C_2H_5OH): λ_{max} 259 (ε=11300), 209 (ε=14000).

Found: C, 49.18; H, 5.31; N, 24.10%. Calcd for $C_{12}H_{15}N_5O_4$: C, 49.15; H, 5.12; N, 23.89%.

9-Adenylmalonic Acid (II). In 200 m*l* of aqueous solution of sodium hydroxide (1.6 g) was dissolved 3.0 g (10 mmol) of I. The mixture was stirred at ambient temperature for 16 hr and then was adjusted to pH 3 with concd. hydrochloric acid. The resulting precipitate was then filtered off and washed thoroughly with water; yield 1.85 g (76%). Colorless crystals. IR (KBr): 3380, 3100 (ν_{N-H}), 2800—2500 (ν_{OH}), 1705, ($\nu_{C=O}$), 1680 ($\nu_{C=N}$), 1605 (δ_{N-H}) cm^{-1}.

Found: C, 40.54; H, 2.95; N, 29.95%. Calcd for $C_8H_7N_5O_4$: C, 40.50; H, 2.95; N, 29.50%.

9-Carboxymethyladenine (III). To a solution of water-ethanol mixture (3:1) containing 0.4 g of sodium hydroxide was added 1.4 g of I, and stirred for 3 days at ambient temperature. The clear solution was then evaporated to dryness. The residue was dissolved in 10 m*l* of water and the solution was adjusted to pH 5 with concd. hydrochloric acid. The resulting precipitate was then filtered off and washed with water and ethanol; yield 0.15 g (16%). Colorless crystals. IR (KBr): 3400, 3150 (ν_{N-H}), 2800—2500 (ν_{OH}), 1705 ($\nu_{C=O}$),

1) E. P. Lira and C. W. Huffman, *J. Org. Chem.*, **31**, 2188 (1966).

2) R. Zelnik and M. Pesson, *Bull. Soc. Chim. France*, **1959**, 1667; *Chem. Abstr.*, **55**, 17641 (1960).

3) N. J. Leonard, K. L. Carraway, and J. P. Helgeson, *J. Heterocycl. Chem.*, **2**, 291 (1965).

4) K. Okumura, T. Oine, Y. Yamada, M. Tomie, T. Nagura, M. Kawazu, T. Mizoguchi, and I. Inoue, *Chem. Commun.*, **1970**, 1045.

1605 (δ_{N-H}), 1680 ($\nu_{C=N}$) cm^{-1}.

Found: C, 43.37; H, 3.46; N, 36.35%. Calcd for $C_7H_7N_5O_2$: C, 43.52; H, 3.62; N, 36.27%.

7-(β-Carboxyethyl)theophylline (IV). 150 m*l* of DMF solution containing 16.2 g (90 mmol) of theophylline hydrate, 9.7 g (135 mmol) of β-propiolactone, and a trace of sodium hydroxide was refluxed for 4.5 hr. The solution was then concentrated under reduced pressure. The oily residue was crystallized with water. Recrystallization from water and ethanol gave a colorless crystal; yield 12.0 g (53%), mp 200—210°C (lit,[2] 204—205°C). (Found: C, 47.74; H, 4.86; N, 22.24%).

7-(β-Ethoxycarbonylethyl)theophylline (V). To an ethanol solution (15 m*l*) containing acetyl chloride (3.5 m*l*) was added 1.0 g of IV. The mixture was shaken vigorously for a few minutes until most of the solid dissolved and kept for 24 hr at ambient temperature. Pyridine (2 m*l*) was then added and after 48 hr at ambient temperature, the mixture was concentrated under reduced pressure. The oily residue was crystallized by trituration with water. Recrystallization from ethanol gave colorless crystals; yield 0.4 g (36%), mp 110°C (lit,[2] 105—106°C). (Found: C, 51.15; H, 5.93; N, 19.40%).

9-β-Carboxyethyladenine (VI). DMF solution (20 m*l*) containing 0.81 g (6.0 mmol) of adenine, 0.69 g (9.6 mmol) of β-propiolactone, and a trace of sodium hydroxide was refluxed for 2 hr. The solution was then evaporated to dryness *in vacuo*, the residue was recrystallized from water; yield 0.51 g (43%). Colorless needles, mp 272—278°C (dec.) (lit,[1] 284—228°C). IR (KBr): 3100, 3200 (ν_{N-H}), 3000—2600 (ν_{OH}) cm^{-1}. UV (H_2O): λ_{max} 260 (ε=10100), 206 (ε=14600). (Found: C, 46.25; H, 4.43; N, 33.69%).

Polymer derived from VI (VII). 0.5 g of 9-(β-carboxyethyl)adenine and 0.4 g of phosphorus pentachloride, protected carefully from moisture, was stirred in 3 m*l* of acetyl chloride at ambient temperature for 24 hr. The crude product was separated by filtration from the mixture and washed with petroleum ether. To this was rapidly added a solution of triethylamine (10 m*l*) in 100m*l* of DMF. After being stirred at ambient temperature for one week, the resulting precipitate was collected and recrystallized from hot water; yield 0.047 g (10%). IR (KBr): 1630 (amide $\nu_{C=O}$), 1680 ($\nu_{C=N}$) cm^{-1}.

Found: C, 50.60; H, 3.55; N, 36.72%. Calcd for $C_8H_7N_5O$: C, 50.52; H, 3.68; N, 36.84%.

BULLETIN OF THE CHEMICAL SOCIETY OF JAPAN, VOL. 44, 2555—2556(1971)

Raman, IR, NMR, and NQR of Chlorofluorosilanes

Keinosuke HAMADA*, G. A. OZIN, and E. A. ROBINSON
Department of Chemistry, University of Toronto, Toronto, Canada

(Received March 1, 1971)

Excellent-quality Raman spectra of chlorofluorosilanes have been observed using a laser Raman spectrometer. These Raman spectra will be reported here and compared with the IR spectra of those compounds. In additon, the fluorine NMR and the chlorine NQR of chlorofluorosilanes have been measured. The fluorine chemical shifts of chlorofluorosilanes increase with an increase in the number of fluorine atoms in each compound. The chlorine quadrupole resonance has been observed only for trichloromonofluorosilane, and the resonance frequency is 19.753 MHz at −196°C.

Experimental

Materials. The chlorofluorosilanes were prepared using the method of Booth and Swinehart,[1] in which a Swarts-type reaction was used. Silicon tetrachloride was partially fluorinated using antimony trifluoride and incorporating antimony pentachloride as a catalyst, and the chlorofluorosilanes were separated using trap-to-trap distillation techniques. The separated fractions were found to be sufficiently pure for Raman and IR spectroscopic measurements.

Measurements. Raman spectra were recorded on a Spex 1401 using an argon or a krypton-ion laser. The infrared measurements were done with a Perkin-Elmer 521 spectrometer whose optic material was silver chloride. The NMR spectra of fluorine for the compounds were obtained with a Varian Associate HR-60 high-resolution spectrometer operating at 56.4 MHz. The NQR measurements of chlorine for the compounds were done with a super-regenerative-type spectrometer.

Results and Discussion

Raman and IR. Table 1 shows the Raman and IR spectra for chlorofluorosilanes in the gas phase. The vibrational data for tetrafluorosilane and tetrachlorosilane have previously been reported,[2-4] and the figures for tetrachlorosilanes are cited from Ref. 4. The vibrational data for chlorofluorosilanes are tabulated in Table 1 with reference to the correlation diagram, the polarization data, the band contours of some infrared spectra, and the vibrational spectra of other SiX_mY_{4-m}-type molecules.

NMR. The fluorine chemical shifts of chlorofluorosilanes relative to an inner standard, trichloromonofluoromethane, are shown in Table 2. The fluorine chemical shifts, δ ppm, increase with an increase in the number of fluorine atoms. This trend in the chemical shifts for $SiCl_mF_{4-m}$ is same as that in the BCl_mF_{3-m}, $POCl_mF_{3-m}$, PCl_mF_{5-m}, and CCl_mF_{4-m} series

* Present address: Faculty of Education, Nagasaki University, Bunkyo-cho, Nagasaki

1) H. S. Booth and C. F. Swinehart, *J. Amer. Chem. Soc.*, **57**, 1333 (1935).

2) E. A. Jones, J. S. Kirby-Smith, P. J. H. Woltz, and A. H. Wilson, *J. Chem. Phys.*, **19**, 242 (1951).

3) T. Shimanouchi, *ibid.*, **17**, 848 (1949).

4) B. Trumpy, *Z. f. Physik*, **66**, 790 (1930).

Table 1. Raman and IR spectra of $SiCl_mF_{4-m}$ in gas state

T_d SiF_4		C_{3v} SiF_3Cl		C_{2v} SiF_2Cl_2	
Raman	IR	Raman	IR	Raman	IR
1025 wbr	1025 s	1004 vw	1010 s	987 vw	990 s
(p) 798 s	*ia*	(p) 878 w	876 s	(p) 915 w	912 s
389 mwbr	*a*	(p) 593 s	590 m	638 w	656 s
260 wbr	*ia*	(p) 351 mw	*a*	(p) 520 s	513 w
		255 vw	*a*	(p) 324 mw	*a*
		222 w	*a*	303 w	*a*
				279 w	*a*
T_d $SiCl_4$		C_{3v} $SiFCl_3$		210 w	*ia*
Raman	IR	Raman	IR	(p) 174 mw	*a*
608		(p) 947 vw	942 s		
(p) 422		638 wbr	634 s		
220		(p) 464 s	*a*		
148		(p) 240 m	*a*		
		283 mw	*a*		
		166 m	*a*		

Raman spectra are obtained at 600 mmHg and 25°C, and IR at 30 mmHg and 25°C.
ia means IR inactive and *a*, IR active, but the IR spectrum did not appear because of AgCl optic material.

Table 2. Chemical shifts of $SiCl_mF_{4-m}$ to CCl_3F

Compound	Chemical shift	
	Hz	δ ppm
SiF_4	−9188	163
$SiClF_3$	−7640	135
$SiCl_2F_2$	−6320	112
$SiCl_3F$	−5316	94

and is opposite to that in the PCl_mF_{3-m} and $P(NMe_2)_mF_{3-m}$ series[5,6] in direction. The chemical shifts in the $Si(Et)_mF_{4-m}$ and $Si(Me)_mF_{4-m}$ series have the minimum value of a chemical shift at 2 or 3 fluorine atoms in each series.

NQR. The only chlorine quadrupole resonance frequency observed for trichloromonofluorosilane at −196°C is a resonance of 19.753 MHz between the running frequencies of 18.8 and 22.0 MHz. Silicon tetrachloride has four resonance lines whose average value is 20.391 MH.[7] It is not sure whether trichloromonofluorosilane has only one resonance line like trichlorosilane,[8] or whether the lines other than the one line have just not yet appeared. The chlorine quadrupole resonance for dichlorodifluorosilane has not yet been found. This might be because the present authors have not been able to get a NQR spectroscopically-pure substance. They have also not been able to obtain NQR spectroscopically-pure trifluoromonochlorosilane.

The authors are grateful to Professor R. L. Armstrong and his collaborators of the University of Toronto for the NQR measurements.

5) R. R. Holmes and W. P. Gallagher, *Inorg. Chem.*, **2**, 433 (1963).
6) P. R. Holmes, R. P. Carter, Jr., and G. E. Peterson, *ibid.*, **3**, 1748 (1964).
7) E. Schnell and E. G. Rochow, *J. Amer. Chem. Soc.*, **78**, 4178 (1956).
8) P. Livingston, *J. Phys. Chem.*, **57**, 496 (1953).

BULLETIN OF THE CHEMICAL SOCIETY OF JAPAN, VOL. 44, 2557—2558(1971)

Proton and Nitrogen-14 Nuclear Magnetic Resonance Study of Pyridine - Water System

Yuri KASUGAI, Yoji ARATA, and Shizuo FUJIWARA

Department of Chemistry, Faculty of Science, The University of Tokyo, Hongo, Tokyo

(Received March 8, 1971)

This note reports the results of ^{1}H and ^{14}N Nuclear Magnetic Resonance (NMR) study of the pyridine-water system. Using ^{1}H and ^{14}N line width data for pyridine, the anomalous concentration dependence of macroscopic quantities such as viscosity and density is discussed in terms of the formation of hydrogen-bonding.

Proton and ^{14}N NMR spectra were collected at room temperature using JEOLCO JNM 4H-100 and Varian VF-16 spectrometers operating at 100 MHz and 4.15 MHz, respectively. Proton NMR samples were vacuum degassed by repeated freeze-pump cycles.

A remarkable dependence on concentration was observed for the line widths of the α protons and ^{14}N of pyridine. The line width of the α protons for the neat pyridine sample is about 1.5 Hz. On adding water, the line width of the α protons decreases until it becomes minimum at $M=0.3$, where M denotes the mole fraction for pyridine, increasing again with further addition of water. In parallel with the behavior of the ^{1}H line widths, the line width for ^{14}N has its maximum at $M=0.3$. Figure 1 shows the change of the ^{14}N relaxation time calculated from the line width by assuming that the line shape is Lorentzian. The variation of viscosity with concentration[1] is also given in Fig. 1, which shows that the viscosity has a maximum at $M=0.3$.

It has been suggested from infrared [2,3] and Raman[4] data that hydrogen-bonded complexes are formed between pyridine and water molecules. When the amount of pyridine is much smaller than that of water, the dominant species is supposed to be [pyridine·H_2O] for which the formation constant has been estimated at 2.8 l/mol.[4]

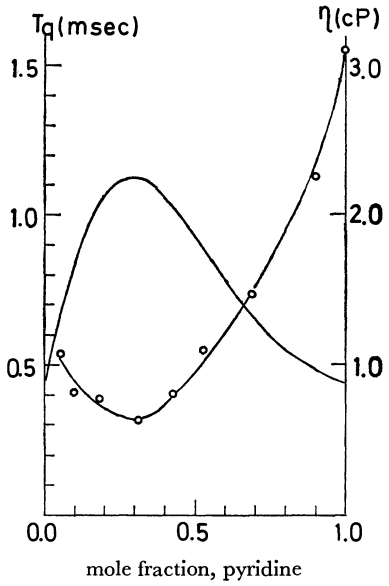

Fig. 1. Concentration dependence of the viscosity and the relaxationtime of ^{14}N.
—○—: Relaxation time of ^{14}N.
———: Viscosity (Ref. 1).

Over the whole range examined, a single line is observed in the ^{14}N spectra, which suggests that there is a rapid exchange of pyridine molecules between free and hydrogen-bonded (to water) sites. In this case, the line width ΔH may be given by

$$\Delta H = p\Delta H_{\text{coord}} + (1-p)\Delta H_{\text{free}}, \qquad \text{(A)}$$

where p is the fractional population of the hydrogen-bonded pyridine molecules, and ΔH_{coord} and ΔH_{free} are the line widths for the hydrogen-bonded and free pyridine molecules, respectively. The fractional population p was calculated with the use of the equilibrium constant $K=2.8$ l/mol;[4] ΔH_{free} was taken as the line width of neat pyridine, and ΔH_{coord} from the region $M \leqq 0.1$ of the mixture. The line widths ΔH_{coord} and ΔH_{free} were divided by the viscosity to eliminate any effect due to viscosity. In Fig. 2, ΔH thus obtained

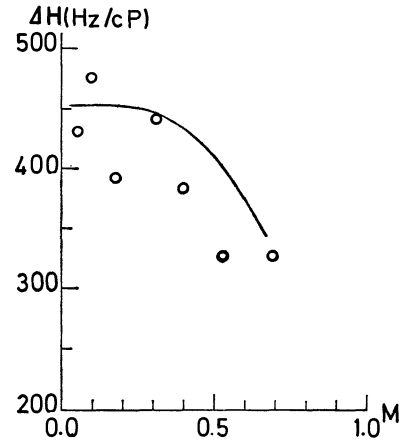

Fig. 2. Calculated and observed line width.
——: Line width calculated from the expression (A).
○: Observed line width corrected for viscosity.

is compared with the observed line width (corrected with respect to the viscosity). Thus in the region $M <$ 0.5, the gross features of the line width are well reproduced by the assumption of the formation of [pyridine·H_2O] complex. These results suggest that the formation of the hydrogen-bonded complex is responsible for the anomalous concentration dependence of the vis-

1) H. Hartley, N. G. Thomas, and M. P. Applebey, *J. Chem. Soc.*, **93**, 538. (1908).
2) A. N. Sidrov, *Optics and Spectroscopy*, **8**, 24 (1960).
3) H. Takahashi, K. Mamola, and E. K. Plyler, *J. Mol. Spectroscopy*, **21**, 217 (1966).
4) J. Rouviere and J. Salvinien, *C. R. Acad. Sci., Paris, Ser. C.*, **265**, 949 (1967).

cosity and density. For the region where M is sufficiently large, complexes other than [pyridne·H_2O] will be formed and the above assumption does not hold.

The authors are grateful to Mr. Keikichi Nakamura, National Research Institute for Metals, for the measurements of the ^{14}N spectra.

BULLETIN OF THE CHEMICAL SOCIETY OF JAPAN, VOL. 44, 2558—2559(1971)

A Convenient Method for Detection of NH Containing Compounds on Thin Layer Chromatograms

Yasuo ARIYOSHI, Naotake SATO, Hideo ZENDA,* and Kikuo ADACHI*

Central Research Laboratories, Ajinomoto Co., Inc., Suzuki-cho, Kawasaki, Kanagawa

**Katsura Chemical Co., Inc., Kurihara, Zama, Kanagawa*

(Received March 16, 1971)

The technique of thin layer chromatography is frequently used to detect various compounds in the course of studies of amino acids or peptides. The compounds with amino or imino group can be easily detected with ninhydrin at μg level on chromatogram. However, the compounds without amino or imino group, such as N-protected amino acids and cyclic peptides, cannot be detected with this reagent. It is known that the compounds with NH group can be detected by chlorination of NH to NCl and subsequent spraying with starch-potassium iodide. As chlorinating reagent, chlorine gas[1-4] and aqueous sodium hypochlorite[5-6] were used. In some cases, they cause background coloration and give indistinct chromatograms. This can be improved by use of tertiary butyl hypochlorite,[7] but this reagent is unstable and expensive.

We will report here a convenient method of chlorinating NH group on a thin layer chromatogram of silica gel. When the silica gel chromatogram was exposed to gas generated from bleaching powder (calcium hypochlorite) and hydrochloric acid, NH group was found to be easily chlorinated in a short period of time at room temperature. Subsequent sprayings of ethanol and aqueous starch-potassium iodide gave a clear violet spot on chromatogram without any background coloration.

This method is recommended for detection of peptides, cyclic peptides, amino acid esters, amino acid amides, N-protected amino acids. It is also applicable to other NH containing compounds such as nucleosides and related compounds and acid amides. The detectable threshold of amino acids or peptides is 0.1—0.25 μg after chromatography. Table 1 shows the results when glass plate coated with silica gel G of 0.25 mm thickness was charged with 0.5 μg of various compounds, developed in butanol-acetic acid-water (4:1:2) system, and stained by this method.

Table 1. Color intensity and R_f value of various compounds

Compound	R_f value	Color intensity
Ala	0.31	W
β-Ala	0.34	S
Arg·HCl	0.14	S
Asp	0.21	S
Cys	0.15	W
Gln	0.27	S
His	0.33	W
Hyp	0.43	S
Leu	0.53	W
Lys·HCl	0.10	S
Ser	0.29	S
Trp	0.65	M
α-Asp-Phe	0.58	M
β-Ala-Tyr	0.41	S
Gly-Leu	0.73	S
Cyclo-(α-Asp-Phe-)	0.78	S
Cyclo-(Phe-Ala-)	0.75	S
Cyclo-(Phe-Val-)	0.86	S
Z-Asp	0.90	M
H-Phe-OMe·HCl	0.67	S
Pyroglutamic acid	0.59	W
Hypoxanthine	0.52	W
5′-Cytidylic acid	0.38	W
Acetanilide	0.85	S

Abbreviations used are: S, strong; M, medium; and W, weak coloration

Experimental

Five μl of sample solution was spotted on a silica gel G plate (5×20 cm) of 0.25 mm thickness. The plate was developed with *n*-butanol-acetic acid-water (4:1:2 v/v). After being dried, the plate was put in a cylinder (22 cm in height and 7 cm in diameter), at the bottom of which a small beaker (1.5 cm in height and 3 cm in diameter) containing 3 g of calcium hypochlorite (available chlorine content is 60%) was placed. The back of the plate was preferably placed to face the beaker to keep the chromatogram from spots caused by

1) H. N. Rydon and P. W. G. Smith, *Nature*, **169**, 922 (1952).
2) F. Reindel and W. Hoppe, *Naturwissenschaften*, **40**, 221 (1953).
3) F. Reindel and W. Hoppe, *Chem. Ber.*, **87**, 1103 (1954).
4) G. Pataki, *J. Chromatog.*, **12**, 541 (1963).
5) S. C. Pan and J. D. Dutcher, *Anal. Chem.*, **28**, 836 (1956).
6) D. E. Nitecki and J. W. Goodman, *Biochemistry*, **5**, 665 (1966).
7) R. H. Mazur, B. W. Ellis, and P. S. Cammarata, *J. Biol. Chem.*, **237**, 1619 (1962).

dispersed bleaching powder on addition of hydrochloric acid. One m*l* of concentrated hydrochloric acid was added to the bleaching powder in the beaker, and the cylinder was covered loosely with a glass plate. Chlorination proceeded at room temperature in 7—10 min. The plate was removed from the cylinder, exposed to a stream of air for 1 min, and then sprayed with a small amount of ethanol. After being dried in a rapid current of air for 1—2 min, the plate was sprayed with a starch-iodide reagent prepared by dissolving 0.5 g of soluble starch and 0.5 g of potassium iodide in 100 m*l* of water. Violet spots of the compounds in the sample appeared immediately on the clear background.

BULLETIN OF THE CHEMICAL SOCIETY OF JAPAN, VOL. 44, 2559—2560(1971)

Nuclear Magnetic Resonance Spectra of Carbanions. VII.[1] 1,1,4,4-Tetraphenylbutadiene Dianion[2]

Masahiro USHIO, Mikio TAKAKI, Kensuke TAKAHASHI, and Ryuzo ASAMI

Department of Synthetic Chemistry, Nagoya Institute of Technology, Gokiso-cho, Showa-ku, Nagoya

(Received March 29, 1971)

The carbanions produced from α-methylstyrene and 1,1-diphenylethylene were studied in our previous reports.[3,4] The studies have now been extended to the carbanion produced from 1,1,4,4-tetraphenylbutadiene (TPB). Furthermore, we have tried, but failed, to observe the spectra of the carbanion produced from 1,4-diphenylbutadiene (DPB).

Experimental

The procedures used in this study are similar to those described in the previous reports.[3,4] Commercially-available TPB and DPB were used as sources of carbanions after two or three recrystallizations from acetone and methanol respectively. The pmr spectra were observed at about 60 MHz with a frequency-swept Hitachi R-20B spectrometer. The chemical shifts of the carbanions were evaluated from the higher-shielding methylene peak of the solvent, THF, used as an internal reference. This peak of THF was taken to be 1.79 ppm from TMS. All the chemical shifts were calibrated by means of a frequency counter (Takeda Riken TR-3824X).

Results and Discussion

The signals appearing in the aromatic-proton region of the carbanion produced from TPB with sodium as counterion are divided into three groups. They show the structures of a doublet, a triplet, and a triplet from lower to higher shielding, with an intensity ratio of about 2:2:1. They can, therefore, easily be identified as the signals of the ortho-, meta-, and para-protons respectively. The chemical shifts of the carbanions are given in Table 1, along with other previously-reported values for the sake of comparison. On treatment with H_2O, the carbanion forms a mixture of 1,1, 4,4-tetraphenylbutene-1 and -2, whose pmr peak positions are 2.82 (2H, triplet, $J=7._5$ Hz), 4.00 (1H, triplet, $J=7._5$ Hz), 5.90 (1H, triplet, $J=7._5$ Hz), 7.00 (weak), and 7.06 (strong) for the former, and 4.72_5 (2H, double doublet, apparently, $J=4$ and $1._5$ Hz), 5.85_5 (2H, double doublet, apparently $J=4$ and $1._5$ Hz), and 7.10_5 ppm for the latter in a CCl_4 solution. The charge localized in the phenyl rings of the carbanion is then estimated to be given in Table 2, taking the reference for the neutral phenyl proton as 7.20 ppm. This charge estimation is not self-consistent because the charge on a carbon with no proton can not be estimated on the proton spectra. However, a series of the data may be compared with each other and may give some information as to the charge distribution of the carbanions. Furthermore, the magnetic anisotropy of the adjacent phenyl ring may contribute to the aromatic proton shifts, especially to the ortho-proton shifts in the carbanion. If we assume the twist angle of the phenyl ring to be 30°, the anisotropy effects will compensate for each other for two far and near ortho-protons, as has been described before.[4] Table 2 shows that the charge localization on the phenyl rings is about 40% for the TPB dianion. The lower charge localization in the phenyl rings of the TPB dianion as compared with that of the 1,1-diphenylethylene dimer dianion is ascribable to the structural difference between I and II, that is, to the presence of a pi-system in the middle part of II:

We have tried, but failed, to observe the spectra of

TABLE 1. THE PROTON CHEMICAL SHIFTS OF CARBANIONS IN ppm

Carbanion	Counterion	Assignment		
		Ortho	Meta	Para
1,1,4,4-Tetraphenyl-butadiene dianion	Na	7.22	6.71	6.00
1,1-Diphenylethylene dimer dianion[a]	Na	7.18	6.61	5.75
Cumyl anion[b]	K	5.16	6.11_5	4.39

a) Ref. 3; b) Ref. 4.

1) Part VI in this series, K. Takahashi, M. Takaki, and R. Asami, Preprint presented at the 9th Symposium on NMR Spectroscopy of the Chemical Society of Japan, Kanazawa, October 1970, p. 124.

2) M. Ushio, K. Takahashi, and R. Asami, Preprint presented shortly at the Tokai District Meeting of the Chemical Society of Japan, Nagoya, October 1970, p. 107.

3) K. Takahashi and R. Asami, This Bulletin, **41**, 231 (1968).

4) K. Takahashi, M. Takaki, and R. Asami, *J. Phys. Chem.*, **75**, 1062 (1971).

TABLE 2. THE CHARGE DISTRIBUTION IN THE CARBANIONS IN UNITS OF THE ABSOLUTE VALUE OF THE CHARGE OF AN ELECTRON

Carbanion	Counterion	Position			Sum for a phenyl ring
		Ortho	Meta	Para	
1,1,4,4-Tetraphenylbutadiene dianion	Na	0.00	−0.05	−0.12	−0.22
1,1-Diphenylethylene dimer dianion[a)]	Na	0.00	−0.06	-0.14_5	-0.26_5
Cumyl anion[a)]	K	-0.20_5	-0.10_5	−0.28	−0.90

a) Ref. 4.

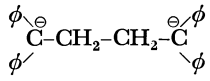

I

II

the carbanion produced from 1,4-diphenylbutadiene, using potassium, sodium, and lithium as counterions. Our failure is ascribable to the contamination of the radical anion formed, because the samples used for the NMR measurements gave strong ESR signals. The pmr spectra of the TPB dianion was observed only with sodium counterions. Even in this case, the NMR sample gave weak ESR signals and the PMR spectra are broader than usual spectra. The TPB dianion with potassium as counterions did not give any resolved spectrum in spite of several trials. No information on the *cis-trans* isomerization of the TPB dianion and 1,1,4,4-tetraphenylbutene-2 can be obtained at present. Further studies along this line are in progress.

BULLETIN OF THE CHEMICAL SOCIETY OF JAPAN, VOL. 44, 2560—2562 (1971)

A Naturally-occurring Bromo-compound, Aplysin-20 from *Aplysia kurodai*

Shosuke YAMAMURA* and Yoshimasa HIRATA
Chemical Institute, Nagoya University, Chikusa, Nagoya

(Received April 6, 1971)

Two bromo-compounds, aplysin and aplysinol, were isolated from *Aplysia kurodai*, whose structures have already been established.[1] We could further isolate a small amount of a third bromo-compound, aplysin-20, from the same materials, which were gathered at Hokkaido (in September.)[1] However, no bromo-compound has been found in the *Aplysia kurodai* which were gathered at Sugashima, Mie-ken (in June).[2] The above different results seem to result from the different kinds of marine plants which were eaten by *Aplysia kurodai*.[3] Especially, the biogenesis of aplysin-20 strongly suggests that its origin must be attributable to the marine plants, as will be discussed later.

Aplysin-20, mp 146—147°C, is regarded as a diterpenoid bromo-compound on the basis of its molecular formula ($C_{20}H_{35}O_2Br$) and spectral data, as will be shown below. In addition to an end absorption in the UV spectrum of aplysin-20, the IR absorption band at 1675 cm^{-1} and a triplet at δ 5.41 ppm (1H, J=7.0 Hz) in the NMR spectrum (see Table 1) indicate the presence of an isolated double bond.

Aplysin-20 was treated with acetic anhydride-pyridine to give a monoacetate (mp 59—62°C; *m/e* 430 and 428 (M^+): ν_{max} 3520, 1730 sh., 1713, 1675 and 1260 cm^{-1}), which could be converted into the starting material with methanolic potassium hydroxide. The acetylation study suggests that aplysin-20 has a primary or secondary hydroxyl group as well as a tertiary one (ν_{max} 3520 cm^{-1}). Furthermore, when the NMR spectra of aplysin-20 and its monoacetate were compared, the doublet at δ 4.16 ppm (2H, J=7.0 Hz) and the triplet at δ 5.41 ppm (1H, J=7.0 Hz) were shifted to the doublet at δ 4.60 ppm (2H, J=7.0 Hz) and the triplet at δ 5.60 ppm (1H, J=7.0 Hz) respectively. The remaining signals are nearly identical in both compounds except for the appearance of the singlet at δ 2.02 ppm (3H, CH_3COO–) in the latter. The above fact, coupled with the observation of the methyl broad

TABLE 1. NMR SIGNALS OF APLYSIN-20

δ-Value	Number of proton and coupling const.	Assignment
0.96	3H (s)	Me+
1.00	3H (s)	Me+
1.08	3H (s)	Me+
1.16	3H (s)	Me+
1.30—2.20	16H (br. m)	
1.70	3H (br. s)	Me–C(=)
3.85	1H (q, J=3.1, 8.5 Hz)	–CH_2–CHBr– (–CH–CHBr–CH–)
4.16	2H (d, J=7.0 Hz)	–C(=)CH–CH_2OH
5.41	1H (br. t, J=7.0 Hz)	–C(=)CH–CH_2OH

* Present address: Faculty of Pharmacy, Meijo University, Showa-ku, Nagoya.

1) S. Yamamura and Y. Hirata, *Tetrahedron*, **19**, 1485 (1963).

2) We can catch them in Sugashima only during the rainy season, and the attempted isolation of bromo-compounds has failed.

singlet at δ 1.70 ppm, indicates the presence of the partial structure (I). Furthermore, when considered in the light of the partial structure (I) and the presence

$$-CMe=CH-CH_2OR$$
(I) R=H; (II) R=Ac

of two hydroxyl groups in aplysin-20 (or the partial structure (II) in a monoacetate with a tertiary hydroxyl group), the appearance of a pair of strong peaks (*m/e* 272 and 270), coupled with the strongest peak in their mass spectra at *m/e* 191, suggests the presence of the partial structure (III) in aplysin-20, as was discussed

$$-CH_2CH_2-CMe=CH-CH_2OH \quad (III)$$

in connection with Scheme I. Accordingly, aplysin-20, which has four tertiary methyl groups (see Table 1) and the partial structure (III),[4] may be regarded as a bicyclic diterpene with a side chain (III); thus, it is analogous to many bicyclic diterpenes with the same number of methyl or potential methyl groups and the same type of side chain as aplysin-20.[5] Manool (IV) and sclareol (V) are typical bicyclic diterpenes; both have the carbon skeleton (VI) with the side chain (VII).[6] Therefore, the structure (VIII) has been proposed for aplysin-20 except for the position of the bromine atom.[7] The tentative structure (VIII) can be satisfactorily explained by means of the mass spectra of both aplysin-20 and its monoacetate (in Scheme I) except for the following point: there are no typical peaks corresponding to the fragmentation, A, which can be found in the spectra of manool, sclareol, and other diterpenes with the exocyclic double bond or equatorial hydroxyl group at the C_8-position (in VI).[8] Accordingly, it seems that aplysin-20 has a configuration different from that of sclareol at the C_8-position or a carbon skeleton different from those of usual bicyclic diterpenes. The final structure was deduced by X-ray analysis,[9] indicating that aplysin-20 has the absolute configuration (IX), which is different from those of manool, sclareol, and streoids. The biogenesis of aplysin-20 is shown in Scheme II. The most interesting point in this study is that aplysin-20 has an axial hydroxyl group at the C_8-position and an equatorial bromine atom located at the C_3-position, a position usually substituted in diterpenes and steroids. From a biogenetic point of view particularly, aplysin-20 is the first bicyclic diterpene with an axial hydroxyl group at the C_8-position

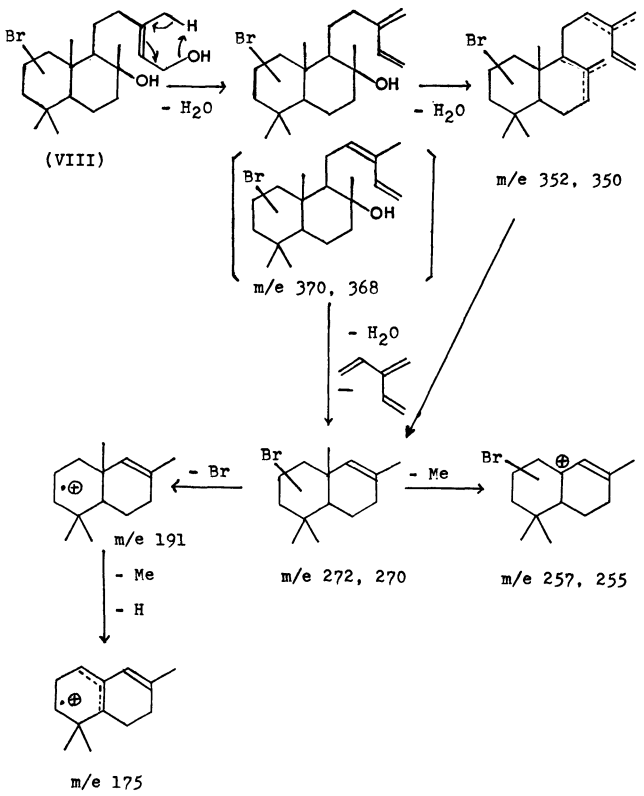

Scheme I. Fragment peaks in the mass spectrum of Aplysin-20.

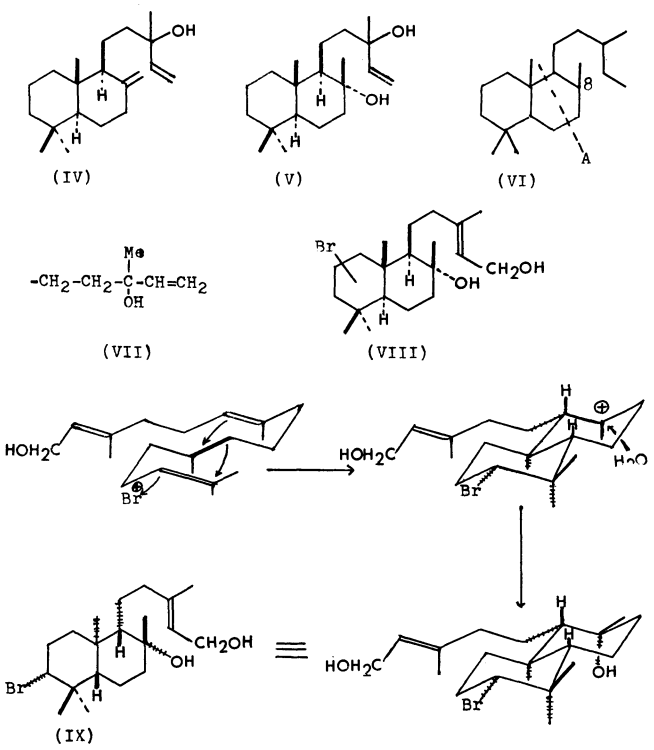

Scheme II. Biogenesis of Aplysin-20.

Experimental

The mps are uncorrected. The IR spectra were taken with a JASCO IR-S spectrophotometer on a potassium bromide disk. The optical rotation was measured in methanol

3) Aplysin-type sesquiterpenes have been isolated from marine plants by T. Irie and his co-workers. (*Cf.* T. Irie, *Nippon Kagaku Zasshi*, **90**, 1179 (1969) and the references cited therein.)

4) Aplysin-20 has two rings which consist of less than ten carbon atoms.

5) D. H. R. Barton, "Chemistry of Carbon Compounds," Vol. II, Elsevier Publishing Co. (1953), p. 696; P. deMayo, "The Higher Triterpenoids," Interscience Publishers, N. Y. (1959), p. 1.

6) The transformation of the side chain (VII) to II has been known (G. Ohloff, *Ann.*, **617**, 134 (1958).

7) S. Yamamura and Y. Hirata, The 16th Annual Meeting of Chemical Society of Japan (Tokyo, April, 1963; Abstract of Papers, p. 84).

8) C. Enzell, *Acta Chem. Scand.*, **15**, 1303 (1961).

9) H. Matsuda, Y. Tomiie, S. Yamamura, and Y. Hirata, *Chem. Commun.*, **1967**, 898.

with a Rudolph and San polarimeter. The NMR spectra were measured in $CDCl_3$ with Nihondenshi JNM-3 and Varian A-60 analytical NMR spectrometers (60 MHz). The values are given in ppm relative to tetramethyl silane as an internal reference (s: singlet; d: doublet; q: quartet; t: triplet: m: multiplet). The mass spectra were measured by the Atlas Werke Co., Ltd., Germany (70 eV).

Isolation of Aplysin-20. Dried *Aplysia kurodai* (2 kg) was treated according to the method described in Ref. 1, and the insoluble materials were removed. The *n*-hexane solution was concentrated to about 100 m*l* and then chromatographed on silica gel (Wakojunyaku Co., Ltd.) (350 g). After elution with *n*-hexane to give debromoaplysin, aplysin, and aplysinol,[1] the second fraction, eluted with *n*-hexane-ether (10:1), was rechromatographed on alumina (Wakojunyaku Co., Ltd.) (15 g). After subsequent elution with *n*-hexane-ether (10:1) to give a yellow liquid, the second fraction, when eluted with *n*-hexane-ether (4:5), afforded a white solid which was then recrystallized from methanol to give colorless needles of aplysin-20 (320 mg),[10] mp 146—147°C; *m/e* 370 and 368 (4) (M^+-18), 352 (19), 350 (19), 289 (2) (M^+-Br), 272 (30), 271 (17), 270 (30), 257 (10), 255 (10), 191 (100, base peak), 175 (13), 149 (16), 147 (10), 135 (29), 134 (32), 133 (11), 123 (19), 121 (18), 119 (12), 109 (22), 107 (21), 105 (10), 98 (39), 97 (12), 96 (11), 95 (41), 94 (11), 93 (22), 91 (10), 84 (15), 83 (20), 82 (18), 81 (62), 79 (14), 71 (46), 69 (64), 68 (17), 65 (20), 57 (14), 55 (43), 43 (39), and 41 (56); ν_{max} 3500—3300 and 1675 cm^{-1} (Found: C, 61.98; H, 9.01%. Calcd for $C_{20}H_{35}O_2Br$: C, 62.00; H, 9.11%).

Acetylation of Aplysin-20. Alpysin-20 (100 mg) was dissolved in a solution of acetic anhydride and pyridine (1:1; 1 m*l*). The reaction solution was allowed to stand at room temperature overnight, and then the unreacted reagent was removed under reduced pressure to give a white solid. Recrystallizaton from methanol afforded colorless crystals of monoacetate (75 mg); mp 59—62°C; *m/e* 430 and 428 (0.4) (M^+), 370 (13), 368 (13), 352 (7), 350 (7), 312 (5), 310 (5), 289 (16) (M^+–Br), 272 (10), 271 (10), 270 (10), 257 (4), 255 (4), 191 (37), 175 (10), 152 (15), 149 (18), 147 (10), 137 (11), 135(23), 134 (16), 133 (10), 123 (19), 121 (20), 119 (15), 118 (17), 109 (26), 107 (23), 105 (11), 99 (13), 98 (15), 97 (10), 95 (41), 94 (10), 93 (23), 84 (15), 83 (12), 82 (12), 81 (50), 79 (14), 71 (37), 69 (68), 68 (12), 67 (20), 57 (17), 55 (39), 43 (100, base peak) and 41 (53); ν_{max} 3520, 1730 sh, 1713, 1675 and 1260 cm^{-1}; δ0.97 (3H, s), 1.00 (3H, s), 1.10 (3H, s), 1.13 (3H, s), 1.30—2.30 (15 H, br.m), 1.66 (3H, br. s), 2.02 (3H, s), 3.75 (1H, br.), 4.60 (2H, d, J=7.0 Hz) and 5.60 ppm (1H, t, J=7.0Hz) (Found: C, 61.20; H, 8.50%. Calcd for $C_{22}H_{37}O_3Br$: C, 61.53; H, 8.68%).

Hydrolysis of the Monoacetate. A solution of the monoacetate (30 mg) in 2N methanolic potassium hydroxide (2 m*l*) was stirred at room temperature for 2hr, poured into a large amount of water, and then extracted with ether. The ethereal solution was washed well with a saturated NaCl solution and dried over anhydrous sodium sulfate. The solvent was removed under reduced pressure to give a crystalline solid (20 mg), which was then recrystallized from methanol to afford colorless needles of aplycin-20 (mp and IR spectrum).

The authors wish to express their thanks to Professor Minoru Yamada, Hokkaido University, for providing us with the *Aplysia kurodai*, and also to Professor Yoshiyuki Toyama, formerly of Nagoya University, for his suggestions.

10) Aplysin-20 was used directly for the X-ray analysis.

BULLETIN OF THE CHEMICAL SOCIETY OF JAPAN, VOL. 44, 2562—2563(1971)

The Mercury-Photosensitized Reaction of Cyclooctene Vapor

Setsuo TAKAMUKU, Kazuyoshi MORITSUGU, and Hiroshi SAKURAI
The Institute of Scientific and Industrial Research, Osaka University, Suita, Osaka

(Received April 12, 1971)

In connection with the studies of the photoelimination of ethylene from cyclooctadienes,[1] we have examined the mercury-photosensitized reaction of cyclooctene and found a unique isomerization into bicyclic compounds, along with the elimination of ethylene. Cyclooctene vapor (99.5%, glc) was irradiated with a low-pressure mercury lamp in the presence of mercury vapor at room temperature. The photolysis products observed were hydrogen, ethylene, 1,5-hexadiene, 1,7-octadiene (I), bicyclo[4.2.0]octane (II), bicyclo[3.3.0]-octane (III), and cyclooctane. Of these products, I, II, and III were isolated by glc (PEG 6000, 80°C) and were identified by a comparison of the NMR, mass spectra, and glc with those of authentic samples which has been independently synthesized (II and III)[2,3] or obtained commercially I[(I)NMR(CCl_4 solution): τ 4.2 (2H, m), 5.0 (2H, m), 5.2 (2H, m), 8.0 (4H, m), and 8.6 (4H, m); mass spectrum; parent peak at *m/e* 110; (II) NMR: τ 7.7 (2H, m), *ca.* 8.2 (4H, m) and 8.5(8H, m), no peaks at τ less than 7.5; mass spectrum: important peaks at *m/e* 110, 82, 81, 67, 54, and 41; (III)NMR: τ 7.6 (2H, m) and *ca.* 8.5 (12H, m), and no peaks at τ less than 7.4; mass spectrum: important peaks at *m/e* 110, 82, 67, 54, and 41]. The product yields are shown in Table 1, together with the effects of added radical scavengers.

Because of the diversity of the photolysis products, several different mechanistic pathways should be considered. Scheme 1 for the formation of ethylene, 1,5-hexadiene, and I may be suggested from the observa-

1) S. Takamuku and H. Sakurai, *J. Phys. Chem.*, **73**, 1171 (1969); S. Takamuku, M. Utsunomiya, and H. Sakurai, *Chem. Commun.*, **1969**, 173; S. Takamuku and H. Sakurai, This Bulletin, **44**, 569 (1971).

2) W. G. Dauben and R. L. Cargill, *J. Org. Chem.*, **27**, 1910 (1962); R. Srinivasan, *J. Amer. Chem. Soc.*, **84**, 4141 (1962).

3) P. R. Stapp and R. F. Kleinschmidt, *J. Org. Chem.*, **30**, 3006 (1965).

Table 1. Mercury-photosensitized reaction of cyclooctene vapor (Cyclooctene 3.9 mmHg; Mercury *ca.* 0.5 g; 5 min; 100 m*l* quartz cell)

Product	None	NO[a]	O_2[b]	C_2H_4[b]
		μmol		
H_2	0.10	c)	c)	c)
C_2H_4	0.11	c)	c)	c)
	0.10	0.09	0.09	0.10
(I)	0.97	0.89	0.69	1.13
(II)	0.98	0.95	0.62	0.90
(III)	0.17	0.18	0.10	0.12
	0.44	0.36	0.21	0.20

a) 5 mol% added, b) 10 mol% added, c) not determined

tions that (i) the products other than cyclooctane were not appreciably affected by the addition of several kinds of radical scavengers (though oxygen affects the formation of almost all products, this effect may be caused by the quenching of triplet cyclooctene), and (ii) the yields of ethylene and 1,5-hexadiene were equal within the limits of experimental error:

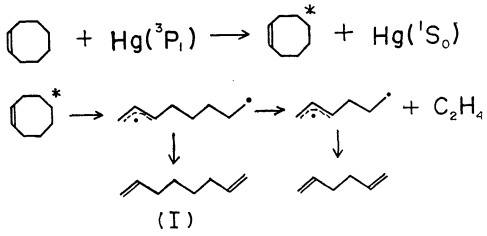

Scheme 1

In Scheme 1, a diradical intermediate, which is produced by the familiar allylic C–C bond cleavage, may undergo unimolecular isomerization to I or further C–C bond cleavage, yielding ethylene and a new diradical resulting in a similar isomerization to 1,5-hexadiene. Such an allylic diradical intermediate has been widely proposed in the mercury-photosensitized reaction of cyclopentene,[4] cyclohexene,[5] cycloheptene,[5] where the ring closure to the respective vinylcycloalkanes has been observed as one of the typical reactions of the intermediate. The yield of vinylcyclohexane expected from the intermediate was very low in the present photolysis of cyclooctene. Thus, the allylic diradical intermediate seems to show different reactivities depending on the vibrational excess energy or the molecular structure.

On the other hand, the most reasonable pathway for the formation of bicyclic compounds (II and III) is presumed to be the hydrogen transfer from an appropriate methylene group to the olefinic double bond with subsequent or simultaneous C–C bond formation. The transannular hydrogen abstraction from C-5 methylene *via* six- (1,5-shift) or five-center (1,4-shift) processes, leading to the formation of II or III through the respective diradical intermediates, is given below:

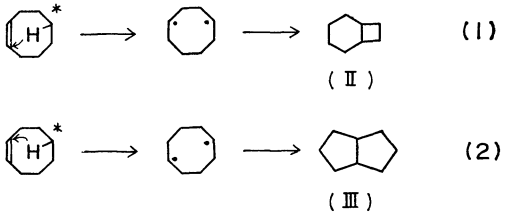

Though the mechanistic details, whether concerted or step-by-step, are not clear, the larger yield of II compared with that of III shows a preference for 1,5-hydrogen transfer *via* a six-center process over other hydrogen transfers.

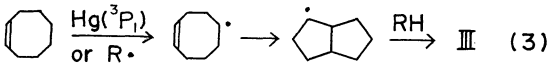

An alternate diradical process (3), which is presumed by an analogy with a free radical transannular cycloaddition to 1,5-cyclooctadiene, thus forming bicyclo[3.3.0]octane derivatives,[6] may be ruled out on the basis of the experiments with radical scavengers.

4) W. A. Gibbons, W. F. Allen, and H. E. Gunning, *Can. J. Chem.*, **40**, 568 (1962).
5) G. R. DeMare, O. P. Strausz, and H. E. Gunning, *ibid.*, **43**, 1329 (1965).
6) R. Dowbenko, *Tetrahedron*, **20**, 1843 (1964).

BULLETIN OF THE CHEMICAL SOCIETY OF JAPAN, VOL. 44, 2564—2565(1971)

The Charge-transfer Complexes of Metal Chelates of 8-Quinolinol with Various Halogen-substituted *p*-Benzoquinones

Yôichi IIDA

Department of Chemistry, Faculty of Science, Hokkaido University, Sapporo

(Received April 23, 1971)

Much attention has been paid to a large number of charge-transfer complexes made from electron donors and acceptors.[1] However, there are few donor molecules that are known to be composed of organic metal chelates. In 1965 the charge-transfer complexes of 8-quinolinol and its copper, palladium, and nickel chelates with *p*-chloranil were first prepared by Bailey *et al.*[2] Recently, we have reported that bis(8-quinolinolato)palladium(II), ($Pd(Ox)_2$), and bis(8-quinolinolato)copper(II), ($Cu(Ox)_2$), form stable crystalline (1:1) charge-transfer complexes with 2,5-diazido-3,6-dichloro-1,4-benzoquinone and 2,5-diazido-3,6-dibromo-1,4-benzoquinone.[3]

In the present work, we found that $Pd(Ox)_2$ and $Cu(Ox)_2$ can also form stable crystalline (1:1) charge-transfer complexes with various halogen-substituted *p*-benzoquinones. Measurements of the diffuse reflection spectra of these solid complexes were attempted in order to study the charge-transfer interaction between the metal chelates of 8-quinolinol and the halogen-substituted *p*-benzoquinones.

The following crystalline complexes were prepared according to a method similar to that described by Bailey *et al.*[2]: $Pd(Ox)_2$-*p*-Bromanil, $Pd(Ox)_2$-*p*-Iodanil, $Pd(Ox)_2$-*p*-QBr_2Cl_2,[4] $Pd(Ox)_2$-*p*-QBr_3Cl,[4] $Cu(Ox)_2$-*p*-Bromanil, $Cu(Ox)_2$-*p*-Iodanil, $Cu(Ox)_2$-*p*-QBr_2Cl_2, and $Cu(Ox)_2$-*p*-QBr_3Cl. The complexes were pulverized and diluted with potassium bromide. The diffuse reflection spectra of these complexes were recorded as the difference in the reflectance between the mixture and pure potassium bromide, as determined by means of a Beckman DK-2A spectroreflectometer. The solid-state spectra were then obtained by plotting the diffuse reflection spectra using the Kubelka-Munk equation, $f(R)=(1-R)^2/2R$, in which R is the reflectance.

The $Pd(Ox)_2$ Complexes

The solid-state spectrum of the $Pd(Ox)_2$-*p*-Bromanil complex (Fig. 1, Curve a) shows the band peaks at 14.6 kK and 23.5 kK and a shoulder around 29 kK. The band at 23.5 kK and the shoulder arise from the absorptions due to the component molecules, while the band at 14.6 kK appears in the low-energy region, where neither of the component molecules are absorbed. The value for this low-energy band was found to be close to that for the band of the $Pd(Ox)_2$-*p*-Chloranil complex at 14.8 kK, which Bailey *et al.* assigned to the charge-transfer transition from $Pd(Ox)_2$ to *p*-chloranil. Therefore, the band at 14.6 kK for the $Pd(Ox)_2$-*p*-Bromanil complex is also attributable to the charge-transfer transition from $Pd(Ox)_2$ to *p*-bromanil. These results seem to indicate that the electron affinity for *p*-bromanil is almost the same as that for *p*-chloranil. Since the molecular sizes and the shapes of these acceptors are almost identical, the crystal structure of the $Pd(Ox)_2$-*p*-Bromanil complex may be similar to that of the $Pd(Ox)_2$-*p*-Chloranil complex determined by Kamenar *et al.*[5]

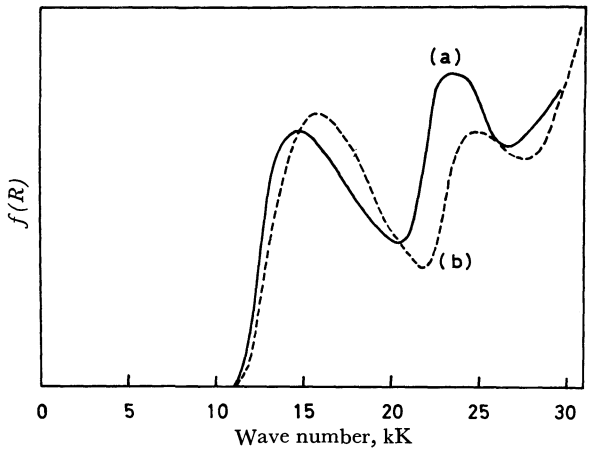

Fig. 1. The solid-state spectra of (a) $Pd(Ox)_2$-*p*-Bromanil and (b) $Cu(Ox)_2$-*p*-Bromanil.

The spectroscopic features for the complexes of $Pd(Ox)_2$ with the other halogen-substituted *p*-benzoquinones are quite analogous to that for the $Pd(Ox)_2$-*p*-

TABLE 1. THE SPECTROSCOPIC DATA ON THE MAXIMUM POSITIONS OF THE CHARGE-TRANSFER BANDS
(in unit of 10^3 cm^{-1})

Acceptor	$Pd(Ox)_2$	$Cu(Ox)_2$
p-Chloranil	14.8[a]	15.9[a]
p-Bromanil	14.6	15.9
p-Iodanil	14.3	15.7
p-QBr_2Cl_2	14.8	16.0
p-QBr_3Cl	14.8	16.0

a) Ref. 2.

1) G. Briegleb, "Elektronen-Donator-Acceptor Komplexe," Springer-Verlag, Berlin-Göttingen-Heidelberg (1961).

2) A. S. Bailey, R. J. P. Williams, and J. D. Wright, *J. Chem. Soc.*, **1965**, 2579.

3) S. Koizumi and Y. Iida, This Bulletin, **44**, 1436 (1971).

4) 2,5-Dibromo-3,6-dichloro-1,4-benzoquinone and tribromomonochloro-*p*-benzoquinone are abbreviated as *p*-QBr_2Cl_2 and *p*-QBr_3Cl respectively.

5) The crystal structure of the $Pd(Ox)_2$-*p*-Chloranil complex has a triclinic symmetry. The planar $Pd(Ox)_2$ and *p*-chloranil molecules, which are alternately stacked, are arranged in planes approximately parallel to the crystallographic (111) plane. See B. Kamenar, C. K. Prout, and J. D. Wright, *J. Chem. Soc.*, **1965**, 4851.

Bromanil complex or for the $Pd(Ox)_2$-*p*-Chloranil complex. The energy values for the charge-transfer bands of the complexes are collected in Table 1. Table 1 shows that the charge-transfer-band positions for the $Pd(Ox)_2$ complexes, practically, do not depend on the acceptors now under investigation. This means that the electron affinities of these halogen-substituted *p*-benzoquinones are very similar to one another.

The $Cu(Ox)_2$ Complexes

The solid-state spectrum of the $Cu(Ox)_2$-*p*-Bromanil complex (Fig. 1, Curve b) shows the band peaks at 15.9 kK and 25.0 kK, and a shoulder around 30 kK. The low-energy band at 15.9 kK can also be assigned to the charge-transfer transition from $Cu(Ox)_2$ to *p*-bromanil; this energy value was found to be in good coincidence with the value for the $Cu(Ox)_2$-*p*-Chloranil complex (15.9 kK).[2] However, we can see that the charge-transfer energy for the $Cu(Ox)_2$-*p*-Bromanil complex is larger than that for the $Pd(Ox)_2$-*p*-Bromanil complex by 1.3 kK. For a common acceptor, the variation in the charge-transfer energy arises mostly from the difference in the ionization potentials of the donor molecules. Therefore, it seems that the ionization potential of $Cu(Ox)_2$ is higher than that of $Pd(Ox)_2$ by about 1.3 kK.

The spectroscopic features of the complexes of $Cu(Ox)_2$ with the other halogen-substituted *p*-benzoquinones are found to be quite similar to those of the $Cu(Ox)_2$-*p*-Bromanil complex. The charge-transfer bands of the complexes are given in Table 1.

Discussion

The solid-state spectra clearly indicate that the ionization potential of a metal chelate of 8-quinolinol is much affected by the species of the central metal ion. The ionization potential of $Cu(Ox)_2$ is appreciably larger than that of $Pd(Ox)_2$. For the above four acceptors, the magnitude of this difference is estimated to be 1.3 ± 0.2 kK (0.16 ± 0.025 eV).

Bailey *et al.* examined the charge-transfer complexes of $Cu(Ox)_2$, $Pd(Ox)_2$ and various aromatic hydrocarbons with common acceptors and compared their charge-transfer energies.[2] By the use of the relationship between the charge-transfer-band energies and the ionization potentials of the donors, they proposed that the values for the ionization potentials of $Cu(Ox)_2$ and $Pd(Ox)_2$ were 7.3 eV and 7.1 eV respectively.[2] The difference in the ionization potentials between $Cu(Ox)_2$ and $Pd(Ox)_2$ is 0.2 eV, which is in good agreement with the value determined by the present investigation.

BULLETIN OF THE CHEMICAL SOCIETY OF JAPAN, VOL. 44, 2565—2566 (1971)

A Remark on the Applicability of the CNDO Calculation to the Chemical Reactivity Theory

Hiroshi FUJIMOTO, Shoichi SUGIHARA, Shinichi YAMABE, and Kenichi FUKUI

Faculty of Engineering, Kyoto University, Sakyo-ku, Kyoto

(Received April 23, 1971)

The usefulness of the CNDO calculation for the interpretation of the chemical and physical properties of organic molecules has been verified in numerous cases.[1] The extended Hückel MO method gave good results with respect to the calculation of the chemical reactivity index, the frontier electron density, of hydrogens in the E2 reaction of some halogenated hydrocarbons, in the base-catalyzed allylic rearrangement of some olefins, and in the halogenation of norbornane.[2-4] It has been reported, however, that the extended Hückel MO method sometimes fails to give satisfactory results when it is applied to a molecule containing polar bonds.[5] The discrepancy may partly be attributed to the unreasonable parametrizations due to the ambiguity of the physical meaning of the one-electron Hamiltonian operator in this method.[6] Hence, it may be expected that the CNDO method can be a convenient means for discussing the chemical reactivity of sizable molecules, since the electron populations are smoothed out by the self-consistent-field iteration procedure. The purpose of this note is to present the results of our CNDO calculation of the chemical reactivity of the hydrogens of some substituted and unsubstituted hydrocarbons. The method of calculation is CNDO/2, using the integrals given in the literature.[1]

Chemical Reactivity of Hydrogens toward Nucleophilic Abstraction. The frontier electron density of a hydrogen for nucleophilic reactions is defined by;[7]

$$f_r^{(N)} = 2(C_r^{(LU)})^2$$

1) J. A. Pople and D. L. Beveridge, "Approximate Molecular Orbital Theory," McGraw-Hill, New York (1970).

2) a) K. Fukui and H. Fujimoto, *Tetrahedron Lett.*, **1965**, 4303. b) K. Fukui, H. Hao, and H. Fujimoto, This Bulletin, **42**, 348 (1969).

3) H. Fujimoto, H. Oba, and K. Fukui, *Nippon Kagaku Zasshi*, **90**, 1005 (1969).

4) H. Fujimoto and K. Fukui, *Tetrahedron Lett.*, **1966**, 5551.

5) See, for instance, M. J. S. Dewar, "The Molecular Orbital Theory of Organic Chemistry," McGraw-Hill, New York (1969).

6) K. Fukui and H. Fujimoto, This Bulletin, **40**, 2787 (1967).

7) K. Fukui, T. Yonezawa, C. Nagata, and H. Shingu, *J. Chem. Phys.*, **22**, 1433 (1954).

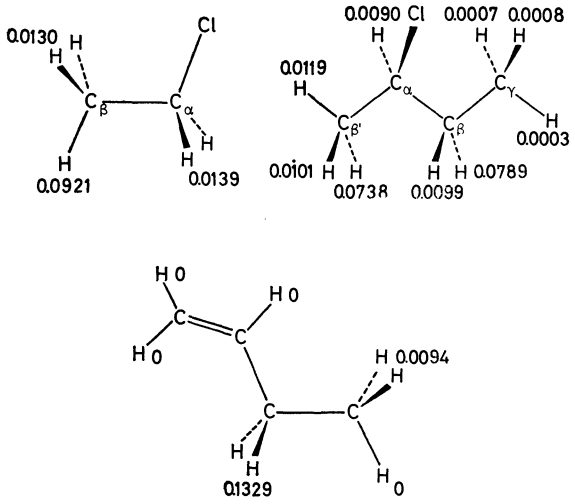

Fig. 1. Frontier electron densities of hydrogens toward nucleophilic abstraction.

where $C_r^{(LU)}$ is the coefficient of the hydrogen, 1s AO r, in the lowest unoccupied (LU) MO. Figure 1 shows that β-hydrogens of ethyl chloride and 2-chlorobutane which are located *trans* to chlorine are most reactive toward the attacking nucleophile, while, in the case of butene-2, the allylic hydrogens have the largest frontier electron density, which is in accordance with the experimental results.[8,9]

Chemical Reactivity of Hydrogens toward Homolytic Abstraction. The frontier electron density of a hydrogen for homolytic reactions is defined by;

$$f_r^{(R)} = (C_r^{(HO)})^2 + (C_r^{(LU)})^2$$

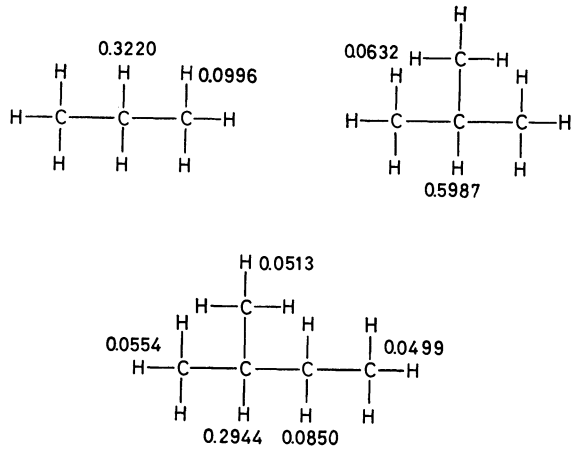

Fig. 2. Frontier electron densities of hydrogens toward homolytic abstraction.

where HO implies the highest occupied MO. Figure 2 shows the $f_r^{(R)}$ values of hydrogens in propane, isobutane, and isopentane. The values indicate the averages with respect to three hydrogens of primary carbons and two hydrogens of secondary carbons. The frontier electron densities decrease in this order:

$$\text{tertiary} > \text{secondary} > \text{primary}$$

showing a good agreement with the well-established experimental results.[10]

In some unfortunate cases, the MO levels calculated by the CNDO method may happen to be in an unrealistic order. The present results suggest, however, that the chemical reactivity index, the frontier electron density, obtained from the CNDO MO wave function can be a suitable measure for an intramolecular comparison of the chemical reactivities in a variety of organic compounds.

8) See, for instance, E. S. Gould, "Mechanism and Structure in Organic Chemistry," Holt, Reinhart and Winston, New York (1959) p. 472.

9) a) A. Schriesheim, R. J. Muller, and C. A. Rowe, Jr., *J. Amer. Chem. Soc.*, **84**, 3164 (1962). b) S. Bank, C. A. Rowe, Jr., and A. Schriesheim, *ibid.*, **85**, 2115 (1963).

10) See Ref. 8, p. 695.

SHORT COMMUNICATIONS

Friedelin and Related Compounds. Part XI.[1] Identification of a Saturated Nor-Aldehyde from Ultraviolet Irradiation of Friedelin

Robert STEVENSON, Takahiko TSUYUKI, Reiko AOYAGI,* and Takeyoshi TAKAHASHI*

Department of Chemistry, Brandeis University, Waltham, Massachusetts, U.S.A.

** Department of Chemistry, Faculty of Science, The University of Tokyo, Hongo, Bunkyo-ku, Tokyo*

(Received May 7, 1971)

In previous works,[2,3] it was reported that the ultraviolet irradiation of friedelin (I) in diethyl ether solution yields a mixture of hydrocarbons, an unidentified aldehyde, ketones,[4,5] and hydroxycarbonyl compounds.

In this communication, we present evidence that the aldehyde has the structure 5α-ethyl-10β-formylmethyl-des-A-friedelane (II). Isolation of a *saturated nor*-secoaldehyde by photochemical degradation of a cyclic ketone is apparently unprecedented.

A solution of friedelin (1.0 g) in diethyl ether (1 *l*) was irradiated at room temperature under a nitrogen atmosphere for 2.25 hr with a high pressure quartz mercury vapour lamp (Hanovia 8A-36). This procedure was repeated and the combined residue, after solvent removal, was chromatographed on silica gel (300 g, Merck). The crude aldehyde fraction (84 mg) was then purified by further chromatography on alumina (Woelm, neutral, 15 g, then repeated on 20 g), and then crystallized from ether to give 5α-*ethyl*-10β-*formylmethyl-des*-A-*friedelane* (II) as needles (18 mg), mp 182°C. The empirical formula, $C_{29}H_{50}O$, was confirmed by mass spectrum determination (*m/e*, relative intensity %): 414 (65%, M^+), 399 (29, M−15), 386 (21, M–28; aldehyde), 385 (8, M–29), 371 (10, M–43; loss of $-CH_2CHO$), 358 (8, M–56; 3,4-seco-friedelane), 273 (69), 261 (18), and 205 (100). Other analytical and spectroscopic data were as previously reported.[3]

The proposed structure(II) was confirmed by comparison (IR, NMR, mass spectrum, analytical TLC) with a specimen, mp 181—181.5°C, prepared by catalytic hydrogenation (palladium-carbon, ethanol) of 5α-vinyl-10β-formylmethyl-des-A-friedelane (IV) produced

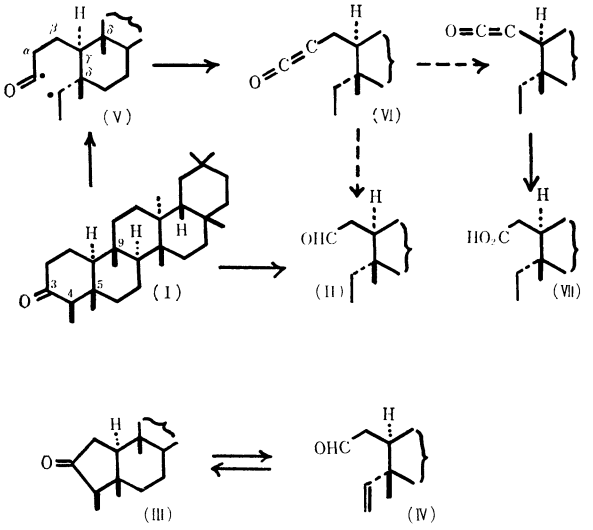

by photo-irradiation of *nor*-friedelin (III) in hexane.[6]

The pathway for the well-documented photo-cleavage of cyclohexanones to yield δ-*unsaturated* aldehydes by α-cleavage followed by transfer of a hydrogen atom from a δ-carbon atom (six-membered transition state) is unavailable for friedelin (quaternary C-5 and C-9). It seems probable, consequently, that the initial di-radical species (V) is stabilized by hydrogen transfer from C-2 to the alkyl radical (six-membered transition state) to yield the ketene (VI) which undergoes the unusual degradation to the *nor*-seco aldehyde (II). It is of interest, in this connexion, that a *nor*-seco carboxylic acid (VII) was identified as a product of irradiation of friedelin in hexane.[7] Experiments aimed at elucidation of the mechanism of formation of II and VII are in progress.[8]

1) Part X. Ref. 2.
2) F. Kohen and R. Stevenson, *Chem. Ind.* (London), **1966**, 1844.
3) F. Kohen, A. S. Samson, and R. Stevenson, *J. Org. Chem.*, **34**, 1355 (1969).
4) T. Tsuyuki, S. Yamada, and T. Takahashi, This Bulletin, **41**, 511 (1968).
5) T. Tsuyuki, R. Aoyagi, S. Yamada, and T. Takahashi, *Tetrahedron Lett.*, **1968**, 5263.
6) R. Aoyagi, T. Tsuyuki, and T. Takahashi, This Bulletin, **43**, 3967 (1970).
7) M. Takai, R. Aoyagi, S. Yamada, T. Tsuyuki, and T. Takahashi,This Bulletin, **43**, 972 (1970).
8) In this connexion, it is significant that the saturated nor-aldehyde (II) is *not* detected on similar irradiation of nor-friedelin (III).

Molecular-weight Determination by the Vapor-pressure-Depression Method using Gas Chromatography[1)]

Yozaburo Yoshikawa, Kimiko Arita, Akira Inaba, and Kiyoko Sasaki
Institute of Chemistry, College of General Education, Osaka University, Machikaneyama Toyonaka
(Received May 10, 1971)

The molecular-weight-determination method based on the principle of vapor-pressure depression has not been widely utilized because of the difficulty of measuring precisely small differences in the vapor pressure.

Now, however, we have been able to measure conveniently the degree of vapor-pressure depression of the solution by means of gas chromatography and determine the molecular weight of the solute within an error of 3%.

The method and the obtained results will be reported here.

According to Raoult's law, the degree of the depression of the solvent vapor in a dilute solution is equal to the mole fraction of the solute. The next equation is thus obtained:

$$(p^\circ - p)/p^\circ = n/(N+n) \qquad (1)$$

p°= vapor pressure of a pure solvent
p= vapor pressure of the solvent in the solution
n= mole number of the solute dissolved in N mol of the solvent

When w grams of a solute is dissolved in W grams of a solvent with a molecular weight of M, the term of $(p^\circ-p)/p^\circ$ can be calculated from the peak height of the chromatograms of the pure solvent (h°) and the solvent in the solution (h).

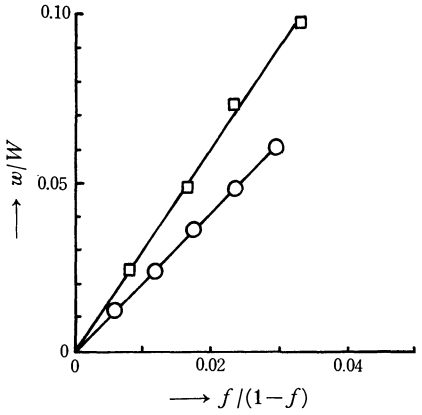

Fig. 1. Relation of molality and depression degree of vapor pressure of benzoic acid in acetone and benzene solution.
○ Benzoic acid in acetone solution
□ Benzoic acid in benzene solution

1) A part of this work was presented at the 23 rd Annual Meeting of the Chemical Society of Japan, Tokyo, April, 1970.

Table 1. Molecular weight data determined by vapor pressure depression method

Solute	Solvent	Experimental value	Theoretical value	Error (%)
Naphthalene	Acetone	128.52	128.17	0.27
	Benzene	127.58		0.46
	Carbon tetrachloride	128.66		0.38
	Ethyl alcohol	130.94		2.16
Benzoic acid	Acetone	123.42	122.12	1.06
	Benzene	236.85*	*dimer 244.24	3.03
	Carbon tetrachloride	234.78*		3.87
	Ethyl alcohol	125.65		2.89
Dipyridin-coppernitrate	Acetone	344.18	345.76	0.46
Benzene	Toluene	79.65	78.11	1.97
n-Hexane	*n*-Heptane	86.39	86.18	0.24
Carbon tetrachloride	Toluene	155.62	153.82	1.17

Hence, the molecular weight of the solute, m, is obtained using this equation:

$$m = w \cdot M/W[1-(h^\circ-h)/h^\circ \,/\, (h^\circ-h)/h^\circ] \qquad (2)$$

Equation (2) can then be transformed to the next equation when $(h^\circ-h)/h^\circ$ is represented as f:

$$m/M = w/W\,/f/(1-f) \qquad (2)'$$

In Fig. 1, the concentration of each solution (w/W) *vs.* $f/(1-f)$ is plotted. From this slope ($=m/M$) of the plot, the molecular weight of the solute can be calculated.

The obtained results are shown in Table 1.

In this experiment, the vapor of a pure solvent or solution was saturated in a glass flask at a constant temperature slightly lower than room temperature. A Teflon stopper was used for this flask. A glass syringe and a stainless-steel pipe were attached to this stopper; the fromer was used for pushing out the sample gas in the flask, while the latter was used for introducing the sample vapor to the gas sampler of the gas chromatograph.

The concentration of the solution used was higher than 0.05 molality. Now, an experiment on the solution of less than 0.05 molality is in progress.

The Facile Reduction of Acyl Halides into Aldehydes *via* Acylcarbonylferrates

Yoshihisa WATANABE, Take-aki MITSUDO, Masato TANAKA, Kazuo YAMAMOTO, Toshiharu OKAJIMA, and Yoshinobu TAKEGAMI

Department of Hydrocarbon Chemistry, Faculty of Engineering, Kyoto University, Sakyo-ku, Kyoto

(Received June 11, 1971)

Previously, we reported that alkyl halides such as *n*-propyl iodide[1] and ethyl α- or β-bromopropionate[2] react with an ethanolic solution of tetracarbonylferrate, $Fe(CO)_4^{2-}$, with the absorption of carbon monoxide, to give a mixture of the corresponding carbonylated products, ethyl *n*-butyrate and *n*-butyraldehyde, and diethyl succinate and diethyl methylmalonate, respectively.

Recently, Cooke carried out an analogous reaction in tetrahydrofuran (THF) in the presence of triphenylphosphine; quenching it with acetic acid, he found that alkyl bromides are carbonylated to the corresponding aldehydes in high yields.[3] In these reactions, it can reasonably be considered that acylcarbonylferrate complexes are formed as the reaction intermediates.[1-3]

In this communication, we wish to report a facile reduction of acyl halides into aldehydes, which is considered to proceed *via* acyltetracarbonylferrates.

Acyl halides react with an equivalent mole of $Na_2Fe(CO)_4$ in THF at 0—60°C to give, after quenching with acetic acid, the corresponding aldehydes in high yields. This fact strongly suggests that sodium acyltetracarbonylferrates (I)[4] are directly formed in high yields by the nucleophilic attack of $Fe(CO)_4^{2-}$ on the acyl carbon atom. Some results of typical reactions are shown in Table 1.

$$R-\underset{\underset{O}{\|}}{C}-Cl + Na_2Fe(CO)_4 \rightarrow \underset{(I)}{Na^+[Fe(CO)_4COR]^-} + Na^+Cl^-$$

$$(I) + AcOH \rightarrow R-\underset{\underset{O}{\|}}{C}-H$$

The reduction of benzoyl chloride to benzaldehyde illustrates a typical procedure. A THF solution of $Na_2Fe(CO)_4$[3,5] (7.3 mmol) was prepared by adding, drop by drop, 1.0 m*l* of $Fe(CO)_5$ in 25 m*l* of THF to 4 m*l* of a 1% sodium amalgam in 25 m*l* of THF under argon at room temperature. After the amalgam had been removed through a side arm, to this solution was added 0.85 m*l* (7.3 mmol) of benzoyl chloride at 30°C; the mixture was stirred vigorously for 1 hr and then treated with 1.2 m*l* of glacial acetic acid. The mixture was stirred for an additional 5 min, then poured into 50 m*l* of water, and extracted with 20 m*l* of pentane and then 20 m*l* of ethyl ether, after which the organic extracts were submitted to glpc analysis.[6]

Aromatic and aliphatic acyl halides are readily reduced to the corresponding aldehydes in high yields, indicating that the corresponding acyltetracarbonylferrates (I) are formed in high yields and that these complexes are thermally stable in the solution, even in the absence of a stabilizing ligand such as triphenylphosphine.[3] The branched acyl complex, isobutyryltetracarbonylferrate, is also stable in the solution even at 60°C and does not isomerize to the normal acyl complex, in contrast with the branched acylcarbonylcobalt, which isomerizes to *n*-acylcarbonylcobalt.[7]

The high yield of the aldehydes and the facility of the reaction procedures enable us to utilize this reaction instead of the Rosenmund reduction[8] and reduction with $LiAlH(OR)_3$.[9]

The acyltetracarbonylferrate (I) can possibly be utilized as a starting material for further organic syntheses. These reactions will be discussed in the near future.

TABLE 1. THE REDUCTION OF ACYL CHLORIDES TO ALDEHYDES WITH $Na_2Fe(CO)_4$ IN THF

Exp. No.	Acyl chloride	Reaction condition		Product	Yield[a] %
		temp. (°C)	time (hr)		
1	Benzoyl chloride	30	1	Benzaldehyde	95
2	*p*-Chlorobenzoyl chloride	0	1	*p*-Chlorobenzaldehyde	74
3	*o*-Chlorobenzoyl chloride	0	1	*o*-Chlorobenzaldehyde	65
4	*n*-Butyryl chloride	30	1	*n*-Butyraldehyde	75
5	Isobutyryl chloride	60	3	Isobutyraldehyde	71

a) Yield determined by glpc analysis using an appropriate internal standard previously calibrated against an authentic sample of pure aldehyde.

1) Y. Takegami, Y. Watanabe, H. Masada, and I. Kanaya, This Bulletin, **40**, 1456 (1967).
2) H. Masada, M. Mizuno, S. Suga, Y. Watanabe, and Y. Takegami, *ibid.*, **43**, 3824 (1970).
3) M. P. Cooke, Jr., *J. Amer. Chem. Soc.*, **92**, 6080 (1970).
4) The analogous acyltetracarbonylferrates have been obtained as their tetramethylammonium (a) and lithium (a and b) salts. a) E. O. Fischer and V. Kiener, *J. Organometal. Chem.*, **23**, 215 (1970). b) Y. Sawa, M. Ryang, and S. Tsutsumi, *J. Org. Chem.*, **35**, 4182 (1970).
5) V. W. Hieber and G. Braun, *Z. Naturforsch.*, **14b**, 132 (1959).
6) The peak of aldehyde appears only after the reaction mixture is treated with acetic acid, not befor the quenching.
7) Y. Takegami, Y. Watanabe, H. Masada, Y. Okuda, K. Kubo, and C. Yokokawa, This Bulletin, **39**, 1495 (1966) and the references in it.
8) K. W. Rosenmund and F. Zetzsche, *Ber.*, **54**, 425 (1921).
9) D. C. Ayers, B. G. Carpenter, and R. C. Denney, *J. Chem. Soc.*, **1965**, 3578.

Mössbauer Spectroscopic Studies of the Oxidation State of ^{57}Fe produced in ^{57}Co-doped and γ-irradiated Trisacetylacetonatoiron(III)

Hirotoshi SANO, Keiko SATO, and Hiroko IWAGAMI

Department of Chemistry, Faculty of Science, Ochanomizu University, Otsuka, Tokyo

(Received July 2, 1971)

A number of cobalt compounds labelled with ^{57}Co used as Mössbauer sources have shown the presence of one or more "anomalous" charge states. The formation of iron-atom charge states less positive than the charge state of the cobalt atom in the parent compound has been interpreted in terms of the "internal pressure hypothesis" by Hazony and Herber,[1] based on the similarity between the Mössbauer spectra of $Fe(acac)_3$ under a high external pressure[2] and that of a $^{57}Co(acac)_3$ source experiment.[3] This hypothesis has also been supported by the fact that such anomalous charge states were not observed in the IT(IC) decay of ^{119m}Sn in the various tin compounds.[1] We have, however, recently reported experimental evidence for the presence of an "anomalous" charge state in the IT(IC) decay of ^{119m}Sn in $K_6Sn_2(C_2O_4)_7 \cdot 4H_2O$.[4] It is debatable, therefore, whether or not the lattice can generate a high local internal pressure. Here we will describe the Mössbauer spectra of the first excited state of ^{57}Fe produced in a $Fe(acac)_3$ host crystal doped with $^{57}Co(acac)_3$. The Mössbauer spectra of γ-irradiated $Fe(acac)_3$ are also shown for comparison.

An (Fe, ^{57}Co)$(acac)_3$ source was prepared from a solution containing 50 mg of ferric iron and 2 mCi of ^{57}Co by following the method described in Ref. 5. Another source was prepared by the extraction method. Carrier-free 2 mCi $^{57}Co(acac)_3$ was extracted from the aqueous solution into the benzene phase by following the method described in Ref. 6. To the benzene phase were added 50 mg of $Fe(acac)_3$ or $^{56}Fe(acac)_3$ prepared from natural iron or ^{56}Fe-enriched iron, and the benzene solution was filtered. After freezing the filtrate in liquid nitrogen, the frozen solution kept at -15°C was pumped out through a liquid nitrogen trap in order to remove the benzene and the excess acetylacetone. The source was then kept in a cryostat, and the Mössbauer spectra were measured against an ^{57}Fe-enriched stainless-steel absorber moving in a constant acceleration mode at room temperature. All the sources showed the same Mössbauer spectrum. The (Fe, ^{57}Co)$(acac)_3$ source prepared from natural iron was also used as an "absorber" against a 10 mCi ^{57}Co(Pt) source in order to confirm the absence of species other than $Fe(acac)_3$. X-ray diffraction data indicate that the doped sample has the same crystal structure as the host $Fe(acac)_3$ if the content of $Co(acac)_3$ incorporated in $Fe(acac)_3$ is less than 10%.

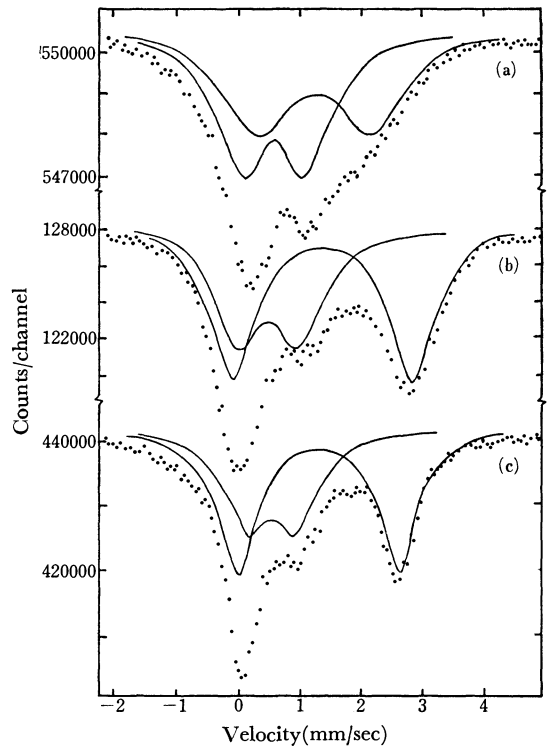

Fig. 1. Mössbauer spectra of (a) (Co, ^{57}Co)$(acac)_3$ source (kept at 78°K) *vs* ^{57}Fe-stainless steel absorber, (b) (^{56}Fe, ^{57}Co)$(acac)_3$ source (kept at 78°K) *vs* ^{57}Fe-stainless steel absorber, and (c) γ-irradiated (10^{10} r) $Fe(acac)_3$ absorber (kept at 78°K) *vs* ^{57}Co(Pt) source. All the velocity scales were normalized with respect to iron.

Typical Mössbauer spectra are shown in Fig. 1. The experiment involving the ^{57}Co(Pt) source and the (Fe, ^{57}Co)$(acac)_3$ "absorber" shows the absence of species other than $Fe(acac)_3$. The experiment using the (Fe, ^{57}Co)$(acac)_3$ source kept at 78°K and a stainless-steel absorber clearly shows the presence of divalent ^{57}Fe species. The experiment using the ^{57}Co (Pt) source and the γ-irradiated $Fe(acac)_3$ absorber kept at 78°K shows the same spectral pattern as that found in the (Fe, ^{57}Co)$(acac)_3$ source experiment.

The results indicate that the divalent ^{57}Fe species are still produced. As ^{57}Co was incorporated into a similar trisacetylacetonatoiron(III) matrix, the "internal-pressure effect" is supposed to be no longer working in the (Fe, ^{57}Co)$(acac)_3$ source. One possible mechanism is auto-radiolysis including an electronic excitation process initiated by the Auger effect. The latter would be followed by the decomposition of the acetylacetonate ligands to various fragments, such as carbon monoxide, carbon dioxide, methane, ethane, and hydrogen, which were detected in the gas chromatography of the γ-irradiated $Fe(acac)_3$.

1) Y. Hazony, R. H. Herber, *J. Inorg. Nucl. Chem.*, **31**, 321 (1969).
2) A. R. Champion, R. W. Vaughan, H. G. Drickamer, *J. Chem. Phys.*, **47**, 2583 (1967).
3) G. K. Wertheim, W. R. Kingston, R. H. Herber, *ibid.*, **37**, 687 (1962).
4) H. Sano, M. Kanno, *Chem. Commun.*, **1969**, 601.
5) G. Urbain, A. Debierne, *Compt. rend.*, **129**, 302, 303(1899).
6) G. H. Morrison, H. Freiser, "Solvent Extraction in Analytical Chemistry", John Wiley, New York (1957), p. 202.

COMMENTS

Explosion during the Preparation of Ethylphenyl Thallic Acetate Perchlorate

Sakae UEMURA, Yoshihiro IKEDA,* Osamu ITOH,* and Katsuhiko ICHIKAWA*

Institute for Chemical Research, Kyoto University, Uji, Kyoto

**Department of Hydrocarbon Chemistry, Faculty of Engineering, Kyoto University, Yoshida, Kyoto*

(Received June 3, 1971)

We have reported a method of preparing arylthallic acetate perchlorate monohydrates[1] ($RC_6H_4TlOAc\text{-}ClO_4\cdot H_2O$), with the syntheses of phenyl, tolyl, three isomeric xylyl, and anisyl derivatives. On applying this method to the preparation of ethylphenyl derivative, a violent explosion occurred in the last stage of concentration of the reaction mixture carried out with a rotary vacuum evaporator. The procedure was as follows. Into acetic acid (180 m*l*) containing $Tl(OAc)_3$ (45 g), 70% $HClO_4$ (18 g), and then ethylbenzene (25 g) were added at 65°C under stirring. After 5 hr the precipitated thallium(I) salts (*ca.* 5 g) were filtered off and the solvent in the filtrate was evaporated slowly at *ca.* 60°C in a vacuum with a rotary vacuum evaporator to give *ca.* 30 m*l* of white pasty residue. Soon after evaporation was stopped, a violent explosion occurred.

Before this experiment, two runs of the same reaction were carried out safely to give the expected product in 14.7% yield and a trace amount. About 150 runs of preparative experiments were carried out without any trouble. However, care should be taken during the process of evaporating the solvent and too much evaporation should be avoided.

We would like to add the following remark with respect to the handling of perchloric acid. When one drop of 70% perchloric acid was added to 10 m*l* of dimethylsulfoxide (DMSO) at room temperature, a violent explosion occurred. Reactions in DMSO with perchloric acid should be avoided.

1) K. Ichikawa, S. Uemura, E. Uegaki, and T. Nakano, This Bulletin, **44**, 545 (1971).

Photoconduction of Polystyrylpyrimidines

Ryo HIROHASHI, Yasushi HISHIKI, and Masahiro HARUTA
Faculty of Engineering, Chiba University, Yayoi-cho, Chiba

(Received August 14, 1970)

Eight polystyrylpyrimidines were synthesized from *p*-xylylpyrimidine with *p*-phenylene diisothiocyanate (DIT), terephthaloylchloride (TPC), *p*-xylylenedibromide (XDB), *p*-phenylenediamine (PDA), 4,4'-diaminodiphenyl (BD), 4,4'-diamino diphenylsulfone (DPS), hexamethylene diamine (HMD), and 4,4'-diaminodiphenylmethane (DPM). These polymer films have a fairly large photoconductive character; using a surface-type photoconductive cell, the logarithmic relation of the photo-current (I_p) to the applied potential was found to be linear. Further, it was found that the slopes (n) obtained from the logarithmic relation ($I_p=kL^n$) of the photocurrent to the light intensity (L) have values from 1.0 to 2.4. The peaks of the spectral response of the photocurrent of the eight samples exit around 500—600 mμ and/or near the ultraviolet wavelength region. The photoconduction of these polymers was enhanced by the bridging groups attached to xylylpyrimidine; the enhancement is in the following order;

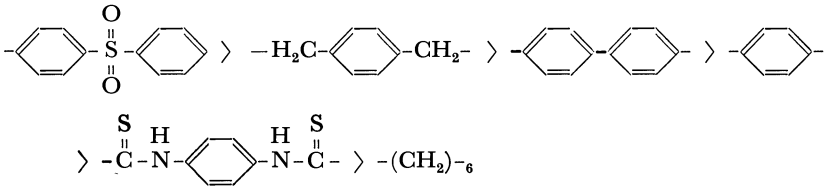

These have in recent years been a large number of reports on the photoconduction of polycyclic aromatics and also of polymers.[1] However, scarcely systematic research on the relation between the photoconduction and the chemical structure has been carried out.[2]

It was been widely noted that polyvinylcarbazole shows quite a large photoresponse, one which is influenced by sensitizers.[3] The cause of this photoresponse is assumed to be that polyvinylcarbazole has a large side group which shows an energy transfer by means of dipole-dipole resonance between carbazole molecules.[4] As other organic photoconductive materials, polystyrene,[5] polyvinylacridine,[6] and polyhalogenated vinyl,[7] and so on have been investigated. However, the photoconduction of the polymer containing a hetero-ring in the main chain has not yet been investigated.

Recently, many sorts of electrophotographic techniques have been developed. The main requirements for good electrophotographic materials are as follows; the ratio between the photoconductivity and the dark conductivity should be large, and the spectral response of the photoconduction should cover a wide visible and ultraviolet wavelength region. If the relation between the molecular structure and the photoconductive character could be find, materials suitable for electrophotographic printing could be prepared.

In this report, we will describe the variation in the photoconductive characters of eight sorts of polystyrylpyrimidines as a function of the molecular structure.

Experimental

1. Synthesis of the Polymers. The polycondensations of *p*-xylylpyrimidine (1.00×10^{-2} mol) with various diamines (1.00×10^{-2} mol) were carried out for 5—10 hr 100 m*l* three-necked flask equipped with a stirrer, a nitrogen gas inlet, and a calcium chloride drying tube at 150°C. Inorganic catalysts were not used, since inorganic impurities obviously affect their electrical properties. Triethylamine (5 wt% for monomer) was used as a catalyst for polycondensation. During the synthesizine procedure, highly polar solvents dimethylformamide and dimethylacetamide were used to accelerate the reaction. The reaction mixture was poured into ethanol, and the precipitated polymer was filtered and washed successively with hot water and alcohol. The powders separated from the reaction mixture were purified by a Soxlet extraction, dried at 100°C under a vacuum, and stored over a desicant.[8] The polymer was found to have no ash content. Table 1 shows the structures and the nitrogen analyses for the polymers obtained from *p*-xylylpyrimidine reacted with and various monomers.

2. Measurement of the Semiconductive Properties and Photoconductivity. The electrical resistivity of the powdered samples compressed between stainless-steel electrodes by a pressure of 50 kg/cm^2 was measured *in vacuo*. The details of this procedure already have been presented.[9] The resistivity decreased with an increase in the temperature, and a good linear relationship was obtained between the logarithm of the resistivity (ρ) and the reciprocal of the temperature, this indicates the applicability of the following formula.[10]

$$\rho=\rho_0\exp(\Delta E_G/2kT)$$

Measurement of the Surface Photo-current: Throughout the experiments described in this report, a sample tablet (1.31

1) "Encyclopedia of Polymer Science and Technology," Vol. 11, ed. by H.H.Mark and N.G.Gaylord, Interscience Publ., New York (1969), p.338.
2) V. Mylnikov and A. Terenin, *J. Polym. Sic., C*, **16**, 3655 (1968).
3) K. Okamoto, Y. Hasegawa, S. Kusabayashi, and H. Mikawa, This Bulletin, **41**, 2563 (1968).
4) W. Klopffer, *J. Chem. Phys.*, **50**, 2337 (1969).
5) M. Ofran, N. Ofran, and A. Weinreb, *ibid.*, **50**, 3131 (1969).
6) B. B. Homer and M. Shinitzky, *Makromol.*, **1**, 469 (1968).
7) M. Kryszeniski, A. Szymanski, and A. Wlochouicz, *J. Polym. Sci., C*, **16**, 3921 (1965).
8) R. Hirohashi, Y. Hishiki, and M. Haruta, *Kogyo Kagaku Zasshi*, **73**, 631 (1970).
9) R. Hirohashi, Y. Hishiki, and S. Ishikawa, *Polymer.*, **11**, 297 (1970).
10) R. Hirohashi, Y. Hishiki, and S. Saito, *Kogyo Kagaku Zasshi*, **72**, 1189 (1969).

Table 1. Structures and nitrogen analyses of polystyrylpyrimidines

No.	Reagent	Structure	Nitrogen analyses Calcd (%)	Found (%)
P1	DIT	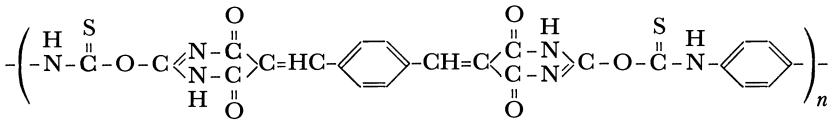	15.38	15.24
P2	TPC	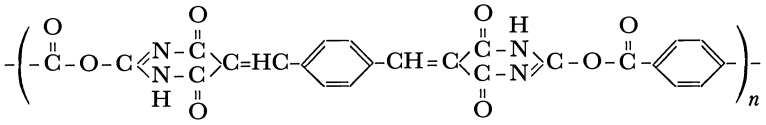	11.57	13.55
P3	XDB	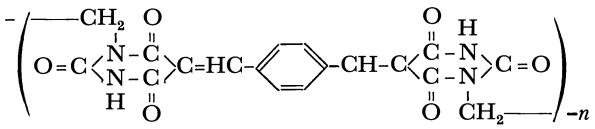	12.28	13.69
P4	PDA	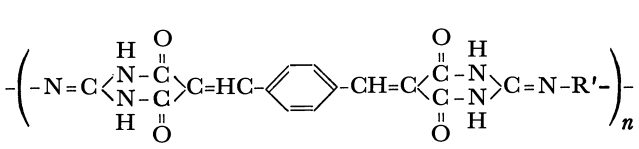	19.71	18.39
P5	BD		16.73	15.28
P6	DPS		15.27	15.64
P7	HMD		19.35	20.72
P8	DPM		16.27	15.55

DIT: *p*-Phenylene diisothiocyanate, TPC: Terephthaloyl chloride, XDB: *p*-Xylylene dibromide, PDA: *p*-Phenylene diamine, BD: Benzidine, DPS: 4,4'-Diamino diphenylsulfone, HMD: Hexamethylene diamine, DPM: 4,4'-diamino diphenylmethane

cm^2 surface area and *ca.* 0.5—1.0 mm thick) was made by the compression of about 0.1 g of a finely-powdered at about 200 kg/cm^2. Silver paste (du Pont conducting silver paint No. 4817) was painted in two stripes on the surface of a tablet with a 1 mm gap. A 750 watt tungsten lamp was used, associated with metallic interference filteres in order to isolate narrow particular wavelength regions. The maximum transmissive wavelengths of the regions, which were 10—61 mμ in the half-band width, ranged from 398 mμ to 1340 mμ, with intervals of 50—100 mμ.[11] The photoconduction of the polymer was measured in a conductivity cell by illumination with a tungsten lamp or a hydrogen-discharge lamp. The electric current was measured by means of the DC amplifier. As the voltage source applied to an organic photocell, we used a DC voltage supply of up to 1000 V.

The absolute measurements of the intensity of the incident light on an organic photocell were made by means of a Nihonbunko vacuum thermopile which was placed at the position of the photocell. The maximum intensity, 3.70—4.73 $\times$ 10^{15} photons/sec·cm^2, was obtained for the light which was isolated by a 848 mμ filter.[12]

Results and Discussion

The voltage dependence of the surface photo-current and the dark-current of the polymers was measured. Most of the observations were made *in vacuo* with a

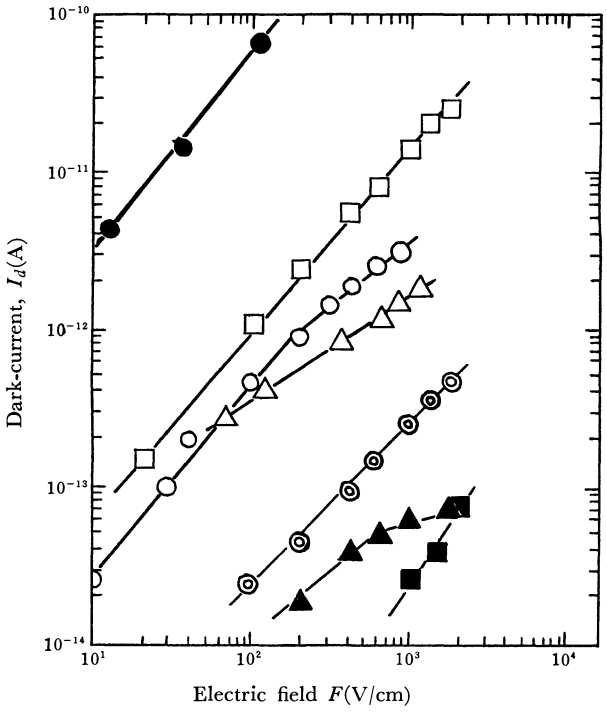

Fig. 1. Surface photo-current *vs.* applied electric field for polystyrylpyrimidines. (at 10^{-6} Torr, by tungsten lamp 750 watt)
○ ● △ ▲ ◎ □ ■
P1 P2 P3 P4 P5 P6 P7

11) R. Hirohashi, Y. Hishiki, and S. Ishii, *J. Sci. Phot. Japan*, **33**, 90 (1970).
12) M. Sano, "Dissertation," The University of Tokyo (1961).

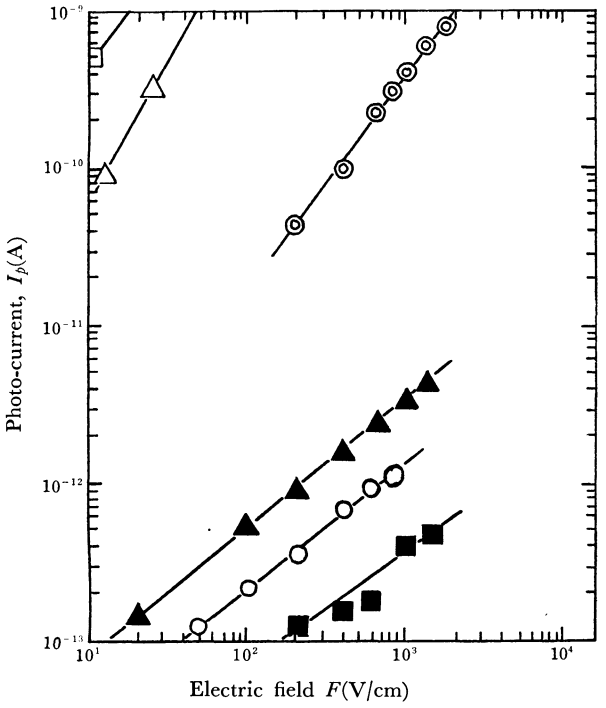

Fig. 2. Surface photo-current *vs.* applied electric field for polystyrylpyrimidines. (at 10^{-6} Torr, by tungsten lamp 750 watt)

○ P1 △ P3 ▲ P4 ◎ P5 □ P6 ■ P7

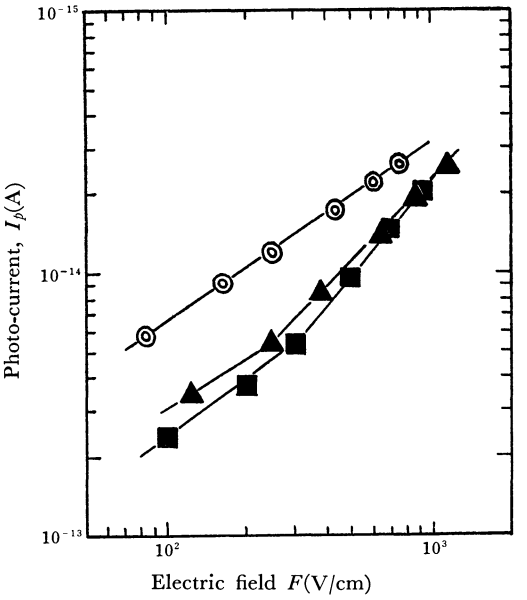

Fig. 3. Surface photo-current *vs.* applied electric field for polystyrylpyrimidines. (at 10^{-6} Torr, by hydrogen discharged tube)

▲ P4 ◎ P5 ■ P7

surface-type photocell in order to avoid the effects of the space charge which are occasionally observed with sandwich-type photocells. The potential dependence for the photocurrent is reproducible, as in the case of the dark-current. Figures 1 and 2 show the electric-field(V) dependence of the dark-current (I_d) and of the photo-current (I_p).

Ohmic behavior derived from the I_d-V relation was observed for all samples except the P7- and P8-samples for the dark-current. On the other hand, ohmic relations for the photo-current against the applied potential were obtained for all samples except P3. Figure 3 shows the I_d-V relation under illumination by a hydrogen-discharge lamp.

Table 2 shows the values of the slopes(α and β) of the I-V relation for polystyrylpyrimidines. The values of α and β were calculated from the $I_d=kV^\alpha$ and $I_p=kV^\beta$ relation respectively. The specific resistivities, the values of the energy gap, and the temperature-possessed kink of the energy gap are shown in Table 2.

A summary of the results for surface-type cells is presented in Table 3. The ratios of the photo-current (I_p) to the dark-current (I_d) reveal the effects of the molecular structures sufficiently well.

The photo-current decreases in air ($I_p=4.5\times10^{-13}$ Å) more than in a vacuum ($I_p=4.3\times10^{-11}$ Å). As a general rule, upon illumination by incandescent lamp the photo-current does not immediately rise to its equilibrium value. Usually the current-time curve shows a peak shortly after the light has been switched

Table 2. The values of slope(α and β) and semiconducting properties of polymers

No.	Specific resistivity ρ(ohm/cm) Temp. (°C)	Energy gap ΔE_G (eV)	Temp. °C	α Field low	α Field high	β Tungsten lamp	HDT[a] Field low	HDT[a] Field high
P1	1.74×10^{13} (18)	0.68	50— 91	1.3	0.9	0.8	—	—
		1.51	91—143					
P2	3.74×10^{13} (17)	0.56	17— 69	1.1		—	—	—
		1.70	69—138					
P3	6.89×10^{13} (12)	0.83	12—114	0.7		1.7	—	—
		1.65	114—143					
P4	4.27×10^{12} (9)	1.52	21—152	1.0	0.4	0.8	0.6	1.1
P5	4.48×10^{12} (12)	1.20	12—147	1.0		1.3	0.8	
P6	4.96×10^{14} (12)	1.91	45—145	1.1		1.4	—	—
P7	3.59×10^{12} (13)	1.23	36—148	2.0		1.0	0.7	1.2
P8	4.82×10^{12} (12)	1.18	12—146	1.6		—	—	—

a) HDT: Hydrogen discharged tube.

Table 3. The ratios of photo-current to dark-current for polymers

No.	Electrical field (V/cm)	I_p (A)	I_d (A)	I_p/I_d (max)
P 1	10	2.67×10^{-14}	2.7×10^{-14}	1
P 3	25	3.32×10^{-10}	2.7×10^{-13}	1230
P 4	400	2.03×10^{-11}	6.5×10^{-14}	310
P 5	400	5.85×10^{-10}	3.5×10^{-13}	1670
P 6	20	1.21×10^{-9}	1.66×10^{-13}	7300

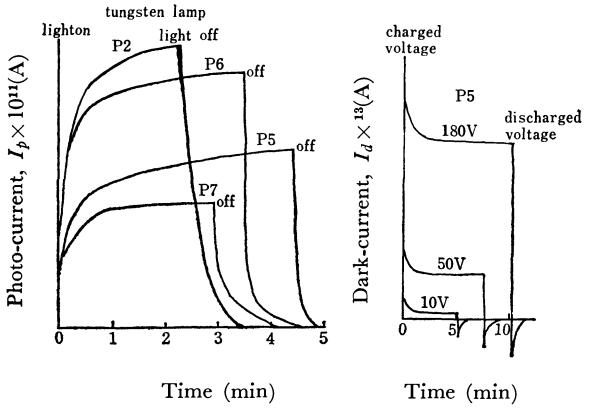

Fig. 4. Dependence of the absorption current on chemical structure and charged voltage.

on as in Fig. 4.

This indicates the formation of a space-charge effect[13] and shows the influence of the contact between electrodes and the specimen. On the other hand, the photo-current upon illumination by the photo-current to its equibrium value. After switching on the field, the currents rises to a peak value, which then slowly decreases to equilibrium. When the supply of the field is stopped, a back current is obtained. The photo-current markedly depends on the voltages and light intensities used.

The Spectral Dependence of the Photo-currents of Polystyrylpyrimidines. A number of investigations of photoconduction in organic solids have been reported. Most of them have been concerned with simple compounds, especially with the anthracene crystal. The spectral response curve of photoconduction was in a closed relation to the absorption spectrum of the anthracene crystal[14] and to those for polycyclic aromatic compounds.[15]

The absorption spectra in the ultraviolet and visible regions of polystyrylpyrimidines, dissolved in concentrated sulfuric acid, were recorded at room temperature. Figure 5 shows the absorption spectra.

Figure 6 shows the spectral dependence of the photo-current of polystyrylpyrimidines. In order to normalize the photo-current, it was divided by the incident-light intensity for each wavelength. The photo-

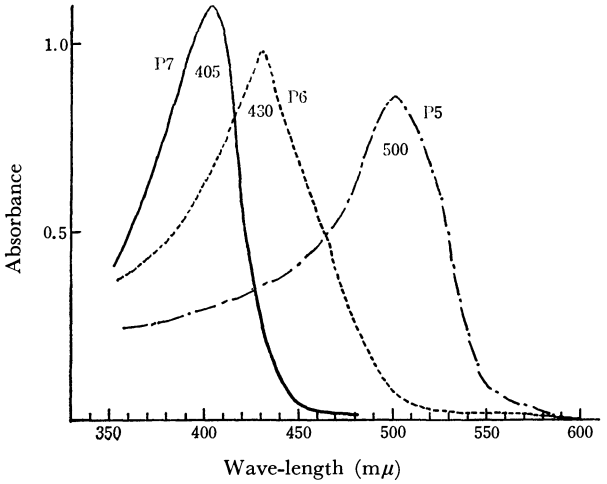

Fig. 5. Absorption spectra of polystyrylpyrimidines. (in concentrated sulfuric acid)

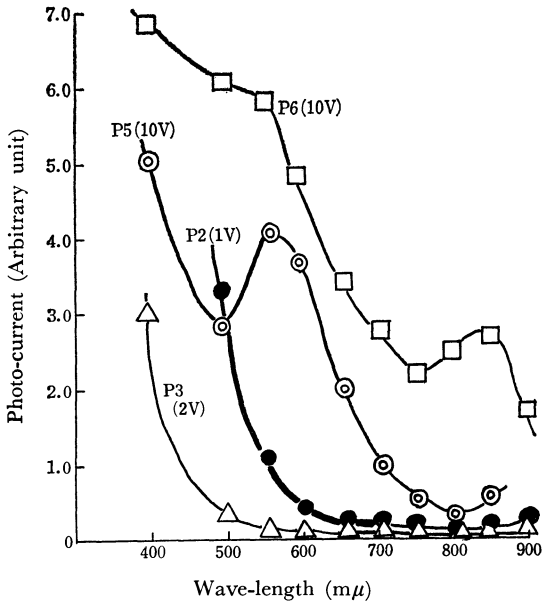

Fig. 6. The spectral dependence of the photo-current of polystyrylpyrimidines. (with metalic interfacial filters.)

current is produced by the light energy which is absorbed into the bulk of the polymeric solid. Generally, the main feature of the spectral response curves is that their peaks correspond to the minima of the absorption spectrum; that is, a higher extinction coefficient will lead to a lower photo-current in the region of the absorption spectrum.

The number of carriers is proportional to the number of photons absorbed into the bulk, with a definite coefficient of the quantum yield. The photo-current curve of polystyrylpyrimidines possesses quite a long tail, one extending to the near-infrared wavelength region. The sensitivity of photoconduction decreases more or less with an increase in the wavelength and continues to extend over the infrared region. In this experiment, the threshold value for photo-conduction could not be found, but the value should be located near the ultraviolet region judging from our results.

The Incident-light-intensity Dependence of the Photo-

13) J. Kommandeur and W. G. Schneider, *J. Chem. Phys.*, **28**, 582 (1958).
14) D. J. Carswell and L. E. Lyons, *J. Chem. Soc.*, **1955**, 1734.
15) H. Akamatu and H. Inokuchi, *J. Chem. Phys.*, **20**, 1481 (1952).

current. The measurements of the photo-current with a variation in the intensity of the incident light indicated that the current observed was almost proportional to the light intensity. The dependence of the photo-current (I_p) on the illumination intensity (L) is expressed by the equation; $I_p=kL^n$. Going to the longer-wavelength region, it approaches more and more linearity until, at 748 mμ, the photo-current is proportional to the light intensity. Table 4 shows the values of n for the tungsten lamp and for each wavelength.

The values of n changed as a function of the applied voltage, the wavelength, and the atmosphere. In the presence of oxygen, the value of n is less than unity; the cause of this decrease is assumed to be the fact that the oxygen absorbs on the polymer films.[16]

16) A. T. Vartanyan and L. D. Rozenstein, *Dokl. Akad. Nauk SSSR*, **124**, 295 (1958).

Table 4. The values of n

Polymer No.			
P1	—	P5	0.8 and 2.4
P2	1.1	P6	1.1
P3	1.0	P7	2.3
P4	2.0	P8	—

a) low light intensity 0.8 and high light intensity 2.4

Sample P5	Wavelength λ_{max} mμ	Applied voltage	n
	551	90	0.73
	653	90	0.96
	749	150	0.98

The authors wish to express their sincere thanks to Professor Hiroo Inokuchi, of the Institute for Solid State Physics, the University of Tokyo, for his valuable suggestions in the course of this work.

BULLETIN OF THE CHEMICAL SOCIETY OF JAPAN, VOL. 44, 2577—2582 (1971)

Conformation of α-Aminobutyric Acid in Aqueous Solution

Toshio AKIMOTO, Masamichi TSUBOI, Masatsune KAINOSHO,* Fumihide TAMURA,* Asao NAKAMURA,* Shuichi MURAISHI,** and Teruo KAJIURA**

Faculty of Pharmaceutical Sciences, The University of Tokyo, Hongo, Bunkyo-ku, Tokyo

** Central Research Laboratory, Ajinomoto Co., Inc., Kawasaki, Kanagawa*

*** Japan Electron Optics Laboratory, Company, Nakagami, Akishima, Tokyo*

(Received September 29, 1970)

Raman spectrum of α-aminobutyric acid has been observed in its 15% aqueous solution (neutral). By comparing it with the Raman and infrared spectra of crystal A (in which 40% of the total molecules are the T-form molecules, 36% G_a-, and 24% G_b-form molecules), crystal B (which consists only of T-form molecules), and a complex crystal of this amino acid with calcium chloride (in which 85% are the G_a-form molecules), it has been shown that the G_a-form molecules are predominant in the aqueous solution. Here, T-, G_a-, and G_b-forms have respectively the amino group, the hydrogen atom, and the carboxy group in the position trans to the methyl group in the internal rotation around the C_α-C_β bond. Proton magnetic resonance spectrum was observed of a C_γ-deuterated product ($CD_3CH_2CH\ NH_3{}^+COO^-$) in its aqueous solution at several temperatures in the −1.5 to 91°C range. It has been indicated that the C_α-form is more stable by about 300 cal/mole than the other two forms.

For DL-α-aminobutyric acid, two crystalline modifications, A and B, were previously found.[1] An analysis of X-ray diffraction[2,3] indicated that in crystal A the methyl group on the β-carbon does not take a fixed position. It was found to be distributed among the three sites in the internal rotation around the C_α–C_β axis. One site is nearly trans to the amino group (designated as T-form), another is nearly trans to the hydrogen atom (G_a-form), and the other nearly trans to the carboxy group (G_b-form) (see Fig. 1). The occupancy factors of these three positions were found to be 40, 36, and 24%, respectively, at room temperature. In crystal B, only T-form was found.[2,3] Recently, Akimoto and Iitaka[4] found that, in a complex crystal of DL-α-amino-*n*-butyric acid with calcium chloride, 85% of the amino acid molecules are in G_a-form. Thus, it is probable that T-, G_a-, and G_b-forms are three stable rotational isomers. The purpose of the present work is to examine which of

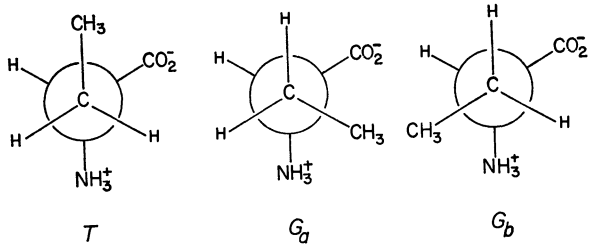

Fig. 1. Three rotational isomers found of DL-α-aminobutyric acid.

1) M. Tsuboi, Y. Iitaka, S. Suzuki, and S. Mizushima, This Bulletin, **32**, 529 (1959).

2) T. Ichikawa, Y. Iitaka, and M. Tsuboi, *ibid.*, **41**, 1027 (1968).

3) T. Ichikawa and Y. Iitaka, *Acta Cryst.*, **B24**, 1488 (1968).

4) T. Akimoto and Y. Iitaka, to be published. See also T. Akimoto, Doctor Thesis, University of Tokyo, 1970.

these three forms are involved in neutral aqueous solution of this amino acid.

Experimental

DL-*α-Aminobutyric Acid and Its Crystals.* The sample of DL-α-aminobutyric acid used in this investigation was obtained from a commercial source and was purified by recrystallization with water and ethanol.

Crystal A was obtained by dissolving the amino acid in water and by adding ethanol. When a small amount of precipitate came out, this was dissolved again by adding a small amount of water. The solution was then placed in a refrigerator at 5—10°C, and, a few days after, crystals were obtained which were found to be all in A-form.

From aqueous solutions with 1 M NaCl, always crystal B was obtained. Crystal B could be also obtained, however, by adding a greater amount of ethanol into an aqueous solution of this amino acid. When a good amount of precipitate came out, this mixture was placed in a refrigerator. The crystals thus obtained were found to be in B form.

The crystal of the complex with $CaCl_2$ was obtained by adding $CaCl_2$ into an aqueous solution of the amino acid so that the mole ratio of amino acid/$CaCl_2$ became about 2/1.5, and then by gradual evaporation of the solvent. What was obtained was a hygroscopic, monoclinic crystal elongated along the c axis. Elementary analysis was made of a sample completely dried by means of an Abderhalden's dryer.

Found: C, 27.4; H, 6.35; N, 8.00%. Calcd for $C_8H_{20}N_2O_6CaCl_2$: C, 27.35; H, 5.70; N. 8.00%.

A crystallographic analysis[4] of this crystal indicated that its chemical unit is $CaCl_2$ - 2(DL-α-amino-*n*-butyric acid) - $2H_2O$.

Raman Spectrum Raman spectrum of DL-α-aminobutyric acid was observed in its neutral aqueous solution by the use of a Perkin-Elmer LR-1 Raman Spectrometer with a 10 milliwatt He–Ne laser. The concentration was about 15% and the solution was placed in a 2.5-m*l* multi-reflection cell.

The Raman spectrum of this aqueous solution was observed also by the use of 5145 Å radiation of an argon ion laser. The results of the measurements with two different light sources agreed well, so that the Raman lines of this amino acid in its neutral aqueous solution could be fixed with a high degree of certainty.

The Raman spectra of the crystals were observed in the form of powder by the use of a JRS-01B spectrophotometer of Japan Electron Optics Laboratory Co., Ltd. with the 4880 Å and/or 5145 Å line of an argon ion laser.

Infrared Spectra. Infrared spectrum of an aqueous solution with the concentration 15% was observed with a CaF_2 cell by the use of a Perkin-Elmer 621 spectrometer.

Infrared spectra of crystals were observed in the forms of the Nujol and hexachlorobutadiene mulls. The spectral region of 4000—300 cm^{-1} was covered by the use of a Perkin-Elmer 621 Spectrometer. Each spectrum was observed not only at a room temperature but also at lower temperatures by the use of dry ice+acetone and of liquid nitrogen as cryogens. At lower temperatures, most absorption bands were observed at slightly higher frequencies, were narrower in their widths, and were observed with a higher resolution than those observed at the room temperature.

Preparation of DL-*α-aminobutyric-4-*d_3 *Acid.* The C-deuterated product $CD_3CH_2CH(NH_3^+)COO^-$ was prepared from acetic acid-d_4 containing over 99% deuterium (purchased from E. Merck and Co.) *via* the following steps:

$$CD_3CO_2D \rightarrow CD_3CH_2OH \rightarrow CD_3CH_2Br \rightarrow$$

$$CD_3CH_2\underset{\displaystyle NHCOCH_3}{\underset{|}{C}}(CO_2C_2H_5)_2 \rightarrow CD_3CH_2\underset{\displaystyle NH_3^+}{\underset{|}{C}}HCOO^-$$

Ethanol-2-d_3: A solution of 11.0 g (0.17 M) of acetic acid-d_4 in 50 m*l* of diethyl carbitol was added to a slurry of 10 g of lithium aluminum hydride in 100 m*l* of diethyl carbitol at room temperature. The reaction mixture was kept stirring for 8 hours at 60—70°C. After the reaction was completed, the mixture was cooled, and 260 m*l* of monobutyl carbitol was added below 20°C with stirring. Stirring was continued for additional 4 hr. The resulting ethanol-2-d_3 was distilled under 10^{-3}—10^{-4} mmHg at the bath temperature of 60—70°C, and collected in a trap chilled with liquid nitrogen. The yield was 7.3 g (87%).

Ethyl-2-d_3 *Bromide*: To 7.3 g of ethanol-2-d_3, prepared as described above, was added 27 g of phosphorus tribromide at −10°C. The reaction mixture was subjected to a fractional distillation, and the product was dried over potassium carbonate. Yield 10.3 g (62%).

Ethyl Acetamido (Ethyl-2-d_3*) Malonate*: In a solution of 16.3 g of ethyl acetamidomalonate plus 30 m*l* of absolute ethanol was dissolved 1.73 g of sodium. To the solution was added the deuterated ethyl bromide dissolved in 20 m*l* of ethanol. The mixture was refluxed for 13 hr, and then poured into ice-cold water. The resulting crystals were collected by filtration, washed with cold water, and recrystallized from ethanol-water. Yield 15 g (86%).

α-Aminobutyric-4-d_3 *Acid*: The deuterated ethyl acetamido (ethyl)malonate was hydrolyzed and decarboxylated by refluxing with 100 m*l* of concentrated hydrochloric acid for 7 hr. The mixture was concentrated to dryness. The residue was dissolved in a small amount of aqueous ethanol and 15 m*l* of pyridine was added dropwise to the solution. By filtration of the precipitate, 3.8 g (57%) of the crude crystals was obtained. It was recrystallized from hot 96% ethanol.

Proton Magnetic Resonance. Proton magnetic resonance of DL-α-aminobutyric-4-d_3 acid, $CD_3CH_2CH(NH_3^+)COO^-$, was observed in D_2O solution by the use of a Varian HA-100 spectrometer. The concentration of the sample was again about 15%. The temperature of the sample solution was controlled with a Varian V6040 Controller.

Results and Interpretations

Raman spectrum of DL-α-aminobutyric acid in its aqueous solution (15%) is shown at the top of Fig. 2 and also of Fig. 3. Raman spectra of the same amino acid in its crystalline states (crystal B, complex with $CaCl_2$, and crystal A) are given in the lower part of Fig. 2. Infrared absorption spectra of the aqueous solution and crystals are given (with absorption upward) in Fig. 3. The infrared spectra of the three crystals given here are all what were observed at about −180°C (with liquid nitrogen). By comparing the Raman spectra of the three crystals with one another, many of the Raman lines can be assigned to the T, G_a, or G_b form molecule. By a similar comparison of the infrared spectra, the assignments of the absorption bands are also made. In addition, by comparing the Raman and infrared spectra, it is shown that each of the broad Raman peaks of crystal A at 650, 770, 875, 1050, 1120, 1170, and 1270 cm^{-1} must consist

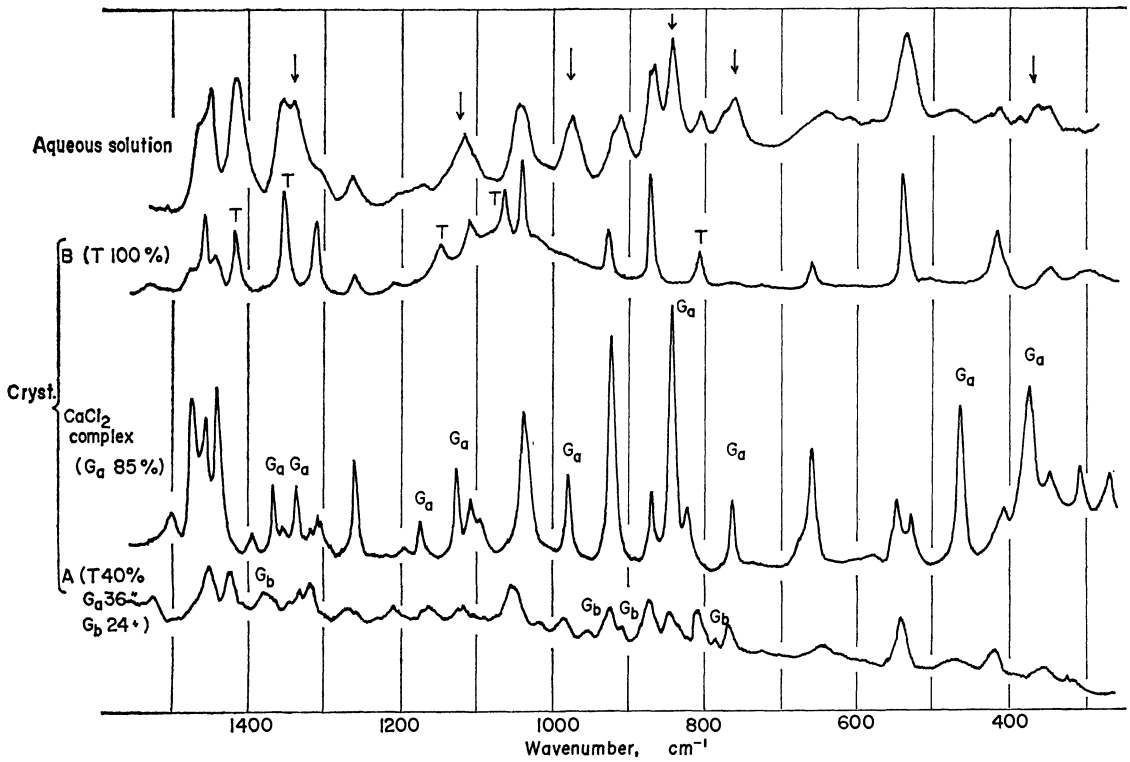

Fig. 2. Raman spectra of DL-α-aminobutyric acid in aqueous solution (top) and of three crystals: B-form, $CaCl_2$-complex, and A-form.

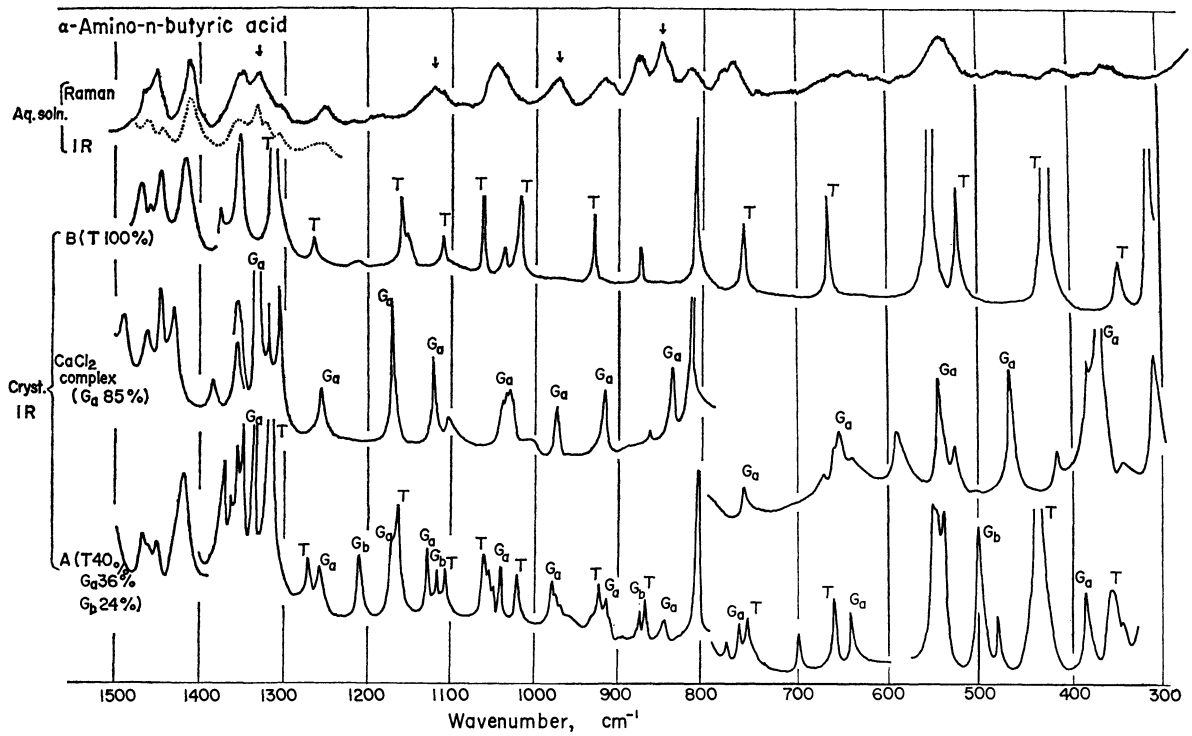

Fig. 3. Raman and infrared spectra of DL-α-aminobutyric acid in aqueous solutions (top) and infrared spectra of three crystals: B-form, $CaCl_2$-complex, and A-form.

of T, G_a, and/or G_b lines. The assignments of the Raman lines and infrared bands to the T, G_a, and G_b forms are given in Figs. 2 and 3. The appearance of strong Raman lines at 765, 843, 970, 1120, and 1340 cm^{-1} (indicated by arrows in Fig. 2) suggests that the G_a form is predominant in the aqueous solution at room temperature. A strong infrared band at 1340 cm^{-1} and a weak Raman line at 375 cm^{-1} give a support to this idea.

Proton magnetic resonance spectrum (Fig. 4) of deuterated α-aminobutyric acid ($CD_3CH_2CH(ND_3^+)COO^-$) in D_2O solution, gives its methylene (AB)

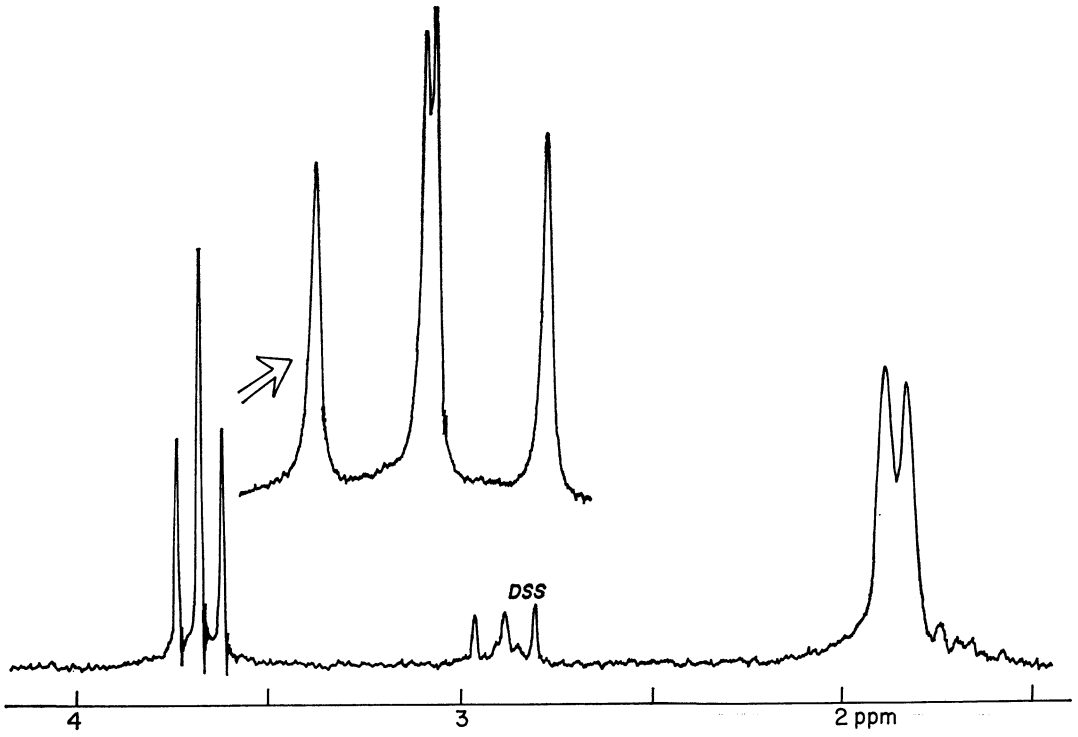

Fig. 4. Magnetic resonance signal of the proton on the α-carbon in α-aminobutyric acid-4-d_3 in D_2O solution.

signal (doublet) at 1.85 ppm (from internal DSS[5]) and the signal of the proton on C_α at 3.68 ppm (X). The latter signal consists of four components (see Fig. 4) which are caused by coupling with the methylene protons. Each value of the coupling constants J_{AX} and J_{BX} cannot easily be determined from the spectrum, but the value of $|J_{AX}+J_{BX}|$ can be determined by measuring the separation between the outermost peaks. As is shown in Table 1 and in Fig. 5, this value was found to change slightly but appreciably with the temperature of the solution.

Table 1. Vicinal coupling constants in α-aminobutyric acid-4-d_3 and the population of G_a form

Temperature °C	$J_{AX}+J_{BX}$ Hz	$\alpha(G_a)$	K	ΔF kcal/mol
−1.5	11.70	0.407	1.37_2	−0.165
8.5	11.82	0.396	1.31_1	−0.152
34	11.92	0.387	1.26_3	−0.142
46.5	11.99	0.381	1.23_1	−0.132
69	12.00	0.380	1.22_5	−0.136
91	12.04	0.376	1.20_5	−0.135

The temperature effect of the $|J_{AX}+J_{BX}|$ value is attributable to a conformational change of the amino acid in the aqueous solution. The fact that the $|J_{AX}+J_{BX}|$ value *increases* with the temperature indicates that G_a form is the most stable form among the three postulated rotational isomers. Thus, in form G_a both of the methylene C-H bonds are at gauche positions with respect to the C_α–H bond around the C_α–C_β axis, whereas in forms T and G_b one at trans and the other at gauche positions (see Fig. 1). As is now well known, the vicinal coupling constant (J_g) is much smaller when the H–C–C–H system is in a gauche form than that (J_t) when it is in a trans form. Therefore, the $|J_{AX}+J_{BX}|$ value should be smaller for G_a form than that for T or G_b form, and the fact that this value increases with the temperature should mean that the population of form G_a decreases and those of form T and/or form G_b increase with the temperature.

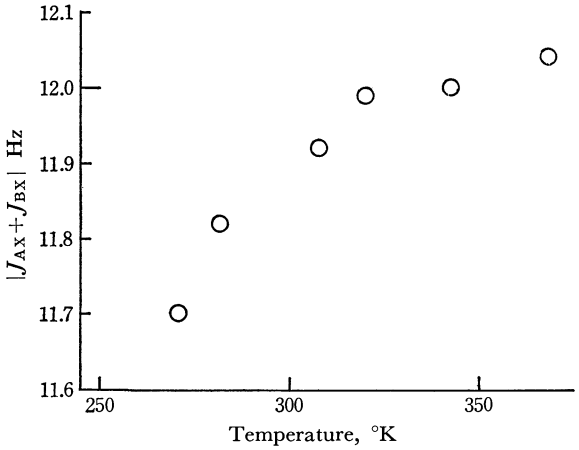

Fig. 5. Temperature dependence of the *vicinal* coupling constants in α-aminobutyric acid-d_3.

If, according to Pachler,[6] the J_g and J_t values are assumed to be 2.60 and 13.56 Hz, respectively, then the mole fraction $\alpha(G_a)$ of G_a form molecules can be calculated by an equation,

$$\alpha(G_a) = [(J_t+J_g) - |J_{AX}+J_{BX}|]/(J_t-J_g) \cdot$$
$$= (16.16 - |J_{AX}+J_{BX}|)/10.96 \quad (1)$$

5) DSS=Sodium-2,2-dimethyl-2-silapentane-5-sulfonate.

The equilibrium constant K between G_a form and the other two forms is given as

$$K = \alpha(G_a) \Big/ \frac{[1-\alpha(G_a)]}{2}. \quad (2)$$

Here, it is tentatively assumed that T and G_b forms have always equal populations to each other. The $\alpha(G_a)$, K and ΔF (free energy difference) values calculated from the $|J_{AX}+J_{BX}|$ value at each temperature are given in the last three columns of Table 1. The energy difference ΔE between the G_a form and the other two forms is to be estimated as usual from the slope of the $\ln K$ *versus* $1/T$ curve. As may be seen in Fig. 6, the $\ln K$-$1/T$ plot does not result in a straight line. This fact may be interpreted as indicating that the ΔE value depends on the temperature. It is also possible, however, that this dependence is merely an apparent one which is caused by neglecting the free energy difference of the T and G_b forms. The apparent ΔE value is obtained as $\Delta E = -0.4$ kcal/mol at 20°C and $\Delta E = -0.2$ kcal/mol at 50°C.

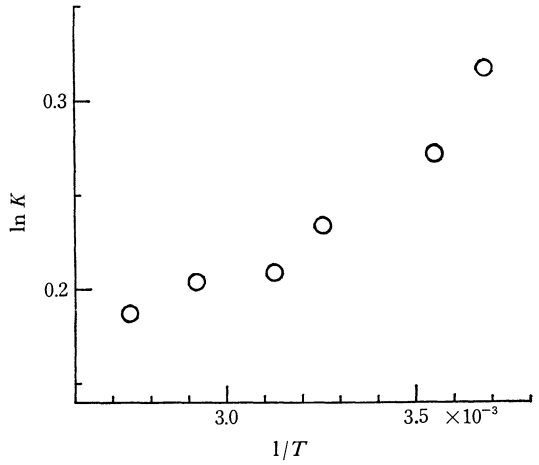

Fig. 6. Natural logarithm of the equilibrium constant K (see Eq. 2) plotted against $1/T$.

Discussion

Rotational isomerism of α-aminobutyric acid in aqueous solution was previously studied by Pachler.[6,7] He drew a conclusion that all of the three isomers have almost equal residence times to one another at about 30°C. This conclusion, however, was based upon the results of his NMR examination of an alkaline and an acidic solutions, while our present study was made of a neutral solution. In addition, he obtained only an approximate (±0.5 Hz) vicinal coupling constant of the CH_2–CH system. A more precise NMR study of undeuterated α-aminobutyric acid should involve a rather elaborate A_3MNX treatment for the CH_3CH_2CH system. Even if a decoupling experiment were done, this would not provide coupling constant values with an accuracy of ±0.02 Hz.

To overcome the difficulties, we have deuterated the methyl group of this amino acid in our present study. The NMR of the CH_2CH group can now be treated as an ABX problem. A precise value of $|J_{AX}+J_{BX}|$ can now be obtained, and a detailed discussion of the temperature effect on this value is now significant. We have also obtained in our present study a quite independent set of data—*i.e.* the vibrational spectrum.

As has been described above, our present NMR study clearly indicated that G_a form is the most stable among the three rotational isomers. Both of our NMR and Raman data showed that, in a neutral aqueous solution at room temperature, G_a form molecules are most abundant. From the NMR data, the mole fraction of G_a form has been estimated to be 0.387 which is only slightly greater than 1/3. It should be pointed out here, however, that this figure is based upon an assumption that every proton in the CH_2–CH system in every rotational isomer is located at an exact trans or an exact gauche position with respect to another proton, so that the proton-proton coupling constant should be 13.56 or 2.60 Hz. It is not improbable that the actual rotational isomers take conformations somewhat deviated from such "standard" conformations. For such deviated conformations, the effective J_t value would be slightly smaller than 13.56 Hz and the effective J_g value would be slightly greater than 2.60 Hz. If so, $\alpha(G_a)$ should be estimated (Eq. (1)) to be somewhat greater than 0.387.

One might be puzzled by our present conclusion that G_a form is the most stable among the three possible rotational isomers, because this form should undergo the strongest intramolecular steric repulsion. The steric repulsion between the methyl group and the carboxyl and/or amino group looks certainly a factor of making G_a form less stable. Thus, when the methyl group is substituted by the OH group (which is smaller than CH_3) the population of G_a form becomes greater (0.61 at room temperature[8]). When the methyl group is substituted by the carboxyl or SH group (which is greater than CH_3), on the other hand, the population of G_a form becomes smaller (0.22 for L-aspartic acid and 0.38 for L-cystein[6,7]). For all of these amino acids, however, it is necessary to postulate a factor which makes G_a form more stable. It is not likely that this factor is related with the electric dipole moment of the molecule or with an electrostatic interaction within the molecule, because the position of the methyl group should not cause great change in the dipole moment or in the electrostatic interaction. It is probable that the factor is related with the extent to which the water structure is disturbed by bringing the amino acid molecule into water. Perhaps it is worthwhile to point out here that G_a form is the most globular among the three rotational isomers. A preliminary examination of a space-filling model has indicated that the largest and smallest radii of the molecule are respectively 6.8 and 5.2 Å in G_a form whereas they are 7.2 and 4.4 Å in both T and G_b forms.

In the present study we could estimate only the

6) K. G. R. Pachler, *Spectrochim. Acta*, **19**, 2085 (1963).
7) K. G. R. Pachler, *ibid.*, **20**, 581 (1964).
8) H. Ogura, S. Fujiwara, and Y. Arata, *J. Mol. Spectry.*, **23**, 76 (1967).

population $\alpha(G_a)$ of G_a form but could not estimate those of T and G_b forms. The latter would be possible if we can deuterate selectively one of the two hydrogens on the β-carbon. An NMR spectrum of such a deuterated product $CD_3CHDCH(NH_3^+)COO^-$ should give J_{AX} or J_{BX} value.

BULLETIN OF THE CHEMICAL SOCIETY OF JAPAN, VOL. 44, 2582—2587 (1971)

The Measurement of Reaction Rates under Pressure by using a Manganin Pressure Gauge

Takashi MORIYOSHI

Department of Chemical Engineering, Faculty of Engineering, Tokushima University, Minamijōsanjima-cho, Tokushima

(Received December 28, 1970)

An apparatus capable of following reaction rates under pressure without sampling has been designed and constructed. The pressure change due to the progress of a reaction in a closed system could be accurately measured to about 0.08 atm by means of a "fixed bridge" combined with a manganin pressure gauge, in which the unbalanced e.m.f. generated at a constant bridge current was potentiometrically determined to 0.1 μV. The rates of the acid-catalyzed inversion of sucrose and the base-catalyzed decomposition of diacetone alcohol, with the expansion in volume and the contraction respectively, were measured in order to verify the applicability of this apparatus. The agreement between the results obtained by this method and those obtained by the analytical method was satisfactory. From these results, it has been confirmed that the method is sufficiently applicable to the measurement of reaction rates under pressure.

The techniques for measuring reaction rates under pressure may be generally classified into two kinds. One is the method usually employed, which requires the sampling of the reaction mixture for analysis with or without the release of pressure, while the other is that which immediately determines the reaction rates without any sampling by following the change in the physical properties of the reaction mixture due to the conversion. The latter method is essentially restricted in the range of its application by the character of the measured reaction, but if a suitable means of following the change is found, then it becomes very useful. A conductance method is typical of this kind of means and has been employed conveniently for the measurement of the rates of several solvolyses under pressure.[1] The technique of following the rate by using a manganin pressure gauge, which is called the piezometric method (or occasionally the dilatometric method), is of the same kind and has recently been used by several workers in studying some liquid-phase reactions.[2-4] Since this method involves measuring the pressure change caused when the reaction takes places in a closed pressure vessel, the desired accuracy should be insured in the measurement of the pressure.

As was pointed out by Withey and Whalley,[3] the pressure change caused by the reaction results in a change in the rate constant, a change dependent on the magnitude of the volume of activation, therefore, the extent of pressure change during the kinetic measurement, which may be allowed for measuring the rate constant with the same accuracy, is entirely limited by the absolute value of this parameter, being small for the reaction with a large value, but large for that with a small one. For instance, in order to obtain the rate constant with an accuracy of 1 per cent for the reaction whose volume of activation is ± 5 cm^3/mol, the total pressure change measured must be less than 50 atm; hence, it is desired that the sensitivity of the pressure in the measurement is greater than 0.5 atm.

The "fixed-bridge" method has been employed in the present work because it is most suitable for measuring by means of a manganin gauge coil, the resistance change dependent on such a small pressure change. This method, first employed by Adams *et al.*,[5,6] is essentially based on the measurement of the unbalanced electromotive force (e.m.f.) generated in a Wheatstone bridge with four fixed arms and containing the gauge coil when at a constant bridge current; it is more accurate than directly measuring the resistance change itself. Withey and Whalley[3] also adopted the same method in principle and made an apparatus capable of measuring the pressure change automatically. The measurements of the e.m.f. in this work were carried out with a potentiometer in order to determine exact absolute values comparable

1) J. Buchanan and S. D. Hamann, *Trans. Faraday Soc.*, **49**, 1425 (1953); J. B. Hyne, H. S. Golinkin, and W. G. Laidlaw, *J. Amer. Chem. Soc.*, **88**, 2104 (1966); H. S. Golinkin, I. Lee, and J. B. Hyne, *ibid.*, **89**, 1307 (1967); A. B. Lateef and J. B. Hyne, *Can. J. Chem.*, **47**, 1369 (1969); B. T. Baliga and E. Whalley, *J. Phys. Chem.*, **73**, 654 (1969); B. T. Baliga and E. Whalley, *Can. J. Chem.*, **48**, 528 (1970); D. L. Gay and E. Whalley, *ibid.*, **48**, 2021 (1970); M. J. Mackinnon, A. B. Lateef, and J. B. Hyne, *ibid.*, **48**, 2025 (1970).

2) F. M. Merrett and R. G. W. Norrish, *Proc. Roy. Soc.* (London), **A 206**, 309 (1951); C. Walling and J. Pellon, *J. Amer. Chem. Soc.*, **79**, 4776 (1957); C. Walling and J. Pellon, *ibid.*, **79**, 4782 (1957).

3) R. J. Withey and E. Whalley, *Trans. Faraday Soc.*, **59**, 895 (1963).

4) R. J. Withey and E. Whalley, *ibid.*, **59**, 901 (1963).

5) L. H. Adams, E. D. Williamson, and J. Johnston, *J. Amer. Chem. Soc.*, **41**, 12 (1919).

6) L. H. Adams, R. W. Goranson, and R. E. Gibson, *Rev. Sci. Instr.*, **8**, 230 (1937).

with those estimated theoretically.

The present paper will describe a technique for following the reaction rate piezometrically and will present some results obtained for the acid- and base-catalyzed reactions under pressure.

Apparatus

A schematic diagram of the high-pressure apparatus used is shown in Fig. 1. It consists principally of four components: a pressure vessel, a manganin pressure gauge, a Bourdon gauge, and a high-pressure hand-operated pump. The pressure vessel, with a capacity of about 180 cm^3, was a cylinder made of SUS-27 stainless steel, 11 cm in diameter and 24 cm in length; it was sealed by means of an O-ring, with a back-up ring made of Teflon. The reaction vessel was a hypodermic syringe with a Teflon plug, with a capacity of about 90 cm^3; it was put in a pressure vessel filled with silicone oil as the pressure-transmitting fluid. The manganin pressure gauge used was that made by the Harwood Engineering Co., Inc.; it consisted of two non-inductively would manganin coils which both had 120±0.1 ohm resistance at atmospheric pressure. The one was a pressure-active coil which had a pressure coefficient of 2.446×10^{-6} atm^{-1}; it was exposed to the pressure system, but was enclosed by a bronze bellows filled with methyl butane in order to isolate it from the pressure fluid. The other, a compensating coil, was located in the cap of the gauge cell. These coils were connected in series to form a Wheatstone bridge with two other precise resistance coils.

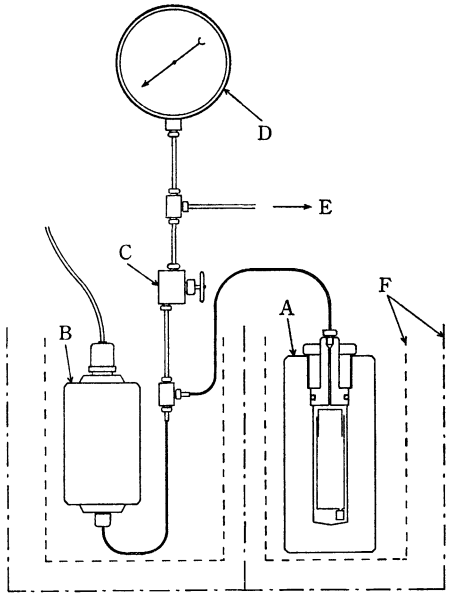

Fig. 1. Schematic diagram of the high pressure apparatus.
A: Pressure vessel, B: Manganin pressure gauge, C: Valve, D: Bourdon gauge, E: Pressure pump, F: Thermostat.

The pressure vessel and the manganin gauge were separately immersed in each thermostat, which was doubly thermostatted and was capable of controlling the temperature to 0.001°C; its temperature was measured to 0.001°C by means of a precise Beckmann thermometer. It has been found that the pressure coefficient of the resistance of manganin may actually be regarded as a function of the temperature and that it increases by about 2×10^{-2} of itself for each degree the temperature rises at 0—70°C.[6] Hence, the manganin gauge in the present work was maintained near 30°C for over a year for ease in controlling; the resistance of manganin was thus relatively less sensitive to the temperature change, because the temperature coefficient of manganin becomes zero in the vicinity of room temperature.[6,7] The connection between the pressure vessel and the manganin gauge was made through a junction of stainless steel tubing 1/8 inch in outer diameter and 0.024 inch in inner diameter in order to make the volume of the unthermostatted part as small as possible. During the measurement of the reaction rate, their components were isolated from the Bourdon gauge and the pressure pump by shutting a valve, as is shown in Fig. 1. Pressure was directly applied by means of the pressure pump and was measured with an accuracy of 7 atm by means of a Heise Bourdon gauge, which was calibrated up to 1400 atm from time to time against a pressure balance made by the American Instrument Co., Inc. The resistance change of the gauge coil caused by the pressure change in the closed system was measured by means of the "fixed-bridge" method.[5,6] The arrangement is shown schematically in Fig. 2, in which R_1 and R_2 represent the active and the compensating coils respectively; these coils are mounted in the gauge cell. R_3 and R_4 are both precise resistance coils of 100±~1 ohm. A constant current through the bridge was supplied by a Takasago model GPO 50-2 DC power supply and was finely adjusted. The unbalanced e.m.f. was measured to 0.1 μV by means of a Yokogawa model P-7 potentiometer.

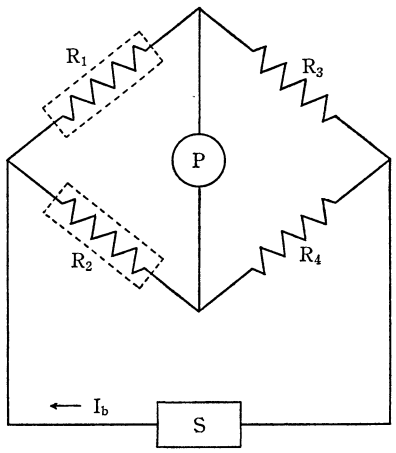

Fig. 2. The "fixed bridge" arrangement.
P: Potentiometer, S: DC power supply.

Fundamentals of Measurement

In the bridge arranged as in Fig. 2, the resistance change, ΔR, with the pressure, P, of the gauge coil,

7) H. E. Darling and D. H. Newhall, *Trans. Amer. Soc. Mech. Engrs.*, **75**, 311 (1953).

R_1, generates across the bridge at a constant current, I_b, an unbalanced e.m.f., E_p, expressed by:

$$E_p = \frac{(R_1 \cdot R_4 - R_2 \cdot R_3 + R_4 \cdot \Delta R) I_b}{R_1 + R_2 + R_3 + R_4 + \Delta R} . \quad (1)$$

Assuming that the pressure coefficient, α, of the gauge coil has no appreciable change over the whole range of applied pressures, ΔR at a constant temperature is given by:

$$\Delta R = \alpha \cdot R_1 \cdot P . \quad (2)$$

Since the ΔR for the coil used of 120 ohm, as estimated from Eq. (2), is only a few ohm even at 10000 atm, and since it is negligible as compared with the other terms in the denominator on the right hand side of Eq. (1), one can convert Eq. (1) to a relation linear with respect to the pressure by using Eq. (2); that is,

$$E_p = E_1 + \frac{\alpha \cdot R_1 \cdot R_4 \cdot I_b \cdot P}{R_1 + R_2 + R_3 + R_4} , \quad (3)$$

where E_1 denotes an unbalanced e.m.f. that will develop when $R_1 \cdot R_4 \neq R_2 \cdot R_3$ at atmospheric pressure, E_1 being given by:

$$E_1 = \frac{(R_1 \cdot R_4 - R_2 \cdot R_3) I_b}{R_1 + R_2 + R_3 + R_4} . \quad (4)$$

Thus, it follows that E_p is proportional to only the pressure acting on the gauge coil at a constant bridge current. This suggests that one can follow the reaction with any pressure change under given conditions by measuring the unbalanced e.m.f. instead of the pressure itself. Substituting the numerical value for each term and the one used, 20.00 mA, for I_b into Eq. (3), and assuming that $R_1 \cdot R_4 = R_2 \cdot R_3$, the following equation is obtained as an approximately calculated one:

$$E_p = 1.334 \times 10^{-3} \cdot P, \quad (5)$$

where E_p is given in mV, and P, in atm. To verify Eq. (5), blank experiments when the pressure vessel entirely filled with the pressure fluid and the gauge cell were controlled at 35.00°C and 29.10°C respectively were carried out at pressures up to 2000 atm. Pressures up to 1250 atm were directly measured with an accuracy of about 0.07 atm by means of a pressure balance, and the higher pressures by means of a calibrated Bourdon gauge; the e.m.f. values were determined by averaging those obtained at increasing and decreasing pressures. The results are shown, together with the calculated line given by Eq. (5), in Fig. 3, in which the increment, $E_p - E_1$, dependent on the pressure is conveniently plotted for purposes of comparison. They are almost exactly proportional to the measured pressure of the system, as is expected from Eq. (3). The most reasonable relationship between the unbalanced e.m.f. and the pressure was obtained from the observed data using the method of least squares; it was expressed by:

$$E_p = 0.0139 + 1.320 \times 10^{-3} \cdot P \text{ mV}, \quad (6)$$

The standard deviation from this relationship was found to be 0.0125. The difference in the pressure dependence from Eq. (5) is about 1 per cent; it is not surprising and is, in fact, quite satisfactory considering that E_1 has a small definite value, as is shown in Eq. (6),

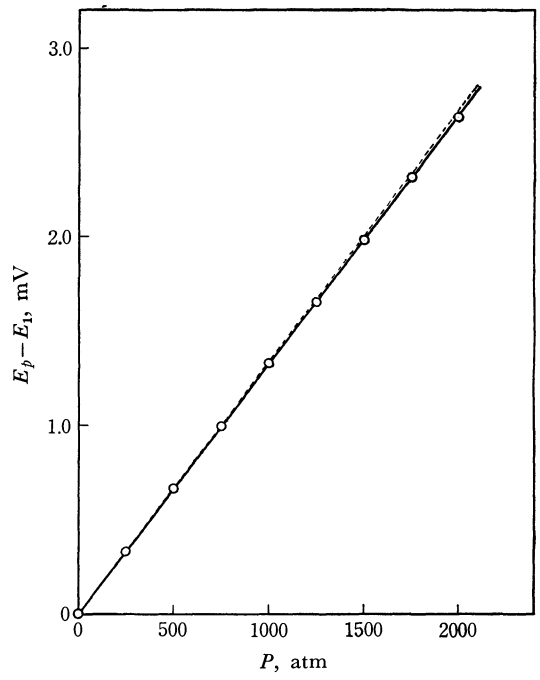

Fig. 3. Relationship between unbalanced e.m.f. and pressure.
Full line: Experimental one.
Dashed line: Calculated one.

because there is a small unbalance ($R_1 \cdot R_4 \neq R_2 \cdot R_3$) between the inherent values of the four resistances at atmospheric pressure. If one assumes that all the resistances have approximately the same extent of error, from which the above difference arises entirely, then the error may be estimated to be ± 0.002 ohm at the most. This value is obviously within the error allowed for their resistances. Otherwise, an uncertainty involved in the pressure coefficient of the gauge coil used must also be considered, but perhaps such a small difference between the pressure dependences of the e.m.f. is predominantly due to the former cause rather than to the latter.

The linearity of the manganin pressure gauge has been well verified from these results; hence, of course, it may undoubtedly be regarded as being established more exactly in a small range of pressure changes (usually below 100 atm) during the actual measurement of the reaction. The potentiometer employed in the present work can be easily read to 0.1 μV, so it is possible to measure the pressure change to 0.08 atm, at least over the pressure range up to a few thousand atmospheres, as was predicted from Eq. (6). Therefore, it is evident that one can determine the reaction rate with a reasonable accuracy by following the e.m.f. change consequent on the pressure change with the progress of the reaction in a closed system.

If a much greater sensitivity is desired in the measurement of the pressure, it may be convenient to place, on opposite sides of the bridge, two gauge coils exposed to the same pressure. When the coils, R_1 and R_4, in the arrangement shown in Fig. 2 are made up of the same material and are both equally subjected to the pressure being measured, one obtains the following approximate equation instead of Eq. (3):

$$E_p = E_1 + \frac{(\alpha_1+\alpha_4)R_1 \cdot R_4 \cdot I_b \cdot P}{R_1+R_2+R_3+R_4}, \quad (7)$$

where α_1 and α_4 are the pressure coefficients of the active coils, R_1 and R_4, respectively. Further, if their coefficients can be taken to be approximately equal to α, then it may be represented by:

$$E_p = E_1 + \frac{2\alpha R_1 \cdot R_4 \cdot I_b \cdot P}{R_1+R_2+R_3+R_4}. \quad (8)$$

Therefore, it follows that the sensitivity in the measurement can be enhanced to 2 times that in the present case when one active coil is used, as is clear from a comparison with Eq. (3).

In the practical measurement of the pressure, it is also necessary to take into account the effect due to the heat of reaction. If the heat evolved by the reaction could not be transferred to the surroundings, the reverse of when it is absorbed, fast enough to retain the isothermal condition, then the temperature of the reaction mixture varies; therefore, the crresponding pressure change must lead to a significant error in the measurement of the reaction rate. Although a theoretical analysis of the thermal effect has been pronounced by Withey and Whalley,[3] it is difficult in general to estimate to what extent the rate constant may be affected because there is no available information on the heat transfer between the reaction mixture and the thermostat in the system concerned. Because such an undesirable effect is essentially dependent upon the amount of conversion in a unit of time under given conditions, it can be experimentally eliminated by seeing whether or not the actually measured rate constants are appreciably affected by varying the concentrations of the reactant and the catalyst or the volume of the reaction mixture, *etc.*

Operation and Determination of the Rate

The reaction mixture, after being prepared, was readily preheated to a temperature somewhat higher than that of the thermostat in order to remove some dissolved air; then it was quietly poured into a glass syringe, from which air had been carefully expelled before it was stoppered with a Teflon plug. The syringe was put into the pressure vessel immersed in the thermostat, and then the vessel was quickly assembled and brought up to the desired pressure by means of the pressure pump. After about 40 min had been allowed for thermal equilibrium and the pressure had been finely adjusted to the required value on the Bourdon gauge, the valve was shut; then the unbalanced e.m.f. across the bridge, through which a constant current was passed, was potentiometrically measured at suitable time intervals. In all runs, an interval of about 2 half-lives of the reaction was taken between the first measuring set and the second one; thus, the obtained e.m.f. data were conveniently analyzed according to the Guggenheim equation:[8]

$$k_1 t + \ln(E_{t+\Delta t} - E_t) = \ln[(E_\infty - E_0)(1 - e^{-k_1 \Delta t})] = \text{constant}, \quad (9)$$

where E's are the observed e.m.f.'s, t is the reaction time and Δt is the time interval. The subscripts 0 and ∞ refer to the start and the equilibrium for reaction respectively. From Eq. (9), the first-order rate constants, k_1, were graphically obtained by plotting $\log(E_{t+\Delta t} - E_t)$ against t. The second-order rate constants, k_a, were calculated by dividing the first-order constants by the concentration of the catalyst used.

Results and Discussion

In order to test the usefulness of this apparatus in the measurement of the reaction rate, two kinds of reactions were chosen. One was the acid-catalyzed inversion of sucrose with a contraction of the volume, and the other was the base-catalyzed decomposition

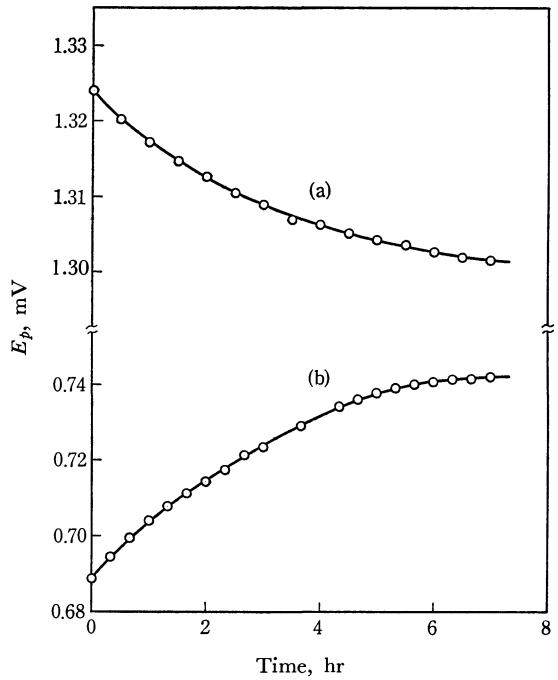

Fig. 4. Plots of E_p against time.
(a): Inversion of sucrose at 25.00°C and 1000 atm.
(d): Decomposition of diacetone alcohol at 30.00°C and 500 atm.

Table 1. Rate constants for the acid-catalyzed inversion of sucrose in water at 25.00°C

P, atm	C_{HCL}[a], mol·l^{-1}	$10^5 \times k_1$, sec^{-1}	$10^4 \times k_a$, $l \cdot mol^{-1} sec^{-1}$
1[b]	0.3134	4.01	1.28
100	0.6127	7.69	1.26
500	0.7829	8.96	1.14
1000	0.8263	8.15	0.986
1500	0.4395	3.86	0.878

a) The concentration of acid denotes the value corrected for compression of the solution by using Bridgman's data[9] for water.
b) The result at 1 atm was obtained from usual dilatometric measurement.

8) E. A. Guggenheim, *Phil. Mag.*, **2**, 538 (1926).

9) P. W. Bridgman, *Proc. Amer. Acad. Arts Sci.*, **48**, 309 (1912).

of diacetone alcohol with, on the contrary, an expansion of the volume.

First, the inversion of sucrose was measured at 25.00°C in aqueous dilute hydrochloric acid which contained initially about 0.5 mol/l of the reactant; here, the total pressure change during the kinetic measurements was in the range of from 9 to 20 atm. A typical curve obtained is shown in Fig. 4, while its Guggenheim plot is shown in Fig. 5. The first-order rate constants, as calculated from similar plots obtained at various pressures, are listed in Table 1, together with the second-order constants.

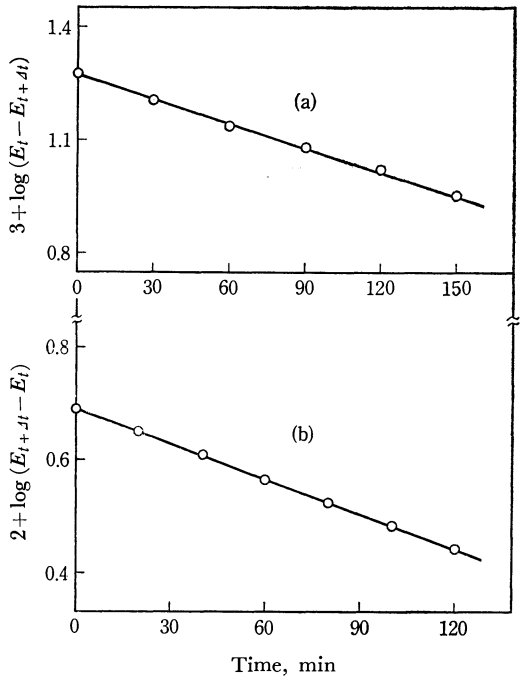

Fig. 5. Guggenheim plots for two e.m.f. data.
(a): Inversion of sucrose.
(b): Decomposition of diacetone alcohol.

The second-order rate constants as a function of the pressure are graphically shown in Fig. 6, together with those calculated from the data of Cohen and de Boer,[10] which were obtained by measurement with a polarimeter. The piezometrically-determined values are less than these by about 15 to 21 per cent, but it is not determined whether such a discrepanct results from the differences in the method of measurement or in the concentration of the acid used (their reaction mixtures were 0.0625 N in hydrochloric acid), or from other causes. The volumes of activation, $\Delta V^{\neq}$, were calculated from the slopes at 1 atm using the usual equation:

$$\left(\frac{\partial \ln k_a}{\partial T}\right)_T = -\frac{\Delta V^{\neq}}{RT}, \qquad (10)$$

where R is the gas constant and T is the absolute temperature. The value determined from the observed data is 6.0 cm³/mol; this is in good agreement with the 5.0 cm³/mol value from the data of Cohen and de Boer and also with the 6.0±~0.3 cm³/mol obtained by Whalley[11] from the same data.

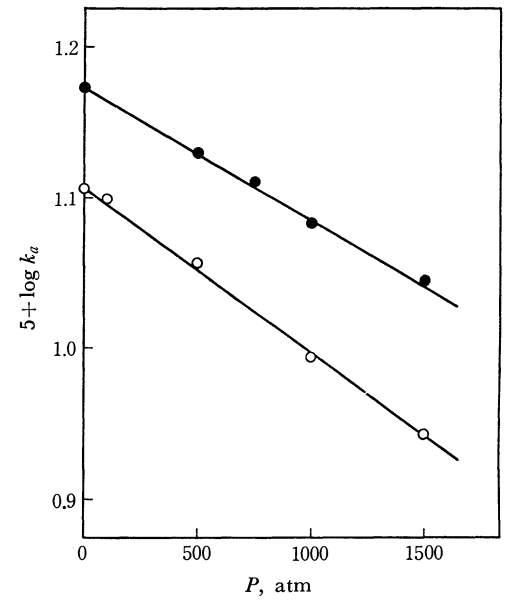

Fig. 6. Effect of pressure on the acid-catalyzed inversion of sucrose in water at 25.00°C.
●: Cohen and de Boer,[10] ○: This work.

The decomposition of diacetone alcohol as another reaction was measured in an aqueous solution involving initially about 0.4 mol/kg of the reactant and an appropriate amount of sodium hydroxide as a catalyst at 30.00°C and at various pressures. There was a pressure change of from 14 to 40 atm during the kinetic measurements. The results for this reaction are shown, along with those of sucrose, in Figs. 4 and 5. For purposes of comparison, the rates of the same reaction were also measured separately using an analytical method based on the oximation of the carbonyl group with hydroxylamine hydrochloride.[12] Both

Table 2. Rate constants for the base-catalyzed decomposition of diacetone alcohol in water at 30.00°C[a]

P, atm	method[b]	$10^3 \times C_{NaOH}$ mol·kg^{-1}	$10^4 \times k_1$ sec^{-1}	$10^2 \times k_a$, kg·mol^{-1} sec^{-1}
1	a	7.222	1.08	1.50
1	b	7.920	1.19	1.50
100	c	11.57	1.79	1.55
500	a	7.181	1.24	1.73
500	c	4.657	0.797	1.71
1000	a	6.173	1.19	1.93
1000	c	8.667	1.71	1.97
1500	a	6.173	1.30	2.11
1500	c	7.753	1.71	2.21

a) The measurements with analytical method were made in a thermostat controlled to within ±0.05°C.
b) a: analytical method, b: usual dilatometric method, c: piezometric method.

10) E. Cohen and R. B. de Boer, *Z. Phys. Chem.* (Leipzig), **84**, 41 (1913).

11) E. Whalley, *Trans. Faraday Soc.*, **55**, 798 (1959).

12) D. M. Smith and J. Mitchell, Jr., *Anal. Chem.*, **22**, 750 (1950).

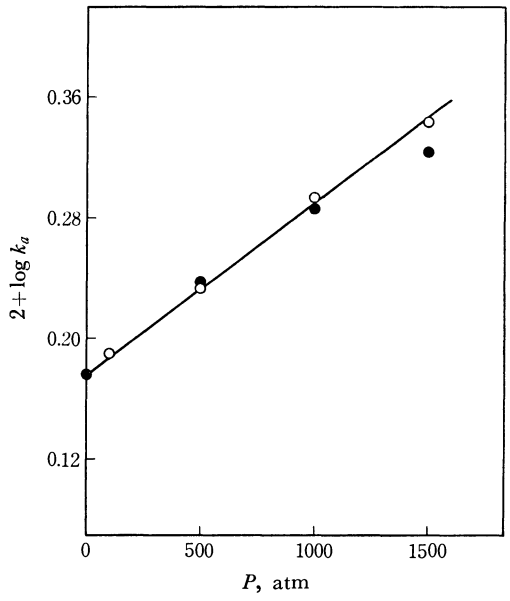

Fig. 7. Effect of pressure on the base-catalyzed decomposition of diacetone alcohol in water at 30.00°C.
●: Analytical method, ○: Piezometric method.

rate constants obtained are listed in Table 2; the agreement between them is very satisfactory. The volume of activation obtained from Fig. 7 was almost the same, -6.6 cm^3/ mol, in both cases, and no appreciable difference could be found graphically. The mechanistic consideration of the observed value of $\Delta V^{\neq}$ for this reaction has not been made here, for it is beyond the present purposes, but it will be reported elsewhere. In addition, the rate of the depolymerization of paraldehyde catalyzed by 0.0991 mol/l perchloric acid was found in the same way to be 7.36×10^{-4} l/mol·sec at 35.00°C and 500 atm; this is in good agreement with the 7.12×10^{-4} l/mol·sec obtained by the piezometric measurements of Withey and Whalley.[4]

From some preliminary measurements for each reaction, it might be presumed that all of the results mentioned above were not significantly affected by the heat of reaction during the measurements.

Consequently, it may be concluded that the apparatus and the technique employed in the present work are sufficiently applicable to the rate measurements of any other reaction with a change in volume.

The author should like to thank Mr. H. Ōto for his help in the construction of the high-pressure apparatus and Mr. J. Ōtsubo for his help in the kinetic measurements.

BULLETIN OF THE CHEMICAL SOCIETY OF JAPAN, VOL. 44, 2587—2590 (1971)

An MO Interpretation of the Chemical Shifts of Inner-shell Electrons

Hiroshi KATO, Kazuhiro A. ISHIDA,* Hiroshi NAKATSUJI,* and Teijiro YONEZAWA*

Department of General Education, Nagoya University, Chikusa-ku, Nagoya

** Department of Hydrocarbon Chemistry, Faculty of Engineering, Kyoto University, Kyoto*

(Received December 31, 1970)

A correlation formula between the chemical shifts of inner-shell electrons and molecular-charge distributions is derived by an MO scheme with CNDO-type approximations. Errors imposed in these schemes are discussed. Reorganization energy terms are briefly discussed in the same level of approximations.

The chemical shifts of inner-shell electrons have been studied in a wide variety of organic and inorganic compounds.[1,2] One interesting feature of the problem is that the chemical shifts change linearly with the charges on the atoms considered. These charges have been estimated by several methods-i.e., methods with using the oxidation number and Pauling's electronegativity differences,[1,3] an iterative extended Hückel method,[4] CNDO method,[5] and several types of non-empirical calculations.[6-11]

In this report, an MO interpretation of the correlation between the chemical shifts of the binding energies of inner-shell electrons in certain molecules and the atomic charges is given by introducing some approximations, and the limitations of these relations are briefly discussed.

Theoretical

By Roothaan's SCF treatment for closed-shell systems, the orbital energy of ith MO, ε_i, is given by:

$$\varepsilon_i = F_{ii} = \sum_{r,t} C_r{}^i C_t{}^i F_{rt} \qquad (1)$$

1) K. Siegbahn *et al.*, ESCA atomic molecular and solid state structure studied by means of electron spectroscopy, Almqvist and Wiksills A. B., Stockholm (1967).

2) D. M. Hercules, *Anal. Chem.*, **42**, 20A (1970).

3) R. G. Albridge, U. Erickson, J. Hedman, C. Nardling, and K. Siebahn, *Ark. Kemi*, **28**, 257 (1968).

4) M. Pelavin, D. Hendrickson, J. M. Hollander, and W. L. Jolly, *J. Phys. Chem.*, **74**, 1116 (1970).

5) J. M. Hollander, D. N. Hendrickson, and W. L. Jolly, *J. Chem. Phys.*, **49**, 3315 (1968).

6) R. Manne, *ibid.*, **46**, 4645 (1967).

7) F. A. Gianturco, and C. A. Coulson, *Mol. Phys.*, **14**, 223 (1968).

8) H. Basch, and L. C. Snyder, *Chem. Phys. Lett.*, **3**, 333 (1969).

9) M. E. Schwartz, C. A. Coulson, and S. D. Allen, *J. Amer. Chem. Soc.*, **92**, 447 (1970).

10) M. E. Schwartz, *Chem. Phys. Lett.*, **5**, 50 (1970).

11) C. A. Coulson, and F. A. Gianturco, *Mol. Phys.*, **18**, 607 (1970).

Where C_r^i and F_{rs} are the rth AO coefficient of the ith MO and the F_{rs}-element of the Fock operator respectively.

Suppose that the ith MO is mainly constructed by inner-shell AO's; the following derivation can then be easily carried out with considerable accuracy, since the diagonal elements of the Fock operator for inner-shell AO's, F_{ss}, is very large compared with that of the off-diagonal ones F_{rs}:[12,13]

$$\varepsilon_i \simeq \varepsilon_s = F_{ss}, \qquad C_s^i \simeq 1.0, \tag{2}$$

$$F_{ss} = \left(s\left|-\frac{1}{2}\Delta-\frac{Z_A}{r_A}\right|s\right) + \left(s\left|-\sum_{B\neq A}\frac{Z_B}{r_B}\right|s\right) + \sum_{r,t} P_{rt}\left\{(ss/rt)-\frac{1}{2}(sr/st)\right\}. \tag{3}$$

In Eq. (3), the first term is the self-core integral, while the second is the nuclear attraction by the other nuclei and the third consists of electronic repulsions. Throughout this report, r, s, t, and u denote atomic orbitals; especially, s denotes the inner-shell AO in question belonging to the A atom. The i and j notations represent occupied MO's, and k and l, vacant ones. The P_{rt} notation is the bond order between r and t AO's.

To connect the orbital energies with the atomic charges, we use the following approximation, using the same notations as in Refs. 14 and 17:

(A), The self-core integral:

$$\left(s\left|-\frac{1}{2}\Delta-\frac{Z_A}{r_A}\right|s\right) = -I_s - (N_s-1)(ss/ss) - \sum_{r}^{\text{on A}} N_r\left\{(ss/rr)-\frac{1}{2}(rs/rs)\right\} \tag{4}$$

and the nuclear attraction:

$$\left(s\left|-\frac{Z_B}{r_B}\right|s\right) = -Z_B(ss/ns_Bns_B) = -Z_B\gamma_{AB}. \tag{5}[15]$$

The above formulae have already been given in a previous paper.[14] (B), The electronic repulsion integrals can be estimated by a CNDO-type approximation[17]:

Thus, Eq. (3) can be re-written as:

$$F_{ss} = -I_s + (P_{AA}-Z_A^{\,v})\gamma_{AA} + \sum_{A\neq B}(P_{BB}-Z_B^{\,v})\gamma_{AB}, \tag{6}$$

where the average Coulomb integrals are:

$$\gamma_{AA} = (ss/ns_Ans_A), \qquad \gamma_{AB} = (ss/ns_Bns_B), \tag{7}$$

and where $Z_A^{\,v}$ denotes the number of valence electrons on the A atom and ns_A denotes valence s-type AO on the A atom.

When a Mulliken approximation with in Eq. (7) is used instead of the above CNDO-type one, and only the term of S(overlap) is considered, an expression similar to that in Eq. (6) is obtained, but in this case the P_{AA}'s in Eq. (6) become atomic populations.

From Eq. (6), the following simplified relation can be obtained by denoting $(P_{AA}-Z_A^{\,v})=-Q_A$ (Q_A is the net charge of atom A):

$$\Delta\varepsilon_s = \varepsilon_s + I_s = -Q_A\gamma_{AA} - \sum_{B\neq A} Q_B\gamma_{AB}. \tag{8}[18]$$

That is, the shift of the inner-shell binding energy from the atomic ionization energy in certain valence state is correlated with the molecular-charge distribution. The shift of the $\Delta\varepsilon_s$ for the A atom in different chemical environments, which are denoted as X and Y, is:

$$\delta\Delta\varepsilon_s(X,Y) = \{Q_A(X)-Q_A(Y)\}\gamma_{AA} - \sum_{B\neq A}^{\text{in Y}} Q_B(Y)\gamma_{AB}(Y) + \sum_{B\neq A}^{\text{in X}} Q_B(X)\gamma_{AB}(X). \tag{9}$$

Eq. (9) indicates that the chemical shifts depend not only on the atomic-charge differences of the A atom in different molecules, but also on the sum of the charges over the other parts of the molecules, since the γ_{AB}/γ_{AA} ratio is not negligibly small. For diatomic molecules of the first-row elements, AB and A_2, $\delta\Delta\varepsilon_s$-(AB, A_2)=0.5, if $Q_A(AB)=-Q_B(AB)=1.0$, $\gamma_{AA}(AB)=1.0$, and $\gamma_{AB}(AB)=0.5$ (in a.u.).[20] The change in the inner-shell binding energy between the molecules is about 14 eV per unit charge. This is in agreement with the previous results.[19]

Results and Discussion

Tables 1 and 2 summarize the values of some atomic integrals involving the $1S_C$ AO of formaldehyde (in a.u.). By means of these tables we can examine the approximations Eq. (5), and (B). Minimal Slater bases with Slater-rule exponents, except for that of 1.2 for hydrogen, are used throughout the calculations in the present paper. The integrals are evaluated by means of the 4-term Gaussian expansion method.[20]

As shown in Table 1, the approximation introduced

Table 1. Comparison of the nuclear attraction integrals $(S_A|(Z_B/r_B)|S_A)$ with $Z_B\gamma_{AB}$ in formaldehyde (in a.u.)

S_A	B	$(S_A\|(Z_B/r_B)\|S_A)$	$Z_B\gamma_{AB}$
$1S_C$	O	2.6240	2.6160
$1S_C$	H	0.4855	0.4727
$1S_O$	C	1.7493	1.7089
$1S_O$	H	0.2655	0.2654

12) e.g., W. E. Palke and W. N. Lipscomb, *J. Amer. Chem. Soc.*, **88**, 2384 (1966).

13) E. Clementi, *Chem. Rev.*, **68**, 341 (1968).

14) T. Yonezawa, H. Kato, and K. Yamaguchi, This Bulletin, **40**, 536 (1967).

15) While this work, was in progress, the same relation was pointed out in Ref. 16.

16) See Ref. 22.

17) J. A. Pople, D. P. Santry, and G. A. Segal, *J. Chem. Phys.*, **43**, S129 (1965).

18) A similar equation, obtained by means of an electrostaic model, is given in Ref. 19; that is, $\delta\Delta\varepsilon_s(XY)=kQ_s+\sum_{j\neq i}\frac{Q_j}{R_{ij}}+l_y$ but here K, which corresponds γ_{AA} in Eq. (8), is taken to be an empirical parameter. The constant, l_y, is determined by means of the reference compound.

19) U. Gelius, B. Roos, and K. Siegbahn, *Chem. Phys. Lett.*, **4**, 471 (1970).

20) As to the integral values, refer to those in Table 2 and also those in Ref. 12.

20) H. Taketa, S. Huzinaga, and K. O-ohata, *J. Phys. Soc. Japan*, **21**, 2323 (1966); S. Huzinaga, *Suppl. Progr. Theor. Phys.*, No. **40**, 52 (1967). R. F. Stewart, *J. Chem. Phys.*, **52**, 431 (1970).

Table 2. Some electron repulsion integrals including carbon 1S orbitals of formaldehyde (in a.u.)[a]

Type		Type	
$(1S_C1S_C/2S_C2S_C)$	0.8073	$(1S_C1S_C/1S_O1S_O)$	0.4373
$(1S_C1S_C/2P_{xC}2P_{xC})$	0.8072	$(1S_C1S_C/2P_{zC}2P_{zO})$	−0.2452
$(1S_C1S_C/2S_O2S_O)$	0.4360	$(1S_C1S_C/2S_O2P_{zO})$	−0.1190
$(1S_C1S_C/2P_{xO}2P_{xO})$	0.4132	$(1S_C1S_C/2S_C2P_{zO})$	−0.2582
$(1S_C1S_C/2P_{zO}2P_{zO})$	0.4817	$(1S_C2S_C/2S_C2S_C)$	0.0812

a) The z axis is taken to be paralled with the C-O bond.

in Eq. (5) is good. Table 2 indicates that the "average Coulomb" approximation is excellent for one-center integrals and is only correct to within about a 10% error for two-center ones. The two-center Coulomb and hybrid integrels, $(1s_A1s_A/2s_B2p_B)$ and $(1s_A1s_A/2s_A2p_B)$ types, however, are not negligible; therefore, the (B) approximation, *i.e.*, the CNDO-type integal which neglects the above type of integrals, may be bad in certain cases where the corresponding off-diagonal elements of the bond-order matrix are not negligible.

Table 3. Calculated shifts for carbon 1S electrons

Compounds	E_{obsd} [a]	Q_A [b]	$\delta\Delta\varepsilon$ [c]
C_2H_2	291.2	−0.064	−0.90
C_2H_4	290.7	−0.33	−0.41
C_2H_6	290.6	−0.006	−0.07
CH_3OH	292.7	+0.129	1.40
CO_2	297.64	+0.536	5.45
HCO_2H	295.79	+0.381	3.40

a) Observed binding energies (in eV), T. D. Yhomas, *J. Chem. Phys.*, **52**, 1373 (1970); D. W. Davis, J. M. Hollander, and D. A. Shirley, and T. D. Thosmas, *ibid.*, **52**, 3295 (1970).
b) Calculated net charges on carbon atom by CNDO/2 method.
c) Calculated by Eq. (9) with CNDO/2 net charges (in eV).

Table 4. Calculated shifts for nitrogen 1S electrons

Compounds	E_{obsd} [a]	Q_A [b]	$\delta\Delta\varepsilon_s$ [c,e]	
N_2	402.45	0.0	0.0	
NH_3	398.1	−0.234	−2.96	(−5.92)
$(CONH_2)_2$	400.0	−0.238	−1.73	
$(CH_3)_3NO$	402.2	+0.157	2.09	
C_5H_5N(pyridine)	398.0	−0.142	−2.04	(−6.27)
C_6H_5CN	398.4	−0.165	−2.99	
$NaNO_3$ [d]	407.4	+0.636	−2.59	
$NaNO_2$ [d]	404.1	+0.083	−10.36	
NaN_3 [d] (middle N)	403.7	+0.447	−6.58	(−13.0)
(terminal N)	399.3	−0.723	−18.04	(−16.3)
KCN [d]	399.0	−0.409	−18.00	(−19.3)

a), b), c) They are the same as in Table 3.
d) Calculated as anion.
e) The values in parenthesis are evaluated by non-empirical gross atomic charges in stead of CNDO/2 net charges in Eq. (9). These gross charges have been given in references; R. Bonaccorsi, C. Petorngolo, E. Scrocco, and J. Tomasi, *J. Chem. Phys.*, **48**, 1497, 1500 (1968); E. Clementi, *ibid.*, **46**, 4731 (1967); W. E. Palke and N. N. Lipscomb, *J. Amer. Chem. Soc.*, **88**, 2384 (1966).

The results calculated by means of Eq. (9) are collected in Tables 3 and 4 for carbon 1s and nitrogen 1s electrons respectively; they are all shown in Figs. 1 and 2 except for anions. Figures 1 and 2 indicate a rather satisfactory correlation between the observed chemical shifts and the values of $\delta\Delta\varepsilon_s$. The solid lines in Figs. 1 and 2 are inclined about 45°; therefore, it seems that the chemical shifts can be evaluated semi-quantitatively in terms of the $\delta\Delta\varepsilon_s$ in neutral molecules, and that a relation between the molecular-charge distributions and the observed shifts may be in the form of $(Q_A\gamma_{AA}+\sum_{B\neq A}Q_B\gamma_{AB})$. For the anious containing

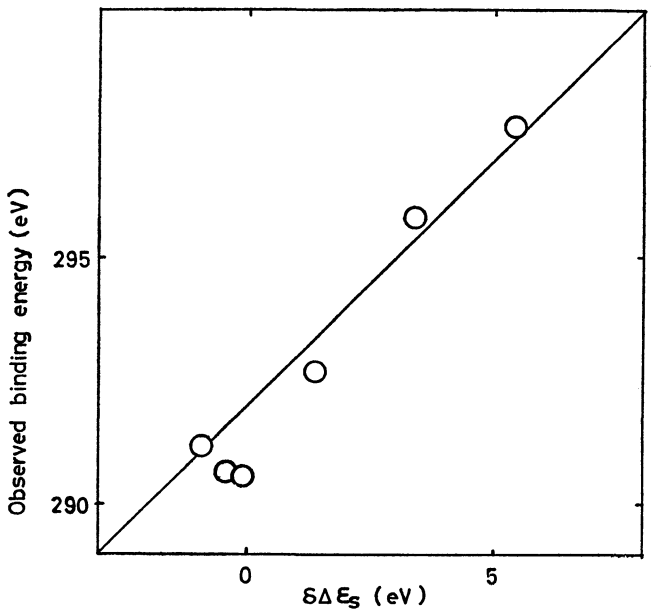

Fig. 1. The observed binding energies of carbon 1s electron plotted against the $\delta\Delta\delta_s$'s.

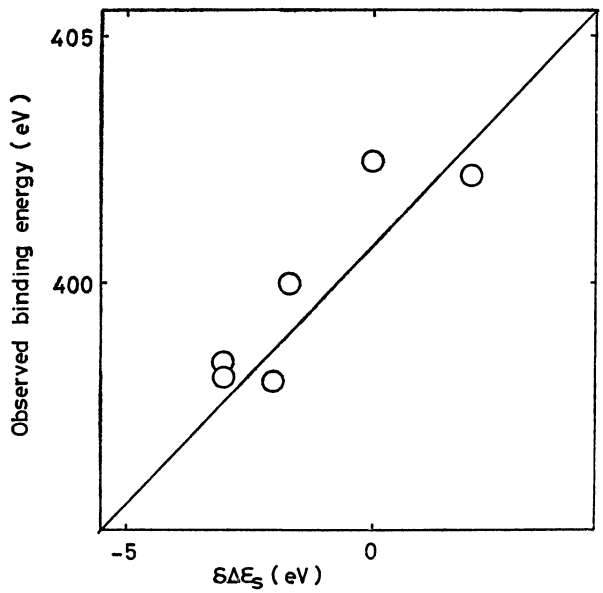

Fig. 2. The observed binding energies of nitrogen 1s electrons plotted against the $\delta\Delta\varepsilon_s$'s.

nitrogen atoms, the above rather good correlation is not observed; that is in these charged species, the crystal effects may be considerable.[5]

It is noticed that the values of ε_s obtained by Roothaan's closed-shell treatment are generally larger than those of the binding energy observed at about 10—20%, and open-shell SCF calculations give better results, as has been pointed out by several authors[7-11,13,21,22]. Further it has been suggested that the main effects of these discrepancies depend on the reorganization energy.[19]

Now, let me examine the reorganization energy in the above approximation scheme. Suppose that MO's i and j are given by Roothaan's closed-shell treatment. Using these MO's, an open-shell wave function with an s hole ($S_z=1/2$), is obtained approximately by a CI scheme;

$$\begin{aligned}\Phi_s{}^0 = {} & |si\bar{i}\cdots jj\bar{j}| + \sum_{j(\neq s)}^{\text{occ.}} \lambda_{is}|s\bar{s}i\bar{i}\cdots j| + \sum_{k}^{\text{vac}} \lambda_{sk}|ki\bar{i}\cdots jj\bar{j}| \\ & + \sum_{j(\neq s)}^{\text{occ}} \sum_{k}^{\text{vac}} \lambda_{jk}(1)\{|si\bar{i}\cdots jk\bar{k}| - |s\bar{i}i\cdots jk\bar{k}|\} \\ & + \sum_{j(\neq s)}^{\text{occ}} \sum_{k}^{\text{vac}} \lambda_{jk}(2)\{2|\bar{s}ii\cdots jk| - |si\bar{i}\cdots j\bar{k}| - |s\bar{i}i\cdots \bar{j}k|\}. \end{aligned} \tag{10}$$ [23]

That is, $\Phi_s{}^0$ is an approximate open SCF function[24] and λ_x is the coefficient of a related configuration, x. By perturbation treatment, these are[25];

$$\begin{aligned} \lambda_{js} &= F_{js}/E_{js} = 0, \qquad \lambda_{sk} = \frac{(ks/ss)}{E_{sk}}, \\ \lambda_{ik}(1) &= \frac{\sqrt{2}\{(ik/ss) - (1/2)(is/ks)\}}{E_{ik}(1)}, \\ \lambda_{ik}(2) &= \frac{-\sqrt{3/2}(is/sk)}{E_{ik}(2)}. \end{aligned} \tag{11}$$

Where E_{sk} is the energy difference between the energy of the $s\rightarrow k$ excited configuration, as shown in Eq. (10), and the ground-state configuration, and so on.

Then, the energy, $E_s{}^0$ becomes;

$$\begin{aligned} E_s{}^0 = (E_0 - \varepsilon_s) + \sum_k \frac{(ks/ss)^2}{E_{sk}} + \sum_{k,i\neq s} \frac{2\{(ik/ss) - (1/2)(is/ks)\}^2}{E_{ik}(1)} \\ + \sum_{k,i\neq s} \frac{\{-\sqrt{3/2}(is/ks)\}^2}{E_{ik}(2)} + \cdots \end{aligned} \tag{12}$$

That is, the reorganization energy is $E_s{}^0 - (E_0 - \varepsilon_s)$, and the dominant contribution comes from the third term, since $E_{sk} \sim \varepsilon_k - \varepsilon_s$(large), $E_{ik}(1) \sim {}^1E_{ik}$ (valence shell $i\rightarrow k$ singlet excitation energy for a closed-shell system, small), and $(ik/ss) \simeq C_r{}^i C_r{}^k (rr/ss)$ is large, and (is/ks) is small as is shown in Table 2.

The magnitude of the third term can be roughly estimated as; E_{sk} (1) $\sim$0.5 a.u., (rr/ss) $\sim$1 a.u., and $\varepsilon_s \sim$10 a.u.; hence, (the third term)$/\varepsilon_s$ $\sim 10^{-1}$ [26]. This order is reasonable when it is compared with the previous results, 10$\sim$20%.[10,13,19,27]

These results indicate that the third part is the most important in reorganization energy. Further, this third term can be approximated:

$$\sum_i \sum_k \frac{2\{\sum_r C_r{}^i C_r{}^k (rr/ss)\}^2}{E_{ik}(1)} \sim \sum_{\text{B}}^{\text{all on B}} \sum_r p_{rr}(2 - p_{rr}) \frac{(\gamma_{\text{AB}})^2}{2E_{\text{aV}}}$$

Where E_{aV} is the average excitation energy.

That is, the reorganization energy is not a linear function for the atomic charges.

As to the other corrections for inner electron binding energies, that is, the correlation correction,[13,28] the relativistic correction[29] and the crystal correction,[3,30] it can be pointed out that these are negligible or are proportional to the charges.

As has been shown in the above discussion, the linear relation between the charges and the inner-shell binding energy is restricted within the imposed approximations; thus, in some cases, this linearities may depend on the cancellations of various effects. We hope this point will be reexamined in the future.

The calculations have been carried out on the FACOM 230—60 Computer of Kyoto University.

21) P. S. Bagus, *Phys. Revs.*, **A619**, 139 (1965).
22) M. E. Schwartz, *Chem. Phys. Lett.*, **5**, 50; **6**, 631; **7**, 78 (1970).
23) The last configuration does not appear in the difference between the zero-th order configuration (the first term) and Roothaan's open SCF configuration. The contribution from this configuration is certainly very small as will be shown later in this report.
24) C. C. J. Roothaan, *Rev. Mod. Phys.*, **32**, 179 (1960).
25) For example, R. Zahradnik, and P. Carsky, *J. Phy. Chem.*, **74**, 1235 (1970).
26) The estimated values of the third term in the level of approximations in the present report are, *e.g.*, 22.7 eV for the N_{1s} of pyridine.
27) For valence-electron systems, the same order values are obtained.
28) E. Clementi, *J. Chem. Phys.*, **47**, 4485 (1967).
29) P. Palmiele, and C. Zauli, *Theor. Chim. Acta*, **7**, 89 (1967).
30) C. S. Fadley, S. B. M. Hagstrom, M. P. Klein, and D. A. Shirley, *J. Chem. Phys.*, **48**, 3779 (1968).

Stochastic Formulation of Entropy Production due to Second-Order Reaction

Kenji ISHIDA

Department of Applied Chemistry, Ibaraki University, Hitachi, Ibaraki

(Received January 11, 1971)

Entropy production, originated from an ideal gas second-order reaction taking place in a closed system, has been stochastically formulated by defining the entropy in a form similar to the conditional entropy used in the theory of information. The entropy is introduced in the natural way as a result of the partial factorization of joint probability for reaction states devised for the approximate solution of the stochastic process of the second-order reaction. The entropy production has also been discussed in comparison with the usual one.

The stochastic nonequilibrium thermodynamics of reaction systems can be studied by the correlation of probability to entropy on the proposition that chemical reaction is a random process. The author has stochastically discussed the nonequilibrium thermodynamics for first-order reactions in closed and open systems.[1] It has been assumed that the entropy change $\Delta_i S$ due to a chemical reaction is of Gibbsian type, *viz.*,

$$\Delta_i S = -k \sum_{\boldsymbol{n}} P(\boldsymbol{n};\ t)\ln[P(\boldsymbol{n};\ t)/P(\boldsymbol{n};\ \infty)] \qquad (1)$$

or

$$S = -k\langle \ln[P(\boldsymbol{n};\ t)/P(\boldsymbol{n};\ \infty)]\rangle + S_e, \qquad (1')$$

where k is Boltzmann's constant, $P(\boldsymbol{n};\ t)$ the probability distribution for the set $\boldsymbol{n}=\{n_\gamma\}$ of all the numbers of molecules of reacting species γ's at time t, $P(\boldsymbol{n};\ \infty)$ the corresponding equilibrium probability distribution, $\Delta_i S=S-S_e$ (S_e is the entropy for the equilibrium probability distribution) and the angular brackets denote the average over all possible reaction states.

As an example, we consider the reaction A⇆B. The probability distribution for reaction states is given by the binomial distribution $P(\boldsymbol{n};\ t)=(n!/\prod_\gamma n_\gamma!)\prod_\gamma \{p_\gamma(t)\}^{n_\gamma}$, in which $n=\sum_\gamma n_\gamma$ (γ=A, B) is the total number of molecules and $p_\gamma(t)$ the probability for a molecule of reacting species γ to be found in the reaction system. According to Eq. (1), the entropy change can be written as

$$\begin{aligned}\Delta_i S &= -k \sum_\gamma \langle n_\gamma\rangle \ln[p_\gamma(t)/q_\gamma] \\ &= -k \sum_\gamma \langle n_\gamma\rangle \ln[\langle n_\gamma\rangle/\langle n_\gamma\rangle_e],\end{aligned} \qquad (2)$$

where q_γ is the probability corresponding to $p_\gamma(t)$ in equilibrium state. This is identified with the result from the usual nonequilibrium thermodynamics, in which the hypothesis of local equilibrium[2] plays an important role. It should be stressed, here, that the hypothesis of local equilibrium is also implicitly involved in Eq. (1), since the equilibrium probability distribution $P(\boldsymbol{n};\ \infty)$ is assumed to be retained throughout the reaction time.

For the system in which a second-order reaction occurs, however, the stochastic formulation of nonequilibrium thermodynamics remains unsettled. This may well be due to the difficulty in finding the probability distribution to facilitate the evaluation of stochastic entropy. When the probability distribution, even though it is approximate, is found at all, the entropy change can be calculated by Eq. (1). The plan of this paper is as follows. We describe a second-order reaction by the stochastic process linearized with the transition probability variable with time on the assumption of the partial factorization of the joint probability distribution for reaction states, and at the same time we define the stochastic entropy in a form similar to the conditional entropy in the theory of information.[3]

Stochastic Model for Second-Order Reaction

For the sake of simplicity, we consider a second-order reaction in ideal gases

$$\mathrm{A} + \mathrm{B} \rightleftarrows \mathrm{C}. \qquad (\mathrm{I})$$

Letting the random variables $X_A(t)$, $X_B(t)$, and $X_C(t)$ represent the numbers of molecules of reacting species A, B, and C at time t, respectively, the stochastic process is then described by the differential-difference equation,

$$\begin{aligned}&\frac{\mathrm{d}}{\mathrm{d}t}P(n_A,\ n_B,\ n_C;\ t) \\ &= \lambda(n_A+1)(n_B+1)P(n_A+1,\ n_B+1,\ n_C-1;\ t) \\ &- (\lambda n_A n_B+\lambda' n_C)P(n_A,\ n_B,\ n_C;\ t) \\ &+ \lambda'(n_C+1)P(n_A-1,\ n_B-1,\ n_C+1;\ t)\end{aligned} \qquad (3)$$

where $P(n_A,\ n_B,\ n_C;\ t)=\mathrm{Prob.}\{X_A(t)=n_A,\ X_B(t)=n_B,\ X_C(t)=n_C\}$ denotes the joint probability that there are n_A, n_B, and n_C molecules of reacting species A, B, and C in the reaction system at time t, respectively, and λ and λ' are the rate constants defined on the assumption that the transition probabilities of reaction processes of A+B→C and A+B←C in the time interval $(t,\ t+\mathrm{d}t)$ are given by $\lambda\, n_A n_B \mathrm{d}t$ and $\lambda' n_C \mathrm{d}t$, respectively.

It is a complicated problem, soluble in principle, to find the probability distribution $P(n_A,\ n_B,\ n_C;\ t)$ from Eq. (3), which is nonlinear with respect to the numbers of molecules. In order to obtain its approximate solution, however, we attempt to reform Eq. (3) into the linear equation of only the number of molecules of reacting species C, n_C. If the reaction system is in the thermodynamic limit such that the total number of molecules taking part in reaction is sufficiently large,

1) K. Ishida, *J. Phys. Chem.*, **70**, 3806 (1966); **72**, 92 (1968).

2) S. R. de Groot and P. Mazur, "Non-Equilibrium Thermodynamics," North-Holland Publishing Co., Amsterdam (1962), p. 23.

3) A. I. Khinchin, "Mathematical Foundations of Information Theory," Dover Publications Inc., New York (1957), p. 35.

it is possible to assume the partial factorization of the joint probability[4]

$$P(n_A, n_B, n_C; t) = P(n_A; t)P(n_B, n_C; t) \quad (4, A)$$

or

$$P(n_A, n_B, n_C; t) = P(n_B; t)P(n_A, n_C; t). \quad (4, B)$$

Such a factorization, as will be shown later, is made to preserve at least the stochastic process of the reaction. Applying the factorization (4, A) to Eq. (3) and taking the summation over all possible values of random variable $X_A(t)$, we obtain

$$\begin{aligned}\frac{d}{dt}P(n_B, n_C; t) &= \lambda\langle n_A\rangle(n_B+1)P(n_B+1, n_C-1; t) \\ &- (\lambda\langle n_A\rangle n_B+\lambda' n_C)P(n_B, n_C; t) \\ &+ \lambda'(n_C+1)P(n_B-1, n_C+1; t). \end{aligned} \quad (5)$$

From Eq. (5), we can easily derive the rate equation with respect to the mean $\langle n_C\rangle$,

$$\frac{d}{dt}\langle n_C\rangle = \lambda\langle n_A\rangle\langle n_B\rangle-\lambda'\langle n_C\rangle. \quad (6)$$

This is of the uncorrelated form of the alternative rate equation derived directly from Eq. (3),

$$\frac{d}{dt}\langle n_C\rangle = \lambda\langle n_A n_B\rangle-\lambda'\langle n_C\rangle, \quad (7)$$

which, in the thermodynamic limit, is practically equivalent to Eq. (6). If the initial numbers of molecules of reacting species A and B are denoted by $n_A^{(0)}$ and $n_B^{(0)}$, respectively, equation (6) is written as

$$\frac{d}{dt}\langle n_C\rangle = \lambda(n_A^{(0)}-\langle n_C\rangle)(n_B^{(0)}-\langle n_C\rangle)-\lambda'\langle n_C\rangle. \quad (6')$$

Solving this differential equation, we obtain, in agreement with the deterministic theory,

$$\langle n_C\rangle = \frac{\alpha\beta(1-\exp[-\lambda(\alpha-\beta)t])}{\alpha-\beta\exp[-\lambda(\alpha-\beta)t]}, \quad (8)$$

where α and β are the roots of

$$\langle n_C\rangle^2 - (n_A^{(0)}+n_B^{(0)}+\lambda'/\lambda)\langle n_C\rangle + n_A^{(0)}n_B^{(0)} = 0. \quad (9)$$

Let us return to Eq. (5). If the transition probability variable with time is defined by

$$\lambda_A(t) = \lambda\langle n_A\rangle, \quad (10)$$

where

$$\langle n_A\rangle = n_A^{(0)} - \frac{\alpha\beta(1-\exp[-\lambda(\alpha-\beta)t])}{\alpha-\beta\exp[-\lambda(\alpha-\beta)t]}, \quad (11)$$

equation (5) becames

$$\begin{aligned}\frac{d}{dt}P(n_B, n_C; t) &= \lambda_A(t)(n_B+1)P(n_B+1, n_C-1; t) \\ &- (\lambda_A(t)n_B+\lambda' n_C)P(n_B, n_C; t) \\ &+ \lambda'(n_C+1)P(n_B-1, n_C+1; t) \end{aligned} \quad (5')$$

or

$$\begin{aligned}\frac{d}{dt}P(n_C; t) &= \lambda_A(t)\{n_B^{(0)}-(n_C-1)\}P(n_C-1; t) \\ &- \{\lambda_A(t)(n_B^{(0)}-n_C)+\lambda' n_C\}P(n_C; t) \\ &+ \lambda'(n_C+1)P(n_C+1; t), \end{aligned} \quad (5'')$$

which is just the same because of Prob. $\{X_B(t)=n_B,\ X_C(t)=n_C\}$=Prob.$\{X_B(t)=n_B^{(0)}-n_C,\ X_C(t)=n_C\}$= Prob. $\{X_C(t)=n_C\}$ on the basis of the introduction of the transition probability $\lambda_A(t)$.

To solve Eq. (5''), let us define the generating function

$$G(z_C; t) = \sum_{n_C} z_C^{n_C}P(n_C; t), \quad 0<|z_C|\leq 1. \quad (12)$$

From Eq. (5''), then, we obtain the partial differential equation

$$\frac{\partial G}{\partial t} = \{\lambda_A(t)+\lambda'\}(1-z_C)\frac{\partial G}{\partial z_C} - n_B^{(0)}\lambda_A(t)(1-z_C)G, \quad (13)$$

where the initial condition is given by $G(z_C; 0)=1$, which corresponds to the initial condition for Eq. (5''), $P(n_C; 0)=\delta_{n_C,0}$. After rather lengthy algebraic manipulations, it can be found that the solution of Eq. (13) is of the form

$$G(z_C; t) = \left\{\frac{\alpha-n_A^{(0)}-(\beta-n_A^{(0)})\exp[-\lambda(\alpha-\beta)t]}{\alpha-\beta\exp[-\lambda(\alpha-\beta)t]} + \frac{n_A^{(0)}(1-\exp[-\lambda(\alpha-\beta)t])}{\alpha-\beta\exp[-\lambda(\alpha-\beta)t]}z_C\right\}^{n_B^{(0)}}. \quad (14)$$

Performing the binomial expansion of the right-hand side of this equation, we have, according to Eq. (12),

$$P(n_C; t) = \binom{n_B^{(0)}}{n_C}\left\{\frac{n_A^{(0)}(1-\exp[-\lambda(\alpha-\beta)t])}{\alpha-\beta\exp[-\lambda(\alpha-\beta)t]}\right\}^{n_C} \times \left\{\frac{\alpha-n_A^{(0)}-(\beta-n_A^{(0)})\exp[-\lambda(\alpha-\beta)t]}{\alpha-\beta\exp[-\lambda(\alpha-\beta)t]}\right\}^{n_B^{(0)}-n_C}. \quad (15)$$

This is the probability distribution on the understanding that the reacting species A takes part in the reaction through the mean number of molecules, $\langle n_A\rangle$. Of course, from the probability distribution (15), we obtain the mean $\langle n_C\rangle$ consistent with Eq. (8).

Let us find the probability $P(n_A; t)$. For this purpose, we introduce again the generating function defined by

$$g(z_A; t) = \sum_{n_A} z_A^{n_A}\{\sum_{n_B, n_C} P(n_A, n_B, n_C; t)\}, \quad 0<|z_A|\leq 1 \quad (16)$$

which may be called a reduced one. Thus, we have from Eq. (3),

$$\frac{\partial g}{\partial t} = (1-z_A)\left\{\lambda\langle n_B\rangle\frac{\partial g}{\partial z_A}-\lambda'\langle n_C\rangle g\right\}, \quad (17)$$

where the factorization (4, A) has been taken into account. Since $\lambda'\langle n_C\rangle_e/\lambda\langle n_B\rangle_e=\langle n_A\rangle_e$ at equilibrium, we find straight from Eq. (17)

$$g(z_A: \infty) = \exp[(z_A-1)\langle n_A\rangle_e]. \quad (18)$$

This shows that the equilibrium probability distribution is Poissonian;

$$P(n_A; \infty) = \exp(-\langle n_A\rangle_e)\langle n_A\rangle_e^{n_A}/n_A!. \quad (19)$$

The time-dependent solution of Eq. (17) is of the same form as Eq. (18),

$$g(z_A; t) = \exp[(z_A-1)\langle n_A\rangle] \quad (20)$$

obtained by means of the initial condition, $g(z_A; 0)=\exp[(z_A-1)n_A^{(0)}]$, in which we have assumed

4) I. Oppenheim, K. E. Shuler, and G. H. Weiss, *J. Chem. Phys.*, **50**, 460 (1969).

$\langle n_A\rangle_{initial}=n_A^{(0)}$. To this generating function corresponds the Poisson distribution,

$$P(n_A;\ t) = \exp(-\langle n_A\rangle)\langle n_A\rangle^{n_A}/n_A!, \tag{21}$$

where the mean $\langle n_A\rangle$ is consistent with the value given by Eq. (11).

It should be mentioned that Eq. (5′) or (5″) describes the stochastic process of the modified second-order reaction as follows:

$$B(\langle A\rangle) \rightleftarrows C, \tag{II, A}$$

where the symbol $\langle A\rangle$ in parentheses indictes the hypothesis that the average change of the number of A molecules is incorporated beforehand in the transition probability $\lambda_A(t)$ at an arbitrarily fixed time t. On the other hand, assuming the factorization (4, B), we may similarly consider the other modified second-order reaction

$$A(\langle B\rangle) \rightleftarrows C. \tag{II, B}$$

Thus, we can symbolically express the probability for the required reaction (I), $\mathcal{P}(A+B\rightleftarrows C)$, by

$$\mathcal{P}(A+B\rightleftarrows C) = \mathcal{P}(A)\,\mathcal{P}(B(\langle A\rangle)\rightleftarrows C) \tag{22, A}$$

or

$$\mathcal{P}(A+B\rightleftarrows C) = \mathcal{P}(B)\,\mathcal{P}(A(\langle B\rangle)\rightleftarrows C). \tag{22, B}$$

In Eq. (22, A), the probability $\mathcal{P}(B(\langle A\rangle)\rightleftarrows C)$ for the modified reaction (II, A) may be regarded as a conditional probability, calculated on the assumption that the average change of the number of A molecules is realized beforehand with the probability $\mathcal{P}(A)$. Equation (22, A) or (22, B), together with the Gibbs entropy postulate (1) or (1′), forms the basis of the stochastic formulation of nonequilibrium thermodynamics of reaction (I).

Stochastic Entropy

Following the Gibbs entropy postulate (1′), we have, as the stochastic entropy for the probability $\mathcal{P}(A+B\rightleftarrows C)$,

$$S(A+B\rightleftarrows C) = -k\langle\ln[\mathcal{P}(A+B\rightleftarrows C)/\mathcal{P}_e(A+B\rightleftarrows C)]\rangle + S_e(A+B\rightleftarrows C). \tag{23}$$

As an example, if we apply the relation (22, A) to Eq. (23), we can write the stochastic entropy $S(A+B\rightleftarrows C)$ in the form

$$\begin{aligned}S(A+B\rightleftarrows C) &= -k\{\sum_A \mathcal{P}(A)\ln[\mathcal{P}(A)/\mathcal{P}_e(A)]\sum_C \mathcal{P}(B(\langle A\rangle)\rightleftarrows C)\\ &\quad + \sum_A \mathcal{P}(A)\sum_C \mathcal{P}(B(\langle A\rangle)\rightleftarrows C)\ln[\mathcal{P}(B(\langle A\rangle)\rightleftarrows C)/\mathcal{P}_e(B(\langle A\rangle)\rightleftarrows C)]\} + S_e(A+B\rightleftarrows C).\end{aligned} \tag{24}$$

However, owing to the normalizations $\sum_A \mathcal{P}(A)=1$ and $\sum_C \mathcal{P}(B(\langle A\rangle)\rightleftarrows C)=1$, this equation now becomes

$$\begin{aligned}S(A+B\rightleftarrows C) &= -k\{\langle\ln[\mathcal{P}(A)/\mathcal{P}_e(A)]\rangle\\ &\quad + \langle\ln[\mathcal{P}(B(\langle A\rangle)\rightleftarrows C)/\mathcal{P}_e(B(\langle A\rangle)\rightleftarrows C)]\rangle\}\\ &\quad + S_e(A+B\rightleftarrows C).\end{aligned} \tag{25}$$

If we furthermore decompose the entropy $S_e(A+B\rightleftarrows C)$ for the equilibrium probability distribution $\mathcal{P}_e(A+B\rightleftarrows C)$ into the two parts, $S_e(A)$ and $S_e(B(\langle A\rangle)\rightleftarrows C)$, we have consequently

$$S(A+B\rightleftarrows C) = S(A) + S(B(\langle A\rangle)\rightleftarrows C), \tag{26, A}$$

which is in a form similar to the conditional entropy in the theory of information. In writing the above equation, we have defined

$$S(A) = -k\langle\ln[\mathcal{P}(A)/\mathcal{P}_e(A)]\rangle + S_e(A) \tag{27}$$

and

$$\begin{aligned}S(B(\langle A\rangle)\rightleftarrows C) &= -k\langle\ln[\mathcal{P}(B(\langle A\rangle)\rightleftarrows C)/\mathcal{P}_e(B(\langle A\rangle)\rightleftarrows C)]\rangle\\ &\quad + S_e(B(\langle A\rangle)\rightleftarrows C).\end{aligned} \tag{28}$$

Proceeding in the same manner, we get also for the relation (22, B),

$$S(A+B\rightleftarrows C) = S(B) + S(A(\langle B\rangle)\rightleftarrows C). \tag{26, B}$$

In order to express explicitly the stochastic entropy (26, A), we start with the evaluation of Eq. (28). Since the probability $\mathcal{P}(B(\langle A\rangle)\rightleftarrows C)$ is given by Eq. (15) and it follows that

$$\mathcal{P}_e(B(\langle A\rangle)\rightleftarrows C) = \binom{n_B^{(0)}}{n_C}(n_A^{(0)}/\alpha)^{n_C}\{(\alpha-n_A^{(0)})/\alpha\}^{n^{(0)}{}_B-n_C}, \tag{29}$$

the stochastic entropy $S(B(\langle A\rangle)\rightleftarrows C)$ takes the form

$$\begin{aligned}S(B(\langle A\rangle)\rightleftarrows C) &= -k\Big\{\langle n_C\rangle\ln\frac{n_A^{(0)}(1-\exp[-\lambda(\alpha-\beta)t])}{\alpha-\beta\exp[-\lambda(\alpha-\beta)t]}\\ &\quad + (n_B^{(0)}-\langle n_C\rangle)\\ &\quad \times\ln\frac{\alpha-n_A^{(0)}-(\beta-n_A^{(0)})\exp[-\lambda(\alpha-\beta)t]}{\alpha-\beta\exp[-\lambda(\alpha-\beta)t]}\\ &\quad - \langle n_C\rangle\ln(n_A^{(0)}/\alpha) - (n_B^{(0)}-\langle n_C\rangle)\\ &\quad \times\ln[(\alpha-n_A^{(0)})/\alpha]\Big\} + S_e(B(\langle A\rangle)\rightleftarrows C).\end{aligned} \tag{30}$$

With the aid of the relations, $\alpha\beta=n_A^{(0)}n_B^{(0)}$, $\beta=\langle n_C\rangle_e$ and $\{\alpha+n_A^{(0)}-(\beta-n_A^{(0)})\exp[-\lambda(\alpha-\beta)t]\}/\{\alpha-\beta\exp[-\lambda(\alpha-\beta)t]\}=n_A^{(0)}(n_A^{(0)}-\langle n_C\rangle)/\alpha\beta$, the above equation is reduced to

$$\begin{aligned}S(B(\langle A\rangle)\rightleftarrows C) &= -k\{\langle n_C\rangle\ln(\langle n_C\rangle/\langle n_C\rangle_e)\\ &\quad + (n_B^{(0)}-\langle n_C\rangle)\ln[(n_B^{(0)}-\langle n_C\rangle)/(n_B^{(0)}-\langle n_C\rangle_e)]\}\\ &\quad + S_e(B(\langle A\rangle)\rightleftarrows C).\end{aligned} \tag{31, A}$$

Similarly, for the modified second-order reaction (II, B), we have

$$\begin{aligned}S(A(\langle B\rangle)\rightleftarrows C) &= -k\{\langle n_C\rangle\ln(\langle n_C\rangle/\langle n_C\rangle_e)\\ &\quad + (n_A^{(0)}-\langle n_C\rangle)\ln[(n_A^{(0)}-\langle n_C\rangle)/(n_A^{(0)}-\langle n_C\rangle_e)]\}\\ &\quad + S_e(A(\langle B\rangle)\rightleftarrows C).\end{aligned} \tag{31, B}$$

Since Eqs. (21) and (19) correspond to the probabilities $\mathcal{P}(A)$ and $\mathcal{P}_e(A)$, respectively, we obtain from Eq. (27)

$$\begin{aligned}S(A) &= -k\{\langle n_A\rangle\ln(\langle n_A\rangle/\langle n_A\rangle_e)\\ &\quad - (\langle n_A\rangle-\langle n_A\rangle_e)\} + S_e(A).\end{aligned} \tag{32, A}$$

Similarly, we have for the probability $\rho(B)$

$$S(\mathrm{B}) = -k\{\langle n_\mathrm{B}\rangle \ln(\langle n_\mathrm{B}\rangle/\langle n_\mathrm{B}\rangle_e) - (\langle n_\mathrm{B}\rangle - \langle n_\mathrm{B}\rangle_e)\} + S_e(\mathrm{B}). \quad (32,\ \mathrm{B})$$

In the final analysis, the substitution of Eqs. (31, A) and (32, A) into Eq. (26, A) leads to

$$\begin{aligned} &S(\mathrm{A}+\mathrm{B} \rightleftarrows \mathrm{C}) \\ &= -k\{\langle n_\mathrm{A}\rangle \ln(\langle n_\mathrm{A}\rangle/\langle n_\mathrm{A}\rangle_e) + \langle n_\mathrm{B}\rangle \ln(\langle n_\mathrm{B}\rangle/\langle n_\mathrm{B}\rangle_e) \\ &\quad + \langle n_\mathrm{C}\rangle \ln(\langle n_\mathrm{C}\rangle/\langle n_\mathrm{C}\rangle_e) + (\langle n_\mathrm{C}\rangle - \langle n_\mathrm{C}\rangle_e)\} \\ &\quad + S_e(\mathrm{A}+\mathrm{B} \rightleftarrows \mathrm{C}), \end{aligned} \quad (33)$$

or by setting $\Delta_i S(\mathrm{A}+\mathrm{B}\rightleftarrows\mathrm{C}) = S(\mathrm{A}+\mathrm{B}\rightleftarrows\mathrm{C}) - S_e(\mathrm{A}+\mathrm{B}\rightleftarrows\mathrm{C})$,

$$\begin{aligned} &\Delta_i S(\mathrm{A}+\mathrm{B} \rightleftarrows \mathrm{C}) \\ &= -k\{\langle n_\mathrm{A}\rangle \ln(\langle n_\mathrm{A}\rangle/\langle n_\mathrm{A}\rangle_e) + \langle n_\mathrm{B}\rangle \ln(\langle n_\mathrm{B}\rangle/\langle n_\mathrm{B}\rangle_e) \\ &\quad + \langle n_\mathrm{C}\rangle \ln(\langle n_\mathrm{C}\rangle/\langle n_\mathrm{C}\rangle_e) + (\langle n_\mathrm{C}\rangle - \langle n_\mathrm{C}\rangle_e)\}, \end{aligned} \quad (33')$$

where $\langle n_\mathrm{A}\rangle = n_\mathrm{A}^{(0)} - \langle n_\mathrm{C}\rangle$ and $\langle n_\mathrm{B}\rangle = n_\mathrm{A}^{(0)} - \langle n_\mathrm{C}\rangle$ have been used. Following the same argument closely we can again find Eq. (33) from Eqs. (26, B), (31, B), and (32, B). We have therefore the symmetrization

$$\begin{aligned} &S(\mathrm{A}+\mathrm{B} \rightleftarrows \mathrm{C}) \\ &= \frac{1}{2}\{[S(\mathrm{A}) + S(\mathrm{B}(\langle \mathrm{A}\rangle) \rightleftarrows \mathrm{C})] \\ &\quad + [S(\mathrm{B}) + S(\mathrm{A}(\langle \mathrm{B}\rangle) \rightleftarrows \mathrm{C})]\} \\ &= \text{r. h. s. of Eq. (33).} \end{aligned} \quad (34)$$

From Eq. (33), the stochastic entropy production $\sigma = \mathrm{d}S(\mathrm{A}+\mathrm{B}\rightleftarrows\mathrm{C})/\mathrm{d}t$ can be readily obtained as

$$\sigma = k(\mathrm{d}\langle n_\mathrm{C}\rangle/\mathrm{d}t)\ln\left(\frac{\langle n_\mathrm{C}\rangle_e}{\langle n_\mathrm{A}\rangle_e\langle n_\mathrm{B}\rangle_e} \Big/ \frac{\langle n_\mathrm{C}\rangle}{\langle n_\mathrm{A}\rangle\langle n_\mathrm{B}\rangle}\right). \quad (35)$$

If it is assumed that temperature T is uniform throughout the reaction system, the chemical affinity a is expressed by

$$a = kT\{\ln(\langle n_\mathrm{A}\rangle/\langle n_\mathrm{A}\rangle_e) + \ln(\langle n_\mathrm{B}\rangle/\langle n_\mathrm{B}\rangle_e) - \ln(\langle n_\mathrm{C}\rangle/\langle n_\mathrm{C}\rangle_e)\} \quad (36)$$

and the reaction velocity by $v = \mathrm{d}\langle n_\mathrm{C}\rangle/\mathrm{d}t$. The stochastic entropy production (35) is reduced to

$$\sigma = (a/T)v \quad (37)$$

a form convenient for comparison with the entropy production in the usual nonequilibrium thermodynamics.[5]

It is instructive to compare the stochastic theory with the usual one. In the latter, the entropy change due to a chemical reaction $\sum_{i=1}^{r} \nu_i \mathrm{A}_i \rightleftarrows \sum_{j=1}^{p} \nu_j' \mathrm{A}_j'$ in ideal gases can be written as

$$\Delta_i S = \int_{\text{arbitrary reaction state}}^{\text{equilibrium state}} (a/T)\mathrm{d}\xi, \quad (38)$$

where the degree of advancement ξ is defined by $-\mathrm{d}\langle n_{\mathrm{A}_i}\rangle/\nu_i = \mathrm{d}\langle n_{\mathrm{A}_j}'\rangle/\nu_j' = \mathrm{d}\xi$ and the chemical affinity a is given by

$$\begin{aligned} a &= \sum_{i=1}^{r} \nu_i \mu_{\mathrm{A}_i} - \sum_{j=1}^{p} \nu_j' \mu_{\mathrm{A}_j'} \\ &= kT\left\{\sum_{i=1}^{r} \nu_i \ln(\langle n_{\mathrm{A}_i}\rangle/\langle n_{\mathrm{A}_i}\rangle_e) - \sum_{j=1}^{p} \nu_j' \ln(\langle n_{\mathrm{A}_j'}\rangle/\langle n_{\mathrm{A}_j'}\rangle_e)\right\}. \end{aligned} \quad (39)$$

In this equation, we have used as the chemical potential of component γ,

$$\mu_\gamma = kT \ln\langle n_\gamma\rangle + \eta_\gamma(T, V),$$

where $\langle n_\gamma\rangle$ is the mean number of molecules of reacting species γ and $\eta_\gamma(T, V)$ a function of volume V and temperature T only. After integration, we obtain

$$\begin{aligned} \Delta_i S = -k\Big\{ &\sum_{i=1}^{r} [\langle n_{\mathrm{A}_i}\rangle \ln(\langle n_{\mathrm{A}_i}\rangle/\langle n_{\mathrm{A}_i}\rangle) - \langle n_{\mathrm{A}_i}\rangle + \langle n_{\mathrm{A}_i}\rangle_e] \\ &+ \sum_{i=1}^{p} [\langle n_{\mathrm{A}'_j}\rangle \ln(\langle n_{\mathrm{A}'_j}\rangle/\langle n_{\mathrm{A}'_j}\rangle_e) \\ &- \langle n_{\mathrm{A}'_j}\rangle + \langle n_{\mathrm{A}'_j}\rangle_e]\Big\}. \end{aligned} \quad (40)$$

In the case of reaction (I), for instance, we have Eq. (33') by using the relation $-(\langle n_\mathrm{A}\rangle - \langle n_\mathrm{A}\rangle_e) = -(\langle n_\mathrm{B}\rangle - \langle n_\mathrm{B}\rangle_e) = \langle n_\mathrm{C}\rangle - \langle n_\mathrm{C}\rangle_e$. Reflecting upon the requirement that the mean numbers of molecules, $\langle n_{\mathrm{A}_i}\rangle$ and $\langle n_{\mathrm{A}'_j}\rangle$, have to be taken with respect to a probability distribution governing the reaction system, we may reform Eq. (40) into

$$\begin{aligned} \Delta_i S = -k\Big\langle \ln\Big\{ &\prod_{i=1}^{r}\left(\frac{\exp(-\langle n_{\mathrm{A}_i}\rangle)\langle n_{\mathrm{A}_i}\rangle^{n_{\mathrm{A}_i}}}{n_{\mathrm{A}_i}!}\right. \\ &\left.\Big/\frac{\exp(-\langle n_{\mathrm{A}_i}\rangle_e)\langle n_{\mathrm{A}_i}\rangle_e^{n_{\mathrm{A}_i}}}{n_{\mathrm{A}_i}!}\right) \\ &\times \prod_{j=1}^{p}\left(\frac{\exp(-\langle n_{\mathrm{A}'_j}\rangle)\langle n_{\mathrm{A}'_j}\rangle^{n_{\mathrm{A}'_j}}}{n_{\mathrm{A}'_j}!}\right. \\ &\left.\Big/\frac{\exp(-\langle n_{\mathrm{A}'_j}\rangle_e)\langle n_{\mathrm{A}'_j}\rangle_e^{n_{\mathrm{A}'_j}}}{n_{\mathrm{A}'_j}!}\right)\Big\}\Big\rangle. \end{aligned} \quad (41)$$

Thus, it turns out that Poisson distribution holds for each reacting species and that it is maintained invariant throughout the reaction process in local equilibrium, which is also assumed in Eq. (38). If we set

$$p(n_\gamma) = \exp(-\langle n_\gamma\rangle)\langle n_\gamma\rangle^{n_\gamma}/n_\gamma! \quad (42)$$

and

$$p_e(n_\gamma) = \exp(-\langle n_\gamma\rangle_e)\langle n_\gamma\rangle_e^{n_\gamma}/n_\gamma! \quad (43)$$

and take the average with respect to the probability distribution $\prod_\gamma p(n_\gamma)$, we can rewrite Eq. (41) in the form

$$\begin{aligned} \Delta_i S &= -k\sum_{\boldsymbol{n}} \prod_\gamma p(n_\gamma)\ln\left(\prod_\gamma [p(n_\gamma)/p_e(n_\gamma)]\right) \\ &= -k\sum_\gamma \sum_{n_\gamma} p(n_\gamma)\ln[p(n_\gamma)/p_e(n_\gamma)]. \end{aligned} \quad (44)$$

If, furthermore, we set $\prod_\gamma p(n_\gamma) = P(\boldsymbol{n})$, we obtain from Eq. (44) the Gibbs entropy postulate

$$\Delta_i S = -k\sum_{\boldsymbol{n}} P(\boldsymbol{n})\ln[P(\boldsymbol{n})/P_e(\boldsymbol{n})] \quad (45)$$

in agreement with Eq. (1). We can therefore conclude that for the entropy change due to a chemical reaction in ideal gases the thermodynamic expression (38) is equivalent to the stochastic one (1).

We can rewrite Eq. (44) corresponding to Eq. (1') as

5) I. Prigogine, "Introduction to Thermodynamics of Irreversible Processes," 3rd ed., Interscience Publishers, New York (1967), p. 23.

$$S = -k \sum_{\gamma} \sum_{n_\gamma} p(n_\gamma) \ln[p(n_\gamma)/p_e(n_\gamma)] + S_e. \quad (44')$$

Assuming $S_e = \sum_{\gamma} S_e(\gamma)$, where $S_e(\gamma)$ denotes the entropy for the equilibrium probability distribution of reacting species γ, we obtain from Eq. (44')

$$S = \sum_{\gamma} S(\gamma), \quad (46)$$

where

$$S(\gamma) = -k \sum_{n_\gamma} p(n_\gamma) \ln[p(n_\gamma)/p_e(n_\gamma)] + S_e(\gamma). \quad (47)$$

This has its origin in the factorization $P(\boldsymbol{n}) = \prod_{\gamma} p(n_\gamma)$. In other words, we can say that the joint probability distribution $P(\boldsymbol{n}; t)$ for reaction states, at all times $0 \leq t \leq \infty$, is factorized as $P(\boldsymbol{n}; t) = \prod_{\gamma} P(n; t)$ in thermodynamic limit. However, so far as thermodynamic considerations are concerned, the probability distribution of reaction states can not be explicitly found through the reaction kinetics. The reason why we have presumed to use the factorization such as Eq. (22, A) or (22, B) is to formulate stochastically the nonequilibrium thermodynamics by considering at least the stochastic process of the modified reaction (II, A) or (II, B), which is of an advantage to the approximate solution of the stochastic process of reaction (I). We emphasize finally that such a theory can systematically deal with the nonequilibrium thermodynamics of chemical reaction together with its stochastic process.

The stochastic theory presented in this paper can be applied to other reactions, *e.g.*, $A+B \rightleftarrows C+D$. The stochastic entropy is given by $S(A+B \rightleftarrows C+D) = S(B(\langle A \rangle) \rightleftarrows C(\langle D \rangle)) + S(A(\langle B \rangle) \rightleftarrows D(\langle C \rangle))$ or $S(A+B \rightleftarrows C+D) = 1/2\{[S(A) + S(D) + S(B(\langle A \rangle) \rightleftarrows C(\langle D \rangle))] + [S(B) + S(C) + S(A(\langle B \rangle) \rightleftarrows D(\langle C \rangle))]\}$. Of course, the former agrees with the latter, assuming the relation (46).

BULLETIN OF THE CHEMICAL SOCIETY OF JAPAN, VOL. 44, 2595—2600 (1971)

Catalytic Oxidation over Molecular Sieves Ion-exchanged with Transition Metal Ions. IV. The Oxidative Dehydrogenation of Cyclohexane

Isao MOCHIDA, Tetsuji JITSUMATSU, Akio KATO, and Tetsuro SEIYAMA

Department of Applied Chemistry, Faculty of Engineering, Kyushu University, Hakozaki, Fukuoka

(Received February 1, 1971)

The oxidative dehydrogenation of cyclohexane over molecular sieves ion-exchanged with cupric ion (Cu(II)-Y) was investigated by means of an ordinary flow reactor with a reactant gas composed of 1.0% cyclohexane, 50% oxygen, and 49% nitrogen. The reaction was studied at temperatures between 210—350°C; here, carbon dioxide and benzene were the main products. The Cu(II)-Y was found to be a very active catalyst for the oxidation of cyclohexane as well as for that of olefins, in comparison with an ordinary cupric oxide catalyst supported on silica gel; the selectivity for benzene formation was as high as 80% below 10% conversion. Both products were found to be formed in competitive reactions. The catalytic activities were also studied on molecular sieves ion-exchanged with other transition metal ions, such as palladium (II), silver (I), and zinc (II). The relations between the catalytic activities and the heats of formation of the corresponding metal oxides per g-atom oxygen were examined; volcano-shaped correlations were observed for both benzene and carbon-dioxide formations for these catalysts. The most active catalyst was Cu(II)-Y for benzene formation, whereas it was Pd (II)-Y for the carbon dioxide formation. The meaning of the correlations was discussed according to Balandin's explanation, based on thermochemistry, although no satisfying explanation was found. The compensation effects were observed between the activation energies and the frequency factors in these oxidations.

In previous papers, it was reported that the molecular sieves ion-exchanged with transition metal ions have very high catalytic activities for the oxidation of olefins.[1-3] It may be interesting to investigate the catalytic activities of these catalysts for the saturated hydrocarbons. Agudo *et al.*[4] reported the oxidations of heptanes on Na-X, Ca-X, and Mn-X, but homogeneous processes were predominant, so the character of the transition metal on the molecular sieve appeared only obscurely.

In the present work, the oxidative dehydrogenation of cyclohexane was studied over molecular sieves ion-exchanged with several transition-metal ions. Although the dehydroisomerization (reforming, in other words) of saturated hydrocarbons by Pd- or Pt-molecular sieves has been reported and applied in industrial processes,[5] regarding oxidative dehydrogenation only a few works have been reported, those using alcohols and alkylbenzenes as the reactants.[6,7]

1) I. Mochida, S. Hayata, A. Kato, and T. Seiyama, *J. Catalysis*, **15**, 314 (1969).

2) I. Mochida, S. Hayata, A. Kato, and T. Seiyama, *ibid.*, **19**, 405 (1970).

3) I. Mochida, S. Hayata, A. Kato, and T. Seiyama, *ibid.*, in press.

4) A. L. Agudo, F. R. Badcock, and F. S. Stone, *Proc. Inter. Congr. Catalysis, 4th Moscow*, No. 59 (1968).

5) J. A. Rado, P. E. Pickert, D. Stmir, and J. E. Bogles, *Actes Congr. Intern. Catalyses, 2e, Paris*, 1960, 2055 (1961); Mays, R. C., *Ind. Eng. Chem.* **53**, 733 (1967).

6) P. N. Galich, A. A. Gutyrya, V. S. Gutyrya, and I. E. Neimark, *Dokl. Akad. Nauk SSSR* **144**, 147 (1962); P. N. Galich, V. S. Gutyrya, O. P. Egorov, I. E. Neimark, Il'in. Golobchenko, and V. S. Frolova, *Neftkhimiya Akad. Nauk, Soedin.* (Ukr. SSR Inst. Khim. Vysckomolekul.), **1964**, 13.

7) J. Turkevich, *Catalysis Rev.* **1**, 1 (1968); P. B. Venuto and P. S. Landnis, *Advan. Catalysis*, **18**, 259 (1968).

Cyclohexane can be thought to be transformed easily into benzene, and the benzene thus produced is relatively stable against further oxidations, so the oxidative dehydrogenation of cyclohexane can be expected to occur with a high activity and selectivity over molecular sieves ion-exchanged with transition-metal ions, since high activities of these catalysts were found with regard to the oxidation of olefinic hydrocarbons.[1,3]

Experimental

Catalyst. The ion-exchanged molecular-sieve catalysts were prepared by the ion-exchange of the Y-molecular sieve (Linde), Na–Y, with an aqueous solution of metal sulfates or nitrate except for the cases of cupric and palladium ions, for which amine complexes were used. A sufficient amount of the metal ion was passed through a cylindrically-shaped column of Na–Y. The ion-exchanged sieves were then washed thoroughly with decationized water, dried at 100°C, and calcined at 400°C for 7 hr in the air. The amount of metal ion-exchanged onto the sieve was determined by extraction with nitric acid and by the titration of the solution. 80—90% of the sodium ions were exchanged. The cupric oxide catalyst supported by silica gel was described in a previous paper.[1]

Reagent. The cyclohexane used was of a G. R. grade and was obtained from the Wako Junyaku Co. It was used without further purification. No benzene or cyclohexene was detected by the gas chromatography.

Apparatus and Procedure The oxidative dehydrogenation was studied by the ordinary flow method, with a fixed catalyst bed diluted with 1% cyclohexane, 50% oxygen, and 49% nitrogen. Cyclohexane was fed by means of a nitrogen flow passed through an alumina bed impregnated with a sufficient amount of cyclohexane kept at 0°C. The cyclohexane, cyclohexene, benzene, and carbon dioxide were analyzed by means of chromatography. For the first three, 2 m TCP (Japan Gaschro Co.) and 1 m PEG (Japan Gaschro Co.) columns were used at 80°C, and for the last, a Porapak Q (Waters Associates, Inc.) column of 2 m was used at room temperature. The conversions and the selectivity were calculated in the following ways:

$$\text{Conversion for carbon dioxide} = \frac{(1/6)\ \text{carbon dioxide}}{\text{cyclohexane fed}}$$

$$\text{Conversion for benzene} = \frac{\text{benzene}}{\text{cyclohexane fed}}$$

$$\text{Selectivity for benzene} = \frac{\text{benzene}}{\text{benzene} + (1/6)\ \text{carbon dioxide}}$$

The activity of the catalyst was corrected to that on a fixed amount of the metal ion.

Results

Oxidation of Cyclohexane on a Y Molecular Sieve Ion-exchanged with Cupric Ions (Cu(II)-Y). The oxidation of cyclohexane over Cu(II)–Y of 300 mg began to occur at 210°C under a flow rate of 50 ml/min. Up to 350°C, benzene and carbon dioxide were the main products, plus a small amount of cyclohexene. The carbon balance was better than 95% (on an inlet cyclohexane basis) after 2 hours' reaction, although a carbon deposit was observed on the catalyst. The catalyst recovered its original color of light blue when the carbon deposited on the catalyst was burned in the air. This means that the cupric ions maintain the ionic state on the molecular sieve during the oxidation reaction, as was previously observed in the oxidation of propylene.[1,2]

Above 350°C, products other than carbon dioxide and benzene were observed. Acetic acid and propionic acid were detected in the products. However, a detailed analysis was not made.

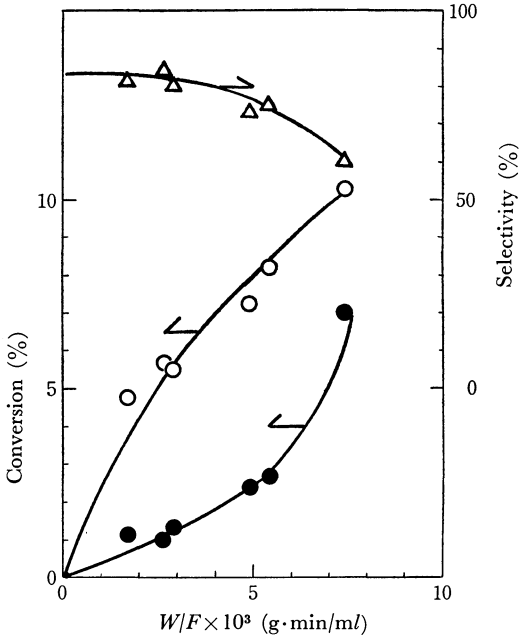

Fig. 1. The oxidation of cyclohexane over Cu(II)-Y at 260°C.
The reactant gas composition; 1% cyclohexane, 50% oxygen, 49% nitrogen.
○: benzene formation, ●: carbon dioxide formation,
△: selectivity of benzene formation.

The oxidation at 260°C is shown in Fig. 1 as a function of the contact time. Benzene and carbon dioxide were formed in linear relations with the contact time below a 10% conversion. Above this conversion, however, the carbon dioxide formation increased rapidly and the benzene formation was surpressed. The former fact may suggest the competitive formations of these products below a 10% conversion, while the latter may do the successive oxidation of benzene into carbon dioxide above a 10% conversion. The selectivity of the benzene formation was as high as 80% in the competitive region. The selectivity in the region of the competitive reactions varied little with the reaction temperature between 210 and 350°C, although the rates increased considerably.

A Comparison of Cu(II)–Y with Cupric Oxide Supported on Silica Gel in the Oxidative Dehydrogenation of Cyclohexane. The catalytic activity of Cu(II)–Y was compared with that of the ordinary cupric oxide mounted on silica gel (Cu(II)–S). The two catalysts had nearly equal surface areas.[1] The reactions on these catalysts in the competitive region at 310°C are shown in Fig. 2 as a function of the contact time. The catalytic

Table 1. Initial rates, activation energies, and frequency factors of molecular sieves ion-exchanged with transition metal ions for the oxidation of cyclohexane

Catalyst	Rate at 290° a) (ml/g·min)		Activation energy (kcal/mol)		Frequency factor (ml/g·min at $T=\infty$)	
	C_6H_6	CO_2	C_6H_6	CO_2	C_6H_6	CO_2
Ag(I)-Y	0.2	2.5	9.6	12.4	3.3	5.2
Pd(II)-Y	4.4b)	7250b)	15.6	35.6	6.6	16.9
Cu(II)-Y	59.0	22	26.9	29·1	12.3	12.5
Ni(II)-Y	1.4	7.3	—	—	—	—
Zn(II)-Y	0.4	3.2	—	—	—	—
Cr(III)-Y	2.3	9.0	14.3	19.5	6.0	8.5
Cu(II)-S	7.4	6.4	20.6	14.5	9.2	6.3

a) (Conversion observed below 10% conversion)/contact time.
b) Estimated from the Arrhenius plots between 200 and 260°C.

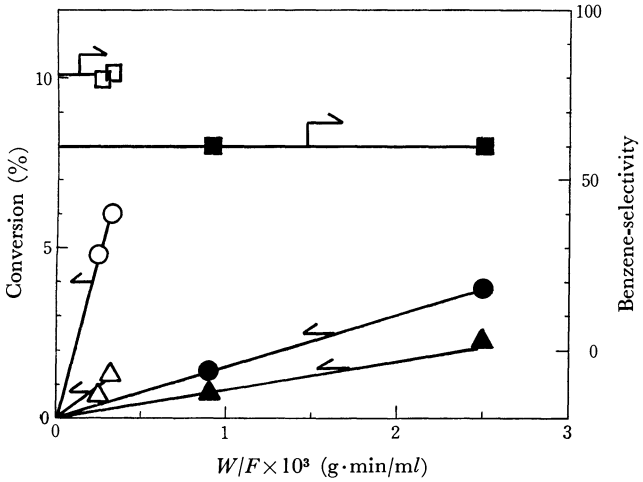

Fig. 2. Comparison between Cu(II)-Y and Cu(II)-S in the oxidation of cyclohexane at 310°C.
○: benzene formation, △: carbon dioxide formation, □: selectivity of benzene formation.
Open plots are for Cu(II)-Y and closed ones are for Cu(II)-S.

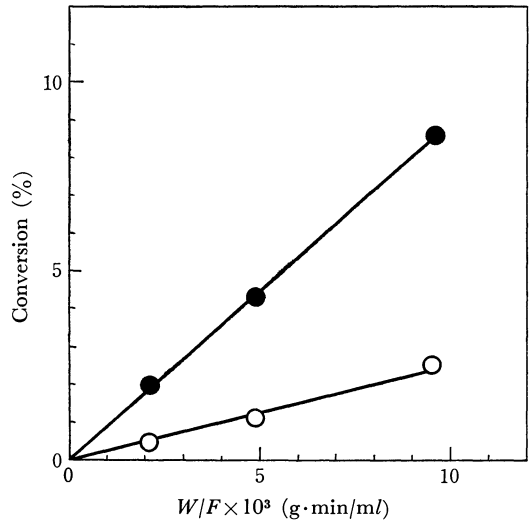

Fig. 3. The oxidation of cyclohexane on Cr(III)-Y at 290°C.
○: benzene formation, ●: carbon dioxide formation.

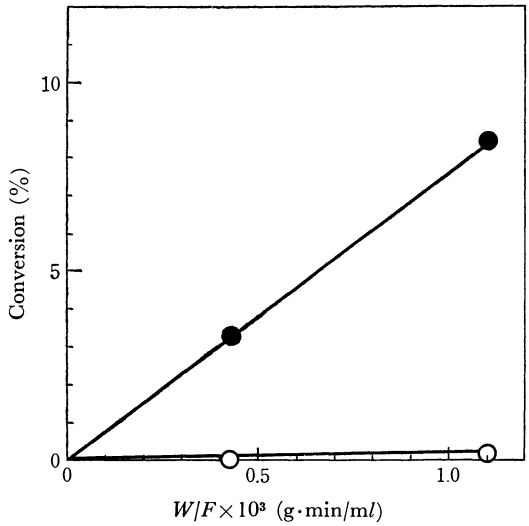

Fig. 4. The oxidation of cyclohexane on Pd(II)-Y at 230°C.
○: benzene formation, ●: carbon dioxide formation.

activity of Cu(II)-Y was much larger than that of Cu(II)-S, being fifteen times as much for the benzene formation and four times as much for the carbon-dioxide formation. The selectivity for the benzene formation in the competitive reactions was also better (80% for Cu(II)-Y, but 60% for Cu(II)-S). The activation energies and frequency factors of these two catalysts are shown in Table 1. It is interesting that Cu(II)-Y had a very high catalytic activity for the oxidations of saturated hydrocarbon as well as of olefinic hydrocarbons at such temperatures.[1-3]

The Oxidations of Cyclohexane over Molecular Sieves Ion-exchanged with Other Transition-metal Ions. The catalytic activities of molecular sieves ion-exchanged with five kinds of transition-metal ions other than the cupric ion were also studied in order to investigate the roles of metal ions in the oxidative dehydrogenation based on the δ_C LFER approach.[8] The reactions over Cr(III)-Y at 290°C and over Pd(II)-Y at 230°C are shown in Figs. 3 and 4 respectively as examples. It should be mentioned that the selectivities for the benzene formation of such sieves were much smaller than that of Cu(II)-Y, although the reactions also seemed competitive on these catalysts below a 10% conversion, as was shown by the linearity of the con-

8) I. Mochida and Y. Yoneda, *J. Catalysis*, **7**, 386 393, **8**, 223 (1967).

version plotted against the contact time. On Pd(II)–Y, the benzene formation was too small to be detected at low conversions, as is shown in Fig. 4, but it became measurable beyond a 10% conversion. This mean that the small value of the selectivity cannot be ascribed to the occurrence of the successive reaction at these conversion levels because of the high activity of this catalyst, and that the formations of benzene and carbon dioxide also take place competitively on Pd(II)–Y.

In Table 1, the rate data of the catalysts used are summarized; the activation energies and frequency factors here were calculated from the rates at reaction temperatures between 230 and 350°C, except for the case of Pd(II)–Y, which was too active for the oxidation rates to be observed in this temperature range, so the observation was made between 200 and 260°C. The catalytic activities of these catalysts at 290°C were in the following orders: Pd>Cu>Cr>Ni>Zn>Ag for the carbon dioxide formation, and Cu>Pd>Cr>Ni>Zn>Ag for the benzene formation (the activity of Pd(II)–Y at this temperature was extrapolated in the Arrhenius plots). The former activity order was analogous to that observed in the deep oxidations of olefins except for the small activity of Ag(I)–Y.[3]

Discussion

The Correlation of the Catalytic Activities with the Heats of Formation of the Corresponding Metal Oxides. The correlation of the catalytic activities for the oxidation of the metal oxides with their heats of formation per oxygen atom was reported on by Moro-oka and Ozaki, Seiyama *et al.*, Komuro *et al.*, and Boreskov and Balandin.[9] Recently, Aonuma and Nakada discussed such a correlation in the oxidative dehydrogenation of cyclohexene on the oxide catalyst.[10] A similar examination of the activities of molecular-sieve catalysts may be of value. In a previous paper,[3] volcano-shaped correlations were found in the oxidations of propylene and ethylene on the molecular-sieve catalysts. Such plots are made for the carbon dioxide and benzene formations in Fig.5, where volcano-shaped correlations were observed for both formations, showing the maximum activity at the palladium ion for carbon dioxide and at the cupric ion for benzene. It is interesting that the heat of the formation of the metal oxide could also be a parameter describing the catalytic activity in the present oxidation.

According to Balandin's explanation of such relations, the most active catalyst can be predicted on the basis of the thermochemical data on the reaction.[11] If the oxidation reaction of cyclohexane can be assumed to proceed through the following two steps, which consist of the dissociative adsorption of oxygen on the metal ion and the successive oxidation of cyclohexane by this adsorbed oxygen, the formation rate of carbon dioxide or benzene is at a maximum when ΔH_1 is equal to ΔH_2 or to ΔH_3 respectively:

$$\mathrm{Me} + 1/2\,\mathrm{O_2} = \mathrm{Me\text{-}O},\ \Delta H_1 \quad (1)$$

$$\mathrm{Me\text{-}O} + 1/24\,\mathrm{C_6H_{12}} = \mathrm{Me} + 1/4\,\mathrm{CO_2} + 1/2\,\mathrm{H_2O},\ \Delta H_2 \quad (2)$$

$$\mathrm{Me\text{-}O} + 1/2\,\mathrm{C_6H_{12}} = \mathrm{Me} + 1/3\,\mathrm{C_6H_6} + \mathrm{H_2O},\ \Delta H_3 \quad (3)$$

(ΔH_1, ΔH_2, and ΔH_3 are the heats of Reactions (1), (2), and (3) respectively.)

Since the sum of ΔH_1 and ΔH_2 or of ΔH_1 and ΔH_3 is equal to the heat of carbon-dioxide formation per g-atom oxygen (ΔH_{CO_2}) or that of benzene formation ($\Delta H_{C_6H_6}$) respectively, the above rule means that the formation rate is at a maximum at $\Delta H_1 = 1/2\,\Delta H_{CO_2}$ for carbon dioxide or at $\Delta H_1 = 1/2\,\Delta H_{C_6H_6}$ for benzene. The values of the heats of oxidation per g-atom oxygen are −42 kcal/mol for the benzene formation and −49 kcal/mol for the carbon-dioxide formation respectively. If the heat of adsorption of oxygen on the metal ion of the molecular sieve, ΔH_1, can be assumed to be equal to that of the formation of the metal oxide, ΔH_f°, the most active catalyst is the one whose ΔH_f° is −21 kcal/mol for the benzene formation and −24.5 kcal/mol for the carbon-dioxide formation respectively. Thus, if the assumptions are appropriate, Pd(II)–Y should be the most active for both formations among the catalysts examined here. The results for the carbon—dioxide formation support the above discussion. However, the cupric ion, not the palladium ion, was most active for the benzene formation. Even if the cyclohexyl radical rather than benzene is considered to be the intermediate product in Eq. (3), the situation is not improved. Other reaction schemes such as dehydrogenation in the first step, followed by the oxidation of the hydrogen with oxygen, may also be considered. However, sufficient thermodynamic data are lacking for further discussion.

Correlation as for Activation energies and Frequency Factors. The reaction rate should be connected with the thermochemical data of the reaction through its activation energy, according to Balandin's explanation.[11] The relations of the activation energies to the parameters used above are shown in Fig. 6 for both formations in order to make possible a discussion of the relations shown in Fig. 5 from another point of view. Similar volcano-shaped correlations were observed for the reaction rates in both formations. Such correlations for activation energies, however, were contradictory to those observed in the usual cases, where the most active catalyst has the smallest value of activation energy.[8,12] The frequency factors are often constant when a linear relation holds between the reaction rate and the thermochemical data.[8] The values of the present case, however, varied considerably from one to another. They were also correlated with the present parameter, as is shown in Fig. 7 for both for-

9) I. Komuro, H. Yamamoto, and T. Kwan, This Bulletin, **36**, 1532 (1963); Y. Moro-oka, and A. Ozaki, *J. Catalysis*, **5**, 116 (1966); T. Seiyama, S. Kagawa and H. Tokunaga, *Shokubai (Catalyst)*, **8**, 306 (1966); G. K. Boreskov, *Advan. Catalysis*, **15**, 285 (1965); A. A. Balandin, *ibid.*, **19**, 1 (1969).

10) T. Aonuma and Y. Nakada, *Shokubai (Catalysts)*, **12**, 20 (1970).

11) A. A. Balandin, *Advan. Catalysis*, **10**, 120 (1957).

12) a) J. E. Leffler, and E. Grunwald, "Rates and Equilibria of Organic Reactions" Wiley, New York (1963), p. 315. b) E. Cramer, *Advan. Catalysis*, **7**, 75 (1955).

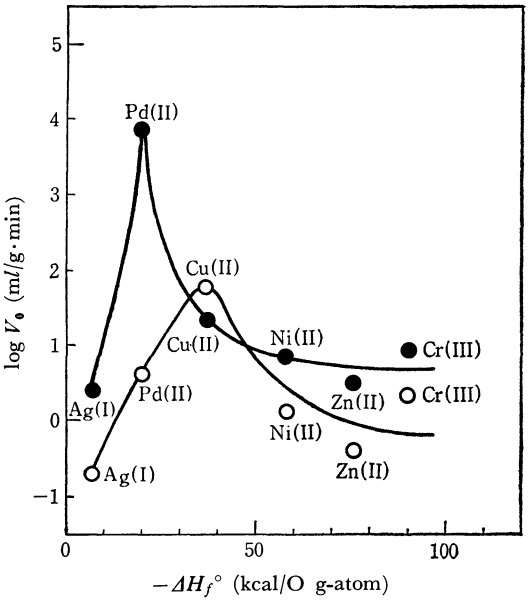

Fig. 5. Correlations of the initial rates of the carbon dioxide and benzene formations with the heats of formation of metal oxides per g-atom oxygen. The reaction temperature was 290°C.
○: benzene, ●: carbon dioxide.

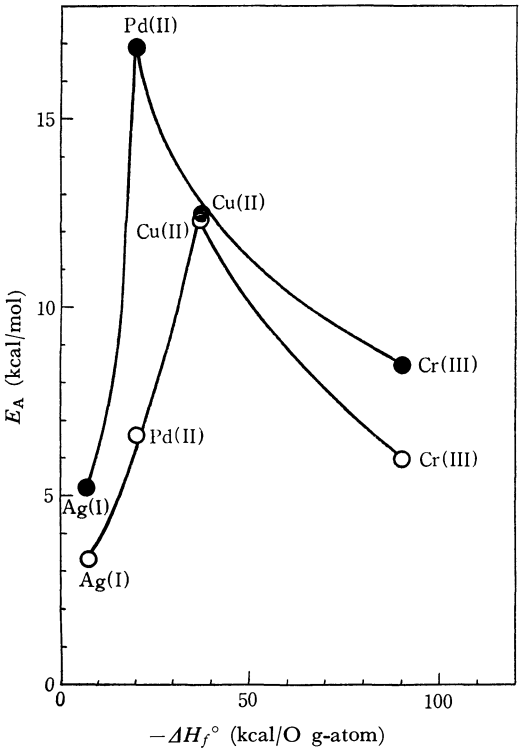

Fig. 6. Correlations of activation energy of the carbon dioxide and benzene formations with the heats of formation of metal oxides per g-atom oxygen.
○: benzene, ●: carbon dioxide.

mations. The relations were in volcano shapes similar to those observed in the activation energies, so that the most active catalyst had the largest frequency factor. This situation was defined as frequency-factor-controlling.[12]

The analogous relations of the activation energy

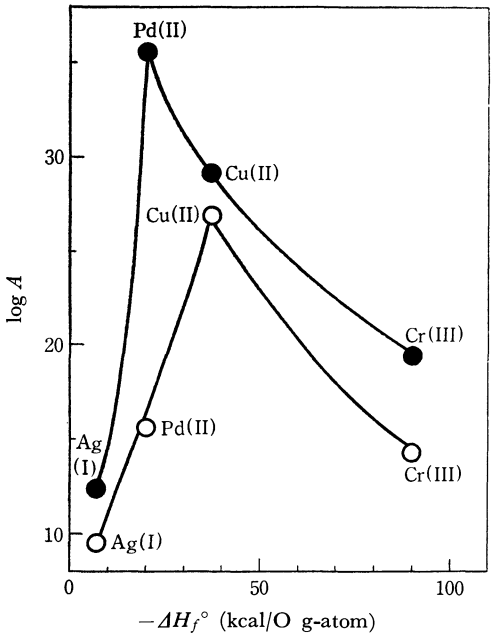

Fig. 7. Correlations of frequency factors of the carbon dioxide and benzene formations with the heats of formation of metal oxides per g-atom oxygen.
○: benzene, ●: carbon dioxide.

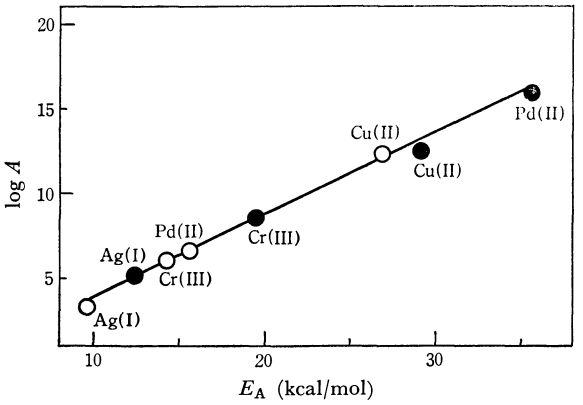

Fig. 8. Compensation effects observed between activation energies and frequency factors in the oxidations of cyclohexane on molecular sieves ion-exchanged with transition metal ions.
○: benzene formation, ●: carbon dioxide formation.

and the frequency factor with the same heat of formation suggest the existence of compensation effects in this oxidation. In fact, the compensation effects in the formations of both carbon dioxide and benzene are shown in Fig. 8. Thus, the frequency-factor-controlling mentioned above implies that the oxidation reaction was observed above the isokinetic temperature.[12]

In a previous paper,[3] the reaction orders as well as the catalytic activity of the ion-exchanged molecular-sieve catalysts for olefin oxidations were reasonably correlated with the parameter of Y,[13] which is thought to represent the softness of the metal ion, but no reasonable relation was found in the present oxidation of

13) M. Misono, E. Ochiai, and Y. Yoneda, *J. Inorg. Nucl. Chem.* **29**, 2685 (1967).

cyclohexane by the use of such a parameter.

In conclusion, the catalytic activities of ion-exchanged molecular-sieve catalysts for the oxidation of cyclohexane into benzene and carbon dioxide can be correlated with the heats of the formation of the corresponding metal oxides per g-atom oxygen at any of the reaction temperatures examined in the present study, because the compensation effects were present. Therefore, the activity of the ion-exchanged molecular sieve can be well estimated from the table values of the metal oxides, although the meaning of such a correlation is yet in question with regard to the reaction mechanism.

We should also mention the possibility of improving the selectivity for the benzene formation, even at the high conversion level, by adopting a better gas-composition of the reactant.

Our thanks are due to Mr. Shinji Hayata for his experimental assistance.

BULLETIN OF THE CHEMICAL SOCIETY OF JAPAN, VOL. 44, 2600—2602 (1971)

Oxidation of *s*-Butyl Alcohol by Cerium(IV)

D. L. MATHUR and G. V. BAKORE*

Department of Chemistry, University of Jodhpur, Jodhpur, India

(Received October 5, 1970)

The oxidation of *s*-butyl alcohol by Ce(IV) in dilute nitric acid medium has been studied. The reaction is of first order with respect to Ce(IV)but of fractional order with respect to *s*-butyl alcohol. A plot of inverse of alcohol concentration against inverse of observed first order rate constant gave a straight line which did not pass through the origin. This suggests an intermediate Ce(IV)-alcohol complex formation. By repeating this procedure at different temperatures the formation constants of the complex and the thermodynamic parameters for the complex formation process have been evaluated. Hydrogen, nitrate, and sulphate ions decrease the rate of oxidation. The results have been explained on the basis of equilibrium $Ce^{4+}+H_2O \overset{K_h}{\rightleftarrows} Ce(OH)^{3+}+H^+$ and assuming $Ce(OH)^{3+}$ as the reactive species of Ce(IV). From the slope-intercept of straight line obtained between inverse of observed rate constant and $[H^+]$, value of $K_h=6.19$ at 35°C has been evaluated in dilute nitric acid at $\mu=2.55$ M. A mechanism in which the first step is the rapid reversible formation of a complex between Ce(IV) and Substrate followed by α–C–H bond rupture in the rate determining step has been suggested.

The oxidation of *s*-butyl alcohol by ceric salts in dilute nitric acid has been examined by Sethuram and Muhammad.[1] The present paper reports some additional data on the oxidation of *s*-butyl alcohol by cerium(IV) in nitric acid to elucidate the mechanism of oxidation.

Experimental

Material. B.D.H. "Analar" *s*-butyl alcohol was used after distillation. Ceric ammonium nitrate A.R. (Atomic Energy Commission, India) and Nitric acid A.R. (Oster, India) were used. All other chemicals used were of analytical grade. All solutions for kinetic studies were prepared in doubly distilled water.

Kinetic Measurements. The reactions were carried out at constant temperature (±0.05°C) with the reaction vessel covered with black paint. The reaction system consisted of ceric ammonium nitrate [$\sim 4.0\times10^{-3}$ M], alcohol [$\sim 5.0\times10^{-2}$ M] and nitric acid [~ 1.08 M] with a total volume of 100 m*l* and at an ionic strength $\mu=1.13$. The ionic strength was kept constant by the addition of sodium perchlorate. It was found that the change in ionic strength (~ 1.13 to 2.63) does not appreciably change the rate of oxidation. Nitric acid was used as a source of hydrogen ions and nitrate ion concentration was adjusted with potassium nitrate solution.

The rate of oxidation was followed by withdrawing aliquots at appropriate intervals of time and quenching the latter in known excess of ferrous ammonium sulphate, back titrating the excess of the latter by standard ceric sulphate using ferroin as an indicator. Reactions were usually conducted for 50—60% conversion of ceric ion.

Results and Discussion

Rate Laws. When *s*-butyl alcohol was in excess, the rate at which cerium(IV) disappears followed the first order rate law, agreeing with the findings of Sethuram and Muhammad.[1] The graphical method was generally used to derive the rate constants.

TABLE 1. VARIATION OF RATE WITH CONCENTRATION OF *s*-BUTYL ALCOHOL

$[Ce(IV)]: 4.0\times10^{-3}$ M; $[HNO_3]: 1.08$ M; Temp.: 25°C. $\mu=1.13$ M

$[Alcohol]\times10^2$ mol/*l*	5.0	10.0	15.00	20.0	25.0
$k_1\times10^3$ min^{-1}	2.23	4.06	5.15	6.66	7.69

In a constant cerium(IV) concentration, it was found that the rate of oxidation rises with increase in alcohol concentration but tends to reach a limiting value at high concentrations of alcohol (Table 1). A plot of the inverse of alcohol concentration against that of observed rate constants gave a straight line. The result suggests that the oxidation proceeds through

* Present address: Department of Chemistry, University of Udaipur, UDAIPUR (India).

1) B. Sethuram and S. S. Muhammad, *Acta Chim. Hung.*, **46**, 115, 125 (1965).

the complex between the alcohol and cerium(IV) as has been suggested by Ardon.[2]

$$\text{Cerium(IV)} + s\text{-butyl alcohol} \overset{K}{\rightleftarrows} \text{complex}$$

$$\text{Complex} \xrightarrow[\text{slow}]{k_s} \text{Cerium(III)} + \text{Free radical} + H^+$$

$$\text{Free radical} + \text{Cerium(IV)} \xrightarrow{\text{fast}} \text{Ketone} + \text{Cerium(III)} + H^+$$

The variation of rate of oxidation with concentration of alcohol is given by the expression

$$-\frac{d[Ce(IV)]}{dt} = \frac{k_s[\text{Alcohol}][Ce(IV)]}{1/K + [\text{Alcohol}]}$$

From the slope-intercept ratio, $K=2.50$ and $K_s = 3.34\times10^{-4}$ sec^{-1} at 25°C have been obtained.

By repeating the procedure at various temperatures, the formation constants (K) have been calculated at different temperatures (Table 2). The thermodynamic data on the cerium(IV)-alcohol complex are listed in Table 3.

Table 2. Effect of temperature on formation of cerium(IV)-*s*-butyl complex

[Ce(IV)]: 4.0×10^{-3} M; [HNO_3]: 1.08 M, $\mu=1.13$ M

Temp., °K	298	303	308
K, l/mol	2.50	1.97	1.62

Table 3. Thermodynamic constants of the cerium(IV) - *s*-butyl alcohol complex

Property	By Sethuran and Muhammad[1] at 22°C	Present work at 25°C and [H^+]: 1.08, μ: 1.13 M
K l/mol	2.213	2.50
$-\Delta H$ kcal/mol	6.75	7.66
$-\Delta F$ cal/mol	465.8	540.8
$-\Delta S$ e. u.	−23.06	−23.90

The difference in the values reported by Sethuram and Muhammad[1] and those obtained in the present investigation might be due to different experimental conditions. The value of the formation constant of the Ce(IV) -alcohol complex probably depends upon hydrogen ion concentration used. The authors[1] gave no idea of the hydrogen ion concentration used by them.

The variation of rate constants with temperature is shown in Table 4.

Table 4. Effect of temperature on the rate of reaction

[Ce(IV)]: 4.0×10^{-3} M: [Alcohol]: 5.0×10^{-2} M; [HNO_3]=1.08 M

Temp., °K	298	303	308	313
$k_1\times10^5$ sec^{-1}	3.71	6.83	10.4	21.6

The apparent energy of activation E was calculated to be 22.0±1.0 kcal by plotting $\log k_1$ *vs.* $1/T$.

2) M. Ardon, *J. Chem. Soc.*, **1957**, 1811.

At constant nitrate ion concentration increase in hydrogen ion concentration causes a slight but distinct decrease in the rate of oxidation. (Table 5).

Table 5. Variation of rate with concentration of hydrogen ions

[Ce(IV)]: 4.0×10^{-3} M, [Alcohol]: 5.0×10^{-2} M; Temp.: 35°C; [NO_3^-]: 2.5 M; $\mu=2.55$ M

[H^+] mol/l	0.50	0.90	1.50	2.0	2.5
$k_1\times10^3$ min^{-1}	7.17	6.76	6.07	5.81	5.48

The effect of hydrogen ion concentration may be explained on the basis of the equilibrium

$$Ce^{4+} + H_2O \rightleftharpoons Ce(OH)^{3+} + H^+ \quad (1)$$

If it is assumed that $Ce(OH)^{3+}$ is a more powerful oxidant than Ce^{4+}, then an increase in the concentration of hydrogen ions should decrease the concentration of $Ce(OH)^{3+}$ and hence the rate of oxidation. The small effect of the concentration of hydrogen ions on the rate of oxidation suggests that the value of the equilibrium constant for reaction (1) is small. At the total concentration of cerium(IV) used, cerium exists mostly as $Ce(OH)^{3+}$ or Ce^{4+}, concentration of the dimer $(Ce\text{–}O\text{–}Ce)^{6+}$ being negligibly small.

If reaction (1) is valid and [Ce(IV)] represents the total concentration of cerium(IV), we have

$$[Ce(OH)^{3+}] + [Ce^{4+}] = [Ce(IV)]$$

$$\text{and} \quad K_h = \frac{[Ce(OH)^{3+}][H^+]}{[Ce^{4+}]} = \frac{[Ce(OH)^{3+}][H^+]}{[Ce(IV)]-[Ce(OH)^{3+}]}$$

$$\text{or} \quad K_h[Ce(IV)] = [Ce(OH)^{3+}]\{[H^+]+K_h\}$$

$$\text{or} \quad [Ce(OH)^{3+}] = \frac{K_h[Ce(IV)]}{[H^+]+K_h}$$

The rate of oxidation will be given by the equation

$$\frac{-d[Ce(IV)]}{dt} = K'\frac{K_h}{[H^+]+K_h}\cdot[Ce(IV)] = k_1[Ce(IV)]$$

$$\text{hence} \quad k_1 = \frac{K'K_h}{[H^+]+K_h}$$

where K_h is the equilibrium constant for reaction (1), k_1 is the observed first order rate constant, and K' is a constant which includes the concentration of alcohol (which is kept constant). Hence we have

$$\frac{1}{k_1} = \frac{1}{K'K_h}\cdot[H^+] + \frac{1}{K'}$$

A plot of $1/k_1$ against [H^+] gave a straight line in the case of *s*-butyl alcohol. The value of K_h was found to be 6.19 at 35°C. The value of K_h found spectrophotometrically by Hardwick and Robertson[3] in $HClO_4$ for reaction (1) was 5.2 at 25°C. This supports the view that in the present investigation $Ce(OH)^{3+}$ may probably be the active species.

It may, however, be pointed out that Sethuram and Muhammad[1] observed that at constant nitrate

3) T. J. Hardwick and E. Robertson, *Can. J. Chem.*, **29**, 818 (1951).

ion concentration, the increase in the H^+ ion concentration was found to accelerate the rate of oxidation. They suggested $[Ce(H_2O)_2(NO_3)_4]$ as the neutral active species. We have not been able to confirm this result.

Table 6. Effect of nitrate ion on the rate of oxidation

[Ce(IV)]: 4.0×10^{-3} M; [Alcohol]: 5.0×10^{-2} M; [HNO]: 0.50 M; Temp.: 35°C.

$[KNO_3]$ mol/l	0.00	0.20	0.40	0.60	0.80	1.00
$k_1\times10^4$ min^{-1}	7.13	6.98	6.71	6.58	6.20	6.01

The nitrate ion was found to inhibit oxidation to a small extent (Table 6). The retardation caused by nitrate ions has also been indicated by Sethuram and Muhammad[1] who observed a linear relationship between observed rate constant and the square of the nitrate ion concentration. The retardation caused by nitrate ions is not so strong as indicated by them. The small retarding effect observed by us can not be attributed to the effect of the ionic strength as well. Shorter[4] explains this inhibiting action of nitrate ions during the oxidation of acetone by ceric ammonium nitrate in nitric acid, by conversion of $Ce(OH)^{3+}$ into a much less reactive species $[Ce(OH)NO_3]^{2+}$:

$$Ce(OH)^{3+} + NO_3^- \rightleftharpoons [Ce(OH)NO_3]^{2+} \quad (2)$$

Addition of sulphate ion retarded the rate of oxidation considerably. The results on the effect of addition of sulphate ions on the rate of oxidation are given in Table 7.

Table 7. Effects of sulphate ions on the rate of oxidation

[Ce(IV)]: 4.0×10^{-3} M; [Alcohol]: 10.0×10^{-2} M [HNO_3]: 1.08 M; Temp.: 25°C.

$[Na_2SO_4]\times10^3$ mol/l	0.00	5.0	10.0	15.0	20.0	25.0
$k_1\times10^3$ min^{-1}	4.06	2.88	2.30	1.92	1.60	1.40

A plot of $1/k_1$ against $[SO_4^{2-}]$ gave a straight line.

The results find an explanation on the assumption that $Ce(OH)^{3+}$ forms complexes with SO_4^{2-} of the type (*cf.* Hargreaves and Sutcliff[5]),

$$Ce(OH)^{3+} + SO_4^{2-} \overset{k_b}{\rightleftharpoons} [Ce(OH)SO_4]^+ \quad (3)$$

and that the complex $[Ce(OH)SO_4]^+$ is a poor oxidant as compared with $Ce(OH)^{3+}$.

If reaction (3) is valid, $[Ce(IV)]=[Ce(OH)^{3+}]+[Ce(OH)SO_4^+]$, the observed rate constant will be related to the concentration of sulphate ions by the expression

$$k_1 = \frac{K''}{1+K_b[SO_4^{2-}]}$$

$$\text{or} \quad \frac{1}{k_1} = \frac{K_b}{K''}\cdot[SO_4^{2-}] + \frac{1}{K''}$$

where k_1 is the observed rate constant and K'' is a constant which includes the concentration of alcohol. From the above relationship, the inverse of the observed rate constant plotted against concentration of sulphate ions should be a straight line as has been observed.

Our results suggest $Ce(OH)^{3+}$ as the reactive species. The colour change of the ceric solution from yellow to reddish brown when alcohol was added indicates the formation of an intermediate complex which has also been established spectrophotometrically.[1]

On the basis of the low value of $k_{CH}/k_{CD}=1.9$ for α-deuterioalcohol during the oxidation of deuterated cyclohexanol by ceric sulphate and $k_{OH}/k_{OD}=1.0$ for oxygen deuterium alcohol, Littler and Waters[6] and Littler[7] suggested that the α-carbon hydrogen fission might be preponderant, though Littler[8] suggested that a concerted mechanism involving both C–H and O–H fissions can not be ruled out. Thus, the mechanism for the oxidation of *s*-butyl alcohol by cerium (IV) in nitric acid may be written as

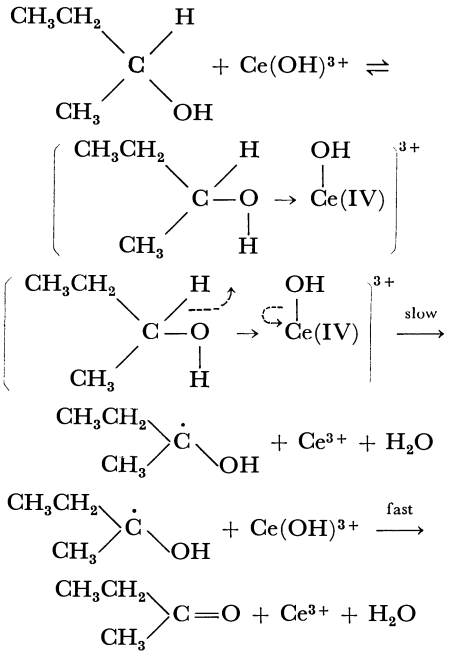

$Ce(OH)^{3+}$ is written as an oxidising species. The ligand groups like NO_3^-, H_2O, *etc.* have not been indicated for the sake of simplicity.

4) J. Shorter, *J. Chem. Soc.*, **1962**, 1868.
5) G. Hargreaves and L. H. Sutcliff, *Trans. Faraday Soc.*, **51**, 1105 (1955).
6) J. S. Littler and W. A. Waters, *J. Chem. Soc.*, **1960**, 2767.
7) J. S. Littler, *ibid.*, **1959**, 4135.
8) J. S. Littler, *ibid.*, **1962**, 2190.

Charge-Transfer Interaction and Fluorescence in Some Tetracyanobenzene Complexes

Takayoshi KOBAYASHI, Keitaro YOSHIHARA,* and Saburo NAGAKURA

The Institute for Solid State Physics, The University of Tokyo, Roppongi, Minato-ku, Tokyo

(Received February 15, 1971)

Fluorescence lifetimes and quantum yields were measured for some tetracyanobenzene complexes with benzene and its methyl derivatives, and the radiative and nonradiative rate constants were determined under various conditions. The results show that the low fluorescence intensities of the complexes in nonpolar fluid media are due to small radiative rate constants and that nonradiative processes become important for the complexes in polar fluid media. From the theoretical consideration of the observed radiative transition probability, it is found that the geometry and the charge distribution in the excited equilibrium state are greatly different from those in the excited Franck-Condon state for the complexes in fluid media at room temperature and that the degree of the charge-transfer in the former state amounts to 96—100%, while it is only 12—45% in the latter state. The stabilization energy due to the reorientation was obtained from the temperature dependence of the fluorescence spectrum.

The fluorescence spectra measured for charge-transfer (hereafter abbreviated to CT) complexes, though rather scanty,[1-9] have the following two characteristics: (1) their Stokes shifts in solution lie between 3500 cm^{-1} and 8500 cm^{-1} at low temperature (−190°C),[1,2] and (2) fluorescence has been observed for only a few CT complexes in solution at room temperature,[3-7] and its intensity is very weak even if it is observed.[10]

Short and Parker[4] determined the quantum yield of fluorescence at room temperature to be ~0.01 or less for the tetrachlorophthalic anhydride and pyromellitic dianhydride complexes with hexamethylbenzene and naphthalene in several solvents. Prochorow and Siegoczyński[5] also measured their fluorescence quantum yields and lifetimes in several solvents and obtained low quantum yields of less than 0.017. Mataga *et al.*[6,7] explained the decrease in the quantum yield with the solvent polarity as due to the decrease in the radiative transition probability. However, Prochorow and Siegoczyński[5] showed that the radiative transition probability might be constant for a series of solvents and that the radiationless transition probability increased with their dielectric constants, though they could not exclude the possibility that, in highly polar solvents, the radiative transition probability might diminish.

It must be emphasized that non-fluorescent CT complexes in fluid solutions at room temperature have fluorescence in the rigid phase.[1,2,11]

In order to explain the above-mentioned characters of CT complexes, we measured the fluorescence lifetimes and quantum yields of tetracyanobenzene complexes with benzene and its methyl derivatives, and determined the radiative and nonradiative rate constants under several conditions. On the basis of the observed results and the theoretical consideration of the radiative rate constants, we interpreted the low quantum yield and the large Stokes shift of CT fluorescence in terms of the reorientation of solvent molecules and the change in the geometry of the complex itself.

Experimental

Materials. Tetracyanobenzene (abbreviated hereafter to TCNB) used as an electron acceptor was purified by recrystallization from ethanol. Dotite spectrograde benzene and toluene were used as donors and solvents without further purification.[12] Commercially-available mesitylene and *m*- and *p*-xylene were purified by distillation. Durene was purified by repeated recrystallizations from benzene and by repeating zone refining about 50 times. Hexamethylbenzene (abbreviated hereafter to HMB) was purified by repeated recrystallizations from ethanol and thereafter by sublimation *in vacuo*.

Ethyl ether was shaken with a 10% aqueous sodium sulfite solution, washed with a saturated aqueous sodium chloride solution containing sodium hydroxide, dried over calcium chloride, and finally distilled over metallic sodium. Cyclo-

* Present address; The Institute of Physical and Chemical Research, Wako, Saitama.

1) J. Czekalla, G. Briegleb, W. Heer, and R. Glier, *Z. Elektrochem.*, **61**, 537 (1957).

2) J. Czekalla, G. Briegleb, and W. Heer, *ibid.*, **63**, 712 (1959).

3) H. M. Rosenberg and E. C. Eimutis, *J. Phys. Chem.*, **70**, 3494 (1966).

4) G. D. Short and C. A. Parker, *Spectrochim. Acta*, **23A**, 2487 (1967).

5) J. Prochorow and R. Siegoczyński, *Chem. Phys. Lett.* **3**, 635 (1969).

6) M. Mataga, T. Okada, and N. Yamamoto, *ibid.*, **1**, 119 (1967).

7) N. Mataga and Y. Murata, *J. Amer. Chem. Soc.*, **91**, 3144 (1969).

8) J. Czekalla, A. Schmillen, and K. J. Mager, *Ber. Bunsenges, Physik. Chem.*, **61**, 1053 (1957).

9) J. Czekalla and K. -O. Meyer, *Z. Physik. Chem.* (Frankfurt), **27**, 185 (1961).

10) The CT complexes which have hitherto been found to be fluorescent at room temperature are as follows:
Tetrachlorophthalic anhydride-substituted methylbenzenes[3,9]
Pyromellitic dianhydride-substituted methylbenzenes[3-5]
Tetracyanobenzene-some aromatic hydrocarbons[7].

11) J. Czekalla, A. Schmillen, and K. J. Mager, *Ber. Bunsenges. Physik. Chem.*, **63**, 623 (1959).

12) We checked, in the initial stage of our experiment, the effect of the purification of benzene and toluene upon fluorescence by comparing the results obtained by the use of the untreated materials with those obtained by the use of the materials purified by shaking with concentrated sulfuric acid, by washing, by drying, and finally by distillation. We could observe no significant effect of purification on the observed results.

hexane was shaken with fuming sulfuric acid, washed with water and aqueous sodium hydroxide, boiled with a mixture of fuming nitric acid and concentrated sulfuric acid, washed with the mixture more than three times, distilled with hydrochloric acid, washed with water, and dried with calcium chloride. After being passed through a newly activated silica gel column, it was finally distilled over metallic sodium.

Methyl methacrylate (MMA) was shaken with 5% aqueous sodium hydroxide several times until no color developed, washed with water more than five times, dried overnight with anhydrous magnesium oxide, and distilled under *ca.* 100 mmHg with nitrogen ebullition. Immediately after the distillation, it was passed through a column of activated silica gel covered with aluminum foil, and redistilled under reduced pressure with nitrogen ebullition. The purified MMA was stored at *ca.* −5°C and was used as a solvent and also as a material for the preparation of a polymer matrix as soon as possible after the above-mentioned purification.

Preparation of Polymer Rigid Solutions Containing Complexes. The rigid solutions of TCNB complexes in polymethyl methacrylate (PMMA) were prepared by polymerizing the MMA solutions in the following way. The MMA solution in a sample tube was deaerated carefully until no bubbling could be detected; then it was polymerized by being kept at 64°C in the dark for about 3 days, and finally slowly cooled to room temperature. No chemical change occurred during the polymerization in the electron donors and acceptors under consideration. We used transparent and completely polymerized rigid solutions with no crack at 77°K.[13] We carefully treated the polymerized samples in order not to expose them to light before measurements.

Measurements. The absorption spectra of TCNB complexes under various conditions were measured by a Cary recording spectrophotometer, Model 14 M. Emission spectra were measured by a JASCO CT-50 grating monochromator with a 100-W high-pressure mercury lamp at a light source, and by an Aminco-Bowman spectrophotofluorometer with a xenon or a mercury-xenon lamp. The emission was detected with an RCA 1P28, an RCA 1P21, or an EMI 9529A photomultiplier. The correct quantum spectra of the complexes were obtained by measuring the sensitivity spectrum of an optical system consisting of lenses, a monochromator, and a photomultiplier by the aid of a standard tungsten filament lamp. Fluorescence quantum yields, η_F's, were measured in the way described by Parker and Rees.[14] The fluorescence quantum yield of the tetrachlorophthalic anhydride-HMB complex was measured by taking the solution of quinine bisulphate in 0.1 N sulfuric acid as the standard. The value thus obtained is in good agreement with that measured by Prochorow and Siegoczyński[5] by using quinine bisulphate or trypaflavine as the standard. For the sake of convenience, the tetrachlorophthalic anhydride-HMB complex was adopted as the secondary standard in determining the quantum yields of the TCNB complexes under consideration, since its fluorescence and absorption are similar to those of the latter complexes in intensity, band shape, and position.

A nitrogen gas laser with a repetition rate of *ca.* 20 Hz, a peak power of ~20 kW, and a pulse width of ~3 nsec was used as the light source for the fluorescence-decay measurements.

Experimental Results

Absorption Spectra and Natural Lifetimes. Absorption spectra were measured for binary solutions containing TCNB in pure benzene, toluene, xylenes, and mesitylene, and also for MMA solutions containing TCNB as an electron acceptor and durene or HMB as an electron donor. The peak wave numbers (ν^A_{max}) and molar extinction coefficients (ε) for the observed CT bands are given in Table 1, together with the ionization potentials of the donors.[15] The natural lifetimes, τ_0's, and the corresponding radiative rate constants, k's, of the complexes were determined by the aid of Eq. (1) presented by Strickler and Berg[16]:

$$k(\mathrm{SB}) = \tau_0^{-1}(\mathrm{SB}) = 2.880 \times 10^{-9} n^2 \langle \nu^{F-3} \rangle_{Av}^{-1} \frac{g_l}{g_u} \int \varepsilon \, d\ln \nu^A \quad (1)$$

Here g_l and g_u represent the degeneracies of the lower and upper states, respectively; ν^A and ν^F are the wave numbers of the absorption and fluorescence spectra, respectively, and n is the refractive index of the solution. In actuality, k(SB) was obtained by the use of the refractive index of the solvent, n_0 instead of that of the solution. This may be expected to have no serious effect to the result, since the concentration of the solution is very small. The evaluated k(SB) values are given in Table 1.

Fluorescence Spectra, Stokes Shifts, Lifetimes, Quantum Yields, and Their Temperature Dependencies. Fluorescence spectra were measured under various conditions for the systems used for the absorption measurements. The total emission spectra are shown in Figs. 1 and 2. As clearly seen in Fig. 1, the fluorescence spectra measured at room temperature for the binary systems containing TCNB in benzene, toluene, *m*-

Table 1. The absorption peak wave number (ν^A_{max}), molar extinction coefficient (ε), and radiative rate constant (k) of TCNB complexes with various electron donors

Donor[a]	I[b] (eV)	n[c]	ν^A_{max} (10^3 cm^{-1})	ε (M^{-1} cm^{-1})	k(SB) (10^7 sec^{-1})
Benzene	9.245	1.5016	32.5	2200	3.8_4
Toluene	8.82	1.4893	31.8	1800	2.3_8
m-Xylene	8.45	1.4973	30.3	1540	1.3_9
p-Xylene	8.56	1.5004	30.5	1680	1.3_5
Mesitylene	8.39	1.4954	28.3	1400	1.1_1
Durene	8.03	1.5015	26.4[d]	660[d]	0.87_0
HMB	7.85	1.5015	24.6	880	0.80_0

a) The measurements were made for the binary systems including a small amount of TCNB in each donor except for the durene-TCNB and HMB-TCNB systems for which the MMA solutions were used.
b) The ionization potential of donor.
c) The refractive index of solvent.
d) The absorption spectrum of the TCNB-durene complex in MMA has no peak but a shoulder. The peak position was estimated by separating the absorption intensity in the concerned wavelength region into the two parts belonging to the strong and weak bands.

13) The incompletely polymerized solution was cracked at the liquid nitrogen temperature.
14) C. A. Parker and W. T. Rees, *Analyst*, **85**, 587 (1960).
15) The equilibrium constants for the CT complex formation were determined to be 0.79 and 2.8 ($l \cdot \mathrm{mol}^{-1}$) by the aid of the usual Stern-Volmer plot for the TCNB complexes with durene and HMB in MMA, respectively.
16) S. J. Strickler and R. A. Berg, *J. Chem. Phys.*, **37**, 814 (1962).

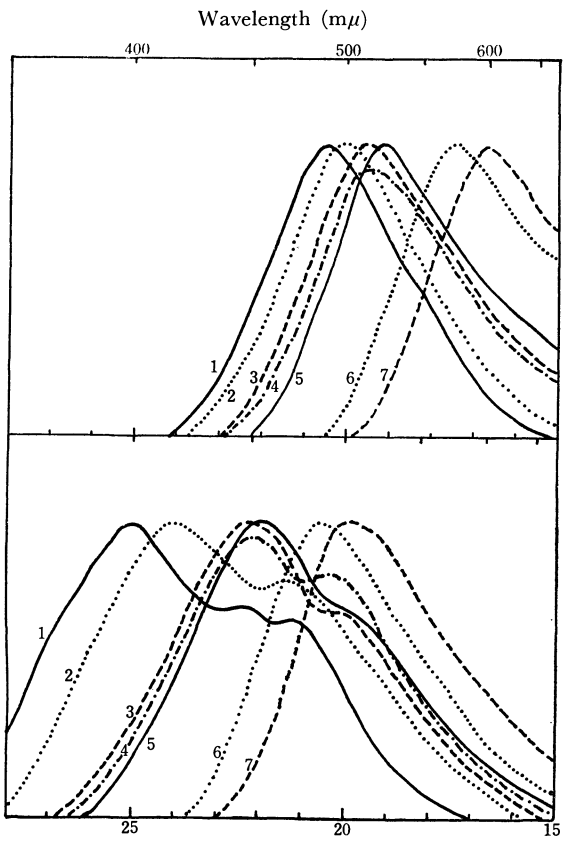

Fig. 1. The total emission spectra of TCNB complexes at room temperature (upper) and at 77°K (lower).

Curve	Donor	Solvent
1	benzene	benzene
2	toluene	toluene
3	*m*-xylene	*m*-xylene
4	*p*-xylene	*p*-xylene
5	mesitylene	mesitylene
6	durene	MMA
7	HMB	MMA

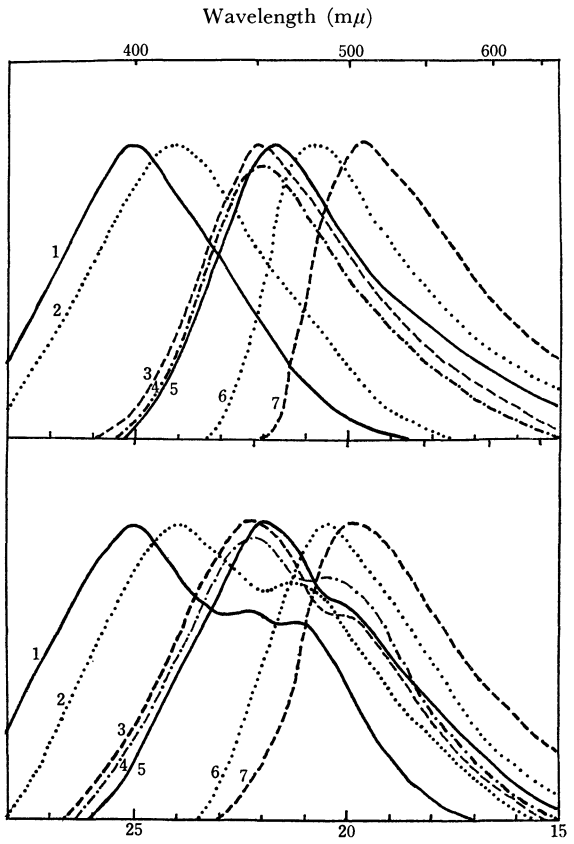

Fig. 2. The total emission spectra of TCNB complexes in PMMA solid solution at room temperature (upper) and at 77°K (lower). The numbering of the curves is the same as in Fig. 1.

xylene, *p*-xylene, and mesitylene (group I) and for the ternary systems of TCNB-durene-MMA and TCNB-HMB-MMA (group II) are different from those at the liquid nitrogen temperature. On the other hand, Fig. 2 shows that the fluorescence spectra of complexes in the PMMA rigid solution (group III) are essentially independent of the temperature, except for the fact that the CT phosphorescence appears at 77°K.

Tables 2 and 3 show the Stokes shifts observed for the TCNB complexes at room temperature and at 77°K, respectively. The observed values at 77°K lie between 8300 cm^{-1} for TCNB-*p*-xylene and 4500 cm^{-1} for TCNB-HMB-MMA, and are close to those previously observed for the other complexes *i.e.*, 8500 cm^{-1} for chloranil-1,2-benzanthracene and 3500 cm^{-1} for 1,3,5-trinitrobenzene-durene.[1,2] At room temperature, however, they are extraordinarily large; that is to say, they are 12000 cm^{-1} for TCNB-benzene

Table 2. The lifetime (τ_F), quantum yield (η_F), rate constans (k^F, k^{FQ}), and stokes shift ($\Delta(\nu^A_{max}-\nu^F_{max})$) at room temperature

Donor[a)]	τ_F (nsec)	η_F	k^F (10^5 sec^{-1})	k^{FQ} (10^6 sec^{-1})	ν^F_{max}	ν^{00} [b)]	Δ^{00}_{FC} [c)]	$\Delta(\nu^A_{max}-\nu^F_{max})$
					(10^3 cm^{-1})			
Benzene	147±3	0.09±0.02	6.1±2.2	6.2±0.3	20.5	23.5	3.0	12.0
Toluene	122±3	0.08±0.02	6.5±1.8	7.5±0.4	20.0	23.0	3.0	11.8
m-Xylene	53±2	0.02±0.01	3.8±2.0	15±3	19.6	22.0	2.4	10.7
p-Xylene	52±2	0.02±0.01	3.9±2.1	15±4	19.6	21.8	2.2	10.9
Mesitylene	43±2	0.01±0.005	2.3±1.3	23±2	19.2	21.5	2.3	9.1
Durene	8±1	0.0003±0.0001	0.38±0.18	120±20	17.2	19.8	2.6	9.2
HMB	5±1	~0.0001	~0.2	~200	16.7	19.0	2.3	7.9

a) See footnote a) in Table 1.
b) The number of 0-0 transition band of fluorescence at room temperature.
c) $\Delta^{00}_{FC}=\nu^{00}-\nu^F_{max}$

TABLE 3. THE LIFETIME (τ_F), QUANTUM YIELD (η_F), RATE CONSTANTS (k^F, k^{FQ}), FREQUENCY DIFFERENCE (Δ^{00}_{FC}) AND STOKES SHIFT ($\Delta(\nu^A_{max}-\nu^F_{max})$) AT 77°K

Donor[a]	τ_F (nsec)	η_F	k^F (10^6 sec^{-1})	k^{FQ} (10^6 sec^{-1})	ν^F_{max} (	ν^{00}[b] 10^3 cm^{-1}	Δ^{00}_{FC}	$\Delta(\nu^A_{max}-\nu^F_{max})$)
Benzene	38±3	0.63±0.05	17	9.5	25.0	27.5	2.5	6.5
Toluene	50±3	0.55±0.05	11	9.0	23.8	26.5	2.7	8.0
m-Xylene	74±3	0.51±0.05	6.9	6.6	22.2	25.0	2.8	8.1
p-Xylene	72±3	0.46±0.05	6.4	7.5	22.2	25.0	2.8	8.3
Mesitylene	85±3	0.47±0.05	5.5	6.5	22.0	24.7	2.7	6.3
Durene	58±3	0.25±0.05	4.3	13	20.4	22.8	2.4	6.0
HMB	39±3	0.16±0.05	4.1	22	20.1	21.8	1.7	4.5

a) See footnote a) in Table 1.
b) The wave number of the 0-0 transition band of fluorescence at 77°K.

and 7900 cm^{-1} for TCNB-HMB-MMA. These facts suggest that the equilibrium state of the lowest excited state is very different from the Franck-Condon state.

The quantum yields were determined at room temperature for the complexes of groups I and II, but at the liquid nitrogen temperature they could not be measured because all the samples except for the TCNB-toluene system became opaque. Therefore, the quantum yields of the complexes of groups I and II at the liquid nitrogen temperature are assumed to be equal to the value of the corresponding TCNB complexes of group III at the same temperature. The validity of this assumption was checked by comparing the fluorescence intensity at 77°K measured for the TCNB-toluene-PMMA system with that for the TCNB-toluene system, which vitrifies in a thin glass tube. The quantum yields derived from the integrated fluorescence intensities observed for the TCNB-toluene and TCNB-toluene-PMMA systems deviate from each other by only 15%. Radiative and nonradiative rate constants were obtained from the quantum yields and lifetimes measured at room temperature and at 77°K; they are listed in Tables 2 and 3.

The fluorescence lifetimes and quantum yields were measured at various temperatures between 77°K and 300°K for the TCNB-toluene and TCNB-HMB-PMMA systems, and their radiative and nonradiative rate constants were obtained; the results are shown in Figs. 3 and 4, together with the temperature dependencies of the wave numbers of the fluorescence maxima, the lifetimes, and the quantum yields. According to Figs. 3 and 4, TCNB-toluene and TCNB-HMB-PMMA show greatly different temperature dependencies of the fluorescence maxima, lifetimes, quantum yields, and radiative rate constants. These quantities change abruptly at about 140°K for the former, while for the latter they vary continuously and the change is small in the whole temperature range.

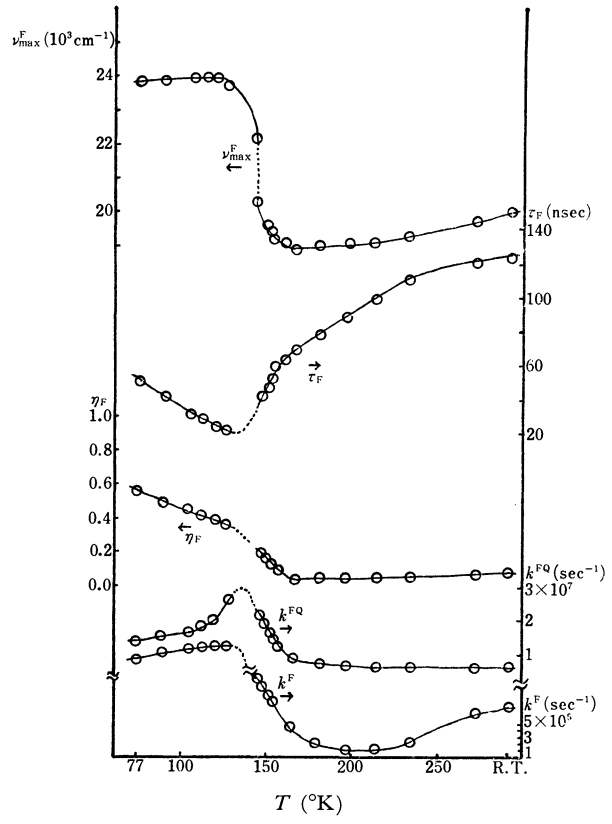

Fig. 3. Temperature dependence of fluorescence maximum (ν^F_{max}), lifetime (τ_F), quantum yield (η_F), and rate constants (k^F, k^{FQ}) for TCNB-toluene.

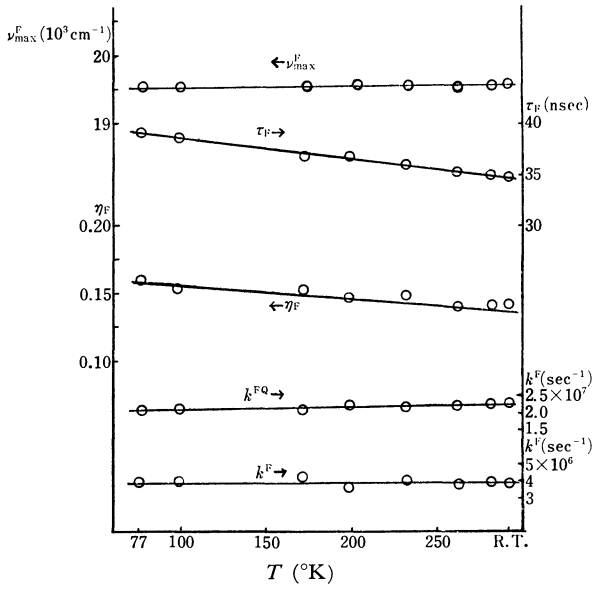

Fig. 4. Temperature dependence of fluorescence maximum (ν^F_{max}), lifetime (τ_F), quantum yield (η_F), and rate constants (k^F, k^{FQ}) for TCNB-HMB-PMMA.

Table 4. The fluorescence maxima (ν^F_{max}), lifetimes (τ_F) quantum yields (η_F), and rate constants (k^F, k^{FQ}) of some TCNB complexes under several conditions

Donor	Solvent	Temp. °C	ν^F_{max} (10^3 cm^{-1})	η_F	τ_F (nsec)	k^F (10^5 sec^{-1})	k^{FQ} (10^7 sec^{-1})
Benzene	Benzene	80	20.5		52		
m-Xylene	*m*-Xylene	−72	19.4		18		
p-Xylene	*p*-Xylene	−72	22.2		70		
Durene	Durene	80	19.0		25		
	Cyclohexane	23	19.0	0.0006	17	0.35	5.9
	Ethyl ether	23	17.2	0.0003	8	0.38	12
	Ethyl ether	74	17.2	0.0002	6	0.33	17
HMB	Cyclohexane	23	18.0	∼0.00027	12	∼0.2	8.3
	Benzene	23	16.7	∼0.00023	11	∼0.2	9.1
	MMA	23	16.7	∼0.0001	5	∼0.2	20
	Ethyl ether	23	16.7	∼0.0001	5	∼0.2	20

Tables 2, 3, and 4 show that the lifetime of the TCNB-*p*-xylene system at the dry ice-ethanol temperature (−72°C) is close to that at 77°K, while in the TCNB-*m*-xylene system the values at both temperatures are different. This is related to the difference in the rigidity of the solutions. At both temperatures, the TCNB-*p*-xylene system is in a rigid state and has a similar lifetime. The TCNB-*m*-xylene system is fluid at dry ice-ethanol temperature and the lifetime at this temperature is shorter than that at 77°K.

Fluorescence Lifetime and Quantum Yield in Polar Solvents. The fluorescence maxima, lifetimes, and quantum yields of several TCNB complexes were measured in various solvents; the results for the TCNB-durene and TCNB-HMB systems are shown in Table 4. This table shows that the fluorescence lifetimes τ_F's, are shorter in polar solvents than in nonpolar solvents. However, the radiative rate constant, $k_F=\eta_F/\tau_F$, for each complex is nearly independent of the solvents used. The situation is the same for the other complexes, though the details will not be presented here.

CT Complexes in the Crystalline State. The fluorescence maximum wave numbers, lifetimes, and relative intensities, I_F's for the TCNB-durene and TCNB-HMB complexes in the crystalline state are given in Table 5. The fluorescence maximum wave numbers and lifetimes given in this table are similar to those of the corresponding complexes in PMMA or in solution at 77°K. The slight difference in the fluorescence maximum wave number between room temperature and 77°K was found by careful measurements to be due to the enhancement of the reabsorption at the higher temperature. The τ_F/I_F values are almost constant between room temperature and 77°K; therefore, the radiative rate constants are almost independent of the temperature.

Table 5. Fluorescence maximum wave numbers (ν^F_{max}), lifetimes (τ_F), and relative intensities (I_F) of the TCNB complexes with durene and hexamethylbenzene in crystalline state

Donor	Temp.	ν^F_{max} (10^3 cm^{-1})	τ_F (nsec)	I_F
Durene	R.T.	20.8	34	1
	77°K	20.4	32	1.1
HMB	R.T.	19.2	26	1
	77°K	19.0	40	1.5

Theoretical Consideration and Discussion

The Possibility of 1 : m Complexes in the Excited State. The large Stokes shift observed for the complexes in the fluid state may be explained by the reorientation of the solvent and solute molecules or by $1:m$ ($m\geq 2$) complex (AD_m) formation in the excited state. According to Table 4, the binary system, for example, TCNB-durene at 80°C, has the fluorescence peak at 19.0×10^3 cm^{-1}. This position is almost the same for the solution containing TCNB-durene in an inert solvent like cyclohexane. This seems to mean that the large Stokes shift for this system in fluid media is not due to the $1:m$ complex formation in the excited state. The situation is the same for the other systems showing a large Stokes shift in fluid media.

Dependence of the Fluorescence Spectrum on the Rigidity of the Medium. The large Stokes shifts observed for fluorescence spectra in fluid solutions are conceivably caused by the stabilization due to the interaction of the excited CT complex with a large dipole moment with the surrounding solvent molecules.[17]

According to Bakshiev, with a decrease in the temperature the fluorescence spectra of polyatomic molecules shift first toward the longer wavelengths and thereafter toward the shorter wavelength as the solvent viscosity increases.[17] Accordingly, a turning point is expected to be observed for the ν^F_{max} *versus* temperature curve. This effect was in fact observed with the TCNB-toluene system, as is shown in Fig. 3. The turning point at ∼140°K is close to the melting point of the toluene solution containing 10^{-3} M of TCNB. This tendency has been found for several systems with intramolecular CT interaction, such as biphenyl, stilbene, and fluorene derivatives in various

17) a) N. G. Bakshiev, *Opt. i Spektroscopiya*, **16**, 821 (1964); *Opt. Spectry.*, **16**, 446 (1964). b) N. G. Bakshiev, *Opt. i Spektroscopiya*, **20**, 976 (1966); *Opt. Spectry.*, **20**, 542 (1966).

solvents.[18]

From Eq. (4) in Reference (17b) and the fluorescence and absorption maxima observed by us and in the literature,[7] we estimate the dipole moment in the excited state of the TCNB-HMB complex to be 8.34 D, by assuming the Onsager radius to be 5.81 Å.[19] This value is rather small compared with 14(±3)D or 10(±1.5)D of the tetrachlorophthalic anhydride-HMB complex.[9,20]

We can now roughly estimate the stabilization energy due to the reorientation of the solute and solvent molecules in the excited state (E_R), the Franck-Condon energies in the ground state before and after reorientation (E_{gb}^{FC} and E_{ga}^{FC}, respectively), and the Franck-Condon energy in the excited state (E_e^{FC}). Their definitions and relations to the wave numbers of the absorption and fluorescence maxima are shown in Fig. 5, while their values are listed in Table 6.

The potential energy curves of the ground and excited states before and after reorientation are shown in Fig. 5, where q means a set of the coordinates which indicates the positions and orientations of the solvent molecules near the solute CT complex. All the q_G's and q_E's adjust themselves to minimize the energies of the ground state, $E_G(R, Q, q)$, and the lowest excited state, $E_E(R, Q, q)$, respectively. Fluorescences in rigid and fluid media take place from the lowest point of the

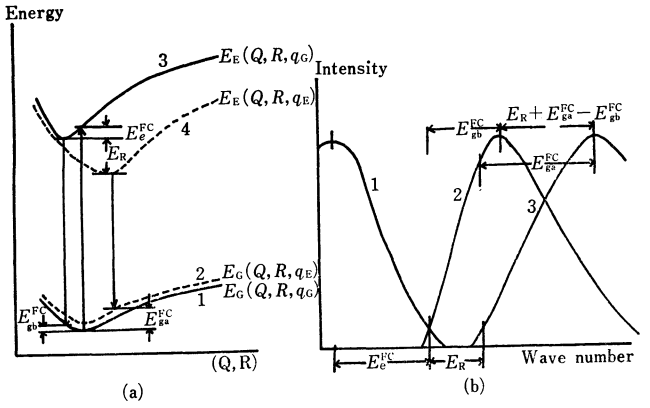

Fig. 5. (a) The potential energy curves of CT complexes. The curves are drawn by plotting the energies *versus* the internal coordinates of the component molecules, Q's and the coordinates concerning the intermolecular distance and orientation, R's. Coordinates of surrounding solvent molecules, q's are determined in such a way as to minimize the energy for a fixed point of the abscissa. 1, ground state before reorientation; 2, ground state after reorientation; 3, first excited singlet state before reorientation; 4, first excited singlet state after reorientation.
(b) The absorption and fluorescence spectra of the CT complex. 1, absorption; 2, fluorescence before reorientation; 3, fluorescence after reorientation.

Table 6. The Franck-Condon destabilization energies in the excited and ground states (E_e^{FC} and E_g^{FC}, respectively) and the reorientation stabilization energy (E^R) (10^3 cm^{-1})

Donor[a]	ν_{max}^F(77°K) $-\nu_{max}^F$(RT)	E_{ga}^{FC}	E_{gb}^{FC}	E_e^{FC}	E_R
Benzene	4.5	3.0	2.5	5.0	4.0
Toluene	3.8	3.0	2.7	5.3	3.5
m-Xylene	2.6	2.4	2.8	5.3	3.0
p-Xylene	2.6	2.2	2.8	5.5	3.2
Mesitylene	2.8	2.3	2.7	3.6	3.2
Durene	3.2	2.6	2.4	3.6	3.0
HMB	3.4	2.3	1.7	2.8	2.8

a) See footnote a) in Table 1.

$E_E(R, Q, q_G)$ and $E_E(R, Q, q_E)$, respectively. The stabilization energy due to the reorientation, E_R, is defined as the energy difference between the two lowest points of the two potential energy curves.

As is shown in this table, the E_R value increases with an increase in the ionization potentials of donors. This may be related to the experimental fact that the difference in the radiative rate constant between room temperature and 77°K increases with the increase in the ionization potential of the donor.

Radiative and Nonradiative Rate Constants. The complexes in a rigid solution, in a nonpolar fluid medium, and in a polar fluid medium are denoted as the complexes in the A, B, and C states, respectively. According to Tables 2, 3, and 4, the radiative rate constants are 10^{6-7} sec^{-1} and 10^{4-5} sec^{-1} for the complexes in the A and B states, respectively. Furthermore, these tables show that the nonradiative rate constants of complexes in the A and B states are 10^{6-7} sec^{-1}, while those in the C state are about 10^8 sec^{-1}. From these facts, it can be concluded that the low fluorescence intensity of the CT complexes in a nonpolar fluid medium is due to the small radiative rate constant and that, for the CT complexes in a polar fluid medium, the nonradiative quenching effect becomes important in addition to the above-mentioned effect. Therefore, it may be said that the discussions made by Mataga and Murata[7] and by Prochorow and Siegoczyński[5] concerning the low fluorescence intensity are correct for the CT complexes in nonpolar and polar media, respectively.

When we compare the radiative rate constant, k(SB), in Table 1, obtained from the absorption intensity, with the rate constant, k^F, in Tables 2 and 3, we can see that the former is larger than the latter for each complex, both at room temperature and at the liquid nitrogen temperature.[21] In particular, the value of k^F at room temperature is extraordinarily small compared with k(SB). This fact, as will be described below, can be explained by considering the great differences in the electron distribution and in the

18) E. Lippert, W. Luder, and F. Moll, *Spectrochim. Acta*, **10**, 585 (1959).

19) The value is given by $(\sqrt{1.7^2+3.96^2}+1.5)$ Å, where 1.7 Å, 3.96 Å, and 1.5 Å are a half of the intermolecular distance, the distance between the center of the TCNB molecule and one of its nitrogen atoms, and the van der Waals radius of nitrogen, respectively.

20) J. Czekalla, *Z. Elektrochem.*, **64**, 1221 (1960); *Chimia* (Switz.), **15**, 26 (1961).

21) Mataga and Murata[7] obtained larger natural lifetimes, 50 and 60 nsec for TCNB-benzene and TCNB-toluene, respectively, than the corresponding values obtained by us, 26 and 43 nsec, respectively. According to our opinion, their values are too great because they disregarded the n^2 in Eq. (1) in their evaluation.

Table 7. The observed and calculated rate constants and the contributions of the CT configuration to the excited state at 77°K and at room temperature (RT)

Donor	$I-A$ (eV)	CT(%) 77°K	k(calc) (10^6 sec^{-1})	k(SB) (10^6 sec^{-1})	$k^F_{77°K}$ (10^6 sec^{-1})	CT(%) RT
Benzene	8.845	12.4	26.0	$38._4$	17	96.7
Toluene	8.42	19.4	18.6	$23._8$	11	96.7
m-Xylene	8.16	28.7	14.7	$13._9$	6.9	98.1
p-Xylene	8.045	30.1	14.8	$13._5$	6.5	98.1
Mesitylene	7.99	32.2	11.8	$11._1$	5.6	99.7
Durene	7.63	41.2	8.38	8.7_0	4.4	99.8
HMB	7.45	44.6	6.14	8.0_0	4.0	99.9

geometrical configuration between the Franck-Condon state and the excited equilibrium state.

The Calculations of the Radiative Rate Constants and the Contribution of the CT Configuration to the Excited State. The wave functions and energies of the ground and excited states of the complex were calculated by considering the configuration interaction among the ground, CT, and locally-excited (abbreviated hereafter to LE) configurations[22,23] constructed by putting electrons into the SCF of MO's of TCNB and benzene. The actual calculations were made by an electronic computer, FACOM 270—30.

The calculations for the system in the rigid solvent were made for the geometrical structure shown in Fig. 6(a), the most stable geometry in the ground state,[24] the ionization potential of the electron donor, I, being taken as a parameter and the electron affinity of the electron acceptor, A, being fixed at 0.4 eV.[25]

By evaluating the matrix element of the dipole moment by the aid of the Mulliken approximation and by taking the diagonal element concerning the CT configuration and the off-diagonal element between the ground and LE configurations to be 3.4 Å and 0.3 Å, respectively, we calculated the transition moment and the natural radiative rate constant, k, which corresponds to k(SB) in Table 1. The results are shown in Table 7. For purposes of comparison, k(SB) and k^F at 77°K ($k^F_{77°K}$) are also tabulated in this table. The k values calculated for the complexes under consideration lie intermediate between the corresponding k(SB) and $k^F_{77°K}$ values. Generally speaking, the calculated k value agrees well with the observed k(SB) or $k^F_{77°K}$ value for each complex. The contribution of the CT configuration to the excited Franck-Condon state changes from 12.4% for the TCNB-benzene complex to 44.6% for the TCNB-HMB complex.

Now let us consider the energy of the lowest excited singlet state in its potential energy minimum. There is no available data on the most stable configuration in the excited state, so we calculated its energy by the method described in the previous paper[23] for various geometrical configurations; the results are shown in Fig. 7. The energy contour map for the lowest excited state shown in this figure was obtained by locating the plane of TCNB parallel to that of benzene with a distance of 3.4 Å and by setting, as is shown in Fig. 6, the a axis of the TCNB molecule parallel to the x axis. It may be worth noting that the main feature in the

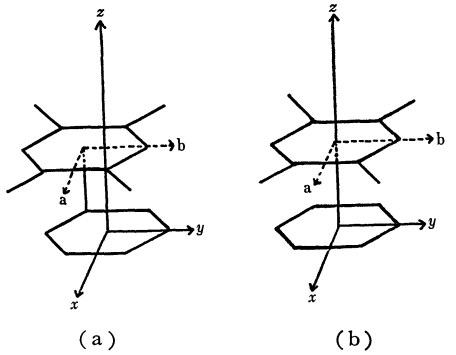

(a) (b)

Fig. 6. The geometrical configuration of the CT complex.
(a) stable configuration in the ground state.
(b) stable configuration in the first excited state.
The distance between the two benzene rings is taken to be 3.4Å.

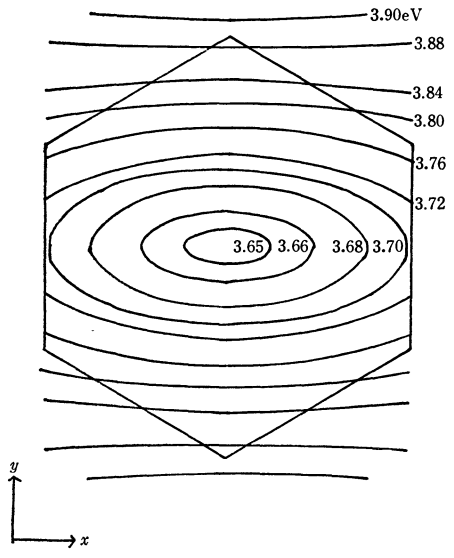

Fig. 7. The energy contour map for the lowest excited singlet state of the TCNB-benzene complex.

22) S. Iwata, J. Tanaka, and S. Nagakura, *J. Amer. Chem. Soc.*, **88**, 894 (1966).
23) T. Kobayashi, S. Iwata, and S. Nagakura, This Bulletin, **43**, 713 (1970).
24) The geometry shown in Fig. 6(a) is very similar to that determined for the TCNB-durene and TCNB-HMB crystals by the X-ray diffraction technique (TCNB-durene: H. Tsuchiya, N. Niimura, and Y. Saito, private communication; TCNB-HMB; N. Niimura, Y. Ohashi, and Y. Saito, This Bulletin, **41**, 1815 (1968)).
25) G. Briegleb, *Angew. Chem. Intern. Ed. Engl.*, **3**, 617 (1964).

energy contour map is common for all the TCNB complexes examined and that in the most stable configuration, the component molecules are located with their centers on the z axis, as is shown in Fig. 6(b).

From the above-mentioned facts, it may be expected that, in fluid media, the component molecules reorient to a great extent and take the geometrical configuration shown in Fig. 6(b). Furthermore, there occur reorientations of the surrounding solvent molecules[26] in addition to those of the electron donor and acceptor molecules. Next, we will describe the wave functions of the ground and excited states of the reoriented system in general forms.

$$\theta_{re}^{G} = a_0^{re}\theta_0(AD)_{re} + \sum_i a_i^{re}\theta_i(A^-D^+)_{re} + \sum_j a_j^{re}\theta_j(A^*D)_{re} \quad (2)$$

$$\theta_{re}^{E} = b_0^{re}\theta_0(AD)_{re} + \sum_i b_i^{re}\theta_i(A^-D^+)_{re} + \sum_j b_j^{re}\theta_j(A^*D)_{re} \quad (3)$$

where θ_0, θ_i's, and θ_j's are the wave functions of the ground, CT, and LE (in acceptor) configurations, respectively, where a_m's and b_m's are the coefficients of the corresponding configurations in the ground and excited states, respectively, and where the superscript or subscript "re" means that the wave function or coefficient is connected with the reoriented system.

In the geometry shown in Fig. 6(b), the overlap integral between electron-donating and -accepting orbitals is equal to zero because of the high symmetricity of the system.[27] This means that the a_i^{re}, a_j^{re}, and b_0^{re} coefficients are nearly equal to zero[28] and that the matrix element, $\langle\theta_i(A^-D^+)_{re}|\vec{er}|\theta_0(AD)_{re}\rangle$, is very small. Here, r represents the coordinate of an electron. Thus, only the following term contributes to k_{RT}^{F};

$$\sum_j a_0^{re}b_j^{re}\langle\theta_0(AD)_{re}|\vec{er}|\theta_j(A^*D)_{re}\rangle \quad (4)$$

where $a_0^{re}\cong 1$. The transition-moment integral in Eq. (4) can be estimated by the aid of the observed absorption spectrum of TCNB itself.

From the observed k^F values at room temperature (k_{RT}^{F}) given in Table 2 and the matrix element shown by Eq. (4), we can obtain the coefficient of the lowest LE (in the acceptor), b_1, which is dominant among b_j's; therefore, we can evaluate the contributions of the LE and CT configurations to the fluorescent state after reorientation. The evaluated values for the CT configuration are given in Table 7. This table shows that, even for the TCNB-benzene and TCNB-toluene complexes, for which the contributions of the CT configuration are less than twenty percent in the Franck-Condon states, they exceed 95% in the excited equilibrium state after reorientation at room temperature. This conclusion as to the TCNB-toluene system is consistent with the result obtained by Masuhara and Mataga from the measurement of the absorption due to the transition from the first excited singlet state to the higher excited state.[29] It is worthy of notice that the degree of the CT between electron donor and acceptor changes greatly upon the reorientation of the component molecules of the complex and of the solvent molecules.

The experimental results given in Table 4 show that the decrease in the fluorescence intensity in a polar solvent is due to the increase in the nonradiative decay. This seems to mean that the scarcity of fluorescence at room temperature for the CT complex in a polar solvent may be due to the rapid nonradiative decay. In view of the great contribution of the CT configuration to the excited equilibrium state after reorientation, the rapid nonradiative process in a polar solvent may be the dissociation process into ions. On the other hand, the scarcity of fluorescence at room temperature for the CT complex in a nonpolar solvent can be mainly due to the small radiative rate constant, as has been described above.

26) In actuality, it is difficult to evaluate the wave functions including surrounding solvent molecules. Therefore, we do not intend to obtain the actual forms of the wave functions from theoretical calculations, alone.

27) The overlap integral between electron-donating and accepting orbitals may be small even when the geometrical configuration of the reoriented system deviates slightly from that shown in Fig. 6(b). This is because the distance between the two component molecules is increased by the increase in the solution energy caused by the reorientation of the solvent molecules.

28) Since $\theta_j(A^*D)_{re}$'s and $\theta_0(AD)_{re}$ mix only through $\theta_i(A^-D^+)_{re}$'s, a_j's are also equal to zero when a_i's vanish.

29) H. Masuhara and N. Mataga, *Chem. Phys. Lett.*, **6**, 608 (1970).

A Theoretical Consideration of the Electron-scavenging Process in Liquid Hydrocarbons. II. Pulse Irradiation

Hideo YAMAZAKI and Kyoji SHINSAKA

Laboratory of Physical Chemistry, Tokyo Institute of Technology, Meguro-ku, Tokyo

(Received February 15, 1971)

A mathematical treatment of the electron recombination process is presented on the basis of the extended Smoluchowski equation, which includes the effects of several positive ions as ion cores in a spur and of a scavenger. The equation is reduced to the usual Smoluchowski equation for the geminate recombination in a special case. The time dependence of the electron concentration is obtained using a successive approximation. The results of numerical calculations for various reaction parameters are presented.

The geminate recombination of the electrons with the parent ions in the primary process in the radiolysis of the liquid phase has been discussed on the basis of a statistical treatment[1-5] and of the basis of the Smoluchowski equation,[6-11] using different approaches. The second method, used by Monchick,[6] Mozumder,[7] and Hummel[8] is based on the approximation of the prescribed diffusion of the Smoluchowski equation. The presence of a singularity at the point of origin in this equation makes it difficult to solve analytically. Numerical calculations using an electronic computer were attempted by Ludwig.[9] In spite of the difficulty of obtaining an accurate solution, the various experimental results, namely, the scavenging effect on the reaction products, the measurement of the electric conduction during irradiation, and the recent development of the spectroscopic tracing of the electron concestration after pulse irradiation, can be interpreted on this theoretical base. However, no unified theory based on a fundamental equation seems to have been proposed in explanation of the various experimental facts. In a previous paper the scavenger effect on the G value of electron recombination has been discussed.[12]

In the present paper, the recombination of the electrons with parent ions after pulse irradiation will be treated by considering the character of a spur and the effect of the scavenger as an extended form of the Smoluchowski equation,[12] which can be reduced to the usual Smoluchowski equation in the absence of a scavenger and in the presence of a single ion in the ion core. The successive approximation was applied to solve the extended form of the Smoluchowski equation, using two extreme cases, namely, the potential-control and diffusion-control cases. To solve the recombination relaxation of the electrons, the determination of the initial distribution of the electrons is important, so various initial distributions were tested in the numerical calculation. Inversely, the initial distribution can be obtained by the inverse Laplace transform from the analysis of the recombination process. In the ion-core model, an ion cluster at the center of the spur and the surrounding electrons are considered. The value of the central ion charge gradually decreases as the neutralization process progresses. The solution can be synthesized by the connection of the solutions for various effective charges in the ion core.

Theory

A) Fundamental Equation and Its Approximations. The fundamental equation for the electron recombination is based on the following form of the extended Smoluchowski equation, (I-12),[13] in a spherical coordinate:

$$\frac{\partial c(r,t)}{\partial t} = D\frac{\partial^2 c(r,t)}{\partial r^2} + \left(\frac{2D}{r} + \frac{\alpha}{r^2}\right)\frac{\partial c(r,t)}{\partial r} - \beta c(r,t) \quad (1)$$

where $C(r, t)$ is the concentration of electrons at a distance r from the center of the ion core and at a time t after the ionization of the central ions. D is the diffusion constant, α is determined by the Coulomb attraction, and β is the rate constant of the scavenger reaction. α decreases with an increase in t by the neutralization of the central ions, and also decreases with an increase in r by means of the screening effect of the electrons outside the ion core, as is shown by Eq. (2):

$$\alpha = N^+(t)eu/\varepsilon \quad (2)$$

where $N^+(t)$ is the number of ions in the ion core, e is the electron charge, u is the mobility of the electrons, and ε is the dielectric constant. However, for the sake of simplicity, α is assumed to be a constant or a step function of time during the neutralization process.

A successive approximation has been used to solve the fundamental equation. An analytical expression of the solution can be obtained in the absence of either the diffusion term or the term of the Coulomb attraction. Therefore, the solutions in which these terms are absent can be used as the zero-th order approximation. For example, in the absence of diffusion term, Eq. (3) is given for the zero-th-order approximation of the potential-control case:

1) G. R. Freeman, *J. Chem. Phys.*, **46**, 2822 (1967).
2) G. R. Freeman and J. M. Fayadh, *ibid.*, **43**, 86 (1965).
3) S. Sato, T. Terao, M. Kono, and S. Shida, This Bulletin, **40**, 1818 (1967).
4) S. Sato, *ibid.*, **41**, 304 (1968).
5) G. R. Freeman, *Adv. Chem. Ser.*, **82**, 339 (1968).
6) L. Monchick, *J. Chem. Phys.*, **24**, 381 (1956).
7) A. Mozumder, *ibid.*, **48**, 1659 (1968).
8) A. Hummel, *ibid.*, **48**, 3268 (1968).
9) P. K. Ludwig, *ibid.*, **50**, 1787 (1969).
10) A. Mozumder, *ibid.*, **50**, 3153 (1969).
11) A. Mozumder, *ibid.*, **50**, 3162 (1969).
12) H. Yamazaki and K. Shinsaka, This Bulletin, **43**, 2713 (1970).

$$\frac{\partial \chi_0(r,t)}{\partial t} = \frac{\alpha}{r^2}\frac{\partial \chi_0(r,t)}{\partial r} - \beta\chi_0(r,t) \tag{3}$$

In the absence of the Coulomb interaction, Eq. (4) is obtained as a diffusion-control case:

$$\frac{\partial \omega_0(r,t)}{\partial t} = D\frac{\partial^2\omega_0(r,t)}{\partial r^2} + \frac{2D}{r}\frac{\partial \omega_0(r,t)}{\partial r} - \beta\omega_0(r,t) \tag{4}$$

or:

$$\frac{\partial r\omega_0(r,t)}{\partial t} = D\frac{\partial^2 r\omega_0(r,t)}{\partial r^2} - \beta r\omega_0(r,t) \tag{4'}$$

The solution for the s-th order approximation can be obtained by means of Eqs. (5) and (6) for the potential control and the diffusion control respectively:

$$\frac{\partial \chi_s(r,t)}{\partial t} = \frac{\alpha}{r^2}\frac{\partial \chi_s(r,t)}{\partial r} + D\frac{\partial^2\chi_{s-1}(r,t)}{\partial r^2} + \frac{2D}{r}\frac{\partial \chi_{s-1}(r,t)}{\partial r} - \beta\chi_s(r,t) \tag{5}$$

and

$$\frac{\partial r\omega_s(r,t)}{\partial t} = D\frac{\partial^2 r\omega_s(r,t)}{\partial r^2} + \frac{\alpha}{r}\frac{\partial \omega_{s-1}(r,t)}{\partial r} - \beta r\omega_s(r,t) \tag{6}$$

By the use of these recurrent equations, the higher-order solutions can be obtained.[14] The zero-th-order solutions are given by Eqs. (7), (8), and (9).[15]

$$\chi_0(r,t) = f(\alpha t + r^3/3)\exp(-\beta t) \tag{7}$$

where f stands for an arbitrary function. Equation (7) is expressed by the integral representation:

$$\chi_0(r,t) = \int_0^\infty K_0(n)\exp(-\beta t - n\alpha t - nr^3/3)\mathrm{d}n \tag{8}$$

where $K_0(n)$ is an arbitrary function of n, which is determined by the initial distribution of electrons. The zero-th-order solution in the diffusion-control case can be written by Eq. (9):

$$\omega_0(r,t) = \frac{\exp(-\beta t)}{2r\sqrt{\pi Dt}}\int_0^\infty \xi\varphi(\xi)[\exp\{-(r-\xi-R_0)^2/4Dt\} - \exp\{-(r+\xi-R_0)^2/4Dt\}]\mathrm{d}\xi \tag{9}$$

where $\varphi(\xi)$ is the initial distribution of the electrons and where R_0 is the radius of the central-ion core. The first- and second-order approximations, χ_1 and χ_2, are given by Eq. (10) and Eq. (11) respectively:

$$\chi_1(r,t) = \int_0^\infty K_1(n)(1+nDr^4/\alpha - n^2Dr^7/7\alpha) \times \exp\{-(\beta+n\alpha)t - nr^3/3\}\mathrm{d}n \tag{10}$$

and

$$\chi_2(r,t) = \int_0^\infty K_2(n)(1+nDr^4/\alpha - n^2Dr^7/7\alpha - 4nD^2r^5/\alpha^2 + 5n^2D^2r^8/2\alpha^2 - 24n^3D^2r^{11}/77\alpha^2 + n^4D^2r^{14}/98\alpha^2) \times \exp\{-(\beta+n\alpha)t - nr^3\}\mathrm{d}n \tag{11}$$

Generally, the s-th order of approximation can be written by:

$$\chi_s(r,r) = \int_0^\infty K_s(n)H_s(n,\alpha,D,r)\exp(-\beta t - n\alpha t - nt^3/3)\mathrm{d}n \tag{12}$$

where H_s is a function of n, α, D, and r. When an approximate electron concentration in the system is expressed as N_s, the approximate electron concentration as a function of the time is given by Eq. (13):

$$\begin{aligned} N_s(t) &= 4\pi\int_{R_0}^\infty r^2\chi_s(r,t)\mathrm{d}r \\ &= 4\pi\int_0^\infty K_s(n)\exp(-\beta t - n\alpha t) \times\left[\int_{R_0{}^3/3}^\infty H_s(n,\alpha,D,\xi)\exp(-n\xi)\mathrm{d}\xi\right]\mathrm{d}n \\ &= 4\pi\int_0^\infty K_s(n)\exp(-\beta t - n\alpha t)G_s(n,\alpha,D,R_0)\mathrm{d}n \end{aligned} \tag{13}$$

where $G_s(n,\alpha,D,R_0)$ is the integral in the brackets, [ ] and is a function of n, α, D, and R_0. The approximate value of $N(t)$ and the time dependence of the electron concentration can be evaluated by using the approximate solutions of $C(r,t)$. Thus, the initial distribution of the electron and the time dependence of the electron concentration in the system are connected by the Smoluchowski equation. The initial distribution of electrons can be estimated from the time behavior of the electron concentration, which is itself determined by the pulse experiment. Therefore, the initial distribution can be expressed by the use of the inverse Laplace transforms[16] of the time dependence of the electron concentration in the system, as is shown in Eq. (14):

$$K_s(n)G_s(n,\alpha,D,R_0) = \frac{1}{8\pi^2 i}\int_{c-i\infty}^{c+i\infty} N_s(p/\alpha) \times \exp\{(\beta/\alpha+n)p\}\mathrm{d}p \tag{14}$$

where the c in the integral is a constant. $G_0(n,R_0)$, $G_1(n,\alpha,D,R_0)$, and $G_2(n,\alpha,D,R_0)$, corresponding to these solutions χ_0, χ_1, and χ_2, are given by Eqs. (15),

---

13) Ref. 12 will be referred to as I, while equations that appear in it will be referred to (I-—).

14) Equation (5) and (6) are solved by the following recurrent equations:

$$\chi_s(r,t) = \exp(-\beta t)\Big[f(t+r^3/3\alpha D) - \frac{D}{\alpha}\int_0^r \exp(-\beta t)\Big\{2r\frac{\partial\chi_{s-1}(r,t)}{\partial r} + r^2\frac{\partial^2\chi_{s-1}(r,t)}{\partial r^2}\Big\}\mathrm{d}r\Big]_{t=c_1-r^3/3\alpha}$$

Where C_1 is a constant, where f is an arbitrary function, and where

$$\omega_s(r,t) = \frac{\exp(-\beta t)}{2r\sqrt{\pi Dt}}\int_0^\infty \xi\varphi(\xi) \times [\exp\{-(r-\xi-R_0)^2/4Dt\} - \exp\{-(r+\xi-R_0)^2/4Dt\}]\mathrm{d}\xi + \frac{\exp(-\beta t)}{2r\sqrt{\pi Dt}}\int_0^t \frac{\exp(\beta\tau)}{\sqrt{t-\tau}}\int_0^\infty \frac{\alpha}{\xi}\frac{\partial\omega_{s-1}(\xi,t)}{\partial\xi} \times [\exp\{-(r-\xi-R_0)^2/4D(t-\tau)\} - \exp\{-(r+\xi-R_0)^2/4D(t-\tau)\}]\mathrm{d}\xi\mathrm{d}\tau$$

Where $\varphi(\xi)$ is the initial distribution of the electrons and where R_0 means the radius of the central-ion core.

15) In the approximation by prescribed diffusion,[7] the product of $\omega_0(r,t)$ and $N^+(t)$ is used for the $C(r,t)$ solution.

16) for example, I. N. Sneddon, "Fourier Transforms," McGrow-Hill Book Co, Inc., New York (1951), p. 30.

(16), and (17) respectively.

$$G_0(n, R_0) = \int_{R_0^3/3}^{\infty} \exp(-n\xi)\mathrm{d}\xi = \exp(-nR_0^3/3)/n \quad (15)$$

$$G_1(n, \alpha, D, R_0) = \int_{R_0^3/3}^{\infty} (1+nD(3\xi)^{4/3}/\alpha - n^2D(3\xi)^{7/3}/7\alpha)\exp(-n\xi)\mathrm{d}\xi \quad (16)$$

$$G_2(n, \alpha, D, R_0) = \int_{R_0^3/3}^{\infty} (1+nD(3\xi)^{4/3}/\alpha - n^2D(3\xi)^{7/3}/7\alpha - 4nD^2(3\xi)^{5/3}/\alpha^2 + 5n^2D^2(3\xi)^{8/3}/2\alpha^2 - 24n^3D^2(3\xi)^{11/3}/77\alpha + n^4D^2(3\xi)^{14/3}/98\alpha^2) \times \exp(-n\xi)\mathrm{d}\xi \quad (17)$$

B) Initial Conditions and Approximate Expressions of the Electron Concentration. From Eqs. (8)-(12) the various types of approximate solutions of electron concentrations can be obtained as a function of the time if the initial distribution of the electrons is given. One of the simplest examples of the initial distribution is the δ-function representation for the weight function, $K_s(n)$. When $K_0(n)$ is expressed by the δ-function in Eq. (8), $K_0(n)=\delta(n\text{-}n_0)$, where n_0 means a positive constant, the solution for the zero-th order approximation in the potential control case can be written as:

$$\chi_0(r, t) = \exp\{-(\beta+n_0\alpha)t - n_0r^3/3\} \quad (18)$$

n_0 can be represented by $2/r_{\max}^3$, where $r_{\max}$ is the distance at the maximum value of initial distribution.[12] Then, the electron concentration normalized by the initial value is given by Eq. (19):

$$N_0(t)/N_0(0) = \exp(-\beta t - n_0\alpha t) \quad (19)$$

Similarly, for the first-order approximation in the case of potential control, the distribution, $\chi_1(r, t)$, is:

$$\chi_1(r, t) = (1+n_0Dr^4/\alpha - n_0^2Dr^7/7\alpha) \times \exp\{-(\beta+n_0\alpha)t - n_0r^3/3\} \quad (20)$$

Then, $N_1(t)/N_1(0)$ is expressed by Eq. (21):

$$N_1(t)/N_1(0) = \exp(-\beta t - n_0\alpha t) \quad (21)$$

The same expression is obtained for the higher-order approximation for the distribution determined by $K_s(n)=\delta(n\text{-}n_0)$. The distribution determined by the superposition of the δ-function can also be considered:

$$K_0(n) = A\delta(n-n_1) + B\delta(n-n_2) \quad (22)$$

where n_1 and n_2 are positive constants and where A and B are constants for superposition. In this case, $N_0(t)/N_0(0)$ is given by Eq. (23):

$$\frac{N_0(t)}{N_0(0)} = \frac{\left(An_2\exp(-\beta t - n_1\alpha t - n_1R_0^3/3) + Bn_1\exp(-\beta t - n_2\alpha t - n_2R_0^3/3)\right)}{An_2\exp(-n_1R_0^3/3) + Bn_1\exp(-n_2R_0^3/3)} \quad (23)$$

Similarly, $N(t)/N(0)$ is expressed by Eq. (24):

$$\frac{N_s(t)}{N_s(0)} = \frac{\left(A\exp(-\beta t - n_1\alpha t)G_s(n_1, \alpha, D, R_0) + B\exp(-\beta t - n_2\alpha t)G_s(n_2, \alpha, D, R_0)\right)}{AG_s(n_1, \alpha, D, R_0) + BG_s(n_2, \alpha, D, R_0)} \quad (24)$$

The same quantities were evaluate for the diffusion-control equation. For the initial distribution, $\varphi(\xi) = \delta(\xi\text{-}r_{\max})/4\pi r_{\max}^2$, the zero-th order approximation solution is:

$$\omega_0(r, t) = \frac{\exp(-\beta t)}{8\pi r_{\max}r\sqrt{\pi Dt}}[\exp\{-(r-r_{\max}R_0)^2/4Dt\} - \exp\{-(r+r_{\max}-R_0)^2/4Dt\} \quad r>R_0 \quad (25)$$

where $r_{\max}$ is the distance between the electron and the ion for maximum distribution. $N_0(t)/N_0(0)$ is given by Eq. (26):[17]

$$N_0(t)/N_0(0) = \exp(-\beta t)\{1+(R_0/r_{\max})\mathrm{Erf}(r_{\max}/\sqrt{4Dt})\}/(1+R_0/r_{\max}) \quad (26)$$

Results and Discussion

The results of numerical calculation using various paremeters are shown in Figs. 1a and 1b and in Fig.

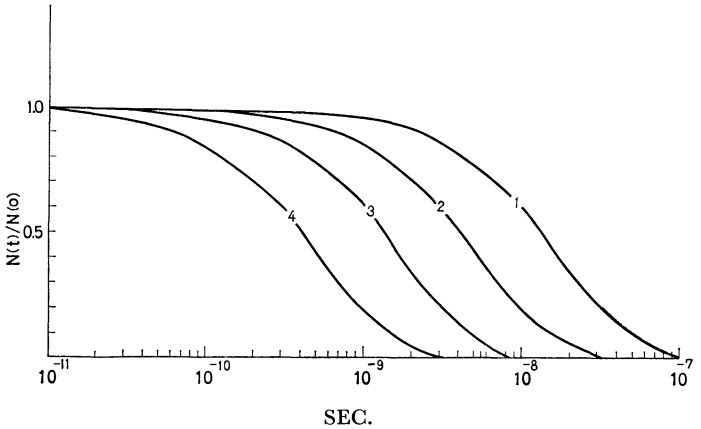

Fig. 1a. Number of electrons in a spur plotted as a function of time in the case of potential control, where the initial value was normalized to be unity. The numerical calculation was carried out using Eq. (23) and the following parameters in CGS unit without scavenger, $\beta=0$.

Curve 1: $A=0.0$, $B=1.0$, $n_1=3.9\times10^{18}$, $n_2=1.2\times10^{18}$, $\alpha=4.3\times10^{-11}$
Curve 2: $A=1.0$, $B=0.0$, $n_1=3.9\times10^{18}$, $n_2=1.2\times10^{18}$, $\alpha=4.3\times10^{-11}$
Curve 3: $A=0.0$, $B=1.0$, $n_1=3.9\times10^{18}$, $n_2=1.2\times10^{18}$, $\alpha=4.3\times10^{-10}$
Curve 4: $A=1.0$, $B=0.0$, $n_1=3.9\times10^{18}$, $n_2=1.2\times10^{18}$, $\alpha=4.3\times10^{-10}$

17) The error function, $\mathrm{Erf}(x)$, is defined by:
$\mathrm{Erf}(x) = \frac{2}{\sqrt{\pi}}\int_0^x \exp(-z^2)\mathrm{d}z$

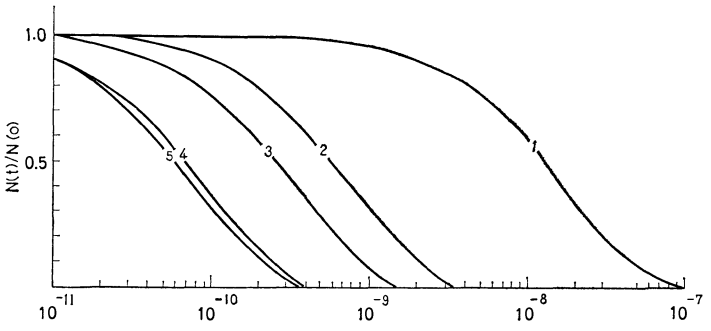

Fig. 1b. Number of electron in a spur plotted as a function of time in the case of potential control in the presence of electron scavenger except for curve 1.

Curve 1: $A=0.0$, $B=1.0$, $n_1=3.9\times10^{18}$, $n_2=1.2\times10^{18}$, $\alpha=4.3\times10^{-11}\sim4.3\times10^{-10}$, $\beta=0.0$, $R=2.0\times10^{-7}\sim1.0\times10^{-7}$
Curve 2: $A=1.0$, $B=0.0$, $n_1=3.9\times10^{18}$, $n_2=1.2\times10^{18}$, $\alpha=4.3\times10^{-11}$, $\beta=1.0\times10^{9}$, $R_0=2.0\times10^{-7}$
Curve 3: $A=1.0$, $B=0.0$, $n_1=3.9\times10^{18}$, $n_2=1.2\times10^{18}$, $\alpha=4.3\times10^{-10}$, $\beta=1.0\times10^{9}$, $R_0=2.0\times10^{-7}$
Curve 4: $A=1.0$, $B=0.0$, $n_1=3.9\times10^{18}$, $n_2=1.2\times10^{18}$, $\alpha=4.3\times10^{-11}$, $\beta=1.0\times10^{10}$, $R_0=2.0\times10^{-7}$
Curve 5: $A=1.0$, $B=0.0$, $n_1=3.9\times10^{18}$, $n_2=1.2\times10^{18}$, $\alpha=4.3\times10^{-10}$, $\beta=1.0\times10^{10}$, $R_0=2.0\times10^{-7}$

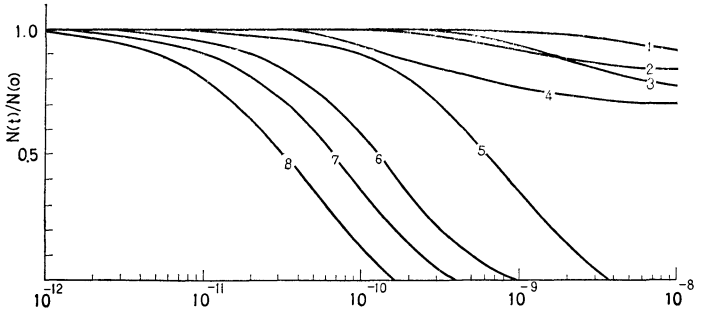

Fig. 2. Number of electrons in a spur plotted as a function of time in the case of diffusion control. The numerical calculation was carried out using Eq. (26) and the following parameters in CGS units.

Curve 1: $D=5\times10^{-5}$, $R_0=2\times10^{-7}$, $r_{max}=8\times10^{-7}$
Curve 2: $D=5\times10^{-4}$, $R_0=2\times10^{-7}$, $r_{max}=8\times10^{-7}$
Curve 3: $D=5\times10^{-5}$, $R_0=2\times10^{-7}$, $r_{max}=4\times10^{-7}$
Curve 4: $D=5\times10^{-4}$, $R_0=2\times10^{-7}$, $r_{max}=4\times10^{-7}$
Curve 5: $D=5\times10^{-5}$, $R_0=2\times10^{-7}$, $r_{max}=4\times10^{-7}\sim8\times10^{-7}$, $\beta=1.0\times10^{9}$
Curve 6: $D=5\times10^{-5}$, $R_0=2\times10^{-7}$, $r_{max}=4\times10^{-7}\sim8\times10^{-7}$, $\beta=5.0\times10^{9}$
Curve 7: $D=5\times10^{-5}$, $R_0=2\times10^{-7}$, $r_{max}=4\times10^{-7}\sim8\times10^{-7}$, $\beta=1.0\times10^{10}$
Curve 8: $D=5\times10^{-5}$, $R_0=2\times10^{-7}$, $r_{max}=4\times10^{-7}\sim8\times10^{-7}$, $\beta=2.0\times10^{10}$

2 for the potential-control process and the diffusion-control process respectively. In Fig. 1a, the time dependence of the electron concentration showed sigmoidal curves. The results of numerical calculation in the scavenger-free case are that the relaxation time of electron recombination is in the range of 10^{-10}—10^{-8} sec, depending mainly on the initial distribution of electron. If the scavenger is present in the system, the value of the relaxation time of the electron disappearance becomes much shorter, as is shown in Fig. 1b.

The case of diffusion control is shown in Fig. 2; here the geminate recombination partially took place, in contrast with the complete recombination in the case of potential control,(Fig. 1a). For the large value of scavenger concentration, the time dependence becomes almost equivalent in the diffusion-control and potential-control processes. Therefore, either method offers a reasonable approximation for the concentrated solution of the scavenger. In these calculations, the value of α was assumed to be constant. In the neutralization process, however, the value should be a step function. If $N^+(t)$ in Eq. (2) decreases from four to one by a step function during the successive neutralization, the time dependence of $N^+(t)/N(0)$ is shown in Fig. 3 with the curves for the fixed values of four and one in $N^+(t)$ in Eq. (2). The relaxation time decreased slightly with an increase in the effective charge of the ion core. The effect of the successive neutralization of the effective charge of the ion core from four to one decreases the rate of the electron recombination, (Fig. 3, Curve 4). The half-life of the electron recombination of the successive neutralization, (Curve 4) showed a intermediate value between that of the effective charge of one (Curve 3) and that of the effective charge of four, (Curve 5). Other calculations, *e.g.*, Mozumder's[7], Ludwig's[9],

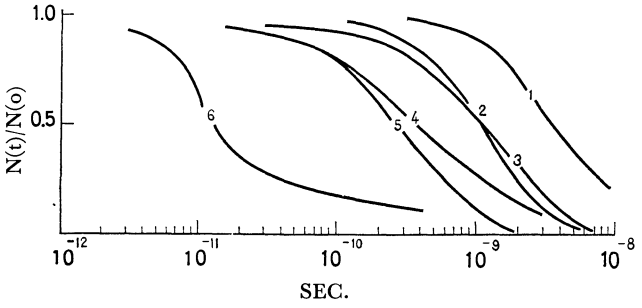

Fig. 3. The electron concentration as a function of time in the various methods of calculation without scavenger.
Curve 1: by Mozumder, (room temperature)
Curve 2: by Ludwig,
Curve 3: core charge to be constants, $N=1$, other parameters are corresponding to the case of curve 3 in Fig. 1a,
Curve 4: core charge to be changed, $N=4\sim1$,
Curve 5: core charge to be constant, $N=4$,
Curve 6: by Freeman

and Freeman's calculations,[5] are also quoted in Fig. 3. The relaxation times of electron recombination are 6×10^{-9}, 1×10^{-9}, 1×10^{-11}, and $4—10\times10^{-10}$ sec for Mozumder, Ludwig, Freeman, and the present calculations respectively, while the corresponding values of r_{max} are 80, 80—112, 20, and 80—120 Å. Thus, the relaxation time of electron recombination largely depends on r_{max}. The relaxation times evaluated by Ludwig, Mozumder, and the present methods are within the same order of magnitude. The slight difference in the relaxation time is due to the difference in the r_{max} and $N^+(t)$ values used in these calculations. The shorter relaxation time in the case of Freeman corresponds to the smaller value of r_{max}. Some examples of these initial distributions were illustrated in a previous paper.[12] The real solution, $C(r, t)$, may be somewhere between the potential-control and diffusion-control cases, it is quite similar to $\chi_s(r, t)$ at the smaller distance of r and can be well approximated by $\omega_s(r, t)$ for a large r distance. Therefore, a linear combination of $\chi_s(r, t)$ and $\omega_s(r, t)$ by using a slowly-changing function of distance will provide a better approximation.

In the numerical calculation, the estimation of the various parameters involved in the theory is important in relative the theory to the experimental results. In this work, the main parameters are n, α, β, and R_0. The value of n is expressed in terms of the distance of the maximum distribution, namely, $n=2/r_{max}^3$. The value of r_{max} can be determined by the thermalization length of the electron ejected from the parent ion by the primary act of radiation. According to Mozumder and Magee,[18] the value of the effective thermalization length is 80 Å. In this work, two values ($r_{max}=80$ Å, 120 Å) are used.

The parameter, $\alpha(=N^+(t)eu/\varepsilon)$, of electron recombination can be estimated from the number of ions in the ion core in a spur, $N^+(t)$, and from the mobility of the electron, u. The fixed values of $N^+(t)(=4, 3, 2, 1)$ and the variable value of $N^+(t)$ from four to one, decreasing with time as a step function, are considered in this work. The value of the mobility of the electron of $2\times10^{-3-4}$ cm^2 v^{-1} sec^{-1} [19] was used in estimating α. The β parameter is defined as the product of the rate constant and the concetration of the scavenger. The rate constants of most scavengers have an order of magnitude of 10^{10} M^{-1} sec^{-1}, and usually an appreciable effect of the scavenger is observed in the concentrations of the scavenger beginning from 10^{-1} M, so the value of β used in this calculation is in the range of $1.0\times10^{9-10}$ in terms of the scavenger effect. The reaction radius of the recombination of the electron and ions is in the range of 10 Å—20 Å, where the electron escape from the recombination seems to be negligible.

The authors wish to thank Professor S. Shida and Dr. S. Sato of the Tokyo Institute of Technology and Dr. K. Fueki of Nagoya University for reading the preliminary manuscript of this paper and for many helpful discussions. They also wish to thank Dr. A. Imamura and Miss H. Fujita of the National Cancer Center Research Institute for their assistance in the computer work.

18) A. Mozumder and J. L. Magee, *J. Chem. Phys.*, **47**, 939 (1967).

19) This value has been used in most calculations. Recently, quite a large value of u ($=2\times10^{-1}$ cm^2 V^{-1} sec^{-1}) was reported by Conrad and Silverman.[20] If this value had been used in the present calculation, Curves 3,4, and 5 in Fig. 3 would have shifted to shorter life times, thus coming to have the same order of magnitude as in Freeman's data, (Curve 6). On the contrary, a small value of u ($\approx1\times10^{-5}$ cm^2 V^{-1} sec^{-1}) can be expected from the experimental results of the pulse radiolysis of viscous squalane[21] at a low temperature and with a lifetime of over 10^{-6} sec, where bound and unbound states of electrons may be in equilibrium.

20) E. E. Conrad and J. Silverman, *J. Chem. Phys.* **51**, 450 (1969).

21) I. A. Taub and H. A. Gillis, *J. Amer. Chem. Soc.*, **91**, 6507 (1970).

The Estimation of the Surface Properties of Metal Oxides by the Use of TCNQ Adsorption

Hiroshi Hosaka, Takao Fujiwara, and Kenjiro Meguro

Department of Applied Chemistry, Faculty of Science, Science University of Tokyo, Kagurazaka, Shinjuku-ku, Tokyo

(Received March 1, 1971)

The electron-donor properties of metal oxides (magnesia, alumina, silica, titania, zinc oxide, and nickel oxide) were investigated by means of TCNQ adsorption. When TCNQ was adsorbed on the surfaces of the metal oxides from its acetonitrile solution, the surfaces of the metal oxides acquired the colorations characteristic of each oxide. The coloration was caused by the formation of TCNQ anion radicals on the metal oxide surfaces. The presence of the TCNQ anion radicals on the colored metal oxide surfaces was confirmed by studying the ESR absorption and electronic spectra. The radicals were formed as a result of electron transfer to TCNQ from the metal oxide surfaces. The order of the radical-forming activity, determined by ESR, was as follows: magnesia> zinc oxide>alumina>titania>silica>nickel oxide. The electron-donor property of the metal oxide surfaces might be dependent on the natures of the semiconductor and the surface hydroxyl ion.

During the past decade, there has been much discussion about the natures of the acid and base present on metal oxide surfaces, and their relevance in catalysis has been extensively investigated. Spectroscopic studies have established the existence of strong electrophilic centers on the silica-alumina surface and the formation of cation radical from hydrocarbons at the same centers.[1-3] On the assumption that cation radicals are formed on Lewis-acid sites, the formation of radical ions at the surface of the silica-alumina catalyst, *i.e.*, the electron-accepting property of the silica-alumina surface, has been widely studied.[1-3] The nature of the site responsible for the electron transfer process is of wide interest. Recently, Flockhart *et al.*[4] studied the formation of the TCNE anion radical at alumina surfaces, *i.e.*, the electron-donor properties of aluminas; however, there have been few reports about the electron-donor properties of metal oxides. In this work, it was demonstrated that when 7,7,8,8-tetracyanoquinodimethan (TCNQ), which was one of the strongest electron acceptors, was adsorbed onto magnesia, alumina, silica, titania, zinc oxide, and nickel oxide, TCNQ anion radicals were formed as a result of electron transfer to TCNQ from the metal oxide surfaces. Comparing the radical-forming activity of the metal oxides, we revealed the electron-donor properties of the metal oxides.

Experimental

Materials. The titania, alumina, and silica were prepared by the hydrolysis of titanium tetra-butoxide, aluminium *s*-butoxide, and silicon ethoxide, purified by distillation. Excess aqueous ethanol was vigorously stirred into the alcoholic solution of alkoxide. Stirring was continued for 10 hr at a temperature near the boiling point. The precipitate was then separated by centrifuging, thoroughly washed with alcohol, finely ground, and then evacuated at 100°C until the residual pressure was less than 10^{-5} Torr. The complete hydrolysis of these alkoxides was confirmed by infrared spectra. The dried products were calcined for 2 hr at 500°C.

The magnesia, zinc oxide, and nickel oxide were obtained by the thermal decomposition of their carbonates (G. R.) at 500°C for 2 hr in an electric furnace.

The crystal structures of the metal oxides, as determined by X-ray diffractometry, were as follows: the titania, anatase; the alumina, γ-alumina; the silica, amorphous. The X-ray diffraction patterns of the magnesia, zinc oxide, and nickel oxide showed typical lines.

The surface areas of the metal oxides, as determined by nitrogen adsorption, were as follows: the titania, 64; the alumina, 263; the silica, 600; the magnesia, 134; the zinc oxide, 7.10 m^2/g.

TCNQ was synthesized from the condensation product of 1,4-cyclohexanedione and malononitrile.[5] This was the purified by repeated recrystallization. The purity was checked by elemental analysis (Found: C, 70.22; H, 2.60; N, 27.8%, Calcd.: C, 70.59; H, 1.97; N, 27.42%), measurement of the melting point (280.0—283.0°C), and spectrophotometry.

Apparatus and Procedure. The metal oxide was placed in a flask which was attached directly to a high-vacuum line and outgassed at 10^{-5} Torr for 1 hr at 100°C, and then cooled to 25°C *in vacuo* prior to the TCNQ adsorption. A solution of TCNQ in acetonitrile (10 mM) was then poured into the flask through a stop cock. Subsequently, the content in the flask was transferred into an L-type test tube and then shaken for 2 hr at 25°C. After shaking, the metal oxide was collected by centrifuging and dried at room temperature *in vacuo*. The dried sample was used for the measurement of the electronic spectrum and was evacuated at 10^{-5} Torr for the ESR measurement.

The ESR spectra were measured by means of a Japan Electrons Optics Laboratory JES-3BS-X-type ESR spectrometer operating at a cavity resonance frequency of 9400 Hz with 100 kHz modulation. The *g*-value was obtained by comparison with the value for Mn^{2+}. The radical concentration (spin conc.) were estimated by comparing the peak-to-peak heights on the first derivative curves with those of an internal-standard Mn^{2+} sample.

The electronic spectra of the metal oxides were measured by means of a diffuse-reflectance spectrophotometer.

Results and Discussion

When TCNQ was adsorbed on the surfaces of the magnesia, alumina, silica, titania, and zinc oxide

1) H. P. Leftin and M. C. Hobson, Jr., *Advan. Catal.*, **14**, 372 (1963).
2) A. Terenin, *ibid.*, **15**, 256 (1964).
3) R. P. Porter and W. K. Hall, *J. Catal.*, **5**, 366 (1966).
4) B. D. Flockhart, I. R. Leith, and R. C. Pink, *Trans. Faraday Soc.*, **65**, 542 (1969).
5) D. S. Acker and W. R. Hertler, *J. Amer. Chem. Soc.*, **84**, 3370 (1962).

from its acetonitrile solution at room temperature, the surfaces of the metal oxides acquired the coloration characteristic of each oxide. The colors were as follows: magnesia, blue green; alumina, blue green; silica, yellow; titania, violet; zinc oxide, greyish green. The same colorations were observed when the metal oxides were ground with TCNQ crystal. The colorations of the metal oxide surfaces suggest that new adsorbed species are formed on the surfaces. This suggestion was confirmed by the evidence that the colored metal oxides show ESR absorptions, indicating the presence of free radical species. The spectra are unresolved (Figs. 1—5; *g*-values, 2.011); this can be explained by the fact that the anisotropy of the hyperfine structure arises from the lack of motional degrees of freedom. The state of the adsorbed species was studied by means of the electronic spectra in addition to the ESR spectra. The electronic spectra of the colored samples are illustrated in Figs. 1—5. The bands appearing below 400 mμ are common to all the oxides and may be supposed to correspond to the physically-adsorbed state of neutral TCNQ, which has the absorption band at 395 mμ.[5] In the cases of titania and zinc oxide, this assignment does not hold completely because the titania

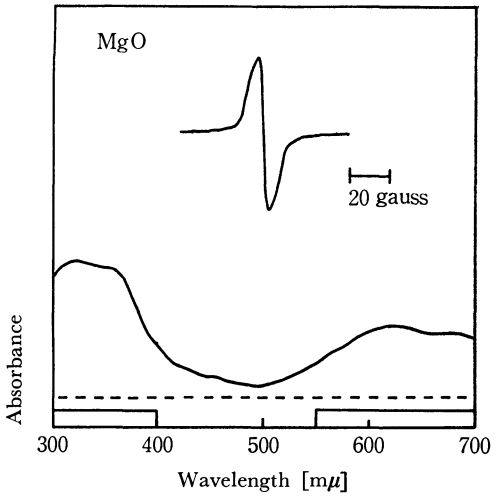

Fig. 1. ESR and electronic spectra from TCNQ adsorbed on the magnesia. Dotted line, MgO prior to adsorption.

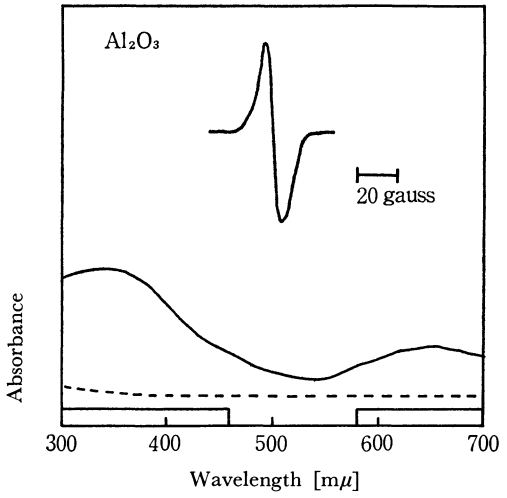

Fig. 2. ESR and electronic spectra from TCNQ adsorbed on the alumina. Dotted line, Al_2O_3 prior to adsorption.

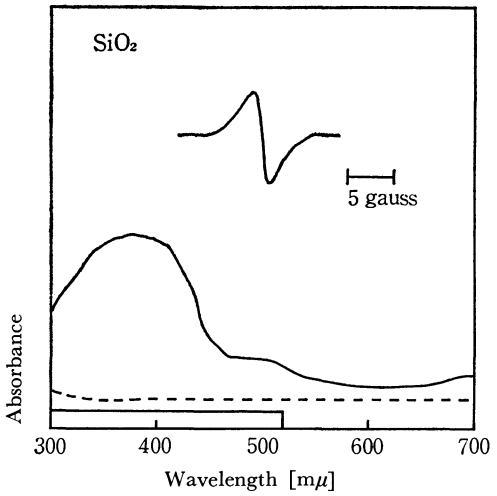

Fig. 3. ESR and electronic spectra from TCNQ adsorbed on the silica. Dotted line, SiO_2 prior to adsorption.

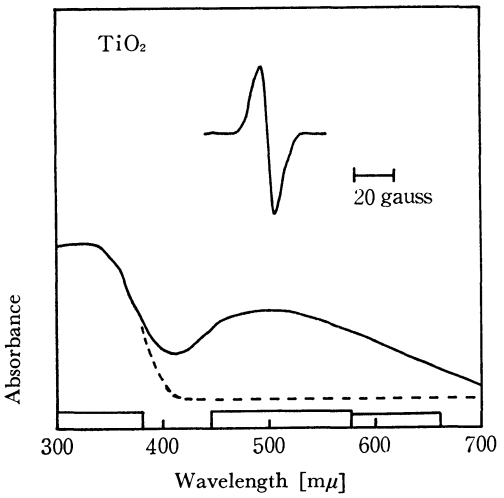

Fig. 4. ESR and electronic spectra from TCNQ adsorbed on the titania. Dotted line, TiO_2 prior to adsorption.

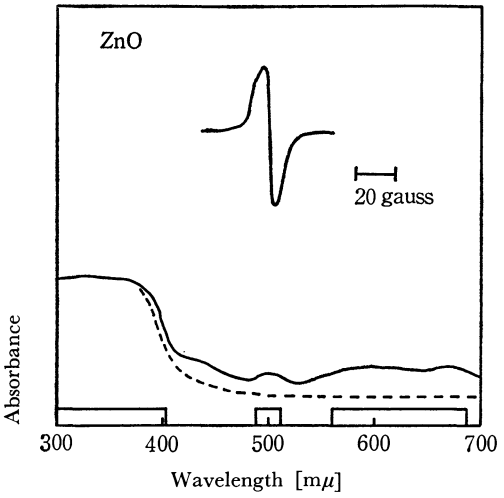

Fig. 5. ESR and electronic spectra from TCNQ adsorbed on the zinc oxide. Dotted line, ZnO prior to adsorption.

Table 1. Summary of the TCNQ adsorption

	Type of semiconductor	The color of the metal oxide surface after TCNQ adsorption	The relative radical concentration (radical conc./m^2)
MgO	insulator	blue green	100
Al_2O_3	insulator	blue green	38
SiO_2	insulator	yellow	0.11
TiO_2	*n*-type semiconductor	violet	1.6
ZnO	*n*-type semiconductor	greyish green	47
NiO	*p*-type semiconductor		0.00

and zinc oxide have characteristic bands in the same region. The absorption bands in the visible region observed in the cases of magnesia, alumina, silica, titania, and zinc oxide can be attributed to neither TCNQ nor the metal oxides. The bands near 600 mμ probably stem from the dimer TCNQ anion radical, which absorbs light at 643 mμ.[6] They are very broad and have not been assigned with certainty, but this tentative attribution is supported by the characteristic features that neutral TCNQ absorbs only at 395 mμ, that TCNQ has a high electron affinity, and that the TCNQ anion radical derivatives are stable even at room temperature.[7-10] The ESR and the electronic spectra confirm that radical ions are formed as a result of electron transfer to TCNQ from the metal-oxide surfaces.

The radical-forming activities of the metal oxide surfaces, estimated by means of the relative radical concentration (spin number/m^2), are as follows: magnesia, 100; zinc oxide, 47; alumina, 38: titania, 1.6; silica, 0.11; nickel oxide, 0.00. The nature of the site responsible for the electron-transfer process is not well understood. However, it may be suggested that two types of active sites exist on the surfaces. One of these has an anion deficiency (*n*-type semiconductor), and the other has a hydroxyl ion on the oxide surface.

The type of surface complex by the mechanism of electron transfer from a semiconductor was found in titania, zinc oxide, and nickel oxide. A major way of introducing donors and acceptors into semiconductors arises from the nonstoichiometry in compounds.[11] The nonstoichiometry can arise either by virtue of vacant lattice sites for one component of the compound, or because of an excess of one component located in interstitial sites. A donor center can result from the trapping of one or more electrons in an anion vacancy. Semiconductors which have an excess of conduction electrons over holes are normally called "*n*-type", because their conductivity arises from negative-current carriers. Those with an excess of holes are called "*p*-type," as the carriers are positive. *n*-Type semiconductors have anion deficiencies (or cation excesses), while *p*-type semiconductors have anion excesses (or cation deficiencies). For example, zinc oxide,[12,13] titania,[14] and nickel oxide are as follows;

$$ZnO \rightleftarrows O_v^{+} + \ominus + 1/2\, O_2(g)$$
$$ZnO \rightleftarrows O_v^{2+} + 2\ominus + 1/2\, O_2(g)$$

where O_v is an O vacancy and where $\ominus$ is a free electron. An O_v in zinc oxide is a donor.

$$2TiO_2 \rightleftarrows Ti_2O_3 + (O_v^{2+}\cdot 2\ominus)^{\circ} + 1/2\, O_2(g)$$
$$(O_v^{2+}\cdot 2\ominus)^{\circ} \rightleftarrows (O_v^{2+}\cdot\ominus)^{+} + \ominus$$

where $(O_v^{2+}\cdot 2\ominus)^{\circ}$ is a neutral, charged O vacancy.

$$1/2\, O_2(g) \rightleftarrows NiO + Ni_{(v)}^{2-} + 2\oplus$$
$$1/2\, O_2(g) \rightleftarrows NiO + Ni_{(v)}^{2-}\cdot\oplus + \oplus$$

where $Ni_{(v)}$ is a Ni vacancy and where $\oplus$ is a positive hole. A Ni vacancy in nickel oxide is an acceptor. From this fact, it is reasonable that nickel oxide has no radical-forming activity. If TCNQ radical ions are formed by interaction with free electrons derived from the intrinsic or extrinsic defects present on the surface or in the bulk of the solid, magnesia, alumina, and silica, which are insulators, they would not normally be expected to participate in a charge-transfer adsorption process because of the lack of a free electron. Flockhart *et al.*[4] have suggested that the electron-donor defect site on the surface of alumina was created at activation temperatures of above 500°C.

The second active site may be the surface hydroxyl ion. Surface hydroxyl groups can be expected on all metal oxides.[15] The ionization potential of hydroxyl ions is comparatively small ($\sim$2.6 eV in the gas phase[16]); therefore, the possibility of its participation in oxidation-reduction processes of the type:

$$OH^{-} + A \rightarrow OH + A^{-}$$

where A is an electron-acceptor, can not be excluded. Indeed, Fomin *et al.*[17] have shown that electron

6) R. H. Boyd and W. D. Phillips, *J. Chem. Phys.*, **43**, 2927 (1965).
7) D. S. Acker, R. J. Harder, W. R. Hertler, W. Mahler, L. R. Melby, R. E. Benson, and W. E. Mochel, *J. Amer. Chem. Soc.*, **82**, 6408 (1960).
8) R. G. Kepler, P. E. Bierstedt, and R. E. Merrifield, *Phys. Rev. Lett.*, **5**, 503 (1960).
9) D. B. Chesnut, H. Foster, and W. D. Phillips, *J. Chem. Phys.*, **34**, 684 (1961).
10) L. R. Melby, R. J. Harder, W. R. Hertler, W. Mahler, R. E. Benson, and W. E. Mochel, *J. Amer. Chem. Soc.*, **84**, 3374 (1962).
11) N. B. Hannay, "Semiconductors," ed. by N. B. Hannay, Reinhold Publishing Co., New York (1959), p. 20.
12) H. H. V. Baumbach and C. Wagner, *Z. Phys. Chem.*, **B22**, 199 (1933).
13) K. Hauffe and J. Block, *ibid.*, **196**, 438 (1950).
14) T. Kawaguchi, *Nippon Kagaku Zasshi*, **75**, 835 (1954).
15) W. Stöber, *Kolloid-Z. Z. Polym.*, **145**, 17 (1956).
16) V. M. Vedeneev, L. V. Gurvich *et al.*, Cleavage Energies of Chemical Bonds. Ionization Potentials and Electron Affinity. Handbook (in Russian), Izd. AN SSSR (1960).
17) G. V. Fomin, L. A. Blyumenfel'd, and V. I. Sukhorukov, *Proc. Acad. Sci.* (U. S. S. R.), **157**, 819 (1964).

transfer from the hydroxyl ion can and does occur in certain solvent systems provided a suitable acceptor molecule is present. Flockhart *et al.*[4] have reported that the electron-donor site on the alumina surface might be associated with the presence on the surface of unsolvated hydroxyl ions. As alumina, magnesia, and silica surfaces are usually covered with hydroxyl groups,[18] the charge-transfer adsorptions of TCNQ on alumina, magnesia, and silica may result from the electron-transfer from surface hydroxyl. Stöber[15] found that, even after thorough outgassing at 100°C, one molecule of externally tightly adsorbed water is retained for each two silanol groups in the amorphous silica. This surprising result was confirmed by Boehm *et al.*[19] using chemical reactions as well as deuterium exchange. Lee and Weller[20] confirmed the existence of surface hydroxyl groups on alumina which had been dehydrated at 500°C. It is reasonable to assume that these electron-transfer from hydroxyl ions on the metal oxides which have been calcined at a high temperature such as 500°C. Surface hydroxyls may exist on all of the samples. However, surface hydroxyls on metal oxides are shown to differ in chemical properties. Surface silanol groups are much more stable than Al–OH groups.[18] Differences in acidity among the hydroxyl groups of several oxide surfaces have been reported.[21] These results suggest that the hydroxyl ions of the metal oxide surfaces have different electron-donor properties (radical-forming activities).

The radical-forming activity, *i.e.*, the electron-donor property of the metal oxide surfaces, may be associated with the natures of the semiconductor and the surface hydroxyl ion. The radical-forming activity determined by TCNQ adsorption is a new convenient method of estimating the electron-donor property of metal oxide surfaces.

We wish to thank Miss Y. Matsumura, National Institute of Industrial Health, for her kindly advice on the measurement of the ESR spectra, and Mr. T. Sekine Government Chemical Industrial Research Institute, Tokyo, for his helpful advice on the measurement of the electronic spectra.

18) H. P. Boehm, *Advan. Catal.*, **16**, 179 (1966).
19) H. P. Boehm, M. Schneider, and F. Arendt, *Z. Anorg. Allg. Chem.*, **320**, 43 (1963).
20) J. K. Lee and S. W. Weller, *Anal. Chem.*, **30**, 1057 (1958).
21) M. L. Hair and W. Hertl, *J. Phys. Chem.*, **74**, 91 (1970).

BULLETIN OF THE CHEMICAL SOCEITY OF JAPAN, VOL. 44, 2619—2626 (1971)

Effect of Phase on Hot Hydrogen Atom Abstraction Reaction with Solid Isobutane as Studied by Electron Spin Resonance Spectroscopy

Terunobu WAKAYAMA, Tetsuo MIYAZAKI, Kenji FUEKI, and Zen-ichiro KURI

Department of Synthetic Chemistry, Faculty of Engineering, Nagoya University, Chikusa-ku, Nagoya

(Received March 10, 1971)

The effect of phase on the hot-hydrogen-atom abstraction reaction with isobutane at 77°K has been studied by electron spin resonance spectroscopy in the photolysis and the radiolysis of solid isobutane containing hydrogen iodide. While only the isobutyl radical is formed by the UV-illumination of isobutane–hydrogen iodide systems in the polycrystalline state, the tertiary butyl radical, accompanied with a small amount of isobutyl radicals, is produced from isobutane-methylcyclohexane-hydrogen iodide systems in the glassy state. The hot hydrogen atom produced by dissociative electron attachment to hydrogen iodide abstracts the tertiary hydrogen atom from isobutane at 77°K, independent of whether the matrix is polycrystalline or glassy. It appears that the H-abstraction reaction from isobutane by hot hydrogen atoms depends upon the energy of the hot hydrogen atoms.

The familiar atomic hydrogen-saturated hydrocarbon abstraction reaction has been extensively investigated at thermal energies under equilibrium conditions,[1] at very high kinetic energies in recoil media,[2] and at intermediate energies in photolytic systems.[3]

In the photolytic technique, hydrogen atoms of different known initial kinetic energies (7—92 kcal/mol) may be selectively generated by the photodissociation of hydrogen iodide (HI) in the presence of a reactant. For example, when activation is induced by a 2537 Å light, the kinetic energy of the hydrogen atom produced is 20 kcal/mol if the iodine atom is produced in the $^2P_{1/2}$ excited state and 41 kcal/mol if it is produced in the $^2P_{3/2}$ ground state.[4] The hot hydrogen atom produced by dissociative electron attachment to HI may have an energy of *ca.* 5—6 kcal/mol.

Although hot atom reactions have been investigated in detail in the gas phase, such reactions in condensed phases[5] are much less well understood. One of the complications in the hot atom reaction in condensed

1) A. F. Trotman-Dickenson, "Gas Kinetics," Butterworth and Co., Ltd., London (1955); V. N. Kondratev, "Chemical Kinetics of Gas Reactions," Addison Wesley Co., Reading, Mass. (1964); I. Amdur and G. G. Hammes, "Chemical Kinetics: Principles and Selected Topics," McGraw-Hill Book Co., Inc., New York, N. Y. (1966).

2) R. Wolfgang, *Ann. Rev. Phys. Chem.*, **16**, 15 (1965); E. K. C. Lee and F. S. Rowland, *J. Amer. Chem. Soc.*, **85**, 897 (1963).

3) R. J. Carter, W. H. Hamill, and R. R. Williams, Jr., *ibid.*, **77**, 6457 (1955); R. M. Martin and J. E. Willard, *J. Chem. Phys.*, **40**, 3007 (1964).

4) S. Aditya and J. E. Willard, *J. Amer. Chem. Soc.*, **88**, 229 (1966).

5) J. R. Nash, R. R. Williams, Jr., and W. H. Hamill, *ibid.*, **82**, 5974 (1960); C. D. Bass and G. C. Pimentel, *ibid.*, **83**, 3754 (1961); R. E. Rebbert and P. Ausloos, *J. Chem. Phys.*, **48**, 306 (1968).

phases is in the possible existence of the cage effect, which is absent in the gas phase. The cage effect explains the characteristically low quantum yield of primary dissociation in a condensed medium.[6] It was found in previous studies that the fragmentation of the excited molecule is an important process in the radiolysis of saturated hydrocarbons in the solid state at 77°K.[7] We reported in a previous paper that different radicals are formed in the radiolysis of solid isobutane at 77°K, depending on whether it is in the glassy or polycrystalline state.[8] In a recent stupy with isobutane-2-d_1 we concluded that such a phase effect cannot be attributed to the isomerization of butyl radicals, such as i-$C_4H_9 \rightleftarrows t$-$C_4H_9$, but must be attributed to the primary process of the C–H bond rupture.[9]

In the present work, we shall examine, by ESR measurements, the phase effect on the hydrogen atom abstraction reaction in the photolysis and the radiolysis of isobutane-HI systems at 77°K, and shall attempt to compare these results with those of hot-hydrogen-atom reaction in the radiolysis of pure isobutane at 77°K.

In this paper, emphasis will be placed on our experimental findings rather than on their interpretation.

Experimental

The isobutane, methylcyclohexane(MCH), and 3-methylpentane (3MP) were more than 99.9%pure. Gas-chromatographic analysis did not show any detectable impurities. They were purified by distillation on a vacuum line and were dried over a sodium mirror. Isobutane-2-d_1, synthesized by the Grignard reaction, was purified by passing it through a column of freshly-activated alumina and then through a column of fresh soda lime. The xenon was used as received, the stated purity being 99.9%.

The hydrogen iodide was prepared from Katayama Chemical reagent-grade aqueous HI by removing the iodine by shaking it with red phosphorus and by then allowing the frozen solution to warm twice in the presence of excess P_2O_5 on the vacuum line.

The samples, prepared on the vacuum line, were sealed in 4.3-mm o.d. Suprasil tubes. They were illuminated by ultraviolet light or γ-rays at 77°K, and then ESR measurements were made by means of a JES-3BX ESR spectrometer.

γ-Irradiation was provided by ^{60}Co at a dose rate of 1.0×10^6 rads/hr, and UV-illumination, by a filtered end-window Toshiba medium-pressure mercury lamp. A Toshiba UV-25 filter was used; it cut off UV-light of wavelengths shorter than 2500 Å.

Results and Discussion

Effects of Phase on Hydrogen-atom Abstraction in the Photolysis of Solid Isobutane Containing HI. Figure 1A shows the ESR spectrum of 0.2 mol% HI in isobutane at 77°K obtained after a 10-min illumination with a medium-pressure mercury lamp. The prolonged photolysis of isobutane without HI produced

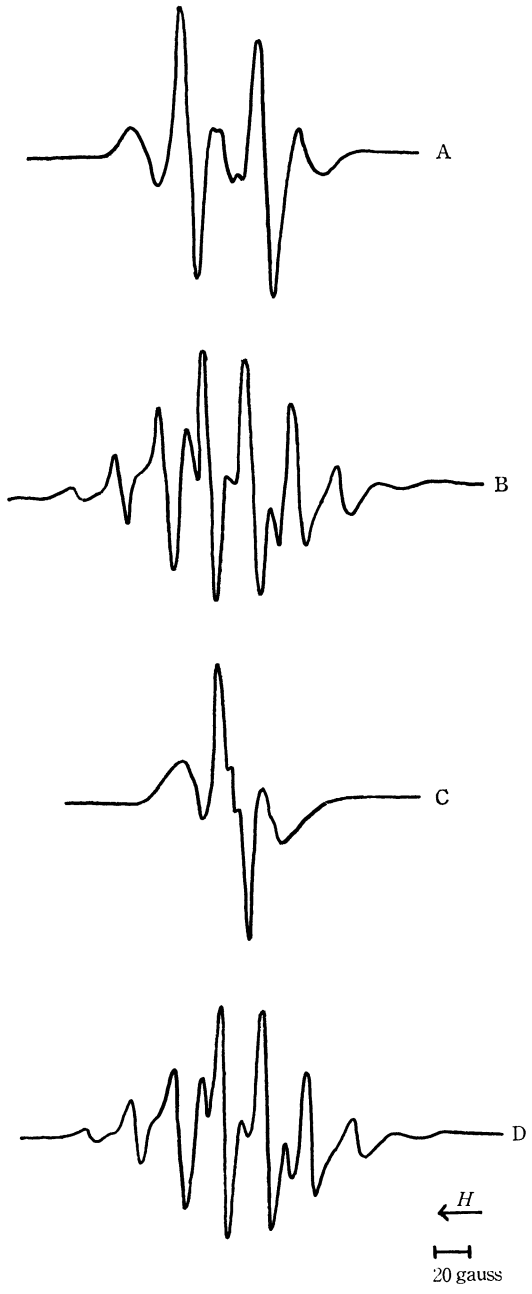

Fig. 1. (A) ESR spectrum of UV-illuminated i-C_4H_{10}-HI (0.2 mol%) at 77°K. UV-illumination time: 10 min.
(B) ESR spectrum of UV-illuminated i-C_4H_{10}-MCH (3.8 mol%)-HI (0.2 mol%) at 77°K. UV-illumination time: 2.5 min.
(C) ESR spectrum of UV-illuminated i-C_4H_9D-2-d_1-HI (0.2 mol%) at 77°K. UV-illumination time: 10 min.
(D) ESR spectrum of UV-illuminated Xe-i-C_4H_{10} (4.6 mol%)-HI (0.2 mol%) at 77°K. UV-illumination time: 10 min.

6) I. Franck and E. Rabinowitch, *Trans. Faraday Soc.*, **30**, 120 (1934).
7) T. Wakayama, T. Miyazaki, K. Fueki, and Z. Kuri, This Bulletin, **42**, 1164 (1969); T. Wakayama, T. Kimura, T. Miyazaki, K. Fueki, and Z. Kuri, *ibid.*, **43**, 1017 (1970).
8) a) T. Miyazaki, T. Wakayama, K. Fueki, and Z. Kuri, *ibid.*, **42**, 2086 (1969); b) T. Wakayama, T. Miyazaki, K. Fueki, and Z. Kuri, *J. Phys. Chem.*, **74**, 3584 (1970).
9) Y. Saitake, T. Wakayama, T. Kimura, T. Miyazaki, K. Fueki, and Z. Kuri, This Bulletin, **44**, 301 (1971).

no detectable radicals. A spectrum identical to Fig. 1A was obtained by the γ-irradiation of the isobutane. This indicates H-abstraction from the primary position in isobutane at 77°K by the photochemically-produced hot H atoms to form the isobutyl radical.

As the HI concentration in an isobutane matrix is increased, the yield of the isobutyl radical increases; it reaches a maximum at *ca.* 0.1 mol% HI concentration, and then decreases (Fig. 2). This result may

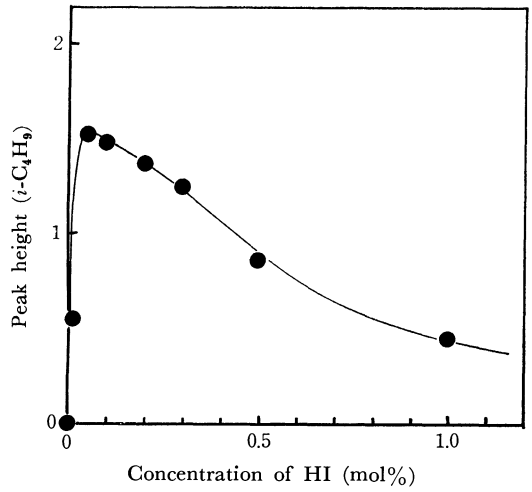

Fig. 2. Effect of HI concentration on the amounts of isobutyl radicals produced in UV-illuminated i-C_4H_{10} at 77°K. UV-illumination time: 10 min.
●—●: i-C_4H_9

be explained in terms of the competitive reactions between HI and isobutane for hot H atoms. A possible kinetic scheme is as follows:

$$HI \xrightarrow{\Phi I_{abs}} H_{hot} + I \quad (1)$$

$$i\text{-}C_4H_{10} + H_{hot} \xrightarrow{k_2} i\text{-}C_4H_9 + H_2 \quad (2)$$

$$i\text{-}C_4H_{10} + H_{hot} \xrightarrow{k_3} i\text{-}C_4H_{10} + H \quad (3)$$

$$HI + H_{hot} \xrightarrow{k_4} H_2 + I \quad (4)$$

where I_{abs} is the rate of light absorption by HI, Φ is the quantum yield of the photodissociation of HI, and k is the rate constant. From these equations we can derive the following kinetic equation:

$$\frac{\Phi I_{abs}\tau}{(R\cdot)} = \left(1 + \frac{k_3}{k_2}\right) + \frac{k_4(HI)}{k_2(RH)} \quad (5)$$

where (R·), (RH), and (HI) are the concentrations of isobutyl radicals, isobutane, and HI respectively. τ is the time of light illumination. (R·) is measured by ESR, and I_{abs} is calculated as a function of (HI), using a value of 75[10] for the molar extinction coefficient of HI and taking the geometrical factor of the sample into account. Since Φ is constant, it can be expected from Eq. (5) that the relative value of $\Phi I_{abs}\tau/(R\cdot)$ also increases linearly with an increase in (HI)/(RH). Figure 3 shows the relative value of $\Phi I_{abs}\tau/(R\cdot)$ *vs.* the value of (HI)/(RH). It can be seem from Fig. 3 that several of the points tested fall on a straight line. This supports our interpretation presented above.

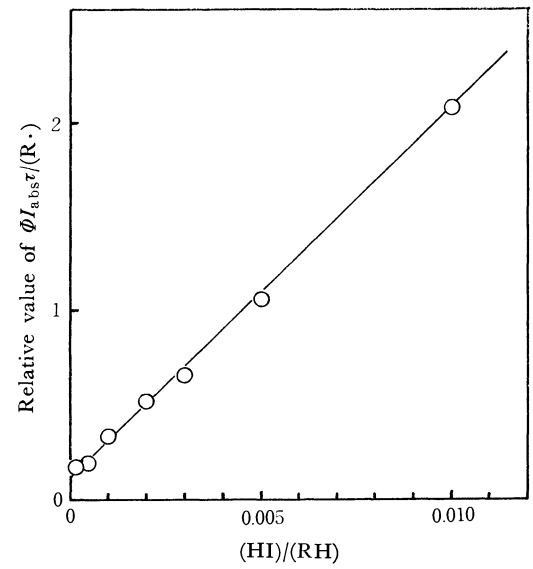

Fig. 3. Relation between $\Phi I_{abs}\tau/(R\cdot)$ and (HI)/(RH).

Pure isobutane is polycrystalline at 77°K, while isobutane containing 3.8 mol% MCH is glassy at 77°K. A quite different ESR spectrum was obtained by the 2.5-min photolysis of an isobutane-MCH mixture containing 0.2 mol%HI in the glassy state (Fig. 1B). This spectrum is identical with that of tertiary butyl radicals produced in γ-irradiated isobutane-3.8 mol% MCH in the glassy state at 77°K. This result indicates that the hot H atoms produced by the photolysis of isobutane-3.8 mol% MCH abstract the tertiary H atoms of isobutane to form tertiary butyl radicals.

The effect of the MCH concentration in an isobutane-0.2 mol% HI solution on the formation of radicals is shown in Fig. 4. Here, the remarkable point is the rapid increase in the yield of the tertiary butyl

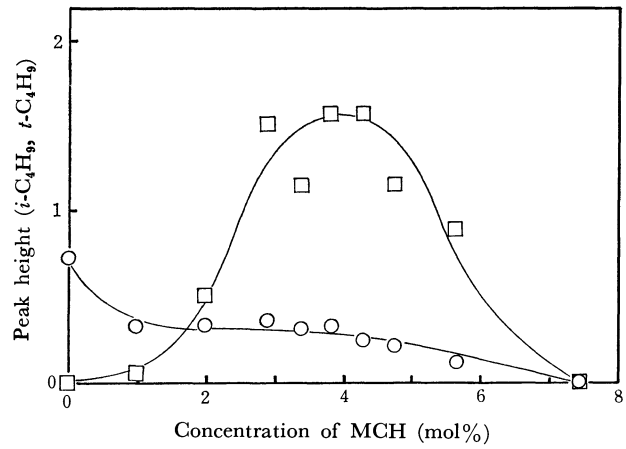

Fig. 4. Effect of MCH concentration on the amounts of butyl radicals produced in UV-illuminated i-C_4H_{10}-HI (0.2 mol%) at 77°K. UV-illumination time: 2.5 min.
○—○: i-C_4H_9
□—□: t-C_4H_9

10) R. M. Martin and J. E. Willard, *J. Chem. Phys.*, **40**, 2999 (1964).

radical, reaching a maximum at *ca.* 4 mol% MCH concentration. The yield of the isobutyl radical, however, does not change as much as that of the tertiary butyl radical. This result may be interpreted in terms of the following effects. As the concentration of MCH is increased, the matrix becomes glassy, so that the tertiary butyl radical is primarily produced by the hot-H-atom abstraction, while the isobutyl radical is secondarily produced by the photo-induced isomerization, $t\text{-}C_4H_9 \xrightarrow{h\nu} i\text{-}C_4H_9$. The yields of both isobutyl and tertiary butyl radicals decrease in the range of MCH concentration above *ca.* 4 mol%, where the matrix becomes so soft that the radicals are trapped less efficiently in the matrix.[11]

Figure 5 shows the dependence of the yields of butyl radicals on the UV-illumination time. As the illumination time is increased, the yield of the isobutyl radical increases almost linearly, while that of the tertiary butyl radical initially increases and then reaches a plateau after a 40-min illumination. This result indicates that the tertiary butyl radical is produced by the hot-H-atom abstraction reaction with isobutane, while the isobutyl radical arises from a secondary process, *i.e.*, the photoisomerization of the tertiary butyl radical to the isobutyl radical upon prolonged UV-illumination,[12] in an isobutane-3.8 mol% MCH solution containing 0.2 mol% HI at 77°K.

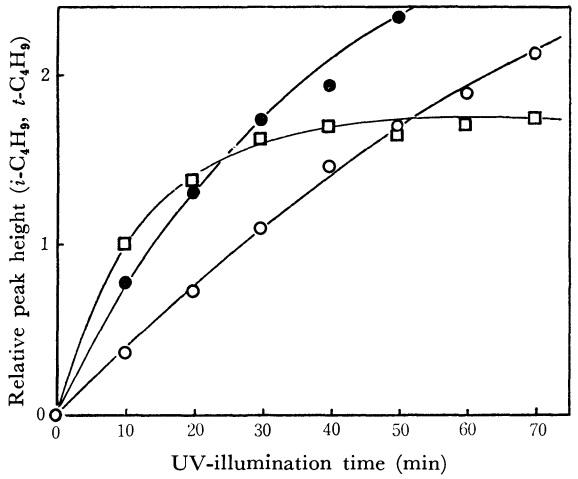

Fig. 5. Effect of UV-illumination time on the amounts of butyl radicals produced in UV-illuminated i-C_4H_{10}-HI (0.2 mol%) and i-C_4H_{10}-MCH (3.8 mol%)-HI (0.2 mol%) at 77°K.
●—●: i-C_4H_9 in an i-C_4H_{10} matrix.
○—○: i-C_4H_9 in an i-C_4H_{10}-MCH (3.8 mol%) matrix.
□—□: t-C_4H_9 in an i-C_4H_{10}-MCH (3.8 mol%) matrix.

Table I shows the butyl radicals produced by the hot-H-atom abstraction from isobutane in various UV-illuminated systems containing HI. Since the isobutyl-2-d_1 radical is produced in the photolysis of isobutane-2-d_1-HI (Fig. 1C), reactions (6) and (7) can be ruled out and reaction (8) occurs predominantly to form the isobutyl-2-d_1 radical:

$$i\text{-}C_4H_9D\text{-}2\text{-}d_1 + H_{hot} \rightarrow t\text{-}C_4H_9 + HD \quad (6)$$

$$t\text{-}C_4H_9 \rightarrow i\text{-}C_4H_9 \quad (7)$$

$$t\text{-}C_4H_9D\text{-}2\text{-}d_1 + H_{hot} \rightarrow i\text{-}C_4H_8D\text{-}2\text{-}d_1 + H_2 \quad (8)$$

In order to investigate the phase effect on the hot-H-atom abstraction reaction with isobutane, we have examined both the thermal isomerization and the decay of radicals. Ayscough and Evans[12] and Iwasaki and Toriyama[13] reported that isobutyl radicals produced in γ-irradiated alkyl halides, on standing at 77°K, isomerize thermally to tertiary butyl radicals. When the isobutyl radical was produced from dissociative electron attachment to i-C_4H_9Cl in the γ-irradiated i-C_4H_{10}-3.8 mol% MCH-1 mol% i-C_4H_9Cl system, the i-$C_4H_9 \rightarrow t$-C_4H_9 isomerization could be observed when it stood in the dark at 77°K for 15 hr.[8b] When an isobutane-3.8 mol% MCH solution containing 0.2 mol% HI is UV-illuminated for 30 min, the isobutyl radical is produced in addition to the tertiary butyl radical. When this sample was stored in the dark at 77°K for about 30 hr, the isomerization of the isobutyl radical could not be observed at all, but both isobutyl and tertiary butyl radicals decayed. The isobutyl radical produced by the photolysis of isobutane containing HI neither isomerizes to the tertiary butyl radical nor decays at all at 77°K (Fig. 6). The same phenomena were observed in γ-irradiated glassy isobutane-3.8 mol% MCH and in polycrystalline isobutane at 77°K.[8b]

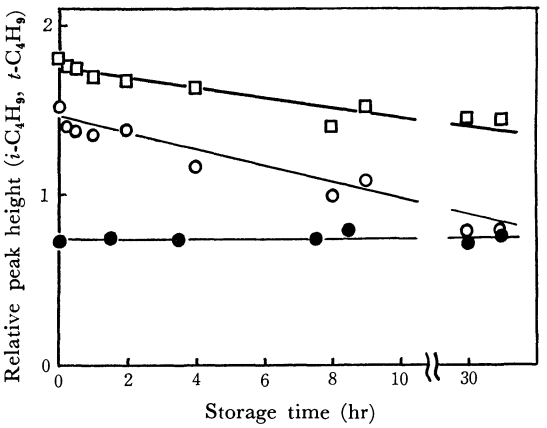

Fig. 6. Effect of storage time on the amounts of butyl radicals produced in UV-illuminated i-C_4H_{10}-HI (0.2 mol%) and i-C_4H_{10}-MCH (3.8 mol%) - HI (0.2 mol%) at 77°K. UV-illumination time: 30 min.
●—●: i-C_4H_9 in an i-C_4H_{10} matrix.
○—○: i-C_4H_9 in an i-C_4H_{10}-MCH (3.8 mol%) matrix.
□—□: t-C_4H_9 in an i-C_4H_{10}-MCH (3.8 mol%) matrix.

An ESR spectrum was obtained for the radicals produced in the radiolysis of a Xe-3.8 mol% isobutane mixture at 77°K; these radicals are identified as tertiary butyl radicals, presumably produced by energy transfer from Xe to isobutane. These tertiary butyl radicals isomerize to isobutyl radicals upon UV-

11) T. Wakayama, T. Miyazaki, K. Fueki, and Z. Kuri, This Bulletin, **43**, 3761 (1970).
12) P. B. Ayscough and H. E. Evans, *J. Phys. Chem.*, **68**, 3066 (1964).
13) M. Iwasaki and K. Toriyama, *J. Chem. Phys.*, **46**, 2852 (1967).

Table 1. Butyl radicals produced in the photolysis of HI in various matrices at 77°K[a)]

System	Phase	Radical
i-C_4H_{10}	Crystal	i-C_4H_9
i-C_4H_9D-2-d_1	Crystal	i-C_4H_8D-2-d_1
i-C_4H_{10}-MCH (3.8 mol%)	Glass	t-C_4H_9
i-C_4H_9D-2-d_1-3MP (7.4 mol%)	Glass	t-C_4H_9
Xe-i-C_4H_{10} (4.6 mol%)		t-C_4H_9

a) Concentration of HI: 0.2 mol%; UV-illumination time: 10 min

Table 2. Effect of matrix on butyl radical formation in the radiolysis at 77°K[a)]

System	Phase	Radical
i-C_4H_{10}	Crystal	i-C_4H_9
i-C_4H_9D-2-d_1	Crystal	i-C_4H_8D-2-d_1
i-C_4H_{10}-MCH (3.8 mol%)	Glass	t-C_4H_9
i-C_4H_9D-2-d_1-MCH (5.7 mol%)	Glass	t-C_4H_9
Xe-i-C_4H_{10} (3.8 mol%)		t-C_4H_9
X-i-C_4H_9D-2-d_1 (4.6 mol%)		t-C_4H_9

a) γ-Irradiation dose: 2.22×10^5 rad

illlumination. When this sample was stored in the dark at 77°K for *ca.* 30 hr, both the isobutyl and the tertiary butyl radicals decayed. These results indicate that the physical state of a Xe-3.8 mol% isobutane mixture at 77°K is rather more similar to the glassy state of an isobutane-MCH mixture than to the polycrystalline state of pure isobutane. This is also consistent with the fact that the primary radicals produced from isobutane in the photolysis and radiolysis are isobutyl radicals in the polycrystalline matrix and tertiary butyl radicals in the glassy matrix at 77°K (Tables 1 and 2). Accordingly, the thermal isomerzation from the isobutyl to the tertiary butyl radical seems to be a phenomenon characteristic of the isobutyl radical produced from alkyl halides. The decay of butyl radicals seems to be related to the physical state of the matrix.

Figure 1D shows the ESR spectrum of radicals produced by the photolysis of 0.2 mol% in Xe-4.6 mol% isobutane at 77°K.

Kagiya *et al.* reported an empirical method of evaluating the activation energies for radical substitution reactions in the gas phase.[14)] Using their method, we have calculated the activation energies for such thermal radical substitution reactions as:

$$H_{thermal} + i\text{-}C_4H_{10} \rightarrow H_2 + t\text{-}C_4H_9 \text{ (or } i\text{-}C_4H_9) \quad (9)$$

and

$$H_{thermal} + i\text{-}C_4H_9D\text{-}2\text{-}d_1 \rightarrow HD \text{ (or } H_2) + t\text{-}C_4H_9 \text{ (or } i\text{-}C_4H_8D\text{-}2\text{-}d_1) \quad (10)$$

The calculated activation energies are shown in Table 3. If we assume that the activation energies for the thermal radical substitution reactions are independent of the temperature, we can say, on the basis of the

14) T. Kagiya, Y. Sumida, T. Inoue, and F. S. Dyachkovskii, This Bulletin, **42**, 1812 (1969).

Table 3. The calculated activation energies of H atom abstraction reactions with isobutanes in the gas phase

Isobutane	Type of the bond	D_i[a)] (kcal/mol)	E_a[b)] (kcal/mol)
Isobutane	t-C-H	85	6.8
Isobutane	i-C-H	89	7.7
Isobutane-2-d_1	t-C-D	85.9	6.6
Isobutane-2-d_1	i-C-H	89	7.7

a) The bond dissociation energy of the initial bond. The C-D bond strength is taken to be 0.9 kcal/mol greater than that of C-H: S. W. Benson, "Foundations of Chemical Kinetics," McGraw-Hill Book Co., Inc., New York, N. Y. (1960), p. 666.
b) The activation energy.

activation energies estimated above, that the tertiary hydrogen atom of isobutane should be abstracted much more easily than the primary one at 77°K. However, this is inconsistent with observations on the polycrystalline samples, indicating that the hot hydrogen atom must be involved in the abstraction reaction in these systems.

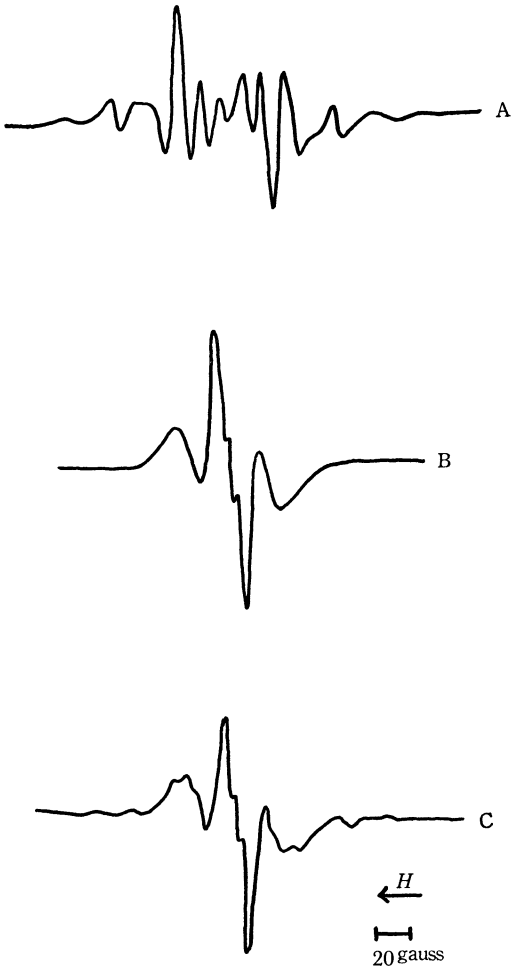

Fig. 7. (A) ESR spectrum of γ-irradiated i-C_4H_{10}-HI (1.0 mol%) at 77°K.
(B) ESR spectrum of γ-irradiated i-C_4H_9D-2-d_1 at 77°K.
(C) ESR spectrum of γ-irradiated i-C_4H_9D-2-d_1-HI (1.0 mol%) at 77°K. Irradiation dose: 2.22×10^5 rad.

Effects of Phase on Hydrogen-atom Abstraction in the Radiolysis of Solid Isobutane Containing HI. γ-Irradiated pure isobutane at 77°K displays a five-line ESR spectrum with a hyperfine coupling constant of $a_{av}=20.7$ G, which can be attributed to the isobutyl radical[15] (Table 2). A quite different ESR spectrum, however, is obtained for radicals produced in the radiolysis of isobutane containing 1.0 mol% HI. This spectrum consists of two components which may be assigned to the tertiary butyl radical (a ten-line spectrum with $a_{av}=22.3$ G)[16] and the isobutyl radical (Fig. 7A) respectively.

Figure 8 shows the dependence of the peak heights

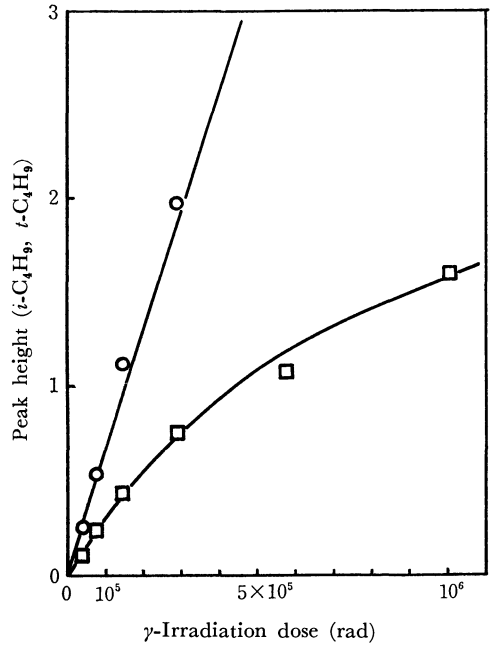

Fig. 8. Effect of dose on the amounts of butyl radicals produced in γ-irradiated t-C_4H_{10}-HI (2.0 mol%) at 77°K.
○—○: i-C_4H_9
□—□: t-C_4H_9

of trapped radicals on the dose in γ-irradiated isobutane containing 2.0 mol% HI at 77°K. The peak intensity of isobutyl radicals is linear in doses over the entire range studied, while that of tertiary butyl radicals is linear in doses up to 1.5×10^5 rad, but deviates from the straight line with doses beyond it. This result can be interpreted in terms of the following reactions:

$$i\text{-}C_4H_{10} \text{ -}\!\!\wedge\!\!\vee\!\!\wedge\text{- } i\text{-}C_4H_{10}^*,\ i\text{-}C_4H_{10}^+ + e^- \quad (11)$$

$$i\text{-}C_4H_{10}^* \rightarrow i\text{-}C_4H_9 + H \quad (12)$$

$$HI + e^- \rightarrow H_{hot} + I^- \quad (13)$$

$$H_{hot} + i\text{-}C_4H_{10} \rightarrow H_2 + t\text{-}C_4H_9 \quad (14)$$

The isobutyl radical is produced by the decomposition of the excited isobutane molecule (reaction (12)),[7] while the tertiary butyl radical is produced in the H-abstraction by the hot H atom which is formed in the dissociative electron attachment (reaction (13)) and has an energy of *ca.* 5—6 kcal/mol.

As the HI concentration in an isobutane matrix is increased, the yield of the isobutyl radical produced in the radiolysis decreases initially and reaches a plateau value at *ca.* a 1.0 mol% HI concentration, while that of the tertiary butyl radical increases rapidly initially and then gradually (Fig. 9). Figure 10

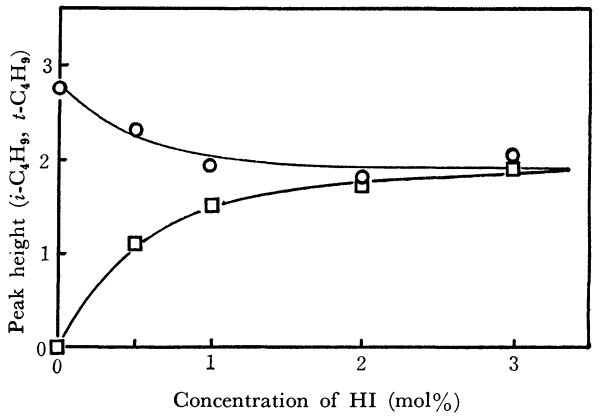

Fig. 9. Effect of HI concentration on the amounts of butyl radicals produced in γ-irradiated i-C_4H_{10} at 77°K. Irradiation dose: 8.9×10^4 rad.
○—○: i-C_4H_9
□—□: t-C_4H_9

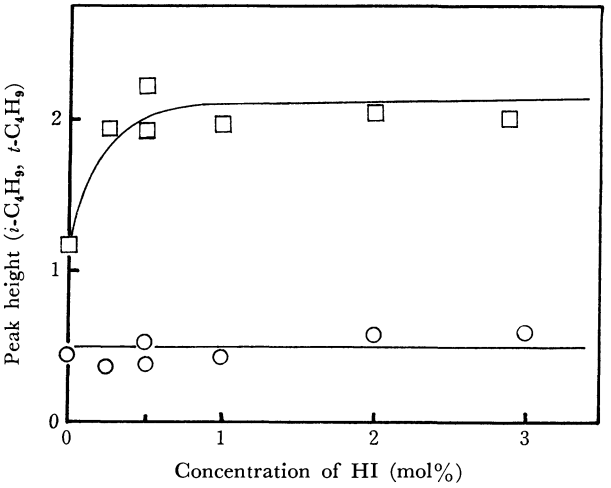

Fig. 10. Effect of HI concentration on the amounts of butyl radicals produced in γ-irradiated t-C_4H_{10}-MCH (3.8 mol%) at 77°K. Irradiation dose: 8.9×10^4 rad.
○—○: i-C_4H_9
□—□: t-C_4H_9

shows the dependence of the yields of trapped radicals on the concentration of HI in a γ-irradiated isobutane-3.8 mol% MCH matrix at 77°K. The yield of the tertiary butyl radical increases with the concentration of HI up to *ca.* 0.5 mol% and reaches a plateau value, while that of the isobutyl radical is constant over the entire range of HI concentrations studied. These results may be interpreted in terms of the energy dependence of the hot-H-atom reaction and on the basis of the electron yield in γ-irradiated hydrocarbons in the solid state; the hot H atom produced from HI by the dissociative electron attachment (reaction

15) J. Lin and F. Williams, *J. Phys. Chem.*, **72**, 3707 (1968).
16) P. B. Ayscough and C. Thomson, *Trans. Faraday Soc.*, **58**, 1477 (1962).

(13)) abstracts an H atom from the tertiary position more easily than from the primary position in isobutane at 77°K, since the hot H atom thus produced has an energy of *ca.* 5—6 kcal/mol, which is much lower than that produced by the photolysis of HI. Such an argument holds for both polycrystalline isobutane and glassy isobutane-MCH matrices (Table 4). The

Table 4. Butyl radicals produced in the radiolysis of HI in various matrices at 77°K[a)]

System	Phase	Radical
i-C_4H_{10}	Crystal	t-C_4H_9
i-C_4H_9D-2-d_1	Crystal	t-C_4H_9
i-C_4H_{10}-MCH (3.8 mol%)	Glass	t-C_4H_9

a) Concentration of HI: 1.0 mol%; γ-irradiation dose: 2.22×10^5 rad

yield of the tertiary butyl radical produced by reaction (14) increases with HI concentration up to *ca.* 1.0 mol%, above which it remains constant, because the yield of electrons which escape from recombination with the parent positive ions in the radiolysis of condensed systems is limited and its maximum value in solid hydrocarbon matrices is $G(e^-)=2$.[17)] The yield of the isobutyl radical is rather insensitive to the concentration of HI, since the isobutyl radical is produced by the decomposition of the excited isobutane molecule.

Figure 7B shows the ESR spectrum of radicals produced in the radiolysis of pure isobutane-2-d_1 at 77°K, which can be attributed to the isobutyl-2-d_1 radical.[9)] In γ-irradiated 1 mol% HI in isobutane-2-d_1, the tertiary butyl radical is produced in addition to the isobutyl-2-d_1 radical (Fig. 7C). The tertiary butyl radical may arise from D-atom abstraction from isobutane-2-d_1 by the hot H atom produced from HI.

Cause of Phase Effect on H-atom-abstraction Reaction by Hot H Atoms. When a diatomic molecule such as HI dissociated by absorbing light with more energy than the dissociation energy of the bond, the atoms produced will be hot. The main advantage of utilizing photochemically-produced hot atoms is that their initial kinetic energy is well known. In the 2537 Å photolysis of HI, hot H atoms have 20 kcal/mol or 41 kcal/mol, depending on whether the iodine atom is produced in the excited state or in the ground state. Since the first excited-state energy of the H atom is about 237 kcal/mol, the energy given to the H atom produced photochemically is the kinetic energy.

The phase effect can be discussed from the following two points of view: (i) whether the phase change affects such primary processes as the fragmentation of the excited HI molecule in the photolysis of solid isobutane containing HI at 77°K, and (ii) whether the phase change affects such secondary processes as the hot-hydrogen-atom abstraction reaction with isobutane. In a diatomic molecule such as HI, the H–I bond rupture of the excited HI molecule (HI*) may occur repulsively in the period of one vibration (less than 10^{-13} sec). Therefore, the phase effect has no important influence upon the primary process of the HI* fragmentation.

One plausible explanation is given by the cage effect on the radiolysis of organic solids, which was reviewed by Willard.[18)] Since the C–C bond of the stable tertiary butyl radical is formed by sp^2-hybrid orbitals, three methyl groups construct a planar structure. Therefore, the structural rearrangement of the C–C bonds would be necessary for the formation of the stable tertiary butyl radical from the isobutane molecule, which such a rearrangement would be unnecessary for the formation of the isobutyl radical. In the radiolysis of isobutane in the polycrystalline state, the formation of the tertiary butyl radical, accompanied by the structural rearrangement of the C–C bonds, may be suppressed in the rigid crystal, and only the primary C–H bond, which is stronger than the tertiary C–H bond, may be ruptured. The effect of the matrix rigidity was observed both in the abstraction of H atom from isobutane by hot H atoms produced from the photolysis of HI and in the decomposition of the excited isobutane molecule produced by the radiolysis of isobutane (Tables 1 and 2). In the radiolysis of the polycrystalline isobutane-HI or isobutane-2-d_1-HI, however, it was found that the hot H atom, which is produced by dissociative attachment to HI, abstracts the tertiary H atom from isobutane or isobutane-2-d_1 (Table 4). Thus, only the cage effect does not explain satisfactorily this H-abstraction reaction in solid hydrocarbons at 77°K. The energy dependence of the hot-H-atom abstraction reaction must be invoked to interpret this observation.

Another effect of the hot-atom reaction is the moderator effect, which was discussed by Hamill,[19)] in the photolysis of HI. On this model, hot H atoms are formed with 20 or 41 kcal/mol of translational energy, which they can lose in the subsequent moderating collisions with an inert gas. Typically, these are rare gases such as He and Ne, but such substances as A, Kr, Xe, and H_2 may act as moderators. We may interpret the present results for a moderator matrix, Xe (Tables 1 and 2), as follows. The hot H atoms (H**) in a Xe matrix may lose translational energy by collisions with the moderator, Xe, and then they may abstract the tertiary H atoms of isobutane to form tertiary butyl radicals (reactions (15), (16), and (17)). This interpretation is consistent with the findings on the radiolysis of isobutane-HI, where hot H atoms have only 5—6 kcal/mol and preferentially abstract the tertiary H atoms. In summary, the H-abstraction reaction by hot H atoms depends upon the energy of the hot H atoms:

17) M. Shirom and J. E. Willard, *J. Phys. Chem.*, **72**, 1702 (1968); T. Kimura, K. Fueki, and Z. Kuri, This Bulletin, **43**, 3090 (1970); T. Kimura, M. Fukaya, M. Hada, T. Wakayama, K. Fueki, and Z. Kuri, *ibid.*, **43**, 3400 (1970); T. Shida, *J. Phys. Chem.*, **74**, 3055 (1970).

18) J. E. Willard, "Fundamental Processes in Radiation Chemistry," P. Ausloos, Ed., Interscience, New York, N. Y. (1968), p. 599.

19) H. A. Schwarz, R. R. Williams, Jr., and W. H. Hamill, *J. Amer. Chem. Soc.*, **74**, 6007 (1952).

$$HI \xrightarrow{h\nu} H^{**} + I \quad (15)$$

$$H^{**} + M \rightarrow H^{*} + M \quad (16)$$

$$H^{*} + i\text{-}C_4H_{10} \rightarrow H_2 + t\text{-}C_4H_9 \quad (17)$$

In reactions (15)—(17) H** and H* represent hot atoms with higher and lower kinetic energies respectively, and M represents a moderator such as Xe. It should be stressed that, although the efficiency of Xe as a moderator is probably lower than that of hydrocarbons, the contribution of H-abstraction by very hot atoms is more greatly reduced in a Xe matrix than in a hydrocarbon matrix, in which H-abstraction by hot atoms inevitably competes with hot-atom moderation.

The authors thank Dr. T. Kimura and Mr. Y. Saitake of Nagoya University, and Professor E. Maekawa of Nagoya Institute of Technology for their assistance in preparing isobutane-2-d_1.

BULLETIN OF THE CHEMICAL SOCIETY OF JAPAN, VOL. 44, 2626—2630 (1971)

The Reactions of Mobile Electrons in the Frozen Solution of Ethylene Glycol-Water at 77°K

Teikichi SASAKI and Shin-ichi OHNO

Japan Atomic Energy Research Institute, Tokai-Mura, Ibaraki-ken

(Received March 11, 1971)

The yield of trapped electrons produced in ethylene glycol-water glass at 77°K increased linearly with the gamma dose up to 1.5×10^{20} eV/g, and the G value was estimated to be 2.8 ± 0.2. The relative reaction rates of mobile electrons with various inorganic ions at 77°K were determined by competition kinetics. The observed relative reaction rates with simple inorganic ions corresponded to those of hydrated electrons obtained at room temperature. For complex ions, however, the reactivities of the mobile electrons were larger than those of hydrated electrons. The reaction products, such as bromine dioxide, Cr(V) species, and the pentacyano Co(II) ion, all of which are unstable at room temperature, could be detected by optical and ESR spectroscopies at 77°K.

A large number of rate constants for the reaction of the hydrated electron, e_{aq}^-, with solutes have been determined by competition kinetics and pulse-radiolysis techniques.[1] For the mobile electron, e_m^-, produced in acidic or alkaline ices at 77°K, some investigators[2-4] have determined the relative rates of reaction with metal cations and oxyanions. The results observed have shown that the relative reactivity of e_m^- with a solute is quantitatively similar to that of e_{aq}^- with the same solute. Based on these correlations, Kevan has postulated e_m^- as a mobile solvated electron in ice.[2] This preposition also implies that the structure of e_m^- at the time of reaction is similar to that of e_{aq}^-.

Dainton and his co-workers[4,5] have demonstrated that, in 5.4 M sulfuric acid at 77°K, an e_m^- can reduce solutes such as transition metal cations and nitrous oxide. The reaction products of lower valency states are trapped in the matrix; they have been studied by both optical and ESR spectroscopies. However, it is difficult to study the reactivity of e_m^- with solutes which are subject to decomposition in concentrated acid or alkaline solutions.

In the present paper, a study on the rate of the reaction of e_m^- with electron scavengers such as simple inorganic and complex ions was made by employing a neutral solution of an ethylene glycol-water mixture as the solvent matrix. The trapped electron, e_t^-, produced in this matrix by gamma irradiation is indefinitely stable in dark at 77°K and has an absorption band in the visible region which can be readily photobleached by exposure to the visible light. It is well-known[6,7] that the G value of the e_t^- produced at 77°K is comparatively high and reaches its maximum in the region of 50—65 vol% ethylene glycol, which is suitable for quantitative investigations of the reactivity of e_m^-. The products resulting from the e_m^- reactions could also detected by optical and ESR spectroscopies. In some cases, the results were correlated with the data obtained by pulse-radiolysis and flash photolysis.

Experimental

Sample Preparation. Water was distilled three times, and ethylene glycol from the Kanto Kagaku Co., Ltd., was fractionally distilled. All of the other chemicals were of analytical reagent grade and were used without further purification. As the solvent matrix, 67 vol% ethylene glycol diluted with pure water was used. Each sample contained 10^{-3}—5×10^{-2} M metal sulphate or potassium salt as an electron scavenger. The solution was degassed and made into the glassy state by the freeze-pump-thaw technique at 77°K.

1) M. Anbar and P. Neta, *Int. J. Appl. Radiat. Isotopes*, **18**, 493 (1967).
2) L. Kevan, *J. Amer. Chem. Soc.*, **89**, 4238 (1967).
3) L. Kevan, P. N. Moorthy, and J. J. Weiss, *ibid.*, **86**, 771 (1964); L. T. Bugaenko and O. S. Povolotskaya, *Khim. Vys. Energ.*, **1**, 480 (1967); B. G. Ershov and A. K. Pikaev, *Radiation Res. Rev.*, **2**, 62 (1968).
4) D. M. Brown and F. S. Dainton, *Trans. Faraday Soc.*, **62**, 1139 (1966).
5) F. S. Dainton and F. T. Jones, *ibid.*, **61**, 1681 (1965).
6) H. Hase, *J. Phys. Soc. Jap.*, **24**, 589 (1968).
7) I. E. Makarov, B. G. Ershov, and A. K. Pikaev, *Izv. Akad. Nauk SSSR, Ser. Khim.*, 2170 (1969).

The cells for the spectrophotometric measurement were made of quartz with rectangular cross-sections and with overall dimensions of $0.10\times1.2\times3.5$ cm. For the ESR study, Spectrosil tubings of 0.45 cm i.d. were used.

Irradiation and Measurement. Gamma irradiations by a ^{60}Co source were carried out in the dark at 77°K. The dose rate was 4.0×10^{18} eV g^{-1} hr^{-1} except where otherwise described.

The optical absorption spectra were obtained with a Shimadzu QV-50-type spectrophotometer by the use of a Dewar flask with quartz windows. The yield of e_t^- was determined from the decrease in the optical density at 530 nm after the photobleaching procedure. The photobleaching of e_t^- was performed with a 400-W tungsten lamp whose UV light of wavelengths shorter than 350 nm was cut off with a Toshiba color filter.

The ESR spectra were scanned on an X-band ESR spectrometer (Japan Electron Optics Laboratory Co., Ltd., JEP-1) operating at ~9.3 kMc/s and employing 100 kc/s magnetic-field modulation and phase-sensitive detection. The gamma-irradiated samples were first transferred into a quartz Dewar flask of the temperature of liquid nitrogen. Then the vessel was placed inside the cavity of ESR spectrometer equipped with a dry N_2 gas-flow system. The *g*-factors were determined by employing nitrogen oxide radicals trapped in 0.6M $NaNO_3$ ice as a standard. Its isotropic splitting constant was taken to be 54.7 *G*, with a *g*-factor of 2.001.[8]

Results and Discussion

Yield of e_t^- in the Ethylene Glycol-Water Mixture. After gamma irradiation in the dark at 77°K, ethylene glycol-water glass developed a deep blue color. The color readily decayed, however, upon exposure to the visible light ($\lambda>350$ nm). The optical absorption spectra were essentially identical with those of e_t^- reported by Ershov *et al.*[9]

A signal due to e_t^- was also detected by ESR measurement, together with those of hydrogen atoms and some different organic radicals. One of the spectra

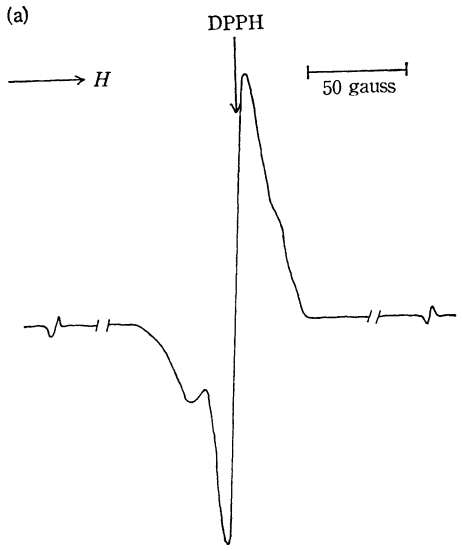

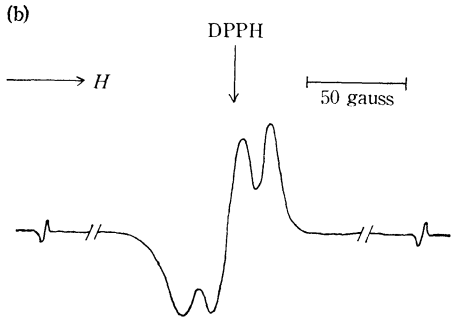

Fig. 1. ESR spectra of ethylene glycol-water glasses irradiated with gamma rays to a dose of 5.0×10^{18} eV/g at 77°K.
(a) before photobleaching, (b) after photobleaching

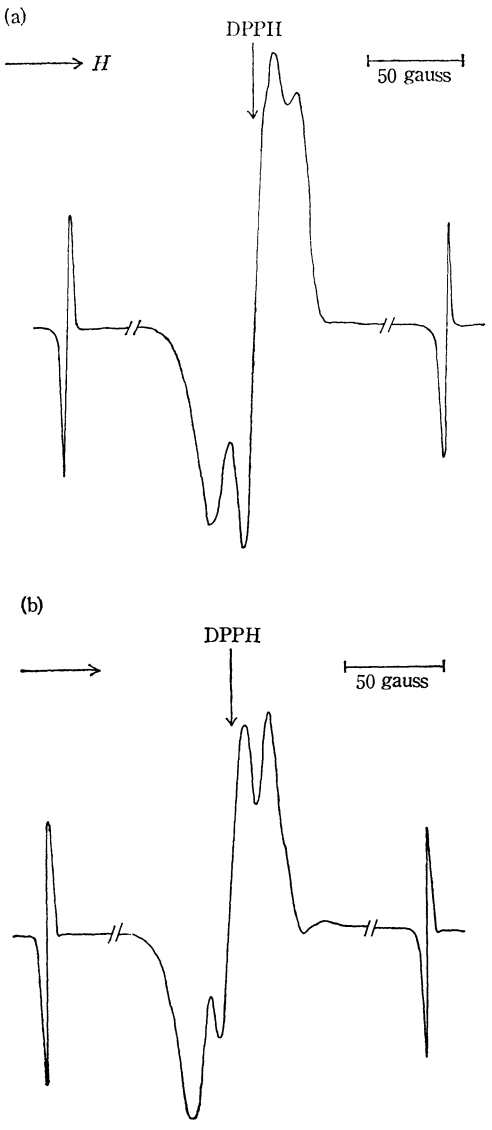

Fig. 2. ESR spectra of ethylene glycol-water glasses irradiated with gamma rays to a dose of 7.3×10^{20} eV/g at 77°K.
(a) before photobleaching, (b) after photobleaching

observed at 77°K is displayed in Fig. 1(a). Besides an H-atom doublet with a splitting of 510 *G*, a signal attributable to e_t^- superimposed by those of the organic

8) L. Kevan, *J. Phys. Chem.*, **68**, 2590 (1964).
9) B. G. Ershov, I. E. Makarov, and A. K. Pikaev, *Khim. Vys. Energ.*, **1**, 404 (1967).

radicals was observed in the central part of the spectrum. The line shape was changed by the photobleaching of e_t^- with the visible light, and the signals due to the organic radicals which have been assigned to the $HOCH_2CH_2\dot{O}$ and $HOCH_2\dot{C}HOH$ radicals[7] clearly appeared, as is shown in Fig. 1(b). For the samples irradiated with gamma doses higher than about 1.5×10^{20} eV/g, a decrease in the ratio of the signal intensity of e_t^- to that of hydrogen atoms was observed. The central part of the spectrum was also changed, as may be seen in Fig. 2.

The yield of e_t^- in the ethylene glycol-water glass increases linearly up to a dose of about 1.5×10^{20} eV/g. Assuming that the extinction coefficient of e_t^- produced in the matrix at 77°K is identical with that of e_t^- in the irradiated alkaline glass, 1.37×10^4 M^{-1} cm^{-1} at 530 nm,[10] the G value of e_t^- can be estimated to be 2.8±0.2. It is noteworthy that this value agrees well with the maximum G value of e_t^- produced in the alkaline glasses (3.0 in 10 M KOH glass[10]). The yield of e_t^- reaches its maximum at *ca.* 1×10^{21} eV/g and then decreases, while those of the hydrogen atoms and organic radicals increase with the absorbed dose, as is shown in Fig. 3. Such a dose dependence of e_t^- is identical with the observations for the 10 M NaOH frozen solutions irradiated with gamma rays of doses higher than *ca.* 2.5×10^{20} eV/g.[11] The characteristics observed may arise from di-electron formation and the disappearance due to the recombination reaction of e_t^- with the positive-ion radicals.

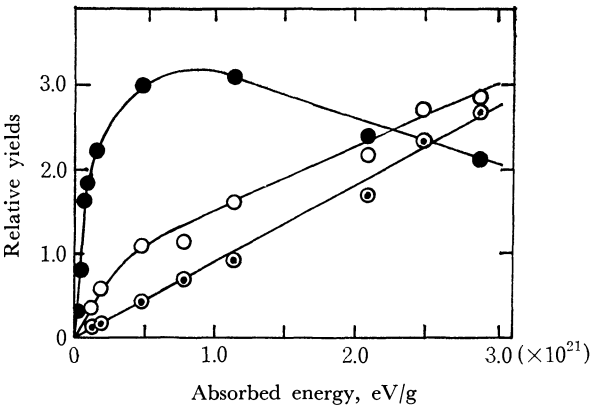

Fig. 3. Relative yields *vs.* absorbed energy of gamma irradiation. In the region of the dose higher than 1.1×10^{21} eV/g, the samples were irradiated at the dose rate of 2.4×10^{19} eV/ghr.
●: trapped electron, ○: organic radicals
⊙: trapped hydrogen atom

Reaction Rates of e_m^- with Electron Scavengers. The relative reaction rates of e_m^- can be determined by a competition reaction, such as:

$$e_m^- + T \xrightarrow{k_1} e_t^- \qquad (1)$$

$$e_m^- + S \xrightarrow{k_2} S^- \qquad (2)$$

where T and S are the electron trap and the electron scavenger respectively. Competition kinetics applied to the e_m^- reaction in the system yields the following expression:

$$\frac{C_o(e_t^-)}{C(e_t^-)} - 1 = \frac{k_2[S]}{k_1[T]} \qquad (3)$$

where $C_o(e_t^-)$ and $C(e_t^-)$ are the e_t^- concentrations in the absence and in the presence of the scavenger. Because the optical density at 530 nm, $D(e_t^-)$, is proportional to the e_t^- concentration, the relative value of k_2 is obtained from the slope of the straight line by plotting $\{D_o(e_t^-)/D(e_t^-)-1\}$ against [S].

The results for NO_3^-, $[Fe(CN)_6]^{3-}$, and $[Co(CN)_6]^{3-}$ ions, corrected for the absorption of the solvent matrix and quartz cell, are shown in Fig. 4. The ordinate values increases linearly with the scavenger concentration, and no effect on the electron-trap concentration was observed upon the addition of the electron scavenger. The relative rates for the e_m^- reactions with various inorganic ions are summarised in Table

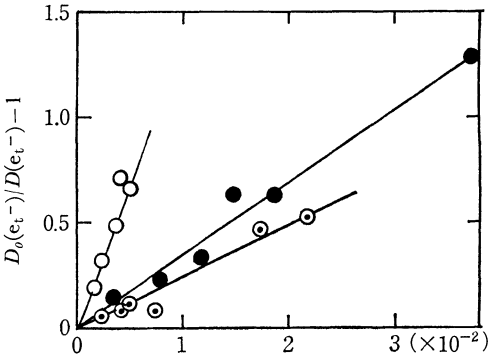

Fig. 4. Relationships between $\{D_o(e_t^-)/D(e_t^-)-1\}$ and scavenger concentration. All samples were irradiated to a gamma dose of 4.0×10^{18} eV/g at 77°K.
●: NO_3^-, ○: $[Fe(CN)_6]^{3-}$, ⊙: $[Co(CN)_6]^{3-}$

TABLE 1. RELATIVE RATES OF e_m^- AND e_{aq}^- REACTIONS WITH VARIOUS IONS

Ion(S)	Relative rates[a]	
	$k(e_m^- + S)$ at 77°K	$k(e_{ap}^- + S)$[b] at ~300°K
NO_3^-	1	1
Cu^{2+}	3.6	3.0
Fe^{3+}	2.8	—
ClO_3^-	≪0.1	3.6×10^{-4}
BrO_3^-	0.2	0.19
IO_3^-	0.6	0.70
CN^-	≪0.1	$<10^{-4}$
$[Fe(CN)_6]^{3-}$	3.9	0.40
$[Fe(C_2O_4)_3]^{3-}$	2.4	—
$[Co(CN)_6]^{3-}$	0.6	0.25
$[Co(C_2O_4)_3]^{3-}$	3.1	1.1

a) All rates were normalized to NO_3^- rate=1.
b) The data were cited from the table compiled by Anbar and Neta.[1]

10) B. G. Ershov, O. F. Khodzhaev, and A. K. Pikaev, *Dokl. Akad. Nauk SSSR*, **179**, 911 (1968).
11) L. Kevan, D. Renneke, and R. J. Friauf, *Solid State Commun.*, **6**, 469 (1968); H. Hase and L. Kevan, *J. Phys. Chem.*, **73**, 3290 (1969).

1; those for the e_m^- reaction obtained at pH 7.0 are also presented for comparison.

In the case of all inorganic ions except the complex ion, the relative values of the e_m^- rates agree with those of the e_{aq}^- rates. The correlations seem to support Kevan's postulations[2,12] that e_m^- in ice acts as a mobile solvated electron and that the entropic effects of the scavenger ions are responsible for the rate differences between the different solutes. On the other hand, the e_m^- rates for complex ions are usually larger than the e_{aq}^- rates for the corresponding ions. This finding is unexpected, and it seems that more experimental data are neccessary to give a definite explanation of the reactivity of e_m^- with complex ions.

Spectra of Reaction Products. After the photobleaching of e_t^-, the irradiated glass containing the bromate ion gave an optical absorption spectra with a tail in the UV region and a peak at 475 nm, as is shown in Fig. 5. This absorption band disappeared

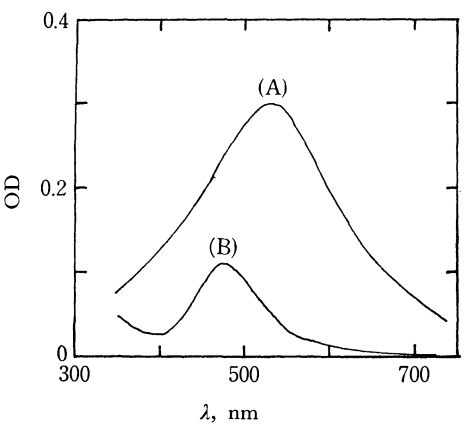

Fig. 5. Optical absorption spectra for glassy specimens irradiated gamma rays at 77°K.
(A): Ethylene glycol-water glass irradiated to a dose of 3.8×10^{18} eV/g (before photobleaching).
(B): Ethylene glycol-water glass containing 0.05 M $KBrO_3$ irradiated to a dose of 5.6×10^{19} eV/g (after photobleaching).

upon thermal annealing at *ca.* 140°K. The peak position is in good agreement with that of the transient species observed in the pulse-radiolysis experiment at room temperature;[13] therefore, it may be thought to be due to the bromine dioxide (BrO_2) which is produced in the reaction:

$$e_m^- + BrO_3^- \rightarrow BrO_2 + O^{2-} \quad (4)$$

An analogous reaction scheme was proposed for the reduction of the bromate ion with e_{aq}^- by flash photolysis.[14] In the irradiated solution containing the iodate ion, however, the clear optical spectrum of dioxide species could not be observed because it was superimposed by a tail of a stronger absorption of the iodine trioxide radical.[15]

The extinction coefficient of the bromine dioxide observed can be determined from the optical density in Fig. 5, assuming that Eq. (3) is correct up to the solute concentration of the order of 0.05 M. Since the bromine dioxide concentration, $C(BrO_2)$, is equal to $C_o(e_t^-)-C(e_t^-)$, it can be expressed as follows:

$$C(BrO_2) = \frac{K[S]C_o(e_t^-)}{1+K[S]} \quad (5)$$

where K is $k_2/(k_1[T])$. Therefore, the extinction coefficient, $\varepsilon(BrO_2)$, is related with the reaction rate of bromate ion by the following expression:

$$\varepsilon(BrO_2) = \frac{D(BrO_2)}{C(BrO_2)\cdot l} = \frac{(1+K[S])\,D(BrO_2)}{K[S]C_o(e_t^-)\cdot l} \quad (6)$$

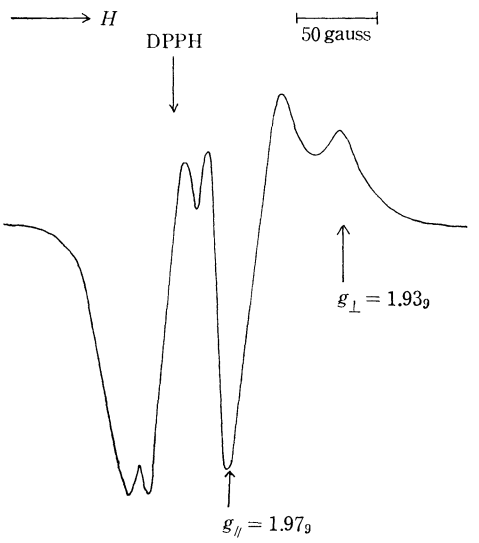

Fig. 6. ESR spectrum of 0.1 M K_2CrO_4 solution irradiated with gamma rays to a dose of 5.0×10^{19} eV/g and photobleached at 77°K.

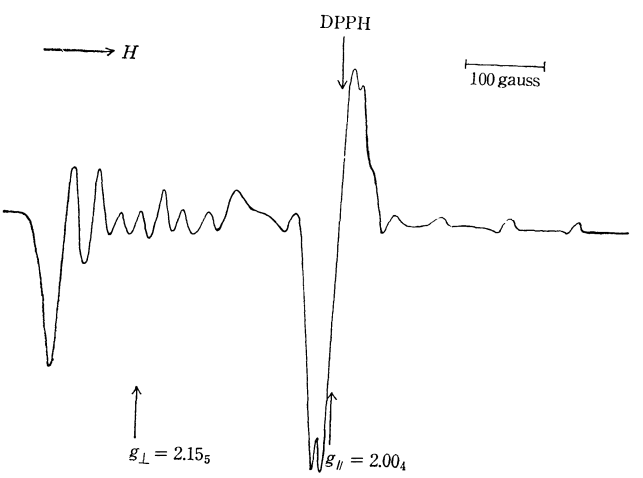

Fig. 7. ESR spectrum of 0.07 M $K_3[Co(CN)_6]$ solution irradiated with gamma rays to a dose of 5.0×10^{19} eV/g and photobleached at 77°K.

12) L. Kevan, "Radiation Chemistry of Aqueous Systems," ed. by G. Stein, Wiley-Interscience, New York (1968); p. 64.
13) G. V. Duxton and F. S. Dainton, *Proc. Roy. Soc. A.*, **304**, 427 (1968); O. Amichai and A. Treinin, *J. Phys. Chem.*, **74**, 3670 (1970).
14) O. Amichai, G. Czapski, and A. Treinin, *Isr. J. Chem.*, **7**, 351 (1969).
15) The trioxide species might be produced in consequence of the following hole reaction:
$M \rightsquigarrow M^+ + e_m^-$
$M^+ + IO_3^- \longrightarrow M + IO_3$
where M denotes the solvent matrix.

where D is the optical density and l is the optical path. The value of K is determined to be 6.5 M^{-1} from the slope of the scavenger curve, and $C_0(e_t^-)$ is 3.2×10^{-3} M in the ethylene glycol-water glass irradiated with a dose of 5.6×10^{19} eV/g. Thus, $\varepsilon(BrO_2)$ can be estimated to be approximately 1.4×10^3 M^{-1} cm^{-1} at 475 nm.

In the presence of the chromate ion as an electron scavenger, an intermediate species was also detected by ESR spectroscopy. The spectrum recorded at 77°K is shown in Fig. 6. An anisotropic signal on the low g-factor side of the free-electron position, which was also observed in the 6 M sulfuric acid matrix, indicates the formation of an electron-rich center. The line shape and the principal g-factors are characteristic of the Cr(V) species formed in the frozen solutions[16] as a result of the electron capture of the chromate ion.

Figure 7 shows the ESR spectrum of a gamma-irradiated glassy specimen containing the 0.07 M hexacyano cobaltate ion. In addition to the central signals resulting from the organic radicals, the specimen gives two eight-line hyperfine patterns. The spectrum is interpreted as consisting of superimposed parallel and perpendicular absorptions; each splits into eight lines, with coupling constants of 30 and 91 G respectively, by means of ^{59}Co ($I=7/2$) nuclear interactions. The respective g-factors and the hyperfine constants are characteristic of those observed for the penta-coordinated Co(II) complex ion rather than the hexa-coordinated Co(II) complex ion in frozen solutions at 77°K by Kataoka and Kon.[17] Therefore, the spectrum obtained strongly suggests the formation of the pentacyano Co(II) ion in consequence of the reaction associated with e_m^-:

$$[Co(CN)_6]^{3-} + e_m^- \rightarrow [Co(CN)_5]^{3-} + CN^- \qquad (7)$$

The authors wish to thank Dr. Mitsuru Koike for his useful suggestions.

16) P. N. Moorthy and J. J. Weiss, *Advan. Chem. Ser.*, **50**, 211 (1965).

17) N. Kataoka and H. Kon, *J. Amer. Chem. Soc.*, **90**, 2978 (1968).

BULLETIN OF THE CHEMICAL SOCIETY OF JAPAN VOL. 44, 2630—2634 (1971)

Gel Filtration of Aqueous Sodium Dodecyl Sulfate

Hitoshi SUZUKI and Tsunetaka SASAKI

Department of Chemistry, Faculty of Science, Tokyo Metropolitan University, Tokyo, Japan

(Received March 17, 1971)

Gel filtration of an aqueous solution of sodium dodecylsulfate (SDS) was carried out using Sephadex G-50 as a gel column, and the overall elution rate (R_f) of SDS was measured. The value of R_f was found to be independent of the concentration C of SDS below a certain point, above which it increased with increasing C. A sharp break point observed coincided with the critical micelle concentration (CMC) of SDS. The intermicellar concentration of SDS was estimated from the shape of the elution curve for the solutions beyond CMC, and shown independent of the total concentration C. The value of R_f for the micelle was further determined by direct measurement. The value was found to increase slightly with C above CMC, becoming practically constant above about 1.4×10^{-2} mol/l. It was concluded from the results that the size of the micelle also increase with the concentration above CMC. Theoretical equations were derived for the relation between R_f and C below and above CMC. Observed R_f *vs.* C relation fitted the equations satisfactorily, from which CMC was calculated. A rapid equilibrium between micelles and monomer ions and the independence of intermicellar concentration on C were also confirmed.

A study on the dissolved state of sodium dodecyl sulfate (SDS) by the gel filtration method using Sephadex G-50 was reported in a previous paper.[1] Equations were proposed which predict a relation between a relative elution rate and the concentration of SDS solution. The observed data fitted the equation from which a rapid equilibrium between micelles and monomer ions, uniformity of micellar size and the independency of intermicellar concentration on the total concentration were concluded.

Further studies made on the direct measurement of the relative elution rate of micelles suggested a slight increase of the micellar size above CMC. This made it necessary to re-examine the former plots. We have derived a revised equation for gel filtration which involves a well defined parameter for the rate of micelle decomposition. Verification was carried out without the method of trial and error which was adopted in the previous case.[1] Constancy of the intermiceller concentration of SDS was also checked experimentally.

Experimental

Materials. Sodium dodecyl sulfate (SDS) was synthesized from dodecyl alcohol and chlorosulfonic acid by the usual method[2] and was purified by solvent extraction using ethyl ether and recrystallization from ethanol. Purity was checked by the absence of a minimum in the surface tension-concentration curve.

1) T. Sasaki and Y. Ogihara, Proceedings of 5th International Congress on Surface Activity, Barcelona (1968).

2) S. J. Rehfeld, *J. Phys. Chem.*, **71**, 738 (1967).

Sodium chloride was purified by recrystallization of the reagent grade product.

The gel used for packing the column was Sephadex G-50[3] fine, manufactured by Pharmacia, Uppsala, Sweden.

Apparatus. The apparatus used for gel filtration is schematically shown in Fig. 1. The main parts of the apparatus consisted of a gel column G prepared in the usual manner[3,4] (diameter 1.2 cm and gel height 32.5 cm), a conductance cell D, a conductometer C and a recorder R. The conductance cell D for detecting SDS recorded the conductance against the elution volume. All experiments were carried out at 30±1°C.

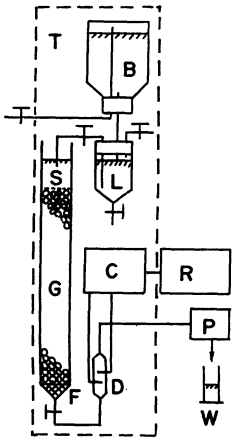

G gel column
S sample solution
F glass wool
D conductance cell
C conductometer
P steady flow pump
R recorder
W weighing vessel
T thermostated chamber
B reservoir
L leveler

Fig. 1. Arrangement for gel filtration.

Methods. To measure the retention volume of SDS, the gel column was previously equilibrated with distilled water and 25.0 m*l* of SDS solutions of varying concentration (C) were put on the gel column. Elution was then started using distilled water at a flow rate of 20 m*l*/hr, and the retention volume (V) was determined from the conductance curve recorded. The results were conventionally expressed as the relative elution rate

$$R_f = V_0/V \qquad (1)$$

where V_0 denotes the retention volume of solvent water.

To measure R_f value of the micelles in the aqueous solution of SDS above CMC, the gel was previously equilibrated with SDS solution of concentration C larger than CMC (C_m), and SDS solution with concentration C' larger than C was added to the gel column. The solution was then eluted with water. From the elution volume $V_m(C')$ thus obtained for the SDS solution of concentration C', the relative elution rate of the micelle $R_f^m(C') = V_0/V_m(C')$ was calculated. $R_f^m(C')$ was then plotted against C' and the value $R_f^m(C)$ was estimated by extrapolating C' to C. The value $R_f^m(C)$ can be considered as the relative elution rate of the micelle flowing through its own intermiceller solution of concentration C without decomposition.

Results and Discussion

Intermiceller concentration of SDS. Figure 2 shows two typical elution curves of SDS solution of concentrations below and above CMC, through the gel column filled with water. We see that the curve of SDS solution of the concentration below CMC shows one plateau and that above CMC two. The higher one corresponds to concentration C of the solution eluted. The lower one might be considered to be the concentration of the intermicellar SDS left after the fast flowing micelles have been eluted, provided that the plateau is sufficiently horizontal and the change between the two plateaus is fairly sharp. Figure 3 shows the plots of the conductance and concentration corresponding to one (solid circles) or two plateaus (open circles and triangles) of the elution curves against the analytical concentration of SDS. We see a straight line passing through the origin and a horizontal straight line starting from CMC. The latter might indicate constant intermicellar concentration which is independent of the SDS concentration and is equal to C_m.

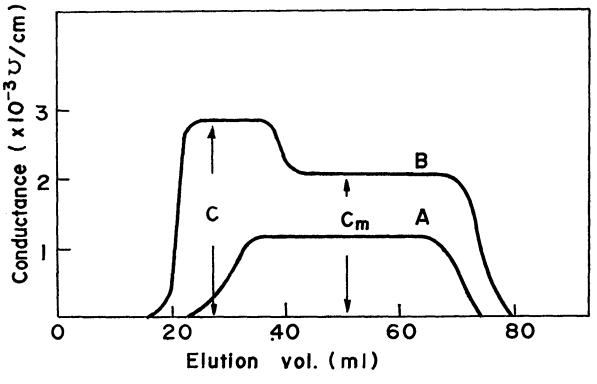

Fig. 2. Elution curve of SDS solution.

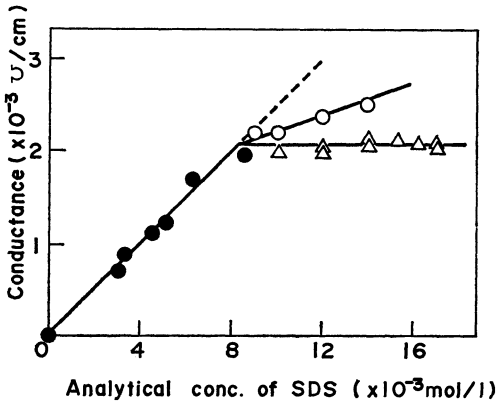

Fig. 3. Conductance of SDS solution.
Conductance of the solution below CMC(●) and above CMC(○); conductance of intermicellar solution(△)

R_f vs. C relation. The observed values of R_f for the aqueous solution of SDS below and above CMC are plotted against the concentration as shown in Fig. 4. Since V_s, the retention volume of the lower concentration region of SDS, was found practically independent of SDS concentration,[1,5,6] its mean value $\bar{V}_s$ was calculated, and $R_f = \bar{V}_s/V$ instead of $R_f = V_0/V$ was used as a relative elution rate. The relative

3) P. Flodin, "Dextran Gels and Their Application in Gel Filtration," Pharmacia, Uppsala, Sweden (1962).
4) H. Determann, "Gel Chromatography," Springer-Verlag, Berlin, Heidelberg, New York (1969), p. 42.
5) T. Sasaki, *Yukagaku*, **16**, (2) 49 (1967).
6) F. Tokiwa, K. Ohki, and I. Kokubo, This Bulletin, **41**, 2285 (1968).

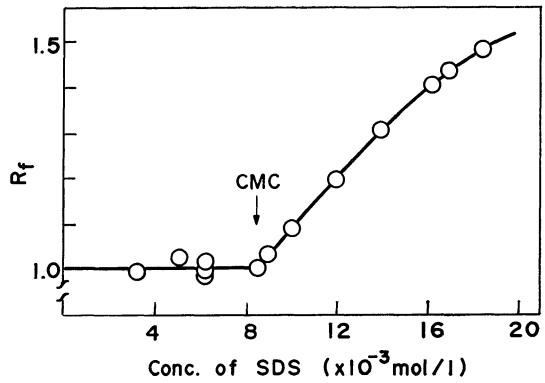

Fig. 4. R_f *vs.* concentration of SDS.

elution rate of monomer ion R_f^s is therefore expressed as

$$R_f^s = \bar{V}_s/V_s \fallingdotseq 1$$

It is evident from Fig. 4 that R_f *vs.* C curve consists of a horizontal straight line $R_f=R_f^s \fallingdotseq 1$ in the lower concentration region and a curve in the higher concentration region, with a break point between them corresponding to the CMC of SDS (8.5×10^{-3} mol/l). The constancy of R_f^s value in the lower concentration region might indicate the presence mainly of monomer molecule of SDS in this region.

The results of the direct measurement of $R_f^m(C')$ together with the process of extrapolation are shown in Fig. 5. The extrapolated $R_f^m(C)$ value (solid circles) increases from about 2.2 near CMC with increasing SDS concentration until it becomes constant, 2.54 above 1.4×10^{-2} mol/l SDS. It is worthy to note that the change in R_f^m is exclusively ascribed to the change in size of solute particle, since the effect of adsorption and other conceivable factors can be excluded from the present experimental conditions, and there is the possibility for a slight increase of micellar size with concentration above CMC.

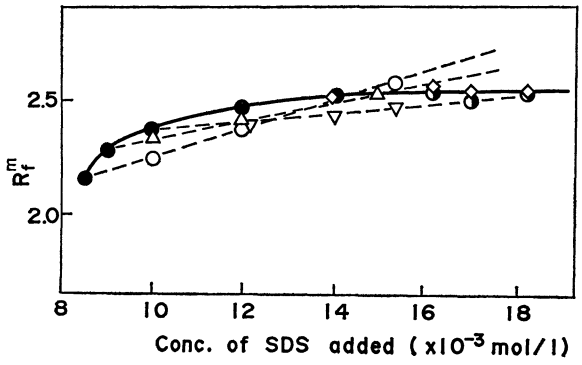

Fig. 5. R_f^m *vs.* concentration of SDS.

Conc. of SDS in gel ($\times10^{-3}$mol/l): ○, 8.5; △, 9.0; ▽, 10.0; ◇, 12.0; ◑, 14.0; ●, extrapolated value of R_f^m for each case.

Let us discuss the relation between R_f and SDS concentration for the solution especially above CMC. For this purpose, it is convenient to use such a diagram as shown in Fig. 6a,[5] for the elucidation of the mechanism of gel filtration and the calculation of R_f as a function of the concentration above CMC. In this diagram, the effective cross sectional area A_m of a packed gel column through which micelles can flow (total cross-section of interspace of gel particles), and a similar area A_s for the passage of sufficiently small molecules (monomer surfactant molecules and solvent water molecules), are taken on OY axis. The distance travelled by the monomer molecules and the micelles during the flow of a solution is taken on OX axis. Thus, the vertical line RS indicates the front of the micelles in sample solution (large circles) just reaching the lower end of the gel column while the solution is continuously supplied and flows down, assuming no decomposition into monomer takes place. The vertical line PQ indicates the front of monomer molecules (small circles) when the front of the micelles reaches RS. Since the volumes occupied by these solute components are equal, we have

$$\square A_sOPQ = \square A_mORS \qquad (3)$$

where □ denotes the area of the square specified which actually expresses the volume. A simple geometry shows that the intersection M of the two straight lines A_mS and PQ lies on the diagonal OU. The micelles in □ MPRS are unstable since they are isolated from monomer molecules which should exist in equilibrium with them. Therefore, such micelles as in □ RR'S'S actually decompose into monomer molecules to fill the space □ QPR'U' with the concentration C_m' ($C_m' \leqq C_m$) as shown by the small circles in this area (Fig. 6b). For further calculation, we put OR=t

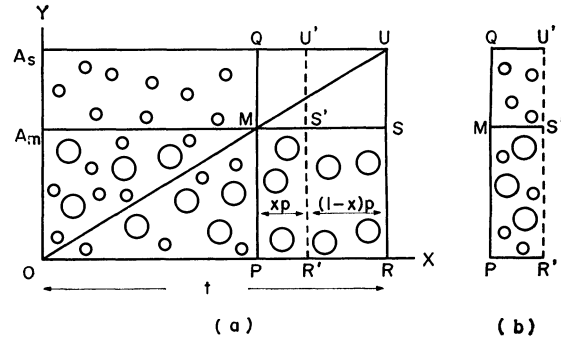

Fig. 6. Mechanism of gel filtration.
○; monomer molecule, ○; micelle

which represents the total length of the gel column, PR'=xp, RR'=$(1-x)p$ as shown in Fig. 6. Then we obtain the relation

$$A_m p(1-x)(C-C_m) = A_s pxC_m' = A_s pxC_m\alpha$$

or

$$A_m(1-x)(C-C_m) = A_s xC_m\alpha \qquad (4)$$

Here α, being equal to C_m'/C_m, denotes a parameter of the rate of micelle decomposition or the rate of equilibration between micelles and monomer. Namely, the decomposition is instantaneous when $\alpha=1$ and no decomposition occurs when $\alpha=0$. Further, the actual retention volume V of the solute is given by

$$tA_m : V = [t-(1-x)p] : t$$

or

$$V[t-(1-x)p] = t^2A_m \tag{5}$$

Eq. (3) is rewritten as

$$(t-p)A_s = tA_m \tag{6}$$

From Eqs. (4), (5), and (6), we obtain

$$\frac{V}{V-tA_m} = \frac{A_mC}{(A_s-A_m)C_m\alpha} + \frac{A_s\alpha-A_m}{(A_s-A_m)\alpha} \tag{7}$$

It can be understood from Fig. 6 that $A_st=V_s$ and $A_mt=V_m$ represent the retention volumes of monomer molecule and micelle (assumed to flow without decomposition), respectively, and the relations

$$R_f = \bar{V}_s/V,\ R_f{}^m = \bar{V}_s/A_mt,\ R_f{}^s = \bar{V}_s/A_st$$

express the relative elution rates of solution and micelle, and mean relative elution rate of monomer molecule, respectively.

Substituting V, A_s, and A_m in Eq. (7) by R_f's, we obtain

$$\frac{R_f{}^m-R_f{}^s}{R_f{}^s}\cdot\frac{R_f}{R_f{}^m-R_f} = \frac{C}{C_m\alpha} - \frac{1-\alpha}{\alpha} \tag{8}$$

Eq. (8) predicts a linear relationship between $\frac{R_f{}^m-R_f{}^s}{R_f{}^s}\cdot\frac{R_f}{R_f{}^m-R_f}$ and C above CMC, from which α and C_m can be calculated. Below CMC we can also express the R_f term in a form similar to Eq. (8) for comparison:

$$\frac{R_f{}^m-R_f{}^s}{R_f{}^s}\cdot\frac{R_f}{R_f{}^m-R_f} = \frac{R_f{}^m-R_f{}^s}{R_f{}^s}\cdot\frac{R_f{}^s}{R_f{}^m-R_f{}^s} \fallingdotseq 1 \tag{9}$$

To verify Eqs. (8) and (9), $\frac{R_f{}^m-R_f{}^s}{R_f{}^s}\cdot\frac{R_f}{R_f{}^m-R_f}$ was plotted against C, using the observed data of $R_f{}^m(C)$, $R_f(C)$, and $R_f{}^s$ (Fig. 7).

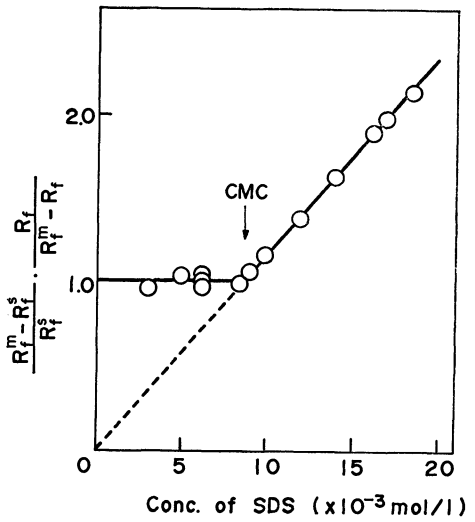

Fig. 7. Concentration dependence of R_f.

We see two straight lines corresponding to Eqs. (8) and (9) with a sharp break point between them which again gives the CMC of SDS. The fact that the plots corresponding to Eq. (8) show a straight line which passes through the origin ($\alpha=1$) indicates the constancy of the intermicellar concentration and a rapid equilibrium between micelles and monomer molecules, at least under the present conditions of the experiment. The value of CMC obtained from the break point was 8.6×10^{-3} mol/l, and the same value was obtained from the inclination of Eq. (8). These values are compared with similar values in literature.[7]

In the above study, the elution volume of SDS monomer molecule was used in place of V_0, the elution volume of solvent water or such a simple substance as sodium chloride. This may be justified since the molecular weight of SDS (about 500) is well below the lower limit of the fractionation range of Sephadex

Table 1. Gel chromatography of SDS and NaCl on sephadex gel

concn. of aq. SDS or NaCl filling gel medium		concn. of SDS solution added afterwards		elution volume
0	mol/l	SDS	3.2 $\sim6.4\times10^{-3}$ mol/l	mean value 31.0 ml
0	mol/l	NaCl	5.0$\sim$ 10.0×10^{-2} mol/l	mean value 28.8 ml
SDS	2.5×10^{-3} mol/l	SDS[a]	2.5×10^{-3} mol/l	
		NaCl	5.0×10^{-3} mol/l	28.45 ml (NaCl)[b]
SDS	2.5×10^{-3} mol/l	SDS[a]	2.5×10^{-3} mol/l	
		NaCl	2.5×10^{-3} mol/l	28.45 ml (NaCl)
NaCl	1.9×10^{-3} mol/l	NaCl[a]	1.9×10^{-3} mol/l	
		SDS	5.0×10^{-3} mol/l	31.58 ml (SDS)
NaCl	2.5×10^{-3} mol/l	NaCl[a]	2.5×10^{-3} mol/l	
		SDS	7.0×10^{-3} mol/l	31.59 ml (SDS)

a) mixed solution.
b) compound in parenthesis indicates the substance for which elution volume was measured.

7) M. Miura and T. Matsumoto, *J. Science of the Hiroshima University*, **21**, 51 (1957); K. Sinoda, "Colloidal Surfactants," Academic Press, New York (1963).

G-50. In a separate experiment, however, the elution volumes of urea, NaCl, and dodecylpyridinium bromide have been measured under the same conditions as for SDS. The retention volumes for urea and NaCl found were 29.1 m*l* and 28.8 m*l*, respectively, while the retention volumes of SDS and dodecylpyridinium bromide obtained were 31.0 m*l* and 30.9 m*l*, respectively, the latter two being slightly but distinctly larger. This presents another problem since an elution volume not larger than 28.8 m*l* is expected for SDS. Various factors can be pointed out to explain the anomalies, such as adsorption of SDS by the gel matrix,[8] swelling or syneresis of the gel by SDS or NaCl respectively, so-called ion exclusion effect,[9] and the effect due to the amphipathic nature of the internal surface of gel matrix.[10] In the present study, however, the effect of adsorption need not be considered since in the measurements above CMC the elution of the solution was made into the gel previously equilibrated with the solution of the same concentration. Elution of the solutions below CMC was also carried out under similar conditions and the possibility of adsorption was also confirmed to be excluded. In order to confirm the effects, if any, of syneresis and swelling, elution volumes of aqueous NaCl and SDS solutions into the gels previously equilibrated with SDS and NaCl, respectively, were measured for comparison with the untreated gels as shown in Table 1. However, the elution volumes were not affected by this gel-treatment. Thus these factors are considered to be insignificant. The possibility of ion exclusion effect which had been expected was also excluded, since the elution volume was independent of the concentration of the electrolyte in the present study. Further study is required concerning the effect of amphipathic nature of the gel matrix as a cause of the anomalies.[10] It may be inferred further that the micelles are uniform in size, since the conductance rise in the elution curve indicating the micellar front is as sharp as that for single ions below CMC.

8) D. G. Herries, W. Bishop, and F. M. Richards, *J. Phys. Chem.*, **68**, 1842 (1964).

9) D. Saunders and R. L. Pecsok, *Anal. Chem.*, **40**, 44 (1968); P. A. Neddermeyer and L. B. Rogers, *ibid.*, **40**, 755 (1968).

10) H. Small and D. N. Bremer, *I & EC Fundamentals*, **3**, 361 (1964).

BULLETIN OF THE CHEMICAL SOCIETY OF JAPAN, VOL. 44, 2634—2638 (1971)

Electron Spin-Spin Interaction in the Multiplet Ground State of Non-planar Methylene Derivatives

Jiro HIGUCHI

Department of Chemistry, Faculty of Engineering, Yokohama National University, Minami-ku, Yokohama

(Received March 20, 1971)

The effect of deviation from the planar structure in electron spin-spin interaction has been semiempirically investigated for spin multiplet ground state of radicals with methylene bonds. If these bonds are not coplanar, a significant influence occasionally appears on the values of D and E, while the influence is very small if the relative orientation among the methylene bonds still does not change.

In previous papers,[1-3] the electron spin-spin interaction of the methylene derivatives was investigated by assuming coplanar methylene bonds with the central benzene ring. From the non-planar structure of the benzophenone molecule (the dihedral angle between the plane of the carbonyl bond [C–(C=O)–C] and that of the phenyl group (α) is 30°, and the bond angle at the carbonyl carbon atom (θ) is 122°),[4] the above assumption does not seem always adequate for higher molecular spin multiplet radicals with several phenyl groups. In the present paper, a semiquantitative study will be reported on the relation between the electron spin-spin interaction and the molecular structure, especially concerning the influence on the deviation from the planar structure.

The ratio of E/D is used for a measure which can be compared with the observed value, since this ratio may be largely affected by the molecular structure but subject to minor influence on the spin density at the methylene carbon –C–. The values of D and E were evaluated according to the formulas

$$D = \left(\frac{3e^2\hbar^2}{4m^2c^2}\right)\frac{2!(2S-2)!}{(2S)}\sum_{i,j}\left\langle \phi_i(1)\phi_j(2) - \phi_j(1)\phi_i(2)\left|\frac{r_{12}^2-3z_{12}^2}{r_{12}^5}\right|\phi_i(1)\phi_j(2)\right\rangle \quad (1)$$

and

$$E = \left(\frac{3e^2\hbar^2}{4m^2c^2}\right)\frac{2!(2S-2)!}{(2S)!}\sum_{i,j}\left\langle \phi_i(1)\phi_j(2) - \phi_j(1)\phi_i(2)\left|\frac{y_{12}^2-x_{12}^2}{r_{12}^5}\right|\phi_i(1)\phi_j(2)\right\rangle \quad (2)$$

where ϕ_i's are the unpaired orbitals. Details of the

1) J. Higuchi, *J. Chem. Phys.*, **38**, 1237; **39**, 1847 (1963).
2) J. Higuchi, *ibid.*, **39**, 1339 (1963). The revised result is given in Appendix of the present paper.
3) J. Higuchi, This Bulletin, **43**, 3773 (1970).
4) E. B. Fleischer, N. Sung, and S. Hawkinson, *J. Phys. Chem.*, **72**, 4311 (1968).

calculation are the same as those in previous papers.[5]

Radicals with Only One Methylene Bond

Diphenylmethylene $(C_6H_5)_2C$ is taken as the simplest example of non-planar triplet radicals with only one methylene bond assuming the symmetry of C_2. In this case, the unpaired orbitals may be expressed as

$$\phi_1 = (4-6\sin^2\alpha\cos\theta)^{-1/2}[2\chi_{l0}-\sin\alpha\,(-\cos\theta)^{1/2} \times(\chi_2-\chi_4+\chi_6-\chi_{2'}+\chi_{4'}-\chi_{6'})] \quad (3)$$

and

$$\phi_2 = (4+6\cos^2\alpha)^{-1/2} \times[2\chi_{\pi 0}-\cos\alpha(\chi_2-\chi_4+\chi_6+\chi_{2'}-\chi_{4'}+\chi_{6'})]. \quad (4)$$

Here, θ and α are, respectively, the –C– bond angle and the dihedral angle between the plane of the –C– bond and that of the phenyl group, χ_{l0} is the s–p hybridized orbital of the –C– atom (0):

$$\chi_{l0} = [(1+\cos\theta)/(1-\cos\theta)]^{1/2}\chi_{2s0} + [-2\cos\theta/(1-\cos\theta)]^{1/2}\chi_{2px0} \quad (5)$$

(x is the symmetry axis of the molecule),

$\chi_{\pi 0}$ is the p orbital of the –C– atom which is perpendicular to the –C– bond plane, and χ_i's ($i\neq 0$) are the p orbitals of atom C_i's which are perpendicular to the phenyl plane concerned.

Figure 1 shows the calculated D and E values of diphenylmethylene as a function of the –C– bond angle (θ) assuming the planar structure ($\alpha=0°$) and the structure with the two phenyl groups to be perpendicular to the plane of the –C– bond ($\alpha=90°$). Similar calculations were carried out at various dihedral angles of α. The deviation of D and E values from those of the planar structure with the same –C– angle is fairly small at angles of α within 60°. In these calculations, we obtain various sets of angles, θ and α, where the ratio of E/D coincides with the observed value of 0.04735 [$D/\boldsymbol{hc}=\pm 0.40505\ \mathrm{cm}^{-1}$, $E/\boldsymbol{hc}=\pm 0.01918\ \mathrm{cm}^{-1}$][6] as shown in Fig. 2. As a result, the probable –C– bond angles are found over a range between 144° and 150°. It should be noted here that the electron spin resonance experiment of diphenylmethylene by Brandon *et al.*[6] was carried out using a host crystal of benzophenone molecule. From the dihedral angle of $\alpha=30°$ in the host molecule with $\theta=122°$, the value of α in the diphenylmethylene might be slightly smaller than 30°, since the steric

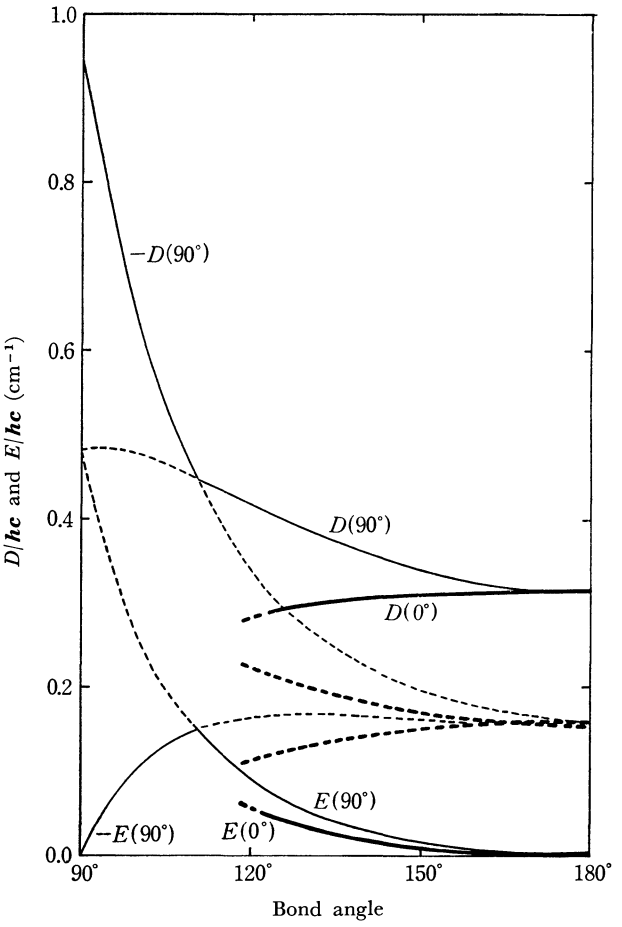

Fig. 1. D and E values of diphenylmethylene with planar structure ($\alpha=0°$) (bold lines) and that with the two phenyl groups perpendicular to the plane of the –C– bond ($\alpha=90°$) (fine lines). For large (small) –C– bond angles, the principal axes of fine-structure tensor [or Eqs. (1) and (2)] are as follows: the x axis is the symmetry axis of the molecule, the y (z) axis is perpendicular to the plane of the –C– bond, and the z (y) axis is perpendicular to the other axis. Fine dotted lines are the extensions in the case of $\alpha=90°$. Bold dotted lines correspond to the case where the z axis in Eq. (1) is taken to be perpendicular to the molecular plane ($\alpha=0°$).

hindrance is expected to be smaller than that of the benzophenone because of its larger θ value. In view of these facts, the most probable –C– bond angle can be estimated to be 145°±1° as in the phenylmethylene (see Appendix). In this case, the influence of non-planar structure does not appear remarkably, although the D and E values increase with increasing dihedral angle of α. This is apparently due to the fact that the terms with α almost cancel each other in the ratio of E/D, since the atomic contribution in D is approximatley proportional to that of E. Similarly, the influence of non-planar structure on the ratio of E/D is expected to be very small for other triplet radicals with only one methylene bond, because of the slight change of their atomic term which has a large contribution to the energy. This is similar to the case of *m*-phenylene-*bis*-phenylmethylene where the change in the orientation of only the side phenyl groups does not significantly affect the relative values of D and E[3].

5) The one-center integrals were those calculated from the self-consistent field atomic orbitals. The two-center integrals were approximately evaluated as follows: the 2*s* electron was replaced by a unit point charge at the nucleus, the 2*p* electron was two half-unit charges located to give the same quadrupole moment, and the atomic dipole effect was added. All the C–C distances were taken to be 1.393 Å as in benzene molecule. Simple LCAO-MO's were used for the π-orbitals. The unpaired σ orbitals were assumed to be hybridized ones located at each –C– atom and directed along the bisector of the –C– bond angle. For the sake of simplicity, configuration interaction was disregarded. [Refs. 2 and 3].

6) R. W. Brandon, G. L. Closs, C. E. Davoust, C. A. Hutchison, Jr., B. E. Kohler, and R. Silbey, *J. Chem. Phys.*, **43**, 2006 (1965). The x and the y axes of this paper correspond to, respectively, the y and the x axes of the present work.

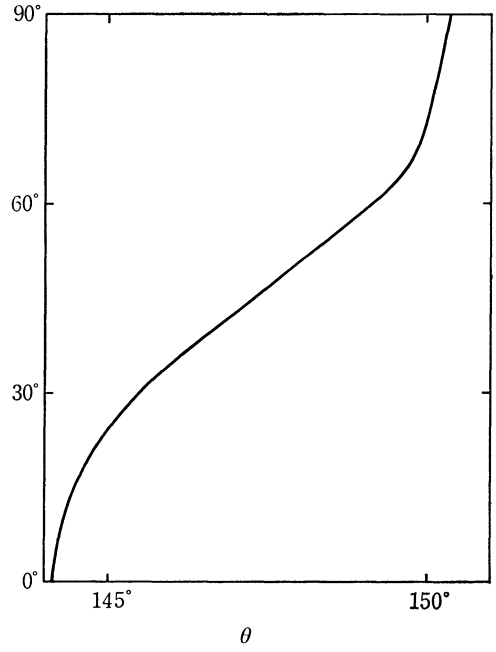

Fig. 2. The -C- bond angle (θ) and the dihedral angle between the plane of the -C- bond and that of the phenyl groups (α) in the diphenylmethylene with the structure where E/D coincides with the experimental value.

Radicals with Several Methylene Bonds

For spin multiplet radicals with more than one methylene bond such as *m*-phenylene-dimethylene, the approximation of the planar structure might not always be adequate for discussing the spin-spin interaction, since the relative orientation of these bonds is expected to have a great influence on the ratio of E/D. In the spin quintet radicals with coplanar methylene bonds, the bond angular dependence of D and E does not differ much between the calculation with all the spin-spin interactions and that with only the atomic contribution.[7] This means that approximation without interatomic interactions might be used for knowing the general tendency of *m*-phenylene-dimethylene radicals, because the main contribution of the D and the E values is due to the atomic term. In view of these facts, a simplified calculation of the D and the E values for only the atomic contribution is carried out by changing dihedral angles between the plane of the central phenylene group and that of each side methylene bond. Hereafter, such angles are denoted by α_1 and α_2, corresponding to the methylene bond with C_7 and that with C_8, respectively. (Fig. 3).

The result obtained for *m*-phenylene-dimethylene shows that the relative orientation of two methylene bonds has a significant influence on the D and E values. In some sets of the –C– bond angles, all the possible values of $|E|/|D|$ appear by changing α_1 and α_2 [*e.g.* in the case of $\theta_1=\theta_2=210°$, the $|E|/|D|$ changes from 0 to 1/3 by varying α_i ($\alpha_1=\alpha_2$) from 0° to 60°]. In such cases, one cannot estimate the –C– bond angles from only the absolute value of E/D, although the possibility of α_i values larger than 45° may be very small. On the other hand, it is not always very easy to calculate the D and E values which can be compared with the experimental values in a quantitative sense. A similar result is obtained for the septet ground state of 1,3,5-$C_6H_3(CX)_3$ without a C_3 axis.

As an example, Figs. 4 and 5 show the ratio of $|E|/|D|$ thus obtained for *m*-phenylene-dimethylene at the dihedral angles of $\alpha_1=30°$ and $\alpha_2=\pm30°$ in the cases of $\theta_1=\theta_2$ and $\theta_1+\theta_2=360°$, respectively. Such dihedral angles might have probable values when the host crystal used is the benzophenone (with $\alpha=30°$). We see that the uncertainty of the –C– bond angles due to the change of $\Delta\alpha_i=\pm30°$ is larger than 10° for some values of E/D. For *m*-phenylene-*bis*-phenylmethylene and *m*-phenylene-*bis*-methylene, however, the direction of principal axes in the fine-structure tensor [or those in Eqs. (1) and (2)] differ from those of the cases where all the possible values

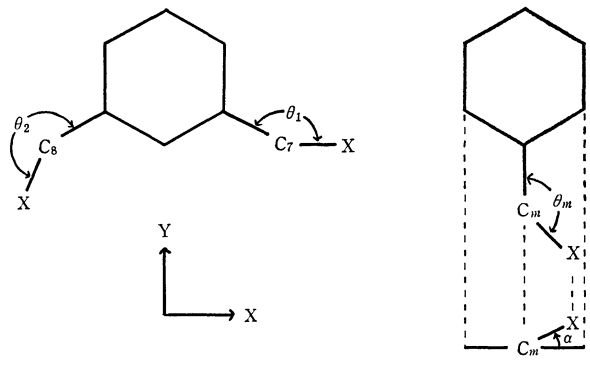

Fig. 3. Coordinate system (right-handed system), the methylene bond angles (θ_i's), and the dihedral angles between the central phenylene group and that of a side methylene bond (α_i's) in *m*-$C_6H_4(CX)_2$.

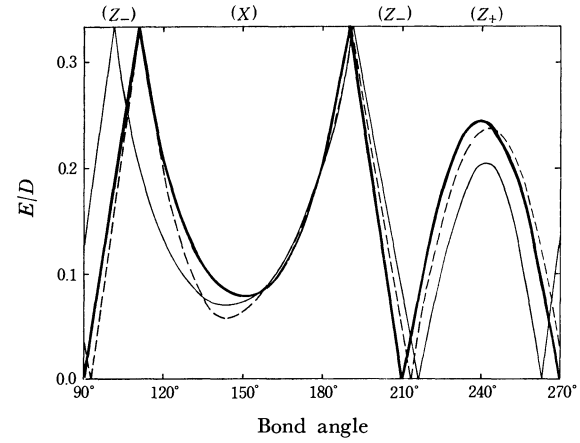

Fig. 4. The ratio of E/D of *m*-$C_6H_4(CX)_2$ calculated with only the intratomic interaction with $\theta_1=\theta_2$ in the cases of $\alpha_1=\alpha_2=0°$ (bold full line), $\alpha_1=\alpha_2=30°$ (fine full line), and $\alpha_1=-\alpha_2=30°$ (fine broken line). The letters X, Z_+, and Z_- on the top of the figure imply that the set of axes (x, y, z) in Eqs. (1) and (2) should take the sets of directions, respectively, (Y, Z, X), (X, Y, Z), and (Y, X, Z) shown in Fig. 3.

7) For example, compare Figs. 4 and 5 of Ref. 3 with the bold lines in Figs. 4 and 5 of this paper.

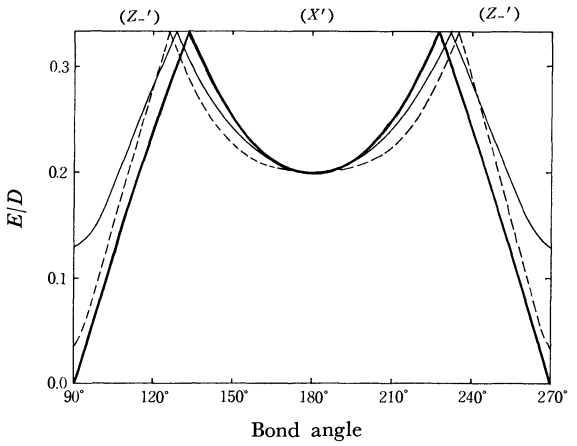

Fig. 5. The ratio of E/D of m-$C_6H_4(CX)_2$ calculated with only the intratomic interaction when $\theta_1+\theta_2=360°$ in the cases of $\alpha_1=\alpha_2=0°$ (bold full line), $\alpha_1=\alpha_2=30°$ (fine full line), and $\alpha_1=-\alpha_2=30°$ (fine broken line). The letters X' and Z_-' on the top of the figure imply that the set of axes (x, y, z) in Eqs. (1) and (2) are close to the sets of directions, (Y, Z, X) and (Y, X, Z) respectively, shown in Fig. 3. In the case of $\alpha_1=\alpha_2=0°$, the z axis ($\theta_1\geq 129°$) or the x axis ($\theta_1<129°$) makes angle of $90°-\theta_1/2$ counterclockwise with the X axis in Fig. 3.

of $|E|/|D|$ appear by changing α_1 and α_2 under the conditions of $|D|\geq 3|E|$ and $E/D\geq 0$. In these cases, the uncertainty is not large near the observed ratio of E/D ($\simeq 0.275$) [*i.e.* $\theta_1=\theta_2\simeq 185°$ and $\theta_1\simeq 140°$, $\theta_2\simeq 220°$]. This might show that the conclusion obtained in the previous work[3] on the spin quintet radicals is fairly reasonable. In general, however, one should take the influence of the relative orientation among methylene bonds into consideration for discussing the electron spin-spin interaction in molecular multiplets with several methylene bonds.

Some Remarks

Recently, Bernheim *et al.*[8] reported values of D and E for the methylene radical (CH_2) in matrix [$|D|/\boldsymbol{hc}=0.69$ cm^{-1}, $|E|/\boldsymbol{hc}=0.003$ cm^{-1}]. A similar result was also obtained by Wasserman *et al.*[9] If the present procedure is applied to these values, the –C– bond angle may be near 170° which is much larger than the estimated values of the triplet ground states of phenylmethylene and diphenylmethylene ($\sim$145°) and the quintet ground states of *m*-phenylene-*bis*-methylene and *m*-phenylene-*bis*-phenylmethylene ($\sim$140°). Wasserman *et al.*[9] showed that if the effect of the partial rotation in the matrix is included the –C– bond angle is 136° which is fairly close to that of these radicals. Further, they reported that the D and especially the E value considerably decrease by such a partial rotation and that the extrapolated $D/\boldsymbol{hc}$ value yields 0.93 cm^{-1} for an immobile methylene radicals. These evidences do not contradict the results we obtained, and suggest the necessity of further investigations of spin multiplet radicals with methylene bonds.

Most of the numerical calculations were carried out on HITAC 5020E at the Computer Centre, The University of Tokyo.

Appendix

Spin-Spin Interaction in Phenylmethylene. There were some numerical errors in the calculation of planar phenylmethylene in a previous paper.[2] The revised result given herewith is closely connected with the present work on diphenylmethylene. As can be seen in Fig. 6, the general

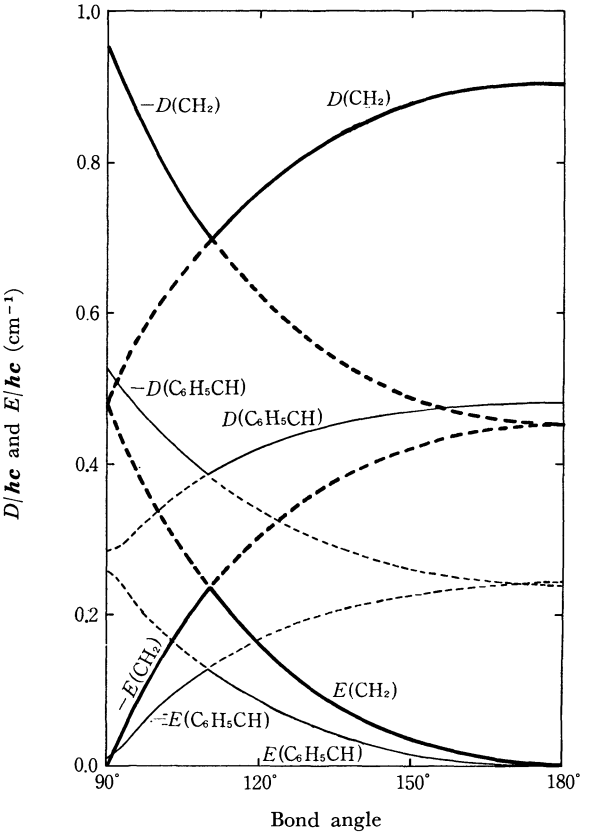

Fig. 6. D and E values of methylene (bold lines) and of phenylmethylene (fine lines). For large (small) –C– bond angles, the y (z) axis of fine-structure tensor [or Eqs. (1) and (2)] is perpendicular to the molecular plane. Dotted lines show their extensions [the revised figure of Fig. 1 in Ref. 2].

tendency of the angular dependence of D and E values does not differ much from the previous result. However, the most possible –C– bond angle is obtained near $\theta=145°$ where the calculated E/D value coincides with the observed ratio of $|E|/|D|=0.046$.[10] For large (small) –C– bond angles, the principal axes of fine-structure tensor [or those in Eqs. (1) and (2)] are as follows: the x axis is closely directed to the bisector of the –C– bond angle, the y (z) axis is perpendicular to the molecular plane, and the z (y) axis is perpendicular to the other axes. The deviation from the z (y) axis from the symmetry axis of the carbon skeleton in the phenylmethylene is given in Table 1.

8) R. A. Bernheim, H. W. Bernard, P. S. Wang, L. S. Wood, and P. S. Skell, *J. Chem. Phys.*, **53**, 1280 (1970).

9) E. Wasserman, W. A. Yager, and V. J. Kuck, *Chem. Phys. Lett.*, **7**, 409 (1970).

10) A. M. Trozzolo, R. W. Murray, and E. Wasserman, *J. Amer. Chem. Soc.*, **84**, 4990 (1962).

TABLE 1. DEVIATION OF $z^{a)}$ (OR $y^{b)}$) AXIS FROM THE SYMMETRY AXIS OF THE CARBON SKELETON IN THE PHENYLMETHYLENE[c)]

-C- bond angle	180°	165°	150°	135°	120°	105°	90°
Deviation	0.0°	8.0°	16.0°	24.0°	32.0°	40.6°	0.0°

a) For large -C- bond angles.
b) For small -C- bond angles.
c) The revised table of Table 1 in Ref. 2.

BULLETIN OF THE CHEMICAL SOCIETY OF JAPAN, VOL. 44, 2638—2642 (1971)

Molecular Structure and Phase-shift of Tetramethyllead as Studied by Gas Electron Diffraction

Takeo OYAMADA*, Takao IIJIMA, and Masao KIMURA
Department of Chemistry, Faculty of Science, Hokkaido University, Sapporo
(Received March 25, 1971)

The molecular structure of tetramethyllead has been determined by the sector-microphotometer method of gas-phase electron diffraction. The structure parameters determined by a least-squares analysis on molecular intensities are, with estimated limits of error, as follows; r_g(Pb–C)=2.238±0.009 Å, r_g(Pb···H)=2.72±0.06 Å, r_g(C···C)=3.66±0.07 Å, and r_g(C–H)=1.08±0.02 Å. The experimental cut-off point was nearly 37 in q value for the 42.0 keV electrons; this was not in sufficient agreement with the theoretical value as calculated from the Thomas-Fermi-Dirac potential for Pb and from the Hartree-Fock potential for C. Moreover, the experimental background showed a significant deviation from its theoretical counterpart in the region of small q values. This discrepancy has not been accounted for even by the use of scattering factors based on a relativistic SCF calculation, or by the correction for the polarization effect available at present.

The electron diffraction study of tetramethyllead (abbreviated to TML) was previously carried out by Wong and Schomaker[1] by use of the visual technique. They pointed out that the use of the complex atomic scattering factors of Ibers and Hoerni,[2] instead of the first Born scattering factors, was essential to the interpretation of the electron-diffraction pattern of TML, which contains both heavy (Pb) and light (C, H) atoms. The effect of the phase-angle difference of the atomic scattering factors, occasionally called the phase-shift, had already been elucidated by Schomaker and Glauber.[3] Wong and Schomaker attempted the first experimental test of the then newly-calculated table of Ibers and Hoerni. They determined the molecular structure of TML to be r(Pb–C)=2.20_3±0.01_0 Å and r(Pb–H)=2.79±0.01 Å. The first cut-off point was determined as q^c_{Pb-C}=38.5±1.5 for the 39.7 keV electrons; they remarked that this was slightly larger than the theoretical value 35.8 obtained from the table of Ibers and Hoerni, which was based on the Thomas-Fermi potential. When the present study was initiated, it was anticipated that the use of the phase angles calculated by the Thomas-Fermi-Dirac (TFD) potential instead of by the Thomas-Fermi potential would improve the consistency between the experimental and theoretical cut-off points. Thus, the present investigation has the purpose of performing a more quantitative examination of the phase-effect as well as making a more precise determination of the structure parameters, which became possible by the use of a modern diffraction unit and by means of the microphotometric processing of the photographic plates.

Experimental

The sample of TML was kindly supplied by Mr. Y. Fujiwara of the Central Technical Research Laboratory, Nippon Oil Co., Ltd., in the form of toluene blend. (Blending with toluene is necessary in order to stabilize the TML. The rate of the blending of TML and toluene was about 2 to 3). The separation of toluene (mp −95°C) from TML was achieved by utilizing the higher melting point of TML (mp −30°C) as follows. In order to protect TML from oxidation by air, the blend was placed in a flask purged with a flow of dry nitrogen gas. It was then slowly cooled in a dry ice-acetone bath under gentle stirring in order to avoid rapid crystallization. This cooling process was continued for about three hours until nearly two-thirds of the total content had solidified. Then the liquid part (toluene) was removed by decantation. This process of separation was repeated three times. The sample thus obtained was then assumed to have sufficient purity, since it has been reported that a series of several freezings and decantations raises the purity of TML to above 99%.[4]

The separated TML was transferred into a glass sample holder in a dry box filled with nitrogen gas. The whole

* Present address: Sumitomo Chiba Chemical Company, Ltd., Anegasaki, Chiba.

1) C. Wong and V. Schomaker, *J. Chem. Phys.*, **28**, 1007 (1958).
2) J. A. Ibers and J. A. Hoerni, *Acta Crystallogr.*, **7**, 405 (1954).
3) V. Schomaker and R. Glauber, *Nature* **170**, 290 (1952).
4) The separation and purification were carried out by referring to a technical report privately communicated by Mr. Fujiwara of Nippon Oil Co., Ltd.

procedure of separation and purification was carried out just before taking photographs. Since TML is a strong toxicant, full caution was used during the experimental procedures by following the advice in the Manual prepared by Ethyl Corporation.

Diffraction patterns were taken by means of a unit reported elsewhere,[5] with an r^3-sector at the camera length of 24.43 cm. The experimental conditions were as follows; accelerating voltage, ~42.0 kV; sample pressure, ~17.5 Torr; exposure time, 40~50 sec; electron-beam current, ~0.2 μA; and room temperature, 18°C. In order to make the calibration of the accelerating voltage, the diffraction patterns of carbon disulfide were taken just before taking those of the sample in the same sequence of exposures.

The optical densities of the diffraction photagraphs were measured by means of a double-beam microphotometer connected to an integral digital voltmeter. The data covered the range of $q=12$—62.

Analysis

The optical densities (0.25—0.50) were converted to the total intensities by assuming the proportionality between density and electron intensity. After the correction for the imperfection of the sector shape had been applied, the total intensities were interpolated at integral q values by Lagrange's method of three-point interpolation and were leveled by the theoretical background function. The experimental backgrounds and molecular intensities were determined by the calculation of the radial distribution curve and its inverse Fourier trans formation in the range of $r \leqq 0.8$ Å. In the calculation of the radial distribution curves, Bartell's correction for non-nuclear scattering[6] was modified in order to avoid difficulty arising from the large phase-angle difference. The method follows that of our previous paper.[7] The factors $\chi_{tj}=\mu_{tj}\cos\Delta\eta_{tj}$ were replaced by the following approximate functions:

$$\chi_{Pb,C} = 1.527 \cos\left\{0.1251\left(\frac{\pi}{10}q\right)\right\}$$

$$\chi_{Pb,H} = 1.933 \cos\left\{0.1488\left(\frac{\pi}{10}q\right)\right\}$$

$$\chi_{C,C} = 4.247 \exp\left\{-0.0143\left(\frac{\pi}{10}q\right)^2\right\}$$

$$\chi_{C,H} = 6.302 \exp\left\{-0.0135\left(\frac{\pi}{10}q\right)^2\right\}$$

$$\chi_{H,H} = 8.569 \exp\left\{-0.0133\left(\frac{\pi}{10}q\right)^2\right\}$$

The b value in the damping factor $\exp(-bq^2)$ was taken to be 0.00065.

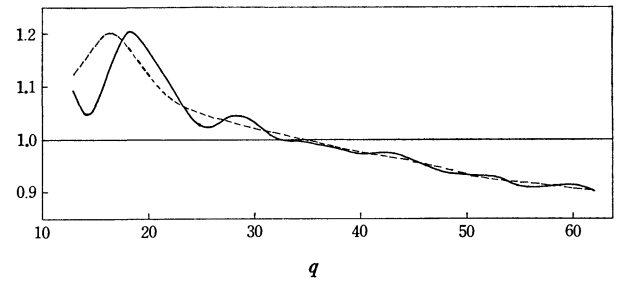

Fig. 1. Total intensity and experimental background of TML leveled by the theoretical background based on the TFD potential for Pb.

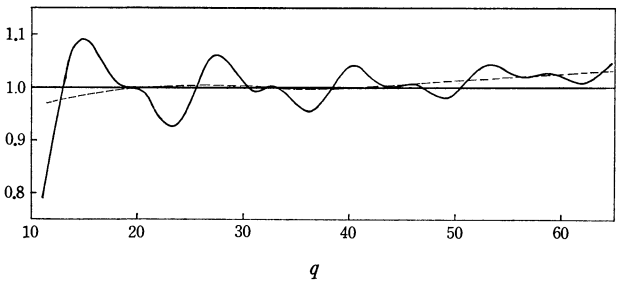

Fig. 2. Total intensity and experimental background of carbon disulfide leveled by the theoretical background.

One of the leveled total intensities and its background thus obtained are shown in Fig. 1 for TML[8] and in Fig. 2 for carbon disulfide, the reference molecule. The theoretical backgrounds were calculated by the use of elastic and inelastic scattering factors taken from the literature.[9-11] As is shown in Fig. 1, the background of TML rises sharply in the region of q values less than 19; this tendency is different from that of the theoretical value, which is a straight horizontal line at 1.00. On the other hand, the background of carbon disulfide, shown in Fig. 2, is not so different from its theoretical counterpart, except for the tailing up at large q values. This discrepancy in the background will be discussed in the next section.

The experimental molecular intensities obtained from the three best plates were analysed by the standard least-squares method.[12] The theoretical molecular intensity was calculated by the following equation, in which the notations have the usual significance:

$$qM(q) = k\sum_{ij}{}' A_{tj}\mu_{tj}\cos\Delta\eta_{tj}\exp\left\{-\frac{1}{2}\left(\frac{\pi}{10}q\right)^2 l_{tj}^2\right\} \times \sin\left[\frac{\pi}{10}q\left\{r_{atj}-\left(\frac{\pi}{10}q\right)^2\kappa_{tj}\right\}\right]$$

The index of resolution k, the distance r_a and the mean amplitude l were determined by the least-squares fitting of the theoretical expression to the experimental intensities. The nine parameters, the index of resolu-

5) Y. Murata, K. Kuchitsu, and M. Kimura, *Japan J. Appl. Phys.*, **9**, 591 (1970).

6) L. S. Bartell, L. O. Brockway, and R. H. Schwendeman, *J. Chem. Phys.*, **23**, 1854 (1955).

7) H. Fujii and M. Kimura, This Bulletin, **43**, 1933 (1970).

8) Numerical experimental data of the leveled total intensity have been deposited with the Chemical Society of Japan. (Document No. 7113). A copy may be secured by citing the document number and by remitting, in advance, ¥ 100 for photoprint. Pay by check or money order payable to: Chemical Society of Japan.

9) a) M. Kimura, S. Konaka, and M. Ogasawara, *J. Chem. Phys.*, **46**, 2559 (1967); b) M. Ogasawara, S. Konaka, and M. Kimura, *ibid.*, **50**, 1488 (1969).

10) C. Tavard, D. Nicolas, and M. Rouault, *J. Chim. Phys.*, **64**, 540 (1967).

11) L. Bewilogua, *Physik. Z.*, **32**, 740 (1931).

12) a) K. Hedberg and M. Iwasaki, *Acta Crystallogr.*, **17**, 529 (1964); b) Y. Morino, K. Kuchitsu, and Y. Murata, *ibid.*, **18**, 549 (1965).

tion, the distances and the mean amplitudes of Pb–C, Pb···H, C···C, and C–H atom pairs were adjusted without any constraint among them. All the non-bonded C···H and H···H pairs were ignored because of the negligibly small contribution of these terms. The asymmetry parameters κ for bonded pairs were fixed at the values estimated by the diatomic approximation:[13]

$$\kappa = \frac{1}{6}al^4\left\{1+\frac{8\varepsilon}{(1+\varepsilon)^2}\right\}, \quad \varepsilon = \exp\left(-\frac{h\nu}{kT}\right).$$

The Morse anharmonicity parameters, a, were assumed to be 1.7 Å^{-1} for the Pb–C atom pair and 2.0 Å^{-1} for the C–H atom pair.[14] The characteristic frequencies ν were taken to be 475 and 2998 cm^{-1} for Pb–C and C–H, respectively.[15] The estimated values were 49×10^{-7} Å^3 for κ_{Pb-C} and 123×10^{-7} Å^3 for κ_{C-H}. The parameters κ for the non-bonded pairs were assumed to be zero.

The results of the least-squares adjustment for the three plates were in excellent consistency with one another, as is shown in Table 1. The error matrix is shown in Table 2. The final values of the interatomic distances r_g and mean amplitudes are given in Table 3. The total limits of error were estimated by following the procedure described in previous papers.[7,16] The experimental molecular intensity and the theoretical one calculated by the best-fit parameters are shown in Figs. 3 and 4.

Table 1. Results of the least-squares analysis[a] (r_a and l in Å units)

		σ_1[b]	σ_2[b]
k	0.947	0.035	0.026
r_a(Pb-C)	2.2364	0.0034	0.0017
l(Pb-C)	0.0550	0.0049	0.0023
r_a(Pb···H)	2.7102	0.0232	0.0065
l(Pb···H)	0.1739	0.0181	0.0081
r_a(C···C)	3.6455	0.0264	0.0117
l(C···C)	0.1726	0.0218	0.0040
r_a(C-H)	1.0791	0.0073	0.0062
l(C-H)	0.0868	0.0099	0.0094

a) The averages of the results of three plates are listed.
b) The definitions of σ_1 and σ_2 are given in Ref. 12(b).

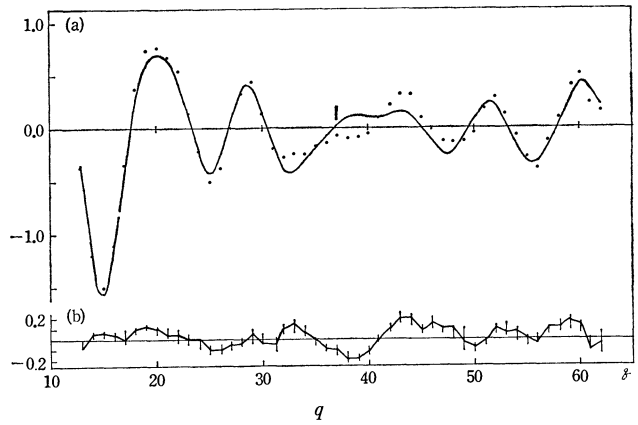

Fig. 3. (a) Molecular intensity of TML. Dots for experimental values and solid curve for the best-fit theoretical intensity. The heavy vertical bar at $q=37$ shows the experimental cut-off point for the Pb-C term. (b) The residuals. Vertical bars indicate the random scattering of residuals among six observed molecular intensities.

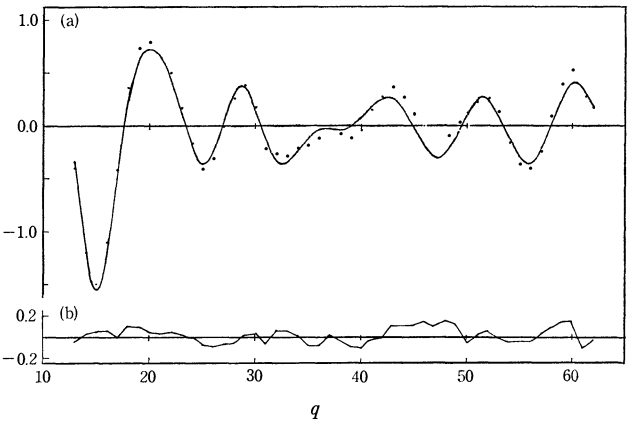

Fig. 4. (a) Molecular intensity of TML. Theoretical curve calculated by use of modified phase-angles for Pb (solid curve) and experimental values (dots). (b) The residuals.

Table 2. Error matrix[a]

	r_a(Pb-C)	l(Pb-C)	r_a(Pb···H)	l(Pb···H)	r_a(C···C)	l(C···C)	r_a(C-H)	l(C-H)	k
r_a(Pb-C)	62	22	130	7	−74	15	16	34	100
l(Pb-C)		87	120	−64	−73	72	16	59	184
r_a(Pb···H)			414	253	−289	152	54	152	469
l(Pb···H)				335	226	−201	15	−116	−341
r_a(C···C)					400	−151	−42	−93	−299
l(C···C)						338	11	95	276
r_a(C-H)							128	−41	65
l(C-H)								171	227
k									657

a) Elements of the matrix are given by $\sigma_{ij}=\mathrm{sgn}(\boldsymbol{B}^{-1})_{ij}\{|(\boldsymbol{B}^{-1})_{ij}|\boldsymbol{V}'\boldsymbol{P}\boldsymbol{V}/(N-m)\}^{1/2}$, where the notations follow Ref. 12(a). Units ($\times10^{-4}$) for r_a and l are Å and for the index of resolution k dimensionless.

13) K. Kuchitsu, This Bulletin, **40**, 505 (1967).
14) E. R. Lippincott and R. Schroeder, *J. Chem. Phys.*, **23**, 1131 (1955).
15) J. A. Jackson and J. R. Nielsen, *J. Mol. Spectrosc.*, **14**, 320 (1964).
16) S. Konaka and M. Kimura, This Bulletin, **43**, 1693 (1970).

Table 3. Distances and mean amplitudes of TML with estimated limits of error (in Å)

	r_g	l
Pb-C	2.238±0.009	0.055±0.012
Pb···H	2.721±0.058	0.174±0.045
C···C	3.656±0.066	0.173±0.055
C—H	1.083±0.020	0.087±0.025

A remarkable result seen in Fig. 3 is that the general features of the experimental molecular intensity are rather different from those of the theoretical curve in the region of q=35—44. This was systematically reproduced in each of the molecular intensities from the three plates. The reproducibility is demonstrated by the vertical bars in Fig. 3(b). Thus, the deviation has been considered to be significant, although its amount at each observed point is roughly twice the random scattering of data observed in current studies of other molecules using the same apparatus and analytical procedure. The cut-off points for the Pb–C and Pb···H bond pairs lie in this region. However, the contributions of the Pb···H and other terms to the molecular intensity are smaller in this region than that of the Pb–C term. The theoretical value for the first cut-off point, q^c_{Pb-C}, defined by $\Delta\eta_{Pb-C}=\pi/2$ at q^c_{Pb-C}, is 39.8 for the 42.0 keV electrons, according to the calculation based on the TFD potential for Pb and the Hartree-Fock potential for C.

Discussion

Structure. The bond angles, θ(CPbC) and θ(PbCH), calculated by use of the final values of the r_g distances are 109.5°±3.6° and 104.6°±5.4° respectively. Although the θ angle does not necessarily correspond to the geometrical conformation,[17] no further refinement was attempted on account of the large uncertainties of the non-bonded distances. The obtained θ(CPbC) value merely indicates the overall consistency of the present results with the symmetry of the molecule.

Mean Amplitudes. The vibrational mean amplitudes of TML were calculated by the following two simplified models: (a) A five-atom molecule with *Td* symmetry, where the methyl group was replaced by a point of mass; (b) A five-atom molecule, $PbCH_3$, with C_{3v} symmetry. In each of these models, a simple Urey-Bradley force field was determined from the normal frequencies observed by Jackson and Nielsen.[15] For the *Td*-model, the skeletal normal modes were selected from the observed frequencies. For the C_{3v}-model, the observed frequencies were assessed by considering the correlation between *Td* and C_{3v}. If nearly equivalent frequencies were found in the A_1 and F_2 species in the original assignment by Jackson and Nielsen, an average of them was taken; it was assumed to be an A_1 mode in the local C_{3v} molecule. Similarly, those found in both E and F_2 were assessed to be E-mode frequencies in the C_{3v}-model.

The values of these *observed* frequencies and those calculated by the use of the determined force constants are listed in Table 4. The calculated values of the mean amplitudes are shown in Table 5. In spite of the above simplification, the calculated values have sufficient accuracy because of the heavy central atom in TML. By comparing Tables 5 and 3, it may be seen that the observed mean amplitudes are in fair agreement with the calculated values.

Table 4. Vibrational frequencies of TML (in cm^{-1})

Td-model	obsd.[a]	calcd.	C_{3v}-model	obsd.[a]	cald.
A_1	462	462	A_1	2918	2931
				1153	1167
E	145	145		462	459
F_2	475	477	E	2998	2985
	130	131		1430	1431
				785	777

a) Values selected from the observed frequencies by Jackson and Nielsen.[15] (see Text)

Table 5. Calculated mean amplitudes of TML at 288°K (in Å)

	l(Pb-C)	l(C···C)	l(C-H)	l(Pb···H)
Td-model	0.0594	0.154	—	—
C_{3v}-model	0.0570	—	0.0782	0.138

Scattering Factors and Phase-angles. It has been found that the discrepancy in the molecular intensity shown in Fig. 3 can be alleviated if the cut-off point of the Pb–C term is moved to q=37, which is indicated by a heavy bar in Fig. 3. The phase-angle η of the Pb atom was modified in such a way as to make $\Delta\eta_{Pb-C}=\pi/2$ at q=37 by simply shifting the whole η *vs.* q curve slightly upwards. As is shown in Fig. 4, the general features of the theoretical intensity as calculated from the modified phase-angles are in better agreement with those of the experimental intensity in the region of q=35—44. This suggests that the phase-angles of Pb as calculated from the TFD potential are slightly smaller than the exact values.

In Table 6 are listed the structure parameters obtained by a least-squares fitting of the theoretical expression by the use of the modified phase-angles. The r_a distances are in agreement with the previous values given in Column II within their standard deviations.

Table 6. Results of the least-squares analysis of plate 3 (r_a and l in Å)

	I[a]	II[b]
k	0.992	0.961
r_a(Pb-C)	2.2368	2.2372
r_a(Pb···H)	2.735	2.720
r_a(C···C)	3.637	3.625
r_a(C-H)	1.077	1.081
l(Pb-C)	0.068	0.055
l(Pb···H)	0.182	0.158
l(C···C)	0.171	0.180
l(C-H)	0.091	0.089

a) By use of modified phase angles (see Text).
b) Previous results by use of unmodified phase angles.

17) K. Kuchitsu, *ibid.*, **44**, 96 (1971).

The mean amplitudes are slightly larger, but they are consistent within the total limits of error.

In the hope of accounting for the discrepancy in the background and the cut-off point, the scattering factors based on the relativistic SCF calculation and the correction for the polarization effect were employed. The background of TML was calculated by the use of the relativistic scattering factor for Pb, which was computed by Schäffer, Yates, and Bonham[18] from Liberman's Dirac-Slater atomic potentials. The phase-angles η taken from their table are graphically shown in Fig. 5. The background is shown in Fig. 6. The original values for the 40 keV electrons were converted to those for 42 keV by assuming that the $|f|$ and η curves, regarded as functions of the scattering angle, show no significant difference between 40 and 42 keV. Therefore, only the scaling of abscissa was corrected for the voltage difference in getting the $|f|$ and η *vs.* q curves for 42 keV. The validity of this assumption was confirmed by comparing the TFD scattering factors for 40 and 42 keV.

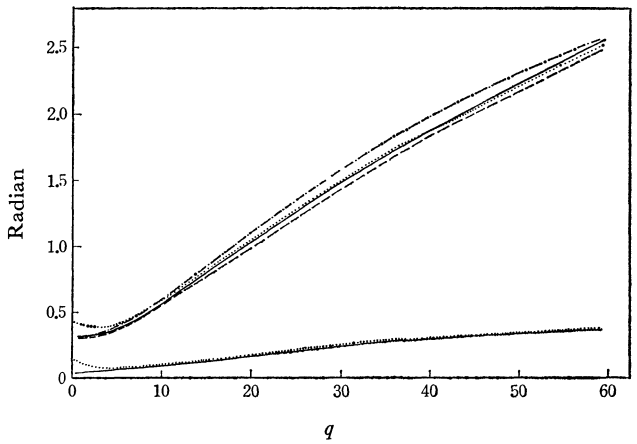

Fig. 5. Comparison of phase-angles; —— TFD for Pb and Hartree-Fock for C, ····· TFD corrected for the polarization effect for Pb and Hartree-Fock corrected for the polarization effect for C, ---- Dirac-Slater for Pb, —·—· modified phase-angle for Pb.

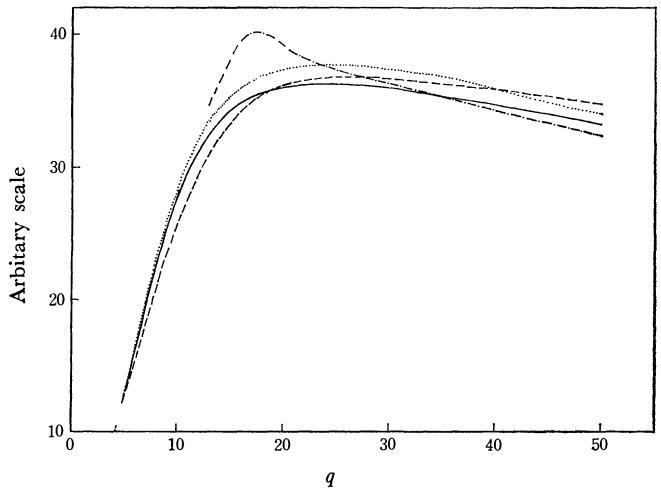

Fig. 6. Comparison of the background functions of TML. The elastic scattering factor of Pb is based on the atomic potential of TFD (——), TFD corrected for the polarization (·····), and Dirac-Slater (----). The observed background normalized to TFD at $q=35$ is shown by (—·—·).

18) L. Schäffer, A. C. Yates, and R. A. Bonham, *J. Chem. Phys.* to be published.

The correction for the polarization effect was computed by a program kindly offered by Professor Bonham.[19] As the numerical parameters for the computation, the following values of the total inelastic scattering cross sections σ_{inel} were employed, namely, $\sigma_{inel}(\mathrm{Pb})=0.2684$ Å^2 and $\sigma_{inel}(\mathrm{C})=0.0531$ Å^2. By this program, the corrections for the real part ΔR^{pol} and the imaginary part ΔIm^{pol} due to the polarization effect were computed. For the Pb atom, these values were added to the real part R^{TFD} and the imaginary part Im^{TFD} of the TFD scattering factors, and the magnitude $|f|$ and the phase angle η of the corrected scattering factors were obtained by:

$$|f| = \{(R^{\mathrm{TFD}}+\Delta R^{\mathrm{pol}})^2 + (Im^{\mathrm{TFD}}+\Delta Im^{\mathrm{pol}})^2\}^{1/2}$$

$$\eta = \tan^{-1}\{Im^{\mathrm{TFD}}+\Delta Im^{\mathrm{pol}})/(R^{\mathrm{TFD}}+\Delta R^{\mathrm{pol}})\}.$$

For the C atom, the same procedure was applied to the Hartree-Fock scattering factors.

The phase-angles and the backgrounds are compared in Figs. 5 and 6. It can be seen from these figures that the theoretical improvement by the use of relativistic scattering factors and the polarization correction is too small to account for the experimental results. The deviation in the background is too large in amount and opposite in direction to be interpreted in terms of the effect of chemical-bond formation.[20] In the diffraction studies of $HgCl_2$[21] and $BiCl_3$[22], however, the experimental results showed no discrepancy from the TFD-based theoretical values in either the cut-off points or the backgrounds. Thus, the possibility that this discrepancy is common in heavy atoms seems to have been excluded. Should the discrepancy observed in the present study be in fact real, then it must presumably be due to something specific to the lead atom. A future investigation of this matter in both experimental and theoretical aspects is to be hoped for.

The authors wish to thank Mr. Yasuo Fujiwara of Central Technical Research Laboratory, Nippon Oil Co., Ltd. for his kind supply of the sample and information on safe handling of the material. They also thank Professor Russell A. Bonham, Indiana University, for his allowing them to use his program and numerical results before publication. The authors are indebted to Dr. Shigehiro Konaka for his helpful discussions, Mr. Koji Igarashi for his help in the early stage of this work and Miss H. Hayasaka for her typing the manuscript. Numerical computations were performed on a FACOM 230—60 of the Hokkaido University Computing Center and also on a FACOM 270—20 of Professor Kimio Ohno's laboratory, Hokkaido University, to whom the authors' thanks are also due.

19) R. A. Bonham, *Phys. Revs. A*, **3**, 298 (1971).

20) a) T. Iijima, This Bulletin, **39**, 843 (1966); b) D. A. Kohl and R. A. Bonham, *J. Chem. Phys.*, **47**, 1634 (1967).

21) K. Kashiwabara and M. Kimura, The 24th Annual Meeting of the Chemical Society of Japan, (April, 1971) Osaka.

22) S. Konaka and M. Kimura, *ibid.*

Molecular Structure of Dimethyltin Dichloride as Studied by Gas-electron Diffraction

Hideji Fujii[1] and Masao Kimura

Department of Chemistry, Faculty of Science, Hokkaido University, Sapporo

(Received March 25, 1971)

The molecular structure of dimethyltin dichloride was determined by the sector-microphotometer method of electron diffraction to be as follows: r_g(Sn-Cl)=2.327±0.003 Å, r_g(Sn-C)=2.108±0.007 Å, and r_g(C-H)=1.113±0.020 Å, and all the valency angles were near 109.5°. In comparison with the Sn-Cl distances in the series of $Sn(CH_3)_{4-n}Cl_n$, as determined previously by the same method, a regular bond contraction in going from $Sn(CH_3)_3Cl$ to $SnCl_4$, as pointed out previously by Skinner and Sutton, was ascertained.

Many structural studies have recently been published of a series of molecules, $Sn(CH_3)_{4-n}Cl_n$(n=0, 1, 2, 3, 4), by various experimental techniques, *e.g.*, dipole moment measurements,[2,3] NMR,[2,4] Mössbauer effects,[5] NQR,[6] X-ray crystal analysis,[7] and studies of the vibrational spectra[8-11] and electron diffraction.[12-14] In these studies, relations between bond lengths and other physical quantities have often been discussed.

As for the interatomic distances in these molecules in the gaseous state, Skinner and Sutton once determined tin-chlorine bond lengths by the visual method and found that the magnitude of bond contraction from the sum of the covalent radii increased with an increase in the number of halogen atoms.[12] However, these data involve large uncertainties inherent in the visual method and may even be incorrect owing to the ignorance of phase differences between Sn and Cl, and Sn and C, atoms.[15]

In order to get a more profound insight into the molecular structures of this series of molecules, it is essential to have more precise, up-to-date information regarding the bond lengths in free molecules. Recently, the present authors have determined the Sn-Cl bond length in $SnCl_4$ to be 2.281±0.004 Å,[13] a value which was 0.03 Å shorter than the value determined by the visual method.[14] In the present paper we will report on the bond lengths of dimethyltin dichloride as determined by the sector-microphotometer method.

Experimental

A pure sample of dimethyltin dichloride (mp 108°C) was kindly provided by Professor Toshio Tanaka of the Osaka University. Photographs were taken by the apparatus in our laboratory equipped with an r^3-sector[16] and a high-temperature nozzle[17] at two camera lengths, 258.90 cm (long camera length) and 123.90 cm (short camera length). The accelerating voltage was about 42.25 kV. The sample was sublimed by maintaining the nozzle temperature at 85—88°C. The scale factors were determined by reference to the diffraction patterns of carbon disulfide taken under the same experimental conditions.[13] The photographs were recorded on Fuji Process Hard Plates with exposure times of 40 to 70 sec and a beam current of 0.3 μA, and were developed at 20°C for 5 min with a FD-131 developer diluted twice. Seven plates from the long camera length and four plates from the short camera length were selected, and their optical densities were measured as reported previously;[13] the observed points covered the range of q=8—60 and q=25—110 for the respective camera lengths. Because of the damping effects due to intramolecular vibrations and the phase differences of scattered beams from the Sn, Cl, and C atoms, the molecular scattering in a range of q beyond about 80 falls in amplitude down to the order of random fluctuations of the observed total intensities. Therefore, the structure parameters were determined by employing the optical densities of the plates from the long camera length.

Analysis and Results

The reductions of the molecular intensities, $qM(q)^{exptl}$, were done following the method described in our previous paper, unless otherwise stated.[13] The experimental leveled intensity, I_T, and the experimental background, I_B, curve, the $qM(q)^{exptl}$ and the difference curve of the experimental and theore-

1) Present address: Central Research Laboratory, Hitachi Ltd., Kokubunji, Tokyo.

2) J. Lorberth and H. Nöth, *Chem. Ber.*, **98**, 969 (1965).

3) E. V. Van Den Berghe and G. P. Van der Kelen, *J. Organometal. Chem.*, **6**, 515 (1966).

4) J. R. Holmes and H. D. Kaesz, *J. Amer. Chem. Soc.*, **83**, 3903 (1961).

5) N. N. Greenwood, P. G. Perkins, and D. H. Wall, *Symposia of the Faraday Society*, **1**, 51 (1967).

6) P. J. Green and J. D. Graybeal, *J. Amer. Chem. Soc.*, **89**, 4305 (1967).

7) J. D. Graybeal and D. A. Berta, *Nat. Bur. Stand. Spec. Publ.*, No 301, 393 (1967).

8) W. F. Edgell and C. H. Ward, *J. Mol. Spectrosc.*, **8**, 343 (1962).

9) a) P. Taimsalu and J. L. Wood, *Spectrochim. Acta*, **20**, 1043 (1964); b) *ibid.*, **20**, 1357 (1964).

10) F. K. Butcher, W. Gerrard, E. F. Mooney, R. G. Rees, H. A. Willis, A. Anderson, and H. A. Gebbie, *J. Organometal. Chem.*, **1**, 431 (1964).

11) a) R. J. H. Clark and C. S. Williams, *Spectrochim. Acta*, **21**, 1861 (1965); b) R. J. H. Clark, A. G. Davies, R. J. Puddephatt, W. Ramsay, and R. Forster Laboratories, *J. Chem. Soc., A*, **1968**, 1828.

12) H. A. Skinner and L. E. Sutton, *Trans. Faraday. Soc.*, **40**, 164 (1944).

13) H. Fujii and M. Kimura, This Bulletin, **43**, 1933 (1970).

14) R. L. Livingston and C. N. R. Rao, *J. Chem. Phys.*, **30**, 339 (1959).

15) Critical importance of the consideration of the phase difference has been pointed out by the present authors in their study of $SnCl_4$.[13]

16) Y. Murata, K. Kuchitsu, and M. Kimura, *Jap. J. Appl. Phys.*, **9**, 591 (1970).

17) M. Ogasawara and M. Kimura, Symposium on Molecular Structure, Chemical Society of Japan, October, 1967.

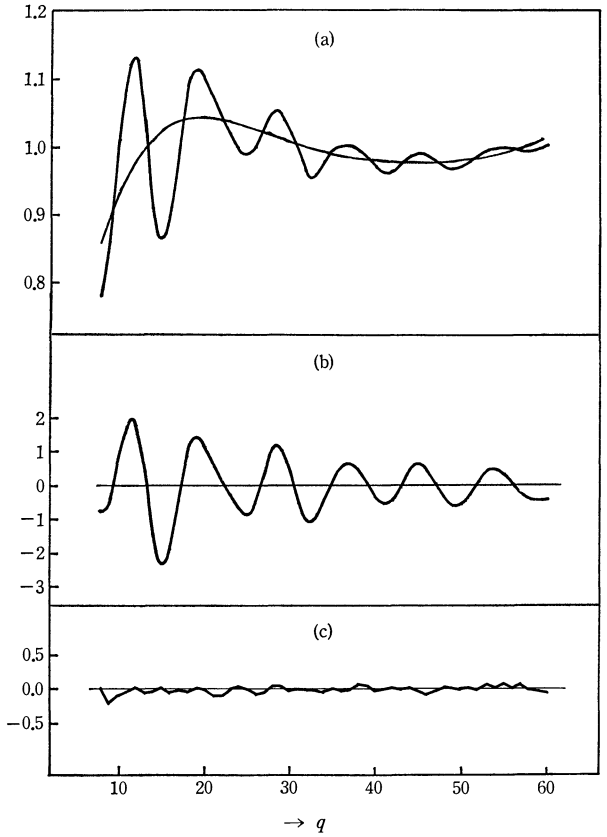

Fig. 1. (a) The experimental leveled intensity and the background curve; (b) The observed molecular intensities $qM(q)^{exptl}$; and (c) The difference curve of the experimental and theoretical molecular intensities.

tical $qM(q)$ values for an arbitrarily selected plate are shown in Figs. 1(a), (b), and (c) respectively.[18] The elastic and inelastic scattering factors used were taken from the references.[19-23]

The radial distributions, $f(r)$, were calculated by the use of the correction term for the non-nuclear scattering:[13]

$$\Delta qM(q) = \sum_{i,j}{}' A_{ij} \sin\left(\frac{\pi}{10} q r_{ij}\right) \exp(-a_{ij}q^2) \times \{\chi_{ij} - \mu_{ij} \cos(\Delta\eta_{ij})\},$$

with the following correction functions, χ_{ij}:

$$\chi_{HH} = 1.20 + 1.65 \exp(-0.00017\, q^2) + 3.1 \exp(-0.0015\, q^2),$$

$$\chi_{HC} = 1.08 + 1.10 \exp(-0.00013\, q^2) + 2.5 \exp(-0.0020\, q^2),$$

$$\chi_{HCl} = 0.20 + 2.80 \exp(-0.0002\, q^2),$$

$$\chi_{HSn} = 0.88 \cos(0.3206\, q) + 0.8 \exp(-0.0020\, q^2),$$

$$\chi_{CC} = 1.32 + 1.78 \exp(-0.0006\, q^2),$$

$$\chi_{CCl} = 0.90 + 1.40 \exp(-0.00034\, q^2)$$

$$\chi_{CSn} = 0.90 \cos(0.02523\, q) + 0.5 \exp(-0.0014\, q^2),$$

$$\chi_{ClCl} = 1.40$$

and

$$\chi_{ClSn} = \cos(0.01415\, q).$$

A trial background was revised after Karles' non-negativity criterion by the Fourier inverse transformation of the difference between the observed and calculated radial distributions, $\Delta f(r)$, below $r=1.10$ Å. In these calculations, it was assumed that the molecule has C_{2v} symmetry, that each methyl group has a three-

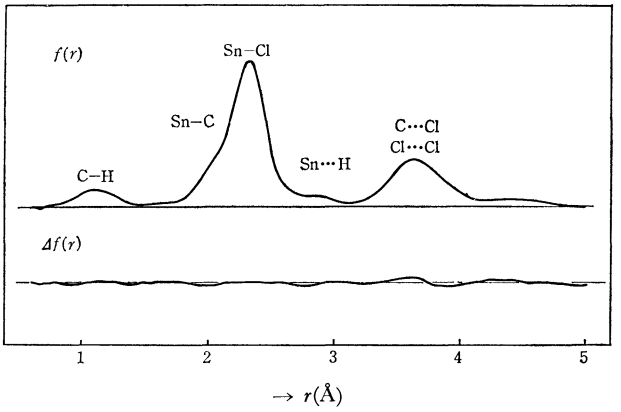

Fig. 2. The experimental radical distribution, $f(r)$, and the difference between the calculated and the experimental radial distributions, $\Delta f(r)$.

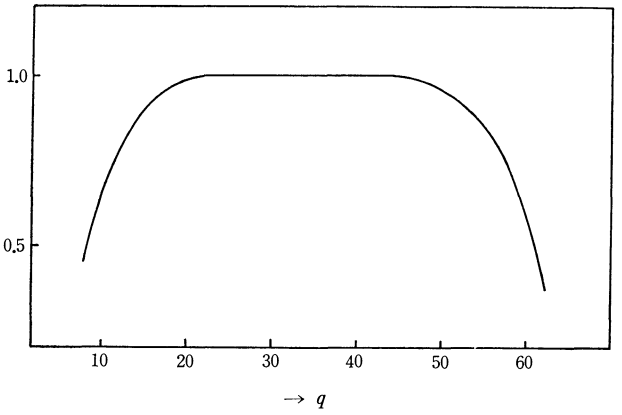

Fig. 3. The weight function used for the least-squares adjustments.

18) The experimental data of the leveled total intensities have been filed with the Chemical Society of Japan (Document Number 7114). A copy may be secured by citing the Document Number and by remitting, in advance, ¥400 for photoprints. Pay by check or money order payable to: Chemical Society of Japan.

19) a) M. Kimura, S. Konaka, and M. Ogasawara, *J. Chem. Phys.*, **46**, 2559 (1967); b) M. Ogasawara, S. Konaka, and M. Kimura, *ibid.*, **50**, 1488 (1969).

20) C. Tavard, D. Nicolas, and M. Rouault, *J. Chim Phys.*, **64**, 540 (1967).

21) L. Bewilogua, *Physik. Z.*, **32**, 740 (1931).

22) R. F. Pohler and H. P. Hanson, *J. Chem. Phys.*, **42**, 2347 (1965).

23) Elastic scattering factors have been calculated by Cox and Bonham on the bases of relativistic wave functions (*J. Chem. Phys.*, **47**, 2599 (1967)). As far as the Sn atom is concerned, these scattering factors are significantly larger than those used by us[19] and also by the Manchester group, and consequently, give a larger phase difference for the Sn–Cl atom pair. However, new scattering factors based upon relativistic wave functions, which are to be published by Schäffer, Yates, and Bonham in the Journal of Chemical Physics. The authors are indebted to Professor Bonham for making use of their table for a comparative purpose.

fold symmetry about the bond joining the methyl group to the Sn atom and is staggered to the opposite Sn–Cl bond, and that all the valence angles are 109.5°. On these assumptions, the molecular parameters were evaluated appropriately from the observed $f(r)$ curve and the results of the least-squares adjustments. The final $f(r)$ and $\Delta f(r)$ values obtained from the I_T's shown in Fig. 1 are depicted in Fig. 2.

The structural parameters were determined by the least-squares method applied to the observed molecular intensities with a diagonal weight matrix (Fig. 3). The asymmetry parameters, κ, for the H···H, C···H, and Cl···H pairs were set equal to zero, while the others were fixed at the following values:

κ_{CH}	122,	κ_{ClCl}	178,
κ_{SnC}	26,	κ_{ClC}	257,
κ_{SnCl}	18,	κ_{SnH}	313, (in 10^{-7} Å^3);
κ_{CC}	281,		

These values were estimated by the method applied to $SiCl_4$ by Morino and Murata.[24,25] The interatomic distances for the non-bonded H···H, C···H, Cl···H, and C···C pairs, which make very little contributions to the scattering intensity, were constrained in the r_a structure, and their mean amplitudes were fixed at values roughly estimated from those in analogous compounds. Least-squares adjustments were then performed for the thirteen parameters listed in Table 1. The fluctuations of the adjusted values during least-squares iterations were the largest for r(Cl···Cl) or l(Cl···Cl). Therefore, the iterations were terminated when the fluctuations of the adjusted r(Cl···Cl) and l(Cl···Cl) values became less than 1.5 percent and when the parameter values for the C–H, Sn–C, and Sn–Cl atom pairs converged within 10, 4, and 1×10^{-4} Å respectively.

The value for each parameter was obtained by averaging the results from the seven plates. The parameter values thus obtained and their estimated standard deviations, σ_1 and σ_2, are shown in Table 1, where the interatomic distances are given in terms of r_g and where the σ_1 and σ_2 have the same significances as in our previous paper.[13]

As may be seen in Table 1, the non-bonded interatomic distances could not be determined with satisfactory accuracy. If the valence angles are evaluated from the r_g values in Table 1, we get the values of 107.5±3.9° for ∠ClSnCl and 109.8±1.2° for ∠ClSnC; hence, they are indistinguishable from the tetrahedral angle. The most probable bonded interatomic distances and mean amplitudes are reproduced in Table 2, together with their limits of error, which include the random errors and the errors due to the uncertainty of the scale factor. The former errors were taken as 2.5 times the larger of σ_1 and σ_2, while the latter were estimated to be 0.1% of the interatomic distances.

Table 1. Results of the least-squares adjustments[a]

Parameter	Average[b]	σ_1[b]	σ_2[b]
k	0.967	0.018	0.019
r_g(C-H)	1.1119	0.0068	0.0088
l (C-H)	0.0792	0.0077	0.0058
r_g(Sn···H)	2.6703	0.0303	0.0120
l (Sn···H)	0.1701	0.0166	0.0085
r_g(C···Cl)	3.6314	0.0101	0.0034
l (C···Cl)	0.1223	0.0062	0.0014
r_g(Sn-C)	2.1089	0.0034	0.0031
l (Sn-C)	0.0748	0.0073	0.0079
r_g(Cl···Cl)	3.7549	0.0366	0.0146
l (Cl···Cl)	0.2248	0.0325	0.0109
r_g(Sn-Cl)	2.3266	0.0010	0.0014
l (Sn-Cl)	0.0607	0.0025	0.0018
∠ClSnCl = 107.5±3.9°[c]			
∠ClSnC = 109.8±1.2°[c]			

a) Index of resolution k is dimentionless; r_g and l in Å.
b) The definitions of σ_1 and σ_2 were given in Ref. 13.
c) Estimated from the r_g values.

Table 2. Bond distances and mean-amplitudes (in Å)

	r_g	l
C-H	1.112±0.022	0.079±0.019
Sn-C	2.109±0.009	0.075±0.020
Sn-Cl	2.327±0.004	0.061±0.006

Calculation of the Mean-square Amplitudes

Since the low-lying fundamental frequencies and their assignments were uncertain,[8–11] the Nujol-mull spectra were measured in the region below 400 cm^{-1}. Some of them are reproduced in Table 3. Edgell and Ward[8] assigned the Raman lines at 344 cm^{-1} and 135 cm^{-1} to accidentally degenerate Sn–Cl stretching modes and skeletal bending modes respectively. However, such degeneracies seem unlikely. Taimsalu and Wood[9b] studied the effect of the environment on the vibrational frequencies of the $Sn(CH_3)_{4-n}Cl_n$ series and concluded that dimethyltin dichloride associated strongly in the solid state and that its Sn–Cl stretching frequencies shifted markedly towards the lower-frequency side. On the contrary, our solid spectra in this range displayed an intense band at 357 cm^{-1} with a shoulder near 349 cm^{-1} and broad, weak bands at 306 and 325 cm^{-1}. It seems that the strong band and its shoulder at 357 and 349 cm^{-1} are to be assigned to the Sn–Cl stretching frequencies, and that the two weak bands at the lower frequencies are overtone and combination bands. The assignment of the $SnCl_2$ deformation mode is also ambiguous. Taimsalu and Wood assigned bands at 124 cm^{-1} and 129 cm^{-1} to the bending and rocking modes respectively,[9a] whereas Butcher *et al.* assigned a band at 121 cm^{-1} to the bending mode.[10] If one follows the assignment made by Taimsalu and Wood, the observed frequencies in our spectra may be assigned as is shown in the last column of Table 3. The general

24) Y. Morino and Y. Murata, This Bulletin, **38**, 104 (1965).
25) The κ values for non-bonded pairs are possibly smaller than the listed values. However, the use of smaller values does not change the results of the present least-squares adjustment substantially.

Table 3. The observed skeletal vibrational frequencies of $Sn(CH_3)_2Cl_2$ (in cm^{-1})

			Edgell[a] and Ward. R. L.	Taimsalu[b] and Wood. IR. Nm.	Butcher[c] *et al.* IR. Sol.[e]	Present[d] study. IR. Nm.
A_1	Sn-C	stretch	521	515 s	524	
	Sn-Cl	stretch	344	307 vs	356 sh	349 sh
	$Sn-Cl_2$	bending	135	124 w	121	116
	SnC_2	bending	135	158 w		158
B_1	Sn-C	stretch	566	567 s	560	
	$SnCl_2$	rocking	135	129 m		126
B_2	Sn-Cl	stretch	344	332 vs	361 s	357 s
	$SnCl_2$	rocking	135	146 s		143

R: Raman; IR: Infrared; L: liquid; Nm: Nujol mull; Sol: solution; vs: very strong; s: strong; m: medium
a) Ref. 8. b) Ref. 9a. c) Ref. 10.
d) In addition to the bands listed in this column, two weak, broad bands were observed at 325 and 306 cm^{-1}. See text.
e) Cyclohexane solutions were used except for the band at 560 cm^{-1}, which was observed in carbondisulfide solution.

pattern of our frequencies is similar to that assigned by Clark *et al.*[11b] Although the frequencies and their assignments of the low-lying fundamental vibrations remain questionable, the mean-square amplitudes were calculated with rigid CH_3 groups and by the use of the Urey-Bradley force field. The results are listed in Table 4. It was necessary to introduce a non-zero force constant, G(SnC.SnC), in order to fit the calculated Sn-C stretching frequencies to the observed ones to the extent shown in Table 4. In spite of some uncertainties in the vibrational spectra and in spite of the approximations involved in the present calculations, the mean amplitudes thus obtained may be considered to have sufficient accuracy for comparative use. The experimental and theoretical values listed in Table 2 and 4 have similar orders of magnitude.

Table 4. The Urey-Bradley force constants, the calculated skeletal vibrational frequencies and the calculated mean amplitudes

Force constants (md/Å)		Frequencies[a] (cm^{-1})			Mean Amplitudes (Å)	
K(Sn-CH_3)	2.188	A_1	515	(515)	Sn-Cl	0.054
K(Sn-Cl)	1.866		116	(116)	Sn-C	0.054
H(ClSnCH_3)	0.036		158	(158)	C···C	0.147
H(CH_3SnCH_3)	0.062		345	(349)	Cl···Cl	0.133
H(ClSnCl)	0.049	B_1	567	(567)	C···Cl	0.146
F(CH_3-Cl)	0.086		123	(126)		
F(CH_3-CH_3)	0.038	B_2	360	(357)		
F(Cl-Cl)	0.109		146	(143)		
κ	0.044					
G(SnC SnC)	−0.168					

a) Values in parentheses are observed frequencies.

Contraction of the Sn–Cl Bonds

Table 5 presents the molecular structures of the $Sn(CH_3)_{4-n}Cl_n$ series (n=0,1,2,3,4) as determined by electron diffraction.

It is evident in Table 5 that there is a regular contraction of Sn-Cl bond lengths from $Sn(CH_3)_3Cl$ to $SnCl_4$; that is, the magnitudes of the contractions of r(Sn-Cl) from the sum of the single-bond covalent radii, 2.39 Å, are 0.04, 0.06, 0.09, and 0.11 Å for the molecules of n=1,2,3, and 4 respectively. The values of the Sn-C distances, except for $Sn(CH_3)_4$, are equal in their marginal errors, while the Sn-C distance in $Sn(CH_3)_4$ is close to those in methyl stannanes, *e.g.*, r_g(Sn-C)=2.150±0.003 Å for $Sn(CH_3)_2H_2$ and 2.147±0.004 Å for $Sn(CH_3)_3H$.[26] The relations between the bond lengths and other physical properties for these compounds present interesting problems which will have to be solved in the future.

Table 5. The bond distances of $Sn(CH_3)_{4-n}Cl_n$ as determined by electron diffraction

Compound	Visual method			Sector-microphotometer method		
	Sn-C (Å)	Sn-Cl (Å)	Ref.	Sn-C (Å)	Sn-Cl (Å)	Ref.
$Sn(CH_3)_4$				2.134±0.007		27
$Sn(CH_3)_3Cl$	2.19±0.03	2.37±0.03	12	2·106±0.006	2.351±0.007	26
$Sn(CH_3)_2Cl_2$		2.34±0.03	12	2.108±0.007	2.327±0.003	present study
$Sn(CH_3)Cl_3$	2.19±0.05	2.32±0.03	12	2.104±0.016	2.304±0.003	26
$SnCl_4$		$2.31\pm0.01_5$	14		2.281±0.004	13

26) K. McAloon, private communication. The authors wish to thank Dr. K. McAloon for permission to quote his results prior to publication.
27) A preliminary result by the present authors.

We would like to thank Professor Toshio Tanaka of Osaka University for providing us with the sample. We are also indebted to Professor Takao Iijima and Dr. Shigehiro Konaka for their helpful suggestions and discussions, and to Mr. Tomoichi Kamo for his help in the infrared work. The calculations were performed with an electronic computer, FACOM 270—20, in the laboratory of Professor Kimio Ohno, to whom our thanks are also due.

BULLETIN OF THE CHEMICAL SOCIETY OF JAPAN, VOL. 41, 2647—2649 (1971)

A New Method of Solubility Determination of Hydrolyzing Solute — Solubility of Benzyl Chloride in Water

Ryuichiro Ohnishi and Kozo Tanabe

Research Institute for Catalysis and Department of Chemistry, Faculty of Science, Hokkaido University, Sapporo

(Received April 1, 1971)

A method of determining the solubility of a solute with a considerable rate of hydrolysis and small solubility in water was devised. The method consists of measurements of the hydrolysis rate below or at saturation solubility, the rate constants and order of reaction, and analysis of kinetic data. The solubility of benzyl chloride in water was found to be 33.1 mg/100 m*l* at 4.5°C, 49.3 at 20°C, and 55.5 at 30°C. Solubility of benzal chloride and benzotrichloride was calculated to be 25 mg/100 m*l* at 30°C and 5.3 at 5°C, respectively, by utilizing the kinetic data given in literature

In a course of a study on the relative reactivity of benzyl chloride, benzal chloride and benzotrichloride,[1] it became necessary to obtain the solubility of the compounds in water. The only datum is the solubility of benzyl chloride at 30°C obtained by means of extraction with ether from the saturated aqueous solution.[2] However, since chlorine compounds having small solubility in water hydrolyze fairly fast during extraction, the extraction method does not seem to be reliable. We therefore attempted to determine the solubility by analyzing the kinetic data of hydrolysis. The rate, the rate constant, and the order of the hydrolysis reaction of benzyl chloride were measured at 4.5, 20, and 30°C and the solubility was determined by a new method. The solubility of benzal chloride and benzotrichloride determined by the same method using known kinetic data is also reported.

Principle of Kinetic Determination of Solubility

Let us express the rate V of a hydrolysis reaction by the equation

$$V = \sum_i k_i[S]^i \qquad (1)$$

where i is the order of reaction, k_i the rate constant of ith order reaction, and $[S]$ the concentration of a solute.

First, a sufficiently large amount of a solute is dissolved in water forming a liquid phase of a solute, the concentration of the solute in water being kept constant at constant temperature with the saturation solubility S_s. The rate V_s at saturation solubility can be measured keeping the solute concentration constant during the rate measurement. The rate V is then measured at various solute concentrations below saturation solubility, and k_i and i are determined from the data by the usual method. Saturation solubility S_s is now obtained from the observed V_s, k_i, and i by the following equation.

$$V_s = \sum_i k_i[S_s]^i \qquad (2)$$

The principle of this method is simple and can be applied to the solubility measurement of a solute whose solubility is so small and solvolysis rate so great that the application of usual methods is difficult. However, there are several restrictions for the measurement. 1) The solubility of a solute must be so small that the phase of the solute can exist together with the solvent phase. 2) The rate of dissolution of a solute into a solvent must be sufficiently fast in comparison with that of solvolysis. 3) The solubility or the rate of solvolysis must not be influenced by any product of solvolysis. If the influence cannot be neglected, correction of the influence should be made. 4) The rate of solvolysis in solute phase must be negligibly small compared with that in solvent phase. If not, correction should be made.

Experimental

Since benzyl chloride decomposes in water to form benzyl alcohol and hydrogen chloride,[1,2] the reaction was followed by observing the increase in proton concentration.

As soon as benzyl chloride was added to water in a glass reaction vessel equipped with a tefron-coated magnetic stirrer and placed in a water bath, the mixture was vigorously stirred in order to dissolve the benzyl chloride and start the reaction immediately. The pH change of the solution due to hydrolysis was measured with a Hitachi-Horiba M-5 type pH meter (accuracy: 0.03 pH) whose glass electrode was dipped in the solution. The temperature of the reaction mixture was maintained at 20±0.01°C, 30±0.01°C, and 4.5±0.2°C. In the measurement of V, the amount of benzyl chloride

1) K. Tanabe, *Nippon Kagaku Zasshi*, **87**, 629 (1966).
2) S. C. J. Olivier, *Rec. Trav. Chim.* **53**, 891 (1934).

which is smaller than that of the saturation solubility was used for the reaction, while a sufficiently large amount above S_s was used for the measurement of V_s.

An approximate value of the saturation solubility necessary to undertake experiments at solute concentration below saturation solubility was obtained by the following method. A certain amount (a mg) of benzyl chloride is dissolved in a certain amount (b ml) of acetone which can dissolve both benzyl chloride and water and in which benzyl chloride does not solvolyze. Some amount (c ml) of water is then added dropwise from a burette into the solution until the solution shows white turbidity. An approximate value of the solubility in acetone-water is thus calculated by the equation, $a/(b+c)\times 100$ (mg/100 ml). An approximate solubility in pure water is obtained by extrapolating the plots of $a/(b+c)\times 100$ against the volume %, $(c/b+c)\times 100$, of added water.

Benzyl chloride (extra pure reagent of Wako Junyaku Co., Ltd.) was distilled in a vacuum. Deionized water was used.

Results and Discussion

Rate V_s at Saturation Solubility. The pH change due to the hydrolysis of benzyl chloride in the saturated aqueous solution plotted against reaction time is shown in Fig. 1. The change is fast in the initial stage of the reaction but slow later. Since the increase in the amount of added benzyl chloride above saturation solubility value caused an increase in the amount of the first sharp pH change but did not change the inclination of the straight line at the later stage, the sharp pH change is considered to be due to the hydrolysis of impurities such as benzal chloride and benzotrichloride whose rate constants,[3] $(292\pm2)\times 10^{-5}$ sec^{-1} at 30°C and $(387\pm5)\times 10^{-5}$ sec^{-1} at 5°C, are much larger than that of benzyl chloride, $(58.3\pm 0.1)\times 10^{-5}$ sec^{-1} at 60°C. The amount of impurities was estimated to be 0.1 mol% from the amount of the sharp pH change. The rate V_s was thus obtained from the inclination of the straight line appearing later, the values being listed in Table 1. The fact that V_s was almost constant independent of the amount of added benzyl chloride indicates that the hydrolysis in the phase of benzyl chloride can be neglected. All calculations were made by employing the method of least square.

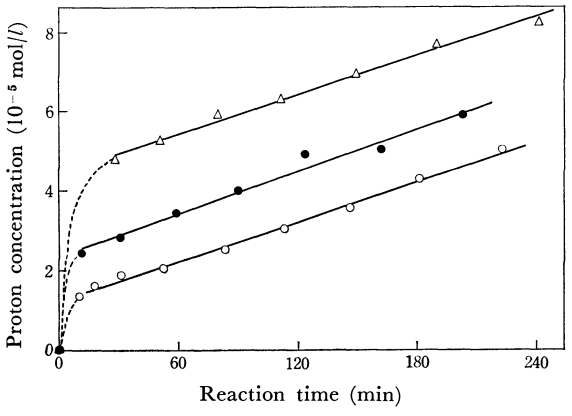

Fig. 1. Proton concentration *vs.* reaction time at 4.5°C.
-○- 0.5 ml of benzyl chloride in 300 ml of water
-●- 1 ml/300 ml -△- 2 ml/300 ml

Rate Constant k_i and Order of Reaction i. An approximate value of the solubility of benzyl chloride was 15 mg/100 ml of water at room temperature (Experimental). The reactions were carried out at several concentrations of benzyl chloride below the approximate solubility, and the initial rates $(dx/dt)_0$ were calculated from the curves obtained by plotting proton concentration against reaction time, where x is the concentration of proton formed by the hydrolysis at time t. The initial rates thus obtained at various initial concentrations a and at several temperatures are given in Table 2.

By plotting $\log(dx/dt)_0$ against $\log a$, the order of reaction was obtained to be 1.00 at 30°C, 1.11 at 20°C, and 1.17 at 4.5°C. At 20 and 4.5°C, second order reaction seems to take place together with first order reaction as represented by the equation

$$\left(\frac{dx}{dt}\right)_0 = k_1 a + k_2 a^2 \qquad (3)$$

where k_1 and k_2 are the rate constants of the first and second order reactions, respectively. Eq. (3) was justified by the fact that the plot of $(dx/dt)_0/a$ *vs.* a gave straight lines as shown in Fig. 2. The values of k_1 and

Table 1. Rate V_s at staturation solubility

Temp. (°C)	Volume (ml) Benzyl chloride	Volume (ml) Water	V_s (M/min)	Averaged values of V_s (M/min)
4.5	0.5	300	$(1.64\pm0.42)\times10^{-7}$	$(1.65\pm0.04)\times10^{-7}$
	1	300	$(1.77\pm0.10)\times10^{-7}$	
	2	300	$(1.62\pm0.07)\times10^{-7}$	
	5	100	$(1.56\pm0.12)\times10^{-7}$	
20	1	300	$(1.62\pm0.03)\times10^{-6}$	$(1.67\pm0.04)\times10^{-6}$
	1	300	$(1.63\pm0.04)\times10^{-6}$	
	2	300	$(1.86\pm0.07)\times10^{-6}$	
	2	300	$(1.71\pm0.06)\times10^{-6}$	
	5	100	$(1.80\pm0.05)\times10^{-6}$	
30	0.44	400	$(5.81\pm0.23)\times10^{-6}$	$(5.59\pm0.07)\times10^{-6}$
	0.55	400	$(5.65\pm0.11)\times10^{-6}$	
	1	400	$(5.57\pm0.10)\times10^{-6}$	
	10	200	$(5.23\pm0.24)\times10^{-6}$	

3) P. M. Laughton and R. E. Robertson, *Can. J. Chem.*, **37**, 1491 (1959).

Table 2. Initial rate

Temp. (°C)	a (M)	$(dx/dt)_0$, (M/min)
4.5	2.54×10^{-3}	$(1.59\pm0.04)\times10^{-7}$
	1.91×10^{-3}	$(1.09\pm0.03)\times10^{-7}$
	1.29×10^{-3}	$(6.42\pm0.24)\times10^{-8}$
	6.08×10^{-4}	$(2.81\pm0.13)\times10^{-8}$
20	2.63×10^{-3}	$(1.01\pm0.01)\times10^{-6}$
	2.53×10^{-3}	$(9.62\pm0.13)\times10^{-7}$
	1.58×10^{-3}	$(5.48\pm0.09)\times10^{-7}$
	1.27×10^{-3}	$(4.26\pm0.08)\times10^{-7}$
	5.95×10^{-4}	$(1.85\pm0.01)\times10^{-7}$
	2.77×10^{-4}	$(8.55\pm0.31)\times10^{-8}$
30	1.76×10^{-3}	$(2.02\pm0.09)\times10^{-6}$
	9.30×10^{-4}	$(1.11\pm0.05)\times10^{-6}$
	4.31×10^{-4}	$(5.65\pm0.44)\times10^{-7}$
	$3\cdot48\times10^{-4}$	$(3.92\pm0.26)\times10^{-7}$

k_2 obtained by Eq. (3) are given in Table 3. The activation energies and frequency factors calculated from the data are also given in Table 3.

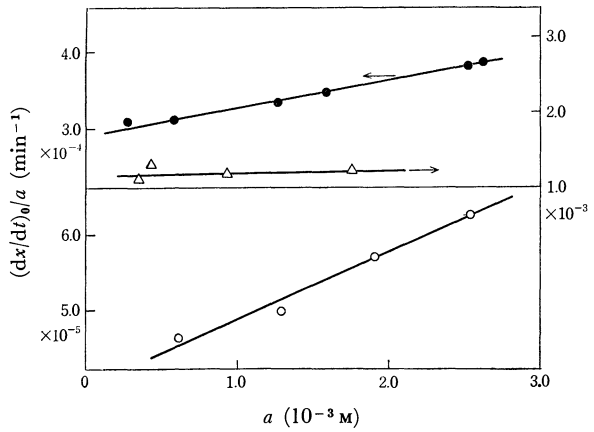

Fig. 2. Plots of $(dx/dt)_0/a$ against a.
-○- 4.5°C, -●- 20°C, -△- 30°C

Determination of Solubility. Solubility S_s of benzyl chloride is now calculated from the values of V_s, k_1, and k_2 according to the following equation.

Table 3. k_1 and k_2 and activation parameter

Temp. (°C)	k_1, (min^{-1})	k_2, ($M^{-1}\,min^{-1}$)
4.5	$(3.98\pm0.17)\times10^{-5}$	$(8.9\pm2.5\ )\times10^{-3}$
20	$(2.90\pm0.02)\times10^{-4}$	$(3.6\pm0.10)\times10^{-2}$
30	$(1.16\pm0.09)\times10^{-3}$	$(2.7\pm7.1\ )\times10^{-2}$
Activation energy (kcal/mol)	21.2±1.1	14.6±1.3
Frequency factor (sec^{-1})	12.2±0.8	9.4±1.0

Table 4. Solubility of benzyl chloride

Temp. (°C)	Solubility	
	M	mg/100 m*l*
4.5	$(2.61\pm0.09)\times10^{-3}$	33.1
20	$(3.89\pm0.08)\times10^{-3}$	49.3
30	$(4.4\ \pm1.0\ )\times10^{-3}$	55.5

$$V_s = k_1S_s + k_2S_s^2 \qquad (4)$$

The results are given in Table 4. The solubility value at 30°C is a little larger than 46.5 mg/100 m*l* obtained by Olivier.[2] The heat of dissolution calculated from the data in Table 4 was 4.05±0.44 kcal/mol.

Equation (4) allows us to calculate the degree of contribution of second order reaction to total hydrolysis reaction. The fractions of second order reaction, $k_2S_s^2/(k_1S_s+k_2S_s^2)$, are 36.9% at 4.5°C, 32.6 at 20°C, and 9.25 at 30°C, the values being higher at lower temperature.

The solubility of benzal chloride and benzotrichloride was calculated similarly by the present method, utilizing the kinetic data obtained by Ohnishi,[4] Tanabe and Sano,[5] and Laughton and Robertson,[3] and is shown in Table 5. Tables 4 and 5 reveal that with the increase of the number of chlorines of chlorinated phenylmethanes, their hydrolysis rate increases, but solubility decreases.

Table 5. Solubility of benzal chloride and benzotrichloride

	Temp. (°C)	V_s (M/min)	i	k_1 (sec^{-1})	S_s, mg/100 m*l*
Benzal chloride	30	2.77×10^{-4} a)	1	297×10^{-5} c)	25
Benzotrichloride	5	6.3×10^{-5} b)	1	387×10^{-5} c)	5.3

a) From Ref. 4, b) From Ref. 5, c) From Ref. 3.

4) R. Ohnishi, unpublished data.

5) K. Tanabe and T. Sano, *J. Res. Inst. Catalysis, Hokkaido Univ.*, **13**, 110 (1966).

A Further Study of the Scavengeable Electron Yield in the Radiolysis of Hydrocarbon Glasses at −196°C

Toyoaki KIMURA, Kenji FUEKI, and Zen-ichiro KURI

Department of Synthetic Chemistry, Faculty of Engineering, Nagoya University, Chikusa-ku, Nagoya

(Received April 8, 1971)

The yield of scavengeable electrons produced by γ-irradiation in mixtures of cyclopentane and methylcyclohexane at −196°C has been determined by electron-scavenging experiments with bromobenzene. It has been found that the maximum yield of scavengeable electrons in these mixture glasses increases with an increase in the cyclopentane concentration and that it reaches the total ionization yield in a liquid hydrocarbon. The implication of these results for the yield of radiation-induced ionization in condensed systems is discussed.

In order to determine the yield of electrons produced by ionizing radiations in nonpolar condensed systems, we must reply upon electron-scavenging experiments with some electron scavenger, because in such systems any direct method of observing solvent-trapped electrons, such as ESR and optical absorption, can only provide information about a small fraction of the electrons produced.

In a previous study[1] we have shown that bromobenzene can be used as an electron scavenger in hydrocarbons and have measured the yield of scavengeable electrons in methylcyclohexane(MCH), 3-methylpentane, cumene, and *t*-butylbenzene in the liquid state at 20°C and in the glassy state at −196°C. In that study it was found that the yield of scavengeable electrons in glassy hydrocarbons is much lower than that in liquid hydrocarbons. The possible causes for this difference in the electron yield were discussed in some detail. In the experiments with mixtures of isopentane and MCH at −196°C, we have shown that the yield of scavengeable electrons depends on the viscosity of the system, and suggested that the electron-solvent interaction would affect the yield of scavengeable electrons. However, because of the limitation of the solubility of bromobenzene in these mixtures, we could not determine the maximum yield of scavengeable electrons in isopentane-MCH glasses.

In this work we will extend such a study to mixtures of cyclopentane and MCH, where bromobenzene dissolves to a higher concentration, and will determine from the Schuler plot the maximum yield of scavengeable electrons in these mixture glasses.

Experimental

Materials. The methylcyclohexane was a product of Tokyo Kagaku Seiki (99.9%) and was used as received. The cyclopentane (a Nakarai Kagaku guaranteed reagent) was shaken with concentrated sulfuric acid in a separating flask, washed with distilled water, and then dried with sodium sulfate. After passage through a silica gel column, the cyclopentane was fractionally distilled before use. The bromobenzene (a Nakarai Kagaku guaranteed reagent) was passed through an activated alumina column and then fractionally distilled.

Sample Preparation. Each sample was degassed in a 10-mm glass tube by the freeze-pump-thaw technique and then sealed off.

Irradiation. Irradiation was performed with γ-rays from a ^{60}Co source. The dose delivered to the sample was 3.6×10^{19} eV/g.

Analysis. The yield of benzene produced was determined by means of a Hitachi K53 gas chromatograph with a flame ionization detector. The column used was *n*-hexatriacontane (4 mm×4 m).

Results and Discussion

A fraction of the electrons produced by γ-irradiation in liquid or glassy hydrocarbons containing bromobenzene are captured by bromobenzene to yield bromide anions and phenyl radicals. The phenyl radical thus produced immediately abstracts a hydrogen atom from a solvent molecule, even at −196°C, to form a benzene molecule and a solvent radical.[2]

$$RH \rightsquigarrow RH^+ + e^- \quad (1)$$

$$e^- + C_6H_5Br \rightarrow C_6H_5 + Br^- \quad (2)$$

$$C_6H_5 + RH \rightarrow C_6H_6 + R \quad (3)$$

It can be seen from Eqs. (2) and (3) that the yield of benzene produced corresponds to that of the electrons scavenged. It has been shown that the abstraction of a bromine atom by the hydrogen atom from bromobenzene does not occur to any appreciable extent.[3] The contribution to benzene formation of the neutralization reaction of the bromobenzene cation with a negative species can also be excluded at bromobenzene concentrations below about 0.1 M.[1]

In the present study we have measured the yield of benzene produced from bromobenzene in mixtures of cyclopentane (CP) and MCH γ-irradiated at −196°C as a function of the bromobenzene concentration. The compositions of these mixtures were varied over a wide range from pure MCH to a volume ratio of CP to MCH=7/4. Such a variation in the composition results in a substantial change in the viscosity of the system, although the viscosity is not known quantitatively. We have also measured the yield of benzene from bromobenzene in MCH at 20°C for comparison with the results obtained at −196°C.

These results are presented in Figs. 1 and 2 in a converted form to be described below. It can be seen from Fig. 1 that the yield of benzene at −196°C increase with an increase in the CP concentration at a

1) T. Kimura, K. Fueki, and Z. Kuri, This Bulletin, **43**, 3090 (1970).

2) S. Noda, K. Fueki, and Z. Kuri, *ibid.*, **41**, 2882 (1968).

3) J. M. Warman, K. -D. Asmus, and R. H. Schuler, *J. Phys. Chem.*, **73**, 931 (1969).

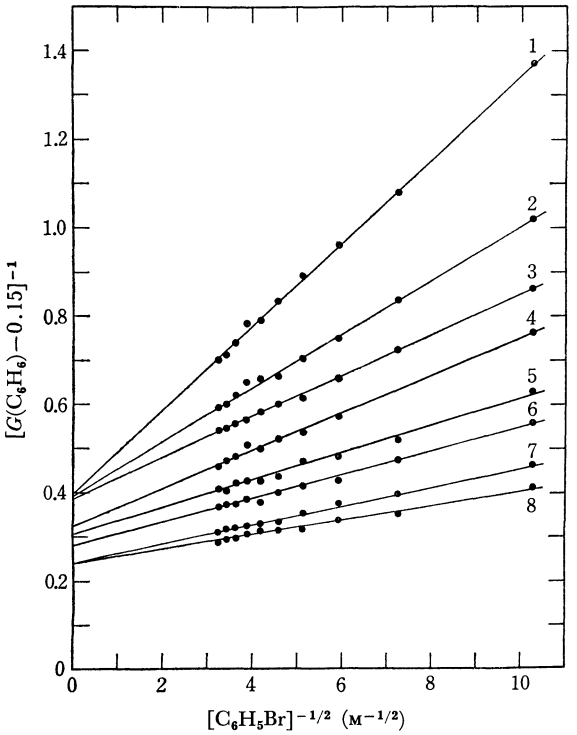

Fig. 1. Plot of $[G(C_6H_6)-0.15]^{-1}$ as a function of $[C_6H_5Br]^{-1/2}$ in CP-MCH mixtures containing bromobenzene at −196°C.
1: pure MCH, 2: CP/MCH=1/10, 3: CP/MCH=2/9, 4: CP/MCH=3/8, 5:CP/MCH=4/7, 6: CP/MCH=5/6, 7: CP/MCH=6/5, 8: CP/MCH=7/4.

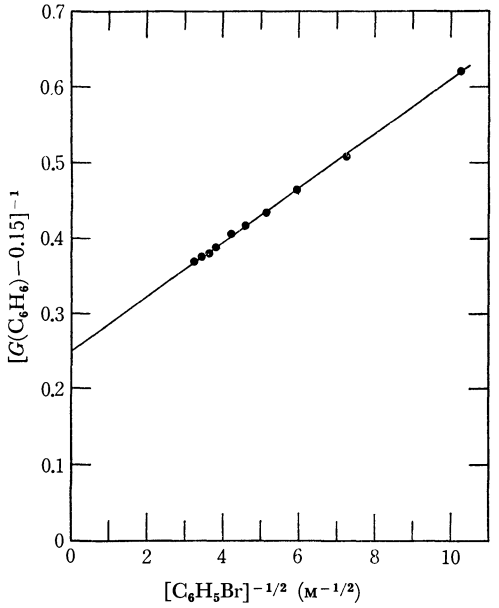

Fig. 2. Plot of $[G(C_6H_6)-0.15]^{-1}$ as a function of $[C_6H_5Br]^{-1/2}$ in MCH containing bromobenzene at 20°C.

specified concentration of bromobenzene. Here we have applied the semiempirical equation developed by Schuler and his coworkers[3] to our data on electron scavenging. The maximum yield of scavengeable electrons can be determined by using the following equation:

$$\frac{1}{G(C_6H_6)-G_{fi}}=\frac{1}{G_{gi}}+\frac{1}{G_{gi}\alpha_s^{1/2}}\frac{1}{[S]^{1/2}} \quad (4)$$

where G_{fi} and G_{gi} are the yield of free electrons and that of electrons which undergo geminate recombination respectively, where α_s is an empirical parameter, and where [S] is the molarity of the scavenger. Taking $G_{fi}=0.15$,[4] the values of $[G(C_6H_6)-0.15]^{-1}$ are plotted against $[C_6H_5Br]^{-1/2}$ in Figs. 1 and 2. The experimental data at both −196°C and 20°C fit straight lines well, as was to be expected from Eq. (4). From the intercepts of the straight lines, the maximum yields (G_m) of scavengeable electrons are determined as $G_m=G_{fi}+G_{gi}$. The values of α_s are obtained from the slopes of the straight lines. These values are listed in Table 1. The value of G_m in the CP-MCH mixtures at −196°C increases with an increase in the CP concentration or with a decrease in the matrix viscosity, reaching 4.28 for the mixtures with volume ratios of CP to MCH>1. This limiting value of G_m at −196°C is in agreement with the value of G_m in MCH at 20°C (4.15 G) within the limits of experimental error. The principal source of error in G_m at −196°C is perhaps in the dosimetry at this temperature.

Table 1. Scavengeable electron yields in CP-MCH mixtures at −196°C and MCH at 20°C

Irradiation temperature	Volume ratio of CP : MCH	G_m	α_s (M^{-1})
−196°C	pure MCH	2.65	18
−196°C	1 : 10	2.69	42
−196°C	2 : 9	2.73	69
−196°C	3 : 8	3.23	59[a]
−196°C	4 : 7	3.41	98
−196°C	5 : 6	3.72	110
−196°C	6 : 5	4.28	140
−196°C	7 : 4	4.28	190
20°C	pure MCH	4.15	48

a) This value is probably underestimated.

Recently, Shida[6] has reported the yields of radiation-induced ionization in a variety of organic systems at −196°C. He measured by optical absorption spectroscopy the disulfide anion produced on scavenging electrons in mixture glasses containing disulfide, obtaining $G=2.10$ for the yield of scavengeable electrons in aliphatic hydrocarbons. This value of 2.10 is compared with our value of 2.65 for MCH at −196°C. It is possible that this discrepancy arises partly from the different methods of extrapolating the experimental data adopted by the two studies. Nevertheless, both of these results indicate that the yield of scavengeable electrons produced in hard hydrocarbon glasses at −196°C is significantly lower than that in liquid hydrocarbons.

As may be seen in Table 1, the value of α_s at −196°C

4) The yield of free electrons was determined by the clearing-field method to be 0.155 for CP and 0.148 for cyclohexane at 23°C.[5]

5) W. F. Schmidt and A. O. Allen, *J. Phys. Chem.*, **72**, 3730 (1968).

6) T. Shida, *ibid.*, **74**, 3055 (1970).

increases with an increase in the CP concentration or a decrease in the matrix viscosity. The parameter, α_s, is given by the ratio of the second-order rate constant, k_s, for the electron scavenging process to the parameter, λ:[7]

$$\alpha_s = \frac{k_s}{\lambda} \tag{5}$$

λ is proportional to $D=D_+ + D_-$, where D_+ and D_- are the diffusion coefficients of the positive ion and the electron respectively. Since D_- is generally much greater than D_+, λ is approximately proportional to the diffusion coefficient of the electron, which is itself related to the electron mobility by the relation:

$$D_- = \frac{kT}{e} u_- \tag{6}$$

where u_- is the mobility of the electron; e, the electronic charge; k, the Boltzmann constant; and T, the absolute temperature. Thus, if k_s is nearly constant in these systems, the variation in values of α_s at -196°C may be ascribed to the change in the electron mobility; *i. e.*, the harder the matrix, the greater the mobility of the electron. We are tempted to state that, in the harder hydrocarbon glasses, the electrons behave more like "quasi-free" electrons, while in the softer glasses the electrons behave more like "solvated" electrons. This might be further related to the rate of molecular relaxation in the matrix, but our present knowledge on this problem is too little to provide any satisfactory explanation for this.

It may also be seen in Table 1 that the α_s for the softer glasses at -196°C is much greater than that for liquid MCH at 20°C. It should be noted, however, that the temperature can affect the diffusion coefficient, given by Eq. (6), if the mobility is kept constant, and can then affect α_s through Eq. (5). Thus, the value of α_s at -196°C is reduced by a factor of 4 for a constant mobility when the temperature is raised to 20°C. For example, a value of $\alpha_s=190$ for the softest glass at -196°C is reduced to 47 at 20°C, which is very close to the α_s for MCH at 20°C. This may indicate that the mobility of the electron in the softest glass studied almost reaches that in liquid MCH.

Such a consideration of α_s may be relevant to the interpretation of the yield of scavengeable electrons. The smaller value of α_s at a specified temperature implies a faster geminate recombination between positive ions and electrons at that temperature. Thus, it is likely that, in hard hydrocarbon glasses at -196°C, a substantial fraction of the electrons recombine with the geminate positive ions too fast to be captured by any electron scavengers, and that the Schuler plot is not necessarily applicable over a wide range of solute concentrations and that its simple extrapolation does not provide the total ionization yield in these systems. It should be noted, however, that the present results do not exclude the possibility that the initial ionization yield is substantially lower in hard hydrocarbon glasses at -196°C than in liquid hydrocarbons.

7) S. J. Rzad, P. P. Infelta, J. M. Warman, and R. H. Schuler, *J. Chem. Phys.*, **52**, 3971 (1970).

BULLETIN OF THE CHEMICAL SOCIETY OF JAPAN, VOL. 44, 2652—2660 (1971)

The Crystal Structure of Ascochlorin *p*-Bromobenzenesulfonate[1)]

Yoshiharu NAWATA* and Yoichi IITAKA

Faculty of Pharmaceutical Sciences, The University of Tokyo, Hongo, Bunkyo, Tokyo

**Research Laboratories, Chugai Pharmaceutical Co., Ltd., Takada, Toshima, Tokyo*

(Received April 20, 1971)

The structure of ascochlorin, $C_{23}H_{29}O_4Cl$, has been determined by the three-dimensional X-ray crystal structure analysis of ascochlorin *p*-bromobenzenesulfonate. The crystal is orthorhombic, space group $P2_12_12_1$, with four molecules in a unit cell of dimensions, $a=13.86$, $b=30.04$, and $c=6.82$ Å. The structure was solved by the heavy atom method and refined by the method of block-matrix least-squares. The final R value was 0.102 for 1627 independent reflexions. Ascochlorin consists of (3-chloro) orcylic aldehyde and (2,3,4-trimethyl) cyclohexanone moieties which are connected with each other through a zigzag chain of *trans*-(3-methyl)penta(2,4) diene. The cyclohexanone ring takes a typical chair form, and the intramolecular hydrogen bond exists in the orcylic aldehyde residue. The absolute configuration was determined by the anomalous dispersion method.

Ascochlorin is a new antibiotics obtained from the filter cake of fermented broth of Ascochyte viciae Libert,[2)] which exhibits significant inhibitory effect on the viral growth in cultured cells.[3)] Since the molecular structure of ascochlorin had not been known, the present X-ray analysis was undertaken. The terpenoid metabolite (named LL-Z1272-γ) with the same chemical structure as ascochlorin has been isolated from an unclassified Fusarium species.[4)] The crude products of ascochlorin containing both α and β forms are easily divided into each component by silica gel column chromatography. While the β form is syrup, the α form crystallizes as extremely fine

1) Presented at the Annual Meeting of the Chemical Society of Japan, Tokyo, April, 1970.

2) G. Tamura, S. Suzuki, A. Takatsuki, K. Ando, and K. Arima, *J. Antibiot.* (Tokyo), **21**, 539 (1968).

3) A. Takatsuki, G. Tamura, and K. Arima, *Appl. Microbiol.*, **17**, 825 (1969).

4) G. A. Ellestad, R. H. Evans, Jr., and M. P. Kunstmann, *Tetrahedron*, **25**, 1323 (1969).

TABLE 1. THE FINAL ATOMIC PARAMETERS AND THEIR STANDARD DEVIATIONS

x, y, and z are the fractional coordinates. The temperature factors are expressed in the form

$$T=\exp[-(\beta_{11}h^2+\beta_{22}k^2+\beta_{33}l^2+2\beta_{12}hk+2\beta_{13}hl+2\beta_{23}kl)].$$

The e.s.d.'s given in parentheses are in the units of the least significant digits given for the correponding parameters. To represent the correct absolute configuration, the parameters should be referred to a right handed set of axes.

Atom	x	y	z	β_{11}	β_{22}	β_{33}	β_{12}	β_{13}	β_{23}
Br	0.1959 (2)	0.1273 (1)	1.0663 (5)	0.0074 (2)	0.0010 (0)	0.0360 (9)	0.0004 (1)	0.0044 (4)	0.0020 (2)
C(1)	0.1822 (16)	0.1792 (7)	0.9059 (37)	0.0043 (14)	0.0012 (3)	0.0201 (76)	-0.0009 (5)	0.0051 (30)	-0.0012 (12)
C(2)	0.1577 (15)	0.1764 (7)	0.7116 (40)	0.0032 (12)	0.0008 (2)	0.0280 (81)	-0.0002 (5)	0.0010 (27)	0.0002 (12)
C(3)	0.1523 (16)	0.2142 (8)	0.5959 (40)	0.0040 (14)	0.0014 (3)	0.0209 (79)	-0.0002 (5)	-0.0003 (28)	0.0010 (13)
C(4)	0.1798 (14)	0.2558 (7)	0.6812 (34)	0.0024 (12)	0.0009 (2)	0.0182 (64)	-0.0012 (5)	0.0008 (25)	0.0003 (11)
C(5)	0.2006 (13)	0.2581 (6)	0.8784 (30)	0.0017 (11)	0.0009 (2)	0.0135 (61)	-0.0006 (5)	-0.0011 (23)	-0.0003 (9)
C(6)	0.2062 (15)	0.2193 (6)	0.9911 (31)	0.0043 (12)	0.0006 (2)	0.0118 (65)	0.0000 (5)	-0.0016 (24)	0.0003 (9)
S	0.1764 (4)	0.3017 (2)	0.5316 (8)	0.0029 (3)	0.0008 (1)	0.0102 (14)	0.0001 (1)	0.0003 (6)	0.0001 (3)
O(1)	0.1431 (10)	0.2910 (5)	0.3418 (25)	0.0032 (9)	0.0015 (2)	0.0193 (47)	0.0010 (4)	-0.0044 (17)	-0.0003 (9)
O(2)	0.1373 (12)	0.3364 (5)	0.6415 (26)	0.0060 (11)	0.0012 (2)	0.0255 (55)	0.0009 (4)	0.0056 (21)	-0.0005 (9)
O(3)	0.2896 (9)	0.3131 (4)	0.5175 (18)	0.0032 (8)	0.0010 (2)	0.0041 (37)	-0.0006 (3)	-0.0009 (14)	-0.0005 (6)
C(7)	0.3377 (13)	0.3126 (6)	0.3365 (30)	0.0013 (10)	0.0009 (2)	0.0066 (51)	-0.0008 (4)	0.0021 (20)	-0.0010 (9)
C(8)	0.3382 (15)	0.3491 (6)	0.2256 (34)	0.0041 (13)	0.0003 (2)	0.0186 (66)	0.0002 (4)	0.0017 (24)	-0.0021 (10)
C(9)	0.3888 (13)	0.3461 (6)	0.0385 (31)	0.0025 (10)	0.0006 (2)	0.0082 (54)	-0.0000 (4)	-0.0010 (22)	0.0020 (9)
C(10)	0.4311 (15)	0.3069 (7)	-0.0196 (32)	0.0048 (13)	0.0008 (2)	0.0096 (63)	-0.0001 (5)	-0.0003 (24)	-0.0009 (10)
C(11)	0.4272 (13)	0.2690 (6)	0.0941 (33)	0.0013 (11)	0.0010 (2)	0.0149 (63)	0.0002 (4)	-0.0011 (22)	-0.0005 (11)
C(12)	0.3788 (16)	0.2731 (7)	0.2728 (35)	0.0044 (14)	0.0011 (3)	0.0133 (66)	-0.0008 (5)	-0.0018 (27)	-0.0014 (12)
O(4)	0.3961 (12)	0.3848 (4)	-0.0650 (27)	0.0080 (11)	0.0006 (2)	0.0258 (49)	-0.0003 (3)	0.0036 (24)	0.0020 (9)
O(5)	0.4868 (11)	0.3388 (5)	-0.3173 (23)	0.0055 (11)	0.0014 (2)	0.0118 (45)	-0.0004 (4)	-0.0007 (19)	-0.0011 (9)
C(13)	0.4770 (15)	0.3041 (8)	-0.2222 (37)	0.0030 (13)	0.0014 (3)	0.0173 (70)	-0.0006 (5)	-0.0044 (26)	-0.0017 (13)
C(14)	0.4643 (17)	0.2232 (7)	0.0284 (37)	0.0067 (16)	0.0010 (3)	0.0168 (73)	0.0004 (6)	0.0004 (31)	-0.0015 (13)
Cl	0.3796 (4)	0.2274 (2)	0.4373 (11)	0.0049 (4)	0.0009 (1)	0.0204 (17)	0.0004 (1)	-0.0017 (8)	0.0006 (3)
C(15)	0.2904 (15)	0.3941 (5)	0.2908 (35)	0.0034 (13)	0.0003 (2)	0.0282 (73)	-0.0004 (4)	0.0012 (27)	-0.0019 (10)
C(16)	0.3691 (18)	0.4230 (7)	0.3728 (35)	0.0065 (17)	0.0010 (3)	0.0138 (72)	-0.0006 (6)	-0.0029 (29)	-0.0007 (12)
C(17)	0.3625 (15)	0.4506 (6)	0.5251 (35)	0.0043 (13)	0.0007 (2)	0.0148 (69)	0.0003 (5)	0.0012 (25)	-0.0005 (11)
C(18)	0.4436 (16)	0.4808 (7)	0.5671 (36)	0.0050 (14)	0.0010 (3)	0.0087 (60)	-0.0002 (5)	0.0011 (28)	0.0008 (12)
C(19)	0.4499 (14)	0.5084 (6)	0.7202 (36)	0.0031 (12)	0.0003 (2)	0.0240 (73)	-0.0002 (4)	-0.0015 (26)	-0.0008 (10)
C(20)	0.2673 (16)	0.4568 (8)	0.6427 (38)	0.0043 (14)	0.0012 (3)	0.0185 (76)	-0.0005 (6)	0.0017 (27)	-0.0011 (13)
C(21)	0.5299 (15)	0.5392 (6)	0.7687 (34)	0.0040 (13)	0.0005 (2)	0.0174 (67)	-0.0004 (5)	-0.0006 (25)	0.0006 (11)
C(22)	0.4906 (15)	0.5903 (6)	0.7590 (38)	0.0031 (12)	0.0005 (2)	0.0257 (73)	0.0000 (5)	0.0032 (26)	-0.0002 (11)
C(23)	0.5662 (16)	0.6245 (7)	0.8251 (36)	0.0057 (15)	0.0006 (2)	0.0206 (69)	-0.0007 (6)	-0.0007 (29)	0.0004 (12)
C(24)	0.5992 (19)	0.6147 (6)	1.0359 (44)	0.0094 (20)	0.0005 (2)	0.0323 (89)	0.0004 (5)	-0.0075 (40)	0.0000 (13)
C(25)	0.6344 (15)	0.5668 (7)	1.0481 (42)	0.0039 (13)	0.0012 (3)	0.0224 (73)	0.0007 (5)	0.0001 (31)	-0.0005 (14)
C(26)	0.5621 (16)	0.5304 (6)	0.9858 (33)	0.0066 (15)	0.0003 (2)	0.0142 (71)	0.0002 (5)	-0.0058 (26)	0.0002 (9)
C(27)	0.4532 (19)	0.6027 (7)	0.5470 (43)	0.0085 (19)	0.0009 (3)	0.0214 (77)	-0.0008 (6)	-0.0023 (37)	0.0011 (14)
O(6)	0.7119 (12)	0.5565 (6)	1.1089 (30)	0.0052 (11)	0.0017 (2)	0.0437 (68)	0.0004 (4)	-0.0066 (25)	-0.0006 (11)
C(28)	0.5976 (16)	0.4825 (6)	1.0208 (39)	0.0064 (15)	0.0003 (2)	0.0279 (85)	0.0003 (5)	-0.0012 (32)	0.0011 (11)
C(29)	0.6165 (14)	0.5341 (6)	0.6297 (34)	0.0023 (12)	0.0008 (2)	0.0197 (71)	-0.0001 (5)	0.0034 (24)	-0.0003 (10)

TABLE 2. OBSERVED AND CALCULATED STRUCTURE FACTORS

H	K	L	F(OBS)	F(CAL)
0	4	0	8.71	5.26
0	6	0	16.94	25.70
0	8	0	53.30	37.99
0	10	0	29.48	33.98
0	12	0	164.72	154.00
0	14	0	23.36	27.12
0	16	0	41.06	44.03
0	18	0	25.06	15.92
0	20	0	63.40	59.02
0	26	0	35.22	35.82
0	28	0	53.67	54.71
0	32	0	21.23	20.82
0	34	0	19.00	17.11
0	36	0	15.94	8.35
1	3	0	37.45	39.08
1	4	0	105.95	101.14
1	5	0	100.67	117.60
1	6	0	80.62	82.85
1	7	0	89.34	82.34
1	8	0	84.17	73.54
1	9	0	78.98	70.78
1	10	0	46.16	45.82
1	11	0	150.44	141.36
1	12	0	15.08	13.56
1	14	0	32.07	32.50
1	15	0	33.65	33.09
1	16	0	25.77	22.79
1	17	0	71.75	67.28
1	18	0	41.06	35.31
1	20	0	14.00	12.30
1	21	0	70.45	74.44
1	22	0	17.70	5.94
1	23	0	101.87	93.32
1	25	0	27.90	34.47
1	27	0	23.27	19.04
1	28	0	19.93	11.99
1	29	0	19.74	10.90
1	30	0	19.37	7.44
1	31	0	26.97	30.13
1	32	0	18.17	20.45
1	33	0	17.24	15.19
1	36	0	19.37	28.99
2	0	0	89.64	94.13
2	1	0	36.09	31.47
2	2	0	107.43	100.05
2	3	0	82.50	80.34
2	4	0	76.47	74.80
2	5	0	132.37	137.76
2	6	0	10.38	13.97
2	8	0	15.11	15.75
2	9	0	34.95	33.02
2	10	0	33.65	31.69
2	11	0	47.27	45.41
2	12	0	77.40	81.51
2	13	0	10.66	4.22
2	14	0	12.88	6.87
2	15	0	11.68	4.96
2	16	0	112.90	108.08
2	17	0	74.06	75.89
2	18	0	15.20	20.53
2	19	0	15.85	15.93
2	20	0	16.41	10.35
2	21	0	22.71	20.07
2	22	0	16.59	9.77
2	23	0	18.04	30.95
2	24	0	24.29	24.51
2	25	0	102.80	96.22
2	26	0	23.17	20.06
2	27	0	23.27	23.37
2	29	0	19.65	20.99
2	31	0	18.72	10.54
2	32	0	17.98	9.79
2	34	0	15.94	12.25
2	36	0	13.26	6.43
3	1	0	31.42	42.10
3	2	0	148.22	143.25
3	3	0	96.49	91.28
3	4	0	62.20	63.49
3	5	0	51.17	44.84
3	6	0	145.99	149.90
3	7	0	52.84	54.84
3	8	0	21.78	27.67
3	10	0	88.59	86.13
3	11	0	14.37	7.78
3	12	0	31.33	32.44
3	13	0	32.63	23.55
3	14	0	43.47	45.11
3	15	0	66.65	62.09
3	16	0	17.51	14.05
3	17	0	12.98	14.80
3	18	0	41.25	45.07
3	20	0	22.43	25.33
3	22	0	59.05	57.26
3	23	0	19.00	17.52
3	24	0	55.52	61.59
3	25	0	19.74	9.42
3	27	0	26.14	27.18
3	28	0	23.08	25.56
3	30	0	19.09	6.45
3	32	0	17.61	11.37
3	34	0	28.74	36.66
3	36	0	12.70	14.89
4	0	0	130.24	134.31
4	1	0	278.77	246.42
4	2	0	81.66	86.14
4	3	0	80.64	71.29
4	4	0	47.46	51.87
4	5	0	18.76	46.19
4	6	0	8.99	15.05
4	7	0	55.52	49.04
4	8	0	13.72	4.55
4	9	0	86.58	83.41
4	11	0	100.57	99.79
4	12	0	12.98	10.17
4	13	0	71.19	70.73
4	14	0	34.20	22.56
4	15	0	38.38	35.94
4	16	0	18.45	25.84
4	17	0	55.71	59.14
4	18	0	32.16	37.13
4	19	0	28.39	15.21
4	20	0	26.51	30.30
4	21	0	58.40	53.60
4	22	0	21.32	21.39
4	23	0	69.61	64.50
4	24	0	28.09	26.49
4	25	0	28.36	21.00
4	26	0	32.91	34.55
4	27	0	23.17	24.46
4	29	0	50.33	45.14
5	1	0	15.02	6.71
5	2	0	107.06	112.23
5	3	0	26.05	30.73
5	4	0	87.02	89.64
5	5	0	9.73	6.44
5	6	0	84.07	85.33
5	7	0	14.46	13.01
5	8	0	31.78	25.65
5	9	0	45.61	41.15
5	10	0	70.82	69.46
5	11	0	36.61	32.74
5	12	0	11.96	9.24
5	13	0	17.43	12.36
5	14	0	45.05	45.14
5	15	0	18.63	24.23
5	16	0	29.38	25.77
5	17	0	46.25	44.03
5	18	0	66.00	55.32
5	19	0	24.01	17.85
5	22	0	22.58	71.10
5	23	0	19.56	15.17
5	24	0	28.36	25.01
5	25	0	30.87	25.75
5	26	0	19.93	13.83
5	27	0	19.74	9.12
5	30	0	21.32	20.71
5	34	0	16.58	16.99
6	0	0	102.98	105.97
6	1	0	75.82	79.25
6	2	0	99.92	131.96
6	3	0	22.62	23.70
6	4	0	43.10	40.49
6	6	0	40.14	35.58
6	7	0	128.94	129.37
6	8	0	60.62	66.28
6	9	0	65.35	65.68
6	10	0	12.65	20.64
6	11	0	12.42	7.80
6	12	0	14.74	8.76
6	13	0	53.30	45.68
6	14	0	15.57	19.96
6	15	0	13.90	6.44
6	16	0	26.05	24.82
6	17	0	34.87	33.23
6	18	0	24.19	29.21
6	19	0	33.18	29.92
6	20	0	21.41	22.74
6	21	0	45.23	36.53
6	24	0	40.23	30.55
6	25	0	19.84	9.03
6	28	0	24.93	12.57
6	30	0	17.61	7.42
7	1	0	16.22	5.10
7	2	0	57.10	55.65
7	3	0	26.41	12.93
7	4	0	34.48	35.06
7	5	0	87.04	87.83
7	6	0	12.05	7.62
7	7	0	60.81	59.39
7	8	0	36.71	39.98
7	9	0	14.74	15.41
7	10	0	55.15	57.83
7	11	0	53.21	55.81
7	17	0	27.90	30.23
7	18	0	25.12	24.57
7	19	0	18.35	12.71
7	20	0	19.00	16.51
7	21	0	43.10	43.94
7	22	0	23.17	19.68
7	23	0	80.55	67.13
7	28	0	18.35	7.32
7	30	0	19.47	19.25
7	32	0	16.96	20.00
7	33	0	13.16	15.25
8	0	0	53.30	51.67
8	1	0	37.08	39.04
8	2	0	17.89	15.40
8	3	0	14.65	10.93
8	4	0	37.73	33.94
8	5	0	12.98	11.05
8	6	0	35.50	33.90
8	8	0	49.22	51.07
8	9	0	44.77	50.24
8	10	0	37.82	40.50
8	11	0	20.11	21.50
8	12	0	57.93	50.57
8	13	0	17.06	17.89
8	14	0	23.36	22.97
8	15	0	19.84	20.25
8	16	0	96.96	91.03
8	17	0	71.69	24.76
8	18	0	61.55	51.63
8	22	0	23.27	13.12
8	24	0	22.80	16.74
8	27	0	18.17	7.12
9	2	0	19.47	23.11
9	3	0	31.80	25.93
9	4	0	19.65	15.39
9	5	0	48.57	45.75
9	6	0	15.48	13.05
9	7	0	64.05	61.23
9	11	0	23.36	21.15
9	12	0	21.69	26.84
9	13	0	21.97	15.41
9	14	0	27.25	23.24
9	15	0	31.89	30.89
9	16	0	27.90	25.25
9	18	0	23.17	18.10
9	22	0	25.77	11.28
9	24	0	31.24	17.15
9	28	0	21.23	7.45
10	0	0	47.64	43.35
10	1	0	69.34	70.58
10	2	0	21.60	15.38
10	4	0	48.85	47.00
10	5	0	28.83	31.06
10	6	0	20.67	22.02
10	7	0	18.45	20.51
10	8	0	55.52	53.64
10	9	0	18.82	5.64
10	10	0	22.25	14.32
10	11	0	19.19	15.43
10	12	0	25.49	18.64
10	13	0	22.80	20.69
10	14	0	19.65	16.02
10	15	0	19.84	19.76
10	16	0	30.87	30.15
10	20	0	22.90	15.05
10	28	0	14.55	18.86
11	1	0	26.23	27.70
11	2	0	24.66	21.11
11	5	0	20.86	19.32
11	6	0	28.18	26.37
11	9	0	27.44	23.80
11	10	0	22.99	23.56
11	11	0	54.23	52.70
11	15	0	19.93	17.82
11	16	0	19.84	11.41
11	18	0	22.71	23.68
11	19	0	22.43	17.92
11	20	0	21.97	22.52
11	22	0	17.80	24.58
12	0	0	46.07	40.25
12	1	0	23.08	19.69
12	3	0	23.00	17.48
12	6	0	26.14	23.90
12	7	0	19.93	5.14
12	8	0	28.46	31.10
12	9	0	19.93	4.73
12	10	0	23.27	22.08
12	14	0	19.56	10.38
12	15	0	25.49	23.16
12	16	0	19.19	5.49
12	17	0	41.16	40.95
12	18	0	24.29	15.30
12	20	0	25.03	24.75
12	22	0	18.91	17.47
13	3	0	23.17	25.79
13	4	0	19.84	11.62
13	6	0	58.86	53.53
13	14	0	21.69	20.58
13	15	0	21.32	20.62
13	16	0	20.86	19.15
13	22	0	16.41	17.66
14	6	0	29.38	12.18
14	15	0	19.19	19.72
14	17	0	17.98	14.62
16	0	0	18.08	17.72
16	10	0	19.37	4.53
0	3	1	59.60	63.05
0	4	1	32.81	19.36
0	5	1	153.78	157.35
0	6	1	30.22	33.24
0	7	1	167.58	164.23
0	8	1	41.06	40.61
0	9	1	124.58	125.92
0	10	1	14.92	13.27
0	11	1	50.43	42.43
0	12	1	59.05	52.92
0	13	1	19.47	10.25
0	14	1	56.00	46.78
0	15	1	16.50	17.33
0	16	1	17.15	14.24
0	17	1	42.64	37.67
0	18	1	30.40	34.71
0	19	1	31.52	36.43
0	21	1	43.01	35.58
0	24	1	18.72	13.44
0	25	1	45.42	40.42
0	26	1	32.54	32.06
0	28	1	22.99	20.47
0	30	1	22.25	23.51
0	31	1	21.60	20.49
0	33	1	19.65	24.43
0	34	1	13.07	12.53
0	37	1	13.14	20.45
1	0	1	53.58	42.03
1	1	1	82.50	79.17
1	2	1	175.01	165.17
1	3	1	115.59	120.56
1	4	1	86.85	90.09
1	5	1	29.01	32.98
1	6	1	47.74	45.29
1	7	1	85.19	65.77
1	8	1	58.58	45.70
1	9	1	60.07	43.67
1	10	1	57.01	43.53
1	11	1	64.70	55.10
1	12	1	91.40	82.42
1	13	1	73.04	69.06
1	14	1	111.97	104.82
1	15	1	39.40	36.97
1	16	1	55.62	57.65
1	17	1	32.81	27.98
1	18	1	40.41	35.28
1	19	1	35.41	33.16
1	20	1	28.36	32.36
1	21	1	16.96	22.35
1	22	1	34.85	33.86
1	23	1	33.93	27.30
1	24	1	36.06	37.80
1	25	1	21.97	25.40
1	26	1	45.98	46.52
1	29	1	19.47	19.72
1	30	1	19.09	15.66
1	31	1	21.60	17.67
1	32	1	17.70	16.99
1	35	1	16.87	14.03
1	36	1	15.11	15.22
1	37	1	13.07	15.13
2	0	1	138.11	126.52
2	1	1	43.01	35.02
2	2	1	102.15	113.20
2	3	1	72.86	75.63
2	4	1	104.10	106.02
2	5	1	99.37	87.93
2	6	1	69.80	65.33
2	7	1	92.23	95.13
2	8	1	89.36	82.06
2	9	1	124.86	130.36
2	10	1	72.12	75.33
2	11	1	40.23	37.25
2	12	1	47.83	36.05
2	13	1	15.57	23.33
2	14	1	26.51	27.65
2	16	1	46.53	45.50
2	17	1	29.85	27.56
2	18	1	30.96	31.33
2	19	1	51.26	52.33
2	20	1	83.01	85.85
2	21	1	53.30	55.08
2	22	1	52.00	45.58
2	23	1	39.86	31.08
2	24	1	19.28	17.27
2	25	1	45.70	41.57
2	26	1	39.66	35.56
2	28	1	19.65	16.87
2	31	1	18.35	21.09
2	32	1	20.49	12.21
3	0	1	205.04	199.35
3	1	1	108.82	105.59
3	2	1	161.75	159.74
3	3	1	166.76	172.39
3	4	1	83.98	81.31
3	5	1	85.00	71.62
3	6	1	62.20	53.98
3	7	1	35.13	32.82
3	8	1	89.91	82.94
3	9	1	101.96	92.44
3	10	1	75.64	79.21
3	11	1	71.00	71.11
3	12	1	79.44	84.28
3	13	1	13.16	7.62
3	14	1	56.17	55.63
3	15	1	54.50	61.06
3	16	1	44.31	35.48
3	17	1	30.59	27.94
3	18	1	40.41	37.74
3	19	1	14.18	8.96
3	20	1	32.07	31.07
3	21	1	36.89	33.97
3	22	1	17.80	14.21
3	23	1	26.05	22.52
3	24	1	26.08	23.71
3	25	1	22.52	15.97
3	26	1	23.08	15.82
3	27	1	28.27	25.11
3	28	1	22.80	14.72
3	29	1	22.43	22.30
3	30	1	21.88	22.72
3	31	1	33.28	30.18
3	32	1	17.15	16.02
3	37	1	14.37	19.04
4	0	1	87.67	91.95
4	1	1	104.93	105.84
4	2	1	72.86	60.99
4	3	1	89.36	81.70
4	4	1	102.61	101.37
4	5	1	55.80	52.70
4	6	1	57.75	55.52
4	7	1	85.19	75.77
4	8	1	49.31	46.12
4	9	1	60.93	55.31
4	10	1	44.49	46.63
4	11	1	22.34	11.09
4	12	1	54.50	47.85
4	13	1	53.11	54.47
4	14	1	17.52	20.29
4	15	1	29.57	29.82
4	16	1	73.04	74.97
4	17	1	15.85	10.90
4	18	1	23.00	23.19
4	19	1	31.47	26.81
4	20	1	56.27	59.16
4	21	1	24.47	28.31
4	22	1	44.77	47.98
4	23	1	18.91	20.82
4	24	1	22.90	22.58
4	25	1	19.74	9.93
4	32	1	23.92	29.24
5	0	1	43.01	39.13
5	1	1	32.35	34.07
5	2	1	54.32	53.46
5	3	1	11.31	9.74
5	4	1	29.11	33.65
5	5	1	45.70	47.01
5	6	1	14.65	15.75
5	7	1	34.20	31.90
5	8	1	14.09	11.27
5	9	1	12.88	7.34
5	10	1	26.60	17.81
5	11	1	40.51	34.01
5	12	1	47.00	51.48
5	13	1	68.32	72.16
5	14	1	64.70	64.12
5	15	1	78.23	90.54
5	16	1	19.56	16.81
5	17	1	16.41	16.41
5	18	1	14.65	10.88
5	19	1	23.27	27.26
5	20	1	34.76	30.46
5	21	1	21.04	13.73
5	22	1	34.67	30.19
5	23	1	45.70	45.14
5	24	1	22.99	29.34
5	25	1	25.27	22.82
5	26	1	22.99	25.92
5	27	1	39.39	39.41
5	28	1	27.25	29.17
6	0	1	102.43	97.28
6	1	1	49.59	49.49
6	2	1	25.21	26.67
6	3	1	61.46	61.16
6	4	1	97.08	96.28
6	5	1	38.10	38.71
6	6	1	65.81	63.07
6	7	1	49.98	50.15
6	8	1	52.84	52.94
6	9	1	84.07	86.61
6	10	1	26.70	26.09
6	11	1	47.09	47.91
6	12	1	46.48	46.78
6	13	1	26.70	27.62
6	14	1	27.44	28.67
6	15	1	22.99	22.94
6	16	1	31.61	28.27
6	17	1	16.68	15.46
6	18	1	24.75	20.56
6	19	1	40.23	37.53
6	20	1	21.88	10.53
6	21	1	42.36	46.02
6	24	1	46.16	38.28
6	25	1	19.65	12.20
6	26	1	32.16	31.42
6	32	1	21.60	29.23
7	0	1	27.07	24.09
7	1	1	49.87	50.65
7	2	1	87.23	90.47
7	3	1	56.54	57.07
7	4	1	69.98	79.00
7	5	1	43.20	43.35
7	6	1	41.43	40.43
7	7	1	25.03	26.16
7	8	1	47.64	48.55
7	9	1	15.02	15.96
7	10	1	48.39	49.34
7	11	1	44.22	48.13
7	12	1	15.94	12.85
7	13	1	30.50	28.77
7	14	1	48.39	49.83
7	15	1	30.50	27.09
7	16	1	20.21	23.79
7	17	1	18.17	11.90
7	18	1	41.43	36.67
7	19	1	22.43	21.19
7	20	1	27.90	32.29
7	21	1	19.65	12.36
7	22	1	19.74	13.75
7	23	1	23.08	26.15
7	24	1	19.65	19.41
7	25	1	19.37	12.71
7	26	1	19.00	18.39
7	27	1	18.54	14.06
7	30	1	23.17	28.66
8	0	1	69.52	67.43
8	1	1	69.52	65.82
8	2	1	51.54	45.30
8	3	1	27.99	22.82
8	4	1	26.14	23.64
8	7	1	60.52	61.29
8	8	1	17.70	19.33
8	9	1	44.03	48.23
8	10	1	20.02	23.37
8	11	1	15.63	19.24
8	12	1	32.07	35.16
8	13	1	41.34	36.47
8	14	1	24.70	21.48
8	15	1	18.26	6.61
8	16	1	35.04	27.73
8	17	1	19.28	13.41
8	18	1	19.47	7.35
8	19	1	62.75	55.20
8	20	1	23.08	21.87
8	21	1	51.63	50.19
8	27	1	17.70	15.77
9	0	1	17.98	20.10
9	1	1	16.04	7.67
9	2	1	41.06	44.33
9	3	1	34.30	35.35
9	4	1	36.43	32.10
9	5	1	30.68	36.99
9	6	1	30.96	31.80
9	7	1	16.68	23.63
9	8	1	18.91	25.67
9	9	1	35.13	32.23
9	10	1	33.37	30.90
9	11	1	27.01	25.99
9	13	1	48.57	45.37
9	14	1	39.77	39.05
9	15	1	24.01	28.38
9	16	1	22.06	24.60
9	17	1	22.15	24.72
9	18	1	32.63	33.26
9	25	1	21.04	25.96
10	0	1	48.11	43.62
10	1	1	36.15	35.78
10	2	1	55.71	65.63
10	3	1	40.23	36.87
10	4	1	52.44	45.59
10	5	1	21.04	10.77
10	6	1	25.42	22.44
10	7	1	21.69	16.97
10	8	1	37.91	35.89
10	9	1	44.22	42.72
10	10	1	25.12	22.36
10	11	1	22.43	22.34
10	12	1	22.62	10.81
10	13	1	27.90	23.84
10	14	1	28.09	25.25
10	18	1	19.65	17.89
10	23	1	18.08	22.69
10	25	1	24.01	21.12
11	1	1	35.22	32.89
11	2	1	25.12	20.09
11	3	1	27.34	23.79
11	4	1	27.44	27.88
11	6	1	22.62	22.41
11	7	1	25.49	25.68
11	8	1	19.47	10.78
11	9	1	22.90	18.70
11	10	1	19.65	15.86
11	13	1	39.95	41.25
11	14	1	23.08	18.71
11	15	1	19.65	19.42
11	18	1	22.34	15.86
11	19	1	21.97	22.29
11	20	1	18.45	14.72
11	21	1	17.98	16.08
11	22	1	22.90	27.15
11	25	1	17.61	15.54
12	2	1	28.18	23.64
12	3	1	19.74	11.91
12	4	1	25.95	18.01
12	5	1	19.74	24.77
13	6	1	27.99	33.02
12	8	1	28.27	31.09
12	11	1	22.99	23.89
12	20	1	22.43	25.12
13	1	1	22.99	23.86
13	3	1	22.99	27.98
13	4	1	22.90	15.86
14	0	1	31.24	35.98
14	3	1	26.97	31.40
14	8	1	24.01	30.31
14	20	1	16.41	14.11
16	0	1	17.43	21.78
17	4	1	13.07	4.40
17	6	1	10.57	13.83
0	0	2	205.41	192.83
0	1	2	33.65	24.62
0	2	2	47.27	47.78
0	3	2	81.48	73.59
0	5	2	103.17	103.35
0	6	2	22.80	19.32
0	7	2	33.09	35.01
0	8	2	29.66	27.51
0	9	2	92.69	97.83
0	10	2	55.06	49.59
0	11	2	13.35	18.28
0	12	2	119.11	122.18
0	13	2	66.09	65.82
0	15	2	92.60	87.99
0	16	2	46.72	50.25
0	19	2	45.05	47.99
0	20	2	43.75	49.39
0	21	2	31.79	29.87
0	22	2	16.31	12.56
0	23	2	38.65	44.13
0	24	2	16.50	16.36
0	25	2	17.06	11.57
0	26	2	20.30	16.54
0	27	2	17.98	19.86
0	20	2	35.87	42.15
0	34	2	13.44	7.04
0	36	2	17.52	9.58
1	0	2	28.83	29.65
1	1	2	82.50	76.27
1	2	2	9.27	9.81
1	3	2	36.06	29.48
1	4	2	96.12	103.55
1	5	2	58.40	54.56
1	6	2	83.70	76.02
1	7	2	44.68	39.06
1	8	2	82.40	78.68
1	9	2	93.34	89.61
1	10	2	37.26	32.95
1	11	2	101.59	97.04
1	12	2	55.34	55.35
1	13	2	45.05	51.43
1	14	2	30.77	26.44
1	15	2	26.14	25.15
1	16	2	35.57	31.02
1	17	2	41.06	38.98
1	18	2	30.96	33.34
1	19	2	28.18	22.02
1	21	2	44.59	43.36
1	22	2	18.63	12.48
1	23	2	31.24	31.51
1	24	2	53.50	46.12
1	25	2	20.95	16.36
1	26	2	36.43	37.82
1	28	2	23.27	26.32
1	32	2	15.39	15.79
1	33	2	16.07	12.08
1	35	2	15.85	14.52
2	0	2	76.57	85.14
2	1	2	19.65	22.85
2	2	2	40.41	34.37
2	3	2	54.50	50.26
2	4	2	46.90	40.85
2	5	2	66.46	69.85
2	6	2	52.74	50.91
2	7	2	67.26	70.24
2	8	2	29.85	25.44
2	9	2	68.59	60.20
2	10	2	97.70	95.49
2	11	2	58.30	54.62
2	12	2	86.21	89.41
2	13	2	40.88	35.83
2	14	2	25.58	22.57
2	16	2	48.76	51.44
2	17	2	37.82	39.08
2	18	2	16.50	21.94
2	19	2	34.11	33.38
2	20	2	17.15	14.69
2	21	2	18.35	15.93
2	22	2	21.51	25.65
2	23	2	24.56	23.56
2	24	2	46.53	46.41
2	25	2	20.95	21.05
2	27	2	20.86	15.53
2	28	2	23.17	28.25
2	29	2	20.11	15.21
2	36	2	11.86	7.89
3	0	2	49.50	40.38
3	1	2	114.38	120.03
3	2	2	27.62	25.70
3	3	2	57.56	52.11
3	4	2	24.29	17.40
3	5	2	95.10	83.60
3	6	2	61.55	67.98
3	7	2	45.05	43.78
3	8	2	28.92	31.49
3	9	2	41.06	35.41
3	10	2	50.33	43.49
3	11	2	20.49	22.04
3	12	2	53.86	59.62
3	13	2	55.99	52.28
3	14	2	36.15	31.81
3	15	2	16.78	17.96
3	16	2	24.47	24.84
3	17	2	17.89	15.59
3	18	2	33.00	29.08
3	19	2	39.21	34.19
3	20	2	26.14	30.65
3	21	2	30.68	32.44
3	22	2	51.91	43.10
3	23	2	23.27	19.68
3	24	2	20.95	15.52
3	27	2	17.80	15.30
3	29	2	24.38	26.77
3	30	2	23.54	12.85
3	34	2	14.74	15.62
3	35	2	16.13	15.63
3	36	2	12.51	22.88
3	37	2	11.12	4.94
4	0	2	80.18	74.05
4	1	2	89.26	89.34
4	2	2	70.91	71.38
4	3	2	18.72	15.77
4	4	2	33.74	37.91
4	5	2	27.53	31.79
4	6	2	60.90	62.44
4	7	2	35.41	33.66
4	9	2	29.65	34.65
4	10	2	63.50	61.57
4	11	2	85.83	87.27
4	12	2	28.83	25.97
4	13	2	48.94	45.20
4	14	2	55.00	61.22
4	15	2	22.43	21.71
4	16	2	25.31	10.09
4	17	2	28.18	25.18
4	18	2	28.92	29.39
4	19	2	17.70	22.67
4	20	2	17.80	17.50
4	22	2	29.11	33.34
4	24	2	20.95	23.43
4	26	2	29.48	27.34
4	27	2	25.21	26.03
4	29	2	19.56	15.51
4	32	2	16.78	11.51
4	35	2	12.33	6.22
5	0	2	59.08	54.81
5	2	2	28.27	23.94
5	3	2	51.26	45.67
5	4	2	40.04	38.03
5	5	2	39.95	44.52
5	6	2	33.37	35.10
5	7	2	16.07	24.44
5	8	2	29.85	31.84
5	9	2	34.20	33.65
5	10	2	53.48	56.92
5	11	2	43.20	46.48
5	12	2	41.71	40.49
5	13	2	51.91	56.55
5	14	2	14.37	9.23
5	15	2	23.36	21.79
5	16	2	3.36	25.97
5	17	2	19.08	53.78
5	18	2	47.74	45.53
5	19	2	16.22	15.48
5	20	2	43.01	37.33
5	22	2	51.03	51.18
5	24	2	21.04	27.97
5	25	2	29.57	31.16
5	29	2	19.00	20.88
5	35	2	11.03	11.53
6	0	2	38.10	34.35
6	1	2	69.71	73.30
6	2	2	37.08	40.33
6	3	2	45.08	42.60
6	4	2	26.05	25.14
6	5	2	29.20	32.97

TABLE 2. (Continued)

needles from methanol solution. Thus, the *p*-bromobenzenesulfonyl derivative of the α form was subjected to the crystal structure analysis. A preliminary report has already been published.[5]

Experimental

The *p*-bromobenzenesulfonyl derivative of ascochlorin was prepared by the esterification of the phenolic hydroxyl group with *p*-bromobenzenesulfonyl chloride in pyridine (heating for 30 min on boiling water bath). The reaction mixture was poured into cold water, and the product was extracted with ether. The crystals obtained from acetone solution were needles developed along the *c*-axis. Two single crystals of 0.20×0.12 and 0.15×0.05 mm in cross section, measured along the diagonal lines, were used for the intensity data collection around the *c*- and *a*-axes, respectively. Precession photographs of (0*kl*) and (*hk*0) were used for the measurements of cell parameters, and the higher layer line spectra of Weissenberg photographs were also used for the determination of the space group.

Crystal data. Ascochlorin-*p*-bromobenzenesulfonate, $C_{29}H_{33}O_6SClBr$, mol wt, 624.4.

Orthorhombic,

$a=13.86\pm0.03$, $b=30.04\pm0.03$, $c=6.82\pm0.01$ Å;

$U=2839.5$ Å^3, $Z=4$, $Dx=1.460$ g.cm^{-3}.

μ(Cu $K\alpha$)$=41.2$ cm^{-1}, F(000)$=1160$.

Absent spectra, *h*00 when *h* is odd, 0*k*0 when *k* is odd, 00*l* when *l* is odd.

Space group, D_2^4—$P2_12_12_1$.

Intensity data were collected with Cu$K\alpha$ radiation on the multiple film packs of Weissenberg photographs with the use of equi-inclination method. Layers from 0th to 5th around the *c*-axis and from 0th to 6th around the *a*-axis were recorded. Intensities were measured visually by comparison with the standard intensity scale. These data were then corrected for Lorentz, polarization and spot elongation factors but not for absorption. The derived structure factors on different layers were correlated and scaled in a common base by comparing the common reflexions. The total number of independent reflexions was 1627.

Determination of the Crystal Structure

The crystal structure was elucidated by the heavy atom method. The positional parameters of bromine atom were determined from the three Harker sections of $P(0.5, v, w)$, $P(u, 0.5, w)$, and $P(u, v, 0.5)$, sharpened to correspond to the atoms at rest. The structure factor calculated for the bromine atom alone gave the *R* value of 0.44. The coordinates of the atoms in

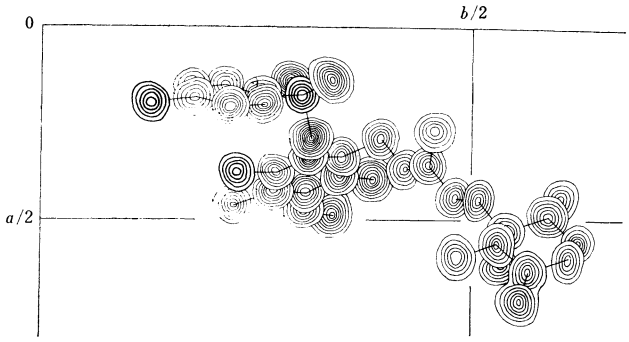

Fig. 1(a). Composite drawing of the final electron density map viewed along the *c*-axis. Contours for carbon and oxygen atoms are drawn at intervals of 1 e.Å^{-3} starting at 1 e.Å^{-3}, and for sulfur and chlorine atoms are at intervals of 3 e.Å^{-3} starting at 3 e.Å^{-3}. Those for bromine atom are drawn by arbitrary scale.

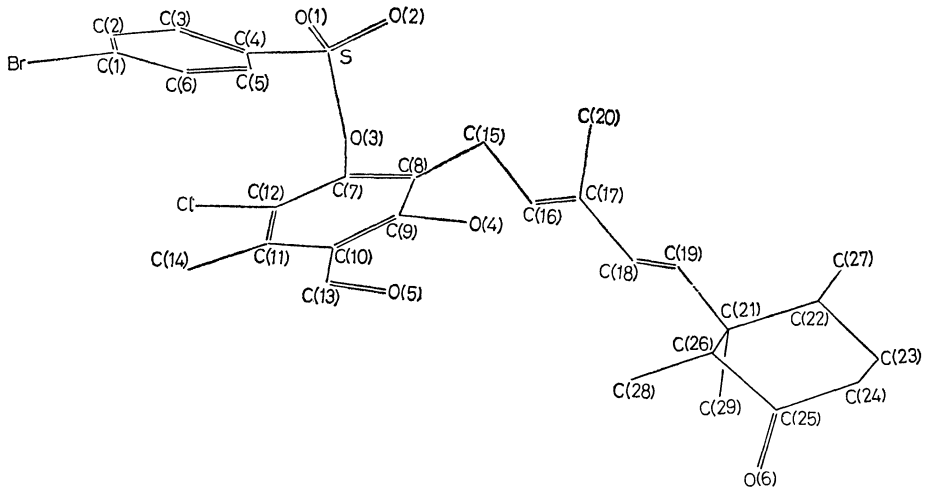

Fig. 1(b). The molecular structure viewed along the *c*-axis.

5) Y. Nawata, K. Ando, G. Tamura, K. Arima, and Y. Iitaka, *J. Antibiot.* (Tokyo), **22**, 511 (1969).

the *p*-bromobenzenesulfonyl group and the chlorine atom were determined on the Fourier map and used for the next structure factor Fourier calculations. The *R* value for the structure factors of these twelve atoms was 0.34. The subsequent Fourier and difference Fourier syntheses revealed all the positions of the atoms at the stage where the *R* value reached 0.24. The four oxygen atoms of the ascochlorin molecule were distinguished easily from the carbon atoms on the difference Fourier map. The molecular structure of ascochlorin elucidated in this way consisted of (3-chloro)orcylic aldehyde and (2,3,4-trimethyl)cyclohexanone moieties linked together through the zigzag chain of *trans*-(3-methyl)penta(2,4)diene. Further refinement of the parameters was carried out by the least-squares method of block matrix approximation with the use of the program HBLS.[6] Anisotropic thermal motions were considered only for bromine atom. The *R* value dropped to 0.123 after four cycles of refinement, and the positions of single and double bonds in the molecule were confirmed. The characters of the four oxygen atoms of ascochlorin molecule were made clear at this stage; one was of keto group in the cyclohexanone moiety, and the others were of two hydroxyl and one aldehyde groups in the orcylic aldehyde moiety. Finally, the least-squares refinement was carried out with the anisotropic temperature factors for all atoms. The *R* value was converged to 0.102 after three cycles of calculations. In these calculations all reflexions were treated with equal weight. Atomic scattering factors used were those given in *International Tables for X-ray Crystallography*.[7] Final values of atomic parameters and anisotropic temperature factors are given in Table 1. Figure 1(a) shows the final three-dimensional Fourier map.

Absolute Configuration

The absolute configuration of ascochlorin-*p*-bromobenzenesulfonate molecule was determined by Bijovet's method with the use of anomalous dispersion of Cu$K\alpha$ radiation by bromine, sulfur, and chlorine atoms. Dispersion corrections of the scattering factors used were those given by Dauben and Templeton.[8] The values of $\Delta f'$ and $\Delta f''$ are as follows:

Br	$\Delta f' = -1.0$	$\Delta f'' = 1.4$
S	0.3	0.7
Cl	0.3	0.6

The structure factors for both hkl and $h\bar{k}l$ were calculated with final atomic parameters. If one takes the left-handed coordinate system, the observed and calculated values of the ratios of the intensities $I(hkl)/I(h\bar{k}l)$ are not coincident for all pairs, as shown in Table 3, and the assumed configuration proves to be reversed. In this report, the molecules are shown by the correct absolute configuration.

Table 3. The determination of the absolute configuration

h	k	l	$\lvert F_c(hkl)\rvert^2/\lvert F_c(h\bar{k}l)\rvert^2$	$I_0(hkl)/I_0(h\bar{k}l)$
5	1	1	1.42	<1
1	6	1	1.22	<1
5	9	1	7.01	<1
6	5	2	1.27	<1
2	6	2	1.22	<1
5	6	2	1.27	<1
5	3	1	0.60	>1
4	8	1	0.79	>1
5	8	1	0.63	>1
1	10	1	0.76	>1
5	10	1	0.83	>1
4	11	1	0.69	>1
3	13	1	0.26	>1
3	4	2	0.59	>1
1	7	2	0.79	>1
1	16	2	0.75	>1

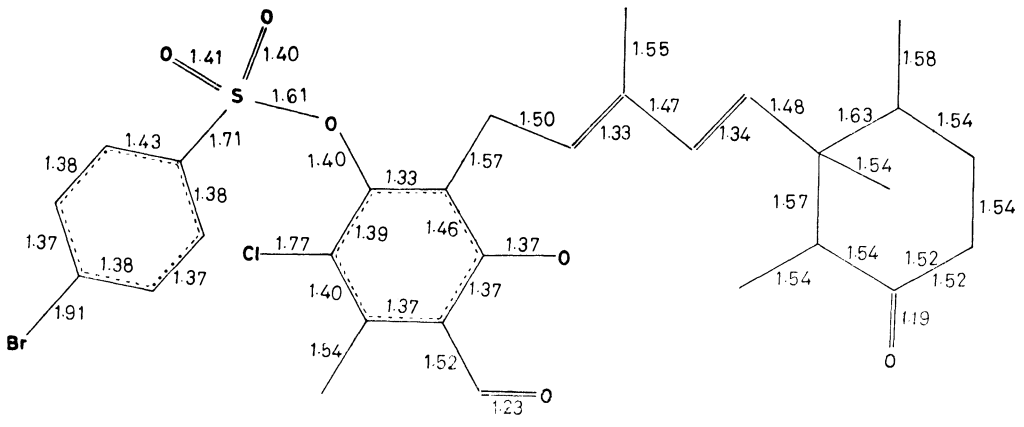

Fig. 2. Bond lengths (Å).

6) Y. Okaya and T. Ashida, *HBLS IV, The Universal Crystallographic Computing System (I)*, p. 65, Japanese Crystallographic Association.

7) "International Tables for X-ray Crystallography," Vol. III, Kynoch Press, Birmingham (1962).

8) C. H. Dauben and D. H. Templeton, *Acta Cryst.* **8**, 841 (1955).

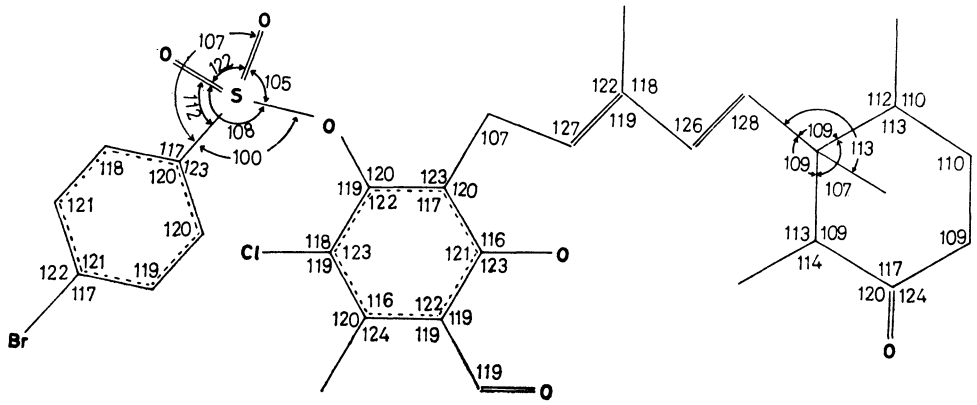

Fig. 3. Bond angles (°).

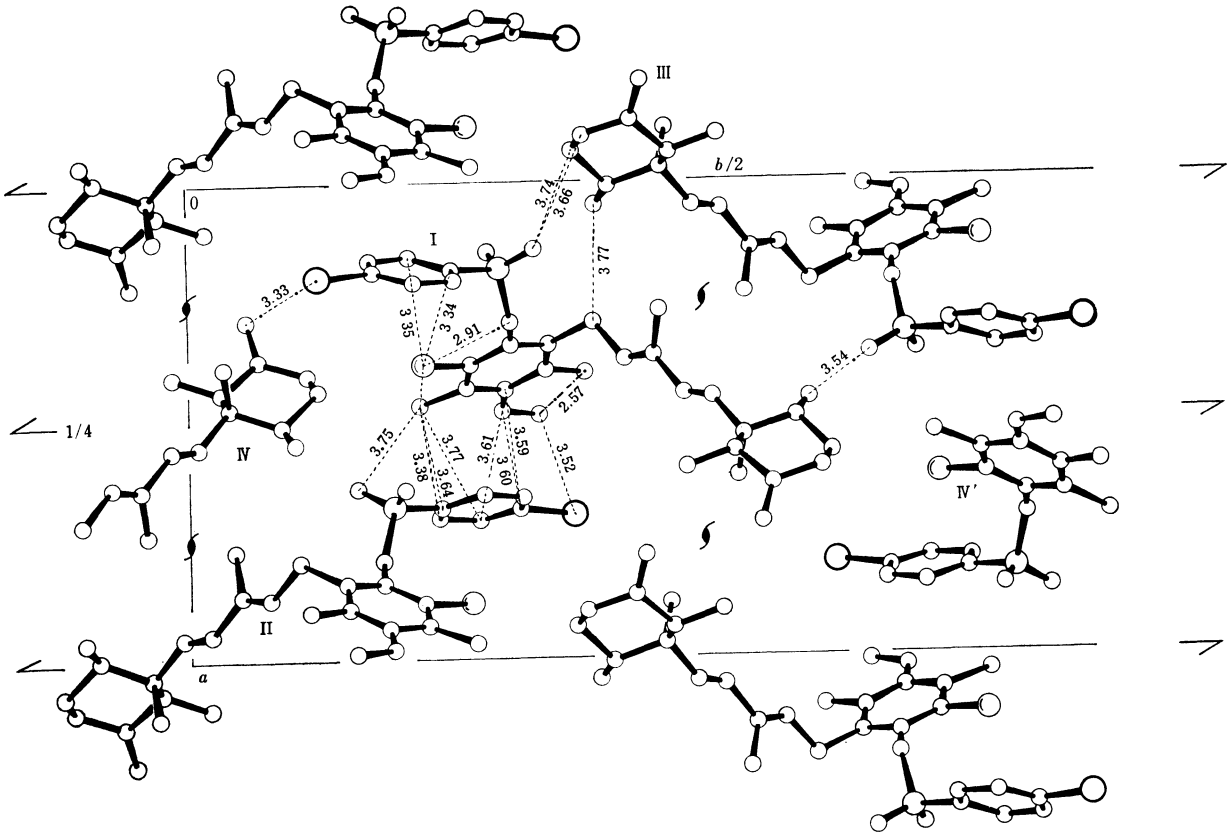

Fig. 4. Arrangement of the molecules in the unit cell viewed down [001].

Discussion of the Structure

The molecular structure of ascochlorin-*p*-bromobenzenesulfonate is illustrated in Fig. 1(b), in which the numbers and symbols of the atoms are also given. Ascochlorin is built up of chloroorcylic aldehyde residue, trimethylcyclohexanone ring and the zigzag chain of *trans*-methylpentadiene. As shown in Table 5, all atoms of chloroorcylic aldehyde residue lie approximately on a plane. Of these, the six carbon atoms of the benzene ring lie on an almost complete plane, the average deviation from the least-squares plane being only 0.009 Å. Chlorine atom and its adjacent methyl group(C(14)), which are separated only by 3.03 Å, deviate by −0.124 and +0.134 Å from the benzene ring in order to balance the repulsive forces between the *ortho*-substituents. The short distance(2.57 Å) between the two oxygen atoms of hydroxyl(O(4)) and aldehyde group (O(5)), indicates the existence of an intramolecular hydrogen bond between them, in consistence with the spectral data of proton magnetic resonance.[5] The four oxygen atoms of the sulfonyl group are arranged in a distorted tetrahedral configuration around the central sulfur atom, and O(1) lies nearly on the plane passing through the benzene ring(perpendicular distance to the plane is +0.027 Å), O(2) lies above the plane(+0.795 Å) and O(3) below the plane(−1.540 Å). As the conformation of O(1)—S—O(3)—C(7) bonds at the ester linkage

TABLE 4. BOND LENGTH AND ANGLES WITH THEIR STANDARD DEVIATIONS (e.s.d.)

Br——C (1)	1.914 Å	(0.023)	C (1)—C (2)	1.370 Å	(0.037)	C (2)—C (3)	1.384 Å	(0.034)
C (3)—C (4)	1.431	(0.031)	C (5)—C (6)	1.400	(0.027)	C (6)—C (1)	1.379	(0.029)
S——C (4)	1.714	(0.022)	S——O (1)	1.411	(0.017)	S——O (2)	1.396	(0.017)
S——O (3)	1.609	(0.013)	S (3)—C (7)	1.402	(0.023)	C (7)—C (8)	1.331	(0.027)
C (8)—C (9)	1.459	(0.030)	C (9)—C (10)	1.374	(0.027)	C (10)-C (11)	1.378	(0.029)
C (11)-C (12)	1.398	(0.032)	C (12)-C (7)	1.386	(0.029)	O (4)—C (9)	1.366	(0.023)
C (10)-C (13)	1.524	(0.033)	O (5)—C (13)	1.234	(0.028)	C (11)-C (14)	1.535	(0.029)
Cl——C (12)	1.773	(0.023)	C (8)—C (15)	1.570	(0.025)	C (15)-C (16)	1.501	(0.031)
C (16)-C (17)	1.332	(0.032)	C (17)-C (20)	1.555	(0.032)	C (17)-C (18)	1.474	(0.029)
C (18)-C (19)	1.335	(0.031)	C (19)-C (21)	1.482	(0.027)	C (21)-C (22)	1.629	(0.026)
C (22)-C (27)	1.581	(0.038)	C (22)-C (23)	1.537	(0.029)	C (23)-C (24)	1.537	(0.038)
C (24)-C (25)	1.523	(0.029)	O (6)—C (25)	1.193	(0.028)	C (25)-C (26)	1.542	(0.029)
C (26)-C (28)	1.539	(0.025)	C (26)-C (21)	1.569	(0.032)			

Br——C (1)—C (2)	121.9°	(1.8)	Br——C (1)—C (6)	116.5°	(1.6)
C (1)—C (2)—C (3)	121.0	(2.2)	C (2)—C (3)—C (4)	118.1	(2.1)
C (3)—C (4)—C (5)	119.8	(1.9)	C (3)—C (4)—S	117.0	(1.6)
C (4)—C (5)—C (6)	120.4	(1.8)	C (5)—C (6)—C (1)	119.0	(1.9)
C (6)—C (1)—C (2)	121.4	(2.1)	O (1)—S——O (2)	122.4	(1.0)
O (1)—S——O (3)	108·2	(0.8)	O (1)—S——C (4)	111.8	(1.0)
O (2)—S——O (3)	104.5	(0.9)	O (2)—S——C (4)	107.0	(1.0)
O (3)—S——C (4)	100.4	(0.9)	S——C (4)—C (5)	123.1	(1.6)
O (3)—C (7)—C (8)	119.6	(1.7)	O (3)—C (7)—C (12)	118.6	(1.7)
C (7)—C (8)—C (9)	116.7	(1.8)	C (7)—C (8)—C (15)	123.1	(1.8)
C (8)—C (9)—C (10)	120.7	(1.8)	C (8)—C (9)—O (4)	115.8	(1.7)
C (9)—C (8)—C (15)	120.3	(1.7)	O (4)—C (9)—C (10)	123.4	(1.8)
C (9)—C (10)-C (11)	122.0	(1.9)	C (9)—C (10)-C (13)	119.1	(1.8)
C (10)-C (11)-C (12)	115.8	(1.9)	C (10)-C (11)-C (14)	124.3	(1.9)
C (10)-C (13)-O (5)	118.5	(2.0)	C (13)-C (10)-C (11)	118.8	(1.9)
C (11)-C (12)-C (7)	123.2	(2.0)	C (11)-C (12)-Cl	118.7	(1.7)
C (14)-C (11)-C (12)	119.7	(1.9)	C (12)-C (7)—C (8)	121.6	(1.9)
Cl——C (12)-C (7)	117.9	(1.6)	C (8)—C (15)-C (16)	107.3	(1.7)
C (15)-C (16)-C (17)	126.9	(2.1)	C (16)-C (17)-C (18)	118.9	(2.0)
C (16)-C (17)-C (20)	122.3	(2.0)	C (17)-C (18)-C (19)	125.7	(2.0)
C (20)-C (17)-C (18)	118.2	(1.8)	C (18)-C (19)-C (21)	127.6	(2.0)
C (19)-C (21)-C (22)	109.2	(1.7)	C (19)-C (21)-C (29)	112.6	(1.7)
C (19)-C (21)-C (26)	108.6	(1.7)	C (21)-C (22)-C (23)	113.0	(1.7)
C (21)-C (22)-C (27)	111.7	(1.8)	C (22)-C (23)-C (24)	110.4	(1.9)
C (27)-C (22)-C (23)	109.5	(1.8)	C (23)-C (24)-C (25)	109.1	(2.0)
C (24)-C (25)-C (26)	116.6	(2.0)	C (24)-C (25)-O (6)	123.5	(2.2)
C (25)-C (26)-C (21)	109.0	(1.7)	C (25)-C (26)-C (28)	114.3	(1.8)
O (6)—C (25)-C (26)	119.8	(2.1)	C (26)-C (21)-C (22)	107.0	(1.6)
C (28)-C (26)-C (21)	113.2	(1.7)			

is *cis* form, the chlorine atom of the chloroorcylic aldehyde residue comes at a position close to the benzene ring of the *p*-bromobenzenesulfonyl residue. The perpendicular line from the chlorine atom to the latter benzene ring drops inside the ring(distance 3.22 Å). This conformation is thus stabilized by the interaction between the benzene ring and the chlorine atom which has a larger electron affinity than the other atoms. These two benzene planes of the same molecule make an angle of 133°25′. In the case of siccanin-*p*-bromobenzenesulfonate,[9] the conformation of O–S–O–C bonds(at the ester linkage) is *trans* form and the ether oxygen atom in *D*-ring of siccanin comes above the benzene ring of *p*-bromobenzenesulfonyl residue.

The zigzag chain of the methylpentadiene residue takes all *trans* conformations, and the internal rotation angle[10] around the C(17)—C(18) bond is 175.9°. The bond lengths of C(17)—C(18) and C(19)—C(21), 1.47 and 1.48 Å, respectively, suggest that the π electrons in the methylpentadiene residue is delocalized.

The cyclohexanone ring adopts a typical chair form. As shown in Table 5, the two carbon atoms,

9) K. Hirai, S. Okuda, S. Nozoe, and Y. Iitaka, *Acta Cryst.*, **B25**, 2630 (1969).

10) The internal rotation angle around the B—C bond of A—B—C—D is defined as the angle between projection of A—B and that of C—D, when the projection is taken along the B—C bond. The positive value is taken in the same sense as that of the turning direction of a right handed screw advancing along the B—C bond.

TABLE 5. THE LEAST-SQUARE PLANES AND THE PERPENDICULAR DISTANCES OF THE ATOMS FROM THE PLANES

p-Bromobenzensulfonyl			
benzene:	$0.9602X-0.1337Y-0.2453Z+1.86488=0$		
C (1)	0.008 Å	C (4)	−0.029
C (2)	−0.023	C (5)	0.013
C (3)	0.033	C (6)	−0.003
Br	0.121	S	0.055
Chlorocyclic aldehyde			
benzene:	$0.8559X+0.2710Y+0.4406Z+4.53956=0$		
C (7)	0.017	C (10)	0.008
C (8)	−0.013	C (11)	−0.005
C (9)	0.000	C (12)	−0.008
Cl	0.124	C (14)	−0.134
C (13)	−0.077	O (5)	0.035
O (4)	0.092	O (3)	−0.005
salicyl aldehyde:	$0.8629X+0.2487Y+0.4399Z+4.37469=0$		
C (7)	0.009	C (10)	0.015
C (8)	−0.046	C (11)	0.026
C (9)	−0.024	C (12)	0.014
C (13)	−0.064	O (5)	0.027
O (4)	0.043		

where X, Y, Z are taken along the crystallographic a, b, and c axes, respectively, and measured in Å units.

C(25) and C(22), deviate by +0.64 and −0.70 Å, respectively, from the plane(A) formed by the four carbon atoms of C(21), C(23), C(24), and C(26). The two planes formed by C(21), C(22), and C(23), and by C(24), C(25), C(26), and O(6), intersect with the plane (A) at angles of 126.6° and 128.5°, respectively. Of the three methyl groups attached to the cyclohexanone ring, two are in equatorial (C(27), C(28)) and the other in axial position (C(29)). The same conclusion was deduced for the terpenoid metabolite (LL-Z1272-γ) from the NMR spectral data.[4]

The structures of the crystal projected along the c and a axes are shown in Figs. 4 and 5, respectively. As is clear from Fig. 5, the orcylic aldehyde and *p*-bromobenzenesulfonyl residues are stacked to construct the columns of aromatic rings along the a-axis and form the layers parallel to the (010) plane. The stacking of the two phenyl groups is such that the Br-ϕ and Cl-ϕ groups are arranged in anti-parallel fashion with respect to the halogen position. The cyclohexanone and the methylpentadiene residues are extended from the aromatic layers and fill up the spaces between them. The shortest intermolecular distances less than 3.8 Å are shown in Fig. 4, in which the molecules are designated by the molecular number I to IV as follows:

I at (x, y, z)
II at $(0.5+x, 0.5-y, 1-z)$
III at $(0.5-x, 1-y, -0.5+z)$
IV at $(1-x, -0.5+y, 2.5-z)$

The distance between the oxygen atom O(6) of keto group (IV) and the bromine atom (I) (3.33 Å) suggests the existence of rather strong van der Waals interaction between them (the sum of the van der Waals radii=3.35 Å).

Thanks are due to C. Itoh Electronic Computing Service for use of a CDC 3600 computer.

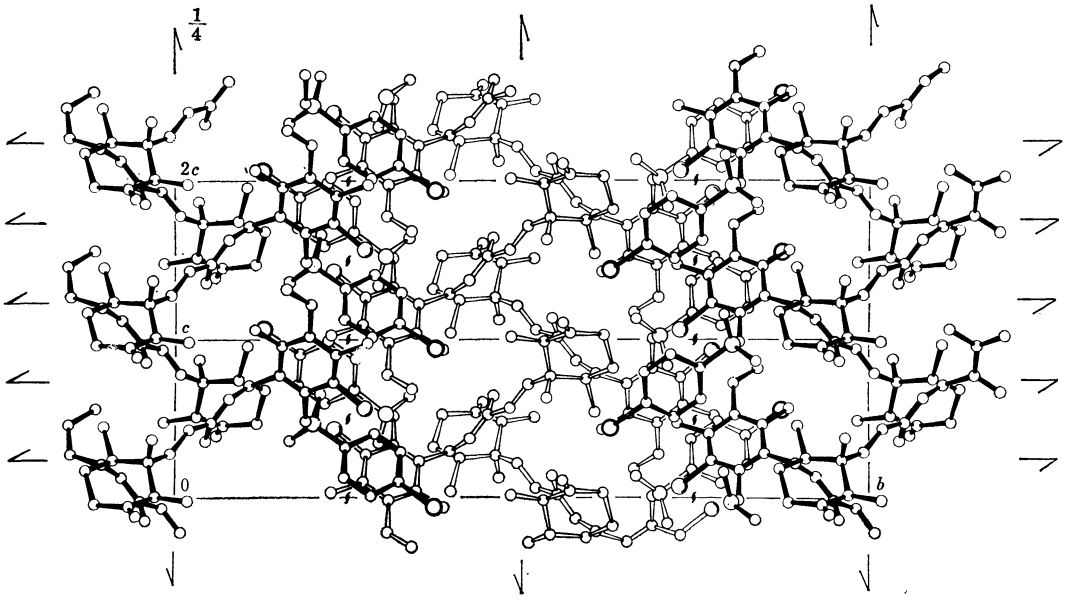

Fig. 5. Arrangement of the molecules in the unit cell viewed down [100].

Electrochemiluminescence of Aromatics in *N,N*-Dimethylformamide

Kenji MORI, Naoto YAMAMOTO, and Hiroshi TSUBOMURA

Department of Chemistry, Faculty of Engineering Science, Osaka University, Toyonaka, Osaka

(Received April 22, 1971)

Electrochemiluminescence (ECL) of aromatics was studied in dimethylformamide. The solutions were electrolyzed with square-wave voltage at various frequencies. For anthracene, emission from species produced by electrochemical reaction was observed together with anthracene fluorescence. These emissions were quenched when water was added to the solution. For rubrene and perylene, fluorescence from the molecules was observed. For phenanthrene, emission differing from phenanthrene fluorescence was observed at 515 mμ.

Many investigations have shown that alternating current electrolysis of aromatics hydrocarbons in conducting fluid media produces chemiluminescence.[1-6] The spectrum of this electrochemiluminescence (ECL) comprises, in most cases, normal or excimer fluorescences of the aromatics,[3] though spectra of different origin have sometimes been observed.[7]

The mechanism of the appearance of normal and excimer fluorescence in the ECL processes is generally recognized to be as follows.

Production of cation and anion

$$A - e^- \rightarrow A^+ \quad (1)$$

$$A + e^- \rightarrow A^- \quad (1)'$$

Combination of the ions yielding singlet or triplet excited states

$$A^+ + A^- \rightarrow {}^1A^* \text{ (or } {}^3A^*) + A \quad (2)$$

Triplet annihilation process

$$2\,{}^3A^* \rightarrow {}^1A^* + A \quad (3)$$

Emission of fluorescence

$${}^1A^* \rightarrow A + h\nu_F \quad (4)$$

Production of excimer

$$A^+ + A^- \rightarrow ({}^1A^*\cdots A) \quad (5)$$

Emission from excimer

$$({}^1A^*\cdots A) \rightarrow 2A + h\nu_{F'} \quad (6)$$

It has been suggested on the basis of energetics[2] that the fluorescent singlet state is generally formed rather from processes (3) and (4) via the triplet state than from the direct combination of cation and anion. To explain the ECL emission band at longer wavelengths than the normal fluorescence, the excimer fluorescence mechanisms (5) and (6) were proposed as well.[3] In some cases, the contribution from species electrochemically formed or from the impurities in the solution cannot be ignored.

In this paper, we report the studies on the ECL emission obtained for anthracence rubrene, perylene phenanthrene and pyrene in dimethylformamide (DMF), applying square-wave voltage at various frequencies.

Experimental

Anthracene and phenanthrene were recrystalized from benzene after passing through a column of silica gel and then sublimed in a vacuum. Commercially obtained rubrene and pyrene were sublimed in a vacuum. Perylene was recrystalized from toluene and then sublimed in a vacuum. Tetra-*n*-butylammonium perchlorate (TBAP) used as a supporting electrolyte was prepared from an aqueous solution of sodium perchlorate and tetra-*n*-butylammonium iodide and repeatedly recrystalized from aqueous solutions. DMF used as solvent was distilled at reduced pressure after standing for two days over potassium carbonate or magnesium sulfate. The distillate was stored in a vacuum desiccator. Acetonitrile was purified in the same way as described elswhere.[8]

The cell used is made of quartz, 30 mm in diameter, and has two platinum electrodes shown in Fig. 1, namely, a slightly curved plate (20×20 mm) and a rod 3 mm in diameter. The electrodes were 5 mm apart.

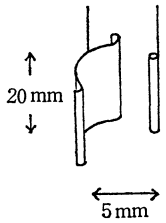

Fig. 1. The shape and arrangement of electrodes.

The solutions containing 10^{-3}—10^{-2} M aromatics and 5×10^{-1} M TBAP in DMF or acetonitrile were deaerated by bubbling with nitrogen gas before electrolysis. All solutions except for the cases of phenanthrene and pyrene were electrolyzed by applying voltage of the square-wave type generated from a transistor switching circuit shown in Fig. 2. Switching was controlled with a signal from a National VP-702B low frequency oscillator. The frequency was varied from 20 to 2×10^5 cps. ECL emission spectra were recorded in most cases using a Nalumi RM 23 monochrometer, an RCA 1P28 photomultiplier tube and a pen recorder. Response of the ECL emission was measured with a photomultiplier tube placed near the cell and a synchroscope (National VP 511B). Frequency dependence of the emission

1) D. M. Hercules, *Science*, **145**, 808 (1964); T. C. Werner, J. Chang, and D. M. Hercules, *J. Amer. Chem. Soc.*, **92**, 763 (1970).
2) G. J. Hoytink, *Discuss. Faraday Soc.*, **45**, 14 (1968).
3) E. A. Chandross, J. W. Longworth, and R. E. Visco, *J. Amer. Chem. Soc.*, **87**, 3259 (1965).
4) A. Zweig, D. L. Maricle, J. S. Brinen, and A. H. Maurer, *ibid.*, **89**, 473 (1967).
5) A. Weller and K. Zachariasse, *J. Chem. Phys.*, **46**, 4984 (1967).
6) M. Sano and F. Egusa, This Bulletin, **41**, 1490 (1968).
7) L. R. Faulkner and A. J. Bard, *J. Amer. Chem. Soc.*, **90**, 6284 (1968).
8) N. Yamamoto, Y. Nakato, and H. Tsubomura, This Bulletin, **39**, 2603 (1966).

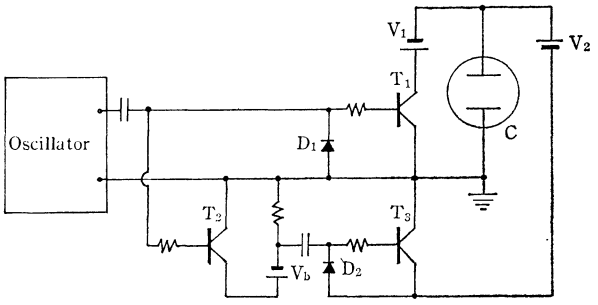

Fig. 2. Switching circuit for generating square-wave voltage.
V_1 and V_2; battery and resistance
V_b; 6—45 V
T_1, T_2 and T_3; 2SC525
D_1 and D_2; IN540
C; reaction cell

intensity was also recorded on the pen recorder through an AC-DC converter(Yokogawa 3142). During electrolysis, the ECL emission changed with time owing to irreversible electrochemical reactions. Measurements were, therefore, carried out immediately after the start of electrolysis. When acetonitrile was used as a solvent, the ECL intensity was found to be weaker than that for DMF. Detailed experiments were performed only for DMF solutions.

Results and Discussion

Anthracene. The ECL of anthracene was reported by two groups. Chandross *et al.* reported a broad spectrum with maximum at 450 mμ,[3,9] while Faulkner and Bard obtained a quite different spectrum having a rather sharp maximum at 400 mμ and another one at 460 mμ.[7] The ECL spectrum of anthracene in DMF we obtained is shown in Fig. 3, where the solution was electrolyzed at a frequency of 20 cps. The broken line shows an ECL spectrum for the applied voltage of 2.5 V.[10] The emission appearing at a wavelength shorter than 470 mμ has a shape similar to that of the normal fluorescence of anthracene and

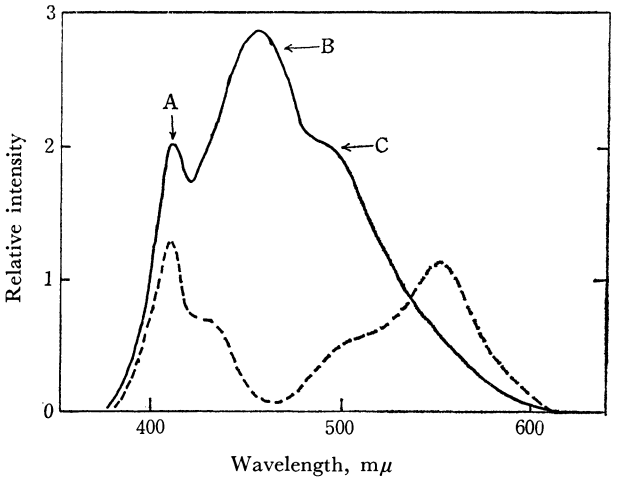

Fig. 3. Emission spectra of anthracence solution electrolyzed at 20 cps. --- at 2.5 V; —— at 3.6 V

9) R. E. Visco and E. A. Chandross, *J. Amer. Chem. Soc.*, **86**, 5350 (1964).

may be assigned to it. It is difficult to determine the species relevant to the 470—600 mμ emission from its spectral shape. The ECL emission spectra obtained at voltages lower than 3.0 V stayed essentially the same as the broken line in Fig. 3. Above 3.0 V, the spectrum changed very much. A typical example is shown by the solid line in Fig. 3 obtained at 3.6 V. The spectrum seems to consist of three components, (A) the fluorescence of anthracence, (B) a strong emission centered at 455 mμ, and (C) a shoulder at 500 mμ. The B band is similar to that previously obtained by Faulkner and Bard[7] who asigned it to the fluorescence of anthranol. When the applied voltage was varied in the range 3.0—6.0 V, the spectral feature did not change. It was found that the intensity ratio of the B band to the A band decreased with increase in the frequency of the applied voltage.

The total ECL response on the photomultiplier was traced with a synchroscope, and is shown in Fig. 4 together with the wave form of the applied voltage. It was confirmed from visual observation that the emission near the earthed electrode was so weak that its contribution to the wave form is negligible. Figure 4a shows a wave form of the ECL intensity obtained

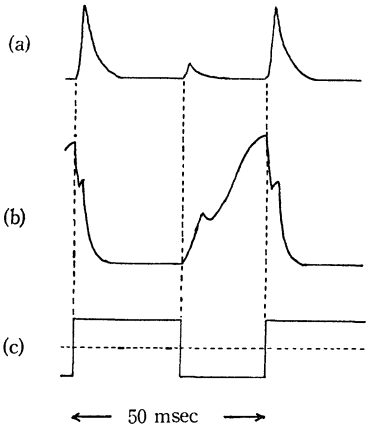

Fig. 4. Wave form of ECL intensity of anthracene solution,
(a) electrolyzed at 2.5 V.
(b) electrolyzed at 3.5 V.
(c) Wave form of the applied voltage.

at 2.5 V. There is a strong peak appearing immediately after the begining of each positive-half cycle, while the peak appearing at the negative-half cycle was very weak. It can be suggested that the emission results, for the most part, from an annihilation reaction of the cation and anion radicals of anthracence, and the marked difference between peak heights at positive- and negative-half cycles is explained by assuming that the cation radical is much more short-lived than the anion radical.[11] It is then expected that as the frequency is increased until its reciprocal is equal to the life-time of the cation radical or less,

10) In this paper, a rod-like electrode was earthed, and positive and negative voltages were alternately applied to the other electrode. The voltage given in the text indicates the absolute value of the voltage applied to the latter.

11) M. E. Peover and B. S. White, *J. Electroanal. Chem.*, **13**, 93 (1967).

the magnitudes of the two peaks should become alike. It was, in fact, found that the two peaks were equal in magnitude at 100 cps. When the solution was electrolyzed at 3.0 V, the ECL intensity increased but the wave form was identical with that obtained at 2.5 V.

At a voltage higher than 3.0 V, the ECL emission had a wave form as shown in Fig. 4b. There is a new strong peak at the negative-half cycle in addition to the peak described before. It can be easily deduced that this peak corresponds to the B band shown in Fig. 3 which appears only at a higher voltage. Since the peak has a long rise time and appears only at the negative-half cycle, it may be concluded that the B band is due to a species formed secondarily from the ionic species. As mentioned before, the higher the frequency, the smaller the intensity of the B band. This tendency may be explained very well by the results obtained in Fig. 4.

Frequency dependence of the ECL intensity was measured at 6.0 V (Fig. 5). Curve a shows a typical result obtained at wavelengths shorter than 405 mμ corresponding to the normal fluorescence of anthracence. The curve is nearly flat in the region up to 150 cps and quickly drops at higher frequencies. The drop at high frequency might be explained by the change of bulk impedance. Curve b in Fig. 5 shows a typical curve for the emission at longer wavelengths than 440 mμ. The curve decreases rapidly with frequency even in the range where curve a is flat. The result confirms also that the slow-rising component in Fig. 4b corresponds to the B band. Addition of water to the same solution as used above was found to quench the ECL emission.

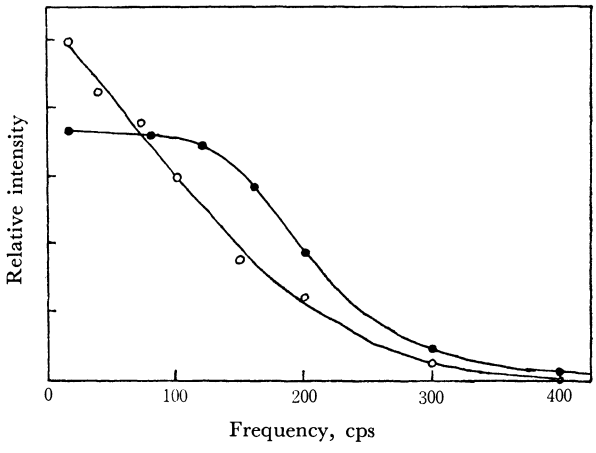

Fig. 5. Frequency dependence of ECL intensity of anthracene solution electrolyzed at 6.0 V. Curve a, emissions at wavelengths longer that 440 mμ (●), curve b, emissions in wavelengths shorter than 405 mμ (○).

From the position and shape of the spectrum, it seems reasonable to assign the B band at 455 mμ in Fig. 3 to the fluorescence of anthranol. As this band has a threshold voltage higher than that yielding the anthracene fluorescence and is observed as a slow-rising peak only at negative-half cycle (Fig. 5b), it may be suggested that anthracene dinegative ion participates in the mechanism yielding the anthranol fluorescence. At present, however, it is difficult to explain details of the anthranol emission process.

With the continuation of electrolysis, the ECL emission gradually changed its intensity as shown in Fig. 6. Here, the electrolysis was performed at an

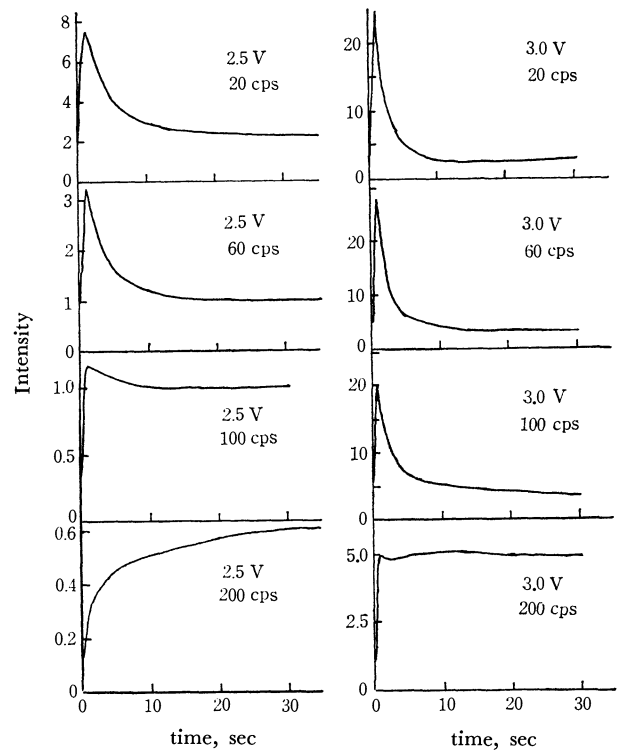

Fig. 6. Time dependence of ECL intensity of anthracene solution.

applied voltage below 3.0 V, and no emission band at 455 mμ appeared. From the curves shown in Fig. 8, the following relationships are derived.

(1) At a given frequency, the higher the voltage, the quicker the decay of emission.

(2) At a constant voltage, the greater the frequency, the slower the decay of emission.

Since the electric current increases with the applied voltage, it is reasonable to consider that irreversible chemical change of anthracene is promoted by increasing the voltage. Relation (1) seems to be based on it. It is expected that if the frequency is high enough, the cation radical formed on a positive-half cycle reacts efficiently with the anion radical and disappears. The annihilation of the cation may decrease the decomposition rate of anthracene. Relation (2) seems to be due to this.

Rubrene. The intense ECL emission of rubrene has been assigned to the normal fluorescence of rubrene.[12,13] All the ECL spectra we obtained at 1.8, and 3.6 V at the frequency of 20 cps had a peak identical with that of the normal fluorescence of rubrene. The wave form was also measured at various voltages. By the electrolysis of solution at 2.0 V, a strong peak

12) D. M. Hercules, R. C. Lansbury, and D. K. Roe, *J. Amer. Chem. Soc.*, **88**, 4578 (1966).

13) D. L. Maricle and A. H. Maurer, *ibid.*, **89**, 188 (1967).

appeared at the positive-half cycle and a weak peak at the negative-half cycle. Their average lifetimes were found to be about 2.5 msec. At 3.0 V, a slow-rising peak appeared at the positive-half cycle as well as sharp-rising peaks. The peak increased with time. It may be suggested that the sharp-rising peaks are the emission due to the annihilation between the cation and the anion radicals of rubrene, while the slow-rising peak is the emission originated from the reaction product from rubrene. In spite of the change of the wave form with the voltage, the spectrum did not change. It is possible that, even if the reaction product participates in the ECL emission, the excited singlet state of rubrene is finally formed by charge transfer process or by energy transfer process.

Perylene. The ECL-intensity of perylene was weak compared with that of anthracence and rubrene. The solution was electrolyzed at 2.5, 3.0, and 3.6 V at 50 cps. Concentration of TBAP was 5.6×10^{-2} M. The solid line in Fig. 7 shows a spectrum obtained at 3.0 V. The broken line shows the spectrum obtained by Chandross *et al.* who assigned it to the excimer fluorescence of perylene.[3] The spectrum we obtained is similar to that of the normal fluorescence of perylene. Wave form of the ECL intensity was also measured at various voltages (Fig. 8). It differs largely from that observed for anthracene or for rubrene. By increasing the voltage, the time lag for the sharp-rising on a negative-half cycle was found to become longer. In addition to the peak, there was a slow-rising peak in the positive-half cycle and even in the negative-half cycle at a higher voltage. Assuming that the ECL emssion is assigned only to the normal fluorescence, these results suggest that there is, in addition to the annihilation reaction, an other one producing the excited singlet state of perylene.

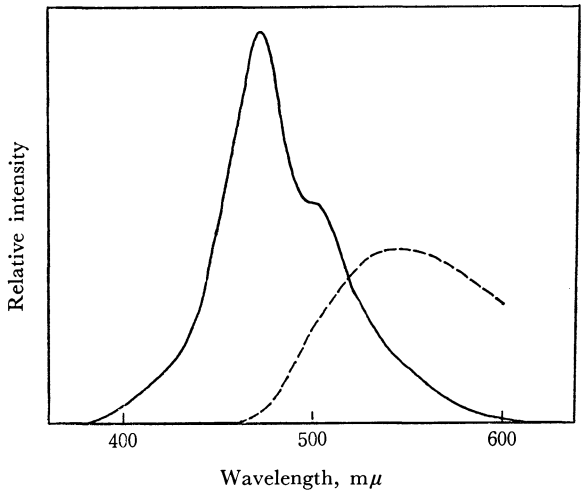

Fig. 7. Emission spectrum obtained from perylene solution electrolyzed at 3.0 V at 50 cps (solid line).
Broken line indicates ECL spectrum from a pyrene solution reported by Chandross *et al.*[3]

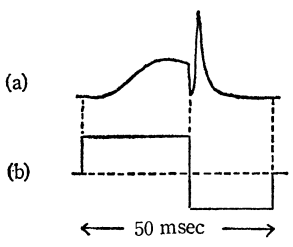

Fig. 8. Curve a, wave form of the ECL intensity of perylene solution electrolyzed at 2.5 V. Curve b, that of the applied voltage.

Frequency dependence of the ECL emission was measured at various voltages. Concentration of TBAP was 2.66×10^{-2} M. Curves (a) and (b) in Fig. 9 obtained at 3.0 and 4.0 V, respectively, decline monotonically with the frequency. Curves (c) and (d) at 5.0 and 6.0 V, respectively, have maxima. As the voltage increases, the maxima tend to shift toward the high frequency side. The shift seems to be related with the slow-rising peak.

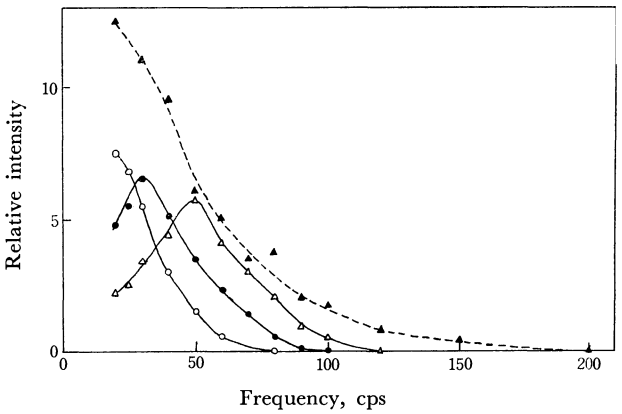

Fig. 9. Frequency dependence of the ECL emission from perylene solution, electrolyzed.
(a) ▲, at 3.0 V, 5.6×10^{-2} M TBAP;
(b) ○, at 4.0 V, 2.3×10^{-2} M TBAP;
(c) ●, at 5.0 V, 2.3×10^{-2} M TBAP;
(d) △, at 6.0 V, 2.3×10^{-2} M TBAP.

Phenanthrene. ECL emission spectrum from phenanthrene solution in DMF is shown in Fig. 10. Electrolysis was carried out with the sinusoidally alternating voltage of 60 cps. The spectrum obtained resembles that of the phosphorescence of phenanthrene. However, it seems unreasonable that the phosphorescence of phenanthrene should be observed so strongly in a solution at room temperature. Therefore, the

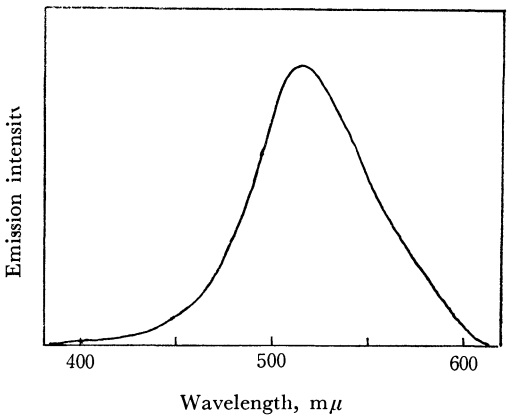

Fig. 10. Emission spectrum from phenanthrene solution.

possibility of an impurity luminescence cannot entirely be neglected.

Pyrene. When pyrene in DMF was electrolyzed with a DC voltage at 6.0 V, white-blue emission was observed at the anodic surface together with gas evolution. The emission intensity was so weak that we could not measure the spectrum.

Concluding Remark. There have been a few studies on the ECL imposing square wave voltage.[14] It may be emphasized that the observation of the wave form of the ECL-intensity as described in this paper is a useful method to study the mechanism of emission and the assignments of the emitting species. Measurement of the frequency dependence of the ECL emission bands may also give valuable information on the electrolytic reaction mechanisms.

14) A. Zweig, G. Metzler, A. H. Maurer, and G. Roberts, *J. Amer. Chem. Soc.*, **88**, 2864 (1966).

BULLETIN OF THE CHEMICAL SOCIETY OF JAPAN VOL. 44, 2665—2670 (1968)

The Crystal Structure of 3-(10,11-dihydro-5*H*-dibenzo[*a*,*d*]cyclohepten-5-ylidene)-1-ethyl-2-methylpyrrolidine Hydrobromide

Yoji Tokuma, Hiroshi Nojima, and Yukiyoshi Morimoto

Research Laboratories, Fujisawa Pharmaceutical Co., Ltd., Kashima-cho, Higashiyodogawa-ku, Osaka, Japan

(Received April 26, 1971)

The crystal structure of 3-(10,11-dihydro-5H-dibenzo[*a*,*d*]cyclohepten-5-ylidene)-1-ethyl-2-methylpyrrolidine hydrobromide, $C_{22}H_{26}NBr$, has been determined. The crystal is monoclinic with space group $P2_1/a$; the unit-cell dimensions are: $a=30.16$, $b=18.78$, $c=7.048$ Å, $\beta=90.53°$. The asymmetric unit contains two molecules. The intensities were estimated visually from the multiple-film equi-inclination Weissenberg photographs. The structure was solved by the heavy atom method. The atomic parameters were refined by the block-diagonal least-squares method, and final R index was reduced to 0.147. It is concluded that the overall geometry of the two independent molecules is similar in every detail The pyrrolidine ring is puckered. The 10,11-dihydro-5*H*-dibenzo[*a*,*d*]cyclohepten-5-ylidene part consists of three planes. The dihedral angles between the planes are 63° for the benzene planes I and II, 59° for the benzene plane I and the ylidene plane, and 76° for the benzene plane II and the ylidene plane.

3-(10,11-dihydro-5*H*-dibenzo[*a*,*d*]cyclohepten-5-ylidene)-1-ethyl-2-methylpyrrolidine hydrochloride (piroheptine hydrochloride) has been found to show antagonism of tremorine tremor by S. Kumada *et al.*[1] S. Umio *et al.*[2] have suggested that both piroheptine hydrochloride and piroheptine hydrobromide seemed to have more than two conformations in the solution on the basis of interpretation of NMR spectra.

From our interest in the relation[3] between structure and drug action, we undertook X-ray determination of the crystal structure of piroheptine hydrobromide in order to obtain useful information on its conformation in the solution.

As a result, conformation in the crystal seems to correspond to the most stable conformation in the solution suggested by NMR study.

Experimental

The crystal of piroheptine hydrobromide was obtained from a methanol-ether solution in the form of colorless prism elongated along the c axis.

Unit-cell dimensions were determined by the least-squares calculation, using 19 $hk0$ and 20 $0kl$ reflections whose Bragg angles were measured on zero-layer Weissenberg photographs taken with Cu$K\alpha$ radiation and calibrated with aluminum powder lines. The density was measured by flotation in a benzene-carbon tetrachloride mixture.

Crystal data:

Piroheptine hydrobromide, $C_{22}H_{26}NBr$; M=384.4; mp=237—240°C

Monoclinic, $a=30.16\pm0.008$, $b=18.78\pm0.014$, $c=7.048\pm0.003$ Å, $\beta=90.53\pm0.03°$, V=3992.0 Å^3

$D_m=1.28$, Z=8, $D_x=1.279$ g/cm^3

Absorption of X-ray, $\lambda=1.5418$ Å (Cu$K\alpha$); $\mu=31.3$ cm^{-1}.

$F(000)=1608$

Absent spectra: $h0l$ when h is odd, $0k0$ when k is odd. Space group is $P2_1/a$.

Since a unit-cell contains eight molecules, an asymmetric unit contains two crystallographically independent molecules.

The three dimensional intensity data of nickel-filtered Cu$K\alpha$ radiation were collected from the multiple-film equi-inclination Weissenberg photographs for the layer line 0—5 about the c axis and 0—2 about the b axis. The intensities of reflections out to spacings of 1 Å were visually estimated by comparison with a standard scale. The values of intensity ranged from 1 to 10,000. They were corrected for Lorentz and polarization factors; no absorption or extinction corrections were applied. Corrections for variation in spot-size on higher-layer photographs were made by the method of Phillips.[4] The intensity data from the b axis photographs were used only for layer scale adjustment of the a axis photo-

1) S. Kumada, M. Hitomi, and N. Kumadaki, private communication.

2) S. Umio, H. Nojima, and Y. Morimoto, private communication.

3) K. Larsson, *Acta Chem. Scard.*, **24**, 1503 (1970).

4) D. C. Phillips, *Acta Crystallogr.*, **7**, 746 (1954).

graphs. 3797 intensity data were obtained of which 800 were too weak to be observed.

Structure Determination

The coordinates of two bromine ions in an asymmetric unit were deduced from the Patterson function. A Fourier synthesis based on the coordinates of the two bromine ions clearly revealed all 46 light atoms. Succesive Fourier synthesis showed no spurious peak except for a few peaks about the bromine ions.

The positional and thermal parameters of the atoms were refined by the block-diagonal least-squares method minimizing $\sum w(|F_o|-|F_c|)^2$. The weighting scheme

Table 1. Final atomic coordinates (fractional), isotropic temperature factors (Å^2) and their standard deviations (Å, Å^2)

Atom	x (x)	y (y)	z (z)	B (B)
Br(A)	0.2057(0.002)	0.1038(0.002)	−0.1446(0.002)	
N(A1)	0.1914(0.012)	0.0982(0.012)	0.2925(0.012)	1.74(0.24)
C(A2)	0.1857(0.015)	0.1759(0.015)	0.3794(0.016)	2.10(0.31)
C(A3)	0.2324(0.016)	0.2033(0.016)	0.3762(0.017)	2.34(0.33)
C(A4)	0.2656(0.018)	0.1426(0.018)	0.3123(0.019)	3.30(0.39)
C(A5)	0.2350(0.017)	0.0748(0.017)	0.3580(0.018)	2.86(0.36)
C(A6)	0.1537(0.016)	0.0511(0.017)	0.3731(0.017)	2.82(0.35)
C(A7)	0.1592(0.022)	−0.0214(0.022)	2.2718(0.023)	5.32(0.51)
C(A8)	0.1516(0.017)	0.2164(0.017)	0.2519(0.018)	2.87(0.36)
C(A9)	0.1879(0.023)	0.4495(0.023)	0.4303(0.023)	5.56(0.52)
C(A10)	0.1648(0.023)	0.4428(0.024)	0.5911(0.024)	5.99(0.54)
C(A11)	0.1647(0.023)	0.3817(0.024)	0.7038(0.024)	5.94(0.55)
C(A12)	0.1940(0.021)	0.3213(0.022)	0.6308(0.022)	4.93(0.49)
C(A13)	0.2159(0.017)	0.3280(0.017)	0.4633(0.018)	3.07(0.36)
C(A14)	0.2461(0.016)	0.2699(0.016)	0.4152(0.017)	2.51(0.34)
C(A15)	0.2926(0.016)	0.2889(0.016)	0.3969(0.017)	2.62(0.34)
C(A16)	0.3237(0.019)	0.2693(0.019)	0.5338(0.020)	4.01(0.42)
C(A17)	0.3689(0.019)	0.2900(0.019)	0.5100(0.020)	4.19(0.43)
C(A18)	0.3810(0.023)	0.3271(0.023)	0.3542(0.024)	5.74(0.54)
C(A19)	0.3496(0.023)	0.3479(0.023)	0·2069(0.024)	5.82(0.54)
C(A20)	0.3062(0.019)	0.3288(0.019)	0.2360(0.019)	3.96(0.41)
C(A21)	0.2694(0.021)	0.3478(0.022)	0.0879(0.022)	5.29(0.49)
C(A22)	0.2396(0.023)	0.4073(0.023)	0.1680(0.024)	5.66(0.54)
C(A23)	0.2155(0.020)	0.3935(0.021)	0.3403(0.021)	4.67(0.45)
Br(B)	0.0288(0.002)	0.1225(0.003)	0.3356(0.002)	
N(B1)	0.0421(0.011)	0.1212(0.011)	0.7763(0.012)	1.38(0.23)
C(B2)	0.0478(0.016)	0.1970(0.016)	0.8692(0.016)	2.22(0.33)
C(B3)	0.0026(0.016)	0.2269(0.016)	0.8593(0.016)	2.38(0.33)
C(B4)	−0.0320(0.017)	0.1677(0.018)	0.8049(0.018)	3.09(0.37)
C(B5)	−0.0032(0.018)	0.0991(0.018)	0.8323(0.018)	3.31(0.38)
C(B6)	0.0795(0.018)	0.0708(0.019)	0.8551(0.019)	3.46(0.40)
C(B7)	0.0745(0.020)	−0.0004(0.021)	0.7517(0.021)	4.46(0.45)
C(B8)	0.0833(0.018)	0.2351(0.018)	0.7325(0.018)	3.30(0.38)
C(B9)	0.0633(0.025)	0.4628(0.026)	0.9316(0.026)	6.42(0.61)
C(B10)	0.0853(0.025)	0.4456(0.025)	1.0980(0.026)	6.79(0.61)
C(B11)	0.0811(0.027)	0.3838(0.028)	1.2043(0.028)	7.67(0.67)
C(B12)	0.0485(0.020)	0.3338(0.021)	1.1252(0.021)	4.47(0.45)
C(B13)	0.0248(0.017)	0.3477(0.017)	0.9642(0.018)	3.18(0.37)
C(B14)	−0.0089(0.016)	0.2927(0.016)	0.9037(0.017)	2.53(0.34)
C(B15)	−0.0552(0.018)	0.3179(0.018)	0.8818(0.018)	3.34(0.38)
C(B16)	−0.0855(0.022)	0.3014(0.022)	1.0301(0.023)	5.23(0.51)
C(B17)	−0.1308(0.027)	0.3304(0.027)	0.9990(0.027)	7.61(0.65)
C(B18)	−0.1390(0.026)	0.3673(0.027)	0.8481(0.027)	7.36(0.64)
C(B19)	−0.1114(0.025)	0.3881(0.025)	0.6974(0.026)	6.62(0.59)
C(B20)	−0.0642(0.021)	0.3616(0.021)	0.7184(0.021)	4.84(0.47)
C(B21)	−0.0288(0.026)	0.3812(0.027)	0.5730(0.027)	7.11(0.65)
C(B22)	0.0049(0.023)	0.4330(0.023)	0.6805(0.023)	5.59(0.52)
C(B23)	0.0303(0.019)	0.4110(0.019)	0.8620(0.019)	3.83(0.40)

Table 2. Anisotropic temperature factors for bromide ions (their standard deviations)

The anisotropic temperature factors are expressed in the from
$\exp[-(\beta_{11}h^2+\beta_{22}k^2+\beta_{33}l^2+\beta_{12}hk+\beta_{13}hl+\beta_{23}kl)]$

Atom	β_{11}	β_{22}	β_{33}	β_{12}	β_{13}	β_{23}
Br(A)	0.0017	0.0043	0.0199	0.0007	0.0004	0.0003
	(0.00003)	(0.00009)	(0.00062)	(0.00005)	(0.00011)	(0.00018)
Br(B)	0.0014	0.0052	0.0187	−0.0009	−0.0004	0.0005
	(0.00003)	(0.00010)	(0.00061)	(0.00005)	(0.00010)	(0.00019)

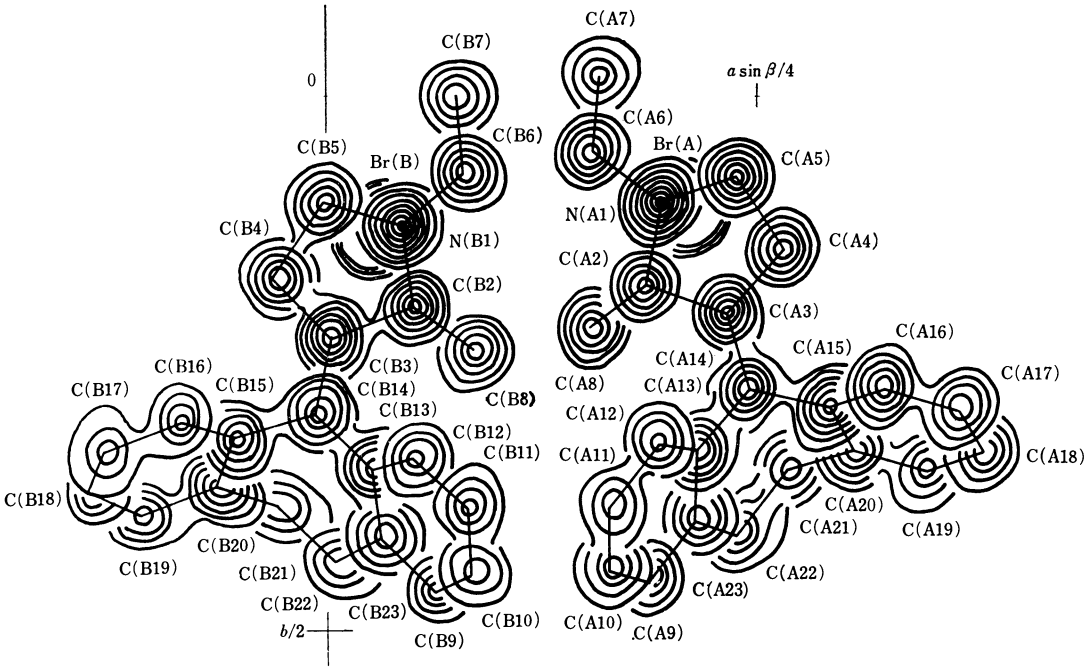

Fig. 1. A composite drawing of the final electron density map, viewed along the c axis. Contours are drawn at 1.5, 2.5, 3.5 e.Å^{-3}...for the light atoms. Contours for the bromide ions are omitted.

was; $w=0.3$ when $|F_o|=0$ and $w=1$ when $|F_o|\neq 0$. The scattering factors for H, C, N, and Br^- were taken from International Tables.[5] Two cycles of the least-squares refinement were carried out, assigning isotropic temperature factors to all atoms and ions. These two cycles decreased the reliability index R to 0.192. Four more cycles of the refinement were performed, assigning anisotropic temperature factors to two bromine ions. The R index was reduced to 0.147, excluding non-observed reflections ($R=0.188$, for all 3797 reflections).

The final atomic coordinates and isotropic temperature factors are given in Table 1, and the anisotropic temperature factors for the bromine ions in Table 2. The two independent molecules are denoted by symbols A and B. A composite drawing of the final electron density map is shown in Fig. 1.

All the numerical computations were carried out on a CDC 3600, C. Itoh Electronic Computing Service Co., Ltd. and a HITAC 8400, Fujisawa Pharmaceutical Co., Ltd. Most computing programs used were the application programs of C. Itoh Electronic Computing Service Co., Ltd.

5) "International Tables for X-ray Crystallography," Vol. III, Kynoch Press, Birmingham (1962), p. 202.

Discussion

Geometry of the molecule. Comparison of the corresponding bond lengths and angles in the two independent molecules are given in Table 3 and 4, and the average values of the corresponding bond lengths and angles in the two independent molecules are shown in Fig. 2. The bond lesgths and angles in the two molecules agree closely with each other, with a few exceptions. The root mean square deviations between the two molecules are 0.052 Å for the bond lengths and 4.0° for the bond angles. The C(3)–C(14) bond length 1.33 Å agrees with the standard C–C double bond length 1.34 Å.

The conformation of the pyrrolidine rings is shown in Fig. 3. Arabic numerals denote the displacements (in Å) of the atoms from the best plane of the pyrrolidine ring. The pyrrolidine rings are puckered. The conformation about the C(2)–N(1) bond by stereographic projection is shown in Fig. 4.

The 10,11-dihydro-5H-dibenzo[*a*,*d*]cyclohepten-5-ylidene part consists of the three planes. The first is benzene plane I through the C(9), C(10), C(11), C(12), C(13), C(23), C(14), and C(22) atom. The second is benzene plane II through the C(15), C(16),

Table 3. Bond lengths and their standard deviations

	A (σ)	B (σ)	Average		A (σ)	B (σ)	Average
N(1)-C(2)	1.59 (0.019)	1.57 (0.019)	1.58 Å	C(12)-C(13)	1.36 (0.028)	1.36 (0.027)	1.36 Å
N(1)-C(5)	1.46 (0.021)	1.49 (0.021)	1.47	C(13)-C(14)	1.46 (0.024)	1.51 (0.024)	1.49
N(1)-C(6)	1.55 (0.020)	1.57 (0.022)	1.56	C(13)-C(23)	1.50 (0.027)	1.40 (0.026)	1.45
C(2)-C(3)	1.50 (0.022)	1.48 (0.022)	1.49	C(14)-C(15)	1.45 (0.023)	1.48 (0.024)	1.47
C(2)-C(8)	1.56 (0.023)	1.61 (0.024)	1.59	C(15)-C(16)	1.39 (0.025)	1.43 (0.029)	1.41
C(3)-C(4)	1.59 (0.024)	1.57 (0.024)	1.58	C(15)-C(20)	1.42 (0.026)	1.44 (0.028)	1.43
C(3)-C(14)	1.34 (0.023)	1.32 (0.023)	1.33	C(16)-C(17)	1.43 (0.027)	1.48 (0.035)	1.46
C(4)-C(5)	1.61 (0.025)	1.57 (0.025)	1.59	C(17)-C(18)	1.35 (0.031)	1.29 (0.038)	1.32
C(6)-C(7)	1.55 (0.027)	1.53 (0.028)	1.54	C(18)-C(19)	1.45 (0.033)	1.41 (0.037)	1.43
C(9)-C(10)	1.34 (0.033)	1.38 (0.036)	1.36	C(19)-C(20)	1.38 (0.030)	1.51 (0.032)	1.45
C(9)-C(23)	1.49 (0.031)	1.47 (0.032)	1.48	C(20)-C(21)	1.56 (0.029)	1.53 (0.034)	1.54
C(10)-C(11)	1.40 (0.034)	1.39 (0.038)	1.39	C(21)-C(22)	1.55 (0.032)	1.59 (0.035)	1.57
C(11)-C(12)	1.53 (0.032)	1.47 (0.034)	1.50	C(22)-C(23)	1.44 (0.032)	1.54 (0.030)	1.49

Table 4. Bond angles and their standard deviations

	A (σ)	B (σ)	Average		A (σ)	B (σ)	Average
C(2)-N(1)-C(5)	105° (1.1°)	104° (1.1°)	104°	C(3)-C(14)-C(13)	123° (1.5°)	122° (1.5°)	123°
C(2)-N(1)-C(6)	107 (1.1)	109 (1.1)	108	C(3)-C(14)-C(15)	120 (1.5)	122 (1.5)	121
C(5)-N(1)-C(6)	112 (1.2)	113 (1.2)	113	C(13)-C(14)-C(15)	116 (1.4)	116 (1.4)	116
N(1)-C(2)-C(3)	102 (1.1)	103 (1.2)	102	C(14)-C(15)-C(16)	121 (1.6)	118 (1.6)	119
N(1)-C(2)-C(8)	107 (1.2)	103 (1.2)	105	C(14)-C(15)-C(20)	119 (1.5)	116 (1.6)	117
C(3)-C(2)-C(8)	116 (1.3)	115 (1.3)	115	C(16)-C(15)-C(20)	120 (1.6)	126 (1.8)	123
C(2)-C(3)-C(4)	111 (1.3)	111 (1.3)	111	C(15)-C(16)-C(17)	119 (1.7)	114 (2.0)	116
C(2)-C(3)-C(14)	127 (1.5)	126 (1.5)	127	C(16)-C(17)-C(18)	120 (1.9)	119 (2.4)	120
C(4)-C(3)-C(14)	122 (1.4)	123 (1.5)	123	C(17)-C(18)-C(19)	123 (2.1)	131 (2.6)	127
C(3)-C(4)-C(5)	98 (1.3)	101 (1.3)	99	C(18)-C(19)-C(20)	116 (2.0)	113 (2.1)	115
N(1)-C(5)-C(4)	103 (1.2)	104 (1.3)	103	C(15)-C(20)-C(19)	123 (1.8)	116 (1.8)	119
N(1)-C(6)-C(7)	105 (1.4)	107 (1.4)	106	C(15)-C(20)-C(21)	117 (1.6)	123 (1.9)	120
C(10)-C(9)-C(23)	126 (2.1)	117 (2.2)	121	C(19)-C(20)-C(21)	121 (1.8)	121 (2.0)	121
C(9)-C(10)-C(11)	124 (2.2)	127 (2.4)	126	C(20)-C(21)-C(22)	110 (1.7)	106 (1.9)	108
C(10)-C(11)-C(12)	114 (2.0)	113 (2.3)	114	C(21)-C(22)-C(23)	118 (1.9)	123 (1.9)	121
C(11)-C(12)-C(13)	121 (1.9)	123 (2.0)	122	C(9)-C(23)-C(13)	109 (1.7)	118 (1.8)	114
C(12)-C(13)-C(14)	116 (1.6)	117 (1.6)	116	C(9)-C(23)-C(22)	121 (1.9)	115 (1.8)	118
C(12)-C(13)-C(23)	125 (1.7)	122 (1.7)	123	C(13)-C(23)-C(22)	129 (1.8)	126 (1.7)	128
C(14)-C(13)-C(23)	119 (1.5)	121 (1.6)	120				

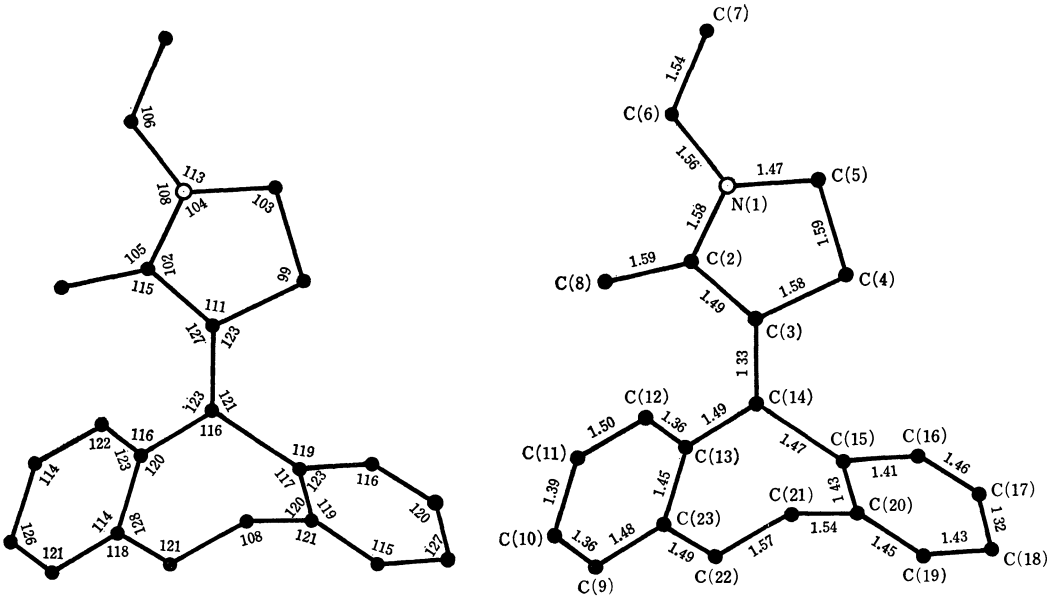

Fig. 2. Average values of the corresponding bond lengths and angles in the two independent molecules.

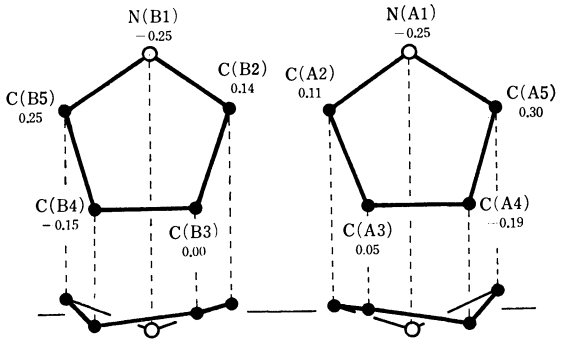

Fig. 3. Conformation of the pyrrolidine rings. Arabic numerals show the displacements (in Å) of the atoms from the best plane of the pyrrolidine rings.

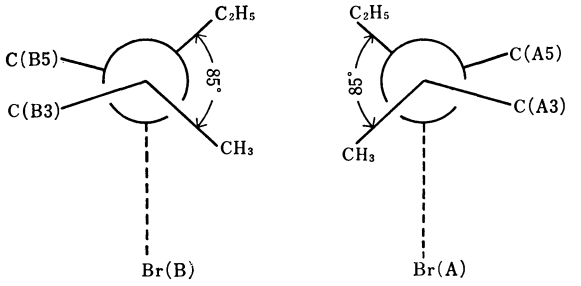

Fig. 4. Stereographic projection of the conformation about the C(2)-N(1) bond.

C(17), C(18), C(19), C(20), C(14), and C(21) atom. The third is the ylidene plane through the C(2), C(3), C(4), C(13), C(14), and C(15) atom. The equations for these planes, displacements of the individual atoms from the planes and the dihedral angles between the planes are given in Table 5.

It is concluded that the overall geometry of the two independent molecules is similar in every detail.

Packing of the Molecules. The drawing of the structure viewed along the *c* axis and the *b* axis are shown in Figs. 5 and 6, respectively. The N(1)···

Table 5. Best planes

(a) Equations[a)]

A molecule	
Benzene plane I	$0.7702X + 0.3770Y + 0.5073Z = 9.051$
Benzene plane II	$-0.1738X + 0.8552Y + 0.4898Z = 4.478$
Ylidene plane	$0.1221X - 0.2424Y + 0.9612Z = 2.460$
B molecule	
Benzene plane I	$-0.7118X + 0.4413Y + 0.5530Z = 6.124$
Benzene plane II	$0.2438X + 0.8247Y + 0.5081Z = 7.710$
Ylidene plane	$-0.1490X - 0.2461Y + 0.9591Z = 4.773$

a) X, Y, and Z in Å units.

(b) Displacements of atoms from the planes

Benzene plane I		Benzene plane II		Ylidene plane	
A molecule					
C(A9)	0.034 Å	C(A15)	−0.001 Å	C(A2)	−0.006 Å
C(A10)	0.025	C(A16)	−0.007	C(A3)	0.019
C(A11)	−0.007	C(A17)	0.006	C(A4)	−0.015
C(A12)	−0.013	C(A18)	0.001	C(A13)	−0.020
C(A13)	−0.057	C(A19)	−0.010	C(A14)	0.031
C(A23)	−0.041	C(A20)	0.013	C(A15)	−0.009
C(A14)	0.062	C(A14)	−0.001		
C(A22)	−0.002	C(A21)	−0.001		
B molecule					
C(B9)	−0.017	C(B15)	−0.034	C(B2)	−0.023
C(B10)	0.018	C(B16)	0.018	C(B3)	−0.025
C(B11)	0.010	C(B17)	0.024	C(B4)	0.036
C(B12)	−0.012	C(B18)	−0.006	C(B13)	0.025
C(B13)	−0.017	C(B19)	−0.021	C(B14)	0.022
C(B23)	−0.009	C(B20)	−0.008	C(B15)	−0.034
C(B14)	0.015	C(B14)	−0.006		
C(B22)	0.012	C(B21)	0.034		

(c) Dihedral angles between the planes

			A	B	Average
Benzene plane I	and	Benzene plane II	64°	62°	63°
Benzene plane I		Ylidene plane	60	59	59
Benzene plane II		Ylidene plane	76	76	76

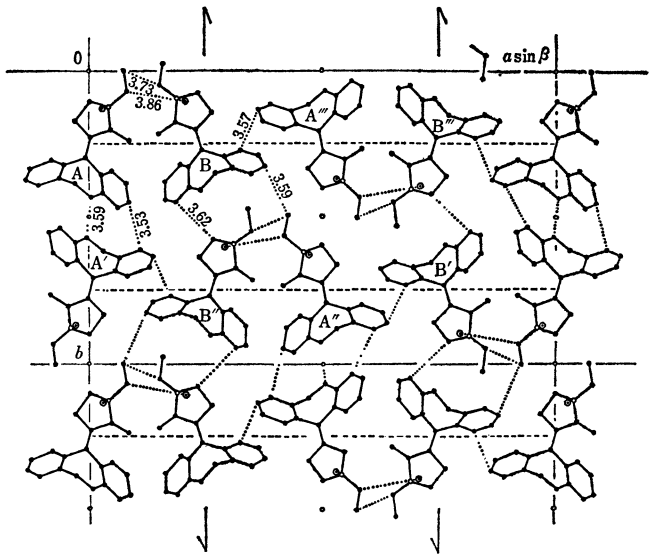

Fig. 5. A drawing of the structure viewed along the *c* axis. Some of the van der Waals contacts are indicated by dotted lines.

Br^- distances are 3.12 Å in the A molecule and 3.13 Å in the B molecule. In both A and B molecules, the C(2), C(5), C(6) atom, and the Br^- ion are approximately on the four vertices of a tetrahedron centered at the N(1) atom. The bond angles involving the N(1) atom and the Br^- ion are:

	A molecule	B molecule
$Br^-\cdots N(1)$-C(2)	111°	115°
$Br^-\cdots N(1)$-C(5)	101	99
$Br^-\cdots N(1)$-C(6)	119	116

The evidence thus obtained suggests that $N(1)\cdots Br^-$ form $N\text{–}H\cdots Br^-$ hydrogen bondings. They are indicated by the broken lines in Fig. 6.

Some shorter intermolecular distances are indicated by dotted lines in Figs. 5 and 6. No unusually short contact is found in this crystal structure.

The complete data of the F_o–F_c table are kept at the office of the Bulletin of the Chemical Society of Japan.[6]

The authors thank Miss Kazuko Nakayama for her assistance in the intensity measurement. They are also indebted to Professor Masao Kakudo and Dr. Tamaichi Ashida for discussions and suggestions.

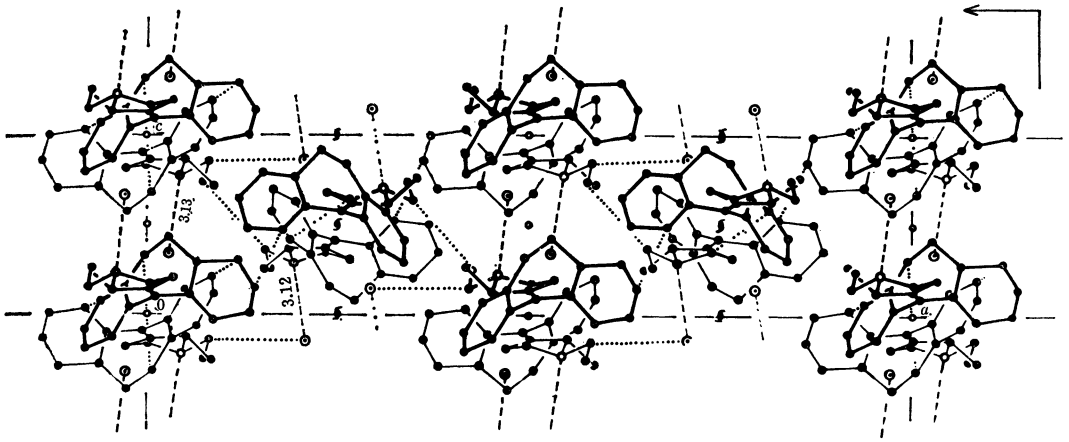

Fig. 6. A drawing of the structure viewed along the *b* axis. The hydrogen bonds and van der Waals contacts are indicated by broken and dotted lines, respectively.

6) Document No. 7115. A copy may be secured by citing the document number and remitting, in advance, ¥500 for photoprints. Pay by check or money order payable to: Chemical Society of Japan.

The Decomposition of Energized Ethylene Formed in the Photolyses of Alkanes

Yuji OGATA, Kinichi OBI, Hajime AKIMOTO, and Ikuzo TANAKA

Department of Chemistry, Tokyo Institute of Technology, Ohokayama, Meguro-ku, Tokyo

(Received May 4, 1971)

The decomposition and the collisional deactivation of energized ethylene formed in the photolyses of ethane, propane, *n*-butane, and cyclobutane at 1470 Å have been studied from the change in ethylene and acetylene yields with varying pressures of alkane or nitrogen added as a deactivator. The rate constants of the collisional deactivation and decomposition of energized ethylene were determined from the experimental data. The unimolecular decomposition theory has been applied to energized ethylene, and the results compared with the experimental rate constants.

In recent years, several studies of the Photolyses of simple alkanes, such as ethane,[1-5] propane,[6-9] *n*-butane,[9-11] and cyclobutane,[12] have been reported in respect of the primary processes. On the other hand, some studies of the photolyses of ethane[13,14] and propane[15] at 1470 Å have been undertaken in order to obtain insight into the nature of intermediate energized ethylene. These works have made it clear that two kinds of energized ethylene should be yielded through the molecular elimination of hydrogen from ethane or that of methane from propane; one undergoes unimolecular decomposition into acetylene and hydrogen, competing with collisional stabilization to ethylene, while the other can not decompose more. In the photolyses of ethane and propane, the following reaction schemes with respect to the ethylene- and acetylene-forming reactions have been proposed:[14,15]

$$C_2H_6 + h\nu \xrightarrow{\phi_{1a}} H_2 + C_2H_4^{**} \xrightarrow{k_d} C_2H_2 + H_2 \quad (1)$$
$$\qquad\qquad\qquad\qquad\qquad\qquad \searrow^{k_s^M[M]} \quad (2)$$
$$\xrightarrow{\phi_{1b}} H_2 + C_2H_4^{*} \longrightarrow C_2H_4$$
$$\xrightarrow{\phi_2} 2H + C_2H_4 \quad (3)$$
$$C_3H_8 + h\nu \xrightarrow{\phi_{1a}} CH_4 + C_2H_4^{**} \xrightarrow{k_d} C_2H_2 + H_2 \quad (4)$$
$$\qquad\qquad\qquad\qquad\qquad\qquad \searrow^{k_s^M[M]} \quad (5)$$
$$\xrightarrow{\phi_{1b}} CH_4 + C_2H_4^{*} \longrightarrow C_2H_4$$
$$\xrightarrow{\phi_2} H + CH_3 + C_2H_4 \quad (6)$$

The k_s^M/k_d values should depend on the energy retained in energized ethylene and the relative deactivation efficiencies of the deactivators. In order to determine the relative deactivation efficiency of energized ethylene, nitrogen was added as a common deactivator to a fixed amount of alkane and the change in the product distribution was studied by means of the change in the pressure of added nitrogen.

Recently, the nonequilibrium decomposition of ethylene has been discussed theoretically using a simple RRKM treatment, especially in the photolysis of 3-methyldiazirine.[16] In this paper, the average rate constants for the decomposition of ethylene produced in the photolyses of several alkanes will be calculated using the unimolecular decomposition theory. The experimental results are compared with the values obtained on a theoretical model for the relative deactivation rates, and a good agreement was found.

Experimental

The experimental procedures used in these experiments were almost the same as have been described previously.[15] A reaction cell with a magnetic circulator was used to prevent the accumulation of the products near the window. C_2H_6, C_3H_8, and *n*-C_4H_{10} were obtained from the Takachiho Chem. Ind. Co., and cyclo-C_4H_8 from Merck, Sharp, & Dohme, Ltd. Samples were purified by means of a gas chromatograph with a silica gel column. A 3 m activated charcoal column was used to detect ethylene and acetylene in a huge amount of unreacted ethane or propane. In the photolysis of *n*-C_4H_{10} or cyclo-C_4H_8, products were analyzed on a 2 m silica gel column with 5% squalane. In order to eliminate radical reactions, experiments were always carried out in the presence of nitric oxide (5—10% of alkanes).

Results and Discussion

A) Experimental Average Rate Constants. The reaction scheme previously established in the photolyses of ethane and propane,[14,15] in which the energized ethylene in two excited states is formed, may be similarly adopted in the photolyses of *n*-butane and cyclobutane:

$$n\text{-}C_4H_{10} + h\nu \xrightarrow{\phi_{1a}} C_2H_6 + C_2H_4^{**} \xrightarrow{k_d} C_2H_2 + H_2 \quad (7)$$
$$\qquad\qquad\qquad\qquad\qquad\qquad \searrow^{k_s^M[M]} \quad (8)$$
$$\xrightarrow{\phi_{1b}} C_2H_6 + C_2H_4^{*} \longrightarrow C_2H_4$$
$$\xrightarrow{\phi_2} H + C_2H_5 + C_2H_4 \quad (\text{and/or } 2CH_3 + C_2H_4) \quad (9)$$

1) H. Okabe and J. R. McNesby, *J. Chem. Phys.*, **34**, 668 (1961).
2) R. F. Hampson, Jr., J. R. McNesby, H. Akimoto, and I. Tanaka, *ibid.*, **40**, 1099 (1964).
3) H. Akimoto, K. Obi, and I. Tanaka, *ibid.*, **42**, 3864 (1965).
4) R. F. Hampson, Jr., and J. R. McNesby, *ibid.*, **42**, 2200 (1965).
5) S. G. Lias, G. J. Collin, R. E. Rebbert, and P. Ausloos, *ibid.*, **52**, 1841 (1970).
6) H. Okabe and J. R. McNesby, *ibid.*, **37**, 1340 (1962).
7) P. Ausloos, S. G. Lias, and I. B. Sandoval, *Discuss. Faraday Soc.*, **36**, 66 (1963).
8) P. Ausloos and S. G. Lias, *J. Chem. Phys.*, **44**, 521 (1966).
9) P. Ausloos and S. G. Lias, *Ber. Bunsenges. Physik. Chem.*, **72**, 187 (1968).
10) M. C. Sauer, Jr., and L. M. Dorfman, *J. Chem. Phys.*, **35**, 497 (1961).
11) H. Okabe and D. A. Becker, *ibid.*, **39**, 2549 (1963).
12) R. D. Doepker and P. Ausloos, *ibid.*, **43**, 3814 (1965).
13) R. F. Hampson, Jr., and J. R. McNesby, *ibid.*, **43**, 3592 (1965).
14) H. Akimoto and I. Tanaka, *J. Phys. Chem.*, **71**, 4135 (1967).
15) H. Akimoto and I. Tanaka, *Ber. Bunsenges. Physik. Chem.*, **72**, 135 (1968).
16) A. W. Kirk and E. Tschuikow-Roux, *J. Chem. Phys.*, **51**, 2247 (1969).

$$\text{cyclo-}C_4H_8 + h\nu \xrightarrow{\phi_{1a}} C_2H_4 + C_2H_4^{**} \xrightarrow{k_d} C_2H_2 + H_2$$
$$\xrightarrow{k_s^M[M]} \quad (10)$$
$$\xrightarrow{\phi_{1b}} C_2H_4 + C_2H_4^{*} \longrightarrow C_2H_4 \quad (11)$$

In the case of cyclobutane, the primary process of radical splitting is not observed.[17]

In the presence of nitrogen, the energized ethylene is deactivated upon collision with alkane itself or nitrogen. Thus, assuming the reaction schemes described above, and neglecting the internal scavenging reaction of hydrogen atoms by products at a very low conversion, the following equations are obtained for ethane, propane, and *n*-butane:

$$\frac{\phi(C_2H_4)}{\phi(C_2H_2)} = \frac{\phi_2+\phi_{1b}}{\phi_{1a}} + \frac{k_s^M}{k_d}\left(1+\frac{\phi_2+\phi_{1b}}{\phi_{1a}}\right)[M] + \frac{k_s^{N_2}}{k_d}\left(1+\frac{\phi_2+\phi_{1b}}{\phi_{1a}}\right)[N_2] \quad (12)$$

and for cyclo-C_4H_8:

$$\frac{\phi(C_2H_4)}{\phi(C_2H_2)} = \frac{\phi_{1a}+2\phi_{1b}}{\phi_{1a}} + \frac{2k_s^M}{k_d}\left(1+\frac{\phi_{1b}}{\phi_{1a}}\right)[M] + \frac{2k_s^{N_2}}{k_d}\left(1+\frac{\phi_{1b}}{\phi_{1a}}\right)[N_2] \quad (13)$$

where $\phi(C_2H_4)$ and $\phi(C_2H_2)$ are the relative yields of ethylene and acetylene respectively, and M is C_2H_6, C_3H_8, or *n*-C_4H_{10} for Eq. (12) and cyclo-C_4H_8 for Eq. (13).

Figure 1 shows the ratios of C_2H_4 to C_2H_2 in the photolyses of pure C_2H_6, C_3H_8, *n*-C_4H_{10}, and cyclo-C_4H_8 as a function of the alkane pressure. Also, varying amounts of nitrogen were added to a fixed amount of alkane (28 Torr), and the ratios were measured as a function of the N_2 pressure, as is shown in Fig. 2. These results show that Eqs. (12) and (13) are satisfied.

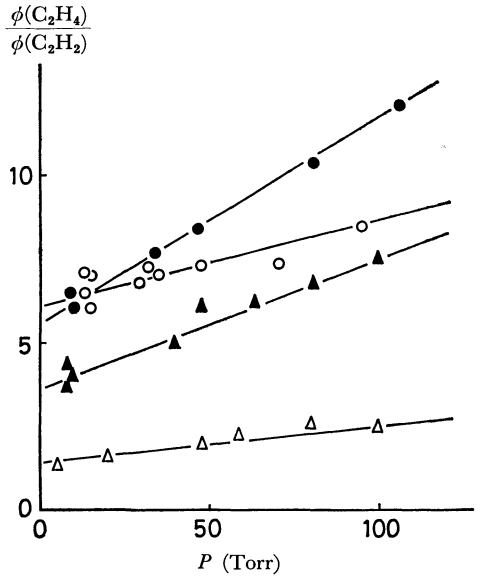

Fig. 1. Ethylene to acetylene ratio *vs.* alkane pressure. C_2H_6 (△), C_3H_8 (▲), *n*-C_4H_{10} (●), and cyclo-C_4H_8 (○)

17) K. Obi, Y. Ogata, H. Akimoto, and I. Tanaka, *J. Chem. Phys.*, in press.

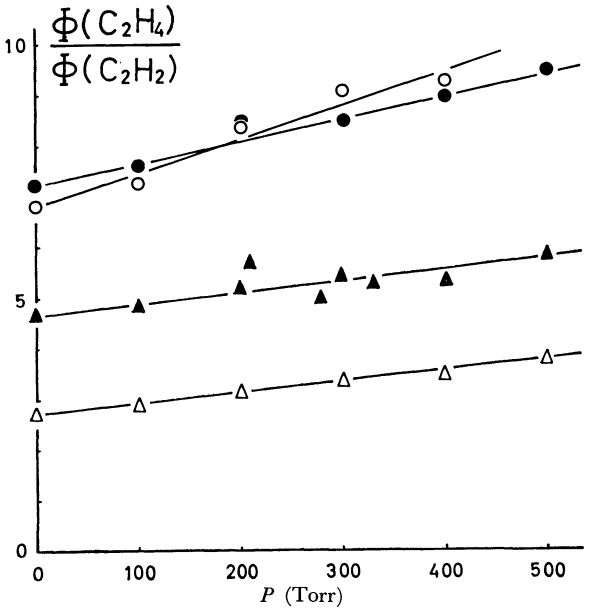

Fig. 2. Ethylene to acetylene ratio *vs.* added nitrogen pressure in the photolyses of alkanes. C_2H_6 (△), C_3H_8 (▲), *n*-C_4H_{10} (●), and cyclo-C_4H_8 (○)

The values of ϕ_2 were determined from the relative yields of methane and ethane in the photolyses of propane and *n*-butane respectively; this will be discussed elsewhere.[17] From the intercepts and the slopes of the plots in Figs. 1 and 2, the values of ϕ_{1a}, ϕ_{1b}, k_s^M/k_d and $k_s^{N_2}/k_d$ can be determined. The results are summarized in Table 1.

Table 1. The relative yields of the primary processes and the ratios of rate constants in the photolyses of alkanes at 1470 Å

	ϕ_{1a}	ϕ_{1b}	ϕ_2	k_s^M/k_d (Torr^{-1})	$k_s^{N_2}/k_d$ (Torr^{-1})
C_2H_6	0.39	0.46	0.15	0.0047	0.00088
C_3H_8	0.20	0.20	0.60	0.0089	0.00051
n-C_4H_{10}	0.15	0.19	0.66	0.0095	0.00064
cyclo-C_4H_8	0.28	0.72		0.0039	0.00097

Since the rate of deactivation would not be equal to the strong collision frequency, the rate constant of deactivation, k_s^M, is written as follows:

$$k_s^M = \frac{\beta Z^{C_2H_4-M}}{[M]} \quad (14)$$

where β is the collisional deactivation probability and $Z^{C_2H_4-M}$ is the collision frequency between the energized ethylene and the deactivator, M. The latter was calculated by means of the gas kinetic theory.

If the unit probability of energy transfer per collision is assumed for propane, the experimental values of k_s^M/k_d and $k_s^{N_2}/k_d$ and the collision frequencies yield values of β for the other deactivators. The values of β and k_s^M are summarized, together with the collision diameters, in Table 2.

The value of β is supposed to be affected by the nature and the degree of internal freedom of the deactivators. It can easily be understood that β increases with the complexity of the molecule from nitrogen to propane. A small decline from propane to *n*-butane would result from the experimental error. An unexpected lower value is found for cyclobutane. This lower value probably cames from the different character of the internal modes of vibrations compared with those of other paraffins or from the formation of energized ethylene with a different nature. The energized ethylene formed from chain alkanes results from the isomerization of the ethylidene produced in the primary processes, while that from cyclobutane is formed directly. The different nature of the energized ethylene can, therefore, be expected to be formed in the case of cyclobutane. If this is the case, it would be reasonable to obtain the lower value of β.

The experimental average rate constants for the decomposition of energized ethylene can be obtained by using the values of k_s^M (in Table 2) and k_s^M/k_d (in Table 1).

Table 2. The collisional diameters, the collisional deactivation probabilities and the rate constants of deactivation

	σ_{M-M} [a] (A)	β	k_s^M (Torr^{-1} sec^{-1})
N_2	3.85	0.063	8.03×10^5
C_2H_6	4.38	0.33	4.77×10^6
C_3H_8	5.24	1	1.58×10^7
n-C_4H_{10}	5.87	0.78	1.34×10^7
cyclo-C_4H_8	5.0	0.25	3.60×10^6
C_2H_4	4.07		

a) Values are taken from J. O. Hirschfelder, C. F. Curtis, and R. P. Bird, "Molecular Theory of Gases and Liquids," John Wiley & Sons, Inc., New York, N. Y. (1964), p. 1214, or are reasonable estimates based on data given in this reference.

B) Calculated Average Rate Constants. It was assumed in this treatment that the energized ethylene molecules decomposing to acetylene and hydrogen were composed of highly vibrational-excited ground-state ethylene.[13] The energized ethylene produced in the photolyses of alkanes may not be monoenergetic. If the energy distribution function of energized ethylene is expressed as $f(E)$, the average rate constant for the decomposition of ethylene is written as follows:[18]

$$k_d = \frac{\int \frac{k_E}{k_E+\omega} f(E)\,dE}{\int \frac{1}{k_E+\omega} f(E)\,dE} \tag{15}$$

where k_E is the specific rate constant for the decomposition of ethylene at energy E (which can be calculated from the RRKM theory), and ω is the rate of the deactivation of energized ethylene (assumed to be independent of the energy), which is equal to $k_s^M[M]$.

18) B. S. Rabinovitch and D. W. Setser, *Advan. Photochem.*, **3**, 1 (1964).

Calculations of the Specific Rate Constant, k_E: The specific rate constant for the decomposition of ethylene at energy E is given by the RRKM theory as follows:[19,20]

$$k_E = \frac{1}{h}\frac{\sigma}{\sigma^+}\left(\frac{I_A{}^+ I_B{}^+ I_C{}^+}{I_A I_B I_C}\right)^{1/2} \frac{\sum P(E-E_0)}{N(E)} \tag{16}$$

where σ and σ^+ are the symmetric numbers of the active molecule and the activated complex, I_i and $I_i{}^+$ are the moments of inertia of the active molecule and the activated complex respectively, and E_0 is the critical energy for the decomposition of ethylene to acetylene and hydrogen.

$N(E)$ is the energy level density for the active molecule at energy E. If there is no active internal free rotation for the active molecule, the expression for $N(E)$ is:

$$N(E) = \frac{(E+aE_z)^{s-1}}{\Gamma(s)\prod_i h\nu_i} \tag{17}$$

which is given by Rabinovitch and Setser,[18] where a is a correcting factor, s is the number of the degrees of freedom for the vibration, and E_z is the zero-point energy (*i.e.* $1/2\sum_i h\nu_i$).

$\sum P(E-E_0)$ is the sum of the energy levels for the activated complex, and in the absence of an active internal free rotation for the activated complex, it is written as follows:[21]

$$\sum P(E-E_0) = \frac{(E-E_0+a^+E_z{}^+)^{s^+}}{\Gamma(s^++1)\prod_i h\nu_i{}^+} \tag{18}$$

Thus, the expression for k_E (*i.e.* Eq. (16)) is:

$$k_E = \frac{1}{h}\frac{\sigma}{\sigma^+}\left(\frac{I_A{}^+ I_B{}^+ I_C{}^+}{I_A I_B I_C}\right)^{1/2} \times \frac{\Gamma(s)\prod h\nu_i}{\Gamma(s^++1)\prod h\nu_i{}^+} \frac{(E-E_0+a^+E_z{}^+)^{s^+}}{(E+aE_z)^{s-1}} \tag{19}$$

In this paper, the rigid and semirigid models were considered as an activated complex. The structure of the activated complex was assumed to be as follows:

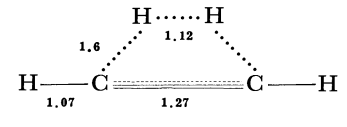

(unit; Å)

The fundamental frequencies and the moments of inertia for the active molecule and activated complexes are given in Table 3. The correlation between the fundamental frequencies is also shown. The frequencies of the fundamental modes of the activated complexes leading to the vibrational modes of products were estimated roughly from the average values of the initial and final systems. The vibrations leading to the free rotation in the final system were taken to have

19) R. A. Marcus and O. K. Rice, *J. Phys. Colloid. Chem.*, **55**, 894 (1951).

20) G. M. Wieder and R. A. Marcus, *J. Chem. Phys.*, **37**, 1835 (1962).

21) R. A. Marcus, *ibid.*, **20**, 359 (1952).

Table 3. Structure parameters

	C_2H_4[a]	Model I	Model II	$C_2H_2+H_2$[a]
frequency (cm^{-1})	3094 (4) (A_{1g}, B_{1g}, B_{2u}, B_{3u})	3200 (2) (A_{1g}, B_{3u})	3200 (2)	4160 (1) H_2
		3094 (1) (B_{1g})	1500 (1)	3330 (2) C-H
	1623 (1) (A_{1g})	1800 (1) (A_{1g})	1800 (1)	1974 (1) C≡C
	1392 (2) (B_{3u}, A_{1g})	2800 (1) (A_{1g})	2800 (1)	
	1024 (3) (B_{1g}, B_{2u}, A_{1u})	850 (4) (B_{3u}, B_{1g}, B_{2u}, B_{2g})	850 (4)	729 (2) (E_g)
		1024 (1) (A_{1u})	510 (1)	612 (2) (E_u)
	946 (2) (B_{2g}, B_{1u})	946 (1) (B_{1u})	470 (1)	free rot.
		trans.	trans.	trans.
zero-point energy (eV)	1.35	1.21	1.05	
moments of inertia				
$I_A=$	33.7×10^{-40}	33.0×10^{-40}	33.0×10^{-40}	
$I_B=I_C=$ ($g\cdot cm^2$)	16.8×10^{-40}	16.5×10^{-40}	16.5×10^{-40}	
number of symmetry	4	2	2	

a) G. Herzberg "Molecular Spectra and Molecular Structure II, Infrared and Raman Spectra," Van Nostrand, Princeton, N. J. (1945). p. 290 and 326.

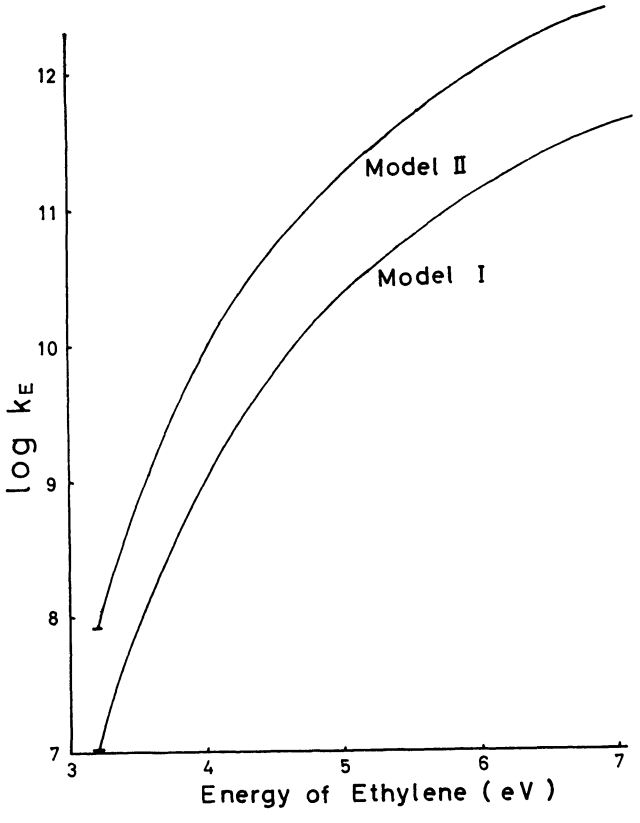

Fig. 3. Variation of the specific rate constant with energy of ethylene.

the same values in the initial system for the rigid model, but were lowered to half those values for the semirigid model.

E_0 was assumed to be 74 kcal/mol (3.2 eV).[22] The correcting factor has a value of 0.7—0.8 when the energy is small, rising to unity at a sufficiently high energy.[18] Since the decomposition reaction would occur near the critical energy, we assumed that $a=1$ and $a^+=0.8$.

Figure 3 shows the plots of log k_E as a function of energy E. The specific rate constant calculated using Model I is rather claser to that obtained by Kirk and Tschuikow-Roux[16] than that calculated using Model II. The difference in the specific rate constants is mainly due to the values of E_0 and the frequencies of the activated complex. These values make it possible to make an arbitrary choice, while there has not previously been any reliable value in the literature.

Calculation of the Energy Distribution Function, $f(E)$: It can be expected that the energized ethylene molecules produced in the photolyses of various alkanes will have energy spreads. However, at present there exists no *a priori* method to determine the energy distribution of the products of the reaction. A simple statistical distribution was used in this paper. If all the internal degrees of freedom for alkane are in an energy equilibrium everwhere on the reaction surface, one can determine the relative concentration of products with energy E simply from the phase-space consideration. The fraction of energized ethylene molecules which have an energy E out of the total available energy, E_t, can be written[23,24] as:

$$f(E)=\frac{N_{C_2H_4}(E)\cdot N_R(E_t-E)}{\sum N_{C_2H_4}(E_i)\cdot N_R(E_t-E_i)} \qquad (20)$$

22) I. D. Gay, R. D. Kern, G. B. Kistiakowsky, and H. Niki, *J. Chem. Phys.*, **45**, 2371 (1966).

Table 4. The ratios of the yields of primary processes and the experimental and calculated rate constants of decomposition

	$\phi_{1b}/(\phi_{1a}+\phi_{1b})$			A (eV)	$k_d(\text{sec}^{-1})\times 10^{-9}$		
	exp.	calc. from Eq. (20)	calc. (corr.) from Eq. (22)		exp.	Model I	Model II
C_2H_6	0.54	0.08	0.50	2.2	1.01	0.33	1.21
C_3H_8	0.50	0.44	0.50	0.4	1.78	1.00	2.90
n-C_4H_{10}	0.56	0.91	0.55	−3.4	1.41	1.02	2.84
cyclo-C_4H_8	0.72	0.55	0.71	1.0	0.92	0.31	1.05

where $N_{C_2H_4}(E)$ is the energy-level density of the ethylene part of alkane, $N_R(E_t-E)$ is that of the remaining degrees of freedom of alkane, and E_t is the total available energy. The energy-level densities were calculated by means of Eq. (17).

The total available energy is written as follows:

$$E_t = E(\text{h}\nu) + E(\text{thermal}) - \Delta H \qquad (21)$$

where $E(\text{h}\nu)$ is the photon energy of the exciting wavelength, which is equal to 8.4 eV at 1470 Å, E(thermal) is the thermal energy of the active molecule at the initial temperature (neglected in this paper), and ΔH is the heat of the reaction. The total available energies are 6.99, 7.57, 7.44, and 7.60 eV for ethane, propane, n-butane, and cyclobutane respectively.

The energy distribution function of the energized ethylene calculated from Eq. (20) is shown in Fig. 4(a), with ethane as the example. As C_2H_4* is thought to have a smaller energy than the critical energy,[16,25] the fraction of C_2H_4* can be estimated from Fig. 4(a). As may be seen in Table 4, the estimated values differ from the experimental values. Therefore, the correcting parameter, A, was introduced into Eq. (20) as follows:

$$f(E) = \frac{N_{C_2H_4}(E)N_R(E_t-A-E)}{\sum N_{C_2H_4}(E_i)N_R(E_t-A-E_i)} \qquad (22)$$

The correcting parameter was determined so that the fractions of C_2H_4* calculated from the energy distribution functions of Eq. (22) were nearly equal to the experimental fractions of C_2H_4*. The experimental fractions, the calculated fractions, and the correcting parameter are summarized in Table 4. The corrected energy distribution of energized ethylene is shown in Fig. 4(b), with ethane as the example.

The correcting parameter expresses the difference between the simple statistical distribution as calculated by Eq. (20), and the real energy distribution of energized ethylene. The correcting parameter is larger than zero in the photolysis of ethane, propane, or cyclobutane, while it is negative for n-butane. It is interpreted that energized ethylene would have a smaller vibrational energy than that to be expected from the simple statistical distribution for the positive A value, in other words, that the relative translation

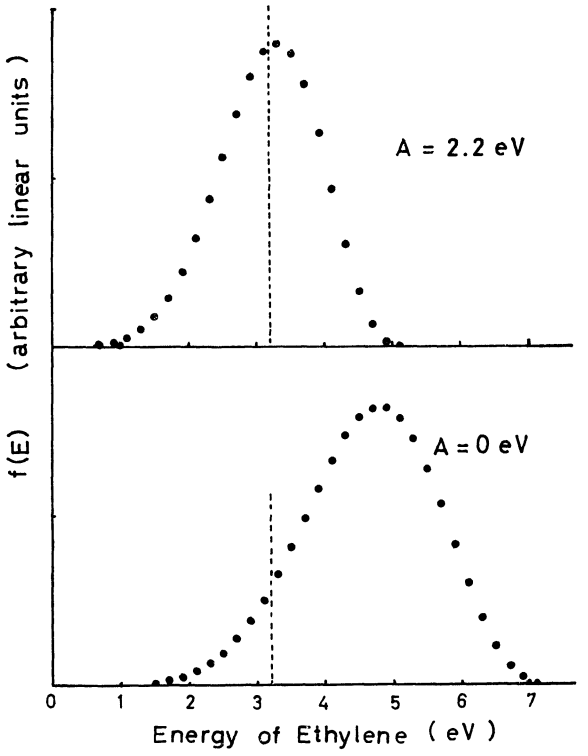

Fig. 4. Energy distributions of ethylene formed in the photolysis of ethane. (a) is calculated without a correcting parameter A; (b) is calculated with a correcting parameter A=2.2 eV.

or rotation of the products would take away a larger energy than that to be expected from Eq. (20). In particular, the correcting parameter is fairly large in the case of ethane. According to the Monte Carlo calculations,[26] this may be explained by the large energy transfer into the relative translational mode, since the hydrogen molecule in the products is quite light.

Calculation of the Average Rate Constants, k_d: A graphical integration procedure consists of approximating the energy distribution above E_0 to a histogram of regular energy intervals (ΔE=0.2 eV). The average rate constants for the decomposition can be calculated by means of Eq. (15) using the values of k_E, $f(E)$ and k_s^M. When the pressure of alkane is 100 Torr, the experimental rate constants and the calculated

23) R. J. Campbell and E. W. Schlag, *J. Amer. Chem. Soc.*, **89**, 5103 (1967).
24) P. Cadman, H. M. Meunier, and A. F. Trotman-Dickenson, *ibid.*, **91**, 7640 (1969).
25) A. Mele and H. Okabe, *J. Chem. Phys.*, **51**, 4798 (1969).
26) P. J. Kuntz E. M. Hemeth, J. C. Polanyi, S. D. Rosner, and C. E. Young, *J. Chem. Phys.*, **44**, 1168 (1966).

ones for the two kinds of the activated complex are summarized in Table 4.

In spite of the fairly simple estimation of the vibrational frequencies of the activated complexes, the calculated rate constants show good agreement with the experimental ones. Although it is not possible to choose between the two model, these simple models yield satisfactory results.

BULLETIN OF THE CHEMICAL SOCIETY OF JAPAN, VOL. 44, 2676—2681 (1971)

Nuclear Quadrupole Resonance Study of Charge Transfer Complexes: Chloranil Complexes

Hideaki CHIHARA and Nobuo NAKAMURA

Department of Chemistry, Faculty of Science, Osaka University, Toyonaka, Osaka

(Received May 4, 1971)

^{35}Cl nuclear quadrupole resonance frequencies were measured in electron donor-acceptor complexes between chloranil (tetrachloro-*p*-benzoquinone) and such donors as aromatic hydrocarbons, polyaromatics and amines. Some correlations between the resonance frequencies and infrared spectra were found and discussed in a qualitative way in terms of the π-electron transfer between donors and the chloranil molecule as acceptor. A Zeeman effect experiment was carried out on a single crystal of the 1:2 chloranil-8-hydroxyquinoline complex. The direction of one of the two non-equivalent C–Cl bonds obtained slightly differs from that determined by an X-ray diffraction study. Possible effects of the charge transfer on the resonance frequency and the asymmetry parameter are discussed according to the Mulliken theory of 'weak' charge-transfer complex. No simple relations could be found between the experimental resonance frequencies and the ionization potential of the donor. This suggests that crystal field effects are rather large in comparison with the effect of charge transfer interaction.

A great number of experimental works have been carried out on various charge transfer (CT) complexes. Most of the data on the electronic and infrared spectra, dipole moments, and electron spin resonances were successfully interpreted by Mulliken's theory of the electron donor-acceptor complexes.[1)]

Recently some questions have been raised about the role of the CT forces in the formation of the CT complexes.[2–4)] Moreover, the extent to which the CT forces contribute to the stability of the CT complexes has not been settled.[5)]

As the electric field gradient (EFG) at a nucleus is a quantity sensitive to a small intermolecular perturbation in a crystal,[6)] one should be able to obtain some information about the existence and/or the degree of charge transfer from the donor (D) to the acceptor (A), by applying the nuclear quadrupole resonance (NQR) method to the CT complexes in a coordinated way. Hooper found that the shift in the NQR frequencies upon the complex formation was so slight that it could reasonably be concluded that there was virtually no CT in the ground state.[7)] On the other hand, Read and others have found that the NQR frequencies both of Br_2 and of C_6H_5Br are influenced when they form a CT complex.[8)]

Gilson and O'Konski pointed out that an NQR frequency at a temperature other than 0°K can not be directly correlated with the CT force because the frequency changes with temperature.[9)] The controversial situation as to whether the charge transfer is in fact responsible for the formation of such complexes seems to arise from differences in the nature of interactions between a particular pair of the donor and the acceptor molecules.

The complexes studied are so called σ-π complexes and analysis of the NQR data may be complicated by a variety of donor-acceptor interactions. The π-π complexes, on the other hand, usually assume rather simple crystal structures in which D and A molecules stack alternately and can be treated as approximately rigid molecules.[10)] Thus information concerning CT interaction could be obtained from the NQR data of weak CT complexes containing one specified acceptor and various donors, since the crystal field effect is not expected to change seriously.

We chose chloranil (CA) as an acceptor and measured the NQR frequencies in its CT complexes. While our work was in progress several authors reported on

1) a) R. S. Mulliken, *J. Amer. Chem. Soc.*, **74**, 811 (1952). b) R. S. Mulliken, *Rec. Trav. Chim.*, **75**, 845 (1956). c) R. S. Mulliken and W. B. Person, *Ann. Rev. Phys. Chem.*, **13**, 107 (1962).

2) M. J. S. Dewar and C. C. Thompson, Jr., *Tetrahedron Suppl.*, **7**, 97 (1966).

3) J. L. Lippert, M. W. Hanna, and P. J. Trotter, *J. Amer. Chem. Soc.*, **91**, 4035 (1969).

4) R. J. W. Lefevre, D. V. Radford, and P. J. Stiles, *J. Chem. Soc.*, **1968**, B 1297.

5) R. S. Mulliken and W. B. Person, *J. Amer. Chem. Soc.*, **91** 3409 (1969).

6) a) T. P. Das and E. L. Hahn, "Nuclear Quadrupole Resonance Spectroscopy," Academic Press, New York (1958). b) E. A. C. Lucken, "Nuclear Quadrupole Coupling Constants," Academic Press, New York (1969).

7) H. O. Hooper, *J. Chem. Phys.*, **41**, 599 (1964).

8) M. Read, R. Cahay, P. Cornil, and J. Duchesene, *Compt. Rend.*, **257**, 1778 (1963).

9) D. F. R. Gilson and C. T. O'Konski, *J. Chem. Phys.*, **48**, 2767 (1968).

10) a) S. C. Wallwork, *J. Chem. Soc.*, **1961**, 494. b) C. K. Prout and J. D. Wright, *Angew. Chem.*, **80**, 688 (1968).

NQR studies on organic CT complexes.[11–13]

Semin and others found that in picryl chloride complexes the ^{35}Cl NQR frequencies can be correlated with the ionization potential of D's.[13]

This paper presents NQR frequencies of CA complexes with aromatic hydrocarbons and amines and gives discussion on the relation of NQR parameters to other quantities pertaining to the CT interactions in the light of Mulliken's CT theory. The result of the Zeeman effect experiment on CA-8-hydroxyquinoline complexes is compared with that of X-ray analysis.[14]

Experimental

Chloranil was purified by recrystallization from a benzene solution. The *N,N*-dimethylaniline complex was obtained by mixing solid chloranil and *N,N*-dimethylaniline directly under stirring followed by washing with ether. Bis-8-hydroxyquinolinatocopper(II) complex was prepared after the method in literature.[15] Other complexes were prepared by mixing the warm benzene solutions of the D- and A-components.

The ^{35}Cl NQR was observed at liquid nitrogen temperature with a Dean-type super-regenerative detector.[16] The resonace frequencies (ν_Q) were determined on an oscilloscope by use of a VHF signal generator (Yokogawa-Hewlett-Packard Model 608C) and a frequency counter (Takeda Riken TR-5578). The error in the frequency measurement was about 1 kHz except for the case of *p*-phenylenediamine complex for which the resonance line was very weak and broad, the uncertainty being about 5 kHz. The Zeeman effect study was carried out at liquid nitrogen temperature with Helmholtz coils and a goniometer designed for low temperature studies.[17] The zero-splitting loci for the ^{35}Cl reosnance lines were determined on an oscilloscope by rotating the sample and the magnetic field about mutually orthogonal axes. A magnetic field strength between 150 and 300 gauss was used.

Unsuccessful attempts were made to find the ^{35}Cl resonance lines in the frequency range 25—42 MHz in the chloranil complexes with the following donors: phenothiazine, *p*-anisidine, benzidine, tetramethyl-*p*-phenylenediamine, *p*-aminodiphenylamine, 1,8-diaminonaphthalene, and K^+-(chloranil)$^-$. Absence of the resonance lines is probably

Table 1. Nuclear quadrupole resonance frequencies, infrared frequencies and the ionization potentials of chloranil complexes

No	Donor	ν_Q at 77°K (MHz)	ν(C–Cl) b_{2u} (cm^{-1})	ν(C=O) (cm^{-1})	I_p (eV)
1	Durene	27.3958	739	1685	8.3[b]
2	Hexamethylbenzene	37.5031	737	1686	7.95[b]
		37.7127			
3	Pyrene	37.735	731	1687	7.45[c]
		37.872			
4	Perylene	37.3448	731	1682	7.1[c]
		37.3595	737		
		37.4102			
		37.4775			
5	*N,N*-Dimethylaniline	36.9039	730	1682	7.3[b]
		37.1373	739		
		37.3612	744		
6	*P*-Phenylenediamine	36.944			
7	Tetramethylbenzidine	37.3561			
8	1,5-Diaminonaphthalene	36.875			
		37.520			
9	8-Hydroxyquinoline(1:2)	37.2808	742	1688	7.9[d]
		37.3904			
10	Bis-8-hydroxyqunolinato-Copper (II)	36.8353	741	1680	7.3[d]
		37.2196	755		
	Chloranil	37.4414	755[a]	1683[a]	
		37.4693		1695[a]	
		37.5134			
		37.5830			

a) Reference 22. b) G. Bregleb and J. Czekalla, *Z. Elektrochem.*, **63**, 6 (1959). c) Reference 15. d) Reference 15.

11) R. A. Bennett and H. O. Hooper, *J. Chem. Phys.*, **47**, 4855 (1967).

12) G. A. Bowmaker and S. Hacobian, *Aust. J. Chem.*, **22**, 2047 (1969).

$\pm 0.2°$ and $x/a=5269(14)$ for the coordinate of O(2) in Table 2 of his paper.

15) A. S. Bailey, R. J. P. Williams, and J. D. Wright, *J. Chem. Soc.*, **1965**, 2579.

due either to some imperfections in the complex or to the effect of the occlusion of the solvent. It is also possible that delocalized unpaired electrons prevent the observation of the NQR lines in the case of the radical salts.

Results and Discussion

The ^{35}Cl NQR frequencies of chloranil in the complexes together with those in the pure chloranil crystal are listed in Table 1. The resonance frequencies in CA-hexamethylbenzene complex slightly differ from those in literature.[18] The number of resonance lines in 8-hydroxyquinoline, hexamethylbenzene, and pyrene complexes coincides with that of the non-equivalent chlorine atoms in these complexes.[14,19,20]

It is to be noted that the resonance signals have been observed in freshly prepared specimens of *N,N,N',N'*-tetramethylbenzidine, 1,5-diaminonaphthalene and *p*-phenylenediamine complexes but they faded out in about a week. This phenomenon is perhaps due to decomposition of the complexes. On the other hand, in hexamethylbenzene, pyrene and perylene complexes the resonance lines became progressively sharper during several months. This might be due to the relaxation of the lattice strain produced in the preparation process.

In Table 1, C–Cl b_{2u} and C=O stretching frequencies are also recorded. They were measured for solid complexes in nujol mull and were assigned according to Prichard[21] and Yamada and Kawamori.[22]

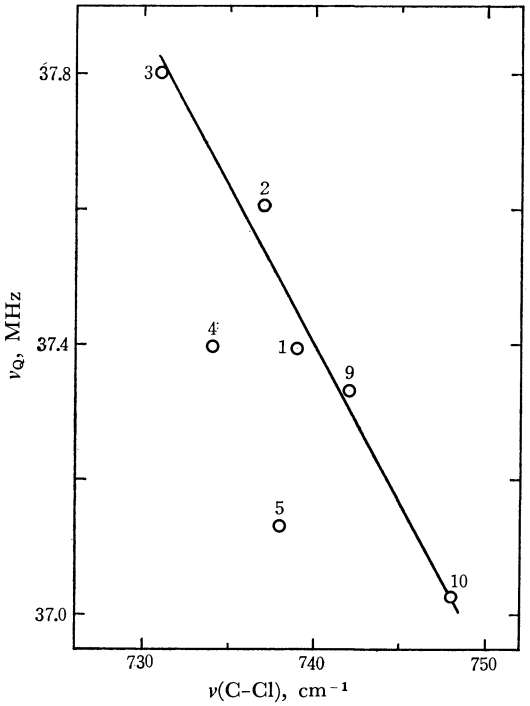

Fig. 1. The average nuclear quadrupole resonance frequency plotted against the C–Cl b_{2u} stretching frequency. For the numbers expressing the complexes cf. Table 1.

18) D. C. Douglass, *J. Chem. Phys.*, **32**, 1882 (1966).
19) T. T. Harding and S. C. Wallwork, *Acta Crystallogr.*, **8**, 787 (1955).
20) K. Ogawa, private communication.
21) F. E. Prichard, *Spectrochim. Acta*, **20**, 127 (1964).
22) H. Yamada and M. Kawamori, to be published.

Correlation between the Quadrupole Resonance Frequencies and Infrared Spectra. In Figs. 1 and 2 the average NQR frequency ν_Q is plotted against the average C–Cl b_{2u} and C=O stretching frequencies for each complex, respectively. Although almost linear relationship between ν_Q and C–Cl b_{2u} mode holds in Fig. 1, the slope inclined in the opposite direction to that found experimentally[23] or predicted theoretically[24] for simple σ-bonded molecules. We see from Fig. 2 that ν_Q changes more rapidly than the C=O stretching frequency in the same direction.

These facts can be interpreted qualitatively as follows: The large inductive effect of an oxygen atom, making its π-electron density increase, increases the partial π-bond character between the carbon and the chlorine atoms in a free CA molecule to make the bond stronger than those in chlorobenzenes. Now, if a charge transfer complex is formed between CA and a molecule acting as an electron donor, the π-electron density on the CA molecule increases. This seems to make the two C=O bonds stronger,[25] whereas the π-bond character in the four C–Cl bonds decreases in

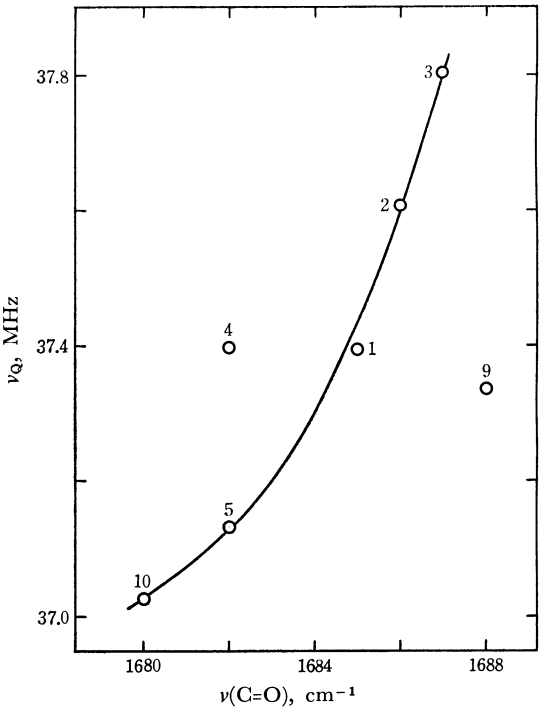

Fig. 2. The average nuclear quadrupole resonance frequency plotted against the C=O stretching frequency. For the numbers expressing the complexes, cf. Table 1.

23) R. Gerdil, *Nature*, **212**, 922 (1966).
24) A. B. Anderson, N. C. Handy, and R. G. Parr, *J. Chem. Phys.*, **50**, 3634 (1969).
25) In view of the very narrow range in which ν(C=O) changes its frequency, the trend appearing in Fig. 2 may not be significant enough for us to state that the charge transfer increases the C=O bond order (strength). In fact, ν(C=O) is displaced to a *lower* frequency by a radical ion formation (*cf.* Y. Matsunaga, *Can. J. Chem.*, **38**, 1172 (1960); Y. Iida, This Bulletin, **43**, 345 (1970); M. A. Slifkin, *Phys. Lett.*, **7**, 195 (1970)). Perhaps in the limit of weak complexes, the transfer of minute quantity of electronic charge might affect the C=O and C–Cl bonds in a different way from that in the case of strong complexes.

comparison with that in the bonds in a free CA molecule. Therefore, ν(C=O) shifts to a higher frequency and ν(C–Cl) to a lower with an increase in the effective number of π-electrons on CA due to the complex formation. ν_Q is expected to increase in such a situation as will be discussed in the next section. Then it seems reasonable to consider that the correlations between ν_Q and infrared frequencies in Figs. 1 and 2 originate from the charge transfer.

Predictions by Theory of Charge Transfer and Comparison with Experiments. The ground state wave function of a CT complex may be given after Mulliken[1b] by

$$\Psi_N = a\psi_0 + b\psi_1 \quad (1)$$

where ψ_0 and ψ_1 are the wave functions for the no-bond and the CT structures, respectively, and both are assumed to have been normalized.

We are interested in the electric field gradient (EFG) q at a chlorine nucleus in the acceptor molecule, which is given by

$$q = \sum_i e_i \int \Psi_N (3\cos^2\theta_i - 1)/r_i^3) \Psi_N d\tau + q_{ex} \quad (2)$$

In this equation the resonant ^{35}Cl nucleus is assumed to be at the origin; the sum represents the contributions to q from the nuclear or the electronic charges e_i at the position r_i and θ_i in the molecule. The summation in Eq. (2) must be carried out over all the nuclei and the electrons in the molecule. The second term q_{ex} is the EFG which comes from all molecules in the crystal except for the acceptor under consideration. Substituting Eq. (1) into Eq. (2), q is written as

$$q = a^2 q_0 + 2abq' + b^2 q_{CT} + q_{ex} \quad (3)$$

where

$$q_0 = \sum_i e_i \int \psi_0 (3\cos^2\theta_i - 1)/(r_i^3)\psi_0 d\tau$$

$$q' = \sum_i e_i \int \psi_0 (3\cos^2\theta_i - 1)/(r_i^3)\psi_1 d\tau$$

and

$$q_{CT} = \sum_i e_i \int \psi_1 (3\cos^2\theta_i - 1)/(r_i^3)\psi_1 d\tau$$

q_0 is the EFG in the no-bond structure and is thought to be approximately equal to that in a free acceptor molecule. q' is the EFG connecting the no-bond and the CT states. It will be roughly proportional to the overlap integral between the donor and the acceptor $S = \int \psi_0 \psi_1 d\tau$. q_{CT} represents the EFG in the CT state where one π-electron has been transfered from the donor to the acceptor.

By using the normalization condition on Ψ_N,

$$a^2 + 2abS + b^2 = 1$$

Eq. (3) can be rewritten as follows.

$$q = q_0 + 2ab(q' - Sq_0) + b^2(q_{CT} - q_0) + q_{ex} \quad (4)$$

If it is assumed that the second term on the right hand side of Eq. (4) is small in comparison with the other terms, and that q_{ex} varies only slightly from one donor to another, we can expect that the EFG is linearly dependent on the amount of contribution of the CT state b^2 to the ground state of the complex. Then it follows that

$$q \fallingdotseq q_0' + b^2 \Delta q_{CT} \quad (5)$$

where $q_0' = q_0 + q_{ex}$ and $\Delta q_{CT} = q_{CT} - q_0$ or in terms or the resonance frequencies

$$\nu_Q \fallingdotseq \nu_0' + b^2 \Delta \nu_{CT} \quad (6)$$

The contribution of the CT structure b^2 can also be related to the ionization potential I_p of a donor through the formula

$$b/a \fallingdotseq cS/(I_p - A) \quad (7)$$

where c and A are constants. Since $a \approx 1$ for a weak complex, it follows that

$$\nu_Q \fallingdotseq \nu_0' + \Delta \nu_{CT}(cS)^2/(I_p - A)^2 \quad (8)$$

A comparison of the experimental results with theoretical predictions is a very crucial matter.

Equation (6) states that ν_Q should increase when chloranil forms a CT complex. However, Table 1 shows that the resonance frequencies for some of the complexes are lower than the frequency for chloranil itself, whereas those for other complexes are higher. This fact may be an indication of the relieved strain of chloranil molecules upon complex formation. Therefore comparison among a family of donors seems more practical. Hydrocarbon donors give higher ν_Q than do the nitrogen- or oxygen-containing donors. Reliable values of b^2 have not been obtained except for hexamethylbenzene[26] and durene[27] complexes which b^2 of the order of 0.04 has been assigned.

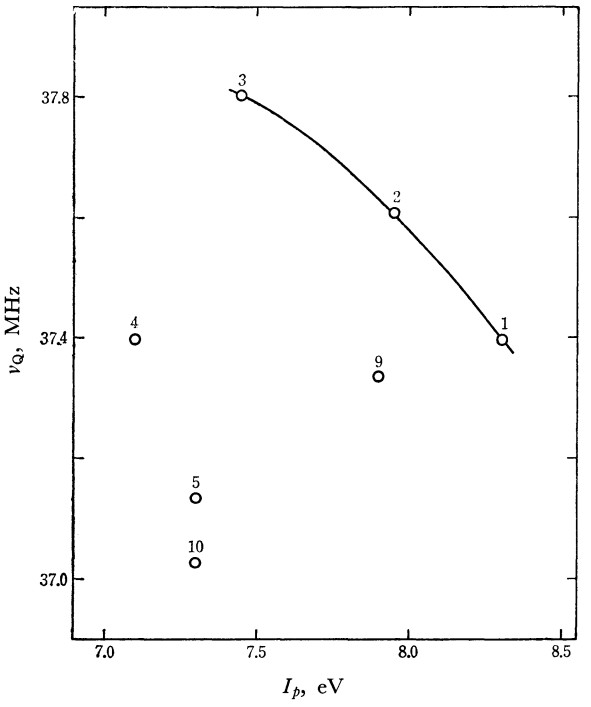

Fig. 3. The average nuclear quadrupole resonance frequency ν_Q *vs.* the ionization potential of the complex.
For the numbers expressing the complexes cf. Table 1.

26) G. Briegleb, J. Czekalla, and G. Reuss, *Z. Phys. Chem.*, **30**, 333 (1961).
27) G. Briegleb and J. Czekalla, *Angew. Chem.*, **72**, 401 (1960).

Correlation of ν_Q with I_p or the CT absorption bands is also very poor as seen in Fig. 3.

The reason for the poor correlation between the quadrupole resonance and the available CT properties is probably twofold. One is that for weak complexes the crystalline field effect (q_{ex}) is often as large as the CT effect. This is shown by the fact that *N,N*-dimethylaniline, for example, gives three resonance lines between 36.9 and 37.4 MHz. The other reason would be that the charge transfer is mainly responsible for the appearance of the so-called CT band but may not be so for the intermolecular interaction. In other words the field of force in which the acceptor molecule is placed consists not merely of the charge transfer interaction but also of other contributions. One evidence of the latter is found in the good relationship between ν_Q and vibrational frequencies as depicted in Figs. 1 and 2.

Zeeman Effect on Chloranil-8-Hydroxyquinoline Complex (1 : 2). Electrons transferred from the donor molecule will enter a π-orbital of the acceptor molecule which will then migrate to some extent to the *p*-orbital of the chlorine atom. Such an effect will cause a change in the asymmetry parameter of the EFG. We have grown a large single crystal of CA-8-hydroxy quinoline complex and carried out a Zeeman effect experiment of the ^{35}Cl resonance lines at room temperature. This crystal belongs to the triclinic space group $P\bar{1}$ and contains one formula unit in the unit cell: There are two crystallographically non-equivalent chlorine atoms and only one equivalent direction exists for each C-Cl bond.[14]

The zero-splitting loci were determined for the two ^{35}Cl lines, ν_1 and ν_2. The directions of the principal axes (X, Y, Z) of the EFG tensor in the laboratory-fixed coordinate system were determined and were transformed to X_c, Y_c, and Z_c in the crystal-fixed coordinate system. Calculation of the directions of X,Y, and Z was carried out by the least squares method programmed for the NEAC-2200 digital computer.

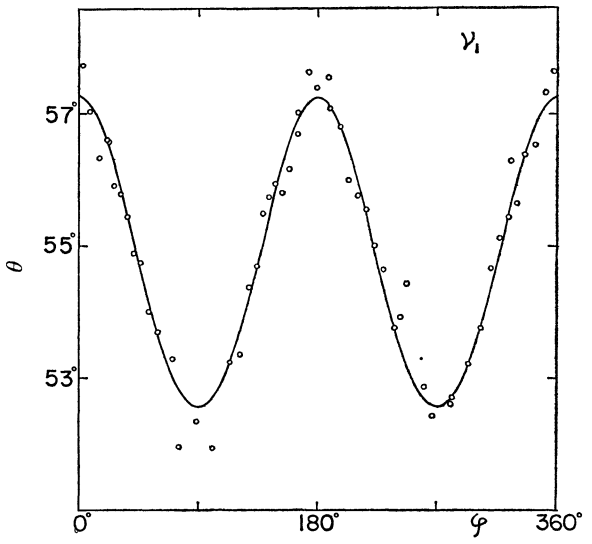

Fig. 4. The zero-splitting locus of ν_1 in 8-hydroxyquinoline complex in the principal axes system of the electric field gradient tensor.

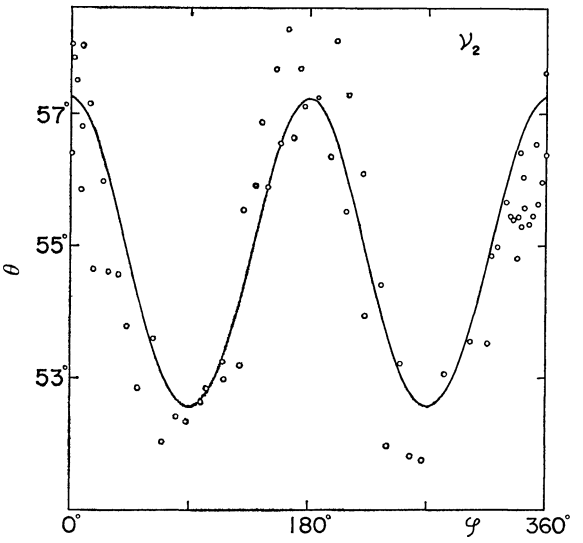

Fig. 5. The zero-splitting locus of ν_2 in 8-hydroxyquinoline complex in the principal axes system of the electric field gradient tensor.

The numbers of the data employed were 55 and 70 for ν_1 and ν_2, respectively.

The results are shown in Figs. 4 and 5. In these figures θ and φ express the direction of the zero splitting locus in the principal axes system of the EFG tensor. The solid curve in each figure corresponds to the theoretical relation[28]

$$\sin^2\theta = 2/(3-\eta\cos^2\varphi) \tag{9}$$

where η was chosen so as to obtain the best fit between experimental data and the theoretical curve.

The direction cosines in the crystal fixed coordinate system are given in Table 2, where the X-axes of the EFG are taken to be perpendicular to the quinone ring. The direction cosines of the Z-axes of the EFG's can be compared with the C-Cl bond directions determined by X-ray analysis.[14] Although the principal Z-axis of the EFG for ν_2 coincides with the direction of the C_2-Cl_{12} bond,[29] that for ν_1 differs from the direction of the C_1-Cl_{11} bond by about 17°. The reason for this discrepancy is not obvious.

η is thus given, in terms of the number of unbalanced *p*-electrons U_X, Y_Y, and U_Z, by the formula[6a]

$$\eta = (3/2)(U_X - U_Y)q_{at}/q \tag{10}$$

where q_{at} is the EFG in an atomic chlorine. If it is assumed that the charge transfer is accompanied only by an increase in the π-electron density of the acceptor molecule, U_Y can be put equal to U_Y^0 corresponding to the free acceptor molecule whereas U_X can be expressed as $U_X = U_X + \delta$, where δ expresses the increase in the excess electrons in the p_X- or the π-orbital of the chlorine. Then, Eq. (10) can be written as

$$\eta = (3/2)(U_X^\circ - U_Y^\circ)q_{at}/q + (3/2)\delta q_{at}/q \tag{11}$$
$$\fallingdotseq \eta_0 + (3/2)\delta q_{at}/q$$

28) C. Dean, *Phys. Rev.*, **96**, 1053 (1954).
29) See Ref. 14 for the numbers affixed to the atoms.
30) a) S. S. C. Chu, G. A. Jeffrey, and T. Sakurai, *Acta Crystallogr.*, **15**, 661 (1962). b) C. B. Richardson, *J. Chem. Phys.*, **38**, 510 (1963).

Table 2. Nuclear quadrupole coupling constants, asymmetry parameters, and the direction cosines of the principal Z-axes of the electric field gradient tensors

The direction cosines are compared with the direction of the C-Cl bond determined by X-ray analysis (Ref. 14).

Bond	Method	R (A)	e^2Qq/h (MHz)	η %	X_c (a^*)	Y_c (b)	Z_c (c')
C_{11}-Cl_1	NQR	—	74.191	17.3	−0.5182	−0.5251	0.6752
	X-ray	1.77	—	—	−0.5680	−0.5448	0.5556
C_{12}-Cl_2	NQR	—	74.416	17.2	0.5420	−0.5591	−0.6274
	X-ray	1.70	—	—	0.5504	−0.5062	−0.6639

	NQR	X-ray
Angle between Cl_1 σ bond and Cl_2 σ bond	65°43′	66°04′
Cl_1 π bond and Cl_2 π bond	2°25′	—

where η_0 is the asymmetry parameter in the free acceptor.

On the other hand, the EFG q is expressed by using the unbalanced electron numbers as

$$q = \left(U_Z - \frac{(U_X + U_Y)}{2}\right)q_{at} + q_{ex}$$
$$= q_0' - (\delta/2)q_{at}$$

By comparing this equation with Eq. (5), we get

$$(\delta/2)q_{at} \fallingdotseq -b^2\Delta q_{CT}$$

and therefore

$$\eta \fallingdotseq \eta_0 - 3b^2\Delta q_{CT}/q$$

Since $\Delta q_{CT} > 0$, η should decrease with an increase in CT. As shown in Table 3, η's in CA-8-hydroxy quinoline complex are significantly small in comparison with those in pure chloranil crystal for which η is about 0.21:[30] and this is consistent qualitatively with Eq. (12). However a quantitative comparison does not seem of any value for reason given in the preceding Section.

Thanks are due to Profs. Haruo Kuroda and Yoshihiko Saito, University of Tokyo, for their valuable discussions. We are also indebted to Prof. Haruka Yamada, Kwansei Gakuin University, for kindly showing us the manuscript of her paper prior to publication.

BULLETIN OF THE CHEMICAL SOCIETY OF JAPAN, VOL. 44, 2681—2684 (1971)

Correlation between the Transition Temperature and the Rotational Potential Barrier in Plastic Crystals

Hideaki CHIHARA and Yoshikata KOGA*

Department of Chemistry, Osaka University, Toyonaka

* *Department of Chemistry, University of British Columbia, Vancouver 8, B. C., Canada*

(Received May 10, 1971)

A linear retationship was found between the transition temperature of plastic crystals and potential energy barrier hindering molecular rotation determined below or above the transition point, with the slope of the line 7.5 R and 4.1 R, respectively, where R is the gas constant. Consideration of the distribution of molecules between the librational and the rotational states showed that the transition starts to occur cooperatively when the fraction of the rotating molecules reaches a value of 1/60 and concludes with a value of 1/3. The model gives the entropies of transition which reasonably agree with the observed values.

Many of the phase transitions in molecular solids are the result of a further acquisition of the degree or degrees of freedom of motion at the transition point. In the case of globular molecules, the additional degrees of freedom are considered to be of rotational or orientational origin.[1] In fact, a previous paper[2] demonstrated an approximately linear relationship between the transition temperature and the height of the potential barrier hindering the molecular rotation in a few molecular crystals of this type. There, the values of the hindering potential was derived from the entropy evaluation and its procedure was subject to an assumption based on the corresponding state principle.

Meanwhile, more reliable values of the hindering potential barrier height have been accumulated by application of the nuclear magnetic resonance techniques; In particular the measurements of the spin-lattice relaxation time by the pulsed NMR methods have proved to give the more meaningful values for such a quantity than does the indirect thermodynamic reasoning.

1) J. Timmermans, *J. Phys. Chem. Solids*, **18**, 1 (1961).
2) H. Chihara and T. Shinoda, This Bulletin, **37**, 125 (1964).

TABLE 1. TRANSITION TEMPERATURE (T_c), ENTROPY OF TRANSITION (ΔS_c), AND BARRIER TO ROTATION ($E^\dagger$) OF SOME PLASTIC CRYSTALS

No. in Fig. 1	Material	T_c	$E^\dagger$(kcal/mol)		$\Delta S_c/R$	
			Phase B	Phase A	Exptl	Calcd
1	CH_4	20.50	0.20[a]	—	0.38[e]	0.88
2	CD_4	26.9	0.53[a]	—	0.62[f]	1.49
3	CF_4	76.221	—	—	2.31[g]	2.29
4	H_2Se	82.3	1.4[b]	0.23[b]	1.88[h]	2.06
5	HCl	98.38	1.4[c]	—	1.45[h]	1.55
6	DCl	105.03	—	0.85[c]	1.52[i]	1.80
7	HI	125.68	1.74[c]	—	1.0[h]	1.79
8	DI	128.28	—	0.97[c]	1.51[l]	1.94
9	$C(CH_3)_4$	140.498	3.0[d]	1.0[d]	2.25[j]	2.44
10	$(CH_3)_2CCl_2$	188.1	—	2.2[d]	—	2.36
11	$(CH_3)_3CCl$	183	2.8[d]	1.5[d]	—	2.00
12	CCl_4	225.5	—	—	2.40[h]	2.38
13	Ar	83.81	1.28[k]	—	1.68[l]	—
14	Kr	115.78	1.77[k]	—	1.69[l]	—

a) Derived from G. A. DeWit, Ph. D. Thesis, University of British Columbia (1966).
b) J. H. Loehlim, P. G. Menaitt, and J. S. Waugh, *J. Chem. Phys.*, **44**, 3912 (1965).
c) D. J. Genin, D. E. O'Reilly, E. M. Peterson, and T. Tsang, *J. Chem. Phys.*, **48**, 4525 (1968).
d) E. O. Stejskal, D. E. Woessner, T. C. Furrar, and H. S. Gustowsky, *J. Chem. Phys.*, **31**, 55 (1959).
e) K. Clusius, and L. Popp, *Z. Physik. Chem.*, **B46**, 63 (1940).
f) J. H. Colwell, E. K. Gill, and J. A. Morrison, *J. Chem. Phys.*, **39**, 635 (1963).
g) H. Enokido, S. Shinoda, and Y. Mashiko, This Bulletin, **42**, 3415 (1969).
h) "Selected Values of Chemical Thermodynamic Properties," NBS Circular 500 (1952).
i) K. Clusius and G. Wolf, *Z. Naturforsch.*, **2a**, 495 (1947).
j) H. Enokido, T. Shinoda, and Y. Mashiko, This Bulletin, **42**, 84 (1969).
k) Enthalpy of vacancy formation; See Ref. 3.
l) Entropy of fusion; See Ref. 3.

In the present paper, we will put forward a revised relationship between the transition temperature and the potential barrier hindering the molecular rotation in solids and also discuss some of its ramifications which will help to understand the nature of the cooperative phenomena.

Potential Energy Barrier and Fraction of Rotating Molecules. Table 1 is a compilation of the experimental values of the barrier height for a number of plastic crystals. Where available, the value for both the high temperature phase and the low temperature phase are given. These barrier values are plotted against the transition temperatures in Fig. 1. Inert gas crystals, Ar and Kr, are also listed at the bottom of the Table, which are the plastic crystals that have no transition points; Their values refer to the triple points and the heats of vacancy formation.[3] The significance of these two points will be discussed in a later Section.

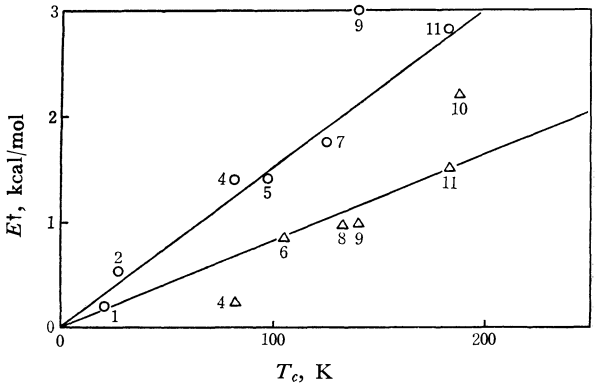

Fig. 1. Linear relationship between the transition temperature (T_c) and the potential energy barrier ($E^\dagger$) hindering molecular rotation: ○ Phase B, △ phase A. Numbers in the figure correspond to those given in Table 1.

It is seem from Fig. 1 that the points corresponding to the high-temperature phase (phase A) and those corresponding to the low-temperature phase (phase B) lie on the two separate straight lines. Both lines pass through the origin as pointed out earlier[2] and the lines are represented by the formula

$$E^\dagger = \alpha R T_c \qquad \begin{matrix} \alpha = 4.1 \text{ for phase A} \\ \alpha = 7.5 \text{ for phase B} \end{matrix} \qquad (1)$$

These relationships may be interpreted as showing that the phase transition takes place when the average thermal energy reaches a certain fraction of the potential barrier and the factor α at which it occurs does not depend on a particular compound.[4] However α depends on the direction in which the transition point is approached and there is a jump in its value at T_c. The jump occurs in a cooperative way but we shall focus our attention on its difference between the two

3) R. H. Beaumont, H. Chihara, and J. A. Morrison, *Proc. Phys. Soc.* (London), **78**, 1462 (1961).
4) The compounds listed in Table 1 assume the face-centered cubic structure in phase A with exceptions of CCl_4 (rhombohedral), CF_4(unknown), and $(CH_3)_2CCl_2$ (unknown).
5) G. B. Guthrie and J. P. McCullough, *J. Phys. Chem. Solids*, **18**, 53 (1961).

phases. Although the cooperative effect does not abruptly come into play at T_c, the transitions under consideration are very close to those of the first order. Therefore, we may extrapolate the properties of the phases A and B to T_c to examine what triggers the cooperative transition.

To evaluate the significance of Eq. (1), we shall take a simplified classical picture. It will be assumed that a crystal consists of two different species of molecules, 'rotational' and 'librational' (abbreviated as R and L, respectively), and that a quasi-chemical equilibrium

$$\mathrm{L} \rightleftarrows \mathrm{R} \tag{2}$$

is established between the two species, with the Helmholtz energy difference $A^\dagger$ given by

$$A^\dagger = E^\dagger - TS^\dagger . \tag{3}$$

$E^\dagger$ will be taken as the potential barrier height and

$$S^\dagger = S_\mathrm{R} - S_\mathrm{L} \tag{4}$$

The transition may now be looked upon as an abrupt displacement of the equilibrium (2) toward the right as T_c is approached from Phase B. This may be achieved by an increase in $S^\dagger$ and/or a decrease in $E^\dagger$ in a cooperative way.

In the present treatment, S_R was calculated in a conventional way from the knowledge of the geometry of molecules and S_L was obtained in the harmonic oscillator approximation from the appropriate values of $E^\dagger$ and the appropriate number of minima ($=4$) of the potential function for both Phases A and B.

Such calculations yielded $S^\dagger/R=3.2\pm0.6$, except for methanes, with a surprisingly small scatter from compound to compound and between the two phases. Therefore, the transitions are associated with a decrease in $E^\dagger$ (as shown in Eq. (1)) rather than with an increase in $S^\dagger$.

The fraction of rotating molecules or the equilibrium constant of the reaction (2) may be written as

$$N_\mathrm{R}/N_\mathrm{L} = \exp(-A^\dagger/\boldsymbol{R}T) = \exp(S^\dagger/\boldsymbol{R})\exp(-E^\dagger/\boldsymbol{R}T) \tag{5}$$

where N_R and N_L denote the number of 'rotational' and 'librational' molecules. Thus at $T=T_c$, Eq. (5) reads

$$N_\mathrm{R}{}^\mathrm{B}/N_\mathrm{L}{}^\mathrm{B} = (30\pm20)\exp(-7.5) \fallingdotseq 1/60 \tag{6}$$

for Phase B and

$$N_\mathrm{R}{}^\mathrm{A}/N_\mathrm{L}{}^\mathrm{A} = (30\pm20)\exp(-4.1) \fallingdotseq 1/2 \tag{7}$$

for Phase A.

This means that only one molecule out of 60 is 'rotating' in phase B, whereas as many as one-third of the molecules are in the 'rotational' state in Phase A at the transition temperature, *i.e.* the transition would be triggered by the fraction of molecules that amounts to 1.7% of the total or one-quarter $(1/60)^{1/3}$ of a one-dimensional extention of the molecular array.

Entropy of Transition

We shall now attempt to calculate the entropy of transition by use of Eqs. (6) and (7).

The entropy of either phase S is given by

$$S = \boldsymbol{k}T\left(\frac{\partial \ln Q}{\partial T}\right)_{V,N} + \boldsymbol{k}\ln Q \tag{8}$$

where Q is the partition function of the phase, which may be written, aside from the configurational part, as

$$Q = q^N \tag{9}$$

q being the molecular partition function,

$$q = \sum_{i=1}^{\infty} \exp(-E_i/\boldsymbol{k}T) = \sum_{i}^{E_i \le E^\dagger} \exp(-E_i/\boldsymbol{k}T) + \sum_{i}^{E_i > E^\dagger} \exp(-E_i/\boldsymbol{k}T) \tag{10}$$

the first sum in Eq. (8) corresponds to the 'librational' state and the second corresponds to the 'rotational' state. If q_L and q_R denote the corresponding partition functions, Eq. (8) can be rewritten as

$$q \fallingdotseq q_\mathrm{L} + [\exp(-E^\dagger/\boldsymbol{k}T)]q_\mathrm{R}. \tag{11}$$

The entropy of the molecules in the two states is given by

$$S_\mathrm{L} = \boldsymbol{R}T\left(\frac{\partial \ln q_\mathrm{L}}{\partial T}\right)_{V,N} + \boldsymbol{R}\ln q_\mathrm{L} \tag{12}$$

and

$$S_\mathrm{R} = \boldsymbol{R}T\left(\frac{\partial \ln q_\mathrm{R}}{\partial T}\right)_{V,N} + \boldsymbol{R}\ln q_\mathrm{R} \tag{13}$$

Therefore,

$$\frac{N_\mathrm{L}S_\mathrm{L}+N_\mathrm{R}S_\mathrm{R}}{N} = \frac{\boldsymbol{R}T}{N}\left[N_\mathrm{L}\left(\frac{\partial \ln q_\mathrm{L}}{\partial T}\right)_{V,N} + N_\mathrm{R}\left(\frac{\partial \ln q_\mathrm{R}}{\partial T}\right)_{V,N}\right] + \frac{\boldsymbol{R}}{N}N_\mathrm{L}\ln q_\mathrm{L} + N_\mathrm{R}\ln q_\mathrm{R}) \tag{14}$$

Now, since

$$\frac{q_\mathrm{L}}{q} = \frac{N_\mathrm{L}}{N} \quad \text{and} \quad \frac{q_\mathrm{R}\exp(-E^\dagger/\boldsymbol{k}T)}{q} = \frac{N_\mathrm{R}}{N} \tag{15}$$

we have

$$\begin{aligned} \ln q_\mathrm{L} &= \ln\frac{N_\mathrm{L}}{N} + \ln q \\ \ln q_\mathrm{R} &= \ln\frac{N_\mathrm{R}}{N} + \ln q + E^\dagger/\boldsymbol{k}T \end{aligned} \tag{16}$$

From Eqs. (8), (9), (14), and (16), the total entropy S is given by

$$S = \frac{N_\mathrm{L}}{N}S_\mathrm{L} + \frac{N_\mathrm{R}}{N}S_\mathrm{R} - \boldsymbol{R}\left(\frac{N_\mathrm{L}}{N}\ln\frac{N_\mathrm{L}}{N} + \frac{N_\mathrm{R}}{N}\ln\frac{N_\mathrm{R}}{N}\right) \tag{17}$$

The entropy of transition ΔS_c is defined by

$$\Delta S_c = S^\mathrm{A} - S^\mathrm{B} \tag{18}$$

where S^A and S^B desote the total entropies of the Phases A and B. $N_\mathrm{R}/N_\mathrm{L}$ values are given by Eqs. (6) and (7). Therefore the entropy of transition may be obtained simply from the knowledge of T_c and the geometry of molecules. The result is given in the last column of Table 1. General agreement with the observed entropy changes is satisfactory except for CH_4 and CD_4.

Discussion

It has been shown that the fraction of rotating molecules changes in a cooperative way from 1/61 in phase B to 1/3 in phase A at least in a class of compounds that undergoes 'rotational' transition. Further experimental evidence may be required to establish this as an empirical rule but it does seem that the intermolecular interaction of the cooperative nature extends as far as the second neighbors in phase B where the crystal field is rather 'hard,' whereas it extends only to the nearest neighbors in phase A in which the crystal field is rather 'soft' because of the large kinetic energy.

It is interesting in this connection to note that the fusion of argon and krypton is governed by the same principle; *i.e.* melting occurs when the fraction of vacancies reaches the same number 1/61, This equality in the number, however, may only be a fortuitous one in the sense that $S^{\dagger}/R$ for both cases happened to be the same and this may have brought about the equality in $E^{\dagger}/RT_c$. Therefore it seems extremely interesting to analyze various kind of phase changes in terms of such two-species model as is developed in the present treatment.

The molecular model adopted here is a crude one which neglects the detailed configurational considerations and deals with a uniform phase as a mixture of the two molecular species, nevertheless the good agreement of the calculated and observed entropies of transition suggests that it should serve a useful picture of such solids. It is certainly more realistic than interpreting the entropy in terms of increased uniform orientational degrees in phase A.[5]

The authors would like to thank Dr. P. S. Allen (University of Nottingham) for stimulating discussions.

BULLETIN OF THE CHEMICAL SOCIETY OF JAPAN, VOL. 44, 2684—2688 (1971)

ESR Studies of Methyl Radicals Stabilized on Silica-gel Surfaces

Shozo KUBOTA, Masamoto IWAIZUMI, and Taro ISOBE

Chemical Research Institute of Non-Aqueous Solutions, Tohoku University, Katahira-nichome, Sendai

(Received May 14, 1971)

The methyl radicals produced on silica-gel surfaces by the photolysis of methyl iodide or methane have been investigated by ESR. When the silica gel is preheated at high temperatures (above *ca.* 300°C), two methyl radicals which have abnormally small hfs constants are trapped on the surfaces. In the case of the photolysis of methyl iodide, these two radicals disappear by continuing uv-irradiation, and instead an ordinary type of methyl radical is produced. The former two radicals have nearly isotropic *g*-values, and these values are approximately equal to that of a free electron and are considered to have a non-planar structure. The adsorption sites for these radicals were estimated to be siloxane groups. On the other hand, when the silica gel is preheated at low temperatures (below *ca.* 300°C) the methyl radicals produced have hfs constants of the same magnitude as that of the ordinary type of methyl radical, but each proton line of the radicals is accompanied by four satellite lines. The outer satellite lines have been confirmed by measurements of the X- and K-band spectra to be a concurrent spin-flip transition of an odd electron and a nearby proton of the silica-gel surface. The models of the adsorption state of the radicals are considered.

Since Kazanskii's work,[1] several interesting investigations[2-7] have been reported on the ESR of methyl radicals stabilized on solid surfaces. As the methyl radical shows a well-resolved hyperfine structure, even in the adsorbed state, it is possible to detect a small perturbation of the methyl radical caused by the interaction with solid surfaces. The studies of the methyl radical, therefore, seem of interest and seem to be useful from the point of view of studies of the nature of radical-solid surface interaction and also studies of the surface structure.

In this work, methyl radicals trapped on silica-gel surfaces were studied by ESR. The methyl radicals on the silica-gel surfaces show characteristics similar in several points to those trapped on porous Vycor glass.[6,7] In this paper, the characteristics of the ESR of the radicals and of radical-surface interactions observed in silica-gel systems pretreated at different temperatures, the effect of the irradiation time on radical formation by the photolysis of methyl iodide, and the satellite lines in the ESR will be presented. Some of our results may be useful in understanding problems of the methyl radicals in the porous Vycor glass system already reported.

Experimental

Methyl radicals were produced by the photolysis of methyl iodide or methane adsorbed on silica-gel surfaces at the temperature of liquid nitrogen. The methyl iodide was ob-

1) V. B. Kazanskii, G. B. Pariiskii, I. V. Aleksandrov, and G. M. Zhidomirov, *Solid State Physics (USSR)*, **5**, 649 (1963).
2) J. Turkevich and Y. Fujita, *Science*, **152**, 1619 (1966).
3) M. Fujimoto, H. D. Gesser, B. Garbutt, and A. Cohen, *Science*, **154**, 381 (1966).
4) M. Fujimoto, H. D. Gesser, B. Garbutt, and M. Shimizu, *Science*, **156**, 1105 (1967).
5) G. B. Garbutt, H. D. Gesser, and M. Fujimoto, *J. Chem. Phys.*, **48**, 4605 (1968).
6) N. Shimamoto, Y. Fujita, and T. Kwan, This Bulletin, **43**, 580 (1970).
7) G. B. Garbutt and H. D. Gesser, *Can. J. Chem.*, **48**, 2685 (1970).

tained from the Koso Chemical Co., Ltd., and purified according to the procedure used by Cowley and Partington.[8] The purified methyl iodide was degassed in a vacuum line and stored over P_2O_5. The methane was obtained from the Takachiho Co. and was used after drying over P_2O_5. The silica gel obtained from the Kanto Chemical Co., Ltd., (60—80 mesh for chromatography) was heated in oxygen at 300°C to remove organic impurities and then stored in a glass bottle. Prior to the adsorption of methyl iodide or methane, this silica gel was heated *in vacuo* to dehydrate the surface. To see the effect of the dehydration on the methyl-radical formation, the silica gel was heated at various temperatures from room temperature to 700°C. After the methyl iodide or methane had adsorbed on the silica gels, the resulting samples were irradiated with the light of a mercury lamp. An Ushio 6-w low-pressure mercury lamp and a Hitachi ultra-high pressure mercury lamp were used as the light sources. The measurements of ESR spectra were carried out with a Hitachi 771 X-band spectrometer. For the measurements of the satellite lines, a Hitachi MES 4001 K-band spectrometer was used as well as the X-band spectrometer. The magnetic field was calibrated with an aqueous solution of potassium nitrosodisulfonate and DPPH powder for the determination of the *g*-values.

Results and Discussion

The Methyl Radicals Stabilized on Silica Gel Preheated at High Temperatures. The ESR spectra for the methyl radicals trapped on the silica-gel surfaces depend on the dehydration temperature of the silica gel. Figure 1 shows the ESR spectra obtained from the methyl radicals produced by the photolysis of methyl iodide when the silica gel was preheated at 600°C *in vacuo* for 5 hr. The spectra obviously show marked changes with the uv-irradiation time. In an early stage of the irradiation, two sets of quartet splittings due to two methyl radicals, $Me(a_1)$ and $Me(a_2)$, are observed. The intensities of these two methyl radicals increase with the progress of the irradiation until about 90 sec.[9] However, upon further irradiation the intensities of the radicals begin to decrease and another quartet ($Me(n_1)$) appears. The intensity of this latter quartet increases as the first two decrease with the continuation of the photolysis, until only the latter radical, $Me(n_1)$, remains. For heating the samples, the former two methyl radicals, $Me(a_1)$ and $Me(a_2)$, are very unstable, but the latter one, $Me(n_1)$, is stable and can be observed even at room temperature. The radical existing at the final stage of irradiation, $Me(n_1)$, has about the same hfs constant and amplitude distribution for the quartet as those already reported by Kazanskii *et al.*[1] On the other hand, $Me(a_1)$ and $Me(a_2)$ radicals have abnormally small hfs constants compared to that of the ordinary methyl radical and have *g*-values close to that of a free electron (see Table 1). The line broadening for the quartets of these methyl radicals, $Me(a_1)$ and $Me(a_2)$, are approximately symmetric

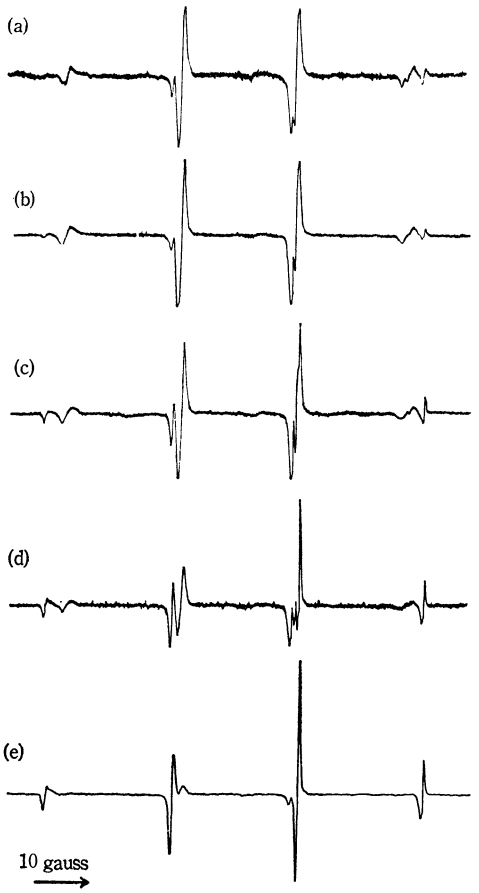

Fig. 1. Change of ESR spectra with uv-photoirradiation time observed for the photolysis of methyl iodide on the silica gel preheated at 600°C *in vacuo*. Irradiation time: (a) 20 sec. (b) 90 sec. (c) 3 min. (d) 6 min. (e) 12 min.; Temp=77°K.

Table 1. Hfs constants and *g*-values for the methyl radicals, $Me(a_1)$, $Me(a_2)$ and $Me(n_1)$, on the silica-gel surface at 77°K

	Hfs constants (in gauss)	*g*-values
$Me(a_1)$	20.7	2.0024
$Me(a_2)$	21.2	2.0023
$Me(n_1)$	23.0	2.0027

to the center of the spectrum, showing a marked contrast to the line-broadening effect in the $Me(n_1)$ radical or the previously-reported normal methyl radicals, which reveal unsymmetric line broadening to the center of the spectrum (see Fig. 2).

Recently Fujimoto,[3] and also Shimamoto,[6] found in the porous Vycor glass system a methyl radical with an abnormally small hfs constant. Shimamoto *et al.* pointed out that this new type of methyl radical shows an inverse line-broadening effect compared to that of the normal methyl radical; that is, in the normal methyl radical the low-field lines are broader than the high-field lines, but in the new methyl radical the higher-field lines are broader than the low-field lines. In the present case, if a large amplitude of

8) E. G. Cowley and J. R. Partington, *J. Chem. Soc.*, **1938**, 977; "Organic Solvents" ed. by A. Weissberger, Interscience Publishers, New York (1955), p. 427.

9) The time is not strict because it changes somewhat with sample.

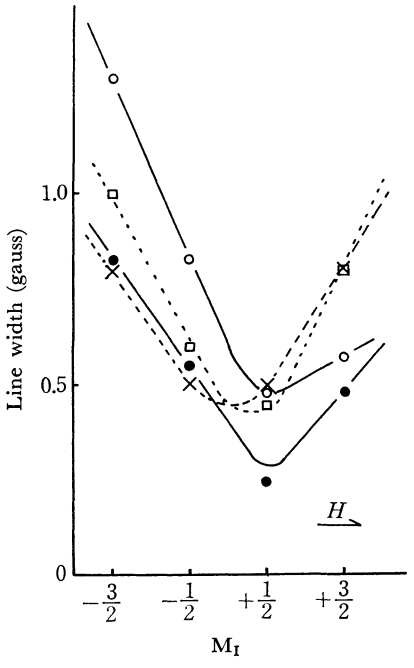

Fig. 2. Line width as a function of M_I at 77°K. X: $Me(a_1)$, □: $Me(a_2)$, ●: $Me(n_1)$, ○: Main proton lines for $Me(n_2)$. The line widths for $Me(a_1)$ and $Me(a_2)$ are evaluated by computer simulation.

field modulation is used for the measurements of ESR, the absorptions for $Me(a_1)$ and $Me(a_2)$ can not be distinguished as two species any more, but shows a hyperfine pattern quite similar to that observed in the porous Vycor glass system. This fact implies that the quartet splitting for the new type of methyl radical observed in the porous Vycor glass system may consist of two overlapped quartets which are due to two species of methyl radicals.

According to the electron-spin-relaxation theory,[10-12] the fact that the line-width-broadening effect is symmetric to the center of the spectra in the $Me(a_1)$ and $Me(a_2)$ radicals implies that the *g*-values of the radicals are nearly isotropic. In the present case, as is indicated in Table 1, the *g*-values for the $Me(a_1)$ and $Me(a_2)$ radicals are also almost equal to the value for a free electron. The *g*-value of the $Me(n_1)$ radical is larger than the value of a free electron and is estimated to be anisotropic from the line-width-broadening effect in the spectrum. From the changes in the *g*-values of the free radicals, it may be estimated that the structures of the new types of methyl radicals, $Me(a_1)$ and $Me(a_2)$, are different from that of the normal type, $Me(n_1)$; *i.e.*, the new one probably has a non-planar structure. The deformation from a planar structure corresponds to the increase in the *s*-character in an odd electron orbital; this in turn leads to a *g*-value close to that of a free electron. The facts that the proton hfs constants of the $Me(a_1)$ and $Me(a_2)$ radicals are smaller than that of the normal methyl radical is also a good indication of the non-planar structure. Although there may be some effect due to charge transfer to the surface sites, the contribution of the charge transfer to the decrease in hfs constants is probably small. If there is any appreciable effect of charge transfer to the surface sites, such as the boroxane groups suggested by Garbutt *et al*,[7] the *g*-value would probably deviate more from the value of a free electron because of the larger effect of spin-orbit coupling at the adsorption sites.

The formation of the nonplanar methyl radicals can be attributed to the strong interaction with the silica-gel surface. The formation of such radicals could not be observed when the silica gel was preheated at low temperatures. This fact suggests that the adsorption sites for the non-planar methyl radicals are siloxane groups formed by the dehydration of surface silanol groups. In the study of methyl radicals in the porous Vycor glass system, Garbutt *et al*, proposed that boroxane groups are adsorption sites for the methyl radical, which has an abnormally small hfs constant. Their conclusion was based on Zammit's experiment, which reported that this new type of methyl radical could not be observed on the pure (boron-free) silica gel. The present result using silica gel implies that siloxane groups are adsorption sites for this new type of methyl radical in the porous Vycor glass system, too. It seems interesting that there are two different adsorption states for the non-planar methyl radicals. From the intensity ratio of the two radicals, $Me(a_1)$ and $Me(a_2)$, it can be estimated that the populations of the two strong adsorption sites on the silica-gel surface are approximately the same.

As has been mentioned above, in the photolysis of the methyl iodide the new methyl radicals, $Me(a_1)$ and $Me(a_2)$, appear at the early stage of irradiation, but as the photolysis continues the intensities of the radicals decrease, and instead an ordinal methyl radical, $Me(n_1)$, appears. In the photolysis of methane, the observed spectra (Fig.3) did not show such a change, indicating that the iodine produced in the photolysis of methyl iodide disturbs the stabilization of the non-planar form of the methyl radical by covering the active sites for adsorption.

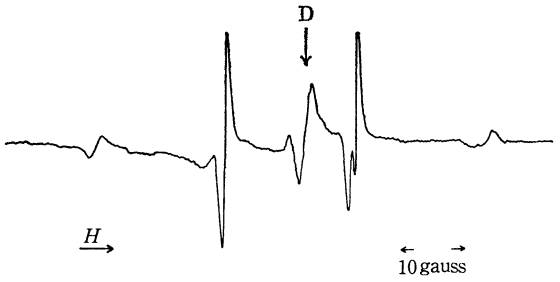

Fig. 3. ESR spectrum of the methyl radicals produced from methane at 77°K. The silica gel was preheated at 600°C *in vacuo* for 5 hr. D: Defect signal.

The Methyl Radical Formed on the Silica Gel Preheated at Low Temperatures, and the Satellite Lines about the Four Proton Lines. When the silica gel is preheated at temperatures below about 300°C, the methyl radicals with abnormally small hfs constants are not ob-

10) H. M. McConnell, *J. Chem. Phys.*, **25**, 709 (1956).
11) D. Kivelson, *ibid.*, **33**, 1094 (1960).
12) J. Freed and K. Fraenkel, *ibid.*, **39**, 326 (1963).

served. The observed quartet for the methyl radical has about the same splitting and amplitude distributions as those of the ordinary methyl radical (Fig.4). In this case, however, each proton hyperfine line is accompanied by four satellite lines, as is shown in Fig. 5. Such satellite lines were not observed when the silica gel was preheated at high temperatures, implying that they are related to the interaction with the proton of the silanol groups on the silica-gel surface. By measurements of both the X- and K-band spectra, it has been found that the outer satellite lines are affected by the magnetic field, although the inner satellite lines are not affected (see Figs. 5 and 6). The separations between the two outer satellite lines were 11.5 and 26.2 gauss at the X- and K-band spectra respectively; the spectra were approximately equal to $2g_N \cdot \beta_N I \cdot H$. That is, the values calculated by the use of $2g_N\beta_N I \cdot H$ are 10.9 and 25.8 gauss respectively and

Fig. 4. ESR spectrum of the methyl radical on the silica gel surface at 77°K. The silica gel was pretreated by evacuating for 15 hr without heating.

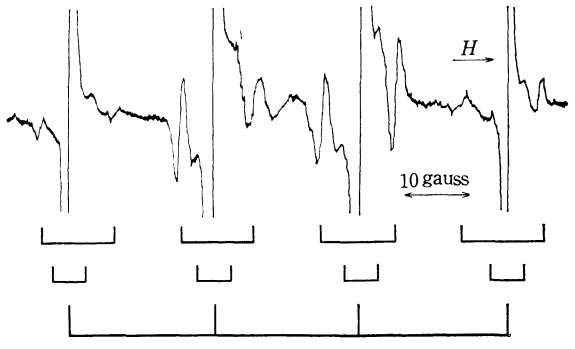

Fig. 5. ESR spectrum showing the satellite lines at X-band. Temp: 77°K.

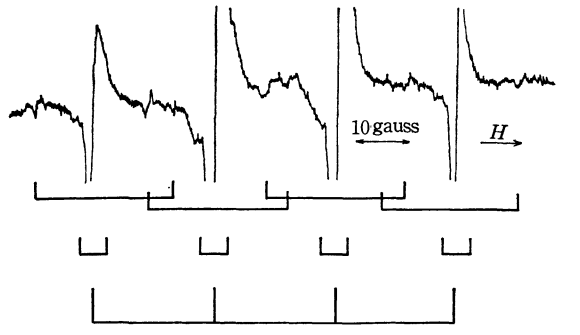

Fig. 6. ESR spectrum showing the satellite lines at K-band. Temp: 77°K.

are in good agreement with the observed values.

Previously Rogers *et al.*[13] explained the two satellite lines observed for the methyl radicals in irradiated single crystals of sodium acetate trihydrate as arising from the concurrent spin flip of the electron of the methyl radical and the proton of the water of crystallization. They showed in their study that the separation of the satellite lines is close to $2g_N\beta_N I \cdot H$, which is to be expected from the theory that there is some second-order effect in the hyperfine interaction.[14,15] In such concurrent spin flip-type transitions of the unpaired electron and a nearby proton, if it is assumed that the central line is associated with satellite lines, as in the above example, the ratio of the intensity of either satellite line, T_1, to that of the central line, $2T_2$, is given by:

$$T_1/2T_2 = (3g^2\beta^2/20\,H^2)\,\langle r^{-6}\rangle \qquad (1)$$

This equation indicates that the $T_1/2T_2$ ratio is inversely proportional to the square of the external field. The $T_1/2T_2$ ratio in the K-band spectrum can, therefore, be expected to be about 1/6 for the case of the X-band spectrum. In the present case, the ratio of the intensity of the outer satellite lines to that of the central line, $T_1/2T_2$, in the K-band spectrum was about 1/3—1/6 of the value in the X-band spectrum, in good agreement with the expectation from Eq. (1).

It may be concluded, therefore, that the outer satellite lines are due to the spin flip-type transition of the unpaired electron and a nearby silanol proton coupled by dipole-dipole interaction. As has been mentioned above, the central line can probably be associated with the outer satellite lines (the Me(n_2) radical), and so the inner satellite lines may be attributed to the other species of methyl radical, which has Fermi-type interaction with protons on the silica-gel surface (the Me(n_3) radical). It seems interesting that in this case, too, there are two different adsorption states for the methyl radicals. Figure 7 is one possible model for Me(n_2) and Me(n_3). By using the $T_1/2T_2$ intensity ratio for the outer satellite lines, the mean distance, $\langle r\rangle$, for the Me(n_2) methyl radical is calculated to be 2 Å from Eq. (1).

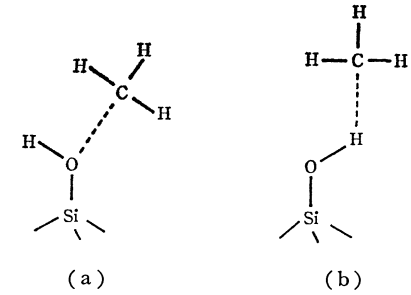

(a) (b)

Fig. 7. Methyl radical-silica gel interaction models.
(a) Model for radical Me(n_2).
(b) Model for radical Me(n_3).

13) M. T. Rogers and L. D. Kispert, *ibid.*, **46**, 221 (1967).
14) G. T. Trammell, H. Zeldes, and R. Livingston, *Phys. Rev.*, **110**, 630 (1958).
15) I. Miyagawa and W. Gordy, *J. Chem. Phys.*, **32**, 255 (1960).

As has been shown, the methyl radicals show well-resolved ESR spectra even in the adsorbed state, although the hyperifine interaction between the $2p_z$ unpaired electron and a α proton has a large anisotropy. This can be well explained by the rapid rotation of the molecules around the three-fold axis. However, the tumbling of the molecules should be greatly restricted by the interaction with solid surfaces, as may be seen from the line-width broadening, showing the deviation of the amplitude distribution from the binomial law. The observation of the satellite lines due to the magnetic dipole-dipole interaction between the electron spin and a neighboring surface proton gives useful information about the lifetime of adsorbed states or the tumbling of the molecules. That is, the tumbling frequency of the $Me(n_2)$ radical was estimated to be lower than 2×10^8 Hz from the relation:

$$\tau_c \gg 1/2\pi\Delta\nu \qquad (2)$$

where τ_c is the correlation time for fluctuation in the interaction between the electron and the proton or a reciprocal of the tumbling frequency, and where $\Delta\nu$ is the separation of the doublet.

BULLETIN OF THE CHEMICAL SOCIETY OF JAPAN, VOL. 44, 2688—2693 (1971)

Gas Chromatography of Aluminum, Gallium, and Indium β-Diketone Chelates

Kei UTSUNOMIYA

Institute for Chemical Research, Kyoto University, Uji, Kyoto

(Received November 30, 1970)

The gas-chromatographic behavior of aluminum(III), gallium(III), and indium(III) chelates with various β-diketones was investigated. The β-diketones studied were acetylacetone and 8 synthesized, alkyl-substituted acetylacetones, benzoylacetone, dibenzoylmethane, trifluoroacetylacetone and its 5 synthesized alkyl derivatives, hexafluoroacetylacetone, benzoyltrifluoroacetone, furoyltrifluoroacetone, and thenoyltrifluoroacetone. The trifluoromethyl group increases the volatility of the chelates, while the aromatic group tends to decrease the volatility. In the alkyl-substituted acetylacetone series, the retention time of the chelates increases with an increase in the molecular weight, but it does not depend upon the volatility. On the other hand, the retention of the chelates containing the trifluoromethyl group is almost inversely correlated with the volatility.

During the past decade, the gas chromatography of volatile metal chelates has attracted much attention; many works were summarized in a monograph[1] in 1965. Beryllium(II) and aluminum(III) chelates with acetylaceton,[2-4] trifluoroacetylacetone,[2-11] and hexafluoroacetylacetone[4,12,13] have been most extensively investigated. The results indicated that the substitution of fluorine for the hydrogen of the methyl group in the ligand increased the volatility and also sometimes the thermal stability of metal chelates.

Other tervalent metals, chromium(III),[3,4,6,7,14,15] gallium(III),[16,17] indium(III),[16,17] and iron(III)[9-11,18] chelates, were well studied, and the separation of these metal ions by means of gas chromatography was also examined using trifluoroacetylacetone[16,17] or hexafluoroacetylacetone.[12] However, little has been published on systematic investigations with various β-diketones which have different terminal groups, except for Tanaka and his co-workers, study[19] of the gas chromatography of some copper β-diketones chelates and Eisentraut and Sievers's study[20] of the thermogravimetry of aluminum, chromium(III), iron(III), and rhodium(III) chelates.

The present investigation was undertaken in order to evaluate the effect of the substitution of acetylacetone for methyl groups on the volatility, the thermal stability, and the gas chromatographic behavior of metal chelates. Aluminum, gallium, and indium were chosen as the central metals so that the present results could be readily compared with the results already reported. As the ligands, 21 β-diketones, acetylacetone and its alkyl derivatives, benzoylacetone dibenzoylmethane, trifluoroacetylacetone and its

1) R. W. Moshier and R. E. Sievers, "Gas Chromatography of Metal Chelates," Pergamon Press, New York (1965).
2) R. D. Hill and H. Gesser, *J. Gas Chromatog.*, **1**, 11 (1963).
3) R. E. Sievers, B. W. Ponder, M. L. Morris, and R. W. Moshier, *Inorg. Chem.*, **2**, 693 (1963).
4) W. D. Ross, *Anal. Chem.*, **35**, 1596 (1963).
5) K. Tanikawa, K. Hirano, and K. Arakawa, *Chem. Pharm, Bull.*, **15**, 915 (1967).
6) D. K. Albert, *Anal. Chem.*, **36**, 2034 (1964).
7) W. D. Ross, R. E. Sievers, and G. Wheeler, Jr., *ibid.*, **37**, 598 (1965).
8) W. D. Ross and R. E. Sievers, *Talanta*, **15**, 87 (1968).
9) P. C. Uden and C. R. Jenkins, *ibid.*, **16**, 893 (1969).
10) R. W. Moshier and J. E. Schwarberg, *ibid.*, **13**, 445 (1966).
11) W. G. Scribner, W. J. Treat, J. D. Weis, and R. W. Moshier, *Anal. Chem.*, **37**, 1136 (1965).
12) K. Arakawa and K. Tanikawa, *Bunseki Kagaku*, **16**, 812 (1967).
13) W. D. Ross and G. Wheeler, Jr., *Anal. Chem.*, **36**, 266 (1964).
14) W. D. Ross and R. E. Sievers, *ibid.*, **41**, 1109 (1969).
15) J. Savory, P. Mushak, F. W. Sunderman, Jr., R. H. Estes, and N. O. Roszel, *ibid.*, **42**, 294 (1970).
16) J. E. Schwarberg, R. W. Moshier, and J. H. Walsh, *Talanta*, **11**, 1213 (1964).
17) G. P. Morie and T. S. Sweet, *Anal. Chem.*, **37**, 1552 (1965).
18) R. E. Sievers, J. W. Connolly, and W. D. Ross, *J. Gas Chromatog.*, **5**, 241 (1967).
19) M. Tanaka, T. Shono, and K. Shinra, *Nippon Kagaku Zasshi*, **89**, 669 (1968).
20) K. J. Eisentraut and R. E. Sievers, *J. Inorg. Nucl. Chem.*, **29**, 1931 (1967).

alkyl derivatives, hexafluoroacetylacetone, benzoyltrifluoroacetone, furoyltrifluoroacetone, and thenoyltrifluoroacetone were compared.

Experimental

Preparation of β-Diketones. The β-diketones were prepared by Claisen condensation, except for eight β-diketones—acetylacetone, benzoylacetone, dibenzoylmethane, trifluoroacetylacetone, furoyltrifluoroacetone, thenoyltrifluoroacetone, benzoyltrifluoroacetone, and hexafluoroacetylacetone—which were obtained from the Dojindo Co., Ltd., Research Laboratories. The alkyl-substituted β-diketones, propionylacetone, isobutyrylacetone, pivaloylacetone, diisobutyrylmethane,[21] isobutyrylpivaloylmethane, dipivaloylmethane, dipropionylmethane, and pivaloylpropionylmethane, were prepared by the condensation of the corresponding esters and ketones in the presence of sodium amide,[22] while the fluorinated β-diketones, trifluoroacetylpropionylmethane, trifluoroacetylisobutyrylmethane, trifluoroacetylpivaloylmethane,[23] trifluoroacetyl-α-methylbutyrylmethane, and trifluoroacetylisovalerylmethane, were prepared from ethyl trifluoroacetate and the corresponding ketones in the presence of sodium methoxide.[24] The crude products were converted to the copper chelates by treatment with a solution of cupric acetate in hot aqueous methanol. After recrystallization from benzene, the copper chelates were dissolved in ether and decomposed with 10% sulfuric acid. The boiling points of these β-diketones are given in Table 1, along with the symbols used in this paper.

Preparation of Aluminum(III), Gallium(III), and Indium(III) Chelates. The β-diketonates were prepared by adding a stoichiometric quantity of β-diketone, dissolved in ethanol or methanol, to an aqueous solution of the metal nitrate. The solution was either buffered with sodium acetate or adjusted to pH 6 with a 1 M ammonia solution. The metal chelate thus precipitated was filtered off, dried, recrystallized from benzene, and then dried in a vacuum desiccator over phosphorus pentoxide. Attempts to synthesize the metal chelates with HPrA, HDPrM and HPiPrM by the same procedure failed. The melting points of the chelates thus prepared are shown in Table 2; the results of the elemental analyses of the alkyl substituted β-diketonates are in good agreement with the values calculated for the (1 : 3) chelate.

The thermogravimetric analysis of metal chelates was made with a Shimadzu thermo-balance. About 20 mg of a sample placed in a platinum dish were heated at a rate of 10°C/min in a nitrogen atmosphere and at a flow rate of 50 ml/min. The gas chromatograms were obtained with a Yanagimoto gas chromatograph GCD-5DH equipped with a thermal conductivity detectar. The column, 75 cm × 3 mm i.d., stainless steel, was packed with 5% (by weight) Dow Corning high-vacuum silicone grease on Chromosorb W AW DMCS (80—100 mesh). Helium was used as the carrier gas. Sample solutions, prepared by dissolving the chelates in benzene, were injected at the optimum column temperature for the chelates. The injection-port temperature was maintained at 30°C above the column temperature.

Results and Discussion

Thermogravimetric Analysis. Thermogravimetric analysis is a well-established technique for surveying the volatility of various metal chelates. It presents information on whether the chelates in question are sufficiently volatile and thermally stable to give

Table 1. β-Diketones investigated

β-Diketone	Symbol	Structural formula	Bp (°C)
Acetylacetone	HAA	$CH_3COCH_2COCH_3$	
Propionylacetone	HPrA	$CH_3COCH_2COC_2H_5$	73—73.5/19 mmHg
Isobutyrylacetone	HIBA	$CH_3COCH_2COCH(CH_3)_2$	71—72/30 mmHg
Pivaloylacetone	HPiA	$CH_3COCH_2COC(CH_3)_3$	74—75/30 mmHg
Diisobutyrylmethane	HDIBM	$(CH_3)_2CHCOCH_2COCH(CH_3)_2$	49—50/4.5 mmHg
Isobutyrylpivaloylmethane	HIBPM	$(CH_3)_3CCOCH_2COCH(CH_3)_2$	77—78/13 mmHg
Dipivaloylmethane	HDPM	$(CH_3)_3CCOCH_2COC(CH_3)_3$	96—98/27 mmHg
Dipropionylmethane	HDPrM	$C_2H_5COCH_2COC_2H_5$	65/18 mmHg
Pivaloylpropionylmethane	HPiPrM	$(CH_3)_3CCOCH_2COC_2H_5$	70/13 mmHg
Benzoylacetone	HBzA	$CH_3COCH_2COC_6H_5$	
Dibenzoylmethane	HDBM	$C_6H_5COCH_2COC_6H_5$	
Trifluoroacetylacetone	HTFA	$CF_3COCH_2COCH_3$	
Trifluoroacetylpropionylmethane	HTPrM	$CF_3COCH_2COC_2H_5$	31—31.5/26 mmHg
Trifluoroacetylisobutyrylmethane	HTIBM	$CF_3COCH_2COCH(CH_3)_2$	42—43.5/26 mmHg
Trifluoroacetylpivaloylmethane	HTPM	$CF_3COCH_2COC(CH_3)_3$	47—47.5/18 mmHg
Trifluoroacetyl-α-methylbutyrylmethane	HTMBM	$CF_3COCH_2COCH(CH_3)C_2H_5$	50—51/22 mmHg
Trifluoroacetylisovalerylmethane	HTIVM	$CF_3COCH_2COCH_2CH(CH_3)_2$	57—58/26 mmHg
Furoyltrifluoroacetone	HFTA	$CF_3COCH_2COC_4H_3O$	
Thenoyltrifluoroacetone	HTTA	$CF_3COCH_2COC_4H_3S$	
Benzoyltrifluoroacetone	HBFA	$CF_3COCH_2COC_6H_5$	
Hexafluoroacetylacetone	HHFA	$CF_3COCH_2COCF_3$	

21) T. Shigematsu, M. Matsui, and K. Utsunomiya, *Bull. Inst. Chem. Res., Kyoto Univ.*, **46**, 256 (1968).
22) J. T. Adams and C. R. Hauser, *J. Amer. Chem. Soc.*, **66**, 1220 (1944).
23) T. Shigematsu, M. Matsui, and K. Utsunomiya, This Bulletin, **42**, 1278 (1969).
24) J. C. Reid and M. Calvin, *J. Amer. Chem. Soc.*, **72**, 2948 (1950).

Table 2. Melting points of aluminum, gallium, and indium chelates

Chelate	Mp (°C)	(Reference)	Chelate	Mp (°C)	(Reference)	Chelate	Mp (°C)	(Reference)
$Al(AA)_3$	192.5	(112,[25] 198[26])	$Ga(AA)_3$	194		$In(AA)_3$	181.5	
$Al(IBA)_3$	oil		$Ga(PiA)_3$	oil		$In(DIBM)_3$	96.0	
$Al(PiA)_3$	oil		$Ga(DIBM)_3$	129		$In(IBPM)_3$	96.5	
$Al(DIBM)_3$	139		$Ga(IBPM)_3$	148.5		$In(DPM)_3$	204—209	
$Al(IBPM)_3$	181		$Ga(DPM)_3$	220.5		$In(BzA)_3$	214	
$Al(DPM)_3$	257	(264—265[27])	$Ga(BzA)_3$	222		$In(DBM)_3$	251	
$Al(BzA)_3$	221	(223.5—224.0[28])	$Ga(DBM)_3$	294		$In(TFA)_3$	122—124	(118—120[29])
$Al(DBM)_3$	295—300		$Ga(TFA)_3$	125—126	(128—129.5[29])	$In(TPrM)_3$	99—102	
$Al(TFA)_3$	120	(117,[25] 120—121[29])	$Ga(TPrM)_3$	63.0		$In(TIBM)_3$	104—107	
$Al(TPrM)_3$	61.5		$Ga(TIBM)_3$	67.0		$In(TPM)_3$	112—119	
$Al(TIBM)_3$	65.0		$Ga(TPM)_3$	67.0		$In(TMBM)_3$	53.0	
$Al(TPM)_3$	71.5	(70—72[19])	$Ga(TMBM)_3$	70.0		$In(TIVM)_3$	oil	
$Al(TMBM)_3$	71.0		$Ga(TIVM)_3$	oil		$In(FTA)_3$	194—196	
$Al(TIVM)_3$	oil		$Ga(FTA)_3$	206—208		$In(BFA)_3$	137—140	
$Al(FTA)_3$	185—188	(204—205[25])	$Ga(BFA)_3$	152—154		$In(TTA)_3$	154—156	(164.6[30])
$Al(BFA)_3$	169—171	(173—174[25])	$Ga(TTA)_3$	181—183	(184—184.2[30])	$In(HFA)_3$	73.0	
$Al(TTA)_3$	198—201	(203—205[25])	$Ga(HFA)_3$	68.5—70.0	(68.0—69.5[12])			
$Al(HFA)_3$	71.5	(70.5—71.3[12])						

good gas chromatograms. The TGA curves of aluminum, gallium, and indium β-diketonates are shown in Figs. 1 to 3.

The aluminum β-diketonates are volatile and are thermally stable, except for $Al(BzA)_3$ and $Al(DBM)_3$, which decompose over 200°C instead undergoing sublimation. The volatility increases in the following order: for alkyl-substituted acetylacetone chelates,

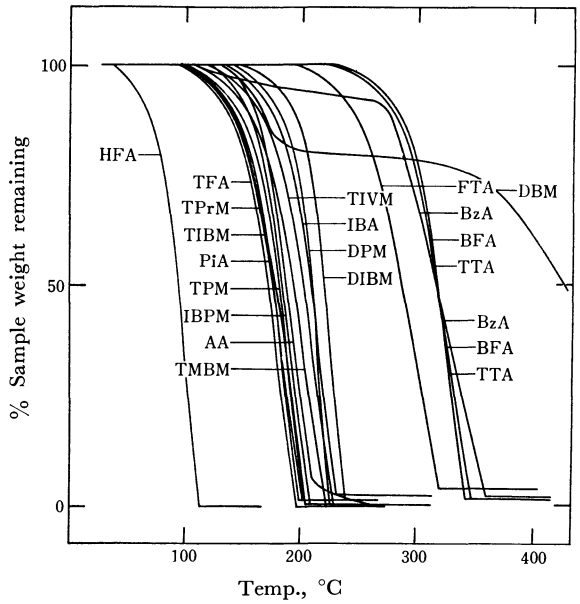

Fig. 1. Thermogravimetric curves of aluminum β-diketonates.

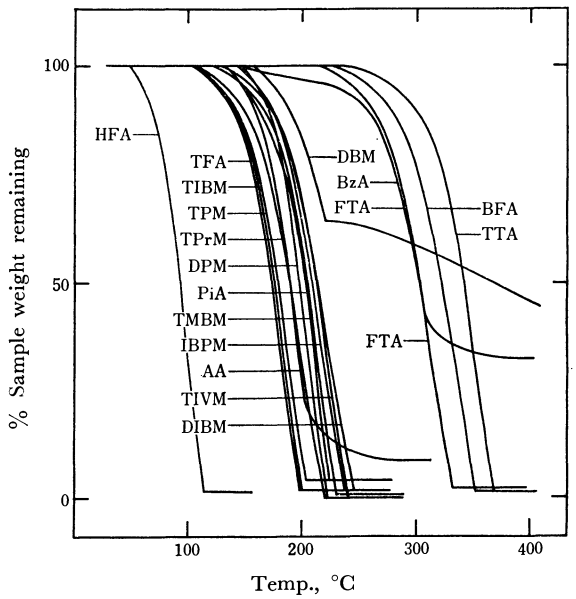

Fig. 2. Thermogravimetric curves of gallium β-diketonates.

$Al(DIBM)_3 < Al(DPM)_3 \leq Al(IBA)_3 < Al(AA)_3 < Al(IBPM)_3 < Al(PiA)_3$; for fluorinated β-diketone chelates, $Al(TTA)_3 \leq Al(BFA)_3 < Al(FTA)_3 \ll Al(TIVM)_3 < Al(TMBM)_3 < Al(TPM)_3 < Al(TIBM)_3 \leq Al(TPrM)_3 < Al(TFA)_3 \ll Al(HFA)_3$ (Fig. 1). Gallium(III) acetylacetonate does not completely sublime, and $Ga(BzA)_3$ and $Ga(DBM)_3$ decompose. The volatility increases in this order: $Ga(DIBM)_3 < Ga(IBPM)_3 < Ga(PiA)_3 < Ga(DPM)_3 < Ga(AA)_3$; $Ga(TTA)_3 < Ga(BFA)_3 < Ga(FTA)_3 \ll Ga(TIVM)_3 < Ga(TMBM)_3 < Ga(TPrM)_3 < Ga(TPM)_3 < Ga(TIBM)_3 < Ga(TFA)_3 \ll Ga(HFA)_3$ (Fig. 2). Many of the indium(III) chelates do not quantitatively sublimate, and $In(AA)_3$, $In(BzA)_3$, $In(DMB)_3$, and $In(HFA)_3$ decompose. The increasing order of the volatility is as follows: $In(DIBM)_3 < In(IBPM)_3 < In(DPM)_3$; $In(TTA)_3 < In(BFA)_3 < In(FTA)_3 \ll In(TIVM)_3 < In-$

25) E. W. Berg and J. T. Truemper, *Anal. Chim. Acta*, **32**, 245 (1965).
26) R. W. Moshier and R. E. Sievers, "Gas Chromatography of Metal Chelates," p. 141, Pergamon Press, New York (1965).
27) *Ibid.*, p. 148.
28) *Ibid.*, p. 147.
29) R. C. Fay and T. S. Piper, *J. Amer. Chem. Soc.*, **84**, 2303 (1962).
30) M. Yamazaki and T. Takeuchi, *Nippon Kagaku Zasshi*, **91**, 965 (1970).

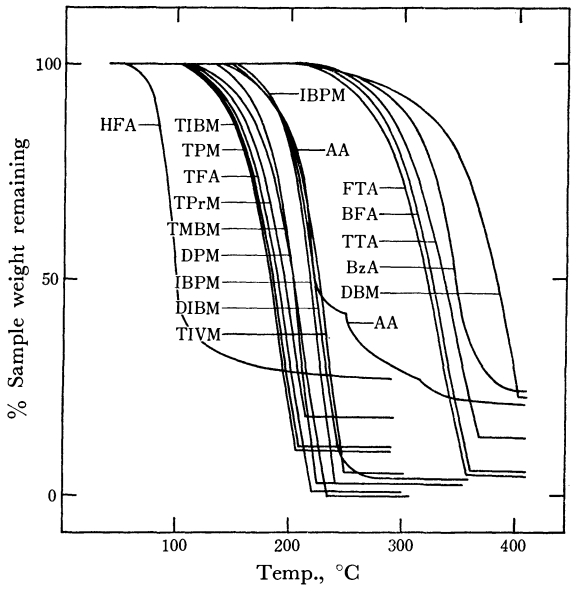

Fig. 3. Thermogravimetric curves of indium β-diketonates.

$(TMBM)_3 < In(TPrM)_3 < In(TFA)_3 < In(TPM)_3 < In(TIBM)_3$ (Fig. 3).

Usually, the substitution of the fluoromethyl group increases the volatility of the chelates, while an aryl group, such as a furyl, phenyl, or thienyl group, tends to decrease the volatility. Accordingly, FTA, BFA, and TTA chelates are less volatile, in spite of the presence of a trifluoromethyl group, and BzA and DBM chelates decompose without sublimation. However, there is no general correlation between the volatility of alkyl-substituted chelates and their substituted groups, except in the one case of indium(III) chelates, where the volatility does seem to increase in the order of substitution: $CH_3- < (CH_3)_2CH- < (CH_3)_3C-$.

Gas Chromatography of Alkyl-substituted β-Diketonates. Figure 4 shows gas chromatograms of the aluminum, gallium, and indium chelates of some β-diketones. The elution is strongly temperature-dependent. Aluminum chelates give optimal chromatograms at a column temperature of 200°C, but at this temperature the peaks of gallium and indium chelates are broad and tailed. The peak sharpens at a higher column temperature. Gallium chelates show good chromatograms at 212°C, and indium chelates, at 220°C. As may be seen in the chromatograms of $Ga(AA)_3$ and $Ga(PiA)_3$ (Fig. 5(a), (b)), a small peak or a shoulder is observed prior to the main peak. Such a confusing peak can not be removed by varying the temperature or by employing another kind of column; it might arise from a thermally-decomposed impurity.

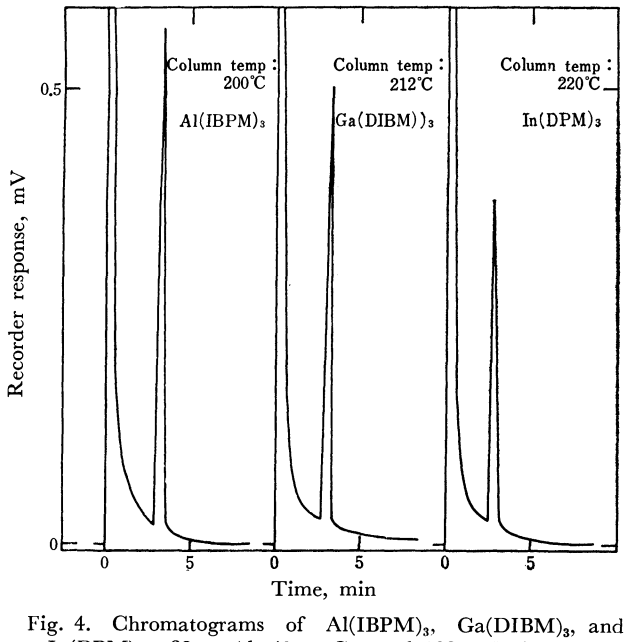

Fig. 4. Chromatograms of $Al(IBPM)_3$, $Ga(DIBM)_3$, and $In(DPM)_3$. 28 μg Al, 49 μg Ga, and 102 μg In in benzene (10 μl).

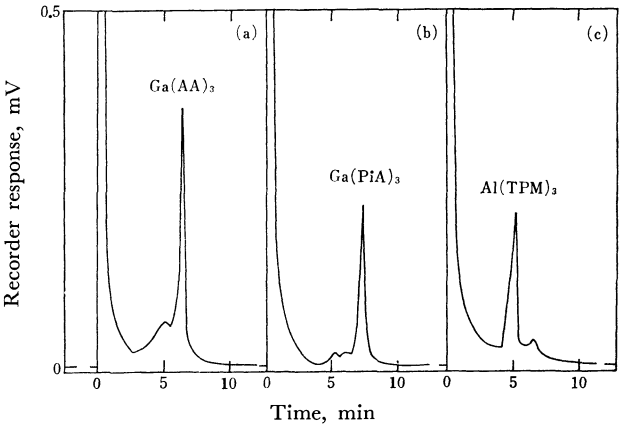

Fig. 5. Chromatograms of $Ga(AA)_3$, $Ga(PiA)_3$, and $Al(TPM)_3$. (a) 120 μg $Ga(AA)_3$, and (b) 152 μg $Ga(PiA)_3$ in benzene (20 μl). Column temperature: programmed from 100 to 250°C at 20°C/min. Helium flow rate: 95 ml/min. (c) 231 μg $Al(TPM)_3$ in benzene (10 μl). Column temperature: 178°C. Helium flow rate: 81 ml/min.

The retention data of the metal chelates with alkyl substituted β-diketones are summarized in Table 3. The retention times of the chelates increase in the following order: $Al(AA)_3 < Al(IBA)_3 < Al(PiA)_3 \approx Al(DIBM)_3 < Al(IBPM)_3 < Al(DPM)_3$, $Ga(AA)_3 < Ga(PiA)_3 < Ga(DIBM)_3 \approx Ga(IBPM)_3 < Ga(DPM)_3$, $In(DIBM)_3 < In(IBPM)_3 < In(DPM)_3$. This order is in good agreement with an empirical rule of gas chromatography that the retention time of organic compounds increases with an increase in the molecular weight. However, no correlation is obtained between the elution behavior and the volatility of the chelates observed in the TGA curve. For the separation of aluminum, gallium, and indium, DIBM, IBPM, and DPM chelates are suitable, but AA, BzA, and DBM chelates can not be used because of their smaller volatility.

Gas Chromatography of Fluorinated β-Diketonates. Aluminum, gallium, and indium chelates with TFA, TPrM, TIBM, TPM, TMBM, and TIVM are eluted at a column temperature between 120 and 200°C. For FTA, BFA, and TTA chelates, the column temperature must rise about 100°C higher than for the above β-diketonates: $Al(FTA)_3$ and $Al(BFA)_3$ are eluted at 230°C, while $Al(TTA)_3$, $Ga(TTA)_3$, and $In(FTA)_3$ are eluted at 250°C with decomposed products. The TGA curves predict that the column temperature for $In(BFA)_3$ and $In(TTA)_3$ will be 300°C or more.

Table 3. Retention time of aluminum, gallium, and indium chelates with nonfluorinated β-diketones (min)

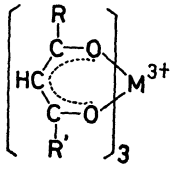

	AA	IBA	PiA	DIBM	IBPM	DPM	BzA	DBM	
R	CH_3-	CH_3-	CH_3-	$(CH_3)_2CH$-	$(CH_3)_3C$-	$(CH_3)_3C$-	CH_3-	C_6H_5-	
R′	CH_3-	$(CH_3)_2CH$-	$(CH_3)_3C$-	$(CH_3)_2CH$-	$(CH_3)_2CH$-	$(CH_3)_3C$-	C_6H_5-	C_6H_5-	
Aluminum	0.4	1.4	2.6	2.6	3.4	4.0	nv	nv	(column temp.: 200°C) (Helium flow rate: 80 ml/min)
Gallium	0.7*	—**	1.8	3.0	3.0	3.8	nv	nv	(column temp.: 212°C) (Helium flow rate: 79 ml/min)
Indium	nv	—**	—**	2.3	2.6	2.8	nv	nv	(column temp.: 220°C) (Helium flow rate: 75 ml/min)

nv: non-volatile. *: partly decomposed. **: chelates could not be synthesized.

Table 4. Retention time of aluminum, gallium, and indium chelates with fluorinated β-diketones (min)

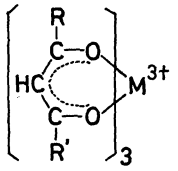

	HFA	TFA	TPrM	TIBM	TPM	TMBM	TIVM	FTA	BFA	TTA
R=CF_3 R′	CF_3-	CH_3-	C_2H_5-	$(CH_3)_2CH$-	$(CH_3)_3C$-	$C_2H_5CH(CH_3)$-	$(CH_3)_2CHCH_2$-			
Aluminum	4.0	1.3	3.2	3.9	5.1	11.8	13.3	1.8	5.2	5.3[a] / 7.1
Gallium	5.3	2.7	4.8	5.9	7.2	15.8	19.7	2.5	6.0	6.2[a] / 9.0
Indium	ne	2.5	4.2	4.6	5.3	6.0	9.5	3.2[b] / 3.6	ne	ne
Operating conditions	column temp.: 90°C Helium flow rate: 47 ml/min.			For Al and Ga chelates, column temp.: 138°C, Helium flow rate: 67 ml/min. For In chelates, column temp.; 154°C Helium flow rate: 50 ml/min.				column temp.: 250°C Helium flow rate: 45 ml/min.		
Order of elution	← fast elution						late elution →			

a) partly decomposed. b) decomposed products. ne: chelates were not eluted.

Therefore a column coated with 3% (by weight) silicone gum SE-30 on Chromosorb W AW DMCS (80—100 mesh) was used for these indium chelates; nevertheless, the chelates were not eluted even at a column temperature between 300 and 340°C. In the chromatograms of $Al(TPrM)_3$, $Al(TIBM)_3$, and $Al(TPM)_3$, a main peak is followed by a smaller peak (Fig. 5(c)); although no detailed study was carried out, this phenomenon might result from the *cis* and *trans* isomers, as has been reported for $Cr(TFA)_3$.[3]

The retention data of fluorinated β-diketone chelates are listed in Table 4. The table indicates that HTFA, HTPrM, HTIBM, HTPM, HTMBM, and HTIVM can be used for the separation of aluminum, gallium, and indium. An example using HTPrM is presented in Fig. 6. The retention time of fluorinated β-diketonates increases in this order: $M(HFA)_3 \ll M(TFA)_3 < M(TPrM)_3 < M(TIBM)_3 < M(TPM)_3 < M(TMBM)_3 < M(TIVM)_3 \ll M(FTA)_3 < M(BFA)_3 < M(TTA)_3$; in contrast with the alkyl-substituted acetylacetonates series, it evidently depends upon the volatility of the chelates. The increasing order of the retention time is quite the same as the decreasing order of the volatility of aluminum chelates; a similar relationship is observed for gallium chelates except for the position of TPrM and for indium chelates except for the position of TFA and TPrM.

In the present research, the substitution on the γ-position of β-diketonates was not investigated, because it had previously been reported that substitution on this position with bromine,[20] methyl,[31] or isopropyl[31] group reduced the volatility of the metal chelates.

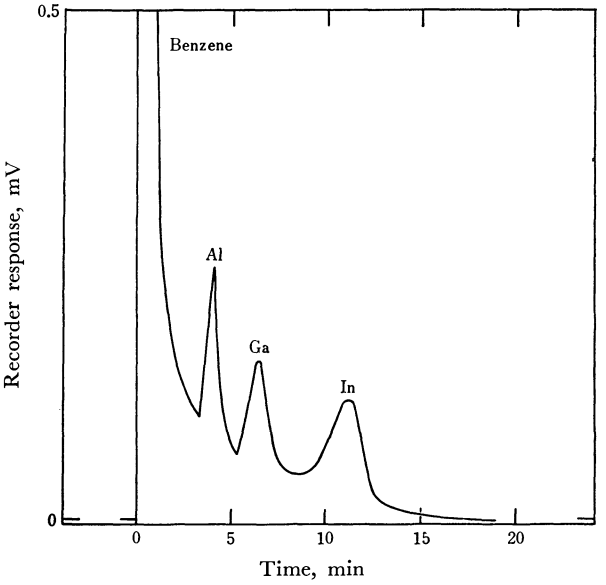

Fig. 6. Separation of aluminum, gallium, and indium TPrM chelates. 29 μg Al, 72 μg Ga, and 230 μg In in benzene (25 μl). Column temperature: 128°C. Helium flow rate: 81 ml/min.

The author wishes to express his thanks to Professor Tsunenobu Shigematsu for his guidance throughout this study. Thanks are also due to Drs. Masayuki Tabushi and Masakazu Matsui for their helpful advice and discussions.

31) G. K. Schweitzer, B. P. Pullen, and Yi-Hung Fang, *Anal. Chim. Acta*, **43**, 332 (1968).

BULLETIN OF THE CHEMICAL SOCIETY OF JAPAN, VOL. 44, 2693—2697 (1971)

The Separation of Aluminum from Iron by the Zone-melting of Their Complexes

Michio MASHIMA and Kazuo MARUYAMA

Faculty of Engineering, Niigata University, Nagaoka

(Received December 16, 1970)

The separation of Al from Fe was attempted as a first step in the chromatographic application of the zone-melting method to metal complexes. *N,N'*-ethylenedianthranilic acid and benzoic acid complexes, and various organic solid solvents were prepared. The experiment was carried out with a zone speed of 6 cm/hr and a molten-zone length of 0.6—1.0 cm at 75°C. When stearic acid was used as the solvent, the recovery percentage of Al was about 75% with the benzoic acid complex and about 99% with the *N'N'*-ethylenedianthranilic acid complex. Furthermore, the effective distribution coefficient and phase diagram supported due idea of the behavior of the complexes.

It has widely been known that pure germanium may be prepared by a zone-melting method.[1] Nowadays, it is used in various fields.[2,3] There are two methods of zone-melting for the separation and condensation of metals. One is used for the metallic state, and the other is used for the metal chelate state. Though the latter is easier than the former, because metal chelates have relatively low melting points and various organic characteristics, good results seem not yet to have been obtained.[4]

1) W. G. Pfann, *Trans. AIME*, **194**, 747 (1952).

2) W. G. Pfann, "*Zone Melting*," John Wiley & Sons, Inc., New York, (1958), 128.

3) H. Schildknecht, "*Zoneschmelzen*," Verlag Chemie, Weinheim, (1964).

4) K. Ueno, *et al. Talanta* **14**, 1403, 1411, (1967); K. Ueno, H. Kaneko, and Y. Watanabe, *Micro. Chem. J.*, **10**, 244 (1966); K. Ueno, H. Kaneko, and N. Fujimoto, *Talanta*, **11**, 1371 (1964).

In this study, in order to separate one metal from other, the chromatographic development[5] by the zone-melting method was carried out with the metal chelates of benzoic acid[6] and *N,N'*-ethylenedianthranilic acid (NEA)[7] as solutes, and with stearic acid, benzoic acid, and naphthalene as their solvents. When stearic acid was used as the solvent, good results in the separation of aluminum from iron were obtained. Furthermore, the effective distribution coefficient[8] and the phase diagram were examined, so that the operation of this method could be discussed.

Experimental

Zone-melting Procedure. A vertical type zone-melting apparatus was used, by which a sample in a glass tube was zone-melted. The apparatus had several ring heaters, and it was cooled with water or air. The apparatus was of our own making. Long glass tubes 5 mm in inner diameter were used as the sample columns. As Fig. 1 shows, about 0.1 mg of the complex with about 250 times as much solid solvent was melted into the bottom of the glass tube and then cooled to solidify it, then the pure solvent was placed on it. Finally, the column length was 20 cm. When a 30-cm column was used, it took very long to zone-melt, and the results were similar to those obtained with the 20-cm column. Therefore, the 20-cm column was mainly used in this experiment. Besides it, the 10-cm column was also used for the sake of comparison. The experiment was carried out at a rate of zone travel of 6 cm/hr. The width of the molten zone was 1 cm in the apparatus with air cooling and 0.6 cm in the one with water cooling. The temperature of the molten zone was about 75°C. At temperatures higher than 75°C, the molten zone became wider and it became unstable at the solid-liquid intersurface.

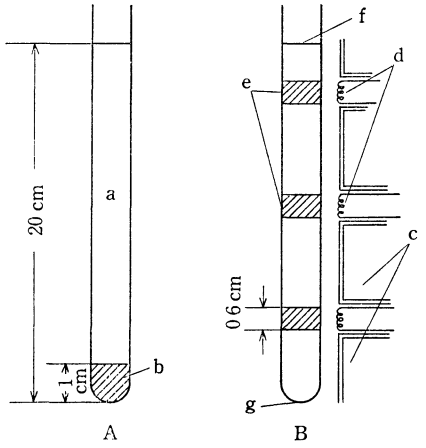

Fig. 1. Diagrammatic representation of sample column(A) and that in zone apparatus with water-cooling(B).
(a) Solid solvent, (b) Complex as solute, (c) Cooler, (d) Heater, (e) Molten zone, (f) Upper end, (g) Bottom

Preparation of Metal Complexes. A metal ion solution was adjusted to pH 4—5 with ammonium acetate; then a 50 : 50 water-alcohol solution which contained a little more excess ligand than the calculated quantity of a solution of NEA[9] or benzoic acid was added to the solution. A precipitate was formed immediately; it was then collected in a suction filter. It was washed with water and sucked to dryness. These precipitates were determined photometrically. In both the benzoic acid complexes and the NEA complexes, we found a 1 : 3 rate of metal to ligand.[6,7] These metal complexes and such organic compounds as stearic acid, benzoic acid, naphthalene, and acetoanilide were solutes and solid solvents respectively.

Analysis of Zone-melted Samples. Zone-melted samples were cut, weighed, and dissolved in chloroform; after these complexes had then been decomposed with 6 N HCl, aluminum and iron ions were removed into the HCl phase. The HCl phase separated from chloroform phase was added to a 1% oxine acetic acid solution, and the solution was adjusted to pH 4.8—5.2 with 2 N ammonia water and ammonium acetate. The oxinates were extracted with 10 m*l* of chloroform. The aluminum and iron were then determined photometrically.[10]

Results and Discussion

At first, the NEA complex in stearic acid solvent was zone-melted with an air-cooling apparatus. The molten zone traveled upwards. The Al and Fe complexes contained 0.3 and 0.6 mg of metal respectively. The zone passes were done 12 and 15 times. One of these chromatograms is shown in Fig. 2. The metal concentration (%), the quantity of metal (mg) per

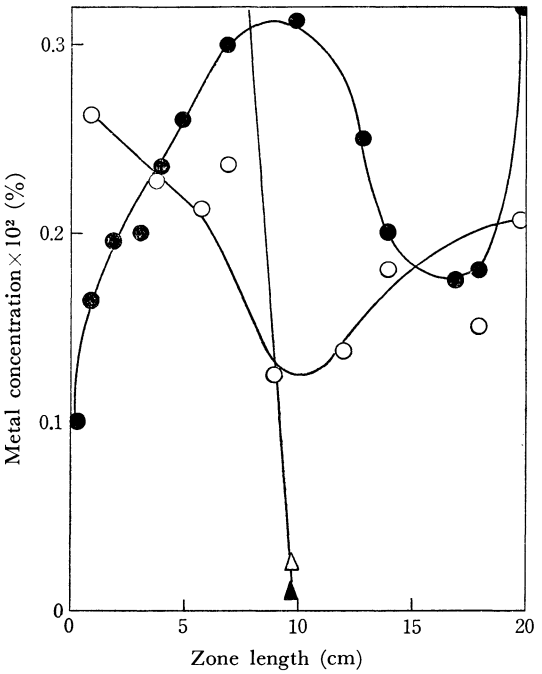

Fig. 2. Distribution of NEA-complexes with 12 and 15 zone passes.
Al: 12 ○, 15 ●, Fe: 12 △, 15 ▲

5) W. G. Pfann, *Anal. Chem.*, **36**, 2231 (1964).
6) I. M. Kolthoff, V. A. Stenger, and B. Maskovitz, *J. Amer. Chem. Soc.*, **56**, 812 (1934); I. Lehrmann and J. Kramer, *ibid.*, **56**, 2648 (1934).
7) B. Amberger and V. Goldberger, *Ann.*, **305**, 362.
8) R. H. Mcfee, *J. Chem. Phys.*, **15**, 856 (1947).
9) M. Mashima, Bunseki Kagaku, **9**, 199 (1960).
10) K. Motojima and H. Hashitani, This Bulletin, **29**, 458 (1956).

gram of the solvent is plotted as the ordinate, and the length from the bottom to the center of a piece of the sample is plotted as the abscissa. Though the Al-complex moved toward the upper end with an increase in the number of zone passes, the Fe-complex moved only to the center of the column even after zone passes. Therefore, it may be possible to separate Al from Fe. If the column was cut at the point where Fe was absent, 40 and 51% of the total Al could be separated with 12 and 15 zone passes respectively. This was defined as the "recovery percentage." As a large quantity of the Al-complex was still present at the bottom in the above case, the experiments were carried out with a smaller amount of complexes later.

Figure 3 shows a chromatogram when 0.02 mg of Al and 0.03 mg of Fe were used. Most of the Al-complex moved to the upper end, while the Fe-complex could not be found more than 9 cm from the bottom; thus, the Al-complex was separated efficiently.

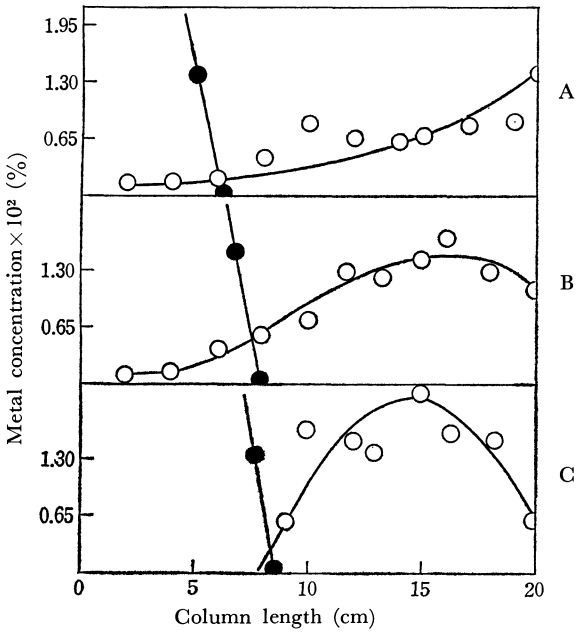

Fig. 3. Distribution of NEA-complex in stearic acid after zone melting process, using 2.0×10^{-2} mg of Al(○) and 3.0×10^{-2} mg of Fe(●).
A: 12 zone passes, B: 16 zone passes,
C: 18 zone passes

Table 1. Recovery percentage of Al as NEA complex

Exp. No.	Column length (cm)	Rate of zone travel (cm/hr)	No. of zone passes	Weight of Al (cm)	Weight of Fe (mg)	Recovery percent (%)
1	10	6	10	1.05	0.47	17
2	10	6	12	1.15	0.54	17
3	10	6	10	1.07	1.09	16
4	10	6	12	1.11	1.09	20
5	20	6	10	1.16	0.62	17
6	20	6	12	1.16	0.62	25
7	20	6	5	3.36	7.15	55
8	20	3	5	2.36	5.21	56
9	20	6	12	0.013	0.025	88
10	20	6	16	0.022	0.041	89
11	20	6	18	0.021	0.038	99

The recovery percentages of Al were 88, 89, and 99% with 12, 16, and 18 zone passes respectively; Al was thus almost completely separated from Fe with 18 zone passes. In Figs. 3B and C, the decrease in the Al concentration at the top of the chromatogram may be attributed to the following cause. Stearic acid evaporated from the top of the charge and condensed on the inner wall of the glass tube, and then this stearic acid was present in the top section of the sample during the analysis.

Table 1 shows the recovery percentage for the quantity of the complexes used, the column length, and the rate of zone travel. A comparison of No.1 with No. 3 reveals that the recovery percentage was not affected by the quantity of the Fe-complex; the recovery percentages were 17 and 16% for about 0.5—1 mg of Fe. Furthermore, a comparison of No. 2 with No. 6 reveals that the recovery percentage increased with the column length; the recovery percentages were 17 and 25% for the column lengths of 10 and 20 cm respectively.

No. 7 and No. 8 show the variation with the rate of zone travel. The recovery percentages were 55 and 57% in 6 and 3 cm/hr respectively.

Figure 4 shows a chromatogram of the Al and Fe complexes of benzoic acid in a stearic acid solvent obtained by the use of the apparatus with water-cooling. Here, the solubility of the benzoic acid complexes in stearic acid was about 2.5%, the same

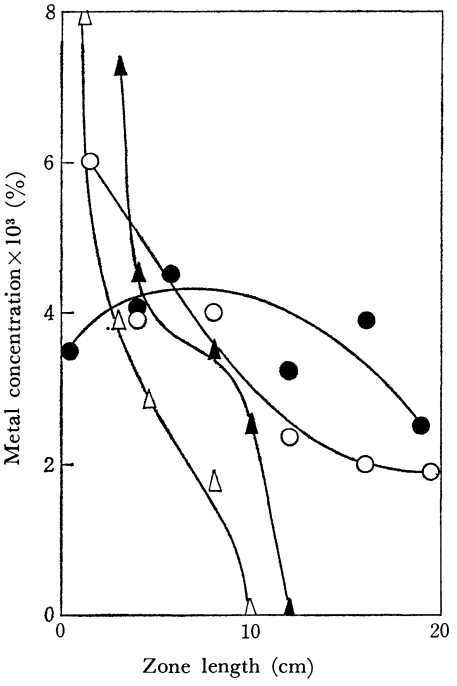

Fig. 4. Distribution of benzoic acid-complex. with 4 and 8 zone passes.
Al {○ 4 zone passes ● 8 zone passes Fe {△ 4 zone passes ▲ 8 zone passes

Table 2. Recovery percentage of Al as benzoic acid complex

Exp. No.	Column length (cm)	Rate of zone travel (cm/hr)	No. of zone passes	Weight of Al $\times 10^2$ mg	Weight of Fe $\times 10^2$mg	Recovery percent (%)
1	20	6	8	7.49	7.22	49
2	20	6	12	9.90	7.16	46
3	20	6	10	8.86	4.75	49
4	20	6	14	7.54	3.82	58
5	20	6	5	2.88	1.77	44
6	20	6	9	3.26	2.03	63
7	10	6	9	2.55	1.47	58
8	10	6	12	2.50	1.86	75

as that of the NEA complex in stearic acid. In this case also, the results obtained were similar to those obtained with the NEA complex. The recovery percentages were 25 and 49% in 4 and 8 zone passes respectively; the percentage thus increased with the number of zone passes.

Table 2 shows the recovery percentage for the Al-complex of benzoic acid, obtained in the same manner as in Table 1. The separation of Al from Fe seems to be efficient in No. 4, 6, 7, and 8.

The normal freezing equation has also been derived theoretically and experimentally by Mcfee *et al.*[2,8] Thus;

$$\log [C_s(x)/C_0] = \log K + (K-1) \log[1-(x/L)]$$

where C_0 is an initial concentration. Both the slope and the intercept at $x=0$ provided a measure of the effective distribution coefficient, K. Figure 5 shows the relationship between $\log C_s(x)$ and $\log[1-(x/L)]$ with the complexes in stearic acid. The initial concentrations were all 0.2%. The effective distribution coefficient was obtained from the slope of the linear line; in normal freezing, the column of the complex and stearic acid mixture was melted, then it was frozen from the bottom by means of a cooler, and the frozen sample was analyzed by the above-mentioned method. The concentration of the complex, $C_s(x)$, at any distance, x, from the bottom along a frozen column with a total length of L was obtained from the normal freezing. The effective distribution coefficients of NEA and benzoic acid complexes of Fe were 1.08 and 1.01, while those of the Al-complex were 0.61 and 0.89 respectively. These results suggest that only the Al-complexes travel to the upper end, while Fe-complexes do not; the results presuppose the possibility of the separation of Al from Fe.

Table 3 shows the effective distribution coefficients of these complexes in other solvents. From the table, it seems that benzoic acid could also be used as a solvent in this method, but it was not used because the column of the benzoic acid solvent was easily broken when several zones were passed.

Figure 6 shows the phase diagrams of these complexes in stearic acid; the concentration of the complex in stearic acid was less than 3%. A Coblle automatic thermoanalyzer was used in this experiment. These results suggest that the tendency of the NEA-complex

Table 3. Effective distribution coefficient

	NEA-complex		Benzoic acid-complex	
	Al	Fe	Al	Fe
Solvent				
Benzoic acid	0.9	1.27	1.3	0.99
Naphthalene	1.27	1.27	1.28	0.98
Cetyl alcohol	0.8	1.50		
Acetoanilide	1.7	1.10		

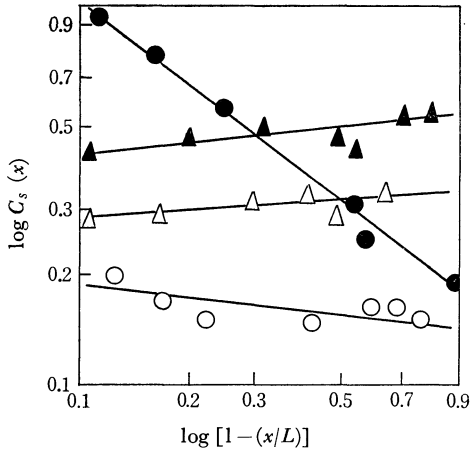

Fig. 5. Distribution coefficient of NEA and benzoic acid complex in stearic acid solvent.
NEA-Al-complex ●, NEA-Fe-complex ▲,
Benzoic acid-Al-complex ○, Benzoic acid-Fe-complex △

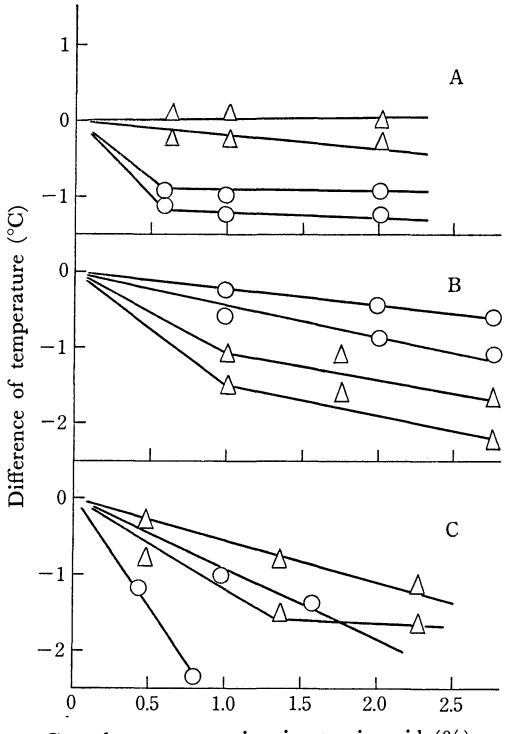

Fig. 6. Phase diagram of Al(○) and Fe(△) complex.
A: Stearic acid-complex, B: NEA-complex,
C: Benzoic acid-complex

was different from that of the benzoic acid complex, and each complex may not change its ligand in this zone-melting method. Here, the difference in temperature is based on the melting point of stearic acid. In each figure 6A, B, and C, the upper curve and lower curve were liquidus and solidus lines respectively. In Fig. 6A, the liquidus curve of Al-complex is not horizontal; it may decrease slightly with the concentration. A more detailed analysis of these phase diagrams will be reported latter.

BULLETIN OF THE CHEMICAL SOCIETY OF JAPAN, VOL. 44, 2697—2702 (1971)

Studies of Aliphatic Hydroxycarboxylic Acids as Antioxidant. V. Complexes of Copper(II) with *erythro*- and *threo*-2-Methyltartaric, and *meso*- and *threo*-2,3-Dimethyltartaric Acids

Kazuo Horikawa and Shinroku Masuyama
The Osaka Municipal Technical Research Institute, Kita-ku, Osaka

(Received December 21, 1970)

The dissociation constants of *erythro*- and *threo*-2-methyltartaric and *meso*- and *threo*-2,3-dimethyltartaric acids were determined by the potentiometric titration method at the ionic strength of $\mu=0.1$ and at 22°C. The values of the dissociation constants were $pK_1=3.54$ and $pK_2=5.03$ for *erythro*-2-methyltartaric acid, and $pK_1=3.28$ and $pK_2=4.70$ for the *threo*-form. For *meso*-2,3-dimethyltartaric acid, the corresponding values were 3.52 and 4.98, while the *threo*-form had values of 3.04 and 5.30. The complex formation of copper(II) with these acids has been investigated using Job's method of continuous variations at the ionic strength of $\mu=0.2$ and at 22°C. Copper-(II) and *erythro*-2-methyltartaric acid react in a 1 : 1 ratio at pH 2.40 and in a 3 : 2 ratio at pH 5.00. On the other hand, the *threo*-form does not combine with copper(II) at pH 2.40, though it does react at pH 5.00 in a 1 : 1 ratio. As for *meso*-2,3-dimethyltartaric acid, the complex formation in a 3 : 2 ratio was observed at pH 5.00. However, the *threo*-form and copper(II) react in a 1 : 2 ratio at pH 5.00. The equilibrium constants (apparent stability constants) were calculated by the method of Turner and Anderson. The values of the equilibrium constant were $\log K=9.71$ (pH 5.00) and $\log K=2.02$ (pH 2.40) for *erythro*-2-methyltartaric acid, $\log K=3.78$ (pH 5.00) for the *threo*-form, $\log K=9.70$ (pH 5.00) for *meso*-2,3-dimethyltartaric acid, and $\log K=5.19$ (pH 5.00) for the *threo*- form. On the basis of these data, the structures of these complexes are discussed.

It is a well-known fact that small quantities of heavy metals have a deteriorating effect on the stability of oils. Especially, copper and iron have long been known to be detrimental to the stability of vegetable oils. Chelating agents, citric or tartaric acids, was added in order to decrease the influence of these metals. In order to study the influence of metal traces on the behaviour and the efficiency of these hydroxycarboxylic acids against the autoxidation of oils, we carried out experiments with a pure substrate, diethyl linoleate, and with soybean oil. These results have been published previously.[1] In a continuation of our study of hydroxycarboxylic acids as antioxidants, the present paper will report the determination of the dissociation constants on methyl derivatives of tartaric acid and of the equilibrium constants with copper(II). It seemed worthwhile to study the stability constants of these methyl derivatives with copper(II), since the composition of the complexes and the stability constants of these chelate compounds might be related to the stabilizing effect on the vegetable oils as antioxidants. Although a great deal of work has been done in the preparation of chelate compounds, for example, copper(II) or iron(III) tartrate and citrate, and upon their structures and formation constants,[2-5] no attempt has yet been made to determine the dissociation constants of methyl derivatives of tartaric acid and the stability constants with copper(II).

In this paper, *erythro*- and *threo*-2-methyltartaric acids were synthesized by the oxidation of diethyl-citraconate and diethylmesaconate respectively with permanganate. *Meso*- and *threo*-2,3-dimethyltartaric acids were prepared according to the procedure of Izumi *et al.*[6] The dissociation constants of these acids was determined by means of the potentiometric titration method. In order to calculate the equilibrium constants (apparent stability constants), we used the Turner and Anderson dilution method.[7] The composition of the complexes was studied Job's method of continuous variation.[8,9]

1) K. Horikawa and S. Masuyama, Paper presented at the 4th. Symposium of the Oxidation-Reaction, Tokyo, Oct. 1970.

2) L. Meites, *J. Amer. Chem. Soc.*, **71**, 3269 (1949), **72**, 180 (1950).

3) R. W. Green and G. M. Parkins, *J. Phys. Chem.*, **65**, 1658 (1961).

4) M. Bobtelsky and J. Jordan, *J. Amer. Chem. Soc.*, **69**, 2286 (1947).

5) C. F. Timberlake, *J. Chem. Soc.*, **1964**, 1229.

6) S. Tatsumi, Y. Izumi, M. Imaida, Y. Fukuda, and S. Akabori, This Bulletin, **39**, 602 (1966).

7) S. E. Turner and R. C. Anderson, *J. Amer. Chem. Soc.*, **71**, 912 (1949).

8) P. Job, *Ann. Chim.*, **11**, 97 (1936).

9) M. Muzaffaruddin and M. W. Roomi, *J. Amer. Oil Chemists' Soc.*, **46**, 368 (1969).

Experimental

All the melting points are uncorrected. The infrared spectra were determined in Nujol mull using a Shimadzu IR-27 spectrometer in the 2—15 μ region. The potentiometric titrations were made with a Metrohm Herisau Potentiograph, E 336. Optical density measurements from 600 to 800 mμ were made on a Hitachi 139 spectrophotometer. The pH of the reaction mixture was measured by means of a Yanagimoto Model 42-A pH-meter. During potentiometric titrations and spectro photometric measurements, constant ionic strenghts of 0.1 and 0.2 respectively were maintained by adding the requisite amount of a sodium perchlorate solution. Buffer solutions were prepared by adding the proper amount of 0.1 N acetic acid to a 0.1 N solution of sodium acetate. Standard copper(II) perchlorate (commercial reagent) in demetalized water and copper(II) was estimated spectrophotometrically (JIS-H-1101—1961). A sodium perchlorate solution was prepared in a concentration of 1 M. The dissociation constants of these acids were determined by the potentiometric titration of 10^{-3} M solutions, while the equilibrium constants of the copper(II) complexes were obtained spectrophotometrically.

Preparation of Ligands. The Preparation of erythro-*2-Methyltartaric Acid* (erythro-*MTA*): A solution of diethylcitraconate (40 g) dissolved in 200 m*l* of ethanol was oxidized with 2% aqueous potassium permanganate for 5 hr from −20 to −5°C. The reaction solution was then allowed to stand at room temperature overnight. The precipitated inorganic salt was removed by filtration; the filtrate was concentrated *in vacuo* to a syrup, which was then extracted with ether. After the evaporation of the solvent *in vacuo*, the residue was refluxed for 8 hr with 3 N hydrochloric acid. The hydrolysate was then evaporated to dryness *in vacuo*. The residue was dissolved in ethylacetate and was crystallized by the addition of a small amount of petroleum ether. Recrystallization from ethylacetate gave *erythro*-MTA. Mp 144—145°C. IR: 2.92, 2.99 μ. Paper chromatography R_f: 0.37 (*n*-BuOH-HCO_2H-H_2O, 4 : 1 : 2)

The Preparation of threo-2-*Methyltartaric Acid* (threo-*MTA*): The *threo*-form was similarly prepared by the oxidation of diethylmesaconate and by subsequent hydrolysis. Recrystallization from ethylacetate gave *threo*-MTA. Mp 159—160°C. IR: 2.89, 2.91 μ. R_f: 0.44.

The Preparation of meso- (meso-*DMT*) *and* threo-2,3-*Dimethyl tartaric Acids* (threo-*DMT*): *meso*-DMT and *threo*-DMT were prepared according to the method described by Izumi *et al.*; that is, these acids were prepared from diacetyl and hydrogen cyanide, and their barium salts were separated by solubility difference in water. *meso*-DMT: mp 179—180°C. *threo*-DMT: mp 187°C.

The Determination of the Dissociation Constants of These Acids. The dissociation constants were determined as follows: about a 100-mg portion of acid was dissolved in 25 m*l* of water. A mixture of the acid solution (5 m*l*) and 1 M sodium perchlorate (5 m*l*) was diluted to 50 m*l* with demetalized water (ionic strength 0.1) and then titrated at 22°C with a 0.1 N sodium hydroxide solution, using a Metrohm Herisau Potentiograph, E 336. The dissociation constants were calculated by the procedure of Speakman;[10] that is, the dissociation constants of a dibasic acid, H_2A, may be difined by the equations:

$$K_1 = a_{H^+}[HA^-]y_1/[H_2A]y_0,\quad K_2 = a_{H^+}[A^{2-}]y_2/[HA^-]y_1$$

where a_{H^+} signifies the activity of hydrogen ions and where y_0, y_1, and y_2 are the activity coefficients of the H_2A, HA^-, and A^{2-} species respectively. In a solution with a total acid concentration of a (molar):

$$a = [H_2A] + [HA^-] + [A^{2-}]$$

and when a strong monoacid base, which may be taken as completely dissociated, has been added to give a molar concentration of b, electrical neutrality requires that:

$$b + [H^+] = [HA^-] + 2[A^{2-}] + [OH^-]$$

If we define L, M, and N by these equations:

$$L = b + [H^+] - [OH^-]$$

$$M = a - b - [H^+] + [OH^-]$$

$$N = 2a - b - [H^+] + [OH^-]$$

it can be shown that:

$$Ly_2[H^+]^2/Ny_0 = My_2[H^+]K_1/Ny_1 + K_1K_2 \qquad (1)$$

where $\log y_1 = -0.5\sqrt{I}$ and $\log y_2 = -2.0\sqrt{I}$, $y_0 = 1$. (I signifies the ionic strength). Therefore, in the case of an ionic strength of 0.1, Eq. (1) may be written as:

$$0.233L[H^+]^2/N = 0.233M[H^+]K_1/0.695N + K_1K_2 \qquad (2)$$

When L, M, and N can be evaluated from the experimental data, the plot of the $(0.233L[H^+]^2/N)$ term against the $(0.233M[H^+]/0.695N)$ term should give a straight line, the slope of which equals K_1, while the intercept on the Y axis should equal K_1K_2.

The Determination of the Equilibrium Constants of the Copper-(II) Complexes. The equilibrium constants (apparent stability constants) of copper(II) with these acids were determined as follows: calculated volumes of copper(II) perchlorate (1.536×10^{-2} mol/*l*) and acid solutions (1.536×10^{-2} mol/*l*) were mixed, and then we added the proper amount of sodium perchlorate (1 mol/*l*) to maintain a constant ionic strength $\mu=0.2$; the whole was diluted to the proper volume (*e.g.*, 25 m*l*, 10 m*l*) by adding a buffer solution and allowed to stand 1 hr at 22°C. The optical density was then measured. The absorption cell was not thermostated, but all the solutions were brought to a constant temperature before measurements were made. Preliminary experiments showed that the copper(II)-acid solutions reached equilibrium within 1 hr and showed no measurable variation thereafter for a period of less than 24 hr. In order to calculate the equilibrium constants, we used the Turner and Anderson dilution method; *i.e.*, complex formation proceeds by this pathway:

$$nM + mA \rightleftarrows M_nA_m \qquad (3)$$

in which M is a metallic ion, and A, an organic molecule or an anion. If a and b are the initial concentrations of M and A respectively and if x is the equilibrium concentration of the chelate complex, then the equilibrium constant:

$$K = x/(a-nx)^n(b-mx)^m \qquad (4)$$

To determine the value of x, Job's method of continuous variations is employed, with different initial concentrations of the reactants. n and m can be determined from the experimental data by means of Job's method. If two concentrations (a_1+b_1) and (a_2+b_2) of the reactants have the same optical density, then the equilibrium constant:

$$K = x/(a_1-nx)^n(b_1-mx)^m = x/(a_2-nx)^n(b_2-mx)^m \qquad (5)$$

This equation can be solved for x. Thus, knowing the value of x, at a known concentration of reactants K can be calculated.

10) J. C. Speakman, *J. Chem. Soc.*, **1940**, 855.

Table 1. Titration of *erythro*-MTA(1.881×10^{-2} M; 10 ml, $NaClO_4$ 1 M; 5 ml. total vol.=50 ml) with 0.1081 M NaOH at 22°C (μ=0.1).

NaOH (ml)	pH	$[H^+]$ ($\times10^{-4}$)	Ly_2 ($\times10^{-3}$)	My_2 ($\times10^{-3}$)	Ny_1 ($\times10^{-3}$)	Ny_0 ($\times10^{-3}$)	$Ly_2[H^+]^2/Ny_0$ ($\times10^{-8}$)	$My_2[H^+]/Ny_1$ ($\times10^{-5}$)
0.6	3.29	5.13	0.4180	0.4480	3.919	5.640	1.95	5.86
0.8	3.40	3.99	0.4895	0.3730	3.685	5.303	1.46	4.04
1.0	3.51	3.09	0.5657	0.2936	3.438	4.948	1.09	2.63
1.2	3.65	2.24	0.6424	0.2134	3.189	4.589	0.702	1.49
1.4	3.79	1.62	0.7237	0.1288	2.927	4.212	0.451	0.71
1.6	3.93	1.18	0.8083	0.0410	2.655	3.821	0.297	0.18

Results and Discussion

The Dissociation Constants of Ligands. erythro-2-*Methyltartaric Acid*: Table 1 represents the titration of *erythro*-MTA (1.881×10^{-2} mol/*l*, 10 ml) with 0.1081 N sodium hydroxide. The plot of the ($Ly_2[H^+]^2/Ny_0$) term against ($My_2[H^+]/Ny_1$) is shown in Fig. 1; the points lie very close to the straight line, from which pK_1 and pK_2 were calculated to be 3.54 and 5.03 respectively at μ=0.1.

threo-2-*Methyltartaric Acid*: The dissociation constants, pK_1 and pK_2, were similarly calculated to be 3.28 and 4.70 respectively. For *meso*-2,3-*dimethyltartaric acid*, the corresponding values were 3.52 and 4.98 (Fig. 2), on the other hand, for the *threo*-form the corresponding values were 3.04 and 5.30 (Fig. 2).

The Equilibrium Constants of Copper(II) Complexes. Complex with erythro-*MTA, at pH* 2.40: Calculated volumes of copper(II) perchlorate (3.840×10^{-2} M) and this acid (3.840×10^{-2} M) solution were mixed; then a sodium perchlorate solution (1 M, 5 ml) was added, and the whole was diluted to 25 ml by adding a buffer solution and was allowed to stand 1 hr at 22°C. The optical density was then measured at 760 mμ. The results are shown in Fig. 3A, where

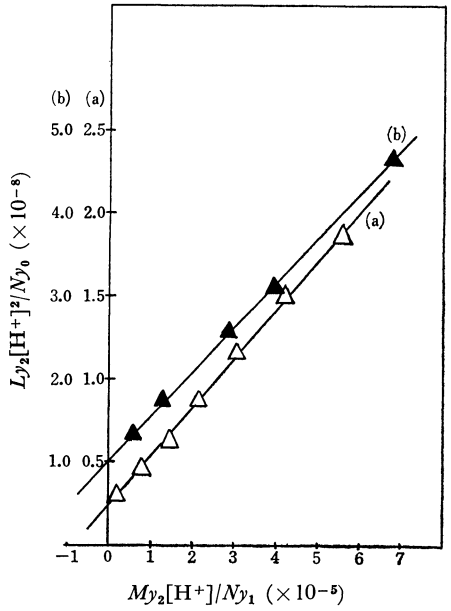

Fig. 1. Correlation of $Ly_2[H^+]^2/Ny_0$ with $My_2[H^+]/Ny_1$.
(a) *erythro*-MTA 1.881×10^{-2} mol/*l*, 10 ml
(b) *threo*-MTA 3.178×10^{-2} mol/*l*, 10 ml

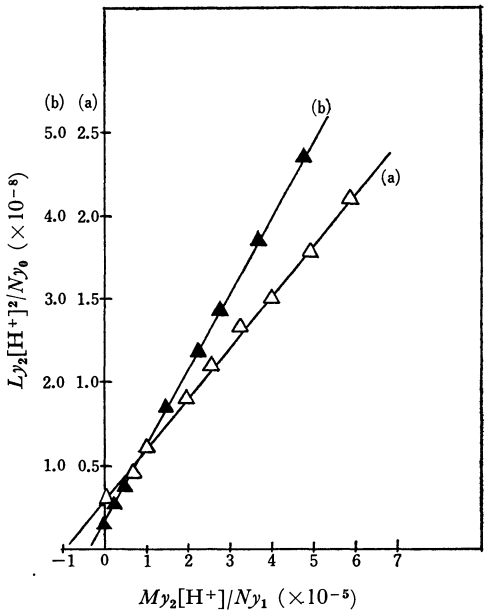

Fig. 2. Correlation of $Ly_2[H^+]^2/Ny_0$ with $My_2[H^+]/Ny_1$.
(a) *meso*-DMT 1.850×10^{-2} mol/*l*, 10 ml
(b) *threo*-DMT 2.002×10^{-2} mol/*l*, 10 ml

the difference in optical density (ΔOD) of the complex and copper(II) perchlorate is plotted against the concentration of the reactants. Maxima are obtained at a mole fraction (copper) value of 0.5 with this acid and indicate a 1 : 1 combination. In order to calculate the eqilibrium constant, therefore, Eq. (4) should become:

$$K = x/(a-x)(b-x) \tag{6}$$

To determine the value of x, Job's method is again employed, but with a different initial concentration of the reactants. That is, an appropriate amount of copper(II) perchlorate (3.840×10^{-2} M) and this acid (3.840×10^{-2} M) solution were mixed; then we added the sodium perchlorate solution (1 M, 2 ml), and the whole was diluted to 10 ml by adding a buffer solution. The optical density was measured at the same wave length (760 mμ). The results are shown in Fig. 3B. From this curve and the data of Fig. 3A, a series of pairs of solutions can be selected with equal optical densities (and thus essentially equal concentrations of the complex), but with different concentrations of reactants. Therefore, Eq. (5) becomes:

$$K = x/(a_1-x)(b_1-x) = x/(a_2-x)(b_2-x) \tag{7}$$

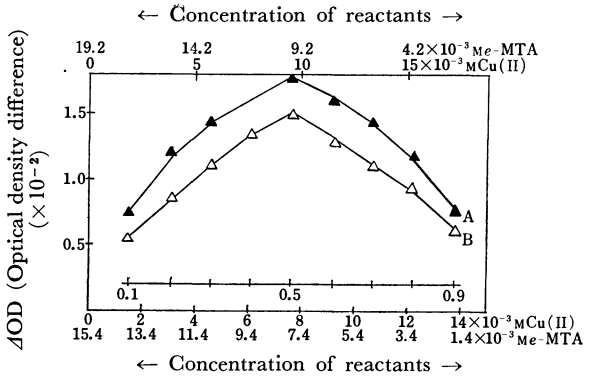

Fig. 3. Variation of ΔOD with varying concentration of Cu(II) and *erythro*-MTA, at pH 2.40, 760 mμ. Upper scale for curve A and lower scale for curve B. (ionic strength μ=0.2)

This equation could be solved for x as follows:

$$x = (a_1b_1 - a_2b_2)/\{(a_1+b_1)-(a_2+b_2)\} \quad (8)$$

In this case, a line at an optical density difference of 0.011 was drawn parallel to the concentration axis which intersects the curves, A and B. A point corresponding to the intersection at curve A gives a_1 and b_1 on the concentration axis, while the point on curve B gives a_2 and b_2 (on the right side of the peak). Similarly, other pairs, a_1 and b_1, and a_2 and b_2, can be selected on the left side of the peak, and x and also the log K value may be calculated for the complex. The results are shown in Table 3.

At pH 5.00: Copper(II) perchlorate (1.464×10^{-2} M) and this acid (1.464×10^{-2} M) solution were mixed similarly, and the optical density was measured. Maxima are obtained at a mole fraction value of 0.6, indicating that copper(II) and this acid react in a 3 : 2 ratio. Therefore, Eq. (4) becomes:

$$K = x/(a-3x)^3(b-2x)^2,$$

Then,

$$x = (a_1^3b_1^2 - a_2^3b_2^2)/\{(9a_1^2b_1^2+4a_1^3b_1)-(9a_2^2b_2^2+4a_2^3b_2)\}$$

The results are shown in Figs. 4A and 4B and in Table 3.

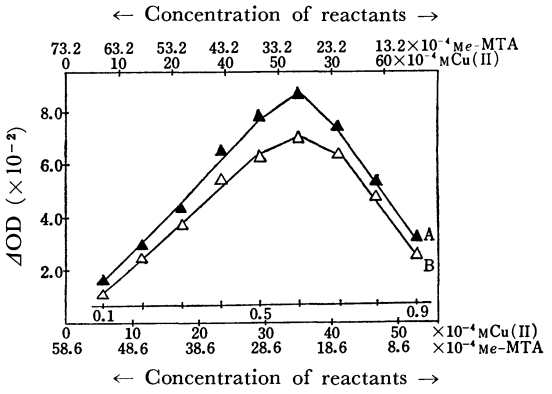

Fig. 4. Variation of ΔOD with varying concentration of Cu(II) and *erythro*-MTA, at pH 5.00, 650 mμ. Upper scale for curve A and lower scale for curve B.

Table 2. Titration of *threo*-MTA(3.178×10^{-2} M; 10 ml, $NaClO_4$ 1 M; 5 ml. total vol.=50 ml) with 0.1081 M NaOH at 22°C (μ=0.1).

NaOH (ml)	pH	$[H^+]$ ($\times10^{-4}$)	Ly_2 ($\times10^{-3}$)	My_2 ($\times10^{-3}$)	Ny_1 ($\times10^{-3}$)	Ny_0 ($\times10^{-3}$)	$Ly_2[H^+]^2/Ny_0$ ($\times10^{-8}$)	$My_2[H^+]/Ny_1$ ($\times10^{-5}$)
1.4	3.16	6.92	0.8472	0.5929	6.065	8.726	4.64	6.76
1.6	3.22	6.03	0.9213	0.5135	5.812	8.362	4.00	5.32
1.8	3.30	5.02	0.9921	0.4373	5.568	8.012	3.12	3.94
2.0	3.37	4.27	1.0681	0.3558	5.308	7.638	2.54	2.86
2.4	3.51	3.09	1.2256	0.1873	4.771	6.865	1.70	1.21
2.6	3.59	2.57	1.3048	0.1027	4.505	6.482	1.33	0.58
2.8	3.67	2.14	1.3854	0.0167	4.232	6.090	1.04	0.08

Table 3. Equilibrium constants of copper(II) with *erythro*- and *threo*-MTA

a_1 ($\times10^{-3}$ M)	b_1 ($\times10^{-3}$ M)	x ($\times10^{-3}$)	log K	a_2 ($\times10^{-3}$ M)	b_2 ($\times10^{-3}$ M)	x ($\times10^{-3}$)	log K
Cu(II) with *e*-MTA at pH 2.40, μ=0.2, 760 mμ.							
3.31	15.89	1.88	1.97	4.00	11.36	1.88	1.97
11.5	3.86	2.03	2.07	15.81	3.39	2.03	2.03
Mean log K 2.02±0.05, Cu : acid=1:1							
Cu(II) with *e*-MTA at pH 5.00, μ=0.2, 650 mμ.							
2.015	5.305	0.210	9.52	1.850	4.010	0.210	9.95
6.281	1.039	0.207	9.46	4.875	0.985	0.207	9.92
Mean log K 9.71±0.25, Cu : acid=3:2							
Cu(II) with *t*-MTA at pH 5.00, μ=0.2, 690 mμ.							
1.906	5.414	1.82	3.75	1.950	3.910	1.82	3.82
Mean log K 3.78±0.03, Cu : acid=1:1							

Complex with threo-*MTA, at pH* 5.00: Equimolar solutions (1.464×10^{-2} M) were similarly mixed, and the optical density was measured. Maxima are obtained at a mole fraction value of 0.5 with this acid, indicating a 1 : 1 combination. The results are shown in Figs. 5A and 5B and in Table 3.

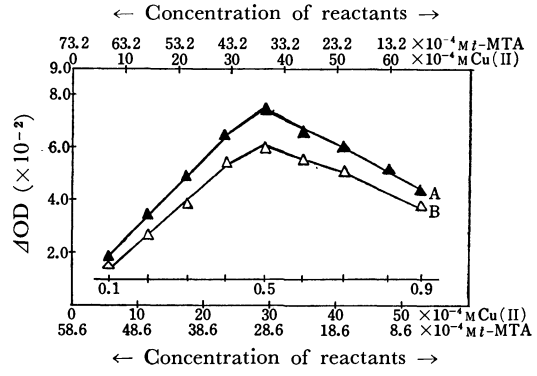

Fig. 5. Variation of ΔOD with varying concentration of Cu(II) and *threo*-MTA, at pH 5.00, 690 mμ. Upper scale for curve A and lower scale for curve B.

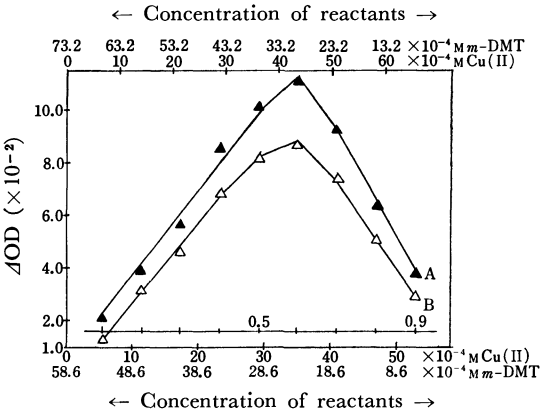

Fig. 6. Variation of ΔOD with varying concentration of Cu(II) and *meso*-DMT, at pH 5.00, 640 mμ. Upper scale for curve A and lower scale for curve B.

Complex with meso-*DMT, at pH* 5.00: Equimolar solutions (1.464×10^{-2} M) were similarly mixed, and the optical density was measured. The results are shown in Figs. 6A and 6B and in Table 4.

Complex with threo-*DMT, at pH* 5.00: The results are shown in Figs. 7A and 7B and in Table 4.

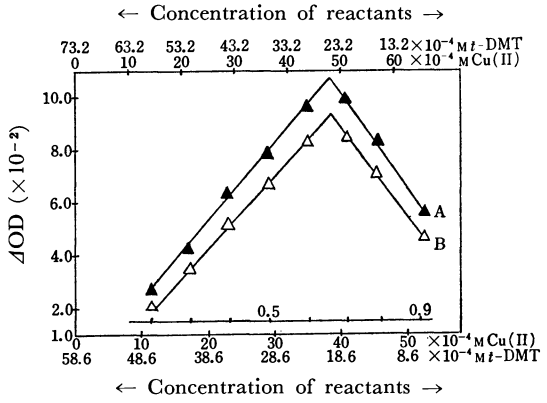

Fig. 7. Variation of ΔOD with varying concentration of Cu(II) and *threo*-DMT, at pH 5.00, 660 mμ. Upper scale for curve A and lower scale for curve B.

It would be reasonable to assume that these hydroxycarboxylic acids function as quadridentate chelating agents, and that both carboxyl and adjacent hydroxyl groups are involved in bond formation, and a tentative structure could be presumed for them (Fig. 8). The most stable conformations in *threo*-MTA and *erythro*-MTA would, respectively, be 1 and 2, where the two carboxyl groups are in anti positions (Fig. 9). Five- and six-membered rings are by far the most common among metal chelates. In *threo*-MTA, if the complex formation with copper(II) occurred at the carboxyl and hydroxyl groups in the vicinal position, as is shown in Fig. 9, the combination ratio would be the same as in the *erythro*-MTA-copper(II). Hence, the chelate formation in this manner does not explain the observed difference in the combination ratio between *threo* and *erythro* forms. Accordingly, it seemed to

Table 4. Equilibrium constants of copper(II) with *meso*- and *threo*-DMT

a_1 ($\times10^{-4}$ M)	b_1 ($\times10^{-4}$ M)	x ($\times10^{-4}$)	log K	a_2 ($\times10^{-4}$ M)	b_2 ($\times10^{-4}$ M)	x ($\times10^{-4}$)	log K
Cu(II) with *m*-DMT at pH 5.00, μ=0.2, 640 mμ.							
19.37	53.83	2.01	9.54	18.37	35.23	2.01	10.08
73.20	10.70	2.15	9.25	47.37	6.23	2.15	9.93
Mean log K 9.67±0.41, Cu : acid=3:2							
Cu(II) with *t*-DMT at pH 5.00, μ=0.2, 660 mμ.							
27.96	45.24	7.33	5.04	26.25	32.35	7.33	5.34
65.00	8.20	6.03	5.19	49.75	8.85	6.03	5.20
Mean log K 5.19±0.15, Cu : acid=2:1							

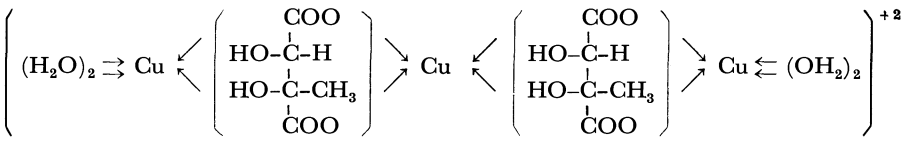

Fig. 8.

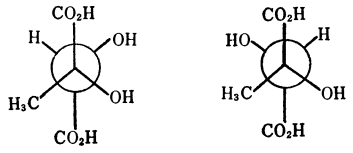

1 2

Fig. 9.

be reasonable to assume that the copper(II) complexes have a 5-membered ring and that copper(II) attaches to geminally-situated carboxyl and hydroxyl groups. In *erythro*-MTA, both sets of carboxyl and hydroxyl groups are set in opposite directions, thus forming the complex in a 2 : 3 ratio. The chelate from *threo*-MTA in this ratio is unstable. Among the equilibrium constants of the acid-copper(II) complexes, the *erythro*-form ligands have larger values, $\log K=9.71$ for *erythro*-MTA and $\log K=9.70$ for *meso*-DMT. It is known that the stability constant difference is correlated with the dissociation constant of the ligand.[11] Strictly speaking, the stability constant does not agree with the equilibrium constant, but the equilibrium constant can be regarded as the apparent stability constant.[7,9] A close parallelism between the equilibrium constant and the dissociation constant is observed also in our case. When comparing the pK values of *threo*-form ligands with those of *erythro*-form ligands, the former are found to have lower values of pK. The pK values of the *erythro*-form are similar to each other, while there is a remarkable difference in the *threo*-form ligands. These tendencies also reflect the values of the equilibrium constants of *erythro*-form ligands; that is, the $\log K$ values of *erythro*-form ligand-copper(II) are also similar to each other.

11) M. Calvin and K. W. Wilson, *J. Amer. Chem. Soc.*, **67**, 2003 (1945).

The stabilizing effect of the substituted tartaric acids, *erythro*- and *threo*-MTA, and *meso*- and *threo*-DMT, on the vegetable oil as antioxidants in o/w-type emulsion has been evaluated in our previous work.[1] The influence of the metallic ion and the effect of these acids as antioxidants on the dissolved oxygen in o/w-type emulsion was investigated by employing a polarographic Beckman Oxygen Analyzer, Model 777. Soybean oil with different P.O.V.'s (peroxide values) and water were emulsified into o/w-type emulsions using Tween-40 as the emulsifiser, and the absorption of dissolved oxygen was measured in the presence of the Cu(II) ion. In order to evaluate the effect of these acids, an acid solution (10^{-1} mol/l, 1 ml) was added to the emulsion. Then, the metallic solution (0.5×10^{-1} mol/l, 1 ml) was added to the same emulsion, and the variation in the dissolved oxygen was measured. The results of these measurements revealed that the oxygen absorption increased in the presence of Cu(II) and, that the deteriorating effect was suppressed by the addition of these acids. When comparing the stabilizing effect of *erythro*-form acid with those of *threo*-form ligands, the former is clearly seen to function as a more effective antioxidant. Moreover, in the test for antioxidant activity by means of AOM (Active Oxygen Method) and the Shaal Oven Test, the results similarly revealed that *erythro*-form acid functions as a more effective antioxidant. On the basis of these data, it cab be concluded that the stabilizing effect on the oil as antioxidant can be attributed to the equilibrium constants of these acid-metal complexes. Detailed results will be published later.

The authors are grateful to Professor T. Kubota, Dr. T. Tokoroyama, and Dr. Y. Nakamura, Osaka City University, and to Professor Y. Izumi, Osaka University, for their valuable discussions and suggestions.

The Electronic Character of the π-Allylic Group of π-Allylic Palladium Complexes

Yasutaka TAKAHASHI, Hiroyuki AKAHORI, Shizuyoshi SAKAI, and Yoshio ISHII

Department of Synthetic Chemistry, Faculty of Engineering, Nagoya University, Chikusa, Nagoya

(Received January 7, 1971)

The substituent constants of the 2- and 1-positions of the π-allylic group of acetylacetonato (a) and cyclopentadienyl (b) derivatives of π-[2-(*p*-substituted phenyl)allyl]-(I) and π-(*p*-substituted cinnamyl)-palladium complexes(II) were estimated from their NMR spectra. The differences in the chemical shift ($\Delta\nu$, Hz) between the *p*-phenylene ring protons H^1 and H^2 of the complexes was found to be dependent upon the ligand and the substituent X. The plot of $\Delta\nu$ against the substituent constant σ_p^+, of X gave a fairly good linear relationship, and from the intercept of the straight line at $\Delta\nu=0$, the substituent constants of the 1-and 2-positions of the π-allylic group in the IIa or IIb complex and the Ia or Ib complex were estimated: σ_p: at the 1-position, 0.27 (IIa) or 0.24 (IIb), and at the 2-position, 0.21 (Ia) or 0.03 (Ib).

Up to now, little evidence suggesting the electronic character of the π-allylic group in π-allylic palladium complexes has been reported. Robinson and Shaw[1] found that 4-methoxy-substituted π-allylic palladium complexes were converted to the corresponding 4-ethoxy derivatives by ethanolysis, in which a carbonium-ion intermediate stabilized with the π-allylic group was assumed. This result suggests that the π-allylic group has an olefinic character even after coordinating with the metal ion. Nesmeyanov and Gubin,[2] on the other hand, suggested that the palladium ion in π-cyclopentadienyl-π-allylpalladium was to be regarded as an electron-attracting atom from an investigation of the electrophilic reaction and from the polarographic study. Bis(π-allylpalladium chloride) is also known to react with a nucleophilic reagent such as alkoxide, acetate, and the malonate anion.[3] The latter two results are evidence that the electron density of the π-allylic group is rather poor. These apparently contradictory observations stimulated us to estimate the electronic character of the π-allylic group.

In the NMR spectra of *p,p'*-disubstituted benzene derivatives, the differences in the chemical shifts, $\Delta\nu$, of *p*-phenylene-group protons depend upon the electronic characters of the X and Y substituents, becoming zero when they are equal.

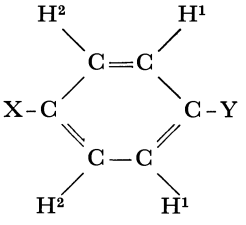

If Y is a π-allylic palladium moiety, its electronic character may be determined from the relation of $\Delta\nu$ to a substituent constant of X. Furthermore, the electron-donating or -withdrawing character of another ligand bonded to a metal may be evaluated at the same time. From this point of view, the NMR spectra of I and II complexes were measured. The results will be presented and discussed in this paper.

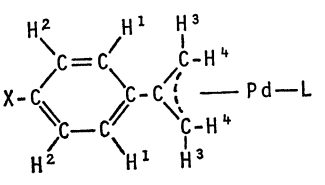

(I)

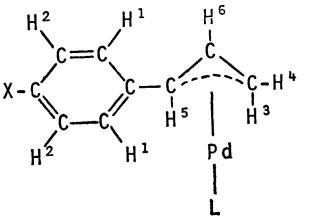

(II)

[L=acac (a), Cp (b), Cl (C); X=Br, Cl, H, CH_3, and CH_3O]

Experimental

The acetylacetonato and cyclopentadienyl derivatives of π-(*p*-substituted cinnamyl)palladium complexes (IIa and IIb) were prepared by the reaction of bis[π-(*p*-substituted cinnamyl)palladium chloride] with thallium acetylacetonate and cyclopentadienide[4] respectively, according to the methods in the literature.[5,6] Bis[π-{2-(*p*-substituted phenyl)-allyl}palladium chloride] complexes were prepared by the reaction of sodium chloropalladite and *p*-substituted α-methylstyrenes in the presence of cupric acetate in acetic acid. The complexes prepared are summarized as follows:

Substituent	Yield (%)	Mp(°C)		Analysis C(%)	H(%)	Pd(%)
Br	93.5	260(d)[a]	Found	31.96	2.31	31.4
			Calcd	31.99	2.39	31.49
Cl[b]	70.4	220(d)	Found	36.66	2.69	36.1
			Calcd	36.83	2.75	36.25
H[b]	78.9	200(d)	Found	41.82	3.42	41.2
			Calcd	41.73	3.50	41.08
CH_3	74.8	260(d)	Found	43.81	3.86	38.7
			Calcd	43.99	4.06	38.97
CH_3O	69.1	230—2	Found	41.56	3.90	36.9
			Calcd	41.55	3.84	36.81

a) Decomposed, b) These compounds have previously been prepared by Hüttel *et al.*[7] and by Volger.[8]

1) S. D. Robinson and B. L. Shaw, *J. Chem. Soc.*, **1963**, 4806.
2) A. N. Nesmeyanov and S. P. Gubin, *Tetrahedron Lett.*, **1964**, 2881.
3) J. Tsuji, H. Takahashi, and M. Morikawa, *Kogyo Kagaku Zasshi*, **69**, 138 (1966).
4) H. Meister, *Angew. Chem.*, **69**, 533 (1957).
5) Y. Takahashi, T. Inagaki, H. Mori, S. Sakai, and Y. Ishii, *Kogyo Kagaku Zasshi*, **73**, 760 (1970).
6) P. M. Maitlis, A. Efrarty, and M. L. Games, *J. Organometal. Chem.*, **2**, 284 (1965).
7) R. Hüttel, J. Kratzer, and M. Bechter, *Chem. Ber.*, **94**, 766 (1961).
8) H. C. Volger, *Rec. Trav. Chim. Pays-Bas*, **88**, 225 (1969).

These complexes were converted to acetylacetonato (Ia) or cyclopentadienyl derivatives (Ib) by treatment with thallium acetylacetonate or cyclopentadienide respectively.

The NMR spectra were measured on JEOL, MH-60 in $CDCl_3$ (or CCl_4), using TMS as the internal standard, and were calibrated by the signal due to $CHCl_3$ contaminated in $CDCl_3$. The $\Delta\nu$ values observed in chloroform were consistent with those observed in carbon tetrachloride.

Results and Discussion

Acetylacetonato (Ia or IIa) and π-cyclopentadienyl derivatives (Ib or IIb) were prepared from the reactions of the corresponding chloro-bridged complexes (Ic or IIc) with thallium cyclopentadienide and acetylacetonate in benzene, and their NMR spectra were measured in $CDCl_3$ except for the case of IIb (CCl_4). The observed spectra of two representative complexes Ib (X=Cl) and IIa (X=Cl) are shown in Figs. 1 and 2 respectively. The spectral data for Ia and Ib are summarized in Tables 1 and 2. In the case of complex IIa, the resonance of the methyl group in the acetylacetonato-ligand appeared as two singlets because of the anisotropic effect of the phenyl ring in the π-cinnamyl moiety.[5] Allylic protons were observed distinctly as three doublets and a multiplet assignable to H^{3-5} and H^6 respectively; these results are consistent with the general features of the NMR spectra for a rigid π-allyl complex. In the case of complex IIb, the NMR spectra for the rigid π-allyl structure were also observed. These observations seem, therefore, to support the assumption that there is no fluxinal behaviour including the Pd-

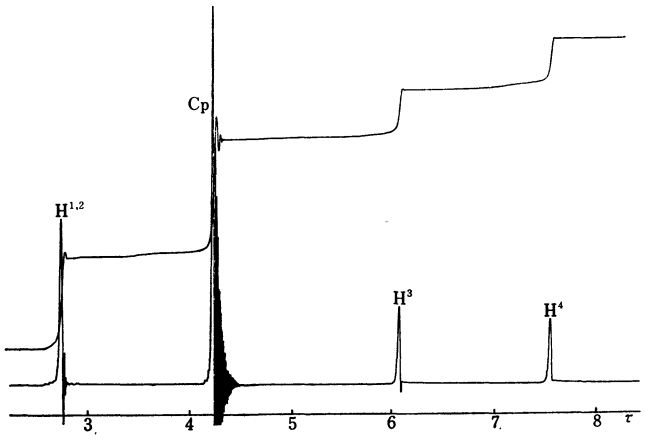

Fig. 1. NMR spectrum of complex Ib (X=Cl) in $CDCl_3$ at 25°.

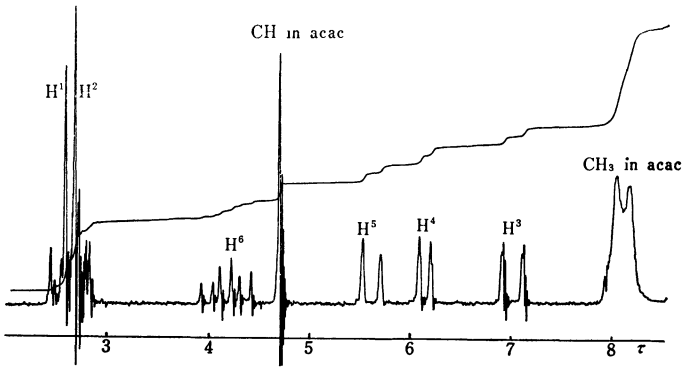

Eig. 2. NMR spectrum of complex IIa in $CDCl_3$ at 25°.

Table 1. NMR Spectra of π-{2-(p-substituted phenyl)allyl}acetylacetonatopalladium complex (Ia)

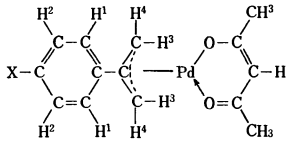

X	τ_3	τ_4	τ_{CH_3}	τ_{CH}	τ_X	τ_1	τ_2	$\Delta\nu_{2-1}$
Br	6.94	5.85	7.93	4.54	—	2.51	2.51	0.0
Cl	6.97	5.89	7.96	4.56	—	6.51	2.64	8.0
H	6.98	5.84	7.94	4.56	—	—	—	*ca.* 8
CH_3	6.99	5.83	7.94	4.56	7.58	2.48	2.78	17.5
CH_3O	7.01	5.83	7.94	4.57	6.06	2.46	3.05	35.5

τ (ppm), $\Delta\nu$ (Hz)

Table 2. NMR Spectra of π-{2-(p-substituted phenyl)allyl}cyclopentadienylpalladium complex (Ib)

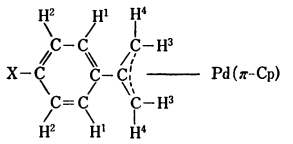

X	τ_3	τ_4	τ_{Cp}	τ_X	τ_1	τ_2	$\Delta\nu_{2-1}$
Br	7.57	6.08	4.25	—	2.76	2.67	−6.5
Cl	7.59	6.10	4.27	—	2.76	2.76	2.0
H	7.59	6.10	4.30	—	—	—	*ca.* 2
CH_3	7.62	6.10	4.29	7.70	2.82	3.02	11.5
CH_3O	7.68	6.13	4.35	6.26	2.85	3.35	30.0

τ (ppm), $\Delta\nu$ (Hz)

ligand bond dissociation or the σ-π interconversion of the π-allylic moiety in the solution of complex IIa.

The chemical-shift difference between H^1 and H^2, $\Delta\nu$, decreased in the order of the *p*-substituent, X: $CH_3O > CH_3 > H > Cl > Br$. The plot of $\Delta\nu$ against the substituent constant, σ_p^+, of X gave a moderately good linear relationship, as is shown in Fig. 3, but the constant other than σ_p^+ did not. The intercept of the straight lines at the axis, $\Delta\nu=0$, were designated as 0.21 (Ia) and 0.03 (Ib). In *p*-substituted toluenes and acetophenones, an analogous correlation between $\Delta\nu$ and σ_p^+ was also found,[9] as is shown in Figs. 4 and 3 respectively. The intercept (−0.30) of the straight line for toluenes at $\Delta\nu=0$, which might be the substituent-constant of the methyl group, was consistent with its σ_p^+ value as it appeared in the literature.[10] Therefore, the results obtained for complex Ia or Ib might be considered to indicate the substituent constant of the 2-position of the π-allylic group of complex Ia or Ib respectively. These results suggest that the substituent constant of the 2-position of the π-allylic group varies with other ligand bonded to the palladium ion, and that cyclopentadienyl group gave a smaller σ_p^+ value than the acetylacetonato group, indicating that the former is a better electron donor than the latter. These results are in accordance with the fact that the $CpRh(CH_2{=}CH_2)_2$ complex is more basic than the $(acac)Rh(CH_2{=}CH_2)_2$.[11]

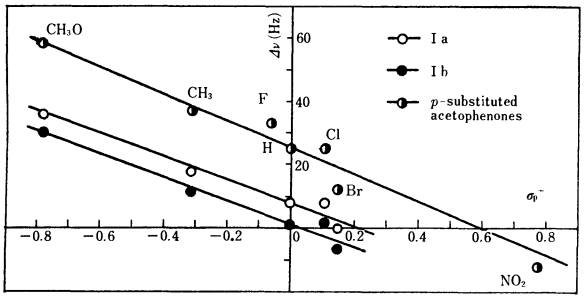

Fig. 3. The relation of $\Delta\nu$ of *p*-phenylene group of complexes Ia and Ib, and of *p*-substituted acetophenones.

In the cases of π-(*p*-substituted cinnamyl)palladium acetylacetonate (IIa) and cyclopentadienide (IIb), linear relationship between $\Delta\nu$ and σ_p^+ of X were also found; the results are illustrated in Fig. 4. The intercepts of the straight lines (σ_p^+ values of the 1-position of the π-allylic group) at $\Delta\nu=0$ were independent of the ligand; 0.27 (IIa) and 0.24 (IIb), unlike as in the observations in the case of I complexes. The relatively large σ_p^+ values estimated for the complexes II indicate that the 1-position of the π-allylic group is so electron-poor to be susceptible to nucleophilic reactions.

In the NMR spectrum of *p*-methoxy- and *p*-methyl-substituted α-methylstyrenes, $\Delta\nu$ was found to be 32.0 or 13.5 Hz respectively. The line through the points

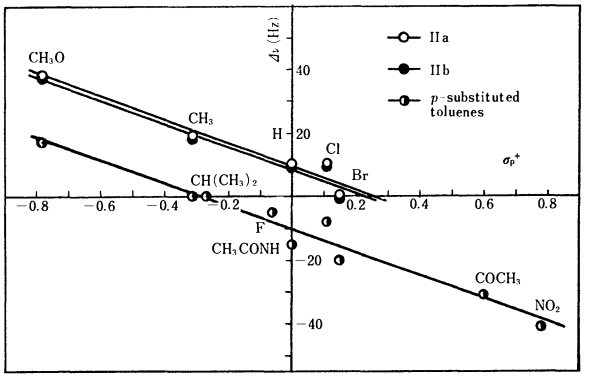

Fig. 4. The relation of $\Delta\nu$ of *p*-phenylene group of complexes IIa and IIb, and of *p*-substituted toluenes to substituent constant σ_p^+.
The σ_p^+ value of acetyl group was eastimated from the result of Fig. 1.

for the methoxy and methyl groups was assumed (parallel with other lines), and the σ_p^+ value for the isopropenyl group was evaluated as 0.05, smaller than that for Ia, IIa, and IIb, and nearly equal to that of Ib. Therefore, except for complex Ib, π-allylic palladium group may be concluded to behave as an electron-attracting substituent, consistent with the qualitative observations of Nesmeyanov and Gubin.[2]

The different dependences of the σ_p^+ of the 1- and 2-position of the π-allylic group on the ligand are closely related to the bonding nature of the π-allylic ligand to the metal ion. Kettle and Mason[12] reported from their theoretical calculations that two lower levels of the molecular orbital (ϕ_1 and ϕ_2) of the allylic radical could be more strongly overlapped with the atomic orbital of palladium than its highest orbital ϕ_3. It may be assumed that ϕ_1 is overlapped with the metal orbital with bonding-manner, and ϕ_2 with backbonding-manner. The bonding of the 1-position of allylic radical with metal is governed by both ϕ_1 (donation) and ϕ_2 (backdonation), but that of the 2-position is governed only by ϕ_1, indicating that the 1-position of the allylic group in the complex is "softer" than the 2-position. Therefore, the substituent constant of the 2-position might be directly reflected by the electron density of the metal atom, that is, the ligand on it, but that of the 1-position is independent of it as a result of compensation between ϕ_1 and ϕ_2.

Throughout, the anisotropic effects of the π-allylic and other ligands have been ignored. Furthermore, the effect of the solvent is very important. The $\Delta\nu$ value of complex IIb (X=Cl) was observed to be 10.5 Hz in CCl_4, but changed to zero Hz in hexadeuterobenzene. In our previous paper[5] concerning the NMR spectra of a substituted π-cinnamylpalladium complex, the specific solvation of benzene molecules to palladium atom had been suggested. However the above observation can not be explained as a result of such a solvation of benzene; a different kind of factor have to account for it. We can not, at present, give a clear explanation.

9) The $\Delta\nu$ values for *p*-substituted toluenes and acetophenones in the literature "NMR Data Tables for Organic Compound," Vol. 1, by F. A. Bovey, Interscience Publishers (1967) and of our measurement were used ignoring the solvent effect.

10) H. C. Brown and Y. Okamoto, *J. Amer. Chem. Soc.*, **79**, 1913 (1957).

11) R. Cramer, *J. Amer. Chem. Soc.*, **89**, 5377 (1967).

12) S. F. A. Kettle and R. Mason, *J. Organometal. Chem.*, **5**, 573 (1966).

The Determination of the Amount of Oxygen in Molten Copper-Nickel and Copper-Silver Alloys by the EMF Method

Iwao TSUKAHARA

Furukawa Electric Co., Ltd., Central Research Laboratory, Futaba, Shinagawa-ku, Tokyo

(Received January 28, 1971)

Using the following solid oxide-electrolyte galvanic cells, Pt/air//ZrO_2 (+CaO) O//(in Cu–Ni alloy)/Mo and Pt/air//ZrO_2 (+CaO) O//(in Cu–Ag alloy)/Mo, the electromotive forces of the cells have been measured as a function of the oxygen concentration in copper-nickel or -silver alloys at oxygen concentrations ranging from several ppm to 1000 ppm, at 1210°C for copper-nickel alloys and at 1100°C or 1200°C for copper-silver alloys respectively. The activity coefficient of oxygen has been determined from the electromotive force for the alloy systems investigated. In the case of copper-nickel, the activity coefficient of oxygen decreases with an increase in the nickel concentration and also with a decrease in the oxygen concentration. The solubility of oxygen in the copper-nickel alloy has also been measured at 1210°C by the use of the following galvanic cell, Pt/air//ZrO_2 (+CaO)//O(in Cu–Ni alloy), NiO/Mo.

The determination of the amount of oxygen in molten metals and alloys is of great importance in the metallurgical process or in controlling the quality of products. In recent years, there have been many studies concerning the direct electrochemical measurement of the oxygen content in molten iron[1–9] or copper.[10–14] These investigations have employed galvanic cells, the electrolytes in which are various solid mixed-oxides which conduct the current through the migration of oxide ion vacancies. Since the work of Kiukkola and Wagner[15] was reported, such electrolytes have been used in numerous cell studies in order to determine the thermodynamic properties of metallic oxides, the partial pressure of oxygen in various atmospheres, and the properties of oxygen dissolved in metals and alloys. The advantage of this electrochemical method is that it make possible the fast, direct, and continuous determination of oxygen.

In a previous paper,[16] the determination of the amount of oxygen in molten copper and copper-tin alloys by the EMF method using lime-stabilized zirconia as the solid electrolyte was reported by the author. In this investigation, a study of the determination of the amount of oxygen in molten copper-nickel and copper-silver alloys has been made by the same method. The main objects of this investigation are to determine the relationship between the electromotive forces of the following cells and the oxygen contents in copper-nickel and copper-silver alloys and to determine the activity coefficients of the oxygen in these alloys.

$$\text{Pt/air//}ZrO_2\text{(+CaO)//O(in Cu-Ni alloy)/Mo} \quad (1)$$

$$\text{Pt/air//}ZrO_2\text{(+CaO)//O(in Cu-Ag alloy)/Mo} \quad (2)$$

Since the transference number of oxide ion in stabilized zirconia is regarded as unity under the experimental conditions of this work,[9,17–19] the electromotive force (E) of the cell, (1) or (2), is:

$$E = (2.303\boldsymbol{R}T/4\boldsymbol{F}) \log (0.21/P_{O_2}) - E_{th}$$
$$= (2.303\boldsymbol{R}T/4\boldsymbol{F}) \log (0.21/a_O^2) - E_{th} \quad (3)$$

where $\boldsymbol{F}$ is the Faraday constant, where P_{O_2} and a_O are the partial pressure and the activity of oxygen in the liquid alloys with respect to a reference state of pure oxygen gas at 1 atmospheric pressure respectively, and where E_{th} is the thermoelectromotive force of the Pt–Mo thermocouple, which has been measured previously and expressed by Eq. (4),[16] where molybdenum is positive and where t is the temperature in °C:

$$E_{th}(\text{in mV}) = 406.3/t^{1/2} + 0.04352t - 29.09 \quad (4)$$

At a given temperature, all the terms of Eq. (3) are constants except E and a_O. Thus, a_O can be determined by the measurement of the electromotive force.

The electromotive force is also related to the mole fraction of oxygen (N_O) by Eq. (5) in the oxygen concentration range over which the activity of oxygen obeys Henry's law:

$$E = (2.303\boldsymbol{R}T/4\boldsymbol{F}) \log 0.21K$$
$$- E_{th} - (2.303\boldsymbol{R}T/2\boldsymbol{F}) \log N_O \quad (5)$$

where K is the equilibrium constant for the reaction:

$$O_2(g) = 2O \text{ (in alloy, liq.)} \quad (6)$$

At a given temperature, the electromotive force of the cell, (1) or (2), is a linear function of $\log N_O$.

1) J. K. Pargeter and D. K. Faurschou, *J. Metals*, **21**, 46 (1969).
2) *Canad. Chem. Process.*, **20**, 78 (1968).
3) J. K. Pargeter, *J. Metals*, **20**, 27 (1968).
4) G. R. Fitterer, *ibid.*, **19**, 92 (1967).
5) W. A. Fischer and W. Ackermann, *Arch. Eisenhuct'enw.*, **36**, 643 (1965).
6) K. Schwerdtfeger, *Trans. Met. Soc. AIME*, **239**, 1276 (1967).
7) M. Ohtani and K. Sanbongi, *Tetsu to Hagane*, **49**, 22 (1963).
8) K. Goto and Y. Matsushita, *ibid.*, **52**, 827 (1966).
9) R. Baker and J. M. West, *J. Iron Steel Inst.*, **204**, 212 (1966).
10) T. C. Wilder, *Trans. Met. Soc., AIME*, **236**, 1035 (1966).
11) H. Rickert and H. Wagner, *Electrochim. Acta*, **11**, 83 (1966).
12) C. M. Diaz and F. D. Richardson, *Trans. Inst. Min. Met. Soc. C*, **75**, C196 (1967).
13) W. Pluschkell and H-J. Engell, *Z. Metallk.*, **56**, 450 (1965).
14) Z. Kozuka, K. Suzuki, T. Oishi, and J. Moriyama, *Nippon Kinzoku Gakkaishi*, **32**, 1132 (1968).
15) K. Kiukkola and C. Wagner, *J. Electrochem. Soc.*, **104**, 379 (1957).
16) I. Tsukahara, *Nippon Kinzoku Gakkaishi*, **34**, 679 (1970).
17) J. W. Patterson, E. C. Bogren, and R. A. Rapp, *J. Electrochem. Soc.*, **114**, 752 (1967).
18) H. Schmalzried, *Z. Elektrochem.*, **66**, 572 (1962).
19) W. D. Kingery, J. Pappis, M. E. Doty, and D. C. Will, *J. Amer. Ceram. Soc.*, **42**, 393 (1959).

Experimental

An internal cell arrangement is shown in Fig. 1. About 600 g of molten Cu–Ni or Cu–Ag alloy was placed in the alumina crucible (66 mm i.d., 100 mm height), in which a stabilized zirconia in the form of a closed-end tube (500 mm long, 13 mm o.d., 8 mm i.d.) and a Pt–Pt/13% Rh thermocouple in an alumina sheath were immersed. A platinum contact wire was pressed (with a spring mechanism) against the inside bottom wall of the electrolyte tube, which was flushed continuously with a stream of air *via* an alumina tube inserted inside the electrolyte tube. The platinum contact wire acted as the reference electrode ($P_{O_2}=0.21$ atm.). A molybdenum contact wire was immersed in the alloy melt only at the times when the measurements were taken, because dissolved oxygen attacked molybdenum and eventually broke the electrical contact if the molybdenum wire was immersed continuously in the melt with a high oxygen content. A radiation shield of inconel or of alundum was placed on the alumina crucible. The whole of the cell was enclosed in an alumina outer tube which was closed gas-tight at the top with a water-cooled brass head.

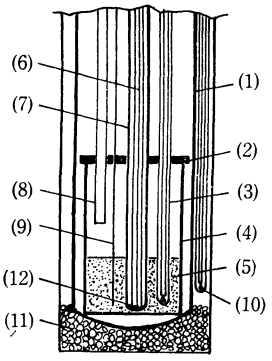

Fig. 1. Experimental cell.
(1) quartz tube, (2) inconel or alundum radiation shield, (3) Pt-Pt/13%Rh thermocouple in alumina tube, (4) alumina crucible, (5) Cu-Ni or Cu-Ag alloy melt, (6) Pt lead in alumina tube, (7) ZrO_2(+CaO) tube, (8) quartz sampling guide and addition tube, (9) Mo lead, (10) thermocouple for temperature control, (11) alumina, (12) Pt electrode

After the system had been evacuated and then filled with purified argon, the entire cell unit was heated in a resistance furnace to the desired temperature. The temperature was controlled by means of a Chino E-500 Controller using a Pt–Pt/13% Rh thermocouple with an accuracy of ±2.5°C. The cell potential was measured with a Yokogawa Electric P-1 Electrometer with an accuracy of ±0.5 mV. Oxygen was added to the melt by dropping reagent-grade copper oxide (CuO) chips through the sampling guide tube. After waiting for equilibrium, as evidenced by a steady cell potential with the time, electromotive force measurements were taken for each oxygen concentration: a sample of about 20 g was taken from the alloy melt by suction into the quartz tube (4 mm i.d.) which was guided through the sampling guide tube. The quartz tube was then immediately removed from the melt and quenched in distilled water. The sample was analyzed for oxygen by the vacuum-fusion method.

The measurements were carried out for the Cu–Ni alloy containing up to 0.22 mole fraction of nickel at 1210°C and for the Cu–Ag alloy containing up to 0.031 mole fraction of silver at 1100°C and 1200°C. The oxygen concentration was changed from several ppm to 1000 ppm.

Table 1. Chemical composition of stabilized zirconia (in wt%)

ZrO_2	CaO	MgO	SiO_2	Al_2O_3	Fe_2O_3	TiO_2
90.98	5.93	0.67	1.59	0.46	0.20	0.14

The stabilized zirconia used was a commercial zirconia tube, ZR-11, of the Nippon Kagaku Kogyo Co., Ltd.; its chemical composition is listed in Table 1.

Results and Discussion

1) Relation between Electromotive Force and Oxygen Content. The relations between the oxygen concentrations in the alloy melts and the electromotive forces measured are shown in Fig. 2—Fig. 4, where N_O, N_{Ni}, and N_{Ag} are the mole fractions of oxygen, nickel, and silver respectively. The relations have also been expressed in the form of Eq. (7), and the values of A and B have been calculated by the least-squares method and are listed in Tables 2 and 3.

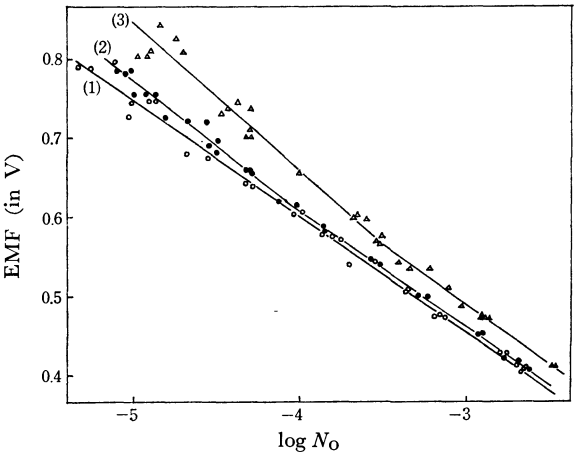

Fig. 2. Relation between the electromotive force of the cell-(1) and oxygen content at 1210°C.
(1) -○- N_{Ni}: 0.0015, (2) -●- N_{Ni}: 0.011, (3) -△- N_{Ni}: 0.10

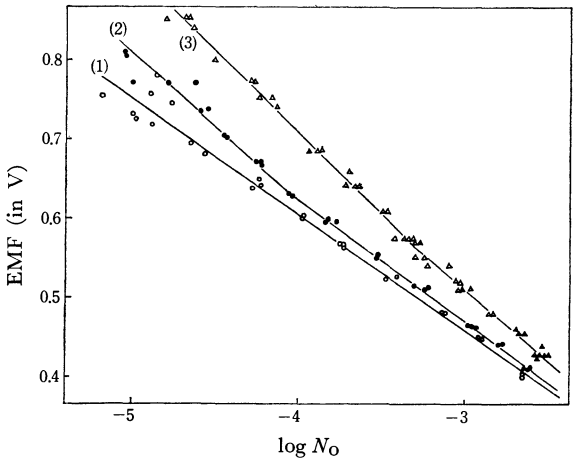

Fig. 3. Relation between the electromotive force of the cell-(1) and oxygen content at 1210°C.
(1) -○- N_{Ni}: 0.0053, (2) -●- N_{Ni}: 0.056, (3) -△- N_{Ni}: 0.22

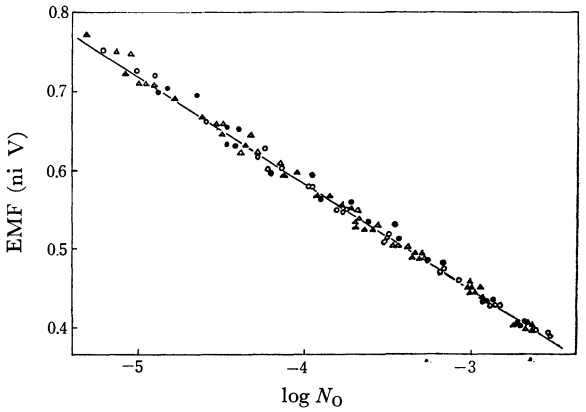

Fig. 4. Relation between the electromotive force of the cell-(2) and oxygen content at 1100°C.
-○- N_{Ag}: 0.00089, -●- N_{Ag}: 0.0029, -△- N_{Ag}: 0.0059, -▲- N_{Ag}: 0.031

TABLE 2. THE VALUES OF A AND B IN Eq. (7) AT 1210°C, Cu-Ni ALLOY

N_{Ni}		A	B
0.0015		0.012	−0.147
0.0053		0.012	−0.148
0.011	$N_O \leqq 7.7\times10^{-5}$	−0.056	−0.166
	$N_O \geqq 7.7\times10^{-5}$	0.022	−0.147
0.056	$N_O \leqq 8.3\times10^{-5}$	−0.128	−0.187
	$N_O \geqq 8.3\times10^{-5}$	0.010	−0.153
0.10	$N_O \leqq 3.0\times10^{-4}$	−0.097	−0.189
	$N_O \geqq 3.0\times10^{-4}$	0.029	−0.153
0.22	$N_O \leqq 5.2\times10^{-4}$	−0.113	−0.206
	$N_O \geqq 5.2\times10^{-4}$	−0.034	−0.182

TABLE 3. THE VALUES OF A AND B IN Eq. (7) AT 1100°C AND 1200°C, Cu-Ag ALLOY

N_{Ag}	1100°C		1200°C	
	A	B	A	B
0.00089	0.040	−0.136	0.010	−0.146
0.0029	0.041	−0.136	0.010	−0.146
0.0059	0.041	−0.136	0.007	−0.146
0.031	0.039	−0.136	0.010	−0.146

$$E = A + B \log N_O \quad (7)$$

As is shown in the results, in the cases of both Cu-Ag and Cu-Ni alloys containing not more than 0.0053 mole fraction of nickel, the relation between the electromotive force and log N_O is shown by a straight line over the oxygen concentration range investigated. On the other hand, in the case of the Cu-Ni alloy containing 0.011 mole fraction of nickel or more, the relation is divided into two regions, lower and higher concentration regions of oxygen, and is shown by a straight line in each region. In the latter case, the majority of the B values in Eq. (7) exhibit deviations from the Nernstian slope (−0.147 at 1210°C). These deviations are due to the lowering of the activity coefficient of oxygen with a decrease in the oxygen concentration as will be discussed later. Phenomena similar to those discussed above were also observed in the Cu-Sn alloy system.[16]

In any case, we can use the relations shown in Fig. 2—Fig. 4 as calibration curves for the determination of the amount of oxygen in molten Cu-Ni and Cu-Ag alloys.

2) Activity of Oxygen. The activity coefficient of oxygen (γ_O), as defined by Eq. (8), has been determined. From Eqs. (8) and (3), we obtain Eq. (9). By substituting E and E_{th}, which have been already given by Eqs. (7) and (4) respectively, into Eq. (9), we can obtain the activity coefficient of oxygen as a function of the mole fraction of oxygen at each temperature

$$a_O = \gamma_O \cdot N_O \quad (8)$$

$$\log \gamma_O = (1/2) \log (0.21/N_O^2) - 2\boldsymbol{F}(E+E_{th})/2.303\boldsymbol{RT} \quad (9)$$

and at each concentration of nickel or silver. The activity coefficient of oxygen thus obtained has been expressed in the form of Eq. (10); the values of A and B in Eq. (10) are listed in Tables 4 and 5. From the results listed in those tables, it can be seen that: (1) in cases of both Cu-Ag and Cu-Ni alloys containing not more than 0.0053 mole fraction of nickel, the activity coefficient of oxygen is independent of the oxygen concentration and the activity of oxygen follows Henry's law. (2) in the Cu-Ni alloy containing 0.011 mole fraction of nickel, the decrease in the activity coefficient of oxygen with a decrease in the oxygen concentration is seen in the lower oxygen concentration region, while in the higher oxygen concentration region, the activity of oxygen follows Henry's law. (3) in Cu-Ni alloys containing 0.056, 0.10, and 0.22 mole fractions of nickel, the activity coefficient of oxygen decreases with a decrease in the oxygen concentration and the activity of oxygen no longer follows Henry's law over the whole oxygen concentration region investigated. Similar phenomena in the activity coefficient of oxygen were also observed in the Cu-Sn-O system.[16] It is worth noting that the lowering of the activity coefficient of oxygen with a decrease in the oxygen concentration was observed in copper alloy with nickel or tin, but not in the case of copper[16] or copper-silver alloy. The origin of these phenomena is not obvious. However, in view of the fact that the affinity of nickel or tin for oxygen is stronger than that of copper or silver, it probably depends on the affinity of the atoms of alloying elements for oxygen atoms, or it may be due to the formation of the molecular species or the dipoles between oxygen atoms and the atoms of the alloying elements, the oxygen atoms in which may be bonded more tightly to nickel or tin atoms as the concentration of oxygen decreases. Kozuka *et al.*[14] have noted that phenomena similar to those described above which were also observed by them in the Cu-O system are probably

$$\log \gamma_O = A + B \log N_O \quad (10)$$

Table 4. The values of A and B in Eq. (10) at 1210°C, Cu-Ni alloy

N_{Ni}	A	B
0.0015	−0.660	0
0.0053	−0.660	0
0.011	$N_O \leqq 7.7\times10^{-5}$: −0.197	0.129
	$N_O \geqq 7.7\times10^{-5}$: −0.728	0
0.056	$N_O \leqq 8.3\times10^{-5}$: 0.293	0.272
	$N_O \geqq 8.3\times10^{-5}$: −0.646	0.041
0.10	$N_O \leqq 3.0\times10^{-4}$: 0.082	0.286
	$N_O \geqq 3.0\times10^{-4}$: −0.775	0.041
0.22	$N_O \leqq 5.2\times10^{-4}$: 0.191	0.401
	$N_O \geqq 5.2\times10^{-4}$: −0.347	0.238

Table 5. The values of A and B in Eq. (10) at 1100°C and 1200°C, Cu-Ag alloy

N_{Ag}	1100°C		1200°C	
	A	B	A	B
0	−0.863	0	−0.654	0
0.00089	−0.863	0	−0.649	0
0.0029	−0.870	0	−0.649	0
0.0059	−0.874	0	−0.672	0
0.031	−0.865	0	−0.649	0

due to impurities in the copper. If this is so, it is probably that the impurities are elements which have a strong affinity for oxygen.

On the other hand, as is shown in Tables 4 and 5, the activity coefficient of oxygen in the Cu–Ni alloy is also affected by the addition of nickel and decreases with an increase in the nickel concentration. This decrease in the activity coefficient of oxygen, as expressed by Eq. (11) in both the nickel concentration range of not more than 0.011 mole fraction and the oxygen concentration range over which the activity coefficient of oxygen is independent of the oxygen concentration, is due to the interaction between oxygen and nickel atoms. The usual way of expressing this

$$\log \gamma_O = -8.06N_{Ni} - 0.636 \quad (11)$$

interaction is in terms of the interaction coefficient, $\varepsilon_O^{(Ni)}$, derived by Wagner.[20] The value of $\varepsilon_O^{(Ni)}$ obtained from the present work, −8.06, that is, the slope of function (11), is in near agreement with the value determined by Oishi *et al.*, −7.00.[21]

3) Solubility of Oxygen. The solubility of oxygen in Cu–Ni melts containing 0.056, 0.10, and 0.22 mole fractions of nickel has been measured at 1210°C. By substituting E_s, which is the electromotive force of Cell (12) measured at 1210°C in a fixed mole fraction of nickel under the equilibrium conditions of Reaction (13), into E in Eq. (7), we can obtain the solubility (in mole fraction) of oxygen in the Cu–Ni melt. The solubilities thus obtained are listed in Table 6.

$$Pt/air//ZrO_2(+CaO)//O(\text{in Cu-Ni, liq.}), NiO/Mo \quad (12)$$

$$Ni(\text{in Cu-Ni, liq.}) + O(\text{in Cu-Ni, liq.}) = NiO(s) \quad (13)$$

The experiments were carried out as follows: after assembling the cell as has been described above, the cell system was evacuated, filled with purified argon, and then heated to 1210°C. Oxygen was added to the Cu–Ni melt until the oxygen concentration near the solubility of oxygen was reached, and then nickel oxide (NiO) powder was added to the melt. After the equilibrium has been reached, the potential (E_s) was measured, at the same time, a sample for oxygen analysis was taken. The oxygen content of the sample taken, that is, the solubility of oxygen, was determined by the vacuum-fusion method; these values are listed in Table 6 and compared with those calculated from E_s and Eq. (7).

The solubility of oxygen, as calculated from E_s and Eq. (7), is in good agreement with that determined by the analysis of oxygen; the solubility of oxygen decreases with an increase in the nickel concentration in the nickel concentration range investigated.

Table 6. Solubility of oxygen in Cu-Ni alloy at 1210°C

N_{Ni}	Solubility (mole fraction)	
	Calculated[a]	Analyzed[b]
0.056	0.00482	0.00478
0.10	0.00392	0.00387
0.17	—	0.00300
0.22	0.00291	0.00284

a) Calculated from E_s and Eq. (7).
b) Analyzed by vacuum-fusion method.

20) C. Wagner, "Thermodynamics of Alloys", Addison-Wesley Publish. Comp., Inc., Reading, Massachusetts, U.S.A.

21) T. Oishi, T. Nagahata, and J. Moriyama, *Nippon Kinzoku Gakkaishi*, **34**, 1103 (1970).

The Chelating Behavior of 1-(2-Phosphonophenylazo)-2-hydroxynaphthalene-3,6-disulfonic Acid with Alkaline Earth Metals

Kenyu KINA, Haruo MIYATA, and Kyoji TÔEI

Department of Chemistry, Faculty of Science, Okayama University, Tsushima, Okayama

(Received March 19, 1971)

A new chelating agent, *o*-phosphonophenylazo-2-hydroxynaphthalene-3,6-disulfonic acid, has been synthesized. The acid dissociation constants of this ligand and the chelate stability constants with alkaline earth metals have been measured by the pH titration method at an ionic strengh of 0.10 and at 25.0±0.1°C. This ligand forms the acido complex, MHL, in the pH 5—7 region. The stability constants of the acido complex decrease in this order: $\log K_{SrHL} \approx \log K_{CaHL} > \log K_{MgHL}$; whereas the decreasing order of the stability constants, $\log K_{ML}$, is as follows: $\log K_{MgL} > \log K_{CaL} > \log K_{SrL}$.

As a link in the chain of the studies of the *o*-substituted phenylazo compound, the present authors have attempted to introduce the phosphonate group into the *o*-position of the azo compound. For this purpose, it is necessary to prepare *o*-aminophenylphosphonic acid, which is produced by the reduction of *o*-nitrophenylphosphonic acid; however, it seemed difficult to introduce the phosphonate group into the *ortho* position of the nitro group. Recently Cadogan *et al.* presented a new method of synthesizing diethyl *o*-nitrophenylphosphonate;[1] the difficulty of the substitution is overcome by this synthetic manner, that is, *o*-nitrophenylphosphonic acid is obtained by the hydrolysis of diethyl *o*-nitrophenylphosphonate. The structural formula for *o*-phosphonophenylazo-2-hydroxynaphthalene-3,6-disulfonic acid disodium salt is:

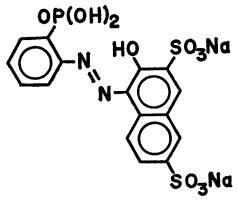

The present paper will describe a method of synthesizing *o*-phosphonophenylazo-2-hydroxylnaphthalene-3,6-disulfonic acid disodium salt and the chelating behavior of this compound.

Experimental

Synthesis of o-*Phosphonophenylazo-2-hydroxynaphthalene-3,6-disulfonic Acid Disodium Salt.* The reagent was obtained by the coupling reaction of diazotized *o*-aminophenylphosphonic acid with the R acid [2-hydroxynaphthalene-3,6-disulfonic acid]. This reaction mixture was allowed to stand overnight, and then it was added, drop by drop to well-chilled concentrated hydrochloric acid. A reddish precipitate was obtained by this procedure. The azo compound thus obtained was recrystallized several times from an acidic solution by the salting-out method. The reagent, which is obtained as disodium salt, consists of fine, reddish needles. *o*-Aminophenylphosphonic acid was synthesized by using *o*-dinitrobenzene as the starting material; the procedure has been described in detail in a previous paper.[2]

Reagent Solutions. The stock solution of the ligand was prepared by dissolving it in distilled water; the concentration, 1.5×10^{-3} M, was standardized by potentiometric titration with standard 0.10 N potassium hydroxide before use. A carbonate-free potassium hydroxide solution was prepared by the method of ion exchange and was standardized titrimetrically by potassium hydrogen phthalate. The concentrations of the Mg(II) and Ca(II) solutions were determined by chelatometric titration, while the concentration of the Sr(II) solution was determined by the usual gravimetric method.

pH Titration Method. All the measurements were carried out by the use of a micro-titration vessel, the volume of which was 5 m*l*. The temperature was kept at 25.0± 0.1°C during the titration by the circulation of water through the jacketed titration vessel; the ionic strength of the solution was adjusted to 0.10 with potassium nitrate. Alkali was added from a calibrated 0.50-m*l* micrometer syringe to the solution in an atmosphere of carbon dioxide-free nitrogen. Potentiometric measurements were performed by using an HRL-Model P pH meter (made by Horiba instruments, Inc., Kyoto), with a combined glass electrode (Metrohm, EA-125 U-type, Herisaw, Switzerland). Further details of the titration have been presented in the previous paper.[2]

Results and Discussion

Titration Curves. The titration curves are illustrated in Fig. 1 for the ligand in the presence and in the absence of alkaline-earth metal ions. The acid-dissociation constants of this ligand can be calculated by the use of the titration curve in the absence of alkaline earth metal ions. As can be seen from Fig. 1, the "ligand only" titration curve shows well-defined inflections at $a=1$ and at $a=2$, where a is equal to the number of moles of bases added per mole of the ligand. Since each of the dissociation steps is separated by such well-defined inflection points, the calculation of the acid dissociation constants can be performed separately, as in the case of monoprotic acid. The calculation formula is as follows:

$$(T_L - T_{OH} - [H] + [OH])/(T_{OH} + [H] - [OH])[H] = 1/K_a$$

where T_L represents the total concentration of the ligand species and where T_{OH} represents the total concentration of the base added to the system. The acid dissociation constants of the reagent are defined as follows:

$$K_{a1} = [H][H_2L]/[H_3L],\ K_{a2} = [H][HL]/[H_2L],$$
$$K_{a3} = [H][L]/[HL],$$

1) J. I. G. Cadogan, D. J. Sears, and D. M. Smith, *Chem. Commun.*, **1966**, 491.

2) K. Kina, H. Miyata, and K. Tôei, This Bulletin, **44**, 1855 (1971).

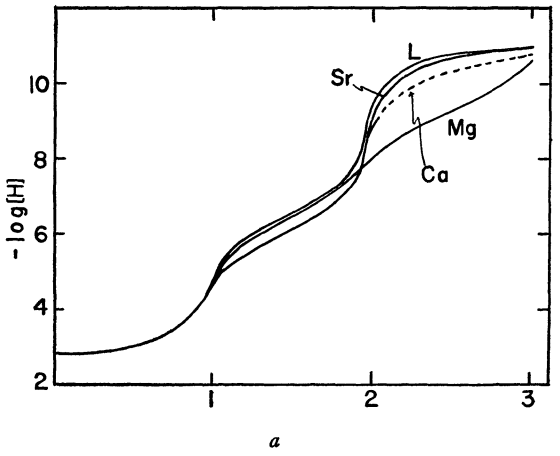

Fig. 1. Titration of 1-(2-phosphonophenylazo)-2-hydroxy-naphthalene-3,6-disulfonic acid disodium salt and its chelate system at 25°C, $\mu=0.10$; L, Ligand only, [Ligand]$=1.555\times10^{-3}$ M, [Mg]$=2.216\times10^{-3}$ M, [Ca]$=2.256\times10^{-3}$ M, [Sr]$=2.078\times10^{-3}$ M,
a=moles of base added per mole of ligand

where the ionic charge is omitted for the sake of convenience. The first and the second steps of the titration curve correspond to the two phosphonic protons, while the third step corresponds to the naphtholic proton. Therefore, the pK_{a1} and the pK_{a2} values were assigned to the phosphonic group; the pK_{a3} value was assigned to the naphtholic hydroxyl group.

The titration curves in the presence of alkaline earth metal ions show a clear pH depression caused by the chelation; the chelate stability constants can be obtained from these curves by the algebraic method. No precipitates, except for the barium chelate system, were found throughout the titration. The calcium and the strontium chelate systems present the same degree of pH depression in the region of $a=1$—2, while this titration curve splits into two lines at $a=2$; the dotted and the solid lines indicate the titrations of the calcium and strontium chelate systems respectively. These chelate systems give well-defined inflections at $a=1$ and at $a=2$ similar to that of the ligand only. This indicates that different reactions occur in the two pH regions separated by such well-defined inflections. In the region of $a=1$—2, the metal-ligand equilibria may be expressed by:

$$M + HL \rightleftarrows MHL, \quad K_{MHL} = [MHL]/[M][HL].$$

That is to say, the acido complex exists in this region; after $a=2$, the reaction may be expressed as:

$$MHL \rightleftarrows H + ML, \quad K_a' = [H][ML]/[MHL],$$

where the dissociation of the complex is observed. The order of the stability constant can be judged roughly by the extent of the pH depression. It is obvious that calcium and strontium ions form more stable acido complexes than does the magnesium ion; their values, $\log K_{SrHL}$ and $\log K_{CaHL}$, may be of much the same magnitude. The decreasing order of the stability constant, K_{ML}, with respect to the metal ions may be as follows: Mg(II)>Ca(II)>Sr(II). The titration curves of the calcium and strontium chelate systems show a clear inflection at $a=2$ similar to that of the ligand only. From this, it can be expected that the pK_a' values of the acido complex will differ little from the pK_{a3} value of the ligand.

Stability Constants. The chelating reaction is separated into two steps; the calculation of the equilibrium constants, except for the case of the magnesium chelate system, can be treated separately as two steps, that is, the acido complex formation and the acid dissociation of this complex. The stability constant of the barium chelate system was not obtained because of the precipitation. At the formation step of the acido complex in the region of $a=1$—2, the calculation formula of the acido complex stability constant is:

$$K_{MHL} = (T_L-F)/[HL](F+T_M-T_L),$$

where $$[HL] = K_{a3}/[H](T_L - T_{OH} - [H] + [OH]),$$

$$F = (1+K_{a2}/[H])(T_L-T_{OH}-[H]+[OH]).$$

The acid dissociation constant of the acido complex was then obtained by the following equation:

$$1/K_a' = (T_{MHL}-A)/[H]A, \quad \text{here } A=T_{OH}+[H]-[OH],$$

where T_{MHL} represents the total concentration of the acido complex species, which is almost equal to T_L when there is an excess of the metal ion. In addition, the following simple relationship holds among the equilibrium constants:

$$K_{MHL}\cdot K_a'/K_{a3} = K_{ML}.$$

Therefore, $\log K_{MHL} - pK_a' + pK_{a3} = \log K_{ML}$

The stability constant, $\log K_{ML}$, of the calcium or strontium chelate system was obtained by the use of the above relationship. The results of these calculations are shown in Table 1. When we suppose the structural formula of the acido complex, first we consider that the metal ion makes a coordination bond with the phosphonate group alone; however, neither phenylphosphonic acid nor the *p*-isomer of the ligand showed a remarkable pH depression such as did the ligand in the region of $a=1$—2. As can be seen from this result, the metal ions form a coordination bond not only with the phosphonate group, but also with the azo group. The naphtholic hydroxyl group of the azo compound is known to make a hydrogen bond with the azo link;[3] the structural formula for the acido complex, therefore, may be represented by Structure I. The magnesium ion forms an unstable chelate, MgHL, therefore, the calculation of the K_{ML} can be adequately approximated by the following equation:

$$K_{ML} = (T_L-F)/[L](F+T_M-T_L)$$

where $$[L] = (2T_L-T_{OH}-[H]+[OH])/([H]/K_{a3} + 2[H]^2/K_{a3}K_{a2})$$

$$F = [L](1+[H]/K_{a3}+[H]^2/K_{a3}K_{a2})$$

In this manner, the stability constant of the magnesium chelate, $\log K_{MgL}$, was obtained; it is also shown in Table 1. As can be seen from the titration curves and Table 1, the acido complex of the magnesium ion has a smaller pK_a' value than the other pK_a' values; it is considered that the acido complex of the magnesium ion, MgHL, has a tendency to become the stable

3) S. Nakashima, H. Miyata, and K. Tôei, This Bulletin, **41**, 2632 (1968).

TABLE 1. ACID DISSOCIATION CONSTANTS OF *o*-PHOSPHONOPHENYLAZO-2-HYDROXYNAPHTHALENE-3,6-DISULFONIC ACID DISODIUM SALT AND STABILITY CONSTANTS OF ITS CHELATE ($t=25.0\pm0.1$°C, $\mu=0.10$; KNO_3)

Ligand	pK_{a1} ***	pK_{a2} 6.49	pK_{a3} 11.10
	Mg	Ca	Sr
$\log K_{ML}$	4.83	3.80	3.06
$\log K_{MHL}$	—	2.98	2.97
pK_a'	—	10.28	11.01

where $K_{ML}=[ML]/[M][L]$, $K_{MHL}=[MHL]/[M][HL]$, $K_a'=[H][ML]/[MHL]$

*** too strong to be measured.

chelate form, MgL, through its own acid dissociation. In other words, since the electron-withdrawing tendency of the magnesium ion is larger than that of the calcium or strontium ion, the basicity of the naphtholic hydroxyl group was lowered by the magnesium ion which was coordinated to the azo link. This relation may be illustrated by Structure I.

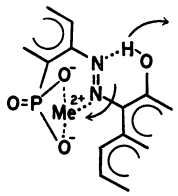

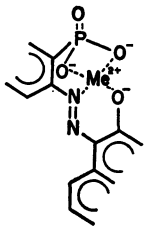

Me^{2+} = Metal Ion

Structure I. MHL Structure II. ML

The decreasing order of the pK_a' values with respect to the metal ions is as follows: Sr(II)>Ca(II)>Mg(II); that is, the electron-withdrawing tendency of the metal ions increases in this order: Sr(II)<Ca(II)<Mg(II). It seems reasonable that the metal ion forms a coordination bond with the dissociated naphtholic hydroxyl group after the dissociation of the acido complex (Structure II).

BULLETIN OF THE CHEMICAL SOCIETY OF JAPAN, VOL. 44, 2712—2716 (1971)

The Chelate Formation of (*o*-Substituted Phenylazo)chromotropic Acids with Alkaline Earth Metals. II

Takeshi KATAYAMA, Haruo MIYATA, and Kyoji TÔEI

Department of Chemistry, Faculty of Science, Okayama University, Tsushima, Okayama

(Received April 20, 1971)

The acid dissociation constants of phenylazochromotropic acid and its *o*-substituted derivatives with $-CH_3$, $-OCH_3$, $-COCH_3$, -COOH, $-CH_2COOH$, -COCOOH, $-OCH_2COOH$, and -CH(OH)COOH in the *ortho* position to the azo group, and the stability constants of their 1 : 1 metal chelates with alkaline earth metals have been measured by potentiometric titation. The measurements have been carried out at 25°C and at $\mu=0.10$ with KNO_3. The effects of these substituents on the acid dissociation constants of the reagents and on the stability constants of these chelates were discussed. The pK_a value for the naphtholic proton of the *o*-substituted reagents was larger than that of phenylazochromotropic acid, and the stability constants of these chelates with alkaline earth metals decreased as follows: Mg>Ca>Sr>Ba, while for the chelates of the *o*-OCH_2COOH reagent the order was Ca>Mg>Sr>Ba, and for the *o*-CH(OH)COOH reagent it was Mg≈Ca>Sr>Ba. The plots of the stability constants, $\log K_1$, against the sum of the acid dissociation constants, $pK_A(=pK_{a1}+pK_{a2})$, were approximately linear except for the above two reagents with calcium, strontium, and barium. From the results obtained, the *o*-OCH_2COOH reagent that behaves as a quadridentate ligand forms a more stable chelate with calcium, strontium, and barium, and the effect of the $-OCH_2COOH$ group, especially that of the coordination of the -O- atom, is remarkable in its calcium chelate.

Many of the (*o*-substituted phenylazo)chromotropic acids are well known as colorimetric reagents and as metal indicators in chelatometry. In a previous paper,[1] the effects of various substituents on the acid dissociation of the reagents and also on the chelate formation with alkaline earth metals were discussed. The present authors have now extended the studies to alkaline earth metal chelates with the eight (*o*-substituted phenylazo)chromotropic acids shown in Fig. 1, and have investigated the effect of the substituents on the dissociation constants and the stability constants by means of the potentiometric-titration method.

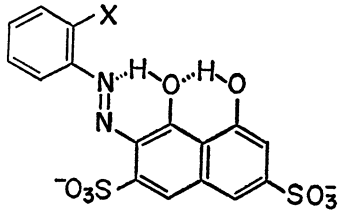

Fig. 1. Structure of reagents.
X: -H, $-CH_3$, $-OCH_3$, $-COCH_3$, -COOH, $-CH_2COOH$, -COCOOH, $-OCH_2COOH$, and -CH(OH)COOH

1) S. Nakashima, H. Miyata, and K. Tôei, This Bulletin, **41**, 2632 (1968).

Experimental

Reagents. The o-H reagent [phenylazochromotropic acid, 2-(phenylazo)-1,8-dihydroxynaphthalene-3,6-disulfonic acid],[2] the o-CH_3 reagent [2-(o-tolylazo)-1,8-dihydroxynaphthalene-3,6-disulfonic acid], the o-OCH_3 reagent [2-(o-anisolazo)-1,8-dihydroxynaphthalene-3,6-disulfonic acid],[3] the o-$COCH_3$ reagent [2-(o-methylbenzoylazo)-1,8-dihydroxynaphthalene-3,6-disulfonic acid,[4] the o-COOH reagent [2-(o-carboxyphenylazo)-1,8-dihydroxynaphthalene-3,6-disulfonic acid],[5] the o-CH_2COOH reagent[2-(o-phenylacetic acidazo)-1,8-dihydroxynaphthalene-3,6-disulfonic acid],[6] the o-COCOOH reagent [2-(o-oxalophenylazo)-1,8-dihydroxynaphthalene-3,6-disulfonic acid],[7] the o-OCH_2COOH reagent [2-(o-phenoxyacetic acidazo)-1,8-dihydroxynaphthalene-3,6-disulfonic acid],[8] and the o-CH(OH)COOH reagent [2-(o-mandelic acidazo)-1,8-dihydroxynaphthalene-3,6-disulfonic acid][9] were synthesized by the coupling reaction of chromotropic acid with the corresponding diazonium compounds. The disodium salt of the reagents was obtained by the salting-out of purified azo sulfonic acids. These reagents are all fine crystals. They are dried at 60°C in a vacuum and stored in a calcium chloride desiccator. The stock solutions of these reagents were standardized by potentiometric titration with a standard 0.10 M potassium hydroxide solution.

Analytical-grade $Mg(NO_3)_2 \cdot 6H_2O$, $Ca(NO_3)_2 \cdot 4H_2O$, $Sr(NO_3)_2$, and $Ba(NO_3)_2$ were used to make the stock solutions, and these solutions were standardized by chelatometric titration or gravimetric analysis.

Potentiometric titration. The apparatus and the procedure for the potentiometric titration were presented in a previous paper[1]; the temperature and ionic strength of a solution were maintained, respectively, at 25°C and at 0.10 with potassium nitrate.

Calculations of Acid Dissociation Constants and Stability Constants. The o-H, o-CH_3, o-OCH_3, and o-$COCH_3$ reagents are considered to be monobasic acids, while the o-COOH, o-CH_2COOH, o-COCOOH, o-OCH_2COOH, and o-CH(OH)COOH reagents are considered to be dibasic acids. The acid dissociation constants, K_{a_1} and K_{a_2}, and the stability constant, K_1, can be calculated by equations similar to those reported by Murakami *et al.*[10] K_{a_1}, K_{a_2} and K_1 are expressed as follows:

$$K_{a1} = \frac{[H][HL]}{[H_2L]}, \quad K_{a2} = \frac{[H][L]}{[HL]}$$

$$K_1 = \frac{[ML]}{[M][L]}$$

where the ionic charge was neglected for the sake of convenience

Results and Discussion

Titration Curves. The potentiometric titration curves for phenylazochromotropic acid (the o-H reagent) chelate system are illustrated in Fig. 2, while those for the o-COOH reagent chelate system are shown in Fig. 3. The clear inflection at $a=1$ in the titration curve of the ligand in Fig. 3 shows the dissociation of the carboxyl proton of the reagent. No inflection was observed at all on the neutralization of the naphtholic hydroxyl proton. The titration curves of the o-CH_3, o-OCH_3, and o-$COCH_3$ reagents were similar to that of the o-H reagent in Fig. 2, while those of the o-CH_2COOH, o-COCOOH, o-OCH_2COOH, and o-CH(OH)COOH reagents resemble the curve in Fig. 3.

Acid Dissociation Constants. The acid dissociation constants of the reagents were calculated from the titration curves and are summarized in Table 1.

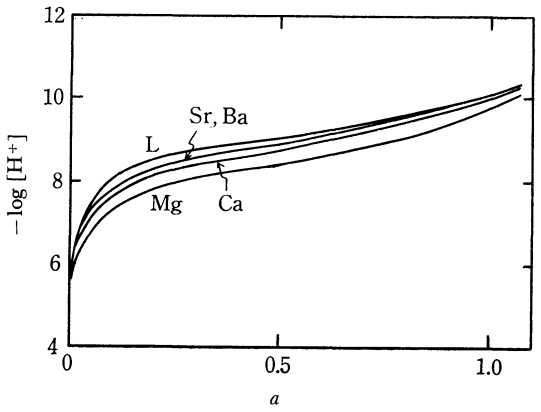

Fig. 2. Titration curves of phenylazochromotropic acid chelate system at 25°C, $\mu=0.10$.
L: ligand only
$[L]=[M]=1.188\times10^{-3}$ M
a: moles of base added per mole of ligand

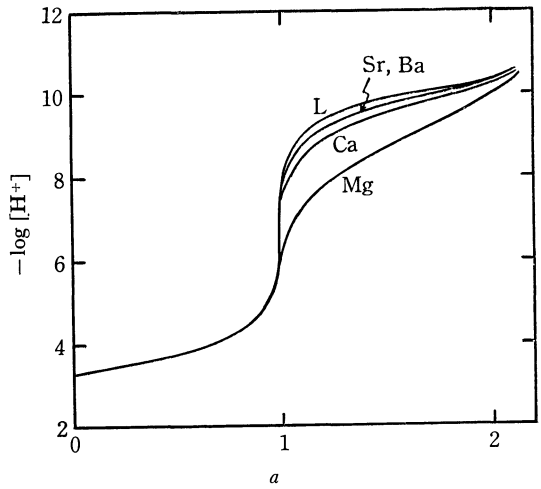

Fig. 3. Titration curves of the o-COOH reagent chelate system at 25°C, $\mu=0.10$.
$[L]=1.255\times10^{-3}$ M
$[Mg]=1.108\times10^{-3}$ M
$[Ca]=1.134\times10^{-3}$ M
$[Sr]=1.092\times10^{-3}$ M
$[Ba]=0.979\times10^{-3}$ M

2) T. Iwachido, H. Miyata, and K. Tôei, *ibid.*, **33**, 95 (1960).
3) S. Nakashima, H. Miyata, and K. Tôei, *ibid.*, **40**, 870 (1967).
4) Y. Inagaki, H. Miyata, and K. Tôei, Presented at the 22nd Annual Meeting of the Chemical Society of Japan, Tokyo, April, 1969.
5) K. Tôei, H. Miyata, and T. Harada, This Bulletin, **40**, 1141 (1967).
6) K. Tôei, H. Miyata, and S. Aoki, unpublished results.
7) T. Ozaki, H. Miyata, and K. Tôei, *Nippon Kagaku Zasshi*, **91**, 1148 (1970).
8) K. Tôei, H. Miyata, T. Shibata, and S. Miyamura, This Bulletin, **38**, 334 (1965).
9) K. Tôei, H. Miyata, and T. Mitsumata, *ibid.*, **38**, 1050 (1965).
10) Y. Murakami, K. Nakamura, and M. Tokunaga, *ibid.*, **36**, 669 (1963); **35**, 52 (1962).

TABLE 1. ACID DISSOCIATION CONSTANTS OF (*o*-SUBSTITUTED PHENYLAZO)CHROMOTROPIC ACIDS AND STABILITY CONSTANTS OF THESE CHELATES
(t=25°C, μ=0.10; KNO_3)

Substituent X	Acid dissociation constant		Stability constant, log K_1			
	pK_{a1}	pK_{a2}	Mg	Ca	Sr	Ba
-H		9.19	3.64	2.70	2.08	1.84
$-CH_3$		9.60	3.47	2.56	—	—
$-OCH_3$		9.92	3.95	3.25	2.40	2.08
$-COCH_3$		9.65	3.66	2.95	2.35	
-COOH	3.60	10.00	4.53	3.37	2.82	2.81
$-CH_2COOH$	3.77	9.64	4.00	3.50	2.75	2.43
-COCOOH	3.54	9.96	4.55	3.41	2.88	2.73
$-OCH_2COOH$	2.84	9.83	4.31	5.13	3.65	3.00
-CH(OH)COOH	3.03	9.39	3.96	3.92	3.40	3.12

The pK_{a1} and pK_{a2} values correspond to the dissociation of the carboxyl group and one of the naphtholic hydroxyl groups respectively. The other naphtholic hydroxyl group is not dissociated under ordinary experimental conditions because of a strong hydrogen bridge between two oxygen atoms of chromotropic acid, as is shown in Fig. 1. The pK_a value of the *o*-H reagent is 9.19. It is suggested that pK_a values of the *o*-CH_3 and *o*-OCH_3 reagents are larger than that of the *o*-H reagent, because the methyl and methoxy groups are *ortho*- and *para*-directing and electron-donating. Because of the effects of these groups, the N···H hydrogen bond should become stronger, as is shown in Fig. 1; in fact, the pK_a values for the *o*-CH_3 and the *o*-OCH_3 reagents are 9.60 and 9.92 respectively. In the case of the *o*-$COCH_3$ reagent, the value is 9.65 in spite of its electron-withdrawing effect. However, the value of the *p*-$COCH_3$ reagent is 9.08 because of this effect. The same phenomenon appears in the case of the *o*- and the *p*-sulfophenylazochromotropic acids, where the pK_a of the *o*-reagent is 9.35, whereas that of the *p*-reagent is 8.95.[1] Thus, the introduction of such electron-withdrawing groups into the *para*-position results in a lowering of the pK_a value, while their introduction into the *ortho*-position leads to a rise in the value. This is due to the *ortho* effect which inhibits the dissociation of the naphtholic proton.

In the *o*-COOH reagent, the resonance of the carboxyl group is so inhibited by the six-membered ring, which contains the N···H hydrogen bond, that the carboxyl group and benzene ring cannot exist on the same plane. The carboxyl proton tends to be dissociated easily for this reason.

The pK_{a1} values of the five reagents which have a carboxyl group are compared with those of the aromatic acids in Table 2. The pK_{a1} values of all the reagents except the *o*-COCOOH reagent are smaller than those of the aromatic acids. This exception is also dependent on the *ortho* effect.

Stability Constants. The stability constants of their 1 : 1 chelates with alkaline earth metals are also tabulated in Table 1. The *o*-H, *o*-CH_3, *o*-OCH_3, and *o*-$COCH_3$ reagents are considered to form a bidentate ligand, the *o*-COOH, *o*-CH_2COOH, and *o*-COCOOH reagents are terdentate, and the *o*-OCH_2-COOH and the *o*-CH(OH)COOH reagents are quadridentate for alkaline earth metal ions.

The strontium and barium chelates of the *o*-CH_3 reagent were so unstable that their stability constants could not be determined. The barium chelate of the *o*-$COCH_3$ reagent also could not be obtained because of its precipitation.

The relation between the stability constants, log K_1, and the reciprocal of alkaline earth metal ionic radii,[16] $1/r$, is given in Fig. 4. The log K_1 values of most metal chelates decrease as follows: magnesium >calcium>strontium>barium, with an increase in

TABLE 2. THE pK_a VALUES OF AROMATIC ACIDS

Acid	pK_a
Benzoic acid	4.01[11]
Phenylacetic acid	4.31[12]
Phenylglyoxylic acid	1.32[13]
Phenoxyacetic acid	2.93[14]
Mandelic acid	3.41[15]

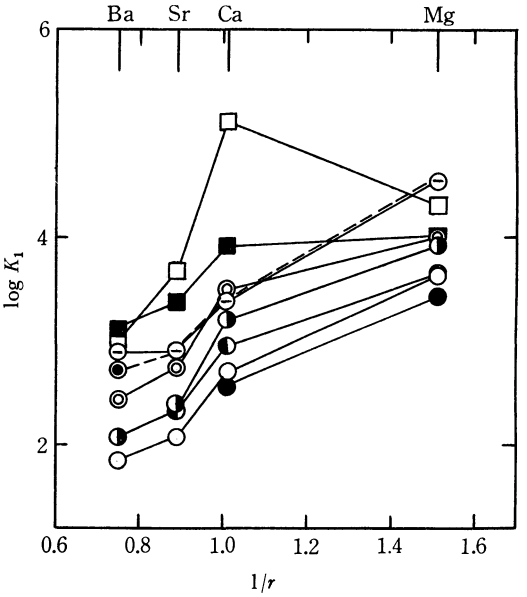

Fig. 4. Plot of log K_1 for (*o*-substituted phenylazo) chromotropic acid chelates against $1/r$ of metal ions.
○ -H ⊖ -COOH
● $-CH_3$ ◎ $-CH_2COOH$
◑ $-OCH_3$ ⊙ -COCOOH
◐ $-COCH_3$ ⊡ $-OCH_2COOH$
■ -CH(OH)COOH

11) M. Yasuda, K. Yamasaki, and H. Otaki, This Bulletin, **33**, 1067 (1960).
12) J. Frederich, J. Dippy, and F. R. Williams, *J. Chem. Soc.*, **1 34**, 161.
13) J. Böeseken, *Rec. Trav. Chim. Pays-Bas.*, **40**, 571 (1921).
14) K. Suzuki and K. Yamasaki, *J. Inorg. Nucl. Chem.*, **24**, 1093 (1962).
15) R. P. Bell and G. M. Waind, *J. Chem. Soc.*, **1911**, 2357.
16) L. H. Ahrens, *Geochim. Cosmochim. Acta*, **2**, 155 (1952).

the ionic crystal radii. However, in the o-OCH_2-COOH and the o-CH(OH)COOH chelates, the order of decreasing stability is calcium≳magnesium> strontium>barium. The values of the o-COOH chelates with strontium and barium are nearly equal, because the chelation in the o-COOH reagent is suitable for the barium ionic radius.

As the relation between metal ions and these ligands is regarded as a Lewis acid-base reaction, the log K_1 value is plotted against the sum of the dissociation constants, pK_A ($=pK_{a_1}+pK_{a_2}$), in Fig. 5. The log K_1 values are nearly proportional to the pK_A values. This implies that the stability of these chelates is mainly dependent upon the basicity, *i.e.*, the pK_A value, of the ligands, except for the calcium, strontium, and barium chelates of the o-OCH_2COOH and the o-CH(OH)COOH reagents.

As for the reagents behaving as monobasic acid, the plots of the log K_1 values of the o-H chelates against

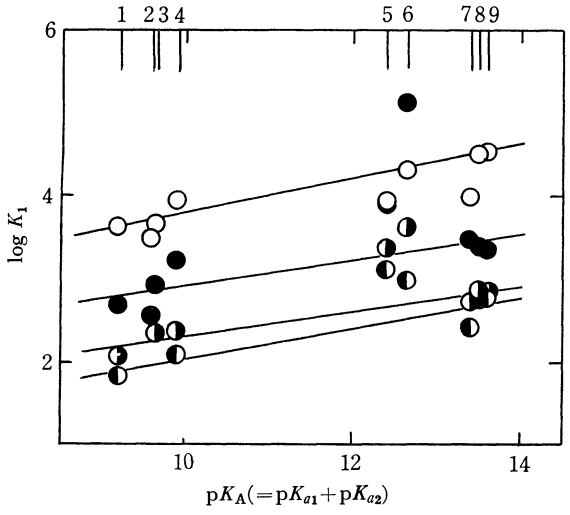

Fig. 5. Relation between pK_A of the reagents and log K_1 of their metal chelates.

1 -H	5 -CH(OH)COOH	9 COOH
2 $-CH_3$	6 $-OCH_2COOH$	
3 $-COCH_3$	7 $-CH_2COOH$	
4 $-OCH_3$	8 -COCOOH	

○ Mg, ● Ca, ◑ Sr, ◐ Ba

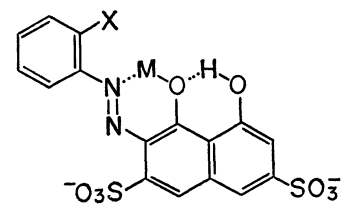

Structural formula 1
X: -H, $-CH_3$, $-OCH_3$

those of the o-OCH_3 or o-$COCH_3$ chelates are shown in Fig. 6(a). These reagents may form a bidentate ligand, and a good linear relation sphip is obtained among the reagents. This suggests that these chelate structures are similar to each other, as is shown in the structural formula (1). The chelate structure of the o-H reagent with an alkaline earth metal ion forms a stable six-membered ring. The bulky methyl group of the o-CH_3 reagent disturbs the chelate formation. Especially, these chelates with strontium and barium are very unstable because of these large ionic radii. The small stable deviation of the o-OCH_3 reagent with calcium is due to the coordination of the oxygen atom of the methoxy group, but those of the acetyl group scarcely coordinate at all with the metal ion.

The same relationship is obtained for the dibasic acid system, as is shown in Fig. 6(b) and (c); these structures are shown in structural formulas (2), (3), and (4). That is to say, the structure of the o-COOH chelate has two chelate rings as a terdentate ligand, but those of the o-OCH_2COOH and the o-CH(OH)-COOH chelates probably have three chelate rings.

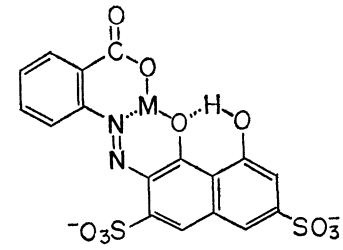

Structural formula 2

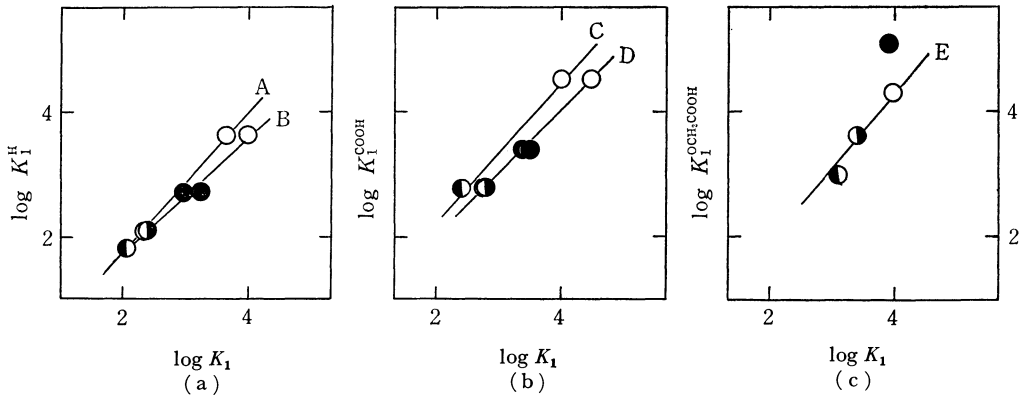

Fig. 6. Relation between log K_1's for pairs of ligands

A: -H～$-OCH_3$	C: -COOH～$-CH_2COOH$	E: $-OCH_2COOH$～-CH(CH)COOH
B: -H～$-COCH_3$	D: -COOH～-COCOOH	

○ Mg, ● Ca, ◑ Sr, ◐ Ba

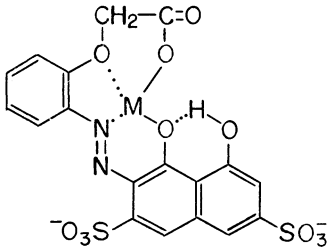

Structural formula 3

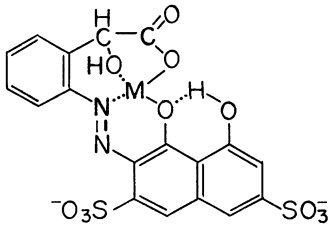

Structural formula 4

Thus, the reagents may behave as a quadridentate ligand. As is shown in Fig. 5, the positive deviation from the straight line for the log K_1 values of these calcium, strontium, and barium chelates is considered to result from this cause. This tendency is so remarkable in the *o*-OCH_2COOH chelate with calcium that the order of the stability is calcium>magnesium. On the other hand, on the magnesium chelates of these reagents, the plots in Fig. 5 lie on or under the straight line. This means that their oxygen atom (–O– or –OH) in the substituent scarcely contributes at all to the coordination, because the ionic radius of magnesium is much smaller than that of the other alkaline earth metals discussed before.

The present work has been supported in part by a Grant for Science Research from the Ministry of Education.

BULLETIN OF THE CHEMICAL SOCIETY OF JAPAN, VOL. 44, 2716—2721 (1971)

The Stability of Fused Rings in Metal Chelates. VIII. Solution Equilibria of the Copper(II) Complexes of Glycinamide and Related Compounds

Osamu YAMAUCHI, Hiroko MIYATA, and Akitsugu NAKAHARA

Institute of Chemistry, College of General Education, Osaka University, Toyonaka, Osaka

(Received May 14, 1971)

The aqueous solution equilibria of the systems containing copper(II) ion and glycinamide, β-alaninamide, glycine-*N*,*N*-diethylamide, or β-alanine-*N*,*N*-diethylamide have been investigated by potentiometric titration at 25°C (μ=0.1 (KNO_3)). The stability constants K_1 and K_2 and the constants of the deprotonation reactions K_1^H, K_{c1}, and K_{c2}, for the glycinamide-copper(II) systems, and K_1 and K_2 for the other ligand-copper(II) systems were calculated by the method of non-linear least-squares with the aid of a computer. The K_1 values were found to be in the order, glycine-*N*,*N*-diethylamide (6.17) > β-alanine-*N*,*N*-diethylamide (5.5) > glycinamide (5.30) > β-alaninamide (5.1). The sequence reveals that the five-membered chelates are more stable than the six-membered ones. The K_1 and K_{c1} values for glycylglycine and β-alanylglycine have been determined anew, and the structures of the chelates formed in acid solution have been discussed from comparative studies of the equilibrium constants, which suggest a tridentate nature of the dipeptides in the chelates of the type $Cu(HL)^+$ where HL denotes free dipeptide.

From comparative studies of the stability constants of various copper(II)-dipeptide chelates, Rabin[1] postulated that in acid solution glycylglycine (Gly·Gly) binds with copper(II) as bidentate ligand through the amino nitrogen and peptide oxygen as indicated by the structure Ia. Since then a considerable number of papers have appeared dealing with the nature of the copper(II)-peptide bonding in the chelates formed in acid solution.

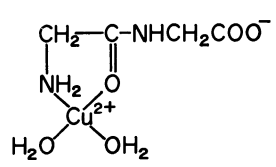

Ia

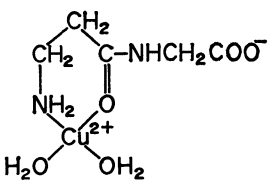

Ib

Nancollas and his co-workers[2-4] confirmed the bidentate nature of Gly·Gly, triglycine, and tetraglycine on the basis of thermodynamic investigations, and

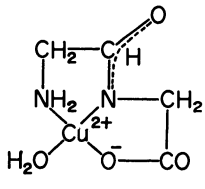

IIa

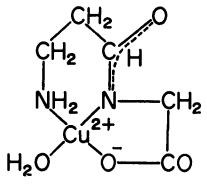

IIb

1) B. R. Rabin, *Trans. Faraday Soc.* **52**, 1130 (1956).

2) A. P. Brunetti, M. C. Lim and G. H. Nancollas, *J. Amer. Chem. Soc.*, **90**, 5120 (1968).

3) G. H. Nancollas and D. J. Poulton, *Inorg. Chem.*, **8**, 680 (1969).

4) G. H. Nancollas, *Coord. Chem. Rev.*, **5**, 407 (1970).

Pagenkopf and Margerum[5] and Pasternack *et al.*[6] also obtained results supporting the view from kinetic studies. Kim and Martell,[7,8] on the other hand, favored the fused-ring structures like IIa from the potentiometric and spectral points of view.

We reported[9] the reactions of copper(II) with some dipeptides composed of glycine and/or β-alanine as studied from the viewpoint of the relative stability of fused-ring chelates, and interpreted the results as indicative of the coordination to copper(II) in acid solution by the amino nitrogen, amide nitrogen, and carboxyl oxygen of the dipeptides as shown by IIa and IIb.

The necessity for further information on the bonding modes in solution prompted us to carry out studies on the interactions of copper(II) with some amino acid amides as fundamental constituents of peptides. In this connection, it seemed significant to investigate comparatively the stabilities and structures of the copper(II) complexes of glycinamide, β-alaninamide, and the corresponding *N,N*-diethylamides in order to get information on the contribution of peptide oxygen and nitrogen atoms to coordination.

The solution equilbria of the copper(II)-glycinamide complexes have been reported by Datta and Rabin,[10] Li *et al.*,[11] and Sigel.[12] Regardh[13] carried out detailed studies on the equilibria involved in a 2 : 1 glycinamide-copper(II) mixture as well as the copper(II) ion-catalyzed hydrolysis of glycinamide, and obtained equilibrium constants by the method of Bjerrum. However, the equilibrium constants for glycinamide reported so far by these investigators were determined under different conditions and do not seem to be complete. It might be of value to reinvestigate the glycinamide-copper(II) systems along with the other amide-copper(II) systems.

This paper deals with the studies on the solution equilibria of the copper(II) complexes of glycinamide (GA), β-alaninamide (β-AA), glycine-*N,N*-diethylamide (GDA), and β-alanine-*N,N*-diethylamide (β-ADA), and a discussion on the structures and stabilities of the complexes.

Experimental

Reagents. GA hydrochloride was purchased from Nakarai Chemicals Co., Ltd., and used without further purification. β-AA hydrochloride,[14] GDA hydrochloride,[15] Gly·Gly,[16,17] and β-alanylglycine (β-Ala·Gly)[18] were prepared according to literature and checked by the melting point and elemental analysis.

*β-Alanine-*N,N*-diethylamide* (β-ADA). To a stirred solution of diethylamine (6.6 g, 90 mmol) in toluene (50 m*l*) was added, under cooling in ice water, carbobenzoxy-β-alanyl chloride[19] in toluene (50 m*l*) prepared from carbobenzoxy-β-alanine (10.0 g, 45 mmol), and the mixture was stirred for 2.5 hr at room temperature. The filtrate from diethylamine hydrochloride was washed successively with dilute aqueous sodium carbonate and water and dried over magnesium sulfate. The yellow oil obtained after evaporation of the solvent *in vacuo* was reduced with Pd-H_2 in methanol (250 m*l*) containing concentrated hydrochloric acid (2 m*l*). After removal of the catalyst and solvent, the oily residue was dried over P_2O_5 *in vacuo* and crystallized by washing with acetone. Yield, 3.0 g. Recrystallization from ethanol-acetone-ether gave the hydrochloride of β-ADA as very hygroscopic leaflets, mp 115—116°C (uncor.). Found: C, 46.38; H, 9.57; N, 15.51%. Calcd for $C_7H_{17}N_2OCl$: C, 46.53; H, 9.48; N, 15.51%.

0.1 N *Potassium Hydroxide.* Prepared according to Armstrong,[20] standardized against potassium hydrogen phthalate, and stored under a nitrogen atmosphere.

0.01 M *Copper(II) Nitrate.* Prepared by dissolving copper (II) nitrate trihydrate in water and standardized by chelatometric titrations.[21]

All the reagents used were of reagent grade and deionized water was used throughout.

pH Titrations. An aqueous solution of a ligand and copper(II) nitrate (0.002—0.008 M) was titrated with 0.1 N potassium hydroxide under a nitrogen atmosphere at 25°C (μ=0.1(KNO_3)). For the calculation of the acid dissociation constants, the ligands were titrated in the absence of copper(II) nitrate. The pH values were measured with a Radiometer PHM 4d pH meter equipped with a G202C glass electrode and a K401 saturated calomel electrode. The system was standardized with a Horiba and a Radiometer standard buffer solution (pH 4.01 and 6.48). Conversion of pH to $-\log[H^+]$, where $[H^+]$ refers to the hydrogen ion concentration, and determination of the apparent ion product of water pK_w' were made by titrating 0.01 N nitric acid with 0.1 N potassium hydroxide under the same conditions. The values $[H^+]=10^{-pH}/0.85$ and $pK_w'=13.88$ were used in the calculations.

Results and Discussion

Titration Curves. The titration curves of the amides both in the absence and presence of copper(II) are shown in Fig. 1. The curves for the GA-copper (II) systems reveal that two protons are liberated from a ligand in the presence of copper(II), whereas only one proton is liberated in the GDA-copper(II) system. The two protons undoubtedly can be ascribed

5) G. K. Pagenkopf and D. W. Margerum, *J. Amer. Chem. Soc.*, **90**, 6963 (1968).
6) R. F. Pasternack, M. Angwin, and E. Gibbs, *ibid.*, **92**, 5878 (1970).
7) M. K. Kim and A. E. Martell, *Biochemistry*, **3**, 1169 (1964).
8) M. K. Kim and A. E. Martell, *J. Amer. Chem. Soc.*, **88**, 914 (1966).
9) O. Yamauchi, Y. Hirano, Y. Nakao, and A. Nakahara, *Can. J. Chem.*, **47**, 3441 (1969).
10) S. P. Datta and B. R. Rabin, *Trans. Faraday Soc.*, **52**, 1123 (1956).
11) N. C. Li, B. E. Doody, and J. M. White, *J. Amer. Chem. Soc.*, **79**, 5859 (1957).
12) H. Sigel, *Angew. Chem.*, **80**, 124 (1968).
13) C.-G. Regardh, *Acta Pharm. Suecica*, **4**, 335 (1967).
14) H. T. Hason and E. L. Smith, *J. Biol. Chem.*, **175**, 833 (1948).
15) A. J. Speziale and P. C. Hamm, *J. Amer. Chem. Soc.*, **78**, 2558, 5583 (1956).
16) C. Sannie, *Bull. Soc. Chim. Fr.*, **9**, 487 (1942).
17) E. Fischer and E. Fourneau, *Ber.*, **34**, 2868 (1901).
18) Y. Nakao, H. Ishibashi, and A. Nakahara, This Bulletin, **43**, 3457 (1970).
19) R. H. Sifferd and V. du Vigneaud, *J. Biol. Chem.*, **108**, 758 (1935).
20) A. Albert and E. P. Serjeant, "Ionization Constants of Acids and Bases," Methuen and Co., Ltd., London (1962).
21) K. Ueno, "Kireto Tekiteiho," Nankodo Co., Ltd., Tokyo (1960).

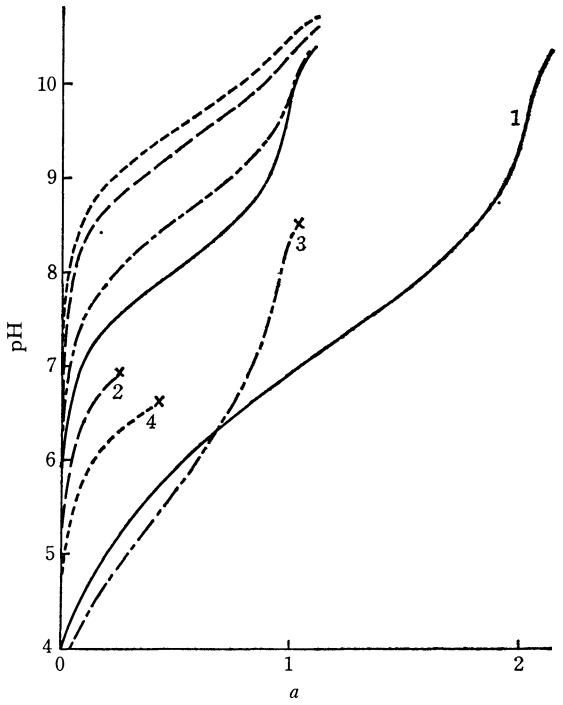

Fig. 1. Titration curves for the amino acid amides in the absence and in the presence of copper(II) ion.
—— GA; ——— β-AA; ·—·—· GDA; ------ β-ADA
Curves 1—4 correspond to the titrations of the following system:
curve 1 GA=0.004182 M; Cu(II)=0.002088 M
curve 2 β-AA=0.004272 M; Cu(II)=0.001044 M
curve 3 GDA=0.003980 M; Cu(II)=0.002046 M
curve 4 β-ADA=0.004000 M; Cu(II)=0.002046 M
a: Moles of alkali added per mole of ligand
×: Precipitate formation

to the dissociation of the ammonium and amide groups of protonated GA. The titrations of the solutions containing copper(II) and the β-alaninamides at various ratios resulted in the precipitations of the hydrolyzed species of copper(II). No sufficient data were obtained. This might indicate that the β-alanine derivatives, in sharp contrast to the glycine derivatives, form unstable complexes with copper(II), where the copper(II)-ligand bonds are susceptible to hydrolytic cleavage.

Calculation of the Equilibrium Constants. We see from the titration curves that the equilibria for the GA-copper(II) systems are somewhat complicated, and the usual Bjerrum method, which is effective for the *N*,*N*-diethylamides, does not seem to be suitable for calculating the constants appearing in these systems. Various computer programs for the non-linear least-squares treatment of data have hitherto been proposed and applied to such complex systems. Recently Sayce[22] reported a general program SCOGS, which evaluates data by this method based on the minimization of the sum of the squares of the residuals in the titer of base, in contrast to the earlier programs which seek to minimize the sum of the squares of the residuals in the analytical hydrogen ion concentrations.

Since the former apparently seems to be easier in the weighing procedure, we also attempted the least-squares refinements as suggested by Sayce. Our program is in principle analogous to SCOGS and earlier programs and consists of the Newton-Raphson iterations, which calculate from the initial estimates of the constants the free ligand and free metal ion concentrations, using the mole balance equations for the total ligand and total metal ion concentrations, the setting up of the matrix for the least-squares treatment, which gives the shifts in the constants by matrix inversion, and the output of the refined constants and their estimated standard deviations. The output also includes the calculated concentration of alkali, the difference of the calculated titer from the experimental, the free ligand and free metal concentrations, and the individual amounts of coordinated species relative to the total metal ion concentration, for each data point. In the present version of the program, partial derivatives were obtained arithmetically for each system, and the calculated shifts in the constants were in the form of the constants and not in their logarithms. The residuals in the concentrations of alkali were calculated from the equation for the electroneutrality of solution. Initial estimates of the constants were obtained by some other methods or taken from literature, and the program accepted up to ten sets of such estimates for a system. The standard deviations of the constants were estimated from the elements of the inverted matrix and the assumed error in the titer of alkali. The subroutine for matrix inversion is conventional and that for least-squares treatment is described elsewhere.[23]

The reaction sequences expected from the titration curves of the 1 : 1 and 2 : 1 GA-copper(II) systems can be expressed by the following equlibria (1) through (5) with the relevant equilibrium constants K_1, K_1^H, K_2, K_{c_1}, and K_{c_2} defined by Eqs. (6) through (10):

$$Cu^{2+} + HL \overset{K_1}{\rightleftharpoons} Cu(HL)^{2+} \quad (1)$$

$$Cu(HL)^{2+} \overset{K_1^H}{\rightleftharpoons} CuL^{+} + H^{+} \quad (2)$$

$$Cu(HL)^{2+} + HL \overset{K_2}{\rightleftharpoons} Cu(HL)_2^{2+} \quad (3)$$

$$Cu(HL)_2^{2+} \overset{K_{c_1}}{\rightleftharpoons} Cu(HL\cdot L)^{+} + H^{+} \quad (4)$$

$$Cu(HL\cdot L)^{+} \overset{K_{c_2}}{\rightleftharpoons} CuL_2 + H^{+} \quad (5)$$

$$K_1 = \frac{[Cu(HL)^{2+}]}{[Cu^{2+}][HL]} \quad (6)$$

$$K_1^H = \frac{[CuL^{+}][H^{+}]}{[Cu(HL)^{2+}]} \quad (7)$$

$$K_2 = \frac{[Cu(HL)_2^{2+}]}{[Cu(HL)^{2+}][HL]} \quad (8)$$

$$K_{c_1} = \frac{[Cu(HL\cdot L)^{+}][H^{+}]}{[Cu(HL)_2^{2+}]} \quad (9)$$

$$K_{c_2} = \frac{[CuL_2][H^{+}]}{[Cu(HL\cdot L)^{+}]} \quad (10)$$

22) I. G. Sayce, *Talanta*, **15**, 1397 (1968).

23) K. B. Wiberg, "Computer Programming for Chemists," W. A. Benjamin, Inc., New York (1965).

TABLE 1. EQUILIBRIUM CONSTANTS (25±0.05°C; μ=0.1 (KNO_3))[a]

Ligand	$pK_{a_{COOH}}$	$pK_{a_{NH_3^+}}$	log K_1	pK_1^H	log K_2	pK_{c_1}	pK_{c_2}
GA[b]		7.96±0.003	5.22±0.005		4.36±0.010	6.95±0.007	8.17±0.004
			5.30±0.002[c]	6.79±0.005[c]			
β-AA[d]		9.23±0.008	5.0_9		4.5		
			5.1_0[e]		4.4[e]		
GDA		8.49±0.005	6.18±0.003		5.12±0.005		
			6.15[e]		5.14[e]		
β-ADA[d]		9.48±0.005	5.51±0.04		5.2_4±0.1		
			5.55[e]		5.1_5[e]		
Gly·Gly	3.14±0.006	8.09±0.006	5.50±0.001			4.10±0.001	
			5.50[f]			4.10[f]	
β-Ala·Gly	3.22±0.009	9.45±0.009	5.45±0.001			4.09±0.001	
			5.45[f]			4.08[f]	
Glycine[g]	2.41	9.63	8.20[e]		6.90[e]		
β-Alanine[g]	3.55	10.15	6.99[e]		5.55[e]		

a) Variances are expressed in standard deviations. For all the data used for calculation, the differences between the observed and calculated titers of 0.1 N potassium hydroxide were within 0.02 m*l* for the titers ranging from 0 to 2.5 m*l*.
b) The following values have been reported:
$pK_{a_{NH_3^+}}$=8.04±0.02; log K_1=5.40±0.04; pK_1^H=7.01±0.04 (25°C; μ=0.1 ($NaClO_4$))[12]
$pK_{a_{NH_3^+}}$=8.19±0.01; log K_1=5.4; log K_2=4.4; pK_{c_1}=7.7; pK_{c_2}=8.6 (25°C; μ=1.0 ($NaClO_4$)).[13]
c) Calculated from the data obtained by titrating a 1 : 1 GA-copper(II) system.
d) The log K_1 and log K_2 values are inaccurate owing to precipitation.
e) Calculated from the $\bar{n}$ values.[24]
f) Calculated by the method of Datta and Rabin.[10]
g) Constants included for comparison and are taken from our previous studies[9] and unpublished results.

where HL and L refer to GA and GA deprotonated from the amide nitrogen atom, respectively. Least-squares adjustment taking the equlibria (1), (3), (4), and (5) into account was satisfactory for the 2 : 1 ligand-copper(II) system over the pH range 4—9. Attempts to include the equilibrium (2) were not successful, indicating that this process is negligible if not improbable in this system. Constant K_1^H was obtained from the titration of a 1 : 1 ligand-copper(II) mixture.

For the β-AA-copper(II) system, evaluation of the data may be inaccurate because of the precipitate formation at a very early stage of titration. Considering the pH range of the data and the expected stability of the complex, deprotonation reactions (2), (4), and (5) seemed to be negligible, and only the calculation of the constants K_1 and K_2 for the equilibria (1) and (3) was attempted. On the other hand, the *N,N*-diethylamides have no dissociable amide hydrogens and form complexes of the types CuL^{2+} and CuL_2^{2+}, where L refers to free ligand, according to equlibria similar to (1) and (3). Thus, the stability constants K_1 and K_2 were calculated by the Bjerrum and the least-squares methods. The amide β-ADA was similar in behavior to β-AA and did not afford sufficient data owing to precipitation.

Interpretation of the Equilibrium Constants. The calculated constants for the amides are shown in Table 1 along with the values for Gly·Gly, β-Ala·Gly, glycine, and β-alanine. The dipeptide-copper(II) systems were titrated under the same conditions, and the K_1 and K_{c_1} values, which describe the reactions analogous to (1) and (2), were calculated by the method of Datta and Rabin[10] and by the present method.

The stability constants log K_1 and log K_2 for GDA and β-ADA calculated by the present method agreed with those obtained by the method of Irving and Rossotti[24] from the $\bar{n}$ values (average number of ligand molecules bound to a metal ion) within 0.1 log unit.

Also, the constants log K_1 and $-\log K_c$ (pK_{c_1}) for the dipetides calculated by the present treatment were in excellent agreement with those obtained by the method of Datta and Rabin.

As regards the GA-copper(II) systems, Regardh[13] obtained the four constants K_1, K_2, K_{c_1}, and K_{c_2} according to the method of Bjerrum by titrating a 2 : 1 ligand-copper(II) system at 25°C (μ=1.0($NaClO_4$)). Considering the differences in the conditions and the method of calculation, they are in good agreement with the present values. As Regardh remarked, however, serious deviations were observed between the calculated and the experimental values in the

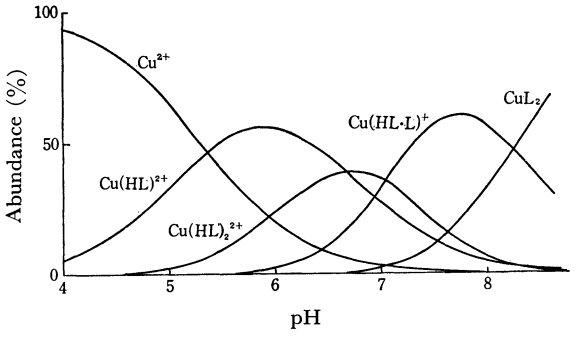

Fig. 2. Abundances of coordinated species in the 2 : 1 GA-copper(II) system; calculated from the constants listed in Table 1.

24) H. Irving and H. S. Rossotti, *J. Chem. Soc.*, **1953**, 3397.

pH region where two or more concomitant reactions take place, because only a limited number of reactions were taken into consideration. According to the least-squares treatment of data, a better fit to the experimental curve could be obtained over the entire pH range in question. The relative amounts of the coordinated species present in a 2 : 1 ligand-copper (II) system at various pH values are shown in Fig. 2. We see that in the pH range 6.2—8.0 at least three of the four species exist in considerable amounts. Constant K_1^H for the equlibrium (2) could not be obtained from the titration of a 2 : 1 ligand-copper(II) system, which indicates the predominance of the formation of the 2 : 1 chelate over that of the deprotonated 1 : 1 chelate.

Stability constants for the β-alaninamides were calculated from a very small number of data as compared with those for the glycinamides and are less reliable. For the β-AA-copper(II) system, the stability constants can be influenced by the probable errors due to hydrolysis reactions.

Komorita *et al.*[25] inferred from the spectral studies that the preferred coordination sites of α-amino acid amides in acid solution are the amino nitrogen and the carbonyl oxygen as shown by structure III and that in alkaline solution the amide nitrogen replaces oxygen (IV). Figure 2 indicates that in the pH range 4—7 the complexes $Cu(HL)^{2+}$ and $Cu(HL)_2^{2+}$ predominate, whereas at higher pH values the amounts of the deprotonated species $Cu(HL\cdot L)^+$ and CuL_2 exceed the amount of $Cu(HL)_2^{2+}$. The finding is consistent with that from the spectral studies.

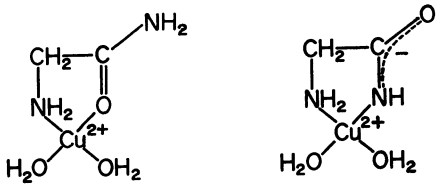

III IV

When compared with the dipeptide-copper(II) chelates, the 1 : 1 GA-copper(II) chelate exhibits a remarkable difference in the pK_{c_1} value (6.95) which is more than 2.8 log units higher than the values for the dipeptides. Therefore, the deprotonated chelates CuL of Gly·Gly and β-Ala·Gly predominate over $Cu(HL)^+$ in wide pH ranges as demonstrated in Figs. 3 and 4. The fact probably points to the difference in stability of the deprotonated chelates.

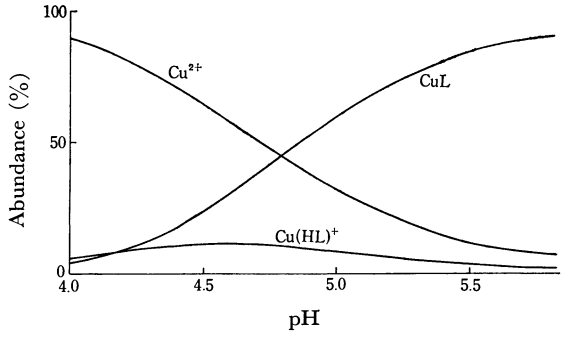

Fig. 3. Abundances of coordinated species in the 1 : 1 Gly·Gly-copper(II) system; calculated from the constants listed in Table 1. Similar curves were reported by Kim and Martell.[7]

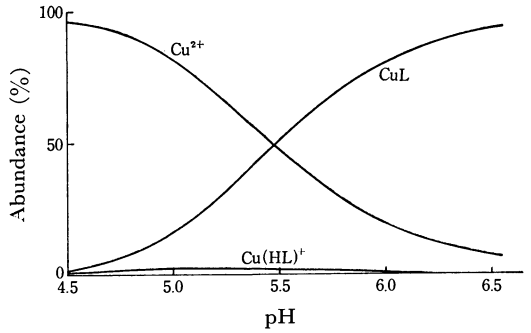

Fig. 4. Abundances of coordinated species in the 1 : 1 β-Ala·Gly-copper(II) system; calculated from the constants listed in Table 1.

Stability constants log K_1 for the glycinamides are now found to be greater than those for the corresponding β-alaninamides. Although the values for β-AA may not be reliable, the hydrolysis reactions observed during the titrations manifest that β-AA-copper(II) chelates are less stable than the GA-copper-(II) chelates. On the other hand, there is practically no difference between the log K_1 values of the Gly·Gly-and β-Ala·Gly-copper(II) chelates in spite of the large difference between those of the glycine- and β-alanine-copper(II) chelates. We explained the fact as due to the formation of the fused-ring structures, IIa and IIb,[9] where the steric requirements of the individual rings might be cancelled or dispersed over the chelate system as a whole to give chelates of equal stability. The present results indicate that the ring size produces a decisive effect on the chelate stability when the substituents on the amide nitrogen do not take part in chelation. Hence, the equal stability of the Gly·Gly- and β-Ala·Gly-copper(II) chelates appears to be better explained by the structures IIa and IIb rather than by Ia and Ib. As suggested by Tanaka *et al.*,[26] there seems to be a linear relationship between the differences in the pK_a values of the amino groups of the glycine derivatives and of the corresponding β-alanine derivatives investigated and the differences in the log K_1 values. Although the small difference observed for the dipeptides can be explained according to this relationship by the Rabin models Ia and Ib as well, we are more inclined to favor the fused-ring structures for the charged dipeptide-copper(II) chelates formed in acid solution, from the findings described above. Very recently Barnet *et al.*[27] determined the crystal structures of cobalt(III) complexes of Gly·Gly, of which bis(glycylglycinato)cobalt(III) perchlorate was shown to have

25) T. Komorita, J. Hidaka, and Y. Shimura, This Bulletin, **42**, 168 (1969).

26) H. Tanaka, A. Yokoyama, Y. Sugiura, and K. Aiba, private communication, 1970.

27) M. T. Barnet, H. C. Freeman, D. A. Buckingham, I-N. Hsu, and D. v. d. Helm, *J. Chem. Soc., D*, **1970**, 367.

two Gly·Gly ions coordinating to cobalt(III) through the amino nitrogen, peptide nitrogen, and carboxyl oxygen with the hydrogen of the peptide group attached to the peptide oxygen. This seems to strongly support our view.

The situation would be somewhat different in the longer peptides, because the carboxyl group is quite apart from the strongly coordinating amino residue, so that it would be rather difficult to arrange the intervening peptide nitrogens around the coordination sphere of copper(II) without dissociation of the peptide hydrogens.

The authors wish to thank the members of the Osaka University Computation Center for the computations. The investigation was supported in part by a grant of the Japanese Ministry of Education.

BULLETIN OF THE CHEMICAL SOCIETY OF JAPAN, VOL. 44, 2721—2724 (1971)

The Crystal Structure of $(+)_{589}$-Dicyanobis(ethylenediamine)cobalt(III) Chloride Monohydrate

Keiji MATSUMOTO, Shun'ichiro OOI, and Hisao KUROYA

Department of Chemistry, Faculty of Science, Osaka City Univetsity, Sumiyoshi-ku, Osaka

(Received May 17, 1971)

The crystal structure of $(+)_{589}$-$[Co(CN)_2en_2]Cl \cdot H_2O$ has been determined from three-dimensional X-ray photographic data. The crystals are monoclinic, with the lattice constants of $a=8.15(1)$, $b=11.69(2)$, $c=6.61(1)$Å, and $\beta=107.1(2)°$, and with the space group of $P2_1$, containing two formula units in the cell. The structure was solved by a conventional Fourier technique and was refined by the least-squares method to an R factor of 0.114. The absolute configuration of the complex ion can be denoted as $\Lambda(\lambda\lambda)$; this is in accordance with the assignment made by Mason *et al.* The complex ion has an approximately two-fold axis, and both of the ethylenediamine chelate rings are of the *ob*-conformation.

The absolute configurations of the several bisethylenediamine cobalt(III) complexes with C_2-symmetry have been studied on the basis of the optical properties, such as CD or ORD spectra.[1-4] However, since no X-ray diffraction study had been made on the bisdiamine complexes, we carried out the direct determination of the absolute structure of $(+)_{589}$-$[Co(CN)_2en_2]Cl \cdot H_2O$ by the X-ray method. The preliminary results of this work have been reported previously.[5,6] In this paper, the complete crystal structure, as refined by the use of the three-dimensional reflection data, will be described.

Experimental

The plate-like, yellow crysatls of $(+)_{589}$-$[Co(CN)_2en_2]Cl \cdot H_2O$ were kindly supplied by Ohkawa and Fujita.[7] Lattice constants were determined by the least-squares refinement of the twenty-eight θ values from the $h0l$ and $hk0$ Weissenberg photographs, on which aluminum-powder diffraction lines were superimposed for calibration.

The observed systematic absences ($0k0$, $k=2n+1$) indicate two possible space groups, $P2_1$ and $P2_1/m$; however, the latter can be excluded, because the compound is optically active, including only the dextrorotatory enantiomer of the complex ions. The crystal data are shown in Table 1.

TABLE 1. CRYSTALLOGRAPHIC DATA

Monoclinic
$a=8.15(0.01)$Å
$b=11.69(0.02)$Å
$c=6.61(0.01)$Å
$\beta=107.1(0.2)°$
Space group $P2_1$
$Z=2$ ($D_m=1.56$, $D_c=1.57$ g·cm^{-3})
$\mu=51.3$ cm^{-1} (for Ni$K\alpha$, $\lambda=1.6591$ Å)

Multiple-film, equi-inclination Weissenberg photographs, $h0l$ through $h6l$, and $hk0$ through $hk3$, were taken with Ni$K\alpha$ radiation. The intensities were estimated by visual comparison with the calibrated intensity scale and were corrected for the Lp factor and spot-shape.[8] Since the crystal specimens used were sufficiently small ($\sim 0.10 \times 0.03 \times 0.4$ mm), the absorption correction was not applied. A total of 860 independent reflections were collected. However, 163 of these were too weak to be measured and so their intensities were assumed to be zero.

Determination of the Crystal Structure

At the early stages of this work, the electronic computer available to us was OKITAC 5090D, with which it was difficult to deal with the three-dimensional data; hence, we started on the structure analysis

1) F. P. Dwyer, T. E. McDermott, and A. M. Sargeson, *J. Amer. Chem. Soc.*, **85**, 661 (1963).
2) T. E. McDermott and A. M. Sargeson, *Aust. J. Chem.*, **16**, 334 (1963).
3) R. D. Gillard and G. Wilkinson, *J. Chem. Soc.*, **1964**, 1368.
4) A. J. McCaffery, S. F. Mason, and B. J. Norman, *ibid.*, **1965**, 5094.
5) K. Matsumoto, S. Ooi, and H. Kuroya, Presented at the 14th Symposium of Coordination Chemistry, Chemical Society of Japan, Nov. 1964, Fukuoka.
6) K. Matsumoto, Y. Kushi, S. Ooi, and H. Kuroya, This Bulletin, **40**, 2988 (1967).
7) K. Ohkawa, J. Fujita, and Y. Shimura, *ibid.*, **38**, 66 (1965).
8) D. C. Philips, *Acta Crystallogr.*, **7**, 746 (1954).

by the two-dimensional method. The positions of the cobalt and chlorine atoms were found from the Patterson functions, $P(UW)$ and $P(UV)$. The remaining atroms were difficult to locate on the Fourier map $\rho(xz)$ phased by the heavy atoms, because of the poor resolution of the atomic peaks. Subsequently, the minimum function, $M(xy)$, was synthesized graphically[9] utilizing the coordinates of the Co and Cl atoms. The x and y coordinates of all the non-hydrogen atoms but the oxygen atom of the water molecule were found on the $M(xy)$ by the use of the scaled model of the complex ion. The oxygen atom could be located on the subsequent Fourier map, $\rho(xy)$. The crystal structure was refined to an R factor of 0.13 for the $hk0$ data by a diagonal least-squares method. At this stage, the z coordinate of each atom was readily obtained from the $\rho(xz)$. The R value for $h0l$ data was reduced to 0.14 by successive difference syntheses.

Further refinements were made by the block-diagonal least-squares method using the three-dimensional reflection data. The weighting scheme employed was as follows:

$$w=0.4 \text{ for } F_o<5.3$$
$$w=1.0 \text{ for } 5.3\leq F_o\leq 40.0$$
$$w=40.0/F_o \text{ for } F_o>40.0$$

The atomic scattering factors were taken from the International Tables for X-ray Crystallography.[10] The real part of the anomalous dispersion correction for Co was taken into account.[11] After four cycles of the refinement with an individual isotropic temperature factor, the R value was reduced to 0.114 for the 697 non-zero reflections. A subsequent refinement in which the Co and Cl atoms were allowed to vibrate anisotropically could improve neither the R factor nor the e.s.d.'s of the parameters. A difference Fourier map calculated at this point confirmed the crystal structure, but did not show peaks corresponding to any of the hydrogen atoms. The final atomic coordinates and temperature factors are listed in Table 2; a complete list of the observed and calculated structure factors is preserved by the Chemical Society of Japan.[12]

Table 2. The final atomic coordinates, temperature factors and their e.s.d.s.

Atom	x	y	z	B
Co	0.0632(6)	0.0000	0.1346(7)	2.38(7)
Cl	−0.2253(9)	0.1815(8)	0.5424(12)	3.4(1)
N_1	0.135(3)	0.087(2)	0.407(3)	2.4(4)
N_2	0.278(3)	−0.081(2)	0.247(4)	2.8(5)
N_3	−0.155(3)	0.086(2)	0.036(4)	3.5(5)
N_4	−0.063(3)	−0.110(2)	0.256(4)	2.6(4)
N_5	0.262(4)	0.179(3)	−0.037(4)	4.3(6)
N_6	−0.026(4)	−0.146(3)	−0.262(5)	4.6(6)
C_1	0.296(4)	0.035(3)	0.548(5)	4.6(7)
C_2	0.400(4)	−0.013(3)	0.419(5)	3.9(6)
C_3	−0.298(4)	0.009(3)	0.038(4)	3.4(5)
C_4	−0.243(4)	−0.064(3)	0.233(5)	3.7(6)
C_5	0.180(4)	0.108(3)	0.018(5)	3.0(5)
C_6	0.007(4)	−0.085(3)	−0.113(4)	2.6(5)
O	0.415(3)	−0.202(2)	−0.084(4)	4.8(5)

In order to determine the absolute configuration of the complex ion, the oscillation photographs were taken around the b axis with Cu$K\alpha$ radiation. The right-handed coordinate system was carefully used in the indexing of photographs throughout the present work. Some Bijvoet pairs are shown in Table 3, together with the observed inequality relationships. In the table, the intensities of the reflections, as calculated on the basis of the atomic coordinates in Table 2, are also listed. A comparison of the observed inequality relationships with the calculated ones indicates that the set of the atomic coordinates shown in Table 2 corresponds exactly to the absolute structure of the crystal.

Table 3. Calculated and observed intensities

$h\ k\ l$	$F_c^2(hkl)$	obsd.	$h\ \bar{k}\ l$	$F_c^2(h\bar{k}l)$
2 1 2	49	<	2 $\bar{1}$ 2	178
2 1 5	140	<	2 $\bar{1}$ 5	307
2 1 1	1857	>	2 $\bar{1}$ 1	1062
3 1 1	615	<	3 $\bar{1}$ 1	1267
4 1 1	71	<	4 $\bar{1}$ 1	238
4 1 5	178	>	4 $\bar{1}$ 5	115
6 1 $\bar{4}$	406	<	6 $\bar{1}$ $\bar{4}$	502
6 1 $\bar{5}$	317	>	6 $\bar{1}$ $\bar{5}$	186
6 1 $\bar{7}$	16	<	6 $\bar{1}$ $\bar{7}$	31
7 1 $\bar{5}$	393	>	7 $\bar{1}$ $\bar{5}$	263
7 1 $\bar{6}$	46	<	7 $\bar{1}$ $\bar{6}$	89

Result and Discussion

The absolute crystal structures viewed along the c and b axes are shown in Figs. 1 and 2 respectively. The crystal is composed of $(+)_{589}$-$[Co(CN)_2en_2]^+$, Cl^- and H_2O, which are held together mainly by ionic forces. In order to find the hydrogen bonds, the positions of the hydrogen atoms in the NH_2 groups were calculated on the assumption that the N–H bond length is 1.03 Å.[13] The data for the N–H···B hydrogen bonds (B=N, O, and Cl) are summarized in Table 4a. In the chelate ring involving N_1 and N_2, all the hydrogen atoms linked to the nitrogen atoms participate in the hydrogen bonding, while in another ring only one hydrogen atom of the individual NH_2

9) M. J. Buerger, "Vector Space," John Wiley & Sons, New York (1959), p. 271.
10) "International Tables for X-ray Crystallography," Vol. III. Kynoch Press, Birmingham (1962), p. 202.
11) R. W. James, "The Optical Principles of the Diffraction of X-rays," G. Bell & Sons, London (1948), p. 608.
12) The complete data of the F_o-F_c table are kept as Document No. 7116 at the office of the Bulletin of the Chemical Society of Japan. A copy may be secured by citing the document number and remitting, in advance, ¥400 for photoprints. Pay by check or money order payable to: Chemical Society of Japan.
13) W. C. Hamilton and J. A. Ibers, "Hydrogen Bonding in Solids," W. A. Benjamin, New York (1968), p. 260.

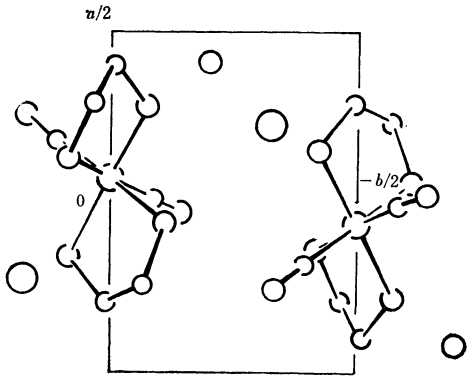

Fig. 1. The structure projected upon the (001) plane

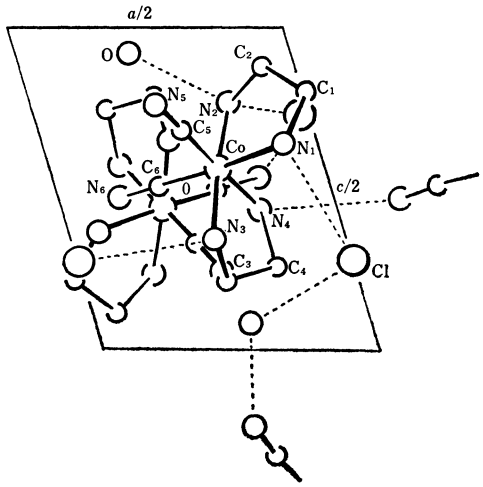

Fig. 2. The structure viewed along the *b* axis.

Tablr 4a. Possible N-H···B bonds with N···B distances less than 3.50 Å
$(+)_{589}$-$[Co(CN)_2en_2]^+$

N	B	N···B	H···B	∠N-H-B
N_1	Cl	3.49 Å	2.58 Å	147°
N_1	$N_6(-x, -1/2+y, -z)$	3.31	2.41	157
N_2	O	3.08	2.12	154
N_2	$Cl(-x, -1/2+y, 1-z)$	3.20	2.17	180
N_3	$Cl(x, y, -1+z)$	3.33	2.30	180
N_4	$N_6(x, y, 1+z)$	3.14	2.24	145

Table 4b.

$(+)_{589}$-$[CoCl_2en_2]^+$ containing Co_1[a] as a central matal atom

N	B	N···B	H···B	∠N-H-B
N_1	$Cl_4(x, y, -1+z)$	3.46 Å	2.72 Å	129°
N_1	$O_2(x, y, -1+z)$	3.31	2.55	130
N_2	Cl_5	3.49	2.65	139
N_3	$Cl_6(1-x, 1/2+y, 1-z)$	3.34	2.39	153
N_3	$O_2(x, y, -1+z)$	3.15	2.51	120
N_4	Cl_5	3.47	2.65	138

$(+)_{589}$-$[CoCl_2en_2]^+$ containing Co_2[a] as a central metal atom

N	B	N···B	H···B	∠N-H-B
N_5	Cl_1	3.40 Å	2.52 Å	143°
N_5	$O_1(x, y, -1+z)$	2.96	2.06	145
N_6	Cl_6	3.30	2.32	159
N_6	Cl_5	3.30	2.38	148
N_7	$O_1(x, y, -1+z)$	3.13	2.23	145
N_8	Cl_6	3.39	2.52	142
N_8	$Cl_2(-x, -1/2+y, 1-z)$	3.36	2.48	143

a) The atoms are labelled in the same way as in the previous paper.[15] There are two crystallographically-independent complex ions in the $(+)_{589}$-$[CoCl_2en_2]Cl \cdot H_2O$ crystal.

group takes part in the hydrogen bonding. The interatomic distance between $O(-x, 1/2+y, -z)$ and $N_5(x-1, y, z)$ is 3.08 Å, and that between $O(-x, 1/2+y, -z)$ and Cl is 3.27 Å, the Cl–O–N_5 angle being 102°. Thus, both of the hydrogen atoms of the water molecule seem to participate in the hydrogen bonding. The hydrogen bonds are shown in Fig.2 by the dashed lines.

The absolute configuration of $(+)_{589}$-$[Co(CN)_2en_2]^+$ is depicted in Fig. 3. This is in accordance with that proposed by Mason *et al.*[4] and can be denoted as $\Lambda(\lambda\lambda)$.[14] In the figure the absolute configuration of $(+)_{589}$-$[CoCl_2en_2]^+$ is also shown as a reference.[15] Both of the ethylenediamine molecules have the *ob* conformation in the present complex; thus, the complex cation can be described as having the *ob-ob* conformation. According to the conformational analysis made by Corey and Bailar,[16] the *ob-ob-ob* conformer is the least stable among the possible conformers of the trisethylenediamine complex. This probably holds true for the case of the *cis*-bisethylenediamine complex as well. As was stated in the previous paper,[15] however, the difference in the intramolecular potential energy between the most stable

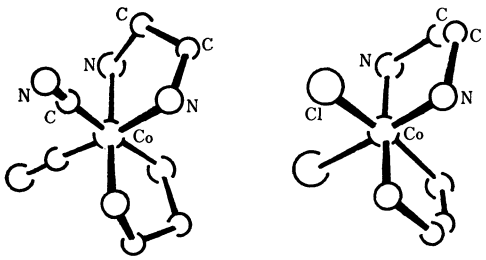

$(+)_{589}$-$[Co(CN)_2en_2]^+$ $\Lambda(\lambda\lambda)$ $(+)_{589}$-$[CoCl_2en_2]^+$ $\Lambda(\delta\delta)$

Fig. 3. The absolute configurations of the complex ions.

14) "Tentative Proposals (of the Commission on the Nomenclature of Inorganic Chemistry of IUPAC) for Nomenclature of Absolute Configurations," *Inorg. Chem.*, **9**, 1 (1970).

15) K. Matsumoto, S. Ooi, and H. Kuroya, This Bulletin, **43**, 3801 (1970).

16) E. J. Corey and J. C. Bailar, Jr., *J. Amer. Chem. Soc.*, **81**, 2620 (1959).

lel-lel conformer and the least stable *ob-ob* conformer is quite small in the bisethylenediamine complex, as compared with the case of the trisethylenediamine complex.

Ibers *et al.*[17] pointed out that the *lel-lel-lel* conformer of $[Cr\ en_3]^{3+}$ has fewer amine hydrogens which are free to form hydrogen bonds than does the *ob-ob-ob* conformer, and that the less stable latter conformer is favoured in the cases where strong hydrogen bonds can be formed. Though, in the bisethylenediamine complex, the situation is different from the case of the trisethylenediamine complex, their results seem also to be applicable to $(+)_{589}$-$[Co(CN)_2en_2]^+$ and $(+)_{589}$-$[CoCl_2en_2]^+$. In Fig. 4 are illustrated the hydrogen bonds coming out of the amine hydrogens of $(+)_{589}$-$[Co(CN)_2en_2]^+$ (*ob-ob*) and $(+)_{589}$-$[CoCl_2en_2]^+$(*lel-lel*), while the numerical data of the latter cation are listed in Table 4b. A comparison of these data with those of $(+)_{589}$-$[Co(CN)_2en_2]^+$ indicates that there are no appreciable differences in number and in length of the hydrogen bonds between these *lel-lel* and *ob-ob* conformers. Thus, the role of the hydrogen bonding in stabilizing the energetically-unfavourable *ob-ob* conformer does not seem so important in the bisethylenediamine complex as in the trisethylenediamine complex.

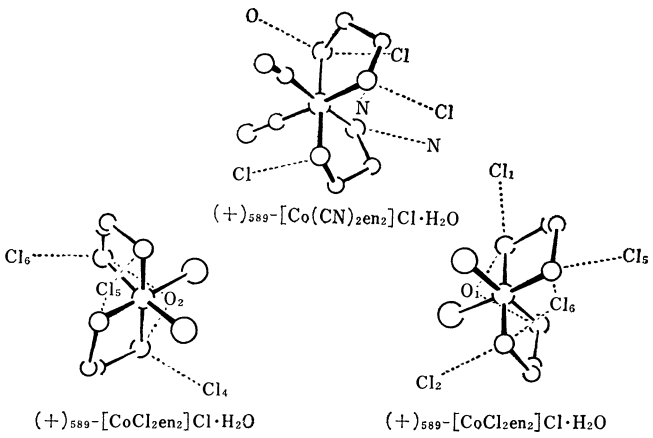

Fig. 4. Possible hydrogen bonds around the complex ions.

TABLE 5. THE BOND DISTANCES AND ANGLES IN THE COMPLEX ION

$Co-N_1$	2.00 (2) Å	N_1-Co-N_2	85 (1) °
$Co-N_2$	1.94 (3)	N_3-Co-N_4	86 (1)
$Co-N_3$	1.98 (3)	$Co-N_1-C_1$	109 (2)
$Co-N_4$	1.96 (2)	$Co-N_2-C_2$	111 (2)
$Co-C_5$	1.88 (3)	$Co-N_3-C_3$	109 (2)
$Co-C_6$	1.85 (3)	$Co-N_4-C_4$	109 (2)
N_1-C_1	1.49 (4)	$N_1-C_1-C_2$	110 (3)
N_2-C_2	1.50 (5)	$N_2-C_2-C_1$	106 (3)
N_3-C_3	1.48 (5)	$N_3-C_3-C_4$	108 (3)
N_4-C_4	1.52 (4)	$N_4-C_4-C_3$	109 (3)
C_1-C_2	1.49 (5)	$Co-C_5-N_5$	174 (3)
C_3-C_4	1.50 (5)	$Co-C_6-N_6$	175 (3)
C_5-N_5	1.18 (4)		
C_6-N_6	1.19 (4)		

The bond distances and angles are given in Table 5. The Co–C bond is nearly collinear with the C–N bond. The average value of the Co–C bond length (1.87 Å) is in good agreement with that (1.869 Å) found in $[Cr\ en_3][Co(CN)_6]\cdot 6H_2O$,[18] but slightly less than the value (1.92 Å) in $(+)_{589}$-$[Co(C_{10}H_{28}N_6)][Co(CN)_6]\cdot 2H_2O$.[19] All the bond distances and angles in the chelate rings are normal.

The authors wish to express their thanks to Dr. K. Ohkawa and Dr. J. Fujita, who provided the crystals of $(+)_{589}$-$[Co(CN)_2en_2]Cl\cdot H_2O$. We are also indebted to Mr. K. Hirotsu, who adapted the HBLS-4 and the RSSFR-3 computer programs to the FACOM 270-30 computer at Osaka City University. This research was aided in part by a Scientific Research Grant from the Ministry of Education, to which the authors' thanks are due. Furthermore, one of authors (K. M.) gratefully acknowledges the financial support of the Matsunaga Science Foundation for his research.

17) K. N. Raymond, P. W. R. Corfield, and J. A. Ibers, *Inorg. Chem.*, **7**, 842 (1968).

18) K. N. Raymond and J. A. Ibers, *ibid.*, **7**, 2333 (1968).

19) A. Muto, F. Marumo, and Y. Saito, *Acta Crystallogr.*, **B26**, 226 (1970).

The Polymerization of Silacyclopentene and -pentane Derivatives

Tsunao ARAKI, Daiyo TERUNUMA, Tamio SATO, Norio NAGAI, Mitsuharu FURUICHI, and Shigeyoshi NAKAMURA

Department of Applied Chemistry, Faculty of Science and Engineering, Saitama University, Urawa

(Received September 11, 1970)

The polymerization of 1,1,3-trimethyl-1-silacyclopentene-3 (I), 1-methyl-, 1-allyl-1,1-diallyl-1-silacyclopentenes and -pentanes with aluminum chloride was carried out. By means of an IR spectroscopic analysis of the resulting polymers, it was established that not only ring opening but also vinyl polymerization due to the C–C double bond occur in this polymerization. Attempts to polymerize I with other catalysts, such as $BF_3 \cdot OEt_2$, AIBN, KOH, and a Ziegler catalyst, were unsuccessful.

Nametkin, Vdovin *et al.*[1] reported the aluminum chloride-catalyzed ring-opening polymerization of silaheterocylic compounds. We have been interested in studying the behavior of silacyclopentene derivatives toward aluminum chloride. Since 1,1,3-trimethyl-1-silacyclopentene-3 (I) contains an unsaturated bond in the ring, it is expected that I can be polymerized either at the C–C double bond or with the opening of the ring. The polymerization of I and its derivatives has been studied in order to obtain some information about the polymerizability of the silacyclo compounds.

Results and Discussion

The silacyclo compounds synthesized in the present work are 1,1,3-trimethyl-1-silacyclopentene-3 (I),[2] 1,3-dimethyl-1-allyl-1-silacyclopentene-3 (II),[3] 1,1-diallyl-3-methyl-1-silacyclopentene-3 (III),[3] 1-methyl-1-allyl-1-silacyclopentane (IV),[3] 1-methyl-1-allyl-2,5-diphenyl-1-silacyclopentane (V),[3] 1,1-diallyl-2,5-diphenyl-1-silacyclopentane (VI), and 1,1,3-trimethyl-1-silacyclopentane (VII).[3]

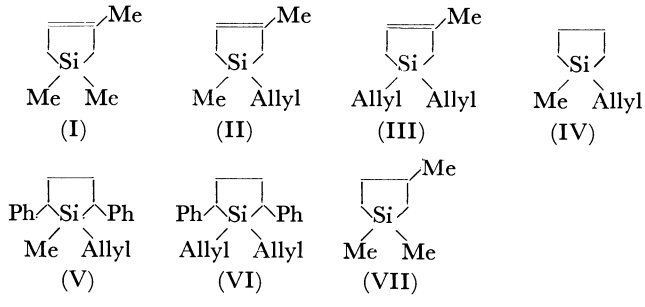

These silacyclopentenes and -pentanes were polymerized in the presence of aluminum chloride under various conditions, and studies of the solubilities and IR absorption spectra were carried out with all the polymers obtained. The IR spectrum of VII (Fig. 1) shows three absorption bands, at 1020, 1030, and 1070 cm^{-1}, attributable to a silicon-containing five-membered ring,[4] whereas polymers obtained from VII exhibit an absorption band only at 1070 cm^{-1} in the above region. The disappearance of the absorption bands at 1020 and 1030 cm^{-1} may be taken as an indication of the occurrence of ring-opening polymerization. Consequently, we used these bands for detecting the presence of the five-membered ring in the polymerization products.

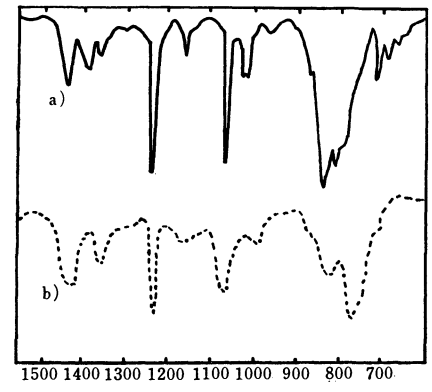

Fig. 1. IR spectra of 1,1,3-trimethyl-1-silacyclopentane (VII) and its polymer.
a) 1,1,3-Trimethyl-1-silacyclopentane (VII)
b) Polymer obtained from VII

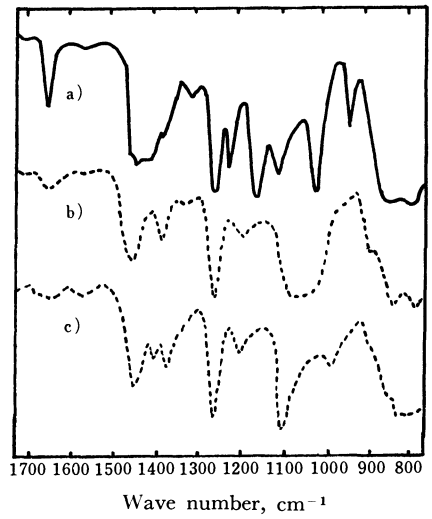

Fig. 2. IR spectra of 1,1,3-trimethyl-1-silacyclopententene-3 and its polymer.
a) 1,1,3-trimethyl-1-silacyclopentene-3 (I)
b) Polymer obtained from I by treating it with $AlCl_3$ at 21°C
c) Polymer obtained from I by treating it with $AlCl_3$ at 120°C

1) N. S. Nametkin, V. M. Vdovin, K. S. Pushchevaya, and V. I. Zav'yalov, *Izv. Akad. Nauk SSSR, Ser. Khim.*, 1453, (8) (1965).
2) D. R. Weyenberg, L. H. Toporcer, and L. E. Nelson, *J. Org. Chem.*, **33**, 1975 (1968).
3) These are new compounds.
4) V. M. Vdovin, K. S. Pushchevaya, N. A. Belikova, and R. Syltanov, *Dokl. Akad. Nauk SSSR.*, **136**, 96 (1961).

The IR spectrum of the polymer prepared from I at 21°C showed somewhat weakened absorption bands at 1020 and 1030 cm^{-1}, while the polymer prepared at 120°C showed no absorption band in this region. (Fig. 2) A similar correlation was found between the temperature of polymerization and the intensity of the IR absorption band of the C–C double bond which appears in the 1600 cm^{-1} region in the spectrum. These observations indicate that I, upon treatment with aluminum chloride at a high temperature, polymerized at the C–C double bond as well as by ring opening. On the other hand, as is shown in Table 1, the yield of the polymer obtained from I increased with an increase in the concentration of aluminum chloride in I up to 20%, beyond which the yield decreased instead. Moreover, the addition of a small amount of water to aluminum chloride was found to have no influence on the yield of polymers (Table 2). Attempts to polymerize I with radical, cationic, and anionic catalyst, such as AIBN, $BF_3 \cdot OEt_2$, and KOH, were unsuccessful (Table 4). Therefore, it is conceivable that the aluminum chloride-catalyzed polymerization of I must be explained in terms of a mechanism which is not involved in ordinary vinyl polymerization.

A mechanism of the ring-opening polymerization of five-membered saturated silaheterocyclic compounds was proposed by Nametkin *et al.*[1] on the base of a metal halide-catalyzed disproportionation.[5] This concept of coordinative attack on the α–C of silacyclopentane may also be applied to the polymerization of the unsaturated silaheterocyclic compound. Further, no noticiable polymerization occurred when I and II were treated with a Ziegler cata-

Table 1. Polymerization of 1,1,3-trimethyl-1-silacyolopentene-3 (I) with $AlCl_3$
effect of catalyst concentration

Exp. no.	Cat. concent. (mol%)	Solvent	Reaction		Yield (%)	Appearance of polymer
			Temp. (°C)	Time (hr)		
1	2.7	CCl_4	15—20	24	0.2	slightly yellow solid
2	4.8	CCl_4	15—20	24	8.6	brown solid
3	13.4	CCl_4	15—20	24	39.0	brown solid
4	21.0	CCl_4	15—20	24	65.6	brown solid
5	31.0	CCl_4	15—20	24	57.1	brown solid
6	42.0	CCl_4	15—20	24	54.7	brown solid

Table 2. Polymerization of I with $AlCl_3$
effect of a little amount of water contained in $AlCl_3$

Exp. no.	Mol% of water contained in $AlCl_3$	Concent. (mol%)	Solvent	Reaction		Yield (%)	Appearance
				Temp. (°C)	Time (hr)		
7	18.4	15.7	CCl_4	27	24	33.5	brown solid
8	28.0	16.0	CCl_4	27	24	35.6	brown solid

Table 3. Polymerization of I with $AlCl_3$
effect of reaction temperature

Exp. no.	Cat. concent. (mol %)	Solvent	Reaction		Yield (%)	Appearance of polymer
			Temp. (°C)	Time (hr)		
9	22.0	—	−70	48	not detectable	
10	20.9	CCl_4	25—30	24	66.7	brown solid
11	22.3	—	122	21	54.2	dark brown solid

Table 4. Polymerization of I with initiators other than $AlCl_3$

Exp. no.	Catalyst	Cat. concent. (mol %)	Reaction		Yield
			Temp. (°C)	Time (hr)	
12	AIBN	10	100	5	not detectable
13	$BF_3 \cdot OEt_2$	2.3	21—28	48	not detectable
14	$BF_3 \cdot OEt_2$	10	100	5	not detectable
15	KOH	37	20	27	not detectable
16	KOH	30.8	122	37	not detectable

5) G. A. Russel, *J. Amer. Chem. Soc.*, **81**, 4815 (1959).

lyst at 60—85°C, although Murahashi *et al.* reported[6] the successful polymerization of allyl derivatives of methylsilanes with a Ziegler catalyst (Table 5). This difficulty in the polymerization of silacyclopentene derivatives may be attributed to the inactivity of the double bond in the ring toward Ziegler polymerization and to that of the allylic double bond resulting from the steric hindrance of the bulky silacyclopentene ring.

In addition, in order to examine the polymerizability of the allylic double bond in silacyclopentane and -pentene derivatives, the polymerizations of II, III, IV, V, and VI were undertaken and the IR spectra of the polymers were obtained. The results of the experiment (Table 6) show that allyl derivatives of silacyclopentane (IV, V, VI) undergo polymerization faster than their methyl derivatives to give insoluble polymers; this shows that they are crosslinked. In Fig. 3 it can be seen that an absorption band of the allylic double bond which would appear at 1640 cm^{-1} is scarcely observable in the IR spectra of the resulting polymers. These facts lead to the conclusions that polymerization occurs by the allylic double bond as well as by ring opening, and that the polymers are crosslinked through allylic linkages (A) and also by linkages produced by ring opening (B):

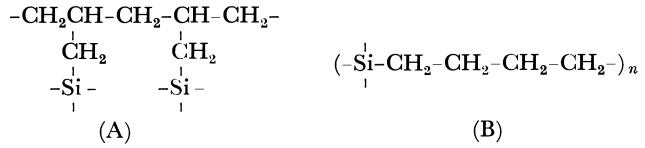

(A) (B)

Furthermore, II and III also undergo polymerization upon treatment with aluminum chloride, giving solid polymers even under such mild conditions where the analogous methyl derivative of silacyclopentene does not polymerize easily (Table 6). Moreover, a remarkable decrease in intensity of the absorption band at 1640 cm^{-1} was observed in the IR spectra of the resulting polymers. Since II and III contain two kinds of double bonds, allylic and endocyclic, the IR absorption bands of which appear in the same region, no decided conclusion about the predominance of allylic polymerization can be drawn from only these experimental data; yet, it may be considered from the foregoing discussion of the facility of the polymerization of allylic derivatives of silacyclopentane, that the allylic polymerization may also play an important role in the case of the polymerization of allyl derivatives of unsaturated silacyclic compounds.

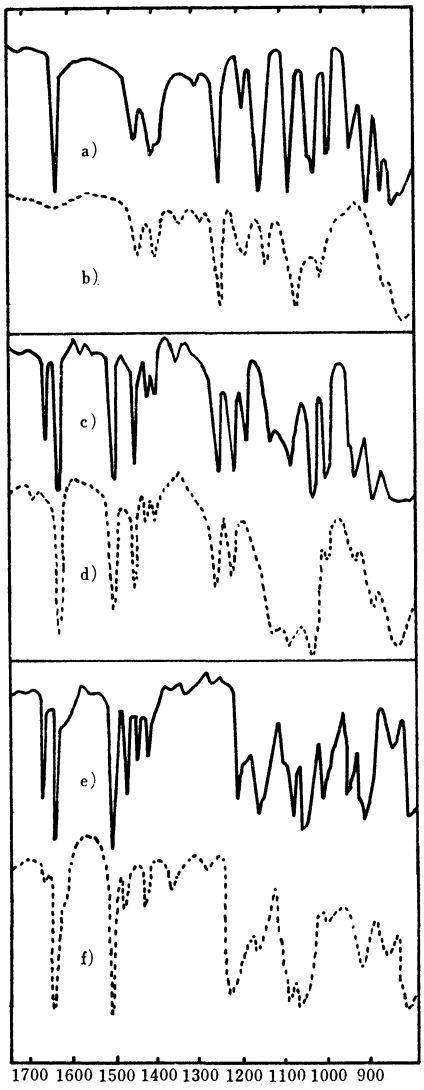

Fig. 3. IR spectra of allyl derivatives of silacyclopentane IV, V, VI, and their polymers.
a) 1-Methyl-1-allyl-1-silacyclopentane (IV)
b) Polymer obtained from IV by treating it with $AlCl_3$
c) 1-Methyl-1-allyl-2,5-diphenyl-1-silacyclopentane (V)
d) Polymer obtained from V by treating it with $AlCl_3$
e) 1,1-Diallyl-2,5-diphenyl-1-silacyclopentane (VI)
f) Polymer obtained from VI by treating it with $AlCl_3$

Table 5. Polymerization of 1,1,3-trimethyl- (I) and 1,3-dimethyl-1-allyl (II)-silacyclopentene with Ziegler catalyst

Exp. no.	Monomer	Monomer used (mmol)	$AlEt_3$ (mmol)	$TiCl_4$ (mmol)	Solvent	Reaction		Yield
						Temp. (°C)	Time (hr)	
17	I	15.9	1.98	0.80	*n*-hexane	60	25	not detectable
18	II	20.0	1.40	0.40	*n*-heptane	85	48	not detectable

6) S. Murahashi, S. Nozakura, and M. Sumi, This Bulletin, **32**, 670 (1959); *ibid.*, **33** 1760 (1960).

Table 6. Polymerization of allyl derivatives of silacyclopentene II, III and -pentane IV, V, VI with $AlCl_4$[a)]

Exp. no.	Monomer	Cat. concent. (mol%)	Reaction		Appearance of polymer
			Temp. (°C)	Time (hr)	
19	II	5	70	7	brown solid
20	III	5	70	5	brown solid
21	IV	6	60	4	brown solid
22	V	18	170	20	slightly yellow solid
23	VI	16	room temp.	5	brown solid

a) Yields were not estimated.

Table 7. Polymerization of 1,1,3-trimethyl-1-silacyclopenane (VII) with $AlCl_3$

Exp. no.	Cat. concent. (mol%)	Solvent	Reaction		Yield (%)	Appearance of polymer
			Temp. (°C)	Time (hr)		
24	17.2	CCl_4	21	24	61.3	dark brown solid
25	21.0	CCl_4	21	24	67.5	dark brown solid

Table 8. Yield and physical properties of I—VII

Monomer	Yield (%)	Bp (°C/mmHg)	n (°C)	d (°C)	Si analysis	
					Found (%)	Calcd (%)
I	28.5	123	1.4462 (25)	0.8144 (25)	22.1	22.2
II	18.4	174	1.4684 (25)	0.8443 (25)	18.3	18.4
III	15.1	209	1.4880 (25)	0.8670 (25)	15.7	15.7
IV	54.0	155	1.4631 (18)	0.8260 (18)	20.4	20.1
V	25.2	152—3/0.1	1.5748 (30)	1.0160 (30)	9.5	9.6
VI	—	170—2/0.4	1.5762 (30)	—	8.6	8.8
VII	88.6	120—123	1.4345 (20)	—	21.9	22.0

Experimental

The infrared spectra were obtained on a Shimadzu IR 27 spectrophotometer.

Preparation of Monomers. Compounds I, II, III, V, and VI were synthesized by the method of Weyenberg *et al.*[2)] Olefins, such as isoprene and styrene, were treated with diorganodichlorosilane $R_1R_2SiCl_2$ (R_1=Me, Allyl; R_2=Me, Allyl) in tetrahydrofuran in the presence of sodium dispersion under a nitrogen atmosphere. After stirring for 20—25 hr at room temperature, filtration and distillation gave I in a 28.5% yield from isoprene and dimethyldichlorosilane, II in a 18.4% yield from isoprene and methylallyldichlorosilane, III in a 15.1% yield from isoprene and diallyldichlorosilane, V in a 25.2% yield from styrene and methylallyldichlorosilane, and VI from styrene and diallyldichlorosilane. IV was synthesized from 1-chloro-1-methyl-1-silacyclopentane, which had itself been synthesized from methyltrichlorosilane and the di-Grignard reagent of 1,4-dibromobutane, by treating it with allylmagnesium bromide in Et_2O. VII was prepared from I by hydrogenating it with hydrogen gas using a Pt–C catalyst in dry *n*-hexane. The yields and physical properties of the above monomers are summarized in Table 8.

Purification of Aluminum Chloride. The $AlCl_3$ catalyst used in this polymerization was obtained from commercial $AlCl_3$ by subliming it and sealing into a glass ampoule.

Polymerization of I and VII with $AlCl_3$. Polymerization was carried out in a three-necked flask equipped with a mechanical stirrer under a nitrogen atmosphere. A monomer and an ampoule containing a given amount of $AlCl_3$ were placed in the flask. Polymerization was started by breaking the ampoule and mixing the ampoule content-$AlCl_3$ with the monomer. After stirring for 4—48 hr at various temperature, polymerization was stopped by the addition of methanol. Dissolving the product in cyclohexane, followed by reprecipitation from a cyclohexane solution, gave a soluble polymer, while an insoluble polymer was obtained from the cyclohexane-insoluble part by washing it with methanol, chloroform, and with dilute alkali.

Polymerization of I and II with a Ziegler catalyst. The triethylaluminum used in this experiment was a product of the Mitsui Toatsu Kagaku Co. *n*-Hexane and *n*-heptane were purified by shaking them with concentrated sulfuric acid, washing them with water and aqueous sodium hydroxide and, after drying over sodium wire, redistilling them under a nitrogen atmosphere just before use. A solution of $AlEt_3$ in *n*-hexane or in *n*-heptane was slowly added, using an injector, to a solution of $TiCl_4$ contained in a flask. A monomer was then added, and polymerization was allowed to proceed for a given period of time. Polymerization was stopped by adding acidic methanol (10 vol. Methanol+1 vol. conc. HCl) to the reaction mixture in the flask. The isolation of the polymer was attempted by pouring the reaction product into a large amount of methanol.

Polymerization of II, III, IV, V, and VI with $AlCl_3$. In a three-necked flask equipped with a mechanical stirrer, aluminum chloride which had been sublimed just before use was placed, a monomer was then stirred into the aluminum chloride under a nitrogen atmosphere. After the reaction flask

had been kept at the polymerization temperature for a given period of time, the resulting product was purified by reprecipitation from a cyclohexane solution into methanol, in just the same manner as has been described before.

Polymerization of I with other than $AlCl_3$. Polymerization was carried out in the same manner as in the case of the polymerization of I and VII with $AlCl_3$ except for the use of catalysts other than $AlCl_3$.

The authors are indebted to Dr. H. Nohira for his valuable discussions, to the Shinetsu Kagaku Co. for providing the dimethyldichlorosilan, and to the Mitsui Toatsu Kagaku Co. for supplying the triethylaluminum.

BULLETIN OF THE CHEMICAL SOCIETY OF JAPAN, VOL. 44, 2729—2732 (1971)

Electrolyses of 2,2-Dichloro-3-phenylcyclopropanecarboxylic Acids in Hydroxylic Solvents with a Platinum Anode*

Akira TAKEDA, Satosi WADA, and Yasuo MURAKAMI

Department of Synthetics Chemistry, School of Engineering, Okayama University, Tusima, Okayama

(Received October 27, 1970)

Electrolysis of 2,2-dichloro-3-phenylcyclopropanecarboxylic acid (**1a**) in hydroxylic solvents such as methanol and acetic acid, or in aqueous methanol with acetic acid in excess, was carried out with a platinum anode. Solvolysis rather than coupling was found to occur yielding 3,3-dichloro-1-phenylallyl methyl ether (**4a**) or 3,3-dichloro-1-phenylallyl acetate (**5a**), or both, depending on the solvent. Electrolysis of 2,2-dichloro-3-methyl-3-phenylcyclopropanecarboxylic acid (**1b**) in aqueous methanol gave ether **4b**. Structural characterization of the products was also discussed.

In the Kolbe reaction of carboxylic acids, alkyl-substitution at the α-position of the carboxyl group causes a decrease in the yield of the coupled product.[1] Similarly, the α-phenyl-substitution of acetic acid hinders the normal Kolbe coupling reaction and favors anodic reactions such as methoxylation in methanol and acetoxylation in acetic acid.[2] Wladislaw and Ayres[3] have found that the electrolysis of α-methoxyphenylacetic acid and α-methoxydiphenylacetic acid in methanol produces benzaldehyde dimethyl acetal and benzophenone dimethyl acetal in good yield. For these anodic reactions, a two electron discharge mechanism to generate carbonium ion, which in turn undergoes solvolysis, has been postulated.[4a] Formation of allylic products in the electrolysis of cyclopropanecarboxylate has been presented as a proof.[4b] We investigated the behavior of 3-substituted 2,2-dichlorocyclopropanecarboxylic acids (**1a**, R=H; **1b**, R=CH_3) in the Kolbe anodic reaction in different hydroxylic solvents to obtain more chemical evidences concerning the reaction mechanism.

Electrolysis of 46 g of **1a** conducted in aqueous methanolic solution of acetic acid partly neutralized with potassium hydroxide, with two platinum foils (1.5 cm×2 cm) as an electrode, gave 44 g of neutral oily product, whose composition obtained by gas chromatography (glc) is shown in Table 1 (Electrolysis-1).

The principal product collected by fractional distillation of the neutral product (97—120°C/2 mmHg, see Experimental) was further purified by preparative thin layer chromatography (tlc). The results (C, 55.25; H, 4.80%), correspond to the formula $C_{10}H_{10}OCl_2$. We suspected that this might be 2,2-dichloro-3-methoxycyclopropylbenzene (**2a**) ($C_{10}H_{10}OCl_2$), since the primary step of the reaction would allow the existence of both 2,2-dichloro-3-phenylcyclopropyl radical and methoxy radical. Attempted synthesis of **2a** by the addition of dichlorocarbene to β-methoxystyrene gave only α-chlorocinnamal-

Table 1. Electrolytic products of 2,2-dichloro-3-phenylcyclopropanecarboxylic acid (**1a**)

Retention time[a] Min	Retention time[a] Sec	Neutral portion Peak area (%)	Constituent
2	18	7.7	Benzaldehyde
3	18	3.1	Methyl benzoate
3	54	0.9	Acetophenone
6	18	0.3	Benzyl alcohol
10	31	66.4	3,3-Dichloro-1-phenylallyl methyl ether (**4a**)
34	24	11.6	3,3-Dichloro-1-phenylallyl acetate (**5a**)
		10.0	Others

a) Hitachi F6-D gas chromatograph; column, 10% polyneopentyl glycol succinate, 4 m/m×1 m; column temp., 150°C; injection temp., 300°C; carrier gas, N_2 (0.5 kg/cm², 50 ml/min); detector, FID.

* Presented in part before the Annual Meeting of the Chemical Society of Japan, April 1, 1968 (Osaka).

1) B. C. L. Weedon "Advances in Organic Chemistry", Vol. 1, ed. by R. A. Raphael, E. C. Taylor and H. Wynberg, Interscience Publishers, New York, N. Y. (1960), p. 1.

2) R. P. Linstead, B. R. Shephard, and B. C. L. Weedon, *J. Chem. Soc.*, **1952**, 3624.

3) B. Wladislaw and A. M. J. Ayres, *J. Org. Chem.*, **27**, 281 (1962).

4) a) E. J. Corey, N. L. Bauld, R. T. LaLonde, J. Casanova, Jr., and E. T. Kaiser, *J. Amer. Chem. Soc.*, **82**, 2645 (1960). b) T. Shono, I. Nishiguchi, S. Yamane, and R. Oda, *Tetrahedron Lett.*, **1969**, 1965.

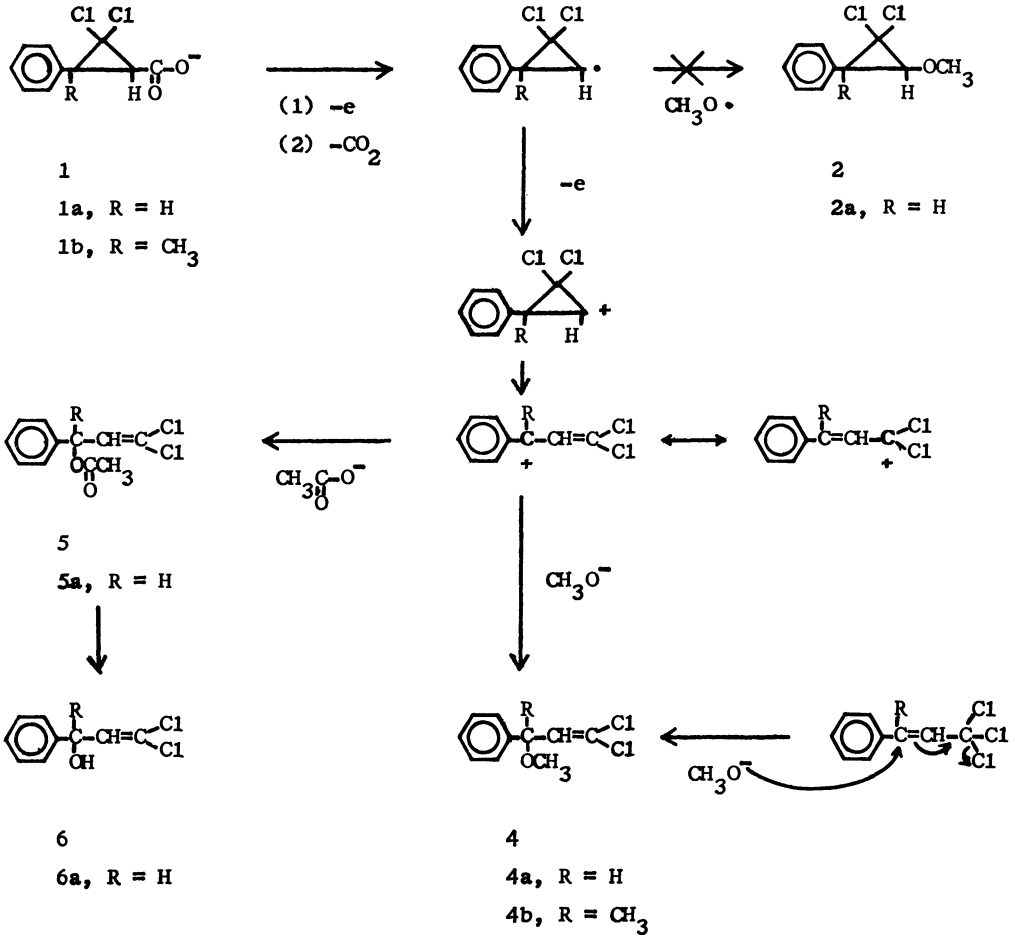

Scheme 1

dehyde (**3**).[14] Compound **3** was identified by its IR spectra, the IR spectra, melting point, and elementary analysis of its 2,4-dinitrophenylhydrazone. This suggests that compound **2a**, if its formation was possible in electrolysis, is so unstable to rearrange to **3** immediately. Actually, the presence of **3** in the electrolyte could not be detected. Thus, 3,3-dichloro-1-phenylallyl methyl ether (**4a**) was considered to be the possible structure of the principal product in Electrolysis-1. The structure has been verified by identity of its spectral data with those of the authentic sample, prepared in a different way. Preparation of 1,1-dichloro-3-methoxy-1-butene by the action of sodium methoxide to 1,1,1-trichloro-2-butene has been reported by Nesmeyanov *et al.*[5] The reaction

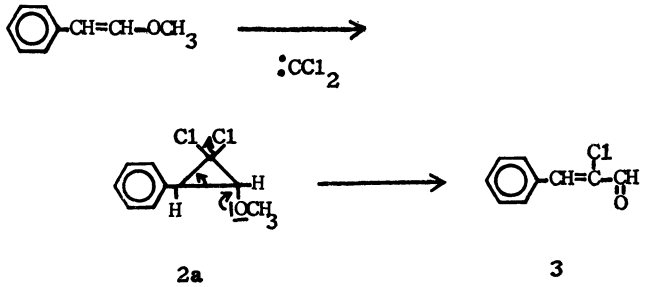

Scheme 2

of sodium methoxide with 1-phenyl-3,3,3-trichloropropene[6] afforded **4a** in 77% yield; IR (cm^{-1}, liquid) 2840 (OCH_3), 1615 (C=C), 765, and 705; NMR(τ, $CDCl_3$) 6.62 (s, 3H, $-OCH_3$), 4.95 (d, 1H, J= 8.2 Hz, C_6H_5-CH-OCH_3), 3.96(d, 1H, J=8.2 Hz, =CH–), and 2.63(s, 5H, C_6H_5–).

Identification of benzaldehyde, acetophenone, benzyl alcohol, methyl benzoate, and 3,3-dichloro-1-phenylallyl acetate (**5a**) present in the electrolyte was made by a comparison of the retention time in glc with that of the authentic sample. We failed to isolate **5a** either by preparative glc (TCD) or by tlc. However, its existence in the neutral product has been confirmed by the retention time of glc (FID), which was determined for the acetate **5a** obtained in Electrolysis-4 (see Experimental).

The anodic reaction of 2,2-dichloro-3-methyl-3-phenylcyclopropanecarboxylic acid (**1b**) carried out in a similar condition, gave products such as acetophenone, α-methylbenzyl alcohol, α-methylbenzyl acetate, and 3,3-dichloro-1-methyl-1-phenylallyl

5) A. N. Nesmeyanov, R. Kh. Fre idlina, L. I. Zakharkin, and A. B. Belyavskii, *Zh. Obshch. Khim.*, **26**, 107 (1956); *Chem. Abstr.*, **50**, 16658 (1956).

6) M. S. Kharasch, O. Reinmuth, and W. H. Urry, *J. Am. Chem. Soc.*, **69**, 1105 (1947).

methyl ether (**4b**) (Electrolysis-2). Compound **4b** was isolated by means of preparative tlc, and its structure has been elucidated by IR spectra, NMR spectra, and elementary analyses. Table 2 summarizes the compositions of the neutral product in Electrolysis-2, which were analyzed by glc (FID) at different reaction times (12 hr and 30 hr).

Table 2. Electrolytic products of 2,2-dichloro-3-methyl-3-phenylcyclopropanecarboxylic acid (**1b**)

Retention time[a] Min	Sec	Neutral portion Peak area (%) 12 hr	30 hr	Constituent
4	6	27.7	48.2	Acetophenone
4	42	0.9	2.1	α-Methylbenzyl acetate
5	45	0.6	4.5	α-Methylbenzyl alcohol
13	48	56.2	22.3	3,3-Dichloro-1-methyl-1-phenylallyl methyl ether (**4b**)
		14.6	22.9	Others

a) Hitachi F6-D gas chromatograph; column, 10% polyneopentyl glycol succinate, 4 m/m×1 m; column temp., 160°C; injection temp., 290°C; carrier gas, N_2 (0.5 kg/cm², 50 ml/min); detector, FID.

Formation of ether **4** and acetate **5** can be interpreted by assuming a two electron discharge mechanism of **1** to generate cyclopropyl cation as an intermediate, which undergoes ring opening followed by solvolysis to **4** and **5**. The reaction sequence is shown in Schemes 1 and 2. The pathway in which the carbonyl compounds such as benzaldehyde and acetophenone were formed could not be ascertained in detail. However, the fact that the content ratio of acetophenone to ether **4b** in the product of Electrolysis-2 was upset between the 12th hr and 30th hr of the reaction strongly supports the assumption that **4b** primarily produced is transformed to acetophenone during electrolysis. Accordingly, it seems reasonable to consider that methyl benzoate, acetophenone, and benzyl alcohol in Electrolysis-1 and α-methylbenzyl acetate and α-methylbenzyl alcohol in Electrolysis-2 are the secondary products from benzaldehyde in the former and from acetophenone in the latter.[7]

Electrolysis of **1a** in methanol gave **4a** in 81% yield, together with benzaldehyde in 5% yield. On the other hand, electrolysis of **1a** in acetic acid containing anhydrous sodium acetate afforded **5a** in 94% yield and benzaldehyde in 4% yield. Compound **5a** tends to be decomposed during distillation or by treatment with either tlc or glc. Therefore, the acetate **5a** was hydrolyzed to α-(2,2-dichlorovinyl) benzyl alcohol (**6a**)[8] with 1 N aqueous sodium hydroxide for structural confirmation.

Experimenal[9]

The melting points and boiling points are uncorrected. Thin layer chromatography was carried out on silica gel G (E. Merck AG, Darmstadt), where the spots of materials were detected by spraying with sulfuric acid solution of potassium permanganate (7 : 3 in wt.). Infrared spectra was determined on a Hitachi IR EPI-S2 spectrophotometer. The electrolysis was carried out using the apparatus described previously.[7b] Standard conditions of electrolysis are as follows [code number of electrolysis experiment, terminal voltage (V), current density (A/cm²), current efficiency (%)]: 1, 6—8, 0.8, 8; 2, 9—12, 0.8, 3; 3, 15, 0.4, 9; 4, 15, 0.2, 3.

Materials. Ethyl ester of **1a** was prepared from ethyl cinnamate and sodium trichloroacetate, bp 135—140°C/4 mmHg (lit. bp 103—106°C/0.3 mmHg).[10] Acid **1a** was obtained from the ester by hydrolysis, mp 101°C (lit. mp 101°C).[10] Ethyl ester of **1b** was prepared from ethyl β-methylcinnamate[11] and sodium trichloroacetate in 57% yield, bp 126—130°C/2 mmHg. Found: C, 57.05; H, 5.13%. Calcd for $C_{13}H_{14}O_2Cl_2$: C, 57.16; H, 5.17%. The acid **1b** was prepared from the ethyl ester by treatment with a mixture of fuming hydrochloric acid and acetic acid (1 : 1 V/V) in 53% yield, mp 136.5°C. Found: C, 53.67; H, 4.17%. Calcd for $C_{11}H_{10}O_2Cl_2$: C, 53.90; H, 4.11%.

Commercially available compounds were used as reference samples for tlc and glc. α-Methylbenzyl acetate was prepared, bp 103—104°C/17 mmHg.[12]

Electrolysis of 2,2-Dichloro-3-phenylcyclopropanecarboxylic Acid (1a) in Aqueous Acetic Acid-Methanol-Potassium Hydroxide Solution (Electrolysis-1). A mixture of **1a** (46.2 g, 0.2 mol) with acetic acid (120 g, 2 mol), methanol (60 ml), water (120 ml), and potassium hydroxide (16.8 g, 0.3 mol) was charged to the cell. Electrolysis was carried out for 58 hr at 30—33°C with magnetic stirring with terminal voltage 6—8 V and a current of 2.0—2.4 A. Platinum electrodes were cleaned every 5 hr to avoid deposition of resinous material on the surface until the electrolyte became weakly acidic (pH 5—6). The reaction mixture was diluted with 300 ml of water and taken up in ether. The extract was separated in the usual manner giving neutral component (43.7 g) and acidic component (0.8 g). The glc analysis of the neutral portion has been summarized in Table 1. It was fractionally distilled under reduced pressure as follows.

Fraction	Bp, °C/mmHg	Weight, g
1	50—97/2	3.5
2	97—110/2	7.9
3	110—120/2	2.1
4	120—145/2	1.3
5	Residue	5.7

By glc analysis each fraction was found to be a mixture but the principal constituent was present in fractions 2 and 3. Product identification was achieved by comparing retention times with those of authentic samples. The analytical sample of the principal constituent (**4a**) was isolated by preparative tlc,[13] bp 110—114°C (bath temp.)/4 mmHg, R_f 0.85, IR

7) a) A. Takeda, S. Torii, and H. Oka, *Tetrahedron Lett.*, **1968**, 1781. b) A. Takeda, S. Wada, S. Torii, and Y. Matui, This Bulletin, **42**, 1047 (1969).

8) D. S. Matteson and R. W. H. Mah, *J. Org. Chem.*, **28**, 2174 (1963).

9) Elementary analyses were carried out by Mr. Eiichiro Amano of our laboratory. We are indebted to Dr. Akira Suzuki, and Mr. Sigezo Simokawa, both of Hokkaido University, Sapporo, for NMR measurements.

10) J. J. K. Novak, J. Farkas and F. Sorm, *Collect. Czech. Chem. Commun.*, **26**, 2090 (1961); *Chem. Abstr.*, **55**, 27125 (1961).

11) S. Lindenbaum, *Ber.*, **50**, 1279 (1917).

12) J. Steigman and L. P. Hammett, *J. Amer. Chem. Soc.*, **59**, 2536 (1937).

13) Conditions of the preparative tlc: support, silica gel G (E. Merck AG, Darmstadt), 0.8 mm; developer, *n*-hexane-acetone (5 : 1 V/V); eluent, acetone.

(cm^{-1}, liquid) 2840 (-OCH_3), 1615 (C=C), 765, and 705; NMR (τ, $CDCl_3$) 6.62 (s, 3H, -OCH_3), 4.95 (d, 1H, J= 8.2 Hz, C_6H_5-CH-OCH_3), 3.96 (d, 1H, J=8.2 Hz, =CH-), and 2.68 (s, 1H, C_6H_5-).

Found: C, 55.25; H, 4.80%. Calcd for $C_{10}H_{10}OCl_2$: C, 55.32; H, 4.64%.

Alternative Synthesis of 3,3-Dichloro-1-phenylallyl Methyl Ether (4a). This compound was prepared in the same manner as in the synthesis of 1,1-dichloro-3-methoxy-1-butene.[5] To a sodium methoxide solution prepared by dissolving sodium (0.07 g, 0.003 g-atom) in methanol (5 m*l*) was added 1-phenyl-3,3,3-trichloropropene[6] (0.7 g, 0.003 mol). After refluxing for 150 min, the mixture was allowed to stand overnight. Water was added and the organic layer was extracted with ether, washed with water, and dried over anhydrous sodium sulfate. Removal of the solvent gave 0.5 g (77%) of the oily product, which was purified by preparative tlc; bp 110—115°C (bath temp.)/4 mmHg; IR (cm^{-1}, liquid) 2840 (-OCH_3), 1615 (C=C), 765, and 705.

Found: C, 55.51; H, 4.63%. Calcd for $C_{10}H_{10}OCl_2$: C, 55.32; H, 4.64%.

Attempted Reaction[14] of β-Methoxystyrene with Dichlorocarbene (α-Chlorocinnamaldehyde). To a stirred solution of β-methoxystyrene[15] (9.4 g, 0.07 mol) and chloroform (56.9 g, 0.48 mol) in petroleum ether (500 m*l*) was added powdered potassium *t*-butoxide (17.4 g, 0.18 mol) in small portions at −35—−40°C. Stirring was continued for additional 5 hr at room temperature. After being allowed to stand overnight, the reaction mixture was diluted with water. The organic layer was separated and washed with water several times, dried over anhydrous sodium sulfate, and concentrated. Distillation of the residue *in vacuo* gave 6.4 g (43%) of oily product boiling at 107—108°C/3 mmHg, which exhibited one large spot at R_f 0.41 and one very small spot at R_f 0.66. The constituent with the R_f value of 0.41 was purified by preparative tlc; IR (cm^{-1}, liquid) 1690 (C=O) and 1610 (C=C).

The oily product gave 2,4-dinitrophenylhydrazone quantitatively; mp 269—270°C (lit. mp 272—273°C);[16] IR (cm^{-1}, Nujol) 1620 (C=N), 1510 (NO_2), and 1340 (NO_2).

Found: C, 52.20; H, 3.44; N, 15.78%. Calcd for $C_{15}H_{11}O_4ClN_4$; C, 51.96; H, 3.20; N, 16.16%.

Electrolysis of 2,2-Dichloro-3-methyl-3-phenylcyclopropanecarboxylic Acid (1b) in Aqueous Acetic Acid-Methanol-Potassium Hydroxide Solution (Electrolysis-2). A mixture of **1b** (9.6 g, 0.04 mol) with acetic acid (24.0 g, 0.4 mol), methanol (40 m*l*), water (40 m*l*), and potassium hydroxide (3.4 g, 0.06 mol) was electrolyzed for 30 hr at 20—26°C with magnetic stirring, with terminal voltage 9—12 V and a current of 2.0—2.4 A. During the electrolysis, a 20 m*l* portion of acetic acid was added every 5 hr to the reaction mixture. It was worked up in a manner similar to that in Electrolysis-1, giving 5.4 g of the neutral portion and 0.3 g of the acidic portion. Glc analysis of the product is summarized in Table 2. Isolation of 3,3-dichloro-1-methyl-1-phenylallyl methyl ether (**4b**) from the non-ketone and non-aldehyde portion was achieved by preparative tlc;[13] bp 103—108°C (bath temp.)/2 mmHg; R_f 0.73; IR (cm^{-1}, liquid) 2840 (-OCH_3), 1610 (C=C), 767, and 705; NMR (τ, $CDCl_3$) 8.30 (s, 3H, CH_3-), 6.93 (s, 3H, -OCH_3), 3.76 (s, 1H, =CH-), and 2.75 (s, 5H, C_6H_5-).

Found: C, 56.87; H, 5.17%. Calcd for $C_{11}H_{12}OCl_2$: C, 57.16; H, 5.23%.

Electrolysis of 1a in Methanol (Electrolysis-3). To a solution of sodium methoxide (0.012 mol) in absolute methanol (200 m*l*) was added 13.8 g (0.06 mol) of **1a**. The mixture was electrolyzed at 30—31°C for 31 hr with magnetic stirring, with terminal voltage 15 V and a current of 0.9—1.2 A. After removal of the solvent under reduced pressure, the residue was dissolved in ether and separated into the neutral portion (12.4 g) and acidic portion (2.5 g) as usual. Glc analysis (FID) of the constituents of the neutral material indicated the presence of 3,3-dichloro-1-phenylallyl methyl ether (**4a**) (81.4%), benzaldehyde (4.9%), and unidentified materials (13.7%).

Electrolysis of 1a in Acetic Acid (Electrolysis-4). A solution of **1a** (4.6 g, 0.02 mol) and anhydrous sodium acetate (9.8 g, 0.12 mol) in acetic acid (144 g, 2.4 mol) was electrolyzed at 27—30°C for 55 hr with magnetic stirring, with terminal voltage 15 V and a current of 0.5—0.6 A. After working up in the usual manner, 3.3 g of neutral portion and 0.1 g of acidic portion were obtained. By glc analysis the neutral portion was found to contain **5a** (93.5%), benzaldehyde (4.3%), and a small amount (2.2%) of unidentified materials. Purification of **5a** by means of preparative tlc or glc was unsuccessful because of decomposition under such treatment. A crude sample of **5a** obtained by preparative tlc gave no correct analysis; IR (cm^{-1}, liquid) 1745 (acetate C=O), 1625 (C=C), and 1235 (ester C-O).

A mixture of 7.4 g (0.03 mol) of the crude ester and 60m*l* of 1 N aqueous sodium hydroxide was heated at 50°C for 42 hr. The hydrolysate was acidified and extracted with ether. The ethereal extract, after being washed with water, dried over anhydrous sodium sulfate, and removal of the solvent, gave 4.0 g (58%) of the crude product, which was distilled under reduced pressure to yield the following fractions.

Fraction	Bp, °C/mmHg	Weight, g
1	50—118/2.5	1.0
2	118—122/2.5	1.8
3	122—150/2.5	0.3
4	Residue	0.9

α-(2,2-Dichlorovinyl)benzyl alcohol (**6a**) was isolated from fraction 2 by preparative tlc;[13] mp 53—55°C (lit. mp 53—54°C);[8] R_f 0.58; IR (cm^{-1}, Nujol) 3200 (OH), 1615 (C=C), 1025, 760, and 705 (lit. IR 1621, 1026, 901, 895, 763, and 699);[8] NMR (τ, $CDCl_3$) 7.55 (s, 1H, -OH), 4.50 (d, 1H, J=8.2 Hz, C_6H_5-CH-OH), and 3.90 (d, 1H, J=8.2 Hz, =CH-).

Found: C, 53.13; H, 3.94%. Calcd for $C_9H_8OCl_2$: C, 53.23; H, 3.97%.

14) The synthesis of alkyl-substituted *gem*-dichlorocyclopropyl ethers has been reported by Skattebøl [L. Skattebøl, *J. Org. Chem.*, **31**, 1554 (1965)]. These ethers, when heated under reflux with an alcohol in the presence of a base, undergo ring opening with formation of acetals.

15) K. Auwers, *Ber.*, **44**, 3514 (1911).

16) G. Märkl, *Chem. Ber.*, **95**, 3003 (1962).

The 3020-cm^{-1} Band in the Infrared Absorption Spectra of Methyl Esters of Unsaturated Higher Fatty Acids

Yoshio HIRABAYASHI, Nobukatsu KATO, Masateru MIZUTA, and Hideharu ISHIHARA

Faculty of Engineering, Gifu University, Kakamigahara, Gifu

(Received November 13, 1970)

Studies were made of the infrared absorption spectra of methyl esters of oleic, elaidic, linoleic, linoelaidic, *trans*-10, *cis*-12-octadecadienoic, α-eleostearic, stearolic, stearic, 9,10-dideutero-oleic, and 9,10-dideutero-elaidic acids in the C–H stretching region. It was further confirmed that the prominent absorption bands at 3020 cm^{-1} occurring in the infrared absorption spectra of methyl esters of unsaturated higher fatty acids are assignable to the =C–H stretching vibrations of a *cis*-ethylenic double bond. The =C–D stretching vibrations of deutero-ethylenic double bonds (–CD=CD–) in methyl 9,10-dideutero-oleate and -elaidate occurred at 2250 and 2225 cm^{-1} respectively.

It is well known that, in the infrared absorption spectra of some unsaturated higher fatty acid methyl esters such as methyl oleate and methyl linoleate, a prominent absorption band occurs at 3020 cm^{-1}, which is on the higher-frequency side of the absorption bands attributable to the stretching vibrations of carbon-hydrogen bonds in the methylene and methyl groups.

Two explanations have been reported of the assignment of the absorption band at 3020 cm^{-1}. Sinclair *et al.*[1] assigned the absorption band at 3020 cm^{-1} to the =C–H stretching vibrations of an ethylenic double bond in their study of the infrared absorption spectra of oleic, linoleic, linolenic, arachidonic, and elaidic acids, and their methyl esters. On the other hand, Adams and Auxier[2] assigned the absorption band at 3020 cm^{-1} to the C–H stretching vibrations of alpha methylene groups adjacent to an ethylenic double bond on the basis of their observations that the intensity of this band diminished simultaneously with the oxidation of dipentaerythritol linoleate, and that the intensity of this band was very small in oleate, greater in linoleate, and still greater in linolenate. Privett *et al.*[3] supported the latter explanation on the basis of their observations that this band was much weaker in the conjugated peroxide-concentrate from autoxidized methyl linoleate than in oleate or in *cis-trans* conjugated linoleate; this is in accordance with the speculation that the expected structure of the peroxide, $-CH_2CH=CHCH=CHCH-$ (OOH), would have only one alpha methylene, compared to two for oleate or conjugated linoleate, and three for linoleate, and that this fact agreed best with the assignment of this band to the alpha methylene group. Fukuzumi and his collaborators[4-19] discussed, by employing this explanation, the infrared absorption spectra in liquids, methyl eicosapentaenoate, methyl docosahexaenoate, and methyl octadecatetraenoate, and further confirmed the assignment of the absorption band at 3020 cm^{-1} to the C–H stretching vibrations of alpha methylene groups adjacent to an ethylenic double bond; they did this on the basis of the observation that the intensity of this band was much smaller in conjugated methyl docosahexaenoate(with different *polytrans* conjugated polyene systems) than in non-conjugated methyl docosahexaenoate(with isolated *cis*-ethylenic double bonds only), in spite of the presence of the same number of ethylenic double bonds in both.[13]

Thus, the assignment of the absorption band at 3020 cm^{-1} seems to be not necessarily established in the field of fat and oil chemistry.

This paper will describe a study of the infrared absorption spectra of methyl esters of unsaturated higher fatty acids, such as oleic, elaidic, linoleic, linoelaidic, *trans*-10,*cis*-12-octadecadienoic, α-eleostearic, stearolic, 9,10-dideutero-oleic, and 9,10-dideutero-eladic acids, in the C–H stretching region; some information will be presented to facilitate a choice between these alternative explanations of the assignment of the absorption band at 3020 cm^{-1}.

Experimental

Materials. Each sample of the methyl esters used for the determinations of the infrared absorption spectra was prepared by the esterification of the corresponding acid (obtained by a process to be described later) with methanol by using *p*-toluenesulfonic acid as a catalyst. Its purity was estimated to be above 99%, except for methyl 9,10-dideutero-

1) R. G. Sinclair, A. F. McKay, G. S. Myers, and R. N. Jones, *J. Amer. Chem. Soc.*, **74**, 2574 (1952).
2) K. Adams and R. W. Auxier, *Official Digest*, **322**, 669 (1951).
3) O. S. Privett, W. O. Lundberg, N. A. Khan, W. E. Tolberg, and D. H. Wheeler, *J. Amer. Oil Chemists' Soc.*, **30**, 61 (1953).
4) K. Fukuzumi, S. Ito, and S. Nakanishi, *Yukagaku*, **12**, 89 (1963).
5) K. Fukuzumi and Y. Iwata, *ibid.*, **12**, 93 (1963).
6) K. Fukuzumi, Y. Iwata, and K. Kawashima, *ibid.*, **12**, 165 (1963).
7) K. Fukuzumi, S. Ito, and T. Hatachi, *ibid.*, **12**, 348 (1963).
8) K. Fukuzumi and I. Ando, *ibid.*, **12**, 351 (1963).
9) K. Fukuzumi and K. Shibata, *Yukagaku*, **12**, 396 (1963).
10) K. Fukuzumi and T. Miyakawa, *Kogyo Kagaku Zasshi*, **66**, 1320 (1963).
11) K. Fukuzumi and T. Yatsuo, *ibid.*, **66**, 1324 (1963).
12) K. Fukuzumi, Y. Iwata, and M. Takada, *ibid.*, **66**, 1675 (1963).
13) K. Fukuzumi and T. Wakita, *ibid.*, **66**, 1846 (1963).
14) K. Fukuzumi and T. Miyakawa, *ibid.*, **67**, 2065 (1964).
15) K. Fukuzumi, T. Miyakawa, and H. Morohira, *ibid.*, **67**, 2070 (1964).
16) K. Fukuzumi and T. Miyakawa, *ibid.*, **67**, 2074 (1964).
17) K. Fukuzumi and T. Maruyama, *ibid.*, **68**, 308 (1965).
18) K. Fukuzumi, *Fette·Seifen·Anstrichm.*, **71**, 104 (1969).
19) K. Fukuzumi, *ibid.*, **71**, 953 (1969).

oleate. The analysis was made by combinations of gas-liquid chromatography, infrared absorption spectrometry, and ultraviolet absorption spectrometry.

Methyl oleate was prepared from oleic acid ($n_D^{17.0}$ 1.4612) fractionated from olive oil fatty acids by the urea-adduct process: iodine value (I. V.) 85.6; $n_D^{14.4}$ 1.4543. The presence of the *trans*-isomer was not detected by means of the infrared absorption spectrum.

Methyl elaidate was prepared from elaidic acid (mp 44.5—45.0°C), which had itself been isolated by the recrystallization of an elaidinized matter obtained by the nitric acid-potassium nitrite isomerization of oleic acid: I. V. 85.6; $n_D^{16.2}$ 1.4529.

Methyl stearolate[20] was prepared from stearolic acid (mp 47.2—47.3°C), which had itself been isolated by the recrystallization of a crude product obtained by the dehydrobromination of dibromostearic acid (prepared by the bromination of oleic acid in ether) with isoamyl alcohol and potassium hydroxide: I. V. 85.7; $n_D^{17.9}$ 1.4578.

Methyl linoleate[21] was prepared from linoleic acid ($n_D^{16.3}$ 1.4711), which had itself been fractionated, by the urea-adduct process in a nitrogen atmosphere, from safflower-oil fatty acids free from unsaponifiable matter: I. V. 172.3; $n_D^{16.0}$ 1.4629. Its ultraviolet and infrared absorption spectra indicated that it contained trace amounts of the conjugated acid ester and of the *trans*-isomer.

Methyl linoelaidate[22] was prepared from linoelaidic acid (mp 27.7—28.1°C), which had itself been isolated by the recrystallization of an elaidinized matter obtained from linoleic acid by the selenium (1%) isomerization at 200—210°C for 6 hr in a nitrogen atmosphere: I. V. 172.4; $n_D^{15.0}$ 1.4620.

Methyl trans-10,cis-12-octadecadienoate[23] was prepared from *trans-10,cis-12*-octadecadienoic acid (mp 22.0—23.0°C), which had itself been isolated from a crude product obtained by the alkali isomerization of linoleic acid: $n_D^{16.0}$ 1.4750; K_{233} 92.6.

Methyl α-Eleostearate was prepared from α-eleostearic acid (mp 48.1—48.8°C) obtained by the crystallization of tung oil fatty acid: $n_D^{20.0}$ 1.5148.

Methyl 9,10-Dideutero-oleate was prepared by the partial deuteration of methyl stearolate with Lindlar's catalyst[24] in the presence of quinoline. A modified type of Herschberg's apparatus for catalytic hydrogenation was used for the deuteration. In a reduction flask were charged 0.522 g of methyl stearolate, 30 ml of cyclohexane, and 0.02 g of quinoline. The air in the apparatus was completely replaced with deuterium (purity: above 99.9 mol%, Showa Denko make). Then, 0.2 g of Lindlar's catalyst was added to the solution, and the deuterium was allowed to be absorbed at 16.5°C under atmospheric pressure with stirring. Deuteration was stopped when the uptake corresponded to one mole of deuterium per mole of methyl stearolate. The catalyst was then filtered off. The cyclohexane solution was washed with dilute hydrochloric acid (1 : 1), and the sample was obtained by distilling away the cyclohexane: I. V. 85.0; $n_D^{8.0}$ 1.4571. The presence of several per cent of *trans*-isomer was detected by studying the infrared absorption spectrum. No other impurities, such as methyl stearolate and methyl 9,9′,10,10′-tetradeutero-stearate, were detected by gas-liquid chromatography or by a study of the infrared absorption spectrum.

Methyl 9,10-Dideutero-elaidate. An elaidinized matter was obtained by the nitric acid-potassium nitrite isomerization of 9,10-dideutero-oleic acid itself prepared by the saponification of methyl 9,10-dideutero-oleate. (The process of the isomerization was the same as that of elaidic acid from oleic acid.) The elaidinized matter was recrystallized from methanol to give 9,10-dideutero-elaidic acid (mp 44.2—44.4°C), from which the sample itself was prepared: $n_D^{18.0}$ 1.4521.

Infrared Absorption Spectra. A JASCO Grating Infrared Spectrophotometer, Model IR-G, with 0.5-mm matched cells was used. The infrared absorption spectrum of each methyl ester was determined in a carbon tetrachloride solution at a concentration of 0.067 mol/l (approximately 2%) or in a liquid film at 20°C.

Results and Discussion

Table 1 shows the characteristics of the structural units possibly associated with the absorption at 3020 cm^{-1} of the methyl esters investigated. Figures 1

TABLE 1. INFRARED ABSORPTION OF UNSATURATED HIGHER FATTY ACID METHYL ESTERS AT 3020 cm^{-1}

Methyl esters	Number and configuration of double bond	Number of alpha methylene group adjacent to unsaturated linkage	Absorption at 3020 cm^{-1}
Oleate	*cis* 1	2	○[a]
Elaidate	*trans* 1	2	×
Linoleate	*cis* 2	3	○
Linoelaidate	*trans* 2	3	×*
trans-10,*cis*-12-Octadecadienoate	*cis* 1, *trans* 1	2	○
α-Eleostearate	*cis* 1, *trans* 2	2	○
Stearolate	-C≡C-	2	×
9,10-Dideutero-oleate (d_2-O)	*cis* 1	2	×
9,10-Dideutero-elaidate (d_2-E)	*trans* 1	2	×
Stearate	0	0	×

a) ○: evident. ×: not observed. ×*: the shoulder occurs at about 3030 cm^{-1}, Ref. 26.

20) K. Kino, *J. Soc. Chem. Ind. Jap.*, **32**, s. b. 187 (1929).
21) D. Swern and W. E. Parker, *J. Amer. Oil Chemists' Soc.*, **30**, 5 (1953).
22) Kass and Burr, *J. Amer. Chem. Soc.*, **61**, 1062 (1939).
23) P. L. Nichols, Jr., S. F. Herb, and R. W. Riemenschneider, *J. Amer. Chem. Soc.*, **73**, 247 (1951).
24) H. Lindlar, *Helv. Chim. Acta*, **35**, 446 (1952).

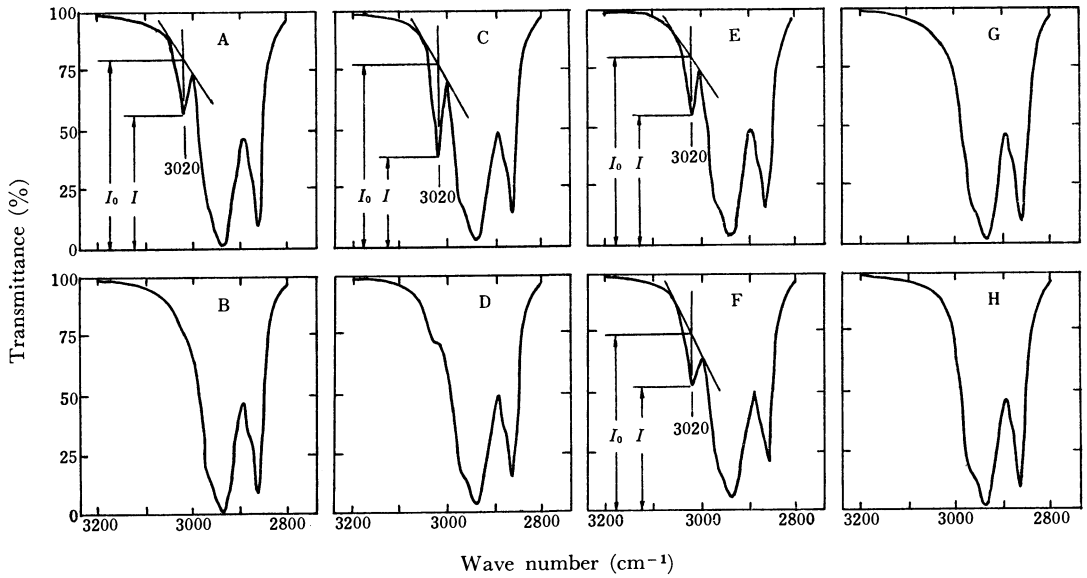

Fig. 1. Infrared spectra of fatty acid methyl esters in the C-H stretching region (in the CCl_4 solution of 0.067 mol/l and with the cell of 0.5 mm thickness).
A: methyl oleate. B: methyl elaidate. C: methyl linoleate. D: methyl linoelaidate.
E: methyl *trans*-10,*cis*-12-octadecadienoate. F: methyl α-eleostearate. G: methyl stearolate.
H: methyl stearate.

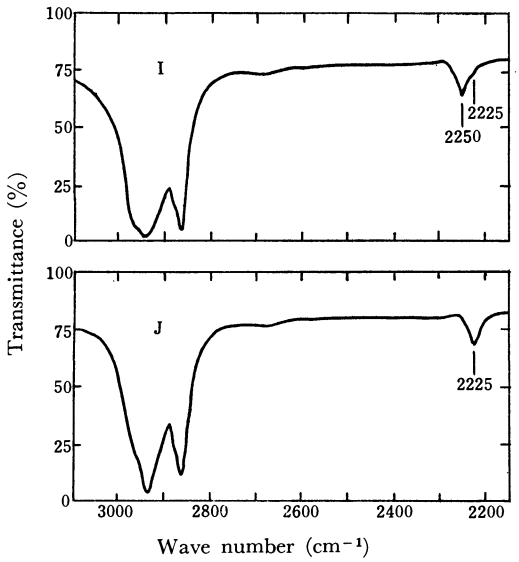

Fig. 2. Infrared spectra of methyl 9,10-dideutero-oleate (I) and methyl 9,10-dideutero-elaidate (J) in the C-H and C-D stretching regions (liquid films).

and 2 show the infrared absorption spectra of the methyl esters in the C–H stretching region.

Among the methyl esters investigated, oleate, linoleate, *trans*-10,*cis*-12-octadecadienoate, and α-eleostearate possess prominent absorption bands at 3020 cm^{-1}.[25] The accurate determination of the optical densities of these esters at the 3020-cm^{-1} bands is difficult because the bands overlap with the C–H stretching bands of the methylene and methyl groups. However, the approximate values of the optical densities, as calculated from the transmittances obtained by the base–line method at the absorption maximum at 3020 cm^{-1} (I/I_0, see Fig. 1), were as follows (in the CCl_4 solution of 0.067 mol/l and with the cell of 0.5-mm thickness): oleate, 0.156; linoleate, 0.315; *trans*-10,*cis*-12-octadecadienoate, 0.160; α-eleostearate, 0.158.

The ratio between the optical densities, 1.00 : 2.02 : 1.03 : 1.01, is almost equal to the ratio of the numbers of the *cis*-ethylenic double bonds present in the molecules, 1 : 2 : 1 : 1; there is thus no difference between isolated and conjugated systems.

On the other hand, elaidate and linoelaidate,[26] in which the ethylenic double bonds are of the *trans*-structure, do not possess prominent absorption bands at 3020 cm^{-1}, though they, like oleate and linoleate, have alpha methylene groups adjacent to the ethylenic double bonds. In addition, stearolate, methyl 9,10-dideutero-oleate (d_2-O), and methyl 9,10-dideutero-elaidate (d_2-E), which all have alpha methylene groups adjacent to a triple bond or dideutero–ethylenic double bonds (–CD=CD–), do not possess an absorption band at 3020 cm^{-1}.

From the above facts, it seems most reasonable to conclude that the absorption bands at 3020 cm^{-1} evident in the absorption spectra of methyl esters of unsaturated higher fatty acids are attributable to the =C–H stretching vibrations of *cis*-ethylenic double bonds, and not to the C–H stretching vibrations of alpha methylene groups adjacent to ethylenic double bonds.

25) Sinclair *et al.*[1] reported that similar bands were observed in oleic, linoleic, linolenic, and arachidonic acids, and proposed the spectrographic method for the determination of the degree of the *cis*-unsaturated acids, basing the procedure on the optical densities of the absorption bands at 3020 and 2920 cm^{-1}.

26) Linoelaidate possesses only a very weak absorption band at about 3030 cm^{-1}; this absorption is not attributable to the trace of the *cis*-isomer in the sample methyl ester. At any rate, its intensity is much lower than that of the absorption band at 3020 cm^{-1} in linoleate.

The propriety of the above view can be more clearly explained by the following results.

Both d_2-O and d_2-E have two alpha methylene groups adjacent to a deutero-ethylenic double bond. The deutero-ethylenic double bond in d_2-O has the *cis*-structure, while that in d_2-E has the *trans*-structure. None of them shows an absorption band at 3020 cm^{-1}. However, the absorption band attributable to the =C-D stretching vibrations of the deutero-ethylenic double bond occurs at 2250 cm^{-1} in d_2-O and at 2225 cm^{-1} in d_2-E. A slight shoulder at 2225 cm^{-1} in d_2-O indicates the formation and mixing of several per cent of the *trans*-isomer after methyl stearolate was subjected to the partial deuteration with Lindlar's catalyst in the presence of quinoline.

If it is true that the absorption band at 3020 cm^{-1} is due to the =C–H stretching vibrations of the *cis*-ethylenic double bond, the absorption at 3020 cm^{-1} will not occur in d_2-O, but the absorption band attributable to the =C-D stretching vibrations of the *cis*-deutero-ethylenic double bond corresponding to the above band must occur in d_2-O. Fortunately, spectroscopic data by Hoffmann[27] are available in this case.

The =C–D stretching frequency of a *cis*-deutero-ethylenic double bond corresponding to 3020 cm^{-1} was calculated to be 2247 cm^{-1} from the ratio of 1.344 : 1 between the stretching frequencies of the =C–H(νC–H) and the =C–D(νC–D) of Hoffmann's data; this value agrees very well with the value of 2250 cm^{-1} for that of d_2-O.

Furthermore, the =C–H stretching frequency corresponding to the 2225 cm^{-1} in d_2-E was calculated in the same way to be 2990 cm^{-1}. Sinclair *et al.*[1] reported that weak bands appeared at 2995, 3015, and 3033 cm^{-1} in the infrared absorption spectrum of elaidic acid. According to the results of the present experiments, the absorption band at 2995 cm^{-1}, among the three bands, corresponds to the =C–H stretching band of a *trans*-ethylenic double bond.

It was, thus, further confirmed that the 3020 cm^{-1} absorption band occurring in the infrared absorption spectra of methyl esters of unsaturated higher fatty acids is due to the =C–H stretching vibrations of *cis*-ethylenic double bonds in the isolated or the conjugated system, and not to the C–H stretching vibrations of alpha methylene groups (including the group existing between the two double bonds, of course) adjacent to the ethylenic double bonds.

Some reports, mentioned in the preface of this paper, have stated that the diminution in intensity of the 3020 cm^{-1} absorption band coinciding with the oxidation of methyl esters of unsaturated higher fatty acids is to be attributed to the loss of alpha methylene groups adjacent to an ethylenic double bond as a result of the formation of a hydroperoxide ($-CH=CH-CH_2- \rightarrow -CH=CH-\underset{\underset{OOH}{|}}{CH}-$),[5-8,12,13,15] as a result of the formation of a conjugated system ($-CH=CH-CH_2-CH=CH- \rightarrow -CH=CH-CH=CH-CH_2-$),[9,12,14,15] or as a result of consumption for polymerization,[10] indicating that the expected structure of the hydroperoxide obtained has the $-CH=CH-CH=CH-\underset{\underset{OOH}{|}}{CH}-$ or the $-CH=CH-\underset{\underset{OOH}{|}}{CH}-CH=CH-$ group.[3,4,12]

However, it seems to be important to consider that the decrease in this band is due to the loss of *cis*-ethylenic double bonds, including that by isomerization to the *trans*-form coinciding with the maintenance of the intact position, with migration to a new position, or with the formation of a conjugated system.

27) E. G. Hoffmann, *Ann.*, **618**, 276 (1958).

	νC-H, cm^{-1}	νC-D, cm^{-1}
cis- $C_2H_5CH=CHC_2H_5$	3010	—
cis- $C_2H_5CD=CHC_2H_5$	3010	2240
cis- $C_2H_5CD=CDC_2H_5$	—	2240

The Stereochemistry of the Reduction of 2-Substituted Cyclopentanones with Complex Aluminum Hydrides

Yasuhisa SENDA, Sekio MITSUI, Ryuko ONO*, and Shizuo HOSOKAWA**

Department of Applied Science, Tohoku University, Sendai

**Department of Science, Miyagi University of Education, Sendai*

***Ichinoseki Technical College, Ichinoseki, Iwate*

(Received November 13, 1970)

Five different 2-substituted cyclopentanones have been reduced by complex aluminum hydrides in various solvents. In the lithium aluminum hydride reduction, the proportion of *cis* 2-substituted cyclopentanols tends to increase with the steric bulkiness of the substituent. The fact that the composition of the products changes with the sort of solvent is discussed in terms of the difference in the coordinating abilities of the solvents. More *cis* 2-substituted cyclopentanols are obtained by lithium trimethoxyaluminum hydride than by the other complex aluminum hydrides used in the present study. Lithium tri-*t*-butoxyaluminum hydride and lithium aluminum hydride-aluminum chloride reduction are also investigated.

Although the stereochemistry of the reduction of substituted cyclohexanones has been studied in detail,[1] there have been only a few investigations of that of simple cyclopentanone derivatives.[1a,2]

In order to ascertain the effects of the substituents, solvents, and complex metal hydrides on the stereochemistry in the reduction of five-membered ring compounds, the reduction of representative 2-substituted cyclopentanones with lithium aluminum hydride and some of its alkoxy derivatives was undertaken in various solvents. The cyclopentanones (2-methyl-, 2-ethyl-, 2-isopropyl-, 2-cyclopentyl-, and 2-phenylcyclopentanones) were reduced with lithium aluminum hydride in diethyl ether, tetrahydrofuran, dimethoxyethane, triethylamine or pyridine, lithium trimethoxyaluminum hydride in tetrahydrofuran, lithium tri-*t*-butoxyaluminum hydride in tetrahydrofuran, and lithium aluminum hydride-aluminum chloride mixture in diethyl ether. In order to confirm the accuracy of the data, experiments were repeated at least twice in all hydride reductions, and the isomeric ratios of the products were quantitatively analyzed by gas chromatography.

Results

Reduction with Lithium Aluminum Hydride. The reduction of 2-methylcyclopentanone(I) in diethyl ether yielded a mixture of *cis* and *trans* 2-methylcyclopentanol(VI) containing 74—78% of the *trans* isomer. This is in good agreement with the result reported by Umland and Jefraim.[2a] The proportion of *trans*-VI changed with the solvents and increased in the order of diethyl ether, tetrahydrofuran, and dimethoxyethane. A similar isomer distribution was obtained in the reduction of 2-ethylcyclopentanone(II). The reduction of 2-isopropylcyclopentanone (III), which is considered to be relatively hindered ketone, gave slightly more *cis* 2-isopropylcyclopentanol (VIII) than *trans* (55—57% of *cis*-VIII) in diethyl ether. Conversely, the formation of *trans*-VIII was preferred in tetrahydrofuran, and 70% of the *trans* isomer was yielded in dimethoxyethane. On the other hand, the reduction of 2-cyclopentylcyclopentanone (IV) proceeded to give slightly more *trans*-2-cyclopentylcyclopentanol (IX) than *cis* (54% of *trans*-IX) in diethyl ether; a similar solvent dependence in the case of III was observed. The reduction of 2-phenylcyclopentanone (V) afforded 61% of *trans* 2-phenylcyclopentanol (X) in diethyl ether, while no appreciable solvent dependence on the isomer distribution was observed.

When triethylamine was used as the solvent, less of the *trans* isomer was obtained than in the ether-type sovents. Compounds I, II, III, IV, and V gave 68, 67, 37, 45, and 44% of the *trans* isomers respectively.

Lansbury and Peterson[3] reported that the reaction of lithium aluminum hydride with excess pyridine fairly rapidly formed a complex, lithium tetrakis-(1,2-dihydropyridyl)aluminate. They also reported that the complex reacted sluggishly with aliphatic ketones. Actually, the reaction of the cyclopentanones which were used in the present study with the complex gave the corresponding cyclopentanols in a yield of less than 1% even after 24 hr. However, when lithium aluminum hydride was added to the ketone-pyridine mixtures at 0°C, cyclopentanols were obtained in a good yield, so the ketone might be reduced by lithium aluminum hydride itself. In this case, the isomer distribution was similar to that obtained in dimethoxyethane. In all cases, the reduction favored the formation of the *trans* isomer.

Reduction with Lithium Tri-t-butoxyaluminum Hydride. In this case, inverse addition method was employed

1) a) H. C. Brown and H. R. Deck, *J. Amer. Chem. Soc.*, **87**, 5620 (1965) and references cited therein; b) H. C. Brown and J. Muzzio, *ibid.*, **88**, 2811 (1966); c) M. Chèrest and H. Felkin, *Tetrahedron Lett.*, **1968**, 2205; d) J. Klein, E. Dunkelblum, E. L. Eliel, and Y. Senda, *ibid.*, **1968**, 6127; e) D. N. Kirk, *ibid.*, **1969**, 1729; f) E. L. Eliel and Y. Senda, *Tetrahedron*, **26**, 2411 (1970); g) D. C. Ayres, D. N. Kirk, and R. Sawdaye, *J. Chem. Soc., B*, **1970**, 505.

2) a) J. B. Umland and M. I. Jefraim, *J. Amer. Chem. Soc.*, **78**, 2788 (1956); b) W. Hückel and G. Näher, *Chem. Ber.*, **91**, 792 (1958); c) J-C. Richer and C. Gilardeam, *Can. J. Chem.*, **43**, 3419 (1965); d) R. G. Haber and B. Fuchs, *Tetrahedron Lett.*, **1966**, 1447; e) D. V. Banthrope and H. ff. S. Davies, *J. Chem. Soc., B*, **1968**, 1356; f) B. V. Baddeley and W. L. Shao, *Tetrahedron*, **24**, 6513 (1968).

3) P. T. Lansbury and J. O. Peterson, *J. Amer. Chem. Soc.*, **85**, 2236 (1963).

TABLE 1. REDUCTION OF 2-SUBSTITUTED CYCLOPENTANONES WITH COMPLEX ALUMINUM HYDRIDES[a]

Cyclopentanone	Order of addition	Products (*trans* %)								
		$LiAlH_4$					$LiAl(OMe)_3H$	$LiAl(O\text{-}t\text{-}Bu)_3H$	$LiAlH_4$-$AlCl_3$	
		(DEE)[b]	(THF)[c]	(DME)[d]	(TEA)[e]	(PYD)[f]	(THF)	(THF)	K[g] (DEE)	T[h] (DEE)
2-Methyl-	N[i]	74[k]	80[l]	83	68	—	54[m]	—[n]	83	100
	I[j]	78	83	—	—	83	54	72	—	—
2-Ethyl-	N	72	76	75	67	—	40	—	73	100
	I	75	81	—	—	82	38	71	—	—
2-Isopropyl-	N	45[o]	66	70	37	—	28	—	47	100
	I	43	72	—	—	72	37	53	—	—
2-Cyclopentyl-	N	54	66	79	45	—	33	—	62	100
	I	—	—	—	—	75	26	68	—	—
2-Phenyl-	N	61	59	64	44	—	30	—	58	99+
	I	61	59	—	—	53	24	52	—	—

a) All are simply average percentages from more than two concordant experiments. b) Diethyl ether c) Tetrahydrofuran d) Dimethoxyethane e) Triethylamine f) Pyridine g) Under the condition of kinetic control h) Under the condition of thermodynamic control i) Normal addition j) Inverse addition k) Umland and Jefraim[2a] reported 75% *trans*, temperature not specified. l) Brown and Deck[1a] reported 76% *trans* at 0°C. m) Brown and Deck[1a] reported 56% *trans* at 0°C. n) Brown and Deck[1a] reported 71% *trans* at 0°C. o) Hückel and Näher[2b] reported 43% *trans* at 20°C.

for all experiments. Compounds I and II gave results very similar to the isomer distribution realized with lithium aluminum hydride itself. Similar results have already been observed in the reduction of substituted cyclohexanones by Haubenstock and Eliel[4] and by Brown and Deck.[1a] In the cases of III and IV, a situation different from that of I and II prevailed and the proportion of the more stable isomer was larger than that realized with lithium aluminum hydride in diethyl ether, the predominant product being the *trans* isomer. The lithium tri-*t*-butoxyaluminum hydride reduction of V gave more of the *cis* isomer than that with the parent hydride, and the ratio of the *cis* to the *trans* isomer became almost unity. In the cases of III, IV, and V, the isomer distribution was not similar to that obtained from lithium aluminum hydride reduction in diethyl ether, but was rather close to that in tetrahydrofuran.

Reduction with Lithium Trimethoxyaluminum Hydride. The replacement of hydrogen in lithium aluminum hydride by methoxyl groups resulted in an isomer distribution of the reduction products different from that resulting from reduction by other reagents. In the case of I, the amount of the more stable isomer decreased as compared to the amounts with other metal hydride reagents, and the isomer ratio became 46% of *cis* and 54% of *trans*-VI. With the increase in the steric requirement of the substituent in the 2 position, in other words, the change in the methyl group into the ethyl group, the predominant product was no longer the *trans* isomer. The *trans* 2-ethylcyclopentanol (VII) thus obtained was 38—40%.

Reduction with Lithium Aluminum Hydride - Aluminum Chloride Mixture. The reduction with a lithium aluminum hydride - aluminum chloride mixture was also performed. Under the conditions of kinetic control (in the presence of excess hydride), the ratio of *trans* 2-substituted cyclopentanols to *cis* isomers was very close to that obtained in the reduction by lithium aluminum hydride alone. However, when acetone was added at the end of the reduction, and when the reaction mixture was then refluxed for 4 hr (in the presence of excess ketone), the products of thermodynamical control, *trans* 2-substituted cyclopentanols, were predominant, probably because equilibriation occurred.

The results of the reduction of 2-substituted cyclopentanones are summarized in Table 1.

Discussion

In 1956 Dauben, Fonken, and Noyce postulated that the steric course of complex metal hydride reduction was controlled by two factors, "product development control" and "steric approach control".[5] Alternative explanations have also been devised. Richer[6] seeks it in the steric interference of the approaching nucleophile with the axial hydrogens in the 2 and 6 positions, and Chêrest and Felkin[1c] ascribe the same interference to bond-eclipsing factors. Eliel and his coworkers deduce, from the kinetic data of the reduction of several cyclohexanones by lithium tri-*t*-butoxyaluminum hydride[1d] and from a competitive rate study of complex metal hydrides,[1f] that product development control plays, at best, a minor role especially in the reduction with aluminum hydrides.

Since it has been suggested[7] that the cyclopentanone exists in the half-chair form with the maximum puckering occurring at the 3 and 4 carbon atoms, the Dreiding model shows the steric environments above and below the plane of the carbonyl group in this molecule

4) H. Haubenstock and E. L. Eliel, *ibid.*, **84**, 2363 (1962).

5) W. G. Dauben, G. J. Fonken, and D. S. Noyce, *ibid.*, **78**, 2579 (1956).

6) J-C. Richer, *J. Org. Chem.*, **30**, 324 (1965).

7) E. L. Eliel, N. L. Allinger, S. J. Angyl, and G. A. Morison, "Conformational Analysis", Interscience Publishers, Inc., New York, N. Y. (1965), p. 202.

to be identical. Consequently, it seems impossible to introduce the steric factors, for example, Felkin's eclipsing factor, to explain the prior formation of the more stable one of the two possible products. Our results indicate that, in contrast to six-membered cyclic ketones, the steric course in the resuction of relatively unhindered cyclopentanone reflects the relative stability of the two isomeric products.

As was pointed out previously, the rates of reaction of the simple cyclic model systems exhibit this order; cyclohexanone>cyclopentanone.[8] This typical I-strain order can be attributed to the influence of bond-opposition forces on the energetics of the initial and final states, reflected in the transition state.

Since it has been suggested that the complex metal hydride reduction of cyclohexanone has a reactant-like transition state,[1c,1g] the results obtained in the present study and the difference in reactivity between cyclohexanone and cyclopentanone implies that the complex aluminum hydride reduction of the latter has a product-like transition state. In the increase in the steric requirement of the substituent in the 2 position of cyclopentanone, steric approach control is also operative in the course of the reaction.

It is also evident from this study that lithium trimethoxyaluminum hydride reduction gives more of the *cis* isomer which is obtained by the hydride attack from the less-hindered side of the carbonyl group than either lithium aluminum hydride or lithium tri-*t*-butoxyaluminum hydride reduction, as has been observed previously.[1a,4] This may mean, of course, that steric approach control becomes important with the trimethoxyaluminum hydride, even in the reduction of II.

The solvent effect on the isomeric ratio of the products was observed in the lithium aluminum hydride reduction. Our results do not permit a definitive statement of the mechanism, but we have adopted the one presented below as a tentative postulate. The solvent effect on the stereochemistry of the reduction is examined in terms of steric approach control, which is the steric interference between the entering metal hydride and the substituent in the 2 position, and product development control, which is the steric interference between the developing alkoxyaluminum function and the substituent in the 2 position at the transition state. Geneste and Lamaty[9] have postulated a transition state for hydride reduction of the type shown in Fig. 1. For convenience, however, these two factors will be discussed separately.

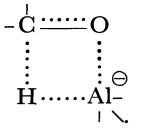

Fig. 1.

Steric Approach Control. Hydride transfer from aluminum to carbonyl carbon is facilitated by the coordination of aluminum with a Lewis base.[10] Since the greater the coordination, the more facile the hydride transfer, the ionic property of hydride may be accentuated and the distance between aluminum and hydride at the transition state seems to be longer in strongly-coordinating solvent than in a weakly-coordinating solvent. Consequently, the steric interaction of the entering hydride reagent with the substituent in the 2 position decreases with an increase in a Lewis base strength; in other words, more of the *trans* isomer will be afforded in a strongly-coordinating solvent than in a weakly-coordinating one.

Product Development Control. When the solvent coordinates on the aluminum atom of the OAl group in the 1 position, the steric strain between this OAl group and the substituent in the 2 position at the transition state may increase with the coordinating ability of the solvents; in other words, more of the *trans* isomer will be obtained in a strongly-coordinating solvent than in a weakly-coordinating one.

Jorgenson and Thacher[11] reported on the basis of a rate study of the reduction of cinnamyl alcohol with lithium aluminum hydride that tetrahydrofuran is more effective than diethyl ether as a solvent medium by a factor of 7.5, and that dimethoxyethane is better than tetrahydrofuran by a factor of 4—6.

Reportedly, the observed Lewis base strengths of the ether-type solvents used in the present study increase in the order: diethyl ether < tetrahydrofuran<dimethoxyethane,[12] an order which is identical with the coordinating ability.

Taking the above discussion of the coordinating ability of the solvents into account, the proportion of the *trans* isomer may increase in the order: diethyl ether<tetrahydrofuran<dimethoxyethane. Actually, the proportion of the *trans* isomers obtained from I, II, III, and IV agrees with the above prediction. Especially in the cases of III and IV, the solvent dependence is very significant.

Pyridine, whose base strength is stronger than that of an ether-type solvent, may behave as a solvent only under the experimental conditions employed. The isomer distributions of the products in pyridine are close to those in dimethoxyethane.

Wiberg and his coworkers[13] found that, when lithium aluminum hydride is treated with an excess of trimethylamine, the molecular compound $LiAlH_4 \cdot 2Me_3N$ is formed in the temperature range between $-40°$ to 0°C. Alternatively, Peters[14] reported that lithium aluminum hydride with one mole of trimethylamine forms $(Me_2N)_2AlH_3$. He observed, however, when an excess of trimethylamine was used, nearly all of the lithium aluminum hydride gave a compound containing lithium and aluminum in an approximately 1 to 1 molar ratio, hydrogen and loosely-bound trimethylamine. He considered that this compound may be the material that Wiberg

8) H. C. Brown and K. Ichikawa, *Tetrahedron*, **1**, 221 (1957).
9) P. Geneste and G. Lamaty, *Bull. Soc. Chim. Fr.*, 669 (1968).
10) E. I. Synder, *J. Org. Chem.*, **32**, 3531 (1967).
11) M. J. Jorgenson and A. F. Thacher, *Chem. Commun.*, **1968**, 973.
12) E. M. Annett and Y. Wu, *J. Amer. Chem. Soc.*, **84**, 1680, 1684 (1962).
13) E. Wibetg, H. Noth, and R. U. Lacal, *Z. Naturforsch.*, *B*, **11**, 486 (1956).
14) F. M. Peters, *Can. J. Chem.*, **42**, 1755 (1964).

and his coworkers observed. However he did not reach any definite conclusion. The formation of the corresponding compound, $LiAlH_4 \cdot 2Et_3N$ or $(Et_2N)_2AlH_3$, can be expected when triethylamine is used instead of trimethylamine. Either way, although triethylamine is the strongest Lewis base among the solvents used in the present study, the molecular structure of lithium aluminum hydride in triethylamine seems to be a bulkier reagent than that in other solvents and so the steric interaction of the entering hydride reagent with the substituent in the 2 position will increase.

In the reduction of 2-substituted cyclopentanones with the lithium aluminum hydride-aluminum chloride mixture, the isomeric ratios differ according to the reaction conditions. In the presence of an excess of the hydride reagent, the isomer distribution is very close to that obtained in the reduction with lithium aluminum hydride. On the other hand, when excess ketone exists in the reaction system, *trans* isomers are yielded exclusively. Presumably the complex of the *trans* isomer is much more stable than that of the *cis* isomer because of the large bulk of the $-AlCl_2$ group, which is possibly swelled further by the solvation of the aluminum with ether. The equilibrium lies certainly very much more on the side of the *trans* isomer than the corresponding equilibrium of the free 2-substituted cyclopentanols.[15]

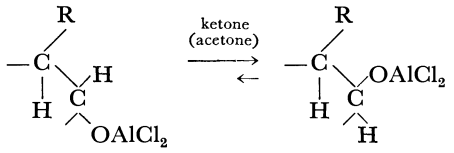

(*cis*) (*trans*)

It is also of interest to relate the conformational equilibrium constant with the steric course of metal hydride reduction. The equilibria of VI, VII, VIII, and IX were studied in dioxane with Raney nickel at 80°C. The composition of the equilibrium mixture is listed in Table 2. The equilibrium compositions of VI and VII are 76 and 75% of the *trans* isomer respectively. However, VIII whose substituent is expected to be of a larger effective size than that of the methyl or the ethyl group gives a proportion of 61% of the *trans* isomer at equilibrium, while IX yields a mixture containing 66% of the *trans* isomer.

Table 2. Equilibrium mixture of 2-substituted cyclopentanols

Cyclopentanol	*Trans* %
2-Methyl-	76[a]
2-Ethyl-	75
2-Isopropyl-	61[b]
2-Cyclopentyl-	66

a) Umland and Williams[16] reported 58% *trans* with aluminum isopropoxide-isopropanol system. b) Hückel and Näher[2a] reported more than 91% *trans* with aluminum isopropoxide-isopropanol system.

Experimental

Materials. The lithium aluminum hydride and the lithium tri-*t*-butoxyaluminum hydride were purchased from Metal Hydride Inc. The lithium trimethoxyaluminum hydride was prepared *in situ* by adding a calculated amount of anhydrous methanol solution to lithium aluminum hydride in tetrahydrofuran. The hydride solution was titrated with iodine and sodium thiosulfate. The 2-methylcyclopentanone (I) was prepared from 1-methylcyclopentene by the method of Brown and his coworkers.[17,18] The 2-ethylcyclopentanone (II) was prepared from 1-ethylcyclopentene as the above ketone (I). The 2-isopropylcyclopentanone (III) was prepared by the aldol-type condensation of cyclopentanone with acetone, followed by the hydrogenation over the palladium catalyst. The 2-cyclopentylcyclopentanone (IV) was prepared by the method reported by Hückel and his coworkers.[19] The 2-phenylcyclopentanone (V) was prepared by the rearrangement of 1-phenylcyclopentene oxide by sulfuric acid. The 1-phenylcyclopentene oxide was dissolved in ether with 5 micro drops of 6 N sulfuric acid, after which the mixture was refluxed for 32 hr.

Reduction Procedures. The gas-chromatographic analysis showed that the yields of isomeric cyclopentanols from the corresponding ketones were in the range between 75—100%.

Reduction with Lithium Aluminum Hydride or Its Alkoxy Derivatives. (*a*) *In the Ether-type Solvent*: Ketone (0.04 mol) which had been dissolved in 15 m*l* of a solvent and an equivalent amount of a hydride solution was mixed at 0°C over a period of 10—15 min. Two orders of addition, normal and inverse addition were employed. After the reaction mixture had been stirred for 30 min, water and crushed ice were added, followed by enough 10% sulfuric acid to dissolve the precipitate. The aqueous layer was extracted with ether which had been washed with saturated sodium hydrogen carbonate, and then by brine, and dried over sodium sulfate. The solution was concentrated, and the residual solution was subjected to gas chromatography.

(*b*) *In Pyridine*: Ketone (0.04 mol) was dissolved in 10 m*l* of pyridine. To this solution, maintained in an ice bath, we then added powdered lithium aluminum hydride (0.01 mol) over a period of 1—2 min. After the reaction mixture had been stirred for 30 min, water and crushed ice were added, followed by enough 10% sulfuric acid to acidify the solution. The solution was extracted with ether which had been washed with saturated sodium hydrogen carbonate, and then by brine, and dried over sodium sulfate. The solution was concentrated, and the residual solution was subjected to gas chromatography.

(*c*) *In Triethylamine*: Lithium aluminum hydride (0.01 mol) was dissolved in 15 m*l* of triethylamine. To this solution, maintained in an ice bath, we then added a ketone (0.04 mol) in 10 m*l* of triethylamine over a period of 10—15 min. After the reaction mixture had been stirred for 30 min, water and crushed ice were added, followed by enough 10% sulfuric acid to acidify the solution. The solution was

15) E. L. Eliel, *Rec. Chem. Progr.*, **22**, 129 (1961) and references cited therein.

16) J. B. Umland and B. W. Williams, *J. Org. Chem.*, **20**, 2788 (1956).

17) H. C. Brown and C. P. Garg, *J. Amer. Chem. Soc.*, **83**, 2951 (1961).

18) H. C. Brown, K. J. Murray, L. J. Murray, J. A. Sonver, and G. Zweifel, *J. Amer. Chem. Soc.*, **82**, 4233 (1960).

19) W. Hückel, M. Maier, E. Jordan, and W. Seeger, *Ann. Chem.*, **616**, 46 (1958).

20) E. L. Eliel and M. Rerick, *J. Amer. Chem. Soc.*, **82**, 1367 (1960).

extracted with ether which had been washed with saturated sodium hydrogen carbonate, and then brine, and dried over sodium sulfate. The solution was concentrated, and the residual solution was subjected to gas chromatography.

Reduction with Lithium Aluminum Hydride - Aluminum Chloride.[20] (*a*) *Under Conditions of Kinetic Control*: To a solution of 0.050 mol of aluminum chloride in 50 m*l* of ether, we added 0.014 mol of lithium aluminum hydride in ether. After stirring the homogeneous solution for 30 min, a solution of ketone (0.050 mol) in 10 m*l* of ether was added, drop by drop, over a period of 30 min. The mixture was stirred for 30 min at 0°C; then the excess hydride was destroyed with water and crushed ice, followed by enough 10% sulfuric acid to dissolve the precipitate. The aqueous layer was extracted with ether which had been washed with saturated sodium hydrogen carbonate, and then by brine, and dried over sodium sulfate. The solution was concentrated, and the residual solution was subjected to gas chromatography.

(*b*) *Under Conditions of Thermodynamic Control*: The mixed hydride was prepared as in (a) from 0.050 mol of aluminum chloride and 0.014 mol of lithium aluminum hydride. A solution of 0.050 mol of ketone in 10 m*l* of ether was added, after which the mixture was stirred for 30 min at 0°C. To this reaction mixture we then added 0.010 mol of acetone and refluxed the mixture for 4 hr; then water and crushed ice were added, followed by enough 10% sulfuric acid to dissolve the precipitate. The aqueous layer was extracted with ether, which had been washed with saturated sodium hydrogen carbonate, and then by brine, and dried over sodium sulfate. The solution was concentrated, and the residual solution was subjected to gas chromatography.

Equilibrium. Raney nickel which had been prepared from the alloy was thoroughly washed with distilled water, absolute ethanol, and dioxane. For equilibriation 0.3 g of 2-substituted cyclopentanol was dissolved in 10 m*l* of the solvent. Raney nickel (*ca* 2 g) was added in the suspension and the mixture was heated at 80°C. From time to time, samples were withdrawn and analyzed by gas chromatography. Equilibrium was deemed to be reached when several consecutive samples gave identical analyses. In all cases, equilibrium was approached from both sides. Equilibriation was usually complete after 250—300 hr.

Gas Chromatography. Hitachi K-53 or F-6 equipped with 45 m PEG goley column (0.25 or 0.50 mm in diameter) was used along with a flame ionization detector.

BULLETIN OF THE CHEMICAL SOCIETY OF JAPAN, VOL. 44, 2741—2744 (1971)

p-Nitrophenyl Phosphates as Phosphorylating Reagents of Alcohols

Kyu-Jang CHONG and Tsujiaki HATA

Department of Chemistry, Tokyo Institute of Technology, Ookayama, Meguro-ku, Tokyo

(Received December 21, 1970)

Phosphorylation of alcohols by means of P^1,P^2-di-*p*-nitrophenyl pyrophosphate and *p*-nitrophenyl phosphate was investigated. Alcohols were phosphorylated in almost quantitative yields by use of P^1,P^2-di-*p*-nitrophenyl pyrophosphate. It was found that *p*-nitrophenyl phosphate acts as an effective phosphorylating reagent for alcohols in dry pyridine to give the corresponding alkyl phosphate.

It is known that tetra-substituted[1] and tri-substituted[2] pyrophosphates can be advantageously used for the syntheses of esters of phosphoric acid and nucleotides. However, P^1,P^2-di-substituted pyrophosphates are not suitable for the phosphorylation of alcohols except when the reaction is carried out in the presence of an activator such as trichloroacetonitrile[3] or dicyclohexylcarbodiimide.[4]

In the present experiment, we tested the phosphorylation of alcohol with various P^1,P^2-di-aryl substituted pyrophosphates with the expection that the usefulness of the method would considerably increase if a generally applicable reagent, P^1,P^2-di-substituted pyrophosphate, could be found. We found that P^1,P^2-di-*p*-nitrophenyl pyrophosphate (**1**) is effctive for the phosphorylation of alcohols without using any activating reagent. As an example, when **1** was treated with excess alcohol at 80°C for three hours, alkyl *p*-nitrophenyl phosphate (**2**) and *p*-nitrophenyl phosphate (**3**) were obtained in almost quantitative yields(Table 1).

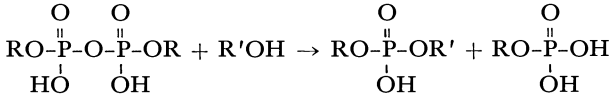

(**1**) (**2**) (**3**)

R = *p*-nitrophenyl, R' = alkyl

In the course of the experiment, it was found that alkyl phosphate (**4**) and *p*-nitrophenol were unexpectedly obtained in high yields along with **2** when the reaction was carried out in dry pyridine.

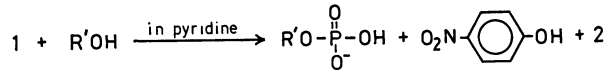

(**4**)

1) a) J. G. Moffatt and H. G. Khorana, *J. Amer. Chem. Soc.*, **79**, 3741 (1957). b) R. W. Chambers, J.G. Moffatt and H. G. Khorana, *ibid.*, **79**, 3747 (1957).

2) a) F. Cramer and K. G. Gärtner, *Chem. Ber.*, **91**, 704 (1958). b) F. Cramer and R. Wittmann, *ibid.*, **94**, 328 (1961). c) F. Cramer and D. Voges, *ibid.*, **92**, 752 (1959). d) A. M. Michelson, *Biochim. Biophys. Acta*, **91**, 1 (1964).

3) a) F. Cramer and H. J. Baldauf, *Angew. Chem.*, **72**, 627 (1960). b) F. Cramer, K. H. Scheit, and H. J. Baldauf, *Chem. Ber.*, **95**, 1657 (1962).

4) a) M. Smith, G. I. Drummond, and H. G. Khorana, *J. Amer. Chem. Soc.*, **83**, 698 (1961). b) G. M. Tener, H. G. Khorana, R. Markham, and E. H. Pol, *ibid.*, **80**, 6223 (1958). c) H. Schaller and H. G. Khorana, *ibid.*, **85**, 3828 (1963).

TABLE 2. PREPARATION OF ALKYL PHOSPHATES (4)

Alkyl	Yield (%)	Mp[a] (°C)	R_f value[b]	Formula	Calcd			Found		
					C	H	N	C	H	N
Ethyl	87	162—163	0.26	$C_8H_{14}NO_4P$	43.85	6.44	6.39	44.03	6.44	6.39
n-Propyl	90	140—142	0.28	$C_9H_{16}NO_4P$	46.34	6.92	6.01	45.82	6.94	5.82
β-Cyanoethyl	73	154.5—155	0.34	$C_9H_{13}N_2O_4P$	44.27	5.36	11.47	45.97	5.76	11.67
n-Butyl	92	141—142	0.40	$C_{10}H_{18}NO_4P$	48.58	7.34	5.66	47.82	7.39	5.51
n-Pentyl	81	136—137	0.52	$C_{11}H_{20}NO_4P$	50.56	7.72	5.36	51.98	7.97	5.67
i-Pentyl	89	140—140.5	0.55	$C_{11}H_{20}NO_4P$	50.56	7.72	5.36	50.95	7.87	5.07
n-Octyl	62	129—130	0.72	$C_{14}H_{26}NO_4P$	55.44	8.58	4.62	55.60	8.75	4.63
n-Hexadecyl	41	108—108.5[c]	0.05	$C_{16}H_{38}NO_4P$	56.64	11.21	4.13	57.84	11.32	3.80
Bornyl	53	178—180	0.64	$C_{16}H_{26}NO_4P$	58.72	8.02	4.28	58.46	8.04	4.08

a) Monoanilinium salt
b) Solvent system used: *i*-propyl alcohol, concentrated ammonium hydroxide, water (7:1:2 v/v).
c) Monoammonium salt

It seems that the formation of **4** and *p*-nitrophenol was caused by the subsequent reaction of alcohol and **3** which was initially formed. The reaction of **3** with alcohol in dry pyridine was tried separately in order to elucidate the mechanism of the formation of **4** and *p*-nitrophenol. When a mixture of **3** and excess ethanol in dry pyridine was heated at 110—120°C for two hours, ethyl phosphate and *p*-nitrophenol were obtained in high yields.

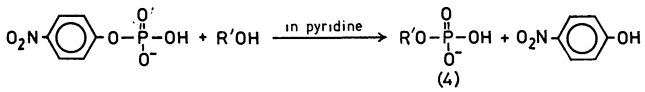

This indicates that *p*-nitrophenyl phosphate (**3**) could be successfully employed as an effective phosphorylating reagent for the synthesis of various alkyl phosphates (**4**). It was established that several alkyl phosphates (**4**) can be prepared in high yields by a simple procedure from **3** and alcohols.[5] The results are summarized in Table 2. In the above reactions, it was shown that the yields of **4** depend on the amount of alcohols. As an example, the yields of **4** remarkably decreased when one equivalent of alcohols was used.

Of various tertiary amines examined, it was shown that pyridine is superior to other amines[6] such as triethylamine, tri-*n*-butylamine and *N*-methylmorpholine. It was also found that *p*-nitrophenyl phosphate (**3**) is the most suitable reagent in comparison with other aryl phosphates such as phenyl-, *p*-tolyl-, and *o*-hydroxyphenyl phosphate.

The reaction seems to proceed through an intermediate, inner salt of *N*-phosphopyridinium hydroxide (**5**), formed from **3** and pyridine. The inner salt (**5**) in turn reacts with alcohol to give alkyl phosphate **4** as shown in the following scheme.

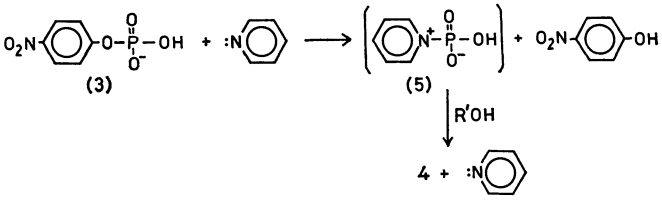

On the other hand, when *p*-nitrophenyl phosphate **3** was heated alone in pyridine, several *p*-nitrophenyl polyphosphates were obtained. These polyphosphates can be detected and determined by UV spectra and phosphorus analysis after being chromatographed on paper (Table 3).

TABLE 1. REACTION OF P^1,P^2-DI-*p*-NITROPHENYL PYROPHOSPHATE (**1**) WITH ALCOHOLS

Alcohol	Yield (%) of **2**	R_f value[a]	Yield (%) of **3**
Ethanol	60	0.83	68
n-Propanol	83	0.84	77
n-Butanol	96	0.86	94
s-Butyl alcohol	99	0.90	98
i-Pentanol	86	0.87	83
n-Octanol	96	0.89	70

a) Solvent system used: *i*-propyl alcohol, concentrated ammonium hydroxide, water (7:1:2 v/v).

5) The reason why 2 can not be used for this type of phosphorylation could not be explained.
6) In the cases of triethylamine and tri-*n*-butylamine, the reactions proceeded very sluggishly.

TABLE 3. REACTION OF *p*-NITROPHENYL PHOSPHATE (**3**) WITH PYRIDINE

(R = *p*-nitrophenyl)

Product	R_f value[a]	Yield[b] (%)	Phosphorus content[c]	$\lambda_{max}^{H_2O}$ (mμ)
Rp	0.36	15	1.00	309
Rp_2	0.24	7	2.01	292
Rp_3	0.12	0.8	3.21	289
Rp_4	0.08	0.7	4.97[d]	288
Rp_2R	0.73	4	1.00	288
Rp_3R	0.58	2	1.49	290
Rp_4R	0.47	0.6	1.90	288

a) Solvent system used: *i*-propyl alcohol, concentrated ammonium hydroxide, water, (7:1:2 v/v).
b) A remaining part was proved to be *p*-nitrophenol and inorganic phosphates.
c) Values are relative to *p*-nitrophenyl group.
d) The compound is contaminated with inorganic phosphate.

In this reaction, intermediate **5** would react with **3** to give *p*-nitrophenyl diphosphate (**6**). Compound **6** would further react with **5** to form *p*-nitrophenyl triphosphate (**7**), whereas inner salt of *p*-nitrophenylphosphopyridinium hydroxide (**8**) and inorganic phosphate would be produced by the immutability reaction of polyphosphates, reported by Moffatt.[7] Compound **8** thus successively reacts with **3**, **6**, or **7** to afford α,ω-di-*p*-nitrophenyl polyphosphates.

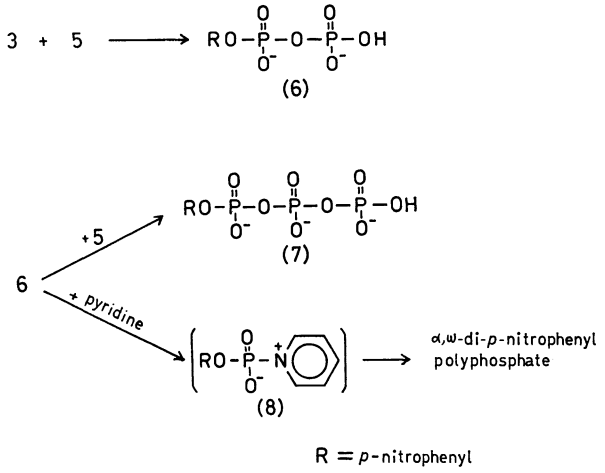

Experimental

General Procedure. Paper chromatography was performed by the descending technique using Toyo Roshi No.51 paper. Solvent system used was: isopropyl alcohol, concentrated ammonium hydroxide, water (7 : 1 : 2 v/v) (Solvent *A*). The phosphorus containing compounds were dected by means of a spray of Hanes-Isherwood reagent[8] on paper. The R_f values of all compounds described are given in Tables 1, 2, and 3. In all reactions, dried materials were employed. Pyridine was purified and dried by distillation over *p*-toluenesulfonyl chloride and stored over calcium hydride for several days. Evaporation was carried out using a rotatory evaporator under reduced pressure. *p*-Nitrophenyl phosphate was prepared by a modified procedure of Cramer[9] as described below. P^1,P^2-Di-*p*-nitrophenyl pyrophosphate was prepared according to a previous paper.[10]

p-Nitrophenyl Phosphate (3). *p*-Nitrophenyl phosphorodichloridate[11] (83.5 g) was added slowly in portions into 400 m*l* of water with vigorous stirring. The temperature was kept below 15°C during the reaction. Water was evaporated under reduced pressure at a temperature below 60°C. After addition of benzene (150 m*l*), the solution was concentrated under reduced pressure until some white crystals appeared and was allowed to stand in a refrigerator overnight. *p*-Nitrophenyl phosphate (40.0 g, 56%) was obtained as pale yellowish crystals. Recrystallization from benzene containing a trace of ether afforded white needles, mp 156—158°C. By recrystallization from the mother liquid, an additional product (14.3 g, 20%) was obtained.

Reaction of P¹,P²-*Di*-p-*nitrophenyl Pyrophosphate (1) with Alcohols.* A mixture of P^1,P^2-di-*p*-nitrophenyl pyrophosphate (**1**) (11.56 mg, 0.02 mmol) and alcohol (2.0 m*l*) was heated at 100°C for 3 hr. The mixture was then concentrated to dryness and the residue was dissolved in water (2.25 m*l*). Chromatography was performed on paper using Solvent *A* for development. Yields of the compounds, **2** and **3**, were determined spectrophotometrically using $\varepsilon_{291m\mu}=1\times10^4$ (pH 7) for alkyl *p*-nitrophenyl phosphate (**2**) and $\varepsilon_{307m\mu}=1\times10^4$ (pH 7) for *p*-nitrophenyl phosphate (**3**). The results are summarized in Table 1.

Reaction of P¹,P²-*Di*-p-*nitrophenyl Pyrophosphate (1) with Alcohols in pyridine. A Typical Procedure*: A solution of di-pyridinium salt of P^1, P^2-di-*p*-nitrophenyl pyrophosphate (**1**) (324 mg, 0.5 mmol) and *s*-butyl alcohol (3 m*l*) in dry pyridine (4 m*l*) was concentrated by heating at 100°C for 4 hr. Chromatography was performed on paper using Solvent *A*. Three products were detected: *s*-butyl *p*-nitrophenyl phosphate (R_f 0.85, 92%), *s*-butyl phosphate (R_f 0.43, 96%) and *p*-nitrophenol (R_f 0.77, 96%). The yields of the compounds were determined spectrophotometrically.

Isolation of s-*Butyl Phosphate.* The oily residue was dissolved in water (10 m*l*) and the solution was washed with three portions of ether (3×20 m*l*) for removal of *p*-nitrophenol. The aqueous layer was concentrated to dryness. The residue was dissolved in dry pyridine (5 m*l*) and pyridine was evaporated for complete removal of moisture. White precipitate was stored in desiccator over phosphorus pentoxide. The percipitate was poured into a solution of freshly distilled aniline (0.5 m*l*) in dry benzene (20 m*l*). The suspension was heated until it became clear. After cooling, the solution separated white crystals which were collected by filtration. Monoanilinium salt of *s*-butyl phosphate (102 mg) was obtained: mp 155.5—156°C. Found: C, 48.84; H, 7.91; N, 5.10%. Calcd for $C_{10}H_{18}O_4NP$: C, 48.55; H, 7.29; N, 5.66%. From the mother liquid, the salt (10 mg) was obtained. Total yield was 112 mg (92%).

Preparation of Alkyl Phosphates (3). To a solution of an anhydrous alcohol (4 m*l*) in dry pyridine (2 m*l*), *p*-nitrophenyl phosphate (438 mg, 2 mmol) was added. The mixture was heated at 120°C for 1.5 hr and then was concentrated under reduced pressure. The gummy residue was dissolved in water (50 m*l*) and washed with three portions of ether (3×10 m*l*). Ethyl, β-cyanoethyl, *n*-propyl, *n*-butyl and *i*-butyl phosphates were obtained according to method A and the other derivatives listed in Table 2 were isolated by method B.

Method A. The aqueous solution was concentrated to dryness under reduced pressure at a temperature below 15°C. The residue was dissolved in 10% of aqueous pyridine (10 m*l*) and 30% aqueous barium acetate solution was added with vigorous stirring. After 2 hr, the precipitate was collected by filtration and washed with ethyl alcohol. Amorphous barium salt of alkyl phosphate was isolated by centrifuging. The barium salt was further suspended in water and then Dowex 50W-X8 (pyridinium form) was added with stirring over a period of 2 hr. After filtration, the resin was washed with water. The filtrate and washings were combined and concentrated to dryness. The syrup was dissolved in dry pyridine and further concentrated to dryness. This was repeated three times for complete removal of moisture. After addition of freshly distilled aniline (0.4 m*l*), the precipitate was collected by filtration and recrystallization from benzene containing a small amount of ethyl alcohol gave a monoanilinium salt of alkyl phosphate (**4**). The yields and the physical properties are shown in Table 2.

7) a) W. E. Wehrli and J. G. Moffatt, *J. Amer. Chem. Soc.*, **87**, 3760 (1965). b) D. L. M. Verheyden, W. E. Wehrli, and J. G. Moffatt, *ibid.*, **87**, 2257 (1965).
8) C. A. Hanes and F. A. Isherwood, *Nature*, **164**, 1107 (1949).
9) F. Cramer and M. Winter, *Chem. Ber.*, **92**, 2761 (1959).
10) K. J. Chong, S. S. Pong, and T. Hata, This Bulletin, **43**, 2571 (1970).
11) M. Y. Kraft and V. V. Katyshkina, *Dokl. Akad. Nauk. S.S.S.R.*, **86**, 726 (1952); *Chem. Abstr.*, **47**, 8032 (1953).

Method B. The aqueous solution was concentrated to dryness. Pyridine (10 m*l*) was added and removed by evaporation. This was repeated three times for complete removal of moisture. The gummy residue was dissolved in dry chloroform (50 m*l*) and allowed to stand at room temperature for 6 hr. The pyridinium salt of inorganic phosphate was removed by filtration. After evaporation of chloroform, this procedure was repeated three times for complete removal of inorganic phosphate. The resulting residue was dissolved in chloroform and freshly distilled aniline (0.4 m*l*) was added. The precipitate was collected by filtration and recrystallization from benzene. A monoanilinium salt of alkyl phosphate (**4**) was obtained as shown in Table 2.

Reaction of p-*Nitrophenyl Phosphate (4) with Pyridine in the Absence of Alcohol.* *p*-Nitrophenyl phosphate (65.7 mg, 0.3 mmol) was dissolved in dry pyridine (0.1 m*l*). The solution was sealed and heated at 110°C for 1.5 hr. After cooling, water (3 m*l*) was added and the aqueous solution was washed with three portions of ether (3×10 m*l*). The aqueous solution was then concentrated to a small volume. Chromatography was performed on paper (Toyo Roshi No. 51) using Solvent *A* for development. The results are summarized in Table 3.

The authors heartily thank Professor Teruaki Mukaiyama for his encouragement and discussions throughout the investigation and also Mr. Masaru Koezuka for his help with elemental analysis.

BULLETIN OF THE CHEMICAL SOCIETY OF JAPAN, VOL. 44, 2744—2749 (1971)

Synthesis and Decomposition of Alkane- and Arenesulfonyl Aryl Disulfides

Yasuo ABE, Takeshige NAKABAYASHI, and Jitsuo TSURUGI

Radiation Center of Osaka Prefecture, Shinke-cho, Sakai, Osaka

(Received December 12, 1970)

Pyridinium alkane- and arenethiolsulfonates were allowed to react with arenesulfenyl chlorides, ClSAr′, to yield sulfonyl disulfides in which R is *n*-dodecyl, benzyl, phenyl, or *p*-tolyl group, and Ar′ *o*-nitrophenyl or *o*-nitro-*p*-chlorophenyl. *p*-Toluenesulfonyl *p*-nitrophenyl disulfide was also prepared by this method. IR and UV spectra of these compounds were determined and compared with those of the corresponding thiolsulfonates. Decomposition of ^{35}S-labeled *p*-toluenesulfonyl *p*-nitrophenyl disulfide, *p*-$CH_3C_6H_4SO_2S^{35}SC_6H_4NO_2$-*p*, gave ^{35}S-labeled *p*-nitrophenyl *p*-toluenethiolsulfonate, *p*-$CH_3C_6H_4SO_2{}^{35}SC_6H_4NO_2$-*p*. Triphenylphosphine was found to attack two oxygen atoms and a sulfur atom of *p*-toluenesulfonyl *o*-nitrophenyl disulfide at the same rate. The reaction of triphenylphosphine with ^{35}S-labeled *p*-toluenesulfonyl *o*- and *p*-nitrophenyl disulfides revealed that the central sulfur atom of these sulfonyl disulfides was desulfurated. This result coincides with that of the decomposition mentioned above. The susceptibility of sulfonyl disulfides containing *p*-nitrophenyl group to the decomposition and the desulfuration of the central sulfur atom of sulfonyl disulfides in general are also discussed.

Very little work has been published on the synthesis and chemistry of organic sulfonyl disulfides (RSO_2SSR', sulfonyl sulfenyl thioanhydride in IUPAC) which are considered as partially oxidized compounds of organic trisulfides. Brooker *et al.*[1] reported synthesis of arenesulfonyl aryl disulfides by the reaction of finely powdered potassium arenethiolsulfonates with arenesulfenyl chlorides in ether. Uhlenbroek and Koopmans[2] examined fungitoxic activity of arenesulfonyl trichloromethyl disulfides which were prepared by the heterogeneous reaction of potassium arenethiolsulfonates in water with trichloromethanesulfenyl chloride.

$$ArSO_2SK + ClSAr' \rightarrow ArSO_2SSAr' + KCl$$

$$ArSO_2SK + ClSCCl_3 \rightarrow ArSO_2SSCCl_3 + KCl$$

In the present work we succeeded in the homogeneous synthetic reaction in organic solvents by using pyridinium alkane- or arenethiolsulfonates and arenesulfenyl chlorides. Since most sulfenyl chlorides are sensitive to hydrolysis, our method will promise synthesis of a variety of the entitled compounds.

Some types of organic sulfonyl disulfides including several novel compounds were successfully prepared by our method, but others were found to decompose during preparation process or recrystallization procedure to give the corresponding thiolsulfonates, RSO_2SAr'. So far as our experiments show, *p*-toluenesulfonyl *p*-nitrophenyl disulfide, was only one stable compound containing *p*-nitrophenyl group as Ar′ in RSO_2SSAr'. This compound specifically labeled with ^{35}S was utilized to confirm which sulfur atom was desulfurated on the spontaneous decomposition, $RSO_2SSAr' \rightarrow RSO_2SAr'$.

In order to obtain further knowledge on sulfonyl disulfides, we allowed nonlabeled and ^{35}S-labeled *p*-toluenesulfonyl *p*- or *o*-nitrophenyl disulfides to react with triphenylphosphine, which has been known to behave as both deoxygenating and desulfurating agents.

Results and Discussion

Synthesis of Alkane- and Arenesulfonyl Aryl Disulfides. A chloroform solution of arenesulfenyl chloride (9 mmol) was added to pyridinium alkane- or arene-

1) L. G. S. Brooker, R. Child, and S. Smiles, *J. Chem. Soc.*, **1927,** 1384.

2) J. H. Uhlenbroek and M. J. Koopmans, *Rec. Trav. Chim. Pays-Bas*, **76,** 660 (1957).

Table 1. The Mp and analysis of the compounds

Compound No.	R	Ar′	Yield (%)	Mp (°C)	Anal, Found (Calcd) C	H	N	S
				RSO_2SAr'				
1	n-$C_{12}H_{25}$	o-$NO_2C_6H_4$	90.5	67— 68	51.49 (51.52)	7.21 (6.97)	3.53 (3.34)	23.2 (22.92)
2	$C_6H_5CH_2$	o-$NO_2C_6H_4$	87.7	132—135	45.87 (45.73)	3.28 (3.25)	4.05 (4.10)	28.1 (28.17)
3	C_6H_5	o-$NO_2C_6H_4$	98.5	151—153	44.31 (44.02)	2.74 (2.78)	4.19 (4.28)	29.2 (29.28)
4	p-$CH_3C_6H_4$	o-$NO_2C_6H_4$	91.4	140—141 (lit,[1] 141)				
5	n-$C_{12}H_{25}$	o-NO_2-p-ClC_6H_3	88.1	49— 51	47.71 (47.61)	6.51 (6.23)	2.71 (3.09)	
6	$C_6H_5CH_2$	o-NO_2-p-ClC_6H_3	85.7	133—134	41.52 (41.41)	2.46 (2.54)	3.62 (3.62)	
7	C_6H_5	o-NO_2-p-ClC_6H_3	93.5	131—134	39.86 (39.83)	2.20 (2.23)	3.73 (3.87)	
8	p-$CH_3C_6H_4$	o-NO_2-p-ClC_6H_3	96.2	110—113 (lit,[1] 114)				
9	p-$CH_3C_6H_4$	p-$NO_2C_6H_4$	66.6	105—106	45.94 (45.73)	3.15 (3.25)	4.28 (4.10)	27.5 (28.17)
				RSO_2SAr'				
1a	n-$C_{12}H_{25}$	o-$NO_2C_6H_4$	98.3	64— 66	55.54 (55.77)	7.48 (7.58)	3.58 (3.61)	16.5 (16.54)
2a	$C_6H_5CH_2$	o-$NO_2C_6H_4$	93.5	89— 91	50.43 (50.47)	3.49 (3.59)	4.47 (4.53)	20.8 (20.73)
3a	C_6H_5	o-$NO_2C_6H_4$	96.7	82— 83 (lit,[3] 84—85)				
4a	p-$CH_3C_6H_4$	o-$NO_2C_6H_4$	96.8	99—100	50.71 (50.47)	3.56 (3.58)	4.28 (4.53)	20.4 (20.73)
5a	n-$C_{12}H_{25}$	o-NO_2-p-ClC_6H_3	91.8	47— 49	50.59 (51.22)	6.77 (6.70)	3.32 (3.32)	
6a	$C_6H_5CH_2$	o-NO_2-p-ClC_6H_3	90.1	107—109	44.89 (45.41)	2.72 (2.94)	4.20 (4.07)	
7a	C_6H_5	o-NO_2-p-ClC_6H_3	93.9	100—102	43.52 (43.70)	2.28 (2.45)	4.41 (4.25)	
8a	p-$CH_3C_6H_4$	o-NO_2-p-ClC_6H_3	90.1	120—121	45.03 (45.41)	2.84 (2.94)	3.95 (4.07)	
9a	p-$CH_3C_6H_4$	p-$NO_2C_6H_4$	55.1	135—136 (lit,[3] 133—134)				

thiolsulfonate (10 mmol) in chloroform at room temperature. The mixture was allowed to stand overnight for completion of the reaction, and washed with water to remove the unchanged pyridinium thiolsulfonate and pyridinium hydrochloride produced. Our experience indicates that an excess

$$RSO_2S^-C_5H_5NH^+ + ClSAr' \rightarrow RSO_2SAr' + C_5H_5NH^+Cl^- \quad (1)$$

sulfenyl chloride should be avoided not to induce undesirable reaction between the sulfonyl disulfide produced and the excess sulfenyl chloride. The results are summarized in Table 1 together with the results of the corresponding thiolsulfonates for comparison. Table 1 clearly indicates that when Ar′ in RSO_2SAr' is o-nitrophenyl or o-nitro-p-chlorophenyl, the sulfonyl disulfides are stable enough to be isolated. With the exception of **9** in Table 1, synthesis of alkane- and arenesulfonyl p-nitrophenyl disulfides failed in spite of all our efforts.

Absorption Spectra of the Sulfonyl Disulfides. In Table 2 are summarized the spectral data of the sulfonyl disulfides together with those of the corresponding thiolsulfonates. As expected from the literatures on sulfones and thiolsulfonates,[4] IR bands of SO_2 group of the sulfonyl disulfides in Table 2 are in a range from 1117 to 1149 and a range from 1325 to 1338 cm^{-1}, respectively.

Leandri *et al.*[5] reported absorption spectra of some thiolsulfonates in near-UV range. The sulfonyl disulfides prepared by us are restricted to only the compounds containing nitro-aromatic rings attached to the thiol sulfur atom, because of the synthetic dif-

3) G. Leandri and A. Tundo, *Ann. Chim. Appl.*, **44**, 74 (1954).

4) L. J. Bellamy, "The Infra-red Spectra of Complex Molecules," John Wiley & Sons, New York (1954), pp. 297—299.

5) G. Leandri, A. Mangini, and A. Tundo, *J. Chem. Soc.*, **1957**, 52.

Table 2. The UV and IR spectra

Compound No.	UV $\lambda_{max}(m\mu)$[a]	UV log ε	IR ν_{SO_2} (cm^{-1})	Compound No.	UV $\lambda_{max}(m\mu)$[a]	UV log ε	IR ν_{SO_2} (cm^{-1})
1	223	4.14	1136	**1a**	228	4.26	1136
	252	4.04	1334		282[s]	3.52	1326
	278[s]	3.88					
	347	3.60					
2	225	4.32	1117	**2a**	233	4.20	1125
	250[s]	4.18	1334				1335
	345	3.61					
3	226[s]	4.32	1135	**3a**	232	4.30	1147
	265[s]	4.04	1332		278[s]	3.63	1335
	344	3.59					
4	233	4.36	1136	**4a**	234	4.36	1145
	269[s]	4.11	1335		279[s]	3.68	1334
	347	3.62					
5	235	4.20	1125	**5a**	234	4.28	1134
	250[s]	4.11	1325				1336
	355	3.51					
6	236	4.32	1125	**6a**	233	4.23	1134
	256[s]	4.20	1335				1335
	360	3.59					
7	238	4.18	1143	**7a**	235	4.32	1149
	263[s]	3.99	1332				1331
	359	3.48					
8	238	4.42	1145	**8a**	237	4.36	1144
	260[s]	4.23	1335				1338
	360	3.60					
9	239[s]	4.18	1149	**9a**	251	4.15	1151
	261[s]	4.15	1338		263	4.11	1350
	314[s]	3.86			304[s]	3.79	

a) s: shoulder

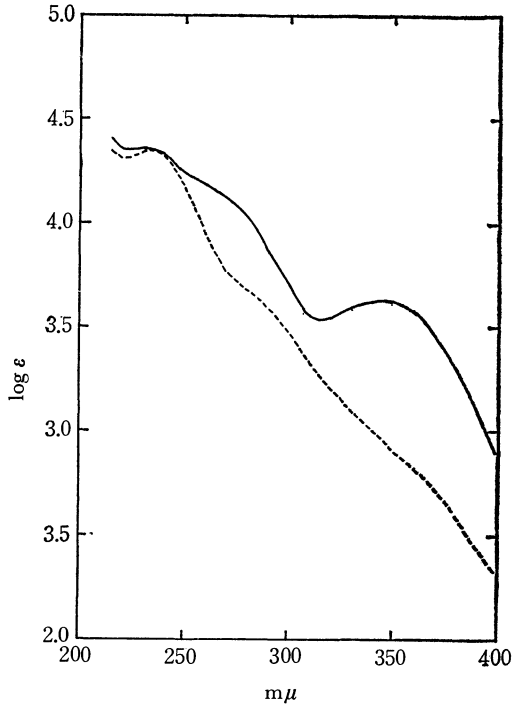

Fig. 1. The UV spectra of **4** and **4a**.
—— **4**, ---- **4a**

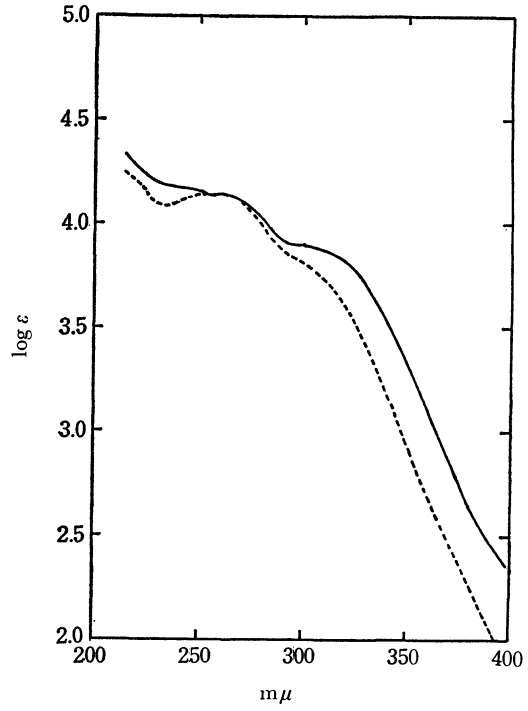

Fig. 2. The UV spectra of **9** and **9a**.
—— **9**, ---- **9a**

ficulty. Therefore, the discussion should be confined to only a limited type of the compounds. As to the UV spectra of thiolsulfonates, Leandri[5] noticed that substituent effects in benzene ring attached to sulfonyl group are comparatively small to affect the general character of the spectra. The same effect as Leandri noticed is observed in the UV spectra of the sulfonyl disulfides in Table 2. (Compare **3** with **4**, and **7** with **8** in Table 2.) Moreover, when the spectra of alkanesulfonyl aryl disulfides (**1**, **2**, **5**, and **6**) were compared with those of arenesulfonyl aryl disulfides (**3**, **4**, **7**, and **8**), prominent difference was not observed. However, the effect of a nitro-substituent in thiol-containing benzene ring is eminent depending on whether the nitro group is in *ortho* or *para* position.

Figure 1 shows UV spectra of **4** and **4a**, and Fig. 2 those of **9** and **9a**. A band at 233 mμ and a shoulder at 269 mμ of **4** in Fig. 1 are attributed to the excitations of benzene ring attached to sulfonyl group as Leandri has assigned for thiolsulfonates. (Refer to those of **4a** in Fig. 1.) However, the broad but well defined band at 347 mμ is considered specific for **4**, because **4a** exhibits only smooth running in this range.[6] We[7] reported already that di-*o*-nitrophenyl sulfide and disulfide have a maximum near 350 mμ and that structure I might contribute to the excitation of these compounds. The specific band at 347 mμ of **4** may be rationalized by the contribution of the structure I,

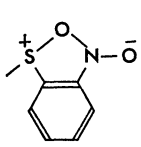
I

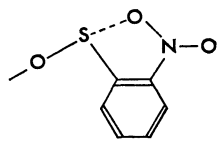
II

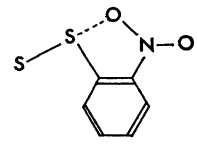
III

in which N, O, and S atoms are coplanar with benzene ring. The similar specific bands are observed in UV spectra of **1**—**3** (sulfonyl *o*-nitrophenyl disulfides), and slight bathochromic shifts are also observed in **5**—**8** (sulfonyl *o*-nitro-*p*-chlorophenyl disulfides). The smooth running down of the spectrum of thiolsulfonate **4a** in this range suggests that coplanarity in structure I disappeared because of steric effect of adjacent SO_2 group or that the electrons of sulfur atom attached to nitrobenzene ring are intensively withdrawn by SO_2 group.

A shoulder near 310 mμ of **9** in Fig. 2 may be assigned to the excited structure of *p*-nitrobenzenesulfenyl group, because di-*p*-nitrophenyl disulfide was reported[8] to exhibit a maximum at 316 mμ. The similar shoulder of **9a** is shifted to shorter wavelength. This suggests that the excited state of *p*-nitrobenzenesulfenyl group is disturbed to some extent by the intensive electron-withdrawing effect of adjacent SO_2 group, while in **9** this effect is weakened to a greater extent by the intervening sulfur atom.

The stability of the sulfonyl disulfides containing *o*-nitrophenyl or *o*-nitro-*p*-chlorophenyl group (compounds **1**—**8**) may be explained as follows. Hamilton and La Placa[9] attributed the stability of *o*-nitrobenzenesulfenate to a resonance stability originated from the coplanarity as indicated in II and a specific nonbonding interaction of S and O atoms of sulfenic acid group with almost linear O—S···O configuration. The stability of the compounds **1**—**8** may be rationalized by the same argument mentioned above (III).

The Decomposition of ^{35}S*-labeled* p-*Toluenesulfonyl* p-*Nitrophenyl Disulfide (labeled* ***9****).* As stated above, **9** was obtained as only one stable compound among sulfonyl *p*-nitrophenyl disulfides. We examined the decomposition of the ^{35}S-labeled **9** by submitting to several recrystallizations from a polar solvent. This labeled compound was prepared as shown below.

$$p\text{-}NO_2C_6H_4{}^{35}S{}^{35}SC_6H_4NO_2\text{-}p + Cl_2 \rightarrow 2\,p\text{-}NO_2C_6H_4{}^{35}SCl$$

$$p\text{-}CH_3C_6H_4SO_2S^-C_5H_5NH^+ + p\text{-}NO_2C_6H_4{}^{35}SCl \rightarrow p\text{-}CH_3C_6H_4SO_2S{}^{35}SC_6H_4NO_2\text{-}p \quad \text{(labeled 9)}$$

This compound, after recrystallizations of more than ten times, was found to be converted into *p*-nitrophenyl *p*-toluenethiolsulfonate (labeled **9a**), of which specific activity was determined as 1,395 dpm/mg. The standard labeled **9a** for radioassay was prepared from the same *p*-nitrobenzenesulfenyl chloride as for the labeled **9**. The specific activity of the standard **9a** was found 1,427 dpm/mg and coincided with that (1,395 dpm/mg) of the decomposition product from the labeled **9** within experimental error. Therefore, we can conclude that the central sulfur atom of **9** is desulfurated on the spontaneous decomposition. This conclusion does not contradict with the explanation on the stability of compounds **1**—**8** mentioned above. The failure to synthesize other compounds than **9** which contain *p*-nitrophenyl as Ar′ in RSO_2-SSAr′ may be ascribed to the extreme susceptibility to spontaneous decomposition.[10]

$$p\text{-}CH_3C_6H_4SO_2S{}^{35}SC_6H_4NO_2\text{-}p \rightarrow p\text{-}CH_3C_6H_4SO_2{}^{35}SC_6H_4NO_2\text{-}p \quad (2)$$
(labeled **9**) (labeled **9a**)

The Reaction of Triphenylphosphine with p-*Toluenesulfonyl* o-*Nitrophenyl Disulfide (****4****).* Hayashi *et al.*[11] subjected thiolsulfonates and disulfonyl sulfides

6) Leandri *et al.*[5] reported that UV spectra of phenyl *o*- and *p*-nitrobenzenethiolsulfonates, when determined in ethanol, have each maximum at 400 and 340 mμ respectively, besides those determined in cyclohexane. They ascribed these additional bands to specific interaction between alcohol and the nitrobenzenethio-group. However, as shown in Figs. 1 and 2 (**4a** and **9a**), we could not observe such additional bands as they reported.

7) T. Nakabayashi and J. Tsurugi, *J. Org. Chem.*, **26**, 2482 (1961).

8) E. Campaigne, J. Tsurugi, and W. W. Meyer, *ibid.* **26**, 2486 (1961).

9) W. C. Hamilton and S. J. La Placa, *J. Amer. Chem. Soc.*, **86**, 2289 (1964).

10) We attempted to prepare also alkanesulfonyl alkyl disulfides like $C_6H_5CH_2SO_2SSCH_2C_6H_5$ and arenesulfonyl aryl disulfides such as $C_6H_5SO_2SSC_6H_5$, but failed in spite of all our efforts. The order of the susceptibility of sulfonyl disulfide to the decomposition to thiolsulfonate is estimated by the numbers of times of recrystallization (from ethanol) to be converted to the corresponding thiolsulfonate. The order is: alkanesulfonyl alkyl> arenesulfonyl aryl>arenesulfonyl *p*-nitrophenyl.

(RSO_2SSO_2R') to deoxygenation and desulfuration with triphenylphosphine and concluded as summarized below. It seems interesting to examine whether or

$$RSO_2SR' \xrightarrow[\text{reflux}]{Ph_3P} RSOSR' \xrightarrow[\text{reflux}]{Ph_3P} RSSR'$$

$$RSO_2SSO_2R' \xrightarrow[\text{reflux}]{4\ Ph_3P} RSSSR' \xrightarrow[\text{reflux}]{Ph_3P} RSSR'$$

not sulfonyl disulfide behaves similarly to thiolsulfonate or disulfonyl sulfide. Benzene solution of **4** (1 mmol) was added to equimolar amount of triphenylphosphine in ethanol. After the mixture was allowed to stand for one hour at room temperature, glc analysis indicated that 0.67 mmol of triphenylphosphine oxide and 0.33 mmol of triphenylphosphine sulfide were produced. This result shows that under these conditions two oxygen atoms of sulfonyl group and a sulfur atom were eliminated with triphenylphosphine, and makes a clear contrast to the stepwise deoxygenation and desulfuration of thiolsulfonate and disulfonyl sulfide.

The Reaction of Triphenylphosphine with ^{35}S-Labeled p-*Toluenesulfonyl* o- *and* p-*Nitrophenyl Disulfides (Labeled* ***4*** *and* ***9***). In order to confirm which sulfur atom of sulfonyl disulfide is desulfurated, we utilized ^{35}S-labeled **4**, which was prepared as shown below. The specific activity of the labeled **4** recrystallized from

$$p\text{-}CH_3C_6H_4SO_2^-C_5H_5NH^+ + {}^{35}S \rightarrow p\text{-}CH_3C_6H_4SO_2{}^{35}S^-C_5H_5NH^+$$

$$p\text{-}CH_3C_6H_4SO_2{}^{35}S^-C_5H_5NH^+ + o\text{-}NO_2C_6H_4SCl \rightarrow p\text{-}CH_3C_6H_4SO_2{}^{35}SSC_6H_4NO_2\text{-}o$$

(labeled **4**)

carbon tetrachloride was 25,634 dpm/mg. One mmol of the labeled **4** in benzene was allowed to react with three mmol of triphenylphosphine in ethanol at room temperature for one hour. An aliquot of the reaction mixture, when determined by GLC, showed 2 : 1 molar ratio of phosphine oxide and sulfide produced. Triphenylphosphine sulfide was separated from the mixture by recrystallization from ethanol. Specific activity of the sulfide obtained was 29,855 dpm/mg. The standard triphenylphosphine sulfide for radioassay was prepared from triphenylphosphine and the same radioactive sulfur as used for the labeled **4**. The specific activity of this standard was found 29,867 dpm/mg and coincided with that (29,855) of the desulfuration product from the labeled **4**. Therefore,

$$p\text{-}CH_3C_6H_4SO_2{}^{35}SSC_6H_4NO_2\text{-}o + 3(C_6H_5)_3P \rightarrow 2(C_6H_5)_3PO + (C_6H_5)_3P{}^{35}S + p\text{-}CH_3C_6H_4SSC_6H_4NO_2\text{-}o \quad (3)$$

The ^{35}S-labeled **9**, $p\text{-}CH_3C_6H_4SO_2S^{35}SC_6H_4NO_2\text{-}p$, which was utilized for the decomposition of sulfonyl disulfide as shown above, was also allowed to react with triphenylphosphine. Triphenylphosphine sulfide separated similarly to the case for the labeled **4** was found nonradioactive.

$$p\text{-}CH_3C_6H_4SO_2S^{35}SC_6H_4NO_2\text{-}p + 3(C_6H_5)_3P \rightarrow 2(C_6H_5)_3PO + (C_6H_5)_3PS + p\text{-}CH_3C_6H_4S^{35}SC_6H_4NO_2\text{-}p \quad (4)$$

Although Eqs. (3) and (4) predict the formation of the nonlabeled *p*-tolyl *o*-nitrophenyl disulfide and labeled *p*-tolyl *p*-nitrophenyl disulfide respectively, their isolation was not carried out, because our intention is to isolate and assay the radioactivity of phosphine sulfide produced. The formation of radioactive phosphine sulfide in Eq. (3) clearly indicates that the central sulfur atom of the sulfonyl disulfide is desulfurated. Eq. (4) also supports this conclusion. In the present paper we noticed that unstable sulfonyl disulfide decomposes into thiolsulfonate by recrystallization from ethanol. The decomposition results in the release of the central sulfur atom. (See Eq. (2).) This analogy suggests that the decomposition may arise from a nucleophilic attack by ethanol.

Experimental

All melting points are uncorrected. Infrared spectra were recorded on a JASCO IR-S spectrometer by KBr disk method and UV spectra were recorded on a Shimadzu RS-27 spectrometer in 99.5% ethanol. Triphenylphosphine oxide and sulfide were identified by comparison of their retention times with those of authentic specimens, and estimated by use of triphenylphosphorothionate as an internal standard, with a Yanagimoto GCG-5DH gas chromatograph using Silicone DC 200 column. Specific activities of all the labeled compounds, which were recrystallized until the respective constant specific activities attained, were counted with a Packard Tri-Carb Liquid Scintillation Spectrometer, Model 314, using a mixture of POPOP and PPO (0.1 g and 4 g in 1 *l* of toluene) as a scintillator.

Materials. Benzene- and *p*-toluenesulfinic acids were prepared by acidification of commercial sodium salts. *n*-Dodecanesulfinic acid was prepared from *n*-dodecylmagnesium bromide and sulfur dioxide.[12] ω-Toluenesulfinic acid was prepared from ω-toluenesulfonyl chloride by reduction with sodium sulfite.[13]

Pyridinium salts of alkane- and arenethiolsulfonic acids were prepared from the corresponding sulfinic acids and elemental sulfur in pyridine.[14] Mp and analysis of the compounds are summarized in Table 3.

Table 3. The Mp and analysis of the pyridinium thiolsulfonates

Pyridinium thiolsulfonate[b]	Mp (°C)	Anal, Found (Calcd)			
		C	H	N	S
n-Dodecane	65— 70	58.76 (59.07)	9.08 (9.06)	3.75 (4.05)	18.4 (18.56)
p-Toluene	88— 94	54.06 (53.91)	5.20 (4.90)	5.23 (5.24)	23.9 (23.98)
w-Toluene	129—131	53.69 (53.91)	4.85 (4.90)	5.08 (5.24)	24.13 (23.98)

b) Since benzenethiolsulfonate was obtained as an oily material, it was used for the succeeding synthesis without isolation.

11) S. Hayashi, M. Furukawa, J. Yamamoto, and K. Hamamura, *Chem. Pharm. Bull.*, **15**, 1310 (1967).
12) C. S. Marvel and R. S. Johnson, *J. Org. Chem.*, **13**, 822 (1948).
13) S. Smiles and C. M. Bere, "Organic Syntheses," Coll. Vol. 1, p. 7.
14) F. Kurzer and J. R. Powell, *J. Chem. Soc.*, **1952**, 3733.

Arenesulfenyl chlorides were prepared from the corresponding disulfides by chlorination.[15,16]

Thiolsulfonates. Compounds **1a**—**8a** were prepared from the arenesulfenyl chlorides and a slight excess of the sulfinic acids both in chloroform. Compound **9a** was prepared from pyridinium sulfinate by the same method as for **1a**—**8a**. Crude products were recrystallized from ethanol.

Alkane- and Arenesulfonyl Aryl Disulfides. To a solution of the pyridinium alkane- or arenethiolsulfonate (10 mmol) in 30 m*l* of chloroform, was added a solution of the arenesulfenyl chloride (9 mmol) in 30 m*l* of chloroform dropwise at room temperature. The mixture was allowed to stand overnight at the same temperature. The reaction mixture was thoroughly washed with water and then dried over anhydrous sodium sulfate. After the removal of the solvent under reduced pressure, the crude sulfonyl disulfide was recrystallized from ethanol. Only **9** was recrystallized from carbon tetrachloride for prevention of the decomposition.

Specifically ^{35}S*-Labeled* p-*Toluenesulfonyl* o-*Nitrophenyl Disulfide (**4**).* Radioactive sulfur (5 mCi) in benzene was diluted with 18 g of nonactive sulfur in 200 m*l* of carbon disulfide. After removal of the solvent under reduced pressure, crystals of elementary sulfur were recrystallized from benzene. The crystals had an appropriate specific activity for the further synthesis. To a solution of *p*-toluenesulfinic acid (7.1 g) in pyridine (50 m*l*) was added 1.5 g of the radioactive sulfur. The mixture was treated by the same method as for nonactive one to yield 8.2 g of pyridinium *p*-toluenethiolsulfonate. The radioactive sulfonyl disulfide was prepared from this compound and *o*-nitrobenzenesulfenyl chloride by the same method as for nonactive compound and recrystallized from carbon tetrachloride (25,634 dpm/mg).

Specifically ^{35}S*-Labeled* p-*Nitrophenyl Disulfide (**9**).* Radioactive sulfur (1 mCi) in benzene was diluted with 10 g of nonactive sulfur in 100 m*l* of carbon disulfide. The solvent was removed under reduced pressure. From the active sulfur was prepared radioactive sodium disulfide, which was allowed to react with *p*-nitrochlorobenzene to give radioactive *p,p'*-dinitrodiphenyl disulfide (12.7 g, mp 182—183°C). The latter compound (1.6 g) was converted to radioactive *p*-nitrobenzenesulfenyl chloride by chlorination. Radioactive **9** was prepared from the radioactive sulfenyl chloride and pyridinium *p*-toluenethiolsulfonate (2.7 g) as for nonlabeled **9**, and recrystallized from carbon tetrachloride (mp 105—106°C, 1,287 dpm/mg).

Specifically ^{35}S*-Labeled* p-*Nitrophenyl* p-*Toluenethiolsulfonate (**9a**).* Radioactive *p*-nitrobenzenesulfenyl chloride which was used for the preparation of the labeled **9** and pyridinium *p*-toluenesulfinate (2.64 g) in chloroform (100 m*l*) was allowed to stand overnight. The mixture was washed with water three times and dried over anhydrous sodium sulfate. Removal of chloroform by a rotary evaporator yielded crystals. After five recrystallizations from ethanol, constant specific activity (1,427 dpm/mg) was obtained.

Standard ^{35}S*-Labeled Triphenylphosphine Sulfide.* To a solution of radioactive sulfur (0.32 g) which was used for the preparation of labeled **4** in benzene was added triphenylphosphine (2.62 g) in ethanol. The mixture was allowed to stand for one hour at room temperature. The solvent was removed under reduced pressure. After four recrystallizations from ethanol, constant specific activity (29,867 dpm/mg) was obtained.

Reaction of p-*Toluenesulfonyl* p-*Nitrophenyl Disulfide (**4**) with Triphenylphosphine.* To a solution of nonactive sulfonyl disulfide (1 mmol) in 10 m*l* of benzene, was added a solution of triphenylphosphine (1 mmol) in 5 m*l* of ethanol.

*Reaction of the Labeled **4** with Triphenylphosphine.* To a solution of radioactive sulfonyl disulfide (1 mmol) in 20 m*l* of benzene, was added a solution of triphenylphosphine (3 mmol) in 15 m*l* of ethanol at room temperature. The mixture was allowed to stand for one hour. An aliquot was analyzed by GLC. The solvent of the remaining portion of the solution was evaporated under reduced pressure, the solid was washed with cold ethanol and then recrystallized from ethanol to constant mp (162.5—163°C) and specific activity (29,855 dpm/mg).

*Reaction of the Labeled **9** with Triphenylphosphine.* Reaction was carried out by the same method as for labeled **4**. Pure triphenylphosphine sulfide obtained indicated no radioactivity.

We wish to thank Mr. Ryuichi Akaki in this laboratory for elemental analysis.

15) M. T. Bogert and A. Stull, "Organic Syntheses" Coll. Vol. 1, p. 220.
16) M. H. Hubacher, *ibid.*, Coll. Vol. 2, p. 455.

Studies of Benzoylsulfene. IV.[1] The Cycloaddition Reactions of Benzoylsulfene with Cinnamylideneamines

Otohiko TSUGE and Sumio IWANAMI

Research Institute of Industrial Science, Kyushu University, Hakozaki, Fukuoka

(Received February 2, 1971)

The reaction of benzoylmethanesulfonyl chloride with cinnamylideneamines in the presence of triethylamine has been investigated; the products were identified, by spectral studies as well as by chemical transformations, as the corresponding Diels-Alder adducts of benzoylsulfene as a dienophile to the α,β-unsaturated anils, 2-substituted 5*H*, 6*H*-6-benzoyl-5-phenyl-1,2-thiazine 1,1-dioxides, in which the phenyl and benzoyl groups are quasi-equatorial and quasi-axial respectively. The cycloadducts underwent inversion, on treatment with sodium methoxide in methanol or with silica gel in chloroform, to the corresponding epimers, in which both the phenyl and benzoyl groups are quasi-equatorial.

Recently, we found that benzoylsulfene PhCO-CH=SO_2), generated *in situ* from benzoylmethanesulfonyl chloride (I) and triethylamine (NEt_3), reacts with the C=N bonds of anils[2] and carbodiimides[3] to give the (2+2) and/or (4+2) cycloadducts, in spite of the fact that the usual sulfenes (RCH=SO_2) did not react with the C=N bond.[4]

This might indicate that the electron-attracting benzoyl group makes benzoylsulfene more reactive than the sulfenes (RCH=SO_2), and that benzoylsulfene behaves as a 1,2- and/or 1,4-dipole.

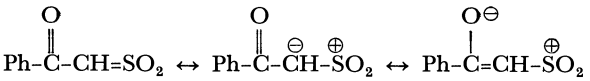

On the other hand, Sakamoto and Tomimatsu[5] found that the adduct obtained from the reaction of phenylketene with cinnamylideneaniline is not the Diels-Alder adduct, as proposed by Pfleger and Jäger,[6] but the corresponding (2+2) cycloadduct of ketene to the C=N bond.

In this connection, it seemed that it would be interesting to investigate the reaction of benzoylsulfene with α,β-unsaturated anils.

In the present paper, we wish to report on the formation of the Diels-Alder adducts by the reaction of benzoylsulfene with cinnamylideneamines.

Results and Discussion

The reaction of benzoylmethanesulfonyl chloride (I) with equimolar amounts of cinnamylideneaniline (IIa) and NEt_3 in dioxane at room temperature for 1.5 hr gave a crystalline compound, IIIa, mp 159—160°C (decomp.), and triethylammonium chloride in 43% and quantitative yields respectively. The elemental analysis and the molecular weight (M^+ *m/e* 389) of IIIa were consistent with those of the expected 1 : 1 adduct of benzoylsulfene and IIa.

The Diels-Alder adduct of benzoylsulfene as a dienophile to IIa, and the (2+2) and (4+2) cycloadducts of benzoylsulfene to the C=C or C=N bond in IIa, are possible for the structure of IIIa.

The IR spectrum of IIIa showed characteristic band at 1686 (νC=O), 1655 (νC=C or νC=N), 1340, and 1140 cm^{-1} (νSO_2), while the PMR spectrum in deuteriochloroform ($CDCl_3$) exhibited the four signals (each 1H) shown in Fig. 1, and also multiplets around τ 2.2—3.1 (15H, aromatic protons). Moreover, a solution of IIIa in benzene absorbed an equimolar amount of bromine.

These observations suggest that the 1 : 1 adduct is either the Diels-Alder adduct (IIIa) or the (2+2) cycloadduct (IIIa′) to the C=N bond.

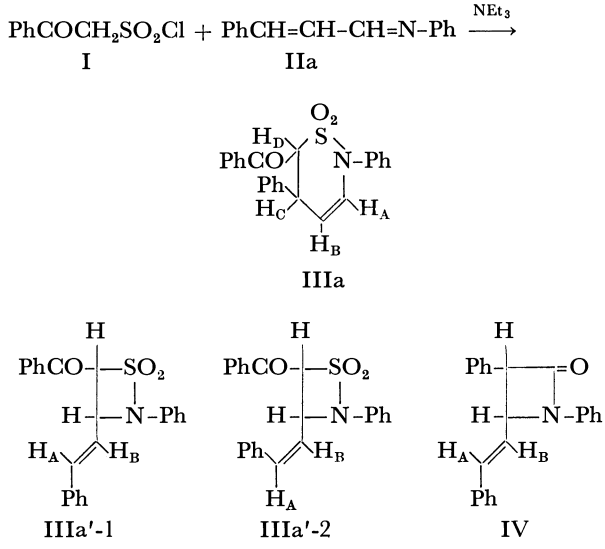

It is well known[7] that *trans* ethylenic coupling constants are always larger than *cis* ethylenic coupling constants for any pairs of 1,2-disubstituted ethylenes. The value of the ethylenic coupling constants, J_{AB} of the β-lactam IV obtained from phenylketene and IIa has been reported to be 17 Hz.[4] Also, the value of the ethylenic coupling constant of *trans*-cinnamaldehyde, the starting material of IIa, is 16.2 Hz.[8]

1) Part III: O. Tsuge and S. Iwanami, *Nippon Kagaku Zasshi*, **92**, 448 (1971).

2) O. Tsuge and S. Iwanami, This Bulletin, **43**, 3543 (1970).

3) O. Tsuge and S. Iwanami, *Nippon Kagaku Zasshi*, **92**, 448 (1971).

4) H. Ulrich, "Cycloaddition Reactions of Heterocumulenes," Academic Press, New York, London (1967), p. 286.

5) M. Sakamoto and Y. Tomimatsu, *Yakugaku Zasshi*, **90**, 1386 (1970).

6) R. Pfleger and A. Jäger, *Chem. Ber.*, **90**, 2460 (1957).

7) L. M. Jackman and S. Sternhell, "Application of Nuclear Magnetic Resonance Spectroscopy in Organic Chemistry," 2nd Ed., Pergamon Press, Oxford, London, Edinburgh, New York, Toronto, Sydney, Paris, Braunschweig (1969), p. 301.

The value of J_{AB} (8.6—8.8 Hz) in IIIa, as obtained its PMR spectrum (see Fig. 1 and Table 2), implies that H_A and H_B in IIIa are *cis*;[9,10] this observation excludes the possible formation of 4-benzoyl-2-phenyl-3-*trans*-styrylthiazetidine 1,1-dioxide (IIIa'-1).

It was very difficult to distinguish between the Diels-Alder adduct, 5*H*,6*H*-6-benzoyl-2,5-diphenyl-1,2-thiazine 1,1-dioxide (IIIa), and the (2+2) cycloadduct, 4-benzoyl-2-phenyl-3-*cis*-styrylthiazetidine 1,1-dioxide (IIIa'-2), on the basis of the spectral data. Since the olefinic hydrogens of IIa are *trans*, however, the predominant formation of the (2+2) cycloadduct with the *cis*-styryl group does not seem reasonable.

On the basis of the above observations and the chemical transformations, which will be discussed below, we can conclude that the most reasonable structure for the reaction product between benzoylsulfene and IIa is the Diels-Alder adduct IIIa.

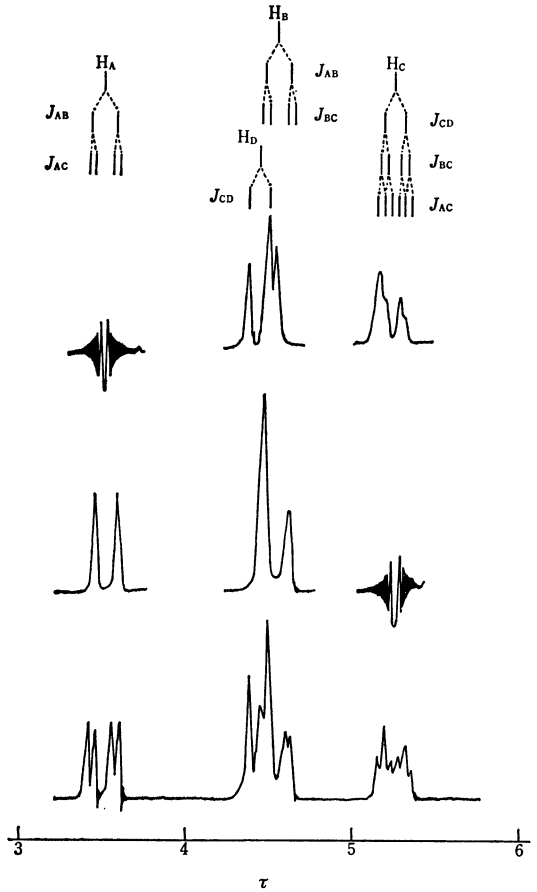

Fig. 1. PMR spectrum of IIIa in $CDCl_3$ at 60 MHz.

When a suspension of IIIa in methanol was treated with sodium methoxide at room temperature for 10 min, a compound Va, mp 175°C, was obtained as colorless needles in an exellent yield. The compound Va was also formed on treating IIIa with silica gel in chloroform.

The compound Va was proved, by the results of elemental analysis as well as by a study of its mass spectrum, to be an isomer of IIIa. The IR spectrum of Va showed characteristic bands at 1678 (νC=O), 1629 (νC=C), 1360, and 1160 cm^{-1} (νSO_2), while the PMR spectrum in $CDCl_3$ exhibited four signals (each 1H), as Fig. 2 shows, besides multiplets around τ 2.2—2.9 (15H, aromatic protons); the J_{AB} value between olefinic protons is 8.1 Hz.

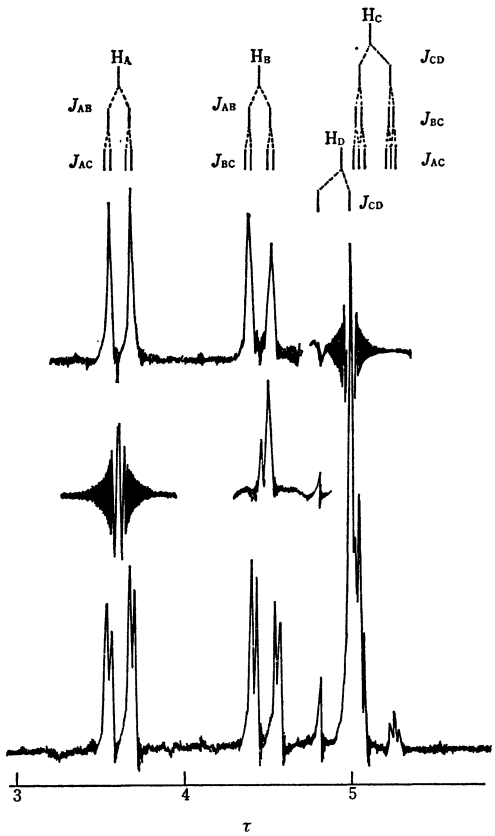

Fig. 2. PMR spectrum of Va in $CDCl_3$ at 60MHz.

From the above observations, it seems that the same ring structure as in IIIa might be involved in Va.

As is illustrated in Fig. 1, the allylic J_{AC} value between the olefinic and the allylic protons is almost equal to the vicinal J_{BC} value (2.5 Hz). This fact suggests that the hydrogen, H_C, in IIIa is quasi-axial.

An inspection of the Dreiding models indicates that the dihedral angle, θ_{CD} between H_C and H_D is about 40° if the benzoyl and phenyl groups in IIIa are *cis*. The observed J_{CD} value of 7.2 Hz is compatible with the value of 7.3 Hz calculated by a modified Karplus equation when θ=40°.[11]

On the other hand, in the PMR spectrum of Va (Fig. 2) the J_{AC} value is also almost equal to the J_{BC} value (1.8 Hz); consequently, the hydrogen, H_C, in Va is quasi-axial.

Furthermore, the observed J_{CD} value of 11.7 Hz implies that the benzoyl and phenyl groups in Va are *trans*-diquasi-equatorial.

8) The olefinic coupling constant of IIa could not be measured, because assignments of the olefinic protons could not be made. While, the olefinic coupling constant of IId was observed to be 16 Hz.

9) G. V. Smith and H. Krilof, *J. Amer. Chem. Soc.*, **85**, 2016 (1963).

10) R. Bramley and M. D. Johnson, *J. Chem. Soc.*, **1965**, 1372.

11) R. J. Abraham, *Mol. Phys.*, **1**, 513 (1962).

On the basis of the above observations, it is evident that IIIa is 5*H*,6*H*-6-benzoyl-2,5-diphenyl-1,2-thiazine 1,1-dioxide, in which the benzoyl and 5-phenyl groups are quasi-axial and quasi-equatorial (*cis*), while Va is its epimer, in which the benzoyl and 5-phenyl groups are both quasi-equatorial (*trans*).

It may be thought that IIIa is easily isomerized into the stable epimer, Va, under such mild conditions, because the hydrogen, H_D, in IIIa is highly activated by the neighboring electron-attracting benzoyl and sulfone groups. The treatment of IIIa with sodium methoxide in deuteriomethanol (CH_3OD) afforded the epimer-6-d (Va-d), mp 175°C, whose structure was established by a study of the PMR and mass spectra.

In general, the Diels-Alder reaction proceeds through the endo addition corresponding to the maximum accumulation of the double bond of the two reagents.

The favorable formation of IIIa can be reasonably explained in terms of the maximum accumulation of double bonds of benzoylsulfene and IIa with the *trans-s-cis-anti* configulation, as is illustrated in Scheme 1.

Furthermore, it may be considered that the active hydrogen, H_D, in IIIa is easily abstracted with a base, leading to the formation of the stable epimer, Va. However, the reaction course is not yet clear in detail.

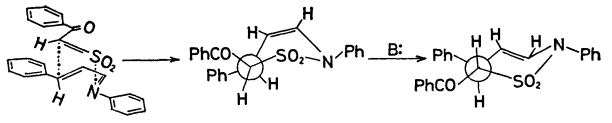

IIa Va

Scheme 1

Both the cycloadducts, IIIa and Va, were hydrolyzed with aqueous sodium hydroxide in boiling methanol; both thus afforded the same compound, VI ($C_{16}H_{15}O_2NS$, M^+ *m/e* 285), mp 86—87°C (decomp.), as colorless plates, whose IR spectrum did not show any bands ascribable to the carbonyl and NH groups, but which did exhibit bands at 1645 (νC=C), 1350, and 1165 cm^{-1} (νSO_2).

The PMR spectrum of VI in $CDCl_3$ exhibited signals due to olefin-, methine- and methylene-protons, as is shown in Fig. 3, besides multiplets (10H, aromatic protons) around τ 2.5—2.9. The values of J_{AB}, J_{AC}, J_{BC}, J_{CD}, J_{CE}, and J_{BD} are found to be 8.3, 2.3, 2.2, 6.0, 12.5, and 1.2 Hz respectively. The long-range coupling (J_{BD}=1.2 Hz) may be due to the W-letter arrangement of H_B-C-C-C-H_D.[12] Furthermore, J_{DE} is 13.0 Hz.

The above observations indicate that the compound VI is 5*H*,6*H*-2,5-diphenyl-1,2-thiazine 1,1-dioxide, in which the 5-phenyl group and hydrogen H_D are both equatorial.

4-Benzoyl-2,3-diphenyl-1,2-thiazetidine 1,1-dioxide was hydrolyzed with aqueous sodium hydroxide as in the following equation,[2] while the ring skeltons

12) A. Rassat, C. W. Jefford, J. M. Lehn, and B. Waegell, *Tetrahedron Lett.*, **1964**, 1233; S. Sternhell, *Rev. Pure Appl. Chem.*, **14**, 15 (1964).

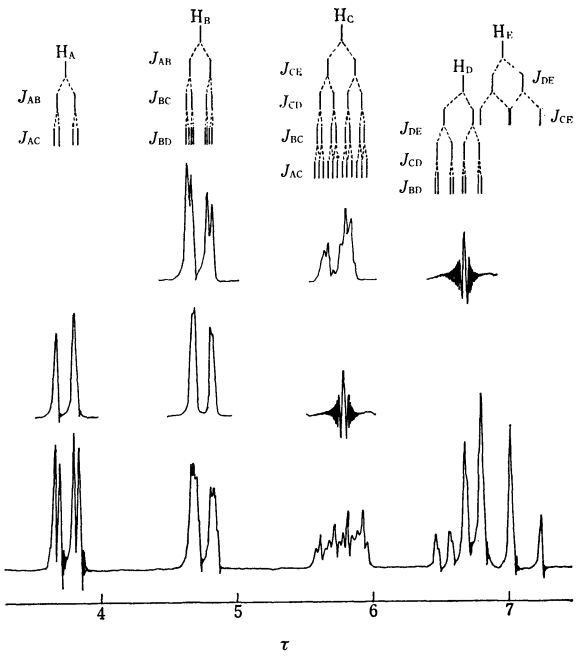

Fig. 3. PMR spectrum of VI in $CDCl_3$ at 60 MHz.

of IIIa and Va were retained under similar conditions. These facts also support the proposed structures for IIIa and Va.

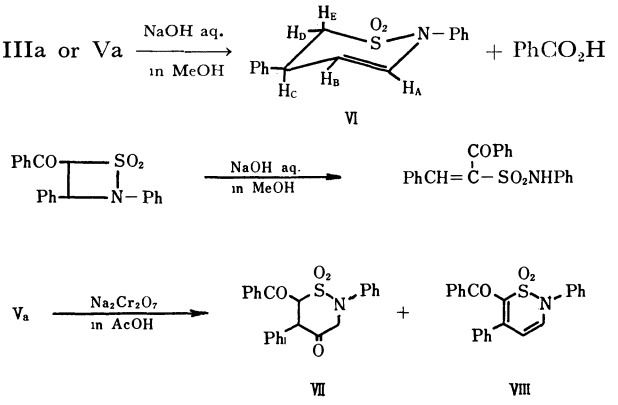

Scheme 2

The following experiment offered additional evidence for the proposed structure for Va. The oxidation of Va with sodium dichromate in acetic acid afforded perhydro-6-benzoyl-2,5-diphenyl-1,2-thiazin-4-one 1,1-dioxide (VII), mp 239—240°C, and 6-benzoyl-2,5-diphenyl-1,2-thiazine 1,1-dioxide (VIII), mp 169—170°C, in 23 and 10% yields respectively. The structures of VII and VIII were confirmed by elemental analyses and spectral studies.

Similar reactions of I with cinnamylidene-*p*-anisidine (IIb), -*p*-chloroaniline (IIc), -*n*-propylamine (IId) and α-methylcinnamylideneaniline (IIe) were investigated in the presence of triethylamine the results are summarized in Table 1.

Althogh the reaction with IIa and IId afforded the initial Diels-Alder adducts, IIIa and IIId, as crystalline compounds, oily substances were formed in the reactions with IIb, IIc, and IIe. However,

TABLE 1. 2,4-DISUBSTITUTED 6-BENZOYL-5-PHENYL-1,2-THIAZINE 1,1-DIOXIDES, III AND V

Compound	Yield (%)	Appearance	Mp (°C)	IR, cm^{-1}				Analysis (%) Found (Calcd)			Mol wt (*m/e*)
				νC=C	νC=C	νSO_2		C	H	N	
IIIa	43	colorless prisms	159 (decomp.)	1686	1655	1340	1140	71.10 (70.94)	5.07 (4.92)	3.73 (3.60)	389
IIId	37	colorless prisms	156 (decomp.)	1670	1642	1320	1130	67.32 (67.59)	6.00 (5.96)	4.00 (3.94)	355
Va	(42) a)	colorless needles	175	1678	1628	1360	1160	71.25 (70.94)	4.68 (4.92)	3.64 (3.60)	389
Vb	43	colorless needles	189—190	1670	1642	1360	1160	68.86 (68.72)	4.88 (5.05)	3.39 (3.34)	419
Vc	26	colorless needles	189	1676	1636	1355	1150	64.98 (65.17)	4.01 (4.28)	3.22 (3.30)	423 425
Vd	(36) a)	colorless needles	182—183	1678	1642	1335	1150	67.83 (67.59)	5.84 (5.96)	4.03 (3.60)	355
Ve	10	colorless needles	149—150 (decomp.)	1678	b)	1335	1150	71.16 (71.45)	5.12 (5.25)	3.60 (3.47)	403

a) Yield from chromatography of reaction mixture over silica gel without isolation of pure IIIa or IIId.
b) A distinct absorption band ascribed to νC=C was not observed.

TABLE 2. PMR SPECTRAL DATA ON III, V AND VIa (60 MHz)

Compound	Chemical shift (τ)					Coupling constant[a] (Hz)					Solvent
	H_A	H_B	H_C	H_D	H_E	J_{AB}	J_{AC}	J_{BC}	J_{CD}	J_{CE}	
IIIa	3.51	4.55	5.27	4.46		8.6	2.5	2.5	7.2		$CDCl_3$
	3.76	4.82	5.24	4.44		8.8	2.6	2.4	7.2		C_6D_6
	3.41	4.43	5.25	4.23		8.7	2.6	2.4	7.2		CD_3NO_2
IIId	3.67	4.71	5.38	4.63		8.4	2.4	2.3	7.4		$CDCl_3$
Va	3.62	4.48	5.08	4.96		8.1	1.8	1.8	11.7		$CDCl_3$
	3.53	4.46	5.23	4.65		8.0	2.1	2.1	11.8		CD_3NO_2
Vb	3.66	4.53	5.10	4.98		8.2	1.8	1.8	12.0		$CDCl_3$
Vc	3.61	4.40	5.04	4.92		8.0	1.8	1.8	11.5		$CDCl_3$
Vd	3.80	4.76	5.20	5.02		8.3	2.0	2.0	11.8		$CDCl_3$
Ve	3.82	8.40[b]	5.31	4.88		—	—	—	11.8		$CDCl_3$
VIa	3.76	4.77	5.77	7.02	6.67	8.3	2.3	2.2	6.0	12.5	$CDCl_3$
	4.14	5.15	5.93[c]	7.36	7.00	8.4	2.2	2.3	6.3	12.3	C_6D_6
	3.60	4.62	5.78[c]	6.83	6.43	8.3	2.2	2.2	6.0	12.5	CD_3NO_2

a) Coupling constant, *J*, was measured with an error of about ±0.3 Hz.
b) Chemical shift of methyl protons.
c) This value is uncorrect, since impurity of the solvent exhibits multiplets around τ 5.6—5.8.

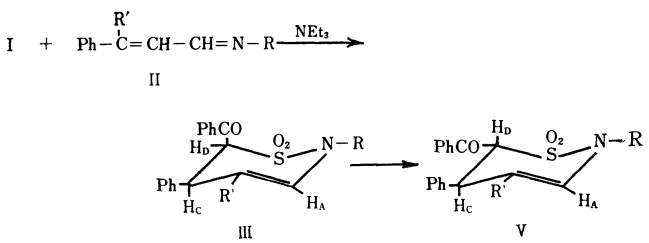

b: R=*p*-$MeOC_6H_4$, R'=H_B; c: R=*p*-ClC_6H_4, R'=H_B; d: R=*n*-Pr, R'=H_B; e: R=Ph, R'=Me

oily substances were transformed, by chromatography on silica gel using chloroform as the eluent, to the corresponding epimers, V, as crystalline compounds. These results suggests that the oily substances contained considerable amounts of III, because IIIa and IIId were quantitatively transformed, as has been mentioned, to Va and Vd.

The structures of III and V were established by elemental analyses and by spectral studies. The yields, physical properties, elemental analyses, and spectral data are summarized in Tables 1 and 2.

Additional reactions of Va with hydrogen halides and bromine were also investigated.

When hydrogen bromide was passed through a solution of Va in benzene, and the resulting solution was then treated with methanol, perhydro-6-benzoyl-2,5-diphenyl-4-methoxy-1,2-thiazine 1,1-dioxide (IX), mp 175°C (decomp.), was obtained quantitatively. The structure of IX was confirmed by the results of the elemental analysis and by the spectral data.

Also, the treatment of Va with concentrated hydrochloric acid in methanol at room temperature gave IX in a quantitative yield. Although an addition

product of hydrogen bromide to Va could not be in a pure form, it is evident that the products from hydrogen halides are the corresponding perhydro-4-halo-1,2-thiazine 1,1-dioxide (Scheme 3).

The bromination of Va, followed by the treatment of a resulting oily dibromo compound with aqueous potassium hydroxide, afforded a crystalline compound, X ($C_{16}H_{14}O_2NSBr$), mp 147°C, in a low yield. The IR spectrum of X showed bands at 1632 (νC=C), 1355, and 1160 cm^{-1} (νSO_2), but not any carbonyl bands. The PMR spectrum in $CDCl_3$ revealed signals at τ 6.15—6.95 (2H, multiplets, >C<u>H</u>$_2$), 5.4—5.9 (1H, multiplet, >C<u>H</u>), 3.32 (1H, doublet, -C<u>H</u>=, J=1.8 Hz), and 2.4—2.7 (10H, multiplets, aromatic protons).

The above observations indicate that the compound X is 5*H*,6*H*-3-bromo-2,4-diphenyl-1,2-thiazine 1,1-dioxide. The structure for X was also supported by the mass spectrum.

On the other hand, the treatment of the dibromo compound with methanol gave a crystalline compound XI, mp 170—171°C (decomp.), in a good yield. The compound XI ($C_{24}H_{22}O_4NSBr$) was assumed to be perhydro-6-benzoyl-3-bromo-2,5-diphenyl-4-methoxy-1,2-thiazine 1,1-dioxide on the basis of the following evidence.

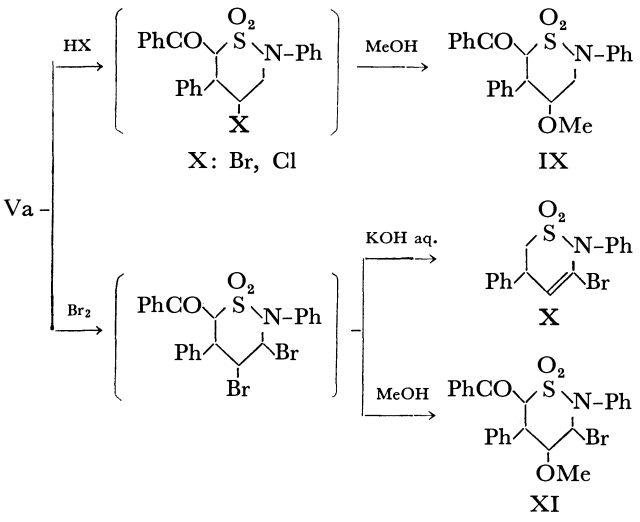

Scheme 3

The IR spectrum of XI showed bands at 1685 (νC=O), 1336, and 1150 cm^{-1} (νSO_2), while the PMR spectrum in $CDCl_3$ revealed signals at τ5.47 (1H, two pairs of doublets, MeO-C<u>H</u><, each J= 2.5 Hz), 4.98 (1H, double doublets, Ph-C<u>H</u><, J= 11.8 and 2.5 Hz), 4.82 (1H, doublet, Br-C<u>H</u><, J= 2.5 Hz), 3.95 (1H, doublet, PhCO-C<u>H</u><, J=11.8 Hz), and 1.8—2.9 (15H, multiplets, aromatic protons). The 4-bromo-3-methoxy isomer is also possible for the structure of XI. However, it may be considered that the 3-bromo-4-methoxy compound is more probable than the isomer, because the 4-bromine is more reactive than 3-bromine in the dibromo compound, as was shown in the formation of X. From the vicinal $J_{4,5}$ and $J_{5,6}$ values, it is evident that the 5-phenyl and benzoyl groups are both equatorial, and that the methoxy group is axial in XI.

Experimental

All the melting and boiling points are uncorrected. The IR spectra were measured in a KBr disk. The PMR spectra were taken on a Hitachi R-20 NMR spectrometer (60 MHz), using tetramethylsilane as the internal standard. The mass spectra were obtained on a Hitachi RMS-4 mass spectrometer, using a direct inlet and an ionization energy of 70 eV.

Materials. Benzoylmethanesulfonyl chloride (I), mp 88°C (lit,[13] mp 87.5—88.2°C) was prepared according to the method of Truce and Vriesen.[13] α,β-Unsaturated anils were prepared from the corresponding cinnamaldehydes and amines: cinnamylideneaniline (IIa), mp 109°C (lit,[14] mp 109°C), -*p*-anisidine (IIb), mp 118—119°C (lit,[15] mp 119°C), and -*p*-chloroaniline (IIc), mp 106—107°C (lit[15] mp 107°C).

Cinnamylidene-*n*-propylamine (IId), bp 140—142°C/0.2 mmHg.

Found: C, 83.40; H, 8.66; N, 7.93%. Calcd for $C_{12}H_{15}N$: C, 83.19; H, 8.73; N, 8.09%. M^+: *m/e* 173.

β-Methylcinnamylideneaniline (IIe); bp 192°C/1.2 mmHg.

Found: C, 87.18; H, 6.79; N, 6.26%. Calcd for $C_{16}H_{15}N$: C, 86.84; H, 6.83; N, 6.33%. M^+: *m/e* 221.

General Procedure for the Reaction of I with II in the Presence of NEt_3. To a vigorously-stirred solution of 0.01 mol of II and 1.0 g (0.01 mol) of NEt_3 in 20 m*l* of dioxane, a solution of 2.2 g (0.01 mol) of I in 30 m*l* of dioxane was added, drop by drop, at room temperature over a period of 30 min. After the reaction mixture had been stirred at the same temperature for 1.5 hr, the triethylammonium chloride was removed by filtration. The filtrate was evaporated *in vacuo* at 40—50°C, leaving an oily substance. The oily substance obtained from the reaction with IIa or IId was triturated with methanol to give the 5*H*,6*H*-6-benzoyl-5-phenyl-1,2-thiazine 1,1-dioxide, IIIa or IIId, as crystals, but the thiazines, IIIb, IIIc, and IIIe, could not be isolated as crystals.

On the other hand, a chloroform solution of III was chromatographed over silica gel to give the epimer V.

The yields, physical properties, results of elemental analyses, and spectral data of III and V are summarized in Tables 1 and 2.

Inversion to V from III with Sodium Methoxide. A suspension of 0.5 g of IIIa in 5 m*l* of methanol was stirred with a few milligrams of metallic sodium at room temperature for 10 min. Subsequent filtration gave 0.49 g (98%) of colorless crystals, which were identical with the epimer, Va, obtained from the treatment of IIIa with silica gel described above. Similarly, IIId was transformed to the epimer Vd in a 97% yield.

A similar reaction of IIIa in deuteriomethanol (CH_3OD) gave the epimer-6-d (Va-d), mp 175°C, as colorless needles in a quantitative yield.

IR: 1673 (νC=O), 1625 (νC=C), 1354, 1158 cm^{-1} (νSO_2). PMR ($CDCl_3$): τ 3.62 (1H, double doublets, >N-C<u>H</u>=, J= 8.2 and 2.1 Hz), 4.49 (1H, double doublets, -C<u>H</u>=C<u>H</u>-N<, J=8.2 and 2.1 Hz), 5.10 (1H, multiplet, Ph-C<u>H</u><). Mass spectrum: M^+ *m/e* 390.

13) W. E. Truce and C. W. Vriesen, *J. Amer. Chem. Soc.*, **75**, 2525 (1953).
14) A. T. Mason, *Ber.*, **20**, 270 (1887).
15) A. Senier and P. H. Gallagher, *J. Chem. Soc.*, **113**, 28 (1918).

Hydrolysis of Va. A solution of 0.26 g of Va in 5 m*l* of 80% aqueous methanol, with 0.1 g of sodium hydroxide dissolved in it, was refluxed for 30 min. To the mixture was added 100 m*l* of water, and then the mixture was extracted with benzene. The benzene extract was washed with water, dried over sodium sulfate, and then evaporated *in vacuo* to give a viscous oil, which crystallized on trituration with petroleum benzine. Recrystallization from petroleum benzine (bp 45—60°C) gave 30 mg (16%) of 5*H*,6*H*-2,5-diphenyl-1,2-thiazine 1,1-dioxide (VI), mp 86—87°C, as colorless plates.

Found: C, 67.26; H, 5.16; N, 4.91%. Calcd for $C_{16}H_{15}O_2NS$: C, 67.36; H, 5.30; N, 4.91%. Mass spectrum: M^+ *m/e* 285.

The water layer was neutralized with concentrated hydrochloric acid to give 20 mg (24%) of benzoic acid.

Oxidation of Va. After a solution of 3.0 g of Va in 30 m*l* of acetic acid had been refluxed with 7.7 g of sodium dichromate dihydrate for 1 hr, the reaction mixture was cooled. To the mixture was added 100 m*l* of water, and then the mixture was extracted with chloroform. The chloroform extract was washed with water, dried over sodium sulfate, and then evaporated *in vacuo*. The residue was triturated with 10 m*l* of methanol to afford crystals. Subsequent filtration and recrystallization from a methanol-benzene mixture gave 0.72 g (23%) of perhydro-6-benzoyl-2,5-diphenyl-1,2-thiazin-4-one 1,1-dioxide (VII), mp 239—240°C, as colorless needles.

Found: C, 68.20; H, 4.66; N, 3.76%. Calcd for $C_{23}H_{19}O_4NS$: C, 68.14; H, 4.72; N, 3.46%. IR: 1710 (νC=O), 1672 (νC=O), 1325, 1143 cm^{-1} (νSO_2). Mass spectrum: *m/e* 405(M^+), 341(M^+-SO_2), 324(341^+-OH), 249(341^+-PhNH), 236(341^+-PhCO), 221(249^+-CO), 105($PhCO^+$).

The methanol filtrate was cooled at 0°C to give yellow crystals. Recrystallization from methanol gave 0.3 g (10%) of 6-benzoyl-2,5-diphenyl-1,2-thiazine 1,1-dioxide (VIII), mp 169—170°C, as yellow needles.

Found: C, 70.99; H, 4.27; N, 3.73%. Calcd for $C_{23}H_{17}O_3NS$: C, 71.31; H, 4.42; N, 3.62%. IR: 1640 (νC=O conjugated with C=C), 1340, 1160 cm^{-1} (νSO_2). PMR ($CDCl_3$): τ 3.12 (1H, doublet, olefinic protons). Mass spectrum: *m/e* 387(M^+), 323(M^+-SO_2), 322(323^+-H), 246(323^+-Ph), 230(322^+-PhNH), 217(322^+-PhCO), 105($PhCO^+$).

Perhydro-6-benzoyl-2,5-diphenyl-4-methoxy-1,2-thiazine 1,1-Dioxide (IX). After a suspension of 0.2 g of Va in 10 m*l* of methanol has been stirred with 2 m*l* of concentrated hydrochloric acid at room temperature for 5 hr, the mixture was evaporated *in vacuo* to leave 215 mg of crystals. Recrystallization from methanol gave IX, mp 175°C (decomp.), as colorless needles.

Found: C, 68.51; H, 5.45; N, 3.25%. Calcd for $C_{24}H_{23}O_4NS$: C, 68.40; H, 5.50; N, 3.33%. IR: 1670 (νC=O), 1340, 1148 cm^{-1} (νSO_2). PMR (deuteronitromethane): τ 7.4 (2H, multiplet, >N–C<u>H</u><), 6.49 (3H, singlet, OCH_3), 5.5 (1H, multiplet, Ph–C<u>H</u><), 4.92 (1H, multiplet, MeO–C<u>H</u><), 4.23 (1H, doublet, PhCO–C<u>H</u>–SO_2–, J=11.9 Hz), 1.9—2.9 (15H, multiplet, aromatic protons). Mass spectrum: *m/e* 421 (M^+), 389 (M^+—MeOH), 265 (M^+-SO_2-PhNH), 233 (265^+-MeOH), 147 ($Ph-N^+\equiv C-\dot{C}HOMe$), 115 ($147^+-MeOH$), 105 ($PhCO^+$).

After hydrogen bromide gas was passed through a solution of 0.39 g of Va in 50 m*l* of benzene at room temperature for 5 hr, the benzene was evaporated *in vacuo* to leave a pale red solid. A methanol solution of the solid was refluxed for 5 min to give 0.2 g of IX.

5H,6H-3-Bromo-2,4-diphenyl-1,2-thiazine 1,1-Dioxide (X). To a solution of 0.8 g of Va in 50 m*l* of benzene was added, drop by drop at room temperature, a solution of bromine in benzene until there was no further disappearance of the reddish color of the bromine. The reaction mixture was then evaporated *in vacuo*, leaving an oily substance. A mixture of the oily substance in 20 m*l* of 0.5 N aqueous potassium hydroxide was heated at 70—80°C for 1 hr, after which the mixture was cooled. After 30 m*l* of concentrated hydrochloric acid had then been added to the mixture, the mixture was extracted with benzene. The benzene extract was washed with water, dried over sodium sulfate, and then evaporated *in vacuo* to leave a residue. A benzene solution of it was chromatographed over alumina and then eluted using chloroform to give colorless crystals. Recrystallization from petroleum benzine (bp 45—60°C) gave 0.1 g (13%) of X, mp 147°C, as colorless needles.

Found: C, 52.36; H, 3.83; N, 3.82%. Calcd for $C_{16}H_{14}O_2NSBr$: C, 52.76; H, 3.87; N, 3.85%. Mass spectrum: *m/e* 365, 363 (M^+, relative intensity 1 : 1), 301, 299, (M^+-SO_2, relative intensity 1 : 1), 220 (301^+ and 299^+-Br).

Perhydro-6-benzoyl-3-bromo-2,5-diphenyl-4-methoxy-1,2-thiazine 1,1-Dioxide (XI). The oily substance obtained from the bromination of 193 mg of Va according to the above mentioned-method was triturated with 5 m*l* of methanol, thus affording colorless crystals. Recrystallization from methanol gave 0.2 g (81%) of XI, mp 170—171°C (decomp.), as colorless needles.

Found: C, 57.36; H, 4.60; N, 2.74%. Calcd for $C_{24}H_{22}O_4NSBr$: C, 57.65; H, 4.44; N, 2.80%. Mass spectrum: *m/e* 501, 499 (M^+, relative intensity 1 : 1), 369, 467 (M^+—MeOH, relative intensity 1 : 1), 420 (M^+-Br), 388 (420^+—MeOH), 356 (420^+-SO_2), 227, 225 (relative intensity 1 : 1).

Chemically Induced Dynamic Nuclear Polarization in the Photochemical Reaction of Phenanthraquinone with Hydrogen Donors. I. Kinetics of Nuclear Spin Polarization[1]

Kazuhiro MARUYAMA, Heisaburo SHINDO,* Tetsuo OTSUKI, and Tetsuo MARUYAMA*

Department of Chemistry, College of Liberal Arts and Science, Kyoto University, Kyoto
**JEOL(USA) Inc., 235 Birchwood Avenue, Cranford, N.J. 07016, USA*

(Received February 23, 1971)

Strongly-enhanced NMR signals were observed in the photo-induced hydrogen abstraction reaction of phenanthraquinone with several hydrogen donors in benzene. Chemically-induced dynamic nuclear polarization was kinetically treated in the photochemical reaction during the course of irradiation by visible light and shut-off. It was found that the relaxation time of the nuclear-spin system under the irradiation is shorter by a factor of 2 to 4 than that in the black-out stage and that the enhancement factor for the methine proton of the 1,2-adduct of phenanthraquinone was evaluated as 1000—2000.

Of the products of the rapid radical reaction, their proton NMR spectra are often observed as an enhanced absorption and/or emission line during the course of the reaction.[2-11] This phenomenon is called "chemically-induced dynamic nuclear polarization (CIDNP)"[3]

Since the discovery of this phenomenon by Fischer and Bargon,[2,3] many kinds of radical reactions have been investigated by several workers from the standpoint of CIDNP.[4-9] Thus, Closs and his co-workers[10] and Kaptein and Oosterhoff[11] recently proposed a model of a radical pair as an intermediate of the reaction, and showed that the CIDNP phenomenon originates from the mixing between the electronic singlet and triplet states of the radical pair. Their theory (CKO theory)[10,11] seems to have been accepted as the explanation of CIDNP phenomenon.

CIDNP is dynamic in its nature; nevertheless, no phenomenological treatments have been made from the point of view of kinetics. For simplicity, we preferred the photo-induced chemical reaction to any other type of radical reaction, that is, the hydrogen abstraction reactions of phenanthraquinone with fluorene, xanthene, diphenylmethane, and 9,10-dihydroanthracene in benzene. In these reactions, the 1,2-type adduct[12] of phenanthraquinone with hydrogen donors mentioned above is known to be mainly produced.[13]

The NMR singlet spectrum of the methine proton of the adduct of each of hydrogen donors revealed a strongly-enhanced absorption; the nuclear-spin polarization of this methine proton will be kinetically discussed.

Experimental

Materials. Phenanthraquinone was prepared by oxidation of phenanthrene with pottassium dichromate and was repeatedly purified by the recrystallization method from its acetic acid solution. It has a mp of 202—206°C and λ_{max} =410—420 mμ in the UV spectrum. Commercially-available guaranteed-grade reagents, used as hydrogen donors to phenanthraquinone, were used without further purification. A benzene solution of 2.3×10^{-2} M of phenanthraquinone and 1.0M of the hydrogen donor was sufficiently degassed in vacuum and submitted to NMR measurements.

Apparatus. The NMR spectra were observed at 60 MHz by the use of a spectrometer of the C-60HL type (JEOL Co. Ltd.). A saw-tooth wave generator (JEOL. Co. Ltd.) was used to measure the variation in the spectrum intensity with the time.

In order to induce a photochemical reaction within the NMR probe, we modified the probe for introducing UV or visible light as follows. The light source (Ushio high-pressure Hg lamp, 500W) is placed above the magnet. The focused light from the source is guided into the probe through a hole, reflects once on the aluminum mirror attached within the probe, and then arrives at the sample. In order to be used effectively, the light is forced to pass to the sample again by means of a concave aluminum mirror.

Theory

Phenanthraquinone (PQ) I in benzene is photochemically excited to a triplet state, II, with a fairly long lifetime, τ; II returns to a singlet ground state with the emission of fluorescence.[14]

1) This work has been done at the Department of Chemistry, College of Liberal Arts and Science, Kyoto University.
2) H. Fischer and J. Bargon, *Z. Naturforsch.*, **22a**, 1551 (1967).
3) J. Bargon and H. Fischer, *ibid.*, **22a**, 1556 (1967).
4) H. R. Ward and R. G. Lawler, *J. Amer. Chem. Soc.*, **89**, 5518 (1967); R. G. Lawler, *ibid.*, **89**, 5519 (1967).
5) H. R. Ward, R. G. Lawler, and H. Y. Loken, *ibid.*, **91**, 736 (1969); H. R. Ward, R. G. Lawler, and R. A. Cooper, *ibid.*, **91**, 746 (1969).
6) A. R. Lepley and R. L. Landau, *ibid.*, **91**, 748 (1969); A. R. Lepley, *ibid.*, **91**, 749 (1969).
7) G. L. Closs and L. E. Closs, *ibid.*, **91**, 4549, 4550 (1969); G. L. Closs, *ibid.*, **91**, 4552 (1969); G. L. Closs and A. D. Trifunac, *ibid.*, **91**, 4554 (1969).
8) A. R. Lepley, P. M. Cook, and G. F. Willard, *ibid.*, **92**, 1101 (1970).
9) M. Cocivera and H. D. Roth, *ibid.*, **92**, 2573 (1970).
10) G. L. Closs and A. D. Trifunac, *ibid.*, **92**, 2183 (1970); G. L. Closs, C. E. Doubleday, and D. R. Paulson, *ibid.*, **92**, 2185 (1970); G. L. Closs and A. D. Trifunac, *ibid.*, **92**, 2186 (1970).
11) R. Kaptein and L. J. Oosterhoff, *Chem. Phys. Lett.*, **4**, 195, 214 (1969).
12) See structure V.
13) These reactions are, in general, very clean, and almost all of the products are 1,2-type adducts. The details of the structure of the photo-adduct will be reported in the near future.
14) Although PQ is activated to an excited singlet state at first through $n\rightarrow\pi^*$ excitation, the molecule is transformed to a triplet state by inter-system crossing.

When a hydrogen donor (III), for instance, fluorene, is present, hydrogen abstraction reaction easily proceeds with a specific rate constant of k_a, simultaneously, a radical pair, IV, may be formed, as was assumed in CKO theory.[10,11]

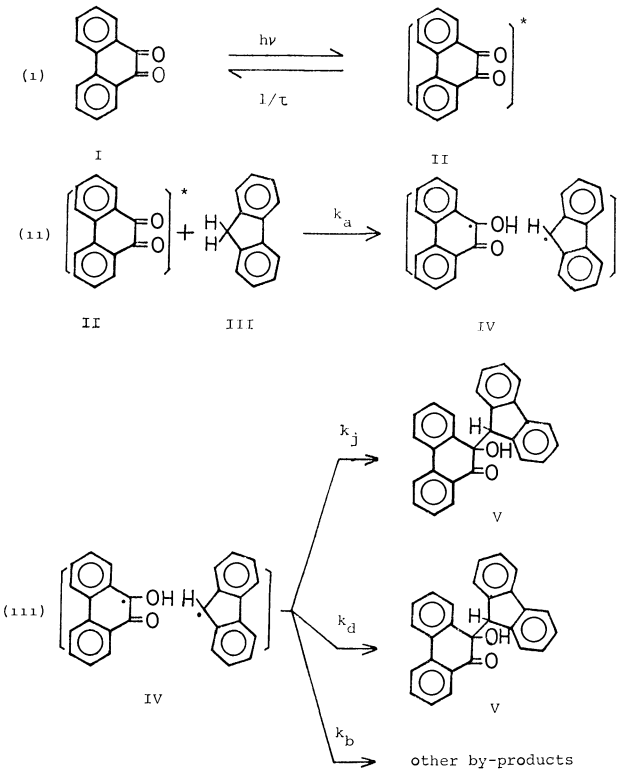

The radical pair, IV, was assumed to yield the products through three processes. One is the process producing the 1,2-adduct V directly from the radical pair. The specific rate constant of this process, k_j, is assumed to depend on the nuclear spin state of the 1,2-adduct, in accordance with the CKO theory. Thus, the nuclear-spin polarization occurring in the adduct is produced only through this process. The second process, occurring with a rate constant of k_d is related to the separation and recombination of the radical pair to give the 1,2-adduct. However, the nuclear-spin polarization of the adduct generated through this process is considered to be less important in our system.[15]

The last process of the three is assumed to be associated with the process giving other by-products.

For convenience, we may rewrite the reaction processes, (i), (ii), and (iii), as follows:

$$X \underset{1/\tau}{\overset{k_0}{\rightleftharpoons}} X^* \xrightarrow{k_a} Y \begin{cases} \xrightarrow{k_j} Z_j^* \\ \xrightarrow{k_d} Z_j' \\ \xrightarrow{k_b} \text{by-products} \end{cases}$$

Also, the nuclear-spin system polarized through the reaction process mentioned above will, with the relaxation time, T_1, approach the thermal equilibrium;

$$Z_j \underset{1/2T_1(k,j)}{\overset{1/2T_1(j,k)}{\rightleftharpoons}} Z_k$$

where the two suffixes, j and k, represent, respectively, jth and kth nuclear spin state of the 1,2-adduct, and where $T_1(j,k)$ is the relaxation time between jth and kth nuclear-spin states. The population of the jth nuclear spin state of the 1,2-adduct, $[Z_j^*]+[Z_j']$, is denoted by $[Z_j]$.

In the case of a sufficiently concentrated solution of PQ, the increase in the rate of X*, k_0, may be considered to be independent of the concentration of PQ, [X]. It depends only on the intensity of the light used; that is, this reaction process is of the zeroth order. The reaction process from X* to Y may be regarded as quasi-first order because of the large excess of the hydrogen donor compared with that of PQ. The other processes are first order in their natures. Thus, we may write the rate of chemical change during the course of the light irradiation as follows;

$$\frac{d[X^*]}{dt} = k_0 - (1/\tau + k_a)[X^*] \tag{1}$$

$$\frac{d[Y]}{dt} = k_a[X^*] - \sum_j (k_j + k_d + k_b)[Y] \tag{2}$$

$$\frac{d[Z_j]}{dt} = (k_d + k_j)[Y] - \sum_k 1/2T_1^*(j,k) \times (\langle [Z_j]-[Z_k]\rangle - \langle [Z_j]-[Z_k]\rangle_0) \tag{3}$$

where $\langle [Z_j]-[Z_k]\rangle_0$ is the difference in populations between the jth and kth energy levels in the thermal euilibrium; the use of T_1^* in place of T_1 indicates the relaxation time during irradiation.

As the signal of photo-adduct in the thermal equilibrium can not be observed even after the chemical change proceeded, the term $\langle [Z_j]-[Z_k]\rangle_0$ may be ignored in Eq. (3). In general, a solution of Eq. (3) can not be analytically obtained, so we will deal with the case of the single spin system alone. In such a case, we can replace Eq. (3) by;

$$\frac{d[Z_1]}{dt} = (k_d + k_1)[Y] - 1/2T_1^*\langle [Z_1]-[Z_2]\rangle \tag{4}$$

$$\frac{d[Z_2]}{dt} = (k_d + k_2)[Y] - 1/2T_1^*\langle [Z_1]-[Z_2]\rangle \tag{5}$$

From Eqs. (4) and (5), we obtain;

$$\frac{d\langle [Z_1]+[Z_2]\rangle}{dt} = \sum_{j=1}^{2} (k_j + k_d)[Y] \tag{6}$$

$$\frac{d\langle [Z_1]-[Z_2]\rangle}{dt} = (k_1 - k_2)[Y] - 1/T_1^*\langle [Z_1]-[Z_2]\rangle \tag{7}$$

On integrating Eqs. (1) and (2), and considering that X* and Y are zero when t is zero, the concentrations of PQ* and the radical pair are given by;

$$[X^*] = \frac{k_0}{1/\tau + k_a}(1 - e^{-t/\tau - k_a t}) \tag{8}$$

$$[Y] = \frac{k_0 k_a}{1/\tau + k_a}\left\{ \frac{1}{\sum(k_j + k_d + k_b)}(1 - e^{-\sum(k_j+k_d+k_b)t}) - \frac{1}{\sum(k_j + k_d + k_b) - 1/\tau - k_a}(e^{-t/\tau - k_a t} - e^{-\sum(k_j+k_d+k_b)t}) \right\} \tag{9}$$

15) This can be concluded from the following two experimental observations: i) the rate of hydrogen abstraction by phenanthraquinone and the successive recombination of radicals formed are usually too fast for intermediate radicals to be observed by the ESR technique, and ii) the fact described in footnote 13).

Since it is reasonable that $\sum(k_j+k_d+k_b) \gg 1/\tau+k_a$ and $1/T_1^*$, the solutions of Eqs. (6) and (7) can be approximated by;

$$\langle[Z_1]+[Z_2]\rangle = \frac{k_0k_d(k_j+k_d)}{(1/\tau+k_a)\sum(k_j+k_d+k_b)} \times \left(t+\frac{1}{1/\tau+k_a}e^{-t/\tau-k_at}\right) \quad (10)$$

$$\langle[Z_1]-[Z_2]\rangle = \frac{k_0k_a(k_1-k_2)T_1^*}{(1/\tau+k_a)\sum(k_j+k_d+k_b)}\left\{(1-e^{-t/T_1^*}) - \frac{1/T_1^*}{1/T_1^*-1/\tau-k_a}(e^{-t/\tau-k_at}-e^{-t/T_1^*})\right\} \quad (11)$$

by using Eq. (9).

Next, let us consider the case when the irradiation is shut off at a certain time, $t=t_0$, after the establishment of a steady-state nuclear polarization. The rate of the chemical reaction (1) is replaced by;

$$\frac{d[X^*]}{dt} = -(1/\tau+k_a)[X^*] \quad (12)$$

On integrating Eqs. (2), (9), and (12) under appropriate initial conditions,[16] the expression of $\langle[Z_1]-[Z_2]\rangle$ is given by Eq. (13);

$$\langle[Z_1]-[Z_2]\rangle = \frac{k_0k_a(k_1-k_2)T_1}{(1/\tau+k_a)\sum(k_j+k_d+k_b)} \times \left\{\frac{1/T_1}{1/T_1-1/\tau-k_a}e^{-(1/\tau+k_a)(t-t_0)} - \frac{1/\tau+k_a}{1/T_1-1/\tau-k_a}e^{-(t-t_0)/T_1}\right\} \quad (13)$$

after being approximated in the same manner as was done in Eqs. (10) and (11). The relaxation time under the off-irradiation is denoted by T_1 in order to distinguish it from the relaxation time under the irradiation, T_1^*.

If $1/T_1^*$ and $1/T_1 \ll 1/\tau+k_a$, the signal intensity in the irradiating stage increases in accordance with the following expression;

$$\langle[Z_1]-[Z_2]\rangle = \frac{k_0k_a(k_1-k_2)T_1^*}{(1/\tau+k_a)(k_1+k_2+2k_d+2k_b)}(1-e^{-t/T_1^*}) \quad (14)$$

as may be found from Eq. (11). On the other hand, the signal after blacking-out is diminished exponentially as follows;

$$\langle[Z_1]-[Z_2]\rangle = \frac{k_0k_a(k_1-k_2)T_1}{(1/\tau+k_a)(k_1+k_2+2k_d+2k_b)}e^{-(t-t_0)/T_1} \quad (15)$$

as may be seen from Eq. (13). We obtain the envelope curve depicted by signal peaks during the irradiation and black-out.

The enhancement factor is defined by;

$$P = \frac{\langle I\rangle-\langle I\rangle_0}{\langle I\rangle_0} \simeq \frac{\langle I\rangle}{\langle I\rangle_0} = \frac{\langle[Z_1]-[Z_2]\rangle}{\langle[Z_1]-[Z_2]\rangle_0} \quad (16)$$

16) The initial conditions, that is, the concentrations of X,* Y, and $\langle[Z_1]-[Z_2]\rangle$ at $t=t_0$ may be given by the respective values at $t=\infty$ in Eqs. (8), (9), and (11); $[X^*]=k_0/(1/\tau+k_a)$, $[Y]=k_0k_a/(1/\tau+k_a)\times\sum(k_j+k_d+k_b)$ and $\langle[Z_1]-[Z_2]\rangle = k_0k_a \times T_1^*/(1/\tau+k_a)\sum(k_j+k_d+k_b)$ were used.

where $\langle I\rangle_0$ is the expectation value of the spin-angular momentum in the thermal equilibrium. The value of $\langle[Z_1]-[Z_2]\rangle_0$ can be obtained from the value of $\langle[Z_1]+[Z_2]\rangle$ on the basis of Boltzmann's law. Thus, the enhancement factor at a certain time in a steady-state can easily be found from Eqs. (10) and (11);

$$P = \frac{(k_1-k_2)T_1^*}{(k_1+k_2+2k_d+2k_b)t}\cdot\frac{2kT}{\Delta E} \quad (17)$$

where ΔE is the energy difference between the two energy levels of the spin system; k, Boltzmann constant, and T, the absolute temperature.

Results

Phenanthraquinone (PQ) is photochemically induced to yield its 1,2-adducts in the presence of hydrogen donors. For example, when a solution of 2.3×10^{-2}M of PQ and 1.0M of fluorene in benzene was irradiated inside the probe, an enhanced singlet line of the methine proton of the 1,2-adduct was observed at a field lower by about 45 Hz from the chemical shift of the methylene protons of fluorene. This is shown for fluorene and xanthene in Fig. 1. That such an absorption line is strongly enhanced is shown by its collapse after the irradiation was shut off.

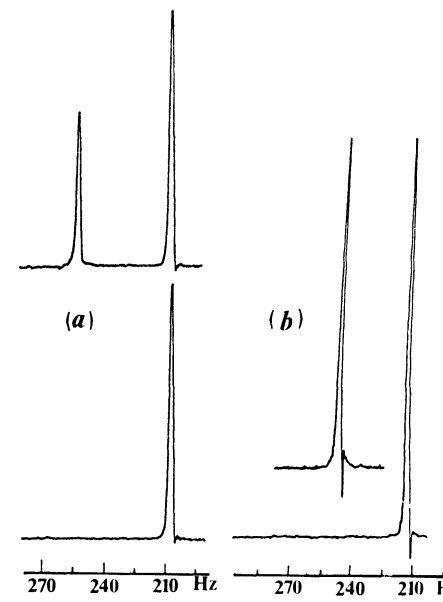

Fig. 1. Enhanced and normal NMR spectra in the photochemical reaction of phenanthraquinone (2.3×10^{-2}M) with hydrogen donor (1.0M) in benzene.

The envelope curves of the singlet lines in Figs. 2 and 3 were obtained at 70°C by field scanning repeated with a saw-tooth wave of 1 Hz for both fluorene and xanthene. Figures 4—6 show the envelope curves for the adducts of fluorene, xanthene, diphenylmethane, and 9,10-dihydroanthracene at 30° and 50°C. As can be seen from these figures, the signal intensity increases exponentially just after the application of light and then establishes its steady-state. When the irradiation is shut off at a certain time, $t=t_0$, signal is diminished exponentially. The values of the loga-

rithms of the signal intensities, $I_\infty - I_t$ and I_{t-t_0}, are plotted against the time (see Fig. 7). Here, I_∞ and I_t represent the signal intensities at the steady-state and at a certain time, t. As may be seen in Fig. 7, the fact that these plots fall on a straight line indicates an exponentially time-dependent nature of the signal intensity. Thus, it may be found that the relaxation times, T_1^* and T_1, in Eqs. (14) and (15) can be determined from the slopes of straight lines in Fig. 7. The values of T_1^* and T_1 are given in Table 1.

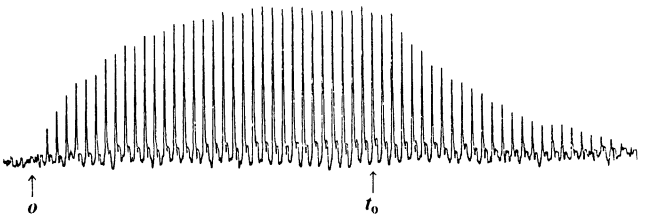

Fig. 2. Envelope curve of enhanced signals due to the methine proton of the adduct of fluorene (field-scanning with saw-tooth wave of 1 Hz, 70°C). Arrows in figure indicate a starting point of the irradiation, $t=0$ and a point of the black-out $t=t_o$.

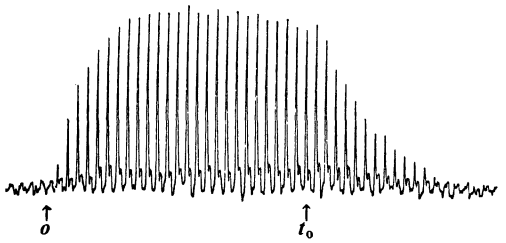

Fig. 3. Envelope curve of enhanced signals due to the methine proton of the adduct of xanthene at 70°C.

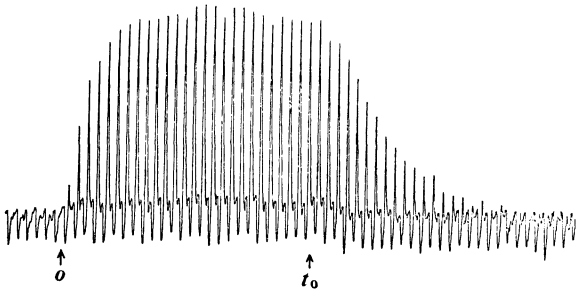

Fig. 4. Envelope curve of enhanced signals due to the methine proton of the adduct of fluorene at 50°C.

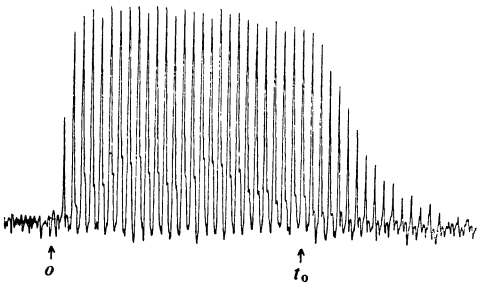

Fig. 5. Envelope curve of enhanced signals due to the methine proton of the adduct of xanthene at 50°C.

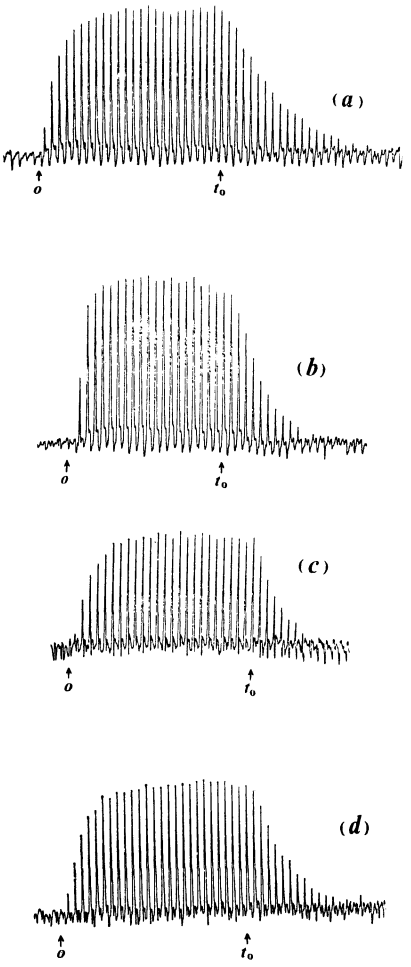

Fig. 6. Envelope curves of enhanced signals due to the methine proton of the adducts of fluorene (a) and xanthene (b) at 30°C, and those of diphenylmethane (c) and 9,10-dihydroanthracene (d) at 50°C.

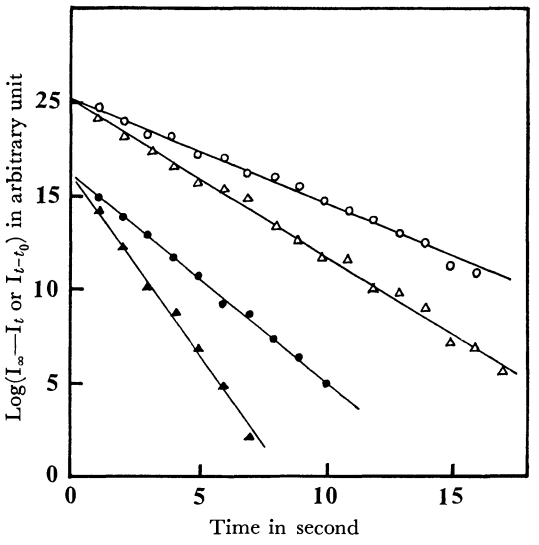

Fig. 7. The time-dependent intensity change of enhanced signals for the adducts of fluorene and xanthene.
△: $\log(I_\infty - I_t)$ for fluorene after the irradiation
○: $\log I_{t-t_0}$ for fluorene after the black-out
▲: $\log(I_\infty - I_t)$ for xanthene after the irradiation
●: $\log I_{t-t_0}$ for xanthene after black-out

TABLE 1. RELAXATION TIMES T_1^* AND T_1 EVALUATED FROM THE ENVELOPE CURVES OF THE ENHANCED SIGNALS

Hydrogen donors	Temperature(°C)	T^*_1 (sec)	T_1 (sec)	Signal intensity[a)]
Fluorene	30	2.1	6.8	
	50	2.6	7.0	2.0
	70	6.6	9.4	
Xanthene	30	1.0	3.6	
	50	0.9	4.3	2.3
	70	3.0	4.6	
Diphenylmethane	50	2.3	3.2	1.8
9,10-Dihydroanthracene	50	2.6	4.4	3.9

a) See the text.

Now, we are interested in the relative values of $\langle[Z_1]-[Z_2]\rangle$, which are proportional to the signal intensity. The intensity ratios of the enhanced signal to the intensity per proton of a methylene group of a given hydrogen donor (concentration; 1.0M) in a benzene solution were evaluated as shown in the last column in Table 1.

Discussion

The envelope curves of enhanced signals are shown in Figs. 2 to 6; the figures represent the typical nature of these photochemical reactions. Contrary to the usual conception of photochemical reactions, in the photo-induced CIDNP examined here the rate constants of nuclear polarization after the irradiation and black-out differed by a factor of about 2 to 4 (see Table 1). It was mentioned in the previous section that the rate constants for nuclear-spin polarization are controlled by the relaxation times of the nuclear-spin system.

For fluorene at 50°C, the relaxation time during the irradiation is 2.6 sec and that under the black-out is 7.0 sec. It is found that the value of T_1^* is generally smaller than that of T_1 and that the ratio of T_1^*/T_1 approaches a unit value with an increase in the temperature. These facts may be responsible for the presence of paramagnetic species during the irradiation, whose concentration must decrease with an increase in the temperature. This is because the relaxation time is inversely proportional to the concentration of paramagnetic species.[17] The steady-state concentration of PQ* is given by (see Eq. (4));

$$[X^*] = \frac{k_0}{1/\tau + k_a}$$

Since the specific rate, k_a, can be considered to increase with an increase in the temperature in the temperature range of 30° to 70°C, the steady-state concentration of PQ* decreases with an increase in the temperature, as may be seen from the last equation. On the other hand, the value of T_1 may well give the usual relaxation time because of the rapid collapse of PQ* just after blacking-out. The facts that the T_1^*/T_1 ratio is smaller than the unit value and that it increases with an increase in the temperature can reasonably be explained in terms of the presence of activated phenanthraquinone PQ* during the irradiation of light.

The enhancement factor, P, is defined as the expression (16); hence, it is experimentally determined from the ratio of the intensity of the enhanced signal to that of the standard solution as follows;

$$P = \frac{[Z]_s}{[Z]_p} \times \frac{I_p}{I_s} \tag{18}$$

where $[Z]_p$ and $[Z]_s$ are the concentration of the proton associated with the enhanced signal and that of the standard methylene protons of hydrogen donors respectively. I_p and I_s represent the signal intensity of the enhanced and that of the standard protons.

In our case, the increase in the rate of the adduct, $[Z]_p=[Z_1]+[Z_2]$, is given by Eq. (10). Since phenanthraquinone exclusively yields 1,2-adducts, $2k_b$ can be neglected compared with $(k_1+k_2+2k_d)$. Thus, one obtains the following expression for the increase in the rate of the 1,2-adduct in the steady-state polarization;

$$[Z]_p = k_0 t$$

The light was very difficult to apply uniformly over the whole of the sample; hence, the exact value of k_0 could not be determined. However, it may be roughly evaluated as below. When the irradiation was kept on continuously, the steady-state polarization was found to be suddenly broken at a certain time, t_b, which was about 100 sec or more at 50°C in all of our experiments. This is the time where the zeroth-order approximation can not hold any longer for the reaction process from X to X*; thus, the concentration of phenanthraquinone at t_b is found to be rather small. Thus, the ratio of the initial concentration of phenanthraquinone to the time, $[X]_0/t_b$, may be taken as the value of k_0. Remembering that $[X]_0=2.3\times10^{-2}$M, we find that $k_0 \gtrsim 2\times10^{-4}$ mol/l/sec.

The value of I_p/I_s is in the range of 2 to 4 (see Table 1). Since $[Z]_s$ is 1.0M, we find that the enhancement factor, P, should amount to the value of 1000—2000 at $t=10$ sec just after the irradiation.

The authors wish to thank Mr. Shozo Shimizu (JEOL (USA), Inc.) for his helpful suggestions for modifying the NMR probe for photochemical reactions.

17) I. Solomon, *Phys. Rev.*, **99**, 559 (1955).

Chemical Constituents of *Alnus sieboldiana* (BETULACEAE)[1] II. The Isolation and Structure of Flavonoids and Stilbenes

Yoshinori ASAKAWA

Department of Chemistry, Faculty of Science, Hiroshima University, Higashisenda-machi, Hiroshima

(Received March 18, 1971)

Four new flavonoids with an unsubstituted B-ring, alnusin, alnetin, alnustin, and alnustinol, isolated from *Alnus sieboldiana* were established to be 3,5,7-trihydroxy-6-methoxyflavone (**1**), 5-hydroxy-6,7,8-trimethoxyflavone (**2**), 5-hydroxy-3,6,7-trimethoxyflavone (**3**), and 3,5,7-trihydroxy-6-methoxyflavanone (**15**) respectively. Some previously-known flavonoids, chrysin (**4**), izalpinin (**5**), tectochrysin (**6**), pinocembrin (**16**), pinobanksin (**17**), strobopinin (**19**) and naringenin (**20**), and some stilbenes, pinosylvin (**24**), pinosylvin monomethyl ether (**25**), and pinosylvin dimethyl ether (**26**), were identified along with the above new flavonoids.

In previous papers,[2] we have reported the isolation and the structure of two new hydroxyketones, *trans*-stilbene (**23**), pinostrobin (**18**), alpinetin (**21**), β-phenylethyl cinnamate, and cinnamic acid from the benzene extract of the male flower of *Alnus sieboldiana*. In the course of continuing the investigation on the viscous substance of the male flower, we further isolated four new flavonoids,[3] accompanied by some previously-known flavonoids and stilbenes. We now wish to report on the structural elucidation, and to present our supposition as to the biosynthetic pathway, of these compounds.

Results and Discussion

The isolation of flavonoids and stilbenes was performed by utilizing their solubility difference in ether and methanol, followed by a combination of column- and preparative thin-layer chromatography on silica gel.

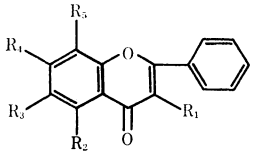

Alnusin(1) $R_1=R_2=R_4=OH$ $R_3=OMe$ $R_5=H$
Alnetin(2) $R_1=H$ $R_2=OH$ $R_3=R_4=R_5=OMe$
Alnustin(3) $R_1=R_3=R_4=OMe$ $R_2=OH$ $R_5=H$
Chrysin(4) $R_1=R_3=R_5=H$ $R_2=R_4=OH$
Izalpinin(5) $R_1=R_2=OH$ $R_3=R_5=H$ $R_4=OMe$
Tectochrysin(6) $R_1=R_3=R_5=H$ $R_2=OH$ $R_4=OMe$
(7) $R_1=R_2=R_4=OAc$ $R_3=OMe$ $R_5=H$
(8) $R_1=R_3=R_4=OMe$ $R_2=OH$ $R_5=H$
(9) $R_1=R_2=R_3=R_4=OMe$ $R_5=H$
(10) $R_1=R_2=R_4=OEt$ $R_3=OMe$ $R_5=H$
(11) $R_1=H$ $R_2=R_3=R_4=R_5=OMe$

Fig. 1

Alnusin (1). Alnusin, the main flavonoid of the plant, was crystallized as yellow plates, mp 239—241°C. Its elemental analysis and the mass spectrum indicated the formula $C_{16}H_{12}O_6$. The compound was shown to be a flavone by alcoholic ferric chloride and magnesium hydrochloric acid tests. The IR spectrum indicated the presence of an α,β-unsaturated carbonyl group (1640 cm^{-1}). The presence of hydroxyl groups were confirmed by the infrared absorption bands at 3350 and 3300 cm^{-1} and by the NMR signal of two singlets at 9.25 and 12.23 ppm. The signal in the far-down field showed the presence of a hydroxyl group which is hydrogen-bonded to the carbonyl group. The acetylation of **1** with acetic anhydride gave the triacetate (**7**), confirming the presence of three hydroxyl groups. The absence of *o*-dihydroxyl groups was indicated by the lack of any appreciable change in the UV spectrum of alnusin on the addition of boric acid-sodium acetate.[4] On the other hand, the presence of the C_7–OH group was suggested by the bathochromic shift on the addition of sodium acetate to the alcoholic solution of **1**.[4] The presence of C_5–OH group was shown by the bathochromic shift in the UV spectrum on the addition of aluminum chloride[4] and by the NMR spectrum of the triacetate, which showed the characteristic resonance of C_5–OAc as a singlet at 2.48 ppm, unlike those of other flavone acetyl groups.[5] The presence of a monosubstituted benzene-ring was shown by the infrared absorption bands at 762 and 680 cm^{-1} and by the A_2B_3 signals of the NMR spectrum at 7.60 and 8.20 ppm. The NMR spectrum of **1** showed a signal for one methoxy proton at 3.89 ppm. The position of the methoxy group was confirmed to be C_6 by the intense quinoid cation (M-15, *m/e* 285) of the mass spectrum, which is characteristic of flavones with the C_6–OMe group.[6] The one-proton singlet at 6.88 ppm was assinged to either the C_3- or the C_8-proton. The treatment of **1** with diazomethane gave trimethylether (**8**), while methylation with dimethyl sulfate resulted in 3,5,6,7-tetramethoxyflavone (**9**).[7] The oxygenation pattern was established by the alkaline degradation of **9** which gave 2-hydroxy-ω-4,5,6-

1) The plant name "*Alnus firma* Sieb. et Zucc." has been given in our previous papers.[2] However, we now wish to correct it to "*Alnus sieboldiana*," due to the identification of *Alnus* species by Professor Hyoji Suzuki of Hiroshima University.

2) a) Y. Asakawa, F. Genjida, S. Hayashi, and T. Matsuura, *Tetrahedron Lett.*, **1969**, 3235. b) Y. Asakawa, This Bulletin, **43**, 575 (1970). c) Y. Asakawa, *ibid.*, **43**, 2223 (1970).

3) Y. Asakawa, F. Genjida, and T. Suga, This Bulletin, **44**, 297 (1971).

4) L. Jurd, "The Chemistry of Flavonoid Compounds," ed. by T. A. Geissman, Pergamon Press, New York (1962),p. 107.

5) C. A. Henrick and P. R. Jefferies, *Aust. J. Chem.*, **17**, 934 (1964).

6) J. H. Bowie and D. W. Cameron, *Aust. J. Chem.*, **19**, 1627 (1966).

7) A. C. Jain, T. R. Seshadri, and K. R. Sreenivasan, *J. Chem. Soc.*, **1955**, 3908.

tetramethoxyacetophenone (**12**) and benzoic acid (**14**). Thus, the structure of alnusin is undoubtedly 3,5,7-trihydroxy-6-methoxyflavone. The NMR solvent shift data[8] obtained on changing the solvent from deuteriochloroform to benzene for alnusin triethylether (**10**) offered further support for the structure of alnusin.

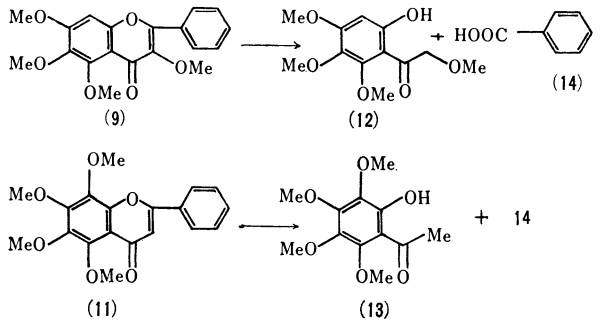

Fig 2.

Alnetin (2). Alnetin was obtained as pale yellow needles (mp 100—101°C). The elemental and mass spectral analyses supported the molecular formula of $C_{18}H_{16}O_6$ (M^+ 328). It showed a positive coloration with ferric chloride. The IR spectrum showed the presence of a hydroxyl group, an α,β-unsaturated carbonyl group, and a monosubstituted benzene-ring. The considerable bathochromic shift of the UV spectrum upon the addition of aluminum chloride to the alcoholic solution of **2** suggested the presence of the C_5–OH group, which was also supported by the NMR signal at 12.45 ppm (s, 1H). The absence of the C_7–OH and *o*-dihydroxyl groups was based on the lack of any appreciable change in the UV spectrum upon the addition of sodium acetate or boric acid-sodium acetate. The NMR spectrum indicated the presence of three methoxy groups (3.95, 3.97, 4.10 ppm, each s, 9H), one aromatic proton (6.69 ppm, s, 1H), monosubstituted benzene-ring protons (7.56, 7.95 ppm, m, 5H), and a chelated hydroxyl group (12.45 ppm, s, 1H). The methylation of **2** with dimethyl sulfate afforded a tetramethoxy derivative (**11**) which was identical with the 5,6,7,8-tetramethoxyflavone reported by Lee *et al.*[9] The hydrolysis of the tetramethoxy derivative (**11**) with aluminum chloride in ether gave the original compound. The treatment of **11** with a 50% potassium hydroxide solution gave 2-hydroxy-3,4,5,6-tetramethoxyacetophenone (**13**) and benzoic acid (**14**). Alnetin has thus been assinged the (**2**) structure. This compound has never been isolated from any natural source; it has been reported only as a synthetic product.[9]

Alnustin (3). Alnustin, $C_{18}H_{16}O_6$, mp 175—176°C, M^+ 328, was obtained as yellow plates. The compound showed a positive coloration with ferric chloride, and all of its spectra were typical of flavoniods. The IR spectum showed the presence of an α,β-unsaturated carbonyl group and a monosubstituted benzene-ring. The UV spectrum, upon the addition of sodium acetate, boric acid-sodium acetate, or aluminum chloride, showed that **3** contained no *o*-dihydroxyl groups and no C_7–OH, but it did contain the free C_5–OH group. The presence of the C_5–OH group was also indicated by the far-down signal at 12.58 ppm (s, 1H) in the NMR spectrum. The other signals in the spectrum were assigned to monosubstituted benzene-ring protons (7.56, 8.10 ppm, m, 5H), three methoxy groups (3.89, 3.94, 3.97 ppm, each s, 9H), and C_8–H (6.54 ppm, s, 1H). On methylation with dimethyl sulfate, Compound (**3**) gave a tetramethoxy derivative (**9**) which was identical with 3,5,6,7-tetramethoxyflavone. The demethylation of **9** with aluminum chloride in ether gave the original compound. Thus, the structure of alnustin was established as 5-hydroxy-3,6,7-trimethoxyflavone.

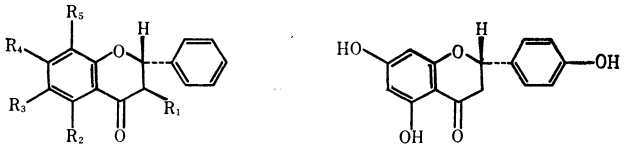

Naringenin (20)

Alnustinol(15)	$R_1=R_2=R_4=OH$ $R_3=OMe$ $R_5=H$
Pinocembrin(16)	$R_1=R_3=R_5=H$ $R_2=R_4=OH$
Pinobanksin(17)	$R_1=R_2=R_4=OH$ $R_3=R_5=H$
Pinostrobin(18)	$R_1=R_3=R_5=H$ $R_2=OH$ $R_4=OMe$
Strobopinin(19)	$R_1=R_5=H$ $R_2=R_4=OH$ $R_3=Me$
Alpinetin(21)	$R_1=R_3=R_5=H$ $R_2=OMe$ $R_4=OH$
(22)	$R_1=R_2=OH$ $R_3=R_4=OMe$ $R_5=H$

Fig 3.

Alnustinol (15).[10] Alnustinol was isolated in a minute quantity as colorless needles, mp 175—176°C, M^+ 302. The compound gave the characteristic coloration of flavanonols with ferric chloride, magnesium hydrochloric acid, and zinc hydrochloric acid and in Pachcós tests. The IR spectrum indicated the presence of hydroxyl groups, an α,β-unsaturated carbonyl group, and a monosubstituted benzene-ring. The lack of the bathochromic shift in the UV spectrum, on the addition of boric acid-sodium acetate, showed the absence of *o*-dihydroxy groups. On the other hand, the considerable bathochromic shift on the addition of aluminum chloride or sodium acetate indicated the presence of the C_7–OH and C_5–OH groups. The latter hydroxyl group was also confirmed by the NMR signal at 11.34 ppm (s, 1H). The NMR spectrum exhibited the signals at 3.86 ppm (s, 3H) assignable to a methoxy group, at 4.40 ppm and 4.97 ppm (typical AB doublet, J=12 Hz, 2H) assignable to the flavanonol structure, and at 5.99 ppm (s, 1H) to C_8–H, and at 7.33 ppm (s, 5H) assignable to monosubstituted benzene-ring protons. The presence of the C_3–OH group was supported by the fragment ions at *m/e* 273 (M–CHO) and 91 (120–CHO) which are characteristic of 3-hydroxyflavanone.[11] Chemical evidence in favor

8) R. G. Wilson, J. H. Bowie, and D. H. Williams, *Tetrahedron*, **24**, 1407 (1968).

9) H. H. Lee and C. H. Tan, *J. Chem. Soc.*, **1965**, 2743.

10) In the previous paper,[3] the structure of alnustinol has been given as 3,5,8-trihydroxy-7-methoxyflavanone. The author now wishes to correct it to 3,5,7-trihydroxy-6-methoxyflavanone from the results of the reexamination of the solvent shift in the UV spectrum and the chemical reactions.

11) H. Audier, *Bull. Soc. Chim. Fr.*, **1966**, 2892.

of the C_5–OH and C_3–OH groups in alnustinol was obtained by its reaction with diazomethane,[12] which gave only a monomethylated compound (**22**). Hence, the structure of 15 may be said to be 3,5,7-trihydroxy-6-methoxy- or 3,5,7-trihydroxy-8-methoxyflavanone. The dehydrogenation of **15** with palladium charcoal gave a flavonol which was shown to be identical with 3,5,7-trihydroxy-6-methoxyflavone (**1**). On the basis of the above chemical and spectral evidence, alnustinol was established to be 3,5,7-trihydroxy-6-methoxyflavanone (**15**). 3,5,6,7-Tetrasubstituted- and fully oxygenated A-ring flavonoids with an unsubstituted B-ring are rare in nature.

The Known Flavonoids and Stilbenes. Nine flavonoids, chrysin (**4**), izalpinin (**5**), tectochrysin (**6**), pinocembrin (**16**), pinobanksin (**17**), pinostrobin (**18**), strobopinin (**19**), naringenin (**20**), and alpinetin (**21**), were identified by the comparison of their physical and chemical properties with those of authentic samples

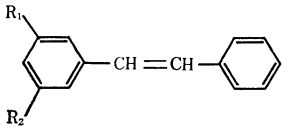

trans-Stilbene (23) $R_1=R_2=H$
Pinosylvin (24) $R_1=R_2=OH$
Pinosylvin monomethyl ether (25) $R_1=OH$ $R_2=OMe$
Pinosylvin dimethyl ether (26) $R_1=R_2=OMe$

Fig 4.

or with those reported previously. Also, three stilbenes, pinosylvin (**24**), pinosylvin monomethyl ether (**25**), and pinosylvin dimethyl ether (**26**), were confirmed by the same methods as above. In the mass spectrum of *trans*-stilbene (**23**), the loss of the methyl radical (M-15) from the molecular ion is observed; this fragmentation process has shown, by the deuterium labelling, that one of the central CH groups, together with an ortho-hydrogen atom from either ring, is eliminated.[13] Similar losses of a methyl radical are also observed in pinosylvin, pinosylvin monomethyl ether, and pinosylvin dimethyl ether. Except for the M-15 ion, all these stilbenes involve the strong fragment ion at *m/e* 165 which was determined to be $C_{13}H_9^+$ by high-resolution mass measurements. Thus, stilbenes isolated from natural source can be detected by the mass spectrum with characteristic fragment ions at *m/e* M-15, and *m/e* 165 ($C_{13}H_9^+$), and the molecular ion appears as a base peak. It is known that the stilbenes of the genus Pinus serve as chemotaxonomic tracers in the *Pinaceae*[14] and that pinosylvin and its monomethyl ether have biological activity and protect the heartwood from wood-rotting fungi and insects.[15] Stilbenes have been found in *Pinaceae*, *Moraceae*, *Saxifragaceae*, *Myrtaceae*, *Polygonaceae*, *Fagaceae*, *Liguminosae*, and *Liliaceae* as free and/or glycoside forms.[16] Hence, it is notable that this paper is reporting the first example of the isolation of the stilbenes (**23**, **24**, **25**, and **26**) from the *Betulaceae*.

Biogenesis. Flavonoids and stilbenes have been found to occur together in the heartwood of various pines,[14] *Morus bomycis*,[17] and *Eucalyptus* species.[18] Apparently, the co-existence of these compounds has never been found in *Betulaceae*. The coexistence of the flavonoids and stilbenes in the same plant and the analogy of the structure of the isolated compounds provide important clues for the elucidation of their biogenesis. Almost all the compounds isolated from *A. sieboldiana* possessed a monosubstisuted benzene-ring in the molecule; only naringenin (**20**) did not. The male flower of this plant contained a large quantity of free cinnamic acid. Accordingly, the above monosubstituted benzene-ring must arise from cinnamic acid. The route of synthesizing pinosylvin (**24**) has recently been established by the isolation of the enzyme, which catalyzes the cyclization of cinnamoyl triacetic acid to pinosylvin (**24**), from *Eucalyptus sideroxylon* leaves,[18] while the formation of various flavonoids from chalkone has been confirmed by means of a parallel competetive feeding experiment.[19]

The flavonoids and stilbenes isolated from *A. sieboldiana* may be formed by a combination of the shikimic acid and acetate (polyketide) pathways. We would like to propose the biosynthetic pathway of the flavonoids and stilbenes shown in Scheme 1.

Experimental

All the melting points are uncorrected. Analytical and preparative tlc were carried out using silica gel GF_{254} and $HF_{254+366}$ (Merck) using a solvent composed of benzene, dioxane, and acetic acid (90:25:4 vol%). The spot was detected by using the UV light (254 and 366 nm) and/or iodine vapor. The mass spectra were recorded on a Hitachi-RMU 6D Mass spectrometer under the following conditions: chamber volt, 70 V; vacuum, 3.0×10^7 mmHg; ion chamber temp., 250°C; direct sample-introduction system. The high-resolution mass spectra were measured on a MS 902 double-focusing instrument. The UV, IR, and NMR spectra were measured by the methods reported in a preceding paper.[2c]

Extraction and Isolation. The *Alnus sieboldiana* was collected near Hiroshima City in March, 1969. The male flower (95 kg) was extracted with benzene for three months. The benzene extract (780 g) was successively extracted with a 5% aqueous sodium bicarbonate solution (Fraction 1), a 5% aqueous sodium carbonate solution (Fraction 2), and a 5% sodium hydroxide solution (Fraction 3).

Alnustinol (15). The neutralization of Fraction 1 with dilute hydrochloric acid and extraction with ether yielded a brown slurry (8 g). It was triturated with ether to give alnustinol (**15**). The crystallization of **15** from *n*-hexane gave colorless needles (58 mg); mp 175—176°C; $FeCl_3$ (dark

12) R. Robinson and K. F. Tseng, *J. Chem. Soc.*, **1938**, 1004.
13) R. A. W. Johnstone and B. J. Millard, *Z. Naturf.*, **21a**, 604 (1966).
14) G. Lindstedt and A. Misiorny, *Acta Chem. Scand.*, **5**, 121 (1951).
15) H. Erdtman and E. Rennerfelt, *Svensk Pappersmasse Tidn*, **47**, 45 (1944).
16) G. Billek, *Fortschr. Chem. org. Naturst.*, **22**, 115 (1964).
17) T. Knodo, H. Ito, and M. Suda, *Nippon Nogeikagaku Kaishi*, **32**, 1 (1958).
18) W. E. Hillis and N. Ishikura, *Phytochem.*, **8**, 1079 (1969).
19) E. Wong, *Chem. Comm.*, **1968**, 395. E. Wong and H. Grisebach, *Phytochem.*, **8**, 1419 (1969).

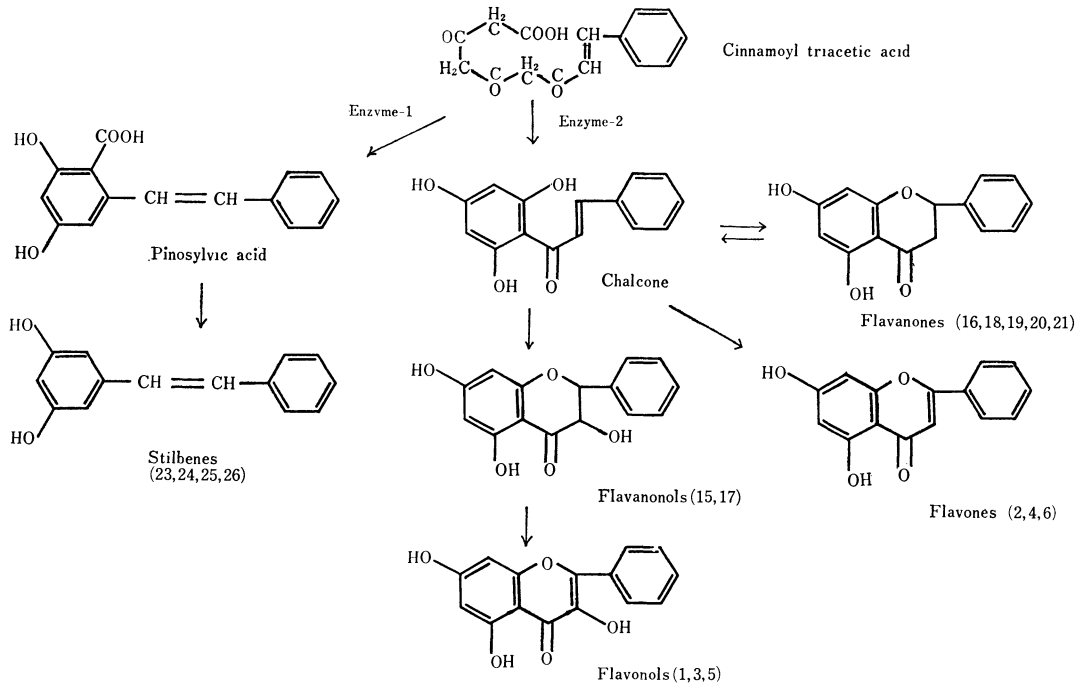

Scheme 1. Biosynthetic pathways of flavonoids and stilbenes isolated from the male flower of *A. sieboldiana*.

green), Mg-HCl (yellow), Zn-HCl (yellow), Pachcós test (reddish brown); UV spectrum λ_{max}^{EtOH} 215 nm (log ε, 4.58), 226_{sh} (4.48), 295 (4.32), 340 (3.65), $\lambda_{max}^{EtOH+AlCl_3}$ 226 (4.36), 318 (4.48), 400 (3.55), $\nu_{max}^{EtOH+NaOAc}$ 216 (4.34), 300 (4.14), 335 (4.41), $\lambda_{max}^{EtOH+NaOEt}$ 215 (4.43), 245 (4.18), 333 (4.41); IR spectrum, λ_{max}^{Nujol} 3480, 3460, 3340 (OH), 1635—1654 (CO), 1588, 1498, 1358, 1298, 1175, 1164, 1126, 1086, 1000, 990, 963, 884, 838, 797, 752, 685 cm^{-1}; NMR signals ($CDCl_3$), δ=3.49 (s, C_3–OH), 3.86 (s, C_6–OMe), 4.40 (d, J=12 Hz, C_3–H), 4.97 (d, J=12 Hz, C_2–H), 5.99 (s, C_8–H), 7.33 (s, 5H, B-ring protons), 11.34 ppm (s, C_5–OH); mass spectrum (prominent) *m/e* 302 (M^+), 273, 195, 183 (base), 182, 167, 156, 120, 91, 77, 69.

Found: C, 63.95; H, 4.87%. Calcd for $C_{16}H_{14}O_6$; C, 63.57; H, 4.67%.

Chrysin (4), Pinocembrin (16), and *pinobanksin (17).* Fraction 2 was acidified with 5% hydrochloric acid and then extracted with chloroform. The refrigeration of the brown viscous material (0.85 g) dissolved in ether diposited a yellow mass. Subsequent crystallization from methanol gave chrysin (**4**) (40 mg); mp 275—277°C, lit,[20] 278—279°C; ν_{max}^{Nujol} 3350—3050 (OH), 1640 (CO), 795 cm^{-1}; *m/e* 254 (M^+, base), 226, 152, 124, 113, 77, 69. On the other hand, more cooling of the mother liquor gave another pale yellow mass. Subsequent crystallization from methanol afforded white needles of pinocembrin (**16**) (150 mg); mp 200—201°C, lit,[21] 193—194°C; ν_{max}^{Nujol} 3250—2500 (OH), 1623 (CO), 1155 cm^{-1}; *m/e* 256 (M^+, base), 179, 153, 152, 124, 104, 103, 96, 78, 77, 69, 51. When the combined mother liquor was subjected to preparative thin-layer chromatography, it yielded pinobanksin (**17**) (8 mg); mp 177—178°C, lit,[21] 177—178°C; ν_{max}^{Nujol} 3465 (OH), 1625 (CO), 815 cm^{-1}.

Alnusin (1), Alnetin (2), Alnustin (3), Tectochrysin (6), Izalpinin (5), Pinostrobin (18), Strobopinin (19), Naringenin (20), Alpinetin (21), Pinosylvin (24), and *Pinosylvin monomethyl ether (25).* Fraction 3 was extracted with chloroform after acidification with dilute hydrochloric acid. The removal of the solvent yielded a brown solid (8.45 g), which was then dissolved in ether and kept in a refrigerator. The major flavonol, alnusin (**1**), was thus deposited as yellow mass (2.85 g); mp 239—241°C (from methanol); $FeCl_3$ (dark green), Mg-HCl (pink); λ_{max}^{EtOH} 238 (3.91), 270 (4.25), 325 (4.26), 362_{sh} (4.20), $\lambda_{max}^{EtOH+AlCl_3}$ 251 (4.33), 278 (4.38), 350 (4.25), 415 (4.26), $\lambda_{max}^{EtOH+NaOAc}$ 271 (4.39), 328 (4.15), 368 (4.20), $\lambda_{max}^{EtOH+NaOEt}$ 212 (4.26), 234 (4.13), 281 (4.00), 347 (3.71), 413 (3.95); ν_{max}^{Nujol} 3350, 3300 (OH), 1640 (CO), 1615, 1590, 1548, 1490, 1480, 1387, 1318, 1295, 1260, 1215, 1200, 1170, 1155, 1098, 1073, 1065, 1033, 1020, 970, 883, 805, 789, 762, 735, 695, 680, 585 cm^{-1}; δ (CD_3COCD_3)=3.89 (s, 3H, C_6–OMe), 6.68 (s, 1H, C_8–H), 9.25 (s, C_3 or C_7–OH), 7.60 and 8.20 (m, 5H, B-ring protons), 12.23 ppm (s, 1H, C_5–OH); *m/e* 300 (M^+), 285 (M-15, 50%), 283 (M–OH), 282 ($M-H_2O$), 271, 257 (M–MeCO, base), 131, 105, 77, 69, 51, 39;

Found: C, 64.88; H, 4.29%. Calcd for $C_{16}H_{12}O_6$: C, 64.00; H, 4.03%.

The removal of the solvent from the mother liquor affored a brown solid, which was then chromatographed on a silica-gel column using a mixture of ether and methanol, thus dividing it into four eluates. The first eluate was further chromatographed on a silica-gel column using chloroform to give pinostrobin (**18**) (0.87 g) and alnetin (**3**) (0.48 g) as yellow needles; mp 100—101°C (from *n*-hexane); $FeCl_3$ (dark green); λ_{max}^{EtOH} 207 (4.52), 282 (4.56), 320 (3.84), $\lambda_{max}^{EtOH+AlCl_3}$ 206 (4.35), 218 (4.29), 300 (4.33), 336 (3.88), 415 (3.14), $\lambda_{max}^{EtOH+NaOEt}$ 216 (4.20), 229 (4.04), 286 (4.37), 410 (3.46); ν_{max}^{Nujol} 3350 (OH), 1660 (CO), 760, 675 cm^{-1} (monosubst. benzene-ring); δ ($CDCl_3$)=3.95, 3.97, 4.10 (s, 9H, 3 OMe), 6.69 (s, 1H, C_3–H), 7.56 and 7.95 (m, 5H, B-ring protons), 12.45 ppm (s, 1H, C_5–OH), δ (benzene)=3.83, 3.64, and 3.80 ppm (s, 3 OMe); *m/e* 328 (M^+), 314, 315 (M-15), 183, 77, 69 (base).

Found: C, 65.85; H, 4.88%. Calcd for $C_{18}H_{16}O_6$: C, 65.85; H, 4.91%.

The second eluate gave alnustin (**3**) (0.65 g); mp 175—176°C (from *n*-hexane); $FeCl_3$ (dark green); λ_{max}^{EtOH} 207 (4.28), 213 (4.28), 245 (4.00), 271 (4.30), 317 (4.09), $\lambda_{max}^{EtOH+AlCl_3}$ 207 (4.28), 224 (4.15), 253 (3.85), 286 (4.28), 337 (4.08),

20) H. Erdtman, *Chem. Abstr.*, **40**, 1309 (1946).
21) V. B. Mahesh and T. R. Seshadri, *J. Sci. Instr. Res.*, **13B**, 835 (1954).

392 (4.01), $\lambda_{max}^{EtOH+NaOEt}$ 215 (4.59), 226 (4.60), 289 (4.54), 385 (3.85); ν_{max}^{Nujol} 1660 (CO), 1590, 1300, 1235, 1215, 1175, 1120, 980, 800, 765, and 695 cm^{-1} (monosubst. benzene-ring); δ ($CDCl_3$)=3.89, 3.94, 3.97 (s, 9H, 3 OMe), 6.54 (s, 1H, C_8–H), 7.56 and 8.10 ppm (m, 5H, B-ring protons), 12.85 ppm (s, 1H, C_5–OH), δ (benzene)=3.23, 3.67, and 3.87 ppm (s, 3 OMe); *m/e* 328 (M^+, base), 327, 313 (M-15), 309, 285, 153, 118, 105, 89, 77, 69.

Found: C, 65.90; H, 4.86%. Calcd for $C_{18}H_{16}O_6$: C, 65.85; H, 4.91%.

The third eluate was further subjected to column chromatography on silica-gel using a mixture of chloroform and methanol; this gave pinosylvin monomethyl ether (**25**) (0.25 g) and izalpinin (**5**) (70 mg).

Pinosylvin monomethyl ether (**25**); mp 119—120°C, lit,[21] 118—120°C; λ_{max}^{EtOH} 303 (4.26); ν_{max}^{Nujol} 3338 (OH), 955 (*trans*-CH=CH), 680 cm^{-1}; *m/e* 226 (M^+, base), 225, 211 (M-15), 210, 195 (M–OMe), 194, 165 ($C_{13}H_9^+$: Found 165.0696; Calcd. 165.0704).

Izalpinin (**5**): mp 190—191°C, lit,[21] 192—193°C; δ (CD_3COCD_3)=3.83 (s, 3H, OMe), 6.38 (d, J=2 Hz, 1H), 6.50 (d, J=2 Hz, 1H), 7.62 and 8.17 (m, 5H, B-ring protons), 12.64 ppm (s, 1H, C_5–OH).

The fourth eluate was repeatedly subjected to preparative thin-layer chromatography, thus isolating tectochrysin (**6**), (25 mg), strobopinin (**19**) (12 mg), naringenin (**20**) (22 mg), alpinetin (**21**) (19 mg), and pinosylvin (**24**) (48 mg).

Tectochrysin (**6**): mp 165—166°C, lit,[21] 163—164°C; ν_{max}^{Nujol} 1660 (CO), 795, 759, 681, 632 cm^{-1}; *m/e* 268 (M^+, base), 255, 240, 166, 138, 123, 95, 77, 39.

Strobopinin (**19**): mp 225—226°C, lit,[20] 225—227°C; λ_{max}^{EtOH} 295 (4.33), 338 (3.70); ν_{max}^{Nujol} 1640 (CO), 810, 700 cm^{-1}; *m/e* 270 (M^+), 269, 193, 166 (base), 138, 120, 104, 69, 51, 39.

Naringenin (**20**): mp 251—252°C, lit,[22] 248°C; λ_{max}^{EtOH} 290 (4.33); ν_{max}^{Nujol} 3300—3110 (OH), 1634 (CO), 820 cm^{-1}; *m/e* 272 (M^+), 271, 179, 166, 153 (base), 152, 124, 120, 107, 91, 69, 31.

Pinosylvin (**24**): mp 156—158°C, lit,[21] 153—155°C; λ_{max}^{EtOH} 305 (4.49); ν_{max}^{Nujol} 953 (*trans* CH=CH), 675 cm^{-1}; *m/e* 212 (M^+, base), 211, 197 (M-15), 195, 194, 165 ($C_{13}H_9^+$: Found 165.0709; Calcd. 165.0704), 141, 128, 77, 69, 55, 51, 39.

Methylation with diazomethane yielded pinosylvin dimethyl ether (**26**).

Pinosylvin Dimethyl Ether (26). A sample of a neutral fraction (50 g) was chromatographed on a silica-gel column using a mixture of *n*-hexane and ether (1:1) to give pinosylvin dimethyl ether (**26**) as a yellow oil (0.225 g); λ_{max}^{EtOH} 305 (4.39); $\nu_{max}^{liq.}$ 950 (*trans* CH=CH), 740, 682 cm^{-1}; *m/e* 240 (M^+, base), 239, 225 (M-15), 209 (M–OMe), 194, 165 ($C_{13}H_9^+$: Found 165.0706; Calcd. 165.0704), 152, 77, 55. The demethylation of **26** with pyridine hydrochloride gave pinosylvin (**24**).

Methylation of Alnusin (1). *A) With Diazomethane*: The treatment of a methanol solution of alnusin (0.1 g) with excess diazomethane at 0°C for 3 hr gave 5-hydroxy-3,6,7-trimethoxy flavone (**8**) (74 mg), mp 175—176°C, which was identical with alnustin (**3**) in all respects.

B) With Dimethyl Sulfate: The refluxing of an acetone solution of alnusin (0.4 g) with dimethyl sulfate (2 m*l*) in the presence of dry potassium carbonate (3.0 g) gave 3,5,6,7-tetramethoxyflavone (**9**) (0.3 g); mp 112.0—112.5°C, lit,[7] 110—111°C; λ_{max}^{EtOH} 213 (4.50), 240 (4.21), 260 (4.30), 310 (4.30); ν_{max}^{Nujol} 1637 (CO), 1627, 1232, 973, 813, 790, 778, 701 cm^{-1}; δ ($CDCl_3$)=3.88, 3.92, 3.97, 4.02 (s, 12H, 4 OMe), 6.78 (s, 1H, C_8–H), 7.55 and 8.22 (m, 5H, B-ring protons), δ (benzene)=3.28, 3.75, 3.80, 4.04 (s, 3 OMe); *m/e* 342 (M^+), 327 (M-15, base), 323, 311, 283, 195, 167, 141, 105, 77, 69.

Found: C, 66.11; H, 5.41%. Calcd for $C_{19}H_{18}O_6$: C, 66.66; H, 5.30%.

Acetylation of Alnusin (1). The acetylation of **1** (76 mg) with acetic anhydride in the presence of pyridine gave the triacetate (**7**) (66 mg); mp 142—144°C (from *n*-hexane-ethyl acetate); λ_{max}^{EtOH} 257 (3.89), 300 (3.80); ν_{max}^{Nujol} 1770 (acetate), 1644 (CO), 1182, 699 cm^{-1}; δ ($CDCl_3$)=2.29 (s, 3H, MeCO), 2.38 (s, 3H, MeCO), 2.45 (s, 3H, C_5–MeCO), 3.86 (s, 3H, C_6–OMe), 7.27 (s, 1H, C_8–H), 7.55 and 7.79 ppm (m, 5H, B-ring protons), δ (benzene)=3.69 (s, OMe); *m/e* 426 (M^+), 384, 342, 300 (base,) 285, 282, 271, 257, 105, 77, 69, 43.

Ethylation of Alnusin (1). The heating of the acetone solution of **1** (68 mg) with ethyl iodide (4 g) and dry potassium carbonate (2 g) for 70 hr gave the triethyl ether derivative (**10**) (40 mg); λ_{max}^{EtOH} 262 (3.69), 312 (3.64); δ ($CDCl_3$)=1.28 (t, J=7 Hz, 3H, Me), 1.51 (t, J=7 Hz, 6H, 2 Me), 3.90 (s, 3H, OMe), 4.18 (q, J=7 Hz, 6H, 3 CH_2), 6.71 (s, 1H, C_8–H), 7.48 and 8.08 ppm (m, 5H, B-ring protons), δ (benzene)=1.09 (t, J=7 Hz, 3H, Me), 1.20 (t, J=7 Hz, 3H, Me), 1.56 (t, J=7 Hz, 3H, Me), 3.48 (q, J=7 Hz, 2H, CH_2), 3.48 (q, J=7 Hz, 2H, CH_2), 3.75 (s, OMe), 4.25 (q, J=7 Hz, 2H, CH_2), 4.28 (q, J=7 Hz, 2H, CH_2).

Methylation of Alnetin (2). The methylation of **2** (0.35 g) with dimethyl sulfate in the same manner as above yielded **11** (0.32 g); 112—113°C, lit,[9] 112—113°C; λ_{max}^{EtOH} 207 (4.40), 270 (4.34), 305 (4.08); ν_{max}^{Nujol} 1660 (CO), 763, 680 cm^{-1}; δ ($CDCl_3$)=3.96 (s, 6H, 2 OMe), 4.04 (s, 3H, OMe), 4.10 (s, 3H, OMe), 6.70 (s, 1H, C_3–H), 7.57 and 7.96 ppm (m, 5H, B-ring protons), δ (benzene)=3.65, 3.73, 3.77, 4.01 ppm (s, 4 OMe); *m/e* 342 (M^+), 327 (M-15, base), 284, 197, 182, 83.

Found: C, 66.27; H, 5.30%. Calcd for $C_{19}H_{18}O_6$: C, 66.66; H, 5.30%.

Methylation of Alnustinol (15). The methylation of alnustinol (18 mg) with diazomethane yielded **22** (15 mg); mp 189.0—189.5°C (from benzene); λ_{max}^{EtOH} 216 (4.28), 234 (4.21), 292 (4.31), 340 (3.52), $\lambda_{max}^{EtOH+AlCl_3}$ 227 (4.29), 316 (4.36), 390 (3.22), $\lambda_{max}^{EtOH+NaOEt}$ 244 (4.42), 295 (4.35), 377 (3.87); ν_{max}^{Nujol} 3498 (OH), 1635 (CO), 765 and 698 cm^{-1}; δ ($CDCl_3$)=3.48 (bs, 1H, C_3–OH), 3.83 (s, 3H, C_6–OMe), 6.12 (s, C_8–H), 4.54 (d, J=12 Hz, 1H, C_3–H), 5.10 (d, J=12 Hz, 1H, C_2–H), 7.49 (s, 5H, B-ring protons), 11.03 ppm (s, 1H, C_5–OH); *m/e* 316 (M^+), 287 (M–CHO), 198, 197, (base), 196, 182, 181, 170, 167, 155, 154, 136, 125, 120, 91, 77, 69, 65, 51, 39.

Found: C, 63.95; H, 4.87. Calcd for $C_{17}H_{16}O_6$: C, 63.57; H, 4.67%.

Alkaline Degradation of 3,5,6,7-Tetramethoxyflavone (9). The flavone (**9**) (0.18 g) was refluxed in a mixture of a 50% potassium hydroxide solution (16 m*l*) and ethanol (7 m*l*) in a current of nitrogen for 20 hr. After acidification, the ether extract was washed with a 5% sodium bicarbonate solution. The ethereal layer provided 2-hydroxy-ω-4,5,6-tetramethoxy-acetophenone (**12**) (68 mg); mp 69—71°C; λ_{max}^{EtOH} 211 (4.14). 228 (4.29), 298 (4.33), 308 (4.37); ν_{max}^{Nujol} 3370 (OH), 1625 (CO), 780 cm^{-1}; δ ($CDCl_3$)=3.50 (s, 3H, ω-OMe), 3.73, 3.85, 3.99 (s, 9H, 3 OMe), 4.61 (s, 2H, -COC$\underline{H}_2$–O–), 6.23 (s, 1H, C_3–H), 13.12 (s, 1H, C_2–OH). On the other hand, the sodium bicarbonate washings gave benzoic acid (**14**); mp 121—122°C.

Alkaline Degradation of 5,6,7,8-Tetramethoxyflavone (11). The alkaline degradation of the flavone (**11**) (41 mg) for 20 hr in the same manner as above gave 2-hydroxy-3,4,5,6-tetramethoxy acetophenone (**13**); λ_{max}^{EtOH} 280 (3.74), 345 (3.16);

22) J. Shinoda and S. Kamieda, *Yakugaku Zasshi*, **49**, 575 (1929).

$\nu_{max}^{liq.}$ 3400 (OH), 1620 (CO), 730 cm^{-1}; δ ($CDCl_3$)=2.66 (MeCO), 3.80, 3.85, 3.85, 4.07 ppm (s, 12H, 4 OMe); the 2,4-Dinitrophenylhydrazone: mp 169—171°C, lit,[9] 168—170°C. Benzoic acid was obtained from the sodium bicarbonate washings.

*Dehydrogenation of Alnustinol (**15**).* The heating of alnustinol (40 mg) with palladium charcoal (10 mg) in the presence of cinnamic acid (0.18 g) gave 3,5,7-trihydroxy-6-methoxyflavone, which was identical to alnusin (**1**) in all respects.

The author wishes to express his hearty gratitude to Dr. Takayuki Suga and Professor Emeritus Tamon Matsuura of Hiroshima University for their guidance and encouragement. The author is also indebted to Professor Hyoji Suzuki of Hiroshima University for his suggestions about identifing *Alnus sieboldiana,* to Professor Shô Itô of Tohoku University for the measurement of the mass spectra, and to Dr. M. E. Wall of the Research Triangle Institute for the measurement of the high-resolution mass spectra. Thanks are also due to Professor H. Erdtman of the Royal Institute Technology for kindly supplying tectochrysin, pinocembrin, chrysin, and pinosylvin monomethyl ether and also for his helpful advice, and to Dr. H. H. Lee of the University of Malaya for his kind gift of the 5,6,7,8-tetramethoxyflavone used in this investigation.

BULLETIN OF THE CHEMICAL SOCIETY OF JAPAN, VOL. 44, 2766—2770 (1971)

The Total Synthesis of (±)-Taxodione, A Tumor Inhibitor[1]

Takashi MATSUMOTO, Yakudo TACHIBANA, Junji UCHIDA, and Kenji FUKUI

Department of Chemistry, Faculty of Science, Hiroshima University, Higashi-sendamachi, Hiroshima

(Received March 19, 1971)

A total synthesis of (±)-taxodione (I) has been achieved. The Friedel and Crafts reaction of 1,2-dimethoxy-3-isopropylbenzene (IV) with succinic anhydride gave β-(4-hydroxy-3-isopropyl-5-methoxybenzoyl)propionic acid (V), which was then converted to γ-(4,5-dimethoxy-3-isopropylphenyl)butyric acid (IX). Since the cyclization of IX gave 6,7-dimethoxy-8-isopropyl-1-tetralone (X), the acid (IX) was subjected to bromination, cyclization, and then debromination. Subsequently, 7,8-dimethoxy-6-isopropyl-1-tetralone (XIII) was converted to (±)-7,8-dimethoxy-6-isopropyl-1-methyl-2-tetralone (XV). The condensation of (±)-XV with the methyl vinyl ketone gave a (±)-hexahydro-2-oxo-phenanthrene derivative (XVI), which was then further converted to (±)-11,12-dimethoxyabieta-5,8,11,13-tetraene (XIX). The introduction of a carbonyl group at the 6 position was achieved by the hydroboration of (±)-XIX, followed by the oxidation of the resulting 6-hydroxyl derivative. Finally, (±)-11,12-dimethoxyabieta-8,11,13-trien-6-one (XXI) was converted to (±)-I, whose IR, UV, and NMR spectra were identical in every respect with those of natural taxodione.

Taxodione, a tumor-inhibitory diterpenoid quinone methide, was recently isolated from *Taxodium distichum* Rich (Taxodiaceae) by Kupchan *et al.*[2,3] On the basis of spectral and chemical studies, they deduced the structure of taxodione to be I. Because of its unique structure and, especially, its significant tumor-inhibitory activity against the Walker carcinosarcoma 256 in rats, we planned the total synthesis of I by the route of C→B→A ring construction. During the course of the present work, Mori and Matsui[4] reported on the synthesis of I starting from podocarpic acid (II) *via* 11,12-dimethoxyabieta-8,11,13-triene (III). The appearance of their publication prompts us to report our own results. The present paper will describe the total synthesis of (±)-taxodione.

1,2-Dimethoxy-3-isopropylbenzene (IV),[5] which corresponds to the C ring in I, was chosen as our starting material. The Friedel and Crafts reaction of IV with succinic anhydride in dichloromethane gave a keto-acid (V), which was then methylated with diazomethane to a methyl ester (VI). The V acid gave a positive ferric chloride reaction in ethanol and showed bands at 1703 (CO_2H) and 1659 cm^{-1} (C=O) in its IR spectrum. The NMR spectrum of V in $CDCl_3$ showed signals at δ 7.41 ppm and δ 7.54 ppm (each 1H doublet and J=2 Hz) due to aromatic protons, thus suggesting the presence of two meta-coupling protons. Further, the signal due to the methine proton of the isopropyl group appeared at δ *ca.* 3.3 ppm in $CDCl_3$ and at δ *ca.* 3.7 ppm in pyridine-d_5. This pyridine-induced solvent shift[6] suggested the presence

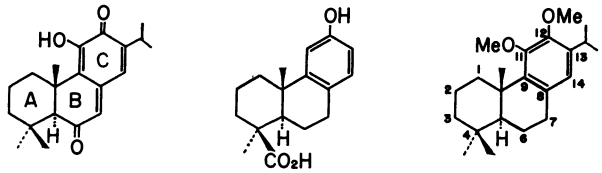

I II III

1) Although the formulas depicted represent only one enantiomer, they are taken to indicate a racemate.

2) S. M. Kupchan, A. Karim, and C. Marcks, *J. Amer. Chem. Soc.*, **90**, 5923 (1968).

3) S. M. Kupchan, A. Karim, and C. Marcks, *J. Org. Chem.*, **34**, 3912 (1969).

4) K. Mori and M. Matsui, *Tetrahedron*, **26**, 3467 (1970).

5) J. D. Edwards, Jr., and J. L. Cashaw, *J. Org. Chem.*, **20**, 847 (1955).

6) P. V. Demarco, E. Farkas, D. Doddrell, B. L. Mylari, and E. Wenkert, *J. Amer. Chem. Soc.*, **90**, 5480 (1968).

of a hydroxyl group at the position ortho to the isopropyl group. From the above results, the structure of V was identified as β-(4-hydroxy-3-isopropyl-5-methoxy benzoyl)propionic acid. The methylation of V with dimethyl sulfate in an alkaline solution, followed by alkaline hydrolysis, afforded the corresponding methyl ether (VII), which gave a negative ferric chloride reaction. The reduction of the carbonyl group in VII to the corresponding methylene group in an almost quantitative yield was carried out in the following manner. That is, the ketone (VII) in aqueous sodium hydroxide was treated with sodium borohydride at room temperature; the resulting crude product was then heated on a steam bath to give a γ-lactone (VIII). The hydrogenolysis of VIII in methanol in the presence of Pd-C gave γ-(4,5-dimethoxy-3-isopropylphenyl) butyric acid (IX). Subsequently, the treatment of IX in benzene with phosphorous pentachloride, followed by the intramolecular cyclization of the resulting acid chloride with anhydrous stannic chloride, gave a 1-tetralone derivative (X), the NMR spectrum of which showed a signal at δ 4.11 ppm due to the methine proton of the isopropyl group. This chemical-shift value indicates that the methine proton in X is deshielded by a newly-formed carbonyl group, because the spectrum of IX showed a signal at δ 3.36 ppm attributable to the methine proton of the isopropyl group. From this spectral evidence, the structure of X was identified as 6,7-dimethoxy-8-isopropyl-1-tetralone, as had been expected. Since this (X) was not a useful intermediate for the synthesis of (±)-I, the

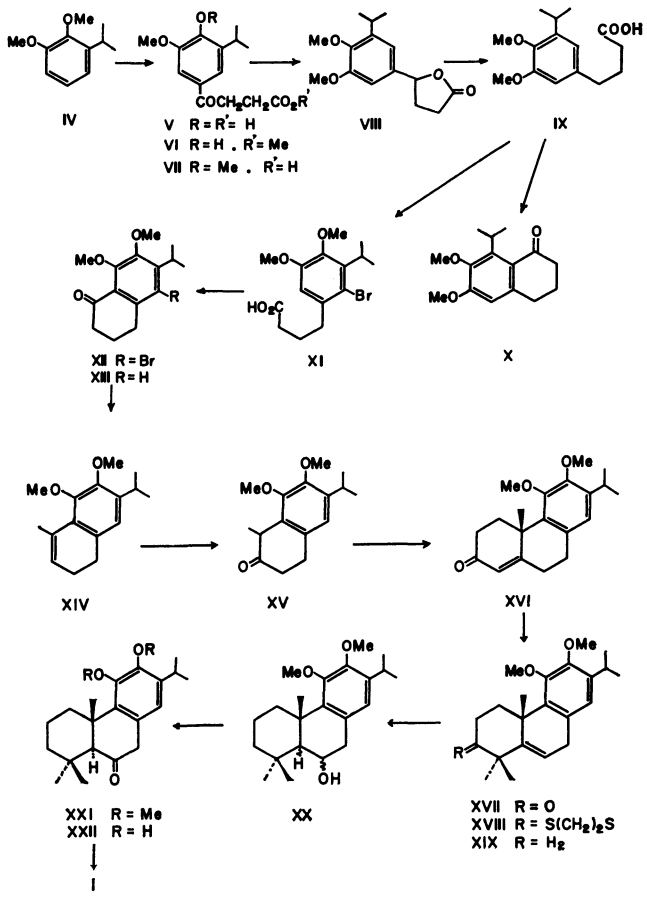

IX acid was subjected to bromination in carbon tetrachloride; γ-(2-bromo-4,5-dimethoxy-3-isopropylphenyl)butyric acid (XI) was thus obtained. The structure of XI was also assigned on the basis of its NMR spectrum, which showed signals, at δ 3.70 ppm and at δ 6.68 ppm, attributable to the methine proton of the isopropyl group and an aromatic proton respectively. The treatment of XI with phosphorous pentachloride and then with stannic chloride gave a 5-bromo-1-tetralone derivative (XII); this was hydrogenated at room temperature in methanolic potassium hydroxide in the presence of Pd-C to give 7,8-dimethoxy-6-isopropyl-1-tetralone (XIII). The Grignard reaction of XIII with methylmagnesium iodide afforded the corresponding alcohol, which was then dehydrated with dilute sulfuric acid to give 3,4-dihydro-7,8-dimethoxy-6-isopropyl-1-methylnaphthalene (XIV). Subsequently, the naphthalene derivative (XIV) was treated with lead tetraacetate in acetic acid; the resulting crude product was then refluxed with ethanol containing concentrated sulfuric acid to give (±)-7,8-dimethoxy-6-isopropyl-1-methyl-2-tetralone (XV). The construction of the A ring was achieved by the condensation of (±)-XV with methyl vinyl ketone in the presence of sodium ethoxide; after chromatographic purification, (±)-2,3,4,9,10,12-hexahydro-5,6-dimethoxy-7-isopropyl-12-methyl-2-oxophenanthrene (XVI) was thus obtained. The methylation of (±)-XVI with methyl iodide in *t*-butanol in the presence of potassium *t*-butoxide gave (±)-11,12-dimethoxyabieta-5,8,11,13-tetraen-3-one (XVII), which was then further converted to (±)-11,12-dimethoxyabieta-5,8,11,13-tetraene (XIX) *via* a thioketal derivative (XVIII). The IR and NMR spectra of (±)-XIX were in good agreement with those of an optically-active sample[3] derived from natural taxodione. The introduction of a carbonyl group at the 6 position was achieved by the hydroboration of (±)-XIX, followed by the oxidation of the resulting 6-hydroxyl derivative (XX) with the Jones reagent.[7] Thus, (±)-11,12-dimethoxyabieta-8,11,13-trien-6-one (XXI) was obtained. Its IR and NMR spectra were also identical with the data reported for an optically-active XXI.[3,4] Mori and Matsui[4] had reported that the demethylation of XXI[8] with boron tribromide in dichloromethane gave 11,12-dihydroxyabieta-8,11,13-trien-6-one (XXII), which was then further oxidized with silver oxide in chloroform to give taxodione (I). On the other hand, the conversion of XXII[8] to I by aerial oxidation on silica gel had also been reported by Kupchan *et al.*[3] Therefore, our final step in the total synthesis of (±)-I was carried out as follows. By the method of Mori and Matsui,[4] (±)-XXI was demethylated with boron tribromide to give (±)-XXII, which was then immediately chromatographed on silica gel according to the method of Kupchan *et al.*[3] to give (±)-I as a yellow oil. The IR, UV, NMR, and mass spectra of the synthetic (±)-I were identical in every respect with those of natural taxodione.[3]

7) A. Bowers, T. G. Halsall, E. R. H. Jones, and A. J. Lemin, *J. Chem. Soc.*, **1953**, 2548.

8) Optically-active substance.

Experimental

All the melting and boiling points are uncorrected. The NMR spectra were taken on a Hitachi Model R-20 NMR spectrometer (60 MHz), using tetramethylsilane as the internal standard. Their chemical shifts are presented in terms of δ values; s: singlet; bs: broad singlet; d: doublet; t: triplet; q: quartet; m: multiplet. The column chromatography was performed on Merck silica gel (0.08 mm).

β-(4-Hydroxy-3-isopropyl-5-methoxybenzoyl)propionic Acid (V). Anhydrous aluminum chloride (6.66 g) was stirred, over a period of 15 min, into a mixture of IV (3.60 g), succinic anhydride (2.10 g), and dry dichloromethane (20 m*l*) with cooling at 5—8°C. After the addition was complete, the mixture was stirred at room temperature for 4 hr and was then gently refluxed for 10 min. The mixture was poured into a mixture of concentrated hydrochloric acid (15 m*l*) and ice (*ca.* 100 g) and extracted with ethyl acetate, after which the ethyl acetate solution was extracted with aqueous sodium hydroxide (5%). After the alkaline extract had been acidified with dilute sulfuric acid, the yellow precipitate was collected, washed with water, and then recrystallized from aqueous methanol to give colorless needles, mp 169—171°C, which gave a green ferric chloride reaction in ethanol; yield, 3.2 g (60%). NMR in $CDCl_3$: 1.26 (6H, d, J=7 Hz, $-CH(C\underline{H}_3)_2$), 2.80 (2H, t, J=6 Hz, $-C\underline{H}_2CO_2H$), 3.32 (2H, t, J=6 Hz, $-COC\underline{H}_2-$), *ca.* 3.3 (1H, m, overlap, $-C\underline{H}(CH_3)_2$), 3.93 (3H, s, $-OC\underline{H}_3$), 7.41 and 7.54 (each 1H d and J=2 Hz, aromatic protons) ppm. NMR in pyridine-d_5: 1.34 (6H, d, J=7 Hz, $-CH(C\underline{H}_3)_2$), 3.08 (2H, t, J=6 Hz, $-C\underline{H}_2CO_2H$), 3.56 (2H, t, J=6 Hz, $-COC\underline{H}_2-$), *ca.* 3.7 (1H, m, overlap, $-C\underline{H}(CH_3)_2$), 3.68 (3H, s, $-OC\underline{H}_3$), 7.71 and 7.91 (each 1H d and J=2 Hz, aromatic protons) ppm.

Found: C, 63.11; H, 6.58%. Calcd for $C_{14}H_{18}O_5$: C, 63.14; H, 6.81%.

The starting IV (1.2 g) was recovered from the ethyl acetate solution.

Methyl β-(4-Hydroxy-3-isopropyl-5-methoxybenzoyl)propionate (VI). A solution of V (500 mg) in acetone (40 m*l*) was methylated with an excess ethereal diazomethane solution at room temperature for 3 hr. After a usual work-up, the product was recrystallized from a mixture of ether and petroleum ether (cooled on dry ice) to give VI as colorless prisms, mp 80.5—81.5°C, which gave a blue ferric chloride reaction in ethanol; yield, 410 mg. NMR in $CDCl_3$: 1.25 (6H, d, J=7 Hz, $-CH(C\underline{H}_3)_2$), 2.74 (2H, t, J=6 Hz, $-C\underline{H}_2CO_2-$), 3.30 (2H, t, J=6 Hz, $-COC\underline{H}_2-$), *ca.* 3.3 (1H, m, overlap, $-C\underline{H}(CH_3)_2$), 3.69 (3H, s, $-CO_2C\underline{H}_3$), 3.92 (3H, s, $-OC\underline{H}_3$), 6.26 (1H, s, $-O\underline{H}$), 7.39 and 7.55 (each 1H d and J=2 Hz, aromatic protons) ppm. NMR in pyridine-d_5: 1.32 (6H, d, J=7 Hz, $-CH(C\underline{H}_3)_2$), 2.87 (2H, t, J=6 Hz, $-C\underline{H}_2CO_2-$), 3.46 (2H, t, J=6 Hz, $-COC\underline{H}_2-$), *ca.* 3.6 (1H, m, overlap, $-C\underline{H}(CH_3)_2$), 3.59 (3H, s, $-CO_2C\underline{H}_3$), 3.68 (3H, s, $-OC\underline{H}_3$), 7.64 and 7.85 (each 1H d and J=2 Hz, aromatic protons) ppm.

Found: C, 64.50; H, 7.33%. Calcd for $C_{15}H_{20}O_5$: C, 64.27; H, 7.19%.

β-(4,5-Dimethoxy-3-isopropylbenzoyl)propionic Acid (VII). Dimethyl sulfate (37.8 g) was stirred, drop by drop at 60—65°C over a period of 1 hr, into a solution of V (26.6 g) in aqueous sodium hydroxide (10%: 100 m*l*). After the stirring had been continued for an additional hour, the mixture was hydrolyzed with aqueous sodium hydroxide (10%: 50 m*l*) at this temperature for 1 hr. The cold solution was then acidified with dilute sulfuric acid, and the precipitate was collected, washed with water, and then recrystallized from aqueous methanol to give VII as colorless needles, mp 131—133°C, which gave a negative ferric chloride reaction in ethanol; yield, 25.0 g (89%). NMR in $CDCl_3$: 1.24 (6H, d, J=7 Hz, $-CH(C\underline{H}_3)_2$), 2.80 (2H, t, J=6 Hz, $-C\underline{H}_2CO_2H$), 3.30 (2H, t, J=6 Hz, $-COC\underline{H}_2-$), 3.37 (1H, m, J=7 Hz, $-C\underline{H}(CH_3)_2$), 3.88 and 3.90 (each 3H and s, 2-$OC\underline{H}_3$), 7.42 and 7.53 (each 1H d and J=2 Hz, aromatic protons), 9.15 (1H, bs, $-CO_2\underline{H}$) ppm.

Found: C, 64.00; H, 7.20%. Calcd for $C_{15}H_{20}O_5$: C, 64.27; H, 7.19%.

γ-Hydroxy-γ-(4,5-dimethoxy-3-isopropylphenyl)butyric Acid γ-Lactone (VIII). A mixture of sodium borohydride (380 mg) and VII (4.8 g) in aqueous sodium hydroxide (2%: 40 m*l*) was allowed to stand at room temperature for 24 hr, after which it was acidified with dilute sulfuric acid. The mixture was heated on a steam bath for 20 min and then cooled. The precipitate was collected, washed with water, and then recrystallized from aqueous methanol to give VIII as colorless needles, mp 128—129°C; yield, 4.2 g (93%). IR in nujol: 1765 cm^{-1} (γ-lactone). NMR in $CDCl_3$: 1.22 (6H, d, J=7 Hz, $-CH(C\underline{H}_3)_2$), 1.8—2.9 (4H, m, $-(C\underline{H}_2)_2-$), 3.38 (1H, m, J=7 Hz, $-C\underline{H}(CH_3)_2$), 3.82 and 3.87 (each 3H and s, 2-$OC\underline{H}_3$), 5.47 (1H, t, J=6 Hz, $-C\underline{H}-O-$), 6.77 (2H, s, aromatic protons) ppm.

Found: C, 68.16; H, 7.62%. Calcd for $C_{15}H_{20}O_4$: C, 68.16; H, 7.63%.

γ-(4,5-Dimethoxy-3-isopropylphenyl)butyric Acid (IX). A solution of VIII (4.2 g) in methanol (150 m*l*) was hydrogenated at room temperature in the presence of Pd-C (10%: 1.4 g). After the absorption of hydrogen had ceased (after *ca.* 40 min), the mixture was filtered and washed with hot methanol; the filtrate was then evaporated. The residue was recrystallized from aqueous methanol to give IX as colorless needles (mp 83.5—84.5°C); yield, 4.1 g (98%). NMR in $CDCl_3$: 1.22 (6H, d, J=7 Hz, $-CH(C\underline{H}_3)_2$), 1.8—2.8 (6H, m, $-(C\underline{H}_2)_3-$), 3.36 (1H, m, J=7 Hz, $-C\underline{H}(CH_3)_2$), 3.81 and 3.87 (each 3H and s, 2-$OC\underline{H}_3$), 6.62 and 6.68 (each 1H d and J=2 Hz, aromatic protons), 8.65 (1H, bs, $-CO_2\underline{H}$) ppm.

Found: C, 67.39; H, 8.37%. Calcd for $C_{15}H_{22}O_4$: C, 67.64; H, 8.33%.

6,7-Dimethoxy-8-isopropyl-1-tetralone (X). A mixture of IX (1.33 g), phosphorous pentachloride (1.04 g), and dry benzene (20 m*l*) was stirred at room temperature for 30 min, and then heated at 50°C for 5 min. After the solution had been cooled, a solution of anhydrous stannic chloride (1.5 m*l*) in dry benzene (5.0 m*l*) was added, drop by drop at 5—10°C, over a period of 15 min. The mixture was then further stirred at room temperature for 75 min, heated at 45—50°C for 1 hr, and then poured into dilute hydrochloric acid (5%: 25 m*l*). The organic layer was separated, washed with aqueous sodium carbonate and water successively, and then dried over sodium sulfate. After the removal of the solvent, the residue was recrystallized from aqueous methanol to give X as colorless prisms, mp 87.5—88.5°C; yield, 1.10 g (89%). NMR in $CDCl_3$: 1.34 (6H, d, J=7.5 Hz, $-CH(C\underline{H}_3)_2$), 2.02 (2H, m, J=6 Hz, $-CH_2C\underline{H}_2CH_2-$), 2.63 and 2.88 (each 2H t and J=6 Hz, 2-$C\underline{H}_2-$), 3.84 and 3.91 (each 3H and s, 2-$OC\underline{H}_3$), 4.11 (1H, m, J=7.5 Hz, $-C\underline{H}(CH_3)_2$), 6.65 (1H, s, aromatic proton) ppm.

Found: C, 72.41; H, 8.41%. Calcd for $C_{15}H_{20}O_3$: C, 72.55; H, 8.12%.

γ-(2-Bromo-4,5-dimethoxy-3-isopropylphenyl)butyric Acid (XI). A solution of bromine (10.9 g) in carbon tetrachloride (30 m*l*) was stirred, drop by drop at 3—5°C over a period of 1.5 hr, into a solution of IX (18.0 g) in carbon tetrachloride (120 m*l*).

After the stirring had then been continued for an additional 1.5 hr, the reaction mixture was washed successively with water, aqueous sodium thiosulfate, and water. The subsequent removal of the dried solvent gave a solid which was recrystallized from cyclohexane to give colorless crystals, mp 77.5—78.5°C; yield, 22.5 g (96%). This gave a positive Beilstein halogen test. NMR in $CDCl_3$: 1.34 (6H, d, J=7 Hz, $-CH(C\underline{H}_3)_2$), 1.95—2.95 (6H, m, $-(C\underline{H}_2)_3-$), 3.70 (1H, m, J=7 Hz, $-C\underline{H}(CH_3)_2$), 3.83 (6H, s, $2\text{-}OC\underline{H}_3$), 6.68 (1H, s, aromatic proton) ppm.

Found: C, 52.32; H, 6.14%. Calcd for $C_{15}H_{21}O_4Br$: C, 52.17; H, 6.09%.

7,8-Dimethoxy-6-isopropyl-1-tetralone (XIII). A solution of XI (20.7 g) in dry benzene (100 m*l*) was treated with phosphorous pentachloride (12.5 g) and then with anhydrous stannic chloride (25 m*l*) by a method similar to that used for X. The crude product was distilled under a vacuum to give XII as an oil, bp 168—174°C/0.85 mmHg; yield, 17.0 g (87%). NMR in $CDCl_3$: 1.36 (6H, d, J=7 Hz, $-CH(C\underline{H}_3)_2$), 2.10 (2H, m, J=6 Hz, $-CH_2C\underline{H}_2CH_2-$), 2.64 and 3.03 (each 2H t and J=6 Hz, $2\text{-}C\underline{H}_2-$), *ca.* 3.8 (1H, m, overlap, J=7 Hz, $-C\underline{H}(CH_3)_2$), 3.87 and 3.93 (each 3H and s, $2\text{-}OC\underline{H}_3$) ppm.

To a solution of the above XII (15 g) in methanol (30 m*l*), methanolic potassium hydroxide (10%: 100 m*l*) and Pd - C (10%: 5.0 g) were added; the mixture was then subjected to hydrogenolysis at room temperature. After the absorption of hydrogen had ceased, the mixture was filtered and the filtrate was evaporated under a vacuum. The residue was extracted with ether, which had been washed with water and then dried over sodium sulfate. After the removal of the solvent, the crude product was distilled under a vacuum to give XIII as an oil, bp 138—143°C/0.8 mmHg, which gave a negative Beilstein halogen test; yield, 10.8 g (95%). NMR in $CDCl_3$: 1.23 (6H, d, J=7 Hz, $-CH(C\underline{H}_3)_2$), 2.05 (2H, m, J=6 Hz, $-CH_2C\underline{H}_2CH_2-$), 2.61 and 2.90 (each 2H t and J=6 Hz, $2\text{-}C\underline{H}_2-$), 3.33 (1H, m, J=7 Hz, $-C\underline{H}(CH_3)_2$), 3.88 (6H, s, $2\text{-}OC\underline{H}_3$), 6.87 (1H, s, aromatic proton) ppm.

Found: C, 72.72; H, 8.12%. Calcd for $C_{15}H_{20}O_3$: C, 72.55; H, 8.12%.

3,4-Dihydro-7,8-dimethoxy-6-isopropyl-1-methylnaphthalene (XIV). A solution of XIII (8.20 g) in dry benzene (50 m*l*) was stirred, drop by drop over a period of 30 min, to a Grignard reagent which had been prepared from magnesium (960 mg), methyl iodide (5.70 g), and dry ether (30 m*l*). The mixture was refluxed for 5 hr, cooled, decomposed with dilute hydrochloric acid (10%: 60 m*l*), and then extracted with ether. The extract was washed with water and dried over sodium sulfate. After the removal of the solvent, the residue was dissolved in dry toluene (60 m*l*) containing *p*-toluenesulfonic acid (0.5 g) and the solution was refluxed for 3 hr. Then, the solvent was slowly distilled off over a period of 3 hr and the residue was extracted with ether. The extract was washed with aqueous sodium hydrogen carbonate and water successively, dried over sodium sulfate, and then evaporated. The product was distilled under a vacuum to give an oil (5.4 g), bp 114—136°C/0.9 mmHg (mainly 118—119°C/0.9 mmHg). This was purified by means of column chromatography on silica gel (220 g), using benzene containing 2% ether as the eluent, to give XIV as a colorless oil (4.49 g). NMR in $CDCl_3$: 1.23 (6H, d, J=7 Hz, $-CH(C\underline{H}_3)_2$), 2.24 (3H, s, $=\overset{|}{C}C\underline{H}_3$), 2.65 (4H, t, J=7 Hz, $-(C\underline{H}_2)_2-$), 3.23 (1H, m, J=7 Hz, $-C\underline{H}(CH_3)_2$), 3.81 and 3.87 (each 3H and s, $2\text{-}OC\underline{H}_3$), 5.90 (1H, bt, J=4 Hz, $=C\underline{H}-$), 6.86 (1H, s, aromatic proton) ppm.

In another experiment, the dehydration of the Grignard reaction product was also carried out by the refluxing of the crude alcohol with dilute sulfuric acid (20 %) for 5.5 hr, similar results were obtained.

Found: C, 78.21; H, 9.11%. Calcd for $C_{16}H_{22}O_2$: C, 78.01; H, 9.00%.

(±)-7,8-Dimethoxy-6-isopropyl-1-methyl-2-tetralone (XV). A solution of XIV (530 mg) in acetic acid (4.0 m*l*) was stirred into a lead tetraacetate solution which had been freshly prepared from red lead oxide (2.06 g) and acetic acid (5.0 m*l*) at 55—60°C. After the stirring had been continued at room temperature for 1.5 hr, a few drops of ethylene glycol were added. The mixture was further stirred for 20 min, diluted with water (40 m*l*), and then extracted with ether which had been washed successively with aqueous sodium hydrogen carbonate and a saturated sodium chloride solution. After the removal of the ether, the residue was refluxed for 3 hr with ethanol (5.0 m*l*) containing concentrated sulfuric acid (0.5 m*l*), diluted with water, and then extracted with ether. The extract was washed successively with aqueous sodium hydrogen carbonate and water, dried over sodium sulfate, and then evaporated. The residue was chromatographed on silica gel (20 g), using benzene containing 2% ether as the eluent, to give XV as an oil (412 mg). IR in $CHCl_3$; 1706 cm^{-1} (C=O). NMR in $CDCl_3$; 1.24 (6H, d, J=7 Hz, $-CH(C\underline{H}_3)_2$, 1.40 (3H, d, J=8 Hz, $-\overset{|}{C}HC\underline{H}_3$), 3.87 and 3.90 (each 3H and s, $2\text{-}OC\underline{H}_3$), 6.88 (1H, s, aromatic proton) ppm.

Found: C, 73.20; H, 8.28. Calcd for $C_{16}H_{22}O_3$: C, 73.25; H, 8.45%.

(±)-2,3,4,9,10,12-Hexahydro-5,6-dimethoxy-7-isopropyl-12-methyl-2-oxophenanthrene (XVI). A solution of XV (3.56 g) in dry ether (20 m*l*) was stirred, at −10°C under a stream of nitrogen, into a sodium ethoxide solution which had been prepared from sodium (400 mg) and absolute ethanol (13 m*l*). After the stirring had been continued at this temperature for 30 min, methyl vinyl keton (1.0 g) was added. The mixture was further stirred at −10°C for 5 hr, at room temperature for 30 min, and then refluxed for 30 min. After cooling, the mixture was poured into dilute hydrochloric acid (10%: 50 m*l*) and extracted with ether. The extract was washed successively with aqueous sodium hydrogen carbonate and water, and then dried over sodium sulfate. After the removal of the ether, the crude product was purified by column chromatography on silica gel (250 g), using benzene containing 5% ether as the eluent, to give XVI as an oil (2.64 g: 61%). IR in $CHCl_3$; 1660 cm^{-1} (C=O). NMR in CCl_4; 1.17 (6H, d, J=7 Hz, $-CH(C\underline{H}_3)_2$), 1.63 (3H, s, $-\overset{|}{C}C\underline{H}_3$), 3.69 and 3.82 (each 3H and s, $2\text{-}OC\underline{H}_3$), 5.64 (1H, s, $-COC\underline{H}=$), 6.56 (1H, s, aromatic proton) ppm.

Found: C, 76.70; H, 8.36%. Calcd for $C_{20}H_{26}O_3$: C, 76.40; H, 8.34%.

(±)-11,12-Dimethoxyabieta-5,8,11,13-tetraen-3-one (XVII). A solution of XVI (2.51 g) in absolute *t*-butanol (20 m*l*) was stirred, at room temperature over a period of 10 min under a stream of nitrogen, to a potassium *t*-butoxide solution which had been prepared from potassium (1.19 g) and absolute *t*-butanol (20 m*l*). The mixture was stirred for 30 min, and to this was added methyl iodide (4.30 g). Under a stream of nitrogen, the mixture was stirred for 2 hr, refluxed for 30 min, cooled, poured into dilute hydrochloric acid (5%: 50 m*l*), and then extracted with ether. The ether extract was washed successively with water, aqueous sodium thiosulfate, and water. The solvent, after drying over sodium sulfate, was evaporated; the residue was then recrystallized from methanol to give XVII as colorless crystals (1.75 g), mp 154—154.5°C. The mother liquor of crystallization was evaporated, and the residue was chromatographed on silica gel (80 g), using benzene containing 3% ether as the eluent to give an addition-

al XVII (0.67 g). IR in $CHCl_3$; 1700 cm^{-1} (C=O). NMR in $CDCl_3$; 1.21 (6H, d, J=7 Hz, $-CH(C\underline{H}_3)_2$), 1.31 (6H, s, 2-$\dot{C}C\underline{H}_3$), 1.37 (3H, s, $-\dot{C}C\underline{H}_3$), 3.43 (2H, d, J=4 Hz, $=CH-C\underline{H}_2-$), 3.77 and 3.88 (each 3H and s, 2-$OC\underline{H}_3$), 5.80 (1H, t, J=4 Hz, $=C\underline{H}CH_2-$), 6.74 (1H, s, aromatic proton) ppm.

Found: C, 77.28; H, 9.06%. Calcd for $C_{22}H_{30}O_3$: C, 77.15; H, 8.83%.

(±)-11,12-Dimethoxyabieta-5,8,11,13-tetraene (XIX). A mixture of XVII (1.90 g), ethanedithiol (1.0 m*l*), and freshly-distilled boron trifluoride etherate (3.0 m*l*) was allowed to stand overnight at room temperature. After a usual work-up, the crude product was recrystallized from a mixture of ether and petroleum ether to give a thioketal (XVIII: 1.72 g), mp 156—157.5°C, which showed no carbonyl absorption band in its IR spectrum. NMR in $CDCl_3$; 1.18 and 1.21 (each 3H d and J=7 Hz, $-CH(C\underline{H}_3)_2$, 1.48 (3H, s, $-\dot{C}C\underline{H}_3$), 1.51 (6H, s, 2-$\dot{C}C\underline{H}_3$), 3.73 and 3.85 (each 3H and s, 2-$OC\underline{H}_3$), 5.94 (1H, t, J=4 Hz, $=C\underline{H}CH_2-$), 6.63 (1H, s, aromatic proton) ppm.

Found: C, 69.08; H, 8.27%. Calcd for $C_{24}H_{34}O_2S_2$: C, 68.87; H, 8.19%.

A solution of XVIII (2.15 g) in hot ethanol (200 m*l*) was refluxed for 3 hr with Raney nickel (W-7) prepared from Raney alloy (50 g), allowed to stand overnight at room temperature, and then filtered. The filtrate was evaporated, and, to the residue dilute hydrochloric acid (10%: 10 m*l*) was added. The mixture was extracted with ether. The extract was washed with water, dried over sodium sulfate, and then evaporated. The crude product was purified by column chromatography on silica gel (150 g), using hexane containing 30% benzene as the eluent, to give XIX as an oil (1.27 g), the IR and NMR spectra of which were identical with the data[3] reported for an optically-active sample. NMR in $CDCl_3$; 1.16 and 1.23 (each 3H and s, $-\dot{C}(C\underline{H}_3)_2$), 1.18 and 1.21 (each 3H d and J=7 Hz, $-CH(C\underline{H}_3)_2$), 1.46 (3H, s, $-\dot{C}C\underline{H}_3$), 3.13 (1H, m, overlap), 3.32 (2H, d, J=4 Hz, $=CHC\underline{H}_2-$), 3.75 and 3.84 (each 3H and s, 2-$OC\underline{H}_3$), 5.84 (1H, t, J=4 Hz, $=C\underline{H}CH_2-$), 6.67 (1H, s, aromatic proton) ppm. Literature.[3,8] NMR in $CDCl_3$: 1.08 (3H), 1.18 (3H), 1.24 (6H), 1.47 (3H, s), 3.12 (1H, septet), 3.28 and 3.37 (2H), 3.78 (3H, s), 3.88 (3H, s), 5.87 (1H, t, J=4 Hz), 6.67 (1H, bs) ppm.

(±)-11,12-Dimethoxyabieta-8,11,13-trien-6-one (XXI). A solution of XIX (1.470 g) in dry tetrahydrofuran (10 m*l*) was added to a suspension of sodium borohydride (210 mg) in dry tetrahydrofuran (10 m*l*). To the stirred and cooled (0—5°C) suspension, a solution of freshly-distilled boron trifluoride etherate (1.1 m*l*) in dry tetrahydrofuran (3.0 m*l*) was added over a period of 5 min. After the stirring had been continued for 3 hr at 0—10°C, a few drops of water were added to decompose the excess diborane, and then aqueous sodium hydroxide (12%: 1.6 m*l*) and hydrogen peroxide (30%: 1.6 m*l*) were added to the stirred solution. The mixture was stirred for 30 min, poured into a saturated sodium chloride solution, and then extracted with ether. The extract was washed with a saturated sodium chloride solution, dried over sodium sulfate, and then evaporated. The residual oil was chromatographed on silica gel (150 g) to give the crude XX as an oil (590 mg), the IR spectrum of which showed a band at 3600 cm^{-1}(OH).

A solution of the above XX (550 mg) in acetone (10 m*l*) was oxidized with the Jones reagent[7] (2N: 1.3 m*l*) at room temperature for 5 min. The mixture was then poured into water, and extracted with ether, after which the extract was washed with aqueous sodium chloride and then dried over sodium sulfate. After the removal of the ether, the residue was chromatographed on silica gel (50 g), using benzene as the eluent, to give XXI as a solid (126 mg). This was recrystallized from ether containing petroleum ether to give colorless crystals, mp 102—103.5°C. The IR and NMR spectra of XXI were identical with the data reported for an optically-active sample. IR in $CHCl_3$; 1718, 1605, 1560, 1470, 1450, 1405, 1363, 1318, 1065, 1020 $cm.^{-1}$ NMR in $CDCl_3$; 1.02 and 1.27 (each 3H and s, $-\dot{C}(C\underline{H}_3)_2$), 1.18 and 1.21 (each 3H d and J=7 Hz, $-CH-(C\underline{H}_3)_2$), 1.36 (3H, s, $-\dot{C}C\underline{H}_3$), 2.60 (1H, s, $-\dot{C}\underline{H}CO-$), 3.16 (1H, m, $-C\underline{H}(CH_3)_2$), 3.55 (2H, q, $-COC\underline{H}_2-$), 3.77 and 3.84 (each 3H and s, 2-$OC\underline{H}_3$), 6.62 (1H, s, aromatic proton) ppm.

Found: C, 76.89; H, 9.25%. Calcd for $C_{22}H_{32}O_3$: C, 76.70; H, 9.36%.

Literature: IR in $CHCl_3$[3] 1724, 1605, 1565, 1471, 1449, 1406, 1362, 1316, 1068, 1025 cm^{-1}. NMR in $CDCl_3$[3] 1.01 (3H), 1.11 (3H), 1.28 (6H, s), 1.36 (3H, s), 2.59 (1H, s), 3.15 (1H, septet), 3.46 and 3.58 (2H), 3.79 (3H, s), 3.87 (3H, s), 6.62 (1H, s) ppm, and NMR in $CDCl_3$[4] 1.08 (3H, s), 1.23 (3H, d, J=7 Hz), 1.25 (3H, d, J=7 Hz), 1.30 (3H, s), 1.40 (3H, s), 2.61 (1H, s), 3.15 (1H, septet, J=7 Hz), 3.50 (2H, q), 3.76 (3H, s), 3.85 (3H, s), 6.56 (1H, s) ppm.

(±)-Taxodione (I). A solution of XXI (110 mg) in dichloromethane (1.5 m*l*) was treated with a solution of boron tribromide (0.6 m*l*) in dichloromethane (1.5 m*l*) by the method of Mori and Matsui[4] to give a crude product (XXII), which was then immediately chromatographed on silica gel (15 g).

According to the method of Kupchan *et al.*,[3] elution with benzene was carried out; (±)-taxodione (I) was thus obtained as a yellow oil (47 mg). The identity of I with natural taxodione was confirmed by a comparison of their spectra. UV; λ_{max}^{EtOH} nm (ε): 322 (21000), 334 (21800), 405 (2700). IR in CCl_4; 3333, 1676, 1644, 1628, 1618, 1425, 1357, 1249, 1145, 1055, 907 cm^{-1} NMR in benzene-d_6; 0.96 and 1.02 (each 3H d and J=7 Hz, $-CH(C\underline{H}_3)_2$), 1.15 and 1.22 (each 3H and s, $-C(C\underline{H}_3)_2$), 1.34 (3H, s, $-\dot{C}C\underline{H}_3$), 2.29 (1H, s, $-\dot{C}\underline{H}CO-$), 2.98 (1H, m, $-C\underline{H}(CH_3)_2$), 5.81 and 6.37 (each 1H and s, $2=C\underline{H}-$), 7.65 (1H, s, $-O\underline{H}$) ppm. Mass; *m/e* 314 (M^+), 299, 287, 286, 272, 271, 245, 232, 231.

The following spectral data have been reported for natural taxodione: UV[3] λ_{max}^{MeOH} nm (ε): 320 (25000), 332 (26000), 400 (2000). IR in CCl_4[3] 3344, 1681, 1647, 1631, 1621, 1427, 1361, 1252, 1149, 1060, 910 cm^{-1}. NMR in benzene-d_6[3] 0.97 (3H, d, J=7 Hz), 1.04 (3H, d, J=7 Hz), 1.18, 1.25, and 1.38 (each 3H and s) 2.32 (1H, s), 2.95 (1H, septet), 5.87 and 6.42 (each 1H and s), 7.70 (1H, s) ppm. Mass[3] *m/e* 314 (M^+), 299, 286, 245, 232, 231. Mass[4] *m/e* 314 (M^+), 299, 287, 286, 272, 271, 245, 232, 231.

The authors are grateful to Professor S. Morris Kupchan, University of Virginia, for his gift of natural taxodione.

The Solvent Effect on the Reaction Selectivity in the Chlorination of Propionic Acid

Toshikazu NAGAI, Yukio HORIKAWA, Hon Son RYANG, and Niichiro TOKURA

Department of Applied Chemistry, Faculty of Engineering, Osaka University, Suita, Osaka

(Received March 25, 1971)

The chlorinations of propionic acid with chlorine were carried out at 70°C in various solvent mixtures with photo-irradiation or with initiation by benzoyl peroxide. Benzene - CCl_4, naphthalene - CCl_4, and anthracene - CCl_4 mixtures, and sulfur dioxide - CCl_4 were used as the solvents. In the benzene - CCl_4 mixtures, the relative reactivity, β/α, of the α and the β positions of propionic acid changed from 1.68 (CCl_4) to 1.11 (benzene), the ratio being inversely proportional to the electron-donor properties of the solvents. In the naphthalene - CCl_4 mixtures, the plot of the relative reactivity, β/α, *versus* the naphthalene content showed a minimun at *ca.* 0.1 mol/*l* of naphthalene; however, the total yield of the chlorinated acids decreased as the content of the naphthalene increased. No chlorinated acids were obtained in the anthracene - CCl_4 system. In the presence of sulfur dioxide, the α-position was more readily substituted than the β-position, the β/α ratio decreasing as the molar ratios of Cl_2/SO_2 were decreased, from 1.3 ($Cl_2/SO_2=0.286/0.036$) to 0.49 (0.286/0.858), by the initiation of benzoyl peroxide. However, dilution with CCl_4 or photo-irradiated chlorination cause no change in the selectivity in spite of the presence of sulfur dioxide. A mechanism to account for such a selectivity has been suggested.

It is well known[1] that the chlorine atom attacks hydrogen atoms more readily in this order: tertiary> secondary>primary hydrogen. However, when a compound bearing an electron-withdrawing substituent, such as propionic acid, is involved, the primary position (β-hydrogen) is more readily substituted than the secondary one (α-hydrogen) because of the lower electron density at the α-position, while the chlorine atom is an electrophilic reagent.

It has been generally assumed that a solvent has little effect upon the course and rate of the free radical reaction. Yet, it has also been accepted that chlorination by a chlorine atom has a remarkable selectivity varying with the solvent used. Chlorine forms a π-complex with the aromatic nucleus by a charge transfer-type interaction.[2] This complexed radical is less reactive and more selective than a free chlorine atom. Thus, the ratio of the relative rates, k_{tert}/k_{prim}, of 2,3-dimethylbutane rises more in benzene or in other donor solvent than in a hydrocarbon.[3]

The present paper is concerned with the study of the reaction and the selectivity of attacking radicals in the chlorination of propionic acid in various solvent mixtures.

Results and Discussion

The chlorination of propionic acid with chlorine was carried out at 70°C in various solvents with photoirradiation or with initiation by benzoyl peroxide (BPO). The solvents used were benzene - carbon tetrachloride mixtures, naphthalene - carbon tetrachloride mixtures, and anthracene - carbon tetrachloride mixtures. The chlorination was also undertaken in the presence of sulfur dioxide and sulfur dioxide - carbon tetrachloride mixtures.

The reactions were performed by passing chlorine gas through the reaction mixtures. As products, α-chloro-, α,α-dichloro-, β-chloro-, and β,β-dichloro- propionic acids and a cyclic anhydride of β-sulfopropionic acid[4] were obtained. A negligible amount of chlorinated aromatic compounds was also formed.

The products were analyzed by the NMR spectral method. In these experiments the authors paid special attention to establishing the relationship between the relative reactivity, β/α, and the concentration of the aromatic compound mixed into the solution or the quantity of sulfur dioxide used.

Table 1 summarizes the results of the chlorination where the effect of benzene in the reaction mixture was examined. The data in this table demonstrate that the relative reactivity, β/α, decreases from 1.68 to 1.11 as the mole fraction of benzene in the solvent (benzene - CCl_4) increases from zero to unity. The values of β/α are not affected by differences in the initiation, the photo-irradiation, or the BPO. The results of the addition of naphthalene to the solvent (CCl_4) are shown in Table 2. The plot of the relative reactivity *vs.* the concentration of naphthalene exhibits a minimum point at *ca.* 0.1 mol/*l* of naphthalene, as is seen in Fig. 2. Moreover, the total yield of the chlorinated products decreases as the concentration of naphthalene is increased.

The addition of anthracene to the solvent (CCl_4) gave no chlorinated propionic acids, even when a very small quantity (0.117 mol/*l*) was present in the reaction mixture. As Table 3 indicates, the decrease in the relative reactivity was more accelerated in the presence of sulfur dioxide. When an equimolar amount of sulfur dioxide or more is mixed with the chlorine, the relative reactivity decreases below unity, indicating the reversal of the reactivities between the α- and β-positions. On the contrary, no change in the selectivity with the sulfur dioxide concentration was observed in the photo-initiated chlorination where the relative reactivity was kept constant, $\beta/\alpha=1.4$; this selectivity is very similar to the relative reactivity in the carbon tetrachloride only.

1) W. A. Pryor, "Free Radicals," McGraw-Hill, New York (1966), p. 181.
2) R. E. Bühler, *Helv. Chim. Acta*, **51**, 1558 (1968).
3) G. A. Russell, *J. Amer. Chem. Soc.*, **80**, 4987 (1958).
4) M. S. Kharasch, T. H. Chao, and H. C. Brown, *ibid.*, **62**, 2393 (1940).

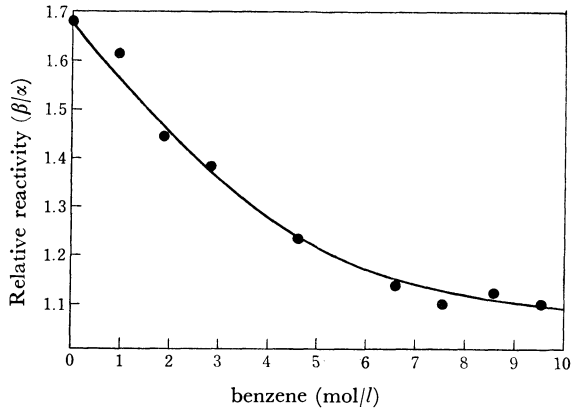

Fig. 1. Relative reactivity (β/α) in the chlorination of propionic acid with chlorine initiated by benzoyl peroxide in benzene - CCl_4 mixtures at 70°C.

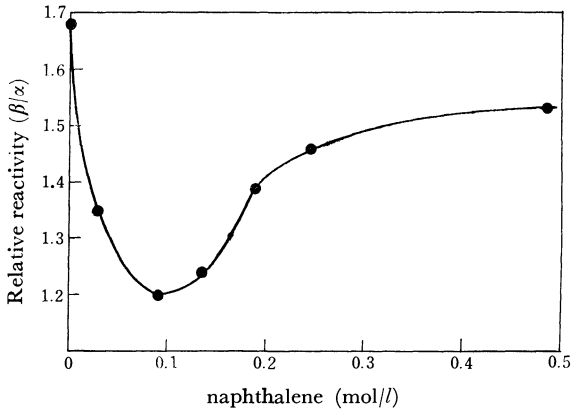

Fig. 2. Relative reactivity (β/α) in the chlorination of propionic acid with chlorine initiated by benzoyl peroxide in naphthalene - CCl_4 mixtures at 70°C.

TABLE 1. CHLORINATION OF PROPIONIC ACID IN BENZENE - CCl_4 AT 70°C

Initiation	Mole fraction of benzene in the mixed solvent	Product yield (mol %)				Relative reactivity(β/α)
		$CH_3CHClCO_2H$	$CH_3CCl_2CO_2H$	$CH_2ClCH_2CO_2H$	$CHCl_2CH_2CO_2H$	
BPO	0.0	10.9	16.0	10.8	56.9	1.68
	0.1	12.9	16.1	14.3	53.4	1.61
	0.2	16.1	12.5	16.8	44.9	1.44
	0.3	15.1	13.2	20.1	35.7	1.38
	0.5	18.0	9.6	25.0	26.4	1.23
	0.7	16.4	10.2	23.5	22.0	1.14
	0.8	16.3	8.0	22.6	18.2	1.11
	0.9	15.8	7.0	24.5	14.0	1.13
	1.0	18.5	7.8	28.9	14.5	1.11
hν	0.0	13.8	1.7	34.3	4.2	1.65
	0.5	14.6	4.3	30.4	3.1	1.23
	1.0	16.3	3.3	30.5	2.6	1.13

TABLE 2. CHLORINATION OF PROPIONIC ACID IN NAPHTHALENE - CCl_4 AT 70°C

Mole fraction of naphthalene in the solvent	Product yield (mol %)				Relative reactivity(β/α)
	$CH_3CHClCO_2H$	$CH_3CCl_2CO_2H$	$CH_2ClCH_2CO_2H$	$CHCl_2CH_2CO_2H$	
0.00	10.9	16.0	10.8	56.9	1.68
0.006	19.1	8.6	26.3	29.8	1.35
0.010	21.0	6.8	32.4	18.1	1.20
0.014	24.5	3.7	39.7	13.0	1.24
0.019	18.1	4.3	33.2	14.6	1.39
0.025	19.2	2.5	38.1	9.8	1.46
0.050	19.6	0.6	40.4	5.7	1.53
0.10	8.2	0	19.7	0	1.59
0.20	0	0	0	0	—

However, the cyclic anhydride of β-sulfopropionic acid was obtained in both photo- and BPO- initiated processes, and neither the free acid nor the cyclic anhydride of α-sulfopropionic acid was detected in the reaction mixture; these results coincide with the earlier results of photochlorination by Kharasch *et al.*[4] This suggests that the formation of the cyclic anhydride of α-sulfopropionic acid is difficult because of the electronical and sterical effects of the carboxyl group.

Table 3 also lists the results of the reaction of propionic acid with sulfuryl chloride at 70°C. The relative reactivity by BPO initiation, $\beta/\alpha=0.76$, resembles the result of equimolar chlorination with SO_2 and Cl_2 by BPO initiation, 0.87.

These data on the various reactions suggest several interesting things. First, the dependence of the relative reactivities upon the concentrations of aromatic compounds or the quantities of sulfur dioxide suggests that not only the chlorine radical, but also another radical species such as complexed radicals, take part in these reactions. Moreover, the species have more selectivities than the free chlorine atom. Secondly, the con-

Table 3. Chlorination of propionic acid in the presence of SO_2 and by SO_2Cl_2 at 70°C

Initiation	Cl_2(mol)	SO_2(mol)	CCl_4(mol)	Product yield (mol%)[c] $CH_3CH(Cl)CO_2H$	$CH_3CCl_2CO_2H$	$CH_2ClCH_2CO_2H$	$CHCl_2CH_2CO_2H$	Cyclic anhydride[a]	Relative reactivity(β/α)
BPO	0.286	0.036		24	2	41	8	3	1.3
	0.286	0.143		20	5	26	3	9	1.0
	0.286	0.286		24	2	15	1	18	0.87
	0.286	0.572		40	0	9	0	22	0.52
	0.286	0.858		20	6	3	0	16	0.49
	0.286	0.572	0.143	24	4	17	3	36	1.4
	0.195	(SO_2Cl_2 mol)		29	0	15	0	18	0.76[b]
$h\nu$	0.143	0.858		10	0	7	0	15	1.4
	0.286	0.858		20	4	13	0	37	1.4

a) The cyclic anhydride of β-sulfopropionic acid
b) Chlorination by SO_2Cl_2
c) No hydrogen rearrangement between the α- and β- position occurred under the present conditions, which was confirmed using propionic-α,α-d_2 acid-d_1 as the starting material.

tributions of these species to the reactions differ greatly among aromatic compounds.

Thirdly, in the presence of sulfur dioxide, the photo-initiated reaction proceeds quite differently from the BPO-initiated reaction, where there is no dependence of the relative reactivity on the concentration of sulfur dioxide used. Consequently, the chlorination mechanism in the former case should be discriminated.

In the aromatic systems, the radical species different from the free radicals are probably complexed radicals between aromatic compounds and a chlorine radical. The formation of this π-complex had been suggested by Russel.[3] For benzene, it could be written as follows:

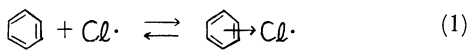

(1)

Recently,[2] such a π-complex was detected by means of the UV spectra as arising from a charge-transfer-type interaction. Thus, we presumed that these π-complexed radicals and free chlorine radicals are competitive in the present reaction series. The chain propagation reactions can be formulated thus, where Ar denotes aromatic compounds:

$$Cl_2 + Ini\cdot \longrightarrow IniCl + Cl\cdot \quad (2)$$

$$Cl\cdot + Ar \overset{K_1}{\rightleftarrows} Cl\cdot \rightarrow Ar \quad (3)$$

$$Cl\cdot + 2Ar \overset{K_2}{\rightleftarrows} Ar\rightarrow Cl\cdot\leftarrow Ar \quad (4)$$

$$CH_3CH_2CO_2H + Cl\cdot \xrightarrow{k_{\alpha 0}} CH_3\dot{C}HCO_2H + HCl \quad (5)$$

$$CH_3CH_2CO_2H + Cl\cdot \xrightarrow{k_{\beta 0}} \dot{C}H_2CHCO_2H + HCl \quad (6)$$

$$CH_3CH_2CO_2H + Cl\cdot\leftarrow Ar \xrightarrow{k_{\alpha 1}} CH_3\dot{C}HCO_2H + HCl + Ar \quad (7)$$

$$CH_3CH_2CO_2H + Cl\cdot\leftarrow Ar \xrightarrow{k_{\beta 1}} \dot{C}H_2CH_2CO_2H + HCl + Ar \quad (8)$$

$$CH_3CH_2CO_2H + Ar\rightarrow Cl\cdot\leftarrow Ar \xrightarrow{k_{\alpha 2}} CH_3\dot{C}HCO_2H + HCl + 2Ar \quad (9)$$

$$CH_3CH_2CO_2H + Ar\rightarrow Cl\cdot\leftarrow Ar \xrightarrow{k_{\beta 2}} \dot{C}H_2CH_2CO_2H + HCl + 2Ar \quad (10)$$

We could not explain the results of the naphthalene - CCl_4 system by considering merely the free chlorine radical or the 1:1 complexed radical between the chlorine radical and naphthalene as the reacting species. This is the reason why we wish to propose the presence of another complex, such as a 1:2 complex between the chlorine radical and the aromatic compound, in the reaction mixture.

The step of hydrogen abstraction must be rate-controlling in the chlorine substitution reaction. The formation rates of α-chloropropionic acid and β-chloropropionic acid are given by Eqs. (11) and (12) respectively:

$$\frac{d[CH_3CHClCO_2H]}{dt} = k_{\alpha 0}[Cl\cdot][Pr] + k_{\alpha 1}[Ar\rightarrow Cl\cdot][Pr] + k_{\alpha 2}[Ar\rightarrow Cl\cdot\leftarrow Ar][Pr] = (k_{\alpha 0}+k_{\alpha 1}K_1[Ar] + k_{\alpha 2}K_2[Ar]^2)[Pr][Cl\cdot] \quad (11)$$

$$\frac{d[CH_2ClCH_2CO_2H]}{dt} = k_{\beta 0}[Cl\cdot][Pr] + k_{\beta 1}[Ar\rightarrow Cl\cdot][Pr] + k_{\beta 2}[Ar\rightarrow Cl\cdot\leftarrow Ar][Pr] = (k_{\beta 0}+k_{\beta 1}K_1[Ar] + k_{\beta 2}K_2[Ar]^2)[Pr][Cl\cdot] \quad (12)$$

Hence, the relative formation rate may be represented as Eq. (13):

$$\frac{d[CH_2ClCH_2CO_2H]}{d[CH_3CHClCO_2H]} = \frac{k_{\beta 0}+k_{\beta 1}K_1[Ar]+k_{\beta 2}K_2[Ar]^2}{k_{\alpha 0}+k_{\alpha 1}K_1[Ar]+k_{\alpha 2}K_2[Ar]^2} \quad (13)$$

If the concentration of the aromatic compounds is constant during the reaction time, the relative reactivity can be expressed as the following Eq. (14):

$$\frac{\beta}{\alpha} = \frac{[CH_2ClCH_2CO_2H]}{[CH_3CHClCO_2H]} \times \frac{2}{3} = \frac{k_{\beta 0}+k_{\beta 1}K_1[Ar]+k_{\beta 2}K_2[Ar]^2}{k_{\alpha 0}+k_{\alpha 1}K_1[Ar]+k_{\alpha 2}K_2[Ar]^2} \times \frac{2}{3} \quad (14)$$

Many interesting suggestions about these reaction series were obtained from the differential equation of Eq. (14) with respect to the aromatic concentration (Eq. (15)):

$$\frac{d\left(\frac{\beta}{\alpha}\right)}{d[Ar]} = \frac{(k_{\alpha0}k_{\beta1}K_1 - k_{\alpha1}k_{\beta0}K_1) + 2(k_{\alpha0}k_{\beta2}K_2 - k_{\alpha2}k_{\beta0}K_2)[Ar] + (k_{\alpha1}k_{\beta2}K_1K_2 - k_{\alpha2}k_{\beta1}K_1K_2)[Ar]^2}{(k_{\alpha0} + k_{\alpha1}K_1[Ar] + k_{\alpha2}K_2[Ar^2])^2} \times \frac{2}{3} \quad (15)$$

First, the relation (16) can be derived for the benzene - CCl_4 system, which shows a monotonous decreasing curve in the β/α *vs.* Ar (aromatic) plot, as is indicated in Fig. 1:

$$\frac{k^B_{\beta0}}{k^B_{\alpha0}} > \frac{k^B_{\beta1}}{k^B_{\alpha1}} > \frac{k^B_{\beta2}}{k^B_{\alpha2}} \quad (16)$$

The relation (16) demonstrates that the relative reactivities decrease in this order: the free chlorine radical, the 1:1 complexed radical, and the 1:2 complexed radical. Such a prediction makes it clear that the reactivities of these radical species diminish in this order, so the reactivity of secondary hydrogen in propionic acid increases as compared with the primary hydrogen according to the above order.

The approximate value of each term in the relation (16) can be obtained from the curve of Fig. 1. That is, in benzene - CCl_4 systems the relative reactivities of the free radical, the 1:1 complex radical, and the 1:2 compelx radical are estimated to be 1.68, 1.12, and 1.01 respectively.

Secondly, in the naphthalene - CCl_4 series a minimum point in the plot is seen as shown in Fig. 2, where the relation (17) may be derived similarly as in the above case:

$$\frac{k^N_{\beta0}}{k^N_{\alpha0}} > \frac{k^N_{\beta1}}{k^N_{\alpha1}} \qquad \frac{k^N_{\beta1}}{k^N_{\alpha1}} < \frac{k^N_{\beta2}}{k^N_{\alpha2}} \quad (17)$$

The relation (17) points out the striking tendency that the relative reactivity of the 1:2 complexed radical is larger than that of the 1:1 complexed radical. Thus, it is anticipated that the hydrogen abstraction in the α-position suffers from more steric hindrance, largely because of the bulk of the 1:2 complexed radical. Accordingly, this steric effect will accelerate the increase in the selectivity, indicating a reversal of the reactivity tendency. Thirdly, the two equilibrium constants in the naphthalene - CCl_4 system, K_1 and K_2, are much larger than those in the benzene - CCl_4 system, because the relative reactivityl of the former changes in a much lower concentration of aromatic compounds than that of the latter. Fourthly, the equilibrium constants of the anthracene - CCl_4 systems are so large that the free chlorine radical could scarcely participate in this reaction. Moreover, the recativity of the formed complexed radicals is too low to be able to abstract a hydrogen atom of propionic acid.

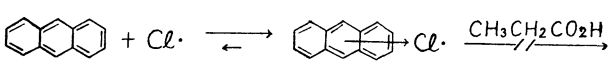

In the presence of sulfur dioxide, a new radical such as $SO_2Cl\cdot$ may be formed, as is seen in Scheme 1:

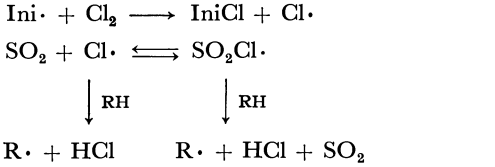

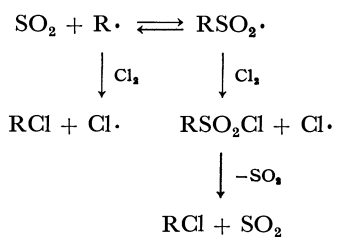

Scheme 1

The chlorine radical has so large an electrophilicity that the reaction is very sensitive to the electron density of the substrate as well as to the solvent used. The relative reactivity (β/α) or the selectivity varies according to the polar effect of the substituent in the substrate and the medium with which the radical may form a complex or a new attacking species.

The present authors have confirmed that propionic acid does not react with chlorine in either *n*-heptane, anisole, or dioxane, where the hydrogens of the solvent molecules have high electron densities. Thus, the relative reactivity (β/α) of propionic acid will diminish upon the decrease in the electrophilicity of the attacking radical, because the electron density at the α-position hydrogen atom is expected to have a lower electron density than that at the β-position in propionic acid.

Ordinarily, a rise in such a selectivity is accompanied by a decrease in the reactivity of the attacking radical.

It has been reported that the sulfochlorine radical is less reactive than the chlorine radical.[5] The increase in the content of the aromatic compound in the reaction mixture results in a proportionate decrease in the total yield of the reaction product. The decrease in the reactivity of the attacking radical will cause an increase in the energy difference due to selectivity (E_s) between primary (β) and secondary (α) hydrogens. On the other hand, the energy difference due to the polar effect (E_p) will decrease as the chlorine radical forms another complex or a new complexed radical, because the nucleophilic character of the latter will increase. The energy difference between the α and the β-positions would be reduced by the compensation of both the effects. If E_s is very large and if E_p is small, as in the sulfochlorine radical, it can be expected that the reversal of the relative reactivity may easily happen.

The energy-level diagram in the reaction course is illustrated in Fig. 3.

In the chlorine - sulfur dioxide system the present authors assumed that a sulfochlorine radical was formed. However, we could not completely rule out the interaction between the carboxyl group of the substrate and the sulfur dioxide molecule. The oxygen atom of sulfur dioxide is bonded with the α-hydrogen atom by a hydrogen bonding, as is indicated in Fig. 4. Thus, the α-hydrogen-carbon bond is weakened and is easily attacked by a chlorine radical to abstract the α-hydrogen atom.

The difference in the results of the photoreactions between the Cl_2 - aromatics - CCl_4 and Cl_2 - sulfur dioxide systems is probably caused by the following factors.

5) G. A. Russell and H. C. Brown, *J. Amer. Chem. Soc.*, **77**, 4031 (1955).

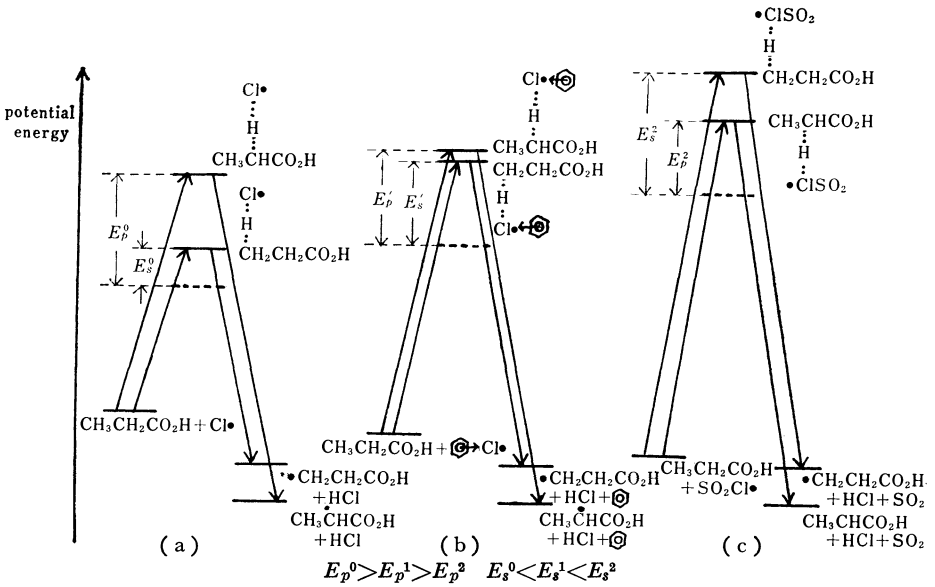

Fig. 3. Schematic energy diagram of chlorination reaction of propionic acid with chlorine, in the absence of solvent (a), in the presence of benzene (b) or sulfur dioxide (c).

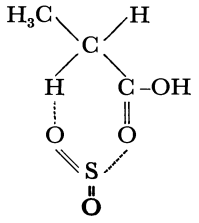

Fig. 4

In the Cl_2-aromatics - CCl_4 system, photo-irradiation has little influenece upon the stabilities of the formed complexed radicals, while photo-irradiation may hinder the formation or may quickly decompose the sulfochlorine radical, as is shown by the following scheme:

$$SO_2 + Cl\cdot \rightleftarrows SO_2Cl\cdot$$

$$SO_2Cl\cdot \xrightarrow{h\nu} SO_2Cl\cdot * \longrightarrow SO_2 + Cl\cdot$$

As has been mentioned above, the relative reactivity in the photoreactions by the $Cl_2 - SO_2$ system was similar to that of the attack by the chlorine radical alone, in spite of the presence of sulfur dioxide.

The selectivity in the reaction of SO_2–Cl_2 diluted with carbon tetrachloride has also indicated no dependence upon the concentration of sulfur dioxide as in the case of the photo-irradiation. The reason for this probably lies in the instability of the $SO_2Cl\cdot$ radical as a result of its dilution by carbon tetrachloride.

The formation of the $SO_2Cl\cdot$ radical as the attacking species in the $Cl_2 - SO_2$ - BPO system may be proved by the results shown in Table 3, where the relative reactivity, β/α, is 0.76, this value being close to the result in the equimolar ($Cl_2 : SO_2 = 1 : 1$) chlorination, $\beta/\alpha = 0.87$.

Experimental

Chlorination of Propionic Acid Initiated by Benzoyl Peroxide in a Benzene - Carbon Tetrachloride Mixed Solvent. Propionic acid (10.59 g, 0.143 mol), a solvent (1.0 mol), and BPO (0.087 g, 0.00036 mol) were placed in a four-necked flask (200 m*l* volume) immersed in a water bath equipped with a thermostat. The solvents used were mixtures of benzene and carbon tetrachloride, mole fractions of benzene varying as 0.0, 0.1, 0.2, 0.3, 0.5, 0.7, 0.8, 0.9, and 1.0. Chlorine gas (0.286 mol), which had been washed and dried by the use of water, concentrated sulfuric acid, calcium oxide and phosphorus pentoxide, was blown into the reaction mixtures at 70°C for three hours. The amount of flowing chlorine gas was set by a flow meter. In these reactions, all the entire reaction apparatus was sheltered from light, and the reaction apparatus was filled with nitrogen gas before the reactions in order to eliminate the effect of oxygen. The solvents were removed by distillation, and the residue was analyzed by means of the NMR spectra. The following compounds were obtained for chlorinated propionic acids.

NMR: $CH_3CHClCO_2H$, τ, 5.70 (quartet) 8.29, (doublet).
$CH_3CCl_2CO_2H$ 7.70 (singlet),
$CH_2ClCH_2CO_2H$ 6.12 (triplet), 7.18 (triplet).
$CHCl_2CH_2CO_2H$ 3.98 (triplet), 6.72 (doublet).

The yields of these compounds were calculated from the areas of their respective peaks. A small white crystal was gained as the by-product. The crystal was recrystallized from ethanol melted at 157—158°C. This product was confirmed as α-benzene hexachloride by a comparison of the IR and NMR spectra, and the retention time in gas-liquid chromatography, with those of an authentic specimen. In addition to this, a very small amount of chlorobenzene was obtained; it was identified by a study of the IR spectrum and by glc.

Chlorination in Naphthalene - Carbon Tetrachloride and Anthracene - Carbon Tetrachloride. The reactions were performed in the same apparatus and using the same procedure as have been described above. The mole fractions of naphthalene in the solvent (CCl_4) used were 0.006, 0.01, 0.014, 0.019, 0.025, 0.05, 0.10, and 0.20, and that of anthracene was 0.0129.

Chlorination with Photo-initiation in Benzene - Carbon Tetrachloride. In a reaction flask we placed propionic acid (10.59 g, 0.143 mol) and solvents (1.0 mol). This reaction flask was then illuminated by a 300-watt unfrosted tungsten light bulb placed near it. The mole fraction of benzene in the mixed solvents were 0.0, 0.5, and 1.0 respectively. Iden-

tification and quantitative analysis were done by the previously-described procedures.

Chlorination Initiated by BPO in the Presence of Sulfur Dioxide. To a four-necked vessel with a volume of 50 m*l* immersed in a water bath and equipped with a thermostat, we added propionic acid (10.59 g, 0.143 mol) and BPO (0.087 g, 0.00036 mol). Dried chlorine gas (0.286 or 0.572 mol) and sulfur dioxide gas were then passed through the reaction mixtures at 70°C for three hours. The total amounts of sulfur dioxide used were 0.036, 0.142, 0.286, 0.572, and 0.858 mol respectively. Soon after the reaction, white crystals were formed. These crystals were separated from benzene - ligroin (1:4) mixtures. The compound was identified as the cyclic anhydride of β-sulfopropionic acid by a comparison of its melting point, NMR, and mass spectra with those of an authentic specimen. Mp, 76—77°C. NMR: centered at 6.97 (multiplet) and 7.38 (multiplet). Mass: exhibited a molecular ion peak at *m/e* 136 with those of fragment ions. The soluble compounds in the solvent were distilled under pressure (10 mm Hg) after the solvents had been removed. The three portions of the distillate at 50—70, 70—80 and 80—90°C were submitted to NMR analyses.

Photochlorination in the Presence of Sulfur Dioxide. Sulfur dioxide (0.858 mol) was passed with chlorine gas (0.143 or 0.286 mol) through a reaction vessel containing propionic acid (0.143 mol). Identification and quantitative analysis were done as has been described in the experimental section concerning initiation with BPO.

Reaction of Propionic Acid with Sulfuryl Chloride. Propionic acid (0.143 mol) was reacted with sulfuryl chloride (0.195 mol) at 70°C with BPO (0.00036 mol).

NMR Spectra. The proton resonance spectra were run on a Nihondenshi spectrometer at 60 MHz.

IR Spectra. The infrared spectra were recorded on an EPI-S2-TYPE Hitachi spectrometer.

Mass Spectra. The mass spectra were run on a Hitachi RMU-6E single-focusing instrument.

Gas-liquid Chromatography. Glc was carried out on a K53-TYPE Hitachi chromatograph, using Silicone SE-30 as the column.

BULLETIN OF THE CHEMICAL SOCIETY OF JAPAN, VOL. 44, 2776—2779 (1971)

The Hofmann Rearrangement. IV. Kinetic Isotope Effect of *N*-Chlorobenzamide

Tsuneo IMAMOTO, Seung-Geon KIM, Yuho TSUNO, and Yasuhide YUKAWA
The Institute of Scientific and Industrial Research, Osaka University, Yamadakami, Suita, Osaka

(Received March 25, 1971)

Kinetic isotope effects in the Hofmann rearrangement of phenyl-1-^{14}C and carbonyl-^{14}C labeled *N*-chlorobenzamides were measured in a sodium hydroxide solution at 15°C. The observed isotope effect on the phenyl-1-carbon is

$$k_{12}/k_{14} = 1.0456 \pm 0.0012$$

and that on the carbonyl-carbon is

$$k_{12}/k_{14} = 1.0447 \pm 0.0006$$

These results strongly support a concerted mechanism for this rearrangement. Attempts have been made to correlate the isotope effect on phenyl-1-carbon to the *r*-value of the linear aromatic substituent-reactivity relationship in related 1,2-rearrangements.

The most important stage in the course of the Hofmann reaction is the rearrangement step in which the conjugate base of *N*-haloamide is converted into isocyanate accompanying the release of a halide ion. With a view to clarifying the precise reaction mechanism of this step, we have investigated this rearrangement kinetically. Kinetic results of the rearrangements of various substituted *N*-bromo- and *N*-chlorobenzamides in an aqueous sodium hydroxide solution have been reported.[1-3] These results could be interpreted by considering a concerted mechanism (path (A)) rather than an alternative two-step mechanism (path (B)).

We have now studied the kinetic isotope effect of this rearrangement using phenyl-1-^{14}C and carbonyl-^{14}C labeled *N*-chlorobenzamides in order to demonstrate this concerted mechanism.

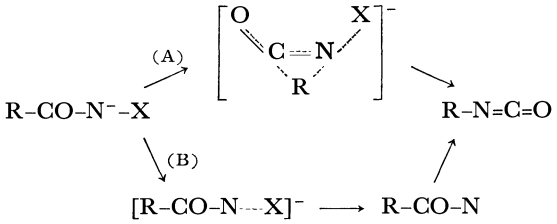

Results and Discussion

The rate of rearrangement of the non-labeled *N*-chlorobenzamide was measured at 15.00±0.01°C by the iodometric method. The initial concentrations of *N*-chloroamide and sodium hydroxide were 0.05 mol/*l*

1) T. Imamoto, Y. Tsuno, and Y. Yukawa, This Bulletin, **44**, 1632 (1971).
2) T. Imamoto, Y. Tsuno, and Y. Yukawa, *ibid.*, **44**, 1639 (1971).
3) T. Imamoto, Y. Tsuno, and Y. Yukawa, *ibid.*, **44**, 1644 (1971).

and 0.5 N, respectively.[4] The first-order kinetic plots formed straight line to at least 85% completion of the reaction. The rate constant obtained from repeated runs was $k_1=7.830\pm0.009\times10^{-5}$ sec^{-1}. This value is larger by *ca.* 1% than the one reported previously.[2] The slight difference in the rate constant refers to the change of the initial concentration of *N*-chloroamide from 0.025 to 0.05 mol/*l*.

Determination of the kinetic isotope effect was carried out under the same reaction conditions by measuring the specific activities of the benzamide derived quantitatively from the remaining reactant *N*-chlorobenzamide. Labeled *N*-chlorobenzamide, prepared from commercial benzoic-^{14}C acid, was dissolved in an aqueous sodium hydroxide solution. A certain amount of the reaction solution was pipetted out at intervals and transferred into hydrochloric acid containing excess potassium iodide. After reduction of the liberated iodine with a sodium thiosulfate solution, the benzamide was extracted and purified by recrystallization. The specific activity of the benzamide thus obtained was determined by an equilibrium voltage method with an ionization chamber and a vibrating reed electrometer connected to a digital integrating voltmeter. These results are listed in Table 2. The kinetic isotope effect was calculated by the least-squares method according to the equation

$$\log A_x = \log A_0 - (1-k_{14}/k_{12}) \log (1-x) \qquad (1)$$

where x is the fraction of reaction calculated from the reaction time and the rate constant ($k_1=7.830\times10^{-5}$ sec^{-1}), and A_x and A_0 are specific activities at $x=x$ and $x=0$ respectively. Figure 1 shows the plots of log A_x *vs.* log$(1-x)$. The calculated kinetic isotope effect on the phenyl-1-carbon is given by

$$k_{12}/k_{14} = 1.0456 \pm 0.0012$$

and that on the carbonyl-carbon by

$$k_{12}/k_{14} = 1.0447 \pm 0.0006$$

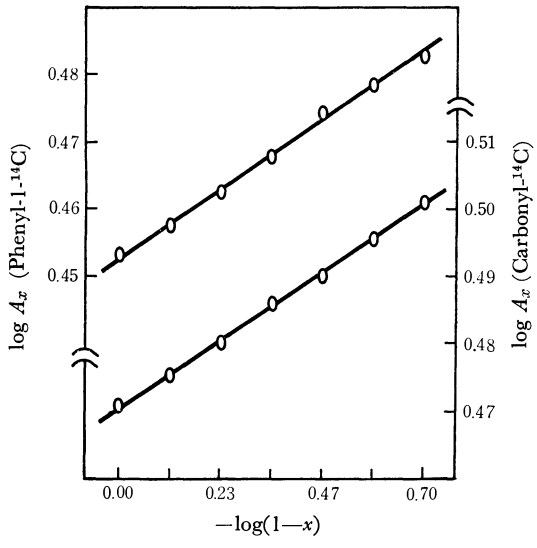

Fig. 1. Plots of log A_x *vs.* −log$(1-x)$

4) From the results of the preliminary experiment on the recovery and the purification of the residual unrearranged benzamide, 0.05 mol/*l* was employed as the most suitable initial concentration of *N*-chloroamide.

Theoretical and experimental studies on the isotope effect lead to the conclusion that the variation of bonding at a labeled position from the initial state to the transition state in the rate-determining step is the most important factor to cause a kinetic isotope effect.[5,6] Thus it is necessary, for elucidation of the precise reaction mechanism of the present Hofmann rearrangement, to examine the variations of the total bondings at respective labeled positions in *N*-chlorobenzamide for the proposed mechanisms.

The initial and transition states for the concerted and two-step mechanisms may be schematically represented as follows.

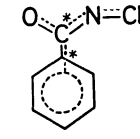

I. S.

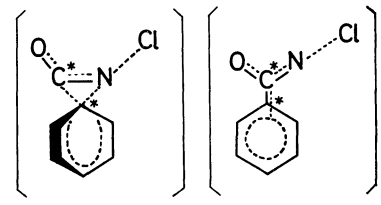

T. S., Concerted T. S., Two-step

In the former mechanism, bondings at the labeled positions change remarkably in proceeding from initial to transition states, and measurable kinetic isotope effects can be expected in this mechanism. On the contrary, if the reaction proceeds through the two-step mechanism, no apparent kinetic isotope effect should be observed, since the transition state resembles the initial state with respect to the bondings at the labeled positions.

Thus the apparent kinetic isotope effects on phenyl-1- and carbonyl-carbons evidently indicate the concerted mechanism for the Hofmann rearrangement.[7]

In addition to the present Hofmann rearrangement, the kinetic isotope effects of Beckmann, Wolff and Schmidt rearrangements have been studied in our laboratory by the use of phenyl-1-^{14}C and carbonyl-^{14}C labeled compounds. The obtained results are summarized in Table 1. An important working hypothesis in the course of these studies is that the apparent observation of the kinetic isotope effect on phenyl-1-carbon indicates the participation of the phenyl group in electron-deficient migration terminus in the transition state. This suggests that the Hofmann and the Beckmann rearrangements proceed through a concerted type transition state. In the cases of other Wolff and Schmidt rearrangements, where kinetic isotope effects

5) J. Bigeleisen and M. Wolfsberg, *Advan. Chem. Phys.*, **1**, 15 (1958).

6) L. Melander, "Isotope Effects on Reaction Rates," Ronald Press Co., New York, N. Y. (1960).

7) Wright and Fry studied the kinetic isotope effect of the Hofmann rearrangement using phenyl-1-^{14}C and carbonyl-^{14}C labeled *N*-bromobenzamides, and also supported the concerted mechanism. A. Fry, private communication.

TABLE 1. KINETIC ISOTOPE EFFECTS AND r-VALUES OF 1,2-REARRANGEMENTS

	Temp. (°C)	Phenyl-1-C k_{12}/k_{14}	Carbonyl-C k_{12}/k_{14}	r-Value
Hofmann rearrangement	15.00±0.01	1.0456±0.0012[a]	1.0447±0.0006[a]	0.41[g] (0.69)[h]
Beckmann rearrangement	60.00±0.01	1.018 ±0.009[b]		
	60.00±0.01	1.025 ±0.008[b]		0.632[i]
	40.00±0.01	1.026 ±0.003[b]		0.600[j]
	71.30±0.01	1.052 ±0.017[c]	1.00 ±0.01[c]	
Wolff rearrangement	30.00±0.01	1.00 ±0.01[d]	1.00 ±0.01[d]	−1.7[k]
Schmidt rearrangement	45.00±0.01	1.00 ±0.02[e]	1.045 ±0.02[e]	
	45.00±0.01		1.066 ±0.022[f]	

a) Present results.
b) Acetophenone oxime, in concd. H_2SO_4. Y. Yukawa, S. G. Kim, T. Ando, and T. Kawakami, unpublished.
c) Acetophenone oxime-acetate, in Beckmann mixture. Y. Yukawa and S. G. Kim, unpublished.
d) α-Diazoacetophenone, in *t*-butyl alcohol containing silver benzoate and triethylamine. Y. Yukawa and T. Ibata, This Bulletin, **42**, 802 (1969).
e) Acetophenone, in aqueous trichloroacetic acid containing sodium azide. Y. Yukawa and K. Toriyama, unpublished.
f) Benzophenone, in aqueous trichloroacetic acid containing sodium azide. Y. Yukawa and K. Toriyama, unpublished.
g) *N*-Chlorobenzamides, in 0.5 N NaOH, at 30°C. Ref. 2.
h) 2-Chloro 4- and 5-substituted *N*-chlorobenzamides, in 0.5 N NaOH, 30°C. Ref. 3.
i) Acetophenone oximes, in sulfuric acid, 51°C. P. J. McNulty and D. E. Pearson, *J. Amer. Chem. Soc.*, **81**, 612 (1959).
j) Acetophenone oxime-picrates, in dichlorobutane, 70°C. R. Huisgen, J. Witte, H. Walz, and W. Jira, *Ann. Chem.*, **604**, 191 (1957).
k) α-Diazoacetophenones, in toluene containing silver benzoate and triethylamine. Y. Yukawa, Y. Tsuno, and T. Ibata, This Bulletin, **40**, 2618 (1967).

on the phenyl-1-carbon were not observed within experimental error, the migration of the phenyl group might not take place in the rate-determining step.

On the other hand, application of the following LArSR relationship (linear aromatic substituent–reactivity relationship) is useful for elucidating the mechanisms of organic reactions.

$$\log k/k_0 = \rho(\sigma^0 + r\Delta\bar{\sigma}_R^+) \qquad (2)$$

In particular, empirical facts on the resonance parameter r have enabled us to evaluate quantitatively the degree of conjugation effect on the reactivity.[8]

The calculated r-values of Hofmann, Beckmann and Wolff rearrangements are given in Table 1. Comparatively large positive r-values of the former two rearrangements indicate the additional conjugation effect to the reaction center with the stabilization of the transition state. In contrast, the large negative r-value of the Wolff rearrangement shows that the resonance stabilization of the initial state is the most important factor in the reactivity.

It is of interest to compare these r-values with the kinetic isotope effects on phenyl-1-carbons. The positive r-value indicates an apparent isotope effect and the large negative r-value no effect. This leads to the conclusion that not only the application of the LArSR relationship but also the isotope effect study on phenyl-1-carbon are useful for the elucidation of the precise reaction mechanism of 1,2-rearrangement.

Experimental

Materials. N-*Chlorobenzamide-(Phenyl-1-*^{14}*C)*: A mixture of 10.0 g of phenyl-1-^{14}C labeled benzoic acid (supplied from NENC, USA) and 27 g of purified thionyl chloride was refluxed for 2 hr. The excess thionyl chloride was removed by azeotropic distillation adding twice 10 m*l* of absolute benzene. The benzoyl chloride obtained was added dropwise to 70 m*l* of 28% aqueous ammonia with stirring at 0—5°C. The benzamide precipitated was collected, washed with water and dried, mp 126.5—127.5°C, yield 8.11 g (82%). This crude amide was recrystallized three times from dichloroethane - ligroin (1:1), 6.60 g, mp 127.5—128.5°C. Specific activity 2.830 mCi/mol. The obtained pure amide (6.37 g) was dissolved in 400 m*l* of 3N HCl and chlorine gas was passed for 2 hr. The *N*-chloro derivative thus precipitated was collected, washed with water and dried *in vacuo*, 6.91 g (84%), mp 114—116°C. This was recrystallized twice from dichloroethane - ligroin (1:2), 5.38 g, mp 117.0—118.0°C (reported 117.0—118.0°C[2]). Active chlorine: found 22.85%, calcd. 22.79%. Specific activity 2.830 mCi/mol.

N-*Chlorobenzamide-(Carbonyl-*^{14}*C)*: Carbonyl-^{14}C labeled benzoic acid (supplied from RCC, England) (10.0 g) was converted into *N*-chlorobenzamide (4.95 g) by the same procedure as described in the preceding part. Benzamide: mp 127.5—128.5°C, specific activity 2.961 mCi/mol. *N*-chlorobenzamide: mp 117.0—118.0°C, specific activity 2.960 mCi/mol, active chlorine; found 22.73%, calcd 22.79%.

No mutual contamination of the phenyl-1-^{14}C and the carbonyl-^{14}C labeled *N*-chlorobenzamides was indicated by comparing the specific activities of the derived acetanilides with those of the respective reactants *N*-chlorobenzamides-^{14}C.

Determination of the Rate Constant. The rate constant of the rearrangement of non-labeled *N*-chlorobenzamide was determined at 15.00±0.01°C by the same procedure described previously.[1,2]

Measurement of the Kinetic Isotope Effect. Kinetic Procedure and Preparation of the Sample for Assay. In a measuring flask was placed 400 m*l* of a standardized aqueous sodium hydroxide solution (0.500N), and the flask was immersed in a constant temperature bath (15.00±0.01°C). Labeled *N*-chlorobenzamide (3.112 g) was weighed into a 500 m*l* Erlenmeyer flask and immersed in the same bath. After being kept for several hr, the sodium hydroxide solution was transferred into the Erlenmeyer flask with vigorous swirling. A certain amount of the reaction solution was pipetted out at intervals

8) Y. Yukawa, Y. Tsuno, and M. Sawada, This Bulletin, **39**, 2274 (1966); Y. Yukawa and Y. Tsuno, *Nippon Kagaku Zasshi*, **86**, 783 (1965).

and transferred into 15 m*l* of 6N HCl containing 700 mg of potassium iodide. A sodium thiosulfate solution (0.3N) was added dropwise until the color of the liberated iodine disappeared. The residual unrearranged benzamide was extracted with five 50 m*l* portions of dichloromethane. The solvent was evaporated and the residue was stirred with 50 m*l* of dichloroethane. A small amount of the undissolved salts was excluded by filtration. The filtrate was evaporated to give pale yellow needles, *ca.* 120 mg, mp 125—127°C. This was recrystallized five times from toluene to afford 40—50 mg of sample for assay, colorless plates, mp 127.5—128.5°C.

Measurements of Specific Activity. About 7—8 mg of accurately weighed benzamide-^{14}C was burned by means of a combustion furnace for micro-elemental analysis, and the carbon dioxide generated was introduced into a 200 m*l* ionization chamber. The chamber was set on a Takeda-Riken RS-84 vibrating reed electrometer connected to a digital integrating voltmeter. The ion current was recorded as relative voltage every ten seconds for 1 hr, and the mean value of the voltage was obtained with the standard deviation of $\pm$0.2%. The radioactivity of the sample was calculated by calibration of the obtained voltage with that of the standard chamber. Specific activity measurements were carried out at least twice for each sample. Reproducibility of the specific radioassay was within 0.25% in every case. The results are given in Table 2. The error indicates the standard deviation from the mean value.

Table 2. Specific activities of residual unrearranged benzamide

No.	Time (min)	Fraction of reaction (%)	Specific activity (mCi/mol) Phenyl-1-^{14}C	Carbonyl-^{14}C
1	0	0	2.8404$\pm$0.0024[a)]	2.9567$\pm$0.0016[a)]
2	57.1	23.5	2.8666$\pm$0.0014	2.9877$\pm$0.0024
3	114.2	41.5	2.9011$\pm$0.0022	3.0257$\pm$0.0033
4	171.3	55.3	2.9357$\pm$0.0024	3.0629$\pm$0.0020
5	228.4	65.8	2.9805$\pm$0.0010	3.0914$\pm$0.0016
6	285.5	73.9	3.0101$\pm$0.0011	3.1287$\pm$0.0004
7	342.6	80.0	3.0389$\pm$0.0029	3.1690$\pm$0.0040

a) The sample was obtained by treatment of pure *N*-chlorobenzamide with potassium iodide in aqueous acetic acid.

The authors express their sincere appreciation to Mr. T. Fujino and Mr. T. Shishido for their kind advice on the operation of the combustion furnace. Thanks are due to Mr. N. Shimizu and Mr. H. Yamataka for their assistance.

BULLETIN OF THE CHEMICAL SOCIETY OF JAPAN, VOL. 44, 2779—2786 (1971)

Synthetic Studies of Amino Acids by the Use of Copper Complex. II.[1] The Condensation Reaction of *N*-Pyruvylideneglycinatocopper(II) Complexes with various Aldehydes

Tetsuya ICHIKAWA, Sadao MAEDA, Toshiro OKAMOTO, Younosuke ARAKI, and Yoshiharu ISHIDO

Department of Chemistry, Faculty of Science, Tokyo Institute of Technology, Ookayama, Meguro-ku, Tokyo

(Received March 31, 1971)

An investigation of the mechanism of the reaction which involves the base-catalyzed condensation of bis(glycinato)copper(II) with aldehydes was carried out with the purpose of improving it so that it can proceed even with lower molar equivalent ratios of aldehydes to the complex and under milder conditions. On the basis of the results reported in the literature and those of this investigation, the reaction has been carried out as expected and has been newly shown to be applicable to *p*-tolualdehyde and *p*-chlorobenzaldehyde, and, moreover, to such aldehydo sugar derivatives as 2,3-*O*-isopropylidene-D-glyceraldehyde by the use of *N*-pyruvylideneglycinatocopper(II) complexes in the reaction in place of bis(glycinato)copper(II). An attempt at further improvement will also be described in the present communication.

The base-catalyzed condensation reaction of bis(glycinato)copper(II) (**1**) and acetaldehyde (**2**) has been known to be important in the preparation of DL-threonine (**3**),[2] and the mechanism[3] involving the carbanion depicted in Scheme I has generally been accepted on the basis of the masking effect of the copper ion on the amino group[4] or of the electronic polarization effect of the copper ion on the methylene carbon.[3] However, no evidence for the former effect has been reported in connection with these systems.[5]

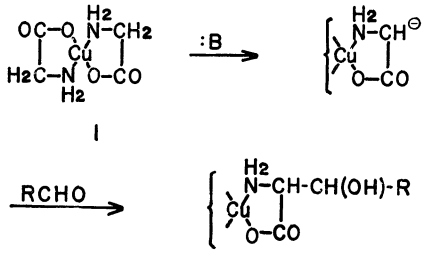

Scheme I

1) T. Ichikawa, S. Maeda, Y. Araki, and Y. Ishido, *J. Amer. Chem. Soc.*, **92**, 5514 (1970).

2) M. Sato, K. Okawa, and S. Akabori, This Bulletin, **30**, 937 (1957).

3) A. Nakahara, *Yuki Gosei Kagaku Kyokaishi*, **27**, 951 (1969).

4) F. P. Dwyer, "Chelating Agents and Metal Chelates," Academic Press, New York, N. Y. (1964), p, 347.

5) M. M. Jones, "Ligand Reactivity and Catalysis", Academic Press, New York, N. Y. (1968), p, 123.

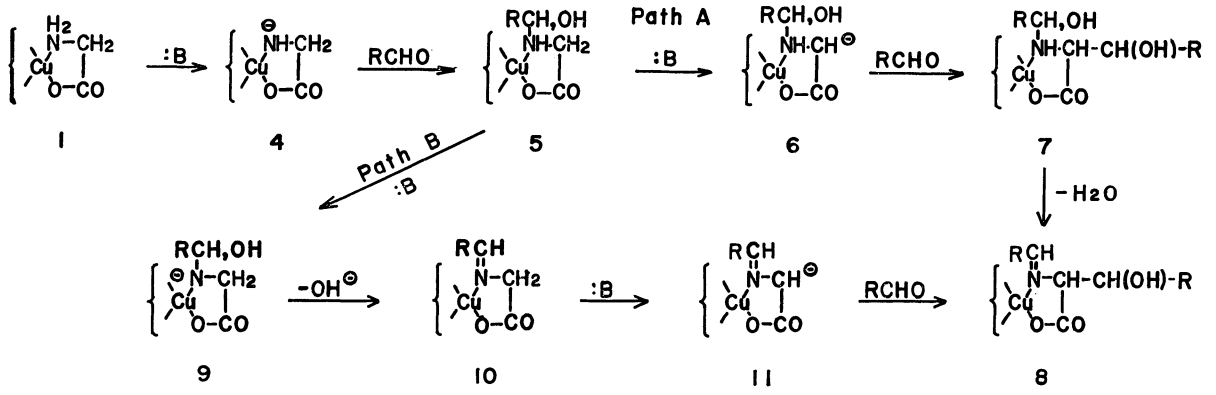

Scheme II

From the synthetic standpoint of view, the reaction is usually carried out under strongly basic conditions in the presence of 2—5 mole equivalents of aldehydes to glycine; it is thus unsuitable for aldehydes which are susceptible to self-condensation or isomerization under basic conditions. The investigation of this series has been undertaken so as to improve the reaction so that it can proceed even under weakly basic conditions and can be used for the aldehydes above mentioned; we have examined the findings on this reaction reported by several groups of investigators.[2-6]

Results and Discussion

Reaction Mechanism. The preferred dissociation of the proton on the nitrogen atom of **1** to that on the methylene carbon atom was explicitly exhibited by the isolation of complexes, *i.e.*, $K[Ni(NHCH_2CO_2)(NH_2CH_2CO_2)]$ and $K_2[Ni(NHCH_2CO_2)_2]$,[7] and by a NMR study of the dissociation of similar complexes of cobalt under slightly alkaline conditions.[8] When mixtures of **1** and **2** (0—2.238 mole equivalents to glycine) were stirred in water at pH 9.5 at room temperature for 5 min, an almost linear relationship was observed between the recovery yield of **1** and the amount of **2** used, as may be in Fig. 1. In this case, it is noticeable that the formation of **3** could not be detected by thin-layer chromatography. This result can be considered to suggest that **2** is not subjected to the attack of the carbanion shown in Scheme I, but to that of the amino group of **1** in the first stage of the reaction. Consequently, the reaction was assumed to proceed *via* a mechanism involving the methylol-type intermediate (**5**), shown in Scheme II. The stability constants of *N*-substituted glycine[9] and ethylenediamine complexes[10] have been known to

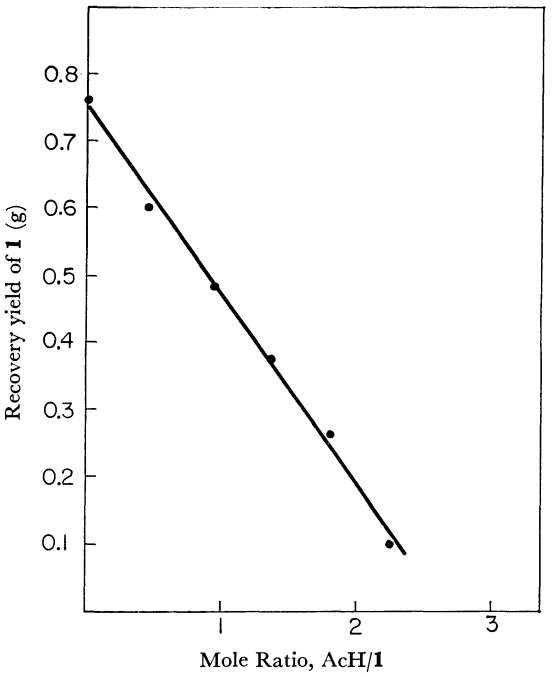

Fig. 1. Plot of recovery yield of bis(glycinato)copper(II)(**1**) *vs.* molar ratio of acetaldehyde (**2**) to glycine in **1** for the reaction of 5 mmol of **1** with **2** which were carried out at pH 9.5 for 5 min at room temperature.

be reduced in proportion to an increment in the bulkiness of *N*-substituent groups. The remarkable difference in reactivity between **2** and propionaldehyde or isobutyraldehyde, which are difficult to condense with **1** in the vicinity of pH 11.0 as far as we examined, may similarly be attributed to the stability or ease of the formation of the intermediate, **5**; *i.e.*, the difference may strongly suggest an important role of **5** in the reaction.

As to the subsequent process of the reaction, two paths, A and B, are conceivable. Path A involves the attack of the **6** carbanion, which is produced from **5** by the dissociation of the proton on the methylene carbon, on aldehydes to give **8** *via* **7**, with a simultaneous dehydration. On the other hand, Path B involves the attack of the Schiff base-type carbanion, **11**, which was produced *via* **9** and **10**, on aldehydes.

If the reaction is assumed to proceed *via* Path A, it can contradictorily be concluded that the dissoci-

6) a) K. Okawa and S. Akabori, Brit. Pat. 814063 (1959). b) Y. Ikutani, T. Okuda, and S. Akabori, This Bulletin, **33**, 582 (1960). c) S. Akabori, T. T. Otani, R. Marshall, M. Winiz, and J. P. Greenstein, *Arch. Biochem. Biophys.*, **83**, 1 (1959). d) T. T. Otani and M. Winitz, *ibid.*, **102**, 464 (1963). e) H. Mix and F. W. Wilke, *Z. Physiol. Chem.*, **337**, 40 (1964). f) M. Ohno and N. Kawabe, Japanese Pat. 6821286 (1968).

7) G. W. Watt and J. F. Knifton, *Inorg. Chem.*, **6**, 1010 (1967).

8) D. H. William and D. H. Busch, *J. Amer. Chem. Soc.*, **87**, 4644 (1965).

9) F. Basolo and Y. T. Chen, *ibid.*, **76**, 953 (1954).

10) H. Irving and J. M. M. Griffiths, *J. Chem. Soc.*, **1954**, 213.

Table 1. An examination of the effect of formaldehyde on the condensation of bis(glycinato)copper(II) with acetaldehyde, and of the regeneration of acetaldehyde from the complex **12**[a)]

Run	$Cu(gly)_2$ (mmol)	CH_3CHO (mmol)	HCHO (mmol)	Complex **12** (mmol)	Yields(%)[12] of Recovered Glycine	Threonine
1	5	5	—	—	75	20
2	5	10	—	—	55	42
3	5	10	10	—	47	30
4	5	10	20	—	56	23
5	2.5	—	—	2.5	46	55

a) All the reactions were carried out by dissolving the reagents in water (50 m*l*) at room temperature for 4 hr in the presence of sodium carbonate (1 g).

ation of the proton on the methylene carbon atom takes preference over that of the proton on the nitrogen atom. However, so large an electron-attracting effect of the copper ion on the methylene carbon atom as to produce the **6** carbanion can not be expected from the structure of **5**. The mechanism *via* Path A can thus be discarded on the basis of these considerations. Consequently, the most important step of this reaction is considered to be that of the formation of **10**; hence, a sufficient electron-attracting effect of the copper ion on the methylene carbon atom can be expected from its structure. The structure of bis(2,5-dimethyloxazolidine-4-carboxylato)copper(II) (**12**),[11] which is easily prepared in a good yield by the reaction of **1** with **2** at pH 11, was confirmed by X-ray analysis; this fact suggests that the masking effect of the copper ion on the amino group is not so large as to prevent the reaction with **2**. **12** may be formed from **8** (R=Me) by the ring closure involving the addition reaction of a β-hydroxy group of threonine to the double bond of the *N*-ethylidene group (Scheme III). As can be seen from Table 1, the addition of formaldehyde (**13**) to the reaction system of **1** and **2** brought about a decrease in the yield of **3** as well as one in that of the total amino acids; the formation of DL-serine was not detected even by the use of an amino-acid analyzer.

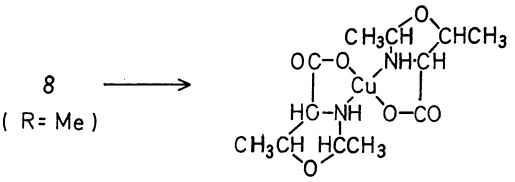

12

Scheme III

Moreover, the regeneration of **2** from **12** on treatment with **1** under the same conditions was experimentally confirmed. It can be thus stated that the formation of carbanion **11** is prevented by the addition of **13**. It is well known, on the other hand, that **13** can not be condensed with **1** so easily as **2**.[6c)] These facts can be explained on the assumption that the product in the first step of the condensation reaction of **1** with **13** is the *N*-methylol-type complex **5** (R=H) and that it remains as it is on account of the instability of the corresponding Schiff base-type intermediate, **10**, under the such conditions. According to Levy[13] and Tomiyama,[14] the monoformyl compound predominates in the pH range above 8.0 in the case of the formol titration. The above consideration is strongly supported by a recent study in which a Schiff base-type intermediate is also assumed in the racemization reaction of bis(L-alaninato)- and bis(*N*,*N*-dimethyl-L-alaninato)copper(II) under basic conditions.[15]

Attempts at Improvement. From the above point of view, it is natural to consider that the application of a complex such as **10**, whose amino group is protected by a proper carbonyl compound, to this reaction in place of **1** may bring about a considerable improvement. An attempted use of *N*-pyruvylideneglycinatoaquocopper(II) (**14**)[16] in the reaction expectedly brought about an improvement in the yields of amino acids and, moreover, made it feasible to condense various aldehydes with **14**. The reaction conditions

11) a) J. P. Aune and P. Maldonado, *Chem. Commun.*, **1970**, 135: the α-form crystal of **12** was analyzed. b) The corresponding β-form crystal of **12** was also analyzed recently by X-ray crystal structure analysis; it was confirmed to have the structure reported in the previous paper. The detailed results will be published elsewhere.

Although Imado reported the preparation of **12** from bis(DL-threoninato)copper(II) and acetaldehyde in the presence of sodium bicarbonate in water, and that it had the structure of bis(*N*-ethylidene-DL-threoninato)copper(II), as is depicted here, this structure can be considered sceptically because **12** does not react with sodium carbonate but nevertheless should be acidic; moreover,

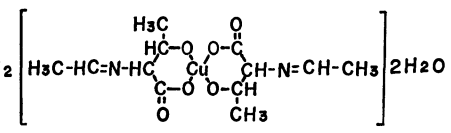

the same complex is obtained from **1** and **2** under strongly basic conditions (pH 11), while it is well known that usual Schiff bases, which are composed of amino acids and aliphatic aldehydes, are unstable under such alkaline conditions [*cf.* S. Imado, *Yakugaku Zasshi*, **81**, 828, 832, and 837 (1961)].

12) No distinct explanation can be given for the drifting change of the yields of total amino acids; they may be arisen from the formation of a structurally-unestablished polymer [*cf.* G. O. Kalland, *Acta Chem. Scand.*, **19**, 2200 (1965)] or other unexpected factors.

13) M. Levy, *J. Biol. Chem.*, **99**, 767 (1933).

14) T. Tomiyama, *ibid.*, **111**, 51 (1935).

15) V. M. Belikov, S. V. Vitt, N. I. Kuznetsova, M. G. Bezrukov, and M. B. Saporovskaya, *Chem. Abstr.*, **72**, 67248s (1970) (*Izv. Akad. Nauk. SSSR, Ser. Khim.*, **1969**, 2536).

16) A. Nakahara, H. Yamamoto, and H. Matsumoto, This Bulletin, **37**, 1137 (1964); the complex could not be obtained in a good yield according to the method described in this article. By the use of cupric hydroxide in place of cupric acetate, it was, however, obtained in a good yield, as has been described in the Experimental section.

Table 2. Reactions of *N*-pyruvylideneglycinatoaquocopper(II) (**14**) with some aldehydes[a)]

R (R-CHO)	Molar ratio (R-CHO:**14**)	Solvent system	pH	Period (hr)	β-Hydroxy amino acids yields(%) under air[b)]	β-Hydroxy amino acids yields(%) under N_2[c)]
H-	1.1	H_2O	8.0	6	28[d)]	—
Me-	1.5	H_2O	9.8	2	61	—
Et	3.0	MeOH	NaOMe[e)]	4	30	76
n-Pr-	3.0	MeOH	NaOMe[e)]	5	48	75
iso-Pr-	3.0	MeOH	NaOMe[e)]	7	—	75
p-NO_2-Ph-	1.0	H_2O - MeOH	9.0	2	80	80
o-NO_2-Ph-	1.0	H_2O - MeOH	9.0	0.5	—	66
Ph-	3.0	MeOH	NaOMe[e)]	9	—	67
p-Cl-Ph-	3.0	MeOH	NaOMe[e)]	10	—	44
p-Me-Ph-	3.0	MeOH	NaOMe[e)]	14	26	41
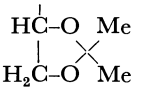	1.1	H_2O	9.5	1	70	—

a) All the reactions were carried out by the use of 10 mmol of **14** [except in the case of 2,3-*O*-isopropylidene-D-glyceraldehyde (9 mmol)] at room temperature (23—26°C) except in the case of *p*-nitrobenzaldehyde (30°C).
b) These results were obtained under atmospheric condition.
c) These results were obtained under nitrogen atmospheric condition.
d) The yield was determined by amino acid analysis with Hitachi KLA 3B amino acid analyzer; An extra peak was observed in this case with almost the same strength in the vicinity of the position where the peak of aspartic acid should be observed.
e) To methanol suspension (40 m*l*), 1N methanolic sodium methoxide solution (7 m*l*) was added.

were greatly improved in the following three ways: 1) The reaction is sufficiently induced in the pH range of 9.0—9.5, in contrast with the above pH value, 10.8, which was used in the reaction of **1**. 2) the reaction satisfactorily proceeds in the presence of 1.0—3.0 mol equivalents of aldehydes to **14**, in comparison with the fact that 2—5 mol equivalents have been utilized in the reaction of **1**. 3) It has come to be possible to condense aldehydes which could not be condensed with glycine in **1** with glycine by the use of **14**. The results, along with the reaction conditions, are summarized in Table 2. The reactions of **14** with **2**, propionaldehyde, *n*-butyraldehyde, and *p*-tolualdehyde were carried out under atmospheric conditions. Except for the reaction with **2**, however, the reactions needed a long period to complete, and not very good results were obtained. In the case of formaldehyde, structurally unestablished amino acid, along with DL-serine, was obtained in a low yield. On the basis of the fact that no glycine could be detected by testing the resultant reaction mixtures thin-layer-chromatographically, and the suggestive report of Nyilasi and Vargha[17)] that glycine in **1** can be subjected to oxidative degradation to give glyoxylic acid and ammonia, it was considered possible that the degradation of glycine in **14** can take place similarly; hence, the above reactions were attempted under a nitrogen atmosphere. The yields of the corresponding β-hydroxy amino acids were thus improved greatly, as may be seen by comparing the data in the 6th and the 7th columns of the table. In the case of highly-reactive *p*-nitrobenzaldehyde (**15**), no difference was observed in the yields of β-(*p*-nitrophenyl)-DL-serine with respect to the atmospheres used. In this connection, the reactions with benzaldehyde and *p*-chlorobenzaldehyde were both carried out under a nitrogen atmosphere. It is remarkable, moreover, that 2,3-*O*-isopropylidene-D-glyceraldehyde (**16**) also gave the corresponding 2-amino-2-deoxypentoaldonic acid in a good yield, even under atmospheric conditions, in spite of the short reaction period, although free sugars are generally known to be susceptible to isomerization or polymerization[18a,b)] under weakly basic conditions. These findings promise to make possible the application of the reaction to the field of carbohydrate chemis-

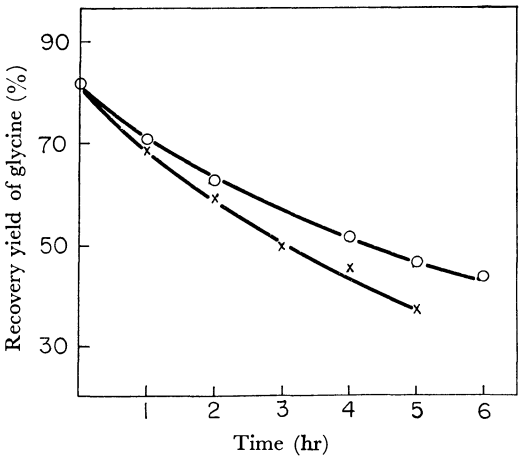

Fig. 2. Plot of recovery yield of glycine *vs.* time for the degradation reaction of *N*-pyruvylideneglycinatoaquocopper(II) (**14**) under nitrogen stream (○) and under atmospheric condition(×).

17) a) J. Nyilasi and E. Vargha, *Acta Chim. Sci. Hung.*, **14**, 113 (1958). b) J. Nyilasi, *ibid.*, **38**, 261 (1963).

18) a) In the reaction with **1**, the corresponding 2-amino-2-deoxyaldonic acid was obtained in a very small yield in spite of the use of 6 equivalents of **15** to each one of **1**. b) C. D. Gutsche, D. Redmore, R. S. Buriks, K. Nowotony, H. Grassner, and C. W. Armbruster, *J. Amer. Chem. Soc.*, **89**, 1235 (1967). c) T. Ichikawa, T. Okamoto, S. Maeda, Y. Ohdan, Y. Araki, and Y. Ishido, *Tetrahedron Lett.*, **1971**, 79.

try as a procedure of synthesizing 2-amino-2-deoxy-aldonic acids involving a chain lengthening by two carbons on aldehydo-sugars.[18c]

To confirm the degradation of glycine in **14**, it was stirred alone in water at pH 9.4—9.6 under both atmospheric and nitrogen atmospheric conditions for comparison, and the recovery yields of glycine were plotted against the reaction period. The results are shown in Fig. 2. The degradation of glycine in **14** may also be explained by the mechanism which was proposed by Nyilasi and Vargha[17] for the degradation of **1**. The observation of a considerable degradation of glycine under nitrogen atmospheric conditions, on the other hand, may suggest the existence of other degradation paths. In the case of the less reactive aldehydes, accordingly, it may be considered that the lower yields of the β-hydroxy amino acids were brought about by the competitive degradation of glycine, especially under atmospheric conditions. The extent of the degradation in the course of the reactions, however, can not be discussed in parallel with that in the examination since the reactions were carried out in methanol in the presence of sodium methoxide. In addition, the degradation test of **14** in methanol could not be performed on account of its insolubility in methanol in the absence of aldehydes.

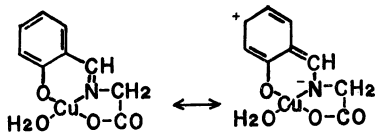

17

On the other hand, *N*-salicylideneglycinatoaquocopper(II) (**17**),[19] which belongs to the same category as **14**, unexpectedly gave no condensation product, even in the reaction with **15**, under the conditions used for the reaction of **14**, although the reaction of **17** with aldehydes[20] is known to proceed provided that 30 mol equivalents of aldehydes are utilized at pH 8.0. These results may be attributed to the resonance effect on the copper ion arising from the inflow of the electron from the benzene ring, as is depicted; hence, protecting the amino group with salicylaldehyde was concluded not to be so advantageous as has been described by Nakahara.[3]

In spite of an attempt to prepare other copper-glycine complexes whose amino groups were protected with acetylacetone or aldol, the corresponding complexes could not be isolated in a pure form; therefore, attempts to use them to the reaction in place of **1** were abandoned.

An attempt at further improvement was undertaken in view of the behavior of **14** upon treatment with an aqueous sodium hydroxide solution. When the alkali solution was added, drop by drop, an aqueous methanolic suspension of **14** and **15**, the mixture turned from blue to bluish green at about pH 6.0, and a gelatinous mass began to separate from the solution.

19) A. Nakahara, This Bulletin, **32**, 1195 (1959).
20) K. Harada and J. Oh-hashi, *J. Org. Chem.*, **32**, 1103 (1967).

A thin-layer chromatographic test of the solution obtained by treating the supernatant of the reaction mixture with hydrogen sulfide showed that it contains only the complex of the resultant amino acid; a corresponding test of the precipitate, on the other hand, showed that it contains only the complex of glycine. It was thus confirmed that the reaction is already induced at about pH 6.0; however, it failed to proceed, presumably on account of the predominant gel formation. The amount of the gel was increased with the addition of the alkali solution, and the mixture was finally turned into gel at about pH 7.5. Even at this point, it was thin-layer-chromatographically confirmed that the condensation reaction made little progress in comparison with the mixture at about pH 6.0. It was confirmed, in addition, that the reaction was not induced by the addition of **15** to the completely-gelled mixture of **14** in aqueous methanol of about pH 7.5. However, the gel began to dwindle over about pH 8.8 upon the further addition of the alkali solution, and the mixture came to be loose enough at pH 9.0 as the reaction proceed smoothly. On the basis of this phenomenon, an equilibrium composed of the species in Scheme IV was assumed; *i.e.*, the entity of the reactant to aldehyde in the vicinity of pH 6.0 may be **18**, and that in the vicinity of pH 9.0 may be **20**, the latter being produced from **14** *via* the salt of hydroxo *N*-pyruvylideneglycinatocopper(II) (**19**).

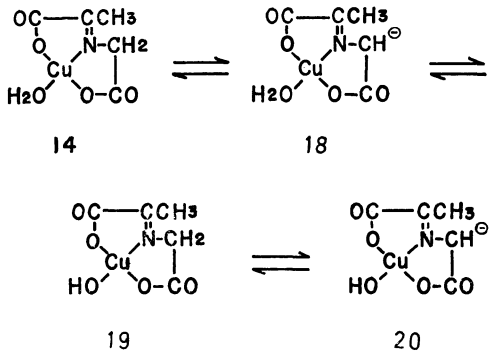

14 18

19 20

Scheme IV

Accordingly, **14** was titrated in water with a 2N aqueous sodium hydroxide solution under nitrogen atmospheric conditions in order to secure evidence of its behavior toward alkali, especially in the pH range of 6.0—9.0. The degradation of glycine in **14** may thus offer no problem since the period required for the titration is short and the pH of the titration mixture is under 9.5. The pH value of the mixture were plotted against the molar ratios of sodium hydroxide to **14** to give the curve shown in Fig. 3. However, the inflection point observed was not clear enough for us to explain the postulated equilibrium. This may arise from a rapid equilibrium among the species in Sheme IV and/or other potential ones. An alteration of the molar concentration of **14** from 5 to 10 mmol had practically no effect on the molar ratio of about 0.15 where the gel formation takes place. These facts presumably suggest the existence of an equilibrium for **14**, although a decisive discussion of this phenomenon is impossible. The dissociation of the α-methylene

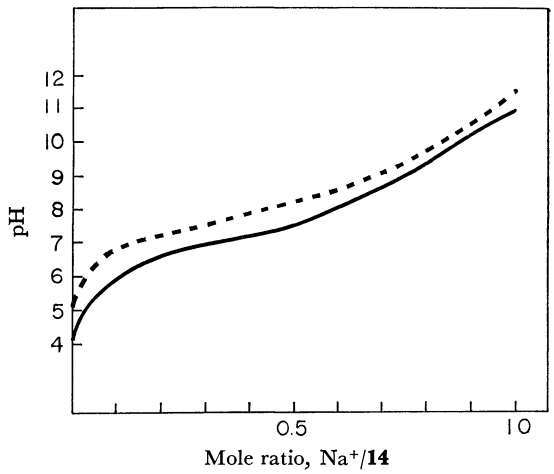

Fig. 3. Titration curves of *N*-pyruvylideneglycinatoaquocopper(II) (**14**) with 2N sodium hydroxide solution in water (50 m*l*) [5 mmol: dotted line; 10 mmol: straight line].

proton of **19** may occur with a certain degree of difficulty compared with that of **14** because of the greater electron density on the copper ion in **18**. However, the active methylene proton of **19** is considered yet to be reactive enough with aldehydes, since an NMR study of sodium chloro *N*-pyruvylideneglycinatopalladium(II) (**21**)[21] established that the α-methylene protons of glycine exclusively dissociate when **21** is dissolved in deuterium oxide. On the basis of these results, it was considered to be favorable for the condensation reaction to replace the aquo ligand in **14** with that which occupies no proton on its coordinating atom; the latter ligand could participate in $p\pi$-$d\pi$ conjugation with copper atom and so minimize the electron density on the copper atom. Pyridine was used as one of the most simple and typical species. *N*-Pyruvylideneglycinatopyridinecopper(II) (**22**) was newly prepared in a good yield by treating equimolar amounts of **14** and pyridine in acetone under vigorous stirring. The equimolar base-catalyzed condensation of **22** with **15** at pH 7.3—7.5 at room temperature was completed within 20 min; it gave β-(*p*-nitrophenyl)-DL-serine in a 67% yield. The reaction conditions in this case are in marked contrast to those used in the reaction of **14**, *i.e.*, at pH 9.5 for 2 hr. Therefore, it is now confirmed that the use of **22** in place of **14** in the condensation reaction with aldehydes brings about so favorable an effect that the reaction proceeds with great ease, even in the vicinity of pH 7.0.

Experimental

All the melting points are uncorrected. Amino acid analyses were carried out by means of a Hitachi KLA-3B Amino Acid Analyzer.

*An Examination of the Recovery of Bis(glycinato)copper (II) (**1**) in Relation to the Mole Equivalents of Acetaldehyde (**2**) Used in the Condensation Reaction.* To a suspension of **1** (1.150 g, 5 mmol) in water (50 m*l*), were added 0—2.238 mol equivalents of **2**; the mixture was then stirred at pH 9.5 for 5 min at room temperature. After the reaction, the undissolved **1** was gathered by filtration, washed with ethanol, and dried by heating *in vacuo*. The melting points (dec) and IR spectra of the recovered **1** were identical with those of the authentic specimen. The results shown below were also presented in Fig. 1.

Run	Acetaldehyde (m*l*)	Acetaldehyde mole equiv. to glycine in **1**	Recovery yield of **1** (g)
1	0	0	0.758
2	0.25	0.448	0.603
3	0.50	0.895	0.485
4	0.75	1.343	0.375
5	1.00	1.790	0.263
6	1.25	2.238	0.100

*An Examination of the Degree of Reactivity between Acetaldehyde (**2**) and Formaldehyde (**13**) with Bis(glycinato)copper(II) (**1**).* A solution of **1** (1.15 g, 5 mmol), **2** (0.5—1.0 mol equivalents), **13** (0—2.0 mol equivalents), and sodium carbonate (1.0 g, 10 mmol) in water (50 m*l*) was stirred at 27°C for 4 hr. After the reaction, concentrated aqueous ammonia (25 m*l*) was added, and the mixture was treated on a column (2.5×9 cm) of Amberlite IR-120B (NH_4 form) and then washed with distilled water (100 m*l*). The effluent and washings were then combined and concentrated to a volume of about 20 m*l* to remove the aldehydes and ammonia. The content of amino acids in the concentrate was determined by amino-acid analysis. The results are summarized in Table 1.

*An Examination of the Regeneration of Acetaldehyde (**2**) from Bis(2,5-dimethyloxazolidine-4-carboxylato)copper(II) (**12**).* A solution of **12** (0.97 g, 2.5 mmol), **1** (0.56 g, 2.5 mmol), and sodium carbonate (1 g, 10 mmol) in water (50 m*l*) was treated in the way described in the previous experiment. The content ratio of the amino acids in the resultant solution was determined by amino-acid analysis; the results are shown in Table 1.

N-*Pyruvylideneglycinatoaquocopper(II) Dihydrate (**14**).* To a suspension of glycine (21.3 g, 284 mmol) in aqueous ethanol (H_2O - EtOH=2:1; 80 m*l*), were added pyruvic acid (25. 0g, 284 mmol). The resultant mixture was stirred at 25°C for 30 min until it become homogeneous. On the addition of freshly-prepared cupric hydroxide, which had been obtained by treating cupric sulfate pentahydrate (71.0 g, 284 mmol) with sodium hydroxide (22.6 g, 568 mmol), a light blue precipitate was formed; the mixture was then allowed to stand overnight with stirring at room temperature. The resultant precipitate was gathered by suctional filtration and dried *in vacuo* over phosphorus pentoxide to give **14** (74.5 g, 75%), mp 195°C(dec).

Found: C, 22.97; H, 4.30; N, 5.32%. Calcd for $C_5H_{11}NO_7Cu$: C, 22.09; H, 4.64; N, 5.39%.

DL-*Serine.* A mixture of **14** (2.60 g, 10 mmol) and formaldehyde (0.9 ml of a 37% aqueous solution, 11 mmol) in aqueous methanol (H_2O - MeOH=3:1; 40 m*l*) was stirred at pH 8.0 for 6 hr at 30°C. After the reaction, the pH of the solution was adjusted to 4 with 3N aqueous acetic acid and the solution was treated with hydrogen sulfide gas. The resultant cupric sulfide was filtered off, and the filtrate was treated on a column (2.5×7 cm) of Amberlite IR-120B (H form) to adsorb the amino acids. After washing with distilled water (5 *l*), the column was eluted with 1N aqueous ammonia (500 m*l*) and the content of amino acids in the eluate was determined by amino-acid analysis. The yield of DL-serine was estimated to be 28%; moreover, an extra peak, one

21) H. Yoneda, Y. Morimoto, Y. Nakao, and A. Nakahara, This Bulletin, **41**, 255 (1968).

observed with almost the same strength, was in the vicinity of the position where the peak of aspartic acid should be observed.

DL-*Threonine.* A mixture of **14** (2.60 g, 10 mmol) and **2** (0.85 m*l*, 15 mmol) in water (50 m*l*) was stirred at pH 9.8 at room temperature for 2 hr. After the reaction, the pH of the resultant mixture was adjusted to 4.5 with 3N aqueous acetic acid; the mixture was then treated with hydrogen sulfide gas and the cupric sulfide was filtered off. The filtrate was concentrated to a volume of about 30 m*l*, and the concentrate was treated on a column (2.5×7 cm) of Amberlite IR-120B (H form), followed by washing with distilled water (5 *l*) and then elution with 1N aqueous ammonia (500 m*l*). The effluent was concentrated almost to dryness, and the residue was treated with ethanol (50 m*l*) to give white crystals of DL-threonine (0.7 g, 61%), mp 216°C (dec).

Found: C, 40.48; H, 7.55; N, 11.51%. Calcd for $C_4H_9NO_3$: C, 40.33; H, 7.62; N, 11.76%.

*β-Hydroxy-*DL-*norvaline.* To a mixture of **14** (2.6 g, 10 mmol) and propionaldehyde (2.1 m*l*, 30 mmol) in methanol (40 m*l*), were added 1N methanolic sodium methoxide (7 m*l*), the mixture was then stirred under a nitrogen atmosphere at 26°C for 4 hr. After the reaction, the resultant mixture was acidified with 3N aqueous acetic acid (5 m*l*), concentrated to a volume of 15 m*l*, and diluted with distilled water (50 m*l*). The solution was washed with diethyl ether (15 m*l*×3 portions) and then with methylene chloride (10 m*l*×2 portions). Then, the aqueous layer was treated with hydrogen sulfide gas, and the resultant cupric sulfide was filtered off. The filtrate was concentrated to a volume of 30 m*l*, and the concentrate was poured onto a column (2.5×7 cm) of Amberlite IR-120B (H form). The column was washed with distilled water (5 *l*) and then eluted with 1N aqueous ammonia (500 m*l*). After the concentration of the effluent *in vacuo* almost to dryness, the residue was treated with ethanol (25 m*l*); the resultant white crystals were gathered by suctional filtration to give *β*-hydroxy-DL-norvaline (1.0 g, 77%), mp 219°C (dec).

Found: C, 44.89; H, 8.14; N, 10.33%. Calcd for $C_5H_{11}NO_3$: C, 45.10; H, 8.33; N, 10.52%.

*β-Hydroxy-*DL-*norleucine, β-Hydroxy-*DL-*leucine, and* DL-*Phenylserine.* These amino acids were obtained by the reaction of *n*-butyraldehyde, isobutyraldehyde, and benzaldehyde respectively with **14** under the conditions described in Table 2 and by the treatment described in the case of propionaldehyde. The melting points and the results of their elemental analyses are shown below:

β-Hydroxy-DL-norleucine, mp 229°C (dec)

Found: C, 48.79; H, 9.20; N, 9.27%. Calcd for $C_6H_{13}NO_3$: C, 48.96; H, 8.90; N, 9.52%.

β-Hydroxy-DL-leucine, mp 225°C (dec)

Found: C, 48.98; H, 9.05; N, 9.61%. Calcd for $C_6H_{13}NO_3$: C, 48.96: H, 8.90; N, 9.52%.

DL-Phenylserine, mp 194.5°C (dec)

Found: C, 60.15; H, 6.47; N, 8.17%. Calcd for $C_9H_{11}NO_3$: C, 59.66; H, 6.47; N, 7.73%.

*β-(*p-*Nitrophenyl)-*DL-*serine.* A suspension of **14** (2.6 g, 10 mmol) and *p*-nitrobenzaldehyde (**15**) (1.5 g, 10 mmol) in aqueous methanol (H_2O - MeOH=1:2; 30 m*l*) was stirred at pH 9.0 for 2 hr at 30°C under a nitrogen stream. After the reaction, water (100 m*l*) was added, the pH of the mixture was adjusted at 5.0 by the addition of 3N aqueous acetic acid, and the resultant suspension was treated with hydrogen sulfide gas and the cupric sulfide was filtered off. The filtrate was treated on a column (2.5×9 cm) of Amberlite IR-120B (H form), washed with distilled water (5 *l*), and then eluted with 1N aqueous ammonia (500 m*l*). The effluent was concentrated almost to dryness and then treated with ethanol (20 m*l*) to give slightly brownish crystals (1.8 g, 80%), mp 181°C (dec). One recrystallization from water gave a pure specimen, mp 182°C (dec).

Found: C, 47.75; H, 4.47; N, 12.30%. Calcd for $C_9H_{10}N_2O_5$: C, 47.79; H, 4.46; N, 12.39%.

*β-(*o-*Nitrophenyl)-*DL-*serine.* *o*-Nitrobenzaldehyde (1.5 g, 10 mmol) and **14** (2.6 g, 10 mmol) were treated in the way described in the previous experiment; the reaction period was 30 min, and the reaction temperature was 20°C. Silghtly brownish crystals (1.5 g, 66%), mp 179°C (dec) were thus obtained.

Found: C, 47.79; H, 4.53; N, 12.52%. Calcd for $C_9H_{10}N_2O_5$: C, 47.79; H, 4.46; N, 12.39%.

*β-(*p-*Chlorophenyl)-*DL-*serine.* To a mixture of **14** (2.6 g, 10 mmol) and *p*-chlorobenzaldehyde (4.2 g, 30 mmol) in methanol (40 m*l*), were added 1N methanolic sodium methoxide (7 m*l*); the mixture was then stirred at 23°C under a nitrogen atmosphere for 10 hr. After the reaction, the mixture was treated with 3N aqueous acetic acid (5 m*l*) and then diluted with distilled water (100 m*l*). The resultant greenish precipitate was filtered off by suction and then washed with benzene (15 m*l*). The filtrate was concentrated *in vacuo* to a volume of 100 m*l*; the concentrate was then washed with diethyl ether (25 m*l*×2 portions) in a separating funnel. The greenish precipitate mentioned above and the aqueous layer were treated together with hydrogen sulfide gas, and the precipitated cupric sulfide was removed by filtration. The filtrate was concentrated to a volume of about 30 m*l*, and the concentrate was treated on a column (2.5×7 cm) of Amberlite IR-120B (H form). Then, the column was washed with distilled water (5 *l*) and eluted with 1N aqueous ammonia (500 m*l*). The effluent was evaporated *in vacuo* almost to dryness, and the residue was triturated with ethanol (10 m*l*). The resultant white crystals were filtered to give *β*-(*p*-chlorophenyl)-DL-serine (0.95 g, 44%), mp 186°C (dec).

Found: C, 50.13; H, 4.65; N, 6.52%. Calcd for $C_9H_{10}NO_3Cl$: C, 50.12; H, 4.67; N, 6.50%.

*β-(*p-*Tolyl)-*DL-*serine.* To a mixture of **14** (2.6 g, 10 mmol) and *p*-tolualdehyde (3.54 m*l*, 30 mmol) in methanol (40 m*l*), were added 1N methanolic sodium methoxide (7 m*l*); the mixture was then stirred at 26°C under a nitrogen atmosphere for 14 hr. After the reaction, the resultant reaction mixture was acidified with 3N aqueous acetic acid (5 m*l*) and diluted with distilled water (100 m*l*). Then, a small amount of the greenish mass washed with diethyl ether (15 m*l*). The filtrate was concentrated *in vacuo* to a volume of 20 m*l*, and the concentrate was washed with diethyl ether (25 m*l*×2 portions) in a seperating funnel. The greenish precipitate and the aqueous layer were treated in the way described in the previous experiment to give *β*-(*p*-tolyl)-DL-serine (0.8 g, 41%), mp 186°C (dec), as white crystals.

Found: C, 61.68; H, 6.98; N, 7.03%. Calcd for $C_{10}H_{13}NO_3$: C, 61.52; H, 6.71; N, 7.18%.

*2-Amino-2-deoxy-4,5-*O*-isopropylidene-*D*-pentoaldonic Acid.* To a solution of 1,2;5,6-di-*O*-isopropylidene-D-mannitol[22] (1.3 g, 5 mmol) in water (50 m*l*), were added sodium metaperiodate (1.1 g, 5 mmol); the solution was then stirred at room temperature for 60 min. The sodium iodate thus precipitated was filtered off, and the filtrate was concentrated *in vacuo* below 40°C almost to a sirup. When the sirup was then treated with ethanol (20 m*l*), the sodium iodate further precipitated was removed by filtration. This

22) D. Horton, J. B Hughes, and J. K. Thompson, *J. Org. Chem.*, **33**, 728 (1968).

operation was repeatedly carried out in order to remove a small amount of the sodium iodate remaining in the sirup. A solution of the sirup thus obtained and an equimolar amount of **14** (2.3 g, 9 mmol) in water (30 m*l*) was adjusted at pH 9.5 by the addition of a 1N aqueous sodium hydroxide solution, and then the mixture was stirred at room temperature for 1 hr. After the reaction, the solution was treated with sodium sulfide ($Na_2S \cdot 9H_2O$: 2.7 g, 11 mmol); the resultant precipitate was filtered off. The filtrate was immediately treated on a column (2.5×9 cm) of Amberlite IR-120B (NH_4 form), after which the column was washed with distilled water (100 m*l*). The combined effluent was concentrated to a volume of 50 m*l* and treated on a column (2.5×5 cm) of Amberlite IR-45 (OH form), after which the column was washed with distilled water (100 m*l*). The effluent was concentrated to a volume of 50 m*l*, and the concentrate was washed with methylene chloride (10 m*l*×3 portions). The aqueous layer was then concentrated to a volume of about 5 m*l*. The white crystals thus precipitated were gathered by filtration and washed with several milliliters of methanol. The filtrate and washings were combined and concentrated almost to a sirup. The white crystals separated on the addition of several milliliters of methanol were similarly gathered by filtration. This procedure was repeated three times more, and then all the crystals were combined and recrystallized from aqueous methanol to give 2-amino-2-deoxy-4,5-*O*-isopropylidene-D-pentoaldonic acid (1.3 g, 70%), mp 198°C (dec).

Found: C, 46.53; H, 7.18; N, 6.96%. Calcd for $C_8H_{15}NO_5$: C, 46.82; H, 7.37; N, 6.83%.

*An Examination of the Degradation of **14** in an Aqueous Alkaline Solution.* Into water (100 m*l*) in a two-necked Erlenmeyer flask (20 m*l*) equipped with a Toa Electronic, Ltd., GC-125 Electrode, were bubbled nitrogen gas more than 1 hr under mechanical stirring; **14** (2600 g, 10 mmol) which had been allowed to stand for 24 hr under a nitrogen atmosphere was then added to the flask. The solution was stirred at 23°C for several hours, its pH value kept at 9.5 by the addition of a 2N aqueous sodium hydroxide solution. After the reaction, the resultant solution was treated in the way described in the reaction of **14** with acetaldehyde. The recoveries of glycine, which were also presented in Fig. 2, were as follows:

Run	Period (hr)	Recovery of glycine (g)	Recovery of glycine (%)
1	0	0.616	82.1
2	1	0.530	70.8
3	2	0.465	62.0
4	4	0.386	51.5
5	5	0.345	46.0
6	6	0.330	43.5

The recoveries of glycine in the examination, obtained under atmospheric conditions in the same way as above, were as follows:

Run	Period (hr)	Recovery of glycine (g)	Recovery of glycine (%)
1	0	0.616	82.1
2	1	0.516	68.8
3	2	0.434	57.9
4	3	0.376	50.1
5	4	0.337	44.9
6	5	0.276	36.8

Titration of N-*Pyruvylideneglycinatoaquocopper(II) (**14**) with an Aqueous Sodium Hydroxide Solution.* *Reagent*: A 2N aqueous sodium hydroxide solution was prepared by the Sörensen procedure to remove the carbon dioxide.

Conditions: A Toa Electronics, Ltd., HM-5A model pH meter with glass and reference electrodes was used to record the hydrogen-ion concentration. The titrations were carried out in a 100 m*l* multi-necked flask with a flat bottom to accommodate gas inlet and outlet tubes, a buret delivery tube, and electrodes. A magnetic stirrer was used for the stirring. In order to obtain a carbon dioxide-free system, nitrogen which had been passed through a 5N aqueous sodium hydroxide solution was bubbled into the system. All the measurements were made at 26°C, and pH values were read 1 min after the addition of one drop of the sodium hydroxide solution.

Titrations: A solution of **14** (1.300 g, 5 mmol and 2.600 g, 10 mmol) in distilled water (50 m*l*) was treated with the 2N aqueous sodium hydroxide solution (f=1.160) under a nitrogen stream; the results are presented in Fig. 3.

N-*Pyruvylideneglycinatopyridinecopper(II) Trihydrate (**21**).* Into a mixture of pyridine (0.8 m*l*, 10 mmol) and acetone (12 m*l*), were stirred **14** (2.6 g, 10 mmol), portion by portion, after which the suspension was stirred at room temperature for 2 hr. Then, blue crystals were precipitated, filtered, and dried to give **21** (3.1 g, 91%), mp 133°C, (a slight coloration began at about 133°C, but the crystals merely turned dark brown without any evolution of gas).

Found: C, 34.98; H, 4.52; N, 7.92%. Calcd for $C_{10}H_{16}N_2O_7Cu$: C, 35.35; H, 4.76; N, 8.24%.

*Preparation of β-(*p*-Nitrophenyl)-*DL*-serine by the Use of **21**.* A solution of **21** (3.4 g, 10 mmol) and *p*-nitrobenzaldehyde (1.5 g, 10 mmol) in aqueous methanol (H_2O - MeOH=1:1; 40 m*l*) was stirred at pH 7.3—7.5 for 20 min at room temperature. The resultant reaction mixture was treated in the way described in the reaction of **14** with the aldehyde; it thus gave slightly brownish crystals. The crystals were recrystallized from water to give β-(*p*-nitrophenyl)-DL-serine (1.5 g, 67%), mp 162°C (dec). The amino acid obtained here was confirmed by paper as well as by thin-layer chromatography to be composed of two amino acids of R_f (paper chromatog) 0.51 and 0.61 (*n*-BuOH: EtCOMe: concd. aq. NH_3: H_2O=5:3:3:1) in a ratio of about 2:3, although it is uncertain which of them corresponds to the *threo* isomer and which to the *allo* isomer.

Found: C, 46.06; H, 4.92; N, 12.37%. Calcd for $C_9H_{10}N_2O_5 \cdot 1/2\ H_2O$ (dried at 65°C over phosphorus pentoxide): C, 45.96; H, 4.72; N, 11.91%.

Studies of Hydroxy Amino Acids. I. Separation of Diastereoisomers of Threonine

Yasuo ARIYOSHI and Naotake SATO

Central Research Laboratories, Ajinomoto Co., Inc., Suzuki-cho, Kawasaki, Kanagawa

(Received April 2, 1971)

It was found that DL-allothreonine forms scarcely any soluble compounds with 5-nitronaphthalene-1-sulfonic acid, α-naphthylphosphoric acid, chlorendic acid,[1] and tetrachlorophthalic acid in water. DL-Threonine formed soluble or unstable compounds in water with these acids. The synthetic threonine mixture was successfully separated into DL-threonine and DL-allothreonine.

L-Threonine is used as medicine or a nutrient-enrichment for foodstuffs. However, allothreonine which is always formed as a by-product in the synthesis of threonine has almost no practical use. Most of the synthetic methods for threonine[2] produce more DL-allothreonine than DL-threonine, except for the reaction of copper glycinate with acetaldehyde[3] and the Strecker reaction of 1-ethoxy-1,2-diacetoxypropane.[4] A few methods of separation of diastereoisomers have been reported, in which threonine was changed to its derivative, Cu-acetaldehyde-threonine complex,[5] *N*-benzoyl-DL-threonine ethyl ester,[6] or sodium DL-threoninate.[7] Some aromatic acids have been used as a specific precipitating reagent for amino acids.[8,9] However, none is found in literature for the diastereoisomers of threonine.

In the course of studies on hydroxy amino acids, it was found that DL-allothreonine forms precipitates scarcely soluble in water with 5-nitronaphthalene-1-sulfonic acid, α-naphthylphosphoric acid, chlorendic acid, and tetrachlorophthalic acid. DL-Threonine, on the contrary, formed soluble or unstable compounds in water with these reagents. This finding was successfully applied to the separation of the two diastereoisomers of threonine. When a threonine mixture was brought into contact with these reagents in water, DL-allothreonine selectively precipitated with the reagents, while DL-threonine remained almost quantitatively in the mother liquor (Table 1).

Elementary analyses showed that the precipitate consists of DL-allothreonine and the reagent in 1:1 molar ratio, except for the precipitate with chlorendic acid. The IR spectra of the precipitates showed the absorption band in a region 1720—1750 cm^{-1} due to the free carboxyl group as the salt of DL-allothreonine with the strong acid.

Table 1. Separation of DL-allothreonine and DL-threonine with various precipitating reagents

Reagent	Grams of aThr and Thr in 100 m*l* of aqueous solution	
	Initial solution	Mother liquor
NNS	aThr 10.0 Thr 10.0	aThr 3.8 Thr 9.8
NP	aThr 10.0 Thr 10.0	aThr 2.0 Thr 8.6
CA	aThr 3.5 Thr 7.0	aThr 1.7 Thr 6.9
TCP	aThr 10.0 Thr 10.0	aThr 0.6 Thr 9.8

Abbreviations used are as follows:
aThr, DL-Allothreonine; Thr, DL-Threonine; NNS, 5-Nitronaphthalene-1-sulfonic acid; NP, α-naphthylphosphoric acid; CA, Chlorendic acid; TCP, Tetrachlorophthalic acid.
1.2 equimolar amount of NNS, NP, and TCP, and 2.4 equimolar amount of CA were used to DL-allothreonine in the initial solution.

In the case of chlorendic acid, the precipitate consisted of DL-allothreonine and chlorendic acid in 1:2 molar ratio. Since its IR spectrum only slightly differed from that of the mechanical mixture of DL-allothreonine and chlorendic acid, it was assumed that the precipitate is formed by the hydrogen bonding between DL-allothreonine and chlorendic acid.

DL-Threonine formed soluble salts with α-naphthylphosphoric acid and tetrachlorophthalic acid, but did not form crystalline compounds with 5-nitronaphthalene-1-sulfonic acid and chlorendic acid in water (Table 2). The salts of DL-allothreonine with 5-nitronaphthalene-1-sulfonic acid, α-naphthylphosphoric acid and tetrachlorophthalic acid were recrystallized from aqueous methanol, whereas the salts of DL-allothreonine with chlorendic acid and of DL-threonine with α-naphthylphosphoric acid and tetrachlorophthalic acid decomposed into the two components on recrystallization from various solvent systems.

When the salt of DL-allothreonine with tetrachlorophthalic acid was gradually heated above its melting point of 117°C, the melted material solidified at 148—150°C, and the solid remelted at 203—204°C. The compound with melting point of 203—204°C was assigned to be *N*-tetrachlorophthaloyl-DL-allothreonine from its IR spectrum, with no NH absorption of the

1) 1,4,5,6,7,7-Hexachloro-*endo*-5-norbornene-2,3-dicarboxylic acid.

2) J. P. Greenstein and M. Winitz, "Chemistry of Amino Acids," Vol. III, John Wiley & Sons, Inc. New York, N. Y. (1961), p. 2240.
3) M. Sato, K. Okawa, and S. Akabori, This Bulletin, **30**, 937 (1957).
4) H. Geipel, J. Gloede, K.P. Hilgetag, and H. Gross, *Chem. Ber.*, **98**, 1677 (1965).
5) T. Fuji, M. Oda, J. Arita, K. Sakai, and M. Takeda, Japanese Pat. Publication, 36-19562 (1961).
6) J. Attenburrow, D. F. Elliott, and G. F. Penny, *J. Chem. Soc.*, **1948**, 310.
7) K. Pfister, C. A. Robinson, A. C. Shabica, and M. Tishler, *J. Amer. Chem. Soc.*, **71**, 1101 (1949).
8) D. G. Doherty, W. H. Stein, and M. Bergmann, *J. Biol. Chem.*, **135**, 487 (1940).
9) N. Sato, N. Uchiyama, and T. Akashi, *J. Agri. Chem. Soc. Japan*, **43**, 504 (1969).

Table 2. Characters of precipitated compounds

Compound	Reagent	Amino acid	Component ratio	Mp °C		Elementary analysis (%)
I	NNS	aThr	1:1	224—225 (dec.)	$C_{14}H_{16}O_8N_2S$	Found C, 45.26; H, 4.18; N, 7.40; S, 8.47
	NNS	Thr	—	——	——	Calcd C, 45.16; H, 4.33; N, 7.52; S, 8.61
II	NP	aThr	1:1	189—190 (dec.)	$C_{14}C_{18}O_7NP$	Found C, 49.11; H, 5.25; N, 3.95; P, 8.71
						Calcd C, 48.98; H, 5.29; N, 4.08; P, 9.02
III	NP	Thr	1:1	160—161 (dec.)	$C_{14}H_{18}O_7NP$	Found C, 49.14; H, 5.21; N, 4.13; P, 8.68
IV	CA	aThr	1:2	136.5—137.5	$C_{22}H_{17}O_{11}NCl_{12}H_2O$	Found C, 28.85; H, 2.09; N, 1.53; Cl, 46.13
						Calcd C, 28.88; H, 2.09; N, 1.52; Cl, 46.51
	CA	Thr	—	——	——	——
V	TCP	aThr	1:1	117	$C_{12}H_{11}O_7NCl_4 2H_2O$	Found C, 31.65; H, 3.08; N, 3.06; Cl, 30.77
						Calcd C, 31.39; H, 3.29; N, 3.05; Cl, 30.89
VI	TCP	Thr	1:1	129—130	$C_{12}H_{11}O_7NCl_4 H_2O$	Found C, 32.97; H, 2.87; N, 3.25; Cl, 32.36
						Calcd C, 32.68; H, 2.97; N, 3.18; Cl, 32.16

compound with melting point of 117°C in the region of 1500—1600 cm^{-1}. The same phenomenon was observed with the salt of DL-threonine with tetrachlorophthalic acid. The compound with a higher melting point of 204—206°C was also assigned to be tetrachlorophthaloyl-DL-threonine from its IR spectrum.

As seen in Table 1, the most effective precipitating reagent was tetrachlorophthalic acid. Separation tests with this acid were made in more detail using the mixtures of the two diastereoisomers with various ratios and a synthetic threonine mixture obtained by the procedure described by Akabori *et al.*[3] (Table 3).

Table 3. Separation of DL-allothreonine and DL-threonine with tetrachlorophthalic acid

No.	Mixture Thr g	Mixture aThr g	TCP[a] g	Water ml	Recovery[b] Thr g(%)	Recovery[b] aThr g(%)
1	14	7	22	150	13.5(96)	5.8(84)
2	10	10	31	135	10 (100)	9.2(92)
3	15	5	16	170	14.7(98)	3.7(74)
4[c]	10.3	6.3	20	110	10 (97)	5.8(92)

a) Tetrachlorophthalic acid as hemihydrate.
b) Purity of all the amino acids not less than 95%.
c) A synthetic mixture containing 0.4 g of glycine.

The precipitate and the mother liquor were separately treated with hydrochloric acid. After removing the liberated tetrachlorophthalic acid by filtration, DL-allothreonine and DL-threonine were recovered in 74—92% and 96—100% yield, respectively, from the acidic solutions using ion-exchange column. Recrystallization gave chromatographically pure DL-allothreonine and DL-threonine.

Experimental

All melting points are uncorrected. The IR spectra were obtained in Nujol mull with a JASCO IR-S spectrometer.

Determination of DL-*Threonine and* DL-*Allothreonine.* Paper chromatographic analysis was carried out by the descending method on Toyo Roshi No. 51 paper with the solvent system, *n*-butanol-methyl ethyl ketone-28% aqueous ammonia-water (5:3:1:1 v/v),[4] and the chromatogram was stained with cadmium-ninhydrin reagent.[10] Two spots corresponding to allothreonine and threonine were individually cut off, and eluted with methanol, and the absorbances of the eluates were measured at 510 mμ.

Salt of DL-*Allothreonine with 5-Nitronaphthalene-1-sulfonic Acid (I).* A solution of 2.0 g of DL-allothreonine and 5.0 g of 5-nitronaphthalene-1-sulfonic acid in 20 ml of water was prepared and stored in a refrigerator overnight. The crystals formed were collected by filtration; yield, 3.5 g (56%). Recrystallization from aqueous methanol gave pure I as platelets. Anal. and mp (Table 2). IR: 3420, 3160 (sh), 3080, 1750, 1615 (sh), 1603, 1530, 1515 cm^{-1}. On the other hand, DL-threonine gave no crystalline salt in analytically pure state when treated with 5-nitronaphthalene-1-sulfonic acid in the same manner.

Salts of DL-*Allothreonine and* DL-*Threonine with α-Naphthylphosphoric Acid (II and III).* To a solution of 5.4 g of disodium α-naphthylphosphate in 20 ml of 2N hydrochloric acid, 2.0 g of DL-allothreonine or DL-threonine was added with stirring at room temperature. The mixture was stirred for 5 hr and kept in a refrigerator overnight. Crystalline II formed was collected by filtration; yield, 4.5 g (78%). Recrystallization from aqueous methanol gave pure II as platelets. Crystalline III was obtained from the concentrated syrupy solution; yield, 3.3 g (57%). Anal. and mp (Table 2). IR of II: 3300, 3080 (sh), 1720, 1620, 1603, 1585, 1525 cm^{-1}. IR of III: 3580, 3220, 3120, 1740, 1620, 1603 (sh), 1580 (sh), 1505 cm^{-1}.

Crystalline Compound of DL-*Allothreonine with Chlorendic Acid (IV).* To a solution of 2.0 g of DL-allothreonine in 20 ml of water, 7.8 g of chlorendic acid was added with stirring at room temperature. The suspension was stirred for 5 hr, and then allowed to stand in a refrigerator overnight. The crystalline compound formed was collected by filtration; yield, 8.2 g (89%). Anal. and mp (Table 2). IR: 3580, 3420, 3100, 1730 (sh), 1710, 1610, 1580, 1515 cm^{-1}. DL-Threonine gave no such crystalline compound with chlorendic acid.

Salts of DL-*Allothreonine and* DL-*Threonine with Tetrachlorophthalic Acid (V and VI).* A mixture of 2.0 g of DL-allothreonine or DL-threonine and 6.3 g of tetrachlorophthalic acid hemihydrate in 20 ml of water was stirred for 5 hr at room temperature, and stored in a refrigerator overnight. The crystals of V formed were collected by filtration; yield, 6.5 g (84%). Recrystallization from aqueous methanol gave pure V as platelets. The crystals of VI were obtained as

10) J. Heilmann, J. Barrollier, and E. Watzke, *Z. Physiol. Chem.*, **309**, 219 (1957).

needles from a concentrated syrupy solution; yield, 5.6 g (75%). Anal. and mp (Table 2). IR of V: 3500 (sh), 3220, 1750, 1710, 1620, 1600, 1550 (sh), 1520 (sh), 1510 cm^{-1}. IR of VI: 3460, 3200, 1735 (sh), 1705, 1595, 1525 cm^{-1}.

Separation of DL-*Allothreonine and* DL-*Threonine with Various Precipitating Reagents (Table 1).* To an aqueous solution containing DL-allothreonine and DL-threonine was added a precipitating reagent in the amount of 1.2 molar equivalent to DL-allothreonine. In the case of chlorendic acid, 2.4 molar equivalent to DL-allothreonine was used. The mixture was stirred for 5 hr and stored in a refrigerator overnight. The precipitate formed was removed by filtration. An aliquot of the filtrate was analyzed by paper chromatography and the contents of DL-allothreonine and DL-threonine in the filtrate were determined. The results are summarized in Table 1.

Separation of DL-*Allothreonine and* DL-*Threonine using Tetrachlorophthalic Acid (Table 3).* A typical run (No. 4. in Table 3) is as follows: To a solution of a synthetic threonine mixture composed of 10.3 g of DL-threonine, 6.3 g of DL-allothreonine, and 0.4 g of glycine in 110 m*l* of water,[3] was added 20 g of tetrachlorophthalic acid hemihydrate with stirring. The mixture was stirred for 5 hr at room temperature, and then kept in a refrigerator overnight. The precipitate was filtered, washed with a small amount of water, and then suspended in 100 m*l* of N hydrochloric acid. The mixture was boiled for 30 min and allowed to stand at room temperature for 3 hr. After removing tetrachlorophthalic acid liberated by filtration, the solution was passed through a column of Dowex 50 W×8 (H form). The column was washed with water and eluted with 2N ammonia. The eluate was concentrated *in vacuo* until crystallization began and a sufficient amount of methanol was added. The crystals were collected by filtration and washed with a small amount of aqueous methanol, giving 5.8 g (92% recovery) of DL-allothreonine. Recrystallized DL-allothreonine from water-methanol was chromatographically pure. The mother liquor, from which the DL-allothreonine salt was removed, was adjusted to pH 1.35 with hydrochloric acid. After removing tetrachlorophthalic acid liberated, the filtrate was treated in the same manner as described above giving 10.0 g (97% recovery) of DL-threonine. Recrystallized DL-threonine from water-methanol was chromatographically pure.

The authors wish to thank Dr. K. Toi of Ajinomoto Co., Inc. for his advice.

BULLETIN OF THE CHEMICAL SOCIETY OF JAPAN, VOL. 44, 2789—2794 (1971)

Chemically Induced Dynamic Nuclear Polarization in the Photochemical Reaction of Phenanthraquinone with Hydrogen Donors. II.[1] A Consideration of Unusual Nuclear Spin Polarization

Heisaburo SHINDO,* Kazuhiro MARUYAMA,** Tetsuo OTSUKI,** and Tetsuo MARUYAMA*

*JEOL(USA) Inc., 235 Birchwood Avenue, Cranford, N.J. 07016, USA

**Department of Chemistry, College of Liberal Arts and Science, Kyoto University, Kyoto

(Received April 12, 1971)

Polarized quartet NMR signals due to methylene protons were observed in the hydrogen-abstraction reactions of phenanthraquinone with *o*-substituted toluenes under the irradiation of light. The relative intensities of these signals could be predicted only by the general treatment of the CKO theory, taking account of the electronic singlet-triplet interactions (S–T_0 and S–T_1) of the radical pair. The scalar electronic-coupling constants, J_e, were evaluated approximately by comparing the theory with the experimental results and were found to be in the order of 7×10^9 sec^{-1}. The rather large value of J_e was discussed in relation to the nature of the reaction system; consequently, the existance of electronic π–π interaction was suggested for the radical-pair intermediate of the reaction.

Fischer and Bargon[2] have proposed a cross-relaxation process between electronic and nuclear-spin systems as the mechanism of the chemically induced dynamic nuclear polarization (CIDNP). However, the observations of combination lines consisting of both absorption and emission lines,[3] and strong nuclear spin polarization[4] over that predicted from the Overhausser effect, can no longer be explained on the basis of the cross-relaxation mechanism alone.

In the present stage, the theory developed by Closs and Trifunac[5] and by Kaptein and Oosterhoff,[6] *i.e.*, the CKO theory, seems to give a more reasonable interpretation of the CIDNP mechanism. This theory is principally based on the formation of a radical-pair intermediate during rapid radical reactions; then reaction products are formed through the radical pair in the electronic-spin singlet state brought about by the mixing of the electronic singlet and triplet states. In the CKO theory as approximated in large magnetic fields, only the mixing between the singlet (S) and triplet state with $m_s=0(T_0)$ is taken into

1) Previous paper, K. Maruyama, H. Shindo, T. Otsuki, and T. Maruyama, This Bulletin, **44**, 2756 (1971). This work has been done at the Department of Chemistry, College of Liberal Arts and Science, Kyoto University.

2) H. Fischer and J. Bargon, *Z. Naturforsch.*, **22a**, 1556 (1967).

3) H. R. Ward and R. G. Lawer, *J. Amer. Chem. Soc.*, **89**, 5518 (1967).

4) G. L. Closs and L. E. Closs, *ibid.*, **91**, 4550 (1969).

5) G. L. Closs, *ibid.*, **91**, 4552 (1969); G. L. Closs and A. D. Trifunac, *ibid.*, **92**, 2183 (1970).

6) R. Kaptein and L. J. Oosterhoff, *Chem. Phys. Lett.*, **4**, 195, 214 (1969).

account; the other two triplet states with $m_s=\pm 1$ (T_1 and T_{-1}) are neglected. Though the aproximate CKO theory has described the major features of CIDNP, it has failed to explain the reactions proceeding in small magnetic fields[7] and, rarely, it could not even predict the nuclear-spin polarization of products resulting from the radical pair, the individual components of which have the same g-value.[8]

The methylene protons of the 1,2-photo-adducts[9] show strongly polarized NMR quartet signals in the photochemical reactions of phenanthraquinone with o-substituted toluenes. The intensities of such quartet signals differed from those predicted from the approximate CKO theory. It was shown, by a more general treatment of the CKO theory, that the S–T_1 interaction as well as the S–T_0 interaction must be taken into account in accounting for the nuclear polarization observed in our experiments.

Experimental

The phenanthraquinone was prepared by the oxidation of phenanthrene with potassium dichromate and was purified by recrystallization from an acetic acid solution. Hydrogen-abstraction reactions of phenanthraquinone (0.04M) in a solution of toluene, o-xylene, o-chlorotoluene or o-bromotoluene were photochemically induced at 70°C inside an NMR probe modified for photochemical reactions; the method of modification has been reported in a previous paper.[10] The NMR spectra were observed at 60 MHz by means of a C-60HL-type spectrometer(JEOL. CO., Ltd.) under light.

Theory

The photochemical reaction of phenanthraquinone occurs through its optically-activated triplet state. In the present case, a weakly-coupled radical pair is formed through the hydrogen abstraction of the excited phenanthraquinone from o-substituted toluenes. A finite fraction of the radical pair yields the 1,2-adduct of phenanthraquinone.[11]

Now, let us examine further the particular protons of the adduct, *i.e.*, the methylene protons (underlined) of the 1,2-adduct;

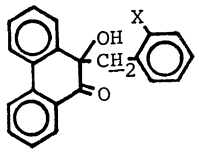

I

a. X=H
b. X=CH_3
c. X=Cl
d. X=Br

As is shown in Figs. 2 to 5, an unusual polarized NMR quartet of signals of the photo-adduct was observed; these signals are not predicted by the CKO theory based on the S–T_0 mixing alone. This finding encouraged us to investigate the more general CKO theory for AB-spin system.

It has been reported that a weakly-interacting radical pair often shows an unusual hyperfine structure of the electron-spin resonance of the triplet state.[12] This is caused by mixing between the electronic-spin singlet and the triplet states of such a radical pair, whose singlet-triplet separation is comparable to the electronic Zeeman energy or less. The effective spin Hamiltonian for such radical-pair tumbling in a fast rate in a solution can be written (if the nuclear Zeeman term is neglected)[6]:

$$\mathcal{H}_0 = \beta H_0(g_1S_1+g_2S_2) - J_e(1/2+2S_1S_2) + \sum_{i,j} A_{ij}I_iS_j + H_d \quad (1)$$

where β is the Bohr magneton, H_0 is the static magnetic field, S and I are the electronic and nuclear-spin operators, J_e is the scalar electronic exchange coupling constant, and A_{ij} is the hyperfine coupling constant between the ith nuclear and the jth electron. The term of dipole-dipole interaction, H_d, is assumed to be negligible because of the establishment of a thermal equilibrium in the electronic-spin system of the triplet precursor.

As the radical pair will have different values of J_e and A_{ij} from one time to another due to the thermal vibration and the collisions, the Hamiltonian, $\mathcal{H}_0$, should be time-dependent. By denoting the total spin-wave function of the radical pair as $\Psi(t)$, the time-dependent Schrödinger equation for the Hamiltonian, $\mathcal{H}_0$, is given by;

$$i\hbar\frac{d\Psi(t)}{dt} = \mathcal{H}_0\Psi(t) \quad (2)$$

The general solution of Eq. (2) produces a linear combination of $U_{ij}{}^0$;

$$\Psi(t) = \sum_{i,j} C_{ij}(t)e^{-iE_{ij}t}U_{ij}^0 \quad (3)$$

where $U_{ij}{}^0$ represents the eigen function describing both ith nuclear and jth electronic states and where E_{ij} is the eigen value of $U_{ij}{}^0$. According to the CKO model, the triplet state of the radical pair does not lie on the reaction coordinate; hence, the rate of population increase to the final product can be assumed to be proportional to the degree of the singlet character of the radical pair (*i.e.*, the probability of the radical pair in the singlet state). Such a probability of the radical pair can be given by the coefficient of the electronic singlet state, $|C_{is}(t)|^2$ for the ith nuclear spin state, where the suffix s refers to the electronic singlet. Thus, by averaging $|C_{is}(t)|^2$ over the lifetime of the radical pair, τ, the rate of the population increase of the ith nuclear spin state follows Eq. (4);

$$k_i = \frac{k_{SE}}{n}\int_0^\infty |C_{is}(t)|^2 e^{-t/\tau}dt \Big/ \int_0^\infty e^{-t/\tau}dt \quad (4)$$

where k_{SE} is the specific rate for the product generated from the radical pair in the pure singlet state and where n is the number of spin states of the nuclear spin system in the problem.

Let us now return to the radical pair in our case;

7) J. F. Garst, R. H. Cox, J. T. Barbas, R. D. Roberts, J. I. Morris, and C. R Morrison, *J. Amer. Chem. Soc.*, **92**, 5761 (1970).
8) H. Iwamura, M. Iwamura, and T. Nishida, 21st Symposium on Organic Reaction Mechanism, Hiroshima, Oct., 1970.
9) See Structure I.
10) K. Maruyama, H. Shindo, T. Otsuki, and T. Maruyama, This Bulletin, **44**, 2756 (1971).
11) The adducts obtained by the reaction of phenanthraquinone with alkyl aromatics are, in general, 1,2-photo-adducts.
12) See, for example, K. Itoh, H. Hayashi, and S. Nagakura, *Mol. Phys.*, **17**, 561 (1969).

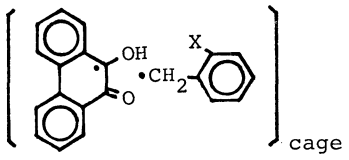

II

which is simply denoted by $[R_1(H_2)\cdot, \cdot R_2]$. Let us evaluate the rate of the population increase of a given nuclear-spin state for methylene protons of the I adduct. Considering the II radical pair, consisting of two electrons and two hydrogen nuclei, one can rewrite Eq. (1) as;

$$\mathscr{H}_0 = \beta H_0(g_1S_1+g_2S_2) - J_e(1/2+2S_1S_2) + (A_{11}I_1+A_{21}I_2)S_1 \quad (5)$$

The four spin functions of the electronic system are taken as $S=1/\sqrt{2}\,(|\alpha\beta>-|\beta\alpha>)$ for the singlet state, and $T_1=|\alpha\alpha>$, $T_0=1/\sqrt{2}\,(|\alpha\beta>+|\beta\alpha>)$, and $T_{-1}=|\beta\beta>$ for the triplet states. Then, the matrix elements of the Hamiltonian, $\mathscr{H}_0$, for these spin functions become as follows;

$$\begin{pmatrix} J_e & -1/2\sqrt{2}\,(A_{11}I_1^+ + A_{21}I_2^+) & 1/2\beta H_0(g_1-g_2)+1/2(A_{11}I_1+A_{21}I_2) & 1/2\sqrt{2}\,(A_{11}I_1^- + A_{21}I_2^-) \\ * & 1/2\beta H_0(g_1+g_2)-J_e+1/2(A_{11}I_1+A_{21}I_2) & 1/2\sqrt{2}\,(A_{11}I_1^- + A_{21}I_2^-) & 0 \\ * & * & -J_e & 1/2\sqrt{2}\,(A_{11}I_1^- + A_{21}I_2^-) \\ * & 0 & * & -1/2\beta H_0(g_1+g_2)-J_e-1/2(A_{11}I_1+A_{21}I_2) \end{pmatrix} \quad (6)$$

where I^+ and I^- are the nuclear-spin operators, I_x+iI_y and I_x-iI_y respectively, and the element * represents the conjugate of the symmetric elements with respect to the diagonal of the matrix. Matrix (6) shows that the mixing between the electronic singlet and triplet states occurs through off-diagonal elements, *i.e.*, hyperifine coupling constants and g values.

Let us denote the four spin states of the nuclear system as ϕ_i $(i=1\cdots,4)$. A solution of Schrödinger's Eq. (2) for the Hamiltonian (5) can be obtained under suitable initial conditions after solving a secular equation of the matrix with dimensions of 16×16. Such a procedure is very tedious, however, so let us now consider two limiting cases: $2|J_e|\cong|A|$ for case (a) and $|\pm\beta gH_0-J_e|\cong|A|$ for case (b).

Case (a); $2|J_e|\cong|A|$. This is a very important case, one in which the electronic singlet, S, and the T_0 triplet are mixing. As the Zeeman energy is much larger than the hyperfine interaction, the mixing between the singlet, S, and the other two triplets, T_1 and T_{-1}, is negligibly small. Then, we can easily solve the secular equation of matrix (6); we get, as the 16 eigen functions;

$$|T_1\phi_i> \quad (7a)$$
$$|T_{-1}\phi_i> \quad (7b)$$
$$(\cos\theta_i|S>+\sin\theta_i|T_0>)\phi_i \quad (7c)$$
$$(\sin\theta_i|S>-\cos\theta_i|T_0>)\phi_i \quad (7d)$$
$$(i=1,\cdots,4)$$

and, as the 16 eigen values;

$$E_{1i} = 1/2\beta H_0(g_1+g_2) - J_e + 1/2M_i \quad (8a)$$
$$E_{2i} = -1/2\beta H_0(g_1+g_2) - J_e - 1/2M_i \quad (8b)$$
$$E_{3i} = [J_e^2+(1/2\beta H_0\Delta g+1/2M_i)^2]^{1/2} \quad (8c)$$
$$E_{4i} = -[J_e^2+(1/2\beta H_0\Delta g+1/2M_i)^2]^{1/2} \quad (8d)$$
$$(i=1,\cdots,4)$$

where $\tan2\theta_i=J_e/M_i$, $\Delta g=g_1-g_2$, and $M_i=<\phi_i|A_{11}I_1+A_{21}I_2|\phi_i>$. By considering that the radical pair, II, was in the triplet state at the initial time, $t=0$, Eq. (2) can be easily solved by means of Eq. (3) in the zeroth-order approximation as follows;

$$\Psi(t) = \frac{1}{2}\sum_{i=1}^{4}\{e^{-iE_{1i}t}|T_1\phi_i>+e^{-iE_{2i}t}|T_{-1}\phi_i>+\sin\theta_i\cos\theta_i \times(e^{-iE_{3i}t}-e^{-iE_{4i}t})|S\phi_i>+(\sin^2\theta_i e^{-iE_{3i}t} +\cos^2\theta_i e^{-iE_{4i}t})|T_0\phi_i>\} \quad (9)$$

The probability that the radical pair transfers after time t from the electronic triplet state to singlet state is given by;

$$|C_{ij}(t)|^2 = \frac{1}{2}\sin^2\theta_i\cos^2\theta_i\{1-\cos(E_{3i}-E_{4i})t\} \quad (10)$$

Then, by using Eq. (4), we obtain k_i as the rate of population increase for the nuclear-spin state, ϕ_i, of the photo-adduct;

$$k_i = \frac{k_{SE}}{2}\,\frac{(1/2\beta H_0\Delta g+1/2M_i)^2\tau^2}{1+(E_{3i}-E_{4i})^2\tau^2} \quad (11)$$

This is a well-known expression derived by Closs and Trifunac[5] and by Kaptein and Oosterhoff.[6] Since the values of M_i in Eq. (11) differ from one nuclear-spin state to another, the increases in the rates of the adduct are different according to the individual nuclear spin states. Thus, polarization occurs in the nuclear-spin system of the adducts.

Case (b); $|\pm\beta gH_0-J_e|\cong|A|$. This is the case in which the electronic singlet, S, does not mix with the T_0 triplet but with the T_1 or T_{-1} triplet. Let us consider the case of the S–T_1 mixing alone. In this case, the Hamiltonian matrix with dimensions of 16×16 may be expressed as the direct sum of nine submatrices, whose dimensions are eight 1×1 and one 8×8. For the sake of simplicity, let us assume a relationship of hyperfine coupling constants, $A_{11}\cong A_{21}$; this is reasonable because two protons of the radical pair, II, in the problem are attached to the same carbon atom. On denoting the two spin functions of a single nuclear spin by $|+>$ and $|->$, we obtain, as the spin functions for AB-spin system, $s=1/\sqrt{2}\,(|+->-|-+>)$, $t_1=|++>$, $t_0=1/\sqrt{2}\,(|+->+|-+>)$, and $t_{-1}=|-->$. The first function, s, may be reffered to the nuclear-spin singlet, while probably the latter three may be reffered to the nuclear-spin triplets. Thus, we obtain the following four eigen functions concerned with the S–T_1 mixing;

$$\cos\gamma|T_1t_0>-\sin\gamma|St_1> \quad (12a)$$
$$\sin\gamma|T_1t_0>+\cos\gamma|St_1> \quad (12b)$$
$$\cos\delta|St_0>-\sin\delta|T_1t_{-1}> \quad (12c)$$

$$\sin\delta\,|St_0\rangle + \cos\delta\,|T_1t_{-1}\rangle \qquad (12d)$$

where $\tan 2\gamma = A/(\beta gH_0 - 2J_e)$ and $\tan 2\delta = A/(\beta gH_0 - 2J_e - 1/2\ A)$. It is acutually found from Eq. (12) that the mixing of the electronic singlet, S, and triplet, T_1, occurs only through the nuclear-spin triplet (t_1, t_0, and t_{-1}), but is not associated with the nuclear-spin singlet(s).

Assuming that the radical pair is in the electronic triplet state at the initial time, $t=0$, just after being produced, then we can obtain the rate of the population increase for a given nuclear-spin state of the adduct in the same manner as in the case of Eq. (9);

$$k(s) = k(t_{-1}) = 0 \qquad (13a)$$

$$k(t_1) = \frac{k_{SE}}{2}\,\frac{A^2\tau^2}{1 + [(\beta gH_0 - 2J_e)^2 + A^2]\tau^2} \qquad (13b)$$

$$k(t_0) = \frac{k_{SE}}{2}\,\frac{A^2\tau^2}{1 + [(\beta gH_0 - 2J_e - 1/2A)^2 + A^2]\tau^2} \qquad (13c)$$

Eq. (13) leads to an unexpected and interesting conclusion. In the limiting case of the S–T_1 mixing, only the adducts in the states of the nuclear-spin triplets (t_0 and t_1) are exclusively generated from the radical pair in the pure electronic singlet state.

If we consider another limiting case of the S–T_{-1} mixing, it may be deduced that the adducts in the states of the nuclear-spin triplets (t_0 and t_{-1}) are preferentially generated from the radical pair.

Results and Discussion

Signal Observed. The hydrogen-abstraction reactions of phenanthraquinone with toluene, *o*-xylene, *o*-chlorotoluene, and *o*-bromotoluene are photochemically induced to yield their 1,2-adducts. For example, as is shown in Fig. 1, methylene protons of the adduct with *o*-xylene indicate the AB-spin system in the NMR pattern; this system was originally observed by one of the present authors (K.M.). The quartet spectrum of the photo-adduct arises from the fact that the two methylene protons are magnetically different from each other due to the unequality in their conformations.[13]

This was confirmed by the fact that the chemical-shift difference between A and B protons decreased with an increase in the temperature. The absorption line at 226 Hz (down field from TMS) in Fig. 1 is due to a hydroxyl proton of the photo-adduct.

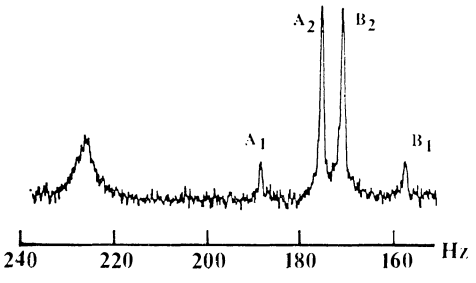

Fig. 1. Normal NMR quartet spectra due to the methylene protons of the 1,2-adduct of phenanthraquinone with *o*-xylene. Chemical shifts are in Hz down-field from TMS.

In Fig. 2 the spectrum (down) was observed for *o*-xylene solution of phenanthraquinone, while the spectrum (up) was recorded in the course of irradiation. The signal at 183 Hz (down-field from TMS) is responsible for a carbon-13 satellite of the methyl group of *o*-xylene, while the small but broad signal at about 180 Hz represents accidental harmonics due to AC power. Strongly-polarized quartet lines are observed during the course of irradiation, where three lines,

Fig. 2. Polarized NMR signals due to methylene protons of the 1,2-adduct of phenanthraquinone with *o*-xylene in photo-induced reaction.

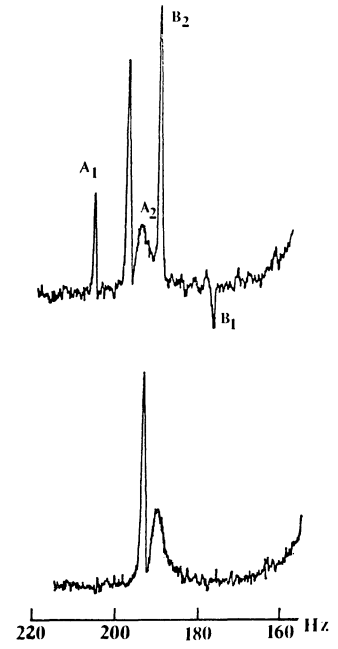

Fig. 3. Polarized NMR signals due to methylene protons of the 1,2-adduct of phenanthraquinone with *o*-chlorotoluene in photo-induced reaction.

13) P. M. Nair and J. D. Roberts, *J. Amer. Chem. Soc.*, **79**, 4565 (1957).

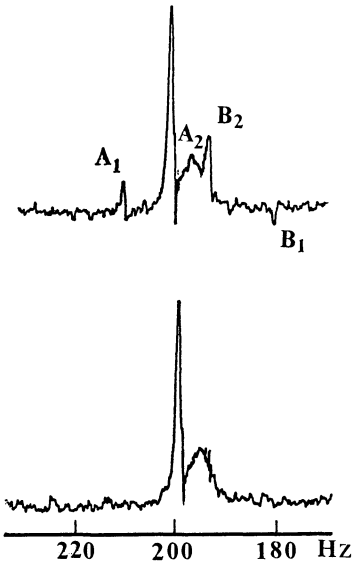

Fig. 4. Polarized NMR signals due to methylene protons of the 1,2-adduct of phenanthraquinone with *o*-bromotoluene in photo-induced reaction.

A_1, A_2, and B_2, at low fields show enhanced absorption, while the remaining line at a higher field (B_1), shows emission.

If the irradiation is shut off, the quartet spectrum promptly decays.

The quartet spectra for adducts of *o*-chlorotoluene and *o*-bromotoluene are illustrated in Figs. 3 and 4. It can be seen from these figures that the A_1 and B_2 lines of the quartet spectra show enhanced absorption, while that the A_2 and B_1 lines show emission. It was observed for the photo-adduct of toluene that the A_2 and B_2 lines are strongly enhanced and that the B_1 line is emission-enhanced. On the other hand, the A_1 line revealed a nearly zero polarization. The parameters of the quartet spectra of these adducts are gived in Table 1.

Table 1. Differences of chemical shifts $\Delta\omega$ spin-spin coupling constants J_n and intensity ratios I_{A_2}/I_{A_1} of quartet spectra of the photo-adducts of phenanthraquinone with hydrogen donors

Hydrogen donor	$\Delta\omega$(Hz)	J_n(Hz)	Intensity ratio, I_{A_2}/I_{A_1}
o-Xylene	12.4	13.1	6.52
o-Chlorotoluene	10.5	12.8	7.81
o-Bromotoluene	11.1	13.5	7.77
Toluene	3.6	8.52	23.0

An Interpretation of Results. As was shown in Eq. (14) of a previous paper[10] the population difference, $[Z_i]-[Z_j]$ between the ith and jth nuclear-spin states of the photo-adduct was thus after light irradiation;

$$[Z_i]-[Z_j] = \frac{k_0 k_a (k_i-k_j) T_1^*}{(k_a+1/\tau_f)\sum_j (k_j+2k_{bd})}(1-e^{-t/T_1^*}) \quad (14)$$

wher k_o and k_a are the specific rate constant for the photo-excited molecule and that for the process of hydrogen abstraction respectively, and where k_i and k_j are the rate constants for the formation of photo-adducts in the ith and jth nuclear spin states respectively. k_{bd} is the rate constant which is associated with the process independent of the nuclear spin. T_1^* is the relaxation time of the nuclear-spin system under the irradiation of light, and τ_f is the lifetime of the excited molecules. On assuming that $k_a \gg 1/\tau_f$, Eq. (14) is reduced to;

$$[Z_i]-[Z_j] = C(k_i-k_j) \quad (15)$$

in the steady-state polarization. Here, C is a constant proper to the reaction system. The relative intensities of the polarized signals of the photo-adduct are proportional to the product of the population difference and to the relative intensities of the normal spectrum (*i.e.*, the transition probability induced by the application of the rf field). Thus, the relative intensities of polarized signals, I_{ij}^*, in steady-state polarization lead to;

$$I_{ij}^* = (k_i-k_j)I_{ij} \quad (16)$$

where I_{ij} is the relative intensity of the spectral line in the thermal equilibrium of the spin system. The (k_i-k_j) factor may be referred to as a relative enhancement factor. One can compare the theoretical results with the experimental results by using Eq. (16).

It must first be investigated whether the polarized quartet signals can or can not be interpreted on the basis of the S–T_0 mixing alone. In the following calculations, it may be reasonable to assume that the hyperfine coupling constant, A_{11}, is nearly eaqual to A_{21} for the reason previously mentioned.

The rates of population increase for the four spin states of the AB-spin system of the photo-adduct can be calculated by means of Eq. (11). The relative intensities of the polarized signals are given by Eq. (17) as follows for the transitions corresponding to the spectral lines, A_1, A_2, B_2, and B_1 in the order of high-resonance frequencies; for lines A_1 and B_2;

$$I^* = \left\{ \frac{1/4(\beta H_0 \Delta g + A)^2\tau^2}{1 + 4[J_e^2 + 1/4(\beta H_0 \Delta g + A)^2]\tau^2} - \frac{1/4(\beta H_0 \Delta g)^2\tau^2}{1 + 4[J_e^2 + 1/4(\beta H_0 \Delta g)^2]\tau^2} \right\} \times I \quad (17a)$$

and for lines A_2 and B_1;

$$I^* = \left\{ \frac{1/4(\beta H_0 \Delta g)^2\tau^2}{1 + 4[J_e^2 + 1/4(\beta H_0 \Delta g)^2]\tau^2} - \frac{1/4(\beta H_0 \Delta g - A)^2\tau^2}{1 + 4[J_e^2 + 1/4(\beta H_0 \Delta g - A)^2]\tau^2} \right\} \times I \quad (17b)$$

It is evident form Eq. (17) that the relative enhancement factor is the same for both the A_1 and B_2 lines and also for both the A_2 and B_1 lines. As was illustrated in Fig. 2, in the polarized quartet signals of the photo-adduct of *o*-xylene, the A_2 line shows a positive polarization, while the B_1 line shows a negative polarization. This fact is substantially inconsistent with the theoretical consideration just mentioned. Thus, we may conclude that the CKO theory approximated to S–T_0 mixing is not satisfactory in discussing the photo-induced reaction examined here.

Now, consider a moderate case; $|A| \ll 2|J_e| < \beta g H_0$. In such a case, the rate of the population increase of the

photo-adduct may be taken as the sum of the contributions from pure S–T_0, S–T_1, and S–T_0–T_1 interactions. Since the contributions from the former two are generally larger than that from the latter, the contribution from the S–T_0–T_1 interaction may be ignored for the sake of simplicity. Therefore, the rates of population increase may be given by Eqs. (11) and (13). Since the A_1,A_2,B_2, and B_1 spectral lines are assumed to correspond to the $t_1 \rightarrow s$, $t_0 \rightarrow t_{-1}$, $t_1 \rightarrow t_{-1}$, and $s \rightarrow t_{-1}$ transitions,[14] the relative intensities of quartet lines are obtained from Eq. (16). On assuming that $2|J_e|$ and $\beta g H_0 \gg |A|$ and $\beta H_0 \Delta g$, they are as follows for individual lines;

$$I^*_{A_1} = \left\{ \frac{1/4A(2\beta H_0 \Delta g + A)\tau^2}{1+4J_e^2\tau^2} + \frac{A^2\tau^2}{1+4(1/2\beta g H_0 - J_e)^2\tau^2} \right\} I_{A_1} \quad (18a)$$

$$I^*_{A_2} = \left\{ \frac{1/4A(2\beta H_0 \Delta g + A)\tau^2}{1+4J_e^2\tau^2} + \frac{A^2\tau^2}{1+4(1/2\beta g H_0 - J_e)^2\tau^2} \right\} I_{A_2} \quad (18b)$$

$$I^*_{B_2} = \frac{1/4A(2\beta H_0 \Delta g + A)\tau^2}{1+4J_e^2\tau^2} \times I_{B_2} \quad (18c)$$

$$I^*_{B_1} = \frac{1/4A(2\beta H_0 \Delta g - A)\tau^2}{1+4J_e^2\tau^2} \times I_{B_1} \quad (18d)$$

The relative intensities of polarized signals in the photo-adduct can be calculated by means of Eq. (18). As for the photo-adducts of *o*-xylene and *o*-chlorotoluene, Fig. 5 (spectra a and b) compares the experimental results with the calculated relative intensities based on the parameters in Table 2; $g=2.0$, $H_0=14000$ gauss, $\tau=10^{-9}$ sec, and A, J_e and Δg were adjusted so as to fit the experimental results. The agreement of the experimental results with the calculations is fairly good. However, the polarized quartet signals of the photo-adduct of toluene could not be interpreted whatever parameter values were used. This discrepancy may be due to the neglect of the S–T_0–T_1 interaction of the radical pair.

The absolute values in Table 2 can not be too significant because of the simplifications adopted in Eq. (18). However, it may be concluded at least that; 1) experimental results are interpreted in terms of the mixing between the electronic singlet (S) and triplet states (T_0 and T_1) of the associated radical pair, and 2) the scalar electronic-exchange coupling constant, J_e, has a positive value intermediate between the Zeeman energy and the hyperfine coupling constant.

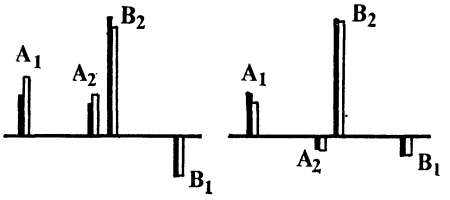

(a) (b)

Fig. 5. Experimental and calculated quartet spectra due to the methylene protons of 1,2-adducts of phenanthraquinone with *o*-xylene(a) and *o*-chlorotoluene(b) in photo-induced reaction.
■; Experimental signal intensity
□; Calculated signal intensity

TABLE 2. PARAMETERS ADJUSTED TO MAKE FIT WITH THE EXPERIMENTAL RESULTS

Hydrogen donor	$\beta H_0 \Delta g/A$	J_e(Hz)$\times 10^9$
o-Xylene	−0.168	7.31
o-Chlorotoluene	−0.053	6.61

The resulting value of J_e is positive and is larger by about one order than the values reported hetherto.[15] As for our present values, it is not unreasonable to consider that an electronic π–π interaction brought about by the aromatic nature of each component of the radical pair may be responsible. There is strong chemical evidence supporting the above considerations.[16,17]

As was pointed out by Garst and his co-workers,[7] the contribution of S–T_1 interaction to nuclear polarization give a chance to observe the polarization from the reactions of diradicals or corresponding radical pairs. The reaction system reported here seems to be an ideal case where both the S–T_0 and S–T_1 interactions are associated with the nuclear-spin polarization.

14) Strictly speaking, this is the case when the limiting factor, $J_n/\Delta\omega \rightarrow \infty$, but this assumption does not lead to fatal errors in the results of the present study.

15) See, for example, G. L. Closs, C. E. Doubleday, and D. R. Paulson, *J. Amer. Chem. Soc.*, **92**, 2185 (1970); G. L. Closs and A. D. Trifunac, *ibid.*, **92**, 2186 (1970).

16) The structural problems of the photo-adducts resulting from the hydrogen-abstraction reactions of phenanthraquinone will be extensively discussed in the near future in this Bulletin by one of the present authors (K. Maruyama).

17) K. Maruyama, H. Shindo, T. Otsuki, and T. Maruyama, This Bulletin, **44**, 2000 (1971).

Solvent Effect in a Partial Asymmetric Synthesis. III

Kazuyoshi NISHIYAMA and Yuzo INOUYE
Institute for Chemical Research, Kyoto University, Uji, Kyoto

(Received April 22, 1971)

The solvent polarity-dependence of asymmetric stereochemistry was unambiguously corroborated in the Michael type cyclopropane formation in a system designed so as to proceed through the transition state conformations of an equal dipole moment not involving any geometrical isomerism: the NaH-catalyzed condensation of (−)-menthyl methacrylate with ethyl chloromalonate in solvent media of varying polarity resulted in the formation of (−)-1-methylcyclopropane-1,2,2-tricarboxylic acid having the same sign of rotation in all cases. The fit of the stereochemistry to the Kirkwood equation was borne out by the linearity found for the plots of log *R*/*S* against the Kirkwood-Onsager parameter. The *R*-configuration of (−)-1-methylcyclopropane-1,2,2-tricarboxylic acid was established by the correlation to (+)-2,2-diphenyl-1-methylcyclopropanecarboxylic acid of the well-defined (*R*)-configuration.

In previous papers,[1a–d] the solvent polarity-dependence of stereochemistry in the base-catalyzed Michael type cyclopropane formation was unequivocally established and a theory was advanced to rationalize the observed solvent effect. The theory asserts that both the *cis*, *trans*-stereochemistry and simultaneous asymmetric induction are the consequence of a delicate balance between the electrostatic and steric stabilities of the transition state conformations: *i.e.* where the electrostatic factor is dominant over the steric one, the transition state having the greater dipole moment is more stabilized by solvation in polar and strongly solvating media, while the situation is just reversed in non-polar media poor at solvation. This is naturally reflected in the rate of formation and leads to the stereochemical outcome that both *cis*/*trans* and *R*/*S* ratios in the cyclopropane products vary regularly depending upon the solvent polarity, and even a conspicuous reversal of the geometric isomer ratio and the sign of rotation of the cyclopropane products takes place at a given polarity of reaction media. The Kirkwood equation strictly holds for the stereochemistry in this type of reaction.

Gemoetrical isomerism necessarily intervened in all the systems investigated so far[1a–d], which sometime caused an argument[2] against our claim of the solvent effect in asymmetric synthesis. The solvent polarity-dependence of stereochemistry in the system designed so as to afford a single compound capable of existing only in enantiomeric forms would confirm the effect and would also enhance the validity of the theory.

For this purpose, we designed a system involving the NaH-catalyzed Michael type condensation of (−)-menthyl methacrylate (I) with diethyl chloromalonate (II) to give 1-methylcyclopropane-1,2,2-tricarboxylic acid ester (III). In contrast to the earlier systems, product (III) in the present system lacks *cis*, *trans*-isomerism by virtue of structural feature and the reaction gives rise to a single compound as mixture of enantiomers in unequal amounts. This not only simplifies the experimental procedure and makes easier the analysis of stereochemical results of the asymmetric reactions, but also suffices for testing the prediction based on the theory.

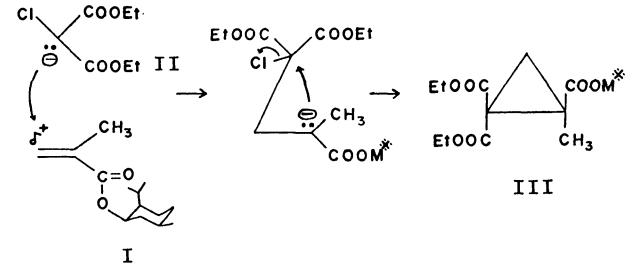

Scheme 1

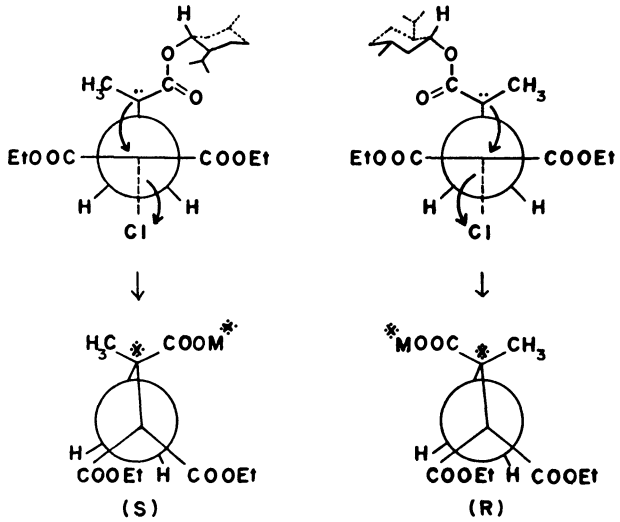

Fig. 1. Transition state conformations leading to *R*- and *S*-1-methylcyclopropane-1,2,2-tricarboxylic acid

Visualized in the Fig. 1 are the transition state conformations (sp^2-model)[1c] which fulfil the stereoelectronic requirements for maximum orbital overlap and charge delocalization and would eventually lead to the enantiomeric *R*- and *S*- products respectively. They have an equal dipole moment (3.2D)[3] and are thus electrostatically equalized to each other. However they differ in steric strain owing to different orientation of the chiral (−)-menthyl moiety.

1a) Y. Inouye, S. Inamasu, M. Ohno, and H. M. Walborsky, *J. Amer. Chem. Soc.*, **83**, 2962 (1961); b) Y. Inouye, S. Inamasu, and M. Horiike, *Chem. Ind.*, **1967**, 1293; c) Y. Inouye, S. Inamasu, M. Horiike, M. Ohno, and H. M. Walborsky, *Tetrahedron*, **24**, 2907 (1968); d) S. Inamasu, M. Horiike, and Y. Inouye, This Bulletin, **42**, 1393 (1969).

2) L. L. McCoy, *J. Org. Chem.*, **29**, 240 (1964).

3) For computation of dipole moment, see ref. 1c.

TABLE 1. ASYMMETRIC SYNTHESIS DATA IN (−)-MENTHYL METHACRYLATE-DIETHYL CHLOROMALONATE SYSTEM

Solvent ratio DMF:benzene	ε	%Yield trimethylester	$[\alpha]_D^{25}$(MeOH) (°)	%Optical yield[a)]	R/S
10:0	37.63	7.8	−5.30	6.81	1.1461
9:1	19.87	6.5	−4.42	5.68	1.1204
8:2	13.05	6.9	−3.49	4.48	1.0938
7:3	9.45	7.3	−3.03	3.89	1.0809
6:4	7.26	5.6	−2.73	3.50	1.0725
5:5	5.77	6.5	−2.44	3.13	1.0646
4:6	4.69	6.0	−2.06	2.64	1.0542

a) Based on the maximum rotation $[\alpha]_D^{25}$ −77.78°

It is seen that the *R*-transition state conformation is sterically more favored than the *S*-counterpart. It may therefore be safely predicted that inasmuch as the steric factor is the controlling factor, the product acid with the same sign[4] of rotation should result from the reactions. The experimental results are summarized in Table 1.

The yields of the cyclopropane product (III) in the present system were found to be rather poor[5], being accompanied by the formation of ethylenetetracarboxylic acid ester as has been observed in analogous non-dissymmetric reactions,[6] but sufficient for the determination of the sign and magnitude of rotation of the product cyclopropane acid which was isolated pure as trimethylester and fully characterized.

As can be seen from the data, the present asymmetric reaction afforded the cyclopropane acid ester (III-a) of levorotation within experimental errors over the range of polarity investigated (from ε 4.69 through 37.63). The plots of log R/S against the Kirkwood-Onsager parameter showed a satisfactory linearity (Fig. 2).

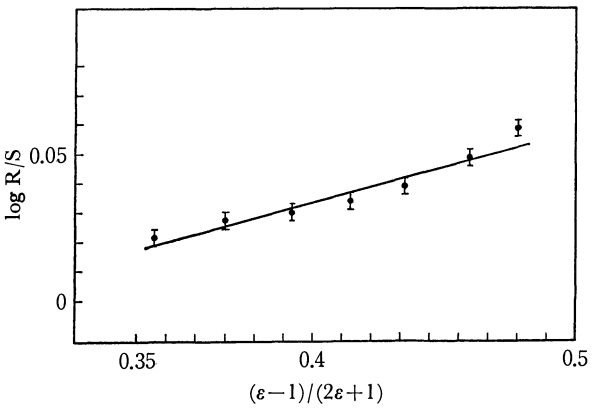

Fig. 2. The plots of logR/S *vs.*Kirkwood-Onsager parameter of reaction medium

A positive slope of the regression line was found for the plots in the present reactions in contrast to the negative ones in the previous systems. The Kirkwood equation, as applied to the present case (eq. 1) and coupled with the positive slope experimentally found, clearly shows $r_R^* < r_S^*$ (the radius of the transition state carbanion), since the dipole moment μ^* is equal to both transition state carbanions (Fig. 1). This is in good agreement with the qualitative prediction based on the mere visual inspection of the scale model that the *R*-transition state carbanion is sterically more favored, *i.e.* more compact, which would manifest itself in a smaller molecular radius or volume.

$$\ln R/S = C_0 - 1/\kappa T \cdot (\varepsilon-1)/(2\varepsilon+1) \cdot \mu^{*2} \cdot (1/r_S^{*3} - 1/r_R^{*3}) \quad (1)$$

The absolute configuration and the maximum rotation of the product acid ester (III-a), which are indispensable for analysis of the steric course as well as estimation of the extent of optical yields, were obtained by the ozonolysis of (+)-2,2-diphenyl-1-methylcyclopropanecarboxylic acid (IV) of the known *R*-configuration[7] leading to (−)-(III-a). The Brewster calculation of conformational asymmetry predicts $[\phi]$ −45° for (*R*)-(III-a), which shows an agreement with the observed value $[\phi]$ −138.6° in the sign of rotation, but not in the magnitude. Considering the empirical nature of the method and since the solvent interaction is not taken into consideration, the value may not be surprising.

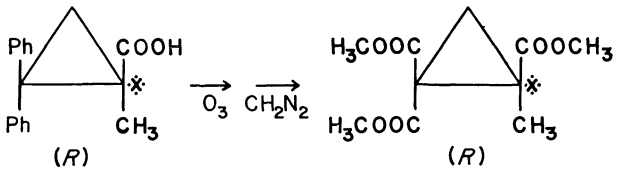

Scheme 2

Experimental

General. Melting and boiling points were uncorrected. Rotations were taken on a Yanagimoto Model ORD-185A recording spectropolarimeter: NMR-spectra were on a Varian A-60.

4) Accumulated knowledge of cyclopropane chirality suggests a levorotation for an *R*-configuration of cyclopropane ring carbon bearing polar groups. This rule of thumb is also in fair agreement with the Brewster conformational asymmetry calculation.

5) This chemical situation may be well understood if one invokes the HSAB principle (R. G. Pearson, *Science*, **151**, 172 (1966) and references cited therein) to the present system: chloromalonate ester carbanion having a moderate base strength comparable to hydroxide anion reacts preferentially with chloromalonate which is harder than (−)-menthyl methacrylate. The self-condensation of chloromalonate thus proceeds *via* the consecutive S_N2 and E2 pathways to give ethylenetetracarboxylate in preponderance.

6) R. Fraisse and R. Jacquier, *Bull. Soc. Chim. Fr.*, **24**, 986 (1957).

7) H. M. Walborsky, L. Barash, A. E. Young, and F. J. Impastato, *J. Amer. Chem. Soc.*, **83**, 2517 (1961); C. Djerassi, K. Undheim, and A. Weidler, *Acta Chem. Scand.*, **16**, 1147 (1962).

Asymmetric Synthesis of 1-Methylcyclopropane-1,2,2-tricarboxylic acid ester (III). The synthetic procedure is exemplified by a typical run in a mixture of benzene and DMF (1:9 by volume ratio). The reaction was repeated in exactly the same manner except that the solvent composition was varied.

(−)-Menthyl methacrylate (22.4 g, 0.1 mol, bp 82°C/0.7 mmHg, n_D^{25} 1.4575) and diethyl chloromalonate (19.4 g, 0.1 mol) were allowed to react in the presence of sodium hydride (4.8 g, 0.1 mol; dispersed in oil from Metal Hydride Inc., 52.9% purity) in 150 m*l* of mixed solvent (benzene: DMF=1:9 by volume) at 25°C for 6 hr with stirring. The reaction temperature was maintained constant throughout the reaction by cooling with ice water when necessary. After the reaction period, sufficient water was added. The organic layer was extracted with ether and the combined extract, after removal of ether, was then hydrolyzed by refluxing with 8% potassium hydroxide in methanol (200 m*l*) for 40 hr. The hydrolyzate was concentrated by evaporation under reduced pressure and was dissolved in water and the liberated menthol was removed with ether. The aqueous layer was acidified with equivalent hydrochloric acid and the cyclopropane acid was thoroughly extracted with ether. The acid was esterified by the standard method with diazomethane, and the crude trimethylester was separated pure by means of preparative vpc (Varian Aerograph Autoprep 700) on a 10 mm×6 m column packed with Silicone SE 30 (15%) at 185°C using helium gas as carrier. *Trimethyl 1-methylcyclopropane-1,2,2-tricarboxylate* n_D^{25} 1.4511; Found: C, 51.95; H, 6.29%. Calcd for $C_{10}H_{14}O_6$: C, 52.17; H, 6.13%. NMR (CCl_4): τ 8.22 (d, J_{gem}=5.0 Hz, cyclopropane methylene 2H); τ 8.60 (s, C-1 methyl 3H); τ 6.26 (s, C-1 ester methyl 3H); τ 6.35 (s, C-2 ester methyl 6H). The IR-spectrum was identical with that of the authentic specimen derived from 1-methyl-2,2-diphenylcyclopropanecarboxylic acid *(vide infra)*. Yield 1.5 g (6.5%); $[\alpha]_D^{25}$ −4.42° (*c* 2.05, MeOH); optical yield 5.66% based on the maximum rotation $[\alpha]_D^{25}$ −77.78°.

Ozonolysis of R-*(+)-1-Methyl-2,2-diphenylcyclopropanecarboxylic acid.* (+)-*R*-1-Methyl-2,2-diphenylcyclopropanecarboxylic acid (mp 189°C, $[\alpha]_D^{25}$ +35° (chloroform); 700 mg), obtained by resolution *via* the brucine salt, was dissolved in acetic acid (100 m*l*). Crude ozone was passed through the solution at room temperature. After prolonged ozonolysis, hydrogen peroxide (30%, 20 m*l*) was added and the mixture was allowed to stand still overnight. Some palladium on carbon was added in order to decompose the remaining peroxide prior to evaporation of the mixture. After acetic acid was removed by evaporation at room temperature, diazomethane was added to the residue. The resulting trimethyl ester was separated pure by means of preparative vpc *(vide supra)*. The IR- and NMR-spectra fully substantiated the structure. Found: C, 52.11: H, 6.18%; Calcd for $C_{10}H_{14}O_6$: C, 52.17; H, 6.13%. n_D^{25} 1.4518; $[\alpha]_D^{25}$ −77.78° (*c* 0.78, MeOH); yield 350 mg (54.8%); NMR (CCl_4): cyclopropane methylene protons τ8.22 (d, 2H, J_{gem}=5.0 Hz); C-1 methyl protons, τ 8.60 (s, 3H); ester methyl protons, τ 6.26 (s, 3H) and τ 6.35 (s, 6H).

The dielectric constants of the binary solvent system consisting of DMF and benzene in continuously varied volume ratios were computed by the mixing rule and the data given in a previous paper.[1c].

The authors are indebted to Professor Walborsky at the Florida State University for the generous gift of samples and also to Professor Griffin at Louisiana State University for his kind suggestions.

BULLETIN OF THE CHEMICAL SOCIETY OF JAPAN, VOL. 44, 2797—2800 (1971)

A Convenient Method for the Preparation of Primary Amines by the Use of Bisbenzenesulfenimide and Bis-*p*-chlorophenylsulfenimide

Teruaki MUKAIYAMA, Takeo TAGUCHI, and Mineo NISHI

Laboratory of Organic Chemistry, Tokyo Institute of Technology, Ookayama, Meguro-ku, Tokyo

(Received April 28, 1971)

A convenient method for the preparation of primary amines by the use of bisarylsulfenimide has been established. Primary amines were obtained in good yields under mild reaction conditions by treating *N*-substituted bisarylsulfenimides with hydrochloric acid or mercaptan. The *N*-substituted bisarylsulfenimides were prepared in good yields by the reactions of lithium bisarylsulfenimide with alkyl halides or alkyl *p*-toluenesulfonates or by the addition reactions of bisarylsulfenimide to olefinic compounds.

It is well known that the Gabriel synthesis[1] is the most general method for the selective preparation of primary amino compounds. However, there is a disadvantage in the method for the preparation of amino compounds with nitrile, ester, amide or carbonyl groups in the same molecule. These functional groups are hydrolyzed to give carboxylic acid or they react with hydrazine at the same time when phthaloyl group is removed from *N*-substituted phthalimide, an intermediate of the Gabriel synthesis.

In the present study, a new route for the convenient preparation of various primary amines from bisarylsulfenimides, such as bisbenzenesulfenimide or bis-*p*-chlorophenylsulfenimide, and alkyl halides or *p*-toluenesulfonates, or olefinic compounds was investigated with the consideration that the sulfur-nitrogen bond of *N*-substituted bisarylsulfenimide is easily cleaved by hydrochloric acid or mercaptan to afford the corresponding primary amine together with sulfenyl chloride or di-

1) a) S. Gabriel, Ber., **20**, 2224 (1887). b) M. S. Gibson and R. W. Bradshaw, *Angew. Chem.*, **80**, 986 (1968).

TABLE 1. YIELDS OF ALKYLAMINES BY THE REACTIONS OF LITHIUM BISBENZENESULFENIMIDE WITH ALKYL *p*-TOLUENESULFONATES OR ALKYL HALIDES

RX (III)	RNH_2(V)[a] $RNHCONHC_6H_5$		Formula	Calcd			Found		
	Yield (%)	mp (°C)		C	H	N	C	H	N
n-C_4H_9OTs	78	128—129	$C_{14}H_{16}ON_2$	68.72	8.39	14.57	68.74	8.19	14.85
n-$C_8H_{17}OTs$	86	74— 75	$C_{15}H_{24}ON_2$	72.54	9.74	11.28	72.28	9.69	11.20
sec-C_4H_9OTs	64	145—149	$C_{14}H_{16}ON_2$	68.72	8.39	14.57	68.54	8.21	14.35
sec-$C_8H_{17}OTs$	63	94— 97	$C_{15}H_{24}ON_2$	72.54	9.74	11.28	72.70	9.49	11.30
n-C_4H_9Br	60	127—128.5							
n-$C_8H_{17}Br$	62	74— 74.5							
sec-$C_8H_{17}Br$	17	94— 96							
$C_6H_5CH_2Br$	86	169	$C_{14}H_{14}ON_2$	74.31	6.24	12.38	74.21	6.25	12.48
p-$NO_2C_6H_4CH_2Br$	67	—	$C_7H_9N_2O_2Cl$[b]	44.58	4.81	14.85	44.72	4.56	15.13

a) The yields of amines were determined from the amounts of *N*-alkyl-*N'*-phenylureas.
b) *p*-Nitrobenzylamine was isolated and identified as its hydrochloride.

TABLE 2. YIELDS OF ALKYLAMINES BY THE REACTIONS OF LITHIUM BIS-*p*-CHLOROPHENYLSULFENIMIDE WITH ALKYL *p*-TOLUENESULFONATES OR ALKYL HALIDES

RX [III]	$(p\text{-}ClC_6H_4S)_2NR$ [IV]		RNH [V] Yield (%)
	Yield (%)	mp (°C)	
$C_6H_5CH_2Br$	79	89—90	100
p-$NO_2C_6H_4CH_2Br$	86	131	91
$C_2H_5O_2CCH_2CH_2OTs$	57[b]	45—46	
n-C_4H_9OTs	—		80
n-$C_8H_{17}OTs$	—		85
n-C_4H_9Br	—		61
n-$C_8H_{17}Br$	—		54

a) These compounds were isolated as their hydrochlorides or picrates to give satisfactory purity.
b) In this case, bis-*p*-chlorophenylsulfenimide was isolated in 8% yield.

sulfide.

It was shown that primary amines are obtained in good yields under mild reaction conditions by treating *N*-substituted bisbenzenesulfenimide with hydrochloric acid or mercaptan.[2] The *N*-substituted bisbenzenesulfenimides are successfully derived from lithium bisbenzenesulfenimide and alkyl halides or alkyl *p*-toluenesulfonates. As an example, benzylamine was obtained in 86% yield by treating *N*-benzyl bisbenzenesulfenimide formed by the reaction of bisbenzenesulfenimide with *n*-butyllithium in tetrahydrofuran at −20°C for 5 min, and the subsequent reaction with benzyl bromide in tetrahydrofuran for 5 hr with 3N hydrochloric acid at room temperature for 3 hr. The yield of the amine was determined from the amount of *N*-benzyl-*N'*-phenylurea obtained by the subsequent reaction with phenyl isocyanate.

$$(ArS)_2NH + n\text{-BuLi} \longrightarrow (ArS)_2NLi$$
[I] [II]

$$[II] + RX \longrightarrow (ArS)_2NR \xrightarrow{HCl} RNH_2 + 2ArSCl$$
[III] [IV] [V]

$Ar = C_6H_5$, *p*-ClC_6H_4

Similarly, various primary amines were prepared from alkyl halides or alkyl *p*-toluenesulfonates and lithium bisbenzenesulfenimide or lithium bis-*p*-chlorophenylsulfenimide. (see Tables 1 and 2).

N-Substituted bisbenzenesulfenimides could not be isolated as pure substances because the imides decomposed on distillation or on silica gel column chromatography. On the other hand, some *N*-substituted bis-*p*-chlorophenylsulfenimide was obtained as crystalline; for example, *N*-benzyl bis-*p*-chlorophenylsulfenimide was obtained in 79% yield as a white crystalline, mp 90°C, by treating lithium bis-*p*-chlorophenylsulfenimide formed by the reaction of bis-*p*-chlorophenylsulfenimide with *n*-butyllithium at −50°C in tetrahydrofuran, with benzyl bromide at room temperature in tetrahydrofuran for 5 hr. Treatment of *N*-benzyl bis-*p*-chlorophenylsulfenimide with dry hydrogen chloride in dry ether gave benzylamine and *p*-chlorophenylsulfenyl chloride in quantitative yields.

Bisbenzenesulfenimide was obtained instead of the corresponding condensation product when lithium bisbenzenesulfenimide was allowed to react with β-carbethoxyethyl *p*-toluenesulfonate. Formation of bisbenzenesulfenimide and acrylonitrile in the above reaction may be explained by considering the abstraction of an acidic hydrogen atom on the α-carbon atom of β-carbethoxyethyl *p*-toluenesulfonate by lithium bisbenzenesulfenimide. On the other hand, lithium bis-*p*-chlorophenylsulfenimide, the acidity of which is higher than that of bisbenzenesulfenimide, reacted with the *p*-toluenesulfonate to give *N*-β-carbethoxyethyl bis-*p*-chlorophenylsulfenimide in 57% yield.

$$(ArS)_2NLi + C_2H_5O_2CCH_2CH_2OTs \longrightarrow \begin{cases} (ArS)_2NH + CH_2{=}CHCO_2C_2H_5 \\ (ArS)_2NCH_2CH_2CO_2C_2H_5 \end{cases}$$

It was found that amines with nitrile group in the same molecule, olefinic amines or highly water-soluble amines were also successfully prepared along with disulfide when the corresponding *N*-substituted bisarylsulfenimide are treated with mercaptan. As an example, β-cyanoethylamine was obtained in 64%

$$(ArS)_2NLi + RX \longrightarrow (ArS)_2NR$$
[II] [III] [IV]

$$(ArS)_2NR + 2R'SH \longrightarrow RNH_2 + 2RSSR'$$
[IV] [VI] [V]

2) T. Mukaiyama and T. Taguchi, *Tetrahedron Lett.*, **1970**, 3411.

Table 3. Reactions of *N*-substituted bisarylsulfenimides with thiols

$(ArS)_2NH$ [I]	RX [III]	R'SH [VI]	Reaction Conditions	RNH_2 [V] Yield (%)	RNH_2 [V] Picrate mp (°C)
$(C_6H_5S)_2NH$	$CNCH_2CH_2OTs$	C_2H_5SH	E.[a] r.temp. 30 min	64	176 —180
	$CH_2=CHCH_2I$	C_2H_5SH	E. r.temp. 10 hr	73	141 —142
	$CH_3OCH_2CH_2OTs$	C_6H_5SH	E. r.temp. 1 hr	74	144.5—145.5
		C_6H_5SH	E. r.temp. 1 hr	46	133 —134.5
$(p\text{-}ClC_6H_4S)_2NH$	$CNCH_2CH_2OTs$	C_6H_5SH cat. $ZnCl_2$[d]	THF[b] r.temp. 3 hr	88[e]	178 —178.5
	$CH_2=CHCH_2I$	C_6H_5SH cat. $ZnCl_2$	THF r.temp. 3 hr	76	138 —141
	$C_6H_5CH=CHCH_2Br$	C_6H_5SH cat. $ZnCl_2$	THF–MeOH–AcOH[c] r.temp. 10 hr	66[e]	182.5—183

a) E: ether b) THF: tetrahydrofuran c) THF: MeOH:AcOH (10:10:1 v/v) d) $ZnCl_2$ was used 5% mol/mol of the imide. e) The yields of amines were determined from *N*-substituted bis-*p*-chlorophenylsulfenimide.

yield as its picrate by the reaction of lithium bisbenzenesulfenimide with β-cyanoethyl *p*-toluenesulfonate in tetrahydrofuran at room temperature for 10 hr and the subsequent treatment with 2 molar equivalents of ethanethiol in ether at room temperature for 1 hr.

Similarly, β-cyanoethylamine was obtained in 88% yield when *N*-β-cyanoethyl bis-*p*-chlorophenylsulfenimide was allowed to react with 2 molar equivalents of benzenethiol in the presence of a catalytic amount of zinc chloride at room temperature in tetrahydrofuran for 3 hr.

On the other hand, *N*-β-cyanoethyl bis-*p*-chlorophenylsulfenimide did not react with benzenethiol even after they were refluxed in tetrahydrofuran for 2 hr.

In a similar way, allylamine, cinnamylamine, β-methoxyethylamine and tetrahydrofurfurylamine were prepared in good yields by the reactions of *N*-substituted bisarylsulfenimides formed from lithium bisarylsulfenimide and alkyl halides or alkyl *p*-toluenesulfonates with mercaptan (see Table 3).

The effects of the solvents on the condensation reactions of lithium bisbenzenesulfenimide with alkyl *p*-toluenesulfonates were studied. It was found that tetrahydrofuran and dimethoxyethane are suitable for this reaction. When diethyl ether or anisole was used as the solvent, diminution in the yield of amine and increase in the yield of unsymmetrical sulfide were observed. This may be due to the rapid decomposition of lithium bisbenzenesulfenimide in comparison with the above mentioned condensation reaction (see Table 4).

The reaction of bisbenzenesulfenimide with *n*-butyllithium in tetrahydrofuran at room temperature for 7 hr, followed by the addition of isoamyl bromide in tetrahydrofuran at room temperature for 5 hr, resulted in the formation of isoamyl phenyl sulfide and diphenyl disulfide in 71% and 67% yields, respectively. This may be explained by considering the decomposition of lithium bisbenzenesulfenimide into lithium thiophenolate and phenylthionitrene. The lithium thiophenolate thus formed reacts with isoamyl bromide to give isoamyl phenyl sulfide and the phenylthionitrene further decomposes to nitrogen and diphenyl disulfide as shown below.

$$(C_6H_5S)_2NH + n\text{-BuLi} \longrightarrow [(C_6H_5S)_2NLi]$$

$$\downarrow$$

$$C_6H_5SLi + [:NSC_6H_5]$$

$$\downarrow i\text{-}C_5H_{11}Br \qquad \downarrow$$

$$i\text{-}C_5H_{11}SC_6H_5 \quad C_6H_5SSC_6H_5 + N_2$$

Table 4. Solvent effect

Solvent	ROTs	RNH_2 Yield (%)	RSC_6H_5 Yield (%)
Tetrahydrofuran	$n\text{-}C_8H_{17}OTs$	86	—
Dimethoxyethane	$n\text{-}C_8H_{17}OTs$	73	—
Ether	$n\text{-}C_4H_9OTs$	15	64
Anisole	$n\text{-}C_4H_9OTs$	19	74

It was also established that primary amines are successfully prepared from bisarylsulfenimide and olefinic compounds. The addition reaction of bisbenzenesulfenimide to acrylonitrile proceeded smoothly in tetrahydrofuran at room temperature in the presence of a catalytic amount of trimethylbenzylammonium hydroxide (Triton B), and β-aminopropionitrile was obtained in 91% yield by treating the adduct with 2 molar equivalents of ethanethiol in ether at room temperature for 1 hr.

$$(C_6H_5S)_2NH + CH_2=CHX \longrightarrow (C_6H_5S)_2NCH_2CH_2X$$
$$\text{[VII]} \qquad \text{[VIII]}$$

$$\text{[VIII]} + 2RSH \longrightarrow NH_2CH_2CH_2X + 2C_6H_5SSR$$

Similarly, ethyl β-aminopropionate, β-aminoethyl methyl ketone and β-aminopropionamide were obtained

Table 5. Yields of amines from bisbenzenesulfenimide and olefinic compounds

Olefinic Compounds [VII]	Amines [V] Yield (%)	Amines [V] Picrate mp (°C)
$CH_2=CHCN$	91	179
$CH_2=CHCO_2C_2H_5$	74	76—77
$CH_2=CHCOCH_3$	38	127.5—129
$CH_2=CHCONH_2$	8	149 —150

from bisbenzenesulfenimide and the corresponding olefinic compounds (see Table 5).[3]

Experimental

*Synthesis of Bis-*p*-chlorophenylsulfenimide.* Into 1000 m*l* of ether solution saturated with dry ammonia, *p*-chlorophenylsulfenyl chloride (51.0 g, in 150 m*l* of ether) was added dropwise under stirring at a temperature below −5°. The reaction mixture was stirred for 2 hr at −5—0°C. After the resulting precipitate, ammonium chloride, was filtered and washed with 100 m*l* of tetrahydrofuran, the filtrate was evaporated under reduced pressure and a crystalline precipitate was obtained. Recrystallization from benzene gave bis-*p*-chlorophenylsulfenimide, 27.5 g (66%), mp 137—140°C (decomp.).

Found: C, 47.76; H, 3.29; N, 4.76; S, 21.42%. Calcd for $C_{12}H_9NS_2Cl_2$: C, 47.70; H, 3.00; N, 4.64; S, 21.18%.

Preparation of Alkylamines from Lithium Bisarylsulfenimide (IIa and IIb) and Alkyl Halides or Alkyl p-*Toluenesulfonates. General Procedure*: *Method A*: A solution of alkyl halide or alkyl *p*-toluenesulfonate (0.005 mol) in tetrahydrofuran was added into a solution of lithium bisarylsulfenimide formed from bisarylsulfenimide (0.005 mol) and *n*-butyllithium (0.005 mol) in tetrahydrofuran at −20——50°C under stirring. The reaction mixture was stirred at −20—0°C for 2 hr and at room temperature for additional 2—8 hr. After removal of the solvent, the residue was stirred in a mixture of ether (20 m*l*) and 3N hydrochloric acid (10 m*l*) for 10 min—3 hr at room temperature.[4] The aqueous solution extracted from the reaction mixture was concentrated to dryness. The residue was dissolved in an aqueous solution of 20% sodium hydroxide (30 m*l*) and extracted with 50 m*l* of ether four times. The ether extract was dried over anhydrous sodium sulfate.

Method A-1: Into the ether extract phenyl isocyanate (0.60 g, 0.005 mol) was added and stirring was continued for 30 min. After removal of ether, a crystalline precipitate was obtained and washed with petroleum ether. Recrystallization from ethanol gave *N*-alkyl-*N'*-phenylurea.

Method A-2: Into the ether extract picric acid (1.15 g, 0.005 mol) was added and ether was removed by evaporation. The picrate of the corresponding alkyl amine was obtained by recrystallization from ethanol or a mixture of ethanol and benzene. By means of either *Method A-1* or *Method A-2*, *n*-butylamine, *n*-octylamine, *sec*-butylamine, *sec*-octylamine benzylamine and *p*-nitrobenzylamine were prepared. The results are summarized in Tables 1 and 2.

Method B: A solution of alkyl halide or alkyl *p*-toluenesulfonate (0.005 mol) in tetrahydrofuran was added under stirring into a solution of lithium bisarylsulfenimide, formed from bisarylsulfenimide (0.005 mol) and *n*-butyllithium (0.005 mol) in tetrahydrofuran at −20——50°C. The reaction mixture was stirred at −20—0°C for 2 hr and at room temperature for additional 2—8 hr. After removal of the solvent, the residue was poured into 30 m*l* of water and the mixture was extracted with ether.[4] The extract was dried over anhydrous sodium sulfate and into the solution excess mercaptan (0.015 mol) was added under stirring. After stirring at room temperature for 30 min—3 hr, a yellowish precipitate was obtained by the addition of picric acid (1.15 g, 0.005 mol), followed by evaporation of the solvent. Recrystallization from ethanol gave the corresponding alkylamine as its picrate. By means of *Method B*, β-cyanoethylamine, β-methoxyethylamine, tetrahydrofurfurylamine, allylamine and cinnamylamine were obtained as their picrates. The results are summarized in Table 3.

Preparation of β-Cyanoethylamine from Bisbenzenesulfenimide and Acrylonitrile. Into a mixture of bisbenzenesulfenimide (1.17 g, 0.005 mol) and acrylonitrile (0.27 g, 0.005 mol) in tetrahydrofuran, a catalytic amount of trimethylbenzylammonium hydroxide (Triton B) was added under stirring. After stirring at room temperature for 30 min, ethanethiol (0.93 g, 0.015 mol) was added and the mixture was stirred at 0°C for 1 hr. After removal of the solvent, a yellowish precipitate was obtained by the addition of picric acid (1.15 g, 0.005 mol) to the residue. Recrystallization from ethanol gave the picrate of β-cyanoethylamine, 1.32 g, (91%), mp 179°C.

Found: C, 36.13; H, 3.03; N, 23.41%. Calcd for $C_9H_9O_7N_5$: C, 36.62; H, 2.98; N, 23.47%.

Similarly, ethyl β-aminopropionate, β-aminoethyl methyl ketone and β-aminoacrylamide were obtained by the reactions of bisbenzenesulfenimide with ethyl acrylate, methyl vinyl ketone and acrylamide, respectively. The results are listed in Table 5.

3) When bis-*p*-chlorophenylsulfenimide was treated with acrylonitrile in tetrahydrofuran at room temperature for 20 hr in the presence of a catalytic amount of Triton B, *N*-β-cyanoethyl bis-*p*-chlorophenylsulfenimide was obtained only in 18% yield.

4) When alkyl *p*-toluenesulfonate was used in place of alkyl halides, lithium *p*-toluenesulfonate precipitated by the addition of ether was removed by filtration and washed with ether.

Synthesis of *cyclo*-Diglycyl-L-tyrosyl-diglycyl-L-tyrosyl and Hydrolysis by Chymotrypsin

Mitsuhiro KONISHI,[1] Norio YOSHIDA, and Nobuo IZUMIYA[2]

Laboratory of Biochemistry, Faculty of Science, Kyushu University, Hakozaki, Fukuoka

(Received May 4, 1971)

A cyclic hexapeptide, *cyclo*-(diglycyl-L-tyrosyl)$_2$, was synthesized by several different routes; the cyclization reactions of a tripeptide active ester, a tripeptide azide, and a hexapeptide azide produced the desired cyclic hexapeptide. The cyclic peptide was hydrolyzed slowly by chymotrypsin to a tripeptide diglycyl-tyrosine, whereas a synthetic linear hexapeptide, diglycyl-L-tyrosyl-diglycyl-L-tyrosine, was hydrolyzed very rapidly to the tripeptide. Since the synthetic *cyclo*-(diglycyl-L-phenylalanyl)$_2$ was insoluble in a buffer, it was not clear whether an incubation mixture of the substrate and enzyme yielded diglycyl-phenylalanine.

For a study of the mode of action of proteolytic enzymes on cyclic peptides, several compounds have been synthesized in this laboratory. In a previous paper, it was shown that *cyclo*-(Gly$_5$-Lys)[3] was completely hydrolyzed to H-Gly$_5$-Lys-OH by trypsin.[4] It was also observed that *cyclo*-(Gly$_2$-Lys)$_2$ was hydrolyzed to H-Gly$_2$-Lys-OH by trypsin though the rate of hydrolysis was extremely slow as compared with that of H-(Gly$_2$-Lys)$_2$-OH.[5] It is known that chymotrypsin hydrolyzes predominantly a peptide bond at the linkage of phenylalanine and tyrosine carbonyl.[6,7] Therefore, it was expected that a cyclic peptide containing Phe or Tyr residue might be hydrolyzed by chymotrypsin.

The present paper describes the syntheses of *cyclo*-(Gly$_2$-Tyr)$_2$ and a linear hexapeptide, H-(Gly$_2$-Tyr)$_2$-OH, and the mode of action of chymotrypsin on these peptides.

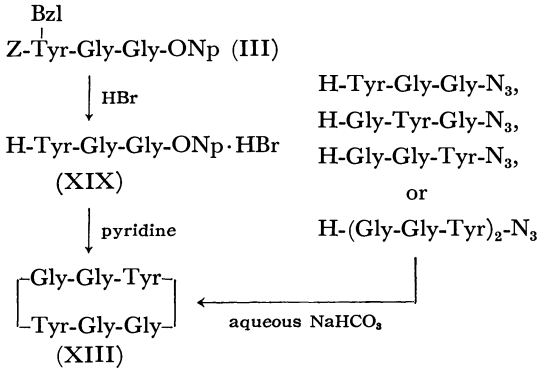

Fig. 1. Synthesis of the cyclic hexapeptide by various reaction sequences.

Five different routes shown in Fig. 1 were undertaken for the synthesis of the cyclic hexapeptide (XIII). In one route, XIII was synthesized *via* a linear tripeptide active ester (XIX), in which Tyr residue occupies the *N*-terminus of a peptide sequence. XIX was treated with a large amount of pyridine, and a pure cyclic hexapeptide was isolated easily though the yield was only 9%. The product was proved to be a dimer by molecular weight determination.

The cyclic peptide was also synthesized *via* linear tripeptide azides, in which Tyr residue occupies three different positions (Fig. 1). Crude cyclic peptide was isolated after the cyclization reaction of the azide in a large amount of water containing sodium bicarbonate. A linear hexapeptide azide was also subjected to the cyclization reaction (Fig. 1). Although the synthetic procedure in azide method to yield a crude cyclic peptide was simpler than that in an active ester method, treatment by a Sephadex LH-20 column with crude cyclic peptide was necessary to isolate a pure cyclic hexapeptide.

TABLE 1. YIELD AND SPECIFIC ROTATION OF CYCLIC HEXAPEPTIDES OBTAINED BY VARIOUS REACTIONS

Starting compound	*cyclo*-(Gly$_2$-Tyr)$_2$[a]	
	Yield, %	$[\alpha]_D^{20}$[b]
Bzl Z-Tyr-Gly$_2$-ONp	9	−63.2°
H-Tyr-Gly$_2$-NHNH$_2$	6	−63.0°
H-Gly-Tyr-Gly-NHNH$_2$	17	−63.5°
H-Gly$_2$-Tyr-NHNH$_2$	15	−62.5°
H-(Gly$_2$-Tyr)$_2$NHNH$_2$	20	−63.1°

a) All samples showed only one spot (R_f 0.80) on the paper chromatogram, and the same mp (decomp.) of 250—255°C. All air-dried samples were assigned to cyclic hexapeptide trihydrate by elemental analyses and molecular weight determinations within experimental errors.
b) *c* 0.2, DMF.

Yields of the cyclic hexapeptide by different routes are summarized in Table 1. It appears that the position of Tyr residue in a tripeptide active ester or azide has an influence on the yield of the cyclic hexapeptide isolated; a lower yield was observed when a bulky Tyr residue occupies *N*-terminus in a tripeptide intermediate.

An incubation mixture of the cyclic hexapeptide (XIII) was analyzed by paper chromatography to check how the susceptibility of XIII toward chymo-

1) Present address: Research Laboratory, Yoshitomi Pharmaceutical Industries, Ltd., Yoshitomi-cho, Fukuoka-ken.
2) To whom requests for reprints should be addressed.
3) Abbreviation: Z, benzyloxycarbonyl; ONp, *p*-nitrophenyl ester; TsOH, *p*-toluenesulfonic acid; TEA, triethylamine; DMF, dimethylformamide; Tyr (Bzl), *O*-benzyl-L-tyrosine residue. Amino acid symbol except Gly denotes L configuration.
4) M. Ohno and N. Izumiya, This Bulletin, **38**, 1831 (1965).
5) O. Abe, H. Takiguchi, M. Ohno, S. Makisumi, and N. Izumiya, *ibid.*, **40**, 1945 (1967).
6) H. Neurath and G. W. Schwert, *Chem. Rev.*, **46**, 69 (1950).
7) N. Yoshida, T. Yamamoto, and N. Izumiya, *Arch. Biochem. Biophys.*, **123**, 165 (1968).

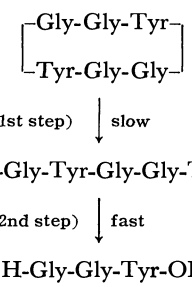

Fig. 2. Hydrolysis of the cyclic hexapeptide by chymotrypsin.

trypsin. It was observed that XIII was completely hydrolyzed to the tripeptide, H-Gly_2-Tyr-OH, after some 6 hr (see Fig. 4). A synthetic linear hexapeptide H-(Gly_2-Tyr)$_2$-OH was also subjected to an enzymatic experiment. The rate of its hydrolysis to the tripeptide was much greater than that of XIII;[8] the linear hexapeptide was completely hydrolyzed after 10 min with the same amount of enzyme used for the cyclic hexapeptide (see Fig. 5). Thus it was deduced that the hydrolysis of the cyclic hexapeptide by the enzyme might proceed in the two steps shown in Fig. 2; the first step, from *cyclo*-(Gly_2-Tyr)$_2$ to H-(Gly_2-Tyr)$_2$-OH, was supposed to be rate-determining.

It was expected that *cyclo*-(Gly_2-Phe)$_2$ (XVIII) would be synthesized more easily than *cyclo*-(Gly_2-Tyr)$_2$ and XVIII would hydrolyzed by chymotrypsin to H-Gly_2-Phe-OH. Since XVIII was insoluble in pH 8.0 buffer, it was not clear whether an incubation mixture of this cyclic hexapeptide and the enzyme yielded the expected tripeptide H-Gly_2-Phe-OH.

Experimental

A spot of material on a paper or plate was detected by spraying ninhydrin, Pauli reagent for Tyr residue or butyl hypochlorite reagent for peptide bond.[9] A spot of an amino group-blocked material on a plate was also detected by spraying 47% by hydrobromic acid and ninhydrin. The R_f refers to paper chromatography on Toyo Roshi No. 52 with a solvent of *n*-butanol-acetic acid-pyridine-water (4:1:1:2, vol). Purity of material was also checked by thin-layer chromatography with the same solvent or chloroform-methanol (5:1, vol).

Z-Tyr(Bzl)-Gly_2-OBzl (I). To a solution of Z-Tyr (Bzl)-ONp[10] (8.4 g) and H-Gly_2-OBzl·TsOH[11] (6.3 g) in chloroform (100 m*l*) was added TEA (2.4 m*l*) at room temperature. The mixture was left to stand overnight, evaporated *in vacuo*, and the oily residue was dissolved in ethyl acetate. It was washed with 2% hydrochloric acid, 4% sodium bicarbonate, and water, successively, dried over sodium sulfate and evaporated. The oil was solidified by the addition of petroleum ether. It was recrystallized from ethyl acetate-ether-petroleum ether; yield, 10.7 g (88%); mp 116—118°C; $[\alpha]_D^{15}$ +4.2° (*c* 1, acetic acid).

Found: C, 68.96; H, 5.77; N, 6.80%. Calcd for $C_{35}H_{35}O_7N_3$: C, 68.95; H, 5.79; N, 6.89%.

Z-Tyr(Bzl)-Gly_2-OH (II). To a solution of I (6.1 g) in a mixture of dioxane-water (2:1; 300 m*l*) was added 2N sodium hydroxide (6 m*l*). After 24 hr, 2N hydrochloric acid (6 m*l*) was added and the solution was evaporated. The residual crystals were collected with the aid of water, and recrystallized from dioxane-ether-petroleum ether; yield, 4.47 g (86%); mp 145—147°C; $[\alpha]_D^{18}$ —21.4° (*c* 1, DMF).

Found: C, 64.42; H, 5.82; N, 7.89. Calcd for $C_{28}H_{29}O_7N_3$: C, 64.73; H, 5.63; N, 8.09%.

Z-Tyr(Bzl)-Gly_2-ONp (III). To a solution of II (1.15 g) in pyridine (7 m*l*) was added di-*p*-nitrophenyl sulfite (3.2 g). After 24 hr, it was evaporated and the residual solid was collected with the aid of a mixture of ether-petroleum ether. The yield was 1.36 g (106%); the *p*-nitrophenyl ester content was estimated to be 93%.[12] The product was used for the preparation of the cyclic peptide (XIII).

Z-Tyr(Bzl)-Gly_2-$NHNH_2$ (IV). A solution of I (1.35 g) and hydrazine hydrate (2.2 m*l*) in DMF (15 m*l*) was allowed to stand for 24 hr, and evaporated *in vacuo*. After the addition of water, the crystals were collected by filtration; yield, 1.35 g (88%); mp 209—212°C; $[\alpha]_D^{21}$ —21.6° (*c* 1, DMF).

Found: C, 62.78; H, 5.92; N, 12.78%. Calcd for $C_{28}H_{31}O_6N_5$: C, 63.02; H, 5.86; N, 13.13%.

H-Tyr-Gly_2-$NHNH_2$·2HCl (V·2HCl). Compound IV (0.89 g, 2 mmol) suspended in 0.43N methanolic hydrogen chloride (7.1 m*l*) was treated with hydrogen in the presence of palladium black. With the progress of reaction the suspended material dissolved into the solution. The filtrate from the catalyst was evaporated; yield of the residual hygroscopic crystal, 0.76 g (approximately 100%); *Rf* 0.50. This was used for the cyclization reaction.

Z-Gly-Tyr-Gly-OBzl (VI). To a chilled solution of Z-Gly-Tyr-$NHNH_2$[13] (2.32 g, 6 mmol) in a mixture of acetic acid (25 m*l*) —N hydrochloric acid (12 m*l*) was added an aqueous solution of sodium nitrite (0.62 g, 9 mmol). After 15 min, water (150 m*l*) was added and the azide was extracted with ethyl acetate. The organic layer was washed with 10% sodium bicarbonate and dried, and the filtrate was added to a mixture of H-Gly-OBzl·TsOH (2.02 g, 6 mmol) and TEA (0.84 m*l*) in chloroform (24 m*l*). After 3 days at O°C, the solution was evaporated, and the oily residue was solidified by trituration with 2% hydrochloric acid and 4% sodium bicarbonate. It was recrystallized from ethyl acetate-ether-petroleum ether; yield, 2.1 g (70%); mp 89—91°C; $[\alpha]_D^{18}$ —5.3° (*c* 1, DMF).

Found: C, 63.69; H, 5.90; N, 8.18%. Calcd for $C_{28}H_{29}O_7N_3\cdot 1/2H_2O$: C, 63.63; H, 5.72; N, 7.95%.

Z-Gly-Tyr-$NHNH_2$ (VII). This was prepared from VI in the same manner as for the preparation of IV; yield, 63%; mp 181—183°C; $[\alpha]_D^{18}$ —10.4° (*c* 1, DMF).

Found: C, 56.64; H, 5.72; N, 15.77%. Calcd for $C_{21}H_{25}O_6N_5$: C, 56.87; H, 5.68; N, 15.79%.

H-Gly-Tyr-Gly-$NHNH_2$·2HCl (VIII·2HCl). A solution of VII (1.05 g) in 0.38N methanolic hydrogen chloride (15 m*l*) was hydrogenated as for the preparation of V·2HCl; yield of hygroscopic crystal, 0.89 g (98%).

H-Gly_2-Tyr-$NHNH_2$·2HCl (IX·2HCl). Z-Gly_2-Tyr-$NHNH_2$[7] (4.56 g) was hydrogenated; yield of hygroscopic crystal, 3.88 g (100%).

Z-(Gly_2-Tyr)$_2$-OEt (X). To azide prepared from Z-Gly_2-Tyr-$NHNH_2$ (1.19 g) was coupled with H-Gly_2-Tyr-OEt·HCl[14] (0.97 g) as described for the preparation of VI.

8) It is of interest to note that H-Gly_2-Tyr-Gly_3-OH or H-Gly_2-Tyr-Gly_4-OH was hydrolyzed by chymotrypsin faster than other homologues, H-Gly_2-Tyr-Gly_n-OH (n=1 and 2).[7]

9) M. Kimura, K. Murayama, M. Nomoto, and Y. Fujita, *J. Chromatogr.*, **41**, 458 (1969).

10) M. Bodanszky and V. du Vigneaud, *J. Amer. Chem. Soc.*, **81**, 5688 (1959).

11) T. Yamashita, *J. Biochem.*, **48**, 651 (1960).

12) R. Schwyzer and P. Sieber, *Helv. Chim. Acta*, **40**, 624 (1957).

13) K. Hofmann, A. Lindenmann, M. Z. Magee, and N. H. Khan, *J. Amer. Chem. Soc.*, **74**, 470 (1952).

The product was recrystallized from hot ethanol; yield, 0.82 g (41%); mp 124—126°C; $[\alpha]_D^{22}$ +19.0° (*c* 1, acetic acid).

Found: C, 57.04; H, 5.76; N, 11.06%. Calcd for $C_{36}H_{42}O_{11}N_6$: C, 57.44; H, 5.89; N, 11.17%.

Z-(Gly$_2$-Tyr)$_2$-NHNH$_2$ (XI). Compound X (0.82 g) was treated with hydrazine hydrate (1.12 m*l*) in DMF (10 m*l*) as described for the preparation of IV; yield, 0.64 g (80%); mp 151—153°C; $[\alpha]_D^{15}$ −6.4° (*c* 0.5, DMF).

Found: C, 54.12; H, 5.81; N, 14.79%. Calcd for $C_{34}H_{40}O_{10}N_8 \cdot 2H_2O$: C, 53.96; H, 5.86; N, 14.81%.

H-(Gly$_2$-Tyr)$_2$-NHNH$_2$·2HCl (XII·2HCl). This was prepared from XI (607 mg); yield of hygroscopic crystal, 570 mg (102%)

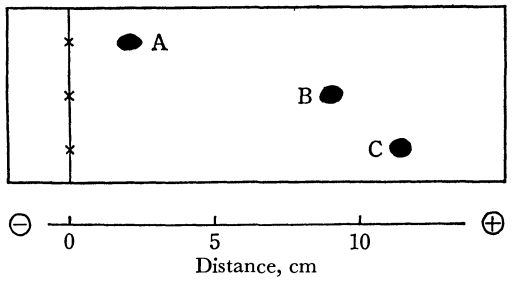

Fig. 3. Paper electrophoresis of *cyclo*-(Gly$_2$-Tyr)$_2$ (A), H-(Gly$_2$-Tyr)$_2$-OH (B) and H-Gly$_2$-Tyr-OH (C). Solvent, 0.01 M citrate buffer (pH 6.7); 600 V/30 cm; 3 hr.

cyclo-*(Gly$_2$-Tyr)$_2$ (XIII)* *(a) From Z-Tyr(Bzl)-Gly$_2$-ONp (III):* III (1.35 g, 2.21 mmol) was dissolved in 25% hydrogen bromide in acetic acid (8 m*l*) at room temperature. After 2 hr, the solution was evaporated and the oily residue (1.1 g), H-Tyr-Gly$_2$-ONp·HBr (XIX), was dissolved in DMF (15 m*l*). It was added to pyridine (600 m*l*) at 55—60°C.[5] After evaporation, the residue was dissolved in a mixture (140 m*l*) of dioxane-methanol-water (7:2:1), and the solution was passed successively through columns of Amberlite IR4B (OH^- form, 1.8×8 cm) and Dowex 50 (H^+ form, 1.8×15 cm). The eluate was evaporated, and the residual crystals were collected by filtration with the aid of ether. It was recrystallized from methanol-ether; yield of an air-dried material, 53 mg (9% from III). Its homogeneity was established by paper electrophoresis (Fig. 3) and paper chromatography (*Rf* 0.80; Fig. 4). The value of specific rotation is shown in Table 1.

Found: C, 51.31; H, 5.90; N, 13.70%; mol wt, 605.[15] Calcd for $C_{26}H_{30}O_8N_6 \cdot 3H_2O$: C, 51.31; H, 5.96; N, 13.81%; mol wt, 609. The air-dried material lost 8.95% of its weight after being dried for 2 hr at 70°C *in vacuo*. Calcd for $3H_2O$: 8.88%.

(b) From Tripeptide Hydrazide (V, VIII or IX): A cyclization reaction of H-Gly-Tyr-Gly-NHNH$_2$ (VIII) is described as an example as follows. To a chilled solution of VIII·2HCl (816 mg, 2.14 mmol) in 0.1 N hydrochloric acid (21.4 m*l*), an aqueous solution of sodium nitrite (162 mg, 2.35 mmol) was added. After 15 min, the solution was poured into cold water (1000 m*l*) containing sodium bicarbonate (2.7 g). After 3 days at 0—4°C, the solution was neutralized with 1 N hydrochloric acid and evaporated. The residue was collected by filtration and washed with water. The product was dissolved in a mixture of dioxane-methanol-water and passed through the columns as described above. Evaporation of the eluate yielded a powder (305 mg) with pale yellow color.[16] A part (100 mg) of the powder dissolved in methanol (1 m*l*) was applied to a column (1.8×35 cm) with Sephadex LH-20, and the development was continued with methanol. Fractions from 39 to 48 m*l* were evaporated, and the crystals were collected with the aid of water; yield of an air-dried product, 40 mg (17%). Data of this product are shown in Table 1.

(c) From Hexapeptide Hydrazide (XII): XII·2HCl (591 mg) was treated in the same manner as described above; yield of an air-dried product, 104 mg (20%). Its properties agreed with those of the products obtained from tripeptide active ester or azides (see Table 1).

Z-(Gly$_2$-Tyr)$_2$-OBzl (XIV). Z-Gly$_2$-Tyr-OBzl[17] (780 mg, 1.5 mmol) was treated with 25% hydrogen bromide in acetic acid (4 m*l*) as described for the preparation of XIX; the H-Gly$_2$-Tyr-OBzl·HBr (XX) (0.7 g) was obtained as an oil. The azide from Z-Gly$_2$-Tyr-NHNH$_2$ (443 mg, 1 mmol) was coupled with XX (0.7 g) as described for the preparation of VI. The product was recrystallized from DMF-ethyl acetate; yield, 509 mg (64%), mp 115—116°C; $[\alpha]_D^{25}$ −5.0°

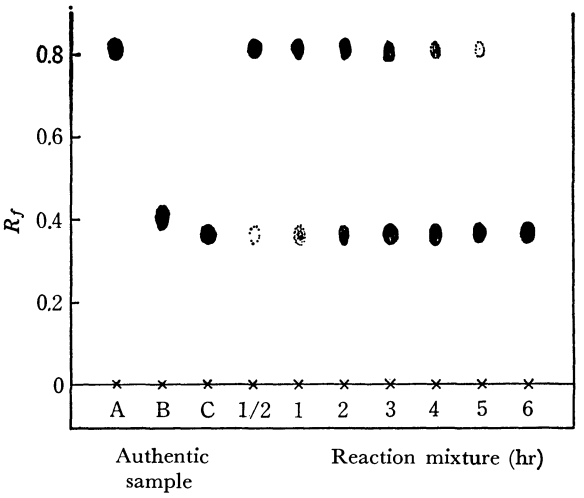

Fig. 4. Paper chromatogram of a reaction mixture (No. 1 of Table 2) of *cyclo*-(Gly$_2$-Tyr)$_2$ and chymotrypsin. A,B, and C, see Fig. 3; solvent, *n*-butanol-acetic acid-pyridine-water (4:1:1:2).

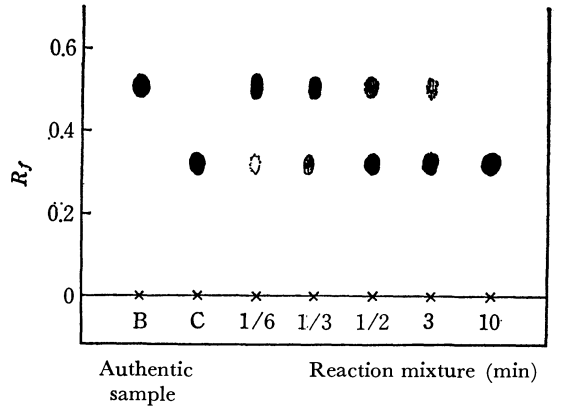

Fig. 5. Paper chromatogram of a reaction mixture (No. 2 of Table 2) of H-(Gly$_2$-Tyr)$_2$-OH and chymotrypsin. B and C, see Fig. 3; solvent, *n*-butanol-acetic acid-pyridine-water (15:3:10:12).

14) T. Yamashita, *J. Biochem.*, **48**, 846 (1960).

15) Methanol was used as a solvent for Hitachi Osmometer, type 115.

16) Recrystallization from metahnol - ether gave no analytically pure cyclic hexapeptide.

17) N. Izumiya and H. Uchio, *J. Biochem.*, **46**, 235 (1959).

TABLE 2. COMPOSITION OF MIXTURE OF THE ENZYMATIC REACTION

No.	Substrate	Weighed amount (0.04 mmol) of substrate	0.2M Tris buffer, pH 8.0	Weighed amount of chymotrypsin	Total volume
1	*cyclo*-$(Gly_2\text{-}Tyt)_2 \cdot 3H_2O$	24 mg	1.0 ml	10 mg	2.0 ml
2	H-$(Gly_2\text{-}Tyr)_2$-OH$\cdot 4H_2O$	26	1.0	10	2.0

(*c* 1, DMF).

Found: C, 59.75; H, 5.64; N, 10.15%. Calcd for $C_{41}H_{44}O_{11}N_4 \cdot 2/3H_2O$: C, 59.77; H, 5.75; N, 10.20%.

H-(Gly_2-Tyr)$_2$-OH (XV). Compound XIV (240 mg) suspended in a mixture (5 ml) of acetic acid - methanol - water (6:3:1) was hydrogenated, and the filtrate was evaporated. The crystals were collected by filtration with the aid of acetone, and recrystallized from water-ethanol; yield, 135 mg (85%); mp 238—242°C (decomp.); $[\alpha]_D^{20}$ −2.8° (*c* 1, water).

Found: C, 48.04; H, 6.07; N, 12.84%. Calcd for $C_{26}H_{32}O_9N_6 \cdot 4H_2O$: C, 48.44; H, 6.25; N, 13.04%.

Action of Chymotrypsin on cyclo-*(Gly_2-Tyr)$_2$ (XIII) and H-(Gly_2-Tyr)$_2$-OH (XV).* α-Chymotrypsin was salt free, crystalline sample from Worthington Biochemical Corp., U.S.A. H-Gly_2-Tyr-OH was prepared as described in literature.[17] Enzymatic experiments were carried out at pH 8.0 and 30°C. The progress of the reactions was checked by paper chromatography as a function of time. Table 2 shows the composition of the reaction mixture. The control experiments showed that no hydrolysis of XIII and XV occurred in the absence of the enzyme. In the presence of the enzyme, XIII was completely hydrolyzed to linear tripeptide after 6 hr, as can be seen in Fig. 4. On the other hand, the linear hexapeptide (XV) was hydrolyzed to the tripeptide within only 10 min in the same condition (Table 2) as seen in Fig. 5.

Z-Gly_2-Phe-OBzl (XVI). This was prepared from Z-Gly_2-OH (2.66 g) and H-L-Phe-OBz·TsOH (4.27 g) by the mixed anhydride method as described previously[5] yield, 3.2 g (64%); mp 81—82°C; $[\alpha]_D^{23}$ +7.0° (*c* 1, acetic acid).

Found: C, 65.59; H, 5.94; N, 8.13%. Calcd for $C_{28}H_{29}O_6N_3 \cdot 1/2H_2O$: C, 65.61; H, 5.90; N, 8.20%.

Z-Gly_2-Phe-$NHNH_2$ (XVII). This was prepared from XVII as described for the preparation of IV; yield, 68%; mp 134—136°C; $[\alpha]_D^{20}$ +13.0° (*c* 1, acetic acid).

Found: C, 58.55; H, 6.00; N, 16.12%. Calcd for $C_{21}H_{25}O_5N_5 \cdot 1/4H_2O$: C, 58.39; H, 5.95; N, 16.21%.

cyclo-*(Gly_2-Phe)$_2$ (XVIII).* Compound XVII (1.07 g, 2.5 mmol) was hydrogenated as described for the preparation of V·2HCl, and the resulting H-Gly_2-Phe-$NHNH_2$·2HCl (0.90 g, 98%) was obtained as hygroscopic crystals. This product (0.9 g) was subjected to cyclization reaction as described for the preparation of XIV from H-Gly-Tyr-Gly-$NHNH_2$. The crude product dissolved in a mixture of dioxane-methanol-water was passed through the columns of Dowex 1 and Dowex 50. The eluate was evaporated, and the residual nice crystals were collected by filtration with the aid of water; yield of an air-dried material, 164 mg (25%); mp 280—285°C (decomp.); $[\alpha]_D^{20}$ −52.0° (*c* 0.5, DMF); R_f 0.93. The material contained no water of crystallization.

Found: C, 59.66; H, 5.89; N, 15.96%; mol wt, 530. Calcd for $C_{26}H_{30}O_6N_6$: C, 59.76; H, 5.79; N, 16.08%; mol wt, 523. This material (XVIII) did not dissolve in pH 8.0 buffer even at a level of 0.002M. It was therefore, not clear whether an incubation mixture of XVIII and chymotrypsin yielded H-Gly_2-Phe-OH by means of paper chromatography.

The authors wish to express their thanks to Mr. Shunichi Takamura for his valuable assistance.

BULLETIN OF THE CHEMICAL SOCIETY OF JAPAN, VOL. 44, 2804—2807 (1971)

Aminocyclitols. XXVII. Preparation of Deoxyinosamines from *vibo*-Quercitol[1]

Tetsuo SUAMI, Seiichiro OGAWA, Kenji YABE,* and Masaru UCHIDA**
Department of Applied Chemistry, Faculty of Engineering, Keio University, Koganei-shi, Tokyo

(Received May 8, 1971)

On bromination with acetyl bromide and acetic anhydride at 130°C, *vibo*-quercitol (**1**) gave tetraacetyl 1-bromo-1-deoxy-*scyllo*-quercitol (**2**) in 23% yield. Treatment of **2** with sodium azide in an appropriate solvent afforded three azido compounds, from which, by hydrogenation, corresponding three deoxyinosamines were obtained: 1-deoxy-*scyllo*-2, 5-deoxy-*chiro*-1 and 1-deoxy-*myo*-2-inosamine. The latter two are new compounds and their structures were established by their proton magnetic resonance (PMR) spectra and the reaction sequences.

We previously described the synthesis of two deoxyinosamines from *vibo*-quercitol (**1**).[2] In the present paper, we wish to report an alternative synthetic route to deoxyinosamines using bromodeoxyquercitol.

When **1** was treated with acetyl bromide and acetic anhydride in a sealed tube at 125—130°C for 8 hr, and subsequently acetylated with acetic anhydride and conc. sulfuric acid, hitherto unknown tetraacetyl bromodeoxyquercitol (**2**), mp 148°C, was obtained as a sole crystalline product in 23% yield. Hydrolysis of **2** by refluxing in 3N hydrochloric acid gave bromodeoxy-

*Present address: Toray Industries, Inc., Ohtsu-shi, Shiga.
**Present address: Ube Kosan, Ichihara-shi, Chiba.

1) All the compounds described in this paper are racemic.
2) T. Suami and K. Yabe, This Bulletin, **39**, 1931 (1966).

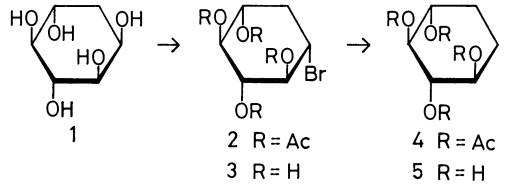

quercitol (**3**). On catalytic hydrogenolysis in the presence of Raney nickel T-4[3] and Amberlite IR-4B (OH^-), **2** afforded tetraacetyl cyclohexanetetrol (**4**), which was converted into known cyclohexanetetrol (1, 3/2,4) (**5**).[4] Therefore, **2** should be either 1-bromo-1-deoxy-*scyllo*- or 1-bromo-1-deoxy-*vibo*-quercitol. This could be easily differenciated on the basis of its PMR spectrum in deuteriochloroform ($CDCl_3$) (Fig. 1). The

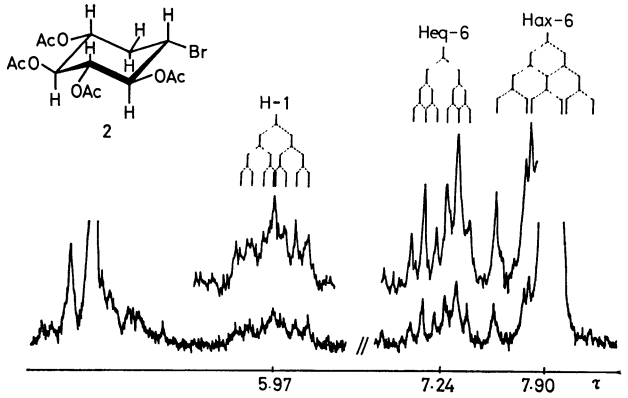

Fig. 1. Partial PMR spectrum of tetraacetyl 1-bromo-1-deoxy-*scyllo*-quercitol (**2**) in $CDCl_3$.

ring proton attached to the carbon atom bearing bromine atom appeared at τ 5.97 as a septet (J=4.5, 9, and 13 Hz), which indicated that the bromine atom should be in equatorial position in the favored conformation and located adjacent to methylene protons. This was further supported by a decoupling experiment. The equatorial methylene proton showed a clearly resolved sextet (J=4.5, 4.5, and 13 Hz) at τ 7.24, which collapsed to a quartet when the septet at τ 5.97 was irradiated at this frequency. While the sextet was irradiated to collapse the septet into a wide triplet. Consequently, **2** was assigned to tetraacetyl 1-bromo-1-deoxy-*scyllo*-quercitol unambigously. The reaction mechanism of the bromination reaction was proposed by assuming an intermediary acetoxonium ion formation between the *cis* hydroxyl groups in *vibo*-quercitol, which was attacked by a bromide ion in a less sterically hindered direction.

When **2** was treated with an excess amount of sodium azide in boiling 90% aqueous 2-methoxyethanol for 40 hr, tetraacetyl 1-azido-1-deoxy-*scyllo*-quercitol (**6**)[2] was obtained in 22% yield. The crude oily product obtained by evaporation of the mother liquor of **6** was hydrogenated in the presence of Raney nickel T-4[3] and subsequently acetylated to afford unknown penta-

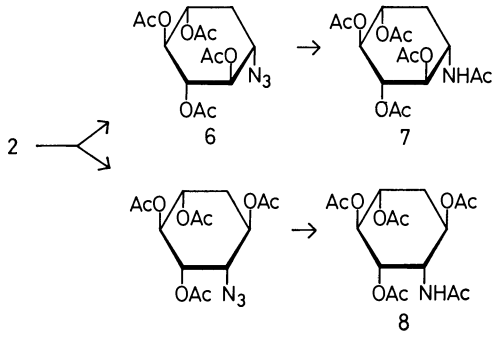

acetyl deoxyinosamine (**8**) in 19% yield. While, **2** was treated with methanolic ammonia in a sealed tube at 120°C for 12 hr and subsequent acetylation gave pentaacetyl 1-deoxy-*scyllo*-inosamine-2 (**7**)[2] and **8** in 14 and 10% yield, respectively.

In the PMR spectrum of **8** in dimethylsulfoxide-d_6 (DMSO-d_6), the acetyl methyl protons revealed four signals at τ 8.14 (1), 8.08 (1), 8.02 (2), and 7.93 (1),[5] which were assigned to one axial acetamido, one equatorial acetoxy, two equatrial acetoxy and one axial acetoxy group, respectively.[6] On the other hand, in the spectrum in $CDCl_3$, four signals due to the acetyl methyl protons were appeared at τ 8.01 (1), 7.96 (1), 7.93 (2), and 7.91 (1), which could be assigned to one equatorial acetamido, one equatorial acetoxy, two axial acetoxy and one axial acetoxy group, respectively.[6] The sextet (J=3, 8, and 8 Hz) at τ 5.50 was attributed to the hydrogen atom attached to the carbon atom bearing the acetamido group, because an addition of deuterium oxide collapsed it into a quartet. Therefore, in $CDCl_3$, **8** seems to take a favored conformation having the acetamido group in an equatorial position. Consequently, according to a reaction sequence and its PMR spectra, **8** was assigned to pentaacetyl 5-deoxy-*chiro*-inosamine-1.

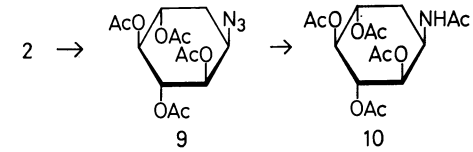

Treatment of **2** with sodium azide in boiling 90% aqueous dimethylformamide for 40 hr and subsequent acetylation gave another tetraacetyl azidodeoxyquercitol (**9**) in 60% yield. Hydrogenation of **9**, followed by acetylation, afforded the corresponding pentaacetyl deoxyinosamine (**10**) in 74% yield. The structures of **9** and **10** were established mainly by way of their PMR spectra. The PMR spectrum of **9** in $CDCl_3$ revealed a narrow quartet (J=3 Hz) at τ 5.83, which was assigned to the equatorial hydrogen atom attached to the carbon atom having azido group[7] and, then, the azido group was proved to be adjacent to the methylene protons. The acetyl methyl protons showed two peaks at

3) S. Nishimura, *ibid.*, **32**, 61 (1959).

4) P. Bedos and A. Ruyer, *Compt. rend.*, **106**, 625 (1933); G. E. McCasland and E. C. Horswill, *J. Amer. Chem. Soc.*, **75**, 4020 (1953).

5) Values in parenthesis show number of acetoxy methyl groups.

6) F. W. Lichtenthaler and P. Emig, *Carbohyd. Res.*, **7**, 121 (1968).

7) T. Suami, S. Ogawa, and M. Uchida, This Bulletin, **43**, 3577 (1970).

τ 8.01 (3) and 7.93 (1). The latter might be considered to be downshifted from the ordinary chemical shift[6] under the influence of the adjacent azido group.[7] While, the PMR spectrum of **10** in DMSO-d_6 indicated two signals at τ 8.11 (1) and 8.04 (4), which were assigned to one axial acetamido and four equatorial acetoxy groups, respectively. Consequently, **9** should be tetraacetyl 1-azido-1-deoxy-*vibo*-quercitol and the corresponding **10** was assignable to pentaacetyl 1-deoxy-*myo*-inosamine-2.

The reaction mechanism was interpreted by a direct S_N2 attack of azide ion in a dipolar aprotic solvent.[7,8]

Experimental

Melting point were determined on a Mitamura Riken micro hot stage and are uncorrected. PMR spectra were measured on a Varian Associate A-60D (60 MHz) spectrometer at a concentration of *ca.* 10% deuteriochloroform or dimethylsulfoxide-d_6 with tetramethylsilane as in internal standard. All solutions were concentrated by a rotary evaporator at 40—50°C under reduced pressure. Whenever pyridine was employed in a reaction, the residual pyridine was removed by repeated codistillation with dry toluene.

Tetraacetyl 1-Bromo-1-deoxy-scyllo-*quercitol (2).* *vibo*-Quercitol (**1**)[2] (3.0 g) was heated in a sealed tube at 125—130°C for 8 hr with acetyl bromide (2.5 m*l*) and acetic anhydride (7.0 m*l*). The reaction mixture obtained from ten sealed tubes evaporated to dryness and the resulting oily product was treated with acetic anhydride (300 m*l*) and conc. sulfuric acid (15 m*l*) at room temperature overnight. Then the mixture was poured into ice and water (1 *l*) and allowed to stand at room temperature overnight. A thick oily product was extracted with chloroform (300 m*l*) and the extracts were washed with 10% aqueous sodium carbonate and water, successively. The solvent was removed by evaporation and the residue was crystallized from ethanol to yield colorless crystals (22.0 g, 23%) of **2**, mp 147—148°C. Recrystallization from ethanol gave an analytical sample, which showed the same melting point.

Found: C, 42.76; H, 5.08; Br, 20.48%. Calcd for $C_{14}H_{19}O_8Br$: C, 42.54; H, 4.85; Br, 20.22%.

1-Bromo-1-deoxy-scyllo-*quercitol (3).* A mixture of **2** (0.50 g) and ethanol (20 m*l*) containing conc. hydrochloric acid (5 m*l*) was refluxed for 90 min. The reaction mixture was evaporated to give a crystalline residue which was recrystallized from ethanol to afford crystals (0.18 g, 62%) of **3**, mp 178—182°C. An analytical sample was obtained by recrystallization from ethanol, mp 185—187°C.

Found: C, 32.28; H, 5.14; Br, 34.72%. Calcd for $C_6H_{11}O_4Br$: C, 31.73; H, 4.88; Br, 35.19%.

Tetraacetyl Cyclohexanetetrol (1,3/2,4) (4). A solution of **2** (0.39 g) in ethanol (20 m*l*) was hydrogenated in the presence of Raney nickel T-4 (one spatula) and Amberlite IR-4B (OH^-) (6 m*l*) in the hydrogen initial pressure of 3 atm for 20 hr. Filtering off the catalyst and resin, the filtrate was evaporated to give a crystalline residue, which was recrystallized from ethanol to afford colorless plates (0.21 g, 68%) of **4**, mp 138.5—139°C (after melting and resolidifying at 126—128°C). Recrystallization from ethanol gave an analytical sample, mp 125.5—127°C.

Found: C, 53.26; H, 6.40%. Calcd for $C_{14}H_{20}O_8$: C, 53.16; H, 6.37%.

Cyclohexanetetrol (1,3/2,4) (5). A mixture of **4** (0.10 g) and 4N hydrochloric acid (6 m*l*) was heated at 90°C for 5 hr. Then the solution was evaporated to give an oily product, which crystallized upon addition of ethanol to afford colorless prisms (37 mg, 78%) of **5**, mp 184—186°C. Recrystallization from methanol gave a pure sample, whose melting point did not change (lit,[4] mp 187—188°C).

Table 1. PMR data[a]

Compd.	Solvent	Acetyl methyl protons	Ring protons
2	$CDCl_3$	7.91 (1)	
		7.95 (1)	
		7.99 (2)	
4	$CDCl_3$	7.98 (4)	
6	$CDCl_3$	7.90 (1)	6.30 (m, H-1)
		7.96 (1)	
		7.99 (2)	
7[2]	DMSO-d_6	8.02 (2)	
		8.06 (2)	
		8.22 (1)	
8	$CDCl_3$	7.91 (1)	5.50 (sextet,
		7.93 (2)	H-1, J=3,
		7.96 (1)	8 and 8 Hz)
		8.01 (1)	
8	DMSO-d_6	7.93 (1)	
		8.02 (2)	
		8.08 (1)	
		8.14 (1)	
9	$CDCl_3$	7.93 (1)	4.52 (t, H-3, J=9.5 Hz)
		8.01 (3)	5.83 (q, H-1, J=3 Hz)
10	DMSO-d_6	8.04 (1)	
		8.11 (4)	
Tetraacetyl 3-azido-3-deoxy-*proto*-quercitol[2]	$CDCl_3$	7.84 (1)	4.59 (t, H-2,
		7.88 (2)	J=10 Hz)
		7.95 (1)	6.17 (q, H-3, J=3 and 10 Hz)

a) Chemical shifts are expressed in τ-values. Values in parenthesis show number of methyl groups. Abbreviations: t (triplet); q (quartet); m (complex multiplet). First-order coupling constants are expressed.

Tetraacetyl 1-Azido-1-deoxy-scyllo-*quercitol (6).* A mixture of **2** (1.8 g), sodium azide (1.5 g), and 90% aqueous 2-methoxyethanol (60 m*l*) was refluxed for 40 hr. The reaction mixture was evaporated to dryness and the residue was treated with acetic anhydride (15 m*l*) and pyridine (15 m*l*) at room temperature overnight. An insoluble material was removed by filtration and the filtrate was evaporated to give an oily product, which crystallized upon addition of ethanol. The crude crystals were recrystallized from ethanol to afford colorless needles (0.35 g, 22%) of **6**, mp 136—138°C. This compound was identified with an authentic sample[2] by a mixed melting point determination and a comparison of infrared spectra.

From the mother liquor of **6**, a small amount of crystals was isolated after long storage in a refrigerator, mp 128—130°C. The infrared spectrum was different from that of **6**, so that this compound might be proposed to be tetraacetyl 4-azide-4-deoxy-*proto*-quercitol.

Found: C, 46.64; H, 5.10; N, 11.39%. Calcd for $C_{14}H_{19}N_3O_8$: C, 47.06; H, 5.36; N, 11.76%.

8) T. Suami, F. W. Lichtenthaler, and S. Ogawa, This Bulletin **38**, 754 (1965).

Pentaacetyl 5-Deoxy-chiro-*inosamine-1 (8).* The mother liquor of **6** was hydrogenated in the presence of Adams' platinum oxide (20 mg) in the initial hydrogen pressure of 3 atm for 12 hr. The hydrogenated product was acetylated with acetic anhydride and pyridine and crystallized from ethanol to give crystals (0.37 g, 22%) of **8**, mp 187—188°C. Recrystallization from ethanol gave an analytically pure sample, which showed the same melting point.

Found: C, 51.56; H, 6.14; N, 3.90%. Calcd for $C_{16}H_{23}NO_9$: C, 51.47; H, 6.21; N, 3.75%.

Ammonolysis of 2 using Methanolic Ammonia. Compound **2** (1.5 g) was heated with methanol (100 m*l*) saturated with ammonia at 0—5°C in an autoclave at 120°C for 12 hr. The reaction mixture was evaporated to dryness and treated with acetic anhydride and pyridine at room temperature overnight. Evaporation of the excess reagent gave a crude mixture, which was fractionally crystallized from ethanol and ether to afford pentaacetyl 1-deoxy-*scyllo*-inosamine-2 (**7**) (0.19 g, 13%), mp 224—226°C, and **8** (0.15 g, 10%), mp 187—188°C.

Tetraacetyl 1-Azido-1-deoxy-vibo-*quercitol (9).* A mixture of **2** (1.5 g), sodium azide (1.0 g) and 90% aqueous dimethylformamide (50 m*l*) was refluxed for 40 hr. The reaction mixture was processed similarly as described in the preparation of **6**. The crude product was crystallized from ethanol to give crystals (0.81 g, 60%) of **9**, mp 142—145°C. Recrystallization from ethanol afforded an analytical sample, mp 143.5—144.5°C.

Found: C, 46.82; H, 5.40; N, 11.79%. Calcd for $C_{14}H_{19}N_3O_8$: C, 47.06; H, 5.36; N, 11.76%.

Pentaacetyl 1-Deoxy-myo-*inosamine-2 (10).* A solution of **9** (0.35 g) in ethanol (50 m*l*) was hydrogenated similarly as described in the preparation of **8**. The crude product was acetylated with acetic anhydride and pyridine and crystallized from ethanol to give colorless crystals (0.27 g, 74%) of **10**, mp 224—225°C. Recrystallization from ethanol afforded an analytical sample, which showed the same melting point.

Found: C, 51.73; H, 6.46; N, 3.77%. Calcd for $C_{16}H_{23}NO_9$: C, 51.47; H, 6.21; N, 3.75%.

The authors are grateful to Professor Sumio Umezawa for his kind advice, and to Mr. Saburo Nakada for his elementary analyses. The financial support from the Ministry of Education for this work is gratefully acknowledged.

BULLETIN OF THE CHEMICAL SOCIETY OF JAPAN, VOL. 44, 2807—2810 (1971)

The Reactions of Complexes of Thioboronite with Compounds Containing Carbon-Nitrogen Multiple Bond

Teruaki MUKAIYAMA, Shoji YAMAMOTO, and Katsuhiko INOMATA

Laboratory of Organic Chemistry, Tokyo Institute of Technology, Ookayama, Meguro-ku, Tokyo

(Received May 10, 1971)

n-Butyl di-*n*-butylthioboronite reacts with isocyanates to give 1 : 2 adducts, and with isothiocyanate or carbodiimide to give a 1 : 1 adduct. It was found that thioboronite forms a 1 : 1 co-ordinated complex with benzyl cyanide, and that the complex reacts with isocyanates to give the corresponding acetamidine derivatives in good yields.

It has been reported by Mikhailov and his co-workers[1] that various thioboronites or thioborates react with carbonyl compounds to give the corresponding mercaptols or mercaptals. The results indicate that the boron-sulphur bond cleavage takes place easily through co-ordinated complexes of carbonyl compounds and boron compounds. The reactions of thioboronites with compounds containing the carbon-nitrogen multiple bond, such as isocyanates, carbodiimide and nitriles, were studied in order to examine the chemical behavior of the boron-sulfur bond.

In the reaction of triethyl orthothioborate with phenyl isocyanate in dry benzene, it was found that *N*-ethylthiocarbonyl-*N*,*N*′-diphenylurea (II) is obtained in a 94% yield (route *B*) instead of the expected mercaptol (I) (route *A*).

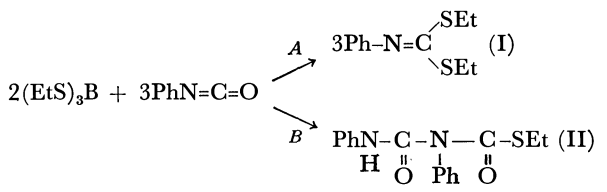

n-Butyl di-*n*-butylthioboronite (0.01 M) in carbon tetrachloride was treated with phenyl isocyanate (0.02 M) in the same solvent under nitrogen atmosphere at room temperature. After stirring for 20 min, it was observed that the infrared spectra of the oily substance obtained by evaporating the solvent *in vacuo* showed no bands at 2250 cm^{-1} ($\nu_{N=C=O}$) and 1110 cm^{-1} assignable to *B*–*S* bond, but new bands at about 1700 cm^{-1} ($\nu_{C=O}$) and 1330—1320 cm^{-1} assignable to *B*–*N* bond. It can be assumed that *n*-butyl di-*n*-butylthioboronite and phenyl isocyanate forms an 1 : 2 adduct. This was further confirmed by the fact that *N*-*n*-butylthiocarbonyl-*N*,*N*′-diphenylurea (V) was isolated as white crystal in a 95% yield by hydrolysis of this adduct. The structure was established by elemental analysis and comparison with the authentic compound prepared from phenyl isocyanate and *S*-*n*-butyl thiocarbanilate according to the method of Lakra *et al.*[2]

1) B. M. Mikhailov and N. S. Fedotov, *Izv. Akad. Nauk SSSR., Otdel. Khim. Nauk*, 999-1000 (1961); *Chem. Abstr.* **57**, 16643 (1962).

2) H. Lakra and F. B. Pains, *J. Amer. Chem. Soc.*, **51**, 2220 (1929).

TABLE 1. REACTION OF THIOBORONITE WITH ISOCYANATES.

R–N=C=O	Product yield (%)	Product mp (bp) (°C)	Formula	Calcd (%) C	Calcd (%) H	Calcd (%) N	Calcd (%) S	Found (%) C	Found (%) H	Found (%) N	Found (%) S
C_6H_5	95	90.0—90.5	$C_{18}H_{20}O_2N_2S$	65.84	6.14	8.53	9.82	65.58	6.18	8.29	9.96
p-$O_2NC_6H_4$	98	128 (decomp.)	$C_{18}H_{20}O_2N_2S$	51.67	4.34	13.39	7.65	51.39	4.06	13.59	7.83
	quant.	65.0—66.0	$C_{18}H_{32}O_2N_2S$	63.50	9.47	8.23	9.40	63.69	9.22	8.53	9.51
C_2H_5	95	(136—140/7 mmHg)	$C_{14}H_{20}O_2N_2S$	51.70	8.68	12.06	13.78	52.04	8.28	12.20	14.64

The reaction is considered to proceed as follows; initially one mole of isocyanate co-ordinates to thioboronite to form a 1:1 complex (III).[3] Then another isocyanate abstracts the mercapto group, activated by the influence of $\overset{\delta-}{B}\leftarrow\overset{\delta+}{N}$ polarization and accompanied by a nucleophilic attack of the nitrogen atom on the carbon atom of initially co-ordinated isocyanate to form (VI).

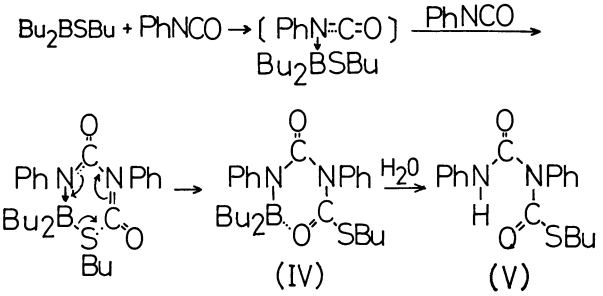

In a similar way, p-nitrophenyl isocyanate, cyclohexyl isocyanate and ethyl isocyanate gave the corresponding ureas in almost quantitative yields. The results are summarized in Table 1.

The reaction of n-butyl di-n-butylthioboronite with phenyl isothiocyanate and with dicyclohexylcarbodiimide was tried. In both cases, formation of the corresponding 1:1 adducts was confirmed by infrared spectra. The adducts were in turn converted into n-butyl dithiocarbanilate (VI 45%) and S-n-butyl-N,N'-dicyclohexylisothiourea (VII 83%) by hydrolysis, respectively.

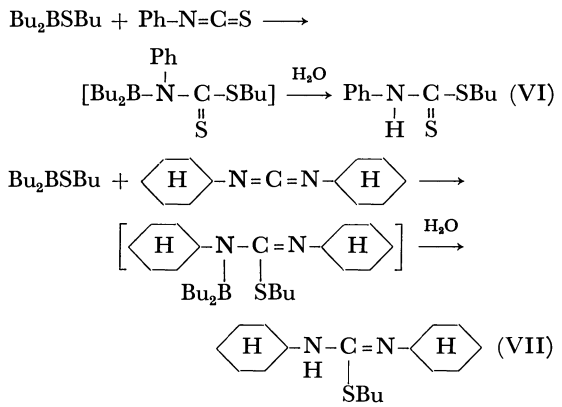

Differing from isothiocyanate and carbodiimide, the formation of the 1:2 adduct in the case of isocyanate, might depend on its strong electrophilic character, which abstracts the mercapto group from the 1:1 complex initially formed.

An attempt to synthesize an analogous adduct of n-butyl di-n-butylthioboronite and benzyl cyanide was made according to the report by Mikhailov *et al.*[4] showing that the stable dimerized adduct $(R_2BN{=}CMeSR')_2$ is obtained by the reaction of acetonitrile with thioboronite (R_2BSR'). Unexpectedly, it was found that a 1:1 complex is produced instead of the dimerized adduct when n-butyl di-n-butylthioboronite (0.01 M) was allowed to react with benzyl cyanide (0.01 M) under nitrogen atmosphere at room temperature for 20 min. After removal of the solvent, the band at 2150 cm^{-1} ($\nu_{C\equiv N}$) disappeared and a new strong band appeared at 1810 cm^{-1} in the infrared spectra of the resulting oily substance. With the addition of ethanol amine, the band at 2150 cm^{-1} reappeared and the band at 1810 cm^{-1} disappeared. It is thus clear that thioboronite and benzyl cyanide form a 1:1 co-ordinated complex, and that the band at 1810 cm^{-1} is assignable to the nitrile group shifted greatly to lower frequency by co-ordination. It was found that the 1:1 complex exists in ether and dioxane, but it dissociates into nitrile with the addition of tetrahydrofuran, amines (pyridine, triethylamine) dimethyl sulfide as shown in the following equation.

$$[PhCH_2C\dot{=}N\rightarrow BBu_2SBu] + :L \rightleftharpoons PhCH_2CN + L{:}BBu_2SBu$$

L: THF, pyridine, triethylamine, dimethylsulfide

When the co-ordinated complex obtained by evaporating the solvent *in vacuo* was stirred for a few days, the band at 1810 cm^{-1} in the infrared spectra disappeared and a new band at 1610 cm^{-1} ($\nu_{C=N}$) appeared, the stable adduct (VIII) being obtained as a white crystal in a 40—50% yield. It was also observed that dry air is effective to accelerate the transfer of mercapto group, but the detailed mechanism is not yet clear.

$$[PhCH_2CN\rightarrow BBu_2SBu] \longrightarrow (PhCH_2C(SBu)=N\text{–}BBu_2)_n \quad \text{(VIII)}$$

The results indicate that formation of the co-ordinated complex of thioboronite and benzyl cyanide facilitates the formation of mercapto anion due to the influence of $\overset{\delta-}{B}\leftarrow\overset{\delta+}{N}$ polarization.

Thus, it is expected that an abstraction of the mercapto group from the complex would occur by the use of isocyanates. An equimolar amount of phenyl isocyanate was added to the 1:1 complex in the presence of a catalytic amount of boron trifluoride etherate in the

3) There is another possible pathway for formation of the complex by the oxygen atom of the isocyanate with the boron atom, but this was excluded by the infrared spectra.

4) B. M. Mikhailov, V. A. Dorokhov and I. P. Yakovlev, *Izv. Akad. Nauk SSSR., Ser. Khim.*, **1966** (2) 332; *Chem. Abstr.*, **64**, 17623 g (1966).

Table 2. Reaction of isocyanates with 1:1 complex of thioboronite and benzyl cyanide

R–N=C=O	Product		Foumula	Calcd (%)				Found (%)			
	Yield (%)	mp (°C)		C	H	N	S	C	H	N	S
p-$O_2NC_6H_4$	83	149.0—149.5	$C_{19}H_{21}O_3N_3S$	61.44	5.70	11.32	8.66	61.14	5.48	11.16	8.96
C_6H_5	74	69.5— 70.5	$C_{19}H_{22}ON_2S$	69.94	6.75	8.59	9.86	69.83	6.74	8.78	9.65
α-$C_{10}H_7$	70	110.5—111.0	$C_{23}H_{24}ON_2S$	73.38	6.43	7.44	8.50	73.08	6.29	7.55	8.24
p-$CH_3OC_6H_4$	69	99.5—100.0	$C_{20}H_{24}O_2N_2S$	67.39	6.79	7.86	8.98	67.31	6.75	7.99	9.24
p-$CH_3C_6H_4$	61	111.0—111.5	$C_{20}H_{24}ON_2S$	70.56	7.11	8.23	9.40	70.42	6.94	8.20	9.34
m-$CH_3C_6H_4$	46	a)									
o-$CH_3C_6H_4$	49	83.0	$C_{20}H_{24}ON_2S$	70.56	7.11	8.23	9.40	70.25	6.96	8.02	9.44
	67	101.0—102.0	$C_{19}H_{28}ON_2S$	68.63	8.49	8.43	9.64	68.38	8.21	8.41	9.94
C_2H_5	59	a)									
t-C_4H_9	35	a)									

a) Oily substances which undergo decomposition during the course of vacuum distillation. This was confirmed by means of infrared spectra and the hydrolysis to acylurea.

minimum amount of ether at 0°C under dry air[5]. After stirring the mixture for 10 hr, the infrared spectra of the oily substance obtained by evaporating the solvent showed the diappearance of the band at 1810 cm^{-1} and 2150 cm^{-1} ($\nu_{N=C=O}$) and the appearance of a new band at 1605 cm^{-1} ($\nu_{C=N}$). By hydrolysis of the reaction mixture, *N*-*n*-butylthiocarbonyl *N*-phenyl phenylacetamidine (IX) was obtained in a 74% yield as expected. The reaction is considered to proceed as shown below.

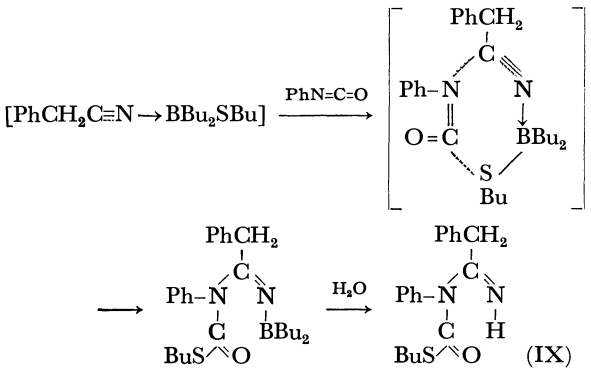

The structure was established by elemental analysis, infrared spectra and NMR spectra. In the case of various isocyanates, a similar reaction took place to give the corresponding acetamidine derivatives. The results are shown in Table II.

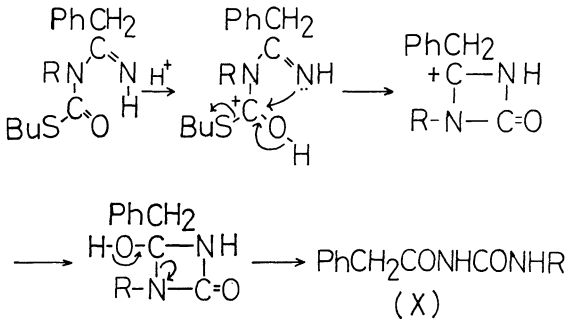

It was found that acetamidine derivatives thus obtained give the corresponding acylureas (X) quantitatively by acidic hydrolysis as shown in the above scheme.

Experimental

Reaction of n-*Butyl Di*-n-*butylthioboronite and Phenyl Isocyanate.* A solution of phenyl isocyanate (2.38 g, 0.02 mol) in carbon tetrachloride was added dropwise with strirring to a solution of *n*-butyl di-*n*-butylthioboronite (2.20 g, 0.01 mol) in the same solvent at room temperature under nitrogen atmosphere. After stirring for 20 min, the oily substance obtained by evaporating the solvent was hydrolyzed in THF-water for 3 hr at room temperature, and saturated with sodium chloride. The THF layer was then separated and the water layer was extracted with ether three times. The THF layer and the ether layer were combined and dried with sodium sulfate. After removal of the solvent, the residue was chromatographed on silica gel. From the elute of benzene a white crystal was obtained. Recrystallization from 95% ethanol gave *N*-*n*-butylthiocarbonyl-*N*,*N*'-diphenylurea, 3.02 g (95%), mp 90—90.5°C.

In a similar way, the corresponding *N*-*n*-butylthiocarbonylurea derivatives were obtained by the reaction of *n*-butyl di-*n*-butylthioboronite with *p*-nitrophenyl isocyanate, cyclohexyl isocyanate, or ethyl isocyanate, respectively. The results are listed in Table 1.

Reaction of n-*Butyl Di*-n-*butylthioboronite and Phenyl Isothiocyanate.* A mixture of phenyl isothiocyanate (1.35 g, 0.01 mol) and *n*-butyl di-*n*-butylthioboronite (2.23 g, 0.01 mol) in carbon tetrachloride was stirred for 3 days at room temperature under nitrogen atmosphere. The oily substance obtained by evaporating the solvent was hydrolyzed in THF-water for 3 hr at room temperature and saturated with sodium chloride. The THF layer was then separated and the water layer was extracted with ether three times. The THF layer and the ether layer were combined and dried with sodium sulfate. After removal of the solvent the residue was chromatographed on silica gel. From the elute of benzene a white crystal was obtained. Recrystallization from petroleum ether gave *n*-butyl dithiocarbanilate, 1.02 g (45%) mp 55.5—56.0°C.

Found: C, 63.43; H, 7.46; N, 6.69; S, 15.18%. Calcd for $C_{11}H_{15}NS_2$: C, 63.14; H, 7.23; N, 6.69; S, 15.29%.

5) When a large amount of ether is used as solvent, free thioboronite liberated from the complex reacts with isocyanate to give the 1:2 adduct (IV) as shown below.

$PhCH_2CN + Bu_2BSBu \rightleftharpoons PhCH_2CN \rightarrow BBu_2SBu$

$\downarrow$ 2RNCO

1:2 adduct (IV)

Table 3. Hydrolysis of phenylacetamidine derivatives. $PhCH_2CONHCONHR$

R	mp (°C)	Fromula	Calcd (%)			Found (%)		
			C	H	N	C	H	N
p-$O_2NC_6H_4$	189.0	$C_{15}H_{13}O_4N_3$	60.19	4.38	14.08	59.94	4.24	14.28
C_6H_5	147.5—148.5	$C_{15}H_{14}O_2N_2$	70.85	5.55	11.02	70.61	5.49	11.11
α-$C_{10}H_7$	202.0	$C_{19}H_{16}O_2N_2$	74.98	5.30	9.21	74.79	5.00	9.40
p-$CH_3OC_6H_4$	165.0—166.0	$C_{16}H_{16}O_3N_2$	67.59	5.67	9·85	67.89	5.96	9.89
p-$CH_3C_6H_4$	186.0—186.5	$C_{16}H_{16}O_2N_2$	71.62	6.01	10.44	71.35	6.05	10.51
m-$CH_3C_6H_4$	154.0—155.0	$C_{16}H_{16}O_2N_2$	71.62	6.01	10.44	71.86	6.26	10.70
o-$CH_3C_6H_4$	159.0—160.0	$C_{16}H_{16}O_2N_2$	71.62	6.01	10.44	71.69	5.74	10.50
	126.0—126.5	$C_{15}H_{20}O_2N_2$	69.20	7.44	10.76	69.35	7.49	10.49
C_2H_5	155.0—156.0	$C_{11}H_{14}O_2N_2$	64.06	6.84	13.58	63.77	6.62	13.41
t-C_4H_9	157.5—158.5	$C_{13}H_{18}O_2N_2$	66.64	7.74	11.96	66.83	7.85	11.68

Reaction of n-*Butyl Di*-n-*butylthioboronite with Dicyclohexylcarbodiimide.* A mixture of *n*-butyl di-*n*-butylthioboronite (2.14 g, 0.01 mol) and dicyclohexylcarbodiimide (2.06 g, 0.01 mol) in methylene chloride was stirred for 1 hr at room temperature under nitrogen atmosphere. By treating the mixture with water, *S*-*n*-butyl-*N,N'*-dicyclohexyl isothiourea was obtained in an 85% yield as an oily substance which undergoes decomposition during the course of vacuum distillation to give dicyclohexylcarbodiimide.

Reaction of n-*Butyl Di*-n-*butylthioboronite and Benzyl Cyanide.* A solution of benzyl cyanide (0.61 g, 0.005 mol) in methylene chloride was added with stirring to a solution of *n*-butyl di-*n*-butylthioboronite (1.11 g, 0.005 mol) in methylene chloride at room temperature under nitrogen atmosphere. After stirring for 20 min, the 1:1 complex of *n*-butyl di-*n*-butylthioboronite and benzyl cyanide was obtained as a yellow oily substance by evaporating the solvent *in vacuo*. After stirring the complex under dry air for a few days, dimerized adduct was obtained as a white precipitate by adding 95% ethanol.

Recrystallization from acetonitrile at a temperature below 50°C gave a white needle 0.77 g (45%), mp 66.0—66.5°C.

Found: C, 72.25; H, 10.31; N, 4.53; S, 9.85%. Calcd for $C_{20}H_{34}NBS$: C, 72.48; H, 10.36; N, 4.23; S, 9.67%.

Reaction of 1:1 Complex between n-*Butyl Di*-n-*butylthioboronite and Benzyl Cyanide with Phenyl Isocyanate.* The 1:1 complex obtained from *n*-butyl di-*n*-butylthioboronite (1.42 g) and benzyl cyanide (0.78 g) was stirred for 1 hr at room temperature under dry air. A solution of phenyl isocyanate (0.79 g) in 3 m*l* ether was then added all at once to the complex in the presence of a catalytic amount of boron trifluoride etherate at 0°C. After stirring for 10 hr at 0°C, the reaction mixture was dissolved in dry THF. The THF solution was added with vigorous stirring to the mixture of THF and pH 7 buffer (9.10 g, KH_2PO_4+18.90 g Na_2HPO_4/*l*). After stirring 3 hr at 25—30°C, the THF layer was separated and the water layer was extracted with ether three times. Both layers were combined and dried with sodium sulfate. The yellow oily substance obtained by evaporating the solvent *in vacuo* was crystallized in a small amount of petroleum ether at −78°C. The crystal was filtered. The filtrate was concentrated by evaporation and the residue was chromatographed on silica gel. From the elute of benzene a white crystal was obtained. Recrystallization from petroleum ether gave *N*-*n*-butylthiocarbonyl *N*-phenyl phenylacetamidine, 1.57 g (74%) mp 69.5—70.5°C.

The corresponding phenyl acetamidine derivatives were obtained in a similar way. The results are listed in Table 2.

Hydrolysis of N-n-*Butylthiocarbonyl* N-*Phenylacetamidine.* Dilute hydrochloric acid solution was added to a solution of *N*-*n*-butylthiocarbonyl *N*-phenyl phenylacetamidine (0.41 g) in THF at room temperature. After removal of the solvent, the acylurea was obtained as a white crystal (0.32 g). The yield of acylurea was quantitative.

In a similar way, various acylureas were obtained in quantitative yields. The results are listed in Table 3.

Ambident Ion. VI. Kinetical and Thermodynamical Control in the Acylation of β-Dicarbonyl Compounds. Acetylation of Benzoylacetone and Benzoylacetonate Anion

Masakazu SUAMA, Yukimichi NAKAO, and Katsuhiko ICHIKAWA

Department of Hydrocarbon Chemistry, Faculty of Engineering, Kyoto University, Yoshida, Kyoto

(Received May 11, 1971)

Kinetically as well as thermodynamically controlled steps have been established in acetylation of ambident ion. Acetylation of sodium benzoylacetonate in pyridine gave initially the kinetically controlled product (I) which isomerized gradually to the thermodynamically controlled (II). *C*-Acetylation product (III) was formed by the reaction of benzoylacetonate ion with *O*-acetylbenzoylacetones at higher temperatures. Comparison of the results in the acetylation of benzoylacetone with those of its sodium salt suggested that enolate anion was the reacting species in both processes of *O*- and *C*-acetylation. Isomerization between I and II was suppressed in α-picoline or 2,6-lutidine solution. Utilizing these results we have prepared three kinds of acetylated products I, II, and III readily in high selectivity.

Alkylation of enolate anions has been extensively studied, but not the acylation of enolates.[1-3]

In this paper we wish to report on the acetylation of benzoylacetone which shows a marked duality in the reaction process, *viz.*, kinetically controlled and thermodynamically controlled processes. Acetylation of the salts of benzoylacetone is expected to give two *O*-acetylated products (I) and (II) and one *C*-acetylated one (III) (Eq. 1). It was found that solvents effected the product distribution remarkably.

$$(PhCOCHCOCH_3)^-Na^+ + AcCl \longrightarrow \underset{\underset{OAc}{|}}{PhCOCH{=}C{-}CH_3} \quad (I)$$

$$+ \underset{\underset{OAc}{|}}{PhC{=}CHCOCH_3} \quad (II) \; + \; \underset{\underset{Ac}{|}}{PhCOCHCOCH_3} \quad (III) \qquad (1)$$

Solvent Effects on the Product Distribution in Acetylation of Sodium Benzoylacetonate. The results of the acetylation of sodium benzoylacetonate with acetyl chloride in several solvents are shown in Table 1.

Total yields including *O*- and *C*-acylated products in ether solvents increased in the order: ethyl ether< dimethoxyethane<diglyme. This suggests that the solvating power to Na^+ plays an important role.[4] The contents of III in the product decreased in the order: ether>dimethoxyethane>diglyme, and those of II increased in the reverse order. This suggests that *O*-acetylation is more favored when the reaction medium is more favorable for the dissociation of the sodium salt to enolate anion. Benzene is distinguished from the others in giving III as the major product. In *N,N*-dimethylformamide, no formation of *C*-acetylated product was detected and the ratio of I/II was 79/21, being much higher than the other cases at 0°C. The ratio, however, changed to 19/81 when acetylation was carried out at 50°C.

Table 1. Solvent effects on the product distribution in the acetylation of sodium benzoylacetonate

Solvent[a]	Reaction temp. °C	Time hr	Yield[b] %	Composition I%	II%	III%
Ether	38	24	31.0	18	45	37
DME	0	24	32.8	21	59	20
DGM	0	24	45.1	22	78	0
Benzene	12	24	26.2	4	6	90
DMF	0	24	32.9	79	21	0
DMF	50	24	26.3	19	81	0

a) DME: 1,2-dimethoxyethane; DGM: diethylene glycol dimethyl ether (diglyme).
b) Based on sodium salt.

Isomerization between the two *O*-acetylated compounds at a higher reaction temperature was confirmed experimentally as shown in Table 2. The same phenomenon was also realized in acetylation in pyridine as mentioned later.

Acetylation of Benzoylacetone and its Sodium Salt in Pyridine at 0°C (O-acetylation). It is well known that the acylation of β-dicarbonyl compounds in pyridine proceeds smoothly and gives *O*-acylation products exclusively, but the reaction mechanism is open to question.[5] By comparing the results in the acetylation of benzoylacetone with those of its sodium salt, the intervention of enolate anion as a reacting species was examined. Changes of the product compositions during the course of the reaction are shown in Figs. 1 and 2.

1) W. R. Gilkerson, W. J. Argersinger, Jr., and W. E. McEwen, *J. Amer. Chem. Soc.*, **76**, 41 (1954), and the references cited therein.
2) W. M. Muir, P. D. Ritchie, and D. J. Lyman, *J. Org. Chem.*, **31**, 3790 (1966), and the references cited therein.
3) M. Suama, Y. Murata, and K. Ichikawa, *Nippon Kagaku Zasshi*, **91**, 162, 168 (1970).
4) H. O. House, and V. Kramer, *J. Org. Chem.*, **27**, 4146 (1962).
5) McEwen *et al.* (*J. Amer. Chem. Soc.*, **76**, 41 (1954).) proposed a reaction mechanism through the intermediate (IV) which has been denied in Ref. 3.

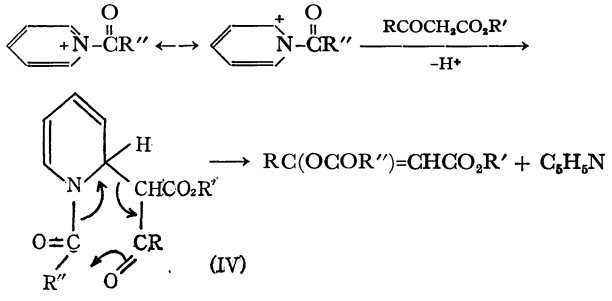

Table 2. Acetylation of sodium benzoylacetonate in DMF at 50°C

Reaction time hr	Yield %	Composition		
		I%	II%	III%
0.25	59	56	24	20
2.0	59	34	41	25

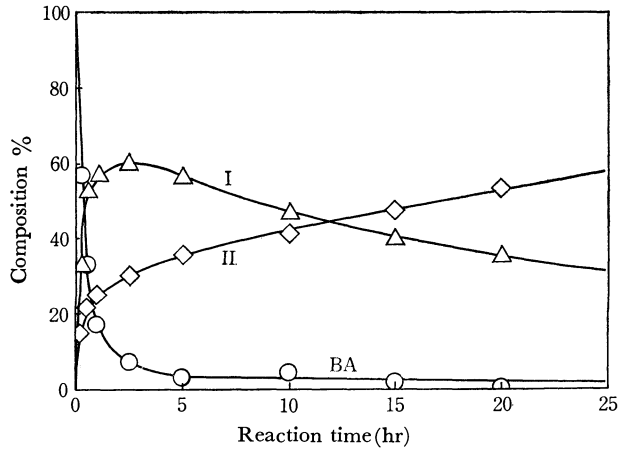

Fig. 1. Acetylation of benzoylacetone (BA) in pyridine at 0°C.

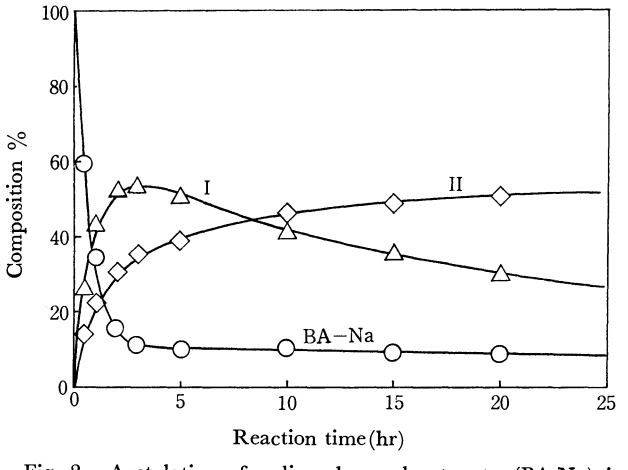

Fig. 2. Acetylation of sodium benzoylacetonate (BA-Na) in pyridine at 0°C.

In each case, acetylation was complete in about 2 hr, and afforded I and II nearly in quantitative yield and only a trace amount of III. Kinetic preference for the formation of I to II can be attributed to the steric hindrance of phenyl group, since no acetylation occurred in the case of dibenzoylmethane under the reaction conditions.

Figures 1 and 2 clearly show that the isomerization of I to II occurred. In the reactions of ambidents, these kinds of isomerization have scarcely been considered so far. However, our data indicate that it is necessary to distinguish the competitive reactions from the isomerization reactions in order to discuss the reactivity of two reaction sites.

Controlled experiments showed that the mutual isomerization between I and II occurred in pyridine and the equilibrium ratio of I to II was about 19/81 at 0°C. The results of the isomerization are shown in Figs. 3 and 4.

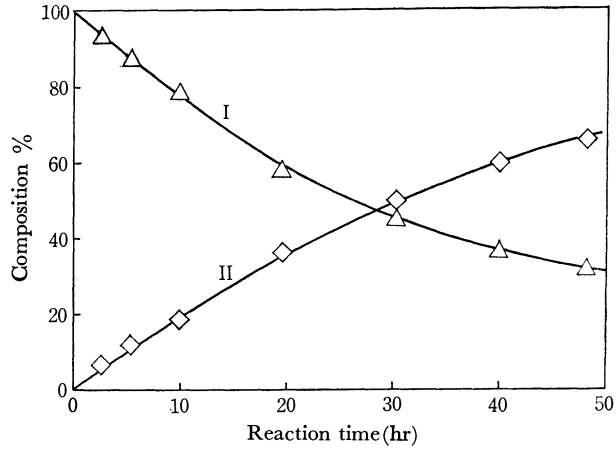

Fig. 3. Isomerization of I to II in pyridine at 0°C.

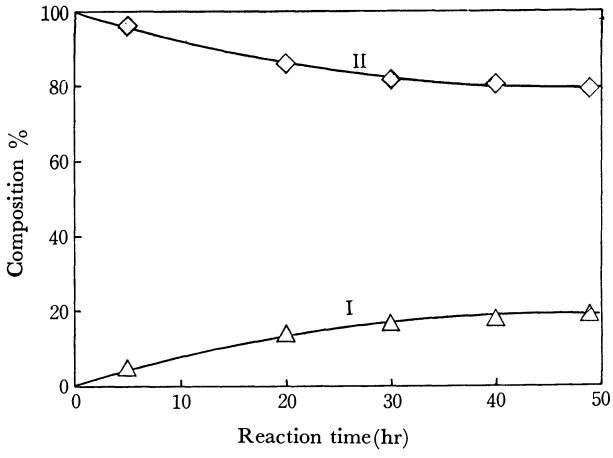

Fig. 4. Isomerization of II to I in pyridine at 0°C.

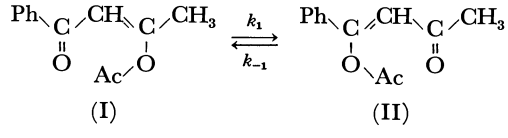

(I) (II)

Isomerization was of first order with respect to both I and II, and the pseudo-first order rate constants were $k_1=0.85\times10^{-5}\,\mathrm{sec}^{-1}$ and $k_{-1}=0.20\times10^{-5}\,\mathrm{sec}^{-1}$, respectively. Considering the absence of any other acylating agents and substrate except solvents in these experiments, the isomerization seems to be an intramolecular rearrangement caused by the assistance of pyridine base.

Under the reaction conditions of Figs. 1 and 2, the rate of isomerization was smaller than that of acetylation, and the effect of the isomerization can be neglected in the early period of the reaction. In the cases of benzoylacetone and its salt, *C*-acetylated product formation was a minor process and the relative ratios of I to II were about 2.0/1.0 in the early stage of the reactions.

The results and similarities in the composition patterns of Figs. 1 and 2 suggest that in the acetylation of benzoylacetone also, enolate anion is the reacting species which is formed by the deprotonation from benzoylacetone by the action of pyridine base. However, the direct acylation process of keto-enol tautomers by acetylpyridinium cation[3] is not yet

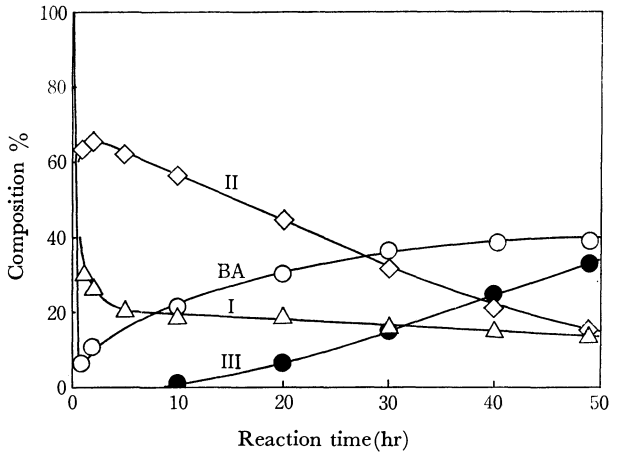

Fig. 5. Acetylation of benzoylacetone in pyridine at 50°C.

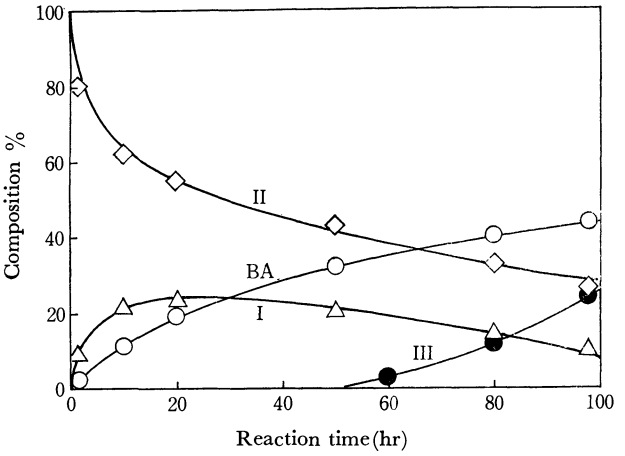

Fig. 6. Isomerization and decompsition of II in pyridine at 50°C.

completely excluded.

Acetylation of Benzoylacetone in Pyridine at 50°C (C-*Acetylated Benzoylacetone Formation).* When acetylation was carried out at 50°C, the composition of the reaction mixtures changed with reaction time as shown in Fig. 5.

During the course of the reaction, III was formed which was a minor product in the acetylation at 0°C as mentioned before. As shown in Fig. 6, when II was kept at 50°C in pyridine, III and benzoylacetone were formed, suggesting that the formation of III and benzoylacetone resulted from the isomerization and decomposition of II. Figures 5 and 6 indicate that the formation of benzoylacetone takes place before the formation of III. When an equimolar mixture of II and benzoylacetone were kept at 50°C in pyridine, formation of III was very slow. However, when sodium salt of benzoylacetone was used instead of benzoylacetone, the formation of III was favored. Consequently, in the process of *C*-acetylation the reacting species is also enolate anion.

Mutual Isomerizations between I and II in Methylpyridines. I and II isomerized mutually in pyridine at 0°C through first order kinetics. The isomerization in methylpyridines was also examined and the results are shown in Tables 3 and 4.

Introduction of methyl group into the 2- and/or

Table 3. Isomerization of I at 0°C in methylpyridines

Solvent	Reaction time hr	Composition			
		BA[a] %	I%	II%	III%
α-Picoline	53	2	89	6	3
γ-Picoline	53	9	25	66	0
2,6-Lutidine	53	1	92	7	0

a) BA: benzoylacetone

Table 4. Isomerization of II at 50°C in methylpyridnes

Solvent	Reaction time hr	Composition			
		BA%	I%	II%	III%
α-Picoline	53	2	13	85	0
γ-Picoline	53	41	10	9	40
2,6-Lutidine	47	0	12	82	0

6-position of pyridine nucleus suppressed the isomerization effectively, but the methyl group in 4-position showed no such inhibition. This indicates that steric bulkiness around the basic nitrogen atom is largely reflected upon the catalytic activity of pyridine base in the isomerization process. However, acetylation of benzoylacetone in α-picoline gave I selectively in high yield (70%) in the reaction at 0°C for 23 hr. Thus, the 2-methyl group which suppresses the isomerization does not effect the first step acetylation rate. The result is very useful for the preparation of I.

Conclusion

The reaction courses of acetylation of benzoylacetone and its sodium salt have been established as follows:

$$(PhCOCHCOCH_3)^-Na^+ + CH_3COCl \xrightarrow{\text{in ethers}} I + II + III$$

$$PhCOCH_2COCH_3 \overset{\text{pyridine}}{\rightleftharpoons} (PhCOCHCOCH_3)^- + \text{N-acetylpyridinium}$$

$$PhCOCH{=}C(OAc)CH_3\ (I) \quad \overset{\text{in pyridine, 0°C}}{\rightleftharpoons} \quad PhC(OAc){=}CHCOCH_3\ (II)$$

$$I \text{ and } II \xrightarrow{\text{pyridine, 50°C}} PhCOCH_2COCH_3 \overset{\text{pyridine, 50°C}}{\rightleftharpoons}$$

$$(PhCOCHCOCH_3)^- \xrightarrow[\text{pyridine, 50°C}]{\text{I or II}} PhCOCHCOCH_3 \quad (III)$$
$$\qquad\qquad\qquad\qquad\qquad\qquad\qquad\qquad\qquad\quad Ac$$

In the acetylation of sodium salt of benzoylacetone in ethers the dissociation into enolate anion favored *O*-acetylation, suggesting that enolate anion is a reacting species in the *O*-acetylation. By comparison of the acylation of benzoylacetone with that of sodium salt, the intervention of enolate anion is also probable in the *O*-acetylation of benzoylacetone itself. The formation of *C*-acetylation product in pyridine at a higher reaction temperature clearly shows that the

enolate anion is acylated by enol ester as pointed out by Muir *et al.*[2]

In the acetylation in pyridine, consecutive mutual isomerizations between I and II proceed even at 0°C. The isomerization is first order reaction with each enol ester I and II and seems to be intramolecular rearrangement reaction. The isomerization can be retarded by the introduction of methyl group into the 2- and/or 6-position of pyridine ring. At a higher temperature further isomerization into III occurred, being an intermolecular migration of acetyl group from the enol ester to enolate anion.

Selection of the reaction condition in the acetylation of benzoylacetone makes it possible to obtain three kinds of acetylated products I, II, and III selectively. Thus, in acetylation in pyridine at 50°C for more than 80 hr, III could be obtained in a selectivity of 83%. Futher, in the acetylation in α-picoline at 0°C, I was formed in 76% selectivity and II was obtained in the selectivity of 77% after a reaction at 0°C for 80 hr. Utilizing these reactions three kinds of acetylated products are readily prepared.

Experimental

Infrared spectra were recorded on a Hitachi EPI-G2. The ultraviolet absorption spectra were determined with a Hitachi EPS-3T spectrophotometer. Nuclear magnetic resonance spectra were recorded on Japan Electronic Optics JNM-3H-60 and JNM-MH-60 using tetramethylsilane as the internal standard in deuteriochloroform. Thin layer chromatography was carried out on silica gel G and developed with benzene or *n*-hexane-ethyl acetate mixtures (90: 10, and 80:20). The spots were detected by standing in an atmosphere of iodine.

Reagents. Benzoylacetone was prepared by the method of Claisen[6] and purified by vacuum distillation and recrystallization from *n*-hexane in 68% yield, bp 104—108°C/2—5mmHg (lit, 132/14 mmHg), mp 56.4—56.6°C (reported 60—61°C). The IR spectrum of the sample was identical with that of Sadtler's data No. 476K and No. 5437. Sodium salt of benzoylacetone was prepared by the reaction of benzoylacetone and sodium metal in dry ether under reflux in the presence of a catalytic amount of ethanol. The white powder precipitated was collected, washed with ether and dried *in vacuo*. Acetyl chloride was purified by distillation of GR grade reagent and stored under nitrogen in a sealed ampule, bp 51.2—51.4°C. Pyridine, α-picoline, γ-picoline, 2,6-lutidine, dimethylformamide, dimethoxyethane, and ethylene glycol dimethyl ether were purified by the procedures described previously.[3]

Analysis of the Composition of the Reaction Mixture. Because of the thermal instability of I, II, and III, glc method was very troublesome. We developed an electronic computer program which determined the concentration of each components by analyzing UV spectra of the reaction mixtures. Aliquots of the reaction mixture were diluted with methanol in order to stop the reaction. UV absorptions were measured and expressed in numerical absorptions in the wave length range 258—334 mμ in every milimicron and the concentration of each component was obtained by the program using computer HARP-5020. The accuracy of the concentration obtained by this method was ±5% in absolute values. It was confirmed that Lambert-Beer's law and the additivity of the absorptions of the components existing in the system holdand the absorptions of the other components except for those cited in Table 5 do not disturb the analysis in this range of concentrations.

Table 5. Ultraviolet absorption of each component

Compound	λ_{max}(mμ)	$\varepsilon_{max} \times 10^{-4}$
Benzoylacetone	309	1.51
	249	0.574
Sodium benzoylacetonate	309	1.05
	247	0.584
I	262	1.89
II	280	1.47
III	280	1.08
	252	1.50

Identification of Acetylated Products. 4-Phenyl-2-acetoxy-2-buten-4-one (I): 16.2 g of benzoylacetone (0.1 mol) was dissolved in 50 g of α-picoline in a flask equipped with a mechanical stirrer, dropping funnel, and a silica gel tube and cooled on an ice-water bath. Acetyl chloride 11.8 g (0.15 mole) was added in portions at a rate which kept the reaction temperature below 4°C. The progress of the reaction was checked by UV spectrum during a period of 10 hr. The reaction mixture was poured into dilute hydrochloric acid. and the neutralized mixture was extracted with ether. After the usual work-up an oily product was obtained which afforded yellow crystals on cooling at −20°C. The crystals were collected and recrystallized from petroleum ether to yield 3.6 g of I, mp 32.5—33.0°C, bp 108—117°C/0.5 mmHg. Found: C, 70.77; H, 5.85%. Calcd for $C_{12}H_{12}O_3$: C, 70.57; H, 5.92%. IR (KBr) 1750 (s, $\nu_{C=O}$ enol ester), 1680 (s, $\nu_{C=O}$ benzoyl), 1630 (s, $\nu_{C=C}$), 1450, 1380 (m, δCH_3), 1230, 1147 (vs, ν_{C-O} ester), 780, and 710 cm^{-1} (s, phenyl). NMR ($CDCl_3$) τ 7.76 (s, 3H, acetoxy), 7.57 (d, 3H, J=1.1 Hz, $-CH=C(OAc)C\underline{H}_3$), 3.17 (q, 1H, J=1.1 Hz, vinyl proton), and 2.0—2.8 (m, 5H, ArH). UV λ_{max}^{MeOH}=281 mμ (ε=1.55×10^4).

1-Phenyl-1-acetoxy-1-buten-3-one (II): The acetylation of benzoylacetone was carried out in pyridine at 0°C for 24 hr. After a similar working-up as above, the oily product was separated into I and II by means of column chromatography (Wakogel C-200, 30φ×420, elutant: benzene and then ethyl acetate). Recrystallization of crude solid from petroleum ether afforded colorless crystals II mp 38.2—38.5°C, bp 119—123°C/0.5 mmHg. Found: C, 70.73; H, 5.93%. Calcd for $C_{12}H_{12}O_3$: C, 70.57; H, 5.92%. IR (KBr) 1770 (s, $\nu_{C=O}$ enol ester), 1690 (s, $\nu_{C=O}$ acetyl), 1600 (s, $\nu_{C=C}$), 1450, 1362 (m, δCH_3), 1200, 1160 (vs, ν_{C-O} ester), 765, and 690 cm^{-1} (s, phenyl). NMR ($CDCl_3$) τ 7.75 (s, 3H, acetoxy) 7.65 (s, 3H, acetyl), 3.48 (s, 1H, vinyl proton), 2.0—2.6 (m, 5H, ArH). UV λ_{max}^{MeOH}=262 mμ (ε=1.98×10^4).

ω,ω-Diacetylacetophenone (III): III was prepared by the Schotten-Baumann reaction[7] and purified by vacuum distillation and recrystallization from methanol or petroleum ether in a yield of 42%, mp 28.9—29.4°C (reported 35.0°C), bp 132—135°C/5 mmHg. Found: C, 70.80; H, 5.93%. Calcd for $C_{12}H_{12}O_3$: C, 70.57; H, 5.92%. IR (KBr) 1655 (*vs*, $\nu_{C=O}$ intramolecular H-bonded), 1590 (s, $\nu_{C=C}$ enol form), 1450, 1360 (m, δCH_3), 730, and 700 cm^{-1} (s, phenyl). NMR ($CDCl_3$) τ 7.92 (s, 6H, two acetyl), 1.8—2.6

6) L. Claisen, *Ber.*, **38**, 695 (1905).

7) L. Claisen, *Ann.*, **291**, 63 (1896).

(m, 5H, ArH), −7.20 (broad s, 0.8H, enol OH). UV λ_{max}^{MeOH} =253 mμ ($\varepsilon=1.59\times10^4$), and 280 mμ ($1.08\times10^4$).

I and II could be decisively identified by means of NMR—the presence of fine long-range coupling between methyl and vinyl ptotons of $-C\underline{H}=C(OAc)C\underline{H}_3$ in I. Purity of the samples could be readily determined by taking advantage of the signals of vinyl protons.

Acetylation of Sodium Benzoylacetonate. The sodium salt (20 mmol) was dissolved in 50 g of solvent and acetyl chloride (22 mmol) was added under cooling when necessary. A similar treatment of the reaction mixture as mentioned above gave an oily product which was analyzed by glpc (OV-17 5%, 2m, 130°C) with *trans*-stilbene as an internal standard. Besides the glpc analysis, UV technique was also applied directly to the reaction mixture.

Acetylation of Benzoylacetone and Sodium Benzoylacetonate in Pyridine at 0°C. 11.8 g of acetyl chloride (0.15 mol) was added to 35.0 g of pyridine under stirring on an ice-water bath. Pyridine (15.0 g) solution of benzoylacetone 16.2 g (0.10 mol) was added into the suspension of acetylpyridinium chloride in pyridine and aliquots were analyzed by means of UV technique. Acetylation of sodium benzoylacetonate at 0°C was carried out in a similar way.

Acetylation of Benzoylacetone and its Sodium Salt in Pyridine at 50°C. Acetyl chloride (0.15 mol) was added to pyridine (50g) solution of benzoylacetone sodium salt (0.10 mol) at 50°C. Previous addition of acetyl chloride as mentioned above in the experiments at 0°C failed to give rise to reproducibility of the results.

Acetylation of Benzoylacetone in α-Picoline at 0° and 50°C. The procedure is described in the preparation of I. The change of composition was followed by means of UV technique. In the reaction at 0°C, the ratios of I/II were constant (4.8± 0.4) all through the reaction for 8 hr up to 90% conversion. In the reaction at 50°C, acylation was complete in 0.5 hr (cf. at 0°C, 75% conversion after the reaction for 2 hr) but slow isomerization of I to II was observed.

Isomerization between I and II in Pyridine at 0°C. Ca. 1g of pyridine solution of I or II (0.1—2.0 mol/*l*) was kept at 0°C and aliquots were analyzed by means of UV technique at proper time intervals. The changes of composition are shown in Figs. 3 and 4. The plot of $\ln[([I]_0-[I]_e)/([I]-[I]_e)]$ *vs.* reaction time gave a common straight line through the origin over the range of twenty times initial concentration of I or II. From the slope of the straight line (1.05×10^{-5} sec^{-1}) and the equilibrium ratio of I to II (19/81), k_1 (0.85×10^{-5}) and k_{-1}(0.20×10^{-5} sec^{-1}) were obtained.

Isomerization between I and II in Methylpyridines. Ca. 180 mg of methylpyridine solution of I or II (2.0 mol/*l*) was kept at 0 or 50°C and aliquots were analyzed in a similar way. Isomerization was also examined in DMF, dimethoxyethane, diglyme, acetonitrile, and benzene at 50°C but no isomerization was detected. In triethylamine, however, II isomerized to a mixture after the reaction at 50°C for 47 hr, whose composition was benzoylacetone 31, I 18, II 43, and III 8%.

BULLETIN OF THE CHEMICAL SOCIETY OF JAPAN, VOL. 44, 2815—2820 (1971)

Studies of Thioiminocarbonates. I. The Formation and Decomposition of *O*-Alkyl *S*-Aryl Thioiminocarbonates in the Reaction of Aryl Thiocyanates with Alcohols in the Presence of the Cyanide Ion[1)]

Kazuhiko TANAKA, Jun-ichi HAYAMI, and Aritsune KAJI

Department of Chemistry, Faculty of Science, Kyoto University, Sakyo-ku, Kyoto

(Received May 17, 1971)

The reactions of aryl thiocyanates (I) with alcohol in the presence of cyanide ion were found to give alkyl aryl sulfides (III). The intermediate was isolated in the case of *p*-tolyl thiocyanate with methanol at 0°C and was determined to be *O*-methyl *S*-*p*-tolyl thioiminocarbonate (IIa) on the basis of NMR and IR spectral studies. The treatment of IIa with the cyanide ion afforded methyl *p*-tolyl sulfide (IIIa) in a high yield. When a mixture of an equimolecular amount of *O*-methyl *S*-*p*-tolyl thioiminocarbonate (IIa) and *O*-ethyl *S*-*p*-chlorophenyl thioiminocarbonate (IId) was treated with sodium cyanide in ethanol, all the anticipated sulfides——methyl *p*-tolyl sulfide (IIIa), *p*-tolyl sulfide (IIIb), methyl *p*-chlorophenyl sulfide (IIIc) and ethyl *p*-chlorophenyl sulfide (IIId)——were isolated. The mechanistic route, which involves the addition of alcohol to aryl thiocyanate, and the dissociation of the resulting *O*-alkyl *S*-aryl thioiminocarbonate (II) into aryl mercaptide ion and aryl cyanate, was proposed.

In the course of the work on the desulfurization of disulfides with the cyanide ion,[2)] an interesting reaction was observed. When bis(2-chloro-5-nitrophenyl) disulfide was treated with potassium cyanide in methanol, methyl 2-chloro-5-nitrophenyl sulfide was isolated (Eq. (1)):

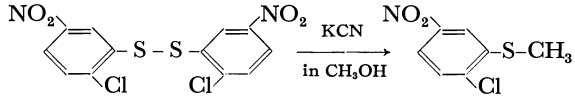

(1)

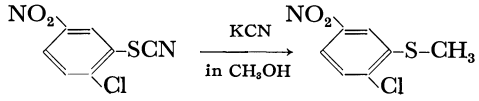

(2)

1) Presented at the 22nd Annual Meeting of the Chemical Society of Japan, Tokyo, April, 1969.

2) To be published elsewhere.

Methyl 2-chloro-5-nitrophenyl sufide was also obtained in the reaction of 2-chloro-5-nitrophenyl thiocyanate with potassium cyanide under the same reaction conditions (Eq. (2)). The formation of alkyl aryl sulfide was ascribed to the reaction of aryl thiocyanate, which is the intermediate postulated for the desulfurization of diaryl disulfide by the cyanide ion.[2)]

The present study was undertaken in order to clarify the reaction mechanism of the formation of sulfide and to isolate the intermediate formed when aryl thiocyanate is treated with alcohol in the presence of the cyanide ion.

Results and Discussion

Formation of Alkyl Aryl Sulfides in the Reaction of Aryl Thiocyanates with Alcohols in the Presence of the Cyanide Ion. When aryl thiocyanate was treated with alcohol in the presence of an equimolecular amount of sodium (or potassium) cyanide, alkyl aryl sulfide was easily obtained in a fairly good yield. The results are summarized in Table 1. In order to examine the general application of this novel reaction, we attempted to prepare benzyl and *n*-butyl aryl sulfide by the same procedure. However, sodium cyanide and potassium cyanide were only slightly soluble in these alcohols. This was overcome by using dimethyl sulfoxide as the solvent or by using tetraethylammonium cyanide as the cyanide-ion precursor in acetonitrile. Thus, benzyl *p*-tolyl sulfide was obtained in a 68% yield in the reaction of *p*-tolyl thiocyanate with benzyl alcohol in the presence of sodium cyanide in DMSO, and *n*-butyl *p*-tolyl sulfide was obtained in a 59% yield by using tetraethylammonium cyanide in a mixture of

TABLE 1. FORMATION OF ALKYL ARYL SULFIDES IN THE REACTION OF ARYL THIOCYANATES WITH ALCOHOLS IN THE PRESENCE OF CYANIDE ION

I III

Aryl thiocyanate 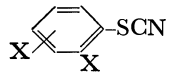 X	Alcohol[a)] ROH R	Cyanide Ion	React. temp. (°C)	React. time (hr)	Product[b)] 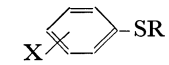 (%)
p-Me–N	Me	NaCN	60	3	50
o-Me	Me	NaCN	50	3	59
m-Me	Me	NaCN	50	3	50
p-Me	Me	NaCN	50	3	55
p-Me	Me	NaCN (2 eq. exess)	50	3	58
p-Me	Me	NaCN	0, 50[c)]	0.5, 3[c)]	66
p-Me	*n*-Bu	Et_4NCN (in CH_3CN)[d)]	r.t.	21	59
p-Me	*n*-Bu	NaCN (in DMSO)[d)]	r.t.	22	60
p-Me	Me	NaCN	50	24	78
p-Me	Bz[e)]	NaCN (in DMSO)[d)]	50	20	68
H	Me	NaCN	r.t.	3	51
o-Cl	Et	NaCN	r.t.	5	47
o-Cl	*n*-Pr	NaCN	50	4	29
o-Cl	*n*-Pr	NaCN (in DMSO)[d)]	50	5	50
o-Cl	*i*-Pr	NaCN (in DMSO)[d)]	50	5	34
m-Cl	Me	NaCN	r.t.	3	61
p-Cl	Me	NaCN	50	1	59
p-Br	Me	NaCN	r.t.	5	59
p-SCN	Me	NaCN (2 eq. exess)	50	4	37
o-NO_2	Me	NaCN	45	1	70
o-NO_2	Et	NaCN	50	2	36
m-NO_2	Me	NaCN	r.t.	0.5	66
m-NO_2	Et	NaCN	r.t.	1	50
p-NO_2	Me	NaCN	50	2	70
2-Cl-5-NO_2	Me	KCN	reflux	4	48
2-NO_2-4-Cl	Et	NaCN	50	4	27

a) Alcohol was used as solvent
b) Isolated yield
c) 0.5 hr at 0°C, then 3 hr at 50°C
d) Mixture of alcohol and DMSO or CH_3CN
e) Benzyl

Table 2. Formation of alkyl aryl sulfides in the reaction of *O*-alkyl *S*-aryl thioiminocarbonates with bases

II	Solvent	Base	React. temp. (°C)	React. time (hr)	Yield of Sulfide (%)
IIa	MeOH	NaCN	50	3	IIIa (55)
IIa	DMSO	NaCN	r.t.	5	IIIa (81)
IIb	EtOH	IR-45[a)]	60	12	IIIb (53)
IIb	EtOH	b	reflux	7.5	c

a) Weak basic ion-exchange resin Amberlite IR-45 (OH-form)
b) Without base
c) 87% of starting material (IIb) was recovered unchanged.

Table 3. Formation of alkyl aryl sulfides in the reaction of *O*-alkyl *S*-aryl thioiminocarbonates with cyanide ion

II	Cyanide Ion	Solvent	Reaction Condition		Yield of Sulfide	
			Temp. (°C)	Time (hr)	IIIa	IIb
IIa (0.05 mol)	NaCN (0.05 mol)	EtOH (200 m*l*)	50	3	67% (100)	0% (0)
IIb (0.05 mol)	NaCN (0.05 mol)	MeOH (200 m*l*)	50	3	7% (90)	64% (10)

n-butyl alcohol (20 m*l*) and acetonitrile (50 m*l*).

Ross[3)] reported the formation of ethyl phenyl sulfide in the reaction of phenyl thiocyanate and sodium ethoxide in ethanol; he proposed the following pathway:

$$2PhSCN + 2EtONa \longrightarrow PhSNa + EtOCN + PhS\text{-}O\text{-}Et \quad (3)$$

$$PhS\text{-}O\text{-}Et \xrightarrow{O} PhSEt \quad (4)$$

(PhSEt with O)

$$PhSEt + 2PhSH \longrightarrow PhSEt + PhSSPh + H_2O \quad (5)$$

(PhSEt with O)

However, he reported that ethyl phenyl sulfide was not obtained in the reaction of ethyl benzenesulfenate and thiophenol in ethanol containing sodium ethoxide. This result shows that sulfenate is not the intermediate. Recently, Mislow *et al.*[4)] reported that methyl *p*-toluenesulfenate does not rearrange to methyl *p*-tolyl sulfoxide. Thus, there remains much doubt about the pathway in Eqs. (3)—(5).

When *p*-tolyl thiocyanate was treated with sodium cyanide in methanol at 0°C, methyl *p*-tolyl sulfide (38%) and a pale yellow oil (2.1 g) were obtained. This oil showed a strong infrared band at 1634 cm^{-1} (C=N) and a weak band at 3360 cm^{-1} (NH), and the NMR peaks at τ 6.40 (OCH_3) and at τ 3.45 (NH), in accordance with the expected formation of *O*-methyl *S*-*p*-tolyl thioiminocarbonate (IIa) as the intermediate.

The *O*-alkyl *S*-aryl thioiminocarbonates (II) were synthesized independently by the following procedure, similar to that reported by Knorr.[5)] The results are reported in Table 5.

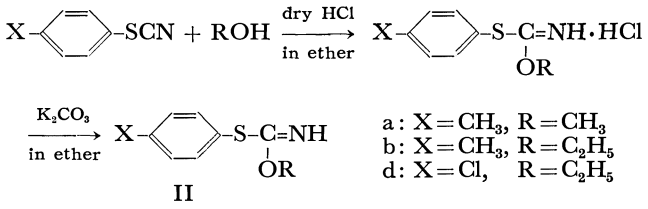

Scheme 1

Formation of Alkyl Aryl Sulfides from O-*Alkyl* S-*Aryl Thioiminocarbonates.* *O*-Alkyl *S*-aryl thioiminocarbonates (II) were treated with sodium cyanide in alcohol. In all the cases studied, alkyl aryl sulfide (III) was isolated in a fairly good yield. In DMSO, IIIa was obtained in an 81% yield, since the basicity of the cyanide ion and the nucleophilicity of the mercaptide ion were enhanced in dipolar aprotic solvents.[6)] The results are reported in Table 2.

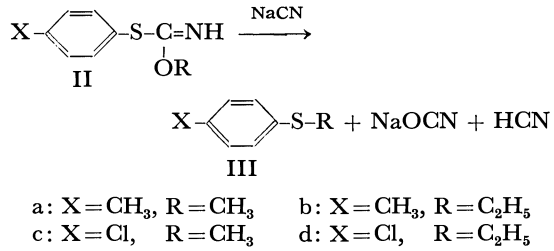

Scheme 2

The reaction of IIa with sodium cyanide in ethanol afforded IIIa exclusively, while the reaction of IIb in methanol gave a mixture of sulfides, which were shown by glc to be IIIb (64%) and IIIa (7%). These results show that the alkyl moiety of III was derived from that of II, not from the alcohol used as a solvent.

3) J. Ross, *J. Amer. Chem. Soc.*, **56**, 727 (1934).
4) E. G. Miller, D. R. Rayner, and K. Mislow, *ibid.*, **88**, 3139 (1966).
5) A. Knorr, *Ber.*, **49**, 1735 (1916).
6) A. J. Parker, "Advances in Organic Chemistry, Methods and Results," Vol. 5, ed. by R. A. Raphael, E. C. Taylor and H. Wynberg, Interscience Publishers, New York, N. Y. (1965), p.l.

TABLE 4. THE ANALYTICAL DATA AND PHYSICAL CONSTANTS OF ALKYL ARYL SULFIDES

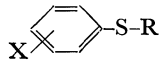

X	R	Mp (°C) (Bp °C/mmHg)	Analysis % Found (Calcd) C	H	N	S	Cl
p-Me_2N	Me	(115/3)	64.39 (64.42)	7.95 (7.83)	8.53 (8.37)	18.89 (19.17)	
p-CH_3	*n*-Bu	(142/27)	73.03 (73.30)	8.86 (8.95)		17.47 (17.75)	
p-CH_3	Bz	42—43	78.15 (78.45)	6.67 (6.58)		15.16 (14.96)	
o-Cl	Et	(123/18)	55.91 (55.64)	5.53 (5.25)		18.63 (18.57)	20.75 (20.53)
o-Cl	*n*-Pr	(135/18)	57.89 (57.90)	6.10 (5.94)		17.21 (17.17)	18.77 (18.99)
o-Cl	*i*-Pr	(130/22)	58.13 (57.90)	5.95 (5.94)		17.33 (17.17)	19.11 (18.99)
m-Cl	Et	(118/18)	55.39 (55.64)	5.16 (5.25)		18.36 (18.57)	20.82 (20.53)
o-NO_2	Me	60—61	49.73 (49.69)	4.10 (4.17)	8.38 (8.28)	18.97 (18.95)	
p-NO_2	Me	69—70	49.62 (49.69)	4.11 (4.17)	8.51 (8.28)	18.83 (18.95)	
2-Cl-5-NO_2	Me	97—99	40.98 (41.28)	2.87 (2.97)	6.92 (6.88)	15.83 (15.74)	17.39 (17.42)
2-NO_2-4-Cl	Et	95—96	44.41 (44.14)	3.64 (3.70)	6.53 (6.44)	15.01 (14.73)	16.46 (16.29)

This was also confirmed by the reaction of IIa with sodium cyanide in DMSO, which gave IIIa exclusively and in a high yield (Table 3).

Crossover Experiment with O-Alkyl S-Aryl Thioiminocarbonates. In order to find a clue to the mechanism of the formation of alkyl aryl sulfide (III) from *O*-alkyl *S*-aryl thioiminocarbonate (II), a crossover experiment using a mixture of *O*-methyl *S*-*p*-tolyl thioiminocarbonate (IIa) and *O*-ethyl *S*-*p*-chlorophenyl thioiminocarbonate (IId) was made. The mixture of IIa and IId was treated with sodium cyanide in ethanol, and the resulting mixture of sulfides was analyzed by glc. All four sulfides, *i.e.*, IIIa (23.8 mol%), IIIb (9.7 mol%), IIIc (22.8 mol%), and IIId (43.7 mol%), were found in the reaction mixture. Since IIa underwent no ester exchange with the ethanol used as the solvent, the ethyl moiety in IIIb is probably derived from that of IId.

On the basis of the observations presented earlier, we propose a following mechanism involving the dissociation of II into the aryl mercaptide ion and alkyl cyanate for the formation of sulfide:

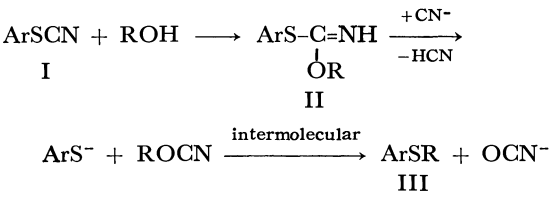

Scheme 3

Direct evidence for the existence of aryl mercaptide was obtained by the reaction of IIa with sodium cyanide in the presence of 2,4-dinitro-chlorobenzene, which is known to be a good mercaptide ion scavenger.[7] Thus the reaction of IIa (0.05 mol) with sodium cyanide (0.05 mol) in the presence of 2,4-dinitro-chlorobenzene (0.05 mol) in methanol afforded 2,4-dinitrophenyl *p*-tolyl sulfide in a 24% yield.

Kinetic studies of the formation and the decomposition of II will be reported in forthcoming papers.

Experimental

The melting points are uncorrected; the glc analyses were carried out with a Yanagimoto GCG-5DH chromatograph (Silicone DC-550, 190°) and with a Hitachi-Perkin-Elmer F-6D chromatograph (BDS-15 capillary column, 110°). The IR spectra were recorded on Nippon Bunko IR-S and DS-402G spectraphotometers. The NMR spectra were obtained on a Nihon-Denshi JNM 3H-60 spectrometer.

Reaction of Bis(2-chloro-5-nitrophenyl) Disulfide with Potassium Cyanide in Methanol. A solution of bis(2-chloro-5-nitrophenyl) disulfide (4.7 g, 0.0125 mol) and potassium cyanide (1 g, 0.0154 mol) in 200 m*l* of methanol was stirred for 4 hr under reflux. The precipitates were then removed by filtration, and water was added to the filtrate. The resulting yellow solid was separated by filtration; subsequent recrystallization from methanol gave 2 g of pale yellow needles (87%); mp 98—99°C; NMR ($CDCl_3$): τ 7.45 (SCH_3).

Found: C, 41.19; H, 2.90; N, 6.99; S, 15.76; Cl, 17.65%. Calcd for $C_7H_6NO_2SCl$: C, 41.28; H, 2.97; N, 6.88; S, 15.74; Cl, 17.42%.

Aryl Thiocyanates. Aryl thiocyanates (I) were prepared by the Sandmeyer reaction of the corresponding anilines.[8]

Formation of Alkyl Aryl Sulfides from Aryl Thiocyanates. General Procedure: Into a mixture of aryl thiocyanate (I, 0.05 mol) and alcohol (200 m*l*), powdered sodium cyanide

7) R. W. Bost, J. O. Turner, and R. D. Norton, *J. Amer. Chem. Soc.*, **54**, 1985 (1932).

Table 5. Preparations and physical properties *O*-alkyl *S*-aryl thioiminocarbonates

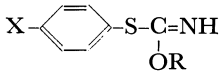

II	X	R	Yield (%)	BP °C/mmHg	Analysis C%	Found H%	(Calcd) N%
IIa	CH_3	CH_3	49	103—106/3	59.89 (59.64)	6.28 (6.12)	7.93 (7.73)
IIb	CH_3	C_2H_5	52	112—114/3	61.60 (61.50)	6.81 (6.71)	7.30 (7.17)
IId	Cl	C_2H_5	35	125—128/5	50.27 (50.11)	4.75 (4.67)	6.28 (6.49)

Table 6. Proton chemical schift τ of *O*-alkyl *S*-aryl thioiminocarbonates
(Solvent: CCl_4; internal standard: TMS)

II	(CH_3–CH_2–O–) CH_3–	(CH_3–CH_2–O–) –CH_2–	(CH_3O–)	(C=NH)	(CH_3Ph)	(aromatic)
IIa			6.40s	3.45s	7.75s	3.10m
IIb	8.72t	5.80q		3.20s	7.66s	2.72m
IId	8.74t	5.80q		3.18s		2.62m

Table 7. Infrared frequencies (cm^{-1}) of *O*-alkyl *S*-aryl thioiminocarbonates

II:	cm^{-1}								
IIa:	3360m,	2970m,	1634vs,	1433s,	1265vs,	1230vs,	1060vs,	930m,	813s
IIb:	3320m,	2980s,	1628vs,	1495m,	1260vs,	1228vs,	1060vs,	1015m,	810s
IId:	3350m,	3000m,	1636vs,	1482s,	1260vs,	1227vs,	1095s,	1013s,	823s

or potassium cyanide (0.05 mol) was stirred. After stirring had been continued for an appropriate period (see Table 1), the sodium (potassium) cyanate was removed by filtration. The filtrate and alcoholic washing were then combined, after which the usual work-up afforded alkyl aryl sulfide.

Preparation of O-*Alkyl* S-*Aryl Thioiminocarbonates. General Procedure*: Into a mixture of aryl thiocyanate (I, 0.134 mol) and absolute alcohol (0.134 mol), a stream of dry hydrogen chloride was introduced at 0°C. After the solution had been solidified, dry ether was added and the pale yellow solid of *O*-alkyl *S*-aryl thioiminocarbonate hydrochloride was pulverized and filtered. The dry hydrochloride was suspended in ether, and an aqueous solution of potassium carbonate was stirred in at 0°C. The ethereal layer was separated and dried with anhydrous sodium sulfate. Distillation *in vacuo* gave II as a transparent liquid. The physical constants and analytical data of II are reported in Table 5, Table 6, and Table 7.

Isolation of the Intermediate in the Reaction of p-*Tolyl Thiocyanate with Sodium Cyanide in Methanol.* Into a mixture of Ia (7.5 g, 0.05 mol) and absolute methanol (170 m*l*), powdered sodium cyanide (2.5 g, 0.05 mol) was stirred. After the stirring had been continued for 1 hr at 0°C, the solution was filtered. The filtrate was concentrated under reduced pressure, and the residue was extracted with ether. The ethereal solution was washed with a saturated aqueous solution of sodium chloride and dried with anhydrous sodium sulfate. Distillation under reduced pressure gave 2.6 g of IIIa (38%) and a pale yellow oil (2.1 g); IR: 3360 cm^{-1} (NH) and 1634 cm^{-1} (C=N).

NMR (TMS): τ 3.20 (aromatic), τ 3.40 (NH), τ 6.40 (OCH_3) and τ 7.83 (CH_3). This oil was identified as IIa.

Formation of Alkyl Aryl Sulfides from O-*Alkyl* S-*Aryl Thioiminocarbonates.* Into a solution of IIa (9.1 g, 0.05 mol) in absolute methanol (200 m*l*), powdered sodium cyanide (2.5 g, 0.05 mol) was added. After stirring had then been continued for 3 hr at 50°C, the precipitated sodium cyanate (1.6 g) was removed by filtration. The filtrate was concentrated under reduced pressure, and the residue was extracted with ether. The distillation of the dried ethereal solution gave IIIa in 55% yield; bp 100—102°C/20 mmHg (lit,[9] bp 104—105°C/20 mmHg). NMR (TMS): τ 3.33 (aromatic), τ 7.80 (S–CH_3) and τ 7.88 (CH_3).

In an analogous way, IIa in ethanol gave 4.6 g of IIIa, while IIb in methanol afforded IIIa and IIIb (90:10) by glc.

Crossover Experiment between O-*Methyl* S-p-*tolyl Thioiminocarbonate (IIa) and* O-*Ethyl* S-p-*Chlorophenyl Thioiminocarbonate (IId).* Sodium cyanide (1.5 g, 0.03 mol) was added to a solution of IIa (2.7 g, 0.015 mol) and IId (3.2 g, 0.015 mol) in absolute ethanol (130 m*l*). After stirring for 3 hr at 50°C, the work-up gave an oil which was found by glc analysis to be a mixture of IIIa (23.8 mol%), IIIb (9.7 mol%), IIIc (22.8 mol%), and IIId (43.7 mol%).

Isolation of 2,4-Dinitrophenyl p-*Tolyl Sulfide.* Into a

8) a) L. Gattermann and W. Haussknecht, *Ber.*, **23**, 738 (1890). b) G. Thurnauer, *ibid.*, **23**, 769 (1890). c) F. Challenger and A. D. Collins, *J. Chem. Soc.*, **125**, 1377 (1924). d) J. W. Dienske, *Rec. Trav. Chim. Pays-Bas*, **50**, 21 (1931). e) F. Challenger, C. Higginbottom, and A. Huntington, *J. Chem. Soc.*, **1930**, 26. f) A. Hantzsch and B. Hirsch, *Ber.*, **29**, 947 (1896). g) K. Brand and H. W. Leyerzapf, *ibid.*, **70**, 284 (1937).

9) H. Gilman and N. J. Beaber, *J. Amer. Chem. Soc.*, **47**, 1449 (1925).

mixture of IIa (9.1 g, 0.05 mol) and 2,4-dinitro-chlorobenzene (10.1 g; 0.05 mol) in absolute methanol (200 m*l*), powdered sodium cyanide (2.5 g, 0.05 mol) was stirred. After stirring had been continued for 3 hr at 50°C, the solution was concentrated under reduced pressure; the residue was then recrystallized from ethanol to afford 3.5 g (24%) of 2,4-dinitrophenyl *p*-tolyl sulfide as yellow needles; mp 102—103°C (lit,[5] mp 103°C).

The authors wish to acknowledge the enthusiastic assistance of Mr. Masao Nishikuri in carrying out this work.

BULLETIN OF THE CHEMICAL SOCIETY OF JAPAN, VOL. 44, 2820—2823 (1971)

Preparation of *p*-Toluenesulfonyl Derivatives of *myo*-Inositol

Tetsuo SUAMI, Seiichiro OGAWA, and Shuichi OKI

Department of Applied Chemistry, Faculty of Engineering, Keio University, Koganei-shi, Tokyo

(Received May 18, 1971)

Six *p*-toluenesulfonyl esters of *myo*-inositol, five of which are new, have been prepared by a selective sulfonylation of *myo*-inositol derivatives and the structures of the new compounds were established by means of their proton magnetic resonance (PMR) spectra and the reaction sequences. Preparation of 1,3-di-*O*-*p*-toluenesulfonyl-*myo*-inositol, an useful intermediary compound for synthesizing *myo*-inosadiamine-1,3, has been improved by the present method.

In the preceding paper,[1] we described the preparations of *p*-toluenesulfonyl esters of *myo*-inositol by selective sulfonylation of 1,2-*O*-cyclohexylidene-*myo*-inositol. In this paper, we wish to report the alternative synthetic route to its positional isomers. Six *p*-toluenesulfonyl esters (1,3-, 1,3,4- 1,3,5-, 1,3,4,5-, 1,3,4,6- and 1,3,4,5,6-) have been prepared by selective sulfonylation of *myo*-inositol derivatives. The structures of the new compounds were confirmed by the PMR spectra of their acetyl derivatives or the reaction sequences. Preparation of 1,3-di-*O*-*p*-toluenesulfonyl-*myo*-inositol,[2] an important intermediary compound for *myo*-inosadiamine-1,3,[3] has been much improved by the present method.

Treatment of 4,5,6-tri-*O*-acetyl-1,2-*O*-cyclohexylidene-3-*O*-*p*-toluenesulfonyl-*myo*-inositol (**1a**)[1] with boiling 80% aqueous acetic acid resulted removal of cyclohexylidene group to give 4,5,6-tri-*O*-acetyl-1-*O*-*p*-toluenesulfonyl-*myo*-inositol (**2a**) in 68% yield. One of the two hydroxyl groups in **2a** was expected to be selectively esterified by *p*-toluenesulfonyl chloride, since they are in an axial and an equatorial orientation, respectively.[4] When **2a** was treated with 2 molar equivalents of *p*-toluenesulfonyl chloride in dry pyridine at 30°C for 4 days, 4,5,6-tri-*O*-acetyl-1,3-di-*O*-*p*-toluenesulfonyl-*myo*-inositol (**3a**) was obtained as a sole product in 88% yield. The structure of **3a** was established by converting it into the known tetraacetyl derivative (**4a**)[2] by the usual manner. Therefore, the equatorial hydroxyl group on C-3 was shown to be selectively esterified. While the axial hydroxyl group on C-2 was found to be extremely unreactive due to being highly sterically hindered by the two vicinal *p*-toluenesulfonyloxy groups in *cis* relationship. Even when the reaction of **2a** with an excess amount of *p*-toluenesulfonyl chloride was carried out over 100°C for prolonged periods, a formation of the tri-ester could not be detected by a thin layer chromatography (tlc).

Similarly, 5,6-di-*O*-acetyl-1,4-di-*O*-*p*-toluenesulfonyl-*myo*-inositol (**2b**) was obtained in 86% yield from 4,5-di-*O*-acetyl-1,2-*O*-cyclohexylidene-3,6-di-*O*-*p*-toluenesulfonyl-*myo*-inositol (**1b**)[1] by refluxing in aqueous acetic acid. Treatment of **2b** with 3 molar equivalents of *p*-toluenesulfonyl chloride gave 5,6-di-*O*-acetyl-1,3,4-tri-*O*-*p*-toluenesulfonyl-*myo*-inositol (**3b**) selectively in 90% yield. Compound **3b** was also obtained from 4,5-di-*O*-acetyl-1,6-di-*O*-*p*-toluenesulfonyl-*myo*-inositol (**2c**) which was derived from 5,6-di-*O*-acetyl-1,2-*O*-cyclo-

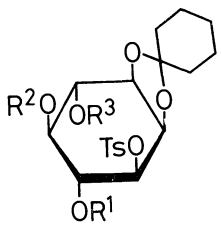

1

	R^1	R^2	R^3
a	Ac	Ac	Ac
b	Ac	Ac	Ts
c	Ts	Ac	Ac
d	Ac	Ts	Ac
e	Ts	Ac	Ts
f	Ac	Ts	Ts

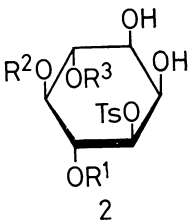

2

	R^1	R^2	R^3
a	Ac	Ac	Ac
b	Ac	Ac	Ts
c	Ts	Ac	Ac
d	Ac	Ts	Ac
e	Ts	Ac	Ts
f	Ac	Ts	Ts
g	Ts	Ts	Ts

1) T. Suami, S. Ogawa, T. Tanaka, and T. Otake, This Bulletin, **44**, 835 (1971).

2) T. Suami, F. W. Lichtenthaler, and S. Ogawa, *ibid.*, **40**, 1488 (1967); S. J. Angyal, P. T. Gilham, and G. J. H. Melrose, *J. Chem. Soc.*, **1965**, 5252.

3) T. Suami and S. Ogawa, This Bulletin, **40**, 1295 (1967); T. Suami, S. Ogawa, S. Naito, and H. Sano, *J. Org. Chem.*, **33**, 2831 (1968).

4) T. Suami and S. Ogawa, This Bulletin, **37**, 1238 (1964).

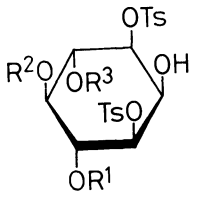

3

	R^1	R^2	R^3
a	Ac	Ac	Ac
b	Ac	Ac	Ts
c	Ac	Ts	Ac
d	Ts	Ac	Ts
e	Ac	Ts	Ts
f	Ts	Ts	Ts

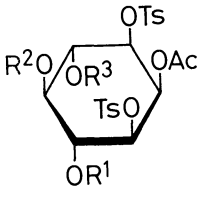

4

	R^1	R^2	R^3
a	Ac	Ac	Ac
b	Ac	Ac	Ts
c	Ac	Ts	Ac
d	Ts	Ac	Ts
e	Ac	Ts	Ts

hexylidene-3,4-di-*O*-*p*-toluenesulfonyl-*myo*-inositol (**1c**).[1] These results confirmed the proposed structure of **3b** unambiguously. Acetylation of **3b** gave the triacetyl derivative (**4b**) which, in PMR spectrum in deuteriochloroform ($CDCl_3$), revealed a narrow triplet (J= 3 Hz) at τ 4.49. Similar triplet was found in the PMR spectrum of **4a** (τ 4.37), and then it was assigned to the hydrogen atom on C-2 bearing acetoxy group.

Preferential sulfonylation of 4,6-di-*O*-acetyl-1,5-di-*O*-*p*- toluenesulfonyl-*myo*-inositol (**2d**). which was obtained by removal of the cyclohexylidene group of 4,6-di-*O*-acetyl-1,2-*O*-cyclohexylidene-3,5-di-*O*-*p*-toluenesulfonyl-*myo*-inositol (**1d**),[1] afforded 4,6-di-*O*-acetyl-1,3,5-tri-*O*-*p*-toluenesulfonyl-*myo*-inositol (**3c**) exclusively in 95% yield. On acetylation, **3c** gave the triacetyl derivative (**4c**), which revealed two signals of 1 : 2 relative intensities in an acetoxy methyl region[5] in its PMR spectrum

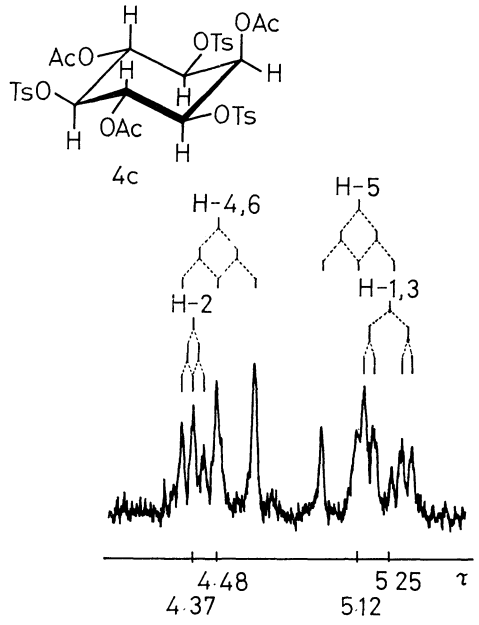

Fig. 1. Partial PMR spectrum of 2,4,6-tri-*O*-acetyl-1,3,5-tri-*O*-*p*-toluenesulfonyl-*myo*-inositol (**4c**) in $CDCl_3$ at 60 MHz: J_{ae}=3 Hz, J_{aa}=10 Hz.

5) F. W. Lichtenthaler and P. Emig, *Carbohyd. Res.*, **7**, 121 (1968).

Table 1. Chemical shifts of methyl protons[a]

Compd. No.	Acetoxy	*p*-Toluenesulfonyloxy
4a	7.95 (1)	7.54 (2)
	8.01 (1)	
	8.10 (2)	
4b	7.93 (1)	7.54 (3)
	8.00 (1)	
	8.12 (1)	
4c	7.97 (1)	7.53 (3)
	8.17 (2)	
4d	7.92 (1)	7.56 (4)
	8.02 (1)	
4e	8.00 (1)	7.56 (4)
	8.15 (1)	

a) Measured at 60 MHz in $CDCl_3$. Values in parenthesis show number of methyl groups. Chemical shifts are expressed in τ-values.

in $CDCl_3$. This result supported the proposed structure of **4c**, because it has a symmetrical structure and the signals due to two acetoxy groups on C–4 and C–6 should be overlapped each other (Table. 1). Furthermore, the signals of the ring protons could be resolved by first-order method and assigned unambiguously to each proton, as shown in Fig. 1.

By the same reaction sequences, 5-*O*-acetyl-1,4,6-tri-*O*-*p*-toluenesulfonyl-*myo*-inositol. (**2e**) and 6-*O*-acetyl-1, 4,5-tri-*O*-*p*-toluenesulfonyl-*myo*-inositol (**2f**) were obtained from 5-*O*-acetyl-1,2-*O*-cyclohexylidene-3,4,6-tri-*O*-*p*-toluenesulfonyl-*myo*-inositol (**1e**)[1] and 4-*O*-acetyl-1,2-*O*-cyclohexylidene-3,5,6-tri-*O*-*p*-toluenesulfonyl-*myo*-inositol (**1f**)[1] in 90 and 93% yield, respectively. On sulfonylation with 5 molar equivalents of *p*-toluenesulfonyl chloride, **2e** and **2f** afforded 5-*O*-acetyl-1,3,4,6-tetra-*O*-*p*-toluenesulfonyl-*myo*-inositol (**3d**) and 6-*O*-acetyl-1,3-4,5-tetra-*O*-*p*-toluenesulfonyl-*myo*-inositol (**3e**) predominantly in 42[6] and 99% yield, respectively. Compound **3d** and **3e** were converted into the diacetyl derivative (**4d**) and (**4e**), respectively, which showed the narrow triplets (J=3 Hz) at τ 4.55 and 4.58, supporting the location of the acetoxy group at C-2.

Sulfonylation of 1,4,5,6-tetra-*O*-*p*-toluenesulfonyl-*myo*-inositol (**2g**)[1] produced 1,3,4,5,6-penta-*O*-*p*-toluenesulfonyl-*myo*-inositol (**3f**) as a sole product in 63% yield. Attempt of acetylation of **3f** by the usual manner failed. Introduction of five *p*-toluenesulfonyl group into all the equatorially orientated hydroxyl groups in *myo*-inositol seemed to make the remaining axial hydroxyl group on C-2 extremely unreactive. Therefore, the structure of **3g** was substantially established by an analogy.

Experimental

Melting points were determined on a Mitamura Riken micro hot stage and are uncorrected. PMR spectra were measured on a Varian Associate A-60D (60 MHz) spectrometer at a concentration of *ca.* 10% deuteriochloroform with tetramethylsilane as an internal standard. Chemical shifts are expressed in τ-values and signals are described as

6) The low yield of **3d** may be due to a partial de-*O*-acetylation of **2d** and/or **3d** during a sulfonylation reaction.

s (singlet), t (triplet), q (quartet), or m (complex multiplet). Values given for coupling constants are first-order. Thin layer chromatography was done with silica gel (Wakogel B-10, Wako pure chemical industries Ltd.) using toluene-methyl ethyl ketone (4:1 or 3:1 volume) as the solvent system. The compounds were detected by exposing the plates to iodine vapor or by heating after spraying 50% sulfuric acid. All solutions were concentrated by a rotary evaporator at 40—50°C under reduced pressure. All the compounds described in this paper are racemic.

4,5,6-Tri-O-*acetyl-1*-O-p-*toluenesulfonyl*-myo-*inositol (2a)*. A mixture of 4,5,6-tri-*O*-acetyl-1,2-*O*-cyclohexylidene-3-*O*-*p*-toluenesulfonyl-*myo*-inositol (**1a**)[1] (1.0 g) and 80% aqueous acetic acid (20 m*l*) was refluxed for 2 hr. The reaction mixture was evaporated to give an oily product which crystallized by trituration with ethanol to afford crystals (0.54 g, 68%) of **2a**, mp 202—204°C. Recrystallization from ethanol gave colorless prisms which showed the same melting point.

Found: C, 50.14; H, 5.26; S, 7.12%. Calcd for $C_{19}H_{24}O_{11}S$: C, 49.55; H, 5.25; S, 6.96%.

4,5,6-Tri-O-*acetyl-1,3-di*-O-p-*toluenesulfonyl*-myo-*inositol (3a)*. To a solution of **2a** (0.46 g) in dry pyridine (5 m*l*) was added *p*-toluenesulfonyl chloride (0.29 g) under ice cooling. The reaction mixture was allowed to stand at 30°C for 4 days, till when the tlc showed the disappearance of **2a**. Poured into ice and water (100 m*l*), the crude crystals (0.64 g) were collected by filtration. A 0.44 g portion of the crude product was recrystallized from ethanol to give colorless needles (0.38 g, 88%) of **3a** monohydrate, mp 207—208.5°C (after melting and resolidifying to plates at 117—125°C).

Found: C, 49.55; H, 5.20; S, 9.62%. Calcd for $C_{26}H_{30}O_{13}S_2 \cdot H_2O$: C, 49.37; H, 5.10; S, 10.14%.

The monohydrate lost water of crystallization when it was dried over phosphorus pentoxide under vacuum at 120°C for 24 hr, mp 207.5—208.5°C.

Found: C, 50.94; H, 4.88; S, 10.46%. Calcd for $C_{26}H_{30}O_{13}S_2$: C, 50.80; H, 4.92; S, 10.43%.

2,4,5,6-Tetra-O-*acetyl-1,3-di*-O-p-*toluenesulfonyl*-myo-*inositol (4a)*. A 0.21 g portion of the crude **3a** monohydrate was treated with a mixture of acetic anhydride (2 m*l*) and pyridine (2 m*l*) at 80°C for 1 hr. Then the mixture was poured into ice and water and the crystals were collected by filtration; yield 0.19 g (90%), mp 220—223°C (lit,[2] mp 220—222°C). This compound was identified with an authentic sample by comparing with IR spectra.

5,6-Di-O-*acetyl-1,4-di*-O-p-*toluenesulfonyl*-myo-*inositol (2b)*. A mixture of 4,5-di-*O*-acetyl-1,2-*O*-cyclohexylidene-3,6-di-*O*-*p*-toluenesulfonyl-*myo*-inositol (**1b**)[1] (1.27 g) and 80% aqueous acetic acid (25 m*l*) was refluxed for 2 hr. Then the mixture was evaporated and the crystalline residue was triturated with ethanol to afford colorless crystals (0.97 g, 86%) of **2b**, mp 201.5—203.5°C. Recrystallization from ethanol gave an analytical sample, colorless needles, mp 207.5—209°C.

Found: C, 50.52; H, 4.86; S, 11.05%. Calcd for $C_{24}H_{28}O_{12}S_2$: C, 50.33; H, 4.94; S, 11.20%.

5,6-Di-O-*acetyl-1,3,4-tri*-O-p-*toluenesulfonyl*-myo-*inositol (3b)*. To a solution of **2b** (0.19 g) in dry pyridine (2 m*l*) was added *p*-toluenesulfonyl chloride (0.18 g, 2.8 molar equiv.) and the reaction mixture was kept at 30°C for 4 days, followed at 85°C for 1 hr. Then the mixture was poured into ice and water (25 m*l*) and the resulting oily product was extracted with chloroform (25 m*l*), washed with water (3×20 m*l*) and dried over anhydrous sodium sulfate. Evaporation gave a colorless oil, which crystallized on treatment with chloroform and ethanol to give crystals (0.21 g, 90%) of **3b**, mp 201—203°C. Recrystallization from chloroform and ethanol afforded an analytical sample, colorless plates, mp 204.5—206°C.

Found: C, 51.32; H, 4.82; S, 13.14%. Calcd for $C_{31}H_{34}O_{14}S_3$: C, 51.23; H, 4.72; S, 13.23%.

2,5,6-Tri-O-*acetyl-1,3,4-tri*-O-p-*toluenesulfonyl*-myo-*inositol (4b)*. A 100 mg portion of **3b** was treated with acetic anhydride (1 m*l*) and pyridine (1 m*l*) at room temperature overnight. The reaction mixture was poured into ice and water and the resulting crystals were collected by filtration. The crude crystals of **4b** weighed 100 mg (96%), mp 147—150.5°C. An analytical sample was obtained by recrystallization from chloroform and ethanol, mp 166—167.5°C. PMR: τ 4.49 (1, t, H-2, J=2.8 Hz).

Found: C, 51.60; H, 4.65; S, 12.72%. Calcd for $C_{33}H_{36}O_{15}S_3$: C, 51.56; H, 4.72; S, 12.49%.

4,5-Di-O-*acetyl-1,6-di*-O-p-*toluenesulfonyl*-myo-*inositol (2c)*. A mixture of 5,6-di-*O*-acetyl-1,2-*O*-cyclohexylidene-3,4-di-*O*-*p*-toluenesulfonyl-*myo*-inositol (**1c**)[1] (0.19 g) and 80% aqueous acetic acid (10 m*l*) was refluxed for 2 hr. Then the reaction mixture was evaporated to give a colorless oil which was induced crystallization on addition of aqueous ethanol to afford crystals (0.15 g) of **2c**. Recrystallization from ethanol gave colorless prisms (0.10 g, 58%), mp 184.5—185°C.

Found: C, 50.42; H, 5.17; S, 11.08%. Calcd for $C_{24}H_{28}O_{12}S_2$: C, 50.33; H, 4.94; S, 11.20%.

Selective p-*Toluenesulfonylation of 2c*. To a solution of **2c** (61 mg) in dry pyridine (0.6 m*l*) was added *p*-toluenesulfonyl chloride (0.10 g, 4.9 molar equiv.) and the reaction mixture was kept at 30°C for 70 hr. Then the mixture was processed similarly as described in **3b** to give colorless crystals (63 mg, 81%) of **3b**, mp 206—207°C, which was identified with the compound derived from **2b** by the mixed melting point and comparing with IR spectra.

4,6-Di-O-*acetyl-1,5-di*-O-p-*toluenesulfonyl*-myo-*inositol (2d)*. A mixture of 4,6-di-*O*-acetyl-1,2-*O*-cyclohexylidene-3,5-di-*O*-*p*-toluenesulfonyl-*myo*-inositol (**1d**)[1] (1.04 g) and 80% aqueous acetic acid (20 m*l*) was refluxed for 2 hr. The mixture was evaporated to give a slightly yellow oil, which crystallized on addition of water to give crude crystals (0.89 g). It was shown to be contaminated with the partly de-*O*-acetylated product by a tlc, then, the crude product was recrystallized two times from ethanol to afford chromatographically pure crystals (0.57 g, 63%) of **2d**, mp 178.5—180.5°C.

Found: C, 49.99; H, 4.95; S, 11.27%. Calcd for $C_{24}H_{28}O_{12}S_2$: C, 50.33; H, 4.94; S, 11.20%.

4,6-Di-O-*acetyl-1,3,5-tri*-O-p-*toluenesulfonyl*-myo-*inositol (3c)*. To a solution of **2d** (155 mg) in dry pyridine (1.5 m*l*) was added *p*-toluenesulfonyl chloride (250 mg, 4.9 molar equiv.) and the mixture was kept at 30°C for 70 hr. Then the reaction mixture was processed similarly as described in **3b** to give crude crystals, which were recrystallized from chloroform and ethanol to afford colorless needles (187 mg, 95%) of **3c**, mp 165—167°C (after sintering at 147°C). Recrystallization from the same solvents gave an analytical sample which showed the same melting point.

Found: C, 51.28; H, 4.72; S, 12.95%. Calcd for $C_{31}H_{34}O_{14}S_3$: C, 51.23; H, 4.72; S, 13.23%.

2,4,6-Tri-O-*acetyl-1,3,5-tri*-O-p-*toluenesulfonyl*-myo-*inositol (4c)*. A 101 mg portion of **3c** was treated with acetic anhydride (1 m*l*) and pyridine (1 m*l*) at room temperature overnight. Then the mixture was poured into ice and water to give crystals (106 mg, 99%) of **4c**, mp 178—185°C. An analytical sample was obtained by recrystallization from ethanol, colorless tiny needles, mp 181.5—183°C (after sintering at 175°C).

Found: C, 51.75; H, 4.73; S, 12.41%. Calcd for $C_{33}H_{36}O_{15}S_3$: C, 51.54; H, 4.72; S, 12.49%.

5-O-Acetyl-1,4,6-tri-O-p-*toluenesulfonyl*-myo-*inositol (2e)*. A mixture of 5-*O*-acetyl-1,2-*O*-cyclohexylidene-3,4,6-tri-*O*-*p*-

toluenesulfonyl-*myo*-inositol (**1e**)[1] (1.0 g) and 80% aqueous acetic acid (50 m*l*) was refluxed for 2 hr. After cooling, the resulting crystals were collected by filtration and washed with ethanol to yield colorless granular crystals (0.79 g, 85%) of **2e**, mp 222.5—224.5°C. Recrystallization from pyridine and ethanol gave an analytical sample, colorless prisms, mp 223—225°C.

Found: C, 51.30; H, 5.19; S, 14.58%. Calcd for $C_{29}H_{32}O_{13}S_3$: C, 50.86; H, 4.72; S, 14.04%.

5-O-*Acetyl-1,3,4,6-tetra*-O-p-*toluenesulfonyl*-myo-*inositol (3d)*. To a solution of **2e** (0.25 g) in dry pyridine (3 m*l*) was added *p*-toluenesulfonyl chloride (0.20 g, 3 molar equiv.) and the mixture was kept at 30°C for 4 days. After heating at 80°C for 1 hr, the reaction mixture was poured into ice and water and the resulting oily product was extracted with chloroform (25 m*l*). The extract was washed with water, dried over anhydrous sodium sulfate and then, evaporated to give a colorless oil which crystallized on addition of ethanol. The crude crystals were shown to be consisted of two major components by a tlc: **3d** and de-*O*-acetylated product, probably 1,3,4,6-tetra-*O*-*p*-toluenesulfonyl-*myo*-inositol. Fractional crystallization from ethanol afforded colorless plates (0.13 g, 42%) of **3d**, mp 194.5—199.5°C. An analytical sample was obtained by recrystallization from chloroform and ethanol, mp 200—201°C.

Found: C, 51.67; H, 4.62; S, 15.33%. Calcd for $C_{36}H_{38}O_{15}S_4$: C, 51.53; H, 4.57; S, 15.29%.

2,5-Di-O-*acetyl-1,3,4,6-tetra*-O-p-*toluenesulfonyl*-myo-*inositol (4d)*. Acetylation of **3d** (33 mg) with acetic anhydride (1 m*l*) and pyridine (1 m*l*) at room temperature gave colorless crystals (28 mg, 74%) of **4d**, mp 205—207°C. Recrystallization from chloroform and ethanol afforded an analytical sample, mp 207—209°C. PMR: τ 5.55 (2, q, H-1,3, J=3 and 8 Hz), τ 4.55 (1, t, H-2, J=3 Hz).

Found: C, 51.75; H, 4.75; S, 14.31%. Calcd for $C_{38}H_{40}O_{16}S_4$: C, 51.82; H, 4.58; S, 14.57%.

6-O-*Acetyl-1,4,5-tri*-O-p-*toluenesulfonyl*-myo-*inositol (2f)*. A mixture of 4-*O*-acetyl-1,2-*O*-cyclohexylidene-3,5,6-tri-*O*-*p*-toluenesulfonyl-*myo*-inositol (**1f**)[1] (1.39 g) and 80% aqueous acetic acid (100 m*l*) was refluxed for 2.5 hr. Then the solution was evaporated to give a crystalline residue. Trituration with ethanol gave crystals (1.16 g, 93%) of **2f**, mp 197—200°C (after melting and resolidifying at 162—168°C). Recrystallization from chloroform and ethanol afforded an analytical sample colorless, needles, mp 202—204°C.

Found: C, 50.90; H, 4.70; S, 13.58%. Calcd for $C_{29}H_{32}O_{13}S_3$: C, 50.86; H, 4.72; S, 14.04%.

6-O-*Acetyl-1,3,4,5-tetra*-O-p-*toluenesulfonyl*-myo-*inositol (3e)*. To a solution of **2f** (0.30 g) in dry pyridine (3 m*l*) was added *p*-toluenesulfonyl chloride (0.27 g, 3.4 molar equiv.) and the mixture was kept at 30°C for 4 days. Then the reaction mixture was processed similarly as described in **3a** to give crude crystals (0.37 g, 99%) of **3e**, mp 197—203°C (after sintering and resolidifying at 170—180°C). Recrystallization from chloroform and ethanol afforded an analytical sample, colorless rods, mp 208—210.5°C.

Found: C, 51.30; H, 4.53; S, 15.55%. Calcd for $C_{36}H_{38}O_{15}S_4$: C, 51.53; H, 4.57; S, 15.29%.

2,6-Di-O-*acetyl-1,3,4,5-tetra*-O-p-*toluenesulfonyl*-myo-*inositol (4e)*. A 0.15 g portion of **3e** was treated with acetic anhydride (1 m*l*) and pyridine (1 m*l*) at room temperature gave crystals (0.15 g, 95%) of **4e**, mp 99—112°C. Recrystallization from ethyl acetate and ethanol gave an analytical sample, colorless needles (0.09 g), mp 180—194°C (after melting and resolidifying at 130—140°C). PMR τ: 4.58 (1, t, H-2, J=3 Hz), τ 4.54 (1, t, H-6, J=9 Hz).

Found: C, 51.92; H, 4.46; S, 15.48%. Calcd for $C_{38}H_{40}O_{16}S_4$: C, 51.82; H, 4.58; S, 14.57%.

1,3,4,5,6-Penta-O-p-*toluenesulfonyl*-myo-*inositol (3f)*. To a solution of 1,4,5,6-tetra-*O*-*p*-toluenesulfonyl-*myo*-inositol (**2g**)[1] (0.15 g) in dry pyridine (1.5 m*l*) was added *p*-toluenesulfonyl chloride (0.25 g, *ca.* 7 molar equiv.) and the mixture was kept at 30°C for 2 weeks. Then the reaction mixture was processed similarly as described in **3d** to give colorless crystals (0.12 g, 63%) of **3f**, mp 184—185°C. An analytical sample was obtained by recrystallization from chloroform and ethanol, colorless granular crystals, which showed the same melting point.

Found: C, 51.79; H, 4.53; S, 17.06%. Calcd for $C_{41}H_{42}O_{16}S_5$: C, 51.77; H, 4.46; S, 16.85%.

The authors are grateful to Professor Sumio Umezawa for his kind advice, and to Mr. Saburo Nakada for his elementary analyses. The financial support from the Ministry of Education for this work is gratefully acknowledged.

Selective *p*-Toluenesulfonylation of *myo*-Inositol Derivatives

Tetsuo SUAMI, Seiichiro OGAWA, and Shuichi OKI

Department of Applied Chemistry, Faculty of Engineering, Keio University, Koganei-shi, Tokyo

(Received May 27, 1971)

Attempt to know the reactivities, toward sulfonylation, of the hydroxyl groups in *myo*-inositol was carried out using partially sulfonylated derivatives of *myo*-inositol. The present studies indicated that the order of reactivity of the hydroxyl groups is 1-OH and 3-OH>4-OH and 6-OH>5-OH>2-OH. From a preparative standpoint, 1,3-di-*O*-*p*-toluenesulfonyl-*myo*-inositol was readily obtained in 59% yield from 1-*O*-*p*-toluenesulfonyl-*myo*-inositol by a selective sulfonylation.

In order to know the reactivities toward sulfonylation of the hydroxyl groups in *myo*-inositol, attempts of a selective sulfonylation of *myo*-inositol derivatives were made. Little information is as yet available on the relative reactivities, toward sulfonylation, of the hydroxyl groups of cyclitols.[1] Because of its insolubility in pyridine, direct esterification of *myo*-inositol could not be conducted, and then five partially sulfonylated *myo*-inositol derivatives (1-, 1,3-, 1,4-, 1,4,5- and 1,4,6-)[2,3] were used for the present studies.

First of all, a selective *p*-toluenesulfonylation of 1-*O*-*p*-toluenesulfonyl-*myo*-inositol (**1**)[2] was attempted. Theoretically, twenty four positional isomers of *p*-toluenesulfonyl derivatives of *myo*-inositol can be obtained from **1**. However, if 2-*O*-*p*-toluenesulfonyl derivatives are excluded in view of the unreactivity of the axial hydroxyl group on C-2,[4] thirteen isomers (diesters 4, triesters 5, tetraesters 3 and pentaester 1) would be expected to be obtainable. When **1** was treated with 4 molar equiv. of *p*-toluenesulfonyl chloride (TsCl) in dry pyridine at 30°C and the progress of the reaction was followed by thin layer chromatography (tlc) using silica gel, after 4 days, at least eight components were detected in the reaction mixture. Six of the products formed could be identified by a direct comparison of *Rf* values on tlc with authentic samples. These were found to be the 1,3- (**2**), 1,3,4- (**3**), 1,3,5- (**4**), 1,3,4,5- (**5**), 1,3,4,6- (**6**) and 1,3,4,5,6-isomers (**7**) (Fig. 1).

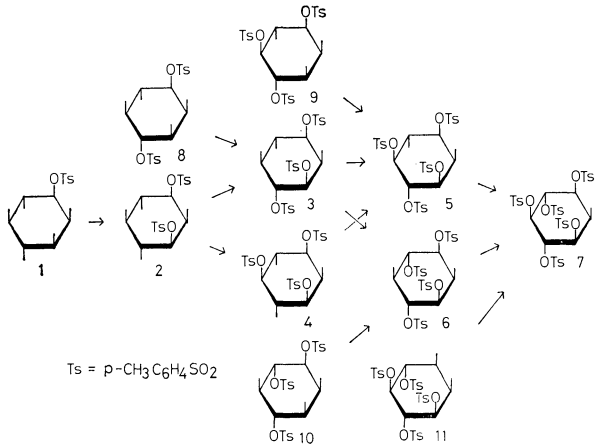

Fig. 1. Course of a selective *p*-toluenesulfonylation of *myo*-inositol[a]

a) All the compounds described in this paper are racemic. In the formulas, the vertical lines represent hydroxyl groups; the hydrogen atoms on the ring carbons are not shown.

Treatment of **1** with 1, 1.2 and 1.5 molar equiv. of TsCl in dry pyridine at 0—30°C for 6—10 days, and subsequent acetylation with acetic anhydride gave 2,4,5,6-tetra-*O*-acetyl-1,3-di-*O*-*p*-toluenesulfonyl-*myo*-inositol (**2a**) in 50, 59, and 49% yield, respectively, in a pure crystalline state by one recrystallization of the crude product from chloroform and ethanol. Accordingly, the hydroxyl group on C-3 is the most reactive among five hydroxyl groups in **1**. This result was in accordance with the fact that, in the case of 1,2-*O*-cyclohexylidene-*myo*-inositol, the C-3 hydroxyl group which is adjacent to *cis*-arranged cyclohexylidene oxygen atom is the most reactive.[3] The high reactivity at C-3 may be explained by hydrogen bonding between the C-2 and C-3 hydroxyl groups in the transition state of esterification.[1]

When a sulfonylation of **1** was carried out using more than 2 molar equiv. of TsCl, a considerable amount of the tetraesters were formed. On treatment with 3, 4 and 5 molar equiv. of TsCl, **1** gave 1,3,4,6-tetra-*O*-*p*-toluenesulfonyl-*myo*-inositol (**6**) in 9, 34, and 28% yield, respectively, which was characterized by converting it into the known diacetate (**6a**).[4]

Then a selective sulfonylation of 1,3- and 1,4-di-*O*-*p*-toluenesulfonyl-*myo*-inositol (**2** and **8**)[3] was attempted. Monitoring by tlc the progress of the reaction of **2** with 2 and 4 molar equiv. of TsCl, almost the same chromatograms as those observed in the case of **1** under the similar sulfonylation condition were obtained, which indicated that the sulfonylation reaction of **1** proceeded through **2**. On the other hand, from **8**, the 1,3,4,5- and 1,3,4,6-isomers were detected to be formed, then, in view of the high reactivity of C-3 hydroxyl group, the tetraesters should be yielded from the 1,3,4-triester apparently. Therefore, the relative yields of the two tetraesters may accord with the reactivity of C-5 and C-6 hydroxyl groups. According to visual observation of a relative intensity of the 1,3,4,5- and 1,3,4,6-tetraesters on a tlc plate, hydroxyl group on C-6 seemed to be about two times more reactive than that on C-5. This fact might be explained by a steric and electronic effects exerted by an axial hydroxyl group on C-2 in a transition state of esterification.

1) D. H. Ball and F. W. Parrish, *Advan. Carbohyd. Chem.*, **23**, 233 (1968); **24**, 139 (1969).
2) S. J. Angyal, V. Bendor, and J. H. Curtin, *J. Chem. Soc. (C)*, **1966**, 798.
3) T. Suami, S. Ogawa, T. Tanaka, and T. Otake, This Bulletin, **44**, 835 (1971).
4) T. Suami, S. Ogawa, and S. Oki, *ibid.*, **44**, 2820 (1971).

In 4 molar esterification of **2** and **8**, when **8** was completely consumed to be converted into the tetraesters *via* the 1,3,4-triester, the 1,3,4- and 1,3,5-triesters, as well as **2**, were still remaining in the reaction mixture. This indicated that the reactivities of the hydroxyl groups on C-4, 5 or 6 were lower than that on C-3. Furthermore, in the case of **2**, when two triesters almost disappeared on a tlc, the relative intensities of the two spots due to two tetraesters were nearly the same as that observed in **8**. Therefore, in **2**, the hydroxyl group on C-5 was shown to be less reactive than that on C-4 (or 6), even if a theoretical treatment were taken into account. Because the 1,3,4,5-tetraester should be formed from the 1,3,5-triester solely, so that if the latter was yielded from **2** more than half of the 1,3,4-isomer, the yield of the 1,3,4,5-isomer should overwhelmed that of the 1,3,4,6-isomer. This was also understood by an influence of the axial hydroxyl group on C-2.

From the reaction of the 1,4,5- (**9**) and 1,4,6-triesters (**10**) with 4 molar equiv. of TsCl, after 24 hr at 30°C, the 1,3,4,5- and 1,3,4,6-tetraesters were obtained, respectively, in good yield, but even after 10 days, only a trace amount of the 1,3,4,5,6-pentaester was detected in the reaction mixture. On the other hand, from the reaction of the 1,4,5,6-tetraester (**11**) with 4 molar equiv. of TsCl, the 1,3,4,5,6-isomer was obtained comparatively in good yield.[4] Consequently, introduction of *p*-toluenesulfonyloxy group into a vicinal position of hydroxyl group was found to make the remaining free hydroxyl group quite unreactive.[5]

Summarizing the results described above, the reaction sequences of *p*-toluenesulfonylation of *myo*-inositol were shown in Fig. 1. The order of reactivity of six hydroxyl groups in *myo*-inositol could be deduced to be 1-OH and 3-OH>4-OH and 6-OH>5-OH>2-OH. In the case of 1,2-*O*-cyclohexylidene-*myo*-inositol,[3] considering from the relative yield of the isomers, the order of reactivity of its four hydroxyl groups is 3-OH>6-OH>4-OH>5-OH, which seems to be in good accordance with the present result.

Along with the present studies, preferential benzoylation of *myo*-inositol is now underway in our laboratory.

Experimental

Melting points were determined on a Mitamura Riken micro hot stage and are uncorrected. Infrared (IR) spectra were taken in KBr disks. Tlc was done with silica gel (Wakogel B-10, Wako Pure Chemical Industries Ltd.) using toluene-methyl ethyl ketone (4:1, 3:1, 2:1 or 1:1) or benzene-ethyl acetate (7:2, 3:1 or 1:1) as the solvent system. The compounds were detected by exposing the plates to iodine vapor or heating at 100°C after spraying 30% sulfuric acid. Identification of the compounds was accomplished mainly by mixed tlc and comparison of *Rf* value on a tlc. All solutions were concentrated by a rotary evaporator at 40—50°C under reduced pressure.

p-*Toluenesulfonylation of 1*-O-p-*toluenesulfonyl*-myo-*inositol (1)*. a) 1 molar sulfonylation: To a solution of **1** (0.2 g) in dry pyridine (2 m*l*) was added TsCl (0.12 g) in one portion under ice cooling. The reaction mixture was kept at 30°C for 10 days, and then acetic anhydride (1 m*l*) was added and heated over boiling water bath for 3 hr. The mixture was poured onto ice and water and the resulting precipitates were collected by filtration. The crude product (0.42 g) was recrystallized from chloroform and ethanol to give colorless needles (0.20 g, 50%) of tetra-*O*-acetyl-1,3-di-*O*-*p*-toluenesulfonyl-*myo*-inositol (**2a**), mp 209—212°C. This compound was identified with an authentic sample[2] by mixed melting point and IR spectra.

b) 1.2 molar sulfonylation: To a solution of **1** (0.20 g) in dry pyridine (2 m*l*) was added TsCl (87 mg) at 0°C and the solution was kept at the same temperature for 24 hr. Then another portion of TsCl (47 mg) was added and the reaction mixture was allowed to stand at 0°C for 2 days. The product was acetylated and processed as described in (a) to afford crystals (0.23 g, 59%) of **2a**, mp 212—213°C.

c) 1.5 molar sulfonylation: Compound **1** (0.21 g) was sulfonylated with TsCl (0.18 g) at 30°C for 10 days and processed as described in (a) to afford crystals (0.20 g, 49%) of **2a**, mp 212—214°C.

d) 2 molar sulfonylation: Compound **1** (0.51 g) was treated with TsCl (0.59 g) in dry pyridine (5 m*l*) at 30°C for 3 days. Then the product was acetylated and processed as described in (a) to give crystals (0.30 g, 30%) of **2a**, mp 213—215°C.

e) 3 molar sulfonylation: Compound **1** (0.50 g) was treated with TsCl (0.88 g) at 30°C for 5 days. The crude product (1.2 g) was fractionated by crystallization from chloroform and ethanol: 0.11 g (the 1,3,4,6-isomer), mp 260—265°C; 0.41 g (the 1,3,4- and 1,3,4,6-isomers); 0.25 g (the 1,3,4-, 1,3,5- and 1,3,4,5-isomers).

f) 4 molar sulfonylation: Compound **1** (0.50 g) was treated with TsCl (1.2 g) in dry pyridine (5 m*l*) at 30°C for 6 days. Then the reaction mixture was poured onto ice and water, and the resulting white precipitates were collected. Recrystallization of the crude product from chloroform and ethanol gave colorless plates (0.40 g, 34%) of 1,3,4,6-tetra-*O*-*p*-toluenesulfonyl-*myo*-inositol (**6**), mp 267—269°C. From the mother liquor, the mixture of the tri- and tetraesters (0.17 g) was isolated.

g) 5 molar sulfonylation: Compound **1** (0.50 g) was treated with TsCl (1.5 g) in dry pyridine (5 m*l*) at 0—5°C for 24 hr, and then at 30°C for 24 hr. After heating at 80°C for 5 hr, the reaction mixture was poured onto ice and water to give white powder (1.1 g), which was fractionated by crystallization from chloroform and ethanol to afford colorless plates (0.33 g, 28%) of **6**, mp 265—268°C.

1,3,4-Tri-O-p-*toluenesulfonyl*-myo-*inositol (3)*. A mixture of 5,6-di-*O*-acetyl-1,3,4-tri-*O*-*p*-toluenesulfonyl-*myo*-inositol[4] (0.20 g), conc. hydrochloric acid (2 m*l*) and ethanol (10 m*l*) was refluxed for 3 hr. After cooling, the resulting oily product was collected by decantation and induced to crystallization by addition of chloroform. The crystals were triturated with ethanol and collected by filtration: colorless needles (0.14 g, 80%) of **3**, mp 229—230°C. Recrystallization from ethanol gave an analytical sample, mp 230—230.5°C.

Found: C, 50.02; H, 4.64; S, 15.09%. Calcd for $C_{27}H_{30}O_{12}S_3$: C, 50.45; H, 4.71; S, 14.96%.

1,3,5-Tri-O-p-*toluenesulfonyl*-myo-*inositol (4)*. A mixture of 2,4,6-tri-*O*-acetyl-1,3,5-tri-*O*-*p*-toluenesulfonyl-*myo*-inositol[4] (40 mg), conc. hydrochloric acid (10 m*l*) and ethanol (10 m*l*) was refluxed for 10 hr. After cooling, the resulting crystals were collected by filtration: colorless prisms of **4**, mp 259—263°C. IR spectrum did not show any absorption at ester carbonyl region. Tlc showed a single spot in several solvent systems and the *Rf* value was shown to be identical with that of one of the components observed in the

5) R. W. Jeanloz, A. M. C. Rapin, and S. Hakomori, *J. Org. Chem.*, **26**, 3939 (1961).

sulfonylation mixture of both **1** and **2**.

p-*Toluenesulfonylation of the 1,3- and 1,4-Diesters.* A 30 mg portion of the diester was dissolved in dry pyridine (0.3 m*l*) and TsCl (52 mg, 4 molar equiv.) was added, and the reaction mixture was allowed to stand at 30°C. The course of the reaction was monitored by tlc (solvent system: benzene-ethyl acetate=7:2 and 1:1). The chromatograms (the 1,3-diester) were found to be almost identical with those of the reaction mixture of **1** and 4 molar equiv. of TsCl in pyridine prepared under the same condition. The component, which corresponds to the 1,3,5-triester, was not observed in the sulfonylation mixture of the 1,4-diester. After 5 days, when all the 1,4-diester had been consumed to be converted into the tri- and tetraesters, the 1,3-diester was still remaining unchanged partly in the reaction mixture. The relative intensities of the tetraesters (the 1,3,4,5- and 1,3,4,6-isomers) derived from the 1,4-diester was approximately in the ratio of 1:2.

1,3,4,5-Tetra-O-p-*toluenesulfonyl*-myo-*inositol (5).* a) To a solution of 1,4,5-tri-*O-p*-toluenesulfonyl-*myo*-inositol (**9**)[3] (30 mg) in dry pyridine (0.3 m*l*) was added TsCl (38 mg, 4.3 molar equiv.) and the mixture was kept at 30°C for 21 hr. Then the solution was poured onto ice and water and the precipitates (40 mg) were collected by filtration. The crude crystals were recrystallized from methyl ethyl ketone and ethanol to give colorless needles (22 mg, 58%) of **5**, mp 253—256°C (after sintering at 246°C).

Found: C, 51.46; H, 4.61; S, 15.86%. Calcd for $C_{34}H_{36}O_{14}S_4$: C, 51.24; H, 4.56; S, 16.09%.

b) A mixture of 6-*O*-acetyl-1,3,4,5-tetra-*O-p*-toluenesulfonyl-*myo*-inositol[4] (34 mg), conc. hydrochloric acid (10 m*l*) and ethanol (10 m*l*) was refluxed for 10 hr. After cooling, the resulting crystals were collected and recrystallized from ethanol: colorless prisms of **5**, mp 247—249°C. This compound was identified with the sample obtained from **9** by comparing with IR spectra.

1,3,4,6-Tetra-O-p-*toluenesulfonyl*-myo-*inositol (6).* a) To a solution of 1,4,6-tri-*O-p*-toluenesulfonyl-*myo*-inositol (**10**)[3] (0.21 g) in dry pyridine (2 m*l*) was added TsCl (0.24 g, 3.9 molar equiv.) and the mixture was kept at 30°C for 22 hr, Then the solution was poured onto ice and water and the resulting crystals were recrystallized from 2-methoxyethanol to give colorless needles (0.25 g, 95%) of **6**, mp 269.5—270.5°C.

Found: C, 51.21; H, 4.35; S, 16.13%. Calcd for $C_{34}H_{36}O_{14}S_4$: C, 51.24; H, 4.56; S, 16.09%.

b) To a solution of 1,4-di-*O-p*-toluenesulfonyl-*myo*-inositol (**8**)[3] (0.15 g) in dry pyridine (1.5 m*l*) was added TsCl (0.29 g, 4.9 molar equiv.) and the mixture was kept at 30°C for 7 days. The reaction mixture was poured onto ice and water and the crude crystals were recrystallized two times from chloroform and ethanol to give pure crystals (0.14 g, 56%) of **6**, mp 270—272°C. This compound was identified with the sample obtained from **10** by comparing with IR spectra and mixed tlc.

2,5-Di-O-*acetyl-1,3,4,6-tetra*-O-p-*toluenesulfonyl*-myo-*inositol (6a).* Compound **6** (0.4 g) was acetylated with acetic anhydride (5 m*l*) and pyridine (5 m*l*) at room temperature overnight. The reaction mixture was poured into water and the resulting crystals were recrystallized from chloroform and ethanol to afford colorless crystals (0.39 g, 88%) of **6a**, mp 207—209°C. This compound was identified with the authentic sample by comparing with IR spectra and mixed melting point.[4]

The authors are grateful to Professor Sumio Umezawa for his kind advice and to Mr. Saburo Nakada for his elementary analyses. The financial support from the Ministry of Education for this work is gratefully acknowledged.

Synthesis and Conformational Studies of [7](2,6)Pyridinophanes

Shinsaku FUJITA and Hitosi NOZAKI

Department of Industrial Chemistry, Kyoto University, Kyoto

(Received March 2, 1971)

[7](2,6)Pyridinophane (V) and the 4-deuterio derivative (V_D) are prepared from cyclododecane-1,5-diones (IV and IV_D). Lithiation at the α-position of V and the subsequent derivation give 1-methoxycarbonyl- (VIII), 1-hydroxy- (IX), 1-oxo- (X), and 1,1-dimethoxy[7](2,6)pyridinophane (XI). A bathochromic shift in UV spectra is observed and ascribed to the nonplanarity of the pyridine ring. The protons on the C_4 of these heterophanes experience strong shielding due to the magnetic anisotropy of the respective pyridine rings. The shielding of the C_4 protons is more pronounced at low temperatures; this can be explained by assuming an extreme conformation such as XII. The temperature dependence of the NMR spectra is examined, and the energy barriers (ΔG_c^*) for the conformational changes (XII⇄XII′) are estimated to be 9.0 for V and 9.6 kcal/mol for XI. [7](2,6)Pyrylophanium perchlorate (VI) is prepared, in which a similar shielding effect of the pyrylium ring is observed.

The chemistry of uniquely strained meta- and paracyclophanes has been the subject of extensive research.[1] Particularly, their conformational changes have been investigated by means of temperature-variable NMR spectrometry.[2] The heteroaromatic analogs (heterophanes[3]) have recently attracted much attention, since two natural products, muscopyridine[4] and metacycloprodigiosin,[5] were characterized as the derivatives of [10](2,6)pyridinophane and [9](2,4)pyrrolophane respectively. In continuation of our studies of [8]-[6] and [9]heterophanes,[7] the present paper will describe [7](2,6)pyridinophanes with the shortest 2,6-polymethylene bridge ever reported.[8]

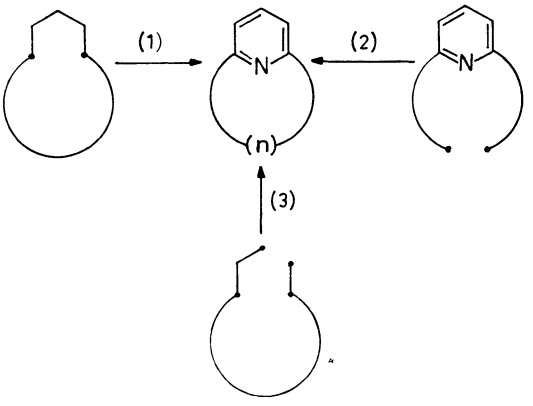

Scheme 1

Synthesis of [7](2,6)Pyridinophanes. Scheme 1 shows three possible ways of constructing [*n*](2,6)pyridinophanes: (1) the aromatization of 1,5-bifunctional cyclic compounds,[4,9] (2) the cyclization of 2,6-disubstituted pyridines,[10] and (3) pyridine-ring synthesis accompanying simultaneous bridge formation.[11,12] We have chosen the first approach and have utilized cyclododecane-1,5-dione (IV) as a precursor (see Scheme 2).

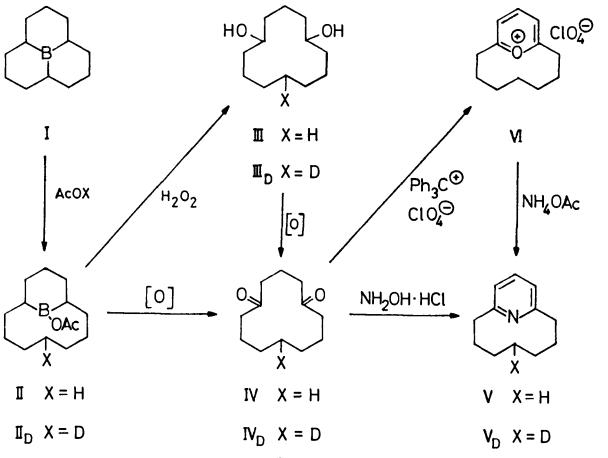

Scheme 2

The treatment of 9*b*-boraperhydrophenalene (I) with an equimolar amount of acetic acid and the subsequent Brown oxidation gave IV in a 30% yield.[13] The 1,5-diketone IV was also obtained by the oxidation of the corresponding diol III, which was in turn prepared by the oxidation of a partially-acetolyzed product II with alkaline hydrogen peroxide.

The heating of an alcoholic solution of IV and hydroxylamine hydrochloride gave [7](2,6)pyridinophane (V) in a 44% yield.[14] 4-Deuterated pyridinophane (V_D) was synthesized in a similar method.

1) a) R. W. Griffin, Jr., *Chem. Rev.*, **63**, 45 (1963); b) B. H. Smith, "Bridged Aromatic Compounds," Academic Press, New York (1964); c) T. Sato, *Kagaku no Ryoiki*, **23**, 672, 765 (1969); d) H. J. Reith and D. J. Cram, *J. Amer. Chem. Soc.*, **91**, 3505 (1969).

2) a) F. Vögtle, *Chem. Ber.*, **102**, 3077 (1969); b) F.A.L. Anet and M. A Brown, *J. Amer. Chem. Soc.*, **91**, 2389 (1969); c) D. H. Hefelfinger and D. J. Cram, *ibid.*, **92**, 1073 (1970).

3) For the nomenclature of this kind of compounds, see F. Vögtle and P. Neumann, *Tetrahedron Lett.*, **1969**, 5329.

4) K. Biemann, G. Büchi, and B. H. Walker, *J. Amer. Chem. Soc.*, **79**, 5558 (1957).

5) a) H. H. Wasserman, G. C. Rodgers, and D. D. Keith, *ibid.*, **91**, 1263 (1969); b) H. H. Wasserman, D. D. Keith, and J. Nadelson, *ibid.*, **91**, 1264 (1969).

6) H. Nozaki, T. Koyama, and T. Mori, *Tetrahedron*, **25**, 5357 (1969).

7) S. Fujita, T. Kawaguti, and H. Nozaki, This Bulletin, **43**, 2596 (1970).

8) A preliminary account of a portion of this work has appeared: H. Nozaki, S. Fujita, and T. Mori, *ibid.*, **42**, 1163 (1969).

9) A. T. Balaban, *Tetrahedron Lett.*, **1968**, 4643.

10) F. Vögtle, *Tetrahedron*, **25**, 3231 (1969).

11) A. T. Balaban, M. Gavat, and C. D. Nenitzescu, *ibid.*, **18**, 1079 (1962).

12) H. Gerlach and E. Huber, *Helv. Chim. Acta*, **51**, 2027 (1968).

13) The 1,5-diketone IV was previously prepared by fermentation technique. See G. S. Fonken, M. E. Herr, H. Murray, and L. M. Reineke, *J. Amer. Chem. Soc.*, **89**, 672 (1967).

14) Treatment of 9-acetoxycyclododecane-1,5-dione with hydroxylamine hydrochloride gave no pyridinophane derivative. See S. Fujita and H. Nozaki, This Bulletin, **43**, 2995 (1970).

The treatment of I with acetic acid-*d*, oxidation with alkaline hydrogen peroxide, and final oxidation afforded cyclododecane-1,5-dione-9*d* (IV_D), the subsequent cyclization of which gave [7](2,6)-pyridinophane-4*d* (V_D). The C–D stretching absorption of V_D appeared at 2140 cm^{-1}.

The dehydration and hydride abstraction[15] of IV with trityl perchlorate gave [7](2,6)pyrylophanium perchlorate (VI). The treatment of the pyrylium salt VI with ammonium acetate yielded the pyridinophane V, which was identical with the sample prepared directly from IV.

The addition of *n*-butyllithium to a solution of V gave an orange-red solution of 1-lithio[7](2,6)pyridinophane (VII), which then afforded methyl [7](2,6)pyridinophane-1-carboxylate (VIII) upon quenching with carbon dioxide and subsequent esterification. The 1-lithio compound VII reacted with oxygen to form the corresponding alcohol, IX. The Cornforth oxidation of IX gave [7](2,6)-pyridinophan-1-one (X). The treatment of X with methyl orthoformate afforded the corresponding dimethyl acetal (XI).

The heating of V with hydrogen peroxide in acetic acid resulted in the recovery of the starting pyridinophane under conditions sufficient for [10](2,6)pyridinophane to afford the corresponding *N*-oxide in a fair yield.[4] This is due to a steric hindrance introduced by the shorter heptamethylene chain.

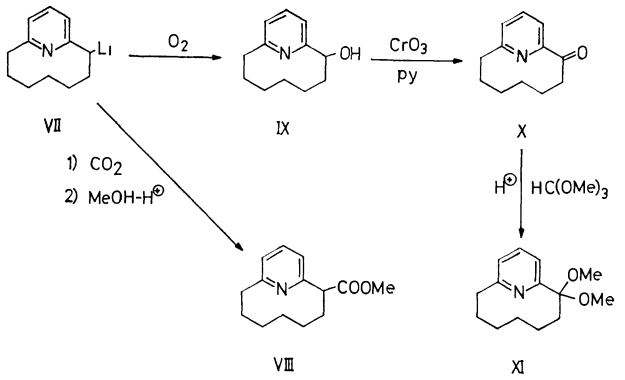

Scheme 3

UV and NMR Spectra of [7](2,6)Pyridinophanes and [7](2,6)-Pyrylophanium Perchlorate. The ultraviolet spectra of the [7](2,6)pyridinophanes are summarized in Table 1, together with those of the decamethylene homologs. Bathochromic shifts were observed upon a comparison of the UV bands (^1L_b bands) of [7]pyridinophanes with those of [10]-homologs. This effect can be explained by assuming a nonplanar pyridine ring bridged by the heptamethylene group.[1b]

Table 1. UV spectra of [*n*](2,6)pyridinophanes[a]

α-Substituent	[7](2,6)-Pyridinophane λ_{max}nm (log ε)	[10](2,6)-Pyridinophane[b] λ_{max}nm (log ε)
None	211.5 (3.87)	213 (3.82)
	272 (3.49)	267 (3.62)
-OH	211.5 (3.86)	212 (3.77)
	271 (3.53)	266 (3.54)
=O	236 (3.85)	236 (3.81)
	279 (3.56)	276 (3.66)

a) Ethanol was used as the solvent.
b) Reported in Ref. 4.

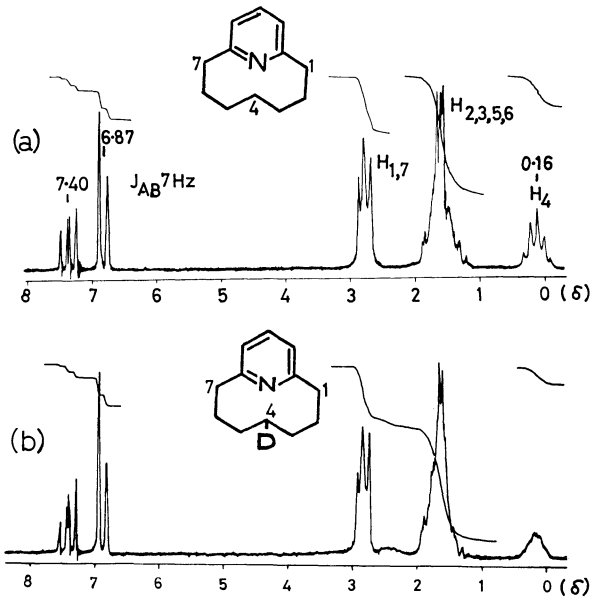

Fig. 1. NMR Spectra of V (a) and V_D (b) (in $CDCl_3$ at 24°C, 60 MHz. TMS as an internal standard).

The NMR spectra of V and V_D are shown in Fig. 1. The aromatic NMR signal of V showed a typical AB_2 pattern, one which resembled the splitting pattern of 2,6-lutidine very closely. The absorptions due to the heptamethylene protons of V were composed of three groups of multiplets (intensity: 4:8:2). In particular, two protons (a quintet at δ 0.16) of the heptamethylene chain were unexpectedly shielded in comparison with usual methylene group linking tetrahedral carbons. The signal at the high field can be ascribed to the C_4 protons, since the 4-monodeuterio-substituted derivative (V_D) showed the corresponding one proton peak which was broadened by a *geminal* H–D coupling. An inspection of the molecular models of V shows that H_a on C_4 is forced close to the π-cloud of the pyridine ring in an extreme conformation, XII. The apparently less crowded conformation, XIII, may be less favored, as the four C–C bonds linking C_2 through C_6 are all in an eclipsed conformation in XIII. The shielding effect in V is ascribed to the magnetic anisotropy of the pyridine ring.[16] Since the peak due to C_1 and C_7 (centered at δ 2.84) and that

15) M. Siemiatycki, *Bull. Soc., Chim. Fr.*, **1961**, 538.

16) The magnetic effect may consist of the diamagnetic ring current of the pyridine ring and/or the anisotropy of the nitrogen atom (Ref. 17). 2,6-Dithia[7]metacyclophane (XVI), in which such magnetic anisotropy of nitrogen atom was absent, was reported to exhibit the signal of C_4 protons at δ 0.45 (in dichloromethane-d_2). See Ref. 18.

17) a) V. M. S. Gil and J. N. Murrell, *Trans. Faraday Soc.*, **60**, 248 (1964); b) K. Sisido, K. Tani, and H. Nozaki, *Tetrahedron*, **19**, 1323 (1963); c) E. V. Donckt, R. H. Martin, and F. Greerts-Evrard, *ibid.*, **20**, 1495 (1964); d) F. Bohlmann, D. Schumann, and C. Arndt, *Tetrahedron Lett.*, **1965**, 2705; e) F. Bohlmann, D. Schumann, and H. Schulz, *ibid.*, **1965**, 173.

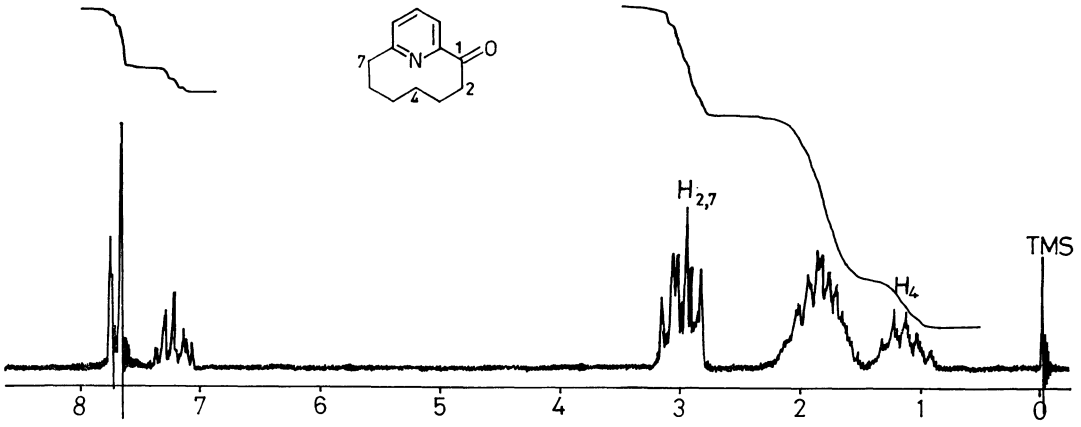

Fig. 2. NMR spectrum of X (in $CDCl_3$ at 24°C, 60 MHz).

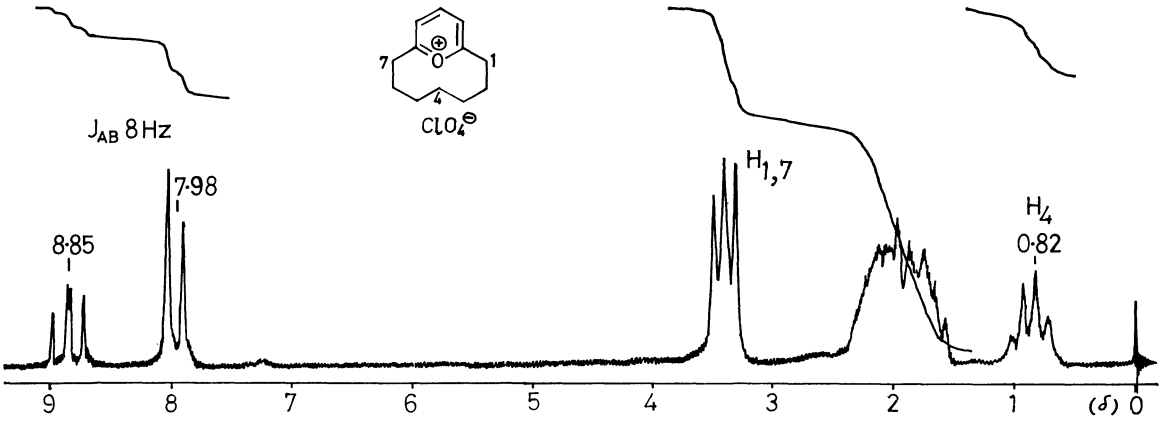

Fig. 3. NMR spectrum of VI (in CF_3COOH at 24°C, 60 MHz).

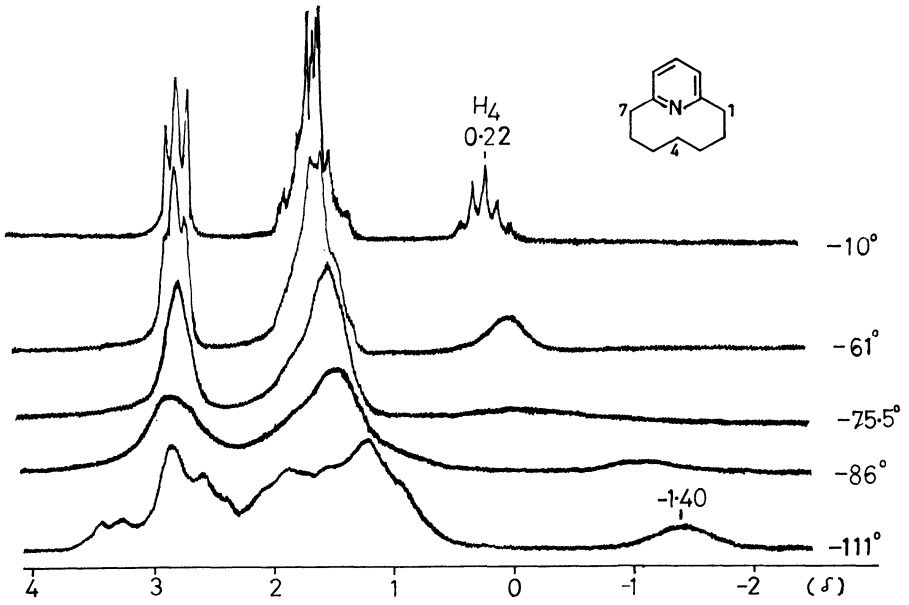

Fig. 4. Dynamic NMR spectra of the heptamethylene chain of V (in $CFCl_3$ at 60 MHz, TMS as an internal standard).

of the C_4 protons can be approximately regarded as a triplet and a quintet respectively, the heptamethylene chain of V possibly flips up and down (XII⇄XII') and its protons show average NMR signals at room temperature (*vide infra*).

The incorporation of a trigonal α-carbon in X resulted in a drastic reduction of the diamagnetic shielding effect as compared with the cases of V, IX, and XI. The conjugation of the pyridine ring of X with the α-carbonyl group should favor a conformer such as XIV, in which C_4 protons are forced out of the center of the pyridine-ring field.

The NMR spectrum of VI (Fig. 3) showed an AB_2-type signal of pyrylium-ring protons. The C_4 methylene of VI was also shielded, appearing at δ 0.82. This is the first example of the diamagnetic shielding effect of a pyrylium ring.

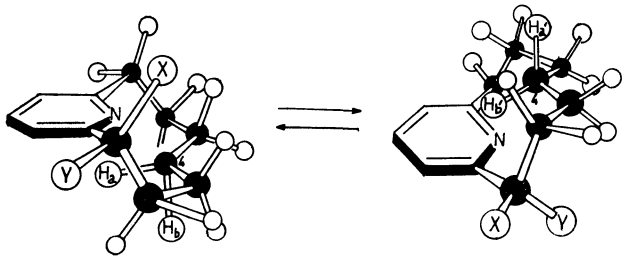

XII XII'

a : X=Y=H
b : X=Y=OMe
c : X=H, Y=COOMe
d : X=H, Y=OH

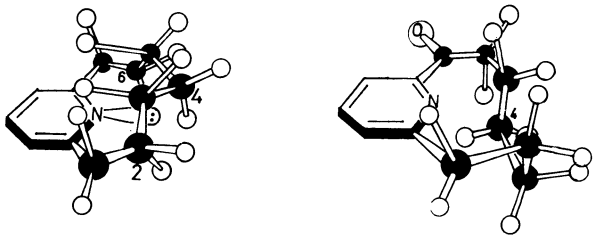

XIII XIV

Conformational Changes of [7](2,6)Pyridinophanes. The temperature dependence of the NMR spectrum of V is shown in Fig. 4. The signal of the C_4 protons of V broadened at −75.5°C and reappeared at δ −1.40; this is consistent with the extreme conformation, XIIa. The low-field counterpart of the signal is possibly concealed behind the multiplets of the other methylenes.

The C_4 protons of the 1,1-dimethoxy derivative (XI) are also shielded by the magnetic anisotropy of the pyridine ring. Fig. 5 shows the temperature dependence of the NMR spectrum of XI. The signal of the C_4 protons of XI broadened at −62.5°C, and then that of methoxy methyl broadened at −77.0°C. The signals at δ 3.21 and δ 2.98 may be assigned to the *pseudo*-equatorial and *pseudo*-axial methoxy groups of XIIb respectively.

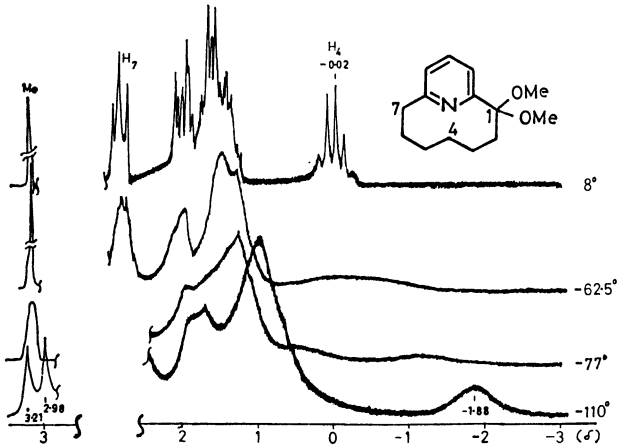

Fig. 5. Dynamic NMR spectra of the heptamethylene chain and methoxy of XI (in $CFCl_3$ at 60 MHz, TMS as an interanl standard).

The estimated energy barriers for the conformational changes (XII⇄XII') of V and XI are shown in Table 2. The ΔG_c^* value reported for 2,6-dithia[7](2,6)pyridinophanes (XV)[10] is smaller than that of our [7](2,6)pyridinophanes. Moreover, even 2,6-dithia[7]metacyclophane (XVI)[18] has a ΔG_c^* value comparable to those of V and XI. The flexibility introduced by S–substitution may be ascribed to the fact that C–S bonds are longer than C–C bonds and C–S–C bending requires much less energy than does C–C–C bending.

Table 2. Energy barriers of the flipping of V and XI[a]

Compd.	Signal	T_c °C	$\Delta\nu$ Hz	k_c[b] sec^{-1}	ΔG_c^*[c] kcal/mol
V	C_4-protons	−75.5	194[d,e]	432	9.0
XI	C_4-protons	−62.5	223[d,f]	495	9.6
	MeO	−77.0	13.8[f]	30.6	10.0

a) The dynamic NMR spectra were determined on a JEOL-C-60-H spectrometer at 60 MHz, using $CFCl_3$ as the solvent and tetramethylsilane (TMS) as the internal standard. See Figs. 4 and 5.
b) $k_c=\pi\Delta\nu/\sqrt{2}$ (Ref. 19)
c) $\Delta G_c^*=2.303RT_c(10.319-\log k_c+\log T_c)$ (Ref. 19)
d) As the signal of the low-field counterpart of the C_4 protons was hidden behind those of other methylenes, $\Delta\nu$ was estimated by the equation, $\Delta\nu=2(\nu_{high}-\nu_{average})$, where ν_{high} was the chemical shift of the high field counterpart at a low temperature and where $\nu_{average}$ was the average chemical shift at room temperature. This approximation may be rough. The discussions in the text may thus be of limited, qualitative meaning. (The authors are grateful to one of the referees for his helpful criticism on this point.)
e) Determined at −111°C.
f) Determined at −110°C.

The two conformers of 1-monosubstituted pyridinophanes (XII and XII') are nonequivalent: the (Y) substituent occupies the *pseudo*-equatorial position in XII and the *pseudo*-axial position in XII'. The NMR spectrum of the 1-hydroxy derivative IX (Fig. 6) showed the multiplet of the two C_4 protons at δ 0.2—δ −0.3. This fact suggests that the conformational change (XIId⇄XIId') is as fast as the NMR time scale at room temperature. On the other hand, even at room temperature, the flipping (XIIc⇄XIIc') of the heptamethylene chain of VIII may be slow enough

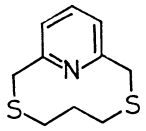

XV
ΔG_c^* <10.2 kcal/mol
T_c<−60°C

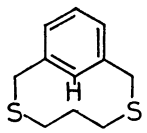

XVI
ΔG_c^* 10.2 kcal/mol
T_c−50°C

18) R. H. Mitchell and V. Boekelheide, *ibid.*, **1969**, 2013.
19) a) G. Binsch, in "*Topics in Stereochemistry.*" ed. by E. L. Eliel and N. L. Allinger, Vol. 3, Interscience Publishers, New York (1968) pp. 97—192; b) I. C. Calder and P. J. Garratt, *J. Chem. Soc., B*, **1967**, 660; c) A. Allerhand, H. S. Gutowsky, J. Jonas, and R. A. Meinzer, *J. Amer. Chem. Soc.*, **88**, 3185 (1966).

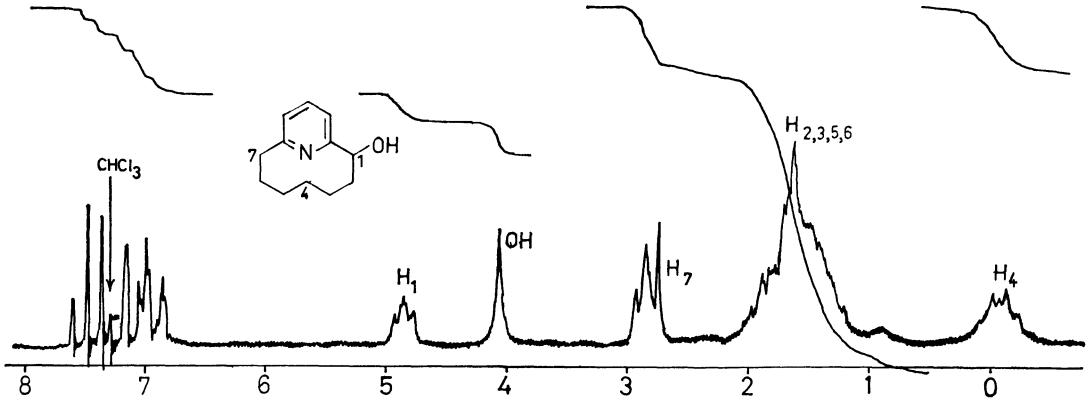

Fig. 6. NMR spectrum of IX (in $CDCl_3$ at 24°C, 60 MHz. TMS as an internal standard).

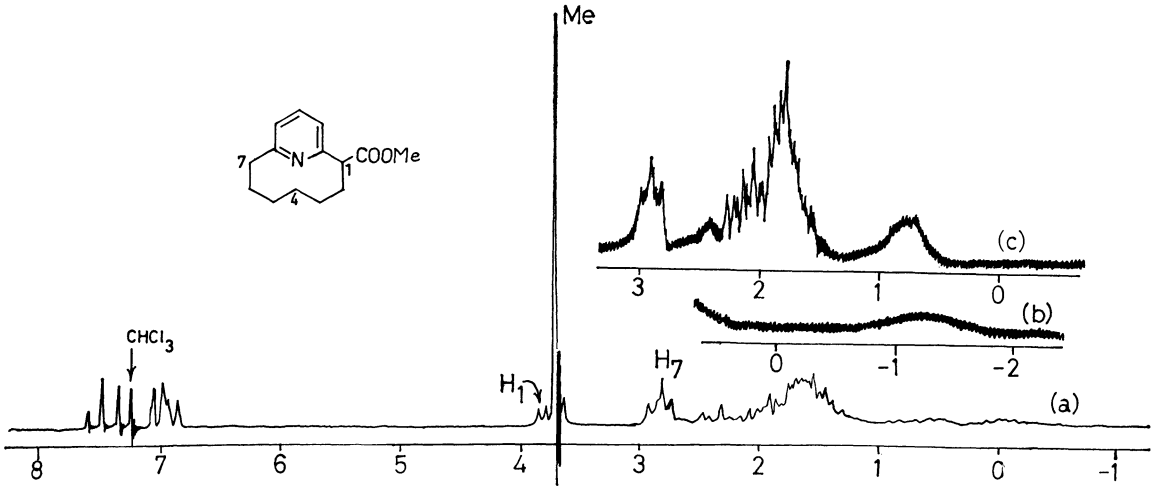

Fig. 7. NMR spectrum of VIII at 60 MHz: (a) in $CDCl_3$ at 24°C; (b) in $CDCl_3$ at −77°C; (c) in hexachlorobutadine at 140°C. TMS as an internal standard.

to induce the observed coalescence of the C_4 proton signal (Fig. 7). The signal of the two C_4 protons appeared at δ 0.70 at 140°C, corresponding to rapid exchange.

Experimental

All the melting points are uncorrected. The NMR spectra were determined on a JEOL C-60-H spectrometer at 60 MHz with deuteriochloroform, fluorotrichloromethane, and/or hexachlorobutadiene as the solvents. The mass spectra were obtained on a Hitachi RMU-6L spectrometer.

9b-Boraperhydrophenalene (I). A previous method of preparation[20] was modified as follows. A mixture of cyclododeca-1*t*,5*t*,9*c*-triene (42.0 g, 0.26 mol), the trimethylamine-borane complex[21] (19.0 g, 0.26 mol), tetrahydrofuran (THF) (50 m*l*), and cumene (110 m*l*) was added, under a nitrogen atmosphere over a 3-hr period, to cumene maintained at 135—150°C. After concentration *in vacuo*, the oily residue was distilled to give I (33.3 g, 73%); bp 122—128°C/16 mmHg.[20]

Cyclododecane-1,5-dione (IV). *(a) The Brown Oxidation of II*: A solution of I (22.2 g, 0.13 mol) and acetic acid (7.61 g, 0.13 mol) in benzene (150 m*l*) was refluxed at 100—110°C for 3 hr. After the evaporation of the solvent under a nitrogen atmosphere, the oily residue was dissolved in dry ether (120 m*l*) and a chromic acid solution (a mixture of sodium dichromate dihydrate (75.6 g), sulfuric acid (56.6 m*l*), and water 380 m*l*)) was added over a 1-hr period. The reaction mixture was extracted with ether, washed, and dried over sodium sulfate. Concentration and column chromatography on silica gel (ether-benzene 1:9) gave the diketone IV (7.47 g, 30%); mp 66.5—67.5°C (*n*-hexane, lit,[13] mp 64—65°C).

(b) The Jones Oxidation of III: The diol III (20.0 g, quantitative) was obtained from I (17.6 g, 0.10 mol) according to the method in Ref. 20a. A mixture of chromium (VI) oxide (11.2 g), sulfuric acid (9.6 m*l*), and water (30 m*l*) was added at 0°C to a solution of III (20.0 g, 0.10 mol) in acetone (700 m*l*). After filtration, 2-propanol (10 m*l*) and sodium hydrogen carbonate were added to the filtrate. The solid was filtered off, and the filtrate was concentrated and extracted with ether. Concentration and recrystallization then afforded IV (12.3 g, 63%).

[7](2,6)Pyridinophane (V). A mixture of IV (3.19 g, 16 mmol), hydroxylamine hydrochloride (2.84 g, 41 mmol), and absolute ethanol (40 m*l*) was heated at 150—175°C in a 100-m*l* autoclave for 15 hr. The reaction mixture was made strongly basic with concentrated sodium hydroxide, and, the ethanol was removed *in vacuo*. The residue was steam distilled. The distillate was extracted with ether and dried over sodium sulfate. Subsequent concentration and

20) a) G. W. Rotermund and R. Köster, *Ann. Chem.*, **686**, 153 (1965); b) H. C. Brown and W. C. Dickason, *J. Amer. Chem. Soc.*, **91**, 1226 (1969); c) N. N. Greenwood and J. H. Morris, *J. Chem. Soc.*, **1960**, 2922.

21) J. Bonham and R. S. Drago, *Inorg. Synth.*, **9**, 8 (1967).

distillation gave the pyridinophane V (1.26 g, 44%), bp 70—73°C/3 mmHg. IR (neat): 3060 2920, 2840, 1588, 1575, 1458, 1317, 1156, 788, 772, 745, and 723 cm^{-1}. The NMR and UV spectra are found in Fig. 1a and in Table 1 respectively. MS *m/e* (relative abundance): 175 (28), 147 (100), 146 (25), 123 (metastable peak for *m/e* 175→147), 121 (21), and 106 (22).

Found: C, 82.5; H, 9.9; N, 7.7%. Calcd for $C_{12}H_{17}N$: C, 82.2; H, 9.8; N, 8.0%.

[7](2,6)Pyrylophanium Perchlorate (VI). A mixture of IV (1.03 g, 5.3 mmol), trityl perchlorate (1.91 g, 5.6 mmol), and acetic acid (13 m*l*) was heated at 110—120°C for 10 min. After cooling, the reaction mixture was treated with dry ether (50 m*l*); the crystals thus precipitated (VI) (0.94 g, 65%) were collected by filtration. Mp 150°C (dec.). IR (Nujol): 3060, 1627, 1550, 1498, 1088 (broad), 868, and 798 cm^{-1}. The NMR of VI is shown in Fig. 3.

Found: C, 52.6; H, 6.0; Cl, 12.6%. Calcd for $C_{12}H_{17}ClO_5$: C, 52.1; H, 6.2; Cl, 12.8%.

[7](2,6)Pyridinophane (V) from VI. The pyrylium salt (VI) (0.31 g, 1.1 mmol) was added to a solution of ammonium acetate (0.56 g, 7.2 mmol) in acetic acid (10 m*l*). The mixture was then heated at 110°C for 5 min. After cooling, the reaction mixture was diluted with water (30 m*l*), neutralized with sodium carbonate, and extracted with ether. Drying (sodium sulfate) and concentration, followed by column chromatography on silica gel (benzene as an eluent), gave V (0.13 g, 66%); this was identical with the sample described above.

*Cyclododecane-1,5-dione-9*d (IV_D). A solution of I (7.76 g, 44 mmol) and acetic acid-*d* (2.71 g, 44 mmol) in benzene (50 m*l*) was heated at reflux for 2.5 hr and then cooled. To the mixture we then added, successively, methanolic potash (10 g potassium hydroxide in 100 m*l* methanol) and 30% aq. hydrogen peroxide (15 m*l*). After the evaporation of the solvent, the diol, III_D (6.05 g), was collected by filtration. The filtrate was extracted with ether and dried over sodium sulfate. Concentration afforded an additional crop of crystals (3.06 g). The total yield was 9.11 g (quantitative).

The oxidation of III_D (5.26 g, 26 mmol) gave cyclododecane-1,5-dione-9*d* (IV_D) (3.72 g, 72%); mp 58.5—59.0°C (*n*-hexane). IR (Nujol): 2150, 1715, 1216, 1186, 1134, 1120, 1046, 1008, 982, 891, 876, 853, 793, 780, 757, and 702 cm^{-1}. The D content as determined by MS: d_0, 8.3%; d_1, 90.6%; d_2, 1.1%.

*[7](2,6)Pyridinophane-4*d (V_D). A mixture of IV_D (1.45 g, 7.4 mmol), hydroxylamine hydrochloride (1.28 g, 18 mmol), and absolute ethanol (30 m*l*) was heated at 160—170°C in an autoclave. Work-up gave V_D as a colorless oil (0.54 g, 42%), bp 103°C (bath temperature)/7 mmHg. IR (neat): 3060, 2140, 1588, 1576, 1457, 1152, 996, 847, 780, 772, and 745 cm^{-1}. The D content as determined by NMR: 0.87 d_1/molecule. The NMR of V_D is found in Fig. Ib.

Attempted Synthesis of the N-*Oxide of V.* A mixture of V (0.15 g, 0.86 mmol), 30% aq. hydrogen peroxide (0.13 g) and acetic acid (2.0 m*l*) was heated at 80°C during 3 days. An additional 0.2 m*l* of peroxide was added in two portions during this time. The usual work-up resulted in the recovery of the starting pyridinophane.

Methyl [7](2,6)Pyridinophane-1-carboxylate (VIII). To THF (10 m*l*) there was added, at room temperature, a solution (5.0 m*l*) of *n*-butyllithium (0.74 N, 3.7 mmol) in *n*-hexane, and subsequently a solution of V (0.52 g, 3.0 mmol) in THF (10 m*l*). After sitrring under a nitrogen atmosphere for 35 min, the orange-red solution was poured onto dry ice and the solvent was evaporated to give lithium [7](2,6)-pyridinophane-1-carboxylate (0.97 g). A solution of the lithium salt in methanol (35 m*l*) was then saturated with dry hydrogen chloride and allowed to stand at room temperature for 2 days. The evaporation residue was dissolved in chloroform (15 m*l*), neutralized with aq. sodium carbonate, and dried over sodium sulfate. Concentration and dry column chromatography on silica gel (benzene as an eluent) afforded VIII as a colorless liquid (0.36 g, 52%), bp 84°C (bath temperature)/0.03 mmHg. IR (neat): 3060, 2930, 2850, 1738, 1588, 1576, 1457, 1233, 1190, 1150, 1066, 1017, 784, 778, 750, 726, and 710 cm^{-1}. MS *m/e* (relative abundance): 233 (34), 218 (100), 205 (57), 174 (53), 173 (23), 172 (35), 147 (25), 146 (46), 145 (31), 144 (43), 133 (77), 132 (33), and 119 (34). The NMR spectrum of VIII is shown in Fig. 7.

Found: C, 72.2; H, 8.1; N, 6.1%. Calcd for $C_{14}H_{19}NO_2$: C, 72.1; H, 8.2; N, 6.0%.

[7](2,6)Pyridinophan-1-ol (IX). To THF (10 m*l*) we added, successively, a solution (8.0 m*l*) of *n*-butyllithium (0.74 N) in *n*-hexane and a solution of V (0.54 g, 3.1 mmol) in THF (10 m*l*). After stirring under a nitrogen atmosphere for 35 min, the orange-red solution was cooled to −75°C and oxygen was passed through the solution for 1.5 hr. The reaction mixture was then treated with aq. ammonium chloride (5 m*l*), extracted with ether, and dried over potassium carbonate. Concentration and dry-column chromatography on silica gel (benzene and ether as eluents) afforded IX as white crystals (0.38 g, 65%); bp 95°C (bath temperature)/0.1 mmHg; mp 53.5—54.0°C (*n*-hexane). IR (KBr disk): 3250, 3060 (shoulder), 1596, 1576, 1467, 1293, 1264, 1087, 1072, 1050, 1000, 880, 853, 797, 786, 750, 723, and 700 cm^{-1}. MS *m/e* (relative abundance): 191 (100), 174 (22), 172 (23), 163 (51), 144 (36), 134 (76), 121 (41), 93 (27), 77 (26), and 65 (26). The NMR spectrum is found in Fig. 6, and the UV data, in Table 1.

Found: C, 75.4; H, 8.9; N, 7.3%. Calcd for $C_{12}H_{17}NO$: C, 75.4; H, 9.0; N, 7.3%.

[7](2,6)Pyridinophan-1-one (X). To cooled pyridine (10 m*l*) we added a solution of chromium(VI) oxide (1.00 g) in water (1 m*l*) and a solution of IX (0.31 g, 1.6 mmol) in pyridine (10 m*l*). The mixture was then allowed to stand overnight at room temperature, poured into water (200 m*l*), and extracted with ether. The combined extracts were thoroughly washed with water and dried over sodium sulfate. Subsequent concentration and dry-column chromatography on silica gel (benzene as an eluent) yielded the ketone X (0.17 g, 55%); mp 33.5—34.5°C (*n*-hexane). IR (KBr disk): 3060, 1693, 1585, 1455, 1446, 1345, 1310, 1263, 1247, 1216, 1141, 1061, 1029, 1017, 1001, 929, 851, 799, 760, 752, 730 cm^{-1}. MS *m/e* (relative abundance): 189 (47), 161 (13), 133 (100), 132 (26), 91 (19), and 89 (19). The NMR is shown in Fig. 2, and the UV data, in Table 1.

Found: C, 76.1; H, 7.9; N, 7.2%. Calcd for $C_{12}H_{15}NO$: C, 76.2; H, 8.0; N, 7.4%.

1,1-Dimethoxy[7](2,6)pyridinophane (XI). A mixture of X (0.15 g, 0.80 mmol), *p*-toluenesulfonic acid (0.24 g), methyl orthoformate (1.29 g), and methanol (30 m*l*) was heated under reflux for 2 hr and then neutralized after cooling with methanolic sodium hydroxide (1 g of sodium hydroxide in 5 m*l* of methanol). After the evaporation of the solvent, the residue was diluted with water (30 m*l*), extracted with ether, and dried over sodium carbonate. Subsequent concentration and distillation gave XI as a colorless liquid (0.16 g, 86%); 85°C (bath temperature)/0.06 mmHg. IR (neat): 3060, 1590, 1579, 1127, 1099, 1083, 1050, 810, 790, 757, 750, 728 cm^{-1}. MS *m/e* (relative abundance): 235 (1), 220 (38), 204 (15), 203 (19), 188 (100), 160 (32). The

NMR spectrum is shown in Fig. 5.

Found: C, 71.3; H, 9.0; N, 5.9%. Calcd. for $C_{14}H_{21}NO_2$: C, 71.5; H, 9.0; N, 6.0%.

The authors are grateful to Professor K. Sisido for his generous help. Financial support from the Ministry of Education, Japanese Government, and from the Toray Science Foundation is also acknowledged with pleasure.

BULLETIN OF THE CHEMICAL SOCIETY OF JAPAN, VOL. 44, 2833—2836(1971)

Stereochemical Studies of Monoterpene Compounds. XII.[1] The Acid-Catalyzed Rearrangements of 2α-Bromo-10β-pinan-3-one

Toshifumi HIRATA and Takayuki SUGA[2]

Department of Chemistry, Faculty of Science, Hiroshima University, Higashisenda-machi, Hiroshima

(Received March 13, 1971)

In connection with the bromination of 3-acetoxy-pin-2-ene (II), the acid-catalyzed rearrangement of 2α-bromo-10β-pinan-3-one (I) was investigated under several conditions. The bromoketone (I) was thus found to yield (+)-6-*endo*-bromocamphor (III), (−)-α-carvone (V), (−)-8-hydroxycarvotanacetone (VI), carvacrol (VII), (+)-dihydro-β-campholenolactone (VIII), and (+)-campholenic acid (IX). It also became clear that the bromocamphor (III) and the (V), (VI), and (VII) products are directly formed from the bromoketone (I), whereas the γ-lactone (VIII) is obtained *via* α-campholenic acid (IX) from the bromocamphor (III). The mechanistic implications of the rearrangements are discussed.

Because 2α-bormo-10β-pinan-3-one (I) was necessary in the course of our study of the stereochemistry of the oxygenated pinane system, the bromination of 3-acetoxy-pin-2-ene (II) was carried out by following the method in the literature,[3] but the literature has reported the formation of only the bromoketone (I). In contrast with the results reported in the literature, however, we found the method to result in the formation of not only the bromoketone (I), but also an isomeric bromoketone, 6-*endo*-bromocamphor (III). We now wish to report on the results of the bromination of II and, further, to deal with the acid-catalyzed rearrangement of the bromoketone (I) and the mechanistic implications of the reaction.

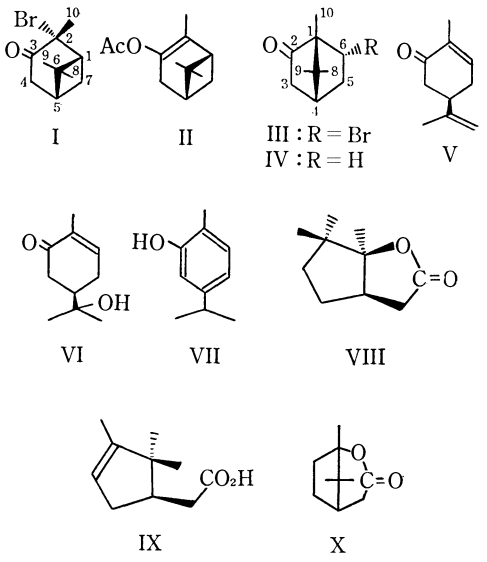

Results and Discussion

Under exactly the same conditions as in the literature,[3] the treatment of a carbon tetrachloride solution of (−)-3-acetoxy-pin-2-ene (II) with bromine in the presence of anhydrous sodium carbonate gave an oily reaction mixture, which was composed of (−)-2α-bromo-10β-pinan-3-one (I) (84% yield) and (+)-6-*endo*-bromocamphor (III) (5.0%), accompanied by unchanged enol-acetate (II) (4.0%). The bromocamphor (III) was confirmed by comparing its spectral data with those reported for 6-*endo*-bromocamphor[4] and by converting it into (+)-camphor (IV) on debromination.

In order to clarify the mechanism of the formation of the bromocamphor (III), the bromoketone (I) was subjected to acid treatments under various conditions. In the literature,[3] the treatment of the bromoketone (I) with 10% acetic acid under reflux for 3 hr has been reported to give only an intractable oil. The re-examination of this reaction clarified that the product consisted of (−)-carvone (V), (−)-8-hydroxycarvotanacetone (VI), carvacrol (VII), and (+)-dihydro-β-campholenolactone (VIII), accompanied by a trace of the bromocamphor (III). On the other hand, the bromoketone (I) was converted into the bromocamphor (III) in a 55% yield on treatment with 10% acetic acid at 50°C for 5 hr. The reaction of the bromoketone (I) with dilute hydrobromic acid at 50°C for 5 hr yielded also the bromocamphor (III) in a

1) Paper XI of this series: T. Suga, T. Hirata, and T. Matsuura, *J. Chem. Soc., C*, submitted for publication.

2) To whom all inquiries regarding to this paper should be addressed.

3) M. P. Hartshorn and A. F. A. Wallis, *Tetrahedron*, **21**, 273 (1965).

4) M. P. Hartshorn and A. F. A. Wallis, *J. Chem. Soc.*, **1964**, 5254.

34% yield, along with the same kinds of products as above. These results show the ready conversion of the bromoketone (I) into the bromocamphor (III) by the acid-catalyzed reaction. Thus, the formation of the bromocamphor (III) in the bromination of the enol-acetate (II) is clearly due to the acid (probably hydrobromic acid)-catalyzed rearrangement of the bromoketone (I) initially produced.

The heating of the bromocamphor (III) with 10% acetic acid afforded only dihydro-β-campholenolactone (VIII). This shows the bromocamphor (III) to be connected only with the formation of the γ-lactone (VIII), not with that of such products as (V), (VI), and (VII). Moreover, the milder reaction of the bromocamphor (III) with aqueous acetic acid indicated the formation of (+)-α-campholenic acid (IX), along with the γ-lactone (VIII) and 1,2-campholide (X). The acid (IX) is expected as an intermediate in the formation of the lactone (VIII). The formation of the acid (IX) was also proved in the reaction of the bromoketone (I) with aqueous hydrobromic acid.

The formation of the products from the bromoketone (I) is best explained by the following three pathways: (a) the alteration of the bicyclo[3.1.1]skeleton to the monocyclic system, (b) the intramolecular rearrangement to the bicyclo[2.2.1]skeleton, and (c) lactonization involving the Wagner-Meerwein rearrangement. The formation of the (V), (VI), and (VII) products can be explained by the (a) pathway and can be explained as initiated by the detachment of the *t*-bromine atom from the bromoketone (I) with the acid, followed by the opening of the bridge to form the carbonium ion, as is shown in Scheme I. The intramolecular rearrangement in the (b) pathway is supported by the ready conversion of the bromoketone (I) into the bromocamphor (III) even under such conditions as in the absence of bromine. The mutual exchange between the *gem*-dimethyl brigde and the bromine atom in the bromoketone (I), followed by intramolecular rearrangement through a transition state (XI), results in the formation of a more stable compound, the bromocamphor (III), as is shown in Scheme II. The transition state (XI) is not so absurd because of the analogy to the transition state in the diaxial-diequatorial rearrangement proposed by Grob[5] and Barton.[6] Finally, the formation of dihydro-β-campholenolactone (VIII) from the bromocamphor (III) can be explained by the same mechanism as the rearrangement of 2-hydroxypinocamphone with anhydrous oxalic acid, which was reported recently by us.[7] The migration of the bromine atom and the (a) bond affords the acid (IX) as an intermediate product. It suffers protonation on an ethylenic bond, the 1,2-shift of a methyl group of the *gem*-dimethyl group, and then the lactonization of the carboxyl group, thus yielding the γ-lactone (VIII) (Scheme III).

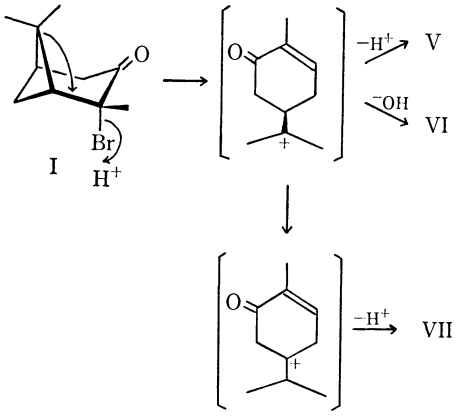

Scheme I

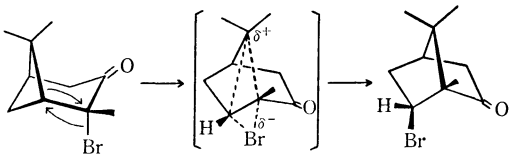

Scheme II

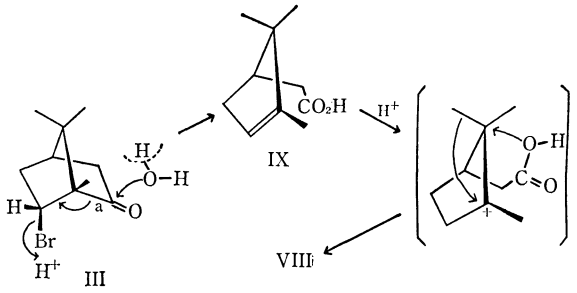

Scheme III

Experimental

The IR spectra were recorded with a Hitachi EPI-S Infrared Spectrophotometer. The NMR spectra were measured with a Hitachi Perkin-Elmer R-20 high-resolution spectrometer, using tetramethylsilane as the internal standard. The mass-spectral analyses were performed by a Hitachi mass-spectrometer, Model RMS-4, ionizing at the order of 80 eV. Vapour-phase chromatographic analyses were made using a Hitachi Perkin-Elmer F6-D gas chromatograph with attached a column packed with 20% PEG-6000 on Celite.

3-Acetoxy-pin-2-ene (II). Following the method in the literature,[3] the treatment of isopinocamphone ($[\alpha]_D^{25}$ −11.1°) with acetic anhydride in the presence of perchloric acid, followed by purification on a silica gel column, afforded II in a 76% yield: $[\alpha]_D^{25}$ −35.0° (*c* 0.29, MeOH), lit[3] $[\alpha]_D^{25}$ +36° (*c* 1.00), derived from (+)-isopinocamphone; $\nu_{max}^{liq.}$ 1760 cm^{-1} (enol-acetate); NMR (CCl_4) δ 0.98 (s, C_9-3H), 1.30 (s, C_8-3H), 1.55 (t, J=1.5 Hz, C_{10}−3H), and 2.09 ppm (s,OAc).

Bromination of 3-Acetoxy-pin-2-ene (II). To a stirred suspension of 1.08 g of II and 1.00 g of anhydrous sodium carbonate in 5 m*l* of carbon tetrachloride, we added 0.94 g of bromine in 4 m*l* of carbon tetrachloride over a 5-min period at 0°C. After stirring for an additional 5 min, the reaction mixture was isolated by ether to give 1.13 g of an

5) C. A. Grob and S. Winstein, *Helv. Chim. Acta*, **35**, 782 (1952).
6) D. H. Barton and J. F. King, *J. Chem. Soc.*, **1958**, 4398.
7) T. Suga, T. Hirata, M. Noda, and T. Matsuura, *Experientia*, **26**, 1192 (1970).

oily product, which was then subjected to column chromatography on silica gel with a mixture of ethyl acetate and *n*-hexane to obtain 0.94 g of I, 0.06 g of III, and 0.05 g of unchanged II. The (I) and (III) products were identified on the basis of the following physical properties and the chemical reaction.

The Bromoketone (I): $[\alpha]_D^{25}$ −101.8° (*c* 1.18, MeOH); $\nu_{max}^{liq.}$ 1722 (C=O), lit[3] 1726 cm^{-1}, and 1376 and 1393 cm^{-1} (*gem*-dimethyl); λ_{max}^{MeOH} 313 nm (ε 135.3), lit[3] 312.5 nm (ε 130). The C-9, C-8, and C-10 methyl proton signals appeared at δ 0.91, 1.41, and 1.93 ppm in a 10% carbon tetrachloride solution, at δ 0.49, 0.93, and 1.88 ppm in a 10% benzene solution, and at δ 0.73, 1.19, and 1.93 ppm in a 10% pyridine solution, respectively, as singlets.

The Bromocamphor (III): mp 132—133°C, lit[4] mp 133—134°C; $[\alpha]_D^{25}$ + 36.6° (*c* 0.63, MeOH), lit[4] $[\alpha]_D^{25}$ + 44° (*c* 1.04); $\nu_{max}^{CCl_4}$ 1751 (C=O), lit[4] 1757 cm^{-1}, and 1381 and 1396 cm^{-1} (*gem*-dimethyl); λ_{max}^{MeOH} 291 nm (ε 40.8); NMR (CCl_4) δ 0.90 (s, C_8- and C_{10}-3H), 0.98 (s, C_9-3H), and 4.11 ppm (d.d, *J*=9.5 and 3.5 Hz, C_6-H); mass spectrum *m/e* (rel. intensity) 232 and 230 (M^+; 4) 217 and 215 (2), 190 and 188 (1), 175 and 173 (13), 151 (66), 135 and 133 (4), 109 (100), 94 (13).

The Debromination of 50 mg of III was carried out in 0.4 m*l* of 70% acetic acid with the addition of 50 mg of zinc powder under reflux over a 1-hr period. Ether extraction of the filtrate freed from the zinc powder afforded 31 mg of (+)-camphor (IV): $[\alpha]_D^{25}$ +30.1° (*c* 0.19, MeOH); $\nu_{C=O}^{KBr}$ 1743 cm^{-1}.

Rearrangement of 2α-Bromo-10β-pinan-3-one (I). *A) With Hydrobromic Acid*: A stirred suspension of 800 mg of the bromoketone (I) in 40 m*l* of 10% hydrobromic acid was heated at 50°C for 5 hr. The reaction product was treated with a 5% sodium carbonate solution, and then it was extracted with ether. The neutral reaction mixture obtained from the ether layer was subjected to column chromatography on silica gel with a mixture of ethyl acetate and *n*-hexane; we thus obtained 153 mg of (+)-6-*endo*-bromocamphor (III), 14 mg of (−)-carvone (V), 158 mg (−)-8-hydroxycarvotanacetone (VI), 24 mg of carvacrol (VII), and 90 mg of (+)-dihydro-β-campholenolactone (VIII). The aqueous layer, after it had been acidified with dilute hydrochloric acid, was extracted with ether to yield 25 mg (+)-α-campholenic acid (IX). Each component was confirmed by comparing its spectra and physical properties with those of an authentic sample[8] and/or by preparing their crystalline derivatives, as is shown below.

(+)-Bromocamphor (III): mp 132—133°C; $[\alpha]_D^{25}$ +37.0° (*c* 0.63, MeOH); ν_{max}^{KBr} 1752 cm^{-1} (C=O).

(−)-Carvone (V): $[\alpha]_D^{25}$ −45.0° (*c* 0.15, MeOH); $\nu_{max}^{liq.}$ 1677 (α,β-unsaturated C=O) and 3063 cm^{-1} (*endo*- methylene); λ_{max}^{MeOH} 236 nm (ε 6900); the 2,4-dinitrophenylhydrazone, mp 187—188°C.

(−)-8-Hydroxycarvotanacetone (VI): $[\alpha]_D^{25}$ −40.5° (*c* 0.15, MeOH); $\nu_{max}^{liq.}$ 1660 (α,β-unsaturated C=O) and 3400 cm^{-1} (OH); λ_{max}^{MeOH} 235 nm (ε 9100); NMR (CCl_4) δ 1.18 (s, C_9- and C_{10}-3H), 1.72 (b.s, C_7-3H), and 6.66 ppm (b.s, C_6-H); the semicarbazone, mp 178—179°C.

Carvacrol (VII): $\nu_{max}^{liq.}$ 1619 and 1584 (aromatic C=C), 1370 and 1385 (isopropyl), and 3400 cm^{-1} (OH); λ_{max}^{MeOH} 277 nm (ε 2150).

(+)-Dihydro-β-campholenolactone (VIII): mp 30°C; $[\alpha]_D^{25}$ +22.8° (*c* 0.15, EtOH); ν_{max}^{KBr} 1775 cm^{-1} (C=O); NMR (CCl_4) δ 0.90, 1.08, and 1.26 ppm (s, 3H, respectively).

(+)-α-Campholenic Acid (IX): $[\alpha]_D^{25}$ +5.3° (*c* 0.10, MeOH); $\nu_{max}^{liq.}$ 1710 (COOH), 1370 and 1392 cm^{-1} (*gem*-dimethyl); NMR (CCl_4) δ 0.78 (s, 3H), 0.99 (s, 3H), 1.58 (b.s, 3H), and 5.17 ppm (b.s, 1H).

B) Under Other Conditions: The reactions were carried out under various conditions, as is shown below. The bracketed figures in the heading show the experimental number in Table 1. (1) A solution of the bromoketone (I) (100 mg) in carbon tetrachloride (5 m*l*) was maintained at 50°C for 5 hr. (2) The bromoketone (300 mg) was stirred into a suspension of bromine (300 mg) and anhydrous sodium carbonate (300 mg) in carbon tetrachloride (15 m*l*) at 50°C over a 5-hr period. (3) The bromoketone (100 mg) was heated in 10% acetic acid-carbon tetrachloride (5 m*l*) at 50°C for 5 hr. (4) A suspension of the bromoketone (100 mg) in 10% aqueous acetic acid (5 m*l*) was stirred at 50°C for 5 hr. (5) The bromoketone (100 mg) was refluxed in 10% aqueous acetic acid (5 m*l*) for 3 hr. (6) A suspension of the bromoketone (100 mg) in 5% hydrobromic acid (5 m*l*) was stirred at 50°C for 5 hr. (7) The bromoketone (100 mg) was maintained in a mixture of 5% hydrobromic acid (5 m*l*) and methanol (10 m*l*) at 50°C for 5 hr. (8) The bromoketone (100 mg) was heated in the stirred suspension of 10% hydrobromic acid (2.5 m*l*) and 10% aqueous acetic acid (2.5 m*l*) at 50°C for 5 hr.

After the reaction, the whole reaction mixture were extracted with ether. The ether solution was washed with a sodium bicarbonate solution, and then water, after which it was dried over anhydrous sodium sulfate. The removal of the solvent from the solution gave a reaction mixture, which was subjected to preparative thin-layer chromatography on silica gel with a mixture of ethyl acetate and *n*-hexane (3:7 by volume) in order to separate the components. Each component was confirmed by comparing its spectra and physical properties with those of an authentic sample. The results of these reactions are summarized in Table 1.

Table 1. Rearrangements of bromoketone (I) under various conditions

Expt. No.	Yield of products (%)					
	III	V	VI	VII	VIII	I (unchanged)
1	trace[a]	—	—	—	—	95
2	2.3	—	—	—	—	94
3	7.6	—	—	—	—	87
4	55	12	21	trace[a]	trace[a]	—
5	trace[a]	3.0	17	41	13	—
6	30	8.0	11	trace[a]	trace[a]	13
7	22	9.5	6.1	trace[a]	5.6	22
8	30	5.1	32	1.0	3.2	—

a) These were only detected by gas chromatographic and thin-layer chromatographic analyses.

Rearrangements of (+)-6-endo-Bromocamphor (III). *A) Under Reflux for 3 hr*: The bromocamphor (III) (50 mg), dissolved in 10% acetic acid (2.5 m*l*) was stirred under reflux for 3 hr. The reaction mixture was extracted by ether to obtain a reaction product (36 mg). Gas-chromatographic analysis showed the product to consist of 93% of the γ-lactone (VIII) and 1.6% of the unchanged bromocamphor (III). The product was subjected to preparative thin-layer chromatography with silica gel with 30% ethyl acetate - *n*-hexane in order to isolate the lactone (VIII) (32 mg): mp 30—31°C; $[\alpha]_D^{25}$ +29.8° (*c* 0.24, EtOH); ν_{max}^{KBr} 1775 cm^{-1} (γ-lactone).

B) Under Milder Conditions: A suspension of III in

8) T. Hirata, T. Suga, and T. Matsuura, This Bulletin, **43**, 2588 (1970).

10% acetic acid was stirred at 105°C for 2 hr in the same manner as above. The ether solution of the reaction mixture was then treated with a 5% sodium carbonate solution in order to isolate (+)-α-campholenic acid (IX) (16%): $[\alpha]_D^{25}$ 5.0° (*c* 0.15, MeOH); $\nu_{max}^{liq.}$ 1710 cm^{-1} (COOH). The neutral reaction mixture freed from the acid was composed of (+)-γ-lactone (VIII) (55%), 1,2-campholide (X) (1.5%), and the unchanged bromocamphor (III) (4.5%). The δ-lactone (X) was only detected by gas-chromatographic and thin-layer chromatographic analyses.

BULLETIN OF THE CHEMICAL SOCIETY OF JAPAN, VOL. 44, 2836—2839(1971)

Studies of *N*-Sulfinyl Compounds. VI.[1] The Preparation of *N*-Sulfinylbenzamide and Its Reaction with Styrene Oxide

Otohiko TSUGE and Shuntaro MATAKA

Research Institute of Industrial Science, Kyushu University, Hakozaki, Fukuoka

(Received March 18, 1971)

The reaction of benzamide with thionyl chloride in the presence of pyridine gave *N*-sulfinylbenzamide and *N,N'*-dibenzoylsulfurdiimide. It has been found that *N*-sulfinylbenzamide reacted with styrene oxide in the presence of tetraethylammonium bromide to give 4-oxo-5-benzoyl-2,6-diphenyl-1,4,3,5-oxathiadiazepine as the main product, accompanied by lesser quantities of two *N*-benzoyl-phenylaminoethanols, 2,5-diphenyloxazoline, benzonitrile, and benzamide. The pathways for the formation of the products are suggested.

In previous papers in which the reactions of *N*-sulfinylanilines (Ar-NSO)[2] and of *N*-sulfinyl-*p*-toluenesulfonamide (Tos-NSO)[3] with styrene oxide in the presence of tetraethylammonium bromide (Et_4NBr) were investigated, the corresponding two tetraarylpiperazines were formed in the reactions of *N*-sulfinylanilines, while the reaction of *N*-sulfinyl-*p*-toluenesulfonamide gave the 1-oxo-1,2,5-thiadiazolidine compound, accompanied by two aminoalcohols.

Recently, it has been reported by Scherer and Schmitt[4] that *N*-sulfinylbenzamide (I) which had been prepared from the reaction of *N,N*-bis-trimethylsilylbenzamide with thionyl chloride, reacted with norbornene to give the (2+4) cycloadduct, 4-oxo-2-phenyl-4a,5,6,7,8,8a-hexahydro-5,8-methano-1,4,3-benzoxathiazine.

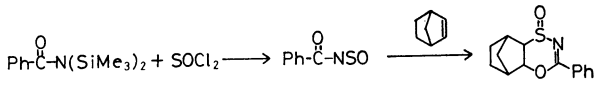

I

On the basis of the above fact, it may be inferred that I is not only more reactive than *N*-sulfinylanilines, but also behaves as the 1,4-dipole in the following resonance structures.

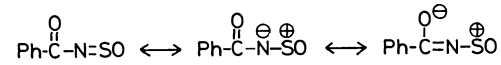

Accordingly, the reaction of I with styrene oxide can be expected to give products of a different type from those in the reactions of *N*-sulfinylanilines and of *N*-sulfinyl-*p*-toluenesulfonamide.

In the present paper we wish to report on the preparation of I by the reaction of benzamide with thionyl chloride, and on the formation of the 1,4,3,5-oxathiadiazepine compound as the main product in the reaction of I with styrene oxide.

Results and Discussion

The Reaction of Benzamide with Thionyl Chloride. It has been found by Olah[5] that benzamide reacted with thionyl chloride to give *N*-sulfinylbenzamide (I), but he failed to isolate I in a pure form.

After the reaction of benzamide with thionyl chloride was conducted in a mixed solvent of benzene and pyridine at temperatures below 10°C, the reaction mixture was rapidly filtered to remove the pyridine hydrochloride; then the filtrate was distilled under reduced pressure to give I, bp 76°C/0.16 mmHg (lit,[4] bp 70°C/0.1 mmHg), as an yellow oil in a 62% yield and dark brown crystals (II), together with a small amount of benzonitrile. It is very important that distillation is carried out at temperatures below 100°C, because an appreciable decomposition of I takes place above 100°C.

As I proved rather unstable and was decomposed by moisture in the air, the elemental analysis of I was not carried out. However, the IR spectrum of I was in agreement with that reported by Scherer and Schmitt.[4] Furthermore, I was easily hydrolyzed to give benzamide, and was violently decomposed at 130°C to yield benzonitrile.

1) Part V of this series: O. Tsuge and S. Mataka, *Nippon Kagaku Zasshi*, **92**, 543 (1971).

2) O. Tsuge and S. Mataka, This Bulletin, **44**, 1896 (1971).

3) O. Tsuge and S. Mataka, *Nippon Kagaku Zasshi*, **92**, 543 (1971).

4) O. J. Scherer and R. Schmitt, *Chem. Ber.*, **101**, 3302 (1968).

5) The authors wish to express their appreciation to Professor G.A. Olah of Case-Western Reserve University for his personal communication.

On the other hand, the compound II which was obtained as a residue on distillation, was also unstable and was easily hydrolyzed to give benzamide. Although II could not be isolated in a pure form, its

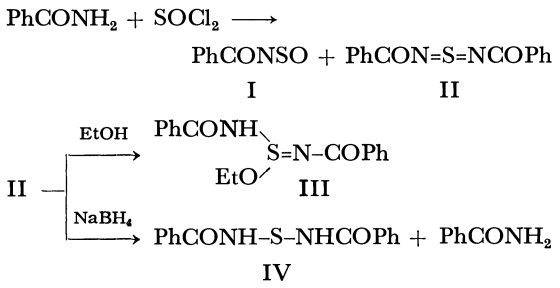

structure was assumed to be *N,N'*-dibenzoylsulfurdiimide (II) on the basis of the following chemical transformations.

The treatment of II with excess amounts of ethanol gave *S*-benzamido-*S*-ethoxy-*N*-benzoylsulfilimine (III), mp 135—140°C (decomp.), which was then gradually decomposed on standing at room temperature to give benzamide in a low yield. The structure of III was confirmed by a study of its IR spectrum as well as by the elemental analysis. Furthermore, II was reduced with sodium borohydride, affording *N,N'*-thiodibenzamide (IV) and benzamide under the elimination of hydrogen sulfide.

It is known[6] that *N*-sulfinyl compounds react with a base to give the corresponding sulfurdiimides under the elimination of sulfur dioxide. Although Scherer and Schmitt[4] reported that attempts to prepare II by the reaction of I with a trace amount of a base were unsuccessful, it may be considered that II was obtained *via* the reaction with pyridine of I formed from benzamide and thionyl chloride.

The Reaction of N-*Sulfinylbenzamide with Styrene Oxide.* When a solution of *N*-sulfinylbenzamide (I) and styrene oxide (V) in benzene was refluxed with Et_4NBr for 1 hr, a colorless crystalline compound VII, mp 171—172°C (decomp.), was obtained as the main product, accompanied by lesser quantities of crystals, VI, mp 126—7°C, a pale green liquid, VIII, benzonitrile and benzamide.

Although VI was proved, by the elemental analysis as well as by a comparison of its IR and NMR spectra with those of authentic samples of *N*-benzoyl-*β*-phenyl-*β*-aminoethanol (VIa), mp 151°C (lit,[7] mp 154—154.5°C), and *N*-benzoyl-α-phenyl-*β*-aminoethanol (VIb), mp 147—148°C (lit,[8] mp 148.6—149.1°C), to be a mixture of nearly equal amounts of VIa and VIb, attempts to isolate VIa and VIb in pure forms were unsuccessful.

The results of the elemental analysis and the molecular weight (M^+ *m/e* 390) of VII were consistent with those of the compound derived from a 2:1 adduct of I and V under the elimination of sulfur dioxide. The IR spectrum of VII showed characteristic bands ascribed to the C=O and/or C=N bonds at 1660 and 1630 cm^{-1}, while the NMR spectrum in deuteriochloroform ($CDCl_3$) exhibited double doublets at δ 4.75 (H_A, 1H), 5.64 (H_B, 1H) and 6.25 ppm (H_X, 1H), with coupling constants of $J_{AB}=8$, $J_{BX}=2$, and $J_{AX}=7$ Hz, besides a signal of aromatic protons (15H).

On the basis of the above observations and inspections of reaction courses, the following compounds (VII-1—VII-7) can be said to be possible for the structure of VII (Chart 1); the compounds VII-1—VII-3 correspond to the apparent cycloadducts of I to 1-benzoyl-2-phenylaziridine,[9] while compounds VII-4—VII-7 correspond to the cycloadducts of I to the sulfurdiimide II.

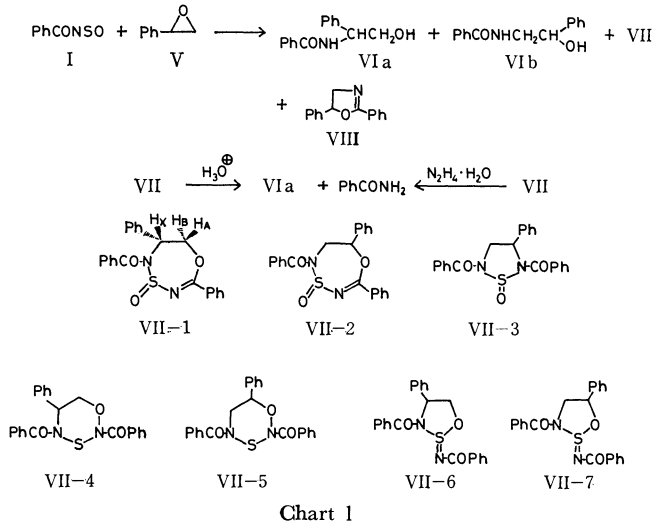

Chart 1

The hydrolysis of VII with hydrochloric acid in methanol gave the aminoethanol VIa and benzamide in 38 and 97% yields respectively. Also, VII reacted with hydrazine hydrate under the elimination of hydrogen sulfide, affording VIa and benzamide in good yields. The production of VIa from VII eliminated the possibility of VII-2, VII-5 and VII-7 for the structure of VII.

On the other hand, the mass spectrum of VII showed peaks at *m/e* 390 (M^+), 389 (M^+–H), 342 (M^+–SO), 238 (342^+–$PhCH=CH_2$), 223 (M^+–PhCONSO and/or 342^+–PhCON, base peak), 193 (223^+–CH_2O), and 105 ($PhCO^+$). The appearance of the peak at *m/e* 342 in the spectrum excluded the compounds VII-4 and VII-6 as the possible structure of VII.

Previously,[3] we reported that 1-oxo-2,5-di(*p*-toluenesulfonyl)-3-phenyl-1,2,5-thiadiazolidine, which had been obtained from the reaction of *N*-sulfinyl-*p*-toluenesulfonamide with V, was hydrolyzed with hydrochloric acid in methanol, thus affording *N,N'*-di(*p*-toluenesulfonyl)-1-phenylethylene-1,2-diamine in a good yield.

If VII is the 1,2,5-thiadiazolidine VII-3, the corresponding ethylenediamine compound should be given

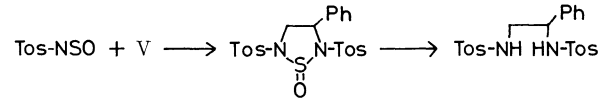

6) G. Kresze and W. Wucherpfennig, *Angew. Chem.*, **79**, 109 (1967).

7) S. Gabriel and J. Colman, *Ber.*, **47**, 1871 (1914).

8) A. J. Castro, D. K. Brain, H. D. Fischer, and R. K. Fuller, *J. Org. Chem.*, **19**, 1444 (1954).

9) 1-Benzoyl-2-phenylaziridine corresponds to the compound derived from the 1:1 adduct of I and V under the elimination of sulfur dioxide.

by the hydrolysis of VII.

Consequently, it may be deduced that the most reasonable structure for VII is 4-oxo-5-benzoyl-2,6-diphenyl-1,4,3,5-oxathiadiazepine (VII-1).

On the other hand, VIII was proved to be 2,5-diphenyloxazoline by the spectral studies as well as by the identification of its picrate with the authentic sample prepared by the method of Wolfheim.[10]

The formation of 4-oxo-1,4,3,5-oxathiadiazepine VII is of interest in connection with the contribution of the 1,4-dipole of I.

Several pathways for the formation of VII and oxazoline VIII are possible.[11] On the basis of the previously reported results,[3,4,12-14] and of the formation of aminoalcohols VIa and VIb, however, we considered that compounds VII and VIII were derived from the 2-oxo-1,2,3-oxathiazolidine intermediates A and B which were formed by the (2+3)cycloaddition of I to 1,3-dipoles arising from the cleavage of the bond *a* or *b* in V, as shown in Chart 2.

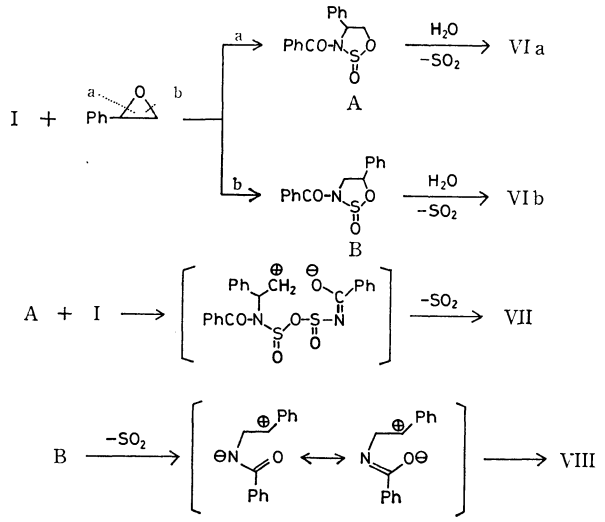

Chart 2

As has previously been reported,[3] reactive *N*-sulfinyl-*p*-toluenesulfonamide reacted with V under similar conditions, giving 1-oxo-1,2,5-thiadiazolidine whose structure corresponded to the compound derived from a 2:1 adduct of the *N*-sulfinyl compound and V under the elimination of sulfur dioxide.

Because I as well as *N*-sulfinyl-*p*-toluenesulfonamide is more reactive than *N*-sulfinylanilines, I will be able to further attack 2-oxo-1,2,3-oxathiazolidine intermediates; the attack of I on A will be preferable to that on B having 5-phenyl group.

As is shown in Chart 2, the reaction of I with A leads to the formation of VII under the elimination of sulfur dioxide. On the other hand, the elimination of sulfur dioxide from the intermediate B and subsequent ring closure results in the formation of VIII. The by-products, benzonitrile and benzamide, may be secondarily formed from I and VII.

Experimental

All the melting and boiling points are uncorrected. The NMR spectra were determined at 60 MHz with a Hitachi-20 NMR spectrometer, using TMS as the internal reference, while the mass spectra were obtained on a Hitachi RMS-4 mass spectrometer, using a direct inlet and an ionization energy of 70 eV.

Reaction of Benzamide with Thionyl Chloride. To a stirred solution of 48.2 g of benzamide and 64.0 g of pyridine in 400 m*l* of benzene, a solution of 47.6 g of thionyl chloride in 200 m*l* of benzene was added, drop by drop, at a temperature below 10°C over a period of 12 hr. After the reaction mixture was allowed to stand overnight at room temperature, the precipitated pyridine hydrochloride was rapidly removed by filtration. The filtrate was evaporated *in vacuo* to remove the solvents and benzonitrile, and then a residue was distilled under reduced pressure to give 41.3 g (62%) of *N*-sulfinylbenzamide (I), bp 76°C/0.16 mmHg (lit,[4] bp 70°C/0.1 mmHg), as an yellow oil, and to leave 10 g of crude *N,N'*-dibenzoylsulfurdiimide (II) as dark brown crystals.

The IR spectrum (neat) of I was in agreement with that reported by Scherer and Schmitt.[4] The main absorption bands are as follows: 3060, 1700, 1675, 1600, 1585, 1490, 1450, 1380, 1320, 1240, 1180, 1140, 1100, 1075, 1030, 1005, 950, 850, 810, 740, 710, 685, 655, 620, and 520 cm^{-1}.

The treatment of crude II, whose IR spectrum was similar to that of I, with an excess of ethanol gave colorless crystals. The crystals were rapidly collected by filtration and washed with ethanol to give *S*-benzamido-*S*-ethoxy-*N*-benzoylsulfilimine (III), mp 135—140°C (decomp.), which gradually decomposed on standing in air to give benzamide.

Found: C, 60.79; H, 4.76; N, 8.87%. Calcd for $C_{16}H_{16}O_3N_2S$: C, 60.75; H, 5.10; N, 8.86%. IR (KBr): 3040 (ν_{NH}), 1683 cm^{-1} (ν_{CO}).

Reduction of N,N'-Dibenzoylsulfurdiimide (II) with Sodium Borohydride. A suspension of 1.74 g of crude II in 20 m*l* of diethyl ether was stirred with 0.25 g of sodium borohydride at room temperature for 24 hr. The reaction mixture was poured into an ice-water mixture and was then extracted with chloroform. The chloroform-extract was washed with water, dried over sodium sulfate, and then evaporated *in vacuo* to give 0.82 g of crystals. Recrystallization from acetonitrile gave 0.28 g (16%) of *N,N'*-thiodibenzamide (IV), mp 191°C (decomp.) (lit,[15] mp 188°C), as colorless needles.

Found: C, 61.58; H, 4.29; N, 10.21%. Calcd. for $C_{14}H_{12}O_2N_2S$: C, 61.76; H, 4.44; N, 10.29%. IR (KBr): 3220 (ν_{NH}), 1655 cm^{-1} (ν_{CO}).

The mother liquor was concentrated *in vacuo* to leave a residue, which was then recrystallized from carbon tetrachloride to give 0.41 g (26%) of benzamide.

Reaction of N-Sulfinylbenzamide (I) with Styrene Oxide (V). After a solution of 1.01 g (0.006 mol) of I and 0.73 g (0.006 mol) of V in 10 m*l* of benzene had been refluxed with 0.06 g (0.0003 mol) of Et_4NBr for 1 hr, the reaction mixture was concentrated *in vacuo* to leave a residue. The residue was

10) F. Wolfheim, *Ber.*, **47**, 1440 (1914).

11) The sulfurdiimide II did not react with V in the presence of Et_4NBr. On the other hand, it has been found that the reaction of I with 1-*p*-toluenesulfonylaziridine did not give a compound of VII type, but 1-oxo-2-benzoyl-5-*p*-toluenesulfonyl-1,2,5-thiadiazolidine and 1,2,3,6-thiatriazine compounds: the results will be reported in detail elsewhere.

12) O. Tsuge, S. Mataka, M. Tashiro, and F. Mashiba, This Bulletin, **40**, 2709 (1967).

13) V. S. Etlis, A. P. Sineokov, and M. E. Sergeeva, *Khim. Geterotskil. Soedin.* **1966**, 682; *Chem. Abstr.*, **66**, 55150s (1967).

14) F. Yamada, T. Nishiyama, M. Kinugasa, and M. Nakatani, This Bulletin, **43**, 3611 (1970).

15) K. G. Naik, *J. Chem. Soc.*, **119**, 1168 (1921).

triturated with 5 m*l* of methanol to give colorless crystals, which on recrystallization from methanol, gave 0.47 g (41%) of 4-oxo-5-benzoyl-2,6-diphenyl-1,4,3,5-oxathiadiazepine (VII), mp 171—172°C (decomp.), as colorless prisms.

Found: C, 67.70; H, 4.39; N, 7.11%. Calcd. for $C_{22}H_{18}O_3N_2S$: C, 67.68; H, 4.65; N, 7.18%. IR (KBr): 1660 (ν_{CO}), 1630 cm^{-1} ($\nu_{C=N}$).

The filtrate was concentrated *in vacuo* to give a residue, which was then chromatographed on alumina using benzene and then methanol as eluents. A trace amount of benzonitrile and 0.23 g (17%) of 2,5-diphenyloxazoline (VIII) were obtained from the benzene-eluent. The methanol-eluent was evaporated *in vacuo* to leave a viscous substance, which was then extracted with hot carbon tetrachloride. The colorless solid obtained from the carbon tetrachloride-extract was treated with 10 m*l* of aqueous hydrochloric acid to dissolve the benzamide (0.1 g). The recrystallization of insoluble crystals from carbon tetrachloride gave 0.05 g (3.5%) of colorless crystals, mp 126—127°C, which were found to be a mixture of nearly equal amounts of *N*-benzoyl-*β*-phenyl-*β*-aminoethanol (VIa) and *N*-benzoyl-α-phenyl-*β*-aminoethanol (VIb) by NMR spectroscopy.

A similar reaction of V with two molar quantities of I gave VI, VII and VIII in yields of 12, 32, and 3% respectively, accompanied by trace amounts of benzonitrile and benzamide.

The IR spectrum of VI mp 126—127°, revealed all the distinctive bands of authentic samples of VIa and VIb, the results of elemental analysis agreed with the calculated values of VI.

Found: C, 74.99; H, 6.26; N, 5.36%. Calcd. for $C_{15}H_{15}O_2N$: C, 74.66; H, 6.27; N, 5.81%.

On the other hand, VIII (M^+ *m/e* 223), a pale green oil whose IR spectrum showed the characteristic band ascribed to $\nu_{C=N}$ at 1650 cm^{-1}, was derived to its picrate, mp 141—142°C. The picrate was identical with the picrate, mp 141—142°C (lit,[10] mp 141—142°C) of 2,5-diphenyloxazoline prepared by the method of Wolfheim.[10]

N-Benzoyl-α-phenyl-β-aminoethanol (VIb). To a suspension of 17 g of a mixture of α-phenyl- and *β*-phenyl-*β*-aminoethanol, bp 119—126°C/6 mmHg (lit.[16] bp 135—144°C/4—6 mmHg), which had been prepared from styrene oxide and ammonia according to the method of Castro *et al.*[8], in 50 m*l* of diethyl ether and 100 m*l* of 10% aqueous sodium hydroxide, 25 m*l* of benzoyl chloride was added, drop by drop, at 0°C. The precipitated solid was collected by filtration, washed with water, and dried. Several recrystallizations from benzene gave 6.3 g of VIb, mp 147—148°C (lit,[8] mp 148.6—149.1°C), as colorless plates.

Found: C, 74.21; H, 6.17; N, 5.73%. Calcd. for $C_{15}H_{15}O_2N$: C, 74.66; H, 6.27; N, 5.81%. IR(KBr): 3440 (ν_{OH}), 3320 (ν_{NH}), 1623 cm^{-1} (ν_{CO}). NMR (DMSO-d_6): δ 3.35—3.6 (multiplet, 2H, $-CH_2-$), 4.7—5.0 (multiplet, 1H, >CH), 5.55 (doublet, 1H,–OH, exchanged with D_2O), 7.2—8.0 (multiplet, 10H, aromatic protons), 8.55 ppm (triplet, 1H, –NH–, exchanged with D_2O).

Reaction of VII with Hydrazine Hydrate. When 2 m*l* of hydrazine hydrate was added to a solution of 0.5 g of VII in 20 m*l* of ethanol at room temperature, hydrogen sulfide evolved immediately. After the reaction mixture had been stirred at room temperature for 1 hr, it was concentrated *in vacuo* to leave crystals. The crystals were washed with benzene and then recrystallized from carbon tetrachloride, thus affording 0.22 g (68%) of *N*-benzoyl-*β*-phenyl-*β*-aminoethanol (VIa), mp 151°C (lit,[7] mp 154—154.5°C), as colorless needles.

Found: C, 74.34; H, 6.06; N, 5.69%. Calcd. for $C_{15}H_{15}O_2N$: C, 74.66; H, 6.27; N, 5.81%. IR (KBr): 3440 (ν_{OH}), 1630 cm^{-1} (ν_{CO}). NMR (DMSO-d_6): δ 3.71 (double doublet, 2H, $-CH_2-$), 4.8—5.4 (multiplet, 2H, >CH, and –OH), 7.2—8.2 (multiplet, 10H, aromatic protons), 8.75 ppm (doublet, 1H, –NH–).

The benzene washings were evaporated *in vacuo*, leaving 0.17 g (100%) of benzamide.

The hydrolysis of 0.3 g of VII with hydrochloric acid in methanol gave 70 mg (38%) of VIa and 90 mg (97%) of benzamide.

16) R. F. Nystrom and W. G. Brown, *J. Amer. Chem. Soc.*, **70** 3738 (1948).

NOTES

BULLETIN OF THE CHEMICAL SOCIETY OF JAPAN, VOL. 44, 2840 (1971)

Preparation of Sodium *o*-(*N*-Hydroxy-*N*-phenylcarbamoyl)benzenesulfonate and Reactions with Metal Ions

S. P. BHARGAVA and N. C. SOGANI
Chemistry Department, University of Rajasthan, Jaipur, India

(Received January 12, 1971)

N-Benzoyl-*N*-phenylhydroxylamine (BPHA) has been recommended as a gravimetric reagent for 16 metal ions including copper, iron, aluminum, and titanium,[1] cobalt and nickel,[2] and uranium.[3] The interest in BPHA and its analogues can be judged from the number of papers and reviews.[4] Bass and Yoe[5] surveyed 33 hydroxamic acids and 3 *N*-substituted hydroxamic acids as reagents for metal ions and concluded that BPHA is the most popular compound for this purpose. We thought it worthwhile to study its sulfonic acid derivative, which should prove a useful spectrophotometric reagent for a number of metal ions. Thus, sodium *o*-(*N*-hydroxy-*N*-phenylcarbamoyl)benzenesulfonate (I) was prepared as water-soluble chelating reagent. The preparation could be easily accomplished by allowing *o*-sulfobenzoic anhydride to react phenylhydroxylamine.

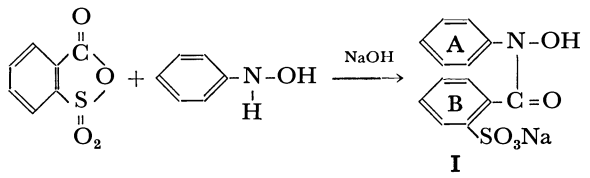

I

With a view to preventing the possibility of steric hindrance in the formation of metal chelates by a sulfonic acid group ortho to the coordinating carbonyl group, attempts were made to introduce it in ring A or meta or para to carbonyl group in ring B, but with no success.

o-Sulfobenzoic anhydride is a weak acylating agent and gives only *N*-acyl derivative. In the preparation of BPHA, however, benzoylation of phenylhydroxylamine yields both *N*-and *o*-substituted products, which must be separated by using ammonium hydroxide solution.

There is no difference in the colours of metal complexes of BPHA and its sulfonic acid derivative, indicating that the sulfonic acid group has not altered the chelating properties.

Conventional procedures were adopted for studying the reactions of the reagent towards various metal ions. Results are recorded in Table 1.

The reagent did not give any colour reactions with Mn(II), Ni(II), Hg(II), Pb(II), Al(III), Sn(IV), Sn(II), Bi(III), Cd(II), Sb(III), Rh(III), Ir(III), Pt(IV), Tl(III), La(III), Ce(IV), Th(IV), Zr(IV), alkali and alkaline earth metals.

TABLE 1. REACTIONS OF THE REAGENT WITH METAL IONS

Metal ion	pH	Colour of complex
Fe(III)	below 1.5	Purple
	1.5—3.8	Wine-red
	3.8—9.5	Orange
Fe(II)	6—7	Brown
V(V)	1—3	Orange-red
Ti(IV)	1—3	Yellow
U(VI)	3.0—9.5	Orange
Mo(VI)	0.5—5.5	Yellow
Co(II)	6—7	Light pink
Cu(II)	4—6	Yellow-green
Ru(III)	3—4	Light violet
W(VI)	2—3	Yellow
Cr(III)	3—4	Dirty yellow
Pd(II)	2—4	Light yellow-orange

The application of I as a spectrophotometric reagent for iron(III), vanadium(V), molybdenum(VI), uranium(VI), *etc.* is in progress.

Experimental

Preparation. *O*-Sulphobenzoic anhydride was prepared by the reaction of ammonium *o*-sulphobenzoate and thionyl chloride.[6]

Dry phenylhydroxylamine (22 g,0.2 mol) was dissolved in 200 m*l* of dry benzene and *o*-sulphobenzoic anhydride 37 g,0.2 mol) in 150 m*l* of dry dioxane was run slowly under continuous mechanical stirring. After the addition was complete, stirring was continued for 15 min. A viscous mass appeared. With a vacuum pump the major bulk of the solvent was removed under reduced pressure. The viscous mass was dissolved in 10% ethanolic sodium hydroxide solution and the pH was maintained between 7.0 and 8.5. Sodium salt was precipitated by addition of ether. The crude material was crystallised by dissolving it in a minimum quantity of water and adding excess of ethanol. The compound came out as white cane-sugar like crystals. Yield: 50%. Dec. point: 118—120°C; $\lambda_{max}^{H_2O}$: 250—255 nm ($\varepsilon = 5.51 \times 10^4$).

Found: C, 49.49: H, 3.10; N, 4.21; S, 10.02%. Calcd for $C_{13}H_{10}NO_5SNa$: C, 49.52; H, 3.17; N, 4.44; S, 10.15%.

The compound is highly soluble in water but insoluble in organic solvents. In solid state it is stable indefinitely, but in solution it starts decomposing in about 24 hr.

The authors express their gratitude to Prof. R. C. Mehrotra for providing facilities in the department.

1) S. C. Shome, *Analyst* (London), **75**, 27 (1950).
2) S. K. Sinha and S. C. Shome, *Anal. Chim. Acta*, **21**, 459 (1959).
3) J. Das and S. C. Shome, *ibid.*, **27**, 58 (1962).
4) I. P. Alimarin, F. P. Sudakov, and B. G. Golovkin, *Russ. Chem. Rev.*, **31**, 466 (1962); A. M. Macdonald, *Ind. Chemist*, **36**, 512 (1960); **37**, 30 (1961).
5) V. C. Bass and J. H. Yoe, *Talanta*, **13**, 735 (1966).
6) H. Gilman and A. H. Blatt, "Organic Syntheses", Coll. Vol. 1, p. 495 (1951).

BULLETIN OF THE CHEMICAL SOCIETY OF JAPAN, VOL. 44, 2841—2842 (1971)

On the Reaction of Limonene with Chloranil[1,2]

Shin-ichi FUJITA,* Yasuo KIMURA, Rikisaku SUEMITSU, and Yasuji FUJITA**

Faculty of Engineering, Doshisha University, Kamikyo-ku, Kyoto

***Government Industrial Research Institute, Osaka, Midorigaoka, Ikeda-shi, Osaka*

(Received June 20, 1970)

In 1942, one of the present authors[3] examined the reaction of *d*-limonene with chloranil and proved the formation of dipentene and *p*-cymene, together with a large amount of polymerized substances. A further study of this reaction will be reported here.

Experimental

Materials. The *d*-limonene (**1**) was found to be 98.2% pure by gas-liquid chromatography (GLC), it had the following properties; bp 177°C/765 mmHg, d_4^{30} 0.8393, n_D^{30} 1.4678, $[\alpha]_D^{15}$+99.75°. The chloranil (**2**) was a commercial product of an extra pure grade; mp 288°C.

Reaction I. A mixture of 5.0 g (0.037 mol) of **1** and 1.1 g (0.005 mol) of **2** was heated at 170°C for 1 hr. The reaction mixture turned brown, and the generation of a small amount of hydrogen chloride was observed. The reaction product was then distilled with steam, and the distilled oil was extracted with ether and subsequently dried over anhydrous sodium sulfate. When the solvent was removed, 4.1 g of oil were obtained.

Reactions II_1, II_2, and II_3. Mixtures of 5.0 g of **1** and 2.2 g (0.009 mol) of **2** were heated at 130°C for 1 hr and 6 hr, and another at 170°C for 1 hr. After the same treatment, 4.4 g, 3.8 g, and 2.7 g respectively of oils were obtained.

Reactions III_1 and III_2. Mixtures of 5.0 g of **1** and 4.5 g (0.018 mol) of **2** were heated at 150°C and 170°C for 1 hr; 2.3 g and 1.4 g of oils respectively were thus obtained.

Reaction IV. A mixture of 5.0 g of **1** and 9.0 g (0.037 mol) of **2** was heated at 170°C for 2 hr, 1.6 g of oil were thus obtained.

Examination of the Reaction Products. The GLC was carried out by using Yanagimoto GC-3D Model equipment equipped with a thermal conductivity detector; the contents of the components were calculated from the peak areas of the gas-chromatograms. The components were isolated by preparative GLC with PEG 6000 column, and were identified by a comparison of their IR spectra with those of authentic samples.

d-*Limonene (1) and Dipentene (6).* Component **1** was isolated from the reaction product of I, and was identified as limonene. However, the specific rotation of this limonene was $[\alpha]_D^{20}$+27.56°, indicating that it contained about 70% of dipentene; this compound also afforded tetrabromide, mp 124°C.

8-p-*Menthene (3)*, *1*-p-*Menthene (4)*, *α-Terpinene (5)*, *γ-Terpinene (7)*, p-*Cymene (8)*, *Terpinolene (9)*, *1-Methyl-4-iso-propenylbenzene (10).* Each component was isolated from the reaction products of II_3—IV and was identified by a comparison of the IR spectrum[4] and retention time of GLC with those of authentic sample.

Reactions V, VI, VII, and VIII. Mixture of 5.0 g (0.037 mol) of *p*-cymene (**8**) (98.7% purity by GLC; bp 176°C/760 mmHg, d_4^{30} 0.8546, n_D^{30} 1.4867), and 1.1 g (0.005 mol), 2.2 g (0.009 mol), 4.5 g (0.019 mol), and 9.0 g (0.037 mol) of chloranil (**2**) were each heated at 170°C for 1 hr. By this treatment, 4.0 g, 3.6 g, 3.3 g, and 1.9 g of oils respectively were obtained. The reaction products consisted of **10** and large amounts of unreacted **8**. These results are shown in Fig. 1 and in Tables 1 and 2.

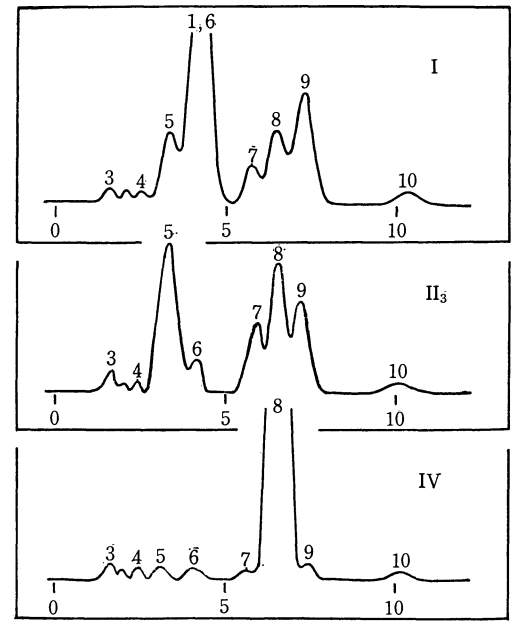

Fig. 1. Gas chromatograms of the volatile products of the reactions I, II_3 and IV.
Condition: PEG 6000 (30%), 2m×5mmϕ, 165°C, 40 ml/min H_2.

Nonvolatile Products. The nonvolatile residues of the steam distillation of the products of the reactions IV and VIII were each extracted with ether; after the separation of the chloranol (mp 233°C) formed, 1.6 g and 1.5 g portions of viscous oils were obtained respectively. These components were examined by GLC. In the case of the reaction VIII, the main component amounted to 76% of the oil. The IR spectrum of this compound showed bands at 1515(s), 1495(m), 1455(s), 1385(m), 1375(m), 1365(m), 1190(m), 1020(m), 815(s),

*Present Address: College of Education, Mukogawa Women's University, Ikebiraki-cho, Nishinomiya-shi, Hyogo.

1) Biogenetical Studies of Essential Oils. XXI.

2) Presented at the 12th Symposium on the Chemistry of Terpenes, Essential Oils, and Aromatics of the Chemical Society of Japan, Hamamatsu, October, 1968.

3) Y. Fujita and S. Ōhashi, *Nippon Kwagaku Kwaishi*, **63**, 1443 (1942).

4) B. M. Mitzner, E. T. Theimer, and S. K. Freeman, *Appl. Spectrosc.*, **19**, 169 (1965); M. J. Murray and W. S. Gallaway, *J. Amer. Chem. Soc.*, **70**, 3867 (1948).

Table 1. Compositions of the volatile products of reactions I—IV

The compounds identified	Compositions (%)						
	I	II_1	II_2	II_3	III_1	III_2	IV
8-*p*-Menthene (**3**)	0.1			3.9	2.8	8.6	0.9
(unidentified)	0.3			1.7	1.2	1.4	0.2
1-*p*-Menthene (**4**)	0.2			2.5	1.5	4.9	0.7
α-Terpinene (**5**)	8.4			23.7	21.1	2.5	0.1
d-Limonene (**1**) and Dipentene (**6**)	54.2	93.3	90.4	1.3	1.8	0.1	0.1
γ-Terpinene (**7**)	3.7			13.2	15.8	1.3	0.1
p-Cymene (**8**)	8.3	1.0	1.4	33.2	34.8	75.6	94.6
Terpinolene (**9**)	20.4	1.7	2.0	16.8	16.9	2.2	2.5
1-Methyl-4-isopropenylbenzene (**10**)	4.1	3.1	5.7	3.5	3.9	3.2	2.5

Table 2. Compositions of the volatile products of reactions V—VIII

The compounds identified	Compositions (%)			
	V	VI	VII	VIII
p-Cymene (**8**)	91.7	94.2	95.2	89.9
1-Methyl-4-isopropenylbenzene (**10**)	7.9	5.5	4.3	9.5
(unidentified compounds)	0.4	0.3	0.5	0.6

and 725(m) cm^{-1}; it was identified as 1,3,3,6-tetramethyl-1-*p*-tolylindan (**11**) by comparison with the IR spectrum of authentic one,[5] though the minor components have not yet been determined. The gas chromatograms of these products are shown in Fig. 2.

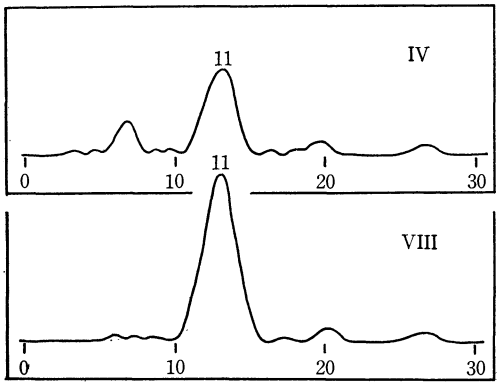

Fig. 2. Gas chromatograms of the nonvolatilve products of the reactions IV and VIII.
Condition: PEG 6000 (30%), 1m×5mmϕ, 175°C, 200 ml/min H_2.

Results and Discussion

When *d*-limonene (**1**) is heated at 150—170°C with chloranil (**2**), there occur several reactions, such as racemization, isomerization, dehydrogenation, disproportionation, and dimerization. Moreover, the formation of 8-*p*-menthene (**3**), 1-*p*-menthene (**4**), α-terpinene (**5**), dipentene (**6**), γ-terpinene (**7**), *p*-cymene (**8**), terpinolene (**9**), 1-methyl-4-isopropenylbenzene (**10**), and 1,3,3,6-tetramethyl-1-*p*-tolylindan (**11**) has been confirmed. These reactions may be concluded to be as is shown in Fig. 3.

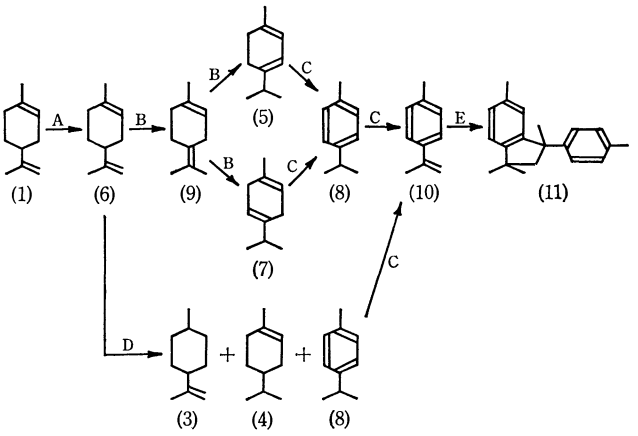

Fig. 3. The schematic mode of formation of the reaction products of *d*-limonene (1) with chloranil (2).
A: Racemization, B: Isomerization, C: Dehydrogenation, D: Disproportionation, E: Dimerization

The monoterpene compounds obtained in these reactions frequently occur in natural essential oils and can be considered in some cases to be formed by similar complex reactions of quinonoid compounds *in vivo*.

In a previous paper,[6] the present authors examined the reaction of citral with chloranil in a benzene solution under refluxing and proved the formation of **6**, **8**, and **10**.

5) V. N. Ipatieff, H. Pines, and R. C. Olberg, *J. Amer. Chem. Soc.*, **70**, 2123 (1948).

6) S. Fujita, Y. Kimura, R. Suemitsu, and Y. Fujita, *Nippon Kagaku Zasshi*, **92**, 175 (1971).

BULLETIN OF THE CHEMICAL SOCIETY OF JAPAN, VOL. 44, 2843—2845 (1971)

The NMR Chemical Shifts of Aromatic Ring Protons. I. The Chemical Shifts of the Ring Protons of Mono-substituted Benzenes

Yasuhide YUKAWA, Yuho TSUNO, and Nobujiro SHIMIZU

The Institute of Scientific and Industrial Research, Osaka University, Yamada-kami, Suita, Osaka

(Received September 25, 1970)

The ring protons of *mono*-substituted benzenes generally give complicated NMR spectra as a result of complex spin-spin coupling with their neighbors. This creates difficulties in determining the chemical shift of the respective ring protons and, subsequently, in examining effects. While recent computer analysis of ordinary spectra has provided a set of parameters,[1] the most practical method easily applicable in a laboratory of organic chemistry to solve this problem seems to be the deuterium-decoupling technique. Spiesecke and Schneider[2] and Schmid[2] determined the chemical shifts of ring protons of *mono*-substituted benzenes in a cyclohexane solution by means of deuterium substitution at specific positions. As a more convenient method, Garnett[3] suggested the application of massive deuteration.

Although the chemical shifts of the ring protons of benzene derivatives have been studied over a wide variety of substituents,[4,5] a comprehensive set of SCS data for *mono*-substituted benzenes under the same conditions is only available in carbon tetrachloride[1] and cyclohexane solutions.[2] Therefore, we determined the chemical shifts of *mono*-substituted benzenes in various solvents.

Our method of chemical-shift determination is essentially an application of Garnett's deuterium decoupling (massive deuteration). A statistical mixture of isomeric *mono*-substituted benzene-d_4, obtained by introducing a substituent to monoprotio deuteriobenzene, gives a highly simplified absorption pattern which consists of three singlets for the *o*-, *m*-, and *p*-proton. Thus, the chemical shifts of the respective protons were directly obtained from the spectra.

Mono-protio pentadeuteriobenzene was prepared from hexadeuteriobenzene by the bromination and subsequent reduction of the Grignard reagent with light water. This starting material was converted by direct substitutions and subsequent reactions to a series of *mono*-substituted monoprotio deuteriobenzenes.

The measurements were carried out with a Hitachi R-20 spectrometer operating at 60 MHz. The chemical shifts were determined relative to TMS as an internal standard at three concentrations below 5.0 mol% and were extrapolated to infinite dilution values. The shift values were determined rather precisely; the uncertainty involved in the infinite dilution values may be estimated as far less than ± 0.5 Hz, except when the signals are coalesced. Since the relative intensity of the signals corresponds to the relative amounts of the existing protio-isomers, 2: 2: 1 for *o*-, *m*-, and *p*-isomers, the signals for *p*-protons could be assigned from their intensities without difficulty. The assignment of the *m*- and *o*-protons for most of the derivatives was confirmed by comparison with existing data.[1,2]

The SCS for the compounds for which no literature data were available were further confirmed by a study of the spectra of specifically-deuterated materials. The chemical shifts determined in carbon tetrachloride were in good accordance with those given by theoretical analysis; the discrepancy did not exceed ± 0.5 Hz. This indicates the reliability of the present sets of data, obtained by the conventional method, as indicating the actual shifts of *mono*-substituted benzenes.

According to the results, the substituent chemical shifts (SCS values) appears to vary to a considerable extent depending on the solvents. Table 1 lists the SCS values in dimethylacetamide (DMA) as a representative polar solvent and in cyclohexane as a non-polar solvent. The *meta*- and *para*-SCS values are magnified in DMA as compared with those in C_6H_{12}, but the *ortho*-SCS values remain approximately the same in both solutions. The SCS in C_6H_{12} is found to be proportional to that in CCl_4. On the contrary, no such linear correlation can be obtained between the SCS's in DMA and in C_6H_{12} or CCl_4. In a DMSO solution, practically the same SCS values as in DMA were reproduced within the order of experimental uncertainty. These findings suggest that the SCS should be treated independently in each solvent.

A number of studies of the correlation of the chemical shifts of substituted benzene dreivatives with the substituent parameters have been successfully made,[4-6] although actual correlations have always suffered from the significant deviations of the anisotropic substituents. However, the direct application of Hammett σ-constants does not necessarily result in satisfactory correlations.

1) K. Hayamizu and O. Yamamoto, *J. Mol. Spectroscopy*, **25**, 422 (1968); S. Castellano, R. Kostelnik, and C. Sun, *Tetrahedron Lett.*, **1967**, 4635, 5205.

2) H. Spiesecke and W. G. Schneider, *J. Chem. Phys.*, **35**, 731 (1961); F. Langenbucher, R. Mecke, and E. D. Schmid, *Ann. Chem.*, **669**, 11 (1963).

3) J. L. Garnett, L. J. Henderson, W. A. Sollich, and G. Van Dyke Tiers, *Tetrahedron Lett.*, **1961**, 516. G. B. Savitsky, L. G. Robinson, W. A. Tallor, and L. R. Womble, *J. Magn. Resonance*, **1**, 139 (1969).

4) For comprehensive review, see L.M. Jackman and S. Sternhell, "Application of Nuclear Magnetic Resonance Spectroscopy in Organic Chemistry" Pergamon press, N.Y. (1969); M.T. Tribble and J. G. Trayham, *J. Amer. Chem. Soc.*, **91**, 379 (1969); Y. Yukawa, Y. Tsuno, and H. Yamada, *Memo. ISIR, Osaka Univ.*, **23**, 79 (1966); K. L. Williamson, N. C. Jacobus, and K. T. Soucy, *J. Amer. Chem. Soc.*, **86**, 4021 (1964); H. Güsten and M. Salzwedel, *Tetrahedron*, **23**, 173 (1967); R. R. Fraser, *Can. J. Chem.*, **38**, 2226 (1960); Y. Nomura and Y. Takeuchi, *Org. Magn. Resonance*, **1**, 213 (1969).

5) Y. Yukawa and Y. Tsuno, *Nippon Kagaku Zasshi*, **86**, 873 (1965); Y. Yukawa, Y. Tsuno, and H. Yamada, *ibid.*, **85**, 501 (1964); Y. Yukawa, Y. Tsuno, and M. Sawada, This Bulletin, **39**, 2274 (1966).

6) J. Niwa, *ibid.*, **42**, 1926 (1969).

TABLE 1. RELATIVE CHEMICAL SHIFT OF THE RING PROTON OF *mono*-SUBSTITUTED BENZENES

Substituent	in DMA			in C_6H_{12}		
	$\Delta\delta_o$	$\Delta\delta_m$	$\Delta\delta_p$	$\Delta\delta_o$	$\Delta\delta_m$	$\Delta\delta_p$
NO_2	−55.7	−23.6	−32.6	−56.8	−11.9	−18.6
CN	−31.4	−17.0	−25.4	−16.9	− 6.0	−12.2
SO_2Cl	−49.7	−32.9	−38.9	−45.2	−14.9	−21.4
CH_3CO	−38.7	−11.7	−15.7	−39.7	− 7.4	−10.4
t-BuCO	−22.9	− 8.8	− 8.8	−26.6	− 3.2	− 3.2
CO_2Et	−40.1	−12.4	−19.4	−47.5	− 4.4	−10.1
CO_2H	−40.3	−10.1	−16.2	−54.2	− 8.9	−16.4
Br	−14.7	− 1.6	− 3.4	−12.0	6.0	3.7
I	−25.1	8.3	− 3.9	−25.0	15.0	1.8
$SiMe_3$	−10.4	0.6	0.6	−12.9	0.9	0.9
Me	10.5		10.5	11.1		11.1
t-Bu	− 3.7	2.8	10.2	− 4.5	2.8	10.3
neo-Pent.	14.1	6.4	16.1			
OPh	20.2	− 2.6	13.4	17.3	3.1	14.0
OMe	25.2	4.3	24.8	25.1	3.7	23.1
OH	32.5	12.1	36.1	31.6	7.0	25.8
NMe_2	37.2	12.9	43.1	35.1	8.2	32.4
NH_2	42.4	21.4	52.5	44.3	14.3	37.6

This failure should be attributed to the changes in the relative importance of the π-electronic delocalization (resonance) effect relative to the non-delocalization polar effect, changes depending on the structure of the systems and also on the nature of the detection variables (*i.e.*, the proton NMR chemical shifts compared to the pK_a of benzoic acids).

We have previously demonstrated[4,5] that the substituent effect on the chemical shift of side-chain protons can be described generally by Eq. (1):

$$\Delta\delta = \rho(\sigma^0 + r^+\Delta\bar{\sigma}_R^+ + r^-\Delta\bar{\sigma}_R^-) \qquad (1)$$

ρ is the reaction constant, and σ^0 is the standard substituent constant. $\Delta\sigma_R^+$ and $\Delta\sigma_R^-$ are the resonance substituent constants measuring the capacity of −R and +R groups respectively for electron donation and attraction through π-electronic delocalization. Either r^+ and r^- is the resonance reaction constant describing the extent of additional π-electronic interaction with conjugatively electron-donating(−R) or electron-attracting (+R) substituents.

Our linear Aromatic Substituent-Reactivity (**LArSR**) relationship (1) can be applied to the SCS's of the ring protons of *mono*-substituted benzenes. By the least-squares treatment, the following correlations were derived for the respective ring protons in DMA solution:

$$\Delta\delta_p = -39.6(\sigma_p^0 + 0.87\Delta\bar{\sigma}_R^+) + 0.24$$
$$(n=13,\ \mathrm{SD}=2.81,\ \mathrm{R}=0.995)$$
$$\Delta\delta_m = -34.5(\sigma_m^0 + 0.42\Delta\bar{\sigma}_R^+) - 0.61$$
$$(n=9,\ \mathrm{SD}=2.03,\ \mathrm{R}=0.993)$$

Equation (1) was also employed successfully for the SCS's in C_6H_{12} solution; $\sigma_p = -25.4$, $r_R^+ = 0.98$ and $\sigma_m = -18.9$, $r_m^+ = 0.48$. Halogens in the *meta*-correlation and dimethylamino group were not included in these calculations. The results are shown in Fig. 1 and 2 for

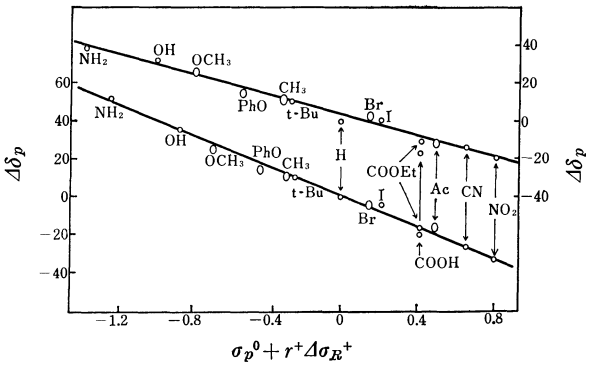

Fig. 1. Application of **LArSR** Eq. (1) to *para*-SCS values; Upper line, SCS in C_6H_{12}, and lower in DMA solutions.

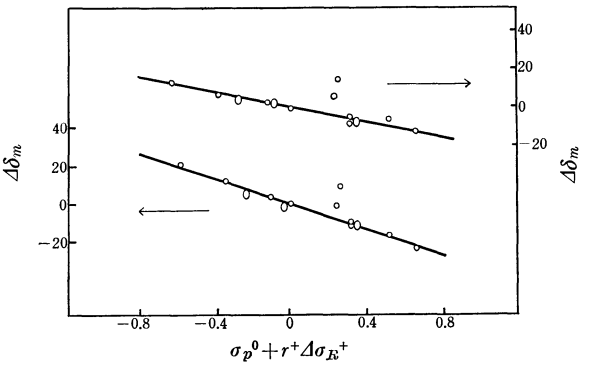

Fig. 2. Application of **LArSR** Eq. (1) to *meta*-SCS values; Upper in C_6H_{12} and lower in DMA solutions.

m- and *p*-protons respectively. Yamamoto *et al.*[1] pointed out that the SCS values in CCl_4 were linearly correlated with σ^+ This means that the shifts in CCl_4 correlate with an r_p^+ value near unity.

From these results, it is evident that our **LArSR** Eq. (1) can be employed as a useful approximation to describe the physical properties mainly brought about

by the electronic distributions of the ground-state molecules.

In para correlations, the resonance contribution of the —R substituents is remarkably exalted to give high r^+ values near unity, while the contribution of the $r^-\Delta\bar{\sigma}_R^-$ term is not significant; in effect, $r^-=0$. This suggests that the benzene ring works more effectively as a π-electron acceptor than as a π-electron donor in the π-delocalization in the ground-state *mono*-substituted benzenes. The change in r from one solvent to another may result in the non-linearity between the *para*-SCS values in different solvents. The significant solvent-variations of σ as well as of r values suggest that the simple sum treatment[1] should be applied only to data obtained in the same solvent or at least in a closely related group of solvents.

It should be noticed that the *meta*-correlation also requires exalted r^+-values, contraty to the negligible additional resonance term ($r_m^+=0$) in the ordinary *meta*-reactivity correlations. This might be caused by certain secondary contributions from the *ortho* and *para* π-charges.[8] Whatever the origin of the exalted resonance contribution,[8] the fact that the r_m value is just a half as much as the corresponding r_p value may be important, as the 1/2 ratio is a characteristic of the resonance contribution in the insulated σ^0-reactivity.

The substantial deviation of certain substituents might be attributed mainly to the specific magnetic effect. It is interesting to note that the effect of anisotropic substituents appears somewhat solvent-dependent (see Table 1). Dimethylamino group was not successfully correlated with the ordinary $\Delta\sigma_R^+$ value. In usual solvents, dimethylamino group was less electron-releasing than amino group, but it was more electron-releasing in carbon tetrachloride. No plausible explanation of this fact is available.

The chemical shift of the *ortho* proton can not be described simply by Eq. (1) alone. This is quite reasonable because the proximity of the *o*-proton to substituents may give rise to predominant non-electronic effects, such as anisotropic, local-field, and steric interactions. However, practically a linear correlation, $\Delta\delta_o=-55.3(\sigma^0{}_p+0.59\Delta\bar{\sigma}_R^+)$, can be obtained in DMA from selected well-behaving substituents. Similar results were obtained in other solvents. This means that the electronic effect predominantly controls the chemical shifts of the *o*-proton despite significant contributions of non-electronic factors.

The same method of determination and a similar type of SCS analysis have been used successfully in the study of particular solvent effects or of the complex formation of substituted benzenes and naphthalenes; the results will be reported in the near future.

7) For reference see G. W. Smith, *J. Mol. Spectroscopy*, **12**, 146 (1964).

8) In a previous report[9] we have treated such an exalted π-electronic contribution of *meta* substituents in terms of the variation of the ring current by localized π-charges with substituents.[10]

9) Y. Yukawa, Y. Tsuno, and H. Yamada, This Bulletin **43** 1459 (1970).

10) H. P. Figeys and R. Flammang, *Mol. Phys.*, **12**, 581 (1967).

BULLETIN OF THE CHEMICAL SOCIETY OF JAPAN, VOL. 44, 2845—2847 (1971)

Electrical Conductivity in Crystalline Hexamethylbenzene

Kazuhiko KUREMATSU, Nagao KANEKO, and Shoichi MATSUMOTO

Toshiba Research and Development Center, Tokyo Shibaura Electric Co., Ltd., Komukai, Kawasaki

(Received December 1, 1970)

The influence on the electrical property of organic crystals of their phase transition has been found for phthalocyanine,[1,2] chlorpromazine,[3] phenanthrene,[4,5] and so on. It has, however, been reported by Kronick and Labes that no change was discernible in the electrical property accompanying the phase transition of hexamethylbenzene crystals at 110°C.[6] Recently, Chojnacki has found an increase in the electrical conductivity of hexamethylbenzene at the transition point, while he has reported no change in the activation energy for conduction at that point.[7]

The crystal structure of hexamethylbenzene below 110°C is a triclinic modification, belonging to the space group of C_1'—$P_{\bar{1}}$. A unit cell whose dimensions are a=8.92Å, b=8.86Å, and c=5.30Å (α=44°27′, β=116°43′, γ=119°34′) at 20°C contains one molecule.[8] Through the phase transition, the molecules within the plane of the molecular rings shift slightly, so that the triclinic symmetry becomes orthorhombic. Here, the unit cell whose dimensions are a=9.06Å, b=15.70Å, and c=7.52Å (at 155°C) belongs to the space group of $D_{2h}^{23}F_{mmm}$ and contains four molecules.[9]

This paper will report on studies of the temperature dependence characteristic of the electrical conductivity

1) D. D. Eley and G. D. Parfitt, *Trans. Faraday Soc.*, **51**, 1529 (1955).
2) K. Wihksene and A. E. Newbick, *J. Chem. Phys.*, **34**, 2184 (1961).
3) F. Gutmann and A. Netschey, *ibid.*, **36**, 2355 (1962).
4) S. Matsumoto and T. Tsukada, This Bulletin, **38**, 2023 (1965).
5) S. Matsumoto, *ibid.*, **40**, 2749 (1967).
6) P. L. Kronick and M. M. Labes, *J. Chem. Phys.*, **38**, 776 (1963).
7) H. Chojnacki, *Acta Physica Polonica*, 715 (1966).
8) L. O. Brockway and J. M. Robertson, *J. Chem. Soc.*, **1939**, 1324.
9) T. Watanabe, Y. Saito, and H. Chihara, *Sci. Papers Osaka Univ.*, **1**, 9 (1949).

of crystalline hexamethylbenzene. The results of the increase in the activation energy through the transition will be discussed in connection with both crystallographic forms.

Experimental

Material. Hexamethylbenzene of an extra pure grade obtained from Tokyo Kasei Kogyo Co., Ltd., was purified by recrystallization from a chloroform solution and then by the zone-melting technique.[10]

Electrical Measurements. The powdered specimen was packed in a rigid Teflon cylinder and compressed between the metal (stainless steel) plungers which were used as electrodes. Their effective area was 1 cm^2. The specimen compressed under a pressure of 120 kg/cm^2 was 1—2 mm thick. The electrical measurements were then carried out by means of a vibrating-reed electrometer (Takeda-TR15) in a vacuum of 10^{-3}—10^{-4} mmHg, while applying a voltage of 100V to the cell.[4,5] The sample heating rate was 0.2—0.4°C per minute.

Dilatometric Measurements. A dilatometric investigation was made by using a modified differential dilatometer of the type originated by Chevenard.[11] Our dilatometer was designed to magnify 2000 times the differential expansion between the specimen and an equal length of fused silica used as the standard.

In this study, the heating rate was about 0.9°C/min, except in the vicinity of the anomalous point, where the temperature was raised as slowly as possible.

Samples were prepared by casting molten rods of zone-refined hexamethylbenzene 11.7 mm in length.

Results and Discussion

In the electrical investigation over the temperature range of 85—130°C, a distinct anomaly was found in the temperature dependence of the electrical resistivity of crystalline hexamethylbenzene. A typical example of the temperature dependence of the electrical resistivity in the heating process by the DC method is shown in Fig. 1. The relation between the logarithm of the resistivity and the reciprocal absolute temperature shows an anomaly at 110±3°C, while the relations both below and above that point are linear. The reproducibility of this amonalous phenomenon was good within the range of experimental error.

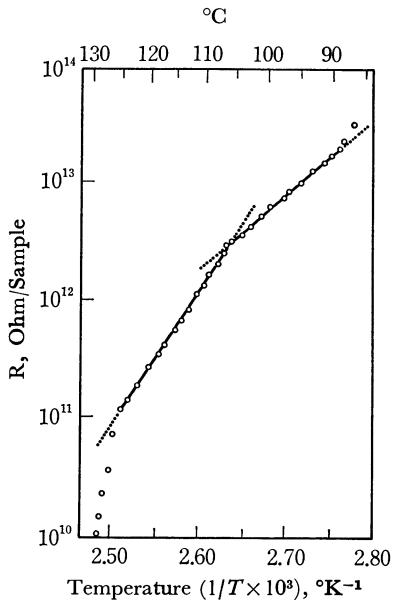

Fig. 1. The temperature dependence of the electrical resistivity of crystalline hexamethylbenzene for heating.

Assuming the resistivity, R, to obey the usual semiconductor relation:

$$R = R_0 \exp(\Delta\varepsilon/2kT) \quad (1)$$

the values of the activation energy for conduction, $\Delta\varepsilon$, obtained from the above relation, were found to be, respectively, 2.5 eV and 4.5 eV below and above the anomalous point.

In the electrical study by Kronick and Labes, using a hexamethylbenzene specimen cast between glass plates, no anomaly was reported. The activation energy was 1.78 eV. According to the report by Chojnacki, the increase in the electrical conductivity of a pellet specimen made from powdered hexamethylbenzene crystal under a pressure of 1000 atm. doubled, the activation energy for conduction did not change, and the activation energy was 2.0 eV.

There seems to have been no anomaly in the results reported by Kronick and Labes caused by their measurement technique. On the other hand, Chojnacki discussed his experimental results, in which no change was found in the activation energy at the phase transition, on the basis of these being no dependence of the $\Delta\varepsilon$ on the crystallographic direction. However, his discussion may be confused because one cannot regard the effect on the electrical conductivity influenced by the crystal-phase transition as being equal with the anisotropy of conductivity.

The intrinsic band-gap energy can be fundamentally induced from the crystal ionization potential, I_c, and the crystal electron affinity, A_c, corresponding to the energy gap between the top of the valence band and the bottom of the conduction band, $\Delta\varepsilon_0$.[5] If the values of I_g and A_g are available, the intrinsic band-gap energy, $\Delta\varepsilon_0$, may be calculated from the following equation:

$$\Delta\varepsilon_0 = I_c - A_c \quad (2)$$

Thus, Eq. (3) is derived from Eq. (2):

$$\Delta\varepsilon_0 = I_g - A_g - P_+ - P_- \quad (3)$$

where I_g and A_g are the gaseous ionization potential and the electron affinity respectively, and where P_+ and P_- are the stabilization energies attributed to polarization by positive and negative centers in the crystal respectively.

If the activation energy for conduction, $\Delta\varepsilon$, is equal to the band-gap energy, $\Delta\varepsilon_0$, the activation energy will vary more or less with the change in the crystallographic form, since the stabilization energy of polarization, P, depends on the crystal structure. However, $\Delta\varepsilon$ probably does not depend on the crystallographic direction, because P would have little anisotropy.

In the dilatometric study, a distinct discontinuity

10) S. Matsumoto, This Bulletin, **39**, 1811 (1966); **41**, 2792 (1968).

11) P. Chevenard, *Rev. Met.*, **14**, 610 (1917).

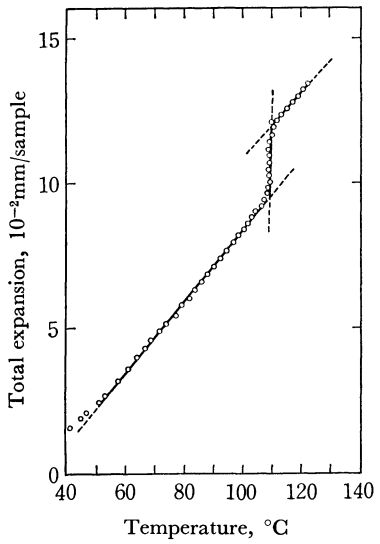

Fig. 2. The linear expansion-temperature relation of hexamethylbenzene crystal for heating.

was found in the linear expansion-temperature relation of the hexamethylbenzene crystal at 110.3°C. Figure 2 gives, as a typical example, a graphical representation of the total linear expansion of Sample No. 2 (listed in Table 1) plotted against the temperature, where the curve consists of three distinct lines. These phenomena were quite reversible with the temperature. These features of the expansion-temperature relation show that the thermal expansion coefficient of the specimen is almost constant below or above 110.3°C, but that it undergoes an abrupt change of linear expansion at the transition point. Each expansion coefficient can be evaluated from the slope of each line. The results are summarized in Table 1, where β_I is the mean coefficient of the linear thermal expansion between the temperatures of 40°C and Ttr. (the transition point) and where β_{II} is the coefficient between Ttr. and 130°C.

Table 1. The mean coefficient of linear thermal expansion of hexamethylbenzene crystal measured with a dilatometer

Trial	Ttr., °C	β_I ($\times 10^{-4}$)	β_{II} ($\times 10^{-4}$)
Sample No. 1	111.2	1.01	0.794
Sample No. 2	110.0	1.06	0.814
Sample No. 3	109.8	1.08	0.811
Average	110.3	1.05	0.806

The molar volumes calculated from the data of the crystal structure,[8,9] using the results obtained from our experiments of the thermal expansion, are 156.11 cm^3/mol in the triclinic system at 110°C and 159.43 cm^3/mol in the orthorhombic system at 110°C. Thus, the increase in the molar volume by the phase transition at 110°C is 2.13% of the molar volume at 110°C in the triclinic system.

Through the transition from a triclinic system to an orthorhombic system at 110°C, the increase in the molar volume would induce a decrease in the stabilization energy of polarization, P. Therefore, it seems reasonable, from Eq. (3), that an increase in the activation energy at the transition point was found in these experiments.

BULLETIN OF THE CHEMICAL SOCIETY OF JAPAN, VOL. 44, 2847—2848 (1971)

The Crystal Structure of *N*-Methylphenothiazine

Nobuko I. WAKAYAMA

Government Chemical Industrial Research Institute, Tokyo, Shibuya-ku, Tokyo

(Received December 8, 1970)

Phenothiazine derivatives are used widely in medical practice. Their actions change entirely with the side chains attached to the phenothiazine nucleus. *N*-substituted phenothiazine can take two different forms, quasi-equatorial and quasi-axial (Fig. 1). According to the calculation based on the molecular orbital theory by Malrieu and Pullman,[1] the electronic states of the two forms are different. The energy state and ionization potential of the quasi-equatorial form are lower than those of the quasi-axial one, the former being more reactive towards electrophilic reagents since the nitrogen lone pair electrons participate in the conjugated electronic system. The N–H bond of phenothiazine (PT) has been found to have a quasi-equatorial orientation by X-ray structure analysis.[2] PT has a

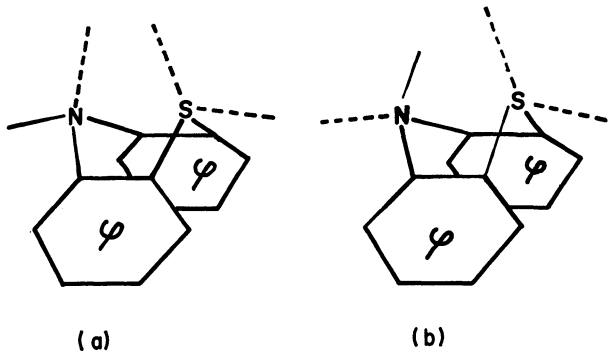

(a) (b)

Fig. 1. Configuration of *N*-substituted phenothiazine derivatives.
(a) quasi-equatorial form (b) quasi-axial form

1) J. P. Malrieu and B. Pullman, *Theor. Chim. Acta*, **2**, 293 (1964).

2) J. D. Bell, J. F. Blount, O. V. Briscoe, and H. C. Freeman, *Chem. Commun.*, **1968**, 1656; C. J. Fritchie, Jr., and B. L. Trus, *ibid.*, **1968**, 833; C. J. Fritchie, Jr., *J. Chem. Soc., A*, **1969**, 1328.

0.24—0.34 eV lower ionization potential[3] and is more reactive[4] towards electrophilic reagents than *N*-substituted derivatives which are supposed to take a quasi-axial form because of the steric hindrance of a large substituent.

We report the configuration of *N*-Methylphenothiazine (NMPT) which is regarded as a model substance of *N*-substituted phenothiazine. NMPT has a 0.15 eV higher ionization potential in the acetonitrile solution[5] and is less reactive towards electrophilic reagents than PT. NMPT cation was reported to take a quasi-axial form from the spin densities obtained from ESR measurement.[1] A single crystal, colorless and a prismatic needle in shape, was prepared by evaporation at room temperature from its benzene solution.

Crystallographic data are as follows:

$C_{13}H_{11}NS$

Orthorhombic: $a=14.9$, $b=11.4$, $c=6.79$Å

Density observed: 1.17_2 g·cm^{-3}

Density calculated: 1.18_2 g·cm^{-3}

Four formula units per unit cell

Space group: $Cmc2_1$

A set of intensity data was collected up to 5th layer around the *c*-axis, and up to 8th layer around the *b*-axis with a Weissenberg camera using Cu$K\alpha$ radiation. In total, 383 independent reflections were observed from 755 possible reflections, the rest being too weak to be observed. The intensities were estimated visually and corrected for Lorenz and polarization factors. The scale factor of each layer was determined by the least square method. From the space group $Cmc2_1$, the nitrogen, sulfur atoms and the carbon atom of the methyl group should be on the mirror plane perpendicular to the *b*-axis. The structure was solved by the Patterson and Fourier methods, and refined by diagonal, isotropic least squares. The final *R* factor was 0.135. The final atomic parameters are given in Table 1. The arrangement of the molecules in the crystal is shown in Figure 2. The bond lengths are C–N 1.43Å (0.026) and C–S 1.82Å (0.017). Bond angles are C–S–C 97° (0.77) and C–N–C 120° (2.5). The figure in parenthesis shows the value of standard deviation. The mean bond length of C–C is 1.41Å (0.033) and the mean bond angle of C–C–C is 120° (2.0). The plane equation of a benzene ring is $0.766x+0.294y+0.572z+4.72=0$. The N and S atoms deviate significantly from the planes of the benzene rings (N; 0.07, S; 0.18Å). The dihedral angle of the two benzene rings is 151° which is as large as that of PT. The configuration of the bonds about the nitrogen atom is a flattened tetrahedron, as is also the case with PT. Thus NMPT is determined to take a quasi-equatorial form in the crystal. This is not strange if we consider the fact that the steric effect of the methyl group is small and the molecule with this form is flattened and can be packed well. However, the present result contradicts the presumption based on the similarity of the chemical property to the other *N*-substituted derivatives. It is interesting to study whether the conversion from a quasi-axial form to a quasi-equatorial one happens in crystallization or not. Measurement of the ionization potential of the crystal of PT and NMPT is in progress to explain the difference in electronic state and structure between PT and *N*-substituted derivatives. All calculations were performed with the use of UNICS programs.

Table 1. Atomic parameters

Atom	*x/a*	*y/b*	*z/c*	B
C(1)	0.1840	0.1193	0.5745	2.076
C(2)	0.1869	0.2182	0.4662	3.153
C(3)	0.1368	0.3250	0.5426	3.773
C(4)	0.0845	0.3117	0.6961	4.169
C(5)	0.0762	0.2072	0.8039	2.464
C(6)	0.1296	0.1085	0.7469	2.647
C(7)	0.0852	0.0000	1.0485	5.935
N	0.1291	0.0000	0.8541	2.315
S	0.2584	0.0000	0.5033	2.422

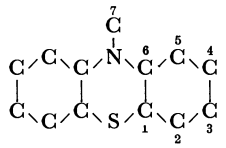

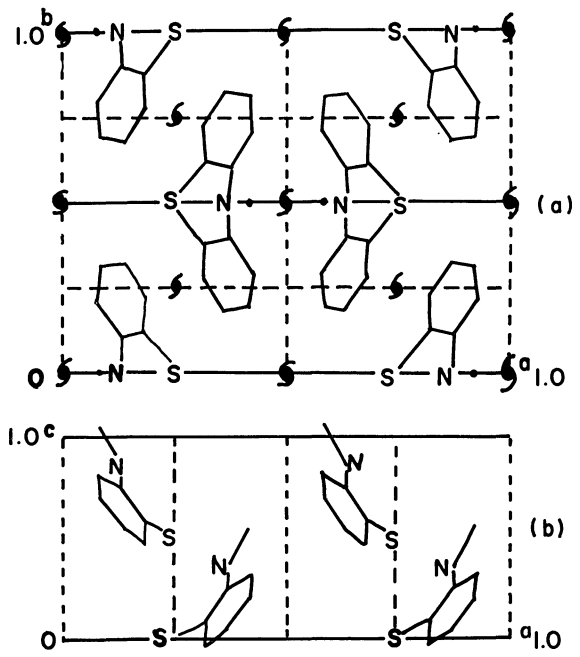

Fig. 2. Arrangement of the molecule in the crystal.
(a) Projection along the *c*-axis
(b) Projection along the *b*-axis

The author thanks Professors S. Hosoya and H. Inokuchi, the University of Tokyo, for their encouragement throughout this work.

3) P. Kabasakalian and J. MacGlotten, *Anal. Chem.*, **31**, 431 (1959).

4) C. Bodea and I. Silberg, *Advan. Heterocyclic Chem.*, **9**, 433 (1968).

5) J. P. Billon, G. Cauquis, and J. Combrisson, *J. Chim. Phys.*, **61**, 374 (1964).

BULLETIN OF THE CHEMICAL SOCIETY OF JAPAN, VOL. 44, 2849—2850 (1971)

A Polarographic Study of the Rates of the Dissociation Reactions of Nickel(II)-Ethylenediaminemonoacetate and -*N*-(2-Hydroxyethyl)ethylenediamine Complexes

Mutsuo KODAMA and Noboru OYAMA*

Department of Chemistry, Ibaraki University, Bunkyo, Mito, Ibaraki

**Chemistry Department, Faculty of Engineering, Ibaraki University, Narisawa, Hitachi, Ibaraki*

(Received December 22, 1970)

In a previous paper,[1] we studied the dissociation reactions of nickel(II)- and cobalt(II)-acetylacetonate complexes and of nickel(II)-glutamate, -aspartate, and -iminodiacetate complexes by investigating systematically the nature of the kinetic currents due to their dissociation at the electrode surface; we also determined their rate constants. The nickel(II) ions in ethylenediaminemonoacetate (EDMA) and *N*-(2-hydroxyethyl)ethylenediamine (EtEN) solutions also gave the kinetic waves due to the dissociation of the nickel(II)-EDMA and -EtEN complexes at the electrode surface preceding the electron-transfer step. In this investigation, we also studied thoroughly the nature of the kinetic waves of nickel(II)-EDMA and -EtEN complexes and determined the dissociation mechanism and their dissociation rate constants. The detailed structure of reaction intermediate was also determined.

Experimental

Reagents. The EDMA was prepared by the method of Fujii, Kyuno, and Tsuchiya.[2] The way of preparing the standard nickel(II) nitrate solution was also described in a previous paper.[3] The EtEN was purified by distillation under reduced pressure. The other chemicals used were of analytical reagent grade and were used without further purification.

Apparatus and Experimental Procedures. All the apparatus and the experimental procedures employed in this study were the same as those described in the previous paper.[1] In the present study, no buffer reagent was used, because all the sample solutions always contained an appreciable amount of uncomplexed EDMA or EtEN.

Results and Discussion

As in the cases of nickel(II) ions in acetylacetonate, glutamate, aspartate, and iminodiacetate solutions,[1] the nickel(II) ions in EDMA and EtEN solutions also exhibited the reduction waves corresponding to the reduction of the nickel(II) ion, which are kinetic-controlled in nature (the first waves). The second waves can be ascribed to the direct reduction of the nickel(II) complexes of EDMA and EtEN. In both EDMA and EtEN systems, the total wave-height was almost constant under the present experimental conditions. The log-plot examination for the first waves of nickel(II)-EDMA and -EtEN complexes gave straight lines with reciprocal slopes of about 60 and 72 mV respectively, corresponding to the two-electron irreversible reduction. Provided that the other experimental conditions are kept constant, the plot of the reciprocal of the limiting current for the first wave, i_l^{-1}, against the $(1+K_2'[X]_f)[X]_f^{1/2}$ or $(1+K_2'[X]_f)/(\alpha_H)_x^{1/2}$ value invariably gave the linear relation. However, the plot of i_l^{-1} against $(1+K_2'[X]_f)/(\alpha_H)_x^{1/2}[H^+]^{1/2}$ did not give a straight line in either system. Typical examples are shown in Fig. 1. Here, K_2' denotes the conditional

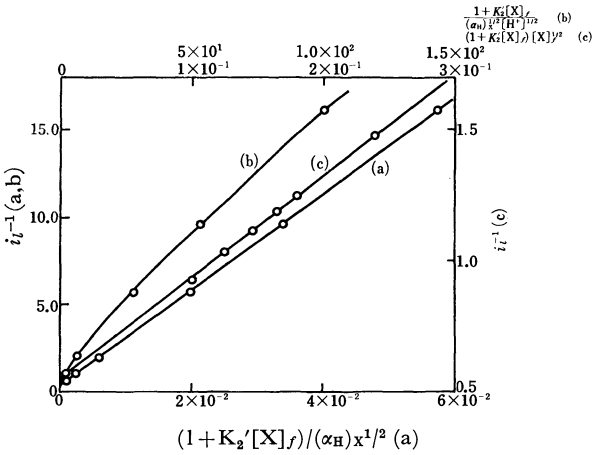

Fig. 1. The plot of $1/i_l$ against $(1+K_2'[X]_f)/(\alpha_H)x^{1/2}$, $(1+K_2'[X]_f)/(\alpha_H)x^{1/2}\cdot[H^+]^{1/2}$, or $(1+K_2'[X]_f)[X]_f^{1/2}$
The concentration of nickel(II) ion=1.0 mM 25.0°C
a) i_l^{-1} *vs.* $(1+K_2'[X]_f)/(\alpha_H)x^{1/2}$ plot
The concentration of uncomplexed EDMA=25.0 mM
b) i_l^{-1} *vs.* $(1+K_2'[X]_f)/(\alpha_H)x^{1/2}\cdot[H^+]^{1/2}$ plot
The concentration of uncomplexed EDMA=25.0 mM
c) i_l^{-1} *vs.* $(1+K_2'[X]_f)\cdot[X]_f^{1/2}$ plot
pH=5.40

second formation constant of the nickel(II)-EDMA or -EtEN complex; $[X]_f$, the concentration of uncomplexed EDMA or EtEN, and $(\alpha_H)_x$, the (α_H) value of EDMA or EtEN, defined as $1+[H^+]/K_n+[H^+]^2/K_nK_{n-1}+\cdots$. Furthermore, in both EDMA and EtEN systems, the plots of the half-wave potential against-log $[X]_f$ or log $(\alpha_H)_x$ gave straight lines, the slopes of which were 30 and 37 mV respectively. As was discussed previously,[1] these facts indicate that the electrode reaction for the first waves observed in nickel(II)-EDMA and -EtEN complexes can be expressed as:

$$NiX_2^{2-2m} \rightleftharpoons NiX^{2-m} + X^{m-} \quad \text{rapid}$$

$$NiX^{2-m} \overset{k_d}{\rightleftharpoons} Ni^{2+} + X^{m-} \quad \text{slow}$$

$$Ni^{2+} + 2e^- + Hg \rightleftharpoons Ni(Hg)$$

where X^{m-} means the completely-deprotonated EDMA

1) M. Kodama, H. Nunokawa, and N. Oyama, This Bulletin, **44**, 2387 (1971).
2) Y. Fujii, E. Kyuno, and R. Tsuchiya, *ibid.*, **43**, 786 (1970).
3) M. Kodama, *ibid.*, **42**, 2532 (1969).

Table 1. Dissociation rate constants (μ=0.20, 25°C) and formation constants

i) Dissociation rate constants	
System	k_d, sec^{-1}
Nickel(II)-*N*-(2-hydroxyethyl)-ethylenediamine complex	0.20
Nickesl(II)-ethyleledíaminemono-acetate complex	$2.4_4\times10^{-4}$
ii) Formation constants (μ=0.20)	
System	log K_{MX}
Nickel(II)-*N*-(2-hydroxyethyl)-ethylenediamine complex	6.66[9]
Nickel(II)-ethylenediaminemono-acetate complex	10.40[8]

anion or EtEN. From the slopes of the linear relation between the i_l^{-1} value and the $(1+K_2'[X]_f)[X]_f^{1/2}$ or $(1+K_2'[X]_f)/(\alpha_H)_x^{1/2}$ value obtained by using Eq. (10_a) in Ref. 1, the dissociation rate constants, k_d's, were determined (Table 1).

The k_d value for the nickel(II)-EtEN complex is nearly equal to the rate constant for the breakage of a nickel(II)-nitrogen bond, which forms part of a five-membered chelate ring in which both ends of the chelate are amino nitrogen atoms.[4] This fact evidently implies that, in the dissociation of a 1:1 nickel-(II)-EtEN complex, the bond breakage of the first nitrogen is the rate-determining step, and that the hydroxyethyl group in the EtEN has little effect on the rate of dissociation of the nickel(II)-EtEN complex.

In the dissociation of the nickel(II)-EDMA complex, it is very hard to believe that all three nickel(II)-EDMA bond breakages are involved in the rate-determining step. Therefore, the dissociation may proceed through one of the three reaction intermediates shown in Fig. 2. The reaction intermediate where the leaving EDMA anion is bonded to the nickel(II) ion through an acetate group can be eliminated, because the nickel-oxygen bond rupture is much faster than the nickel-nitrogen bond rupture.[5] As was discussed in the previous paper,[1] by relating the observed rate constant to the rate constant calculated on the basis of the proposed reaction intermediate, we determined the correct reaction intermediate. The rate constants calculated on the basis of the reaction intermediates in Fig. 2 by using the following relation are given in Table 2. Here, K_{MX} is the formation constant of the nickel(II)-EDMA complex with a 1:1 ratio; k_{rds},[4,6,7] the rate constant for

$$k_d = \frac{K_{int}}{K_{MX}} k_{rds}$$

the rate-determining step, and $K_{int.}$, the stability constant of the reaction intermediate prior to the rate-determining step. In the calculation, the electrostatic contribution to the stability of the reaction intermediate was also taken into consideration. The rate constant calculated on the basis of the reaction intermediate I agreed best with the observed one. We have already mentioned that the substitution reaction of the nickel-(II)-EDMA complex with cyclohexane-1,2-diamine-*N*,*N*,*N*′,*N*′-tetraacetic acid (CyDTA) proceeds through the reaction intermediate in which the displaced EDMA anion is bonded to the nickel(II) ion through an ethylenediamine five-membered chelate ring.[8] Therefore, the finding that the dissociation of the nickel(II)-EDMA complex proceeds through the reaction intermediate with an ethylenediamine five-membered chelate ring suggests that, in the nucleophilic substitution reaction involving the nickel(II)-EDMA complex, the attacking group just assists the dissociation of the EDMA anion from the nickel(II) ion, without effecting any change in the detailed dissociation mechanism of the nickel(II)-EDMA complex.

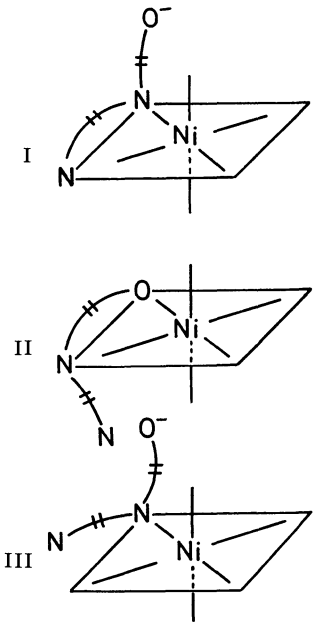

Fig. 2. Reaction intermediates for the dissociation of nickel (II)-EDMA complex

Table 2. The k_d values calculated

Reaction intermediate	k_d
I	4.5×10^{-4}
II	3.7×10^{-6}
III	1.3×10^{-6}

4) A. K. S. Ahmed and R. G. Wilkins, *J. Chem. Soc.*, **1959**. 3700.

5) T. J. Bydalek and D. W. Margerum, *Inorg. Chem.*, **2**, 678 (1963).

6) G. G. Hammes and J. I. Steifeld, *J. Amer. Chem. Soc.*, **84**, 4639 (1962).

7) D. W. Margerum, D. B. Rorabacher, and J. F. G. Clarke, Jr., *Inorg. Chem.*, **2**, 667 (1963).

8) M. Kodama, Y. Fujii, and T. Ueda, This Bulletin, **43**, 2085 (1970).

9) J. L. Hall, W. G. Dean, and E. A. Pacofsky, *J. Amer. Chem. Soc.*, **82**, 3303 (1960).

BULLETIN OF THE CHEMICAL SOCIETY OF JAPAN, VOL. 44, 2851—2852 (1971)

Tertiary Amine *N*-Oxide XXXIII. Reaction of α,*N*-Diphenylnitrone with Acylating Reagents

Seizo TAMAGAKI and Shigeru OAE

Faculty, of Engineering Osaka City University, Sugimoto-cho, Sumiyoshi-ku, Osaka

(Received February 1, 1971)

In the preceding paper of this series,[1] it was proposed on the ground of oxygen-^{18}O tracer experiments and kinetic studies that the mechanism of the reaction of aldonitrone with acetic anhydride cannot be represented by the intramolecular cyclic rearrangement alone as suggested by Umesawa,[2] but by the intramolecular rearrangement in which both the cyclic and sliding migrations of the acetoxy group take place concomitantly:

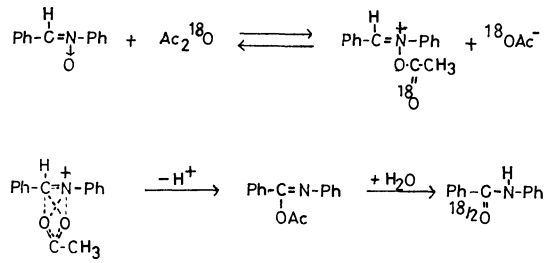

Krohenke[3] suggested that the rearrangement reaction of aldonitrone to amide proceeded *via* addition-elimination. According to his mechanism the reaction of aldonitrones with benzoyl chloride, benzenesulfonyl chloride, and phosphoryl chloride could be written as follows.

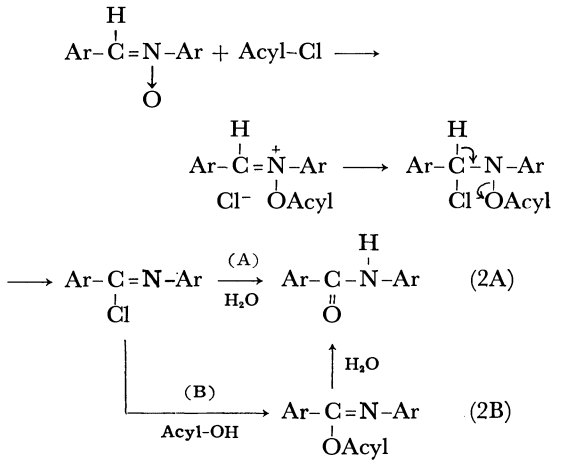

It was observed[2] that even less than one mol equivalent of acyl halide is sufficient to complete the reaction, and that in the reaction system there is not enough water to hydrolyze either the iminochloride or the acyloxyimine. Umesawa ruled out the two possibilities (2A and 2B) and postulated the following intramolecular cyclic rearrangement mechanism taking benzoyl chloride as an example.

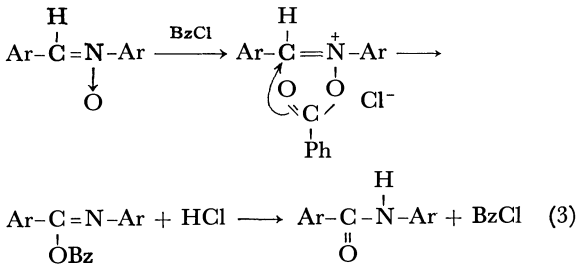

There are still controversies concerning the mechanistic interpretation of these rearrangement reactions.

In order to disclose the mechanistic picture of these reactions, we carried out ^{18}O-tracer experiments for the reactions of α,*N*-diphenylnitrone with benzoyl chloride, benzenesulfonyl chloride, and phosphoryl chloride enriched with excess ^{18}O.

Mechanism (3) would require the benzanilide to be completely scrambled with ^{18}O-distribution of all the oxygens incubated into the system when uniformly ^{18}O-labeled acyl halide is used, because, when the mechanism is operative the benzoyl chloride or other halides would be used repeatedly. Results of ^{18}O-analysis are given in Table 1. We see that the use of a greater amount of benzoyl chloride results in increasing incorporation of oxygen-^{18}O in benzanilide. The results are in line with the fact that benzoyl chloride in the system is used repeatedly, where the oxygen-^{18}O content in benzoyl chloride is diluted gradually with natural oxygen originated from the unlabeled nitrone.

Since benzoyl chloride can be recovered without decomposition, this reaction take place satisfactorily with only a catalytic amount of benzoyl chloride and affords benzanilide even when water is not present in the reaction mixture. Thus, the reaction likely proceeds through the initial formation of adduct and subsequent intramolecular cyclic or sliding transition state, as in the case for the reaction with acetic anhydride,[1] to give the **C**-benzoyloxyimine which is then attacked by chloride ion, rather than the cyclic rearrangement suggested by Umesawa.

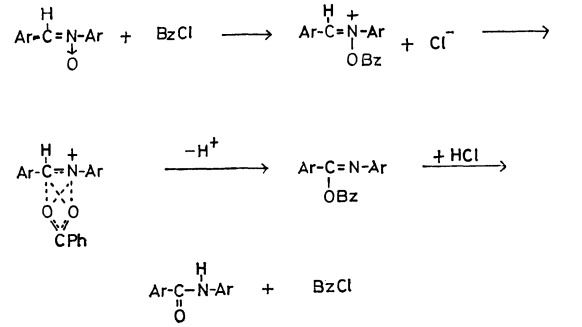

(Successively used) (4)

1) S. Tamagaki and S. Oae, *Tetrahedron*, **26**, 1795 (1970).
2) B. Umesawa, *Chem. Pharm. Bull.*, (Tokyo), **8**, 697, 967 (1960).
3) F. Krohenke, *Ann. Chem.*, **604**, 203 (1957).

TABLE 1. ^{18}O-ANALYTICAL DATA FOR REACTION OF α,N-DIPHENYLNITRONE WITH VARIOUS CHLORIDES

Chloride	Solvent	Mole ratio, (chloride)/(nitrone)	^{18}O-excess atom % chloride (used)	benzanilide exptl.	benzanilide theoretically calcd a)	b)	c)	d)
BzCl	none	1.0	1.33	0.64	0.67	1.33	0	0.67
	$CHCl_3$	1.0	1.33	0.65	0.67	1.33	0	0.67
	$CHCl_3$	3.75	1.38	1.04	1.07	1.38	0	0.69
$C_6H_5SO_2Cl$	$CHCl_3$	1.0	1.00	0.01	0.50	1.00	0	0.50
	$CHCl_3$	1.0	1.00	0.00	0.50	1.00	0	0.50
$POCl_3$	$CHCl_3$	1.0	1.33	0.09	0.67	1.33	0	0.67

a) Chlorides were repeatedly used during the reaction.
b) Based on intramolecular cyclic mechanism
c) Based on intramolecular sliding mechanism
d) Based on scrambling mechanism

The other acyl chlorides, such as benzenesulfonyl and phosphoryl chlorides were treated in a similar way with α,N-diphenylnitrone. Data of ^{18}O-analysis show that the ^{18}O-results are not incompatible with all the previous mechanisms. The benzanilide obtained was found to contain no excess oxygen-18. Thus, the most reasonable mechanism for these reactions appears to involve the formation of the initial acyl adduct and the subsequent intramolecular sliding shift with no scrambling of the oxygens in the acyloxy group.

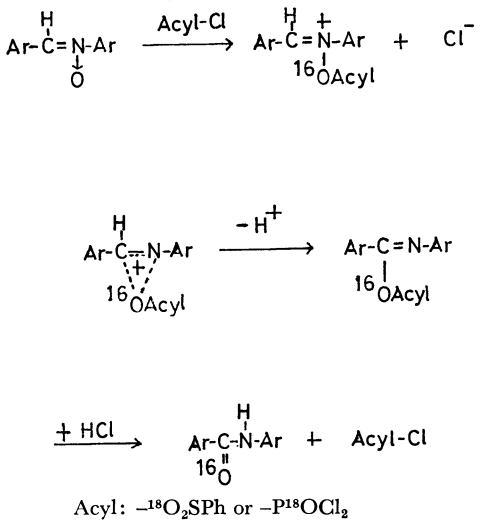

Acyl: $-{}^{18}O_2SPh$ or $-P^{18}OCl_2$

Experimental

Reaction with Benzoyl Chloride. To 3.0 g of α,N-diphenylnitrone without solvent or in chloroform, 2.14 g of benzoyl chloride was added portionwise under ice-cooling. The reaction mixture was then heated on a boiling water bath for 15 min. The mixture was cooled to room temperature and then solidified. The solids obtained were recrystallyzed from benzene or benzene-hexane.

This was identified as benzanilide by mixed melting point with the authentic sample, mp 163—164°C (lit, 163°C).

The yield was quantitative.

Reaction with Benzenesulfonyl Chloride. To a solution of 2.56 g α,N-diphenylnitrone in 7 cc of $CHCl_3$, 2.27 g of benzenesulfonyl chloride was added carefully.

The whole mixture was refluxed on a boiling water bath for 15 min. After it was cooled and an aqueous sodium hydrogen carbonate solution was added, the aqueous layer was extracted with chloroform. The solvent was evaporated to dryness. The residue was chromatographed on alumina eluted with benzene.

First elution product of pale yellow crystals, mp 155°C was recrystallized from benzene-hexane. Yield: 0.51 g(20%)

Reaction with Phosphoryl Chloride. To a solution of 3.20 g of α,N-diphenylnitrone in chloroform, 2.50 g of phosphoryl chloride was added. The column chromatographic treatment gave benzanilide, yield 6.5%.

BULLETIN OF THE CHEMICAL SOCIETY OF JAPAN, VOL. 44, 2853—2854 (1971)

The Beckmann Rearrangement of *p*-Nitrobenzophenone Oxime with Thionyl Chloride

Tsuyoshi OGATA, Sakuya TANAKA, Hiroshi YOSHIDA, and Saburo INOKAWA

Department of Synthetic Chemistry, Faculty of Engineering, Shizuoka University, Johoku, Hamamatsu

(Received February 24, 1971)

As is well known, many works on the Beckmann rearrangement have been reported.[1] Generally, it has been shown that the rearrangement is brought about by acids including Lewis acids, and that the mechanism proceeds in the migration of the *trans*-substituent for the hydroxyl group into the nitrogen atom (*trans*-migration).

Recently, Yukawa has reported the migratory aptitude in the Beckmann rearrangement varies according to the kind of catalysts.[2] However, the details have not yet been published. The authors are interested in this point and have done the present work seeking a clue to elucidate the effect of a migrating catalyst on the Beckmann rearrangement.

p-Nitrobenzophenone oxime I was chosen as the starting material, because it can be purified and separated into *syn*- and *anti*-isomers readily. The Beckmann rearrangements of this oxime with phosphorus pentachloride[3] and phosphoryl chloride[4] have been reported in the migration of the *trans*-substituent for the hydroxyl group. For the present paper, the authors chose thionyl chloride as the migrating catalyst, and the reactions were carried out in both benzene and chloroform.

Results and Discussion

p-Nitrobenzophenone oxime I was separated into *syn*- and *anti*-isomers (Ia and Ib) by the method of Sutton.[3] To the solution of Ia or Ib we then slowly stirred three equivalent moles of thionyl chloride. The given amides II were hydrolysed with an aqueous sodium hydroxide solution, and then aromatic acids were separated. These aromatic acids, IIIa and IIIb, were silylated with trimethylchlorosilane and hexamethyldisilazane to form volatile derivatives. That procedure is shown in Scheme 1. These silyl esters, IVa and IVb were determined quantitatively by gas-liquid chromatography, using methyl *p*-nitrobenzoate as the internal standard substance.[5]

The results are shown in Table 1. On the basis of these results, the following conclusions are deduced.

1) On using thionyl chloride as a migrating catalyst, only phenyl group which is situated in the *trans* position for the hydroxyl group in Ia migrated (*trans* migration), while in Ib either a *trans* or a *cis* migration took place simultaneously. It appears that Ib isomerized into Ia, along with a small amount of hydrogen chloride which

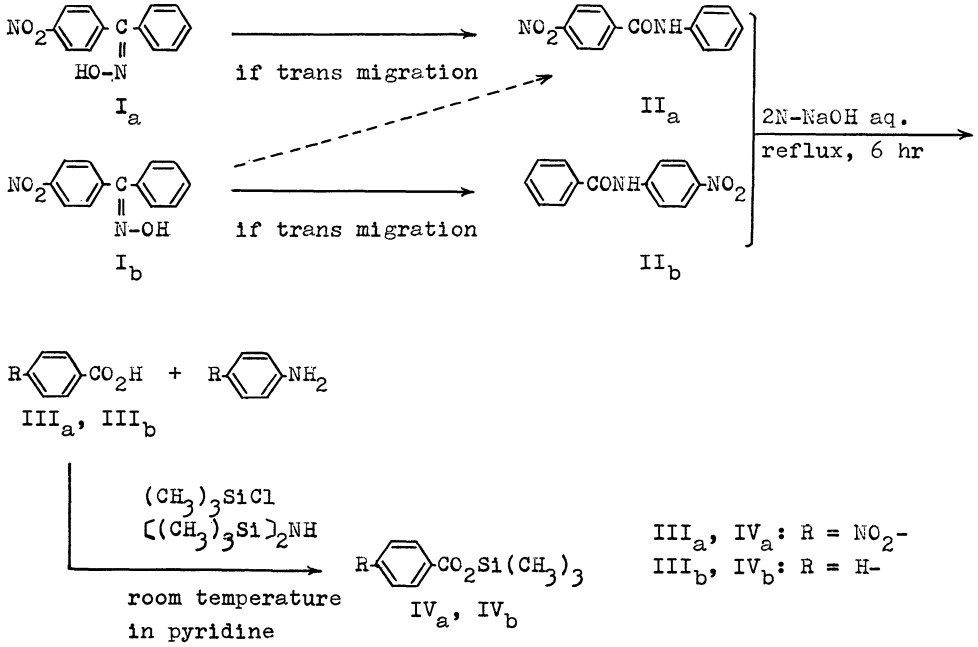

Scheme 1

1) a) A. H. Blatt, *Chem. Rev.*, **12**, 215 (1933); b) E. C. Franklin, *ibid.*, **14**, 219 (1934); c) B. Jones, *ibid.*, **35** 335 (1944); d) M. Kotake, "Jikken Kagaku, Koza," Vol. 18, Maruzen Co., Tokyo (1957), p. 417; e) M. Murakami, "Yukihannokikō no Shinpo," Vol. 1, Maki Shoten, Tokyo (1958), p. 189; f) L. G. Donaruma and W. Z. Heldt, "Organic Reactions," Vol. 11, John Wiley & Sons, New York and London (1960), p. 1.

2) See 1) d) Y. Yukawa, p. 426.

3) L. Brady and R. P. Mehta, *J. Chem. Soc.*, **125**, 2297 (1924); L. E. Sutton and T. W. J. Taylor, *ibid.*, **1931**, 2190.

4) J. Meisenheimer and G. Gaiser, *Ann. Chem.*, **539**. 95 (1939).

5) Z. Horii, M. Makita, I. Takeda, Y. Tamura, and Y. Ohnishi, *Chem. Pharm. Bull.* (Tokyo), **13**, 636 (1965).

Table 1. Migratory aptitude of *p*-nitrobenzophenone oxime

Oxime	Migrating catalyst	Solvent	Reaction temperature °C	Ratio of TMS ester of acid IVa:IVb	Migratory aptitude
Ia	$SOCl_2$	Benzene	10	only IVa[a)]	*trans*
			26	only IVa[a)]	*trans*
		Chloroform	10	only IVa[a)]	*trans*
			26	only IVa[a)]	*trans*
	PCl_5	Benzene	29	only IVa[a)]	*trans*
Ib	$SOCl_2$	Benzene	10	82:18	*cis* : *trans*
			26	80:20	*cis* : *trans*
			20	81:19	*cis* : *trans*
		Chloroform	−8	50:50	*cis* : *trans*
			26	69:31	*cis* : *trans*
			58	45:55	*cis* : *trans*
	PCl_5	Benzene	29	only IVb	*trans*

a) The given amide was identical with authentic sample which was prepared from aniline and *p*-nitrobenzoic acid.

was produced in the reaction system; then Ia was rearranged into IIa with thionyl chloride.[6] At any rate, it is necessary to measure both the isomerizing and migrating rates of Ib in order to clarify the mechanism in detail.

2) The *cis* migrating ratio in benzene predominates over that in chloroform. It appears that the migration proceeds faster than the isomerization in chloroform, because generally the migrating rate in the Beckmann rearrangement increases in a polar solvent.[7]

3) Within the limits of these experiments, the migrating aptitudes are independent of the reaction temperature.

4) Regardless of whether the oxime is of the *syn*- or *anti*-form, only the *trans* migration took place with phosphorus pentachloride.

It is clear from the above conclusions that the migratory aptitude varies greatly with the migrating catalyst and that it is affected by the stability of "*anti*-oxime" for a catalyst.

Experimental

p-*Nitrobenzophenone.* *p*-Nitrobenzophenone was prepared by the method of Schroether.[8] Mp 138°C (recrystallized from acetic acid); yield, 80%.

syn- *and* anti-p-*Nitrobenzophenone oxime Ia, Ib.* *p*-Nitrobenzophenone oxime I was prepared by the method of Brady.[3] Mp 108—116°C. *syn*- and *anti*-Oximes were separated by the method of Sutton.[3] Ia: mp 158°C; yield, 25%; NMR spectrum, 11.69 ppm in DMSO (*syn*-=N-OH). Ib: mp 136°C; yield, 25%; NMR spectrum, 11.88 ppm in DMSO (*anti*-=N-OH). The IR spectrum of Ia was identical with that of Ib.

Purification of Thionyl Chloride. Commercial-grade thionyl chloride was further purified by the method of Fieser.[9] Bp 76°C; colorless.

The Beckmann Rearrangement of p-*Nitrobenzophenone Oxime.* Into 1.2 g (0.005 mol) of oxime in anhydrous benzene (5 m*l*) we stirred thionyl chloride (1.1 m*l*, 0.015 mol) in benzene (2.5 m*l*). The reaction was carried out for 30 min at the temperatures shown in Table 1. After the solution has then been left standing for a night, the excess amount of thionyl chloride was decomposed with water, and the benzene was removed. The precipitate was filtered and used for the following procedure. In each case, the product was obtained quantitatively.

Hydrolysis of the Given Amide. To a given amide (0.6 g) we added a 2N sodium hydroxide aqueous solution (13 m*l*), after which the mixture was refluxed in an oil bath at 140°C for 6 hr. The solution was then cooled to room temperature and neutralized with hydrochloric acid. The precipitate was filtered and dried in a desiccator. The aromatic acid was obtained quantitatively.

Silylation and Quantitative Determination of Aromatic Acids. III. The aromatic acids were convertedi nto their volatile trimethylsilyl derivatives and were determined quantitatively by a modification of the method of Horii.[5] To crude III (0.04 g) in dry pyridine (0.6 m*l*), we added trimethylchlorosilane (0.2 m*l*) and then hexamethyldisilazane (0.2 m*l*). The formation of their trimethylsilyl derivatives occurred very rapidly at room temperature; after the pyridine hydrochloride has been removed by means of centrifuge, within a few minutes the entire reaction mixture was injected directly into the chromatograph.

Instrument: Yanagimoto GCG-550T.
Conditions: Column, 2 m×3 mmϕ
Column packing, 40% Silicone DC-Hv grease on 60-80 mesh Celite 545.
Column temperature, 170°C (Determination for IVa) 150°C (Determination for IVb)
H_2 flow rate, 40 m*l* per min.

6) The oxime Ib was isomerized into Ia with hydrogen chloride at room temperature, but Ib did not rearrange into amide under the same conditions.

7) J. Meisenheimer, *Ber.*, **54**, 3206 (1921); A. W. Chapman *et al.*, *J. Chem. Soc.*, **1933**, 806; **1934**, 1550; **1935**, 1223.

8) G. Schroether, *Ber.*, **42**, 3360 (1909).

9) L. F. Fieser, "Experiments in Organic Chemistry," 3rd ed., D. C Heath and Co., Boston (1955), p. 345.

BULLETIN OF THE CHEMICAL SOCIETY OF JAPAN, VOL. 44, 2855—2856 (1971)

Self-Diffusion Coefficients of Carbon Tetrachloride and Cyclohexane in the Carbon Tetrachloride-Cyclohexane System

Akio NISHI, Yoshinobu KAMEI, and Yasumichi OISHI
Department of Nuclear Engineering, Faculty of Engineering, Kyushu University, Fukuoka

(Received February 25, 1971)

The carbon tetrachloride-cyclohexane system shows relatively small compositional dependence of density,[1] viscosity, and interdiffusion coefficient[2,3] compared with other organic binary systems. Equilibrium vapour pressures[1,4] determined indicate a high thermodynamical ideality of this binary system.[2] This suggests that the self-diffusion coefficients of both components also show small and simple compositional dependence. This was confirmed by determining the self-diffusion coefficients of both components for the whole composition range of the system by a capillary-cell technique.

Experimental

An apparatus with a cell of 8 cm diameter, a capillary of 0.8 mm I.D. and 40 mm length, and a stirrer similar to Wang's[5] was used. All determinations were made at 25± 0.02°C. The carbon tetrachloride and cyclohexane used were of spectrum analysis reagent grade. A sample solution having a certain composition in the cell was adjusted to a radioactivity of about 0.06 μCi/cc with the ^{14}C-labelled CCl_4 or C_6H_{12}. The capillary filled with an unlabelled solution of the same chemical composition was dipped in the cell solution to a depth of 5 mm. The velocity of the stirrer was 30 rpm. The diffusion time of 20—25 hr was so scheduled as to result in the diffusion of an amount corresponding to about one third of the final uptake. After the diffusion run the radioactivities of the solutions in the capillary and the cell were determined in toluene solutions of 2,5-diphenyloxazole and *p*-bis-[2-(5-phenyloxazolyl)]-benzene with a liquid scintillation counter. In scintillation counting, difference in the concentration of sample in scintillator solution generally causes a different degree of quenching effect on counting. A correction was made in calculating the concentration of tracer so as to give different sample solutions an equal counting efficiency. Equation (1) gives the ratio of amounts diffusing at time t and infinite time under the above boundary conditions.[6]

$$\frac{M_t}{M_\infty} = 1 - \sum_{n=1}^{\infty} \frac{2\alpha(1+\alpha)}{1+\alpha+\alpha^2 q_n^2} \cdot \exp(-Dq_n^2 t/l^2) \qquad (1)$$

$$\tan q_n = -\alpha q_n \qquad (2)$$

where M_t and M_∞ are the amounts diffusing at time t and infinite time, α the ratio of volumes of solutions in the capillary and in the cell, l the length of the capillary, and D the diffusion coefficient which is to be determined. q_n in Eq. (1), not being zero, is the solution of Eq. (2).

Results and Discussion

Figure 1 shows both the self-diffusion coefficients of carbon tetrachloride, $D(CCl_4)$ and cyclohexane, $D(C_6H_{12})$ determined at 25°C, and the reported viscosity, η[2] as a function of mole fraction of CCl_4,

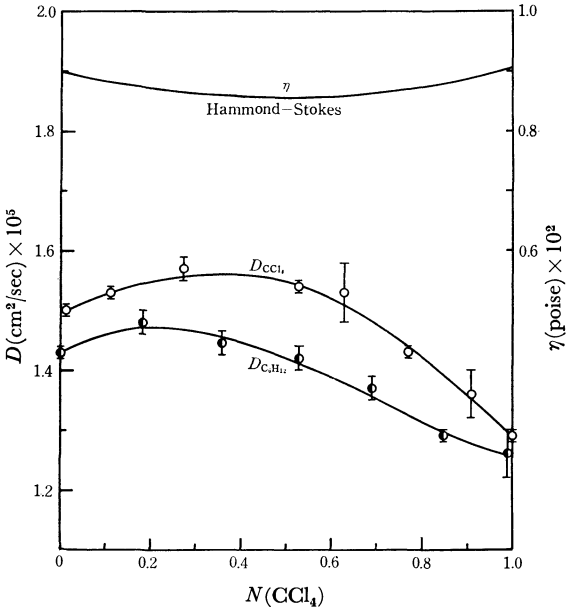

Fig. 1. Self-diffusion coefficients and viscosity as a function of composition for the CCl_4–C_6H_{12} system at 25°C.

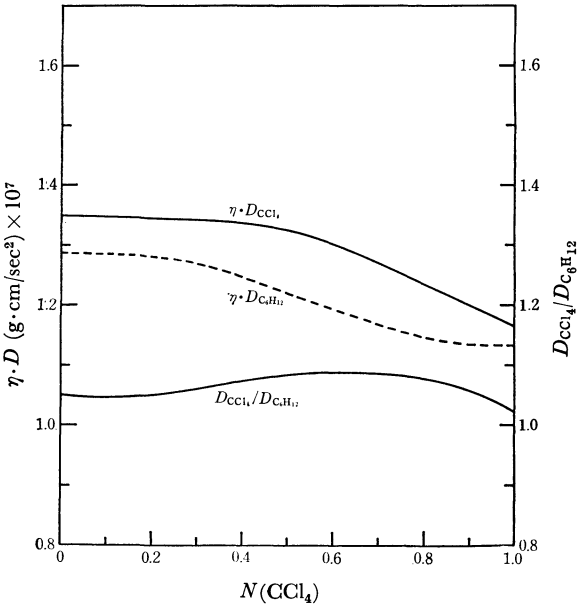

Fig. 2. The ratio of self-diffusion coefficients and the products of self-diffusion coefficients and viscosity as a function of composition for the CCl_4–C_6H_{12} system.

1) G. Scatchard, S. E. Wood, and J. M. Mochel, *J. Amer. Chem. Soc.*, **61**, 3206 (1939).
2) B. R. Hammond and R. H. Stokes, *Trans. Faraday Soc.*, **52**, 781 (1956).
3) M. V. Kulkarni, G. F. Allen, and P. A. Lyons, *J. Phys. Chem.*, **69**, 2491 (1965).
4) I. Brown and A. H. Ewald, *Aust. J. Phys.*, **3**, 306 (1950).
5) J. H. Wang, *J. Amer. Chem. Soc.*, **73**, 510 (1951).
6) J. Crank, "The Mathematics of Diffusion," Clarendon Press, Oxford (1956), p. 53.

$N(CCl_4)$. All are the averaged values of more than four determinations. Both self-diffusion coefficients show similar, relatively small compositional dependence as predicted. The compositional dependence is in reverse trend to that for the viscosity as seen in Fig. 1. Figure 2 shows the ratio of $D(CCl_4)$ and $D(C_6H_{12})$ and the products of viscosity and respective self-diffusion coefficients as a function of composition. The compositional dependence of the ratio $D(CCl_4)/D(C_6H_{12})$ is small compared with many other organic binary systerms. The ratio is close to that of molar volumes for pure cyclohexane and pure carbon tetrachloride: $V(C_6H_{12})/V(CCl_4)=1.12$, which means that Bearman's relation[7] holds. Compositional dependence of $\eta \cdot D(CCl_4)$ and $\eta \cdot D(C_6H_{12})$ is also small compared with water-acetone[8] and many other organic binary systems. The results together with the small compositional dependence of density, viscosity, and equilibrium vapour pressure[1,4] indicate the thermodynamical ideality of the system. In consequence, molecular association will be negligible and the diffusing species for both components will be essentially single molecules in the carbon tetrachloride-cyclohexane system at 25°C.

7) R. J. Bearman, *J. Chem. Phys.*, **32**, 1308 (1960).
8) Y. Kamei and Y. Oishi, *Nippon Kagaku Zasshi*, **91**, 403 (1970).

BULLETIN OF THE CHEMICAL SOCIETY OF JAPAN, VOL. 44, 2856—2858 (1971)

The Paal-Knorr Condensation of Acetonylacetone with 5-Aminopyrazoles

Isaburo HORI* and Minoru IGARASHI*,**

*The Institute of Physical and Chemical Research, Wako, Saitama

**Department of Chemistry, Faculty of Science, Ibaraki University, Mito, Ibaraki

(Received March 8, 1971)

There are very few reports on the Paal-Knorr condensation using heterocyclic amine. The reaction was undertaken with the expectation of formation of pyrazolo-1,3-diazepine ring, but it gave rise to only normal condensation.

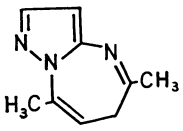

This paper deals with the condensation of acetonylacetone with several 5-aminopyrazoles (**1**, **2a,b** and **3**) in the presence of acetic acid to form a new series of 1-(pyrazol-5-yl)-2,5-dimethylpyrroles (**4**, **5a,b** and **6**). 1,4-Disubstituted 5-aminopyrazole such as **2c** and **2d** could not be condensed under these conditions, due perhaps to steric requirements.

The structure of **4** obtained from 1,2-unsubstituted 5-aminopyrazole (**1**) was confirmed by means of NMR spectral data and chemical evidence. All NMR spectra of **4**, **5**, and **6** show two sharp singlets in the ranges δ 1.92—2.05(6H) and 5.61—5.90(2H) corresponding to the α-methyl protons and β-protons of pyrrole nucleus, respectively. Methylation of **4a—d** with methyl iodide gave the corresponding 1-(1-methylpyrazol-5-yl)-2,5-dimethylpyrroles (**5**). Support for the structures **5c** and **5d** was provided by NMR spectra, in which the *N*-methyl protons are located at high magnetic field than that of the corresponding 1-(2-methylpyrazol-5-yl)-2,5-dimethylpyrroles (**6**) similar to other cases. Furthermore, with two moles of methyl iodide, **4a** reacted to give methiodide (**7**), which could be also derived from either **5a** or **6a** by similar methylation.

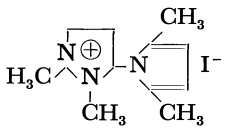

7

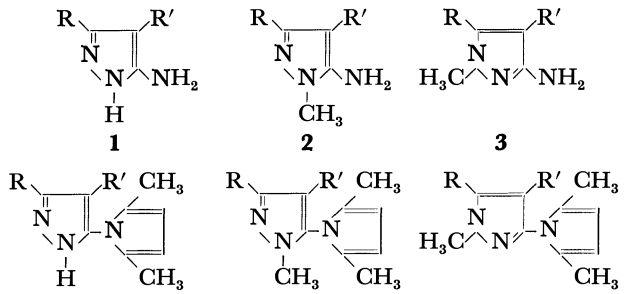

1	2	3	4	5	6	R	R′
1a	**2a**	**3a**	**4a**	**5a**	**6a**	H	H
1b	**2b**	**3b**	**4b**	**5b**	**6b**	CH_3	H
1c	**2c**	**3c**	**4c**	(**5c**)	**6c**	H	$COOC_2H_5$
1d	**2d**	**3d**	**4d**	(**5d**)	**6d**	CH_3	$COOC_2H_5$
1e			**4e**			C_6H_5	H

Experimental

All melting points and boiling points are uncorrected. The NMR spectra were taken with a JNM-C-60 high-resolution NMR spectrometer, using TMS as an internal standard.

5-Aminopyrazoles. 1,2-Unsubstituted 5-aminopyrazoles (**1a–d**) were prepared by the use of a method described in a previous paper.[1] 3-Phenyl-5-aminopyrazole (**1e**) was obtained as described in literature.[2] *N*-Methyl-5-aminopyrazoles (**2a,b** and **3a,b**) were obtained by hydrolysis of 4-ethoxycarbonyl derivatives (**2c,d** and **3c,d**), prepared by

1) H. Baba, I. Hori, T. Hayashi and H. Midorikawa, This Bulletin, **42**, 1653 (1969).

2) A. Takamizawa and Y. Hamashima, *Yakugaku Zasshi*, **84**, 1113 (1964).

Table 1. Physical properties, yields, analytical and NMR data of 1-(pyrazol-5-yl)-2,5-dimethylpyrroles

Compd.	Mp °C (Bp °C/mmHg)	Yield %	Formula	Analysis Found (Calcd) C%	H%	N%	NMR (CCl_4) δ ppm Pyrazole nucleus R	R′	N–CH_3	Pyrrole nucleus α-2CH_3	β-2H
4a	205—208	87.6	$C_9H_{11}N_3$	67.13 (67.05	6.60 6.88	26.02 26.07)	[6.27$_d$(H) (J=2.4 Hz)	7.89$_d$(H)		2.22	6.08][a]
4b	140—142	48.5	$C_{10}H_{13}N_3$	68.81 (68.54	7.39 7.48	24.08 23.98)	1.76 (CH_3)	5.83 (H)		2.05	5.62
4c	136	78.5	$C_{12}H_{15}O_2N_3$	61.57 (61.78	6.49 6.48	18.19 18.02)	7.16 (H)	1.19, 4.12 ($COOC_2H_5$)		2.00	5.90
4d	102—105 (205—208/5.5)	85.0	$C_{13}H_{17}O_2N_3$	63.31 (63.14	6.86 6.93	17.09 16.99)	1.98 (CH_3)	1.02, 4.00 ($COOC_2H_5$)		2.00	5.72
							[2.68 (CH_3)	1.06, 4.15 ($COOC_2H_5$)		2.18	6.03][a]
4e	150—152	62.3	$C_{15}H_{15}N_3$	75.83 (75.92	6.79 6.37	18.01 17.71)	7.24$_m$(C_6H_5)	6.37 (H)		2.02	5.67
5a	(95—99/15)	63.8	$C_{10}H_{13}N_3$	68.92 (68.54	7.49 7.48	24.40 23.98)	[6.21$_d$(H) (J=1.8 Hz)	7.54$_d$(H)	3.48	1.97	5.91][b]
5b	(75/2)	78.0	$C_{11}H_{15}N_3$	69.39 (69.81	7.49 7.99	22.42 22.20)	2.21 (CH_3)	5.88 (H)	3.33	1.94	5.74
5c	(115—116/2)		$C_{13}H_{17}O_2N_3$	62.78 (63.14	6.88 6.93	17.22 16.99)	7.83 (H)	1.12, 4.06 ($COOC_2H_5$)	3.50	1.92	5.80
5d	(105—111/10)		$C_{14}H_{19}O_2N_3$	63.68 (64.34	7.58 7.33	16.23 16.08)	2.42 (CH_3)	1.05, 4.01 ($COOC_2H_5$)	3.44	1.92	5.76
6a	62—63 (135—137/9.5)	66.5	$C_{10}H_{13}N_3$	68.17 (68.54	7.50 7.48	23.85 23.98)	[6.14$_d$(H) (J=2.1 Hz)	7.36$_d$(H)	3.89	2.10	5.85][b]
6b	67—69	92.3	$C_{11}H_{15}N_3$	69.37 (69.81	7.91 7.99	22.57 22.20)	2.27 (CH_3)	5.80 (H)	3.72	2.03	5.61
6c	(140—145/2)	58.5	$C_{13}H_{17}O_2N_3$	62.84 (63.14	6.74 6.93	16.96 16.99)	7.97 (H)	1.11, 4.08 ($COOC_2H_5$)	3.73	1.97	5.71
6d	65—68	37.6	$C_{14}H_{19}O_2N_3$	63.49 (64.34	7.25 7.33	16.52 16.08)	2.55 (CH_3)	1.02, 4.00 ($COOC_2H_5$)	3.77	1.93	5.63

a) in C_5H_5N b) in $CDCl_3$

the procedure of Schimdt *et al.*.[3] **1a**: bp 140—142°C/7 mmHg (lit[4] 115—116°C/1.5 mmHg, mp 38—40°C). **1b**[1]: mp 47—48°C, bp 146.5—147°C/4 mmHg. **1c**: mp 104.5—105.5°C (lit[5] 102—103°C). **1d**[1]: mp 109—110°C. **1e**: mp 127—128°C). (lit.[2] 120—122°C). **2a**: mp 71—73°C (lit[6] 67°C, bp 110°C/4 mmHg). **2b**: mp 77—78°C (lit[7] 78—79°C). **2c**: mp 99—101°C (lit[3] 101°C, bp 121°C/0.05 mmHg). **2d**: mp 108—109°C (Found: C, 52.63; H, 6.98; N, 23.14%. Calcd for $C_8H_{13}O_2N_3$: C, 52.44; H, 7.15; N, 22.94%). **3a**: bp 95—100°C/10 mmHg (lit[6] 92—98°C/9 mmHg). **3b**: mp 66—67°C (Found: C, 54.26; H, 7.98; N, 37.85%. Calcd for $C_5H_9N_3$: C, 54.03; H, 8.16; N, 37.81%). **3c**: mp 88—90°C (lit[3] 92—93°C). **3d**: mp 101—103°C (Found: C, 52.35; H, 7.13; N, 22.87%. Calcd for $C_8H_{13}O_2N_3$: C, 52.44; H, 7.15; N, 22.94%).

Condensation of Acetonylacetone with 5-Aminopyrazoles. To a solution of acetonylacetone (0.02 mol) and 5-aminopyrazole (0.02 mol) dissolved in benzene (50 m*l*), acetic acid (0.5 m*l*) was added, and the mixture was refluxed with a water-separator until the formation of water ceased. After the reaction mixture had been evaporated on a rotary evaporator at 50°C, the residue was purified by washing or recrystallization from an appropriate solvent or by distillation under reduced pressure to give 1-(pyrazol-5-yl)-2,5-dimethylpyrroles (**4**, **5a**, **b** and **6**).

Both **2c** and **2d** did not react and were quantitatively recovered. The results along with the NMR data are summarized in Table 1.

Methylation of 4a–d with Methyl Iodide. A mixture of **4** (5.0 mmol) and methyl iodide (5.0 mmol) in methanol (5 m*l*) was heated in a sealed tube at 100°C for 5 hr. After cooling the reaction mixture was evaporated on a rotary evaporator at 40°C. The dark-reddish residue was distillated under reduced pressure to give mono-methylated products as colorless oil.

The products thus obtained from **4a** and **4b** were identical with the corresponding **5** prepared by the above condensation (yields 40.0 and 32.5%, respectively). The products obtained from **4c** and **4d** were inferred to be the corresponding **5** from NMR spectral study (yields 36.6 and 38.0% respectively). The physical properties, analyses and NMR data are shown in Table 1.

Formation of Methiodide (7). *a)* From **4a**: A mixture of **4a** (0.40 g, 2.5 mmol) and methyl iodide (0.71 g, 5.0 mmol) in methanol (3 ml) was heated in a sealed tube at 100°C for 12 hr. After cooling the reaction mixture was evaporated on a rotary evaporator at 40°C. The dark-reddish residue was triturated with ether-methanol to yield brown crystals. Gel filtration (Sephadex LH-20) with methanol gave the methiodide (**7**) (0.55 g, 70.0%) as nearly colorless needles; mp 159—161°C (dec). NMR (CD_3COCD_3): δ 2.08(s, 6H), 4.03(s, 3H), 4.56(s, 3H), 5.96(s, 2H), 7.04(d, J=3 Hz, 1H),

3) P. Schmidt, K. Eichenberger, M. Wilhelm, and J. Druey, *Helv. Chim. Acta*, **42**, 349 (1959).

4) H. Reimlinger, A. V. Overstreten, and H. G. Viehe, *Chem. Ber.*, **94**, 1036 (1961).

5) J. Druey and P. Schmidt, Ger. 1065421 (1959); *Chem. Abstr.*, **55**, P18786c (1961).

6) S. Hayashi, *Yakugaku Zasshi*, **85**, 442 (1965).

7) C. F. Boehringer and Soehne G.m.b.H., Brit. 863060 (1961); *Chem. Abstr.*, **55**, P18776a (1961).

8.89(d, J=3 Hz, 1H). Found: C, 41.50; H, 5.07; N, 13.57; I, 39.93%. Calcd $C_{11}H_{16}N_3I$: C, 41.66; H, 5.08; N, 13.25; I, 40.01%.

b) From ***5a*** *or* ***6a***. A mixture of **5a** or **6a** (2.5 mmol) and methyl iodide (2.5 mmol) in methanol (2 m*l*) was worked up by the method mentioned above. Both products thus obtained were identical with **7** (yields 56.5 and 52.7%, respectively).

The authors wish to thank Dr. Hiroshi Midorikawa of this Institute for helpful discussion and Mr. Norimichi Suzuki for technical assistance.

BULLETIN OF THE CHEMICAL SOCIETY OF JAPAN, VOL. 44, 2858—2859 (1971)

Photolytic Cyclodehydrogenation Reactions of [2.2]Metacyclophane by Means of Aryl Ketones and Alkoxyl and Thiyl Radicals[1]

Takeo SATO, Kozaburo NISHIYAMA, Shigeru SHIMADA, and Kazuo HATA
Department of Chemistry, Faculty of Science, Tokyo Metropolitan University, Setagaya, Tokyo

(Received March 12, 1971)

The irradiation of [2.2]metacyclophane (I) in benzene or cyclohexane solutions containing iodine through a quartz vessel led to a transannular dehydrogenation reaction to give 4,5,9,10-tetrahydropyrene (II) as the major product.[2,3] As a result of subsequent dehydrogenation processes occurring at a slower rate, the reaction mixture contained 4,5-dihydropyrene (III) and pyrene (IV).[3] Several alkyl derivatives of I were similarly converted into the corresponding 4,5,9,10-tetrahydropyrenes.[4]

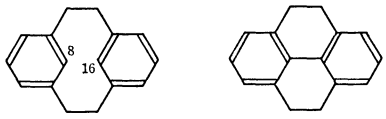

I II

The quantum yield of the initial dehydrogenation step for I was found to be 0.006.[3] The reaction mechanism was suggested to involve the photoexcitation of charge-transfer complex between I and iodine followed by dehydroiodination.[3] The formation and dissociation constants of the charge-transfer complexes involving I were studied spectroscopically.[5,6]

Oxygen is less effective as oxidant. The irradiation of an aerated solution of I in benzene using a high-pressure lamp produced only trace amounts of II and III after 45 hr.[7]

From mechanistic view, we wished to know whether photocyclodehydrogenation was possible with oxidants other than iodine or oxygen.[8] In this paper we will describe the attempts using aryl ketones, di-*t*-butyl peroxide (DTBP), and dibenzyl disulfide.

A benzene solution of I in the presence of a three-fold excess of benzophenone was irradiated under a nitrogen current using a 100-W low-pressure lamp for 25 hr. A 41% yield of II together with further dehydrogenation products were produced (Table 1). Formation of pinacol during the reaction was noticed.

Similar results were obtained by irradiation with a 1-kW high-pressure lamp using a quartz vessel though the conversion was less complete. 4,4'-Dimethoxybenzophenone was also found to bring about the dehydrogenation reaction, while acetophenone, desoxybenzoin and fluorenone were less effective.[9]

The results are surprising since the abstraction of aryl hydrogens instead of benzylic ones is just the reverse of what is to be expected. The photoreduction of benzophenone is known to occur only with good hydrogen donors but never with aromatic hydrogens.[10] In the present case, the loss of aryl hydrogens at $C_{8,16}$ occurred more rapidly than the following aromatization steps leading to III and IV.

No cyclodehydrogenation with benzophenone took place when the reaction was carried out in a Pyrex vessel, where the excitation of only the carbonyl compound was possible since shorter wavelength regions required for I (λ_{max} 266 nm) were cut by a filter.

Cyclodehydrogenation with benzophenone was effectively quenched by naphthalene (E_T=61 kcal/mol) or by triphenylene (E_T=67 kcal/mol)(Table 1).[7]

These results suggest that direct photoexcitation of both the substrate and the aryl ketone is necessary for transannular reaction and no energy transfer from the aryl ketone to I occurs. If a triplet state of I is to be

1) Photo-Aryl Coupling and Related Reactions. IX. Part VIII: T. Sato and T. Morita, This Bulletin, in press.

2) T. Sato, E. Yamada, Y. Okamura, T. Amada, and K. Hata, *ibid.*, **38**, 1049 (1965).

3) T. Sato, M. Wakabayashi, S. Hayashi, and K. Hata, *ibid.*, **42**, 773 (1969).

4) T. Sato, S. Akabori, S. Muto, and K. Hata, *Tetrahedron*, **24**, 5557 (1968); H. Shizuka, K. Sorimachi, T. Morita, K. Nishiyama, and T. Sato, This Bulletin, **44**, 1983 (1971). Other dimethyl- and tetramethyl[2.2]metacyclophanes were similarly cyclodehydrogenated (unpublished results).

5) S. Hayashi and T. Sato, *Nippon Kagaku Zasshi*, **91**, 950 (1970).

6) S. Hayashi and T. Sato, unpublished results.

7) The cyclodehydrogenation reaction of I was noticed with aerated and degassed solutions [Y. Takayama, K. Sorimachi, H. Shizuka, and T. Morita, Abstracts of Papers, the 23rd Annual Meeting of the Chemical Society of Japan, April, 1970 (Tokyo)]. The reaction rate appears to be lower compared with the case in which iodine is used.

8) *p*-Benzoquinone was found to be effective for the conversion of I to II.[6]

9) As a control experiment a benzene solution of I was irradiated for 45 hr under nitrogen. Only trace amounts (less than 1%) of II and III were detected.

10) N. J. Turro, "Molecular Photochemistry," W. A. Benjamin, Inc., New York (1965), p. 137.

Table 1. Photocyclodehydrogenation of [2.2]metacyclophane (I) with aryl ketones

Aryl ketone	>C=O/I	Additive	Irrad. time, hr	Filter	Product, %			
					II	III	IV	Recovery
Benzophenone	3		25	Vycor[b]	41	13	4	42
Benzophenone	3		44	quartz	24	9	3	64
Benzophenone	2		44.5	quartz	8	2	0	90
Benzophenone	2		45	Pyrex	0	0	0	100
Benzophenone	2	naphthalene	44.5	quartz	trace	trace	0	100
Benzpphenone	2	triphenylene	45	quartz	0	0	0	100
Benzophenone	2	acetophenone	45	quartz	trace	0	0	100
4,4′-Dimethoxybenzophenone	2		45	quartz	15	0	0	85
Acetophenone	2		45	quartz	3	trace	0	97
Desoxybenzoin	2		44	quartz	3	trace	0	97

a) Dilute benzene solutions of I (4×10^{-3} M) containing appropriate aryl ketones were irradiated with a 1-kW high-pressure lamp. The reaction mixture was analyzed by gas chromatography using 1 m XE-60 silicone gum rubber on Chromosorb W column. The yields are shown in product ratios.

b) A 100-W low-pressure lamp was used as the light source.

involved, E_T must be higher than that of benzophenone, namely, 69 kcal/mol. We propose that the reaction proceed through an excited singlet state since the iodine-induced reaction is not quenched by oxygen. Recently, Takayama, Sorimachi, Shizuka, and Morita[7] suggested a singlet-state mechanism for the photoreaction of I on basis of quenching experiments and emission spectra measurements.

The results with benzophenone led us to examine the photoreactions of I toward alkoxy and thiyl radicals. Whereas no reaction occurred when I was reacted with *t*-butoxy radicals generated by the thermal decomposition of DTBP at 140°C, the irradiation of a benzene solution of I containing DTBP under nitrogen produced II (7.4%), III (2.3%), and IV (trace). *t*-Butoxy radicals are believed not to abstract hydrogens on an aromatic ring.

The photolysis of a benzene solution containing I and dibenzyl disulfide also gave II (10.8%), III (6.1%), and IV (trace).

The inertness of the methylene groups in I toward radical attack can be ascribed to steric restrictions, rigidity of the molecule and bond angle deformation, which restrict usual charge stabilization associated with a benzylic radical. Tendency of I to undergo transannular reactions is explained by large angle and bond-distance changes. An enhanced reactivity of the aryl hydrogens upon photoexcitation appears to be explainable only by postulating an intermediate that possesses a transannular bonding between C_8 and C_{16} positions.

Experimental

Photolysis of I with Aryl Ketones. The results are summarized in Table 1. For quenching experiments three-molar equivalent of an additive was employed. A typical example is shown below.

A solution of 25.4 mg (0.12 mmol) of I and 68.7 mg (0.38 mmol) of benzophenone in 30 m*l* of benzene was irradiated under nitrogen using a 100-W low-pressure lamp for 25 hr. By gas chromatographical analysis using 1 m XE-60 on Chromosorb W column II (41%), III (13%), and IV (4%) were identified by comparing retention times with those of authentic materials.

Photolysis of I with DTBP. Irradiation of a benzene solution (30 m*l*) of 30.0 mg (0.14 mmol) of I and 57.3 mg (0.39 mmol) of DTBP contained in a quartz vessel using a 1-kW high-pressure lamp for 45 hr under nitrogen produced II (7.4%), III (2.3%), and IV (trace) as analyzed by gas chromatography.

Photolysis I with Dibenzyl Disulfide. Irradiation of a benzene solution (30 m*l*) of 26.0 mg (0.13 mmol) of I and 93.3 mg (0.38 mmol) of dibenzyl disulfide as above gave II (10.8%), III (6.1%), and IV (trace). The rest of the material was recoverable as I.

BULLETIN OF THE CHEMICAL SOCIETY OF JAPAN, VOL. 44, 2860—2861 (1971)

The Gas-Phase Radiolysis of Cyclopropane

Jun-ichi TANAKA, Yoshihiko HATANO, and Shoji SHIDA

Laboratory of Physical Chemistry, Tokyo Institute of Technology, Meguro-ku, Tokyo

(Received March 19, 1971)

Cyclopropane is used as a good positive-ion scavenger in the radiolysis of hydrocarbons[1] and it can undergo an H_2 transfer reaction with a hydrocarbon positive ion.[2] On the radiolysis of cyclopropane itself, however, only a few reports have been published.[3-6] In the present study, the effects of additives, such as SF_6 and C_2H_4, on the formation of hydrogen and various hydrocarbon products in the gas-phase radiolysis of cyclopropane have been examined. The results are rather similar to those in the radiolysis of olefins, although cyclopropane apparently belongs to paraffinic hydrocarbons in chemistry. The olefinic properties of cyclopropane have also been pointed out elsewhere.[7] The effects of some paraffinic hydrocarbons added to cyclopropane have also been examined: a large increase of propane formation has been observed and ascribed to ion-molecule reaction involving H^- and H_2^- transfer processes.

Experimental

All the materials in the experiment were supplied by the Takachiho-Shoji Co. The gas-chromatographic analysis of cyclopropane using a dimethyl sulfolane column showed a purity of 99.96%. The cyclopropane contains 0.024% of propane and 0.016% of propylene. It was used after usual degassing and distillation in a vacuum line. The sulfur hexafluoride and some paraffins used as additives were of a high purity and were used without further purification. The cell for irradiation was a glass ampule with a volume of 50m*l*. The total gas pressure was 760 mmHg. The samples were irradiated by Co^{60} γ-rays at room temperature. The dose rate was 5.0×10^{19} eV/g·hr, and the total dose was 6.0×10^{20} eV/g. The quantitative analysis of hydrogen and methane was carried out by means of a Toepler pump equipped with a gas burette. Hydrocarbon products were analysed by gas chromatography using a dimethyl sulfolane column and by mass spectrometry.

Results and Discussion

Table 1 shows the *G*-values of products in the gas-phase radiolysis of cyclopropane. The relative yields of C_2 and C_3 hydrocarbon products are different from those reported by Ausloos *et al.*[6] This difference may be due to the large difference in the sample pressure in the experiments. The *G*-value of hydrogen is almost equal to that of Yang.[4] It is known in general that the *G*-values of hydrogen from paraffinic hydrocarbons in the gas-phase radiolysis are about 5—8,[8-12] while they are about 1 from olefins.[13] As is evident from Table 1, the yield of hydrogen from cyclopropane is very near to those from olefins. In the gas-phase radiolysis of paraffins, a rapid decrease in $G(H_2)$ is observed upon the addition of a small amount of an electron scavenger.[10] In this experiment, however, $G(H_2)$ from cyclopropane is scarcely suppressed at all by the addition of SF_6 as an electron scavenger, even at high concentrations, ~1 mol%. This hydrogen yield is also unaffected by the addition of C_2H_4 (~1 mol%). The experimental results described above are rather similar to those of olefins. Thus, the primary process of the hydrogen formation in the gas-phase

Table 1. *G*-Values[a] of products from the gas-phase radiolysis of cyclopropane

Product	*G*-value
Hydrogen	1.36
Methane	0.38
Ethylene	2.40
Propane	0.52
Propylene	0.27
Isobutane	0.03
n-Butane	0.37
Acetylene	b)
Allene	b)
trans-2-Butene or Isopentane	0.14
Methylcyclopropane	0.18
n-Pentane	0.10
Allylene	0.03
1-Pentene	0.03
2,3-Dimethylbutane or 2-Methyl pentane	0.13
3-Methylpentane	0.06
n-Hexane	0.03
C_6(others)	0.07

a) Initial values. These values were almost independent of total dose up to 1.0×10^{21} eV/g.

b) These products could not be determined quantitatively upon this column in gas chromatography.

1) See, for example, K.-D. Asmus, J. M. Warman, and R. H. Schuler, *J. Phys. Chem.*, **74**, 246 (1970).
2) P. Ausloos, A. A. Scala, and S. G. Lias, *J. Amer. Chem. Soc.*, **89**, 3677 (1967).
3) C. F. Smith, B. G. Corman, and F. W. Lampe, *ibid.*, **83**, 3559 (1961).
4) K. Yang, *J. Phys. Chem.*, **65**, 42 (1961).
5) H. Umezawa and F. S. Rowland, *J. Amer. Chem. Soc.*, **84**, 3077 (1962).
6) A. A. Scala and P. Ausloos, *J. Chem. Phys.*, **49**, 2282 (1968).
7) See, for example, L. Joris, P. von R. Schleyer, and R. Gleiter, *J. Amer. Chem. Soc.*, **90**, 327 (1968) and references cited in.
8) R. W. Hummel, *Discuss. Faraday Soc.*, **36**, 75 (1963).
9) K. Yang and P. J. Gant, *J. Phys. Chem.*, **65**, 1861 (1961).
10) G. R. A. Johnson and J. M. Warman, *Trans. Faraday Soc.*, **61**, 1709 (1965); N. Fujisaki, S. Shida, and Y. Hatano, *J. Chem. Phys.*, **52**, 556 (1970).
11) S. Shida, N. Fujisaki, and Y. Hatano, *ibid.*, **49**, 4571 (1968).
12) T. J. Hardwick, *J. Phys. Chem.*, **66**, 1611 (1962).
13) Y. Hatano and S. Shida, unpublished results; M. C. Sauer, and L. M. Dorfman, *J. Phys. Chem.*, **66**, 322 (1962).

radiolysis of cyclopropane may be interpreted, similarly to the case of olefins,[14] in terms of the following two processes: the molecular detachment of the hydrogen molecule and the hydrogen-atom abstraction of hot hydrogen atoms formed by the direct excitation which may involve superexcitation.

Table 2. Effect of addition of hydrocarbons on the yields of propane and propylene in the gas-phase radiolysis of cyclopropane

n-C_6H_{14}			c-C_6H_{12}		
mol%	$G(C_3H_8)$	$G(C_3H_6)$	mol%	$G(C_3H_8)$	$G(C_3H_6)$
0	0.52	0.27	0	0.52	0.27
0.4	1.1	0.50	0.7	0.94	0.42
1.0	0.92	0.49	2.1	1.1	0.46
1.5	1.0	0.50	3.0	1.1	0.46
2.1	1.1	0.50			

The addition of small amounts of some paraffinic hydrocarbons, C_2H_6, n-C_4H_{10}, n-C_5H_{12}, n-C_6H_{14}, and c-C_6H_{12}, caused a definite increase in the propane formation; *e.g.*, in the case of n-C_6H_{14} or c-C_6H_{12}, as is shown in Table 2, the yield of propane increases by as much as that from pure cyclopropane. This increase may be interpreted neither in terms of the direct radiolysis of the additive hydrocarbons nor in terms of simple charge-transfer processes from cyclopropane to the additives. Since, as is also shown in Table 2, the increase in propylene formation due to the addition of c-C_6H_{12} is not very large, the large increase of propane can not be interpreted only by the simple free-radical mechanism, the disproportionation of propyl radicals.

The isotopic distribution of the propane produced in the radiolysis of the following two mixtures was examined; c-C_3H_6- 3 mol% c-C_6D_{12} and c-C_3H_6- 3 mol% c-C_6D_{12}- 5 mol% O_2. In each case, the formation of $C_3H_6D_2$ and C_3H_7D was observed and the quantity of C_3H_7D was more than that of $C_3H_6D_2$. The ratio of these two quantities, about 2.0, is not affected by the presence of O_2. The above results have led us to conclude that the increase in the propane formation may be interpreted in terms of the following ion-molecule reactions:

$$c\text{-}C_3H_6^+ + RH_2 \longrightarrow C_3H_8 + R^+ \quad (1)$$

$$c\text{-}C_3H_6^+ + c\text{-}C_3H_6 \longrightarrow C_3H_7^+ + C_3H_5 \quad (2)$$

$$C_3H_7^+ + RH_2 \longrightarrow C_3H_8 + RH^+ \quad (3)$$

where RH_2 is an additive hydrocarbon. Judging from the results of the isotopic experiments, the H^--transfer reaction (3) is more important for the increase of the propane formation than the H_2^--transfer reaction (1). The occurrence of reaction (2), *i.e.*, the presence of $C_3H_7^+$, was observed in the mass-spectrometric experiment on cyclopropane.[15] The H_2^--transfer to the $C_3H_6^+$ ion produced by the photoionization of propylene[16,17] or by the gas-phase radiolysis of c-C_5H_{10}[18] has already been investigated. In the case of the cyclopropane parent ion, c-$C_3H_6^+$, however, the H_2^--transfer reaction in radiolysis has not been reported in detail, although this process was suggested by Ausloos *et al.*[19] in connection with the gas-phase radiolysis of c-C_6H_{12} with c-C_3D_6 as an additive. The H_2^--transfer reaction of c-$C_3H_6^+$ in a mass spectrometer was reported by Futrell *et al.*[15]

14) Y. Hatano and S. Shida, *J. Chem. Phys.*, **46**, 4784 (1967); Y. Hatano, S. Shida, and M. Inokuti, *ibid.*, **48**, 940 (1968); Y. Hatano, S. Shida, and S. Sato, This Bulletin, **41**, 1120 (1968).

15) L. W. Sieck and J. H. Futrell, *J. Chem. Phys.*, **45**, 560 (1966).

16) R. Gorden, Jr., R. Doepker, and P. Ausloos, *ibid.*, **44**, 3733 (1966).

17) L. W. Sieck and S. K. Searles, *J. Amer. Chem. Soc.*, **92**, 2937 (1970).

18) R. D. Doepker and P. Ausloos, *J. Chem. Phys.*, **44**, 1951 (1966).

19) P. Ausloos and S. G. Lias, *ibid.*, **43**, 127 (1965).

BULLETIN OF THE CHEMICAL SOCIETY OF JAPAN, VOL. 44, 2861—2863 (1971)

Alkylation of 2,6-Lutidine

Ichiro KAWASAKI, Isao KUSUMOTO,* and Takeo KANEKO**

Faculty of Science, Osaka University, Toyonaka, Osaka

(Received March 20, 1971)

For a study of the intramolecular oxidative coupling of phenolic compounds, we tried to prepare 2,6-bis(*p*-hydroxyphenyl)alkyl- and alkenylpyridine.

Attempts to condense 2,6-lutidine with cinnamaldehyde and hydrocinnamaldehyde by heating or with acetic anhydride were unsuccessful.

Some reactions of 6-methyl-2-picolyllithium have been reported, but discrepancies are found in literature regarding the possibility of generating and using a dilithium derivative of 2,6-lutidine.[1)]

The reaction of lutidyllithium with cinnamaldehyde afforded no simple reaction products. 1-(6-Methyl-2-pyridyl)-4-phenyl-2-butanol (Ia) was formed by the action of hydrocinnamaldehyde along with 3,3-di(6-methyl-2-pyridylmethyl)-1-phenylpropane (II), which was formed from two moles of lutidine with one mole of aldehyde. Further treatment of lithium derivative of tetrahydropyranyl ether Ib with aldehyde gave no

* Present address: Central Research Laboratories, Ajinomoto Co. Inc., Suzuki-cho, Kawasaki.

** Present address: Research Laboratory of Shiseido Co. Ltd., Nippa-cho, Kohoku-ku, Yokohama.

1) K. Schofield, "Hetero-Aromatic Nitrogen Compounds," Butterworth & Co. Ltd., London (1967), p. 381.

reaction products, only the starting material Ib and Ia being recovered.

The product obtained from 2,6-lutidine and benzyl chloride with two equivalents of phenyllithium has been reported as 2-dibenzylmethyl-6-methylpyridine.[2)]

The same results were obtained by the action of lutidyllithium on cinnamyl chloride. The product ($C_{25}H_{25}N$) was assigned to 2-dicinnamylmethyl-6-methylpyridine by NMR spectra (2.50 ppm, 3H singlet of α-methyl proton of pyridine).

On the other hand, symmetrical dialkylation occurred by using γ-phenylpropyl bromide. The product IVa ($C_{25}H_{29}N$) showed no absorption at 2.50 ppm in NMR spectra. This prompted us to try the reaction with γ-(*p*-methoxyphenyl)-propyl bromide. The structure of IVb is supported by NMR and MS which has a parent ion peak at *m/e* 403. Fragmentation peaks at *m/e* 255, 121, and 107 are assigned to ions $[CH_3O\text{-}C_6H_4\text{-}(CH_2)_4\text{-}C_5H_4N\text{-}CH_2]^+$, $[CH_3O\text{-}C_6H_4\text{-}CH_2]^+$ and $[CH_3\text{-}C_5H_4N\text{-}CH_2]^+$ respectively. Phenolic compound IVc was produced by boiling IVb with 48% hydrobromic acid.

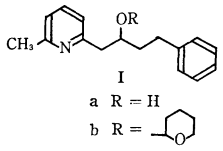

I

a R = H

b R =

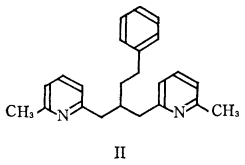

II

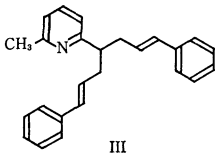

III

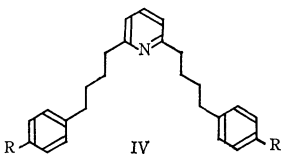

IV

a R = H

b R = OCH_3

c R = OH

Experimental

Reaction of 2,6-lutidine with hydrocinnamaldehyde.

1) To a solution of phenyllithium (0.2 mol) in ether (200 m*l*) was added dropwise 2,6-lutidine (21.4g, 0.2 mol) at room temperature and stirred for 3 hr. A solution of hydrocinnamaldehyde (26.8g, 0.2 mole) in ether (30 m*l*) was then added and the reaction mixture was stirred overnight at room temperature. The cooled reaction mixture was decomposed by addition of ice-water. The aqueous layer was extracted with ether and the ethereal extracts were washed with water, and dried. The residual oil obtained by evaporation of the solvent was distilled to give 37g (78%) of Ia, bp 137—142°C/0.001 mmHg. NMR: δ (CCl_4) 1.75 (m, 2), 2.52 (s, 3), 2.60-3.00 (broad, 4), 3.92 (quintet, 1, *J*=*ca.* 6 Hz), 4.97 (broad s, 1), 6.8—7.6 ppm (8). IR: 3400, 1600, 1585 cm^{-1}.

Found: C, 79.74; H, 7.96; N, 5.84%. Calcd for $C_{16}H_{19}ON$: C, 79.63; H, 7.94; N, 5.80%.

Tetrahydropyranyl ether of Ia, bp 170—175°C/0.001 mmHg.

Found: C, 77.47; H, 8.39; N, 4.23%. Calcd for $C_{21}H_{27}O_2N$: C, 77.50; H, 8.36; N, 4.30%.

2) The reaction was effected by 0.05 mol of 2,6-lutidine and 0.18 mol of hydrocinnamaldehyde and the product was extracted with ether. The organic layer was extracted with 6N hydrochloric acid and the acidic extract was made basic with sodium carbonate and then reextracted with ether. The ethereal extracts were washed with sodium hydrogen sulfite solution and water, and dried. The solvent was removed and the residual oil was distilled at 180—190°C/0.001 mmHg, 2.2 g. The oil showed two spots (R_f 0.60, 0.69: ethyl acetate) on TLC (silica gel G). One (R_f 0.69) was identical with that of Ia. Chromatography over 40 g of silica gel and elution with benzene-ether (99: 1) afforded 700 mg of II: R_f 0.60, bp 220—250°C/0.001 mmHg. NMR: δ(CCl_4) 1.37—1.77 (broad, 3), 2.45 (s, 6), 2.48—2.90 (broad, 6), 6.65—7.42 ppm (11).

Found: C, 82.84; H, 8.01; N, 8.15%. Calcd for $C_{23}H_{26}N_2$: C, 83.59; H, 7.93; N, 8.48%.

Picrate: mp 174°C (from ethanol).

Found: C, 53.45; H, 4.13; N, 14.23%. Calcd for $C_{35}H_{32}O_{14}N_8$: C, 53.30; H, 4.09; N, 14.21%.

2-Dicinnamylmethyl-6-methylpyridine (III). To a stirred solution of lutidyllithium (0.06 mol) in ether was added dropwise cinnamyl chloride (21.2 g, 0.16 mol) at −15°C during a period of 2.5 hr. After standing overnight at 0°C, the reaction mixture was refluxed for 1 hr. The product obtained in the usual way was distilled to give 9.8 g (48%) of III, bp 215—217°C/0.001 mmHg. NMR: δ (CCl_4), 2.50 (s, 3), *ca.* 6.2 (2), 6.7—7.4 ppm (15).

Found: C, 88.33; H, 7.35; N, 4.12%. Calcd for $C_{25}H_{25}N$: C, 88.45; H, 7.42; N, 4.13%.

2,6-Bis-(δ-phenylbutyl)pyridine (IVa). To a stirred solution of lutidyllithium (0.05 mol) in ether (100 m*l*) was added a solution of γ-phenylpropyl bromide (20 g, 0.1 mol) in ether (50 m*l*) at 0°C. After stirring for 2 hr at room temperature and for 30 min under reflux, the reaction was quenched by addition of water. The separated ethereal layer was washed with water and dried. The residue obtained by evaporation of the solvent was distilled to give two kinds of oily products. The first fraction amounted to 5.1 g (45%) of 6-methyl-2-(δ-phenylbutyl)pyridine, bp 107°C/0.1 mmHg. NMR: δ (CCl_4) 1.7 (m, 4), 2.5 (s, 3), 2.65 (m, 4), 6.67—7.6 (8).

Found: C, 84.95; H, 8.56; N, 6.03%. Calcd for $C_{16}H_{19}N$: C, 85.28; H, 8.50; N, 6.22%.

The second fraction was 8.3 g (48%) of IVa, bp 183°C/0.1 mmHg. NMR: δ (CCl_4) 1.7 (m, 8), 2.65 (m, 8), 6.67—7.6 ppm (13).

Found: C, 87.14; H, 8.48; N, 4.10%. Calcd for $C_{25}H_{29}N$: C, 87.41; H, 8.51; N, 4.08%.

2,6-Bis[δ-(p-methoxyphenyl)butyl]pyridine (IVb). To a stirred solution of lutidyllithium (0.1 mol) in ether (170 m*l*) was added a solution of γ-(*p*-methoxyphenyl)propyl bromide[3)] (45.8 g, 0.2 mol) in ether (100 m*l*) at 0°C. After further stirring for 3 hr at 0°C, 2 hr at room temperature and 1 hr under reflux, the reaction was quenched by addtion of water and the products obtained in the usual way were fractionally distilled. The main fraction was 17.3 g (43%) of IVb, bp 230—235°C/0.001 mmHg. NMR: δ (CCl_4), 1.3—2.0 (broad, 8), 2.3—2.9 (broad, 8), 3.65 (s, 6), 6.5—7.5 ppm (11). IR: 1610, 1585, 1580 cm^{-1}. MS: *m/e* 403(3), 268 (5), 255(21), 121(100), 120(75), 107(48), 91(9), 79(5), 78(9), 77(12%).

Found: C, 80.14; H, 8.26; N, 3.47%. Calcd for $C_{27}H_{33}O_2N$: C, 80.36; H, 8.24; N, 3.47%.

The low boiling fraction (bp 132—135°C/0.001 mmHg) was 6.1 g of 2-[δ-(*p*-methoxyphenyl)butyl]-6-methylpyridine.

Found: C, 79.83; H, 8.22; N, 5.53%. Calcd for $C_{17}H_{21}ON$: C, 79.96; H, 8.29; N, 5.49%.

Further treatment of the lithium derivative of this compound with equimolecular amount of bromide yielded IVb, 60%.

2) J.I. de Jong and J.P. Wibaut, *Rec. Trav. Chim.*, **70**, 962 (1951).

3) Ki-U Kim, *J. Pharm. Soc. Japan*, **63**, 376 (1943).

*2,6-Bis[δ-(*p*-hydroxyphenyl)butyl]pyridine (IVc).* IVa (26 g) was dissolved in 48% hydrobromic acid (1 *l*) and heated for 8 hr under reflux. The residue obtained by evaporation of the solution *in vacuo* was crystallized from alcoholic water to give 16 g(54 %) of IVc-hydrobromide, mp 181—182°C.

Found: C, 65.74; H, 6.54; N, 3.02; Br, 17.30%. Calcd for $C_{25}H_{30}O_2NBr$: C, 65.79; H, 6.65; N, 3.07; Br, 17.51%.

The solution of IVc-hydrobromide in methanol was treated with sodium carbonate solution and evaporated to dryness *in vacuo*. The residue was extracted with hot ethyl acetate. The crystal obtained by evaporation of the solvent was recrystallized from ethanol, mp 124—126°C. NMR: δ (pyridine-d_5), 1.5—2.0 (broad, 8), 2.56 (t, 4, J=*ca.* 7 Hz), 2.82 (t, 4, J=*ca.* 6 Hz), 7.02 (s, 8), 6.8—7.9 (t, 3), 8.6 ppm (broad s, 2). IR: 3320—2300 cm^{-1}.

Found: C, 79.89; H, 7.77; N, 3.68%. Calcd for $C_{25}H_{29}O_2N$: C, 79.96; H, 7.79; N, 3.73%.

BULLETIN OF THE CHEMICAL SOCIETY OF JAPAN, VOL. 44, 2863—2864 (1971)

Preparation and Properties of Metal Complexes in Non-aqueous Solutions. III. Preparation of Tetrammine-monoethylenediamine- and -monopropylenediamine-cobalt(III) Complexes in Dimethyl Sulfoxide

Hayami YONEDA, Masayuki MUTO, and Kyoko TAMAKI
Department of Chemistry, Wakayama University, Masagocho, Wakayama

(Received March 24, 1971)

Tetramminemonoethylenediaminecobalt(III) complex is prepared by an indirect route[1]:

$$NH_4[Co(SO_3)_2(NH_3)_4] \xrightarrow{en} NH_4[Co(SO_3)_2(NH_3)_2en] \xrightarrow{HCl} [CoCl_2(NH_3)_2en]Cl \xrightarrow{KNCS} [Co(NCS)_2(NH_3)_2en]^+ \xrightarrow{H_2O_2} [Co(NH_3)_4en]^{3+}$$

Such a roundabout method of preparation is necessary because of the lability of cobalt(III)ammine complexes in an alkaline solution. Even the basicity of ethylenediamine is enough to expel the coordinated ammonia from the coordination sphere. Previously Yoneda[2] suggetsed that cobalt(III)ammines are decomposed *via* the proton dissociation of the coordinated ammonia. That is, ammonia is linked to the cobalt(III) ion fairly firmly as long as it keeps its three hydrogen atoms and remains as NH_3, but it becomes labile when it loses a proton to form NH_2. If this interpretation is valid, we can expect that the monoethylenediamine complex can be prepared directly from the diacidotetrammine complex by using some non-aqueous solvent which prevents the proton dissociation of the coordinated ammonia. Thus, we tried to use dimethyl sulfoxide (DMSO) in the preparation of $[Co(NH_3)_4en]^{3+}$ and $[Co(NH_3)_4pn]^{3+}$ and obtained the expected results. The present paper will describe the details of the preparation and the PMR spectra of these two complexes.

Experimental

Preparation of the Complexes. Five grams (1/63 mol) of $[Co(NO_3)_2(NH_3)_4]NO_3$ were dissolved in 30 m*l* of DMSO, and to this solution there was added 0.95 g (slightly less than 1/63 mol) of ethylenediamine in 10 m*l* of DMSO. The solution was then kept at 60°C for three hours. Then, 130 m*l* of ethanol was added to precipitate the desired complex. Yield, 3.3 g. Orange crystals were obtained by recrystallization from a hot aqueous solution acidified with acetic acid. Found: C, 6.33; H, 5.47; N, 33.47%. Calcd for $[Co(NH_3)_4en](NO_3)_3$: C, 6.44; H, 5.41; N, 33.78%.

The monopropylenediamine complex was prepared in a similar way. Found: C, 9.09; H, 5.65; N, 32.68%. Calcd for $[Co(NH_3)_4pn](NO_3)_3$: C. 9.30; H, 5.74; N, 32.56%.

PMR Measurements. The spectra reported here were recorded on a Varian A60 Analytical NMR spectrometer. The spectra were run in trifluoroacetic acid (TFA), and the chemical shifts were measured relative to tetramethylsilane as an internal reference.

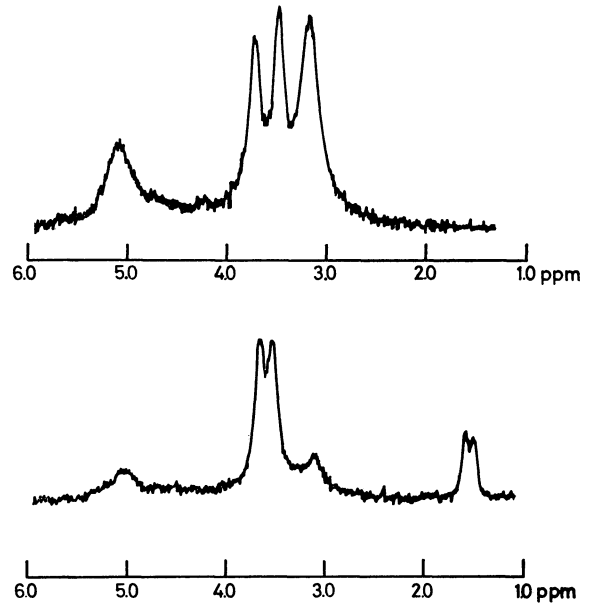

Fig. 1. The PMR spectra of $[Co(NH_3)_4en](NO_3)_3$ (above) and $[Co(NH_3)_4pn](NO_3)_3$ (below) in TFA.

1) K. Ohkawa, J. Fujita, and Y. Shimura, This Bulletin, **38**, 66 (1965).
2) H. Yoneda, *ibid.*, **31**, 74 (1958).

TABLE 1. ASSIGNMENTS OF PMR SIGNALS OF $[Co(NH_3)_4en](NO_3)_3$ AND $[Co(NH_3)_4pn](NO_3)_3$ IN TFA MEASURED AT 60MHz (PPM UNIT)

	CH_2CH_2	NH_3		NH_3			
$[Co(NH_3)_4en]^{3+}$	3.18	3.50	3.57	5.10			
	CH_3		CH_2	CH	NH_3		NH_2
$[Co(NH_3)_4pn]^{3+}$	1.50	1.58	3.08	*ca.* 3.33	3.53	3.67	5.0

Interpretation of the PMR Spectra

The PMR spectra of $[Co(NH_3)_4en](NO_3)_3$ and $[Co(NH_3)_4pn](NO_3)_3$ are shown in Fig. 1. The intensity ratios of the PMR signals in these spectra snd the comparison of these spectra with those of $[Co\ en_3]^{3+}$ and $[Co\ pn_3]^{3+}$ complexes lead to unambiguous assignments of these signals, as is shown in Table 1. Both spectra have the NH_3 signal in two separate peaks of equal intensity, which confirms that the complexes prepared are in fact $[Co(NH_3)_4en]^{3+}$ and $[Co(NH_3)_4pn]^{3+}$.

BULLETIN OF THE CHEMICAL SOCIETY OF JAPAN, VOL. 44, 2864—2865 (1971)

Convenient Synthesis of Chloroiodomethane from Dichloromethane and Sodium Iodide in DMF

Sotaro MIYANO and Harukichi HASHIMOTO

Department of Applied Chemistry, Faculty of Engineering, Tohoku University, Aramaki, Sendai

(Received March 24, 1971)

Organozinc reagent obtained from chloroiodomethane and zinc-copper couple is useful for the synthesis of α-olefins from aldehydes.[1] Chloroiodomethane is usually synthesized from dichloromethane and sodium iodide by refluxing in acetone for several days.[2] The reaction period can be shortened to several hours by the use of an autoclave.[1] However, the procedure is not suitable for a large scale synthesis. It is well known that dipolar-aprotic solvents accelerate S_N2 type reaction remarkably.[3] Suitable solvents and reaction conditions for the synthesis of chloroiodomethane were investigated.

Results and Discussion

Table 1 shows the effect of solvent on the reaction of dichloromethane and sodium iodide. Chloroiodomethane was obtained in only poor yield with acetone, while DMSO, DMF, and HMPA gave much better results. From its availability and the yield of chloroiodomethane, DMF seems to be the most suitable solvent. When the reaction was carried out in DMF for 10 hr, the yield of chloroiodomethane amounted to 83% based on the used sodium iodide, accompanying the formation of 10% of diiodomethane. In the synthetic procedure, pure chloroiodomethane was isolated by distillation in 63% yield, providing a convenient method for the synthesis. In a similar way, bromoiodomethane was also obtained from dibromomethane and sodium iodide.

Table 2 shows that water retards the reaction, presumably because of the solvation of iodide ion. Preliminary experiments have shown that commercially available dichloromethane, DMF, and sodium iodide can be used without significant decrease in the yield of chloroiodomethane.

Table 3 shows the effects of the cation on the yield of chloroiodomethane. The degree of the solvation of cation by DMF seems to decrease in the order Li>Na

TABLE 1. EFFECT OF THE SOLVENT ON THE REACTION OF CH_2Cl_2 AND NaI[a]

Solvent	(ml)	Reaction temp. (°C)	Product Yield[b] CH_2ClI (%)	Product Yield[b] CH_2I_2 (%)
Actone	30	51	2.6	0
Acetonitrile	30	55—56	1.6	0
Methanol	30	41	0.5	0
DMSO	30	56—59	24.1	0
DMF	30	55—66	48.0	3.8
		55—75[c]	82.8	10.2
HMPA	30	51—61	54.6	2.9
Acetone[d] / DMF	30 / 10	54—56	18.7	<1.0
THF[d] / DMF	30 / 10	58—59	22.3	1.0
DMF[e]	30	70[f]	CH_2BrI 84.5	14.8
DMF[g]	30	63—68	CH_2ClBr 4.3	—

a) NaI 0.100 mol, CH_2Cl_2 0.47 mol. Reactions were carried out under gentle reflux for 5 hr.
b) Based on NaI.
c) Reaction was continued for 10 hr.
d) Mixed solvents were used.
e) CH_2Br_2 (0.47 mol) was used in place of CH_2Cl_2.
f) Reaction was carried out at constant temperature.
g) NaBr (0.100 mol) was used in place of NaI.

1) S. Miyano, M. Hida, and H. Hashimoto, *J. Organometal. Chem.*, **12**, 263 (1968).
2) For example, E. M. Kosower, and I. Schwager, *J. Amer. Chem. Soc.*, **86**, 5528 (1964).
3) For example, A. J. Parker, *Chem. Rev.*, **69**, 1 (1969).

Table 2. Effect of water on the reaction of CH_2Cl_2 and NaI[a]

Added water (ml)	Reaction temp. (°C)	Product yield[b] CH_2ClI (%)	Product yield[b] CH_2I_2 (%)
0	55—66	48.0	3.8
0.3	55—64	46.6	3.1
0.6	54—63	38.4	1.9
1.0	54—61	38.9	1.8

a) NaI 0.100 mol, CH_2Cl_2 0.47 mol, DMF 30 ml. Reactions were carried out under gentle reflux for 5 hr.
b) Based on NaI.

>K.[4] This seems to account for the fact that sodium iodide gives a better yield of chloroiodomethane than potassium iodide. On the other hand, the lower yield of chloroiodomethane in case of lithium iodide can be ascribed to an occurrence of the reverse reaction. This is supported by the fact that the reaction of chloroiodomethane with lithium chloride is so fast that only 27% of initial chloroiodomethane is detected after 5 hr.

Table 3. Effect of the cation on the reaction of CH_2Cl_2 and NaI[a]

Alkali Metal Halide	CH_2Cl_2 (mol)	Reaction temp. (°C)	Product yield[b] CH_2ClI (%)	Product yield[b] CH_2I_2 (%)
NaI	0.47	55—66	48.0	3.8
KI	0.47	60—65	32.4	1.5
LiI[c]	0.47	53—58	24.6	1.8
LiCl	0.37 CH_2ClI 0.100	62—59	27.0[d]	1.4[d]

a) Alkali metal halide, 0.100 mol, DMF 30 ml. Reactions were carried out under gentle reflux for 5 hr.
b) Based on alkali metal halide.
c) Contained 0.12 g of water.
d) Based on CH_2ClI initially used.

Experimental

Materials. All solvents were purified by the usual methods before use. Alkali metal halides except for lithium iodide were dried at 150°C for 10 hr under reduced pressure (2mm Hg). Commercial lithium iodide trihydrate was dehydrated at temperatures up to 150°C for 20 hr under reduced pressure. The Vorhard titration showed that the resulting cake contained 91.8% of lithium iodide, the rest appearing to be water. Commercial dihalomethanes were dried with calcium chloride and fractionated before use.

Typical Experimental Procedure. As a typical reaction procedure, the reaction of dichloromethane and sodium iodide in DMF is described. The reaction was carried out in a 100 ml round-bottomed flask equipped with a magnetic stirrer, reflux condenser topped with drying tube, thermometer and dropping funnel. Sodium iodide (15.0g, 0.100 mol) and dichloromethane (40g, 0.47 mol) were placed in the flask and stirred at room temperature. DMF (30ml) was added in about 3 min, whereupon the temperature of the reaction mixture rose from 20°C to 50°C. The reaction mixture became almost homogeneous, but precipitation of sodium chloride was soon observed. After the addition of DMF, the flask was heated to maintain gentle reflux for 5 hr under stirring. At the end of the reaction period, 30 ml of water was added to the chilled reaction mixture. The organic layer was separated, and the aqueous layer was extracted several times with portions of dichloromethane. The combined organic layer was analysed by glc for the determination of resulting chloroiodomethane and diiodomethane using bromobenzene as an internal standard.

Synthesis of Chloroiodomethane. The reaction was carried out according to the same procedure as avobe, except that the reaction scale was 8 times larger, and was continued for 10 hr, during which period, the reflux temperature rose from 51°C to 71°C. The reaction mixture was allowed to stand overnight at room temperature. The content was then steam distilled. The organic layer was separated from the distillate, and washed with several portions of water. The aqueous layer was extracted with CH_2Cl_2, and the extract was washed with water. The combined organic layer was dried with calcium chloride. Distillation through a 20 cm Vigreux column yielded 93.5 g (63% based on NaI) of pure chloroiodomethane boiling at 108—109°C (lit,[2] bp, 108°C). The residue contained chloroiodomethane, DMF, and diiodomethane.

Dibromomethane (82.0 g, 0.472 mol) and sodium iodide (15.0 g, 0.100 mol) was allowed to react in DMF (30 ml) for 5 hr.

A similar work up gave 7.5 g of bromoiodomethane boiling at 138—139°C (lit,[5] bp 137.8—141.2°C), which was contaminated with 3% of diiodomethane (34% yield based on NaI).

Identity of each product was confirmed by comparison of the chemical shift of NMR with that of authentic sample: CH_2ClI, τ, 5.00; CH_2BrI, τ, 5.41 (TMS, 5 mol% solution in CCl_4).

4) Y. Yamashita and K. Ito, *Yuki Gosei Kagaku Kyokai Shi*, **25**, 1098 (1967).

5) W. Bacherand and J. Wagner, *Z. Phys. Chem.* (Leipzig), **43**, 193 (1939).

BULLETIN OF THE CHEMICAL SOCIETY OF JAPAN, VOL. 44, 2866—2867 (1971)

Stereochemical Studies in Friedel-Crafts Reactions. IV. The Reactions of *cis*-1,2-Disubstituted 4-Cyclohexenes with Benzene

Kaichiro SUGITA and Shuzi TAMURA

Department of Chemistry, Ritsumeikan University, Kita-ku, Kyoto

(Received March 26, 1971)

In a previous paper,[1] we reported that the aluminum chloride-catalyzed reactions of benzene with *trans*-1,2-disubstituted 4-cyclohexenes, such as *trans*-2-benzoyl-4-cyclohexene-1-carboxylic acid and its methyl ester and methyl *trans*-2-chloroformyl-4-cyclohexene-1-carboxylate, give stereoselectively *r*-1, *c*-2, *t*-5-trisubstituted cyclohexane in all cases. The present paper will describe two reactions, those of benzene with methyl *cis*-2-chloroformyl-4-cyclohexene-1-carboxylate (**1**) and with *cis*-2-benzoyl-4-cyclohexene-1-carboxylic acid (**3**) in the presence of aluminum chloride.

The reaction of methyl *cis*-2-chloroformyl-4-cyclohexene-1-carboxylate (**1**) with benzene gave methyl *c*-2-benzoyl-*t*-5-phenylcyclohexane-*r*-1-carboxylate (**2**)[1,2] in a 54% yield. In the reaction of *cis*-2-benzoyl-4-cyclohexene-1-carboxylic acid (**3**) with benzene, a carboxylic acid (**4A**) was obtained in an 11% yield. The acid **4A** was converted to *c*-2-benzoyl-*t*-5-phenylcyclohexane-*r*-1-carboxylic acid (**4B**)[1,2] by treatment with sodium ethoxide in ethanol, followed by acidification. This epimerization indicates that the two acids, **4A** and **4B** are stereoisomeric with each other. When **4A** was treated with bromine in acetic acid, the bromine color disappeared, while in the case of **4B** the bromine color did not change under similar conditions.[2] Since the ease of bromination depends on the rates of enolization,[3] the difference in the behavior of **4A** and **4B** should be attributed to the presence of the axial benzoyl group in **4A**. These results support the **4A** structure.

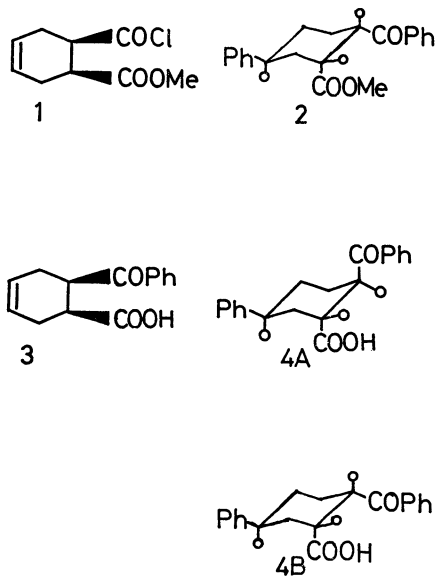

Fig. 1.

Experimental[4]

Material. The *cis*-methoxycarbonyl-4-cyclohexene-1-carboxylic acid was prepared by the procedure reported by Nazarov and Kucherov.[5] The *cis*-2-benzoyl-4-cyclohexene-1-carboxylic acid (**3**) was prepared by the procedure reported by Fieser and Nevello.[6]

Methyl cis-*Chloroformyl-4-cyclohexene-1-carboxylate (1).* A mixture of *cis*-2-methoxycarbonyl-4-cyclohexene-1-carboxylic acid (18 g) and thionyl chloride (18 g) was treated in a manner similar to that described previously. Methyl *cis*-2-chloroformyl-4-cyclohexene-1-carboxylate (**1**) was thus obtained quantitatively. The crude product was used without distillation. IR: (neat) 1795 (acid chloride), 1740 (ester), and 1655 cm^{-1} (olefin). NMR: δ ($CDCl_3$) 2.65—2.25 (m, 4H, $2CH_2$), 3.40—2.85 (m, 2H, 2CH), 3.72 (s, 3H, CH_3), and 5.70 ppm (m, 2H, CH=CH).

Reaction of Methyl cis-*2-Chloroformyl-4-cyclohexene-1-carboxylate (1) with Benzene.* Into a suspension of aluminum chloride (29 g) in dry benzene (90 m*l*) the ester chloride (**1**) (20 g) was vigorously stirred, drop by drop, below 10°C. The stirring was continued for one hour without further cooling and then for five additional hours reflux. Then the reaction mixture was poured onto ice-water. The resulting benzene solution was separated, washed with water, and dried over anhydrous magnesium sulfate. The benzene solution was finally evaporated to dryness. The distillation of the reaction residue gave **2** (17 g, 54%); bp 210—212°C/4 mmHg. The IR and NMR spectra of the ester **2** are identical with those of authentic methyl *c*-2-benzoyl-*t*-5-phenylcyclohexane-*r*-1-carboxylate. (Found: C, 78.59; H, 7.02%).

Reaction of cis-*2-Benzoyl-4-cyclohexene-1-carboxylic Acid (3) with Benzene.* Into a solution of the acid **3** (20 g) in dry benzene (90 m*l*) we stirred aluminum chloride (23 g) over a five-minute period below 10°C; the stirring was then continued for one hour without further cooling and for two hours under reflux. Then the reaction mixture was poured onto ice-water. The resulting benzene solution was separated, washed with water, and dried over anhydrous magnesium sulfate. The benzene solution was finally evaporated to dryness. A crystalline solid was thus obtained (25 g, 82%); mp 105—145°C. Recrystallization from 45% alcohol gave **4A** as colorless

1) K. Sugita and S. Tamura, This Bulletin, Submitted.
2) K. Sugita and S. Tamura, This Bulletin, in press.
3) H. E. Zimmerman, *J. Org. Chem.*, **20**, 549 (1955).

4) All the melting points and boiling points are uncorrected. The IR spectra were taken on a Hitachi EPI-S spectrometer. The NMR spectra were obtained on a Japan Electron Optics C-60-H spectrometer.

5) I. N. Nazarov and V. F. Kucherov, *Ordel. Khim. Nauk*, **1954**, 329; *cf. Chem. Abstr.*, **49**, 5328 (1955). It is reported that methyl *cis*-2-chloroformyl-4-cyclohexene-1-carboxylate (**1**) was isomerized to a mixture of **1** and methyl *trans*-2-chloroformyl-4-cyclohexene-1-carboxylate under the conditions used for distillation (118—119°C/7 mmHg).

6) L. F. Fieser and F. C. Nevello, *J. Amer. Chem. Soc.*, **64**, 802 (1942).

prisms (3.4 g, 11%); mp 156—157°C. The IR spectra of **4A** is different from that of *c*-2-benzoyl-*t*-5-phenyl-cyclohexane-*r*-1-carboxylic acid (**4B**).[1] The melting point of **4A** was depressed by mixing it with **4B**. IR: (KBr) 2800—2500 (-OH), 1700 (carboxyl), 1680 (ketone) and 1600 cm^{-1} (aromatic). Found: C, 77.83; H, 6.44%. Calcd for $C_{20}H_{20}O_3$: C, 77.90; H, 6.54%.

*Conversion of **4A** to **4B**.* To a sodium ethoxide solution prepared from absolute ethanol (50 m*l*) and sodium (100 mg), we added **4A** (500 mg). The solution was refluxed for five hours and then cooled. After the subsequent addition of water (100 m*l*) to the reaction mixture, the resulting mixture was acidified and filtered. The precipitates thus collected were washed with water and dried; 450 mg of a white product was thus yielded; 95%; mp 179—181°C. The IR spectrum of the product was identical with those of **4B**. The melting point of the product, without any purification, was not depressed by mixing it with **4B**.

BULLETIN OF THE CHEMICAL SOCIETY OF JAPAN, VOL. 44, 2867—2868 (1971)

A MO-theoretical Account for the Molecular Structure of the Grignard Reagent

Katsutoshi OHKUBO and Fumio WATANABE

Department of Synthetic Chemistry, Kumamoto University, Kurokami-machi, Kumamoto

(Received April 8, 1971)

Concerning the molecular structure of the Grignard reagent,[1] two representative chemical formulae (RMgX and $R_2Mg \cdot MgX_2$) have been proposed by Ashby[2] and Dessy.[3] However, the structure has not yet been strictly established. In view of the association of the reagent in such a solvent as ether, the structure of the reagent can also be characterized by the following equilibrium:

$$\underset{\text{I}}{(RMgX)_2} \rightleftarrows \underset{\text{II}}{2RMgX} \rightleftarrows$$

$$\underset{\text{III}}{R_2Mg + MgX_2} \rightleftarrows \underset{\text{IV}}{R_2Mg \cdot MgX_2}$$

We intend to clarify which is the most plausible structure among the reagents expressed by the above chemical formulae. The extended Hückel method[4] was applied to the discussion of this feature. For the discussion from the energetic point of view, R and X were taken to be C_2H_5 and Cl respectively.

First, let us discuss the change in the total energy (E_{EH}) of the symmetrical dimer, $(RMgCl)_2$, with the variation in the angle of Cl–Mg–Cl (named by θ) at the fixed distance of Mg–Cl (2.39 Å), together with the variation in the distance of Mg–Cl at the fixed angle ($\theta=90°$). As Fig. 1 indicates, the most energetically stable structure of the symmetrical dimer can be found in the configuration of $\theta=130°$ (Mg–Cl=2.39 Å).

Second, it is of interest to discuss this problem with respect to the structure of the anti-symmetrical dimer, $R_2Mg \cdot MgX_2$. The Mg–Cl distance of 1.80 Å gives the most stable structure of the anti-symmetrical dimer, as may be seen from Fig. 2.

Third, the extended Hückel-MO calculations were also performed on RMgX ($R=C_2H_5$ and X=Br),

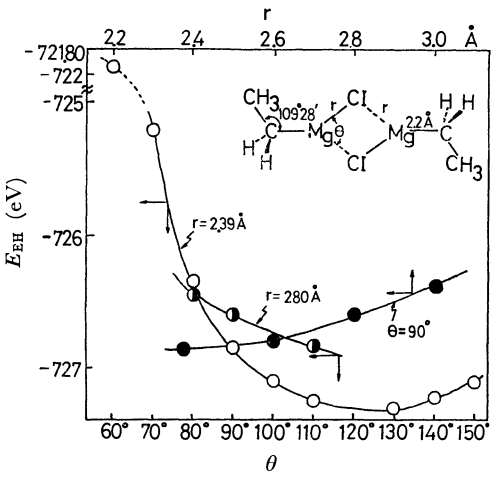

Fig. 1. Changes in the total energy (E_{EH}) of the symmetrical dimer, $(C_2H_5MgCl)_2$. (The bond length of Mg-C was cited from Ref. 8).

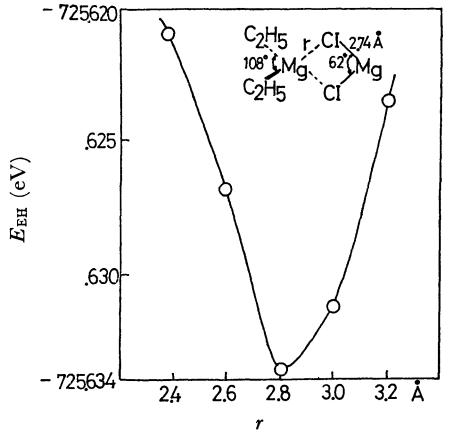

Fig. 2. Change in the total energy (E_{EH}) of the anti-symmetrical dimer, $(C_2H_5)_2Mg \cdot MgCl_2$. (The bond lengths and angles were cited from Ref. 9).

which is considered to take two distinct configurations, *i.e.*, an angular-type RMgX[5] and a linear-type RMgX. These configurations are presented below, together with

1) V. Grignard, *Ann. Chim. Phys.*, **24**, 433 (1901); Grignard has suggested the structure of the reagent by the chemical formula of RMgX.

2) E. C. Ashby, *Quart. Rev.* (London), **21**, 259 (1967), and the references cited therein.

3) R. E. Dessy, *J. Org. Chem.*, **25**, 2260 (1960).

4) R. Hoffmann, *J. Chem. Phys.*, **39**, 1397 (1963); *ibid.*, **40**, 2474 (1964). The Coulomb intergrals of Mg are −8.95 eV (for 3*s*) and −4.52 eV (for 3*p*).

their atomic charges and total energies (E_{EH}).

Angular-type RMgX

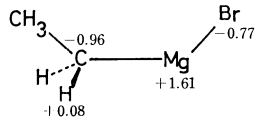

$E_{EH}=-359.55$ eV

Linear-type RMgX

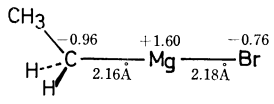

$E_{EH}=-359.67$ eV

In view of the orientation effect of the solvent surrounding RMgX, the former structure of RMgX seems more possible than the latter one, although the value of E_{EH} in the latter structure is lower than that in the former. Accordingly, the angular-type RMgX ($R=C_2H_5$, X=Cl, and $E_{EH}=-365.11$eV) was adopted for the structure of II.

Finally, we studied the system involving R_2Mg and MgX_2. Their atomic charges and total energies are shown below:

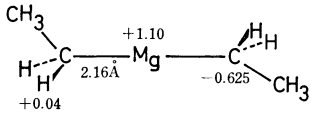

$E_{EH}=-470.05$ eV

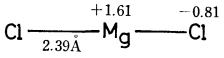

$E_{EH}=-258.04$ eV

On the basis of the above discussions, the order of the energetic stability of the Grignard reagents expressed by I, II, III, and IV is as follows: II(−730.22eV)> III(−728.09eV)>I(−727.09eV)>IV(−725.63eV). In other words, the monomer-type structure of II is the most stable and the Schlenk's equilibrium reaction[6] between II and III can be accepted on the basis of some evidence.[7] However, the equilibrium mentioned before can be expected at a low concentration of the Grignard reagent (at least, below 0.3 mol/l). In the case of a high concentration, the reagent is apt to take a dimeric structure in a solvent, in particular in ether. Table 1 indicates the stabilization energy of RMgX as solvated by several solvents. Considering that RMgX exists as a monomer in tetrahydrofuran or triethylamine while, in ether, RMgX is present as a dimer at a high concentration, the number of the molecules interacting with the reagent may be different between the solvents according to the values of E_{EH} listed in Table 1.

Table 1. The stabilization energy (ΔE_{EH}) in the system of RMgX and solvents

RMgX[a] solvated	Mg–O or Mg–N (Å)	∠CMgO or ∠CMgN	ΔE_{EH} (eV)	ΔE_{calcd}[c] (eV)
RMgX monoetherate[b]	2.04	110°	1.13	1.19
RMgX monotetrahydrofuranate	2.04	110°	1.06	—
RMgX monotrimethylaminate	2.1	110°	1.18	0.87

a) R=C_2H_5 and X=Br.
b) Methyl derivative was used for the simplicity of computations.
c) This stands for the stabilization energy estimated from a rough approximation: $\Delta E_{calcd}=e^2(1-1/\varepsilon)/2a$, where a is taken to be 5.0 Å and ε is the dielectric constant of the solvent. The assumed value of 5 Å was estimated from the ionic radii of Mg and Br and van der Waals radius of CH_3CH_2 group.

5) R. E. Rundle and L. J. Guggenberger, *J. Amer. Chem. Soc.*, **86**, 5344 (1964).
6) W. Schlenk and W. Schlenk, Jr., *Ber.*, **62**, 920 (1929).
7) E. C. Ashby and W. E. Berker, *J. Amer. Chem. Soc.*, **85**, 118 (1963).
8) E. Weiss, *J. Organometal. Chem.*, **4**, 101 (1965).
9) H. Schibilla and G. T. Le Bihan, *Acta Cryst.*, **23**, 332 (1967).

BULLETIN OF THE CHEMICAL SOCIETY OF JAPAN, VOL. 44, 2868—2869 (1971)

On the Enantiotropic Transitions in the Phenanthrene Picrate

Yoshio MATSUNAGA

Department of Chemistry, Faculty of Science, Hokkaido University, Sapporo

(Received April 12, 1971)

Phenanthrene has long been known to form an equimolecular addition compound with picric acid.[1] The presence of an enantiotropic transition at 106°C in this compound was noted by Kofler in 1944.[2] We newly observed the presence of another transition in the phenanthrene picrate. Contrary to the one reported by Kofler, the change from the high-temperature form to the low-temperature one is very slow in the new transition located at 77°C. As ordinary phenanthrene is often contaminated with an appreciable amount of anthracene, the effect of the impurity on the transitions was also examined. As will be described later, a reason why Kofler missed one of the transitions can be proposed on the basis of this examination.

Phenanthrene, Eastman white label, was boiled with maleic anhydride in xylene to remove any anthracene.[3] The picrate crystallized from benzene was mixed with anthracene picrate separately prepared, in various ratios (0.97—10.0 mol%) and then fused together. After annealing at room temperature for three days or longer, the specimens were examined by means of a Rigaku Denki differential scanning calorimeter, Model 8001 SL/C, at a heating rate of 3°C/min. The heats of transition were estimated by comparing the peak areas with that for the transition in hexamethyl-

1) C. Graebe, *Ann. Chem.*, **167**, 137 (1873).
2) A. Kofler, *Z. Elektrochem.*, **50**, 200 (1944).
3) J. Feldman, P. Pantages, and M. Orchin, *J. Amer. Chem. Soc.*, **73**, 4341 (1951).

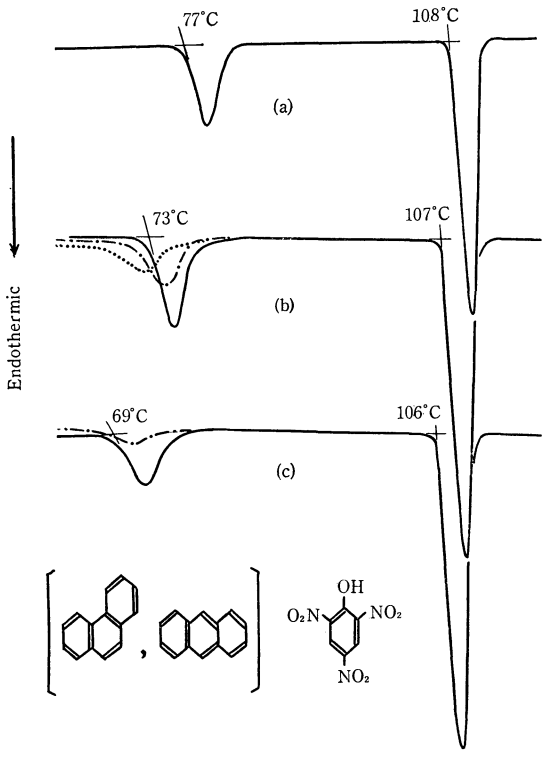

Fig. 1. The DSC thermograms of phenanthrene picrate annealed over one month (—), for one day (····), and for three days (-·-·-): (a) 18.8 mg of the pure specimen, (b) 22.3 mg of the specimen containing 0.97 mol% of anthracene picrate and (c) 22.8 mg of the specimen containing 3.12 mol% of anthracene picrate.

benzene, which is known to take place at 110.6°C with ΔH=0.422 kcal/mol.[4]

The transitions in pure phenanthrene picrate are located at 77°C with ΔH=1.1 kcal/mol and at 108°C with ΔH=3.1 kcal/mol. The first transition cannot be observed in the second run if it is recorded immediately after the first heating. A similarly slow transition has been known to occur in anthracene picrate at about 85°C.[2] As is shown in Fig. 1, both the first and second transition points move to lower temperature upon the addition of anthracene picrate. Although the heat of transition due to the second phase-change stays almost constant up to a 5 mol% addition of anthracene picrate, that due to the first phase-change decreases slightly to 0.8—0.9 kcal/mol in the range of 2—3 mol%. Furthermore, the higher the contamination with anthracene, the slower the rate of the recovery of the low-temperature form. After annealing for three days, which is long enough for pure phenanthrene picrate, the specimens containing 0.97—3.12 mol% anthracene picrate produce a peak area due to the first phase-change much smaller than that obtained after a prolonged annealing. In addition, it must be noted that the peak observed after a partial recovery appears at temperatures lower than that observed after the complete recovery. Above a 5 mol% addition of anthracene picrate, the first phase-change is no longer detectable even after over-one-month storage at room temperature. Thus, not only the magnitude of the heat of the newly-found transition, but also the rate of the recovery of the low-temperature form are very sensitive to contamination with anthracene. From these observations it would appear that the visual examination of this transition employed by Kofler is difficult if the phenanthrene contains anthracene in the order of one mol percent. On the other hand, the second phase-change in phenanthrene picrate remains even in the presence of 10 mol% anthracene picrate. Therefore, it seems likely that the discrepancy between the present observation and Kofler's can be ascribed to the difference in purity of the phenanthrene used.

4) M. E. Spaght, S. B. Thomas, and G. S. Parks, *J. Phys. Chem.*, **36**, 882 (1932).

BULLETIN OF THE CHEMICAL SOCIETY OF JAPAN, VOL. 44, 2869—2871 (1971)

Electronic Structures of Dialkyl Peroxides

Katsutoshi OHKUBO and Masahide OKADA

Department of Synthetic Chemistry, Kumamoto University, Kurokami-machi, Kumamoto

(Received April 12, 1971)

Dialkyl peroxides (ROOR) have often been postulated as intermediates in hydrocarbon oxidations. The chemical properties of the said peroxides are closely akin to those of alkyl hydroperoxides (ROOH) in terms of the bond-dissociation energies[1] of their O–O linkages and their reactivities to nucleophiles[2] or electrophiles.[3] The bond character of the O–O linkage in ROOR, however, has not yet been established strictly. The present study intends to illuminate the electronic structures of ROOR in connection with those of ROOH by the use of the extended Hückel method.[4]

Calculation Method

The geometries of ROOR used for the calculations were set up similarly to those of ROOH,[5] as is indicated below:

1) A. D. Kirk and J. H. Knox, *Trans. Faraday Soc.*, **56**, 1296 (1960).

2) For instance, L. S. Silbert, and D. Swern, *J. Amer. Chem. Soc.*, **81**, 2365 (1959); J. K. Kochi, *ibid.*, **85**, 1958 (1963).

3) F. Haber and P. Weiss, *Proc. Roy. Soc.*, London, **A147**, 233 (1939); N. Uri, *Chem. Rev.*, **50**, 375 (1952).

4) R. Hoffmann, *J. Chem. Phys.*, **39**, 1397 (1963); **40**, 2474, 2480, 2745 (1964).

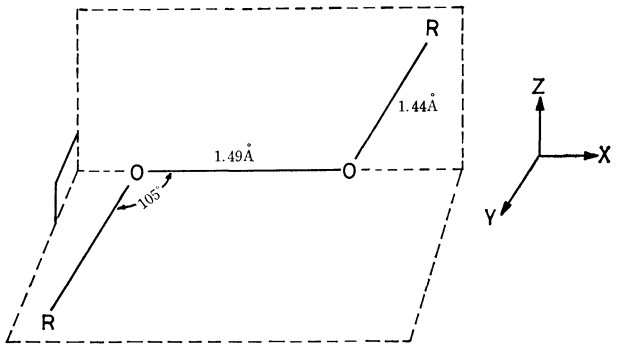

R=H, CH_3, C_2H_5, n-C_3H_7, n-C_4H_9, and t-C_4H_9

The orbital exponents and Coulomb intergrals ($H_{\mu\mu}$) were supplied by Clementi[6] and Jaffé[7] respectively. Especially, as the $H_{\mu\mu}$ values of the oxygen atom, the following values were taken:
$H_{\mu\mu}$(eV)=−36.07 (O 2s) and −15.85(O 2p).
The resonance integrals ($H_{\mu\nu}$) were evaluated by the Wolfsberg-Helmholtz approximation[8]: $H_{\mu\nu}=0.875(H_{\mu\mu}+H_{\nu\nu})S_{\mu\nu}$, where $S_{\mu\nu}$ is the overlap intergral between AO's.

Results and Discussion

First, let us discuss the bond character of the O–O linkage in ROOR. As Table 1 indicates, the bond population of the O–O (M_{oo}) is relatively small, falling in the range, 0.353—0.369. This range of M_{oo} is the same as or slightly smaller than that of ROOH.[5] From this result, it can be deduced that the energy required for the homolytic scission of the O–O linkage (E_{dec}) in ROOR is much the same as that in ROOH; In fact, the observed values are 37.9± 0.4 kcal/mol for the former and 41.1 kcal/mol for the latter, on the average. A parallelism between M_{oo} and E_{dec} could be observed with some exceptions. This close resemblance in the bond character of the O–O linkage between ROOR and ROOH can also be observed in the orbital energy (see Table 1). The lowest unoccupied molecular orbitals (LU MO) of both peroxides are localized in O–O, as is illustrated by the following examples:[9]

$$\varphi^{LU}(RO_\alpha O_\beta R) = 0.823X_\alpha + 0.823X_\beta + 0.207S_\alpha - 0.207S_\beta - 0.132Y_\alpha + 0.016Y_\beta - 0.016Z_\alpha + 0.132Z_\beta + \cdots$$

and

$$\varphi^{LU}(RO_\alpha O_\beta H) = 0.833X_\alpha + 0.813X_\beta + 0.217S_\alpha - 0.201S_\beta - 0.139Y_\alpha + 0.017Y_\beta - 0.009Z_\alpha + 0.145Z_\beta + \cdots$$

where R denotes CH_3. These wave functions show that the LU MO's are mainly the 2p AO's of oxygen atoms.

Table 1. Bond character of the O–O linkage and orbital energies in dialkyl peroxides (ROOR)

ROOR (R)	M_{oo}	N_{oo} ($p\sigma$)	Orbital energy (eV) HO	Orbital energy (eV) LU	E_{dec}[a] (kcal/mol)
H	0.369	0.359	−15.12	−9.19	48.0[b]
CH_3	0.360 (0.361)	0.344 (0.346)	−13.58 (−14.03)	−9.00 (−9.10)	36.9[c] (——)
C_2H_5	0.355 (0.358)	0.342 (0.345)	−12.89 (−13.60)	−8.99 (−9.10)	34.1[b] (37.7[b])
n-C_3H_7	0.353 (0.357)	0.341 (0.345)	−12.82 (−13.18)	−8.99 (−9.10)	36.5[d] (——)
n-C_4H_9	0.353 (0.357)	0.341 (0.345)	−12.82 (−12.97)	−8.99 (−10.85)	—— (——)
t-C_4H_9	0.354 (0.354)	0.329 (0.343)	−11.78 (−12.72)	−9.05 (−9.09)	34±2[e] (37.8[b])

a) Activation energies of decomposition.
b) Cited from Ref. 1.
c) Cited from Y. Takezaki and C. Takeuchi, *J. Chem. Phys.*, **9**, 1527 (1954).
d) Cited from E. J. Harris, *Proc. Roy. Soc.* (London), **A173**, 126 (1939).
e) Cited from J. Murawski, J. S. Roberts, and M. Szwarc, *J. Chem. Phys.*, **19**, 698 (1951).
Values in parentheses stand for those in ROOH.

Next, let us examine the reactivity of ROOR to nucleophiles or electrophiles. The LU MO and the HO MO play an important role in weakening the O–O linkage by means of interaction with nucleophiles and electrophiles respectively. The LU MO is strongly localized in the O–O linkage, as has been mentioned before, and has an antibonding character with respect to the O–O bond, whereas the HO MO is occupied predominantly by the nonbonding oxygen orbitals. Consequently, nucleophiles attack ROOR in the direction of the O–O axis, while electrophiles approach the nonbonding oxygen orbital expansion from the opposite side of R.

As the reactivity indices we employed the value of

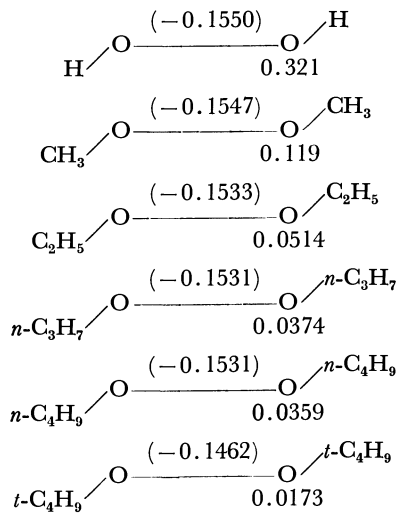

Fig. 1. Reactivity indices in ROOR.
(The figures without parentheses stand for $1/2N_{nbo}^{HO}$; th figures with parentheses indicate $1/4N_{p\sigma}^{LU}$.)

5) T. Yonezawa, O. Yamamoto, H. Kato, and K. Fukui, *Nippon Kagaku Zasshi*, **87**, 26 (1966).
6) E. Clementi and D. L. Raimondi, *J. Chem. Phys.*, **38**, 2686 (1963).
7) J. Hinze and H. H. Jaffè, *J. Amer. Chem. Soc.*, **84**, 540 (1962).
8) M. Wolfsberg and L. Helmholtz, *J. Chem. Phys.*, **20**, 837 (1952).
9) The notations of X_α, X_β, S_α, *etc.* denote $O_\alpha p_x$, $O_\beta p_x$, $O_\alpha s$ orbitals *etc.* respectively.

the partial AO bond population of the antibonding $p\sigma$-orbital of the O–O in the LU MO, $\frac{1}{4}N_{P\sigma}^{LU}$, and that of the partial AO population of the nonbonding oxygen orbital in the HO MO, $\frac{1}{2}N_{nbo}^{HO}$, both of which are given in Fig. 1. A presumption can be made that the reactivity of ROOR to nucleophiles or electrophiles lessens with the bonding of the larger alkyl groups to the O–O.

Finally, it is of interest to compare the reactivity indices to nucleophiles in ROOR with those in ROOH. Three alkyl hydroperoxides selected for the sake of comparison, CH_3OOH, n-C_3H_7OOH, and t-C_4H_9OOH, have the following values of $-N_{P\sigma}^{LU}$: -0.1547, -0.1539, and -0.1528 respectively. On the basis of the facts derived above, we may conclude that ROOH is more reactive than ROOR to the nucleophilic attack.

BULLETIN OF THE CHEMICAL SOCIETY OF JAPAN, VOL. 44, 2871—2873 (1971)

Direct Iodination of Trimethylbenzoic Acids and Tetramethylbenzoic Acids with Iodine-Periodic Acid[1]

Hitomi SUZUKI

Department of Chemistry, Faculty of Science, Kyoto University, Sakyo-ku, Kyoto

No report seems to be found in literature on the preparation and properties of iodotrimethyl- and iodotetramethylbenzoic acids. In view of the high propensity for iodine atom to undergo displacement, an attempt to introduce carboxylic group into the nucleus of reactive iodopolymethylbenzenes seems to be practically meaningless. The commonly used indirect method wihch involves the replacement of amino group by iodine atom is unsuitable in the present case, since most of the required polymethylaminobenzoic acids are unknown and not readily available. In previous papers,[2,3] *iodine used with periodic acid* has been proposed as a convenient iodinating agent for polyalkylbenzenes because of the simple procedure, excellent yield, and high purity of products. Although the reagent has not been used extensively for the iodination of polyalkyl compounds other than hydrocarbons, satisfactory results recently obtained with less activated compounds, such as halopolyalkylbenzenes and halobiphenyls,[4] seem to promise a successful use of this reagent for one-step synthesis of iodopolymethylbenzoic acids from the corresponding polymethylbenzoic acids. Thus, some trimethylbenzoic acids and tetramethylbenzoic acids were treated with the above reagent in aqueous acetic acid containing a small amount of sulfuric acid as catalyst.

Trimethylbenzoic acids were readily iodinated with iodine-periodic acid to give the monoiodo derivatives in a high yield of 85% or higher. General character of the reaction suggests an ionic scheme, with the ease of iodination in the decreasing order 2,4,6>2,4,5> 2,3,4~2,3,6> 3,4,5-trimethylbenzoic acid. 2,4,5-Trimethylbenzoic acid gave almost exclusively 3-iodo-2,4,5-trimethylbenzoic acid. 5-Iodo-2,3,4-trimethylbenzoic acid was obtained from 2,3,4-trimethylbenzoic acid. The meta position to the carboxylic group was in every case preferred to ortho position. The position occupied by iodine atom in these systems was established by spectral comparison with the chloro or bromo analogs. Replacement of chlorine or bromine atom by iodine atom led to only a slight change in the general patterns of infrared and PMR spectra of these compounds.

With the use of excess reagent, 2,4,6-trimethylbenzoic acid (mesitoic acid) was readily converted into 3,5-diiodo-2,4,6-trimethylbenzoic acid, but diiodination of other isomeric acids was quite slow and usually accompanied by an appreciable extent of iododecarboxylation, giving diiodotrimethylbenzenes as an alkaline-insoluble part. 2,4,5-Trimethylbenzoic acid was especially hard to be diiodinated.

Iodination of tetramethylbenzoic acids proceeded with much ease. Of three isomeric acids, 2,3,4,6-tetramethylbenzoic acid was the most reactive, followed by 2,3,5,6-tetramethylbenzoic acid and 2,3,4,5-tetramethylbenzoic acid. The reaction was also subjected to iododecarboxylation to some extent, although iodotetramethylbenzoic acid was stable towards further action of the reagent (Fig. 1).

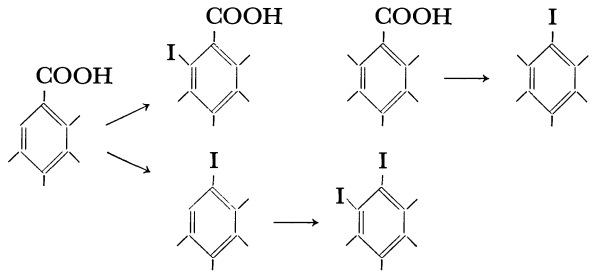

Fig. 1

In order to find a substitutional process on the alkyl side-chain, pentamethylbenzoic acid was treated with the above iodinating agent. The fully methylated benzoic acid readily underwent iodination to give a white crystalline solid, which, however, contained no acidic function and proved to be identical with iodopentamethylbenzene by direct comparison with the authentic specimen (Fig. 1). Spectral inspection of

1) The Reaction of Polysubstituted Aromatics. XXIII. Part XXII: This Bulletin, **44**, 2248 (1971).

2) H. Suzuki, K. Nakamura, and R. Goto, This Bulletin, **39**, 128 (1966).

3) H. Suzuki, "Organic Syntheses," Vol. 51, in press (1971).

4) H. Suzuki and N. Yamamoto, This Bulletin, in press (1971).

Table 1. Physical properties of some monoiodo and diiodopolymethylbenzoic acids

Compound	Mp (°C)	PMR spectra ArH	PMR spectra CH_3 (τ)	IR spectra[a] (cm^{-1})	Elementary analysis, % Found	Elementary analysis, % Calcd
5-Iodo-2,3,4-trimethylbenzoic acid	252—253	1.82	7.68 (1)[b] 7.56 (1) 7.51 (1)	769 860 893 910 1031 1073 1246 1281 1704	C: 41.40 H: 3.89	41.41 3.82
3-Iodo-2,4,5-trimethylbenzoic acid	182—183	2.39	7.64 (1) 7.50 (1) 7.30 (1)	732 775 821 895 910 989 1252 1286 1696	C: 41.75 H: 4.02	41.41 3.82
3-Iodo-2,4,6-trimethylbenzoic acid	196—197	3.00	7.75 (1) 7.55 (1) 7.52 (1)	725 790 862 922 966 1026 1099 1211 1287 1690	C: 41.31 H: 4.11	41.41 3.82
2-Iodo-3,4,5-trimethylbenzoic acid	186—189	2.72	7.75 (1) 7.70 (1) 7.47 (1)	701 766 890 941 1198 1248 1292 1694	C: 42.25 H: 3.99	41.41 3.82
4,5-Diiodo-2,3,6-trimethylbenzoic acid	266—268		7.72 (1) 7.41 (1) 7.33 (1)	889 937 1034 1062 1164 1270 1284 1691 1712	C: 29.01 H: 2.66	28.87 2.42
3,5-Diiodo-2,4,6-trimethylbenzoic acid	242—243		7.56 (3)	784 869 954 1102 1248 1695	C: 28.78 H: 2.61	28.87 2.42
2,6-Diiodo-3,4,5-trimethylbenzoic acid	266—268		7.62 (1) 7.52 (2)	695 737 773 931 942 1003 1226 1316 1697	C: 28.95 H: 2.53	28.87 2.42
6-Iodo-2,3,4,5-tetramethylbenzoic acid	232—233		7.83 (1) 7.76 (1) 7.71 (1) 7.53 (1)	677 717 769 833 913 970 1197 1233 1300 1667	C: 43.26 H: 4.38	43.45 4.31
5-Iodo-2,3,4,6-tetramethylbenzoic acid	232—235		7.81 (1) 7.73 (1) 7.57 (1) 7.47 (1)	729 779 827 933 1043 1176 1269 1693 1712	C: 43.37 H: 4.39	43.45 4.31
4-Iodo-2,3,5,6-tetramethylbenzoic acid	274—276		7.70 (2) 7.50 (2)	682 742 899 937 994 1038 1084 1247 1298 1692 1712	C: 43.73 H: 4.18	43.45 4.31

a) Principal peaks in the regions, 650—1350 and 1500—2000 cm^{-1}.
b) Numerals in parentheses refer to the number of methyl groups. PMR spectra were determined in dioxane solutions.

the crude reaction product had no indication of the side-chain substitution.

All the iodotrimethylbenzoic acids, diiodotrimethylbenzoic acids and iodotetramethylbenzoic acids are well crystallized solids with high melting points. They dissolve very slightly in light petroleum, benzene, carbon tetrachloride, and cold aqueous ethanol, and are moderately or readily soluble in hot ethanol, dioxane and tetrahydrofuran. Some physical properties of these iodopolymethylbenzoic acids are summarized in Table 1.

Experimental

2,4,6-Trimethylbenzoic acid (mesitoic acid), 2,4,5-trimethylbenzoic acid, and three isomeric tetramethylbenzoic acids were prepared by the Friedel-Crafts carboxylation of the corresponding hydrocarbons with oxalyl chloride.[5,6] A similar treatment of 1,2,3-trimethylbenzene gave a mixture of 2,3,4-trimethylbenzoic acid and 3,4,5-trimethylbenzoic acid. Fractional crystallization of the product mixture from aqueous ethanol gave the former acid as a more soluble and the latter acid as a less soluble part. 3,4,5-Trimethylbenzoic acid was also prepared by the oxidation of 3,4,5-trimethylacetophenone with sodium hypochlorite.[7] 2,3,6-Trimethylbenzoic acid was obtained by carbonation of the Grignard reagent from 3-bromo-1,2,4-trimethylbenzene.[8] Pentamethylbenzoic acid was prepared from hexamethylbenzene through side-chain nitrooxylation followed by potassium permanganate-pyridine oxidation.[9]

Infrared spectra were measured on Nujol mulls with a Jasco 402G spectrophotometer and only prominent peaks are recorded. PMR spectra were determined in dioxane solutions with a JEOLCO 3H-60 spectrometer against internal TMS.

Procedure for the Iodination of Polymethylbenzoic Acids. The general procedure is illustrated below by the reaction of mesitoic acid.

3-Iodo-2,4,6-trimethylbenzoic Acid (Iodomesitoic Acid). A mixture of mesitoic acid (4.1 g), iodine (2.55 g), periodic acid dihydrate (1.14 g), and 80% acetic acid (40 ml) containing catalytic amounts of sulfuric acid was heated with stirring at 70—75°C for about 15—20 min until the color of iodine disappeared. After cooling, water was added and the crystalline deposit was collected. The crude product was dissolved into aqueous sodium hydroxide and any trace of

5) G. A. Varvoglis and N. E. Alexandrou, *Chimika Chronika*, **26A**, 137 (1961).
6) H. Suzuki, *Nippon Kagaku Zasshi*, **91**, 484 (1970).
7) H. Suzuki, This Bulletin, **42**, 2618 (1969).
8) H. A. Smith and J. A. Starfield, *J. Amer. Chem. Soc.*, **71**, 81 (1949).
9) H. Suzuki, *Nippon Kagaku Zasshi*, **91**, 179 (1970).

insoluble by-product was removed over decolorizing charcoal. The clear filtrate was made acidic with concentrated hydrochloric acid and the precipitate was collected, thoroughly washed with water, and crystallized from aqueous ethanol to give *iodomesitoic acid* as colorless fine needles, mp 196—197°C. Yield, 6.2 g (86%).

When mesitoic acid was treated with twice the amount of the reagent under the same conditions, white crystals soon deposited from the mixture. They were collected and crystallized from aqueous ethanol to yield *diiodomesitoic acid* in 78% yield. Colorless large leaflets, mp 242—243°C.

Iododecarboxylation of Pentamethylbenzoic Acid. Pentamethylbenzoic acid (3.2 g) was suspended in 80% aqueous acetic acid (40 m*l*) containing a small amount of sulfuric acid as catalyst, and treated with iodine (1.7 g) and periodic acid dihydrate (0.75 g) in a similar manner as above. After several hours, iodine was mostly consumed and white crystalline powder deposited from the solution. It was filtered and crystallized from dilute ethanol to give colorless prisms (3.8 g), mp 139—141°C. It was identified as iodopentamethylbenzene (mp 141—142°C)[10] by direct comparison with the authentic specimen. IR: 901, 996, 1010, 1060, and 1197 cm^{-1}. PMR (CCl_4): 7.95 (Me), 7.86 (2 Me), and 7.63τ (2 Me).

10) H. Suzuki, T. Sugiyama, and R. Goto, This Bulletin, **37**, 1858 (1964).

BULLETIN OF THE CHEMICAL SOCIETY OF JAPAN, VOL. 44, 2873—2875 (1971)

The Oxidation of Phenols by Potassium Disulfonate Nitroxyl

Kazuhiro MARUYAMA and Tetsuo OTSUKI

Department of Chemistry, College of Liberal Arts and Science, Kyoto University, Sakyo-ku, Kyoto

(Received April 30, 1971)

The oxidation of phenols is one of the most stimulating subjects in the chemical and biochemical fields. When potassium disulfonate nitroxyl (Fremy's salt; $\cdot ON(SO_3K)_2$)[1] is used as an oxidizing agent, phenols are oxidized to produce benzoquinones in high yields. Teuber and his co-workers[2] have investigated the reaction through product analysis, but no details on the reaction mechanism have been published. The reaction is characteristic in that benzoquinones (*i.e.*, *o*-benzoquinones and *p*-benzoquinones) are produced exclusively, accompanied by no coupling products, and the yields are relatively high. Moreover, whereas *p*-benzoquinones are selectively produced when the para position of phenols is not occupied by any substituents, *o*-benzoquinones are the sole products in high yields when the para position is substituted.

Because of our interest in this high selective oxidation of phenols by Fremy's salt, we attempted to elucidate the reaction mechanism.

Results and Discussion

We will now investigate the relative reactivity of phenols to Fremy's salt. The substrates examined here are phenols with no substituents at the position para to their hydroxyl group, such as phenol, 2-methylphenol, 3-methylphenol, 2,5-dimethylphenol, 2,6-dimethylphenol, 2-*t*-butylphenol, 2,6-di-*t*-butylphenol, 2-chlorophenol, and 2-nitrophenol.

The course of the reaction and the subsequent spectrophotometric determination of *p*-benzoquinones produced are depicted in Fig. 1. The amount of *p*-benzoquinones produced 10 min after the beginning of the reaction is determined as a measure of the relative rates of the oxidation of phenols (Table 1).

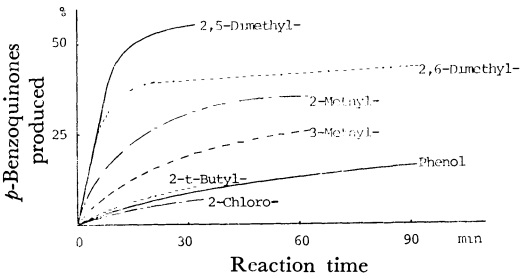

Fig. 1. Relative oxidation rates of phenols.

TABLE 1. RELATIVE REACTIVITIES OF PHENOLS AND THEIR NMR CHEMICAL SHIFT OF HYDROXYL PROTONS

Phenols	*p*-Benzoquinones	Yields after 10 min (%)	Chemical shift of OH[a] (ppm)
Phenol	*p*-Benzoquinone	4	4.31
2-Methyl-	2-Methyl-	19	4.33
3-Methyl-	2-Methyl-	9	4.21
2,5-Dimethyl-	2,5-Dimethyl-	44	4.22
2,6-Dimethyl-	2,6-Dimethyl-	35	4.30
2-*t*-Butyl-	2-*t*-Butyl-	5	4.47
2,6-Di-*t*-butyl-	no reaction		4.96
2-Chloro-	2-Chloro-	3	5.38
2-Nitro-	no reaction		10.57

a) The values are measured in infinite dilution with CCl_4.

From these results, it can be deduced that the rate of this reaction is enhanced by electron-donating substituents and that it is depressed with strong electron-withdrawing substituents, such as the nitro group. 2-Nitrophenol, for instance, is not oxidized and is recovered quantitatively after being treated with Fremy's salt for 30 min. When the reaction rates of monomethylphenols are compared with those of di-

1) D. J. Cram and R. A. Reeves, *J. Amer. Chem. Soc.*, **80**, 3099 (1958).

2) a) H. J. Teuber and G. A. Jellinek, *Chem. Ber.*, **85**, 95 (1952). b) H. J. Teuber and W. Rau, *ibid.*, **86**, 1036 (1953).

methylphenols, dimethylphenols such as 2,5-dimethylphenol and 2,6-dimethylphenol are found to be more reactive than monomethylphenols. According to Teuber and Rau,[2b] 2-chlorophenol could not be oxidized to 2-chloro-*p*-benzoquinone by Fremy's salt. However, in this work, 2-chlorophenol is found to be oxidized to the corresponding *p*-benzoquinone, although the reaction rate is considerably slow, because of the electron-withdrawing nature of the chlorine atom.

Although the reaction rate of 2-*t*-butylphenol is nearly the same as that of non-substituted phenol, 2,6-di-*t*-butylphenol is not oxidized under the same conditions. That is; the reaction rate of phenols with the *t*-butyl group at the *o*-position is rather slower than would be expected only from the above-mentioned electronic effects. The observed effect of the *t*-butyl group may be explained as the steric hindrance to the attack of the reagent on the hydroxyl group in phenols.

The molar ratio of phenols to Fremy's salt varies from 0.4 to 4.0. Within this range, the reaction rate is changed linearly with the molar ratio. The reaction between phenols and Fremy's salt can thus be described as follows:

$$\text{Rate} = k[\text{Phenols}][\text{Fremy's salt}]$$

$k = 2.01 \times 10^{-2}$ *l*/mol·sec for 2,6-dimethylphenol at 0°C

On the other hand, the decay of Fremy's salt in the reaction system was followed by using ESR spectroscopy, as is shown in Fig. 2. The peak height of the ESR absorption signal is proportional to the concentration of Fremy's salt, because the ESR absorption signal of Fremy's salt has the same half-height width at every stage of the reaction. Thus, in view of the decay rate of the peak height of the ESR absorption signal, Fremy's salt in the reaction system decreases in first order to time. This result is also in good agreement with the rate equation presented above.

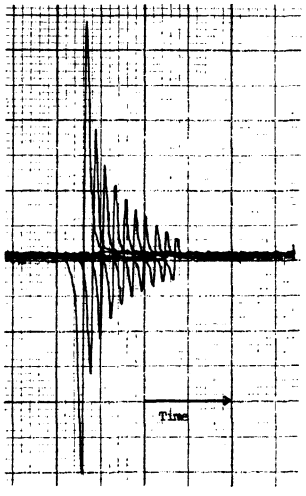

Fig. 2. Decay of Fremy's salt in its reaction with 2,6-dimethylphenol. Time interval; 170 sec

These results indicate that the electrophilic attack of Fremy's salt on phenols is the rate-determining process in this reaction. As a matter of fact, the steric factor of the substituents to the hydroxyl group of phenols should be considered at the same time. Moreover, whether or not the reaction proceeds is well correlated with the NMR chemical shift of the hydroxyl proton and, consequently, with the acidity of phenols. The NMR chemical shifts of the hydroxyl protons are shown in Table 1. Considering from the NMR data, the fact that 2-nitrophenol is not oxidized may be explained by its high acidity.

In the reaction described above, no coupling products were isolated, and the ESR spectra of free phenoxy radicals could not be observed. Thus, no free phenoxy radicals with a fairly long lifetime may exist under those reaction conditions; that is, the phenoxy radicals produced decay too rapidly to establish their existence by ESR spectroscopy. These results also indicate that the rate-determining process may be the stage of the first attack of Fremy's salt on phenols.

The decay of Fremy's salt, as followed by ESR measurements, is considerably fast if the phenols have no substituent on the *o*- and/or *p*-position to their hydroxyl group, such as 2,6-dimethylphenol. In the case of 2,4,6-trimethylphenol, however, the decay of Fremy's salt is rather slow. Although the ESR spectra of free phenoxy radicals could not be observed at any stage of the reaction, the ESR spectra corresponding to Fremy's salt are broadened and the coupling constant due to nitrogen, a_N, becomes slightly smaller than that of free Fremy's salt (Fig. 3). The above-mentioned

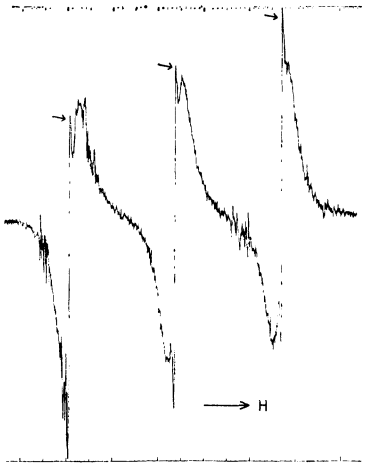

Fig. 3. ESR spectra observed in the reaction of 2,4,6-trimethylphenol with Fremy's salt. Three lines indicated by arrows are due to free Fremy's salt as an external standard.

deformation may be ascribed to a complex formation between Fremy's salt and 2,4,6-trimethylphenol. Considering a_N, some part of the free spin of Fremy's salt may be delocalized onto 2,4,6-trimethylphenol, thus making a labile molecular complex. In the case of phenols with free *o*- and/or *p*-positions, therefore, the formation of such a complex would make the subsequent attack of Fremy's salt easier than the first attack on phenols; this would be the origin of the high selectivity of this reaction.

Considering the above results, the course of the reaction may be described as follows:

Table 2. Physical properties of *p*-benzoquinones

p-Benzoquinones	Mp (°C)	$\lambda^{a)}$ (nm)	ε ($CHCl_3$)	Chemical shift (CCl_4)	
				Substituents (ppm)	Benzene ring (ppm)
p-Benzoquinone	111	437	20.4	—	6.70
2-Methyl-	66	436	28.2	2.05	6.50—6.70
2,5-Dimethyl-	123—124	430	27.0	2.03	6.50—6.60
2,6-Dimethyl-	71	430	42.5	2.04	6.48
2-*t*-Butyl-	53	440	24.0	1.28	6.50—6.65
2-Chloro-	55	415	24.0	—	6.75—6.95

a) The wavelength used for determination for *p*-benzoquinones.

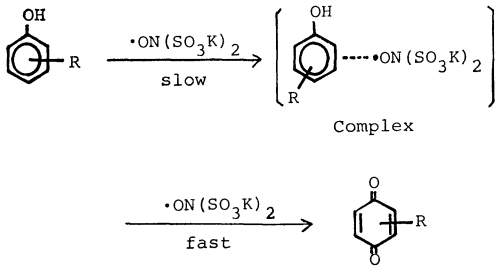

Experimental

2.5×10^{-3} mol of Fremy's salt[1] was dissolved into 50.0 m*l* of water buffered with sodium acetate (pH 8.2), after which the solution was cooled to about 2°C. To the solution, 1.0×10^{-3} mol of phenols dissolved in 2.0 m*l* of ether was then added all at once (0—3°C). After the reaction had stopped, the products were separated by using TLC and were determined spectroscopically. The physical properties of *p*-benzoquinones thus produced are shown in Table 2. An ME-3X-type ESR spectrometer with 100 kHz modulation was used in this experiment.

BULLETIN OF THE CHEMICAL SOCIETY OF JAPAN, VOL. 44, 2875—2876 (1971)

Mechanism of the Oxygen Exchange Reaction of Diaryl Sulfoxides in Hydrochloric Acid[1]

Hiroshi YOSHIDA,* Tatsuo NUMATA, and Shigeru OAE

Department of Applied Chemistry, Faculty of Engineering, Osaka City University, Sugimoto-cho, Sumiyoshi-ku, Osaka

(Received May 4, 1971)

Mislow *et al.*[2] showed that sulfoxides undergo stereomutation together with oxygen exchange in hydrochloric acid-dioxane media. While the rate of oxygen exchange of *p*-tolyl phenyl sulfoxide was equal to that of racemization, the rate of racemization was found to be affected markedly by the steric requirement of the group attached to the central sulfur atom. The rate-determining step of the reaction was assumed to be the interconversion of the enantiomorphic chlorosulfonium chloride to the other.

Landini *et al.*[3] studied the acid-catalyzed stereomutation of sulfoxides with chloride ion and found that the rate of racemization of *p*-tolyl methyl sulfoxide was accelerated by the increase of chloride ion concentration in aqueous perchloric acid media, while the logarithms of the rates of racemization were nicely correlated with the Hammett acidity function (*Ho*). They suggested that the rate-determining step of the reaction is the formation of chlorosulfonium salt.

The two investigations seem to deal with the same reaction system. However, there is a disagreement as to the rate-determining step of the reaction. In order to correlate the two investigations and to find the rate-determining step of the oxygen exchange and racemizations of sulfoxide with hydrochloric acid, and also to confirm the importance of the steric effect of this reaction, we have carried out a kinetic study on the oxygen exchange and racemization reactions of both ^{18}O-labeled and optically active *p*-tolyl phenyl sulfoxide, and also a more sterically hindered *p*-tolyl mesityl sulfoxide in 3.93N HCl in 80% dioxane-water mixture. We also reinvestigated the correlation of the rates of racemization of both sulfoxides with the Hammett acidity function (*Ho*). The rates of racemization of both sulfoxides were determined in hydrochloric acid with various concentrations of hydrogen chloride in 80% dioxane-water solution, and the logarithms of k_{rac}/[HCl] were plotted against the Hammett acidity function (*Ho*). Strainght lines with a slope 0.80 and 0.81 were obtained for *p*-tolyl phenyl and *p*-tolyl mesityl sulfoxides, respectively, as shown in Table 1.

*Faculty of Engineering, Shizuoka University.

1) Paper XL on Sulfoxides

2) K. Mislow, T. Simmons, J. T. Melillo and A. L. Ternay, Jr., *J. Amer. Chem. Soc.*, **86**, 1452 (1964)

3) a) D. Landini and F. Montanari, *Chem. Commun.*, **1968**, 86 b) D. Landini, G. Modena, F. Montanari and G. Scorrano, *J. Amer. Chem. Soc.*, **92**, 7168 (1970)

Table 1. Rates of racemization of *p*-Tol-S(O)-Ar[a] in hydrochloric acid of various concentrations

HCl (*N*)	$-Ho$	Temp (°C)	$10^6k_{rac}(sec^{-1})$ Phenl	Mesityl	k_{ph}/k_{Mes}
3.16	1.07	25	104		
3.55	1.30	25	169	0.798	212
3.93	1.49	25	276[b]	1.25[c]	216
3.93	1.49	30	430[b]	2.03[c]	212
3.93	1.49	35	645[b]	2.98[c]	216
4.51	1.84	25	510	2.29	222
4.89	1.96	25	798		

a) Sulfoxide; 0.1 mol/*l*; *p*-Tol=*p*-$CH_3C_6H_4$
b) E_a=15.4 kcal/mol $\Delta S^{\ddagger}$=−23.3 *e.u.*
c) E_a=15.8 kcal/mol, $\Delta S^{\ddagger}$=−30.9 *e.u.*

This means that the protonated species are involved in the transition state of the reaction, indicating that the reaction is of the A-1 type mechanism according to Zucker-Hammett's hypothesis.[4]

The rates of oxygen exchange of both sulfoxides in 3.93N hydrochloric acid were determined. The results are listed in Table 2 together with rates of racemization.

Table 2. Kinetic data of oxygen exchange and racemization reactions of *p*-Tol-S(O)Ar[a] at 25°C

Ar	$10^6k_{ex}(sec^{-1})$	$10^6k_{rac}(sec^{-1})$	k_{ex}/k_{rac}
Phenyl	326	276	1.18
Mesityl	1.55	1.25	1.24

a) Sulfoxide; 0.1 mol/*l*

The results reveal that the rate of oxygen exchange is nearly the same as that of racemization in both cases. This means that the two reactions share a common rate-determining step which is presumed to be the A-1 type S-O bond cleavage in view of the Hammett acidity correlation.

The rate of oxygen exchange of *p*-tolyl mesityl sulfoxide was about 210 times smaller than thet of *p*-tolyl phenyl sulfoxide. The marked rate retardation by the *ortho* substituents is for the most part due to the difference in the activation entropies of racemization reactions of both sulfoxides (Table 1). This is steric hindrance at either one of the two conceivable steps or both steps of the reactions; namely, the nucleophilic attack of chloride ion at the sulfur atom of the hydroxysulfonium salt to form the chlorosulfonium intermediate and the prior second protonation to form the diprotonated species. The steric hindrance for the double protonation was suggested to be responsible for the substantial retardation of the rates of racemization of *p*-tolyl mesityl sulfoxide in concentrated sulfuric acids.[5]

The fact that the rate of HCl-catalyzed racemization is markedly greater than that of H_2SO_4 catalyzed reaction suggests that the attack of chloride ion facilitates the S-O bond cleavage in the rate-determining step. We have found that the acid-catalyzed oxygen exchange and racemization reactions in concentrated sulfuric acids is markedly accelerated by the addition of chloride ion.[6] A plausible scheme of the oxygen exchange reaction of sulfoxide in hydrochloric acid can be illustrated as follows.

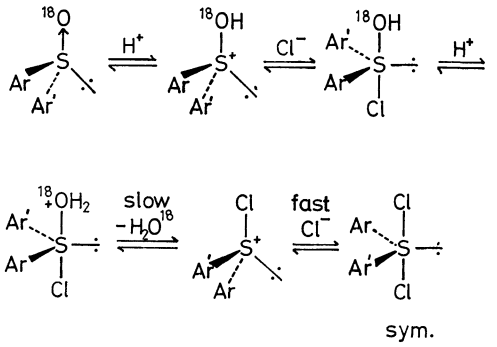

The reaction seems to proceed through the nucleophilic attack of chloride ion at the sulfur atom of protonated sulfoxide, followed by the rate-determining S-O bond cleavage to afford an unstable chlorosulfonium intermediate.

The subsequent step of either the formation of sulfonium dichloride or the hydrolysis of chlorosulfonium salt should be very fast.

Experimental

Optically Active Sulfoxides and ^{18}O*-Labeled* p-*Tolyl Phenyl Sulfoxide* were synthesized in the usual procedure as described.[5a]

^{18}O*-Labeled* p-*Tolyl Mesityl Sulfoxide* was prepared from the ^{18}O-labeled methyl *p*-toluenesulfinate with the Grignard reagent of mesityl bromide in tetrahydrofuran. 55% yield mp 75—77°C.

The Values of Ho were determined with *p*-nitro, *o*-chloroaniline as an indicator in UV spectrometry by the method of Jorgenson and Harter.[7]

Kinetic Procedures of Oxygen Exchange and Racemization Reaction. The procedures were similar as those described previously.[8]

4) M. A. Paul and F. A. Long, *Chem. Revs.*, **51**, 935 (1957)
5) a) S. Oae and N. Kunieda, This Bulletin, **41**, 696 (1968) b) S. Oae, *Quart. Rept. Sulfur Chem.*, **5**, 53 (1970)
6) N. Kunieda and S. Oae, unpublished work.
7) J. Jorgenson and D. R. Harter, *J. Amer. Chem. Soc.*, **85**, 878 (1963)
8) T. Numata, K. Sakai, M. Kise, N. Kunieda, and S. Oae, *International J. Sulfur Chem.* **1**, 1 (1971).

BULLETIN OF THE CHEMICAL SOCIETY OF JAPAN, VOL. 44, 2877 (1971)

Basicities of Formamide, Acetamide, and Their Alkyl Derivatives in Aqueous Solution

Goro WADA and Takako TAKENAKA

Department of Chemistry, Nara Women's University, Nara

(Received May 10, 1971)

The basicity constants pK_a of formamide, acetamide and their alkyl derivatives, generally represented by $R_1CONR_2R_3$ where R_1, R_2, and R_3 stand for H, CH_3, C_2H_5, CH_2Cl, or $CHCl_2$ respectively, were measured in aqueous solution spectrophotometrically,[1] using *o*-nitroaniline as indicator. Measurements were carried out at 25°C for wavelengths of 380, 410, and 440 nm, and ionic strength of μ=0.55M. The acid dissociation constant of *o*-nitroaniline, $K_{In}=[H^+][In]/[HIn^+]$, was taken to be 1.27M.[1]

The results of the determination of pK_a related to various amides are listed in Table 1, together with the values of their donor numbers $DN(SbCl_5)$[2] and dielectric constants D. The thermodynamical constants pK_a^0 can be approximately estimated by the following equation.

$$pK_a^0 = pK_a - 0.5\sqrt{\mu}$$

According to recent NMR studies,[3] the protonation of most amides was found to occur predominantly at O-atom and not at N-atom, as revealed by the fact that the double bond character between C and N atoms and the barrier to rotation around the C–N bond increase with the protonation of amides.[4] The nature of amides is thus acidic and far less basic than ammonia and alkylamines.

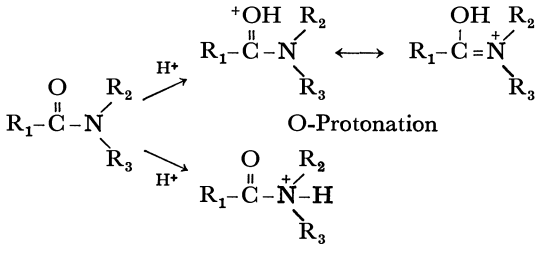

Alkylamines usually exhibit pK_a values 9—11, in remarkable contrast to -0.1 ± 0.2 as the mean value of pK_a^0 of the nine amides in Table 1. The values of pK_a^0 of some amides given in Table 1 were separately measured by potentiometric titration with perchloric acid in acetic scid with chloranil electrode and coincide well with our results within the mean discrepancy ±0.4[5]

Although the pK_a does not seriously vary with the substitution of H by alkyl radicals in both formamide and acetamide, there is a slight tendency for pK_a to grow higher as R_2 or R_3 changes in the direction H→ CH_3→C_2H_5. The effect of chlorine atom in R_1 in acetamide upon pK_a is distinct, making the compound less basic. No close relationship of pK_a with the donor numbers and the dielectric constants is noticed, as far as our data are concerned.

TABLE 1. BASICITY CONSTANTS, DONOR NUMBERS AND DIELECTRIC CONSTANTS OF VARIOUS AMIDES

Compound	R_1	R_2	R_3	pK_a	pK_a°	DN ($SbCl_5$)	D
Formamide	H	H	H	0.12	−0.25		109
N-Methylformamide	H	H	CH_3	0.52	0.15		177
N,*N*-Dimethylformamide	H	CH_3	CH_3	0.18	−0.19	26.6	36.1
N,*N*-Diethylformamide	H	C_2H_5	C_2H_5	0.36	−0.01	30.9	
Acetamide	CH_3	H	H	−0.025	−0.40		
N-Methylacetamide	CH_3	H	CH_3	0.26	−0.11		179
N,*N*-Dimethylacetamide	CH_3	CH_3	CH_3	0.62	0.25	27.8	38.9
Chloroacetamide	CH_2Cl	H	H	−0.26	−0.63		
Dichloroacetamide	$CHCl_2$	H	H	−0.26	−0.63		

1) G. Wada, This Bulletin, **42**, 890 (1969).

2) V. Gutmann and E. Wychera, *Inorg. Nucl. Chem. Letters*, **2**, 257 (1966); V. Gutmann, "Coordination Chemistry in Non-Aqueous Solutions," Springer-Verlag, Wien and New York (1968), p. 19.

3) A. Berger, A. Loewenstein, and S. Meiboom, *J. Amer. Chem. Soc.*, **81**, 62 (1959); G. Fraenkel and C. Franconi, *ibid.*, **82**, 4478 (1960); R. J. Gillespie and T. Birchall, *Can. J. Chem.*, **41**, 148 (1963); W. E. Stewart and T. H. Siddall, III, *Chem. Rev.*, **70**, 517 (1970); B. G. Cox, *J. Chem. Soc.*, B, **1970**, 1780.

4) In the cases of urea and its alkyl derivatives, the protonation probably occurs at both O and N atoms. G. A. Olah and M. Calin, *J. Amer. Chem. Soc.*, **90**, 401 (1968).

5) R. Huisgen and H. Brade, *Chem. Ber.*, **90**, 1432 (1957).

BULLETIN OF THE CHEMICAL SOCIETY OF JAPAN, VOL. 44, 2878—2879 (1971)

Effect of the Number of Sulfur Atoms on the Chemical Shifts of Mercapto Protons in Aralkyl Hydropolysulfides

Shunichi KAWAMURA, Toyokazu HORII, and Jitsuo TSURUGI
Radiation Center of Osaka Prefecture, Shinke-cho, Sakai, Osaka

(Received May 25, 1971)

Chemical shift of group X in organic polysulfides $X(S)_nY$ has been observed to be sensitive to the character of far distant group Y and the number of sulfur atoms.[1-5] This phenomenon is useful for the analyses of polysulfide mixtures.[2-4] However, little information is available on protons directly attached to sulfur except for that on sulfanes[6] [$H(S)_nH$]. We wish to report on the PMR study on aralkyl hydropolysulfides [$R(S)_nH$, n=1—3].

TABLE 1.[a] CHEMICAL SHIFTS OF $R(S)_nH$ (n=1—3)

No.	R	Thiols, RSH	Hydrodisulfides, RSSH	Hydrotrisulfides, RSSSH
1	$C_6H_5CH_2$	1.51[b]	2.74[d]	3.38
2	$(C_6H_5)_2CH$	2.05[b]	2.72[d]	3.17
3	$(C_6H_5)_3C$	2.90[c]	2.48	2.63

a) Values are in δ ppm, 7 w/w% in CCl_4. All SH peaks of course disappear by addition of D_2O. In benzyl and benzhydryl hydrodisulfides, each singlet peak accompanies beats, from which long range coupling constants with methylene or methine proton, J=0.4 and 0.6 Hz, are estimated. In hydrotrisulfides, peaks are singlet.
b) J. Tsurugi, T. Horii, T. Nakabayashi, and S. Kawamura, *J. Org. Chem.*, **33**, 4133 (1968).
c) J. Tsurugi, Y. Abe, T. Nakabayashi, S. Kawamura, T. Kitao, and M. Niwa, *ibid.*, **35**, 3263 (1970).
d) S. Kawamura, Y. Abe, and J. Tsurugi, *ibid.*, **34**, 3633 (1969).

Table 1 shows the PMR data obtained for dilute carbon tetrachloride solutions; chemical shifts of sulfhydryl groups of thiols, hydrodisulfides and hydrotrisulfides, in which R groups are the series of benzyl, benzhydryl and triphenylmethyl. Fig. 1 presents a graphical explanation of the results. In thiols, the chemical shift of benzhydryl compound is in a lower field than that of benzyl, triphenylmethyl being in the lowest, whereas a reverse relation is noted in hydrotrisulfides. As to the triphenylmethyl derivatives, their chemical shifts are not lowered with the increase of the number of sulfur atoms.

We see that at least two factors are required for explanation of the relation of the chemical shifts. One which clearly originates from the length of sulfur chain is anisotropy or inductive effect by sulfur atoms, and the other anisotropy and/or inductive effect of R group. In the PMR study of alkyl polysulfides or analogous compounds, Van Wazer and Grant[1] reported on C_y and C_z values (These are defined as follows; for the molecule $X(S)_nY$, C_y is the shift contribution of the terminal group Y separated from the group X, containing the magnetic nucleus, by n sulfur atoms, and C_z is the shift contribution of each sulfur atom.), which is calculated based on the theory for so-called "neighbor anisotropy effect." For our data, a similar calculation is possible.[7] In Table 2 are cited C_y values for each aralkyl group and C_z. The relation of the chemical shifts to calculated curves is also shown in Fig. 1.

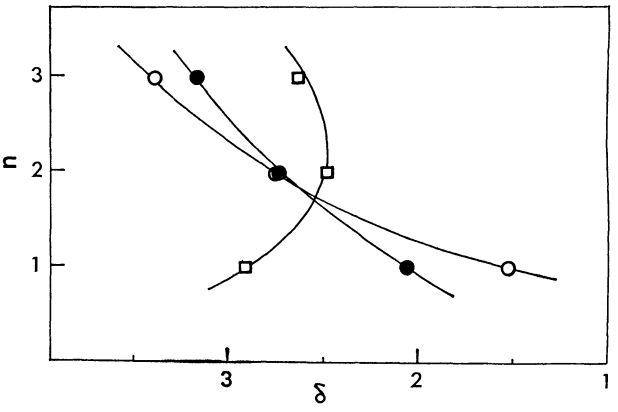

Fig. 1. Relationship between the chemical shifts and the number of sulfur atoms(n).
○ $C_6H_5CH_2(S)_nH$ ● $(C_6H_5)_2CH(S)_nH$ □ $(C_6H_5)_3C(S)_nH$
—— Calculated curve

7) C_y and C_z values were obtained by computer-programmed calculation. The computation was performed by the least mean square method, using the following linear equation,

$$\Delta\delta = C_y(1)\cdot U_1(n) + C_y(2)\cdot U_2(n) + C_y(3)\cdot U_3(n) + C_z\cdot V(n) \quad (1)$$

where $\Delta\delta=\delta_2-\delta_n$, and $C_y(1)$, $C_y(2)$, $C_y(3)$ and C_z correspond to coefficients which designate the magnitudes of neighbor anisotropy effects of benzyl, benzhydryl, and triphenylmethyl groups, and of sulfur atom, respectively. Variables $U_i(n)$ and $V(n)$ which are the functions of the number of sulfur atoms n are derived from the Van Wazer's equation;[1]

$$U_i(n) = 1/R_{n+1}^3 - 1/R_3^3$$

$$V(n) = \sum_{j=1}^{n} 1/R_j^3 - \sum_{j=1}^{3} 1/R_j^3$$

where R denotes the distance between the center of contributing group or atom and the nucleus in question, which is obtained by the random-flight calculation. In Eq. (1), $U_i(n)$ is taken as zero, except when the chemical shifts of a series of compounds are referred to. As an example, when the value of $\Delta\delta$ of α-toluenethiol, 2.74 −1.51=1.23, is replaced in Eq. (1), one would obtain $1.23=C_y(1)\cdot U_1(1)+0.0+0.0+C_z\cdot V(1)$.

1) J. R. Van Wazer and D. Grant, *J. Amer. Chem. Soc.*, **86**, 1450 (1964).
2) D. Grant and J. R. Van Wazer, *ibid.*, **86**, 3012 (1964).
3) D. J. Martin and R. H. Pearce, *Anal. Chem.*, **38**, 1604 (1966).
4) T. L. Pickering, K. J. Saunders, and A. V. Tobolsky, *J. Amer. Chem. Soc.*, **89**, 2364 (1967).
5) T. Fujisawa and G. Tsuchihashi, This Bulletin, **43**, 3615 (1970).
6) E. Muller and J. B Hyne, *J. Amer. Chem. Soc.*, **91**. 1907 (1969).

Table 2. Anisotropic parameters for R(S)H (n=1—3)

No.	R	C_y	C_z
1	$C_6H_5CH_2$	−8.0	−9.7
2	$(C_6H_5)_2CH$	−12	−9.7
3	$(C_6H_5)_3C$	−21	−9.7

The large negative C_z value in Table 2 means that divalent sulfur atoms markedly deshield the directly attached neighboring protons. The fact that the value of C_y is also negative and increases in its absolute value with the number of benzene nucleus in the aralkyl group may imply that the sulfhydryl proton is mainly present near the plane of benzene nucleus. The reverse winding of the curve for triphenylmethyl series in Fig. 1 or the large negative C_y value of triphenylmethyl group compared with that of benzyl or benzhydryl, seems to suggest a sterically significant relation. In benzyl or benzhydryl derivatives, sulfhydryl protons have the chance to project over the surface of benzene nuclei. On the other hand, an extremely restricted rotation of benzene nuclei in triphenylmethyl groups diminishes the possibility, or the bulky groups prevent the real random-flight motion, and chemical shifts might be much lowered.

Van Wazer's equation gives an excellent fit for the relative position of the chemical shifts, but does not determine their absolute values. Therefore, some other effects such as the inductive effect should be taken into consideration to elucidate the fact that the chemical shift of diphenylmethanethiol is lower than that of α-toluenethiol, *etc.*

Experimental

PMR spectra were taken on a JNM 3H-60 spectrometer with tetramethylsilane as an internal standard (7 w/w% in CCl_4). Values of C_y and C_z in Table 2 were obtained by computer-programmed least squares calculation using Eq. (1) in Ref. 7 and data in Table 1. Benzyl,[8] benzhydryl,[8] and triphenylmethyl[9] hydrodisulfides, and benzyl[10] and triphenylmethyl[9] hydrotrisulfides were prepared by known procedures. Benzhydryl hydrotrisulfide (86% purity) was obtained as a carbon tetrachloride solution by the following procedure. To a solution of acetyl benzhydryl trisulfide (1 g) in *n*-propyl alcohol (20 m*l*) was added 1N *n*-propyl alcoholic hydrogen chloride (5 m*l*). The solution was kept at 29°C for 1 hr. Volatiles were evaporated under reduced pressure, and carbon tetrachloride was added to the residual oil. Acetyl benzhydryl trisulfide was prepared by the same method as that given in literature.[9] 77% of crude material, mp 53—57°C was obtained. This was purified by repeated recrystallization from ether to obtain white crystals, mp 57—58.5°C.

Found: C, 58.49; H, 4.82; S, 31.64%. Calcd for $C_{15}H_{14}OS_3$: C, 58.79; H, 4.60; S, 31.38%.

The authors wish to thank Dr. T. Nakabayashi for the synthesis of acetyl benzhydryl trisulfide and Mr. R. Ito for his assistance in computer calculation.

8) J. Tsurugi and T. Nakabayashi, *J. Org. Chem.*, **24**, 807 (1959).
9) T. Nakabayashi, J. Tsurugi, and T. Yabuta, *ibid.*, **29**, 1236 (1964).
10) H. Böhme and G. Zinner, *Ann. Chem.*, **585**, 152 (1954).

SHORT COMMUNICATIONS

Admittance Behavior of Electrode Reaction of Water at a Dropping Mercury Electrode

Kiyoshi MATSUDA, Katsuo TAKAHASHI, and Reita TAMAMUSHI
The Institute of Physical and Chemical Research, Wako-shi, Saitama
(Received June 4, 1971)

The DC and AC polarographic behavior of dropping mercury electrode (DME)/dilute aqueous electrolyte solution systems was studied in the potential region from zero to ± 5V. In AC polarography, conductance and susceptance components of the cell admittance were measured by a phase-sensitive AC polarograph constructed in our laboratory.[1]

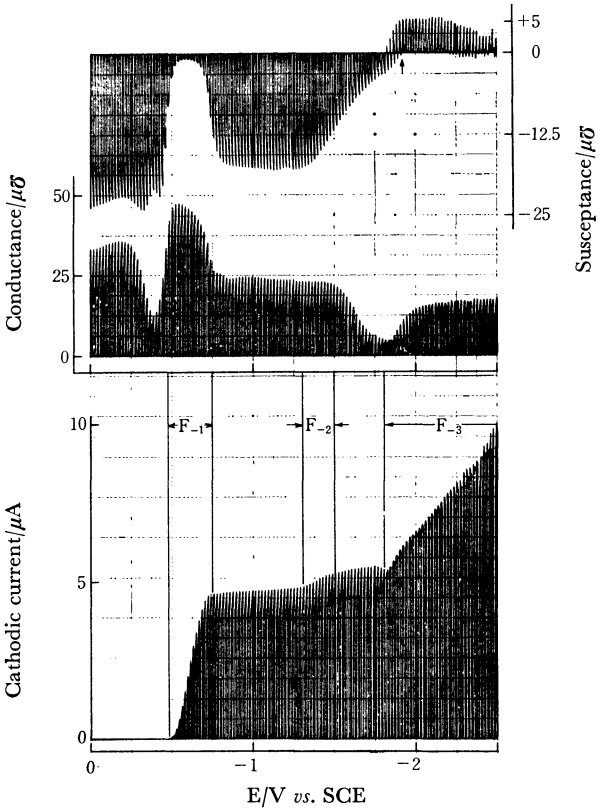

Fig. 1. DC polarogram, conductance-potential and susceptance-potential curves of a DME/0.5 mM $Cd(NO_3)_2$ system in negative potential region at 25°C, the conductance and susceptance being measured at 31 Hz.

Figure 1 shows typical DC and AC polarograms of a DME/0.5 mM $Cd(NO_3)_2$ system (pH=4—5) in the negative potential region. The reduction waves of cadmium and hydrogen ions were observed on the DC polarogram in potential regions F_{-1} and F_{-2}, respectively. The cathodic current increased almost linearly with potential in the more negative potential region F_{-3}. This increase in cathodic current is attributed to the reduction of water.[2]

In the potential region F_{-3}, a remarkable change in the direction of the susceptance vector was observed as indicated by an arrow in Fig. 1, when the admittance was measured at relatively low frequencies. This type of anomaly in the susceptance component was also observed in solutions of various cations such as H^+, Na^+, K^+, Ag^+, Hg_2^{2+}, Tl^+, Ca^{2+}, Co^{2+}, Ni^{2+}, Zn^{2+}, Cd^{2+}, and Pb^{2+}. Exceptions were solutions containing Mg^{2+}, NH_4^+, $(CH_3)_4N^+$ and $HgCl_2$; in case of Mg^{2+} the DC reduction wave of Mg^{2+} and that of water overlapped, and in NH_4^+-, $(CH_3)_4N^+$- and $HgCl_2$-systems the DC and AC polarograms were strongly disturbed in the potential region F_{-3}, which prevented us from making further analysis of susceptance components.

The analysis of the frequency dispersion suggested the contribution of some inductive components to the electrical equivalent circuit of the cell system in the potential region F_{-3}. The admittance behavior of this nature has been reported by Epelboin and his coworkers[3] in the electrochemical dissolution of iron and nickel electrodes. In case of cathodic processes, the possibility of the contribution of inductive components to the faradaic admittance has been suggested theoretically for hydrogen evolution.[4] It seems, however, that this paper provides the first experimental evidence for the contribution of an inductive susceptance to the equivalent circuit of the cathodic reduction of water at a DME.

In solutions containing hydroxide and thiocyanate ions, inductive susceptances were also detected in the positive potential region where anodic currents are observed. Details of the experimental results and the theoretical consideration will be reported elsewhere.

1) K. Matsuda, K. Takahashi, and R. Tamamushi, *Sci. Papers Inst. Phys. Chem. Res.*, **64**, 62 (1970).

2) D. Ilkovič, *Coll. Czech. Chem. Commun.*, **4**, 480 (1932); T. Okada and S. Yoshizawa, *Kogyo Kagaku Zasshi*, **49**, 183 (1964).

3) For example: I. Epelboin, M. Keddam and J.-C. Lestrade, *Revue Générale de l'Electricité*, **76**, 777 (1967); R. Wiart, *Oberfläch-Surface*, **9**, 213, 241, 275 (1968); I. Epelboin and M. Keddam, *J. Electrochem. Soc.*, **117**, 1052 (1970).

4) H. Gerischer and W. Mehl, *Z. Elektrochem.*, **59**, 1049 (1955); I. M. Novosel'skii and N. N. Gudina, *Elektrokhim.*, **5**, 820 (1969).

Infrared Spectra of Crystalline Chloroform at High Pressure

Mitsuko KOYAMA and Haruka YAMADA
Department of Chemistry, Kwansei Gakuin University, Nishinomiya
(Received March 31, 1971)

Infrared absorption spectra of polycrystalline chloroform were measured at 100°K and the results were discussed in comparison with the X-ray diffraction data.[1] In order to justify the previous analysis and to determine the assignment of components of internal mode splittings in the crystal field, measurements of spectra of single crystals or oriented crystals are most desirable.

In the present work, single crystals of chloroform have been produced in a diamond high-pressure cell at room temperature. Sample crystals were grown from liquid chloroform sealed between a molybdenum gasket and diamond anvils in a high-pressure cell (High Press. Optics, Co.). Pressure was increased up to about 30 kbar on the sample until solidification to a polycrystal occurred (the pressure in the cell was roughly estimated by counting the rotations of the screw as shown in its catalogue). The pressure was then decreased gradually until the crystal melted, and the pressure was again increased rapidly until single crystals were grown. By repeating the procedure, the single crystals as shown in Fig. 1 were obtained. Although the crystals grown in the cell consisted not of one block but of several blocks, the polarization effect on the spectra was observed, indicating some orientation of the single crystals.

Infrared spectra were recorded on a modified Jasco DS-301 prism (triple-pass) spectrometer, whose beam was first focussed on the sample using a mirror of long focal length. An AgBr grid wire polarizer was employed. No polarization effect from the diamond cell was detected at 1 atm and also at high pressures.

Spectra of samples 1 and 2 are shown in Figs. 2 and 3, respectively. Sample 1 shows two peaks at 3053 and 3008 cm^{-1} in the ν_1 region and three peaks at 1226, 1207 and 1198 cm^{-1} in the ν_4 region, while sample 2 has two peaks at 3048 and 3008 cm^{-1} in the ν_1 region as well as two peaks at 1225 and 1210 cm^{-1} in the ν_4 region without the lowest frequency peak. In these figures the dotted lines represent the spectra in ploarized light. The polarizer was used in such a way that the most significant spectral changes from the unpolarized spectra might be observed. For polycrystals the spectra obtained at high pressures are very similar to those reported for the polycrystalline film at 100°K, though the crystal field splittings for the ν_4 vibration are somewhat larger for the crystals at high pressures than for that at 100°K. The peak at 3050 cm^{-1} was not reported for the polycrystalline film, but we have observed it by making a thicker film at 100°K.

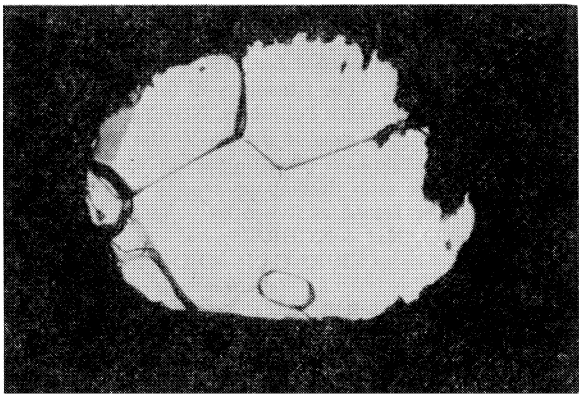

Fig. 1. $CHCl_3$ single crystals grown in diamond cell at *ca.* 30 kbar (sample 2).

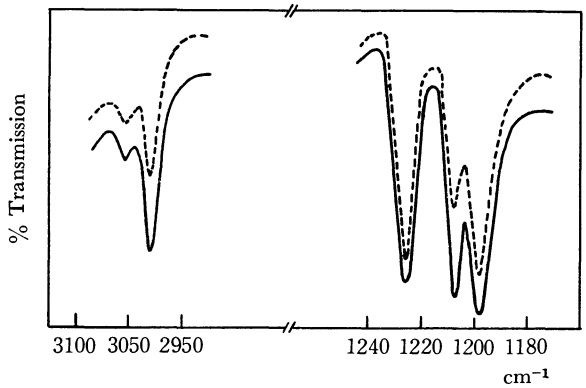

Fig. 2. ν_1 and ν_4 bands of $CHCl_3$ for sample 1.
—— unpolarized, ------ polarized

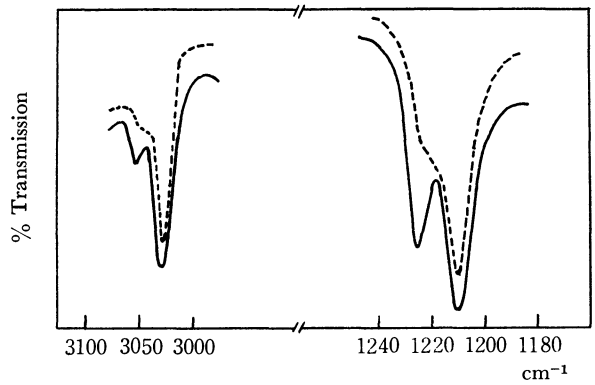

Fig. 3. ν_1 and ν_4 bands of $CHCl_3$ for sample 2.
—— unpolarized, ------ polarized

As can be seen from Figs. 2 and 3, the central peak at 1207 cm^{-1} in the ν_4 band and the peak at 3008 cm^{-1} in the ν_1 band are ascribed to one crystal axis component while the peaks at 1225 cm^{-1} and at 3050 cm^{-1} are assigned to another crystal axis component. Since the chloroform crystal belongs to D_{2h}^{16} and the CH bonds lie on the ac plane, making an angle of 14° with the *a* axis, the peak at 3008 cm^{-1} is assigned to the *a* axis component. The three peaks in the ν_4 band can then be assigned to the *c*, *a*, and *b* axis components, respectively, from high to low frequencies, supporting the previous analysis.

1) A. Kimoto and H. Yamada, This Bulletin, **41**, 1096 (1968).

Synthesis of 4-Substituted Isoxazole-3,5-dicarboxylic Acids from 2-Substituted-1,3-dinitroglutarates and the Reaction Mechanism therefrom[1,2]

Shonosuke ZEN and Masao KOYAMA

School of Pharmaceutical Sciences, Kitasato University, Shirokane, Minato-ku, Tokyo

(Received May 29, 1971)

A solution of 1 mol of 2-substituted-1,3-dinitroglutarates[3] (**1**) in absolute ethanol was added to about 10 mol of a primary amine, such as *n*-butylamine or *n*-propylamine. The reaction mixture was refluxed for several hours, and upon concentration crude 4-substituted bis-carbamoylisoxazoles (**5**) were obtained as oils, which were crystallized after washing, digesting or extracting with suitable solvents. Compounds **5**, listed in Table 1 were identified by comparison with authentic samples[4] (except 5-E and 5-F). They were hydrolysed with aqueous sodium hydroxide to give free acids[5] (**6**).

1 was decomposed in the presence of the amines. After liberation of nitrous acid, it gave isoxazoline-*N*-oxide (**3**) which might be produced *via* an olefin intermediate (**2**), followed by the intramolecular addition as suggested by Nielsen and Archibalt.[6]

Since compound (**3**) is also classified as "*Cyclic Nitronic Esters*,[7,8] the following mechanism seems to be reasonable. (a) Compound **3** is decomposed into an oximino-ketone (**4**), and (**4a**), the enol-form of **4** yields a dehydrated product, an isoxazole (**5**) as observed by Worrall.[9] (b) Two ester groups of (**4a**) form diamide of the corresponding primary amine in the final step.

The mechanism was confirmed by the following results. (i). An isoxazoline-*N*-oxide (**3a**, $R^1=C_6H_5$, $R^3=CO_2CH_3$ of **3**), mp 94.5—96°C; IR (KBr), 1730 (ester CO), 1610 (phenyl), 1340 cm^{-1} (*N*-oxide); NMR ($CDCl_3$), 2.61 (s. 5H phenyl), 5.02 (d, 1H ring), 5.12 (d, 1H ring), 6.06 (s. 3H methyl), 6.24 τ (s. 3H methyl), could be obtained from a solution of a diethylamine salt of 2-phenyl-1,3-dinitroglutarate in methanol at room temperature. (ii). When an excess of *n*-butylamine was added to an ethanol solution of **3a**, it was converted into isoxazole (**5**, $R^1=C_6H_5$, $R^2=C_4H_9$) in a 97% yield. As emphasized in previous papers,[4,5] compound **1** should be regarded as a key compound for the reaction of α,β-unsaturated α-nitroesters with *n*-butylamine to give **5**.

The postulated mechanism is shown in Chart 1.

All new compounds reported above (**3a**, 5-B($R^2=n$-C_3H_7), 5-E, and 5-F) gave satisfactory results in C, H, and N analyses.

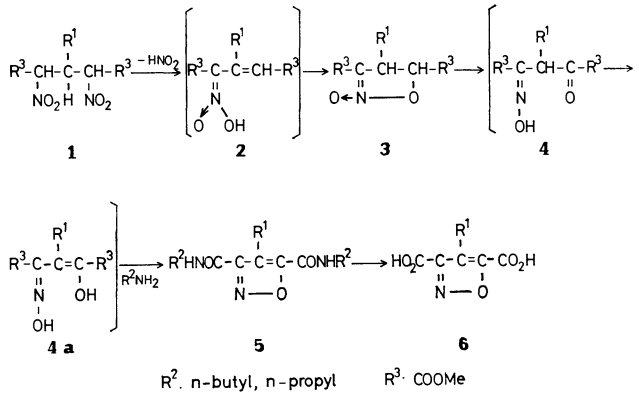

Chart 1.

TABLE 1. 4-SUBSTITUTED 3,5-BIS(*n*-BUTYLCARBAMOYL)ISOXAZOLES (**5**) FROM 2-SUBSTITUTED 1,3-DINITROGLUTARATES (**1**)

5, R^1:	n-C_3H_7	C_6H_5	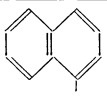				
	(5-A)[a]	(5-B)[b]	(5-C)[a]	(5-D)[a]	(5-E)[c]	(5-F)[d]	(5-G)[a]
Yield, %	39	80	76	56	41	48	50

a) Ref. 4 b) Ref. 5; $R^2=n$-C_3H_7: mp 165—166°C (ethanol-water) c) mp 81—84°C (*n*-hexane) d) mp 83—85°C (*n*-hexane)

1) Part VI in the series, "The Synthetic Reactions of Aliphatic Nitro Compounds," Part V: S. Zen, M. Koyama, and S. Koto, *Kogyo Kagaku Zasshi*, **74**, 70 (1971).

2) This work was presented in part at the 91st Annual Meeting of the Pharmaceutical Society of Japan, Fukuoka, April, 1971; Abstracts of Presentation, p. 689 (1971).

3) Prepared by the methods described by A. Dornow and G. Wiehler (*Ann.*, **578**, 113 (1952)) and A. Dornow and A. Frese, (*Ann.*, **581**, 211 (1953)). Monodiethylamine salts were employed because of their better stability than the free acids.

4) S. Zen and S. Umezawa, This Bulletin, **34**, 890 (1961); **36**, 1146 (1963); **36**, 1150 (1963).

5) S. Umezawa and S. Zen, *ibid.*, **33**, 1016 (1960).

6) A. T. Nielsen and T. G. Archibalt, *J. Org. Chem.*, **34**, 984 (1969).

7) A. T. Nielsen, *Tetrahedron Lett.*, **1968**, 3375: *Tetrahedron*, **26**, 3475 (1970); H. Feuer, "The Chemistry of the Nitro and Nitroso Groups," Part 1, Interscience Publishers, New York (1969), p. 417.

8) Generally, nitronic ester is given as *O*-alkylated product by the reaction of metallic salts of nitroparaffins with alkyl halides. This acyclic nitronic ester decomposes readily to form an oxime and an aldehyde or ketone as shown by

$$R^1R^2\cdot C{=}NO_2^-Na^+ + XCHR^3R^4 \longrightarrow R^1R^2\cdot C{=}N(\rightarrow O)OCHR^3R^4 \longrightarrow$$

(*acyclic nitronic ester*)

$$R^1R^2\cdot C{=}N{-}OH + R^3R^4\cdot C{=}O$$

9) Dibenzoyl phenyl monoxime is readily converted into triphenylisoxazole (D. E. Worrall, *J. Amer. Chem. Soc.*, **57**, 2299 (1935)).

The Crystal and Molecular Structure of *trans*-Bis(dinitrogen)bis[1,2-bis(diphenylphosphino)ethane]molybdenum(0)

Tokiko UCHIDA, Yasuzo UCHIDA,* Masanobu HIDAI,* and Teruyuki KODAMA*

Department of Industrial Chemistry, Faculty of Science and Technology, The Science University of Tokyo, Noda, Chiba

**Department of Industrial Chemistry, Faculty of Engineering, The University of Tokyo, Hongo, Tokyo*

(Received June 16, 1971)

Since the discovery of the dinitrogen-coordinated complex of a transition metal,[1] attention has been drawn to dinitrogen complexes of transition metals in relation to nitrogen fixation in biological systems. Molybdenum-dinitrogen complexes are especially interesting because of the key role of molybdenum in both chemical and biological nitrogen fixation. In previous papers[2] we reported briefly the preparation of molybdenum-dinitrogen complexes of the types $Mo(N_2)(PPh_3)_2 \cdot C_6H_5CH_3$ and *trans*-$Mo(N_2)_2(Ph_2PCH_2CH_2PPh_2)_2$ obtained by the reduction of molybdenum(III) acetylacetonate with trialkylaluminum in the presence of triphenylphosphine or 1,2-bis(diphenylphosphino)-ethane under a nitrogen atmosphere. In this communication we wish to report the crystal and molecular structure of the latter molybdenum-dinitrogen complex, *trans*-bis(dinitrogen)bis[1,2-bis(diphenylphosphino)-ethane]molybdenum(0), determined by three-dimensional X-ray analysis.

Orange crystals suitable for X-ray analysis were obtained by recrystallization of the complex from toluene/*n*-hexane. The specimen was sealed off in a thin-walled Pyrex capillary in a nitrogen atmosphere. Crystals are triclinic, space group $P\bar{1}$ with one molecule in a unit cell of dimensions, $a=10.64$, $b=12.63$, $c=10.51$Å, $\alpha=92.47$, $\beta=118.91$, and $\gamma=71.20°$. Intensity measurements were carried out on the four-circle diffractometer using monochromatized Mo$K\alpha$ radiation. A total of 3253 reflections were recorded in the range of $2\theta \leq 55°$. Lorentz and polarization corrections were made, absorption correction being neglected. The positions of molybdenum atom and two phosphorus atoms were determined from three-dimensional Patterson map. All other light atoms except hydrogen atoms then revealed their positions on three-dimensional electron density map calculated on the basis of molybdenum and phosphorus contributions. Structure was refined by block-diagonal least-squares with isotropic temperature factors, to an R factor of 0.148.

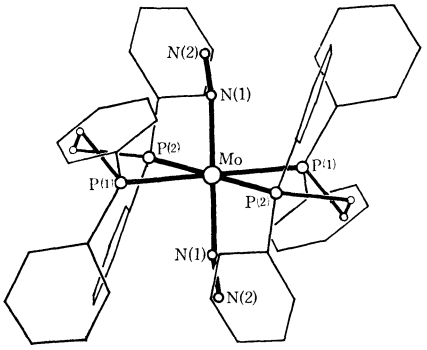

TABLE 1. BOND LENGTHS AND ANGLES

Bond length			Bond angle	
Mo–P(1)	2.50 Å	(0.004)	P(1)–Mo–P(2)	80.9°(0.1)
Mo–P(2)	2.45	(0.005)	N(1)–Mo–P(1)	87.3 (0.4)
Mo–N(1)	2.01	(0.012)	N(1)–Mo–P(2)	84.3 (0.5)
N(1)–N(2)	1.10	(0.02)	N(2)–N(1)–Mo	171.8 (1.1)

Values in parentheses indicate standard deviation.

Molybdenum atom occupies the center of symmetry, and four phosphorus atoms and *trans* two nitrogen molecules form a distorted octahedron. The end view along the b axis is shown above. The bond lengths and angles at this stage are summarized in Table 1. There is no significant elongation of the N–N bond upon coordination, as in the case of ruthenium- and cobalt-dinitrogen complexes.[3] The Mo–N bond length of 2.01 Å is not significantly shorter than a metal-nitrogen (M–N) single bond distance (1.95—2.15 Å). It is of great interest that the Mo–N–N entity is slightly bent in contrast to the M–N–N entities of ruthenium- and cobalt-dinitrogen complexes which are almost linear.[3]

Calculations were carried out at the Computer Center, the University of Tokyo, with programs of UNICS.

1) A. D. Allen and C. V. Senoff, *Chem. Commun.*, **1966**, 621.

2) M. Hidai, K. Tominari, Y. Uchida, and A. Misono, *ibid.*, **1969**, 814; *ibid.*, **1969**, 1392.

3) B. R. Davis, N. C. Payne, and J. A. Ibers, *Inorg. Chem.*, **8**, 2719 (1969); I. M. Treitel, M. T. Flood, R. E. Marsh, and H. B. Gray, *J. Amer. Chem. Soc.*, **91**, 6512 (1969); B. R. Davis and J. A. Ibers, *Inorg. Chem.*, **9**, 2768 (1970).

The Photosensitized Decomposition of Methane Adsorbed on Porous Vycor Glasses Coated with Metal Oxides at 77°K

Yuzaburo FUJITA, Keiichiro HATANO, Michiyasu YANAGITA, Takashi KATSU, Mitsuo SATO, and Takao KWAN

Faculty of Pharmaceutical Sciences, The University of Tokyo, Hongo, Bunkyo-ku, Tokyo

(Received June 18, 1971)

As has been reported previously, it has been found that various types of methyl radicals have been trapped at 77°K on the surface of porous Vycor glass (PVG).[1,2]

We were interested in the influence of the metal oxides coated on the surface of PVG on the photodecomposition mechanisms of methane, and so we studied the photolysis of methane at 77°K on various PVG surfaces (abbreviated PVG(V_2O_5) and so on) by the technique of ESR spectroscopy.[1] We have found an interesting new effect of these metal oxides; that is, the photosensitivity of these metal oxides for the formation of methyl radicals at 77°K was quite different from one metal oxide to the other.

Though some of these metal oxides are catalytically active for the oxidation of organics,[3] their photosensitivities have not yet been revealed.

In this communication we will report briefly some results on the photosensitivities of various oxides coated on the PVG for the formation of the methyl radical at 77°K.

Oxide-coated PVG samples were prepared as follows: after the leaching of a PVG rod (Corning #7930, 4 mmϕ, 1 cm in length, 38 m^2/sample) with concentrated nitric acid, an appropriate metal salt, for example, ammonium meta-vanadate (NH_4VO_3) for vanadium oxide, was absorbed from an aqueous solution in an amount sufficient for a coverage of θ=0.01—0.001%; the PVG thus treated was ignited at 500—600°C in air to convert the salt into an oxide.

A tenth of the monolayer amount of methane was then introduced at room temperature, followed by repeated oxidation and degassing at 500—600°C in a quartz sample tube. Irradiation of the sample tube was carried out at 77°K directly in a Dewar vessel inserted in the cavity of an ESR apparatus with a filtered light of an ultra-high-pressure mercury lamp (USH-500D, Ushio Electric Co., Ltd.).

Some representative results on the wavelength characteristics of the oxide-coated PVGs for the methyl radical formation at 77°K are shown in Fig. 1.

On these oxide-coated PVGs, the CH_3(II) or CD_3-(II), the so-called abnormal methyl radical (g=2.002, $A^H_{CH_3}$=19.3 G, $A^D_{CD_3}$=3.0 G),[1] was observed preferentially by the photolysis at 77°K; this methyl radical showed the characteristic linewidth alternation with a sharper line in the lower magnetic field.

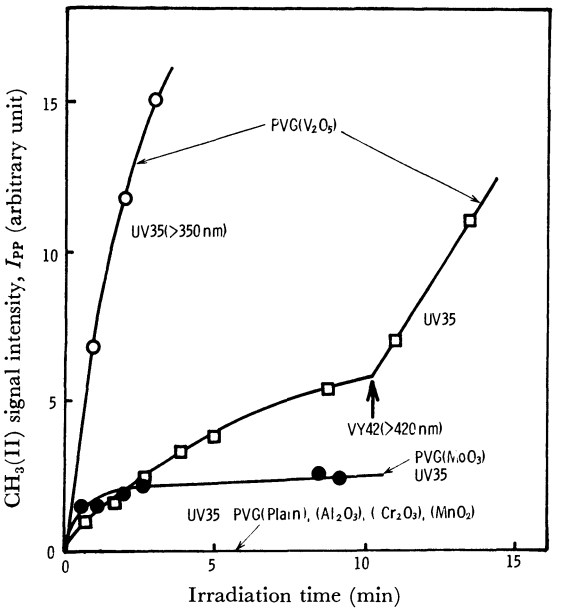

Fig. 1. Photosensitized formation of CH_3(II) radical on metal oxide coated PVGs.

The second hf line from the lower field (m_I=−½) with the largest peak-to-peak intensity, I_{pp}, was used as a monitor for the CH_3(II) radical concentration; its change with the irradiation time is plotted in Fig. 1.

The largest photosensitization was observed on the PVG(V_2O_5), and even a visible light larger than 420 nm showed a relatively large photosensitizing effect on the radical formation. Although the PVG(MoO_3) also showed the photosensitizing activity, its activity was less than that of the PVG(V_2O_5). On the PVG(plain) and PVG(Al_2O_3), no photosensitization was observed, and the CH_3(II) radical was observed only with the full light of a low-pressure mercury lamp. Here, it is very interesting that, on the PVG(MnO_2) and PVG-(Cr_2O_3), a "photodesensitization" was clearly observed, and that, in these cases, none of the methyl radical could be observed even with the full light of a low-pressure mercury lamp.

It may be worthy of note here that the oxides showing the "photodesensitization" are well known active oxidation catalysts, while, on the other hand, V_2O_5 and MoO_3 are considered to be weak oxidizing catalysts for the complete oxidation of methane.[4] Therefore, one can deduce that there is a reverse correlation between the radical trapping efficiencies and the oxidizing abilities of the oxide-coated PVGs.

When a trace of oxygen was present in the PVG-(V_2O_5)-CH_4 system, a large signal of a peroxyradical (g_1=2.002, g_2=2.01, g_3=2.03) was observed in place of the CH_3(II).

1) N. Shimamoto, Y. Fujita, and T. Kwan, This Bulletin, **43**, 580 (1970).

2) G. B. Garbutt and H. D. Gesser, *Can. J. Chem.*, **48**, 2685 (1970).

3) L. Ya. Margolis, *Adv. in Catalysis*, **14**, 429 (1963); H. H. Voge and C. R. Adams, *ibid.*, **17**, 151 (1967).

4) R. B. Anderson, K. C. Stein, J. J. Feenan, and L. J. E. Hofer, *Ind. Eng. Chem.*, **53**, 809 (1961).

Reaction of Photo-excited Phenanthraquinone with Dibenzyl Ether. Formation of an Adduct and its Decomposition studied by CIDNP Method.

Kazuhiro MARUYAMA and Tetsuo OTSUKI

Department of Chemistry, College of Liberal Arts and Science, Kyoto University, Kyoto

(Received June 18, 1971)

Whereas photo-excited phenanthraquinone reacts with alkyl aromatics showing enhanced PMR absorption signals for 1,2-adducts,[1] it reacts with dibenzyl ether showing an enhanced PMR emission signal for 1,4-adduct (Fig. 1-A). Dibenzyl glycol, phenyl benzyl ether, and hydroquinone dibenzyl ether undergo the same type of reaction showing all the enhanced PMR emission signals. Protons giving the enhanced signals are indicated in (1) and (2) (underlined). All these

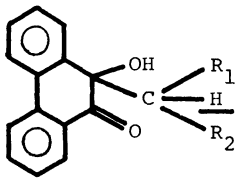

1,2-adduct
(1)

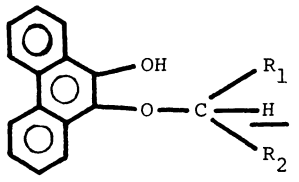

1,4-adduct
(2)

reactions are rationalized if we consider the hydrogen abstraction by photo-excited phenanthraquinone in n-π^* triplet state followed by recombination of the resulting radicals in a solvent cage, because none of the reactions are affected even if we use a UV-cut filter.[2] By comparing their PMR and/or IR spectra one can easily differentiate the 1,2-adduct and 1,4-adduct.[3]

1,4-Adduct which is transparent in visible region shows a slightly enhanced absorption signal (2 to 10 times) when it is irradiated with UV light and decomposes photochemically at an elevated temperature to give phenanthraquinhydrone, benzaldehyde, *sym*-diphenylethane, toluene and unidentified products.[4] During the course of photochemical decomposition we can observe the enhanced PMR absorption signal of the resulting benzaldehyde (due to formyl proton) (Fig. 1-B). When light was cut off, the enhanced signal decayed promptly. Thus, it is confirmed that the neutral molecule, *i.e.* benzaldehyde, produced by fragmentation of radical can take the nuclear spin polarized state. The photochemical decomposition is effective only with UV light. No such enhanced signal of benzaldehyde could be observed when we applied a UV-cut filter.[5]

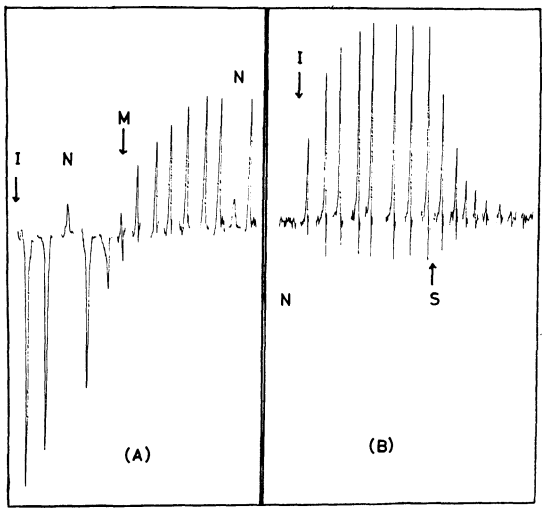

Fig. 1. (A) Enhanced PMR signals of 1,4-adduct (τ: 4.12) observed in the photochemical reaction of phenanthraquinone with dibenzyl ether (70°C). I: Irradiation initiated. N: The normal signal of the accumulated adduct under no irradiation. I→M: Enhanced emission signals. M: Enhanced emission and absorption signals balance, and nearly all of the phenanthraquinone in the reaction system is consumed.
(B) Enhanced PMR signals of benzaldehyde (τ: 0.35) observed in the photochemical decomposition of the 1,4-adduct (90°C). N: No irradiation. I: Irradiation initiated. I→S: enhanced absorption signals of benzaldehyde. S: Irradiation stopped.

1) K. Maruyama, H. Shindo, and T. Maruyama, This Bulletin, **44**, 585 (1971); K. Maruyama, T. Otsuki, H. Shindo, and T. Maruyama, *ibid.*, **44**, 2000 (1971).

2) A 500 W high pressure Hg lamp as a light source and a Toshiba V-Y 42 filter were used. A 60 MHz C-60HL NMR spectrometer manufactured by JEOL was used.

3) 1,2-Adducts show the following characteristic spectra;
IR, ν_{OH}: sharp ~3500 cm^{-1}, $\nu_{C=O}$: 1690 cm^{-1}
PMR, τ_{OH}: ~6.0 region, $\tau_{methine\ or\ methylene}$: ~7.0 region
1,4-Adducts show the following characteristic spectra;
IR, ν_{OH}: broad ~3300 cm^{-1}, $\nu_{C=O}$: none
PMR, τ_{OH}: in phenolic OH region, $\tau_{methine\ or\ methylene}$: 4.0—5.0 region

4) These decomposition products were identified by PMR, TLC, GLC, and chemical analyses.

5) 1,4-Adduct can decompose also thermally very slowly without any light. However, no PMR enhanced signal could be observed during the course of the reaction.

ESR Spectrum of Triplet Species in Würster's Red Perchlorate

Michiya Itoh

Faculty of Pharmaceutical Sciences, The University of Tokyo, Bunkyo-ku, Tokyo

(Received June 23, 1971)

Numerous investigations have been carried out on the electronic and magnetic properties of Würster's salts in both solution and solid. Thomas *et al.*[1] reported a triplet species in a single crystal of Würster's blue perchlorate (WBP) below the temperature of the phase transition (186°K), and suggested the dimerization of the cation through small molecular displacement in the crystal below transition point. Sakata and Nagakura[2] showed that the intensity of the charge transfer band between the cation in the solid WBP increased remarkably below transition temperature. Oohashi *et al.*[3] reported the extremely strong charge transfer band in solid Würster's red perchlorate (WRP), compared with those of WBP and of Würster's red bromide (WRB). No crystal sturcture of WRP was reported, while the cation in the solid WRB was reported by Tanaka and Mizuno[4] to be stacked at equal distances from each other.

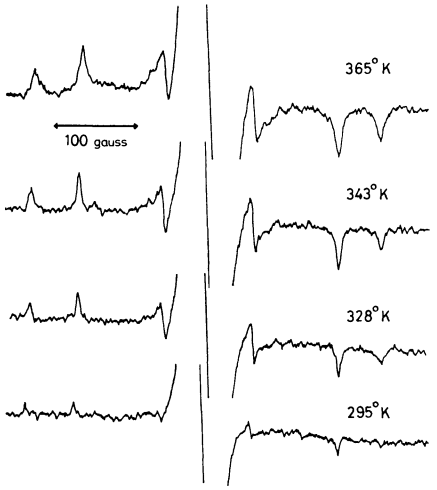

Fig. 1. The ESR spectra of the solid Würster's red perchlorate with random orientation at various temperatures.

We observed the ESR spectrum of triplet species in the powdered WRP[5] for the first time at various temperatures ranging from 290°K to 370°K. The results suggest the dimer structure of the cation in the solid WRP. Figure 1 shows a strong signal at $g=\sim 2.002$, and weak signals characteristic to the triplet species with random orientation at various temperatures. The ESR signals due to the triplet species showed reversible increment with increasing temperature up to the melting point of the crystal, while the central signal increased irreversibly with temperature. This might be due to the paramagnetic impurity decomposed in the crystal with increasing temperature. From three pairs of lines in ESR spectrum the zero-field splitting parameters were obtained to be $D=0.0189\ \mathrm{cm^{-1}}$ and $E=0.0098\ \mathrm{cm^{-1}}$ with $2D=406$ gauss.[6] The D value is consistent with a spin-spin dipolar interaction for an average distance of 5.1 Å.[7]

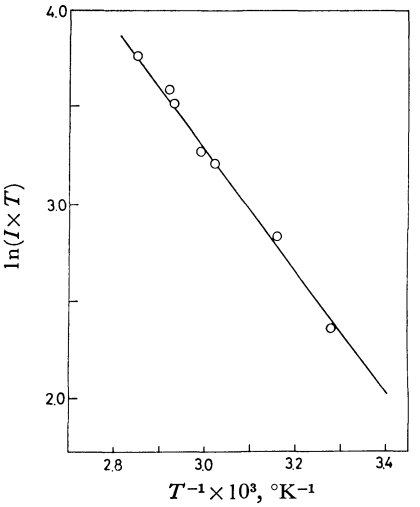

Fig. 2. Temperature dependence of the ESR spectrum due to the triplet species. Intensity of the signal obtained actually from the Y component[6] is in arbitary unit.

Figure 2 shows a linear relationship of $\ln(IT)$ against $1/T$, where I is the intensity of the ESR signal due to the triplet at various temperatures. From a slope of the straight line in Fig. 2, a singlet-triplet separation J was obtained to be $2100\pm 200\ \mathrm{cm^{-1}}$, where $I\propto \exp(-J/kT)$ was assumed because of $J\gg kT$. The value of J so obtained was compared with that in WBP (235—$246\ \mathrm{cm^{-1}}$).[1,2] The present results suggest that the WRP crystal consists of the dimer structure of the cation *at room temperature*. The large singlet-triplet separation is consistent with the extremely strong charge transfer band in WRP, and with the first observation of the ESR spectrum due to the triplet in the ion radical salts *at room temperature*.

1) D. D. Thomas, H. Keller, and H. M. McConnell, *J. Chem. Phys.*, **39**, 2321 (1963).
2) T. Sakata and S. Nagakura, This Bulletin, **42**, 1497 (1969).
3) Y. Oohashi, T. Sakata, and S. Nagakura, The work was presented at the Symposium of Molecular Structure and Spectra, Tokyo (October, 1970).
4) J. Tanaka and M. Mizuno, This Bulletin, **42**, 1841 (1969).
5) The author is indebted to Drs. T. Sakata and Y. Oohashi for supplying a pure sample of WRP.
6) E. Wasserman, L. C. Snyder, and W. A. Yager, *J. Chem. Phys.*, **41**, 1763 (1964).
7) N. Hirota and S. I. Weissman, *J. Amer. Chem. Soc.*, **86**, 2538 (1964).

Glassy Liquid Crystal of the Nematic Phase of *N*-(*o*-Hydroxy-*p*-methoxybenzylidene)-*p*-butylaniline

Michio Sorai and Syûzô Seki

Department of Chemistry, Faculty of Science, Osaka University, Toyonaka, Osaka

(Received June 25, 1971)

In general, glass transition takes place through a delicate balance between the relaxation time of molecular motion and the time scale of observation. The ordinary glassy state can be established by quenching many supercooled liquids below their glass transition points without crystallization, and by other suitable procedures.[1-3] Adachi *et al.*[4] reported the possible existence of glassy state even in crystalline materials as the non-equilibrium state of many plastic crystals. We also reported the new finding of glassy state in the metastable liquid crystal of cholesteryl hydrogen phthalate (CHP) and proposed to designate this state as "**glassy liquid crystal.**"[5]

N-(*p*-Methoxybenzylidene)-*p*-butylaniline (MBBA)[6] is a rare example of nematic liquid crystal at room temperature and has widespread applications to display devices, but the material is relatively unstable against cleavage or reaction of the anil linkage. In contrast, OHMBBA, an *o*-hydroxy analog of MBBA which was recently synthesized,[7] has an intramolecular hydrogen bonding stabilizing the anil linkage. The melting point T_m of OHMBBA is 44°C and the enantiotropic transition T_{tr} from the nematic mesophase to the isotropic liquid is 64.5°C.

OHMBBA of special grade obtained from Tokyo Ohka Kogyo Co., Ltd. was dried in a vacuum by a freeze-and-thaw technique for 24 hr. Differential thermal analysis (DTA) was carried out. Typical results are illustrated in Fig. 1. Run 1 shows a heating curve of crystalline OHMBBA with a rate of 2.5K/min. Run 2 gives a cooling curve of the isotropic liquid with a rate of −12K/min. The transition from the isotropic

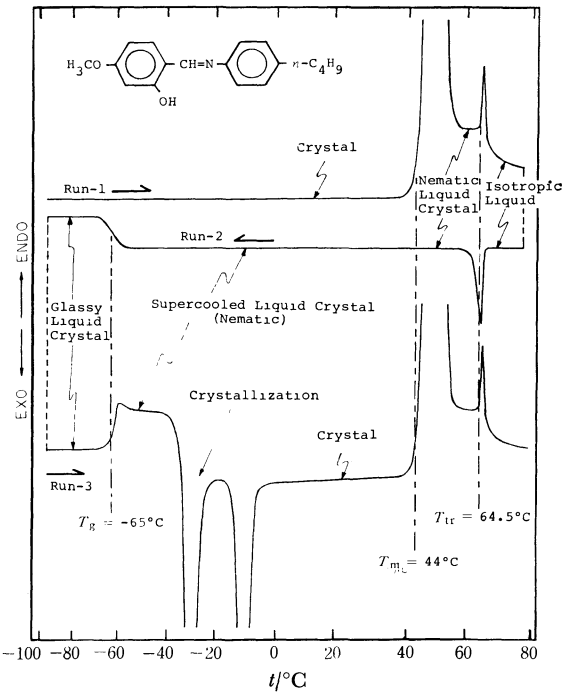

Fig. 1. DTA curves for *N*-(*o*-hydroxy-*p*-methoxybenzylidene)-*p*-butylaniline.

liquid to the nematic phase was observed even in a rapid cooling as fast as −80K/min. When the cooling rate was greater than −10K/min, the nematic mesophase was easily quenched to give a glassy state. Run 3 shows a heating curve of the glassy liquid crystal with a rate of 2.5K/min. A clear glass transition phenomenon was observed at −65°C. On further heating, the supercooled nematic liquid crystal was transformed into a stable crystal through a crystallization process around −30°C. The values of T_m and T_{tr} agree well with the previous data.[7]

Thus we found a glass transition phenomenon for a *stable* liquid crystal, but in the case of CHP it was observed only for a *metastable* one. In this respect, OHMBBA may be more appropriate material than CHP for studying the glass transition phenomenon in liquid crystals.

1) M. Sugisaki, H. Suga, and S. Seki, This Bulletin, **41**, 2581, 2591 (1968).
2) N. Onodera, H. Suga, and S. Seki, *J. Non-Cryst. Solids*, **1**, 331 (1969).
3) N. Onodera, H. Suga, and S. Seki, This Bulletin, **41**, 2222 (1968).
4) K. Adachi, H. Suga, and S. Seki, *ibid.*, **41**, 1073 (1968); **43**, 1961 (1970); **44**, 78 (1971).
5) K. Tsuji, M. Sorai, and S. Seki, *ibid.*, **44**, 1452 (1971).
6) H. Kelker and B. Scheurle, *Angew. Chem.*, **81**, 903 (1969).
7) I. Teucher, C. M. Paleos, and M. M. Labes, *Mol. Cryst. and Liq. Cryst.*, **11**, 187 (1970).

A Mass Spectrometric Study of the Reaction of Hydrogen Atom with Butadiene

Seiichiro KODA and Tsutomu HIKITA

Department of Reaction Chemistry, Faculty of Engineering, University of Tokyo, Hongo, Bunkyo-ku, Tokyo

(Received June 25, 1971)

The reaction of hydrogen atom with simple olefins has been extensively investigated,[1-4] but few studies have been published on the reaction kinetics of hydrogen atom with conjugated dienes. In this communication, we describe the evidence for the existence of butenyl radical in the reaction of hydrogen atom with 1,3-butadiene, and suggest the reaction mechanism in a low pressure reaction with a relatively high concentration of hydrogen atom, in comparison with the reaction of butenes with hydrogen atom now under investigation.

Hydrogen atoms produced by a 2450 MHz microwave discharge in the mixture of about 20% hydrogen in agron, are introduced into a Pyrex reaction tube with a flow velocity of about 4 m/sec at 0.38 Torr (total pressure: Ar, 0.31 Torr: H_2, 0.07 Torr). Butadiene is added *via* a movable inner tube to control the reaction time in the range of 2—30 msec. The reaction is studied at room temperature. The reaction products are fed into a time-of-flight-type mass spectrometer through a pin hole positioned at the end of the reaction tube.

The analysis of the mass spectra shows that butenes (1-, *trans*-2-, and *cis*-2-butene), propylene, ethane, and methane are the main reaction products, and that *n*-butane, propane, and ethylene are minor ones. For example, the reaction at the initial concentration of butadiene of 4.6×10^{-8} mol/*l* and of hydrogen atom[1] of 2.0×10^{-7} mol/*l* at the total pressure of 0.38 Torr is explained at the reaction time of 8.1 msec as $C_4H_6 \rightarrow 0.70C_4H_8 + 0.19C_3H_6 + 0.04C_2H_6 + 0.04CH_4 +$ other minor products. Some pentenes and several species which have an eight-carbon-structure are also detected.

In this analysis, the peak intensities of $m/e=55$ in the spectrum are in excess compared with those calculated from the standard mass spectral patterns of the above products. In order to decide what product contributes to the $m/e=55$ peak, the ionization efficiency curve was observed as shown in Fig. 1. The appearance potential is 7.7 eV lower than the ionization potential of argon atom,[5] *i.e.*, 15.8—7.7=8.1 eV. This value agrees fairly well with that of 2-butenyl(α-methylallyl) radical[6] 7.7 eV our data, 8.1 eV is considered to be slightly higher than the true value, because our method gives slightly higher potentials than true ones, for example, that of butadiene is measured to be 9.3 eV (9.0—9.2 eV[5]). It was slso reported that 2-butenyl radical was detected by means of electron spin resonance in the reaction of butadiene with hydrogen at 77°K.[7]

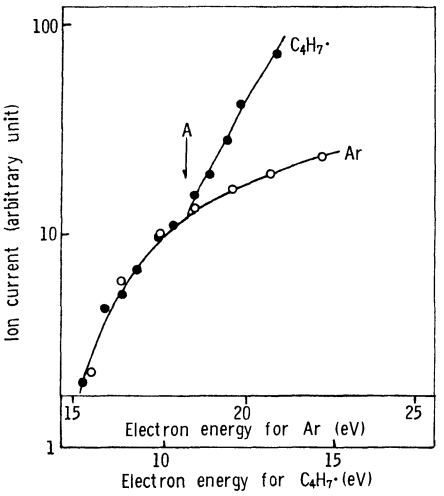

Fig. 1. Ionization efficiency curve of butenyl radical in the reaction mixture
reaction conditions
$[\text{butadiene}]_{\text{initial}}=1.0\times10^{-7}$ mol/*l*
$[\text{hydrogen}]_{\text{initial}}=1.3\times10^{-7}$ mol/*l*
reaction time, 2.7 msec; total pressure, 0.38 Torr at room temperature.
Point A shows the beginning of the contribution of fragment ions from other species in the reaction mixture.

From the above results and consideration on the reactions of butenes, propylene and ethylene[1] with hydrogen atom, the following successive reactions are concluded to be dominant in the present condition. The ratios of decomposition reactions *vs.* stabilization reactions from the hot species (hot butenyl radial and hot butenes) are considered to be small, from the distribution of the reaction products.

$$C_4H_6 + H \longrightarrow C_4H_7\cdot{}^* \longrightarrow C_4H_7\cdot$$
$$\qquad\qquad\qquad\qquad\qquad\qquad\quad \downarrow \longrightarrow \text{decomposition (minor)}$$
$$C_4H_7\cdot + H \longrightarrow C_4H_8{}^* \longrightarrow C_4H_8$$
$$\qquad\qquad\qquad\qquad\qquad\qquad\quad \downarrow \longrightarrow \text{decomposition (minor)}$$
$$C_4H_8 + H \longrightarrow C_3H_6,\ C_2H_6,\ CH_4, \text{ and others}$$

(* means hot species)

The apparent second-order reaction rate constant of butadiene with hydrogen atom was determined to be $(1.1—1.7)\times10^9$ *l*/mol·sec at the above total pressure, by measuring the decreasing rate of butadiene.

1) S. Tsuchiya, F. Ishihara, S. Tashiro, and T. Hikita, This Bulletin, **42**, 847 (1969).
2) J. R. Barker, D. G. Keil, J. V. Michael, and D. T. Osborne, *J. Chem. Phys.*, **52**, 2079 (1970).
3) M. P. Halstead, D. A. Leathard, R. M. Marshall, and J. H. Purnell, *Proc. Roy. Soc.*, **316**, 575 (1970).
4) E. E. Daby and H. Niki, *J. Chem. Phys.*, **51**, 1255 (1969).
5) J. L. Franklin, J. G. Dillard, H. M. Rosenstock, J. T. Herron, and K. Draxl, "Ionization Potentials, Appearance Potentials, and Heat of Formation of Gaseous Positive Ions," National Bureau of Standards, Washington (1969).
6) C. A. McDowell, F. P. Lossing, I. H. S. Henderson, and J. B. Farmer, *Can. J. Chem.*, **34**, 345 (1956).
7) C. U. Morgan and K. J. White, *J. Amer. Chem. Soc.*, **92**, 3309 (1970).

Reaction Kinetics of the Redox Decomposition of Hydroxymercurated Propylene in Aqueous Solution Followed by Time-Sequential NMR Spectroscopy

Masashi MATSUO and Yasukazu SAITO

Department of Synthetic Chemistry, Faculty of Engineering, The University of Tokyo, Bunkyo-ku, Tokyo

(Received December 15, 1970)

The redox decomposition process of hydroxymercurated propylene in aqueous solution yielding acetone has been followed by time-sequential NMR spectroscopy *in situ*. No reaction intermediates and reaction products other than acetone were observed. Stoichiometric relationship holds between the reactant and the product during the reaction, which was verified by NMR spectra. The reaction rate was confirmed to be of first order with respect to mercurial. Although the rate was accelerated at higher acidity in solution, a similar rate enhancement took place by addition of neutral salts. At a certain ionic strength, no close linear correlation between the apparent rate constants and proton concentration was observed. In contrast, excellent linear dependence was obtained by the thermodynamic activities of the added electrolytes including acid. Since the apparent rate constant was independent of the concentration of free mercuric ion, a monomolecular mechanism is proposed. Taking into account the rate dependence upon added electrolytes, the redox decomposition of the hydroxymercurated olefins to give carbonyl compounds seems to proceed only when an aquo ligand is removed from the carbon-bonded mercuric ion.

Olefin oxidation by metal ions in aqueous solution has long been investigated from the industrial, synthetic, and mechanistic viewpoints, with a good deal of knowledge compiled for Pd(II)[1] and Tl(III)[2] as well as for Hg(II).[3-5] Similarities and contrasts were pointed out by Henry between Pd(II) and Tl(III) in olefin oxidation.[6] Although common reaction products, *i.e.*, saturated carbonyl compounds, are obtainable,[5] little attention has been paid to Hg(II) oxidation. In order to elucidate the catalytic oxidation of olefins with metal ions, comparison from the mechanistic viewpoint seems to be indispensable between Pd(II), Tl(III), and Hg(II) oxidation. The reaction schemes of the σ-complex formation *via* π-complex intermediates are commonly postulated for these metal ions toward olefins. In the case of Hg(II), σ-complex is considered to be formed *via* mercurinium ion, a π-complex intermediate.[7] The redox decomposition of the σ-complexes is known to proceed fast for both Pd(II) and Tl(III) oxidation, but slowly for Hg(II) oxidation, which is ascribed to the stability of β-hydroxyalkylmercury(II) complexes. Thus information concerning the redox decomposition step of σ-complexes can only be afforded by studying Hg(II) oxidation.

The first order kinetics with respect to free mercuric ion was confirmed for the formation of unsaturated carbonyl compounds.[3] However, proton dependence on the rates of redox decomposition has never been investigated in spite of the following facts. (1) The rate of hydroxymercuration of olefins[8] is independent of proton concentration. (2) The rate of deoxymercuration yielding original olefins[7] is dependent on proton concentration, since proton is incorporated in the pre-equilibrium step of deoxymercuration. In the present work, kinetics on both proton and free mercuric ion as well as neutral salt effects were studied in order to elucidate the reaction mechanism of the redox decomposition of hydroxymercurated olefins yielding saturated carbonyl compounds. The time-sequential NMR spectroscopy was adopted to monitor the reaction, since it affords the possibility for detecting reaction intermediates, if any.

Experimental

Materials. All the reagents were of G.R. grade, prepared by Kojima Kagaku Co., Ltd. (Tokyo), and were used without further purification. Absence of impurities was confirmed by gas chromatography using a β,β′-dioxypropionitrile column for each gaseous olefin prepared by Takachiho Kagaku Kogyo Co., Ltd. (Tokyo). Mercuric solutions were prepared by dissolving mercuric nitrate into concentrated nitric acid, which was diluted with ion-exchanged water up to a given concentration. The concentration of mercuric ion was determined by titration with potassium thiocyanate.

Procedure. Propylene was introduced from the cylinder for 2 min at room temperature into 10 m*l* of the aqueous solution consisting of 6.5 g (20 mmol) of mercuric nitrate and 0.69 g (11 mmol) of nitric acid with or without additional electrolytes. The concentration dependence of the free mercuric ion was studied for the series of solutions consisting of a certain amount of hydroxymercurated propylene and of various amounts of free mercuric ion. The concentration of hydroxymercurated propylene, which is stable at room temperature, was determined from the NMR peak intensity by comparing it with that of the external tetramethylsilane reference.

The time-sequential NMR spectra were obtained at a given temperature with a JEOL C-60 NMR spectrometer constructed by Japan Electron Optics Laboratory Co. Ltd. The reaction temperature was regulated by blowing cooled nitrogen gas and determined by the relative chemical shifts of 1,3-propanediol. The reaction was thus followed by NMR spectroscopy *in situ*.

1) a) E. W. Stern, "Catalysis Reviews," Vol. I. (1968), p. 74; b) A. Aguilo, "*Adv. Organometal. Chem.*," Vol. V. (1967), p. 321.
2) P. M. Henry, *J. Amer. Chem. Soc.*, **87**, 990, 4423 (1965); **88** 1597 (1966).
3) B. C. Fielding and H. Roberts, *J. Chem. Soc., A*, **1966**, 1627.
4) J. C. Strini and J. Metzer, *Bull. Soc. Chem. Fr.*, 3145, 3150 (1966).
5) Y. Saito and M. Matsuo, *J. Organometal. Chem.*, **10**, 524 (1967).
6) P. M. Henry, *Adv. Chem. Ser.*, **52**, 126 (1968).
7) W. Kitching, *Organometal. Chem. Rev.*, **3**, 61 (1968) and references therein.
8) J. Halpern and H. B. Tinker, *J. Amer. Chem. Soc.*, **89**, 6427 (1967).

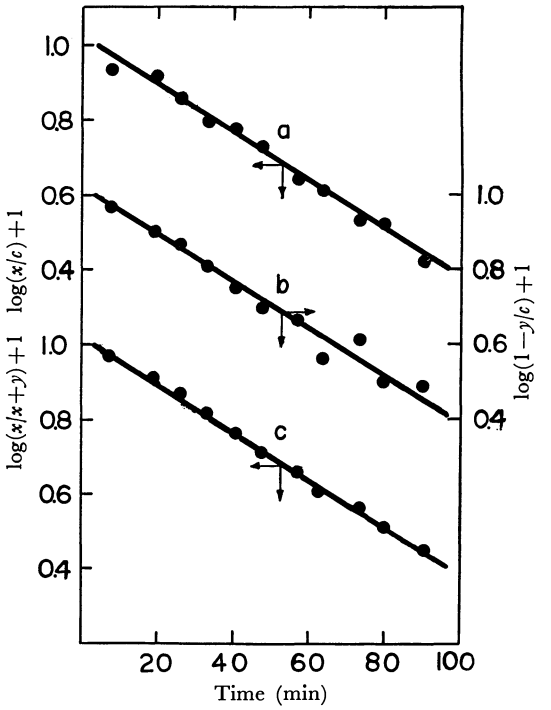

Fig. 1. Reaction kinetics represented by the following three equations.
a. $\ln[x/c]=-kt$
b. $\ln[1-(y/c)]=-k't$
c. $\ln[x/(x+y)]=-k''t$
where x and c are the concentrations of hydroxymercurated propylene at time t and $t=0$, respectively, and y is that of acetone at time t.

The first order rate equation for the redox decomposition with respect to hydroxymercurated olefin was ascertained previously[5] by comparing three kinds of parallel straight lines, obtained from the peak decrease of the reactant mercurial *versus* the external reference, from the peak increase of the product ketone *versus* the reference, and from mercurial *versus* ketone without intermediary of tetramethylsilane. A typical example of the analysis is shown in Fig. 1.

Calculation of thermodynamic activities of electrolytes. With regard to the estimation of thermodynamic activities, the square root of ionic strength is not a good measure of concentrations higher than *ca.* 0.1 molality in aqueous solution. However, it was verified at elevated temperatures that the logarithms of the activity coefficient of hydrogen chloride in aqueous solution mixed with sodium chloride or of hydrogen bromide mixed with potassium bromide varied linearly with concentration up to about 3 molality.[9]

It is assumed, therefore, that a linear relationship holds between the logarithm of the activity coefficient of a certain electrolyte in aqueous solution and the concentration of the added electrolyte in the present solutions as well. Since the activity coefficients of electrolytes such as nitric acid, lithium nitrate, sodium nitrate, potassium nitrate, and sodium perchlorate in aqueous solution as a single component are all available up to highly concentrated regions,[10] the values of the activity coefficients of each electrolyte in the mixed aqueous solution can thus be calculated on the basis of the above-mentioned assumption.

9) M. L. Lietzke, *J. Phys. Chem.*, **69**, 2395 (1965).
10) R. Parsons, Handbook of Electrochemical Constants, Butterworths, New York (1959), p. 20.

Results

Dependence of Reaction Rates on Acid and Salt Concentration. Although the rate of the redox decomposition of hydroxymercurated propylene yielding acetone[5] was determined to be first order with respect to the concentration of hydroxymercurated propylene, no kinetic investigation concerning the concentration of either proton or free mercuric ion has been carried out. At a certain ionic strength, *i.e.*, $\mu=9.49$, regulated by adding either lithium nitrate, sodium nitrate, or potassium nitrate, the concentration of nitric acid increased and monotonous enhancement of rate constants was obtained at 45.6°C as shown in Fig. 2.

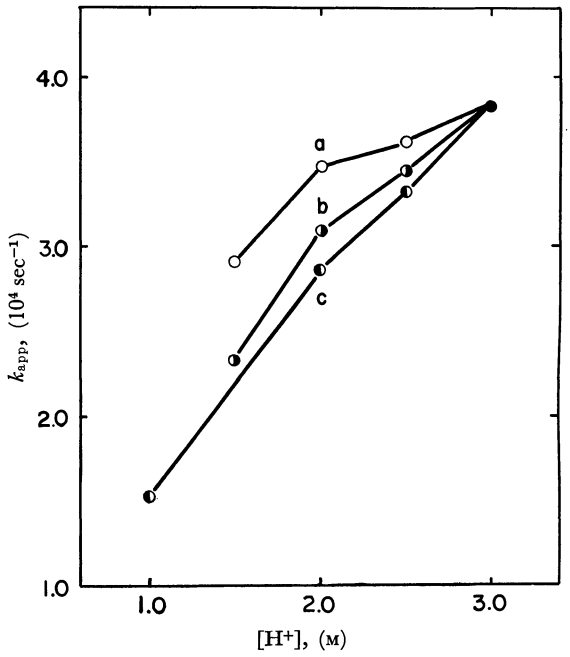

Fig. 2. Apparent rate constants of hydroxymercurated propylene yielding acetone as a function of proton concentration at constant ionic strength regulated by nitrates.
a. $LiNO_3$, b. $NaNO_3$, c. KNO_3

When the concentrations of nitric acid and the neutral salts cited above increased with no control in ionic strength, a similar monotonous enhancement was observed (Fig. 3).

Dependence of the Reaction Rates on Acid and Salt Activity. Excellent linear relationship between the rate constants and the estimated thermodynamic activities of added electrolytes were found for nitric acid, lithium nitrate, sodium nitrate, potassium nitrate, and sodium perchlorate (Fig. 4).

A better linearity is found in Fig. 4 than in Fig. 3. The apparent rate constants are, therefore, not correlated to the concentrations but to the activities of added electrolytes. All the results are summarized in Table 1.

The rate equation to yield acetone from hydroxymercurated propylene, given previously as

$$v = k_{app}\,[\text{mercurial}], \qquad (1)$$

should be expressed as

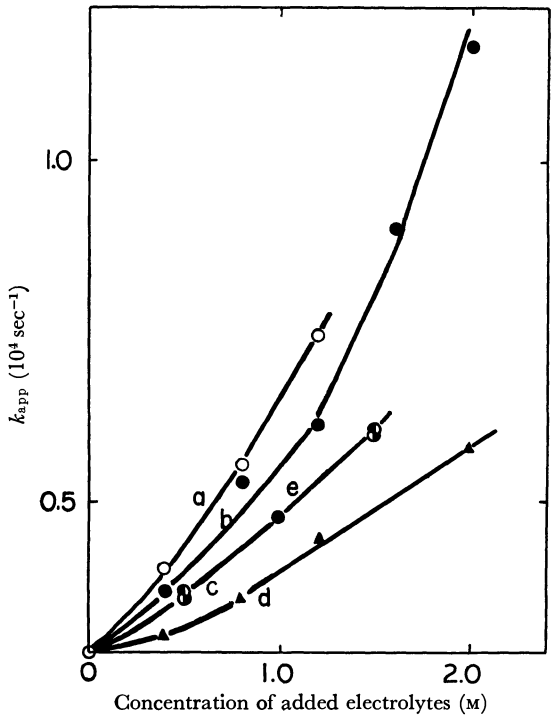

Fig. 3. Plots of apparent rate constants of hydroxymercurated propylene yielding acetone as a function of the concentrations of added electrolytes.
a. HNO_3, ○ b. $LiNO_3$, ● c. $NaNO_3$, ◑
d. KNO_3, △ e. $NaClO_4$, ◐

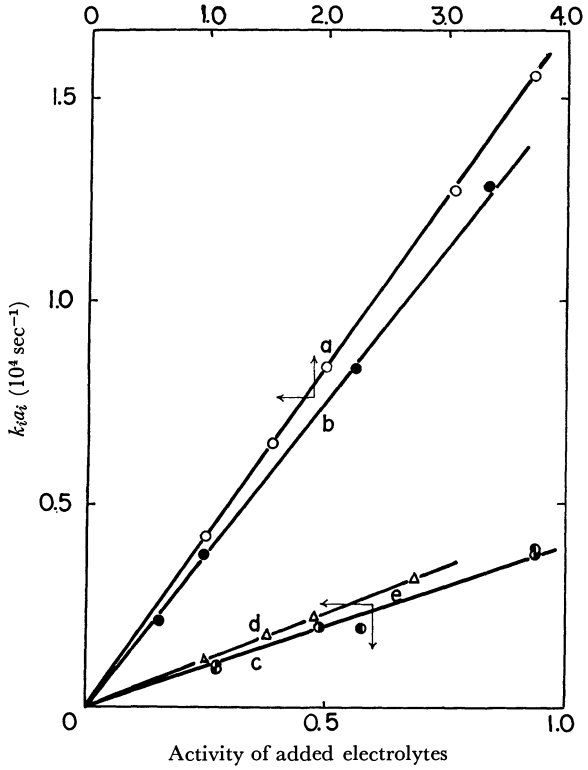

Fig. 4. Correlation of apparent rate constants of hydroxymercurated propylene yielding acetone with the thermodynamic activities of added electrolytes.
a. HNO_3, ○ b. $LiNO_3$, ● c. $NaNO_3$, ◑
d. KNO_3, △ e. $NaClO_4$, ◑

Table 1. Apparent rate constants of the redox decomposition of hydroxymercurated propylene in correlation to the concentration and the activity of added electrolytes

Added acid Concentration	activity (M)	Added salts Concentration	activity (M)	k_{app} (sec^{-1})
HNO_3		$LiNO_3$		
1.60	1.67	0.04	0.48	9.8×10^{-3}
	1.78	0.80	1.00	13.4
	2.17	1.60	2.38	20.3
	2.58	2.00	3.32	26.0
HNO_3		$NaNO_3$		
1.60	1.69	0.50	0.29	10.3
	1.87	1.00	0.51	12.3
	2.13	1.50	0.91	15.2
HNO_3		KNO_3		
1.60	1.67	0.40	0.27	8.3
	1.87	0.80	0.39	9.2
	1.98	1.20	0.49	10.7
	2.58	2.00	0.69	14.2
HNO_3		$NaClO_4$		
1.60	1.69	0.50	0.30	10.8
	1.87	1.00	0.61	12.0
	2.13	1.50	0.93	15.4
HNO_3				
1.20	1.08			5.2
1.60	1.52			7.3
2.00	2.16			9.3
2.40	2.96			12.1
2.80	3.65			16.3

$$v = (k_0 a_0 + k_i a_i)\ [\text{mercurial}], \qquad (2)$$

where k_0 and a_0 are the rate constant and the thermodynamic activity of HNO_3, and k_i and a_i are the corresponding quantities of added neutral salts. The rate constant k_0 for HNO_3 was obtained as 4.5 g/sec·mol and k_i for $LiNO_3$, $NaNO_3$, KNO_3, and $NaClO_4$ as 4.0, 4.8, 5.2, and 4.8 g/sec·mol, respectively. The effect of nitric acid on rate enhancement was thus eventually equal to that of neutral salts.

Dependence of Reaction Rates on Free Mercuric Ion Concentration. The apparent rate constants given in Eq. (1) were independent of the concentrations of free mercuric ion as shown in Fig. 5. The first order kinetics with respect to free mercuric ion was established for acrolein formation from hydroxymercurated propylene.[3] The reaction kinetics of acetone formation from the same reactant is in contrast to that of acrolein formation. Although both are redox decomposition products of hydroxymercurated propylene, it is to be noted that the change of oxidation state of the former is four, while that for the latter is two.

Time-sequential NMR Spectra for Monitoring the Reaction. No reaction intermediates or products other than acetone were recognized and no chemical shifts of the mercurial signals during the reaction process were observed in the time-sequential NMR spectra. Stoichiometric relationships between the reactant mercurial and the product acetone were confirmed from peak heights.

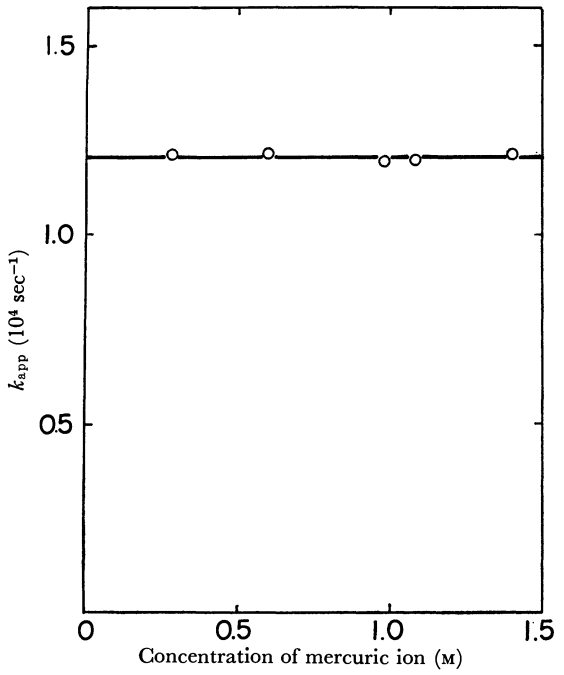

Fig. 5. Apparent rate constants of hydroxymercurated propylene yielding acetone as a function of the concentration of free mercury(II) ions.

Discussion

Influence of the Activities of Added Electrolytes on Reaction Rates. It should be noted that the concentration level of the electrolytes adopted in the present work is far higher than the values ordinarily used for the reactions in aqueous solutions[11] due to the need of NMR observation. This is why considerations were made not only on concentrations but also on activities, and the activity coefficients of electrolytes were calculated by the above-mentioned method.

As far as a reaction of first order with respect to a reactant A (including a pre-equilibrium step $A+B \rightleftharpoons C \rightarrow X+Y$) is concerned, the rate equation is given by

$$v = k_{app}[A] = k_0[C], \quad (3)$$

where k_{app} and k_0 are apparent and true rate constants, respectively. Since the equilibrium constant K is given as the ratio of activities,

$$K = \frac{a_C}{a_A a_B} = \frac{[C]}{[A][B]} \frac{\gamma_C}{\gamma_A \gamma_B} \quad (4)$$

the following rate equation is derived.

$$v = k_0 K \frac{\gamma_A \gamma_B}{\gamma_C}[A][B] = k a_B[A] \quad (5)$$

where $k=k_0 K \gamma_A/\gamma_C$ is used for brevity. By comparing Eqs. (3) and (5), a linear relationship between k_{app} and a_B would be anticipated for the runs of different high concentration levels of B, as far as the participation of the substance B to the reaction is expected at the pre-equilibrium step.

With regard to the redox decomposition reaction of hydroxymercurated propylene followed by NMR spectroscopy *in situ*, it has been ascertained in Fig. 3 and Fig. 4 that a linear correlation with the reaction rates is not obtained for the concentrations but for the activities of the added electrolytes. This would suggest the participation of these added electrolytes to the reaction at a pre-equilibrium step, since the electrolytes can reduce water activities of the solutions, with an aquo ligand replaced from the mercurial to the electrolyte. In other words, the step of an aquo ligand removal from the carbon-bonded mercuric ion would be assumed prior to its redox decomposition as follows.

$$CH_3CH(OH)CH_2Hg^+(OH_2) + MX \rightleftharpoons CH_3CH(OH)CH_2Hg^+ + MX(OH_2) \quad (6)$$

$$CH_3CH(OH)CH_2Hg^+ \longrightarrow CH_3COCH_3 + Hg(0) + H^+ \quad (7)$$

Although water activities in the solutions can be calculated by use of the Gibbs-Duhem equation, no additional data processing was made, as undesirable decrease in reliability might take place in high concentration region.

It is known that the rate of ethylene oxidation by Tl(III) in aqueous solution is of first order in the concentration of both Tl(III) and ethylene.[2] The rate is considerably accelerated by increasing salt concentration, the effect being related also to changes in the activity of water. It was presumed that more complexing between the metal ions and olefins would occur at lower water activity,[12] since the lower the activity of water in the solution, the more vacant the ligand sites for the metal ions.

A similar acceleration with the increase of the ionic strength of the solution is also recognized in aromatic mercuration.[13]

No Rate Dependence on Free Mercuric Ion. First order kinetics with respect to the concentrations of both the mercurial and the free mercuric ion were reported for acrolein formation from hydroxymercurated propylene in similar acidic aqueous media.[3] As for acrolein formation, the four equivalent oxidation is necessary in total, whereas acetone is made by two equivalent oxidation. It seems, therefore, reasonable that zero order dependence on the free mercuric ion was found in the present reaction. Moreover, lack of incorporation of free mercuric ion in either pre-equilibrium steps or the rate-determining process for this two-equivalent oxidation reaction would suggest a monomolecular mechanism in which two-electron transfer takes place. It does not necessarily mean that metallic mercury is found in the reaction products, because the following disproportionation reaction is fast and the equilibrium is much favored to Hg^{2+} side.[14]

$$Hg(0) + Hg^{2+} \rightleftharpoons Hg_2^{2+} \quad (8)$$

11) S. Glasstone, K. J. Laidler, and H. Eyring, "The Theory of Rate Processes", McGraw-Hill, New York (1941), p. 400.

12) F. Basolo and R. G. Pearson, "Mechanism of Inorganic Reactions," 2nd ed., John Wiley and Sons, New York, (1967) p. 598.

13) C. Perrin and F. H. Westheimer, *J. Amer. Chem. Soc.*, **85**, 2773 (1963).

14) F. A. Cotton and G. Wilkinson, "Avanced Inorganic Chemistry," Intsci. Publ., New York, (1962) p.481.

Reaction Process Followed by Time-sequential NMR Spectroscopy. Generally speaking, chemical species prevailing in spectroscopy are not necessarily prevailing kinetically for reaction processes. As for spectroscopic approach to reaction analysis, monitoring the reaction process *in situ* is important for this reason. The time-sequential NMR spectroscopy is advantageous not only in qualitative discrimination or quantitative identification but also in molecular characterization of chemical species concerned, especially for reaction intermediates, if they exist above the detection level of high resolution NMR spectroscopy.

In the present reaction the concentration of the reaction intermediate of the successive type, $R \rightarrow I \rightarrow P$, was concluded to be sufficiently low, since no signals other than the reactant's and product's were found in each of the time-sequential spectra. Moreover, coincidence was recognized between the rate constants obtained from the reactant decrease and the product increase independently for the total period of the reaction. The contribution of reaction intermediates of the pre-equilibrium type, $R \rightleftharpoons I \rightarrow P$, would also be sufficiently small, since no change in chemical shifts during the reaction was observed.

The authors are grateful to Professor Y. Yoneda for his encouragement and helpful discussion. Financial support from the Kawakami Memorial Fund is acknowledged.

BULLETIN OF THE CHEMICAL SOCIETY OF JAPAN, VOL. 44, 2893—2899 (1971)

Reaction of Methanol with Accelerated Rare Gas Ions

Takashi KOTOYORI,* Makoto TAKAHASI, and Akira ICHINOSE**

Department of Pure and Applied Sciences, College of General Education, The University of Tokyo, Komaba, Meguro, Tokyo

(Received December 31, 1970)

Reaction of methanol with accelerated rare gas ions was studied. The yields of the reaction products, H_2, CO, CH_4, HCHO, and ethylene glycol, were determined, varying the initial kinetic energy of ion (2—6 kV), ionic species, (Ar, Xe, and Kr), and pressure of methanol ($(2—14)\times 10^{-3}$ Torr). No appreciable effect on the product yields was observed by adding carbon tetrachloride as electron scavenger or propylene as radical scavenger. The product yields are found to be linear against ln E_i, (E_i is initial kinetic energy of ions). Although the detailed reaction mechanism is left for future investigation, the reaction seems to be interpreted in terms of billiard model, momentum of ion being transferred directly to a local part of the target molecule at the contact time.

Studies on the chemical reaction of neutral compounds with accelerated ions have been rather few except in the field of mass spectrometric studies and radiation chemistry. It is well known that the ion-molecule reaction takes an important part in the processes of radiation chemistry and plasma chemistry in electrical discharge, but the studies on the reaction initiated directly by accelerated ions are few, apart from the radiation chemical studies with α-particles. In these recent years, a remarkable progress has been achieved in elucidating the characteristics of ion-molecule reaction using single or tandem-type mass spectrometer technique. Study of ion-molecule reaction with mass spectrometer has a pronounced advantage, in observing directly the behavior of the secondary ions produced by impact of primary ions. However, we consider it is also important and interesting to get the information on the final reaction products obtained by ion impact. For this purpose, a small chemical accelerator was constructed which is furnished with an ion source of relatively strong beam intensity and enables us to obtain enough amount of reaction products to be analysed by the conventional analytical methods. With this apparatus we studied the reaction of methanol with accelerated rare gas ions and obtained some preliminary results on the reaction mechanism.

Experimental

Apparatus and Procedures. Figure 1 shows a schematic drawing of the apparatus. Details of the construction and performance of this apparatus is describred elsewhere.[1] Impact ions are generated by electrical discharge of 70 MHz radio waves. Discharge tube is made of Pyrex glass, and is similar to that used in some neutron generator. Gas pressure in discharge tube is adjusted to obtain maximum ion intensity, and the optimum rate of gas feeding is about 10 m*l* STP per hour. The ions are accelerated by DC voltage from 2 to 6 kV. The efficiency of ion extraction is found to be very sensitive to the shape and size of quartz tube for ion exit. The ion extraction efficiency from discharge tube increases with increase of DC voltage, and maximum intensity of ion obtained is about 70 μA. F is an ion focussing lens to which DC voltage is applied, and the optimum ratio of ion focussing voltage to source voltage in the present apparatus is about 1.16. The reaction tube is made of Pyrex glass of 30 cm of length and 3 cm in diameter. A cold trap C is provided to collect condensable vapours and methanol

* Present address: Research Institute of Industrial Safety, Ministry of Labor.

** Present address: Matsushita Research Institute, Tokyo Incorporation.

1) T. Kotoyori and M. Takahasi, *Mass Spectrometry*, **17**, 619 (1969).

and reaction products (formaldehyde and ethylene glycol) can be collected almost quantitatively in the trap. Incondensable gases such as argon, hydrogen, methane, and carbon monoxide are collected in an evacuated bulb of 2 *l* through oil diffusion pump, closing the valve V during the irradiation time. It was checked beforehand that oil diffusion pump does not give any decomposition products, although mercury diffusion pump may be more preferable. Ion current is measured by a Faraday cup attached at the end of the reaction tube, and auxiliary electrodes are furnished to remove charge accumulated on the glass wall. At present, the reaction tube of 5 cm in diameter instead of that of 3 cm in diameter is used, and in this case, it is found that these auxiliary electrodes are unnecessary. Target vapour is supplied from the end of the reaction tube, and the rate of feeding is regulated by a needle valve, monitoring the pressure with Pirani gauge. The gauge was calibrated for methanol in the range of 0.001 to 10 Torr. The working pressure of methanol in the experiment is $(2—14)\times10^{-3}$ Torr. Methanol is purified by refluxing with magnesium metal and distilled in the vacuum line. The irradiation time is 5 min for collecting condensable products, and 2 min for collecting incondensable gases. Incondensable gases collected in an evacuated bulb are compressed by a Toepler pump and analysed by gas chromatography with Molecular Sieve 5 A column. The amount of formaldehyde was determined by spectrophotometric method after being treated with chromotropic acid.[2] The amount of ethylene glycol was determined separately after being oxidized with periodic acid to formaldehyde.[3] To collect these reaction products quantitatively, it is necessary to heat the reaction tube with electrical heater of nichrome wire wound on outside of the reaction tube. Water may also be produced, but its analysis was not attempted in the present experiment.

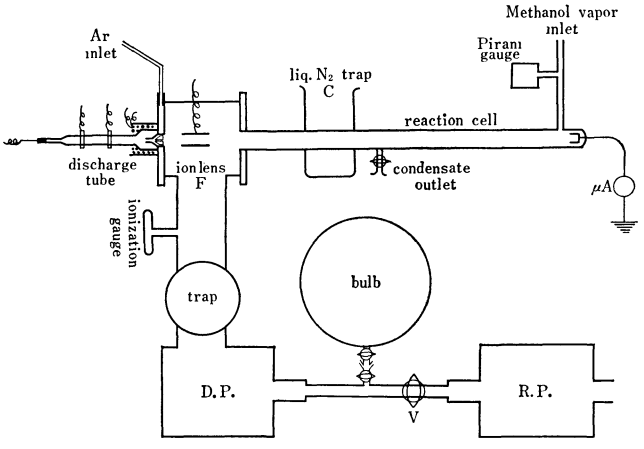

Fig. 1. Diagram of ion impact apparatus.

Results

Spread of Energy of Incident Ar Ion and Abundance of Double Charged Ion. It is generally known that the spread of energy of ion beam generated by electrical discharge is fairly large, and in order to determine the magnitude of the energy spread under the present experimental condition, the ion source is installed to a mass spectrometer which is 60° sector type with analysing tube of 20 cm radius. The maximum beam intensity of Ar at the ion accelerating voltage of 5kV is about 6μA, but the intensity fluctuates slowly. Since it can be easily recovered by adjusting the magnetic field, this fluctuation must be due to that of the energy, which seems to be caused by the periodic slow instability of plasma in the discharge tube. Due to this fluctuation of beam intensity, it is difficult to determine the exact shape of the beam against magnetic field, but the approximate energy spread of Ar at 5 kV is estimated to be about 150 V. The relative abundance Ar^{2+} to Ar^{+} is also estimated to be about 1 to 40 by scanning the magnetic field. In the actual impact experiments, the ion source is directly attached to the reaction tube as shown in Fig. 1, to obtain enough intensity of the ion beam, without eliminating double charged ions, assuming that their contribution is negligible.

Proportionality of Product Yields with Ion Intensity and Product Distribution Pattern. In order to confirm the reliability of our apparatus and the reproducibility of the product yields, the proportionality of the yields of the reaction products per unit irradiation time with the intensity of impact ion was investigated in the range from 20 to 40 μA in the impact experiment of methanol with Ar ion. The proportionality of the yields is satisfactory.

As will be described later, the product distribution in the methanol impact experiment depends to some extent on the pressure of methanol and the energy of impact ions, but an example of the product distribution under a specified condition is presented in Table 1, including the photochemical and radiation chemical results obtained by the other authors for comparison.[4,5]

Table 1. Product distribution patterns in the reaction of methanol with 5 kV Ar^{+} at[6] 8.5×10^{-3} Torr of methanol and other data for comparison

	Unit	H_2	CO	CH_4	$(CH_2OH)_2$	HCHO
5kV Ar^{+}	molecule per Ar^{+}	41.0	10.7	2.7	3.2	1.0
Co γ-ray[4]	*G* value	10.4	0.84	0.26	3.1	5.6
1849 Å photon[5]	mole per cc sec, 10^{-13}	86	2	1.5	60	16

Hitherto, in interpreting the product distribution patterns of the radiolysis of organic compounds, calculations have been made by several authors[7,8] on the basis of the relative abundance of ions observed in mass spectra. In the case of methanol radiolysis,

2) C. E. Bricker and H. R. Johnson, *Ind. Eng. Chem. Anal. Ed.*, **17**, 400 (1945).

3) N. N. Lichtin, *J. Phys. Chem.*, **63**, 1449 (1959).

4) J. H. Baxendale and R. D. Sedgwick, *Trans. Faraday Soc.*, **57**, 2157 (1961).

5) J. Hagege, S. Leach, and C. Vermeil, *J. Chem. Phys.*, **62**, 736 (1965).

6) The atom ratio (H:C:O) calculated from the experimental result from Table 1 is 25:5:4.4. From the material balance, the ratio 4:1:1 should be expected. The incomplete material balance may be due to some missing of carbon products or to hydrogen production by some unknown reaction with contaminated water or oil of diffusion pump.

7) G. G. Meisels, W. H. Hamil, and R. R. Williams, *J. Phys. Chem.*, **61**, 1456 (1957).

8) J. H. Futrell, *J. Amer. Chem. Soc.*, **81**, 5921 (1959).

TABLE 2. PRODUCT DISTRIBUTION PATTERNS CALCULATED ON THE BASIS OF VARIOUS ASSUMPTIONS OF THE PRIMARY ION PRODUCT DISTRIBUTIONS AND SUCCESSIVE ION-MOLECULE REACTION SCHEMES

Assumption adopted		Final products ratio[a]					
Distribution of primary ions	Secondary ion-molecule reaction scheme	H_2	$(CH_2OH)_2$	HCHO	CO	CH_4	H_2O
Proposed values by Lindholm	Proposed scheme by Lindholm	10	8.3	5.7	0.51	4.0	4.0
Observed values by Lindholm(10VAr$^+$)	Lindholm	10	9.1	11.2	2.8	9.6	9.6
Same as above	Baxendale	10	3.4	5.3	1.2	1.0	—
Observed values in electron impact	Baxendale	10	3.4	5.1	0.9	0.3	—
Present experimental values		10	0.78	0.25	2.6	0.66	—

a) normalized to hydrogen

calculations by Lindholm *et al.*[9] and Baxendale *et al.* show fairly good agreement with the experimental results. We attempted the similar calculation to our ion impact case, assuming that the primary ion distribution in the present case is same as that of ion impact spectrum of 10 V Ar$^+$ reported by Lindholm.[9] This assumption may be acceptable because it is known that the ion impact spectra do not vary so much with the kinetic energy of ion in the case of charge transfer. Since Lindholm and Baxendale assumed slightly different reaction schemes for the successive secondary processes, we made calculations on the both reaction schemes. As shown in Table 2, the calculated results do not agree with our experimental result. The distiguished feature in our observed result is very low yields of formaldehyde and ethylene glycol, and the calculation cannot give high yield of carbon monoxide, unless a fundamentally different mechanism is introduced.

Variations of Yields of the Reaction Products with Different Incident Ionic Species. Several authors[9-11] proposed that the secondary ion spectra of organic compounds obtained by ion impact may be explained assuming that the most part of energy required to produce secondary ions from the original target molecule comes from the charge neutralization energy of the incident ions due to the charge transfer process. Lindholm observed the ion impact mass spectra of methanol due to charge transfer with various positive ions of low kinetic energy (4—900 V). He concluded that for most ions the mass spectra of methanol are almost independent of the kinetic energy of the incident ions, and that the energy transferred to methanol equals the electron recombination energy of the incident ions. If this could be applied to the present impact case, we would expect the variation of yields of the reaction products with ionic species of various electron recombination energies. To investigate the effect of recombination energy of impact ions, Ar (I_p=15.75, 15.95 eV), Kr (I_p=14.0, 14.67 eV), and Xe (I_p=12.15, 13.44 eV) are used as source gas. Since the ionization potential of methanol is 10.88 eV, the gain of energy due to the charge transfer is at most 4.87 eV for Ar$^+$, 3.12 eV for Kr$^+$, and 1.27 eV for Xe$^+$ for each ground state of ions. As Fig. 2 shows, the yields of the reaction products per ion at a fixed translational energy are almost the same within the experimental errors irrespective of the species of ion used.

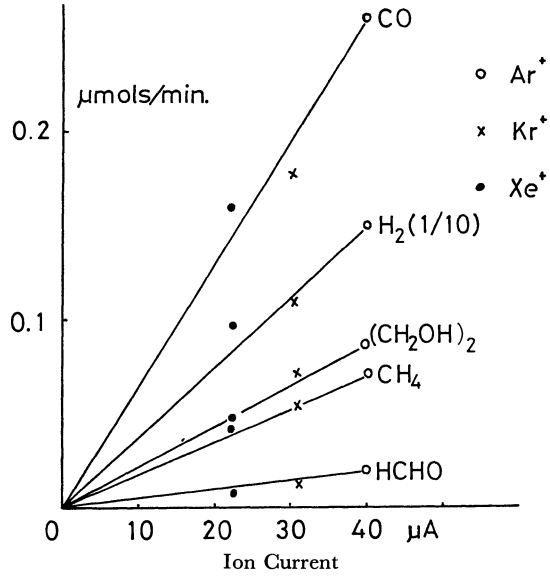

Fig. 2. The yields of the reaction products per ion with Ar$^+$, Xe$^+$, and Kr$^+$.

This figure shows that the product yields of five components, if normalized to ion intensity, do not show any appreciable difference. (In Fig. 2, the beam intensities are not normalized, since the extraction efficiencies of ions from ion source depend on the ionic species). Therefore, the present result cannot be interpreted in terms of charge transfer process. It can be understood if we consider that our experimental conditions (high energy of incident ion, long reaction path, and higher pressure of methanol in the reaction chamber than in the ionization chamber of mass spectrometer) result in the multiple collisions of incident ion. Table 1 shows that a single ion reacts with more than one molecule of methanol, although we have not definite evidence that all of these products are produced by the reaction with initial ions. At any rate, we may conclude that the charge transfer process does not contribute predominantly, although it may be involved in the initial step to some extent.

The Effect of Initial Kinetic Energy of Impact Ion and of Pressure of Methanol. The variation of product

9) P. Wilmenius and E. Lindholm, *Arkiv Fysik*, **21**, 97 (1962).
10) J. B. Homer, R. S. Lehrle, J. C. Robb, M. Takahasi, and D. W. Thomas, "Advances in Mass Spectrometry," Vol. 2, Pergamon Press, London (1961), p. 503.
11) V. Čermák and Z. Herman, *Nucleonics*, **19**, 106 (1961).

yields with the initial kinetic energy of ion (2 to 6 kV) was investigated. The plot of product yields with logarithm of the initial energy E_i shows a fairly good linear relationship, as Fig. 3 shows. Another interesting point to be noted is that the extrapolations of slopes for carbon monoxide, ethylene glycol, and methane intercept the abscissa nearly at the same position. Interpretation of these results will be given in discussion part.

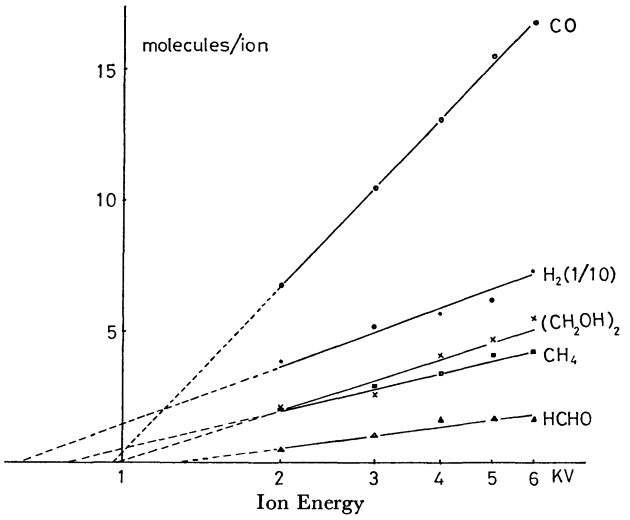

Fig. 3. The plots of the yields of the reaction products against logarithm of the initial energy, ln E_i.

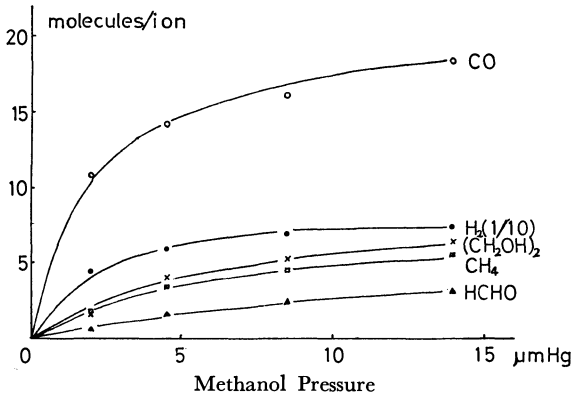

Fig. 4. The variation of the reaction product yields with the increase of the pressure of methanol.

The variation of the reaction product yields with the increase of the pressure of methanol was also investigated in the range $(2—14)\times10^{-3}$ Torr. (Fig. 4). When the pressure of methanol is increased, the yields of all the reaction products increase, approaching to constant values. Five components of the reaction products do not show the same behavior, particularly the yields of hydrogen and carbon monoxide increasing more rapidly with methanol pressure than those of the other reaction products. If the simple bimolecular collision of methanol with ion is assumed, we would expect for the product yields to be proportional to flux of incident ions, length of the reaction tube and pressure of methanol. It is already shown that the product yields are proportional to the ion intensity. The fact that the product yields increase first and approach to limiting values with the increase of methanol pressure indicates some more complicated mechanism is involved in the present reaction. We have not yet definite interpretation for the pressure effect, but some ideas will be given later.

Effect of the Addition of Carbon Tetrachloride and Propylene. It is well known that in the radiolysis of organic compounds with γ-ray the energetic secondary electrons produced by Compton scattering take an important role. However, in the present case, the average energy of the electrons produced by ionizing penetration of heavy charged particles is supposed to be very near to the thermal energy, since the kinetic energy of incident ion is at most 6 kV. Therefore, the direct excitation of methanol by energetic electrons is unlikely, but the production of excited methanol by charge neutralization of methanol ion might be possible, resulting the decomposition of excited methanol.

$$CH_3OH^+ + e \longrightarrow CH_3OH^*$$
$$CH_3OH^* \longrightarrow \text{Products}$$

Meaburn and Mellows[12] found the reduction of the yield of hydrogen in the radiolysis of methanol vapour with the addition of 0.01% of carbon tetrachloride ($G(H_2)=4.1$), and assumed that carbon tetrachloride interrupts the following process, scavenging slow electrons.

$$CH_3OH^+ + CH_3OH \longrightarrow CH_3OH_2^+ + CH_3O\cdot$$
$$CH_3OH_2^+ + e \longrightarrow CH_3OH + H$$

To know whether these processes play any role in the present case, we examined the effect of the addition of carbon tetrachloride. As Fig. 5 shows, no appreciable effect in the product yields was observed except in formaldehyde, and it is concluded that these processes seem not to contribute appreciably in the production of hydrogen. The increase of the yield of formaldehyde with the addition of carbon tetrachloride was noticed. Any conclusive interpretation for this

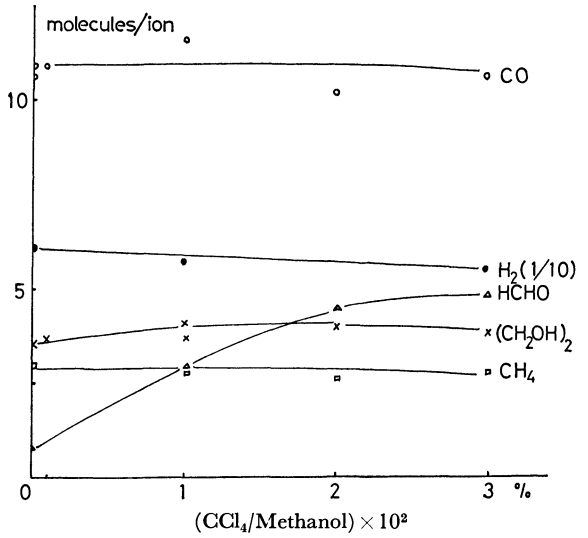

Fig. 5. The effect of the addition of carbon tetrachloride on the yields of the reaction products.

12) M. Meaburn and P. W. Mellows, *Trans. Faraday Soc.*, **61**, 1701 (1965).

finding is not available at present, but if chlorine atom is assumed to be produced by impact of carbon tetrachloride, it may induce the abstraction of hydrogen from methanol, resulting $\cdot CH_2OH$ or $CH_3O\cdot$ which may be finally converted into formaldehyde.

In view of the existence of ethylene glycol among the reaction products, the formation of free radicals (hydrogen atom and methylol radical $\cdot CH_2OH$) is supposed to be quite probable, and propylene was added as radical scavenger to find the extent of the contribution of free radicals to the whole reaction. Contrary to out expectation, no remarkable decrease of yields of the reaction products was observed, as Fig. 6 shows. It seems to be difficult to assume that the whole hydrogens were produced by molecular mechanism, so that an alternative possible explanation may be that produced hydrogen atoms are hot. Hatano and Shida[13] found that hot hydrogen atoms produced in irradiation of liquid olefins with Co 60 γ-rays do not add to olefins and rather abstract hydrogen. No reduction of ethylene glycol with addition of propylene may be understood, if we consider the fact that methylol radical is stabilized by conjugation of odd electron with oxygen and cannot add to propylene at room temperature.

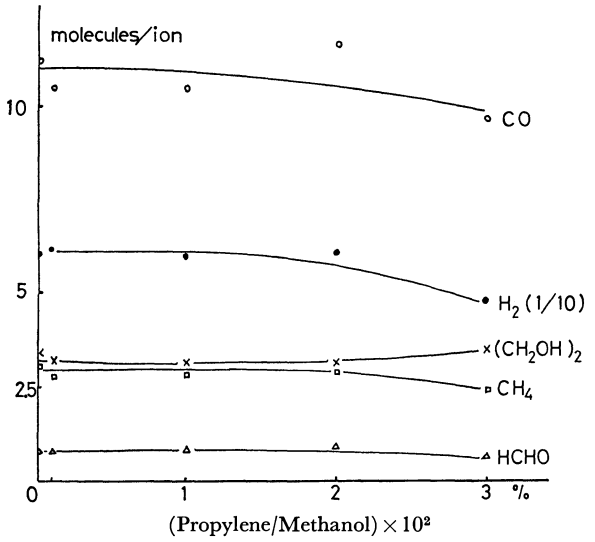

Fig. 6. The effect of the addition of propylene on the yields of the reaction products.

Luminescence by Ion Impact. Faint purple luminescence was observed in the reaction tube, when methanol vapour was introduced. Spectra in the visible region were taken by a spectrograph, with exposure time of 30 min. The spectra consisted of line spectra of hydrogen Balmer series and some unidentified bands (band heads at 4311.8 Å, 3978 Å, and 3955 Å). More detailed investigations for the interpretation of these spectra are left for future study.

Discussions

Summarizing the above experimental results, the contributions of the possible processes are considered and evaluated.

(1) Charge Transfer Process.

$$X^+ + CH_3OH \longrightarrow X + CH_3OH^{*+}$$

$$CH_3OH^{*+} \longrightarrow \text{Products}$$

As described in experimental results, no variation of the yields of the reaction products with different ionic species was observed. As excess energy left on methanol ion, CH_3OH^{*+}, must depend on the amount of recombination energy of incident ion X^+, different product distribution patterns would be expected, depending on the ionic species used. Present results are incompatible with this expectation, and the charge transfer process appears not to play an important role under the present conditions.

(2) Complex Formation Process as Considered in Ion-molecule Reaction. Now it is generally admitted that the complex formation mechanism in ion-molecule reaction takes place only in the very low translational energy range,[14,15] and the energy range of the present experiment is well above this energy range. Therefore, the contribution of this type of reaction may not be necessary to be considered.

(3) Excitation Process by Secondary Electrons. At present, we have no direct experimental evidence whether the excitation of methanol by secondary electrons produced by ionizing penetration of heavy charged particles is involved or not. The data of cross sections for the ionization of methanol by rare gas ions in the energy range of several kV are not available, but the cross sections reported in the case of accelerated ion with various atomic particles are in 10^{-16} cm^2 range,[16,17] indicating that the probability of ionization by charged heavy particles in several kV range is generally large. However, it is less likely that the electrons produced have enough energy to excite methanol, since the relative velocity of ion is fairly low compared with the velocity of orbital electron.

(4) Dissociative Excitation of Methanol Ions by Charge Neutralization. If methanol ion is produced by ionization, excited methanol may be formed through charge neutralization, resulting in its decomposition. However, our experimental result on the effect of addition of carbon tetrachloride seems not to favour this process.

(5) Direct Dissociation Process by Momentum Transfer.

$$X^+ + M \longrightarrow X^+ + R_1 + R_2,$$

or

$$X^+ + M \longrightarrow X^+ + M^* \longrightarrow X^+ + R_1 + R_2.$$

The collision dynamics by classical or semiclassical treatment has been recently developed for interpreting the product yields, the isotope effect and the moderator

13) Y. Hatano, S. Shida, and S. Sato, This Bulletin, **41**, 1120 (1968).

14) "Ion-Molecule Reactions in the Gas Phase," Advances in Chemistry Series 58, Amer. Chem. Soc., (1966).

15) *Discussions Faraday Soc.* **44** (1967).

16) J. B. Hasted, "Physics of Atomic Collisions," Butterworth, London (1964).

17) E. W. McDaniel, "Collision Phenomena in Ionized Gases," John Wiley & Sons, New York, N. Y. (1964), p. 238.

effect in hot atom chemistry.[18-20] The main characteristic of this type of reaction is transfer of momentum of hot atom to molecule in the collision process. The same type of collision is also observed in molecular beam experiment of alkali atom with halogen[21] and ion-molecule reaction in relatively high energy impact.[22] In these experiments, only the reactions to give stable association products such as HT in the reaction, $T+H_2$, MX in the reaction, M (alkali metal) $+X_2$, and ArH^+ in the reaction, Ar^++H_2 have been considered. However, if the energy of incident particles is high, more drastic reactions to give fragmental products must be considered. We presume that this type of reaction takes an important role in the present ion impact experiment, considering that the processes (1)—(4) mentioned above are rather less likely. To interprete the relation of the product yields with the initial kinetic energy of ions, a similar formula as derived for the relative yields of hot atom products is considered.

Miller and Dodson[23] gave the following formula for the yield of hot product,

$$N_{\mathrm{hot}j} = N_s\int f_j p_j(E)n(E)\mathrm{d}E, \qquad (1)$$

where N_{hot} is the number of hot product, N_s is the total number of hot atoms available for the reaction, f_j, the relative probabilty of collision, $p_i(E)$, the probability of hot combination reaction in such collision at energy E, and $n(E)$ is the average number of collision per unit energy at E (collision density). Estrup and Wolfgang[24] derived the following equation for the number of collisions between energies E and $E+\mathrm{d}E$ of a hot atom not undergoing hot combination reaction, assuming elastic and reactive collisions are taking place competitively,

$$n(E)\mathrm{d}E = -\frac{\mathrm{d}E}{\alpha E}\left\{1-\sum_j\int_{E_1}^{E} f_j p_j(E)n(E)\mathrm{d}E\right\}, \qquad (2)$$

where $\alpha=\sum f_i\alpha_i$, and for hard sphere collision,

$$\alpha_j = 1+\frac{\beta_j\ln\beta_j}{1-\beta_j} \quad \text{and} \quad \beta_j=\left[\frac{(M_j-m)}{(M_j+m)}\right]^2,$$

where m is the mass of hot atom and M_j, that of the particle struck. The quantity in the bracket of Eq. (2) is the probabiliy that the hot atom has escaped reaction in the energy interval E_2 to E. Here, the reactions to form stable products by hot atom combination (such as CH_3T in the reaction, $T+CH_4$) are only considered.

In the present ion impact system, the incident ions are not lost, since they do not form any stable products by collision, and therefore we may simply assume that the number of ion impact products N_j is proportional to the collision number of methanol with incident ions in the energy range between E_i (initial energy of ion) and E_f (final energy). In this case, the formula similar to the equation (1) can be used, redifining N_s as the total number of incident ions.

$$N_j = N_s\int_{E_f}^{E_i} p_j n(E)\mathrm{d}E \qquad (3)$$

Since the form of scattering function for reactive and nonreactive collision is not known, the exact form of $n(E)$ cannot be derived. However, if we simply assume that the collision density function approaches rapidly to the following well known asymptotic solution[23]

$$n(E) = 1/\alpha E, \qquad (4)$$

the equation (3) can be simplified,

$$N_j = N_s\int_{E_f}^{E_i} p_j\left(\frac{1}{\alpha E}\right)\mathrm{d}E = N_s\frac{p_j}{\alpha}\ln(E_i/E_f), \qquad (5)$$

assuming p_j and α are both independent of energy, although this is obviously an approximation.[25] From the experimental point of view, since Fig. 3 shows that the yields per ion, (N_j/N_s) are proportional to logarithm of initial ion energy E_i, p_j/α can be determined as slope and $\ln E_f$ as intercepts with abscissa. Here, E_f can be interpreted as the lowest limits of energy to give appreciable reaction products.

In Table 3, the values calculated by least squares method are given. Here, it is interesting to compare

Table 3. Average logarithmic energy loss α and minimum energy to give reaction rpoduct calculated by the least squares method from the experimental results shown in Fig 3.

	α/p_j	$\ln E_f$	E_f, volt
H_2	0.035	6.2	490
CO	0.11	6.9	980
$(CH_2OH)_2$	0.24	6.9	980
CH_4	0.51	6.6	740

Table 4. Calculated α values for several sets of collision pair in the case of isotropic scattering for $\alpha=1+\frac{\beta\ln\beta}{1-\beta}, \beta=\left(\frac{m_1-m_2}{m_1+m_2}\right)^2$

	Ar	Kr	Xe
H	0.05	0.02	0.02
He	0.19	0.09	0.06
Ne	0.73	0.23	0.16
Ar	1.00	0.70	0.50
Kr	0.70	1.00	0.85
Xe	0.50	0.85	1.00
CH_3OH	0.94	0.60	0.41

18) R. Wolfgang, "Progress in Reaction Kinetics," Vol. 3, Pergamon Press, London (1965), p. 97.
19) R. N. Porter and S. Kunt, *J. Chem. Phys.*, **52**, 3240 (1970).
20) C. Hsiung, K. L. Verosub, and A. A. Gordus, *ibid.*, **41**, 1595 (1964).
21) R. Herschbach, "Molecular Beams," Advances in Chemical Physics, Vol. X, Interscience, New York, N. Y. p. 319.
22) A. Henglein, K. Lacmann, and G. Jacobs, *Ber. Bunsenges. Phys. Chem.*, **69**, 279, 286, 292 (1965).
23) J. M. Miller and R. W. Dodson, *J. Chem. Phys.*, **18**, 865 (1950).
24) P. J. Estrup and R. Wolfgang, *J. Amer. Chem. Soc.*, **82**, 2665 (1960). See also, for example, S. Glasstone, "The Elements of Nuclear Reactor Theory," Van Nostrand, Inc., New York, N. Y. (1955), p. 147.
25) In a strict sense, the asymptotic equation (4) cannot be applied to the region near E_i. However, Placzek (*Phys. Rev.* **67**, 423 (1964)) and Hsiung, Verosub, and Gordus (*J. Chem. Phys.*, **41**, 1595 (1964) have shown that $n(E)$ approaches rapidly to $1/\alpha E$, if β is much less than 1.

p_j/α with values α calculated for isotropic elastic scattering for several collision pairs.

The values of p_j are not known, but they must be less than unity, so the values of α in the experiment must be below 0.035, indicating that the average energy fraction lost in reactive collision is rather small corresponding to a small value of β. This seems to suggest that momentum is transferred to a part of light mass in a molecule (possibly to hydrogen atom), not to the whole molecule at the collision instant. After collision, the struck atom may depart from molecule, carrying kinetic energy, or dissipate energy to the whole molecule as in unimolecular decomposition. The latter process is taken into consideration, in view of the pressure effect on the product yields described below.

Pressure Effect on the Product Yields. Apparently, the pressure effect shown in Fig. 4 might be explained in terms of exponential law like Lambert-Beer type as

$$N_j = N_s \exp(-n_{CH_3OH}\sigma_j l) \quad (6)$$

However, under the present experimental conditions, "so-called single collision condition" is not the case, and our experimental result of pressure dependency itself does not fit to Lambert-Beer type law. Although plot of logarithm of product yields against pressure of methanol is linear, the extrapolation of plot does not pass through origin at pressure zero, but rather intercepts the ordinate at much larger values. Instead, if the reciprocals of the product yields per ion are plotted against the reciprocal of pressure, again linear relationships are obtained. This type of linear relationship is known in the unimolecular decomposition mechanism, fluorescence and photochemical quenching, indicating the involvement of deactivation process of excited species by collision. Since the detailed reaction mechanism is not yet established, the following reaction scheme might be oversimplified one, but it may be helpful for understanding the feature of the reaction.

$$X^+ + CH_3OH \xrightarrow{\sigma_j l} X^+ + CH_3OH^* \quad 1$$

$$CH_3OH^* + CH_3OH \xrightarrow{k_{2j}} 2CH_3OH \quad 2$$

$$CH_3OH^* \xrightarrow{k_{3j}} \text{Product } j \quad 3$$

The rate of formation of primary products to give j-th final product per ion, R_j may be as follows,

$$R_j = n_{CH_3OH}\sigma_j l\left(\frac{k_{3j}}{k_{3j}+n_{CH_3OH}k_{2j}}\right), \quad (7)$$

or

$$1/R_j = \frac{1}{\sigma_j l}(k_{2j}/k_{3j} + 1/n_{CH_3OH}),$$

assuming steady state condition. n_{CH_3OH} is the number of methanol per ml, l, the length of reaction tube (30 cm), σ_j, macroscopic cross section for the process 1, and k_{2j} and k_{3j} are the rate constants for the processes 2 and 3, respectively.[26] The values σ_j[27] and k_{2j}/k_{3j} determined from the experimental values are given in Table 5. We consider a very large cross section for hydrogen production is an apparent one, since more than one hydrogen molecule must be produced per single collision. Relating to our observation, it is interesting that Tachikawa and Kahara[28] recently reported the similar pressure dependence of the reaction of recoil Br produced from ^{80m}Br with CH_4 and CD_4. They concluded the lifetime of the excited species is in the range of 10^{-8} to 10^{-9} sec. In the present case, much longer life-time (10^{-3} sec) must be assigned on the basis of our experimental values of k_{2j}/k_{3j}.

Table 5. Slopes and intercepts calculated from the plots of $1/R_j$ against $1/p$, cross sections σ_j, and k_{2j}/k_{3j}

Product	Slope (molecule ion)$^{-1}$/(10^{-3} Torr)$^{-1}$	Intercept (molecule/ion)$^{-1}$	σ_j (10^{-14} cm^2)	k_{2j}/k_{3j} (10^{-14}cc/molecule)
H_2	0.023	0.012	4.2	1.5
CO	0.086	0.051	1.1	1.7
$(CH_2OH)_2$	0.601	0.12	0.16	0.55
CH_4	0.743	0.13	0.09	0.34
HCHO	1.955	0.19	0.05	0.27

We are now undertaking the experiment in the presence of moderator, and more definite scheme for ion impact process will be obtained in near future.

26) In order to introduce the pressure effect into the equation (5), Eq. (7) must be combined with Eq. (5), but this is left for future investigation. We point out here only that it is necessary to modify the meaning of p_j to some extent.

27) As Table 5 shows, σ for each reaction product is not constant. This seems to be peculiar, but the appropriate interpretation is not available at present.

28) E. Tachikawa and T. Kahara, This Bulletin, **43**, 1293 (1970).

Near Ultraviolet Absorption Spectrum of Pyridine-d_5 Vapor

Yoshinori HASEGAWA

College of General Education, Tohoku University, Kawauchi, Sendai

(Received March 2, 1971)

The near ultraviolet absorption spectrum of pyridine-d_5 vapor due to n–π^* transition was measured and analyzed. The origin is at 34951 cm^{-1} and higher than that of pyridine-h_5 by 182 cm^{-1}. The ground-state frequencies 582 and 1019 cm^{-1} and their counterparts of 511 and 953 cm^{-1} in the upper state dominate the progressions in the spectrum. Besides the above frequencies, several active frequencies were obtained.

The near ultraviolet absorption spectrum of pyridine-h_5 vapor has been observed by Henri and Angenot[1] and by Sponer and Stücklen.[2] Assuming that the electronic transition is polarized in the molecular plane perpendicular to a twofold axis passing through the nitrogen atom, Sponer and Stücklen have assigned many bands in the region to the progressions with several totally and nontotally symmetric frequencies. In the spectrum of Sponer and Stücklen, the origin and the progressional members with the totally symmetric frequencs 542 cm^{-1} have been observed to belong to the parallel bands of an oblate symmetric top. The electronic transition has, therefore, been assigned to the A_1–B_1 transition with the electronic transition moment perpendicular to the molecular plane.[3] Although Sponer and Stücklen have reported on several fundamental frequencies in the ground and upper states, ambiguity remains on the character of the vibrations.

The infrared and Raman spectra of pyridine and deuteropyridines and their vibrational analyses have been extensively studied by many workers.[3–7] Their works provide us with much information on the n–π^* absorption spectrum of pyridine.

The purpose of the present study is to analyze the n–π^* absorption spectrum of pyridine-d_5 vapor in relation to that of pyridine-h_5 vapor.

Experimental

The spectrum was photographed in the second order of a Shimadzu GE-100 Ebert type grating spectrograph with a 500 W xenon arc lamp as light source. The reciprocal dispersion was 4.1 Å/mm. A Toshiba UV-D2 filter was used to eliminate all radiation in the other orders. Fuji spectroscopic plates were used. The wavelengh calibration was made by an iron arc. The absorption cells with quartz windows had light path lengths 20 and 60 cm. The 20 cm cell had a side arm in which the sample was kept during exposures at temperatures varying from −16°C to room temperature. The 60 cm cell into which the sample was introduced was helically wound with nichrome wire over an asbestos sheet and covered with an asbestos sheet. The cell temperature could be regulated between room temperature and 50°C.

The 99% pure pyridine-d_5 was a Merk product. The sample was twice distilled in a vacuum and then introduced into the absorption cell in a vacuum. The spectrum of pyridine-d_5 showed no spectrum of pyridine-h_5.

Results and Discussion

The n–π^* absorption bands of pyridine-d_5 vapor observed at −16°C appear in the wavelength region 2860—2620 Å. The bands have narrow line-like shapes in the longer wavelength region, but become diffuse in the shorter wavelengths and finally are submerged in a strong continuum. The strongest band at 34951 cm^{-1} in the longest wavelength region is taken as the origin, which is shifted by 182 cm^{-1} toward the blue compared

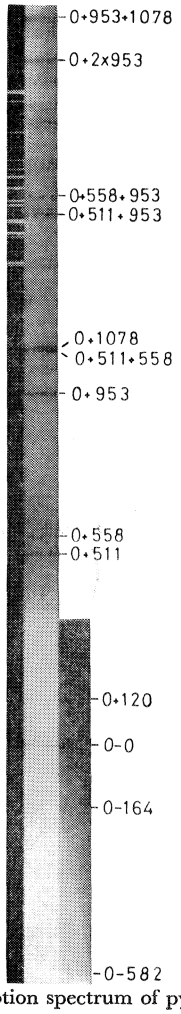

Fig. 1. Absorption spectrum of pyridine-d_5 vapor.

1) V. Henri and P. Angenot, *J. de Chim. Phys.*, **33**, 641 (1936).
2) H. Sponer and H. Stücklen, *J. Chem. Phys.*, **14**, 101 (1946).
3) K. K. Innes, J. P. Byrne, and I. G. Ross, *J. Mol. Spectrosc.*, **22**, 125 (1967).
4) L. Corrsin, B. J. Fax, and R. C. Lord, *J. Chem. Phys.*, **21**, 1170 (1953).
5) J. K. Wilmshurst and H. J. Bernstein, *Can. J. Chem.*, **35**, 1183 (1957).
6) D. B. Cunliffe-Jones, *Spectrochim. Acta*, **21**, 747 (1965).
7) D. A. Long, F. S. Murfin, and E. L. Thomas, *Trans. Faraday Soc.*, **59**, 12 (1963).

TABLE 1. ABSORPTION BANDS OF PYRIDINE-d_5

Wave number	Separation from origin	Intensity		Assignment
		tube 60 cm		
		50°C	40°C	
33353	−1598	w		0−582−1019
33473	−1478	w		0−582−1019+120
33544	−1407	w		0−582−828
33616	−1335	w		0−1335
33626	−1325	w		0−1325
33692	−1259	vw		0−582−680
33719	−1232	vw		
33788	−1163	s	m	0−2×582
33853	−1098	w		0−2×582+62
33876	−1075	w		0−1019−56
33906	−1045	m		0−2×582+120
33932	−1019	s	m	0−1019
33938	−1013		vw	
33967	−984		vw	0−1019+34
33993	−958		vw	0−958
				0−1019+62
34053	−898		m	0−1019+120
				0−582−(316)
34060	−891		vw	0−891
34089	−862		vw	0−1019+120+34
				0−582−(316)+34
34123	−828		wd	0−828
				0−1335+511
34145	−806		vw	0−1325+511
34186	−765		vwd	0−765
34202	−749		w	0−582−680+511
34205	−746		s	0−582−164
34271	−680		s	0−680
34312	−639		s	0−582−56
34329	−622		w	0−622
34338	−613		wd	
34369	−582		s	0−582
34403	−548		vwd	0−582+34
34431	−520		w	0−520
				0−582+62
34445	−506		w	0−1019+511
		tube 60 cm		
		40°C	20°C	
34488	−463	s	m	0−582+120
34492	−459	vw		0−1019+558
34517	−434	vw		
34526	−425	m		0−582+120+34
34545	−406	vw		
34572	−379	w		0−1335+953
34580	−371	wd		0−371
				0−1325+953
34590	−361	w		
34603	−348	w		
34621	−330	s		0−2×164
34635	−316	vs	s	0−(316)
				0−828+511
34668	−283	s	m	0−(316)+34
				0−828+511+34
34686	−265	md		0−828+558
34710	−241	w		0−1325+1078
34726	−225	s	w	0−1019+802
				0−164−56
34743	−208	s	w	
34764	−187	s	w	0−582+558−164
				0−164−20
		tube 60 cm	20 cm	
		20°C	−16°C	
34783	−168	w		0−680+511
34787	−164	s		0−164
34803	−148	vw		
34821	−130	m		0−164+34
34826	−125	w		0−680+558
34832	−119	w		
34866	−85	vw		
34882	−69	m		0−582+511
34885	−66	m		0−1019+953
34895	−56	vs		0−56
34911	−40	m		0−2×20
34931	−20	s		0−20
				0−582+558
34951	0	vs	s	0−0
34985	34		vw	0+34
35013	62		w	0+62
35071	120		m	0+120
				0−680+802
35127	176		vw	
35153	202		vw	
35160	209		vw	
		tube 20 cm		
		−16°C		
35192	241		vw	0+2×120
35222	271		w	0−680+953
35252	301		w	
35318	367		vw	0−582+953
35327	376		vw	
35445	494		w	0−582+1078
35462	511		s	0+511
35509	558		s	0+558
35581	630		w	0+511+120
35622	671		m	0+558+120
35732	781		w	0−680+511+953
35739	788		w	0+953−164
35753	802		vw	0+802
35770	819		w	
35783	832		w	0−680+558+953
35904	953		vs	0+953
35977	1026		vw	0+2×511
35982	1031		vw	
35999	1048		vw	
36021	1070		vs	0+511+558
36029	1078		vs	0+1078
36166	1215		w	
36183	1232		w	
36197	1246		w	

Table 1 (Continued)

Wave number	Separation from origin	Intensity	Assignment	Wave number	Separation from origin	Intensity	Assignment
36260	1309	m	0+511+802	37413	2462	md	0+558+2×953
36410	1459	vs	0+511+953	37474	2523	wd	
36460	1509	vsd	0+558+953	37507	2556	wd	
36539	1588	w	0+511+1078	37560	2609	vwd	
36544	1593	w		37617	2666	vwd	
36727	1776	m	0−680+558+2×953	37665	2714	wd	0+802+2×953
36854	1903	s	0+2×953	37806	2855	md	0+3×953
36926	1975	wd	0+2×511+953	37835	2884	vwd	
36975	2024	vsd	0+953+1078	37888	2937	vwd	0+2×511+2×953
37216	2265	wd	0+511+802+953	37928	2977	md	0+511+558+2×953
37358	2407	sd	0+511+2×953	38176	3225	wd	0+511+802+2×953

Notes: Intensities are roughly estimated from plates.
Abbreviations: v=very, w=weak, m=moderate, s=strong, and d=diffuse.

Table 2. Active frequencies of pyridine-h_5 and pyridine-d_5 (cm^{-1})

Symmetry	Mode	Pyridine-h_5			Pyridine-d_5		
		IR, Raman[a]	Ground[b] state	Excited[b] state	IR, Raman[a]	Ground state	Excited state
a_1	1	992	992	968	962	958	
	6a	605	601	542	582	582	511
	9a	1218	1218		887	891	
	12	1029	1031	995	1006	1019	953
	18a	1068	1063		823	828	
	19a	1482	1491		1340	1335	
b_1	6b	652	649		625	622	
	14	1375	1372		1322	1325	1078
	15	1148	1141		(887)		
a_2	10a	886	891		690	680	558
b_2	4	675[c]	676?		(625)[d]		
	5	942	945		762[d]	765	
	11	703[c]	712		530	520	
	16b	405	405		371	371	

a) The values taken from Corrsin *et al.*[4]
b) The values by Sponer and Stücklen.[2]
c) Cunliffe-Jones has assigned the frequencies 700 and 746 cm^{-1} to the modes 4 and 11, respectively.[6]
d) Wilmshurst and Bernstein have assigned the frequencies 567 and 823 cm^{-1} to the modes 4 and 5, respectively.[5]

with that of pyridine-h_5.[2] With the rise of temperatures, many line-like bands appear in the longer wavelength side of the origin.

Table 1 represents our measurements with visually estimated intensities and assignments of the bands. Table 2 shows the active frequencies of the pyridine-d_5 spectrum together with those of the pyridine-h_5 spectrum.[2]

The interval 582 and 1019 cm^{-1} are most prominent in the longer wavelength region of the origin. These are identical with the frequencies 582 and 1006 cm^{-1} assigned to the totally symmetric in-plane ring bending modes 6a and 12, respectively, in the vibrational spectra.[4,5] The frequency 582 cm^{-1} corresponds to the prominent frequency 601 cm^{-1} in the pyridine-h_5 spectrum and has a counterpart of 511 cm^{-1} (542 cm^{-1} in pyridine-h_5) in the upper state. The frequency 1019 cm^{-1} has a counterpart of 953 cm^{-1} in the upper state. The frequencies 1031 and 995 cm^{-1} in the ground and upper states, respectively, in the pyridine-h_5 spectrum correspond to the frequencies.

The separation 680 cm^{-1} of the strong hot band at 34271 cm^{-1} from the origin might coincide with a frequency of 690 cm^{-1} in the vibrational spectra. This frequency is assigned to the out-of-plane hydrogen bending mode 10a with species a_2. It may be expected that the bands caused by a nontotally symmetric vibration of species a_2 show a perpendicular type.[8] The shape of the band is, however, line-like and can not be distinguished from those of the parallel bands. The frequency 680 cm^{-1} corresponds to 891 cm^{-1} in the pyridine-h_5 spectrum and has a counterpart of

8) A. C. Albrecht, *J. Chem. Phys.*, **33**, 156 (1960).

558 cm^{-1} (probably 672 cm^{-1} in pyridine-h_5) in the upper state.

Separations 371, 520, 622, 765, and 828 cm^{-1} of weak bands to the red from the origin coincide with the respective frequencies in the vibrational spectra as shown in Table 2 and assigned as in Table 1.

Separations 891, 958, 1325, and 1335 cm^{-1} of very weak bands to the red from the origin are identical with the respective frequencies in the vibrational spectra and assigned as in Table 1.

Separation 316 cm^{-1} of the strong hot band at 34635 cm^{-1} from the origin might coincide with the frequency 329 cm^{-1} in the vibrational spectra. The analogous band separated from the origin in the pyridine-h_5 spectrum by 378 cm^{-1} is, however, extremely weak. Thus ambiguity of the band remains.

The most characteristic feature of the pyridine-d_5 spectrum is the prominence of frequency 953 cm^{-1} in the upper state. Vibration 953 cm^{-1} makes overtone bands with three members and dominates progressions in combination with other vibrations. In the pyridine-h_5 spectrum, the 542 cm^{-1} progression starting from the origin appears up to the fourth member, but the analogue of 511 cm^{-1} in pyrinine-d_5 has only two progressional members.

The other fundamental frequencies in the upper state are 558 and 1078 cm^{-1}. The frequency 558 cm^{-1} seems to make no overtone and is a counterpart of the ground-state frequency 680 cm^{-1}. The frequency 1078 cm^{-1} probably corresponds to the ground-state frequency 1325 cm^{-1}.

On both sides of the origin, satellites appear with separations −164, −56, −40, −20, 34, 62, and 120 cm^{-1}. The satellite band separated from the origin by 120 cm^{-1} corresponds to the band separated from the origin by 139 cm^{-1} in the pyridine-h_5 spectrum, which disappears from the spectrum in solid solution at low temperature.[9] This satellite might be due to a v–v transition of a low frequency vibration. The other satellites might be due to v–v transitions of some vibrations.

The author is particularly indebted to Prof. H. Azumi for use of the spectrograph.

9) *Cf.* Ref. 3.

BULLETIN OF THE CHEMICAL SOCIETY OF JAPAN, VOL. 44, 2903—2911 (1971)

Kinetic Studies of the Solvent Extraction of Metal Complexes. I. The Extraction of the Beryllium(II)-TTA Chelate from Aqueous Perchlorate Media into Carbon Tetrachloride and Methyl Isobutyl Ketone

Tatsuya SEKINE, Yasuaki KOIKE, and Yū KOMATSU

Department of Chemistry, Science University of Tokyo, Kagurazaka, Shinjuku-ku, Tokyo

(Received March 8, 1971)

The rate of extraction of beryllium ions from aqueous 4.0M or 0.1M sodium perchlorate-chloride or -nitrate ionic media into carbon tetrachloride or MIBK (methyl isobutyl keton) as a chelate complex with TTA (thenoyltrifluoroacetone) has been determined at 25°C. The rate of extraction in the carbon tetrachloride system is first-order with respect both to the beryllium ion and the dissociated TTA anion in the aqueous phase. The rate constant for this reaction is about 2×10^{4}M^{2}min^{-1}. The rates in these systems are not influenced by the replacement of perchlorate ions by nitrate or chloride ions in the ionic media when the ionic concentration is kept constant. On the other hand, it was found that three extraction reactions take place in the MIBK systems. The rate of these extractions is in all cases first-order with respect both to the beryllium ion and the dissociated TTA anion, but is zeroth-, first, or second-order with respect to the perchlorate ions in the aqueous phase. Because of this, the extraction is much faster when the perchlorate concentration is larger; for example, when the concentration of the TTA anion is kept constant, the extraction from a 4.0M sodium perchlorate solution is about 200 times faster than that from the 4.0M sodium chloride solution. From these experimental results, the following conclusions were reached. In the carbon tetrachloride system, the beryllium ion first forms the TTA chelate in the aqueous phase, and then the complex is extracted into the organic phase. The rate-determining step is the 1:1 complex formation in the aqueous phase. In the MIBK system, on the other hand, the formation of the TTA complex in the aqueous phase, followed by its extraction into the organic phase (zeroth-order reaction with respect to the perchlorate ion), also occurs, but at the same time, the beryllium ion in the aqueous phase is first extracted into the organic phase as ion-pairs, such as $BeCl(ClO_4)$ or $BeNO_3(ClO_4)$ and $Be(ClO_4)_2$ (first- and second-order reactions with respect to the perchlorate ions respectively), and the ion-pairs then react with the TTA anions in the organic phase. The enhancement of the rate of extraction by the perchlorate ions in the MIBK system seems to be explained by the overall effect of these extraction mechanisms.

The solvent extraction of the beryllium(II)-TTA (thenoyltrifluoroacetone) chelate complex has been known as a slow reaction. It was reported that the rate of this extraction is dependent on the hydrogen-ion concentration and that a prolonged agitation is necessary until the distribution equilibrium is estab-

lished, especially when the pH is not high;[1] an agitation for one week was carried out in order to obtain the distribution equilibrium of the beryllium(II)-TTA chelate between *o*-xylene and aqueous solutions,[2] for instance. A slow beryllium(II) extraction with TTA has been also observed in our laboratory; it took one week or more to obtain the distribution equilibrium when beryllium(II) in perchlorate media was extracted with 0.01M to 0.1M TTA in chloroform or in carbon tetrachloride by the mechanical agitation of the two phases in glass tubes placed on a rotating framework at 20 rpm.[3] At the same time, it was also observed that the extraction is much faster when MIBK (methylisobutyl ketone) is used as the organic solvent; the extraction equilibrium was achieved within 12 hr by the same mechanical agitation.[3,4]

In this paper, the present authors have carried out a kinetic study of the beryllium(II) extraction with TTA in order to ascertain further details on this remarkable difference in the rate of extraction when these two organic solvents are used. The aqueous phase employed was 4.0M or 0.1M constant ionic media containing sodium perchlorate and sodium chloride or sodium nitrate. From these experimental data, the rate of extraction was given as a function of the concentration of the components and the important role of the perchlorate ions in the extraction mechanism has been established. The results were further discussed by comparing them with these of a distribution equilibrium study carried out under the same conditions.[4]

Experimental

Reagents. A radioactive tracer, beryllium-7, has always been used in order to determine the distribution ratio. It was obtained as a hydrochloric acid solution and was diluted with 0.01M perchloric acid in order to prepare the stock tracer solution. A reagent-grade beryllium hydroxide was dissolved in perchloric acid, and the concentration was determined by gravimetry after beryllium(II) 2-methyloxinate had been precipitated. The stock carrier solution was prepared by the dilution of this solution. It contained 5×10^{-3}M beryllium and 0.01M perchloric acid. The TTA was obtained from the Dōjindō Co. The MIBK was obtained from the Tokyo Kasei Co.; it was washed with 0.1M perchloric acid, water, and a 0.1M aqueous sodium hydroxide solution successively, and then several times with water. The sodium perchlorate was prepared from sodium carbonate and perchloric acid. It was recrystallized three times from water. All of the other reagents were of a reagent grade and were used without further purification.

Procedures. All of the procedures were carried out in a thermostatted room at 25±0.3°C. Stoppered glass tubes (volume, 20 m*l*) were always used in order to equilibrate the two phases. The organic solution of TTA prepared was stored overnight before the experiments. The aqueous phase initially contained 1.0×10^{-4}M labeled beryllium, sodium perchlorate, and, in some cases, sodium chloride or sodium nitrate and a 0.01M sulfanilate buffer. The total ionic concentration was 4.0M or 0.1M. A 5.0-m*l* portion of the organic solution and a 5.0-m*l* portion of the aqueous solution were placed in the glass tube, and the two phases were agitated vigorously by means of a mechanical shaker. In order to ascertain the effect of the material diffusion on the rate of extraction, a series of experiments were carried out as follows: a 5.0-m*l* portion of the aqueous solution and a 5.0-m*l* portion of the organic solution were taken, each from a certain batch, and placed in a glass tube. The tube was placed on the mechanical shaker and was shaken for 5 min at a certain shaking speed. The distribution ratio of beryllium(II) was then determined in a manner which will be described later. Several experiments were carried out by changing the shaking speed, and the distribution ratio thus obtained was plotted against the speed. It was found that the distribution ratio was dependent on the speed when it was low. However, beyond a certain speed (which was dependent on the nature and the volume of the two phases), the distribution ratio (which was much lower than the value at equilibrium) became no longer dependent on the speed. Such a "plateau region" of the shaking speed was determined before each series of experiments, and the shaking of that series of experiments was always carried out under those conditions.

In order to determine the rate of extraction, a series of experiments were carried out at different shaking intervals, but otherwise under the same experimental conditions. When the agitation was stopped, the two phases in the tube were immediately centrifuged and a certain portion was pipetted from each phase and transferred into small test tubes. The γ-radioactivity of each phase was counted by means of well-type (NaI) scintillation counter. Another portion was also taken from the aqueous phase and transferred into a glass vessel. The hydrogen-ion concentration (the stoichiometric unit) was determined by potentiometry by using standard perchloric acid, in which the ionic concentration was 0.1M or 4.0M.

The beryllium content in the two phases was determined from the initial beryllium concentration and the γ-radioactivity of the two phases as:

$$[\mathrm{Be(II)}]_{org} = [\mathrm{Be(II)}]_{initial} \times (\gamma\text{-count-rate})_{org}/(\gamma\text{-count-rate})_{initial}$$

$$[\mathrm{Be(II)}] = [\mathrm{Be(II)}]_{initial} \times (\gamma\text{-count-rate})_{aq}/(\gamma\text{-count-rate})_{initial}$$

Statistical

The rate of extraction could be influenced by many factors. As has been described, the agitation of the two phases in this study was always done in the plateau region, where the rate was independent of the speed of the two-phase agitation. Thus, the diffusion or the transport of materials could be eliminated from consideration; the rate is dependent only on the concentrations of the materials in the system.

On the basis of these facts, the extraction rate may be generally described as follows:

$$-\frac{d[Be^{2+}]}{dt} = k^*[Be^{2+}]^a[HA]_{org}^b[H^+]^c[ClO_4^-]^d \qquad (1)$$

Here, the term of water is omitted because it is not possible to change the water activity without influencing the other factors.

1) R. A. Bolomey and L. Wish, *J. Amer. Chem. Soc.*, **72**, 4483 (1950).
2) H. J. Debruin and R. B. Temple, *Aust. J. Chem.*, **15**, 153 (1962).
3) T. Sekine and M. Sakairi, This Bulletin, **40**, 261 (1967).
4) T. Sekine, Y. Komatsu, and M. Sakairi, *ibid.*, **44**, 1480 (1971).

The dissociation and the distribution constants of the chelating acid are described as:

$$K_a = \frac{[H^+][A^-]}{[HA]} \quad (2)$$

$$K_D = \frac{[HA]_{org}}{[HA]} \quad (3)$$

$$\frac{K_D}{K_a} = \frac{[HA]_{org}}{[H^+][A^-]} \quad (4)$$

When b is equal to c^{-1}, Eq. (1) can also be described as:

$$-\frac{d[Be^{2+}]}{dt} = k[Be^{2+}]^a[A^-]^e[ClO_4^-]^d \quad (5)$$

where $k=k^*K_DK_a^{-1}$.

As the perchlorate and the extractant (HA) are in a large excess in relation to beryllium, and as the aqueous phase is buffered, the rate can be described as follows:

$$-\frac{d[Be^{2+}]}{dt} = q[Be^{2+}]^a \quad (6)$$

Here q is the multiplication of the rate constant, k^*, and the other concentrations which are kept at certain values. When the reaction order with respect to beryllium is unity, as it is in the present study, the following simplified statistical treatments are possible.

Equation (6) can be rewritten as:

$$-\frac{d[Be^{2+}]}{dt} = q[Be^{2+}] \quad (7)$$

$$-\log[Be^{2+}] = qt + c_0 \quad (8)$$

Equation (8) shows that the above assumption should stand if the $\log[Be^{2+}]$ *vs.* t plot is a straight line with a slope of $-q$.

The reaction order with respect to the other species can be determined from the rate measurements when two of the concentrations out of these three are kept at certain values. For example, when the concentrations of the extractant and perchlorate ions are kept at B and D, then the quantity q_{H^+} can be defined as follows:

$$\log q_{H^+} = \log k^*B^bD^d + c\log[H^+] \quad (9a)$$

As can be seen from Eq. (9a), the $\log q_{H^+}$ *vs.* $-\log[H^+]$ plot should be a straight line with a slope of $-c$ under such conditions; thus, the reaction order with respect to the hydrogen ion, c, can be determined.

By similar procedures, the rest of the values of the b and d reaction orders can be determined from the slope of the plot given by the following equations:

$$\log q_{HA} = \log k^*C^cD^d + b\log[HA]_{org} \quad (9b)$$

$$\log q_{ClO^-} = \log k^*B^bC^c + d\log[ClO_4^-] \quad (9c)$$

However, as will be seen below, the reaction order with respect to the perchlorate ions, d, was not a constant in some systems, but changed as the perchlorate concentration was changed; this was, therefore, further treated.

The reaction order with respect to the perchlorate can, then, be generally described as:

$$-\frac{d[Be^{2+}]}{dt} = k^*[Be^{2+}][HA]_{org}^b[H^+]^c(1+k_1[ClO_4^-] + \cdots + k_n[ClO_4^-]^n) \quad (10)$$

or

$$= k[Be^{2+}][A^-]^e(1+k_1[ClO_4^-] + \cdots + k_n[ClO_4^-]^n) \quad (11)$$

In such cases, the following equation should be used instead of Eq. (9c):

$$\log q_{ClO_4^-} = \log k^*B^bC^c + \log(1+k_1[ClO_4^-] + \cdots + k_n[ClO_4^-]^n) \quad (12)$$

Thus, the $\log q_{ClO_4^-}$ *vs.* $\log[ClO_4^-]$ plot is not a straight line but a curve with two asymptotes:

$$[ClO_4^-] \to 0 \quad \log q_{ClO_4^-} = \log k^*B^bC^c$$

$$[ClO_4^-] \to \infty \quad \log q_{ClO_4^-} = n\log[ClO_4^-]$$

As the limiting slope was found to be $+2$ in the present study, the k_1 and k_2 constants were determined by a curve-fitting of the $\log q_{ClO_4^-}$ *vs.* $\log[ClO_4^-]$ with the following family of standard curves, as has been described in other papers:[5,6]

$$Y = \log(1+pv+v^2) \qquad X = \log v \quad (13)$$

The above treatments are probably valid only when the effect of the reverse reaction or the back extraction is negligible.

Results

In the present study, beryllium was always added to the aqueous phase, and the data used for the analysis were obtained only from the early stage of the extraction; therefore, the statistical treatments given above can be adopted without any corrections for the back extraction.

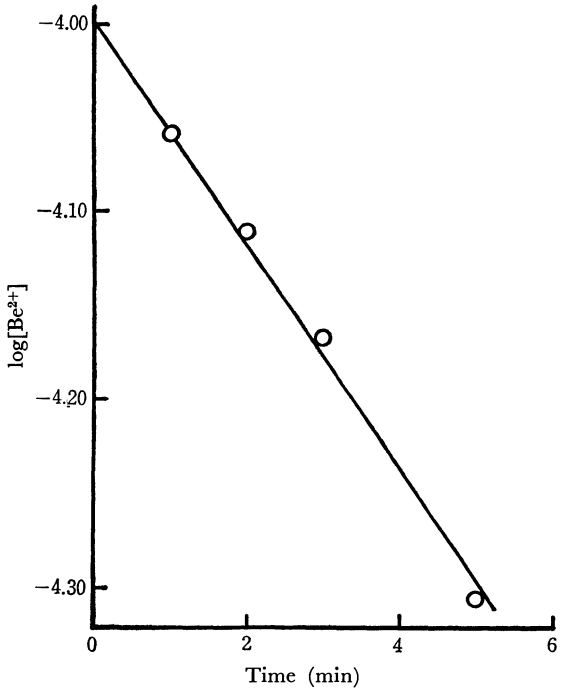

Fig. 1. Dependence of the rate of Be(II) extraction as TTA chelate on the Be^{2+} concentration.
Org. phase. MIBK containing 0.1M TTA.
Aq. phase. 4.0M $NaClO_4$ at $-\log[H^+]=3.00$.

5) T. Sekine and M. Ono, This Bulletin, **38**, 2087 (1965).
6) T. Sekine, M. Sakairi, and Y. Hasegawa, *ibid.*, **39**, 2141 (1966).

In all of the experiments, the TTA concentration in the initial organic phase was 0.1M and the perchlorate concentration was 0.1M or 4.0M, except when the dependence of the rate on these concentrations was determined. The hydrogen-ion concentration was, in general, 1.0×10^{-3}M. However, when the rate was too small or too large for accurate measurement, the experiments were carried out at a somewhat higher or lower hydrogen-ion concentration and the q_{HA} and $q_{ClO_4^-}$ values in Eqs. (9b) and (9c) were normalized to those at $-\log[H^+]$ 3 by assuming that they are inversely proportional to the hydrogen-ion concentration.

Extraction of Beryllium Perchlorate. Beryllium(II) in sodium perchlorate solutions is extracted even into MIBK in the absence of any chelating ligand, as has been pointed out (Ref. 4 Fig. 1). This extraction proceeds very rapidly, and the distribution equilibrium is reached within 30 sec under the present experimental conditions. The distribution ratio of beryllium(II) between MIBK and 4.0M sodium perchlorate is $10^{-1.16}$.

Reaction Order with Respect to Be^{2+}. In most experiments, the $-\log[Be^{2+}]$ *vs.* *t* plot under certain conditions was a straight line. Figure 1 gives an example of this. As can be seen from Eq. (8), this shows that the reaction order with respect to the beryllium ion is unity. However, when the two-phase agitation was carried out for a very long time, a deviation of the plot from a straight line was observed. The deviation is probably caused by the back extraction.

(A) Extraction into Carbon Tetrachloride. Reaction Order with Respect to the Hydrogen Ions: The rate of extraction was determined when the TTA concentration in carbon tetrachloride was 0.1M, the aqueous sodium perchlorate concentration was 0.1M or 4.0M and the hydrogen-ion concentration was between $10^{-2.5}$ and $10^{-3.5}$M. The value of *q* in Eq. (8) at a certain hydrogen-ion concentration was determined from the slope of the $-\log[Be^{2+}]$ *vs.* *t* plot; the series of log *q* values thus obtained at different hydrogen-ion concentrations, log q_{H^+}, are plotted against $-\log[H^+]$ in Fig. 2a. In the 4.0M ionic media, the plot is a straight line with a slope of +1, although the results are somewhat erroneous; it would be possible to conclude that the rate of extraction is inversely proportional to the hydrogen-ion concentration in this system. In the 0.1M ionic media, the plot is also almost a straight line with a slope of +1 in the higher $-\log[H^+]$ region. However, it deviates from the line as $-\log[H^+]$ decreases. The present authors cannot yet explain this deviation in the lower $-\log[H^+]$ region, but still it could be concluded that the reaction order with respect to the

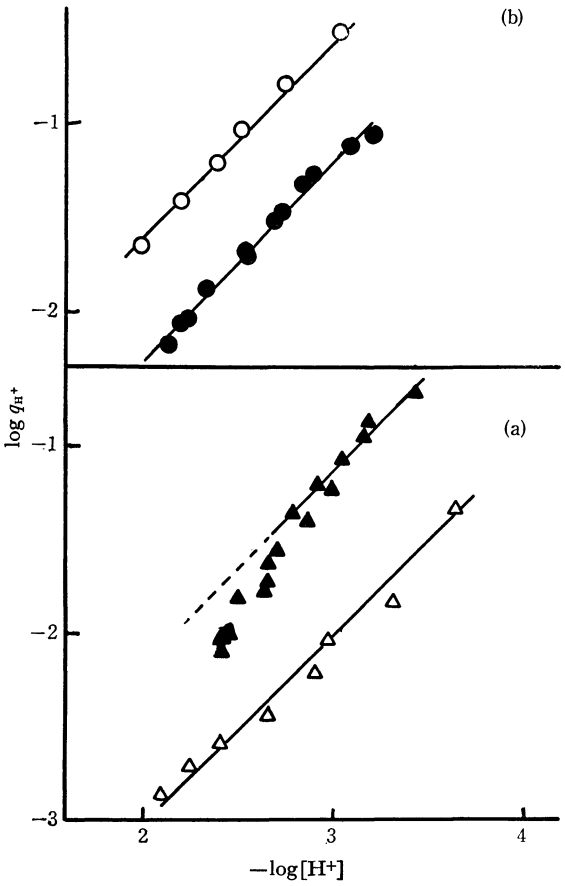

Fig. 2. Dependence of the Be(II) extraction as TTA chelate on the hydrogen ion concentration. The notation q_{H^+} on the ordinate is given in Eq. (9a).
(a) Org. phase. CCl_4 containing 0.1M TTA.
Aq. phase. 4.0M $NaClO_4$ (open triangles).
0.1M $NaClO_4$ (closed triangles).
(b) Org. phase. MIBK containing 0.1M TTA.
Aq. phase. 4.0M $NaClO_4$ (open circles).
0.1M $NaClO_4$ (closed circles).

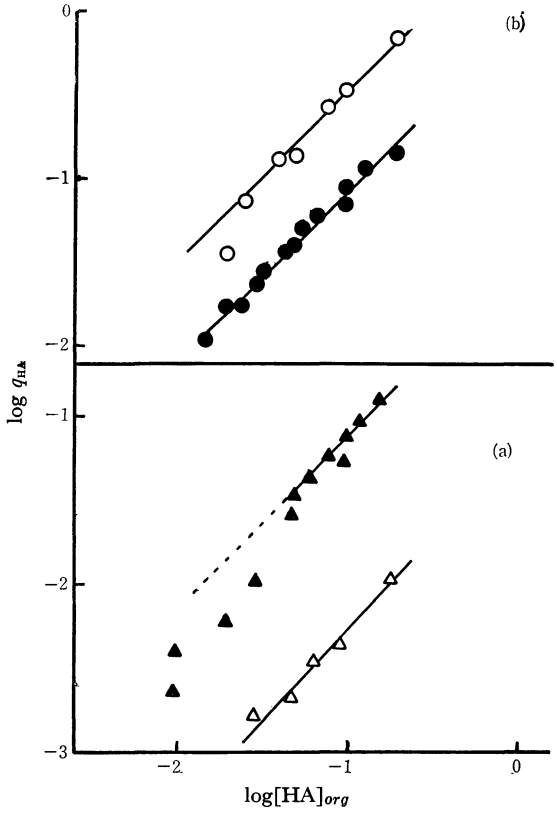

Fig. 3. Dependence of the rate of Be(II) extraction as TTA chelate on the TTA concentration in the organic phase. The notation q_{HA} on the ordinate is given in Eq. (9b).
(a) Org. phase. CCl_4 containing TTA.
Aq. phase. 4.0M $NaClO_4$ (open triangles).
0.1M $NaClO_4$ (closed triangles).
(b) Org. phase. MIBK containing TTA.
4.0M $NaClO_4$ (open circles).
0.1M $NaClO_4$ (closed circles).

hydrogen-ion concentration is -1 when the hydrogen-ion concentration is around 1×10^{-3}M or less.

Reaction Order with Respect to TTA: The rate of extraction was determined when the hydrogen-ion concentration was $10^{-2.9}$M in the 0.1M ionic media and $10^{-3.1}$M in the 4.0M ionic media. The results are given in Fig. 3a. In the 4.0M ionic media, the plot is a straight line with a slope of $+1$, it was concluded that the extraction is proportional to the TTA concentration. In the 0.1M media, the plot is also almost a straight line with a slope of $+1$ in the higher TTA concentration region. However, it deviates from the line as the concentration decreases. The authors also cannot explain this deviation now, but they believe that it could be concluded that the reaction order with respect to TTA is $+1$ when the TTA concentration is about 5×10^{-2}M or more.

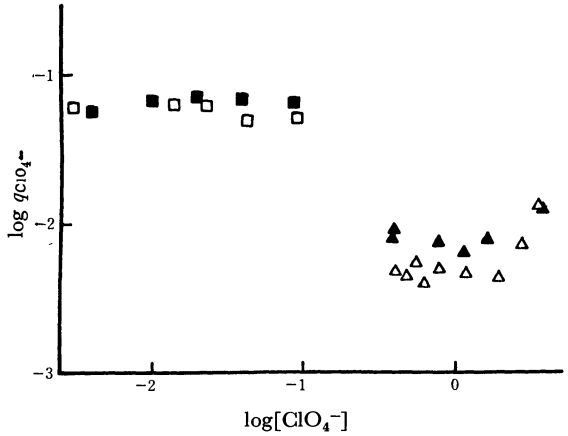

Fig. 4. Dependence of the rate of Be(II) extraction as TTA chelate on the aqueous perchlorate concentration when it is replaced by sodium nitrate (closed symbols) or by sodium chloride (open symbols). The notation $q_{ClO_4^-}$ on the ordinate is given in Eq. (9c).
Org. phase. CCl_4 containing 0.1M TTA.
Aq. phase. 4.0M Na(Cl, ClO_4) (open triangles)
4.0M Na(NO_3, ClO_4) (closed triangles)
0.1M Na(Cl, ClO_4) (open squares)
0.1M Na(NO_3, ClO_4) (closed squares)

Reaction Order with Respect to Perchlorate Ions. The rate of extraction was determined when the TTA concentration was 0.1M and the perchlorate ion concentration was changed. The hydrogen-ion concentration in these experiments was $10^{-3.5}$M in the 4.0M or 0.1M Na(NO_3, ClO_4) media, $10^{-3.6}$M in the 4.0M Na(Cl, ClO_4) media, and $10^{-2.8}$M in the 0.1M Na(Cl, ClO_4) media. Figure 4 gives the results (*cf.* Eq. (9c)). From Fig. 4, it can be seen that the rate of extraction is almost constant in the 0.1M media, that it decreases somewhat in the 4.0M media when the perchlorate ions are replaced by chloride or nitrate ions, but that it becomes almost constant when the concentration of these ions is above 2.0M. Thus, it can be concluded that the rate of extraction is practically independent of the composition of the salt in the aqueous phase.

From these findings, it was concluded that the rate of beryllium extraction into carbon tetrachloride with TTA is expressed by the following equation (*cf.* Eq. (1)):

$$-\frac{d[Be^{2+}]}{dt}=k^*[Be^{2+}][HA]_{org}[H^+]^{-1}[ClO_4^-]^0 \quad (14)$$

As may be seen from Eqs. (2) to (5), Eq. (14) can also be rewritten as:

$$-\frac{d[Be^{2+}]}{dt}=k[Be^{2+}][A^-] \quad (15)$$

The rate constants calculated from these results are given in Table 1.

Table 1. A summary of the rate constants for the extraction of beryllium(II)-TTA chelate complexes at 25°C

(A) Extraction into carbon tetrachloride

$$-\frac{d[Be^{2+}]}{dt}=k[Be^{2+}][A^-][ClO_4^-]^0$$

	0.1M $NaClO_4$	4.0M $NaClO_4$
log k	4.5	4.3

(B) Extraction into MIBK

$$-\frac{d[Be^{2+}]}{dt}=k[Be^{2+}][A^-](1+k_1[ClO_4^-]+k_2[ClO_4^-]^2)$$

	0.1M ionic media		4.0M ionic media	
	Na (NO_3, ClO_4)	Na (Cl, ClO_4)	Na (NO_3, ClO_4)	Na (Cl, ClO_4)
log k	4.8	4.7	4.9	4.4
log kk_1	6.5	6.3	5.8	5.7
log kk_2	5.9	5.7	4.9	5.2

The dissociation and distribution constants at 25°C used for the calculation of $[A^-]$ from $[HA]_{org}$ and $[H^+]$ are as follows. (taken from unpublished data by T. Sekine *et al.*)

		0.1M $NaClO_4$	4.0M $NaClO_4$
$\log\frac{[H^+][A^-]}{[HA]}$		−6.46	−6.57
$\log\frac{[HA]_{org}}{[HA]}$	CCl_4	1.30	1.93
	MIBK	2.25	2.62

(B) Extraction into MIBK. The distribution ratio of beryllium(II) between MIBK and 0.1M sodium perchlorate media is estimated to be $10^{-4.5}$ from the extrapolation of the data in Fig. 1, Ref. 4. Thus, the perchlorate extraction is negligible in the 0.1M ionic media. However, in the 4.0M ionic media, the distribution ratio into MIBK is already $10^{-1.16}$ in the absence of TTA. As has been described, the rate of extraction of the perchlorate ion-pairs is very large; thus, the beryllium(II) extraction with TTA from 4.0M perchlorate media is proceeded by the much faster perchlorate extraction.

On the basis of these findings, the rate of beryllium(II) extraction with TTA in MIBK was calculated after a correction for this beryllium(II) perchlorate extraction made as follows. In a preliminary experment, an aqueous phase initially containing the same amounts of beryllium, hydrogen, and perchlorate ions as in the systems to be studied had been equilibrated with an MIBK phase containing no TTA, and the beryllium concentrations in the two phases were measured. The extraction into MIBK containing TTA was

assumed to be started from these phases; that is, the aqueous beryllium(II) concentration measured above was used as the initial aqueous beryllium(II) concentration, and the organic beryllium(II) concentration preliminarily determined (which should correspond to the organic beryllium perchlorate fraction) was substracted from the organic concentration obtained in the presence of TTA.

Reaction Order with Respect to Hydrogen Ions: The rate of extraction was determined when the hydrogen-ion concentration was between $10^{-2.0}$ and $10^{-3.5}$M. The results are given in Fig. 2b. Both in the 0.1M and in the 4.0M media, the plot is a straight line with a slope of +1, as can be seen from Fig. 2b. Thus, it was concluded that the extraction is inversely proportional to the hydrogen-ion concentration in the aqueous phase.

Reaction Order with Respect to TTA: The rate of extraction was determined when the hydrogen-ion concentration was $10^{-2.5}$M in the 0.1M ionic media and $10^{-2.4}$M in the 4.0M media. In both these ionic media, the log q_{HA} *vs.* log$[HA]_{org}$ plot is a straight line with a slope of +1, as is shown in Fig. 3b. Thus, it was concluded that the extraction rate is proportional to the TTA concentration in the organic phase.

Reaction Order with Respect to Perchlorate Ions: The rate of extraction was determined when the TTA concentration was 0.1M and the hydrogen-ion concentrations were $10^{-3.0}$M (0.1M $Na(NO_3, ClO_4)$), $10^{-3.4}$M (0.1M $Na(Cl, ClO_4)$), $10^{-2.7}$M (4.0M $Na(NO_3, ClO_4)$), and $10^{-3.3}$M (4.0M $Na(Cl, ClO_4)$). In all of the experiments, the log $q_{ClO_4^-}$ *vs.* log$[ClO_4^-]$ plot was not a straight line. The slope always increased as the perchlorate concentration increased. Figures 5 and 6 show the results.

The data in these figures were analyzed by the curve-fitting, and it was concluded that the limiting slope for each plot was always +2; the plot can be represented by the following equation (*cf.* Eq. (12)):

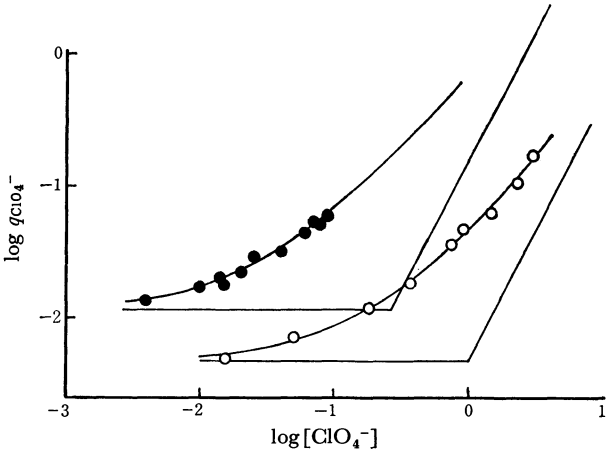

Fig. 5. Dependence of the rate of Be(II) extraction as TTA chelate on the perchlorate concentration in the sodium perchlorate-nitrate systems.
Org. phase. MIBK containing 0.1M TTA.
Aq. phase. 4.0M $Na(ClO_4, NO_3)$ (open circles).
0.1M $Na(ClO_4, NO_3)$ (closed circles).
The solid curve for the open circles gives
$Y=4.9\times10^{-3}(1.0X^2+8.0X+1)$
and for the closed circles gives
$Y=1.2\times10^{-2}(15X^2+48X+1)$.

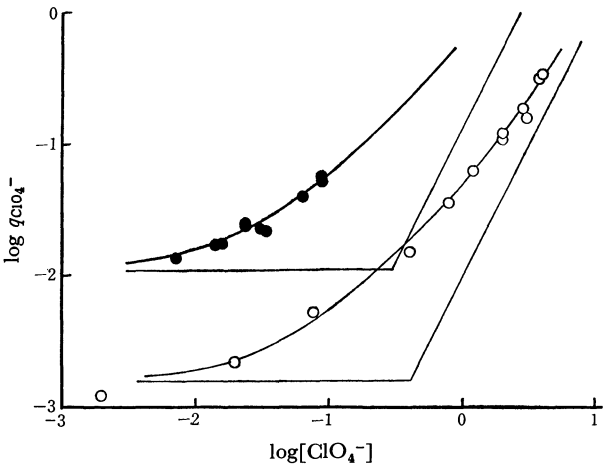

Fig. 6. Dependence of the rate of Be(II) extraction as TTA chelate on the perchlorate concentration in the sodium perchlorate-chloride systems.
Org. phase. MIBK containing 0.1M TTA.
Aq. phase. 4.0M $Na(ClO_4, Cl)$ (open circles).
0.1M $Na(ClO_4, Cl)$ (closed circles).
The solid curve for the open circles gives
$Y=1.6\times10^{-3}(5.9X^2+19X+1)$
and for the closed circles gives
$Y=1.1\times10^{-2}(11X^2+44X+1)$.

$$\log q_{ClO_4^-} = \log k[A^-] + \log(1+k_1[ClO_4^-] + k_2[ClO_4^-]^2) \quad (16)$$

The constants, k^*, k_1, and k_2, in Eq. (10) (and, at the same time, k_1 and k_2 in Eq. (16)) were determined from the parameters of the best-fit standard curve, and the values of k in Eq. (16) were calculated from these values of k^* and the dissociation and distribution constants of TTA in Eqs. (2) and (3) by using Eqs. (4) and (5). The constants are listed in Table 1.

(C) *Effect of the Rate of TTA Distribution.* As has been pointed out, the rate of the distribution of TTA in the organic phase into aqueous solutions is rather slow. For example, the distribution equilibrium is established after 18 hr of two-phase agitation when carbon tetrachloride containing 0.1M TTA is placed in contact with 0.1M sodium perchlorate at pH 2[7] (by a rotating framework at 20 rpm on which stoppered glass tubes containing the two phases were placed. The two-phase agitation in the present study is much more vigorous than this). In order to see the effect of this slow distribution of TTA into the aqueous phase on the rate of beryllium extraction, carbon tetrachloride containing TTA was agitated with aqueous solutions containing no beryllium, but otherwise the same as in the experiments shown in Fig. 1. After the two phases had been agitated vigorously for 5 min, the tracer and carrier were added to the aqueous phase, the agitation was started again, and the extraction was determined as a function of the interval of the agitation after this addition of beryllium to the aqueous phase. However, it was found that the results were practically identical with those in Fig. 1: that is, no difference was observed in the rate of beryllium(II) extraction when the TTA

7) T. Sekine and Y. Hasegawa, "Solvent Extraction Research," ed. by A. S. Kertes and Y. Marcus, Wiley-Interscience, New York (1969), p. 289.

has been distributed between the two phases beforehand and when the TTA was initially added to the organic phase and the beryllium(II) was initially added to the aqueous phase: thus, the distribution of the TTA started at the same time as the metal extraction.

Discussion

Freiser and his co-workers have presented a series of papers on the kinetics of the solvent extraction of divalent metal ions with dithizone and its derivatives.[8-11] They have established that the rate-determining step of the solvent extraction in these system is the formation of the first metal chelate in the aqueous phase (with the exception of zinc extraction with di-α-naphthyldithiocarbazone)[9] if the two phases are vigorously shaken; thus, the effect of the diffusion of materials is eliminated.

In these papers, it was suggested that the rate of metal dithionate formation increases in an approximately linear fashion with the rate of dissociation of water from various metal ions, and that a loss of coordinated water is involved in the rate-determing step.[8-9] However, it was also suggested that, as a relatively minor variation in large ligand anions changes the rate constant for the complex formation considerably in some cases, the initial complex involves a metal-ligand bonding of some sort; in other words, the first complex which is formed rapidly can not be a simple ion-pair.[10]

There have been also some studies of the rate of solvent extraction.[12] It was pointed out that the rates of extraction of chelating systems containing TTA, *N*-benzyl-*N*-phenyl-hydroxylamine, or pyridylazonaphthol seem to be controlled by the chelate formation.[13]

Enhancements of the rate of extraction by the addition of other ligands to the aqueous phase have been pointed out. Finston and his co-workers[14-16] have reported that the rate of extraction of iron(III) and zirconium with TTA in benzene enhanced by the addition of ammonium thiocyanate to the aqueous perchlorate media and that the enhancement is larger when MIBK is added to the organic phase. They suggested in these papers that the enhancements of the extraction caused by the thiocyanate is due to a change in the mechanism of the extraction; the thiocyanate formed in the aqueous phase is first extracted into the organic phase, and then the thiocyanate ions are replaced by TTA in the organic phase. The enhancement of the rate caused by the addition of the thiocyanate is probably due to the fact that above two processes are faster than the TTA chelate formation in the aqueous phase, which is the rate-determining step when the thiocyanate is absent in the system. They also suggested that the synergic enhancement of metal chelate extraction can, at least in some cases, be explained in terms of this kind of kinetic effect.

The addition of acetate ions was found to enhance the rate of zinc dithizonate extraction; $ZnOAc^+$ reacts 25 times as fast as Zn^{2+}, whereas the formation of $NiOAc^+$ does not accelerate the nickel dithizonate extraction.[12] It was also reported that the extraction of chromium(III) with TTA is accelerated by the addition of fluoride ions;[17] this was explained in terms of the intermediate fluoride complexes, which destroy the hydrate shell of Cr^{3+} but do not prevent the formation of extractable chromium(III)-TTA complexes.

The extraction and complex formation equilibria in the systems studied in the present paper have already been reported in another paper.[4] It was observed that nitrate and chloride form relatively weak complexes with beryllium(II); the stability constants are log $\beta_1=-0.63$ for the $BeNO_3^+$ and log $\beta_1=-0.35$ and log $\beta_2=-0.70$ for the $BeCl^+$ and $BeCl_2$ species. At the same time, it was found that beryllium(II) in the aqueous phase containing 4.0M sodium perchlorate is extracted into MIBK containing TTA in three forms, $Be(ClO_4)_2$, $BeAClO_4$, and BeA_2. The extraction of beryllium(II) into MIBK containing no TTA is very small; the distribution ratio is almost proportional to the square of the aqueous sodium perchlorate concentration, which is lower than 4.0M (*cf.* Fig. 1 in Ref. 4).

As has been described, the two phases in this study were agitated so vigorously that the diffusion of materials had no effect on the rate of extraction; the rate-determining step in the system is probably a chemical reaction in one of the phases. This rate-determining reaction could be concluded from the results to be shown below.

The data in Figs. 2 and 3 indicate that the rate of extraction in the carbon tetrachloride systems can be described by $-d[Be^{2+}]/dt=k[Be^{2+}][A^-]$ except for the following data. It can be seen from Figs. 2a and 3a that the plot of the extraction from 0.1M ionic media into carbon tetrachloride deviates from the straight line with a slope of +1 in the lower $-\log[H^+]$ or $[HA]_{org}$ region. From the distribution and dissociation constants of TTA given in Table 1, it can be concluded that the rate of extraction is practically proportional to $[A^-]$ when it is higher than $10^{-6.0}$M, but that the apparent reaction order with respect to the TTA anions becomes larger than +1 for some unknown reasons when $[A^-]$ is lower than this.

The complex formation with nitrate or chloride ions seems to have no remarkable influence on the rate of extraction, for, as can be seen from Fig. 4, the rate in the carbon tetrachloride systems somewhat decreases when 4.0M sodium perchlorate is replaced by chloride

8) C. B. Honaker and H. Freiser, *J. Phys. Chem.*, **66**, 127 (1962).
9) B. E. McClellan and H. Freiser, *Anal. Chem.*, **36**, 2262 (1964).
10) J. S. Oh and H. Freiser, *ibid.*, **39**, 295 (1967).
11) H. Freiser, "Solvent Extraction Chemistry," ed. by D. Dyrssen, J.-O. Liljenzin, and J. Rydberg, North-Holland Pub. Co., Amsterdam (1967), p. 85.
12) H. Freiser, *Anal. Chem.*, **40**, 522R (1968).
13) Yu. A. Zolotov, Khim. Osuovy Ekstraksion, Metoda Razdeleniya Elementov, *Akad. Nauk SSSR, Inst. Geokhim. i Analit. Khim* 1666, 44. cited in Ref. 12.
14) H. L. Finston and Y. Inoue, *J. Inorg. Nucl. Chem.*, **29**, 199 (1967).
15) H. L. Finston and Y. Inoue, *ibid.*, **29**, 2431 (1967).
16) H. L. Finston and E. Gnizi, "Solvent Extraction Research," ed. by A. S. Kertes and Y. Marcus, Wiley-Interscience (1969), p. 333.
17) O. M. Petrukhin, L. A. Izosenkova, I. N. Marov, Tu. N. Dubrov, and Yu. A. Zolotov, *Zh. Neorg. Khim.*, **12**, 1407 (1967), *Chem. Abstr.*, **67**, 57668 (1967).

or nitrate. At the same time, it can also be seen that the rate is practically independent of the ligand concentration when it is higher than 2.0M, in which region the concentration of the complexes and, consequently, that of free beryllium decreases. The authors have not yet found any reasonable explanation of this.

Although there are such exceptions, we may still conclude that the rate of extraction is generally represented by Eq. (15); this indicates that the rate-determining step is the first 1:1 complex formation in the aqueous phase, as Freiser *et al.* have pointed out with regard to the divalent metal dithizonate extractions. The unit reactions for the extraction can be described as:

$$HA(org) \rightleftarrows HA \quad (17a)$$
$$HA \rightleftarrows H^+ + A^- \quad (17b)$$
$$Be^{2+} + A^- \longrightarrow BeA^+ \quad (17c)$$
$$BeA^+ + A^- \rightleftarrows BeA_2 \quad (17d)$$
$$BeA_2 \rightleftarrows BeA_2(org) \quad (17e)$$

Probably only the unit reaction in Eq. (17c) is responsible for the rate given by Eq. (15). As carbon tetrachloride is a nonpolar solvent, the extraction of beryllium species other than the bis-TTA complex is probably very poor. At the same time, the dissociation of TTA in this nonpolar solvent into A^- should be very small (the presence of the TTA anion is necessary in order to explain the rate of extraction in the MIBK systems, as will be shown below). Thus, only the above mechanism is dominant in the carbon tetrachloride system where $[A^-]$ is larger than $10^{-6.0}$M in the 0.1M media and in all the regions studied in the 4.0M ionic media.

In Fig. 4, a difference is observed in the apparent rate of extraction from 0.1M and 4.0M ionic media; the apparent rate constant in Eq. (9c) is ten times larger in the 0.1M media than that in the 4.0M media. However, this is due to the differences in the acid dissociation and two-phase distribution constants, K_a and K_D, in Eqs. (2) and (3). The rate constants for the unit reaction in Eq. (17c), given in Table 1, are not very different in these two ionic media.

In the MIBK systems, the rate of extraction is very much enhanced by the perchlorate ions in the aqueous phase. It seems that this can be explained in terms of the extraction of beryllium ion-pairs with perchlorate ions.

When the ionic concentrations in the aqueous phase is 0.1M and no perchlorate is present, the rate constants in the MIBK systems given by Eq. (15) are practically the same as that in the carbon tetrachloride systems. Thus, the rate-determining step should be the formation of the first complex in the aqueous phase, both in the MIBK systems containing no perchlorate in the aqueous phase and in all the cases in the carbon tetrachloride systems. When sodium perchlorate is added to the aqueous phase instead of the nitrate or chloride, ion-pairs such as $Be(NO_3)(ClO_4)$ or $BeCl(ClO_4)$ and $Be(ClO_4)_2$ are extracted. If these extracted ion-pairs react with the dissociated TTA anion in the organic phase, and if this reaction in the organic phase is faster (although the authors cannot give any reasonable explanation for the faster reaction in the organic phase) than the reaction in the aqueous phase, the enhancements of the rate which are proportional to $[ClO_4^-]$ and $[ClO_4^-]^2$ can be explained; the over-all extraction rate should be given by the sum of these rates, as is described by Eq. (12).

In the MIBK systems, the rate of extraction in the absence of perchlorate ions, that is, k, is already larger than the rate in the carbon tetrachloride systems containing the same aqueous solutions. As was pointed out in a previous paper,[4] the extraction of beryllium in these nitrate or chloride solutions could not be measured within the limits of experimental accuracy ($D_{Be} < 10^{-2}$). However, still it is possible to assume that an extraction of the ion-pairs, $BeCl_2$ or $Be(NO_3)_2$, occurs from such salt solutions into MIBK. This extracted beryllium nitrate or chloride in MIBK (this extraction should be negligible into carbon tetrachloride or from a 0.1M ionic solution into MIBK) could react with TTA anions in the organic phase; the overall effect of that reaction in the aqueous phase which should occur simultaneously may explain why the rate is larger in this solvent than in carbon tetrachloride.

As has been pointed out,[4] the extraction of beryllium perchlorate in the aqueous phase increases with the increase in the aqueous perchlorate concentration. The first-order dependence of the rate on the perchlorate concentration is probably due to the extraction of the mixed species, $Be(NO_3, ClO_4)$ or $Be(Cl, ClO_4)$, while the second-order dependence is probably due to the extraction of the perchlorate, $Be(ClO_4)_2$. These ion-pairs may react in the organic phase and form TTA complexes by exchanging the inorganic anion with the TTA anion.

It is remarkable that the extraction reaction in the MIBK systems is always dependent on the first order of $[A^-]$ and not on $[HA]_{org}$. Until now, no information has been available about the dissociation constant of TTA and the hydrogen-ion concentration in the MIBK phase in an equilibrium with the aqueous phase, and the authors have no knowledge whether or not a portion of the TTA in the MIBK phase is in the dissociated anion, or whether or not the concentration of this TTA fraction, $[A^-]_{org}$, is proportional to that in the aqueous phase, $[A^-]$. However, it may be reasonable to assume that a part of weak acid, TTA, the concentration of which is more than two orders higher than that in the aqueous phase, is also in the dissociated anionic form or is in other forms such as NaA, than the HA form, and that this fraction of TTA reacts with the extracted beryllium ion-pairs in the MIBK phase. When this assumption is accepted, the enhancement of the rate of extraction can be explained as occurring when the rate of this 1:1 complex formation in the organic phase is larger than that in the aqueous phase. It is also reasonable that the complex formation in the organic phase is not assumed in the carbon tetrachloride system, for in this nonpolar solvent, not only does the extraction of the ion-pairs occur, but also the concentration of the TTA anion, which is indispensable for the complex formation in the organic phase, is probably very low.

Eigen,[18] has pointed out that Be^{2+}, Al^{3+}, and other

18) M. Eigen, *Pure Appl. Chem.*, **6**, 97 (1963).

strongly-hydrolysing trivalent metal ions show quite a slow substitution rate of water with a ligand and that the splitting of a water molecule (hydrolysis) is faster than the substitution. Thus, a ligand specificity (basicity) on the rate may be observed in these metal ions. The characteristic rate constants for water substitution in the inner coordination sphere of Be^{2+} given by Eigen is $10^{1.5}$—$10^{2.5}$ (sec^{-1}) or $10^{3.3}$—$10^{4.3}$ (min^{-1}) (Fig. 5 in Ref. 19). The reaction constants for the 1:1 beryllium-TTA complex in the carbon tetrachloride systems in the present study (which is independent of the concentration of the perchlorate ion and can thus be assumed to take place in the aqueous phase) are $10^{4.3}$ and $10^{4.5}$ (min^{-1}). As the pH in the present study is 2.0—3.5 and the metal concentration is very low, the hydrolysis of this metal ion may not be important.[19]

As has been pointed out, the distribution of the TTA in the organic phase into the aqueous phase has been recognized as a slow reaction. In the present study, TTA was initially added to the organic phase and beryllium(II) was initially added to the aqueous phase, and the agitation was started just after the two phases had come in contact in the vessels. When the distribution of this TTA into the aqueous phase in which the reaction between Be^{2+} and A^- occurs is very slow, the concentration, $[A^-]$, at a certain pH should be lower than the value at the equilibrium if the agitation has been carried out for such a short interval as 10 min or less, as in the present experiments. When this occurs, the apparent value of the rate constant, k, calculated by using the value of K_D at the equilibrium should be smaller than the true value, which could be calculated if the K_D value after such a short interval (this value of K_D should be larger than that at the equilibrium) were available. However, as has been described, the present authors have observed that the rate of the extraction of beryllium(II) obtained when the TTA has been distributed between the two phases before the addition of the metal ions is identical with the values obtained when the distribution of TTA is started at the same time as the metal extraction. The authors cannot yet explain why the results of these two series of experiments agree with each other. Further information seems to be necessary before a full explanation of this situation can be given.

The early stage of this work was carried out by Mr. Mitsuo Sakairi. The authors are grateful to him. They are also grateful to Messers Yukio Arai, Teijūrō Ariu, and Yasuki Obi of the present laboratory for their experimental aid. Part of this work was done at the Laboratory of Nuclear and Analytical Chemistry, Institute of Physical and Chemical Research; the authors are grateful to Professor Nobufusa Saito, the head of the Laboratory.

19) L. G. Sillén and A. E. Martell, "Stability Constants," The Chemical Society spec. pub. No. 17 (1964); H. Kakihana and L. G. Sillén, *Acta Chem. Scand.*, **10** 985 (1956); G. Schwarzenbach, *Pure Appl. Chem.*, **5**, 377 (1962).

BULLETIN OF THE CHEMICAL SOCIETY OF JAPAN, VOL. 44, 2911—2915 (1971)

Studies on Microcapsules. XI. Electrophoretic Behavior of Polyphthalamide Microcapsules Containing Aqueous Solution of Bovine Serum Albumin

Motoharu SHIBA, Yasuaki KAWANO, Suiichi TOMIOKA, Masumi KOISHI,* and Tamotsu KONDO*

Research Laboratory, Chugai Pharmaceutical Co., Ltd., Toshima-ku, Tokyo,
**Faculty of Pharmaceutical Science, Science University of Tokyo, Shinjuku-ku, Tokyo*

(Received March 8, 1971)

Electrophoretic measurements were made on polyphthalamide microcapsules containing aqueous solution of bovine serum albumin and their membrane at various hydrogen ion concentrations. The microcapsules moved toward the anode at any pH, while the membrane migrated to the anode above pH 3.5 and to the cathode below this pH. These results were explained on the assumption that a fraction of albumin molecules is chemically incorporated into the microcapsule membrane through the microencapsulation and that the net electrical charge of the microcapsules is highly dependent on the charge of the outer surface of their membrane.

A previous paper of this series[1] has reported the electrophoretic behavior of polyphthalamide microcapsules containing aqueous solution of various polyelectrolytes. The microcapsules containing anionic or cationic polyelectrolyte, such as sodium heparinate or poly(1,2-dimethyl-5-vinyl pyridinium methyl sulfate), were found to move towards the anode or cathode according to the sign of charge on the polyelectrolyte encapsulated. When the microcapsules contained aqueous solution of amphionic polyelectrolyte, such as 2-methyl-5-vinylpyridine methyl acrylate-methacrylic acid copolymer, they migrated either to the anode or the cathode depending on the pH of the medium, showing the existence of an isoelectric point.

1) M. Shiba, Y. Kawano, S. Tomioka, M. Koishi, and T. Kondo, *Kolloid-Z. Z. Polym.*, submitted.

On the other hand, it was strongly suggested that bovine serum albumin, a typical amphoteric polyelectrolyte, participates in the interfacial polycondensation reaction between diamine and acid dichloride because albumin molecules, contrary to the amphionic polyelectrolyte molecules used in the previous paper,[1] have many amino groups which are able to react readily with acid chloride.[2] If it is really the case, a different electrophoretic behavior may be expected for microcapsules containing aqueous solution of bovine serum albumin from that for those containing aqueous solution of the polyampholyte.

This paper describes the experimental results on the electrophoresis of polyphthalamide microcapsules containing aqueous solution of bovine serum albumin and their possible implications.

Experimental

Preparation of Microcapsules. Polyphthalamide microcapsules containing aqueous bovine serum albumin solution used in this work were prepared by the same method as described in the previous paper[2] by making use of the interfacial polycondensation reaction between terephthaloyl dichloride and piperazine, and dispersed in water with the aid of dispersing agent. The microcapsule dispersion so obtained was dialyzed in a cellulose tubing (Visking) against distilled water at 40°C with shaking until a constant specific conductance of the dispersion was attained in order to remove any remaining ionogenic impurities. The dialyzed microcapsule dispersion could be conveniently stored in a refrigerator at 2—4°C before use. A fraction of the stored microcapsules was broken by subjecting to a high centrifugal field. This was done because it was expected that there may be a difference in surface charge between the outside and the inside of the membrane in view of the possibility that some of the albumin molecules encapsulated participate in the interfacial polycondensation reaction. The membranes thus obtained was washed and dispersed in buffer solution.

Measurement of Electrophoretic Mobility. Electrophoretic measurements of the microcapsules and their membrane were taken in a quartz flat microelectrophoretic cell. The media for the measurements were acetate buffer (pH 3—6) and HCl-sodium acetate buffer (pH 2—3), the ionic strength of which was maintained at 0.01 by the addition of NaCl throughout the measurement unless otherwise stated. For each measurement 40 specimens were timed in each direction to eliminate the polarization effect of the electrodes. Mobilities were taken at room temperature and corrected to water at 25°C.

Calculation of Zeta-Potential. At first sight, mobilities seemed to be convertible into zeta-potentials (ζ) by means of the simple Smoluchowski-Henry equation,[3]

$$\zeta = \frac{f \cdot \pi \cdot \eta}{D \cdot X} \cdot U$$

where U is the mobility, η the viscosity of the medium, D the dielectric constant, X the potential gradient, and f the numerical factor depending on the product of the reciprocal thickness of double layer and the particle diameter. However, some correction was necessary because the surface conductance was found to be of the order of $10^{-7}\Omega^{-1}$ which could not be neglected in the calculation. Zeta-potentials of the microcapsules were, therefore, calculated by the Henry equation,[4]

$$\zeta = \frac{6 \cdot \pi \cdot \eta}{D \cdot X} \cdot U[1 + \lambda'\{3f(\kappa a) - 2\}]$$

where κ represents the reciprocal thickness of double layer, a the microcapsule diameter, and $f(\kappa a)$ a function of κa. λ' is given by the following equation,

$$\lambda' = \frac{\mu_0 - \frac{2\mu_s}{a}}{2\left(\mu_0 + \frac{\mu_s}{a}\right)}$$

where μ_s is the surface conductance and μ_0 the specific conductance of the suspending medium. The surface conductance was evaluated by the method proposed by Fricke and Curtis.[5]

The Henry equation was also used for calculating the zeta-potential of microcapsule membrane. In this case, the value of a was assumed to be the same as the average diameter of the microcapsules though the shape of the membrane was not necessarily spherical. Therefore, the zeta-potential of the membrane should be regarded as being apparent.

Results and Discussion

Figure 1 shows the change in the specific conductance of the microcapsule dispersion during dialysis in a cellulose tubing against the volume of distilled water used. As the ionogenic impurities diffused out through the microcapsule membrane and the cellulose tubing, the specific conductance of the microcapsule dispersion decreased and then levelled off. The final value of specific conductance increased with increasing concentration of albumin encapsulated, being presumably due

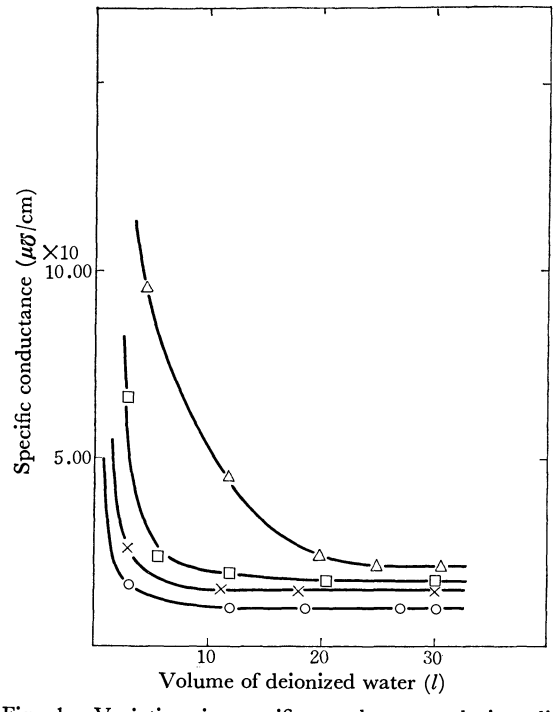

Fig. 1. Variation in specific conductance during dialysis against water of microcapsule dispersions.
Albumin Concentration:
(○) 0.5%, (×) 1%, (□) 2%, (△) 5%

2) M. Shiba, S. Tomioka, M. Koishi, and T. Kondo, *Chem. Pharm. Bull. (Tokyo)*, **18**, 803 (1970).
3) D. C. Henry, *Proc. Roy. Soc. London*, **133**, 106 (1931).
4) D. C. Henry, *Trans. Faraday Soc.*, **44**, 1021 (1948).
5) H. Fricke and H. J. Curtis, *J. Phys. Chem.*, **40**, 715 (1936).

to the dissociation of albumin molecules in water.

The microcapsule dispersions used in this work were those having the final specific conductance given in the figure.

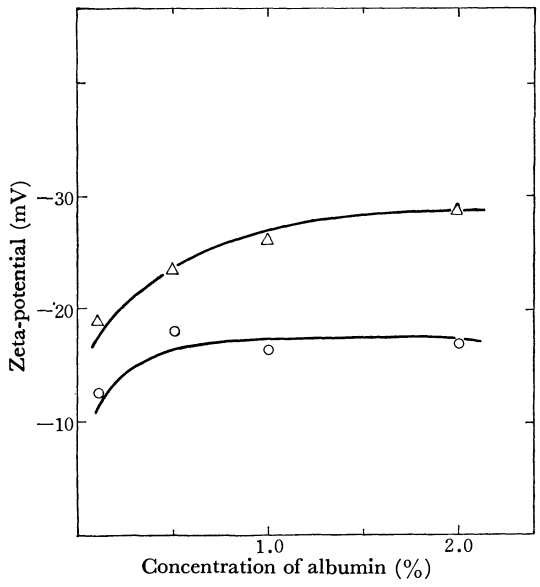

Fig. 2. Zeta-potential of microcapsules containing aqueous albumin solution as a function of albumin concentration in acetate buffers.
(○) pH 4.7, (△) pH 5.7

The zeta-potential of the microcapsules is given in Fig. 2 as a function of the concentration of albumin solution used in their preparation. The potential increased as the concentration of albumin increased and then became nearly constant above a concentration of 1% albumin irrespective of the pH of the medium. This tendency is quite similar to that observed for the microcapsules containing aqueous polyelectrolyte solution.[1)]

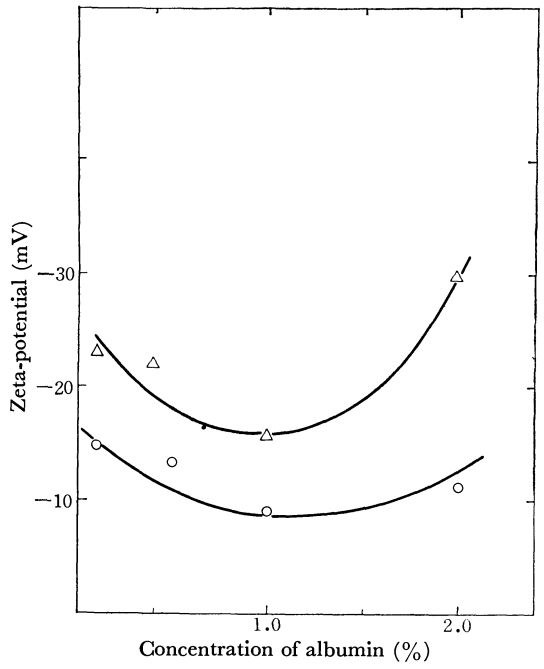

Fig. 3. Zeta-potential of microcapsule membrane as a function of albumin concentration used for preparing microcapsules in acetate buffers.
(○) pH 4.7, (△) pH 5.7

In Fig. 3 is plotted the zeta-potential of microcapsule membrane against the concentration of albumin solution. In contrast to the microcapsule themselves, the membrane showed a minimum zeta-potential when the albumin concentration varied. The appearance of the minimum may be interpreted as follows. An increase in the albumin concentration will increase the number of albumin molecules chemically incorporated in the membrane, causing an increase in the number of dissociable carboxyl groups. The increase in the number of dissociable carboxyl groups will facilitate the fixation of counter ions, thereby lowering the zeta-potential. However, it may outweigh the fixation of counter ions at high albumin concentration, resulting in an increase of negative charge of the microcapsule membrane.

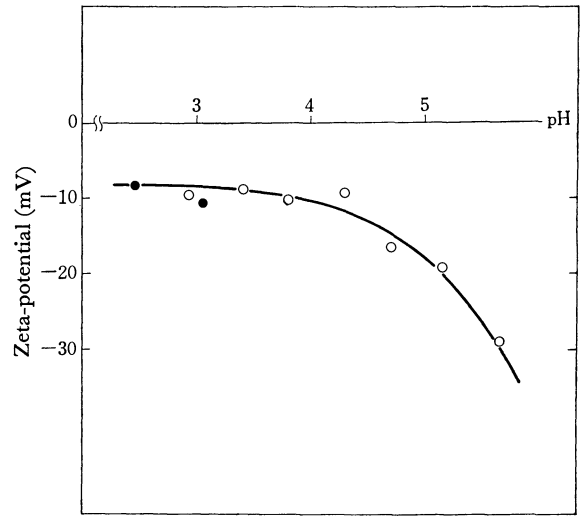

Fig. 4. Zeta-potential of microcapsules containing aqueous 1 wt% albumin solution as a function of pH in CH_3COONa–CH_3COOH (○) and CH_3COONa–HCl (●) buffers at a constant ionic strength of 0.01.

Figure 4 illustrates the zeta-potential *versus* pH curve of the microcapsules. They were negatively charged at all pH, even at lower pH than that of the isoelectric point of albumin (pH 4.8). This differs from what has been reported in the previous paper[1)] in that the microcapsules do not necessarily bear a charge of the same sign as that of albumin molecules encapsulated. The polyphthalamide microcapsules containing aqueous solution of cationic or anionic polyelectrolyte always moved towards the cathode or anode in an electric field in accordance with the sign of charge on the encapsulated polyelectrolyte.[1)]

The dependence of apparent zeta-potential of the microcapsule membrane on the pH of the medium is shown in Fig. 5. What is evident from this figure is a charge reversal of the membrane occurred in the vicinity of pH 3.5, indicating the existence of isoelectric point. This should be related to the chemical incorporation of albumin molecules into the membrane through the reaction with acid chloride.[2)]

Of the dissociable groups of albumin, the carboxyl groups of aspartic and glutamic acids give negative

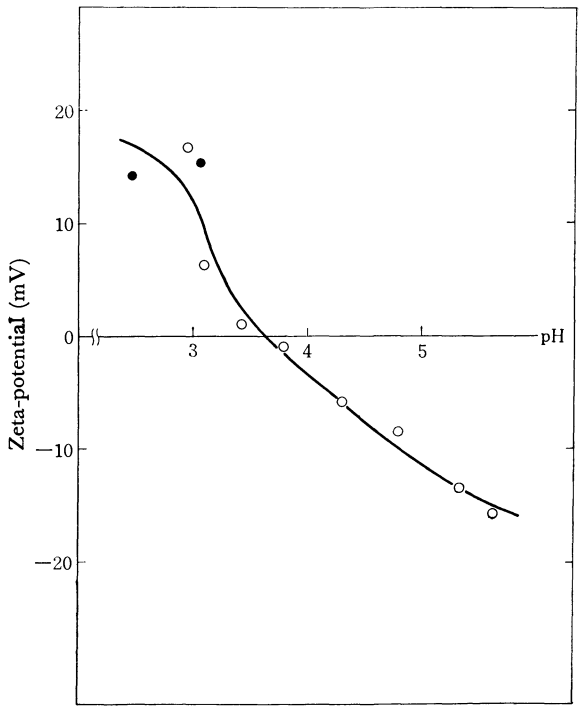

Fig. 5. Zeta-potential of microcapsule membrane as a function of pH in CH_3COONa–CH_3COOH (○) and CH_3COONa–HCl (●) buffers at a constant ionic strength of 0.01.

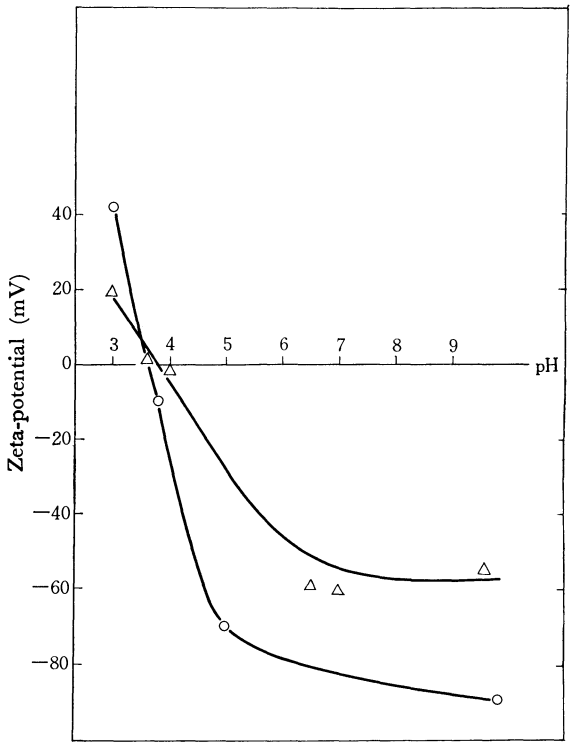

Fig. 6. Zeta-potential of microcapsules containing aqueous 1 wt% MPM solution as a function of pH in acetate buffers. Ionic strength: (△) 0.01 and (○) 0.001

charge (the dissociation of the hydroxyl groups of tyrosine and the sulfhydryl groups of cystein may also contribute to the negative charge at high pH) while the amino groups of lysine and arginine, and imino groups of histidine can produce positive charge. In view of this and the pK of each group,[6] it may be assumed that about 60% of the amino groups of lysine and arginine have reacted with acid chloride to shift the isoelectric point of the chemically incorporated albumin from pH 4.8 to 3.5.

As to the albumin molecules in the encapsulated solution, preliminary tests were made to check whether they were modified or not during the microencapsulation process. The Ouchterlony method,[7] which is frequently used in immunochemistry, and paper-electrophoresis proved that the albumin molecules are not subjected to any detectable changes immunochemically or electrophoretically during the microencapsulation process as compared with native albumin molecules.

Before making an attempt to elucidate the difference in the pH dependence of zeta-potential between the microcapsules and their membrane, an examination is made of the electrophoretic behavior of polyphthalamide microcapsules containing solution of a copolymer of 2-methyl-5-vinylpyridine-methyl acrylate and methacrylic acid (Fig. 6). This polymer (abbreviated as MPM) is practically insoluble in water in the range of pH 4—7.5.[8] However, the polymer is readily soluble in water outside of this pH region and has a net negative charge above pH 7.5 and a net positive charge below pH 4. Moreover, the polymer is unable to react with acid chloride. As is seen from the figure, the microcapsules containing aqueous MPM solution are negatively charged above pH 7.5 and positively charged below pH 4. It may be inferred, therefore, that the sign of charge of microcapsules is determined solely by that of amphoteric polyelectrolyte unless the membrane acquires electrical charge by chemically incorporating the polyelectrolyte.

TABLE 1. SIGN OF CHARGE OF ALBUMIN MOLECULES, MICROCAPSULES, AND THEIR MEMBRANE

Species	pH region		
	Below 3.5	3.5—4.8	Above 4.8
Encapsulated albumin	+	+	−
Microcapsules	−	−	−
Microcapsule membrane	+	−	−

In Table 1 are summarized the sign of charge of the encapsulated albumin, microcapsules, and their membrane in three pH regions. When the pH of the medium was above 4.8, all of the encapsulated albumin molecules, microcapsules, and their membrane were negatively charged. In the region of pH 4.8—3.5, the microcapsules and their membrane had a negative charge while the albumin molecules bore a positive charge. This may result from the screening of the positive charge of albumin molecules in the encapsulated solution by the negative charge of the membrane. Very curiously, however, the microcapsules were negatively charged below pH 3.5 in spite of

6) J. Steinhart and S. Beychok, "The Proteins," Vol. 2, Academic Press, New York (1964), p. 162.
7) O. Ouchterlony, *Pror. Allergy*, **5**, 1 (1958).
8) T. Ida, S. Kishi, S. Takahashi, and I. Utsumi, *J. Pharm. Sci.*, **51**, 1061 (1962).

positive charges on the encapsulated albumin molecules and the membrane. This makes it necessary to consider the distribution of charged sites in the membrane.

It is evident that polyphthalamide molecules constituting the microcapsule membrane form and grow on the organic solvent side of the organic solvent-water interface.[9] The presence of albumin molecules in the water phase to be encapsulated will not change the features of the polycondensation reaction except that albumin molecules may participate in the polymerization. The amino groups of albumin molecules are very likely to react at the interface with acid chloride molecules coming from the interior of the organic phase to form amide linkages since albumin molecules can spread in a more expanded state at the oil-water interface than at the air-water interface[10] with the amino groups directing towards the oil phase.[11] As the polycondensation reaction proceeds, the amount of acid chloride reaching the interface will decrease with time and thereby will increase the number of amino groups remained unreacted of the following albumin molecules. The number of dissociable amino groups in the microcapsule membrane will increase, therefore, in the direction from the outside to the inside of microcapsules whereas the dissociable carboxyl groups are uniformly distributed in the membrane. As the result, the negative charge on the outer surface of the membrane may screen and surpass the positive charge on the inner surface and albumin molecules in the encapsulated solution. Based on this assumption, the positive zeta-potential observed for the microcapsule membrane below pH 3.5 (Fig. 5) may be interpreted as indicating that the breakdown of the microcapsules by centrifugation turned their membrane inside out, probably because the inner surface is likely to be more hydrophilic than the outer surface, thus making prevail the positive charge due to the amino groups of albumin incorporated in the membrane over the negative charge arising from the dissociation of the carboxyl groups.

9) P. W. Morgan and S. L. Kwolek, *J. Polymer Sci.*, **40**, 299 (1959).
10) A. E. Alexander and T. Teorell, *Trans. Faraday Soc.*, **35**, 727 (1939).
11) J. T. Davis, *Biochem. J.*, **56**, 509 (1954).

BULLETIN OF THE CHEMICAL SOCIETY OF JAPAN, VOL. 44, 2915—2918 (1971)

Photochemical Reactions of Uranyl Ions with Organic Compounds. IV. The Uranyl Fluorescence Quenching by Aliphatic Alcohols

Shukichi SAKURABA and Ryoka MATSUSHIMA
Faculty of Engineering, Shizuoka University, Hamamatsu

(Received March 15, 1971)

The relative rates for uranyl fluorescence quenching by aliphatic alcohols (methyl, ethyl, *n*-propyl, isopropyl, *n*-butyl, isobutyl, and *s*-butyl alcohols) were measured under various conditions. The rates were increased in proportion to the perchloric acid concentration at pH <1, whereas the rates were smaller and nearly constant at the pH's between 1—4; thus showing the involvement of both acid-dependent and acid-independent processes. Though the rates for both processes changed with the change in the alcohol structure (the polar substituent effect), the ratio of the two rate constants was nearly constant. The inhibitory effects of cupric ions (as a scavenger for the one-equivalent redox intermediates) suggested that the acid-dependent quenching process involves a two-equivalent redox or two consecutive one-equivalent redox steps between the same partners. The mechanisms of these quenching processes are discussed.

A kinetic study has been made of the photo-redox reaction of the uranyl ions with alcohols in solution with pH's ranging from 1 to 3, where the rates seemed to be insensitive to the acidity of the medium.[1] However, in the course of the investigation of the effects of the acid concentration (up to 2M in perchloric acid) on the rates, it appeared that the rates of both the quenching and the photo-redox reactions were increased with the acid concentration in the pH region below 1, suggesting the involvement of an acid-catalyzed process as well as an acid-independent process. Further, the former process seemed to involve a two-equivalent redox or two consecutive one-equivalent redox steps between the same partners, while the latter process features *via* α-hydrogen abstraction (followed by proton liberation) *i.e.*, a one-equivalent redox process, followed by the disproportionation reactions to produce the photo-redox products. The quenching mechanisms are discussed in connection with photo-redox reaction mechanisms.

1) S. Sakuraba and R. Matsushima, This Bulletin, **43**, 2359 (1970).

Experimental

Guaranteed reagents and doubly-distilled water were used. Preliminary experiments showed that traces of such impurities as halogen ions and aldehydes or ketones which might be present in the reagents were negligible under the present conditions.

Aqueous solutions of the 0.02M uranyl nitrate containing various concentrations of the substrates and perchloric acid

were prepared. After the desired temperature (usually 20°C) was attained, the relative fluorescence intensities were rapidly measured. The fluorescence measurements were carried out using a fluorescence spectrophotometer (Hitachi 204 Type) without an attachment for temperature control. The errors in the determination of the temperature inherent in the procedure were estimated to be within ±1°C. De-oxygenation with oxygen-free nitrogen (keeping air-tight) produced no change in the fluorescence intensities. The relative intensities at the 510 nm peak of the uranyl fluorescence were measured with 405 nm excitation, though no significant changes in the quenching constants were observed with the changes in the analyzing (490, 510, 533 nm) and the excitation (313, 366, 405 nm) wavelengths with the exception of a slight lowering in the quenching constants with the 436 nm excitation. The methods for the analysis of the photo-redox products and the measurements of their quantum yields were previously described.[1]

Results and Discussion

Effects of pH and Ionic Strength on the Rate. The quenching constants of the uranyl fluorescence by some alcohols at various pH's are shown in Fig. 1. In the pH region below 1 the quenching constant was markedly increased with the increase in acidity, while it was nearly constant in the pH region from 1 to 4. Perchloric acid did not quench the fluorescence of a 0.02M uranyl solution in the absence of alcohols. Thus, the quenching reaction involves both acid-dependent and acid-independent processes. The rates of these processes, then, can be expected to result in a difference in their sensitivities to ionic strength. The effects of the ionic strength on the rates at different acid concentrations are shown in Fig. 2. The slope of the plot for the 0.5M $HClO_4$ solution was 0.28, larger than that for the solutions of pH 1 and 2, 0.07. Since the quenchers (alcohols) have no net charge, the rate for a simple bimolecular quenching process between the excited uranyl ion and the quencher should not be affected largely by the ionic strength, while the rate of the quenching process in which the hydrogen ions participate should show a greater sensitivity to the ionic strength.[2]

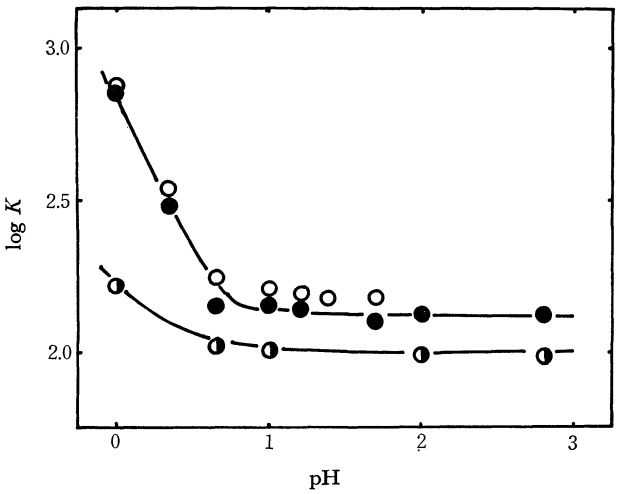

Fig. 1. Variation in the quenching constant with pH.
$[UO_2(NO_3)_2]=0.02$M, [substrate]=0.005—0.05M,
λ(excitation)=405 nm, λ(emission)=510 nm.
◑: *n*-Propyl alcohol, ●: *s*-Butyl alcohol,
○: Glucose.

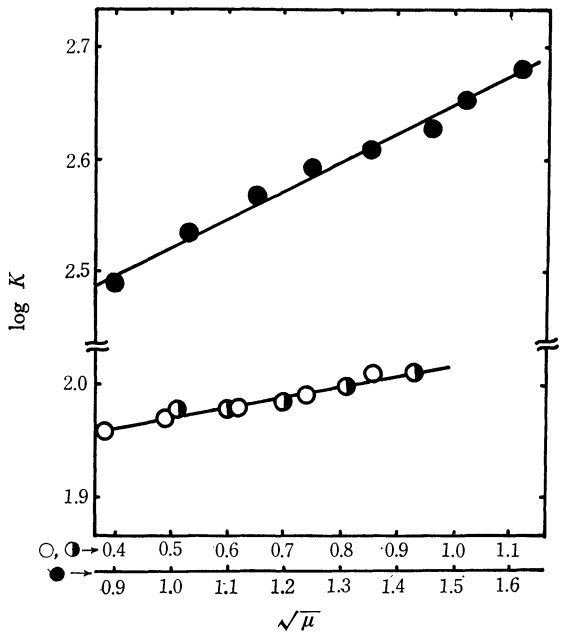

Fig. 2. Effects of ionic strength on the quenching constant (*n*-Propyl alcohol).
$[UO_2(NO_3)_2]=0.02$M, [*n*-Propyl alcohol]=0.005—0.05M,
λ(excitation)=405 nm, λ(emission)=510 nm,
●: $[HClO_4]=0.5$M (pH≒0), ○: pH=2.0,
◑: pH=1.0.

Inhibitory Effects by Cupric Ions. Table 1 shows the inhibitory effects of cupric ions (as scavengers for one-equivalent redox intermediates[1,3]) on the formation of the photo-redox products. The direct quenching of the uranyl fluorescence by cupric ions was negligible. Cupric ions can only scavenge the one-equivalent redox intermediates, U(V) and/or R· species; the effect should be less sensitive to the two-equivalent redox process. Therefore the change in the effects on the ratio of the products, [U(IV)]/[Ox], with the acid concentration suggests that the acid-dependent chemi-

Table 1. Inhibitory effects of cupric ions on the product ratio [U(IV)]/[Ox] at different acid concentration[a]

$[HClO_4]$, M	$[U(IV)]\times10^3$M	$[Ox]\times10^3$M	[U(IV)]/[Ox]
0.02	0.47	3.00	0.16
0.04	1.34	2.98	0.45
0.16	1.72	3.17	0.54
0.30	3.10	3.20	0.97
0.08	3.39	3.23	1.05[b]

Initial concentrations of $UO_2(NO_3)_2$, *n*-propyl alcohol, and $CuSO_4$ were 0.02, 0.20, and 0.005M, respectively.
a) Solutions to be photolyzed were de-oxygenated with oxygen-free nitrogen and kept air-tight.
b) In the absence of cupric ions.

2) K. J. Laidler, "Chemical Kinetics," McGraw Hill, New York (1965), pp. 219—222.
3) a) A. C. Harkness and J. Halpern, *J. Amer. Chem. Soc.*, **81**, 3526 (1959); b) F. A. Jones and E. S. Amis, *J. Inorg. Nucl. Chem.*, **26**, 1045 (1964).

cal quenching process involves a two-equivalent redox or two consecutive one-equivalent redox steps between the same partners within a solvent cage. Table 1 also shows that cupric ions mainly scavenge the U(V) species, since the amount of the oxidation product, [Ox], is only slightly decreased in the presence of cupric ions.

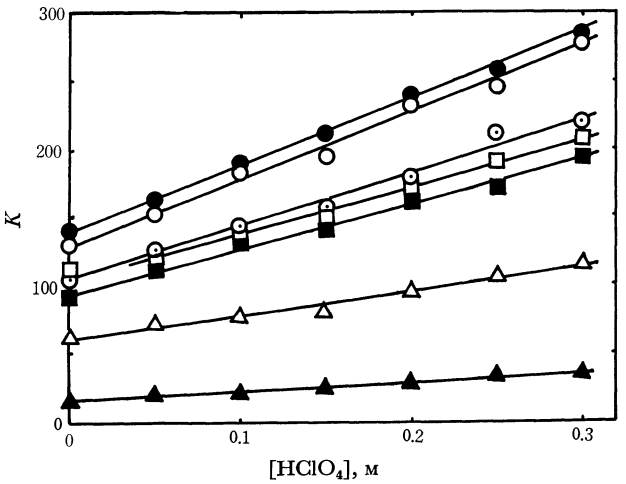

Fig. 3. Linear relationship between the quenching constant and the acid concentration.
$[UO_2(NO_3)_2]=0.02$M, [Alcohol]$=0.005-0.5$M,
λ(excitation)$=405$ nm, λ(emission)$=510$ nm,
Temperature$=20\pm1$°C.
●: *s*-Butyl alcohol,
○: Isobutyl alcohol, ⊙: *n*-Butyl alcohol,
□: Isopropyl alcohol, ■: *n*-Propyl alcohol,
△: Ethyl alcohol, ▲: Methyl alcohol.

Separation of the Quenching Constants. The quenching constants, K's, in the Stern-Volmer equation[4] (1), were measured as a function of the perchloric acid concentration (Fig. 3):

$$I_f^0/I_f = 1 + K[\mathrm{R}] \quad (1)$$

Figure 3 shows that the quenching constants, K, can be represented by the following equation:

$$K = K_1 + K_2[\mathrm{H}^+] \quad (2)$$

where K_1 and K_2 refer to the quenching constants for the acid-independent and the acid-dependent processes respectively. In Table 2, K_1 (the intercept) and K_2 (the slope) obtained from the plot of K *vs.* $[H^+]$ are listed. It may be noticed that the ratio of the quenching constant for the acid-dependent process to that for the acid-independent process, K_2/K_1, is nearly constant, whereas both K_1 and K_2 vary considerably, with the variation in the alcohol structure.

TABLE 2. THE QUENCHING CONSTANTS, K_1 AND K_2 IN Eq.(2), FOR ALIPHATIC ALCOHOLS (from Fig. 3).

Alcohols	K_1, M^{-1}	K_2, M^{-2}	K_2/K_1, M^{-1}
Methyl	16	60	3.8
Ethyl	60	180	3.0
n-Propyl	90	340	3.8
Isopropyl	107	340	3.2
n-Butyl	105	400	3.8
Isobutyl	130	480	3.7
s-Butyl	140	490	3.5

The Mechanism. The following mechanism may be assumed for the quenching reaction of the uranyl fluorescence by aliphatic alcohols in an acidic aqueous solution:

$$\mathrm{U} + h\nu \xrightarrow{I_a} \mathrm{U} \quad (3)$$

$$\mathrm{U}^* \xrightarrow{k_f} \mathrm{U} + h\nu' \quad (4)$$

$$\mathrm{U}^* \xrightarrow{k_d} \mathrm{U} + \text{heat} \quad (5)$$

$$\mathrm{U}^* + \mathrm{U} \xrightarrow{k_s} 2\mathrm{U} + \text{heat} \quad (6)$$

$$\mathrm{U}^* + \mathrm{R} \xrightarrow{k_1} \mathrm{U(V)} + \mathrm{R}\cdot + \mathrm{H}^+ \quad (7)$$

$$\mathrm{U}^* + \mathrm{R} \xrightarrow{k_1'} \mathrm{U} + \mathrm{R} + \text{heat} \quad (8)$$

$$\mathrm{U}^* + \mathrm{R} + \mathrm{H}^+ \xrightarrow{k_2} \mathrm{U(IV)} + \mathrm{Ox} + 3\mathrm{H}^+ (\text{or } \mathrm{U(V)} + \mathrm{R}\cdot + 2\mathrm{H}^+) \quad (9)$$

$$\mathrm{U}^* + \mathrm{R} + \mathrm{H}^+ \xrightarrow{k_2'} \mathrm{U} + \mathrm{R} + \mathrm{H}^+ + \text{heat} \quad (10)$$

Here, U, R, U(V), R·, U(IV), and Ox refer to $(UO_2^{2+})_{aq}$, R_1R_2CHOH, $(UO_2^{+})_{aq}$ $R_1R_2\dot{C}OH$, U(IV) species, and R_1R_2CO respectively; I_a is the rate of the light absorption in einsteins$\cdot l^{-1}$sec^{-1}; k_1 and k_2 refer to the rate constants for the acid-independent and the acid-dependent quenching processes respectively. Process (7) has been shown to involve a one-equivalent redox (α-hydrogen abstraction[1,5]), followed by fast disproportionation reactions:

$$2\mathrm{U(V)} \xrightarrow{\mathrm{H}^+} \mathrm{U(IV)} + \mathrm{U}, \text{ and } 2\mathrm{R}\cdot \longrightarrow \mathrm{R} + \mathrm{Ox}.$$

The acid-dependent chemical quenching process (9) may involve a two-equivalent redox or two consecutive one-equivalent redox steps between the same partners. This is suggested by the facts that (i) the product quantum yield is higher than 0.5 in the 1N $HClO_4$ solution (the maximun quantum yield for the photoredox products expected from the one-equivalent transfer is 0.5), and (ii) the cupric ions have minor inhibitory effects. However, the initial reacting species in the process has not yet been clarified, and the description drawn here may not be valid; alternative mechanisms, such as those involving a fast pre-equilibrium of proton-addition on the uranyl ion or of the formation of a complex or an ester-intermediate, may explain the results equally well.

Since neither the change in the concentration of alcohol nor that of perchloric acid resulted in a change in the absorption of the system (pH<2), the steady state assumption for U* leads to the following expression:

$$I_f^0/I_f = 1 + \tau_0\{k_1+k_1'+(k_2+k_2')[\mathrm{H}^+]\}[\mathrm{R}] \quad (11)$$

$$= 1 + \tau_0(k_1+k_1')[\mathrm{R}] + \tau_0(k_2+k_2')[\mathrm{R}][\mathrm{H}^+] \quad (12)$$

$$\tau_0 = \{k_f+k_d+k_s[\mathrm{U}]\}^{-1} \quad (13)$$

From Eqs. (1), (2), (11), and (12), the following equations result:

$$K_1 = \tau_0(k_1+k_1') \quad (14)$$

4) O. Stern and M. Volmer, *Physik. Z.*, **20**, 183 (1919).

5) To be published.

$$K_2 = \tau_0(k_2+k_2') \quad (15)$$

$$K_2/K_1 = (k_2+k_2')/(k_1+k_1') \quad (16)$$

While both K_1 and K_2 in Table 2 decrease with the increase in the polar substituent effect, $\sum\sigma^*$[6] of the substrate (alcohol), the K_2/K_1 ratio is nearly constant; *i.e.*, the sensitivities of the rates of the two processes (acid-dependent and independent processes) are similar. This suggests that the rate-determining steps of the two processes involve the same primary act, *i.e.*, α-hydrogen abstraction. The two processes, however, differ in their secondary steps: the secondary step of the acid-dependent process involves a second one-equivalent redox reaction between the same partners, whereas that of the acid-independent process involves the disproportionation reaction of the UO_2^+ species, each of which is formed in a separate solvent cage.[1] The change in the rate with the acid concentration may be attributable to the change in the species of the uranyl ions excited or to be excited. One can assume, for example, that the protonated uranyl ions are formed through a fast equilibrium[7]: $UO^{2+}+H^+ \rightleftharpoons UO_2H^{3+}$, and have stronger oxidation power in their excited states (and/or intermediate states) than the unprotonated uranyl ions. The formation of a complex[8] or an ester-like intermediate[9] (as has been proposed for the thermal oxidations by many transition metal ions) prior to the photolysis is also conceivable. However, no evidence for such pre-equilibria was found from absorption, emission, and excitation spectra. At this stage we cannot decide the initial species in the acid-dependent process; hence, only a tentative stoichiometry has been outlined here. These problems will be discussed later in detail, with more experimental date.

6) M. S. Newman, "Steric Effects in Organic Chemistry," John Wiley and Sons, New York (1956), p. 619.

7) Analogous to that of the thermal oxidations with the vanadyl ions: J. S. Littler and W. A. Waters, *J. Chem. Soc.*, **1959**, 4046.

8) a) G. E. Heckler, A. E. Taylor, C. Jensen, D. Percival, R. Jensen, and P. Fung, *J. Phys. Chem.*, **67**, 1, (1962); b) K. Venkatarao and M. Santappa, *Indian J. Chem.*, **5**, 304 (1967); c) *Chem. Abstr.*, **66**, 9476 (1967); d) S. Sakuraba and R. Matsushima, This Bulletin, **43**, 1950 (1970);

9) a) F. H. Westheimer and N. Nicolaides, *J. Amer. Chem. Soc.*, **71**, 25 (1949); b) W. A. Waters, "Mechanisms of Oxidation of Organic Compounds," Methuen and company, London (1964); c) K. B. Wiberg and H. Schöfer, *J. Amer. Chem. Soc.*, **91**, 933 (1969).

BULLETIN OF THE CHEMICAL SOCIETY OF JAPAN, VOL. 44, 2918—2921 (1971)

Desorption of Spread Monolayer of 1-Dodecanol into Aqueous Sodium Dodecyl Sulfate Substrate

Tsutomu SEIMIYA, Kazuo OHBU,* Akio NAKAMURA, and Tsunetaka SASAKI

Department of Chemistry, Faculty of Science, Tokyo Metropolitan University, Setagaya, Tokyo

(Received March 19, 1971)

The process of desorption of dodecanol monolayer into the aqueous sodium dodecyl sulfate (SDS) solutions of varying concentrations was studied by the surface tension measurement. The rate of desorption in its early stage obeyed the simple diffusion law and the plot of logarithms of surface pressure against the square root of time showed a linear relationship. The rate constant of desorption decreased slightly and linearly with an increasing concentration of SDS up to CMC. Beyond CMC it increased rapidly and linearly owing to the increase of dodecanol solubility due to the solubilization. Further, from these rate constants and the surface tension *vs.* concentration curve, the diffusion coefficient of dodecanol in water and in aqueous SDS solutions, its solubilization in aqueous SDS solution and the partition coefficient of dodecanol between water and SDS micelles were calculated. Critical micelle concentration of sodium dodecyl sulfate was also determined as a break point of desorption constant *vs.* concentration curve.

The dissolution of and penetration into a monolayer spread on an aqueous surface have been studied by many investigators referring to the state of monolayer or the mechanism of interaction between the monolayer constituents,[1] reaction kinetics of the monolayer,[2] and the mechanism of desorption.[3-5]

In the present report, the mechanism of the rate of dissolution of spread dodecanol monolayer into an underlying aqueous solution of sodium dodecyl sulfate (SDS) was studied by measuring the change of surface tension due to its dissolution. When the rate constant

* Preseot address, Lion Fat and Oil Co. Ltd., Edogawa, Tokyo.

1) J. T. Davies, "Surface Phenomena in Chemistry and Biology," ed. by F. J. Danielli, K. G. A. Pankhurst, and A. C. Riddford, Pergamon Press, London, New York, Paris, Los Angeles (1958), p. 60; D. G. Dervichian, *ibid.*, p. 70.

2) K. G. A. Pankhurst, *ibid.*, p. 100; M. Muramatsu and H. Sobotka, *J. Colloid Sci.*, **18**, 636 (1963).

3) L. Saraga, *C. R. Acad. Sic., Paris.*, **233**, 135 (1951).

4) L. Ter. Minassian-Saraga, *J. Colloid Sci.*, **11**, 398 (1956).

5) H. L. Rosano and G. Karg, *J. Phys. Chem.*, **63**, 1692 (1959); N. L. Gershfeld and C. S. Patlak, *J. Phys. Chem.*, **70**, 286 (1966); J. T. Davies, *Trans. Faraday Soc.*, **48**, 1052 (1952).

of dissolution was expressed as a function of SDS concentration, two straight lines were obtained which intersected with each other at the critical micelle concentration (CMC) of SDS. Saraga's equation for the monolayer dissolution[3] was extended to explain the rate of dissolution of the monolayer into SDS solution below and above CMC.

Experimental

Materials. Dodecanol used was fractionally distilled and its purity was checked by the gas chromatography to be 98%. It contained no higher homologues. SDS was synthesized by the usual method[6] and was purified by repeated extraction with ether and recrystallization from ethanol until a minimum in the surface tension *vs.* concentration curve disappeared. Benzene used as a spreading solvent was purified by shaking with concentrated sulfuric acid and distilling over sodium hydroxide. Water used as a substrate was purified first by refluxing with an alkaline permanganate solution and then distilling thrice using a Hysil flask.

Apparatus. The Wilhelmy's vertical plate method was adopted for the surface tension measurement. A small displacement of the glass plate due to the change of surface tension was recorded by means of a differential transformer, which was driven by 13 V alternating current input supplied from a 1 kHz oscillator, stabilized by a Zenar diode. The output current from the differential transformer was rectified, properly attenuated, biassed and recorded on a Hitachi QPD recorder. The surface tension change of about 28 dyn/cm could be measured by this apparatus with the error of ± 0.14 dyn/cm, when a ground glass plate of 4 cm in perimeter was used.

Procedure. From 5 to 10 μl of benzene solution of dodecanol (5.3×10^{-4} mol/l) was spread from a 50 μl microsyringe on an aqueous surface of SDS solution contained in a glass dish of 7 cm in diameter and 1 cm in depth, and the change in the surface tension was recorded. Typical example of the surface tension change when the benzene solution was spread on the aqueous surface is schematically shown in Fig. 1, where the line AB represents the initial surface tension of the aqueous solution. The surface tension fell to C when the dodecanol solution was spread on the aqueous surface from a single drop at B. The surface tension remained constant from C to D during which period the benzene solution continued to spread, then the surface tension suddenly decreased from D to E and it gradually returned to the value of the substrate solution (AB) as the desorption of dodecanol monolayer proceeded. Five microliter of the spreading solution was confirmed best for the instantaneous completion of the spreading on the aqueous surface. The time required from C to D was a few seconds. So the time for the spreading was negligible compared with the whole period of desorption measurement and the point E was safely taken as the start of the desorption. The evaporation loss during the surface tension measurement was minimized by covering the aqueous surface with a glass plate having a small opening for the passage of the rod attached to the Wilhelmy plate. To facilitate the evaporation of benzene, the monolayer was exposed to open air during the initial period of 30 sec. A special care was taken to ensure the zero contact angle in the advancing meniscus condition. This was confirmed by a slight pushing-down of the plate from an equilibrium position into the solution and checking it to return to the original position when left free.

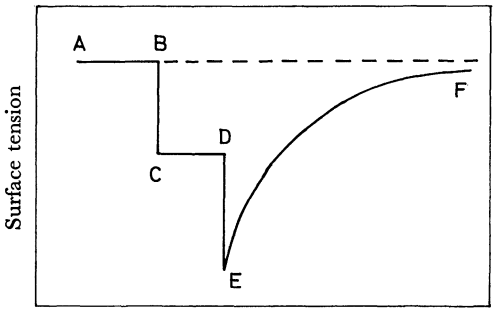

Fig. 1. Surface tension change due to spread benzene.

Results and Discussion

According to the theory proposed by Saraga,[3] a monolayer spread on an aqueous surface partly desorbs to form a sublayer with which the rest of the monolayer establishes a temporary equilibrium, and the rate determining process of desorption is the diffusion of solute from the subsurface through the stagnant layer to the bulk of the solution where the convection current makes the concentration uniform.[7] Thus, the following equation was derived,

$$-\mathrm{d}\Gamma/\mathrm{d}t = C(D/\pi t)^{1/2} \quad (1)$$

where Γ expresses the amount of adsorption (mol/cm^2) at time t (sec), C the subsurface concentration of the solute (mol/1000 g) in equilibrium with Γ and D the diffusion coefficient (cm^2/sec). Assuming $C/\Gamma = k$ and $C/F = q$ (F being the surface pressure of the spread monolayer) to be constant throughout the period of desorption, Eq. (1) after integration gives the following relation, which is in accordance with the relation shown experimentally by Roylance.[8]

$$\ln F/F_0 = -2k(D/\pi)^{1/2} \cdot t^{1/2} \quad (2)$$

where F_0 is the value of F at $t=0$. Equation (2) predicts a linear relationship between the logarithm of the surface pressure F and the square root of time t. The observed plot of $\ln F$ against $t^{1/2}$ for varying concentrations of aqueous SDS substrate is shown in Fig. 2. Here, the difference in surface tension between the aqueous SDS solutions with and without dodecanol monolayer was taken as the surface pressure F of dodecanol monolayer, the assumption being valid for the mixed films containing dodecanol of such low surface pressure as in the present experiment.

In Fig. 2, a good linear relationship was observed to hold between $\ln F$ and $t^{1/2}$. The rate constant of desorption was calculated from the slope of these straight lines and plotted against the concentration of SDS as shown in Fig. 3. In this figure, the value of G for lower concentration of SDS in the substrate ($=G_s$) is seen to decrease slightly and linearly from

6) E. E. Dreger., *Ind. Eng. Chem.*, **36**, 610 (1944).

7) J. H. Brooks and A.E. Alexander, *Proc. 3rd Int. Congr. Surface Activity*, Cologne, Vol. 2, 196 (1960).

8) A. Roylance and T. G. Jones, *Proc. 3rd Int. Congr. Surface Activity*, Cologne, Vol. 2, 123 (1960).

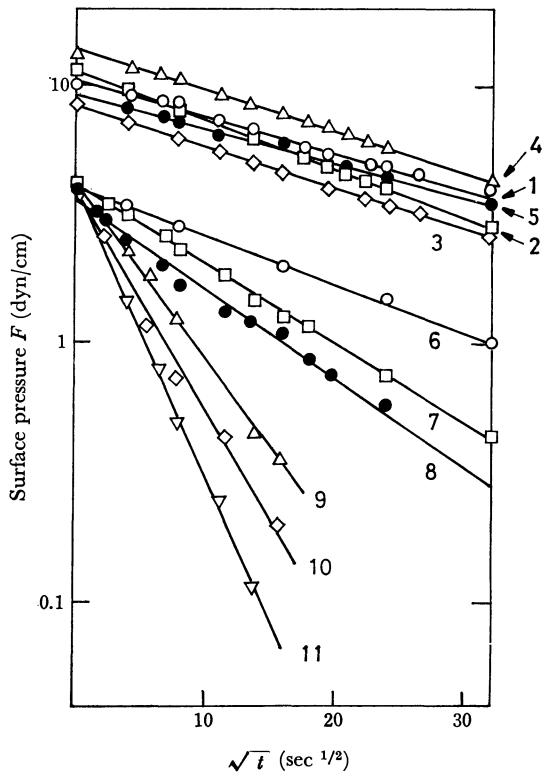

Fig. 2. Surface pressure decrease due to dissolution of surface film.

Conc. of SDS ($\times 10^{-3}$ mol/l)

1; 0	2; 2.52	3; 5.05	4; 6.05
5; 7.05	6; 8.07	7; 9.09	8; 9.51
9; 10.09	10; 12.90	11; 15.35	

the value for water up to a point, beyond which G ($=G_m$) increased linearly and steeply with the concentration of SDS. The break point of the curve, 7.7×10^{-3} mol/l, agreed with CMC reported by others.[9] The value of G_s is given by

$$G_s = 2k(D/\pi)^{1/2} \tag{3}$$

The linear increase of G_m above CMC may reasonably be explained by the solubilization of dodecanol by SDS micelles. According to Eq. (2), the increase of G_m may be due to the increase of k and/or D. However, the solubilization of dodecanol cannot be expected to increase the coefficient of diffusion from the subsurface into the bulk of the solution appreciably, while actual value of $k=C/\Gamma$ is considered to increase to $k'=(C+\Delta C)/\Gamma$, provided that the solubilization equilibrium is instantaneous like surface/subsurface equilibrium. Here, $\Delta C=CC_mPM\times 10^{-3}$ is the increase of dodecanol concentration due to the solubilization, C_m being the concentration of SDS micelles in mol/1000 g water, M the molecular weight of SDS, and P the partition coefficient of dodecanol expressed by

$$\frac{\text{intramicellar concn. of dodecanol (mol/1000 g micelles)}}{\text{intermicellar concn. of dodecanol (mol/1000 g solution)}}$$

Then the following relation holds

$$k' = k(1+C_mPM\times 10^{-3})$$

and Eq. (2) is replaced by

$$\ln F/F_0 = -2k(1+C_mPM\times 10^{-3})(D/\pi)^{1/2}t^{1/2} \tag{4}$$

where

$$2k(1+C_mPM\times 10^{-3})(D/\pi)^{1/2} = G_m \tag{5}$$

Equations (4) and (5) well explain the linear relationship above CMC shown in Figs. 2 and 3.

From the Eqs. (3) and (5) we obtain

$$G_m = G_{sm}(1+C_mPM\times 10^{-3}) \tag{6}$$

Here G_{sm} expresses the value of G_s for SDS solution of critical micelle concentration. According to Eq. (6), P can be calculated from G_{sm} and the slope of G_m *vs.* C_m plot shown in Fig. 3. The value of P thus obtained was 3.62×10^3, which may be compared with similar data obtained for other substances by Herries.[10]

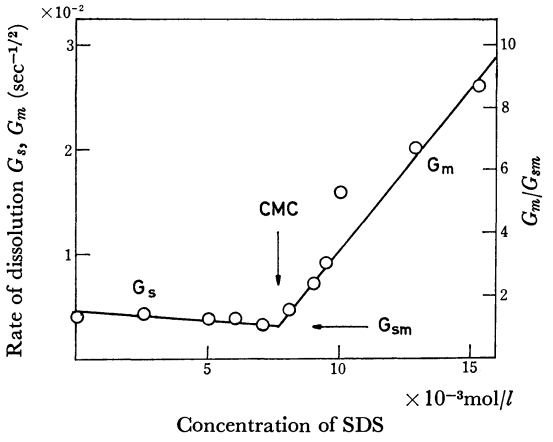

Fig. 3. Rate of dissolution of DOH monolayer into aqueous SDS.

Using this value of P, the amount of solubilization of dodecanol, C_{DOH}, was calculated from the following relation,

$$C_{DOH} = C_s(1+C_mPM\times 10^{-3}) \tag{7}$$

where C_s denotes the solubility of dodecanol in the aqueous SDS solution of CMC.

For the measurement of C_s, the solutions were prepared by adding varying amounts of DOH as small volumes of alcoholic solutions to the aqueous SDS solutions of CMC, and the transmittance of the solutions measured at the wave length of 350 mμ was plotted against DOH concentration. The value of C_s was evaluated as the DOH concentration corresponding to the intersection of two straight lines for the transparent and the turbid solutions. $C_s=2.2\times 10^{-4}$ mol/l was obtained at 25°C which is in agreement with the value estimated from the published data,[11] and with the data obtained by surface tension method.[12] Using this value and 7.7×10^{-3} mol/l for the CMC of SDS, C_{DOH} for instance of 7.9×10^{-4} mol/l, for SDS solution of 1×10^{-2} mol/l concentration, was obtained which agrees with 8×10^{-4} mol/l, calculated from the published data.[11,13]

The diffusion coefficients D of DOH in pure water

9) H. V. Tartar, *J. Colloid Sci.*, **14**, 115 (1959).

10) G. Herries, W. Bishop, and M. Richards, *J. Phys. Chem.*, **68**, 1842 (1964).

11) M. G. Epstein and J. Ross, *J. Phys. Chem.*, **61**, 1578 (1957).

12) to be published in a near future.

13) M. Miura and S. Arichi, *J. Sci. Hiroshima Univ.*, **A 22**, 57 (1958).

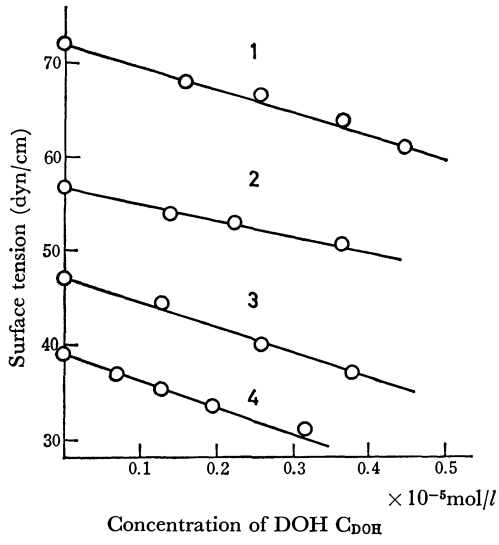

Fig. 4. Surface tension of aq. DOH solution containing SDS.
Conc. of SDS ($\times 10^{-3}$ mol/l)
1; 0 2; 0.77 3; 4.0 4; 7.7

and in aqueous SDS solution were estimated according to the Eq. (3). For this purpose, the measurements of surface tension σ against concentration C were made for the aqueous solutions of dodecanol containing SDS of a given concentration as shown in Fig. 4, from which k was calculated from the linear part of the curve at sufficiently dilute concentration, by applying the Gibbs adsorption isotherm,

$$1/k = \Gamma/C = -\frac{1}{RT}\frac{d\sigma}{dC}$$

From these values of k and the rate constant G_s for aqueous SDS solution, the diffusion coefficients of 16×10^{-6}, 6.9×10^{-6}, 12×10^{-6}, and 8.4×10^{-6} cm^2 sec^{-1} were obtained for 0, 0.77×10^{-3}, 4.0×10^{-3}, and 7.7×10^{-3} mol/l SDS solutions, respectively. Two of these values, especially the value for water, seem too high, presumably due to the evaporation of DOH not being negligible when we consider a fairly small solubility of DOH in pure water. Other values of diffusion constant are considered to be of right order of magnitude, compared with the value for a similar substance.[14]

The authors are grateful to the Ministry of Education for a grant in aid of scientific research.

14) F. Van Voorst Vader, Th. F. Erkens, and M. Van Den Tempel, *Trans. Faraday Soc.*, **60**, 1170 (1964).

BULLETIN OF THE CHEMICAL SOCIETY OF JAPAN, VOL. 44, 2921—2925 (1971)

Evidence of a Preresonance Raman Effect of the Base Residue in a Nucleic Acid

Masamichi TSUBOI and Seizo TAKAHASHI
Faculty of Pharmaceutical Sciences, The University of Tokyo, Hongo, Bunkyo-ku, Tokyo
Shuichi MURAISHI and Teruo KAJIURA
Japan Electron Optics Laboratory, Company, Nakagami, Akishima, Tokyo

(Received March 22, 1971)

The Ramam spectra of β-uridine-5′-phosphoric acid (UMP), its deuterated product, β-uridine-3′-β-uridine-5′-phosphoric acid (U_pU), and polyribouridylic acid (poly U) have been observed in their aqueous solutions; and the Raman lines assignable to the phosphate group and to the base residue have been indicated. For UMP, the intensity ratio of a Raman line of the base residue *versus* that of the phosphate group was found to become greater on changing the exciting line from the 6328 Å line of a helium-neon laser to the 4880 Å line of an argon ion laser. This fact has been taken as indicating that a preresonance Raman effect takes place of the base residue with the effective absorption at 2600 Å.

In the course of our investigation on the Raman effects of the nucleic acids, we noticed that the apparent intensity ratio of a Raman line assignable to a base residue *versus* that assignable to the phosphate group was often found to be markedly greater in the spectrum obtained with an argon ion laser than that in the spectrum obtained with a helium-neon laser. We suspected that this fact is ascribed to the so-called preresonance Raman effect. As is now well known, each base residue in a nucleic acid has a strong absorption band at about 2600 Å (molar extinction coefficient at 2600 Å is about 10^4), whereas the phosphate group has no strong absorption band in the spectral region from 7000 Å down to 1800 Å. Therefore, it seems quite probable that a great contribution comes from the electronic excited state corresponding to the 2600 Å band (*i.e.* a preresonance with the 2600 Å band takes place) in some Raman lines of base residues while it does not in the Raman lines of the phosphate group. In general, the intensity (I) of a Raman line is given, in an approximation,[1] by

$$I = C\mu^4_{eg}(\nu_0-\nu)^4(\nu^2_{eg}+\nu_0^2)^2/(\nu^2_{eg}-\nu_0^2)^4. \quad (1)$$

Here, C is a constant, ν_0, ν, and ν_{eg} are the frequencies

1) J. Behringer, in "Raman Spectroscopy", ed. by H. A. Szymanski, Plenum Press, New York (1967), p. 191.

respectively of the exciting light, of a molecular vibration, and of the transition from the ground state to the lowest exicted electronic state; and μ_{eg} is the corresponding transition moment. If ν_{eg} is assumed to be 3.846×10^4 cm^{-1} (2600 Å) for the base residue and 5.556×10^4 cm^{-1} (1800 Å) for the phosphate group, the intensity ratio I(base)/I(phosphate) may be greater for $\nu_0=2.0487\times10^4$ cm^{-1} (4879.9 Å) line of argon ion laser than that for $\nu_0=1.5798\times10^4$ cm^{-1} (6328.2 Å) line of helium-neon laser. If the same value of μ_{eg} is assumed for the phosphate group as that for the base, for example, the value of ϕ defined by

$$\phi = \frac{[I(\text{base})/I(\text{phosphate})]_{Ar^+}}{[I(\text{base})/I(\text{phosphate})]_{He-Ne}} \qquad (2)$$

should be 1.6. Thus, the ϕ value is expected to be useful in characterizing each Raman line observed—it would tell whether the 2600 Å band is responsible for the Raman line in question, and if so how much. We attempted, in the present work, a measurement of these quantities for several Raman lines of β-uridine-5′-phosphoric acid in a neutral aqueous solution.

Experimental

In the present paper the following three compounds are subjected to our examination: di-sodium salt of β-uridine-5′-phosphoric acid (5′ UMP),

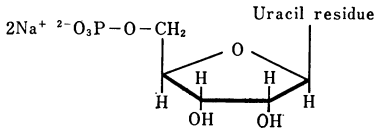

sodium salt of β-uridine-3′-β-uridine-5′-phosphoric acid (U_pU),

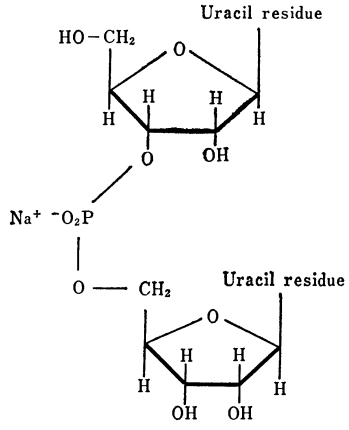

and polyribouridylic acid,

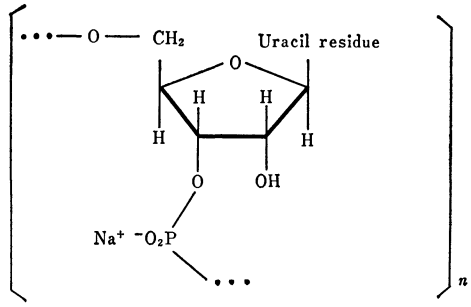

The sample of 5′UMP was a gift from Takeda Chemical Industries, Ltd., and that of U_pU was purchased from Miles Chemical Company. The purity of these samples was confirmed by a chromatographic method. Poly U with the sedimentation constant $S_{20,w}=6.95$ S was purchased from Miles Chemical Company. For the observation of the Raman spectrum, about 0.2 m*l* of an aqueous solution of each nucleic acid was prepared. The concentration was about 5%. A small amount of NaOH was added in the solvent, and the pH of the solution was adjusted to 7.5 in every case. Each solution was placed in a cylindrical glass tube of 2 mm in inside diameter and 15 mm in length. The tube was placed vertically, and the laser beam was sent along the length of the tube through the flat glass plates at the lower and upper ends of the cylinder (see Fig. 1). The

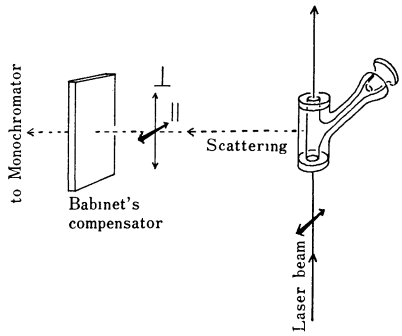

Fig. 1. Raman cell for aqueous solutions of nucleic acids. Polarization directions of excited light and scattered light.

Raman light scattered along a direction perpendicular to the excited beam (*i.e.* along a horizontal direction) was examined by the use of a JRS-Ul spectrophotometer of Japan Electron Optics Laboratory Co., Ltd. The polarization directions of the excited and scattered beam are shown in Fig. 1. The depolarization ratio ρ is defined by $\rho=I_\perp/I_{//}$, where $I_\perp$ and $I_{//}$ are the intensities of the scattered beams whose polarization directions are $\perp$ and // to that of the excited beam (see Fig. 1).

Results and Interpretations

First, in order to provide the data of assignments of the Raman lines of uridylic acids, those of 5′UMP, U_pU, and poly U (*i.e.* monomer, dimer, and polymer of uridylic acid) are shown in Fig. 2. For 5′UMP, Raman spectrum was observed not only in a H_2O solution but also in a D_2O solution, and the result is given in Fig. 2b. Frequencies, approximate intensities, and depolarization ratios of the Raman lines observed are listed in Table 1.

In a solution of pH (or pD)=7.5, the phosphate group of 5′UMP takes the form PO_3^{2-} with three P⋯O bonds having equal amounts (about one-third) of double-bond character. The phosphate group of U_pU or poly U, on the other hand, takes the form PO_2^- with two P⋯O bond having equal amounts (about one-half) of double-bond character. The characteristic vibrations of these PO_3^{2-} and PO_2^- groups were previously examined in detail,[2,3] and it was shown that symmetric

2) M. Tsuboi, *J. Amer. Chem. Soc.*, **79**, 1351 (1957).
3) T. Shimanouchi, M. Tsuboi, and Y. Kyogoku, in Advances in Chemical Physics, Vol. VII, "The Structure and Properties of Biomolecules and Biological Systems," ed. by J. Duchesne, Wiley-Interscience, New York (1964), pp. 435—498.

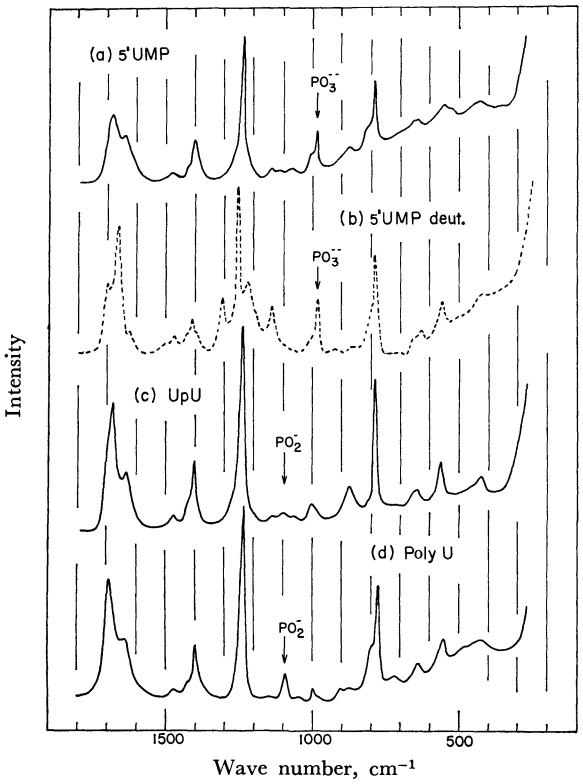

Fig. 2. Raman spectra of (a) 5'UMP, (b) deuterated 5'UMP, (c) U_pU, and (d) poly U in their 5% aqueous solutions at room temperature and at pH 7.5. Observed by the use of an argon ion laser (4880 Å line).

stretching vibrations of the PO_3^{2-} and PO_2^- groups give strong Raman lines respectively at 980 and 1100 cm^{-1}. This is found to be the case for 5'UMP, U_pU, and poly U. Thus, a sharp Raman line at 980 cm^{-1} is found for both of undeuterated and deuterated 5'UMP but not for U_pU and poly U, while a peak at 1100 cm^{-1} is observed only for U_pU and poly U. It is certain that the former is assignable to the PO_3^{2-} symmetric stretching vibration and the latter to the PO_2^- symmetric stretching vibration. The relative intensity of the 1100 cm^{-1} line is lower in U_pU than that in poly U. This is understandable because in U_pU only one half PO_2^- group is involved per uracil residue, whereas in poly U one PO_2^- group per uracil residue.

Most of the other Raman lines observed for 5'UMP are found also for U_pU and poly U at nearly the same frequencies (Fig. 2). Their relative intensities and depolarization ratios are also almost equal to those of the corresponding Raman lines of 5'UMP (Fig. 2, Table 1). This fact may be taken as indicating that these Raman lines are all assignable to vibrations in the uracil residue. At the same time, the fact indicates that the intra-molecular interactions, if any, are so weak between the uracil residues in the U_pU and poly U molecules, that they are hardly detected in the Raman spectra.

In Fig. 3, the result of our experiment for determining the ϕ values (defined by Eq. 2) of these Raman lines due to the base residue is shown. The two curves were recorded for the Raman scatterings from the same sample (20% 5'UMP in H_2O) by the use of the same

Table 1. Raman lines observed for neutral H_2O solution of 5'UMP, D_2O solution of 5'UMP, H_2O solution of U_pU, and H_2O solution of poly U

5' UMP			5'UMP deuterated		U_pU			Poly U		
Frequency (cm^{-1})	Intensity	Depolarization ratio	Frequency (cm^{-1})	Intensity	Frequency (cm^{-1})	Intensity	Depolarization ratio	Frequency (cm^{-1})	Intensity	Depolarization ratio
395	0	0.8[a]								
425	1	0.8[a]	425	1	422	1		430	0	0.6[a]
563	1	0.6[a]	553	2	559	2	0.4	559	1	
			623	1						
651	1	?	639	0	640	1	0.5[a]	640	1	0.5[a]
								724	0	
785	6	0.2	784	8	785	7	0.1	786	6	0.1
815	2	?	806	3				802	3	0.1[a]
873	1	~0	868	0	873	2	0.2	868	0	
			916	0				906	0	
980	4	0.1	979	4						
1002	1	~0[a]	1000	1	999	1	0.3	999	0	0[a]
1066	0				1053	0		1053	0	0.4[a]
					1093	1	~0[a]	1093	1	~0[a]
1133	0	0.8[a]	1138	2	1142	0	0.4[a]	1142	0	0[a]
			1214	3						
1233	10	0.4	1249	10	1235	10	0.3	1234	10	0.3
			1305	3						
1399	4	0.4	1405	2	1399	4	0.5	1400	3	0.2
1474	0	0.8[a]	1464	1	1473	0	0.5[a]	1472	0	0.4[a]
			1620	0						
1634	4	0.4	1659	9	1634	3	0.4	1631	3	0.3
1679	7	0.3	1696	6	1683	7	0.3	1689	6	0.2

a) The value of the depolarization ratio is less accurate than others.

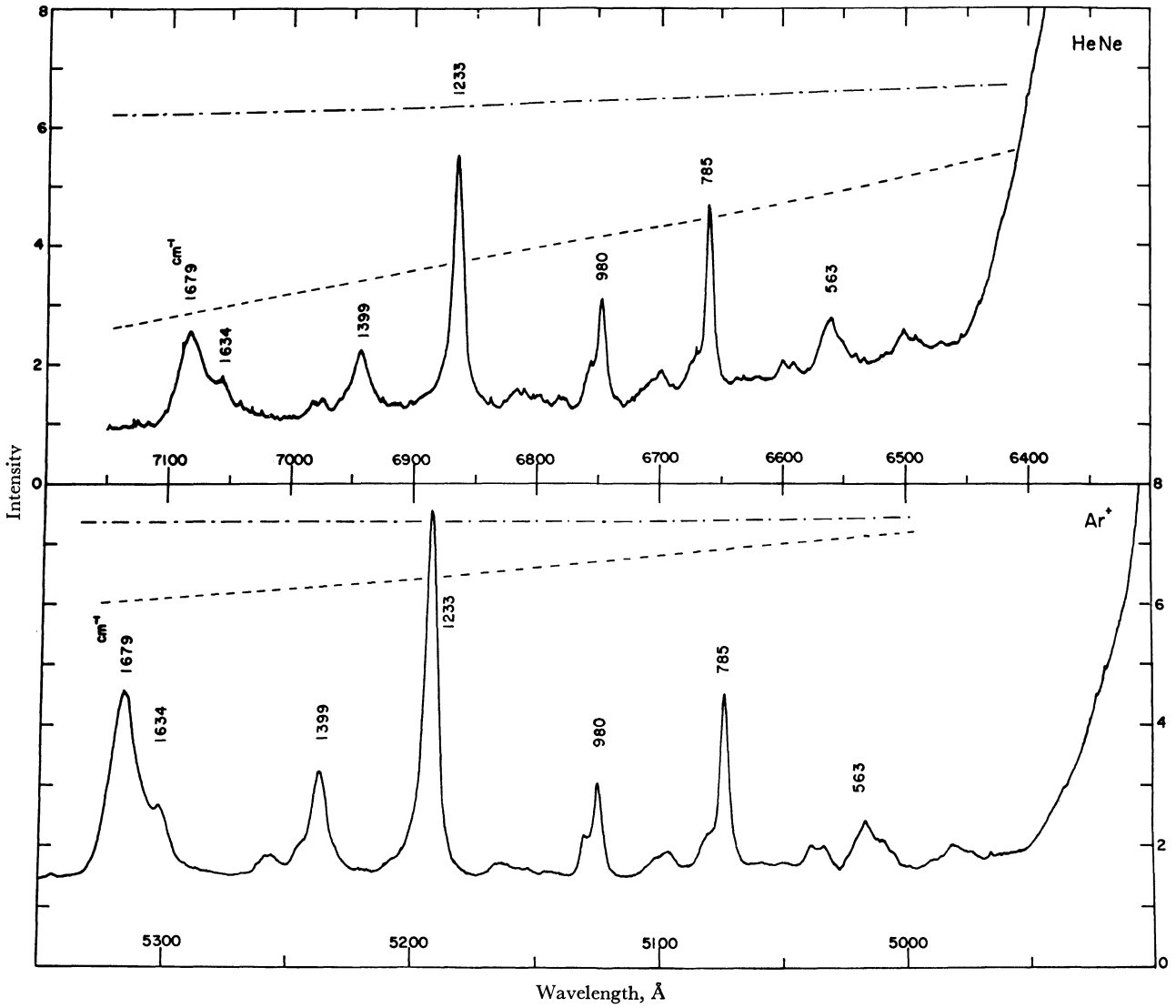

Fig. 3. A reproduction of the recorded curves for the Raman scattering from an aqueous solution (20%) of 5′UMP.
Upper: a helium-neon laser was used as the source of the exciting light (6328 Å beam).
Lower: an argon ion laser was used as the source of the exciting light (4880 Å beam).
Spectral slit width: 10.7 cm^{-1}. -·-·- shows the efficiency of the diffraction grating in the monochromator, and ------ shows the spectral response of the photomultiplier used.

spectrophotometer. One of them (upper) was obtained on exciting with the 6328 Å line of a helium-neon laser, whereas the other (lower) with the 4880Å line of an argon ion laser. The slit widths were adjusted (400 μ for the run with the helium-neon laser and 235 μ for that with argon ion laser) so that the spectral slit widths were approximately equal (10.7 cm^{-1}) for the two runs. As is readily seen in Fig. 3, the relative intensity of the 1233 cm^{-1} peak (base residue), for example, with respect to the 980 cm^{-1} peak (PO_3^{2-}) is greater in the curve (lower) with Ar^+ than that (upper) with He-Ne.

For obtaining the ϕ values (Eq. 2), corrections have been made for the efficiency of the diffraction gratings in the monochromator and for the spectral response of the photomultiplier. The monochromator contains two Jarrell-Ash No. 1297 Gratings (Cat. No. 980-45-20-22, 1180 grooves/mm 5000 Å blaze) and the efficiency-wavelength curve for each grating (reproduced by -·-·- in Fig. 3) was given by the manufacturer. The efficiency of the two gratings at each wavelength was assumed to be the square of the efficiency of one grating. The spectral response of the photomultiplier used (EMI 9558B) is given in EMI Technical Data and is reproduced by ------ in Fig. 3.

In Table 2, the ϕ values thus determined for six

Table 2. The values of ϕ defined by Eq. (2) for some Raman lines of 5′UMP.

Frequency, cm^{-1}	ϕ
563	1.1_2
785	1.2_1
980	(1.00)
1233	1.5_6
1399	1.6_0
1634	1.4_2
1679	1.6_3

stronger Raman lines (all assignable to vibrations in the uracil residue) are given. The ϕ values for the 1233, 1399, 1634, and 1679 cm^{-1} lines are approximately equal to the value 1.6 predicted above on the basis of Eq. (1) with $\nu_{eg}=3.846\times10^4$ cm^{-1} (2600 Å), and therefore it is now evident that a preresonance Raman effect takes place in each of these lines. All of these Raman lines are strongly polarized (depolarization ratio $\ll$ 0.75) and they are assignable to in-plane vibrations in the uracil residue.

For the strong Raman line at 785 cm^{-1}, on the other hand, the ϕ value is found to be much smaller (1.2). The depolarization ratio is very small for this line (0.2), and therefore this line is also assignable to an in-plane vibration in the uracil residue. Lord and Thomas[4] suggested that this line is caused by a ring-breathing type of motion. Eaton and Lewis[5] observed a vibrational structure in the 2600 Å band of a 1-methyluracil crystal with a spacing of 750 cm^{-1}, and they suggested that this frequency corresponds to the ground state frequency, 785 cm^{-1}. Thus, it is probable that the excited electronic state corresponding to the 2600 Å band of the uracil residue has its potential minimum at a position appreciably shifted from that of the ground state along the normal coordinate corresponding to the 785 cm^{-1} line. If so, one would expect a rather stronger preresonance effect and therefore rather greater ϕ value for the 785 cm^{-1} Raman line, in contrast to what is actually found. Professor T. Miyazawa (Osaka University), in his private communication, suggested that in the normal vibration corresponding to the Raman line at 785 cm^{-1} the atomic movements are not necessarily localized in the base residue. If the 785 cm^{-1} vibration consists of movements of the uracil and ribose groups, for example, and if an appreciable contribution to the intensity of the 785 cm^{-1} Raman line comes from the ribose part, the observed low ϕ value is certainly understandable.

A low ϕ value is found also for the 563 cm^{-1} line. This line shows somewhat greater depolarization ratio (Table 1), and it is probable that this is caused by an out-of-plane vibration of the uracil residue.

It has now been shown that the intensities of the Raman lines at 1233, 1399, 1634, and 1679 cm^{-1} are caused almost exclusively by the excited state of the uracil residue corresponding to the 2600 Å band, while the intensity of the 785 cm^{-1} Raman line is caused only partly by the 2600 Å excited state. In other words, Eq. (1) is nearly valid for the first four Raman lines while it is not for the 785 cm^{-1} line (other terms are necessary in the right side of Eq. (1)). If Eq. (1) is valid, the intensity of the Raman line should be proportional to μ^4_{eg}, *i.e.*, to the square of the ultraviolet absorption intensity of the 2600 Å band. Therefore, when an inter-base interaction (such as a hydrophobic stacking interaction[6]) causes a hypochromicity in the 2600 Å band of a uracil residue, it should cause a much more marked lowering in the intensities of the Raman lines at 1233, 1399, 1634, and 1679 cm^{-1}. Tomlinson and Peticolas[7] made a similar prediction on the basis of their theory,[8] but they actually found the intensity of the Raman line at 720 cm^{-1} of adenine residue to show a rather linear dependence on the ultraviolet absorbance.[7] We suspect that the 720 cm^{-1} line of the adenine residue has a similar nature to the 785 cm^{-1} line of the uracil residue. If so, what they found is understandable, because only a part of its intensity comes from the 2600 Å excited state, and only that portion of the intensity is proportional to μ^4_{eg} (2600 Å).

4) R. C. Lord and G. J. Thomas, Jr., *Spectrochim. Acta*, **23A**, 2551 (1967).

5) W. A. Eaton and T. P. Lewis, *J. Chem. Phys.*, **53**, 2164 (1970).

6) See for example I. Tinoco, Jr., *J. Amer. Chem. Soc.*, **82**, 4785 (1960).

7) B. L. Tomlinson and W. L. Peticolas, *J. Chem. Phys.*, **52**, 2154 (1970).

8) W. L. Peticolas, L. Nafie, P. Stein, and B. Fanconi, *J. Chem. Phys.*, **52**, 1576 (1970).

Structure and Rotational Isomerism of Ethylenediamine as Studied by Gas Electron Diffraction

Akimichi YOKOZEKI and Kozo KUCHITSU

Department of Chemistry, Faculty of Science, The University of Tokyo, Hongo, Tokyo

(Received March 22, 1971)

The structure and the rotational isomerism of ethylenediamine have been investigated by means of gas electron diffraction. Evidence has been given for the presence of one conformer (*gauche*) in the vapor phase (at 50—120°C); the N–C–C–N dihedral angle measured from the *cis* position is $64._0 \pm 4°$, and the fraction of any other isomer, if present, is estimated to be less than 5%. A theoretical prediction based on the SCF-CNDO/2 method has essentially accounted for this finding. The r_g distances and the angles based on the r_a structure determined by a least-squares analysis on molecular intensities, with estimated limits of error, are as follows: C–C=1.545± 0.008 Å, C–N=1.469 ±0.004 Å, ∠C–C–N=110.2 ±0.7°, C–H=1.10_9 ±0.01 Å, ∠C–C–H=$111._9$ ±5°, and ∠H–C–H=$112._7$ ±8°.

A previous paper[1] has reported on the molecular structure of triethylenediamine. One of the characteristic aspects is that this molecule has a twisting motion around the N···N axis, where the ethylenediamine bridges have a large-amplitude torsion about the *cis* conformation. Moreover, the C–C distance in the bridge is longer than those in normal alkanes by more than 0.02 Å.

On the other hand, the structure of free ethylenediamine has not been studied in detail, in contrast with extensive studies of its complexes by X-ray crystallography,[2] and the existing assignment of the vibrational data (infrared and Raman) to a single (*cis*) conformer was only tentative[3] (see Fig. 1). Under these circumstances, an electron-diffraction study was initiated in order to elucidate the structure and rotational isomerism of ethylenediamine in the gas phase. A preliminary result[4] has given evidence for a dominant *gauche* conformer. In the present paper a further analysis has been made in consideration of the hydrogen positions of the amino groups.

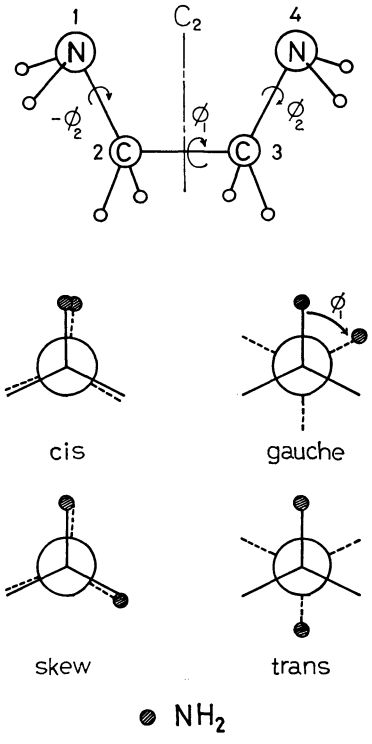

Fig. 1. Rotational isomerism for ethylenediamine. (See text).

Experimental

Anhydrous ethylenediamine (Guaranteed Reagent) obtained from the Tokyo Chemical Industry Co., Ltd. was used in this work. Diffraction photographs were taken on Fuji Process Hard plates at 55, 65, 90, and 118°C using an apparatus equipped with an r^3 rotating sector.[5] The sample was introduced into the diffraction chamber through a heated nozzle assembly,[1] and the above-mentioned temperatures were kept within ±1°C at the nozzle tip and in the sample flask during the experiment. The accelerating voltage was about 40 kV and was stabilized to within 1×10^{-4}. Two camera lengths of 114 and 249 mm were used, and the scale factors of the diffraction patterns were calibrated with reference to the r_a(C–O) distance of carbon dioxide (1.1646 Å)[5] for the shorter camera length and to the r_a(N–N) distance of nitrogen (1.1007 Å)[6] for the longer camera length. Four plates taken at each camera length with photographic densities ranging from 0.19 to 0.57 were used for the analysis. A typical experimental

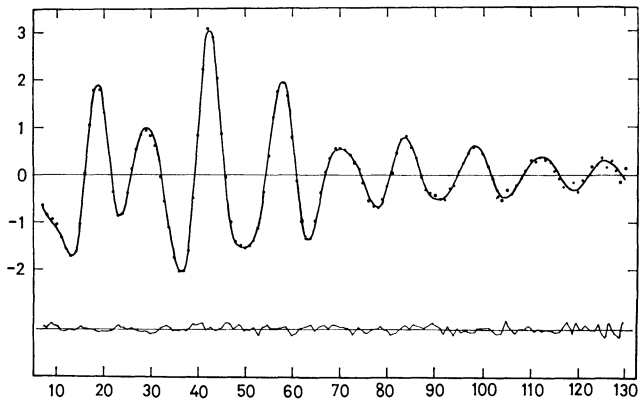

Fig. 2. Molecular intensity $qM(q)$ curve for ethylenediamine. Upper solid curve: best-fit theoretical; dots: experimental; lower curve: experimental minus theoretical.

1) A. Yokozeki and K. Kuchitsu, This Bulletin, **44**, 72 (1971).
2) For example, M. Iwata, K. Nakatzu, and Y. Saito, *Acta Crystallogr.*, **B25**, 2562 (1969).
3) A. Sabatini and S. Califano, *Spectrochim. Acta*, **16**, 677 (1960).
4) A. Yokozeki and K. Kuchitsu, This Bulletin, **43**, 2664 (1970).
5) Y. Murata, K. Kuchitsu, and M. Kimura, *Jap. J. Appl. Phys.*, **9**, 591 (1970).
6) K. Kuchitsu, This Bulletin, **40**, 498 (1967).

molecular intensity $qM(q)$ ($q=7-130$ Å^{-1}) is illustrated in Fig. 2.[7] The intensity curves[8] derived from plates taken at different temperatures were not distinguishable from one another beyond the uncertainties in the measurement. Most of the calculations were carried out by the HITAC-5020E in the Computer Centre of the University of Tokyo.

Analysis

Ethylenediamine has two axes of internal rotation (C–C and C–N) as illustrated in Fig. 1. The parameters ϕ_1 and ϕ_2 represent, respectively, the dihedral angle between the N_1–C_2–C_3 and C_2–C_3–N_4 planes measured from the *cis* position and that between the planes which bisect the H–N_1–H and the H–C_2–H angles measured from the eclipse position.

In order to make the analysis tractable, the following assumptions were made.

1) The bond lengths and bond angles are independent of internal rotation.

2) The C–C–N plane is perpendicular to the H–C–H plane and bisects the H–C–H angle.

3) The C–N–H and H–N–H angles are equal to those in methylamine:[9] ∠C–N–H=112.1° and ∠H–N–H=105.9°.

4) The N–H bond distance is equal to that in ammonia,[10] r_g (N–H)=1.0302 Å.

5) The molecule has C_2 symmetry; *i.e.*, the ϕ_2 angles for the amino groups have equal values with opposite signs (Fig. 1).

On the above assumptions, seven parameters were chosen for the subsequent analysis: the C–C, C–N, and C–H bond distances, the C–C–N and H–C–H bond angles, and the ϕ_1 and ϕ_2 dihedral angles.

In addition, the mean amplitudes of vibration and shrinkage corrections[11] for all the atom pairs were calculated by a normal-coordinate analysis based on the force constants listed in Table 1, where the torsional force constants Y(C–C) (0.16 md·Å) and Y(C–N) (0.12 md·Å) were estimated so as to roughly reproduce the observed torsional frequencies[3] of 186 cm^{-1} for the C–C axis and 327 cm^{-1} for the C–N axis. The estimated value of Y(C–C) is justified in a later section. The calculated vibrational frequencies based on a staggered conformation ($\phi_1=\phi_2=60°$) by the use of the above force constants are given in Table 2. No refine-

Table 1. Estimated force constants for ethylenediamine[a]

K(C-C)	2.3	H(C-C-N)	0.30	F(C-C-N)	0.70
K(C-H)	4.3	H(C-C-H)	0.25	F(C-C-H)	0.47
K(C-N)	5.5	H(N-C-H)	0.28	F(N-C-H)	0.52
K(N-H)	5.6	H(C-N-H)	0.32	F(C-N-H)	0.46
Y(C-C)[b]	(0.16)	H(H-N-H)	0.40	F(H-N-H)	0.00
Y(C-N)[b]	(0.12)				

a) Force constants for ethylenediamine estimated from those for normal alkanes and amides (See Ref. 1). Y's in units of md·Å and others in md/Å.
b) See text.

Table 2. Vibrational frequencies of ethylenediamine (cm^{-1})

	Calcd[a]	Obsd[b]	Calcd	Obsd	Calcd	Obsd
A	3259	3246	1367	—	904	761
	3200	—	1299	1298	383	468
	2977	2891	1236	—	331	—
	2936	2858	1196	1104	167	186
	1486	1597	1065	980		
	1401	1469	973	920		
B	3259	3335	1459	1456	1041	951
	3201	3171	1369	1360	877	775
	2983	2930	1299	1305	590	510
	2951	2917	1207	1249	309	327
	1493	1608	1166	1065		

a) Frequencies for a *gauche* conformation (C_2) calculated by the use of the force constants given in Table 1. (See text).
b) Observed values by infrared and Raman spectra listed in Ref. 3, where a tentative assignment for a *cis* conformer (C_{2v}) was made. The correspondence of the observed and calculated frequencies is, therefore, mostly ambiguous.

Table 3. Calculated mean amplitudes for ethylenediamine[a]

C—N	0.0451	$C_2\cdots H_1$[b]	0.1057
C—C	0.0517	$C_2\cdots H_3$	0.1053
C···N	0.0686	$N_1\cdots H_2$	0.1018
C—H	0.0784	$C_2\cdots H_4$(S)[c]	0.1676
N—H	0.0746	$C_2\cdots H_4$(L)	0.1019
$l(\phi_1)$[d]	0°	60°	180°
N···N	0.1795	0.1471	0.0677
$N_1\cdots H_3$(S)	0.1408	0.1582	0.1570
$N_1\cdots H_3$(L)	0.1408	0.1003	0.1570
$N_1\cdots H_4$(S)	0.2942	0.2578	0.1173
$N_1\cdots H_4$(L)	0.1375	0.1577	0.1850
$l(\phi_2)$[e]	a_i	b_i	c_i
$C_2\cdots H_4$(S)	0.0170	−0.0166	0.1248
$C_2\cdots H_4$(L)	−0.0170	−0.0162	0.1248
$N_1\cdots H_4$(S)	0.0409	−0.0373	0.2055
$N_1\cdots H_4$(L)	−0.0436	−0.0269	0.2055

a) Mean amplitudes calculated for 90°C by the use of the force constants given in Table 1 (in Å units). Those for the H···H pairs are not listed. Values listed in the first section are independent of the N_1–C_2–C_3–N_4 dihedral angle ϕ_1 (for $\phi_2=60°$).
b) Subscript of the hydrogen atom denotes the number of the atom to which the hydrogen atom is bonded.
c) Atom pairs denoted as S and L have shorter and longer distances, respectively.
d) Mean amplitudes calculated for three conformers (for $\phi_2=60°$) (See Fig. 1).
e) Parameters of the mean amplitudes dependent on ϕ_2 (for $\phi_1=60°$), given in Eq. (1).

7) Numerical experimental data of the leveled total intensity have been deposited with the Chemical Society of Japan (Document No. 7117). A copy may be secured by citing the document number and by remitting, in advance, ¥200 for photoprints. Payment by check or money order payable to: the Chemical Society of Japan, 5, 1-Chome, Kanda-Surugadai, Chiyodaku, Tokyo.

8) Y. Morino, K. Kuchitsu, and T. Fukuyama, This Bulletin, **40**, 423 (1967).

9) D. R. Lide, Jr., *J. Chem. Phys.*, **27**, 343 (1957).

10) K. Kuchitsu, J. P. Guillory, and L. S. Bartell, *ibid.*, **49**, 2488 (1968).

11) K. Kuchitsu and S. Konaka, *ibid.*, **45**, 4342 (1966).

ment of the force constants was made, since only a provisional assignment of the observed frequencies[3] was available. The mean amplitudes calculated for a number of conformers are given in Table 3. They were treated as constants until the final stage of the conformational analysis.

Conformational Analysis (I). The structural parameters were first estimated from a preliminary analysis of the molecular intensity on the assumption that the ϕ_2 angle was 60°. As a result of a least-squares analysis,[4] the following parameters were derived: C–C=1.55 Å, C–N=1.47 Å, and ∠C–C–N=110°. This analysis also gave the ϕ_1 angle of about 60°, *i.e.*, the "*gauche*" conformation about the skeleton.

This conformation was also evidenced in the radial distribution (RD) curve for $r \gtrsim 2.5$ Å. For the calculation of the RD curve with a damping factor of exp $(-0.00014q^2)$, a small-angle region (q=0—7 Å^{-1}) of the molecular intensity curve was spliced by a set of theoretical intensity curves computed for different ϕ_1 angles: 0° (*cis*), 60° (*gauche*), 120° (*skew*), and 180° (*trans*). As for the hydrogen positions in the NH_2 groups, contributions from three staggered positions were averaged. The experimental and theoretical RD curves for *cis*, *gauche*, *skew*, and *trans* forms are compared in Fig. 3. The N···N peak shown by vertical lines shows that the *gauche* form is dominant in the vapor phase. A further conformational analysis is made in later sections.

Refinements of Structural Parameters. In the preceding section, the skeletal parameters were determined on the basis of the ϕ_2 angle fixed to 60°. This parameter was now treated as an additional variable. When the analysis was started from 60, 180, and 300° (three staggered positions), it converged to 81, 200, and 308° with standard deviations of about 9°, and hence, the equilibrium hydrogen positions of the amino groups about the C–N axes seem to be staggered.

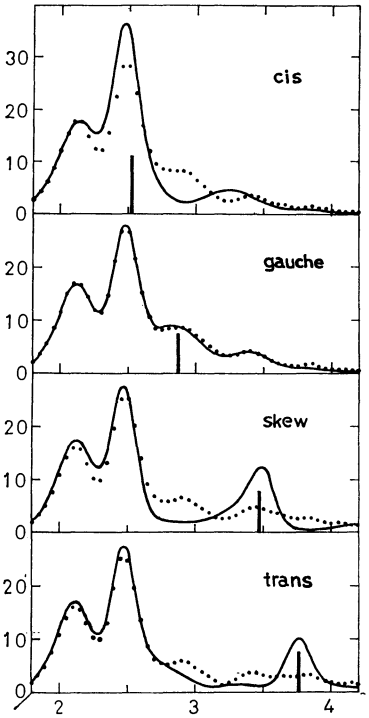

Fig. 3. Radial distribution curves for ethylenediamine. Dots: experimental; solid lines: corresponding theoretical curves for *cis*, *gauche*, *skew*, and *trans* conformers about the C–C axis with the index of resolution of 100%. Vertical line indicates the nonbonded N···N distance for each conformer.

In order to refine the structural parameters, the contribution to the scattering intensity from the atom pairs dependent on the internal rotation about the C–N axis was calculated by taking a weighted average of the intensity at every position of the ϕ_2 angle.[12,13] The weight was given by the Boltzmann distribution with a three-fold potential, $V(\phi_2)=\frac{1}{2}H_3(1+\cos 3\phi_2)$, where the barrier height H_3 was assumed to be 3.8 kcal/mol from the torsional force constant Y(C–N) of 0.12 md·Å mentioned above. In this treatment a rotation-inversion coupling was ignored, since the frequency of the NH_2 wagging motion is much higher than that of the torsion about the C–N axis.[3] Contributions from the skeletal vibrations to the mean amplitudes, $l(\phi_2)$, were obtained as a function,

$$l_i = a_i \sin\phi_2 + b_i \cos\phi_2 + c_i, \quad (1)$$

and the three parameters given in Table 3 were determined so as to reproduce the mean amplitudes calculated for several ϕ_2 angles.[12,13]

On the above-mentioned assumptions, the independent parameters and some of the mean amplitudes were determined by a least-squares analysis on the molecular intensity curves. The error matrix[14] derived from the analysis is given in Table 4. The results are listed in Tables 5 and 6 with the estimated limits of error including possible systematic errors. The experimental systematic errors primarily depend on the uncertainty in the electron wavelength (0.07%) and sector imperfection (0.05%),[15] whereas the systematic errors due to the assumptions made in the above analysis were estimated by the method described elsewhere[16] with moderate changes in the assumed values to be of the order of the corresponding random standard errors.

Conformational Analysis (II). For a quantitative examination of the fractions of the *gauche* conformer and other possible candidates, a background analysis[17] was undertaken by the use of the scattering intensity observed in a small-angle region (q=7—20 Å^{-1}). The background function $I_b(q)$ is given by $I_b(q)=I_0(q)/[1+kM_c(q)]f(q)$. "Smoothness" of the $I_b(q)$ function, which should have no systematic fluctuation with a period similar to that of the molecular intensity, was taken as a criterion for the choice of a correct structural model. The index of resolution k was assumed to be unity, and an empirical quartic function $f(q)$ was used

12) A. Yokozeki, K. Kuchitsu, and Y. Morino, This Bulletin, **43**, 2017 (1970).
13) Y. Morino and E. Hirota, *J. Chem. Phys.*, **28**, 185 (1957).
14) K. Hedberg and M. Iwasaki, *Acta Crystallogr.*, **17**, 529 (1964).
15) K. Kuchitsu, T. Fukuyama, and Y. Morino, *J. Mol. Structure*, **1**, 463 (1968).
16) A. Yokozeki and K. Kuchitsu, This Bulletin, **44**, 2356 (1971).
17) Y. Morino and K. Kuchitsu, *J. Chem. Phys.*, **28**, 175 (1958); M. Abe, K. Kuchitsu, and T. Shimanouchi, *J. Mol. Structure*, **4**, 245 (1969).

Table 4. Error matrix[a)]

	x_1	x_2	x_3	x_4	x_5	x_6	x_7	l_1	l_2	l_3	l_4	l_5	l_6	l_7	l_8	k
x_1	30	−6	−7	−30	37	25	61	−10	11	−17	19	−17	−24	−16	−11	30
x_2		13	8	−12	−11	31	50	15	10	25	17	17	14	4	16	39
x_3			31	4	−32	18	64	10	7	17	7	25	9	9	11	44
x_4				48	−78	−63	−108	−13	−11	−22	−27	16	54	53	106	−53
x_5					265	190	−174	18	−36	12	39	−127	−120	−146	−204	−34
x_6						302	−130	48	−32	72	64	−150	−176	−69	−201	131
x_7							553	56	76	97	78	216	−123	46	226	207
l_1								23	15	35	28	16	−21	−14	−24	59
l_2									22	22	21	32	21	25	66	45
l_3										56	39	33	−33	−16	−23	90
l_4											46	9	−32	−24	−37	79
l_5												137	89	34	125	79
l_6													137	45	122	−65
l_7														150	253	−31
l_8															333	−44
k																199

a) x_1=C-C, x_2=C-N, x_3=C-H, x_4=∠C-C-N, x_5=ϕ_1, x_6=∠C-C-H, and x_7=∠H-C-H. The mean amplitudes l_1—l_8 follow the order listed in Table 6. Units ($\times 10^{-4}$) for the distances are Å, those for the angles are rad., and the index of resolution k is dimensionless.

Table 5. Structural parameters for ethylenediamine[a)]

C—C	1.545±0.008
C—N	1.469±0.004
∠C-C-N	110.2±0.7°
ϕ_1[b)]	$64._0\pm4._5°$
C—H	$1.10_9\pm0.01$
∠C-C-H	$111._9\pm4._6°$
∠H-C-H	$112._7\pm8._5°$
k[c)]	1.02±0.05

a) Experimental r_g distances in Å units and r_α angles determined in the present study with estimated limits of error (See text).
b) The N-C-C-N dihedral angle measured from the *cis* position (See Fig. 1).
c) Index of resolution (dimensionless).

Table 6. Mean amplitudes in ethylenediamine (Å)

Atom Pair	Obsd[a)]	Calcd[b)]
C—N	$0.046_1\pm0.006$	0.045_1
C···N	$0.074_7\pm0.006$	0.069_2
C—C	$0.05_3\pm0.01_4$	0.051_7
C—H	$0.08_2\pm0.01_1$	0.078_4
$C_2\cdots H_1$	$0.11_1\pm0.03_4$	0.106
$C_2\cdots H_3$	$0.10_2\pm0.03_4$	0.105
N···N	$0.14_5\pm0.03_7$	0.147
$N_1\cdots H_3$(S)	$0.14_8\pm0.08$	0.158

a) Experimental root-mean-square amplitudes of vibration determined in the present study with estimated limits of error (See text). Subscripts of the atom pairs follow those listed in Table 3.
b) Theoretical mean amplitudes for the *gauche* conformer given in Table 3.

for leveling the total intensity $I_0(q)$. Theoretical molecular intensities $qM_c(q)$ were based on the structural parameters determined above, except that the ϕ_1 parameter was taken to be 0, 60, 120, and 180°. Typical I_b curves are illustrated in Fig. 4. The I_b curve corresponding to 100% *gauche* population is flat to within 0.5% of I_b, while other models are definitely unacceptable because of the systematic oscillations in the I_b curves.

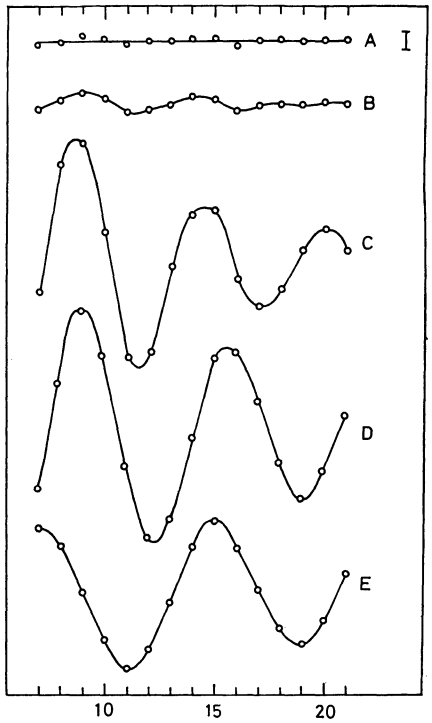

Fig. 4. Background functions I_b for different compositions of the *gauche* and other conformers. (See text).
(A) *gauche* (100%); (B) *gauche-trans* (95%: 5%); (C) *trans* (100%); (D) *skew* (100%); (E) *cis* (100%). The vertical bar represents the magnitude of 0.5% of I_b.

The limit of uncertainty in the above results was estimated from two principal sources of errors:[17] (A) random errors in the intensity measurement and (B) uncertainties in the structural parameters assumed in the analysis. The noise levels in I_b due to (A) was estimated to be 0.2% from the reproducibility of photographic measurements. Furthermore, the I_b function of nitrogen obtained by the same procedure had no fluctuation exceeding 0.2%. On the other hand, the

uncertainties due to (B) originated principally from the assumption of the ϕ_2 parameter. In this analysis, the amino-hydrogen positions were averaged with a threefold potential $V(\phi_2)$ as mentioned in the preceding section. The systematic error due to this assumption was estimated to be 0.3% of I_b from similar analyses using the ϕ_2 parameter fixed to the staggered positions.

Therefore, the total uncertainty level of I_b was estimated to be 0.4%, corresponding to the limit of uncertainty in the concentration of 5%. Hence, in the temperature range from 50 to 120°C at least 95% of the molecule takes the *gauche* conformation in the gas phase.

Discussion

Structural Parameters. The C–C bond distance, 1.545 Å, seems to be about 0.01 Å longer than that in ethane, 1.534 Å,[18] while the C–N bond distance, 1.469 Å, is similar to that in methylamine, 1.467 Å.[19] The C–C–N bond angle, 110.2°, is nearly equal to the tetrahedral angle and is smaller than the C–C–C angles in normal alkanes (*e.g.*, 112° for butane).[20] The azimuthal angle ϕ_1, found to be 64°, is similar to that in butane[20] and is about 10° smaller than those in 1, 2-dichloroethane[21] and ethylene glycol.[22]

A related bicyclic compound, triethylenediamine,[1] has analogous C–C–N angle and C–N distance, whereas the C–C distance in triethylenediamine, 1.562 Å, is significantly longer than that in ethylenediamine. A similar lengthening in the C–C bond in a bicyclic compound as compared with normal alkanes has also been suggested for bicyclo[2.2.2]octane.[12]

The observed mean amplitudes, listed in Table 6, agree with the calculated values, which have comparable uncertainties. The calculated N···N amplitude is sensitive to the choice of Y(C–C): *e.g.*, 0.1641 Å for Y=0.11 md·Å and 0.1805 Å for Y=0.083 md·Å[23] (corresponding to that in ethane). Therefore, from the observed N···N amplitude of $0.145_4 \pm 0.037$ Å one can estimate Y(C–C) to be 0.16_7 md·Å. The Y value determined in this way[24] is about twice as large as that for ethane and is nearly equal to that for the *gauche* form of 1,2-dichloroethane, 0.16 md·Å.[25]

Rotational Isomerism. The *gauche* conformer is found to be by far the most stable in the gas phase; the fractions of any other conformers, if present, should not exceed 5%. This is analogous to the case of ethylene glycol[22] and contrasts with that in 1,2-dichloroethane,[21,26] where the *trans* form is about 1.14 kcal/mol more stable than the *gauche* form.

In order to examine the rotational isomerism in this molecule, a conformational analysis was carried out by a SCF-MO (CNDO/2) method[27] by the use of a program written by Segal.[28] The azimuthal angles ϕ_1 and ϕ_2 were varied systematically in all directions. Other structural parameters were fixed to the values determined in the present study. The results are illustrated in Fig. 5 as a contour map. The areas where

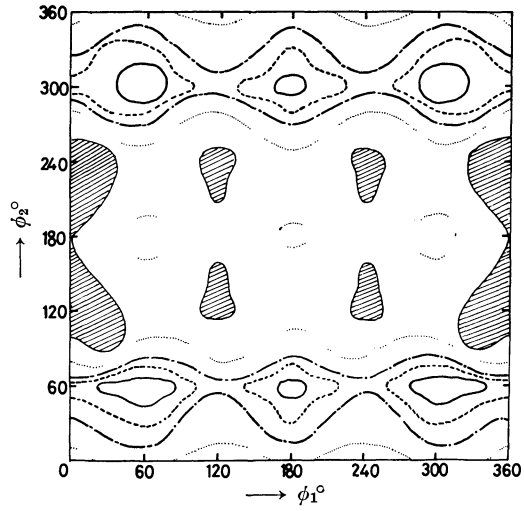

Fig. 5. Contour map for the potential energy of internal rotation of ethylenediamine calculated by the SCF-CNDO/2 method. (See text).
——: limits within 1 kcal/mol above the deepest minimum; ------: 2 kcal/mol; —·—: 3 kcal/mol; ·····: 5 kcal/mol. Shaded regions indicate local maxima 10 kcal/mol above the minimum.

the energies are less than 1 kcal/mol above the deepest minimum, enclosed in solid lines, are located in the neighborhood of ϕ_1=60° (*gauche*) and 180° (*trans*), with ϕ_2=60° or 300° (staggered). The cross sections of the energy surface at ϕ_2=60° or 300° show that the *gauche* form (ϕ_1=60°) is about 0.9 kcal/mol more stable than the *trans* form (corresponding to the equilibrium fraction of about 10% around 100°C) and that the barrier heights at ϕ_1=0° and 120° are about 1.5 and 2.8 kcal/mol, respectively. The theoretical prediction about the *gauche*-minimum agrees with the present experiment, whereas the predicted energy difference between the *trans* and *gauche* forms is much too small. This discrepancy seems to be due to the fault in the theory, since the CNDO/2 method often gives proper estimates of molecular geometry but fails to predict correct energies.[29] More reliable information on the potential function should await future spectroscopic measurements.

18) L. S. Bartell and H. K. Higginbotham, *J. Chem. Phys.*, **42**, 851 (1965).
19) H. K. Higginbotham and L. S. Bartell, *ibid.*, **42**, 1131 (1965).
20) K. Kuchitsu, This Bulletin, **32**, 748 (1959); R. A. Bonham and L. S. Bartell, *J. Amer. Chem. Soc.*, **81**, 3491 (1959).
21) J. Ainsworth and J. Karle, *J. Chem. Phys.*, **20**, 425 (1952); O. Bastiansen and K. Kveseth, Private communication (1971).
22) O. Bastiansen, *Acta Chem. Scand.*, **3**, 415 (1949).
23) E. J. Jacob, H. B. Thompson, and L. S. Bartell, *J. Chem. Phys.*, **47**, 3736 (1967).
24) E. Hirota, This Bulletin, **31**, 130 (1958).
25) T. Miyazawa and K. Fukushima, *J. Mol. Spectrosc.*, **15**, 308 (1965).
26) K. Kuratani, T. Miyazawa, and S. Mizushima, *J. Chem. Phys.*, **21**, 1411 (1953).
27) J. A. Pople and G. A. Segal, *ibid.*, **44**, 3289 (1966).
28) G. A. Segal, "Molecular Calculations with Complete Neglect of Differential Overlap," Program 91, Quantum Chemistry Program Exchange, Indiana University, 1966. This program was rewritten at the Computer Centre of the University of Tokyo in FORTRAN-IV by Drs. Toshiyasu L. Kunii and Toshiaki Ohta, to whom the authors are grateful for allowing them to use the program.
29) M. J. S. Dewar and E. Haselbach, *J. Amer. Chem. Soc.*, **92**, 590 (1970).

Solvent Effects on the Spin-Lattice Relaxation Times and Chemical Shifts of *N*-Methylacetamide and *N*,*N*-Dimethylacetamide in Hydrogen Bonding Solvents

Kazuo SATO and Atsuo NISHIOKA

Department of Polymer Engineering, Tokyo Institute of Technology, Meguro-ku, Tokyo

(Received April 3, 1971)

The proton spin-lattice relaxation and the chemical shift were studied in *N*-methylacetamide (NMA) and *N*,*N*-dimethylacetamide (DMA) in *p*-dioxane and chloroform. In the *p*-dioxane solution, it has been found that the self-association of NMA does affect its spin-lattice relaxation, whereas the amide-solvent association does not affect it entirely. This was interpreted in terms of the lifetime of the inter-amide ($\simeq 10^{-11}$—10^{-12} sec) and the amide-solvent association (much shorter than 10^{-11}—10^{-12} sec). On the other hand, the effect of the amide-solvent association on the spin-lattice relaxation is pronounced in chloroform, as is the effect of the self-association of NMA. The inter-amide interaction which leads the double-bond character of DMA to be more stable was not reflected distinctly in the concentration dependence of the spin-lattice relaxation times of DMA.

The inter-molecular interactions and self-association phenomena of amides in solutions have been the subjects of a considerable number of experimental and theoretical discussions, and have been studied quantitatively by using IR, the NMR-chemical shift, the thermodynamic technique, *etc.*[1]

In our previous paper,[2] we studied the proton spin-lattice relaxation and chemical shift of *N*-methylacetamide (NMA) and *N*,*N*-dimethylacetamide (DMA) in aqueous (D_2O) and non-polar (CCl_4) environments, and pointed out that, in addition to the chemical shift, the spin-lattice relaxation time (T_1) measurements are useful in providing basic information for understanding the molecular motion, the non-equilibrium properties, and the inter-amide interactions.

In this paper, we will report on T_1 and chemical-shift measurements of NMA and DMA as well as of solvent molecules, *p*-dioxane, and chloroform, which have been well known to act as hydrogen-bonding proton acceptors and donors respectively. We will discuss the molecular motion and the inter-amide and amide-solvent interactions in these solutions on the basis of our experimental results on the T_1's and chemical shifts of the protons of solute and solvent molecules. Moreover by comparing the results of the NMA solutions with those of the DMA solutions, further information on the peptide-bond character will be obtained.

It is useful to compare the results of the T_1's with those of the chemical shifts on amide solutions in order to understand the hydrogen-bonding phenomena in detail, for the former depends on non-equilibrium properties, whereas the latter depends on equilibrium properties.

Experimental

Materials. The NMA, DMA, *p*-dioxane, and chloroform were reagent-grade samples purchased from the Tokyo Kasei Co., Ltd. The chloroform-*d* and *p*-dioxane-d_8 were provided by E. Merck A G., Darmstadt. The atmospheric oxygen dissolved in the samples was carefully removed by several freeze-pump-thaw cycles in a NMR tube; then, under a vacuum, the sample tube was sealed off.

NMR Measurements. The NMR instrument used was a JNM-C-60H spectrometer operated at 60MHz; the measurements of T_1 were performed at 25 ± 1°C by adiavatic-rapid-passage or saturation-recovery methods. The experimental errors were smaller than $\pm5\%$ in every case. Two T_1's of the non-equivalent *N*-methyl protons of DMA were in agreement with each other within the range of experimental errors, so we adopted the T_1 of *N*-methyl as the average value. The chemical shifts were measured at 25 ± 1°C by the usual side-band-technique, using tetramethylsilane as the internal reference. Other experimental details appeared in the previous paper.

Results and Discussion

Before discussing the results of the spin-lattice relaxation and chamical-shift measurements, we should like to mention the method of analyzing the data. The obserbed spin-lattice relaxation time, $(T_1)_{obs}$, is expressed as follows for solute and solvent molecules respectively, taking all the possible contributions into account:

$$(T_1^{-1})_{obs}^{solute} = (T_1^{-1})_{intra} + (T_1^{-1})_{inter}^{solute\text{-}solute} + (T_1^{-1})_{inter}^{solute\text{-}solvent} \quad (1)$$

$$(T_1^{-1})_{obs}^{solvent} = (T_1^{-1})_{intra} + (T_1^{-1})_{inter}^{solvent\text{-}solvent} + (T_1^{-1})_{inter}^{solvent\text{-}solute} \quad (2)$$

where $(T_1^{-1})_{intra}$ and $(T_1^{-1})_{inter}^{solute\text{-}solute}$ represent the intramolecular and the solute-solute intermolecular magnetic dipolar contributions respectively, and where $(T_1^{-1})_{inter}^{solute\text{-}solvent}$ refers to the solute-solvent intermolecular contribution, which indicates the magnetic effects of the solvent protons on the spin-lattice relaxation of solute protons. Deuteron and chlorine are considered to contribute negligibly to the relaxation of the protons because of their small magnetogyric ratios. Each term in Eq. (2) represents a similar contribution.

$(T_1^{-1})_{intra}$ and $(T_1^{-1})_{inter}$ depend on the rotational and the relative translational motions of the molecules. $(T_1^{-1})_{intra}$ can be expressed as Eq. (3) in terms of

1) For example, S. Mizushima, "Structure of Molecules and Internal Rotation," Academic Press, New York (1954), Chap. 6; G. C. Pimentel and A. L. McClellan "The Hydrogen Bond," W. H. Freeman and Company, San Francisco, California (1960), Chap. 3.

2) K. Sato and A. Nishioka, This Bulletin, **44**, 52, (1971).

the interprotonic distance, r_{ij}, and the rotational correlation time, τ_c: [3,4]

$$(T_1^{-1})_{\text{intra}} = \frac{3}{2}\hbar^2\gamma^4\sum_j\langle r_{ij}^{-6}\rangle\cdot\tau_c \qquad (3)$$

where $\hbar$ is Plank's constant divided by 2π, and where γ is the magnetogyric ratio of the proton. We estimated the $(T_1^{-1})_{\text{intra}}$ of NMA and DMA by the extrapolation procedure to infinite dilution, and calculated τ_c by Eq. (3), taking into account the molecular geometries of NMA and DMA.[5]

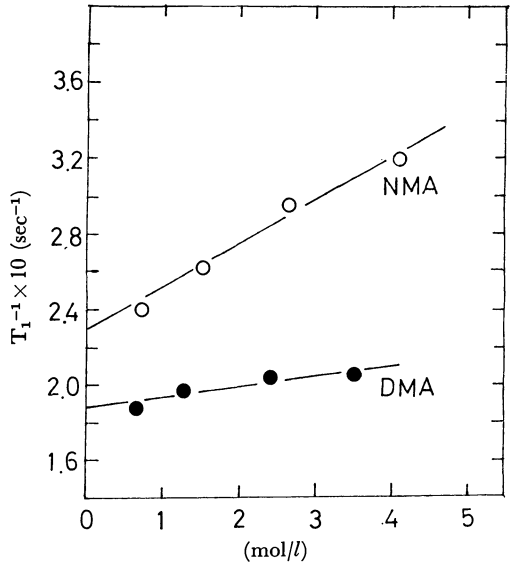

Fig. 1. Relaxation rate of methyl protons of amides *vs.* concentration of NMA (○) and DMA (●); *p*-dioxane solutions.

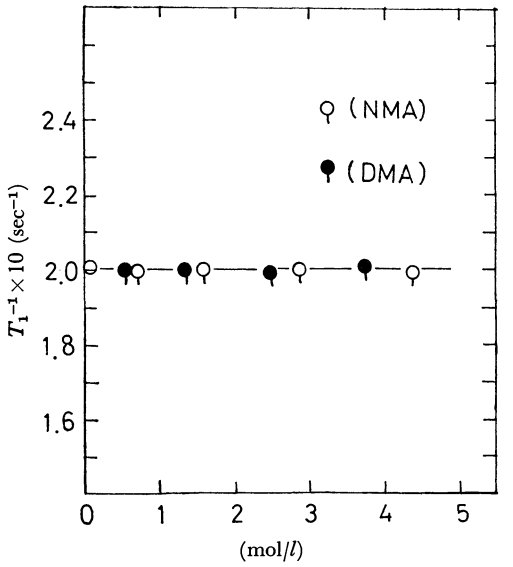

Fig. 2. Relaxation rate of solvent protons *vs.* solute concentration; *p*-dioxane solutions.
solute; NMA-♀, DMA-♀

p-Dioxane Solution. The concentration dependences of the spin-lattice relaxation rates, T_1^{-1}, of NMA, DMA, and the solvent are shown in Figs. 1 and 2 respectively. The T_1 values of the *C*-methyl protons are almost equal to those of *N*-methyl in both amides within the limits of experimental error. From the observed linear plot of T_1^{-1} *vs.* the concentration of the amide, we can extrapolate the results to infinite dilution. The T_1's of the solvent are almost independent of the concentration of the amide. This means that $(T_1^{-1})^{\text{solvent-solute}}_{\text{inter}}\simeq 0$ and $(T_1^{-1})_{\text{intra}}$, $(T_1^{-1})^{\text{solvent-solvent}}_{\text{inter}}$ are not affected by the amide-solvent interactions. It is interesting to note that the hydrogen bonding with NMA does not affect the spin-lattice relaxation of *p*-dioxane.

The spin-lattice relaxation is governed by the microscopic molecular motions and the ratio of the correlation times of the motion to the lifetime of molecular association. Recently, Anderson and Fryer[6,7] and Marshall[8] have discussed theoretically and experimentally the effect of molecular association on the spin-lattice relaxation, and concluded that, if the lifetime of the associated molecules moving as a unit is longer than the correlation times of motion (for most liquids, the correlation times are of the order of 10^{-11}—10^{-12} sec), the effect of association is pronounced, whereas the effect is small if the lifetime is shorter. In view of this, the lifetime of the hydrogen bonding between NMA and *p*-dioxane is probably much shorter than 10^{-11}—10^{-12} sec. We have previously studied the effects of the molecular association on the spin-lattice relaxation in mixtures of chloroform and proton-acceptor solvents, such as dimethyl sulfoxide, pyridine, acetone, and benzene, and shown that the association with a larger association constant does more remarkably affect the spin-lattice relaxation of chloroform, while the weak association has no effect at all.[9] Thus, it is considered that the association between NMA and *p*-dioxane through the hydrogen bonding is very weak and that the association constant may be small.

LaPlanche, Thompson, and Rogers[10] have studied theoretically the chain-association equilibria based on the model that the solute molecules form chain-like polymers through self-association, and that either the solvent molecules associate with the solute or do not. They have also applied the theory to the chemical-shift measurements of *N*-monosubstituted amides in solutions. From the equilibrium constants found for *N*-isopropylacetamide in *p*-dioxane and chloroform, they have concluded that chloroform and *p*-dioxane

3) N. Bloembergen, E. M. Purcell, and R. V. Pound, *Phys. Rev.*, **73**, 679 (1948).
4) A. Abragam, "The Principle of Nuclear Magnetism," Clarendon Press, Oxford (1961), Chap. 8.
5) L. Pauling, "The Nature of the Chemical Bond," Cornell University Press, Ithaca (1960), Chap. 8, p. 281. As in previous paper, we assumed that the geometry of DMA is the same as that of NMA except for the substituted *N*-methyl group, and internal rotation of methyl is almost free.
6) J. E. Anderson and P. A. Fryer, *J. Chem. Phys.*, **50**, 3784, (1969).
7) J. E. Anderson, *ibid.*, **51**, 3578 (1969).
8) A. G. Marshall, *ibid.*, **52**, 2527 (1970).
9) K. Sato and A. Nishioka, This Bulletin, **44**, 1506, (1971).
10) L. A. LaPlanche, H. B. Thompson, and M. T. Rogers, *J. Phys. Chem.*, **69**, 1482 (1965).

Table 1. Intramolecular relaxation times and the rotational correlation times of NMA and DMA estimated from extrapolating to infinite dilution

solvent	solute					
	NMA			DMA		
	observed protons	$(T_1)_{intra}$	$\tau_c \times 10^{12}$	observed protons	$(T_1)_{intra}$	$\tau_c \times 10^{12}$
$CDCl_3$	$-\overset{O}{\overset{\|\|}{C}}-CH_3$	6.3_0 sec	2.8_5 sec	$-\overset{O}{\overset{\|\|}{C}}-CH_3$	7.1_1 sec	2.4_5 sec
	$-\overset{\|}{N}-CH_3$	6.3_0	2.7_8	$-N\langle CH_3)_2$	7.1_1	2.4_0
$C_4H_8O_2$	$-\overset{O}{\overset{\|\|}{C}}-CH_3$	4.2_7	4.1_4	$-\overset{O}{\overset{\|\|}{C}}-CH_3$	5.4_2	$3\cdot2_9$
	$-\overset{\|}{N}-CH_3$	4.2_7	4.0_5	$-N\langle CH_3)_2$	5.4_2	3.2_3

compete with approximately the same efficiency for the hydrogen bonding of *N*-isopropylacetamide. They have also studied NMA in chloroform, and found that chloroform associates with NMA; however, they have not examined it in *p*-dioxane. There is no guarantee that their conclusion about *N*-isopropylacetamide mentioned above holds also in the case of NMA in *p*-dioxane. Moreover, we must give attention to the fact that they measured the chemical shift on the basis of an internal reference. It has been established that the resonance frequncies of internal-reference compounds are often considerably influenced by solvent effects.[11] In order to discuss the results in detail and quantitatively, it will be necessary to measure the chemical shifts on the basis of an external reference and to correct for differences in the bulk diamagnetic susceptibility between the sample and the reference compound. It seems necessary to reexamine this problem over a wide range of experimental conditions for both the T_1 and the chemical shift.

From the experimental facts mentioned above, that $(T_1^{-1})_{inter}^{solvent\text{-}solute} \simeq 0$, and that the amide-solvent association does not affect the spin-lattice relaxation of *p*-dioxane, it can reasonably be assumed that the T_1's of amide protons are also not affected by *p*-dioxane. We measured the T_1 of NMA in *p*-dioxane-d_8(2.7 mol/*l* of NMA) and found that $T_1^{-1}=2.8\times10^{-1}(sec^{-1})$. This value is almost equal to that in *p*-dioxane, and the assumption that $(T_1^{-1})_{inter}^{solute\text{-}solvent} \simeq 0$ holds. Therefore, the values extrapolated to infinite dilution are identical to the $(T_1^{-1})_{intra}$ of amides. The values of $(T_1)_{intra}$ and τ_c of NMA and DMA are shown in Table 1. The τ_c's of *C*-methyl and *N*-methyl protons in the same molecule are almost equal for both NMA and DMA, but the values of NMA are longer than those of DMA by a factor of about 1.2—1.3. We consider that this is the effect of the self-association of NMA in solutions. Klotz and Fransen[12] also con-

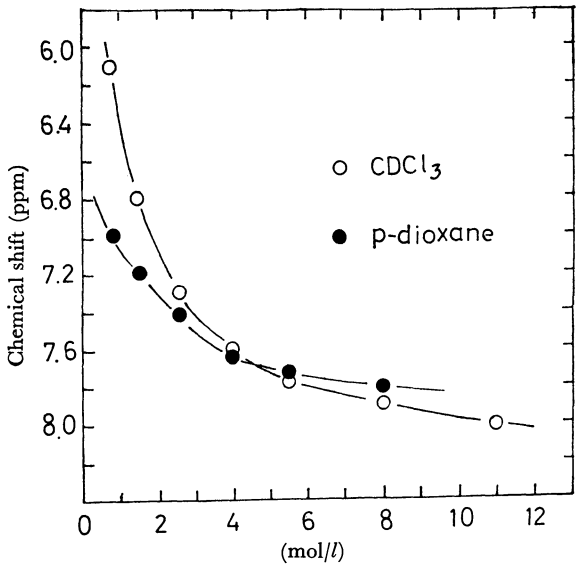

Fig. 3. Concentration dependence of N-H proton chemical shift of NMA in deuteriochloroform (○) and *p*-dioxane (●). Chemical shift were measured downfield from internal TMS.

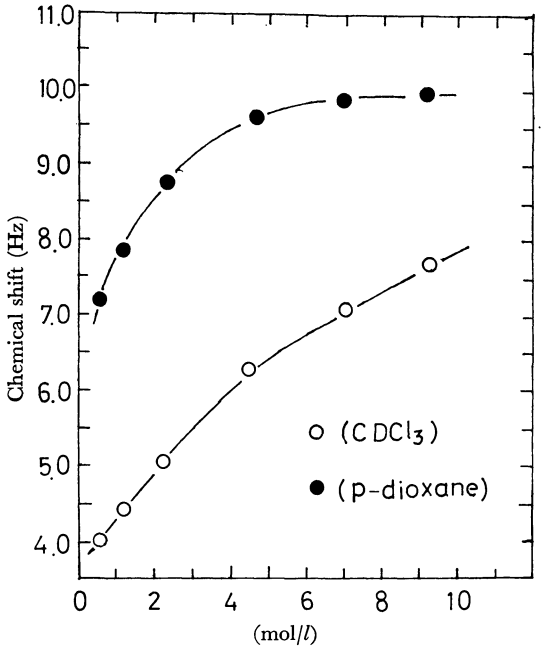

Fig. 4. Concentration dependence of the chemical shift between the two N-CH_3 signals of DMA in deuteriochloroform (○) and *p*-dioxane (●).

11) J. W. Emsley, J. Feeny, and L. H. Sutcliffe, "High Resolution Nuclear Magnetic Resonance Spectroscopy," Pergamon Press, Oxford (1965), Chap. 7.

12) I. M. Klotz and J. S. Fransen, *J. Amer. Chem. Soc.*, **84**, 3461 (1962).

cluded, on the basis of IR measurements, that, in *p*-dioxane, the self-association of NMA is appreciable at moderate concentrations. The low-field shift of the N–H proton with an increase in the concentration of NMA is considered to support the self-association of NMA in *p*-dioxane (Fig. 3).

The τ_c's of NMA estimated in the present study are considered to characterize the rotational motions of NMA restricted slightly in a weakly-associated chain. Moreover, it is concluded that the lifetime of the inter-amide hydrogen bonding may be of the order of 10^{-11}—10^{-12} sec. The larger concentration dependence of the T_1^{-1} of NMA than that of DMA also means that the rotational and translational mobilities of NMA are reduced through the hydrogen bonding.

In Fig. 4, the concentration dependence of the chemical shift between the two *N*-methyl protons of DMA is shown in *p*-dioxane as well as in chloroform. The origin of the nonequivalence of the two *N*-methyl groups has been understood to be due to the double-bond character of the central C–N linkage.[13] The increase in the chemical shift with an increase in the concentration of amide has been considered to be due to the inter-amide interaction, which leads the double-bond character to be more stable.[14–16] This inter-amide interaction has no appreciable effect on the concentration dependence of T_1, which is almost linear over the experimental range of the concentrations of amide. In carbon tetrachloride, remarkable effects of the inter-amide interaction on T_1 of DMA have been observed, and the concentration dependence of T_1 at moderate concentrations differs from that at dilute concentrations.[2] The absence of the effects of the inter-amide interaction on T_1 is considered to be due to the fact that, in *p*-dioxane, the lifetime of the inter-amide interaction is shorter than that in carbon tetrachloride. The chemical shift between two *N*-methyl protons in *p*-dioxane is smaller than in carbon tetrachloride; we consider this also to be due to the weak inter-amide interaction in *p*-dioxane. The slight increase in the relaxation rate with an increase in the concentration of amide may be the result of the increase in the spin-densities of the solutions.

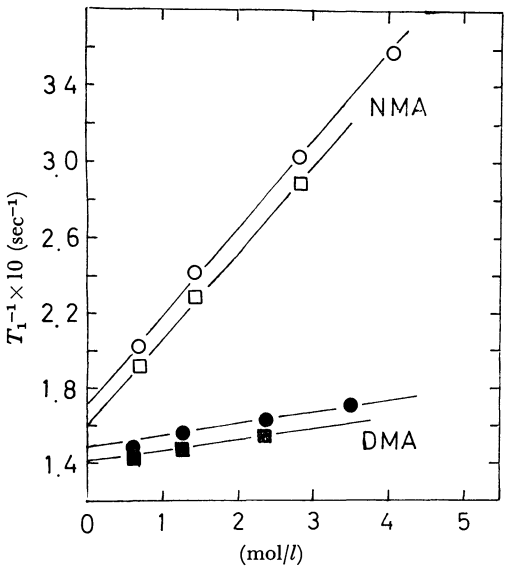

Fig. 5. Relaxation rate of methyl protons of amides *vs.* concentration of NMA (○-chloroform solutions, □-deuteriochroform solutions) and DMA (●-chloroform solutions, ■-deuteriochloroform solutions).

Chloroform Solution. The concentration dependences of the T_1^{-1}'s of NMA and DMA are shown in Fig. 5. As in the case of *p*-dioxane solutions, the T_1's of *C*-methyl and *N*-methyl protons in the same molecule are identical with each other, and the plot of T_1^{-1} *vs.* the concentration of the amide is also linear. By extrapolation in chloroform-*d* solutions, we obtained $(T_1)_{\text{intra}}$ and calculated the values τ_c of both amides (Table 1). The fact that the τ_c's of NMA are longer than those of DMA by a factor of about 1.2, and the large concentration dependence of T_1^{-1} of NMA are attributable to the self-association. Moreover, the lifetime of the association is considered to be almost identical to that in the *p*-dioxane solution. The effect of the association on the N–H proton chemical shift can easily be seen; it moves to a low field with an increase in the concentration of amide (Fig. 3).

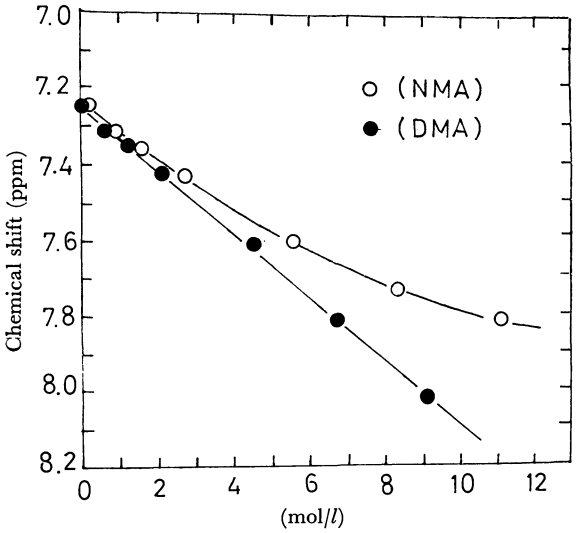

Fig. 6. Chemical shift of chloroform proton *vs.* solute concentration. solute; NMA-○, DMA-●. Chemical shift were measured downfield from internal TMS.

The chemical shifts of the chloroform proton depend upon the concentrations of the amides, as is shown in Fig. 6. A linear relation is observed in the DMA solution, but not in the NMA solution. The low-field shift of the chloroform proton is caused by the formation of hydrogen bonding with amides and the magnetic anisotropy effect due to the carbonyl group. The linear low-field shift in the DMA solution may be the result of the approximate 1 : 1 amide-solvent association. On the other hand, the smaller and non-linear change in the NMA solution suggests that the inter-amide hydrogen bonding becomes predominant over the amide-solvent hydrogen bonding with an increase

13) Ref. 11, Chap. 9.
14) M. Rabinovitz and A. Pines, *J. Chem. Soc. B*, **1968**, 1110.
15) M. Rabinovitz and A. Pines, *J. Amer. Chem. Soc.*, **91**, 1585 (1969).
16) R. C. Neuman, Jr., W. R. Woolfenden, and V. Jonas, *J. Phys. Chem.*, **73**, 3177 (1969).

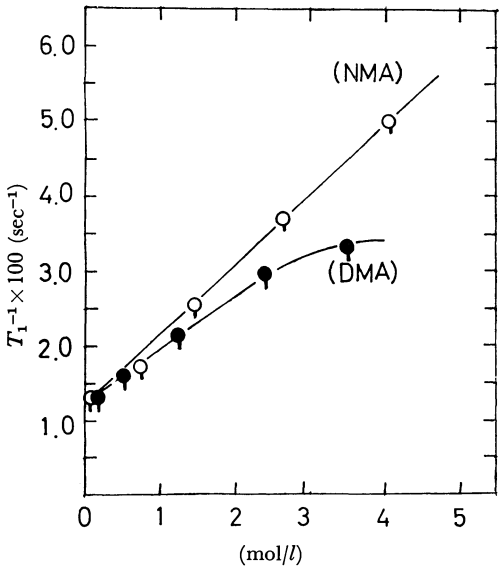

Fig. 7. Relaxation rate of solvent proton *vs.* solute concentration; chloroform solutions. solute; NMA-○, DMA-●

in the concentration and, consequently, decreases the fraction of the solvent molecules participating in the hydrogen bonding with amide.

In Fig. 7 the dependence of T_1^{-1} of the chloroform proton on the concentrations of the amides is shown. The spin-lattice relaxation of the solvent is considerably affected by the presence of amides; this is strikingly different from the case with *p*-dioxane solutions. This pronounced effect of amides can be interpreted in terms of the amide-solvent association, whose lifetime is almost equal to or longer than 10^{-11}—10^{-12} sec. As has been mentioned above, in the NMA solution the fraction of solvents participating in the hydrogen bonding with amides is considered to be smaller than in the DMA solution. Nevertheless, the effect of the NMA on the T_1's of the chloroform proton is more remarkable. In the NMA solution, chloroform associates with amide and breaks up the self-associated chain to some degree, and it must interact with the terminal carbonyl group of the broken chain. The molecular motion of chloroform associating with the chain-terminal is restricted to a greater degree than that in the DMA solution. Thus, the effect of the hydrogen bonding with NMA on the spin-lattice relaxation of the chloroform proton is considered to be more pronounced in spite of the samller fraction of associated chloroform molecules. As in the case of the *p*-dioxane solution of DMA, the effect of the inter-amide interaction of DMA which leads the double-bond character to be more stable is not observable distinctly over the range of experimental concentrations.

In our previous paper, we have estimated the τ_c's of NMA and DMA in D_2O solutions: $\tau_c=2.5\times10^{-12}$ sec. These values are almost equal to those in chloroform solutions. The BPP theory predicts $\tau_c=4\pi\eta a^3/3kT$ for the rigid molecules, where η and a represent solution viscosity and the radius of a spherical molecule respectively.[3] The solution viscosities of D_2O solutions are larger by a factor of about 2 than those of chloroform solutions;[17] therefore, according to this theory, the τ_c's in chloroform must be shorter than those in D_2O. This can be explained by considering that, in chloroform, the molecular motion of amides is reduced through the amide-solvent association and the self-association of amide (NMA), which may in turn lead the micro-viscosities of the solutions to be higher.

17) unpublished data.

An MO-theoretical Interpretation of the Nature of Chemical Reactions III. Bond Interchange

Hiroshi FUJIMOTO, Shinichi YAMABE, and Kenichi FUKUI
Faculty of Engineering, Kyoto University, Sakyo-ku, Kyoto

(Received April 5, 1971)

The wave functions of a system composed of two mutually-interacting molecules have been expressed in terms of configuration interaction wave functions. The electron configurations have been taken into account with respect to the states of adiabatic interaction, delocalization interaction, and polarization interaction. The electron populations in all of these states have been obtained separately. It has been demonstrated that the adiabatic interaction between two closed-shell molecules can not be the origin of the bond interchange in chemical reactions. The inclusion of charge-transferred states has been shown to be of great importance in explaining the formation of new bonds and the weakening of old bonds in the case of chemical interaction between two molecules. On the basis of the results of numerical calculations on some typical reaction models, the important role of the orbital overlapping interaction of the highest occupied molecular orbital and the lowest unoccupied molecular orbital has been pointed out.

The interaction energy between two mutually-reacting molecules has been investigated by partitioning it into the Coulomb-interaction, exchange-interaction, delocalization, and polarization terms on the assumption of no nuclear configuration change.[1] Expressions for these four energy terms have been derived. The important role of electron delocalization in determining the favorable position and spatial direction of chemical interaction with respect to each of the two reacting molecules has been pointed out on the basis of the three governing principles of chemical interaction.[2] The significance of the cooperation of the charge-transfer and the nuclear configuration change has been stressed in relation to the nodal properties of the highest occupied (HO) molecular orbital (MO) and of the lowest unoccupied (LU) MO. The purpose of the present paper is to show how and why the formation of new bonds and the cleavage of old bonds take place in chemical reactions. This seems to be one of the most fundamental problems in understanding the nature of chemical reactions.

Wave Functions

Let us consider the chemical interaction between the molecules A and B. Here we set limits to the case in which both A and B have closed-shell structures in the isolated state. Only a slight modification should be needed for other systems. We represent the wave function of the combined system of the two molecules, A and B, by the configuration interaction (CI) wave function;

$$\Psi = C_0\Psi_0 + \sum_i^{\text{occ}}\sum_l^{\text{uno}} C_{i\to l}\Psi_{i\to l} + \sum_k^{\text{occ}}\sum_j^{\text{uno}} C_{k\to j}\Psi_{k\to j} + \sum_i^{\text{occ}}\sum_j^{\text{uno}} C_{i\to j}\Psi_{i\to j} + \sum_k^{\text{occ}}\sum_l^{\text{uno}} C_{k\to l}\Psi_{k\to l} + \cdots \quad (1)$$

The meanings of the wave functions Ψ_0, $\Psi_{i\to l}$, $\Psi_{i\to j}$, $\cdots$ are the same as those in Ref. 1. These wave functions are constructed by means of the Slater determinants, composed of the MO's, a_i's, and a_j's of the molecule A and the b_k's and b_l's of the molecule B, according to each electron configuration. Other highly-transferred and highly-excited configurations can be neglected, provided the interaction is not too strong. The coefficients, C_0, $C_{i\to l}$, $C_{i\to j}$, $\cdots$, can be obtained by solving the secular equations. The integrals which are necessary in constructing the secular determinant have already been derived in Ref. 1. The coefficients of the wave function, Ψ, are taken so as to satisfy the normalization condition:

$$\int \Psi^2 d\tau = 1 \quad (2)$$

In order to obtain the expressions of the electron populations of the interacting systems by the use of Ψ, it is convenient to represent them as the sum of the electron populations in each of the terms appearing in Eq. (1). For this purpose, we present the first-order density matrices[3] of some of the terms in Appendix. In the following

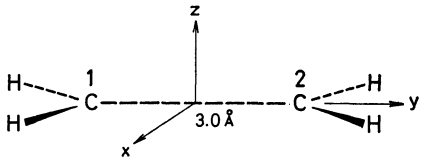

MODEL I

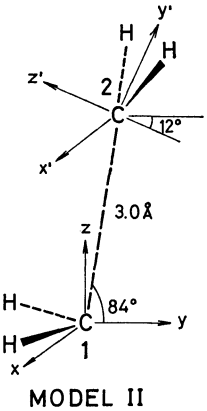

MODEL II

Fig. 1. A schematic representation of assumed models of the dimerization of methylenes.

1) K. Fukui and H. Fujimoto, This Bulletin, **41**, 1989 (1968).
2) K. Fukui and H. Fujimoto, *ibid.*, **42**, 3399 (1969).
3) R. McWeeny, *Proc. Roy. Soc.* (London), **A223**, 63 (1954); **A232**, 114 (1955).

discussions, the contribution from polarized configurations may be disregarded so long as we concentrate our attention on the intermolecular charge-transfer between A and B. The off-diagonal terms $\rho_{JJ'}$ $(J \neq J')$ (see Appendix), in which neither J nor J' is 0, are put equal to zero in a first approximation.

The example taken here to show the numerical results is the dimerization of singlet methylenes to form ethylene. This system was discussed by Hoffmann and his coworkers in order to demonstrate the preference of the non-least motion to the least motion in the mutual approach of methylenes by the use of the extended Hückel calculation.[4] We will compare the two modes of approach by means of our method, from the standpoint of mutual electron-donating and electron-accepting interactions. The two models are schematically illustrated in Fig. 1. The relative nuclear positions of the two methylenes are the same as those determined by Hoffmann. In Tables 1 and 2 we present the coefficients, C_0, $C_{i\to l}$'s, and $C_{k\to j}$'s, with respect to the two models in Fig. 1. The method of calculation and the approximations employed are the same as those adopted in our previous calculation.[5] It is clear that the charge-transfer interaction is by far more effective in Model II than in Model I.

Table 1. The coefficients of the ground-state CI wave function of model I

$C_0=0.9925$

		π'	σ_4'	σ_5'
$\lvert C_{i\to l}\rvert$	σ_1	0	0.0223	0
	σ_2	0	0	0.0025
	σ_3	0	0.0544	0

		π	σ_4	σ_5
$\lvert C_{k\to j}\rvert$	σ_1'	0	0.0223	0
	σ_2'	0	0	0.0025
	σ_3'	0	0.0544	0

The MO's of methylenes are termed as follows.

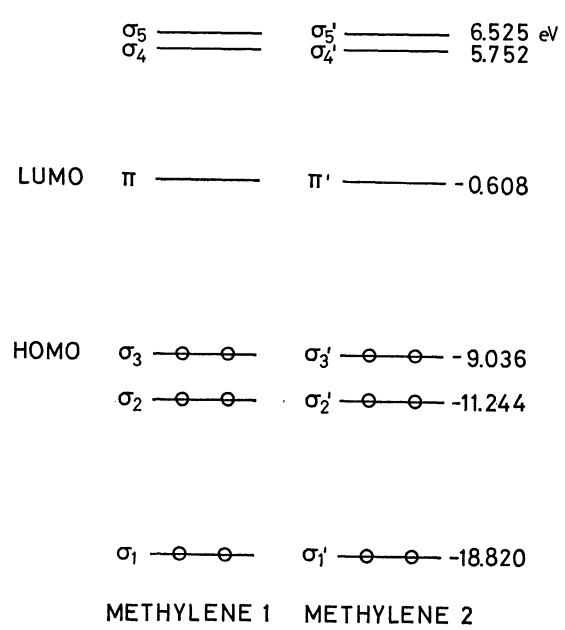

Table 2. The coefficients of the ground-state CI wave function of model II

$C_0=0.9231$

		π'	σ_4'	σ_5'
$\lvert C_{i\to l}\rvert$	σ_1	0.0038	0.0240	0
	σ_2	0	0	0.0039
	σ_3	0.0601	0.0035	0

		π	σ_4	σ_5
$\lvert C_{k\to j}\rvert$	σ_1'	0.0466	0.0266	0
	σ_2'	0	0	0.0111
	σ_3'	0.2879	0.0480	0

Formation of New Bonds

Let us divide the electron populations into two parts, intermolecular and intramolecular. First, let us try to connect this concept to the origins of the formation of new bonds between A and B. The AO bond population between the AO t of A and the AO u of B is given by:

$$\phi_{tu} = \phi_{tu}^{(E)} + \phi_{tu}^{(D)} \tag{3}$$

$\phi_{tu}^{(E)}$ is the AO bond population between t and u due to the exchange interaction:

$$\phi_{tu}^{(E)} \cong C_0^2(\phi_{tu}^{(E)})_0 + \sum_i^{\text{occ}} \sum_l^{\text{uno}} C_{i\to l}^2(\phi_{tu}^{(E)})_{i\to l} + \sum_k^{\text{occ}} \sum_j^{\text{uno}} C_{k\to j}^2(\phi_{tu}^{(E)})_{k\to j} \tag{4}$$

$$(\phi_{tu}^{(E)})_0 \cong -4(M!)\mathcal{N}_0^2 \sum_i^{\text{occ}} \sum_k^{\text{occ}} c_t^{(i)} c_u^{(k)} s_{tu} S_{ik} \tag{5}$$

where $c_t^{(i)}$ is the coefficient of the AO t in the MO a_i and where s_{tu} is the overlap integral between the AO's, t and u.

$$(\phi_{tu}^{(E)})_{i\to l} \cong -2(M!)\mathcal{N}_{i\to l}^2 \Big(2\sum_{i'}^{\text{occ}} \sum_k^{\text{occ}} c_t^{(i')} c_u^{(k)} s_{tu} S_{i'k} - \sum_k^{\text{occ}} c_t^{(i)} c_u^{(k)} s_{tu} S_{ik} + \sum_{i'}^{\text{occ}} c_t^{(i')} c_u^{(l)} s_{tu} S_{i'l} - 2c_t^{(i)} c_u^{(l)} s_{tu} S_{il}\Big) \tag{6}$$

$(\phi_{tu}^{(E)})_0$, $(\phi_{tu}^{(E)})_{i\to l}$, and $(\phi_{tu}^{(E)})_{k\to j}$ indicate the AO bond populations of a bond newly formed between the AO t of A and the AO u of B due to the electron exchange in Ψ_0, $\Psi_{i\to l}$, and $\Psi_{k\to j}$ states respectively.

The quantity $\phi_{tu}^{(D)}$ implies the AO bond population between t and u due to the electron delocalization:

$$\phi_{tu}^{(D)} \cong \sum_i^{\text{occ}} \sum_l^{\text{uno}} \{(\phi_{tu}^{(D)})_{0,i\to l} + (\phi_{tu}^{(D)})_{i\to l,0}\} C_0 C_{i\to l} + \sum_k^{\text{occ}} \sum_j^{\text{uno}} \{(\phi_{tu}^{(D)})_{0,k\to j} + (\phi_{tu}^{(D)})_{k\to j,0}\} C_0 C_{k\to j} \tag{7}$$

$$(\phi_{tu}^{(D)})_{0,i\to l} \cong \sqrt{2}\, c_t^{(i)} c_u^{(l)} s_{tu} \tag{8}$$

In Table 3 are given $(\phi_{tu}^{(E)})_0$ and $\phi_{tu}^{(E)}$ with respect

4) R. Hoffmann, R. Gleiter, and F. B. Mallory, *J. Amer. Chem. Soc.*, **92**, 1460 (1970).

5) H. Fujimoto, S. Yamabe, and K. Fukui, This Bulletin, **44**, 971 (1971).

Table 3. The intermolecular AO bond populations due to the exchange

		Carbon of Methylene 1			
		s	x	y	z
Carbon of Methylene 2	s'	−0.0038 (−0.0035)	0 (0)	−0.0000 (−0.0000)	−0.0001 (0)
	x'	0 (0)	−0.0001 (−0.0001)	0 (0)	0 (0)
	y'	−0.0051 (−0.0048)	0 (0)	−0.0000 (−0.0000)	0.0005 (0)
	z'	0.0000 (0)	0 (0)	0.0000 (0)	0 (0)

The values in parentheses indicate $(\phi_{tu}^{(E)})_0$.

Table 4. The intermolecular AO bond populations due to the electron delocalizations from methylene 1 to methylene 2 and from methylene 2 to methylene 1

		Carbon of Methylene 1			
		s	x	y	z
Carbon of Methylene 2	s'	−0.0021 −0.0035	0 0	0.0000 0.0003	0 0.0139
	x'	0 0	0.0001 −0.0002	0 0	0 0
	y'	0.0015 −0.0052	0 0	0.0000 0.0003	0 0.0372
	z'	0.0002 0	0 0	0.0014 0	0 0

The upper value in each set indicates the AO bond population due to the electron delocalization from methylene 1 to methylene 2 and the lower value that arising from the electron delocalization from methylene 2 to methylene 1.

to Model II. The contribution of mono-transferred states to $\phi_{tu}^{(E)}$ is negligibly small. It can be seen that the sum of $\phi_{tu}^{(E)}$'s over all the pairs of the t of A and the u of B is negative. This demonstrates an antibonding contribution of the exchange interaction in the chemical interaction between two methylenes. Table 4 shows the $\phi_{tu}^{(D)}$ due to the electron delocalization from methylene 1 to methylene 2 and that due to the electron delocalization from methylene 2 to methylene 1. Adding $\phi_{tu}^{(D)}$ to $\phi_{tu}^{(E)}$, we can find the positive atomic bond population arising in the region between the carbon atoms of two methylenes. It should be noted that the greatest contribution comes from the combination of the p_z orbital of methylene 1 and $p_{y'}$, orbital of methylene 2, and that the next largest is that of the p_z orbital of methylene 1 and the $2s$ orbital of methylene 2.

The intermolecular chemical bonding can be interpreted in terms of the mixing of charge-transferred states into the Ψ_0 state. Thus, the importance of delocalization interaction in the process of bond formation is clear.

Weakening of Old Bonds

The changes in the bond populations of the intramolecular AO pairs in A and B due to the electron-exchange interaction may be given by:

$$\varphi_{tt'}^{(E)} = C_0^2(\varphi_{tt'}^{(E)})_0 + \sum_i^{\text{occ}}\sum_l^{\text{uno}} C_{i\to l}^2(\varphi_{tt'}^{(E)})_{i\to l} + \sum_k^{\text{occ}}\sum_j^{\text{uno}} C_{k\to j}^2(\varphi_{tt'}^{(E)})_{k\to j} \tag{9}$$

$$\varphi_{uu'}^{(E)} = C_0^2(\varphi_{uu'}^{(E)})_0 + \sum_i^{\text{occ}}\sum_l^{\text{uno}} C_{i\to l}^2(\varphi_{uu'}^{(E)})_{i\to l} + \sum_k^{\text{occ}}\sum_j^{\text{uno}} C_{k\to j}^2(\varphi_{uu'}^{(E)})_{k\to j} \tag{10}$$

$$(\varphi_{tt'}^{(E)})_0 \cong 4(M!)\mathcal{N}_0^2\sum_i^{\text{occ}}\sum_k^{\text{occ}} c_t^{(i)}c_{t'}^{(i)}s_{tt'}S_{ik}^2 \tag{11}$$

$$(\varphi_{tt'}^{(E)})_{i\to l} \cong 2(M!)\mathcal{N}_{i\to l}^2\{\sum_{i'}^{\text{occ}} c_t^{(i')}c_{t'}^{(i')}s_{tt'}(2\sum_k^{\text{occ}} S_{i'k}^2 + S_{i'l}^2) - c_t^{(i)}c_{t'}^{(i)}s_{tt'}(\sum_k^{\text{occ}} S_{ik}^2 + 2S_{il}^2)\} \tag{12}$$

$$(\varphi_{tt'}^{(E)})_{k\to j} \cong 2(M!)\mathcal{N}_{k\to j}^2\{\sum_i^{\text{occ}} c_t^{(i)}c_{t'}^{(i)}s_{tt'}(2\sum_{k'}^{\text{occ}} S_{ik'}^2 - S_{ik}^2) + c_t^{(j)}c_{t'}^{(j)}s_{tt'}(\sum_{k'}^{\text{occ}} S_{jk'}^2 - 2S_{jk}^2)\} \tag{13}$$

The changes in the AO bond populations of A and of B due to the mixing of charge-transferred states into Ψ_0 are given by:

$$\varphi_{tt'}^{(D)} \cong 2(-\sum_i^{\text{occ}}\sum_l^{\text{uno}} C_{i\to l}^2 c_t^{(i)}c_{t'}^{(i)}s_{tt'} + \sum_k^{\text{occ}}\sum_j^{\text{uno}} C_{k\to j}^2 c_t^{(j)}c_{t'}^{(j)}s_{tt'} - 2\sqrt{2}C_0\sum_i^{\text{occ}}\sum_l^{\text{uno}} C_{i\to l}c_t^{(i)}c_{t'}^{(i)}s_{tt'}S_{il}) \tag{14}$$

$$\varphi_{uu'}^{(D)} \cong 2(-\sum_k^{\text{occ}}\sum_j^{\text{uno}} C_{k\to j}^2 c_u^{(k)}c_{u'}^{(k)}s_{uu'} + \sum_i^{\text{occ}}\sum_l^{\text{uno}} C_{i\to l}^2 c_u^{(l)}c_{u'}^{(l)}s_{uu'} - 2\sqrt{2}C_0\sum_k^{\text{occ}}\sum_j^{\text{uno}} C_{k\to j}c_u^{(k)}c_{u'}^{(l)}s_{uu'}S_{kj}) \tag{15}$$

Table 5. The changes in the AO bond populations of the C–H bond of methylene 1 and methylene 2

Methylene 1

	Carbon			
	s	x	y	z
Hydrogen s	−0.0035	0.0000	−0.0012	0

Methylene 2

	Carbon			
	s'	x'	y'	z'
Hydrogen s'	0.0053	0.0000	−0.0083	0

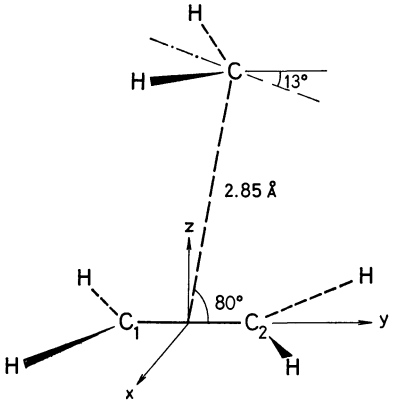

Fig. 2. A schematic representation of assumed model of the addition of methylene to ethylene.

Table 6. The changes in the bond populations of the carbon-carbon bond of ethylene due to the interaction with methylene

		Carbon 1			
		s	x	y	z
Carbon 2	s	−0.0020	0	0.0002	0
	x	0	0.0003	0	0
	y	−0.0002	0	−0.0003	0
	z	0	0	0	−0.0397

Table 5 shows the changes in the AO bond populations in methylenes. However, the numerical values are too small to show the importance of the bond weakening caused by electron delocalization, since carbon-hydrogen bonds in methylenes never break down in the process of dimerization to form an ethylene molecule. In order to obtain a more distinct result, we had better proceed to the addition of singlet methylene to ethylene[6] (Fig. 2). The results of the calculation of the changes in the AO bond populations of the carbon-carbon bond of ethylene are shown in Table 6. We can find that the AO bond population between the $2p_z$ orbital of the carbon 1 and the $2p_z$ orbital of the carbon 2 decreases conspicuously, while the others remain almost unchanged. This demonstrates the start of the disappearance of the π bond in ethylene to form σ bonds with methylene.

Extending Mulliken's concept of population analysis[7] to an AO pair between two interacting molecules, the electrons flow into the intermolecular region through the orbital overlapping between the AO t of A and the AO u of B may be divided into two, one of which reverts to the AO t, and the other, to the AO u. Therefore, the changes in the AO populations of AO t and AO u due to the electron delocalization are given by:

$$\Delta N_t^{(D)} = \frac{1}{2}\left(\sum_u^B \phi_{tu}^{(D)} + \sum_{t'}^A \varphi_{tt'}^{(D)}\right) \tag{16}$$

$$\Delta N_u^{(D)} = \frac{1}{2}\left(\sum_t^A \phi_{tu}^{(D)} + \sum_{u'}^B \varphi_{uu'}^{(D)}\right) \tag{17}$$

Table 7 shows the changes in the AO populations of methylenes in Model II. We can see that methylene 2 serves as an electron donor, and methylene 1, as an electron acceptor.

Table 7. The changes in AO populations of methylene 1 and methylene 2

Methylene 1

Carbon				Hydrogen
s	x	y	z	
−0.0053	0.0000	−0.0034	0.1088	0.0042

Methylene 2

Carbon				Hydrogen
s'	x'	y'	z'	
−0.0070	0.0000	−0.0961	0.0045	−0.0050

6) a) R. Hoffmann, *J. Amer. Chem. Soc.*, **90**, 1475 (1968). b) K. Fukui, H. Fujimoto, and S. Yamabe, to be published.

7) R. S. Mulliken, *J. Chem. Phys.*, **23**, 1833, 1841, 2338, 2343 (1955).

Intramolecular Electron Rearrangement Due to Interaction

The other terms in the diagonal elements of Eqs. (A. 1), (A. 3), and (A. 5), which have not appeared in Eqs. (4)—(17), stand for the reorganization of the electron populations in both A and B caused by the mutual interaction. We may define the partial AO populations of the AO t as:

$$n_t^{(ii')} + n_t^{(i'i)} = (p_t^{(ii')} + v_t^{(ii')}) + (p_t^{(i'i)} + v_t^{(i'i)}) \tag{18}$$

$$p_t^{(ii')} = c_t^{(i)} c_t^{(i')} \qquad (i \neq i')$$

$$v_t^{(ii')} = \sum_{t'}^A c_t^{(i)} c_{t'}^{(i')} s_{tt'} \qquad (t \neq t')$$

where $p_t^{(ii')}$ stands for the valence-inactive part, and $v_t^{(ii')}$ for the valence-active part.[8] The quantity $n_t^{(ii')} + n_t^{(i'i)}$ gives a non-zero value, in general, although the sum over all the t's of the molecule A vanishes. We represent the changes in the AO bond populations in the molecules A and B by $\varphi_{tt'}^{(R)}$ and $\varphi_{uu'}^{(R)}$ respectively. Therefore, the changes in the AO populations of the AO's t and u resulting from the intramolecular electron rearrangement may be given by:

$$\Delta N_t^{(R)} = \frac{1}{2}\sum_{t'}^A \varphi_{tt'}^{(R)} \tag{19}$$

$$\Delta N_u^{(R)} = \frac{1}{2}\sum_{u'}^B \varphi_{uu'}^{(R)} \tag{20}$$

The changes in the AO populations and AO bond populations caused by the electron rearrangement are shown in Table 8 with respect to Model II. Although the changes in the electron populations due to the intramolecular electron rearrangement are small in comparison with the other terms discussed above, they are hardly negligible in the systems where one or both of the reactants involve highly-polarized bonds. In Fig. 3 we present the changes in the atomic popula-

Table 8. The changes in AO populations and in AO bond populations of methylene 1 and methylene 2 due to the intramolecular electron rearrangement

Methylene 1

	Carbon				Hydrogen
	s	x	y	z	
Hydrogen	0.0046	0.0003	−0.0002	0	−0.0024
	−0.0035	0.0000	0.0001	0	—

Methylene 2

	Carbon				Hydrogen
	s'	x'	y'	z'	
Hydrogen	−0.0059	−0.0001	0.0025	0	0.0018
	0.0006	0.0000	0.0012	0	—

8) K. Ruedenberg, *Rev. Mod. Phys.*, **34**, 326 (1962).

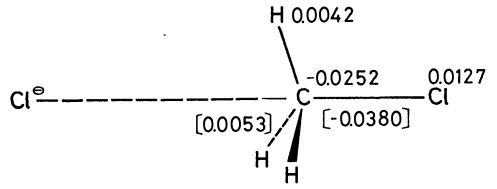

(C—Cl⊖ 2.8 Å, C—Cl 1.9 Å, C—H 1.09 Å, ∠HCCl 105°)

Fig. 3. The changes in atomic populations and in atomic bond populations due to the intramolecular electron rearrangement. The values in [ ] indicate the changes in atomic bond populations.

tions and in the atomic bond populations due to the intramolecular electron rearrangement with regard to the chemically-interacting system shown in the figure.[5] It is interesting to see that the carbon-chlorine bond is loosened and that electron migration takes place in the direction from carbon to chlorine.

Changes in Electron Populations

The difference in the population of the AO t before and after interaction will be:

$$\Delta N_t \cong \frac{1}{2}\sum_{u}^{B}\phi_{tu} + \frac{1}{2}\sum_{t'}^{A}(\varphi_{tt'}^{(D)}+\varphi_{tt'}^{(E)}+\varphi_{tt'}^{(R)}) \qquad (21)$$

Similarly, the change in the AO bond population between the AO's t and t' of A is given by:

$$\varphi_{tt'} \cong \varphi_{tt'}^{(D)} + \varphi_{tt'}^{(E)} + \varphi_{tt'}^{(R)} \qquad (22)$$

Summing up the changes in AO populations and AO bond populations discussed above gives the final results on Model I and Model II for the dimerization of methylenes shown in Fig. 4.

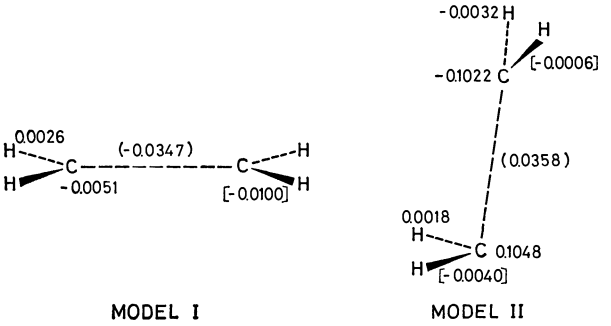

MODEL I MODEL II

Fig. 4. The changes in atomic populations and in atomic bond populations due to the interaction. The values in ( ) indicate the intermolecular atomic bond populations and the values in [ ] stand for the changes in atomic bond populations.

As has been discussed above, the delocalization interaction has a close connection to the bond-interchange in chemical reactions of two closed-shell molecules. It has been demonstrated that the formation of new bonds between reagent and reactant and the weakening of old bonds in both can be interpreted only by the inclusion of charge-transferred configurations. Among various charge-transferred terms, the orbital interaction between the HO MO of the reactant and the LU MO of the reagent, and the reverse interaction, play the most dominant role. Those electron configurations which have been omitted in the present calculation can also be included in a similar fashion in the population calculation, although it will take too much computer time to be performed. It is believed that the main consequences would not be seriously different from those presented here.

This calculation has been limited to the cases in which both reactant and reagent are closed-shell systems. Extension to other cases is now in progress.

The authors wish to express their appreciation to the Data Processing Center of Kyoto University for the generous permission to use the FACOM 230–60 computer.

Appendix

Taking the terms up to the second order of the overlap integrals S_{ab} between the MO's, a's of the molecule A and b's of the molecule B, we have the first order spinless density matrix given by:

$$\begin{aligned}\rho(1'|1)_{0,0} &= M\int \Psi_0(1', 2, \cdots, M)\Psi_0(1, 2, \cdots, M)\mathrm{d}\xi_1\mathrm{d}\tau_2\cdots\mathrm{d}\tau_M \\ &\cong 2\sum_{i}^{occ} i(1')i(1) + 2\sum_{k}^{occ} k(1')k(1) \\ &\quad + \{2\sum_{i}^{occ}\sum_{i'}^{occ}\sum_{k}^{occ} i(1')i'(1)S_{ik}S_{i'k} \\ &\quad + 2\sum_{k}^{occ}\sum_{k'}^{occ}\sum_{i}^{occ} k(1')k'(1)S_{ik}S_{ik'} \\ &\quad - 2\sum_{i}^{occ}\sum_{k}^{occ}(i(1')k(1)+k(1')i(1))S_{ik}\}\mathcal{N}_0^2(M!)\end{aligned} \qquad (A.1)$$

where M is the total number of electrons of the system composed of A and B, $i(1')k(1)$, for instance, is the abbreviation of $a_i(1')b_k(1)$, and the normalization factor for Ψ_0 is:

$$\mathcal{N}_0 \cong (1-2\sum_{i}^{occ}\sum_{k}^{occ}S_{ik}^2)^{-1/2}(M!)^{-1/2} \qquad (A.2)$$

With respect to $\Psi_{i\to l}$, we have

$$\begin{aligned}\rho(1'|1)_{i\to l, i\to l} &\cong 2\sum_{i'}^{occ} i'(1')i'(1) \\ &\quad + 2\sum_{k}^{occ} k(1')k(1) - i(1')i(1) + l(1')l(1) \\ &\quad + \{i(1')i(1)(\sum_{k}^{occ}S_{ik}^2+2S_{il}^2) + l(1')l(1)(\sum_{i'}^{occ}S_{i'l}^2-2S_{il}^2) \\ &\quad - 2\sum_{i'}^{occ}\sum_{k}^{occ}(i'(1')k(1)+k(1')i'(1))S_{i'k} \\ &\quad + \sum_{k}^{occ}(i(1')k(1)+k(1')i(1))S_{ik} \\ &\quad - \sum_{i'}^{occ}(i'(1')l(1)+l(1')i'(1))S_{i'l} + 2(i(1')l(1)+l(1')i(1))S_{il} \\ &\quad + \sum_{i'}^{occ}\sum_{i''}^{occ} i'(1')i''(1)(2\sum_{k}^{occ}S_{i'k}S_{i''k}+S_{i'l}S_{i''l}) \\ &\quad - \sum_{i'}^{occ}(i(1')i'(1)+i'(1')i(1))(\sum_{k}^{occ}S_{ik}S_{i'k}+2S_{il}S_{i'l}) \\ &\quad + \sum_{k}^{occ}\sum_{k'}^{occ} k(1')k'(1)(2\sum_{i'}^{occ}S_{i'k}S_{i'k'}-S_{ik}S_{ik'}) \\ &\quad + \sum_{k}^{occ}(k(1')l(1)+l(1')k(1))(\sum_{i'}^{occ}S_{i'k}S_{i'l}-2S_{ik}S_{il})\}\mathcal{N}_{i\to l}^2(M!)\end{aligned} \qquad (A.3)$$

and

$$\mathcal{N}_{i\to l} \cong (1-2\sum_{i'}^{\mathrm{occ}}\sum_{k}^{\mathrm{occ}} S_{i'k}^2+\sum_{k}^{\mathrm{occ}} S_{ik}^2-\sum_{i'}^{\mathrm{occ}} S_{i'l}^2+2S_{il}^2)^{-1/2}(M!)^{-1/2} \tag{A.4}$$

The next to be considered is the term which represents the mixing in of monotransferred configuration into zero-configuration. Neglecting the terms smaller than S_{ab}^2, we have:

$$\begin{aligned}\rho(1'|1)_{0,i\to l} \cong{}& \sqrt{2}\,S_{il}(2\sum_{i'}^{\mathrm{occ}} i'(1')i'(1)+2\sum_{k}^{\mathrm{occ}} k(1')k(1))\\ &-\sqrt{2}\,(\sum_{i'}^{\mathrm{occ}} i(1')i'(1)S_{i'l}+\sum_{k}^{\mathrm{occ}} k(1')l(1)S_{ik}-i(1')l(1))\end{aligned} \tag{A.5}$$

Similar expressions are obtained from $\Psi_{k\to j}$. The elements of the density matrix due to the mixing in of the monoexcited states are:

$$\begin{aligned}\rho(1'|1)_{i\to j,i\to j} \cong{}& 2\sum_{i'}^{\mathrm{occ}} i'(1')i'(1)\\ &+2\sum_{k}^{\mathrm{occ}} k(1')k(1)-i(1')i(1)+j(1')j(1)\\ &+\{j(1')j(1)\sum_{k}^{\mathrm{occ}} S_{jk}^2+i(1')i(1)\sum_{k}^{\mathrm{occ}} S_{ik}^2\\ &+2\sum_{i'}^{\mathrm{occ}}\sum_{i''}^{\mathrm{occ}}\sum_{k}^{\mathrm{occ}} i'(1')i''(1)S_{i'k}S_{i''k}\\ &-\sum_{i'}^{\mathrm{occ}}\sum_{k}^{\mathrm{occ}}(i(1')i'(1)+i'(1')i(1))S_{ik}S_{i'k}\\ &+\sum_{i'}^{\mathrm{occ}}\sum_{k}^{\mathrm{occ}}(j(1')i'(1)+i'(1')j(1))S_{jk}S_{i'k}\\ &-2\sum_{k}^{\mathrm{occ}}(j(1')i(1)+i(1')j(1))S_{jk}S_{ik}\\ &+\sum_{k}^{\mathrm{occ}}\sum_{k'}^{\mathrm{occ}} k(1')k'(1)(2\sum_{i'}^{\mathrm{occ}} S_{i'k}S_{i'k'}-S_{ik}S_{ik'}+S_{jk}S_{jk'})\\ &-2\sum_{i'}^{\mathrm{occ}}\sum_{k}^{\mathrm{occ}}(i'(1')k(1)+k(1')i'(1))S_{i'k}\\ &+\sum_{k}^{\mathrm{occ}}(i(1')k(1)+k(1')i(1))S_{ik}\\ &-\sum_{k}^{\mathrm{occ}}(j(1')k(1)+k(1')j(1))S_{jk}\}\mathcal{N}_{i\to j}^2(M!)\end{aligned} \tag{A.6}$$

and:

$$\mathcal{N}_{i\to j} \cong (1-2\sum_{i'}^{\mathrm{occ}}\sum_{k}^{\mathrm{occ}} S_{i'k}^2+\sum_{k}^{\mathrm{occ}} S_{ik}^2-\sum_{k}^{\mathrm{occ}} S_{jk}^2)^{-1/2}(M!)^{-1/2} \tag{A.7}$$

and;

$$\begin{aligned}\rho(1'|1)_{0,i\to j} \cong{}& \sqrt{2}\,\{(2\sum_{i'}^{\mathrm{occ}} i'(1')i'(1)\\ &+2\sum_{k}^{\mathrm{occ}} k(1')k(1))(-\sum_{k}^{\mathrm{occ}} S_{ik}S_{jk})\\ &+\sum_{i'}^{\mathrm{occ}}\sum_{k}^{\mathrm{occ}} i(1')i'(1)S_{jk}S_{i'k}+\sum_{i'}^{\mathrm{occ}}\sum_{k}^{\mathrm{occ}} i'(1')j(1)S_{ik}S_{i'k}\\ &+\sum_{k}^{\mathrm{occ}}\sum_{k'}^{\mathrm{occ}} k(1')k'(1)S_{ik}S_{jk'}-\sum_{k}^{\mathrm{occ}} i(1')k(1)S_{jk}\\ &-\sum_{k}^{\mathrm{occ}} k(1')j(1)S_{ik}\}+\sqrt{2}\,i(1')j(1)\,(1-2\sum_{i'}^{\mathrm{occ}}\sum_{k}^{\mathrm{occ}} S_{i'k}^2)^{1/2}\\ &\times(1-2\sum_{i'}^{\mathrm{occ}}\sum_{k}^{\mathrm{occ}} S_{i'k}^2+\sum_{k} S_{ik}^2-\sum_{k}^{\mathrm{occ}} S_{jk}^2)^{-1/2}\end{aligned} \tag{A.8}$$

and similar formulas corresponding to the contributions from $\Psi_{k\to l}$.

Studies of the Liquid-Liquid Partition Systems. VIII. Stabilities and Extractabilities of Copper(II) and Zinc(II) Complexes with Acetylacetone, Trifluoroacetylacetone, and Hexafluoroacetylacetone in Aqueous Sodium Perchlorate Solution-Carbon Tetrachloride Systems

Tatsuya SEKINE and Naohiko IHARA

Department of Chemistry, Science University of Tokyo, Kagurazaka, Shinjuku-ku, Tokyo

(Received April 7, 1971)

The distribution of copper(II) and zinc(II) chelates with three β-diketones, acetylacetone (AA), trifluoroacetylacetone (TFA), and hexafluoroacetylacetone (HFA) between carbon tetrachloride and aqueous sodium perchlorate solutions at 0.1M, 1M, and 3M has been determined at 25°C as a function of the concentration of the dissociated chelate anions. The stability constants for the metal chelates in the aqueous phase and the two phase-distribution constants for the uncharged complexes have been determined by a graphic analysis of the distribution data. The distribution was also measured when the carbon tetrachloride phase was added with tributylphosphate (TBP) or trioctylphosphine oxide (TOPO) and the adduct-formation constants of the uncharged chelate with these ligands have been determined by a graphic analysis of the increase in the distribution ratio as a function of the ligand concentration. The results are as follows: (i) Copper(II) forms first and second complexes with these chelating ligands in the aqueous phase, whereas zinc(II) forms the third complex (except with HFA) besides the first and the second ones; the complexes are more stable in the ligand order of AA>TFA>HFA. (ii) The stability constants of the copper(II) complexes are much higher than those of the corresponding zinc(II) complexes. (iii) The distribution constant of the uncharged copper(II) complex is higher than that of the corresponding zinc(II) complex. (iv) No remarkable relation has been found among the distribution constants of the chelating acid and those of the uncharged metal chelates. (v) The adducts of the metal chelates are more stable in the ligand order of HFA>TFA>AA. The zinc(II) complex forms more stable adducts than does the corresponding copper(II) complex, and TOPO forms more stable adducts than does TBP. (vi) Changes in the concentration of the background salt alter the stability constants of the metal chelates and the distribution constants of the uncharged chelate (salting-out); the effects are, however, very complicated. On the basis of these results, the distribution constants of the uncharged chelates were discussed from the standpoint of the interactions of the central metal ions in the complexes with the water molecules, and a qualitative relationship between these interactions and the stabilities of the adduct chelate complexes was pointed out.

The solvent extraction of metal ions with various weakly acidic chelating reagents has been studied by many authors from the standpoint of the chemical equilibria involved in the extraction processes. The distribution ratios of the metal ions in these systems have been determined as a function of the concentration of the extractants, and the statistical treatments of the distribution data are now very well established.

As will later be discussed in detail, the distribution ratio in metal-chelate extraction systems is represented by the successive complex formations in the aqueous phase and the distribution of the uncharged complex among them.

The stability constants of metal complexes with various chelating anions are an important chemical characteristic of the complexes, and they have been studied by many coordination chemists. However, the two-phase distribution behavior of the uncharged complex is rather a special problem of solvent-extraction chemistry, and, as it is difficult to determine the distribution constant of the uncharged complex in many systems directly, not very much has been established.

In this investigation, the present authors have studied the extraction of copper(II) and zinc(II) mainly from this standpoint. Three β-diketones, acetylacetone (AA), trifluoroacetylacetone (TFA), and hexafluoroacetylacetone (HFA) have been used as the extractants. They were chosen because we desired to know how the distribution behavior of chelate complexes is changed by the substitution of the trifluoromethyl group for the methyl group in acetylacetone; they were also chosen because of the practical reason that the distribution constants are not too high to make an accurate measurement.

Sodium perchlorate solutions were used as the aqueous phase. The concentration of this salt was adjusted at 0.1M, 1.0M, or 3.0M in order to observe the effect of this "*inert*" salt on the stability and the extractability of the metal complexes. In some experiments, the carbon tetrachloride phase was added with tributylphosphate (TBP) or triocytlphosphine oxide (TOPO) in order to determine the enhancements of the distribution due to the adduct-chelate formation and in order to determine the equilibrium constants of the complexes more accurately. The equilibrium constants were determined by a curve-fitting method, on the basis of these data, and some discussion was made of the extractability from the standpoint of the interactions of the metal complexes in the aqueous phase.

Experimental

Reagents. A radioactive tracer, copper-64, and zinc-65 were used in order to determine the distribution ratio of the metal ions. The three β-diketones were obtained from Dojindo & Co. The TBP was obtained from the Tokyo Kasei Co. It was washed perchloric acid, water, and an aqueous sodium hydroxide solution, and then several times with water. The TOPO was obtained from Dojindo & Co.

Standard sodium hydroxide solutions were prepared from a 50% sodium hydroxide solution and decarbonated water. It was standardized to potassium acid phthalate. The sodium perchlorate was prepared from sodium carbonate and perchloric acid. It was recrystallized three times from water. The other reagents were of an analytical grade and were used without further purification.

A certain amount of a β-diketone was dissolved in carbon tetrachloride. The concentration was determined by a two-phase titration; a 5 m*l* portion of the organic solution was pipetted and transferred into a flask containing a certain amount of water, after which the solution was titrated with a standard sodium hydroxide solution by using a suitable indicator (phenolphthalein or azoblue). The concentration of the TBP or TOPO solution was calculated from the weight of the reagent dissolved. The water-saturated TBP was regarded as $TBP \cdot H_2O$. The concentration of the sodium perchlorate stock solution was calculated from the weight of the residue left after a certain amount of the stock solution had been evaporated in an air-bath at 120°C.

Procedures. All of the experiments were carried out in a thermostatted room at 25±0.3°C. An aqueous solution initially containing sodium perchlorate, sodium hydroxide, and 1.0×10^{-5}M copper ions labeled by copper-64 or 1.2×10^{-6}M zinc ions labeled by zinc-65 and carbon tetrachloride containing one of the extractants was placed in the tube. In the highest $-\log[H^+]$ region, the chelating acid distributed into buffered the aqueous phase, and no other buffering reagent was added. In the lower region, however, acetate was used for the experiments with copper(II) and an acetate or acid carbonate buffer was used for the experiments with zinc(II). The initial concentration of the buffer was 0.01M in the aqueous phase, and practically no difference in the distribution ratio was observed when the buffer concentration was changed to a half: it was thus concluded that the effect of the buffer was negligible. The initial volume of the two phases was always 5 m*l*.

The two phases in the tubes were settled on a rotating framework, agitated mechanically for one hour, and centrifuged. A 2-m*l* portion was pipetted from each phase, and the portions were transferred into small test tubes. The γ-radioactivities of the samples were measured with a scintillation counter, and the distribution ratio was calculated as;

$$D = \frac{\gamma\text{-count-rate per m}l\text{ of the org. phase}}{\gamma\text{-count-rate per m}l\text{ of the aq. phase}}$$

Some portion was also pipetted from the aqueous phase and transferred into a small glass vessel. The hydrogen-ion concentration in the stoichiometric scale was determined by potentiometry using solutions containing 1.00×10^{-2}M perchloric acid and 0.09M, 0.99M, or 2.99M sodium perchlorate as the standard of $-\log[H^+]=2.00$ in a 0.1M, 1M, or 3M constant ionic medium.

Statistical

When a weak acid, HA, is distributed between an organic and an aqueous phase, the distritution constant is described as:

$$HA \rightleftarrows HA_{(org)}$$

$$K_D = \frac{[HA]_{org}}{[HA]} \quad (1)$$

The acid dissociation of HA in the aqueous phase is described as:

$$HA \rightleftarrows H^+ + A^-$$

$$K_a = \frac{[H^+][A^-]}{[HA]} \quad (2)$$

If the volumes of the two phases are the same, the initial concentration of the acid in one phase (in the present study, it was the organic phase), C_{HA}, is described, on the basis of the concentrations after the equilibrium is established, as:

$$C_{HA} = [HA]_{org} + [HA] + [A^-] \quad (3)$$

By introducing Eqs. (1) and (2) into Eq. (3), we obtain:

$$C_{HA} = [A^-]\left(\frac{K_D+1}{K_a}[H^+]+1\right) \quad (4)$$

Equation (4) shows that the aqueous concentration of the anion from the acid in a liquid-liquid distribution system can be calculated from the initial acid concentration, from the hydrogen-ion concentration at the equilibrium, and from the distribution constant and the dissociation constant of the acid.

The complex formation of a divalent metal ion, M^{2+}, with a ligand anion, A^-, is described as follows:

$$M^{2+} + nA^- \rightleftarrows MA_n^{2-n}$$

$$\beta_n = \frac{[MA_n^{2-n}]}{[M^{2+}][A^-]^n} \quad (5)$$

Among these complexes, the uncharged one, MA_2, could be extracted into a non-polar organic solvent. The distribution constant of this metal complex is described as:

$$MA_2 \rightleftarrows MA_{2(org)}$$

$$K_{DM} = \frac{[MA_2]_{org}}{[MA_2]} \quad (6)$$

When the organic phase contains only the MA_2 species, and when the aqueous phase contains a series of metal complexes, the distribution ratio is described as follows:

$$D = \frac{[MA_2]_{org}}{[M^{2+}]+[MA^+]+[MA_2]+[MA_3^-]+\cdots} \quad (7)$$

By introducing Eqs. (5) and (6), Eq. (7) can be rewritten as:

$$D = \frac{K_{DM}\beta_2[A^-]^2}{1+\beta_1[A^-]+\beta_2[A^-]^2+\beta_3[A^-]^3+\cdots} \quad (8)$$

When the complex, MA_2, in the organic phase undergoes further complex formation with a neutral organophilic ligand, L, the equilibrium is described as:

$$MA_{2(org)} + nL_{(org)} \rightleftarrows MA_2L_{n(org)}$$

$$\beta_{n(org)} = \frac{[MA_2L_n]_{org}}{[MA_2]_{org}[L]^n_{org}} \quad (9)$$

When this type of adduct formation occurs in the organic phase, the distribution ratio can be described as follows:

$$D = \frac{K_{DM}\beta_2[A^-]^2(1+\beta_{1(org)}[L]_{org}+\beta_{2(org)}[L]^2_{org}+\cdots)}{1+\beta_1[A^-]+\beta_2[A^-]^2+\beta_3[A^-]^3+\cdots} \quad (10)$$

If the distribution ratio under a certain $[A^-]$ and $[L]_{org}$ is denoted by D, and when that under the identical $[A^-]$, but in the absence of L, is denoted by D_0, the following can be obtained from Eqs. (8) and (10):

$$D/D_0 = 1 + \beta_{1(org)}[L]_{org} + \beta_{2(org)}[L]^2_{org} + \cdots \quad (11)$$

When the distribution constant, K_{DM}, into a non-polar solvent is very small, it is very difficult to deter-

mine the stability constants of the metal complexes in the aqueous phase from the extraction data by using Eq. (8). However, if a certain amount of an adduct-forming ligand is added to the organic phase, the distribution ratio is increased. When the concentration of the adduct-forming ligand is kept constant throughout a series of experiments, the value in the parentheses in Eq. (10) is always constant. In such a case, the $K_{DM}(1+\sum\beta_{n(org)}[L_1]^n_{org})$ value, where $[L_1]_{org}$ is the concentration of the adduct-forming ligand, can be used instead of the K_{DM} value, in Eq. (8) and the stability constants can be determined from these data.

In many papers, the extraction equilibrium of M^{2+} with a chelating extractant is described as:

$$M^{2+} + 2HA_{(org)} \rightleftarrows MA_{2(org)} + 2H^+$$

$$K_{ex} = \frac{[MA_2]_{org}[H^+]^2}{[M^{2+}][HA]^2_{org}} \quad (12)$$

When the distribution ratio can be described as:

$$D = \frac{[MA_2]_{org}}{[M^{2+}]} \quad (13)$$

$$= K_{ex}[HA]^2_{org}[H^+]^{-2} \quad (14)$$

Thus, when no aqueous chelate complex is formed, the distribution ratio is proportional to the square of the concentration of the chelating extractant in the organic phase or is inversely proportional to the square of the hydrogen ion concentration in the aqueous phase. However, when the distribution ratio is given by Eq. (7), it can be described as:

$$D = \frac{K_{ex}[HA]^2_{org}[H^+]^{-2}}{1+\beta_1[A^-]+\beta_2[A^-]^2+\beta_3[A^-]^3+\cdots} \quad (15)$$

as $K_{DM}\beta_2[A^-]^2 = K_{ex}([HA]_{org}/[H^+])^2$;

$$K_{ex} = K_{DM}\beta_2 K_a^2 K_D^{-2} \quad (16)$$

The equilibrium constants in the above equations may be determined from the following graphic method.[1,2]

When the distribution ratio given by Eq. (8) is plotted as log D *vs.* log$[A^-]$:

$$Y = \log K_{DM}\beta_2 - \log([A^-]^{-2}+\beta_1[A^-]^{-1}+\beta_2+\beta_3[A^-]+\cdots) \quad (17)$$

If the complexes higher than the MA_2 are negligible, Eq. (17) can be rewritten as:

$$Y = \log K_{DM} - \log(\beta_2^{-1}[A^-]^{-2}+\beta_1\beta_2^{-1}[A^-]^{-1}+1) \quad (17')$$

The plot should have the following two asymptotes:

$$\lim_{[A^-]\to 0} Y = \log K_{DM}\beta_2 + 2\log[A^-] \quad (18\text{-}1)$$

$$\lim_{[A^-]\to \infty} Y = \log K_{DM} \quad (18\text{-}2)$$

The plot in Eq. (17′) could be fitted with the following family of standard curves:

$$Y = \log(1+pv+v^2) \quad (19\text{-}1)$$

$$X = \log v \quad (19\text{-}2)$$

From the two asymptotes, Eqs. (18-1) and (18-2), the K_{DM} and β_2 values can be obtained, and from the parameter, p, of the best-fit standard curve, β_1 is obtained as:

$$p = \beta_1\beta_2^{-1/2}$$

When the aqueous phase also contains the MA_3^- complex, the graphic analysis of the data was made as follows. In the lower $[A^-]$ region, the log D *vs.* log$[A^-]$ plot was first fitted with the standard curves in Eqs. (19-1) and (19-2). From this, approximate values of K_{DM}, β_1, and β_2 were determined. Then, by using these constants and an assumed value of β_3, a calculated curve was made and compared with the observed experimental data in the higher $[A^-]$ region. After several trials, the best-fit β_3 was found from the parameter of the best-fit curve.

When a set of constants were thus obtained, the extraction curve was calculated from these constants; it was then compared with the experimental points in order to check whether or not they are reasonable.

When a log D/D_0 *vs.* log $[L]_{org}$ plot, where factors other than $[L]_{org}$ are always kept constant, is made for an adduct-formation system, the data can also be analyzed by the curve-fitting as follows.[3] If the data are represented by:

$$D/D_0 = 1 + \beta_{1(org)}[L]_{org} \quad (20)$$

that is, if only the first complex is formed, the data could be fitted with the standard curve:

$$Y = \log(1+v) \quad (21\text{-}1)$$

$$X = \log v \quad (21\text{-}2)$$

When the data are represented by:

$$D/D_0 = 1 + \beta_{1(org)}[L]_{org} + \beta_{2(org)}[L]^2_{org} \quad (22)$$

they could be fitted with the standard curves given by Eqs. (19-1) and (19-2). If the asymptote for the log-D/D_0 *vs.* log$[L]_{org}$ plot of the data given by Eq. (20) intersects the X axis at $(X_1, 0)$, the value of log $\beta_{1(org)}$ should be $-X_1$. If the asymptote for the log D/D_0 *vs.* log $[L]_{org}$ plot of the data given by Eq. (22) intersects with the X axis at $(X_2, 0)$, the value of log $\beta_{2(org)}$ should be $-2X$; $\beta_{1(org)}$ can then be obtained from this $\beta_{2(org)}$ and the p of the best-fit standard curve as:

$$p = \beta_{1(org)}\beta_{2(org)}^{-1/2} \quad (23)$$

Results

The results of the measurements were, in general, reproducible. The recovery of the γ-radioactivity from the two phases was always quantitative within the limits of experimental accuracy. The concentration of the chelating anion in the aqueous phase was calculated by using Eq. (4); the dissociation and the distribution constants of these reagents, reported in another paper,[4] are also given in Table 1 of the present paper.

Figure 1 shows the dependence on the hydrogen-ion concentration of the distribution of copper(II) between carbon tetrachloride and a 1 M sodium perchlorate solution. Figure 2 shows the dependence on the hydrogen-ion concentration of the distribution of zinc(II) between carbon tetrachloride (open symbols) or carbon tetrachloride containing a certain amount of TBP (closed

1) D. Dyrssen and L. G. Sillén, *Acta Chem. Scand.*, **7**, 668 (1953).
2) L. G. Sillén, *ibid.*, **10**, 186 (1956).
3) T. Sekine and M. Ono, This Bulletin, **38**, 2087 (1965).
4) T. Sekine and N. Ihara, This Bulletin, to be published.

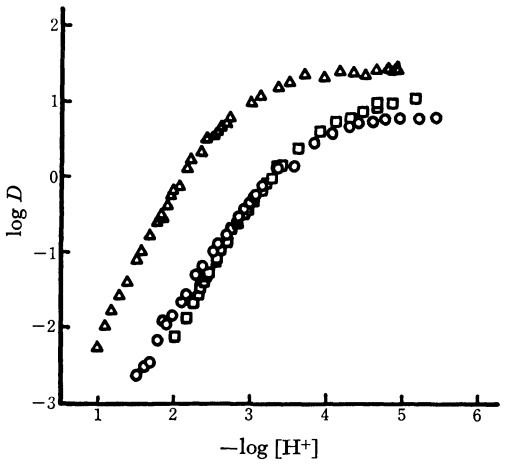

Fig. 1. Extraction of copper(II) complexes with AA(circles), TFA(triangles) and HFA(squares) as a function of the hydrogen ion concentrations.
organic phase: carbon tetrachloride
aqueous phase: 1M $Na(ClO_4)$

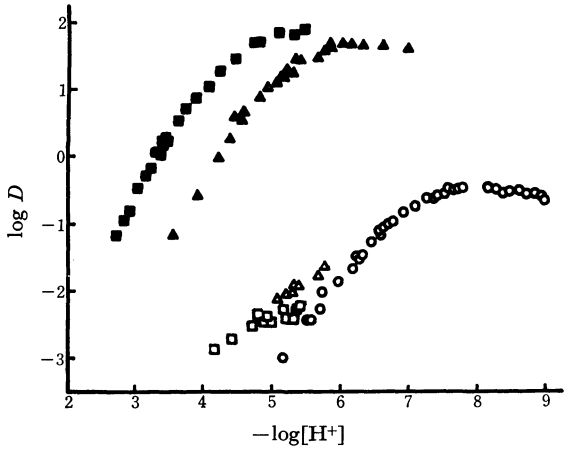

Fig. 2. Extraction of zinc(II) complexes with AA(circles), TFA(triangles) and HFA(squares) as a function of the hydrogen ion concentrations.
organic phase: (open symbols) carbon tetrachloride, (closed symbols) carbon tetrachloride containing 1×10^{-1}M TBP for the TFA or 6×10^{-3}M TBP for the HFA extractions.
aqueous phase: 1M $Na(ClO_4)$

symbols) and a 1M sodium perchlorate solution.

As may be seen from Fig. 2, the distribution ratio of zinc(II) in the TFA or HFA extraction is very low in the absence of TBP. However, the distribution ratio is much enhanced by the addition of TBP, and the extraction curves could be determined accurately in these systems. The stability constants of the zinc(II) complexes with TFA and HFA were obtained from these data; they are indicated by the closed symbols in Figs. 2 and 4.

The curves of zinc(II) extraction with TFA and HFA in the absence of TBP in the organic phase are indispensable in determining the distribution constants of the uncharged complexes, K_{DM}, in Eq. (6). Although the distribution ratios were low, the results of the extraction with TFA (open triangles) were reproducible and, as will be shown later, resonable values of K_{DM} and the formation constants of the adducts with TBP

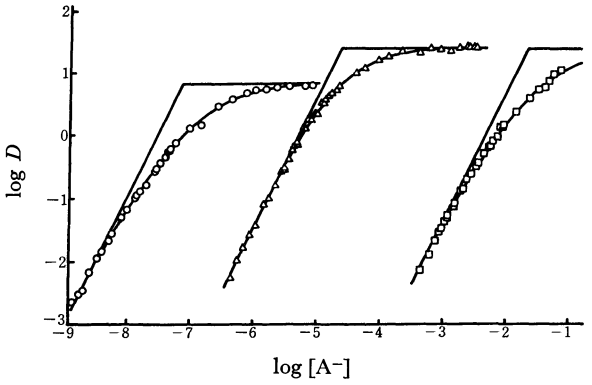

Fig. 3. Extraction of copper(II) complexes with AA(circles), TFA(triangles) and HFA(squares) as a function of the concentrations of the chelate anions.
organic phase: carbon tetrachloride
aqueous phase: 1M $Na(ClO_4)$
The solid curves are drawn by the equation,
$\log D=\log K_{DM}\beta_2[A^-]^2-\log(1+\beta_1[A^-]+\beta_2[A^-]^2)$

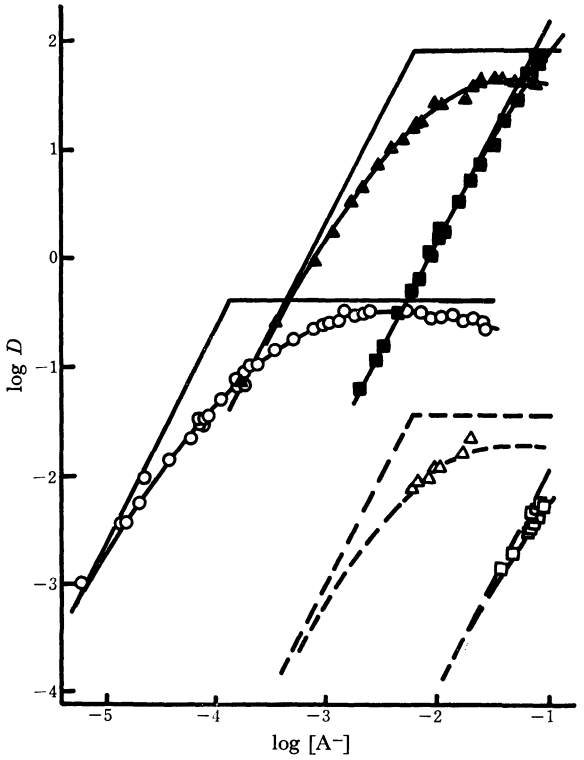

Fig. 4. Extraction of zinc(II) complexes with AA(circles), TFA(triangles) or HFA(squares).
organic phase: (open symbols) carbon tetrachloride, (closed symbols) crabon tetrachloride containing 1×10^{-1}M TBP for the TFA extraction or 6×10^{-3}M TBP for the HFA extractions.
aqueous phase: 1M $Na(ClO_4)$
The solid curves are drawn by the equation,
$\log D=\log K_{DM}\beta_2 f[A^-]^2-\log(1+\beta_1[A^-]+\beta_2[A^-]^2+\beta_3[A^-]^3)$
here, f is the enhancement factor due to the synergism, that is, D/D_0 in Eq. (22). When TBP is absent, f is unity and when 1×10^{-1}M TBP is present in the TFA extractions, f is $10^{3.35}$ and when 6×10^{-3}M TBP is persent in the HFA extractions, f is $10^{4.2}$.

TABLE 1. EQUILIBRIUM CONSTANTS FOR THE β-DIKETONES AND THE METAL β-DIKETONATES AT 25°C
aqueous phase: sodium perchlorate solution
organic phase: carbon tetrachloride

	ionic medium	pK_a[a]	$\log K_D$[a]	Cu(II)				Zn(II)				
				$\log \beta_1$	$\log \beta_2$	$\log K_{DM}$	$\log K_{ex}$	$\log \beta_1$	$\log \beta_2$	$\log \beta_3$	$\log K_{DM}$	$\log K_{ex}$
AA	0.1M	8.62	0.51	7.74	14.28	0.70	−3.47	4.85	8.22	9.43	−0.65	−10.69
	1 M	8.99	0.40	7.81	14.22	0.83	−3.73	4.58	7.76	9.16	−0.38	−11.40
	3 M	9.75	0.22	8.41	15.42	1.04	−3.52	4.93	8.46	10.26	0.17	−11.35
TFA	0.1M	6.09	−0.22	5.17	9.38	1.24	−1.12	3.18	5.28	6.14	−1.84	−8.30
	1 M	6.09	−0.19	4.80	9.14	1.40	−1.26	2.72	4.48	5.42	−1.44	−8.76
	3 M	6.52	0.06	5.56	10.04	1.81	−1.31	3.24	5.52	5.68	−1.01	−8.75
HFA	0.1M	4.42	−1.92	2.52	3.84	0.90	−0.26	1.6	—	—	—[c]	−4.9
	1 M	4.34	−1.74	2.25	3.20	1.39	−0.61	1.0	—	—	—[c]	−5.2
	3 M	4.42	−1.40	2.68	4.16	1.76	−0.12	1.1	—	—	—[c]	−5.0

The literature values for the extraction of copper (II) and zinc (II) in 1 M $NaClO_4$ with AA in benzene are as follows[11];

	$\log \beta_1$	$\log \beta_2$	$\log K_{DM}$
Cu(II)	8.05(8.22)[b]	14.75(14.81)[b]	1.10(1.10)[b]
Zn(II)	4.63	8.59	−0.19

a) The values of pK_a and $\log K_D$ are taken from another work[4] in which they are determined by a titration and a spectrophotometry.
b) Experiments at varying acetylacetone concentration.
c) The $\log K_{DM} \times \beta_2$ for the extraction of zinc(II) with HFA are 0.2(0.1M), 0.0(1M), and 1.1(3M).

or TOPO, $\beta_{n(org)}$ in Eq. (9), could be determined for the zinc(II)-TFA chelate. However, the extraction with HFA into carbon tetrachloride containing no TBP is scattered for some unknown reason; only representative data of these extractions are given in Fig. 2 (open squares). Thus, the extraction constant of zinc(II) with HFA, K_{ex} in Eq. (12), in Table 1 and the adduct-formation constants of the HFA chelate, which can be determined only by using the data of the extraction into carbon tetrachloride containing no TBP, may be somewhat erroneous.

In order to analyze these extraction data by using Eq.(8) or Eq.(10), the distribution ratios are plotted against the chelating-anion concentration in the aqueous phase. Figures 3 and 4 show the plot. In Fig. 3, it may be seen that each plot has an asymptote with a slope of +2 and an asymptote with a slope of zero. By the curve-fitting, the constants, β_1, β_2, and K_{DM}, were determined to be as is shown in Table 1. The solid curves in the figures are those calculated by introducing these constants into Eq.(8). The values of K_{ex} defined by Eq.(12) for these extractions were also calculated by using the K_a and K_D values of the chelating acid and Eq.(16).

Figure 4 gives the log D *vs.* log[A^-] plot of the zinc(II) extractions. As the extraction with HFA into carbon tetrachloride is too low to determine the equilibrium constants, the analysis was made by using the plot when the organic phase contains 1×10^{-1}M TBP for the TFA and 6×10^{-3}M TBP for the HFA extractions. As is shown in Eq.(10), the figure of the log D *vs.* log[A^-] plot should be the same even when the organic phase contains a certain amount of the adduct-forming ligand, L (here it is TBP); in this case, $K_{DM} \times (1 + \beta_{1(org)}[L_1]_{org} + \beta_{2(org)}[L_1]^2_{org} + \cdots)$, where $[L_1]_{org}$ is the concentration of the adduct-forming ligand, is the apparent distribution constant, which should be used instead of K_{DM} in Eq.(8), as has already been described.

The equilibrium constants for the extraction zinc(II) with AA were obtained by an analysis of the data given by the open circles, whereas those for the extractions with HFA or TFA were obtained by an analysis of the data given by the closed symbols.
The distribution constants, K_{DM}, for these extractions were obtained from these apparent distribution constants and the enhancements of the extraction by the TBP, which are given in Fig. 6.

It may be seen from Fig. 4 that the curve for the zinc(II) extraction with HFA is quite close to a straight line with a slope of +2. As can be seen from Eqs. (8) or (10), and (17), the log D *vs.* log[A^-] plot should deviate from a straight line with a slope of +2 when the MA^+ and MA_2 complexes are formed. However, in the [A^-] range studied in this paper ([A^-]<0.1M), the range where the MA_2 species is formed in an appreciable amount could not be covered; in other words, the deviation is too small to determine the stability constants for the second complex, β_2, and consequently, it was not possible to devide the $K_{DM} \times \beta_2$ value into the two constants. Thus, only the values for β_1 and $K_{DM} \times \beta_2$, together with K_{ex}, are listed in Table 1 for the zinc(II) complexes with HFA.

As can be seen from Fig. 4, the extraction curve with AA or TFA does not approach an asymptote with a slope of zero, but it decreases somewhat after the maximum. It was assumed to be due to the formation of the third complex, ZnA_3^-; the constants were changed until the best-fit of the calculated curve with the experimental data was obtained. The constants given in Table 1 were thus obtained. The solid curves in Fig. 4 were calculated by the use of these constants.

The above results are for the systems containing 1M sodium perchlorate solutions as the aqueous phase. In order to ascertain the effect of the concentrations of the coexisting salt on these constants, similar experiments

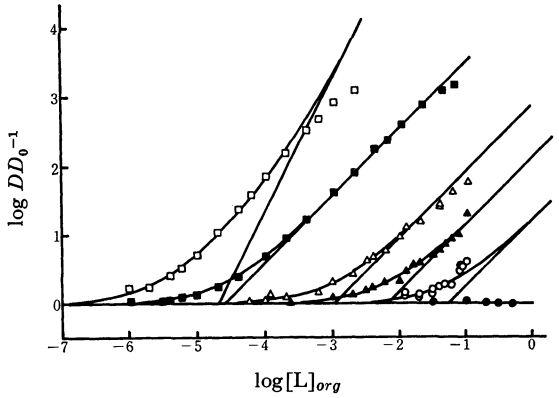

Fig. 5. The enhancement of copper(II) extractions with AA(circles), TFA(triangles) and HFA(squares) by additions of TBP or TOPO.
organic phase: (open symbols) carbon tetrachloride containing TOPO.
(closed symbols) carbon tetrachloride containing TBP.
aqueous phase: 1M Na(ClO_4)

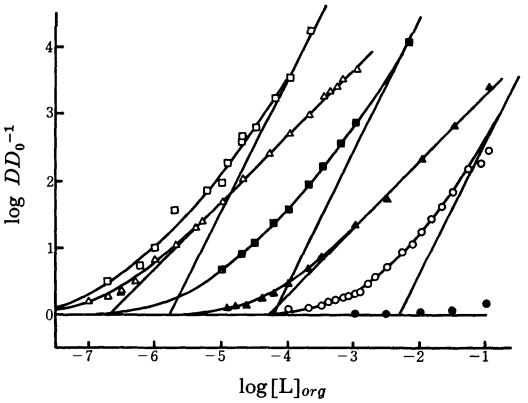

Fig. 6. The enhancement of zinc(II) extractions with AA-(circles), TFA(triangles) and HFA(squares) by addition of TBP or TOPO.
organic phase: (open symbols) carbon tetrachloride containing TOPO.
(closed symbols) carbon tetrachloride containing TBP.
aqueous phase: 1M Na(ClO_4)

Table 2. Adduct formation constants of the metal chelates with TBP and TOPO in CCl_4
aqueous phase: 1.0M (Na,H)ClO_4
organic phase: carbon tetrachloride containing 0.1M of HA and various amounts of TBP or TOPO.

	ligand	Cu(II)		Zn(II)	
		$\log\beta_{1(org)}$	$\log\beta_{2(org)}$	$\log\beta_{1(org)}$	$\log\beta_{2(org)}$
$M(AA)_2$	TBP	n.c.[a]	n.c.[a]	n.c.[a]	n.c.[a]
	TOPO	1.28	—	3.07	4.66
$M(TFA)_2$	TBP	2.16	—	4.29	—
	TOPO	2.96	—	6.70	—
$M(HFA)_2$	TBP	4.60	—	5.5[b]	8.5[b]
	TOPO	5.63	9.36	7.0[b]	11.6[b]

$$\beta_{n(org)} = \frac{[MA_2L_n]_{org}}{[MA_2]_{org}[L]^n_{org}}$$

a) n.c. no complex formation ($\beta_{1org}<0.1$)
b) As the distribution ratio of Zn-HFA chelate into carbon tetrachloride, D_0 in Eq.22, could not be determined accurately, these values would be somewhat erroneous.

were also carried out in systems containing 0.1M or 3M sodium perchlorate solutions, while the equilibrium constants were also obtained by a similar graphic analysis. The constants are also given in Table 1.

The enhancements of these extractions by the addition of a neutral organophilic ligand, TBP or TOPO, which are due to the adduct formations (*cf.* Eq. (9)), were determined as a function of the concentration of the neutral ligand. Figure 5 gives the results of the copper(II) extractions, while Fig. 6 gives those of the zinc(II) extractions. In both cases, the addition of TBP did not enhance the extraction with AA. The data were also analyzed by means of curve-fitting; the formation constants of the adduct-chelate complexes were determined to be as is shown in Table 2. The solid curves were calculated by introducing the constants in Table 2 into Eq. (11).

The effect of the background salt on the stability

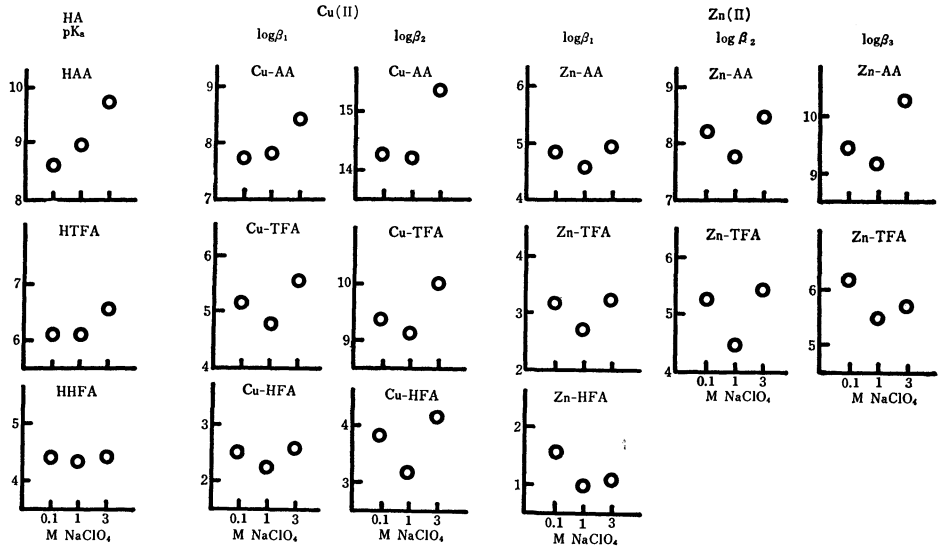

Fig. 7. Effect of the coexisting sodium perchlorate in the aqueous phase on the acid dissociation constant of the chelating agents and the stability constants of the metal chelates. The ordinate gives pK_a or $\log\beta_n$ and the abscissa gives the concentration of sodium perchlorate in the aqueous phase.

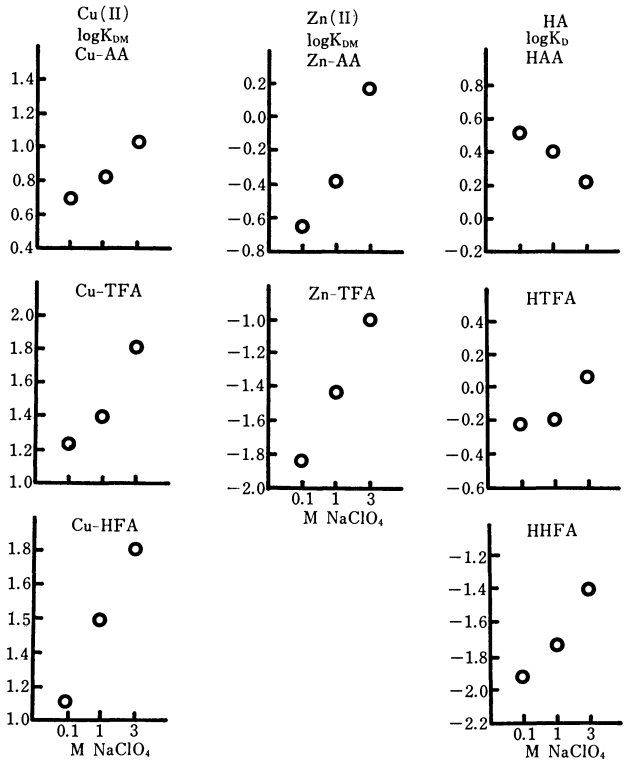

Fig. 8. Effects of the coexisting sodium perchlorate in the aqueous phase on the distribution constant of the reagent (K_D in Eq. (1)) or of the MA_2 chelate complex (K_{DM} in Eq. (6)). The ordinate gives log K_D or log K_{DM} and the abscissa gives the concentration of sodium perchlorate in the aqueous phase.

constants and on the distribution constants is complicated. Figures 7 and 8 summarize these results.

Discussion

As can be seen from Figs. 1 and 2, the $-\log[H^+]$ range studied in the present paper is from 1 to 5.5 for the copper(II) extraction and from 2.5 to 9 for the zinc(II) extraction; the hydrolyses of these metals in the aqueous phase should be negligible.[5,6] Thus, the decrease in the distribution ratio of zinc(II) in the highest $-\log[H^+]$ region after the maximum can not be due to the hydrolysis, but must be due to the formation of the third complex.

Acetylacetone and its derivatives have been used for the extraction of various metal ions.[7] The extraction of copper(II) with AA in benzene,[8] in chloroform,[9] or in carbon tetrachloride,[10] and the extraction of zinc(II) with AA in benzene[8] have been reported not to be complete. Recently, Liljenzin, Stary, and Rydberg[11] made a very comprehensive study of the AA extraction of these metal ions in a 1.0M sodium perchlorate solution into benzene in the range from 10°C to 40°C. Their results can be compared directly with the present results except for K_{DM} (they used benzene, while the present authors used carbon tetrachloride as the organic phase). These recent data almost completely agree with the present results, although the former are somewhat higher than the latter (the values of K_a and K_D of acetylacetone used for the calculation were not given in Ref. 11). The other two β-diketones, TFA and HFA, have also been used for the extraction of various metal ions,[12] but no systematic studies of the extraction equilibria of these metal ions seem to have been made and no constants which can be compared with the present results seem to be available.

The well-known general tendency of the order of the stability constants also appears in the present results shown in Table 1; that is, copper(II) forms more stable complexes than does zinc(II), and the weaker bases which are produced by the substitution of the trifluoromethyl group for methyl groups form less stable complexes.

It can be seen from Table 1 that the highest complexes for copper(II) are the second ones, while those for zinc(II) are the third ones. The four coordination for copper(II) and zinc(II) seem to have been well established; the six coordination for zinc(II) in some cases has been also pointed out. The coordination number of zinc(II) in the third complex with AA or TFA should be six, but it is not possible to confirm the coordination number from only the distribution data.

The effect of the coexisting sodium perchlorate on the stability constants is complicated. However, it can be pointed out, on the basis of Table 1 and Fig. 7, that the stability constants are, in most cases, lowest in the 1M ionic medium and highest in the 3M ionic medium (the exceptions are β_1 for the Cu(II)-AA complex, β_1 for the Zn(II)-HFA complex, and β_3 for the Zn(II)-TFA complex).

Suzuki and his co-workers have made a series of studies of the distribution constant of metal-chelate complexes, MA_m, in liquid-liquid systems.[13-21] They

5) L. G. Sillén and A. E. Martell, "Stability constants," The Chemical Soceity, Spec. Publ. (1964), p. 17.
6) T. Sekine, *Acta Chem. Scand.*, **19**, 1526 (1965).
7) J. Stary, "The Solvent Extraction of Metal Chelates," Pergamon Press., Oxford (1964).
8) J. Stary and E. Hladky, *Anal. Chim. Acta*, **28**, 227 (1963).
9) T. Shigematsu and M. Tabshi, *Bull. Inst. Chem. Res. Kyoto. Univ.*, **39**, 35 (1961).
10) S. Stene, *Tidskr. Kjemi. Bergvesen. Met.*, **19**, 6 (1939), cited in Ref. 5.
11) O. Liljenzin, J. Stary, and J. Rydberg, "Solvent Extraction Research," ed. by A. S. Kertes and Y. Marcus, Wiley-Interscience., New York, (1969), p. 21.
12) T. V. Healy, *ibid.*, (1969), p. 257.
13) T. Wakabayashi, S. Oki, T. Omori, and N. Suzuki, *J. Inorg. Nucl. Chem.*, **26**, 2255 (1964).
14) T. Omori, T. Wakabayashi, S. Oki, and N. Suzyki, *ibid.*, **26**, 2265 (1964).
15) S. Oki, T. Omori T. Wakabayashi, and N. Suzuki., *ibid.*, **27**, 1141 (1965).
16) T. Wakabayashi, This Bulletin, **40**, 2836 (1967).
17) T. Wakabayashi, K. Takaizumi, K. Seto, N. Suzuki, and K. Akiba, *ibid.*, **41**, 1854 (1968).
18) N. Suzuki, A. Akiba, and T. Kanno, *Anal. Chim. Acta.*, **43**, 311 (1968).
19) N. Suzuki, K. Akiba, T. Kanno, and T. Wakabayashi, *J. Inorg. Nucl. Chem.*, **30**, 2521 (1968).
20) N. Suzuki, K. Akiba, T. Kanno, T. Wakabayashi, and K. Takaizumi, *ibid.*, **30**, 3047 (1968).
21) K. Akiba, N. Suzuki, and T. Kanno, *ibid.*, **42**, 2537 (1969).

have pointed out that the distribution constants of metal-chelate complexes can be well explained by the regular solution theory.[22] They have demonstrated how the distribution constants of a certain metal-chelate into various non-solvating solvents are parallel to that of the chelating acid, HA, for scandium(III) with some β-diketones and zinc(II) chelates with TTA. Furthermore, they have suggested that the distribution of scandium(III)-β-diketonates are satisfactorily explained in the various solvent systems by:

$$\log K_{DM} = \frac{V_{MA_m}}{V_{HA}} \log K_D + \text{constant} \qquad (24)$$

where V_{HA} and V_{MAm} denote the molar volume of the chelating reagent and that of the metal chelate complex respectively.[14,17,18,20] This relation was also pointed out for the distribution of Zn(II)-TTA chelates into various solutions.[21]

In the present study, only one organic solvent, carbon tetrachloride, has been used, and so no comparison of the distribution constants into different organic solvents is possible. Thus, only the comparison of the distribution constant of a certain chelating acid, K_D, with that of the bis-complex of copper(II) or zinc(II) with the same chelating acid, K_{DM}, may be made. As may be seen from Table 1 and Fig. 8, the distribution constants of the chelating reagents and of the chelate complexes of the two metal ions change in a very complicated manner upon the change in the coexisting salt concentration. The salt effect is parallel neither among three different reagents nor among a certain reagent, HA, and its metal-chelates, CuA_2 and ZnA_2. Actually, the relation given in Eq. (24) is seen only in the extraction of copper(II) in the 1M ionic medium with AA. Except for this, the relation between K_D and K_{DM} is very irregular. Even for the copper(II) extraction with AA, the relation in Eq. (24) is not observed in the extraction from a 0.1M or 3M ionic medium. The distribution constants, K_{DM}, of the copper(II) chelates are here higher than that of the chelating reagents, K_D, whereas they are much lower in the zinc(II) chelates.

The treatments by the regular solution theory are made on the assumption that there is no special strong interaction between the solute and the solvent molecules. As far as the interactions in the carbon tetrachloride phase are concerned, this assumption can be accepted for all the reagents and metal-chelates. However, in aqueous solutions, it is difficult to assume that the central metal ions in the copper(II) and zinc(II) chelates with a certain ligand have the same interactions with water molecules. It can also be supposed that the interactions of the coexisting salt on the two metal complexes with different central metal ions and the same ligand are somewhat different. As will be considered below, the central copper(II) ion in a chelate complex with a certain ligand should interact with polar molecules weaker than those with which the central zinc(II) ion in the complex with the same ligand interacts. Thus, the zinc(II) complex is retained in the aquoues phase more than is the copper(II) complex.

Until now, not many K_{DM} values in chelate-extraction systems have been reported. Dyrssen has, however, reported the K_{DM} values for a series of divalent metal-chelates with β-isopropyltropolone (IPT) between chloroform and a 0.1M sodium perchlorate ionic medium.[23] He reported, for example, that the K_{DM} of the copper(II)-IPT chelate ($\log K_{DM}=4.12$) is much higher than that of the zinc(II)-IPT chelate ($\log K_{DM}=2.25$), and he described how the K_{DM}^{-1} value presumably shows the affinity of the uncharged chelate for the aqueous phase, that is, the tendency for MA_2 to form a hydrate in the aqueous phase, and how this tendency of hydration reveals a fundamental difference in the remaining coordinating power of the central metal ion in the chelate complex.

It seems that the above hypothesis can be adopted even for the present results. The extraction of copper(II) chelates into carbon tetrachloride is always better than that of zinc(II) chelates; this can be explained in terms of the lower K_{DM} of the latter, which in turn is due to the larger interactions of the central zinc(II) ion with water molecules (hydration) than those of the central copper(II) ion in the complex with the same ligand. This may also be seen in the following discussions.

There have been many studies of the adduct formation of metal-chelates with various organophilic neutral ligands, as has been reviewed by Irving[24] and Healy.[12] A general tendency has been observed in the stabilities of the adduct-chelates in the organic phase—those chelates which are extracted better—(or which are extracted in a lower pH region or in a lower chelating reagent concentration) form less stable adducts than do other metal-chelates with the same ligand, but when the central metal ion is the same but the ligand is different, those extracted better form more stable adducts. At the same time, it has been known that more basic neutral ligands form more stable adduct-chelates.

This tendency can also be observed in the results shown in Table 2; zinc(II) chelates form more stable adducts than do the corresponding copper(II) chelates. The chelates of copper(II) or of zinc(II) form more stable adducts in the ligand order of AA<TFA<HFA, which is the inverse of the order of the stabilities of the complexes in the aqueous phase, but the same order as the extraction constants, K_{ex}, in Eq. (12).

The stability of an adduct-chelate should be influenced by many factors, and a too simplified consideration of this problem would lead to an erroneous conclusion. However, as far as the results shown in Tables 1 and 2 are concerned, it may be possible to make the following conclusions: (i) the central metal ion retains more ability to accept further coordination with the neutral ligands in the zinc(II) chelate complexes than in the copper(II) complexes, and (ii) the

22) J. H. Hildebrand and R. L. Scott, "Solubility of Nonelectrolyte," 3rd. ed. Reinhold, New York (1964).

23) D. Dyrssen, *Trans. Royal Inst. Technol. Stockholm, No.* 188 (1962).

24) H. M. N. H. Irving, "Solvent Extraction Chemistry, "North-Holland (1967), p. 105.

central metal ion among the complexes with the same metal ion retains more ability to accept further coordination with other ligands if the stability of the chelate in the aqueous phase is lower.

When the ability of the central metal ion to accept a further ligand is larger, the stability of the adduct should be larger. At the same time, it would interact with water molecules more strongly; this seems to explain the stability order of the adduct-chelates. The molar volumes of CuA_2 and ZnA_2 would not be very much different from each other, and, as was assumed by Suzuki and his co-workers,[13,14] the solubility parameters of the reagent and of the chelate are practically the same. Thus, the lower K_{DM} value of zinc(II) chelates than that of the copper(II) chelates is probably due to the stronger interactions of the central metal ion in the zinc(II) chelates with water molecules than those in the copper(II) chelates. However, further information seems to be necessary if we are to make a detailed consideration of this problem.

The authors are very grateful to Misses Nobuko Saito, Katsue Asami, and Etsuko Yamaguchi for their experimental aid. Part of the work has been carried out in the Laboratory of Nuclear and Analytical Chemistry, Institute of Physical and Chemical Research. The authors are especially grateful to Professor Nobufusa Saito, the head of the Laboratory.

BULLETIN OF THE CHEMICAL SOCIETY OF JAPAN, VOL. 44, 2950—2954 (1971)

Electron Spin Resonance Study of Short-Lived Free Radicals in Photoreduction of Benzophenone

Hiroshi YOSHIDA and Tetsuo WARASHINA*

Faculty of Engineering, Hokkaido University, Sapporo
**Research Reactor Institute, Kyoto University, Kumatori-cho, Osaka*

(Received April 13, 1971)

By observing electron spin resonance spectra during photolysis at room temperature, kinetic behaviors of short-lived free radicals are studied in photoreduction of benzophenone in alcohols, especially in ethanol, with and without sodium methoxide. In neutral solution, diphenylhydroxymethyl radicals and hydroxyethyl radicals are observed simultaneously. This is a firm evidence, obtained from ESR, of hydrogen abstraction of excited benzophenone from ethanol. Results indicate that (1) free radicals are the most efficiently generated by the light of ~350 nm, (2) hydroxyethyl radicals transform into diphenylhydroxymethyl radicals if the concentration of benzophenone is high, and (3) the latter radicals disappear following the second order reaction. In the presence of sodium methoxide, diphenylhydroxymethyl radicals transform into benzophenone ketyl anions.

Rate constants are determined, being 3×10^7 and $\sim10^4$ $mole^{-1}\cdot l\cdot sec^{-1}$ for the combination reaction between diphenylhydroxymethyl radicals and the proton transfer reaction from diphenylhydroxymethyl radical to methoxide ion, respectively.

Photoreduction of benzophenone in alcohols is one of the most extensively studied subjects in photochemical reactions. Triplet excited benzophenone abstracts hydrogen from the solvent molecule to form diphenylhydroxymethyl radicals, which combines with each other to benzpinacol in neutral solutions.[1] Porter and Wilkinson proved directly by flash photolysis technique that the diphenylhydroxymethyl radicals were formed as intermediates in the photoreduction of benzophenone, and also that they converted to benzophenone ketyl anions in alkaline solutions.[2] Beckett and Porter determined the rate constant of reactions involving the diphenylhydroxymethyl radicals and ketyl anions.[3]

Since Livingston and Zeldes developed a technique of observing electron spin resonance (ESR) spectra of transient free radicals in liquids during photolysis,[4] the technique has been successfully employed to several photochemical reactions. Among them, Wilson studied free radicals photolytically generated from aromatic carbonyl compounds,[5-9] and found that diphenylhydroxymethyl radical was formed from benzophenone in alcohols, tetrahydrofuran,[6] and triethylamine.[9] From the observed hyperfine coupling constants, the structure of the free radical, especially the effect of hydrogen bond on the coupling constant of hydroxy proton, was studied in detail in referring to a molecular orbital calculation. The ESR observation gave an evidence that the photoreduction process involves the transient diphenylhydroxymethyl radical,

1) For example, (a) J. N. Pitts, Jr., B. L. Letsinger, R. T. Taylor, J. M. Patterson, G. Rectenwald, and R. B. Martin, *J. Amer. Chem. Soc.*, **81**, 1068 (1959); (b) W. M. Moore, G. S. Hammond, and R. P. Foss, *ibid.*, **83**, 2789 (1961).
2) G. Porter and F. Wilkinson, *Trans. Faraday Soc.*, **57**, 1686 (1961).
3) A. Beckett and G. Porter, *ibid.*, **59**, 2038 (1963).
4) R. Livingston and H. Zeldes, *J. Chem. Phys.*, **44**, 1245 (1966)
5) R. Wilson, *Can. J. Chem.*, **44**, 551 (1966).
6) R. Wilson, *J. Chem. Soc. (B)*, **1968**, 84.
7) R. Wilson, *ibid.*, **1968**, 1581.
8) R. S. Davidson, P. F. Lambeth, F. A. Younis, and R. Wilson, *J. Chem. Soc. (C)*, **1969**, 2203.
9) R. S. Davidson and R. Wilson, *J. Chem. Soc. (B)*, **1970**, 71.

though the counterpart radical formed from solvent was unable to be detected.

These investigations encouraged us to extend ESR study to kinetical behavior of transient free radicals during photolysis. In the present investigation, the ESR technique is employed to study the photoreduction of benzophenone in alcohols with the intention of elucidating the kinetical behavior of radicals, their formation and decay, in neutral and alkaline solutions.

Experimentals

Apparatus used was essentially the same as described by Livingston and Zeldes.[4] Illuminating light from a superhigh pressure mercury lamp (Philips, SP-500, 500 watts) passed throuth a quartz lens and a grid plate of a resonance cavity (Varian, Model E-4531), connected to a conventional ESR spectrometer (Varian, E-3), to a quartz flat cell. A glass cut-off filter or a mesh was inserted between the lens and the grid plate, if necessary, to regulate the illuminating light.

Analytical grade chemicals were used without further purification. Air dissolved in solutions was removed by bubling helium gas for at least half an hour before photolysis.

Flow rate of solutions was 4.3 m*l* per min. As the effective volume of the cell was 0.052 m*l*, the resident time of the solution in the cell was estimated to be 0.7 sec, during which free radicals were generated by light, and their ESR spectra were detected. Flowing through the cell, the solutions were heated by the light to about 5° higher than the room temperature (20°±2°C).

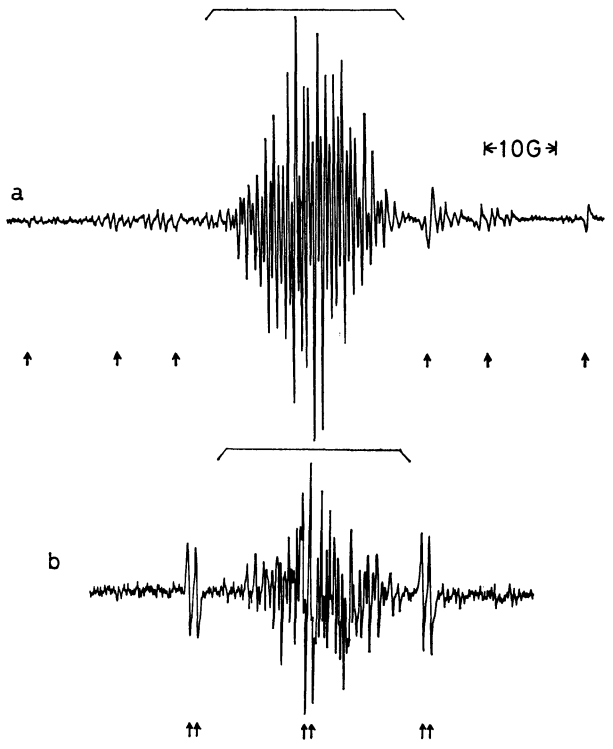

Fig. 1. Electron spin resonance spectra observed during the photolysis of benzophenone (0.44 mol·l^{-1}) in (a) ethanol and (b) methanol at room temperature. Brackets and arrows indicate the spectra of free radicals formed from benzophenone and those formed from alcohols, respectively. Amplitude of magnetic field modulation: 0.5G.

Results

Figure 1 shows the ESR spectra observed from solutions of benzophenone in ethanol and methanol. They are composed of three components: the spectra indicated with arrows due to free radicals, $CH_3\dot{C}HOH$ and $\dot{C}H_2OH$, formed by hydrogen abstraction from ethanol and methanol, respectively, central complex spectra indicated with blackets due to free radicals formed from benzophenone, and other spectra which are rather weak and are not identified. The free radicals fromed from solvent molecules are identical with those reported by Livingston and Zeldes.[4]

The yield of free radicals was larger in ethanol than in methanol. Therefore, ethanol is used as solvent in all experiments described below.

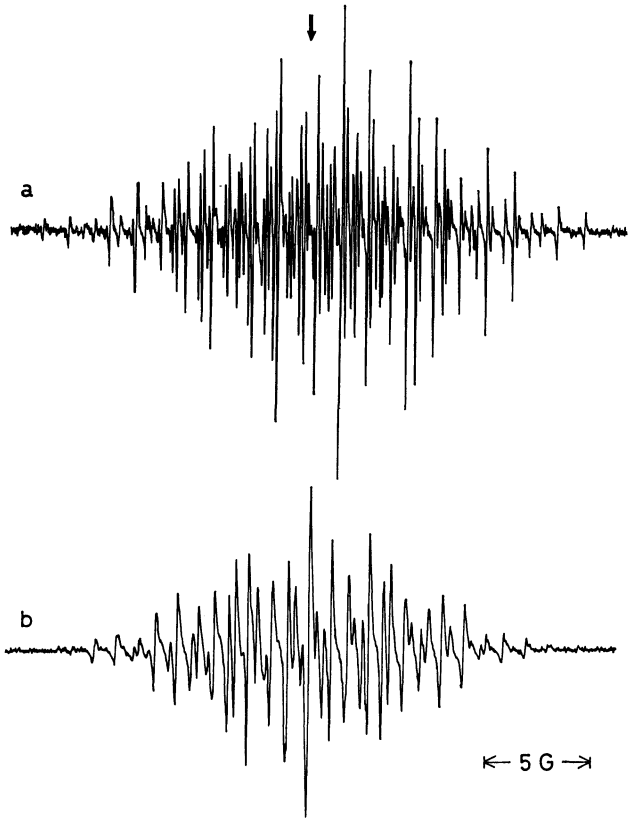

Fig. 2. Electron spin resonance spectra observed during the photolysis of benzophenone (0.44 mol·l^{-1}) in ethanol at room temperature. Amplitude of magnetic field modulation: 50 mG. (a) Diphenylhydroxymethyl radical formed in neutral solution and (b) benzophenone ketyl anion formed in the presence of sodium methoxide. Arrow indicates the center of spectra.

When the central spectrum is recorded with a small amplitude of magnetic field modulation, well resolved hyperfine structure is observed as shown in Fig. 2, *a*. The structure is described by equivalent four protons at the ortho-positions of the rings with hyperfine coupling constant of 3.1G, four protons at meta-positions with the coupling constant of 1.2G, two protons at the para-positions of the rings with the constant of 3.6G, and a proton in hydroxy group with the constant of 2.9G, and it is reasonably attributed to diphenyl-

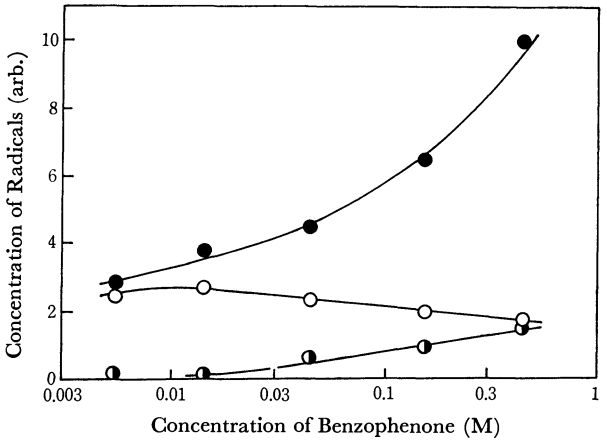

Fig. 3. Dependence of observed concentration of free radicals formed during the photolysis of benzophenone in ethanol on the concentration of benzophenone. ●; Diphenylhydroxymetyl radical, ○; hydroxyethyl radical, ◑; unidentified radical.

hydroxymethyl radical. The observed hyperfine coupling constants are compared with those reported, 3.23, 1.23, 3.64, and 2.91G, respectively.[6] The spectrum of $CH_3\dot{C}HOH$ vanishes if recorded with the small amplitude of field modulation, because of its larger width of hyperfine lines.

Observed intensity of the three spectra are plotted as a function of the concentration of benzophenone in solution, as shown in Fig. 3. At the lowest concentration examined, the observed yield of diphenylhydroxymethyl radical is about the same as that of $CH_3\dot{C}HOH$. With the increasing concentration of benzophenone, the yield of diphenylhydroxymethyl radical increases remarkably, while that of hydroxyethyl radical reaches the maximum and then gradually falls down.

The unidentified spectrum also increases in its intensity with the increasing concentration of benzopheneone. It is probably due to free radicals formed by the reaction between the primarily formed radicals and benzophenone.

The intensity of observed spectra was calibrated with reference to that of diphenylpicrylhydrazyl solution in ethanol. The concentration of diphenylhydroxymethyl radical was estimated to be 4.5×10^{-7} mol·l^{-1} for the highest concentration of benzophenone examined (0.44 mol·l^{-1}), though the value includes the uncertainty factor of 2.

The yield of diphenylhydroxymethyl radical was studied as a function of light intensity, at the benzophenone concentration of 0.14 mol·l^{-1}. It was found to be proportional to the 0.37th power of the light intensity. The radicals disappear probably in combining with each other following the second order kinetics rather than the first order one. The deviation of exponent from 0.5 may have been caused by the fact that the resident time of solution in the resonance cavity is so short that the steady state concentration of the radicals is not completely attained.

The lifetime of diphenylhydroxymethyl radical was determined, for the benzophenone concentration of 0.44 mol·l^{-1} by recording the transient change of the intensity of its spectrum, when the illuminating light was rapidly shut off and lit on repeatedly. Representative results are shown in Fig. 4, *a*. The most probable curve of transient change is obtained as Fig. 4, *b*, which gives the rise and decay times of 0.8 and 0.2 sec, respectively. Difference between the rise time and the decay time is resulted from an effective lifetime due to the flowing of radicals out of the cell, t_f. They are approximated by the following relations:

$$1/t_d = 1/\tau + 1/t_f \quad (1)$$

$$1/t_r = 1/\tau - 1/t_f, \quad (1')$$

where t_d and t_r stand for the decay and rise time, and τ is true half life of the radical.[10] The half life is determined from Fig. 4, *b*, being 0.3 sec. The calculated t_f is 0.5 sec, which is in agreement with the resident time of solution in the cell (a half of the resident time, 0.7/2=0.35 sec, is the expected value for t_f).

To determine the wavelength of light effective to

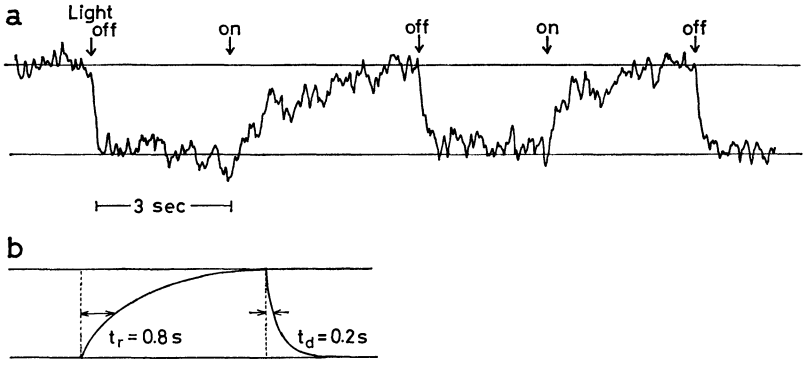

Fig. 4. Transient change in the intensity of electron spin resonance specta due to short-lived free radicals during the photolysis of benzophenone (0.14 mol·l^{-1}) in ethanol, when the light is shut off and lit on rapidly, recorded with response time of 0.1 sec. (a) An example of recorded curves, (b) the most probable curve estimated from several observations.

10) When the plateau of curves in Fig. 4 indicates the steady state concentration under the photo-illumination, the relations (I) and (I′) enable us to estimate the value of $\tau(\approx 1/\sqrt{k_5 R}$, R is the rate of radical formation and k_5 is the rate constant of bimolecular decay of free radicals, as seen in eq. (7)) and t_f. If the plateu value is much less than the steady state concentration, the relations should be replaced by $1/t_d > 1/\tau + 1/t_f$ and $1/t_r < 1/\tau - 1/t_f$. However, in this experiment, the calculated t_f of 0.5 sec is rather close to the expected value of 0.35 sec. Therefore, the relations are thought to be valid for rough estimation of τ.

generate free radicals, the intensity of ESR spectra was examined by inserting a cut-off filter to the light path. The relative values of intensity were 100, 92, 83, 60, and 14 for $\lambda>250$ (without filter), >270, >310, >350, and >390 nm, respectively. Referring a factory-provided datum of the lamp, relative quantum efficiencies are estimated, being 0.3, 1.0, and 1.0 for the wavelength region of 270~310, 310~350, and 350~390 nm. The light of wavelength around 350 nm is the most effective.

When the solution was made alkaline by adding sodium methoxide, the spectrum of diphenylhydroxymethyl radical was replaced by the spectrum shown in Fig. 2, *b*. The latter has the hyperfine structure due to four equivalent protons with the coupling constant of 2.8G, four protons with 1.0G and two protons with 3.5G, and is identical with that of benzophenone ketyl anion reported previously.[11] The *g*-factor of ketyl anion is found to be larger than that of diphenylhydroxymethyl radical by 0.0003. Therefore, $g=2.0033$ for the ketyl anion, because $g=2.0030$ for the latter radical.[6]

At small concentration of sodium methoxide added, ESR spectra show the coexistence of both diphenylhydroxymethyl radical and bonzophenone ketyl anion. With the increasing concentration of sodium methoxide, the former decreases and the latter increases in their concentration. Concurrently, the sum of them increases from 4.5×10^{-7} mol·l^{-1} to a plateau value of 4×10^{-6} mol·l^{-1}, for 0.44 mol·l^{-1} of benzophenone, as shown in Fig. 5.

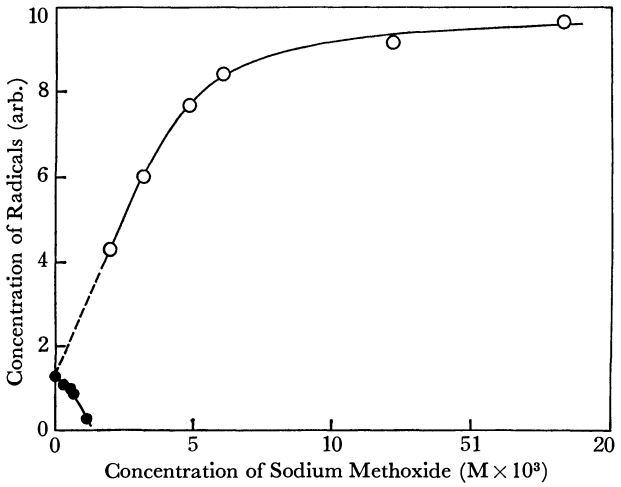

Fig. 5. Observed concentration of diphenylhydroxymethyl radical (●) and benzophenone ketyl anion (○) formed during the photolysis of benzophenone (0.44 mol·l^{-1}) in ethanol as a function of sodium methoxide added to the solution.

Discussion

Photoreduction of benzophenone in alcohols has been studied by means of conventional photochemical analysis method and, later on, by flash photolysis technique. Generally accepted mechanism, for ethanol as solvent, is as follows:[1,3]

11) P. B. Ayscough and R. Wilson, *J. Chem. Soc.*, **1963**, 5412.

$$(C_6H_5)_2C{=}O \xrightarrow{h\nu} (C_6H_5)_2{=}O^* \quad (2)$$

$$(C_6H_5)_2C{=}O^* + CH_3CH_2OH \longrightarrow (C_6H_5)_2\dot{C}OH + CH_3\dot{C}HOH \quad (3)$$

$$CH_3\dot{C}HOH + (C_6H_5)_2C{=}O \longrightarrow CH_3CH{=}O + (C_6H_5)_2\dot{C}OH \quad (4)$$

$$2(C_6H_5)_2\dot{C}OH \xrightarrow{k_5} (C_6H_5)_2COHCOH(C_6H_5)_2 \quad (5)$$

Very primary process is the excitation of benzophenone. Radicals are generated the most efficiently by the light of wavelength around 350 nm, which indicates that $n\rightarrow\pi$ transition of benzophenone is responsible for the hydrogen abstraction reaction (3), as the transition has the band maximum at about 340 nm in alcoholic solutions. The reaction (3) is directly evidenced by observing simultaneously the ESR spectra of both diphenylhydroxymethyl radical from benzophenone and hydroxyethyl radical from ethanol.

Results shown in Fig. 3 strongly suggest the conversion of hydroxyethyl raidcal to diphenylhydroxymethyl radical, by the reaction (4). If the concentration of benzophenone, and therefore that of diphenylhydroxymethyl radical, is enough high, the radical disappear following the second order reaction, as expected from the reaction (5). In the presence of sodium methoxide, the reaction competes with its conversion to benzophenone ketyl anion,

$$(C_6H_5)_2\dot{C}OH + CH_3O^- \xrightarrow{k_6} (C_6H_5)_2CO^- + CHO_3H. \quad (6)$$

As the ketyl anion is much more stable than diphenylhydroxymethyl radical,[3,5] the sum of both the anion and the radical increases in their yield with the increasing concentration of added sodium methoxide. The plateau of curve in Fig. 5 is thought to be attained by the complete conversion to the ketyl anion without loss of diphenylhydroxymethyl radical; $k_5[(C_6H_5)_2\dot{C}OH]\ll k_6[CH_3O^-]$.

The competing reactions are described by the following kinetical relations:

$$\frac{d[(C_6H_5)_2\dot{C}OH]}{dt} = R - k_5[(C_6H_5)_2\dot{C}OH]^2 - k_6[(C_6H_5)_2\dot{C}OH][CH_3O^-] \quad (7)$$

$$\frac{d[(C_6H_5)_2CO^-]}{dt} = k_6[(C_6H_5)_2COH][CH_3O^-], \quad (8)$$

where R stands for the rate of formation of diphenylhydroxymethyl radical. In the absence of sodium methoxide, the concentration of diphenylhydroxymethyl radical follows eq. (9) obtained by integrating eq. (7) with the initial condition of null concentration for $t=0$,

$$[(C_6H_5)_2\dot{C}OH] = \sqrt{\frac{R}{k_5}}\cdot\frac{\exp(2\sqrt{k_5R}\cdot t)-1}{\exp(2\sqrt{k_5R}\cdot t)+1}, \quad (9)$$

For the concentration of sodium methoxide enough high, the loss of free radical may be ignored, and

$$[(C_6H_5)_2CO^-] = R\cdot t. \quad (10)$$

Flowing solutions are photolyzed for their resident time in the cell, t_0. Therefore, the observed intensity of spectra is proportional to

$$\int_0^{t_0}[(C_6H_5)_2\dot{C}OH]dt = \frac{1}{k_5}\cdot\ln\{\exp(2\sqrt{k_5R}\cdot t_0)+1\} - \sqrt{\frac{R}{k_5}}\cdot t_0 \quad (11)$$

and

$$\int_0^{t_0}[(C_6H_5)_2CO^-]dt = \frac{R}{2}\cdot t_0^2. \quad (12)$$

The observed concentration without sodium methoxide (the left hand side of eq. (11), 4.5×10^{-7}) and that at the plateau of curve (the left hand side of (12), 4×10^{-6}) both indicated in Fig. 5 and $t_0=0.7$ sec lead to $k_5=3\times10^7$ mol$^{-1}\cdot l\cdot$sec^{-1}. Thus obtained k_5 is compared with the value derived from flash photolysis study, 5.9×10^7 mol$^{-1}\cdot l\cdot$sec^{-1}, in 50 vol% isopropanol-water mixture.[3]

On the other hand, the value of k_5 can be roughly estimated from the true half life of diphenylhydroxymethyl radical in the absence of sodium methoxide (see Fig. 4). From the relation,

$$k_5 = 1/[(C_6H_5)_2\dot{C}OH]_0\cdot\tau, \quad (13)$$

$[(C_6H_5)_2\dot{C}OH]_0\approx4.5\times10^{-7}$ mol$\cdot l^{-1}$ and $\tau\approx0.3$ sec, k_5 is calculated to be 0.7×10^7 mol$^{-1}\cdot l\cdot$sec^{-1}. If one consider local sensitivity of ESR depending on the sinusoidal distribution of microwave magnetic field, H_1, along the flow of solution, which is ignored in the above treatments, and the uncertainty involved in eqs. (1) and (1'), this value of k_5 is thought to agree rather well with the value of 3×10^7 mol$^{-1}\cdot l\cdot$sec^{-1}.

The yield of benzophenone ketyl anion reaches to 50% of its plateau value at 2.5×10^{-3} mol$\cdot l^{-1}$ of sodium methoxide. At this concentration, the following reaction can be used to evaluate the rate constant, k_6;

$$k_5[(C_6H_5)_2COH] = k_6[\dot{C}H_3O^-], \quad (14)$$

Assuming that sodium methoxide dissociates completely in ethanol at this low concentration, estimation of the order of magnitude gives 10^4 mol$^{-1}\cdot l\cdot$sec^{-1} for the rate constant of proton transfer from diphenylhydroxymethyl radical to methoxide ion, reaction (6).

The authors express their sincere thanks to Prof. Koichiro Hayashi of Hokkaido University and Prof. Takenobu Higashimura of Kyoto University, for their continual encouragement and valuable discussion throughout this work.

BULLETIN OF THE CHEMICAL SOCIETY OF JAPAN, VOL. 44, 2954—2959 (1971)

The Crystal Structure of 1,4-Bis(*p*-bromophenoxy)butane

Toshihiko ISHIKAWA, Seiichi KARINO, Susumu NAGAI, Noritake YASUOKA,*
Nobutami KASAI,* and Masao KAKUDO**

The Osaka Municipal Technical Research Institute, Kitaogimachi, Kita-ku, Osaka
**Department of Applied Chemistry, Faculty of Engineering, Osaka University, Yamadakami, Suita, Osaka*
***Institute for Protein Research, Osaka University, Joancho, Kita-ku, Osaka*

(Received April 21, 1971)

The structure of 1,4-Bis(*p*-bromophenoxy)butane has been determined by means of a single-crystal X-ray analysis. The compound crystallizes in the monoclinic space group *Cc*, with four molecules per unit cell: $a=13.426$, $b=15.249$, $c=7.650$ Å, and $\beta=89.39°$. The structure has been solved by the heavy-atom method. The final discrepancy index is 0.068 for 970 non-zero reflections. The conformation of the methylene chain in the $-O(CH_2)_4O-$ group is *gauche-trans-gauche*, with internal rotation angles of 61.0, 181.0, and 55.2° respectively.

High polymers consisting of the repeating unit $X-C_6H_4-O-(CH_2)_n-O-C_6H_4-X$ generally show high melting and glass-transition points and high elastic moduli. It is generally accepted that this behavior is not only due to the rigidity of the benzene rings in the molecular chains, but also to the length and conformation of the methylene chain between the phenoxy groups.[1-4]

As a crystallographic approach to this problem, Yasuoka *et al.* have determined the crystal structures of a series of model compounds of the above type of polymer. Among the compounds are 1,2-Bis(phenoxy)-ethane,[5] 1,2-Bis(*p*-chlorophenoxy)ethane,[6] and 1,3-Bis-(*p*-bromophenoxy)propane.[7] As a part of this series of studies, the crystal structure analysis of 1,4-Bis(*p*-bromophenoxy)butane, $BrC_6H_4O(CH_2)_4OC_6H_4Br$ was undertaken by means of X-ray diffraction.

Experimental

Single crystals of 1,4-Bis(*p*-bromophenoxy)butane were recrystallized from a methanol-benzene solution. From oscil-

1) T. Ando and S. Kataoka, *Kogyo Kagaku Zasshi*, **65**, 2057 (1962).
2) T. Ando and S. Kataoka, *ibid.*, **66**, 1724 (1963).
3) T. Ando and S. Kataoka, *Nippon Kagaku Zasshi*, **87**, 764 (1966).
4) I. Sakurada, I. Ito, and K. Nakamae, *Makromol. Chem.*, **75**, 1 (1964).
5) N. Yasuoka, T. Ando, and S. Kuribayashi, This Bulletin **40**, 270 (1967).
6) N. Yasuoka, T. Ando, and S. Kuribayashi, **40**, *ibid.*, 265 (1967).
7) Preprints for the 22nd Annual Meeting of the Chemical Society of Japan, Tokyo (April, 1969), and unpublished work.

lation and Weissenberg photographs, the approximate dimensions of the unit cell were determined; they were later redetermined precisely by using a Rigaku on-line controlled four-circle diffractometer. The crystal belongs to the monoclinic system. The systematic absences of reflections, $h+k\neq 2n$ for hkl and $l\neq 2n$ for $h0l$, indicate that the probable space group is $C2/c$ or Cc. The density of the crystal was measured by the flotation method in a carbon tetrachloride-bromoform solution at room temperature. The crystal data are listed in Table 1.

Table 1. Crystal data

$Br_2C_{16}H_{16}O_2$	Mol wt 400.1
	mp 118—120°C
$a=13.426$ Å	$D_m=1.70$g·cm^{-3}
$b=15.249$	$D_x=1.69$g·cm^{-3}
$c=7.650$	$Z=4$
$\beta=89.39°$	Space group Cc

The three-dimensional intensity data were at first collected by multiple-film equi-inclination Weissenberg photographs. Subsequently, the redetermination of the intensity data was carried out using a Rigaku single-crystal diffractometer. A total of 1034 independent reflections (970 non-zero reflections) were collected by means of zirconium-filtered Mo$K\alpha$ radiation. The dimensions of the crystal used were $0.1\times 0.12\times 0.20$ mm. The intensities were corrected for usual Lorentz and polarization factors, but the absorption correction was ignored (the linear absorption coefficient was $\mu=54.6$ cm^{-1} for Mo$K\alpha$).

Structure Determination and Refinement

Though $C2/c$ or Cc was postulated for the structure at the beginning, the space group is determined to be Cc, since the center of symmetry is not found by the N(z) test and since it is impossible to solve the Patterson map if the space group is $C2/c$.

The approximate coordinates of the two bromine atoms were determined from two-dimensional Patterson maps, $P(u,v)$ and $P(u,w)$. The coordinates of the other non-hydrogen atoms were determined by the successive use of Fourier syntheses. Thus, the molecular shape was determined at this stage, and the discrepancy index, $R=\Sigma||F_o|-|F_c||/\Sigma|F_o|$ was 0.21. Further refinement was carried out by using the counter data.

The atomic and isotropic thermal parameters were refined by a block-diagonal least-squares procedure. After seven cycles, the R index was reduced to 0.136 for 970 non-zero reflections. At this stage, anisotropic thermal parameters for non-hydrogen atoms were introduced; six subsequent cycles of the refinement gave $R=0.076$. The function minimized was $\Sigma w\Delta^2$, where the weighting scheme used was:

$$w = 200.0/|F_0| \quad (|F_0|\geqq 200.0),$$
$$w = 1 \quad (200.0>|F_0|>4.0), \text{ and}$$
$$w = 0.2 \quad (|F_0|\leqq 4.0).$$

The atomic scattering factors for all atoms were taken from the International Tables for X-ray Crystallography.[8]

8) "International Tables for X-ray Crystallography," Vol. III, The Kynoch Press, Birmingham (1961), p. 202.

A difference Fourier synthesis (ρ_o-ρ_c) was computed; however, several hydrogen atoms among the total of sixteen could not be found as sharp peaks. Therefore, the coordinates of the hydrogen atoms were fixed; all the C–H bond lengths were taken as 1.08 Å. The anomalous dispersion of the bromine atoms ($\Delta f'=-0.30$ and $\Delta f''=2.60$) was introduced in the refinement, and the R index reached 0.068. At this stage, it was found that the parameter shifts were insignificant compared to the estimated standard deviations, and so the refinement was terminated.

Table 2. The atomic parameters in fraction of cell edges and their estimated standard deviations (in Å)

Atom	x	$\sigma(x)$	y	$\sigma(y)$	z	$\sigma(z)$
Br(1)	0.0000	0.003	0.0838	0.002	−0.5000	0.003
Br(2)	0.1563	0.003	0.1507	0.002	1.1534	0.003
C (1)	0.8899	0.021	0.1030	0.019	−0.3364	0.017
C (2)	0.9161	0.017	0.1311	0.017	−0.1714	0.021
C (3)	0.8359	0.024	0.1468	0.021	−0.0546	0.017
C (4)	0.7420	0.013	0.1281	0.021	−0.1010	0.019
C (5)	0.7183	0.020	0.0991	0.022	−0.2695	0.020
C (6)	0.7968	0.018	0.0867	0.020	−0.3853	0.019
C (7)	0.2466	0.016	0.1410	0.015	0.9706	0.016
C (8)	0.2284	0.020	0.0947	0.022	0.8310	0.022
C (9)	0.2985	0.020	0.0869	0.018	0.6830	0.018
C (10)	0.3846	0.018	0.1288	0.017	0.6986	0.021
C (11)	0.4093	0.019	0.1778	0.021	0.8454	0.021
C (12)	0.3392	0.020	0.1829	0.019	0.9803	0.021
C (13)	0.6740	0.021	0.1740	0.017	0.1690	0.024
C (14)	0.5765	0.023	0.1755	0.018	0.2775	0.020
C (15)	0.5325	0.019	0.0827	0.020	0.3065	0.021
C (16)	0.4405	0.020	0.0850	0.019	0.4127	0.020
O (1)	0.6578	0.014	0.1388	0.014	0.0024	0.014
O (2)	0.4575	0.013	0.1285	0.015	0.5747	0.012

Table 3. The anisotropic thermal parameters, of the form:
$\exp\{-(B_{11}h^2+B_{22}k^2+B_{33}l^2+B_{12}hk+B_{23}kl+B_{13}hl\}$

Atom	B_{11}	B_{22}	B_{33}	B_{12}	B_{13}	B_{23}
Br(1)	0.0088	0.0076	0.0287	−0.0006	0.0115	0.0012
Br(2)	0.0087	0.0060	0.0209	−0.0013	0.0076	−0.0017
C(1)	0.0092	0.0041	0.0110	−0.0021	0.0089	−0.0008
C(2)	0.0044	0.0036	0.0255	−0.0021	−0.0053	−0.0073
C(3)	0.0100	0.0061	0.0102	0.0016	0.0040	−0.0033
C(4)	0.0008	0.0080	0.0213	0.0029	−0.0051	0.0014
C(5)	0.0058	0.0062	0.0204	0.0009	−0.0067	−0.0038
C(6)	0.0046	0.0057	0.0163	0.0023	−0.0033	−0.0008
C(7)	0.0054	0.0014	0.0168	−0.0008	0.0015	0.0036
C(8)	0.0056	0.0065	0.0260	−0.0011	0.0147	−0.0021
C(9)	0.0078	0.0038	0.0144	0.0039	−0.0041	−0.0008
C(10)	0.0049	0.0028	0.0258	0.0029	−0.0020	0.0088
C(11)	0.0052	0.0058	0.0208	0.0000	−0.0071	0.0059
C(12)	0.0068	0.0040	0.0226	−0.0007	−0.0081	0.0007
C(13)	0.0062	0.0033	0.0269	0.0040	−0.0057	−0.0009
C(14)	0.0095	0.0029	0.0188	0.0014	0.0096	0.0034
C(15)	0.0055	0.0047	0.0242	0.0023	0.0087	0.0076
C(16)	0.0064	0.0047	0.0200	−0.0035	0.0025	−0.0018
O(1)	0.0063	0.0063	0.0195	0.0027	−0.0009	0.0035
O(2)	0.0058	0.0075	0.0159	−0.0008	0.0027	0.0101

Table 4. The observed and calculated structure factors

K	FO	FC
H=L= 0		
2	12	12
4	355	363
6	0	10
8	0	5
10	15	19
12	51	49
14	28	26
16	3	15
H=L= 1		
1	84	80
3	64	64
5	93	90
7	46	45
9	31	32
11	16	15
13	37	40
15	12	4
H=L= 2		
0	39	39
2	78	79
4	41	41
6	125	125
8	43	42
10	63	65
12	20	24
14	14	14
16	12	15
H=L= 3		
1	28	30
3	64	65
5	45	46
7	104	103
9	26	24
11	48	47
13	15	13
15	0	2
H=L= 4		
0	123	124
2	105	106
4	97	94
6	155	153
8	54	52
10	63	62
12	18	22
14	15	11
H=L= 5		
1	78	82
3	53	54
5	37	43
7	43	46
9	34	34
11	21	23
13	25	25
15	0	0
H=L= 6		
0	123	126
2	1	4
4	59	61
6	7	13
8	24	24
10	27	25
12	32	34
14	13	18
H=L= 7		
1	90	90
3	51	49
5	40	43
7	18	19
9	18	17
11	0	15
H=L= 8		
0	77	77
2	27	26
4	48	51
6	47	46
8	9	9
10	22	23
12	0	8
H=L= 9		
1	30	35
3	40	38
5	34	36
7	58	58
9	11	12
11	27	31
H=L= 10		
0	9	9
2	35	33
4	17	18
6	56	59
8	19	22
10	26	32
H=L= 11		
1	36	33
3	14	13
5	30	31
7	10	13
9	6	12
H=L= 12		
0	50	52
2	12	8
4	30	31
6	9	17
8	13	10
H=L= 13		
1	32	25
3	0	13
5	20	19
7	7	4
H=L= 14		
0	33	28
2	8	6
4	19	20
H=L= 0		
2	10	12
4	243	236
6	45	43
8	152	148
10	49	46
12	38	38
14	27	22
16	0	2
H=L= 1		
1	79	80
3	98	100
5	69	69
7	42	42
9	44	45
11	34	31
13	19	13
15	15	21
H=L= 2		
2	347	385
4	94	84
6	105	104
8	44	41
10	28	28
12	25	29
14	25	24
16	21	17
H=L= 3		
1	92	95
3	132	131
5	64	64
7	38	37
9	34	33
11	39	42
13	0	12
15	35	38
H=L= 4		
2	141	143
4	72	68
6	37	34
8	67	64
10	28	27
12	26	28
14	13	19
H=L= 5		
1	31	30
3	48	50
5	85	84
7	38	39
9	55	55
11	16	14
13	4	5
15	0	6
H=L= 6		
2	92	93
4	92	95
6	48	46
8	66	68
10	26	25
12	0	11
14	4	7
H=L= 7		
1	46	48
3	46	48
5	34	36
7	20	22
9	31	31
11	25	21
13	1	9
H=L= 8		
2	65	61
4	15	17
6	16	16
8	17	20
10	20	23
12	20	16
H=L= 9		
1	50	48
3	45	42
5	15	18
7	0	1
9	9	8
11	21	20
H=L= 10		
2	52	48
4	29	28
6	14	12
8	6	16
10	11	10
H=L= 11		
1	15	14
3	19	15
5	34	34
7	11	10
9	30	31
H=L= 12		
2	15	12
4	37	33
6	18	15
8	30	28
H=L= 13		
1	9	11
3	13	11
5	11	8
7	15	10
H=L= 14		
2	21	16
H=L= 0		
0	103	101
2	51	50
4	71	68
6	69	69
8	21	23
10	33	32
12	14	14
14	14	17
H=L= 1		
1	49	49
3	92	91
5	62	60
7	152	148
9	22	23
11	77	77
13	15	7
15	12	12
H=L= 2		
0	104	104
2	112	110
4	19	20
6	167	159
8	48	46
10	70	65
12	36	40
14	0	7
H=L= 3		
1	72	75
3	75	75
5	32	35
7	85	88
9	27	23
11	42	47
13	19	21
15	4	8
H=L= 4		
0	139	146
2	11	6
4	97	99
6	24	23
8	21	22
10	31	33
12	18	14
14	14	18
H=L= 5		
1	102	106
3	61	62
5	65	68
7	55	53
9	9	13
11	33	33
13	37	40
H=L= 6		
0	123	121
2	37	35
4	69	64
6	62	61
8	15	12
10	36	35
12	21	17
14	0	12
H=L= 7		
1	16	18
3	55	55
5	32	33
7	50	48
9	17	19
11	12	11
13	12	6
H=L= 8		
0	36	38
2	26	26
4	26	27
6	40	42
8	20	20
10	10	17
12	6	7
H=L= 9		
1	30	29
3	26	23
5	21	22
7	26	27
9	11	11
11	0	12
H=L= 10		
0	40	42
2	17	10
4	21	22
6	15	15
8	0	11
10	12	10
H=L= 11		
1	33	31
3	17	24
5	2	12
7	6	7
9	4	7
H=L= 12		
0	28	28
2	3	12
4	13	17
6	21	18
8	5	7
H=L= 13		
1	7	8
3	20	17
5	10	5
H=L= 14		
0	8	10
H=L= 0		
2	112	109
4	18	17
6	13	15
8	22	22
10	27	27
12	19	21
14	17	19
H=L= 1		
1	121	121
3	139	133
5	36	34
7	29	25
9	13	15
11	37	39
13	0	2
15	23	28
H=L= 2		
2	108	111
4	60	59
6	35	31
8	41	41
10	19	15
12	14	9
14	5	14
H=L= 3		
1	35	38
3	38	37
5	96	95
7	39	40
9	68	69
11	15	16
13	22	20
H=L= 4		
2	48	48
4	69	69
6	11	11
8	53	53
10	27	29
12	10	12
14	14	16
H=L= 5		
1	49	47
3	55	54
5	72	71
7	4	14
9	74	75
11	12	17
13	29	31
H=L= 6		
2	70	70
4	28	29
6	24	29
8	25	25
10	12	15
12	3	16
H=L= 7		
1	52	52
3	36	37
5	38	37
7	0	6
9	31	34
11	26	26
13	18	18
H=L= 8		
2	41	43
4	34	37
6	6	6
8	29	29
10	8	9
12	0	8
H=L= 9		
1	21	22
3	24	25
5	31	29
7	22	21
9	5	16
11	11	9
H=L= 10		
2	13	7
4	17	19
6	21	11
8	17	17
10	9	9
H=L= 11		
1	11	7
3	0	9
5	10	16
7	14	9
H=L= 12		
2	24	26
4	0	6
6	0	5
H=L= 13		
1	15	17
3	17	13
H=L= 0		
0	65	63
2	39	37
4	43	44
6	67	64
8	25	25
10	37	35
12	8	11
14	0	9
H=L= 1		
1	59	62
3	66	67
5	36	36
7	56	56
9	21	23
11	18	17
13	24	25
H=L= 2		
0	98	102
2	0	2
4	57	56
6	15	10
8	8	11
10	13	15
12	23	22
14	12	8
H=L= 3		
1	96	97
3	54	53
5	54	53
7	19	17
9	3	8
11	0	11
13	17	19
H=L= 4		
0	86	84
2	26	29
4	51	49
6	47	48
8	5	1
10	18	20
12	0	11
H=L= 5		
1	25	24
3	44	45
5	23	22
7	45	43
9	11	12
11	18	17
13	21	12
H=L= 6		
0	20	23
2	28	27
4	4	8
6	46	46
8	9	7
10	23	23
12	0	7
H=L= 7		
1	37	39
3	39	38
5	30	37
7	49	49
9	15	7
11	31	30
H=L= 8		
0	51	51
2	0	13
4	31	32
6	24	19
8	16	7
10	9	10
H=L= 9		
1	22	20
3	29	27
5	12	9
7	15	14
9	18	17
H=L= 10		
0	21	20
2	13	12
4	19	11
6	19	17
8	0	2
H=L= 11		
1	13	10
3	0	8
5	12	10
7	13	14
H=L= 12		
0	3	3
2	12	5
4	0	7
H=L= 0		
2	54	53
4	58	57
6	29	25
8	53	53
10	17	14
12	24	25
H=L= 1		
1	15	15
3	25	27
5	59	54
7	20	25
9	44	42
11	19	14
13	14	11
H=L= 2		
2	34	33
4	50	49
6	28	29
8	41	42
10	19	16
12	18	15
H=L= 3		
1	27	33
3	30	32
5	40	40
7	14	15
9	22	23
11	18	23
H=L= 4		
2	55	58
4	15	13
6	14	11
8	12	10
10	15	18
12	4	5
H=L= 5		
1	29	32
3	22	24
5	0	14
7	9	5
9	0	4
11	12	7
H=L= 6		
2	53	58
4	21	26
6	17	20
8	21	19
10	0	4
H=L= 7		
1	16	19
3	25	28
5	18	20
7	16	15
9	15	19
H=L= 8		
2	22	21
4	19	21
6	13	6
8	21	21
H=L= 9		
1	25	25
3	15	21
5	19	23
7	13	11
H=L= 10		
1	13	17
3	14	10
H=L= 0		
0	84	81
2	11	8
4	47	45
6	17	15
8	0	5
10	11	13
H=L= 1		
1	45	44
3	34	32
5	22	26
7	4	8
9	7	11
11	16	6
H=L= 2		
0	42	42
2	12	16
4	30	28
6	28	31
8	8	9
10	25	27
H=L= 3		
1	3	7
3	24	24
5	17	16
7	31	31
9	20	14
H=L= 4		
0	11	11
2	21	19
4	12	15
6	36	34
8	16	16
10	18	18
H=L= 5		
1	0	17
3	19	18
5	10	8
7	16	11
9	5	10
H=L= 6		
0	32	33
2	0	5
4	18	17
6	13	10
8	11	9
H=L= 7		
1	12	6
3	7	5
5	0	3
7	14	8
H=L= 8		
0	39	37
2	17	10
4	27	26
6	22	15
H=L= 9		
1	18	11
3	0	6
5	0	8
H=L= 10		
0	0	3
2	40	41
4	0	6
6	10	13
8	16	9
H=L= 3		
1	25	24
3	23	25
5	15	10
7	9	10
H=L= 4		
2	19	24
4	9	10
6	17	11
H=L= 5		
1	4	11
3	11	3
5	13	18
H=L= 6		
2	0	5
4	12	14
H=L= 7		
1	0	7
3	4	0
H=L= 8		
0	15	16
2	7	5
4	15	11
H=L= 1		
1	10	5
3	13	11
H=L= 2		
0	11	16
2	17	13
H=L= 3		
1	13	9
H=L= -1		
1	31	31
3	33	33
5	147	142
7	18	19
9	120	115
11	14	12
13	32	32
15	0	11
H=L= -2		
2	69	71
4	148	141
6	65	61
8	105	101
10	28	25
12	33	33
14	0	6
16	14	11
H=L= -3		
1	96	94
3	84	82
5	54	53
7	31	29
9	31	36
11	40	40
13	8	8
15	17	19
H=L= -4		
2	157	153
4	18	18
6	20	21
8	7	12
10	52	49
12	28	25
14	32	33

Table 4. (Continued)

K	FO	FC
H,L= -5		1
1	121	119
3	107	107
5	38	37
7	13	12
9	21	19
11	32	35
13	0	6
15	21	22
H,L= -6		1
2	78	82
4	91	90
6	50	48
8	68	66
10	15	14
12	21	18
14	9	5
H,L= -7		1
1	48	48
3	68	69
5	89	86
7	46	43
9	67	65
11	17	15
13	16	15
H,L= -8		1
2	47	47
4	56	55
6	36	33
8	55	52
10	11	16
12	18	22
H,L= -9		1
1	32	32
3	60	59
5	36	36
7	32	31
9	27	27
11	18	17
H,L=-10		1
2	92	93
4	0	5
6	25	24
8	0	9
10	16	16
H,L=-11		1
1	46	47
3	50	50
5	14	14
7	18	15
9	0	2
H,L=-12		1
2	29	30
4	19	17
6	4	19
8	17	13
H,L=-13		1
1	13	10
3	19	14
5	16	15
H,L=-14		1
2	0	4
H,L= -1		2
1	131	132
3	77	75
5	64	60
7	25	27
9	40	37
11	2	7
13	43	42
15	6	6
H,L= -2		2
0	185	187
2	19	19
4	106	101
6	20	21
8	21	18
10	16	19
12	39	41
14	15	17
H,L= -3		2
1	133	136
3	94	94
5	64	63
7	45	45
9	24	23
11	8	9
13	32	32
15	9	7
H,L= -4		2
0	107	112
2	77	75
4	73	72
6	104	104
8	34	31
10	46	42
12	17	15
14	12	12
H,L= -5		2
1	78	76
3	91	89
5	82	77
7	103	101
9	33	34
11	39	42
13	12	12
H,L= -6		2
0	138	135
2	30	32
4	75	74
6	69	68
8	26	26
10	45	43
12	19	15
14	16	14
H,L= -7		2
1	69	71
3	51	51
5	57	57
7	52	54
9	15	16
11	23	25
13	25	26
H,L= -8		2
0	117	116
2	12	10
4	63	63
6	13	13
8	0	11
10	4	13
12	22	25
H,L= -9		2
1	81	81
3	50	50
5	43	42
7	0	6
9	12	9
11	0	2
H,L=-10		2
0	25	19
2	34	34
4	12	20
6	57	56
8	24	20
10	23	24
H,L=-11		2
1	7	15
3	22	22
5	18	17
7	41	37
9	11	4
H,L=-12		2
0	7	15
2	16	16
4	10	10
6	26	28
8	11	10
H,L=-13		2
1	11	16
3	16	18
5	14	16
H,L=-14		2
0	26	27
H,L= -1		3
1	104	105
3	102	99
5	77	77
7	29	26
9	36	36
11	27	30
13	2	1
15	21	19
H,L= -2		3
2	84	82
4	81	82
6	35	34
8	69	69
10	24	23
12	22	21
14	17	12
H,L= -3		3
1	61	59
3	46	46
5	105	103
7	45	46
9	70	69
11	16	16
13	17	16
H,L= -4		3
2	135	131
4	98	94
6	34	32
8	82	79
10	24	31
12	29	30
14	14	13
H,L= -5		3
1	85	89
3	92	94
5	63	66
7	29	30
9	46	45
11	28	30
13	0	12
H,L= -6		3
2	86	88
4	17	14
6	11	13
8	9	6
10	31	30
12	12	18
H,L= -7		3
1	73	73
3	60	60
5	42	43
7	3	8
9	26	25
11	26	20
13	4	12
H,L= -8		3
2	38	39
4	79	80
6	19	18
8	63	62
10	24	27
12	15	13
H,L= -9		3
1	10	11
3	32	32
5	48	47
7	22	21
9	35	38
11	12	9
H,L=-10		3
2	2	3
4	30	31
6	18	16
8	29	25
10	20	19
H,L=-11		3
1	22	26
3	26	23
5	26	25
7	0	10
H,L=-12		3
2	43	43
4	5	15
6	11	10
H,L=-13		3
1	28	26
3	29	24
H,L= -1		4
1	13	14
3	69	66
5	44	42
7	85	81
9	24	24
11	34	34
13	8	9
H,L= -2		4
0	84	90
2	61	59
4	55	52
6	95	93
8	26	26
10	43	49
12	18	21
14	15	14
H,L= -3		4
1	89	92
3	73	73
5	50	52
7	47	44
9	26	27
11	23	19
13	27	26
H,L= -4		4
0	111	115
2	24	22
4	60	60
6	23	21
8	17	17
10	12	13
12	29	31
H,L= -5		4
1	60	62
3	55	56
5	37	36
7	62	62
9	8	13
11	40	40
13	16	19
H,L= -6		4
0	74	76
2	44	44
4	45	42
6	71	72
8	25	26
10	36	32
12	24	22
H,L= -7		4
1	5	10
3	33	33
5	33	27
7	39	40
9	0	14
11	18	15
H,L= -8		4
0	31	31
2	28	32
4	1	12
6	51	53
8	31	24
10	22	20
H,L= -9		4
1	47	47
3	34	34
5	24	24
7	25	24
9	17	8
H,L=-10		4
0	54	60
2	17	12
4	35	35
6	21	20
8	0	3
H,L=-11		4
1	30	33
3	24	23
5	11	14
7	0	5
H,L=-12		4
0	33	36
2	15	12
4	25	23
H,L= -1		5
1	66	65
3	51	52
5	37	35
7	24	21
9	11	8
11	16	21
13	5	3
H,L= -2		5
2	98	96
4	20	20
6	21	19
8	13	11
10	26	25
12	14	15
H,L= -3		5
1	56	58
3	69	68
5	59	57
7	33	30
9	46	50
11	14	16
H,L= -4		5
2	49	50
4	52	53
6	24	26
8	44	44
10	16	18
12	13	13
H,L= -5		5
1	17	18
3	28	29
5	32	30
7	19	20
9	21	17
11	0	6
H,L= -6		5
2	31	33
4	64	64
6	16	16
8	53	50
10	14	18
H,L= -7		5
1	46	48
3	42	45
5	22	26
7	10	8
9	26	22
H,L= -8		5
2	56	58
4	6	14
6	14	13
8	4	12
H,L= -9		5
1	27	28
3	22	23
5	16	19
7	2	6
H,L=-10		5
2	36	39
4	27	26
6	23	18
H,L=-11		5
1	0	7
3	16	18
H,L= -1		6
1	49	50
3	44	43
5	33	33
7	29	32
9	9	9
11	23	16
H,L= -2		6
0	26	24
2	24	25
4	24	23
6	44	44
8	14	15
10	19	23
H,L= -3		6
1	43	44
3	18	17
5	44	44
7	27	29
9	10	13
H,L= -4		6
0	43	44
2	32	31
4	31	30
6	53	51
8	11	12
10	28	24
H,L= -5		6
1	31	35
3	22	25
5	17	14
7	20	18
9	16	13
H,L= -6		6
0	61	65
2	14	3
4	39	37
6	9	5
8	15	7
H,L= -7		6
1	34	31
3	24	22
5	22	21
7	21	20
H,L= -8		6
0	42	42
2	23	17
4	28	30
6	29	30
H,L= -9		6
1	12	7
3	23	22
H,L= -1		7
1	21	18
3	32	33
5	25	22
7	21	19
H,L= -2		7
2	35	32
4	26	27
6	17	15
8	23	23
H,L= -3		7
1	20	23
3	21	19
5	7	10
7	0	3
H,L= -4		7
2	45	44
4	11	10
6	16	15
H,L= -5		7
1	28	28
3	28	31
5	13	18
H,L= -6		7
2	26	28
4	25	23
H,L= -7		7
1	14	10
3	0	13
H,L= -1		8
1	26	21
3	14	11
H,L= -2		8
0	28	32
2	1	6
H,L= -3		8
1	19	20

The final atomic coordinates, along with their estimated standard deviations, are listed in Table 2. The thermal parameters are listed in Table 3. The observed and calculated structure factors are given in Table 4.

The computations of the Patterson function were performed on a NEAC 2200—500 computer at Osaka University, while the Fourier syntheses, least-squares refinements, and other calculations were carried out on a FACOM 230—60 computer at Kyoto University with programs written by Dr. T. Ashida.

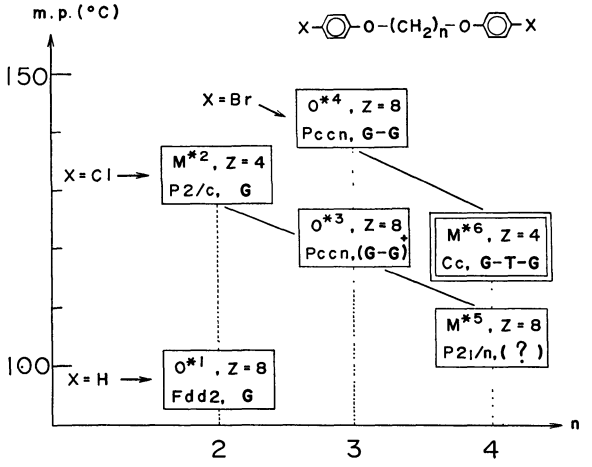

Fig. 1. Crystal data of a series of compounds, X-⬡-O-$(CH_2)_n$-O-⬡-X, correlated with the number of methylene groups, n as well as melting points.

*1 n: 2, X: H, Orthorhombic, Dm=1.22 g·cm^{-3}, mp: 97.3°C
a=34.74, b=12.04, c=5.58 Å[8]

*2 n: 2, X: Cl, Monoclinic, Dm=1.45 g·cm^{-3}, mp: 132.5°C
a=12.79, b=9.89, c=10.37 Å, β=98.2°[9]

*3 n: 3, X: Cl, Orthorhombic, Dm=1.36 g·cm^{-3}, mp: 121.5°C
a=16.83, b=17.64, c=9.60 Å

*4 n: 3, X: Br, Orthorhombic, Dm=1.75 g·cm^{-3}, mp: 142.5°C
a=17.13, b=17.76, c=9.61 Å[10]

*5 n: 4, X: Cl, Monoclinic, Dm=1.32 g·cm^{-3}, mp: 105.8°C
a=12.19, b=20.01, c=12.84 Å, β=92.9°

*6 n: 4, X: Br, Monoclinic, Dm=1.70 g·cm^{-3}, mp: 118—120°C
a=13.43, b=15.25, c=7.65 Å, β=89.4°

+ Supposed conformation on the bases of the fact that Br- and Cl-derivatives are isostructural in the case of n=3.

Discussion

Figure 1 shows the crystal and physical data of a series of homologous compounds, X-C_6H_4-O-$(CH_2)_n$-O-C_6H_4-X (X=H or halogen atom). The crystal structures of the homologues with n=2 had previously been determined.[5,6] For n=3, only the crystal structure of the Br-derivative[7] has been determined; however, the Cl-derivative can be expected to have a similar structure, since they have the same space group, similar unit-cell parameters, and an equal number of chemical units per unit cell, Z, suggesting that these crystals are isostructural.

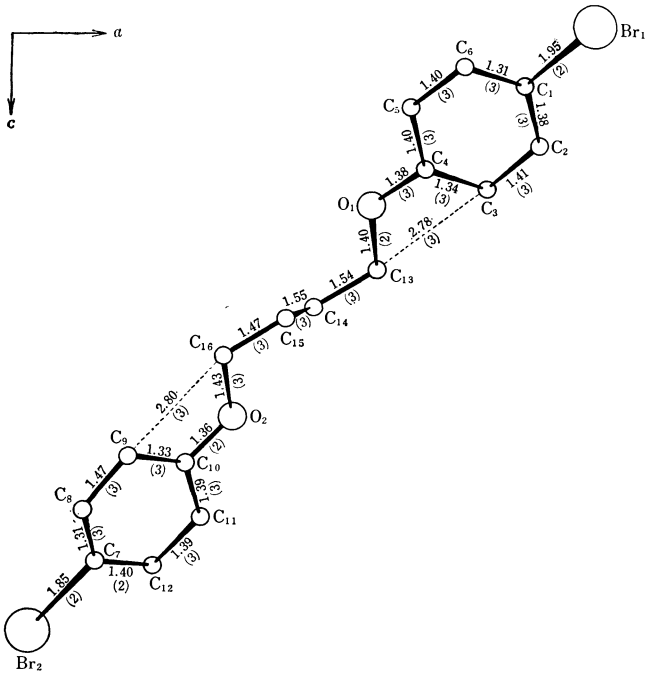

Fig. 2. The molecular shape viewed along the b axis, and bond lengths (Å) with estimated standard deviations ($\times 10^{-2}$Å) in the molecule.

In the case of n=4, there is a difference between the crystal data of the Cl- and Br-derivatives. Thus, the space group and the value of Z are $P2_1/n$ and eight respectively, for the Cl-derivative, while they are Cc and four for the Br-derivative. Therefore, it must be noticed that the information on the packing of molecules in the unit cell and the molecular conformation of the Br-derivative obtained in the present study is not always applicable to that of the Cl-derivative.

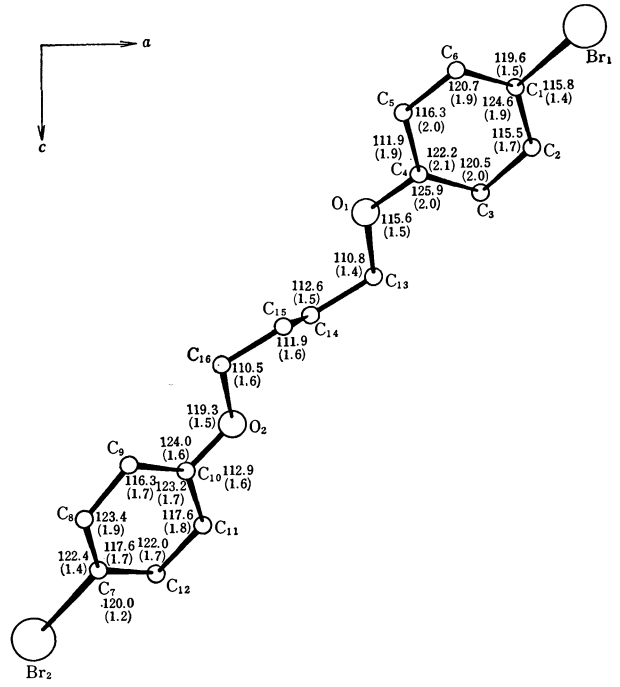

Fig. 3. The molecular shape viewed along the b axis, and bond angles with estimated standard devistions (°) in the molecule.

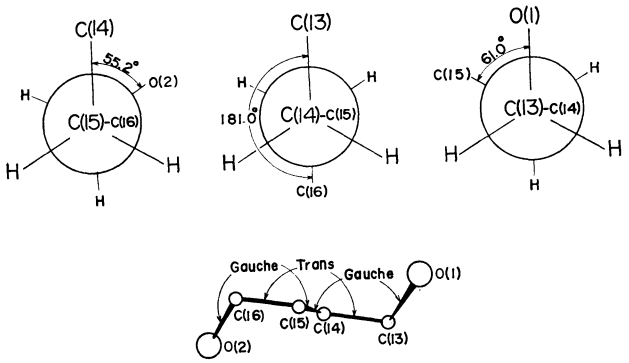

Fig. 4. The conformation of the methylene groups and the internal rotation angles (°).

The molecular shape viewed along the *b* axis is shown in Fig. 2. In Fig. 2 the bond lengths are also given, along with their estimated standard deviations. The bond angles are listed in Fig. 3.

The most remarkable feature of the molecular structure is that the conformation of the methylene groups is in the *gauche-trans-gauche* form (Fig. 4). The internal rotation angles are also shown in Fig. 4. On the other hand, the conformations of the methylene groups found in other, shorter homologues are *gauche* for $n=2$ in $XC_6H_4O(CH_2)_nOC_6H_4X$ and *gauche-gauche* for $n=3$.

The benzene rings are approximately planar, and the best least-squares planes are:

$$0.09254X + 0.94475Y + 0.31445Z + 2.42683 = 0$$

(benzene 1)

and:

$$0.40188X + 0.81185Y + 0.42354Z + 2.62451 = 0$$

(benzene 2)

where $X=ax+cx\cos\beta$, $Y=by$, and $Z=cz\sin\beta$. The maximum deviation of the atom from the plane is 0.024 Å for C(3). As is shown in Fig. 2, the nonbonded intramolecular distance from C(3) to C(13) is 2.78 Å, and that one from C(9) to C(16) is 2.80 Å. C(13) and C(16) lie almost on the plane containing the benzene ring, the displacements from the plane being 0.08 and 0.10 Å respectively.

The crystal structure, as viewed along the *b* and *c* axes, is shown in Fig. 5 and 6 respectively. In these figures short intermolecular atomic contacts of less than 4.0 Å are given. As may be seen in Fig. 5, molecules are piled up along the *b* axis; the benzene ring, 1, of a molecule is above the benzene ring, 2, of the other molecule, and the dihedral angle between two benzene rings in a molecule is 20.39°.

The authors wish to express their deep thanks to Dr. Tadanao Ando of Government Industrial Research Institute, Osaka for supplying crystals. Their thanks are also due to Mr. Yasushi Kai of Osaka University for helping a part of experiment. The authors are also indebted to Dr. Tamaichi Ashida of Institute for Protein Research of Osaka University for his computer programs.

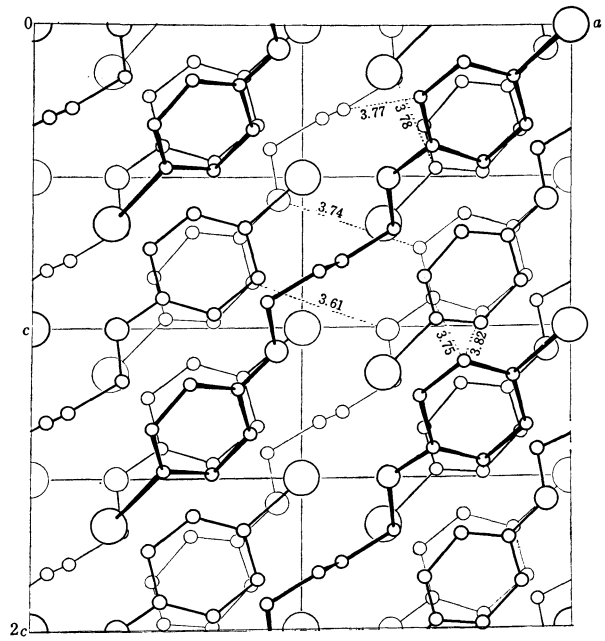

Fig. 5. The crystal structure in the unit cell projected onto the *ac* plane, with some short intermolecular distances (Å).

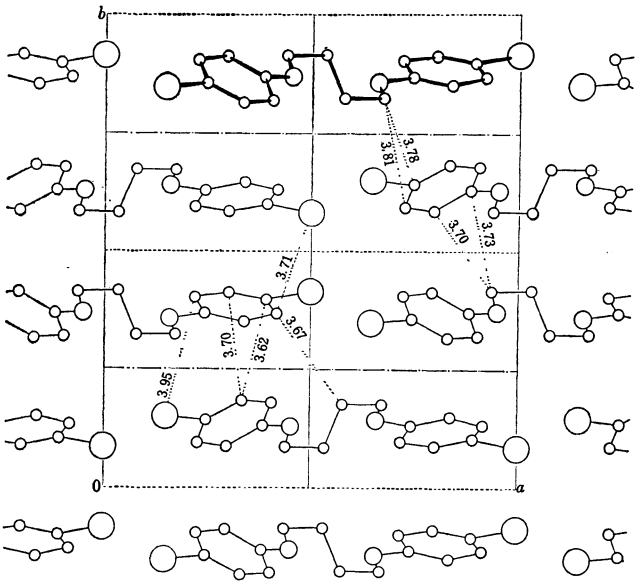

Fig. 6. The crystal structure in the unit cell projected onto the *ab* plane, with some short intermolecular distances(Å).

Anodic Oxidation of Aniline in Aqueous Alkaline Solution

Yoshiharu MATSUDA, Akira SHONO, Chiaki IWAKURA, Yoshiki OHSHIRO, Toshio AGAWA, and Hideo TAMURA

Department of Applied Chemistry, Faculty of Engineering, Osaka University, Yamadakami, Suita, Osaka

(Received April 21, 1971)

The anodic oxidation of aniline in an aqueous alkaline solution was studied. The anode materials were Ni, C, Pt, and Pb. An organic deposit (film) was formed on the anodes. The reaction mechanism was estimated through electrochemical measurements, chemical analysis, thin-layer chromatography, and UV, NMR, and IR spectrometries. The de-electronation of lone-pair electrons of the N atom in an aniline molecule caused the radical cation to be produced,  , and this process was the rate-determining step. Some of the radical cations were found to couple together to produce azo-benzene *via* hydrazobenzene. The other radical cations led to *p*-amino diphenylamine by head-to-tail coupling; this product was de-electronated again to give the polymer with a quinoid structure.

Since Letheby[1] obtained aniline black through the anodic oxidation of aniline, many works have been presented on the anodic oxidation of aromatic compounds. Yasui[2] reported that aniline black was obtained from *p*-amino-diphenylamine and emeraldine in aqueous hydrochloric acid. Recently, discussion[3,4] was focussed on the reaction mechanism of the anodic oxidation of aniline derivatives in aqueous acidic solutions and also in nonaqueous solvents. Adams and his co-workers[5] observed the amino radical in the process of the anodic oxidation of aromatic amines. However, in an aqueous alkaline solution, the anodic oxidation of aniline has not been investigated. The present authors found film formation on the anode in an aqueous alkaline solution containing aromatic amines in their study of the electrochemical behavior of aniline derivatives.[6] In the present work, the anodic oxidation of aniline in an aqueous alkaline solution was carried out in order to elucidate the mechanism of this process by the analysis of the product and by electrochemical measurements.

Experimental

Test Electrode. The test electrodes were platinum, nickel, lead, and carbon. The metal electrodes were plates, 1 cm × 1 cm, equipped with a wire and sealed in glass tube. The carbon electrode was a carbon rod for spectroscopic analysis whose available area was made 1 cm^2 by blinding with Daifloil. The test electrodes were polished with emery paper, rinsed with a 1N aqueous solution of potassium hydroxide and a 1N aqueous solution of hydrochloric acid, and then immersed in a 10% aqueous solution of hydrazine. However, in the case of the lead electrode, the treatments with alkaline and acid were omitted.

Electrolytic Cell. The electrolytic cell was a H cell (100 m*l*) with a sintered glass disk diaphragm and a Luggine capillary connected to a reference electrode (Hg/HgO/1N KOH). The counter electrode was a platinum plate (2 cm × 2.5 cm). Triangular potential waves were generated by using a potentiostat HP-E and a frequency function generator NS_2 (by Nichia Keiki Co., Ltd.). The temperature was 30°C.

Materials. An alkaline solution was prepared with a commercial, analytical-grade reagent and deionized water. The aniline was commercial and at an analytical grade, too.

Results and Discussion

Current-potential Curves of Aniline by Cyclic Voltammetry. A typical current-potential curve of aniline in 1N potassium hydroxide, determined by cyclic voltammetry with a platinum electrode, is shown in Fig. 1.

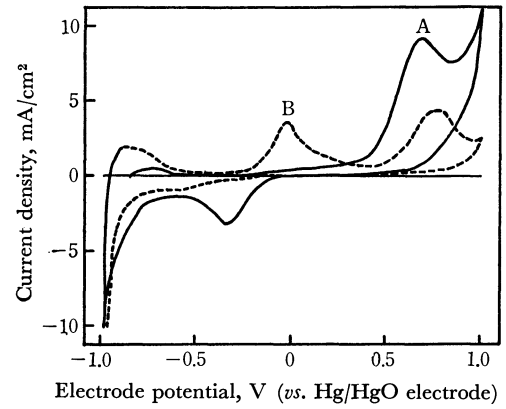

Fig. 1. Voltamgram of aniline in aqueous KOH solution. Potential sweep rate: 0.2 V/sec, 30°C, Electrode: Platinum plate, Electrolyte solution: 1N KOH + 10^{-2}M aniline.

The potential sweep range was −1.0—+1.0 V (*vs.* Hg/HgO electrode); the potentials for the reactions of hydrogen and oxygen evolutions were outside this potential sweep range. The potential was anodically swept first from −1.0 V (*vs.* Hg/HgO electrode); then the direction of the current was reversed at +1.0 V, and the same procedures were repeated.

When aniline was absent in the solution, the current peaks, A and B in Fig. 1, were not observed. At the first anodic sweep with the existence of aniline, only the current peak A was ovserved; after the second sweep, both current peaks, A and B, were obtained.

1) H. Letheby, *J. Chem. Soc.*, **15**, 161 (1862).
2) T. Yasui, This Bulletin, **10**, 305 (1935).
3) S. Wawzonek, T. W. McIntyre, *J. Electrochem. Soc.*, **114**, 1025 (1967).
4) T. Mizoguchi and R. N. Adams, *J. Amer. Chem. Soc.*, **84**, 2058 (1962).
5) E. T. Seo, R. F. Nelson, J. M. Fritsch, L. S. Marcoux, D. W. Leedy, and R. N. Adams, *ibid.*, **88**, 3498 (1966).
6) H. Tamura, Y. Matsuda, and M. Iijima, *Kogyo Kagaku Zasshi*, **72**, 1077 (1969).

When the cyclic voltammetry was applied, the current peaks corresponding to A and B became lower and reddish-brown film was precipitated on the electrode as time passed. When the potential sweep range was only between −1.0 and +0.4 V, the B peak was not observed on the current-potential curve. From the results mentioned above, the two current peaks, A and B, might be assumed to be caused by the anodic reaction of aniline or the intermediate products. The anodic oxidation of aniline, therefore, might be initiated with the electrochemical reaction corresponding to the current peak A. Moreover, it can be assumed that the decrease of the current with cyclic sweeps might be caused by the increase in the resistance on the electrode resulting from the film formation. Therefore, as will be discussed later, this initial reaction is shown by Eq. (1):

$$C_6H_5\ddot{N}H_2 - e^- \longrightarrow C_6H_5\dot{\overset{+}{N}}H_2 \qquad (1)$$

Moreover, the B peak may be assumed to correspond to the anodic oxidation of *p*-amino-diphenylamine, the intermediate product. Mohilner and his co-workers[7] have already observed this phenomenon at *ca.* 0.1 V (*vs.* SCE) in dilute sulfuric acid containing aniline.

Anodic Oxidation of Aniline at a Controlled Potential. As has previously been mentioned, the initial electrochemical reaction corresponded to the A peak in Fig. 1. In this potential range, a Tafel relation was observed when the current was measured 1 min later after setting the potential; the relation between the current and the concentration of aniline was found to be as is shown in Fig. 2. The electrochemical reaction order was found to be one from the slope of the line in Fig. 3.

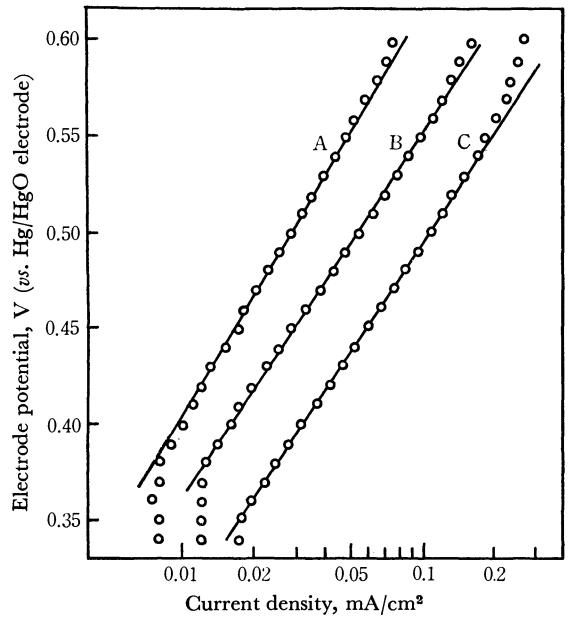

Fig. 2. Tafel lines for anodic oxidation of aniline in aqueous KOH solution.
Under stationary state, Electrode: platinum plate, 30°C
A: 1N KOH+1×10^{-3}M aniline
B: 1N KOH+2.5×10^{-3}M aniline
C: 1N KOH+5×10^{-3}M aniline

7) D. M. Mohilner, R. N. Adams, and W. J. Argersinger, Jr., *J. Amer. Chem. Soc.*, **84**, 3618 (1962).

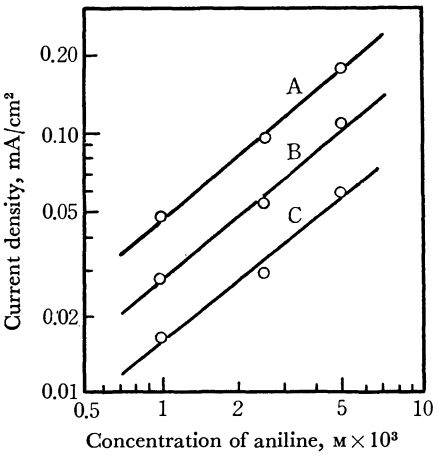

Fig. 3. Relation between current density and concentration of aniline for anodic oxidation of aniline in aqueous KOH solution.
Electrode: platinum plate, 30°C
A: 550 mV (*vs.* Hg/HgO electrode)
B: 500 mV (*vs.* Hg/HgO electrode)
C: 450 mV (*vs.* Hg/HgO electrode)

Mohilner and his co-workers[7] reported that the initial anodic reaction of aniline in an acidic solution was the formation of the cation radical, shown in Eq. (1). Other reports[3-5] on the anodic oxidation of aromatic amines in nonaqueous solvents have pointed out mechanisms similar to Eq. (1). For Eq. (1) to proceed in an acidic solution, a protonated aniline molecule must be de-hydrogenated, as in Eq. (2), because aniline in an acidic solution is usually protonated:

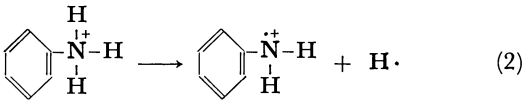

(2)

However, in an alkaline solution, an aniline molecule is only to be de-electronated as in Eq. (3), which is the same as Eq. (1), because aniline is a free amine in an aqueous alkaline solution:

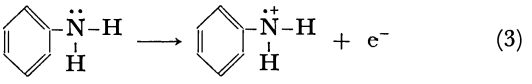

(3)

If we compare the two mechanisms, the reaction shown by Eq. (3) should be easier than the reaction shown by Eq. (2) because the de-electronation is usually easier than the de-hydrogenation. At the same time, the reaction order, one, suggests that the reaction shown by Eq. (1) is the initial anodic reaction.

Furthermore, this process is the rate-determining process for the anodic oxidation in an aqueous alkaline solution, because a Tafel relation was observed at the potential for the current peak A in Fig. 1.

Materials for the Anode. By using carbon, nickel, and lead electrodes, cyclic voltammetric measurements were made at the alkaline solution containing aniline. The current peak potentials corresponding to the A peak in Fig. 1 for these systems are shown in Table 1. This table also shows the slopes of the Tafel lines which were measured by the procedures described in the previous section.

The potential of the current peak and the slope of

TABLE 1. PEAK POTENTIALS AND SLOPES OF TAFEL LINES ON VARIOUS ELECTRODES

Electrode	Peak potentials corresponding to the peak A in Fig. 1 (*vs.* Hg/HgO electrode)	Slope of Tafel line V/log *i*
Ni	0.52 V	0.100
C	0.55	0.131
Pt	0.71	0.188
Pb	0.73	0.501

Tafel line give measures of the electrochemical reaction rate, and nickel is the most active electrode in an aqueous alkaline solution for the initial anodic reaction of aniline corresponding to the A peak in Fig. 1, with carbon and platinum following next. From the data in Table 1, the lead electrode can be said to be the most inactive electrode among them.

Characterization of the Deposit (film) on the Anode. The anodic oxidation of aniline was made by using nickel electrode (3×4 cm^2) and a beaker-type electrolytic cell. The anode potential was +0.5 V (*vs.* Hg/HgO electrode), the electrolyte solution was an aqueous solution of 1N potassium hydroxide with 10^{-2}M aniline, and the temperature was 30°C±0.1°C. The samples for UV and NMR spectrometries, the measurement of the molecular weight, the elementary analysis, and thin-layer chromatography were obtained by the extraction of the film on the electrode with benzene.

After the electrolysis, the IR spectrum of the film on the anode was taken with a polarized IR spectrometer.

TABLE 2. ANALYTICAL RESULTS BY IR SPECTROMETRY FOR DEPOSIT ON THE ELECTRODE

(Nickel anode potential: +500 mV *vs.* Hg/HgO/1N KOH, Polarized reflective IR spectrum)

1560—1580 cm^{-1}	(–C=C–, –C=N– conjugate)
1480 cm^{-1}	(–N=N–)
830 cm^{-1}	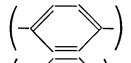
750 cm^{-1}, 690 cm^{-1}	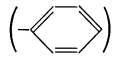

There was no absorption corresponding to $-NH_2$ or –NH– in the range of 3200—3500 cm^{-1}.

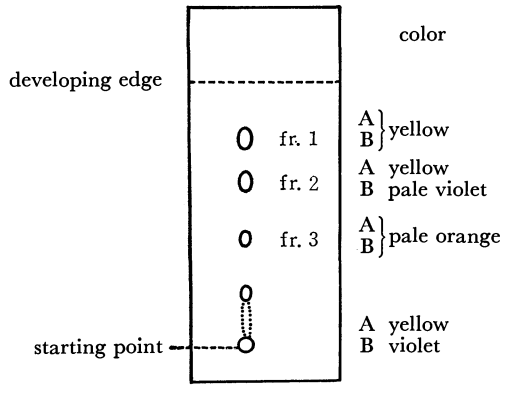

Fig. 4. Thin layer chromatogram of the deposit on the electrode.
A: Colour during the development,
B: Colour after spraying dilute H_2SO_4.

The results are shown in Table 2. The absorption band at 1560—1580 cm^{-1} was found to correspond to the –C=C– and –C=N– bonds with a quinoid structure, while that at 1480 cm^{-1}, and, those at 750 and 690 cm^{-1}, were caused by the –N=N– group of azobenzene and the mono-substituted phenyl ring respectively. Moreover, the absorption at 830 cm^{-1} was probably due to the disubstituted phenyl ring.

The results of thin-layer chromatography are shown in Fig. 4. The thin-layer consisted of silica gel, and the developing agent was benzene. As is shown in Fig. 4, two different groups were detected when the sample was developed and sulfuric acid was sprayed on the chromatogram. The R_f values of fraction 1 were identical with those of the authentic sample.

TABLE 3. ANALYTICAL RESULTS THROUGH COLUMN CHROMATOGRAPHY FOR THE DEPOSIT ON THE ELECTRODE

Fraction 1 (eluted with hexane)
IR: 1480 cm^{-1} (–N=N–)
780 cm^{-1}, 690 cm^{-1} 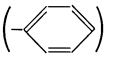
UV: 450 mμ, 320 mμ
mp: 65.5—67 °C
agreed with the mp of authentic sample of azobenzene
Yield: 30%

Fraction 1′ (eluted with benzene)
UV: 450 mμ, 365 mμ, 310 mμ

Fraction 2 (eluted with benzene)
UV: 375 mμ, 298mμ (–C=N–)
cf. UV: 288 mμ Ph_2NH
292 mμ PhNHNHPh

Furthermore, the sample of the film was divided into 3 fractions by column chromatography, and these fractions were analysed by UV spectrometry. These results are shown in Table 3. When the fraction 1 was

TABLE 4. ANALYTICAL RESULTS OF THE FRACTION BY BENZENE EXTRACTION OF THE DEPOSIT ON THE ELECTRODE

Mean molecular weight: 440 (V.P.O. -benzene)

NMR: 2.0—2.4ppm 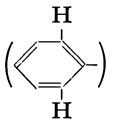

2.5—2.8ppm 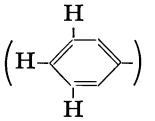

2.7—3.4ppm 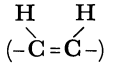

Elementary analysis:

	C	H	N	
Found	76.99	5.25	14.03	$C_{12.2}H_{10}N_{1.9}$
Calculated				
for aniline	77.38	7.58	15.04	
for azobenzene	79.09	5.53	15.38	

eluted with hexane, reddish-orange crystals were isolated. The IR and UV spectra and the melting point agreed with those of the authentic sample of azobenzene. The fraction 1′ was the first fraction with a benzene eluant; this fraction was determined by UV spectrometry to be a mixture of a substance containing an azo group and a quinoid structure. For the fraction 2, the UV spectrum showed λ_{max} at 375 mμ and 298 mμ corresponding to the n-π^* transition of the –C=N– group in the quinoid structure and the n-π^* transition of –N–H respectively; this fraction was assumed to consist of polymers with a quinoid structure and an N–H group.

The mean molecular weight of the film was 440, as is shown in Table 4. Because the azo-benzene content in the film, which was separated by column chromatography, was about 30%, the mean molecular weight of the residual polymer should be about 1100; this was assumed to be the dodecamer of the aniline.

The results of NMR spectrometry are shown in Table 4. The signals of the NMR spectrum were observed at τ 2.0—2.4, 2.5—2.8, and 2.7—3.4. These signals were identified as the signals of protons at the ortho position of azo benzene, the protons at the *meta* and *para* positions of azo benzene, and the protons at the quinoid ring respectively.

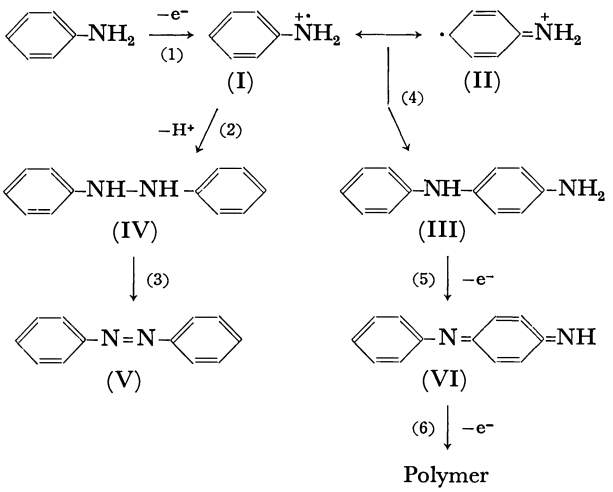

Scheme 1

From the results presented above, it seems that the film was formed on the anode during the electrolysis of aniline in the aqueous alkaline solution; its composition consisted of azo benzene and of polymers with a quinoid structure, but its structure was not clear in detail.

Reaction Mechanism. The reaction mechanism of the anodic oxidation of aniline in an aqueous alkaline solution is assumed to be as in Scheme 1.

At first, the de-electronation of lone-pair electrons of the nitrogen atom in the aniline molecule caused the production of the radical cation, 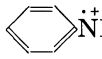 ; this process is the rate-determining step. Some of the radical cations are coupled together and form azobenzene *via* hydrazobenzene. The other radical cations led to *p*-amino-diphenylamine by head-to-tail coupling between the radical cation and its resonance form, 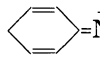 ; this product is de-electronated again and changed to the polymer step by step. The formation of phenyl-hydroxylamine may be considered in this reaction between the radical cation and hydroxyl ion. However, it is not probable, because the current-potential curve of phenyl-hydroxylamine was quite different from that of aniline in cyclic voltammetry. There are many radical cations on the electrode, and so the probability for the coupling is high and paths (2) and (4) in Scheme 1 must proceed simultaneously. In view of other experiments in which hydrazobenzene oxidized easily to azobenzene with air or alkali, the path (3) must proceed chemically.

On the anodic oxidation of aniline in an acidic solution, the formation of the octamer, emeraldine, had been reported by Mohilner and his co-workers.[7] However, in the anodic oxidation of aniline in an alkaline solution, the mechanism was different from that in an acidic solution, and the products were azo benzene and the polymer with a quinoid structure.

Thermoelectric Powers of Molten I_2+Te Solutions

Kazuhiko ICHIKAWA and Mitsuo SHIMOJI

Department of Chemistry, Faculty of Science, Hokkaido University, Sapporo

(Received April 23, 1971)

The initial and steady-state potentials of thermocells of the liquid I_2+Te system were measured at temperatures 250—600°C. Cells with a vapor path were used, together with those in which a vapor transport was forbidden. The difference due to these types of cells was found in the values of not the initial thermoelectric powers but the steady-state ones for only solutions with low Te compositions. In the I_2-rich region, the mechanism is discussed by using the model of charge-transfer due to I_3^- as in the case of conductivities and absorption spectra. The thermoelectric data in both the Te-rich and intermediate composition regions suggest that electronic contributions are highly predominant and a transition to delocalized states continuously appears with increasing Te concentration. Some experiments were carried out in order to examine the formation of concentration gradient due to the thermal effect in low Te compositions.

In this paper we report measurements of thermoelectric powers on the molten I_2+Te system, for which the conductivity measurements[1] have been made over the entire composition range. For the measurements cells in which a vapor transport was completely forbidden and those in which it was slightly permitted were used. The effect of vapor transport is negligible usually for the initial thermoelectric power measured before the concentration gradient due to thermal effects is formed. However, it is important for the stationary-state thermoelectric power of a system containing highly volatile components, as demonstrated in the case of molten Bi+$BiBr_3$ solutions by Kelner *et al.*[2] The data we obtained (with or without a vapor shunt) also indicate a marked difference in the stationary-state values in the region of low Te compositions, but no difference in the other regions. Experiments were carried out in order to examine the transport number of electron in the TeI_4 liquid and the formation of the concentration gradient in the low Te composition range.

The conductivity data[1] suggest that this system shows a transition from ionic transport to electronic transport; in the I_2-rich region the electrical conduction can be determined largely by the migration of the I_3^- ion, the presence of which could be confirmed by absorption spectra,[3] and by the movement of electron in the Te-rich and intermediate concentration region. The thermoelectric data are discussed by means of the same mechanisms, together with formulas[4] based upon thermodynamics of irreversible process.

Experimental

Materials. The purity of the tellurium and iodine used was described previously.[3]

Apparatus and Procedure. (i) Thermoelectric power: Measurements were carried out with three different thermocells. The Hario thermocell (cell A) with a gas shunt was of the same type as described.[5] For cell A′, all the upper surface of the solution was kept in equilibrium with a gaseous phase across the desired small temperature difference. The horizontal cell (cell B) of J-type, was designed in such a manner that no vapor path between the electrodes was permitted.

The initial thermoelectric power θ_{in} was determined from the slope of a curve of cell emf plotted against ΔT in the range 0.5°—5°. The measurements were carried out at 2 min intervals. In the case of stationary-state thermoelectric power θ_{st} all the emf values were checked to be constant by the recorder. The thermoelectric powers were measured at temperatures 300—550°C and for the compositions 3, 10, 20, 30, 40, 50, 60, 70, 80, 90, 95, and 100 at.% Te in I_2.

(ii) Electronic transport number: Wagner's polarization technique[6,7] was used to determine the electronic transport numbers of molten TeI_4. A constant current (0.1—0.3 mA) supplied by an automatic current regulator was passed through the cell, represented by

$$W|Te(S)|TeI_4(L)|C|W,$$

where W denotes a tungsten lead, Te(S) a solid tellurium cathode and C a graphite rod. The stoichiometric TeI_4 liquid prepared from the samples crystallized by Bridgman's method was enclosed in a capillary with length 60 mm and inner diameter 0.5 mm. The potential applied was so low that the decomposition of the TeI_4 melt could be avoided.

Results

The thermocell used in this work can be regarded as a symmetrical cell $W|I_2+Te|W$.[5] The temperature effects on θ_{st} for the I_2+Te solutions are shown in Figs. 1—4. For the iodine solutions containing 30, 40, 50 at.% Te, the magnitude and temperature dependence of θ_{st} measured with cells A and A′ differ significantly from those measured with cell B. On the other hand, no difference was found in the values of θ_{in} for the three types of thermocells. In Fig. 5 θ_{in} and θ_{st} (measured with cell B), are plotted against the Te concentrations, giving minima at about 50 at.% Te. Figure 6 shows that the difference between the initial and stationary values, $\Delta(\equiv\theta_{in}-\theta_{st})$, reaches a maximum at about 30 at.% Te composition, and continuously approaches zero with increasing Te concentration.

1) K. Ichikawa, T. Ōkubo, and M. Shimoji, *Trans. Faraday Soc.*, **67**, 1426 (1971).
2) J. D. Kellner, S. J. Yosim, and L. E. Topol, *J. Phys. Chem.*, **73**, 4419 (1969).
3) K. Ichikawa and M. Shimoji, in press.
4) S. R. de Groot, Thermodynamics of Irreversible Process (North-Hallond Publishers, Amsterdam, 1963) p. 136.
5) K. Ichikawa and M. Shimoji, *Ber. Bunsenges. physik. Chem.*, a); **71**, 1149 (1967); b); **73**, 302 (1969).
6) C. Wagner, *Z. Elecktrochem.*, **60**, 4 (1956).
7) B. Reuter and K. Hardel, *Ber. Bunsenges. physik. Chem.*, **70**, 82 (1966).

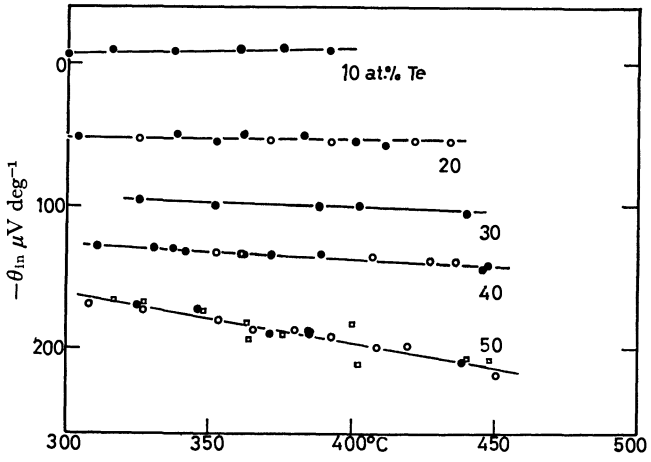

Fig. 1. Initial thermoelectric power θ_{in} (μV/deg) (●, ○, and □, measured with the thermocells A, B, and A′, respectively).

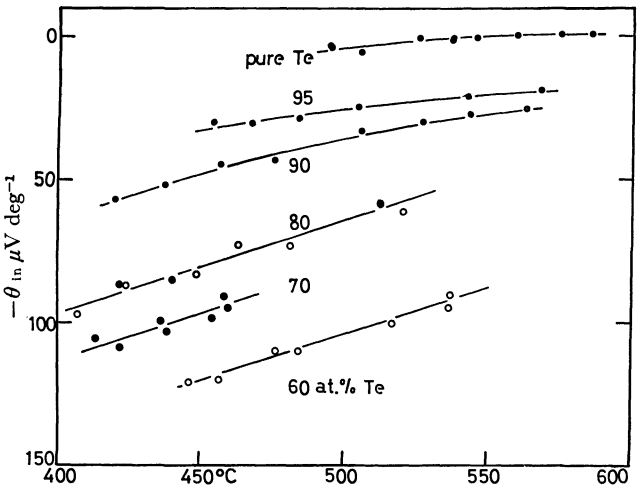

Fig. 2. Initial thermoelectric power θ_{in} (μV/deg) (● and ○, measured with the thermocells A and B, respectively).

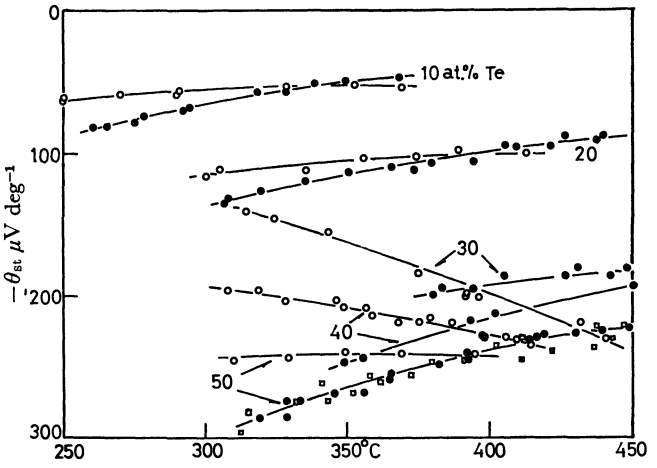

Fig. 3. Stationary-state thermoelectric power θ_{st} (μV/deg) (●, ○, and □, measured with the thermocells A, B, and A′, respectively).

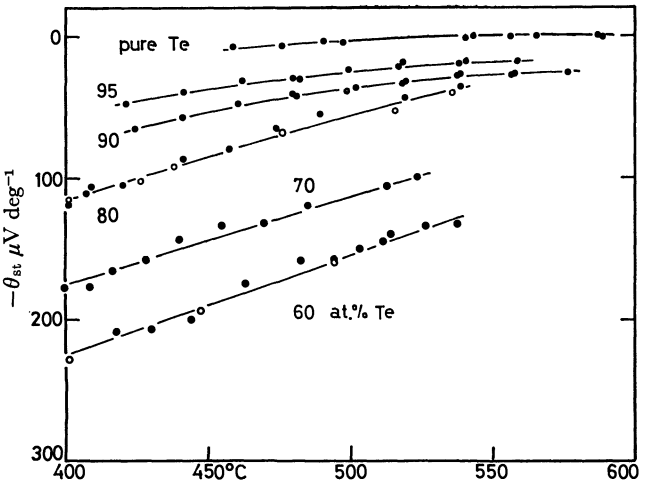

Fig. 4. Stationary-state thermoelectric power θ_{st} (μV/deg) (● and ○, measured with the thermocells A and B, respectively).

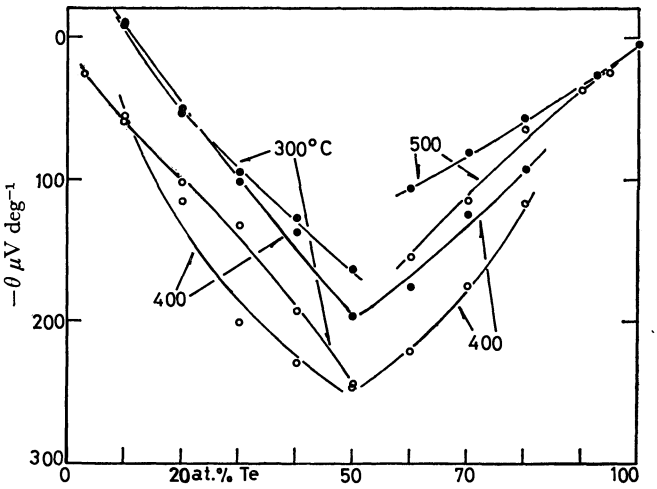

Fig. 5. Initial and stationary-state thermoelectric powers $\theta_{in}(\equiv$ ●) and $\theta_{st}(\equiv$ ○) (μV/deg), measured with the thermocell B, as a function of compositions.

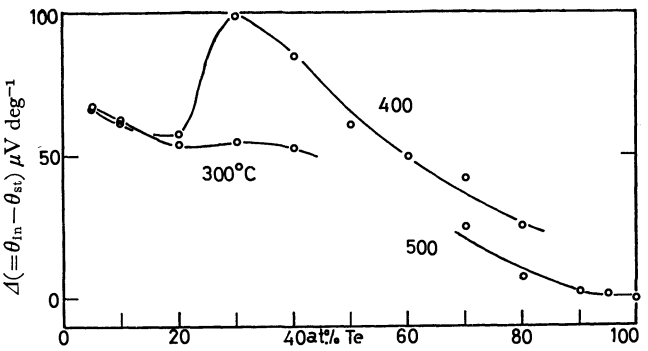

Fig. 6. Dependence of difference $\Delta(=\theta_{in}-\theta_{st})$ (μV/deg) on composition, obtained with the thermocell B.

The electronic transport number t_e in the TeI_4 liquids varies from 0.03 to 0.08 at 300—350°C.

Discussion

The stationary-state data obtained using cells A and A′ seem inadequate for discussing uniquely the thermoelectric powers of the some iodine solutions (*i.e.*, 30, 40, 50 at.% Te), since in these cells with gas shunts the effect of mass transport (mainly due to the I_2 molecule), taking place simultaneously through the gaseous space, is too large to be neglected. Thus, we confine our attention to the results of thermoelectric powers to which no gaseous transport contributes.

As has been pointed out in our conductivity work, the electrical properties of the present system should be examined with three kinds of models applied to the solutions of limited composition ranges.

Charge-Transfer due to I_3^-. In the I_2-rich region (above 95 at.% I), where the contribution of the I_3^- ion to the electrical conduction is predominant, the thermoelectric power θ can be represented by[5]

$$\theta = \theta(\text{hom}) + \theta(\text{het}) + Q. \tag{1}$$

Here, the homogeneous contribution θ (hom) arising from thermal diffusion of the I_3^- ion is approximately given by

$$\theta(\text{hom}) = [\text{grad}\,\mu(I_3^-)]_T/e\,\text{grad}\,T + q^{**}(I_3^-)/eT, \tag{2}$$

where the notation is the same as in our previous paper[5] (except for $q^{**}(k)$ in place of $Q^{**}(k)$). Heterogeneous contribution of the solution θ (het) can be written using the entropy factors of electron arising from some chemical reaction at the surface of electrodes (as proposed for the case of a contact between a solid electrolyte and inert electrodes[8]), and Q represents the absolute thermoelectric power of metal leads. The factor containing $[\text{grad}\,\mu(i)]_T$ is zero for the initial state. Thus we get

$$\theta_{\text{in}}(\text{hom}) = q^{**}(I_3^-)/eT. \tag{3}$$

For the stationary state the concentration gradient formed in the melt can be in local equilibrium.

$$\theta_{\text{st}}(\text{hom}) = [h_V(I_3^-) + q^{**}(I_3^-)]/eT, \tag{4}$$

where $h_V(I_3^-)$ is the heat of formation for the I_3^- ion.

The application of the Fokker-Planck equation to the thermoelectric phenomena predicts[5,8,9] that the heat of transport is equal to the heat of activation for migration. Inferring from the temperature dependence of mobilities of I_3^-, we can estimate the value of $q^{**}(I_3^-)$ to be 0.12 eV.[1] The value of $h_V(I_3^-)$, which may be equivalent to $-eT\Delta$ with the condition that the heterogeneous value is unchanged in both cases, is found to be negative as seen in Fig. 6. This fact $[h_V(I_3^-)<0]$ is reasonably expected also in our works on the conductivities[1] and the absorption spectra[3] for these compositions. The negative value of θ (het) (*e.g.*, at 300°C for 5 at.% Te θ (het) $=-192\ \mu\text{V deg}^{-1}$) is sufficiently probable in the case of inert electrodes. As an example, θ (het) for molten $PbCl_2$ in contact with graphite, tungsten or platinum electrodes was estimated[10] to be negative (their average value of about $-300\ \mu\text{V deg}^{-1}$), with the aid of data obtained from cells with reversible electrodes.

Electronic Conduction. Case I, Te-rich Region: We showed that the 90 at.% Te solution may be on the borderline of the hopping conduction,[1] and the transition to nonlocalized states may continously appear with increasing Te concentration. As seen in Fig. 6, above the 90 at.% Te composition Δ is negligible within experimental error, and the electronic transport number can be exepcted to be nearly equal to unity. Thus, the total thermopower can be given by

$$\theta = -Q(\text{sample}) + Q(\text{leads}), \tag{5}$$

with the absolute thermoelectric power Q(sample) of the solutions

$$Q(\text{sample}) = -(\pi^2 k_B^2 T/3e)[\partial \ln \kappa_e(\varepsilon)/\partial\varepsilon]_{\varepsilon=\varepsilon_F}, \tag{6}$$

where the notation is the same as in our previous paper.[5] According to Mott,[11] for some disordered structures a minimum or pseudogap is expected in the curve of the density of states $N(\varepsilon)$. If the Fermi energy ε_F has a chance of being located at the side lower than the minimum, then the positive values of Q(sample) will be obtained. On the other hand, a negative Hall effect may be expected as in the case of the pure Te liquid.[12] This contradicts the conclusion of the conventional band model. No conduction electrons in liquid Te can, however, be interpreted in terms of a localized model due to Tiéche and Zareba.[12] It is well-known[13] that the sign of thermoelectric power in many electron-conducting liquids is not always in agreement with that of the Hall coefficient, although no satisfactory theoretical interpretations have been proposed.

Electronic Conduction. Case II, Intermediate composition region: In the 60—80 at.% Te solutions, conductivity κ varies from 1 to 300 $\text{ohm}^{-1}\cdot\text{cm}^{-1}$ and $d\kappa/dT>0$. The transport number of electron t_e is considerably small in the TeI_4 liquid. The magnitude of ionic conductivity in the 20—40 at.% Te solutions can be regarded as nearly constant (*i.e.* 0.4 $\text{ohm}^{-1}\cdot\text{cm}^{-1}$ from the conductivity data at 300—400°C). The rapid increase in κ above the 60 at.% solutions should mainly be interpreted in terms of some electron transport mechanism. In other words, the electron-pair exchnage between the ionicpairs (*e.g.* Te^{2+}, Te^{4+}, Te^{6+} etc.) may be responsible for the electrical conduction under conditions where the composition flunctuations in their environments bring the ions to a level of equal energy.[5]

For the homogeneous part of thermoelectric power at the initial state we can write

$$\theta_{\text{in}}(\text{hom}) = q^{**}(2e)/2eT \tag{7}$$

8) M. Shimoji and H. Hoshino, *J. Phys. Chem. Solids*, **28**, 1155 (1967).
9) M. Shimoji, *Nippon Kagaku Zasshi*, **91**, 505 (1970).
10) unpublished work.
11) N. F. Mott, *Phil. Mag.*, **19**, 835 (1969).
12) Y. Tiéche and A. Zareba, *Phys. kondens. Materie*, **1**, 402 (1963).
13) R. S. Allgaier, *Phys. Rev.*, **185**, 227 (1969).

and for that at the stationary state

$$\theta_{st}(\text{hom}) = [h_V(2e)+q^{**}(2e)]/2eT, \quad (8)$$

which are analogous to Eqs. (3) and (4). Here, $h_V(2e)$ is the heat needed to form the site containing the electron-pair, and $q^{**}(2e)$ the heat of transport of the electron-pair. As in Case I, the value of $h_V(2e)$ can be estimated by the experimental data of Δ. Thus we have $h_V(2e)=-0.03$ eV at 70 at.% Te and at 500°C. No magnitude of $q^{**}(2e)$ can, however, be evaluated only from the data of the thermoelectric powers, since the temperature dependence of the heterogeneous part might be so large that it masks that of the homogeneous part. The heterogenous quantity of the solution can be considered to have a configurational entropy term[14] involving permutation of electron pairs among available states such as $Te^{(n-2)+}$ and Te^n, the concentrations of which might depend significantly on temperature. On the other hand, the value of $q^{**}(2e)$, using the Fokker-Planck equation from the slope $(\Delta h_s+\Delta h^*)$ of $\log(\kappa_e T)$ *vs.* $1/T$ (see Eq. (15) in Ref. (5a)), can be estimated to be 0.33 eV at 70 at.% Te and 500°C.

Formation of concentration gradient In the course of time t the concentration gradient, resulting from the term of $[\text{grad}\,\mu(i)]_T/\text{grad}\,T$ in the expression such as Eq. (2) for the species i, is represented by[4,15]

$$\text{grad}\,c_i = (\text{grad}\,c_i)_\infty[1-\exp(-t/\Theta_i)], \quad (10)$$
$$\Theta_i = l^2/\pi^2 D_i$$

in which $(\text{grad}\,c_i)_\infty$ denotes the concentration gradient in the stationary state, Θ_i a characteristic time, l the length of diffusing species taking in the cell, and D_i the interdiffusing coefficients. Equation (10) states that the time needed to reach the stationary state becomes longer as l becomes longer. For example, in this work it was observed that the time required for attainment of stationary state in the cells (cell B) with $l=32$ and 59 mm, containing the 30 at.% Te solution, is 20 and 65 (—95) min, respectively, after the temperature difference across the cell was kept constant.

Formation of the concentration gradient in cell B also can be confirmed also by observing the absorption spectra, characteristic to some species, for the quenching samples. For instance, the I_2 solution containing 30 at.% Te, which had been in the stationary state under conditions where the temperature difference ΔT is 15° at the average temperature 298°C, was rapidly quenched at the liquid nitrogen temperature, and cut into three parts, corresponding to the cool (C), average (A) and hot (H) regions. The absorption spectra of these parts, measured with a diffuse reflectance method, show an increase in relative peak intensity arising from the existence of the I_3^- ion[3] in the order (C), (A), and (H) (or numerically 1 : 1.14 : 1.36).

The authors wish to express their gratitude to Mr. A. Yoshida for his help at an early stage of this experiment, and to Mr. Kiya for technical services related to the apparatus.

14) D. O. Raleigh and L. E. Topol, *J. Chem. Phys.*, **41**, 3179 (1964).

15) S. R. de Groot, *Physica*, **9**, 699 (1942).

BULLETIN OF THE CHEMICAL SOCIETY OF JAPAN, VOL. 44, 2967—2971 (1971)

Properties of Water in Macromoleular Gels. III. Dilatometric Studies of the Properties of Water in Macromolecular Gels

Masuo AIZAWA and Shuichi SUZUKI

Research Laboratory of Resources Utilization, Tokyo Institute of Technology, Meguro-ku, Tokyo

(Received April 22, 1971)

The dilatometric properties of W_1, W_2, and W_3, which were proposed by the present authors, for the classification of water in macromolecular gels, are studied over the range from −30 to 60°C. From the results of the thermal expansion of agarose gels and Sephadex (cross-linked dextrans), higher water contents of gel were found to show an extremely sharp volume change at 0°C; on the contrary, lower water contents of gel exhibited no anomalous change in the specific volume in the range from −30 to 0°C, and a gradual decrease in the specific volume was detected with an increase in the temperature in the range from −20 to 0°C for medium water contents of the gel, though the gel was expected to increase in its volume in that temperature range. Thus, the new classification for the states of water in macromolecular gels was shown to be reasonable, at the same time, the transition temperatures of W_1, W_2, and W_3 were evaluated on the basis of the above results.

The thermal expansion of water in macromolecular gels, even of W_1, was found to be extremely depressed by the polymers of such gels.

In contrast with the conventional classification of water in macromolecular gels, namely, bound water and free water, the present authors previously proposed that water in gels be classified into three groups, W_1, W_2, and W_3, according to its electrochemical properties, where both W_1 and W_2 correspond to conventional free water, and W_3, to bound water.[1,2]

Most physicochemical properties of ordinary water

1) J. Mizuguchi, M. Takahashi, and M. Aizawa, *Nippon Kagaku Zasshi* **91**, 723 (1970).

2) J. Mizuguchi, M. Takahashi, and M. Aizawa, *ibid.*, **91**, 961 (1970).

are well known to change markedly at 0°C. For example, the electric conductivity for high water contents of agarose gel was found to change greatly at 0°C and to decrease gradually with a decrease in the temperature below 0°C, while that for lower water contents of gel shows no marked change at 0°C, but decreases linearly with a decrease in the temperature. Therefore, various states of water with different transition temperatures are speculated to coexist in gels.[1)]

Since W_1, W_2, and W_3 are all supposed to have different transition temperatures, the thermal expansion for varied water contents of agarose gels is expected to be quite different from case to case. In addition, the above W_2 and W_3 were found to have different properties from those of ordinary water, but no difference from ordinary water was detected in W_1 throughout the electrochemical investigations. In W_1, however, the gels are prevented from flowing out. Therefore, the thermal expansion of water is considered to be obstructed in macromolecular gels, which are constructed of a network of macromolecules.

In view of the above facts, the dilatometric properties, especially those of water at lower temperatures, for typical polysaccharide gels, such as agarose gels and cross-linked dextran gels have been investigated over the range from −30 to 60°C, and this has been with the thermal expansion of ordinary water.

Experimental

Materials. The agarose for immuno-electrophoresis, Sephadex G-10, G-50, and G-200 (cross-linked dextrans purchased from Pharmacia) were prepared for gels with various water contents.

The gels were assayed for their water contents by weighing them after drying at 105°C for 24 hr.

Glossary of Principal Symbols. The definition of the principal symbols used in the report are as follows: s, the capillary sectional area of the dilatometer (cm^2); v_{Hg25}, the volume of mercury at 25°C (cm^3); α_{Hg}, the thermal expansion coefficient of mercury (1.34×10^{-5} $degree^{-1}$); t, the temperature (°C); m_s, the weight of the sample (g); p, and w, the weight fractions of polymer and water respectively in the sample, $p+w=1$; h, the mercury height difference in the dilatometer between t and 25°C (cm); $\Delta\Phi_g$, $\Delta\Phi_{wg}$, and $\Delta\Phi_w$, the specific volume changes in the gel, in the water in the gel, and in pure water respectively, as compared with the corresponding specific volume at 25°C (cm^3/g).

Methods. In the thermal-expansion measurements, the above gels were determined for their volume over the range from 25 to −30°C by means of a dilatometer filled with the sample and mercury. The apparent specific volume change, $\Delta\Phi_g$ of the gel was calculated in accordance with the following equation.[3)]

$$\Delta\Phi_g = \{h-(1/s)\alpha_{Hg}V_{Hg25}(t-25)\}s/m_s \qquad (1)$$

Results and Discussion

Hysteresis in the Thermal Expansion of Macromolecular Gels. To profile the general features of the thermal expansion of macromolecular gels, Sephadex G-200, G-50, and G-10 at the same water fraction ($w=0.50$) were measured for their volume changes with an increase and with a decrease in the temperature over the range from 25 to −30°C. The results are presented in Figs. 1, 2, and 3. The specific volume change is de-

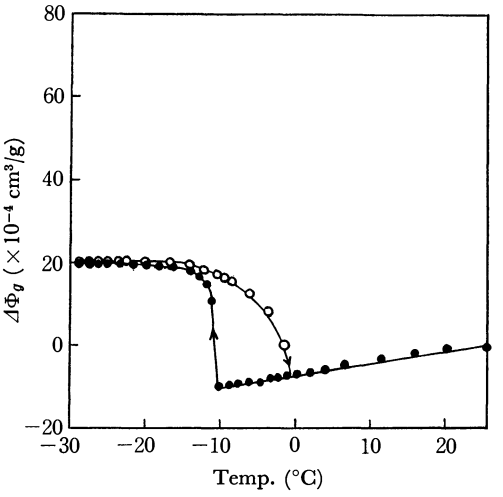

Fig. 1. Hysteresis in thermal expansion of Sephadex G-200 gel ($w=0.50$)

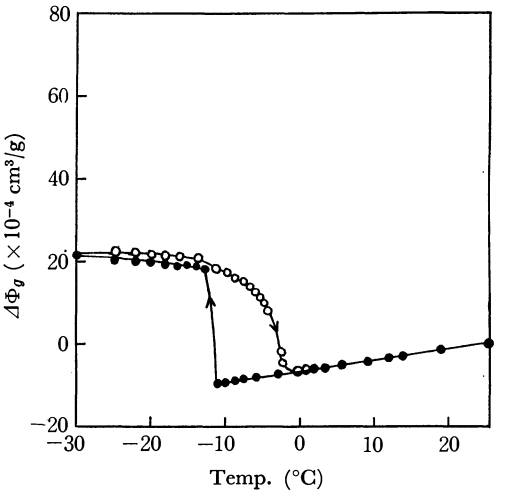

Fig. 2. Hysteresis in thermal expansion of Sephadex G-50 gel ($w=0.500$)

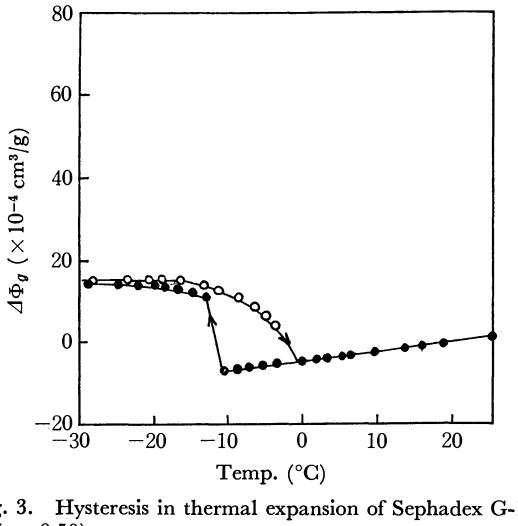

Fig. 3. Hysteresis in thermal expansion of Sephadex G-10 gel ($w=0.50$)

3) Soc. Polymer Sci. Japan, ed., "Experimental Polymer Science. IV", Kyoritsu, Tokyo (1961) p. 43.

noted by the coordinate, taking 25°C as the standard temperature. The specific volume for each gel decreases upon cooling, there is an abrupt increase at approximately −10°C and a gradual decrease with a decrease in the temperature to −30°C. The specific volume of the above gel cooled at −30°C shows a gradual increase with an elevation in the temperatures, even around −10°C, though it decreases markedly near 0°C.

Sephadex gels were found to show hysteresis in thermal expansion over the range of approximately −10 to 0°C.

Relationship between Water Content and the Thermal Expansion of Macromolecular Gels. The thermal expansion of gels is expected to be extremely dependent on the water content as has been described above.

The specific volume changes for agarose are presented in Figs. 4, 5, and 6. The curve with closed circles shows the specific volume change with a decrease in the temperature, while the curve with open circles indicates that with an increase in the temperature. In agarose gel with a higher water content (w=0.974),

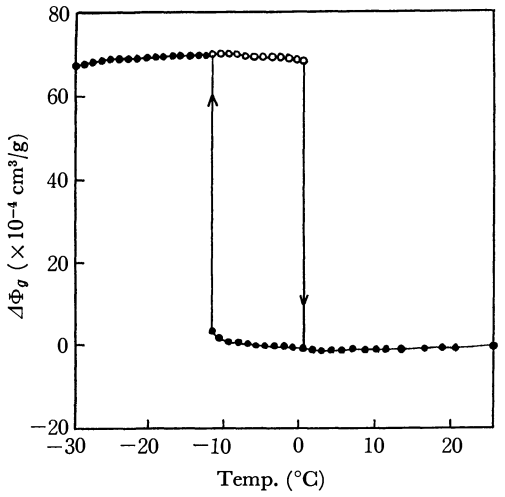

Fig. 4. Hysteresis in thermal expansion of agarose gel (w= 0.974)

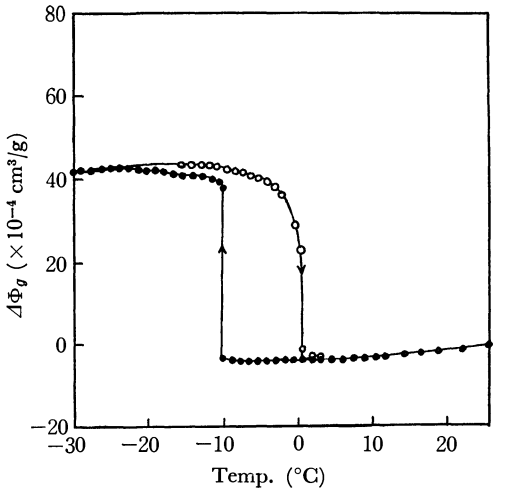

Fig. 5. Hysteresis in thermal expnsion of agarose gel (w= 0.772)

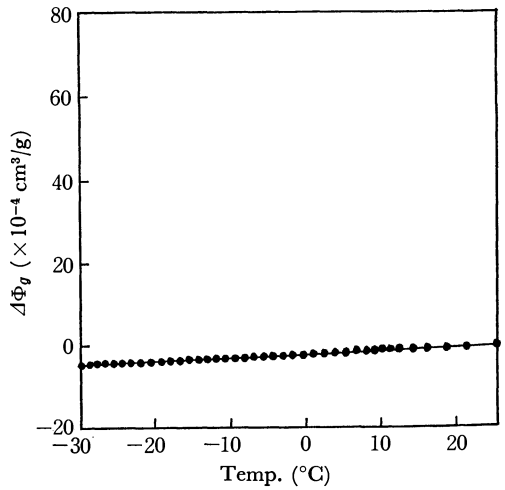

Fig. 6. Hysteresis in thermal expansion of agarose gel (w= 0.290)

the specific volume changes sharply at about −10°C with a decrease in the temperature and at 0°C with a decrease in the temperature. As for the gel whose water fraction is 0.974, it is notable that the specific volume decreases gradually with an increase in the temperature over the range from −20 to 0°C, though it was expected to increase in this temperature range. On the contrary, the agarose gel with a lower water content (w=0.290) shows neither hysteresis in thermal expansion nor any anomalous change in the specific volume around 0°C.

In Fig. 7, the thermal expansions of Sephadex G-50 at various water contents (w=0.833, 0.500, and 0.288) with an increase in the temperature from −30°C up to 25°C are shown. The gel with a lower water content (w=0.288) shows no marked change around 0°C, much like the agarose gel with a lower water content. On the other hand, the specific volumes for the other two gels (w=0.500 and 0.833) decrease gradually over the range from −20 to 0°C.

Since no anomalous change was detected for gels with lower water contents, the water in such gels is considered to show no transition in this temperature range. Most

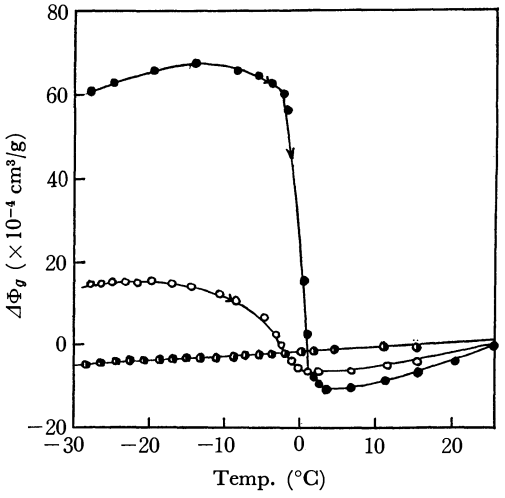

Fig. 7. Thermal expansion of Sephadex G-50 gels -●- w=0.833, -○- w=0.500, -◑- w=0.288

of the water in such lower-water-content gels is supposed to be w_3, as is indicated previously. Therefore, w_3 may have no transition over the range from −30 to 0°C.

Judging from the extremely sharp change in the specific volume for higher water contents of the gel, the transition temperature of w_1 may be 0°C, for w_1 is presumed to be the main component of the gel in higher water contents.

The gradual decrease in the specific volume with an increase in the temperature over the range from −20 to 0°C is considered to indicate that the transition temperatures, perhaps for w_2, should be distributed over this temperature range.

These results lead us to conclude that: (1) the transition temperature of w_1 may be 0°C, (2) that of w_2 may be distributed over the range from −20 to 0°C, and (3) w_3 may have no transition temperature in the range from −30 to 0°C. The above conclusions quite agree with those of electrochemical studies.

Thermal Expansion of Water in Macromolecular Gels. The apparent specific volume changes for agarose gels are shown in Fig. 8. The dotted curve in Fig. 8 presents the specific volume change for pure water. The thermal expansion of agarose gels was found to depend greatly on their water contents and to be extremely retarded as compared with that of ordinary water. In order to evaluate the thermal expansion of water in gels, the apparent specific volume changes, $\Delta\Phi_{w_g}$ were calculated on the basis of the following equation;[4]

$$\Delta\Phi_{wg} = (\Delta\Phi_g - p\Delta\Phi_p)/w \qquad (2)$$

Where the symbols are as defined in the glossary. The specific volume change, $\Delta\Phi_w$, for ordinary water was determined from its specific volume,[5] Φ_w, at the temperature t, which was expressed by

$$\Phi_w = (1+b_1t)/(\sum_{n=0}^{5} a_nt^n) \qquad (3)$$

$a_0 = 0.9998396$ $10^3a_1 = 78.224944$ $10^6a_2 = -7.922210$
$10^9a_3 = -55.44846$ $10^{12}a_4 = 149.7562$ $10^{15}a_5 = -393.2952$
$10^3b_1 = 18.159725$,

$\Delta\Phi_p$ was measured for dried agarose or Sephadex.

The calculated specific volume changes in the water in agarose gels are listed in Tables 1, 2, and 3. The data in the fifth column in each table concern the apparent specific volume change in the water in the gel relative to that of ordinary water at the temperature t.

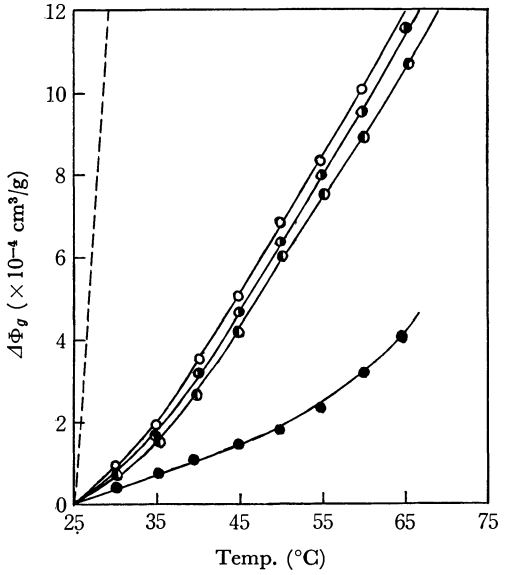

Fig. 8. Thermal expansion of agarose gels
------ ordinary water,
-○- agarose gel (w=0.974)
-◑- agarose gel (w=0.952)
-◐- agarose gel (w=0.772)
-●- agarose gel (w=0.290)

Table 1. Thermal expansion of water in agarose gel (w=0.974)

t(C°)	$\Delta\Phi_g$ ($\times 10^{-4}$ cm³/g)	$p\Delta\Phi_p$ ($\times 10^{-4}$ cm³/g)	$\Delta\Phi_{w_g}$ ($\times 10^{-4}$ cm³/g)	$\Delta\Phi_{w_g}/\Delta\Phi_w$
25.0	0	—	—	—
30.0	0.97	0.01	0.99	0.07
35.0	1.90	0.02	1.94	0.07
40.0	3.51	0.02	3.58	0.07
45.0	4.93	0.03	5.03	0.07
50.0	6.83	0.04	6.99	0.07
55.0	8.02	0.05	8.18	0.07
60.0	10.30	0.06	10.50	0.07

Table 2. Thermal expansion of water in agarose gel (w=0.772)

t(°C)	$\Delta\Phi_g$ ($\times 10^{-3}$ cm³/g)	$p\Delta\Phi_p$ ($\times 10^{-4}$ cm³/g)	$\Delta\Phi_{w_g}$ ($\times 10^{-4}$ cm³/g)	$\Delta\Phi_{w_g}/\Delta\Phi_w$
25.0	0	—	—	—
30.0	0.83	0.05	1.01	0.07
35.0	1.76	0.13	2.12	0.07
40.0	2.70	0.18	3.28	0.07
45.0	4.22	0.25	5.12	0.07
50.0	5.98	0.32	7.35	0.07
55.0	7.57	0.41	9.28	0.07
60.0	8.75	0.56	10.60	0.07

Table 3. Thermal expandsion of water in agarose gel (w=0.290)

t(°C)	$\Delta\Phi_g$ ($\times 10^{-4}$ cm³/g)	$p\Delta\Phi_p$ ($\times 10^{-4}$ cm³/g)	$\Delta\Phi_{w_g}$ ($\times 10^{-4}$ cm³/g)	$\Delta\Phi_{w_g}/\Delta\Phi_w$
25.0	0	—	—	—
30.0	0.35	0.16	0.66	0.05
35.0	0.70	0.40	1.04	0.03
40.0	1.05	0.55	1.75	0.03
45.0	1.40	0.78	2.14	0.03
50.0	1.75	1.00	2.59	0.03
55.0	2.30	1.26	3.60	0.03
60.0	2.14	1.74	4.85	0.03

For agarose gels, the $\Delta\Phi_{w_g}/\Delta\Phi_w$ ratios in all cases deviate greatly from 1.0. The thermal expansions of water in gels with high water contents may be retarded to approximately 7%, and that in lower-water-content gels, to approximately 3%, as compared with that in ordinary water.

4) S. Pocsik, *Acta Biochim. Biophys. Acad. Sci. Hung.*, **4**, 395 (1969).
5) G. S. Kell, *J. Chem. Eng. Data*, **12**, 66 (1967).

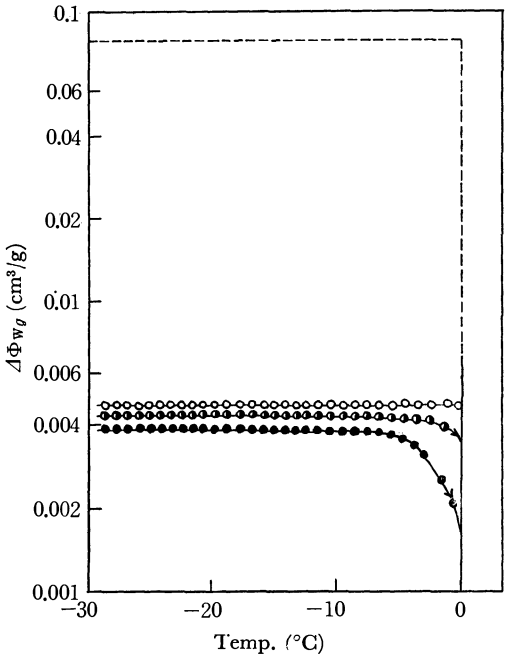

Fig. 9. Thermal expansion of water in agarose gels on the comparison with that of ordinary water.
------ ordinary water
-○- agarose gel (w=0.974)
-◑- agarose gel (w=0.867)
-●- agarose gel (w=0.772)

Since most of the water in lower-water-content gels (w=0.290) may be W_3, thermal expansion coefficient for W_3 can be evaluated as about 3% of that for ordinary water. On the other hand, high-water-content gels (w=0.974 and 0.772) may be occupied much by W_1, and W_2 and little by W_3. Thus, it may be reasonable to conclude that the thermal expansion of most water, even of W_1, is extremely depressed in agarose gels, as was expected.

Volume Change in the Transition of Water in Gels as Compared with That of Ordinary Water. The apparent specific volume change for water in agarose gels is shown in Fig. 9 and compared with that of ordinary water. As is indicated in the figure, the apparent specific volume change in the transition at 0°C for water in gels is extremely retarded to less than 10% of that for ordinary water. Therefore, most of the water in gels may be considered to be obstructed, even in thermal expansion at the transition, by the network of the polymer.

Summary

The dilatometric properties of water in macromolecular gels indicate that our proposed new classification for the states of water, namely, W_1, W_2, and W_3, is reasonable, and that the transition temperature of W_1 may be 0°C, that of W_2 may be distributed over the range from −20 to 0°C, and W_3 may have no transition temperature in the range from −30 to 0°C.

The thermal expansion of most water, even W_1, was found to be extremely depressed in macromolecular gels.

BULLETIN OF THE CHEMICAL SOCIETY OF JAPAN, VOL. 44, 2971—2975 (1971)

Reactions of Aliphatic Amines with *p*-Benzoquinone and Its Chloro Derivatives

Tsuguo YAMAOKA* and Saburo NAGAKURA

The Institute for Solid State Physics, The University of Tokyo, Roppongi, Minato-ku, Tokyo

(Received May 8, 1971)

The reactions of various aliphatic amines with *p*-benzoquinone and its chloro-derivatives were studied by detecting reaction intermediates by means of the rapid scan spectrophotometric method. A detailed kinetic study on the reaction intermediate and the final product was made for the system including *n*-butylamine and chloranil in ethanol; the result shows that the system produces 2,5-di-*n*-butylamino-3,6-dichloro-*p*-benzoquinone *via* the chloranil anion and the *n*-butylamine cation with the rate constant of 9.8×10^2 $sec^{-1}mol^{-1}l$ at 275.2°K. On the basis of reaction mechanisms, the reactions of various aliphatic amines with *p*-benzoquinone and its chloro-derivatives were classified into five types. Stabilization energies due to the amino-substitution of *p*-benzoquinone were calculated by the composite molecule method; the result shows that the 2,5-derivative is most stable among the disubstituted *p*-benzoquinones.

In previous papers,[1] we reported on the interactions of aniline and its *meta*-derivatives with chloranil and concluded that the substitution reactions occur through the outer(π)- and inner(σ)-complexes as reaction intermediates. In these cases, we could find no ion radical as a reaction intermediate. On the other hand, there are many systems consisting of electron donors and acceptors which are led to ionization and produce

* Present address: Department of Printing, Faculty of Engineering, Chiba University, Yayoi-cho, Chiba.

1) T. Nogami, K. Yoshihara, H. Hosoya, and S. Nagakura, *J. Phys. Chem.*, **73**, 2670 (1969); T. Nogami, T. Yamaoka, K. Yoshihara, and S. Nagakura, This Bulletin, **44**, 380 (1971); T. Yamaoka and S. Nagakura, *ibid.*, **43**, 355 (1970).

the anion and cation radicals.[2] Furthermore, in some cases, the substitution or other reactions occur *via* these ion radicals. As an example, Eastman[3] reported that the reaction of *N,N*-dimethylaniline with chloranil proceeds through the ionized state to yield crystal violet.

In a previous paper[4] concerning the interactions of aliphatic amines with quinones, we demonstrated that ionization occurs and a quinone anion exists stably as a final product or transiently as a reaction intermediate. In the present paper, we focus our attention on reaction processes following ionization.

Studies have been carried out to clarify the mechanism of the reaction between alkylamine and quinone,[5] but details are not yet known. The S_N2 mechanism has hitherto been presented[5c] for the reactions of *p*-benzoquinone or its derivatives with alkylamines which act as nucleophilic reagents. In this mechanism, the ionization process is disregarded in the consideration of the reaction mechanism. However, the fact that the anion radicals of quinones exist transiently as a result of the interaction with alkylamines suggests that the reaction can proceed through ionized states. In view of this, we have undertaken to study the reaction mechanism with various systems including aliphatic amines as electron donors and *p*-benzoquinone or its chloro-derivatives as electron acceptors.

Experimental

Materials. *p*-Benzoquinone and chloranil were purified by recrystallization and sublimation at reduced pressure. Commercially available *n*-butylamine and tri-*n*-butylamine of GR grade were used without further purification. Their purities were checked by means of gas chromatography technique. Ethanol used as a solvent was refluxed with magnesium ethylate and was distilled. Ethyl ether was distilled after being kept with sodium metal.

Measurement. Electronic absorption spectra at various stages of a reaction path in solution were measured by a Hitachi rapid scan spectrophotometer RSP-2 located at the Institute of Industrial Science, The University of Tokyo. The apparatus is equipped with an automatically controlled mixing cell. Spectra could be measured every 1/3 sec in the wavelength range from 200 nm to 700 nm.

Results and Discussion

Rapid Scan Spectra of Systems Consisting of Alkylamines and Quinones. In order to clarify the mechanisms of reactions of aliphatic amines with *p*-benzoquinone and its chloro-derivatives in polar solvents, we measured the changes of absorption spectra with time by the rapid scan spectrophotometric method. First, let us explain the results obtained with the ethanol solution containing *p*-benzoquinone and *n*-butylamine ($BuNH_2$). As is seen in Fig. 1, the system shows a couple of peaks at 320 nm and 420—440 nm in the spectrum 1/3 sec after mixing. The peak intensities increase in parallel with each other up to 1 sec after mixing and afterward decrease gradually. As these peaks decrease in intensity, new absorption bands appear at 350 and 480 nm. The initial absorption spectrum is undoubtedly due to the *p*-benzoquinone anion radical judging from its position and shape in literature.[6] The final spectrum coincides with that of 2,5-dibutylamino-*p*-benzoquinone given in literature.[7] These facts show that electron transfer occurs from amine to quinone prior to the formation of 2,5-dibutylamino-*p*-benzoquinone. It should be noticed that the spectrum due to mono-butylaminated *p*-benzoquinone can not be observed. A similar time dependency of absorption spectra was also observed for the ethanol solutions including *n*-butylamine-2,5-dichloro-*p*-benzoquinone, *n*-butylamine-chloranil, and methylamine-*p*-benzoquinone. The reaction mechanism was studied in detail for the *n*-butylamine-chloranil system.

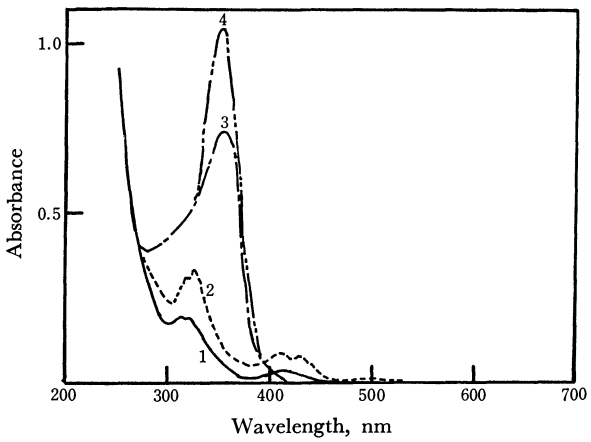

Fig. 1. Rapid scan spectra observed with the ethanol solution containing *n*-butylamine (5.1×10^{-2} mol/*l*) and *p*-benzoquinone (3.1×10^{-5} mol/*l*). Curves 1, 2, and 3 are the spectra measured 1/3 sec, 1 sec, and 10 sec, respectively, after the mixing, and curve 4 is the spectrum of the final product.

When trimethylamine is mixed with chloranil in ethanol, the absorption due to the chloranil anion radical rapidly appears. With the decrease of this absorption, an intense absorption occurs at 545 nm, which is due to 2-dimethylamino-3,5,6-trichloro-*p*-benzoquinone judging from its position and intensity.[7] As this absorption decreases in intensity, there appears the spectrum of the final product. This spectrum is the same as that of 2,5-bis(dimethylamino)-3,6-dichloro-*p*-benzoquinone given in literature.[7] This system is an example in which the absorptions due to the anion radical, the mono-alkylaminated quinone, and the final dialkylaminated product are separately observed with the progress of the reaction. Similar changes in ab-

2) Z. Rappoport, *J. Chem. Soc.*, **1963**, 4498; E. M. Kosower, "Progress in Physical Organic Chemistry," Vol. 3, ed. by S. G. Cohen *et al.*, Interscience Publisher, New York (1965), p. 81.

3) J. W. Eastman, G. Engelsma, and M. Calvin, *J. Amer. Chem. Soc.*, **84**, 1339 (1962).

4) T. Yamaoka and S. Nagakura, This Bulletin, **44**, 1780 (1971).

5) a) B. K. Das and B. Majee, *J. Indian Chem. Soc.*, **45**, 1054 (1968); b) J. Kumanotani, F. Kagawa, A. Hikosaka, and K. Sugita, This Bulletin, **41**, 2118 (1968); c) L. Fieser and M. Fieser, "Advanced Organic Chemistry," Reinhold, New York (1961), p. 853.

6) R. Foster and J. V. Thomson, *Trans. Faraday Soc.*, **59**, 296 (1963).

7) D. Buckley, H. B. Henbest, and P. Slade, *J. Chem. Soc.*, **1957**. 4891.

sorption spectra were also observed for the ethanol solutions containing dimethylamine-*p*-benzoquinone and the diethylamine-*p*-benzoquinone, and for the ethereal solution of methylamine-*p*-benzoquinone.

Tri-*n*-butylamine is ionized by *p*-benzoquinone, 2,5-dichloro-*p*-benzoquinone, and chloranil in such a polar solvent as ethanol but does not cause the substitution reaction.[4] However, trimethylamine reacts with chloranil gradually in ethanol to give 2,5-bis(dimethylamino)-3,6-dichloro-*p*-benzoquinone. This difference in the chemical reactivity between tri-*n*-butylamine and trimethylamine might be due to the great steric hindrance of the *n*-butyl group.

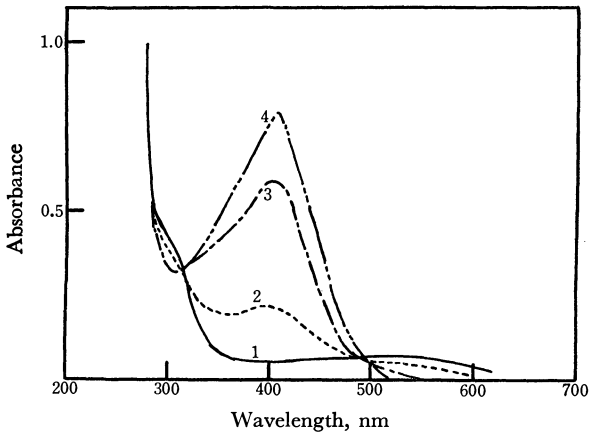

Fig. 2. Rapid scan spectra observed with the ethereal solution containing chloranil (7.9×10^{-5} mol/*l*) and an excess amount of dimethylamine. Curves 1, 2, and 3 are the spectra measured 1/3 sec, 2 sec, and 10 sec respectively, after the mixing, and curve 4 is the spectrum of the final product.

When we use ethyl ether as a solvent instead of ethanol, systems containing electron donors and acceptors show a general tendency for ionization to be difficult. When dimethylamine was mixed with chloranil in ethyl ether, the spectra shown in Fig. 2 were obtained. The absorption peaks appear at 300 and 500 nm in the spectrum 1/3 sec after mixing. These peaks are attributed to 2-dimethylamino-3,5,6-trichloro-*p*-benzoquinone.[7] As their intensities decrease, a new peak due to 2,5-bis(dimethylamino)-3,6-dichloro-*p*-benzoquinone[7] appears at 420 nm. In this case, the absorption of the chloranil anion radical could not be observed. A similar phenomenon was also observed for the ethereal solution containing *n*-butylamine and *p*-benzoquinone.

The ethereal solutions including methylamine-chloranil and *n*-butylamine-2,5-dichloro-*p*-benzoquinone give nothing but the absorption due to the final product, 2,5-dimethyl(or 2,5-di-*n*-butyl)aminated-*p*-benzoquinone.

Classification of the Amine-Quinone Reaction. The spectroscopic changes due to the progress in the reactions between alkylamines and quinones used as electron donors and acceptors, respectively, are greatly dependent on their properties as well as the polarity of the solvent. According to the present spectroscopic study, the reactions were phenomenologically[8] classified as shown in Table 1. The table clearly shows a general tendency for the spectra of the anion radicals of quinones to be easily observed in some stages of the reactions in ethanolic solutions, but not so in ethereal solutions. This may be due to the fact that the anion radical can be stabilized in such a polar solvent as ethanol. It may be noticed that the dimethylamine-chloranil system does not show the absorption of the

Table 1. Classification of the interactions of aliphatic amines with *p*-benzoquinone and its chloro-derivatives

Type of interaction[a]	System[b]
1) D+A→(D⁺)+A⁻ →(MS)→DS	$BuNH_2$-Q, QCl_2, QCl_4(EtOH) $MeNH_2$-Q(EtOH)
2) D+A→(D⁺)+A⁻ →MS→DS	Me_2NH-Q(EtOH) Me_3N-Q(EtOH) Et_2NH-Q(EtOH) $MeNH_2$-Q(Et_2O)
3) D+A→(D⁺)+A⁻	Bu_3N-Q, QCl_2, QCl_4(EtOH)(Et_2O)
4) D+A→MS→DS	$BuNH_2$-Q(Et_2O) Me_2NH-Q, QCl_2, (Et_2O) Me_2NH-QCl_4(EtOH)
5) D+A→(MS)→DS	Me_2NH-QCl_4(Et_2O) $BuNH_2$-QCl_2(Et_2O)

a) D, A, D⁺, A⁻, MS, and DS represent the electron donor, the electron acceptor, the donor cation, the acceptor anion, the monosubstituted species, and disubstituted species, respectively. The specimen in parentheses has not yet been observed directly by the spectrophotometric method.

b) Q, QCl_2, and QCl_4 indicate *p*-benzoquinone, 2,5-dichloro-*p*-benzoquinone, and chloranil, respectively. (EtOH) and (Et_2O) indicate that ethanol and ethyl ether are used as solvents.

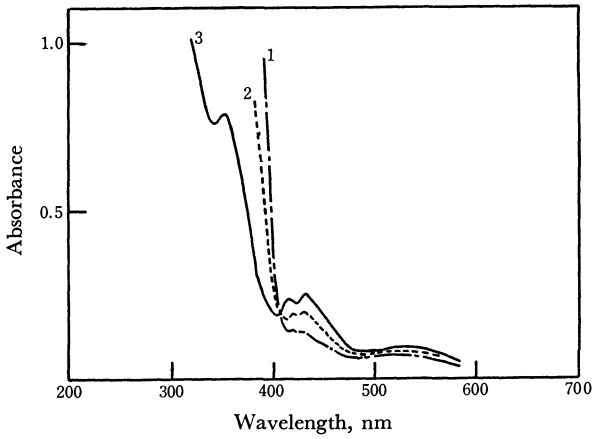

Fig. 3. Rapid scan spectra observed with the ethanol solution containing *n*-butylamine (5.1×10^{-2} mol/*l*) and chloranil (5.0×10^{-5} mol/*l*). Curves 1, 2, and 3 are the spectra measured 1/3 sec, 10 sec, and 40 sec respectively, after the mixing.

8) This classification is made on the basis of the spectroscopic behaviors observed for the systems containing aliphatic amines and *p*-benzoquinone or its chloro-derivatives. This is inevitable at the present stage when the reaction mechanism for the systems belonging to classes (4) and (5) is not yet clarified. Some minor modifications might be necessary when we succeed in clarifying it, though very difficult. For example, the Me_2NH-QCl_4(EtOH) system might move to class (2).

chloranil anion radical even in ethanol, in spite of the fact that the system containing dimethylamine and benzoquinone which is weaker as an electron acceptor than chloranil is ionized in ethanol. Although the reason for this is not clear, it may probably be due to the fact that the ionization process is slower than the succeeding substitution reaction process.

Reaction of n-*Butylamine and Chloranil.* Let us explain the reaction processes in detail, taking the ethanol solution containing *n*-butylamine and chloranil as an example. The time-dependence of the spectrum observed for this system is shown in Fig. 3. In the spectrum 1/3 sec after the mixing, the absorption of the chloranil anion radical[6] can clearly be observed at 420—450 nm. With the decrease in absorption intensity, a new peak due to 2,5-di-*n*-butylamino-3,6-dichloro-*p*-benzoquinone[7] appears, andthe isosbestic point is found at 410 nm. Thus, the following mechanism is proposed for the reaction of *n*-butylamine with chloranil. Here the first step of the reaction is

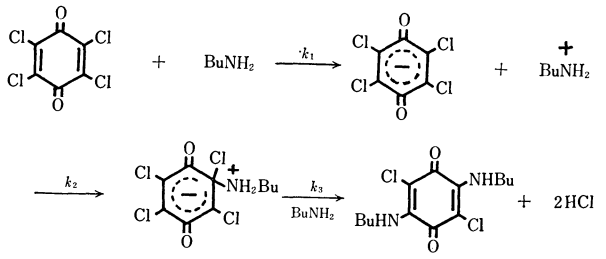

the electron transfer from *n*-butylamine to chloranil to form the anion radical. In the second step, the chloranil anion radical reacts with the *n*-butylamine cation to produce 2-*n*-butylamino-3,5,6-trichloro-*p*-benzoquinone,[7] which reacts further with *n*-butylamine to yield 2,5-di-*n*-butylamine-3,6-dichloro-*p*-benzoquinone.

In order to confirm the mechanism, we carried out a kinetic study for the *n*-butylamine-chloranil system. According to the above mechanism, the rate equation concerning the chloranil anion is given as follows:

$$\begin{aligned} d[Q^-]/dt &= k_1[A][Q] - k_2[Q^-]^2 \\ &= k_1'[Q] - k_2[Q^-]^2 \end{aligned} \quad (1)$$

where [A], [Q], and [Q^-] are the concentrations of *n*-butylamine, chloranil, and the chloranil anion radical, respectively. In our system, [A]>[Q] is satisfied and [A] may be regarded as constant during the reaction. From the time dependence of the peak intensity of the chloranil anion radical, the rate constant for the first step k_1, is known to be apparently much larger than that for the second step k_2. Therefore, after some stage of the reaction, the k_1[A][Q] term in Eq. (1) may be disregarded and we obtain the following equation:

$$k_2t = 1/[Q^-] - 1/[Q_0^-] \quad (2)$$

where [Q_0^-] is the apparent concentration of the chloranil anion radical at $t=0$, the reciprocal of which can be obtained by extrapolating the $1/[Q^-]-t$ relation to the initiation time of the reaction, and may be expected to be almost equal to the initial concentration of chloranil.[9] In the present system, [Q^-] can be determined spectroscopically with considerable accuracy. This is because its absorption spectrum in the 420—450 nm region is not overlapped with the absorptions of the other specimens in this system and the molar extinction coefficient is known.[10] Plotting the observed $1/[Q^-]$ values against reaction time t, we can obtain a straight line as is shown in Fig. 4. This means that Eq. (2) is satisfied and supports the proposed mechanism given by this equation. From the slope of the straight line, the value of k_2 was estimated to be $9.8(\pm0.5)\times10^2$ sec^{-1} mol^{-1} l at 275.2°K.[9]

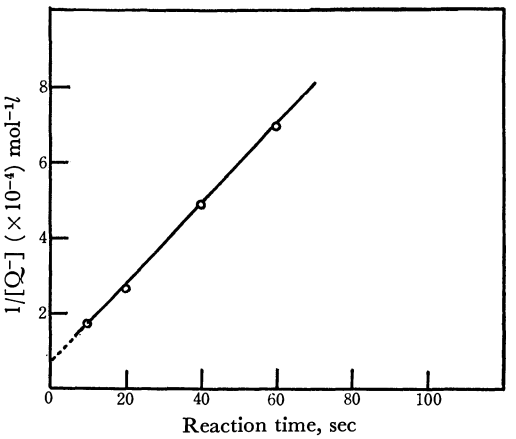

Fig. 4. Plots of the reciprocal of the concentration of the chloranil anion radical against the reaction time. The concentrations of *n*-butylamine and chloranil are 5.05×10^{-2} mol/l and 1.80×10^{-4} mol/l, respectively.

The value of k_2 was also obtained from the rate of the formation of the final product by the aid of the following equation:

$$k_2t = [P]/([Q_0^-]^2 - [Q_0^-][P]) \quad (3)$$

where [P] is the concentration of the final product. Equation (3) can be derived by combining Eq. (2) with the relation $[Q^-]=[Q_0^-]-[P]$ which is reasonable from the reaction mechanism presented by us. The value of k_2 obtained from the time dependence of the observed [P]'s by the aid of Eq. (3) is $8.5(\pm0.4)\times10^2$ sec^{-1} mol^{-1} l at 275.2°K and is consistent with the value obtained by the aid of Eq. (2) within experimental errors.

It is concluded that the replacement reaction observed for the chloranil-*n*-butylamine system proceeds through the ionic species, the chloranil anion and the *n*-butylamine cation, as reaction intermediates. Thus it may be said that the present study gives experimental support to the electron transfer mechanism for the substitution reaction proposed by one of the authous (S.N.) and Tanaka from the consideration of the molecular orbitals of substrates and reagents.[11]

9) The [Q^-] value obtained from the intercept of the straight line with the ordinate is almost equal to the initial concentration of chloranil. This shows the adequateness of the present treatment and supports the reaction mechanism.

10) N. Sakai, I. Shirotani, and S. Minomura, This Bulletin, **44**, 675 (1971).

11) S. Nagakura and J. Tanaka, This Bulletin, **32**, 734 (1959).

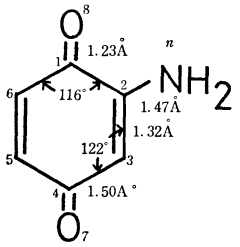

Fig. 5. Geometrical structure and numbering of 2-amino-benzoquinone.

Stabilization Energies of the Aminated p-*Benzoquinones.* The stabilization energies of aminated *p*-benzoquinones were calculated by the composite molecule method.[12] Let us explain the calculation procedure taking 2-amino-*p*-benzoquinone as an example. The system was divided into two components; *p*-benzoquinone and the amino group. The numbering of the atoms and geometry of the molecule are shown in Fig. 5. The Hückel orbitals of *p*-benzoquinone were taken as the component orbitals[13] since they do not differ appreciably from the SCF MO's evaluated by the P-P-P method.[14] The interaction between *p*-benzoquinone and the amino group was taken into account by the configuration interaction between the ground (G), several locally-excited (LE), and charge-transfer (CT) configurations.

The energy of the ground configuration was taken to be standard. The energies of the lowest two locally excited configurations (LE_1, LE_2) were taken to be equal to the observed transition energies corresponding to the first and second bands of *p*-benzoquinone. The energies of CT configurations were calculated by the relation, $I-A+\Delta C$, where I, A, and ΔC represent the ionization potential of amino group (8.40 eV),[15] the electron affinity of *p*-benzoquinone (2.02 eV),[16] and the electrostatic interaction energy between the positive and negative charges caused by an electron transfer from the amino group to *p*-benzoquinone, respectively. The Pariser-Parr approximation[17] was used for evaluating the two center Coulomb repulsion integrals necessary for the evaluation of ΔC. The energies of the configurations are shown in Fig. 6.

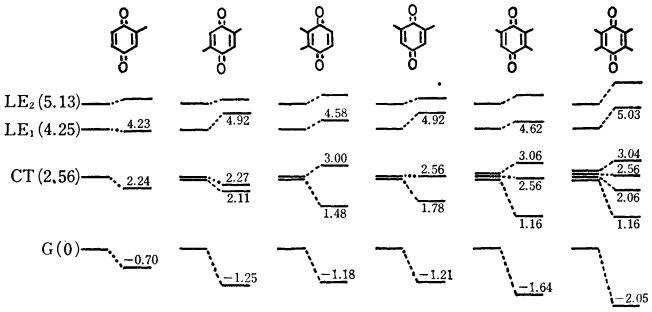

Fig. 6. Configurations used for the composite molecule calculation and the calculated energies (eV) of amino-substituted *p*-benzoquinones. For example, the configurations for 2-amino-*p*-benzoquinone are represented as follows:
$G=|1\,\bar{1}\,2\,\bar{2}\,3\,\bar{3}\,n\,\bar{n}|$ $LE_1=0.9794\,\Phi\,(3\to5)-0.2021\,\Phi(4\to6)$
$LE_2=\Phi\,(3\to6)$
$CT=\Phi\,(n\to4)$
where, $\Phi\,(a\to b)=\{|1\ldots a\bar{b}\ldots\bar{n}|+|1\ldots b\bar{a}\ldots\bar{n}|\}/\sqrt{2}$
and 1, 2,... are the Hückel MO's of *p*-benzoquinone, and n is the 2p AO of amino-nitrogen.

The non-zero off-diagonal matrix elements for each of the interactions between the CT configurations and the G or LE configurations can be represented by the aid of the resonance integral β_{CN} between the neighboring nitrogen and carbon atoms. The value was taken to be −2.0 eV after several trial calculations.

The stabilization energies of *p*-benzoquinone caused by the amino substitutions were evaluated as the difference in energy between the ground configuration and the calculated lowest state. The results are shown in Fig. 6. We see that the 2,5-isomer is most stable among diaminobenzoquinones. This may be related to the fact that the substitution reaction preferably occurs on the 2,5-positions of *p*-benzoquinone.

We are greatly indebted to Prof. Shigeo Hayano and Dr. Masamichi Fujihira, the Institute for Industrial Science, the University of Tokyo, for permitting us to use the rapid scan spectrophotometer and also for their advice about the rapid scan absorption measurement. One of the authors (T.Y.) would like to thank Prof. Takahiro Tsunoda, Chiba University, for encouragement throughout the study.

12) S. Nagakura, *Mol. Phys.*, **3**, 105 (1960).
13) T. Anno, I. Matsubara, and A. Sado, This Bulletin, **30**, 168 (1957).
14) Private communication from Dr. A. Kuboyama, the Government Chemical Industrial Research Institute, Tokyo.
15) K. Watanabe, T. Nakayama, and J. Mottl, *J. Quant. Spectrosc. Radiat. Transfer.*, **2**, 369 (1962).
16) The Chemical Socieyt of Japan, "Kagaku-Binran, Kiso-hen II," Maruzen, Tokyo (1966), p. 1132.
17) P. Pariser and R. G. Parr, *J. Chem. Phys.*, **21**, 767 (1953).

Semiclassical Calculation of the Vibrational Transition Probabilities of Diatomic Molecules in Collision. The Effect of Vibrational Anharmonicity

Yoshiro YONEZAWA and Takayuki FUENO

Department of Chemistry, Faculty of Engineering Science, Osaka University, Toyonaka, Osaka

(Received May 10, 1971)

The multi-state semiclassical method proposed by Sharp and Rapp for calculating the vibrational transition probabilities of harmonic oscillators in collision was extended to Morse oscillators. Model calculations have been carried out for the excitation of a vibrational ground-state hydrogen molecule colliding with a helium atom at varying relative velocity. It has been shown that the Morse oscillator model gives greater transition probabilities than the corresponding harmonic oscillator model.

The basic problem in quantitative investigations of molecular excitation processes involved in chemical reactions is to calculate the vibrational transition probabilities P_{ij} for a target molecule undergoing a transition from an initial state i to a final state j due to perturbation by incident particles. For the calculation of such probabilities, several theoretical treatments based on the classical, semiclassical, and quantum-mechanical approximations have been published.[1)]

The purpose of the present work is to examine the effects of anharmonicity of molecular vibration on the transition probability. To this end, the multi-state semiclassical theory presented by Sharp and Rapp[2)] has been extended to the treatment of Morse-type diatomic oscillators. A computer program was written out and applied to the vibrational excitation of a ground-state hydrogen molecule colliding with a helium atom at temperatures 1000—5000°K. It has been shown that even for lower level transitions a Morse oscillator model leads to transition probabilities several times greater than those obtained from the harmonic oscillator model.

Method of Calculation

We shall deal with a head-on collision between a mass point A and a diatomic molecule BC. The coordinate system is defined in Fig. 1. Two coordinates which characterize the collision are x, the distance between A and the center of mass of BC, and y, the internuclear separation of BC. The intramolecular potential $U(y)$ is approximated by the harmonic or Morse potential, both of which have well-known energy eigenvalues and eigenfunctions.

Let us denote the engenvalues and eigenfunctions of unperturbed oscillator hamiltonian H_0 by E_n and ϕ_n.

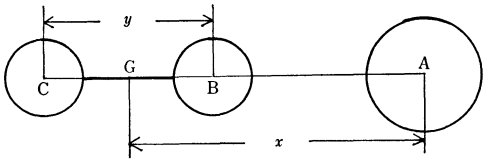

Fig. 1. Coordinate system for the one-dimensional collision between a BC molecule and an incident particle A.

When BC is a harmonic oscillator, we have

$$U_H(y) = \frac{1}{2}\mu\omega^2(y-y_e)^2 \tag{1}$$

$$E_n = \left(n+\frac{1}{2}\right)\hbar\omega \tag{2}$$

$$\phi_n(q) = M_n H_n(\sqrt{\alpha}q)\exp\left(-\frac{1}{2}\alpha q^2\right), \tag{3}$$

where ω is the angular frequency of the oscillator, y_e the equilibrium distance, H_n the Hermite polynomial, $q=y-y_e$ the instantaneous displacement of the oscillator, and μ, α, and M_n are quantities defined as follows:

$$\mu = m_B m_C/(m_B+m_C) \tag{4}$$

$$\alpha = \mu\omega/\hbar \tag{5}$$

$$M_n = (\alpha/\pi)^{1/4}/(2^n n!)^{1/2}. \tag{6}$$

When BC is a Morse oscillator, we can write[3)]

$$U_M(y) = D_e[\exp\{-a(y-y_e)\}-1]^2 \tag{7}$$

$$E_n = \frac{4}{\beta}D_e\left\{\left(n+\frac{1}{2}\right)-\left(n+\frac{1}{2}\right)^2/\beta\right\} \tag{8}$$

$$\phi_n(s) = N_n(-1)^n\Gamma(\beta-n)\exp(-s/2)s^{(\beta/2-n-1/2)} \tag{9}$$

$$\text{for } n = 0, 1, \cdots < (\beta-1)/2.$$

In Eq. (9), Γ(x) is the gamma function and

$$\beta = (8\mu D_e)^{1/2}/\hbar a \tag{10}$$

$$s = \beta\exp(-aq) \tag{11}$$

$$N_n = \{(\beta-1-2n)a/n!\Gamma(\beta-n)\}^{1/2}. \tag{12}$$

The intermolecular potential $V(x, y)$ is assumed to be of the simple exponential repulsion type:

$$V(x,y) = C\exp\left\{-\left(X-\frac{m_C}{m_B+m_C}y\right)/R\right\} \tag{13}$$

with the collision length R. In the semiclassical method the effect of energy transfer upon the trajectory of A is usually ignored, so that $V(x, y)$ is reduced to the following form:

$$V(X, Y) = E\exp\left(-\frac{X(t)}{R}\right)\exp\left(\frac{m_C}{m_B+m_C}\cdot\frac{Y}{R}\right) \tag{14}$$

where

$$X = x - x_T \tag{15}$$

$$Y = y - y_T \tag{16}$$

$$E = \frac{1}{2}mv^2 \tag{17}$$

1) For review, see D. Rapp, and T. Kassel, *Chem. Revs.*, **69**, 61 (1969).

2) T. E. Sharp and D. Rapp, *J. Chem. Phys.*, **43**, 1233 (1965).

3) F. H. Mies, *ibid.*, **40**, 523 (1964).

$$m = m_A(m_B+m_C)/(m_A+m_B+m_C), \quad (18)$$

x_T and y_T being the values of x and y at the classical turning point in the relative motion of A to BC, and v the relative incident velocity. Reduction of Eq. (13) to Eq. (14) is justified when the total energy exchange ΔE is a small fraction of the relative translational energy E.

The classical trajectory $X(t)$ as a function of time t for the present collision model is obtained by neglecting the vibration of BC and solving the classical equation of motion

$$\frac{1}{2}m\left(\frac{dX}{dt}\right)^2 + E\exp(-X/R) = E. \quad (19)$$

The analytical solution of this equation is well-known, but we have made a computation program to solve it numerically, as we intend it to be useful for any assumed form of intermolecular potential between A and BC.

The behavior of the oscillator under the influence of intermolecular interaction can be traced by solving the time-dependent Schrödinger equation

$$\{H_0+V(t, Y)\}\Psi = i\hbar\frac{\partial\Psi}{\partial t}, \quad (20)$$

where $V(t, Y)$ involving t instead of X as a variable constitutes the time-dependent perturbation toward the oscillator.

The time-dependent wavefunction $\Psi(t)$ of the oscillator can be expanded with the complete set $[\phi_n(q)]$. Thus

$$\Psi(t) = \sum_n a_n(t)\phi_n(q)\exp(-iE_nt/\hbar). \quad (21)$$

Insertion of Eq. (21) into Eq. (20) gives

$$\frac{da_j}{dt} = \frac{1}{i\hbar}\sum_n a_n(t)V_{nj}(t)\exp\{-i(E_n-E_j)t/\hbar\}, \quad (22)$$

where $V_{nj}(t)$ is defined by

$$V_{nj}(t) = \int\phi_n(q)V(t, Y)\phi_j(q)dq. \quad (23)$$

In order to evaluate Eq. (23), Y must be related to the oscillator coordinate q for every collision of varying initial phase angle of the oscillator. To avoid this complexity in procedure, we have made use of an averaging convention by setting

$$Y = q - \langle q\rangle_n \quad (24)$$

for the initial nth vibrational state of the oscillator, where

$$\langle q\rangle_n = \int\phi_n(q)q\phi_n(q)dq, \quad (25)$$

which represents the average displacement from the equilibrium nuclear separation of the oscillator in the nth level. Integration of Eq. (25) was carried out numerically for the Morse oscillator using Simpson's integration formula. Note that for a harmonic oscillator $\langle q\rangle_n=0$.

On the above assumption, the factor $V_{nj}(t)$ can be written as

$$V_{nj}(t) = U_{nj}E\exp\{-X(t)/R\}\exp\left(-\frac{m_C}{m_B+m_C}\cdot\frac{\langle q\rangle_n}{R}\right), \quad (26)$$

where U_{nj} is a vibrational matrix element defined by

$$U_{nj} = \int\phi_n(q)\left\{\exp\left(\frac{m_C}{m_B+m_C}\cdot\frac{q}{R}\right)\right\}\phi_j(q)dq. \quad (27)$$

When BC is a harmonic oscillator, Eq. (27) is reduced to[2]

$$U_{ij} = \{\exp(\Delta^2)\}(2^{i-j}i!/j!)^{1/2}\Delta^{i-j}L_i^{(j-i)}(-2\Delta^2), \quad (28)$$

where $L_i^{(j-i)}$ is a generalized Laguerre polynomial and

$$\Delta = \{m_C\hbar/m_B(m_B+m_C)\omega\}^{1/2}/2R. \quad (29)$$

When BC is a Morse oscillator, Eq. (27) takes the form[3]

$$U_{ij} = \{\beta^\eta N_iN_ji!\Gamma(\beta-i)/a\} \times\sum_{m=0}^{i}\frac{(-1)^{m+i-j}\Gamma(1+\eta+i-m)\Gamma(\beta-1-\eta-i-j+m)}{m!(i-m)!\Gamma(1+\eta+i-j-m)\Gamma(\beta-2i+m)}, \quad (30)$$

where

$$\eta = m_C/(m_B+m_C)Ra. \quad (31)$$

To obtain the transition probability P_{ij}, we must solve Eq. (22) for a_i.

For this purpose we used the Runge-Kutta-Gill method retaining lower N vibrational states of the oscillator. If before collision ($t=-\infty$) the molecule BC is in state i, the initial condition for Eq. (22) is $|a_j(-\infty)|^2=\delta_{ij}$. The probability of molecule undergoing the transition to the state j on collision is $P_{ij}=|a_j(+\infty)|^2$.

We have applied the above method of calculation to the excitation of a vibrational ground-state hydrogen molecule colliding with a helium atom at varying incident velocity. The appropriate molecular constants are $m_A=6.64\times10^{-24}$ g, $m_B=m_C=1.673\times10^{-24}$ g, $y_e=0.741$ Å, $\omega=9.378\times10^{14}$ sec^{-1}, $D_e=7.6\times10^{-12}$ erg, and $a=(\mu\omega^2/2D_e)^{1/2}=2.2$ Å^{-1}. R was assumed to be 0.2 Å.

All the numerical procedures were programmed in FORTRAN and calculations were carried out on the FACOM Computer at the Kyoto University Computation Center. Integration of Eq. (22) was started with a distance of 3 Å from the classical turning point and continued until the mass point A passed the 3 Å point on its departure. The integration step size was held below 1.0×10^{-16} sec, which required 1000 to 3000 steps to complete tracing one collision. The number of lower vibrational levels N included for solving Eq. (22) was 6. The incident velocity v was varied between 1.0×10^6 and 4.0×10^6 cm/sec.

Results and Discussion

For calculating the transition probability P_{ij}, it is necessary to evaluate the average displacements $\langle q\rangle_n$ and the vibration matrix elements U_{ij} of the oscillator.

Table 1. The energy levels, E_n, and average displacements, $\langle q\rangle_n$, of H_2

Vibrational state, n	E_n, 10^{-12} erg		$\langle q\rangle_n$, Å	
	Harmonic	Morse	Harmonic	Morse
0	0.4942	0.4862	0	0.0227
1	1.4827	1.4104	0	0.0707
2	2.4711	2.2702	0	0.1229
3	3.4595	3.0659	0	0.1800
4	4.4480	3.7972	0	0.2430
5	5.4364	4.4642	0	0.3130

TABLE 2. VIBRATION MATRIX ELEMENTS, U_{ij}, OF H_2

i	U_{ij}					
	$j=0$	1	2	3	4	5
			Harmonic			
0	1.0212					
1	2.0925×10^{-1}	1.0641				
2	3.0319×10^{-2}	3.0214×10^{-1}	1.1079			
3	3.5869×10^{-3}	5.3249×10^{-2}	3.7776×10^{-1}	1.1526		
4	3.6749×10^{-4}	7.2490×10^{-3}	7.6356×10^{-2}	4.4524×10^{-1}	1.1982	
5	3.3675×10^{-5}	8.2862×10^{-4}	1.1582×10^{-2}	9.9946×10^{-2}	5.0803×10^{-1}	1.2447
			Morse			
0	1.0823					
1	-2.3461×10^{-1}	1.2742				
2	4.3899×10^{-3}	-3.8356×10^{-1}	1.5176			
3	4.3230×10^{-4}	8.8579×10^{-3}	-5.4973×10^{-1}	1.8322		
4	8.0994×10^{-5}	1.0222×10^{-3}	1.4777×10^{-2}	-7.5354×10^{-1}	2.2478	
5	2.1238×10^{-5}	2.1801×10^{-4}	1.9362×10^{-3}	2.2837×10^{-2}	-1.0173	2.8110

Table 1 lists the values of $<q>_n$ together with the energy E_n of the lowest six vibrational levels of a hydrogen molecule in its harmonic and Morse oscillator models. Table 2 gives U_{ij} pertinent to these levels in the harmonic and Morse oscillators.

The fractional populations $|a_j(t)|^2$ of various vibrational levels in a Morse oscillator H_2 molecule are shown in Fig. 2 as a function of time during its collision with an He atom incident with an initial velocity of 1.0×10^6 cm/sec. The H_2 molecule was assumed to be initially on the ground vibrational level. Thus the population of each given level at infinity of time should correspond to the transition probability from zero level to the level in question. It can be seen that P_{01} takes a value of approximately 0.01 on this collision, but the probabilities of transitions to higher levels are negligibly small. This is natural, since the initial velocity chosen in this specific example corresponds to $E_{tr}=1.112\times10^{-12}$ erg, which exceeds the vibrational quantum only slightly, so that none of the 0—2, 0—3, and 0—4 transitions is an energetically attainable transition in a classical-mechanical sense. Quantum-mechanically, however, the 2, 3, and 4 levels are all populated appreciably for some short period around $t=0$, which produces an important contribution to the final magnitude of P_{01}.

The transition probabilities P_{01} calculated for the harmonic model of H_2 are shown in Fig. 3 as the functions of collision velocity v. Figure 4 represents similar results obtained for the Morse model. All these probabilities initially increase with increasing v until they attain maximum values, and then decrease oscillatingly with v. Such a behavior is also observed in

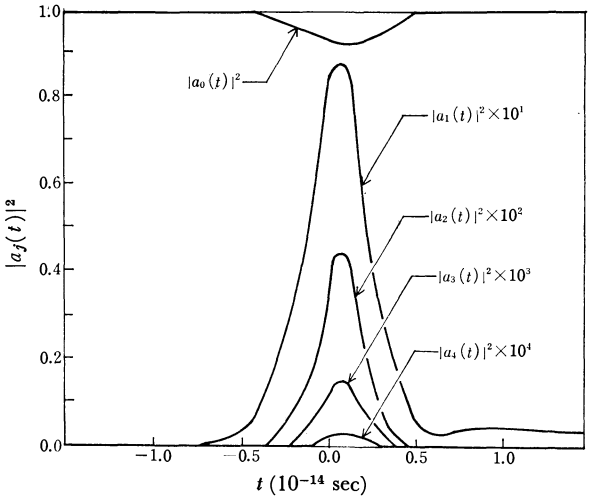

Fig. 2. Population of vibration levels, $|a_j(t)|^2$, as a function of time during a collision of a Morse oscillator H_2 molecule with an incident He.
$|a_j(-\infty)|=\delta_{0j}$; $v=1.0\times10^6$ cm/sec.

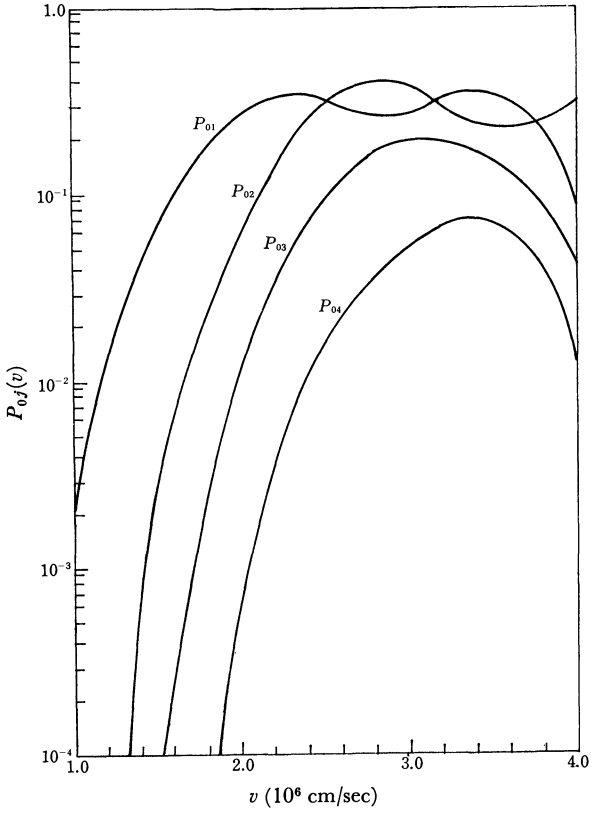

Fig. 3. Vibrational transition probabilities, $P_{1j}(v)$, of a ground-state H_2 (harmonic) molecule on collision with an He atom as the functions of velocity.

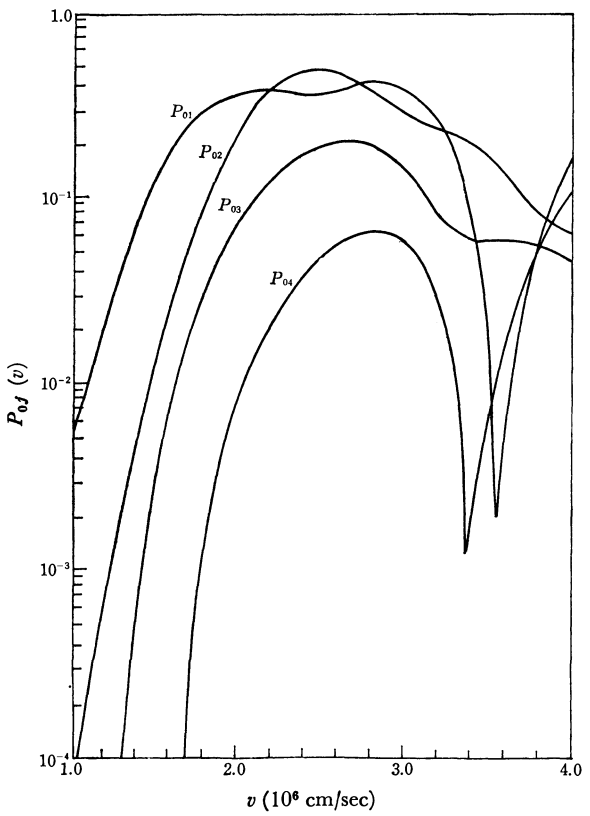

Fig. 4. Vibrational transition probabilities, $P_{ij}(v)$, of a ground-state H_2 (Morse) molecule on a collision with an He atom as the functions of velocity.

both the "exact" classical[4] and quantum-mechanical[5] transition probabilities.

Comparison of Fig. 4 with Fig. 3 shows that the Morse oscillator model leads to greater P_{0j} values than the harmonic model, until the P_{0j}'s calculated from the former model reach maximal values. The results are apparently contradictory to the theoretical demonstration of Mies,[3] who claims that the anharmonicity of diatomic molecules generally reduces the "usually" calculated P_{01} values by a factor of 10^{-1} to 10^{-2}. In order to avoid confusion between these two results, some comments are desirable.

The "anharmonicity factor" proposed by Mies is essentially a correction factor for the conventional adiabaticity assumption $U_{ii}=U_{jj}$, which was invoked in the original two-state distorted-wave approximation (DWA) of Jackson and Mott.[6] In the harmonic oscillator model the assumption is tolerably satisfied. However, if a Morse model is adopted, the assumption becomes no longer justifiable as can be seen in Table 2. Calculations show that use of precisely evaluated U_{ii}'s generally tends to reduce the P_{ij} values. Even in the case of harmonic oscillators, the Jackson-Mott transition probabilities need to be corrected by a factor of 10^0 to $10^{-1.7}$. Thus, in this sense the "anharmonicity factor" might better be termed the "nonadiabaticity correction factor."

In the case of the two-state approximation, the effects of nonadiabaticity are certainly more conspicuous in Morse oscillators than in harmonic oscillators, as Mies emphasizes. Such nonadiabaticity corrections have authomatically been embodied in our multi-state semiclassical treatments. Auxiliary calculations made by forcing all the U_{ii} elements to be 1 have led to the P_{0j} values which are 10^0 to 10^1 times greater than those of more precise calculations. The P_{01} values for the Morse model relative to the harmonic were not altered materially from those given in Figs. 3 and 4. That the Morse model gives greater P_{0j} values than the harmonic model is due primarily to the narrower spacings of the vibrational levels in the former.

The effects of narrow energy level spacings may become clearer in the energy exchange of a highly excited oscillator. We calculated P_{ij} of excited Morse oscillator ($i=10$) at the initial velocity of 1.0×10^{-6}cm/sec. The multi-state semiclassical method gave $P_{10\text{–}11}=0.820$, $P_{10\text{–}12}=0.158$, $P_{10\text{–}13}=0.281$ and $P_{10\text{–}14}=0.102$. The two-state approximation (Jackson-Mott-Mies), on the other hand, resulted in $P_{10\text{–}11}=4.79\times10^{-3}$, $P_{10\text{–}12}=6.22\times10^{-6}$, $P_{10\text{–}13}=9.21\times10^{-4}$, and $P_{10\text{–}14}=1.47\times10^{-4}$. It seems that these values are unreasonably small.

The effects of anharmonicity are thus reflected in both the vibrational matrices U_{ij} and the level heights E_i. Whether the anharmonicity enhances or diminishes the calculated transition probabilitics depends on the approximation used as well as the collision ve-

Table 3. Average transition probabilities, $\langle P_{ij}\rangle$

Transition $i\rightarrow j$	$\langle P_{ij}\rangle$				
	$T=1000$	2000	3000	4000	5000°K
			Harmonic		
0→1	1.544×10^{-6}	1.520×10^{-4}	1.043×10^{-3}	3.210×10^{-3}	6.820×10^{-3}
0→2	7.261×10^{-10}	1.728×10^{-6}	3.505×10^{-5}	2.030×10^{-4}	6.657×10^{-4}
0→3	1.682×10^{-12}	4.254×10^{-8}	1.992×10^{-6}	1.810×10^{-5}	7.872×10^{-5}
0→4	2.852×10^{-15}	9.871×10^{-10}	1.009×10^{-7}	1.303×10^{-6}	6.905×10^{-6}
			Morse		
0→1	3.787×10^{-6}	3.486×10^{-4}	2.256×10^{-3}	6.572×10^{-3}	1.326×10^{-2}
0→2	3.075×10^{-8}	1.405×10^{-5}	1.848×10^{-4}	8.612×10^{-4}	2.447×10^{-3}
0→3	1.505×10^{-11}	3.218×10^{-7}	1.321×10^{-5}	1.090×10^{-4}	4.301×10^{-4}
0→4	1.457×10^{-14}	8.569×10^{-9}	1.090×10^{-6}	1.367×10^{-5}	6.555×10^{-5}

4) J. D. Kelley and M. Wolfsberg, *J. Chem. Phys.*, **44**, 324 (1966).
5) D. Secrest and B. R. Johnson, *ibid.*, **45**, 4556 (1966).
6) J. M. Jackson and N. F. Mott, *Proc. Roy. Soc.*, **A137**, 703 (1932).
7) R. E. Roberts, *J. Chem. Phys.*, **49**, 2880 (1968).

locity chosen.

The 0—j vibrational transition probability averaged over thermal velocity distributions for collisions at a temperature T may be written as

$$\langle P_{0j} \rangle = \int_{v_c}^{\infty} P_{0j}(v) \mathrm{d}n(v), \tag{32}$$

where

$$\mathrm{d}n(v) = (m/kT)v \exp(-mv^2/2kT)\mathrm{d}v \tag{33}$$

and

$$v_c = \{2(E_j - E_0)/m\}^{1/2}. \tag{34}$$

We calculated the $\langle P_{0j} \rangle$ at temperatures 1000—5000°K for every 1000°. The results are given in Table 3, where it may be seen that the $\langle P_{0j} \rangle$ values calculated for the Morse oscillator are always larger than the corresponding values obtained from the harmonic oscillator model.

Our value of $\langle P_{01} \rangle$, 3.486×10^{-4}, calculated for the Morse model at 2000°K agrees well with the value 3.7×10^{-4} which McElwain and Pritchard[8] assumed (based on DWA method) for an anharmonic H_2 molecule at the same temperature. Although the agreement may be fortuitous, the $\langle P_{01} \rangle$ value of *ca.* 10^{-4} will probably be in a correct order of mganitude for the H_2—He system at 2000°K. The $\langle P_{0j} \rangle$ values decrease with the increasing quantum number j of the final state. The decrease is, however, much more moderate than that derived from the usual two-state approximations. The conclusion stresses the need of care in the choice of the $\langle P_{ij} \rangle$ values to be used for high-energy collision processes.

It should be noted that we have used the classical trajectories for the present inelastic collision processes. In the "exact" semiclassical method proposed by Locker and Wilson,[9] the effect of energy exchange on the $X(t)$ and hence on the P_{ij} is evaluated properly. However, the method gives different transition probabilities for different initial phase angles, so that an appropriate averaging procedure is required, if the method is to be really useful for obtaining the average probability on a collision. In our method, on the other hand, such an averaging process is included automatically, though in a crude manner. Thus, our method may be less rigorous but is certainly more tractable than the method of Locker and Wilson.

Conclusion

The multi-state semiclassical method coupled with a proper procedure of averaging the initial vibration phase angles provides a tractable means of evaluating the vibrational transition probabilities of diatomic molecules. When the H_2 molecule is assumed to be a Morse oscillator the probabilties calculated for the H_2 (i=0)—He system at 1000—5000°K are greater than when it is assumed to be harmonic. This seems to have an important bearing with the kinetics of the bimolecular dissociation process of diatomic molecules.

8) D. L. S. McElwain and H. O. Pritchard, *J. Amer. Chem. Soc.*, **91**, 7693 (1969).

9) D. J. Locker and D. J. Wilson, *J. Chem. Phys.*, **52**, 271 (1970).

The Crystal and Molecular Structure of Bis(*o*-ethoxyphenyl)butadiyne

Tooru TAGA,* Norio MASAKI,* Kenji OSAKI,* and Tokunosuke WATANABÉ**

Faculty of Sciences, Osaka University, Osaka

(Received May 15, 1971)

The crystal structure of bis(*o*-ethoxyphenyl)butadiyne has been determined by the statistical method of X-ray analysis. The space group is $P2_1/a$ with two molecules in the unit cell of dimensions $a=14.64$, $b=11.27$, $c=5.19$ Å, and $\beta=105.6°$. The crystal structure is built up from columns of the molecules packed along the *c*-axis. The molecule has a center of symmetry and is almost planar. The diacetylene group is slightly twisted and the three conjugated bond distances of the diacetylene group are 1.434, 1.201, and 1.371 Å.

This is the first paper of a series on the crystal structure of ω,ω'-diphenylpolyynes and their derivatives. A short note on the crystal structure of ω,ω'-diphenyltetrayne and ω,ω'-diphenylpentayne has been repotred by Watanabé, Taguchi, and Masaki.[1]

In a number of papers dealing with the molecular structure of compounds containing the diacetylene group,[2-11] it was reported that the carbon atoms of the diacetylene group are almost linear, and the three conjugated diacetylene bonds lie between 1.44—1.47 Å for the side C–C, 1.18—1.21 Å for the triple C–C and 1.33—1.39 Å for the central C–C bonds, respectively.

The aim of this investigation is to provide accurate values for bond distances and angles in the molecule of bis(*o*-ethoxyphenyl)butadiyne using three-dimensional data. The influence of the ethoxy group substituted in the phenyl ring on the molecular structure as well as on the molecular packing was also investigated.

Experimental

Crystals for the experiment were obtained from ethanol solution. They are monoclinic, colorless needles elongated along the direction of the *c*-axis. The crystallographic data and some physical properties are listed in Table 1. The cell dimensions were determined from Weissenberg and oscillation photographs about the *c*-axis and the space group was determined unambiguously from the systematic absence of reflections. The crystal density was measured by the flotation method in ammonium chloride solutions, and was in good agreement with the calculated density value assuming two molecules per unit cell.

Table 1. CRYSTALLOGRAPHIC DATA

Bis(*o*-ethoxyphenyl)butadiyne $C_{20}H_{18}O_2$	
Molecular Weight=290.4	
Monoclinic, Melting Point=72°C	
Space Group $P2_1/a$ (No.14), $Z=2$	
Cell Dimensions	$a=14.64\pm0.01$ Å
	$b=11.27\pm0.06$ Å
	$c=5.194\pm0.003$ Å
	$\beta=105.6\pm0.3°$
	$V=825.9$ Å^3
$D_m=1.17$ g·cm^{-3}, $D_x=1.168$ g·cm^{-3}	
$\mu=6.16$ cm^{-1} (for *Cu* $K\alpha$), $F_{000}=308$	
Systematic absences of the reflections;	
$h0l$ for $h=2n+1$, $0k0$ for $k=2n+1$	

Intensities of the reflections $hk0$ to $hk4$ were visually estimated from the Weissenberg photographs, recorded with nickel-filtered *Cu* $K\alpha$ radiation. They were reduced to 1033 independent structure factors after corrections for the layer scale, the Lorentz, polarization and spot shape factors being applied. No absorption corrections were applied, since the size of the crystal was small ($0.12\times0.15\times1.3$ mm). The scale factors for each layer, used in the above correction, were estimated from a preliminary examination in which the reflections of the different layers were recorded on the same film, using the anti-equi-inclination Weissenberg technique. The normalized structure factors were calculated from the observed structure factors, using the scale and overall temperature factors obtained by the Wilson method. The average values of $|E|$ and $|E^2-1|$ are 0.852 and 0.981, respectively. The maximum value of $|E|$ is 3.99 and the number of the reflections with $|E|$ value above 1.7 is 124.

Structure Determination

The structure was determined by the statistical method.[12] The origin was specified by assinging positive signs to three reflections, 121, 211, and $86\bar{3}$.[13] For the sign-determining procedure, the sign relation formula $S(E_h)=S(\sum_k E_k E_{h-k})$ was applied to the reflections with $|E|$ value above 1.7. In this procedure the value of the triple product $E_h E_k E_{h-k}$ was required to exceed 8.1 if a single sign indication was accepted, and the new signs were added to the list of known signs and subsequently used to determine other signs. At the end of the procedure, signs of 124 reflections were

* Present address: *Faculty of Pharmaceutical Sciences, Kyoto University, Kyoto*

** Present address: *Faculty of Sciences, Kwansei Gakuin University Nishinomiya*

1) T. Watanabé, I. Taguchi, and N. Masaki, *Acta Crystallogr.*, **12**, 347 (1959).
2) L. Pauling, H. D. Springall, and K. J. Palmer, *J. Amer. Chem. Soc.*, **61**, 927 (1939).
3) A. A. Westenberg and E. B. Wilson, *ibid.*, **12**, 199 (1950).
4) A. V. Jones, *J. Chem. Phys.*, **20**, 860 (1952).
5) G. D. Craine and H. W. Thompson, *Trans. Faraday Soc.*, **49**, 1273 (1953).
6) J. H. Callomon and B. P. Stoicheff, *Can. J. Phys.*, **35**, 373 (1957).
7) G. A. Heath, L. F. Thomas, E. I. Sherrerd, and J. Sheridan, *Discuss. Faraday Soc.*, **19**, 38 (1955).
8) A. Almenningen, O. Bastiansen, and T. Munthe-Kaas, *Acta Chem. Scand.*, **10**, 261 (1956).
9) R. C. Himes, *Discuss. Abs.*, **18**, 1619 (1958).
10) J. D. Dunitz and J. M. Robertson, *J. Chem. Soc.*, **1947**, 1145.
11) E. H. Wiebenga, *Z. Krist.*, **102**, 193 (1940).
12) I. L. Karle and J. Karle, *Acta Crystallogr.*, **21**, 849 (1966).
13) H. Hauptman and J. Karle, *ibid.*, **9**, 45 (1956).

determined and an E-map was synthesized from them. The highest eleven peaks in this map correspond to all the nonhydrogen atoms in the structure.

The structure was refined first by the isotropic diagonal least squares method. After three cycles of refinement the R index was 0.179. The positions of the hydrogen atoms were found from the difference Fourier map calculated at this stage. Further refinements were carried out by the block diagonal least squares method, including the positional parameters of the hydrogen atoms and the anisotropic thermal parameters of the nonhydrogen atoms. Five cycles of this refinement with the Cruickshank weighting scheme reduced the R index to 0.084 for all the observed reflections.[14] The parameter shifts of all the nonhydrogen atoms in the last cycle were less than 2σ.

TABLE 2. POSITIONAL PARAMETERS IN FRACTIONAL COORDINATES

The estimated standard deviations are given in parentheses

Atom	x/a	y/b	z/c
C(1)	0.0401(3)	0.4659(3)	0.0367(8)
C(2)	0.1105(3)	0.4062(3)	0.1004(8)
C(3)	0.1956(3)	0.3367(3)	0.1656(8)
C(4)	0.2676(3)	0.3601(4)	0.0389(9)
C(5)	0.3491(3)	0.2914(5)	0.0979(9)
C(6)	0.3599(3)	0.2009(4)	0.2834(9)
C(7)	0.2895(3)	0.1745(4)	0.4088(8)
C(8)	0.2067(3)	0.2420(3)	0.3492(7)
C(9)	0.1390(3)	0.1223(4)	0.6348(8)
C(10)	0.0498(3)	0.1222(4)	0.7315(8)
O	0.1327(2)	0.2228(2)	0.4575(5)
H(1)	0.2549(28)	0.4269(39)	−0.0887(82)
H(2)	0.4004(30)	0.3148(40)	0.0307(87)
H(3)	0.4188(29)	0.1498(41)	0.3298(87)
H(4)	0.3012(30)	0.1108(40)	0.5458(86)
H(5)	0.1957(30)	0.1296(40)	0.7979(87)
H(6)	0.1433(29)	0.0451(39)	0.5234(85)
H(7)	0.0599(29)	0.0589(40)	0.8746(86)
H(8)	0.0417(30)	0.1980(40)	0.8109(86)
H(9)	−0.0098(30)	0.1072(40)	0.5655(87)

TABLE 3. THERMAL PARAMETERS OF NONHYDROGEN ATOMS

β as given here is defined by

$$T = \exp(-10^{-4} \times (h^2\beta_{11}+k^2\beta_{22}+l^2\beta_{33}+2hk\beta_{12}+2hl\beta_{13}+2kl\beta_{23}))$$

Their estimated standard deviations referred to the last decimal positions of the respective values are given in parentheses.

Atom	β_{11}	β_{22}	β_{33}	β_{12}	β_{13}	β_{23}
C(1)	59(2)	66(3)	454(2)	−3(2)	51(5)	14(5)
C(2)	55(2)	67(3)	475(2)	−10(2)	42(4)	−2(6)
C(3)	47(2)	71(3)	438(2)	−7(2)	39(4)	−31(5)
C(4)	64(2)	94(4)	540(2)	−18(2)	69(5)	−51(7)
C(5)	53(2)	138(5)	662(3)	−19(2)	77(6)	−102(8)
C(6)	51(2)	123(4)	592(2)	10(2)	36(5)	−94(8)
C(7)	48(2)	99(4)	472(2)	12(2)	22(5)	−36(6)
C(8)	44(2)	76(3)	337(2)	5(2)	28(4)	−24(5)
C(9)	60(2)	78(3)	358(2)	−1(2)	32(4)	14(5)
C(10)	64(2)	101(4)	469(2)	−7(2)	53(5)	5(6)
O	50(1)	83(2)	434(1)	12(1)	49(3)	40(4)

TABLE 4. OBSERVED AND CALCULATED STRUCTURE FACTORS

(The values are tabulated on ten times absolute scale)

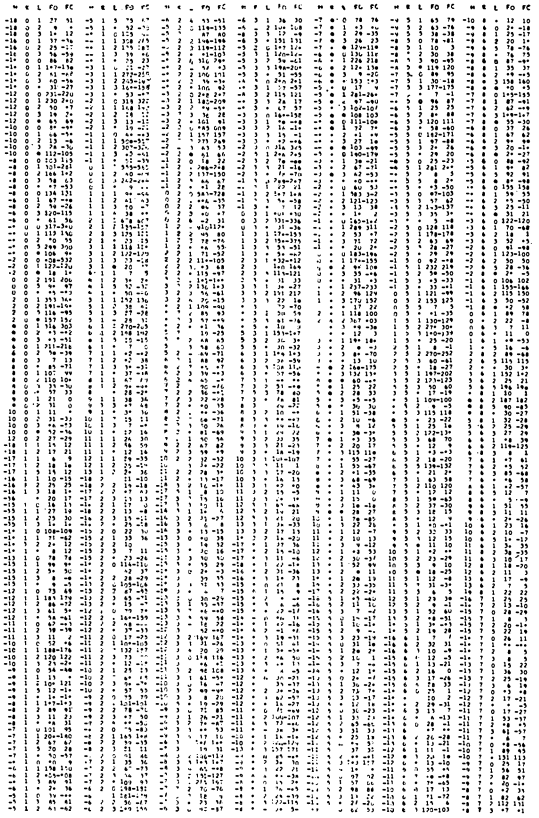

Table 4. (Continued)

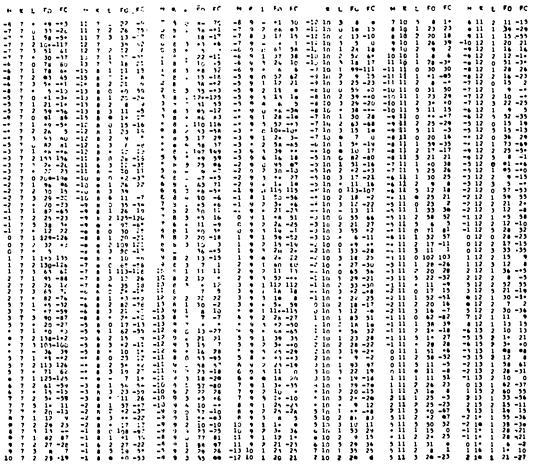

The final positional and thermal parameters are given in Tables 2 and 3, respectively. The observed and calculated structure factors are listed in Table 4.

Results and Discussion

The resulting crystal structure is shown in Figs. 2 and 3, as viewed in the projections along the c- and b-axes, respectively. The center of the molecule lies

14) D. W. J. Cruickshank, "Computing Methods and the Phase Problem in X-ray Analysis," ed. by Pepinsky *et al.*, Pergamon Press, New York (1961), p, 45.

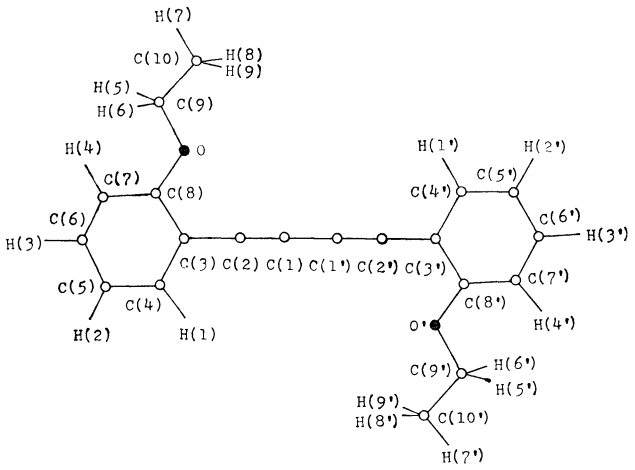

Fig. 1. Conventional numbering and identification of the atoms in bis(*o*-ethoxyphenyl)butadiyne molecule.

at the special position of crystal symmetry ($\bar{1}c$), so that the molecule has a center of symmetry and is almost planar (Fig. 1). The diacetylene chain lies approximately on a plane perpendicular to the *c*-axis and the plane of the phenyl ring is inclined about 49.5° to this plane. The crystal structure is built up from columns of the molecules packed along the *c*-axis, since a large number of short contacts occur between atoms of the molecules related by translation along the *c*-axis, *viz*; 3.49 Å between C(4) and O, 3.59 Å between C(3) and C(9) and 3.59 Å between C(3) and C(10). Only one very short intermolecular distance is found between the columns, namely 3.50 Å between C(4) and C(9). However all other intermolecular distances between the columns are larger than 3.7 Å. These intermolecular distances are considered to be the normal van der Waals distances.

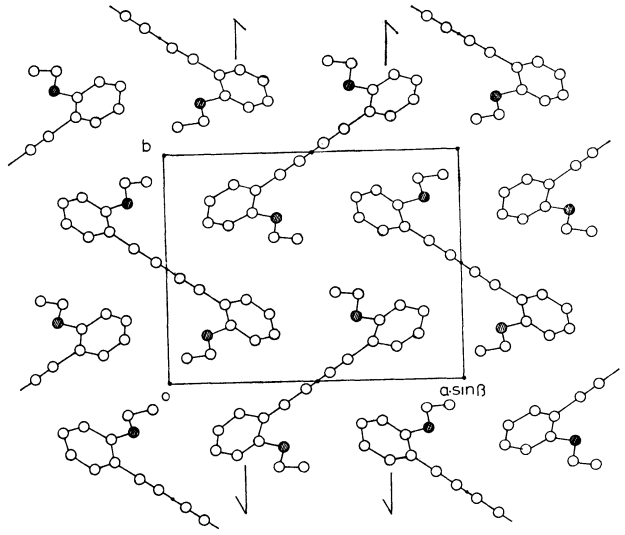

Fig. 2. Projection of the crystal structure along the *c*-axis.

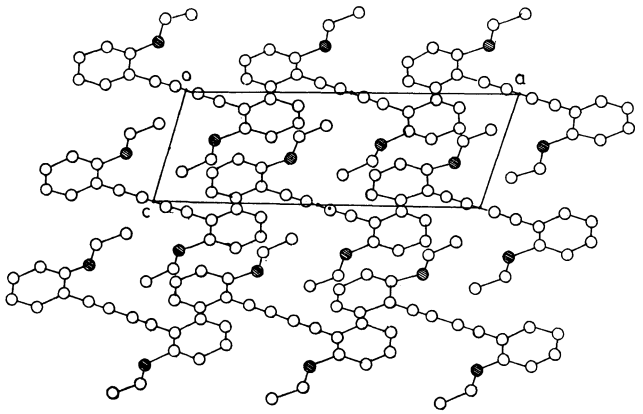

Fig. 3. Projection of the crystal structure along the *b*-axis.

The covalent bond distances and angles in the molecule are listed in Table 5. The carbon-carbon distances of the diacetylene group were corrected for the effect of the thermal motion. The mean square displacement of each atom from its equillibrium position was calculated from the anisotropic thermal parameters given in Table 3. The results indicate that the thermal motion of the molecule cannot be treated as a rigid body motion, and the dominant motion of the atoms of the diacetylene group are considered to be caused by the torsional oscillation about the axis perpendicular to the bond vector, plus the translational motion of the molecule as a whole. Since atoms C(1) and C(1′) are related by the center of symmetry, the C(1)–C(1′) distance was corrected on the basis of the assumption of the upper limit model of Johnson, which corresponds

Table 5. Covalent bond lengths (Å) and angles (°)
Estimated standard deviations are given in parentheses.

Bond	Length	Bond	Angle
C(1)–C(1′)	1.371(6)	C(1′)–C(1)–C(2)	179.6(0.6)
C(1)–C(2)	1.201(6)	C(1)–C(2)–C(3)	177.4(0.5)
C(2)–C(3)	1.434(6)	C(2)–C(3)–C(4)	120.0(0.4)
C(3)–C(4)	1.411(7)	C(2)–C(3)–C(8)	120.5(0.5)
C(4)–C(5)	1.388(7)	C(4)–C(3)–C(8)	119.5(0.4)
C(5)–C(6)	1.379(7)	C(3)–C(4)–C(5)	120.0(0.4)
C(6)–C(7)	1.396(8)	C(4)–C(5)–C(6)	119.8(0.5)
C(7)–C(8)	1.394(6)	C(5)–C(6)–C(7)	121.6(0.4)
C(8)–C(3)	1.411(5)	C(6)–C(7)–C(8)	119.2(0.4)
C(9)–C(10)	1.520(7)	C(3)–C(8)–C(7)	119.9(0.5)
C(8)–O	1.367(6)	C(3)–C(8)–O	116.0(0.4)
C(9)–O	1.447(5)	C(7)–C(8)–O	124.1(0.4)
C(4)–H(1)	0.987(43)	C(8)–O–C(9)	117.7(0.3)
C(5)–H(2)	0.946(49)	C(10)–C(9)–O	107.3(0.4)
C(6)–H(3)	1.011(42)	C(3)–C(4)–H(1)	115.3(2.7)
C(7)–H(4)	0.992(45)	C(5)–C(4)–H(1)	124.7(2.7)
C(9)–H(5)	1.018(40)	C(4)–C(5)–H(2)	118.9(2.6)
C(9)–H(6)	1.057(45)	C(6)–C(5)–H(2)	120.6(2.5)
C(10)–H(7)	1.012(45)	C(5)–C(6)–H(3)	121.1(2.8)
C(10)–H(8)	0.969(46)	C(7)–C(6)–H(3)	117.3(2.8)
C(10)–H(9)	1.063(38)	C(6)–C(7)–H(4)	118.9(2.7)
		C(8)–C(7)–H(4)	121.8(2.7)
		C(10)–C(9)–H(5)	107.9(2.8)
		O–C(9)–H(5)	111.4(2.6)
		C(0)–C(9)–H(6)	111.3(2.5)
		O–C(9)–H(6)	107.4(2.5)
		H(5)–C(9)–H(6)	111.5(3.3)
		C(9)–C(10)–H(7)	105.9(2.7)
		C(9)–C(10)–H(8)	110.8(2.8)
		C(9)–C(10)–H(9)	108.9(2.8)
		H(7)–C(10)–H(8)	108.6(3.7)
		H(7)–C(10)–H(9)	114.2(3.4)
		H(8)–C(10)–H(9)	108.5(3.7)

to the out-of-phase displacement of these-atoms perpendicular to the bond.[15] The corrections to distances C(1)–C(2) and C(2)–C(3), although small, were also calculated by the lower limit model.

The central C(1′)–C(1) bond distance 1.371 Å and the triple C(1)–C(2) bond distance 1.201 Å found in this investigation, agree with the corresponding values 1.376 and 1.205 Å, for diacetylene reported by Callomon and Stoicheff and the values 1.375 and 1.199 Å, for dimethyldiacetylene reported by Himes within experimental errors,[6,9] while the side C(2)–C(3) bond distance 1.434 Å, is close to that of diphenyldiacetylene, 1.44 Å, given by Wiebenga.[11] From these values, the bond order of the C(1′)–C(1) and C(2)–C(3) bonds are estimated to be about 1.63 and 1.27, respectively, indicating that the C(1′)–C(1) bond has considerable double bond character.[16] Concerning the bonds in the ethoxy group, the C(8)–O bond of 1.367 Å has a partial double bond character through the influence of the aromatic ring, while the C(9)–O bond of 1.447 Å and the C(9)–C(10) bond of 1.520 Å are normal paraffinic single bonds. The mean value of the carbon-carbon distances in the phenyl ring is 1.396 Å, which is in good agreement with the normal value 1.395 Å. The mean value of the C–H distances is 1.006 Å.

Table 6. Deviations of each atom from the best plane (see text) and their estimated standard deviations in the direction of the plane normal

Atom	Deviation(Å)	E.S.D.(Å)
C(1)	0.011	0.006
C(2)	0.028	0.006
C(3)	0.030	0.006
C(4)	0.007	0.007
C(5)	−0.020	0.007
C(6)	−0.008	0.007
C(7)	−0.005	0.006
C(8)	0.006	0.006
C(9)	−0.111	0.006
C(10)	−0.078	0.007
O	−0.010	0.004

The best plane equation of the molecule except for the four atoms of the ethyl groups is expressed by

$$0.2224x + 0.6368y + 0.7376z = 3.589,$$

where x, y, and z are the orthogonal coordinates in Ångstrom unit. Deviations of each atom from this plane are given in Table 6. Atoms C(9) and C(10) of the ethyl group deviate from this plane about 0.111 Å and 0.078 Å, respectively, and the plane through these atoms and the nearest oxygen atom is inclined about 4.7° to the above best plane. The deviations of atoms C(2) and C(3) from the best plane are about 0.028 Å and 0.030 Å, respectively, which are significantly large in comparison with their estimated standard deviations of positions. Four atoms of the diacetylene group lie approximately on the straight line, while atoms C(2), C(3), and C(6) also are almost linear. However, atoms C(3) and C(6) do not lie on the line connecting atom C(2) to the center of the molecule, so that the diacetylene chain is slightly bent at atoms C(2) and C(2′), and the ethoxy groups are kept away from the center of the molecule. The diacetylene group has no short intermolecular contacts in the crystal, while the ethoxy and phenyl groups have a large number of short contacts with the nearest molecules. Thus the diacetylene chain can be bent by the intramolecular interactions based upon asymmetry of the molecule about the diacetylene group. It may be also affected by steric effects induced from the side groups which are closely packed in the crystal.

The authors wish to express their gratitude to Dr. F. Toda and Prof. M. Nakagawa for the supply of the specimen. They also thank Mr. H. Iizuka for his assistance in the experiment. The computations were performed with the use of the block diagonal least squares program, HBLS, written by Dr. T. Ashida, UNICS, and the symbolic addition procedure program and others written by one of the authour (T. T.) on the FACOM 230-60 of the Data Processing Center, Kyoto University.

15) C. K. Johnson, "Crystallographic Computing," Munksgaard, Copenhagen (1969), p. 220.
16) L. Pauling, "The Nature of the Chemical Bond," 3rd edition, Cornell University Press, New York (1962), p. 240.

Effects of External Pressure on the Light Absorption and Fluorescence of s-Tetracyanobenzene Complexes

Yoshikazu TORIHASHI, Yoshifumi FURUTANI, Kiyoshi YAGII, Noboru MATAGA,[1] and Akira SAWAOKA*

Faculty of Engineering Science, Osaka University, Toyonaka, Osaka

**Research Laboratory of Engineering Materials, Tokyo Institute of Technology, Ookayama, Meguro-ku, Tokyo*

(Received May 19, 1971)

The effects of high pressure on the charge-transfer (CT) absorption and fluorescence spectra of tetracyanobenzene (TCNB) complexes at room temperature have been examined. The pressure-induced change in the absorption intensity indicated the reduction of the distance between donor and acceptor in the complex and the increase in the overlap between their electron clouds. The pressure-induced red shifts of the absorption and fluorescence spectra were almost equal to each other in the case of the TCNB-toluene system, but the former shift was larger than the latter shift in the case of the TCNB-mesitylene system. These results were interpreted in terms of the reduction of the donor-acceptor distance in the complex as well as in terms of electrical solute-solvent interactions. It has been confirmed that the fluorescence quantum yield and the decay time of the complex decrease with the increase in the pressure, and that the rate of the decrease of the former is much larger than that of the latter, in the case of TCNB-toluene system. These results have been interpreted as being due to the pressure-induced increase in the quenching process at the Franck-Condon excited state as well as in the course of the relaxation process from the excited Franck-Condon state to the equilibrium fluorescent state.

It is well-known from recent experimental results that, on going from vapor to the condensed phase, optical-absorption spectra of weak EDA (electron donor-acceptor) complexes undergo quite remark able changes.[2-5] That is, the CT absorption bands of such complexes as tetracyanoethylene-aromatic and iodine-aromatic systems show red shifts of 1000—4000 cm^{-1} and an intensity enhancement of 200—800% upon this phase change. Furthermore, these effects can be facilitated by an external high pressure added to the condensed phase.[5,6]

It should be noted that the above spectral changes are much larger in the case of weak complexes than in the case of strong complexes or free molecules. It has been argued[4,5,7-9] that these spectral changes in the weak EDA complexes may be related to the reduction in the distance between the component molecules in the complex, which is itself caused by the internal compressional force of the solvent or the host and also by the external pressure. For example, Trotter[7] has pointed out on the basis of statistical mechanical calculations, that liquids exert an internal mechanical pressure of the order of 10^3—10^4 atm on dissolved molecules, and this pressure causes a very large vapor-to-liquid change in the spectra of weak complexes.

It seems that it would be interesting and important to study the effect of high pressure not only on the absorption spectra but also on the fluorescence spectra of EDA complexes. Offen and his co-workers[8,9] have examined the high pressure effect on the absorption and fluorescence spectra of some EDA complexes contained in high polymer matrices. According to their results, *e.g.*, in the case of the TCPA (tetrachlorophthalic anhydride) complexes with aromatic hydrocarbons in a polymethylmethacrylate matrix, the fluorescence spectra showed a much smaller pressure-induced red shift than the absorption spectra. This difference was explained in terms of the potential energy curves for the ground and excited states characterizing the molecular complex. Moreover, the absorption intensity increased, while the fluorescence intensity decreased, as the pressure was increased. The extent of the decrease in the fluorescence intensity was larger than that of the enhancement of the absorption intensity. At any rate, this fact appears to indicate an increase in the quenching process due to the external pressure, though its mechanism is not clear.

As far as we know, there has been no quantitative study of the EDA complex in a liquid solution in which the pressure effects upon both fluorescence and absorption spectral shifts, and upon the fluorescence quantum yields and decay times are investigated. We have, therefore, undertaken a systematic study concerning the high pressure effects on the EDA interactions in the electronic ground state as well as in the excited state, including the weak EDA complex formation, the contact CT interactions, and the exciplex formation in solution. In the present report, we shall describe the results of our study of the TCNB-toluene system, the fluorescence behavior of which has been studied previously in some detail under 1 atm,[10] and also the results of some studies of the TCNB-mesitylene system.

Experimental

The TCNB was the same sample as was used before.[10]

1) To whom all correspondence should be addressed.
2) F. L. Lang and R. L. Strong, *J. Amer. Chem. Soc.*, **87**, 2345 (1965).
3) M. Kroll and M. L. Ginter, *J. Phys. Chem.*, **69**, 3671 (1965).
4) J. Prochorow and A. Tramer, *J. Chem. Phys.*, **44**, 4545 (1966).
5) H. W. Offen and A. H. Kadhim, *ibid.*, **45**, 269 (1966).
6) J. R. Gott and W. G. Maisch, *ibid.*, **39**, 2229 (1963).
7) P. J. Trotter, *J. Amer. Chem. Soc.*, **88**, 5721 (1966).
8) H. W. Offen and J. F. Studebaker, *J. Chem. Phys.*, **47**, 253 (1967).
9) A. H. Kadhim and H. W. Offen, *ibid.*, **48**, 749 (1968).
10) N. Mataga and Y. Murata, *J. Amer. Chem. Soc.*, **91**, 3144 (1969).

The toluene was purified by the method described in the literature.[11] The mesitylene was distilled carefully under reduced pressure. The fluorescence spectra were measured with an Aminco-Bowman spectrophotofluorometer which had been calibrated to obtain the correct fluorescence quantum spectrum, while the absorption spectra were measured by means of a Cary 15 spectrometer. The fluorescence spectra were excited exclusively at the wavelength of the first CT absorption band. The fluorescence decay times were measured with a giant pulse ruby laser which has an output powder of 1.5 J and a 15—20 nsec pulse width, or with a pulsed nitrogen gas laser. The exciting light pulse from the ruby laser was produced by an ADP frequency doubler which converted *ca.* 8 per cent of the energy of the 694 nm beam to that of the 347 nm beam. The light pulse of the nitrogen gas laser had an output power of 10 kW and a duration of 3 nsec. Its repetition rate was *ca.* 50 Hz. The fluorescence emission was observed with a travelling wave-pulsed photomultiplier. The outputs from the photomultiplier with a delay line were displayed on an X-Y recorder.

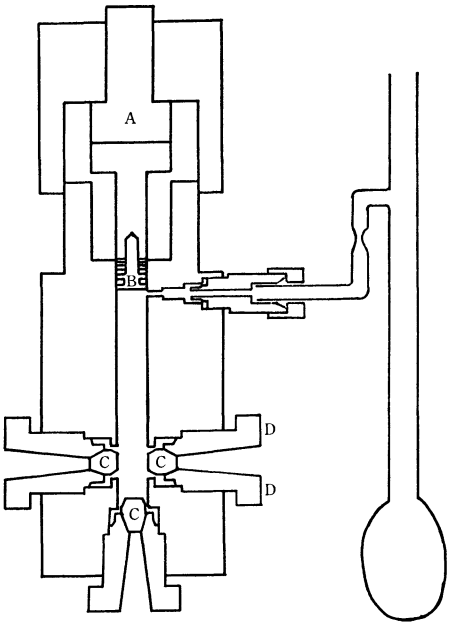

Fig. 1. High pressure optical cell.
A. Low pressure piston, B. High pressure piston
C. Sapphier window, D. Window plug.

Figure 1 shows a cross section of the high-pressure optical cell, the cell is reasonably small, is portable, and can be introduced into various spectrometers and other optical setups. All the metallic parts of the cell, including the pistons and window plugs, are made of copper-beryllium alloy. In order to prevent the leakage of solutions through gaps in the regions of the sapphire-metal contact and metal-metal contacts at the windows and piston parts, various packings, such as teflon, lead, and Viton A of du Pont, were used. The deaeration of the solution was conducted as follows. The solution in an ampoule, which was connected with the high-pressure cell, was deaerated by freeze-pump-thaw cycles. The deaerated solution was then transferred to the high-pressure cell and the transfer glass tube was sealed off. The highest pressure which could be applied to the solution in our high-pressure optical cell was *ca.* 8000 atm.

11) A. Weissberger, Ed., "Technique of Organic Chemistry," Vol. VII, Interscience Publishers, New York, N. Y. (1955). p. 318

Results and Discussion

The absorption and fluorescence spectra of the TCNB-toluene system under various external pressures are indicated in Fig. 2. The first absorption band of the TCNB-toluene complex appears only as a shoulder at *ca.* 29000 cm^{-1}; one cannot observe any distinct peak, even under 7000 atom. However, as is shown in Fig. 3, the rate of the pressure-induced increase in its absorbance is much larger than that of the density of the solvent. Moreover, the rate of the absorbance increase is much larger at longer wavelengths than at shorter wavelengths. The latter fact indicates that the pressure-induced red shift of the first absorption band occurs. We have estimated the wave numbers of the first absorption maximum at various external pressures by subtracting the contributions of the strong second band from the spectra. The results are shown in Fig. 4, where a similar spectral shift of the fluorescence band is also indicated.

We have also carried out quite similar studies of the spectra of the TCNB-mesitylene two-component system. The TCNB-mesitylene complex is stronger than the TCNB-toluene complex and shows a distinct CT

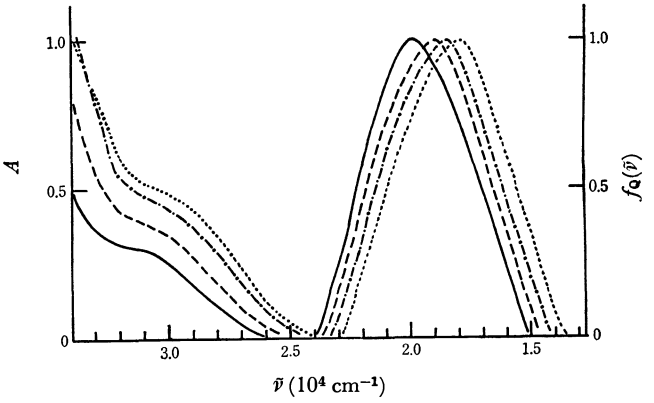

Fig. 2. Absorption and fluorescence spectra of TCNB-toluene system under various external pressures.
——; 1 kg/cm² – – –; 1970 kg/cm² —·—; 5230 kg/cm²
– – – –; 7020 kg/cm²

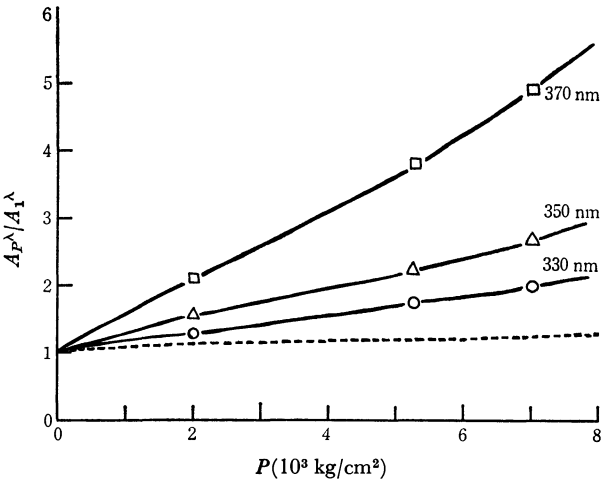

Fig. 3. The pressure induced increase of the absorbance of TCNB-toluene system in comparison with that of the density of toluene. A_P^λ represents the absorbance under pressure P (at λ nm). – – – –density of toluene.

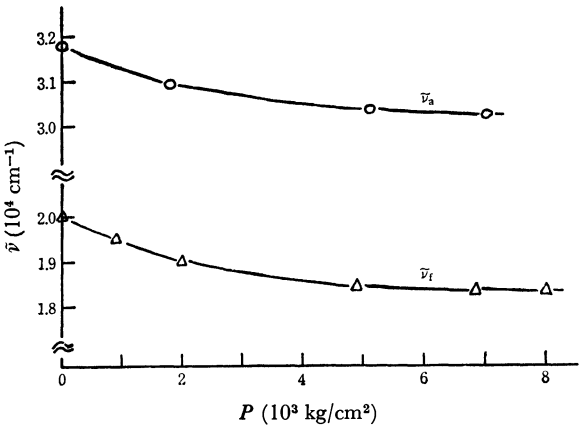

Fig. 4. Dependence of the wave numbers of absorption ($\bar{\nu}_a$) and fluorescence ($\bar{\nu}_f$) band maxima of TCNB-toluene system on the external pressure.

absorption maximum at *ca.* 28200 cm^{-1}. The effects of the external high pressures (at most,~3000 atm, since the solidification of mesitylene occurs at higher pressures) are indicated in Figs. 5 and 6. One may

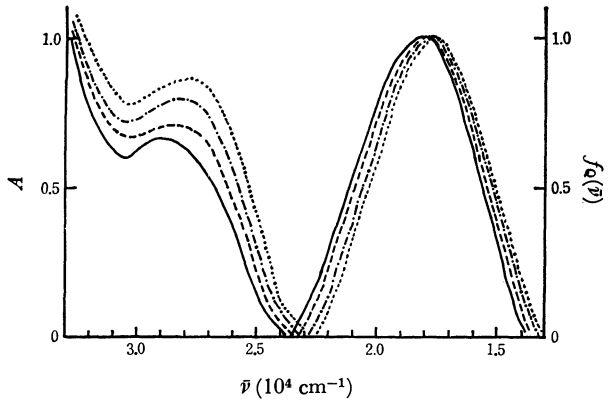

Fig. 5. Absorption and fluorescence spectra of TCNB-mesitylene system under various external pressures.
——; 1 kg/cm^2 ——; 790 kg/cm^2 –·–·; 2100 kg/cm^2
------; 2990 kg/cm^2

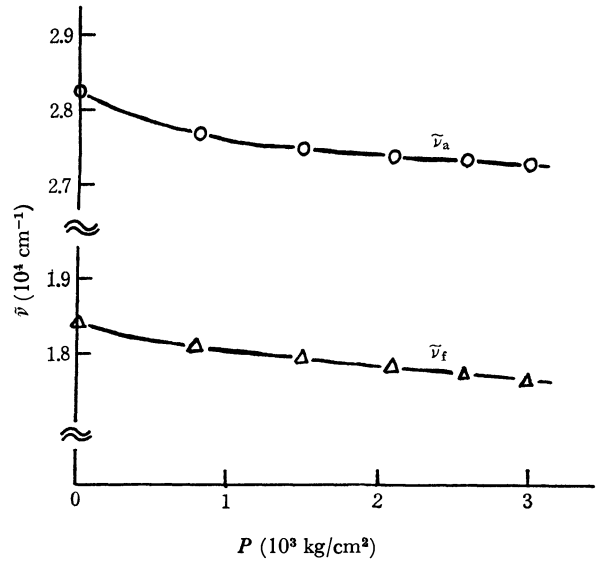

Fig. 6. Dependence of $\bar{\nu}_a$ and $\bar{\nu}_f$ values of TCNB-mesitylene system on the external pressure.

see that the results are rather different from those in the TCNB-toluene system.

The pressure-induced change in the absorbance corrected for the volume contraction might be attributed to the increase in the solvent refractive index, n, at high pressures. Although n values of mesitylene[12] have been observed under various external pressures, we have no such values for toluene. We have estimated the n values for toluene by means of the Debye equation as well as by means of the Onsager equation for dielectric polarization,[13] using the observed values of density and the dielectric constant of toluene under various external pressures.[14,15] The two equations gave practically the same values. By employing these n values, we have made a rough estimation of the pressure-induced absorbance change according to Chako's simplified equation;[16]

$$A \propto f(n) \equiv \left(\frac{n^2+2}{3}\right)^2 / n$$

Table 1. Comparison of the integrated absoption intensity (A) with Chako's function $f(n)$

P(kg/cm^2)	A_P/A_1	$f_P(n)/f_1(n)$
TCNB-toluene system		
1970	1.09	1.04
5230	1.13	1.08
7020	1.19	1.11
TCNB-mesitylene system		
790	1.03	1.02
1480	1.06	1.03
2100	1.07	1.04
2580	1.08	1.05
2990	1.12	1.06

A_P: integrated absorbance under pressure P.
$f_P(n)$: Chako's function under pressure P.

One can see from Table 1 that the pressure-induced absorbance increases as corrected for the change in the refractive index, are rather small. However, the corrected increase for the TCNB-mesitylene system appears a little larger than that of the TCNB-toluene system.

One should note here that there are opposing effects of the external pressure upon the intensity of the CT absorption band of TCNB complexes. That is, there occurs a reduction in the donor-acceptor distance in the complex; this reduction, on the one hand, increases the orbital overlap between the partners in the complex, causing the enhancement of the CT absorption intensity. On the other hand, the decrease in the donor-acceptor distance in the complex presumably makes the excited state more ionic, thus reducing the con-

12) D. W. Langer and R. A. Montalvo, *J. Chem. Phys.*, **49**, 1836 (1968).
13) H. Fröhlich, "Theory of Dielectrics," Oxford at the Clarendon Press (1949), p. 33; S. Oka, "Theory of Dielectrics" (in Japanese), Iwanamishoten, Tokyo (1954), p. 135.
14) J. F. Skinner, E. L. Cussler, and R. M. Fuoss, *J. Phys. Chem.*, **72**, 1057 (1968): W. E. Danforth, Jr., *Phys. Rev.*, **38**, 1224 (1931).
15) Z. T. Chang, *Chinese J. Phys.*, **1**. 1 (1933).
16) N. Chako, *J. Phys. Chem.*, **2**, 644 (1934).

tribution from the locally-excited configuration, which in turn decreases the absorption intensity because of the decrease in the intensity borrowing from the locally-excited state of TCNB. Moreover, if a pressure-induced change in the geometrical structure of the complex from an unsymmetrical structure to a symmetrical overlapping one occurs, the CT transition probability is decreased.[17,18] Becasuse these effects cancel each other out, the appearent increase in the absorption intensity may be rather small. Therefore, one should not exclude the possibility of the pressure-induced reduction of the donor-acceptor distance in the complex in interpreting the other spectral behavior of these complexes, even if the pressure-induced net increase in the absorbance is small.

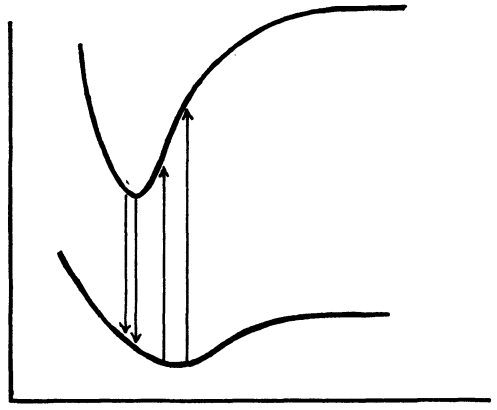

Fig. 7. Potential energy curves for the excited and ground state of an EDA complex.

The above-described circumstances are illustrated in Fig. 7, where one can see also that the decrease in the distance, R_{AD}, between the partners in the complex may cause the red shift of the fluorescence as well as the absorption band. One may suppose from Fig.7 that the amount of the fluorescence red shift is smaller than that of the absorption red shift for the same added external pressure, as a result of the difference between the potential energy curves for the excited and ground states of the complex. Such an example was actually observed, as we have previously described, in the case of TCPA complexes in high polymer matrices.[8,9] In the case of a liquid solution, however, dielectric polarization interactions between the surrounding solvent molecules and the complex in the fluorecent state may be larger than in the case of solid solution, leading to a stronger fluorescence red shift. Nevertheless, the extent of the fluorescence red shift is considerably smaller than that of the absorption in the case of the TCNB-mesitylene system (Fig. 6). The solute-solvent dielectric interaction seems to be larger in the case of the TCNB-toluene system than in the case of the TCNB-mesitylene system. Thus, for the former system, the magnitude of the pressure-induced red shift of the fluorescence spectrum is almost the same as that of the absorption spectrum. On the other hand, the fact that both the absorption and fluorescence spectral shifts became almost saturated at about 6500 atm in the case of the TCNB-toluene does not seem to be interpreted satisfactorily by the ordinary theory of the solvent shift of spectra, since the solvent refractive index and the dielectric constant do not show such a strong saturation effect at pressures of 6000—7000 atm. We can also observe, in the case of the TCNB-mesitylene system (Fig. 6), a tendency for the spectral shifts to become saturated, even at 3000 atm. These results can be explained, at least qualitatively, as due to the structure change in the complex caused by the external pressure. That is, when R_{AD} becames smaller, the complex becomes stronger, and the pressure effect on the spectral shift becomes smaller, because of the enhanced blue-shift contribution from the resonance interaction between the no-bond and CT structure, as has been suggested by Kadhim and Offen.[9] Thus, the pressure-induced spectral shift in our present system may be ascribed to combined effects due to CT forces and potential energy curves appropriate for weak complexes as well as to dielectric polarization interactions between the complex and surrounding solvent molecules.

TABLE 2. FLUORESCENCE QUANTUM YIELDS (η_F) AND DECAY TIMES (τ_F) AT VARIOUS PRESSURES

P(kg/cm^2)	η_F[a)]	τ_F(nsec)
	TCNB-toluene system	
1	1.00(0.080)	109
2070	0.54(0.035)	82
5010	0.13(0.010)	44
6920	0.07(0.006)	35
	TCNB-mesitylene system	
1	1.00(0.010)	45
790	0.84(0.0084)	41
1480	0.69(0.0069)	34
2100	0.65(0.0065)	30
2590	0.60(0.0060)	28
2990	0.596(0.0059)	25

a) The values in parenthesis are absolute quantum yield. The values of the absolute quantum yield at 1 atm were taken from: T. Kobayashi, Y. Yoshihara, and S. Nagakura, The Symposium on EDA Complex (Osaka), 1970, Preprint.

For a closer examination of the behavior of the excited complex, it is necessary to measure the fluorescence quantum yields and decay times under various external pressures. The results of our measurements are indicated in Table 2. One can see from Table 2 that both the relative fluorescence quantum yield and the fluorescence decay time decrease with the increase in the external pressure. In the case of the TCNB-toluene system, where the fluorescence decay time was measured by means of the giant pulse laser, the rate of decrease in the quantum yield is considerably larger than that of the decay time. Therefore according to the $K_F=\eta_F/\tau_F$ equation, the radiative transition probability decreases with the pressure increase. However, it should be noted here that the above statement is valid only if the quenching process at the excited

17) S. Iwata, J. Tanaka, and S. Nagakura, *J. Amer. Chem. Soc.*, **88**, 894 (1966).
18) H. Masuhara and N. Mataga, *ibid.*, to be published.

Franck-Condon (F.C.) state as well as in the course of the relaxation from the excited F.C. state to the equilibrium (e.q.) fluorescent state is not affected by the added pressure.

On the other hand, as has been elucidated in previous works,[10,19,20] the energy and the electronic structure of the excited F.C. state of the TCNB-toluene system are very different from those of the e.q. excited state. It has been confirmed that the observed fluorescence decay time is much longer than the radiative lifetime calculated from the intensity of the absorption band, and there must occur a change in the electronic structure in the course of the relaxation from the excited F.C. state to the e.q. state. It was assumed that the anomalously long fluorescence decay time was due to the very polar structure of the excited e.q. state.[10] This assumption has been proved to be correct by measuring the absorption spectra of the complex in the fluorescent state, using the nanosecond laser photolysis method.[18,19,21] The relaxation from the excited F.C. state to the e.q. state is accompanied by a change in the geometrical structure of the complex from an asymmetrical structure to a symmetrical overlapping sandwich one as well as by a rearrangement of the surrounding solvent molecules, leading to stronger solvation, which in turn makers the probability of radiative transition smaller. Since the dielectric constant of the solvent increases with the pressure, it seems that the fluorescent state of the complex will become more strongly solvated under higher external pressure, leading to a decrease in the probability of radiative transition. However, this statement is not wholly valid, since the pressure-induced red shifts of the spectra cannot be interpreted satisfactorily in terms of the pressure-induced change in the macroscopic dielectric constant and the refractive index of the solvent, as has been discussed already.

According to the interpretation indicated in Fig. 7, the probability of radiative transition for the fluorescence will be enhanced by an increase in the external pressure, as a result of the increase in the orbital overlap between donor and acceptor. Then, it seems to be necessary to assume that the inner quenching processes at the excited F.C. state as well as in the course of the F.C.→ e.q. relaxation are enhanced by the external pressure.

According to the measurement of the time-resolved fluorescence spectra of the TCNB-toluene system under 1 atm,[20] the excited F.C.→ e.q. relaxation is very rapid (relaxation time $<10^{-9}$ sec) and the fluorescence can be regarded as being emitted exclusively from the e.q. state at room temperature. The time-resolved fluorescence spectrum becomes measurable only in a quite viscous, almost rigid solution at 147°K, by means of an apparatus with nanosecond time-resolving power.[20] Since the external pressure enhances the viscosity of the solution, the F.C.→ e.q. relaxation process might be slowed under high pressure. However, the fluorescence decay times of the TCNB-toluene system measured under 7500 atm at different wavelengths of the fluorescence band agreed with each other. Moreover, although we have tried to measure the time-resolved fluorescence spectrum of the TCNB-toluene system under 7500 atm by exciting the solution with nitrogen-gas laser, the spectra observed at various delay times from exciting pulse were not essentially different from each other. Thus, the F.C.→ e.q. relaxation under the high pressures applied here occurs rather rapidly during times smaller than nanosecond. Therefore, the pressure-induced inner quenching process at the F.C. state, and that in the course of the F.C.→ e.q. relaxation process, may occur far more rapidly than that at the e.q. state, which has a lifetime of 10^{-7}—10^{-8} sec.

Contrary to the case of the TCNB-toluene system, the rate of the decrease in the fluorescence quantum yield and that of the decay time caused by the external pressure are not very different from each other in the case of the TCNB-mesitylene system, where the decay time is measured by means of the nitrogen-gas laser. Therefore, the pressure-induced fluorescence quenching of the TCNB-mesitylene system may be said to occur mainly at the excited e.q. state.

Although the explanation for the different behavior of the TCNB-toluene and TCNB-mesitylene systems with respect to the pressure-induced fluorescence quenching is not clear at the present stage of investigation, the difference in the quenching process might be ascribed to the essential difference in electronic structures between the two system. That is, the energy difference and the difference in electronic structure between the excited F.C. and e.q. states are much greater in the case of the TCNB-toluene system than in the case of the TCNB-mesitylene system.

19) H. Masuhara and N. Mataga, *Chem. Phys. Lett.*, **6**, 608 (1970).
20) K. Egawa, N. Nakashima, N. Mataga, and C. Yamanaka, *ibid.*, **8**, 108 (1971).
21) R. Potashnik and M. Ottolenghi, *ibid.*, **6**, 525 (1970).

Mercury Photosensitized Reaction of Deuterio-Propylene Studied by Microwave Spectroscopy

Yuzo Sakurai, Takaharu Onishi, and Kenzi Tamaru
Department of Chemistry, The University of Tokyo, Hongo, Bunkyo-ku, Tokyo

(Received May 25, 1971)

The mercury photosensitized reaction of propylene-*cis*-1-d_1 and 1-butene-*cis*-1-d_1 was studied by means of microwave spectroscopy combined with gas chromatography and mass spectrometry. At pressures above 100 mmHg *cis-trans* isomerization was the main reaction for both the propylene and 1-butene. The number of the absorbed quanta of photons and the number of molecules reacted was almost equal. However, at lower pressures, this condition was not satisfied. At pressures less than 30 mmHg, substantial amounts of the 2-d_1 and 3-d_1 propylene species were detected in the reaction mixtures. Decomposition of propylene into an allylic radical and a hydrogen atom with subsequent "recombination," was proposed to account for this observation. Similar results were obtained with 1-butene-*cis*-1-d_1.

Several investigations on the mercury photosensitized reaction of simple olefins such as *cis*- or *trans*-dideuterioethylene,[1-3] 2-butene,[4,5] and 1-butene[6] have been reported. Usually the reaction was followed by means of gas chromatography, and in the reaction of dideuterioethylene infrared spectroscopy was employed to determine the extent of the reaction. Quite recently another application of infrared spectroscopy to this type of reactions, *e.g.*, photosensitized reaction propylene-1,3,3,3-d_4 has been reported by Hirokami and Sato.[7] In this paper an attempt has been made to apply microwave spectroscopy to the study of the mercury photosensitized reaction of propylene-*cis*-1-d_1 and 1-butene-*cis*-1-d_1.

Experimental

Methylacetylene was treated with weakly alkaline deuterium oxide to replace its acetylenic hydrogen with deuterium. By repeating this procedure several times, the concentration of methylacetylene-1-d_1 was made greater than 90%. The methylacetylene-1-d_1 thus obtained was selectively hydrogenated to propylene-*cis*-1-d_1 by the procedure developed by Rabinovitch and Looney.[8] 1-Butene-*cis*-d_1 was synthesized from ethylacetylene by a similar method. Deuterium contents in the synthesized olefins were determined by mass spectrometry, while the *cis-trans* distribution was analyzed by means of microwave spectroscopy.

Microwave spectra of propylene and its mono-deuterated species were observed by Lide and Christensen,[9] and applied to the quantitative determination of the deuterium contents at each hydrogen position of propylene-d_1 by Hirota and Morino.[10] Microwave spectra of 1-butene and its mono-deuterated species have been reported by Kondo, Hirota, and Morino[11] and were employed as a useful tool to study *n*-butene isomerization over solid acid catalysts.[12] Analysis by means of microwave spectroscopy revealed that more than 96% of the mono-deuterated species of both the propylene and the 1-butene was *cis*-1-d_1, the remainder was *trans*-1-d_1. Other mono-deuterated species such as 2-d_1 and 3-d_1 (and also 4-d_1 in the case of 1-butene) were not observed within the detection limits of the microwave spectroscopy. The prefixes *cis* and *trans* represent the configuration of deuterium relative to the methyl or ethyl group attached to the C_2 atom.

The 10 W low pressure mercury lamp and the quartz-made cylindrical reaction vessel employed in this work were of a conventional type. The light intensity of the 2537 Å resonance line was estimated by the amounts of hydrogen produced in the decomposition reaction of ethylene under the same reaction conditions. The quantum yield of this reaction was assumed to be 0.351 at an ethylene pressure of 13.3 mmHg.[13]

The reaction products were analyzed mainly by means of microwave spectroscopy and mass spectrometry. In some cases gas chromatography was employed in order to identify the reaction products of the decomposition process and also to determine their composition.

Results and Discussion

Table 1 shows some of the results obtained in the mercury photosensitized reaction of propylene-*cis*-1-d_1. The deuterium concentration of the starting propylene was about 80%, but it did not change appreciably in the course of the reaction. (The change in the deuterium content was less than 0.3%.) Table 1 shows the relative, not the absolute concentrations of each mono-deuterated species. The starting reactant listed at the top of the Table contained neither the 2-d_1 nor 3-d_1 species. Especially at pressures less than 15 mmHg, considerable amounts of both the 2-d_1 and 3-d_1 species were formed as the reaction progressed, as well as the *trans*-1-d_1

1) A. B. Callear and R. J. Cvetanovic, *J. Chem. Phys.*, **24**, 873 (1956).
2) A. B. Callear, D. W. Placzek, R. J. Cvetanovic, and B. S. Rabinovitch, *Can. J. Chem.*, **40**, 2179 (1962).
3) D. W. Sester, B. S. Rabinovitch, and D. W. Placzek, *J. Amer. Chem. Soc.*, **85**, 862 (1963).
4) R. B. Cundall and T. F. Palmer, *Trans. Faraday Soc.*, **57**, 1211 (1961).
5) S. Tsunashima and S. Sato, This Bulletin, **41**, 284 (1968).
6) J. R. Majer, B. Mile, and J. C. Robb, *Trans. Faraday Soc.*, **57**, 1336 (1961).
7) S. Hirokami and S. Sato, This Bulletin, **43**, 2389 (1970).
8) B. S. Rabinovitch and F. S. Looney, *J. Amer. Chem. Soc.*, **75**, 2652 (1953).
9) D. R. Lide, Jr., and D. Christensen, *J. Chem. Phys.*, **35**, 1374 (1961).
10) Y. Morino and E. Hirota, *Nippon Kagaku Zasshi*, **85**, 535 (1964).
11) S. Kondo, E. Hirota, and Y. Morino, *J. Mol. Spectrosc.*, **28**, 471 (1968).
12) Y. Sakurai, Y. Kaneda, S. Kondo, E. Hirota, T. Onishi, and K. Tamaru, This Bulletin, **41**, 1496 (1968); *Trans. Faraday Soc.*, in press.
13) B. Deb. Darwent, *J. Chem. Phys.*, **20**, 1673 (1952).

Table 1. Deuterium distribution in propylene in the case of Hg photosensitized reaction of propylene-*cis*-1-d_1

Pressure mmHg	Photons absorbed μ einstein	d_0 %	d_1 %	*cis*-1-d_1 %	*trans*-1-d_1 %	2-d_1 %	3-d_1 %
		20.0	80.0	96.5	3.5	0.0	0.0
3.3	36	20.2	79.8	74.8	10.2	2.5	12.5
7.2	36			85.7	8.4	1.1	4.8
7.6	48	20.3	79.7	84.0	8.9	1.2	5.9
11.9	72	20.0	80.0	83.4	10.5	1.1	5.0
13.1	108	20.3	79.7	80.1	11.7	1.4	6.8
16.6	72	20.3	79.7	86.4	10.3	0.6	2.7
28.8	72			90.9	7.8	0.2	1.1
42.4	72			92.6	7.4	0.0	trace
76.3	216			90.2	9.4	0.0	0.4

species produced by the *cis-trans* isomerization. The fraction of the 2-d_1 species was always smaller than that of the 3-d_1 species, and both became negligible at pressures above 40 mmHg. The quantum yield of the *cis-trans* isomerization was calculated on the basis of the following reaction scheme (A), and the results are plotted against the pressure of propylene in Fig. 1:

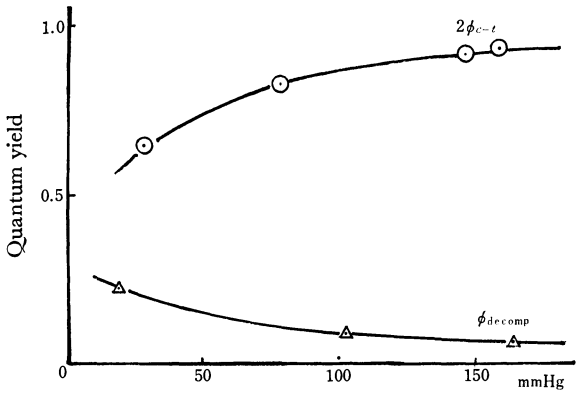

Fig. 1. Pressure dependence of quantum yield of Hg photosensitized *cis-trans* isomerization of propylene-*cis*-1-d_1. (ϕ_{decomp} is for C_3H_6.)

Scheme (A)

$$cis\text{-P} + Hg^* \longrightarrow P^* + Hg$$

$$trans\text{-P} + Hg^* \longrightarrow P^* + Hg$$

$$P^* + M \longrightarrow 1/2\ trans\text{-P} + 1/2\ cis\text{-P} + M$$

Here P* represents an excited state of propylene, possibly the lowest triplet state, and M a third body. The quantum yield of the decomposition reaction, ϕ_{decomp} was calculated for normal propylene after the method of Hirokami and Sato,[7] and the results are shown in Fig. 1 together with $2\phi_{c-t}$.

The pressure dependence of $2\phi_{c-t}$ and ϕ_{decomp} agrees rather well with the results reported by Hirokami and Sato,[7] and the balance between the number of the absorbed quanta of photons and the number of molecules which underwent either isomerization or decomposition is nearly satisfied above 100 mmHg. At pressures less than 100 mmHg, however, this balance can not hold owing to the significant decrease in the quantum yield of the *cis-trans* isomerization. This phenomenon

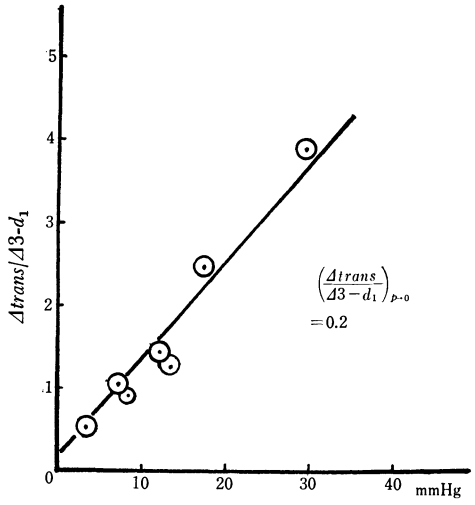

Fig. 2. Hg photosensitized isomerization of propylene-*cis*-1-d_1. Pressure dependence of the ratio ($\Delta trans$-1-$d_1/\Delta 3$-d_1)

was also observed in the mercury photosensitized reaction of 2-butene[5] and propylene-1,3,3,3-d_4.[7] The formation of vibrationally excited propylene or 2-butene, which could not contribute to the isomerization, was assumed in order to explain these observations. However, as is shown in Table 1, 3-d_1 and 2-d_1 species were formed in considerable amounts from propylene-*cis*-1-d_1 at pressures less than 30 mmHg. When the increase in the fraction of *trans*-1-d_1 species ($\Delta trans$-1-d_1) to that of 3-d_1 ($\Delta 3$-d_1) was plotted against the pressure of propylene, the ratio $\Delta trans$-1-$d_1/\Delta 3$-d_1 gave a *linear curve* with a zero intercept of about 0.2 (Fig. 2). On the other hand, the ratio $\Delta 2$-$d_1/\Delta 3$-d_1 was constant and equal to about 0.2 in the pressure region less than 30 mmHg, as shown in Fig. 3.

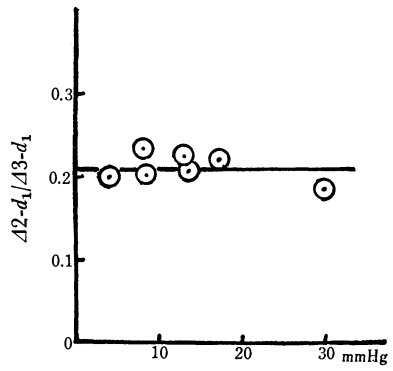

Fig. 3. Hg photosensitized isomerization of propylene-*cis*-1-d_1. Pressure dependence of the ratio ($\Delta 2$-$d_1/\Delta 3$-d_1)

The results in Fig. 2 suggest that the calculation of the quantum yield of the *cis-trans* isomerization on the basis of scheme (A) is open to question at pressures less than 30 mmHg, where the fraction of 3-d_1 species is nearly comparable to that of *trans*-1-d_1. Due attention being paid to the considerable contributions of 2-d_1 and 3-d_1 species in the low pressure region, it was assumed that the mercury photosensitized reaction of propylene-*cis*-1-d_1 proceeds in the following way.

Scheme(B)
Main reaction at high pressures:

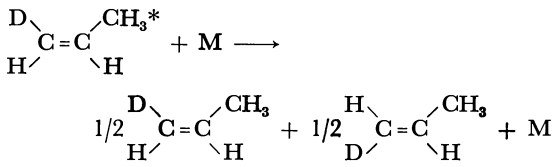

At low pressures:

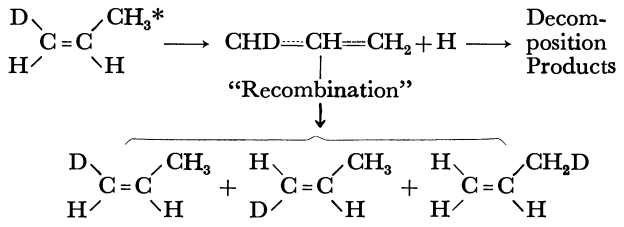

In a rough approximation, the "recombination" reaction of an allylic radical and a hydrogen atom may be expected to yield *cis*-1-d_1, *trans*-1-d_1, and 3-d_1 species in the ratio of 1:1:2. Hydrogen abstraction by an allylic radical from another propylene molecule may also lead to similar results. As this reaction can not be ruled out completely, the term "recombination" is here rather tentatively employed to express the reaction of an allylic radical with a hydrogen atom either in the free or bound state in a hydrocarbon molecule.

The fraction of 3-d_1 species was 1.1% at a pressure of 28.8 mmHg. This suggests that the *trans*-1-d_1 fraction of 0.6% may have resulted from a "recombination" reaction. When this fraction and the original portion of *trans*-1-d_1 in the starting material were substracted, the fraction of *trans*-1-d_1 in the reaction mixture was found to be about 3.7%. In this case the contribution of *cis-trans* isomerization and "recombination" reaction was estimated to be approximately in the ratio of 3.4:1. The $2\phi_{c-t}$ under these conditions was about 0.65 (Fig. 1), and this gave rise to a value of about 0.19 for the quantum yield of the "recombination" reaction.

The quantum yields of *cis-trans* isomerization, "recombination" and decomposition were summed and gave a value of about 1.0, showing that the balance between the number of the absorbed quanta and the number of the reacted molecules was nearly satisfied. Similar results were obtained for reaction at 16.6 mmHg, with a quantum yield of *cis-trans* isomerization being taken from Fig. 1 as 0.55. At pressures less than 15 mmHg the fraction of Δ3-d_1 may become comparable to, or even exceed that of Δ*trans*-1-d_1, as can be seen in Fig. 2. In this pressure region even such very qualitative discussions as described above may not hold.

The above mentioned discussions are rather crude in nature, but they still serve to elucidate the reaction paths involved in the mercury photosensitized reaction of propylene-*cis*-1-d_1. Decomposition of propylene into an allylic radical and a hydrogen atom with subsequent "recombination" to yield the 3-d_1 species of propylene as well as the *cis*- and *trans*-1-d_1 species can not be neglected in the low pressure regions. The formation

Table 2. Deuterium distribution in 1-butene in the case of Hg photosensitized reaction of 1-butene-*cis*-1-*d*

Pressure mmHg	Photons absorbed μ eistein	*cis*-1-d_1 %	*trans*-1-d_1 %	3-d_1 %	d_0 %	d_2 %
		87.2	2.7	0.0	9.1	1.0
6.1	43	75.7	10.3	3.5	10.3	1.6
13.2	64	79.1	8.5	2.0	9.5	0.9
22.7	64	80.9	7.7	1.3	9.3	0.8
34.3	86	83.9	6.7	0.0	9.1	0.9
62.4	143	83.2	6.8	0.0	9.2	1.0
		83.5	1.7	0.0	14.1	0.7
5.0	72	70.1	9.3	3.8	15.3	1.5
7.8	72	75.9	7.1	2.5	14.1	0.4
15.2	110	73.9	8.9	1.9	14.7	0.6
19.8	120	73.5	10.0	1.6	14.3	0.6

of 2-d_1 species was tentatively explained by an intramolecular hydrogen shift within the allylic radical resulting in $CH_2{=}CD{=}CH_2$, which then reacted with a hydrogen atom to yield $CH_2{=}CD{-}CH_3$.

Some of the results obtained in the mercury photosensitized reaction of 1-butene-*cis*-1-d_1, especially those

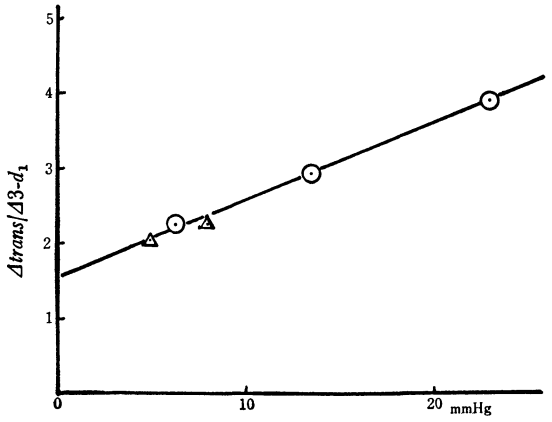

Pressure of 1-butene

Fig. 4. Hg photosensitized reaction of 1-butene-*cis*-1-d_1. Pressure dependence of the ratio (Δ*trans*/Δ3-d_1)

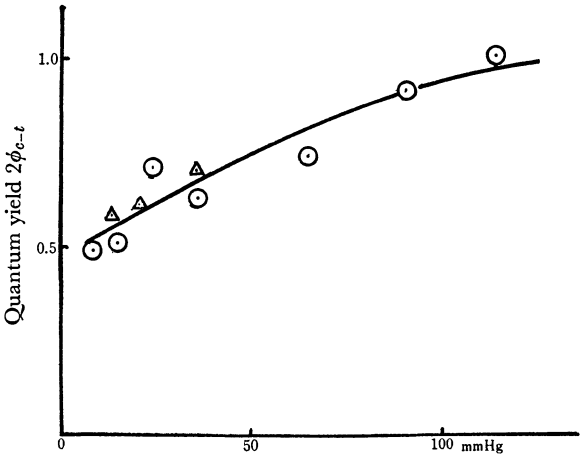

Pressure of 1-butene

Fig. 5. Pressure dependence of quantum yield of Hg photosensitized *cis-trans* isomerization of 1-butene-*cis*-1-d_1.

in the low pressure regions, are given in Table 2. The 3-d_1 species of 1-butene (CH_2=$CHCHDCH_3$) was formed in appreciable amounts after reaction at lower pressures. The 2-d_1 species (CH_2=$CDCH_2CH_3$) was not detected within the limits of the microwave spectroscopy. When the ratio *Δtrans*-1-d_1/*Δ*3-d_1 was plotted against the pressure of 1-butene, a *linear curve* with a zero intercept of about 1.5 was obtained (Fig. 4).

The pressure dependence of the quantum yield of *cis-trans* isomerization, $2\phi_{c-t}$, gave a curve which is shown in Fig. 5; the quantum yield was calculated with a reaction scheme similar to scheme (A) for the reaction of propylene. Owing to the considerable inherent difficulties in the analyses of 1-butene and its mono-deuterated species by microwave spectroscopy, the experimental data showed considerable scattering. Nevertheless Fig. 5 clearly showed that $2\phi_{c-t}$ continuously decreasesed with decreasing pressure and attains a value of 0.45 at the zero pressure intercept. The results in Fig. 4 and Table 2 lead to the conclusion that the mercury photosensitized reaction of 1-butene-*cis*-1-d_1 proceeds *via* scheme (C) which is quite similar to scheme (B) for the reaction of propylene-*cis*-1-d_1.

Scheme(C)

Main reaction at high pressure:

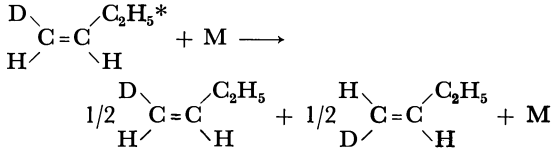

At low pressure:

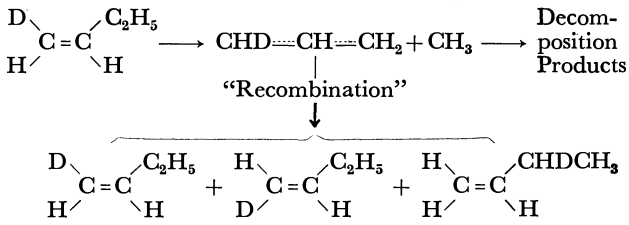

In the reaction of 1-butene-*cis*-1-d_1 the decomposition products were not analyzed accurately, and the pressure dependence of ϕ_{decomp} or an estimation of the quantum yield of the "recombination" reaction was not available for discussion. However, when the data for the deuterium distribution within 1-butene was compared with that for propylene, their similarity strongly suggested that the same conclusion concerning the balance between the number of the reacted molecules and the absorbed photons may also be derived for 1-butene-*cis*-1-d_1.

Thus, microwave spectroscopy was applied to the study of the mercury photosensitized reactions of propylene-*cis*-1-d_1 and 1-butene-*cis*-1-d_1, and some of the reaction paths involved in these reactions were revealed.

The authors are grateful for the assistance of Dr. A. C. Herd in preparing this manuscript.

BULLETIN OF THE CHEMICAL SOCIETY OF JAPAN, VOL. 44, 2993—3000 (1971)

Re-examination of the Cycloaddition of Cycloheptatriene with Maleic Anhydride

Hiroyuki ISHITOBI, Hiroshi TANIDA, Kazuo TORI, and Teruji TSUJI

Shionogi Research Laboratory, Shionogi & Co., Ltd., Fukushima-ku, Osaka

(Received May 28, 1971)

Cycloaddition of cycloheptatriene to maleic anhydride was re-examined and found to produce, in addition to the reported main product *anti*-tricyclo[3.2.2.$0^{2,4}$]non-6-ene-*endo*-8,*endo*-9-dicarboxylic anhydride (**1**), the exo, exo isomer of this compound (**4**) and bicyclo[3.2.2]nona-2,6-diene-*endo*-8,*endo*-9-dicarboxylic anhydride (**5**). Evidence for these structures involving the orientation of the cyclopropane ring in **1** and **4** and the configuration of the carboxylic anhydride was provided by PMR spectroscopy using the intramolecular nuclear Overhauser effect and paramagnetic induced shift due to tris(dipivalomethanato)europium(III). The structure assignment by Alder and Jacobs for **1** was found to be correct, but not the one by Schenk *et al.* The difference in free energies of activation leading to **1** and **4** was determined.

An addition reaction of cycloheptatriene to maleic anhydride was first reported by Kohler and his coworkers.[1] For this adduct, the structure of *anti*-tricyclo[3.2.2.$0^{2,4}$]non-6-ene-*endo*-8,*endo*-9-dicarboxylic anhydride (**1**) was assigned by Alder and Jacobs.[2] Although the structure of the ring system seems to be

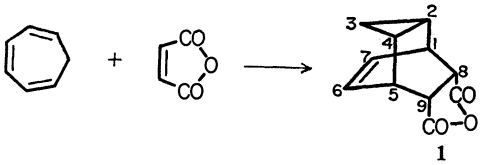

1

unequivocal from the data on chemical transformations, conclusive evidence has not yet been obtained for the *anti* orientation of the cyclopropane ring and the *endo*

1) E. P. Kohler, M. Tishler, H. Potter, and H. T. Thompson, *J. Amer. Chem. Soc.*, **61**, 1057 (1939).

2) K. Alder and G. Jacobs, *Chem. Ber.*, **86**, 1528 (1953).

configuration of the carboxylic anhydride group.[3,4] An important result by Alder and Jacobs[2] favourable to the *endo* configuration of the carboxylic group is the fact that the adduct could be lactonized to the bromolacto acid (**2**) by treatment with bromine in water and,

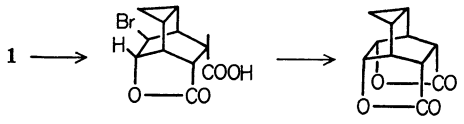

2 **3**

furthermore, to the dilactone (**3**). It was, however, pointed out that such a reaction causes Wagner-Meerwein rearrangements whereby even an *exo* acid forms lactone.[5,6] More recently, Schenk and his co-workers found that the photosensitized addition between cycloheptatriene and maleic anhydride gave mainly Alder's adduct, in addition to two minor compounds, and they assigned the *exo* configuration for the carboxylic anhydride group on the grounds that treatment of the adduct with a basic iodine-potassium iodide solution did not cause iodolactonization.[7,8] However, such a result is worthless for a stereochemical determination unless it is proven that in the treatment one isomer is positive and the other negative. However, this other isomer is still unknown. Prematurely accepting the Alder and Jacobs's structure, one of us (K.T.) used the adduct as a model for the investigation of anisotropic long-range shielding effects of a cyclopropane ring in PMR spectroscopy.[9]

Accordingly, we undertook a re-examination of the cycloaddition reaction and a determination of the configuration of the adduct, mainly by means of PMR spectroscopy. It was found that the reaction produces, besides the reported adduct, another carboxylic anhydride isomer and a bicyclo[3.2.2]nona-2,6-diene derivative, the last compound indicating a new behavior of cycloheptatriene in cycloaddition.

Products. The reaction mixtures were prepared at the indicated reaction temperature by mixing a slight excess of cycloheptatriene and a 0.1 M solution of maleic anhydride in xylene. The reaction at 120°C took about 3 hr for completion. Sampling from the reaction mixture was carried out at given time intervals in order to analyze the products by VPC. The analysis revealed the formation of three products which were isolated for structure determination by a combination of recrystallization and elution chromatography. Relative yields of these products were determined by VPC as a function of reaction temperature and are presented in Table 1. The melting point of the predominant product (**1**), 100.5—101°C, was identical with that reported by Kohler[1] and Alder[2] for their adduct and that by Schenk *et al.* for their most important product.[7] Hydrolysis of the second major product (**4**), mp 112—113°C, in methanol containing a drop of sulfuric acid, followed by epimerization with

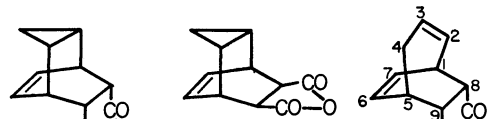

1 **4** **5**

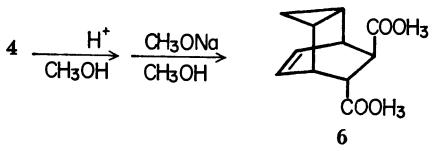

6

sodium methoxide in methanol, yielded a *trans*-dicarboxylic ester (**6**), which was identical with the compound obtained by the cycloaddition of cycloheptatriene to fumaryl chloride followed by methanolysis.[2]

Table 1. Reaction temperature-dependence of product ratio

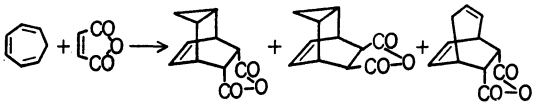

1 **4** **5**

Temp (°C)	Reaction time (hr)	**1** (%)	**4** (%)	**5** (%)	log **1**/**4**
80	2.0	90.20	9.30	~0.5	0.987
80	4.0	91.26	8.24	~0.5	1.044
120	1.0	88.16	11.18	0.66	0.897
120	2.0	88.19	11.32	0.49	0.892
120	3.0	87.59	11.70	0.73	0.874
149.5	0.5	87.72	13.66	0.62	0.798
149.5	1.0	86.12	12.96	0.92	0.822
176.5	0.5	82.03	16.85	1.12	0.687
176.5	1.0	83.83	15.01	1.16	0.747

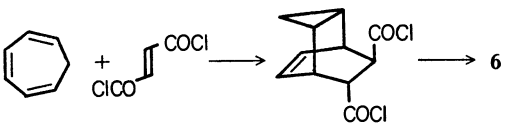

Since **6** was also obtained from the adduct of Alder and Jacobs, the compounds of mp 100—101°C and 112—113°C are concluded to be *exo* and *endo* carboxylic anhydride isomers and to have an identical orientation concerning the cyclopropane ring. The standard procedure of iodolactonization[7,10] was found to be unsuccessful for both **1** and **4**, so that the assignment of

3) A. S. Onishchenko, "Diene Synthesis," Israel Program for Scientific Translations, Jerusalem (1964), pp. 373—375.

4) M. J. Goldstein and A. H. Gevirtz, *Tetrahedron Lett.*, **1965**, 4417.

5) R. B. Woodward and H. Baer, *J. Amer. Chem. Soc.*, **70**, 1161 (1948).

6) C. D. Ver Nooy and C. S. Rondestvedt, Jr., *ibid.*, **77**, 3583 (1955).

7) G. O. Schenk, J. Kuhls, and C. H. Krauch, *Ann. Chem.* (Justus Liebigs), **693**, 20 (1966).

8) Iodolactonization in the absence of Wagner-Meerwein rearrangement has been demonstrated. cf. 5).

9) K. Tori and K. Kitahonoki, *J. Amer. Chem. Soc.*, **87**, 386 (1965).

10) H. Stockmann, *J. Org. Chem.*, **26**, 2025 (1961).

configuration of the carboxylic anhydride by Schenk *et al.* is inconclusive. Bromolactonization with **1** proceeded smoothly with the formation of colorless crystals, but the reaction with **4** gave a viscid tar. The structure of the bromolactone from **1** and the possibility of Wagner-Meerwein rearrangement in this reaction were not investigated. Confirmatory evidence for the tricyclic nature, the orientation of the cyclopropane ring, and the configuration of the carboxylic anhydride group in the structures of **1** and **4** was obtained from their PMR spectroscopic studies.

The minor third product (**5**) showed a melting point, 112—113°C, identical with that recorded by Schenk *et al.* for their bicyclic adduct.[7] Iodolactonization of **5** gave an iodolactone, whose melting point was the same as that reported.[7] The bicyclic structure of **5** was evident on integrating the vinyl proton signals in its PMR spectrum. The thermal conversion of **1** into **5** was observed on heating 1 at 220°C, but not under the mild conditions employed for the present cycloadditon.[11] To our knowledge, **5** is the first cycloadduct from cycloheptatriene which is formed without precedence of the norcaradiene transition state or intermediate.

Kinetic Treatment. Since the relative yields of products in Table 1 were confirmed to be independent of the reaction time within maximum experimental error of 0.9%, they are kinetically controlled ones. If we assume that the formation of all three products in a given run follows rate laws of the same form, the yield ratios are equal to those of the specific rate coefficients, $k_1 : k_4 : k_5$. Since the ground state reactants leading to the transition states in the independent pathways (k_1, k_4, and k_5) are identical, $\log(k_1/k_4)$ is

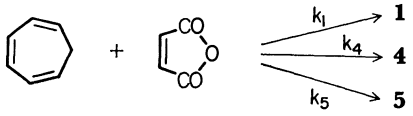

directly proportional to the free energy difference between the two transition states in the k_1 and k_4 pathways. The k_5 pathway is omitted from this treatment because of experimental errors which are unavoidable owing to the very small yield of **5**. The temperature dependence

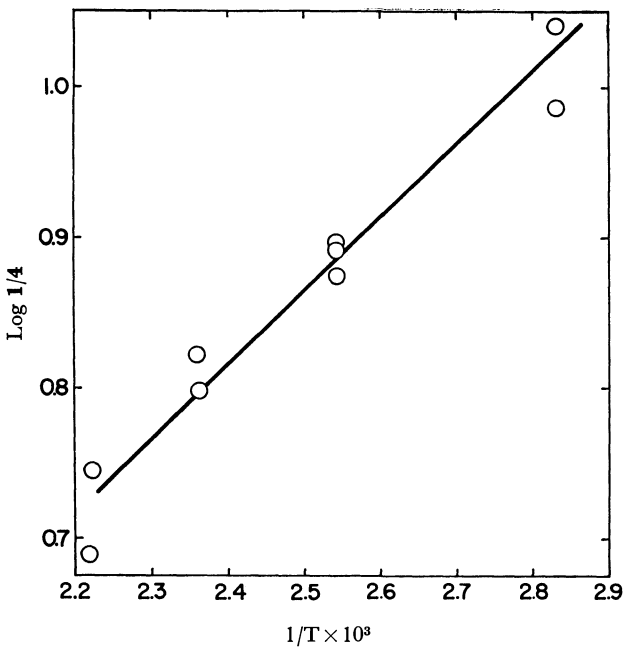

Fig. 1. Arrhenius plots of product ratios, **1/4**.

of the product ratio, expressed in the Arrhenius form gives

$$\log(k_1/k_4) = \log(A_1/A_4) + (E_4 - E_1)/2.303RT \quad (1)$$

for the ratio of the pre-exponential factors and for the difference in empirical activation energy from the intercepts and slope, respectively, of plots of $\log(k_1/k_4)$ *vs.* 1/T. The difference in entropy of activations is given by

$$\Delta S_1^{\ddagger} - \Delta S_4^{\ddagger} = 2.303R \log(A_1/A_4) \quad (2)$$

while the difference in enthalpy of activation is identical with the difference in the Arrhenius activation energy.[12] Regression analysis of logarithms of the relative yields of **1** and **4** on 1/T gave a good linear relationship with a slope of 0.481×10^3 (correlation coefficient 0.9760) as shown in Fig. 1. The equations gave 2.20 ± 0.18 kcal/mole for $\Delta H_1^{\ddagger} - \Delta H_4^{\ddagger}$ and -1.6 ± 0.5 cal/deg for $\Delta S_1^{\ddagger} - \Delta S_4^{\ddagger}$. Since the relative yields in Table 1 were

Table 2. Chemical shift (δ in ppm downfiled from TMS) and coupling constant (J in Hz) in $CDCl_3$ and C_6D_6 (in parentheses)

Compd.	δ						J		
	$H_{1(5)}$	$H_{2(4)}$	H_{3s}	H_a	$H_{6(7)}$	$H_{8(9)}$	$J_{2,3a}$	$J_{2,3s}$	$J_{3a,3s}$
1	3.43	1.13	0.25	0.35	5.88	3.27	7.3	4.0	(−) 6.1
	(3.02)	(0.46)	(−0.12)	(−0.07)	(5.38)	(2.56)			
4	3.41	1.10	0.14	0.22	5.95	3.09	7.5	4.0	(−) 5.5
	(2.88)	(0.70)	(−0.26)	(−0.32)	(2.23)	(2.22)			
7	2.57	1.11	0.86	0.65	~1.34	3.28	7.5	3.4	(−) 6.5
	(2.12)	(0.38)	(~0.3)	(~0.1)	(0.75)	(2.42)			
					(0.95)				
8	2.62	0.97	0.62	0.46	~1.33	3.11	7.6	3.4	(−) 6.0
	(2.11)	(0.55)	(0.03)	(−0.15)	~1.49	(2.13)			
					(~0.76)				
					(~0.52)				

11) T. Tsuji, H. Ishitobi, and H. Tanida, This Bulletin, **44**, 2447 (1971).

12) Substantially the same treatment was carried out for the reaction of cyclopentadiene with some dienophiles. J. A. Berson, Z. Hamlet, and W. A. Mueller, *J. Amer. Chem. Soc.*, **84**, 297 (1962).

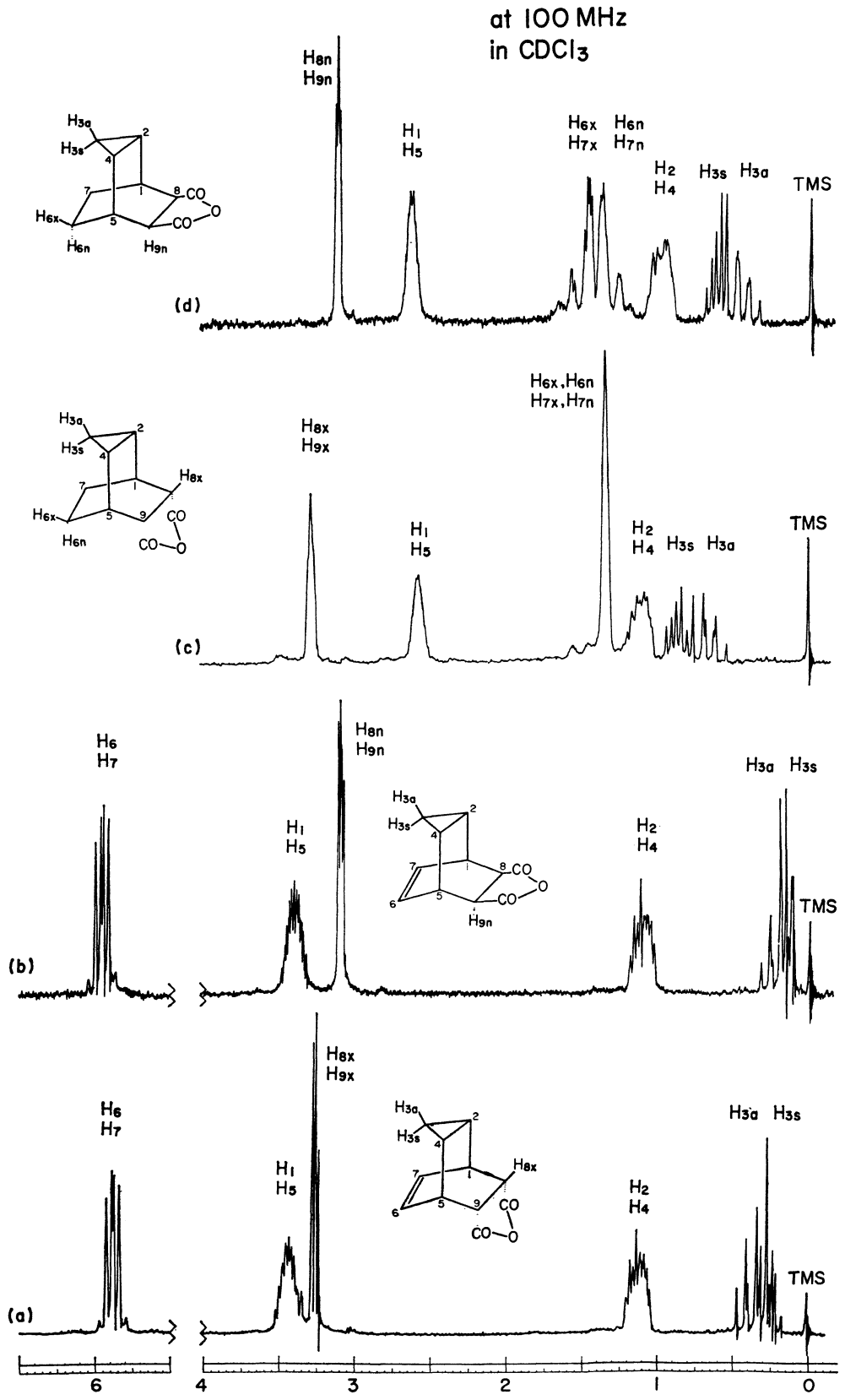

Fig. 2. The 100-MHz PMR spectra of (a) **1**, (b) **4**, (c) **7**, and (d) **8** in $CDCl_3$.

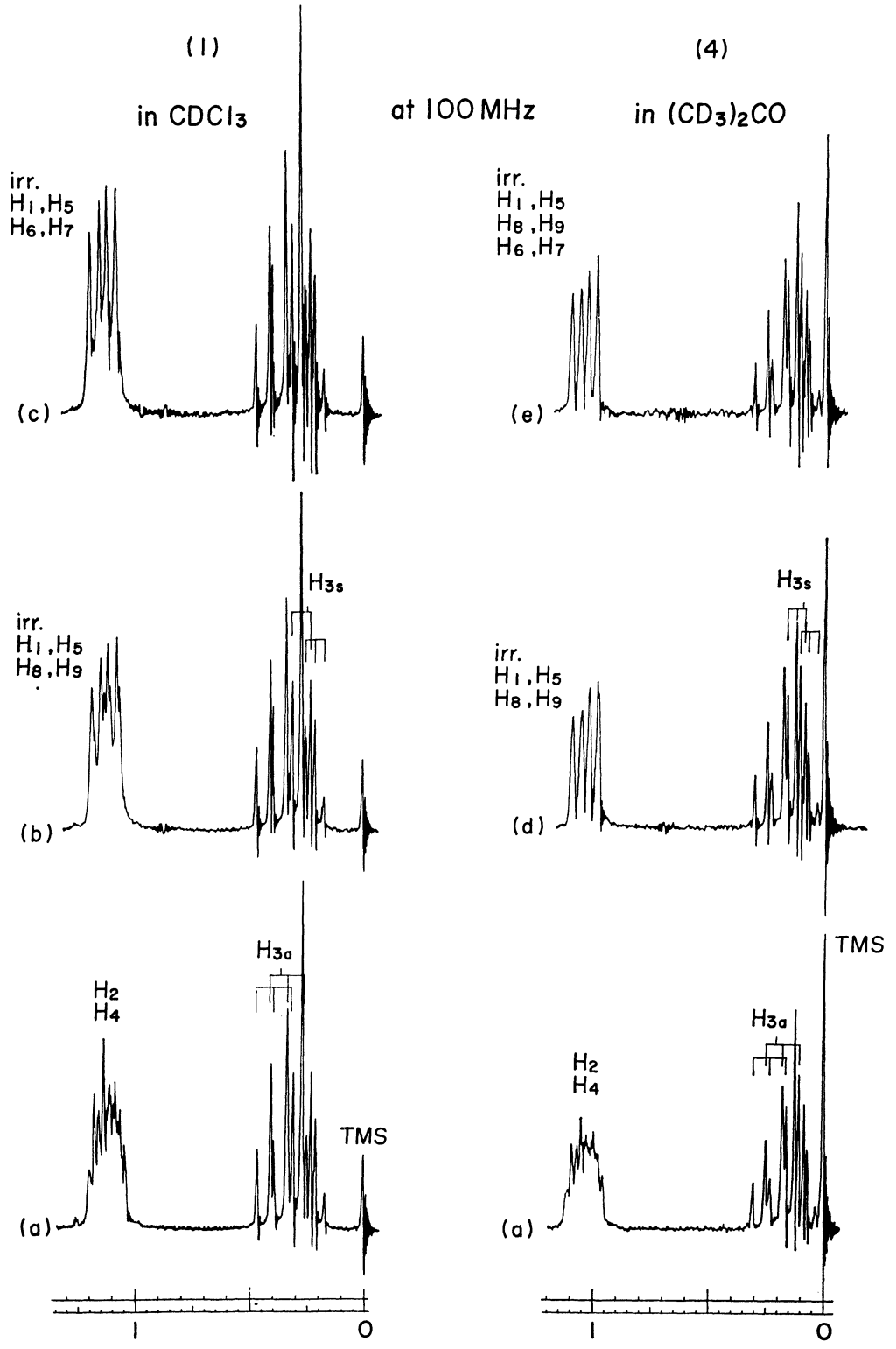

Fig. 3. The 100-MHz PMR (a), PMDR (d), and PMTR (b, c, e) spectra of **1** in $CDCl_3$ and of **4** in acetone-d_6.

constant during the reaction periods with in $\pm 0.9\%$, the values for $\log(k_1/k_4)$ are reliable for 0.02—0.06 units.

It has been reported by Diels and Alder[13] that cyclopentadiene and 1,3-cyclohexadiene show extreme stereospecificity in their additions with maleic anhydride by the formation of a single endo adduct. We traced the reaction with 1,3-cyclohexadiene by means of VPC and confirmed the absence of the exo adduct in amounts greater than 0.2%. Therefore, the decreased stereospecificity of cycloheptatriene presently observed is very notable.

PMR studies. The 100-MHz PMR spectra of **1**, **4**, and their hydrogenation products, **7** and **8**, in

13) O. Diels and K. Alder, *Ann. Chem.* (Justus Liebigs), **460**, 98 (1928). Also, see M. C. Kloetzel "Organic Reactions," Vol. IV, John Wiley & Sons, Inc., New York, N. Y. (1948), p. 1.

$CDCl_3$ are shown in Fig. 2. The spectra of these compounds were also measured in benzene-d_6. The data obtained are listed in Table 2. Signals due to H_{3s} and H_{3a} were assigned according to the known general sequence of the J values between cyclopropane ring protons.[14] The assignment of other signals though simple was confirmed by spin-decoupling experiments.

The anisotropic long-range shielding effect of a cyclopropane ring is well understood,[14] and it is apparent that the cyclopropane rings in **1** and **4** are *syn* to their double bonds in view of the abnormally high-field positions of their olefinic-proton signals. Accordingly, **1** and **4** are determined to be *endo*-8,*endo*-9- and *exo*-8,*exo*-9-isomers, respectively, from the fact that the $H_{8(9)}$ signal of **7** appears at a lower field than that of **8** (see Table 2). The anisotropic shielding effect of the C-6: C-7 double bond[15] upon H_{3s} and H_{3a} and that of the two carbonyl groups[16] upon $H_{6(7)}$ are also consistent with the molecular configurations.

However, the use of chemical shift difference to determine molecular structure is sometimes risky, particularly for bridged bicyclic compounds.[17,18] Therefore, intramolecular nuclear Overhauser effect (NOE)[19] measurements and paramagnetic shifts induced by tris-(dipivalomethanato)europium(III). $Eu(DPM)_3$,[20] have been applied to assign the configurations of the cyclopropane and the acid-anhydride rings of **1** and **4**.

The NOE measurements on **1, 4, 7,** and **8** in $CDCl_3$ are summarized in Table 3. The nuclear Overhauser effects observed for the H_{3s} signals on saturating the $H_{6(7)}$ signals and *vice versa* by double irradiation evidence the *syn* configurations of the cyclopropane rings to the double bonds. The fact that the NOE's between the $H_{2(4)}$ and $H_{8(9)}$ signals were observed for **1** and **7**, but not for **4** and **8**, show that the configurations of the acid-anhydride rings are as illustrated by their formulas. Further, the five-bond long-range spin-couplings[21] observed between H_{3a} and $H_{8(9)}$ ($|J|=0.2$ Hz) in **4** and **8** are consistent with their assigned configurations. Figure 3 shows some results with double and triple resonance experiments on **1** and **4**; the experiments on **4** are shown with the spectra taken in acetone-d_6 because the H_{3s} and H_{3a} signals appeared as the first-order patterns in this solvent.

Table 3. Nuclear overhauser effect values (%)

Observed signal	Saturted signal	Compound 1	4	7	8
$H_{1(5)}$	$H_{2(4)}$	6	6	9	8
$H_{1(5)}$	$H_{6(7)}$	8	10	15	a)
$H_{2(4)}$	$H_{1(5)}$	8	7	a)	a)
$H_{2(4)}$	$H_{6(7)}$	nil	nil	a)	a)
$H_{2(4)}$	$H_{8(9)}$	10	nil	b)	nil
H_{3s}	$H_{6(7)}$	5	5	b)	a)
$H_{6(7)}$	$H_{1(5)}$	11	10	a)	a)
$H_{6(7)}$	$H_{2(4)}$	nil	nil	a)	a)
$H_{6(7)}$	H_{3s}	3	3	a)	a)
$H_{8(9)}$	$H_{2(4)}$	8	nil	7	nil
$H_{8(9)}$	$H_{6(7)}$	nil	nil	nil	a)

a) Unmeasurable
b) Positive but undeterminable

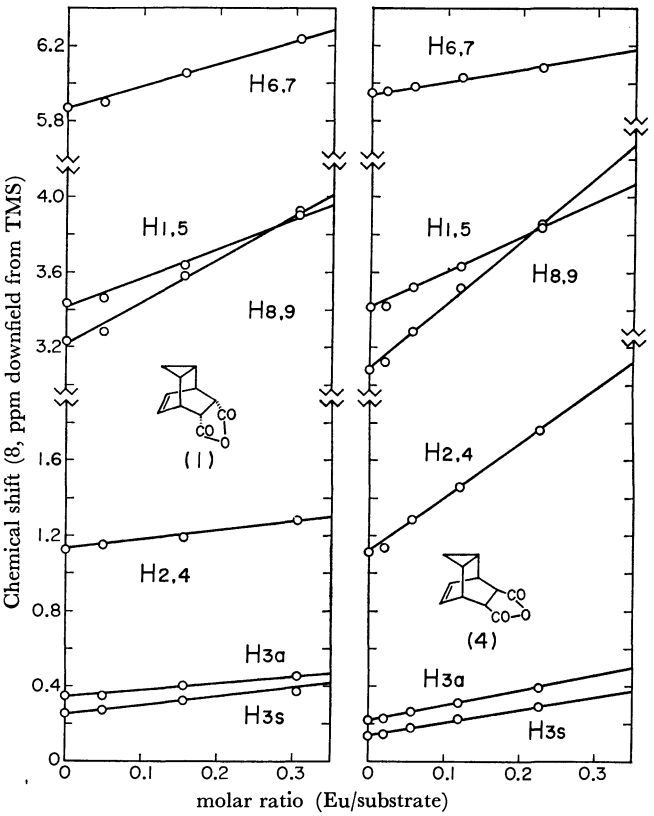

Fig. 4. Paramagnetic induced shift measurements for **1** and **4** using $Eu(DPM)_3$ in $CDCl_3$.

Much interest has been shown in the application of paramagnetic shifts induced by lanthanide complexes such as $Eu(DPM)_3$ in the PMR spectra of molecules having substituents with lone-pair electrons.[20] The paramagnetic shifts caused by $Eu(DPM)_3$ has been considered to result mainly from the pseudocontact shift.[20,22] Therefore, the stereostructure of a compound

Table 4. S-Values for $Eu(DPM)_3$ in $CDCl_3$ (in ppm; +sign denotes a downfield shift)

Compd.	$H_{1(5)}$	$H_{2(4)}$	H_{3s}	H_{3a}	$H_{6(7)}$	$H_{8(9)}$
1	+1.51	+0.49	+0.49	+0.31	+1.14	+2.26
4	+1.90	+2.93	+0.80	+0.93	+0.67	+3.37

14) a) L. M. Jackman and S. Sternhell, "Applications of Nuclear Magnetic Resonance Spectroscopy in Organic Chemistry," 2nd ed., Pergamon Press, Oxford (1969), p, 98; b) F. A. Bovey, "Nuclear Magnetic Resonance Spectroscopy," Academic Press, New York, N.Y. (1969), p. 71.
15) J. W. ApSimon, W. G. Craig, P. V. Demarco, D. W. Mathieson, L. Saunders, and W. B. Whalley, *Tetrahedron*, **23**. 2357 (1967), and references therein.
16) J. W. ApSimon, P. V. Demarco, D. W. Mathieson, W. G. Craig, A. Karim, L. Saunders, and W. B. Whalley, *ibid.*, **26**, 119 (1970), and references therein.
17) K. Tori, A. Aono, Y. Hata, R. Muneyuki, T. Tsuji, and H. Tanida, *Tetrahedron Lett.*, **1966**, 9.
18) a) R. G. Foster and M. C. McIvor, *J. Chem. Soc., B*, **1969**, 188; b) R. G. Foster and M. C. McIvor, *Org. Mag. Res.*, **1**, 203 (1969).
19) F. A. L. Anet and A. J. R. Bourn, *J. Amer. Chem. Soc.*, **87**, 5250 (1965).
20) a) J. K. M. Sanders and D. H. Williams, *ibid.*, **93**, 641 (1971); b) K. Tori, Y. Yoshimura, and R. Muneyuki, *Tetrahedron Lett.*, **1971**, 333, and references therein.
21) K. Tori and M. Ohtsuru, *Chem. Commun.*, **1966**, 886.
22) D. R. Eaton, *J. Amer. Chem. Soc.*, **87**, 3097 (1965).

Table 5. Benzene induced solvent shift
($\Delta\delta_{C_6D_6-CDCl_3}$ in ppm; −sign denoted an upfield shift)

Compd.	$H_{1(5)}$	$H_{2(4)}$	H_{3s}	H_{3a}	$H_{6(7)}$	$H_{8(9)}$
1	−0.41	−0.67	−0.37	−0.42	−0.50	−0.71
4	−0.53	−0.40	−0.40	−0.54	−0.72	−0.87
7	−0.45	−0.73	∼−0.55	∼−0.55	−0.39 −0.59	−0.86
8	−0.51	−0.42	−0.59	∼−0.61	−0.73 −0.81	−0.98

can sometimes be determined by a consideration of paramagnetic shift parameters, *S*-values,[23] measured for each proton signal.[24] The *S*-value is represented by the equation $\delta_E=\delta+S\cdot\mathrm{Eu(DPM)_3/substrate}$ (molar ratio), where δ_E and δ are the chemical shifts of a proton in complexed and uncomplexed molecules, respectively.[23]

Examinations of Dreiding models show that S-values for $H_{2(4)}$ and $_{6(7)}$ in **1** should be respectively smaller and larger than those in **4**. Figure 4 shows the relationships between the chemical shifts of proton in **1** and **4** and the molar ratios of $Eu(DPM)_3$ added to the substrates. The *S*-values obtained are listed in Table 4.

Table 4 shows that the S-value of $H_{2(4)}$ is considerably larger in **4** than in **1**, and the value of $H_{6(7)}$ is smaller in **4** than in **1**. The *S*-values of H_{3s} and H_{3a} in both compounds are small, as was expected. These facts confirm the stereostructutes of **1** and **4**. It should be noted that the complexing ability of the acid-anhydride function with $Eu(DPM)_3$ is fairly weak. The difference in the *S*-values of $H_{8(9)}$ between **1** and **4** cannot immediately be explained.

The benzene induced shift, $\Delta\delta_{C_6D_6-CDCl_3}$,[25] also supports the structures of the present compounds, because thay have an acid-anhydride function. Table 5 lists the benzene-induced shifts for **1**, **4**, **7**, and **8**. The high-field shift values of $H_{2(4)}$ for **1** and **7** are larger than those for **4** and **8**, respectively, whereas the corresponding shift values of $H_{6(7)}$ show opposite trends. These facts are consistent with the structure of the compounds.

Experimental

All melting points were determined in capillary tubes and are corrected. Infrared spectra were determined with a Nippon Bunko IR-S spectrometer. VPC analysis was carried out on a Hitachi-Perkin-Elmer gas chromatograph F-6D equipped with a hydrogen flame ionization detector, using a 1 m×3 mm stainless steel column packed with 5% XE 60 on Chromosorb W.

The 100-MHz PMR spectra were taken with a Varian HA-100 spectrometer using about 5% (w/v) carefully degassed solutions in $CDCl_3$, benzene-d_6, and(or) acetone-d_6 in the frequency-swept and internal $CHCl_3$-locked mode. Calibration of the charts was carried out by direct readings of resonance frequencies, using a Hewlett-Packard HP-5212A electronic counter to an accuracy of ±0.1 Hz. PMDR and PMTR experiments were performed using the spectrometer and two Hewlett-Packard HP-200ABR audiooscillators. Chemical shifts are expressed in δ, ppm downfield from tetramethylsilane as an internal standard with an accuracy of ±0.01 ppm, and coupling constants are in Hz with an accuracy of ±0.1 Hz.

Reaction of Maleic Anhydride with Cycloheptatriene. A solution of 24.4 g of cycloheptatriene and 20 g of maleic anhydride in 100 m*l* of xylene was refluxed for 3 hr. VPC analysis of the reaction solution, operated at 180°C with a flow pressure of 1.3 kg/cm², showed three peaks at retention times of 6 min 30 sec, 7 min 20 sec, and 11 min and with relative areas of 11: 1: 88. The solvent was evaporated under reduced pressure and the residue was recrystallized from ligroin to give 27 g of *anti*-tricyclo[3.2.2.0^{2,4}]non-6-ene-*endo*-8,*endo*-9-dicarboxylic anhydride (**1**) in 69.7% yield, mp 100.5—101°C (lit.,[2] mp 101°C), corresponding to the peak at 11 min. The mother liquor was concentrated to dryness and subjected to elution chromatography on 150 g of silica gel using ether-pentane to give 3.8 g of a mixture of the two minor products in a ratio of 13: 1 as the first fraction eluted. Absence of of the *endo* product in this mixture was confirmed by VPC. The mixture was recrystallized twice from hexane to afford 2.1 g (5.4%) of *anti*-tricyclo[3.2.2.0^{2,4}]non-6-ene-*exo*-8,*exo*-9-dicarboxylic anhydride (**4**), mp 112—113°C, which corresponded to the peak at 6 min 30 sec; IR (CCl_4) 1870, 1782, and 1220 cm^{-1} (C=O), NMR ($CDCl_3$) τ 9.85 (m, 2H at C-3), 8.85 (m, 2H at C-2 and 4), 6.95 (t, J=1.5 Hz, 2H at C-8 and 9), 6.6 (m, 2H at C-1 and 5), and 3.08 (d-d, J=5 and 3.3 Hz, 2H at C-6 and 7).

Found: C, 69.74; H, 5.46%. Calcd for $C_{11}H_{10}O_3$: C, 69.46; H, 5.30%.

Catalytic reduction in a mixed solution of acetic acid and acetic anhydride (15: 1) gave *anti*-tricyclo[3.2.2.0^{2,4}]nonane-*exo*-8,*exo*-9-dicarboxylic anhydride, which was recrystallized from ligroin to give a pure sample, mp 153—154°C.

Found: C, 68.54; H, 6.25%. Calcd for $C_{11}H_{12}O_3$: C. 68.73; H, 6.29%.

Quantitative Products Distribution. Cycloheptatriene sealed in a thin-walled glass capillary, a clean iron bar and 3 m*l* of a 0.1M solution of maleic anhydride dissolved in xylene were placed in a heavy-walled glass ampoule and sealed. The ampoule was immersed in a constant temperature bath (±0.03°C). After temperature equilibrium had been reached, the cycloheptatriene capillary was crushed with the iron bar and the reaction allowed to proceed. Analysis of the products was carried out by VPC, and relative yields of the three adducts were determined by integration of the component peaks with a planimeter with correction for the relative sensitivity of the detector. The control experiments showed that the proportions of adducts were strictly independent both of the yields of the products and of initial proportions of the reactants. The reaction time necessary for detection of the products by VPC varied from 10 min at at 176.5°C to 1 hr at 80°C, but further heating did not affect the relative proportions of the product. Table 1 gives the

23) A. F. Cockerill and D. M. Rackham, *Tetrahedron Lett.*, **1970**, 5149.
24) J. Briggs, F. A. Hart, and G. P. Moss, *Chem. Commun.*, **1970**, 1506.
25) P. Laszlo, *Progr. Nucl. Magn. Resonance Spectrosc.*, **3**, 231 (1967).

data thus obtained.

Dimethyl anti-*Tricyclo*[3.2.2.$0^{2,4}$]*non-6-en-8,9*-trans-*dicarboxylate (6)*. A solution of 300 mg of the anhydride (**4**) and 0.3 m*l* of concentrate sulfuric acid in 8 m*l* of methanol was refluxed for 2.5 hr. After the usual work-up, the *exo-exo* dimethylcarboxylate obtained was dissolved in 8 m*l* of basic methanol, prepared by dissolving 60 mg of sodium into methanol and then refluxed for 5 hr. After removal of the solvent the reaction product was diluted with water and extracted with ether. Evaporation of the ether gave 280 mg of **6** which was identical with an authentic sample[2] obtained by quenching cycloheptatriene-fumaryl chloride adduct with methanol.

Iodolactonization of Adducts. A mixture of 1.0 g of the bicyclic adduct (**5**), 1.8 g of sodium bicarbonate and 30 ml of water was stirred for 20 min at room temperature, and then 13.5 m*l* of a iodine-potassium iodide solution (prepared by dissolving 5 g of iodine and 15 g potassium iodide into 50 m*l* of water) was added to the mixture. During the course of the reaction the initially suspended **5** gradually dissolved and the red colour of the mixture faded. After 4 hr the reaction mixture was made acidic with hydrochloric acid and extracted with dichloromethane. The extract was washed with aqueous sodium thiosulfate and water, and dried over sodium sulfate. After removal of the solvent, 1.3 g of the iodolactone was recrystallized from benzene to give a pure sample, mp 147°C (lit,[7] 147—148°C).

Similar attempts to prepare iodolactones from **1** and **4** failed, the red colour of iodine remaining almost unchanged even after treatment for 24 hr.

Bromolactonization of the Tricyclic Adducts. A solution of 500 mg of the *endo* tricyclic adduct and 230 mg of sodium hydroxide in 7.5 m*l* of water was stirred for 30 min under ice-cooling, and bromine was added slowly until the colour of the bromine persisted. The resulting milky solution was further stirred for 30 min and acidified with hydrochloric acid to give 450 mg of the bromolactone which was recrystallized from ether-hexane to give a pure sample mp 197—198°C (lit,[2] 185°C).

Found: C, 46.29; H, 3.93; Br, 27.55%. Calcd for $C_{11}H_{11}O_4Br$: C, 46.02; H, 3.86; Br, 27.84%.

The same procedure for the *exo* anhydride resulted in the formation of a high molecular product.

BULLETIN OF THE CHEMICAL SOCIETY OF JAPAN, VOL. 44, 3000—3003 (1971)

Kinetics of Silver(I) Ion Catalysed Oxidation of Glycine by Peroxodisulphate Ion

G. CHANDRA and S. N. SRIVASTAVA
Chemical Laboratories, Agra College, Agra, India

(Received December 10, 1970)

The kinetics of Ag(I) ion catalysed oxidation of glycine by peroxodisulphate in aqueous medium has been studied. The reaction is found to be first order in peroxodisulphate and Ag(I) ions and almost independent of glycine concentration. The rate constant is found to decrease with the increase in the concentration of peroxodisulphate ion. Addition of neutral salts shows a retarding effect. A suitable mechanism has been proposed and a theoretical rate law has been derived to account for the results.

The peroxodisulphate ion is one of the strongest oxidizing agents known in aqueous solution. The standard oxidation-reduction potential for the reaction

$$2SO_4^{2-}\,(aq.) \longrightarrow S_2O_8^{2-}\,(aq.) + 2e^-$$

is estimated to be -2.01 V.[10] The reactions involving this ion are generally very slow in the absence of suitable catalysts.[2] The most thoroughly investigated catalyst is Ag(I) ion although reactions involving Cu(II) and Fe(III) ions also have been studied.[3]

Only a very few kinetic studies have been made so far on organic nitrogen compounds. The kinetics of oxidation of urea and acetamide[4] has been studied by Agarwal and Mushran. Ag(I) ion catalysed oxidation of formamide[5] by peroxodisulphate was also investigated by the above authors. Recently Bacon and his coworkers[6] studied certain aspects of Ag(I) ion oxidation of primary aliphatic amines and α-amino acids.

This paper deals with the kenetics of Ag(I) catalysed oxidation of glycine by peroxodisulphate. A mechanism has been proposed and a theoretical rate law has been derived to account for the kinetic data.

Experimental and Results

Potassium peroxodisulphate of G.R.E. Merck quality, glycine and silver nitrate A.R. B.D.H. quality were dissolved in redistilled water for preparing standard solutions. All other chemicals used were also of analytical grade. Potassium peroxodisulphate solution was always prepared fresh. The standard solutions were stored in Jena glass bottles and the same solutions were used throughout the course of investigation.

1) W. M. Latimer, "The Oxidation States of Elements and Their Potentials in Aueuous Solutions," Prentice Hall, N.Y.(1952).
2) H. Marshall, *J. Chem. Soc.*, **59**, 771 (1891).
3) R. Woods, I. M. Kolthoff, and E. J. Meehan, *Inorg. Chem.*, **4**, 697 (1965)
4) M. C. Agarwal and S. P. Mushran, *J. Indian Chem. Soc.*, **42**, 629 (1965); **43**, 343 (1966).
5) M. C. Agarwal and S.P. Mushran, *Chim. Anal.*, **50**, 310 (1968).
6) a) R. G. R. Bacon and D. Stewart, *J. Chem. Soc., C*, **1966**, 1384. b) R. G. R. Bacon, W. J. W. Hanna, and D. Stewart, *ibid.*, **1966**, 1388.

Table 1

Glycine=0.01M, $AgNO_3$=0.0005M, Temp.=35°C

Time in min	$K_2S_2O_8$=0.005M		$K_2S_2O_8$=0.01M		$K_2S_2O_8$=0.02M	
	$Na_2S_2O_3$ ml	$k/2.303\times10^3$ min^{-1}	$Na_2S_2O_3$ ml	$k/2.303\times10^3$ min^{-1}	$Na_2S_2O_3$ ml	$k/2.303\times10^3$ min^{-1}
0	5.00	—	5.00	—	10.00	—
10	3.89	10.91[a]	3.90	10.79[a]	9.06	4.29[a]
20	3.16	9 97	3.56	7.38	8.42	3.74
30	2.51	9.97	3.05	7.16	7.68	3.82
40	2.01	9.89	2.61	7.06	7.00	3.87
50	1.60	9.90	2.16	7.29	6.41	3.86
60	1.29	9.81	1.80	7.04	6.09	3.59
70	1.04	9.74	1.67	6.80	5.67	3.52
80	0.84	9.68	1.42	6.83	5.18	3.57
90	0.63	9.98	1.21	6.85	4.78	3.56
Average		9.87		7.05		3.68

a) neglected

All reactions were carried out in pyrex conical flasks coated outside with black japan. Calculated volumes of silver nitrate and glycine were taken in a reaction vessel and were put in a thermostat maintained at 35±0.1°C. To start the reaction the calculated quantities of potassium peroxodisulphate solution were added to the reaction flasks. The progress of the reaction was studied by estimating the remaining peroxodisulphate iodometrically by a slightly modified method of Bartlett and Cotman[7] adopted by Saxena and Singhal.[8] First order rate constants with respect to peroxodisulphate were calculated and the order with respect to glycine was obtained by changing the concentration of glycine keeping the concentrations of other reactants constant.

Effect of Peroxodisulphate Concentration. The results obtained at three different initial concentrations of $K_2S_2O_8$ on the oxidation of glycine are shown in Table 1. First order rate constants were calculated and found to be fairly constant.

The rate constants k calculated from the Table 1 for three different concentrations of $K_2S_2O_8$ *viz.* 0.005M, 0.01M, and 0.02M are 22.70×10^{-3}, 16.22×10^{-3}, and 8.49×10^{-3} min^{-1}, respectively.

It is evident that the reaction is first order in peroxodisulphate at all concentrations of peroxodisulphate. However, as the concentration of $K_2S_2O_8$ is increased, the value of the first order rate constant decreases due to the specific inhibitory effect of K^+ ion.[4,9]

From the data shown in the last row of the 6th column of Table 1 it may be concluded that the equimolecular consumption of $S_2O_8^{2-}$ and glycine takes place. The stoichiometry can be given as

$$S_2O_8^{2-} + NH_2CH_2COO^- + H_2O \xrightarrow{Ag^+} CO_2 + HCHO + NH_3 + SO_4^{2-} + HSO_4^-$$

Effect of Changing Glycine Concentration. Results showing the effect of the change of initial concentrations of glycine on reaction rate are shown in Table 2.

Table 2

$K_2S_2O_8$=0.01M, $AgNO_3$=0.0005M, Temp.=35°C

Initial concentration of glycine (M)	Rate constant $k\times10^3$ min^{-1}
0.005	16.22
0.010	16.22
0.015	16.01
0.020	15.91
0.025	15.98

We see that the rate is uneffected by a chang in glycine concentration and that the reaction is zero order with respect to glycine concentration because the total order is one at equimolecular concentrations of the reactants.

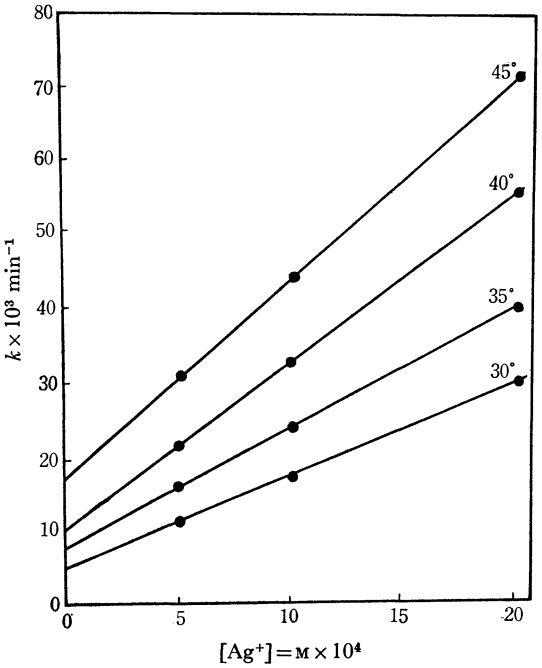

Fig. 1. Variation of rate constant k with the change in the concentration of Ag(I) ion at different temperatures.
$K_2S_2O_8$=0.01 M Glycine=0.01 M

7) P. D. Bartlett and J. D. Cotman, *J. Amer. Chem. Soc.*, **71** 1419 (1949).

8) L. K. Saxena and C. P. Singhal, *Agra Univ. J. Res. Sci.*, **6**, 43 (1957)

9) M. M. Khan and S. P. Srivastava, *J. Indian Chem. Soc.*, **46**, 574 (1969).

Effect of Ag(I) Ion Concentration. The reaction is carried out with different initial concentrations of silver nitrate (the concentrations of other reactants are kept constant) to find the order of reaction with respect to silver ion. In order to show the catalytic activity a graph is plotted between the concentrations of silver ion and rate constants at different temperatures. The plots obtained are straight lines showing direct dependence of reaction rate on silver ion concentration (Fig. 1). As these strainght lines do not pass through origin, it is evident that the uncatalysed oxidation of glycine by peroxodisulphate is also possible. It has been observed that the reaction is slower in absence of Ag(I) ion.

The reaction has also been studied at various temperatures to obtain energy of activation, entropy of activation, frequency factor, *etc.* The results are given in Table 3.

TABLE 3

$K_2S_2O_8$=0.01M, Glycine=0.01M, $AgNO_3$=0.0005M

$k_{35}\times10^3$ min^{-1}	$k_{45}\times10^3$ min^{-1}	Temp. Coeff.	E kcal	A sec^{-1}	S e.u.
16.22	31.32	1.93	12.76	3.27×10^5	−33.45

The entropy of activation is negative. This can be explained on the basis of reaction sequence (5) of the proposed reaction scheme, where a water molecule is incorporated. This will decrease the entropy of activation.[10] A graph showing linear relationship between $\log k$ and $1/T$ has been plotted (Fig. 2).

Effect of Various Neutral Salts. The results of the addition of various neutral salts on the reaction rate are shown in Table 4.

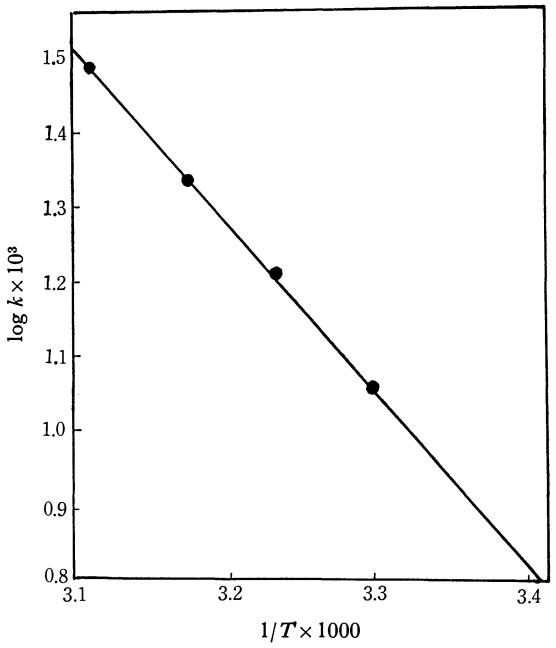

Fig. 2. Linear relationship between $\log k$ and $1/T$.
$K_2S_2O_8$=0.01M, Glycine=0.01M, $AgNO_3$=0.0005M

10) K. J. Laidler, "Chemical Kinetics," McGraw-Hill, London (1965), p. 500.

TABLE 4

$K_2S_2O_8$=0.01M, Glycine=0.01M, $AgNO_3$=0.0005M, Temp.=35°C

Neutral salt	Concentration M×10³	Ionic strength contributed $\mu\times10^3$	Rate constant $k\times10^3$ min^{-1}
NH_4NO_3	1.0	1.0	16.12
	2.0	2.0	16.01
	4.0	4.0	15.82
KNO_3	1.0	1.0	16.07
	2.0	2.0	15.92
	4.0	4.0	15.71
K_2SO_4	1.0	3.0	15.12
	2.0	6.0	14.75
	4.0	12.0	14.12
$Al(NO_3)_3$	1.0	6.0	15.53
	2.0	12.0	15.31
	4.0	24.0	14.89

This shows the retarding effect of some ions on the reaction rate of Ag(I) ion catalysed oxidation of glycine by peroxodisulphate. The rate constants in the presence of 4×10^{-3}M NH_4NO_3, K_2SO_4, and $Al(NO_3)_3$ are 15.82, 14.12, and 14.89×10^{-3} min^{-1}, respectively, and the ionic strength contributed by these salts are 4.0, 12.0, and $24.0\times10^{-3}\mu$, respectively. The decrease in the rate constant is not strictly related to the increase in ionic strength and evidently there is a considerable specific effect of the ions. Similar observations have been obtained by Levitt and Malinowski,[11] and Bartlett and Cotman.[7]

Discussion

Peroxodisulphate oxidation of some organic and inorganic compounds has been reported.[12] It was suggested by Bartlett and Cotman that the initial step in peroxodisulphate oxidation is the formation of two sulphate free radical ions as follows:

$$S_2O_8^{2-} = 2SO_4^-$$

The decomposition may be initiated by dust or impurities present in the solution.

The catalytic activity of silver(I) ion is due to the formation of higher valent silver species. In the case of peroxodisulphate oxidation of oxalate ion catalysed by Ag(I) Allen and Kalb[13] have proposed the formation of bivalent silver. In silver catalysed oxidation of several organic compounds the active species is trivalent silver.[14] However, single electron change in oxidation state of silver ion as catalyst is known.[15,16]

There is a first order dependence of reaction rates with respect to both silver(I) ion and peroxodisulphate concentrations and zero order dependence on glycine. Thus the rate determining step seems to be bimolecular

11) L. S. Levitt and E. R. Malinowki, *J. Amer. Chem. Soc.*, **72**, 4517 (1955).
12) D. A. House, *Chem. Rev.*, **62**, 185 (1962).
13) T. L. Allen and A. J. Kalb, *J. Amer. Chem. Soc.*, **86**, 5107 (1964).
14) D. M. Yost, *ibid.*, **48**, 160 (1926).
15) W. C. Higginson and J. W. Marshall, *J. Chem. Soc.*, **1957**,447
16) S. K. Singhal and S. P. Srivastava, *J. Indian Chem. Soc.*, **46**, 705 (1969).

but gives first order rate constant at constant Ag(I) concentration. The following scheme has been proposed.

$$Ag^+ + S_2O_8^{2-} \xrightarrow{k_1} Ag^{2+} + SO_4^- + SO_4^{2-} \quad (1)$$

The sulphate free radical further reacts with silver ion to produce higher valent silver[17] as follows:

$$SO_4^- + Ag^+ \xrightarrow{k_2} Ag^{2+} + SO_4^{2-} \quad (2)$$

The bivalent silver reacts with glycine and regenerates Ag(I)

$$Ag^{2+} + NH_2CH_2COO^- \xrightarrow{k_3} Ag^+ + NH_2CH_2COO\cdot \quad (3)$$

Like similar radicals[18] $NH_2CH_2COO\cdot$ also decomposes and evolves carbon dioxide

$$NH_2CH_2COO\cdot \xrightarrow{k_4} NH_2\dot{C}H_2 + CO_2 \quad (4)$$

followed by

$$NH_2\dot{C}H_2 + H_2O \xrightarrow{k_5} NH_3 + CH_2O + H\cdot \quad (5)$$

Hydrogen free atom reacts with $S_2O_8^{2-}$ as follows:

$$S_2O_8^{2-} + H\cdot \xrightarrow{k_6} HSO_4^- + SO_4^- \quad (6)$$

The chain terminating step may be

$$SO_4^- + H\cdot \xrightarrow{k_7} HSO_4^- \quad (7)$$

From the foregoing mechanism the rate law is given by equation

$$-\frac{d}{dt}[S_2O_8^{2-}] = k_1[S_2O_8^{2-}][Ag^+] + k_6[H\cdot][S_2O_8^{2-}] \quad (8)$$

Applying the steady state to Eqs. (1)—(7) the following equation can be derived:

$$[H\cdot] = (k_1k_2/k_6k_7)^{1/2}[Ag^+] \quad (9)$$

Substituting this value of $[H\cdot]$ into Eq. (8) we obtain the final rate expression:

$$-\frac{d}{dt}[S_2O_8^{2-}] = \{k_1 + (k_1k_2/k_6k_7)^{1/2}\cdot k_6\}[Ag^+][S_2O_8^{2-}] \quad (10)$$

which is a satisfactory representation of the kinetic rate law, for it explains the observed first order kinetics of peroxodisulphate and zero order dependence on glycine concentration. It is also evident that there is a linear relationship between silver ion concentration and reaction rate when the concentrations of other reactants are kept constant.

Reaction sequence (6) is also supported by the observed increase in the reaction rate caused by the addition of reductant (glycine). Furthermore, the reaction rate is also increased by 20% in N_2 medium. This difference in reaction rate may be explained on the basis of the formation of peroxo radical in presence of air[19] as follows:

$$H\cdot + O_2 = HO_2$$

In this case Eqs. (6) and (7) take the following forms, and k_6' and k_7' will be different from k_6 and k_7.

$$S_2O_8^{2-} + HO_2 \xrightarrow{k_6'} SO_4^- + HSO_4^- + O_2$$

$$SO_4^- + HO_2 \xrightarrow{k_7'} HSO_4^- + O_2$$

Deamination is characteristic of amino acids. Kovats[20] has oxidatively deaminated glycine in the presence of KOH and Cu, the oxidant being KIO_4. The kinetics of reaction between glycine and $KMnO_4$ has been investigated by Pokrovskya.[21] The products were NH_3 and HCN. However, in the present investigation the evolution of CO_2 indicates the degradation of glycine. Identification of formaldehyde was not successful probably because of the reaction with NH_3. However, in the presence of NaOH, formaldehyde has been identified by preparing 2,4-dinitrophenyl hydrazone and determining its melting point.

Thanks are due to the Council of Scientific and Industrial Research, New Delhi, India for the award of a Junior Research Fellowship to one of the authors (G. C.).

17) D. Bacon, "Mechanism of Inorganic Reactions in Solution," McGraw-Hill, London (1968) p. 193.
18) W. A. Water, "Mechanism of Oxidation of Organic Compounds," Methuen & Co. Ltd., London (1964), p. 9.
19) W. A. Water, "Mechanism of Oxidation of Organic Compounds," Methuen & Co., Ltd., London (1964), p. 36.
20) K. Zoltan, *Magyer Kem. Polyoirat.*, **66**, 181 (1960).
21) O. G. Pokrovskaya, *Tr. Novosile. Med. Inst.*, **33**, 156 (1959).

The Dehydrogenation of Butyl Alcohols by the Molten-metal Catalysts

Ken KASHIWADATE, Yasuo SAITO, Akira MIYAMOTO, and Yoshisada OGINO
Department of Chemical Engineering, Faculty of Engineering, Tohoku University, Aramaki, Aoba, Sendai
(Recieved May 29, 1971)

In order to investigate the catalytic activity of molten metals, the dehydrogenation reactions of *n*-butyl alcohol, *iso*-butyl alcohol, and *sec*-butyl alcohol were carried out in the presence of molten zinc and molten indium (molten gallium was also used for the dehydrogenation of *iso*-butyl alcohol). According to the experimental results, all of these molten metals showed persistent catalytic activities and high selectivities for all the test reactions, and the decreasing order of the reactivity of the butyl alcohol isomers was found to be *sec*-butyl alcohol > *iso*-butyl alcohol > *n*-butyl alcohol. Among the three molten metals, *i.e.* Zn, Ga, and In, the activity and the selectivity of the molten zinc catalyst was outstandingly high. Further, kinetic analyses of the data showed that a compensation effect exists between the apparent activaiton energy, E_a, and the logarithmic frequency factor, log A.

Since the pioneer work of Ipatiew[1] was published, only a few works[2,3] about the catalysis of molten metals have appeared in the literature. However, it was expected that the use of molten metals as catalysts would have many advantages in studying the catalysis. Thus, the present authors undertook a systematic study of the catalysis of the molten metal. According to the preceding work,[4] which is the first of this series, some molten metals, such as zinc, gallium, aluminum, indium, and thallium, showed considerable activities for the dehydrogenation of methanol. This finding prompted an investigation with some other alcohols as reactants. It is the purpose of the present paper to show the catalytic activities of such molten metals as zinc and indium for the dehydrogenation of *n*-butyl alcohol (*n*-butanol), *iso*-butyl alcohol (*iso*-butanol), and *sec*-butyl alcohol (*sec*-butanol).

Experimental

Catalysts. Molten zinc (Zn-L) and molten indium (In-L) were used as catalysts (sometimes molten gallium was also used). They were of the highest quality among the commercially available metals, and no purifications were carried out.

Alcohols. *n*-Butanol, *iso*-butanol, and *sec*-butanol were obtained commercially. The gas chromatographic analyses showed that no significant amounts of impurities were present in these alcohols. Therefore, the purifications of these alcohols were not carried out.

Apparatus. The apparatus shown in Fig. 1 was used in the measurement of the catalytic activity of the molten metal. The reactor was made from Pyrex glass; its dimensions are given in Fig. 2.

Procedures. After a given amount (50 g) of a desired metal was charged into the reactor, ③, the air in the reactor as well as in the whole reaction system was driven out by streaming helium. Then, the temperature of the reactor was raised and the melting of the catalyst metal was confirmed directly by sight. (The electric furnace was constructed from two concentric Pyrex tubes, with a nichrome heater wound on the outer wall of the inner tube. Therefore, the interior of the reactor could be observed.) After the desired temperature was reached, the stream of helium was stopped and alcohol was fed in at a rate of 0.088—0.094 mol/hr from a micro-feeder, ①. The preheater, ②, which was packed with glass-wool and maintained at a temperature of ~200°C, served for the vaporization of alcohol. The vapor of alcohol

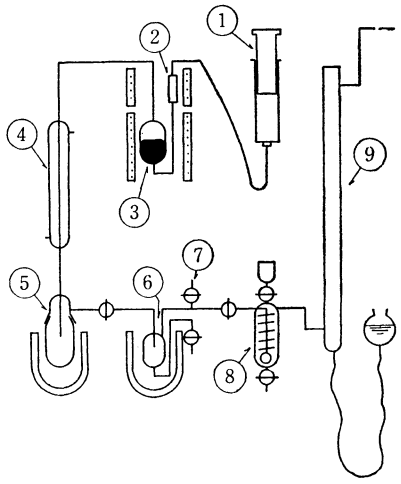

Fig. 1. Flow diagram of the reaction apparatus:
①: microfeeder, ②: preheater, ③: reactor,
④: condenser, ⑤: first separator, ⑥: second separator,
⑦: port for gas sampling, ⑧: scrubber,
⑨: soap film flow meter.

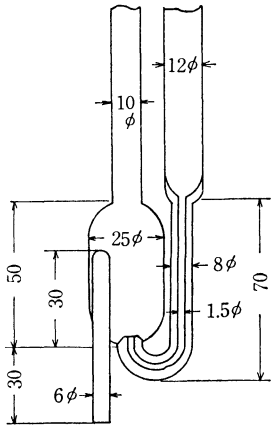

Fig. 2. Details of the reactor (dimensions are given in mm).

* Studies of Catalysis by Molten Metals. II.

1) W. Ipatiew, *Ber. Deut. Chem. Ges.*, **34**, 3579 (1901).
2) E. W. R. Steacie and E. M. Elkin, *Proc. Roy. Soc.*, **A142**, 457 (1933).
3) G. M. Schwab, *Dechema Monographiën*, **38**, 205 (1960).
4) Y. Saito, A. Miyamoto, and Y. Ogino, *Kogyo Kagaku Zasshi*, **74**, 1521 (1971)

was led to the bottom of the reactor and made to bubble from a small opening into the molten metal. The effluent containing the reaction products and unreacted alcohol was cooled by a condenser, ④; the condensable materials were separated from the gaseous products and collected in separators, ⑤ and ⑥, which were immersed in ice baths. The gaseous products were led to a scrubber, ⑧. Then, the flow rate of the gas was measured by means of a soap film-meter, ⑨. Finally, the gas was purged into the atmosphere.

The liquid products collected in the separators were weighed and analyzed by gas chromatography. The gaseous products were collected from a port, ⑦, and analyzed by gas chromatography.

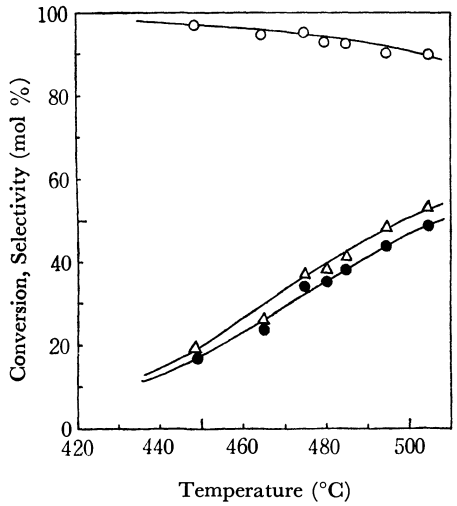

Fig. 3. Temperature dependencies of the catalytic activity of Zn-L for the dehydrogenation of *n*-Butanol:
-○- selectivity for the formation of *n*-butyraldehyde,
-△- total conversion of *n*-butanol,
-●- conversion to *n*-butyraldehyde.

Results and Discussion

Dehydrogenation of n-*Butanol.*

Activity of Zn-L. As can be seen in Fig. 3, molten zinc (Zn-L) showed a catalytic activity for the dehydrogenation of *n*-butanol. The main liquid product was *n*-butyraldehyde, but very small amounts of butylbutyrate, butyl ether, and water were also obserbed. From these results, the following reactions were considered to occur;

$$n\text{-}C_4H_9OH \longrightarrow H_2 + n\text{-}C_3H_7CHO \quad (I)$$

$$2n\text{-}C_4H_9OH \longrightarrow C_4H_9OC_4H_9 + H_2O \quad (II)$$

$$2C_3H_7CHO \longrightarrow C_3H_7CO_2C_4H_9 \quad (III)$$

Reaction I is the main reaction, while Reaction II and III are the side reactions.

The compositions of the gaseous products are given in Fig. 4. As can be seen in this figure, the hydrogen content was very high. This fact supports the idea that Reaction I is the main reaction. Further, the existence of CO, CH_4, C_2H_4, and C_2H_6 in the gaseous products suggests that the following decomposition reaction;

$$C_3H_7CHO \longrightarrow CH_4 + C_2H_4 + CO \quad (IV)$$

occurred together with the reaction;

$$C_2H_4 + H_2 \longrightarrow C_2H_6 \quad (V)$$

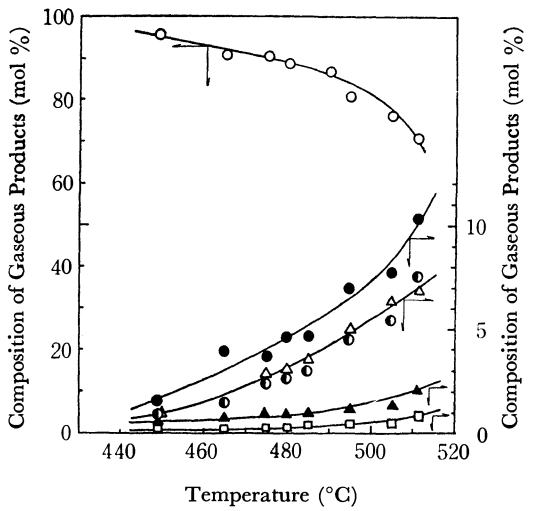

Fig. 4. Temperature dependencies of the compositions of gaseous products produced by the Zn-L catalyst from *n*-butanol:
-○- H_2, -●- CO, -△- CH_4, -◐- C_2H_4,
-▲- C_2H_6, -□- CO_2.

According to these reactions, *i.e.* IV—V, the ratio of CO: CH_4: $C_2H_4+C_2H_6$ should be 1: 1: 1. The experimental results shown in Fig. 4 indicate a somewhat higher CO content than the above-mentioned stoichiometric ratio. In addition, the existence of small amounts of CO_2 in the products seems to suggest that some unknown side reactions also occurred. At any rate, however, the side reactions were small, and the selectivity of the main reaction was higher than 90%.

Activity of In-L. As can be seen in Fig. 5, molten indium (In-L) also showed a catalytic activity for the butanol dehydrogenation, though the conversion was considerably smaller than the value obtained by the use of Zn-L catalyst (Fig. 3). The main liquid product was *n*-butyraldehyde, and the same sorts of by-products as those produced by the Zn-L catalyst were also found in the liquid products. Therefore, the main reaction may be I, and the same sorts of side reactions as for the Zn-L catalyst may be considered to occur.

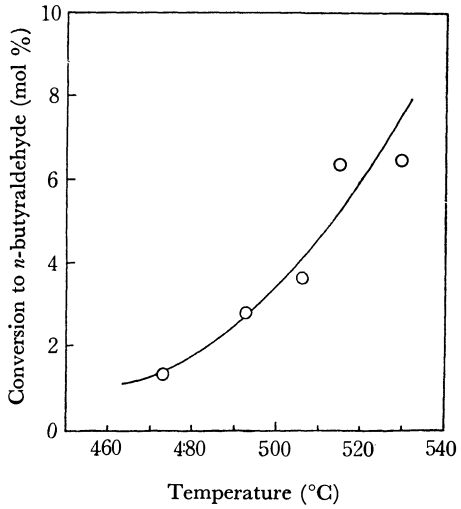

Fig. 5. Temperature dependency of the catalytic activity (conversion to *n*-butyraldehyde) of In-L for the dehydrogenation of *n*-butanol.

Comparison with Solid Catalysts. Dunbar[5] investigated the dehydrogenation of *n*-butanol, using copper chromite as a catalyst. According to his work, the conversion of *n*-butanol was 30—60% in the temperature range of 330—350°C. As can be seen in Fig. 3, nearly the same conversion value as above was obtained in the present work by employing the Zn-L catalyst. However, the reaction temperature employed in the present work is about 150°C higher than that employed by Dunbar. Thus, with respect to the reaction temperature, the copper chromite catalyst is preferable to the Zn-L catalyst. On the contrary, according to Dunbar, the selectivity for the formation of *n*-butyraldehyde was 40—80%, while the selectivity obtained in the present work was higher than 90%.

Excellent copper-containing catalysts have also been proposed by some other workers.[6,7] It is said that the catalysts are effective at temperatures lower than 300°C, and that selectivities higher than 90% are obtainable with these catalysts. However, it must be noted that the activities of copper-containing catalysts are specially sensitive to sintering and poisons. Further, great care is necessary for the preparation of a highly effective solid catalyst. On the contrary, no such difficulties as those described above are encountered in the use of a molten-metal catalyst. Of course, efforts to make more active molten metal catalysts are necessary. The application of molten-alloy catalysts seems to be hopeful.

Dehydrogenation of iso-*Butanol.*

Activity of Zn-L. As can be seen in Fig. 6, molten zinc (Zn-L) showed a catalytic activity for the dehydrogenation of *iso*-butanol, and this activity was found to persist for a long time. Figure 7 shows the relations between the reaction temperature and the degree of conversion as well as the composition of gaseous products. As can be seen in this figure, the conversion increased with the increase in the reaction temperature and reached ~80% at 500°C. Isobutyraldehyde was the main product, while the content

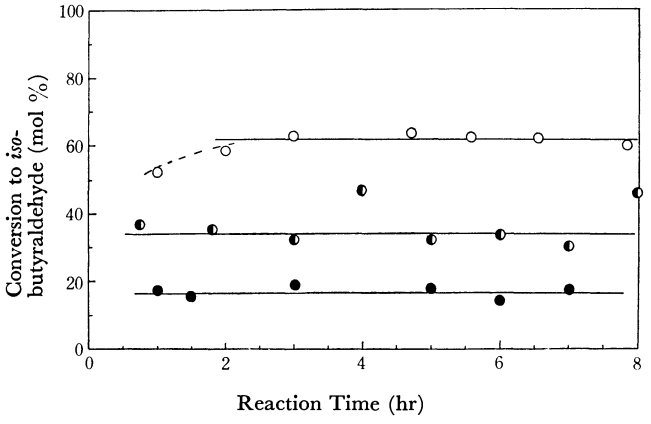

Fig. 6. Relations between the conversion to *iso*-butyraldehyde and the reaction time: -○- Zn-L 500°C, -◐- Zn-L 450°C, -●- In-L 550°C. (Zn 50 g, butanol feed rate=0.089 mol/hr, In 50 g, butanol feed rate=0.089 mol/hr).

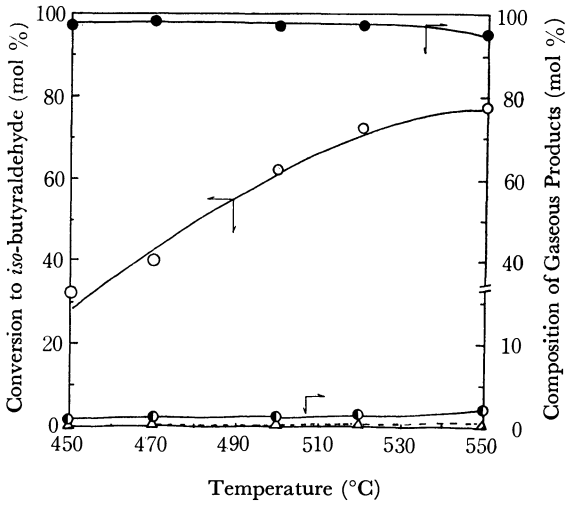

Fig. 7. Temperature dependencies of the catalytic activity of the Zn-L catalyst for the dehydrogenation of *iso*-butanol and the compositions of the produced gas; -○- conversion to *iso*-butyraldehyde, -●-H_2, -◐- CO, -△- CH_4.

of the other products in the liquid products was very small (smaller than 2%). Further, the hydrogen content in the gaseous products was very high, while the contents of CO and CH_4 were very small. On the basis of these results, the selectivity for the reaction;

$$iso\text{-}C_4H_9OH \longrightarrow iso\text{-}C_3H_7CHO + H_2$$

was calculated in order to obtain Fig. 8. This figure demonstrates a very high selectivity (higher than 95%) of the Zn-L catalyst.

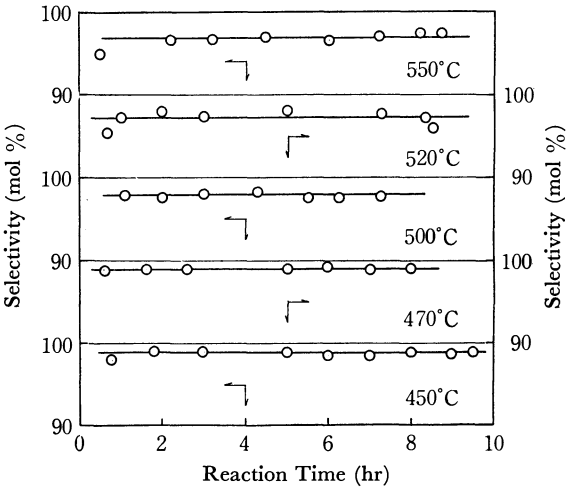

Fig. 8. Selectivities of the Zn-L catalyst for the *iso*-butyraldehyde at various temperatures.

Activity of In-L. As can be seen in Fig. 6, molten indium (In-L) also gave a persistent catalytic activity for the dehydrogenation of *iso*-butanol. The relation between the conversion and the reaction temperature is given in Fig. 9. Over the whole range of reaction temperatures, the conversion value was considerably lower than the value obtained by the use of the Zn-L catalyst.

Further, a comparison of Fig. 7 with Fig. 9 shows that the hydrogen content in the gaseous products for

5) P. E. Dunbar, *J. Org. Chem.*, **3**, 242 (1938).

6) "Monograph on the Science and Engineering of Catalysis." edited by the Catalysis Society of Japan, Vol. 7, Chijinshokan Co. Ltd., Tokyo, Japan (1964), p. 209.

7) S. Yata and S. Kudo, *Kagaku Kogaku*, **28**, 687 (1964).

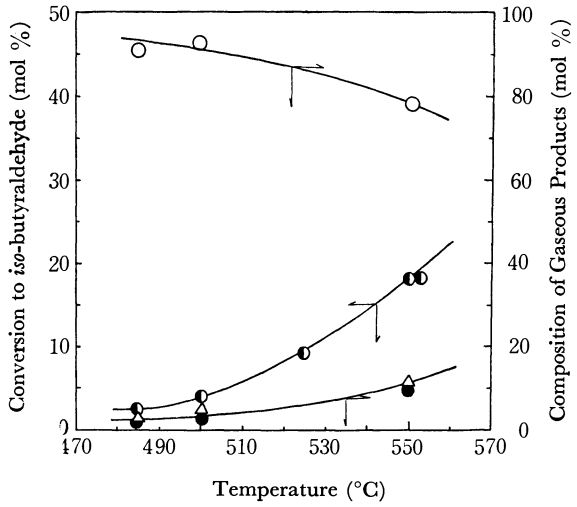

Fig. 9. Temperature dependencies of the catalytic activity of the In-L catalyst for the dehydrogenation of *iso*-butanol and the compositions of the produced gas:
-◐- conversion to *iso*-butyraldehyde, -○- H_2, -△- CO, -●- CH_4.

the In-L catalyst is lower than the content for the Zn-L catalyst. This is due to the higher contents of CO and CH_4 in the gaseous products for the In-L catalyst. From these facts, it can be said that the selectivity of the In-L catalyst is somewhat lower than that of the Zn-L catalyst.

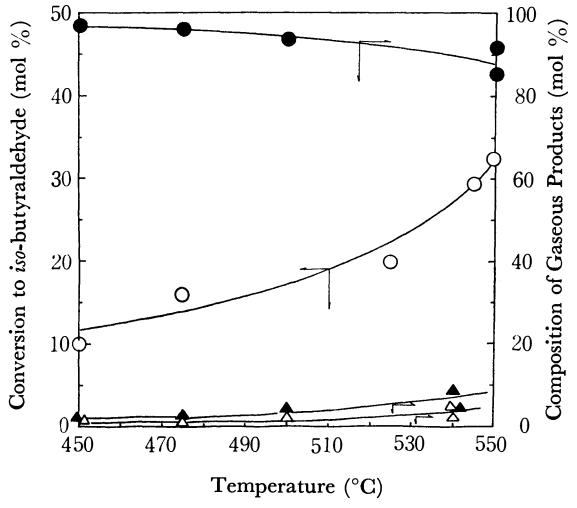

Fig. 10. Temperature dependencies of the catalytic activity of the Ga-L catalyst for the dehydrogenation of *iso*-butanol and the compositions of the produced gas:
-○- conversion to *iso*-butyraldehyde, -●- H_2, -▲- CO, -△- CH_4.

Activity of Ga-L. As can be seen in Fig. 10, Ga-L also showed a catalytic activity. The conversion value was higher than that obtained by the use of the In-L catalyst, while it was lower than the conversion value obtained by the use of the Zn-L catalyst. The hydrogen content in the gaseous products was somewhat higher than the value obtained by the use of the In-L catalyst. Further, the CO content and the CH_4 content were both lower than the corresponding values obtained by the use of the Zn-L catalyst. From these results, it was expected that the *iso*-butyraldehyde content in the liquid products would be higher than that obtained by the use of the In-L catalyst. However, as can be seen in Fig. 11, the selectivity for the formation of the *iso*-butyraldehyde of the Ga-L catalyst was the lowest among the three molten metal catalyst, *i.e.*, Zn-L, In-L, and Ga-L. This may be attributed to the higher content of an unidentified component (presumably isobutylene dissolved in the liquid phase) in the liquid products produced by the Ga-L catalyst.

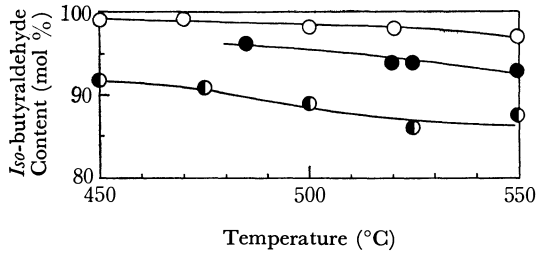

Fig. 11. Temperature dependencies of *iso*-butyraldehyde contents in the liquid products produced by dehydrogenating *iso*-butanol by the molten metal catalysts:
-○- Zn-L, -●- In-L, -◐- Ga-L.

Dehydrogenation of sec-*Butanol.*

Activity of Zn-L. As can be seen in Fig. 12, and

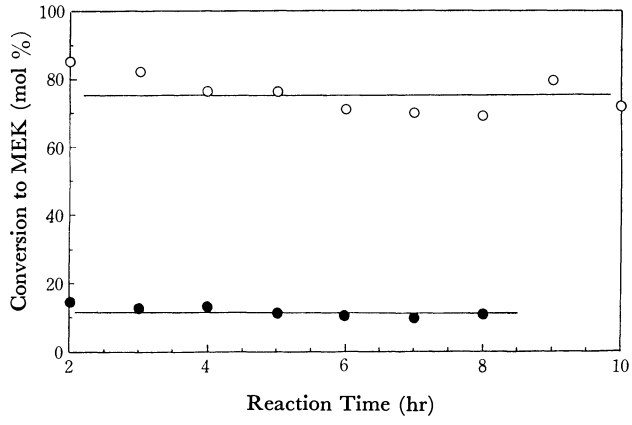

Fig. 12. Relations between the reaction time and the catalytic activities (conversion to MEK) of the Zn-L catalyst (-○-, 462°C) and the In-L catalyst (-●-, 500°C).

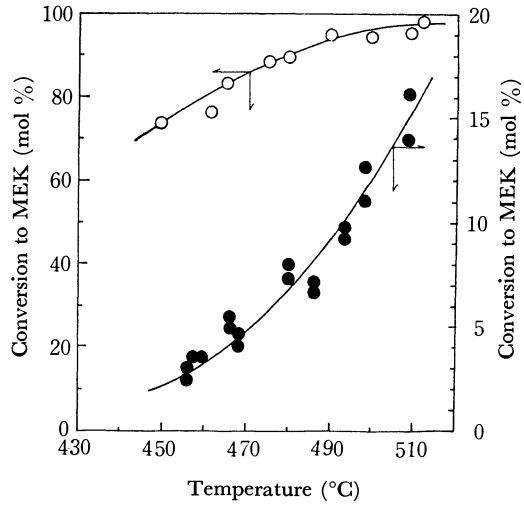

Fig. 13. Temperature dependencies of the catalytic activities (conversion to MEK) of the Zn-L catalyst (-○-) and the In-L catalyst (-●-).

Fig. 13, Zn-L showed a persistent and very high catalytic activity for the dehydrogenation of *sec*-butanol. Further, the liquid products were mainly methylethylketone (MEK). The by-products were acetone and propionaldehyde, and the total content of these materials was less than 1%. Further, the hydrogen content in the gaseous products was very high, and only a small amount of CH_4 was produced at reaction temperatures higher than 500°C. All of these facts indicate that the main reaction may be written as;

$$\begin{matrix} CH_3 \\ C_2H_5 \end{matrix}\!\!>\!CHOH \longrightarrow \begin{matrix} CH_3 \\ C_2H_5 \end{matrix}\!\!>\!CO + H_2$$

and that the selectivity of the Zn-L catalyst for the dehydrogenation of *sec*-butanol is satisfactory.

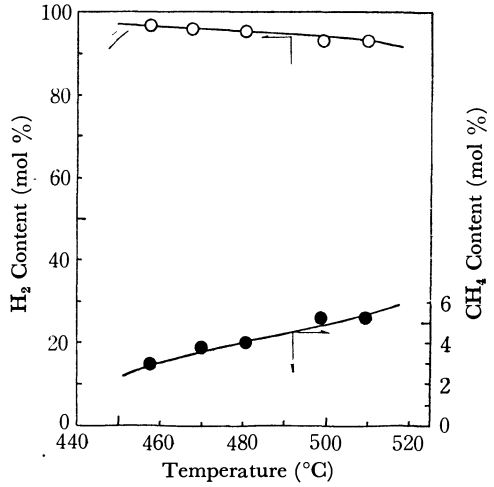

Fig. 14. Temperature dependencies of the composition of the gaseous products produced by the In-L catalyst:
-○- H_2, -●- CH_4.

Activity of In-L. As can be seen in Fig. 12, and Fig. 13, In-L also showed a persistent activity for the dehydrogenation of *sec*-butanol. The main liquid product was MEK, and the main gaseous product was hydrogen, as in the case of the Zn-L catalysts. However, compared with the Zn-L catalyst, the activity of the In-L catalyst was quite low. In addition, the selectivity of the In-L catalyst was somewhat lower than that of the Zn-L catalyst. That is, the content of CH_4 in the gaseous products was considerable (Fig. 14). Further, 2—3% of acetone was found in the liquid products. In addition, a small amount of propionaldehyde was also contained in the liquid products. Considering from these facts, the over-all reaction may be written as follows:

$$\begin{matrix} CH_3 \\ C_2H_5 \end{matrix}\!\!>\!CHOH \longrightarrow \begin{matrix} CH_3 \\ C_2H_5 \end{matrix}\!\!>\!CO + H_2 \longrightarrow \begin{matrix} CH_3 \\ CH_3 \end{matrix}\!\!>\!CO + CH_4$$

$$\begin{matrix} CH_3 \\ C_2H_5 \end{matrix}\!\!>\!CO \longrightarrow CH_3CH{=}CO + CH_4$$

$$CH_3CHCO + H_2 \longrightarrow CH_3CH_2CHO$$

Comparison with Solid Catalyst. The manufacturing of MEK by the dehydrogenation of *sec*-butanol is an industrially important reaction. Thus, several catalysts which can be used for this process have been proposed. For instance, Dunbar and his co-workers[8] proposed the copper chromite catalyst. According to their data, the conversion of *sec*-butanol to MEK was ~68% at 300—325°C. Kolb and his co-workers[9] used the Ni-Cu catalyst, which converted 84% of *sec*-butanol at a pressure of 308 mmHg and at a temperature of 472.2°K. As can be understood from these

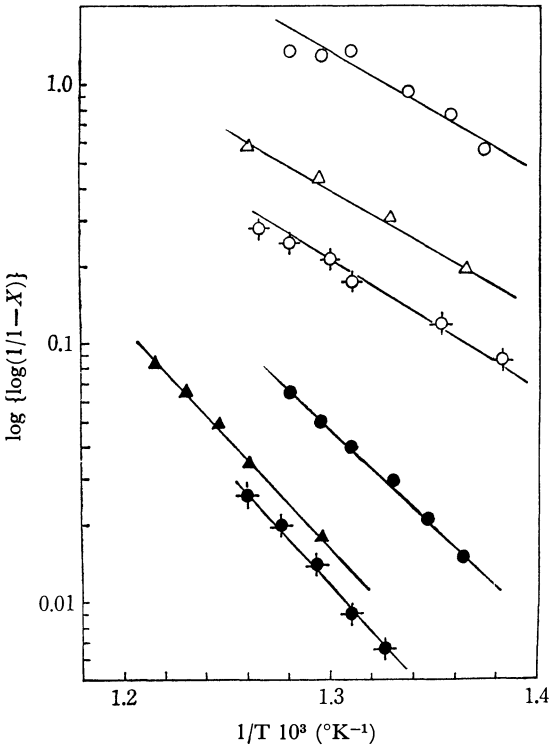

Fig. 15. Arrhenius plots for various reactions:
-○- Zn-L, *n*-butanol, -△- Zn-L, *iso*-butanol,
-○- Zn-L, *sec*-butanol, -◆- In-L, *n*-butanol,
-▲- In-L, *iso*-butanol, -●- In-L, *sec*-butanol.

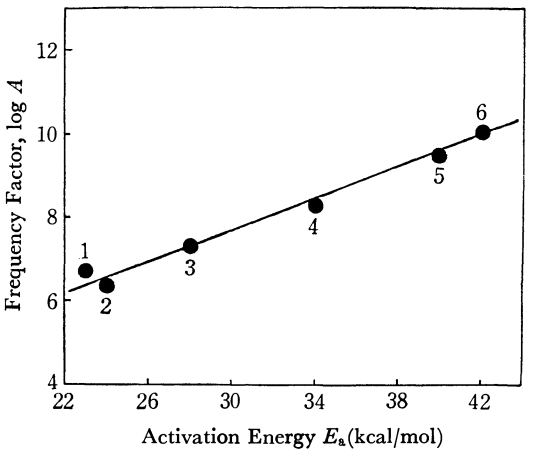

Fig. 16. Compensation effect between the apparent activation energy and the logarithmic frequency factor:
1; Zn-L, *sec*-butanol, 2; Zn-L, *iso*-butanol,
3; Zn-L, *n*-butanol, 4; In-L, *sec*-butanol,
5; In-L, *iso*-butanol, 6; In-L, *n*-butanol.

8) P. E. Dunbar and M. R. Arnold, *J. Org. Chem.*, **10**, 501 (1945).
9) H. J. Kolb and K. Z. Burwell, *J, Amer. Chem. Soc.*, **67**, 1084 (1945).

data, the reaction temperature for the solid catalyst is lower than that for the molten-metal catalyst.

At first sight, this seems to indicate a superiority of the solid catalysts. However, it must be noted that the selectivity of the molten metals, especially the Zn-L catalyst, was very high. Further, the merit of the easier method of the preparation of the molten-metal catalyst must also be taken into consideration.

Kinetic Treatments. As has been described in the preceding sections, the selectivities of the molten-metal catalysts were generally high. This permits us to assume that the side reactions can be disregarded for an approximate kinetic treatment. Further, it may be assumed that the dehydrogenation of alcohol on the metallic catalyst is first order with respect to alcohol,[10] and that the reaction will be approximately irreversible under the present experimental conditions. Thus, the first order rate constant, k, will be proportional to $\log(1/1-X)$, where X is the conversion.

On the basis of the above considerations, $\log\{\log(1/1-X)\}$ was plotted against $1/T$. The results are shown in Fig. 15. As can be seen in this figure, good linear relationships were obtained, and it was possible to evaluate the apparent activation energies, E_a, as well as the frequency factors, A. Interestingly, the apparent activation energy, E_a, was found to be proportional to the logarithmic frequency factor, $\log A$ (Fig. 16). That is, the so-called "compensation effect"[11] was observed. This relation seems to suggest that the catalysis of the liquid metal obeys a simple rule; Schwab's work[3] seems to throw some light on this problem. However, considering the qualitative nature* of the present experiments, this effect will not be discussed further.

10) A. C. Neish, *Can. J. Res.*, **23**, 49 (1945).

11) E. Cremer, "Advances in Catalysis," edited by W. G. Frankenburg, V. I. Komarewsky, and E. K. Rideal, Vol. 7, Academic Press, New York (1955), p. 75.

* In order to discuss the kinetic data further, the following problems must be clarified: i) the relations between the catalytic activity and the size of the bubble, which is affected by the experimental conditions (temperature, pressure, feed rate, catalyst, etc.); ii) the catalysis of metal vapor; iii) the catalysis of the metal film which is formed on the inner wall of the reactor, and iv) the extent of the oxidation of the molten metal and the catalysis of the oxide.

The i) problem is important not only from the scientific point of view but also from the engineering point of view, in which the practical use of the molten-metal catalyst is taken into consideration. Unfortunately, however, little information on this point is available at present, separate investigations to solve the problem seem to be necessary.

Concerning the ii)—iv) problems, somewhat detailed discussions have been given in the preceding paper;[4] these effects have been considered to be minor, though they can not be ignored. The reasons are given briefly in the following table.

Catalyst	Reasons which support to consider the minor effects of		
	ii	iii	iv
In-L	Very low vapor pressure.	Very low vapor pressure and little formation of the film.	Easily-reduible property of indium oxide.
Ga-L	Very low vapor pressure.	Very low vapor pressure and little formation of the film.	No significant oxidation was detected by X-ray diffraction study.
Zn-L	Comparison of the data with the data of Cd vapor and Zn vapor (a).	High activities observed at the initial reaction stage, wherein little metal films were found.	No significant oxidation was detected by X-ray diffraction. Different selectivity of ZnO from that of Zn-L.

(a) N.I. Kobozev and M.N. Danchevskaya, *Zhur. Fiz. Khim.*, **34**, 1728 (1960).

Vibrational Spectra and Normal Coordinate Calculations of $HgNH_2Cl$ and $HgNH_2Br$*

Kiyoshi NIWA, Hiroaki TAKAHASHI, and Keniti HIGASI
Department of Chemistry, School of Science and Engineering, Waseda University, Shinjuku-ku, Tokyo
Teruo KAJIURA
Japan Electron Optics Laboratory Co. Ltd. Akishima-shi, Tokyo
(Received May 29, 1971)

Infrared spectra of $HgNH_2Cl$ and $HgNH_2Br$ and the Raman spectrum of $HgNH_2Cl$ have been measured in the region from 4000 cm^{-1} to 30 cm^{-1}. Effects of changing the X(X=Cl,Br) ion were observed mainly in N–H stretching bands and in lattice vibrations. Calculations of normal frequencies were carried out using a force field which includes inter-molecular forces. An assignment of the lattice vibrations was proposed and the force constants were also calculated. The force constants of the inter-molecular hydrogen bonds N–H···Cl and N–H··· Br were obtained as 0.212 mdyn/Å and 0.142 mdyn/Å, respectively.

The structure of orthorhombic crystal of mercuric amidohalide $HgNH_2X$ (X=Cl, Br) consists of halogen ions and infinite chains of alternating Hg and NH_2 with linear bonds about Hg and tetrahedral bonds about N.[1-3] The vibrational assignment of the infrared bands observed between 4000 to 400 cm^{-1} has already been given for the infinite chain of $(HgNH_2^+)_n$ by Nakagawa *et al.*[4,5] And the force constants associated with the $(HgNH_2^+)_n$ chain have also been computed.[4]

However, the lattice vibrations of these compounds have not been studied. It is considered interesting to examine the effects of changing the halogen ion on the vibrational frequencies. The effects are expected to appear mainly in the lattice vibrations and also in the N–H stretching vibrations because of the possible N–H ···X type hydrogen bonds.

We have measured the infrared spectra of $HgNH_2X$ (X=Cl, Br) and the Raman spectrum of $HgNH_2Cl$ in the region from 4000 to 30 cm^{-1}. The calculation of the normal frequencies was carried out including Cl^- and Br^- ions, and hence both the intra-molecular force constants and the inter-molecular ones were obtained. It then becomes possible to discuss quantitatively about the hydrogen bond N–H···X (X=Cl, Br) and its effects on the N–H stretching force constant.

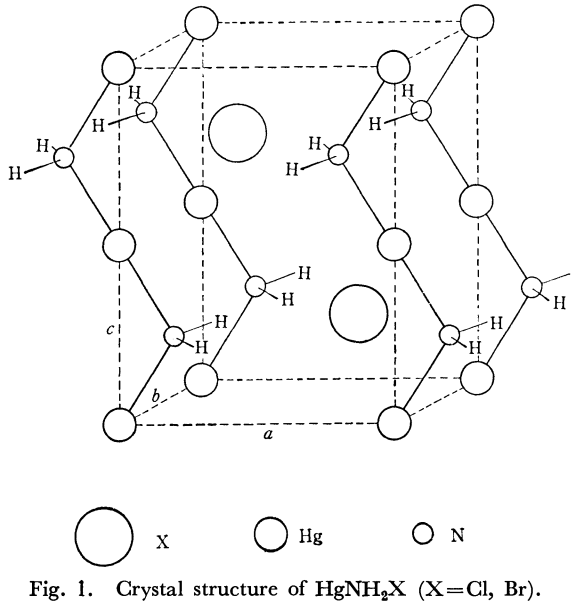

Fig. 1. Crystal structure of $HgNH_2X$ (X=Cl, Br).

Experimental

Mercuric amidochloride $HgNH_2Cl$ of special grade (Sanko Seiyaku Kogyo Co. Ltd.) was used without further purification. Although mercuric amidobromide $HgNH_2Br$ has two types of modifications, namely orthorhombic and cubic, only the orthorhombic one was prepared by the reaction of 150 m*l* of 14 N aqueous ammonia with 2 g of mercury bromide Hg_2Br_2.[2,6] The infrared spectrum of the prepared $HgNH_2Br$ coincided with that of the orthorhombic modification reported by Nakagawa et al.[5]

The infrared spectra of these substances dispersed in Nujol and in KBr disks were recorded by a Hitachi EPI G3 spectrometer (4000—400 cm^{-1}) and these in Nujol by a Hitachi FIS 3 spectrometer (400—30 cm^{-1}). However, the KBr disk method was not adequate for $HgNH_2Cl$ because it was found that a part of chlorine ions in the sample were exchanged by bromine ions in KBr. The Raman spectrum of $HgNH_2Cl$ crystal powder pressed to a disk was obtained by a laser Raman spectrometer (Japan Electron Optics Laboratory Co. Ltd.). The 5145 Å line of argon ion was used as the light source for excitation.

Observed spectra

The infrared spectra of $HgNH_2Cl$ and $HgNH_2Br$ observed from 4000 to 400 cm^{-1} are shown in Figs. 2 and 3, respectively. The far-infrared spectra from 400 to 30 cm^{-1} are given in Figs. 4 and 5. In Fig. 6, the Raman spectrum of $HgNH_2Cl$ is reproduced.

Vibrations of $HgNH_2$. Nakagawa *et al.*[4,5] have

* This work was supported in part by a research grant from the Matsunaga Science Foundation and by the Group Project organized by Science and Engineering Research Laboratory Waseda University 1969—1970

1) W. N. Lipscomb, *Acta Crystallogr.*, **4**, 266 (1951).
2) L. Nijssen and W. N. Lipscomb, *ibid.*, **5**, 604 (1952).
3) W. N. Lipscomb, *Anal. Chem.*, **25**, 737 (1953).
4) S. Mizushima, I. Nakagawa, and D. M. Sweeny, *J. Chem. Phys.*, **25**, 1006 (1956).
5) I. Nakagawa, R. B. Penland, S. Mizushima, T. J. Lane, and J. V. Quagliano, *Spectrochim. Acta*, **9**, 199 (1957).
6) V. K. Brodersen and W. Rudorff, *Z. Anorg. Chem.*, **275**, 141 (1954)

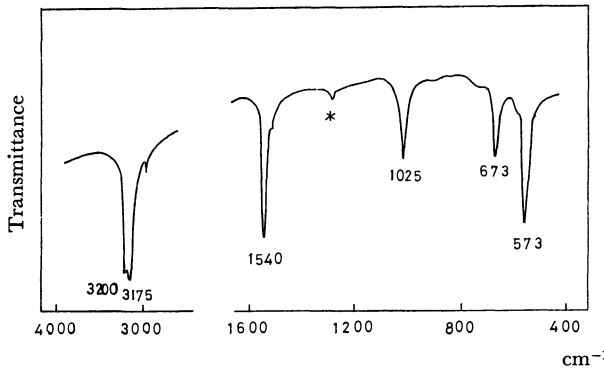

Fig. 2. Infrared spectrum of $HgNH_2Cl$ in nujol mull (nujol bands eliminated). * is due to $Hg(NH_3)_2Cl_2$.[4]

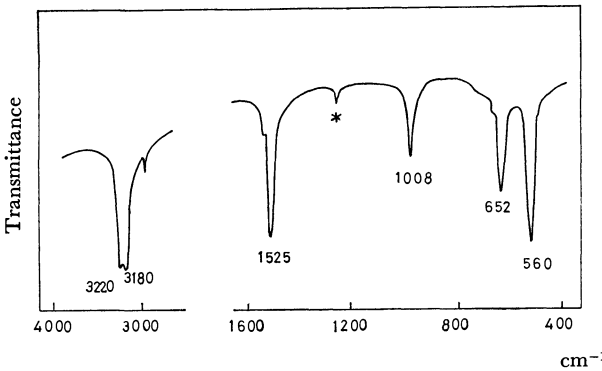

Fig. 3. Infrared spectrum of $HgNH_2Br$ in nujol mull (nujol bands eliminated). * is due to $Hg(NH_3)_2Br_2$.[5]

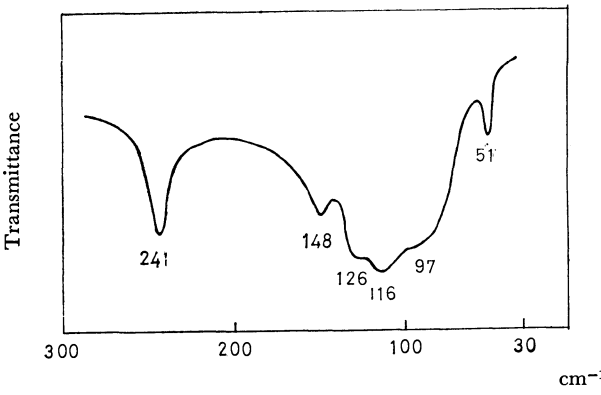

Fig. 4. Far-infrared spectrum of $HgNH_2Cl$ in nujol mull.

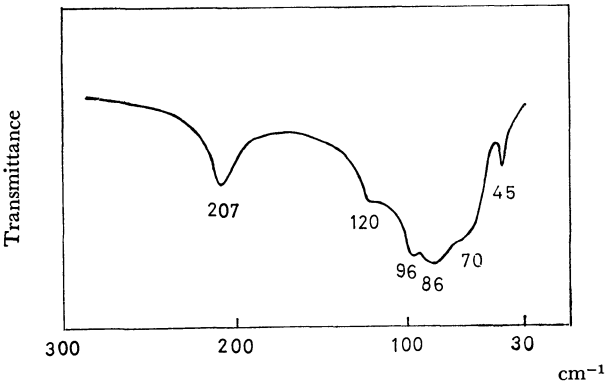

Fig. 5. Far-infrared spectrum of $HgNH_2Br$ in nujol mull.

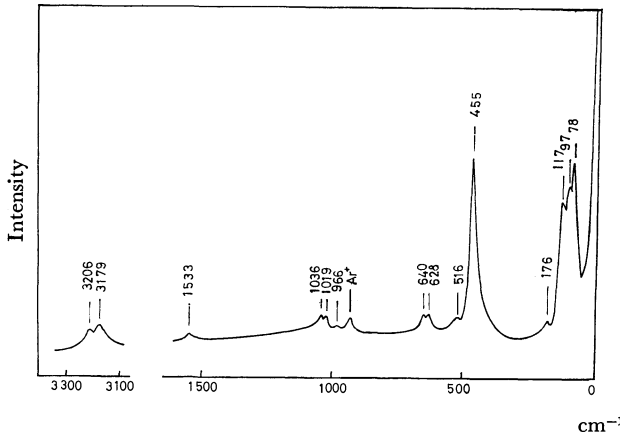

Fig. 6. Raman spectrum of $HgNH_2Cl$ powders (pressed disk).

already measured the infrared spectra of $HgNH_2Cl$ and $HgNH_2Br$ from 4000 to 400 cm^{-1} and have given the assignment of the infrared active vibrations (B_{1u}, B_{2u} and B_{3u} symmetry species) of $HgNH_2^+$. The frequencies which we observed and the assignment which we have made are in substantial agreement with theirs, hence the complete list is not reproduced here. Our contribution is to measure Raman spectrum which was not reported previously and to present the assignment of the Raman active vibrations (A_g, B_{1g}, B_{2g}, and B_{3g} symmetry species).

One interesting feature in the infrared spectra, however, should be pointed out. The NH_2 anti-symmetric stretching vibration is observed at 3200 cm^{-1} in $HgNH_2Cl$ while it is observed at 3220 cm^{-1} in $HgNH_2Br$. The same phenomenon is observed in the NH_2 symmetric stretching also: 3175 cm^{-1} for $HgNH_2Cl$ and 3180 cm^{-1} for $HgNH_2Br$. These high-frequency shifts in N–H stretching vibrations when Cl^- is substituted by Br^- are explained by the existence of the N–H···X (X=Cl, Br) hydrogen bond. All the other vibrations shift to the side of lower frequencies when Cl^- is exchanged by Br^-.

In the Raman spectrum of $HgNH_2Cl$, ten bands are observed above 400 cm^{-1}. The assignment of these Raman bands presented in Table 2 was made by analogy with that of the infrared bands. However, the observed two doublets of NH_2 wagging and of NH_2 rocking vibrations are not explained unambiguously at present. They may be either due to combination bands or to impurities in the sample.

Chain bending and lattice vibrations. There has been no work of the far-infrared spectra below 400 cm^{-1} of these compounds. We have observed the bands due to chain bending vibrations and lattice vibrations of $HgNH_2Cl$ and $HgNH_2Br$ for the first time. They are shown in Figs. 4 and 5, respectively. In the spectrum of $HgNH_2Cl$, six bands are observed at 241, 148, 126, 116, 97, and 51 cm^{-1}. The corresponding bands in $HgNH_2Br$ spectrum are 207, 120, 96, 86, 70, and 45 cm^{-1}. These bands are considered to be due to chain bending vibrations and lattice vibrations or the mixture of these.

In the low frequency region of the Raman spectrum of $HgNH_2Cl$, four bands are observed at 176, 117, 97,

and 78 cm^{-1}. The assignment of these low frequency bands observed in the infrared and Raman spectra are made according to the results of the normal frequency calculations.

Normal coordinate treatment

The crystal structure of $HgNH_2X$ (X=Cl, Br) is orthorhombic with two $HgNH_2X$ units in a Bravis unit cell as shown in Fig. 1. The lattice parameters and the bond-lengths are summarized in Table 1.[1,2]

Table 1. Lattice parameters and bond lengths[1,2]

	$HgNH_2Cl$	$HgNH_2Br$
Lattice parameter	a=5.167 Å	a=5.439 Å
	b=4.357	b=4.487
	c=6.690	c=6.761
Bond length		
N—H	1.04 Å	1.04 Å
Hg—N	2.05	2.07
H···H	1.70	1.70
H···Hg	2.59	2.61
Hg···Hg	3.35	3.38
H···X	2.18	2.36
Hg···X	3.21	3.30
X···X	3.83	3.91

The calculation of the normal frequencies[7] was made assuming a modified Urey-Bradly type force field[8] and a few coordinates corresponding to inter-molecular forces were also taken into account. These coordinates are given below.

	X=Cl	X=Br
q (H···X)	2.18 Å	2.36 Å
q (Hg···X)	3.21 Å	3.30 Å
h (N-H···X)		

The coordinate q(X···X) was omitted because of the large X···X distance: 3.83 Å for X=Cl and 3.91 Å for X=Br.

The potential function was expressed as

$$U = U_l + U_1$$

$$\begin{aligned} U_l = 1/2\{&\sum K_{N-H}(\Delta r_{N-H})^2 + \sum K_{Hg-N}(\Delta r_{Hg-N})^2 \\ &+ \sum F_{H\cdots H}(\Delta q_{H\cdots H})^2 + \sum F_{H\cdots Hg}(\Delta q_{H\cdots Hg})^2 \\ &+ \sum H_{H-N-H}(\Delta\alpha_{H-N-H})^2 + \sum H_{H-N-Hg}(\Delta\alpha_{H-N-Hg})^2 \\ &+ \sum H_{Hg-N-Hg}(\Delta\alpha_{Hg-N-Hg})^2 + \sum H^{\perp}_{N-Hg-N}(\Delta\alpha^{\perp}_{N-Hg-N})^2 \\ &+ \sum H^{//}_{N-Hg-N}(\Delta\alpha^{//}_{N-Hg-N})^2 + \sum Y_{N-Hg-N}(\Delta\tau_{N-Hg-N})^2\} \\ &+ \sum \text{angle interaction constant } l_{ij} \text{ term}^{9} \end{aligned}$$

$$\begin{aligned} U_1 = 1/2\{&\sum f_{H\cdots X}(\Delta q_{H\cdots X})^2 + \sum f_{Hg\cdots X}(\Delta q_{Hg\cdots X})^2 \\ &+ \sum h_{N-H\cdots X}(\Delta\phi_{N-H\cdots X})^2\} \end{aligned}$$

where

U_l is the potential function associated with the $(HgNH_2^+)_n$ chain.

U_1 is that of the lattice vibration.

K, F, H, and Y denote bond-stretching, repulsive, angle-bending and torsional force constants, respectively. f and h are, respectively, stretching and angle-bending force constants associated with the lattice vibrations.

The calculation of the normal frequencies was carried out by the Cartesian coordinate method.[7] The coordinates, with which the potential function is expressed, are transformed into Cartesian displacement coordinates X. And then the optically active potential energy matrix F_{op} is set up in terms of the optically active Cartesian displacement coordinates. The secular equation

$$|M^{-1}F_{op} - E\lambda| = 0$$

gives the eigenvalues and eigenvectors which correspond to the frequencies and the vibrational modes respectively, where M is a diagonal mass matrix and E is a unit matrix.

Results and Discussions

Normal frequency calculation. Lipscomb *et al.* have reported from X-ray studies that the space groups of both $HgNH_2Cl$[1] and $HgNH_2Br$[2] belong to C^1_{2v}-P2mm. However, as can be seen in Table 2, there are very few infrared frequencies which correspond to Raman fre-

Table 2. Observed and calculated frequencies in cm^{-1}

Species	$HgNH_2Cl$		$HgNH_2Br$		Assignment
	Obsd.	Calcd.	Obsd.	Calcd.	
A_g	3179	3176		3185	NH_2 sym. str.
	1533	1539		1535	NH_2 scis.
	455	459		449	Hg-N sym. str. +Hg–N–Hg def.
	117	130		77	lattice
B_{1g}	3206	3204		3215	NH_2 anti. str.
	640, 628	642		615	NH_2 rock.
	176	165		119	lattice
	97	93		66	lattice
B_{2g}	1036, 1019	1018		1004	NH_2 wag.
	516	524		525	Hg–N anti. str.
	78	76		47	lattice
B_{3g}	966	960		921	NH_2 twist.
A_u	inact.	967	inact.	928	NH_2 twist.
		68		66	N–Hg–N bend.($\perp$)
B_{1u}	1025	1019	1008	1006	NH_2 wag.
	573	564	560	565	Hg–N anti. str.
	97	93	70	76	N–Hg–N bend. (//)
	51	53	45	44	lattice
B_{2u}	3200	3204	3220	3215	NH_2 anti. str.
	673	675	652	649	NH_2 rock.
	241	234	207	216	N–Hg–N bend.($\perp$)
	126	135	96	90	lattice
B_{3u}	3175	3176	3180	3185	NH_2 sym. str.
	1540	1540	1525	1535	NH_2 scis.
	—	508	—	499	Hg–N sym. str.
	148	141	120	116	lattice
	116	117	86	91	N–Hg–N bend.(//) +Hg–N–Hg def.

7) T. Shimanouchi, M. Tsuboi, and T. Miyazawa, *J. Chem. Phys.*, **35**, 1597 (1961).
8) T. Shimanouchi, *Pure Appl. Chem.*, **7**, 131 (1963).
9) T. Shimanouchi and I. Suzuki, *J. Mol. Spectrosc.*, **6**, 277 (1961); **8**, 222 (1962).

quencies. This fact would suggest that the vibrational spectra of $HgNH_2Cl$ (and also $HgNH_2Br$) are explained more adequately by a D_{2h} symmetry than a C_{2v}. Therefore we have carried out normal frequency calculations assuming a D_{2h} symmetry instead.

The calculated frequencies listed in Table 2 are in good agreement with the observed values. As the Bravis unit cell contains one $(HgNH_2^+)_n$ chain and two X atoms, one rotational and six translational lattice vibrations are expected to appear. The assignment of lattice vibrations and also of chain bending vibrations are given in the same table. The L_x matrices of lattice vibrational modes and chain bending modes are shown schematically in Figs. 7, 8, and 9. L_x is the transformation matrix between the Cartesian coordinates X and the normal coordinates Q. These figures demonstrate that the low frequency bands cannot be distinctly classified into either lattice vibrations or chain bending vibrations; rather, they are more or less coupled with each other. The low-frequency shifts in the chain bending vibrations, when Cl^- is substituted by Br^-, are well understood from this viewpoint. The chain bending vibrations in the A_u species of $HgNH_2Cl$ and $HgNH_2Br$, however, are both calculated to be almost of the same value: 68 cm^{-1} for $HgNH_2Cl$ and 66 cm^{-1} for $HgNH_2Br$. As can be seen in Table 2 and in Fig. 9, this mode is a pure chain bending vibration so that the effect of changing the halogen ion is negligible. Low-frequency shifts in the lattice vibrations when Cl^- is exchanged by Br^- are explained mainly both by the difference of atomic weight of halogen and by the difference of inter-molecular force constants which will be discussed below.

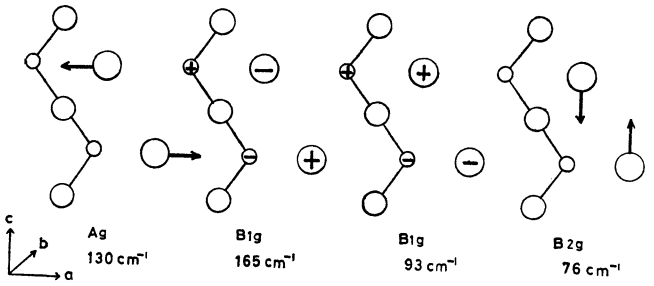

Fig. 7. Displacements of atoms for the Raman active lattice vibrational modes, with calculated frequencies of $HgNH_2Cl$.

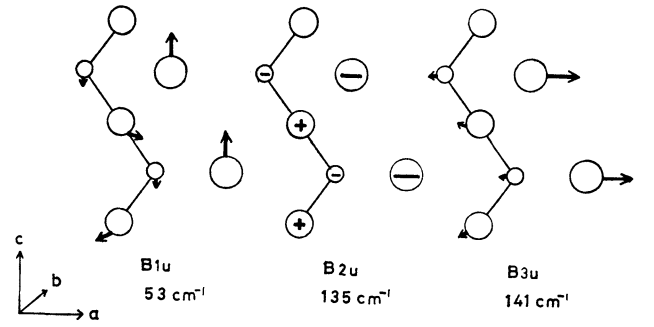

Fig. 8. Displacements of atoms for the infrared active lattice vibrational modes, with calculated frequencies of $HgNH_2Cl$.

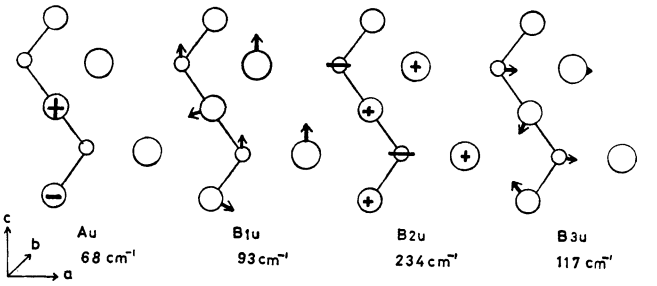

Fig. 9. Displacements of atoms for the chain bending modes, with calculated frequencies of $HgNH_2Cl$.

TABLE 3. FORCE CONSTANTS IN mdyn/Å

	$HgNH_2Cl$	$HgNH_2Br$
K(N–H)	5.276	5.371
K(Hg–N)	1.775	1.775
F(H···H)	0.100	0.100
F(H···Hg)	0.160	0.160
f(H···X)	0.212	0.142
f(Hg···X)	0.111	0.101
H(H–N–H)	0.555	0.555
H(H–N–Hg)	0.105	0.105
H(Hg–N–Hg)	0.081	0.081
h(N–H···X)	0.016	0.011
$H^{\perp}$(N–Hg–N)	0.083	0.083
$H^{//}$(N–Hg–N)	0.077	0.077
Y(N–Hg–N)	0.030	0.030[a]
l(Hg, H, H)	−0.003	0.002[a]
l(H, H, Hg)	0.009	0.009[a]
l(H, Hg, Hg)	−0.035	−0.024[a]

a) mdyn·Å

N–H···X (X=Cl, Br) hydrogen bond. The values of the force constants obtained by the least squares method are shown in Table 3. In the course of the calculation, all the force constants except for K (N–H), f (H···X), f (Hg···X), h (N–H···X) and four kinds of angle interaction constant l[9] were set to be equal for $HgNH_2Cl$ and $HgNH_2Br$ in spite of the slight difference of the bond lengths summarized in Table 1. Nakagawa *et al.* determined F (H···H) to be 0.06 mdyn/Å[4], however, in this calculation it was fixed to 0.10 mdyn/Å according to Harada and Shimanouchi.[10]

The force constants K(N–H) are calculated as 5.276 mdyn/Å for $HgNH_2Cl$ and 5.371 mdyn/Å for $HgNH_2Br$. High-frequency shifts in the N–H stretching vibrations when Cl^- is substituted by Br^- are explained by the fact that K (N–H) of $HgNH_2Br$ is larger than that of $HgNH_2Cl$. This difference in K (N–H) between $HgNH_2Cl$ and $HgNH_2Br$ may suggest that the hydrogen bond of H···Cl is stronger than that of H···Br. And actually, the calculated values of the force constant f (H···Cl) and h (N–H···Cl) become larger than those of f (H···Br) and h (N–H···Br), respectively, as shown in Table 3. Therefore, low-frequency shifts in the lattice vibrations when Cl^- is exchanged by Br^- are understandable. All the other force constants obtained are considered reasonable.

The authors are grateful to Shimanouchi laboratory of the University of Tokyo for the permission to use the computer programs.

10) I. Harada and T. Shimanouchi, *J. Chem. Phys.*, **44**, 2016 (1966)

Far-infrared Reflection Spectra, Optical and Dielectric Constants, and Lattice Vibrations of Some Fluoride Crystals

Ichiro NAKAGAWA

Department of Chemistry, Faculty of Science, The University of Tokyo, Hongo, Tokyo

(Received June 11, 1971)

The reflection spectra of the crystals of the NaCl structure (LiF, NaF, and NiO), the fluorite structure (CaF_2, BaF_2, and CdF_2), and the rutile structure (MgF_2 and MnF_2) were measured. The optical and dielectric constants were derived from the measured reflectivities using the Kramers-Kronig transformation. The absorption indices (k) for these crystals are rather large and the peak values of the imaginary dielectric constants amount to 30.0 or more. However, unlike the ferroelectric substances such as oxide perovskites and rutile, these fluoride crystals do not show any anomalous dielectric behaviour. From the real and imaginary dielectric constants $\varepsilon'(\nu)$ and $\varepsilon''(\nu)$, the transverse and longitudinal frequencies for the lattice modes are determined. These frequencies are reasonably interpreted on the basis of the crystal structures and satisfy the Lyddane-Sachs-Teller relation. The effective charge on the positive and negative ions and the force constant associated with the short-range elastic force against the ion displacement are obtained for the cubic crystals.

Several investigations on the optical and dielectric properties of the fluoride crystals have been made using reflection data as well as transmission spectra by Hunt and Perry,[1] Perry,[2] Barker,[3] Axe and Pettit,[4] Balkanski *et al.*,[5] Bosomworth,[6] and Denham *et al.*[7] In the course of our studies on the lattice vibrations of inorganic salts, we have investigated the transmission spectra of some fluoride perovskites.[8,9] On the basis of the dynamical model we obtained the potential constants associated with the short-range repulsive force without taking into account the long-range interaction. The longitudinal frequencies as well as the transverse frequencies supply further information on the interionic forces in the crystal, specifically on the long-range, electrostatic interaction.

The purpose of the present study is to establish the optical and dielectric constants of various kinds of fluoride crystals from the reflectivity data and to determine the longitudinal frequencies as well as the transverse frequencies for the crystal lattice modes, by which the effective charge on the positive and negative ions can be obtained.

The crystals investigated are those of the NaCl structure (LiF, NaF, and NiO), the fluorite structure (CaF_2, BaF_2, and CdF_2), and the rutile structure (MgF_2 and MnF_2). Reflection and transmission measurements for crystals other than MnF_2 and NiO have been made by several researchers. Except for the fluorites, however, the data are rather old and the observed frequency range and procedure for obtaining the frequencies are not always satisfactory. It is therefore worth while to make a remeasurement for these crystals also and compare the optical and dielectric constants and the lattice frequencies determined in different laboratories with one another, since the procedure for obtaining these parameters is not straightforward and contains a wide variety of technique.

Experimental

The room temperature reflectivity at near normal incidence was measured down to 30 cm^{-1} with a Hitachi FIS-21 single-beam vacuum far infrared spectrometer attached with a specular reflectance accessary (incidence angle 11°). The reflectivity measurement in the region 700—300 cm^{-1} was made with a Hitachi EPI-L double-beam infrared spectrometer attached with a IRR-3 type reflectance accessary (incidence angle 12°).

For the measurement of a crystal of small dimension (~5 mm × 5 mm), a reflectance attachment with two spherical mirrors and two plane mirrors was designed for the use of a Hitachi FIS-1 vacuum infrared spectrometer as a single-beam use, as shown in Fig. 1 (incidence angle 10°).

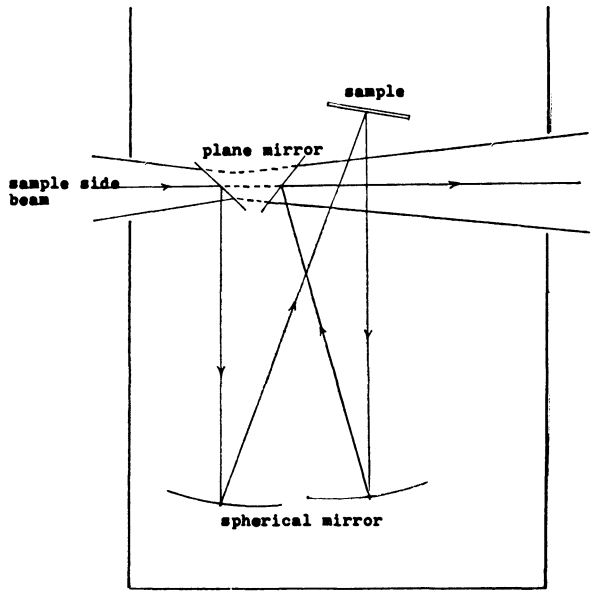

Fig. 1. Specular Reflectance Accessary for a Crystal of Small Dimension Attached to a Hitachi FIS-1 Spectrometer.

1) G. R. Hunt and C. H. Perry, *Phys. Rev.*, **134**, A188 (1964).
2) C. H. Perry, *Japanese J. Appl. Phys.*, **4**, **Suppl. I**, 565 (1965).
3) A. S. Barker, *Phy. Rev.*, **136**, A1290 (1964).
4) J. D. Axe and G. D. Pettit, *Phys. Rev.*, **157**, A435 (1967).
5) M. Balkanski, P. Moch, and G. Parisot, *J. Chem. Phys.*, 44, 940 (1966).
6) D. P. Bosomworth, *Phys. Rev.*, **157**, A709 (1967).
7) P. Denham, G. R. Field, P. L. R. Morse, and G. R. Wilkinson, *Proc. Roy. Soc. London, Ser. A*, **317**, 55 (1970).
8) I. Nakagawa, A. Tsuchida, and Shimanouchi, *J. Chem. Phys.*, **47**, 982 (1967).
9) K. Kohn and I. Nakagawa, This Bulletin **43**, 3780 (1970).

Determination of Optical Constants

The optical and dielectric constants, n(refractive index), k(absorption index), ε' and ε''(real and imaginary dielectric constants), are derived from the measured reflectivity using the Kramers-Kronig relation.[10] At normal incidence it is possible to proceed from a measurement of R(the reflectivity for unpolarized radiation), since the distinction between R_s and R_p (the reflectivities for perpendicular and parallel polarized radiations) is meaningless. The complex reflected amplitude ($\hat{r}$) is expressed in terms of its phase angle θ as

$$\hat{r} = |r| \exp(i\theta) = \sqrt{R} \exp(i\theta) = \frac{n-ik-1}{n-ik+1}, \quad (1)$$

from which one obtains

$$n = \frac{1-R}{1+R-2\sqrt{R}\cos\theta}, \quad (2)$$

$$k = \frac{-2\sqrt{R}\sin\theta}{1+R-2\sqrt{R}\cos\theta}, \quad (3)$$

$$\varepsilon' = n^2 - k^2, \quad (4)$$

$$\varepsilon'' = 2nk. \quad (5)$$

The phase angle θ at any particular frequency ν_0 is calculated by the Kramers-Kronig transformation

$$\theta(\nu_0) = \frac{2\nu_0}{\pi}\int_0^\infty \frac{\ln R(\nu)}{\nu^2-\nu_0^2}d\nu. \quad (6)$$

The reflectivity measurements are limited to some finite spectral region(ν_L to ν_H), and the correction terms due to the contributions from all the frequencies above the high-frequency limit(ν_H) and below the low-frequency limit(ν_L) were calculated according to the procedure proposed by Roessler.[11] The value of $\theta(\nu_0)$ is given as

$$\theta(\nu_0) = \frac{2\nu_0}{\pi}\int_{\nu_L}^{\nu_H}\frac{\ln R(\nu)-\ln R(\nu_0)}{\nu^2-\nu_0^2}d\nu + \frac{1}{2\pi}\ln\left|\frac{\nu_0-\nu_L}{\nu_0+\nu_L}\right|\ln\left[\frac{R(\nu_L)}{R(\nu_0)}\right] - \frac{1}{2\pi}\ln\left|\frac{\nu_H-\nu_0}{\nu_H+\nu_0}\right|\ln\left[\frac{R(\nu_H)}{R(\nu_0)}\right]. \quad (7)$$

Numerical integration of Eq. (7) and subsequent calculations of the optical and dielectric constants were performed with a HITAC 5020E Computer of the Computation Center, the University of Tokyo. The measured reflectivity data and the obtained optical and dielectric constants are shown in Figs. 2~9.

Transverse and Longitudinal Optical Frequencies

On the basis of the damped oscillator model with several modes, the dielectric constants are expressed as

$$\varepsilon'(\nu) = \varepsilon_\infty + \sum_j 4\pi\rho_j\nu_j^2\frac{\nu_j^2-\nu^2}{(\nu_j^2-\nu^2)^2+\gamma_j^2\nu^2}, \quad (8)$$

$$\varepsilon''(\nu) = \sum_j 4\pi\rho_j\nu_j^2\frac{\gamma_j\nu}{(\nu_j^2-\nu^2)^2+\gamma_j^2\nu^2}, \quad (9)$$

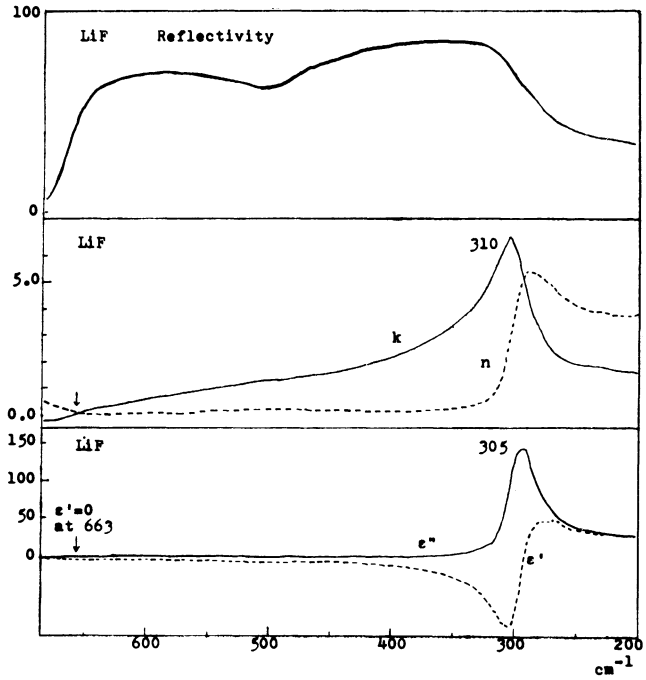

Fig. 2. Reflectivity, Optical Constants (n and k), and Dielectric Constants (ε' and ε'') of LiF.

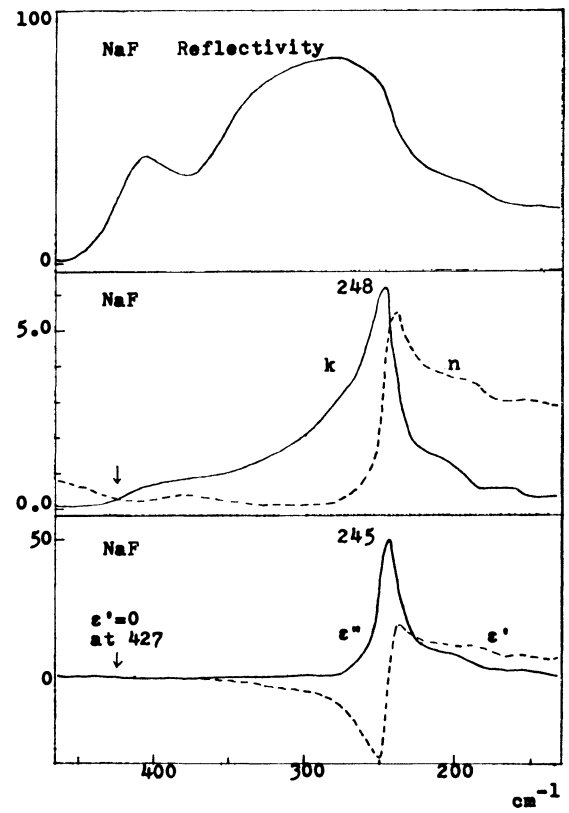

Fig. 3. Reflectivity, Optical Constants (n and k), and Dielectric Constants (ε' and ε'') of NaF.

10) T. S. Robinson and W. C. Price, *Proc. Phys. Soc., Ser. B*, **66**, 969 (1953).

11) D. M. Roesller, *Brit. J. Appl. Phys.*, **16**, 1119 (1965); **17**, 1313 (1966).

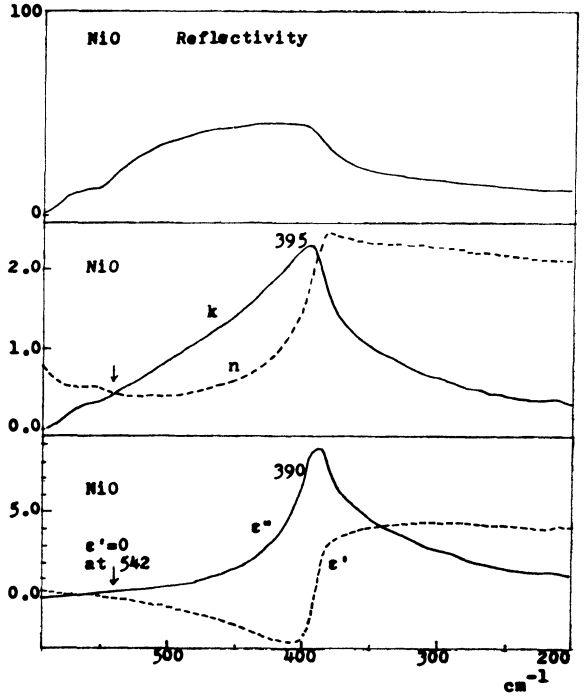

Fig. 4. Reflectivity, Optical Constants (n and k), and Dielectric Constants (ε' and ε'') of NiO.

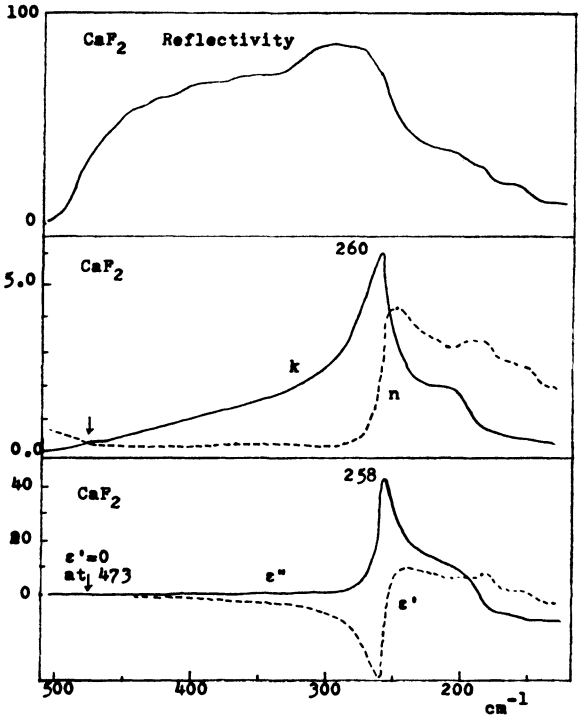

Fig. 5. Reflectivity, Optical Constants (n and k), and Dielectric Constants (ε' and ε'') of CaF_2.

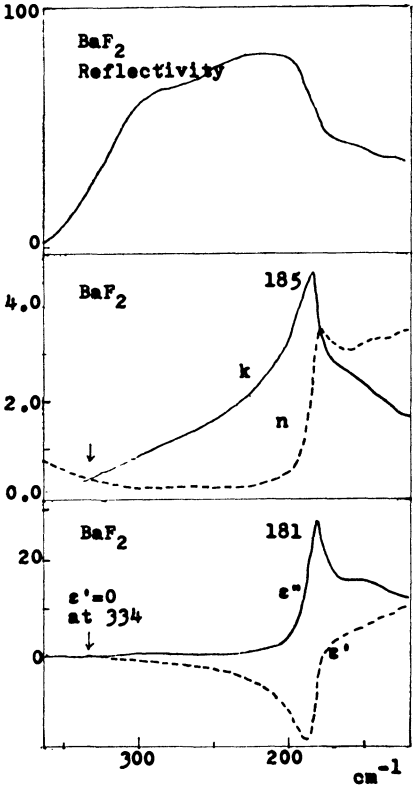

Fig. 6. Reflectivity, Optical Constants (n and k), and Dielectric Constants (ε' and ε'') of BaF_2.

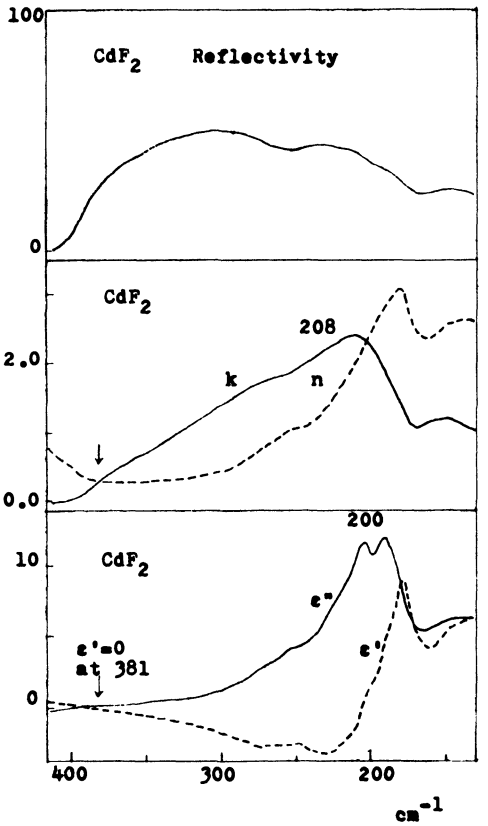

Fig. 7. Reflectivity, Optical Constants (n and k), and Dielectric Constants (ε' and ε'') of CdF_2.

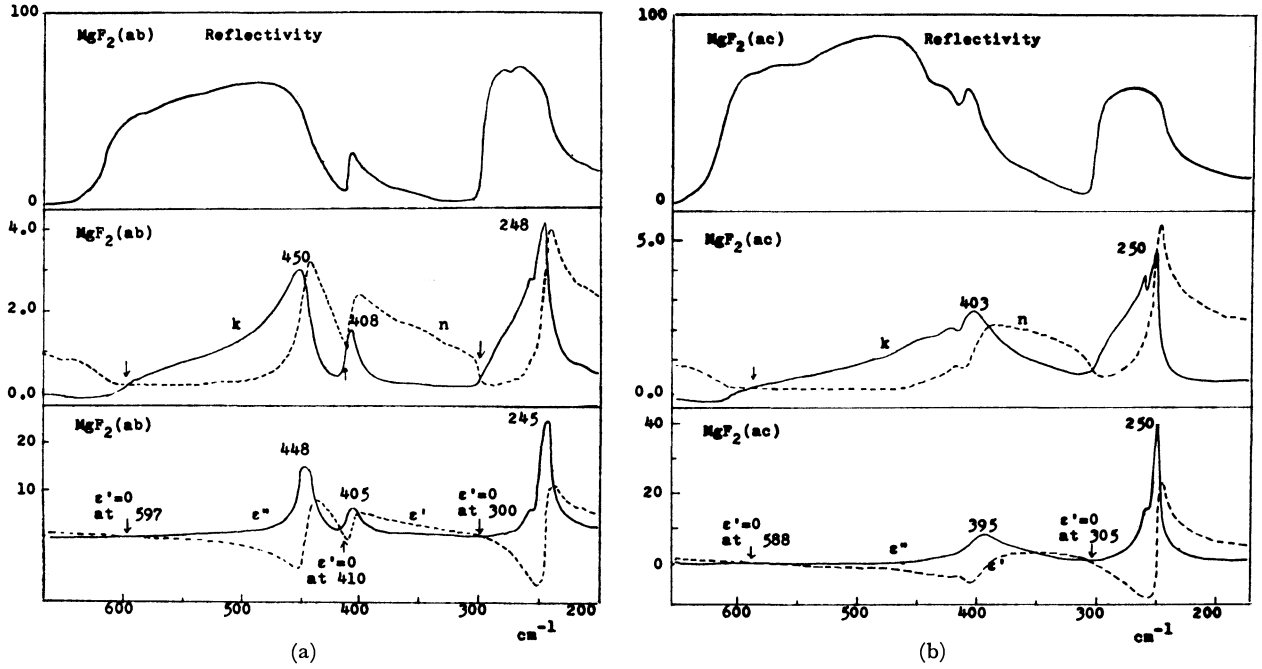

Fig. 8. Reflectivity, Optical Constants (n and k), and Dielectric Constants (ε' and ε'') of MgF_2. (a) Reflection of ab-plane (b) Reflection of ac-plane.

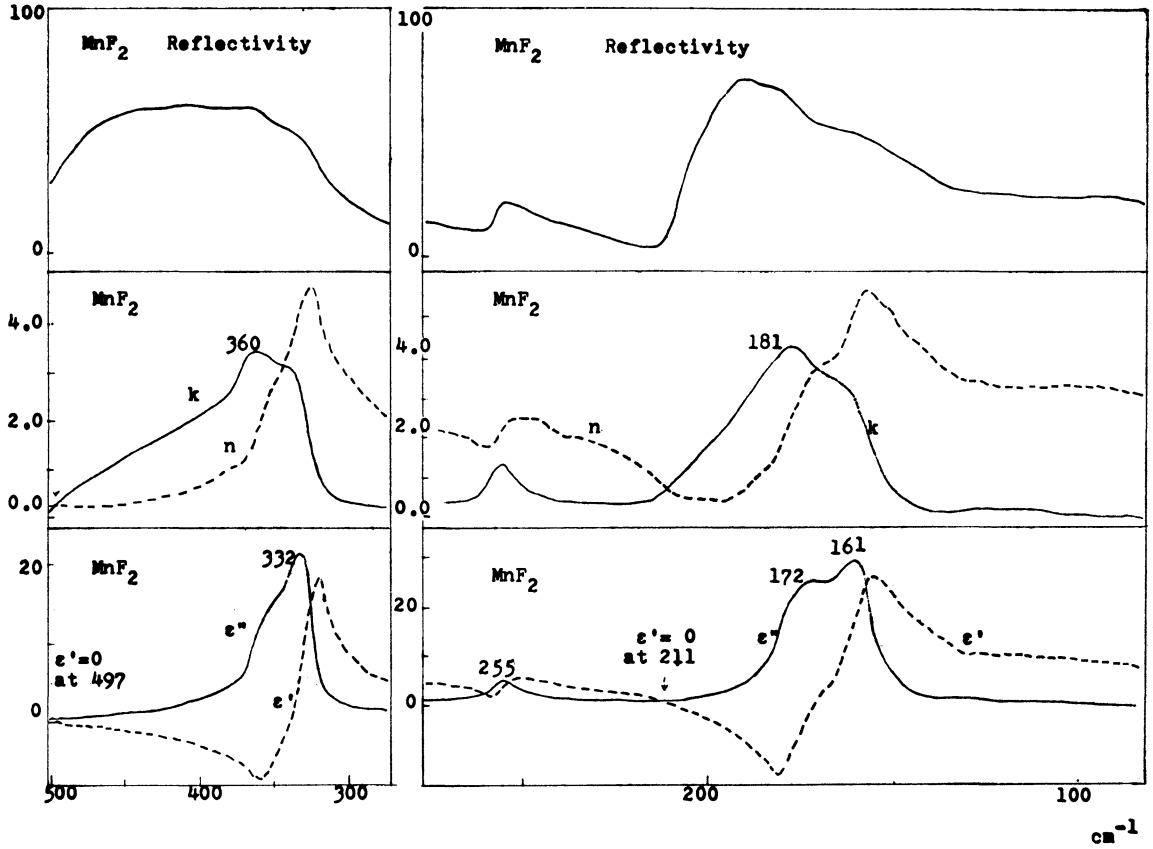

Fig. 9. Reflectivity, Optical Constants (n and k), and Dielectric Constants (ε' and ε'') of MnF_2.

where ν_j, ρ_j and γ_j are the resonance frequency, oscillator strength and damping constant, respectively, of the j-th mode. It is found from Eqs. (8) and (9) that for the small damping γ_j the poles of $\varepsilon'(\nu)$ curve and the maxima of $\varepsilon''(\nu)$ curve coincide and they are located around $\nu=\nu_j$. These frequencies give the optically active lattice frequencies of the long-wavelength transverse modes.[3,4] The corresponding longitudinal frequencies are given by the frequencies where $\varepsilon'(\nu)$ becomes zero in changing from negative to positive values.[3,4,12]

TABLE 1. SUMMARY OF TRANSVERSE AND LONGITUDINAL FREQUENCIES IN cm^{-1}

Crystals	ν_T	ν_{pole}	σ_{max}	ν_L
LiF	305	305	305	663
LiF	304			660 Ref. (13)
NaF	245	245	245	427
NaF	246			424 Ref. (13)
NiO	390	392	390	542
CaF_2	258	255	258	473
CaF_2	266		266	474 Ref. (7)
CaF_2	257			463 Ref. (6)
BaF_2	181	180	181	334
BaF_2	189		189	330 Ref. (7)
BaF_2	184			331 Ref. (6)
CdF_2	200	200	205	381
CdF_2	209		209	404 Ref. (7)
CdF_2	202			380 Ref. (6)
MgF_2	448	446	448	597
	405	(406)	405	410
(*ab*-plane)	(258sh)			
	245	246	245	300
MgF_2	395	390	395	588
(*ac*-plane)	(260sh)			
	250	250	250	305
MgF_2	435			
	405			
	280			Ref. (1)
	265			
$MgF_2(E\perp c)$	450			617 Ref. (3)
	410			415
	247			303
$MgF_2(E//c)$	399			
	not observed			Ref. (3)
MnF_2	(357sh)			
	332	340	332	497
	255			
	172	172	173	211
	161		161	

ν_T: transverse frequencies, ν_L: longitudinal frequencies, ν_{pole}: pole of $\varepsilon'(\nu)$ curve, σ_{max}: peak of conductivity, sh: shoulder.

The transverse and longitudinal frequencies determined by the procedure mentioned above are listed in Table 1. This table also includes the results of other researchers for some of the crystals, since a comparison of the frequencies from different sources is significant to justify various methods for the determination of the transverse and longitudinal frequencies. The argument for each type of crystal listed in Table 1 will be given in the following.

Crystals of NaCl structure. For this type of crystal one infrared active mode is observed as a transverse component and a longitudinal component. The peak values of absorption index(k) and imaginary dielectric constant(ε'') are very large for LiF and NaF, while those for NiO are rather small.

Crystals of fluorite structure. The crystal of this type has the space group O_h^5 with one formula unit and one f_{1u} mode is infrared active. The transverse frequencies of CaF_2, BaF_2 and CdF_2 obtained by this study are in agreement with those by Denham *et al.*[7] and by Bosomworth.[6] The longitudinal frequency of CdF_2 by Denham *et al.* which was determined using the Berreman method[14] by depositing a thin film on a mirror surface differs slightly from that by the present study and by Bosomworth.

Crystals of rutile structure. MgF_2 and MnF_2 have this structure with the space group D_{4h}^{14} and the Bravais primitive cell contains two formula units. This type of crystal is not cubic but uniaxial and 1 $a_{2u}(E//c\text{-axis})$ and 3 $e_u(E\perp c\text{-axis})$ lattice modes are infrared active. As is shown in Fig. 8 the reflectivities of the *ab*-plane and *ac*-plane for MgF_2 are somewhat different. The transverse and longitudinal frequencies obtained in both cases also differ to some extent as is seen in Table 1. From the result of the *ab*-plane measurement shown in Fig. 8(a), the e_u mode frequencies are determined as 448 cm^{-1}, 405 cm^{-1}, and 245 cm^{-1}, which are in good agreement with those obtained by Barker using a $E\perp c$ polarized radiation.[3] In the *ac*-plane measurement, if the crystal is set properly so that the *c*-axis may take a direction perpendicular to the incidence plane, the two peaks of $k(\nu)$ and $\varepsilon''(\nu)$ around 400 cm^{-1} observed in the *ab*-plane spectrum do not appear clearly and instead one peak at 395 cm^{-1} is observed as shown in Fig. 8(b). This *ac*-plane spectrum of Fig. 8(b) is similar to that of $E//c$ by Barker, superimposed with a small amount of *ab*-plane spectrum, though Barker only carried out measurement down to 280 cm^{-1} and could not observe the peak around 250 cm^{-1}. From the above result it is concluded that the peak at 395 cm^{-1} is related to the a_{2u} species and the one around 250 cm^{-1} may also arise from the a_{2u} mode.

For MnF_2 crystal, a sample having sufficient area for the *ab*-plane and *ac*-plane could not be obtained, and accordingly the symmetry species of the observed transverse frequencies have not been determined experimentally. However, the plane for which the reflectivity measurement was performed was found to be almost 101 plane by crystal analysis. Due to the closeness of the transverse frequencies of 172 cm^{-1} and 161 cm^{-1}, two corresponding longitudinal frequencies could not be determined.

Discussion

The dielectric constants $\varepsilon'(\nu)$ and $\varepsilon''(\nu)$ were well interpreted on the basis of the lattice modes expected from the crystal symmetry, except for very weak extra

12) M. Born and K. Huang, "*Dynamical Theory of Crystal Lattices*," (*Oxford University Press, New York, 1954*).

13) D. H. Martin, *Advan. Phys.*, **14**, 39 (1965).

14) D. W. Berreman, *Phys. Rev.*, **130**, 2193 (1963).

bands or shoulders contributed from another extra oscillators which may arise from (a) a forbidden transition, (b) a two-phonon process, or (c) a localized mode due to impurities or a crystal surface. The observed data of ν_T and ν_L frequencies are checked by the Lyddane-Sachs-Teller relation,[15]

$$\prod_j \frac{(\nu_L)_j}{(\nu_T)_j} = \left[\frac{\varepsilon_0}{\varepsilon_\infty}\right]^{1/2} \tag{10}$$

where ε_0 is a static dielectric constant and ε_∞ is a high-frequency dielectric constant and can be obtained from the refractive index for the visible light, n^2. In Table 2 the values of $\prod_j[(\nu_L)_j/(\nu_T)_j]$ calculated from the ν_T and ν_L frequencies determined in Table 1 are compared with $(\varepsilon_0/\varepsilon_\infty)^{1/2}$. The agreement is satisfactory.

Table 2. Application of Lyddane-Sachs-Teller relation to some fluoride crystals

	$\prod_j(\nu_L/\nu_T)_j$	$(\varepsilon_0/\varepsilon_\infty)^{1/2}$
LiF	2.17	2.20
NaF	1.74	1.86
CaF_2	1.83	1.81
BaF_2	1.84	1.82
CdF_2	1.90	1.88
MgF_2 (e_u)	1.65	1.68

A short comment will be made concerning the peak values of $k(\nu)$ and $\varepsilon''(\nu)$. As described before there is some approximation in the procedure to get $k(\nu)$ and $\varepsilon''(\nu)$ curves, due to the limited range of the observed reflectivity data. According to the procedure utilized, the peak values of $k(\nu)$ and $\varepsilon''(\nu)$ are more or less affected but not those of ν_T and ν_L. Thus, no quantitative discussion on the peak values of $k(\nu)$ and $\varepsilon''(\nu)$ will be given. Nevertheless, it should be noted that for these ionic crystals of fluorides the values of the absorption indices(k) are rather large compared with those for liquid samples such as $CHCl_3$ and C_6H_6 (organic compounds)[16,17] and may take values larger than 2.0. ε'' may amount to 30.0 or more for the strong peaks, which are also much larger than the value of the order of 5.0 for liquid samples of organic compounds. However, it should be emphasized that the fluoride crystals studied here do not reveal any anomalous dielectric behavior, as compared with the dielectric constants of the oxide perovskites and rutile which amount to the order of 500.

Splitting of Transverse and Longitudinal Frequencies and Effective Charge

The transverse frequencies of some fluorides were analysed previously,[8,9] on the basis of the normal coordinate treatment of the dynamical model, taking into account the short-range interactions. Therefore, in the present treatment only the elastic force or restoring force against the ion displacement has been taken. The availability of the longitudinal frequencies as well as the transverse frequencies makes it possible to get information on factors other than the elastic force, such as electrostatic interaction.

On the basis of a polarizable ion model for the cubic diatomic crystals given by Born and Huang,[12] the transverse and longitudinal frequencies are derived as

$$4\pi^2\nu_T^2 = \frac{\beta}{\bar{M}} - \frac{4\pi}{3}\frac{1}{v}\left[\frac{Z^2e^2}{\bar{M}}\right]\left[1-\frac{4\pi}{3}\frac{\alpha^+ + \alpha^-}{v}\right]^{-1} \tag{11}$$

$$4\pi^2\nu_L^2 = \frac{\beta}{\bar{M}} + \frac{8\pi}{3}\frac{1}{v}\left[\frac{Z^2e^2}{\bar{M}}\right]\left[1+\frac{8\pi}{3}\frac{\alpha^+ + \alpha^-}{v}\right]^{-1} \tag{12}$$

where $\bar{M}$ is the reduced mass of unit cell ions$=M^+M^-/(M^+ + M^-)$, α^+ and α^- the ionic polarizabilities of the positive and negative ions, $\pm Ze$ the effective charge, β the force constant associated with the elastic force against the ion displacement, and $v=2(r_0/2)^3$ the volume of unit cell (r_0=cell constant). When the ions are assumed to be non-polarizable, this is reduced to a rigid ion model discussed by Denham *et al.*[7]

Eqs. (11) and (12) can be written in terms of ε_∞ instead of α^+ and α^- as

$$4\pi^2\nu_T^2 = \frac{\beta}{\bar{M}} - \frac{4\pi(Z^2e^2)(\varepsilon_\infty+2)}{9v\bar{M}}, \tag{13}$$

$$4\pi^2\nu_L^2 = \frac{\beta}{\bar{M}} + \frac{8\pi(Z^2e^2)(\varepsilon_\infty+2)}{9v\bar{M}\varepsilon_\infty}, \tag{14}$$

using Clausius Mosotti's relation

$$\frac{4\pi}{3}\frac{\alpha^+ + \alpha^-}{v} = \frac{\varepsilon_\infty - 1}{\varepsilon_\infty + 2}. \tag{15}$$

Eqs. (13) and (14) are reduced to the expressions based on a shell model developed by Cochran[18] and Axe.[19] Using the observed values of ν_T and ν_L listed in Table 1, the effective charges are obtained for both non-polarizable and polarizable ion models as shown in Table 3.

Table 3. Effective ionic charge (Z)

	I	II	III
LiF	0.77	0.81	0.82
NaF	0.80	0.85	0.93
NiO	0.81	a	a
CaF_2	0.80×2	0.85×2	0.83×2
BaF_2	0.84×2	0.90×2	0.88×2
CdF_2	0.77×2	0.82×2	0.80×2

I : Calculated based on a rigid ion model.
II : Calculated based on a shell model.
III: Calculated by Szigeti's formula.
a) The values of ε_∞ and ε_0 of NiO are not available.

Furthermore the following relation derived by Szigeti,[20] between ν_T and Ze expressed in terms of ε_0 and ε_∞

$$\nu_T^2 = \frac{1}{9\pi}\frac{(Z^2e^2)}{\bar{M}v}\frac{(\varepsilon_\infty+2)^2}{\varepsilon_0-\varepsilon_\infty}, \tag{16}$$

enables us to obtain Ze from the ν_T frequency for the crystals for which both ε_0 and ε_∞ are available. The

15) R. H. Lyddane, R. G. Sachs, and E. Teller, *Phys. Rev.*, **59**, 673 (1941).
16) T. Fujiyama and B. Crawford, Jr., *J. Phys. Chem.*, **72**, 2174 (1968).
17) B. Crawford, Jr., A. C. Gilby, A. A. Clifford, and T. Fujiyama, *Pure Appl. Chem.*, **18**, 373 (1969).
18) W. Cochran, *Advan. Phys.*, **9**, 387 (1960).
19) J. D. Axe, *Phys. Rev.*, **139**, A1215 (1965).
20) B. Szigeti, *Proc. Roy. Soc. London, Ser. A*, **204**, 51 (1950).

result is also given in Table 3.

In the infrared active mode of the XF_2 cubic crystal of fluorite structure, the reduced mass $\bar{M}=2M_FM_X/(2M_F+M_X)$ is used in Eqs. (11—16). $-Ze/2$, $-Ze/2$ and $+Ze$ correspond to the effective charges, respectively, on the two fluorine ions and on the metal ion.

In Table 3 it is found that the effective charge may be 15—20% below the formal charge for the fluoride crystals. However, for NiO the effective charge is 0.81 against the formal charge 2.0, which means that the electron delocalization is much larger in NiO than in the fluorides.

The contribution of factors other than the elastic force to the lattice frequencies can be estimated from the ratio of the second term of Eq. (11) to the first term for a rigid ion model. The ratio is given in Table 4 which also includes the short-range interionic elastic force constant $K(M\text{-}X)$. $K^*(M\text{-}X)$ is the calculated interionic force constant when the electrostatic term (second term) is neglected in Eqs. (11) and (13). It should be noted that the short-range elastic force constant between the positive and negative ions, calculated without taking into account the long-range electrostatic interaction, $K^*(M\text{-}X)$, is somewhat smaller than the true value $K(M\text{-}X)$.

TABLE 4. INTERIONIC RESTORING FORCE CONSTANTS IN mdyn/Å

	LiF	NaF	NiO	CaF_2	BaF_2	CdF_2
K(M-X)[a)]	0.31	0.31	0.74	0.51	0.39	0.47
K^*(M-X)	0.14	0.18	0.56	0.29	0.22	0.25
Ratio of Electrostatic term to Short-range Term	0.55	0.40	0.24	0.44	0.45	0.47

a) $K(\text{M-X})=\frac{1}{2}\beta$ for MX crystals and $K(\text{M-X})=(3/8)\beta$ for MX_2 crystals.

The author wishes to express his sincere thanks to Prof. Takehiko Shimanouchi, the University of Tokyo, for his encouragement and guidance. Thanks are also due to Prof. Akiyoshi Mitsuishi and Dr. Tetsuro Kawamura, Osaka University, for their kind instruction and suggestion on the Kramers-Kronig program and reflectivity measurement. A part of this work was supported by the RCA research grant.

BULLETIN OF THE CHEMICAL SOCIETY OF JAPAN, VOL. 44, 3020—3027 (1971)

The Crystal and Molecular Structure of Miyaconitine Hydrobromide Dihydrate

Hirotaka SHIMANOUCHI, Yoshio SASADA, and Tatsumichi TAKEDA

Laboratory of Chemistry for Natural Products, Tokyo Institute of Technology, Ookayama, Meguro-ku, Tokyo

(Received June 1, 1971)

The structure of an *Aconitum* alkaloid, miyaconitine, $C_{23}H_{29}O_6N$, has been determined by the X-ray analysis of crystals of the hydrobromide dihydrate, which are monoclinic with four formula units in a unit cell of the dimensions; $a=10.41$, $b=13.85$, $c=9.63$ Å and $\beta=113.8°$; space group, $P2_1$. The structure was solved by the heavy-atom method and was refined by the least-squares method. The final R index was 0.151. The absolute configuration was determined using the anomalous dispersion effect of the bromine atom. It was thus established that miyaconitine is a novel type of *Aconitum* alkaloid.

Introduction

Miyaconitine, $C_{23}H_{29}O_6N$, was isolated from *Aconitum miyabei* Nakai as a major alkaloid; the first preliminary investigation of its structure by chemical methods was reported in 1950.[1] Since then the structure has been investigated by many workers,[2-4] but certain reactions still remained uninterpretable, thus precluding a conclusive elucidation of the structure. Miyaconitine seemed to have an unusual skeleton, capable of a facile cyclization. In view of this, an X-ray structure analysis was undertaken in cooperation with the chemical work by Ichinohe, Yamaguchi, Katsui, and Kakimoto.[5]

A heavy-atom derivative, miyaconitine hydrobromide dihydrate, was prepared and supplied by Professor Ichinohe. A preliminary report of the present X-ray work has already been published.[6]

Experimental

Crystals of miyaconitine hydrobromide dihydrate are colorless scales, the (001) plane being well developed. The unit-cell dimensions were determined from zero-layer Weissenberg photographs about the a and the b axes, calibrated with superimposed Al-powder photographs.

Multiple-film equi-inclination Weissenberg photographs were taken at room temperature for the layer lines from 0 to

1) H. Suginome, S. Furusawa, Y. Chiba, and S. Kakimoto, *J. Fac. Sci. Hokkaido Univ. Ser. III, Chem.*, **4**, 1 (1950).
2) S. Kakimoto, This Bulletin, **32**, 349 (1959).
3) H. Suginome and S. Kakimoto, *ibid.*, **32**, 352 (1959).
4) S. Kakimoto, N. Katsui, and Y. Ichinohe, *ibid.*, **32**, 1153 (1959).
5) Y. Ichinohe, M. Yamaguchi, N. Katsui, and S. Kakimoto, *Tetrahedron Lett.*, **1970**, 2323.
6) H. Shimanouchi, Y. Sasada, and T. Takeda, *ibid.*, **1970**, 2327.

7 about the a axis and from 0 to 9 about the b axis, using Cu$K\alpha$ radiation. The crystals used were square in cross-section, with rectangular dimensions of 0.02×0.002 cm and 0.05×0.002 cm for the a and b axis rotation respectively. Almost no reflections were observed with $2\theta>100°$. Therefore, only 1342 were indexed out of the 2900 possible independent reflections within the limiting sphere for Cu$K\alpha$. The intensities of those 1342 reflections were estimated by visual comparison with a standard scale prepared with the same crystal, of which 211 were unobserved above the background. The accuracies of the intensity data were rather low, because only very thin crystals were available. The corrections for the Lorentz and polarization factors were made in the usual way, and those for the spot-size variation in the high-layer photographs, by the method of Phillips.[7] The correction for absorption was omitted.

Crystal Data

The crystallographic and physical data obtained are: Miyaconitine hydrobromide dihydrate $C_{23}H_{29}O_6N\cdot HBr\cdot 2H_2O$, mp 270°C (decomp.). Monoclinic, $a=10.41$ Å, $b=13.85$ Å, $c=9.63$ Å and $\beta=113.8°$. Absent spectra, $(0k0)$ when k is odd. Space group, $P2_1$. Two molecules per unit cell. Volume of the unit cell, 1270.5 Å^3. Density (by flotation), 1.399 g·cm^{-3}. Density (calculated), 1.391 g·cm^{-3}. Linear absorption coefficient for Cu$K\alpha$ radiation, $\mu=28.4$ cm^{-1}. Total number of electrons per unit cell, $F(000)=556$.

Table 1. Final atomic coordinates and temperature factors

The anisotropic temperature factors are expressed in the form of

$$\exp\{-(B_{11}h^2+B_{22}k^2+B_{33}l^2+B_{12}hk+B_{13}hl+B_{23}kl)\}.$$

Atom	x/a	y/b	z/c
Br	0.1017	0.0000	0.1711
Atom	B_{11}	B_{22}	B_{33}
Br	0.01676	0.00446	0.02593
Atom	B_{12}	B_{13}	B_{23}
Br	0.00205	0.02904	0.00071

Atom	x/a	y/b	z/c	B(Å^2)
O(1)	0.4864	0.4022	0.3369	4.14
O(2)	0.1601	0.5844	0.6034	2.30
O(3)	0.2090	0.4567	0.8366	2.26
O(4)	0.0220	0.2954	0.4435	2.47
O(5)	0.5542	0.2117	0.7295	4.01
O(6)	0.5289	0.2757	0.2128	9.60
OW(1)	−0.0835	0.1781	0.1885	4.56
OW(2)	−0.2241	0.3130	−0.0098	11.37
N	0.3650	0.4897	0.6325	1.19
C(1)	0.2753	0.3216	0.3201	3.33
C(2)	0.3363	0.3907	0.2379	2.55
C(3)	0.2617	0.4902	0.2086	3.62
C(4)	0.2469	0.5300	0.3611	2.19
C(5)	0.1613	0.4618	0.4210	1.53
C(6)	0.2108	0.4886	0.5850	1.98
C(7)	0.1655	0.4241	0.6933	1.55
C(8)	0.2249	0.3173	0.6864	1.09
C(9)	0.1717	0.2880	0.5217	1.45
C(10)	0.2534	0.3559	0.4574	1.53
C(11)	0.2112	0.1744	0.5220	1.00
C(12)	0.3116	0.1502	0.6667	2.58
C(13)	0.4336	0.2222	0.7108	−0.84
C(14)	0.3830	0.3219	0.7334	1.21
C(15)	0.1847	0.2515	0.7933	2.73
C(16)	0.2607	0.1470	0.7904	4.62
C(17)	0.2554	0.0771	0.8885	3.58
C(18)	0.1439	0.6239	0.2817	4.05
C(19)	0.3824	0.5566	0.4981	3.05
C(20)	0.3868	0.3801	0.5970	2.27
C(21)	0.5935	0.3480	0.3265	7.78
C(22)	0.7281	0.3609	0.4408	10.50
C(23)	0.4570	0.5273	0.7868	4.02

7) D. C. Phillips, *Acta Cryst.*, **7**, 746 (1954).

Structure Determination

The three-dimensional sharpened Patterson function was synthesized, and the bromine atom was easily located. A three-dimensional Fourier synthesis was subsequently carried out using the phases of the bromine atom. The resulting map necessarily exhibited the space group symmetry of $P2_1/m$, causing the superposition of the real atoms with their related mirror-image peaks. The 108 peaks were picked out within the asymmetric unit; we then tried to assemble them together to give a three-dimensional molecular model. By studying the distances and angles between peaks, the twenty-three peaks were tentatively assigned to

Table 2. Estimated standard deviations ($\sigma(x)$, $\sigma(y)$, and $\sigma(z)$ in Å, $\sigma(B)$ in Å^2)

Atom	$\sigma(x)$	$\sigma(y)$	$\sigma(z)$
Br	0.005	0.000	0.005
Atom	$\sigma(B_{11})$	$\sigma(B_{22})$	$\sigma(B_{33})$
Br	0.0006	0.0002	0.0008
Atom	$\sigma(B_{12})$	$\sigma(B_{13})$	$\sigma(B_{23})$
Br	0.0008	0.0011	0.0009

Atom	$\sigma(x)$	$\sigma(y)$	$\sigma(z)$	$\sigma(B)$
O(1)	0.025	0.025	0.026	0.53
O(2)	0.021	0.020	0.020	0.39
O(3)	0.021	0.019	0.021	0.39
O(4)	0.021	0.020	0.021	0.41
O(5)	0.026	0.024	0.025	0.52
O(6)	0.040	0.042	0.040	1.02
OW(1)	0.028	0.025	0.027	0.56
OW(2)	0.045	0.048	0.046	1.22
N	0.021	0.024	0.020	0.39
C(1)	0.037	0.034	0.036	0.72
C(2)	0.034	0.031	0.033	0.64
C(3)	0.034	0.043	0.033	0.71
C(4)	0.032	0.027	0.031	0.63
C(5)	0.030	0.026	0.029	0.54
C(6)	0.028	0.034	0.027	0.56
C(7)	0.030	0.027	0.029	0.55
C(8)	0.028	0.025	0.028	0.49
C(9)	0.029	0.026	0.028	0.52
C(10)	0.030	0.027	0.029	0.54
C(11)	0.028	0.025	0.027	0.48
C(12)	0.034	0.032	0.033	0.63
C(13)	0.025	0.021	0.023	0.41
C(14)	0.029	0.026	0.028	0.50
C(15)	0.034	0.032	0.034	0.66
C(16)	0.043	0.040	0.041	0.87
C(17)	0.038	0.036	0.036	0.74
C(18)	0.041	0.038	0.038	0.81
C(19)	0.036	0.033	0.035	0.70
C(20)	0.033	0.031	0.033	0.60
C(21)	0.056	0.053	0.057	1.31
C(22)	0.067	0.068	0.068	1.80
C(23)	0.040	0.035	0.038	0.82

TABLE 3. OBSERVED AND CALCULATED STRUCTURE FACTORS ($\times$ 7)

f K FO FC	K FO FC	K FO FC	K FO FC	K FO FC	K FO FC	K FO FC	K FO FC	K FO FC	K FO FC
H,L= 0 8	1 100 115	11 0 21	10 61 75	12 0 52	10 139 137	9 0 72	2 229 242	H,L= -7 2	
0 78 84	2 95 48	12 61 50	11 0 10	13 44 101	11 0 41	10 67 110	3 33 19	0 184 161	
1 123 151	3 139 181	13 55 33	12 50 62	H,L= 6 2	12 0 79	11 89 66	4 212 215	1 184 179	
H,L= 2 8	4 89 67	H,L= 5 4	H,L= 6 3	0 95 78	13 72 86	12 100 108	5 89 99	2 117 85	
0 72 54	5 72 71	0 83 35	0 83 77	1 95 81	H,L= 6 1	13 72 52	6 229 232	3 206 192	
H,L= 3 8	6 123 129	1 78 64	1 83 90	2 83 87	0 87 72	H,L= 6 0	7 106 107	4 184 194	
0 0 37	7 100 113	2 106 124	2 162 201	3 100 83	1 80 58	0 156 145	8 117 84	5 139 105	
1 72 59	8 83 104	3 95 71	3 83 66	4 184 178	2 111 129	1 240 249	9 128 103	6 134 139	
2 72 27	9 78 71	4 111 107	4 111 138	5 128 100	3 83 74	2 95 96	10 195 187	7 206 166	
3 0 41	H,L= 3 5	5 78 87	5 95 71	6 111 101	4 0 24	3 139 141	11 83 117	8 134 138	
H,L= 0 7	0 72 26	6 0 9	6 95 83	7 95 27	5 106 105	4 139 126	12 100 112	9 0 65	
0 0 35	1 167 131	7 0 45	7 0 2	8 95 27	6 145 137	5 156 166	13 72 54	10 123 90	
1 72 41	2 95 106	8 0 17	8 111 97	9 89 71	7 117 120	6 324 294	H,L= -7 1	11 89 59	
2 55 75	3 167 146	9 100 141	9 0 20	10 0 44	8 100 95	7 134 100	0 178 186	H,L= -1 3	
3 128 150	4 0 69	10 0 29	10 0 77	11 0 28	9 0 15	8 111 112	1 83 23	0 632 672	
4 95 23	5 72 78	11 0 59	11 50 22	12 0 16	10 67 57	9 0 82	2 128 157	1 268 215	
H,L= 1 7	6 117 26	12 44 24	12 44 63	H,L= 7 2	11 0 85	10 0 52	3 123 103	2 302 308	
0 67 59	7 117 64	H,L= 6 4	H,L= 7 3	0 89 46	12 67 28	11 78 61	4 201 215	3 318 327	
1 78 92	8 0 31	0 95 29	0 78 47	1 89 51	13 72 42	12 83 56	5 167 185	4 274 233	
2 67 40	9 111 69	1 95 118	1 89 56	2 134 169	H,L= 7 1	13 78 59	6 111 79	5 206 144	
3 83 91	H,L= 4 5	2 72 72	2 100 76	3 100 62	0 67 51	14 67 37	7 218 176	6 268 247	
4 0 64	0 72 57	3 126 133	3 83 63	4 95 92	1 151 180	H,L= 7 0	8 123 99	7 223 216	
5 67 85	1 100 145	4 95 118	4 95 65	5 83 51	2 162 168	0 89 55	9 0 22	8 279 246	
H,L= 2 7	2 0 46	5 100 100	5 95 101	6 100 88	3 95 33	1 156 155	10 0 39	9 156 99	
0 72 42	3 139 200	6 0 22	6 95 55	7 100 91	4 156 145	2 128 120	11 67 39	10 357 324	
1 78 74	4 0 47	7 0 33	7 0 14	8 95 54	5 156 166	3 117 140	H,L= -1 2	11 234 238	
2 95 113	5 0 22	8 0 83	8 61 51	9 0 48	6 0 87	4 111 73	0 453 492	12 139 141	
3 134 71	6 0 47	9 0 56	H,L= 0 2	10 0 70	7 173 142	5 117 93	1 302 241	H,L= -2 3	
4 0 20	7 78 76	10 67 49	0 643 669	11 72 29	8 123 114	6 95 104	2 408 332	0 50 34	
5 55 33	8 0 36	H,L= 7 4	1 408 395	H,L= 0 1	9 0 41	7 0 18	3 542 535	1 374 370	
H,L= 3 7	9 0 98	0 78 8	2 178 121	0 520 569	10 67 24	8 0 33	4 229 143	2 257 224	
0 78 87	10 67 78	1 95 51	3 201 198	1 313 336	11 0 11	9 100 120	5 413 387	3 234 225	
1 55 103	11 50 21	2 61 10	4 346 347	2 285 249	H,L= 6 0	10 95 79	6 100 90	4 509 470	
2 89 111	H,L= 5 5	3 83 87	5 458 373	3 721 711	2 464 473	11 55 58	7 408 315	5 257 200	
3 0 35	0 61 18	4 83 76	6 201 151	4 313 284	3 0 0	H,L= -1 1	8 117 67	6 290 258	
4 0 69	1 72 54	5 89 44	7 223 227	5 419 354	4 447 427	0 44 4	9 285 254	7 223 170	
5 0 43	2 55 92	H,L= 0 3	8 206 181	6 95 77	5 0 0	1 341 306	10 246 206	8 0 65	
6 0 66	3 0 29	0 318 301	9 67 91	7 279 250	6 598 520	2 520 582	11 167 100	9 100 98	
7 72 32	4 55 51	1 246 207	10 223 209	8 156 113	7 0 0	3 469 434	12 95 105	10 162 164	
H,L= 4 7	5 0 32	2 402 339	11 139 71	9 95 82	8 190 166	4 262 273	13 117 134	11 123 116	
0 50 66	6 0 45	3 139 80	12 134 125	10 89 76	9 0 0	5 313 259	H,L= -2 2	12 78 89	
1 0 30	7 61 74	4 441 418	13 0 35	11 268 268	10 262 272	6 531 418	0 223 163	13 83 144	
H,L= 0 6	8 55 73	5 78 63	H,L= 1 2	12 78 90	11 0 0	7 335 228	1 357 383	H,L= -3 3	
0 167 175	9 50 46	6 279 226	0 83 24	13 0 88	12 190 182	8 380 347	2 447 432	0 206 199	
1 128 132	10 44 30	7 0 22	1 341 332	H,L= 1 1	H,L= 1 0	9 167 104	3 369 348	1 324 374	
2 123 104	11 39 40	8 156 166	2 503 526	0 447 412	0 95 64	10 240 197	4 318 250	2 0 72	
3 0 52	H,L= 6 5	9 206 193	3 61 18	1 822 915	1 542 575	11 78 75	5 402 327	3 676 671	
4 100 104	0 72 11	10 223 195	4 95 105	2 139 71	2 332 406	12 0 75	6 223 165	4 363 334	
5 0 70	1 55 37	11 0 57	5 318 340	3 178 154	3 117 91	13 95 86	7 134 116	5 223 230	
6 139 147	2 61 88	12 95 102	6 251 270	4 290 233	4 290 299	14 0 85	8 139 110	6 324 268	
7 0 12	3 89 39	13 95 70	7 139 113	5 363 387	5 67 58	15 67 34	9 335 320	7 408 368	
8 0 80	4 83 44	H,L= 1 3	8 268 208	6 139 62	6 497 414	H,L= -2 1	10 156 163	8 78 35	
9 78 117	5 83 49	0 251 311	9 0 25	7 0 34	7 274 236	0 453 573	11 257 277	9 234 231	
10 0 30	6 55 50	1 246 249	10 190 164	8 106 77	8 56 82	1 341 355	12 151 147	10 111 73	
11 0 8	7 78 32	2 178 164	11 139 149	9 268 297	9 89 99	2 447 461	13 100 108	11 83 99	
H,L= 1 6	8 72 78	3 134 109	12 173 223	10 139 111	10 178 161	3 89 65	H,L= -3 2	12 78 64	
0 89 59	H,L= 0 4	4 229 269	13 111 65	11 134 159	11 0 63	4 285 333	0 503 610	H,L= -4 3	
1 72 69	0 39 14	5 218 225	H,L= 2 2	12 123 98	12 111 146	5 178 143	1 268 252	0 178 156	
2 0 26	1 357 382	6 234 251	0 246 238	13 145 180	13 139 145	6 626 584	2 419 446	1 156 142	
3 72 72	2 408 435	7 100 68	1 206 188	H,L= 2 1	H,L= 2 0	7 380 389	3 302 292	2 201 195	
4 89 56	3 268 226	8 0 69	2 229 175	0 195 166	0 430 450	8 419 369	4 374 382	3 380 384	
5 0 62	4 83 75	9 184 167	3 218 167	1 391 377	1 257 308	9 173 149	5 223 175	4 206 187	
6 78 78	5 151 141	10 0 84	4 246 262	2 240 215	2 102 157	10 0 116	6 128 112	5 408 331	
7 78 112	6 89 53	11 134 145	5 156 142	3 318 296	3 409 497	11 78 33	7 190 143	6 234 197	
8 100 115	7 178 156	H,L= 2 3	6 212 198	4 290 294	4 240 237	12 78 133	8 234 259	7 223 196	
H,L= 2 6	8 123 122	0 72 53	7 123 138	5 102 177	5 436 428	13 78 46	9 0 38	8 72 85	
0 72 44	9 151 175	1 302 295	8 72 92	6 262 220	6 262 204	14 50 104	10 95 127	9 0 79	
1 100 132	10 0 84	2 111 109	9 0 18	7 352 322	7 369 364	H,L= -3 1	11 100 95	10 195 193	
2 0 59	11 78 70	3 251 274	10 145 165	8 218 202	8 102 110	0 111 146	12 55 82	11 0 47	
3 128 172	12 78 71	4 123 106	11 0 36	9 72 107	9 218 231	1 374 406	13 78 74	12 78 78	
4 0 48	H,L= 1 4	5 117 94	12 111 157	10 139 146	10 156 159	2 363 377	H,L= -4 2	13 78 90	
5 111 139	0 95 103	6 117 114	13 78 63	11 78 99	11 102 210	3 352 355	0 251 284	H,L= -5 3	
6 0 90	1 67 61	7 178 192	14 72 119	12 78 82	12 89 35	4 234 235	1 107 132	0 335 380	
H,L= 3 6	2 190 188	8 83 86	H,L= 3 2	13 100 104	13 78 83	5 190 179	2 268 276	1 139 75	
0 0 12	3 229 210	9 134 159	0 178 140	14 0 88	14 72 57	6 145 124	3 107 168	2 257 214	
1 111 163	4 55 46	10 78 52	1 296 328	H,L= 3 1	H,L= 3 0	7 178 161	4 206 239	3 0 11	
2 89 151	5 123 92	11 78 133	2 251 263	0 139 177	0 503 484	8 117 110	5 134 111	4 285 241	
3 0 35	6 128 88	12 55 18	3 324 347	1 95 114	1 296 355	9 78 86	6 279 267	5 67 65	
4 0 39	7 151 101	H,L= 3 3	4 78 71	2 206 216	2 145 142	10 123 134	7 145 111	6 318 282	
5 78 85	8 89 81	0 0 36	5 190 194	3 173 140	3 475 549	11 100 132	8 262 249	7 151 70	
6 0 30	9 78 91	1 128 138	6 156 172	4 240 222	4 274 260	12 78 95	9 134 112	8 296 259	
7 78 73	H,L= 2 4	2 67 47	7 111 123	5 89 76	5 335 328	13 78 88	10 0 85	9 61 32	
H,L= 4 6	0 111 89	3 134 164	8 106 130	6 201 208	6 151 127	H,L= -4 1	11 0 49	10 190 218	
0 72 57	1 78 94	4 106 109	9 123 131	7 0 25	7 290 297	0 324 333	12 0 92	11 61 50	
1 72 90	2 195 251	5 100 140	10 83 80	8 184 185	8 0 39	1 324 410	13 0 68	12 83 106	
2 83 108	3 151 190	6 111 130	11 0 91	9 106 108	9 107 149	2 257 261	H,L= -5 2	13 0 12	
3 0 52	4 195 240	7 134 160	12 55 59	10 78 85	10 78 52	3 206 235	0 0 43	H,L= -6 3	
4 55 75	5 83 82	8 95 129	H,L= 4 2	11 55 49	11 78 105	4 240 231	1 363 411	0 268 253	
5 0 18	6 0 44	9 145 180	0 0 50	12 55 70	12 43 84	5 380 344	2 83 64	1 151 162	
H,L= 0 5	7 139 172	H,L= 4 3	1 195 149	H,L= 4 1	13 95 114	6 212 174	3 262 232	2 223 225	
0 145 170	8 89 39	0 78 65	2 167 172	0 363 342	H,L= 4 0	7 201 234	4 201 156	3 178 173	
1 218 226	9 117 143	1 156 162	3 162 164	1 341 376	0 61 48	8 117 100	5 285 290	4 128 60	
2 262 260	H,L= 3 4	2 156 142	4 162 160	2 318 287	1 341 381	9 145 163	6 162 194	5 195 175	
3 184 144	0 134 124	3 134 122	5 178 209	3 0 67	2 324 336	10 0 27	7 218 202	6 123 130	
4 201 202	1 89 53	4 139 139	6 83 63	4 262 258	3 268 302	11 173 195	8 134 117	7 83 38	
5 195 196	2 173 225	5 100 111	7 106 145	5 123 119	4 190 165	12 55 68	9 123 128	8 106 73	
6 128 124	3 0 42	6 89 82	8 78 94	6 156 166	5 117 115	13 123 135	10 89 110	9 0 84	
7 100 95	4 117 119	7 0 34	9 0 17	7 89 58	6 89 99	H,L= -5 1	11 240 217	10 0 93	
8 151 192	5 0 54	8 0 79	10 100 80	8 145 134	7 117 100	0 285 292	12 55 31	11 67 41	
9 111 141	6 95 51	9 0 124	11 95 111	9 123 106	8 173 185	1 173 116	13 0 64	12 106 139	
10 111 151	7 111 25	10 100 103	12 61 69	10 111 138	9 89 72	2 123 144	H,L= -6 2	13 0 29	
11 0 40	8 0 66	11 72 47	13 0 62	11 106 122	10 111 121	3 134 133	0 162 122	H,L= -7 3	
12 0 51	9 123 147	12 0 46	H,L= 5 2	12 89 101	11 55 54	4 151 120	1 173 221	0 145 143	
H,L= 1 5	H,L= 4 4	13 44 28	0 357 308	13 72 87	12 67 90	5 307 279	2 83 71	1 234 268	
0 156 151	0 128 143	H,L= 5 0	1 156 147	H,L= 5 1	13 55 51	6 167 147	3 173 137	2 44 83	
1 178 206	1 78 56	0 0 23	2 178 155	0 257 254	H,L= 5 0	7 190 168	4 111 91	3 268 277	
2 123 99	2 117 91	1 100 102	3 72 48	1 218 234	0 44 15	8 123 88	5 246 249	4 162 164	
3 123 108	3 100 124	2 139 119	4 83 64	2 151 107	1 106 85	9 89 124	6 145 136	5 234 237	
4 162 182	4 106 119	3 100 144	5 0 5	3 246 238	2 234 247	10 111 100	7 184 159	6 55 28	
5 72 74	5 83 112	4 123 140	6 95 87	4 195 188	3 89 73	11 78 75	8 106 70	7 246 200	
6 123 127	6 78 109	5 61 29	7 162 157	5 167 154	4 95 100	12 0 19	9 89 76	8 55 31	
7 0 66	7 78 59	6 139 114	8 134 134	6 106 104	5 178 176	13 78 93	10 145 87	9 162 149	
8 55 19	8 123 148	7 0 57	9 128 129	7 55 76	6 195 178	H,L= -6 1	11 128 146	10 72 48	
H,L= 2 5	9 0 63	8 0 95	10 139 140	8 0 13	7 95 96	0 425 405	12 61 70	11 95 91	
0 117 84	10 95 138	9 106 112	11 55 80	9 110 129	8 229 222	1 184 154	13 111 120	H,L= -1 4	

TABLE 3. (Continued)

K	FO	FC	K	FO	FC	K	FO	FC	K	FO	FC	K	FO	FC	K	FO	FC	K	FO	FC	K	FO	FC
0	240	205	7	262	245	9	100	32	3	117	126	7	195	165	2	78	89	7	78	82	8	55	64	H,L=	-3	8
1	229	173	8	123	96	10	173	138	4	156	144	8	100	56	3	184	223	8	72	50	9	0	72	4	128	158
2	335	248	9	184	177	11	67	66	5	78	39	9	72	28	4	156	196	9	139	145	10	0	35	5	83	114
3	279	275	10	0	22	H,L=	-1	5	6	151	138	10	95	54	5	100	130	10	0	40	11	50	89	6	0	91
4	212	260	11	139	147	0	206	213	7	139	100	11	95	85	6	139	165	11	89	65	H,L=	-5	7	H,L=	-4	8
5	257	221	12	0	24	1	257	259	8	151	185	H,L=	-1	6	7	134	130	H,L=	-1	7	0	55	58	0	83	0
6	167	167	13	0	116	2	72	34	9	134	138	0	156	126	8	67	51	0	100	112	1	173	206	1	0	93
7	206	189	H,L=	-5	4	3	67	60	10	83	114	1	134	149	9	106	139	1	128	126	2	134	150	2	162	188
8	100	116	0	212	226	4	151	119	11	100	86	2	117	89	10	78	87	2	190	234	3	128	152	3	0	53
9	100	100	1	262	294	5	190	157	12	78	96	3	151	145	11	78	40	3	100	99	4	111	82	4	167	121
10	134	131	2	55	66	6	100	19	13	0	33	4	139	162	12	0	50	4	139	157	5	106	125	H,L=	-5	8
11	78	109	3	206	183	7	95	116	H,L=	-5	5	5	72	70	13	44	51	5	0	89	6	0	77	0	0	60
12	0	92	4	145	129	8	156	158	0	162	189	6	128	135	H,L=	-5	6	6	0	65	7	128	125	1	128	122
H,L=	-2	4	5	257	228	9	195	208	1	128	147	7	117	114	0	212	199	7	95	98	8	0	38	2	95	110
0	95	79	6	173	151	10	0	46	2	151	206	8	111	34	1	50	81	H,L=	-2	7	9	89	95	3	0	71
1	240	237	7	162	151	11	0	106	3	251	238	9	111	120	2	106	109	0	78	78	10	0	20	4	95	28
2	380	390	8	201	128	12	78	53	4	145	128	10	95	120	3	67	66	1	128	160	11	78	78	5	89	100
3	262	274	9	61	89	H,L=	-2	5	5	195	197	11	78	16	4	100	95	2	123	145	H,L=	-6	7	6	61	91
4	139	120	10	0	61	0	156	160	6	156	150	H,L=	-2	6	5	78	69	3	123	69	0	145	135	7	83	64
5	218	208	11	201	216	1	111	93	7	178	155	0	0	20	6	167	193	4	100	128	1	145	140	8	0	34
6	223	208	12	55	79	2	223	227	8	145	93	1	128	110	7	89	12	5	111	23	2	100	64	9	83	92
7	67	61	13	78	96	3	162	140	9	145	144	2	206	245	8	145	152	6	78	89	3	139	149	10	0	58
8	218	219	H,L=	-6	4	4	229	248	10	0	81	3	223	267	9	61	47	7	95	73	4	123	105	11	67	82
9	151	128	0	123	142	5	229	260	11	89	95	4	95	80	10	123	121	8	89	127	5	55	43	H,L=	-6	8
10	145	158	1	83	53	6	117	115	H,L=	-6	5	5	0	10	11	61	34	H,L=	-3	7	6	55	68	0	0	38
H,L=	-3	4	2	268	279	7	106	102	0	100	91	6	89	64	H,L=	-6	6	0	95	59	7	55	35	1	100	134
0	240	275	3	83	81	8	229	249	1	212	214	7	111	139	0	218	173	1	117	144	8	0	72	2	0	67
1	296	377	4	262	252	9	279	284	2	111	94	8	123	122	1	145	141	2	0	68	9	83	46	3	128	82
2	72	39	5	145	108	10	0	100	3	167	152	9	111	144	2	195	211	3	128	69	10	0	71	4	0	16
3	234	184	6	128	120	H,L=	-3	5	4	162	152	10	78	98	3	234	268	4	123	126	11	78	65	5	128	166
4	363	347	7	128	76	0	229	221	5	201	206	H,L=	-3	6	4	195	205	5	128	190	H,L=	-7	7	6	0	54
5	307	303	8	240	206	1	123	139	6	95	72	0	128	214	5	100	112	6	0	75	0	145	147	7	106	118
6	290	265	9	0	44	2	274	304	7	257	228	1	184	226	6	128	120	7	0	82	1	100	85	8	61	37
7	100	87	10	0	90	3	251	276	8	151	117	2	117	129	7	123	99	8	117	126	2	139	185	H,L=	-7	8
8	178	173	11	67	32	4	234	265	9	251	161	3	134	121	8	134	151	9	0	36	3	111	113	0	0	44
9	89	142	12	61	63	5	67	26	10	95	8	4	72	44	9	67	26	10	78	74	4	128	107	1	128	173
10	78	94	13	78	30	6	123	135	11	89	92	5	123	134	10	89	108	11	0	16	5	0	54	2	0	107
11	83	90	H,L=	-7	4	7	78	83	12	0	39	6	0	37	11	61	22	12	67	43	6	156	158	3	139	140
12	0	59	0	234	271	8	134	166	13	50	107	7	117	138	12	78	58	H,L=	-4	7	7	72	32	4	111	44
H,L=	-4	4	1	44	64	9	139	142	H,L=	-7	5	8	106	133	H,L=	-7	6	0	0	72	8	89	109	5	139	141
0	184	178	2	251	242	10	83	24	0	100	93	9	83	89	0	234	220	1	162	197	9	0	19	6	0	18
1	363	395	3	134	115	11	83	96	1	145	164	10	100	118	1	139	143	2	72	97	10	89	46	7	0	40
2	151	141	4	302	306	12	0	110	2	139	146	11	0	91	2	134	109	3	134	174	H,L=	-2	8	8	89	36
3	117	80	5	123	142	H,L=	-4	5	3	162	170	12	0	24	3	111	81	4	111	147	5	0	32	9	83	63
4	156	128	6	167	166	0	151	158	4	89	90	H,L=	-4	6	4	145	158	5	117	155	6	78	63	10	78	59
5	262	257	7	167	89	1	123	118	5	102	101	0	123	85	5	117	131	6	78	75	7	0	20	H,L=	-7	9
6	111	78	8	296	236	2	240	267	6	128	109	1	167	175	6	0	42	7	0	145	8	72	56	3	139	123

light atoms after many trials; nine of them were later found to be incorrect. The difficulty was the presence of many spurious peaks, probably because of the low accuracies of the diffraction data mentioned in the previous section. To find the remaining atoms, a successive Fourier synthesis and the least-squares refinement were executed in combination. The atoms whose temperature factors became unreasonably large in the least-squares refinement were abandoned. The atoms of the molecular skeleton were revealed step by step, but some of the atoms in the acetoxyl group and a water of crystallization did not appear in this stage. Finally, difference syntheses gave all the non-hydrogen atoms. The oxygen atoms were easily distinguished from the carbon atoms by inspecting the electron-density, the bond lengths, and the hydrogen bonding scheme, as will be described later.

Since the evidence for assigning the nitrogen atom was not conclusive at this stage, the electron-density values at the peaks and the chemical information were taken into account. This assignment is consistent with that of other related diterpenoid alkaloids of a known structure.[8-10]

The atomic parameters were refined by the block-diagonal matrix least-squares method. Anisotropic temperature factors, of the form $\exp\{-(B_{11}h^2+B_{22}k^2+B_{33}l^2+B_{12}hk+B_{13}hl+B_{23}kl)\}$, were applied to the bromine atom, while the thermal motion of the light atoms was assumed to be isotropic. The final discrepancy index, $R=\Sigma||F_o|-|F_c||/\Sigma|F_o|$, was 0.151 for the observed reflections. The atomic scattering factors used were taken from International Tables for X-ray Crystallography (1962).[11] The final atomic coordinates and temperature factors are given in Table 1, and their standard deviations, in Table 2. The ob-

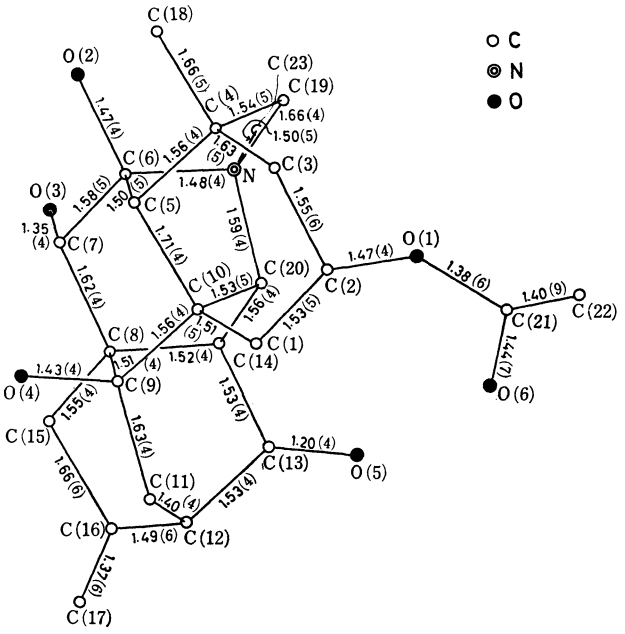

Fig. 1. Bond lengths (Å). The corresponding e.s.d.'s, given in parentheses, refer to the last decimal positions.

8) M. Przybylska, *Acta Cryst.*, **16**, 871 (1963).
9) S. W. Pelletier, L. H. Wright, M. G. Newton, and H. Wright, *Chem. Comm.*, **1970**, 98.
10) K. B. Birnbaum, *Tetrahedron Letters*, 5245 (1969).
11) "International Tables for X-ray Crystallography", Vol. 3, Kynoch Press, Birmingham, England (1962), p. 202.

TABLE 4. BOND ANGLES (deg.)
The corresponding e.s.d.'s, given in parentheses, refer to the last decimal positions.

C(21)	O(1)	C(2)	125(3)	C(9)	C(8)	C(15)	117(2)
C(23)	N	C(6)	119(3)	C(14)	C(8)	C(15)	112(2)
C(6)	N	C(20)	99(2)	C(8)	C(9)	O(4)	113(2)
C(19)	N	C(20)	107(2)	C(8)	C(9)	C(10)	103(2)
C(6)	N	C(19)	102(2)	C(10)	C(9)	C(11)	114(2)
C(19)	N	C(23)	111(2)	C(11)	C(9)	O(4)	107(2)
C(23)	N	C(20)	117(2)	O(4)	C(9)	C(10)	114(2)
C(2)	C(1)	C(10)	120(3)	C(11)	C(9)	C(8)	106(2)
O(1)	C(2)	C(1)	107(3)	C(5)	C(10)	C(9)	104(2)
O(1)	C(2)	C(3)	110(3)	C(5)	C(10)	C(20)	103(2)
C(1)	C(2)	C(3)	112(3)	C(1)	C(10)	C(20)	116(3)
C(2)	C(3)	C(4)	111(3)	C(1)	C(10)	C(9)	117(3)
C(3)	C(4)	C(19)	118(3)	C(9)	C(10)	C(20)	103(2)
C(3)	C(4)	C(5)	114(3)	C(1)	C(10)	C(5)	111(2)
C(5)	C(4)	C(18)	107(3)	C(9)	C(11)	C(12)	109(2)
C(18)	C(4)	C(19)	114(3)	C(11)	C(12)	C(13)	109(3)
C(19)	C(4)	C(5)	107(3)	C(11)	C(12)	C(16)	116(3)
C(3)	C(4)	C(18)	97(3)	C(13)	C(12)	C(16)	109(3)
C(4)	C(5)	C(10)	104(2)	O(5)	C(13)	C(12)	131(3)
C(6)	C(5)	C(4)	104(2)	O(5)	C(13)	C(14)	119(2)
C(6)	C(5)	C(10)	94(2)	C(12)	C(13)	C(14)	109(2)
N	C(6)	O(2)	111(2)	C(8)	C(14)	C(13)	108(2)
N	C(6)	C(5)	101(2)	C(8)	C(14)	C(20)	99(2)
C(5)	C(6)	C(7)	119(3)	C(13)	C(14)	C(20)	103(2)
C(7)	C(6)	O(2)	102(2)	C(8)	C(15)	C(16)	104(3)
O(2)	C(6)	C(5)	111(3)	C(12)	C(16)	C(15)	108(3)
N	C(6)	C(7)	112(3)	C(12)	C(16)	C(17)	135(4)
C(6)	C(7)	C(8)	106(2)	C(15)	C(16)	C(17)	117(3)
C(6)	C(7)	O(3)	115(2)	C(4)	C(19)	N	101(2)
C(8)	C(7)	O(3)	112(2)	N	C(20)	C(10)	104(2)
C(14)	C(8)	C(7)	110(2)	C(10)	C(20)	C(14)	108(3)
C(15)	C(8)	C(7)	107(2)	N	C(20)	C(14)	105(2)
C(9)	C(8)	C(14)	103(2)	O(1)	C(21)	O(6)	107(4)
C(9)	C(8)	C(7)	108(2)	O(1)	C(21)	C(22)	117(5)
				O(6)	C(21)	C(22)	134(5)

served and calculated structure factors are listed in Table 3.

The computations were done on a HITAC 5020E computer in the University of Tokyo, with programs written by Tamaichi Ashida [12]

TABLE 5. SOME LEAST-SQUARES PLANES

	Plane I		Plane II		Plane III
l	−0.667		0.157		−0.445
m	−0.334		0.207		−0.634
n	−0.666		−0.966		0.632
p	5.054		5.140		3.350
	Deviation of atoms (Å)				
C(12)	0.01	O(5)	−0.00	O(1)	0.02
C(16)	−0.03	C(12)	−0.00	O(6)	0.03
C(15)	0.01	C(13)	0.00	C(21)	−0.07
C(17)	0.01	C(14)	−0.00	C(22)	0.02

The equations of the planes are expressed in the form of $lx'+my'+nz'+p=0$ where $x'=x+z\cos\beta$, $y'=y$ and $z'=z\sin\beta$.

12) T. Ashida, "HBLS-4, The Universal Crystallographic Computing System (I)", Japanese Crystallographic Association, Tokyo (1967), p. 65.

Validity of Assignment of Atomic Species

The intramolecular bond lengths and angles are shown in Fig. 1 and Table 4 respectively. Although the standard deviations were quite large, it is possible to distinguish the exocyclic C–O bonds from the C–C

TABLE 6. COMPARISON OF THE STRUCTURE FACTORS IN BIJVOET PAIRS

h	k	l	Calcd. $\lvert F(hkl)\rvert$		Calcd. $\lvert F(h\bar{k}\bar{l})\rvert$	Obs. $\lvert I(hkl)\rvert$		Obs. $\lvert I(h\bar{k}\bar{l})\rvert$
2	1	2	26.4	<	27.5		>	
2	1	4	13.2	>	12.6		<	
2	3	4	26.2	<	27.8		>	
3	1	4	7.6	>	7.5		<	
4	1	3	22.5	<	23.3		>	
4	2	1	39.1	<	42.1		>	
4	3	5	28.1	<	28.2		>	
5	1	2	20.2	<	20.8		>	
5	2	3	15.0	<	15.3		>	
6	3	4	18.5	<	19.1		>	
7	2	2	23.4	<	24.7		>	

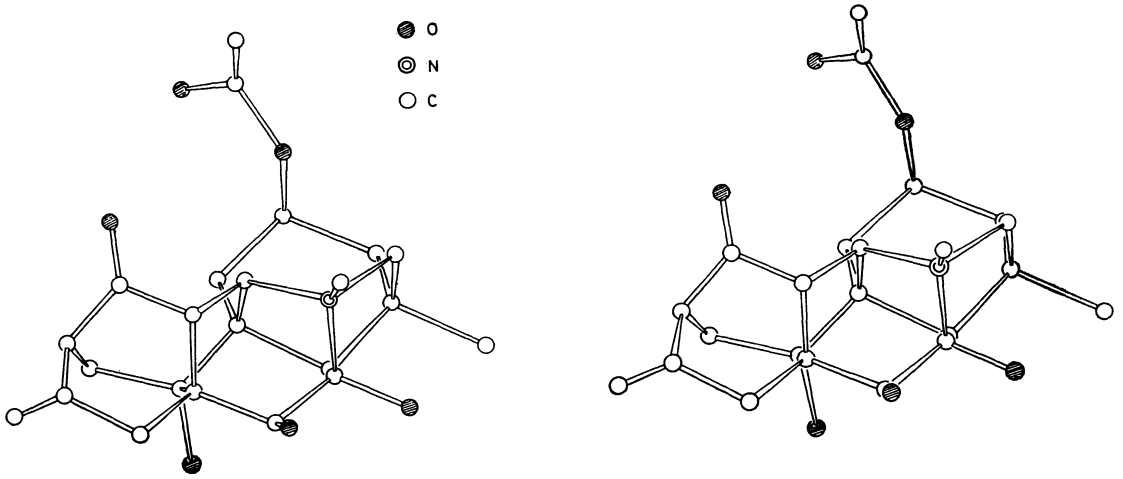

Fig. 2. Stereoscopic drawing of the structure.

bonds. That is, the C(sp^3)–O bond lengths are in the range of 1.35—1.47 Å, while the length of the C(4)—C(18) bond is 1.66 Å.

The equations for the least-squares planes of the planar groups are summarized in Table 5. The C(12), C(16), C(15), and C(17) atoms are essentially planar within the limits of error, and the O(5), C(12), C(13), and C(14) atoms are completely planar, showing that the C(13) and C(16) atoms are in the sp^2 hybridization. The bond lengths, 1.20 Å for C(13)–O(5) and 1.37 Å for C(16)–C(17), clearly distinguish the C=O group from the C=C bond.

The O(1), O(6), C(21), and C(22) atoms are also nearly planar, compatible with the identification of the acetoxyl group. Although there is no significant difference between the C(21)–O(6) and C(21)–C(22) distances, the peak of the electron-density of O(6) was higher than that of C(22) throughout all the stages of Fourier synthesis, so the oxygen atom can tentatively be assigned to the O(6).

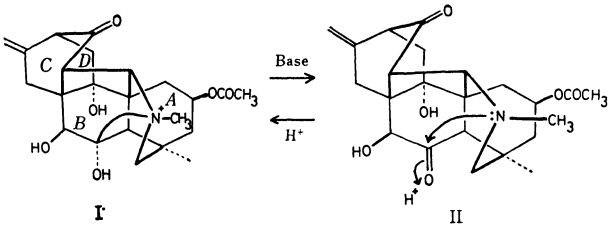

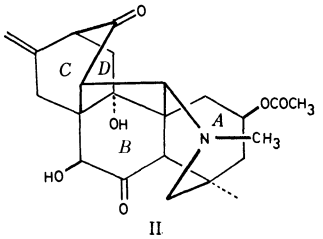

Determination of Absolute Configuration

The absolute configuration of the present compound was determined by means of the anomalous scattering of the Cu$K\alpha$ radiation by the bromine atom. The Bijvoet pairs selected as most advantageous for visual comparison are given in Table 6. From these observations, it can be concluded that the atomic coordinates in Table 1 should be referred to a left-handed coordinate system. All the drawings in this paper are based on the correct absolute configuration. The absolute configuration found is in agreement with those of related compounds.[8–10]

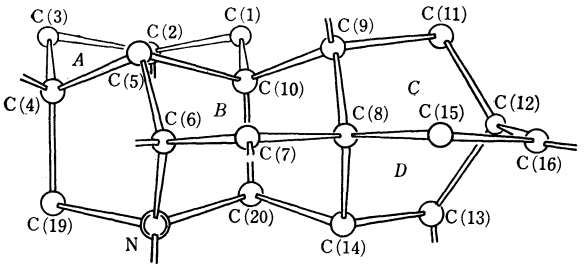

Fig. 3. Molecular skeleton, viewed down the vector between C(7) and the midpoint of C(10)–C(20).

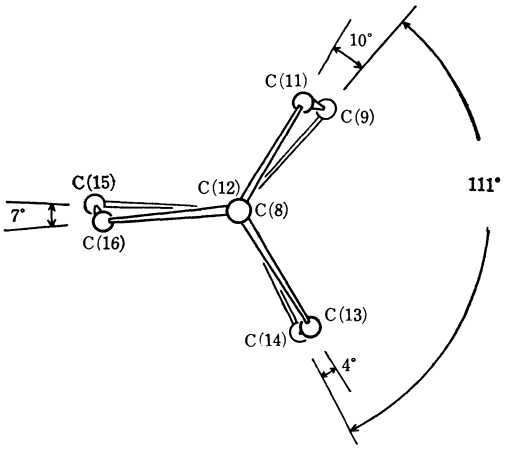

Fig. 4. Rings *C* and *D*, viewed down the C(12)···C(8) vector showing the twisting of the carbocycle.

Results and Discussion

From the X-ray analysis described in the preceding sections, the structure of the present molecule has been determined to be I, including the absolute configuration. A three-dimensional view of the molecule can be obtained from the stereodrawings in Fig. 2. On the basis of the present results, the structure of miyaconitine itself can be deduced to be II, which can easily be converted to I in acidic media.[5] Although the skeleton of the resultant hydrobromide molecule (I) is identical with those of hetisine[8] and kobusine methiodide,[9] the free alkaloid, miyaconitine itself (II), has a new type of skeleton. This is the first substance isolated as a biogenetic intermediate in the transformation from an atisine to a hetisine skeleton in *Aconitum* alkaloids.[5]

The drawing of the skeleton viewed along the vector between the C(7) and the midpoint of the C(10)–C(20) bond is shown in Fig. 3. The *A* ring takes the chair form, with the acetoxyl group in the axial position. If the fusion of the *A* ring and the difference in atomic species are disregarded, the main skeleton possesses an approximate mirror plane through the C(6), C(7), and C(8) atoms. The *C* and *D* rings make a bicyclo-[2,2,2]octane-like system, as is shown in Fig. 4. The conformation of this system is slightly staggered, with the projected angles ranging from 4° to 10°. The presence of a bridge between C(9) and C(14) through the C(10)–C(20) bond causes an appreciable closing of the projected angle, C(9)–C(8)–C(14) (111°). These indicate a significant deviation from D_3 symmetry.[13]

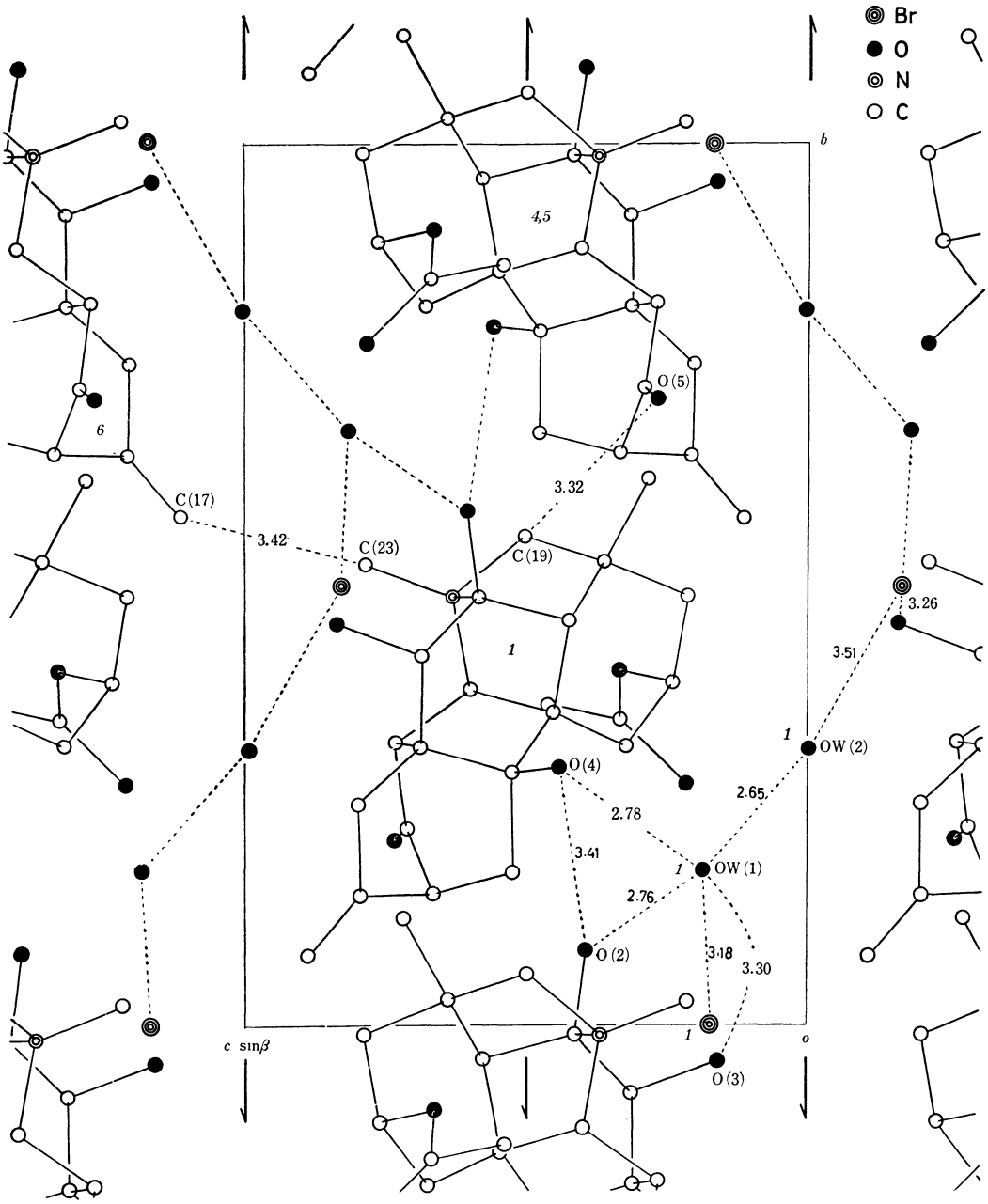

Fig. 5. The crystal structure projected along the a axis with some short intermolecular contacts in Å.

13) A. F. Cameron, G. Ferguson, and D. G. Morris, *J. Chem. Soc. (B)*, **1968**, 1249.

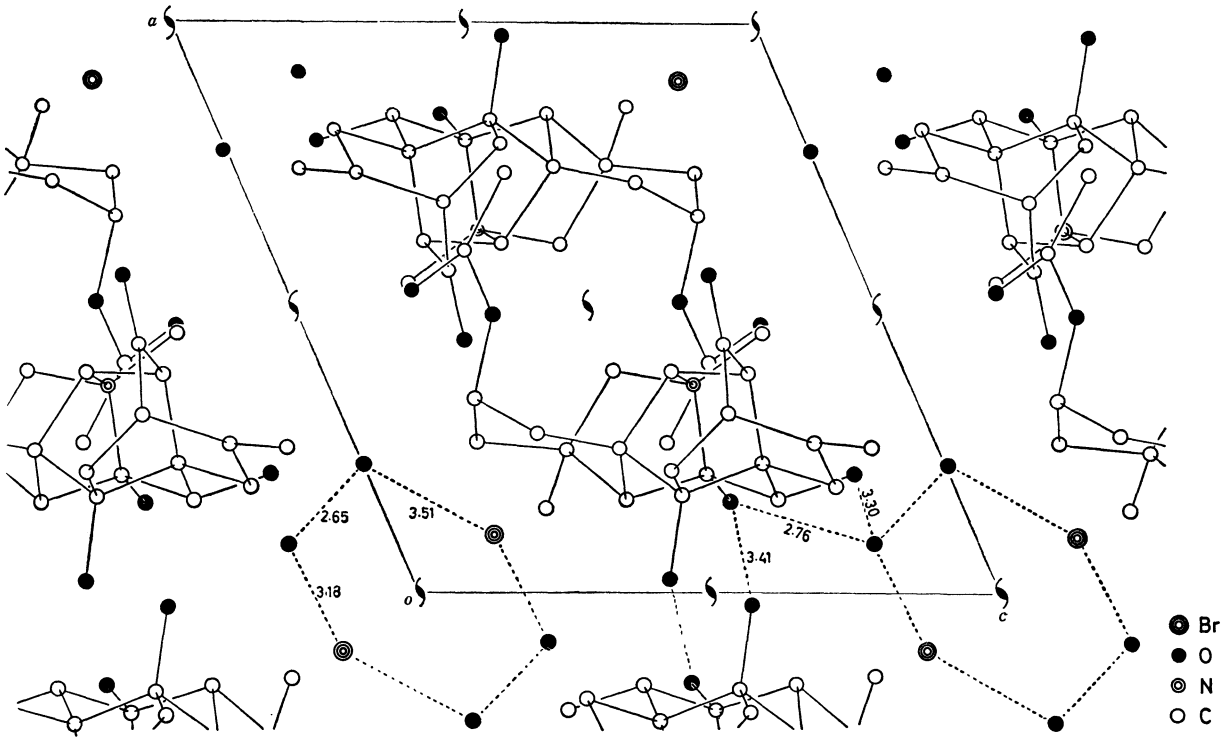

Fig. 6. The crystal structure projected along the b axis.

Table 7. Short intermolecular distances

Atom (position 1)	Atom	in position	Distance
	C···C shorter than 4.00 Å		
C(18)	C(16)	*4*	4.00 Å
C(18)	C(15)	*4*	3.66
C(18)	C(17)	*4*	3.86
C(23)	C(17)	*6*	3.42
	C···O shorter than 3.50 Å		
C(11)	OW(1)	*1*	3.43
O(3)	C(3)	*2*	3.43
C(19)	O(5)	*5*	3.32
C(23)	O(6)	*5*	3.44
C(18)	O(5)	*5*	3.41
	Br^-···C shorter than 4.00 Å		
Br	C(11)	*1*	3.93
C(17)	Br	*2*	3.82
C(7)	Br	*4*	3.67
C(22)	Br	*5*	3.93

Atom (position 1)	Atom	in position	Distance
	Br^-···O shorter than 4.00 Å		
Br	OW(1)	*1*	3.18
OW(2)	Br	*3*	3.51
O(3)	Br	*4*	3.26
	O···O shorter than 4.00 Å		
O(4)	OW(1)	*1*	2.78
OW(2)	OW(1)	*1*	2.65
O(3)	OW(1)	*4*	3.30
O(2)	O(4)	*4*	3.41
O(2)	OW(1)	*4*	2.76
Position[a)]	General coordinates		
1	x,	y,	z
2	x,	y,	$1+z$
3	$\bar{x}$,	$\frac{1}{2}+y$,	$\bar{z}$
4	$\bar{x}$,	$\frac{1}{2}+y$,	$1-z$
5	$1-x$,	$\frac{1}{2}+y$,	$1-z$
6	$1-x$,	$\frac{1}{2}+y$,	$2-z$

a) These are also indicated in Fig. 5.

The UV spectrum of this compound shows a somewhat higher intensity at 295 nm than that of normal saturated ketones.[5] This may correlate with the distance between, and the relative orientation of, the carbonyl and the exocyclic methylene groups; the C(13)···C(16) distance is 2.46 Å ,and the tilt of the C=O bond with respect to the C=C bond is 62°.

The packing diagrams of the crystal viewed along the a and b axes are shown in Figs. 5 and 6 respectively. The intermolecular distances are listed in Table 7.

All the C···C intermolecular distances can be considered to be normal: only four of them are shorter than 4 Å, the shortest being 3.42 Å of the C(sp^3)···C(sp^2) approach shown in Fig. 5. The closest C···O distance is 3.32 Å ,while the Br^-···C distances are all larger than 3.67 Å. The close Br^-···O and O···O approaches are also given in Fig. 5, suggesting that the hydrogen bonds may play an important role in the packing. The shortest N^+···Br^- distance is 5.09 Å, which might indicate no simple cation-anion interaction in the crystal structure.

The authors are grateful to Professor Yoshiyuki Ichinohe for supplying the sample and for his helpful discussions, and to Dr. Tsukasa Iwadare for his continued encouragement. Thanks are also due to Miss Makiko Yamaguchi for her assistance.

The Extraction of the Cesium Ion with Some Nitrophenols into Nitrobenzene. II. Homoconjugation Studies by Means of Conductivity Measurements

Osamu TOCHIYAMA,* Mutsuo KOYAMA, and Taitiro FUJINAGA

Department of Chemistry, Faculty of Science, Kyoto University, Sakyo-ku, Kyoto

**Department of Nuclear Engineering, Faculty of Engineering, Tohoku University, Aramaki-aza-aoba, Sendai*

(Received December 19, 1970)

In connection with the liquid-liquid extraction study of alkali metal nitrophenolates, ionic equilibria taking place in the systems were studied by means of conductivity and solubility measurements. It was revealed that the adduct formation of *p*- and *m*-nitrophenolates consisted of homoconjugation, that is, free nitrophenols are attached not to cations, but to the nitrophenolate anions, thus forming the larger anions and being stabilized in the organic phase. Homoconjugation constants of the nitrophenolates, which are independent of the cations present, were measured. The difference in extraction behaviors was interpreted in terms of the solubilities in both aqueous and organic phases and in terms of the homoconjugation constants.

In the previous paper,[1] it was demonstrated that the process of extracting cesium as nitrophenolates could be interpreted in terms of the dissociation of cesium phenolates and in terms of conjugation or adduct formation with free nitrophenols in the nitrobenzene phase. In that study, the interpretation was based on the fact that the experimental data agreed well with the equations which were postulated; no direct evidence has been given for the existence of dissociated forms of extracted species in the nitrobenzene phase. Besides, no confirmation was possible whether anions or cations participate with free nitrophenol molecules.

Kolthoff *et al.*[2-4] have demonstrated a method of estimating anion conjugation constants, in which the solubility product of the slightly soluble salt and the total ionic solubility were measured in the presence of varying concentrations of conjugating reagents.

In the present study, the method[2-4] was applied in order to clarify the ionic equilibria in the organic phase. As a result, it was found that the mono-nitrophenols are conjugated with anions present in the organic phase, whereas di- and tri-nitrophenols are less conjugated, in this order. The conjugation constants and solubilities of several salts in both organic and aqueous phases were determined. The extraction mechanisms and the participation of the solvent are discussed.

Experimental

Reagents. The alkali nitrophenolates were prepared by adding a slight excess of the alkali hydroxide to aqueous solutions of nitrophenols, concentrating the resulting solutions with a rotary evaporator, filtering off the precipitates, and recrystallizing them from acetone or ethanol solutions. The precipitates were dried for about an hour at 50°C *in vacuo* and then stored in a silica-gel desiccator. Nitrophenols and alkali hydroxides used were of reagent grade purity. The nitrobenzene was prepared by vacuum-distilling special-grade nitrobenzene. Titration with Karl-Fisher reagent using dead-stop indication showed a water content of 0.0035 wt% in the nitrobenzene. The nitrobenzene had a specific conductance of *ca.* 4×10^{-9}.

Apparatus. The conductivity measurements were performed in a glass cell equipped with platinized platinum electrodes by the use of a universal bridge, Type BV-Z-13B, supplied by Yokogawa Electric Works, Ltd. During the measurements, the temperature of the cell was controlled at 25 ± 1°C in a thermostat.

Procedure. The ionic mobility of cesium picrate in nitrobenzene was measured by dissolving a standard cesium picrate solution with nitrobenzene; because of the slight solubility, the concentration of the standard solution was of the order of 10^{-4} M (see Fig. 1).

The ionic mobilities of cesium *p*-nitrophenolate (*p*-NP(Cs)), cesium *m*-nitrophenolate (*m*-NP(Cs)), cesium *o*-nitrophenolate (*o*-NP(Cs)), and cesium 2,4-dinitrophenolate (α-DNP(Cs)) were measured in nitrobenzene in the presence of 0.1 M nitrophenol; the salt was dissolved in a 0.1 M nitrophenol solution and diluted with a 0.1 M nitrophenol solution.

The conductivity measurements of a saturated solution in the presence of nitrophenols were carried out as follows; 100—200 mg of salt, which had previously been washed with nitrobenzene, were introduced into the conductivity cell, 10 m*l* of nitrobenzene were added, and the conductance was measured. The nitrophenol dissolved in nitrobenzene was added from a microsyringe, and after each addition of the reagent, the cell and the contents were shaken until the conductance remained constant within a 1% deviation.

The solubilities of nitrophenolates in distilled water were obtained by the use of ^{137}Cs; a labeled salt was saturated in water at 25 ± 1°C, and the concentration was determined by measuring the γ-ray activities of ^{137}Cs.

Theoretical

(1) Dissociation of Cesium Nitrophenolates in Nitrobenzene. The dissociation of cesium nitrophenolates was ascertained by plotting the equivalent conductances, Λ, against the square roots of the concentration, C, of cesium nitrophenolates.

The relation between λ and $\sqrt{C}$ can be represented by the following expression:[5]

1) T. Fujinaga, M. Koyama, and O. Tochiyama, This Bulletin, **44**, 1591 (1971).

2) M. K. Chantooni, Jr., and I. M. Kolthoff, *J. Amer. Chem. Soc.*, **89**, 1582 (1967).

3) I. M. Kolthoff and M. K. Chantooni, Jr., *ibid.*, **91**, 25 (1969).

4) I. M. Kolthoff and M. K. Chantooni, Jr., *ibid.*, **91**, 4621 (1969).

5) H. S. Harned and B. B. Owen, "The Physical Chemistry of Electrolyte Solutions," Reinhold Publishing Corporation, New York, N.Y., (1958) pp. 164, 178, 286.

$$\Lambda = \Lambda^0 - (B_1 \cdot \Lambda^0 + B_2)\frac{\sqrt{\alpha C}}{1 + B\mathring{a}\sqrt{\alpha C}} \quad (1)$$

where B_1, B_2, and B are the constants for the solvent; α, the degree of the dissociation; C, the concentration, and $\mathring{a}$, the distance of the approach of the ions in angstrom units.

The dissociation constants of the salts were obtained by the method of Shedlovsky.[5]

(2) Homoconjugation of Nitrophenolate Anions. If the chemical form of the species is a free ion in the solvent, the method reported by Kolthoff can be employed to determine the degree of the dissociation and participation of the nitrophenol in nitrobenzene.

The solubility product, $K_{sp,o}$, in nitrobenzene is obtained by measuring the conductivity of the saturated solution of the one-to-one salt MOR:

$$K_{sp,o} = [M^+]_o[OR^-]_o \cdot f^2 \quad f = f_{M^+} = f_{OR^-} \quad (2)$$

where f is the activity coefficient. When free nitrophenol ROH is added to this solution, the homoconjugation of the anion occurs and the new equilibrium represented below must be considered:

$$(OR^-)_o + n(ROH)_o = (OR \cdot nROH^-)_o \quad (3)$$

$$K_n^f = \frac{[OR \cdot nROH^-]_o}{[OR^-]_o[ROH]_o^n} \qquad f_{OR^-} = f_{OR \cdot nROH^-} \quad (4)$$

The shifts of the equilibrium to the right direction cause a rise in the solubility of the cesium ion, according to the demands of the electrical neutrality relation:

$$\begin{aligned}[M^+]_o &= [OR^-]_o + [OR \cdot ROH^-]_o \\ &\quad + [OR \cdot 2ROH^-]_o + \cdots \\ &= [OR^-]_o(1 + \sum_n K_n^f[ROH]_o^n) \end{aligned} \quad (5)$$

Supposing that $K_{sp,o}$ is constant over the concentration range of the nitrophenol examined, the next expression can be obtained:

$$\begin{aligned} f^2[M^+]_o^2/K_{sp,o} &= 1 + K_1^f[ROH]_o \\ &\quad + K_2^f[ROH]_o^2 + \cdots \end{aligned} \quad (6)$$

This expression means that homoconjugation constants can be estimated from the plots of $f^2[M^+]_o^2/K_{sp,o}$ against $[ROH]_o$.

In the application of Eq. (6), the following assumptions have to be made:

(i) Nitrophenol is considered monomeric, and the activity of nitrophenol is taken to be equal to the equilibrium concentration; this assumption was verified previously by the results of the distribution studies of nitrophenols.[1]

(ii) Only the unconjugated salt MOR is present in the solid phase, and the solubility product, $K_{sp,o}$, is considered to be constant. The water in the salt and nitrobenzene has little effect on the $f^2[M]_o^2/K_{sp,o}$ value.

(iii) The independent anion conjugation of the nitrophenol is assumed; that is the K_n^f values of anions are independent of the nature of the cations. This assumption was ascertained by the experiments shown in Fig. 3.

(iv) The limiting Debye-Hückel relation was used to evaluate ionic activity coefficients:[5]

$$\log f_\pm = -A|z_+||z_-|\sqrt{I} \quad (7)$$

$$A = \frac{1.8246 \times 10^6}{(DT)^{3/2}} \quad (8)$$

where D: dielectric constant of nitrobenzene (34.5)

T: Kelvin temperature (273+25)

$|Z_+||Z_-|$: magnitudes of valences of ions (1)

I: ionic strength

(v) The limiting equivalent conductances of the anions, $(OR^-)_o$, $(OR \cdot ROH^-)_o$, and $(OR \cdot 2ROH^-)_o$, are assumed to be equal to the value obtained from Fig. 1. In fact, $\Lambda^0_{OR^-}$, $\Lambda^0_{OR \cdot ROH^-}$, and $\Lambda^0_{OR \cdot 2ROH^-}$ are not equal and the obtained value are mixtures of these values. If, however, $[ROH]_o$ is constant in Eqs. (4) and (5), the ratio of $(OR^-)_o$, $(OR \cdot ROH^-)_o$, and $(OR \cdot 2ROH^-)_o$ remains constant. Therefore, the experimental value can be used in place of each equivalent conductance unless the values, $\Lambda^0_{OR^-}$, $\Lambda^0_{OR \cdot ROH^-}$, and $\Lambda^0_{OR \cdot 2ROH^-}$ differ too much from each other.

(vi) In order to calculate the true conjugation constants, the following mathematical treatments have been made.

First, the relationship between $f^2[M^+]_o^2/K_{sp,o}$ and the total concentration of added nitrophenol, $[ROH]_t$, is obtained experimentally.

Then the relationship between $[ROH]_t$ and $[ROH]_o$ described below is used for the calculation of the concentration, $[ROH]_o$, of free nitrophenol.

$$\begin{aligned}[ROH]_t &= [ROH]_o + [OR \cdot ROH^-]_o \\ &\quad + 2[OR \cdot 2ROH^-]_o + \cdots \\ &= [ROH]_o + [OR^-]_o \sum_n n K_n^f [ROH]_o^n \end{aligned} \quad (9)$$

As the first approximation, the values of K_n^f are estimated from Eq. (6), assuming that $[ROH]_t$ is equal to $[ROH]_o$. By using the K_n^f value thus obtained, $[ROH]_o$ can be calculated according to Eq. (9). The new relationship between $f^2[M^+]_o^2/K_{sp,o}$ and the calculated $[ROH]_o$ gives improved K_n^f values. This procedure was repeated until the calculated value settles to give a converged curve which can be taken to represent a true $f^2[M^+]_o^2/K_{sp,o}$ against $[ROH]_o$.

Results and Discussion

(1) Dissociation of Cesium Nitrophenolates in Nitrobenzene. The relationships between the equivalent conductance and the square root of the concentration of cesium nitrophenolates are shown in Fig. 1. In the experiment, cesium nitrophenolates were dissolved and diluted in a 0.1M free nitrophenol solution except in the case of cesium picrate. When the concentration of a dissolved salt is quite small compared with that of 0.1M free nitrophenol, $[ROH]_o$ can be considered to be constant in Eq. (6).

This means that the ratio of the free anion $(OR^-)_o$ and the conjugated anions $(OR \cdot nROH^-)_o$ is constant in the experiment. Under these conditions, the limiting conductances, Λ^0, were estimated by the following relationship:[5]

$$\Lambda = \Lambda^0 - A\sqrt{C}, \quad (1')$$

The results are shown in Table 1.

In the case of cesium picrate, no picric acid was added in nitrobenzene, and the dissociation constant

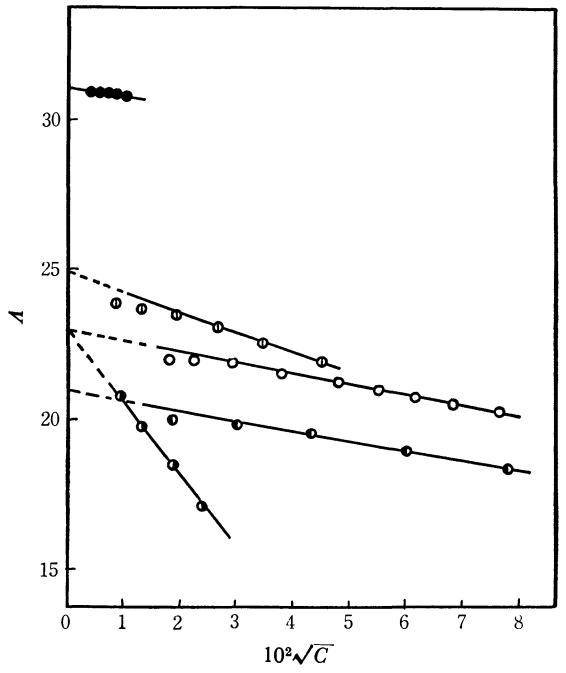

Fig. 1. Λ—$\sqrt{C}$ Plots of cesium nitrophenolates in nitrobenzene.
○ *p*-NP, ◐ *m*-NP, ◑ *o*-NP, ⓘ α-DNP, ● PA

Table 1. Dissociation constants and limiting equivalent conductances.

	pK_o	λ_+^0	λ_-^0
p-NP(Cs)	—		23.0 (0.1M HOR)
m-NP(Cs)	—		21.0 (0.1M HOR)
o-NP(Cs)	—		23.0 (0.1M HOR)
α-DNP(Cs)	—		25.0 (0.1M HOR)
PA(Cs)	2.24		31.5
PA(K)	3.15[6]	17.8[6]	16.0[6]
PA(Na)	4.55[6]	16.3[6]	
PA(Li)	7.2[6]		
PA(H)	7.4[7]	23.0[8]	

was determined from the results to be $pK_o=2.2$. This value is compared with the dissociation constants of other alkali picrates given by Kraus.[6] In Fig. 1, the Λ *vs.* $\sqrt{C}$ plots of cesium *p*-nitrophenolate, cesium *m*-nitrophenolate, and cesium α-dinitrophenolate present fairly gentle slopes. This may perhaps be attributed to the formation of larger conjugated anions, thus giving the larger $\mathring{a}$ value in Eq. (1).

The dissociation of all cesium salts in nitrobenzene can be concluded from these data.

(2) Homoconjugations of Nitrophenolate Anions. Plots of $f^2[M^+]_o^2/K_{sp,o}$ *vs.* $[ROH]_o$ on a logarithmic scale are presented in Figs. 2 and 3, where f is the activity coefficient of the dissociated metal ions in nitrobenzene. $[ROH]_o$ is the concentration of the added nitrophenol minus the concentration of the conjugated

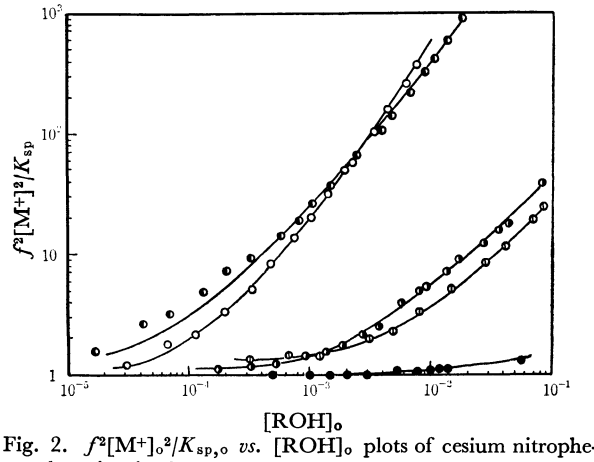

Fig. 2. $f^2[M^+]_o^2/K_{sp,o}$ *vs.* $[ROH]_o$ plots of cesium nitrophenolates in nitrobenzene.
○ *p*-NP, ◐ *m*-NP, ◑ *o*-NP, ⓘ α-DNP, ● PA

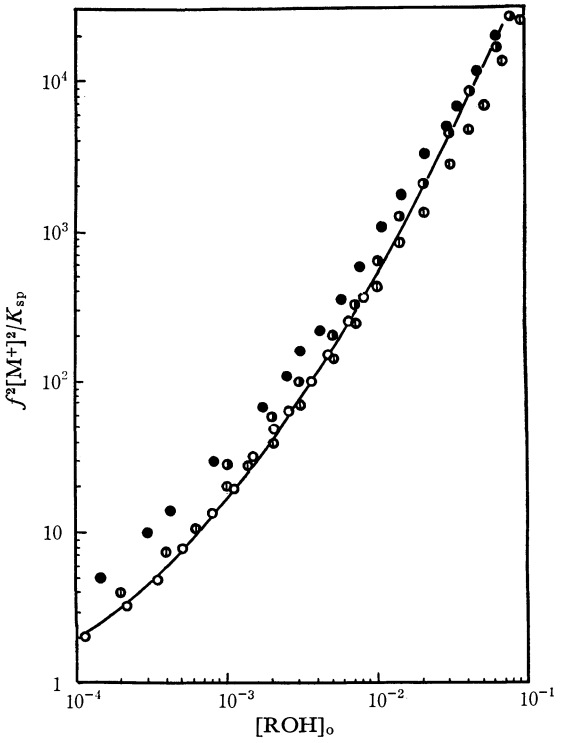

Fig. 3. $f^2[M^+]_o^2/K_{sp,o}$ *vs.* $[ROH]_o$ plots of alkali *p*-nitrophenolates in nitrobenzene.
○ Cs, ● K, ◑ Na, ⓘ Li
curve; $K_f^i=10^4$ $K_f^i=5\times10^6$

nitrophenol. $K_{sp,o}$ represents the solubility product, which was calculated from the conductance of the saturated solution and the limiting equivalent conductance. The $K_{sp,o}$ values of metal nitrophenolates were calculated on the assumption that the Λ^0 value of metal nitrophenolates were equal to those of cesium nitrophenolates. The $K_{sp,o}$ values and homoconjugation constants obtained from Figs. 2 and 3 are summarized in Table 2. The results shown in the table give some suggestions for extraction studies; the $K_{sp,o}$ values increase in the order Na<K<Cs in any nitrophenolate. This difference is the cause of the difference in the distribution behavior. On the contrary, the values do not differ much among cesium nitrophenol-

6) C. R. Witschonke and C. A. Kraus, *J. Amer. Chem. Soc.*, **69**, 2472 (1947).
7) I. M. Kolthoff, D. Stŏcesocá, and T. S. Lee, *ibid.*, **75**, 1834 (1953).
8) "Kagaku Binran," Maruzen Co., Tokyo (1966).

Table 2. Solubility constants, solubilities, and conjugation constants of alkali nitrophenolates

		p-NP	*m*-NP	*o*-NP	α-DNP	PA
$K_{sp,o}$	Li	6.7×10^{-12}	2.9×10^{-13}	1.5×10^{-10}	8.9×10^{-10}	1.6×10^{-8}
	Na	1.1×10^{-10}	1.1×10^{-10}	1.0×10^{-10}	1.0×10^{-10}	7.4×10^{-9}
	K	7.5×10^{-9}	3.0×10^{-8}	1.3×10^{-9}	2.2×10^{-8}	4.1×10^{-8}
	Cs	6.4×10^{-7}	1.0×10^{-6}	2.0×10^{-7}	7.5×10^{-7}	5.5×10^{-7}
S_a	Na	3.5×10^{-1} [9]			1.9×10^{-1} [9]	1.57×10^{-1} [9]
	Cs	1.55			9.7×10^{-2}	1.5×10^{-2}
K_n^f	K_1^f	1.0×10^{4}	2.0×10^{4}	4.5×10^{2}	2.4×10^{2}	$<10^{2}$
	K_2^f	5.0×10^{6}	2.0×10^{6}	—	—	—

ates of different kinds. Only cesium *o*-nitrophenolate gives a little smaller value. This similarity must be caused by the fact that nitrobenzene is a basic solvent and, therefore, combines with cations, but not with anions.

A bare anion which has a localized charge can be stabilized by homoconjugation. Figure 3 shows that the degree of the conjugation is independent of the species of cations.

This fact demonstrates that only the anion conjugation expressed by Eq. (4) takes place preferentially and that free nitrophenols have little capability of interacting with cations in nitrobenzene. In Table 2, it is shown that *p*-and *m*-nitrophenols have homoconjugation constants of considerable extents. *Ortho*-substituted phenols are, however, poor hydrogen-bond donors and form only monoconjugates $(OR\cdot ROH^-)_o$, whereas *p*- and *m*-nitrophenols can form higher conjugates, *e.g.*, $(OR\cdot 2ROH^-)_o$. This seems to be the main reason why there is less possibility of extracting cesium with *o*-nitrophenol.

(3) A Comparison of Solubility Measurements with Extraction Studies. Cesium nitrophenolates which are present as one-to-one salts are not extracted appreciably into nitrobenzene except in the case of cesium picrate, as is reported previously.[1] In the expression of the extraction of cesium:

$$D_{Cs} = K_{Cs}^{*1/2}(1+\sum_n K_n^f[ROH]_o^n)^{1/2}\frac{[OR^-]_a^{1/2}}{[Cs^+]_a^{1/2}} \quad (10)$$

n was obtained from the slope of log D_{Cs} *vs.* log $[ROH]_{total}$, and $K_{Cs}^* K_n^f$ was also calculated as the extraction constant.

These values are shown in Table 3. It was also shown in the previous paper that cesium ions are extracted to a considerable extent with picric acid or α-dinitrophenol, whereas the conductivity experiments have shown that both have small K_n^f values and that

Table 3. Extraction constants and extraction exchange constans (25°C)

		p-NP	*m*-NP	α-DNP	PA
$K_{Cs}^* K_n^f$	$n=0$	—	—	4.7×10^{-5}	2.8×10^{-3}
	$n=1$	—	—	1.6×10^{-2}	4.6×10^{-2}
	$n=2$	1.4	0.83	—	—
K_{Cs}^*/K_{Na}^*		1.1×10^{3}	1.3×10^{3}	2.2×10^{3}	5.0×10^{3} (20°C)

9) W. M. Fischer, *J. Physik. Chem.*, **92**, 581 (1918).

their cesium salts show values of $K_{sp,o}$ similar to those of other nitrophenolates.

These facts imply that cesium picrate and cesium α-dinitrophenolate have a very small solubility in water if the distribution equilibria are determined solely according to the ratio of the solubilities of the solutes in both organic and aqueous solutions. In Table 2, the solubilities, S_a, of sodium or cesium nitrophenolates in water are shown. The S_a values of cesium salts were obtained by the use of ^{137}Cs, while those of sodium salts were taken from the literature.[9]

From the solubility and conjugation data, the extraction constants can be estimated according to the following equation.

$$K_M^{**} = S_o^2/S_a^2,\ S_o^2 = K_{sp,o}/f^2 \quad (11)$$

Table 4. Calculated distribution coefficients and exchange constans

		p-NP	α-DTP	PA
K_{Cs}^{**}	$n=0$	2.7×10^{-7}	8.1×10^{-5}	2.3×10^{-3}
K_{Na}^{**}		9.0×10^{-10}	2.8×10^{-9}	3.0×10^{-7}
$K_{Cs}^{**}K_n^f$	$n=1$	—	1.9×10^{-2}	—
	$n=2$	1.4	—	—
K_{Cs}^{**}/K_{Na}^{**}		3.0×10^{2}	2.9×10^{4}	7.7×10^{3}

The values of K_{Cs}^{**}, $K_{Cs}^{**}K_n^f$, K_{Na}^{**}, and K_{Cs}^{**}/K_{Na}^{**} which are the constants calculated from the solubility and conjugation data, are shown in Table 4. These values can be compared with those shown in Table 3, which were obtained from the extraction studies. In the case of *p*-nitrophenol, only $K_{Cs}^* K_2^f$ ($n=2$) can be obtained from the extraction studies, while in the cases of α-dinitrophenol and picric acid, both $K_{Cs}^* K_1^f$ ($n=1$) and K_{Cs}^* ($n=0$) were obtained from the data when the pH was small and when the pH was very large ($[ROH]_o=0$), respectively. In Tables 3 and 4, K_{Cs}^* and K_{Cs}^{**}, $K_{Cs}^* K_n^f$ and $K_{Cs}^{**}K_n^f$, are in good agreement. For example, in the case of α-dinitrophenol, K_{Cs}^* was obtained as 4.7×10^{-5} from the extraction study when the pH was very large. This value is in fairly good agreement with the value of $K_{Cs}^{**}=8.1\times10^{-5}$ obtained as the square of the ratio of the solubilities of one-to-one cesium α-dinitrophenolate in the organic and aqueous phases.

When the pH was quite small, $K_{Cs}^* K_1^f$ was obtained as 1.6×10^{-2}. This value indicates the distribution constant of one-to-two cesium α-dinitrophenolate CsORROH; the value is also in good agreement with

$K^{**}_{Cs}K^{f}_{1}=1.9\times10^{-2}$, which is the product of $K^{**}_{Cs}=8.1\times10^{-5}$ and $K^{f}_{1}=2.4\times10^{2}$. These facts suggest that water molecules distributed in the nitrobenzene phase have little effect on the distribution of cesium ions. The K^{*}_{Cs}/K^{*}_{Na} values and K^{**}_{Cs}/K^{**}_{Na} values are different in the cases of *p*-nitrophenol and α-dinitrophenol. This disagreement may be attributed to the difference between K^{*}_{Na} and K^{**}_{Na}; the fairly high solubility of sodium salt in water and the very slight solubility of the salt in nitrobenzene seem to have given unsatisfactory data; the extracted water in nitrobenzene affects the solubility seriously.

The agreement of extraction constants and of the *n* value obtained from the extraction experiments with those obtained from the conductivity measurements indicates that Eq. (10) and Eq. (6) are equally meaningful and correlate with each other. Therefore, it must be emphasized that both methods offer equivalent information about the chemical interaction in organic solvents.

BULLETIN OF THE CHEMICAL SOCIETY OF JAPAN, VOL. 44, 3032—3035 (1971)

Anomalous Gas Chromatogram Due to the Oxidation of Porous Polymer Beads by a Sample Containing Oxygen Gas

Reisuke SODA

National Institute of Industiral Health, Kizukisumiyoshi, Kawasaki

(Received March 29, 1971)

By the gas-chromatographic analysis of the organic vapor in the air by means of a Porapak column, a broad peak accompanied by long tailing was observed at column temperatures above a certain value with a flame-ionization or an electron-capture detector. The cause of that peak was investigated using various gases and columns by changing the column temperature. The conclusion was that oxygen in air reacted with polymer beads even at temperatures lower than that cited in the catalogue as temerature to be employed, and the reaction products gave the anomalous broad peaks. The reaction was considered to consist of the oxygenation of polymer beads to produce carbon monoxide, carbon dioxide, formic acid, and the other organic compounds. For Porapak Q and P, the maximum temperature which can be used in safety may be 120°C for an analysis of a sample which consists in greater part of air.

In the field of occupational health, the analysis of toxic gases in very low concentrations is necessary in order to estimate the contamination of the ambient air by the gases, and many analytical methods have been developed. Of these methods, gas chromatography is one of the most reliable and useful methods.[1-6] For the analysis of relatively higher concentrations of toxic gases in the air, a gas sampler attached to a gas chromatograph can be used to introduce the sample air directly into the column. For example, 1 m*l* of air which contains 1 ppm of benzene is sufficient to obtain a satisfactory chromatogram with an ordinary flame-ionization detector. A Porapak column is suitable for the analysis of those samples.[7] Furthermore, the characteristics of columns are not weakened, for no stationary liquid phase is used. Stationary liquid frequently is eluted, even if very slowly, and causes noise.[8] Therefore, a Porapak column is very useful for an analysis of gases in the ambient air in an industrial environment and in the atmosphere.

By the practical use of a Porapak column for the analysis of gases in the air, sometimes an anomalous broad peak has been observed, and it has interfered with the other peaks of the minor components to be determined. For instance, in a sample of organic solvent vapors in the air, a satisfactory chromatogram has been observed at relatively lower temperatures, but with a rise in the temperature an anomalous broad peak has been found, as is shown in Fig. 1. With a Porapak Q column, a few ppm of hexane present in the air has shown a good chromatogram with a clear peak at a column temperature of 132°C. However, for the xylene air sample a broad peak has followed the xylene peak at 183°C. That broad peak has appeared under those experimental conditions at temperatures higher than 160°C and has been enhanced with an increase in the column temperature.

The cause of that broad peak has been investigated in order to avoid such an unfavorable phenomena.

Experimental

Materials. The gases used were nitrogen, carbon monoxide, air, and oxygen, all of which were supplied from a gas cylinder without any purification except in special cases, when air was purified by several methods. The

1) R. Van Houten and G. Lee, *Am. Ind Hyg. Ass. J.*, **30**, 465 (1969).
2) H. W. Lang and R. W. Freedman, *ibid.*, **30**, 523 (1969).
3) L. D. White, D. G. Taylor, P. A. Mauer, and R. E. Kupel, *ibid.*, **31**, 225 (1970).
4) F. H. Reed and W. R. Halpin, *ibid.*, **29**, 390 (1968).
5) J. Novak, V. Vasak, and J. Janak, *Anal. Chem.*, **37**, 660 (1965).
6) I. H. Williams, *ibid.*, **37**, 1723 (1965).
7) O. L. Hollis *ibid.*, **38**, 309 (1966).
8) S. J. Hawkes and E. F. Mooney, *ibid.*, **36**, 1473 (1964).

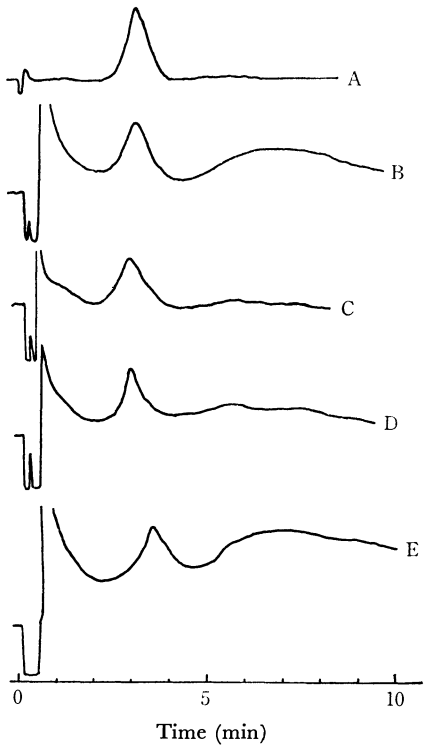

Fig. 1. Gas chromatogram of organic solvent vapor in the air by Porapak Q column of 1/8 in (o.d.) with flame ionization detector.

Flow rate of carrier gas was 30 m*l*/min and volume of gas sampler 4 m*l*.

Samples and column temperatures were with (1) column length of 47 cm, (A) *n*-hexane and 132°C; and (B) *o*-xylene and 183°C; with (2) column of 3 ft, (C) 2,3-dimethyl butane and 164°C; (D) benzene and 174°C; and (E) toluene and 192°C, respectively.

polymer beads were Porapak P and Q (50 to 80 mesh) of Water Associates Co.

Gas Chromatograph. Two types of gas chromatographs were used in the present experiment. The main experiment on the oxygen effect on the column was carried out by means of an Ohkura gas chromatograph Model 6000 equipped with a flame-ionization detector. The column used was made of U-shaped stainless steel tubing. The sample was injected into a chromatograph with an automatic gas sampler (1 m*l*), the temperature of which was regulated at 60°C. A few chromatograms were obtained by means of a Perkin Elmer Model 800 Vapor Fractometer equipped with a dual flame-ionization detector or an electron-capture detector. The column used consisted of coiled stainless steel tubing. The volume of the gas sampler was 4 m*l*. The latter instrument was also used to analyze the pyrolytic products of Porapak P and Q. The column was washed with hydrochloric acid and water, and then dried by nitrogen flushing. Polymer beads were packed into the column by means of a vibrator.

Infrared Spectrometer. A Hitachi EPI G 2 infrared spectrometer was equipped with a 10-cm gas cell and used to identify the gaseous components of pyrolytic products.

Differential Thermal Analysis. The differential thermal analysis and thermogravimetric analysis of polymer beads were done by means of a Rigakudenki DTA, compact-type TGA thermoflex. The temperature was programmed from room temperature to about 500°C at the rate of 5°C/min. For each polymer beads, one curve was observed in a nitrogen-gas flow environment and another in an air flow in the same temperature range.

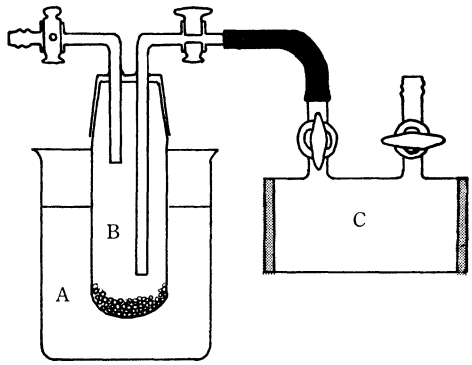

Fig. 2. Schematic diagram of vessel for pyrolysis and sampling of products in a gas cell.

A, Silicone oil bath; B, Vessel for pyrolysis of polymer beads; C, Infrared gas cell.

Analysis. Polymer beads were pyrolyzed in the specially-prepared vessel shown in Fig. 2. The vessel was immersed in an oil bath heated at from 190 to 210°C. The gaseous product in the vessel was introduced into a infrared gas cell which had previously been evacuated at 1 mmHg. The product was also collected in a 10-m*l* hypodermic syringe in order to be introduced into the gas sampler of the gas chromatograph. In this case, the column temperature was maintained at about 120°C, because below 120°C the anomalous chromatogram was not observed by means of a Porapak column.

Results

Any sample the major component of which was air showed an anomalous chromatogram with a highly sensitive detector like a flame ionization or an electron capture at column temperatures above a certain limiting value. As a chromatogram obtained with a flame ionization detector was similar to that obtained with an electron capture detector at the column temperature of 170°C, this paper summarized the results obtained with a flame ionization detector. Air was introduced only into the gas chromatograph with a gas sampler, and chromatograms were taken at various column temperatures. The experimental results are summarized in Fig. 3 for the Porapak Q and P columns. Chromatograms of column temperatures lower than about 140°C did not show any anomalous peaks. For the Porapak Q column, above 170°C broad and long tailed peaks were observed, while for Porapak P above 160°C a large and broad peak with a long tail was observed. If those peaks were caused by a pressure drop or by some other shock of the sampling process, similar phenomena might be observed upon the use of nitrogen gas through a gas sampler. However, that possibility can be excluded on the basis of Fig. 4, where the chromatogram of nitrogen gas shows a little peak with a short interval by injection and no other large or broad peaks appeared. It was considered reasonable that no impurity in the sample or contaminant in the gas sampler caused the anomalous chromatogram, because inactive gases, like nitrogen or carbon monoxide, did not show a broad peak and the braod peak with the air sample could not be removed by the purification of the air.

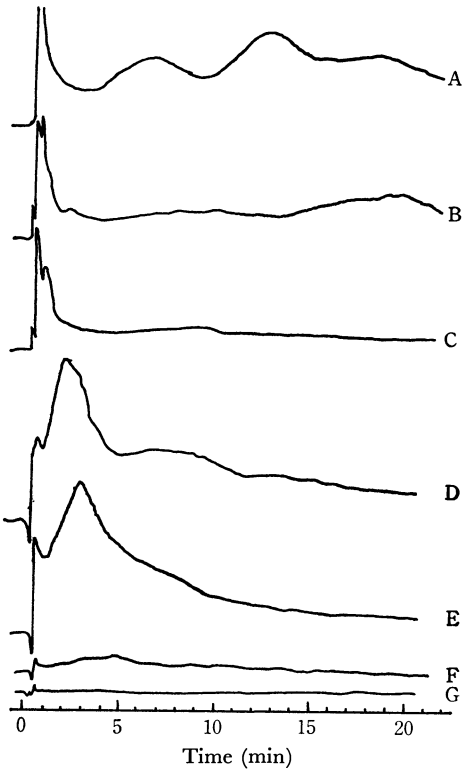

Fig. 3. Anomalous chromatogram by air and column temperature.

Porapak Q column of 6 mm (o.d.) and 200 cm (length) was used for (A), (B), and (C), and Porapak P column of 6 mm and 150 cm for the others. Volume of the gas sampler was 1 m*l*. Column temperature and carrier flow rate were, (A) 182°C and 50 m*l*/min; (B) 170°C and 48 m*l*/min; (C) 137°C and 45 m*l*/min; (D) 180°C and 62 m*l*/min; (E) 164°C and 46 m*l*/min; (F) 144°C and 52 m*l*/min; and (G) 122°C and 48 m*l*/min, respectively.

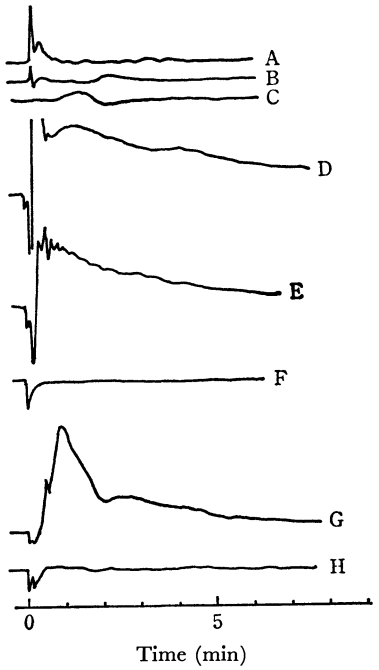

Fig. 4. Chromatograms of a few kinds of gases by Porapak P column, and gas sampler of 1 m*l*.

Column temperature, column size and carrier flow rate were; (1) 116°C, 6 mm (o.d.) and 50 cm (length), and 36 m*l*/min, respectively for samples of (A) oxygen, (B) air, and (C) nitrogen; (2) 170°C, 1/8 in and 6 ft, and 30 m*l*/min, respectively for samples of (D) oxygen, (E) air, and (F) nitrogen; (3) 192°C, 6 mm and 150 cm, and 47 m*l*/min, respectively for samples of (G) air and (H) nitrogen.

The main components of air are oxygen and nitrogen. The former reacts possibly with polymer beads to cause an anomalous broad peak. In fact, the peak with an air sample was enhanced by oxygen at 170°C, as is shown in Fig. 4. The anomalous chromatogram was considered to be due to the pyrolytic product of the polymer beads in the column produced by oxygen at higher temperatures, as organic acid, aldehydes and degraded compounds. The elution of those products could be changed by connecting the Porapak column and another column, like an active carbon, a molecular-sieve, or a silica gel column, in series. The connection of those columns before the Porapak column did not produce any chromatogram different from that produced by the Porapak column only, but in connection after the Porapak column, the active carbon column did not show any detectable broad peaks in the present experiment, and the molecular sieve column greatly delayed the elution of the main broad peaks.

In order to confirm the above estimation, polymer beads were pyrolyzed and the product was analyzed. The temperature at which polymer beads were pyrolyzed was determined by a DTA experiment. By the DTA of a sample in a nitrogen atmosphere, the degradation or decomposition started about 250°C for Porapak Q and about 230°C for Porapak P. However, in oxygen or air the decomposition was observed above 160°C for both polymers. The DTA curve passed a maximum near 210°C. Therefore the pyrolysis was carried out at from 190 to 210°C, and the gaseous product was analyzed by gas chromatography and infrared spectrometry. The infrared spectrum is shown in Fig. 5. The spectrum showed bands of water near 3800, 1600, and 600 cm^{-1}, bands of carbon dioxide near 3800, 2350, and 660 cm^{-1}, band of carbon monoxide near 2100 cm^{-1}, and bands of formic acid near 1780, 1100, and 630 cm^{-1}. Peaks of other many components were observed by gas chromatography, as is shown in Fig. 6. At present, not each component has been identified gas-chromatographically.

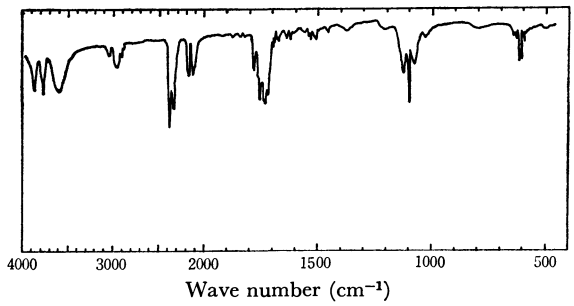

Fig. 5. Infrared spectrum of gaseous product from pyrolysis of Porapak Q.

Temperature of pyrolysis was 210°C.

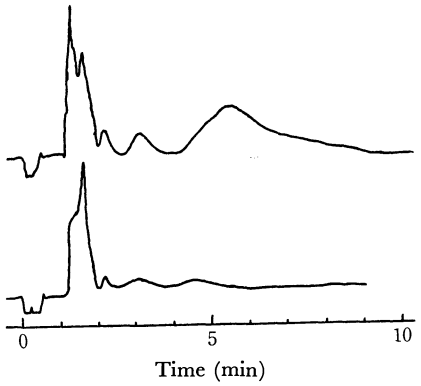

Fig. 6. Chromatograms of gaseous product by pyrolysis of polymer beads at 195°C.

Porapak Q column of 1/8 in (o.d.) and 3 ft (length) was used at 125°C. Flow rate of carrier gas was 30 m*l*/min and volume of gas sampler 4 m*l*. Flame ionization detector was used.

Upper chromatogram was observed with gaseous product of pyrolysis of Porapak P and lower with Porapak Q.

Discussion

An anomalous chromatogram of a sample containing air has been observed with a Porapak column at temperatures higher than about 160°C. Considering the cause of the chromatogram in the basis of the experimental results, it is deduced that the oxygen in the air reacts with polymer beads. Some of the reaction products (mainly oxides) may be identified as carbon monoxide, carbon dioxide, formic acid and other oxidized organic compounds. The Porapak column is stable below the temperature cited in the catalogue only when an inactive carrier gas is used. However, if a sample contains more air or oxygen gas than the components to be analyzed, the chromatogram inevitably produces an anomalous broad peak with a long tailing at temperatures which do not exceed the maximum temperature cited in the catalogue as stable.[9] That chromatogram is not successful for use in determining minor components because of the interference of the broad peak.

Barta and Gordon have reported that Porapak Q has active sites which caused an exchange of hydrogen in ketones.[10] Active sites may also possibly react with oxygen to produce the pyrolytic compounds.

At present not all substances produced by pyrolysis have been identified and experiments are easy in only a few cases. Nevertheless, several significant pieces of information can be obtained from the results. Below 120°C, Porapak P and Q columns apparently do not react with oxygen and no anomalous chromatogram is found. More precisely, the temperature limit of no anomalous peak may be 130°C for the Porapak Q column and 120°C for the Porapak P column, both column materials of 50 to 80 mesh.

The cause of the anomalous peak is apparently the reaction of the polymer beads in the column with oxygen. Several procedures are considered to avoid such unfavorable chromatograms, which frequently interfere with the peak to be observed. These considerations are necessary in making an analysis to monitor the concentration of gas in the air continuously. One procedure is a temperature programming, *i.e.*, air passes through the column at a lower temperature, 120°C or so, and then the temperature is raised at a suitable rate. This temperature programming procedure may avoid the effect of oxygen on the chromatogram when the Porapak column is used. Another method is to make the column shorter. When the particular components to be analyzed are one or two, and when their retention times are far from those of the other peaks, it is possible to make the column shorter than that used usually for the analysis of a sample containing many components, and the column temperature can be lowered. Figure 1 shows one example. When the Porapak Q column 3 ft long is used, the retention time of 2,3-dimethylbutane is about 3 min when the temperature is 164°C and the carrier gas flow rate is 30 m*l*/min. However, the present results show that the retention time becomes shorter (2.6 min) with the 47-cm column at 132°C, and the separation of the peaks is sufficient. By lowering the column temperature with shorter column, it is thus possible to suppress the anomalous chromatogram.

The process of concentrating a sample in the air may also preclude those effects of oxygen on the chromatogram, but the process is rather complicated compared with the direct analysis of the air without any concentration procedures. Furthermore, the procedure of concentrating the samples to be determined involves several problems, such as the efficiency of concentration for each component, the contamination of the sampling apparatus, and the recovery process of the collected compounds.[3-6]

9) The booklet on Porapak, Water Associates, Inc., Framingham Mass. (1965), pp. 5, 19.

10) C. I. Barta and A. S. Gordon, *J. Chromatog. Sci.*, **8**, 63 (1970).

Hot-atom Chemistry of Cobalt-60 Atoms in Neutron Irradiated Organic Solutions of Tris(acetylacetonato)cobalt(III)

Takeshi TOMINAGA, Takuhiko SAKAI, and Kitao FUJIWARA

Department of Chemistry, Faculty of Science, The University of Tokyo, Hongo, Tokyo

(Received April 15, 1971)

Thermal neutron irradiation has been carried out on the solutions of tris(acetylacetonato)cobalt(III) in benzene, ethanol, acetone and acetic acid containing various additives such as metallic salts and mineral acids. The ^{60}Co retention in the irradiated solutions has been found to decrease sharply with the increase in the concentration of various metallic salts. This indicates that the thermal diffusive reactions which contribute greatly to the apparent retention in the irradiated solutions can be suppressed by the addition of adequate metallic salts as scavengers. Salts of the metals which can form more stable complexes with acetylacetone (*i.e.*, Fe(III), Cu(II), Al(III), *etc.*) work as more effective scavengers in these systems. The upper limit for the primary retention of tris(acetylacetonato)cobalt(III) in the benzene solutions has been estimated as $0.00\pm0.02\%$. The use of adequate scavengers appears to be a useful technique to determine the primary retention in the irradiated solution systems. The ^{60}Co retention of the solid complex irradiated at dry ice temperature was 1.4—1.5% irrespective of the organic solvents used for dissolution if they contain ferric chloride, while it increased to 2.0% in the absence of the scavenger.

While a lot of detailed works have been made on the recoil and subsequent reactions of metal complexes in solid state, only a few studies have been reported for such reactions in solutions of these compounds.[1-5]

In 1970 we initiated a systematic study to irradiate the organic solutions of metal complexes with thermal neutrons in order to elucidate the mechanism of hot-atom reactions in these systems.[6] Our results on the irradiated benzene solutions of tris(acetylacetonato) cobalt(III)[7] indicated that the thermal diffusive reactions in the irradiated solutions could be suppressed effectively by the addition of ferric chloride as scavenger for free acetylacetone. Since the addition of scavengers appears to be a useful technique for investigating the hot-atom chemistry of complexes in solutions, we have studied the influence of various scavengers and solvents in more detail. This paper deals with our recent data on the ^{60}Co hot-atom reactions and the scavenger effect in the neutron irradiated solutions of tris(acetylacetonato)cobalt(III) in organic solvents.

Experimental

Reagents. Tris(acetylacetonato)cobalt(III), $Co(acac)_3$, was prepared as described in literature.[8] This was further purified by repeating recrystallization from acetone. Found: C, 50.6%; H, 5.71%. Calcd for $Co(C_5H_7O_2)_3$: C, 50.6%; H, 5.94%.

All the solvents and scavengers (metallic salts, acids, *etc.*) used in the experiments were purchased from Wako Pure Chemical Industries Ltd. as of G.R. grade.

Preparation of $Co(acac)_3$ Organic Solutions with Scavengers. Various $Co(acac)_3$ solutions containing scavengers were prepared for neutron irradiation.

Benzene Solutions: $Co(acac)_3$ benzene solutions containing anhydrous $FeCl_3$ were prepared by simply adding various amounts of $FeCl_3$ to $Co(acac)_3$ benzene solutions. To prepare $Co(acac)_3$ benzene solutions containing other metallic salts or inorganic acids as scavengers, various amounts of the scavengers were dissolved first in ethanol and then they were added to $Co(acac)_3$ benzene solutions so that the resulting solutions contained 10% by volume of ethanol.[9] To investigate the influence of the other organic solvents as additives, they were directly added to $Co(acac)_3$ benzene solutions.

Ethanol, Acetone and Acetic Acid Solutions: Ferric chloride, $FeCl_3\cdot6H_2O$, was added directly to the solutions of $Co(acac)_3$ in ethanol, acetone or acetic acid.

Neutron Irradiation. About 1 m*l* each of the $Co(acac)_3$ organic solutions was placed in a quartz tube with a Teflon stopper and irradiated with slow neutrons for 5 min at room temperature in the rotary specimen rack of a TRIGA Mark II reactor at Rikkyo University. Thermal neutron flux was 5×10^{11} n/cm^2·sec. The accompanying γ dose was 7×10^4R. The solutions were frozen 15—20 min after the completion of the irradiation and stored in dry ice for 2—3 hr before chemical separation.

For making a comparison with the solution systems, solid $Co(acac)_3$ samples were irradiated for 5 min at dry ice or room temperature. After the irradiation they were stored in dry ice until chemical separation.

Chemical Separation. The solvent extraction method was mainly employed in chemical separation of the irradiated complex in order to determine the ^{60}Co retention.[10]

Solutions: One milliliter of the irradiated organic solutions

1) G. Kayas and P. Süe, *J. Chim. Phys.*, **45**, 188 (1948); *Bull. Soc. Chim. France*, **17**, 1145 (1950).

2) A. W. Adamson and J. M. Grunland, *J. Amer. Chem. Soc.*, **73**, 5508 (1951).

3) A. Zuber, USAEC Document NYO-6142 BNL (1954).

4) N. Saito, H. Sano, and T. Tominaga, This Bulletin, **33**, 20 (1960).

5) S. Kaufman, *J. Amer. Chem. Soc.*, **82**, 2963 (1960).

6) The study of hot-atom reactions in the irradiated organic solutions of metal complexes had not been reported before our previous work,[7] although several works have been made on the solutions of organometallic compounds (U. Zahn, *Radiochim. Acta*, **7**, 170 (1967); I. C. Yang and D. R. Wiles, *Can. J. Chem.*, **45**, 1357 (1967).

7) T. Tominaga and K. Fujiwara, This Bulletin, **43**, 2279 (1970).)

8) T. Moeller, "Inorganic Syntheses," Vol. 5, McGraw-Hill Book Co., Inc., New York (1957), p. 188.

9) The scanvenger-free $Co(acac)_3$ solutions also contained 10% of ethanol. It was confirmed that the scavenger effect of metallic salts and acids was not affected by the presence of about 10% of ethanol in the benzene solutions.

10) The retention obtained corresponds to the percentage of the ^{60}Co activity retained in the form of $Co(acac)_3$.

was diluted to 5 m*l* with benzene and extracted with three 5-m*l* portions of 3% EDTA aqueous solution containing 0.8% sodium potassium tartrate and 10 mg of $CoSO_4 \cdot 7H_2O$ as carrier. On mixing with Co^{2+} carrier and EDTA aqueous solution, all the ^{60}Co-labeled species other than $^{60}Co(acac)_3$ are extracted into the aqueous phase, whereas only $^{60}Co(acac)_3$ remains in the organic phase.[11] For the irradiated solutions of $Co(acac)_3$ in ethanol, acetone, or acetic acid, the ion exchange method was also used for the purpose of comparison: after being mixed with water containing Co^{2+} carrier, the irradiated solution was passed through a cation exchange column. The effluent contains only the neutral ^{60}Co-labeled species which does not exchange with Co^{2+} (*i.e.*, $^{60}Co(acac)_3$). Since the radiochemical yield of the neutral fraction by the ion exchange separation was in good agreement with that of the organic phase by the solvent extraction, it is evident that the retention as $^{60}Co(acac)_3$ can be determined by either method for the solutions in these solvents.

Solid Samples: The irradiated solid samples (30—50 mg) were dissolved in 5 m*l* of benzene (containing 10% of ethanol) ethanol, chloroform, carbon tetrachloride, or acetic acid, all with or without ferric chloride additive, and analyzed by means of solvent extraction or ion exchange.

Radioactivity Measurement. The radioactivity of each fraction was counted with a well-type NaI scintillation counter at least one week after neutron irradiation. All the solvents and scavengers (metallic salts and acids) used in the experiments were irradiated separately and the radioactivity of the organic phase after solvent extraction was measured to check the upper limit of induced radioactivity other than ^{60}Co. It was confirmed that the possible contribution to organic phase activities (*i.e.*, retention) from induced activities other than ^{60}Co did not exceed 0.03% when measurements were carried out at least one week after irradiation. Since this contribution was generally smaller than the statistical errors in counting, no correction was necessary.

Results and Discussion

Recoil Species Formed in the Irradiated $Co(acac)_3$ Systems. Various metastable recoil species can be formed as a result of hot-atom reactions in the irradiated solid $Co(acac)_3$ systems. As an example, existence of ligand deficient species such as [bis(acetylacetonato)cobalt (III)]$^+$ has been suggested in the irradiated and unannealed solid $Co(acac)_3$ systems.[11,12] However, all the chemical procedures of separation involving aqueous media (*i.e.*, ion exchange, solvent extraction and paper electrophoresis) have revealed only two ^{60}Co-labeled species which are identified as $Co(acac)_3$ and Co^{2+}.[7,11,12] This indicates that the metastable recoil species are converted into more stable entities on dissolution in an organic solvent and mixing with an aqueous medium.

Although similar metastable recoil species might be produced through hot-atom reactions in the irradiated solutions of $Co(acac)_3$ in organic solvents, only two ^{60}Co-labeled species (*i.e.*, $Co(acac)_3$ and Co^{2+}) were found after chemical separation by means of solvent extraction or ion exchange, both of which involved aqueous media. It is presumed that all the metastable recoil species are finally converted into the stable species in aqueous solutions (*i.e.*, Co^{2+}). Accordingly, the ^{60}Co recoil reactions and scavenger effect in the $Co(acac)_3$ systems have been studied in terms of the ^{60}Co retention which is not perturbed by the procedures of chemical separation.

Retention and Scavenger Effect in the Irradiated Solutions of $Co(acac)_3$ in Benzene Containing 10% of Ethanol. In the absence of scavengers, the apparent ^{60}Co retention in the irradiated 0.2M solutions of $Co(acac)_3$ in benzene (containing 10% of ethanol) was found to be about 7± 1% which was higher than the retentions in the irradiated solid samples. No appreciable concentration dependence was observed for 0.01—0.25M solutions of $Co(acac)_3$ in benzene. The apparent retention increases gradually when the irradiated solutions are kept at room temperature[7] whereas it remains nearly unchanged at dry ice temperature. When acetylacetone was added to the solutions before irradiation, the apparent retention was found to increase with acetylacetone concentration. Thus the ^{60}Co retention in the irradiated benzene solutions containing 50% by volume of acetylacetone was about 25%. A retention value of 90% was observed in the irradiated solution of $Co(acac)_3$ in pure acetylacetone after being kept standing for three days at room temperature. Thus it can be concluded that thermal diffusive reactions taking place during and after the irradiation contribute greatly to the apparent retention in the irradiated solutions without scavengers. The higher apparent retention in solutions than in solid can be explained by assuming that the thermal diffusive reactions proceed more rapidly in irradiated solutions than in irradiated solid.

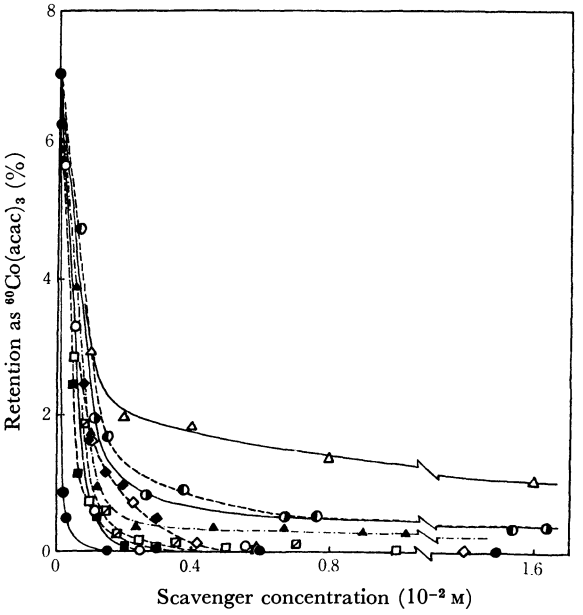

Fig. 1. Scavenger effect of various metallic salts and mineral acids on ^{60}Co retention in the irradiated 0.2M solutions of $Co(acac)_3$ in benzene containing 10% of ethanol.

-●- $FeCl_3 6H_2O$; -○- $FeCl_3$; --⊠-- $AlCl_3$; --■-- $CuCl_2 \cdot 2H_2O$; --□-- $Cu(CH_3CO_2)_2 \cdot H_2O$; --▲-- $NiCl_2 \cdot 6H_2O$; -◑-$CoCl_2 \cdot 6H_2O$; --◐-- $CoCl_2$; -△- $MgCl_2 \cdot 6H_2O$; --◆-- HCl; --◇-- HNO_3.

11) J. Shankar, K. Venkateswarlu, and A. Nath, "Chem. Effects Nucl. Transform., Proc. Symp. Prague," Vol. 1, 309 (1961).

12) J. Shankar, K. S. Venkateswarlu, and M. Lal, *Radiochim. Acta*, **4**, 52 (1965).

In order to study the hot-atom reactions in these systems, the thermal diffusive reactions should be suppressed so that the true primary retention can be determined. Although the scavenger technique has been used successfully to suppress thermal diffusive reactions in organic systems, it has seldom been applied to the hot-atom reactions in inorganic systems. We found that ferric salts could be used as good scavengers to minimize the thermal reactions in the irradiated $Co(acac)_3$ solutions.[7] In the present work we have studied the effect of the addition of various metallic salts on the ^{60}Co retention in the irradiated 0.2M solutions of $Co(acac)_3$ in benzene containing 10% of ethanol (Fig. 1).

We see that the ^{60}Co retention in the irradiated solutions decreases sharply on addition of most metallic salts as scavengers although no decomposition of the parent complex is detected spectrophotometrically. Ferric chloride appears to be the most effective scavenger while magnesium chloride is the least effective. The hydrate might be slightly more effective as scavenger than the anhydride of the corresponding salt. However, the ^{60}Co retention was not influenced by the presence of water up to 0.5% (about 0.25M) in the irradiated benzene solutions. For the convenience of comparison, the scavenging power may be expressed in terms of the percentage of the thermal diffusive reactions scavenged by the addition of an equal molar concentration of the salt. The scavenger curves in Fig. 1 reveal that the scavenging power of the metallic salts generally increases in the order:

$$Mg(II)<Co(II)<Ni(II)<Cu(II)\sim Al(III)<Fe(III)$$

Although the stability constants of the acetylacetonates of these metals in benzene or benzene-ethanol solutions are not known, it has been reported that the stability constants in aqueous media (and in 50% or 75% dioxane) increase in the order:

$$Mg(II)<Co(II)<Ni(II)<Cu(II)<Al(III)<Fe(III)$$[13-18]

Thus the scavenging power of the salts of these metals are correlated well with the stability constants of their acetylacetonates in aqueous media,[19] that is, salts of the metals which can form more stable complexes with free acetylacetone work as more effective scavengers. Thus a probable mechanism of the metal scavenger effect in the irradiated solutions of $Co(acac)_3$ in benzene-ethanol is as follows. The metallic salt competes with the ^{60}Co recoil species (ligand deficient species, *etc.*) in thermal diffusive reactions to combine with free acetylacetone in solutions, thus minimizing the apparent ^{60}Co retention effectively.

Since the ^{60}Co retention in the well-scavenged solutions shows a minimum value of $0.00\pm0.02\%$, this can be considered as an upper limit for the primary retention in the irradiated $Co(acac)_3$ benzene solutions. In other words, the probability of the rupture of at least one ligand of this complex is nearly 100% in the solution systems.

Mineral acids such as HCl and HNO_3 are also good scavengers to reduce the apparent retention (Fig. 1). Acetic acid appears to be less effective in the concentration range below 0.1M, yet it can be used as a good scavenger if its concentration exceeds about 0.2M (Fig. 2).

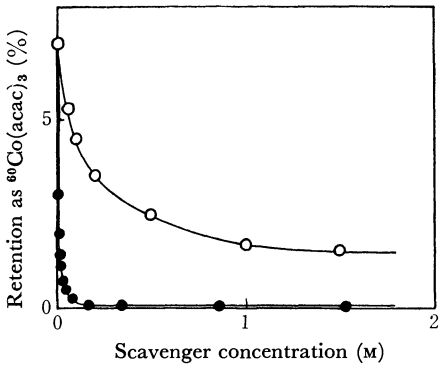

Fig. 2. Scavenger effect of acetic acid and carbon tetrachloride on ^{60}Co retention in the irradiated 0.2M solutions of $Co(acac)_3$ in benzene.
-●- CH_3CO_2H; -○- CCl_4.

We see that the addition of carbon tetrachloride (well-known electron scavenger) gradually decreases the apparent retention. However, the effect is slight as compared with the scavenger effect of metallic salts: the retention cannot be reduced to below 1% even if 1.6M (several hundred times as concentrated as the metallic scavengers) of carbon tetrachloride is present in the irradiated solutions. The results suggest that a different mechanism may be proposed to account for the effect of carbon tetrachloride on the ^{60}Co retention.

The ^{60}Co retention was not influenced significantly by the addition of ethanol (up to 15% by volume) or acetone (up to 100%).

Retention in the Irradiated Solutions of $Co(acac)_3$ in Ethanol, Acetone and Acetic Acid. The effect of ferric chloride on the ^{60}Co retention in the irradiated solutions of $Co(acac)_3$ in ethanol (0.017M) or acetone (0.03M) was similar to the effect observed in the benzene solutions. The apparent retention decreases sharply with the increase in the ferric chloride concentration and reaches nearly 0% if more than 3×10^{-4}M of ferric chloride is present in the solutions.

A different behavior was observed with the irradiated 0.1M $Co(acac)_3$ solutions in acetic acid. The ^{60}Co retention remains at 0%, independent of the ferric chloride concentration since acetic acid can work as both scavenger and solvent.

Retention in the Irradiated Solid $Co(acac)_3$ Samples. Table 1 summarizes the ^{60}Co retentions in the irradi-

13) L. G. Van Uitert, W. C. Fernelius, and B. E. Douglas, *J. Amer. Chem. Soc.*, **75**, 457, 2736 (1953).
14) B. E. Bryant, *J. Phys. Chem.*, **58**, 573 (1954).
15) R. M. Izatt, C. G. Haas, Jr., B. P. Block, and W. C. Fernelius, *ibid.*, **58**, 1133 (1954).
16) R. M. Izatt, W. C. Fernelius, and B. P. Block, *ibid.*, **59**, 80 (1955).
17) R. M. Izatt, W. C. Fernelius, C. G. Haas, Jr., and B. P. Block, *ibid.*, **59**, 170 (1955).
18) H. A. Droll, B. P. Block, and W. C. Fernelius, *ibid.*, **61**, 1000 (1957).
19) We have recently obtained a similar correlation for the irradiated solutions of tris(nitrosonaphtholato)cobalt(III) in benzene. The results will be published shortly.

TABLE 1. ^{60}Co RETENTIONS IN IRRADIATED SOLID $Co(acac)_3$

Temp. of irradiation	Solvent[a)]	Method of separation[b)]	^{60}Co retention (%)	
			Immediately after dissoln.	After standing in solution
Dry ice	C_6H_6+Fe(III)	S.E.	1.4±0.1	1.4±0.1[c)]
Dry ice	C_6H_6	S.E.	2.0±0.1	2.6±0.1[c)]
Dry ice	0.4M acetylacetone in C_6H_6	S.E.		7.8±0.1[d)]
Dry ice	$CHCl_3$+Fe(III)	S.E.	1.7±0.1	1.5±0.1[c)]
Dry ice	$CHCl_3$	S.E.		2.5±0.1[c)]
Dry ice	C_2H_5OH+Fe(III)	I.E.	1.4±0.1	1.4±0.1[c)]
Dry ice	C_2H_5OH	I.E.	2.0±0.1	2.3±0.1[c)]
Dry ice	CH_3COOH+Fe(III)	I.E.	1.5±0.1	
Room	C_6H_6+Fe(III)	S.E.	2.4±0.1	
Room	C_6H_6+CH_3COOH	S.E.	2.3±0.1	
Room	C_6H_6	S.E.		10.0±0.1[e)]
Room	CCl_4	S.E.		6.8±0.1[e)]

a) C_6H_6: Benzene containing 10% of ethanol.
b) S.E. : Solvent extraction; I.E.: ion exchange.
c) Standing for 3 days in solutions.
d) Standing for 2 days in solutions.
e) Standing for 6 days in solutions.

ated solid $Co(acac)_3$ samples. Retentions of the samples irradiated at dry ice temperature generally fall within the range 1.4—1.5% irrespective of solvents used for dissolution, if they contain $3—5\times10^{-3}$M ferric chloride. The ^{60}Co retention remains unchanged even after standing the solutions of the irradiated solid complex for three days if they contain ferric chloride. In the absence of ferric chloride, however, the ^{60}Co retention is 2.0±0.1% for irradiations at dry ice temperature and increases further after the solutions of the irradiated solid samples were kept standing for three days.[20] The increment of the retention is accelerated considerably when the irradiated complex is dissolved in a benzene-acetylacetone mixture. The results indicate that the thermal reactions after the dissolution of the irradiated solid complex contribute appreciably to the apparent retention. Therefore, the retention obtained in the presence of an adequate scavenger can be considered to be a true retention of the irradiated solid systems.

It is concluded that the thermal reactions taking place in the irradiated organic solutions of the complex or after the dissolution of the irradiated solid complex are effectively suppressed by using adequate scavengers such as metallic salts which can form more stable complexes with the free ligand molecules, ions or radicals. We believe that this technique will be useful for determining the primary retention in solution systems or the initial retention in solid systems.

The authors wish to thank Prof. Nobufusa Saito, the University of Tokyo, for his encouragement and support.

20) A similar increase of retention after dissolution has been observed in the methanol and benzene solutions of irradiated solid tris(acetylacetonato)chromium(III) (I. Găinar and A. Ponta, *Rev. Roum. Chem.*, **13**, 401 (1968); T. Omori and T. Shiokawa, *Radiochem. Radioanal. Lett.*, **3**, 39 (1970)).

A Comparison of 4-Hydroxynaphthalene-2,7-disulfonic Acid with Chromotropic Acid as a Coupling Component of Azo-type Metallochromic Indicators

Takeshi KATAYAMA, Haruo MIYATA, and Kyoji TÔEI

Department of Chemistry, Faculty of Science, Okayama University, Tsushima, Okayama

(Received May 6, 1971)

In order to clarify the effect of the hydroxyl group at the 5-position of chromotropic acid on the chelate stabilization, the following six reagents were synthesized by the coupling with 4-hydroxynaphthalene-2,7-disulfonic acid or 4,5-dihydroxynaphthalene-2,7-disulfonic acid(chromotropic acid): 2-(*m*-sulfophenylazo)-1-hydroxynaphthalene-3,6-disulfonic acid(I), 2-(*o*-methoxy-*m*-sulfophenylazo)-1-hydroxynaphthalene-3,6-disulfonic acid(II), 2-(*o*-hydroxy-*m*-sulfophenylazo)-1-hydroxynaphthalene-3,6-disulfonic acid(III), 2-(*m*-sulfophenylazo)-1,8-dihydroxynaphthalene-3,6-disulfonic acid(IV), 2-(*o*-methoxy-*m*-sulfophenylazo)-1,8-dihydroxynaphthalene-3,6-disulfonic acid (V), and 2-(*o*-hydroxy-*m*-sulfophenylazo)-1,8-dihydroxynaphthalene-3,6-disulfonic acid(VI). The acid dissociation constants of these reagents and the stability constants of their metal chelates with magnesium and calcium were measured by the pH titration method at an ionic strength of 0.10 and at 25°C. From the results obtained, it has become apparent that the hydroxyl group at the 5-position exerts a remarkable influence on the chelation of metal ions with the bidentate ligand, such as 2-(*m*-sulfophenylazo)-chromotropic acid, but that it has very little effect on those ions with the terdentate ligand, such as 2-(*o*-hydroxy-*m*-sulfophenylazo)-chromotropic acid. Such an effect appears even in the bidentate ligand with the methoxy group at the *ortho*-position of the benzene ring. That is to say, it may be concluded that the effect of the number of the chelate ring formed with a metal ion is preferred to stabilize the metal chelate over the effect of the hydroxyl group at the 5-position in the terdentate ligand.

Heller and Schwarzenbach[1] have reported that the values of the acid dissociation constants for the two hydroxyl groups of chromotropic acid are 5.36 and 15.6 respectively (pK_a values). The larger value of the latter dissociation of hydroxyl group results from a strong hydrogen bond between two oxygen atoms of chromotropic acid. On the other hand, the pK_{a_1} value of phenylazochromotropic acid is 9.15,[2] which corresponds to the 5.36 value of chromotropic acid; the pK_{a_2} value could not be determined under ordinary experimental conditions because of a strong intramolecular hydrogen bond. It is considered that the phenylazochromotropic acid and its metal chelate have the structures indicated by Formulas (1) and (2) respectively, and that the hydroxyl group at the 5-position of the naphthalene ring probably does not produce chelation with metal ion.

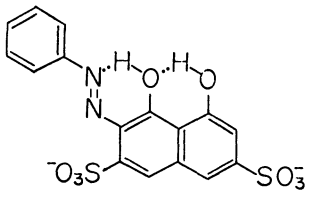

Formula (1)

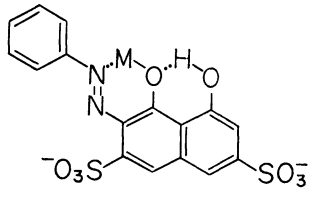

Formula (2)

The present work will compare the chelate formation ability of 4-hydroxynaphthalene-2,7-disulfonic acid with that of chromotropic acid (4,5-dihydroxynaphthalene-2,7-disulfonic acid) as a coupling component. Namely, 2-(*m*-sulfophenylazo)-, 2-(*o*-methoxy-*m*-sulfophenylazo)- and 2-(*o*-hydroxy-*m*-sulfophenylazo)-1-hydroxynaphthalene-3,6-disulfonic acids as well as 2-(*m*-sulfophenylazo)-, 2-(*o*-methoxy-*m*-sulfophenylazo)- and 2-(*o*-hydroxy-*m*-sulfophenylazo)-chromotropic acids were synthesized, and the acid dissociation constants and the stability constants of their chelates with magnesium and calcium were determined by the pH titration method at an ionic strength of 0.10 and at 25°C. The effect of the hydroxyl group at the 5-position will be discussed in comparison with the constants thus obtained.

Experimental

Reagents. The azo compounds, 2-(*m*-sulfophenylazo)-, 2-(*o*-methoxy-*m*-sulfophenylazo)-, and 2-(*o*-hydroxy-*m*-sulfophenylazo)-1-hydroxynaphthalene-3,6-disulfonic acids, and 2-(*m*-sulfophenylazo)-, 2-(*o*-methoxy-*m*-sulfophenylazo)-, and 2-(*o*-hydroxy-*m*-sulfophenylazo)-chromotropic acids, were synthesized by the coupling reaction of 4-hydroxynaphthalene-2,7-disulfonic acid or chromotropic acid with each diazotized *m*-aminophenylsulfonic acid, 2-aminophenol-4-sulfonic acid and *o*-anisidine-*p*-sulfonic acid respectively. After the purification of these six reagents, their disodium salt were obtained as fine crystals by salting out. The stock solutions of these reagents were standardized by pH titration with a standard 0.10N potassium hydroxide solution.

The stock solutions of magnesium and calcium were prepared by dissolving $Mg(NO_3)_2 \cdot 6H_2O$ and $Ca(NO_3)_2 \cdot 4H_2O$ of a guaranteed reagent grade in distilled water; these solutions were then standardized by chelatometric titration.

pH Titration Method. The apparatus and the procedure

1) J. Heller and G. Schwarzenbach, *Helv. Chim. Acta*, **34**, 1876 (1951).

2) S. Nakashima, H. Miyata, and K. Tôei, This Bulletin **41** 2635 (1968).

for the pH titration were described in a previous paper[2]; the temperature and ionic strength of a solution were maintained at 25°C and at 0.10 respectively with potassium nitrate.

Calculations

Acid Dissociation Constants of the Reagents. The reagents I(2-(*m*-sulfophenylazo)-1-hydroxynaphthalene-3,6-disulfonic acid), II(2-(*o*-methoxy-*m*-sulfophenylazo)-1-hydroxynaphthalene-3,6-disulfonic acid), IV(2-(*m*-sulfophenylazo)-chromotropic acid), and V(2-(*o*-methoxy-*m*-sulfophenylazo)-chromotropic acid) are considered to be monobasic acids, while the reagents III(2-(*o*-hydroxy-*m*-sulfophenylazo)-1-hydroxynaphthalene-3,6-disulfonic acid) and VI(2-(*o*-hydroxy-*m*-sulfophenylazo)-chromotropic acid are considered to be dibasic acids. The acid dissociation constants, K_a, of these reagents are defined as follows:

(1) Monobasic acid.

$$HL \rightleftarrows H + L$$

$$K_a = \frac{[H][L]}{[HL]} = \frac{[H](T_{OH}+[H]-[OH])}{T_L - T_{OH} - [H] + [OH]}$$

where T_L and T_{OH} represent the total concentrations of the ligand and the alkali added to the system respectively; the ionic charge is disregarded for the sake of convenience.

(2) Dibasic acid,

$$H_2L \rightleftarrows H + HL \qquad K_{a_1} = \frac{[H][HL]}{[H_2L]}$$

$$HL \rightleftarrows H + L \qquad K_{a_2} = \frac{[H][L]}{[HL]}$$

$$1/K_{a_1} = AK_{a_2} + B$$

where:

$$A = \frac{2T_L - T_{OH} - [H] + [OH]}{[H]^2(T_{OH}+[H]-[OH])}$$

$$B = \frac{T_L - T_{OH} - [H] + [OH]}{[H](T_{OH}+[H]-[OH])}$$

Stability Constants of the Chelates. The stability constants, K, of the chelates are defined as follows:

$$M + L \rightleftarrows ML$$

$$K = \frac{[ML]}{[M][L]} = \frac{T_L - F}{[L](F + T_M - T_L)}$$

where T_M represents the total concentration of the metal ion, and where [L] and F represent as follows:

(1) Monobasic acid

$$[L] = \frac{K_a}{[H]}(T_L - T_{OH} - [H] + [OH])$$

$$F = \left(\frac{K_a}{[H]} + 1\right)(T_L - T_{OH} - [H] + [OH])$$

(2) Dibasic acid

$$[L] = \frac{2T_L - T_{OH} - [H] + [OH]}{\frac{[H]}{K_{a_2}} + \frac{2[H]^2}{K_{a_1}K_{a_2}}}$$

$$F = [L]\left(1 + \frac{[H]}{K_{a_2}} + \frac{[H]^2}{K_{a_1}K_{a_2}}\right)$$

Results and Discussion

Titration Curves. The titration curves for Reagent I in the presence and in the absence of calcium and magnesium ions are illustrated in Fig. 1, while for Reagents II and III the curves are shown in Figs. 2 and 3 respectively. The titration curves for Reagents

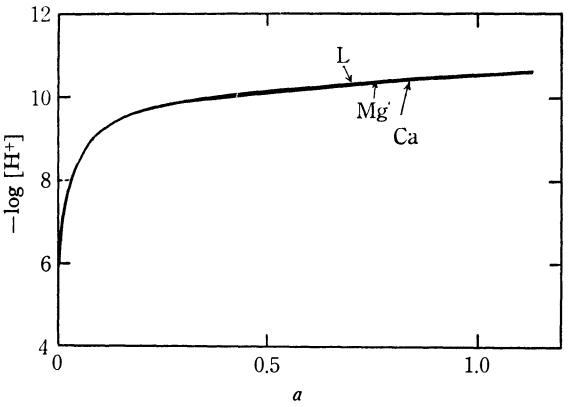

Fig. 1. Titration of 2-(*m*-sulfophenylazo)-1-hydroxynaphthalene-3,6-disulfonic acid chelate system at 25°C and at μ=0.10 L; ligand only, [L]=1.265×10^{-3}M, [Mg]=1.677×10^{-3}M, [Ca]=1.824×10^{-3}M.
a: mols of base added per mol of ligand.

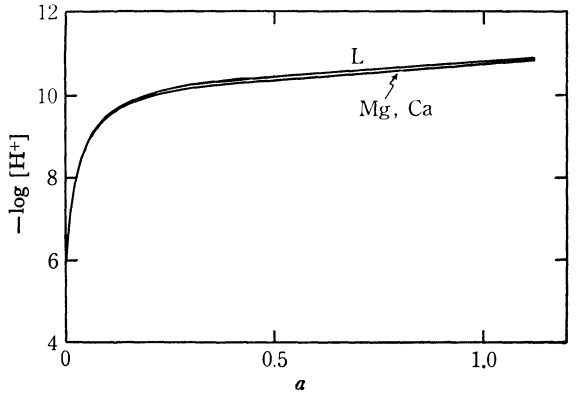

Fig. 2. Titration of 2-(*o*-methoxy-*m*-sulfophenylazo)-1-hydroxynaphthalene-3,6-disulfonic acid chelate system at 25°C, μ=0.10 [L]=1.228×10^{-3}M, [Mg]=1.677×10^{-3}M, [Ca]=1.824×10^{-3}M.

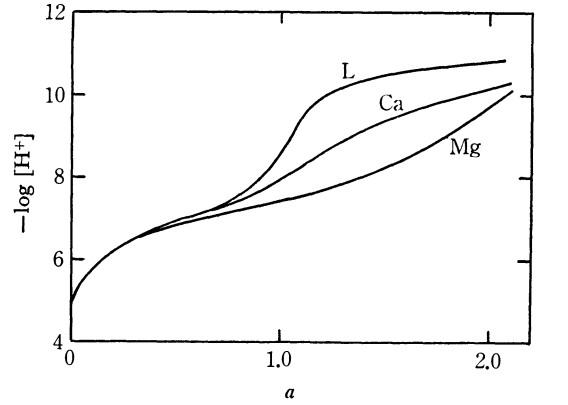

Fig. 3. Titration of 2-(*o*-hydroxy-*m*-sulfophenylazo)-1-hydroxynaphthalene-3,6-disulfonic acid chelate system at 25°C, μ=0.10 [L]=1.143×10^{-3}M, [Mg]=1.108×10^{-3}M, [Ca]=1.134×10^{-3}M.

TABLE 1. ACID DISSOCIATION CONSTANTS OF THE REAGENTS AND THE STABILITY CONSTANTS OF THEIR MAGNESIUM AND CALCIUM CHELATES (t=25°C, μ=0.10)

Reagents	Acid dissociation constant		Stability constant, log K	
	pK_{a_1}	pK_{a_2}	Mg	Ca
2-(*m*-Sulfophenylazo)-1-hydroxynaphthalene-3,6-disulfonic acid (I)		10.33	1.8	1.4
2-(*o*-Methoxy-*m*-sulfophenylazo)-1-hydroxy-naphthalene-3,6-disulfonic acid (II)		10.88	2.30	2.70
2-(*o*-Hydroxy-*m*-sulfophenylazo)-1-hydroxy-naphthalene-3,6-disulfonic acid (III)	6.92	10.94	6.08	4.87
2-(*m*-Sulfophenylazo)-1,8-dihydroxynaphthalene-3,6-disulfonic acid (IV)		8.97	3.62	2.89
2-(*o*-Methoxy-*m*-sulfophenylazo)-1,8-dihydroxy-naphthalene-3,6-disulfonic acid (V)		9.64	4.00	2.90
2-(*o*-Hydroxy-*m*-sulfophenylazo)-1,8-dihydroxy naphthalene-3,6-disulfonic acid (VI)	6.68	10.20	6.08	5.04

IV, V and VI are similar to those of Reagent I, II, and III in Figs. 1, 2, and 3 respectively. The acid dissociation constants of these reagents can be calculated by the use of the titration curve of the ligand only. As is shown in Figs. 1, 2, and 3, those curves for Reagents I and II are almost the same as that of phenylazochromotropic acid,[2] and the curve for Reagent III corresponds to that of phenolazochromotropic acid.[2] The inflection at a=1 in the titration curve of the ligand in Fig. 3 shows the dissociation of the phenolic proton of Reagent III. No inflection is observed at all on the neutralization of the naphtholic proton of the reagents. The titration curve in the presence of the metal ion shows a lower pH value than that of the ligand only. Such a depression of the titration curves indicates the formation of the metal chelate species; the chelate stability order, calcium< magnesium, can easily be expected from the extent of the depression of pH. Evidently, Reagents III and VI formed a more stable chelate with calcium and magnesium than did the other reagents investigated.

Acid Dissociation Constants. The acid dissociation constants of the six reagents are summarized in Table 1. In Table 1, the pK_{a_1} and pK_{a_2} values correspond to the dissociation of the phenolic and naphtholic protons respectively. The other naphtholic proton of chromotropic acid in the reagents is not dissociated by the presence of a strong hydrogen bridge between two oxygen atoms. The basicities of these reagents are expressed as a sum of the dissociation constants, $pK_A = pK_{a_1} + pK_{a_2}$; these values for the reagents decrease as follows: Reagent III>VI>II>I>V>IV. On the effect of the substituents, the sulfo group at the 5-position of the benzene ring decreases the pK_a value for the reagent by means of its electron-withdrawing effect, as is shown in Table 2. On the other hand, the elimination of the naphtholic hydroxyl group at the 5-position of Reagent IV, V, and VI shows a depression of the dissociation of the naphtholic proton at the 4-position of the reagent. This means that the oxygen atom at the 4-position will become more electron-rich than that of chromotropic acid, as is indicated by the following scheme;

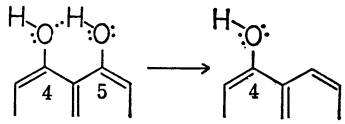

The dissociation of the hydroxyl group is disturbed for this reason.

Stability Constants. The chelate stability constants of their 1:1 chelates with magnesium and calcium ions are also listed in Table 1. Reagents I, II, IV, and V are considered to be bidentate ligands, and Reagents III and VI are considered to be terdentate ligands for metal ions. In these studies, the stabilization of the metal chelate depends mainly on the following factors: (1) the basicity of the reagent, (2) the number of rings formed with a metal ion, and (3) the stabilizing resonance interaction. As for Factor (1), from the concept of Lewis acids and bases, it seems that the strong basic ligand would form the more stable chelate. However, the order of the stability constants of these reagents, VI>III>V>IV>II>I, is not proportional to the basicities of the reagents, III>VI>II>I>V>IV. (2): In the case of Reagents III and VI, the pK_a values of the reagents and the stability

TABLE 2. THE EFFECT OF *m*-SO_3H GROUP ON THE pK_a OF THE REAGENTS

Reagents	pK_a	Reagents	pK_a
2-(Phenylazo)-1-hydroxynaphthalene-3,6-disulfonic acid	10.48	→ I	10.33
2-(*o*-Methoxyphenylazo)-1-hydroxynaphthalene-3,6-disulfonic acid	11.05	→ II	10.88
Phenylazochromotropic acid	9.19	→ IV	8.97
o-Methoxyphenylazochromotropic acid	9.92	→ V	9.64
o-Hydroxyphenylazochromotropic acid	7.60	→ VI	6.68
	10.60		10.20

constants, log K, of magnesium and calcium chelates is almost the same as shown in Table 1. This means that the number of chelate rings exerts a remarkable influence upon the stabilization of their chelates. (3): The effect of the oxygen atom as a donor atom is considered to be almost the same in each reagent. However, the very large difference in the values of log K between Reagents I and IV appeared as the effect of having or not having the naphtholic hydroxyl group at the 5-position. This may be caused by a stabilizing resonance of the chelate ring. The same tendency appears in the difference in the stability constants between the copper chelate of phenylazochromotropic acid and that of 2-(phenylazo)-1-hydroxynaphthalene-3,6-disulfonic acid; these log K's values are 17.23 and 8.84 respectively.[3] In the case of Reagents II and V, the values of the stability constants are between Reagents I and III, or Reagents IV and VI, respectively. Such a stable deviation of the reagent with the OCH_3 group at the *o*-position would be due to the coordination of the oxygen atom of the group to metal ions; this coordination is more suitable for calcium ionic radii than for magnesium ones, as is shown in the following scheme:

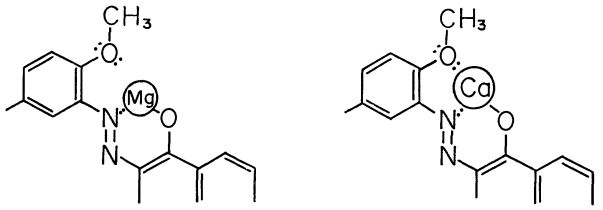

Therefore, the calcium chelate with Reagent II behaves a bidentate ligand or, rather, a terdentate one. In fact, from the comparison of the stability constants of the magnesium or calcium chelate of Reagent II with those of Reagent IV, it can be assumed that the effect of the number of the chelate ring is preferable to the calcium chelate with Reagent II; on the contrary, the effect of the stabilizing resonance interaction by the hydroxyl group at the 5-position is preferred to that of the magnesium chelate with the same reagent.

The present work has been supported in part by a Grant for Science Research from the Ministry of Education.

3) J. Bjerrum *et al.*, "Stability Constants" (Part I, Organic), The Chemical Society, London (1957), p. 95.

BULLETIN OF THE CHEMICAL SOCIETY OF JAPAN, VOL. 44, 3043—3046 (1971)

The Phase Equilibria in the FeO-Fe_2O_3-V_2O_3 System at 1500°K

Masataka WAKIHARA and Takashi KATSURA

Department of Chemistry, Tokyo Institute of Technology, Ookayama, Meguro-ku, Tokyo

(Received May 7, 1971)

The phase equilibria in the FeO–Fe_2O_3–V_2O_3 system have been determined at 1500°K by varying the oxygen partial pressure. The following three oxide phases have been stable in equilibrium: a sesquioxide solid solution with a corundum-type structure (approximate composition Fe_2O_3–V_2O_3), a ternary solid solution with a spinel-type structure (approximate composition $FeO \cdot Fe_2O_3$–$FeO \cdot V_2O_3$), and a ternary wüstite solid solution with a periclase-type structure which dissolves vanadium ions up to about 10 mol per cent. The extent of the solid-solution areas and the location of the oxygen isobars have been determined. The spinel phase coexisted partly with metallic iron and partly with the wüstite solid solution, corresponding to lower and higher iron contents respectively. The standard free energies of the $Fe+V_2O_3+{}^1/_2O_2=FeV_2O_4$ and $0.05\ Fe+V_2O_3+Fe_{0.95}O=FeV_2O_4$ reactions to produce FeV_2O_4 have been calculated to be -45500 ± 200 cal and -5800 ± 400 cal respectively at 1500°K on the basis of the equilibrium oxygen partial pressure.

The Fe–V–O system is of a great deal of interest to metallurgists as well as to ceramists and geochemists. The accurate phase equilibria, however, have not yet been presented, particularly at high temperatures. Binary systems of Fe–O and V–O have been studied by Darken and Gurry[1] and many other investigators.[2–9] Vanadium is a minor element in the earth's crust, and it is often found in magnetite (Fe_3O_4) upon the replacement of iron ions. Burdese[10] studied the phase equilibria of the Fe–V–O system and synthesized FeV_2O_6, FeV_2O_4, and $FeVO_4$. Vorob'ev *et al.*[11] investigated Fe_3O_4–FeV_2O_4 and wüstite solid solutions at 1000°K.

1) L. S. Darken and R. W. Gurry, *J. Amer. Chem. Soc.*, **67**, 1398 (1945); *ibid.*, **68**, 798 (1946).
2) W. Klemm and L. Grimm, *Z. anorg. u. allgem. Chem.*, **250**, 42 (1942).
3) E. Hoschek and W. Klemm, *ibid.*, **242**, 63 (1939).
4) G. Andersson, *Acta Chem. Scand.*, **8**, 1559 (1954); *ibid.*, **10**, 623 (1956).
5) S. Andersson, *ibid.*, **14**, 1161 (1960).
6) K. Kosuge, *J. Phys. Chem. Solids*, **28**, 1613 (1967).
7) T. Katsura and M. Hasegawa, This Bulletin, **40**, 561 (1967).
8) M. Wakihara and T. Katsura, *Met. Trans.*, **1**, 363 (1970).
9) J. S. Anderson and A. S. Khan, *J. Less Common Metals*, **22**, 209 (1970).
10) A. Burdese, *Ann. Chim.* (Rome), **47**, 785 (1957).
11) Yu. P. Vorob'ev, V. N. Bogoslovskii, E. G. Bogachova, and G. I. Chufarov, *Dokl. Akad. Nauk, S.S.S.R.*, **166**, 664 (1966).

Kunnmann *et al.*[12] synthesized some transition metal oxides in the temperature range from 1073° to 1380°K and calculated the standard free energy of FeV_2O_4. Recently, Schmahl and Dillenburg[13] studied the phase equilibria of the Fe–V–O system at 900°C and calculated the activities for the Fe_3O_4–FeV_2O_4 solid-solution series and the standard free energy of FeV_2O_4. Also, they recognized that the Fe_2O_3–V_2O_3 solid solution has an immiscible region in the range of 78—93 mol per cent V_2O_3 at 900°C. In this solid-solution series, Cox *et al.*[14] also found an immiscibility gap in the range of 80—90 mol per cent V_2O_3 on the basis of their magnetic data collected at 1000°C. Wakihara *et al.*[15] synthesized the Fe_3O_4–FeV_2O_4 spinel solid solution at 1500°K and measured the magnetic properties. They proposed these cation distributions: $Fe^{3+}(Fe^{2+}Fe^{3+}_{\mu}V^{3+}_{1-\mu})O_4$ $(0\leqq\mu\leqq1)$ for the Fe_3O_4–Fe_2VO_4 series, and $Fe^{3+}_{\lambda}Fe^{2+}_{1-\lambda}(Fe^{2+}_{\lambda}V^{3+}_{2-\lambda})O_4$ $(0\leqq\lambda\leqq1)$ for the Fe_2VO_4–FeV_2O_4 series.

In the present study, accurate phase equilibria of the FeO–Fe_2O_3–V_2O_3 system has been determined at 1500°K by varying the oxygen partial pressure. The standard free energy of the reaction to produce FeV_2O_4 has been calculated at 1500°K on the basis of the equilibrium oxygen partial pressure.

Experimental

1) General Procedure. Different experimental methods were used in the present study; the quenching and thermogravimetric methods have previously been described by Katsura and Muan[16] and by Katsura and Kimura.[17]

In the quenching method, oxide samples were heated at 1500°K and at a chosen oxygen partial pressure until equilibrium was attained among the gas and condensed phases. The samples were then quenched rapidly to the temperature of cold water and the phases present were determined by the X-ray diffraction method. The total compositions were determined by means of the gravimetric weight-gain method.

In the thermogravimetric method, a pellet of an oxide mixture was suspended in a vertical tube-quenching furnace by means of a thin platinum wire stretched from the bottom of the quick weighing balance. The weight changes were recorded as a function of the oxygen partial pressure at 1500°K.

The furnace temperatures were kept constant to approximately ±3°K throughout this investigation.

2) Materials. The V_2O_5 was obtained by the decomposition of the reagent grade of ammonium meta vanadate at 450°C in air for 12 hr. Analytical-grade Fe_2O_3 was fired at 700°C in air for 12 hr. Mixtures of the desired ratios of the above two oxides were then prepared. The mixture was loosely pressed into a small-size platinum crucible, and then heated at 650°C in a mixed gas of $CO_2/H_2=1$ for 20 min. The griding, pressing, and heating were repeated to obtain an uniform mixture. An error in the atomic ratio of V/Fe in the mixture was estimated to be within ±0.1 per cent. The prepared sample was a mixture of reduced forms of vanadium and iron oxides. The pellet of the oxide sample was suspended in a furnace tube; here it was heated at 1500°K in a desired CO_2–H_2 gas mixture for 10—18 hr until equilibrium was attained among the gas and the solid phases. The details of the procedure have been described by Katsura and Kimura.[17]

3) Analysis of Total Compositions. The total compositions of the quenched samples were determined by the gravimetric weight-gain method. About 1 g of the quenched sample was accurately weighed. Then, the sample was completely oxidized to the mixture of V_2O_5 and Fe_2O_3 at 800°C in air for 24—48 hr, and then again it was weighed. As the Fe_2O_3/V_2O_5 mol ratio of starting materials was known, the total compositions of the quenched sample were evaluated by means of the difference in weight between before and after the oxidation. The vaporization of V_2O_5 was insignificant during heating within the present limits of accuracy. The error in the total compositions was estimated to be within ±0.2 per cent.

4) Control of Atmosphere. A desired partial pressure of oxygen was provided by using a gas mixture of CO_2 and H_2 or CO_2 and O_2. The mixed gas was prepared by a gas mixer similar to that used by Darken and Gurry.[1] The actual oxygen partial pressure was measured by means of a solid electrolyte cell composed of stabilized zirconia, $(ZrO_2)_{0.85}(CaO)_{0.15}$. The principles and procedure have been described previously.[7,8]

5) Thermogravimetry. The rate of the approach to equilibrium was observed thermogravimetrically. Also, the method was used to determine the ranges of the oxygen partial pressure and the composition in which both spinel and wüstite solid solutions exist in equilibrium. The technique was described in detail in previous papers.[7,8,17]

6) Identification of Phases. The phases present in the quenched samples were identified by an X-ray diffraction method using FeK_α radiation.

The presence of metallic iron in the phase assemblages was evidenced by the liberation of hydrogen gas when samples were dipped in hydrochloric acid. This test is sensitive enough to detect iron in amounts as small as 0.2 per cent, as has been described in a previous study.[17]

Results and Discussion

1) Phase Equilibria. The equilibrium data obtained at 1500°K are summarized in Table 1 and are illustrated graphically in Fig. 1.

Three solid solution phases are stable under the present expreimental conditions: the sesquioxide solid solution, the spinel solid solution, and the wüstite solid solution. The compositions of the sesquioxide phase were stoichiometric within the limits of experimental error and were well represented by the formula $(Fe\cdot V)_2O_3$. Sesquioxides of 80—90 mol per cent Fe_2O_3 were prepared by using a gas mixture of CO_2 and O_2. Each phase of the sesquioxide solid solution was identified by the X-ray diffraction method.

The spinel phase is a ternary solid solution with a stable existence at 1500°K within the composition area, Fe_3O_4–FeV_2O_4–Fe_2O_3. The range of oxygen partial pressure in which the spinel solid solution exists in equilibrium is shown in Fig. 2. The figure illustrates

12) W. Kunnmann, D. B. Rogers, and A. Wold, *J. Phys. Chem. Solids*, **24**, 1535 (1963).
13) G. Schmahl and H. Dillenburg, *Z. Phys. Chem.*, **65**, 119 (1969).
14) D. E. Cox, W. J. Takei, R. C. Miller, and G. Shirane, *J. Phys. Chem. Solids*, **23**, 863 (1962).
15) M. Wakihara, Y. Shimizu, and T. Katsura, *J. Solid State Chem.*, (In Press).
16) T. Katsura and A. Muan, *Trans. A.I.M.E.*, 230, 77 (1964).
17) T. Katsura and S. Kimura, This Bulletin, **38**, 1664 (1965).

Table 1. Results of equilibration experiments at 1500°K at various oxygen partial pressures

mol % x: FeO y: Fe_2O_3 z: V_2O_3 ses: sesquioxide solid solution
sp: spinel solid solution wü: wüstite solid solution

$-\log P_{O_2}$ ±0.05	x	y	z	phases present
13.13	50.3	0	49.7	ses+sp
11.71	9.8	4.5	85.7	ses+sp
	27.1	3.7	69.2	ses+sp
	41.2	3.2	55.6	ses+sp
	45.8	2.8	51.4	ses+sp
11.61	49.6	16.5	33.8	sp
	57.9	13.7	28.4	sp+wü
11.48	51.1	19.1	29.8	sp+wü
	66.0	13.9	20.1	sp+wü
	72.7	11.4	15.9	sp+wü
	78.4	9.4	12.2	sp+wü
	84.0	7.2	8.7	sp+wü
	88.7	5.8	5.6	wü
	92.0	5.3	2.7	wü
11.36	50.2	19.8	30.0	sp+wü
	59.4	17.1	23.4	sp+wü
	63.8	15.8	20.4	sp+wü
	70.8	13.0	16.2	sp+wü
	76.9	10.8	12.3	sp+wü
	82.5	8.7	8.8	sp+wü
	87.4	6.9	5.6	sp+wü
	91.5	5.8	2.7	wü
10.94	5.3	6.9	16.2	ses+sp
	24.7	5.3	70.0	ses+sp
	39.4	4.3	56.3	ses+sp
	44.4	3.8	51.8	ses+sp
	48.6	4.1	47.3	ses+sp
	48.8	5.9	45.4	sp
	49.7	20.3	30.0	sp
	52.6	22.9	24.5	sp+wü
	57.9	20.8	21.3	sp+wü
	65.3	17.8	16.9	sp+wü
	73.0	14.3	12.7	sp+wü
	79.2	11.8	9.1	sp+wü
	85.4	8.9	5.7	sp+wü
	90.1	7.1	2.8	wü
	93.5	6.5	0	wü
10.04	50.3	30.9	18.7	sp+wü
	61.5	24.7	13.8	sp+wü
	71.0	19.4	9.6	sp+wü
	78.7	15.3	6.0	sp+wü
	82.2	13.4	4.4	sp+wü
	85.5	11.6	2.8	wü
	89.3	10.7	0	wü
9.75	49.5	35.4	15.1	sp
	61.4	28.2	10.4	sp+wü
	71.9	21.8	6.4	sp+wü
	81.4	15.6	3.0	sp+wü
9.01	49.6	40.9	9.4	sp
	49.6	42.8	7.5	sp
	49.7	44.7	5.6	sp
	61.4	35.1	3.5	sp+wü
	82.6	17.4	0	wü
8.59	0	20.0	80.0	ses
	12.1	17.4	70.4	ses+sp
	23.4	14.8	61.8	ses+sp
	30.1	13.3	56.6	ses+sp
	41.9	10.6	47.5	ses+sp
	48.9	13.3	37.8	sp
	49.2	16.9	34.0	sp
	49.5	35.4	15.0	sp
	49.3	43.2	7.5	sp
	49.5	46.7	3.8	sp
7.61	2.0	28.8	69.3	ses+sp
	13.4	24.4	62.1	ses+sp
	29.4	19.5	51.1	ses+sp
	39.1	16.6	44.3	ses+sp
6.30	11.6	36.6	51.8	ses+sp
	25.7	30.7	43.6	ses+sp
	35.9	27.2	37.0	ses+sp
	46.9	22.5	30.6	sp
	47.0	30.0	23.0	sp
4.41	3.0	52.6	44.4	ses+sp
	20.2	43.9	36.0	ses+sp
	35.1	37.4	27.5	ses+sp
	42.2	34.2	23.6	ses+sp
2.94	8.8	72.1	19.1	ses+sp
	24.7	62.2	13.1	ses+sp
	39.7	52.4	8.0	ses+sp

the relationship between the oxygen partial pressure and the compositional parameter, x, for the general formula of the spinel: $Fe_{1+2x}V_{2-2x}O_4$ ($0 \leqq x \leqq 1$). The solid lines in the range indicate the values of the atomic ratio of 4(Fe+V)/O. No spinel with a greater metal-to-oxygen ratio than 3:4 was found in the present study. These situations are quite similar to the case of the other spinel solid solutions, Fe_2TiO_4–Fe_3O_4[18] and $FeCr_2O_4$–Fe_3O_4[16].

The wüstite phase has a extensive homogeneous range with some V^{3+} ions in the structure. The extent of these compositional ranges is shown in Fig. 1.

The results in the present study at 1500°K on the binary FeO–Fe_2O_3 system are consistent with those obtained by Darken and Gurry[1] within the limits of experimental error.

Schmahl and Dillenburg[13] and Cox *et al.*[14] reported an immiscible gap of the sesquioxide phase with a rhombohedral (corundum-type) structure in the range about from 80 to 90 mol per cent V_2O_3 at 900°C and 1000°C respectively. The gap, however, was not found in the present study throughout the Fe_2O_3–V_2O_3 system at 1500°K, within our limits of experimental error.

The phase equilibria of the FeO–Fe_2O_3–V_2O_3 system were similar to those of the FeO–Fe_2O_3–Cr_2O_3 system previously investigated.[16] Some characteristic differences were these: no deviation of the oxygen-to-cation ratio below the stoichiometric 3:2 ratio in the sesquioxide phase was found in the present study, and the

18) R. W. Taylor, *Amer. Mineral.*, **49**, 1016 (1964).

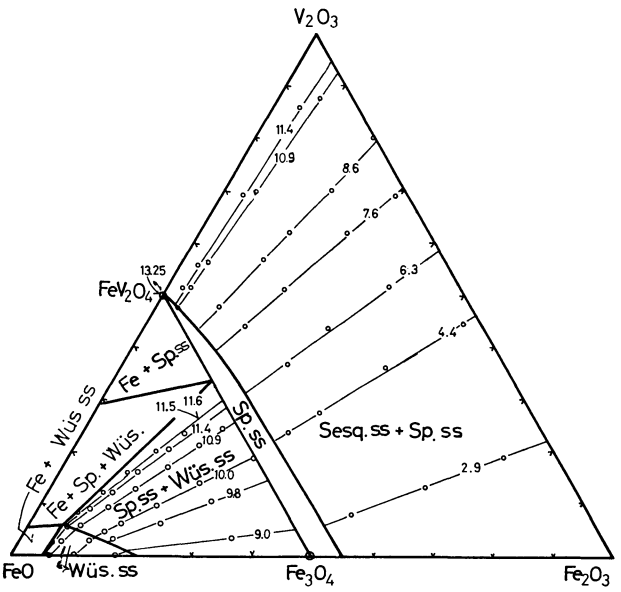

Fig. 1. Graphical representation of equilibrium data obtained for the FeO–Fe_2O_3–V_2O_3 system at 1500°K (mol per cent). Lines in the composition triangle indicate oxygen isobar and numbers on the lines are values of $-\log P_{O_2}$.

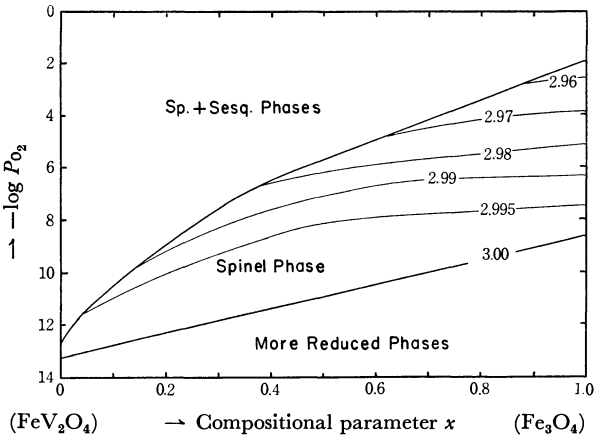

Fig. 2. Relationship between log P_{O_2} and compositional parameter x for $Fe_{1+2x}V_{2-2x}O_4$ at 1500°K; here, lines in the spinel phase region indicate the value of mole ratio, 4(Fe+V)/O.

spinel-phase region in equilibrium with metallic iron (almost from FeV_2O_4 to Fe_2VO_4) was larger than those of the magnetite–iron chromite solid solution series.[16] The latter result may be partly due to the difference in the experimental temperature between the present and previous studies.[16]

2) Thermodynamic Calculations. The oxygen partial pressure at which metallic iron, FeV_2O_4, and V_2O_3 coexist in equilibrium was determined in this investigation ($\log P_{O_2} = -13.25 \pm 0.05$). This value was obtained thermogravimetrically, as is shown in Fig. 2. Therefore, the standard free energy of the reaction to produce FeV_2O_4 from metallic iron and sesquioxide components at 1500°K may be calculated as follows:

$$Fe + V_2O_3 + 1/2O_2 = FeV_2O_4 \qquad (A)$$

The standard free energy of Reaction (A) is given by the following equations:

$$\Delta G^\circ(A) = -RT\ln\frac{a_{FeV_2O_4}}{a_{Fe}\cdot a_{V_2O_3}\cdot P_{O_2}^{1/2}} = 1.152RT\log P_{O_2} \qquad (A')$$
$$= -45500 \pm 200 \text{ cal}$$

where the a_{Fe}, $a_{V_2O_3}$, and $a_{FeV_2O_4}$ activities are equal to unity because these components are pure compounds at the oxygen partial pressure of $\log P_{O_2}(A) = -13.25$.

The standard free energy of Reaction (A) was determined by Kunnmann *et al.*[12] over the temperature range from 1073° to 1380°K by varying the oxygen partial pressure using CO_2/CO gas mixtures. The standard free energy resulting from the present investigation at 1500°K was reasonably consistent with the extrapolated value of their data. According to the data of Darken and Gurry,[1] the oxygen partial pressure at which metallic iron and wüstite phases are stable in equilibrium was logarithmically estimated to be $\log P_{O_2} = -11.58 \pm 0.05$ at 1500°K. Thus, the standard free energy of the formation of wüstite from metallic iron can be readily calculated:

$$0.95Fe + 1/2O_2 = Fe_{0.95}O \qquad (B)$$

$$\Delta G^\circ(B) = -RT\ln\frac{a_{Fe_{0.95}O}}{a_{Fe}^{0.95}\cdot P_{O_2}^{1/2}} = 2.303/2RT\log P_{O_2}(B) \qquad (B')$$
$$= -39700 \pm 200 \text{ cal}$$

where $\log P_{O_2}(B) = -11.58 \pm 0.05$, and where the a_{Fe} and $a_{Fe_{0.95}O}$ activities are unity.

The substraction of Eq. (B) from Eq. (A) gives the following equation:

$$0.05Fe + V_2O_3 + Fe_{0.95}O = FeV_2O_4 \qquad (C)$$

while the standard free energy of Reaction (C) is given by:

$$\Delta G^\circ(C) = \Delta G^\circ(A) - \Delta G^\circ(B) = RT\ln\frac{P_{O_2}(A)}{P_{O_2}(B)} \qquad (C')$$
$$= -5800 \pm 400 \text{ cal}$$

Kinetics of the Reaction of Americium(III) with Peroxydisulfate[1]

Akira OHYOSHI, Akinori JYO, and Tetsuo SHINOHARA

Department of Industrial Chemistry, Faculty of Engineering, Kumamoto University, Kumamoto

(Received May 17, 1971)

Kinetic studies of the americium(III) oxidation have been made in aqueous solutions. The reaction rates are dependent on the concentrations of hydrogen, peroxydisulfate and the silver ion as catalyzers, and on the reaction temperature. The period of induction observed in the initial stage of reaction varies with the concentration of the reactant and with the reaction temperature. The data follow this rate expression:

$$-\frac{d[Am(III)]}{dt} = K_h(k_1+k_2[Ag^+])[S_2O_8^{2-}][Am(III)]\cdot 1/[H^+]$$

where K_h is the dissociation constant of hydrogen peroxydisulfate, and where k_1 and k_2 refer to the silver-ion uncatalyzed and catalyzed paths respectively. The energies of activation were determined to be 28.6 kcal/mol for k_1 and 17.4 kcal/mol for k_2.

The oxidation of americium(III) with the peroxydisulfate ion in the presence of the silver ion is well known.[2,3] This reaction is used to prepare americium isotopes from the spent reactor fuels. Although many papers on the oxidation of Am(III) have been published,[4-7] our knowledge concerning the reaction kinetics of oxidation is rather limited, especially when a tracer concentration is involved. In previous papers[1,8] it was found that the rate data obtained by the tracer technique using the coprecipitation method were in good agreement with those measured specctrophotometrically and that the rate of oxidation appeared to be influenced by the concentrations of the reactants and the acidity of the reaction media. Kinetic studies of this reaction were carried out in order to obtain further information and in order to determine the reaction-rate law.

Experimental

Reagent. Americium-241 oxide which had been obtained from the Radiochemical Centre, Amersham, was dissolved in nitric acid. The solution was then evaporated to dryness, and the residue was dissolved in 0.1 M of a desirable acid. This solution served as the stock solution of americium. Before use, an aliquot of the stock solution was diluted to a suitable concentration with respect to americium and definite acids. The absorption spectrum indicated the tripositive state.[9] The radiochemical purity of ^{241}Am was confirmed by gamma-ray spectrometry.

Ammonium peroxydisulfate, silver nitrate and, all the other chemicals used were of an analytical reagent grade. The solution of ammonium peroxydisulfate was prepared freshly before use.

Apparatus. In order to check the radiochemical purity of ^{241}Am, the gamma-ray spectra were measured with a $2''\times 2''$ NaI(Tl) detector connected with a TMC 400-channel pulseheight analyzer. For the determination of the distribution ratio of ^{241}Am by the coprecipitation method, the gamma-activity of ^{241}Am was counted with a $2''\times 2''$ well-type NaI(Tl) detector connected with an Aloka scaler, Model TDC-5. A Hitachi Model EPS-2U and 124 spectrophotometer were used to determine the absorption spectra of americium. The samples were contained in silica cell which had a 1-cm path length and which contained about 0.8 m*l* of the solution. The silica cell was set in a cell holder thermostated with circulating water of a constant temperature. A Hitachi-Horiba pH meter, Model M-5, was used for the pH measurements.

Procedures. The solutions studied were made up from weighed amounts of ammonium peroxydisulfate, standardized nitric or perchloric acid, and an analyzed stock solution of americium salt. Solutions of ammonium peroxydisulfate containing silver nitrate and Am(III), which upon mixing would give the desired initial composition, were prepared separately and brought to the reaction vessel in a thermostat maintained to within ± 0.2°C of the desired temperature. The reactions were followed by radiometry by means of the lanthanum trifluoride coprecipitation method.[8] In a typical experiment, the reaction mixture was pipetted out into a 10-m*l* centrifuge tube containing a cold solution of the lanthanum carrier and nitric acid. The unoxidized Am(III) was coprecipitated with the lanthanum trifluoride by the addition of an ammonium fluoride solution. The lanthanum trifluoride was centrifuged, and the americium content of the supernatant was determined by the measurement of the gamma-activity of ^{241}Am. The fraction of Am(III) may be described as:

$$1-\frac{\text{Am-remaining}}{\text{Am-taken}}$$

This determination was made for three samples at the same time. The mean value of the three measurements was employed for the kinetic data.

Results and Discussion

Changes in Absorption Spectra during the Reaction. The changes in the absorption spectra of americium during the course of oxidation were measured under

1) Studies of the Actinide Elements. Part IV. part III: A. Ohyoshi, A. Jyo, T. Kanaya, and T. Shinohara, *Radiochem. Radioanal. Lett.*, **7**, 7 (1971).

2) L. B. Asprey, S. E. Stephanou, and R. A. Penneman, *J. Amer. Chem. Soc.*, **72**, 1425 (1950).

3) E. K. Hyde, Proc. Intern. Conf. Peaceful Uses AT. Energy, Geneva, **1955**, 7, paper 728, p. 281, United Nations, New York (1956).

4) M. Ward and G. A. Welch, *J. Chem. Soc.*, **1954**, 4038.

5) R. A. Penneman and T. K. Keenan, "The Radiochemistry of Americium and Curium," NAS-NS-3006 (1960).

6) F. L. Moore, *Anal. Chem.*, **35**, 715 (1963).

7) M. Hara, This Bulletin, **43**, 89 (1970).

8) A. Ohyoshi, A. Jyo, T. Shinohara, and E. Ohyoshi, *Radiochem. Radioanal. Lett.*, **6**, 121 (1971).

9) G. R. Hall and P. D. Herniman, *J. Chem. Soc.*, **1954**, 2214.

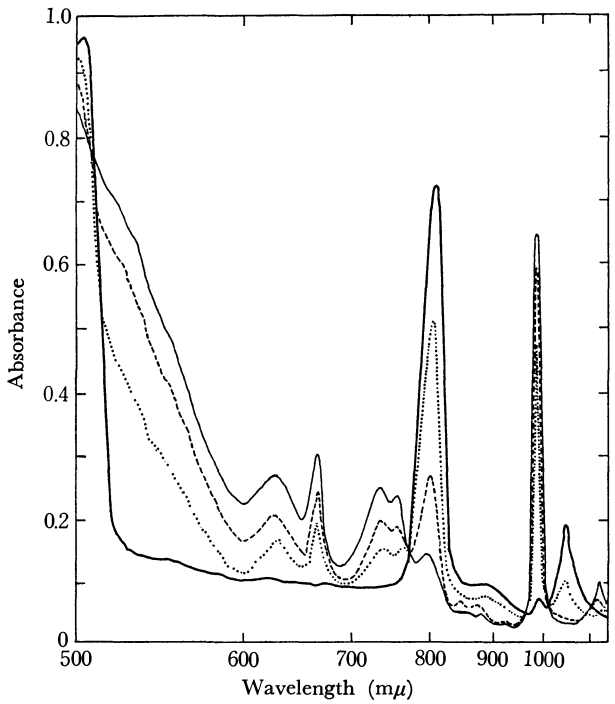

Fig. 1. Change of absorption spectrum of oxidizing americium solution with reaction time.
$[Am(III)]_0=6.4\times10^{-3}$M, $[(NH_4)_2S_2O_8]_0=5.0\times10^{-2}$M, $[AgNO_3]_0=5.0\times10^{-3}$M, $[HNO_3]_0=2.0\times10^{-2}$M, at 60°C.
Reaction time: —— 4 min, ····· 25 min, ---- 55 min, —— 125 min.

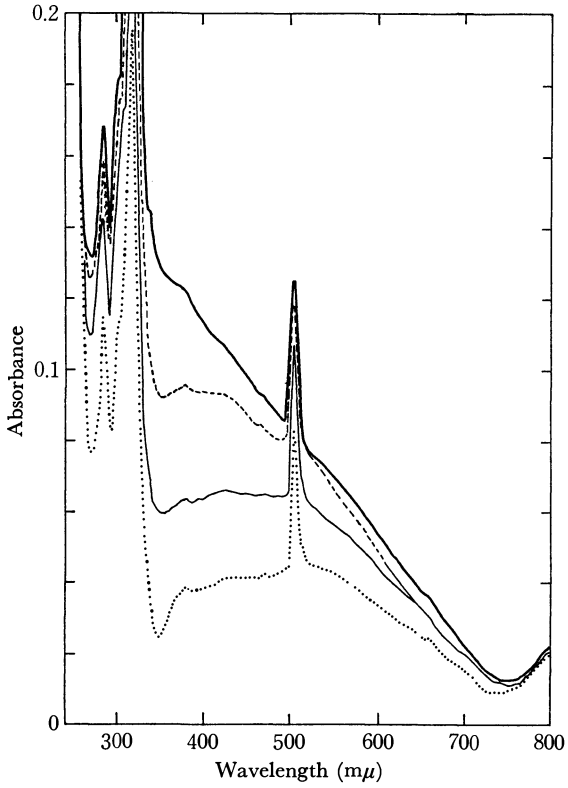

Fig. 2. Change of absorption spectrum of oxidizing americium solution at high acid concentration—I.
$[Am(III)]_0=3.2\times10^{-4}$M, $[(NH_4)_2S_2O_8]_0=5.0\times10^{-2}$M, $[AgNO_3]_0=1.0\times10^{-4}$M, $[HNO_3]_0=0.10$M Temp.=60°C.
Reaction time: —— 1 min, ---- 6 min, —— 11 min, ····· 18 min.

two different sets of experimental conditions. The spectral changes in the visible region of a weak acidic solution are given in Fig. 1. It may be seen that Am(III) exhibits λ_{max} at 814 and 1050 mμ, and that the absorbances at 995 and 666 mμ due to Am(VI) increase with the decrease in those of Am(III) during the reaction time elapsed. In a highly acidic solution, the absorption peak of 503 mμ due to Am(III) does not change immediately after the reactants are mixed, but the broad absorptions in the UV and visible regions obviously change, as is shown in Fig. 2. These absorption band decreased for about 30 min; then, the absorption at 503 mμ began to decrease and a new broad absorption began to appear over the range from 600 to 800 mμ. After this absorption band reached a maximum, it then decreased with the longer reaction time, as is shown in Fig. 3. These changes can be attributed to both the disintegration of Am(III) and the formation of some intermediate compounds. This absorption band shifted towards the lower wavelength region with its increase. After about one hour, this broad band began to decrease, and the absorption peak at 660 mμ due to Am(VI) appeared, though it was not visible because of the low extinction coefficient. The plot of log D_{814} (absorbance at 814 mμ) against the reaction time shows a linear relationship. The same relation was found in the results obtained from the radiochemical measurements.[8] The plots on the

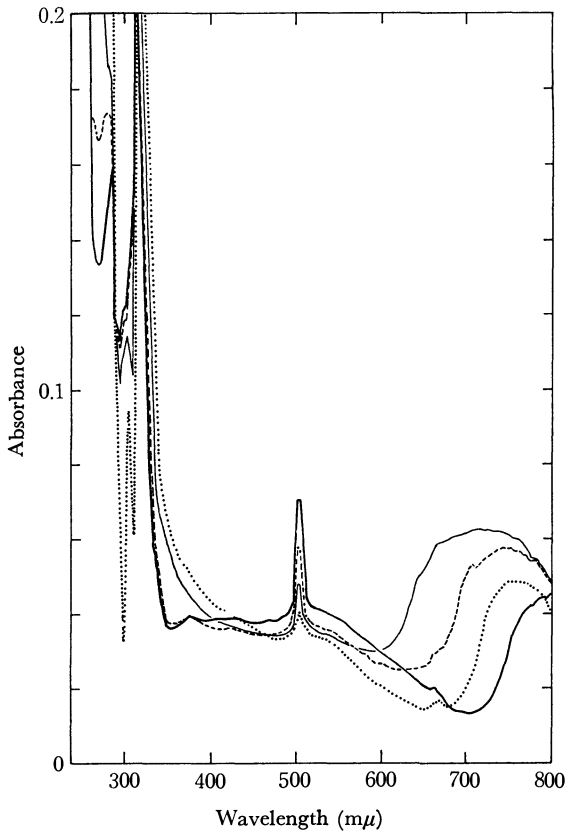

Fig. 3. Change of absorption spectrum of oxidizing americium solution at high acid concentration—II.
$[Am(III)]_0=3.2\times10^{-4}$M, $[(NH_4)_2S_2O_8]_0=5.0\times10^{-2}$M, $[AgNO_3]_0=1.0\times10^{-4}$M, $[HNO_3]_0=0.10$M, Temp.=60°C.
Reaction time: —— 39 min, ---- 50 min, —— 60 min, ····· 70 min.

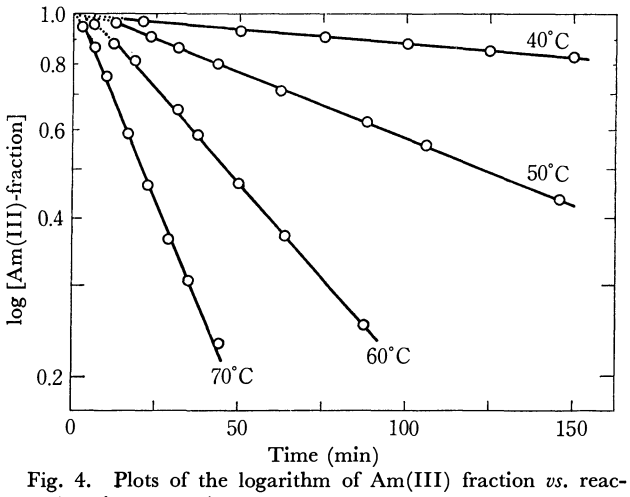

Fig. 4. Plots of the logarithm of Am(III) fraction *vs.* reaction time at various temperatures.
$[Am(III)]_0=4.0\times10^{-6}$M, $[(NH_4)_2S_2O_8]_0=2.0\times10^{-2}$M, $[AgNO_3]_0=1.0\times10^{-3}$M, $[HNO_3]_0=6.0\times10^{-2}$M, $\mu=0.50$.

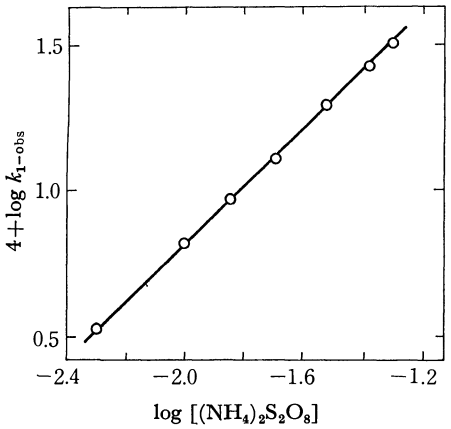

Fig. 5. The plot of log k_{1-obs} *vs.* log$[(NH_4)_2S_2O_8]$
$[Am(III)]_0=3.3\times10^{-7}$M, $[AgNO_3]_0=5.0\times10^{-4}$M, $[HNO_3]_0=8.0\times10^{-2}$M, $\mu=0.50$, Temp.=50°C.

straight lines indicate that the oxidation of Am(III) is first-order with respect to Am(III) over the temperature range of 40—70°C, as is shown in Fig. 4. Thus, the rate of oxidation may be expressed as follows:

$$\text{Rate} = k_{1-obs}[Am(III)] \quad (1)$$

Effects of Other Reactant Concentrations. The variation in the rates as a function of the concentration of the peroxydisulfate ion was studied at 50°C. Assuming the observed rate constants, k_{1-obs}, to be k_{2-obs} $[S_2O_8^{2-}]^n$, the slope of the straight line (Fig. 5) obtained by plotting log k_{1-obs} against log$[S_2O_8^{2-}]$ indicated that n was equal to unity; thus, the rate of oxidation may be expressed by the following equation:

$$\text{Rate} = k_{2-obs}[Am(III)][S_2O_8^{2-}] \quad (2)$$

In order to ascertain the role of the silver-ion catalyst in the kinetics of the oxidation, the study was carried out using $AgNO_3$ of different concentrations. The plots of $[k_{2-obs}-k_1]$ *vs.* $[AgNO_3]$ give curves, as is illustrated in Fig. 6, where the k_1 value is the rate constant obtained in the case of $[AgNO_3]=0$. It appears that the effect of the silver nitrate concentration makes the reaction rate increase and approach a limiting value. Therefore, the k_{2-obs} is given by the following equation under the limiting conditions.

$$k_{2-obs} = k_1 + k_2[Ag^+] \quad (3)$$

where the k_1 is the rate constant of the uncatalyzed reaction and where the k_2 obtained from the initial slope of the linear part of the curve in Fig. 6 corresponds to the rate constant of the catalyzed path of the oxidation. These values are exhibited in Table 1.

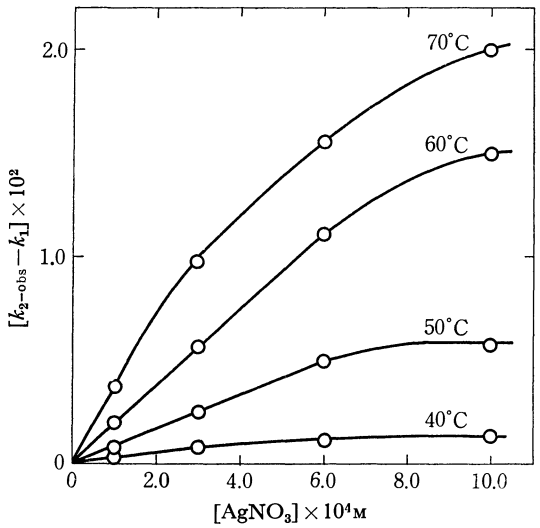

Fig. 6. Difference of total and uncatalyzed reaction rate constants for Am(III) oxidation as a function of the silver nitrate concentration at various temperatures.
$[Am(III)]_0=4.0\times10^{-6}$M, $[(NH_4)_2S_2O_8]_0=2.0\times10^{-2}$M, $[HNO_3]_0=6.0\times10^{-2}$M, $\mu=0.50$.

Table 1. The values of rate constants for silver catalyzed (k_2) and uncatalyzed path (k_1).
$[Am(III)]_0=4.0\times10^{-6}$M, $[(NH_4)_2S_2O_8]_0=2.0\times10^{-2}$M, $[HNO_3]_0=6.0\times10^{-2}$M, $\mu=0.50$.

Temp., °C	k_2 $M^{-2}min^{-1}$	k_1 $M^{-1}min^{-1}$
40	162	0.013
50	420	0.093
60	915	0.36
70	1820	1.45

Effect of the Hydrogen-ion Concentration on the Rate. The experiment were performed at a constant ionic strength and temperature. The hydrogen-ion concentration was varied by the addition of nitric acid. The ionic strength was maintained constant with sodium nitrate. At concentrations of the hydrogen ion higher than 0.4M, no oxidation of Am(III) was observed. The rate increases with the decrease in the hydrogen ion concentration and reaches a constant value at $[H^+]=0.06$M.

A kinetic study of the decomposition of peroxydisulfates has been made by Kolthoff and Miller.[10] It decomposes according to the reaction(4) in a dilute acid solution:

$$S_2O_8^{2-} + H_2O = 2HSO_4^- + 1/2O_2 \quad (4)$$

10) K. I. M. Kolthoff and I. K. Miller, *J. Amer. Chem. Soc.*, **73**, 3055 (1951).

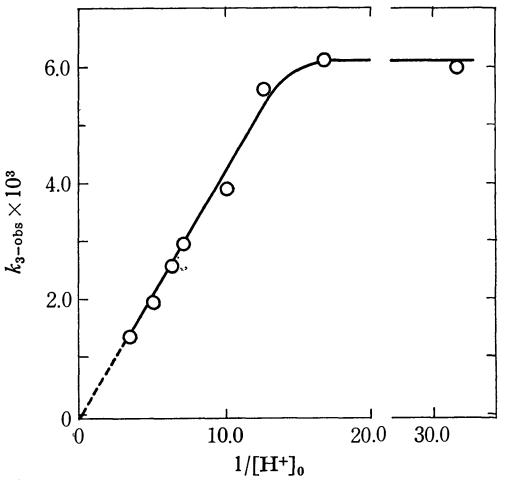

Fig. 7. A plot of the observed rate constants *vs.* reciprocal of the initial hydrogen ion concentration.
$[Am(III)]_0=4.0\times10^{-6}$M, $[(NH_4)_2S_2O_8]_0=2.0\times10^{-2}$M, $[AgNO_3]_0=1.0\times10^{-3}$M, $\mu=0.50$, Temp.=60°C.

In highly acidic solutions, though, reactions(5) and (6) occur:

$$H_2S_2O_8 + H_2O = H_2SO_5 + H_2SO_4 \quad (5)$$

$$H_2SO_5 + H_2O = H_2O_2 + H_2SO_4 \quad (6)$$

The oxidation of Am(III) with the peroxydisulfate ion may be disturbed by the H_2O_2 produced in Eq. (6) because the hydrogen peroxide is an efficient reductant of Am(VI). Figure 7 represents the plot of the observed rate constants against $1/[H^+]_0$. The rate increases with the decrease in the hydrogen-ion concentration but eventually reaches at a constant value, $k_{3-obs}=6.0\times10^{-3}$ min^{-1} at $[H^+]=0.06$M. The results shown in Fig. 7 clearly indicate an inverse first-order dependence of the oxidation rate on the hydrogen-ion concentration. The reaction can thus be expressed by a relation of the type:

$$k_{3-obs} = A\cdot K_h/[H^+] \quad (7)$$

where A is the constant defined by the experimental conditions. The K_h constant, which has the dimension of molarity, was determined from the slope of straight line in Fig. 7 as follows: $K_h=1.4\times10^{-2}$M. This value is close to the secondary dissociation constant of H_2SO_4 ($K_2=1.2\times10^{-2}$M). Thus, it is possible to consider that K_h is the dissociation constant of the hydrogen peroxydisulfate ion, $HS_2O_8^-$.

From the results obtained by the effects of the reaction variables, the over-all rate equation of the Am(III) oxidation reaction may be expressed as follows:

$$-\frac{d[Am(III)]}{dt} = K_h(k_1+k_2[Ag^+])[Am(III)][S_2O_8^{2-}]\cdot 1/[H^+] \quad (8)$$

where k_2 and k_1 refer to the reaction paths catalyzed and uncatalyzed by the silver ion respectively.

From the kinetic relationship, it may be concluded that Am(III) disappears upon reaction with the SO_4^- produced in the decomposition reaction. The kinetics are consistent with the following mechanism:

$$S_2O_8^{2-} \longrightarrow 2SO_4^- \quad (9)$$

$$SO_4^- + Am(III) \longrightarrow Am(VI) \quad (10)$$

If the radicals produced in the reaction(9) react rapidly with Am(III), then the rate is proportional to the concentration of the peroxydisulfate ion and it follows that the measured rate law refers to the unimolecular dissociation of the peroxydisulfate ion. Kolthoff and Miller[10] have shown that a second decomposition reaction occurs in acid media:

$$H^+ + S_2O_8^{2-} \rightleftharpoons HS_2O_8^- \longrightarrow HSO_4^- + SO \quad (11)$$

The fact that the rate of the disappearance of Am(III) was dependent of the reversed hydrogen-ion concentration showed conclusively that Am(III) did not react with SO_4; furthermore, the oxidation of Am(III) might be hindered by the reaction (11). This is in agreement with the above-described mechanism that the two modes of dissociation occur at a comparable rate at these particular hydrogen-ion concentrations.

A mixture of the silver ion and the peroxydisulfate ion forms more powerful oxidizing system than $S_2O_8^{2-}$ alone. The existence of the divalent silver ion is well established,[11] and the influence of Ag^+ in the decomposition of the peroxydisulfate ion can be accounted for by the formation of Ag^{2+} according to the reaction:

$$Ag^+ + S_2O_8^{2-} \longrightarrow Ag^{2+} + SO_4^{-\cdot} + SO_4^{2-} \quad (12)$$

The Period of Induction. When the Am(III) solution was added to a solution containing the ammonium peroxydisulfate and silver nitrate, the oxidation reaction did not start immediately, but after a certain time interval following the mixing of the reactants. This time interval is termed the induction period and is listed in Table 2 for various experimental conditions.

Table 2. Variations of the induction period

		Induction Period, min					
$[AgNO_3]\times10^3$M		0	0.1	0.3	0.5	0.6	1.0
Temp, °C	40	1800	100	35	—	10	0
	50	385	60	25	—	16	1
	60	41	28	8	—	7	6
	70	9	8	5	—	2	2
$[(NH_4)_2S_2O_8]$ $\times10^2$M	0.5				11		
	1.4				7		
	2.0				5		
	3.0				5		
	4.2				10		
	5.0				6		
μ[a]	0.12	25	15	5	—	2	1
	0.25	47	18	8	—	3	2
	0.50	41	28	8	—	7	6
	0.75	120	35	15	—	13	7
	1.00	68	34	10	—	4	6

a) μ was adjusted by the addition of sodium nitrate.

No change in the absorption spectrum due to Am(III) was observed at 503 mμ; however, visible changes were observed in the wavelength region lower than 503 mμ during the induction period (Fig. 2). An increase in the concentration of any of the reactants or an increase in the temperature decreased the period of induction. Thus, it appears that the induction period is related to

11) C. E. H. Bawn and D. Margerison, *Trans. Faraday Soc.*, **51**, 925 (1955).

the mechanism of the oxidation of Am(III). In view of the mechanism, the induction period is the time required for the thermal activation of the peroxydisulfate ion to split into SO_4^- radicals, which then produce the Ag^{2+} responsible for the oxidation of Am(III). An increase in the temperature increases the rate of the chain-initiating process, resulting in a decrease in the induction period. Similarly, an increase in the concentration of either the silver ion or the peroxydisulfate ion increases the rate of SO_4^- radical production by means of reaction (12) or (13) respectively, thereby decreasing the period of induction.

$$S_2O_8^{2-} \rightleftarrows S_2O_8^{2-*} \longrightarrow 2SO_4^- \qquad (13)$$

where (*) denotes the activated state; therefore,

$$SO_4^- + Am(III) \longrightarrow SO_4^{2-} + Am(VI) \qquad (14)$$

Energies of Activation. The plots of log k_1 and k_2 against $1/T$ have been represented in Fig. 8. From the slopes of the straight lines, the activation energies of the silver-ion-catalyzed and uncatalyzed reactions were calculated to be 17.4 ± 0.6 kcal/mol and 28.6 ± 0.8 kcal/mol respectively.

These values are the same as the activation energies calculated in the decomposition of the peroxydisulfate ion[11] in the absence or presence of a silver-ion catalyzer. Such an agreement of values suggests that the same mechanism may be involved in the rate-determining steps of the reactions.

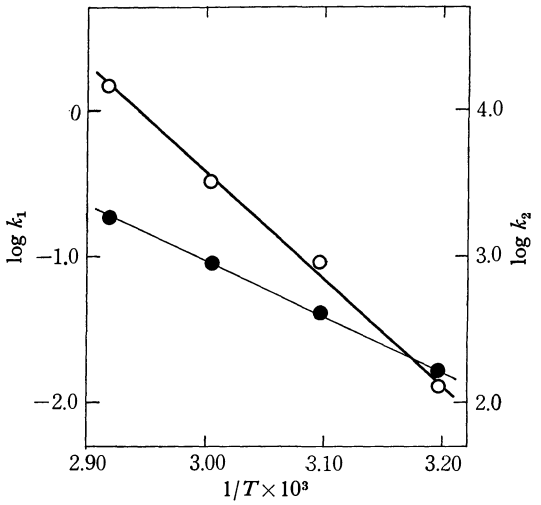

Fig. 8. Arrhenius plots for the silver ion uncatalyzed (k_1) and catalyzed (k_2) reactions.
○ ··· log k_1 ● ··· log k_2

BULLETIN OF THE CHEMICAL SOCIETY OF JAPAN, VOL. 44, 3051—3055 (1971)

Metal Complexes Containing Six-Membered Chelate Rings. I. Preparation and Structure of 2,4-Pentanediaminetetraacetato Complexes of Cobalt(III)

Fujio MIZUKAMI, Haruko ITO, Junnosuke FUJITA, and Kazuo SAITO
Department of Chemistry, Faculty of Science, Tohoku University, Sendai

(Received May 31, 1971)

New cobalt(III) complexes with 2,4-pentanediaminetetraacetate (2,4-ptnta^{4-}) have been prepared. The optically active 2,4-ptnta^{4-} (RR or SS) forms a sexadentate complex and determines the absolute configuration around the metal ion. The *meso*-2,4-ptnta^{4-} (RS) coordinates to the metal ion as a quinquedentate with a free acetate branch. Such stereospecific formations of sexa- and quinquedentate complexes from the optically active and the *meso* 2,4-ptnta^{4-} have been attributed to the steric regulation coming from the methyl groups on the α-carbon atoms.

Recently van Saun and Douglas[1] and Ogino *et al.*[2] prepared and resolved cobalt(III) complexes of trimethylenediaminetetraacetate (trdta^{4-}), and suggested that the ligand acts as a sexadentate with less strain as compared with the sexadentate ethylenediaminetetraacetate (edta^{4-}) in an octahedral complex.

The trdta^{4-} complex involves a six-membered chelate ring with puckered skeletal structure in the trimethylenediamine part, for which the following four conformers are possible; chair, two twist (δ) and (λ), and boat form, as shown in Fig. 1. Molecular models clearly indicate that when trdta^{4-} forms a stable octahedral complex as sexadentate, the six-membered chelate should have twist form,[2] and that the δ twist should give a complex with Λ configuration and the λ twist that with Δ configuration. The trdta^{4-} in chair form can not behave as sexadentate, but does as quinquedentate ligand with a free acetate branch. (Fig. 2)

It is generally understood that methyl groups on carbon atoms in puckered chelate rings always tend to take equatorial position.[3] Hence a stereospecific or stereoselective complex formation may be expected by use of such ligands as *l*-propylenediaminetetraace-

1) C. W. Van Saun and B. E. Douglas, *Inorg. Chem.*, **8**, 1145 (1969).

2) H. Ogino, M. Takahashi, and N. Tanaka, This Bulletin, **43**, 424 (1970).

3) See for example, A. M. Sargeson, "Conformations of Coordinated Chelates" in "Transition Metal Chemistry", R. L. Carlin, Ed., Marcel Dekker, New York (1966), Vol. **3**, pp. 303—343.

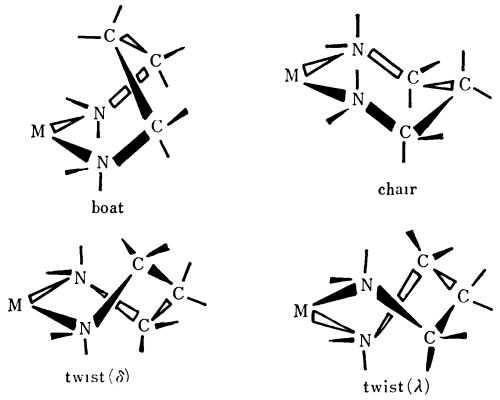

Fig. 1. Possible conformations of six-membered 1,3-diamine chelates. (The notations, δ and λ are by *Inorg. Chem.*, **9**, 1 (1970)).

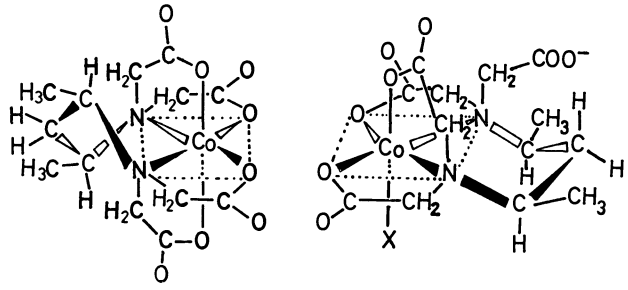

Fig. 2. Cobalt(III) complexes of (a) RR-2,4-ptnta^{4-}, and (b) RS-2,4-ptnta^{4-} with equatorial methyl groups.

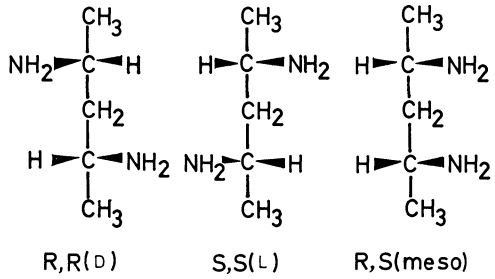

Fig. 3. Isomers of 2,4-pentanediamine.

tate.[4] In this paper, we report the preparation of cobalt(III) complexes of 2,4-pentanediaminetetraacetate (2,4-ptnta^{4-}) which has two methyl groups on the α-carbon atoms adjacent to the amino nitrogen, and discuss the relationship between the structure of these complexes and the optical isomerism of 2,4-pentanediamine, from which the 2,4-ptnta^{4-} ligand is derived.

Experimental

Preparation of Ligands. *2,4-Pentanediamine*: This diamine exists in three isomers, *meso* (RS) and a pair of racemic (RR) and (SS), as shown in Fig. 3. Very recentlyAppleton and Hall[5] reported the separation and the resolution of these isomers. The present method was almost the same as theirs.

Acetylacetone dioxim was reduced with metallic sodium in ethanol by Harries and Haga's [6] and Dippel's[7] metod, and the product was collected by steam distillation. The aqueous ethanol solution of the diamine was acidified with hydrochloric acid and evaporated almost to dryness under reduced pressure. The product, a mixture of *meso* and racemic diaminedihydrochloride, was separated by the following method; a suspension of 100 g of the mixture in 500 m*l* of 95% ethanol was heated to boiling with stirring, and then filtered in hot. The insoluble material was treated further twice with ethanol in the same way, the volume of ethanol being adjusted according to the amount of insoluble material. The residue was almost pure racemic dihydrochloride. Its purity can be examined by the PMR spectrum in deuterium oxide. (Fig. 4) The filtrate was united, cooled to room temperature, the precipitate filtered off, washed with absolute ethanol and ether, and air dried. This product consists of mostly racemate, but contains a small amount of *meso* isomer, which can be removed by repeating the method described above. Ether was added slowly to the filtrate with stirring until the solution became turbid, which was kept in a refrigerator over night. A mixture of racemic and *meso* isomer was precipitated. Here the *meso* isomer formed large prismatic crystals, while the racemate gave fine needle crystals. Thus, these two isomers can be easily separated by decanting the latters with absolute ethanol repeatedly. A small amount of almost pure *meso* isomer was obtained by evaporating all the filtrates under reduced pressure.

Found: racemic isomer C, 34.69; H, 9.27; N, 15.99%. meso isomer C, 34.19; H,9.34; N, 15.99%. Calcd for $C_5H_{16}Cl_2N_2$: C,34.30; H, 9.21; N, 16.00%

The dihydrochloride was converted into free diamine by the following method. An aqueous solution containing a slight excess of potassium hydroxide was added to the dihydrochloride in a small amount of water below 5°C with stirring. The solution was filtered to remove potassium chloride. Free diamine was obtained in aqueous solution by distilling the filtrate under reduced pressure. The concentration was determined by titrating with aqueous 0.1N perchloric acid solution.

As was pointed out by Appleton and Hall,[5] Dippel's assignment of these isomers should be reversed; his racemic (α-isomer) is meso and his meso (β-isomer) is racemic, since his meso was resolved into optical isomers.

Resolution of racemic 2,4-pentanediamine: This was resolved by Appletonand Hall's method as *d*-tartrate. Effective resolution was also substantiated by use of *trans*-1,2-cyclohexanedicarboxylic acid. The specific rotation was the same as that by use of *d*-tartrate.

The tartrates were converted into free diamines by the following method; a small excess of aqueous barium hydroxide solution (1:1) was added to an aqueous solution of the tartrate. The precipitate was filtered off, washed with a small amount of water and the filtrate and the washings were distilled under reduced pressure. The product contained a significant amount of water, and the diamine concentration was determined by titration with 0.1N perchloric acid solution.

The specific rotation of the enantiomers in water are as follows; $[\alpha]_D = -8.33°$ from crystalline *d*-tartrate

$[\alpha]_D = +8.46°$ from oily *d*-tartrate

$(+)_D$-Isomer can be assigned to (SS) configuration, and $(-)_D$-isomer to (RR) configuration, as discussed later.

2,4-Pentanediaminetetraacetate: Free acid and the barium salt of RR-2,4-pentanediaminetetraacetate were synthesized according to a similar method to that for trimethylenediaminetetraacetate by Weyh and Hamm.[8] Monochloroacetic

4) F. P. Dwyer and T. E. MacDermott, *J. Amer. Chem. Soc.*, **85**, 2916 (1963).
5) T. G. Appleton and J. R. Hall, *Inorg. Chem.*, **9**, 1807 (1970).
6) C. Harries and T. Haga, *Ber.*, **32**, 1191 (1899).
7) C. J. Dippel, *Rec. Trav. Chim.*, **50**, 525 (1931).
8) J. A. Weyh and R. E. Hamm, *Inorg. Chem.*, **7**, 2431 (1968).

acid (13.9 g) in 14 m*l* of water was neutralized with 9 g of potassium hydroxide in 15 m*l* of water below 20°C with stirring, and treated with 3.16 g of $(-)_D$-diamine in 5 m*l* of water. The solution was heated at 80°C for 2 hr and 9 g of potassium hydroxide in 10 m*l* of water was added. The solution was evaporated to about 30 m*l* at 80°C, cooled to 0°C and filtered to remove potassium chloride. To the filtrate was added 15.4 g of barium chloride dihydrate in 30 m*l* of hot water with stirring, and the solution was evaporated at 80°C to about 35 m*l*. The barium salt was filtered off, washed with hot water (80°C) several times and air dried.

Found: C, 23.38; H, 3.50; N, 4.37%. Calcd for $C_{13}H_{24}N_2O_{11}Ba_2=Ba_2$(RR-2,4-ptnta)$\cdot 3H_2O$: C, 23.69; H, 3.67; N, 4.25%.

Barium salts of racemic- and meso-2,4-pentanediaminetetraacetate were prepared similarly, but the latter was obtained as powder by adding methanol to its concentrated aqueous solution. Both barium salts give only approximate coincidence between found and calculated analytical results, but their cobalt complexes give very satisfactory analytical results.

Preparation of Metal Complexes. Cobalt(III) complexes of isomers of 2,4-ptnta^{4-} were prepared from $Na_3[Co(NO_2)_6]$[9]. The yields of the complexes were rather low because cobalt(III) was reduced to cobalt(II) during the reaction. Preparation from cobalt(II) salt, 2,4-ptnta^{4-} and an oxydizing agent such as hydrogen peroxide and lead dioxide yielded a large amount of cobalt(II) complex, which could hardly be removed.

The racemic barium salt was treated with an equivalent amount of dilute sulfuric acid, centrifuged and the supernatant evaporated to dryness. The residue was extracted with ethanol and the ethanol evaporated off.

H[Co(RR- and SS-2,4-ptnta)]$\cdot 3H_2O$: An aqueous solution (100 m*l*) containing 6.6 g of racemic $H_4$2,4-ptnta (prepared from 13 g of barium salt) and 8 g of $Na_3[Co(NO_2)_6]$ was warmed at 50°C for 3 hr, cooled to room temperature and filtered. The filtrate was passed through a column of the anion exchanger Dowex 1-X4 in chloride form. The column was washed with water to remove the cobalt(II) ion and the adsorbed purple band was eluted with 0.1N hydrochloric acid. The eluate was condensed in a vacuum desiccator over potassium hydroxide to about 10 m*l*. Purple crystals were deposited by adding ethanol under cooling, which were filtered off, washed with ethanol, air dried and recrystallized from water by cooling together with ethanol.

Found: C, 34.77; H, 5.33; N, 6.13%. Calcd for $C_{13}H_{25}N_2O_{11}Co$: C, 35.14; H, 5.67; N, 6.31%.

K[Co(RR-2,4-ptnta)]$\cdot H_2O$: This complex was prepared from RR-H_4-2,4-ptnta and $Na_3[Co(NO_2)_6]$ by a similar method to that for the racemic-2,4-ptnta complex. Acid complex was converted into potassium salt by treating with aqueous potassium iodide and ethanol. The product was recrystallized from water by adding ethanol.

Found: C, 34.16; H, 4.41; N, 6.02%. Calcd for $C_{13}H_{20}N_2O_9KCo$: C, 34.98; H, 4.55; N, 6.28%.

The rotation of this complex in water shows plus sign at Na D line.

Resolution of H[Co(RR- and SS-2,4-ptnta)]$\cdot 3H_2O$ A solution containing 1.5 g of H[Co(RR- and SS-2,4-ptnta)]$\cdot 3H_2O$ in 25 m*l* of water was stirred with a slight excess of silver oxide, and filtered. The filtrate was added to a suspension containing 1.2 g of $(+)_D$-$[Co(NO_2)_2en_2]Br$[10] in 60 m*l* of water. The mixture was stirred for 20 min, filtered to remove silver bromide, and condensed in a vacuum desiccator over phosphorus pentoxide. When the volume of the filtrate became about 50 m*l*, the first fraction of crystalline diastereomer (0.5 g) was obtained with specific rotation of +887° at Na D line (fraction 1). Recrystallization from water did not increase the rotation. The filtrate was evaporated again to decrease the volume to about 42 m*l*. The second fraction (0.5 g) was obtained with specific rotation of −696° at Na D line (fraction 2). The recrystallized sample from water showed the same specific rotation. By repeating such a fractional crystallization, three more fractions were obtained, but their specific rotations showed smaller absolute values than those of the fractions 1 and 2. Pure diastereomers were further obtained from these three fractions by repeated fractional crystallization from water.

$(+)_D$-*d*-$[Co(NO_2)_2en_2][Co$(2,4-ptnta)$]\cdot 2H_2O$, $[\alpha]_D=+887°$, Found: C, 28.98; H, 5.36; N, 16.28%. Calcd for $C_{17}H_{38}N_8O_{14}Co_2$: C, 29.32; H, 5.36; N, 16.09%.

$(-)_D$-*d*-$[Co(NO_2)_2en_2][Co$(2,4-ptnta)$]\cdot 6H_2O$, $[\alpha]_D=-696°$, Found: C, 26.63; H, 5.95; N, 14.71%. Calcd for $C_{17}H_{46}N_8O_{18}Co_2$: C, 26.57; H, 6.03; N, 14.58%.

These diastereomers were converted into potassium salts by the following method. A solution containing 0.67 g of either $(+)_D$- or $(-)_D$-isomer in 15 m*l* of water was treated with 0.53 g of potassium iodide, warmed at 70°C for 10 min, kept at 0°C for 2 hr and filtered to remove the precipitated $(+)_D$-$[Co(NO)_2en_2]I$. Addition of ethanol to the filtrate gave violet crystals (0.37 g), which were recrystallized from aqueous solution by adding ethanol.

$(+)_D$-[Co(2,4-ptnta)]$\cdot H_2O$, $[\alpha]_D=+1446°$, Found; C, 34.40; H, 4.55; N, 6.31%.

$(-)_D$-[Co(2,4-ptnta)]$\cdot H_2O$, $[\alpha]_D=-1420°$, Found: C, 34.61; H, 4.53; N, 6.27%. Calcd for $C_{13}H_{20}N_2O_9KCo$: C, 34.98; H, 4.55; N, 6.28%.

H[CoCl(RS-2,4-ptntaH)]: Barium salt of *meso*-2,4-ptnta was similarly converted into $H_4$2,4-ptnta. When an aqueous solution containing 7 g of this *meso*-$H_4$2,4-ptnta and 8 g of $Na_3[Co(NO_2)_6]$ was warmed at 60°C for 3 hr, a reddish brown solution was obtained. This was treated with dilute hydrochloric acid at 60°C for 30 min to give a blue solution. This was evaporated almost to dryness in a vacuum desiccator over potassium hydroxide. The residue was dissolved in a small amount of water and passed through a column containing the anion exchanger Dowex 1-X4 in chloride form. The column was washed with water and the adsorbed blue band was eluted with 0.1N hydrochloric acid. The eluate was condensed in a vacuum desiccator over potassium hydroxide and treated with ethanol. Blue crystals were precipitated on cooling, filtered off, washed with ethanol, air dried and recrystallized from 0.1N hydrochloric acid by adding ethanol.

Found: C, 36.35; H, 5.58; N, 6.55%. Calcd for $C_{13}H_{19}N_2O_8ClCo$: C, 36.59; H, 4.72; N, 6.57%.

When the reddish brown solution was submitted to the anion exchange and then treated with 0.1N hydrochloric acid *in situ*, the brown band changed the color into blue with evolution of bubbles and eluted. The same blue crystals were obtained on a similar treatment of the eluate.

K[CoCl(RS-2,4-ptntaH)]: H[CoCl(RS-2,4-ptntaH)] was dissolved in a small amount of 0.1N hydrochloric acid and an excess of potassium acetate was added. Blue crystals obtained on adding ethanol to the solution were filtered off, washed with ethanol, air dried and recrystallized from 0.1N hydrochloric acid by adding ethanol.

Found: C, 33.35; H, 4.07; N, 6.06%. Calcd for $C_{13}H_{19}N_2O_8ClKCo$: C, 33.59; H, 4.12: N, 6.03%.

Elemental analysis and the pH measurement of the aqueous solution suggest that the product is in the given form with free acetic acid branch.

Measurements. Visible and ultraviolet absorption spec-

9) E. Billman, *Z. Anal. Chem.*, **39**, 284 (1900).
10) *Inorganic Syntheses*, **6**, 194 (1960).

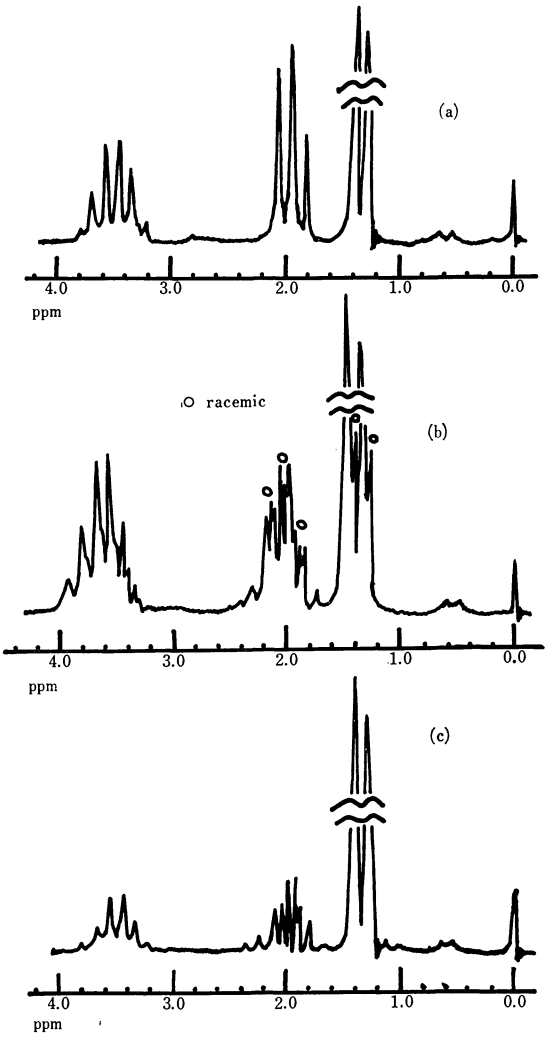

Fig. 4. PMR spectra of (a) racemic 2,4-ptn·2HCl, (b) mixture of racemic- and *meso*-2,4-ptn·2HCl, (c) *meso*-2,4-ptn·2HCl, in D_2O (60 MHz).

tra were recorded with a Hitachi 124 recording spectrophotometer. The CD curves were recorded with a Model ORD/UV-5 spectrophotometer of Japan Spectroscopic Co. with its CD attachment. PMR spectra were obtained with a Varian T-60 spectrometer using Na-TMS as an internal standard. Infrared spectra were recorded with a Hitachi EPI-2G spectrophotometer. All the measurements were made at room temperature.

Results and Discussion

Structure of the Complexes

As Fig. 5 and Table 1 show, the absorption spectrum of [Co(RR- and SS-2,4-ptnta)]$^-$ is very similar to that of [Co(trdta)]$^-$ [1,2], in which the trdta^{4-} coordinates to the cobalt(III) ion as a sexadentate ligand. The infrared spectrum of H[Co(RR- and SS-2,4-ptnta)]·$3H_2O$ exhibits no absorption of free carboxylate. It is thus clear that the complex contains sexadentate ligand (RR- or SS-ptnta^{4-}) with twist form of the six-membered chelate as stated previously. Studies with molecular models made it clear that both RR- and SS-2,4-ptnta^{4-} could form two possible configurational isomers, Δ and Λ-complex. The orientation of both

Table 1. Numerical data of absorption (AB) and circular dichroism (CD) $\bar{\nu}$ in 10^3 cm^{-1}, (log ε) and (ε_l-ε_r)

Complex	AB	CD
$(+)_D$-Δ-K[Co(RR-2,4-ptnat)]·H_2O	18.02(2.09)	17.04(−2.19) 18.94(+2.02)
	26.18(2.00)	24.55(−0.70) 32.26(+0.13)
	43.86(4.38)	40.32(−6.38) 44.44(+8.30)
$(-)_{546}$-Λ-Na[Co(trdta)]·$3H_2O$[a]	18.20(2.12)	17.00(+1.91) 19.00(−2.41)
	26.40(2.06)	24.60(+0.69)
$(-)_{546}$-Λ-K[Co(edta)]·$2H_2O$[a]	18.60(2.54)	17.10(+1.50) 19.80(−0.69) 23.80(+0.28)
	26.65(2.39)	25.60(−0.09) 27.60(+0.29)
K[CoCl(RS-2,4-ptntaH)]	17.24(2.16) 25.71(2.21) 42.55(4.30)	
K_2[CoCl(edta)][b]	17.09(2.38) 24.83(2.43) 41.50(4.27)	

a) Ref. 1)
b) J. Fujita and Y. Shimura, This Bulletin, **36**, 1281 (1963).

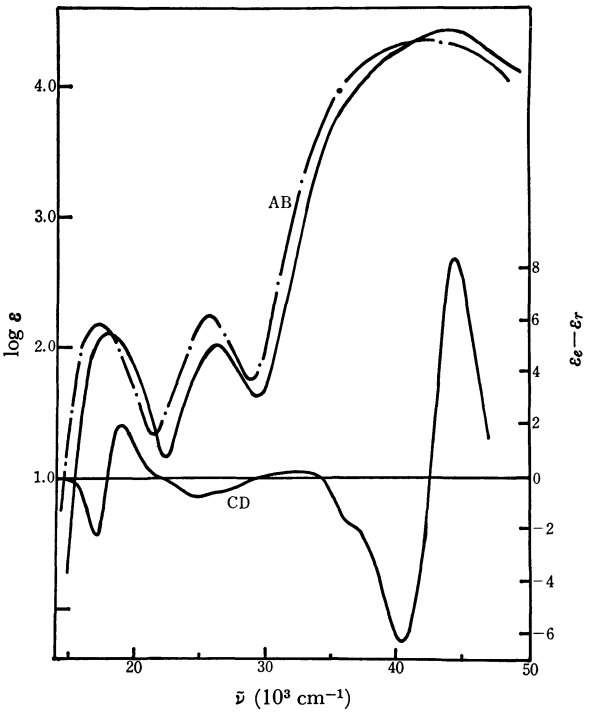

Fig. 5. Absorption (AB) and circular dichroism (CD) spectra of (+)D-K[Co(RR-2,4-ptnta)]·H_2O in H_2O (——), and AB spectrum of H[CoCl(RS-2,4-ptntaH)] in dil. HCl (—·—·).

methyl groups of the Δ complex of RR-2,4-ptnta^{4-} is equatorial to the six-membered ring (λ twist), while that of its Λ complex is axial to the chelate ring (δ twist) (Table 2). However, the existence of the diastereoisomer with the axial methyl groups has not been known so far in such chelate complexes. Thus, the complex which was prepared from racemic 2,4-ptnta^{4-} consists most likely of only a racemic pair, Δ-[Co(RR-2,4-

Table 2. Conformations of diamine part in 2,4-pentanediaminetetraacetates

Ligand	Conformation		
	chair	δ-twist	λ-twist
RR-2,4-ptnta^{4-}	a,e	a,a	e,e
SS-2,4-ptnta^{4-}	a,e	e,e	a,a
RS-2,4-ptnta^{4-}	a,a e,e	a,e	a,e

e: methyl equatorial, a: methyl axial

ptnta)]$^-$ and Λ-[Co(SS-2,4-ptnta)]$^-$. Fig. 5 shows the CD spectrum of $(+)_D$-[Co(2,4-ptnta)]$^-$ in water. This isomer gives a CD pattern very similar to that of Δ-[Co(trdta)]$^-$ in the region of the first absorption band (18000 cm^{-1})[1,2]. It seems that the $(+)_D$-isomer has Δ-configuration and the 2,4-ptnta^{4-} ligand must have RR-configuration. The reaction of $Na_3[Co(NO_2)_6]$ with 2,4-ptnta^{4-} which was prepared from $(-)_D$-2,4-pentanediamine produced only $(+)_D$-Δ-[Co(2,4-ptnta)]$^-$ under the given condition. These results indicate that the complex formation between the cobalt(III) ion and the optically active ptnta^{4-} is stereospecific. It is also clear that the absolute configuration of the carbon atoms of the $(-)_D$-2,4-pentanediamine could be assigned to RR.

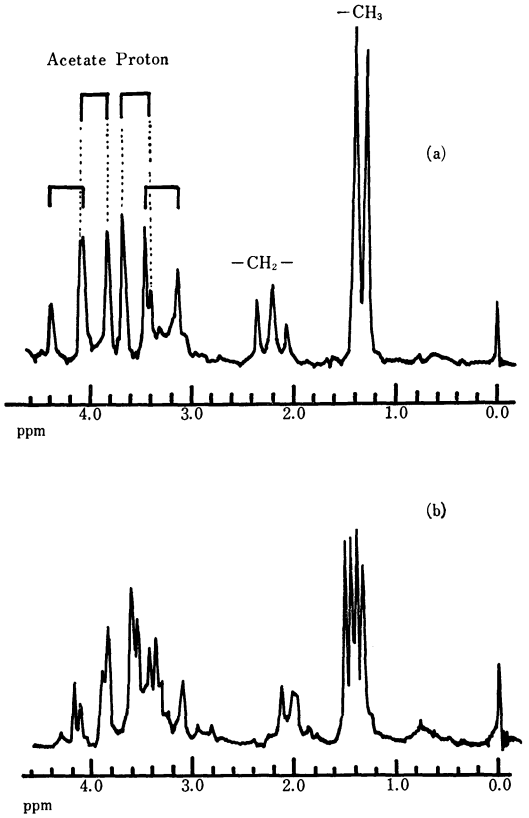

Fig. 6. PMR spectra of (a) [Co(RR- and SS-2,4-ptnta)]$^-$ (D_2O), (b) [CoCl(RS-2,4-ptntaH)]$^-$ (DCl-D_2O), (60 MHz).

The PMR spectrum of the [Co(RR- and SS-2,4-ptnta)]$^-$ in deuterium oxide provides useful information. The spectrum exhibits only one methyl signal and two kinds of acetate methylene signal. (Fig. 6). In this figure is given a tentative assignment for the observed signals.[2] The complex ion, [Co(RR- and SS-2,4-ptnta)]$^-$ has a two-fold axis through the cobalt ion and the β-carbon atom of the six-membered ring, and therefore, the two methyl groups are in an equivalent environment.

The complex, [CoCl(RS-2,4-ptntaH)]$^-$ on the other hand, is considered to involve a quinquedentate ligand. Its infrared absorption spectrum at about 1600 cm^{-1} is much broader than that of the violet complex with sexadentate RR- or SS-2,4-ptnta^{4-}. The free carboxylate absorption may overlap the strong band due to the coordinated carboxyl stretching vibration.

Figure 5 compares the visible and ultraviolet absorption spectra of the quinquedentate and the violet sexadentate complex. The first absorption band of the former complex shows at lower wave number than that of the latter complex. This is in good accord with the spectrochemical series,[11] indicating that the chloride ion coordinates to the cobalt(III) ion in the meso-2,4-ptnta complex.

The PMR spectrum of the chloro complex will also support the quinquedentate coordination of RS-ptnta^{4-}. As Fig. 6 shows, the [CoCl(RS-2,4-ptntaH)]$^-$ in DCl-D_2O gives two kinds of methyl signal, and the signals of acetate methylenes are much more complicated than those of the violet sexadentate complex with racemic or optically active 2,4-ptnta^{4-}. Such a quinquedentate coordination of the meso ligand may be caused by a steric requirement due to the methyl groups on the six-membered ring as stated previously. Molecular models indicate that so far as the methyl groups orientate equatorially to the chelate ring, the six-membered ring should take the chair form and only three out of four acetate branches seem to be allowed to coordinate to the cobalt(III) ion. Figure 2 illustrates this structure schematically. Its structure has no symmetry element and gives a racemic pair which depends on the coordination of either of the two out-of-plane acetate branches. Attempts for optical resolution of this pair have been unsuccessful so far.

Such a stereospecific formation of sexa- and quinquedentate complex from racemic and meso ptnta^{4-} clearly indicates that the steric regulation coming from the methyl group on the α-carbon atom is very strong in the six-membered rings as well as in the five-membered rings

We wish to thank the Ministry of Education for the financial support granted to this research.

11) Y. Shimura and R. Tsuchida, This Bulletin, **29**, 311 (1956).

Kinetic Studies of the Electron Transfer Reaction in Iron(II) and Iron(III) Systems. IV. The Reaction in Mixed Solvents of Dimethyl Sulfoxide and Water[1]

Goro WADA and Michiko AOKI

Department of Chemistry, Faculty of Science, Nara Women's University, Nara

(Received July 5, 1971)

The rate constants, k_{app}, of the electron transfer reaction between iron(II) and iron(III) in mixed solvents of DMSO and water were measured at various acid and DMSO concentrations at μ=0.50M and 25°C. The k_{app} decreased linearly with the increase in [DMSO] at a constant [H^+] and increased linearly with the increase in 1/[H^+] at a constant [DMSO]. The reaction is considered to proceed through two paths: $Fe^{2+}+{}^*Fe^{3+}\rightarrow Fe^{3+}+{}^*Fe^{2+}$ and $Fe^{2+}+{}^*FeOH^{2+}\rightarrow FeOH^{2+}+{}^*Fe^{2+}$, with the rate constants of k_O and k_H respectively. Both k_O and k_H were suppressed by the addition of DMSO to water because of the occurrence of molecular association between DMSO and water. The hydration number of DMSO in a very dilute aqueous solution was approximately six, as revealed by the cryoscopic measurements. The suppression of k_O and k_H was proportional to [DMSO], with a common proportional constant. Consequently, DMSO was deduced to destroy the chains of water molecules connected by hydrogen bondings and to interfere with the ease of hydrogen atom transfer between the reducing and oxidizing iron species. DMSO itself did not serve as a ligand to catalyze the reaction as *N*-methylacetamide, *N*,*N*-dimethylacetamide, and various other anions do.

In aqueous media, the electron transfer reaction between iron(II) and iron(III), Fe(II)+*Fe(III)→Fe(III)+*Fe(II), has been concluded to proceed generally *via* the hydrogen atom transfer mechanism[2] except when the iron species were complexed with some catalytic ligands with a bridging nature or with conjugate double bond systems, in which cases the reaction occurred predominantly *via* the inner- or outer-sphere mechanism respectively instead.[3]

In pure dimethyl sulfoxide (DMSO), however, the reaction between the simply solvated iron species was found to occur faster than in water in the absence of any complexing ligands, although DMSO had no exchangeable hydrogen atoms which might have promoted the reaction to proceed *via* the hydrogen atom transfer mechanism;[4] therefore, the electron transfer reaction between the solvated iron species may occur not only at a different rate, but also through a different path, as the reaction medium changes.

When either *N*-methylacetamide or *N*,*N*-dimethylacetamide was added to water, the reaction was slightly accelerated in quite a similar way. This can be accounted for by the fact that the coordination of one of these substances to the iron ion favored the transfer of hydrogen atoms of water molecules, as a non-bridging ligand attaching to the central ions at the opposite side of the reactive site.[5]

The reaction in mixed solvents of DMSO and water was first observed by Menashi and others,[4] who recognized that the reaction rate exhibited a broad minimum at a certain mole fraction range of DMSO when the hydrogen ion concentration was not very low. In the present paper, the effect of the addition of a small amount of DMSO on the reaction mechanism was investigated in more detail in order to clarify the cause of the decrease in the reaction rate. This phenomenon seems to be related to the strong associative nature of DMSO with water molecules.

Experimental

The methods of preparing the chemical materials used and of the kinetic measurements were quite the same as have been described previously.[1,4] The temperature and the ionic strength of the reaction systems were kept at 25°C and μ=0.50M respectively, unless otherwise noted.

Since the iron(III) species was initially labelled with ^{59}Fe, the iron(II) species gradually became radioactive as time passed after the initiation of the reaction. If the total concentrations of the iron(II) and iron(III) species in the reaction system are represented as [Fe(II)] and [Fe(III)] respectively, and the radioactivities of the iron(II) species at time, t, and infinite time, t_∞, as x and x_∞ respectively, the McKay relation will hold as follows:

$$\ln\left(1-\frac{x}{x_\infty}\right)=-\frac{[Fe(II)]+[Fe(III)]}{[Fe(II)][Fe(III)]}Rt \qquad (1)$$

where R is the total rate of the electron transfer reaction.[6]

The freezing-point depression of water by the addition of DMSO was measured by the usual method in order to determine the hydration number of DMSO in their mixtures.

Results and Discussion

A typical plotting of the linear relation of $\log(x_\infty-x)$ against t is shown in Fig. 1. The slope of the straight line gives the half-life period of the reaction, $t_{1/2}$; thus, the total rate of the electron transfer reaction, R, is obtained:

$$R=\frac{0.693[Fe(II)][Fe(III)]}{([Fe(II)]+[Fe(III)])t_{1/2}} \qquad (2)$$

1) Part III: G. Wada, N. Yoshizawa, and Y. Sakamoto, This Bulletin, **44**, 1018 (1971).

2) W. L. Reynolds and R. W. Lumry, *J. Chem. Phys.*, **23**, 2460 (1955).

3) F. Basolo and R. G. Pearson, "Mechanisms of Inorganic Reactions," John Wiley and Sons, Inc., New York, N. Y. (1967), p. 454.

4) J. Menashi, W. L. Reynolds, and G. Van Auken, *Inorg. Chem.*, **4**, 299 (1965).

5) G. Wada and R. Yoshihara, *Kogyo Kagaku Zasshi*, **73**, 2309 (1970).

6) H. A. C. McKay, *Nature*, **42**, 997 (1938).

Table 1. Variation of the rate with [DMSO] and [H+] at μ=0.50M and 25°C

[H+] M	[DMSO] M	[Fe(II)] $\times 10^4$ M	[Fe(III)] $\times 10^5$ M	$t_{1/2}$ sec	k_{app} (obsd) M^{-1} sec^{-1}	k_{app} (calcd) M^{-1} sec^{-1}
0.45	0.601	3.439	2.88	126	14.7	15.7
0.30	0	1.999	2.50	134	22.9	23.6
	0.188	2.635	2.11	108	22.7	22.9
	0.395	1.809	2.23	169	20.2	20.7
	0.601	1.445	1.95	233	18.0	19.4
	0.940	1.630	1.74	228	16.9	17.7
	1.22	2.749	2.55	166	13.9	15.0
	1.35	1.206	2.12	363	13.5	14.5
	1.50	1.358	2.01	345	12.9	13.4
	1.75	2.211	2.83	252	11.0	12.0
	2.00	2.205	2.17	287	9.9	9.7
	2.00	2.064	2.61	321	9.3	9.7
0.20	0	2.053	2.34	108	28.4	31.8
	0	1.825	1.58	111	31.5	31.8
	0	1.439	1.85	134	31.9	31.8
	0.094	2.488	1.36	87	30.2	31.0
	0.188	1.146	1.96	163	31.7	30.0
	0.188	1.206	1.41	182	28.3	30.0
	0.188	1.434	1.74	136	31.8	30.0
	0.188	2.450	1.25	81	33.7	30.0
	0.301	2.140	1.85	97	30.4	28.9
	0.507	1.499	2.50	169	23.9	26.9
	0.507	1.608	1.96	149	25.8	26.9
	0.940	1.250	2.55	132	22.1	23.0
	0.940	1.782	1.90	148	23.7	23.0
	1.22	3.085	0.76	98	22.2	20.2
	1.22	1.738	1.63	168	20.9	20.2
	1.50	2.499	2.06	141	17.9	17.6
	1.75	4.346	1.63	86	17.8	15.6
	2.00	2.559	1.47	194	13.2	12.7
	2.00	2.401	1.68	202	13.4	12.7
0.15	0.601	2.401	2.61	76	34.5	32.2
	0.940	1.711	2.23	131	27.3	28.2
0.10	0	0.380	1.96	227	53.2	54.3
	0	0.527	2.06	174	54.2	54.3
	0	1.124	2.17	90	56.7	54.3
	0	1.450	2.07	68	60.9	54.3
	0.188	1.228	1.96	96	52.8	51.2
	0.395	0.511	1.96	198	49.7	47.7
	0.601	0.951	1.96	129	46.6	44.5
	0.940	0.983	2.17	146	39.5	39.2
	1.22	1.070	2.17	143	36.9	34.4
	1.35	1.032	2.34	174	31.6	32.3
	1.50	1.331	2.06	155	29.2	29.9
	1.75	1.059	1.96	213	25.8	26.3
	2.00	1.032	2.06	234	23.8	21.7
0.07	0.601	1.423	2.28	70	60.0	60.1
	0.940	1.380	2.17	82	53.0	52.6
	1.22	2.272	2.60	58	47.7	46.7
	1.50	0.999	2.28	137	41.2	40.4
0.05	0.601	0.462	2.28	126	79.8	80.4
	0.601	0.652	2.45	93	83.6	80.4
	0.940	1.179	2.01	69	72.8	70.5
	1.22	0.842	2.66	100	62.3	62.1
	1.50	1.776	2.28	60	57.5	54.0
	2.00	1.619	2.61	83	43.8	39.4

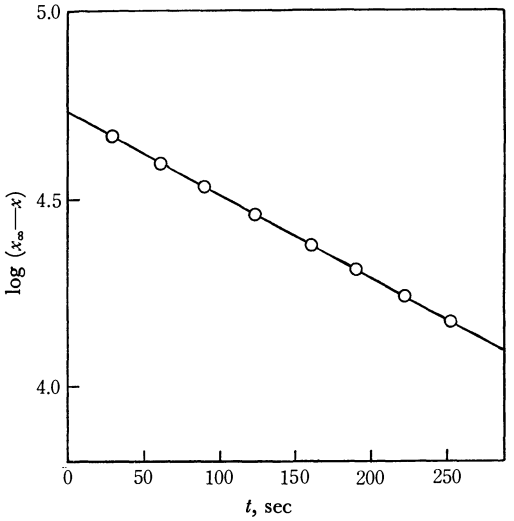

Fig. 1. Plot of log (x_∞—x) *vs.* time at μ=0.50M and 25°C.
[Fe(II)]=9.99×10^{-5}M [Fe(III)]=2.28×10^{-5}M
[DMSO]=1.50M [H+]=0.07M

The results of the measurements are listed in Table 1. In the table, there are some groups of data on the cases in which both the [H+] and [DMSO] used were kept constant; for example, there is a set of data for four kinetic runs performed at [H+]=0.20M and [DMSO]=0.188M, with the half-lives of the respective runs being different from one another. If the rate is proportional to both [Fe(II)] and [Fe(III)], the second-order rate

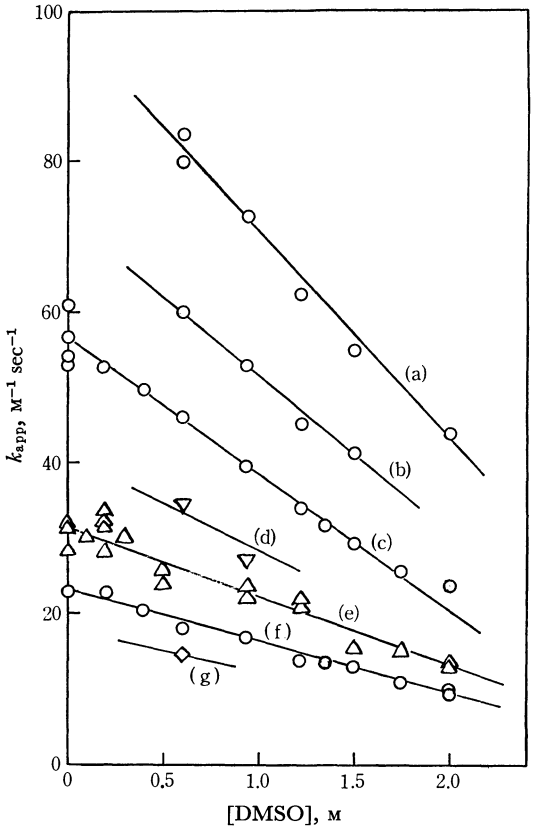

Fig. 2. Plot of k_{app} *vs.* [DMSO] at various [H+] at μ=0.50M and 25°C.
(a) [H+]=0.05M (b) [H+]=0.07M (c) [H+]=0.10M
(d) [H+]=0.15M (e) [H+]=0.20M (f) [H+]=0.30M
(g) [H+]=0.45M

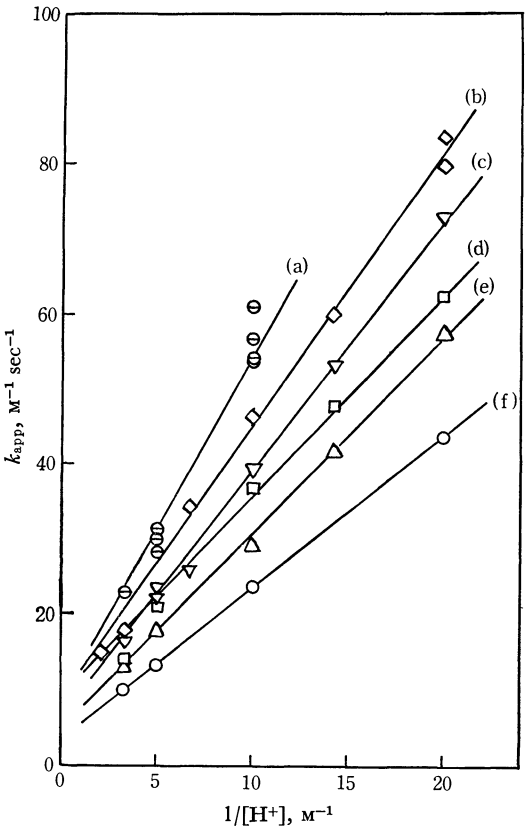

Fig. 3. Plot of k_{app} *vs.* 1/[H$^+$] at various [DMSO] at μ= 0.50M and 25°C.
(a) [DMSO]=0M (b) [DMSO]=0.601M
(c) [DMSO]=0.940M (d) [DMSO]=1.22M
(e) [DMSO]=1.50M (f) [DMSO]=2.00M

constant, k_{app}, is obtained by the following equations:

$$R = k_{app}[Fe(II)][Fe(III)] \quad (3)$$

$$k_{app} = \frac{0.693}{([Fe(II)]+[Fe(III)])t_{1/2}} \quad (4)$$

The values of k_{app} obtained in this way at fixed [H$^+$] and [DMSO] values show a good constant value within the range of experimental error. Therefore, this fact indicates that the reaction can be considered to be of the first order with respect to both [Fe(II)] and [Fe(III)]. In Table 1, the k_{app}'s derived by means of Eq. (4) are shown as the observed values.

It is noticeable that the values of k_{app} in Table 1 vary as the concentration of the hydrogen ion or of DMSO varies. Fig. 2 shows that the k_{app} decreases linearly as the DMSO concentration increases at a constant [H$^+$], and Fig. 3, that the k_{app} is also linear with respect to the reciprocal hydrogen-ion concentration at a constant [DMSO].

When *N*-methylacetamide or *N,N*-dimethylacetamide was added to water instead of DMSO, the matter was quite different from the case of DMSO, with the result that the k_{app} grew larger as the concentration of *N*-methylacetamide or *N,N*-dimethylacetamide became higher.[5] In other words, *N*-methylacetamide and *N,N*-dimethylacetamide are accelerators, while DMSO acts as an inhibitor, of the present reaction.

In aqueous solvents, the main paths of the electron transfer between iron(II) and iron(III) species are the following two reactions:

$$Fe^{2+} + *Fe^{3+} \xrightarrow{k_0} Fe^{3+} + *Fe^{2+} \quad (5)$$

$$Fe^{2+} + *FeOH^{2+} \xrightarrow{k_H} FeOH^{2+} + *Fe^{2+} \quad (6)$$

The respective rate constants are represented as k_0 and k_H. Fe^{2+} and Fe^{3+} represent solvated species, and $FeOH^{2+}$, an iron(III) one of whose solvating water molecules has been hydrolyzed to lose a proton.

When a foreign substance is added to the reaction system, the possibility of the occurrence of an electron transfer between the species coordinated with the substance as a ligand must be taken into account in addition to the paths of (5) and (6). This consideration has been successful in the cases of various anions and mono- and di-methylacetamide, where these substances promote the reaction, while in the present case of DMSO, this kind of procedure can not interpret the decrease in k_{app} at all. The decrease in k_{app} due to the addition of DMSO seems to be attributable to the depression of the activity of water in the mixed solvent.

It is well known that the electron transfer processes expressed by (5) and (6) occur predominantly *via* the hydrogen atom transfer mechanism, in which water molecules used as the solvent play an important role through the chains connected by hydrogen bondings.[2] When DMSO is added to water, it strongly interacts with water, depressing the water activity, as will be described below. If the rate constants, k_0 and k_H, are assumed to be lowered in proportion to the concentration of DMSO, these constants in the mixed solvent may be expressed in the following forms where k_0^0 and k_H^0 represent the constants in the absence of DMSO and where a and b are proportional constants:

$$k_0 = k_0^0(1-a[DMSO]) \quad (7)$$

$$k_H = k_H^0(1-b[DMSO]) \quad (8)$$

Then, according to the usual method of calculation, the k_{app} can be expressed as a function of [H$^+$] and [DMSO]:

$$k_{app} = \frac{k_0^0(1-a[DMSO])+k_H^0K_H(1-b[DMSO])/[H^+]}{1+K_H/[H^+]} \quad (9)$$

in which K_H is an equilibrium constant for the hydrolysis, $Fe^{3+} \rightleftharpoons FeOH^{2+}+H^+$, being equal to 1.59×10^{-3}M.[7] Even at the lowest value of [H$^+$]=0.05M used in the present experiment, the denominator on the right-hand side of Eq. (9) may reasonably be regarded as unity. Thus, the rearrangement of Eq. (9) leads us to the following:

$$k_{app} = \left(k_0^0+\frac{k_H^0K_H}{[H^+]}\right)-\left(ak_0^0+\frac{bk_H^0K_H}{[H^+]}\right)[DMSO] \quad (10)$$

$$= k_0^0(1-a[DMSO]) + \frac{k_H^0K_H(1-b[DMSO])}{[H^+]} \quad (11)$$

Eq. (10) demonstrates the linear relationship between the k_{app} and [DMSO] as is pictured in Fig. 2, and Eq. (11), that between the k_{app} and 1/[H$^+$], as is pictured in Fig. 3. If the slope of a straight line in Fig. 2 is

7) A. S. Wilson and H. Taube, *J. Amer. Chem. Soc.*, **74**, 3509 (1952).

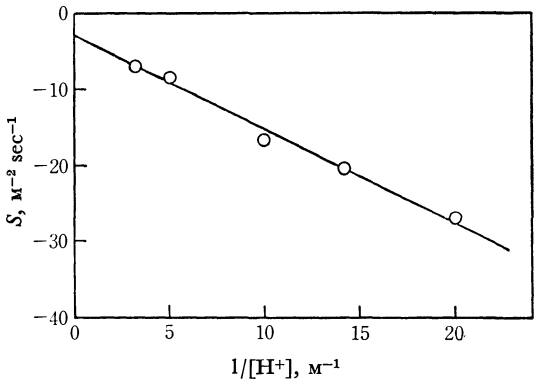

Fig. 4. Plot of slopes of straight lines in Fig. 2 *vs.* $1/[H^+]$.

denoted by S, S is expressed by this equation:

$$S = -ak_0^0 - \frac{bk_H^0K_H}{[H^+]} \tag{12}$$

which also indicates the linear relationship between the S and $1/[H^+]$, as is shown in Fig. 4, with an intercept of $-ak_0^0 = -3\,M^{-2}sec^{-1}$ and with a slope of $-bk_H^0K_H = -1.4\,M^{-1}sec^{-1}$. Since k_0^0 and $k_H^0K_H$ are known from the intercept and the slope of the straight line at [DMSO]=0 in Fig. 3 as $k_0^0 = 9\,M^{-1}sec^{-1}$ and $k_H^0K_H = 4.6\ sec^{-1}$ respectively,[8] a and b can be approximately calculated as follows:

$$a \doteqdot 0.3\,M^{-1}$$

$$b \doteqdot 0.3\,M^{-1}$$

These numerical results for a and b suggest that the addition of DMSO to water equally depresses the rates of both reactions, (5) and (6). Thus, the calculated values of k_{app} using the various constants obtained above are listed in the last column in Table 1. The agreement between the observed and the calculated results is pretty good.

The characteristic interactions between DMSO and water have been recognized from several points of view; the viscosities and local liquid structures in DMSO-water mixtures[9] and the heat of solution of DMSO in water[10] were especially investigated, indicating that a molecular association occurs between DMSO and water.

If there were no molecular association between them, the ideal freezing-point depression of water, ΔT_f^0, would be expected to be given by the following equation:

$$\Delta T_f^0 = \frac{1000gK_f}{GM} \tag{13}$$

in which G and g are the weights of water and DMSO contained in the system respectively, M, the molecular weight of DMSO, and K_f, the molar depression of freezing point of water. However, the actually observed depression of the freezing point of water, ΔT_f, was always much larger than the expected value by Eq. (13). This is because DMSO associates with water; therefore, there occurs a decrease in the amount of water as the solvent, by as much as p:

$$\Delta T_f = \frac{1000gK_f}{(G-p)M} \tag{14}$$

Consequently, the hydration number of DMSO, h, can be defined from Eq. (14) as follows:

$$h = \frac{p}{18m_{DMSO}} = \frac{m_W}{m_{DMSO}} - \frac{55.5K_f}{\Delta T_f} \tag{15}$$

where m_W and m_{DMSO} represent the numbers of the moles of water and DMSO contained in the system, being equal to $G/18$ and g/M respectively. The observed h is plotted against the mole fraction of DMSO in Fig. 5. Although the hydration numbers are slightly scattered, they seem to decrease gradually with the increase in the concentration of DMSO. At a very dilute concentration, a DMSO molecule associates with approximately five or six molecules of water, the structure of the associate being not known yet. This kind of interaction of DMSO with water seems to be quite characteristic, because a similar experiment done with dimethylformamide in place of DMSO exhibited only a small number of hydration, about 0.7. Thus, the strong formation of molecular associates may depress the activity of water and suppress the ease of the hydrogen atom transfer along the chains of hydrogen bondings.

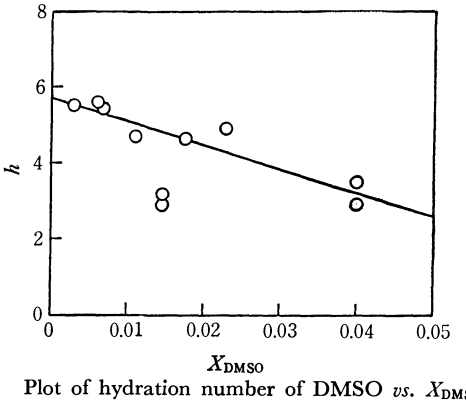

Fig. 5. Plot of hydration number of DMSO *vs.* X_{DMSO}.

Depending upon the NMR investigation concerned with the ionic solvation,[11] Al^{3+} was found to be preferentially solvated with water when water is present in a larger amount than DMSO and with DMSO when DMSO is present in a larger amount than water, in the mixed solvents of DMSO and water. A similar phenomenon may be supposed to occur in the case of Fe^{3+}; it may be solvated overwhelmingly with water in a dilute aqueous solution of DMSO. According to our unpublished data on the optical densities of the systems containing Fe^{3+}, H^+, and DMSO in water, iron(III) was observed to be solvated with DMSO in no noticeable amount, at least not by the optical method.

8) Values appearing in the literature[7] are $k_0^0 = 4.0\,M^{-1}\,sec^{-1}$, $k_H^0 = 3.0\times10^3\,M^{-1}\,sec^{-1}$, $K_H = 1.59\times10^{-3}\,M$ and therefore $k_H^0K_H = 4.8\ sec^{-1}$.

9) S. A. Schichman and R. L. Amey, *J. Phys. Chem.*, **75**, 98 (1971).

10) J. M. Corkill, J. F. Goodman, and J. R. Tate, *Trans. Faraday Soc.*, **65**, 1742 (1969).

11) S. Thomas and W. L. Reynolds, *Inorg. Chem.*, **9**, 78 (1970).

This is the reason why any reaction paths in which the solvated iron species with DMSO take part have been ignored in the present case, only the (5) and (6) reactions being paid much attention to.

Summarizing the above-mentioned considerations, the electron transfer reaction between iron(II) and iron(III) in mixed solvents of DMSO and water when the DMSO concentration is less than 2M proceeds predominantly through the hydrogen atom transfer mechanism, which is retarded by the addition of DMSO to the reaction system because of the strong formation of molecular associates between DMSO and water and, consequently, because of the depression of the activity of water, the depression being proportional to the concentration of DMSO.

At higher DMSO concentrations, DMSO begins to coordinate with iron and to participate in the electron transfer as a catalytic ligand through the inner- or outer-sphere mechanism. In pure DMSO,[4] the latter path only is of importance, with a higher reaction rate than that through the hydrogen atom transfer mechanism in pure water.

BULLETIN OF THE CHEMICAL SOCIETY OF JAPAN, VOL. 44, 3060—3062 (1971)

Mass Spectrometry of Dyes. IV.[1] Electron Impact Reaction of Nitrophenyl Phenyl Ethers and Their Charge Migration

Kazutoshi YAMADA, Takeo KONAKAHARA, and Hirotada IIDA

Department of Synthetic Chemistry, Faculty of Engineering, Chiba University, Yayoicho, Chiba

(Received April 13, 1970)

By the electron impact reaction of substituted 4-nitrodiphenyl ethers (1), the substituents on ring B of (1) cause a reasonable change in the intensity of fragment ions which result from the nitro→nitrite ester rearrangement. There is a linear correlation of the M^+–NO fragment ion intensity of (1) with the ionization potential of the molecules, and with Hammett σ constants. These evidences suggest that the charge of ring B will be free to migrate to ring A in the ion state, even if they are separated by O-atom.

In elucidating the mass spectral fragmentation mechanism, two concepts about the mobility of charge, that is, localization and migration, have been reported. The first concept of localized charge as a driving force for unimolecular decomposition reactions induced by electron impact has been used by a number of authors to explain and correlate a large variety of reactions observed in mass spectra.[2] As an extention of this concept, it has been proposed that most decomposition reactions which yield abundant ions can be interpreted as being initiated by the positive charge or the unpaired electron at a particular site.[2c,3]

Biemann and Mandelbaum, however, have documented the mobility of a charge in the mass spectral fragment ions of a series of substituted 1-(valerylphenyl)-3-phenylcyclopentanes,[4] of which two aromatic rings are separated by a cyclopentane ring. On the other hand, Kinstle and Oliver have reported a charge localization by the fact that substituents on ring B of 4-nitrodiphenyl ethers (1) cause a considerable change in the intensity of fragment ions which result from the nitro→nitrite ester rearrangement.[5] However, their examination seemed to indicate some dissatisfaction.

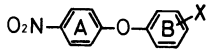

(1)

We will now attempt to re-examine their results. This is based on the fact that there is a linear correlation of the M^+–NO fragment ion intensity in the electron impact reactions of (1) with the ionization potential I_M of the molecules, which are calculated by simple LCAO MO method, and with Hammett σ constants, and that the M^+–NO (or M^+–NO_2) ions, fragment further by the action of substituents X on the other ring B. These evidences suggest that the charge will be free to migrate to the other ring in the ion state.

Experimental

Materials. 4,4′-Dinitrodiphenyl ether was obtained commercially, while 4-nitrodiphenyl ether, 4-chloro-4′-nitrodiphenyl ether, and 4-methoxy-4′-nitrodiphenyl ether were prepared by a known method.[6] Mp and the spectral propeties (UV and mass spectra) confirm the structure.

Electron Impact Reactions. The reactions were carried out using a Hitachi RMU-6E double-focusing mass spectrometer and operating under the following conditions for the

1) Previous papers, Part III: K. Yamada, A. Noguchi, T. Konakahara, and H. Iida, *J. Fac. Eng. Chiba Univ.*, **21**, 47 (1970); Part V: K. Yamada, K. Hayashida, and H. Iida, *Kogyo Kagaku Zasshi.* **74**, 952 (1971); Part VI: K. Yamada, A. Noguchi, and H. Iida, *J. Fac. Eng. Chiba Univ.*, **21**, 149 (1970).

2) See, for example: a) T. Wachs and F. W. McLafferty, *J. Amer. Chem. Soc.*, **89**, 5044 (1967) and references cited therein. b) H. Budzikiewicz, C. Djerassi, and D. H. Williams, "Mass Spectrometry of Organic Compounds," Holden-Day, Inc., San Francisco, Calf., (1967), and references cited therein. c) F. W. McLafferty, "Interpretation of Mass Spectra," W. A. Benjamin, Inc., New York, N. Y., (1966).

3) F. W. McLafferty and T. Wachs, *J. Amer. Chem. Soc.*, **89**, 5043 (1967).

4) A. Mandelbaum and K. Biemann, *ibid.*, **90**, 2979 (1968).

5) T. H. Kinstle and W. R. Oliver, *ibid.*, **91**, 1864 (1969).

6) R. Q. Brewster and T. Groening, "Organic Syntheses," Coll. Vol. II, p. 445 (1966).

above materials: ionizing voltage 80, 70, and 20 eV, heated inlet system at 130—150°C except for 4,4'-dinitrodiphenyl ether (direct inlet system at 180°C), total emission current 80 and 10μA. Other electron impact reaction data were quoted from Ref. 5.

Calculation. The ionization potential I_M values were calculated by simple LCAO MO method,[7] according to the following equation

$$I_M = -\varepsilon_{H.O.}$$

where $\varepsilon_{H.O.}$ is the energy of the highest occupied orbital for the molecule.

The least-squares value of the plot (M^+–NO ion intensity *vs.* Hammett σ) was computed by the usual program.

Results and Discussion

Electron impact reactions are considered as a set of competing consecutive unimolecular decompoiton reactions under highly reduced pressure. The quasi-equilibrium theory (QET) of the electron impact reactions[8] in its simplest form predicts that the rate constant k varies with internal energy E, according to the following equation

$$k = \nu\left(\frac{E-E_0}{E}\right)^{s-1}$$

where ν is a frequency facter, E_0 is the activation energy, and s is the effective numbers of oscillators. In our reaction, Bentley's treatment gives the following

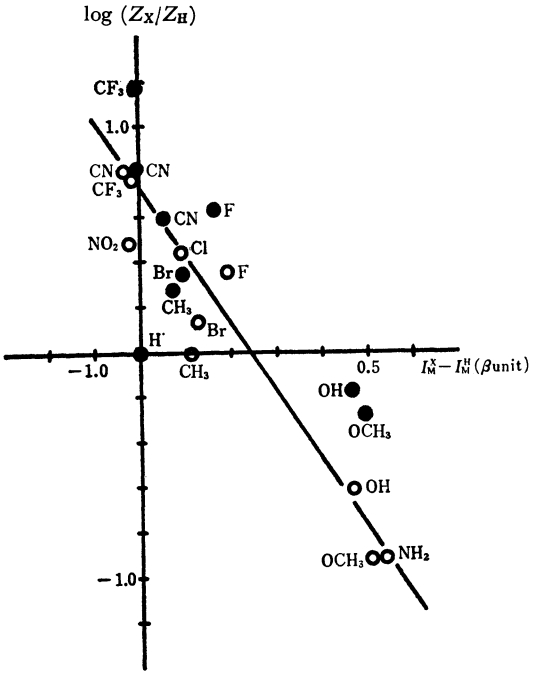

Fig. 1. Correlation of M^+—NO ion intensity with the ionization potential I_M.

$$Z_H = \frac{[OC_6H_4OC_6H_5]^+}{3[O_2NC_6H_4OC_6H_5]^+};\quad Z_X = \frac{[OC_6H_4OC_6H_4X]^+}{[O_2NC_6H_4OC_6H_4X^+]^+}$$

$I_M = -\varepsilon_{H.O.}$; Calculated by simple LCAO MO method.
○: *para*; ●: *meta*

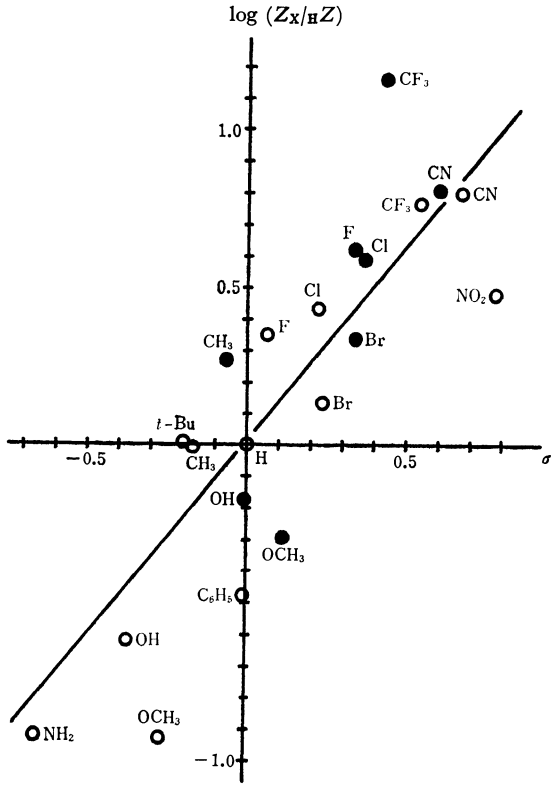

Fig. 2. Correlation of M^+—NO ion intensity with Hammett σ. Least-squares slope (ρ) = +1.24 ($0.85 \leqq \rho \leqq 1.63$), standard deviation=0.29. ○: *para*; ●: *meta*

relationship theoretically[9,10]

$$\log (k_X/k_H) = \log (Z_X/Z_H) \cong [(s-1)/E][(I_M^X - I_M^H) - (I_B^X - I_B^H)]$$

$$\log (Z_X/Z_H) \cong [(s-1)/E](K_M - K_B)\sigma = K\sigma$$

$$(Z = [A]/[M])$$

where [A] and [M] are the relative abundances of the peaks due to the M^+–NO fragment and the molecular ion respectively, I_M and I_B are the ionization potentials, K, K_M, and K_B are constants. The subscripts and/or the superscripts, X and H, refer to substituted and parent compound, and the subscripts M and B to the molecule and the M^+–NO ion. The log (Z_X/Z_H) *vs.* ($I_M^X - I_M^H$) plot, ignoring the effect of I_B, was shown in Fig. 1. I_M values were calculated by simple LCAO MO method. In Fig. 2, which are the correlation between log(Z_X/Z_H) and Hammett σ, the use of σ constants gave a plot with slightly less scatter than did Brown's σ^+ values and the least-squares value of the slope (ρ) is +1.24. This value for our reaction ($M^+ \rightarrow$ M^+–NO) represents a larger numerical reaction constant than most of those previously reported for the rate of an electron impact reaction.[11] Thus, it appears that the reaction is enhanced by an increased positive charge at the reaction site, that is, that the nature of

7) Kikuchi's program and usual parameters were used in this paper.

8) H. M. Rosenstock, M. B. Wallstein, A. L. Wahrhaftig, and H. Eyring, *Proc. Natl. Acad. Soc., U. S.*, **38**, 667 (1952).

9) T. W. Bentley, R. A. W. Johnstone, and D. W. Payling, *J. Amer. Chem. Soc.*, **91**, 3978 (1969).

10) $I_M^X - I_M^H = K_M\sigma$; A. Streitwieser, Jr., *Progr. Phys. Org. Chem.*, **1**, 27 (1963), $I_B^X - I_B^H = K_B\sigma$; A. G. Harrison, P. Kebarle, and F. P. Lossing, *J. Amer. Chem. Soc.*, **83**, 777 (1961).

11) P. Brown and C. Djerassi, *ibid.*, **89**, 2711 (1967).

the substituent greatly affects the ionization of the molecule and/or the electronic distribution in the molecular ion. Indeed, the decomposition of the molecular ions seems to depend on the substituents X as described in Ref. 2. It is clear in Fig. 2, that the formation of M^+–NO ion is inhibited by electron-donating substituents X on ring B and facilitated by electron-withdrawing groups X with a large, often "flat-topped" metastable ion, which has been observed in this NO loss from some nitroaromatics.[12]

The ionization potential of the polyfunctional molecule is determined by the functional group with the lowest ionization potential,[13] and the ionization potential of nitrobenzene is the highest in all of the monosubstituted benzenes.[14] Therefore, I_M^X of substituted 4-nitrodiphenyl ethers is determined by the substituent X, and it seems, the initial site of ionization to be localized on substituted ring B. The more electron-withdrawing is the substituent, the more intense is the M^+–NO ion peak. This is undoubtedly the effect of the substituents X. The electron-withdrawing X groups facilitate the charge and/or radical migration to electron-deficient ring A in the odd-electron fragment ions. Initially, this seemed surprising in view of the results of Kinstle *et al.* who documented the localization of a charge in the odd-electron fragment ions.[5] However, unlike their study, in electron impact reaction (both 70 and 20 eV) of 4-nitrodiphenyl ethers with the electron-withdrawing X groups (*e.g.* X=4′-NO_2, 4′-Cl), M^+–NO (or M^+–NO_2) fragment ions displayed, with considerable intensity, further decompositions because of the substituents X on ring B (Scheme I and II). Likewise, in the case of the electron-donating groups X, it seemed that the initial fragment ions due to the substituents X further decomposed by nitro group on ring A (Scheme III).

The remainder of the ionization potentials between nitro- and chloro- or methoxybenzene (20 and 30 kcal) shows the ease of ionization on ring B. This process

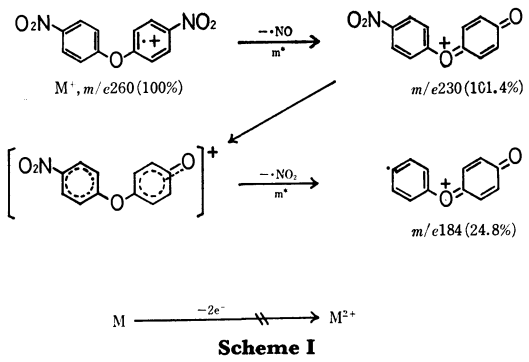

Scheme I

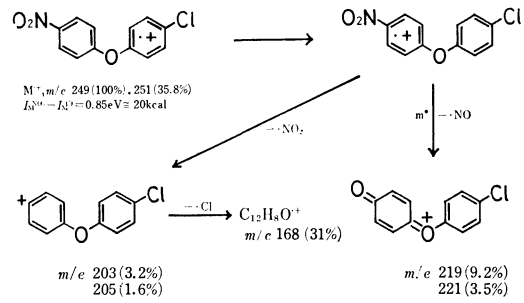

Scheme II

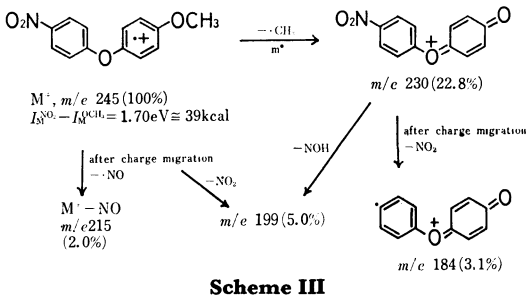

Scheme III

is the same as that of Biemann's report.[4]

These results suggest that the substituent X on ring B of substituted 4-nitrodiphenyl ethers (1) has an important effect on the electronic state of ring A, and that the charge and/or radical migration to electron-deficient ring A in the odd-electron fragment ion is possible by through-conjugation of oxygen *p*-orbital.

12) J. H. Beynon, R. A. Saunders, and A. E. Williams, *Z. Naturforsch.*, **20a**, 180 (1965); M. M. Bursey and F. W. McLafferty, *J. Amer. Chem. Soc.*, **88**, 5023 (1966).
13) G. A. Junk and H. J. Svec, *ibid.*, **89**, 790 (1967).
14) I. Howe and D. H. Williams, *ibid.*, **91**, 7137 (1969).

The Reactions of Grignard Reagents with Transition Metal Halides: Coupling, Disproportionation, and Exchange with Olefins

Masuhiko TAMURA* and Jay K. KOCHI

Department of Chemistry, Indiana University, Bloomington, Indiana 47401, U. S. A.

(Received December 26, 1970)

The reactions of transition metal halides (Mn, Fe, Co, Ni, Pd, Cu, and Ag) with the low-molecular-weight alkyl Grignard reagents in tetrahydrofuran and diethyl ether, especially in the presence of styrene were reinvestigated. An alkyl transition metal species formed *in situ* by metathesis decomposed to a dialkyl (oxidative dimerization) or to an alkene and an alkane (oxidative disproportionation). Silver(I) and copper(II) were particularly effective in oxidative dimerization of primary alkyl groups. Alkyl groups which contain no β-hydrogen were also coupled by iron, cobalt, nickel, palladium, and copper(I) halides with varying degrees of efficiency. Oxidative disproportionation was generally the more common route to decomposition for alkyl groups which have β-hydrogens. It seemed to proceed directly *via* a bimolecular interaction of alkylmetals or indirectly by elimination of a hydrido-metal species. If the latter added to an alkene reversibly, exchange was observed between Grignard reagent and alkene. Styrene was reduced to ethylbenzene during the reaction both in tetrahydrofuran and in diethyl ether in varying yield with transition metal halide and Grignard reagent. In addition to alkyl exchange, dehydrogenation of the ethereal solvent by active (reduced) metal species complicated the stoichiometry of decomposition as measured by the value of the empirical parameter, Q(R). The selection of transition metal in addition to the temperature, solvent and triphenylphosphine was effective variables in promoting the efficiency of the exchange process.

The reactions of various transition metal salts and Grignard reagents in which alkane, alkene and coupling dimer are obtained as products have been studied for some time.[1] In some cases, there is evidence for stable and isolable organometallic compounds.[1] However, the transition metal salt is generally reduced to the metallic state in the presence of excess Grignard reagent, and the stoichiometry of the reaction is represented

$$n\mathrm{RMgX} + \mathrm{MY}_n \longrightarrow [\mathrm{RH},\ \mathrm{R(-H)},\ \mathrm{R\text{-}R}] + n\mathrm{MgXY} + \mathrm{M}^\circ \qquad (1)$$

as follows:

$$Q(R) = \frac{\mathrm{R(-H)} + \mathrm{RH} + 2\mathrm{R\text{-}R}}{\mathrm{MY}_n} = n \qquad (2)$$

The distribution of products is dependent on the transition metal salt as well as the Grignard reagent, and also varies with the reaction conditions. Most of the studies reported for these reactions are so fragmentary that the differences in reactivity of various transition metal salts cannot be compared directly.[1] We have examined the mechanism of the Kharasch reaction catalyzed by various transition metal salts in which we postulated organometallic compounds as intermediates.[2,3] To provide support for our studies of the mechanism of the Kharasch reaction we felt that it was desirable to learn about the chemical properties of such organometallic compounds under the reaction conditions.

Metathesis of transition metal salts and organometallic compounds such as organolithium species and Grignard reagents is often the simplest method of obtaining σ-bonded transition metal alkyl complexes.[1] In this study we examined the reactions

$$n\mathrm{RMgX} + \mathrm{MY}_n \longrightarrow \mathrm{R}_n\mathrm{M} + n\mathrm{MgXY} \qquad (3)$$

of transition metal halides and Grignard reagents in tetrahydrofuran (THF) and diethyl ether ($\mathrm{Et_2O}$) under comparative conditions. The reactions were also examined in the presence of styrene and other olefins in order to probe for exchange processes.

Results

The Reactions of Transition Metal Halides and Grignard Reagents in Tetrahydrofuran. The reactions of transition metal halides with various Grignard reagents in THF are summarized in Table 1 and Table 2, which show clearly that the distribution of products was greatly dependent on the transition metal halide and the Grignard reagent. The yield of coupling dimer was almost quantitative independently of the Grignard reagent in the cases of argentous and cupric halides. It was also generally larger with the higher oxidation state of a given metal, *i.e.*, cupric chloride$\gg$cuprous chloride and ferric chloride$>$ferrous chloride.

Coupling dimer was also formed in fairly good yield almost independently of the transition metal halide from the reaction with methyl, neopentyl, benzyl, vinyl or phenylmagnesium bromide which has no available β-hydrogens. For a given transition metal salt, the yield of coupling dimer increased generally in the sequence: methyl$>$neopentyl, benzyl.

The yield of ethyl chloride was negligibly small and the formation of *n*-butane was predominated in the reaction of cupric chloride and ethylmagnesium bromide. This result was quite different from that in the

* Present address; Central Research Laboratories, Kuraray Co., Ltd., Sakazu, Kurashiki, Okayama, Japan. To whom correspondence should be addressed.

1) F. A. Cotton, *Chem. Rev.*, **55**, 551 (1955); G. W. Parshall and J. J. Mrowca, *Advan. Organometal. Chem.*, **7**, 157 (1968); C. D.M. Beverwijk and G. J. M. Van der Kerk, *Organometal. Chem. Rev.*, **A5**, 215 (1970); G. E. Coates, M. L. H. Green, and K. Wade "Organometallic Compounds" Vol. 2, Third ed., Methuen and Co., Ltd., London (1968).

2) M. Tamura and J. Kochi to be published.

3) M. S. Kharasch and O. Reinmuth, "Grignard Reagents of Nonmetallic Substances," Prentice-Hall Co., New York, N. Y. (1954).

TABLE 1. THE REACTIONS OF FERROUS, FERRIC, COBALTOUS, NICKELOUS, AND PALLADOUS HALIDES WITH GRIGNARD REAGENTS IN TETRAHYDROFURAN[a)]

Transition Metal Salt MX_n	Grignard Reagents RMgBr	Q(R)	Products %[b)]			EtPh[c)] mmol
			R(-H)	RH	R-R	
$FeCl_3$	Et	3.7	22.5	59.6	17.9	
$FeCl_2$	Et	2.1	25.9	67.6	6.5	
$FeCl_3$	Me	3.0		32	68[f)]	
$FeCl_2$	Me	2.0		70	30[f)]	
$FeCl_3$	Neopentyl	3.0		62	38	
$FeCl_2$	Benzyl			n.d.[e)]	38	
$FeCl_2$	Ph			n.d.[e)]	98	
$CoBr_2$	Et	2.8	17.1	78.7	4.2	
$CoBr_2$[d)]	Et	2.7	47.0	49.0	4.0	1.15
$CoBr_2$	Me	2.2		90	10[f)]	
$CoBr_2$[d)]	Me	2.0		70	30[f)]	0.40
$CoBr_2$	Neopentyl	2.0		94	4	
$CoBr_2$	Benzyl			n.d.[e)]	0	
$CoBr_2$	Vinyl	2.0		36	64[g)]	
$CoBr_2$[d)]	Ph			n.d.[e)]	92	0.22
$CoBr_2$	Ph			n.d.[e)]	91	
$NiCl_2$	Et	2.6	36.4	61.2	2.4	
$NiCl_2$	Me	2.1		94	6[f)]	
$NiCl_2$	Neopentyl	2.1		74	26	
$NiCl_2$	Benzyl			n.d.[e)]	27	
$NiCl_2$	Vinyl	1.9		20	80[g)]	
$NiCl_2$	Ph			n.d.[e)]	99	
$PdCl_2$	Et	2.2	48.4	51.6	0	
$PdCl_2$	Me	2.0		49	51[f)]	
$PdCl_2$[d)]	Me	2.1		37	63[f)]	0.23
$PdCl_2$	Neopentyl	2.0		89	11	
$PdCl_2$[d)]	Neopentyl	2.0		55	45	0.12
$PdCl_2$	Benzyl			n.d.[e)]	59	
$PdCl_2$	Vinyl	2.0		12	88	
$PdCl_2$	Ph			n.d.[e)]	93	

a) In 21 *ml* THF containing 1.0 mmol of transition metal halide and excess Grignard reagents (4.0~9.0 mmol) for 60 minutes at 2.0°C. All reactions were complete under these reaction conditions.
b) Based on Q(R), % of R-R was doubled.
c) After acidic hydrolysis
d) In the presence of 26.1 mmol styrene
e) No determination
f) Varying amount of ethylene (less than 30%) was included in R-R.
g) After hydrolysis

same reaction in Et_2O (see below).

On the other hand, the yield of coupling dimer was negligibly small and ethane and ethylene were main products in the reactions of ferrous, cobaltous, nickelous, palladous, manganous and cuprous halides with ethylmagnesium bromide which has β-hydrogens. The ratio of ethane to ethylene obtained was almost 1 : 1 with palladous, cupric and cuprous chlorides. Conversely, this ratio was approximately 2—5 with ferric, ferrous, cobaltous, nickelous and manganous halides.[4)] When excess of styrene was added to the reaction in order to learn about the heterolytic cleavage of alkyl-transition metal bond and to check the material balance of hydrogen, the ratio of ethane : ethylene approached one. Under these conditions styrene was partially reduced to ethylbenzene. Styrene was also partially reduced to ethylbenzene even in the reactions of cobaltous and palladous halides with methyl, neopentyl, and phenylmagnesium bromides which have no β-hydrogens.

Q(R) given by Eq. 2 was independent of the presence of styrene in all cases. Q(Et) was also somewhat higher than n when ferric, cobaltous and nickelous halides were used. The high value of Q(Et) may be related to the abstraction of hydrogen from solvent.[2)]

In those reactions involving argentous, cupric, cuprous and manganous halides, a black precipitate was formed and a colorless supernatant solution appeared after the reaction was completed. On the other hand, ferric, ferrous, cobaltous, nickelous, and palladous halides produced black-brown solutions in addition to varying amounts of black precipitate.[5)]

4) Sneeden and Zeiss have also observed these phenomena. R. P. A. Sneeden and H. H. Zeiss, *J. Organometal. Chem.*, **22**, 713 (1970).

5) H. H. Abraham and H. J. Hogarth *ibid.*, **12**, 1 (1968) and references cited therein; G. Costa, G. Mestroni, and G. Boscarato, *Ric. Sci.*, **7**, 315 (1964).

Table 2. The reactions of manganous, cuprous, cupric, and argentous halides with Grignard reagents in tetrahydrofuran[a)]

Transition Metal Salt MX_n	Grignard Reagents RMBr	Temp. (C°)	Period (min)	Q(R)	Products (%)[b)]		
					R(−H)	RH	R–R
$MnCl_2$	Et	30	60	2.2	28.2	71.8	0
$MnCl_2$[c)]	Et	30	600	2.2	43.6	56.4	0
$MnCl_2$	Me	25	8100[d)]			91	9
$MnCl_2$	Benzyl	60	1440		No	decompd	
$MnCl_2$	Vinyl	25	60[e)]			30	70[f)]
$MnCl_2$	Ph	60	1440		No	decompd	
$CuCl_2$	Et	25	60	2.1	26.1	28.1	45.8[g)]
$CuCl_2$	Et	25	60	1.0	50.9	49.1	0
CuCl	Me	25	900	0.9		7	93
CuCl	Neopentyl	25	5760	1.0		47	53
CuCl	Benzyl	25	30			n.d.[h)]	88[h)]
CuCl	Vinyl	25	180	0.9		19	81
CuCl	Phenyl	60	1440			n.d.[h)]	90
AgBr	Et	25	60	1.0	2.1	6.2	91.7
AgBr	Me	2	30	1.0		4	96
AgBr	Neopentyl	2	60	1.0		17	83
AgBr	Benzyl	2	60			n.d.[h)]	95[h)]
AgBr	Vinyl	2	60	1.0		5	95
AgBr[i)]	Ph	65	120			n.d.[h)]	97[h)]

a) In 21 m*l* THF containing 1.0 mmol of transition metal halide and excess Grignard reagent (3.0—8.0 mmol). All reactions were complete under these reaction conditions unless otherwise mentioned.
b) Based on Q(R). % of R–R was doubled.
c) In the presence of 8.7 mmol styrene, 0.17 mmol of ethylbenzene was obtained after hydrolysis.
d) Partial decomposition; *ca.* 20%
e) Partial decomposition; *ca.* 50%
f) After hydrolysis
g) Included 6% of EtCl in R–R
h) No determination, Calculated from $Q(R)=n$
i) In the presence of 26.1 mmol styrene, none of ethylbenzene was detected after hydrolysis.

The results in Table 1 and Table 2 show that the yield of coupling dimer was generally higher in the presence of styrene, and this effect may be attributed to styrene as a π-ligand. In order to support this point, the reactions of palladous chloride and Grignard reagents were carried out in the presence of triphenylphosphine, since the bis-triphenylphosphine complex with palladous chloride is readily formed.[6)] Table 3 shows that the yield of coupling dimer was indeed increased in the presence of triphenylphosphine.

Q(R) was not altered by the presence of triphenylphosphine.

The Reactions of Lithium Chlorocuprate and Grignard Reagents in Tetrahydrofuran. The reaction of cupric chloride and Grignard reagent is obscure because the reaction is occurring mainly on the surface (Table 2).

Table 3. The reactions of palladous chloride with alkyl Grignard reagents in tetrahydrofuran in the presence of triphenylphosphine[a)]

Grignard Reagent RMgBr	RMgBr / $PdCl_2$	Ph_3P (mmol)	Q(R)	Products (mol %)[b)]		
				R(−H)	RH	R–R
Et	7.5		2.2	48.4	51.6	0
Et	7.0	4.0	2.0	31.0	47.6	21.4
n-Pr	7.0		2.2	45.1	51.9	3.0
n-Pr	7.0	4.0	2.1	31.0	43.0	26.0
i-Pr	7.0		2.2	47.0	47.4	5.6
i-Pr	7.0	4.0	2.1	33.9	39.3	26.8
t-Bu	6.0		2.1	48.6	48.9	2.5
t-Bu	6.0	4.0	2.1	40.7	46.0	13.3

a) In 21 m*l* THF containing 1.0 mmol $PdCl_2$ at 2.0°C for 60 min. The reaction of $PdCl_2$ with Ph_3P was carried out in THF at room temperature for 2 hrs (yellow precipitate was formed) before Grignard reagent was added.
b) Based on Q(R)

Table 4. The reactions of lithium chlorocuprate with Grignard reagents in tetrahydrofuran[a)]

Grignard Reagent RMgBr	RMgBr[b)] / Cu(II)	Temp. (°C)	Distribution of Products[c)]	
			R-R(%)	R-Cl(%)
Et	0.6	2	50.6	49.4
Et	1.2	2	53.9	46.1
Et	2.5	2	73.7	26.3
Et	1.2	−78	75.7	24.3
Et	1.2	25	61.5	38.5
Me	1.2	2	81.3	18.7
Neopentyl	1.2	2	19.0	81.0
Ph	1.2	2	45.3	54.7

a) In 21 m*l* THF containing 2.5 mmol $CuCl_2$ and 5.8 mmol LiCl for 20 minutes.
b) Molar ratio
c) $\frac{\text{R–R or R–Cl}}{\text{R–R+R–Cl}} \times 100$. Total yield of R–R and R–Cl was more than 80% based on RMgBr or Cu(II) in all runs. R–R and R–Cl did not form from Cu(I) in the case of ethylmagnesium bromide (Table 2).

6) F. G. Mann and A. F. Wells, *J. Chem. Soc.*, **1938**, 702; J. Chatt and L. M. Venanzi, *ibid.*, **1957**, 2351.

Cupric chloride became soluble by the formation of lithium chlorocuprate[7] (λ max. 444 mμ, ε: *ca.* 10^3) when two or more equivalent lithium chloride was mixed in THF. The reactions of lithium chlorocuprate with Grignard reagents were examined in THF in order to find the differences in the mechanisms of the formations of coupling dimer and alkyl chloride in the reaction of cupric chloride and Grignard reagent. It is obvious from Table 4 that the yield of ethyl chloride was larger at the smaller ratio of ethylmagnesium bromide to lithium chlorocuprate. Temperature also influenced the distribution of products.

Ethane was major product in the reaction with methylmagnesium bromide and neopentyl chloride was favorably formed from neopentylmagnesium bromide.

Evolutions of *n*-butane and ethyl chloride were completed immediately and the resulting solution turned to purple gradually in the case of ethylmagnesium bromide (molar ratio: 2.5). At this stage, none of ethane or ethylene was evolved.

Both total yield and distribution were not altered by the presence of excess styrene.

A following competitive mechanism may be applicable to the explanation of these results.

$$\underset{\text{(I)}}{[Cu^{II}Cl_4]^{-2}} + RMgBr \longrightarrow \underset{\text{(II)}}{[RCuCl_3]^{-2}} + MgBrCl \quad (4)$$

$$\text{(II)} \xrightarrow{\text{(I)}} R\text{-}Cl + 2[Cu^{I}Cl_2]^{-} + 2Cl^{-}$$
$$\text{(II)} \xrightarrow{\text{(II)}} R\text{-}R + 2[Cu^{I}Cl_2]^{-} + 2Cl^{-} \quad (5)$$

A predominant yield of *n*-butane in the reaction of cupric chloride and excess ethylmagnesium bromide (Table 2) can also be explained by this mechanism.

The Reactions of Transition Metal Halides with a Mixture of Two Grignard Reagents in Tetrahydrofuran. The reactions of transition metal halides with a mixture of Grignard reagents in THF were also examined in order to learn about the mechanism of the disproportionation of alkyl transition metal complex which is assumed to be formed in the Kharasch reaction. The results are summarized in Table 5. In the combination con-

TABLE 5. THE REACTIONS OF TRANSITION METAL SALTS WITH A MIXTURE OF TWO GRIGNARD REAGENTS IN TETRAHYDROFURAN[a)]

Transition Metal Salt MX_n	Combination of Grignard Reagent[b)]	RMgBr+R'MgBr/MX_n	Period (min)	Q(R,R')[c)]	Products (mol %)[d)]							R(-H)/RH	R'(-H)/R'H
					R-R	R-R'	R'-R'	R(-H)	RH	R'(-H)	R'H		
$CoBr_2$	A	3.6	30	2.8	0	0	0		47.0	31.2	21.8		1.4
$CoBr_2$[e)]	A	3.6	30	2.7	0	0	0		41.1	43.8	15.1		2.9
$PdCl_2$	A	3.6	30	2.0	19.3	0	0		32.7	29.6	18.4		1.6
$PdCl_2$[f)]	A	3.6	30	1.9	27.8	0	0		26.8	30.4	15.0		2.0
CuCl[g)]	A	1.4	1200	1.0	4.0	34.7	0		26.0	22.7	12.6		1.8
$CuBr_2$[g)]	A	3.6	720	2.2	4.4	26.3	30.0		9.2	20.6	10.5		2.0
AgBr	A	3.6	30	1.0	23.5	30.2	40.4		1.7	0.8	3.4		0.3
$FeCl_3$	B	5.3	30	3.3	3.3	4.9	3.2	0.4	37.6	39.7	11.8	0.0	3.4
$CoBr_2$	B	2.3	30	2.0	0	0	0	0.0	48.0	15.3	36.7	0.0	0.4
$CoBr_2$[h)]	B	2.3	30	2.2	5.9	2.4	1.2	16.2	22.3	33.5	18.5	0.7	1.8
$NiCl_2$	B	2.3	30	2.0	0	0	0	0.0	41.0	34.9	24.1	0.0	1.4
$PdCl_2$	B	2.3	30	2.1	0	0	0	22.3	25.7	24.1	27.9	0.9	0.9
CuCl	B	0.8	60	0.8	0	0	0	20.6	30.3	31.2	17.9	0.7	1.7
$CuBr_2$	B	4.0	120	2.0	15.6	23.4	12.3	11.5	15.6	14.6	7.1	0.7	2.0
AgBr	B	3.1	60	1.0	46.5	33.7	11.6	1.2	3.5	1.2	2.3	0.3	0.5
$FeCl_3$	C	5.3	30	3.4	2.3	2.8	3.2	2.4	39.7	32.8	16.8	0.1	2.0
$CoBr_2$[i)]	C	2.3	30	2.3	8.2	0	0	15.6	23.3	33.8	19.1	0.7	1.8
$PdCl_2$	C	2.3	30	2.0	0	0	0	14.7	39.4	33.2	12.7	0.4	2.6
CuCl	C	1.1	60	1.0	0	0	0	32.7	14.8	18.3	34.2	2.2	0.5
$CuBr_2$	C	4.0	85	2.0	3.9	7.9	19.8	17.8	7.3	18.2	25.1	2.5	0.7
AgBr	C	3.1	60	1.0	40.5	28.1	10.1	1.7	2.2	7.3	10.1	0.7	0.7

a) In 21 m*l* THF containing 1.0 mmol transition metal salt and an equimolar mixture of two Grignard reagents at 2.0°C.

b) A; RMgBr=MeMgBr, R'MgBr=*n*-PrMgBr
B; RMgBr=EtMgBr, R'MgBr=*n*-PrMgBr
C; RMgBr=EtMgBr, R'MgBr=*i*-PrMgBr

c) $\dfrac{2(R\text{-}R+R\text{-}R'+R'\text{-}R')+R(\text{-}H)+RH+R'(\text{-}H)+R'H}{MX_n}$

d) Based on Q(R,R')

e) In the presence of 8.7 mmol styrene, the yield of ethylbenzene was 1.07 mmol after hydrolysis

f) In the presence of 8.7 mmol styrene, the yield of ethylbenzene was 0.38 mmol after hydrolysis

g) 25°C

h) In the presence of 8.7 mmol styrene, the yield of ethylbenzene was 1.10 mmol after hydrolysis.

i) In the presence of 8.7 mmol styene, the yield of ethylbenzene was 1.14 mmol after hydrolysis.

7) R. P. Eswain, E. S. Howald, R. A. Howald, and D. P. Keeton, *J. Inorg. Nucl. Chem.*, **29**, 437 (1967).

sisting of methyl and *n*-propylmagnesium bromides, disproportionation afforded methane from the methyl moiety and propylene from the *n*-propyl group. The selectivity was more pronounced when styrene was added to the reaction consisting of cobaltous or palladous halide. Styrene was partially reduced to ethylbenzene. The formation of cross coupling dimer (*n*-butane) was facilitated by cuprous chloride. On the other hand, more random coupling occurred with ferric, argentous, and cupric halides.

In the combinations involving ethyl/*n*-propyl and ethyl/isopropyl, ethane was formed mainly from the ethyl group and propylene mainly from the propyl group. Furthermore, in these combinations, the trend became more conspicuous when styrene was added to the reaction. In the reaction of palladous chloride with a mixture of ethylmagnesium bromide and *n*-propyl or isopropylmagnesium bromide, the yield of alkene (ethylene and propylene) and the yield of alkane (ethane and propane) were approximately equal. The further hydrogenation of the initially formed olefin was not significant. In fact, the amount of ethylbenzene was much smaller from the reactions carried out with palladous chloride compared to cobaltous bromide (Table 5).

In the combination of ethyl/*n*-propylmagnesium bromide, the ratio of ethylene: ethane was 0.9 and the ratio of propylene: propane was also 0.9. On the other hand, in the combination of ethyl/isopropylmagnesium bromide, the ratio of ethylene: ethane was 0.4, whereas the ratio of propylene: propane was 2.6. That is, the tendency for alkane to be formed mainly from the ethyl group and alkene from the propyl group was more conspicuous in the latter combination. With cuprous or cupric halide, ethane was formed mainly from the ethyl group and propylene from *n*-propyl group: Conversely, propane was formed mainly from the isopropyl group and ethylene from the ethyl group. This observation has been discussed previously.[2)]

The Reactions of Transition Metal Halides with Grignard Reagents in Diethyl Ether. All the reactions discussed above were carried out in THF. In most studies examined heretofore, Et_2O has usually been the medium of choice. For comparison, a number of the same reactions were carried out in Et_2O, especially in the presence of styrene. As seen in Table 6, the yield of ethylene was much higher in the presence of styrene than that in the absence of styrene with all transition metal halides except argentous and cupric bromides. At the same time, styrene was reduced to ethylbenzene in high yield, especially with ferric, ferrous, cobaltous, and nickelous halides. In the reaction of methylmagnesium bromide with nickelous chloride, the amount of ethylbenzene was also small. In the reactions of cupric chloride with methyl and ethylmagnesium bromides, methyl and ethyl chlorides, respectively, were formed in fairly good yields.[2,8)] The higher yield of ethyl chloride and the formations of ethane and ethylene from copper(II) complex (based on Q(Et)) were sharp contrast with the results in THF (Table 2). The ratio of ethane to ethylene was closer to one in Et_2O than in THF (Table 1) with most of transition metal halides, in the reaction with ethylmagnesium bromide, in the absence of styrene. The

Table 6. The reactions of transition metal salts with ethylmagnesium bromide in diethyl ether in the presence of styrene[a)]

Transition Metal Salt MX_n	Styrene (mmol)	Period (min)	Q(Et)	Products(mol%)[d)]			PhEt[f)] (mmol)
				R(−H)	RH	R–R	
$FeCl_3$		10	3.5	40.4	45.3	14.3	
$FeCl_3$	26.1	60	3.9	62.6	26.0	11.4	1.88[g)]
$FeCl_2$		120	2.0	41.4	51.1	7.5	
$FeCl_2$	26.1	120	4.2	78.0	18.6	3.4	2.53
$CoBr_2$		10	2.2	34.1	65.0	0.9	
$CoBr_2$	26.1	30	3.4	56.4	34.9	8.7	1.49
$NiCl_2$		120	2.3	47.6	52.4	0	
$NiCl_2$	26.1	180	5.2	75.6	22.9	1.5	3.02
$NiCl_2$[b)]	26.1	90	1.9		57.3	42.7[e)]	0.18
$PdCl_2$		30	2.2	49.8	50.2	0	
$PdCl_2$	26.1	30	1.9	53.0	47.0	0	0.17
$MnCl_2$		140	1.9	40.1	59.9	0	
$MnCl_2$	26.1	120	2.0	49.3	50.7	0	0.26
CuCl		180	1.0	52.1	47.9	0	
$CuCl_2$		120	2.1[h)]	40.8	37.8	5.8	
$CuCl_2$	26.1	180	2.0[i)]	42.1	35.8	5.3	0.07
$CuCl_2$[b,c)]		1000	2.0[j)]		9.2	73.8	
AgBr		30	1.0	0.7	1.0	98.3	

a) In 21 m*l* of Et_2O solution containing sytrene, 1.0 mmol of transition metal salt and 5.7 mmol of EtMgBr at 2.0°C b) Methylmagnesium bromide c) 25°C d) Based on Q(Et). e) C_2H_4; 36.6% in R–R f) After hydrolysis g) PhEt was 1.05 mmole before hydrolysis. h) Ethyl chloride was 15.6% based on Q(Et). i) Ethyl chloride was 16.8% based on Q(Et) j) Methyl chloride was 17.0% based on Q(Me).

8) H. Gilman and J. M. Straley, *Rec. Trav. Chim. Pays-Bas*, **55**, 821 (1936).

TABLE 7. THE EXCHANGE BETWEEN ETHYLMAGNESIUM BROMIDE AND STYRENE BY FERRIC CHLORIDE[a)]

$FeCl_3$ conc. $\times 10^4$ M	Solvent	Temp. (°C)	Period (min)	C_2H_4 (mmol)	C_2H_6 (mmol)	PhEt (mmol) Before hydrolysis	PhEt (mmol) After hydrolysis
24	Et_2O	2.0	90	0.55	0.01	0.18	0.57
12	Et_2O	2.0	90	0.57	0.01	0.17	0.60[f)]
2.4	Et_2O	2.0	90	0.51	0.01	n.d.[e)]	0.50
2.4	Et_2O[c)]	2.0	90	0.40	0.01	n.d.	0.42
2.4	Et_2O	25	90	0.06	0.00	n.d.	0.06
2.4	Et_2O[d)]	2.0	480			0.04	0.04
2.4[b)]	Et_2O	2.0	90	0.34	0.01	0.10	0.37
2.4	THF	2.0	100	0.05	0.00	n.d.	0.03
2.4	THF	25	60	0.61	0.06	n.d.	0.59

a) In 21 m*l* solvent containing 1.24M styrene and 0.18M EtMgBr
b) $CoBr_2$ instead of $FeCl_3$ c) 0.09M EtMgBr
d) Methylmagnesium bromide e) No determination
f) Composition of ethylbenzene after deuterolysis with D_2O (NMR analysis) $PhCHCH_3$ (71%), $PhCH_2CH_2D$ (5%), $PhCH_2CH_3$ (24%)

rates of decompositions of diethylmanganese and ethylcopper were approximately 6 times faster in Et_2O than in THF.[2)] These solvent dependencies will be discussed later in this paper.

The mixture on completion of reaction was usually a seemingly black-brown solution[5)] (at least partially) except when argentous, cuprous, cupric, and manganous halides were used. The latter gave colorless solutions and black precipitates. These observations were similar to those obtained in THF.

The rate of conversion of ethylmagnesium bromide with nickelous and ferrous chlorides to ethylene and ethane is shown in Fig. 1, which shows that the yield of ethane rapidly reached a plateau, but the yield of ethylene continued to increase with time, in the presence of styrene. The yield of ethylene shown in Fig. 1 and Table 6 was greater than the stoichiometric amount based on Q(Et) and indicated that part of the ethylene was produced from the exchange between ethylmagnesium bromide and styrene (see below). In order to confirm this point, the exchange between ethylmagnesium bromide and styrene was studied in the presence of catalytic amounts of ferric and cobaltous halides. It can be seen in Table 7 that equivalent amounts of ethylene and ethylbenzene were obtained at 2.0°C in Et_2O. The amount of ethane was negligibly small in both cases. At 25°C, the yields of ethylene and ethylbenzene were quite small. Furthermore, the yields of ethylene and ethylbenzene were negligibly small in THF at 2.0°C, but at 25°C they were almost the same as those formed in Et_2O at 2.0°C. Thus, the effect of temperature on the exchange reaction was highly dependent on the solvent. In the case of methylmagnesium bromide, the amount of ethylbenzene was quite small even in Et_2O at 2.0°C.

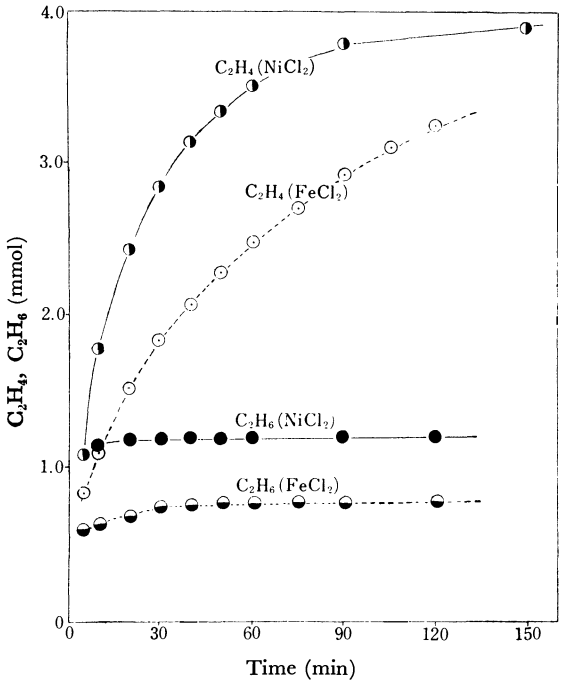

Fig. 1. The rate of formation of ethylene in the reaction of ferrous chloride (0.8 mmol) or nickelous chloride (1.0 mmol) with EtMgBr (5.7 mmol) in Et_2O (18 m*l*) in the presence of 26.1 mmol styrene at 2.0°C
◑ ethylene ($NiCl_2$) ● ethane ($NiCl_2$)
⊙ ethylene ($FeCl_2$) ◓ ethane ($FeCl_2$)

TABLE 8. THE IRON-CATALYZED EXCHANGE BETWEEN GRIGNARD REAGENT AND OLEFIN[a)]

Grignard Reagent RMgBr	Olefin R'(-H)	Solvent	Temp. (°C)	Products (mmol) R(-H)	Products (mmol) R'H after hydrolysis
Et	C_3H_6	THF	25	0.03	0.03
Et	C_3H_6	Et_2O	2.0	<0.01	<0.01
n-Pr	C_2H_4	THF	25	0.68	0.70
n-Pr	C_2H_4	Et_2O	2.0	0.45	0.45
i-Pr	C_2H_4	THF	25	1.20	1.33
i-Pr	C_2H_4	Et_2O	2.0	0.31	0.33
t-Bu	C_2H_4	THF	25	0.15	0.16

a) In 21 m*l* solution containing 3.0 mmol Grignard reagent, 2.0 mmol olefin and 0.025 mmol ferric chloride for 60 min. No appreciable amounts of R'H was detected before hydrolysis in all runs.

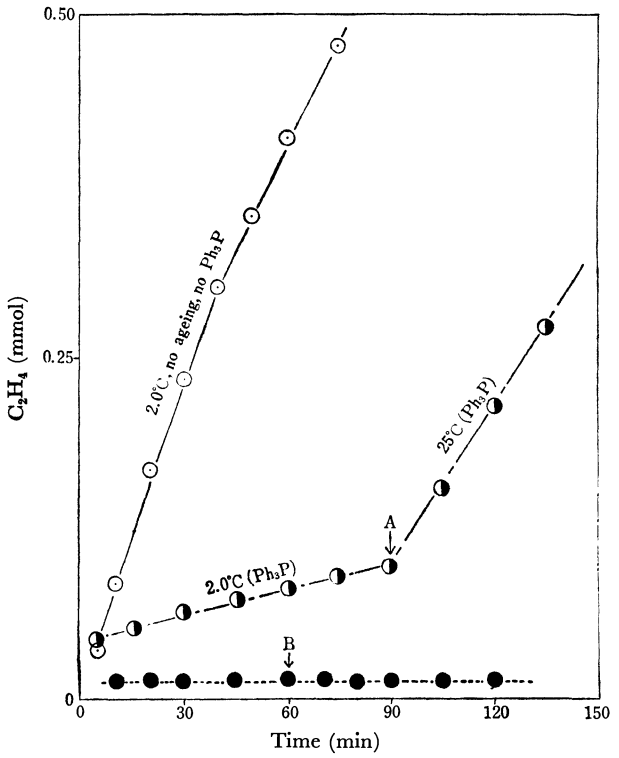

Fig. 2. The iron-catalyzed exchange between EtMgBr and styrene in Et_2O (Et_2O+styrene 21 ml, 0.18M EtMgBr, 1.24M styrene, 2.4×10^{-4}M $FeCl_3$) at 2.0°C.
⊙ 2.0°C, no Ph_3P, no ageing, ◑ In the presence of Ph_3P (0.18M), A; Warmed up to 25°C at this point, ● 2.0°C, no Ph_3P, B; Styrene was added at this point (ageing).

Ethylene and propylene were also used in the iron-catalyzed exchange with various Grignard reagents in THF at 25°C and in Et_2O at 2.0°C. The results are summarized in Table 8 which shows that olefins were formed in high yields from *n*-propyl, isopropyl, and *t*-butylmagnesium bromides in THF at 25°C and in Et_2O at 2.0°C when ethylene was present in the reaction. The amount of ethane after acidic hydrolysis was exactly equal to the yield of olefin derived from the Grignard reagent. On the other hand, the yields of ethylene and propane from ethylmagnesium bromide and propylene were low in Et_2O at 2.0°C and in THF at 25°C. Exchange between Grignard reagent and olefin is, thus, dependent on the particular combination chosen. Additional experiments were performed in order to probe the mechanism of this reaction. The rate of formation of ethylene from the iron-catalyzed exchange of ethylmagnesium bromide and styrene is shown in Fig. 2. No ethylene was formed if styrene was added to an aged catalyst solution, that is 60 minutes after ethylmagnesium bromide and ferric chloride were mixed. The rate of formation of ethylene in the presence of a large excess of triphenylphosphine was also very slow at 2.0°C, but was accelerated when the temperature was raised to 25°C. The effect observed with triphenylphosphine is consistent with those obtained by variation of the temperature and the solvent (Table 7). Finally, the composition of ethylbenzene formed after deuterolysis was shown by NMR analysis (Table 7), to consist of the following:

$PhCHCH_3$	$PhCH_2CH_2D$	$PhCH_2CH_3$
D	5%	24%
71%		

The deuterium content in the ethylbenzene was much smaller at high concentrations of catalyst (Table 6) than at low concentrations (Table 7).

Discussion

I The Distribution of Products from the Reactions of Transition Metal Halides with Grignard Reagents

The Formation of Coupling Dimer. The yield of coupling dimer is strongly dependent on the transition metal halide and the Grignard reagent. The coupling dimer is formed quantitatively from argentous bromide almost independently of the structure of the alkyl of the Grignard reagent except for secondary and tertiary alkyl Grignard reagents.[2] We have proposed a bimolecular mechanism for the silver-catalyzed coupling of a Grignard reagent and an alkyl bromide in order to explain the effects of catalyst concentration, the reaction temperature and the presence of styrene on the yield and stereochemistry of coupling.[2]

$$RAg + R'Ag \longrightarrow R\text{-}R'(R\text{-}R,\ R'\text{-}R') + 2Ag^{\circ} \quad (6)$$

Methyl and ethyl chlorides are formed together with coupling dimers from the reactions of cupric chloride with methyl and ethylmagnesium bromides in Et_2O and that of lithium chlorocuprate with these Grignard reagents in THF. The yield of alkyl chlorides are dependent on the solvent and the molar ratio of Grignard reagent to lithium chlorocuprate and the reaction may also proceed by a bimolecular mechanism expressed by Eq. 5.

Radical mechanism can be neglected for coupling since large excess of styrene does not influence $Q(R)$. Whitesides have also emphasized this point for the decompositions of alkenylcopper and alkenylsilver complexes.[9]

The reaction of ethylmagnesium bromide and ferrous, cobaltous, nickelous, palladous or cuprous halide produces little or no coupling dimer. The coupling dimer is formed, however, in fairly good yields when the Grignard reagent is methyl, neopentyl, phenyl, vinyl, and benzylmagnesium bromides which have no available β-hydrogens.

The yield of coupling dimer is also dependent on the structure of the alkyl group because for a given transition metal salt, the yield of coupling dimer increases generally in the sequence: methyl>neopentyl, benzyl, and ethane and neopentyl chloride are preferably formed in the reactions of lithium chlorocuprate with the corresponding Grignard reagents.

The yield of coupling dimer is enhanced by styrene and triphenylphosphine (Table 3) and it is generally higher in THF than in Et_2O. The salutary effect of these compounds on the yield of coupling dimer may be attributed to the stabilization of the transition metal-carbon bond[10] and or occupation of the coordination

9) G. M. Whitesides and C. P. Casey *J. Amer. Chem. Soc.*, **88**, 4541 (1966).
10) J. Chatt and B. L. Shaw, *J. Chem. Soc.*, **1959**, 4020.

sites necessary for elimination or disproportionation. A similar effect may be applicable to vinyl and phenylmagnesium bromides.[11]

As a conclusion the coupling reaction is thought to proceed by a following bimolecular mechanism.

$$RMX_{n-x} + RMX_{n-x} \longrightarrow R\text{-}R + 2MY_{n-x} \quad (7)$$

Thus the stability of transition metal-carbon bond (transition metal, solvent, ligand as well as reaction temperature), the availability of β-hydrogen and bulkiness of alkyl group are effective factors for coupling. The higher yield of coupling dimer with a higher oxidation state of a given metal may be due to the formation of stable MY_{n-x} salt (Cu and Fe). This mechanism is also supported by the facts that the order of the yield of coupling dimer is primary>secondary> tertiary for argentous bromide and three coupling dimers are formed in the reaction of cupric, argentous or ferric halide with a mixture of two Grignard reagents (Table 5).

The Disproportionation. The disproportionation to afford alkene and alkane is also strongly dependent on the transition metal, the availability of β-hydrogens and the presence of styrene. Styrene is reduced to ethylbenzene except when the reactions are carried out with argentous and cuprous halides. For example, the ratio of ethylene to ethane is 1.0 in the presence of styrene when cobaltous bromide reacts with ethylmagnesium bromide in THF. This ratio is approximately 0.2 in the absence of styrene (Table I). The yield of ethylbenzene is also high when Grignard reagents which have β-hydrogens reacts with cobaltous bromide but it is low from methyl, neopentyl and phenylmagnesium bromide. We deduce from the value of Q(Et) and the ratio of ethylene to ethane (Table 1 and Table 7) that the exchange between ethylmagnesium bromide and styrene can be neglected under these reaction conditions. Thus, *both* hydrogens in ethylbenzene could not have been derived only from the ethyl moiety. Furthermore, the formation of ethylbenzene from methyl, neopentyl, and phenyl Grignard reagents indicates that the hydrogen was derived partially from the solvent.[2] Since the yield of ethylbenzene is much higher with those Grignard reagents possessing β-hydrogens, at least *one* of the hydrogens in ethylbenzene is derived from an alkyl group present in an intermediate.

In the reaction of transition metal halides with a mixture of two Grignard reagents, the trend is for the alkane to be formed mainly from one alkyl group and the alkene to be derived from the other alkyl group (Table 5). This selectivity is more conspicuous when one alkyl group has no β-hydrogen. In all of our experiments, Q(R) is not changed by the presence of styrene and indicates that alkyl radicals does not complicate the interpretation of the mechanism.[2]

Two mechanisms are plausible for the formation of alkane and alkene in the reaction of transition metal halides with Grignard reagents:

A. "Hydride Mechanism"[12]

$$RCH_2CH_2M \longrightarrow RCH{=}CH_2 + HM \quad (8)$$

$$RCH_2CH_2M + HM \longrightarrow RCH_2CH_3 + 2M \quad (9)$$

B. "Direct Hydride Migration (or Bimolecular) Mechanism"

$$RCH_2CH_2M + RCH_2CH_2M \longrightarrow RCH{=}CH_2 + RCH_2CH_3 + 2M \quad (10)$$

These two mechanisms have been discussed in the light of the decompositions of alkylcopper and alkylmanganese species.[2]

We infer that hydride mechanism is generally more common for Mn, Fe, Co, Ni, and Pd. On the other hand, bimolecular mechanism is more plausible for Cu(I) and Ag (especially for secondary and tertiary alkyls). The former groups possess great hydrogenation activity and the latter groups do not have it for olefins under the comparative condition. However, even in the former groups, participation of bimolecular interaction between alkyl metals for decomposition should also be considered in the case of special alkyl groups. The formation of cross coupling dimer in the reaction of cuprous chloride with a mixture of methyl and *n*-propylmagnesium bromides, the higher stability of neopentylcopper than methylcopper (bulkiness) and the adverse relationship between *n*-propyl and isopropylcoppers[13] (Table 5) may support this mechanism.

Thus bimolecular interaction between alkyl metals is very important for both coupling and disproportionation. Direct hydride mignation may not be easily occurred when THF is used as a solvent because THF has a great coordination affinity for metal[14] (occupation of coordination site). This effect of THF may be similar to that of triphenylphosphine. In fact, THF as a solvent and the addition of triphenylphosphine render the high yield of coupling dimer. The ratio of alkane: alkene also becomes greater than one in these cases. Dehydrogenation of coordinated ligand is known in analogous situation.[15] Organocopper clusters in ethereal solvent has been reported recently.[16] We have also observed the interaction between two copper nuclei during the decomposition of alkylcopper species.[2] Moreover, degradation of catalytic activity by aging in the Kharasch reaction is more pronounced in Et_2O than in THF. The ratio of alkane to alkene is greatly dependent on the catalyst concentration in the iron-catalyzed Kharasch reaction.[2] Metal-metal interaction (formation of aggregates), therefore, must be considered in these reactions.

II The Exchange between Grignard Reagent and Olefin by Iron Catalyst

Exchange reactions between Grignard reagents and

11) M. Tsutsui, *The New York Acad. Sci.*, **1961** 135.

12) G. M. Whitesides, E. R. Stedronsky, C. P. Casey, and J. San Fillipo Jr., *J. Amer. Chem. Soc.*, **92**, 1426, (1970).

13) The α,β-elimination of metal hydrides from various main group and transition metal alkyls generally follow the trend tertiary>secondary$\gg$primary [G. E. Coates, M. L. H. Green, and K. Wade, "Organometallic compounds," Vol. I, Methuen and Co., Ltd., London (1967), p. 298], H. H. Zeiss (private communication).

14) E. C. Ashby, *Quart. Revs.*, **21**, 259 (1967); F. W. Walker and E. C. Ashby, *J. Amer. Chem. Soc.*, **91**, 3845 (1969).

15) W. H. Knoth and R. A. Schumn, *ibid.*, **91**, 2400 (1969) and references cited therein.

16) A. Cairncross and W. A. Sheppard, *ibid.*, **93**, 247 (1971).

olefins catalyzed by transition metals including titanium,[17] nickel and cobalt[18] salts have been reported. The mechanism of this reaction has remained unclear, but transition metal hydrides have been postulated as catalysts.

$$\mathrm{RCH{=}CH_2 + R'CH_2CH_2MgBr \xrightarrow{\text{catalyst}} R'CH{=}CH_2 + \underset{\mid \atop MgBr}{RCHCH_3} + RCH_2CH_2MgBr} \quad (11)$$

Table 7 and 8 show that the exchange between Grignard reagent and olefin is induced by catalytic amounts of ferric chloride. Thus, the amount of olefin produced from the Grignard reagent is equal to the alkane formed from the olefin. The combination of *n*-propyl or isopropylmagnesium bromide and ethylene affords propylene and ethylmagnesium bromide. On the other hand, the combination of ethylmagnesium bromide and propylene produces no significant exchange (Table 8).

$$\mathrm{CH_3CH_2CH_2MgBr + CH_2{=}CH_2 \overset{\text{Fe catalyst}}{\rightleftarrows} CH_3CH{=}CH_2 + CH_3CH_2MgBr} \quad (12)$$

As shown in Fig. 2 and Table 7, no appreciable exchange is detected when styrene is added after the catalyst is aged for 60 minutes at 2.0°C in Et_2O. The catalytic activity is also poor at 25°C even without ageing or at 2.0°C in the presence of excess triphenylphosphine. The effects of ageing and temperature have also been observed in the exchange between Grignard reagent and olefin by nickelous chloride.[18]

We postulate that an iron hydride, *e.g.*, HFe,[19] is the catalytically active species in the exchange reaction, and the following mechanism is proposed:

$$\mathrm{FeCl_3 + RCH_2CH_2MgBr \xrightarrow{\text{solvent}} RCH{=}CH_2 + RCH_2CH_3 + HFe + MgBrCl} \quad (13)^{20)}$$

$$\mathrm{HFe + R'CH{=}CH_2 \rightleftarrows \underset{\mid \atop Fe}{R'CHCH_3} \rightleftarrows R'CH_2CH_2Fe} \quad (14)$$

$$\mathrm{\underset{\mid \atop Fe}{R'CHCH_3} + RCH_2CH_2MgBr \rightleftarrows \underset{\mid \atop MgBr}{R'CHCH_3} + RCH_2CH_2Fe} \quad (15)$$

We relate the effect of ageing the catalyst and the temperature dependence of the exchange to the deactivation of the catalytic species, *e.g.*

$$\mathrm{2HFe \longrightarrow H_2 + Fe_2} \quad (16)$$

The adverse effect of triphenylphosphine and the temperature requirements for exchange in Et_2O and in THF can be related to coordination of the active metal species by these ligands in competition with the olefin. The addition of metal hydride to alkenes has been observed in a variety of situations.[21] The decomposition of alkylmanganese to alkenes has been shown to proceed *via* a facile α,β-elimination of a hydridomanganese species.[2] The latter process, however, is not readily reversible under these reaction conditions. In order to obtain catalytic activity in the exchange of alkylmagnesium halides and alkenes, both addition as well as elimination must be facile. Iron, cobalt, and nickel species apparently fulfill both requirements.

Experimental

Materials. Triply sublimed magnesium was supplied from Dow Chemical Co., (analysis; Cu, $<$0.001; Fe, $<$0.003; Mn, $<$0.001; Ni, $<$0.0005; Pb, $<$0.003; Co, $<$0.005; Cr $<$0.005; Ag, $<$0.001; Rh, $<$0.005; Pd, $<$0.001; Mo, $<$ 0.005; Ti, $<$0.005%). Anhydrous nickelous chloride was prepared from the reaction of its hexahydrate and thionyl chloride.[22] Anhydrous ferrous chloride was prepared from metallic iron and anhydrous ferric chloride in THF.[23] Commercial anhydrous manganous chloride was dried *in vacuo* at 130°C for 50 hrs. Anhydrous cobaltous bromide, palladous chloride, ferric chloride, cupric chloride, cuprous chloride, argentous bromide, and lithium chloride were commercial grade substances and used without further purification. Styrene and all organic halides were purified by distillation before use. Triphenylphosphine was commercial grade and used without further purification. Neopentyl bromide was prepared from neopentyl alcohol and tri-*n*-butylphosphine dibromide.[24]

Solvents. THF was refluxed over lithium aluninum hydride under nitrogen over 2 days, fractionated under a nitrogen atmosphere and stored under helium. Et_2O was refluxed over metallic sodium under nitrogen for 24 hrs, distilled under a nitrogen atmosphere and stored over metallic sodium under helium.

Preparation of Grignard Reagent. All Grignard reagents were prepared using excess of magnesium metal (1.5~2.0 times excess of the theoretical amount) in order to minimize the amount of unreacted organic halide. Reaction temperature was varied from 5 to 35°C according to the reactivity of organic halide. All solutions of Grignard reagent were filtered under a nitrogen atmosphere and were almost colorless. The exception, vinylmagnesium bromide, had a red brown color. The concentrations of all Grignard reagents were determined by titration and by quantitative analysis of the hydrocarbon produced on acidic hydrolysis (0.5—1.8 M).

Product Analysis. All products were analyzed by gas chromatography using the internal standard method.

17) G. D. Cooper and H. I. Finkbeiner, *J. Org. Chem.*, **27**, 1439, 3395 (1962).

18) F. Ungváry, B. Babos, and L. Marko, *J. Organometal. Chem.*, **8**, 329 (1967); L. Farady, L. Bencze and L. Marko *ibid.*, **10**, 505 (1967), **17**, 107 (1969).

19) Coordination by ligand around iron is assumed, but not specifically included. The oxidation state of iron may be monovalent despite of the lack of clear evidence.

20) Equation not balanced. Part of hydrogen no doubt comes from the solvent (Table 1).

21) H. C. Brown, "Hydroboration," W. A. Benjamin, Inc., New York (1962); K. Ziegler, *Angew. Chem.*, **64**, 323 (1952); J. Chatt and B. L. Shaw, *J. Chem. Soc.*, **1962**, 5075; R. Cramer, *J. Amer. Chem. Soc.*, **86**, 217 (1964), **87**, 4717 (1965), **88**, 2272 (1966); R. Cramer and R. V. Lindsey. Jr., *ibid.*, **88**, 3534 (1966).

22) G. Brauer, "Handbuch der Präparative Anorganischen Chemie," Ferdinard Enke Verlag, Stuttgart (1954) p. 1154.

23) G. Wilkinson, "Organic Synthesis," Coll. Vol. IV, p. 473, (1963).

24) G. A. Wiley, R. L. Hershkowitz, B. M. Rein, and B. C. Chung, *J. Amer. Chem. Soc.*, **86**, 964 (1964).

Compound	Column	Temperature °C	Internal Standard
Methane	2F′-PorapakQ	Room Temp.	Ethylene or Ethane
Ethylene	2F′-PorapakQ	Room Temp.	Methane
Ethane	2F′-PorapakQ	Room Temp.	Methane
Propylene	15F′-Dowtherm	Room Temp.	Isobutane
Propane	15F′-Dowtherm	Room Temp.	Isobutane
Isobutane	15F′-Dowtherm	Room Temp.	*n*-Butane
Isobutylene	15F′-Dowtherm	Room Temp.	*n*-Butane
n-Butane	15F′-Dowtherm	Room Temp.	Isobutane
Neopentane	15F′-Dowtherm	Room Temp.	Isobutane
Butadiene	15F′-Dowtherm	Room Temp.	*n*-Butane
Isopentane	15F′-FFAP	65	*n*-Heptane
n-Pentane	15F′-FFAP	65	*n*-Heptane
n-Hexane	15F′-FFAP	65	*n*-Heptane
1-Hexene	15F′-FFAP	65	*n*-Heptane
1,5-Hexadiene	15F′-FFAP	65	*n*-Octane
2,2,3,3-Tetramethylbutane	15F′-FFAP	65	*n*-Octane
2,3,5,5-Tetramethylhexane	15F′-FFAP	100	*n*-Decane
2,3-Dimethylbutane	15F′-SF96	90	*n*-Hexane
Benzene	15F′-FFAP	120	Toluene
Toluene	15F′-FFAP	120	Benzene
Ethylbenzene	15F′-FFAP	150	Toluene
Biphenyl	4F′-XF1150	180	Bibenzyl
Bibenzyl	4F′-XF1150	180	Biphenyl
Methyl chloride	15F′-Dowtherm	Room Temp.	Isobutane
Ethyl chloride	15F′-SF96	Room Temp.	Isobutane
Neopentyl chloride	15F′-FFAP	70	*n*-Heptane
Chlorobenzene	15F′-FFAP	160	Isopropylbenzene

Reaction of Cobaltous Bromide with Ethylmagnesium Bromide in Tetrahydrofuran in the Presence of Styrene (A Representative Example). A 250 m*l* round-bottom flask was equipped with a magnetic stirrer bar and a rubber septum. The flask was flushed with nitrogen and 0.224 g (1.0 mmol) cobaltous bromide was added. After the apparatus was tightly sealed, the atmosphere within the flask was swept with helium for 30 min. To this flask, 14.25 m*l* of THF, 1.0 m*l* of standard solution of toluene in THF (1.0M, 1.0 mmol) and 3.0 m*l* of styrene (26.1 mmol) were added with hypodermic syringes. The flask was then immersed in a dry-ice acetone bath and 25 m*l* of methane and 25 m*l* of isobutane were added with syringes. The flask was transferred to an ice-water bath, and after 5 minutes agitation 2.75 m*l* of ethylmagnesium bromide solution (4.0 mmol) was added to the mixture with a syringe. The color of solution changed from sky blue to dark brown immediately. The evolutions of ethane and ethylene was complete within 5 min after the addition of ethylmagnesium bromide. After 30 min agitation at the same temperature (2.0°C), a small sample of gas was taken out and analyzed by gas chromatography (ethylene; 1.26 mmol, ethane; 1.32 mmol, *n*-butane; 0.05 mmol). An aliquot of the reaction mixture was removed with a microsyringe purged with nitrogen. The amount of ethylbenzene (before hydrolysis)[25] was measured immediately by gas chromatography (1.15 mmol). After hydrolysis with 1.0 m*l* of dilute sulfuric acid solution, the amount of ethylbenzene (after hydrolysis) was again analyzed by gas chromatography (1.16 mmol).

25) Part of ethylbenzene may be formed from the thermal decomposition of phenethylmagnesium bromide in gaschromatography. M. Lefrançois and Y. Gault, *J. Organometal. Chem.*, **16**, 7 (1969).

Exchange between Ethylmagnesium Bromide and Styrene in Diethyl Ether with Catalytic Amounts of Ferric Chloride. In a similar experiment, 14.0 m*l* of Et_2O, 3.0 m*l* of styrene, 2.0 m*l* of a solution of EtMgBr in Et_2O (3.8 mmol), 1.0 m*l* of a solution of toluene in Et_2O (1.0 mmol) and 25 m*l* of methane were added to the reaction vessel. After the flask was immersed in an ice-water bath and the mixture agitated for 10 min, 1.0 m*l* of a solution of ferric chloride in Et_2O (0.025 mmol) was added. The color of the solution changed from colorless to pale brown immediately. The rate of evolution of ethylene was determined by periodically removing a small aliquot of gas followed by gas chromatographic analysis. After 90 min the amount of ethylene was 0.57 mmol and the amount of ethylbenzene after hydrolysis was 0.60 mmol (Table 7). Isolation of deuterated ethylbenzene from the reaction mixture was made by the following method. To the reaction mixture obtained in the exchange between ethylmagnesium bromide and styrene (see above), 1.0 m*l* of deuterium oxide was added and the mixture was agitated for 30 min at the same temperature. The resulting mixture was extracted with Et_2O and the ethereal layer was dried over anhydrous sodium sulfate. After filtration, Et_2O was removed *in vacuo*. Ethylbenzene was separated from the residue by preparative gas chromatography (10F′–FFAP, 150°C). The distribution of isomers in deuterated and undeuterated ethylbenzene was determined by NMR. (see Table 7).

Exchange between n-Propylmagnesium Bromide and Ethylene in Tetrahydrofuran with Ferric Chloride Catalyst THF (18.5 m*l*) and 2.5 m*l* of *n*-propylmagnesium bromide (3.0 mmol), 25 m*l* of methane, 50 m*l* of ethylene and 25 m*l* of isobutane were added to the flask in dry-ice acetone bath. The flask was immersed in a temperature controlled water bath (25°C) and the mixture agitated for 10 min. 1.0 m*l* of solution of ferric chloride in THF (0.025 mmol) was added to the mixture

under agitation. The color of the solution changed to pale brown immediately. The rates of formations of propylene and propane were followed by gas chromatography. The evolution of propylene was almost complete within 10 min after the addition of ferric chloride solution. After 60 min the amount of propylene was 0.68 mmol and the amount of propane was 0.06 mmol. None of ethane was detected before hydrolysis whereas 0.70 mmol of ethane was recovered after acidic hydrolysis.

We wish to thank the National Science Foundation for generous financial support, the Du Pont Company for the THF and the Dow Chemical Company for the billet of magnesium used in this work.

BULLETIN OF THE CHEMICAL SOCIETY OF JAPAN, VOL. 44, 3073—3077 (1971)

The Stereochemistry of 5-Substituted 2-Oxo-3-aryl-1,2,3-oxathiazolidines

Tomihiro NISHIYAMA and Fukiko YAMADA

Department of Applied Chemistry, Faculty of Engineering, Kansai University, Senriyama, Suita, Osaka

(Received February 4, 1971)

New six 2-oxo-3-aryl-5-methyl-1,2,3-oxathiazolidines and six 2-oxo-3-aryl-5-chloromethyl-1,2,3-oxathiazolidines have been prepared in good yields by the reactions of *N*-sulfinylanilines with propylene oxide and epichlorohydrin respectively in the presence of catalysts. The compounds obtained exist in isomeric *cis* and *trans* forms at the S=O bond. The configurations of their stereoisomers were discussed by means of NMR.

Recently, a few studies have been reported on the preparations of some oxathiazolidines. For example, Etlis *et al.*[1] reported that, in the presence of NEt_4Br, *N*-sulfinylanilines (**1**) reacted with alkene oxides at 95—100°C to give 2-oxo-3-aryl-1,2,3-oxathiazolidines. On the other hand, Deyrup and Moyer[2] have prepared oxathiazolidines by the reactions of β-amino alcohols with thionyl chloride in the presence of a base; the stereochemical structures of the compounds thus obtained have also been determined by means of their NMR spectra. In a previous paper, we reported that, in the absence of a catalyst, **1** reacted with ethylene oxide at a low temperature to form the corresponding oxathiazolidines.[3] The studies have now been extended to some substituted oxathiazolidines with a view to obtain a clearer picture of the stereoisomers.

In this paper, we wish to describe the reaction of **1** with propylene oxide (**2**) or epichlorohydrin (**3**) in the presence of catalysts and the configurations of the reaction products, oxathiazolidines (**4**), by means of a study of their NMR spectra.

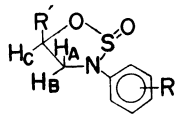

4 *cis*
R=H, CH_3, Cl

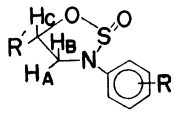

4 *trans*
R′=CH_3, CH_2Cl

Experimental

Measurements. All the melting and boiling points are uncorrected. All the NMR spectra were recorded at 60 MHz with a Japan Electron Optics Model JNM-3H-60 spectrometer. The chemical shifts were described in parts per million downfield from the internal TMS (δ). The IR spectra were recorded on a Hitachi Model EPI-2 grating spectrophotometer. GLC analysis was carried out on a Yanagimoto Gas Chromatograph, Model GCG-550-T, using a 2.15-m column packed with Silicone SE-30 (10 wt%). The percentage composition of the products was estimated by means of the relative peak areas (uncorrected).

Materials. *N*-Sulfinylanilines, *N*-sulfinylaniline (R=H), *N*-sulfinyltoluidines (R=*o*-CH_3, *m*-CH_3, and *p*-CH_3), and *N*-sulfinylchloroanilines (R=*o*-Cl, *m*-Cl, and *p*-Cl) were prepared as has been described in the literatute.[4] **2** and **3** were commercially-available and were of pure in grade. All the reagents used were of an analytical grade.

General Procedure for the Reaction of 1 with 2 or 3. To a vigorously-stirred mixture of **1** with **2** or **3**, a solution of the catalyst in dimethylformamide (DMF) was added. After the mixture had been stirred for an appropriate time at a constant temperature, the residual catalyst was either filtered off or was washed off with water. The removal of DMF left a red-brown colored oily product which, on distillation *in vacuo*, gave oxathiazolidine. The progress of the reaction was periodically checked by measuring the NMR spectrum and glc of the reaction mixture.

Acid Hydrolysis of 2-Oxo-3-phenyl-5-methyl-1,2,3-oxathiazolidine (5). A mixture of 2.9 g of oxathiazolidine (**5**) in 10 m*l* of ethylalcohol and hydrochloric acid (60 mg, 1.64 mmol in 10 m*l* of water) was refluxed for 4 hr. The reaction mixture was extracted in methylene chloride, and then the solution was washed with water. The organic layer was dried; the subsequent removal of methylene chloride left a pale yellow product which, on distillation *in vacuo*, gave a clear pale yellow liquid (122—123°C/3 mmHg, 1.9 g, 83%) and which was identified as *N*-(β-hydroxypropyl)aniline by comparing its infrared spectrum with that of an authentic sample.[5] IR spectrum: 3375, 2970, 1603, 1501, 745, 688 cm^{-1}

1) V. S. Etlis, A. P. Sineokov, and M. E. Sergeeva, *Khim. Geterotskil. Soedin*, 682 (1966); *Chem. Abstr.*, **66**, 55150s (1967).
2) J. A. Deyrup and C. L. Moyer, *J. Org. Chem.*, **34**, 175 (1969).
3) F. Yamada, T. Nishiyama, M. Kinugasa, and M. Nakatani, This Bulletin, **43**, 3611 (1970).
4) A. Michaelis and R. Herz, *Ber.*, **23**, 3480 (1890).
5) K. D. Petrov, *Sbornik Statei Khim., Akad. Nauk S. S. S. R.*, **1**, 374 (1953); *Chem. Abstr.*, **49**, 997g (1955).

Results and Discussion

The Reaction. The products of these reactions and their physical properties are summarized in Tables 1 and 2. The conversion rate of each reaction can be determined by means of the data of the integrated ring protons in its NMR spectrum. These results indicate that the rate is influenced by the composition of the catalyst and by the reaction temperature. The rate of the reaction in the presence of lithium chloride (LiCl) is almost the same as that in the presence of lithium bromide (LiBr), but the rate in the presence of tetraethylammonium bromide (NEt_4Br) is slower than that in the presence of LiCl. This is also brought out clearly by a comparison of the values of the yields (Tables 1 and 2).

General Structure and Assignment of the Configuration. Let us now discuss how the general structure of the reaction products was determined. For example, the compound **5** (Table 1) can be converted to *N*-(β-hydroxypropyl)-aniline by acid-catalyzed hydrolysis. *N*-(β-hydroxypropyl)-aniline was further identified by comparing its infrared spectrum with that of an authentic sample, prepared by another route,[5] and by the results of the elemental analysis. All of the above facts, the results of the elemental analyses, and the spectral data (Tables 1 and 2) support the idea that the products have the structure of **4**.

The structure of **4** indicates the possibility that the reaction product consists of a pair of isomers, namely, the *cis* and *trans* configurations between the S=O group and the substituent, R'. After the reaction had been completed, the NMR spectrum of the reaction mixture always indicated the presence of the two isomers in the product. Therefore, we considered that the two isomers in the reaction product coincide with the *cis* and *trans*

TABLE 1. REACTIONS OF **1** WITH **2**

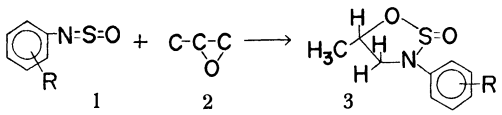

1 2 3

Compd. no.	R	2/1 mol. ratio	Cat.[a] mol	Temp. °C	Time hr	Yield %	Mp °C or Bp (mmHg)	*trans/cis*	% C	% H	% N	% Cl
5	H	1.49	—	25	300	0						
5	H	1.40	0.02	40	6.5	83	59.3—59.8[c,d]	1.44	54.68	5.58	7.12	
5	H	1.40	0.03	40	5.5	70			(54.82)	(5.58)	(7.11)[e]	
6	*o*-CH_3	1.40	0.02	40	13.3	85	129—130(3)[c]	3.00	56.79	6.17	6.72	
									(56.88)	(6.16)	(6.64)	
7	*m*-CH_3	1.40	0.03	35	12.0	78	42.2—45.7[c]	2.62	56.77	6.17	6.73	
8	*p*-CH_3	1.40	0.02	40	13.0	80	83.2—85.0[b]	2.22	56.87	6.22	6.62	
9	*o*-Cl	1.40	0.01	40	7.2	75	76.8—78.0[b]	2.14	46.72	4.38	6.05	15.30
									(46.65)	(4.32)	(6.05)	(15.33)
10	*m*-Cl	1.40	0.015	40	3.9	76	69.0—70.4[c]	2.22	46.69	4.32	6.03	15.30
10	*m*-Cl	1.40	0.036	40	2.5	80						
11	*p*-Cl	1.40	0.01	40	7.1	85	91.8—92.6[c]	2.57	46.54	4.45	6.05	15.30

a) LiCl. b) Mp of *cis* isomer. c) Mp of *trans* isomer.
d) lit[1] mp 57°C. e) Calcd value.

TABLE 2. REACTIONS OF **1** WITH **3**

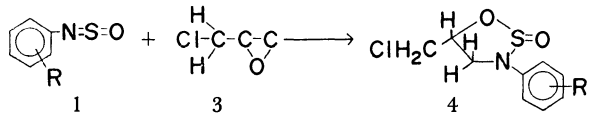

1 3 4

Compd. no.	R	3/1 mol. ratio	Cat mol	Temp. °C	Time hr	Yield %	Mp °C	*trans/cis*	% C	% H	% N	% Cl
12	H	4.0	—	40	450	0		—				
12	H	1.40	0.01[a]	50	3.8	55	98.6—99.1[d,f]	—	46.62	4.22	6.05	15.27
12	H	1.40	0.01[b]	50	3.8	61			(46.75)	(4.35)	(6.17)	(15.06)[g]
13	*o*-CH_3	1.51	0.01[c]	65	9.2	78	76.5—77.1[d]	0.75	48.95	4.86	5.94	14.58
									(49.02)	(4.93)	(6.48)	(14.45)
14	*m*-CH_3	1.40	0.02[a]	40	6.0	76	59.8—60.6[e]	0.68	48.90	4.88	6.23	14.50
15	*p*-CH_3	1.51	0.008[c]	62	15.0	62	76.7—77.1[d]	0.67	48.93	4.89	6.38	14.58
16	*o*-Cl	1.51	0.005[c]	62	5.5	77	101.6—102.0[d]	0.68	40.62	3.32	5.32	26.72
									(40.68)	(3.43)	(5.23)	(26.61)
17	*m*-Cl	1.02	0.02[a]	40	2.5	72	88.3—89.3[e]	1.00	40.76	3.27	5.31	26.78
18	*p*-Cl	1.40	0.01[a]	40	2.6	72	79.2—81.5[d]	0.69	40.68	3.43	5.35	26.74
18	*p*-Cl	1.40	0.02[a]	40	2.0	70		0.64				

a) LiCl. b) LiBr. c) NEt_4Br. d) Mp of *cis* isomer. e) Mp of *trans* isomer.
f) lit,[1] mp 95°C, g) Calcd value.

isomers of the oxathiazolidine. The *cis* or *trans* configuration was assigned by means of NMR spectroscopy.

In each reaction product, the *cis* or *trans* isomer can be separated by recrystallization from carbon tetrachloride. As can be seen in Table 1, the *cis* configuration was assigned to the products **8** and **9**, and the *trans* one, to the products **5**, **6**, **7**, **10**, and **11**. On the other hand, in Table 2, the *trans* configuration is assigned to the products **14** and **17**, and the *cis* one, to the products, **12**, **13**, **15**, **16**, and **18**. As is shown by these results, in each case only one of the isomeric pair can be separated; the other could not be isolated in a pure grade.

The ratio of the *cis* to the *trans* isomer in the reaction product can be determined by comparing the data of the integrated signal due to the methyl (in the case of the reaction of **1** with **2**) or methyne protons (in the reaction of **1** with **3**). The results obtained are also listed in Tables 1 and 2. The ratios are dependent mainly upon the substituents R and R′. The electron-releasing nature of R′ seems to be unfavorable to the formation of the *cis* isomer. The ratios are practically unaffected by the amount and the structure of the catalyst.

NMR Spectra of Oxathiazolidines. The chemical shifts of the oxathiazolidines are listed in Tables 3 and 4. The results show that a pair of isomeric 2-oxo-3-aryl-5-methyl (or chloromethyl)-1,2,3-oxathiazolidines was yielded by each reaction of **1** with **2** or **3**. The sulfoxide bond is well known to have acetylenic-like anisotropy.[6] For this reason, the deshielding of oxathiazolidine-ring substituents which are *cis* to the sulfoxide bond results. As can be seen in Table 3, **5a** and **5b** are identified as a pair of isomers. The methyl-proton signal in the *trans* isomer (**5b**) appeared at δ 1.42 ppm, while those in the *cis* isomer (**5a**) were observed at δ 1.59 ppm. On the other hand, the chloromethyl-proton signal in the *trans* isomer (**12b**) appeared at δ 3.65 ppm and, in the *cis* isomer (**12a**), further

Table 3. Spectral properties of 2-oxo-3-aryl-5-methyl-1,2,3-oxathiazolidines

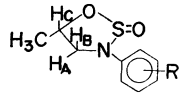

Compd. no.	R	Config	IR(S=O) cm^{-1}	NMR data, δ, ppm in CCl_4	
				H_C	H_A
5a	H	*cis*		4.78—5.15 (m)	3.80 (d, J=10.5)
5b	H	*trnas*	1174	5.19—5.53 (m)	3.24 (t, J *trans*=8.5, J *gem*=8.5)
6a	*o*-CH_3	*cis*		4.58—4.99 (m)	3.74 (d, J=10.0)
6b	*o*-CH_3	*trans*	1168	5.09—5.47 (m)	3.24 (q, J *trans*=7.2, J *gem*=8.8)
7a	*m*-CH_3	*cis*		4.75—5.11 (m)	3.69 (d, J=10.2)
7b	*m*-CH_3	*trans*	1168	5.20—5.52 (m)	3.24 (t, J *trans*=8.8, J *gem*=8.8)
8a	*p*-CH_3	*cis*	1161	4.57—5.08 (m)	3.68 (d, J=6.3)
8b	*p*-CH_3	*trans*		5.08—5.42 (m)	3.13 (t, J *trans*=8.3, J *gem*=8.3)
9a	*o*-Cl	*cis*	1160	4.66—5.05 (m)	3.78 (d, J=6.7)
9b	*o*-Cl	*trans*		5.03—5.53 (m)	3.38 (q, J *trans*=7.0, J *gem*=8.7)
10a	*m*-Cl	*cis*		4.85—5.23 (m)	3.80 (d, J=7.8)
10b	*m*-Cl	*trans*	1163	5.26—5.68 (m)	3.31 (t, J *trans*=8.5, J *gem*= 8.5)
11a	*p*-Cl	*cis*		4.25—4.73 (m)	3.87 (d, J=7.7)
11b	*p*-Cl	*trans*	1171	5.23—5.58 (m)	3.26 (t, J *trans*=8.7, J *gem*=8.7)

	NMR data, δ, ppm in CCl_4			
	H_B	CH_3	R	Ring Proton
5a	3.79 (d, J=8.1)	1.75 (d, J=6.0)	—	6.8 —7.3 (m)
5b	3.85 (q, J *cis*=5.4)	1.58 (d, J=6.0)	—	6.84—7.31 (m)
6a	3.61 (d, J=5.8)	1.60 (d, J=6.2)	2.44 (s)	7.23 (s)
6b	4.09 (q, J *cis*=7.5)	1.50 (d, J=6.2)	2.24 (s)	7.23 (s)
7a	3.66 (d, J=7.8)	1.73 (d, J=5.7)	2.43 (s)	6.6 —7.2 (m)
7b	3.83 (q, J *cis*=5.4)	1.57 (d, J=5.7)	2.43 (s)	6.66—7.22 (m)
8a	3.66 (d, J=8.7)	1.68 (d, J=6.2)	2.40 (s)	7.00 (q)
8b	3.71 (q, J *cis*=6.8)	1.46 (d, J=6.0)	2.40 (s)	7.0 (q)
9a	3.80 (d, J=9.0)	1.72 (d, J=6.0)	—	7.00—7.53 (m)
9b	4.06 (q, J *cis*=7.6)	1.50 (d, J=6.0)	—	7.07—7.48 (m)
10a	3.78 (d, J=6.3)	1.79 (d, J=6.0)	—	6.8 —7.3 (m)
10b	3.93 (q, J *cis*=5.2)	1.65 (d, J=6.0)	—	6.84—7.34 (m)
11a	3.83 (d, J=4.4)	1.77 (d, J=6.0)	—	7.0—
11b	3.86 (q, J *cis*=5.4)	1.63 (d, J=6.0)	—	7.05 (q)

6) J. G. Pritchard and P. C. Lauterbur, *J. Amer. Chem. Soc.*, **83**, 2105 (1961).

TABLE 4. SPECTRAL PROPERTIES OF 2-OXO-3-ARYL-5-CHLOROMETHYL-1,2,3-OXATHIAZOLIDINES

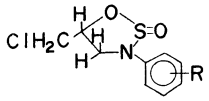

Compd. no.	R	Confign	IR(S=O) cm^{-1}	NMR data, δ, ppm in CCl_4			
				CH	CH_2 and $-CH_2Cl$	R	Ring proton
12a	H	*cis*	1154	4.78—5.22 (m)	3.82 (d, J=6.6) 3.96 (d, J=6.6)	—	6.99—7.48 (m)
12b	H	*trans*		5.15—5.64 (m)	3.80 (d, J=6.0)	—	6.9 —7.4 (m)
13a	*o*-CH_3	*cis*	1156	4.70—5.16 (m)	3.85—4.28 (m)	2.49 (s)	7.21 (s)
13b	*o*-CH_3	*trans*		5.10—5.40 (m)	3.71 (d, J=6.0)	2.49 (s)	7.21 (s)
14a	*m*-CH_3	*cis*		4.72—5.14 (m)	4.13 (d, J=7.2)	2.45 (s)	6.8 —7.3 (m)
14b	*m*-CH_3	*trans*	1177	5.13—5.53 (m)	3.50—4.12 (m)	2.45 (s)	6.84—7.30 (m)
15a	*p*-CH_3	*cis*	1146	4.70—5.17 (m)	3.92 (d, J=6.6)	2.41 (s)	7.02 (q)
15b	*p*-CH_3	*trans*		5.11—5.41 (m)	3.75 (d, J=4.8)	2.41 (s)	7.0 (q)
16a	*o*-Cl	*cis*	1162	4.74—5.21 (m)	4.07 (d, J=6.0)	—	7.12—7.53 (m)
16b	*o*-Cl	*trans*		5.07—5.39 (m)	3.70 (d, J=6.6)	—	7.1—7.5 (m)
17a	*m*-Cl	*cis*		4.88—5.23 (m)	3.76—4.17 (m)	—	6.8—7.2 (m)
17b	*m*-Cl	*trans*	1177	5.25—5.68 (m)	3.55—4.17 (m)	—	6.81—7.26 (m)
18a	*p*-Cl	*cis*	1156	4.81—5.31 (m)	3.96 (d, J=6.0)	—	7.12 (q)
18b	*p*-Cl	*trans*		5.23—5.64 (m)	3.81 (d, J=4.8)	—	7.1 (q)

downfield at δ 3.83 ppm.

Several NMR spectra of oxathiazolidines are first-order spectra and show *cis* and *trans* coupling constants which can be interpreted in terms of the geometry around C–4 and C–5 single bonds. The coupling constants are shown in Tables 3 and 4.

Moyer reported that the coupling constants, J *trans*, J *cis*, and J *gem*, for *trans* 2-oxo-3-*t*-butyl-5-phenyl-1,2,3-oxathiazolidine are 6.5, 6.5, and 8.5 Hz respectively.[7] These values are very close to those of the compounds, as is shown in Table 3.

Solvent Effects. The signal of the methylene protons (C–4) of **18a** appeared as a two-proton doublet in a carbon tetrachloride solution. In a methylene chloride solution, the doublet form was transformed to a quartet form, as is shown in Fig. 1. This phenomenon indicates that the signal of the C–4 methylene protons overlaps that of the C–5 chloromethyl protons. The coupling constant of the C–4 methylene protons was 6.0 Hz in a carbon tetrachloride solution as well as in a methylene chloride solution.

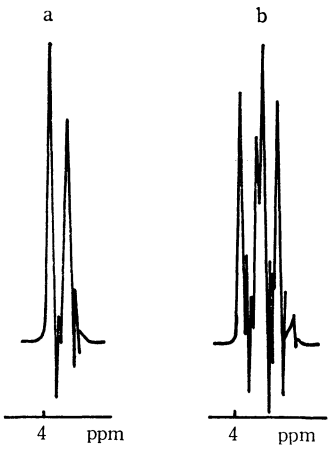

a. CCl_4 solution b. CH_2Cl_2 solution

Fig. 1. NMR spectra for methylene protons of **18a**.

In the carbon tetrachloride solution, the equilibrium composition of the compound **11** was 42% *cis* and 58% *trans*, based on the integration of the NMR spectra of the methyl protons. After this solution had been heated at 80—85°C for 13 hr, the *trans* isomer composition increased from 58% to 72%. The *cis* isomer, however, did not entirely disappear. In the case of the carbon disulfide solution, no change in the composition was observed even upon heating under the same conditions. It is clear that both the solvent and temperature effects may markedly affect the equilibration of the *cis* and *trans* isomers. This suggests that the oxathiazolidine ring interacts with a solvent such as carbon tetrachloride and that then the *cis*-form is turned into the *trans*-form at a suitable temperature.

On the other hand, the NMR spectral data of the *cis* and *trans* isomers of some oxathiazolidines in a benzene solution exhibit benzene-induced shifts, as is shown in Table 5. Figure 2 shows the proposed geometry of the benzene-solute collision complex of the oxathiazolidines. As for the aromatic solvent effect on the sulfoxides, recent papers have described studies con-

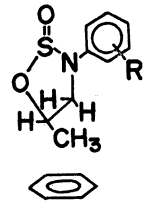

Fig. 2. Proposed geometry of benzene-solute collision complex of the oxathiazolidines.

7) C. L. Moyer, "2-Oxo-1,2,3-oxathiazolidines", Dissertations, II, Harvard University (1968) (Avail. Univ. Microfilms, Ann Arbor, Mich., Order No. 68—16878), p. 95; *Chem. Abstr.* **70**, 77677d(1969).

TABLE 5. SOLVENT EFFECTS ON THE NMR SPECTRA OF THE OXATHIAZOLIDINES

Compd. no.	R	Confign	Concn, mmol/ml	Δ, ppm=$\delta(CCl_4)-\delta(C_6H_6)$			
				H_A	H_B	H_C	CH_3
5b	H	*trans*	0.75	+0.61	+0.62	+0.31	+0.53
6b	*o*-CH_3	*trans*	0.75	+0.55	+0.39	+0.36	+0.47
7b	*m*-CH_3	*trans*	0.75	+0.59	+0.59	+0.29	+0.51
8a	*p*-CH_3	*cis*	0.75	—	—	+0.38	+0.35
9a	*o*-Cl	*cis*	0.75	+0.75	+0.30	+0.50	+0.45
10b	*m*-Cl	*trans*	0.75	+0.87	+0.89	+0.40	+0.59
11b	*p*-Cl	*trans*	0.75	+0.75	+0.77	+0.38	+0.58

cerning the stereochemistry of the penicillin sulfoxides[8] or the methylthiolane oxides.[9] In these compounds, the situation of the methyl group in question is the α-position relative to the sulfoxide group. In the case of the oxathiazolidines, in spite of the situation of the methyl group in the β-position, it was found that the stereochemical assignment is nearly in line with the arguments presented in the above papers. As can be seen in Table 5, however, the shifts of the protons of the compound **6b** were somewhat different. This difference may be ascribed to some effect of the *o*-methyl substituent.

The authors are grateful to the members of the Laboratory of Analysis, Faculty of Science, of Osaka University and the staff of the Research Laboratories, Fujisawa Pharmaceutical Co., Ltd. for the elementary analyses.

8) R. D. G. Cooper, P. V. DeMarco, J. C. Cheng, and N. D. Jones, *J. Amer. Chem. Soc.*, **91**, 1408 (1969).

9) J. J. Rigau, C. C. Bacon, and C. R. Johnson, *J. Org. Chem.*, **35**, 3655 (1970).

BULLETIN OF THE CHEMICAL SOCIETY OF JAPAN, VOL. 44, 3077—3080 (1971)

The Reactions of Pyridinium Bromides with Sulfenamides

Teruaki MUKAIYAMA and Kazuhiko SAIGO

Laboratory of Organic Chemistry, Tokyo Institute of Technology, Ookayama, Meguro-ku, Tokyo

(Received February 5, 1971)

It was found that three different types of products, phenylthiomethylpyridinium bromide, ethoxy-bis(phenylthio)-methane and ethyl ethoxy-bis(phenylthio)acetate were obtained by the reactions of pyridinium bromides, such as phenacylpyridinium bromide, acetonylpyridinium bromide and ethoxycarbonylmethylpyridinium bromide, with sulfenamides in ethanol, depending on the nature of the carbonyl carbon of the starting pyridinium bromides.

Recently, it was reported that α-hydroxyiminopyridinium bromides were obtained in good yields by the reactions of pyridinium bromides such as phenacylpyridinium bromide and acetonylpyridinium bromide with alkyl nitrite.[1] The results indicate that hydrogen atom attached to α-carbon of pyridinium bromide becomes acidic by the influence of both positively charged nitrogen atom and carbonyl group. It was also found that active methylene compounds react with sulfenamides to give mono- or di-sulfenylated products in good yields.[2]

In the present experiment, the reactions of pyridinium bromides with sulfenamides were investigated with the expectation that α-sulfenylated pyridinium bromides would be obtained as in the formation of α-hydroxyiminopyridinium bromide. When phenacylpyridinium bromide (I) was allowed to react with *N*-phenylthiophthalimide (II) in the presence of triethylamine (III) in ethanol for 2 hr, phenylthiomethylpyridinium bromide (VIII) and ethyl benzoate (VII) were obtained in quantitative and 64% yields, respectively, instead of the expected α-phenylthiophenacylpyridinium bromide. Similary, phenylthiomethylpyridinium bromide was obtained in quantitative yield by the reaction of phenacylpyridinium bromide with *N*-phenylthiosuccinimide and triethylamine or *N,N*-diethylbenzenesulfenamide in the absence of triethylamine.

The result indicates that pyridinium salt (VI) and ethyl benzoate are produced by way of a nucleophilic attack of ethoxide anion to carbonyl carbon of the initially formed intermediate (IV) with active carbonyl carbon induced by an electronegative phenylthio group attached to the α-carbon. The subsequent anion exchange between pyridinium salt (VI) and triethylammonium bromide (V) results in the formation of phenylthiomethylpyridinium bromide.

The reactions of acetonylpyridinium bromide with

1) T. Mukaiyama, K. Saigo, and H. Takei, This Bulletin, **44**, 190 (1971).

2) T. Mukaiyama, S. Kobayashi, and T. Kumamoto, *Tetrahedron Lett.*, **1970**, 5115.

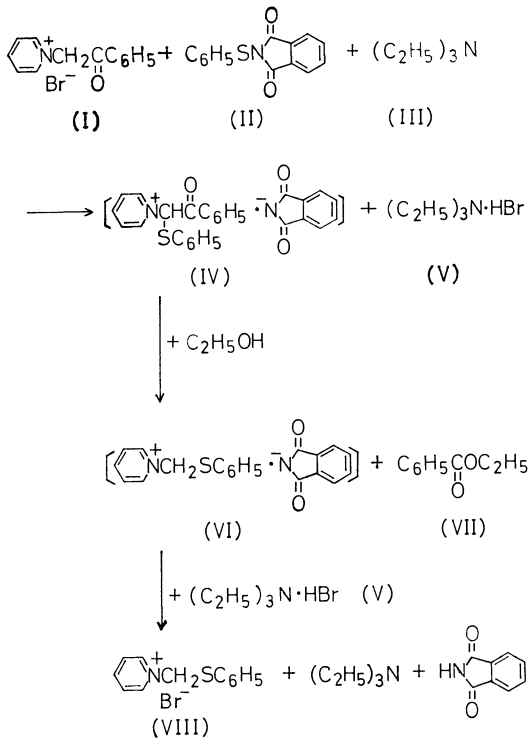

sulfenamides were tried. When an equimolar amount of acetonylpyridinium bromide (IX) was allowed to react with *N*-phenylthiophthalimide (II) and triethylamine (III), α-phenylthioacetonylpyridinium bromide could not be isolated and a tarry product resulted. On the other hand, when the same reaction was carried out in the presence of two equimolar amounts of *N*-phenylthiophthalimide, ethoxy-bis(phenylthio)methane (XIV) was obtained in 20% yield. Similarly, ethoxy-bis(phenylthio)methane (XIV) was isolated in 40% yield by the reaction of acetonylpyridinium bromide with two equimolar amounts of *N*-phenylthiosuccinimide.

This result can be explained as follows; the intermediate (X) is produced as expected from acetonylpyridinium bromide and *N*-phenylthiophthalimide. In this stage, deprotonation of X by imide anion predominates over the nucleophilic attack of ethoxide anion to the carbonyl carbon to form pyridinium ylide (XI), probably due to the slightly higher electron density of the carbonyl carbon of X in comparison with that of IV. XI reacts with another phenylthiophthalimide to give pyridinium salt (XII). The nucleophilic attack of ethoxide anion to the carbonyl carbon of XII followed by the nucleophilic attack by ethoxide anion to the α-carbon of pyridinium salt (XIII) gives ethoxy-bis(phenylthio)methane (XIV).

It was found that the reaction of ethoxycarbonylmethylpyridinium bromide (XV) with two equimolar amounts of *N*-phenylthiophthalimide (II) in the presence of triethylamine (III) gave ethyl ethoxy-bis(phenylthio)acetate (XIX) in 84% yield. In a similar way, ethyl ethoxy-bis(phenylthio)acetate was obtained in 77% yield by the reaction of ethoxycarbonylmethylpyridinium bromide with two equimolar amounts of *N*-phenylthiosuccinimide in the presence of triethylamine.

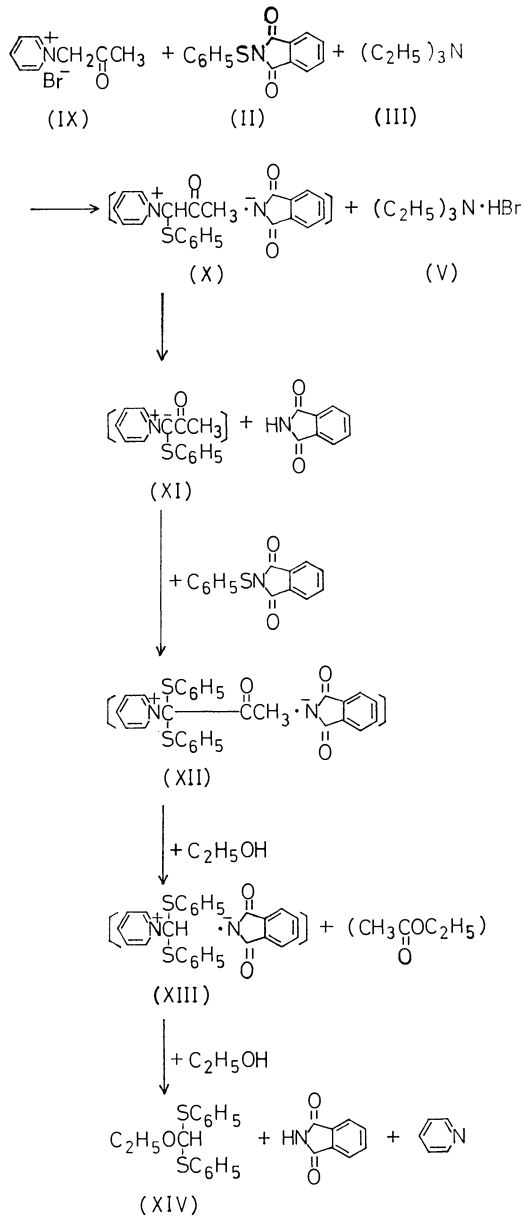

This result may be explained by considering the initial formation of intermediate (XVIII) in a similar manner to the case of the reaction of acetonylpyridinium bromide with sulfenamide. The nucleophilic displacement of ethoxide anion to the α-carbon of XVIII predominates over the nucleophilic attack to carbonyl carbon to form ethyl ethoxy-bis(phenylthio)-acetate.

The different types of products, phenylthiomethylpyridinium bromide, ethoxy-bis(phenylthio)methane and ethyl ethoxy-bis(phenylthio)acetate were obtained according to the nature of the carbonyl carbon of the starting pyridinium salts, by the reactions of phenacylpyridinium bromide, acetonylpyridinium bromide and ethoxycarbonylmethylpyridinium bromide, respectively, with sulfenamide.

The reaction of ethoxycarbonylmethylpyridinium bromide with *N*-phenylthiophthalimide and triethylamine in dichloromethane was investigated in order

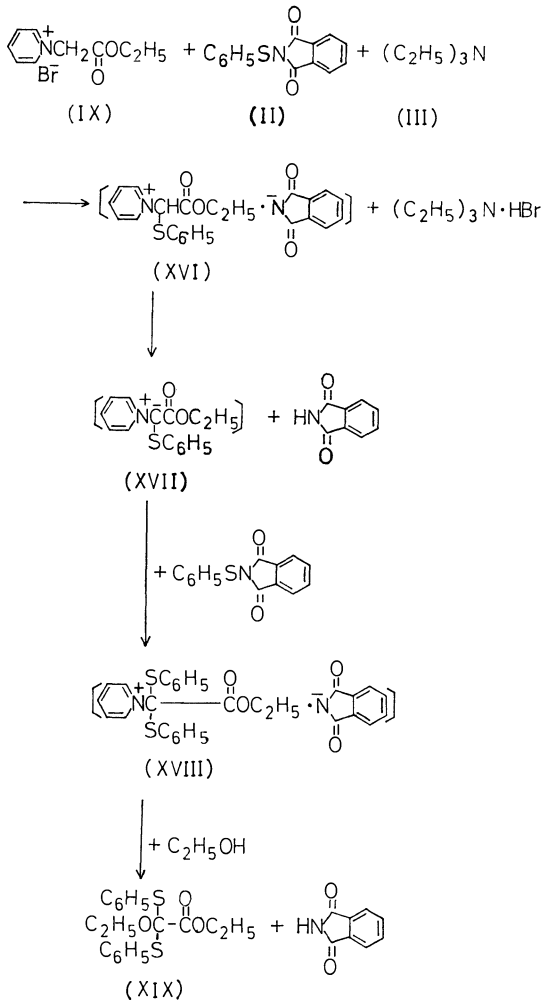

to isolate α-sulfenylated pyridinium ylide. When ethoxycarbonylmethylpyridinium bromide (XV) was allowed to react with *N*-phenylthiophthalimide (II) in the presence of triethylamine (III), 1,2-bis(ethoxycarbonyl)-1,2-bis(phenylthio)ethylene (XXI) was unexpectedly obtained in 50% yield. In contract to the above mentioned reaction at 0°C, carbene (XX) was formed by the thermal decomposition of unstable pyridinium ylide (XVII) at a temperature above 20°C. Carbene (XX) might be dimerized to form 1,2-bis-(ethoxycarbonyl)-1,2-bis(phenylthio)ethylene (XXI).[3]

The reaction of ethoxycarbonylmethylpyridinium bromide, triethylamine and two equimolar amounts of *N*-phenylthiophthalimide in dichloromethane was tried with the purpose of isolating α,α-di-sulfenylated pyridinium bromide. It was found that under the above mentioned conditions, ethoxycarbonyl-bis(phenylthio)-methylpyridinium salt could not be obtained but only a tarry product. When aniline was added the above mentioned reaction mixture, ethyl α-phenylimino-α-phenylthioacetate (XXIII, R=OC_2H_5) was obtained in 49% yield accompanied by the elimination of benzenethiol from the intermediate (XXII), formed by the nucleophilic displacement of aniline to the α-carbon of ethoxycarbonyl-bis(phenylthio)methylpyridinium salt

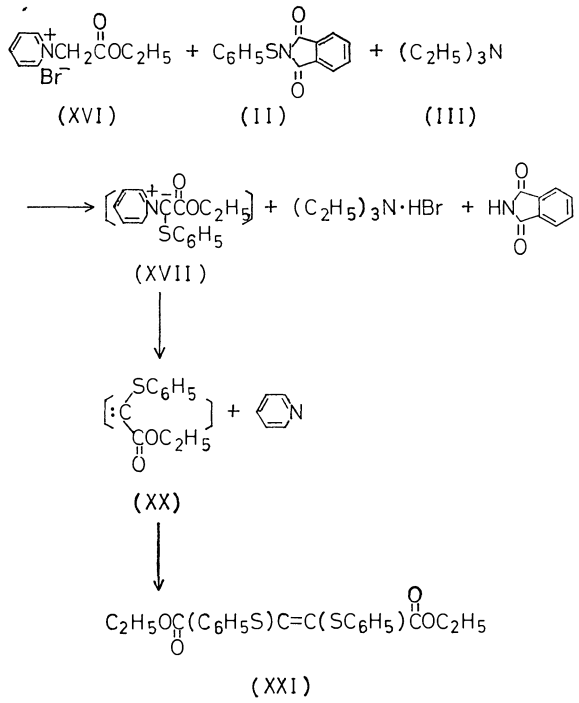

(XVIII). Similarly, α-phenylimino-α-phenylthioacetophenone (XXIII, R=C_6H_5) was obtained in 48% yield by the reaction of phenacylpyridinium bromide.

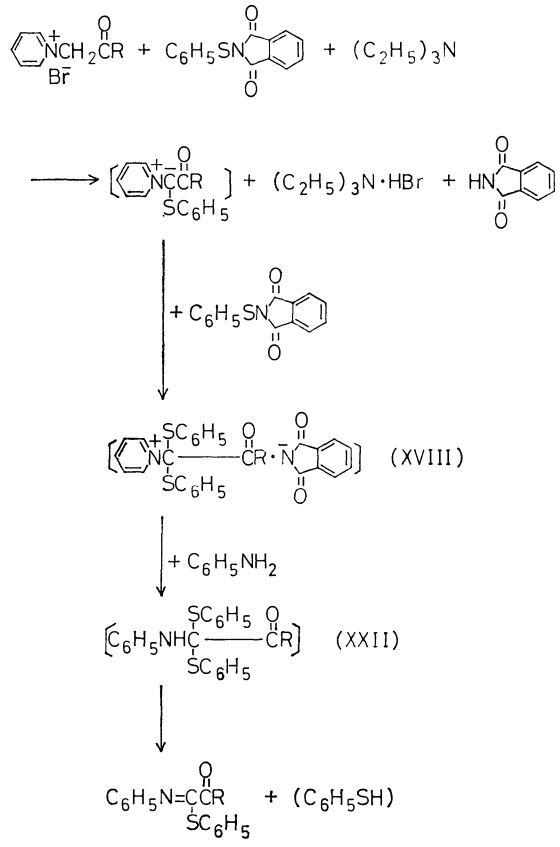

Experimental

Reaction of Phenacylpyridinium Bromide with N-*Phenylthiophthalimide in the Presence of Triethylamine.* Into a solution of

3) The compound is assigned to a mixture of *trans* and *cis* isomers by gas-liquid phase chromatography.

phenacylpyridinium bromide (2.78 g, 0.01 mol) and *N*-phenylthiophthalimide (2.55 g, 0.01 mol) in ethanol (100 m*l*), triethylamine (1.01 g, 0.01 mol) in ethanol (10 m*l*) was added drop by drop under ice cooling and the reaction mixture was stirred for 2 hr. After removal of the solvent, a mixture of water and ether (1:1) was poured into the residue and resulting crystals, phthalimide, were filtered off. The filtrate was separated into water and ether layers. From the water layer, white crystals, phenylthiomethylpyridinium bromide (mp 121.5—123.0°C) were obtained in quantitative yield after removal of the solvent.

Found: C, 51.59; H, 4.30; N, 4.92; S, 11.20%. Calcd for $C_{12}H_{12}BrNS$: C, 51.81; H, 4.29; N, 4.96; S, 11.34%.

The ether layer was evaporated under reduced pressure to give oily residue. Distillation *in vacuo* gave ethyl benzoate (bp 88—90°C/15 mmHg), 0.96 g (64%), identified by IR spectrum.

Reaction of Acetonylpyridinium Bromide with Two Equimolar Amounts of N-*Phenylthiophthalimide in the Presence of Triethylamine.* Into a solution of acetonylpyridinium bromide (1.06 g, 0.005 mol) and *N*-phenylthiophthalimide (1.28 g, 0.005 mol) in ethanol (100 m*l*), triethylamine (0.51 g, 0.005 mol) in ethanol (10 m*l*) was added dropwise and the reaction mixture was stirred for 30 min under ice cooling. Another one mol of *N*-phenylthiophthalimide (1.28 g, 0.005 mol) was added to the reaction mixture with stirring. After a few minutes, the color of the reaction mixture changed from red brown to yellow and the precipitate of phthalimide increased in amount rapidly. The reaction mixture was stirred for additional 3 hr under ice cooling. After the solvent was evaporated under reduced pressure, the residue was extracted with ether. Removal of the ether gave oily residue. The residue was chromatographed on silica gel. Elution with benzene gave ethoxy-bis(phenylthio)methane (mp 88.0—89.5°C), 0.28 g (20%), recrystallized from cyclohexane, and identified by IR and NMR spectra.

Found: C, 65.49; H, 5.93; S, 22.98%. Calcd for $C_{15}H_{16}OS_2$: C, 65.21; H, 5.84; S, 23.16%.

Similarly, by the reaction of ethoxycarbonylmethylpyridinium bromide (1.23 g, 0.005 mol) with two equimolar amounts of *N*-phenylthiophthalimide (2.55 g, 0.01 mol) in the presence of triethylamine (0.51 g, 0.005 mol), ethyl ethoxy-bis(phenylthio)acetate was obtained, 1.47 g (84%), mp 54.0—54.5°C, identified by IR and NMR spectra.

Found: C, 61.87; H, 5.84; S, 17.88%. Calcd for $C_{18}H_{20}O_3S_2$: C, 62.02; H, 5.79; S, 18.37%.

Reaction of Ethoxycarbonylmethylpyridinium Bromide with N-*Phenylthiophthalimide in the Presence of Triethylamine in Dichloromethane.* Into a solution of ethoxycarbonylmethylpyridinium bromide (2.46 g, 0.01 mol) and *N*-phenylthiophthalimide (2.55 g, 0.01 mol) in dichloromethane (100 m*l*), triethylamine (1.01 g, 0.01 mol) in dichloromethane (10 m*l*) was added at room temperature and the reaction mixture was stirred for 3 hr. After removal of the solvent, the residue was extracted with ether. The ether layer was evaporated under reduced pressure and the resulting oily product was chromatographed on silica gel. Elution with benzene, gave 1,2-bis(ethoxycarbonyl)-1,2-bis(phenylthio)ethylene, 0.82 g (50%).

Found: C, 65.33; H, 5.96; S, 19.58%. Calcd for $C_{18}H_{20}O_2S_2$: C, 65.05; H, 6.07; S, 19.26%.

Formation of Ethyl α-Phenylimino-α-phenylthioacetate. By a similar procedure as in the formation of ethoxy-bis(phenylthio)methane, ethoxycarbonylmethylpyridinium bromide (1.23 g, 0.005 mol) was allowed to reacted with triethylamine (0.51 g, 0.005 mol) and two equimolar amounts of *N*-phenylthiophthalimide (2.55 g, 0.01 mol) in dichloromethane (100 m*l*). After stirring for 30 min under ice cooling, aniline (0.47 g, 0.005 mol) in dichloromethane (10 m*l*) was added to the reaction mixture. The solvent was evaporated under reduced pressure after stirring for additional 6 hr under ice cooling, and the residue was extracted with ether. After removal of ether, the resulting oily product was chromatographed on silica gel. Elution with benzene gave ethyl α-phenylimino-α-phenylthioacetate (mp 78—79°C), 0.70 g (49%), identified by IR and NMR spectra.

Found: C, 67.58; H, 5.54; N, 5.19; S, 11.33%. Calcd for $C_{16}H_{15}O_2NS$: C, 67.36; H, 5.30; N, 4.91; S, 11.21%.

Similarly, in the reaction of phenacylpyridinium bromide, α-phenylimino-α-phenylthioacetophenone was obtained in 48% yield, mp 75—76°C, identified by IR and NMR spectra.

Found: C, 75.40; H, 4.58; N, 4.52; S, 10.18%. Calcd for $C_{20}H_{15}ONS$: C, 75.69; H, 4.76; N, 4.41; S, 10.09%.

We thank Dr. H. Takei and Dr. T. Kumamoto for valuable discussions.

A Study of the Catalytic Partial Oxidation of Hydrocarbons. XI. The Catalytic Activity of the MoO_3-P_2O_5 and the MoO_3-Bi_2O_3-P_2O_5 in the Selective Oxidation of Butene, Butadiene, and Furan

Mamoru Ai and Sadao Suzuki

Research Laboratory of Resources Utilization, Tokyo Institute of Technology, Ookayama, Meguro-ku, Tokyo

(Received March 18, 1971)

In the present work, the vapor-phase partial oxidation of *cis*-2-butene, butadiene, furan, and maleic anhydride was carried out over MoO_3–P_2O_5 (1 : 0.2 atomic ratio) and MoO_3–Bi_2O_3–P_2O_5 (1 : 1 : 0.2) with a contact time of 1.6 sec, at a concentration of 0.6—1.0%, and in air, in order to elucidate the difference between the two catalysts in their catalytic specificity for the oxidation of these reactants to maleic anhydride. Over the MoO_3–P_2O_5 catalyst, the selectivities of butene, butadiene, and furan to maleic anhydride were 13, 50, and 78% respectively. Over the MoO_3–Bi_2O_3–P_2O_5 catalyst, the formation of maleic anhydride from the reactants was very small, that of CO_2 was important, and the rate of maleic anhydride destruction was fairly high. It is considered that the MoO_3–Bi_2O_3–P_2O_5 catalyst has almost the same catalytic specificity as the MoO_3–P_2O_5 in the $C_4H_8 \rightarrow C_4H_2O_3$ step, but that its activity for maleic anhydride destruction is so high that maleic anhydride cannot be accumulated.

In a previous paper,[1,2] the selective oxidation of crotonaldehyde and butadiene over various vanadium- and molybdenum-type catalysts has been investigated from the viewpoint of furan production. Among the catalysts tested, the MoO_3–P_2O_5 catalyst system (P/Mo= 0.1—0.3 atomic ratio) showed the best selectivity to furan in the oxidation of the both reactants; in addition, this system showed a fairly stable activity even at 500°C.

Regarding the ternary catalyst system of MoO_3–Bi_2O_3–P_2O_5, this is well-known as a catalyst which has an excellent selectivity for such an allylic oxidation of olefins as 1-butene to butadiene and propylene to acrolein. Therefore, a good deal of work has been devoted to the investigation of the two reactions mentioned above and that of the physicochemical properties of the catalyst system. However, no literature gives definitive data on the important difference in the catalytic specificity between MoO_3–P_2O_5 and MoO_3–Bi_2O_3–P_2O_5, and past studies over molybdenum-type catalysts were limited to investigations under low oxygen concentrations.

In the present work, we compared the results over MoO_3–P_2O_5 and MoO_3–Bi_2O_3–P_2O_5 catalysts on the relative rate and selectivity in the oxidation of butene, butadiene, furan, and maleic anhydride in excess oxygen, and attempted to clarify the difference between the two catalysts in the catalytic features for each reaction step in the step-by-step oxidation of butene to maleic anhydride, and to elucidate how far the mechanism and the selectivity of the partial catalytic oxidation of these reactants depend on the presence of Bi_2O_3 in the MoO_3–P_2O_5 system.

Experimental

The vapor-phase air oxidation of *cis*-2-butene, butadiene, furan, and maleic anhydride was performed over MoO_3–P_2O_5 (Mo: P=1:0.2 atomic ratio) and MoO_3–Bi_2O_3–P_2O_5 (Mo: Bi:P=1:1:0.2) oxide catalysts in an ordinary flow-type reaction system, as has been shown in previous papers.[3,4]

The volume concentrations of the reactants were 0.6—1.0% in air, the flow rate (at 25°C) was kept at 1.5 *l*/min, and the catalyst volume was 40 m*l* (contact time=1.6 sec). The reaction temperature was varied from 200 to 600°C. The experimental and analytical procedures were the same as those employed in pervious works.[1-6]

The catalysts used in the experiments were prepared as follows: the required quantities of $(NH_4)_6Mo_7O_{24}\cdot 4H_2O$ and H_3PO_4 were dissolved in hot water, and in the case of the MoO_3–Bi_2O_3–P_2O_5 catalyst, an acidified $Bi(NO_3)_3$ solution was mixed with the former solution; pumice of a mesh size of 10 to 20 was added to the above mixture, and then the solution was evaporated with constant stirring and finally dried in an oven at 130°C. The amount of pumice was 500 m*l*/g atom of molybdenum. The catalyst was calcined under flowing air at 550°C for 5 hr.

The color of the MoO_3–P_2O_5 after sintering or use in the experiment was black, while that of the MoO_3–Bi_2O_3–P_2O_5 was light-yellow. This indicates that the state of molybdenum in the former catalyst is more reduced than that in the latter. The surface areas, measured with nitrogen by the BET method at −195°C, were about 3 m^2/g for both the catalysts.

Results and Discussion

Oxidation of cis-*2-Butene.* The oxidation of *cis*-2-butene was carried out over the MoO_3–P_2O_5 and the MoO_3–Bi_2O_3–P_2O_5 catalysts in order to clarify the difference in the catalytic features between the two catalysts. The relationship of overall conversion (excluding isomerization) *vs.* the temperature is shown in Fig. 1. The MoO_3–P_2O_5 and the MoO_3–Bi_2O_3–P_2O_5 have almost the same catalytic activity for the overall oxidation of butene.

The oxidation of butene is always accompanied by its isomerization. Oxygen is necessary in the isomerization as well as in the oxidation.[6] The sum of the conversion of *cis*-2-butene to such isomers as *trans*-2-

1) M. Ai and M. Ishihara, *Kogyo Kagaku Zasshi*, **73**, 2152 (1970).
2) M. Ai, *ibid.*, **74**, 183 (1971).
3) M. Ai, K. Harada, and S. Suzuki, *ibid.*, **73**, 524 (1970).
4) M. Ai, T. Niikuni, and S. Suzuki, *ibid.*, **73**, 165 (1970).
5) M. Ai, This Bulletin, **43**, 3490 (1970).
6) M. Ai, *ibid.*, **44**, 761 (1971).

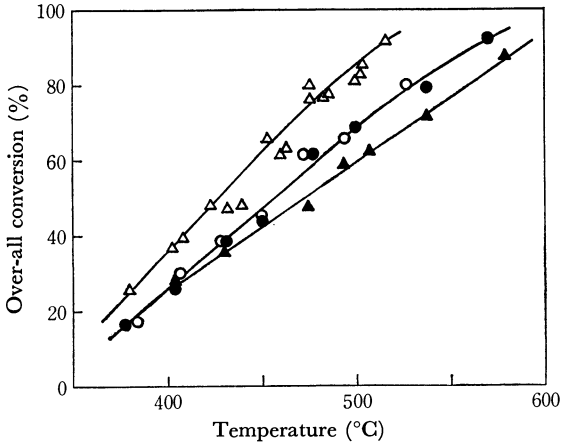

Fig. 1. Over-all conversion of butene and butadiene as a function of temperature.
contact time: 1.6 sec, C_4H_8 or C_4H_6: air=0.65: 100,
MoO_3–P_2O_5: C_4H_8, ○ C_4H_6, △
MoO_3–Bi_2O_3–P_2O_5: C_4H_8, ● C_4H_6, ▲

butene and 1-butene is plotted as a function of the reaction temperature in Fig. 2. It rises to a maximum due to the further oxidation of the isomers. The MoO_3–P_2O_5 has a higher isomerization activity than the MoO_3–Bi_2O_3–P_2O_5. This is in agreement with the data of Echigoya *et al.*[7,8] obtained by the use of MoO_3 and MoO_3–Bi_2O_3 in the oxidative dehydrogenation.

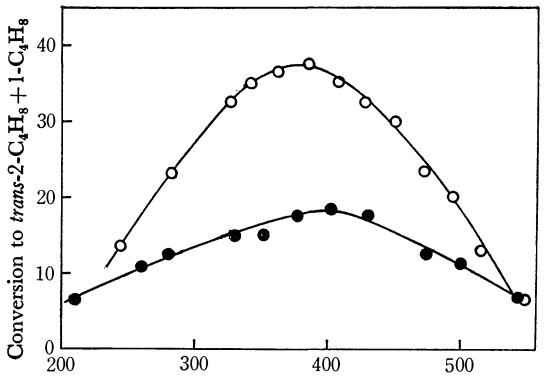

Fig. 2. Formation of isomers of *cis*-2-butene as a function of temperature.
MoO_3–P_2O_5: ○ MoO_3–Bi_2O_3–P_2O_5: ●

The formation of butadiene, which may be considered to be a primary intermediate in the step-by-step oxidation of butene to maleic anhydride, is shown as a function of the over-all conversion of butene (excluding isomerization) in Fig. 3. The slopes of these plots correspond to the differential selectivity at each conversion. Over the MoO_3–Bi_2O_3–P_2O_5 catalyst, the amount of butadiene passed through a maximum at a butene conversion of about 70% and was three times higher than that over the MoO_3–P_2O_3. It can thus be assumed that butadiene is less reactive than butene on the MoO_3–Bi_2O_3–P_2O_5, and that the catalyst is less

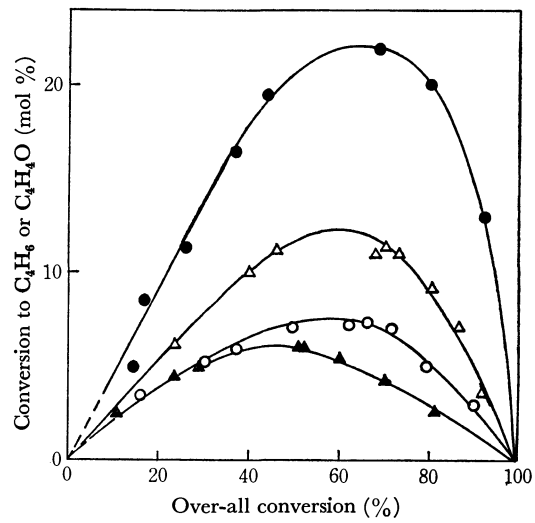

Fig. 3. Formation of intermediates (butadiene and furan) as a function of over-all conversion.
MoO_3–P_2O_5: C_4H_6, ○ C_4H_4O, △
MoO_3–Bi_2O_3–P_2O_5: C_4H_6, ● C_4H_4O, ▲

active than MoO_3–P_2O_5 for butadiene oxidation, probably because butadiene is adsorbed weakly on the MoO_3–Bi_2O_3–P_2O_5 catalyst.[5,9,10]

The formation of maleic anhydride over the MoO_3–P_2O_5 and the MoO_3–Bi_2O_3–P_2O_5 catalysts is shown as a function of over-all conversion of butene in Figs. 4 and 5 respectively. Over the MoO_3–P_2O_5 catalyst, the maximum selectivity to maleic anhydride is 13% at the butene conversion of about 80%, and the amount of maleic anhydride does not exceed 10%. It is found

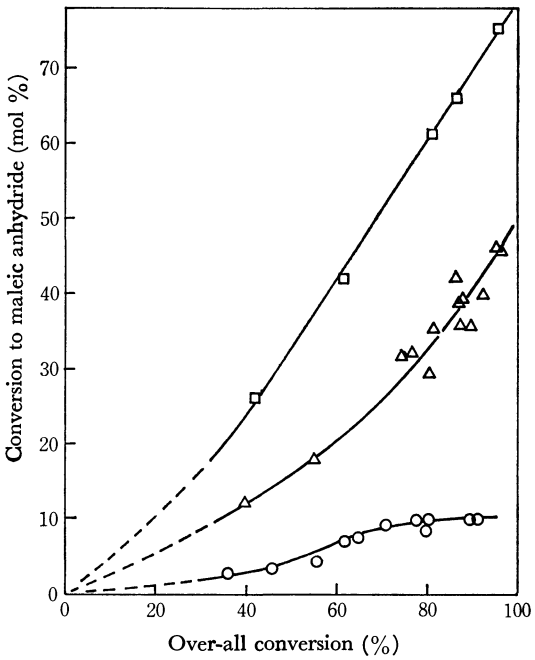

Fig. 4. Formation of maleic anhydride over MoO_3–P_2O_5
Reactant: C_4H_8, ○ C_4H_6, △ C_4H_4O, □

7) E. Echigoya, T. Watanabe, and R. Nakamura, *Kogyo Kagaku Zasshi*, **72**, 1092 (1969).
8) Ph. A. Batist, B. C. Lippens, and G. C. Schuit, *J. Catal.*, **5**, 55 (1966).
9) J. H. de Boer and R. J. A. M. van der Borg, Actes du Deuxieme Congress Internationale de Catalyse, Edition Thechnip, Paris, (1961), p. 919.
10) P. Zwietering and F. Hartog, *J. Catal.*, **2**, 79 (1963).

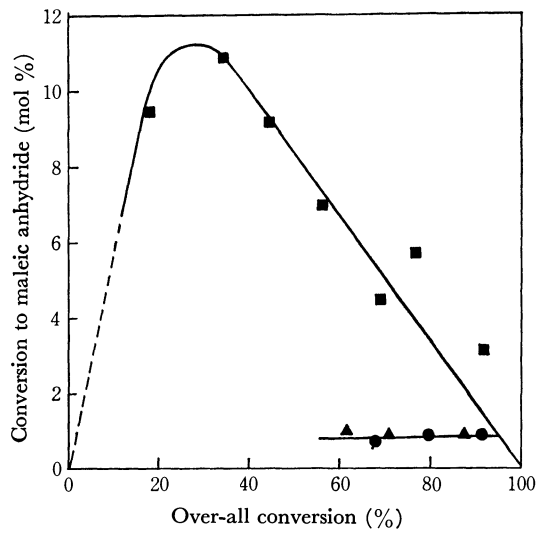

Fig. 5. Formation of maleic anhydride over MoO_3–Bi_2O_3–P_2O_5.
Reactant: C_4H_8, ● C_4H_6, ▲ C_4H_4O, ■

that the result is much inferior to that obtained by the use of vanadium-containing catalysts.[4-6] On the other hand, the MoO_3–Bi_2O_3–P_2O_5 shows a much lower maleic anhydride formation; it is less than 1% even at a butene conversion of 80—90%.

Figure 6 shows the formation of carbon dioxide (CO_2) and carbon monoxide (CO). Over the MoO_3–P_2O_5 catalyst, the formation of CO is superior to that of CO_2, while over the MoO_3–Bi_2O_3–P_2O_5, that of CO is inferior to that of CO_2, and the MoO_3–Bi_2O_3–P_2O_5 gives more CO_2 and less CO than the MoO_3–P_2O_5. The results indicate that, on the MoO_3–Bi_2O_3–P_2O_5 catalyst, a relatively good butadiene formation is obtained even in the presence of a large excess of oxygen, but the further oxidation of butadiene may proceed to complete oxidation. It may be concluded that neither the MoO_3–P_2O_5 nor the MoO_3–Bi_2O_3–P_2O_5 catalyst is adequate for the selective oxidation of butene to maleic anhydride.

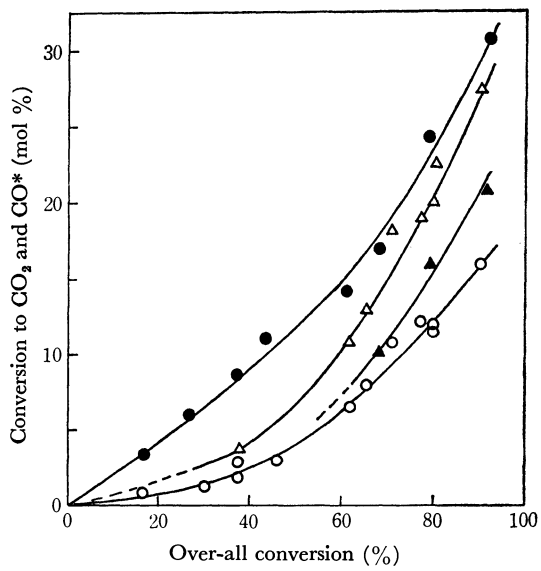

Fig. 6. Conversion of butene to CO_2 and CO as a function of over-all conversion.
MoO_3–P_2O_5: CO_2, ○ CO, △
MoO_3–Bi_2O_3–P_2O_5: CO_2, ● CO, ▲
* 1/4 of the real amount of the formation.

Oxidation of Butadiene. Butadiene conversion-temperature data for both the catalysts are shown in Fig. 1. The MoO_3–P_2O_5 has a considerably higher activity for butadiene oxidation than the MoO_3–Bi_2O_3–P_2O_5. Figure 1 indicates also that, on the MoO_3–Bi_2O_3–P_2O_5 catalyst, butadiene is less reactive than butene, while, on the MoO_3–P_2O_5, butadiene is more reactive than butene. These results agree with the data of butadiene formation from butene (Fig. 3).

The formation of furan, a primary intermediate of butadiene oxidation, is shown in Fig. 3. Contrary to the case of butadiene formation from butene, the amount of furan produced over the MoO_3–Bi_2O_3–P_2O_5 was only half that obtained over the MoO_3–P_2O_5 catalyst.

Over the MoO_3–P_2O_5 catalyst, the selectivity to maleic anhydride increases slightly with an increase in the butadiene conversion, reaching 50% at a butadiene conversion of about 100% (Fig. 4). It is found that the catalyst shows almost the same selectivity of butadiene to maleic anhydride as does the MoO_3–V_2O_5 catalyst (Mo/V=1—4), although its oxidation rate is far lower than that of the latter.[6,11] On the other hand, over the MoO_3–Bi_2O_3–P_2O_5 catalyst, only a small amount of maleic anhydride was obtained (less than 1%) (Fig. 5), much as in the case of butene oxidation.

As is shown in Fig. 7, the formation of CO_2 and CO is not so great in the case of the MoO_3–P_2O_5 catalyst,

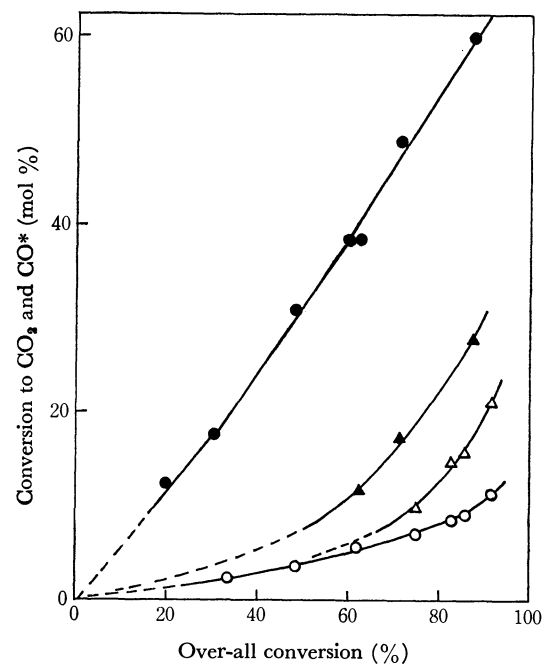

Fig. 7. Conversion of butadiene to CO_2 and CO as a function of over-all conversion.
MoO_3–P_2O_5: CO_2, ○ CO, △
MoO_3–Bi_2O_3–P_2O_5: CO_2, ● CO, ▲
* 1/4 of the real amount of the formation.

11) M. Ai, *Kogyo Kagaku Zasshi*, **73**, 950 (1970).

but in the case of the MoO_3–Bi_2O_3–P_2O_5 catalyst, both of them, especially CO_2, are produced to a significant extent. From these results, it may be concluded that the MoO_3–P_2O_5 catalyst shows relatively good results in the selective oxidation of butadiene to furan and maleic anhydride, but that the MoO_3–Bi_2O_3–P_2O_5 catalyst is not adequate to these formations, especially maleic anhydride formation.

Oxidation of Furan. Furan is considered as an intermediate in the consecutive oxidation of butene or butadiene to maleic anhydride.[2,3,5,10] Thus, the oxidation of furan was tested over the MoO_3–P_2O_5 and the MoO_3–Bi_2O_3–P_2O_5 catalysts in order to ascertain the catalytic action of the catalysts on this reaction step. The relationship between the furan conversion and the temperature is shown in Fig. 8. The MoO_3–P_2O_5 catalyst has a higher activity than the MoO_3–Bi_2O_3–P_2O_5 for furan oxidation, much as in butadiene oxidation. We cannot explain why the two catalysts show different results in the formation of furan from butadiene (Fig. 3). It can be estimated, though, that this difference probably results from the character of the adsorption on the catalyst surface.

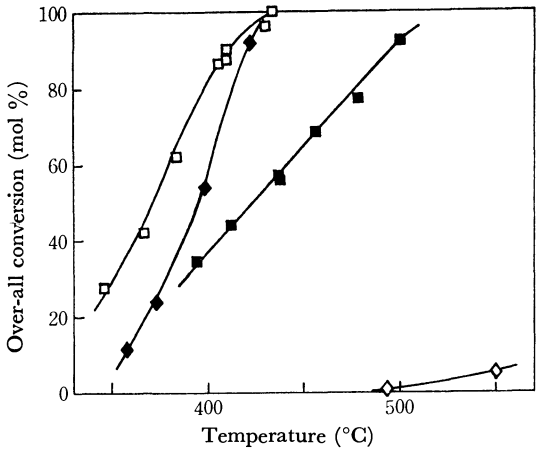

Fig. 8. Over-all conversion of furan and maleic anhydride as a function of temperature.
contact time; 1.6 sec,
C_4H_4O: air=1: 100, $C_4H_2O_3$: air=0.6: 100,
MoO_3–P_2O_5: C_4H_4O, □ $C_4H_2O_3$, ◇
MoO_3–Bi_2O_3–P_2O_5: C_4H_4O, ■ $C_4H_2O_3$, ◆

The conversion of furan to maleic anhydride is shown in Figs. 4 and 5. Over the MoO_3–P_2O_5 catalyst, the selectivity to maleic anhydride is quite good, reaching about 78% at a furan conversion of 80—90%. These results are superior to those obtained from V_2O_5, V_2O_5–P_2O_5, and V_2O_5–MoO_3 catalysts.[3,5,6,11] The MoO_3–Bi_2O_3–P_2O_5 catalyst gives a considerably smaller formation of maleic anhydride than does the MoO_3–P_2O_5 catalyst, and the amount of maleic anhydride passed through a maximum at a furan conversion at about 30%. These results reveal that, under the reaction conditions used here, the degradation of maleic anhydride occurs on the catalyst—that is, maleic anhydride is an intermediate in the oxidation of furan to CO_2 and CO, and that the rate of maleic anhydride decomposition is about 6 times faster than that of its formation.[9,10]

For lack of a suitable method of analysis, the amount of the polymer was obtained as the remainder in the mass-balance of the other products (Fig. 9). The formation of the polymer is higher on the MoO_3–Bi_2O_3–P_2O_5 catalyst than on the MoO_3–P_2O_5 catalyst. It is considered that the greater part of the reaction in this step preceeds on a side pathway on the MoO_3–Bi_2O_3–P_2O_5 catalyst rather than on the MoO_3–P_2O_5. The formation of CO_2 and CO is very low over the MoO_3–P_2O_5, while over the MoO_3–Bi_2O_3–P_2O_5 considerably great amount of them are formed and CO_2 is a major product (Fig. 10).

Oxidation of Maleic Anhydride. The oxidation of maleic anhydride was examined in order to ascertain the activity of the MoO_3–P_2O_5 and the MoO_3–Bi_2O_3–

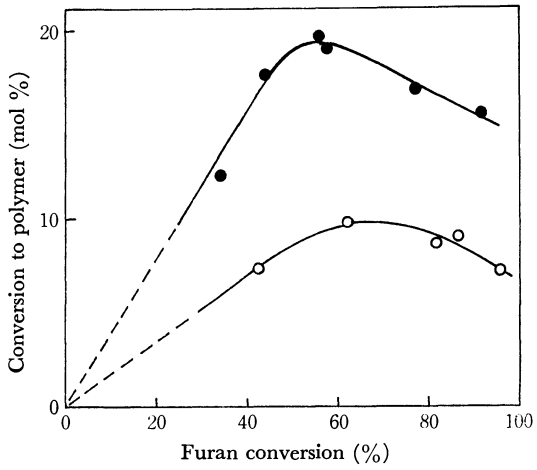

Fig. 9. Polymer formation *versus* furan conversion.
MoO_3–P_2O_5, ○ MoO_3–Bi_2O_3–P_2O_5, ●

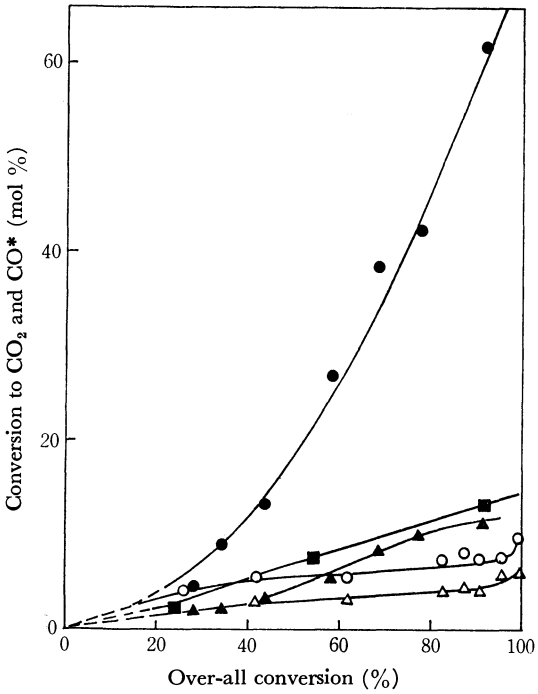

Fig. 10. Conversion of furan and maleic anhydride to CO_2 and CO as a function of over-all conversion.
C_4H_4O oxidation: MoO_3–P_2O_5; CO_2, ○ CO, △
MoO_3–Bi_2O_3–P_2O_5; CO_2, ● CO, ▲
$C_4H_2O_3$ oxidation: MoO_3–Bi_2O_3–P_2O_5; CO, ■
* 1/4 of the real amount of the formation.

P_2O_5 catalysts in the oxidation. Over the MoO_3–P_2O_5 catalyst, maleic anhydride was scarcely oxidized, even at 550°C. This indicates that the MoO_3–P_2O_5 catalyst was almost inactive for maleic anhydride degradation. On the other hand, the MoO_3–Bi_2O_3–P_2O_5 was considerably active in the reaction (Fig. 8). It is also found that, on the catalyst, maleic anhydride is more liable to be oxidized than are butene, butadiene, and furan. Besides CO_2 and CO, no other products were detected. In the degradation of maleic anhydride, the formation of CO was not important; the major product was CO_2 (85%) (Fig. 10).

A Discussion of the Effect of Bi_2O_3 Addition to MoO_3–P_2O_5 on the Reaction Mechanism. The selectivities of the reactants to maleic anhydride over the MoO_3–P_2O_5 catalyst may be summarized as follows: C_4H_8, 13; C_4H_6, 50; and C_4H_4O, 78%. An assumption has been made that the main reaction in the oxidation of butene to maleic anhydride proceeds as follows, in the same manner as over V_2O_5–P_2O_5: $C_4H_8 \rightarrow C_4H_6 \rightarrow C_4H_4O \rightarrow C_4H_2O_3$.[3,5] The selectivites towards the main reaction pathway in each consecutive step have been calculated from the data of selectivity to maleic anhydride in a manner similar to that used in earlier works:[5,6] $C_4H_8 \rightarrow C_4H_6$; 26, $C_4H_6 \rightarrow C_4H_4O$; 64, and $C_4H_4O \rightarrow C_4H_2O_3$; 78%. It has been concluded that this catalyst has an excellent selectivity for the furan-to-maleic anhydride step and a relatively good one for the butadiene-to-furan step, but a low selectivity for the butene-to-butadiene step, much like the V_2O_5-alone catalyst.[4,6]

On the other hand, over the MoO_3–Bi_2O_3–P_2O_5 catalyst, it is hard to get any information about the reaction scheme, from the data on maleic anhydride. Therefore, we will attempt to discuss the reaction on the basis of the data on CO_2 and CO. As regards CO_2 and CO, over such catalyst as V_2O_5, V_2O_5–P_2O_5, V_2O_5–MoO_3, and MoO_3–P_2O_5, whose activity for maleic anhydride oxidation, is very low, the amount of CO_2 formed in the oxidation of butene, butadiene, and furan was always less than that of CO,[1-6,10] but in the case of maleic anhydride oxidation, the main product was CO_2—that is, maleic anhydride undergoes destructive oxidation to CO_2. Margolis and others[12] indicate that, over the MoO_3–Bi_2O_3–P_2O_5 catalyst, the oxidation of CO to CO_2 is difficult and that the main sources of CO_2 formation are acids, while those of CO formation are aldehydes, and that this catalyst has a high activity for acid destruction.

12) A. P. Gorshkov, I. K. Kolchin, A. M. Gribov, and L. Ya. Margolis, *Kinet. Katal.*, **9**, 1089 (1967).

In the first approximation, an assumption is made that, over the MoO_3–Bi_2O_3–P_2O_5 catalyst, the amount of CO_2 formed in each step from C_4H_8 to $C_4H_2O_3$ is the same as that of CO. From the data of the selectivities to CO_2 and CO for each reactant (Table 1), the portion of each reactant destined to maleic anhydride and decomposed immediately to CO_2 and CO is roughly calculated; for example, in the case of butene, the selectivities to CO_2 and CO are 37 and 27% respectively. As those in the oxidation of maleic anhydride are 85 and 15%, the balance of CO_2 and CO can be expressed by the equation:

$$37 = 0.85x + A$$

$$27 = 0.15x + A$$

where x is the portion of butene destined to maleic anhydride ($0.85x$ and $0.15x$ indicate the CO_2 and CO originated from the decomposition of maleic anhydride) and where A is the CO_2 and CO formed in the steps before $C_4H_2O_3$. After the elimination of A, x is 14%. If the amount of CO_2 formed in the steps before $C_4H_2O_3$ is less than that of CO, the value of x becomes a little higher. The results are shown in Table 1.

Table 1. Maximum selectivity to CO_2 and CO and value of x

Reactant	C_4H_8	C_4H_6	C_4H_4O	$C_4H_2O_3$
Selectivity to CO_2	37	68	70	85
Selectivity to CO	27	37	13	15
x	14	44	82	(100)

These results indicate that the approximate selectivity of each reactant to maleic anhydride is: C_4H_8, 14; C_4H_6, 44; and C_4H_4O, 82%. This means that the MoO_3–Bi_2O_3–P_2O_5 catalyst has about the same selectivity to maleic anhydride as the MoO_3–P_2O_5 catalyst. It is considered that the MoO_3–BiO_3–P_2O_5 catalyst has nearly the same catalytic specificity as the MoO_3–P_2O_5 catalyst in the oxidation step from C_4H_8 to $C_4H_2O_3$, but its activity for maleic anhydride oxidation is so very high that maleic anhydride cannot be accumulated. The difference in the catalytic features between the MoO_3–P_2O_5 and the MoO_3–Bi_2O_3–P_2O_5 catalysts may be mainly attributed to that in the activity of maleic anhydride destruction. Thus, we can conclude that no satisfactory maleic anhydride yield can be expected by the use of the MoO_3–Bi_2O_3–P_2O_5 catalyst.

Imidazole Catalyses in Aqueous Systems. VIII. Spontaneous Hydrolysis and Michaelis-Menten-type Catalytic Hydrolysis of Phenyl Esters in the Presence of Cholic Acid and Its Histamine Derivative[1]

Seiji SHINKAI and Toyoki KUNITAKE*

Department of Organic Synthesis, Faculty of Engineering, Kyushu University, Fukuoka

(Received March 22, 1971)

Spontaneous hydrolyses of cationic and anionic phenyl esters in the presence of cholic acid (VI) and their catalytic hydrolyses with a histamine amide of cholic acid (VII) were investigated using a pH-stat at 30°C in 1.0M aqueous KCl. The rates of spontaneous hydrolysis decreased by 30—70% upon binding of substrates with cholic acid. The variation of the apparent binding constant (7-3650M^{-1}) was considered to reflect the magnitude of hydrophobic forces between cholic acid and substrates, although the values may have to be corrected for the possible involvement of self-association of cholic acid molecules. Imidazole derivative VII catalyzed the hydrolysis of phenyl esters according to Michaelis-Menten kinetics. The long methylene chain in the substrate molecule contributed appreciably to the binding of substrate with cholic acid and its derivative. The magnitude of substrate binding with VII appears to be comparable to the true binding constant with cholic acid. The intra-complex rate constants did not differ much from those expected with other enzyme-like catalysts. Thus, the steroid ring seems to provide a non-specific hydrophobic binding site for the substrates used.

We showed that some imidazole derivatives catalyzed the hydrolysis of *p*-acetoxybenzoic acid (ABA) by second-order kinetics (Eq. (1)) or by the Michaelis-Menten kinetics (Eq. (2)):[2,3]

$$C + S \xrightarrow{k'} C + P \quad (1)$$

$$C + S \underset{K_m}{\rightleftharpoons} CS \xrightarrow{k_{cat}} C + P \quad (2)$$

where C, S, and P denote catalyst, substrate, and product, respectively.

The Michaelis-Menten kinetics were observed when imidazole catalysts contained naphthalene ring (I, II, III). The catalysis by less hydrophobic imidazole compounds (IV, V) followed second-order kinetics. Substrate binding in the enzyme-like catalysis was concluded to be ascribable to the hydrophobic interaction. This was also supported by the thermodynamic data obtained for formation of the catalyst-substrate complex.

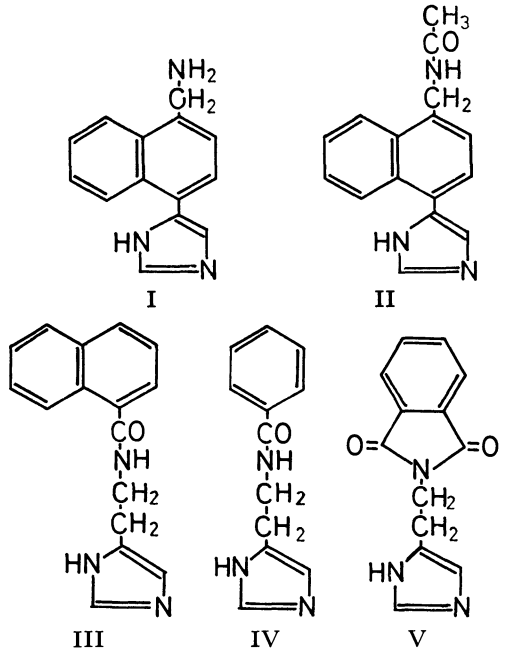

The intra-complex product formation in the Michaelis-Menten pathway was not very efficient because of extraordinarily large negative $\Delta S^{\ddagger}$ values (*ca.* −50 eu). The unfavorable $\Delta S^{\ddagger}$ term was conceivably related to destruction of the hydrophobic interaction between catalyst and substrate in the transition state of the intra-complex reaction.[3]

Since the intra-complex process would be affected by the structure of the binding site it is interesting to study the catalytic behavior of imidazole compounds with different hydrophobic groups. The steroid ring might provide an interesting binding site as considered from its physiological role. In particular, desoxycholic acid and related compounds are known to form stable inclusion compounds in aqueous solutions.[4] Thus,

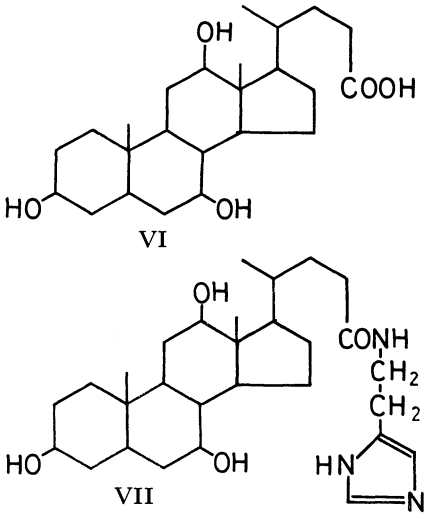

1) Contribution No. 234 from this department. Presented at the 24th annual meeting of the Chemical Society of Japan, April, 1971, Osaka.

* Responsible co-author.

2) a) C. Aso, T. Kunitake, and S. Shinkai, *Chem. Commun.*, **1968**, 1483. b) T. Kunitake and S. Shinkai, This Bulletin, **43**, 1109 (1970).

3) T. Kunitake and S. Shinkai, *ibid.*, **43**, 2581 (1970).

4) See for a general reference, K. Takemoto, "Hosetsu Kagobutsu no Kagaku," Tokyo Kagaku Dojin, Tokyo (1969).

imidazole derivatives of these steroids would give rise to interesting catalytic systems. In this paper we report the influence of complexation of cholic aicd (VI) on the spontaneous hydrolysis of several phenyl esters and the catalytic hydrolysis of these phenyl esters by a histamine derivative of cholic acid (VII). Attempts to synthesize a similar catalyst have been reported by French workers.[5]

Experimental

Materials. Commercial cholic acid (Nakarai Chemicals Ltd., Guaranteed Reagent) was used without further purification. Imidazole catalyst VII was prepared from cholic acid (VI) and histamine. Cholic acid (5.1 g, 12.5 mmol) was dissolved in a mixture of tetrahydrofuran (150 m*l*) and acetonitrile (50 m*l*) containing 10 m*l* of triethylamine. The reaction mixture was cooled in an ice bath and 1.5 g (16 mmol) of methyl chloroformate was added with stirring. After stirring for 36 hr, precipitates (triethylamine hydrochloride) were filtered and the filtrate was evaporated to dryness *in vacuo*. The solid residue was dissolved in 60 m*l* of ethanol containing 2 m*l* of 4N aqueous NaOH and was allowed to stand at room temperature for 2 hr. The solvent was again removed *in vacuo* and the residue was dissolved in absolute alcohol in order to separate inorganic materials. Alcohol was evaporated, and the residue which was dissolved in 1N hydrochloric acid was reprecipitated by pouring into a saturated solution of aqueous sodium carbonate. Reprecipitation was repeated once more. Yield 66%. The infrared spectrum showed an amide peak at 1640 cm^{-1} and characteristic peaks of imidazole at 1440 and 1530 cm^{-1}. Another reprecipitation gave a product of mp 117—120°C in 48% overall yield: $pK_a=7.14$ (1.0M KCl, 30°C).

Found: C, 72.12; H, 9.43; N, 7.19%. Calcd for $C_{29}H_{47}N_3O_4$: C, 69.43; H, 9.44; N, 8.38%.

Two spots were observed at $R_f=0.07$ and 0.52 on a silica-gel thin layer chromatogram with acetic acid as developing solvent. The weak spot at $R_f=0.52$ was due to cholic acid. Purity based on the nitrogen content was 85.8%. This preparation containing cholic acid as probably the sole organic contaminant was used as catalyst. When the reprecipitation was repeated five more times, the product showed mp 122—124°C.

Found: C, 70.69; H, 9.47; N, 7.99%; Calcd for $C_{29}H_{47}N_3O_4$: C, 69.43; H, 9.44; N, 8.38%.

Precipitation and characterization of *p*-acetoxybenzoic acid (ABA, mp 192—194°C), 3-nitro-4-acetoxybenzoic acid (NABA, mp 156—158°C), *m*-acetoxy-*N*-trimethylanilinium iodide (ANTI, mp 223—224°C) and *m*-nonanoyloxy-*N*-trimethylanilinium iodide (NNTI, mp 134—135°C) were described previously.[3,6] *p*-Nonanoyloxybenzoic acid (NBA) was prepared from *p*-hydroxybenzoic acid and nonanoyl chloride: 8.4 g (30 mmol) of *p*-hydroxybenzoic acid and 2.8 g (65 mmol) of NaOH were dissolved in water, and 5.3 g (30 mmol) of nonanoyl chloride (bp 126—130°C/30 mmHg. lit,[7] bp 93—96°C/11 mmHg) was added dropwise with stirring. The reaction flask was immersed in an ice bath. White precipitates were formed at the end of the addition. Stirring was continued for 1 hr and pH of the reaction mixture was adjusted to 2—3 by concentrated hydrochloric acid. The precipitates were filtered, washed with water, dried, and recrystallized two times from benzene, yield 76%, mp 113—115°C, IR(KBr): 1750 cm^{-1}(ester), 1675 cm^{-1}(carboxyl).

Found: C, 68.95; H, 7.90%. Calcd for $C_{16}H_{22}O_4$: C, 69.04; H, 7.97%.

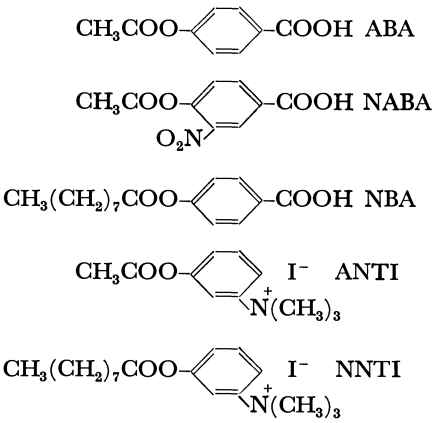

Titration and Hydrolysis Procedures. Titration and hydrolysis were carried out at 30.0±0.05°C using a pH-stat connected with a recorder (TOA Electronics Ltd., Models HS-1B and EPR-2T, respectively). The reaction rate was determined from the amount of alkali automatically added to the reaction mixture in order to neutralize the acid formed. The degree of dissociation of the product phenols under the reaction conditions was taken into account in determining the rate of reaction. Details of the procedure have been described.[8]

Results and Discussion

Spontaneous Hydrolyses in the Presence of Cholic Acid. Phenyl esters are hydrolyzed spontaneously in an alkaline medium by the pseudo-first-order kinetics.[3,6,8]

$$v_{spont} = k_s[S] \quad (3)$$

The rate of spontaneous hydrolysis decreased upon addition of cholic acid. Figures 1 and 2 show the effect of cholic acid on the relative rate of spontaneous hydrolysis of five substrates: ABA, NBA, NABA, ANTI, and NNTI. Hydrolysis of NBA was carried out at pH 9.4, because v_{spont} was too small at pH 8.0 to be determined accurately. The relative rate v/v_0 decreased with increasing concentration of cholic acid, and in the case of NBA it decreased to a saturation value with a small amount of cholic acid. The results can be explained by assuming that phenyl esters form complexes with cholic acid and that the resulting complexes show decreased reactivity.

Retardation (or inhibition) of spontaneous hydrolyses of esters in the presence of additives has been studied by some groups of researchers. In particular, Connors and his coworkers made a detailed study on the effect of theophylline and related heterocyclic compounds in the alkaline hydrolysis of several esters.[9-11]

5) G. Defaye and M. Fétizon, *Bull. Soc. Chim. Fr.*, **1969** 1632.
6) T. Kunitake and S. Shinkai, *Makromol. Chem.*, in press.
7) H. E. Fierz-David and W. Kuster, *Helv. Chim. Acta*, **22**, 86 (1939).
8) T. Kunitake, F. Shimada, and C. Aso, *J. Amer. Chem. Soc.*, **91**, 2716 (1969).
9) J. A. Mollica, Jr., and K. A. Connors, *ibid.*, **89**, 308 (1967).
10) P. A. Kramer and K. A. Connors, *ibid.*, **91**, 2600 (1969).
11) K. A. Connors, M. H. Infeld, and B. J. Kline, *ibid.*, **91**, 3597 (1969).

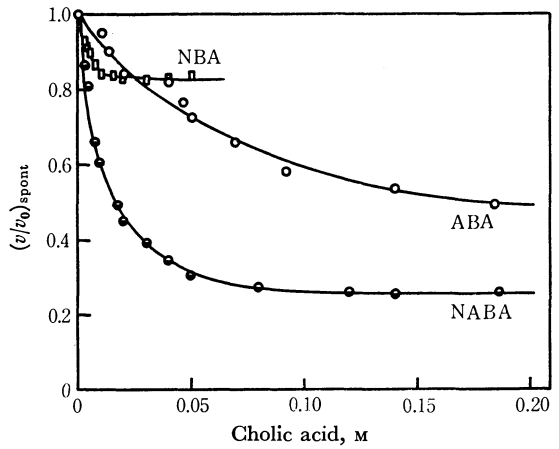

Fig. 1. Spontaneous hydrolysis of phenyl esters in the presence of cholic acid.
ABA: 0.030M, $v_0=1.27\times10^{-5}$M min^{-1} (30°C, 1.0M KCl, pH 8.0)
NABA: 0.015M, $v_0=3.75\times10^{-5}$M min^{-1} (30°C, 1.0M KCl, pH 8.0)
NBA: 0.020M, $v_0=3.22\times10^{-6}$M min^{-1} (30°C, 1.0M KCl, pH 9.4)

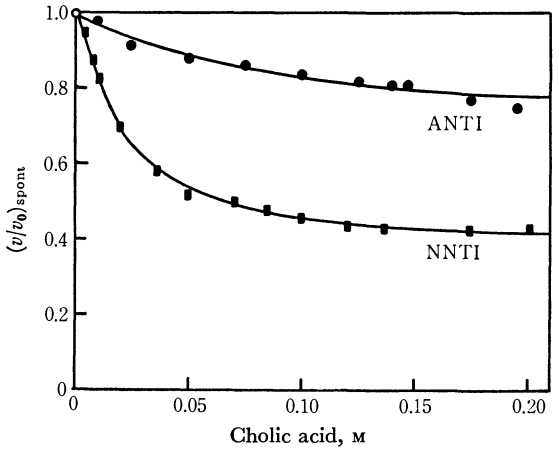

Fig. 2. Spontaneous hydrolysis of phenyl esters in the presence of cholic acid.
ANTI: 0.020M, $v_0=3.18\times10^{-5}$M min^{-1} (30°C, 1.0M KCl, pH 8.0)
NNTI: 0.020M, $v_0=2.34\times10^{-5}$M min^{-1} (30°C, 1.0M KCl, pH 8.0)

The spontaneous hydrolysis of phenyl esters in the presence of cholic acid may be described by the following equations, if substrate S and additive A (cholic acid) interact to form a 1:1 complex SA.

$$S + A \overset{K_c}{\rightleftharpoons} SA \quad (4)$$

$$S \xrightarrow{k_s} \text{products} \quad (5)$$

$$SA \xrightarrow{k_{SA}} \text{products} + A \quad (6)$$

where K_c is the binding constant of phenyl esters and cholic acid and k_{SA} is the pseudo-first-order rate constant for spontaneous hydrolysis of phenyl esters in the complexed state.

The following equation has been obtained according to Connors *et al.* for [A]≫[S]:

$$\frac{k_s}{k_s-k'} = \frac{1}{qK_c[A]} + \frac{1}{q} \quad (7)$$

where k' is the apparent pseudo-first-order rate constant and $q=1-k_{SA}/k_S$. K_c and q are determined by plotting $k_s/(k_s-k')$ against $1/[A]$.

On the other hand, when the simplifying assumption ([A]≫[S]) cannot be made, the overall rate is expressed by

$$v = k_s[S] + k_{SA}[SA]$$
$$= k_s[S] + k_{SA}\{[S]_0-[S]\} \quad (8)$$

where $[S]_0$ is the total concentration of substrate and [S] is the concentration of free substrate. The following equation holds simultaneously.

$$K_c = \frac{[SA]}{[S][A]} = \frac{[S]_0-[S]}{[S]\{[A]_0-([S]_0-[S])\}} \quad (9)$$

where $[A]_0$ is the total concentration of cholic acid.

We see from Figs. 1 and 2 that the additive concentration is not small compared to the substrate concentration. Therefore, Eqs. (8) and (9) were employed and the values of K_c and k_{SA} were determined by computational trial-and-error as follows. Approximate K_c and k_{SA} values were first estimated from Eq. (7). The corresponding rate v_{calcd} was calculated for respective additive concentrations from the known k_s, $[S]_0$ and $[A]_0$ values and compared with the observed rate v_{obsd}. Then a set of K_c and k_{SA} values was sought which minimized the relative error.

$$\text{relative error} = \sum\left\{\frac{(v_{calcd}/v_{obsd}-1)^2}{n}\right\}^{1/2} \quad (10)$$

where n is the number of experimental runs.

Kinetic constants for the spontaneous hydrolysis of phenyl esters and their complexes with cholic acid are summarized in Table 1. As can be expected from Fig. 1, NBA showed a much greater tendency of binding ($K_c=3650$M^{-1}) than other substrates. This might be attributed to hydrophobic forces between the steroid skeleton of cholic acid and the long methylene chain of the substrate. The increased binding due to the long alkyl chain is also evident in the different K_c values between ANTI and NNTI. The carboxyl group in cholic acid is dissociated completely at pH 8 or 9.4. Therefore, it is possible that both hydrophobic and electrostatic forces contribute to binding of cationic substrates ANTI and NNTI. However, their K_c values were lower than those of related anionic sub-

Table 1. Spontaneous hydrolyses with and without cholic acid[a)]

Substrate	M	K_c[b)] M^{-1}	k_s min^{-1} $\times10^3$	k_{SA}[b)] min^{-1} $\times10^3$	k_{SA}/k_s	relative error[c)] %
ABA	0.030	16	0.423	0.13	0.31	2.9
NBA[d)]	0.020	3650	0.161	0.12	0.73	2.1
NABA	0.015	270	2.50	0.60	0.24	3.7
ANTI	0.020	6.8	1.59	0.88	0.55	1.4
NNTI	0.020	106	1.17	0.47	0.40	1.6

a) Hydrolysis conditions, 30°C, pH 8.0, 1.0M KCl, unless otherwise stated.
b) Obtained by assuming that there is no self-aggregation of chloric acid.
c) *Cf.* Eq. (10).
d) Hydrolysis conditions, 30°C, pH 9.4, 1.0M KCl.

strates (ABA and NBA, respectively). This suggests that the carboxylate group of cholic acid did not contribute noticeably to the binding of the cationic substrates.

In the above experiments, high concentration of cholic acid was employed relative to the substrate concentration except for NBA. Cholic acid molecules might be associated at high concentrations as considered from its tendency to form molecular compounds.[4] If, this is the case, the kinetic analysis based on Eqs. (4) (5), and (6) becomes unreliable for high concentrations of cholic acid. Therefore, it is possible that K_c values are underestimated except for NBA because association of cholic acid is assumed to be absent. Nevertheless, the relative tendency of substrates to form molecular complexes is probably not altered by the occurrence of association.

Underestimation of K_c necessarily leads to that of k_{SA} of the 1 : 1 complex according to Eqs. (8) and (9). As shown in Table 1, retardation of the spontaneous hydrolysis due to complexation was the smallest for NBA substrate. If k_{SA} is underestimated because of the neglect of association of cholic acid, the true k_{SA} value will be greater except for NBA substrate, and the extent of retardation might be closer with each other than that given in Table 1.

In any way, the retardation was not very efficient, k_{SA}/k_s being 0.24 to 0.73. On the other hand, in the alkaline hydrolysis of methyl cinnamate in the presence of theophylline, the corresponding relative rate was close to zero, indicating almost complete inhibition of hydrolysis due to complexation.[9] This contrast is interesting in connection with the nature of the binding site. The chemical environments of the ester group of substrates complexed with cholic acid do not appear to differ much from those of the ester group of free substrates. In the case of inhibition by theophylline, Connors *et al.* suggested that the molecular complexes of theophylline with cinnamate esters were formed in such a way as to permit extensive local dipole and induced dipole interactions in the face-to-face orientation.[11] The electronic interaction of the ester group may be much greater with a dipolar, flat theophylline molecule than with a hydrocarbon-like skeleton of cholic acid.

Catalytic Hydrolysis. Catalyst VII was not completely free from cholic acid as shown by elemental analysis and thin layer chromatography. However, cholic acid present as contaminant (*ca.* 10^{-5}M) would show negligible influence. Catalyst concentration was corrected for the purity of the catalyst. The results of catalytic hydrolysis are shown in Figs. 3 and 4. The catalytic rate v_{cat} clearly tends to level off at high substrate concentrations. The results are similar to those previously observed with imidazole catalysts containing naphthalene rings,[2,3] and can be described by the Michaelis-Menten kinetics. In the case of the enzyme-like catalytic pathway (Eq. (2)), the catalytic rate is given by

$$v_{cat} = \frac{k_{cat}[C][S]}{K_m + [S]} \qquad (11)$$

The kinetic constants K_m and k_{cat} can be determined from Lineweaver-Burk plotting between $1/v_{cat}$ and $1/[S]$.[12]

$$\frac{1}{v_{cat}} = \frac{1}{k_{cat}[C]} + \frac{K_m}{k_{cat}[C]} \cdot \frac{1}{[S]} \qquad (12)$$

The Lineweaver-Burk plots of the data of Figs. 3 and 4 were linear, and K_m and k_{cat} values for respective substrates were obtained from the slope and the intercept as given in Table 2. The binding tendency varied with substrates in approximately the same manner as with K_c values. The catalyst concentrations were much smaller than the cholic acid concentration of the spontaneous hydrolysis. In addition, substrates were used in excess of the catalyst in all the catalytic hydrolyses. Therefore, association of the catalyst molecules can be neglected in catalytic hydrolysis in contrast to spontaneous hydrolysis, and $1/K_m$ will reflect the true binding capacity of the catalyst.

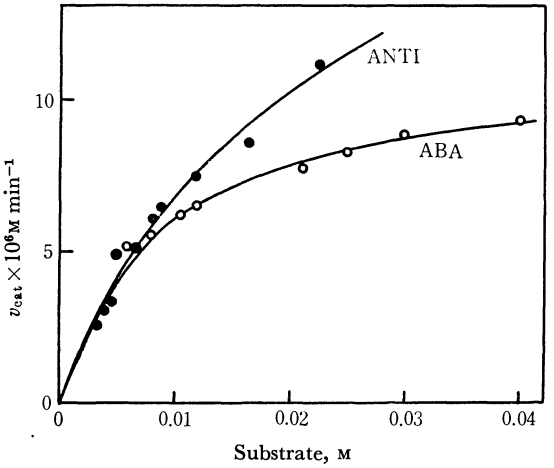

Fig. 3. Catalytic hydrolysis of phenyl esters.
○: substrate ABA, catalyst 4.54×10^{-4}M, 30°C, 1.0M KCl, pH 8.0
●: substrate ANTI, catalyst 2.27×10^{-4}M, 30°C, 1.0M KCl, pH 8.0

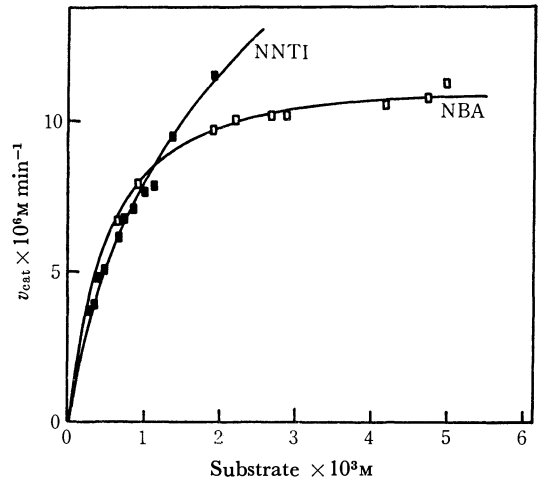

Fig. 4. Catalytic hydrolysis of phenyl esters.
□: substrate NBA, catalyst 5.04×10^{-4}M, 30°C, 1.0M KCl, pH 9.4
■: substrate NNTI, catalyst 2.27×10^{-4}M, 30°C, 1.0M KCl, pH 8.0

12) H. Lineweaver and D. Burk, *J. Amer. Chem. Soc.*, **56**, 658 (1934).

TABLE 2. CATALYTIC HYDROLYSES[a)]

Substrate	Catalyst M × 10^4	K_m mM	k_{cat} min^{-1}	k_{cat}/K_m $min^{-1}M^{-1}$	$1/K_c$ mM
ABA	4.05	8.0	0.028	3.0	63
NBA[b)]	4.50	0.53	0.033	62	0.27
ANTI	2.02	20	0.099	5.0	150
NNTI	2.02	0.94	0.075	80	9.4
ABA	8.2[c)]	16.4	0.021	1.3	—

a) Hydrolysis conditions: 30°C, pH 8.0, 1.0M KCl, unless otherwise stated.
b) Hydrolysis condtions: 30°C, pH 9.4, 1.0M KCl.
c) Catalyst, III. From Ref. 3.

It is obvious that the nonanoyl group enhanced substrate binding due to hydrophobic interaction. The binding tendency of cationic substrates was smaller relative to that of the anionic substrates (ABA *vs.* ANTI, NBA *vs.* NNTI). Since the catalytic species VII does not carry a negative charge, it is not necessary to take into account the electrostatic interaction between the opposite charges in the catalytic hydrolysis. Table 2 includes the rate data of ABA with naphthoylhistamine III. From a comparison of K_m values it is indicated that the steroid skeleton is twice as effective as the naphthalene ring as a hydrophobic binding site. As for the k_{cat} term, these catalysts showed very similar efficiencies, suggesting that the reactivity of the histamine moiety is not affected by this extent of difference in the binding site.

The binding capacities of cholic acid and its histamine derivative can be compared by using $1/K_c$ and K_m given for each substrate in Table 2. As mentioned above, K_c may be underestimated except for NBA. If this is taken into consideration, the $1/K_c$ values for ABA, ANTI, and NNTI will be smaller than those given in Table 2, and K_m and $1/K_c$ values may become close in the respective substrate. It is probable that the nature of the binding site is not greatly altered by incorporation of the histamine moiety.

TABLE 3. FREE ENERGIES OF SUBSTRATE BINDING

Substrate	ΔG_u kcal/mol	$\Delta\Delta G_u$ kcal/mol	Free energy of binding per methylene group, $\Delta\Delta G_u/7$, kcal/mol.
ABA	−5.33	−1.63	−0.23
NBA	−6.96		
ANTI	−4.78	−1.84	−0.26
NNTI	−6.62		

The unitary free energy change ΔG_u (kcal/mol) for substrate binding is defined as follows.[13)]

$$\Delta G = -RT\ln(1/K_m) \quad (13)$$

$$\Delta G_u = \Delta H - T\Delta S_u = \Delta H - T(\Delta S + 7.98) \quad (14)$$

ΔG_u values in the catalytic hydrolysis are summarized in Table 3. The $\Delta\Delta G_u$ value reflects the contribution of the nonanoyl group to substrate binding, and is similar in the anionic and cationic substrates. The contribution of the methylene unit to binding, *ca.* −0.25 kcal/mol, was in the same range as observed with some polymer catalysts.[6)] The hydrophobic contribution of the methylene group has been estimated to be *ca.* −0.75 kcal/mol. The smaller contribution of the methylene unit in the present case suggests that the alkyl chain is not fully available for the hydrophobic interaction with the catalyst.

In conclusion, the steroid ring in cholic acid and its derivative was shown to constitute a substrate binding site based on hydrophobic forces. This hydrophobic region did not show specific interactions at least with the substrates used, contrary to our expectation.

The authors are deeply grateful to Professor Chuji Aso, head of our research group, for his unfailing encouragement and advice.

13) W. Kauzmann, *Advan. Protein Chem.*, **14**, 1 (1959).

S_N2 Reactions in Dipolar Aprotic Solvents. Chlorine Isotopic Exchange Reactions of 2-Arylethyl Chlorides, Chloromethyl Aryl Ethers, and Chloromethyl Aryl Sulfides in Acetonitrile[1)]

Jun-ichi HAYAMI,[2)] Nobuo TANAKA, Syuji KURABAYASHI, Yasuhiro KOTANI, and Aritsune KAJI

Department of Chemistry, Faculty of Science, Kyoto University, Sakyo-ku, Kyoto

(Received March 29, 1971)

The S_N2 reactions having a symmetrical transition state were studied in a dipolar aprotic solvent. A good Hammett correlation was found for the chlorine isotopic exchange reactions in acetonitrile between tetraethylammonium chloride and three types of substituted methyl chlorides, 2-arylethyl chlorides, chloromethyl aryl ethers, and chloromethyl aryl sulfides. The reaction constant was positive for 2-arylethyl chlorides and negative for the methyl chlorides possessing an α-heteroatom. The presence of oxygen and sulfur atom on the α-position to the reaction center resulted in a rate enhancement of about 10^5 times and 10^3 times, respectively. Features of the transition states of these S_N2 reactions are discussed.

Nucleophilic substitution at a saturated carbon atom has been extensively studied.[3)] As compared to abundant studies on unimolecular reactions, not much has been carried out on the features of the S_N2 reactions. Timing of bond-breaking and bond-forming and also the electronic requirement of the transition state are less extensively studied. Parker examined the solvent effect on bimolecular reactions.[4)] However, little information is presented concerning the effect of the structures of the substrates.

In the present study, attempts were made to bring about a clean S_N2 reaction of which the examination of the Hammett relationship is feasible.

Methyl chlorides with a substituent at the α-position were prepared and subjected to isotopic exchange reaction in dry acetonitrile. Smaller solvation of anions in a dipolar aprotic solvent implies a slight change in anion solvation, minimizing the difficulties due to desolvation-solvation phenomena of anionic entities involved in an S_N2 displacement.[5)] As is proved in this communication, kinetics suffered little from the change of ion-pair dissociation equilibria of the quaternary ammonium salt. In solvent acetonitrile, such a salt shows fairly good dissociation and little trouble is anticipated.

Results and Discussion

Three substituted methyl chlorides, 2-arylethyl chlorides, aryloxymethyl chlorides (chloromethyl aryl ethers), and arylthiomethyl chlorides (chloromethyl aryl sulfides) were prepared. These substrates were treated in dry acetonitrile with tetraethylammonium chloride-^{36}Cl. The reactions are summarized as follows.

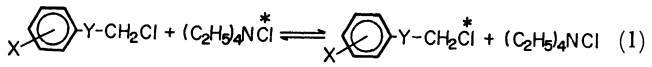

(1)

I Y: CH_2, X: a) *p*-NO_2, b) *m*-Cl, c) *p*-Cl, d) H, e) *p*-CH_3, f) *p*-OCH_3, g) *p*-OC_3H_7-*i*

II Y: O, X: a) *p*-NO_2, b) *m*-Cl, c) *p*-Br, d) *p*-Cl, e) H, f) *p*-CH_3, g) *p*-OCH_3

III Y: S, X: a) *p*-NO_2, b) *p*-CN, c) *m*-CN, d) *p*-$COCH_3$, e) *m*-Cl, f) *p*-Cl, g) H, h) *m*-CH_3, i) *p*-CH_3, j) *p*-OCH_3

Rates of the bimolecular substitution reactions with a symmetrical transition state were followed by examining the radioactivities incorporated in the organic compounds and also the radioactivities remaining in the ionic chloride. In every case, a good first order kinetics was observed. Second order rate coefficients were deduced by dividing the observed first order rate constants by pertinent chloride concentrations. Typical kinetic data are given in Table 1.

Examination was made of the effect of ion-pair dissociation of the quaternary ammonium chloride in

Table 1. Chlorine exchange between chloromethyl phenyl sulfide and tetraethylammonium chloride at 20°C[a)]

Run	Time min	Radioactivity (cpm) benzene layer	Radioactivity (cpm) water layer	X_e[b)]	$k\times10^2$ l/mol min
1	25	1,510	15,720	8,620	3.84
	50	2,700	14,480	8,590	3.77
	75	3,740	13,370	8,560	3.83
	100	4,590	12,570	8,580	3.82
2	60	2,880	12,780	7,830	3.82
	90	3,830	11,670	7,750	3.79
	120	4,670	10,970	7,820	3.79
					av. 3.81

a) [Chloromethyl phenyl sulfide]=[Tetraethylammonium chloride]=0.10M

b) The difference between Run 1 and Run 2 was due to the difference of specific radioactivity of used tetraethylammonium chloride.

1) Presented at the 23rd Annual Meeting of the Chemical Society of Japan, Tokyo, April, 1970.

2) To whom correspondences should be addressed.

3) a) C. K. Ingold, "Structure and Mechanism in Organic Chemistry," 2nd Edition., Cornell Univ. Press, Ithaca, New York (1969), p. 418. b) C. A. Bunton, "Nucleophilic Substitution at a Saturated Carbon Atom," Elsevier Pub. Co., London (1963). c) A. Streitwieser, Jr., "Solvolytic Displacement Reactions," McGraw-Hill Book Co., New York (1962).

4) A. J. Parker, *Chem. Rev.*, **69**, 1 (1969).

5) a) A. J. Parker, *Advan. Org. Chem.*, **5**, 1 (1965). b) A. J. Parker, *Quart. Rev.* (London), 163 (1962).

acetonitrile. A slight but not serious change in k_2 was observed in changing the concentration of the ammonium chloride present. This shows that a slight change in ion-pair dissociation equilibrium took place in the concentration range studied (an implication of essentially complete dissociation). The results are in contrast to reactions in dimethylformamide, where the rate increment of about 30% was observed for the seven fold variation in chloride ion concentration.[6] A slight decrease in the rate observed in the presence of an inert salt may be attributed to a common ion effect which affects the ion-pair dissociation equilibrium in the reaction system.

The reaction was essentially of second order, first order in the substrate and also in tetraethylammonium chloride. Second order rate coefficients calculated were constant, the deviation being within the experimental error for the change in the ten fold variation of chloride concentration. The results for chloromethyl aryl ethers and sulfides present a rare case where molecularity of the reaction is well defined for the reaction of this class of compound. The results are shown in Table 2.

TABLE 2. EFFECT OF THE CHLORIDE ION CONCENTRATION ON THE RATE OF THE CHLORINE EXCHANGE IN THE PRESENCE AND ABSENCE OF TETRAETHYLAMMONIUM PERCHLORATE

	Y	X	T°C	$[Cl^-]_M$	$[ClO_4^-]_M$	k l/mol min
Id	CH_2	H	50.0	0.10	—	1.85×10^{-3}
				0.05	—	1.86
				0.01	—	1.87
				0.05	0.05	1.76
				0.01	0.09	1.66
IIa	O	*p*-NO_2	−15.9	0.10	—	4.73×10^{-2}
				0.05	—	4.89
				0.01	—	5.05
				0.05	0.05	4.59
				0.01	0.09	4.47
IIIg	S	H	20.0	0.10	—	3.81×10^{-2}
				0.05	—	3.87
				0.01	—	3.90
				0.05	0.05	3.77
				0.01	0.09	3.80

Hammett relationship holds for these second order rate coefficients. Typical examples are given in Fig. 1 and the results are summarized in Tables 3, 4, and 5.

These tables clearly show that the reaction constant ρ was positive for the 2-arylethyl chlorides and negative for both the chloromethyl aryl ethers and sulfides. Such a trend is not without precedent but the present instance is perhaps the first case where linear free energy relationship holds. Negative ρ which holds for the varieties of the substituents is rarely reported.

As pointed out by Jaffé,[7] S_N2 reactions of 2-arylethyl chlorides with iodide ion in acetone gave ρ= 0.590 with a correlation coefficient r=0.870. An example of 2-chloroethyl aryl sulfides was also reported,

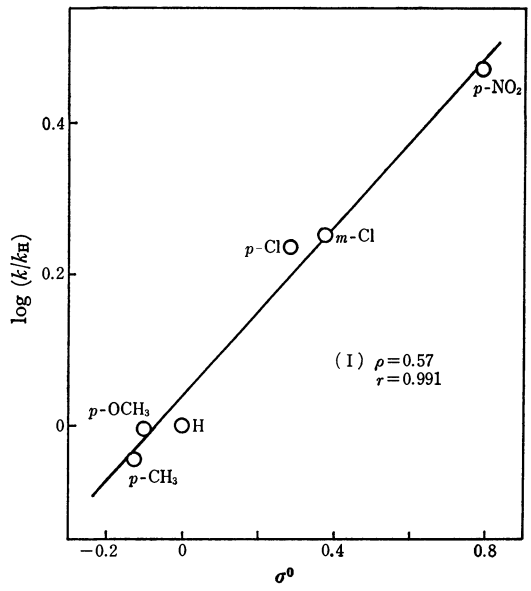

Fig. 1. a) Hammett plot for the chlorine exchange of 2-arylethyl chlorides (I) at 60°C.

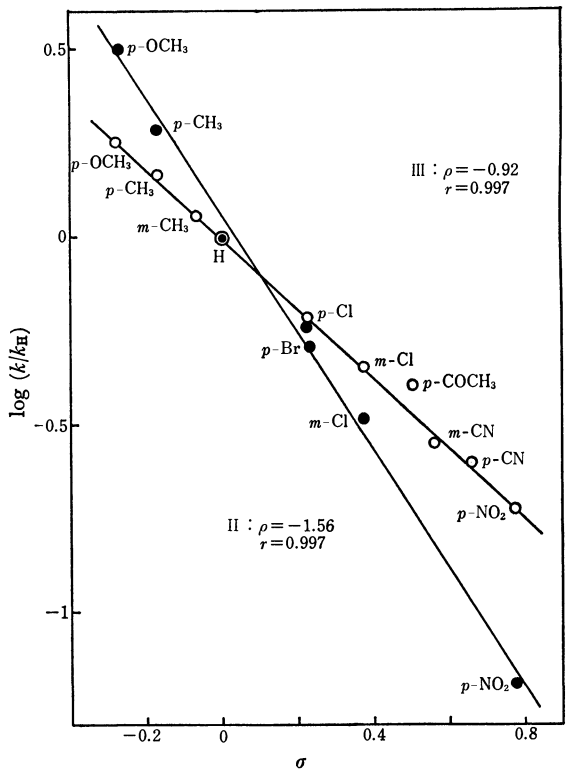

Fig. 1. b) Hammett plot for the chlorine exchange of chloromethyl aryl ethers (II: ●) and sulfides (III: ○) at −15.9°C and 20.0°C, respectively.

where electron-withdrawing substituents accelerate the reaction, ρ being 0.626 with r=0.918.

In the present instance, the rate accelerating effect of the heteroatom located on α-position to the reaction center is fairly large. The oxygen accelerates the reaction by a factor of 10^5—10^6 and the sulfur atom by a factor of 10^2—10^3 compared to the 2-arylethyl system. These values are compatible with the one reported in

6) D. Cook and A. J. Parker, *J. Chem. Soc., B*, **1968**, 142.
7) H. H. Jaffé, *Chem. Rev.*, **53**, 191 (1953).

Table 3. Rate constants for the chlorine exchange of 2-arylethyl chlorides[a)]

	X	$k\times10^3$ l/mol min		
		40.0°C	50.0°C	60.0°C
Ia	*p*-NO_2	1.63	5.68	16.7
Ib	*m*-Cl			10.1
Ic	*p*-Cl			9.76
Id	H	0.564	1.85	5.65
Ie	*p*-CH_3			5.11
If	*p*-OCH_3			5.60
Ig	*p*-OC_3H_7-*i*			5.54

a) [2-Arylethyl chloride]=[Tetraethylammoninm chloride] =0.10M

Table 4. Rate constants for the chlorine exchange of chloromethyl aryl ethers[a)]

	X	k l/mol min			
		−21.3°C	−15.9°C	−10.0°C	0°C
IIa	*p*-NO_2		0.0473	0.112	0.362
IIb	*m*-Cl		0.241		
IIc	*p*-Br		0.374		
IId	*p*-Cl		0.425		
IIe	H	0.413	0.737	1.38	
IIf	*p*-CH_3		1.41		
IIg	*p*-OCH_3		2.33		

a) [Chloromethyl aryl ether]=[Tetraethylammonium chloride]=0.10M

Table 5. Rate constants for the chlorine exchange of chloromethyl aryl sulfides[a)]

	X	$k\times10^2$ l/mol min		
		20.0°C	30.0°C	40.0°C
IIIa	*p*-NO_2	0.715	2.27	6.46
IIIb	*p*-CN	0.939		
IIIc	*m*-CN	1.07		
IIId	*p*-$COCH_3$	1.55		
IIIe	*m*-Cl	1.71		
IIIf	*p*-Cl	2.31		
IIIg	H	3.81	10.9	27.3
IIIh	*m*-CH_3	4.29		
IIIi	*p*-CH_3	5.55		
IIIj	*p*-OCH_3	6.79		

a) [Chlololoromethyl aryl sulfide]=[Tetraethylammonium chloride]=0.10M

literature.[3c,8)] Ballinger and his co-workers[8c)] showed the accelerating effect of the α-heteroatom to be 10^5 for oxygen in a methoxy group in an S_N2 solvolysis of methoxymethyl chloride.

The acceleration may be ascribed to the electron deficiency of the reaction center caused by the presence of an electronegative heteroatom. This can be ruled out by the negative ρ found for the isotopic exchange reactions. The results show definitely that the effects

8) a) M. Murakami and S. Oae, *Nippon Kagaku Zasshi*, **72**, 595 (1951). b) H. Böhme and A. Dörries, *Chem. Ber.*, **89**, 719 (1956). c) P. Ballinger, P. B. D. De La Mare, G. Kohnstam, and B. M. Prestt, *J. Chem. Soc.*, **1955**, 3641.

Table 6. Activation parameters for the chlorine exchange reactions of alkyl chlorides

X-C_6H_4-Y-CH_2Cl

X	Y	*E* kcal/mol	ΔS^* e.u.(20°C)
H	CH_2	24.0	−6.8
	O	14.0	−14.9
	S	18.0	−13.8
p-NO_2	CH_2	24.2	−4.1
	O	17.7	−5.6
	S	20.1	−10.0

of the α-oxygen and of the α-sulfur atom are due to electron-donation. The electron-donating conjugation of oxygen and sulfur seems to surpass the electron-withdrawing inductive effect in this case.

In other words, in the case of the S_N2 reaction of chloromethyl aryl ethers and sulfides, the important factor should be the stabilization of the transition state by the electron-donating conjugation of an α-heteroatom with the reaction center. The conjugation brings about the delocalization of the developing fractional positive charge on the central carbon atom. The $2p$–$2p$ overlap between carbon and oxygen may exert a larger effect than $2p$–$3p$ overlap provided by sulfur.[8a)] The smaller activation energy for the ethers may support this interpretation. An electron-donating group can facilitate the bond dissociation in a nucleophilic displacement, and also can retard the bond formation to the incoming nucleophile. Accordingly, the effect of such a group should be self-canceling and should not reflect on the rate of the bimolecular symmetrical substitution.

In the case of 2-arylethyl chlorides, the ease of approach of the entering chloride ion seems to be essential.[9)] The effect of substituents is essentially polar (inductive), and the linear free energy relationship with a positive ρ holds for Taft's σ^0,[10)] a polar parameter.

It should be noted that as far as the S_N2 reactions in the present instance are concerned, there seems to be no clue to the fact that the ion-pair mechanism of Sneen[11)] is operative. Potential cation from 2-arylethyl chlorides may accept the participation of aryl group (*cf.* ethylenephenonium cation), showing the accelerating effect by electron-donating substituents which generally obeys the ρ–σ^+ relationship. However, this is not the case. Also in the other two cases, where electron-donating substituents accelerated the reaction, ion-pair mechanism is less probable. Hammett ρ values were −1.56 and −0.92 for these compounds. These values seem too small to imply the interaction of an α-heteroatom with the fully developed

9) The polar effect observed in the present study is tentatively ascribed to the importance of bond formation at the transition state. The interpretation based on a field effect proposed by Holtz and Stock is noteworthy. However, the establishment of ρ-σ^0 rather than ρ-σ_I relationship seems to prefer the present interpretation. H. D. Holtz and L. M. Stock, *J. Amer. Chem. Soc.*, **87**, 2404 (1965).

10) a) R. W. Taft, Jr., *J. Phys. Chem.*, **64**, 1805 (1960). b) Y. Yukawa and Y. Tsuno, *Nippon Kagaku Zasshi*, **86**, 878 (1965).

11) R. A. Sneen and J. W. Larsen, *J. Amer. Chem. Soc.*, **91**, 362 (1969).

positive center.[12]

A report was given by the authors showing that the E2 reaction from 2-arylethyl chlorides in acetonitrile gave a ρ value close to 2.[13] This implies that electronic requirement of the S_N2 reaction with chloride ion is quite different from that of the E2 reaction promoted by fluoride ion.

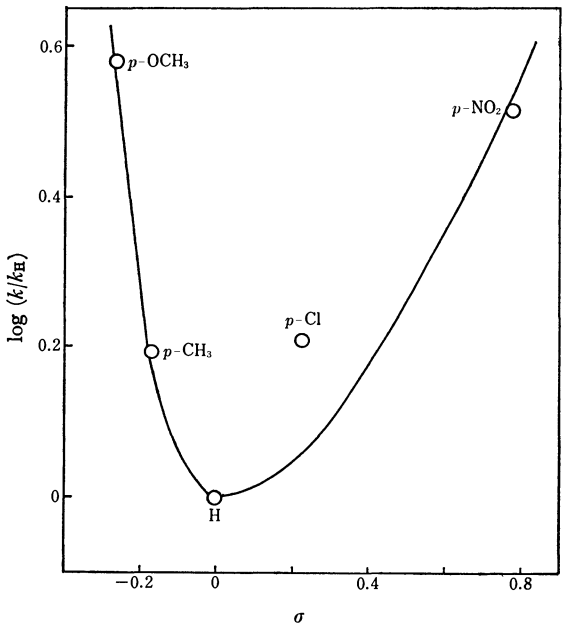

Fig. 2. Hammett plot for the chlorine exchange of benzyl chlorides at 40.0°C.

The U-shaped Hammett plots were reported for the S_N2 reactions of benzyl halides in some cases.[14] The authors carried out the chlorine exchange reaction between substituted benzyl chlorides and tetraethylammonium chloride. The symmetrical S_N2 reaction showed an ordinary U-shaped Hammett plot as shown in Fig. 2. The result implies that the tightening factor in a symmetrical transition state after Parker[15] is not effective enough to make the intrinsically loose transition state tighter.

12) The observed rate constants, or ρ values, can be affected by the ion-pair return that makes the interpretation of ρ values ambiguous.[a] It is quite plausible, however, that the solvent separated ion-pair intermediate is effectively intercepted by chloride and/or perchlorate ion, and external ion-pair return from this intermediate is minimized by the presence of tetraethylammonium salt in a concentration range studied.[b] It is difficult to confirm or disprove the intervention of an intimate ion-pair. However the enhanced internal return should result in a high ρ value reaching the limiting value for S_N1 reactions. Bordwell and his coworkers reported that an S_N1 reaction of chloromethyl aryl sulfides gave $\rho=-2.6$ at 34.85°C.[c] a) S. G. Smith and D. J. W. Goon, *J. Org. Chem.*, **34**, 3127 (1969). b) S. Winstein and A. H. Fainberg, *J. Amer. Chem. Soc.*, **80**, 459 (1958); E. F. Jenny and S. Winstein, *Helv. Chim. Acta*, **41**, 807 (1958). c) F. G. Bordwell, G. D. Cooper, and H. Morita, *J. Amer. Chem. Soc.*, **79**, 376 (1957).

13) J. Hayami, N. Ono, and A. Kaji, This Bulletin, **44**, 1628 (1971).

14) a) S. Sugden and J. B. Willis, *J. Chem. Soc.*, **1951**, 1360. b) G. M. Benett and B. Jones, *ibid.*, **1935**, 1815. c) H. Franzen and I. Rosenberg, *J. Prakt. Chem.*, (2) **97**, 82 (1918).

15) A. J. Parker, Ref. 4, p. 15.

Experimental

Preparation of materials. a) 2-Arylethyl chlorides (Ib—Ig) were prepared from corresponding 2-arylethyl tosylates by heating to reflux with tetraethylammonium chloride in acetonitrile. The products were purified by distillation under reduced pressure. 2-*p*-Nitrophenylethyl chloride (Ia) was obtained by nitration of 2-phenylethyl chloride (Id).

b) Chloromethyl aryl ethers (IIa—IIg) were prepared from sodium aryloxymethanesulfonates with phosphorus pentachloride, and purified by vacuum distillation except for chloromethyl *p*-nitrophenyl ether (IIa) and chloromethyl *p*-bromophenyl ether (IIc) which were recrystallized from petroleum ether containing a small amount of benzene.[16]

c) Chloromethyl aryl sulfides (III) were prepared by either of the two following methods. (A). Corresponding thiophenols were allowed to react with paraformaldehyde and gaseous hydrogen chloride in methylene chloride. (B). Corresponding methyl aryl sulfides were chlorinated with sulfuryl chloride in methylene chloride.[17] Chloromethyl *p*-nitrophenyl sulfide (IIIa) and chloromethyl *p*-cyanophenyl sulfide (IIIb) were purified by recrystallization from methylene chloride. Chloromethyl *m*-cyanophenyl sulfide (IIIc) and chloromethyl *p*-acetylphenyl sulfide (IIId) were recrystallized from methylene chloride after distillation under reduced pressure. The structures of new compounds were confirmed by their NMR and IR spectra and by elemental analyses.

Physical constants of alkyl chlorides (I, II, III) are summarized in Tables 7,8, and 9.

Table 7. Physical constants of 2-arylethyl chlorides

	X	Bp °C/mmHg (Mp °C)	(lit)
Ia	*p*-NO_2	(49.0)	(48—49)[a]
Ib	*m*-Cl	130—131/35	
Ic	*p*-Cl	84.0/4	82—83/3[b]
Id	H	86.0/18	90/25[c]
Ie	*p*-CH_3	66.5/3	67/4[c]
If	*p*-OCH_3	94.0/3	95/4[c]
Ig	*p*-OC_3H_7-*i*	106.0/5	

a) Ref. 18 b) Ref. 19 c) Ref. 13

Table 8. Physical constants of chloromethyl aryl ethers

	X	Bp °C/mmHg (Mp °C)	(lit)[a]
IIa	*p*-NO_2	(34.0—34.5)	(36—37)
IIb	*m*-Cl	82.0—83.0/6	112—113/18
IIc	*p*-Br	(52.0—52.5)	(55—56)
IId	*p*-Cl	87.0—88.0/6	120—124/18
IIe	H	86.0—87.0/17	88—89/15
IIf	*p*-CH_3	98.5—99.0/16.5	106—108/20
IIg	*p*-OCH_3	98.5—99.0/5.5	140—141/18

a) Ref. 16

16) H. J. Barber, R. F. Fuller, M. B. Green, and H. T. Zwartouw, *J. Appl. Chem.* (London), **1953**, 266.

17) F. G. Bordwell and B. M. Pitt, *J. Amer. Chem. Soc.*, **77**, 572 (1955).

18) E. Ferber, *Ber.*, **62**, 187 (1929).

19) C. H. Depuy and C. A. Bishop, *J. Amer. Chem. Soc.*, **82**, 2535 (1960).

Table 9. Physical constants and analytical data of chloromethyl aryl sulfides

	X	Bp °C/mmHg (Mp °C)	Analysis found (calcd) C%	H%	N%	Method	(lit.)
IIIa	*p*-NO_2	(63.5—64.0)				B	(62—64)[a]
IIIb	*p*-CN	(60.5—61.0)	52.50 (52.32	3.16 3.29	7.38 7.63)	B	
IIIc	*m*-CN	120.0—121.0/0.4 (31.5—32.0)	52.28 (52.32	3.07 3.29	7.37 7.63)	B	
IIId	*p*-$COCH_3$	140.5/0.75 (43.0)	54.04 (53.86	4.50 4.52)		A	
IIIe	*m*-Cl	94.5/0.7				B	115—116/5[a]
IIIf	*p*-Cl	109—111/4.0				A	128—129/12[a]
IIIg	H	115.5—116.0/20				A	106—109/12[b]
IIIh	*m*-CH_3	88.5—89.0/1.3				B	125/16[a]
IIIi	*p*-CH_3	87.0/0.8				A	125—126/15[a]
IIIj	*p*-OCH_3	105.0/0.7				A	141—142/12[b]

a) Ref. 12 b) Ref. 17

d) Tetraethylammonium chloride labeled with Cl-36 was prepared by titration of tetraethylammonium hydroxide with hydrochloric acid labeled with Cl-36. Tetraethylammonium chloride having suitable specific radioactivity was obtained by dilution and recrystallization with non-active tetraethylammonium chloride from chloroform containing a small amount of petroleum ether. Essentially no loss of radioactivity due to exchange reaction between chloroform and the chloride was observed. The reagent was dried *in vacuo* at 110°C before use. Acetonitrile was purified according to the procedure described previously.[20]

Kinetic measurements. Batch method was used for kinetic runs. Aliquots of the acetonitrile solutions of an alkyl chloride and tetraethylammonium chloride were put separately into an ampoule with double stems, and the tube was flame-sealed. After the temperature equilibrium was attained, the kinetic run was initiated by inverting and shaking the ampoule. The reactions of 2-arylethyl chlorides and chloromethyl aryl sulfides were quenched by cooling with an acetone-dry ice bath at appropriate intervals. Organic chloride was taken up in benzene while ammonium chloride was extracted in water. The reaction of chloromethyl aryl ethers was carried out in an ampoule equipped with a double rubber septum. The reaction was quenched by addition of a mixture of diisopropyl ether and *n*-hexane (10:1) precooled in an acetone-dry ice bath. The resulting mixture was extracted with three 5 m*l* portions of water. In all cases, the organic layer containing alkyl chlorides, and the aqueous layer containing tetraethylammonium chloride was made up to 25 m*l*. Chlorine-36 radioactivity was measured by liquid scintillation counting.[21] Exchange rates were calculated by the equation[22]

$$k = \frac{1}{t}\frac{1}{a+b}\ln\frac{X_e}{X_e - X},$$

where t, time; a, b, initial concentration; X, radioactivity of organic layer at time t; X_e, radioactivity of organic layer at infinite time.

Blank tests were performed with the non-active materials. Titration proved that alkyl chlorides underwent essentially no hydrolysis during extraction.

The tracer experiments were carried out at Radioisotope Research Center of Kyoto University. Sincere thanks are due to the staff of this institution.

20) R. U. Lemieux and J. Hayami, *Can. J. Chem.*, **43**, 2162 (1965).

21) Nuclear Chicago 6801 liquid scintillation counter was utilized with dioxane base organic phosphor solution (7 g PPO, 0.050 g POPOP, 120 g naphthalene, and 1000 m*l* of dioxane). Radioactivity measurements were made long enough to secure the standard errors below ±1%.

22) A. A. Frost and R. G. Pearson, "Kinetics and Mechanism," John Wiley and Sons, Inc., New York (1961), p. 192.

The Effects of Solvents and Acid Catalysts on the Rearrangement of 2-Benzylidenecyclohexanone Oxide

Kenichi HINOUE, Masatomo NOJIMA, and Niichiro TOKURA

Department of Applied Chemistry, Faculty of Engineering, Osaka University, Suita, Osaka

(Received April 12, 1971)

The rearrangement of 2-benzylidenecyclohexanone oxide (I) to 2-phenylcycloheptane-1,3-dione (II) was carried out in the presence of a Lewis acid or a Brønsted acid in various media-liquid sulfur dioxide, benzene, and ether. The only reaction product of I with a Brønsted acid in these solvents was the rearranged compound, II. In addition to II, 2-(α-halobenzyl)-2-hydroxycyclohexanone, (III) or (IV), was also obtained in the reaction of I with a Lewis acid in solutions. Drastic solvent effects were observed on the rate and the distribution of products in this reaction; however, no solvent effect was observed when a Brønsted acid, which could donate a proton to I, was used as the catalyst. From the variations in the concentrations of the reactant, the intermediate, and the product during the reaction course, the solvent effects upon the reaction pathways were discussed.

In a preceding paper[1] the rearrangement of 2-cyclohexylidenecyclohexanone oxide in the presence of a Lewis acid or Brønsted acid in a solvent, cyclohexane or liquid sulfur dioxide, was reported. The yield of the derived spiro [5.6]-dodecane-7,12-dione was discussed on the basis of its dependence on the solvent and the acid catalyst used. The combined use of a Lewis acid as the catalyst and liq. SO_2 as the solvent gave an excellent conversion, as large as a 93% yield of the spiro compound.

Although the rearrangement of α,β-epoxyketones under acidic conditions has been studied comprehensively from the synthetic point of view,[2] only a few studies have been undertaken to clarify the effects of the solvents and the catalysts.[3]

In the present communication, the results of the reaction of 2-benzylidenecyclohexanone oxide with an acidic catalyst in benzene, ether, or liq. SO_2 will be reported. As was reported previously, 2-cyclohexylidenecyclohexanone oxide has a hydrogen atom which can be eliminated as the proton during the reaction. The purpose of the present work is to study the solvent effects and also the role of the Lewis or the Brønsted acid on the α,β-epoxyketone rearrangement by selecting another compound, 2-benzylidenecyclohexanone oxide (I), which has no hydrogen atom to be drawn off during the reaction. In the reaction of 2-benzylidenecyclohexanone oxide (I), a procedure[1] similar to that used in the case of cyclohexylidenecyclohexanone oxide was followed.

Results and Discussion

The rearrangement of I was carried out at 20°C in sulfur dioxide, in benzene, and in ether. The reaction proceeds instantaneously in liq. SO_2, while in benzene the reaction is completed within thirty minutes. The reaction product of I with Brønsted acids in various solvents consisted only of the rearranged compound, 2-phenylcycloheptane-1,3-dione (II), mp 76.5—78.0°C.

Two products were obtained by the reaction with a Lewis acid, boron trifluoride etherate in benzene or ether. One was the rearranged product (II), while the other was 2-(α-fluorobenzyl)-2-hydroxycyclohexanone (III). The reaction of I with another Lewis acid, antimony pentachloride in benzene or ether, also gave two products, the rearranged compound, II and 2-(α-chlorobenzyl)-2-hydroxycyclohexanone (IV).

In Table 1 the results of experiments under various conditions are listed.

TABLE 1. ACID-CATALYZED REACTIONS OF I AT 20°C FOR 30 MIN

Catalyst	Solvent	Products, %		
		II	III	IV
H_2SO_4	SO_2	90.2	—	—
H_2SO_4	Benzene	90.1	—	—
FSO_3H	SO_2	80.7	—	—
FSO_3H	Benzene	83.2	—	—
$BF_3 \cdot OEt_2$	SO_2	70.3	0	—
$BF_3 \cdot OEt_2$	Benzene	36.1	50.6	—
$SbCl_5$	SO_2	50.0	—	8.7
$SbCl_5$	Benzene	6.7	—	73.9

II: 2-Phenyl-cycloheptane-1,3-dione.
III: 2-(α-Fluorobenzyl)-2-hydroxycyclohexanone.
IV: 2-(α-Chlorobenzyl)-2-hydroxycyclohexanone.

As is indicated in Table 1, when a Brønsted acid, H_2SO_4 of FSO_3H, was used, the product was exclusively the rearranged product (II), and the yields in the two solvents, liq.SO_2 and benzene, were almost the same.

However, the use as the catalyst of a Lewis acid, $BF_3 \cdot OEt_2$ or $SbCl_5$, which has no protonic hydrogen to donate, causes a drastic change in the solvent effects, affording a large quantity of III or IV in benzene. A similar trend was also observed when ether was used as the solvent.

It has well been established that fluorohydrins are formed by the reaction of epoxide with boron trifluoride etherate if the experimental conditions are right.[4,5] H.O.House showed that the treatment of I with boron

1) M. Nojima, K. Hinoue, and N. Tokura, This Bulletin, **43**, 827 (1970).

2) R. E. Parker and N. S. Issacs, *Chem. Rev.*, **58**, 737 (1959), and the references cited there.

3) W. Reusch, D. F. Anderson, and C. K. Johnson, *J. Amer. Chem. Soc.*, **90**, 4988 (1968).

4) B. N. Blackett, J. M. Coxon, M. P. Hartshorn, and K. E. Richards, *Tetrahedron*, **25**, 4999 (1969).

5) J. M. Coxon, M. P. Hartshorn, A. J. Lewis, K. E. Richards, and W. H. Swallow, *ibid.*, **25**, 4445 (1969).

trifluoride etherate in ether led to the formation of the fluorohydrin (III).[6] The reaction of III with boron trifluoride etherate in ether to produce II was also examined; II was obtained directly from the reaction of I with boron trifluoride etherate in benzene. However, there was no conclusive evidence to indicate whether III was an intermediate in the formation of the carbonyl compound or merely a by-product. We examined the concentrations-time curves for the reactant and three products, I, II, and III, in an effort to decide whether or not III is an intermediate in the formation of 1,3-dione, boron trifluoride etherate being used as the catalyst.

Figure 1 reveals the concentration-time relationship between the constituents of the reaction mixture and the reaction process in the reaction in ether. In this case, only fluorohydrin (III) was formed at the early stage of the reaction; it reached a maximum value of 36%, and then slowly decreased with the reaction time. The yield of 1,3-dione (II) increased with an increase in the reaction time, and after 48 hr the yield reached 74%. These results seems to show that III is the intermediate for the formation of 1,3-dione under these conditions.

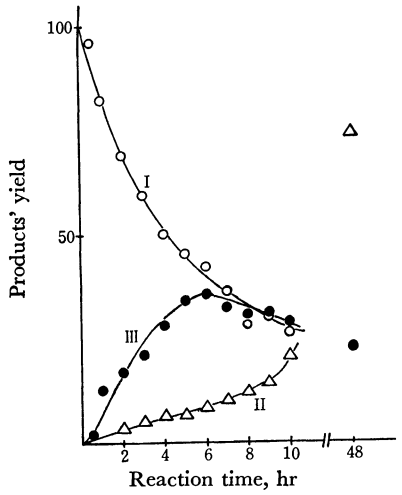

Fig. 1. The reaction of I with $BF_3 \cdot OEt_2$ in ether.

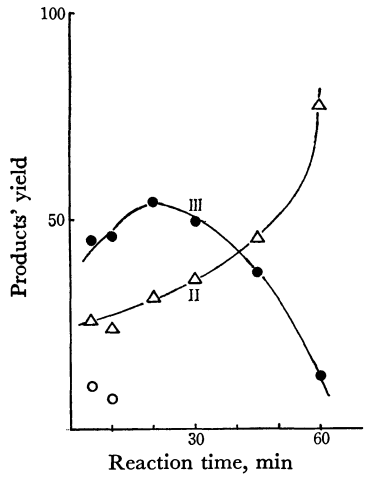

Fig. 2. The reaction of I with $BF_3 \cdot OEt_2$ in benzene.

6) H. O. House and D. J. Reif, *J. Amer. Chem. Soc.*, **77**, 6525 (1955).

Figure 2 illustrates the behavior of I in a benzene solution. These curves indicate that III is produced at the first stage of the reaction and is then converted to 1,3-dione. However, at the early stage of the reaction periods *ca.* a 20% yield of 1,3-dione was formed; this result indicates that onestep (direct) formation of 1,3-dione may contribute in some degree.

In liquid sulfur dioxide the following results were obtained. At 20°C only the rearranged product (II) was formed. To explain these results, two mechanisms seem to be plausible. One is that, as the reaction rate of III is rapid in liquid sulfur dioxide, II is obtained as the sole product, although III is produced as the short-lived intermediate. The other possible explanation for these results is the one-step formation of II from I. To distinguish between the above two pathways, we carried out a reaction at −70°C. Under these reaction conditions we could not detect the formation of III, the only product being II at any reaction period. These results seem to show that the reaction of I with Boron trifluoride etherate in liquid sulfur dioxide proceeds directly to form 1,3-dione.

From these data, Scheme I may be taken to illustrate the probable reaction process. When Brønsted acid is used as the catalyst, I is attacked by a proton to form the intermediate, I_B, after the ring opening, and the migration of the acyl group may subsequently produce 1,3-dione, (II). Since the nucleophilicities of HSO_4^- and FSO_3^- in liq.SO_2 are very small, the intramolecular reaction (rearrangement) must occur predominantly.

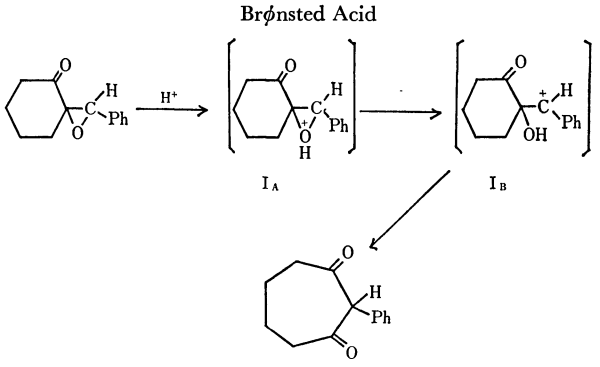

Scheme I

Contrary to the above results, however, halohydrins were formed by the intermolecular epoxide cleavage reaction when Lewis acid was used as the catalyst in ether or benzene. Thus, the reaction pathways with boron trifluoride etherate are greatly dependent on the differences in the solvents. These results may indicate that the reaction rate is slowed down by the decrease in the electrophilicity of the catalyst for the formation of the cordinated complex and that the ionization necessary for the formation of 1,3-dione may be inhibited; the alternative reaction leading to fluorohydrin can then be operative, as is shown in Scheme II.

The fluorohydrin formed in an ether solution seems to arise through a cationic intermediate, I_A' (Scheme II), in which the carbon-oxygen bond is, for the most

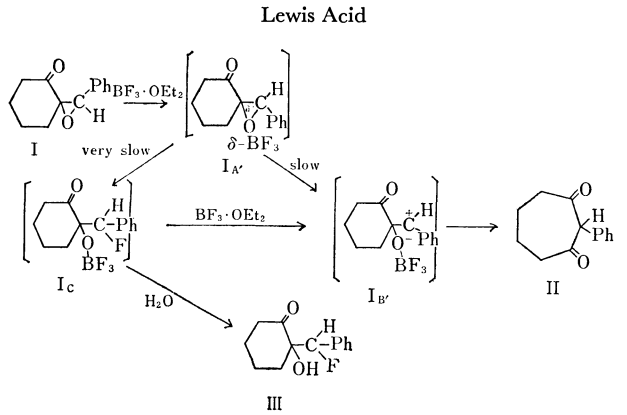

Scheme II

part, maintained. The opening of the epoxide ring of I in benzene seems to involve a transition state of a greater ionic character than the reaction in ether. It seems likely that the rearrangement of the intermediate, I_B', to form II is accelerated by the stabilization of the intermediate due to the solvation of the counter anion by liquid sulfur dioxide. When benzene or ether is used as the solvent, however, there is little means to stabilize the transition state and the displacement to form III seems to be competitive.

To examine further the reactivity of the reactant in this rearrangement, 2-*p*-chloro (IV) and 2-*p*-methyl derivatives (VI) of benzylidenecyclohexanone oxide were prepared and subjected to the same reaction. The reaction was carried out as has been described above, and the same procedure was used to separate the products.

In liquid sulfur dioxide, both the compounds gave over 90% yields of rearranged products, V and VII, when boron trifluoride etherate was used as the catalyst. In benzene, the same catalyst gave 94.7% of V; however, VI (*p*-chlorobenzylidenecyclohexanone oxide) gave 57.7% of the rearranged product, VII, and 28.3% of a fluorohydrine, VIII.

Thus, the electrodonative *p*-methyl group may facilitate the formation and stabilization of a carbonium ion of such a type as I_B' in Scheme II, which is a prime requisite for the rearrangement.

Experimental

Materials. The liquid SO_2 was dehydrated with H_2SO_4 and P_2O_5 successively and distilled. The benzene and ether were purified by ordinary methods.

Apparatus. The IR spectra were run on an EPIS2-type Hitachi IR Spectrometer. The NMR spectra were obtained with a Japan Electron Optics Spectrometer, JNM3H-60.

The mass spectra were recorded on a Hitachi RMU-6E single focusing instrument.

2-Benzylidenecyclohexanone Oxide (I). 2-Benzylidenecyclohexanone oxide was prepared by the method of House.[6] From 30.0 g of 2-benzylidenecyclohexanone and 60 m*l* of a 30% hydrogen peroxide solution, 10.0 g (32.6% yield, based on 2-benzylidenecyclohexanone) of 2-benzylidenecyclohexanone oxide was obtained; mp 124.5—125.0°C (lit,[6] mp 124.5—125.0°C).

2-p-Methylbenzylidenecyclohexanone Oxide (IV). 2-*p*-Methylbenzylidenecyclohexanone was prepared by the condensation of 2-*p*-methylbenzaldehyde with cyclohexanone, using sodium hydroxide as the catalyst. IV was obtained by the reaction of 2-*p*-methylbenzylidenecyclohexanone with 30% H_2O_2 according to the directions of House.[6] Mp 117°C (recryst. from *n*-hexane), IR(KBr), 1710 cm^{-1}; NMR($CDCl_3$), τ, 6.0(1H), 2.85(4H), 7.65(3H). Found: C, 77.52; H, 7.50%. Calcd for $C_{14}H_{16}O_2$: C, 77.75; H, 7.46%

2-p-Chlorobenzylidenecyclohexanone Oxide (VI). VI was prepared by the condensation of 2-*p*-chlorobenzaldehyde and cyclohexanone, followed by epoxidation. Mp 116.0—116.5 (rec. from *n*-hexane), IR(KBr), 1710 cm^{-1}; NMR ($CDCl_3$), τ, 6.0(1H), 2.69(4H). Found: C, 66.05; H, 5.53%. Calcd for $C_{13}H_{13}O_2Cl$: C, 65.95; H, 5.54%.

The General Procedure of the Reaction of I with the Acid Catalyst. To 200 mg of I and 10 m*l* of a solvent, we added 0.1 m*l* of the acid catalyst, after which the mixture was allowed to react at 20°C for 30 min. The reaction mixture was cooled, diluted with water, and extracted three times with ether. The combined organic layers were washed with saturated brine and dried over anhydrous sodium sulfate. The light yellow solid remaining after the evaporation of the solvent was analyzed by NMR spectroscopy. The relative integrals at the τ values 6.05 (I), 5.20 (II), 4.25 (III), and 4.6 (IV), were used to estimate the constituents in the products.

The Measurement of the Concentration-Time Relationship of the Reactant and of the Products in the Rearrangement. The Reaction with Boron Trifluoride Etherate as the Catalyst. To 2.0 g of I and 200 m*l* of the solvent, we added 2.0 m*l* of boron trifluoride etherate, after which the mixture was allowed to react at 20°C. A 10-m*l* aliquot was withdrawn periodically and diluted with water. Then it was worked up as has been described previously, and the relative ratios of the components were calculated from the relative integrals of the NMR spectra as has been described above.

Identification of the Reaction products. Reaction Products of I with Boron Trifluoride Etherate in Benzene. I(2.0 g), 1 m*l* of freshly-distilled boron trifluoride etherate, and 100 m*l* of benzene were maintained at 20°C for 30 min and then worked up as in the previous case. The residue after the removal of the solvent was chromatographed on 50 g of silica gel. After elution with five 50-m*l* portions of petroleum ether, elution with ten 50-m*l* portions of benzene gave 0.6 g (yield%) of a solid, which was then recrystallized from *n*-hexane. 2-Phenylcycloheptane-1,3-dione, (II); mp 76.5—78.0°C (lit,[6] mp 76.5—78.0°C). Mass; *m/e*, 202, Calcd for $C_{13}H_{14}O_2$, 202. NMR($CDCl_3$); τ, 2.73(5H singlet), 5.20(1H, singlet), 5.20(1H singlet), 7.40 and 8.00(8H multiplet). The physical data were also identical with those in the literature.[6]

Elution with ten 50-m*l* portions of benzene gave 1.2 g (yield%) of a solid, which was then recrystallized from *n*-hexane; 2-(α-fluorobenzyl)-2-hydroxycyclohexanone, (III), mp. 129—130°C (lit,[6] mp 129.5—130°C). IR(KBr), 1720, 3460 cm^{-1}; NMR($CDCl_3$), τ, 2.70(5H singlet), 4.25(1H, J: 40.2 Hz), 5.90(1H, singlet), 7.4 and 8.2(multiplet); Mass, *m/e*, 222, Calcd for $C_{13}H_{15}O_2F$, 222.

Reaction Products with Antimony Pentachloride in Benzene. The products was treated as above. Elution gave 1,3-dione (II) and a product, a white crystalline solid, (IV). IV was recrystallized from *n*-hexane and identified as 2-(α-chlorobenzyl)-2-hydroxycylcohexanone (IV); mp 103.5—105.0°C; IR (KBr) 1710, 3460 cm^{-1}; NMR ($CDCl_3$); τ, 4.6 (1H), 5.3(1H singlet); Mass, *m/e*, 238, Calcd for $C_{13}H_{15}O_2Cl$, 238.

The authors wish to thank the Seitetsu Kagaku K.K. for its donation of liquid sulfur dioxide. The present work was made possible by the support of the Scientific Research Fund of the Ministry of Education.

Polymerization of Methyl Methacrylate by the Bis(benzoylacetonato)-Copper(II)-1,10-Phenanthroline System

Kyoji KAERIYAMA and YUKIO YAMAZAKI*

Research Institute for Polymers and Textiles, Sawatari-4, Kanagawa-ku, Yokohama
**Okamoto Riken Rubber Co. Ltd., Hongo 3-27-12, Bunkyo-ku, Tokyo*

(Received April 15, 1971)

The addition of 1,10-phenanthroline accelerates the polymerization of methyl methacrylate by a β-diketonato chelate of Cu(II), Mn(II), Mn(III), Co(II), Co(III), and Fe(III), but has no effect on the chelate of Ni(II). The effect of 1,10-phenanthroline, which is composed of two pyridine units, is much greater than that of pyridine. The polymerization rate of methyl methacrylate by the bis(benzoylacetonato)Cu(II)-1,10-phenanthroline system may be represented as follows:

$$R_p \propto [\text{MMA}]\{[\text{Cu(II)}][\text{1,10-phenanthroline}]\}^{1/2}$$

The initiation reaction is assumed to be by a ligand-exchange reaction of bis(benzoylacetonato)Cu(II) with 1,10-phenanthroline, where a benzoylacetonyl ligand is displaced by 1,10-phenanthroline and Cu(II) is simultaneously reduced to Cu(I).

In has been reported that many additives accelerate vinyl polymerization by metallic chelates of β-diketone. Some additives, such as pyridine[1] and carbonyl compounds,[2] have been shown to coordinate to the central metal of chelate compounds through the lone-pair electrons and to increase the initiation rate of vinyl polymerization by tris(acetylacetonato)Mn(III) ($Mn(acac)_3$, where acac represents an acetylacetonyl ligand). This implies that the greater the ability for coordination to metal, the greater the effect. The chelating agents form a class of compounds which have the greatest ability for coordination. Recently, Bamford and Ferrar have briefly mentioned that ethylene and propylene diamines have a remarkable effect on polymerization by $Mn(acac)_3$. It has been found that 1,10-phenanthroline (phen) has much greater effects on the polymerization of methyl methacrylate (MMA) by metallic chelates of β-diketone than pyridine does. Phen is a chelating agent which is composed of two pyridine units. The effect of phen on bis(benzoylacetonato)Cu(II) ($Cu(ba)_2$, where ba denotes a benzoylacetonyl ligand) is studied in some detail.

Experimental

Reagent. The pyridine, MMA, and solvents were dried over **3A** molecular sieves and were distilled under reduced pressure just before use. The chelate compounds were commercially obtained and were used without further purification. The metallic chelates of acetylacetone were manufactured by the Dojindo Co., Ltd. The $Cu(ba)_2$ was supplied by Eastman Organic Chemicals. The recrystallization of phen was carried out from a benzene solution (mp 94°C). The dipyridyl was recrystallized from an ethanol-water system(mp 69°C).

Procedure. The chelate, the chelating agent, MMA, and benzene were mixed under atmospheric conditions. After the mixture had been placed in a glass tube and degassed by repeated freezing, evacuating, and thawing, it was sealed off. Polymerization was then carried out in the dark. The temperature was controlled within ±0.1°C. The polymer thus produced was precipitated in methanol containing a small amount of hydroquinone and hydrogen chloride, filtered, and dried *in vacuo* to a constant weighs. Conversions were then calculated on the weight of the polymer.

Results and Discussion

1. *Effect of Chelating Agent.* The effects of phen and dipyridyl are compared with those of pyridine in Table 1. Phen has an accelerative effect on the polymerization of MMA by all the chelates of β-diketone examined other than $Ni(acac)_2$. Dipyridyl has an effect on $Mn(acac)_2$, $Mn(acac)_3$, $Cu(ba)_2$, $Co(acac)_2$, and $Co(acac)_3$, but has no effect on $Fe(acac)_3$ and $Ni(acac)_2$. Pyridine accelerates the polymerization of MMA by $Mn(acac)_2$, $Mn(acac)_3$, $Co(acac)_2$, and $Co(acac)_3$, but has no effect on $Cu(ba)_2$, $Fe(acac)_3$, and $Ni(acac)_2$. Pyridine, however, has greater effects on the chelates of Mn and Co than dipyridyl does.

TABLE 1. EFFECTS OF CHELATING AGENT

Chelate		Conversion (%)			
type	concentration $\times 10^2$ mol/l	no additive	phen 2×10^{-2} mol/l	dipyridyl 2×10^{-2} mol/l	pyridine 4×10^{-2} mol/l
$Cu(ba)_2$	2.07	trace	16.9	1.97	0
$Mn(acac)_2$	1.19	3.42	35.6	7.02	13.4
$Mn(acac)_3$	0.568	13.8	59.5	15.6	34.7
$Co(acac)_2$	3.11	2.36	10.7	6.96	8.41
$Co(acac)_3$	2.25	4.79	5.35	5.82	7.29
$Fe(acac)_3$	2.27	0	3.67	0	0
$Ni(acac)_2$	3.11	trace	trace	0	0

[MMA]=2.82 mol/l; solvent: benzene; at 60°C for 8 hr

It has been described that the effect of ketones is dependent on the nucleophilicity.[2] The effects of pyridine homologs on the polymerization of styrene decreases in this order: pyperidine>pyridine>2,6-lutidine.[1] This order is consistent with the ability of coordination to the central metal. In the present case also, it is reasonable to assume that the effects of pyridine homologs are dependent on the ability of coordi-

1) K. Uehara, Y. Kataoka, M. Tanaka, and N. Murata, *Kogyo Kagaku Zasshi*, **70**, 1945 (1967).
2) K. Kaeriyama, This Bulletin, **43**, 1511 (1970). K. Kaeriyama and Y. Yamazaki, *Kogyo Kagaku Zasshi*, **74**, 1718 (1971).
3) C. H. Bamford and A. N. Ferrar, *Chem. Commun.*, **1970**, 315.

nation to the central metal, as can be anticipated from the viewpoint of nucleophilicity and steric hindrance. The average pK values for pyridine, dipyridyl, and phen are 5.21, 4.36, and 4.87 respectively.[4] Pyridine is the most nucleophilic. Steric hindrance of coordination to the central metal of chelate compounds probably decreases in this order: phen>dipyridyl>pyridine. Nevertheless, phen is the most effective. Pyridine has smaller effects than phen. The noticeable effect of phen, which has two coordination sites in a molecule, is attributable to the chelating effect of phen.

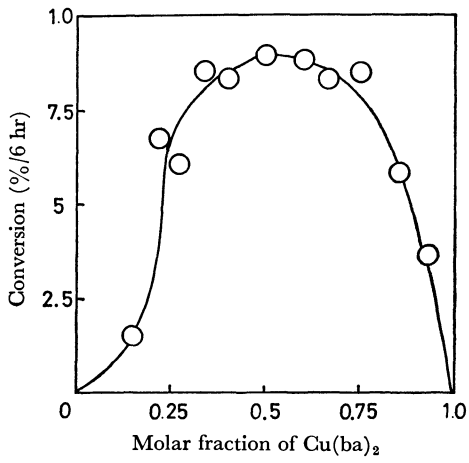

Fig. 1. Dependence of conversion on molar fraction of chelate.
[Cu(ba)$_2$]+[phen]=2.1×10^{-2} mol/l
[MMA]=2.82 mol/l; at 60°C in benzene

2. *Dependence on Molar Fraction of Cu(ba)$_2$.* Conversions at a constant polymerization time are shown as a function of the molar fraction of Cu(ba)$_2$ in Fig. 1. It is apparent from the figure that the binary system is very active in the initiation of MMA polymerization, although neither component shows any appreciable effect. In the case of the Mn(acac)$_3$-phen system,[5] a clear peak is observed at the molar fraction of 0.5. In the present combination, no sharp peak appears, but a wide plateau can be seen in the range of the molar fractions from 0.33 to 0.75.

3. *Dependence on Initiator Concentration.* The dependence of the polymer yield on the polymerization time is shown at different concentrations of the initiator in Fig. 2. No linear relation between the yield and the time can be observed even in the initial stage of polymerization. Therefore, according to the Aoki-Matsumura-Otsu method,[6] the rate of polymerization was estimated approximately from the ratio of the polymer yield and the time at a 5% polymer yield.

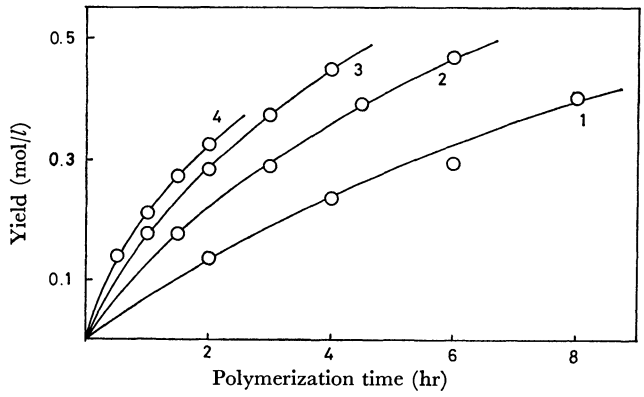

Fig. 2. Dependence of yield on polymerization time.
[MMA]=3.57 mol/l; at 70°C in benzene
{[Cu(ba)$_2$][phen]}$^{1/2}$
1. 3.89×10^{-3} mol/l 2. 7.77×10^{-3} mol/l
3. 11.7×10^{-3} mol/l 4. 15.5×10^{-3} mol/l

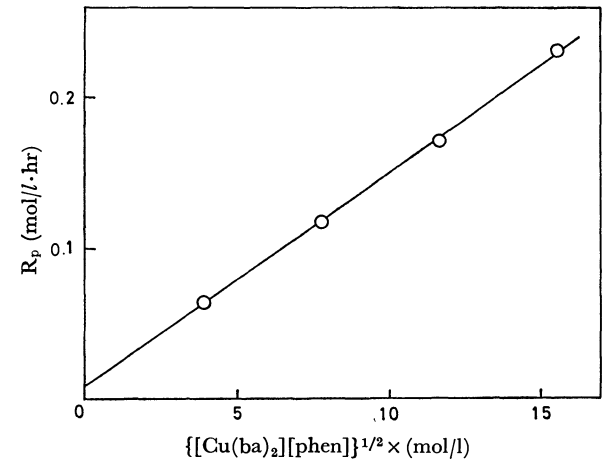

Fig. 3. Dependence of polymerization rate on initiator concentration.
[MMA]=3.57 mol/l; at 70°C in benzene

The rate of polymerization thus obtained is shown as a function of the concentrations of Cu(ba)$_2$ and phen in Fig. 3. The molar concentration of Cu(ba)$_2$ is equal to that of phen in each run. The rate of polymerization is linearly dependent on the square root of [Cu(ba)$_2$][phen]. This suggests that termination is not by a reaction of a polymer radical with the chelate, but by a bimolecular reaction of polymer radicals. This conclusion is also supported by the experimental evidence that Cu(ba)$_2$ has no effect on the polymerization of MMA initiated by azo-bis-isobutyronitrile.

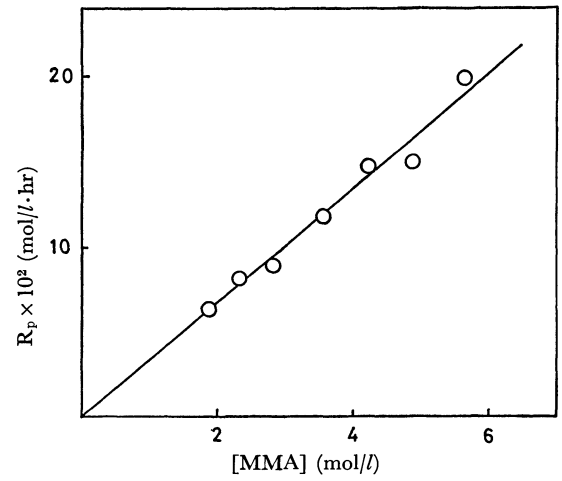

Fig. 4. Dependence of polymerization rate on concentration of MMA.
[Cu(ba)$_2$]=[phen]=7.77×10^{-3} mol/l at 70°C in benzene

4) D. D. Perrin, "Dissociation Constants of Organic Bases in Aqueous Solution," Butterworths, London (1965).
5) K. Kaeriyama, *Makromol. Chem.*, in press.
6) S. Aoki, S. Matsumura, and T. Otsu, This Bulletin, **42**, 2574 (1969).

The line does not pass through the point of origin. This deviation is probably attributable to the fact that the rate is not strictly determined at the initial stage of polymerization from the linear relation between the time and conversion.

4. *Dependence on the Monomer Concentration.* The dependence of the polymerization rate on the MMA concentration is shown in Fig. 4. It is apparent that the rate of polymerization is linearly proportional to the concentration of MMA. The monomer does not participate in the initiation reaction at all. This is the first case, in which MMA does not participate in the initiation reaction of the polymerization by metallic chelates of β-diketones.

5. *Initiation Reaction.* It has been reported by many workers that the initiation reaction of vinyl polymerization by metallic chelates of β-diketone proceeds by means of the elimination of a ligand from the chelate, which accompanies the reduction of the central metal.[1,2,7,8] Electron-donating additives coordinate to the metal of the chelate and accelerate the elimination of the β-diketonyl radical from the chelate.[1-3] This increases the initiation rate of polymerization. Phen also coordinates to Cu and accelerates the polymerization of MMA. Phen is a chelating agent and coordinates at two sites. The initiation reaction can be represented as follows:

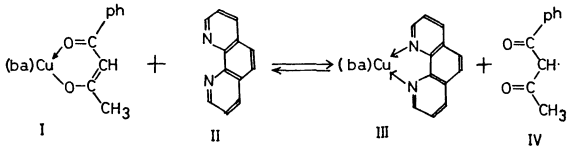

I II III IV

where ph represents a phenyl group. The reaction is a ligand-exchange reaction between the benzoylacetonyl group and phen, and Cu(II) is simultaneously reduced to Cu(I). Radical polymerization is initiated by the benzoylacetonyl radical thus produced. This exchange reaction reasonably explains why phen has a greater effect on $Cu(ba)_2$ than pyridine. It also supports the initiation reaction that the carbonyl group can be detected by IR spectroscopy in polystyrene produced by the initiator system. One of the driving forces for the formation of the radical is the precipitation of III from the polymerizing mixture, which shifts the equilibrium toward the right side.

The authors are grateful to Dr. M. Suzuki, Dr. A. Okada, and Mr. Y. Shimura for their interest and encouragement during this work.

7) C. H. Bamford and D. J. Lind, *Proc. Roy. Soc.*, **A302**, 145 (1968).

8) T. Otsu, Y. Nishikawa, and S. Aoki, *Kogyo Kagaku Zasshi*, **71**, 1067 (1968).

BULLETIN OF THE CHEMICAL SOCIETY OF JAPAN, VOL. 44, 3101—3106 (1971)

The Photoreactions of Phenazines *via* a Semiquinone Radical. The Photoreductive Deacylation of 1- or 2-Acyloxyphenazine[1)]

Hiroo INOUE, Tadao OCHIAI, Akira SUGIMOTO, and Eiji IMOTO

Department of Applied Chemistry, College of Engineering, University of Osaka Prefecture, Sakai, Osaka

(Received April 19, 1971)

The Photo-irradiation of a solution of 1- or 2-benzoyloxyphenazine in 2-propanol, followed by aeration, affords 1- or 2-hydroxyphenazine, benzaldehyde, isopropyl benzoate, and/or benzoic acid as the reaction products. The spectral change of the solution in the reaction process gives evidence of the fission of the acyl-to-oxygen bond. The addition of ferric chloride or dimethyl sulfate to the reaction system containing 1-benzoyloxyphenazine in 2-propanol leads to the formation of isopropyl benzoate. When methanol instead of 2-propanol is used as the solvent, methyl benzoate is produced mainly. In cyclohexene as a hydrogen-donating solvent, benzaldehyde and an oxetane are obtained. The irradiation of a solution of 1-benzoyloxyphenazine in *t*-butyl alcohol or benzene gives no product, and the starting material is recovered in a 90—100% yield. 1-Benzoyloxyphenazhydrin, a photo-reduction intermediate, does not contribute to the formation of benzaldehyde. The intermediary formation of a semiquinoid form during irradiation brings about the fission of the acyl-to-oxygen bond, thus affording the corresponding aldehyde.

The oxidation-reduction through a semiquinone radical is the subject of considerable interest in relation to that in a biological system, particularly in flavoprotein catalysis, and in oxidation-reduction by dehydrogenases involving pyridine nucleotides.[2)]

The photo-reduction of phenazine in alcoholic media produces the semiquinone radical (I) or molecular complexes (II) of phenazine and 5,10-dihydrophenazine of varying stoichiometry.[3,4)] We attempted to investigate a reaction which proceeds through the intermediary

1) Presented partly at the 22nd Annual Meeting of the Chemical Society of Japan, Tokyo, April 1969.

2) H. R. Mahler and E. H. Cordes, "Biological Chemistry," Harper and Row, New York (1966), pp. 354, 575.

3) D. N. Bailey, D. K. Roe, and D. M. Hercules, *J. Amer. Chem. Soc.*, **90**, 6291 (1968).

4) G. A. Russell, R. Konaka, E. T. Strom, W. C. Danen, K. Y. Chang, and G. Kaupp, *ibid.*, **90**, 4646 (1968).

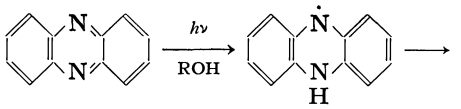

I

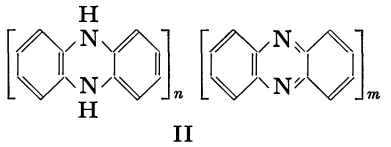

II

formation of the semiquinone radical about phenazines with a substituent. The present paper will indicate that the irradiation of a solution of 1- or 2-acyloxyphenazine in 2-propanol, followed by aeration, leads to the fission of the acyl-to-oxygen bond, thus affording 1- or 2-hydroxyphenazine (IV), and that in the case of 1- or 2-benzoyloxyphenazine (III), the benzoyl group is converted to benzaldehyde, isopropyl benzoate, and/or benzoic acid.

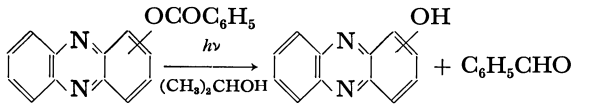

III IV

$+ C_6H_5COOCH(CH_3)_2 + C_6H_5COOH$

Experimental

Materials. 1- or 2-Hydroxyphenazine was synthesized by the method described in the literature.[5-7] 1-Hydroxyphenazine, mp 157—158°C. 2-Hydroxyphenazine, mp 253—254°C. The acyloxyphenazines were prepared by the reaction of acetic anhydride or benzoyl chloride with 1- or 2-hydroxyphenazine in pyridine, followed by recrystallization from ethanol.[8] 1-Acetoxyphenazine, mp 119—120°C. 2-Acetoxyphenazine, mp 151—152°C. 1-Benzoyloxyphenazine, mp 172—173°C.

Found: C, 75.95; H, 3.94; N, 9.61%. Calcd for $C_{19}H_{12}N_2O_2$: C, 75.99; H, 4.03; N, 9.33% 2-Benzoyloxyphenazine, mp 144—145°C.

Found: C, 75.95; H, 4.01; N, 9.05%. Calcd for $C_{19}H_{12}N_2O_2$: C, 75.99; H, 4.03; N, 9.33%.

The benzaldehyde, isopropyl benzoate, methyl benzoate, anhydrous ferric chloride, and dimethyl sulfate were purchased from commercial sources. The methanol, 2-propanol, *t*-butyl alcohol and cyclohexene used as solvents were purified by distilling them two times on anhydrous cupric sulfate, calcium oxide, calcium oxide and sodium respectively.

General Procedure of Photoreaction. Spectral Change: The reactions were carried out in a quartz spectrophotometer cell which was irradiated with light from a 100-W high-pressure mercury arc lamp at a distance of 6 cm and at room temperature. The lamp characteristics, and the procedure for carrying out the reactions, were the same as have been described in detail in a previous paper.[9] At the concentration of 1- or 2-acetoxyphenazine of $(1—1.5)\times10^{-4}$ mol/*l*, the change in the visible absorption spectra corresponding to substrate-disappearance or product-appearance was followed with the period of irradiation. After the reaction, oxygen was admitted into the reaction system, and the spectra of the resulting solution were measured.

Photoreaction: The photoreactions were carried out by the methods described in a previous paper.[10] A dispersed solution of $(3—5)\times10^{-5}$ mol of 1- or 2-benzoyloxyphenazine in 10 m*l* of 2-propanol, unless otherwise stated, was placed in a quartz or Pyrex tube with an inside diameter of 15—20 mm and a wall thickness of 1 mm, and was cooled with liquid nitrogen; the air was removed under the reduced pressure of 1 mmHg, and then the tube was filled with nitrogen gas. The procedure of the replacement by nitrogen gas was repeated 4—5 times. The tube was then sealed and irradiated with a 100-W high-pressure mercury arc lamp in a distance of 4 cm and at room temperature. In order to isolate the reaction products, another procedure was attempted on a large scale by using a cylinderical, 300-m*l* reaction vessel.

Analyses of Products. After the reaction, the visible absorption spectrum of the reaction mixture was measured. The amount of 1- or 2-hydroxyphenazine produced was determined from the optical density of the absorption at 440 mμ, where the starting material has no absorption. After measuring the spectrum, the solution was concentrated to about one-tenth of the original volume in order to analyze the products. The benzaldehyde and isopropyl benzoate were identified by a comparison of their retention times in gas chromatography with those of authentic materials. The amounts of these compounds were determined by means of gas chromatography (gc), using a Yanagimoto 5 DH gas chromatograph; a column containing polyethylene glycol-20M and/or silicone grease-30 was used. Helium gas was used as the carrier gas. Benzoic acid was converted to methyl benzoate by introducing diazomethane into a part of the concentrated solution,[11] after measuring the amounts of benzaldehyde and isopropyl benzoate, and was determined by measuring the amount of methyl benzoate by gc analysis.

Isolation of 1-Hydroxyphenazine. A dispersed solution of 0.4 g of 1-benzoyloxyphenazine in 250 m*l* of 2-propanol, containing partially the crystal of 1-benzoyloxyphenazine, was placed in a cylinderical, 300-m*l* reaction vessel, and then the vessel was irradiated with a 100-W high-pressure mercury arc lamp for 100 hr after nitrogen gas had been bubbled into the solution. The resulting solution was concentrated up to a half volume *in vacuo* at room temperature, and the concentrated solution was poured into about 500 m*l* of water. A white precipitate deposited (0.15 g) was collected with filtration; subsequent recrystallization from ethanol afforded 1-hydroxyphenazine (mp 152—154°C), the IR spectrum of which was identical with that of the authentic meterial.

1-Benzoyloxy-5,10-dihydrophenazine (VI) and Its Phenazhydrin (V). An aqueous saturated solution of sodium hydrosulfite was added to a solution of 30 mg of 1-benzoyloxyphenazine in ethanol. A white powder precipitated. The precipitate (VI) (25 mg) was filtered off, washed repeatedly with water, and dried *in vacuo*. Immediately after the powder had been dried, it was submitted to the reaction, for it was unstable in air. The IR spectrum of the powder (KBr) is shown in Fig. 4. When the powder stood for 2—3 days, it changed to a greenish powder (V), the IR spectrum of which

5) A. R. Surrey, "Organic Syntheses," Coll. Vol. III, p. 753 (1955).

6) I. Yosioka, *J. Pharm. Soc. Jap.*, **72**, 1128 (1952).

7) E. Matsumura and H. Takeda, *Nippon Kagaku Zasshi*, **81**, 515 (1960).

8) F. Wrede and E. Strack, *Z. Physiol. Chem.*, **140**, 1 (1924); F. Kehrmann and F. Cherpillod, *Helv. Chim. Acta*, **7**, 973 (1924).

9) H. Inoue, K. Tamaki, N. Komakine, and E. Imoto, This Bulletin, **39**, 1577 (1966).

10) H. Inoue, K. Komakine, and E. Imoto, *ibid.*, **41**, 2726 (1968).

11) M. Maruyama, "Zoku Jikken Kagaku Koza," Vol. 9, Maruzen, Tokyo (1965), p. 340.

had the absorptions at 3300 and 3400 cm^{-1} characteristic of phenazhydrin.[12]

Results and Discussion

Spectral Aspects. 1-Acetoxyphenazine was used for the measurement of the spectral change under irradiation with ultraviolet light, since it is more easily soluble in 2-propanol than 1-benzoyloxyphenazine. A solution of 1-acetoxyphenazine in 2-propanol, which had been placed in a quartz cell, was irradiated with light after degassing under the reduced pressure of 10^{-5} mmHg. As is shown in Fig. 1, the absorption of 1-acetoxyphenazine at 363 mμ disappeared rapidly and a new broad band appeared in the 490—500 mμ region. The new broad band also disappeared gradually. Immediately after irradiating for 5 min, oxygen gas was admitted to the system. The visible absorption spectrum of the resulting solution had absorptions at 368 and 420—430 mμ, which agreed with those of 1-hydroxyphenazine, as is shown in Fig. 1. The results show that 1-hydroxyphenazine is obtained quantitatively. This means that the acetyl group is cleaved, but does not rearrange on the phenazine ring during the photo-reduction or the oxidation process. Furthermore, the absorption in the 490—500 mμ region may be attributed to that of a phenazhydrin-type compound, such as a molecular complex between 1-hydroxyphenazine or its keto form and 1-hydroxy-5,10-dihydrophenazine. The irradiation of 1-acetoxyphenazine in methanol also showed a spectral change similar to that in the case of 2-propanol.

The spectral change of 2-acetoxyphenazine in 2-propanol by irradiation with ultraviolet light was similar to that of 1-acetoxyphenazine. However, the absorption in the 490—500 mμ region in the case of 2-acetoxyphenazine became larger than that of 1-acetoxyphenazine, indicating the easier formation of a

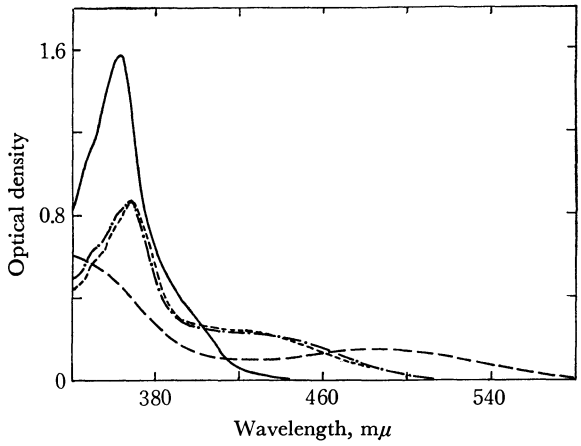

Fig. 1. Spectral change of 1-acetoxyphenazine in 2-propanol under irradiation of ultraviolet light: Concentration of 1-acetoxyphenazine; 1.22×10^{-4} mol/*l*.
—— Before irradiation, - - - after 5 min of irradiation, —·— after 1 hr of oxidation after irradiating for 5 min and ------ spectrum of 1-hydroxyphenazine after 15 min of irradiation, followed by oxidation.

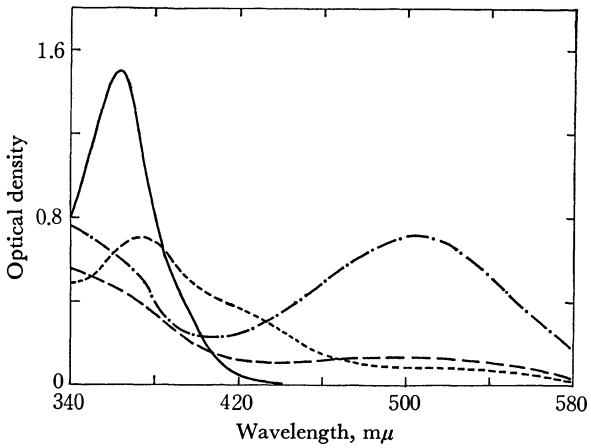

Fig. 2. Spectral change of 2-acetoxyphenazine in 2-propanol under irradiation of ultraviolet light: Concentration of 2-acetoxyphenazine; 1.18×10^{-4} mol/*l*.
—— Before irradiation, —·— after 11 min of irradiation, — — after 3 hr of irradiation and ------ after 1 hr of oxidation after irradiating for 3 hr.
The shape of the absorption spectrum of ----- was similar with that of the keto form of 2-hydroxyphenazine which has the extension of the absorption as far as about 540 mμ.

phenazhydrin-type compound, as is shown in Fig. 2. Immediately after the large peak appeared, the introduction of oxygen resulted in an absorption spectrum represented by the sum of the spectra of 2-acetoxyphenazine and 2-hydroxyphenazine. For example, the introduction of oxygen after irradiating for 11 min, resulted in the molar ratio of 2-acetoxyphenazine to 2-hydroxyphenazine of 3/7. This must mean that the phenazhydrin-type compound contains either 2-acetoxyphenazine or its dihydrophenazine. The difference between the optical densities at 490—500 mμ in the spectral changes of 1- and 2-acetoxyphenazine may be caused by the difference in the ease of the formation of their phenazhydrin-type compounds. The oxidation after the absorption at 490—500 mμ region disappeared completely resulted in the generation of the absorption spectrum of the keto form of 2-hydroxyphenazine, which has been reported by Badger, Pearce and Pettit,[13] as is shown in Fig. 2. Thus, also in the case of 2-acetoxyphenazine, it was confirmed that the fission of the acyl-to-oxygen bond occurs during irradiation with ultraviolet light. However, the acetyl group of 1-acetoxyphenazine was removed more readily than that of 2-acetoxyphenazine. This was caused by the greater difficulty of reducing a semiquinone radical of 1-acetoxyphenazine to its dihydrophenazine as compared with the case of 2-acetoxyphenazine because of the steric retardation of the acetoxy group of 1-acetoxyphenazine.

Photo-reduction of 1-Benzoyloxyphenazine. The benzoyl group was selected as the acyl group in order to make easier analyses of the photoreaction products. A dispersed solution of 1-benzoyloxyphenazine in 2-propanol was degassed in a Pyrex vessel, irradiated with light at room temperature, and then aerated. The yields of the reaction products are shown in Table 1.

12) A. Sugimoto, Y. Yokota, S. Kusaka, H. Inoue, and E. Imoto, to be published.

13) G. M. Badger, R. S. Pearce, and R. Pettit, *J. Chem. Soc.*, **1951**, 3204.

Table 1. Photo-reduction of 1-benzoyloxyphenazine in alcohols and subsequent oxidation[a)]

ROH	Irradiated time, hr	Yield of product (%)			
		1-HOPh[b)]	C_6H_5-CHO	C_6H_5-COOR	C_6H_5-COOH
$(CH_3)_3COH$	160	10	0	0	0
$(CH_3)_2CHOH$	260	72	14	9	20—30
CH_3OH	140	55	0	40	5—10

a) The amount of 1-benzoyloxyphenazine was $(4.4—4.6)\times10^{-5}$ mol in 10 ml of alcohols. Irradiated distance: 4 cm. Reaction vessel: Pyrex glass.
b) 1-HOPh means 1-hydroxyphenazine.

The spectral change in 1-benzoyloxyphenazine was similar to the results obtained by directly irradiating a solution of 1-acetoxyphenazine in 2-propanol with ultraviolet light for a short time, as has been described above. The spectral yield of 1-hydroxyphenazine, as calculated from the optical density of the absorption at 440 mμ, was 72%; the analytical yields of benzaldehyde, isopropyl benzoate, and benzoic acid by gc analysis were 14, 9, and 20—30% respectively. The generation of gas was not observed. In addition to these products, the presence of pinacol and acetone was confirmed by gc. The formation of pinacol and acetone indicates the occurence of the photo-reduction of 1-benzoyloxyphenazine. Furthermore, 1-hydroxyphenazine was isolated from the residue after distilling out the resulting solution, and was identified by a comparison with the IR spectrum of the authentic material. The formation of bezaldehyde means that the homolytic fission of the acyl-to-oxygen bond occurs in the photo-reduction process.

The yields of benzaldehyde and benzoate changed depending on the kinds of alcohols used as the solvents, as Table 1 shows. When methanol was used as the solvent, methyl benzoate was obtained as the main product. On the irradiation of 1-benzoyloxyphenazine in *t*-butyl alcohol for 160 hr, benzaldehyde and *t*-butyl benzoate were not obtained, but 1-benzoyloxyphenazine was recovered in a 90—100% yield. That is, the requirement for the formation of benzaldehyde is that the solvent is a hydrogen donor. Furthermore, a protic solvent tended to decrease the yield of benzaldehyde and, contrarily, to increase that of the corresponding ester.

When 1-benzoyloxyphenazine in cyclohexene with a hydrogen-donating property was irradiated with light, an oxetane (8-phenyl-7-oxabicyclo[4.2.0]octane),[14] benzaldehyde, bicyclohexenyl, and 1-hydroxyphenazine were confirmed by gc analysis, though the amount of the oxetane could not be analyzed quantitatively because it is unstable to heat. The results are shown in Fig. 3. The formation of the oxetane supports the idea that benzaldehyde is produced during the irradiation of 1-benzoyloxyphenazine in a hydrogen-donating solvent.

The reduction of 1-benzoyloxyphenazine with aqueous sodium hydrosulfite did not result in the fission of the acyl-to-oxygen bond. That is, 1-benzoyloxyphenazine was reduced to 1-benzoyloxy-5,10-dihydrophenazine (VI) by an aqueous sodium hydrosulfite solution, and then the resulting solution was heated at about 80°C

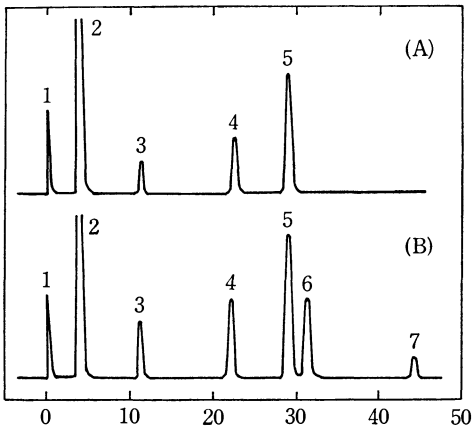

Fig. 3. Gas chromatogram of the products in the photoreaction of 1-benzoyloxyphenazine(A) or benzaldehyde(B) in cyclohexene: Conditions; absorbent, 150 cm, high-vacuum silicone grease-30; carrier gas, helium gas; programmed temperature rate, 6°C/min and temperature range, 80—320°C.
1 air, 2 cyclohexene, 3 benzaldehyde, 4 bicyclohexenyl, 5 8-phenyl-7-oxabicyclo[4.2.0]octane, 6 cyclohexenylphenylcarbinol, and 7 1,2-diphenyl-1,2-ethanediol.

under a nitrogen atmosphere for 6 hr. The color of the solution changed from yellow to greenish-black. The oxidation of the solution with oxygen resulted in the recovery of 1-benzoyloxyphenazine. Furthermore, 1-benzoyloxyphenazhydrin (V) was prepared by the reduction of 1-benzoyloxyphenazine with an aqueous sodium hydrosulfite solution,[12] and was characterized by its IR spectrum (Fig. 4), which has the absorptions of the –NH– group at 3300 and 3400 cm^{-1} and of the –CO–O– group at 1725 and 1740 cm^{-1}. The oxidation of V in 2-propanol with oxygen did not give benzaldehyde and isopropyl benzoate, but resulted in the quantitative recovery of 1-benzoyloxyphenazine. On the

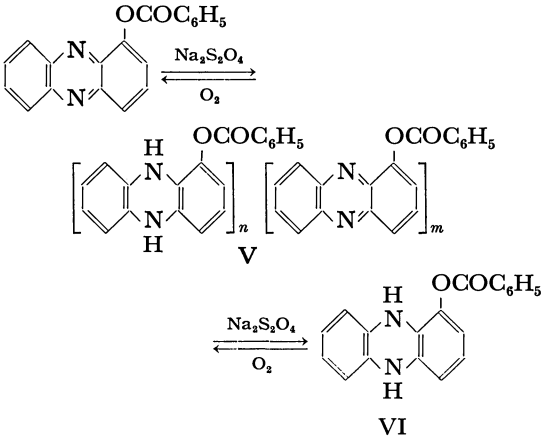

other hand, the irradiation of 1-benzoyloxyphenazine in the presence of 5,10-dihydrophenazine in 2-propanol for 140 hr gave 1-hydroxyphenazine and isopropyl benzoate in 35 and 5% yields respectively. A considerable amount of 1-benzoyloxyphenazine remained, although the amount was not obvious because of the contamination of phenazine. Thus, the formation of a phenazhydrin- or dihydrophenazine-type compound (V or VI), which is considered to be one of the photo-reduction

14) J. S. Bradshaw, *J. Org. Chem.*, **31**, 237 (1966).

products of 1-benzoyloxyphenazine, was ineffective in the fission of the acyl-to-oxygen bond. Therefore, the intermediary formation of a semiquinone radical during the photo-reduction must exert a profound effect on the fission of the acyl-to-oxygen bond. That is, the formation of benzaldehyde can be explained by a homolytic β-fission of the acyl-to-oxygen bond from a canonical structure (VII') of the semiquinone (VII):

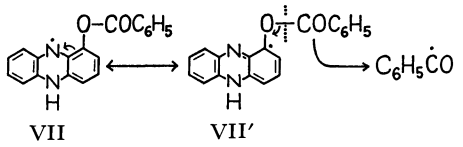

VII VII'

The mechanism of the formation of the benzoate ester is not yet clear. However, the possibility of the formation of isopropyl benzoate from benzaldehyde diisopropyl acetal (VIII)[15] can be ruled out, since benzaldehyde and VIII in 2-propanol do not change to isopropyl benzoate under similar conditions. The mechanism of the formation of benzoic acid will be reported later.

$$C_6H_5CHO \longrightarrow \underset{\text{VIII}}{C_6H_5CH(OCH(CH_3)_2)_2} \xrightarrow{h\nu} C_6H_5COOCH(CH_3)_2$$

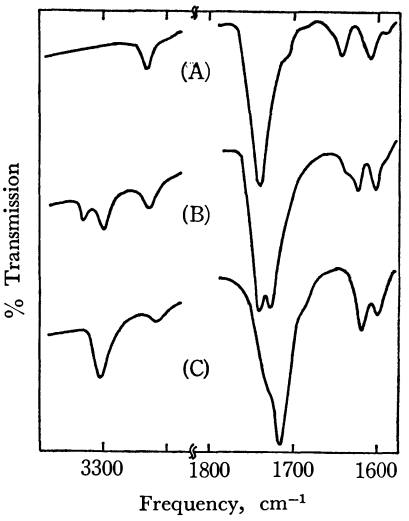

Fig. 4. Infrared spectra of 1-benzoyloxyphenazine (A), 1-benzoyloxyphenazhydrin (B), and 1-benzoyloxy-5,10-dihydrophenazine (C).

Effects of Ferric Chloride and Dimethyl Sulfate. When a solution of 1-acetoxyphenazine in 2-propanol containing ferric chloride with the molar ratio of 1: 1 was irradiated, the absorption of 1-acetoxyphenazine at 363 mμ disappeared rapidly; after irradiation for 2—3 min, a broad new peak appeared at 440 mμ similar to that of the semiquinoid form of pyocyanine.[16] This new band also disappeared upon further irradiation, leading to the appearance of the absorption at 480—490 mμ. After the absorption in the visible region had disappeared completely, oxidation was accomplished by oxygen and resulted in the appearance of a major peak at 368 mμ, as well as a tail up to about 660 mμ, which corresponds to the absorption of the mixture of 1-hydroxyphenazine and ferric chloride. However, there was no spectral change without irradiation of light. Thus, the occurence of the fission of the acyl-to-oxygen bond was established by investigating the spectral change of the reaction system. Also, in the case of dimethyl sulfate, the abosrption at 440 mμ was observed during the photo-reduction, and oxidation by oxygen resulted in the appearance of an absorption spectrum having absorptions at 368 and 430 mμ, absorptions which corresponded to those of 1-hydroxyphenazine, as is shown in Fig. 5.

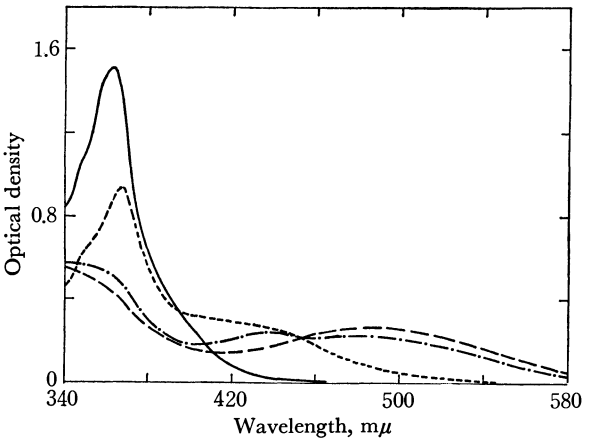

Fig. 5. Spectral change of 1-acetoxyphenazine in the presence of dimethyl sulfate under irradiation of ultraviolet light: Concentration of 1-acetoxyphenazine and dimethyl sulfate; 1.02×10^{-4} mol/*l* and 1.4×10^{-4} mol/*l*.
—— Before irradiation, —·— after 2 min, —— 3 min of irradiation, and ------ after 1 hr of oxidation after irradiating for 3 min.

The photo-irradiation of a solution of 1-benzoyloxyphenazine in 2-propanol, which has been placed in a Pyrex vessel, resulted in the formation of isopropyl benzoate, as is shown in Table 2. The spectral change in the reaction mixture was similar to the results in the case of 1-acetoxyphenazine described above. Although the irradiation of 1-benzoyloxyphenazine in *t*-butyl alcohol did not result in the fission of the acyl-to-oxygen bond, the addition of dimethyl sulfate to the reaction system

Table 2. Effect of the added compounds on the photoreaction of 1-benzoyloxyphenazine in 2-propanol[a]

Added compound	Irradiated time, hr	Yield of product (%)			
		1-HOPh	C_6H_5-CHO	C_6H_5-COOCH-$(CH_3)_2$	C_6H_5-COOH
None	260	72	14	9	20—30
$(CH_3)_2SO_4$	120	—	0	30	—
$FeCl_3$	95	—	0	45	—
Ph-H_2[b]	140	35	0	5	—

a) The starting amounts of 1-benzoyloxyphenazine, dimethyl sulfate, ferric chloride and 5,10-dihydrophenazine were $(4.3—4.6)\times10^{-5}$, 4.9×10^{-4}, 4.9×10^{-5}, and 1.3×10^{-4} mol, respectively. The volume of 2-propanol was 10 m*l*. Irradiated distance: 4 cm. Reaction vessel: Pyrex glass.
b) Ph-H_2 means 5,10-dihydrophenazine.

15) D. Elad and R. D. Youssefyeh, *Tetrahedron Lett.*, **1963**, 2189.
16) W. S. Zaugg, *J. Biol. Chem.*, **239**, 3964 (1964).

gave 1-hydroxy- phenazine and *t*-butyl benzoate as the products. The yield of 1-hydroxyphenazine was 70%. The amount of *t*-butyl benzoate could not be measured because it decomposed so readily in gc analysis.

Photo-reduction of 2-Benzoyloxyphenazine. A solution of 2-benzoyloxyphenazine in 2-propanol was irradiated with light for 50 hr according to the procedure used in the case of 1-benzoyloxyphenazine. 2-Hydroxyphenazine, benzaldehyde, and isopropyl benzoate were obtained in 66, 6, and 2% yields respectively. No other products derived from the benzoyl group could be detected by gc analysis in spite of recording up to about 300°C. Furthermore, the photochemical Fries rearrangement[17] of the benzoyl group to the phenazine ring was not observed. The benzoyl group would be converted to the dark brown polymeric material by a secondary photochemical reaction.

17) D. A. Plank, *Tetrahedron Lett.*, **1968**, 5423; R. A. Finnegan and D. Knutson, *ibid.*, **1968**, 3429; D. Bellus and P. Hrdlovic, *Chem. Rev.*, **67**, 599 (1967).

BULLETIN OF THE CHEMICAL SOCIETY OF JAPAN, VOL. 44, 3106—3108 (1971)

The Conversion of Some Alkylxanthates to the Corresponding Trithiocarbonates. The Nucleophilic Reaction of $^{-}$SCSSR

Hiroshi YOSHIDA, Tsuyoshi OGATA, and Saburo INOKAWA

Department of Synthetic Chemistry, Faculty of Engineering, Shizuoka University, Hamamatsu

(Received April 19, 1971)

The reaction of *O*-methyl-, ethyl-, and benzylxanthates with a catalytic amount of triethylamine in the presence of excess carbon disulfide gave the corresponding trithiocarbonate in good yields. The products were formed by the nucleophilic reaction of $^{-}$SCSSR with xanthates. The kinetic study showed the following order of nucleophilicity toward xanthates in DMF:

$$^{-}SCOSMe > {}^{-}SCSSMe > Me_3N$$

Dialkyl trithiocarbonates are generally prepared from mercaptans and thiophosgene[1]:

$$RSH + ClCSSR' \longrightarrow RSCSSR'$$

$$RSH + CS_2 \longrightarrow KSCSSR \longrightarrow RSCSSR'$$

$$2RSH + CSCl_2 \longrightarrow RSCSSR$$

In the course of the studies of the reaction of xanthates with tertiary amines,[2] the present authors have found a convenient route for the preparation of trithiocarbonates from xanthates.

In a previous paper,[2] the authors reported that xanthates reacted with tertiary amines to give quaternary ammonium salts at room temperature, and dithiolcarbonates at elevated temperatures. It was then shown that these reaction products were formed by the following paths. As an example, the reaction of methyl methylxanthate and triethylamine will be shown:

$$MeOCSSMe + Et_3N \longrightarrow \underset{\underset{Me}{|}}{Et_3N^+} {}^{-}SCOSMe$$

$$MeOCSSMe + {}^{-}SCOSMe \longrightarrow MeSCOSMe + {}^{-}SCOSMe$$

The salt thus formed reacted easily with carbon disulfide to yield the corresponding trithiocarbonate salt:[3]

$$\underset{\underset{Me}{|}}{Et_3N^+} {}^{-}SCOSMe + CS_2 \longrightarrow \underset{\underset{Me}{|}}{Et_3N^+} {}^{-}SCSSMe + COS$$

Results and Discussion

When O-alkylxanthates was treated with triethylamine in the presence of carbon disulfide at higher temperatures, the corresponding trithiocarbonate was obtained in a good yield (Table 1) and gaseous carbon oxysulfide was detected by vpc. Moreover, when methyl methylxanthate was reacted with triethylamine in carbon disulfide at room temperature, diemethyl trithiocarbonate and a small amount of triethylmethylammonium methyltrithiocarbonate were found. These observations seem to show that $^{-}$SCSSR reacts with xanthate to yield trithiocarbonate.

Table 1. The reaction of xanthates with triethylamine in the presence of carbon disulfide[a]

Xanthate	Reaction condition		Yield of trithiocarbonate(%)
	°C	hr	
MeOCSSMe	100	0.7	94
MeOCSSEt	100	0.7	93
MeOCSS*n*-Pr	100	0.7	81
EtOCSSMe	130	6	76[b]
EtOCSSEt	130	7	77
$C_6H_5CH_2OCSSMe$	100	0.5	84

a) Mole ratio, xanthate: CS_2: Et_3N = 1: 2: 0.2
b) Dimethyl and diethyl trithiocarbonate were also produced.

Methyl methylxanthate reacted vigorously with a catalytic amount of KSCSSMe to give dimethyl trithiocarbonate. Even ethyl-, *n*-propyl-, and *i*-propylxanthates gave trithiocarbonates. *i*-Propylxanthate was recovered in about an 80% yield by a 20-minute reac-

1) H. C. Godt, and R. E. Wann, *J. Org. Chem.*, **26**, 4047(1961).
2) H. Yoshida, This Bulletin, **42**, 1948 (1969).
3) H. Yoshida, *Nippon Kagaku Zasshi*, **89**, 883 (1968).

Table 2. The reaction of xanthates with KSCSSMe in the presence of carbon disulfide[a)]

Xanthate	Reaction condition		Yield (%)		
	°C	min	MeS-CSSMe	MeS-CSSR	RS-CSSR
MeOCSSMe	130	1	93		
EtOCSSMe	130	15	26	47	22
n-PrOCSSMe	130	20	25	49	20
i-PrOCSSMe	130	240	28	41	13
EtSCSSMe	130	20	27	49	23

a) Mol ratio, xanthate: CS_2: KSCSSMe=1: 2: 0.2. DMF was added as a homogeneous solvent by about 20 wt %.

tion at 130°C, while heating for about 4 hours gave trithiocarbonates in a good yield. The results are summarized in Table 2. The order of reactivity of xanthates (Me>Et>*n*-Pr≫*i*-Pr) seems to show the reaction proceeds *via* the nucleophilic attack of $^-$SCSSMe on the *O*-alkyl group of xanthates.

When ethyl methyl trithiocarbonate was heated at 130°C with KSCSSMe, crossed products, dimethyl and diethyl trithiocarbonates, were found (Table 2, the bottom line). Without KSCSSMe, however, no crossed product was found under similar reaction conditions. Thus, the crossed products were supposed to be yielded by the transesterification catalysed by the mercaptide ion,[2)] which was itself formed by the thermal decomposition of $^-$SCSSMe.

Thus, the reaction of xanthate with triethylamine in the presence of carbon disulfide may be simplified as follows:

$$ROCSSR' + Et_3N \longrightarrow Et_3\overset{\overset{Me}{|}}{N}{}^+ \ ^-SCOSR' \quad (1)$$

$$^-SCOSR' + CS_2 \longrightarrow {}^-SCSSR' + COS \quad (2)$$

$$ROCSSR' + {}^-SCSSR' \longrightarrow RSCSSR' + {}^-SCOSR' \quad (3)$$

$$ROCSSR' + {}^-SCOSR' \longrightarrow RSCOSR' + {}^-SCOSR' \quad (4)$$

The first reaction is the alkylation of triethylamine with xanthate to yield a quaternary ammonium salt, which was then changed to the corresponding trithiocarbonate salt (reaction (2)). The reactions (3) and (4) are the nucleophilic attack of $^-$SCSSR' and $^-$SCOSR' on xanthate to yield trithio- and dithiolcarbonate respectively. Since no dithiolcarbonate was detected in the reaction, the reaction (2) may be said to proceed faster than the reactions (3) and (4).

In order to clarify the mechanism, the reaction of $^-$SCSSMe with xanthate was investigated kinetically in DMF. The rate constant was first-order with xanthate and was independent of the concentration of carbon disulfide. These results show that the reaction (2) proceeds much faster than the reactions (3) and (4). As Fig. 1 shows, the apparent first-order rate consttants (k_1') are proportional to the concentration of $^-$SCSSMe. The slope of the line gives a second-order rate constant, k_2. The data are summarised in Table 3.

It is well known that thiolate anions have strong nucleophilicities toward tetrahedral carbons in protic solvents.[4)] Although the nucleophilicities of some thiolate anions have been investigated in DMF,[5)] no work on the thiocarbonate ion has been presented.

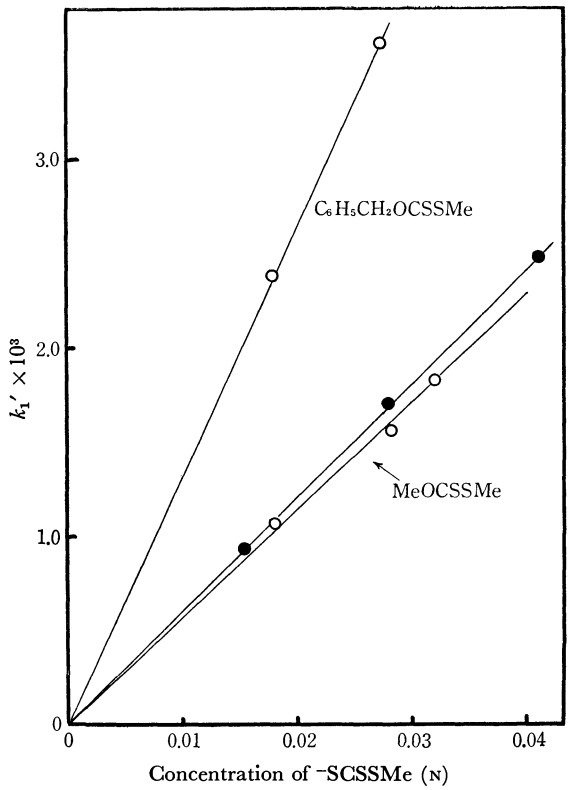

Fig. 1. The relation between the apparent first-order rate constant (k_1') and the concentration of $^-$SCSSMe for the reaction (3).
○ $Me_4NSCSSMe$ ● KSCSSMe

Table 3. Second-order rate constants for the reaction of xanthates with nucleophiles
(30°C k: l/mol·min)

Xanthate	Nucleophile	in DMF	in C_6H_6
MeOCSSMe	Me_3N[a)]	0.036	0.0012
	Et_3N[a)]		0.000097
	$Me_4NSCOSMe$[a)]	0.186	
	$Me_4NSCSSMe$	0.0573	
	KSCSSMe	0.0601	
$C_6H_5CH_2OCSSMe$	Me_3N[a)]		0.0028
	$Me_4NSCSSMe$	0.132	

a) Taken from Ref. 2.

Table 3 shows that $^-$SCSSMe and $^-$SCOSMe have larger nucleophilicities toward xanthate than trimethylamine and obviously than triethylamine has in DMF. The smaller reactivity of $^-$SCSSMe than that of $^-$SCOSMe may be attributed to the resonance stabilization of the ion.

The greater reactivity of benzylxanthate than that of methylxanthate supports the S_N2 mechanism. Once the reaction (1) proceeds, the reactions (2) and (3) recurr to give trithiocarbonate.

Experimental

All the reactions were carried out in stoppered test tubes. The reaction mixture was treated with cold aqueous hy-

4) R. G. Person, H. Sobel, and J. Songstand, *J. Amer. Chem. Soc.*, **90**, 319 (1968).

5) D. Cook, I. P. Evans, E. C. F. Co. and A. J. Parker, *J. Chem. Soc., B*, **1966**, 404.

drochloride and then extracted with carbon disulfide. The carbon disulfide extract was dried over calcium chloride, and was analyzed by vpc and NMR.

Materials. $Me_4NSCSSMe$ was prepared according to the previously described method.[3] KSCSSMe was prepared from methylmercaptan and carbon disulfide in a cold aqueous potassium hydroxide solution. After drying, the salt was recrystallized from acetone - ether. The purity was determined by acid-base titration.

Kinetic Run. A DMF solution containing ^-SCSSMe (0.015—0.04N), xanthate (0.05—0.08N), and carbon disulfide (0.1—0.4N) was allowd to stand in a constant-temperature bath. The rate was followed at suitable time intervals by analyzing the NMR spectrum of the S-Me groups.

BULLETIN OF THE CHEMICAL SOCIETY OF JAPAN, VOL. 44, 3108—3112 (1971)

The Properties and Assignment of Isomers of 2,4-Dinitrophenylhydrazones of Some Aliphatic α-Keto Acids

Hirohiko KATSUKI, Tsuya YOSHIDA,* Jun NAGAI, and Shozo TANAKA**
Department of Chemistry, Faculty of Science, Kyoto University, Sakyo-ku, Kyoto
(Received April 19, 1971)

Visible and infrared spectra and some other properties of *cis* and *trans* isomers of 2,4-dinitrophenylhydrazones of some aliphatic α-keto acids have been studied. It was observed that absorption maximum of the *cis* isomer in visible region occurred at a longer wavelength than that of the *trans* isomer in ethyl acetate as well as in bicarbonate solution and *vice versa* in sodium hydroxide solution. In infrared region, N–H and C=O stretching bands of the *cis* isomer were found at longer wavelengths than the corresponding bands of the *trans* isomer. It was concluded that a hydrogen bond is formed between C=O and N–H groups in the *cis* isomer. Further evidence which supports the above conclusion was given by the difference between both isomers in the nickel complex forming reaction, sodium carbonate reaction and in the properties of sodium salt. Instability of the *trans* isomer appeared to increase as the number of carbon atoms in the keto acid molecule increased. 2,4-Dinitrophenylhydrazones of some other α-keto acids were found to give polymorphs but not geometrical isomers.

2,4-Dinitrophenylhydrazine has been widely used as a reagent for the analysis of carbonyl compounds. A number of studies have been made on physical and chemical properties of the hydrazone derivatives. With α-keto acids, some of which are important metabolites in intermediary metabolism of organisms, investigations on the separation of geometrical isomers of the hydrazones were first carried out by us[1] and others[2–4] in 1955—6. We pointed out the importance of studies on both the isomerization between the *cis* and *trans* isomers of α-keto acid hydrazones and their properties for analysis, and a method for photometric determination of pyruvic acid irrespective of the existence of their isomers was reported.[5]

However, separation of the isomers of hydrazones of other α-keto acids other than those reported was not always possible because of lack of knowledge concerning isomerization between both isomers. The isomerization reaction was investigated and the first large scale separation became feasible by combining the salting-out method with isomerization treatment.[6]

In general, there should exist geometrical isomers in most condensation products of carbonyl compounds with carbonyl reagents including 2,4-dinitrophenylhydrazine. Spectroscopic studies in visible region have been reported since 1913 on the assignment of geometrical isomers of semicarbazones,[7] oximes,[8] and substituted[9,10] or non-substituted[11] phenylhydrazones of carbonyl compounds.

Studies on the infrared spectra were also made with the isomers of various hydrazone derivatives of α-keto acids.[1–4,12] The results indicated that a hydrogen bond was formed between C=O and N–H groups in the *cis* isomer but not in the *trans* isomer.

Proton nuclear magnetic resonance has also been applied successfully to the elucidation of structural isomerism involving restricted rotation. Karabatsos *et al.* studied NMR spectra of phenylhydrazones, semicarba-

* Deceased May 4th, 1970.

** Present address; Kyoto Women's University, Higashiyama-ku, Kyoto.

1) T. Moriwaki, H. Katsuki, and S. Tanaka, *Nippon Kagaku Zasshi*, **76**, 1367 (1955).

2) F. A. Isherwood and R. M. Johnes, *Nature*, **175**, 419 (1955).

3) A. Matsuyama, *J. Agr. Chem. Jap.*, **29**, 736, 977, 982 (1955).

4) I. Hayashi, *Nature*, **178**, 40 (1956).

5) H. Katsuki, C. Kawano, T. Yoshida, H. Kanayuki, and S. Tanaka, *Anal. Biochem.*, **2**, 433 (1961).

6) H. Katsuki, C. Tanegashima, M. Tokushige, and S. Tanaka, This Bulletin, in press.

7) F. J. Wilson and I. M. Heilbron, *J. Chem. Soc.*, **103**, 377 (1913).

8) R. E. Raffauf, *J. Amer. Chem. Soc.*, **68**, 1765 (1946).

9) H. Bredereck, *Ber.*, **65**, 1863 (1932).

10) F. Ramirez and A. F. Kirby, *J. Amer. Chem. Soc.*, **75**, 6026 (1953).

11) R. Kuhn and W. Munzing, *Chem. Ber.*, **85**, 29 (1952).

12) M. Yamaguchi, "Infrared and Raman Spectra," Bunshi-bunkokenkyukai, Tokyo (1949), p.41.

zones, of aldehydes and ketones.[13-16]

It was reported that 2,4-dinitrophenylhydrazones of some α-keto acids such as glyoxylic (I), pyruvic (II), α-ketobutyric (III), α-ketovaleric (IV), α-ketocaproic (V), and α-ketoisocaproic acid (VI) could be separated into two isomers by utilizing the solubility differences in 1N sodium carbonate.[6] These hydrazones were tentatively classified into group A. The hydrazones of α-ketoisovaleric (VII), α-keto-β-methylvaleric (VIII) and α-keto-β-dimethylbutyric acid (IX) could not be separated into two isomers by the above method and gave *x*- and *y*-forms by recrystallization from nonpolar and polar solvent, respectively. These hydrazones were classified into group B.

The present communication describes visible and infrared spectra and some properties of these isomers and forms, and deals with the assignment of the compounds. The study was successfully applied to the characterization,[17] determination[18,19] of α-keto acids which appear in biological materials by 2,4-dinitrophenylhydrazine method.

Experimental

Separation and Purification of Isomers and Forms of the Hydrazones. These were described previously.[6]

Sodium Salts of the Hydrazones. The *cis* hydrazones of keto acids which belong to group A or the hydrazones of keto acids of group B were converted into their sodium salts by treating them with an excess amount of 1N sodium carbonate. The sodium salts of the hydrazones, scarcely soluble in 1N sodium carbonate, were filtered and washed twice with 1N sodium carbonate and twice with a small amount of water. They were recrystallized from 50% aqueous acetone.

Some kinds of *trans* hydrazones of keto acids of group A, such as I and II, were dissolved in 1N sodium carbonate, and the solution was saturated with sodium chloride. The precipitated sodium salts were filtered and washed twice with a small amount of 1N sodium carbonate saturated with sodium chloride, and once with a small amount of water.

The *trans* hydrazones of III, IV, V, and VI were dissolved in a small amount of absolute ethanol. An excess amount of 1N sodium carbonate was added to it. Sodium salts, thus precipitated, were washed with 1N sodium carbonate and water, then recrystallized in the same way as for the *cis* isomers of the hydrazones.

Absorption Spectra in Visible Region. The hydrazones were dissolved in 0.1N sodium bicarbonate or ethyl acetate. The spectra were taken with fresh solutions with the use of a Beckman Spectrophotometer, Model DU, and a Hitachi Recording Spectrophotometer, Model EPS. The spectra of the hydrazones in alkali were taken as follows: to the bicarbonate solution of the hydrazone, an equal volume of 2.0N sodium hydroxide was added and the mixture was shaken thoroughly. After the mixture was left to stand for 10 min at 30°C, the spectra were taken within 10 min. The spectra showed no noticeable change during this period.

Infrared Spectra. Infrared spectra of the hydrazones were taken with a Nihonbunko Infrared Spectrophotometer, Model Koken DS 301 by the Nujol mull method, and also by the potassium chloride disc method in the case of the keto acid hydrazones which belong to group B.

Results and Discussion

Absorption Spectra in Visible Region. In Table 1 are shown the wavelengths at which absorption maxima were observed and the molecular extinction coefficients of the hydrazones at those wavelengths in ethyl acetate, 0.1N sodium bicarbonate and 1N sodium hydroxide containing 0.05N sodium bicarbonate.

Table 1. Absorption spectra of the hydrazones in visible region

Hydrazones of keto acids		0.1N Sodium bicarbonate		Ethyl acetate		1N Sodium hydroxide[a]	
		λ_{max}	ε_{max}	λ_{max}	ε_{max}	λ_{max}	ε_{max}
I	*trans*	365	2.45	350	2.48	453	2.63
	cis	373	2.57	360	2.54	380	1.75
II	*trans*	370	2.14	348	2.11	445	2.09
	cis	380	2.43	365	2.14	430	1.65
III	*trans*	373	2.32	348	2.13	440	1.97
	cis	383	2.45	368	2.33	435	1.70
IV	*trans*	373	2.33	348	2.10	440	1.93
	cis	383	2.48	363	2.34	430	1.75
V	*trans*[b]	(373)	(2.35)	—	—	(435)	(1.81)
	cis	378	2.48	—	—	430	1.74
VI	*trans*	373	2.40	350	2.10	440	1.97
	cis	383	2.44	368	2.37	430	1.75
VII	*x*, *y*	380	2.38	355	2.55	430	1.79
VIII	*x*, *y*	380	2.32	363	2.78	430	1.76
IX	*x*, *y*	375	2.31	365	2.50	430	1.79

a) Containing 0.05M sodium bicarbonate.
b) Contaminated with trace amounts of the *cis* isomer.

It is evident from the spectra of the free hydrazone and the sodium salt (taken in ethyl acetate and sodium bicarbonate solution, respectively) that absorption maximum of the *cis* isomer is at a longer wavelength than that of *trans* isomer, and that the molecular extinction coefficient of the *cis* isomer is greater than that of the *trans* isomer. This holds in all isomeric pairs of the hydrazons tested. These results would be expected from the stable six-membered ring structure of the *cis* isomer as follows:[1-4]

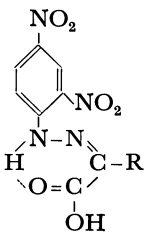

(*cis* isomer)

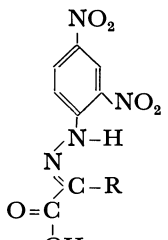

(*trans* isomer)

13) G. J. Karabatsos, J. D. Graham, and F. M. Vane, *J. Amer. Chem. Soc.*, **84**, 753 (1962).
14) G. J. Karabatsos, B. L. Shapiro, F. M. Vane, J. S. Fleming, and J. S. Ratka, *ibid.*, **85**, 2784 (1963).
15) G. J. Karabatsos, R. A. Taller, and F. M. Vane, *ibid.*, **85**, 2326 (1963).
16) G. J. Karabatsos, F. M. Vane, R. A. Taller, and N. Hsi, *ibid.*, **86**, 3351 (1964).
17) H. Katsuki, T. Yoshida, C. Tanegashima, and S. Tanaka, *Anal. Biochem.*, **24**, 112 (1968).
18) C. Kawano, H. Katsuki, T. Yoshida, and S. Tanaka, *ibid.*, **3**, 361 (1962).
19) H. Katsuki, T. Yoshida, C. Tanegashima, and S. Tanaka, *ibid.*, (1971) in press.

It seems reasonable to assume that in sodium bicarbonate solution, only carboxyl group of the hydrazone of keto acid is dissociated, whereas both carboxyl and N–H groups are ionized in strong alkaline solution, giving red coloration. The fact that the addition of alkali to *N*-methyl-phenylhydrazones does not produce a red color[20] seems to support this assumption. The red coloration of alkaline solution is due to the formation of an unstable intermediate or intermediates. Some typical one are assumed to be as follows:

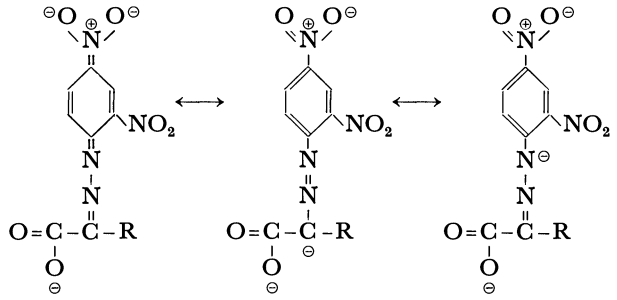

The *trans* isomer would be expected to give a deeper red than the *cis* isomer in alkaline solution since the hydrogen atom of N–H group of the latter is involved in a hydrogen bond formation and not easily ionizable. As a support of this hypothesis the results of spectral analyses of sodium hydroxide solution might be presented. The absorption maximum of the *trans* isomer was found to be at a longer wavelength than that of the *cis* isomer without exception and the molecular extinction coefficient of the *trans* isomer was greater than that of the *cis* isomer.

From the structure described above, a *cis-trans* interconversion would be expected to occur in alkaline solution. The observation that the red coloration produced in the *cis* isomer deepened as the concentration of sodium hydroxide was increased is in agreement with such a prediction.[21] Thus it is suggested that gradual breakage of the hydrogen bond in the *cis* isomer leads to conversion of the *cis* isomer into the *trans* isomer through the intermediate(s) described above.

In order to prove the interconversion of the two isomers in alkaline solution, as suggested by the development of red coloration under such conditions, the isomers were isolated as free hydrazone by the addition of hydrochloric acid to the alkaline solution. Further separation of the isomers was achieved by paper chromatography. Two spots corresponding to the *cis* and *trans* isomers were detected besides one spot presumably representing a decomposition product.

Two forms of the hydrazones of keto acids which belong to group B behaved differently in a solid state, but their solubilities, R_f values and partition coefficients were identical.[6] These two forms showed the same absorption spectra. Thus, they apparently behaved as the same substance in solution. From the spectral data in three different solvents, the form in solution seems to have the *cis* structure.[22]

Reaction with Sodium Carbonate. Although the spectra of the hydrazones in visible region in sodium carbonate solution and of those in sodium bicarbonate solution were nearly the same, the molecular extinction coefficient in the longer wave length region had slightly higher values in sodium carbonate than in sodium bicarbonate. It is difficult to differentiate the *cis* isomers from the corresponding *trans* isomers by visual inspection of the colored solution without comparing the spectra of isomeric pairs. However, a remarkable difference between the *cis* and *trans* isomers was found when the hydrazones reacted with sodium carbonate in ethanol. On the basis of this fact, a test for assigning the *cis* and *trans* isomers of α-keto acid hydrazones was devised as follows: A few milligrams of the hydrazone is dissolved in several drops of ethanol and to this solution is added one drop of 1N sodium carbonate. The *trans* isomer produces red coloration, and the *cis* isomer none.

As shown in Table 2, the *trans* isomers gave a positive reaction and the *cis* isomers a negative reaction with one exception. Although all the hydrazones of the keto acids of group B were expected to give a negative reaction, those of IX gave a positive reaction.

Nickel Complex Formation. The nickel complex forming test[23] was applied to the series of isomers of

TABLE 2. SOME REACTIONS AND PROPERTIES OF THE HYDRAZONES

Hydrazones of keto acids		Sodium carbonate reaction	Nickel complex formation	Color of dehydrated sodium salt
I	*trans*	+	−	black brown (decomp.)
	cis	(−)[a]	+	orange
II	*trans*	+	−	dirty brown
	cis	−	+	red
III	*trans*	+	−	yellow
	cis	−	+	red
IV	*trans*	+	−	yellow
	cis	−	+	yellow
V	*trans*	+	−	yellow
	cis	−	+	red
VI	*trans*	+	−	yellow
	cis	−	+	orange red
VII	*x*, *y*	(−)[a]	+	orange red
VIII	*x*, *y*	(−)[a]	+	red brown
IX	*x*, *y*	+	+	dirty brown (decomp.)

a) Faint orange color

20) F. Bohlmann, *Chem. Ber.*, **84**, 490 (1951).
21) H. B. Stewart, *Biochem. J.*, **55**, xxvi (1953).
22) A shift of the absorption maximum of VII with increasing water content in ethanol solution had been attributed to isomerization. *Cf.* H. Katsuki, K. Sumizu. T. Moriwaki, and S. Tanaka, This Bulletin, **31**, 665 (1958). However, it appears that shift is due to a non-specific solvent effect, since such a phenomenon was also observed with the *cis*- as well as the *trans* hydrazone of II. The absorption maximum of the *cis* hydrazone of II shifted from 363 mμ to 378 mμ and that of the *trans* isomer from 348 mμ to 365 mμ under these conditions.
23) H. Katsuki, K. Sumizu, T. Moriwaki, and S. Tanaka, *Nature*, **181**, 639 (1958).

hydrazones mentioned above. As shown in Table 2, the *cis* hydrazones of keto acids of group A and both forms of the hydrazones of keto acids of group B showed a positive reaction without exception, whereas the *trans* hydrazones of keto acids which belong to group A showed a negative reaction. The results of the nickel complex forming test were in line with the proposed structures of the isomers of keto acid hydrazones.

Properties of Sodium Salt. The characteristic properties of sodium salt of the *cis* hydrazone of II were reported.[1] The hydrated form of its sodium salt had a yellow color, but its color changed to red when dehydrated by standing *in vacuo* or by heating. The dehydrated form was extremely hygroscopic. It turned yellow as soon as it was exposed to air. The dehydrated sodium salt of the *trans* isomer had a dirty brown color and was not hygroscopic. These characteristic properties were also observed with sodium salt of the hydrazone of VII, which had a few molecules of water of crystallization and the dehydrated form showed an orange-red color. According to Hayashi,[24] sodium salt of *cis* isomer of phenylglyoxylic acid 2,4-dinitrophenylhydrazone also showed a similar behavior. In that case the hydrated form was orange, but the dehydrated form had a deep red color.

The characteristic color formation would be expected upon dehydration for the sodium salts of all of the *cis* isomers mentioned above. Inspection of Table 2 reveals that most keto acid hydrazones fulfilled this requirement. Exceptions were sodium salt of the *cis* hydrazone of IV, which was yellow, and that of IX, which decomposed when dehydrated.

Infrared Spectra. As N–H stretching band, each *trans* hydrazone of I, V, and VI showed a single absorption band and that of II, III, and IV showed two bands in the region 3500—3200 cm^{-1}, whereas each of all the *cis* hydrazones of these keto acids showed a single N–H stretching band which occurred at a longer wavelength than the corresponding band of the *trans* isomer. These results are shown in Figs. 1, 2, and 3.

We see that infrared spectra of most hydrazones showed a single stretching band for C=O group 1664—1750 cm^{-1}) except for the case of the *trans* hydrazones of III and IV, for which two and three bands were observed, respectively. The band for the *cis* isomer was seen at a longer wavelength than the corresponding band of the *trans* isomer. The difference in the positions of the stretching bands for C=O group between *cis* and *trans* isomers of the hydrazones of group A was the smallest for VI.

In the case of the hydrazones of keto acids which belong to group B, both *x* and *y* forms seemed to be polymorphic to each other because they showed identical spectra in Nujol mull (Fig. 4) as well as in potassium chloride disc except for those of VII. Both of the two forms of VIII hydrazones showed *cis* type N–H and C=O stretching bands. Absorption spectra in visible region and other properties of the two forms of VIII

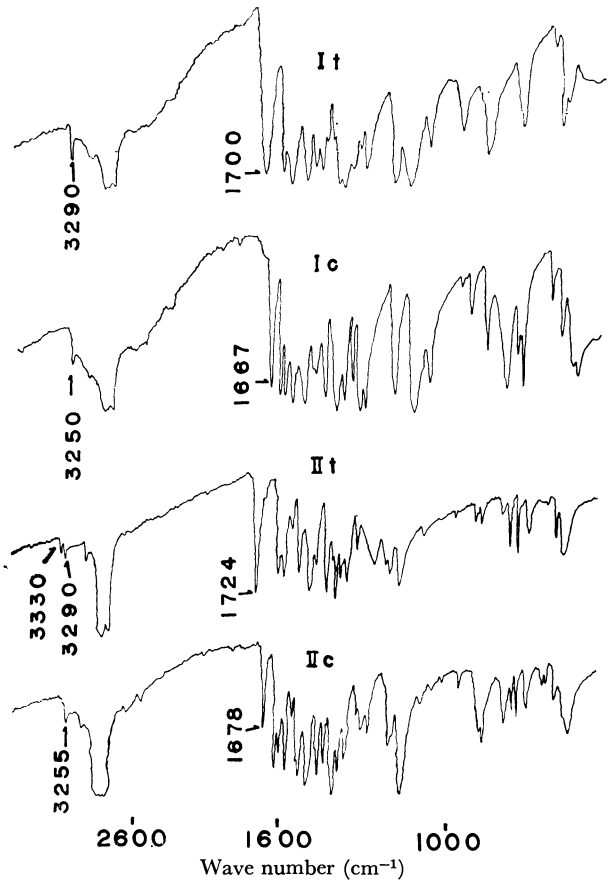

Fig. 1. Infrared spectra of the α-keto acid hydrazones (group A) (1).
by Nujol mull method.

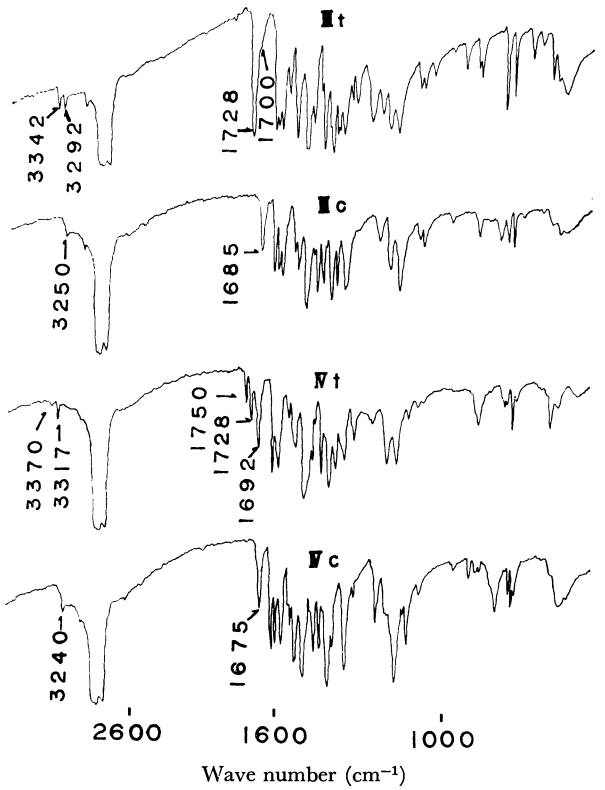

Fig. 2. Infrared spectra of the α-keto acid hydrazones (group A) (2).
by Nujol mull method.

24) I. Hayashi, private communication.

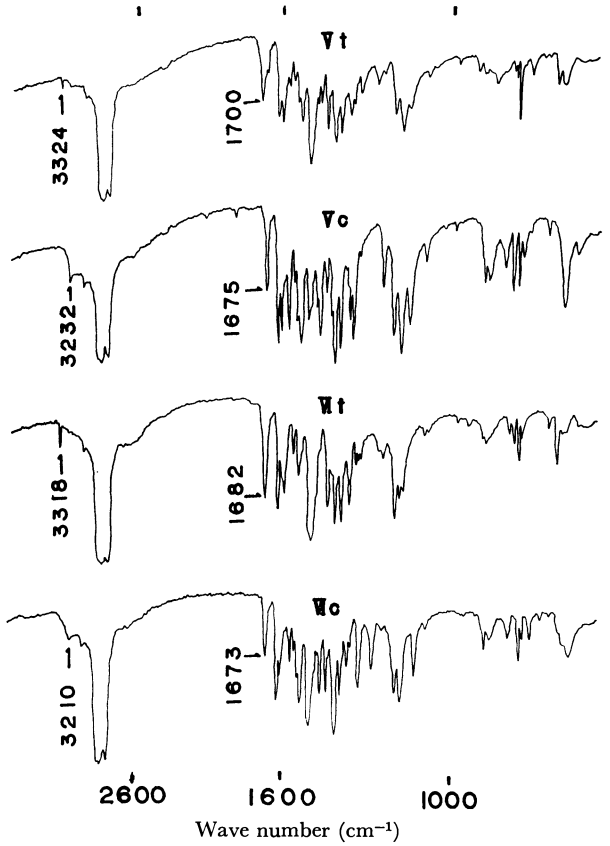

Fig. 3. Infrared spectra of the α-keto acid hydrazones (group A) (3).
by Nujol mull method.

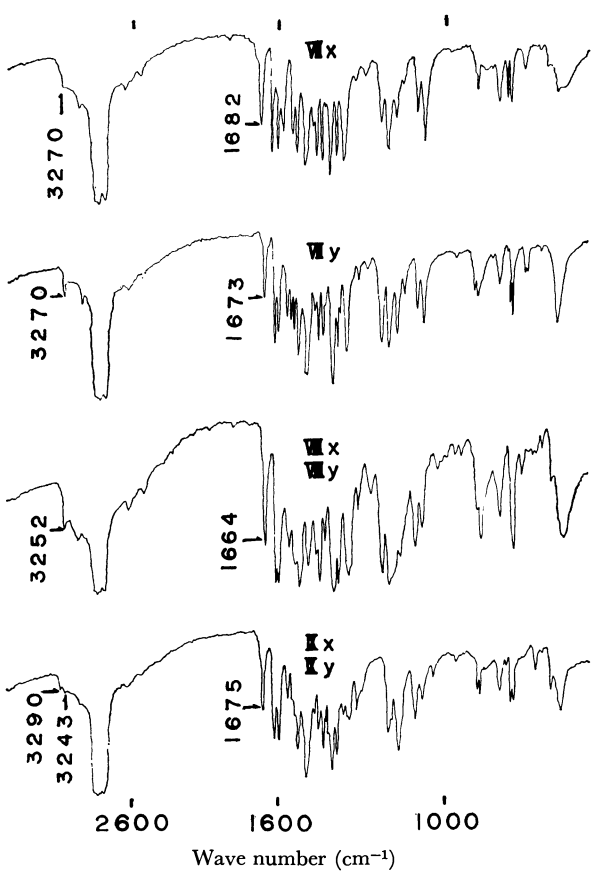

Fig. 4. Infrared spectra of the α-keto acid hydrazones (group B).
by Nujol mull method.

hydrazones supported their *cis* structure. Thus, it was concluded that the two hydrazones of VIII have *cis* structure in solid state as well as in solution.

In the case of IX, it was not possible to assign the hydrazone in solid state, since it showed an abnormal N–H band. Judging from the position of absorption maximum in visible region, the hydrazones of IX in solution seem to have *cis* structure but the result of the sodium carbonate reaction which is normally specific for the *trans* structure does not seem to be in line with it. No explanation could be given for this inconsistency.

The two forms of VII hydrazones, which showed quite different infrared spectra from each other, seem to be *trans* and *cis* isomers, respectively, but not polymorphs, because they showed similar stretching bands for C=O group to those of *cis* and *trans* hydrazones of VI, respectively. However, in solution, they behaved as the same substance to each other and they had the characteristics of *cis* type in all respects. If we assume that the *x* form (*trans* isomer) is stable only in solid state and isomerizes to the *y* form (*cis* isomer) as soon as it is dissolved in solution as reported by Abramovitch and Spenser for pyruvamide phenylhydrazone,[25] the behavior of VII hydrazones might be explained. Judging from its behavior in solid state, VII could be considered a member of group A, though it was classified as belonging to group B according to its behavior in solution.

It appears that the structures of the *cis* and *trans* isomers are stable with the hydrazones of lower keto acids. With the hydrazones of higher keto acids, however, the structure of the *trans* isomer seems to be less stable.

This seems to be supported also by the results of the isomerization of the hydrazones in solution as well as in melting state.[6]

The authors wish to thank Prof. Toru Takenaka, Institute for Chemical Research, Kyoto University, for his useful suggestion and Dr. Chizuko Tanegashima, Mukogawa Women's University, for her technical assistance.

25) R. A. Abramovitch and I. D. Spenser, *J. Chem. Soc.*, **1957**, 3767.

Free-Radical Chlorination of Alkylsilanes. VI.* The Hydrogen Abstraction from α-Substituted Hydrosilanes by Chlorinated Methyl Radicals

Yoichiro NAGAI, Hideyuki MATSUMOTO, Masaki HAYASHI, Eiji TAJIMA, and Hamao WATANABE

Department of Chemistry, Gunma University, Kiryu, Gunma

(Received April 23, 1971)

Relative rates of hydrogen abstraction from Si-H bonds of α-substituted hydrosilanes by the trichloromethyl or the dichloromethyl radical were determined by allowing the hydrosilanes to compete in pairs for a chlorocarbon compound, carbon tetrachloride or chloroform, at 80°C in the presence of benzoyl peroxide. Results show that relative rates of the investigated hydrosilanes toward the trichloromethyl and the dichloromethyl radicals are satisfactorily correlated with the summation of Taft σ* values for the substituent on the central silicon atom, giving ρ* values of −0.11 and −0.08, respectively. Linear correlations are also found to exist between the relative rates and the ^{29}Si-H coupling constants.

Previously,[1-3] it has been shown that a chain reaction occurs when a hydrosilane is allowed to react with an aliphatic halide in the presence of a radical generator, *e.g.* benzoyl peroxide. The chain carrying steps[1-6] are likely to be:

$$\equiv Si\cdot + \equiv CX \longrightarrow \equiv SiX + \equiv C\cdot \quad (1)$$

$$\equiv C\cdot + \equiv SiH \longrightarrow \equiv CH + \equiv Si\cdot \quad (2)$$

(X=Cl or Br)

The reaction makes it feasible to measure both the relative rates of halogen atom abstraction from C-Hal bonds by silyl radicals[2,5-9] and those of hydrogen abstraction from Si–H bonds by carbon radicals.

The present investigation deals with the latter reaction employing several α-substituted hydrosilanes in connection with our earlier work[10] on reactions of nuclear substituted phenylsilanes with carbon tetrachloride under free radical conditions. It was hoped that some correlation would emerge between the relative rates for reactions of the α-substituted hydrosilanes with carbon tetrachloride or with chloroform and structural variables in the substrates or in the attacking carbon radicals.

Results and Discussion

In the present study, triethylsilane, phenyldimethylsilane, diethylchlorosilane, ethyldichlorosilane and trichlorosilane were selected for the α-substituted hydrosilanes. The counter reactant was carbon tetrachloride or chloroform, so that the trichloromethyl or the dichloromethyl radical was to be generated in the system being considered. The investigated hydrosilanes were allowed to compete in pairs at 80°C toward an appropriate chlorinated methane, benzoyl peroxide being used as catalyst. The relative rates of reactions (2) were conveniently calculated by the Ingold-Shaw equation[11]

$$\frac{k_A}{k_B} = \frac{\log [A]_i/[A]_f}{\log [B]_i/[B]_f}$$

where $[A]_i$, $[B]_i$ represent the initial concentrations of two hydrosilanes, $[A]_f$, $[B]_f$ the final concentrations and k_A/k_B the ratio of rate constants for the attack of the abstracting reagent on the two species.

Table 1 summarizes the results of the analysis of the various competitive reaction mixtures. Included in the tabulation are the initial, $[A]_i$ and $[B]_i$, and final, $[A]_f$ and $[B]_f$, amounts of the hydrosilanes competing for the chlorinating reagent. The latter quantities were determined by means of vapor phase chromatography. Figure 1 indicates summaries of all the competitive experiments of Table 1 in which probable errors are included. Examination of Fig. 1 shows the results of the cross-checks on the relative rate constants for reactions of the α-substituted silanes investigated both with carbon tetrachloride and with chloroform to be satisfactory. For example, the relative rate for trichlorosilane relative to triethylsilane can be calculated *via* three possible pathways involving different compounds and the agreement between the values so calculated appears to be reasonable. The averages of the k_A/k_{Et_3SiH} values are summarized in Table 2, in which the experimental uncertainties are not included because the cross-check experiments make it difficult to estimate these quantities.

It is seen from Table 2 that the successive introduction of electron-withdrawing groups on the central silicon atom decreases the reactivity of the Si-H bonds

* For Part V see ref. 10.

1) Y. Nagai, K. Yamazaki, N. Kobori, and M. Kosugi, *Nippon Kagaku Zasshi*, **88**, 793 (1967).

2) Y. Nagai, K. Yamazaki, I. Shiojima, N. Kobori, and M. Hayashi, *J. Organometal. Chem.*, **9**, P. 21 (1967).

3) Y. Nagai, K. Yamazaki, and I. Shiojima, *ibid.*, **9**, P. 25 (1967).

4) R. N. Heszeldine and J. C. Young, *J. Chem. Soc.*, **1960**, 4503.

5) J. A. Kerr, B. J. A. Smith, A. F. Trotman-Dickenson, and J. C. Young, *Chem. Commun.*, **1966**, 157.

6) D. Cooper, *J. Organometal. Chem.*, **10**, 447 (1967).

7) J. A. Kerr, B. J. A. Smith, A. F. Trotman-Dickenson, and J. C. Young, *J. Chem. Soc.*, A, **1968**, 510.

8) P. Cadman, G. M. Tilsley, and A. F. Trotman-Dickenson, *ibid.*, **1969**, 1370.

9) Y. Nagai, K. Yamazaki, I. Shiojima, M. Hayashi, and H. Matsumoto, *Yuki Gosei Kagaku Kyokai Shi*, **26**, 1004 (1968).

10) Y. Nagai, H. Matsumoto, M. Hayashi, E. Tajima, M. Ohtsuki, and N. Sekikawa, *J. Organometal. Chem.*, **29**, 209 (1971).

11) C. K. Ingold and F. R. Shaw, *J. Chem. Soc.*, **1927**, 2918.

TABLE 1. COMPETITIVE CHLORINATIONS WITH CHLORINATED METHANES (80°C)

A	B	$[A]_{i'}$ mmol	$[A]_{f'}$ mmol	$[B]_{i'}$ mmol	$[B]_{f'}$ mmol	$[CCl_4]_{i'}$ mmol	$[CHCl_3]_{i'}$ mmol	k_A/k_B
Et_2SiClH	$PhMe_2SiH$	1.587	0.724	1.000	0.160	10.49	—	0.428
Et_2SiClH	$PhMe_2SiH$	1.615	0.719	1.029	0.176	11.29	—	0.458
$EtSiCl_2H$	Et_3SiH	1.648	1.283	0.826	0.225	7.50	—	0.192
$EtSiCl_2H$	Et_3SiH	1.493	1.154	0.562	0.170	8.00	—	0.215
Cl_3SiH	Et_2SiClH	1.181	0.694	1.031	0.149	6.00	—	0.275
Cl_3SiH	Et_2SiClH	1.172	0.803	1.033	0.193	6.18	—	0.225
Cl_3SiH	Et_2SiClH	1.214	1.068	1.228	0.738	7.72	—	0.251
Cl_3SiH	$EtSiCl_2H$	1.461	1.100	0.930	0.449	6.41	—	0.390
Cl_3SiH	$EtSiCl_2H$	2.490	1.850	1.000	0.469	8.54	—	0.392
$PhMe_2SiH$	Et_3SiH	1.103	0.682	1.175	0.664	8.40	—	0.843
$PhMe_2SiH$	Et_3SiH	1.367	0.599	1.387	0.532	6.33	—	0.861
Et_2SiClH	Et_3SiH	2.066	0.756	1.903	0.156	9.23	—	0.402
Et_2SiClH	Et_3SiH	2.137	1.059	1.758	0.300	9.39	—	0.397
$PhMe_2SiH$	Et_3SiH	1.198	0.994	1.050	0.862	—	6.04	0.946
$PhMe_2SiH$	Et_3SiH	1.357	1.030	1.195	0.902	—	7.45	0.981
Et_2SiClH	$PhMe_2SiH$	1.554	0.920	1.011	0.400	—	13.03	0.565
Et_2SiClH	$PhMe_2SiH$	1.846	1.310	1.027	0.592	—	12.89	0.622
Et_2SiClH	Et_3SiH	1.893	1.340	1.017	0.527	—	13.39	0.525
Et_2SiClH	Et_3SiH	2.657	1.560	1.032	0.380	—	13.27	0.533
$EtSiCl_2H$	Et_3SiH	1.728	1.144	1.026	0.273	—	10.30	0.311
$EtSiCl_2H$	Et_3SiH	2.058	1.135	1.013	0.198	—	10.46	0.365
Cl_3SiH	$EtSiCl_2H$	1.277	0.920	1.050	0.558	—	7.94	0.519
Cl_3SiH	$EtSiCl_2H$	1.502	1.096	1.046	0.563	—	7.56	0.509
Cl_3SiH	Et_2SiClH	1.351	0.694	1.189	0.201	—	8.69	0.375
Cl_3SiH	Et_2SiClH	0.996	0.401	1.016	0.070	—	9.65	0.340

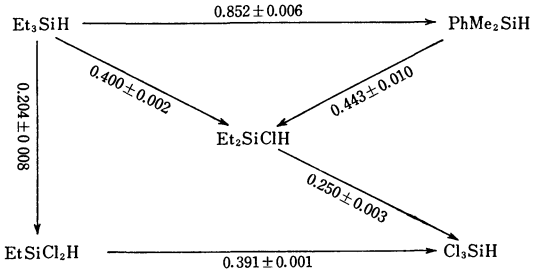

(i) Relative rates toward $\cdot CCl_3$ (80°C).

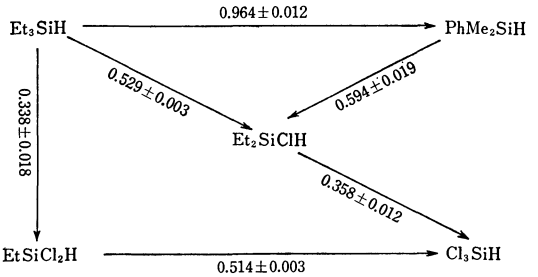

(ii) Relative rates toward $\cdot CCl_2H$ (80°C).

Fig. 1. Summary of competitive chlorinations.[a)]

a) Arrows indicate direct competitions and numbers stand for the rate of the compound at the head of an arrow relative to that at the tail.

toward either the trichloromethyl or the dichloromethyl radical. This trend is in keeping with electron-seeking character of the presumed attacking radical, the trichloromethyl or the dichloromethyl radical, serving as an electron acceptor from the hydride hydrogen atom.

TABLE 2. RELATIVE RATES FOR REACTIONS OF α-SUBSTITUTED HYDROSILANES (80°C)

Silane	k_{rel} (with CCl_4)	k_{rel} (with $CHCl_3$)	$\Sigma\sigma^{*a)}$
Et_3SiH	1.0	1.0	−0.30
$PhMe_2SiH$	0.84	0.89	+0.60
Et_2ClSiH	0.37	0.53	+2.7
$EtSiCl_2H$	0.24	0.37	+5.8
Cl_3SiH	0.093	0.19	+8.8

a) The summation of Taft σ^* values for three substituents on silicon. The value for Cl is calculated from multiplying the value for CH_2Cl by 2.8.

$$[\equiv Si{:}H{\cdot}C\equiv] \longleftrightarrow [\equiv Si^{+}\ H{:}C^{-}\equiv] \longleftrightarrow [\equiv Si{\cdot}H{:}C\equiv]$$

Kinetic data listed in Table 2 are plotted in Fig. 2 against the summation of Taft σ^* values[12] for three substituents on silicon. As will be shown in Fig. 2, the plots for reactions with carbon tetrachloride afford an excellent correlation with a slope of −0.11 and a correlation coefficient of 0.992. A linear correlation is also found to exist for reactions with chloroform with a slope of −0.08 and a correlation coefficient of 0.995. The observed linear correlations may imply that, within this class of substrates, polar factor is of primary importance in determining the rate for the Si-H hydrogen abstraction and that steric or other contributions for a set of the intermediate silyl radicals are nearly constant or vary linearly with changes in electronic effects of the substituents. The reaction constant (in

12) R.W. Taft, Jr., "Steric Effects in Organic Chemistry," ed. by M. S. Newman, John Wiley and Sons, New York, 1956, p. 556.

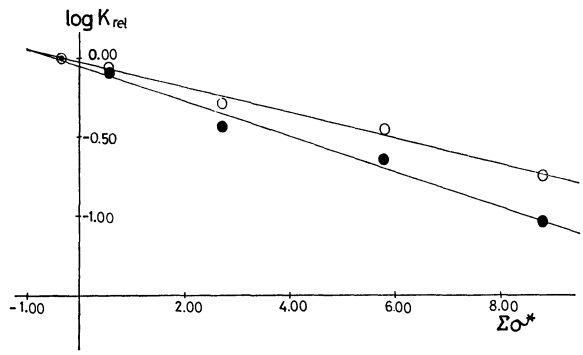

Fig. 2. Plots of relative rates *versus* $\sum\sigma^*$. Open circles represent reactions of carbon tetrachloride and solid circles those of chloroform.

absolute magnitude) is slightly larger for reactions with the trichloromethyl radical than for those with the dichloromethyl radical. Although such a comparison of the ρ^* values may be valid only if allowance is made as to the different solvents in which results have been obtained, the trend found in this study is expected from the polarity of the attacking radicals.

Importance of polar effects in the reaction of hydrosilanes with radicals can be seen in other instances.[13,14] For example, Morris and Thynne[14] reported that trimethylsilane is more reactive toward attack of the trifluoromethyl radical than is trichlorosilane by a factor of about 5 (at 164°C).

It is noteworthy that points for phenyldimethylsilane fall on the straight lines and from this fact the conjugation between the reaction site and phenyl substituent in the transition state is considered to be of only minor importance. This conclusion is reasonable since $3p_\pi$(Si)—$2p_\pi$(C) orbital overlap seems to be ineffective.[15]

It has recently been quoted that linear correlations emerge between the ^{13}C–H coupling constants and CH reactivities toward the abstracting reagents such as the chlorine atom[16,17] or the methyl radical.[18] By analogy, it might be expected that similar correlations would exist between the ^{29}Si-H coupling constants and SiH reactivities toward the attacking radicals employed in the present investigation (See Fig. 3). Although the factors governing the magnitude of $J(^{29}\text{Si-H})$ values are not yet fully understood,[19] the observed correlations are of interest and may imply correlations between change in the fraction of *s* character employed by silicon in a Si-H bond reflecting change in the electron density around the hydrogen and the ease of removal of the hydrogen by the abstracting radical.

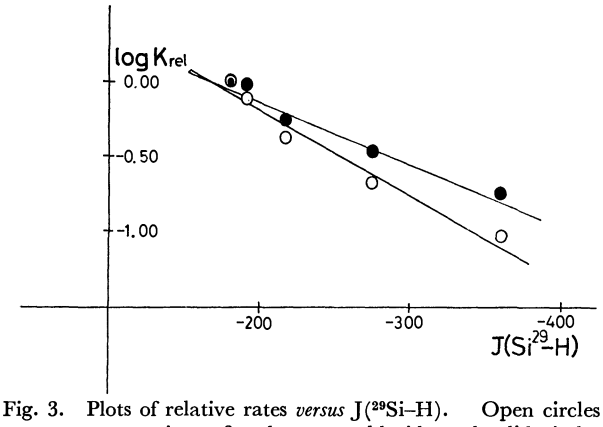

Fig. 3. Plots of relative rates *versus* $J(^{29}\text{Si–H})$. Open circles represent reactions of carbon tetrachloride and solid circles those of chloroform.

Experimental

Starting Materials. Triethylsilane (bp 106.0—106.5°C, lit.[20] 107°C/733 mm.), phenyldimethylsilane (bp 155.0—155.3°C, lit.[21] 158°C), diethylchlorosilane (bp 96—98°C, lit.[22] 99.2°C), ethyldichlorosilane (bp 73.5—74.0°C, lit.[22] 74.2°C) and trichlorosilane (bp 30.5°C, lit.[20] 31.5—32.0°C/729 mmHg) were prepared as described in the literature. Carbon tetrachloride and chloroform were purified according to the standard procedures.[23] VPC analysis of these materials showed negligible impurities. Benzoyl peroxide was commercially obtained as a special grade.

Products. Among the samples necessary for identification of the reaction products, triethylchlorosilane (bp 147°C, lit.[20] 147°C/729 mmHg), phenyldimethylchlorosilane (bp 190—191°C, lit.[21] 192—194°C), diethyldichlorosilane (bp 130°C, lit.[24] 131°C/740 mmHg) and ethyltrichlorosilane (bp 96.5—97.0°C, lit.[25] 97.9°C) were prepared according to the literature. Silicon tetrachloride and dichloromethane were commercially available.

Structures of reaction products were confirmed by comparing infrared spectrum of the respective sample which had been collected by preparative VPC from a reaction mixture with that of the corresponding authentic sample.

Procedure for Kinetic Runs. A solution of two different hydrosilanes was mixed in approximately 3—5 fold excess of an appropriate chloromethane with a catalytic amount of benzoyl peroxide and the resulting solution introduced into a tube which was sealed after the mixture was degassed several times. Then, the reaction tube was maintained at 80°C in a constant temperature bath for 3—5 h. It was found that about 15—90% of the hydrosilanes had reacted during the period of time. The reaction mixtures were subjected to VPC analysis, using column materials such as Silicone DC 550, 710 and so on. It was found by VPC analysis that with all the competitive experiments polydechlorination of carbon tetrachloride or of chloroform had occurred to

13) J. A. Kerr, D. H. Slater, and J. C. Young, *J. Chem. Soc.*, **1966**, 104; **1967**, 134.

14) E. R. Morris and J. C. J. Thynne, *Trans. Faraday Soc.*, **66**, 183 (1970).

15) C. Earbon, "Organosilicon Compound," Buttreworths, London, 1960, p. 86.

16) W. Mack, *Tetrahedron Lett.*, **1967**, 4993.

17) Y. Nagai, M. Kosugi, K. Takeuchi, and T. Migita, *Tetrahedron*, **26**, 2791 (1970).

18) A. U. Chaudhry and B. G. Gowenlock, *J. Organometal. Chem.*, **16**, 221 (1969).

19) C. Juan and H. S. Gutowsky, *J. Chem. Phys.*, **37**, 2198 (1962).

20) F. C. Whitmore, E. W. Pietrusza, and L. H. Sommer, *J. Amer. Chem. Soc.*, **69**, 2108 (1947).

21) M. Maienthal, M. Hellmann, C. P. Haber, L. A. Hymo, S. Carpenter, and A. J. Carr, *ibid.*, **76**, 6392 (1954).

22) H. J. Emeléus and S. R. Robinson, *J. Chem. Soc.*, **1947**, 1592.

23) J. A. Riddick and E. E. Toops, Jr., "Organic Solvents," Interscience Publishers, New York, 2nd ed., 1955, p. 410, 413, 414.

24) J. F. Hyde and R. C. DeLong, *J. Amer. Chem. Soc.*, **63**, 1194 (1941).

25) H. S. Booth and P. H. Carnell, *ibid.*, **68**, 2650 (1946).

negligible extent. Corrections were made for the thermal conductivity of the various components. The relative rates were calculated from original data with equation (3).

NMR Spectra. $J(^{29}Si\text{-}H)$ data were determined from spectra obtained on a Varian Model A-60D high resolution nuclear magnetic resonance spectrometer. NMR spectra were studied in the pure liquid phase. The coupling constants were evaluated from the satelite bands produced by the ^{29}Si in natural abundance which are symmetrically disposed about the main Si-H proton signals. The numerical values obtained are shown in Table 3.

TABLE 3. THE ^{29}Si-H COUPLING CONSTANTS

Compound	Et_3SiH	$PhMe_2SiH$	Et_2SiClH	$EtSiCl_2H$	Cl_3SiH
$J(^{29}Si\text{-}H)$, Hz	−179	−188	−216	−275	−363
Ref.	26)	26)	a	a	27)

a) Present work

26) M. A. Jensen, *J. Organometal. Chem.*, **11**, 423 (1968).
27) E. A. V. Edsworth and J. J. Turner, *J. Chem. Phys.*, **36**, 2628 (1962).

BULLETIN OF THE CHEMICAL SOCIETY OF JAPAN, VOL. 44, 3116—3120 (1971)

The Constituents of Hops. VI[1] Studies of the Volatile Composition of *Humulus lupulus* L. during Ripening

Yoko NAYA and Munio KOTAKE

The Institute of Food Chemistry, Dojimanaka 2-43, Kita-ku, Osaka

(Received April 23, 1971)

Evidence is presented for the volatile constituents of hops, not only in the resin glands, the so-called lupulin, but also in the stalk with leaves and in the three crops of cones during ripening. Lupulin shows a specific accumulation of myrcene, and the amount of the volatile constituents increases from fifty times to eight hundred times that in any other part of the plant in the course of ripening. While ripe cones contain neither any germacratrienes, the precursors of several sesquiterpenes, nor any aliphatic aldehydes, the stalk with leaves and the young cones have quite high concentrations of them respectively. Observation suggests that some of the volatile constituents are formed at an early stage of growth, whilst others are formed later.

The steam-volatile constituents of the cultivated Japanese hop, "Shinshu-wase" (*Humulus lupulus* L.), have previously been studied.[2-6] In the present paper, the isolation and the identification of volatile compounds from different plant tissues during ripening will be reported.

The part with the highest concentration of volatile components is well-known to be the "lupulin" glands of the cones, whilst the other parts of plant have also been found to include the major constituents to some extent. Germacrene D,[7] which is a key intermediate of cadinene-group compounds, and nonanal are found to be formed at an early stage of growth, whilst myrcene is formed in a remarkable amount at a later stage of growth. This observation suggests the compartmentalization effect of biogenesis in the plant tissue on the accumulation of volatile compounds. However, such a technique of the direct volatilization of individual plant tissue for GLC analysis[8] as will avoid numerous ill effects that the experimental samples will suffer after harvest is required before further detailed study can be done. The positive correlation with the size of the cones, or the formation of lupulin, and the quantity of aroma compounds are shown to be in agreement with the results of the recent study of Hautke *et al.*[9]

Experimental

The seedless Shinshu-wase used for the experiment was all cultivated in the same hop yard in Iwate Prefecture. The experimental samples were twice harvested on July 25th and again on August 31st when the cones were their final size, after dried in an oast below 50°C for several hrs, they were tansported by air each time. The analytical samples of various plant parts at different periods and the contents of the neutral volatile components are listed in Table 1. Lupulin for the sample VI was separated from the other cone parts by grinding in liquid nitrogen.

Each of the six samples was extracted with ether, the extract was then steam-distilled to obtain the essential oil for analysis. The distillate was extracted with ether, and the oil thus obtained was separated into the hydrocarbons and the fraction of the oxygenated constituents by selective adsorption on neutral alumina. The proportions of these two fractions from the six samples examined are also shown

1) Previous paper of this series: Y. Naya and M. Kotake, This Bulletin, **43**, 3594 (1970).

2) N. Shigematsu and Y. Kitazawa, *Bull. of Brew. Sci.*, **8**, 23 (1962).

3) R. G. Buttery, R. E. Lundin, and L. Ling, *Agri. Food Chem.*, **15**, 58 (1967).

4) Y. Naya and M. Kotake, *Nippon Kagaku Zasshi*, **88**, 1302 (1967).

5) Y. Naya and M. Kotake, *ibid.*, **89**, 1113 (1968).

6) Y. Naya and M. Kotake, *ibid.*, **91**, 275 (1970).

7) K. Yoshihara, Y. Ohta, T. Sakai, and Y. Hirose, *Tetrahedron Lett.*, **1969**, 2263.

8) E. von Rudoloff, *J. Gas Chromatogr.*, **3**, 390 (1965).

9) P. Hautke and D. Petricek, *Monatsschrift für Brauerei*, **23**, 241 (1970).

Table 1. Analytical samples from the different plant parts of "shinshu-wase" at different periods and the contents of the volatile compounds

Sample	Plant parts	Harvested date (1970)	Yield (%)	Constituents (%)	
				HC	Oxy.
I	Stalk with leaves	25/July	0.045	54.0	46.0
II	Stalk with leaves	31/Aug.	0.027	69.0	31.0
III	Cones with no lupulin (1/8 size)	25/July	0.087	54.5	45.5
IV	Cones with lupulin (1/4 size)	25/July	0.11	96.7	3.3
V	Cones with lupulin (final size)	31/Aug.	0.805	93.7	6.3
VI	Lupulin only	31/Aug.	41.4	94.1	5.9

in Table 1. Analysis was carried out by a combination of adsorption chromatography (silica gel), preparative GLC (Carbowax 20M), and the temperature-programmed capillary GC–MS method. The identification of the compounds was verified by the agreement of the mass spectra as well as by that of the retention time on GLC with those of authentic samples or of published standard references. Furthermore, the major constituents were isolated using the combined method described above, and the identity of the constituents was confirmed by comparing their IR spectra with those of authentic samples.

Apparatus and Operating Conditions. The preparative GLC conditions, using a model 90-P Varian Aerograph fitted with a thermal conductivity detector, were as follows: a 10-ft. × 3/8 in. aluminum column containing 20% Carbowax 20M on 60—80 mesh Diasolid-L. Helium was used as the carrier gas, and the column temperature was set at 100—220°C.

For the analytical GLC, a Hitachi Model K-53 apparatus equipped with a flame ionization detector was used. The capillary column used for the analysis was 45m × 0.25 mm, made of stainless steel and coated with HB 2000; the column temperature was programmed non-linearly from 100 to 150°C. The helium-carrier gas-inlet pressure was set at 1 kg/cm² for initiation and at 2.5 kg/cm² at the end.

The GC–MS were measured with the direct combination of GLC fitted with a Golay column (45m × 0.5 mm, HB 2000) and mass spectrometry using a Hitachi Model RMU-6 Mass Spectrometer; the operating conditions were as follows: ionization energy, 80 eV; acceleration voltage, 2000 V. The column temperature was programmed non-linearly at 60—150°C under a gas-inlet pressure of 0.6—2.0 kg/cm².

Results and Discussion

The identified constituents of the examined oils of "Shinshu-wase" are listed in Table 2, together with the peak number on the programmed GLC (Fig. 1—6).

Significant differences in the composition during the course of ripening may be seen in the gas chromatograms (Fig. 1—6) and in Table 2. The proportion of the oxygenated constituents to hydrocarbons is approximately 1: 1—2 in the samples I—III, whilst in the samples IV—VI it appears to be 1: 15—29 (Table 1). In the sample IV, the common major hydrocarbons, *i.e.*, caryophyllene, α- and β-humulenes, α- and β-selinenes, δ-cadinene, and myrcene, increase in almost the same ratio (Table 3), while the amount of myrcene in the samples V and VI increases almost 20 times more than in the other samples. It is very interesting to note that the annual plant *H. japonicus*[1] which has

Table 2. The constituents of the examined six samples (I-VI) with the peak number on the programmed GLC (Fig. 1–6)

Identity of Constituent	I	II	III	IV	V	VI
α-Pinene	4				4	
Isobutyl isobutyrate		5			5	5
β-Pinene	7	7		7	7	7
Sabinene	7					
Myrcene	8	8	8	8	8	8
2-Methylbutyl propionate					8	8
n-Undecane				9		
2-Methylbutyl isobutyrate		10			10	10
Limonene					11	11
β-Phellandrene	12	12			12	12
α-Phellandrene	13				13	13
2,2,7,7-Tetramethyl-1,6-dioxaspiro-[4.4]nona-3,8-diene		14	14	14	14	
Octanal			15	15		
Nona-2,4-dienal[a]	15					
Methyl heptanoate		16		16	16	16
n-Dodecane	18		18	18		
trans-3-Hexenol-1	18	18	18	18		
2-Methylbutyl 2-methylbutyrate		18			18	18
Methyl 4-methyl-2-hexenoate					18	
2-Methylbutyl isovalerate		19			19	19
2-Hexenol-1	20					
Methyl 6-methylheptanoate		21			21	21
2-Nonanone	22	22		22	22	22
Nonanal	23		23	23		

Identity of Constituent	I	II	III	IV	V	VI
Methyl octanoate		24			24	24
1-Octen-3-ol	25	25				
m/e 184, 106(B)[a]	26	26		26		
trans-2-Methyl-2-vinyl-5-hydroxy-isopropyl-tetrahydrofuran		27			27	
n-Tridecane	28	28	28	28		
cis-2-Methyl-2-vinyl-5-hydroxy-isopropyl-tetrahydrofuran		29				
4,4-Dimethylcrotonolactone			30	30		
2-Decanone	31	31			31	31
Linalool	32	32	32	32	32	32
Methyl nonanoate					33	
Decanal	33		33	33		
Decenal[a]			34			
n-Tetradecane	35		35			
Octyl alcohol					36	
9-Methyl-2-decanone	39	39		39	39	39
Terpinen-4-ol	39	39	39			
α-Ylangene	40	40	40	40	40	40
α-Copaene	41	41	41	41	41	41
Methyl 8-methylnonanoate					41	41
2-Undecanone	45	45		45	45	45
4-Undecen-2-one					45	
Undecanal			46	46		
Methyl 4-decenoate					47	

TABLE 2. Continued

Identity of Constituent	I	II	III	IV	V	VI
α-Terpineol	48	48	48	48	48	48
β-Elemene	49			49		
n-Pentadecane	49	49				
Caryophyllene	51	51	51	51	51	51
β-Farnesene		51		51		
Methyl geranate		53			53	53
α-Humulene	55	55	55	55	55	55
β-Humulene		55	55	55	55	55
Benzyl alcohol	55	55	55	55		
α-Farnesene		55				
Dodecanal			56			
γ-Muurolene	57	57	57	57	57	57
Nerol	57					57
Geranyl acetate					58	58
Germacrene-D	59	59	59			
n-Hexadecane	59		59			
Phenethyl alcohol	60		60	60		
β-Selinene	60	60		60	60	60
α-Selinene	61	61	61	61	61	61
Geraniol		62			62	62
δ-Cadinene	65	65	65	65	65	65
γ-Cadinene				65	65	65
δ_2-Cadinene[a)]		68	68	68	68	68
Heptadecane (branched)[a)]	68		68			
α-Cadinene		69	69	69	69	69
2-Tridecanone	69			69	69	69
Geranyl isobutyrate		70	70		70	70

Identity of Constituent	I	II	III	IV	V	VI
Calamenene	71	71	71	71	71	71
n-Heptadecane	72		72			
m/e 210, 126(B)[a)]		73				
m/e 220, 205 (B)[a)]	74		74	74		
m/e 220, 177(B)[a)]	74	74	74	74		
γ-Calacorene					74	74
α-Calacorene		75		75	75	75
Perrillyl alcohol					76	
Caryophyllene-oxide	78	78	78	78	78	78
Humulene-epoxide-I		80	80	80	80	80
Humulene-epoxide-II	81	81	81	81	81	81
Caryophyllene-alcohol					82	82
Nerolidol	83			83	83	83
Junenol						84
epi-Cubenol	85	85		85	85	85
m/e 222, 43(B) (ketone)[a)]						89
m/e 222, 43(B) (juniper camphor type)[a)]		90		90	90	90
Humulol				91	91	91
γ-Eudesmol		93				
T-Cadinol	94	94	94	94	94	94
T-Muurolol				95	95	95
δ-Cadinol	96			96	96	
α-Eudesmol		98			98	
α-Cadinol	99	99	99	99	99	99
Juniper camphor		100		100	100	100
Humulenol-II			101	101	101	101

a) tentatively identified or unknown compunds.

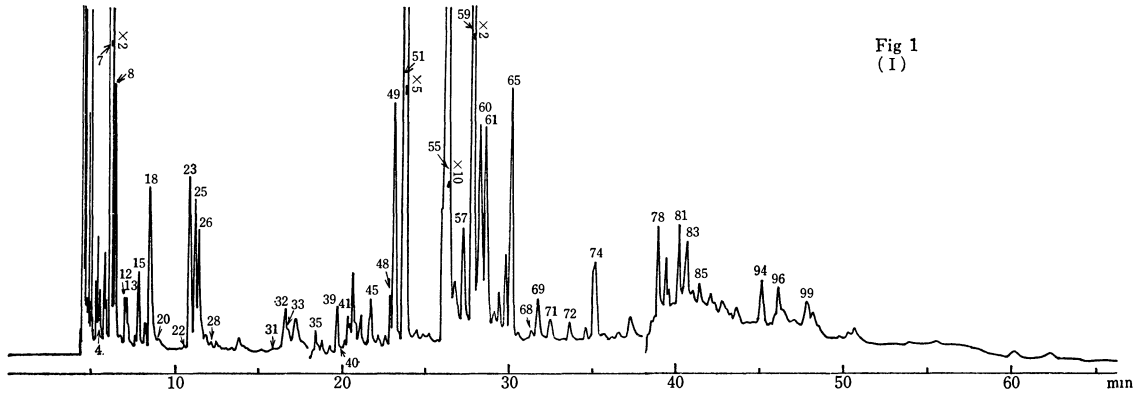

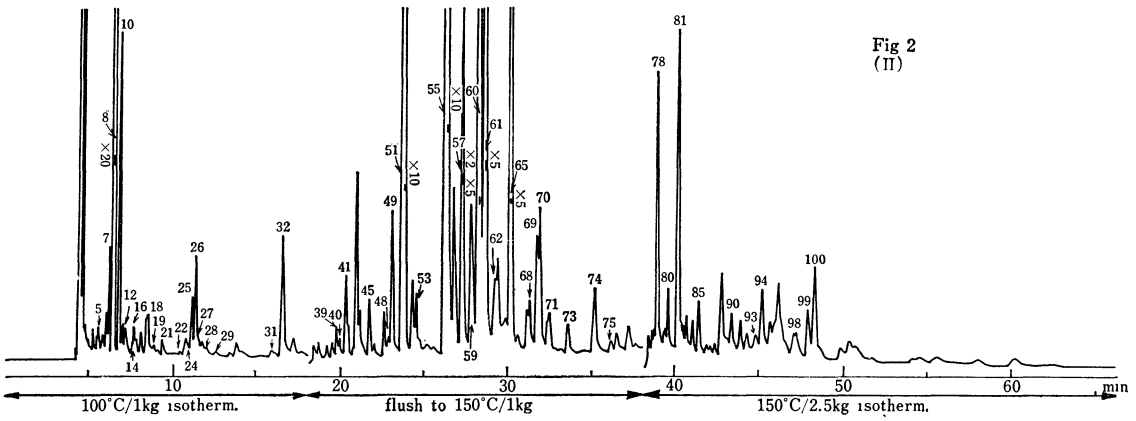

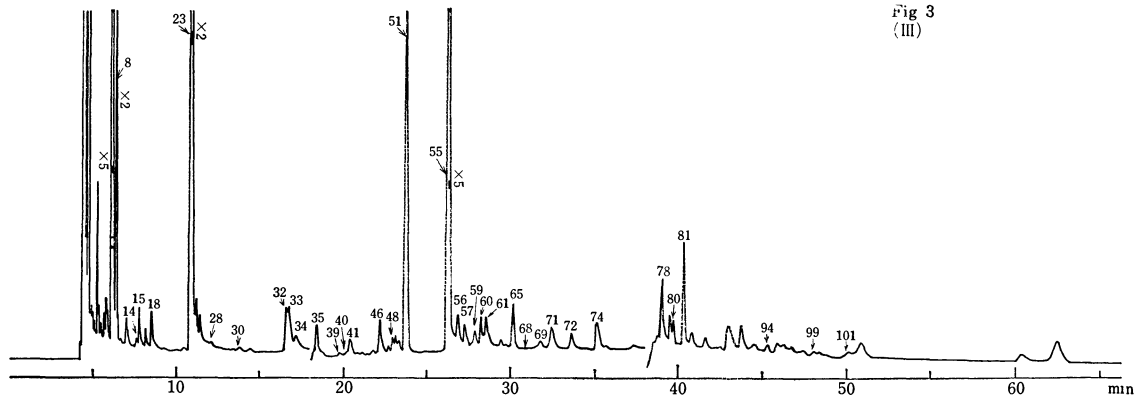

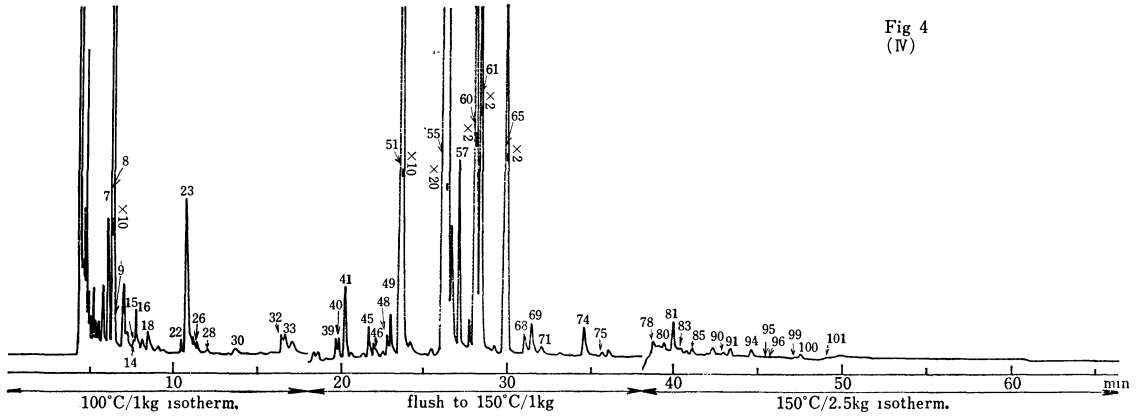

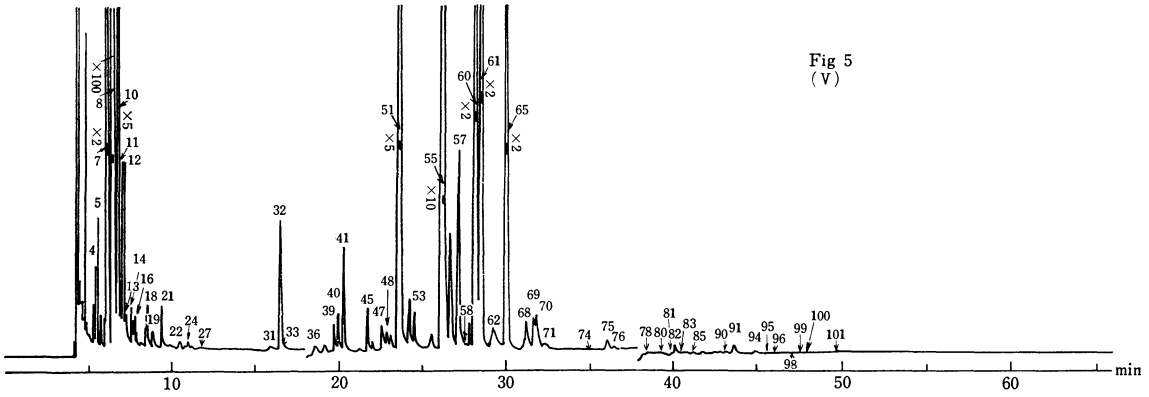

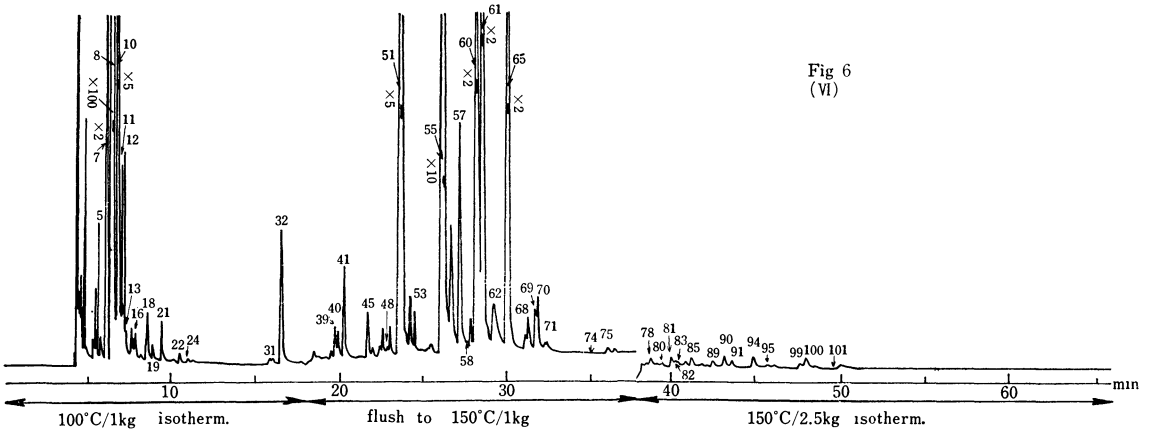

Fig. 1—6. Gas chromatograms of the steam-volatile oil from the examined samples (I—VI). Column 45 m × 0.25 mm coated with HB 2000.

Table 3. Relative abundance of characteristic constituents calculated from the peak area of GLC

Sample	C	H	β-S	α-S	Cd	M	N	G-D
I	1	1.24	0.15	0.15	0.19	0.20		0.45
II	1	1.36	0.42	0.54	0.42	2.32		0.08
III	1	2.50	0.08	0.08	0.13	0.36	1.92	+
IV	1	1.84	0.24	0.26	0.22	0.97	0.09	
V	1	1.45	0.45	0.49	0.38	18.2		
VI	1	1.42	0.42	0.50	0.38	20.6		

C: caryophyllene, H: humulene, β-S: β-selinene, α-S: α-selinene, Cd: cadinenes (δ,γ), M: myrcene, N: nonanal G-D: germacrene-D.

no lupulin, contains only a little amount of myrcene although in other respects it is similar to the volatile constituents of *H. lupulus* previously reported. Therefore, myrcene might be a characteristic compound in the lupulin of fully-ripened hops. Thus, the size of the cones is naturally correlated to the quantity of aroma compounds. The most predominant sesquiterpenic hydrocarbon is humulene, and the next is caryophyllene, in all the examined samples (I—VI), in the ratio of 2: 1. These two hydrocarbons are characteristic of the whole hop plant and are not connected with the differences in the plant tissue and the course of ripening.

A considerable amount of germacrene-D is detected in the sample I at an earlier stage of growth, and a little of it in the samples II and III, but none of it is detected in the samples IV—VI. The contents of selinenes and cadinenes increase considerably at later stages of growth. These compounds are known also to be produced chemically[7] through the germacratrienes. In addition, β-elemene produced by a Cope rearrangement of germacrene-A[10] is found a notable amount in the sample I. The above evidence strongly suggests that the labile germacrene-A, the precursor of β-elemene, α-, and β-selinenes, is present at an earlier stage of growth.

Aliphatic aldehydes, particularly nonanal are specifically accumulated in young cones (the sample III). It is interesting to consider the biological meaning of this compound at that stage of growth. It might be a repellent against insects, with its homologues the stink substances of *Pentatomidae* and *Coreidae*.[11]

10) A. J. Weinhaimer, W. W. Youngblood, P. H. Washecheck, T. K. B. Karns, and L. S. Ciereszko, *Tetrahedron Lett.*, **1970**, 497.

11) T. Tsuyuki, Y. Ogata, I. Yamamoto, and K. Shiomi, *Agr. Biol. Chem.* (Tokyo), **29**, 419 (1965).

BULLETIN OF THE CHEMICAL SOCIETY OF JAPAN, VOL. 44, 3120—3123 (1971)

Studies on the Baudisch Reaction. IV. The Reaction Mechanism[1)]

Kazuhiro MARUYAMA* and Iwao TANIMOTO**

*Department of Chemistry, College of Liberal Arts and Science, Kyoto University, Sakyo-ku, Kyoto

**Faculty of Home Economics, Kyoto Women's University, Higashiyama-ku, Kyoto

(Received April 28, 1971)

Mechanism of the Baudisch reaction was investigated using semicarbazide hydrochloride in lieu of hydroxylamine hydrochloride which is one of the reacting components. It was suggested that pyrocatechol-copper-hydroxylamine complex formed as a reaction intermediate is oxidized to *o*-benzoquinone-copper complex by hydrogen peroxide and one of the carbonyl groups of *o*-benzoquinone reacts with hydroxylamine hydrochloride to give *o*-benzoquinone monooxime, *i.e.* 2-nitrosophenol.

The Baudisch reaction is of interest with respect to the direct production of *o*-nitrosophenols from the corresponding hydrocarbons by the reaction with hydroxylamine hydrochloride, hydrogen peroxide and copper(II) salt.[2,3)] We found that the copper-hydroxylamine complex combined with the phenol formed at the first stage of reaction played a key role in the reaction.[1a,b)] In our recent studies,[1c)] it was demonstrated that *p*-cresol gave 5-methyl-2-nitrosophenol and 3,5-dimethylphenol gave 4,6-dimethyl-2-nitrosophenol; the hydroxy group of *p*-cresol or 3,5-dimethylphenol was replaced by nitroso group and a new hydroxy group was introduced into the position *ortho* to this nitroso group. Furthermore, 2-nitroso-1-naphthol which is the product starting from 1-naphthol was also produced exclusively in the Baudisch reaction of 2-naphthol. These results suggest the essential contribution of pyrocatechol-copper(II) complex (Fig. 1) as a reaction intermediate. For the sake of confirmation we examined whether pyrocatechols, in lieu of phenol, give *o*-nitrosophenols under the same conditions of the Baudisch reaction or not. It was found that pyro-

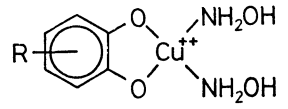

Fig. 1. Pyrocatechol-copper(II) complex.

1) a) Part I: K. Maruyama, I. Tanimoto, and R. Goto, *J. Org. Chem.*, **32**, 2516 (1967). b) Part II: I. Tanimoto, This Bulletin, **43**, 139 (1970). c) Part III: I. Tanimoto, *ibid.*, **43**, 1182 (1970).

2) a) O. Baudisch, *Naturwissenschaften*, **27**, 768 (1939). b) O. Baudisch and S. H. Smith, *ibid.*, **27**, 769 (1939). c) O. Baudisch, *Science*, **92**, 336 (1940). d) O. Baudisch, *Arch. Biochem.*, **5**, 301 (1944).

3) G. Cronheim, *J. Org. Chem.*, **12**, 1 (1947).

Table 1. Formation of hydroxyphenylazoformamides and nitrosophenols from catechols

Pyrocatechols	Nitrosophenols	Hydroxyphenylazoformamides	Elemental analysis, %	Mp °C
Pyrocatechol	2-Nitrosophenol[1c]	2-Hydroxyphenylazoformamide	Found: C, 50.74; H, 4.14; N, 25.19% Calcd for $C_7H_7N_3O_2$: C, 50.91; H, 4.27; N, 25.44%	99.5—101.5
4-Methylpyrocatechol	5-Methyl-2-nitrosophenol[1c]	4-Methyl-2-hydroxyphenylazoformamide	Found: C, 53.36; H, 5.11; N, 23.20% Calcd for $C_8H_9O_2N_3$: C, 53.63; H, 5.06; N, 23.45%	152—153.5
4-Chloropyrocatechol	5-Chloro-2-nitrosophenol	4-Chloro-2-hydroxyphenylazoformamide	Found: C, 42.36; H, 3.33; N, 20.79% Calcd for $C_7H_6O_2N_3Cl$: C, 42.12; H, 3.03; N, 21.05%	164—165
3-Methylpyrocatechol	6-Methyl-2-nitrosophenol	3-Methyl-2-hydroxyphenylazoformamide		122—124

catechols rapidly change into *o*-nitrosophenol-copper (II) complexes. All the mechanisms so far postulated[2c,d,3,4] failed to give an explanation. In this paper we would like to discuss the route by which *o*-nitrosophenol was produced from the pyrocatechol-copper(II) complex and try to elucidate the whole mechanism of the Baudisch reaction.

Results and Discussion

Pyrocatechol did not react with semicarbazide hydrochloride as well as hydroxylamine hydrochloride at pH 2.50 even in the presence of copper(II) ion. The reaction was started, however, by the addition of hydrogen peroxide. After the reaction was completed, the red solution was acidified and the product was extracted with a solvent. The elemental analysis of the purified products coincided with the calculated value for 2-hydroxyphenylazoformamide, *i.e.* semicarbazone of *o*-benzoquinone. The semicarbazone formed a characteristic reddish violet complex with copper(II) ion in water. Electronic spectra of the semicarbazone and of its copper(II) complex are shown in Fig. 2. The absorption peak of semicarbazone at 325 nm is ascribed to the azo group conjugating with aromatic ring, and the peak observed in copper salt at 527 nm seems to indicate the formation of an *o*-hydroxyazo copper chelate. By a similar procedure semicarbazones of substituted *o*-benzoquinones were obtained from the corresponding pyrocatechols. The results are summarized in Table 1. As one of the two hydroxy groups is apparently substituted by an azoformamide group, two isomeric products may result from substituted pyrocatechols. As an example, 4-methyl-2-hydroxyphenylazoformamide and 3-methyl-6-hydroxyphenylazoformamide can be produced from 4-methyl pyrocatechol. However, since the reduction of the product by tin(II) chloride gave only 6-amino-*m*-cresol, it can be deduced that 4-methyl-2-hydroxyphenylazoformamide was produced exclusively. Table 1 shows that in every case the hydroxy group replaced by the azoformamide group was the same as the one which was replaced by the nitroso group in the Baudisch reaction. These results imply that hydroxylamine hydrochloride or semicarbazide hydrochloride reacts with pyrocatechol in a similar manner.

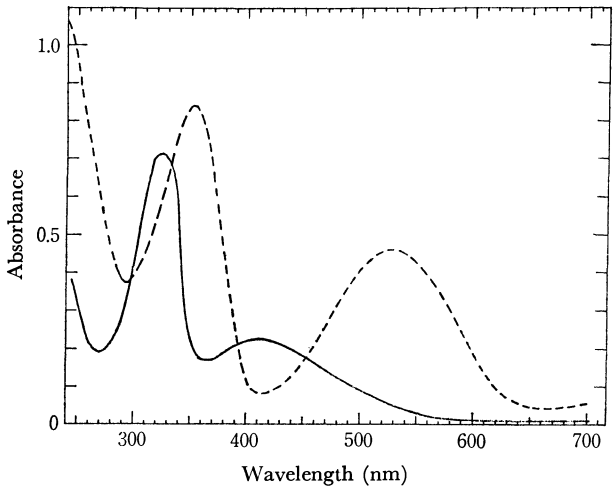

Fig. 2. Absorption spectra.
——: 2-hydroxyphenylazoformamide in chloroform
– – –: Cu^{2+} salt of 2-hydroxyphenylazoformamide in water

According to Horner and Drückheimer,[5] *o*-benzoquinonediazides are obtained by the reaction between *o*-benzoquinones and *p*-toluenesulfonyl hydrazide. Reduction of quinonediazides by hypophosphorus acid gives a mixture of isomeric phenols. Utilizing this reaction, one can determine which carbonyl group of substituted *o*-quinone was preferentially attacked. As an example, 4-chloro-*o*-benzoquinone gives 3-chlorophenol (91%) and 4-chlorophenol (8%); the carbonyl group *para* to chlorine atom is preferentially attacked by hydrazine.[5] Thus, we recognize that the position of the carbonyl group attacked by hydrazide in Horner and Drückheimer's reaction corresponds to the position of the hydroxy group replaced by nitroso or azoformamide group in our reaction. The results seem to indicate the following possible reaction sequence. Pyrocatechol-copper complex is oxidized to *o*-benzoquinone-copper complex and then one of the carbonyl groups of *o*-benzoquinone is attacked by hydroxylamine (or semicarbazide). In line with the above consideration, *o*-benzoquinones gave *o*-nitrosophenols under Baudisch reaction conditions, and no reaction of pyrocatechols with hydroxylamine(or semicarbazide) hydrochloride started until addition of hydrogen peroxide even in the

4) J. O. Konecny, *J. Amer. Chem. Soc.*, **77**, 5748 (1955).

5) L. Horner and W. Drückheimer, *Chem. Ber.*, **95**, 1206 (1962).

presence of copper(II) ion. Examination of the electron density using simple HMO method gave no fruitful guide for the preferential attack of Schiff bases(hydroxylamine, semicarbazide or *p*-toluenesulfonyl hydrazide) to one of two carbonyl groups of *o*-quinones.

On the other hand, the Baudisch reaction in methanol does not take place when no hydroxy group exists in a molecule,[1a] and the reaction of benzene, for example, might proceed *via* phenol formation. Thus, we examined the effect of copper(I) ion on the Baudisch reaction. A mixture of copper(I) and copper(II) in various molar ratio was used in the reaction, the total molar quantity of both ions being kept constant. The result is shown in Fig. 3. *o*-Nitrosophenol formation

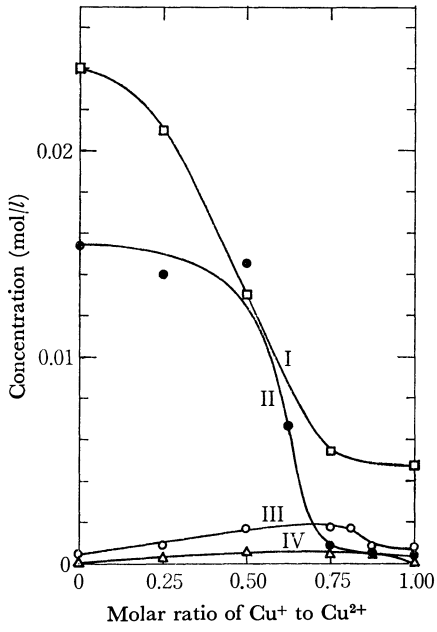

Fig. 3. Effect of copper(I) on the production of *o*-nitrosophenols from phenols or benzenes.
I: *p*-chlorophenol, II: phenol, III: benzene
IV: chlorobenzene

from the phenols decreased gradually with the increase of molar ratio of copper(I) ion. However, in the case of aromatic hydrocarbons the amounts of *o*-nitrosophenols produced was somewhat increased with the increase of the relative molar ratio of copper(I). This is conceivable by considering that copper(I) ion is essential for the decomposition of hydrogen peroxide to form hydroxy radical which attacks aromatic hydrocarbons to afford phenols.

The whole sequence of the Baudisch reaction can be summarized as follows.

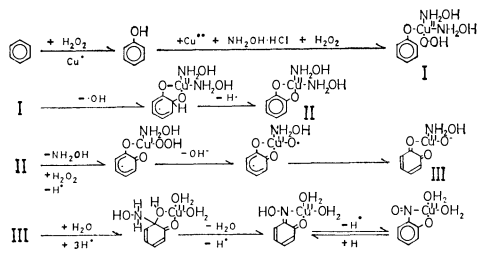

A part of copper(II) ion is reduced at first to copper(I) by hydroxylamine and copper(I) reacts with hydrogen peroxide to produce hydroxy radical. Complex I is then formed from phenol, copper(II), hydroxylamine and hydrogen peroxide, and the complex produces pyrocatechol-copper complex II. In the next stage, complex II may be oxidized to *o*-benzoquinone-copper complex III. In this stage, hydrogen peroxide will substitute the hydroxylamine ligand of complex II and then successive oxidation proceeds. As copper species can easily change their oxidation states,[6] electron of pyrocatechol can be transferred with no difficulty to peroxide through copper atom.[7] Finally, complex III might be oximated to *o*-nitrosophenol-copper(II) complex.

Experimental

Materials. 4-Chlorocatechol was prepared by the chlorination of pyrocatechol.[8] Copper(I) chloride was prepared by the reduction of copper(II) sulfate.[9] After being washed with glacial acetic acid, the crystal was dried and used. Other reagents were the same as described previously.[1a,b,c]

Formation of Hydroxyphenylazoformamide. A typical example is the following: In a 1*l* three-necked flask, equipped with a stirrer, were placed copper(II) nitrate (8 g, 0.033 mol), 4-methyl pyrocatechol (3.7 g, 0.030 mol), semicarbazide hydrochloride (5.6 g, 0.05 mol) and 500 m*l* of hydrochloric acid-sodium acetate buffer (pH 2.5). To this mixture was added 5 m*l* of 30% hydrogen peroxide solution diluted with 200 m*l* of water in 2 hr. The solution was stirred for 2.5 hr at 20°C. The reaction mixture was acidified after the filtration of the residue, and extracted with ethyl ether. The red product in ethyl ether was extracted as a copper salt of the product with an aqueous solution of copper(II) acetate. After the reddish violet aqueous solution was extracted repeatedly with ethyl ether and chloroform, the solution was acidified and extracted with chloroform. The extract was evaporated under a reduced pressure and orange red crude crystals, 4-methyl-2-hydroxyphenylazoformamide, were obtained (*ca.* 800 mg). After being eluted with acetone-ethanol (1:1) on an alumina column, the pure product was obtained, mp 152—153.5°C. The result of elemental analysis is shown in Table 1.

The product was confirmed as follows. The hydroxyphenylazoformamide was dissolved in an acidic tin(II) chloride solution. After the color of the solution had almost faded away, the solution was refluxed for 30 min. After being cooled and extracted with ethyl ether, the solution was made alkaline with aquous 6N NaOH solution. *O,N*-Dibenzoyl derivative of 5-methyl-2-aminophenol, mp 144.5—145.5°C, was obtained. No melting point depression was observed in admixture with an authentic sample.[10]

The Effect of Copper(I) on the Production of o-*Nitrosophenols.*

6) R. G. R. Bacon and H. A. O. Hill, *Quart. Rev.* (London), **19**, 95 (1965).

7) In the Baudisch reaction, copper(II) ion forms a stable complex with *o*-nitrosophenol or monooxime of *o*-benzoquinone. The complex can protect the product against further oxidation or oximation. This might be another important role of copper(II) ion in the Baudisch reaction.

8) R. Willstätter and H. E. Müller, *Ber.*, **44**, 2182 (1911).

9) C. S. Marvel and S. M. McElvain, *Org. Syn.*, *Coll. Vol.*, **1**, 170 (1941).

10) The melting point of this compound (162°C) was reported by K. V. Auwers *et al.* (*Ber.*, **54**, 1314 (1921)), but their report should be corrected.

A mixture of copper(I) chloride and copper(II) chloride was used. The total amount of copper ions was kept 0.005 mol. This mixture and hydroxylamine hydrochloride (0.695 g, 0.01 mol) were dissolved in 100 m*l* of a Walpole buffer (pH 2.55). To the solution, benzene (0.5 m*l*) or chlorobenzene (1.0 m*l*) dissolved in 20 m*l* of *n*-hexane was added. After the addition of 30% hydrogen peroxide (1 m*l*), the mixture was stirred at 30°C for 20 min under a nitrogen atmosphere. Aliquot of the mixture (20 or 50 m*l*) was removed and was acidified with 3 m*l* of 6N HCl. The determination of *o*-nitrosophenol produced was described previously.[18]

Spectrophotometry. The electronic spectra of hydroxyphenylazoformamide in chloroform and its copper(II) salt in water were measured. The aqueous solution of hydroxyphenylazoformamide-copper(II) was obtained by shaking an ethereal solution of hydroxyphenylazoformamide with an aqueous copper(II) sulfate solution.

This work was supported in part by a Research Grant from Kyoto Women's University.

BULLETIN OF THE CHEMICAL SOCIETY OF JAPAN, VOL. 44, 3123—3126 (1971)

Carboxylation of Phenol Derivatives. XX. Syntheses of Phenolpolycarboxylic Acids by the Carboxylation of Alkali Phenoxide in the Presence of Alkali Alkyl Carbonate[1]

Taketoshi KITO and Ichiro HIRAO

Laboratory of Industrial Chemistry, Department of Chemical Engineering, Kyushu Institute of Technology, Tobata-ku, Kita-kyushu

(Received April 30, 1971)

Phenolpolycarboxylic acids, especially hydroxytrimesic acid, were obtained in good yields by heating alkali phenoxide under a carbon dioxide pressure in the presence of alkali alkyl carbonate. Hydroxytrimesic acid was obtained in the best yield by the reaction of potassium phenoxide and potassium alkyl carbonate. In this reaction, neither a superatmospheric pressure nor a high reaction temperature was needed. The formation processes of phenolcarboxylic acids are also discussed.

Phenolcarboxylic acids are usually prepared by heating alkali phenoxide under a carbon dioxide pressure. In this reaction, salicylic acid (SA) is produced mainly from the sodium salt, and *p*-hydroxybenzoic acid (POB) mainly from potassium salt, while 4-hydroxyisophthalic acid (4-OIP) is formed only as a minor product from both the salts.[2]

Although phenolcarboxylic acids are also obtained from the reaction of alkali phenoxide and alkali alkyl carbonate in an atmosphere of nitrogen or carbon dioxide, 4-OIP is similarly a minor product.[3,4]

On the other hand, the methods to produce 4-OIP and hydroxytrimesic acid (OT) have been reported.[5,6] For example, 4-OIP is obtained when dipotassium salicylate or dipotassium salt of POB is heated under a superatmospheric pressure of carbon dioxide at temperatures from 300° to 500°C, and OT is obtained when phenol, SA, POB, 4-OIP, or 2-hydroxyisophthalic acid (2-OIP) or alkali salts of these compounds are heated at carbon dioxide pressures greater than 100 atm at temperatures higher than 250°C in the presence of potassium carbonate. By these methods, phenolpolycarboxylic acids are obtained in good yields, but a high pressure and a high temperature are needed.

However, it has now been found that when the carboxylation of alkali phenoxide is carried out in the presence of an excess of alkali alkyl carbonate, phenolpolycarboxylic acids, such as 4-OIP and OT, are obtained in good yields under mild conditions. The present investigation deals with this newer method for preparing phenolpolycarboxylic acids, especially OT.

Experimental

Alkali Alkyl Carbonate. Carbon dioxide was vigorously introduced into a solution of alkali alcoholate, derived from pure aliphatic alcohol and alkali metal. From the resulting mixture, the excess alcohol was distilled off in a vacuum at a temperature lower than 120°C.

Reaction of Alkali Phenoxide and Alkali Alkyl Carbonate. In a 300-m*l* autoclave, equipped with an electromagnetic stirrer, we placed 0.02 mol of alkali phenoxide, the prescribed amount of alkali alkyl carbonate, and 100 m*l* of a light oil (bp>250°C). After the air had been replaced by carbon dioxide (unless otherwise mentioned, the carbon dioxide pressure means the starting pressure), the autoclave was heated to the prescribed temperature. This took about 30 min. When the reaction was carried out in a flask, a 300-m*l* three-necked flask, equipped with a mechanical stirrer, a thermometer, a gas inlet-tube, and a 10-cm glass tube whose top was connected to a gas-flow meter, was used in place of an autoclave. The flow rate of carbon dioxide was regulated at about 25 *l*/h. After reaction had been stopped, 200 m*l* of water was added and a light oil was separated from the aqueous solution. The aqueous solution was

1) This paper was presented at the 24th Annual Meeting of the Chemical Society of Japan, Osaka, 1971.
2) A. S. Lindsey and H. Jeskey, *Chem. Rev.*, **57**, 583 (1957).
3) J. I. Jones, *Chem. Ind.* (London), **1958**, 228.
4) T. Kito, T. Kondo, H. Ago, S. Yamamoto, and I. Hirao, *Kogyo Kagaku Zasshi*, **73**, 742 (1970).
5) J. C. Wygant, U. S. 3089905 (1963).
6) Henkel, Brit. 968829 (1963).

adjusted to pH 7 with hydrochloric acid and washed with ether. Then, phenolcarboxylic acids were acidified with hydrochloric acid and extracted with ether. After the removal of the ether, SA, POB, 4-OIP, 2-OIP, and OT were found to be present in the residue.

Analysis of the Products by the Ultraviolet Technique. After the removal of the SA by washing with chloroform, the residue was dissolved in water; the solution was then buffered at pH 11 with disodium hydrogen phosphate and sodium hydroxide and at pH 2.8 with disodium hydrogen citrate and sodium hydroxide. The absorptivities of the components are given in Table 1. By using the four key wavelengths the amounts of POB, 4-OIP, 2-OIP, and OT may be determined. The SA can also be determined by the ultraviolet technique after the evaporation of the chloroform from the chloroform solution.

TABLE 1. ABSORPTIVITIES OF COMPONENTS

Wavelength (mμ)	231	252	280	300	340
Slit width (mμ)	0.26	0.24	0.24	0.24	0.24
pH	11.0	11.0	11.0	2.8	2.8
Components	Absorptivity[a]				
SA	4.764	0.310	1.370	2.453	0
POB	1.860	4.055	12.46	0	0
4-OIP	5.820	5.040	1.000	1.382	0
2-OIP	4.785	1.238	0.777	1.637	1.532
OT	10.03	4.181	0.623	1.045	1.698

a) Concentration; 100 γ/ml.

Results and Discussion

Phenolcarboxylic acids are formed by heating potassium phenoxide and an equimolar quantity of potassium alkyl carbonate in an atmosphere of nitrogen or carbon dioxide, but the main product is always POB or SA.

We have further investigated this reaction in the presence of an excess amount of potassium aklyl carbonate. The results are summarized in Table 2. In this reaction, one of the most remarkable features is that considerable amounts of OT and 4-OIP are obtained under mild conditions. Although the latter compound is also obtained from the reaction of potassium phenoxide and carbon dioxide or an equimolar quantity of potassium alkyl carbonate, it is always a minor product. However, by the reaction of potassium phenoxide and potassium 1-pentyl carbonate in a 1 : 3 molar ratio at 220°C for 2 hr, 4-OIP was formed in a 36% yield even at an atmospheric pressure. The total yield of phenolcarboxylic acids (POB+SA+4-OIP+2-OIP+OT) was nearly independent of the reaction temperature and the molar ratio of potassium alkyl carbonate to potassium phenoxide, that is, the carbonate ratio. On the contrary, the carboxylation yield, which is defined as the mole per cent of carbon dioxide introduced into a phenyl nucleus, increased with a rise in the reaction temperature or with an increase in the carbonate ratio. If the reaction proceeds according to Eq. (1), the theoretical values of the carbonate ratio

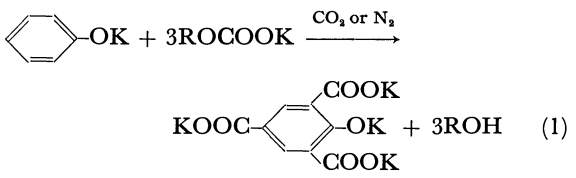

(1)

and of the carboxylation yield must be 3 and 300% respectively. However, the maximum carboxylation yield was only 198% (66% of the theoretical value), even at a carbonate ratio of 5 : 1 and at 240°C.

The reaction was again examined in an autoclave under carbon dioxide pressure. The results are summarized in Table 3. From the results shown in Tables 2 and 3, it is evident that the reaction temperature, the carbonate ratio, and the carbon dioxide pressure have a great effect on both the composition of phenolcarboxylic acids and the carboxylation yield. For example, the carboxylation yield amounted to 284% in the reaction of potassium phenoxide and three times as much potassium 1-pentyl carbonate at 260°C and 5 kg/cm² of carbon dioxide; in other words, OT was nearly the only product. Although other kinds of potassium alkyl carbonates, such as potassium ethyl-, *n*-butyl-, and *n*-octyl carbonate, were used in place of potassium 1-pentyl carbonate (Table 3), no remarkable effects of the alkyl group on the yield of OT was observed. Moreover, the superatmospheric pressure of carbon dioxide was not needed in this reaction.

The effect of the atmosphere was also examined (Table 4). It has been reported that potassium alkyl carbonate reacts with potassium phenoxide to yield phenolcarboxylic acids, especially POB, in good yields. In this reaction, the carbonate is regarded as a car-

TABLE 2. REACTIONS IN A STREAM OF CARBON DIOXIDE

Carbonate (ROCOOK) R	ratio[a]	Reaction temp.[b] (°C)	Total yield of acids (%)	Carboxylation yield (%)	Yield of each acid (%) POB	SA	4-OIP	2-OIP	OT
C_2H_5	2	240	96	151	45	6	28	7	10
n-C_5H_{11}	1	240	80	104	45	11	24	0	0
n-C_5H_{11}	2	240	82	135	34	8	27	0	13
n-C_5H_{11}	3	180	98	130	18	50	28	0	2
n-C_5H_{11}	3	200	86	146	22	18	30	2	14
n-C_5H_{11}	3	220	86	160	15	14	36	4	17
**n*-C_5H_{11}[c]	3	240	85	174	19	5	33	0	28
n-C_5H_{11}	5	240	85	198	10	12	13	0	50

a) ROCOOK/PhOK (mol/mol). b) Reaction time; 2 hr. c) Compare with the asterisked result in Table 4.

Table 3. Reactions under carbon dioxide pressure

Carbonate (ROCOOK) R	ratio[a)]	Conditions press.[b)] (kg/cm²)	temp.[c)] (°C)	Total yield of acids (%)	Carboxylation yield (%)	Yield of acid (%) POB	SA	4-OIP	2-OIP	OT
—	0	5[d)]	240	34	38	23	7	3	1	0
C_2H_5	3	5	240	84	244	0	4	0	0	80
n-C_4H_9	3	5	240	89	263	0	2	0	0	87
n-C_5H_{11}	1	5	240	67	98	41	5	9	2	10
n-C_5H_{11}	2	5	240	81	198	12	4	13	0	52
n-C_5H_{11}	3	5	220	88	195	4	13	28	7	36
n-C_5H_{11}	3	5	240	88	262	0	1	0	0	87
n-C_5H_{11}	3	5	260	96	284	0	2	0	0	94
n-C_5H_{11}	3	50[e)]	240	97	287	0	2	0	0	95
n-C_8H_{17}	3	5	240	88	256	0	4	0	0	84

a), c) See Table 1. b) Starting pressure of CO_2. d) Reaction pressure; about 15 kg/cm² at 240°C.
e) Reaction pressure; 195 kg/cm².

Table 4. Reactions in an atmosphere of nitrogen

Carbonate (ROCOOK) R	ratio[a)]	Reaction temp. (°C)[b)]	Total yield of acids (%)	Carboxylation yield (%)	Yield of each acid (%) POB	SA	4-OIP	2-OIP	OT
C_2H_5	1	220	76	81	66	5	5	0	0
n-C_5H_{11}	1	220	78	89	55	12	11	0	0
C_2H_5	3	240	96	138	63	2	18	2	11
*n-C_5H_{11}	3	240	82	183	11	3	31	4	33

a) b) See Table 2.

boxylating agent. The results listed in Table 4 are consistent with the above idea. However, it must be a weak carboxylating agent. In other words, the first carboxy group is easily introduced into the *ortho* or *para* position to the hydroxy group, but it is difficult to introduce the third one. Although the best-known carboxylating agent is carbon dioxide, the asterisked result in Table 2 is somewhat analogous to the asterisked one in Table 4. Therefore, carbon dioxide is also a weak carboxylating agent, but the yield of OT increased considerably when the carboxylation reaction was carried out under a carbon dioxide pressure. Consequently, in the reactions under a carbon dioxide pressure potassium alkyl carbonate may act as an alkali supplying agent rather than as a carboxylating agent to the carboxy groups introduced.

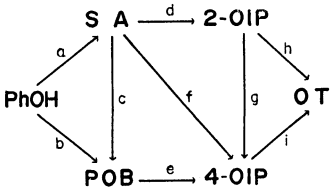

Scheme 1

There are nine routes that are considered to be possible formation processes of the five kinds of acids (Scheme 1). Potassium phenoxide, on being heated for 2 hr in the presence of an equimolar quantity of potassium 1-pentyl carbonate in a stream of carbon dioxide, gave 31% of POB and 48% of SA at 180°C, together with minor amounts of 4-OIP, but it gave 57% of POB, 11% of SA, and 12% of 4-OIP at 220°C. The increase in the amount of POB at 220°C must be due to the rearrangement of the dipotassium salicylate to the dipotassium salt of POB, which is known to be an important process in producing POB. The rearrangement of the tripotassium salt of 2-OIP to the tripotassium salt of 4-OIP may similarly occur at high temperatures. Then, the tripotassium salt of 2-OIP was heated at 180°C or 240°C for 2 hr in an atmosphere of nitrogen; the resulting solid was analysed by the ultraviolet spectral technique, whereas 4-OIP was not obtained even at 240°C. Consequently, the (g) route can be disregarded.

There are three routes, that is, (d)—(h), (e)—(i), and (f)—(i), for yielding OT. Therefore, the dipotassium salt of POB or dipotassium salicylate was heated with twice as much potassium ethyl carbonate at 200° or 240°C for 2 hr in an autoclave at 5 kg/cm² of carbon dioxide. The results were as follows; 1 mol of dipotassium salt of POB gave, at 240°C, 0.89 mol of OT and 0.01 mol of POB, and at 200°C, 0.76 mol of POB, 0.20 mol of 4-OIP, and 0.02 mol of OT, while 1 mol of dipotassium salicylate gave, at 240°C, 0.81 mol of OT and 0.09 mol of SA, and at 200°C, 0.53 mol of SA, 0.28 mol of 4-OIP, and 0.14 mol of 2-OIP. From these results, it was found that neither the dipotassium salt of POB nor dipotassium salicylate give OT at temperatures lower than 200°C, although they give OT as the main product in a good yield at high temperatures. In these reactions, OT must be formed predominantly *via* Route (i), because dipotassium salt of POB can not give 2-OIP and dipotassium salicylate rearranges to dipotassium salt of POB or is carboxylated mainly at the position *para* to the hydroxy group rather than at

TABLE 5. REACTIONS IN THE VARIOUS COMBINATIONS OF ALKALI SALTS

PhOM$_1$ Carbonate (n-$C_5H_{11}OCOOM_2$)			Reaction temp. (°C)[b]	Total yield of acids (%)	Carboxylation yield (%)	Yield of each acid (%)				
M_1	M_2	ratio[a]				POB	SA	4-OIP	2-OIP	OT
K	K	2	220	82	178	17	9	12	4	40
Na	K	2	220	84	189	1	10	35	6	32
K	Na	2	220	76	140	4	24	20	12	16
Na	Na	2	220	81	122	0	49	11	12	9
K	K	3	240	88	262	0	1	0	0	87
Na	K	3	240	75	219	0	3	0	0	72
K	Na	3	240	71	186	0	6	15	0	50
Na	Na	3	240	71	152	0	17	17	10	27

a) n-$C_5H_{11}OCOOM_2$/PhOM$_1$ (mol/mol), where M_1 and M_2 refer to Kand Na, respectively.
b) Reaction time; 2 hr.
Starting pressure of CO_2; 5 kg/cm^2.

the position *ortho*. Then, it became clear that both the dipotassium salt of POB and dipotassium salicylate give 4-OIP, which is further carboxylated to OT at high temperatures.

SA gives 4-OIP *via* two routes. It is known that dipotassium salicylate rearranges to the dipotassium salt of POB,[7] but the rearrangement is influenced by the presence of carbon dioxide. For example, although dipotassium salicylate, on being heated at 240°C and 5 kg/cm^2 of carbon dioxide, rearranges to give 24% of POB and 28% of 4-OIP, 46% of the starting material, dipotassium salicylate, remains unreacted. Therefore, Route (f) is also of importance as the process for yielding 4-OPI. On the other hand, both the tripotassium salt of 2-OIP and that of 4-OIP, on being heated at 240°C and 5 kg/cm^2 of carbon dioxide in the presence of twice as much potassium ethyl carbonate, gives OT in a good yield, but 2-OIP was a minor product in any of the reactions listed in Tables 2, 3, and 4.

On the basis of these data, it seems that the main processes for 4-OIP are the (a)—(c)—(e), (a)—(f), and (b)—(e) routes and that the main process for OT is Route (i).

Sodium salt was used in place of potassium phenoxide or potassium 1-pentyl carbonate. The results are summarized in Table 5. OT was obtained in the best yield when both M_1 and M_2 were potassium. The yield of OT was lowered when either M_1 or M_2 was replaced by sodium, but better results were obtained in the reactions using sodium phenoxide (M_1=sodium). The structures of the products are designated (I) when potassium phenoxide is used and (II) when sodium phenoxide.

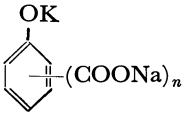

(I)

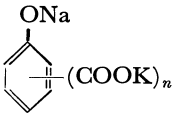

(II)

The reactivity of potassium phenoxide is generally greater than that of sodium phenoxide in the carboxylation of alkali phenoxide. On the other hand, as the COONa group is a more powerful electron attractor than the COOK group, the former makes the phenyl nucleus inactive to a greater extent than the latter. Consequently, the carboxylation yields in the reactions using sodium 1-pentyl carbonate are lower than that in the reactions using the potassium salt of the corresponding carbonate.

Thanks are due to Mr. Y. Hokamura for his assistance in the experimental work.

7) A. J. Rostron and A. M. Spivey, *J. Chem. Soc.*, **1964**, 3092.

The Copolymerization of 2-Chloroacrylaldehyde with Styrene[1]

Yoshio MATSUBARA, Parimal R. KAVI, Masakuni YOSHIHARA, and Toshihisa MAESHIMA

Department of Applied Chemistry, Faculty of Science and Engineering, Kinki University, Kowakae, Higashi-Osaka

(Received May 4, 1971)

The copolymerization of α-chloroacrolein (M_1) with styrene (M_2) has been investigated. An alternating copolymer was obtained without an initiator in dimethyl sulfoxide at 60°C. The formation of a charge-transfer complex between the respective monomers was observed by the continuous-variation method, and it was found that this complex plays an important role in the polymerization. Meanwhile, in the case of the BF_3OEt_2-catalyzed system, it was observed that the polymerization temperature strongly affected the copolymerizability and the structure of the copolymer.

In the course of our research on the polymerization of acrolein and its derivatives,[2-4] the copolymerization of α-chloroacrolein (CAL) with styrene (St) was investigated. Our work on the copolymerization CAL with pyridazinone derivatives[5] has already been reported.

Recently, Elias *et al.*[6] investigated the radical polymerizations of CAL, α-chloroacrolein diacetate, and α-chloroacrolein dimethyl acetal, and also reported the radical copolymerizations of CAL with St and vinyl chloride. It was also indicated by these workers that α-chloroacrolein dimethyl acetal formed a 1:2 complex with boron trifluoride etherate at −60°C *via* the acetal oxygen atoms, which then gave oligomers at 25° to 30°C through cationic mechanism. However, this work did not contain any data on the cationic copolymerization.

In the present paper, we intend to discuss the formation and the polymerization of the 1:1 charge transfer complex due to some donor-acceptor-type interaction between CAL and St both in the absence of and in the presence of boron trifluoride etherate.

Experimental

Materials. The CAL was synthesized from acrolein according to Moureu's method[7] and purified by vacuum distillation (bp 29°C/17 mmHg, d_{25} 1.193, n_D^{25} 1.458).

The St was purified by distillation under a vacuum before use. The boron trifluoride etherate was purified by distillation in the usual manner.

Copolymerization Procedure. The copolymerization was carried out under the dry nitrogen atmosphere in a glass ampoule. Given amounts of the monomer and the solvent were placed in an ampoule, a catalyst solution was added at required temperature, and the ampoule was sealed. After the reaction, the resulting mixture was poured into a large amount of methanol to precipitate the copolymer.

Characterization of the Copolymer. The composition of the copolymer was determined by elemental analysis. The nuclear magnetic resonance (NMR) spectra of the copolymer were measured in carbon tetrachloride with a HITACHI R-20 spectrometer. The infrared(IR) spectra reported in this paper were taken with a YANAGIMOTO LSG-25 infrared spectrometer. The X-ray diffraction spectra of the copolymer were obtained by using nickel-filtered Cu*Kα* radiation with a RIGAKU DENKI geiger flex. The viscosity measurements were carried out with an Ostwald viscometer using toluene as the solvent and at 25°C. The number-average molecular weight of the copolymer was determined by vapour-pressure osmometry using benzene as a solvent at 40.5°C with HITACHI PERKIN ELMER MODEL 105 apparatus. The continuous-variation method[8] applied to the CAL-St system was carried out in dimethyl sulfoxide or toluene using a quartz cell with a path length of 10 mm and at room temperature.

Results and Discussion

Copolymerization without a Catalyst. The results of the copolymerization of CAL with St in the absence of a catalyst are summarized in Table 1. The copolymer obtained was a white powder, soluble in toluene, pyridine, and tetrahydrofuran, and insoluble in methanol and diethyl ether. Figure 1 shows that the maximum values of both the copolymerization rate and the limiting viscosity number of the copolymer were observed at the CAL mole fraction with a monomer-feed com-

TABLE 1. COPOLYMERIZATION OF CAL (M_1) WITH St (M_2) WITHOUT INITIATOR IN DIMETHYL SULFOXIDE AT 60°C, $[M_1]+[M_2]=4$ mol/*l*

M_1 (mol%)	Time (hr)	Conversion (%)	m_1 (mol%)	$[\eta]^{25°C}_{benzene}$
0	10	0.93	0	0.28
10	10	3.59	44.73	0.29
20	10	4.79	46.86	0.36
30	10	7.29	48.04	0.38
40	5	4.28	50.70	0.40
50	4	4.04	52.03	0.44
60	5	4.10	54.41	0.37
70	8	3.49	58.26	0.29
80	10	5.39	63.08	0.20
90	10	3.57	70.38	0.12
100	10	1.26	100	0.08

1) Polymerization of Acrolein and Its Derivatives. VII.
2) N. Yamashita, H. Sumitomo, and T. Maeshima, *Kogyo Kagaku Zasshi*, **71**, 1723 (1968).
3) Y. Matsubara, H. Sumitomo, and T. Maeshima, *ibid.*, **71**, 1726 (1968).
4) Y. Matsubara, J. Asakura, N. Yamashita, H. Sumitomo, and T. Maeshima, *ibid.*, **72**, 2658 (1969).
5) Y. Matsubara, M. Yoshihara, and T. Maeshima, *ibid.*, **74**, 477 (1971).
6) H. G. Elias and W. Nengweiler, *Makromol. Chem.*, **113**, 115 (1968).
7) C. Moureu, *Ann. Chim.*, **15**, 158 (1921).
8) P. Job, *Ann. Chim.*, [10], **9**, 113 (1938).

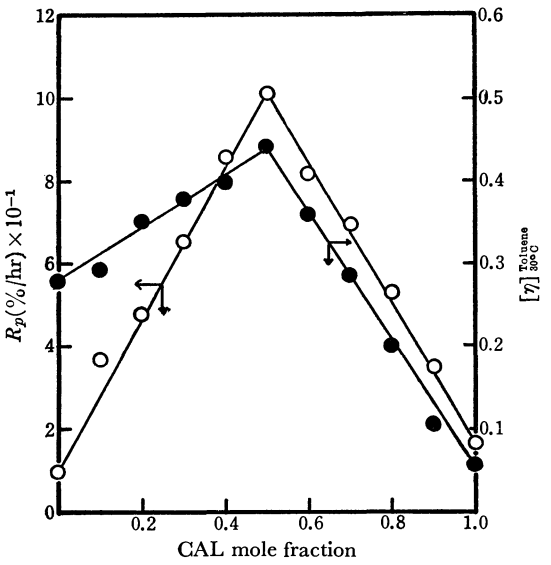

Fig. 1. Copolymerization rate and limiting viscosity numbers for copolymerization of α-chloroacrolein (CAL) with styrene (St) without initiator.

position of 0.5, indicating that there may be some interaction between CAL and St. Meanwhile, the initial copolymerization rate was proportional to the 1.88 order of the monomer concentration, suggesting that the initiation takes place as a result of the interaction between the two monomers.[9] In order to estimate the over-all activation energy for the copolymerization of CAL with St, the polymerization was carried out at 60, 70, and 80°C in the monomer-feed composition of 0.5. Plots of the logarithm of the copolymerization rate against the reciprocal of the absolute temperature gave a linear relation, and from its slope the activation energy was given as 11.37 kcal/mol. This value of the activation energy is much lower than that obtained for usual radical polymerization. The Fineman-Ross plot gave monomer reactivity ratios of r_1=0.18 and r_2=0.06 for the non-catalyzed copolymerization of CAL (M_1) with St (M_2). These values of r_1 and r_2 are less than those for the radical copolymerization reported by Elias (r_1=0.18, r_2=0.078).[6]

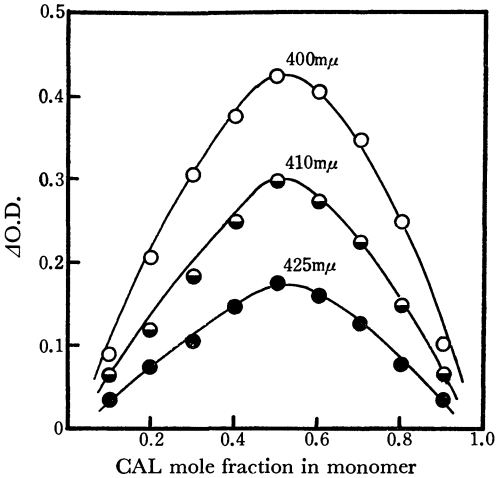

Fig. 2. Continuous variation method in CAL and St system. [CAL]+[St]=0.1 mol/l in DMSO at room temperature

All these results indicate that this copolymerization might take place through a charge-transfer complex. This theory is critically supported by the fact that electronic spectra obtained by means of the continuous variation method gave a maximum value in the optical density when an equimolar mixture was employed (Fig. 2).

Copolymerization in the Presence of Boron Trifluoride Etherate. CAL was copolymerized with St, using boron trifluoride etherate as the catalyst and toluene as the solvent, at −78, 0, 30, and 60°C.

The results of the copolymerization at −78°C are as shown in Table 2. The copolymer obtained as a white powder had a molecular weight in the range of 2300—2800 and was soluble in most organic solvents, such as acetone, carbon tetrachloride, benzene, tetrahydrofuran, and dimethylformamide. Figure 3 shows that an in-

TABLE 2. COPOLYMERIZATION OF CAL(M_1) WITH St(M_2) BY BF_3OEt_2 IN TOLUENE AT −78°C, [M]=2 mol/l, [BF_3OEt_2]=1 mol%/monomer

M_1 (mol%)	Time (hr)	Conversion (%)	m_1 (mol%)	Molecular weight ($\bar{M}_n$)
0	0.5	15.23	0	2880
10	0.5	10.62	5.01	2800
20	0.5	7.05	10.37	2730
30	1	8.78	15.89	2690
40	1	3.69	23.75	2620
50	1	1.58	30.87	2570
60	10	4.67	43.32	2490
70	50	4.89	58.13	2450
80	50	1.18	77.31	2410
90	50	0.11	88.41	2380
100	100	—	—	—

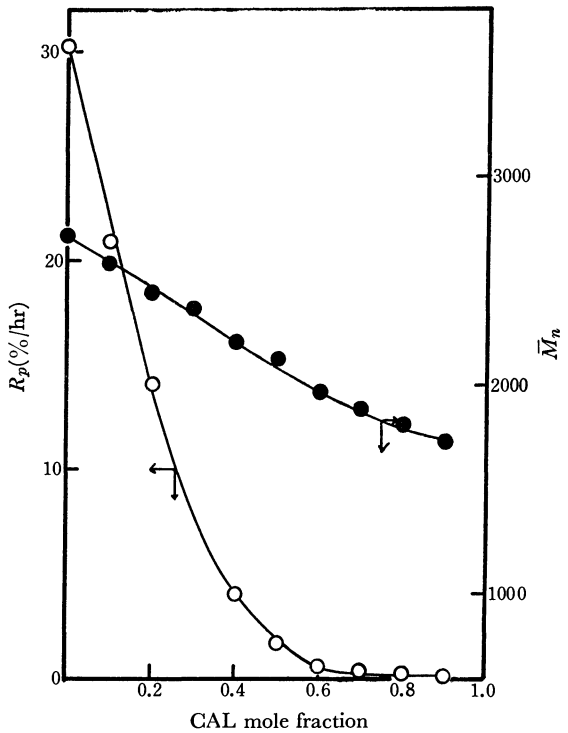

Fig. 3. Copolymerization rates and molecular weights for copolymerization of CAL with St by BF_3OEt_2. [M]=2 mol/l, [BF_3OEt_2]=1 mol%/monomer in toluene at −78°C

9) A. D. Jenkins, *J. Polymer Sci.*, **29**, 245 (1958).

crease the CAL mole fraction of the monomer-feed composition clearly decreases both the copolymerization rate and the number-average molecular weight of the copolymer. These facts are well in accord with the reluctance of CAL to homopolymerize in the presence of BF_3OEt_2.

A colour change from colourless to reddish-brown during polymerization in this system was observed in every case except at −78°C, and the colour became darker with an increase in the time and the temperature. This appearance of the colour at room temperature was recorded by electronic absorption spectra at suitable time intervals; the results are shown in Fig. 4. The A spectrum, obtained without a catalyst, had a shoulder at 400 mμ, while, the B spectra, obtained when BF_3OEt_2 was added, showed a new peak at 486 mμ, the intensity of which tended to be enhanced as time passed. Moreover, it was found that the continuous-variation method gave a maximum peak for the CAL-St ratio of 1:1 (Fig. 5). However, the optical density in this case was quite large as compared to that of the CAL-St system. These observations imply that the strong appearance of a colour in the presence of BF_3OEt_2 might be caused by the formation of a coordina-

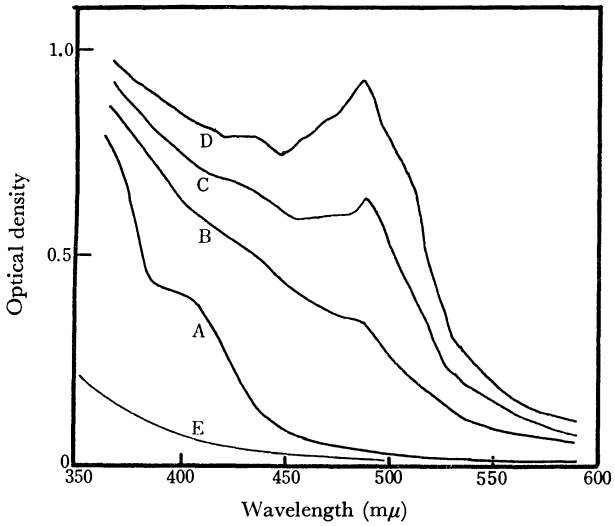

Fig. 4. Electronic absorption spectra.
A: CAL-St system 60 min
B: CAL-St-BF_3OEt_2 system 20 min
C: CAL-St-BF_3OEt_2 system 60 min
D: CAL-St-BF_3OEt_2 system 120 min
E: Copolymer from CAL-St-BF_3OEt_2 system

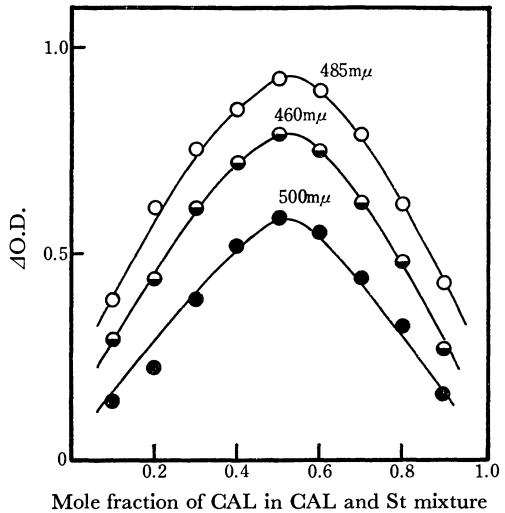

Fig. 5. Continuous variation method in CAL-St-BF_3OEt_2 system.
[CAL]+[St]=0.1 mol/*l* in toluene,
[BF_3OEt_2]=1 mol%/monomer at room temperature

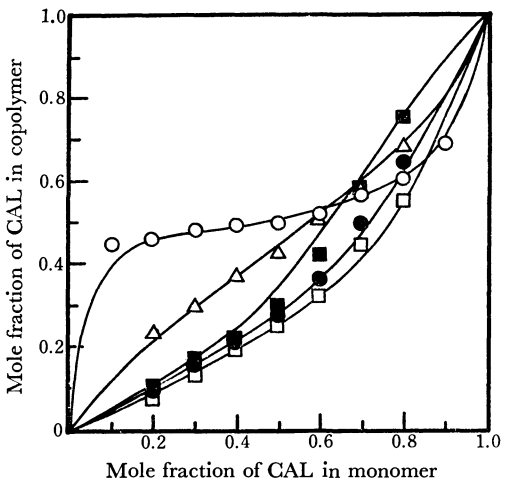

Fig. 6. Composition of copolymer in CAL(M_1)-St(M_2) system.
-○- Non-catalyzed system at 60°C
-△- BF_3OEt_2 system at 60°C
-■- BF_3OEt_2 system at 30°C
-●- BF_3OEt_2 system at 0°C
-□- BF_3OEt_2 system at −78°C

Table 3. Monomer reactivity ratios of copolymerization of CAL(M_1) with St(M_2) by BF_3OEt_2 at various temperature

Temperature (°C)	r_1	r_2	$r_1 \cdot r_2$
−78	0.9	2.8	2.52
0	0.5	2.8	1.40
30	0.4	2.8	1.12
60	0.4	0.7	0.28
60[a)]	0.18	0.06	0.11

a) Without catalyst.

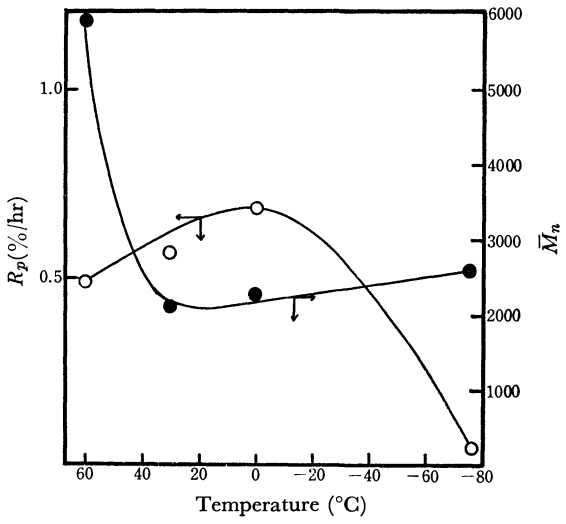

Fig. 7. Correlation between copolymerization rates or molecular weights and temperature.

tion bond between BF_3OEt_2 and the aldehyde group of CAL, this would decrease the electron density of its vinyl group, and, hence, the charge-transfer complex would be intensified. A few investigations have shown that such an interaction appeared in the reaction of a carbonyl compound with an inorganic metallic compound.[10-13] It is noted that the peak due to the complex disappeared when water or alcohol was added to the system.

Figure 6 shows monomer-copolymer composition curves obtained at various temperatures, and Table 3 tabulates the monomer-reactivity ratios obtained from the Fineman Ross plots. One of the most interesting manifestations in Table 3 is the fact that the value of $r_1 \cdot r_2$ gradually decreased with a rise in the polymerization temperature. This observation suggests that a radical polymerization through the charge-transfer complex takes place in some portion at higher temperatures. The same phenomenon has been observed by Sumitomo *et al.*[14] in the formation of the charge-transfer complex between α-cyanomethyl acrolein and zinc chloride, whose copolymerization with styrene gave an alternating copolymer.

It is interesting to note that the copolymerization rate reached its maximum value at about 0°C (Fig. 7). It is also indicated in Fig. 7 that the molecular weight of the copolymer decreased with a rise in the temperature, but increased after reaching a minimum value at about 30°C. This also suggests that a change in the temperature caused a different type of polymerization process to occur as has been described above.

Structure of the Copolymer. The IR, NMR, and X-ray diffraction spectra of the copolymer obtained with a CAL mole fraction of 0.5 in the monomer-feed composition are shown in Figs. 8, 9, and 10 respectively. The spectra of the copolymer obtained from a non-catalyzed system are marked A, whereas those obtained from a catalyzed system at 60, 30, 0, and −78°C are marked B, C, D, and E respectively.

The IR spectra, remarkably, contained the characteristic peaks of both CAL and St. A and B were

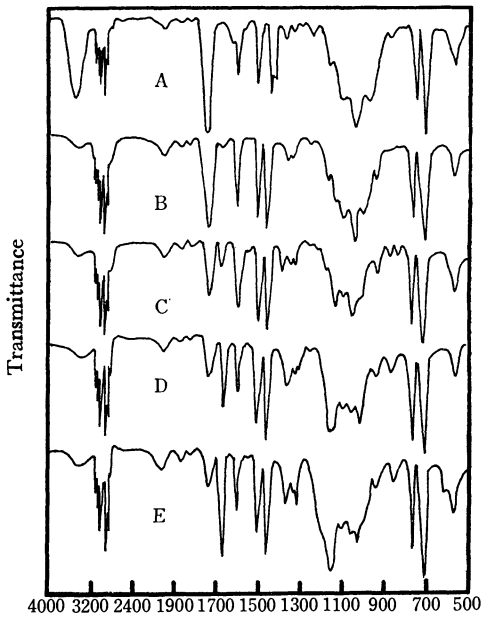

Fig. 8. Infrared spectra of copolymers obtained in CAL mole fraction of 0.5 (KBr disk).
A: Non-catalyzed system at 60°C
B: BF_3OEt_2 system at 60°C
C: BF_3OEt_2 system at 30°C
D: BF_3OEt_2 system at 0°C
E: BF_3OEt_2 system at −78°C

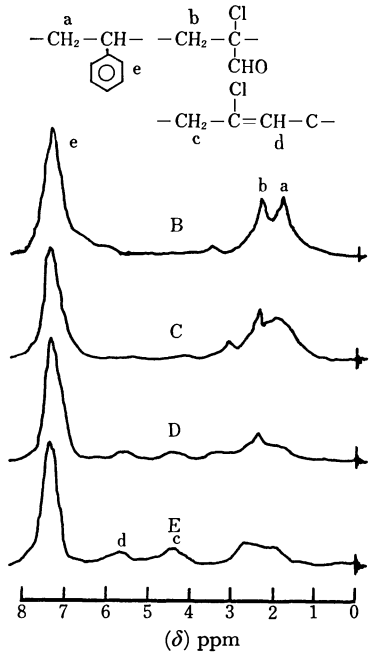

Fig. 9. NMR spectra of copolymers obtained using BF_3OEt_2 at various temperature (solvent DMSO-d_6).
Symbols are same as in Fig. 8.

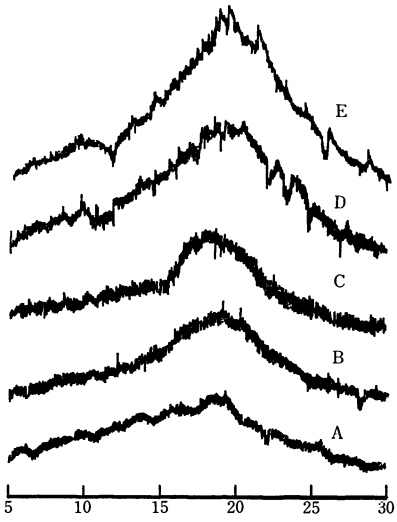

Fig. 10. X-Ray diffraction spectra of copolymers (CuK_α, Ni filter).
Symbols are same as in Fig. 8.

10) C. H. Bamford, A. D. Jenkins, and R. Jhoston, *Proc. Roy. Soc.* London, **A241**, 364 (1957).
11) V. A. Kabanov and P. K. Medelskaya, *Vysokomol. Soyed.*, **2**, 165 (1960).
12) F. A. Bovey, *J. Polymer Sci.*, **47**, 480 (1960).
13) M. Imoto, T. Ootsu, and S. Shimizu, *Makromol. Chem.*, **65**, 175 (1963).
14) I. Takemura and H. Sumitomo, 19th Annual Meeting at the Society of Polymer Science of Japan.

found to contain very similar absorption peaks. However, in the spectra obtained from a BF_3OEt_2-catalyzed system, namely, B, C, D, and E, the intensities of the peaks due to the C=O of the aldehyde groups decreased as the temperature decreased. On the other hand, the decrease in the temperature was found to increase the intensities of the peaks at 1670 cm^{-1} due to C=C and those at 1170 cm^{-1} due to the C–O of C=C–O in the order of B, C, D, and E.

This fact is in good agreement with the results of the NMR spectra. The peak at 4.2 and 5.7 ppm in the D and E spectra might be caused by the methylene proton signals, c and d respectively, as Fig. 9 shows.

In the X-ray diffraction spectra (Fig. 10), the intensities of the peaks were found to decrease in the order of B, C, D, and E. However the A and B spectra had similar peaks.

All these results lead to the conclusion that the BF_3OEt_2-catalyzed system gave a crystalline copolymer with Structure II at lower temperatures, while a noncrystalline polymer with Structure I was obtained at higher temperatures. This may be explained by taking account of the stability of the terminal CAL cation with the counter anion, as is indicated below.

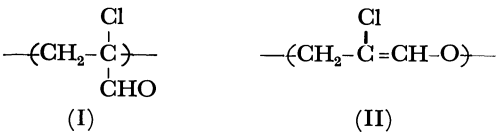

(I) (II)

Thus, when the polymerization occurs *via* the polymer cation A, the higher the temperature, the easier it will be for the reaction to proceed *via* vinyl polymerization, B, than *via* carbonyl Polymerization, C, the carbonyl cation may be destabilized at higher temperatures.[15]

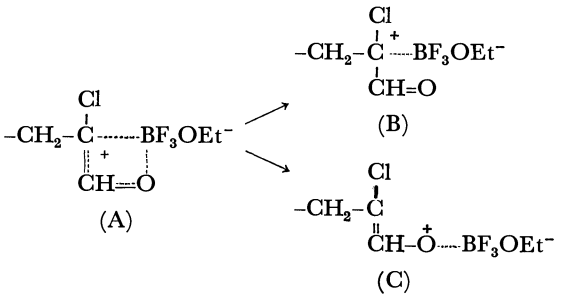

(A) (B) (C)

15) G. Ham, "Vinyl Polymerization," Vol. I, Marcel Dekker, N. Y. (1967), p. 427.

BULLETIN OF THE CHEMICAL SOCIETY OF JAPAN, VOL. 44, 3131—3136 (1971)

Syntheses of *N*-Substituted Carbamimidoylformic Acids

Juji YOSHIMURA, Kunihiko FUJIMORI,* Yuichi SUGIYAMA, and Hiroaki ANDO

Laboratory of Chemistry for Natural Products, Faculty of Science, Tokyo Institute of Technology, Meguro-ku, Tokyo

(Received May 4, 1971)

A few synthetic methods of *N*-substituted-carbamimidoylformic acid (**6**) were examined. Among them, condensation of ethyl 1-carbethoxyformimidate or ethyl thiooxamidate with amines and followed by partial hydrolysis gave unsuccessful results, except of the case of benzylamine in the latter reaction. Direct substitution of potassium thiooxamidate (**9**) with alkylamines in water gave **6**, potassium and/or alkylammonium *N*-substituted-thiooxamidate in fairly good yield, depending on conditions used. The presence of heavy metal ions in the reaction system caused an extensive decomposition of **9**, however, the substitution proceeded smoothly by treatment of alkyl- and aryl-ammonium *N*-unsubstituted- or *N*-substituted-thiooxamidate in methanol with mercuric oxide or lead oxide to give in a good yield **6** or *N,N*-disubstituted-carbamimidoylformic acid, respectively.

N-Substituted-carbamimidoylformic acid which is known only as a partial structure of kasugamycin[1-3] is unique as regards a carboxyl group attaches directly to the carbon atom of formamidine, and kasugamycin has been synthesized in *ca.* 10% yield by condensation of kasuganobiosamine with diethyl ester of oxalimidic acid and followed by partial hydrolysis.[4] However, such a partial hydrolysis was considered to proceed non-selectively, and consequently, to be not profitable for a synthesis of *N*-substituted- or *N,N'*-disubstituted-carbamimidoylformic acid.

In this paper, the authors examined the condensation of ethyl 1-carbethoxyformimidate or ethyl thiooxamidate with amines and successive partial hydrolysis, and direct substitution of potassium thiooxamidate or its free acid with amines.

Results and Discussion

Reaction of Ethyl 1-Carbethoxyformimidate or Ethyl Thiooxamidate with Amines. Although the formation of 1-carbethoxyformamidine hydrobromide from ethyl 1-carbethoxyformimidate (**1**) and ammonium bromide is

* Present address: Central Research Laboratory of Kumiai Chemical Industry Co. Ltd., Shibukawa, Shimizu-shi.

1) H. Umezawa, Y. Okami, T. Hashimoto, Y. Suhara, M. Hamada, and T. Takeuchi, *J. Antibiotics*, **18A**, 101 (1965).

2) Y. Suhara, K. Maeda, H. Umesawa, and M. Ohno, *Tetrahedron Lett.*, **1966**, 1239.

3) T. Ikekawa, H. Umezawa, and Y. Iitaka, *J. Antibiotics*, **19A**, 49 (1966).

4) Y. Suhara, F. Sasaki, K. Maeda, H. Umezawa, and M. Ohno, *J. Amer. Chem. Soc.*, **90**, 6559 (1968).

known,[5] condensation of **1** with amine hydrochlorides at room temperature was unsuccessful, excepting that the reaction of **1** and 2-amino-2-deoxy-D-glucose (**8**) hydrochloride in methanol at elevated temperature gave 2-carbomethoxy-4-(D-*arabino*-1′,2′,3′,4′-tetrahydroxybutyl)-imidazole (**2**) in 10% yield, together with 3, 6-diethoxy-2,5-dihydro-2,5-dioxo-pyrazine (**3**) as a by-product. Condensation of **1** and free amines (*p*-toluidine and **8**) gave complicated products, however, the presence of *N*-substituted-1-carbethoxyformamidine (**4**) was proved by different ways. In the case of **8**, the reaction mixture in methanol was refluxed in the presence of catalytic amount of hydrogen chloride to give **2**, and moreover, decomposition of it with water yielded 2-deoxy-2-oxalylamino-D-glucose methyl ester (**5a**: RNH_2=**8**) which was converted to the corresponding amide by treatment with methanolic ammonia. However, direct partial hydrolysis of the reaction mixture in 0.1 *N*-hydrochloric acid at room temperature gave only a intractable sirup. In the case of *p*-toluidine, direct partial hydrolysis of reaction mixture gave unknown white crystals in 39% yield, $C_{10}H_{10}O_3N_2$, and an attempted ester-exchange reaction with acetic or formic acid gave methyl *N*-*p*-tolyl-oxamidate (**5b**: R=*p*-tolyl) and *N*,*N*′-di-*p*-tolyl-carbamimidoylform-*p*-toluidide.

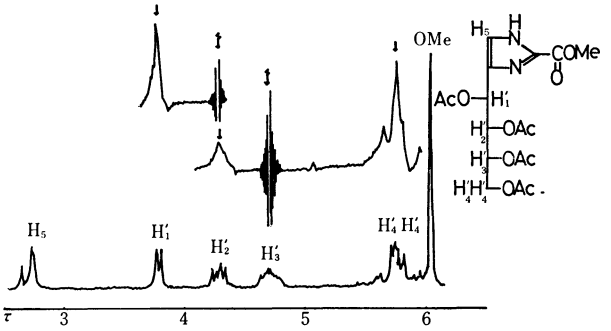

Fig. 1. NMR spectrum of 2-carbomethoxy-4-(D-*arabino*-1′,2′,3′,4′-tetraacetoxybutyl)-imidazole (100 MHz, $CDCl_3$).

The structure of **2** was determined from the following facts: it shows λ_{max}^{MeOH} 267 nm (ε 1.25×10^4), consumes 3.08 equimolar amount of sodium periodate, and gave the corresponding tetraacetate by a usual acetylation, whose NMR spectrum was shown in Fig. 1. In the NMR spectrum, signals at τ 2.74 (*s*, 1H), 3.78 (*d*, 1H), 4.28 (*q*, 1H), 4.71 (*m*, 1H), and 5.6—6.0 (*m*, 2H) were assigned by the double-resonance technique to H_5, H_1', H_2', H_3', and H_4', respectively. The lower chemical shift of H_5 than usual ring protons in sugar moiety indicates the presence of imidazole ring, and the change of chemical shifts of H_5 and H_1' to τ 2.54 and 3.67 by addition of trifluoroacetic acid supports this deduction. Recently, Fischer and Lewis[6] reported that the reaction of **8** and ethyl iminoacetate hydrochloride in dimethylformamide gave D-glucopyrano[1′,2′: 4,5]-2-methylimidazoline which had a lactol ring in the sugar portion. The reason for the difference between these facts is now under studying.

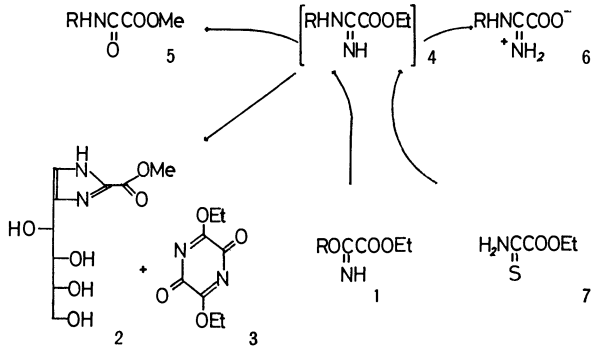

Scheme 1

On the other hand, it has been known that the reaction of thioamides and amines give amidines[7] and the presence of metal salts such as mercuric chloride assists in driving the reaction to completion, owing to the formation of insoluble metal sulfides.[8] Direct substitution of equimolar amount of ethyl thiooxamidate (**7**) and benzylamine in ethanol at room temperature for an hour gave only *N*,*N*′-dibenzyl-thiooxamidic acid amide as precipitates, however, a solution of equimolar amount of **7** and mercuric chloride in methanol showed a strong acidity, indicating a chelate formation, and further addition of two mol of amine induced the precipitation of the sulfide. Thus, the partial hydrolysis of the product in *N*-hydrochloric acid liberated *N*-benzylcarbamimidoylformic acid (**6j**: R=benzyl) in 32% yield. Similar treatment of the chelate solution with **8** gave again **2** in 8% yield, but, other usual amines could not be condensed successfully. From these results presented in Scheme 1, it is concluded that the two methods mentioned above are not recommendable, because the formation of **4** is accompanied with side reaction and is not realized in the case of usual amines.

Substitution of Potassium Thiooxamidate or Its Free Acid with Amines. Thiooxamidic acid is stable in a salt state, but potassium salt decomposes by refluxing in dioxane with liberation of hydrogen sulfide, and the free acid decomposes gradually in acidic solution to carbon dioxide, hydrogen sulfide and hydrogen cyanide. Moreover, it was found that potassium thiooxamidate (**9**)[9] decomposed extensively by addition of Ag^+, Hg^{2+}, or Pb^{2+} ion with liberation of the corresponding metal sulfide, and formed corresponding chelate compounds by addition of Cu^{2+}, Fe^{3+}, or Zn^{2+} ion. Consequently, the substitutions were examined in the absence or presence of metal ion, and metal oxides such as mercuric oxide and lead oxide were found to be the best accelerator on the substitutions.

Direct substitution of **9** with four equivalent of ammonia in absolute methanol under vigorous stirring at room temperature gave carbamimidoylformic acid (**6a**: R=H) in 90% yield, whose structure was supported by characteristic IR absorptions of amidine (3350, 3310, and 3020 cm^{-1}) and intramolecular carboxylate (1640 cm^{-1}), and by its hydrolysis to oxalic acid in alkaline conditions. However, other amines

5) F.C. Schaefer, *J. Org. Chem.*, **27**, 3608 (1962).
6) M.H. Fischer and B.A. Lewis, *Chem. Ind.* (London), **1967**, 192 (1967).
7) A. Bernthsen, *Ann.*, **184**, 321 (1876).
8) A. Bernthsen, *ibid.*, **192**, 1 (1878).
9) A. Weddige, *J. Prakt. Chem.*, **9**, 132 (1874).

Table 1. *N*-Substituted-carbamimidoylformic acid (**6**)

No.	Compound R	Formula	Method	Time (hr)	Yield (%)	Mp. (°C, dec.)	Found (%) C	Found (%) H	Found (%) N	Calcd (%) C	Calcd (%) H	Calcd (%) N
a	hydrogen	$C_2H_4N_2O_2$	A	1	90	230	27.05	4.78	31.87	27.27	4.58	31.81
b	ethyl	$C_4H_8N_2O_2$	B	7	63	177—178	41.28	6.93	24.33	41.37	6.94	24.13
c	hydroxyethyl	$C_4H_8N_2O_3$	B	7	53	186—187	36.62	6.38	20.98	36.36	6.10	21.20
d	*i*-propyl	$C_5H_{10}N_2O_2$	B	7	65	182—183	45.94	7.80	21.84	46.14	7.75	21.53
e	*n*-butyl	$C_6H_{12}N_2O_2$	A	1	48	192	50.61	8.32	19.63	49.98	8.39	19.43
f	*i*-butyl	$C_6H_{12}N_2O_2$	A	1	45	191—192	50.18	8.15	19.20	49.98	8.39	19.43
g	*sec*-butyl	$C_6H_{12}N_2O_2$	B	5	67	180—182	49.58	8.39	19.58	49.98	8.39	19.43
h	*n*-hexyl	$C_8H_{16}N_2O_2$	A	1	46	164—165	55.57	9.22	16.26	55.79	9.36	16.27
i	cyclohexyl	$C_8H_{14}N_2O_2$	B	5	75[d]	173	56.28	8.31	16.28	56.45	8.29	16.46
j	benzyl	$C_9H_{10}N_2O_2$	A	1	64	172—173	60.66	5.97	15.43	60.66	5.66	15.72
k	*p*-tolyl	$C_9H_{10}N_2O_2$	B	3	51	210—213	61.56	5.68	15.93	60.66	5.66	15.72
l	*o*-tolyl	$C_9H_{10}N_2O_2$	B	3	55	162—163	60.57	5.88	15.77	60.66	5.66	15.72
m	a)	$C_{14}H_{24}N_2O_7$	B	3	66	203—204	50.51	7.37	8.42	50.59	7.28	8.43
n	b)	$C_{15}H_{20}N_2O_7$[c]	B	3	53	180—181	51.32	6.13	8.09	51.57	6.06	8.02

a) **6m**: RNH_2=cyclohexyl 2-amino-2-deoxy-α-D-glucopyranoside; $[\alpha]_D^{23}$ +114° (*c* 0.1, water).
b) **6n**: RNH_2=benzyl 2-amino-2-deoxy-α-D-glucopyranoside; $[\alpha]_D^{23}$ +164° (*c* 0.1, water).
c) Compound **6n** was analyzed as 1/2 hydrate.
d) The yield was 35% in the case of Method A.

did not react in the same conditions, probably due to the greater insolubility of **9** than products in methanol. The same substitution with alkylamines in water proceed much faster than in methanol, and gave **6**, potassium *N*-substituted-thiooxamidate (**11**) and/or the corresponding alkylamine salt (**12**) in fairly good yield, respectively, depending on conditions used (Method A). The formation of each product could be controlled by adjustment of the amount of water and amine, reaction period, and pH of the reaction mixture. And the mixture of the products was sometimes separated by crystallization.

In general, **6** is formed at first, the use of large amount of water accumulate **11**, and deposition of **12** is accelerated by use of large amount of amine and by neutralization of potassium ion. For example, the reaction of each 50 mmol of **9** and benzylamine in minimum amount of water (25 m*l*) for 15 min at room temperature deposited **6j** in 61% yield, then standing the filtrate overnight gave **11a** (R=benzyl) in 9% yield, and further neutralization of the filtrate caused the deposition of **12a** (R=benzyl) in 10% yield. A similar phenomenon was also observed in the case of cyclohexylamine.

The existence of an equilibrium in this reaction[10] was ascertained by the following experiment; *i. e.*, reaction of **11a** with seven equivalents of ammonia gave **6a**, **6j**, and **12a** in 22, 37, and 11% yield, respectively. From this result, it is obvious that α-alkylamino-α-amino-α-mercaptoacetic acid (**10**) should be exist as an intermediate in the equilibrium between **6**, **9**, and **11**, as shown in Scheme 2. Such a tetrahedral intermediate was deduced in the hydrolysis of thioimidate esters,[11] and also in the hydrolysis of amidines to amides from a kinetic study.[12]

As an attempted acceleration with a metal ion, Zn^{2+} was examined. Addition of zinc chloride to a suspended solution of **9** in methanol made a homogeneous brown solution. However, addition of amines to this brown solution caused the precipitation of a white chelate composed of **9** and zinc (1: 1), which did not show the tendency of reaction with large excess amount of amines under stirring for a week at room temperature. A homogeneous mixture of equimolar amount of **9**, cylcohexylamine or benzylamine, and zinc cyanide or equimolar mixture of zinc chloride and sodium methoxide gave **6i** (R=cyclohexyl) or **6j** in 18 and 17% yield, respectively, under stirring for ten days. These facts indicate that the affinity of zinc to sulfur is very weak in the systems used.

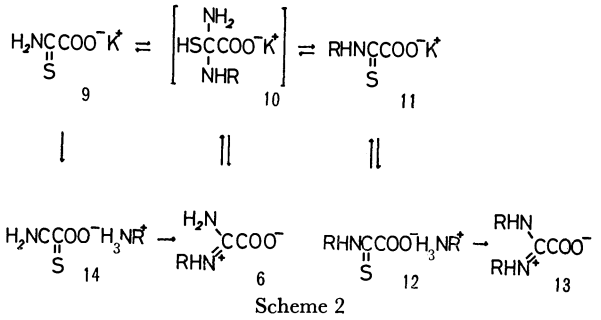

Scheme 2

On the other hand, the structure of **12** was at first deduced to be α,α-bisalkylamino-α-mercaptoacetic acid, from the facts that **12b** (R=cyclohexyl) showed a intense peak *m/e* 187 ($C_8H_{13}NO_2S$) in the mass spectrum which indicates the presence of C–S bond, and the treatment of **12b** with mercuric oxide in methanol gave *N*,*N*′-dicyclohexyl-carbamimidoylformic acid (**13b**: R=cyclohexyl) in 85% yield. However, the deduction was discarded by the facts that it showed $\lambda_{max}^{H_2O}$ 270 nm (ε 8.04×10^3) instead of an end-absorption in usual amidine, and electrophoresis of **12a** at pH 8 showed two ninhydrin-positive spots, where benzylamine moved to the direction of the cathode and **11a** to the

10) R. L. Shriner and F. W. Neumann, *Chem. Rev.*, **35**, 351 (1944).
11) R. K. Chaturvedi and G. L. Schmir, *J. Amer. Chem. Soc.*, **91**, 737 (1969).
12) D. R. Robinson, *ibid.*, **92**, 3138 (1970).

anode. Successful conversion of **12** to **13** indicated the possibility of a synthesis of **6** by treatment of alkylammonium thiooxamidate (**14**) with metal oxides in methanol. In fact, **14** obtained from **9** and amine hydrochlorides or free thiooxamidic acid[13] and amines were smoothly converted to **6** by stirring at room temperature with mercuric oxide or lead oxide in methanol. This method (Method B) was successfully applied to alkyl- and arylamines, and also amino-sugars, as was summarized in Table 1. Among them, benzyl and cyclohexyl 2-amino-2-deoxy-α-D-glucopyranoside were newly prepared from the corresponding 2-acetamido derivatives by an improved method of Gross and Jeanloz.[14]

Contrary to common amidines, exchange-reaction of *N*-substituent in **6** or **13** was generally unsuccessful. For example, reaction of *N*-(*n*-butyl)-carbamimidoylformic acid (**6e**: R=*n*-butyl) and benzylamine at 200°C gave a decarboxylated product: *N,N'*-dibenzylformamidine in 64% yield, and reaction of **6j** and benzylamine in ethanol by refluxing for 5 hr gave *N*-benzylformamide in 37% yield. Direct condensation of **6a** and large excess amount of benzylamine at room temperature for 2 days gave **6j** in 2.8% yield.

Application of the new method mentioned here to the preparation of unsymmetric *N,N'*-disubstituted-carbamimidoylformic acid is now undertaking.

Experimental

All the melting points are uncorrected. The solutions were evaporated under diminished pressure at a bath temperarure not exceeding 45°C. Optical rotations were measured in a 0.5-dm tube at 578 and 546 nm with Carl-Zeiss Polarimeter. The infrared spectra were measured in KBr discs, and the NMR spectra were determined at 100 MHz with a JNM-100H spectrometer, using TMS as an internal reference. The mass spectra were obtained on a Hitachi RMU6E mass spectrometer, using a direct inlet and an ionization energy of 70 eV.

Reaction of Ethyl 1-Carbethoxyformimidate (1) and 2-Amino-2-deoxy-D-glucose (8) Hydrochloride. A suspended solution of 2-amino-2-deoxy-D-glucose hydrochloride (7 g, 33 mmol) and ethyl 1-carbethoxyformimidate (5 g, 34 mmol) in methanol (200 m*l*) was refluxed for 5 hr, and the hydrochloride unchanged was filtered off. Addition of two-fold of ether to the filtrate gave a white crystals, 2-carbomethoxy-4-(D-*arabino*-1',2',3',4'-tetrahydroxybutyl)-imidazole (**2**) which was recrystallized from methanol, in 10% yield (0.8 g). Mp 177.5—176°C; $[\alpha]_D^{23}$ −32° (*c* 1.0, water); UV (nm): λ_{max}^{MeOH} 267 (ε 1.25×10^4); IR (cm^{-1}): 1725 (C=O).

Found: C, 43.46; H, 5.58; N, 11.64%. Calcd for $C_9H_{14}N_2O_6$: C, 43.90; H, 5.73; N, 11.38%.

Concentration of the mother liquor gave a small amount of 3,6-diethoxy-2,5-dihydro-2,5-dioxo-pyrazine (**3**) which was recrystallized from methanol. Mp 167.5—168.2°C; NMR (τ): 5.37 (*q*, 2H, *J*=7.4 Hz), 8.50 (*t*, 3H); IR (cm^{-1}): 1725 (C=O).

Found: C, 49.18; H, 5.13; N, 14.32%. Calcd for $C_8H_{10}N_2O_4$: C, 48.48; H, 5.09; N, 14.14%.

The compound **2** showed negative Fehling test, and the structure was determined as described before. Among them, the periodate oxidation was performed by the method of Fleury and Lange[15], using methyl α-D-glucopyranoside as a reference. The compound **2** consumed 3.23 mol of periodate at room temperature for 15 hr and 3.08 mol at 2.5°C for 18 hr, and the reference 2.30 and 1.94 mol, respectively.

2-Carbomethoxy-4-(D-arabino-1',2',3',4'-tetraacetoxybutyl)-imidazole. To a solution of acetic anhydride (1.74 g, 17 mmol) and pyridine (30 m*l*) was added **2** (0.7 g, 2.8 mmol) with shaking at room temperature, and the reaction mixture was concentrated, after standing for 3 hr. Crystallization of the residual precipitate from methanol gave 0.7 g (60.5%) of white crystals. Mp 171°C; $[\alpha]_D^{23}$ −9° (*c* 1.0, methanol); UV (nm): λ_{max}^{MeOH} 260 (ε 1.05×10^4); IR (cm^{-1}): 3250 (NH), 1745, and 1715 (C=O).

Found: C, 49.20; H, 5.33; N, 6.86%. Calcd for $C_{17}H_{22}N_2O_{10}$: C, 49.27; H, 5.36; N, 6.76%.

2-Oxalylamino-2-deoxy-D-glucose Methylester (5a). To a cooled solution of **1** (3.4 g, 23 mmol) in methanol (20 m*l*) was added dropwise a solution of **8** (5 g, 28 mmol) in methanol (200 m*l*), and the mixture was allowed to stand at room temperature for one day. To the resulted pale yellow solution was added half a volume of ether to give a yellow sirup which could not be crystallized. After a treatment of the sirup once with water, a part of it was crystallized from methanol-ether. Yield, 0.9 g (15%). Mp 188.5—189°C (dec.); $[\alpha]_D^{23}$ +49°→+22° (*c* 1.0, water, 24 hr).

Found: C, 40.99; H, 5.91; N, 5.86%. Calcd for $C_9H_{15}NO_8$: C, 40.75; H, 5.70; N, 5.28%.

2-Oxamidoylamino-2-deoxy-D-glucose. To a cooled solution of **5a** (0.1 g, 3.8 mmol) in methanol (50 m*l*) was passed an excess amount of ammonia, and the solution was evaporated to give a white powder which was crystallized from water-ethanol. Yield, 0.08 g (84%). Mp 190°C (dec.); $[\alpha]_D^{25}$ +24°→+21° (*c* 1.0, water, 45 hr).

Found: C, 38.51; H, 5.50; N, 10.96%. Calcd for $C_8H_{14}N_2O_7$: C, 38.40; H, 5.64; N, 11.20%.

Reaction of p-Toluidine and 2. A solution of *p*-toluidine (2.14 g, 20 mmol) and **1** (2.9 g, 20 mmol) in methanol (40 m*l*) was stood at room temperature for one hr, and then concentrated. The sirup obtained could not be crystallized. A solution of the sirup in N-hydrochloric acid was heated for 1.5 hr at 65°C, neutralized to pH 4.6, and concentrated to about half volume to give a white powder which was crystallized from water. The product melts at 158°C (dec.), and the structure could not be characterized. Yield, 1.6 g (39%). IR (cm^{-1}): 3270, 3160, 1655.

Found: C, 58.46; G, 5.35; N, 13.97%. Calcd for $C_{10}H_{10}N_2O_3$: C, 58.25; H, 4.89; N, 13.58%.

On the other hand, treatment of the sirup with acetic or formic acid and evaporation were repeated twice to give a small amount of *N,N'*-di-(*p*-tolyl)-carbamimidoyl-*p*-toluidide. Mp 178—178.5°C (lit.[16] mp 182°C).

Found: C, 76.82; H, 6.46; N, 10.84%. Calcd for $C_{23}H_{23}N_3O$: C, 77.28; H, 6.49; N, 11.76%. From the mother liquor, a small amount of methyl *N*-(*p*-tolyl)-oxamidate (**5b**), mp 144.5—145.5°C (lit.[17], mp 145°C) was obtained.

Found: C, 62.34; H, 5.62; N, 7.38%. Calcd for $C_{10}H_{11}NO_3$: C, 62.16; H, 5.74; N, 7.25%.

When the above ester-exchange was performed in the presence of hydrochloride, a small amount of *N,N'*-di-*p*-tolyloxamide was obtained. Mp 264°C (lit.[18], mp 269°C).

Found: C, 71.69; H, 5.89; N, 9.75%. Calcd for $C_{16}H_{16}N_2O_2$: C, 71.62; H, 6.10; N, 10.44%.

13) R. Rätz and H. Schroeder, *J. Org. Chem.*, **23**, 1931 (1958).
14) P. H. Gross and R. W. Jeanloz, *ibid.*, **32**, 2759 (1967).
15) P.F. Fleury and J. Lange, *J. Pharm. Chim.*, **107**, 196 (1933).
16) R. Anschütz and T. Charke, *Ann.*, **306**, 21 (1899).
17) R. Anschütz and T. Charke, *ibid.*, **306**, 14 (1899).
18) E. Willm and C. Cirard, *Ber.*, **8**, 1196 (1875).

N-Benzylcarbamimidoylformic Acid from Ethyl Thiooxamidate and Benzylamine. To an ice-cooled solution of mercuric chloride (13.5 g, 50 mmol) in ethanol (100 ml) was added ethyl thiooxamidate[9] (6.7 g, 50 mmol) to give white precipitates, and then further addition of benzylamine (10.7 g, 0.1 mol) in ethanol (10 ml) caused the precipitation of mercuric sulfide. The reaction mixture was filtered, and the filtrate was concentrated after addition of concentrated hydrochloric acid (5 ml) and water (100 ml), to give a sirup. After standing this sirup at room temperature for one day, it was dissolved in water and the solution was neutralized to pH 7.0 with N-sodium hydroxide to give white crystals. Yield, 3.0 g (32%), mp 170—171°C (dec.).

Found: C, 57.52; H, 6.03; N, 14.88%. Calcd for $C_9H_{10}N_2O_2 \cdot 1/2H_2O$: C, 57.74; H, 5.92; N, 14.97%.

When a solution of **7** (6.7 g, 50 mmol) and benzylamine (5.4 g, 50 mmol) in ethanol (100 ml) was stood at room temperature in the absence of metal oxide, a small amount of yellow crystals (*N,N'*-dibenzyl-thiooxamic acid amide) were precipitated, which was recrystallized from ethanol. Yield, 0.9 g (12%), mp 118—121°C. IR (cm^{-1}): 3260 (N-H), 1665 (C=O).

Found: C, 67.70; H, 5.55; N, 9.95%. Calcd for $C_{16}H_{16}N_2OS$: C, 67.59; H, 5.67; N, 9.85%.

General Preparation of N-Substituted-carbamimidoylformic Acid (6) by Substitution of Potassium Thiooxamidate (9) with Amines in Water (Method A). Addition of equimolar amount of amines to **9** in the minimum amount of water caused the deposition of **6** within 15 min–1 hr. If the product is soluble in water, **Method B** must be used, because the enforcement of deposition of **6** by neutralization of the reaction mixture yielded sometimes **12**, which was isolated in the case of benzylamine and cyclohexylamine. Results obtained were summarized in Table 1.

Potassium N-Benzyl-thiooxamidate (11a). To a solution of **9** (7.2 g, 50 mmol) in water (200 ml) was added benzylamine (5.4 g, 50 mmol) in water (100 ml), and then concentrated after standing for half an hour to give yellow crystals which was recrystallized in ethanol-water. (2:1 v/v). Yield, 10.0 g (86%), mp 235—238°C.

Found: C, 46.61; H, 3.60; N, 6.04%. Calcd for $C_9H_8KNO_2S$: C, 46.33; H, 3.46; N, 6.02%.

Alkylammonium N-Substituted-thiooxamidate (12). *a) Benzylammonium N-Benzylthiooxamidate (12a)*: A solution of **9** (4.3 g, 30 mmol) and benzylamine (4.3 g, 40 mmol) in water (50 ml) was stood for one day to deposit yellow crystals. Yield, 2.7 g (30%), mp 166—167°C (dec.).

Found: C, 63.32; H, 5.76; N, 9.56; S, 10.68%. Calcd for $C_{16}H_{18}N_2O_2S$: C, 63.56; H, 6.00; N, 9.27; S, 10.59%.

b) Cyclohexylammonium N-Cyclohexylthiooxamidate (12b): A solution of **9** (14.3 g, 0.1 mol) and cyclohexylamine (25 g, 0.25 mol) in water (100 ml) was stood at room temperature for 15 hr, and neutralized to pH 5.0 with N-hydrochloric acid. The pale yellow crystal separated was purified from ethanol. Yield, 9.2 g (32.2%), mp 181—182°C (dec.). MS (*m/e*): 187 ($C_8H_{13}NO_2S$), 141 ($C_7H_{11}NS$), 112, 106, 99 ($C_6H_{13}N$; cyclohexylamine).

Found: C, 59.04; H, 9.05; N, 9.69; S, 11.25%. Calcd for $C_{14}H_{26}N_2O_2S$: C, 58.72; H, 9.15; N, 9.78; S, 11.18%.

The structure of **12** was determined as described before. Among which, electrophoresis was carried out on Toyo Filterpaper No. 51 at pH 8 and 20 Volt/cm for 2 hr with phosphate buffer. In the case of **12a**, *N*-benzylthiooxamidic acid moved 9.7 cm to anode and benzylamine 4.6 cm to cathode, whereas reference substances moved as the same distance.

N,N'-Disubstituted-carbamimidoylformic Acid (13). *a) Benzyl Derivative (13a)*: A suspended solution of **12a** (6 g, 20 mmol) and mercuric oxide (4.8 g, 22 mmol) was stirred for 15 hr at room temperature, and filtered. Concentration of the filtrate gave white crystals which was purified from water-methanol (1:1). Yield, 3.2 g (60%), mp 143—144°C.

Found: C, 71.89; H, 5.94; N, 10.31%. Calcd for $C_{16}H_{16}N_2O_2$: C, 71.62; H, 6.01; N, 10.44%.

b) Cyclohexylamine Derivative (13b): A similar treatment of **12b** with mercuric oxide gave **13b** in 85% yield, which was purified from ethanol. Mp 139°C.

Found: C, 66.40; H, 9.77; N, 10.93%. Calcd for $C_{14}H_{24}N_2O_2$: C, 66.63; H, 9.59; N, 11.10%.

General Preparation of 6 by Treatment of 14 with Lead Oxide (Method B). A mixture of **14**, which was prepared from equimolar amount of **9** and amine hydrochlorides or free thiooxamidic acid[13] and amines, and about four equimolar amount of lead oxide in suitable amount of methanol was shaked at room temperature for 3 to 7 hr, and lead sulfide was filtered off. Concentration of the filtrate gave *N*-monosubstituted-carbamimidoylformic acids usually in 50—80% yield, as shown in Table 1.

Benzyl 2-Amino-2-deoxy-α-D-glucopyranoside Hydrochloride. A solution of benzyl 2-acetamido-2-deoxy-α-D-glucopyranoside (31 g, 0.1 mol) and potassium hydroxide (60 g, 1.1 mol) in ethanol (150 ml) was refluxed in an oil-bath for 5 hr at 120—125°C, neutralized with concentrated hydrochloric acid (95 ml) under cooling, and potassium chloride precipitated was then filtered off. Evaporation of the filtrate gave crystals in 85% yield, which was recrystallized from methanol. Mp 235—236°C (dec.); $[\alpha]_D^{23}$ +122° (*c* 1.0, water).

Found: C, 50.84; H, 6.43; N, 4.97%. Calcd for $C_{13}H_{19}NO_6HCl$: C, 51.06; H, 6.59; N, 4.58%.

Cyclohexyl 2-Amino-2-deoxy-α-D-glucopyranoside Hydrochloride. A similar treatment of cyclohexyl 2-acetamido-2-deoxy-α-D-glucopyranoside, which was prepared from 2-acetamido-2-deoxy-D-glucose by the method of the authors[19] in 60% yield (Mp 184—186°C; $[\alpha]_D^{23}$ +126° (*c* 1.0, water); Found: C, 55.39; H, 8.03; N, 4.78%. Calcd for $C_{14}H_{25}NO_6$: C, 55.43; H, 8.31; N, 4.62%), with potassium hydroxide gave crystals in 35% yield, which was recrystallized from methanol. Mp 250°C (dec.); $[\alpha]_D^{23}$ +120° (*c* 1.0, water).

Found: C, 48.28; H, 8.34; N, 4.62%. Calcd for $C_{12}H_{23}NO_5HCl$: C, 48.39; H, 8.13; N, 4.70%.

Attempted Substitutions of 6 with Amines. a) A suspended solution of **6a** (0.88 g, 10 mmol) in benzylamine (30 ml) was stirred for two days to give pale yellow homogeneous solution. This solution was neutralized with acetic acid, and mixed with a small amount of water. Filtration of the insoluble material gave **6j** in 2.8% yield. Mp 170°C.

b) A mixture of **6e** (1.4 g, 10 mmol) and benzylamine (2.1 g, 20 mmol) was heated at 200°C for 1 hour, and crystals appeared after cooling was filtered and recrystallized from ligroin. This crystals was determined to be *N,N'*-dibenzylformamidine from elemental analysis and mp. Yield, 1.4 g, (63.5%). Mp 76—77°C (lit.[20] mp 79°C) (Found: C, 80.59; H, 7.10; N, 12.51%. Calcd for $C_{15}H_{16}N_2$: C, 80.32; H, 7.19; N, 12.49%).

c) A solution of **6j** (1.8 g, 10 mmol) and benzylamine (1.1 g, 10 mmol) in the ethanol was refluxed for 5 hr, and concentrated. The residue was dissolved in ether, and insoluble materials (**6j**, 0.8 g) was filtered off. Concentration of the filtrate gave *N*-benzylformamide, which was recrystallized from ligroin - ether. Yield, 0.5 g (37%). Mp 61—62°C

19) J. Yoshimura, H. Ando, Y. Takahashi, H. Ono, and T. Sato, *Nippon Kagaku Zasshi*, **85**, 142 (1964).

20) O. Mathieson, Brit. 807767 (1959).

(Lit.[21]), mp 61°C) (Found: C, 71.33; H, 6.47; N, 10.40%. Calcd for C_8H_9NO: C, 71.09; H, 6.71; N, 10.36%).

21) Houben-weyl, "Methoden der Organischen Chemie," Vol. XI-12, ed. by Eugen Müller, Georg Thieme Verlag, Stuttgart, Germany (1958), p. 29.

The authors are indebted to Mr. K. Fukukawa for NMR measurement, and members of Laboratory of Organic Analysis for microanalysis.

BULLETIN OF THE CHEMICAL SOCIETY OF JAPAN, VOL. 44, 3136—3139 (1971)

Studies of the Synthesis of Furan Compounds. XXV.[1] 2-[2-(5-Nitro-2-furyl)-1-(4-cyanophenyl)vinyl]-1,3,4-oxadiazoles and -1,3,4-thiadiazoles[2]

Ichiro HIRAO and Yasuhiko KATO

Laboratory of Organic Synthesis, Department of Chemical Engineering, Kyushu Institute of Technology, Tobata-ku, Kita-Kyushu

(Received May 10, 1971)

5-Amino-2-[2-(5-nitro-2-furyl)-1-(4-cyanophenyl)vinyl]-1,3,4-oxadiazoles and -1,3,4-thiadiazoles have been synthesized from 3-(5-nitro-2-furyl)-2-(4-cyanophenyl)acrylic acid according to a procedure previously described.[3] All of these compounds exhibit strong antibacterial activity against *Staphylococcus aureus*, but they exhibit a weak activity, or almost no activity, against the other microorganisms tested.

2-[2-(5-Nitro-2-furyl)-1-substituted]vinyl-1,3,4-oxadiazole derivatives have been synthesized in order to investigate the influence of β-substituents at a –C=C– side chain of the furan ring upon the antibacterial activity. In the course of the investigation, the present authors have previously reported compounds whose β-carbon at a –C=C– side chain of the furan ring were bound to hydrogen,[4] methyl,[5] phenyl,[6] 2-furyl,[7] and 4-nitrophenyl[3] groups. This paper will deal with the introduction of a 4-cyanophenyl group into that position.

Results and Discussion

3-(5-Nitro-2-furyl)-2-(4-cyanophenyl)acryloylhydrazine (I) was prepared from the chloride of 3-(5-nitro-2-furyl)-2-(4-cyanophenyl)acrylic acid[8] with hydrazine hydrate by the use of methylene chloride as the solvent and without the formation of 1,2-bis[3-(5-nitro-2-furyl)-2-(4-cyanophenyl)acryloyl]hydrazine as a by-product.

1-[3-(5-Nitro-2-furyl)-2-(4-cyanophenyl)acryloyl]-thiosemicarbazide (II) and its 4-substituted derivatives (IIa: R=CH_3, IIb: R=C_2H_5, and IIc: R=C_6H_5) were obtained respectively, by the treatment of the corresponding acid chloride with thiosemicarbazide and by the reaction of I with the corresponding isothiocyanates. The treatment of II and IIa—IIc with methyl iodide afforded the corresponding *S*-methylisothiosemicarbazide (III) and its 4-substituted derivatives (IIIa—c).

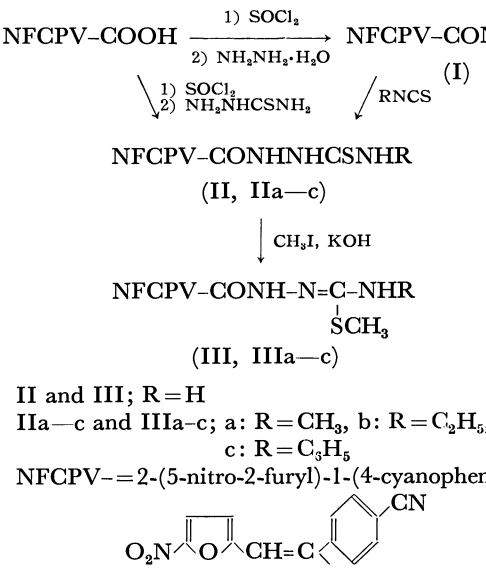

II and III; R=H

IIa—c and IIIa-c; a: R=CH_3, b: R=C_2H_5, c: R=C_3H_5

NFCPV-=2-(5-nitro-2-furyl)-1-(4-cyanophenyl)vinyl;

The introduction of phosgene into a solution of I in dioxane-water produced 2-[2-(5-nitro-2-furyl)-1-(4-cyanophenyl)vinyl]-1,3,4-oxadiazolone (IV) in a good yield. This compound was confirmed to have the keto-structure from the infrared absorption bands[9] at 3350 (N–H) and 1772 cm^{-1} (C=O). The treatment of IV with a large excess of acid anhydrides or with 2—3

1) Part XXIV of this series: I. Hirao, Y. Kato, and T. Hirota, This Bulletin, (Submitted).

2) Presented at the 23rd Annual Meeting of the Chemical Society of Japan, Tokyo, April, 1970.

3) I. Hirao, Y. Kato, and T. Hirota, This Bulletin, **44**, 1923 (1971).

4) I. Hirao and Y. Kato, *Nippon Kagaku Zasshi*, **85**, 693 (1964); **86**, 633 (1965).

5) Y. Kato, Y. Hara, and I. Hirao, *ibid.*, **86**, 957 (1965).

6) Y. Kato and I. Hirao, *ibid.*, **87**, 1336 (1966).

7) I. Hirao, *ibid.*, **88**, 574 (1967); **89**, 713 (1968). Y. Kato, H. Nakajima, and I. Hirao, *ibid.*, **89**, 955 (1968). Y. Kato, This Bulletin, **44**, 489 (1971).

8) I. Hirao and Y. Kitamura, *Bull. Kyushu Inst. Technol.*, No. **18**, 27 (1968).

9) The infrared absorption spectra in this experiments were obtained with a Shimadzu IR-27S spectrophotometer with KBr method.

equimolar acid anhydrides in dioxane gave the corresponding monoacyl derivatives (IVa: R=$COCH_3$, IVb: R=COC_2H_5, and IVc: R=COC_3H_7). These compounds seems to be the *N*-acyl compounds, since the IR spectra contained two C=O absorptions, one near 1770 and the other near 1790 cm^{-1}, thus eliminating the posibility of *O*-acylation.

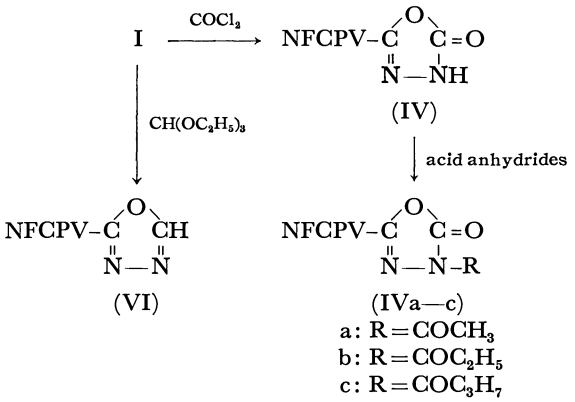

When heated in ethanol, III was cyclized to 5-amino-2-[2-(5-nitro-2-furyl)-1-(4-cyanophenyl)vinyl]-1,3,4-oxadiazole (V) in a good yield. Compound V was also produced from I and cyanogen bromide. Similar treatment of IIIa—IIIc in refluxing ethanol afforded 5-substituted amino-derivatives (Va: R=CH_3, Vb: R=C_2H_5, and Vc: R=C_6H_5). 5-Acylamino derivatives (Vd: R=$COCH_3$, Ve: R=COC_2H_5, Vf: R=COC_3H_7) were similarly prepared by the heating of V with acid anhydrides. 2-[2-(5-Nitro-2-furyl)-1-(4-cyanophenyl)vinyl]-1,3,4-oxadiazole (VI) was obtained by refluxing I in ethyl orthoformate.

5-Amino-2-[2-(5-nitro-2-furyl)-1-(4-cyanophenyl)-vinyl]-1,3,4-thiadiazole (VII) was obtained by the dehydration-cyclization of II with surplus phosphoryl

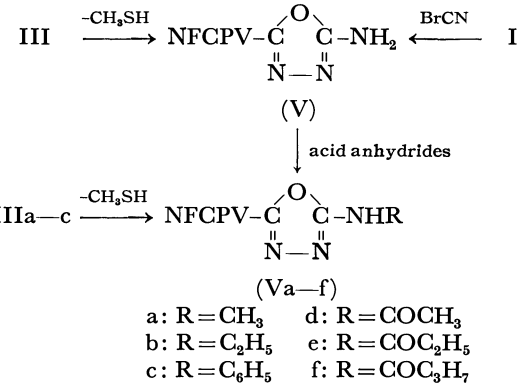

chloride. 5-Alkyl and 5-phenyl-amino-1,3,4-thiadiazoles (VIIa: R=CH_3, VIIb: R=C_2H_5, and VIIc: R=C_6H_5) were prepared by the similar treatment of IIa—IIc with phosphoryl chloride, while the treatment of VII with acid anhydrides afforded 5-acylamino derivatives (VIId: R=$COCH_3$, VIIe: R=COC_2H_5, and VIIf: R=COC_3H_7). All of these compounds are listed in Tables 1 and 2.

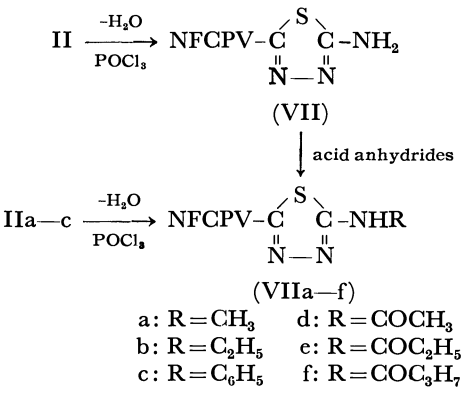

Table 1. 1-[3-(5-Nitro-2-furyl)-2-(4-cyanophenyl)acryloyl]-substituted thiosemicarbazides and *S*-methylisothiosemicarbazides

Compound No.	R	Mp, °C (decomp)	Yield %	Recryst solvent[a]	Appearance[b]	Analysis, % Found (Calcd) C	H	N	
Thiosemicarbazides									
II	H	194—195	78	DMF-W	Y Pm	49.92	3.17	19.20	
						(50.42	3.08	19.61	for $C_{15}H_{11}N_5O_4S$)
IIa	CH_3	219—220	80	MOH	Y Gr	51.80	3.35	18.96	
						(51.75	3.50	18.87	for $C_{16}H_{13}N_5O_4S$)
IIb	C_2H_5	187—188	77	MOH	Y Pm	52.91	3.64	18.64	
						(52.99	3.90	18.18	for $C_{17}H_{15}N_5O_4S$)
IIc	C_6H_5	183—184	69	MOH	O Nd	58.19	3.22	15.79	
						(58.20	3.46	16.17	for $C_{21}H_{15}N_5O_4S$)
S-Methylisothiosemicarbazides									
III	H	174—175	93		Y Pd	52.11	3.17	18.59	
						(51.75	3.50	18.87	for $C_{16}H_{13}N_5O_4S$)
IIIa	CH_3	183—185	87		Y-O Pd	53.07	3.81	17.95	
						(52.99	3.90	18.18	for $C_{17}H_{15}N_5O_4S$)
IIIb	C_2H_5	175—176	77		Y Pd	54.07	4.53	17.79	
						(54.14	4.26	17.54	for $C_{18}H_{17}N_5O_4S$)
IIIc	C_6H_5	184—186	87		Y Pd	58.98	3.66	15.94	
						(59.06	3.80	15.66	for $C_{22}H_{17}N_5O_4S$)

a) Abbreviations; DMF, *N*,*N*-dimethylformamide; W, water; MOH, methanol
b) Abbreviations; Y, yellow; O, orange: Pm, prisms; Gr, granules; Pd, powder; Nd, needles.

10) The authors are indebted to Dr. R. Ueno and his staff of Ueno Pharmaceutical Company, Ltd., for the assay.

TABLE 2. 2-[2-(5-NITRO-2-FURYL)-1-(4-CYANOPHENYL)VINYL]-SUBSTITUTED 1,3,4-OXADIAZOLES AND 1,3,4-THIADIAZOLES

Compound No.	R	Mp, °C (decomp)	Yield %	Recryst solvent[a]	Appearance[b]	Analysis, % Found (Calcd) C	H	N	IR spectrum (KBr) cm^{-1} $\nu_{C\equiv N}$	$\nu_{C=O}$	ν_{C-H}
1,3,4-Oxadiazol-5-ones											
IV	H	175—176	65	EOH	Y Nd	55.67	2.23	17.53	2215	1772	3150, 3050
						(55.56	2.47	17.28 for $C_{15}H_8N_4O_5$)			
IVa	$COCH_3$	228—230	89	Dx-W	Y Gr	55.61	2.98	15.39	2220	1790	3150, 3050,
						(55.74	2.73	15.30 for $C_{17}H_{10}N_4O_6$)		1768	2850—2800
IVb	COC_2H_5	224—225	83	MOH	Y Pd	56.57	3.40	14.99	2220	1790	3150, 3050,
						(56.84	3.16	14.74 for $C_{18}H_{12}N_4O_6$)		1765	2900—2800
IVc	COC_3H_7	163—164	80	MOH	Y Pd	57.74	3.19	14.37	2220	1790	3150, 3050,
						(57.87	3.55	14.21 for $C_{19}H_{14}N_4O_6$)		1765	2900—2800
5-Amino-1,3,4-oxadiazoles											
V	H	248—249	76	MOH	Y Pm	56.02	2.55	21.51	2225		3130
						(55.73	2.85	21.67 for $C_{15}H_9N_5O_4$)			
Va	CH_3	262—263	15	MOH	Y Nd	57.04	2.98	20.44	2220		3140, 3050,
						(56.97	3.26	20.77 for $C_{16}H_{11}N_5O_4$)			2950—2900
Vb	C_2H_5	242—243	37	MOH	O Fb	58.12	3.40	20.05	2220		3140, 3045,
						(58.13	3.70	19.94 for $C_{17}H_{13}N_5O_4$)			2950—2870
Vc	C_6H_5	264—265	34	MOH	Y-O Pm	63.01	3.52	17.45	2215		3150, 3050
						(63.16	3.26	17.54 for $C_{21}H_{13}N_5O_4$)			
Vd	$COCH_3$	245—246	62	MOH	Y Lf	55.89	3.01	19.18	2220	1740	3125, 3045,
						(55.89	2.99	19.31 for $C_{17}H_{11}N_5O_5$)			2950—2890
Ve	COC_2H_5	241—242	54	MOH	Y Fb	56.63	3.30	18.01	2225	1742	3150, 3050,
						(56.99	3.43	18.47 for $C_{18}H_{13}N_5O_5$)			2980—2800
Vf	COC_3H_7	220—221	37	MOH	Y Pm	57.86	3.88	17.71	2225	1740	3150, 3050,
						(58.02	3.82	17.81 for $C_{19}H_{15}N_5O_5$)			2980—2800
5-Amino-1,3,4-thiadiazoles											
VII	H	304—306	21	MOH	Re Nd	52.96	2.83	20.43	2220		3130
						(53.10	2.65	20.65 for $C_{15}H_9N_5O_3S$)			
VIIa	CH_3	239—240	37	MOH	Re Pl	54.41	3.05	19.78	2220		3150
						(54.39	3.12	19.83 for $C_{16}H_{11}N_5O_3S$)			2980—2900
VIIb	C_2H_5	247—248	45	MOH	Re Pd	55.26	3.36	18.80	2220		3130, 3030,
						(55.59	3.54	19.07 for $C_{17}H_{13}N_5O_3S$)			2970—2850
VIIc	C_6H_5	267—269	10	MOH	Re Pd	60.85	2.84	16.51	2220		3145, 3050
						(60.72	3.13	16.87 for $C_{21}H_{13}N_5O_3S$)			
VIId	$COCH_3$	283—284	54	DMF-W	Y Fb	53.09	3.20	18.12	2220	1695	3150, 3030,
						(53.54	2.89	18.37 for $C_{17}H_{11}N_5O_4S$)			2920—2850
VIIe	COC_2H_5	280—282	40	DMF-W	Y-O Gr	54.78	3.49	17.31	2225	1690	3120, 3030,
						(54.78	3.29	17.72 for $C_{18}H_{13}N_5O_4S$)			2920—2830
VIIf	COC_3H_7	269—270	55	Dx	Y Pm	55.41	3.57	16.78	2225	1690	3120, 3030,
						(55.75	3.67	17.12 for $C_{19}H_{15}N_5O_4S$)			2920—2850

a) Abbreviations; EOH, ethanol; Dx, dioxane; W, water; MOH, methanol; DMF, *N,N*-dimethlformamide.
b) Y, yellow; O, orange; Re, red; Nd, needles; Gr, granules; Pd, powder; Pm, prisms; Fb, fibers; Lf, leaflets; Pl, plates.

TABLE 3. INHIBITORY ACTIVITY OF EIGHT COMPOUNDS ON MICROORGANISMS

Minimum inhibitory concentration, μg/ml

Compound	*Diplococcus pneumoniae* Dp-1	*Streptococcus hemolyticus* Group A 089	*Staphylococcus aureus* 209 P	*Bacillus subtilis* pcl 219	*Salmonella enteritidis* 1891	*Salmonella pullorum* Chuyu 114	*Escherichia coli* 0—55	*Klebsiella pneumoniae* ST-101	*Proteus vulgaris* HX 19	*Pseudomonus aeruginosa* 347
II	>25	>25	>25	>25	>25	>25	>25	>25	>25	>25
V	25	12	3.1	12	>25	>25	>25	>25	>25	>25
Vd	12	6.2	6.2	25	>25	>25	>25	>25	>25	>25
Ve	12	12	3.1	12	>25	>25	>25	>25	>25	>25
Vf	6	6	1.5	6	>25	>25	>25	>25	>25	>25
VII	12.5	6.2	1.6	3.1	>25	>25	>25	>25	>25	>25
VIId	>12	>12	1.5	6	>12	>12	>12	>12	>12	>12
VIIe	>3	>3	1.5	>3	>3	>3	>3	>3	>3	>3
Contrast[a]	12	0.4	1.5	1.5	0.8	1.5	1.5	3	6	25

a) 3-(5-Nitro-2-furyl)-2-(2-furyl)acrylic amide was used in the test.

Microbiological Assays.[10] The antibacterial activities of the compounds toward ten microorganisms were examined. The minimum amount of each compound necessary for the complete inhibition of growth was determined by dilution method, using the usual bouillon agar medium (pH 6.8—7.0); some of the results are shown in Table 3. The antibacterial activity of this type of compound showed a behavior similar to that of the compounds possessing a 4-nitrophenyl group[3] previously reported on. All of the compounds tested exhibited a strong activity against *Staphylococcus aureus*, but showed only a weak antibacterial activity at best against the other microorganisms employed. In conclusion, the introduction of a 4-cyanophenyl group into the β-carbon of the –C=C– side chain did not increase the activity.

Experimental[11]

3-(5-Nitro-2-furyl)-2-(4-cyanophenyl)acryloyl Chloride A mixture of 3-(5-nitro-2-furyl)-2-(4-cyanophenyl)acrylic acid[8] (19.9g, 0.07 mol), thionyl chloride (12 g, 0.1 mol), *N,N*-dimethylformamide (1 g), and chlorobenzene (300 m*l*) was stirred at 65—70°C for 1 hr. The resulting solution was cooled with an ice-salt bath, and the acid chloride was separated as yellow crystals, filtrered, washed with dry ether, and used in the following experiments without further purification.

3-(5-Nitro-2-furyl)-2-(4-cyanophenyl)acryloylhydrazine (I). To a stirred, cooled (—5—0°C) mixture of 80% hydrazine hydrate (10.1 g, 0.2 mol), water (10 m*l*), and methylene chloride (90 m*l*), we added, drop by drop a solution of the acid chloride (15.2 g, 0.05 mol) in 350 m*l* of methylene chloride in 30 min. After the addition, the temperature was allowed to rise to room temperature, after which stirring was continued for an additional hr. The resulting suspension was filtered, and the residue was washed with aqueous methanol and then dried to afford 11.4 g (76.5%) of a yellow product melting with decomposition at 217—218°C. Recrystallization from methanol gave yellow leaflets; mp 219°C dec. The yield was 9.7 g (65.1%).

Found: C, 56.21; H, 3.21; N, 18.77%. Calcd for $C_{14}H_{10}N_4O_4$: C, 56.38; H, 3.36; N, 18.79%.

1-[3-(5-Nitro-2-furyl)-2-(4-cyanophenyl)acryloyl]thiosemicarbazide (II). A solution of the acid chloride (9.1 g, 0.03 mol) in dry dioxane (700 m*l*) was stirred slowly into a suspension of thiosemicarbazide (3.28 g, 0.036 mol) and sodium bicarbonate (10 g, 0.12 mol) in 70 m*l* of dioxane. The suspension was stirred for 1 hr at room temperature and then heated at 80°C for 3 hr. After cooling, yellow precipitates were filtered out and poured into aqueous hydrochloric acid. The insoluble product was collected on a filter, washed with water, and then dried. In this way was obtained 8.4 g (77.6%) of a crude product melting with decomposition at 196—197°C. Crystallization from *N,N*-dimethylformamide-water (5: 3, vol/vol) gave yellow prisms (Table 1).

4-Substituted 1-[3-(5-Nitro-2-furyl)-2-(4-cyanophenyl)acryloyl]-thiosemicarbazides (IIa-c). A mixture of I (2 g, 6.7 mmol), alkyl (or phenyl) isothiocyanate (10 mmol), and methanol (100 m*l*) was refluxed for 2—3 hr. The resulting solution was cooled or concentrated, and the precipitated product was collected by filtration. Recrystallization from methanol gave a pure product, as is shown in Table 1.

1-[3-(5-Nitro-2-furyl)-2-(4-cyanophenyl)acryloyl]-S-methylisothiosemicarbazide (III) and Its 4-Substituted Derivatives (IIIa–c). To a stirred mixture of 5 mmol of II (or IIa-c), methyl iodide (15 mmol), and ethanol (30—45 m*l*) was added, drop by drop, a solution of potassium hydroxide (5 mmol) in 40 m*l* of ethanol. After the addition, stirring was continued for 10—12 hr at room temperature. The resulting suspension was filtered, and the residue was washed with a small amount of cold ethanol and dried. When the products were heated in solvents, decomposition occurred with the evolution of methyl mercaptan, but these products were pure enough, as is shown by the results of elemental analyses (Table 1).

2-[2-(5-Nitro-2-furyl)-1-(4-cyanophenyl)vinyl]-1,3,4-oxadiazol-5-one (IV). To a stirred solution of I (5.96 g, 20 mmol) in 400 m*l* of dioxane-water (3:2, vol/vol), phosgene was introduced under cooling at 15—17°C. After 2 hr, the precipitated product was collected and washed with water to give 6.4 g (quantitative) of crude IV; mp 182—184°C. Recrystallization was then carried out (Table 2).

4-Acyl-2-[2-(5-nitro-2-furyl)-1-(4-cyanophenyl)vinyl]-1,3,4-oxadiazol-5-ones (IVa–c). A mixture of IV (0.32 g, 1 mmol) and 5 m*l* of acid anhydride (or 0.4 g of acid anhydride and 5 m*l* of dioxane) was heated on a steam bath for 1—2 hr. The resulting solution was taken to dryness *in vacuo*, and the residue was washed with water, dried, and recrystallized. The yields and mps of the products are given in Table 2.

2-[2-(5-Nitro-2-furyl)-1-(4-cyanophenyl)vinyl]-1,3,4-oxadiazole (VI). A suspension of I (2.98 g, 10 mmol) in ethyl orthoformate (70 m*l*) was heated at 100—105°C for 8—10 hr. The resulting solution was concentrated *in vacuo*, and the product was filtered and washed with cold ethanol. Recrystallization from methanol gave VI as ochreous prisms; mp 225—226°C dec. The yield was 2.68 g (87.2%).

Found: C, 58.23; H, 2.42; N, 17.80%. Calcd for $C_{15}H_8N_4O_4$: C, 58.44; H, 2.60; N, 18.18%.

5-Amino-2-[2-(5-nitro-2-furyl)-1-(4-cyanophenyl)vinyl]-1,3,4-oxadiazole (V). *Procedure A*: A suspension of III (3.71 g, 10 mmol) in ethanol (80 m*l*) was refluxed until the evolution of methyl mercaptan had ceased (*ca.* 4.5 hr). The resulting solution was taken to dryness *in vacuo*, and the residue was crystallized from methanol to give 2.76 g (85.4%) of V as yellow prisms.

Procedure B: A mixture of I (1.49 g, 5 mmol), cyanogen bromide (0.85 g, 8 mmol), and 100 m*l* of methanol was heated under reflux for 2 hr. Cooling then provided 1.46 g (90%) of yellow crystals, mp 167—169°C dec. Recrystallization from methanol raised the melting point to 246—247°C dec; this melting point was undepressed on admixture with a sample prepared by *Procedure A* as above for V.

5-Substituted Amino-2-[2-(5-nitro-2-furyl)-1-(4-cyanophenyl)vinyl]-1,3,4-oxadiazoles (Va–c). These were prepared in the same way as V above (*Procedure A*) using 5 mmol of 4-substituted *S*-methylisothiosemicarbazide derivatives (IIIa–c).

5-Amino-2-[2-(5-nitro-2-furyl)-1-(4-cyanophenyl)vinyl]-1,3,4-thiadiazole (VII) and 5-Substituted Amino Derivatives (VIIa–c). A mixture of 5 mmoles of II (or IIa-c) and phosphoryl chloride (10 m*l*) was heated under refiux for 2–3 hr. The solution was then poured onto crushed ice, and the solidified product was filtered, washed with water, and dried. Two or three recrystallizations gave a pure product (Table 2).

5-Acylamino Derivatives of V and VII. Compound V (or VII) (2 mmol) was covered with the acid anhydride (7 m*l*) and heated on a steam bath for 2—3 hr. Water (30 m*l*) was then added to the resulting solution to decompose the excess acid anhydride. The product was collected, washed with water, and dried. In this way, the corresponding acyl products were obtained; recrystallizations were achieved from solvents or solvent pairs, as is shown in Table 2.

11) All the melting and decomposition points are uncorrected. The elemental analyses were performed on a Yanagimoto CHN Corder MT-2 type.

Retardation Effect Induced by Pyridine in the Radical Copolymerization of Styrene and Liquid Sulfur Dioxide

Tsutomu ENOMOTO,* Masashi IINO, Minoru MATSUDA, and Niichiro TOKURA*

Chemical Research Institute of Non-Aqueous Solutions, Tohoku University, Sendai

(Received May 12, 1971)

We have found that the radical copolymerization of styrene and liquid sulfur dioxide (liq. SO_2) is retarded when a basic solvent such as pyridine is used; we also investigated the mechanism of the retardation induced by pyridine. The polymerization in pyridine was most strongly retarded when the styrene mole fraction in the feed, $[St]_0/([St]_0+[SO_2]_0)$, was small (below about 0.2) and when the pyridine mole fraction in pyridine-liq.SO_2, $[Py]_0/([Py]_0+[SO_2]_0$, was 0.4—0.5. Moreover, from the results in the reaction of the phenylsulfonyl radical (the model radical for the propagating sulfonyl radical) in pyridine or in a pyridine - liq. SO_2 mixture, it may be concluded that the end unit of the polymer has the pyridinium sulfonate structure ($-SO_3^-HPy^+$) and that the retardation may occur by means of the reaction of the propagating sulfonyl radical with the pyridine-SO_2 complex.

We have been investigating the solvent effect on the compositions of copolymers obtained by the radical copolymerization of styrene and liquid sulfur dioxide (liq. SO_2). The following results have so far been obtained; the copolymer compositions depend on the total monomer concentration and on the nature of the solvent, but hardly on feed composition; that is, the styrene content in the copolymer increases with an increase in the volume fraction of the solvent and by the addition of a basic solvent such as pyridine.[1)]

Furthermore, we have found that this polymerization is retarded when a basic solvent such as pyridine, triethylamine, or furan is used.

In this paper, we will dicsuss the mechanism of the retardation induced by pyridine.

Results and Discussion

Retardation of the Radical Copolymerization of Styrene and Liq. SO_2 by Pyridine. In Table 1 the qualitative results are summarized. Table 1 shows that; (1) the polysulfone (methanol-insoluble polymer) is not obtained in pyridine, but is obtained in dichloromethane under the same experimental condition (runs 1 and 2); (2) by increasing the styrene mole fraction in the feed or the azobisisobutyronitrile (AIBN) concentration, polysulfone is obtained, even in pyridine (runs 3, 4, 5, and 6); (3) retardation is also observed in the radical copolymerization of hexene-1 and liq. SO_2 (runs 7 and 8); (4) by the evaporation of the methanol solutions of runs 1, 4, and 5, methanol-soluble (low-molecular weight) styrene polysulfone is obtained.

These results suggest that retardation may occur by the deactivation of the propagating sulfonyl radical (by degradative chain transfer or addition reaction which forms an inactive radical).

Next, we have investigated the rate of copolymerization in pyridine with AIBN under the experimental conditions in which methanol-insoluble polymer was obtained. The styrene mole fraction in the feed and the total concentration of pyridine and liq.SO_2 were kept constant at 0.2 and 12.0 mol/*l* respectively, while the mole fraction of liq.SO_2 in pyridine-liq.SO_2, $[SO_2]_0/([SO_2]_0+[Py]_0)$, was varied from 0.2 to 0.8, using cyclohexane as an inert solvent.[1)] The polymerization rates (mol conv./hr) were calculated using both the initial slope of the time-conversion curves and the copolymer compositions, as is shown in Table 2. Rates relative to the rate of run 7 (Table 2) are plotted against $[SO_2]_0/([SO_2]_0+[Py]_0)$ in Fig. 1. From Fig. 1 it is clear that polymerization was most strongly retarded when comparable amounts of pyridine and

TABLE 1. THE QUALITATIVE RESULTS IN RETARDATION BY PYRIDINE[a)]

No.	Styrene (m*l*)	SO_2 (m*l*)	Pyridine (m*l*)	Dichloro-methane (m*l*)	$\frac{[St]_0}{[St]_0+[SO_2]_0}$[b)]	AIBN (g)	Polymer[c)] yield (g/hr)
1	6.2	24.0	59.8		0.1	0.1	0/4
2	6.2	24.0		59.8	0.1	0.1	0.13/3
3	18.7	18.7	52.6		0.3	0.1	0.26/2
4	6.6	25.0	47.9		0.1	0.15	0/14.5
5	6.6	25.0	47.9		0.1	0.15	0/21
6	6.6	25.0	47.9		0.1	1.0	3.5/46.5
	Hexene-1 (m*l*)						
7	2.5	7.9	5.0			0.02	0/0.5
8	2.5	7.9		5.0		0.02	1.36/0.5

a) Polymerization temperature, 50°C (No. 1—6), 30°C (No. 7 and 8).
b) Styrene mole fraction in feed.
c) Methanol-insoluble polymer.

* Present address: Department of Applied Chemistry, Faculty of Engineering, Osaka University, Suita-shi, Osaka.

1) M. Matsuda and M. Iino, *Macromolecules*, **2**, 216 (1969).

Table 2. Polymerization rates in pyridine[a]

No.	Styrene (ml)	SO_2 (ml)	Pyridine (ml)	Cyclohexane (ml)	$[St]_0$[b] / $[St]_0+[SO_2]_0$	$[SO_2]_0$[c] / $[SO_2]_0+[Py]_0$	Styrene mol% in copolymer	Rate[d] (mol%/hr)	Relative rate
1	2.8	4.8	31.1	1.3	0.2	0.2	91.3	0.077	0.48
2	4.1	7.1	27.2	1.6	0.2	0.3	83.0	0.068	0.42
3	5.5	9.5	23.3	1.7	0.2	0.4	73.7	0.040	0.25
4	6.9	11.9	19.4	1.8	0.2	0.5	69.9	0.006	0.04
5	8.3	14.2	15.5	2.0	0.2	0.6	65.3	0.014	0.09
6	9.7	16.6	11.7	2.0	0.2	0.7	66.3	0.089	0.55
7	11.1	19.0	7.8	2.1	0.2	0.8	66.2	0.162	1.00

a) Polymerization temperature 50°C, $[AIBN]_0=1.52\times10^{-3}$ mol/l, total volume 40 ml, $[SO_2]_0+[Py]_0=12.0$ mol/l.
b) Styrene mole fraction in feed.
c) SO_2 mole fraction in pyridine-liq.SO_2.
d) Mol% = [polymer(mole)/charged monomer(styrene + SO_2) (mole)] × 100.

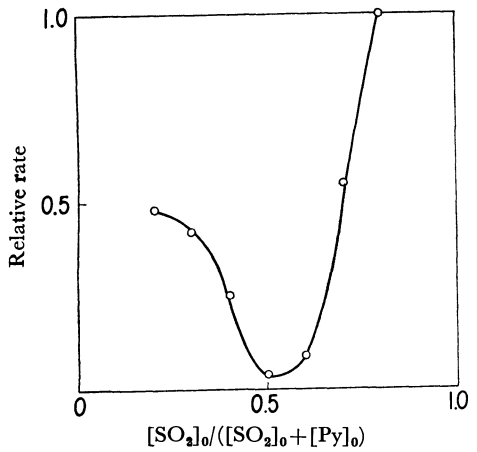

Fig. 1. The plot of relative rate (Table 2) of copolymerization in pyridine against liq. SO_2 mole fraction in liq. SO_2-pyridine, $[SO_2]_0/([SO_2]_0+[Py]_0)$.

liq.SO_2 were present ($[SO_2]_0/([SO_2]_0+[Py]_0)\approx0.5$—$0.6$) and was less retarded when there was an excess of pyridine.

From this fact we can speculate that retardation may occur as a result of the reaction of the propagating sulfonyl radical and the pyridine-SO_2 complex. It is well known that SO_2 behaves as an electron acceptor and forms charge-transfer complexes with pyridine and various amines. Although it has been reported[2] that SO_2 forms a 1:1 (mole) complex with pyridine, our finding,[3] obtained by the continuous-variation method in UV spectra, has shown that the complex consists of one mole of pyridine and two moles of SO_2.

Thermal and Photochemical Decompositions of Phenyl Phenylsulfonyl Diimide (PPD) in Pyridine or in a Pyridine-Liq.SO_2 Mixture. To make clear the retardation mechanism speculated as above, we have carried out a model reaction using the phenylsulfonyl radical.

The α-phenylethanesulfonyl radical is better than the phenylsulfonyl radical as a model radical for the propagating sulfonyl radical in the copolymerization of styrene and liq.SO_2, but attempts to prepare it in a solution containing pyridine were unsuccessful.

As the source of the phenylsulfonyl radical, we have used phenyl phenylsulfonyl diimide (PPD), which has been reported by Rosenthal and Overberger[4] to form this radical by thermal decomposition. Phenylsulfonyl halide was inadequate because of its ionic reaction with pyridine.

The results obtained are summarized in Table 3. Table 3 shows that pyridinium benzenesulfonate ($PhSO_3^-HPy^+$,PBS) was obtained in a good yield in the reaction in the pyridine-liq.SO_2 mixture; on the other hand, in pyridine this product was not obtained. PBS is water-soluble and was obtained from the water-soluble part of the reaction mixture, as will be described in the Experimental section. From the ether-soluble part, we obtained azobenzene; its yield was best in the reaction in pyridine. We could not identify

Table 3. Thermal decomposition of phenyl phenylsulfonyl diimide (PPD)[a]

PPD g(mole)	SO_2 (ml)	Pyridine (ml)	$[SO_2]_0$[b] / $[SO_2]_0+[Py]_0$	PBS[c] g(mole%)	Product Azobenzene g(mol%)	N_2 (mol%)
9.84(0.04)	0.0	50.0	0.0	0.0[d]	0.30(4.1)	
9.84(0.04)	0.0	80.0	0.0	0.0[d]	0.39(5.4)	53
9.84(0.04)	8.4	51.6	0.2	5.54(58.4)	0.03(0.4)	99
9.84(0.04)	23.7	36.3	0.5	5.20(54.8)	0.03(0.4)	87
9.84(0.04)	43.4	16.6	0.8	2.87(30.2)	0.06(0.8)	95

a) 70°C, 24 hr.
b) SO_2 mole fraction in pyridine —liq.SO_2.
c) Pyridinium benzene sulfonate, mole% based on PPD.
d) About 0.8 g of water-soluble product (unidentified) was obtained.

2) A. Tramer, *Bull. Acad. Polon. Sci.*, **5**, 501 (1957).
3) M. Matsuda and T. Hirayama, *J. Polym. Sci.*, **5**, 2769 (1967).
4) A. J. Rosenthal and C. G. Overberger, *J. Amer. Chem. Soc.*, **82**, 108 (1960).

Table 4. Photo-chemical decomposition of phenyl phenylsulfonyl diimide (PPD)[a)]

	PPD g(mol)	SO_2 (m*l*)	Pyridine (m*l*)	$\frac{[SO_2]_0}{[SO_2]_0+[Py]_0}$ [b)]	PBS[c)] g(mol%)	N_2 (mol%)
Irradiation	4.92(0.02)	11.8	18.2	0.5	1.49(31.4)	96
Dark	4.92(0.02)	11.8	18.2	0.5		0.0

a) Room temperature, 36 hr.
b) SO_2 mole fraction in pyridine-liq.SO_2.
c) Pyridinium benzene sulfonate, mol% based on PPD.

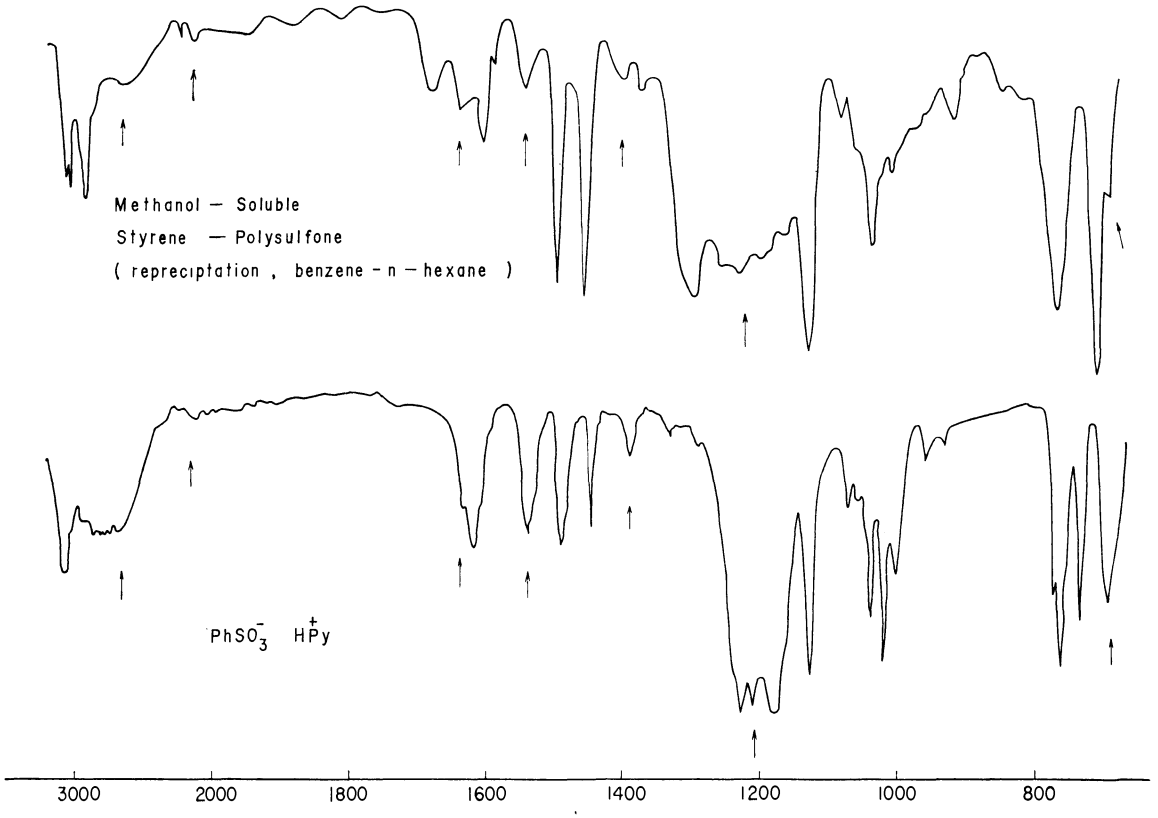

Fig. 2. IR spectra of methanol-soluble styrene-polysulfone obtained by copolymerization in pyridine and $PhSO_3^-$ HPy^+.

any product other than azobenzene from the ether-soluble part.

Table 4 shows that the photolysis of PPD at room temperature in the pyridine-liq.SO_2 mixture gave PBS, while in the dark the reaction did not occur. It is well known that an azo-compound such as PPD is subject to homolysis by light and forms two radicals and nitrogen. Therefore, the results in Table 3 indicate that PBS arises from the phenylsulfonyl radical.

The infrared spectra of methanol-soluble styrene polysulfone described in the preceeding section and PBS are shown in Fig. 2. The arrow in the spectra of polysulfone indicates a peak which does not exist in ordinary styrene polysulfone obtained in bulk or in a non-basic solvent. It is clear that these peaks arise from the end unit of this polymer, formed by termination. The peak at 2200 cm^{-1} indicates the presence of the moiety of the initiator (AIBN) as another end unit of this polymer. All the peaks denoted by arrows also exist in the spectra of PBS. This fact indicates that the end unit of this polymer has a structure similar to that of PBS, namely, $-SO_3^-HPy^+$. In fact, the aqueous solution of this polymer (it is dissolved for the most part in water) is acidic, as is PBS. From the above results, it seems certain that retardation occurs by the deactivation of the propagating sulfonyl radical and that pyridinium sulfonate is formed ultimately. Moreover, the fact that PBS is obtained in a pyridine-liq.SO_2 mixture, but not in pyridine, suggests that the propagating sulfonyl radical is deactivated by the reaction with the pyridine-SO_2 complex.

The results in the thermal decompositions of phenyl *p*-methylphenylsulfonyl diimide (*p*-methylPPD) and phenyl *p*-chlorophenylsulfonyl diimide (*p*-chloroPPD) are summarized in Table 5. In *p*-methylPPD, though the yield was low, pyridinium *p*-toluenesulfonate (*p*-methylPBS) was obtained in the reaction in pyridine. Its formation may be considered to be due to the reaction of pyridine and *p*-toluenesulfinic acid, which is itself formed by the following hydrogen abstraction reaction, because *p*-methylPPD has very reactive hydrogen atoms (a methyl group attached to a phenyl group) toward abstraction, while PPD and *p*-chloroPPD, in which no pyridinium sulfonates were obtained in pyridine, have no such hydrogen atoms;

$$CH_3C_6H_4SO_2\cdot + CH_3C_6H_4SO_2N_2C_6H_5 \longrightarrow CH_3C_6H_4SO_2H + \cdot CH_2C_6H_4SO_2N_2C_6H_5$$

Table 5. Thermal decomposition of phenyl *p*-methylphenylsulfonyl diimide (*p*-methyl PPD) or phenyl *p*-chlorophenylsulfonyl diimide (*p*-chloro PPD)[a]

SO_2 (ml)	Pyridine (ml)	$[SO_2]_0$[b] / $[SO_2]_0+[Py]_0$	*p*-MethylPPD g(mol)	*p*-MethylPBS[c] (g)	N_2 (mol%)[d]	*p*-ChloroPPD g(mol)	*p*-ChloroPBS +PBS (g)	N_2 (mol%)
0.0	30.0	0.0	5.20(0.02)	0.26	57	5.61(0.02)	0.0	79
4.2	25.8	0.2	5.20(0.02)	1.34	99	5.61(0.02)	0.67	97
11.8	18.2	0.5	5.20(0.02)	1.79	82	5.61(0.02)	1.10	74
21.7	8.3	0.8	5.20(0.02)	0.71	70	5.61(0.02)		86

a) 70°C, 24 hr. b) SO_2 mole fraction in pyridine-liq.SO_2.
c) It includes a small amount of PBS (from its NMR spectra). d) Based on diimide.

In fact, we have carried out the reaction of benzene sulfinic acid with pyridine and obtained PBS, as will be described in the Experimental section. In *p*-chloro-PPD, pyridinium *p*-chlorobenzenesulfonate (*p*-chloro-PBS) and PBS were obtained in the pyridine-liq.SO_2 mixture, but not in pyridine. PBS probably arises from the phenylsulfonyl radical formed by the addition reaction of the phenyl radical and SO_2. These results also support the idea that the sulfonyl radical is deactivated by the reaction with the pyridine-SO_2 complex.

We can suggest the following two mechanisms as possible for the deactivation of the sulfonyl radical;

(1) $\sim SO_2\cdot$ + complex $\longrightarrow$
$\sim SO_2H$ + inactive radical $\xrightarrow{+Py}$
$\sim SO_3^-HPy^+$

(2) $\sim SO_2\cdot$ + complex $\longrightarrow$
$\sim SO_2$ − complex·(inactive radical) $\longrightarrow$
$\sim SO_3^-HPy^+$

It is well known that when a radical attacks an aromatic ring, an addition reaction (mechanism 2) usually occurs, but not hydrogen abstraction reaction (substitution reaction on hydrogen, mechanism 1).[5] Accordingly, it seems reasonable to consider that retardation occurs by the addition reaction of the sulfonyl radical to the complex and the formation of an inactive (stable) radical (mechanism 2).

Experimental

Materials. Styrene, AIBN, pyridine, dichloromethane, and cyclohexane were purified by the usual method. Liq. SO_2 was dehydrated by phosphorus pentoxide and distilled *in vacuo*. PPD was prepared[6] from sodium benzenesulfinate and benzenediazonium chloride and was recrystallized from ethanol (mp 74—76°C; lit,[6] 78°C). *p*-MethylPPD and *p*-chloroPPD were prepared using the same method (*p*-methyl PPD: mp 93—95°C; lit,[7] 95°C, *p*-chloroPPD: mp 102—103°C; lit,[6] 106°C).

Copolymerization of Styrene and Liq.SO_2. Polymerization was carried out using a method previously reported.[8] The polymerization rates were measured by the gravimetric method, and the copolymer compositions were determined from the elementary analyses of carbon.

Thermal Decomposition of PPD in Pyridine or in a Pyridine-Liq.SO_2 Mixture. 9.84 g (0.04 mol) of PPD were reacted at 70°C for 24 hr in pyridine (50 or 80 ml) or in a pyridine-liq.SO_2 mixture. The mole fraction of liq.SO_2 in the pyridine-liq.SO_2 mixture was varied from 0.2 to 0.8 (pyridine +liq.SO_2=60 ml; Table 3). After the reaction the liq.SO_2 was evaporated and the pyridine was distilled off under reduced pressure (1—2 mmHg). The residue thus obtained was extracted with water and ether. In the case of the reaction in the pyridine-liq.SO_2 mixture, the evaporation of the water of the water layer and recrystallization from acetone gave PBS (2.9—5.5 g; Table 3): hygroscopic, mp 129.5—132°C; lit,[9] 125—130°C. Its IR and NMR spectra coincided with those of an authentic sample prepared from benzene sulfonic acid and pyridine. PBS could also be obtained by extraction with dehydrated acetone instead of water. This fact indicates that PBS is not formed by the addition of water. On the other hand, in the case of the reaction in pyridine, the evaporation of the water from the water layer gave no PBS, but did give an unidentified product in only a small yield (0.8 g): nonhygroscopic, mp 200—202°C. In either pyridine-liq.SO_2 or pyridine systems, the ether layer was chromatographed on a silica gel column; subsequent elution with a petroleum ether-benzene mixture gave azobenzene in a yield such as is shown in Table 3: mp 65—68°C, identified by comparison with an authentic sample.

In *p*-methylPPD, *p*-methylPBS was identified by comparison with an authentic sample: hygroscopic, mp 117—123°C (recrystallized from acetone); lit,[10] 119—121°C. In the case of *p*-chloroPPD, the IR spectrum of the product shows, when compares with that of authentic *p*-chloroPBS, that a mixture of *p*-chloroPBS and PBS was obtained.

Photo-decomposition of PPD. The reactants in a quartz-reaction vessel were irradiated at room temperature by means of a high-pressure mercury lamp about 5 cm from the vessel.

The Reaction of Benzenesulfinic Acid with Pyridine. 5.26 g (0.03 mol) of benzenesulfinic acid and pyridine (30 ml) were reacted at 70°C for 24 hr. By the same procedure as in the case of PPD, 1.38 g (19.3%) of PBS were thus obtained. 0.3 g of PBS was also obtained in the reaction in the pyridine −liq.SO_2 mixture (mole ratio 1:1) instaed of in pyridine.

Measurement of the Nitrogen Volume Evolved. The volume of the nitrogen evolved was measured from the difference in the volumes at 20°C and 1 atm before and after the reaction, using a mercury manometer. The reaction vessel was filled with nitrogen at 1 atm and 20°C prior to the reaction. In the measurement, the reaction vessel was cooled by liquid nitrogen to prevent any effect of the liq.SO_2.

5) W. A. Pryor, "Free Radicals," McGraw-Hill Book Company, New York (1966), Chap. 16.
6) A. Hantzsch and M. Singer, *Ber.*, **30**, 312 (1897), **31**, 641 (1898).
7) P. K. Dutt, H. R. Whitehead, and A. Wormall, *J. Chem. Soc.*, **119**, 2088 (1921).
8) N. Tokura and M. Matsuda, *Kogyo Kagaku Zasshi*, **64**, 501 (1961).
9) L. Field, *J. Amer. Chem. Soc.*, **74**, 394 (1952).
10) W. E. Rosen, *J. Org. Chem.*, **26**, 5190 (1961).

Conformations of the Esters. II.[1] The Conformation of Alkyl Acetates

Michinori Ōki and Hiroshi Nakanishi

Department of Chemistry, Faculty of Science, The University of Tokyo, Hongo, Bunkyo-ku, Tokyo

(Received May 13, 1971)

Alkyl acetates which carry secondary and tertiary alkyl groups have been found to have bifurcated bands in the carbonyl region of the infrared spectra. The origin of the bifurcated bands has been studied carefully, and it has been concluded that the Fermi resonance is the most probable origin of the phenomenon.

The conformation of the ester group has long been believed to be *s-trans*. The conformation of acetates is not an exception; it has been reported that alkyl acetates take the *s-trans* conformation, judging from the results of dipole-moment measurements,[2] electron diffraction,[3] and infrared spectroscopy.[4] The only exception is the report by Monaham[5] which postulates that the *s-cis* conformer exists in poly(*t*-butyl acrylate) and *t*-butyl acetate after irradiation by light, as revealed by the temperature dependence of the infrared spectra in the lower-frequency region. In the light of the fact that the *s-cis* conformer can exist together with the *s-trans* in some esters of formic acid which carry a bulky alkyl group,[1] it seems that it would be interesting to reinverstigate the situation of the acetate esters. Since it is believed that the *s-cis* conformation can exist in formates, because hydrogen is the smallest alkyl group in *n*-alkanoic acids and the steric repulsion between the alkyl group of an alcoholic part and hydrogen must be the least, the methyl group in acetates serves as a critical example in diagnosing the conformations of the ester group derived from the higher alkanoic acids: if no *s-cis* conformation exist in acetates, other higher alkanoic acid esters can not possibly show signs of the existence of the stable *s-cis* conformer. Thus, the infrared and nuclear magnetic resonance spectra of acetates have been reexamined. The purpose of this paper is to report the results of this investigation.

Fig. 1. Two conformers of acetate.

Experimental

Materials. Various alkyl acetates were prepared according to the standard method. The purity of the samples was checked by means of their physical constants, infrared spectra, nuclear magnetic resonance spectra, and results of gas chromatography. *t*-Butyl acetate-d_3 (CD_3CO_2t-Bu) was prepared from *t*-butyl alcohol and acetyl-d_3 chloride in the presence of pyridine.

Spectra. The infrared spectra were measured by using a Hitachi EPI-G2 grating infrared spectrophotometer (4000——400 cm^{-1}) and a Perkin Elmer 112G single-beam grating spectrophotometer (3600—3300 cm^{-1}, 1800—1700 cm^{-1}). The latter instrument is more precise; the error is estimated to be 0.4 cm^{-1} at 1750 cm^{-1}. The absorption curves due to the carbonyl stretching of alkyl acetates were graphically separated, and it was confirmed that almost all the peaks were in good agreement with the calculated Lorenzian curves. The nuclear magnetic resonance spectra were recorded on a JNM-4H-100 spectrometer.

Results and Discussion

As has previously been described,[1] the chief factors governing the preference of the conformations of the ester group can be considered to include the following three: 1) the dipole-dipole interaction between C=O and O–R bonds, 2) the repulsion between lone-pair electrons of two oxygen atoms, and 3) the steric repulsion between either C=O and R or CH_3 and R (Fig. 2).

As to the first two factors, the *s-trans* conformer is favored over the *s-cis*. However, the third factor, which makes the existence of the *s-cis* conformer in *t*-butyl formate possible, may also operate in acetates so that the *s-cis* conformer exists. Although, of course, the repulsion between methyl and R groups cannot be overcome by that between R and carbonyl oxygen in a usual sense, there is a possibility that the ester group becomes non-planar because of the severe repulsion in

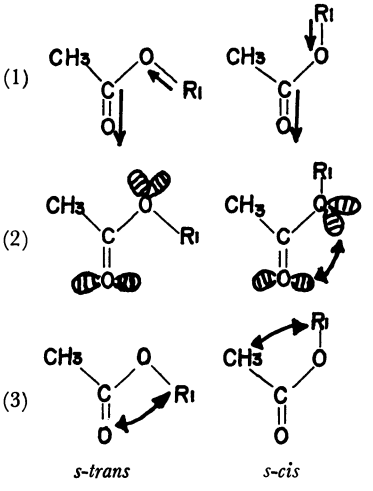

Fig. 2. Factors governing the conformations of acetate.

1) M. Ōki and H. Nakanishi, This Bulletin, **43**, 2558 (1970).

2) a) R. J. B. Marsden and L. E. Sutton, *J. Chem. Soc.*, **1936**, 1383. b) R. J. W. LeFevre and A. Sundaram, *ibid.*, **1962**, 3904.

3) J. M. O'Gorman, W. Schand, Jr., and V. Schmaker, *J. Amer. Chem. Soc.*, **72**, 4222 (1950).

4) a) S. Ichikawa and T. Shimanouchi, Tokyo University, private communication. b) J. K. Wilmshurst, *J. Mol. Spectry.*, **1**, 201 (1957).

5) A. R. Monoham, *J. Polym. Sci. Part A-1*, **5**, 2333 (1967).

6) The correction for the intensity and for the shapes of the infrared absorption bands of esters, as measured with this spectrometer, has been discussed in detail by Kuratani and Minegishi; see K. Kuratani and A. Minegishi, This Bulletin, **31**, 586 (1958).

Table 1. Absorption maxima due to carbonyl stretching vibration of alkyl acetates and solvent effect

	Compound	Solvent					
		CCl_4 (2.23)[a] (c=0.0005 mol/l)		CH_3CN (37.5)[a] (c=0.05 mol/l)		DMSO (48.9)[a] (c=0.05 mol/l)	
I	CH_3CO_2Me	1749.0 cm^{-1} [c]	(824)[b]	1742.2 cm^{-1}	(963)[b]	1738.0 cm^{-1}	(874)[b]
II	CH_3CO_2Et	1741.2[c]	(696)	1736.4	(679)	1732.3	(759)
III	CH_3CO_2n-Pr	1742.9	(473)	1734.1[d]	(328)		
IV	CH_3CO_2n-Bu	1741.9	(736)	1734.2[d]	(874)		
V	CH_3CO_2i-Pr	1728[c]	(87)	1728	(740)	1722	(842)
		1737.2	(1000)	1739	(72)	1736	(11)
VI	CH_3CO_2c-C_6H_{11}	1728[c]	(49)	1717	(97)	1719	(264)
		1735.7	(650)	1729.4	(576)	1728	(844)
VII	$CH_3CO_2CHEt_2$	1729	(175)	1727.5[d]	(504)	1725	(697)
		1736.6	(845)	1738	(45)	(broad)	
VIII	CH_3CO_2t-Bu	1727	(314)	1728.7	(559)	1723.0	(572)
		1738.4	(764)	1741	(80)	1736	(144)
IX	CD_3CO_2t-Bu	1728	(129)	1720	(364)	1717	(576)
		1735.4	(521)	1733	(297)	1731	(324)
X	CH_3CO_2t-Am	1727[c]	(142)	1725.4	(685)	1722.0	(646)
		1735.6	(701)	1737	(124)	1733	(162)

a) Numericals shown in parentheses are dielectric constants at 20°C.
b) Numericals shown in parentheses are molar absorption coefficients.
c) c=0.05 mol/l in CS_2.
d) c=0.007 mol/l.

the planar conformation and that, in such a conformation, the *s-cis* becomes relatively favored.

Infrared Spectra. From the results obtained with formates[1] it is expected that the *s-cis* and *s-trans* conformations of acetates are reflected in the carbonyl stretching vibration absorptions. Many authors have reported on the infrared C=O stretching spectra of acetates,[7,8] but none has discussed the shapes of the absorptions, most of the attention being devoted to the frequencies and intensities of the bands. The results obtained in this study are shown in Table 1. It can be pointed out immediately that methyl and ethyl acetates give only one absorption (which is sharp and symmetrical) in the solvents studied, whereas isopropyl and *t*-butyl acetates give rise to two absorptions. Clearly those acetates which are derived from primary alcohols give only one absorption, while those derived from secondary and tertiary alcohols give two absorption peaks.

The solvent effect (see Fig. 3) on these absorptions is remarkable. With only one exception (cyclohexyl acetate), the absorption at the higher frequency, which is the stronger one in such nonpolar solvents as carbon tetrachloride and carbon disulfide, becomes the minor absorption in such polar solvents as acetonitrile and dimethyl sulfoxide. In order to make the situation clearer, the solvent effect on the carbonyl-stretching absorption of acetates was studied by changing the mixing ratio of carbon tetrachloride to acetonitrile.

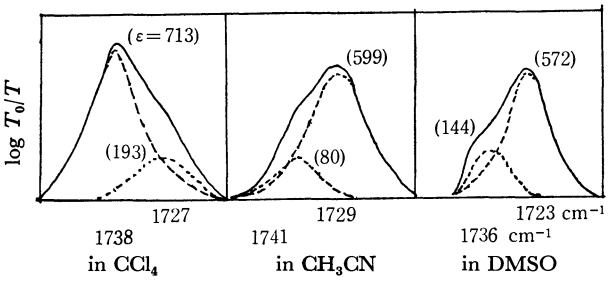

Fig. 3. Solvent effect on ν_{CO} of *t*-butyl acetate.

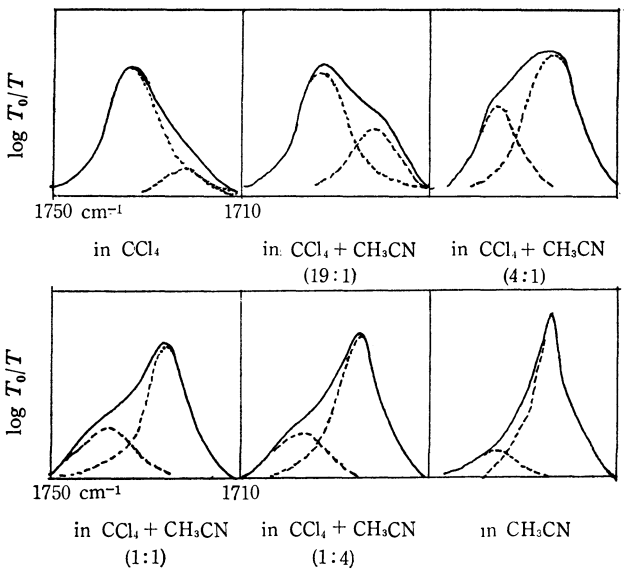

Fig. 4. Effect of solvent on the C=O stretching absorption of *t*-butyl acetate.

7) a) H. W. Thompson and P. Torkington, *J. Chem. Soc.*, **1945**, 640. b) E. J. Hartwell, R. E. Richards, and H. W. Thompson, *ibid.*, **1948**, 1436. c) G. M. Barrow, *J. Chem. Phys.*, **21**, 2008 (1953). d) D. G. I. Felton and S. F. D. Orr, *J. Chem. Soc.*, **1955**, 2170. e) T. L. Brown, *J. Amer. Chem. Soc.*, **80**, 3513 (1958). f) L. J. Bellamy and R. L. Williams, *Trans. Faraday Soc.*, **55**,14(1959). g) A. R. Katritzky, J. M. Lagowski, and J. A. T. Beard, *Spectrochim. Acta*, **16**, 964 (1960). h) H. A. Ory, *Anal. Chem.*, **32**, 509 (1960). i) K. Bowden, N. B. Chapman, and J. Shorter, *Can. J. Chem.*, **41**, 2154 (1963). j) N. Mori, Y. Asano, and Y. Tsuzuki, This Bulletin, **41**, 1871 (1968).

8) K. J. Morgan and N. Unwin, *J. Chem. Soc., B*, **1968**, 880.

Table 2. Effect of solvent on ν_{CO} of *t*-butyl acetate (c=0.05 mol/l)

Solvent CCl_4 %	Solvent CH_3CN %	Band A cm^{-1} (ε)	Band B cm^{-1} (ε)	A/B
100	0	1738.4 (764)	1727 (314)	2.43
95	5	1736.4 (639)	1725 (340)	1.88
75	25	1739 (301)	1727 (620)	0.49
50	50	1737 (266)	1725.5 (698)	0.38
25	75	1735 (213)	1726 (678)	0.31
0	100	1738 (80)	1725.5 (599)	0.13

The results obtained with *t*-butyl acetate are shown in Fig. 4 and Table 2. Apparently, as the polarity of the mixed solvent increases, the absorption at higher wave number diminishes, whereas the absorption at lower wave number increases, in intensity.

The bifurcation of the carbonyl bands of the acetates which carry secondary or tertiary alkyl groups could be explained as resulting from any one of the following causes: 1) solute-solvent interaction, 2) solute-solute interaction, 3) equilibrium between *s-cis* and *s-trans* conformational isomers, and 4) Fermi resonance (including a fairly strong overtone or combination tone).

The first two possibilities may be ruled out for the following reasons: 1) The bifurcation of the carbonyl band in nonpolar solvents because, in these solvents, solute-solvent interactions are negligibly samll. 2) It is very difficult to explain, from the intermolecular interaction, why methyl and ethyl acetates show only one band, whereas secondary and tertiary alkyl acetates show two bands. 3) The concentration of the solution is so low that the intermolecular solute-solute interaction is hardly possible. 4) *t*-Butyl acetate gives essentially the same absorption curves at 0.5, 5, and 50 mmol/l concentration.

If the populations of the rotational isomers change according to the polarity of the solvents, this change must be reflected in the skeletal vibrations. Thus, the infrared spectra of *t*-butyl acetate at lower frequencies (1100—400 cm^{-1}) were recorded in the range of 23°C and −150°C, the three phases being covered by this technique. The results are shown in Figs. 5 and 6. No clear change in the absorptions could be found.

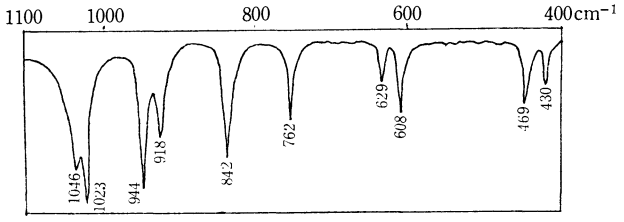

Fig. 5. Infrared spectra of *t*-butyl acetate in the range of 1100—400 cm^{-1} in liquid state.

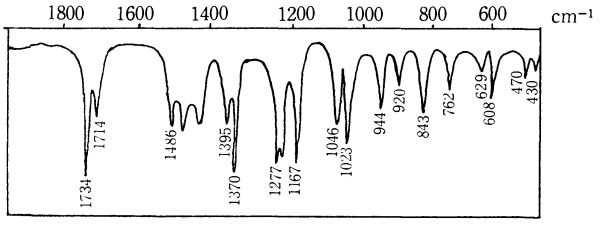

Fig. 6. Infrared spectra of solid state *t*-butyl acetate at lower temperature.

The *s-cis* conformer of the ester is considered to be more polar than the *s-trans*, because the arrangement of bond dipoles implies the more polar nature and because the calculated dipole moments, calculated using the usual C–O and C=O bond dipoles, are 3.40 and 1.53D for the *s-cis* and *s-trans* conformers respectively. These considerations necessarily mean that the population of the *s-cis* conformer will become denser in a polar solvent relative to a non-polar solvent. Thus, the infrared spectra in 1100—400 cm^{-1} region were again scanned with solutions made by dissolving *t*-butyl acetate in solvents of various polarities (CS_2, $CHCl_3$, CH_3CN, DMSO, and $HCONMe_2$). The results showed essentially no change in the spectra, the one exception being a band at 918 cm^{-1} which became stronger in polar solvents.

Since the *s-cis* conformer of the formates is known to give an absorption at a higher frequency than the *s-trans* in the carbonyl-stretching absorption region, and since this arrangement agrees with the consideration of intramolecular dipolar interactions, it is natural to assume that it is the *s-cis* conformer of the acetate which gives rise to an absorption at a higher frequency. However, this consideration leads to a conclusion which is the reverse of actuality: namely, the absorption band which is enhanced in polar solvents is the one located at the lower frequency (see Fig. 4).

All these discussions favor the absence of the *s-cis* conformer of the acetates.[9] Thus, the third possibility may be disregarded also.

Further support for ruling out the possibility of conformational heterogeneity as being the reason for the bifurcation of the carbonyl band could be obtained by studying the overtone region of the carbonyl stretching. Thus, the infrared spectrum of *t*-butyl acetate in the region of 3600—3400 cm^{-1} was carefully recorded. It was made clear that *t*-butyl acetate has only one symmetrical sbsorption, at 3447.6 cm^{-1} (ε=4.00), in carbon tetrachloride at the low concentration of 0.01 mol/l. This result suggests that the most probable cause of the

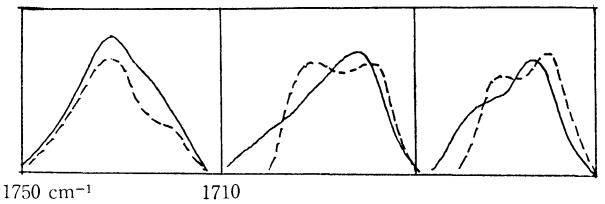

in CCl_4 (c=0.0005 mol/l) in CH_3CN (c=0.05 mol/l) in DMSO (c=0.05 mol/l)

Fig. 7. Infrared spectra of ν_{CO} of *t*-butyl acetate and *t*-butyl acetate-d_3.
—— line: CH_3CO_2t-Bu
---- line: CD_3CO_2t-Bu

9) Morgan and Unwin[8] recently suggested that the *s-cis* conformer might be present in isopropyl and *t*-butyl acatetes, judging from the abnormal solvent effect on the carbonyl-stretching vibration in the infrared spectra. However, since their discussion assumed that these compounds show only one carbonyl absorption, their results must be reinvestigated in the light of the fact reported above.

Table 3. Infrared spectra absorptions of lower region of alkyl acetates (in CS_2)

I CH_3CO_2Me	II CH_3CO_2Et	V CH_3CO_2i-Pr	VIII CH_3CO_2t-Bu	IX CD_3CO_2t-Bu	X CH_3CO_2t-Am
1247 (s)		1240 (s)	1277 (s)	1274 (s)	1253 (s)
1180 (w)		1066 (s)	1255 (s)	1260 (s)	1204 (m)
1156 (w)		1049 (s)	1174 (s)	1165 (s)	1158 (s)
1049 (s)	1097 (s)	1026 (s)	1046 (m)	1108 (m)	1140 (s)
981 (m)	1040 (s)	970 (m)	1023 (s)	1079 (m)	1066 (m)
846 (m)	1003 (m)	909 (m)	944 (m)	1035 (m)	1051 (s)
639 (m)	938 (m)	897 (m)	918 (m)	901 (m)	1018 (m)
604 (m)	914 (m)	856 (m)	842 (s)	875 (m)	950 (m)
431 (m)	846 (m)	777 (m)	762 (m)	825 (s)	940 (s)
	787 (m)	651 (s)	629 (s)	757 (m)	926 (s)
	635 (m)	625 (s)	608 (m)	728 (m)	830 (m)
	609 (m)	503 (s)	467 (m)	666 (s)	784 (s)
	463 (m)		430 (s)	614 (s)	750 (s)
	440 (m)			564 (s)	747 (s)
				536 (s)	625 (s)
				442 (s)	609 (s)
					505 (s)
					460 (s)

s=strong, m=medium, w=weak

bifurcation of the carbonyl band is not the confromational heterogeneity, but the overtone or combination tone, which is enhanced by Fermi resonance.

After establishing the origin of the bifurcation of the carbonyl band of some acetates, it seemed that it would be interesting to know what kind of vibration is responsible for the Fermi resonance. Thus, the deuteration of the acetyl methyl of *t*-butyl acetate was carried out and the infrared spectra were measured. The reason for this deuteration was the fact that there are numerous examples of carbonyl compounds which show Fermi resonance in the carbonyl region attributed to the resonance between the carbonyl fundamental and the overtone of the α C–H deformations.[10-14] The results with *t*-butyl acetate-d_3 are shown in Fig. 7, together with the curves of undeuterated samples for the sake of comparison. As may be seen in Fig. 7 and also in Table 1, *t*-butyl acetate-d_3 also has two absorptions in the carbonyl region in both polar and nonpolar solvents, this behavior being similar to that of the nondeuterated specimen; the only difference between the deuterated and nondeuterated compounds is the fact that the former always give a somewhat stronger band on the higher-frequency side. Thus, it is unlikely that any of the vibrational modes involving hydrogen is responsible for the Fermi resonance.

The infrared spectra of some acetates in carbon disulfide at the lower frequencies are given in Table 3. The skeletal vibrations are expected to be sensitive to the mass of R in CH_3CO_2R; the results shown in Table 3 conform with this expectation. Nevertheless, all the secondary and tertiary alkyl acetates studied so far give rise to a bifurcated band. Thus, we prefer that a common band at 1280—1240 cm^{-1}, which may be assigned to the antisymmetric stretching mode of the C–O–C of the esters, be chosen as one of the origins for the bifurcation in the carbonyl region. Then another band which is responsible for this phenomenon should be found at *ca.* 460 cm^{-1}. Indeed, we can see that those substances which give two bands in the carbonyl region have a fairly strong absorption at 505—430 cm^{-1}, although the assignment of these bands is still obscure. Thus, it can tentatively be concluded that the bifurcation of the carbonyl bands of some acetates can be attributed to the Fermi resonance between the carbonyl fundamental and a combination tone arising from the antisymmetric C–O–C stretching mode and an unknown mode of vibration which gives absorption at 505—430 cm^{-1}.

Nuclear Magnetic Resonance Spectra. The proton magnetic resonance spectra of *t*-butyl acetate in a mixed solvent of carbon disulfide and dichloromethane were measured at various temperatures. The *t*-butyl and acetyl methyl signals appear at 1.40 and 3.07 ppm downward from TMS at room temperature. The chemical shifts are almost the same at −50, −70, and −95°C. No sign of a decrease in the peak heights of these peaks is found as the temperature is lowered.[15] Thus, the results conform with those obtained by the infrared spectral study in that the conformational heterogeneity is not observed with *t*-butyl acetate.

The authors wish to express their hearty thanks to Professor T. Shimanouchi and S. Ichikawa for their helpful discussions.

10) a) R. N. Jones, C. L. Angell, T. Ito, and R. J. D.Smith, *Can. J. Chem.*, **37**, 2007 (1959). b) R. N. Jones and B. S. Gallagher, *J. Amer. Chem. Soc.*, **81**, 5242 (1959).

11) C. L. Angell, P. J. Krueger, R. Lauzon, L. C. Leitch, K. Koack, R. J. D. Smith, and R. N. Jones, *Spectrochim. Acta*, **1959**, 926.

12) R. P. M. Bond, T. Cairns, J. D. Connolly, G. Eglinton, and K. H. Overton, *J. Chem. Soc.*, **1965**, 3958.

13) P. Yates and L. L. Williams, *J. Amer. Chem. Soc.*, **80**, 5896 (1958).

14) L. J. Bellamy and R. L. Williams, *Trans. Faraday Soc.*, **55**, (1959).

15) Lojo *et al.* measured the NMR spectra of methyl acetate in the range of 120°——40°C and found no outstanding change. O. R. Lojo, C. K. Hancock, and A. Danti, *J. Org. Chem.*, **31**, 1899 (1966).

Conformations of the Esters. IV. The Conformations of Carbamates

Michinori Ōki and Hiroshi Nakanishi

Department of Chemistry, Faculty of Science, The University of Tokyo, Hongo, Bunkyo-ku, Tokyo

(Received May 13, 1971)

It has been confirmed from an infrared spectral study of the C=O, N–H, and N–D stretching regions that primary, secondary, and tertiary carbamates take the *s-cis* and *s-trans* conformations with respect to the ester group. The nuclear magnetic resonance spectra and the results of dipole-moment studies support this conclusion.

The conformation of the ester has long been claimed to be *s-trans*, and the conformation of carbamates has been reported to be no exception (Fig. 1). Van der

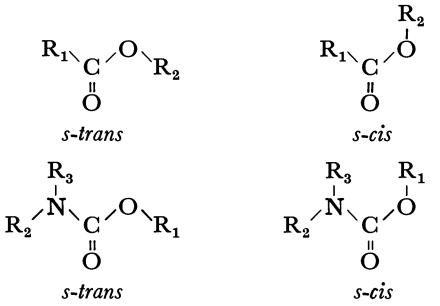

Fig. 1. The conformations of ester and carbamate.

Werf reported[1] two conformations of the ester group in methyl *N*-methyl-*N*-alkylsulfonylcarbamates, but this conclusion has since been proved by NMR study to be not the case.[2] Since we have recently shown that the *s-cis* conformation can exist in some formates,[3] the search for the *s-cis* conformation in carbamates has been undertaken as an extention. The purpose of this paper is to present the results of such a study using infrared and nuclear magnetic resonance spectral techniques and dipole-moment measurements.

Experimental

Materials. The simple carbamates were prepared by the reaction of methyl chloroformate or ethyl chloroformate with aqueous or neat amine with cooling. Methyl *N*-phenylcarbamate was prepared by refluxing a mixture of aniline and methyl chlorofomate in chloroform for an hour. Methyl *N*-deuterio-*N*-methylcarbamate ($MeNDCO_2Me$) was prepared by mixing methyl *N*-methylcarbamate with thirty molar deuterium oxide overnight at room temperature and by subsequent distilling under nitrogen. The physical constants of the compounds used in this study agree with those previously reported in the literature. The purity of the compounds was checked by studying their infrared and nuclear magnetic resonance spectra.

Apparatus. The infrared spectra were measured by using a Perkin Elmer 112G single-beam grating spectrometer (3600—3300 cm^{-1}, 2700—2400 cm^{-1}, 1800—1650 cm^{-1}) and a Hitachi EPI-G2 grating infrared spectrophotometer (4000—400 cm^{-1}). The nuclear magnetic resonance spectra were recorded on a JNM-4H-100 spectrometer. The dipole moment was obtained by the solution method, using benzene as the solvent. The dielectric constant (ε) was measured by the heterodyne-beat method. The electronic polarizations (P_E) were computed from the table of bond refraction, and the atomic polarization (P_A) was taken as 5% of the electronic polarization. The values of the observed dipole moment include an inaccuracy of ± 0.02D.

Results and Discussion

In disussing the conformations of carbamates, two conformers (*s-cis* and *s-trans*) may be considered when the nitrogen atom carries two identical substituents (Ia, Ib, IIIa, and IIIb in Fig. 2), whereas it is necessary to take four conformations into account when the nitrogen of the carbamate carries non-identical substituents, as is exemplified by the secondary amides, IIa, IIb, IIc, and IId, in Fig. 2.

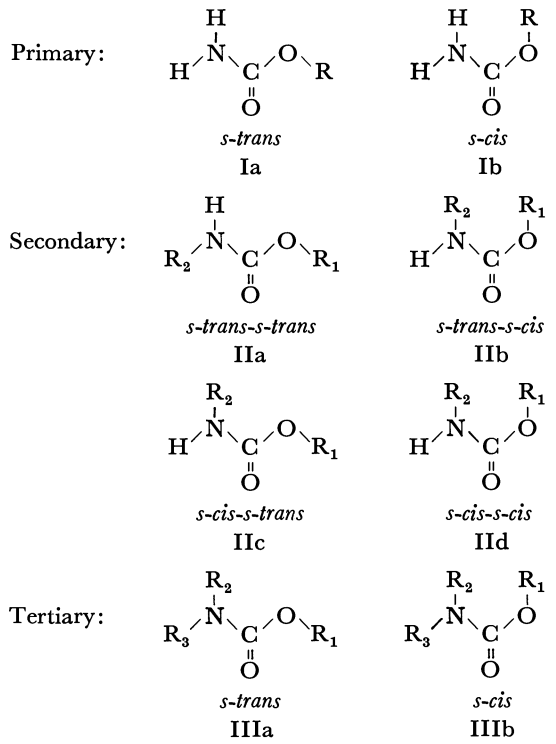

Fig. 2. The conformations of carbamate.

It is well known that the *s-trans* conformation is more stable than the *s-cis* in ordinary secondary amide. LaPlanche reported[4] that *N*-methylformamide (HCONHMe) has only an 8% *s-cis* conformer, and even *N*-*t*-butylformamide (HCONH*t*-Bu) has only a 12% *s-cis* conformer, although in the latter compound the

1) S. van der Werf, T. Olinjnma, and J. B. F. N. Engberts, *Tetrahedron Lett.*, **1967**, 689.
2) S. van der Werf and J. B. F. N. Engberts, *ibid.*, **1968**, 3311.
3) M. Ōki and H. Nakanishi, This Bulletin, **43**, 2558 (1970).
4) L. A. LaPlanche and M. T. Rogers, *J. Amer. Chem. Soc.*, **86**, 337 (1964).

Fig. 3. The conformations of secondary amide.

R_1 is hydrogen, which is sterically small, and the steric repulsion between H and the *t*-butyl group in the *s-cis* conformer is considered to be smaller than that between C=O and the *t*-butyl group in the *s-trans* (Fig. 3) (thus, the *s-cis* conformer is expected to form the majority).

On the other hand, *N*-methyl acetamide (MeCONHMe) exists as the *s-trans* conformer only,[5] probably because the repulsion between two methyl groups in the *s-cis* conformer is too large for the *s-cis* conformer to exist. Comparing the situation of the carbamate with that of the amide, the alkoxy group in carbamate is larger than the hydrogen of the formyl group in formamide. Therefore, the repulsion between R_2 and OR_1 in IIc and IId (Fig. 2) must be larger than that between formyl hydrogen and R_2 in formamide (Fig. 3. IVb, R=H). The dipole-dipole interaction between H–N and the C–OR_1 bond is more favorable for IIa than that for IIc as far as the conformations of the amide part are concerned (see below). These considerations lead to the conclusion that the ratio of the population of the *s-trans* conformer with respect to the amide part of this carbamate (IIa and IIb) to that of the *s-cis* conformers (IIc and IId) is probably larger in carbamates than in ordinary amides. Therefore, it may be expected that the existence of the IIc and IId conformers at least can be neglected.

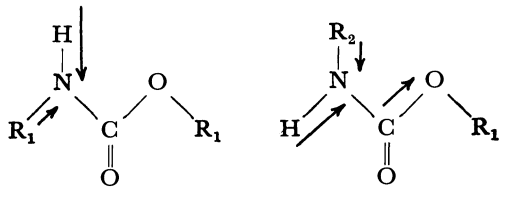

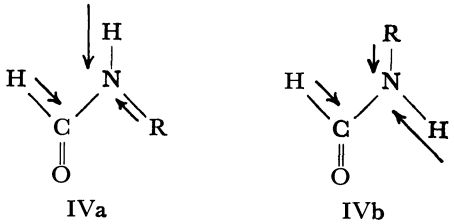

If both the *s-trans* and *s-cis* conformers of the amide group of carbamates should exist, two methyl peaks will appear in the NMR spectra of methyl *N*-methylcarbamate when the temperature of the measurement is lowered enough, because the rotation of the N–CO bond of the amide group has been reported to be slow enough for the NMR time scale.[6,7] For example, methyl *N,N*-dimethylcarbamate (Me_2NCO_2Me) has been reported to have two *N*-methyl peaks in the NMR spectra at temperatures lower than −13°C.[8] On the other hand, methyl *N*-methylcarbamate ($MeNHCO_2Me$) shows only one *N*-methyl peak from 23°C to −100°C at 2.86 ppm from TMS in the CS_2–CH_2Cl_2 solvent at 100 MHz. This fact may be taken as suggesting that the exchange between conformers is not taking place on the NMR time scale. From the standpoint of steric considerations, it may be assumed that the IIa conformation is the most stable. Therefore, the IIa conformation is most probably the one which exists as a sole isomer. It may be argued that the chemical shift between *N*-methyls of IIa and IIb is too small to be resolved at present. However, from the above considerations, together with the discussion of the infrared spectral data to be given below, such a case can be considered rare.

Table 1. Carbonyl absorptions of carbamates

	Compound	Solvent CCl_4 $c=0.0002$ mol/*l*		Solvent CH_3CN $c=0.005$ mol/*l*	
I	H_2NCO_2Me	1728cm^{-1}	(200)	1729cm^{-1}	(274)
		1751	(1293)	1742	(614)
II	H_2NCO_2Et	1742.1	(657)	1725	(73)
		broad		1731	(649)
III	$MeNHCO_2Me$	1736	(777)	1726.4	(861)
		1748	(81)		
IV	$EtNHCO_2Me$	1725	(200)	1714	(104)
		1735	(1189)	1724	(1100)
V	*i*-$PrNHCO_2Me$	1724	(200)	1712	(90)
		1732	(1885)	1722	(803)
VI	*t*-$BuNHCO_2Me$	1721	(190)	1715	(62)
		1737	(1695)	1726	(870)
VII	$MeNHCO_2Et$	1730	(638)	1710	(73)
		1740	(43)	1721	(838)
VIII	$PhNHCO_2Me$	1734	(73)	1722	(41)
		1748	(1007)	1735	(913)
IX	Me_2NCO_2Me	1711	(1333)	1696	(99)
		1720	(93)	1705	(1147)
X	Et_2NCO_2Me	1696	(147)	1698	(1251)
		1706	(1140)		
XI	Me_2NCO_2Et	1706	(961)	1696	(970)

Infrared Spectra of Carbonyl-stretching Vibration. It is natural to anticipate that the *s-trans* and *s-cis* conformers of carbamates will have different carbonyl absorptions in their infrared spectra. Some authors have reported,[9–12] on the carbonyl absorption of carbamates, but no one has reported the observation of two carbonyl absorptions. Using a high-resolution infrared spectrophotometer, the carbonyl absorptions of

5) a) S. Mizushima, K. Kuratani, M. Tsuboi, H. Baba, and O. Fujioka, *J. Amer. Chem. Soc.*, **72**, 3490 (1950). b) I. Suzuki, This Bulletin, **35**, 540 (1962).

6) L. C. Breliere and J. M. Lehn, *Chem. Commun.*, **1965**, 426.

7) B. J. Price, R. V. Smallman, and I. O. Sutherland, *ibid.*, **1966**, 319.

8) E. Lustig, W. R. Benson, and N. Duy, *J. Org. Chem.*, **32**, 851 (1967).

9) S. Pinchas and D. Ben-Ishai, *J. Amer. Chem. Soc.*, **79**, 4099 (1957).

10) A. R. Katritzky and R. A. Jones, *J. Chem. Soc.*, **1960**, 676.

11) M. Sato, *J. Org. Chem.*, **26**, 770 (1961).

12) R. A. Nyquist, *Spectrochim. Acta*, **19**, 509 (1963).

several methyl and ethyl carbamates were measured in carbon tetrachloride and acetonitrile. The results are shown in Table 1. It is apparent that almost all the primary (I, II), secondary (III—VIII), and tertiary (IX, X) carbamates have two carbonyl absorptions in both nonpolar and polar solvents. Since the concentrations of the measurement are dilute enough to exclude the solute association, this bifurcation of the absorptions can be said not to be due to the association effect. The intensity of the higher frequency absorption is stronger than that of the lower one in these two solvents with most compounds; compounds III, VII, and IX are exceptions. It is well known[13] that, in may cases of Fermi resonance, the intensities of bifurcated carbonyl absorption bands change dramatically when the polarity of the solvent is changed. In this case, however, the solvent effect is not so strong (except for III, VII, and IX). Therefore, Fermi resonance may not be the origin of the bifuraction of the carbonyl absorptions in the carbamates. Thus, it is most probable to assume that the existence of conformational isomers is the real origin of this bifurcation of carbonyl absorptions. As the calculated dipole moment values (as will be described later) of the *s-cis* conformer, IIb, are larger than those of the *s-trans* conformer, IIa, the population ratio of IIb to IIa can be expected to increase in polar solvents such as acetonitrile in comparison with in nonpolar carbon tetrachloride, as is the case of formates.[2] However, the solvent effect has been found to be very small in reality on the carbonyl absorptions of carbamates. The higher wave number band can be assigned to the *s-cis* conformer (Ib, IIb, and IIIb) and the lower one, to the *s-trans*, because the direction of the two dipoles of C=O and O–R is parallel in the *s-cis* conformer and is roughly antiparallel in the *s-trans* (Fig. 4); the latter necessitates less energy for stretching the carbonyl bond. Table 1 shows that the higher wave number band is stronger than the lower one in primary and secondary carbamates. This may be taken as evidence for the concept that, in these compounds, the *s-cis* conformer of carbamates with respect to the ester group is more stable than the *s-trans*.

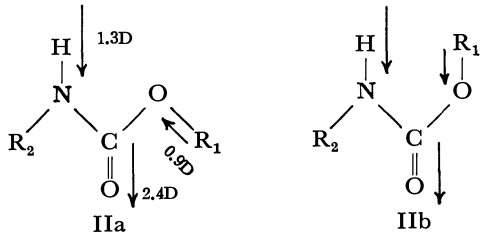

Fig. 4. The directions of the bond dipoles of carbamates.

Infrared Spectra of the N–H and N–D Stretching Vibrations and the First Overtone Band of the Carbonyl Absorption.

In order to obtain more information about the conformations of carbamates, the N–H stretching vibration absorptions in the infrared spectra were measured. The results are shown in Table 2. It is well known that

13) M. Ōki and H. Nakanishi, Part II. This Bulletin, **44**, 3144 (1971), and the references cited therein.

Table 2. ν_{NH} of carbamates

	Compound	Solvent CCl_4 $c=0.0003$ mol/l		$2\nu_{CO}$
I	H_2NCO_2Me	3433cm^{-1}	(30)	3456cm^{-1}
		3444	(96)	3502
		3537	(33)	
		3558	(117)	
II	H_2NCO_2Et	3432	(34)	3484
		3443	(130)	
		3542	(41)	
		3559	(129)	
III	$MeNHCO_2Me$	3468	(24)	3472
		3476	(213)	3496
IV	$EtNHCO_2Me$	3462	(219)	3451
				3471
V	i-$PrNHCO_2Me$	3444	(18)	3448
		3452	(159)	3463
VI	t-$BuNHCO_2Me$	3445	(17)	3442
		3451	(201)	3473
VII	$MeNHCO_2Et$	3468	(21)	3460
		3476	(188)	3480
VIII	$PhNHCO_2Me$	3438	(19)	3468
		3447	(249)	3496

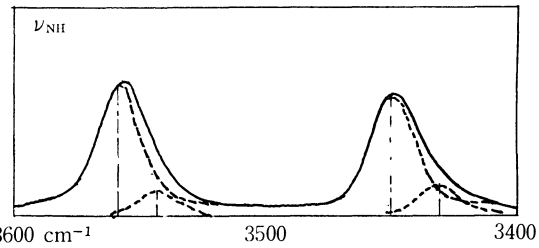

Fig. 5. Infrared spectra of ν_{NH} of methyl carbamate(H_2NCO_2-Me).

the primary amide has two N–H stretching vibration absorptions, an antisymmetrical stretching mode at about 3550 cm^{-1} and a symmetrical one at about 3450 cm^{-1}. Compounds I and II have four bands; both anitsymmetric and symmetric N–H stretching vibration bands are bifurcated. Secondary carbamates (III—VIII) have two N–H stretching vibration bands. In this region of 3600—3400 cm^{-1}, the first overtone of the carbonyl stretching vibration may appear. Therefore, the values of 2 ν_{CO} are listed in the last column of Table 2. Indeed, for example, the first overtone of the fundamental carbonyl absorptions of compound VIII appear at 3459 cm^{-1} (ε=4.2) and 3487 cm^{-1} (ε=5.1), but the intensity is much weaker than that of the fundamental tones. Generally speaking, the molecular extinction coefficient of the first overtone of carbonyl bands of carbamates is less than *ca.* 7. Since the intensities of the weaker bands in compounds I—VIII lie in the range of 41—17 (ε), the possibility of these weaker bands being the first overtones of carbonyl stretching absorptions is very small.

Further support for this assignment may be obtained by avoiding the influence of the overtone of carbonyl absorptions. Thus, the infrared spectra of the N–D stretching vibration were measured. Methyl *N*-deuterio-*N*-methylcarbamate ($MeNDCO_2Me$) shows also

two absorptions, at 2571 cm^{-1} (ε=16) and 2578 cm^{-1} (ε=71), at the low concentration of c=0.0007 mol/l in carbon tetrachloride. This fact can most easily be explained assuming the existence of two conformational isomers.

In Table 2 the difference in the location between the higher and the lower N–H stretching absorptions in wave numbers is about 10 cm^{-1}. On the other hand, it has been reported[14] that the difference in the N–H stretching vibration of the *s-trans* and *s-cis* conformers of amide is about 30—40 cm^{-1}. Therefore, this small difference in the locations of the two absorptions may be taken as indicating that, in secondary carbamates, the conformers with respect to the amide group (IIc and IId) do not exist; this conclusion is in agreement with the NMR results. These small wave-number differences may be attributed to several factors, including the dipole-dipole interaction between H–N and R_1–O bonds through a somewhat long distance (*cf.* Fig. 4). By analogy with the considerations used in the assignment of the carbonyl absorptions, the directions of the two dipoles (H–N, R_1–O) in the *s-cis* conformer (Ib or IIb) probably give rise to the absorption of the N–H stretching at the higher wave number; therefore, the lower one must be assigned to the *s-trans* conformer (Ia or IIa). The intensity of the higher band is stronger than the lower band (Table 2); from these N–H stretching band studies, also, it is confirmed that the *s-cis* conformer (Ib or IIb) is more stable than the *s-trans* conformer (Ia or IIa). The results of the infrared study of N–H and N–D stretching vibration absorptions apparently shows that compound III has two conformations and that the *s-cis* conformer is more stable than the *s-trans*. The abnormality of the carbonyl bands of this compound, that is, the fact that it gives a stronger absorption at lower wave number, may be attributed to the Fermi resonance. The same may also be said about compound VII.

As to the tertiary carbamates, IX, X, and XI, the carbonyl absorptions are complicated. The intensity ratio of the two bands is reversed in compounds IX and X, and compound XI has only one symmetrical band in these two solvents. In order to know more about the conformation of tertiary carbamates, the first overtone spectra of compounds IX and X were measured. Compound IX has only one peak, at 3407.1 cm^{-1} (ε=8.18), and compound X has two peaks, at 3360 cm^{-1} (ε=0.23) and at 3393 cm^{-1} (ε=3.42), at the concentration of 0.013 mol/l in carbon tetrachloride. These results may mean that the Fermi resonance is one of the factors causing the complication of the spectra at the carbonyl region, but it is impossible to draw a solid conclusion without reservation at the present time.

Dipole Moment. The dipole-moment values of methyl *N,N*-dimethylcarbamate (IX) are found to be 2.55D at 16°C and 2.59D at 31°C in a benzene solution. The calculated dipole moment values are 1.38D for the *s-trans* with respect to the ester group and 3.48D for the *s-cis* (bond moment: C=O: 2.4D,C–H: 0.4D, C–N:0.4D, C–O: 0.9D). This calculation was made assuming that these conformations are all on one plane, but the O–Me group may be considered to be out of the plane of the amide group because of the steric repulsion between *N*-methyl and *O*-methyl groups. Since the error is estimated to be ±0.02D, these results may be taken as indicating that the *s-cis* conformer is more stable than the *s-trans* conformer in this compound.

Nuclear Magnetic Resonance Spectra. To obtain information about the conformations of carbamates, the nuclear magnetic resonance spectra of methyl *N*-methylcabamate ($MeNHCO_2Me$) were measured from 23°C to −100°C in the CS_2–CH_2Cl_2 solvent. Only at about −100°C the peak of the methoxy methyl group began to broaden, while the peak of the *N*-methyl group was almost unchanged throughout this temperature range. These phenomena may be taken as further evidence for the existence of the conformational equilibrium of the ester group in this carbamate.

From the infrared and nuclear magnetic resonance spectra and the dipole-moment study, it can be concluded that, in primary and secondary carbamates, two conformers with respect to the ester group exist and the *s-cis* conformer is more stable than the *s-trans*, and that the same may be true in tertiary carbamates. Judging from the steric effect, this fact is very surprising, particularly in connection with the tertiary carbamate, for in these compounds the steric repulsion between *N*-alkyl and *O*-alkyl groups is expected to be large. This phenomenon may be explained partially by two factors; the first is the stabilization of the *s-cis* conformation due to C–N and O–R_1 bond dipolar interaction, and the second is the destabilization of the *s-trans* conformation due to the repulsion between the lone-pair electrons of ether-oxygen and nitrogen (the so-called "Rabbit Ear"; *cf.* E. L. Eliel (Fig. 6)[15] in heterocyclic compounds.).

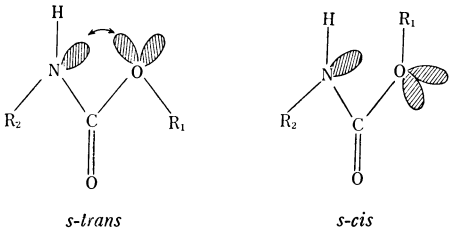

s-trans *s-cis*

Fig. 6. "Rabbit Ear" effect in carbamate.

14) a) V. R. A. Russel and H. W. Thompson, *Spectrochim. Acta*, **8**, 138 (1956). b) R. L. Jones, *J. Mol. Spectry.*, **11**, 411 (1963).

15) a) R. O. Hutchins, L. D. Kopp, and E. L. Eliel, *J. Amer. Chem. Soc.*, **90**, 7174 (1968). b) E. L. Eliel, *Kemisk. Tidskrift*, (1969), No. 6—7, 22.

Aromatic Arylation with Aryl Radicals. III. Gomberg Reaction in Dimethyl Sulfoxide

Nobumasa KAMIGATA, Teruyoshi KURIHARA, Hiroshi MINATO, and Michio KOBAYASHI

Department of Chemistry, Faculty of Science, Tokyo Metropolitan University, Fukazawa, Setagaya, Tokyo

(Received May 18, 1971)

Benzenediazonium tetrafluoroborate in dimethyl sulfoxide decomposed instantaneously with evolution of nitrogen upon addition of a dimethyl sulfoxide solution of choline or tetramethylammonium hydroxide. Orientations and partial rate factors for the phenylation of substituted benzenes indicated that the phenylating agent is not phenyl cation but phenyl radical. Hammett's plots of partial rate factors for *meta* and *para* substitutions were good straight lines with $\rho_m=0.34$, $\rho_p=1.63$ (in choline) and $\rho_m=0.48$, $\rho_p=1.69$ (in tetramethylammonium hydroxide solutions). Decomposition of benzenediazonium tetrafluoroborate by tetramethylammonium hydroxide in aqueous solution was also studied, and the orientation and partial rate factors for the phenylation of substituted benzenes were determined.

Arenediazonium salts decompose with evolution of nitrogen in aprotic polar solvents, and phenyl cation is considered to be the intermediate on the basis of the kinetic studies[1] and the partial rate factors for the competitive arylation of benzene and substituted benzenes.[2]

$$ArN_2^+ \longrightarrow Ar^+ + N_2 \quad (1)$$

However, it has been reproted that arenediazonium salts undergo homolytic decomposition in methanol[3] or pyridine.[4]

$$ArN_2^+ + CH_3O^- \longrightarrow Ar\text{-}N{=}N\text{-}OCH_3 \longrightarrow Ar\cdot + N_2 + \cdot OCH_3 \quad (2)$$

or

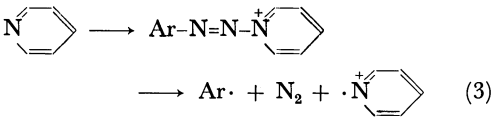

When an arenediazonium solution was added to a dimethyl sulfoxide solution of sodium nitrite, the diazonium salt decomposed instantaneously with evolution of nitrogen, and a homolytic decomposition mechanism was proposed.[5]

$$ArN_2^+ + NO_2^- \longrightarrow Ar\text{-}N{=}N\text{-}O\text{-}N{=}O \longrightarrow Ar\cdot + N_2 + NO_2 \quad (4)$$

or

$$2Ar\text{-}N{=}N\text{-}O\text{-}N{=}O \longrightarrow Ar\text{-}N{=}N\text{-}O\text{-}N{=}N\text{-}Ar + N_2O_3 \longrightarrow Ar\cdot + N_2 + Ar\text{-}N{=}N\text{-}O\cdot \quad (5)$$

As a continuation of our investigations on the decomposition of arenediazonium salts in aprotic polar solvents, addition of quaternary ammonium hydroxide to diazonium salts has been studied. It has been found that a reaction similar to the Gomberg reaction has taken place. With quaternary ammonium hydroxides the medium is homogeneous, whereas the ordinary Gomberg reactions are carried out in heterogeneous mixtures of water and aromatics.

In this paper, the results of this investigation will be described, and the evidence for the homolytic decomposition will be presented.

Experimental

Materials. Dimethyl sulfoxide was purified according to the method described in a previous paper.[1b] Benzene, ethylbenzene, and chlorobenzene were washed with concentrated sulfuric acid and water successively, dried over calcium chloride, and distilled. Boiling points were 80, 135.7, and 131°C, respectively. Anisole was washed with an aqueous sodium hydroxide solution and water, dried over calcium chloride, and distilled; bp 153°C. Benzonitrile was purified by steam distillation. The distillate was washed with sodium carbonate solution and water, dried over calcium chloride, and distilled under reduced pressure; bp 123.4°C/100 mmHg. Nitrobenzene was washed repeatedly with a potassium dichromate solution, dried over calcium chloride, and distilled; bp 95.5°C/18 mmHg. Choline of Tokyo Kasei Limited was used without further purification. A 20% methanolic solution of tetramethylammonium hydroxide obtained from Aldrich Chemical Co., Inc. was evaporated under reduced pressure, and the residue was used.

Benzenediazonium tetrafluoroborate was prepared according to the directions described previously.[6]

Isomeric ethylbiphenyls, methoxybiphenyls, chlorobiphenyls, cyanobiphenyls, and nitrobiphenyls were prepared as the reference compounds by the methods described in the literature.[7] They were purified by elution chromatography, distillation or recrystallization, and their melting points and boiling points agreed with the values in the literature.

Phenylation of Monosubstituted Benzenes in DMSO. Under a nitrogen atmosphere a solution of 2.00 g of benzenediazonium tetrafluoroborate in 20 g of DMSO was added

1) a) E. S. Lewis, *J. Amer. Chem. Soc.*, **80**, 1371 (1958); b) K. Ishida, N. Kobori, M. Kobayashi, and H. Minato, This Bulletin, **43**, 285 (1970).

2) a) R. A. Abramovitch and F. F. Gadallah, *J. Chem. Soc., B*, **1968**, 497; b) M. Kobayashi, H. Minato, E. Yamada, and N. Kobori, This Bulletin, **43**, 215 (1970).

3) D. F. DeTar and M. N. Turetzky, *J. Amer. Chem. Soc.*, **77**, 1745 (1955); **78**, 3925 (1956).

4) R. A. Abramovitch and J. G. Saha, *Tetrahedron*, **21**, 3297 (1965).

5) M. Kobayashi, H. Minato, N. Kobori, and E. Yamada, This Bulletin, **43**, 1131 (1970).

6) E. B. Starkey, "Organic Syntheses," Coll. Vol. 2, p. 225 (1943).

7) R. Adams, "Organic Reactions," Vol. II., John Wiley & Sons, Inc., London (1957); P. E. Fanta, *Chem. Rev.*, **64**, 613 (1954).

drop by drop at 20°C into a vigorously stirred solution of choline or tetramethylammonium hydroxide (3 mol/mol of PhN_2BF_4) and equimolar mixture of benzene and a substituted benzene (total aromatics, 50 mol/mol of PhN_2BF_4) in 60 g of DMSO. Evolution of nitrogen was instantaneous upon addition of each drop of the diazonium salt solution, and the addition was completed in about ten minutes. Ether was added to the solution, and the mixture was washed with water in order to remove DMSO and excess quaternary ammonium hydroxide. After it was dried over anhydrous magnesium sulfate, ether and about 70% of the aromatic solvents were evaporated, and biphenyl isomers in the residue were analyzed by gas chromatography with a Hitachi Gas Chromatograph K-53. Biphenyl isomers were identified by comparison of the retention times with those of the authentic samples on a 1 m to 6 m column (depending upon the ease of separation) packed with Chromosorb W (10% Apiezon L). Quantitative determinations were made by use of calibration curves.

Not benzene but chlorobenzene was used as the standard for the competitive phenylation, since unsubstituted biphenyl easily sublimes during the evaporation of substituted benzenes. The reactivity of each position of substituted benzenes was calculated relative to the reactivity of the *ortho* position of chlorobenzene. The partial rate factor of the *ortho* position of chlorobenzene was determined by a competitive phenylation of benzene and chlorobenzene without evaporation of the unchanged aromatics. The partial rate factors of various substituted benzenes were calculated by the following equation.

$$k_x/k = (k_x/k_{o\text{-Cl}}) \times (k_{o\ Cl}/k)$$

where,

k_x/k: partial rate factor for phenylation of PhX at the x (*o*-, *m*-, or *p*-) position

$k_x/k_{o\text{-Cl}}$: relative rate of phenylation at the x position of PhX against that of the *ortho* position of chlorobenzene

$k_{o\text{-Cl}}/k$: partial rate factor for phenylation at the *ortho* position of chlorobenzene

Phenylation of Monosubstituted Benzenes in Water. Under a nitrogen atmosphere a solution of 2.20 g of benzenediazonium tetrafluoroborate in 35 g of water was added drop by drop at 20°C into a vigorously stirred solution of tetramethylammonium hydroxide (3 mol/mol of PhN_2BF_4) and equimolar mixture of benzene and a substituted benzene (total aromatics, 50 mol/mol of PhN_2BF_4) in 35 g of water. The reaction mixture was treated in a manner similar to that described above for the experiments in DMSO, and the product isomers were analyzed.

Results and Discussion

Benzenediazonium tetrafluoroborate in dimethyl sulfoxide (DMSO) decomposed instantaneously with evolution of nitrogen upon addition of a DMSO solution of choline ($HOCH_2CH_2(CH_3)_3N^+OH^-$) or tetramethylammonium hydroxide. Although the diazonium salts slowly decomposes even in the absence of these quaternary ammonium hydroxide, the rates of the first order decomposition yielding phenyl cation[2b] is much smaller than those observed in the presence of quaternary ammonium hydroxides. Therefore the mechanism of this rapid decomposition must be different from that involving phenyl cation. The difference of the mechanisms is also suggested by the absence of 1,3-benzoxathian in the products, which was always produced when phenyl cation was generated in DMSO.[2b]

Table 1. Orientation (%) and partial rate factors for the phenylation of PhX with PhN_2BF_4 in DMSO at 20°C

X in PhX	Additive	Orientation(%)			Partial Rate Factors		
		o-	*m*-	*p*-,	k_o/k	k_m/k	k_p/k
-OMe	A	62.7	24.2	13.1	3.21	1.23	1.33
	B	71.3	15.7	13.1	6.12	1.38	2.30
-Et	A	45.4	35.7	18.9	1.64	1.28	1.36
-Cl	A	55.9	24.2	19.9	3.69	1.60	2.63
	B	58.8	26.7	14.5	3.85	1.10	1.27
-CN	A	57.5	9.9	32.6	8.61	1.47	9.76
	B	67.2	11.3	21.5	18.8	3.51	12.0
$-NO_2$	A	59.8	6.7	33.5	16.6	1.87	18.7
	B	65.5	6.8	27.7	18.3	1.91	15.7

A: Choline=$HOCH_2CH_2(CH_3)_3N^+OH^-$
B: $(CH_3)_4N^+OH^-$

Table 1 shows the orientations and partial rate factors for the phenylation of substituted benzenes with benzenediazonium tetrafluoroborate and choline or tetramethylammonium hydroxide in DMSO. All the substituents behaved as *o,p*-directors, and the partial rate factors were always larger than 1. These data are similar to those of phenylation with phenyl radical produced from benzoyl peroxide[8] or *N*-nitrosoacetanilide[9] and quite different from those of phenylation with phenyl cation.[2,10] These findings indicate that the benzenediazonium salt reacts with quaternary ammonium hydroxide to produce phenyl radical.

It is likely that the following mechanism proposed by Rüchardt and Merz[11] for the Gomberg reaction is also

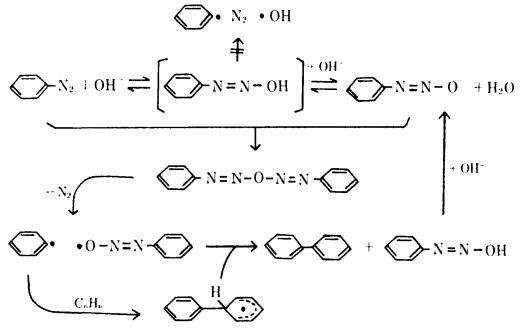

Table 2. Orientation (%) and partial rate factors for the phenylation of PhX with PhN_2BF_4 in the presence of $(CH_3)_4N^+OH^-$ in H_2O at 20°C

X in PhX	Orientation (%)			Partial rate factors		
	o-,	*m*-,	*p*-,	k_o/k	k_m/k	k_p/k
-OMe	70.5	18.8	10.7	4.36	1.14	1.31
-Et	53.3	28.1	18.6	1.69	0.90	1.17
-Cl	63.1	19.7	17.2	3.21	1.02	1.76
-CN	65.4	13.3	21.3	11.9	2.43	7.77
$-NO_2$	64.0	9.1	26.9	13.9	1.83	11.2

8) G. H. Williams, "Homolytic Aromatic Substitution," Pergamon Press, Oxford (1960), p. 73.
9) R. Ito, T. Migita, N. Morikawa, and O. Simamura, *Tetrahedron*, **21**, 955 (1965).
10) M. Kobayashi, H. Minato, and N. Kobori, This Bulletin, **43**, 219 (1970).
11) C. Rüchardt and E. Merz, *Tetrahedron Lett.*, **1964**, 2431.

TABLE 3. ρ_p VALUES[a] FOR THE PHENYLATION WITH PHENYL RADICALS

Exp. No.	Source of Ph·	Solvent	Temp. (°C)	H-Abstractor	ρ_p
1	PhN_2BF_4-$Me_4N^+OH^-$	Aromatics-DMSO	20	Ph-N=N-O·	1.69[b]
2	PhN_2BF_4-$NaNO_2$	Aromatics-DMSO	20	Ph-N=N-O· or NO_2	1.67[c]
3	PhN_2BF_4-Choline	Aromatics-DMSO	20	Ph-N=N-O·	1.63[b]
4	PhN_2BF_4-$Me_4N^+OH^-$	Aromatics-H_2O	20	Ph-N=N-O·	1.38[b]
5	PhN(NO)$COCH_3$	Aromatics	20	Ph-N=N-O· or Ph-N(-$COCH_3$)-O·	1.27[d]
6	$(PhCO_2)_2$	Aromatics	80	BPO or disproportionation	1.15[e]
7	PhN=N-CPh_3	Aromatics-DMSO	60	Ph_3C·	0.93[f]

a) ρ Values for the reaction reported in the literature were calculated by ploting the observed *para* partial rate factors against σ_p. b) this work, c) Ref. 5, d) Ref. 9, e) Ref. 8, f) to be published

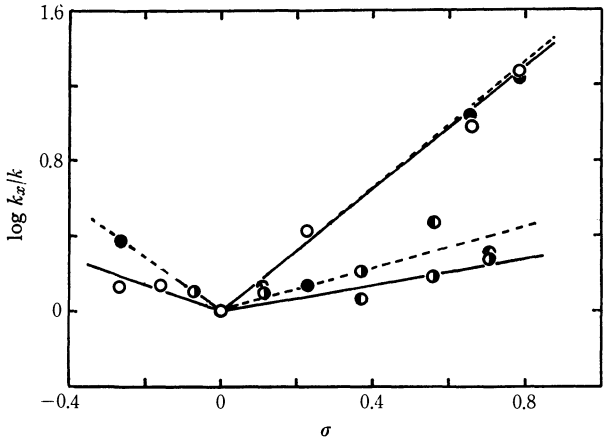

Fig. 1. The Hammett plots for the phenylation of PhX with PhN_2BF_4 in DMSO at 20°C.
—◑—◑— log k_m/k, ρ_m=0.34 } with choline
—○—○— log k_p/k, ρ_p=1.63 }
---◐---◐--- log k_m/k, ρ_m=0.48 } with $(CH_3)_4N^+OH^-$
---●---●--- log k_p/k, ρ_p=1.69 }

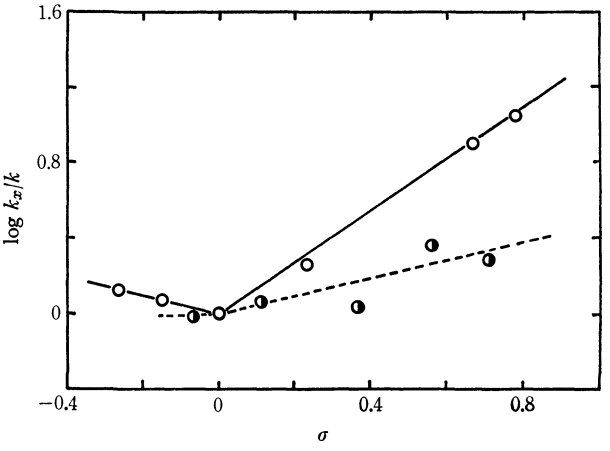

Fig. 2. The Hammett plots for the phenylation of PhX with PhN_2BF_4 in the presence of $(CH_3)_4N^+OH^-$ in H_2O.
---◑---◑--- log k_m/k, ρ_m=0.46
—○—○— log k_p/k, ρ_p=1.38

applicable to the homogeneous reaction between PhN_2^+-BF_4^- and $R_4N^+OH^-$ in DMSO.

Although the Gomberg reaction has been used extensively for synthetic purposes, the partial rate factors for phenylation of substituted benzenes by the Gomberg reaction have not been determined yet. Therefore, the partial rate factors and orientation were determined under the ordinary Gomberg reaction conditions (*i. e.*, heterogeneous mixtures of aromatics and water) using tetramethylammonium hydroxide as a strong base instead of sodium hydroxide commonly used. The results are shown in Table 2.

Figures 1 and 2 are the Hammett's plots of the partial rate factors of the *meta* and *para* positions. Satisfactory V-shape relationships are observed for *meta* and *para* data with ρ_m=0.34, ρ_p=1.63 (with choline, in DMSO), ρ_m=0.48, ρ_p=1.69 (with tetramethylammonium hydroxide, in DMSO) and ρ_m=0.46, ρ_p=1.38 (with tetramethylammonium hydroxide, in H_2O). The ρ values were calculated from the right half of the V-shape which contained larger number of experimental data than the left half.

Table 3 summarized the ρ_p values for the phenylation under various reaction conditions. It is interesting to compare the ρ_p values in Table 3. In PhN_2BF_4–$NaNO_2$, -Choline, and -Me_4NOH in DMSO, the ρ_p values are in the range of 1.63–1.69. The smaller ρ value (1.38) observed in PhN_2BF_4—Me_4NOH in H_2O may be ascribed to the change in solvents. In these four systems, the hydrogen abstractor is probably the same, *i.e.*, Ph–N=N–O·.

In three other systems listed in Table 3, the ρ_p values are much smaller. If the hydrogen abstractor in *N*-nitrosoacetanilide is Ph–N=N–O·, the smaller ρ_p value (1.27) compared with those in Expt. 1—3, must be ascribed to the difference in solvents. However, if the hydrogen abstractor in this system is Ph–N(–$COCH_3$)–O· as Chalfont and Perkins proposed,[12] the smaller ρ value can be ascribed to the difference in solvents and hydrogen abstractors.

In benzoyl peroxide and phenylazotriphenylmethane the temperatures are higher (80 and 60°C), and it is likely that reactions are less selective and ρ values are smaller at higher temperatures. The hydrogen abstractor in these systems are also different from those in Expts. 1—4.

Clear interpretation of these different ρ values, however, can be made only after more detailed studies are carried out.

12) C. R. Chalfont and M. J. Perkins, *J. Amer. Chem. Soc.*, **89**, 3054 (1967).

Syntheses and Reactions of 2-Ethylthio- or 2-Phenylthio-2-cycloalkenones

Teruaki MUKAIYAMA, Takeshi ADACHI, and Takanobu KUMAMOTO
Laboratory of Organic Chemistry, Tokyo Institute of Technology, Ookayama, Meguro-ku, Tokyo
(Received May 25, 1971)

2-Ethylthio- or 2-phenylthio-2-cycloalkenones (five-, six-, or seven-membered ring) were obtained in high yields by the reactions of alicyclic β-ketosulfonium salts with sulfenamides. It was found that dihydrofuran derivatives were obtained in good yields from the sulfonium salts of the cycloalkenones and active methylene compounds.

Recently we found that α-phenylthioacrylophenone was obtained in quantitative yield by the reaction of dimethyl-α-methylphenacyl sulfonium bromide with *N*, *N*-diethylbenzenesulfenamide.[1]

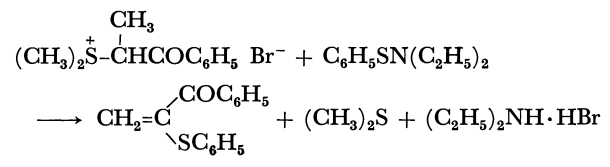

Scheme 1

This indicates that 2-alkylthio- or 2-arylthio-2-cycloalkenones, valuable synthetic intermediates, would be produced from alicyclic β-ketosulfonium salts and sulfenamides.

The preparation of alicyclic β-ketosulfonium salts and the reactions of the salts with sulfenamides were investigated. It is well-known that sulfonium salts are prepared by the reactions of alkyl halides with dimethyl sulfide. However, it was found that the reaction of 2-bromocycloalkanones such as 2-bromocyclohexanone with dimethyl sulfide afforded no corresponding sulfonium salts, except when the reaction was carried out in the presence of silver tetrafluoroborate.[2] Thus, the preparation of the sulfonium salts was attempted by the reactions of β-keto-sulfides with dimethyl sulfate or methyl *p*-tosylate.

When 2-ethylthiocyclohexanone was treated with dimethyl sulfate at room temperature for 1—2 days or with methyl tosylate at 75—85°C for 7—8 hr, the corresponding sulfonium salts were obtained in almost quantitative yields as viscous oil. In a similar way, cyclopentanone and cycloheptanone analogs were prepared in high yields.

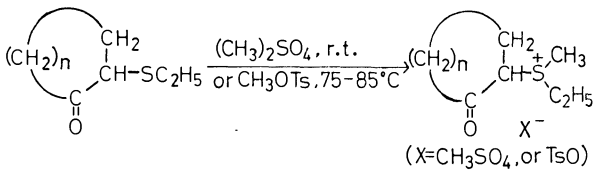

Scheme 2

The reactions of sulfonium salts (IIa—c) thus obtained with several sulfenamides were examined. When methylethyl-2-oxocyclohexylsulfonium tosylate (IIb′) was treated with *N*-phenylthiopyrrolidine[3] (sulfenamides of type *A* in Scheme III) in dichloromethane at room temperature for a day, 2-phenylthio-2-cyclohexenone (IVc) was obtained in 54% yield along with diphenyl disulfide (31%).

The result can be explained as follows. Sulfonium salt (IIb′) reacts with *N*-phenylthiopyrrolidine to afford α-sulfenylated intermediate (III) and pyrrolidine. III is in turn converted to IVc with the elimination of β-hydrogen atom and methyl ethyl sulfide by the influence of pyrrolidine produced at the same time. It was established that IVc was obtained in 78% yield by the reaction of IIb′ with *N*-phenylthiophthalimide (sulfenamides of type *B* in Scheme III) in the presence of triethylamine. These results indicate that sulfenamides of type *B* are preferable to those of type *A* for the synthesis of 2-alkylthio- or 2-arylthio-2-cycloalkenone. In a similar way, reactions of the five- or the seven-membered sulfonium salt with *N*-phenylthio- or *N*-ethylthiophthalimide gave the corresponding 2-phenylthio- or 2-ethylthio-2-cycloalkenones (IVa—f) in good yields (Tabel 1).

TABLE 1. SYNTHESES OF 2-ETHYLTHIO- OR 2-PHENYLTHIO-2-CYCLOALKENONES

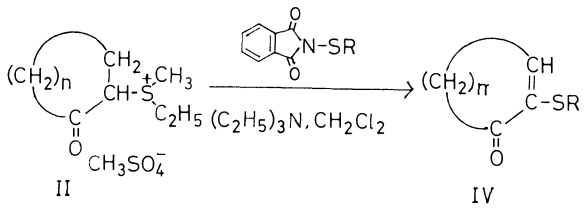

	n	R	Yield (%)	Mp °C (Bp °C/mmHg)	Analyses (%) Found (Calcd) C	H	N
IVa	2	C_6H_5	59	65—66	69.58 (69.46)	5.39 (5.30)	17.12 (16.85)
b	2	C_2H_5	81	(127—128/15)	58.88 (59.14)	7.12 (7.09)	22.30 (22.54)
c	3	C_6H_5	70	57—58	70.31 (70.57)	6.10 (5.92)	15.50 (15.70)
d	3	C_2H_5	80	(110—112/4)	61.57 (61.52)	7.77 (7.75)	20.80 (20.51)
e	4	C_6H_5	76	148—149[a]	71.83 (71.54)	6.29 (6.47)	14.50 (14.69)
f	4	C_2H_5	76	(115—118/5.5)	63.64 (63.51)	8.26 (8.29)	18.79 (18.83)

a) Mp of 2,4-dinitrophenylhydrazone

1) T. Mukaiyama, K. Hosoi, S. Inokuma, and T. Kumamoto, This Bulletin, **44**, 2453 (1971).
2) T. Mukaiyama and M. Higo, *Tetrahedron Lett.*, **1970**, 5297.
3) T. Mukaiyama, S. Kobayashi, and T. Kumamoto, *ibid.*, **1970**, 5115.

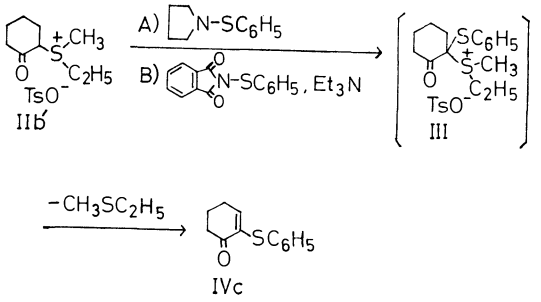

Scheme 3

Reactions of the sulfonium salts (Va—c) of the cycloalkenones with active methylene compounds, such as ethyl acetoacetate or acetylacetone, were attempted. When 2-ethylthio-2-cyclohexenone (IVd) or 2-ethylthio-2-cycloheptenone (IVf) was treated with dimethyl sulfate at 40—50°C for 5 hr, the corresponding sulfonium salts were obtained in almost quantitative yields. In the case of the five-membered analog, the yield of the sulfonium salt (Va) was low.

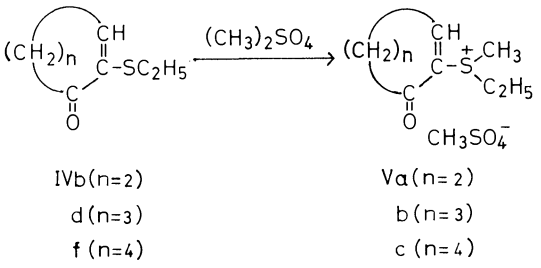

Scheme 4

It was found that when the sulfonium salt (Vb) was treated with ethyl acetoacetate in the presence of triethylamine or sodium ethoxide under ice-cooling for 5 hr, the compound, mp 58—59°C, $C_{12}H_{16}O_4$, was obtained along with methyl ethyl sulfide. Its IR spectrum showed the presence of ester group at 1725 cm^{-1}, carbonyl group of cyclohexane ring at 1695 cm^{-1} and the C=C stretching of enol ether at 1640 cm^{-1}, but not a band for acetyl group. The NMR spectrum (60 MHz) exhibited characteristic peaks of two angular hydrogens at 6.1—6.6 τ (1*H*, multiplet) and at 5.4 τ (1*H*, doublet, J=10 Hz), and the UV spectrum in ethanol showed absorption maximum at 255 mμ (ε=12200). Thus, the structure is assigned to the dihydrofuran derivative, 9-ethoxycarbonyl-8-methyl-7-oxabicyclo[4.3.0]-8-nonen-5-one (Xb).

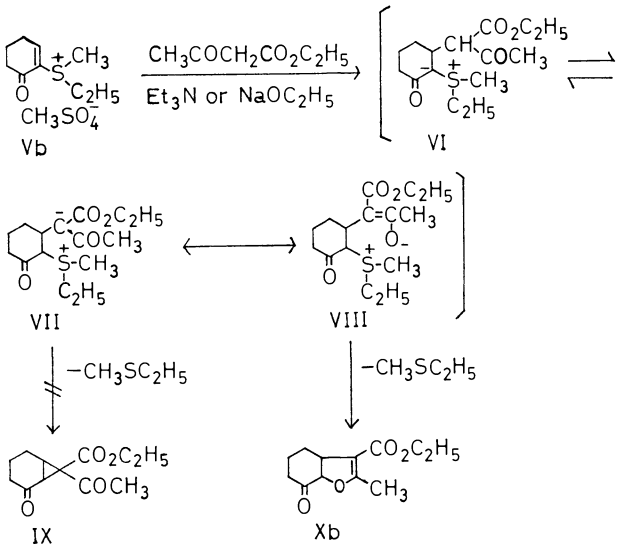

Scheme 5

This result may be explained as follows. First, the intermediate ylide (VI) is produced from the sulfonium salt (Vb) and ethyl acetoacetate by the Michael addition. The ylide (VI) is in turn changed to the betaine form (VII or VIII) by the proton transfer. Subsequent intramolecular nucleophilic attack of enolate anion (VIII) at the α-carbon of sulfonium group affords Xb with the elimination of methyl ethyl sulfide. There is an alternative route for a possible formation of the cyclopropane derivative (IX) involving an attack of the carbanion (VII) at the α-carbon.[4] However, no

Table 2. Preparation of dihydrofuran derivatives

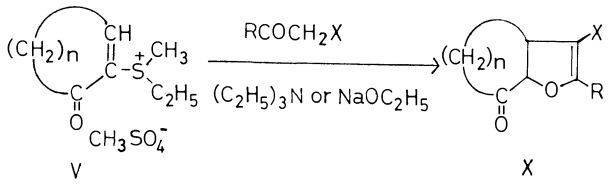

	n	R	X	Yield (%)	Mp °C (Bp °C/mmHg)	λ_{max}^{EtOH} mμ ($\varepsilon\times10^{-4}$)	Analyses (%) Found (Calcd) C	H
Xa	2	CH_3	$CO_2C_2H_5$	18	(127—130/4)		62.55 (62.84)	6.62 (6.71)
b	3	CH_3	$CO_2C_2H_5$	91—98	58—59[a]	255 (1.22)	64.51 (64.27)	7.26 (7.19)
c	3	CH_3	$COCH_3$	70	90—91[a]	274 (1.29)	67.79 (68.02)	6.98 (7.27)
d	3	H	$CO_2C_2H_5$	50	(115—118/4.5)	252 (1.03)	63.11 (62.84)	6.74 (6.71)
e	4	CH_3	$CO_2C_2H_5$	85	64—65[a]	255 (1.21)	65.83 (65.53)	7.63 (7.61)
f	4	CH_3	$COCH_3$	67	86—87[a]	273 (1.36)	68.92 (69.21)	7.44 (7.74)

a) Recrystallized from cyclohexane

4) J. Gosselck, H. Ahlbrecht, F. Dost, H. Schenk, and G. Schmidt, *Tetrahedron Lett.*, **1968**, 995.

such compound could be isolated from the reaction mixture.

Similarly, dihydrofuran derivatives (Xa—f) were obtained from the sulfonium salts of cyclopentenone or cycloheptenone analog and active methylene compounds as shown in Table 2.

Experimental

Materials. 2-Ethylthiocyclopentanone (Ia, bp 57—59°C/4 mmHg) and 2-ethylthiocycloheptanone (Ic, bp 96.5—97.5°C/5 mmHg) were prepared according to the method of Mousseron.[5]

Preparation of Methylethyl-2-oxocycloalkylsulfonium Salts (II). A mixture of 2-ethylthiocyclohexanone (Ib)[5] (1.58 g, 0.01 mol) and freshly-distilled dimethyl sulfate (1.39 g, 0.011 mol) was stirred at room temperature. After stirring for 1—2 days, methylethyl-2-oxocyclohexylsulfonium methylsulfate (IIb) was obtained in almost quantitative yield as a slightly yellowish viscous oil. Similarly, methylethyl-2-oxocyclopentylsulfonium methylsulfate (IIa) and methylethyl-2-oxocycloheptylsulfonium methylsulfate (IIc) were obtained in good yields. Methylethyl-2-oxocyclohexylsulfonium tosylate (IIb′) was prepared by the treatment of Ib (4.75 g, 0.03 mol) with methyl tosylate (6.15 g, 0.033 mol) at 75—85°C for 7—8 hr as a slightly brownish viscous oil. All of these oily salts were used for the reaction with sulfenamides without further purification, and identified by transformation into their picrates.

Table 3. Methylethyl-2-oxocycloalkyl-sulfomium picrates

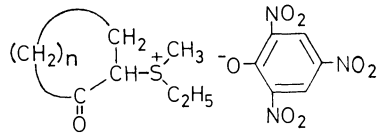

n	Mp °C (dec.)	Analyses, Found (Calcd) (%) C	H	N	S
2	109—110	43.90 (43.41)	4.41 (4.42)	10.80 (10.58)	8.14 (8.28)
3	158	45.17 (44.89)	4.61 (4.77)	10.72 (10.47)	8.29 (7.99)
4	129.5	46.51 (46.26)	5.25 (5.10)	10.28 (10.12)	7.68 (7.77)

Preparation of 2-Phenylthio-2-cyclohexenone (IVc). (A) The Reaction of IIb′ with N-Phenylthiopyrrolidine: A solution of *N*-phenylthiopyrrolidine (5.37 g, 0.03 mol) in dichloromethane (5 m*l*) was added dropwise to a solution of IIb′ (10.9 g, 0.03 mol) in dichloromethane (10 m*l*) under ice-cooling. The reaction mixture was stirred continuously at room temperature for a day. After removal of the solvent, the resulting dark brown syrup was extracted with ether and the ether layer was chromatogaphed on silica gel. Elution with petroleum ether gave diphenyl disulfide 1.0 g (31%) and that with benzene gave slightly yellowish-green crystals, mp 52—54°C, 3.3 g (54%), which were crystallized from isopropyl alcohol to afford colorless needles (IVc), mp 57—58°C.

(B) The Reaction of IIb′ with N-Phenylthiophthalimide: Into a mixture of IIb′ (7.26 g, 0.02 mol) and *N*-phenylthiophthalimide (5.1 g, 0.02 mol)[6] in dichloromethane (25 m*l*), a solution of triethylamine (2.02 g, 0.02 mol) in dichloromethane (2 m*l*) was added dropwise with stirring under ice-cooling. After additional stirring at room temperature for a day, the precipitate of phthalimide (2.11 g, 72%) was filtered off. The filtrate was concentrated under reduced pressure and the resulting oil was chromatographed on silica gel. Elution with benzene gave slightly brownish crystals, mp 52—55°C, 3.2 g (78%). Recrystallization from isopropyl alcohol gave colorless needles (IVc), mp 57—58°C. In a similar manner, 2-phenylthio-2-cyclopentenone (IVa) or 2-phenythio-2-cycloheptenone (IVe) was obtained by the reaction of the corresponding sulfonium salt (IIa or IIc respectively) with *N*-phenylthiophthalimide as shown in Table 2.

Preparation of 2-Ethylthio-2-cyclohexenone. Into a mixture of IIb (29.7 g, 0.1 mol) and *N*-ethylthiophthalimide (20.7 g, 0.1 mol)[6] in dichloromethane (60 m*l*), a solution of triethylamine (10.1 g, 0.1 mol) in dichloromethane (10 m*l*) was added dropwise under ice-cooling. After additional stirring at room temperature for a day, the white precipitate of phthalimide (14 g) was filtered off and the filtrate was concentrated. The residue was extracted with ether and ether layer was washed with 10% sodium hydroxide, 10% hydrochloric acid and water, and dried over sodium sulfate. After removal of the solvent, the residual liquid was distilled to afford a slightly yellowish-green liquid (IVd), bp 110—112°C/4 mmHg, 12.5 g (80%). Similarly, 2-ethylthio-2-cyclopentenone (IVb) or 2-ethylthio-2-cycloheptenone was obtained. The results are listed in Table 1.

Preparation of the Sulfonium Salt of 2-Ethylthio-2-cycloalkenone. A mixture of 2-ethylthio-2-cycloalkenone and dimethyl sulfate (1:1.1 molar ratio) was stirred at 40—50°C for 5 hr or at room temperature for 3—4 days. The corresponding sulfonium salt was obtained as a viscous oil, which turned crystalline on transformation into its 2,4,6-trinitrobenzenesulfonate or picrate.

Table 4. Sulfonium salts of alicyclic β-ketosulfides

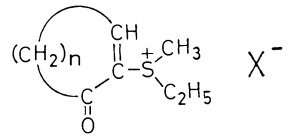

n		Mp °C (dec.)	Analyses, Found (Calcd) (%) C	H	N	S
2	TNBS[a]	191	37.13 (37.41)	3.45 (3.36)	9.45 (9.35)	14.14 (14.27)
3	Pic[b]	113	45.01 (45.12)	4.14 (4.29)	10.50 (10.52)	8.12 (8.03)
4	TNBS	156—157	40.04 (40.24)	4.12 (4.01)	8.58 (8.80)	13.18 (13.43)

a) TNBS: 2,4,6-trinitrobenzenesulfonate
b) Pic: picrate

Preparation of 9-Ethoxycarbonyl-8-methyl-7-oxabicyclo[4.3.0]-*8-nonen-5-one (Xb).* Into a mixture of ethyl acetoacetate (0.98g, 0.0075 mol) and sodium ethoxide [prepared from 0.115 g (0.005 mol) of sodium] in absolute ethanol (5 m*l*), a solution of the sulfonium slat (Vb) (1.47g, 0.005 mol) in absolute ethanol (5 m*l*) was added dropwise under ice-cooling and stirring for 5 hr. White crystals were precipitated during the stirring. After removal of the solvent, water

5) M. Mousseron, R. Jacquier, and A. Fontaine, *Bull. Soc. Chim. Fr.*, **1952**, 767.

6) M. Behforouz and J. E. Kerwood, *J. Org. Chem.*, **34**, 51, (1969).

(10 m*l*) was added to the residue, and the resulting oil was extracted with ethyl acetate. Ethyl acetate layer was dried over sodium sulfate, followed by evaporation of the solvent giving slightly yellowish brown crystals (Xb), mp 53—55°C, 1.1 g (98%), which were recrystallized from cyclohexane to afford colorless needles, mp 58—59°C. When the sulfonium salt (Vb) was treated with a small excess of ethyl acetoacetate in dichloromethane in the presence of equimolar amount of triethylamine under ice-cooling, Xb was obtained in 91% yield. Similarly, the dihydrofuran derivatives (Xa), (Xc), (Xe) and (Xf) were produced from the corresponding sulfonium salt and active methylene compound. The results are listed in Table 2.

Preparation of 9-Ethoxycarbonyl-7-oxabicyclo[4.3.0]*-8-nonen-5-one (Xd).* Into a suspension of the sodium salt (2.07 g, 0.015 mol)[7] of ethyl formylacetate in absolute ethanol (10 m*l*), a solution of Vb (2.94 g, 0.01 mol) in ethanol (10 m*l*) was added dropwise under ice-cooling. After additional stirring for 5 hr, the solvent was evaporated, and the residue was extracted with ethyl acetate. Ethyl acetate layer was chromatographed on silica gel. Elution with benzene-chloroform (1:1) gave the pale yellow oil (Xd), 1.05 g (50%), which was distilled to afford the colorless oil, bp 115—118°C/4.5 mmHg.

7) W. Wislicenus, *Ber.*, **20**, 2930 (1887).

BULLETIN OF THE CHEMICAL SOCIETY OF JAPAN, VOL. 44, 3158—3160 (1971)

A Dianthr[14]annulene

Shuzo AKIYAMA and Masazumi NAKAGAWA

Department of Chemistry, Faculty of Science, Osaka University Toyonaka, Osaka

(Received May 28, 1971)

1,2,3,4,5:8,9,10,11,12-Di(1′,8′-anthr)[14]annulene (III) has been synthesized by the Wittig reaction of 1,8-diformylanthracene (IV) and the bis-ylide (VIII) derived from 1,8-bis(bromomethyl)anthracene (VI).

We previously reported the syntheses and properties of dianthratetradehydro[18]- and dianthroctadehydro-[26]annulenes (I and II).[1,2] It seemed to be of interest to synthesize dianthrannulene and compare its properties with those of dianthradehydroannulenes (I and II). On inspection of a molecular model of the dianthr[14]annulene (III), we realized that the molecule should be twisted owing to the steric repulsion between the hydrogen atoms at 9′-positions of the aromatic nuclei and those of the ethylenic bonds. Thus, a comparison of the electronic spectra of III and related compounds seemed to be of considerable interest. We wish to report the synthesis of the dianthr[14]annulene (III), a lower analogue of I and II.

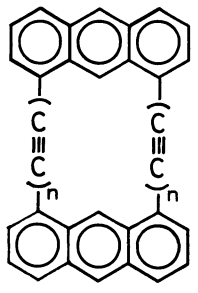

I n=2, II n=4

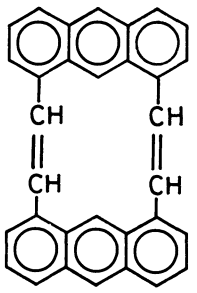

III

Synthesis. Preparation of III was performed according to an analogous sequence of the reaction used in the synthesis of 1,2,3:6,7,8-di(1′,8′-naphth)[10]-annulene.[3]

1,8-Diformylanthracene (IV)[2] was reduced by means of sodium borohydride to give 1,8-bis(hydroxymethyl)-anthracene (V). Glycol (V) was converted quantitatively to bis-bromomethyl derivative (VI). Bis-triphenylphosphonium salt (VIII) was obtained in a high

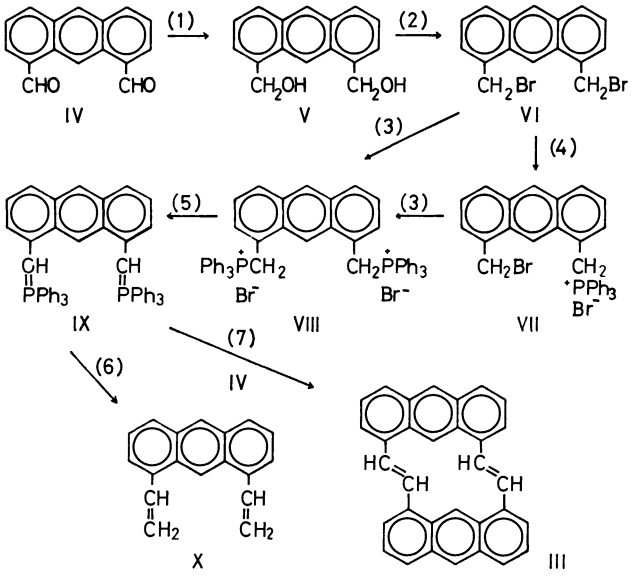

Scheme. Synthesis of dianthr[14]annulene and 1,8-divinylanthracene.

(1) $NaBH_4$/THF; (2) PBr_3-pyridine/THF; (3) Ph_3P/DMF; (4) Ph_3P/benzene; (5) PhLi/toluene; (6) $(CHO)_n$/toluene; (7) toluene.

1) S. Akiyama, S. Misumi, and M. Nakagawa, This Bulletin, **33**, 1293 (1960).

2) S. Akiyama, S. Misumi, and M. Nakagawa, *ibid.*, **35**, 1826 (1962).

3) R. H. Mitchell and F. Sondheimer, *J. Amer. Chem. Soc.*, **90**, 530 (1968).

yield by treatment of VI with 3 molar equivalents of triphenylphosphine in dimethylformamide at *ca.* 100°C. The reaction of the phosphine in benzene gave exclusively monophosphonium salt (VII) which could be converted to VIII in a good yield by further treatment with the phosphine in dimethylformamide. Phenyllithium in toluene transformed VIII to bis-ylide (IX). The Wittig reaction of 1,8-diformylanthracene IV and bis-ylide IX in toluene afforded dianthr[14]annulene III as bright yellow needles in a moderate yield. The crystals of III exhibit light green fluorescence. III gave satisfactory results of elemental analysis and the mass spectrum of III gave a molecular ion peak (M^+=404) exactly corresponding to the molecular weight of III.

1,8-Divinylanthracene (X), a reference substance of III, was prepared by the reaction of bis-ylide (XI) with an excess of paraformaldehyde in toluene.

Properties. Dianthr[14]annulene III thus prepared was found to be an extremely stable compound. It decomposed above 360°C. Annulene III is sparingly soluble in common organic solvents. The solubility in chlorobenzene was found to be 20 mg per 100 m*l* at room temperature. The configuration of ethylenic bonds in III was confirmed to be *trans*, because, as is shown in Fig. 1, the infrared spectrum of III exhibits a band at 975 cm^{-1} which is characteristic of *trans*-ethylene linkage.

The electronic spectrum of III is recorded in Fig. 2 together with those of the related compounds. The spectra of 1,8-diethynyl-[1] and 1,8-divinylanthracenes

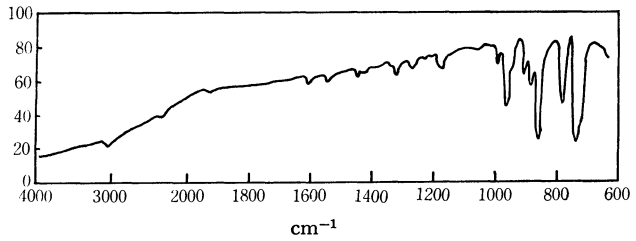

Fig. 1. The infrared spectrum of dianthr[14]annulene.

exhibit distinct vibrational fine structure characteristic of anthracene derivatives. However, disappearance of the fine structure and broadening of both absorption bands (250 nm and 340—450 nm regions) were observed in the spectrum of III. Broadening of the fine structure in the spectrum of X as compared with that of 1,8-diethynylanthracene can reasonably be attributed to the steric hindrance between the hydrogen atoms at 2- and/or 9-positions of anthracene nucleus and those of olefinic linkage. The same trend has been observed in the spectrum of 1,2-di-1′-anthrylethylene,[4] *i.e.*, the ethylene exhibits a broad spectrum in contrast to that of 1,1′-dianthrylacetylene[5] which shows a well-defined fine structure. The electronic spectrum of I also exhibits a sharp fine structure,[1] and vibrational sub-peaks are still observed in the broad and intense absorption bands of II.[2] Thus, the broadening and disappearance of the fine structure in the spectrum of III seem to be attributed mainly to the non-planar geometry of the annelated[14]annulene (III).

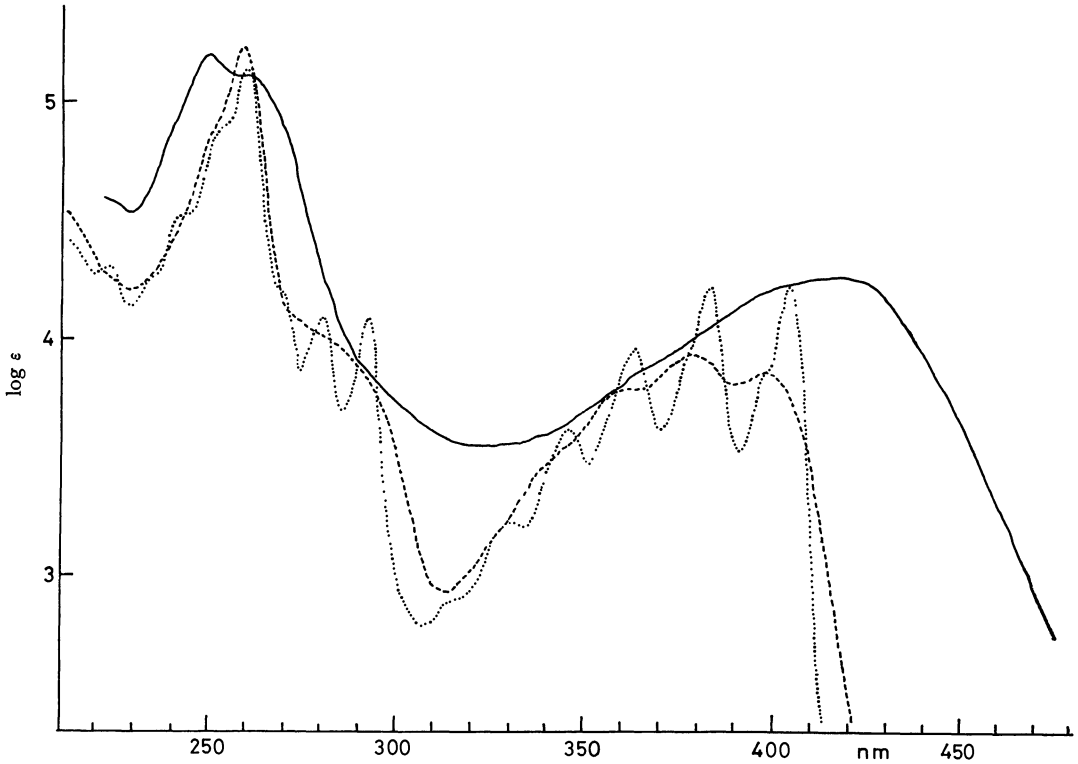

Fig. 2. The electronic spectra of dianthr[14]annulene (III, ——), 1,8-divinylanthracene (X, ——), and 1,8-diethynylanthracene (------).

4) Unpublished result.

5) S. Akiyama, K. Nakasuji, and M. Nakagawa, This Bulletin, **44**, 2231 (1971).

The NMR spectrum of III could not be measured owing to the poor solubility of III in various NMR solvents.

Experimental

All melting points are uncorrected. The electronic spectra were obtained on a Hitachi EPS-3T spectrophotometer. The infrared and the mass spectra were measured on a Hitachi EPI-2 spectrophotometer and a Hitachi RMU-6D mass spectrometer, respectively.

1,8-Bis(hydroxymethyl)anthracene (V). The dialdehyde[2] (IV, 11.72 g, 0.05 mol) was reduced by means of sodium borohydride (1.90 g, 0.05 mol) in tetrahydrofuran (150 m*l*) employing a Soxhlet technique. Reflux was continued for 4 hr. Water was then added to deposit yellow crystals in a quantitative yield. Glycol V thus prepared was found to be identical with the specimen previously prepared.[2]

1,8-Bis(bromomethyl)anthracene (VI). To a stirred mixture of the diol (V, 2.38 g, 0.01 mol), pyridine (0.40 g, 5 mmol) and tetrahydrofuran (50 m*l*), was added a solution of phosphorus tribromide (4.07 g, 0.015 mol) in tetrahydrofuran (10 m*l*) over a period of 20 min. After stirring for further 2 hr at room temperature, cracked ice was added to the reaction mixture. The organic layer was separated, and worked up according to the usual procedure. The solvent was evaporated under reduced pressure. The residue was collected by filtration, and washed successively with an aqueous solution of sodium hydrogen carbonate and water. The yellow crystals obtained in a quantitative yield were recrystallized from benzene to afford yellow needles, mp 230—232°C (dec.). Found: C, 52.94; H, 3.31; Br, 43.69%. Calcd for $C_{16}H_{12}Br_2$: C, 52.78; H, 3.32; Br, 43.90%.

1-Bromomethyl-8-triphenylphosphoniomethylanthracene Bromide (VII). A solution of dibromide (VI, 3.64 g, 0.01 mol) and triphenylphosphine (3.90 g, 0.015 mol) in dry benzene (120 m*l*) was refluxed for 3 hr. The precipitate formed was collected, washed with benzene, and then dried to yield VII, mp 260—265°C (dec.), 6.05 g (97%). Found: C, 66.20; H, 4.34%. Calcd for $C_{34}H_{27}Br_2P$: C, 65.20; H, 4.34%. Unsatisfactory results in the analysis of carbon might be due to contamination with a small amount of bis-phosphonium salt VIII.

1,8-Bis(triphenylphosphoniomethyl)anthracene Dibromide (VIII).
1) From the Monophosphonium Salt (VII): A mixture of VII (2.10 g, 3.35 mmol), triphenylphosphine (1.30 g, 5 mmol) and dimethylformamide (15 m*l*) was refluxed for 30 min. The precipitate formed by the addition of benzene (10 m*l*) was collected and then washed with a small amount of benzene, resulting in yellow fine cubes, 2.48 g (84%). The second crop (0.17 g, 6%) was obtained from the mother liquor. Decomposition of VIII was observed above 360°C.

2) From the Dibromide (VI): A solution of VI (0.364 g, 1 mmol) and triphenylphosphine (0.786 g, 3 mmol) in dimethylformamide (2 m*l*) was heated on a boiling water-bath for 2 hr. The precipitate formed on cooling the reaction mixture in an ice-water bath was collected by filtration and washed with a small amount of benzene. Bis-phosphonium bromide VIII, thus prepared, showed an identical IR spectrum with that of VIII derived from VII and decomposed also above 360°C. Found: C, 70.04; H, 4.78; Br, 17.49%. Calcd for $C_{52}H_{42}Br_2P_2$: C, 70.28; H, 4.76; Br, 17.98%.

1,2,3,4,5:8,9,10,11,12-Di(1',8'-anthr)[14]annulene (III). To a suspension of the bis-phosphonium salt (VIII, 5.334 g, 6 mmol) in toluene (200 m*l*), was added an ethereal solution of phenyllithium (0.85 N, 14.1 m*l*, 12 mmol) at 80°C over a period of 15 min under nitrogen atmosphere. After the mixture had been stirred for 15 min at 80°C, a solution of the dialdehyde (IV, 1.404 g, 6 mmol) in toluene (210 m*l*) was added, and stirred for 2 hr at the same temperature. The insoluble material was collected by filtration, and washed with water and alcohol successively to remove triphenylphosphine oxide. The residue was then digested repeatedly with boiling chlorobenzene (total 1.2 *l*). A brown resinous powder insoluble in chlorobenzene (*ca.* 0.7 g) remained. The hot extract was passed through a column of alumina (60 g) to give yellow filtrate with green fluorescence. The solvent was removed under reduced pressure to afford yellow needles, 0.412 g (17%). The original filtrate of the reaction mixture was passed through a thin layer of alumina (10 g), and the filtrate was concentrated *in vacuo* to afford the second drop of III (0.101 g, 4%). The slightly crude crystals of III thus obtained were dissolved in chlorobenzene and passed through a short column of alumina, affording pure III as bright yellow fine needles with green fluorescence. III was found to decompose above 360°C. Found: C, 94.78; H, 5.00%. Calcd for $C_{32}H_{20}$: C, 95.02; H, 4.98%. IR: 975 cm^{-1} (*trans* double bond). Mass: 404 (M^+), Calcd 404.5. The ratio of $M^+/M^+ + 1$ was found to be consistent with the theoretical value (obs. 0.331. theor. 0.349). UV: $\lambda_{max}^{tetrahydrofuran}$ (ε) 249 (157900), 257 (131300), and 418 (18300) nm.

1,8-Divinylanthracene (X). To a stirred solution of the bis-ylide IX [from VIII, 1.778 g, 2 mmol and phenyllithium, 4 mmol in toluene (50 m*l*)], was added a large excess of paraformaldehyde [dried over phosphorus pentoxide for 3 days] at 70°C. Rapid disappearance of the characteristic red color of the ylide solution was observed. After stirring for 2 hr the solvent was evaporated under reduced pressure and extracted with cyclohexane (150 m*l*). The extract was percolated through a thin layer of alumina (3 g), affording a faint yellow solution with blue-violet fluorescence. Concentration of the solvent under reduced pressure resulted in pale yellow plates, 0.270 g (57%), mp 68—70°C. The material was recrystallized twice from methanol to give analytical specimen, mp 70—71.5°C. Found: C, 93.66; H, 6.06%. Calcd for $C_{18}H_{14}$: C, 93.87; H, 6.13%. IR: 1240, 910 ($=CH_2$), 990 ($=C\langle_H$) cm^{-1}. Mass: 230 (M^+), Calcd 230. UV: $\lambda_{max}^{n\text{-hexane}}$ (ε) 256 (165600), 360 (6100), 378 (8700), and 398 (7300) nm.

The Reduction of *gem*-Dibromocyclopropanes by Means of Chromium(II) Acetate or Potassium Pentacyanocobaltate

Tamio SHIRAFUJI, Koichiro OSHIMA, Yasusi YAMAMOTO, and Hitosi NOZAKI

Department of Industrial Chemistry, Kyoto University, Yosida, Kyoto

(Received May 28, 1971)

The reduction of *gem*-dibromocyclopropane(I) with Cr^{II} acetate in DMSO gives monobromocyclopropanes (II and III) exclusively, whereas the same components in aq DMF afford cyclopropyl acetates(IV and V) as the major products in addition to II and III. A similar substitution on cyclopropane carbon is observed in the reduction of I with $K_3Co(CN)_5$ in DMSO, furnishing cyclopropyl cyanides (IX and X) mainly. The stereochemistry of II, III, IV, and V is determined by the NMR coupling constants and chemical shifts, and that of IX and X, by transformation to the corresponding cyclopropyl methyl ketones derived from cyclopropanecarboxylic acids of known configurations. The reaction of II or III with $K_3Co(CN)_5$ is also described.

The reduction of *gem*-dibromocyclopropanes (I) with chromium(II) (Cr^{II}) sulfate produces *endo*-monobromocyclopropanes (II), along with allenes and completely reduced cyclopropanes (Scheme 1, route A).[1] We now wish to report on the behavior of I toward Cr^{II} acetate or potassium pentacyanocobaltate ($K_3Co(CN)_5$) in polar solvents (Scheme 1, route B or C). The reaction of these reductants with organic halides is not without precedent,[2] but the observed semireduction of I and the accompanying substitution reaction on cyclopropane carbon appear to be novel. The semireduction to monobromocyclopropanes[3] has been effected by means of Cr^{II} acetate in DMSO (system B), whereas substitution products such as cyclopropyl acetates or cyclopropyl cyanides have been obtained as major products in the reaction of I with Cr^{II} acetate in aqueous DMF (system C) and in that of I with $K_3Co(CN)_5$ in DMSO respectively. Such behavior is in remarkable contrast with that of Cr^{II} sulfate in aqueous DMF (system A[1]).

Table 1 summarizes the yields of the isomeric monobromocyclopropanes obtained in the reaction of I with the system B, which proceeded smoothly to afford only

Table 1. Reduction of *gem*-dibromocyclopropanes with Cr^{II} acetate in DMSO (0.3 M)

	Substrate I R^1, R^2	Reaction Temp. (°C)	Reaction Time (hr)	Products (Yield in %)[a] II *endo cis*	Products (Yield in %)[a] III *exo trans*
a	$(CH_2)_4$	45	15	75	7
b	$(CH_2)_6$	50	16	57	18
c	*n*-hexyl, H	50	17	27	46
d	Ph, H	r.t.	20	62	13

a) Yields were based on the consumed I.

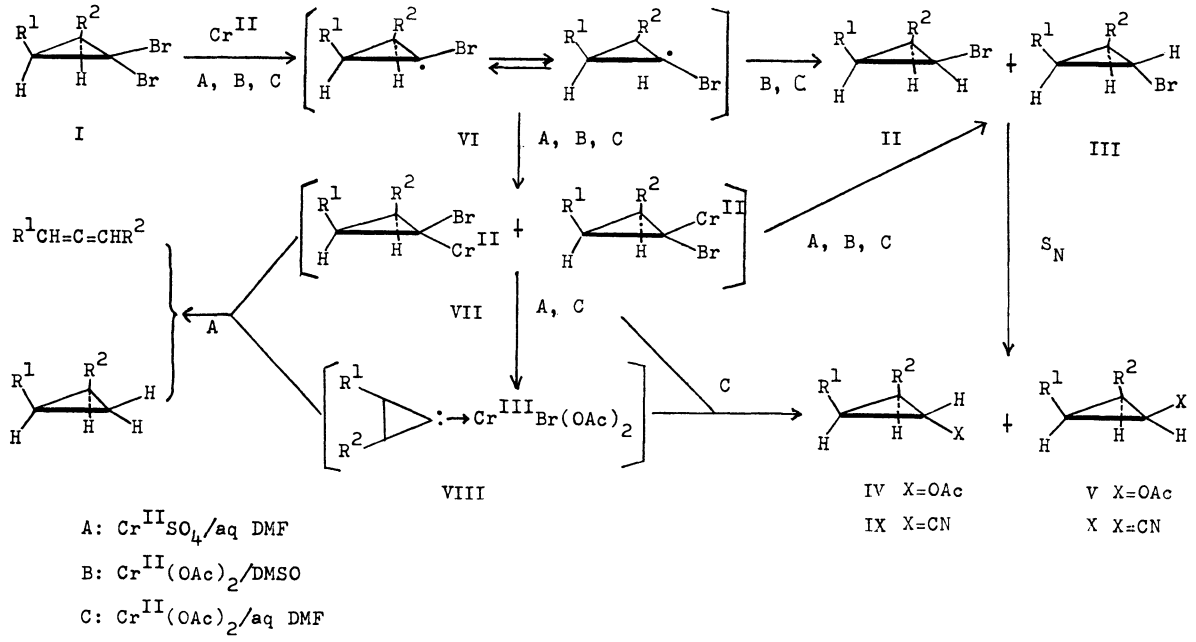

Scheme 1

1) a) H. Nozaki, T. Aratani, and R. Noyori, *Tetrahedron*, **23**, 3645 (1967); b) C. E. Castro, and W. C. Kray, Jr., *J. Amer. Chem. Soc.*, **88**, 4447 (1966) and the refs cited therein; c) J. K. Kochi, and P. E. Mocadlo, *ibid.*, **88**, 4094 (1966).

2) a) D. H. R. Barton, N. K. Basu, R. H. Hesse, F. S. Morehouse, and M. M. Pechet, *ibid.*, **88**, 3016 (1966); b) K. Tarama and T. Funabiki, *Nippon Kagaku Zasshi*, **89**, 88 (1968).

3) a) D. Seyferth, H. Yamazaki, and D. L. Alleston, *J. Org. Chem.*, **28**, 703 (1963); b) D. Seyferth and B. Prokai, *ibid.*, **31**, 1702 (1966); c) T. Ando, H. Yamanaka, F. Namigata, and W. Funasaka, *J. Amer. Chem. Soc.*, **89**, 5719 (1967).

negligible amounts of byproducts, such as allenes and cyclopropanes. The isomer distribution followed the same lines as were observed with other reductants[3]; that is, the predominance of *endo* (or *cis*) products, II, over the stereoisomers, III, holds with the exception of the case of Ic. Unexpectedly, the treatment of 1,1-dibromo-2,2-diphenylcyclopropane (I') with Cr^{II} acetate in DMSO gave 1,1-diphenylallene (II') as the sole isolable product. This is the only case where an allene is obtained.

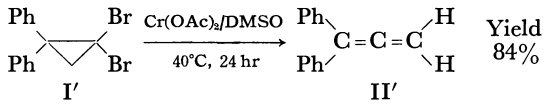

I' II'

The reaction of I with Cr^{II} salts would probably proceed according to Scheme 1, but several remarkable points of difference have been observed between the two systems, A and B. (1) A more rigorous preference of II over III is observed with the system A. (2) Better yields of allenes are obtained in the system A with the exception of the above-mentioned case of 1, 1-dibromo-2,2-diphenylcyclopropane. (3) Totally-reduced cyclopropanes are obtained only in the system A. Rapidly flipping radicals (VI) may be responsible, in part at least, for the formation of II and III in the system B, whereas organochromium intermediates (VII) probably account for the exclusive formation of II in the system A. Allenes and cyclopropanes may originate from the postulated inverse ylides (VIII), which can not be important in the system B.

Unexpectedly, the treatment of I with the system C gave cyclopropyl acetates (IV and V) in addition to monobromocyclopropanes (II and III), as is shown in Table 2.[4] The stereochemistry of IV and V was determined by means of the NMR chemical shifts and coupling constants of the acetoxy methyl protons and the acetoxy-substituted methine protons.[5]

Table 3 summarizes the reactions of I with $K_3Co(CN)_5$ in DMSO.[6] The stereochemistry of the resulting cyclopropyl cyanides (IX and X) was determined by transformation to the corresponding cyclopropyl methyl ketones (XI and XII), as is shown in Table 4.[5] The authentic samples were obtained by the reaction of methyllithium with cyclopropanecarboxylic acids (XIII and XIV) of know configurations (Table 5).[7]

The *endo*/*exo* ratios of monobromocyclopropanes given in Tables 2 and 3 are nearly the same as those obtained in the reduction of I with the system B and are consistently larger than one. Reversely, the *endo*/*exo* or *cis*/*trans* ratios of the substitution products, V/IV and X/IX, were smaller than one. The attempted reaction of two isolated monobromocyclopropanes, II and III, with Cr^{II} or Cr^{III} acetate in DMSO or in aqueous DMF afforded no cyclopropyl acetates, IV and V, but only complex mixtures, which could not be investigated

Table 2. Reduction of *gem*-dibromocyclopropanes with Cr^{II} acetate in aqueous DMF (0.3 M)

	Substrate I R¹, R²	Reaction Temp. (°C)	Reaction Time (hr)	Products (Yield in %)[a] II	III	IV *exo trans*	V *endo cis*
a	$(CH_2)_4$	80	14	5	1	53	15
b	$(CH_2)_6$	80	14	25	0	45	4
c	*n*-hexyl, H	75	18	12	20	27	4
d	Ph, H	70	17	34	7	11	1

a) Yields were based on the consumed I.

Table 3. Reduction of *gem*-dibromocyclopropanes with $K_3Co(CN)_5$ in DMSO (0.3 M)

	Substrate I R¹, R²	Reaction Temp. (°C)	Reaction Time (hr)	Products (Yield in %)[a] II	III	IX *exo trans*	X *endo cis*
a	$(CH_2)_4$	70	16	11	1	46	20
b	$(CH_2)_6$	80	16	nil[c]	nil[b]	44	30[c]
c	*n*-hexyl, H	75	16	27	32	8	6
d	Ph, H	70	16	27	9	26	7[d]

a) Yields were based on the consumed I.
b) Not isolated.
c) As the stereochemistry of IXb and Xb could not be determined because of the absence of the corresponding cyclopropanecarboxylic acid of known configuration, the assignment was made on the basis of glc retention times and NMR chemical shifts of acetyl methyl protons of the corresponding cyclopropyl methyl ketones derived from IXb and Xb as shown in Table 4.
d) Phenylallene was also obtained in a 17% yield.

Table 4. Transformation of cyclopropyl cyanides to cyclopropyl methyl ketones

	R¹, R²	IX *exo trans*	X *endo cis*	XI *exo trans*	XII *endo cis*	Yield %[a]
a	$(CH_2)_4$	70 :	30	81 :	19	62
b	$(CH_2)_6$	60 :	40	85 :	15	65
c	*n*-hexyl, H	57 :	43	60 :	40	67
d	Ph, H	100 :	0	100 :	0	67

a) Yields were based on the consumed IX and X.

Table 5. Transformation of cyclopropanecarboxylic acids to cyclopropyl methyl ketones

	R¹, R²	XIII *exo trans*	XIV *endo cis*	XI *exo trans*	XII *endo cis*	Yield %[a]
a	$(CH_2)_4$	88 :	12	85 :	15	48
c	*n*-hexyl, H	68 :	32	66 :	34	65
d	Ph, H	57 :	43	60 :	40	75

a) Yields were based on the consumed XIII and XIV.

4) On the synthesis of cyclopropanols, see: a) U. Schöllkopf, *Angew. Chem. Intern. Ed. Engl.*, **7**, 588 (1968); b) C. H. Depuy, *Accounts Chem. Res.*, **1**, 33 (1968); c) D. T. Longone and W. D. Wright, *Tetrahedron Lett.*, **1969**, 2859.

5) a) C. H. Depuy, G. M. Dappen, K. L. Eilers, and R. A. Klein, *J. Org. Chem.*, **29**, 2813 (1964); b) Jean-Louis Pierre, *Ann. Chim.*, **1966** 383; c) Idem., *Bull. Soc. Chim. Fr.*, **1966** 1040; d) J. P. Freeman, *J. Org. Chem.*, **29**, 1379 (1964); e) H. Weitkamp and F. Korte, *Tetrahedron*, **20**, 2125 (1964).

6) The reduction of Ib with $K_3Co(CN)_5$ in aqueous DMF gave *endo*-IIb exclusively, but Ia, Ic, and Id gave complex mixtures which were not investigated.

7) a) P. S. Skell and R. M. Etter, *Proc. Chem. Soc.*, **1961**, 443; b) K. Hofman, O. Tucker, W. R. Miller, A. C. Young, Jr., and F. Tausig, *J. Amer. Chem. Soc.*, **76**, 1799 (1954); c) A. Burger and W. L. Yost, *ibid.*, **70**, 2198 (1948).

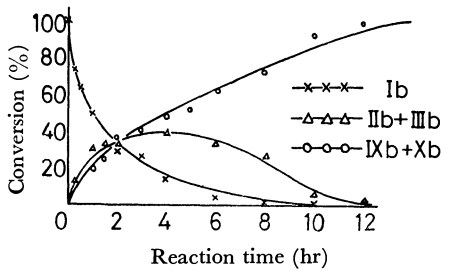

Fig. 1. Reduction of Ib with $K_3Co(CN)_5$ in DMSO followed by glc (HVSG 10%, 1.5 m, 130°C).

Table 6. Transformation of monobromocyclopropanes to cyclopropyl cyanides with $K_3Co(CN)_5$ in DMSO (0.1M)

	R^1, R^2	II *endo cis*	III *exo trans*	IX *exo trans*	X *endo cis*	Total yield %[b]
a	$(CH_2)_4$	100 : 0		83 : 17		88
		0 : 100		77 : 23		67
b	$(CH_2)_6$	100 : 0		56 : 44		60
		0 : 100		43 : 57		65
c	*n*-hexyl, H	100 : 0		63 : 37		62
		0 : 100		42 : 58		78
d	Ph, H	100 : 0		61 : 39		60
		0 : 100		68 : 32		70

a) All reactions were performed at 70—80°C for 15—20 hr.
b) Yields were based on the consumed amount of II or III.

further. We are tempted to assume that IV and V originate from chromium carbenoids (VII) or from chromium inverse ylides (VIII).

The reaction of Ib with $K_3Co(CN)_5$ in DMSO was monitored by means of glc. The results, shown in Fig. 1, indicated the initial formation of IIb and IIIb from Ib followed by the subsequent conversion of IIb and IIIb to cyclopropyl cyanides, IXb and Xb. In fact, the treatment of isolated II or III with $K_3Co(CN)_5$ in DMSO afforded a mixture of IX and X, as is shown in Table 6. The observed formation of a mixture, IX and X, from either II or III possibly involves an S_N-type reaction on a cyclopropane ring, accompanied by no ring-cleavage.[8] We may point out that the isomer ratios in this kind of S_N reactions are largely controlled thermodynamically, but a full explanation must await further investigations in the future.

Experimental

All the boiling points are uncorrected. Glc analyses and separations were performed using a 2-*m* column of HVSG (30%) and He as the carrier gas. The NMR spectra were obtained on a 60 MHz instrument (JEOL C-60-H spectrometer), and the chemical shifts are given in ppm from a TMS internal standard. The mass spectra were obtained on a Hitachi RMU 6D spectrometer. The microanalyses were performed by Mrs. K. Fujimoto at Prof. Sisido's Laboratory and by the Elemental Analyses Center of Kyoto University. The $K_3Co(CN)_5$[2b] and anhydrous Cr^{II} acetate[11] were prepared by the recorded methods.

General Procedure of the Reactions of gem*-Dibromocyclopropane Derivatives with Cr^{II} Acetate or $K_3Co(CN)_5$ in DMSO or Aqueous DMF.* In a nitrogen atmosphere, Cr^{II} acetate (or KCN and Co^{II} chloride) was dissolved in freshly-distilled (over CaH_2) DMSO or in aqueous DMF (1: 1) so as to give *ca.* a 0.3M solution by heating with stirring at 60—70°C for 30 min; then, the solution was maintained at an appropriate reaction temperature (20—80°C). To this we added, drop by drop, a solution (*ca.* 1.5M) of *gem*-dibromocyclopropanes in the same solvent. The atomic ratio of bromine: Cr^{II} (or Co^{II}) was taken to be 1: 1.5—2.0 unless otherwise stated. Heating and stirring were continued until the reddish-brown solution (or blue solution) turned green (or colorless). The mixture was then treated with water and extracted with *n*-hexane, ether, or benzene. The extract was washed with water, dried (Na_2SO_4), and concentrated *in vacuo*. The products were separated and identified as usual. The following description is concerned with cases which are not sufficiently covered by Tables 1, 2, and, 3. Incidentally, the reactions of monobromocyclopropanes with $K_3Co(CN)_5$ in DMSO shown in Table 6 were also performed by this procedure.

*Reaction of 1,1-Dibromo-2-*n*-hexylcyclopropane (Ic) in DMSO.* Dibromide Ic (0.10 g, 0.35 mmol) was treated with a solution of Cr^{II} acetate (0.25 g, 1.5 mmol) in DMSO (30 ml) at 50°C for 17 hr. The glc separation of the reaction mixture gave *cis*-1-bromo-2-*n*-hexylcyclopropane (0.02 g, 27%) and a *trans* isomer 0.035 g, 46%). The *cis*-bromide formed an oil; bp 75°C/18 mmHg (bath temp.), IR (neat): 1248 cm^{-1}, NMR $\delta(CCl_4$, 10%): 2.99 (*m*, 1H, >C<u>H</u>Br, J_{cis}=6.6 Hz), 1.37 (*m*, 10H, methylenes), 0.89 (*m*, 4H, methyl and methine), and 0.44 (*m*, 2H, -C<u>H</u>$_2$CHBr-).

Found: C, 52.9; H, 8.2%. Calcd for $C_9H_{17}Br$: C, 52.7; H, 8.4%. The *trans*-bromide also formed an oil; bp 70°C/18 mmHg (bath temp.), IR (neat): 1234 cm^{-1}, NMR $\delta(CCl_4$, 20%): 2.48 (*m*, 1H, >C<u>H</u>Br, J_{trans}=3.3 Hz), 1.32 (*m*, 11H, methylenes and methine), and 0.87 (*m*, 5H, methyl and -C<u>H</u>$_2$CHBr-).

Found: C, 52.7; H, 8.3%. Calcd for $C_9H_{17}Br$: C, 52.7; H, 8.4%.

Identification of Substitution Products (IV, V, IX, and X). The substitution products, IV, V, IX, and X, were unstable, so that the isolation of each stereoisomer was hard to accomplish. Each mixture of IV and V, or of IX and X, was obtained in an analytically-pure form by preparative tlc; the results of the analyses are shown in Table 7. High-sensitivity glc analyses of the mixtures gave the isomer ratio, which was in accord with the NMR analyses of the mixtures (Table 7). The ratios have been given above in Tables 2, 3, and 6. The attempted isolation of stereoisomers by preparative glc did not give satisfactory results.

Transformation of Cyclopropyl Cyanides (IX and X) to the Corresponding Cyclopropyl Methyl Ketones (XI and XII). A mixture of IX and X was treated with excess amounts of methylmagnesium iodide in ether under gentle refluxing. The reaction mixture was then worked up as usual. A

8) S_N-type reactions of vinylic halides with $K_4Ni_2(CN)_6$ in methanol have been recorded to give α,β-unsaturated nitriles in good yields. See Ref. 9. The S_N-type reaction of *endo*-rich cyclopropyl halides with Ag^I nitrate in methanol gave almost equimolar mixtures of *exo*-rich methoxycyclopropanes and ring-opened methanolysates See Ref. 10.

9) a) E. J. Corey and L. S. Hegedus, *J. Amer. Chem. Soc.*, **91**, 1233 (1969); b) I. Hashimoto, N. Tsuruta, M. Ryang, and S. Tsutsumi, *J. Org. Chem.*, **35**, 3748 (1970).

10) a) D. B. Ledlie and E. A. Nelson, *Tetrahedron Lett.*, **1969**, 1175; b) U. Schöllkopf, E. Ruban, P. Tonne, and K. Riedel, *ibid.*, **1970**, 5077.

11) J. H. Balthis, Jr., and J. C. Bailar, Jr., "Inorganic Syntheses." Coll. Vol., 1, p. 122 (1939).

TABLE 7. PHYSICAL PROPERTIES OF SUBSTITUTION PRODUCTS OBTAINED

Compd	Bp °C/mmHg (bath temp.)	IR (cm^{-1})	NMR (δ ppm, in CCl_4)	Ratio
IVa+Va[a]	60/2	1741, 1230	3.93 (*t*, J_{cis}=7.5 Hz)+3.68 (*t*, J_{trans}=2.8 Hz), 2.04 (*s*, *edno*-OAc)+1.94 (*s*, *exo*-OAc), 1.77—1.20 (*m*, methylenes and methines)	2 : 8
IVb+Vb[b]	75/1	1748, 1225	3.99 (*t*, J_{cis}=7.6 Hz)+3.42 (*t*, J_{trans}=3.0 Hz), 1.99 (*s*, *endo*-OAc)+1.94 (*s*, *exo*-OAc), 1.50—0.89 (*m*, methylenes and methines)	1 : 9
IVc+Vc[c]	65/1	1748, 1232	4.06 (*m*, J_{cis}=6.3 Hz)+3.72 (*m*, J_{trans}=3.8 Hz), 1.99 (*s*, *cis*-OAc)+1.97 (*s*, *trans*-OAc), 1.34—0.10 (*m*, methylenes and methines)	1 : 9
IVd+Vd[d]	80/2	1746, 1235	7.12 (*m*, aromatic), 4.15 (*m*), 2.30—2.15 (m), 1.21 (*m*), 2.00 (*s*, *trans*-OAc)+1.70 (*s*, *cis*-OAc)	11 : 1
IXa+Xa[e]	85/4	2235, 2210 (*exo*-CN) (*endo*-CN)	2.30—1.03 (*m*, methylenes and methines)	
IXb+Xb[f]	90/3	2245, 2215 (*exo*-CN) (*endo*-CN)	2.11 (*m*, methines), 1.46 (*m*, methylenes), 0.70 (*m*, methine)	
IXc+Xc[g]	75/1	2245, 2225 (*trans*-CN) (*cis*-CN)	2.08 (*m*, methine), 1.33 (*m*, methyl, methylenes and methine), 0.90 (*m*, methine)	

a) Found: C, 69.9; H, 9.1%. Calcd for $C_9H_{14}O_2$: C, 70.1; H, 9.2%. MS *m/e* (relative abundance): 154 (4), 112 (28), and 43 (100).
b) Found: C, 72.7; H, 9.8%. Calcd for $C_{11}H_{18}O_2$: C, 72.5; H, 10.0%. MS *m/e* (relative abundance): 154 (3), 140 (68), and 80 (100).
c) Found: C, 71.7; H, 11.1%. Calcd for $C_{11}H_{20}O_2$: C, 71.7; H, 10.9%. MS *m/e* (relative abundance): 184 (3), 142 (10), and 68 (100).
d) Found: C, 75.1; H, 6.8%. Calcd for $C_{11}H_{12}O_2$: C, 75.0; H, 6.9%. MS *m/e* (relative abundance): 176 (5), 134 (50), and 105 (100). For another route to IVd+Vd, see Ref. 5d.
e) Found: C, 79.2; H, 9.1; N, 11.4%. Calcd for $C_8H_{11}N$: C, 79.3; H, 9.2; N, 11.6%. MS *m/e* (relative abuudance): 121 (23) and 67 (100).
f) Found: C, 80.9; H, 9.9; N, 9.4%. Calcd for $C_{10}H_{15}N$: C, 80.5; H, 10.1; N, 9.4%. MS *m/e* (relative abundance): 149 (18) and 54 (100).
g) Found: C, 79.6; H, 11.1; N, 9.1%. Calcd for $C_{10}H_{17}N$: C, 79.4; H, 11.3; N, 9.3%. MS *m/e* (relative abundance): 151 (2) and 54 (100).

TABLE 8. PHYSICAL PROPERTIES OF CYCLOPROPYL METHYL KETONES

Compd	Bp °C/mmHg (bath temp.)	IR (cm^{-1})	NMR (δ ppm, in CCl_4)	Ratio
XIa+XIIa[a]	54/0.5	1689	2.17 (*s*, *endo*-acetyl)+2.14 (*s*, *exo*-acetyl), 1.95—1.05 (*m*, methylenes and methines)	2 : 8
XIb+XIIb[b]	64/0.5	1689	2.17 (*s*, *endo*-acetyl)+2.14 (*s*, *exo*-acetyl), 2.00—0.70 (*m*, methylenes and methines)	1 : 5
XIc+XIIc[c]	52/0.5	1700	2.18 (*s*, *cis*-acetyl)+2.14 (*s*, *trans*-acetyl), 1.98—0.91 (*m*, methylenes and methines)	4 : 6

a) Found: C, 78.1; H, 10.3%. Calcd for $C_9H_{14}O$: C, 78.2; H, 10.2%. MS *m/e* (relative abundance): 138 (24) and 95 (100). For analytical data of XIa+XIIa from the corresponding acids, Found: C, 78.3; H, 10.2%. Calcd for $C_9H_{14}O$: C, 78.2; H, 10.2%.
b) Found: C, 79.2; H, 11.1%. Calcd for $C_{11}H_{18}O$: C, 79.5; H, 10.9%. MS *m/e* (relative abundance): 166 (6) and 95 (100).
c) Found: C, 78.4; H, 11.9%. Calcd for $C_{11}H_{20}O$: C, 78.5; H, 12.0%. MS *m/e* (relative abundance): 168 (4) and 55 (100). For analytical data of XIc+XIIc from the corresponding acids, Found: C, 78.5; H, 12.0%. Calcd for $C_{11}H_{20}O$: C, 78.5; H, 12.0%.

mixture of XI and XII was obtained in an analytically-pure form by preparative glc. The physical properties are shown in Table 8. High-sensitivity glc analyses of the mixture gave the isomer ratio, which was in accord with the NMR analyses of the mixture (Table 8). The ratios have been given above in Tables 4 and 5.

Transformation of Cyclopropanecarboxylic Acids (XIII and XIV) to the Corresponding Cyclopropyl Methyl Ketones (XI and XII). A mixture of XIII and XIV was treated with excess amounts of methyllithium in ether under gentle refluxing. The reaction mixture was then worked up as usual. A mixture of XI and XII was obtained in an analytically-pure form by preparative glc. The analytical data are shown in Table 8.

The authors are grateful to Professor Keiiti Sisido for his generous help. The financial support from the Ministry of Education, the Japanese Government, and from the Toray Science Foundation is also acknowledged with pleasure.

The Structure of Petasitolone, a New Constituent of *Petasites japonicus* Maxim[1]

Keizo NAYA, Fumio YOSHIMURA, and Ichiro TAKAGI

Department of Chemistry, Faculty of Science, Kwansei Gakuin University, Uegahara, Nishinomiya, Hyogo

(Received May 29, 1971)

Petasitolone(I), a new sesquiterpene isolated from *Petasites japonicus* Maxim. has been shown to be 8-oxo-11-hydroxy-$\Delta^{6(7)}$-eremophilene by a physico-chemical method, and synthesized from the known fukinone(VI).

The constituents of flower stalks of *Petasites japonicus* Maxim. have been studied.[2-4] We reported the isolation of fukinone (VI) from the methanolic extract of a cultivated variety "Aichiwasebuki" of this plant. We also isolated a new sesquiterpene named petasitolone from the extract.

Petasitolone (I), $C_{15}H_{24}O_2$, bp 92°C/0.15 mmHg, $[\alpha]_D^{24}+16.7°$, a colorless oil, was obtained by steam and vacuum distillation, and chromatography on silica gel. The two oxygen atoms and one double bond were readily characterized by spectroscopic data: IR bands (Fig. 1) at 3480, 1170 (OH), 1665 cm^{-1} and an UV

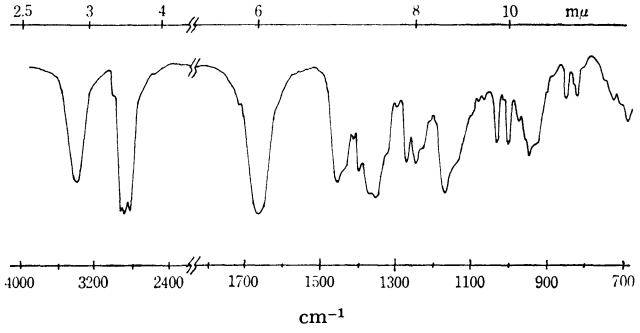

Fig. 1. IR spectrum of petasitolone.

maximum at 237.5 mμ (α,β-unsaturated C=O). Its NMR spectrum indicates one isolated olefinic proton at 6.6[5] due to a β-hydrogen of an α,β-unsaturated ketone, one hydroxyl proton at 3.52, two methyls attached to a carbon bearing a hydroxyl at 1.30, one tertiary methyl at 1.11 and one secondary methyl at 0.93 (d, J=7 Hz). Petasitolone I failed to yield a semicarbazone but afforded a mixture of two 2,4-dinitrophenylhydrazones, $C_{21}H_{28}O_5N_4$, mp 159—160°C and $C_{21}H_{26}O_4N_4$, mp 173—174°C, by Brady's method. The latter $C_{21}H_{26}O_4N_4$ shows no OH band in its IR spectrum and was found to be identical with anhydropetasitolone (II) by mixed melting point determination.

From the above results, petasitolone is strongly presumed to be a bicyclic sesquiterpene containing an α,β-unsaturated carbonyl and a dimethylcarbinol group. The conclusion concerning the structure was confirmed by the following reactions.

Petasitolone was dehydrated with phosphorus oxychloride-pyridine in the cold to yield anhydropetasitolone (II), $C_{15}H_{22}O$, which exhibits an IR band at 1675 cm^{-1} and an UV maximum at 254 mμ (α,β-unsaturated C=O). Its NMR spectrum shows new signals: *i.e.*, a slightly split singlet at 1.86 for a vinyl methyl and two signals at 5.02 and 4.88, respectively for an end-methylene group.

Catalytic hydrogenation of petasitolone with platinum oxide-acetic acid yielded a mixture of dihydropetasitolone (III), $C_{15}H_{26}O_2$ and desoxydihydropetasitolone (IV), $C_{15}H_{26}O$ in the approximate ratio of 2: 3. Upon hydrogenation with palladium charcoal in ethanol, petasitolone furnished predominantly dihydropetasitolone III. Hydrogenolysis to the desoxydihydro compound IV implies that the hydroxyl group of petasitolone can be assumed to be located in the allylic position to the double bond. The desoxydihydro compound IV was found to be identical with the known dihydrofukinone (IV)[3] by comparison of IR spectra and ORD (-Cotton effect) curves, and mixed melting point determination of the two 2,4-dinitrophenylhydrazones.

Thus, from the above evidence the structure of petasitolone, dihydropetasitolone and desoxydihydro compound can be assigned as shown in stereoformulas I, III, and IV.

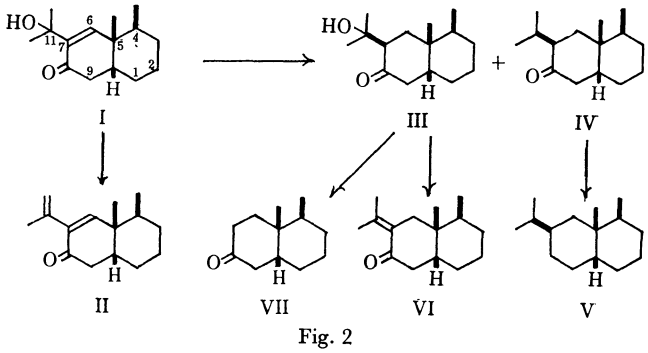

Fig. 2

Along with the above work, the following reactions were examined.

The desoxydihydro compound IV was converted into the known 7β-eremophilane (V)[3,6] *via* ethylene thioketal followed by desulfurization with Raney nickel. On the other hand, when dihydropetasitolone III was subjected to preparative glc for purification, it gave a de-

1) K. Naya, H. Yoshimura and M. Kobayashi, 22nd Annual Meeting of Chemical Society of Japan (1969), Collective Papers Vol. 3, p. 1885.

2) K. Naya and I. Takagi, *Tetrahedron Lett.*, **1968**, 629.

3) K. Naya, I. Takagi, Y. Kawaguchi, Y. Asada, Y. Hirose, and N. Shinoda, *Tetrahedron*, **24**, 5871 (1968).

4) K. Naya, I. Takagi, M. Hayashi, S. Nakamura, M. Kobayashi, and S. Katsumura, *Chem. Ind.* (London), **1968**, 318.

5) All chemical shifts are reported in ppm as δ-values.

6) L. Novotny, J. Jizba, V. Herout, F. Sorm, L. H. Zalkow, S. Hu, and C. Djerassi, *Tetrahedron*, **19**, 1101 (1963).

composition product $C_{12}H_{20}O$ with loss of the dimethylcarbinol unit. The product was identical with desisopropylidenefukinone (VII) obtained previously by base catalyzed retro-aldol reaction from fukinone VI. Dehydration of dihydropetasitolone III with phosphorus oxychloride-pyridine yielded the known fukinone VI as expected.

Synthesis of Petasitolone (I). We postulated that naturally occurring intermediate for petasitolone I is fukinone VI which is converted in the plant to petasitolone I by photochemical oxidation. Little is known about the photosensitized addition of oxygen to an α,β-unsaturated carbonyl system. In fact, the mode of addition to the double bond conjugated with the carbonyl group was found to be similar to that found by Schenck in simple olefinic systems.[7]

When fukinone was irradiated in the presence of rose bengal in atmospheric oxygen followed by reduction with sodium sulfite, petasitolone I was obtained as the main product (45%). The details of the oxidation products will be reported later.

Experimental

All the melting and boiling points are uncorrected. Mass spectra were measured with a Hitachi RMU-6 mass spectrometer; ion source temperature 250°C; evaporation temperature 150°C. IR spectra were recorded with a JASCO DS-402G spectrophotometer and UV spectra were obtained with a Cary Model 14 spectrophotometer. ORD curves were measured with a JASCO spectropolarimeter Model ORD-5. NMR spectra were determined with a Japan Electron Optics JNM-C-60 spectrometer, using TMS as an internal standard ($\delta=0$) and $CDCl_3$ as solvent. Analytical and preparative glc were performed with a Shimadzu GC-1C apparatus on a stainless steel column ($\phi=3$ mm). Tlc were run on silica gel (Merck Kieselgel G). Microanalyses were carried out in the microanalytical section of Shionogi Research Laboratory, Shionogi and Co., Ltd.

Isolation of Petasitolone (I). The dried flower stalks of *P. japonicus* Maxim. (4.5 kg) cultivated in Osaka Prefecture were extracted with methanol at room temperature for 2 weeks. The extract was evaporated *in vacuo* and the residue was extracted with ether to give a dark brown oil (100 g). The oil was chromatographed on silica gel (1 kg). Elution with benzene gave crude fukinone (VI) (40 g) and further elution with methanol afforded an oil (50 g) which was subjected to steam distillation. The distillate was extracted with ether to give an oil (10 g) which contained petasitolone (I) as a major component. The crude petasitolone was purified by silica gel column chromatography using light petroleum-acetone (50: 1) as eluent and by vacuum distillation to give an almost pure sample (1 g) as a colorless oil, bp 92°C/0.15 mmHg; MS: M$^+$ion *m/e* 236, base peak *m/e* 43; IR (film): 3480, 1665, 1170 cm^{-1}; UV: λ_{max}^{MeOH} 237.5 mμ (ε, 8279); $[\alpha]_D^{24}$ +16.7° (*c*, 0.99, MeOH); NMR: 0.93 (d, $J=7$ Hz, 3H), 1.11 (s, 3H), 1.30 (s, 6H), 3.52 (br s, 1H), 6.6 (s, 1H).

Petasitolone (I) was recovered unchanged on both attemted acetylation and Jones' oxidation. The crude product obtained from petasitolone and 2,4-dinitrophenylhydrazine by Brady's method was chromatographed on silica gel and eluted with light petroleum-ether (50: 1) to afford II- and then I-2,4-dinitrophenylhydrazones.

Anhydropetasitolone (II) 2,4-dinitrophenylhydrazone, red needles, mp 173—174°C.

Found: C, 63.30; H, 6.52; N, 13.85%. Calcd for $C_{21}H_{26}O_4N_4$: C, 63.30; H, 6.58; N, 14.06%.

Petasitolone (I) 2,4-dinitrophenylhydrazone, red needles, mp 159—160°C.

Found: C, 60.40; H, 6.85; N, 13.47%. Calcd for $C_{21}H_{28}O_5N_4$: C, 60.56; H, 6.78; N, 13.45%.

Preparation of Anhydropetasitolone (II). Phosphorus oxychloride (3 m*l*) was added slowly to a solution of petasitolone (470 mg) in pyridine (4 m*l*). After being kept standing for 2 days the reaction mixture was added dropwise into ice water, extracted with ether, washed with water and dried over anhydrous sodium sulfate. The solvent was then evaporated. The residue was chromatographed on silica gel (10 g) with light petroleum-ether (50: 1) as eluent to give pure anhydropetasitolone (II) (140 mg) ; MS: M$^+$ion *m/e* 218, base peak *m/e* 147; UV: λ_{max}^{hexane} 254 mμ (ε, 4110); IR (film): 1675, 895 cm^{-1}; NMR: 1.86 (s, 3H), 5.02 and 4.88 (2H). Anhydropetasitolone 2,4-dinitrophenylhydrazone, $C_{21}H_{26}O_4N_4$, mp 173—174°C.

Found: C, 63.62; H, 6.71; N, 13.99%. Calcd for $C_{21}H_{26}O_4N_4$: C, 63.30; H, 6.58; N, 14.06%.

Catalytic Hydrogenation of Petasitolone. a) Platinum Oxide as Catalyst: Petasitolone I (1 g) in acetic acid (10 m*l*) was hydrogenated over Adams' catalyst (80 mg) at room temperature and atmospheric pressure to yield dihydropetasitolone (III) (300 mg) and a desoxydihydro compound (IV) (450 mg). Dihydropetasitolone III : a colorless oil, IR (film): 3340, 1690 cm^{-1}. IR spectrum and glc retention time of compound IV were identical with those of dihydrofukinone obtained from fukinone.[3] ORD in MeOH (*c*, 0.125): $[\phi]_{311}$ −904, $[\phi]_{272}$+1848, $a=-27.5$; 2,4-Dinitrophenylhydrazone, mp 170.5—171°C (authentic sample, [3] mp 171—171.5°C, mixed mp 170.5—171°C).

b) Palladium Charcoal as Catalyst: Petasitolone (600 mg) in ethanol (10 m*l*) was hydrogenated over 10% palladium charcoal (150 mg) at room temperature and atmospheric pressure for 16 hr. About 70 m*l* of hydrogen was absorbed and crude dihydropetasitolone III (560 mg) was obtained as the main product.

Conversion of Desoxydihydro Compound (IV) into 7β-Eremophilane(V). A mixture of IV (25 mg), ethanedithiol (2 m*l*), and BF_3-etherate (4 drops) was allowed to stand for 1 hr, and extracted with ether affording crude thioketal (40 mg). The crude thioketal in ethanol (2m*l*) was refluxed with Raney nickel (1 g) to give 7β-eremophilane (24 mg), which is identical with the authentic sample[3] by glc (PEG-20M, 2.6 m; 30 m*l*/min H_2, column temperature 180°C; retention time 6 min 20 sec).

Conversion of Dihydropetasitolone (III) into Desisopropylidenefukinone (VII) in Glc Column. Dihydropetasitolone III was passed through a glc column (PEG-20M; column temperature 180°C) to give desisopropylidenefukinone (VII), identical with the authentic sample[3] by comparison of IR spectra and glc.

Conversion of Dihydropetasitolone (III) into Fukinone (VI). Dihydropetasitolone III (250 mg) and phosphorus oxychloride (1 m*l*) was dissolved in pyridine (2 m*l*). After being kept standing for a week, the reaction mixutre was poured into ice-water and extracted with ether affording crude fukinone VI (200mg), which was purified by preparative glc (SPE, 2.6 m; 86 m*l*/min H_2; column temperature 190°C; retention time 8 min 20 sec).

Preparation of Petasitolone from Fukinone by Photosensitized Oxidation. A mixture of fukinone (2 g) and rose bengal (50 mg) dissolved in absolute methanol (250 m*l*) was irradiated with a fluorescent lamp (30 watt) under bubbling

7) G. O. Schenck, K. Gollnick, G. Buchwald, S. Schroeter, and G. Ohloff, *Ann. Chem.*, **674**, 93 (1964).

of air for 4 days, when all fukinone was consumed (on tlc analysis). A solution of sodium sulfite (4 g) and water (60 m*l*) was added to the reaction mixture and stirred for 10 hr. The solvent was evaporated *in vacuo*, and the residue was extracted with ether to give a crude oil (1.75 g). The crude oil was chromatographed repeatedly over silica gel eluted with benzene or light petroleum-ether (10 : 1) to afford pure petasitolone (0.9 g) which was identical with the natural specimen by comparison of IR and glc (SE-30, 2.6 m; 60-*ml*/min H_2; column temperature 130°C; retention time 8 min).

The authors wish to thank the staff of Shionogi Research Laboratory, Shionogi and Co., Ltd., for microanalysis and the Institute of Food Chemistry for the measurements of MS and NMR spectra.

BULLETIN OF THE CHEMICAL SOCIETY OF JAPAN, VOL. 44, 3167—3170 (1971)

Photolytic and Thermal Decompositions of 5-Substituted 1,2,3,4-Thiatriazoles in the Presence of Olefins. Reactions of Sulfur Atoms

Renji OKAZAKI, Kazumi OKAWA, Seiji WAJIKI, and Naoki INAMOTO

Department of Chemistry, Faculty of Science, The University of Tokyo, Hongo, Bunkyo-ku, Tokyo

(Received June 15, 1971)

Photochemical decompositions of 5-phenyl- and 5-amino-1,2,3,4-thiatriazoles in the presence of cyclohexene or tetramethylethylene led to the formation of the corresponding episulfide, the production of which has been explained in terms of sulfur atom reactions with the olefins. Kinetic measurements revealed the limitation of the reactions as a synthetic method of an episulfide from an olefin. Mechanism of the episulfide formation was briefly discussed. Thermal decompositions of these thiatriazoles in the presence of olefins gave rise to no episulfides.

Reactions of sulfur atoms have been extensively studied by Strausz and Gunning[1-3] using the photolysis of carbonyl sulfide. Almost all the reactions, however, have been carried out in gas phase and the precursor of sulfur atoms has been restricted only to carbonyl sulfide. Although carbonyl sulfide is probably the most useful source of sulfur atoms for mechanistic studies, the gaseous sulfide is an inconvenient precursor for synthetic studies. There are a few data on reactivities of sulfur atoms in solution,[4,5] and very recently Leppin and Gollnick reported direct photolysis of carbonyl sulfide in diverse organic solvents and reactions of sulfur atoms, thus formed, in solution.[6-8]

This paper describes the reactions of sulfur atoms generated from 5-substituted 1,2,3,4-thiatriazoles in organic solvents and their applicability as a synthetic method of episulfides from olefins.

Results and Discussion

5-Phenyl-1,2,3,4-thiatriazole (I) has been reported to decompose thermally into nitrogen, benzonitrile, and sulfur, and photochemically into the above three compounds and phenyl isothiocyanate.[9]

We found that photolysis of I in the presence of cyclohexene yielded cyclohexene episulfide (II). Results are summarized in Table 1. Identification and yield determination of the reaction products were carried out by means of gas chromatography (g.l.c.). Episulfide (II) was a sole product derived from reactions of sulfur atoms with cyclohexene, no cyclohexene thiols, insertion products, being formed.

Irradiation with high pressure or low pressure mercury lamp (HP or LP lamp) gave rise to II in a similar yield. Irradiation time was chosen so that the amount of II monitored by glc became approximately maximum, since II was found to decompose partially under these reaction conditions. Decomposition rates of I (rate constant k_1) were determined spectrophotometrically by following the decrease in the absorption ($\lambda_{max}^{CH_2Cl_2}$ 283 nm, ε 12000) and the decomposition was found to obey good first-order kinetics (see Table 1 for k_1 values).

Episulfide (II) was found to decompose also according to the first-order kinetics with rate constants (k_2) of 0.218 hr^{-1} (LP lamp) and 0.0848 hr^{-1} (HP lamp). Using these rate constants (k_1 and k_2) and assuming that k_3 and k_3' (rate constants of formation of II and

1) H. E. Gunning and O. P. Strausz, "Advances in Photochemistry," Vol. 4, ed. by N. A. Noyes, Jr., G. S. Hammond, and J. N. Pitts, Jr., Interscience Publishers, New York, N. Y. (1966), p. 143.

2) O. P. Strausz, "Organosulfur Chemistry," ed. by M. J. Hanssen, Interscience Publishers, New York, N. Y. (1967), Chapter 2.

3) O. P. Strausz and H. E. Gunning, "The Chemistry of Sulfides," ed. by A. V. Tobolsky, Interscience Publishers, New York, N. Y. (1968), Part I, p. 23.

4) U. Schmidt, K. Kabitzke, I. Boie, and C. Osterroth, *Chem. Ber.*, **98**, 3819 (1965).

5) M. Luria and A. Tereinin, *J. Phys. Chem.*, **72**, 305 (1968).

6) K. Gollnick and E. Leppin, *J. Amer. Chem. Soc.*, **92**, 2217 (1970).

7) E. Leppin and K. Gollnick, *ibid.*, **92**, 2221 (1970).

8) E. Leppin and K. Gollnick, *Chem. Ber.*, **103**, 2894 (1970).

9) W. Kirmse, *ibid.*, **93**, 2353 (1960).

Table 1. Products, rate constants (k_1), and α values[a] of photodecomposition of the thiatriazole (I) in the presence of cyclohexene

Solvent (dichloromethane): 150 ml; cyclohexene: 50 ml; I:5.00 g (30.7 mmol); reaction temperature: 20°C; reaction time: 18 and 10 hr for irradiation with HP[b] and LP,[b] respectively.

Ligth source[b]	Run	Products (%)				Recovered I (%)	k_1 (hr^{-1})	α
		$C_6H_{10}S$	PhCN	PhNCS	S_8			
LP	1	11	70	7	23	0	0.147	0.35
	2	11	87	11	—[c]	0	0.148	0.35
HP	1	8	44	4	30	—[c]	0.0395	0.26
	2	8(12)[d]	39(55)	5(7)	33(46)	29	0.0428	0.25

a) For definition, see Text.
b) HP and LP denote high pressure and low pressure mercury lamps, respectively.
c) Not determined.
d) Yield in parenthese based on I decomposed.

molecular sulfur, respectively) are much larger than k_1 and k_2, we can derive equation (1) on the basis of the following scheme and accordingly can estimate a hypothetical mole ratio (α) of II formed to I decomposed[10] when II is assumed not to photodecompose.

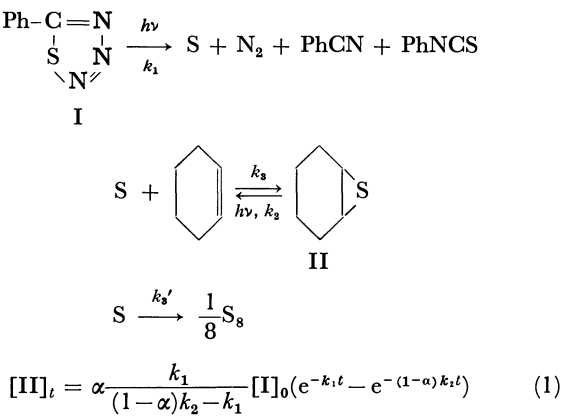

$$[\mathrm{II}]_t = \alpha\frac{k_1}{(1-\alpha)k_2-k_1}[\mathrm{I}]_0(e^{-k_1 t}-e^{-(1-\alpha)k_2 t}) \qquad (1)$$

where $[I]_0$ and $[II]_t$ stand for the concentration of I before irradiation and that of II at time t, respectively. The α values thus obtained (Table 1) indicate that, even if II were stable under these photochemical conditions, the yields might not exceed 35% and 26% under irradiation conditions with LP lamp and HP lamp, respectively. The low values of α seem to reveal the limitation in using sulfur atoms in solution as a reagent for episulfide syntheses.

Comparison of the present data with those of triplet sulfur atom reactions in gas phase deserves some mention. A triplet sulfur atom in gas phase has been reported to react with cyclopentene, structurally similar to cyclohexene, forming cyclopentene episulfide in 54% yield. In the case of other olefins such as ethylene, propylene and butene, the corresponding episulfides have been obtained in more than 80% yield.[11] The great difference in the yield of episulfides is probably attributable to the fact that sulfur atoms generated in solution become less reactive due to deactivation by collision with solvent molecules and readily polymerize into molecular sulfur instead of reacting with cyclohexene.

In this connection, the following two observations are noteworthy. First, the thermal decomposition of I in the presence of an olefin gave no episulfide. This is probably explicable in terms of low excess kinetic(translational) energy of sulfur atoms generated in the thermal reaction. Second, no thiols were formed in the photochemical reactions with cyclohexene. This suggests that the reactive species formed in the photodecomposition of I is a triplet sulfur atom.[1,8] According to Leppin and Gollnick, a singlet sulfur atom generated from carbonyl sulfide is effectively deactivated into a triplet species in alcohol, alkyl cyanide and aromatic hydrocarbon solvents.[6] It is reasonable that dichloromethane, used as solvent in the present study, might be also a solvent favorable for the intersystem-crossing because of heavy atom effect of the chlorine atoms.

Table 2. Quenching of photodecomposition of thiatriazole (I) with naphthalene or piperylene in dichloromethane-cyclohexene (3:1)

Quencher	Products (%)			Recovered I (%)
	$C_6H_{10}S$	PhCN	PhNCS	
Naphthalene[a]	12	80	6	0
Piperylene[b]	5[c]	74[c]	6[c]	20[c]

a) With LP lamp. See Experimental.
b) With HP lamp. See Experimental.
c) Yield based on I decomposed.

Quenching experiments were carried out with naphthalene and piperylene which are known as efficient quenchers for a triplet species. Comparison of the results listed in Table 2[12] with those in Table 1 leads to the conclusion that the reactions were not affected by the quenchers and accordingly the triplet state of I would not be involved in the photoreactions, though the possibility that a short-lived triplet state might be involved cannot be excluded completely.

On the basis of the observations described so far, the

10) Since a small amount of phenyl isothiocyanate was actually formed, the exact value is equal to $\alpha/(1-P/100)$, where P is a percentage yield of phenyl isothiocyanate based on I decomposed. However, here we use the approximate value of α for simplicity.

11) E. M. Lown, E. L. Dedio, O. P. Strausz, and H. E. Gunning, *J. Amer. Chem. Soc.*, **89**, 1056 (1967).

12) Although the yield of II in the reaction with piperylene as quencher is lower than that in one without the quencher, this can be readily explained from the fact that a diene also reacts with sulfur atoms.[1]

following scheme is plausible for formation of II.[13]

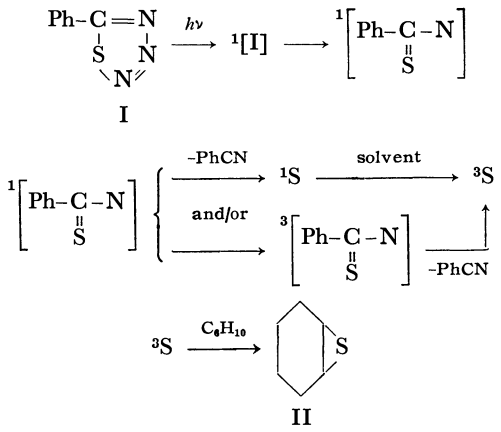

Difference in α values (0.35 and 0.26) caused by change of irradiation conditions can be accounted for probably by the difference in energy content of sulfur atoms; the triplet sulfur atom generated under irradiation with LP lamp might have much more energy than that generated under irradiation with HP lamp.

Table 3. Effect of cyclohexene concentration upon the yield of cyclohexene episulfide[a]

C_6H_{10}/CH_2Cl_2 (ml/ml)	Products (%)[b]			
	$C_6H_{10}S$	PhCN	PhNCS	S_8
10/190	7	78	11	—[c]
50/150	11	70	7	23
150/50	20	63	9	51

a) I used, 5.00 g (30.7 mmol); light source, LP lamp; reaction time, 10 hr; reaction temperature, 20°C.
b) Yield based on I decomposed.
c) Not determined.

Attempts were made to increase the α value and consequently the yield of II by increasing the concentration of cyclohexene in the reaction solution. Results are given in Table 3. In 75% (v/v) cyclohexene solution the yield of II amounted to 20%. This value, though not satisfactory for synthetic purpose, is larger than other ones reported for episulfide formation with sulfur atoms in liquid phase; in the presence of cyclohexene, photodecomposition of ethyl isothiocyanate,[4] thermal decomposition of diethyl tetrasulfide,[14] and photodecomposition of carbonyl sulfide[8] have been reported to give the episulfide (II) in 7, 8, and 2% yields, respectively.

Table 4. Yields of episulfide in photodecompositions of thiatriazoles (I and III) in the presence of olefin

Thiatriazole	Light source	Olefin[c] (ml)	Solvent (ml)	Reac. time (hr)	Episulfide (%)
I[a]	HP	C(50)	150	18	6
I[a]	LP	C(80)	110	5	7
I[a]	HP	T(10)	190	16	1
I[a]	LP	T(10)	190	12	6
III[b]	HP	C(50)	150	10	0.4
III[b]	LP	C(50)	150	6	7
III[b]	HP	T(20)	140	19	0.5
III[b]	LP	T(20)	140	9	6

a) 5.00 g (30.7 mmol) in benzene.
b) 2.70 g (26.5 mmol) in methanol.
c) C and T stand for cyclohexene and tetramethylethylene, respectively.

13) Attempts to trap Ph–C(=S)–N fragment with maleic anhydride were unsuccessful.

When the photodecomposition of I was carried out in the presence of cyclohexene or tetramethylethylene with benzene as solvent, similar results were obtained though the yields of the episulfide were somewhat low (Table 4). The reason for the low value in the reaction with tetramethylethylene is not clear.

5-Amino-1,2,3,4-thiatriazole (III) (λ_{max}^{MeOH} 267 nm, ε 4600), which is quite easily accessible from semicarbazide, could be employed as sulfur atom precursor (Table 4). In this case again, however, the yields of the episulfide were low, especially when irradiated with HP lamp.

Experimental

5-Phenyl-[15] and 5-amino-1,2,3,4-thiatriazoles,[16] cyclohexene episulfide,[17] and tetramethylethylene episulfide[18] were prepared by the methods described in literature. Gas chromatographic analyses were carried out using diethylene glycol polysuccinate column at 100°C.

Photodecomposition of 5-Phenyl-1,2,3,4-thiatriazole (I) in Dichloromethane. A General Procedure: Dichloromethane solution of the thiatriazole (5.00 g, 30.7 mmol) and cyclohexene was irradiated with high pressure (HP lamp) (Rikosha, 100 W) or low pressure mercury lamp(LP lamp) (Rikosha, 160 W). All the reactions were carried out under nitrogen atmosphere at 20°C. Rate measurements were performed spectrophotometrically by following the decrease of absorption at 283 nm (ε 12000). Product analyses were made as follows. The residue obtained after evaporation of the excess olefin and the solvent was dissolved again in dichloromethane. The insoluble part was sulfur. The soluble part was decanted into a volumetric flask and subjected to gas chromatographic analyses.

Photodecompositions of 5-Phenyl- (I) or 5-Amino-1,2,3,4-thiatriazole (III) in Benzene or Methanol. The reactions were carried out in a similar manner to that in the reactions in dichloromethane. Product analyses were not made except for episulfide (II).

Photodecomposition of Cyclohexene Episulfide (II). The episulfide (1.04 g) dissolved in a mixture of dichloromethane (150 ml) and cyclohexene (50 ml) was irradiated with LP or HP lamp. The decomposition rate was determined by following the decrease of II using glc.

Quenching Experiments. a) Quenching with Piperylene: The thiatriazole (I) (2.00 g, 12.3 mmol), cyclohexene (20 ml), and piperylene (6.8 g, 100 mmol) were dissolved in dichloro-

14) S. O. Jones and E. E. Reid, *J. Amer. Chem. Soc.*, **60**, 2452 (1938).
15) K. A. Jensen and C. Pedersen, *Acta Chem. Scand.*, **4**, 1349 (1950).
16) E. Lieber, E. Oftedahl, C. N. Pillai, and R. D. Hites, *J. Org. Chem.*, **22**, 441 (1957).
17) E. E. van Tamelen, "Organic Syntheses," Coll. Vol. IV, p. 232 (1963).
18) M. A. Youtz and P. P. Perkins, *J. Amer. Chem. Soc.*, **51**, 3508 (1929).

methane (60 m*l*), and the solution was irradiated with HP lamp for 18 hr. After similar work-up to that in the other experiments for (I), product analyses were made by glc.

b) Quenching with Naphthalene: The thiatriazole (I) (5.00 g, 30.7 mmol), cyclohexene (50 m*l*), and naphthalene (3.85 g, 30.1 mmol) were dissolved in dichloromethane (150 m*l*) and the solution was irradiated with LP lamp for 10 hr. Product analyses were performed similarly.

Thermal Decomposition of the Thiatriazole (I) or (III) in the Presence of Cyclohexene. The thiatriazole (I) (5.00 g, 30.7 mmol) in a cyclohexene(90 m*l*)-toluene(100 m*l*) mixture was heated at about 100°C for 20 hr. After usual work-up, no cyclohexene episulfide was formed. The thiatriazole (III) (2.70 g, 26.5 mmol) and cyclohexene (50 m*l*) were dissolved in methanol (150 m*l*), and the solution was refluxed for 7 hr. No formation of II was observed.

BULLETIN OF THE CHEMICAL SOCIETY OF JAPAN, VOL. 44, 3170—3174 (1971)

Adsorptive Properties of Decationated Zeolite for Some Aromatic Hydrocarbons as Observed by Gas Chromatography

Hiroshige MATSUMOTO,* Hideo FUTAMI,** Fumiyoshi KATO, and Yoshiro MORITA

Department of Applied Chemistry, School of Science and Engineering, Waseda University, Nishiokubo, Shinjuku-ku, Tokyo

(Received March 20, 1971)

The adsorptive properties of decationated zeolite for simple aromatic hydrocarbons, such as benzene, toluene, ethylbenzene, and xylenes were investigated by means of gas chromatography at 270—330°C. The specific retention volumes of these alkylbenzenes increased with the increase in the sodium ion content and the rise in the pretreatment temperature of zeolite. The adsorption heat was substantially independent of the sodium content, but slightly increased with the rise in pretreatment temperature above 550°C. A linear relationship was found between the decrease in the ionization potential of aromatic hydrocarbons and the increase in the heat of adsorption. For comparison, the adsorption of ethylene was also examined. With the rise of pretreatment temperature of zeolite, the retention volume of ethylene decreased. On introduction of water to the system, the retention volume of ethylene reversibly increased, whereas that of aromatic hydrocarbons decreased. In accordance with the decationation process of zeolite proposed by Hall *et al.*, these aromatic hydrocarbons are adsorbed preferably on tricoordinated aluminum site as well as on sodium ion to form the charge transfer complex, while ethylene interacts with hydroxyl group to form the carbonium ion or hydrogen-bonded complex.

In spite of the widespread use of decationated zeolite as a catalyst for the reactions of aromatic hydrocarbons, its adsorptive properties are still open to question. Adsorption measurement at an elevated temperature is improtant in elucidating the kinetics and mechanisms of catalysis. Little information, however, is available on high temperature adsorption of aromatic hydrocarbons on decationated zeolite. Difficulty in experiment seems to arise from the decomposition and poor volatility of the adsorbate. Gas chromatography might be of use to overcome this difficulty.[1,2] In this work, the apparent adsorption constant and apparent adsorption heat of several aromatic hydrocarbons on decationated zeolite were determined using a simple gas chromatographic technique.

Significant advance has been made in understanding the acid property of decationated zeolite by spectroscopic observations, particularly by infrared absorption. Most investigators agree that the acidic sites on this solid consist of the Brönsted and Lewis acids and that the former can be converted into the latter by thermal treatment. The adsorptive properties of decationated zeolite for some aromatic hydrocarbons was discussed in accordance with this concept.

Experimental

Materials. Sodium zeolite used in this work was Linde Y Molecular Sieve (SK-40). The ammonium form was prepared by the ion exchange of sodium zeolite with 0.05—0.5N solution of ammonium acetate at 50°C. The exchange levels of ammonium zeolite, defined as the percentage of the original sodium ion replaced, were determined to be 14, 25, 37, 59, and 67. The zeolite was preliminary dried at 110°C for 4 hr, pelletized, and ground to the size 48—60 mesh. X-ray examination revealed good crystallinity in these materials. Aromatic hydrocarbons (commercial guaranteed grades) were dehydrated with metallic sodium, distilled and passed through a silica gel column before use.

Apparatus and Procedure. The apparatus was similar to that of the usual gas chromatogragh reported by Everly.[1] The unit consisted of a pulse injection system connected in series to a gas chromatographic column packed with 0.2 g of zeolite and a thermal conductivity cell. The column made from stainless steel was settled in an iron block to keep the temperature constant. The maximum temperature variation over the column was less than 1°C. The carrier gas (hydrogen) was passed through a purification train of Pd and 5A Molecular Sieve. No appreciable change in peak width and retention volume of aromatic hydrocarbons was observed with carrier gas (helium, agron, and nitrogen), its flow rate, and

* Present address: Chemistry Department, Memorial University St. John's, Newfoundland, Canada.

** Present address: General Laboratory of Tokyo Gas Co., Ltd., Shibaura, Minato-ku, Tokyo.

1) P. E. Eberly Jr., *J. Phys. Chem.*, **65**, 68 (1961); **66**, 812 (1962).

2) H. W. Habgood, "The Solid-Gas Interface," Marcel Dekker, New York (1967).

particle size of zeolite.

The weight change of zeolite with thermal treatment was measred by a micro-thermobalance under the condition similar to those in gas chromatography. The effect of water vapor on the retention volume were examined by using a sideline in which the carrier gas passed through a saturator system, consisting of three bubble-vessels filled with water.

Prior to each measurement, fresh zeolite was treated at the desired temperature for 2 hr in a stream of carrier gas. A small amount of argon, as a non-adsorbable gas, was added into a pulse in order to determine the net retention volume of hydrocarbons. The corrected specific retention volume V_r was calculated by means of the equation[3]

$$V_r = (t-t_0)\frac{T}{298}\cdot\frac{3}{2}\cdot\frac{(P_i/P_0)^2-1}{(P_i/P_0)^3-1}\cdot\frac{F}{W}$$

where t and t_0 are the retention times (min) of a hydrocarbon and inert gas, respectively, T is the column temperature (°K), P_i and P_0 are the pressures at the column inlet and outlet, respectively, F is the flow rate of carrier gas (ml/min), and W is the weight of zeolite packed (g).

When a linear isotherm is expected, the apparent equilibrium constant of adsorption K can be obtained by

$$K = \frac{V_r}{RT}$$

where R represents the gas constant.[4] Linearity of an isotherm may be indirectly confirmed by the fact that the specific retention volume is independent of the partial pressure of adsorbate. The result is shown in Fig. 1, in terms of the relation between V_r and the pulse volume of hydrocarbon.

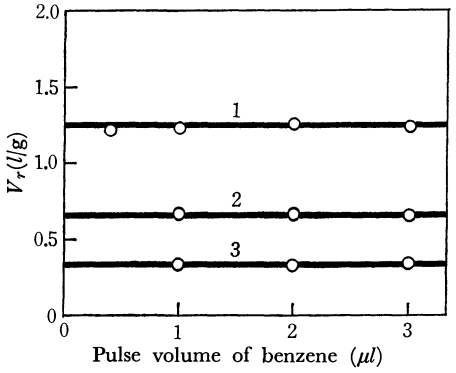

Fig. 1. Effect of injected pulse volume on the specific retention volume.
37% Exchanged zeolite treated at 500°C
Adsorption temperature: 1, 270°C; 2, 300°C; 3, 330°C

Results

Effect of Sodium Ion. Zeolite cation plays an important role for the adsorptive property of zeolite. In the adsorption of aromatic hydrocarbon on decationated zeolite with various degree of ion exchange, the retention volume markedly decreased with the increase of exchange level. The logarithms of V_r/RT for benzene and *o*-xylene are plotted against the reciprocal of the absolute temperature in Figs. 2 and 3, respectively. The data show linear relationships which

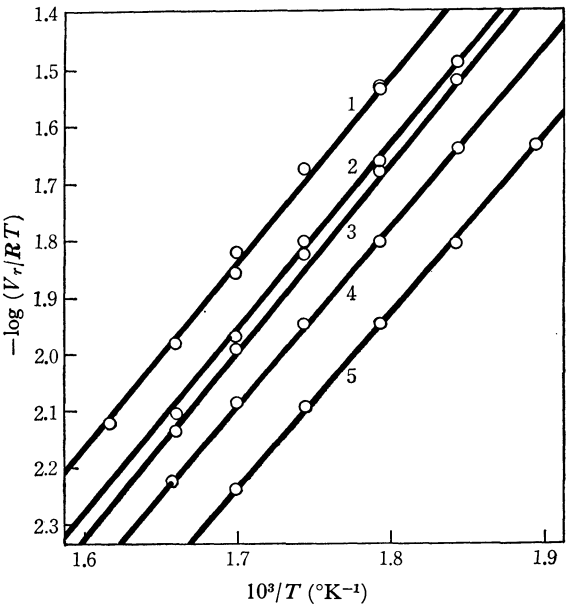

Fig. 2. Temperature dependence of the retention volume of benzene on the zeolites with various degrees of ion exchange.
Pretreatment temperature; 500°C
Ion exchange level: 1, 0 and 14%; 2, 25%; 3, 44%; 4, 59%; 5, 67%

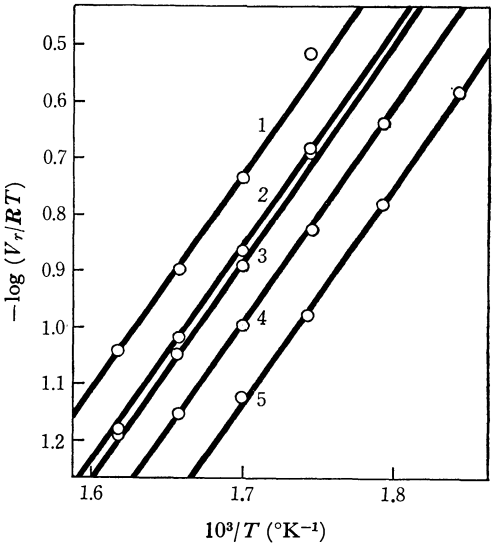

Fig. 3. Temperature dependence of the retention volume of *o*-xylene on the zeolites with various degrees of ion exchange.
Pretreatment temperature: 500°C
Ion exchange level: 1, 0 and 14%; 2, 25%; 3, 44%; 4, 59%; 5, 67%

have practically the same slopes. The apparent heats of adsorption are derived from the tangent of these plots. We see that the apparent adsorption heats of benzene and *o*-xylene are independent of the sodium ion content in the zeolite treated at 500°C, being estimated to be 14.9 and 18.3 kcal/mol, respectively. The former value is rather small in comparison with 15.5 kcal/mol for sodium X zeolite.[1] In similar examinations of other hydrocarbons such as toluene, ethylbenzene and *m*- and *p*-xylene, no appreciable change in the adsorption heat was observed with the change in ex-

3) A. J. M. Keulemans, "Gas Chromatography," Reinhold, New York (1959).

4) J. J. Yan Deemter, F. J. Zwiderweg, and A. Klinkenberg, *Chem. Eng. Sci.*, **5**, 271 (1956).

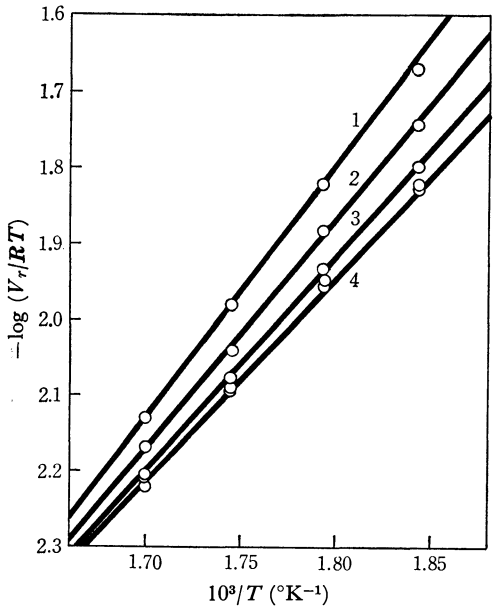

Fig. 4. Temperature dependence of the retention volume of benzene on the zeolite treated at various temperatures.
Ion exchange level: 67%
Pretreatment temperature: 1, 650°C; 2, 600°C; 3, 550°C; 4, 500, 450, 400, and 350°C

change level of zeolite. Thus, it might be expected that ion exchange influences not the strength but the number of the adsorptive sites on zeolite surface.

Effect of Thermal Treatment. Thermal treatment also influences adsorptive properties of decationated zeolite. Figure 4 shows the temperature dependence of benzene adsorption on 67% exchanged zeolite treated at various temperatures. Hardly any variation was observed in adsorptive properties of the zeolite subjected to the treatment at 350—500°C. In the higher temperature range of the treatment, both the specific retention volume and the apparent adsorption heat increased with the rise in the pretreatment temperature.

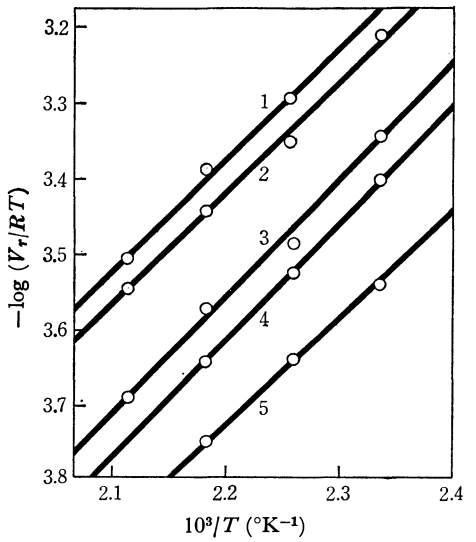

Fig. 5. Temperature dependence of the retention volume of ethylene on the zeolite treated at various temperatures.
Ion exchange level: 67%
Pretreatment temperature: 1, 400°C; 2, 350°C; 3, 450°C; 4, 500°C; 5, 600°C

This might indicate that the thermal treatment at a higher temperature changes the adsorption sites on decationated zeolite.

For comparison, similar examinations were carried out for ethylene adsorption. The results are shown in Fig. 5. There is a marked difference between the adsorption of ethylene and that of benzene. With the rise of temperature of heat treatment, the specific retention volume of ethylene decreased, whereas that of benzene increased. The apparent adsorption heat of ethylene is amlost independent of the pretreatment temperature, while that of benzene depends on the pretreatment temperature above 550°C. It seems that benzene and ethylene are adsorbed on different sites.

TABLE 1. EFFECT OF WATER ADDITION ON THE RETENTION VOLUME OF BENZENE AND ETHYLENE

Condition	V_r of benzene at 225°C (l/g)	V_r of ethylene at 155°C (ml/g)
After calcination at 600°C[a)]	3.41	9.80
On introduction of water	2.22[b)]	14.4[c)]
After calcination at 600°C	3.45	9.00
On reintroduction of water	2.08[b)]	12.0[c)]

a) 67% exchanged zeolite
b) 18.9 mmHg of water pressure
c) 4.6 mmHg of water pressure

Effect of Water Vapor. The effect of thermal treatment on adsorptive properties is presumably due to the water content in zeolite, since a major portion of ammonia seems to evolve below 300°C.[5] The effect of water was examined by introducing water vapor to the system. The results are shown in Table 1. For 67% exchanged zeolite calcined at 600°C, the specific retention volumes of benzene and ethylene are 3.41 l/g at 225°C and 9.8 ml/g at 155°C, respectively. On introduction of water to the system, the retention volume of benzene decreased and reached the stationary value of 2.22 l/g under 18.9 mmHg of water pressure, whereas that of ethylene increased to the level of 14.4 ml/g under 4.6 mmHg of water pressure. When addition

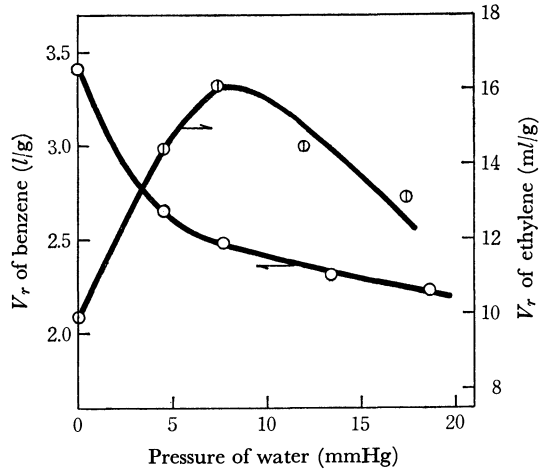

Fig. 6. Retention volume of benzene and ethylene under various pressures of water.

5) J. W. Ward, *J. Catal.*, **9**, 225 (1967).

of water was stopped and the zeolite was treated at 600°C, the original levels of the retention volumes were restored. Again on further introduction of the same pressure of water, each retention volume showed almost the same value as that on the first introduction.

For the adsorption of benzene and ethylene, poisoning and promotive effects of water vapor increased with the increase of its vapor pressure in carrier gas as shown in Fig. 6. A low retention volume of ethylene under a high pressure of water seems to be due to poisoning by the adsorption of excessive water on the surface.

Table 2. The retention volume and the adsorption heat of several aromatic hydrocarbons

Hydrocarbons	V_r at 330°C (l/g)	Q (kcal/mol)
Benzene	0.267	14.9
Toluene	0.947	16.1
Ethylbenzene	2.40	17.4
o-Xylene	3.74	19.1
m-Xylene	2.47	17.8
p-Xylene	2.80	19.2

Sample: 67% exchanged zeolite treated at 600°C

Effect of Alkyl Substituent. Similar measurements were carried out for several alkylbenzenes such as toluene, ethylbenzene, and xylenes in order to confirm the influence of alkyl groups. No chemical reaction of these compounds occurred. The specific retention volume and apparent heat of these hydrocarbons are shown in Table 2. The retention volume increased with the number of alkyl substituents. It can be seen that the larger the retention volume, the larger the heat of adsorption. In the case of cumene and higher alkylbenzene, dealkylation and disproportionation occurred under similar conditions. Adsorption of these alkylbenzenes was not examined, since sorption mechanism might be influenced by the adsorption of reaction products.

Discussion

In the adsorption of π-base such as aromatic hydrocarbons, there is no doubt that the adsorptive sites of decationated zeolite are acidic. It is, however, still obscure whether such sites are the Brönsted acid or Lewis acid. Following Uytterhoeven, Christner, and Hall,[6] decationation process of zeolite can be visualized as follows

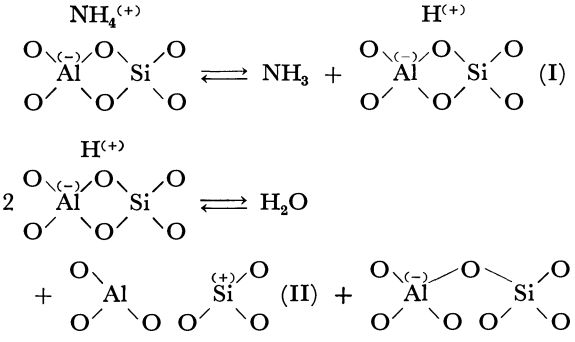

6) J. B. Uytterhoeven, J. B. Christner, and W. K. Hall, *J. Phys. Chem.*, **69**, 2117 (1965).

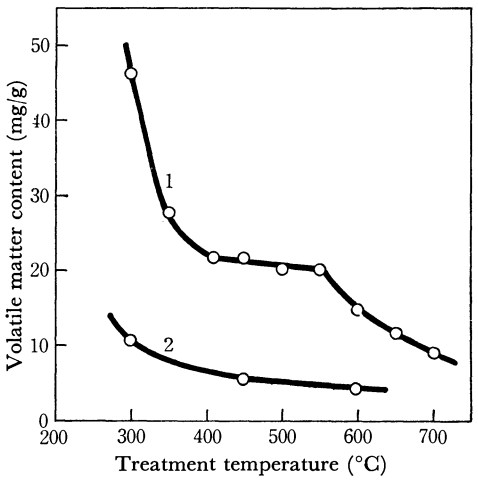

Fig. 7. Weight changes of decationated and sodium zeolite as a function of temperature.
1, Decationated zeolite (67% exchanged)
2, Sodium zeolite

The Brönsted acid site is given by I and the Lewis acid site by II.

Figure 7 shows weight changes of 67% decationated and the original sodium zeolite as a function of the temperature of heat treatment. The results are expressed in terms of the amount of volatile component (water and ammonia) of the samples after each calcination, assuming that the zeolite treated at 1000°C contains no volatile matter. For the decationated zeolite, a marked weight loss takes place below 400 and above 550°C. Effluent gas analysis shows that the initial weight decrease is due to the evolution of ammonia and of water (probably physically adsorbed water). Although the evolution is still continued little by little until 550°C, only that of water is observed above 550°C. It might be that below 400°C the greater part of ammonium ions has been decomposed to ammonia and proton to produce the Brönsted acid sites, and that the removal of the protons as water to generate the Lewis acid sites starts around 550°C. On the other hand, no appreciable weight change of sodium zeolite is detected above 400°C.

It might be considered that aromatic hydrocarbon is adsorbed more preferably on the Lewis acid site than on the Brönsted acid site, since the specific retention volume markedly increased by the treatment above 550°C (Fig. 8). The retention volume of ethylene decreased with the rise of temperature of heat treatment of decationated zeolite. This trend is similar to that of catalytic activity in the reactions *via* carbonium ion intermediate.[7,8] Ethylene seems to be adsorbed on the Brönsted acid site to form carbonium ion or strong hydrogen-bonded complex as a precursor to carbonium ion.[6] Ward[5] and Hattori *et al.*[9] have recognized in infrared measurements of adsorbed pyridine on decationated zeolite that the strong Lewis acid site can be

7) P. B. Venuto, L. A. Hamilton, and P. S. Landis, *J. Catal.*, **5**, 484 (1966).

8) J. Turkevich, Japan-U. S. A. Seminer on Catalytic Sci. (Tokyo, 1968).

9) H. Hattori and T. Shiba, *J. Catal.*, **12**, 111 (1968).

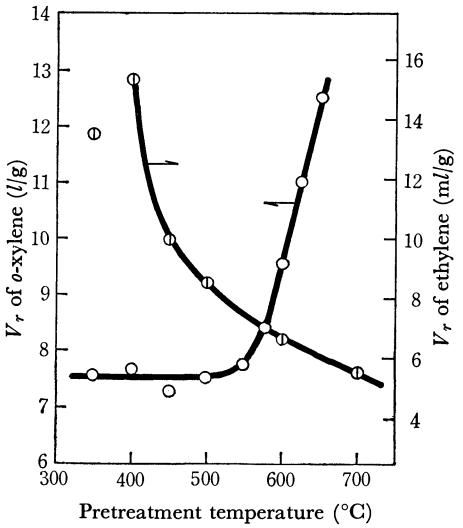

Fig. 8. The retention volume of *o*-xylene and ethylene as a function of pretreatment temperature of zeolite.
Ion exchange level: 67%
Adsorption temperature: *o*-xylene, 285°C; ethylene, 185°C

converted into the Brönsted acid site by the addition of water. We see in Table 1 and Fig. 6 that the specific retention volume of ethylene increased and that of benzene decreased by the introduction of water. Thus, the adsorptive sites of decationated zeolite available for ethylene and benzene seem to be the Brönsted acid and the Lewis acid, respectively.

Alkylbenzene are probably adsorbed not only on tricoordinated aluminum atoms (the Lewis acid) but also on sodium cations, since the sodium ions on the zeolite are almost exposed by heat treatment above 400°C (Fig. 7) and the specific retention volume increases with the increase in the sodium ion content (Figs. 2 and 3). The apparent adsorption heat of benzene is practically independent of the sodium ion content. The adsorptive strength of sodium sites, therefore, does not appear to be affected by a change in the concentration. On the other hand, the adsorption heat of benzene increased with the rise of the temperature of heat treatment above 550°C. This probably indicates that tricoordinated aluminum sites are stronger than sodium sites for the adsorption of benzene.

The interaction between π-base and electrophilic site would be due to charge transfer. It can be seen that both the retention volume and the adsorption heat of benzene derivatives increased with the extent of alkyl substitution (Table 2). The electron-releasing alkyl groups increase the electron density of aromatic ring, making it more susceptible to interact with tricoordinated aluminum atom or sodium ion. This might be confirmed quantitatively with the ionization potential sequence of adsorbates. Figures 9 and 10 show the linear correlations of logarithmic adsorption constant and adsorption heat, respectively, with the ionization

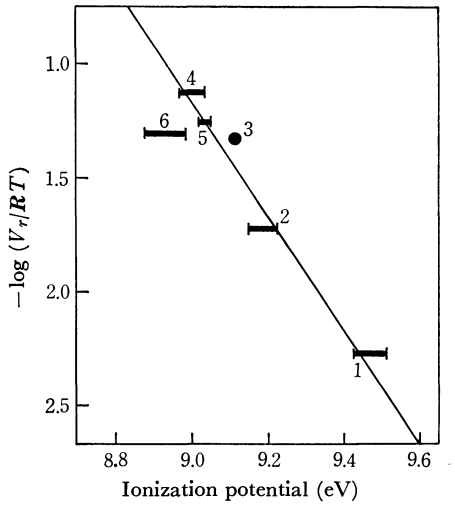

Fig. 9. Relation between the apparent adsorption constant and the ionization potential of aromatic hydrocarbons.
1, benzene; 2, toluene; 3, ehtylbenzene; 4, *o*-xylene; 5, *m*-xylene; 6, *p*-xylene

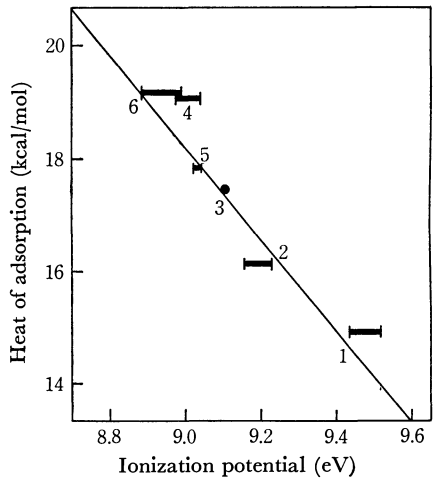

Fig. 10. Relation between the apparent adsorption heat and the ionization potential of aromatic hydrocarbons.
1, benzene; 2, toluene; 3, ethylbenzene; 4, *o*-xylene; 5, *m*-xylene; 6, *p*-xylene

potential of aromatic hydrocarbons. The values of the ionization potential (measured by the electron impacting method) are taken from literature,[10] thick lines indicating the variations of these values. It can be seen that the higher the ionization potential, the smaller the adsorption constant and adsorption heat. These correlations suggest the charge transfer interaction between aromatic hydrocarbon and decationated zeolite.

10) P. E. Honing, *J. Chem. Phys.*, **16**, 105 (1948); J. D. Morrison and A. J. C. Nicholson, *ibid.*, **20**, 1021 (1952); F. H. Field and J. L. Franklin, *ibid.*, **22**, 1895 (1954); I. Omura, H. Baba, and K. Higashi, *J. Phys. Soc. Japan*, **10**, 317 (1955); G. F. Grable and G. L. Kearns, *J. Phys. Chem.*, **66**, 436 (1962).

NOTES

BULLETIN OF THE CHEMICAL SOCIETY OF JAPAN, VOL. 44, 3175—3176 (1971)

The NMR Chemical Shifts of Aromatic Ring Protons. II. The Substituent Chemical Shift of the Ring Protons of 1-Substituted Naphthalenes

Yasuhide YUKAWA, Yuho TSUNO, and Nobujiro SHIMIZU

The Institute of Scientific and Industrial Research, Osaka University, Yamada-kami, Suita, Osaka

(Received September 25, 1970)

We have shown, in the preceding paper, that the chemical shift of *o*-, *m*-, and *p*-ring protons of a number of monosubstituted benzenes could be determined without any difficulty and that they could be assigned without ambiguity by means of the statistically-distributed deuterium substitution method.[1] In the present paper, we will report the application of the same technique to the naphthalene-series, for which few systematic studies seem to have been reported.[2]

Ring hydrogens of naphthalene were about 85% statistically replaced by deuteriums through the hydrogen-deuterium exchange reaction of naphthalene in the presence of a small amount of aluminum trichloride as a catalyst. The extent of the substitution was checked by IR analysis at appropriate intervals. The NMR spectrum of the deuterated naphthalene showed only two singlets corresponding to α and β protons; the intensities of both signals were nearly the same. Since there is little possibility that more than two hydrogens remain at vicinal positions, the spectra are very much simplified to give only two signals, without any splitting of the signals caused by spin-spin interactions. Although the direct assignment of two peaks from the spectrum was impossible, it was made possible by changing chemically their relative intensities up to *ca.* 3: 2, as is shown in Fig. 1-A. This modification was done by heating the above deuterio-naphthalene under reflux with trifluoroacetic acid. As the dedeuteration occurs much more rapidly at the α-position than at the β-position in trifluoroacetic acid, the more intense signal must be assigned to α-protons, and the less intense one, to β-protons. A series of 1-substituted naphthalenes (X in 1-X-Naph-d_6; NO_2, CN, Br, COOH, H, OH, NH_2) were prepared from this partially-deuterated naphthalene. The NMR spectra of Naph-X are generally made up of seven singlets, four of which are little smaller in their intensities than the other three singals, as is shown in Fig. 1-B and 1-C. From this difference in intensity, the smaller four signals can be assigned to β-protons, or 2, 3, 6, and 7-protons, and the rest, to α-protons, or 4, 5, and 8-protons. In some cases, more than two signals overlapped, but it was still possible to analyse the spectra rather precisely by considering the ratio of the intensities of the signals in detail. All the measurements were carried out with a Hitachi R-20 NMR spectrometer at 60 MHz. The chemical shifts were measured at 5 mol% in a *N*,*N*-dimethylacetamide solution from the internal standard TMS. The chemical shifts of each signal can be determined precisely, within ±0.5 Hz in most cases, but the accuracy may fall as much as to ±1.5 Hz in the worst case. The equal intensities of the four signals belonging to the β-protons unfortunately provided us with a serious disadvantage in making further unambiguous assignments of the individual signals, and the same is also true for the three signals corresponding to the α-protons. Nevertheless, plausible assignments can be done by comparison with the data for mono-substituted benzenes and also with their solvent effects.

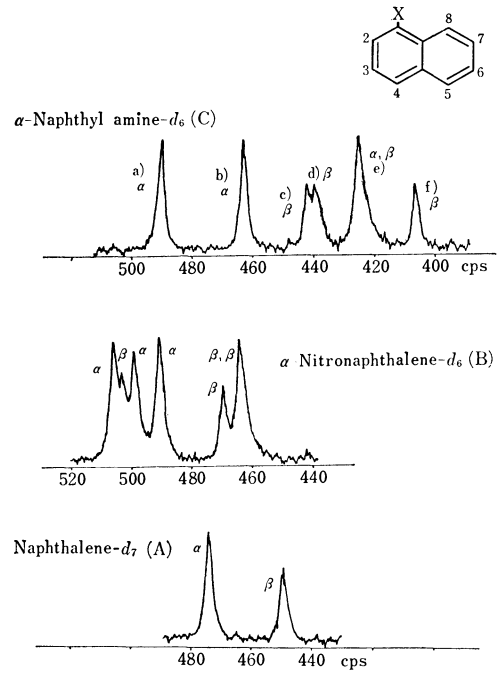

Fig. 1. NMR spectra of deuterated naphthalenes.

In the case of α-naphthylamine in a *N*,*N*-dimethylacetamide solution, for instance, the individual signals could be assigned as follows; one (signal *a*) of the three signals belonging to the α-protons is more deshielded than that of unsubstituted naphthalene ($\Delta = -15.8$ Hz). Since the amino group has a large shielding effect in the benzene series, the *a* signal must be assigned to the 8-proton, of the other two, *e* (two signals overlapped) at a high field ought to be assigned to the 4-proton, and *b*, to the 5-proton. The *f* and *e* signals referred to β-protons can be assigned to 2- and 3-protons respectively by analogy with the relative chemical shifts of the aniline protons. It should also be possible to assign the *d* signal to the proton at the conjugate 7-

1) Y. Yukawa, Y. Tsuno, and N. Shimizu, This Bulletin, **44**, 2843 (1971).

2) P. R. Wells, *Aust. J. Chem.*, **17**, 967 (1964). Y. Sasaki, M. Suzuki, T. Hibino, K. Karai, M. Hatanaka, and I. Shiraishi, *Chem. Pharm. Bull.* (Tokyo), **16**, 1367 (1968).

Table 1. Relative chemical shift of the ring protons of α-monosubstituted naphthalenes

Subst.	2	3	4	5	6	7	8
NO_2	−54.1	−21.0	−27.0	−17.0	−15.2	−15.2	−30.2
CN	−39.7	−19.8	−26.0	−14.0	−11.4	−13.4	−14.9
COOH	−47.1	−8.9	−15.7	−7.1	−4.9	−4.9	−69.2
Br	−22.6	4.0	−4.8	−4.8	−7.0	−10.4	−16.3
OH	31.0	9.8	34.6	7.6	4.2	9.8	−21.6
NH_2	41.2	22.9	47.7	11.4	7.6	9.6	−15.8

Relative values of 2,3,6, and 7-protons were determined from the chemical shift of the β-proton of naphthalene and those of 4, 5, and 8-protons from that of α-proton.

position, and *c*, to the 6-proton, considering the fact that the resonance effect is mostly responsible for the determination of the chemical shifts. The assignments for the other compounds were obtained in a similar manner. In most cases, the resulting assignment for the protons on the substituted ring is believed to be highly reliable, because of the rigorous agreement of the relative variations of the substituent chemical shifts between the corresponding protons of benzene and naphthalene. However, for the β-protons on the other ring, certain ambiguities might unfortunately be involved in the tentative assignment. The relative chemical shifts are listed in Table 1.

The substituent effects in the substituted ring of the naphthalene serise are linearly correlated with those of the corresponding protons in the benzene series; $\Delta\Delta\delta^2 = 1.09\,\Delta\Delta\delta^0$, $\Delta\Delta\delta^3 = 0.98\,\Delta\Delta\delta^m$, and $\Delta\Delta\delta^4 = 0.89\,\Delta\Delta\delta^p$. This may indicate that there is not much difference in the substituent effect on the ring proton chemical shift between the benzene and naphthalene series. The substituent effects on the respective protons are expressed in terms of the σ_p^0 and $\Delta\bar{\sigma}_R^+$ in just the same way as for the benzene series;

$$\Delta\Delta\delta^3 = -27.7(\sigma_p^0 + 0.29\Delta\bar{\sigma}_R^+)$$
$$\Delta\Delta\delta^4 = -38.7(\sigma_p^0 + 0.87\Delta\bar{\sigma}_R^+)$$
$$\Delta\Delta\delta^5 = -22.7(\sigma_p^0 + 0.13\Delta\bar{\sigma}_R^+)$$
$$\Delta\Delta\delta^6 = -19.1(\sigma_p^0)$$
$$\Delta\Delta\delta^7 = -19.7(\sigma_p^0 + 0.17\Delta\bar{\sigma}_R^+)$$

In these treatments, σ_p^0 is used as a conventional measure of the unexalted polar effect throughout the series, since no σ^0 values for the respective naphthalene position are available. Perhaps, in view of the analogy to the benzene system, $\Delta\Delta\delta^3$ should be described in terms of the σ_m^0 parameter. This results in the correlation;

$$\Delta\Delta\delta^3 = -32.1(\sigma_m^0 + 0.45\Delta\bar{\sigma}_R^+)$$

Similarly, the chemical shifts of the non-conjugate 6-proton are given by;

$$\Delta\Delta\delta^6 = -21.0(\sigma_m^0 + 0.23\Delta\bar{\sigma}_R^+)$$

It is evident from these correlations that the protons on the substituted ring are more susceptible to both the polar and resonance effects of substituents than those on the other ring. The same treatment cannot be applied to the chemical shifts of the 8-proton. As the ordinary electronic effects of substituents could not be transmitted so effectively to this position, the behavior of this proton may give many valuable information about the particular interactions with substituents at the closest position.[3]

From the theoretical point of view, it should be more reasonable to treat these results in terms of the inductive σ_i and π-electronic σ_π parameters.[4] The results of this treatment and a comparison with recent results obtained by means of Taft and Dewar treatments[5] will be the subjects of a forthcoming paper.

3) R. H. Martin, N. Defay, and F. Greets-Evard, *Tetrahedron*, **20**, 1505 (1964).
4) Y. Yukawa and Y. Tsuno, *Nippon Kagaku Zasshi*, **86**, 873 (1965).
5) P. R. Wells, S. Ehrenson, and R. W. Taft, "Progress in Physical Organic Chemistry," Vol. **6**, Interscience Publishers, N. Y. (1964), p. 147.

BULLETIN OF THE CHEMICAL SOCIETY OF JAPAN, VOL. 44, 3177—3178 (1971)

The Observation of Surface Hydroxyl Groups on Metal Oxides by Means of Infrared Reflectance Spectroscopy

Nobutsune TAKEZAWA*

Research Institute for Catalysis, Hokkaido University, Sapporo

(Received January 16, 1971)

Much work has been carried out applying the transmission method to the infrared spectral study of adsorption.[1-3] In most cases, the catalyst used as an adsorbent has been supported on a carrier which transmitted the infrared radiation, and has been pressed into a disc. However, since the activity of the catalyst is occasionally affected by the presence of the carrier[1] and the pressure applied on the disc,[4] we cannot simply compare the results with those obtained on a powdered catalyst without a carrier.

Recently, it has been shown, however, that the diffuse reflectance method can be applied to the study of the powdered bulk compounds without using any carrier such as KBr or nujol mull.[5] In this respect, we attempted to study the adsorption on metal oxides in powder form. There have already been a few reports studying the adsorption.[6,7]

Experimental

A Nippon Bunko (Japan Spectroscopic Co. Ltd.) Model DR-1 reflectance apparatus was modified so that the catalyst could be prepared in a cell at an elevated temperature without exposing it to air. The optical system was similar to that used by Mamiya,[7] but the cell could be placed horizontally.

The catalysts used were magnesium oxide (J. T. Baker Chem. Co.), silica (Aerosil, Degussa Co.), stannic oxide (Koso Chemical Co.), zinc oxide (Kanto Chemical Co.), germanium oxide (Nakarai Chem., Ltd.), and titanium oxide (E. Merck A. G.). They were placed in a cell (2 mm in depth and 7 mm in diameter) in the form of a powder without using the disc technique. The average particle size of each sample was as follows: silica ($<1\ \mu$), stannic oxide ($8\ \mu$), zinc oxide ($25\ \mu$), germanium oxide ($7\ \mu$), and titanium oxide ($20\ \mu$).

The spectra during the dehydration and the adsorption of water or deuterium oxide were recorded with a Nippon Bunko Model IR-G infrared spectrophotometer. The dehydration was carried out at temperatures ranging from 50 to 310°C in a stream of prepurified nitrogen. Prior to the experiments, it was determined that the reflectivity of the catalysts was unaffected by the amount of the catalysts.[8]

Water or deuterium oxide vapor saturated at room temperature was carried with the nitrogen stream into the cell during the adsorption experiments.

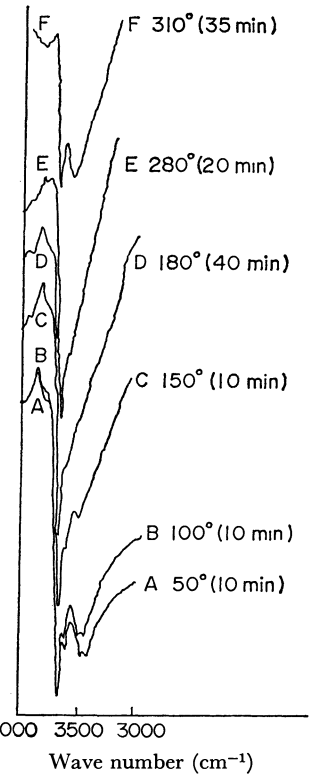

Fig. 1. Dehydration of magnesium oxide at various temperatures.
In brackets in the figure, the time for the dehydration is indicated. (The ordinates are displaced to avoid overlapping of traces.)

Results and Discussion

Figure 1 illustrates the spectra during the dehydration of magnesium oxide at various temperatures. The absorption bands were observed near 3700, 3630, 3500, 3450, and 1630 cm^{-1} at 50°C.[9] When the catalyst was heated at 150°C, the 3450 and 1630 cm^{-1} bands disappeared simultaneously. Since the bands occurred at 3445 and 1627 cm^{-1} in liquid water[10]

* Present address: Department of Chemical Process Engineering, Faculty of Engineering, Hokkaido University, Sapporo.

1) R. P. Eischens and W. A. Pliskin, "Advance in Catalysis," Vol. X, ed. by W. G. Frankenburg, D. D. Eley, and V. I. Komarevsky, Academic Press, New York (1958).

2) L. H. Little, "Infrared Spectra of Adsorbed Species," Academic Press, New York (1966).

3) N. Takezawa and M. J. Low, to be published.

4) W. Osanami, S. Baba, T. Kawakami, and Y. Ogino, Preprints for the 22nd Annual Meeting of the Chemcal Society of Japan, Tokyo (1969), No. 06424.

5) M. Mamiya, *Hyomen (Surface)*, **7**, 45 (1969).

6) G. Kortuem and H. Delfs, *Spectrochim. Acta*, **20**, 405 (1964).

7) M. Mamiya, Preprint for the Analytical Chemistry Meeting, Japan (1968), 11307.

8) With reference to the reflectance of magnesium oxide, the relative reflectivities of the samples were estimated to be 1.78, 1.06, 1.52, 1.78, and 1.48 for silica, stannic oxide, zinc oxide, germanium oxide, and titanium oxide respectively at the wave number of 4000 cm^{-1}.

9) The catalyst was heated to 50°C by infrared radiation.

10) J. E. Hibben, *J. Chem. Phys.*, **5**, 166 (1937).

BULLETIN OF THE CHEMICAL SOCIETY OF JAPAN, VOL. 44, 3179—3181 (1971)

Nuclear Magnetic Resonance Studies of Nitrosonaphthols

Toshiyuki SHONO, Yoshikatsu HAYASHI, and Koichiro SHINRA

Department of Applied Chemistry, Faculty of Engineering, Osaka University, Yamada-kami, Suita, Osaka

(Received February 17, 1971)

In solution, nitrosophenols are in tautomeric equilibrium[1-5] with quinone monoximes. Fischer *et al.*,[6] using nuclear magnetic resonance and infrared spectra, found that 4-nitrosophenol exists in the phenolic form in a dilute dimethyl sulfoxide solution. On the basis of nuclear magnetic resonance spectra, supported by UV and IR data, Norris and Sternhell[7] suggested that 4-nitrosophenol exists predominantly in the quinone monoxime form in an organic solvent. Jaffé[8] has calculated, by the molecular orbital method, that the oxime form of 4-nitrosophenol should be the more stable. As for nitrosonaphthols, Buraway[1] and his associates, on the basis of electronic spectra, have shown that 1-nitroso-2-naphthol exists in the oxime form only.

Hadži[9] investigated the monoximes of *p*-benzoquinone and 1,2-naphthoquinone (1-oxime and 2-oxime) by means of their infrared spectra. It has been found that the oxime formulation correctly represents the structure of these compounds in the solid state, and that this structure predominates also in their chloroform solutions. However, 2-nitroso-1-naphthol (1,2-naphthoquinone 2-oxime) seems to exist in the chelated nitroso form in solution in carbon tetrachloride. With the exception of a brief mention of the nuclear magnetic resonance spectrum of 4-nitroso-1-naphthol, the literature contains no reference to nuclear magnetic resonance investigation of the tautomeric nitrosonaphthols; this has prompted us to examine 1- and 2-nitrosonaphthols and their derivatives.

Experimental

Compounds. The 1-nitroso-2-naphthol which has been taken as the sample was a commercial product, mp 109—110°C, recrystallized from ligroin. The 2-nitroso-1-naphthol, mp 153—154°C, was synthesized by the method of Henriques.[10] 1-Methyloximino-2-naphthoquinone,[11] mp of 74—75°C. Found: C, 70.57; H, 4.79; N, 7.45%. Calcd for $C_{11}H_9O_2N$: C, 70.58; H, 4.81; N, 7.48%. 2-Methyloximino-1-naphthoquinone;[12] mp 89—90°C. Found: C, 70.60; H, 4.85; N, 7.51%. Calcd for $C_{11}H_9O_2N$: C, 70.58; H, 4.81; N, 7.48%. Both were prepared by the reaction of nitrosonaphthol with methyl iodide and were recrystallized from ligroin.

Nuclear Magnetic Resonance Spectra. The proton magnetic resonance spectra (PMR) of the compounds were measured by means of a JNM-3H-60 spectrometer; the results are summarized in Table 1.

Infrared Spectra. A Hitachi model EPI-S2 infrared recording spectrophotometer was used.

Results and Discussion

If detectable amounts of both isomeric forms, I and

TABLE 1. PMR RESULTS FOR THE NITROSONAPHTHOLS
(Chemical shift are given in τ value)

Compound	Solvent	Concentration (%)	Chemical shift of aromatic protons			Chemical shift of hydroxyl proton	Isomer ratio (%)	
			(3)	(4)	(8)		oxime,	phenol
1-Nitroso-2-naphthol	Dimethylsulfoxide (DMSO)	5	3.52	2.21	1.18	—	100	—
	Hexamethylphosphoramide (HMPA)	5	3.72	2.27	1.12	−7.00	100	—
	$CDCl_3$	5	3.53	2.36	1.80	−7.73	100	—
	Dioxane	5	3.48	2.35	1.70	—	100	—
	DMSO-acetic acid (5%)	10	3.57	2.33	1.28	—	100	—
1-Methyloximino-2-naphthoquinone	DMSO	5	3.66	2.34	1.45	—	100	—
2-Nitroso-1-naphthol	DMSO	10	3.01	2.80	1.95	−3.7	100	—
	DMSO-dioxane (5%)	5	3.11 3.41	2.80 —	1.95	—	80	20
	DMSO-acetic acid (5%)	10	3.09 3.39	2.82 —	1.95	—	80	20
2-Methyloximino-1-naphthoquinone	DMSO	5	3.03	2.84	2.00	—	100	—

1) A. Buraway, M. Cais, J. T. Chamberlain, F. Liversedge, and A. R. Thompson, *J. Chem. Soc.*, **1955** 3727.
2) W. R. Vaughan and G. K. Finch, *J. Org. Chem.*, **21** 1201 (1956).
3) W. Lüttke, *Z. Electrochem.*, **61**, 302, 976 (1957).
4) A. W. Baker, *J. Phys. Chem.*, **62** 744 (1958),
5) B. G. Gowenlock and W. Lüttke, *Quart. Rev.*, (London), **12** 321 (1958).
6) A. Fischer, R. M. Golding, and W. C. Tennant, *J. Chem. Soc.*, **1965** 6032.
7) R. K. Norris and S. Sternhell, *Aust. J. Chem.*, **19**, 841 (1966).
8) H. H. Jaffé, *J. Amer. Chem. Soc.*, **77**, 4448 (1955).
9) D. Hadži, *J. Chem. Soc.*, **1956** 2725.
10) R. Henriques and J. Ilinsky, *Ber.*, **18**, 706 (1885).
11) M. Ilinski, *Ber.*, **17**, 2585 (1884).
12) F. Fuchs, *Ber.*, **8**, 627 (1875).

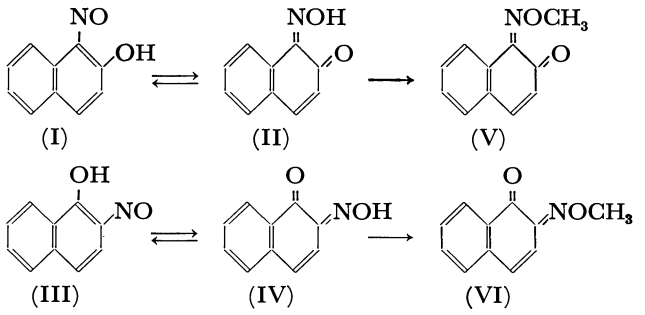

II or III and IV, were present, the spectral pattern would be either a superposition of both forms, or be composed of an independent pattern for each one, depending upon the rate of exchange between the two isomers. If there was any difference between the chemical shifts of the two hydroxyl protons (phenol and oxime) of each tautomer, it should be possible to establish the equilibrium isomer ratio from the signal area. Unfortunately, as is shown in Table 1, the hydroxyl proton gave only one broad peak. The PMR spectrum of both the methyl ethers of nitrosonaphthol, V and VI, are shown in Fig. 1. The difference in the spectra of V and VI is remarkable, particularly at the chemical shifts of the (3) and (4) protons. This difference may be attributed to the existence of the conjugation between the double bond and the carbonyl group. Both compounds, V and VI, seem to exist in the same quinoid form, for the wave numbers of the C=O bands (1670, 1660 cm^{-1} respectively) of V and VI in solution are not much different from those for quinones[13] (benzoquinone 1667, 1,2-naphthoquinone 1678 and 1,4-naphthoquinone 1675 cm^{-1}), and no nitroso group was detected by the Liebermann reaction.

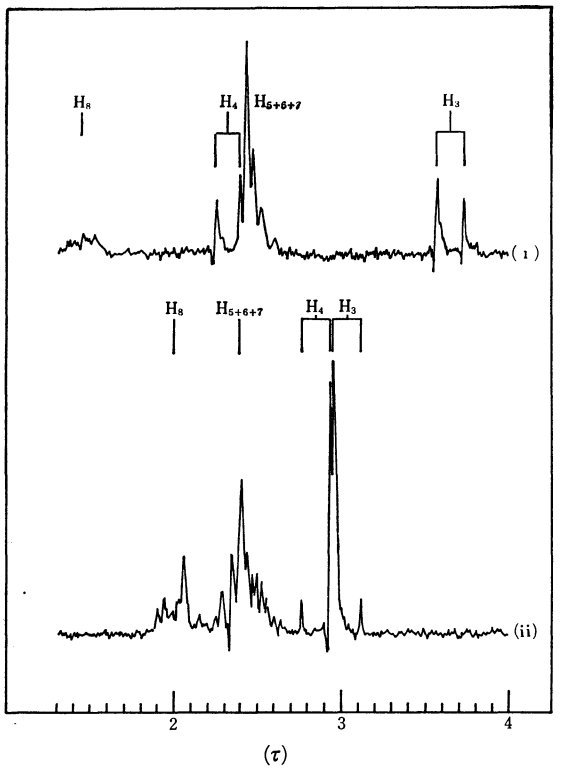

Fig. 1. NMR spectra of methyloximino-naphthoquinone in DMSO (5%), (18°C).
(i) 1-nitroso-2-naphthol (ii) 2-nitroso-1-naphthol

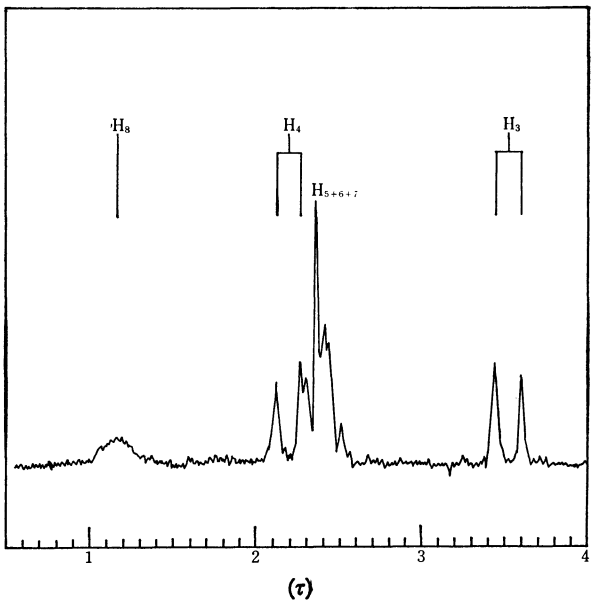

Fig. 2. NMR spectrum of 1-nitroso-2-naphthol in DMSO (5%), (20°C).

In 1-nitroso-2-naphthol, the aromatic protons at (3) and (4) show the AX pattern ($J_{3,4}=10$ Hz) and are very similar to the methyl ether protons, as is shown

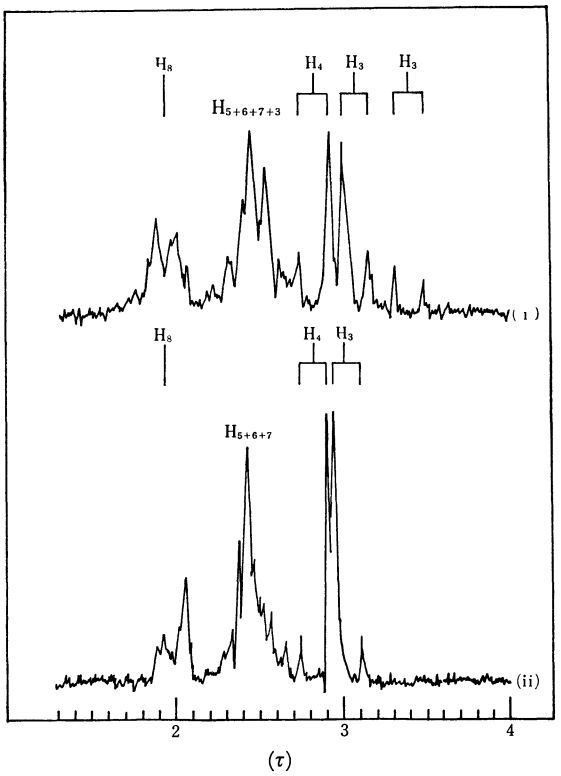

Fig. 3. NMR spectra of 2-nitroso-1-naphthol, (20°C).
(i) in DMSO-acetic acid (5%) (ii) in DMSO (10%)

13) M. Josien, N. Fuson, J. Lebas, and T. Gregory, *J. Chem. Phys.*, **21**, 331 (1953).

in Fig. 2. As has been mentioned above, Buraway[1] and Hadźi[9] have shown that 1-nitroso-2-naphthol exists in the oxime form on the basis of only the electronic and infrared spectra. The chemical shift of the aromatic proton at (3) appeared in a very high field, (τ=3.48—3.72). These facts show that the oxime formulation (II) correctly represents the structure of 1-nitroso-2-naphthol. On the contrary, in 2-nitroso-1-naphthol the aromatic protons at (3) and (4) show a mixture of the AB ($J_{3,4}$=9.8 Hz) and AX ($J_{3,4}$=10 Hz) patterns depending upon the solvent, as is shown in Fig. 3.

This fact shows that detectable amounts of the two forms, III and IV, are both present. From the singal area, the equilibrium isomer ratio is determined to be as is shown in Table 1. In assigning the aromatic protons at (3) and (4) of nitrosonaphthols and their methyl ethers, we have decided that the downfield signal is a (4) proton by analogy with the results obtained with α,β-unsaturated cyclic carbonyl compounds. In a planar cycloalk-2-en-1-one with efficient conjugation between the double bond and carbonyl group, the C-3 proton is strongly deshielded relative to the C-2 proton by mesomeric electron withdrawal.[14]

It is worth noting that the chemical shift of the aromatic proton at (8) appeared in a very low field as a broad line. This seems to be a deshielding effect of the carbonyl and oxime groups of the α-position.

14) L. M. Jackman and S. Sternhell, "Applications of Nuclear Magnetic Resonance Spectroscopy in Organic Chemistry," 2nd Edition, Pergamon Press, Oxford (1969), pp. 188—189.

BULLETIN OF THE CHEMICAL SOCIETY OF JAPAN, VOL. 44, 3181—3182 (1971)

Carbon Products Prepared from Variant Pitch Materials. VI. Pitch Carbon Prepared from Naphtha Cracking Pitch

Sugio Ōtani and Asao Ōya

Faculty of Technology, Gunma University, Kiryu Gunma

(Received February 23, 1971)

It was previously reported that a carbon rod or tablet could be prepared from specific variant pitch materials alone instead of from coke powder and a pitch binder.[1-5] The carbon-shaped articles prepared by this method were referred to as Pitch Carbon, and coal-tar pitch was used as the raw pitch material in the previous experiments. In this case, some special, very trouble some pre-treatments[1-3,5] were required in preparating the pitch carbon in order to elevate the softening point of the raw coal-tar pitch and/or to increase its reactivity in the heating process.

This work was undertaken in order to search for better raw pitch materials for the preparation of pitch carbon, it was found that the pitch produced in the naphtha cracking process is an interesting raw material for pitch carbon.

Experimental

The raw pitch material used here was naphtha cracking pitch (Ligare-N) supplied by the Kureha Chemical Ind. Co., this pitch had a softening point of 193—196°C and had the elemental composition shown in Table 1. The raw pitch was crushed to under 100 mesh and then pressed with 400 kg/cm^2 into tablets of 20 mm in diameter and about 4 mm thick. The tablets were pre-heated in air up to 300°C over a 7-hr period. When the heating rate of this process was too fast, the tablets fused or blistered. Consequently, in the range of temperatures from 180° to 230°C, the heating rate was controlled to 0.3°C/min. The resulting tablets were heated under a stream of N_2 gas at the desired temperatures below 2600°C for 10 min. The heating rate was 5°C/min up to 1000°C and 50°C/min at temperatures higher than 1000°C. The measurement of the properties of the resulting pitch carbon was carried out according to the procedures previously described.[2]

Table 1. Changes in elemental compositions of naphtha cracking pitch and coal-tar pitch by heating in air

Kind of pitch		C(%)	H(%)	diff.(%)[b]
Naphtha	Raw	94.3	4.5	1.2
	After pre-heating	79.4	3.8	16.8
Coal	Raw	91.5	4.6	3.9
	After pre-treatment[a]	92.0	3.9	4.1

a) Raw pitch was distilled at 400°C for 80 min by bubbling air, powdered after cooling, and then heated in air up to 200°C.[3]

b) diff. (%)=100 −C(%) −H(%)

Results

Four characteristic phenomena were observed in the present experiments compared with the case of using coal-tar pitch.

(1) The pre-treatment on the raw pitch material as reported in the previous papers[2-3,5] could be eliminated from the process of preparing pitch carbon without any trouble.

1) S. Ōtani, G. Kubota, A. Ōya, and T. Koitabashi, *Tanso*, No. 52, 13 (1968).
2) S. Ōtani, A. Ōya, and T. Fukabori, *Kogyo Kagaku Zasshi*, **72**, 317 (1969).
3) S. Ōtani, A. Ōya, I. Nakagawa, and T. Fukabori, *ibid.*, **72**, 323 (1969).
4) S. Ōtani and A. Ōya, *ibid.*, **73**, 1110 (1970).
5) S. Ōtani, A. Ōya, and T. Nagashima, *ibid.*, **73**, 2095 (1970).

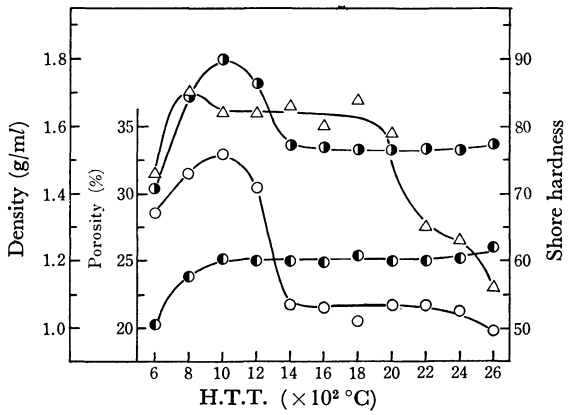

Fig. 1. Changes of density, porosity, and hardness with H.T.T. (—○— Apparent porosity, —◐— Bulk density, —◑— Apparent density, —△— Shore hardness)

(2) As is shown in Fig. 1, the most characteristic feature of the pitch carbon obtained here was its much greater hardness for its low-bulk density as compared with that of the pitch carbon prepared from coal-tar pitch[2-3] or conventional artificial graphite.[6] The pitch carbon finally obtained was non-graphitizable.

(3) Considerable amounts of oxygen were incorporated into the pitch by pre-heating up to 300°C. This phenomenon was not observed at all in the case of coal-tar pitch, as is shown in Table 1. From its infrared spectra and elemental analysis, it was found that the oxygen incorporated is in the form of C=O (1700 cm^{-1}) and C–O (1200 cm^{-1}) and is eliminated during the further heating process under a N_2 gas atmosphere.

(4) In the tablets heated above 600°C, the closed pores formed in most of the larger particles, as is shown in Fig. 2.

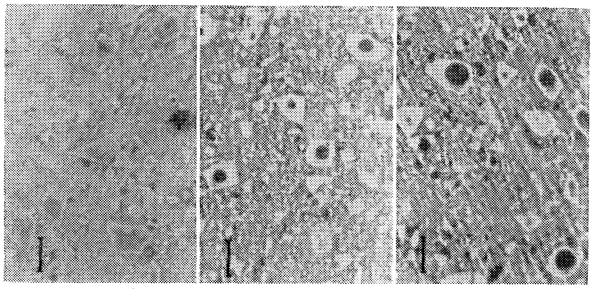

(a) After heating up to 300°C in air (b) 800°C (c) 1600°C

Fig. 2. The microscopic textures of the pitch carbon. (|——| 100μ)

Discussion

The fact described in (3) indicates that the naphtha cracking pitch has a higher reactivity to oxygen in air than does coal-tar pitch. This reactivity accelerates to sinter or bridge among the pitch particles and/or molecules. The high softening point and this reactivity of the pitch may it possible to eliminate the pre-treatment required in the case of coal-tar pitch. It seems that the rigid layers from at the surface of the particle at an early stage of heating and result in the closed pores in the large particles during the subsequent carbonization process. The characteristic feature pointed at in (2) is probably due to those closed pores.

6) M. Ichinose, *Tanso*, **1**, 7 (1949).

BULLETIN OF THE CHEMICAL SOCIETY OF JAPAN, VOL. 44, 3182—3183 (1971)

The Cyclization of Polyenes.[1] VII. The Cyclization of Labda-13-ene-8,12,15-triol

Tadahiro KATO, Susumu KANNO, Mitsuru TANEMURA, Akira KUROZUMI, and Yoshio KITAHARA[2]

Department of Chemistry, Faculty of Science, Tohoku University, Sendai

(Received March 18, 1971)

12α-Hydroxy epimanoyl oxide[3] (I), a labdane-type diterpene, was isolated by Giles *et al.* from Turkish tobacco, which also produces diterpene lactones, α- and β-levantenolides[4] (II, III).

As we have already reported the synthesis of II and III on the basis of biogenetical consideration,[5] it does not seem absurd to expect the conversion of triol (IV) to I or its stereoisomers. This paper will describe the acid-catalyzed cyclization of IV.

The reduction of synthesized α-levantenolide (II) with lithium aluminum hydride afforded the relatively unstable triol (IV), which was then treated with several Lewis acids, such as iodine, *p*-toluenesulfonic, sulfuric, and camphorsulfonic acids, and stannic chloride under various conditions. The reactions were followed by silica-gel thin-layer chromatography using natural 12α-hydroxyepimanoyl oxide (I) as a reference. The treatment of IV with stannic chloride gave, among the examined acids, the simplest mixture, from this mixture an oily compound (V) was isolated in a 37% yield by silica-gel chromatography.

1) Part V of this series, T. Kato, S. Kanno, and Y. Kitahara, *Tetrahedron*, **26**, 4287 (1970).

2) To whom inquiries regarding this paper should be addressed.

3) J. A. Giles, J. N. Schumacher, S. S. Mims, and E. Bernasek, *Tetrahedron*, **18**, 169 (1962).

4) J. A. Giles, and J. N. Schumacher, *ibid.*, **14**, 246 (1961).

5) a) T. Kato, M. Tanemura, T. Suzuki, and Y. Kitahara, *Chem. Commun.*, **1970**, 28. b) M. Tanemura, T. Suzuki, T. Kato, and Y. Kitahara, *Tetrahedron Lett.*, **1970**. 1463.

The gross structure of the product (V) was determined on the basis of the following observations. The NMR spectrum[6] of V exhibits signals of a doublet and a triplet at 4.05 and 5.48 ppm, with $J=7.2$ Hz due to C_{15}- and C_{14}-protons, a sharp singlet at 1.15 (C_8–Me), and broad multiplet at 4.77 (C_{12}–H). The hydroxyl group of V was easily oxidized with manganese dioxide to give the corresponding unsaturated aldehyde (VI), which showed a conjugated carbonyl group at 1672 cm^{-1} in the IR spectrum. The NMR spectrum of VI shows two kinds of formyl groups in *ca.* a 3: 1 ratio, indicating that VI is a mixture of either C_{12}-epimers or double-bond isomers at C_{13}–C_{14}. The former is more probable, since the 13-methyl group appears at 1.95 ppm, showing the *trans* relation of the methyl group with respect to the formyl group.[7] The destruction of the asymmetry at the 12 position of IV might occur prior to the ring formation.[8] Our objective, I, could not be isolated, although the formation, in quite a small amount, of a substance having the same R_f value on thin-layer chromatography with natural I was observed.

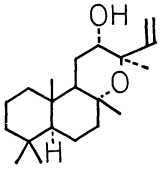

I

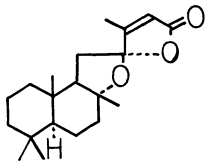

II

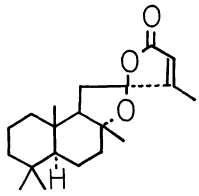

III

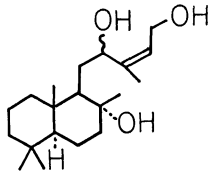

IV

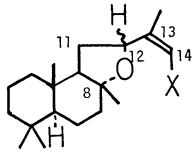

V X = CH_2OH

VI X = CHO

6) NMR spectra were measured with Varian T-60 in carbon tetrachloride and expressed with ppm from an internal standard of tetramethylsilane.

7) M. Ohtsuru, M. Teraoka, K. Tori, and K. Takeda, *J. Chem. Soc.*, **1967**, 1033.

8) E. Wenkert and Z. Kumazawa, *Chem. Commun.*, **1968**, 140.

Experimental

Reduction of dl-α-*Levantenolide.* To a stirred, absolute ether solution (10 m*l*) of α-levantenolide (200 mg), we added lithium aluminum hydride (30 mg) under ice cooling. After stirring for an hour at 0°C, the reaction mixture was further stirred at room temperature for another hour and then poured onto ice water. Ether extracts from the reaction mixture were washed with cold hydrochloric acid and water, and then dried over magnesium sulfate in a refrigerator. Triol (IV) (200 mg) was thus obtained from the ether solution. Although the triol (IV), which should be stored in a refrigerator, could not be purified because of its unstability, the physical evidence supported the structure of the reduction product. NMR (δ) of the crude triol (IV) (D_2O was added) 1.13 (C_8–Me), 1.74 (C_{13}–Me), 4.05 (C_{15}-protons), 4.77 (C_{12}-proton), and 5.40 (C_{14}-proton). IR (film) 3400 cm^{-1} (strong), no absorption in the carbonyl region.

Cyclization of Triol (IV). Stannic chloride (0.1 m*l*) was added to a chloroform solution (10 m*l*) of the triol (200 mg) at −40——−60°C and the mixture was kept for an hour at the same temperature. The temperature of the reaction mixture was gradually raised to 25°C by removing the cooling bath. It took about an hour. After being diluted with ether, the ether solution was washed with aqueous sodium bicarbonate and then water, dried over magnesium sulfate, and then evaporated. The residued oil thus obtained was chromatographed on silica gel with a mixed solvent of benzene - isopropyl ether (8:1) to give V (70 mg). Found, C, 77.86; H, 10.85%. Calcd for $C_{20}H_{34}O_2$: C, 78.38; H, 11.18%.

Although four methyl groups at C_4, C_8, and C_{10} were observed as a sharp singlet in the NMR spectrum of V, the signals due to C_{12}-, C_{14}-, and C_{15}-protons appeared broadly, suggesting that the alcohol (V) is an epimeric mixture. NMR (δ), 0.85 (tert Me×2), 0.87 (tert Me), 1.15 (sharp s, C_8–Me), 1.73 (C_{13}–Me), 3.12 (bs, OH, disappeared on the addition of D_2O), 4.05 (bd, $J=7.2$ Hz, C_{15}–H_2), 4.77 (m, C_{12}–H), and 5.48 (br. t, $J=7.2$ Hz, C_{14}–H). IR (film), 3375 (OH), 1653 (C=C) cm^{-1}.

Oxidation of V. Active manganese dioxide (500 mg) was added to an ether solution (5 m*l*) of V (60 mg) and the reaction mixture was stirred for two hr at room temperature. The subsequent filtration and washing of the solid and evaporation of the combined ether afforded unsaturated aldehyde (VI).

The pair of doublets at 10.23 and 10.20 ppm, which appear in the ratio of 3: 1, corresponds to one formyl proton in the NMR spectrum of VI. The appearance of two kinds of formyl protons may be due to the presence of an epimeric mixture, which could not be separated by usual chromatography. VI; NMR (δ), 1.20 (s, C_8–Me), 1.95 (C_{13}–Me), 5.83 (bd, $J=7$ Hz, C_{14}–H), 10.23 (d, $J=7$ Hz), and 10.20 (d, $J=7$ Hz). IR (film) 1672 (conjugated formyl) cm^{-1}.

The authors wish to thank to Dr. J. A. Giles (12α-hydroxyepimanoly oxide) and the Takasago Perfumery Co. (β-ionone) for their generous gifts of valuable materials.

BULLETIN OF THE CHEMICAL SOCIETY OF JAPAN, VOL. 44, 3184 (1971)

Syntheses of Aromatic Dicarbamates and Their *N,N'*-Dihydroxymethyl Derivatives

Shigeya TAKEUCHI and Eisaku NINAGAWA

Department of Chemistry, Faculty of Education, Toyama University, Gofuku, Toyama

(Received March 18, 1971)

In previous papers,[1-3] aromatic monocarbamates, their *N*-monohydroxymethyl carbamates, and *N,N'*-methylenebis(carbamates) were synthesized. This paper will deal with the syntheses of aromatic dicarbamates and their *N,N'*-dihydroxymethyl derivatives.

p-Xylylene dicarbamate (Ia) and 4,6-dimethyl-*m*-xylylene dicarbamate (IIIa) were synthesized by the method of Kraft[4]:

$$R\text{-}(CH_2OH)_2 + 2C_2H_5OCONH_2 \xrightarrow{Al(OC_3H_7)_3} R\text{-}(CH_2OCONH_2)_2 + 2C_2H_5OH$$
(Ia, IIa)

These dicarbamates (Ia, IIa) react with 2 mol of formaldehyde, in the presence of potassium hydroxide as a catalyst, to form *N,N'*-dihydroxymethyl derivatives (Ib, IIb):

$$R\text{-}(CH_2OCONH_2)_2 + 2CH_2O \xrightarrow{OH^-} R\text{-}(CH_2OCONHCH_2OH)_2$$
(Ia, IIa) (Ib, IIb)

From the analytical data, the structures of these products were determined to be as follows:

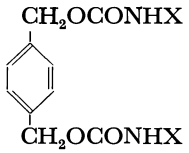

Ia (X=H)
Ib (X=CH_2OH)

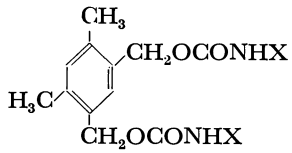

IIa (X=H)
IIb (X=CH_2OH)

Experimental

The melting points are uncorrected. The IR spectra were recorded with a KBr disk on a JASCO Model IR-S infrared spectrometer. The NMR spectra were recorded on a Japan Electron Optics 60 MHz spectrometer in d_6-DMSO (*ca.* 10%); the δ values (ppm) were given against tetramethylsilane as an internal standard.

Preparation of p-*Xylylene Dicarbamate (Ia).* To 53.5 g (0.60 mol) of ethyl carbamate (recrystallized from benzene) in a 300 m*l* four-necked flask fitted with a stirrer, a thermometer, a condenser, and a 30 cm asbestoslagged column, we added 34.5 g (0.25 mol) of *p*-xylylene glycol (mp 115—116°C, from methanol) and 160 m*l* of ethylbenzene. The reaction mixture was heated at 110°C in an oil bath to remove any water in the reagents and was then cooled to 100°C. Subsequently, aluminum isopropoxide (about 10 g) was added and the reaction temperature was held at 134—137°C. The reaction mixture was subsequently stirred for 15 hr. The ethanol-ethylbenzene azeotropic mixture was removed through the column. The crude product thus obtained was recrystallized from DMF to give 28.3 g (50.5%) of a white powder melting at 211—213°C. IR (cm^{-1}): 3430—3230 ($\nu(NH_2)$, *etc.*), 1700 (ν(C=O)), 1620 ($\delta(NH_2)$). NMR (ppm): 7.27 (s, 4H, C_6H_4–), 6.5 (s, 4H, $-NH_2$), 4.93 (s, 4H, $-CH_2$–). Found: C, 53.70; H, 5.53; N, 12.36%. Calcd for $C_{10}H_{12}N_2O_4$: C, 53.56; H, 5.4; N, 12.5%.

*Preparation of 4,6-Dimethyl-*m*-xylylene Dicarbamate (IIa).* To 49.0 g (0.55 mol) of ethyl carbamate we added 33.2 g (0.20 mol) of 4,6-dimethyl-*m*-xylylene glycol and 160 m*l* of ethylbenzene. The reatcion mixture was stirred for 11 hr at 135°C and then treated as has been described above. Mp 199—200°C. Yield, 14.0 g (27.7%). IR (cm^{-1}): 3427—3207 ($\nu(NH_2)$, *etc.*), 1687 (ν(C=O)), 1605 ($\delta(NH_2)$). NMR (ppm): 7.22 and 7.02 (s, each one proton, C_6H_2–), 6.5 (s, 4H, $-NH_2$), 4.93 (s, 4H, $-CH_2$–), 2.23 (s, 6H, $-CH_3$). Found: C, 57.38; H, 6.40; N, 11.12%. Calcd for $C_{12}H_{16}N_2O_4$: C, 57.12; H, 6.41; N, 11.10%.

Reaction Product of Ia with Formaldehyde. A mixture of Ia (5.6 g, 0.025 mol), paraformaldehyde (2.0 g, 0.067 mol), dioxane (30 m*l*), and water (15 m*l*) was stirred at 74°C and pH 11.4 for 80 min, and then to the reaction mixture we added 200 m*l* of water. The solid thus formed was filtered and recrystallized from methanol-water to afford Ib as a white powder; 2.9 g (40.8%); mp 172—173°C. A test with a Tollens reagent was positive. IR (cm^{-1}): 3317 (ν(NH), ν(OH)), 1695 (ν(C=O)), 1530 (ν(CN)+δ(NH)). NMR (ppm): 7.8 (t, 2H, –OH), 7.29 (s, 4H, C_6H_4–), 5.5 (t, 2H, –NH–), 5.0 (s, 4H, $-CH_2OC$–), 4.43 (t, 4H, $-N-CH_2O$–). Found: C, 50.94; H, 5.84; N, 9.66%. Calcd for $C_{12}H_{16}N_2O_6$: C, 50.69; H, 5.68; N, 9.86%.

Reaction Product of IIa with Formaldehyde. A mixture of IIa (2.1 g, 0.008 mol), paraformaldehyde (0.8 g, 0.025 mol), dioxane (30 m*l*), and water (15 m*l*) was stirred at 70°C and pH 13.2 for 30 min and then treated as has been described above. Mp 145—147°C. Yield, 0.57 g (18.3%). A test with a Tollens reagent was positive. IR (cm^{-1}): 3250 (ν(NH), ν(OH)), 1690 (ν(C=O)), 1530 (ν(CN)+δ(NH)). NMR (ppm): 7.8 (t, 2H, –OH), 7.23 and 7.0 (s, each one proton, C_6H_2–), 5.5 (t, 2H, –NH–), 4.97 (s, 4H, $-CH_2OC$–), 4.45 (t, 2H, $-N-CH_2O$–), 2.24 (s, 6H, $-CH_3$). Found: C, 53.67; H, 6.68; N, 8.82%. Calcd for $C_{14}H_{20}N_2O_6$: C, 53.85; H, 6.47; N, 8.97%.

The authors wish to express their thanks to Professor Minoru Imoto of Kansai University for his kind direction, to Professor Masayoshi Kinoshita of Osaka City University for his valuable suggestions and continuous encouragement, and to Dr. Chingyun Huang of the Kobunshi Laboratory of the Nihon Gas Co. for his helpful guidance.

1) S. Takeuchi, M. Kinoshita, C. Huang, and M. Imoto, *Kogyo Kagaku Zasshi*, **73**, 2524 (1970).
2) S. Takeuchi, T. Takahashi, and E. Ninagawa, *Kogyo Kagaku Zasshi*, **74**, 512 (1971).
3) S. Takeuchi, *Memoirs of Faculty of Education, Toyama Univ.*, **18**, 119 (1971).
4) W. M. Kraft, *J. Amer. Chem. Soc.*, **70**, 3569 (1948).

BULLETIN OF THE CHEMICAL SOCIETY OF JAPAN, VOL. 44, 3185—3186 (1971)

Single-Photon Ionization in the Flash Photolysis of *N,N,N',N'*-Tetramethyl-*p*-phenylenediamine in Solution

Takeshi IMURA, *Naoto YAMAMOTO, *Hiroshi TSUBOMURA, and Kazuo KAWABE

Department of Electrical Engineering, Faculty of Engineering, Osaka University, Suita, Osaka
**Department of Chemistry, Faculty of Engineering Science, Osaka University, Toyonaka, Osaka*

(Received March 25, 1971)

The photo-ionization of *N,N,N',N'*-tetramethyl-*p*-phenylenediamine (TMPD) in solution was reported to take place by double-photon process through the triplet state.[1,2] Recently, it was reported that the formation of TMPD cation passing through no triplet state also takes place,[3,4] and that no evidence of double-photon process was obtained in other experiments using the method of laser photolysis.[5]

As a result of our investigation of the effect of light intensity on the photocurrent induced by the ionic species and caused by the flash photolysis of TMPD in acetonitrile at a room temperature, we obtained evidence of ionization by the single-photon rather than the double-photon process.

Experimental details were given previously.[6] Light intensity was regulated by setting the brass wire-gauzes of various transmittances. The photocurrent was measured at the initial maximum peak.

Figure 1 (A) shows the photocurrent *vs.* relative light intensity logarithmically. The linear relation in the formation of ionic species is obvious. The lower curve(b) was obtained when only the light with wavelengths greater than 3100 Å was irradiated with a cut-off filter.

The initial concentration of the generated ionic species should be proportional to the initial value (i_0) of the photocurrent as measured at the maximum peak, and should depend only on the total light intensity (L), since the decay of the photocurrent ($>10^{-2}$ sec) was extremely slow compared with the duration of a flash ($<10^{-5}$ sec). The recombination of the ionic species and the other decay processes may be practically neglected during the flash firing. Therefore, the relation $i_0 \propto L^n$ will hold directly, where $n=1$ and 2 according to the ionization for the single- and the double-photon process, respectively. The experimental results indicate that $n=1$.

When the whole body of the sample including the electrodes was uniformly irradiated by removing the slit, the linear curves in Fig. 1 (B) were again obtained notwithstanding the fact that the exchange of charges between the electrodes and excited TMPD, or the additional generation of the ionic species near the electrodes, can easily take place.

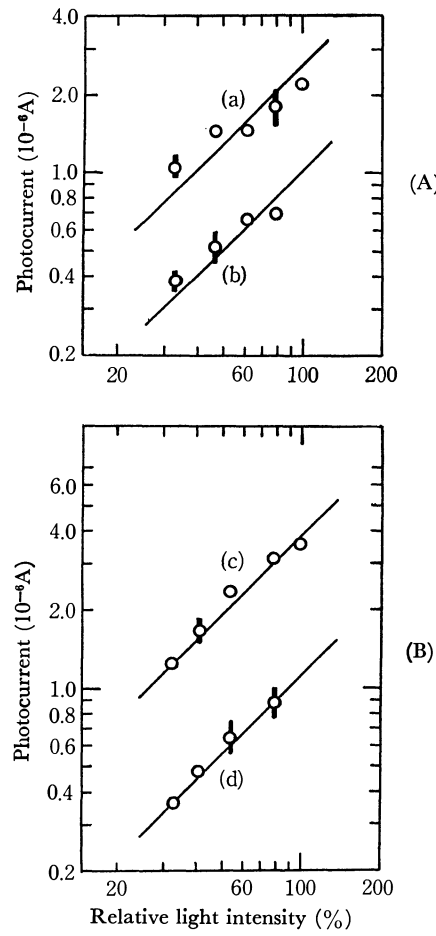

Fig. 1. Effect of light intensity on the photocurrent of TMPD in acetonitrile.
Solid lines correspond to the slope 1.0.
Cut-off filter ($\lambda>3100$ Å) was used in (b) and (d).
(A) Slit was used. Flash input: 275 J.
(a) 3.7×10^{-3}M, (b) 3.8×10^{-3}M.
(B) No slit was used. Flash input: 210 J, 2.7×10^{-4}M.

A sort of semi-ionized state (I) having the CT character can be considered for the ionization.

$$\text{TMPD} \xrightarrow{h\nu} \text{TMPD}^* \longrightarrow [\text{TMPD}^{\delta+} \cdots (\text{CH}_3\text{CN})_m{}^{\delta-}]^* \quad (m \geqq 1)$$

I

It seems that TMPD cation and the counter-anionic species[7] are liberated so spontaneously from state I that no more photon is needed. Examples of the fragmen-

1) Y. Nakato, N. Yamamoto, and H. Tsubomura, This Bulletin, **40**, 2480 (1967).
2) H. S. Pilloff and A. C. Albrecht, *J. Chem. Phys.*, **49**, 4891 (1968).
3) R. Potashnik, M. Ottolenghi, and R. Bensasson, *J. Phys. Chem.*, **73**, 1912 (1969).
4) M. Tamir and M. Ottolenghi, *Chem. Phys. Lett.*, **6**, 369 (1970).
5) J. T. Richards and J. K. Thomas, *Trans. Faraday Soc.*, **66**, 621 (1970).
6) T. Imura, N. Yamamoto, and H. Tsubomura, This Bulletin, **43**, 1670 (1970).
7) Though the initial anionic species was not confirmed, it may be a solvated electron. *cf.* A. Singh, H. D. Gesser, and A. R. Scott, *Chem. Phys. Lett.*, **2**, 271 (1968).

tation into cation and anion from the excited CT state are found.[6,8] As acetonitrile easily accepts electrons from Na metal (ionization potential of Na atom=5.138 eV), the same kind of reaction can be expected by the transfer of electron from TMPD in the excited state (ionization potential of TMPD(gas phase)≒6 eV[9]) to acetonitrile through CT interaction.

Photoconductive measurements were also tried in ethanol solution, where the ionization through a double-photon process was demonstrated by the effect of light intensity on the optical density of generated TMPD cation,[1] but the photocurrent could hardly be detected.[5,6]

8) H. Leonhardt and A. Weller, *Z. Physik. Chem. N. F.*, **29**, 277 (1961); H. Leonhardt and A. Weller, *Ber. Bunsenges. Phys. Chem.*, **67**, 791 (1963); K. Kawai, N. Yamamoto, and H. Tsubomura, This Bulletin, **42**, 369 (1969); M. Koizumi and H. Yamashita, *Z. Phys. Chem. N. F.*, **57**, 103 (1968); H. Masuhara, M. Shimada, and N. Mataga, This Bulletin, **43**, 3316 (1970).

9) H. Tsubomura, "Chemistry of the Excited State," Tokyo Kagaku Dozin, Tokyo (1967), p. 160.

BULLETIN OF THE CHEMICAL SOCIETY OF JAPAN, VOL. 44, 3186—3187 (1971)

Vinyl Polymerization. 272. Synthesis and Polymerization of 9-*O*-Methacryloylquinine

Kiyoshi YAMAUCHI, Masayoshi KINOSHITA, and Minoru IMOTO

Department of Applied Chemistry, Faculty of Engineering, Osaka City University, Sumiyoshi-ku, Osaka

(Received March 25, 1971)

There have been various studies aimed at incorporating drugs into polymeric materials.[1] The most challenging aspect of the problem has been the search for systems, in which the polymer might receive advantages, such as increased pharmacological activities and reduced undesirable side effects.

The present study was undertaken for the synthesis and the polymerization of 9-*O*-methacryloylquinine (II) with the hope that the polymer (III) derived from II might show an increased effectiveness against the usual quinine (I) formulations, such as antifebrile and antimalarial activities.[2]

Further, III would be useful as an optically active resin, since quinine holds four asymmetric carbons. Grubhofer and Schleith[3] performed a resolution of manderic acid, using the reaction product of Amberlite XE 64 reisn with thionyl chloride and then with I (16% content of I). The polymer (III), which we wish to discuss in this paper, might be attractive in this field, too, since it contains one resolving agent per monomer unit.

The synthesis of II was performed by the reaction of I with methacryloyl chloride; it was obtained in a 70% yield. The stereospecific configuration of the quinine part was not altered during the esterification, since an alkaline hydrolysis of II reproduced I in a good yield.

The ester (II) could be converted into a water-soluble dihydrochloride quantitatively, during which time a racemization and a fission of the ester bond of II had not taken place. The compound (II) was also optically stable toward heating in benzene. On the basis of these chemical properties of II, the polymerization was carried out in benzene at 80°C, using AIBN as an initiator. The polymer (A) obtained in the lower concentration of II was soluble in chloroform, benzene, and pyridine, whereas the polymer (B) produced in the higher concentration was insoluble in most organic solvents, but swelled in DMF and DMSO. The difficulty in solubility may be caused by cross-linking through the participation of the vinyl group on the quinuclidinyl ring, and a coupling of radicals produced by chain-transfer reactions.

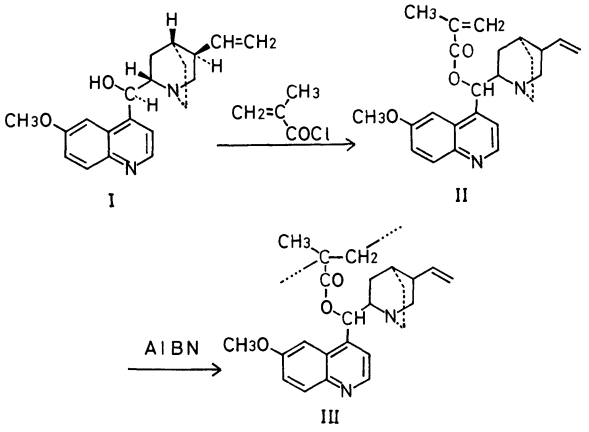

For the studies of the pharmacological activities of the polymer, it would be desirable to modify the polymer into a water-soluble one. This was performed by converting III to its hydrochloride. The introduction of dry hydrogen chloride gas into a benzene solution of polymer (A) generated a hygroscopic salt, and it became very soluble in water, as expected. On the other hand, the salt formation of polymer (B) was difficult because of the lack of appropriate solvents.

The use of the polymer as a high-molecular-weight drug and as an optical-active resin is now being studied; the studies will be described later.

1) G. W. Hastings, *Angew. Chem.*, **82**, 367 (1970).
2) "The Merck Index of Chemicals and Drugs," 7th ed., Merck and Co., Inc., New Jersey (1960), p. 888.
3) N. Grubhofer and L. Schleith, *Hoppe Seylers Z. Physiol. Chem.*, **296**, 262 (1954).

Table 1. Physical constants and analytical data

Compd.	Mp °C	$[\alpha]_D^{19}$ (c)	λ_{max} mμ (ε)	Formula		Analyses (%) C	H	N	Cl
II	125.5—126.5	+29.7 (1.6)[a] +30.4 (9.5)[b]	335.0 (4600)[a]	$C_{24}H_{28}N_2O_3$	Calcd	73.44	7.19	7.14	
					Found	73.22	7.22	7.00	
polymer (A)	>250	−32.2 (1.6)[a]	336.1 (5500)[a]	$(C_{24}H_{28}N_2O_3)_n$	Calcd	73.44	7.19	7.14	
					Found	72.65	7.30	6.87	
Polymer (B)	>300	——	——	$(C_{24}H_{28}N_2O_3 \cdot 1.5H_2O)_n$	Calcd	68.70	7.44	6.67	
					Found	68.93	6.94	6.61	
II-HCl*	170 (decomp)	−16.0 (4.0)[c]	335.0 (5000)[c]	$C_{24}H_{28}N_2O_3 \cdot 2HCl \cdot 2H_2O$	Calcd	57.48	6.83	5.58	14.14
					Found	57.64	6.52	5.69	14.31
Polymer (A)-HCl*	235 (decomp)	+ 9.1 (7.3)[c]	336.0 (5300)[c]	$(C_{24}H_{28}N_2O_3 \cdot 2HCl \cdot 3H_2O)_n$	Calcd	55.48	6.96	5.36	13.65
					Found	54.54	6.39	5.45	13.95
Poylmer (B)-HCl*	>300	——	——	$(C_{24}H_{28}N_2O_3 \cdot 2HCl \cdot 2H_2O)_n$	Calcd	57.48	6.83	5.58	14.14
					Found	57.70	6.09	6.14	13.13

Solvent: a, chloroform; b, benzene; c, water.
* Hygroscopic properties of samples were taken into account for calculation of analytical data.

Experimental

The melting points were uncorrected. The infrared spectra (IR) were run on a Jasco Model IR-G Spectrometer. The ultraviolet absorption spectra (UV) were measured with a Hitachi Recording Spectrometer, Model EPS-3T. The optical rotations were recorded with a Yanagimoto Photo-Magnetic Polarimeter, Model OR-10. The molecular weight was determined using a Hitachi Vapor Pressure Osmometer, Model 115. The physical constants and analytical data of the compounds are listed in Table 1.

9-O-Methacryloylquinine (II). A mixture of quinine monohydrochloride dihydrate (13.0 g, 0.032 mol) and chloroform (60 ml) was treated with 4N sodium hydroxide to transfer quinine into the chloroform layer, which, after dring with anhydrous sodium sulfate, was mixed with methacryloyl chloride (3.3 g, 0.032 mol) and triethylamine (3.2 g, 0.032 mol). After the reaction mixture had been kept at room temperature for one day, it was washed with 10% sodium bicarbonate and dried over anhydrous sodium sulfate. The organic solution was concentrated and then chromatographed on alumina (2 cm × 70 cm, 300 mesh, neutral). Elution with ethyl acetate gave 9.2 g of crystalline 9-*O*-methacryloylquinine, which was recrystallized from ether to afford 9.0 g (70%) of the pure product.

IR (KBr); 2960, 1710, 1620, 1590, 1500, 1225, and 1150 cm^{-1}.

The optical rotation of II was not changed after heating at 80°C for ten hours in benzene; $[\alpha]_D^{19}$+30.4° (*c* 10, benzene).

Hydrolysis of II. A mixture of II (0.39 g, 1 mmol), methanol (10 ml), and 4N potassium hydroxide (10 ml) was allowed to stand for two hours at room temperature. Subsequent extraction with chloroform and evaporation of the solvent gave 0.27 g (76%) of a white solid, the optical ratation of which showed $[\alpha]_D^{19}$−104° (*c* 1.5, chloroform). An authentic sample had $[\alpha]_D^{19}$−108° (*c* 1.5, chloroform). The solid gave only one spot in thin layer chromatography in several solvent systems. IR, UV, and NMR spectra were all identical with those of quinine (I); mp 176°C (lit,[2] 177°C).

Polymerization of II. *Polymer (A):* The ester (II) (2.00 g, 5.1×10^{-3} mol), AIBN (4.5×10^{-3} g, 2.8×10^{-5} mol), and benzene (12 ml) were placed in a glass tube, which was then degassed and sealed. The tube was immersed in a waterbath thermostatted at 80°C and shaken for eight hours, after which it was opened; the reaction mixture was then poured into diethyl ether to precipitate a white polymer, 0.98 g (49%).

The polymer is soluble in chloroform, benzene, DMF, DMSO, and conc. hydrochloric acid, and insoluble in water, methanol, and acetone. Mw=4380 (benzene, 30°C).

Polymer (B): A mixture of II (0.84 g, 2.1×10^{-3} mol), AIBN (2.1×10^{-3} g, 1.3×10^{-5} mol), and benzene (1.6 ml) was treated in a manner similar to that used for polymer (A), producing 0.78 g (93%) of a yellow solid which had an identical IR spectrum with that of polymer (A).

The polymer did not dissolve in any organic solvents and concentrated hydrochloric acid, but swelled in DMF and DMSO.

Preparation of Hydrochloride. II-HCl: Dry hydrogen chloride gas was passed through a benzene solution of II (0.69 g) to produce 0.63 g (70%) of the white hydrochloride. The salt is hygroscopic, and is soluble in water, methanol, and pyridine, but insoluble in tetrahydrofuran and ether.

IR (KBr): 3400, 2500, 1723, 1615, 1500, 1250, and 1135 cm^{-1}.

The ester (II) was recovered from II-HCl (0.30 g) by mixing it with 10% sodium bicarbonate and extracting it with chloroform; 0.21 g (83%), $[\alpha]_D^{19}$+29.7° (*c* 9.0, chloroform), mp 125—126°C.

Polymer (A)-HCl: The introduction of hydrogen chloride gas into a mixture of polymer (A) (0.10 g) and benzene yielded 0.11 g (85%) of the salt. The product is hygroscopic and is soluble in water and methanol, but insoluble in ether, chloroform, and acetic acid.

IR (KBr): 3400, 2600, 1735, 1620, 1600, 1500, 1250, 1140, and 1110 cm^{-1}.

Polymer (B)-HCl: Polymer (B) (0.1 g) in benzene afforded 0.1 g (83%) of the hygroscopic hydrochloride, which was insoluble in any organic solvents and water. Its IR spectrum was similar as that of polymer (A)-HCl.

BULLETIN OF THE CHEMICAL SOCIETY OF JAPAN, VOL. 44, 3188 (1971)

Magnetic Properties of Organic Stable Radicals. III. Diphenyl Nitric Oxide

Osamu TAKIZAWA,* Jun YAMAUCHI,** Hiroaki OHYA-NISHIGUCHI,* and Yasuo DEGUCHI*

*Department of Chemistry, Faculty of Science, Kyoto University, Sakyo-ku, Kyoto

**The Institute for Chemical Research, Kyoto University, Uji, Kyoto

(Received March 26, 1971)

We have already reported on the magnetic property of 2,2,6,6-tetramethyl-4-hydroxypiperidine-1-oxyl (TANOL), which can be explained fairly well by theoretical calculations based on the one-dimensional Heisenberg model.[1] On the other hand, from the findings on the temperature dependence of the susceptibility of the porphyrexide radical, it has been proposed that this radical forms an Ising-type antiferromagnetic chain.[2] The difference between the magnetic properties of TANOL and porphyrexide is considered to be due to their different molecular structures; the former has a nonplanar molecular framework and a localized spin distribution, while the latter is somewhat planar and has a small delocalized spin distribution over the whole molecular frame. In order to examine the effect of the delocalization of spin on the magnetic exchange interaction, another organic stable radical with a more delocalized spin in the π-orbital has been chosen as the next sample. In the present paper we shall report the results of our susceptibility measurements of the diphenyl nitric oxide (DPNO) radical. In this radical the unpaired spin is delocalized in the conjugated π-electron system spreading over the whole molecule,[3] and the molecule is presumed to have a planar framework similar to those of benzophenone and di-*p*-anisyl-nitric-oxide.[4] Cambi has reported the magnetic susceptibility data of DPNO at room temperature only.[5] In the present paper, the magnetic measurements were extended to the temperature range between 1.5°K and 293°K.

A DPNO radical prepared by the method of Wieland and Roth[6] was recrystallized from ether, the melting point being 59.5—60.5°C. Its radical concentration was determined to be 96% by comparing it with the calculated value, using the Curie-Weiss law and the Weiss constant of $\theta = -3.5$°K at 77°K. The measurements were carried out by means of a magnetic torsion balance[7] in the magnetic field about 8 kOe. The diamagnetic correction was made employing -1.21×10^{-4} emu/mol. The results, shown in Fig. 1, obeyed the Curie-Weiss law in the temperature range above 30°K. After deviating from the Curie-Weiss law when the temperature was lowered, the magnetic susceptibility reached a broad maximum at 6.2°K. Thereafter, it decreased successively toward a finite value of 140×10^{-4} emu/mol. The broad maximum in the susceptibility can be attributed to the short-range magnetic ordering, for no intrinsic anisotropy of magnetic susceptibility could be found from the measurement of a single crystal of DPNO. In order to clarify the magnetic property of DPNO, it was compared with the theoretical results of the one-dimensional Heisenberg model ($T_m = 6.2$°K) calculated by Bonner and Fisher,[8] which are also shown in Fig. 1. The theoretical results agree quite well with the present experimental results in the available temperature region.

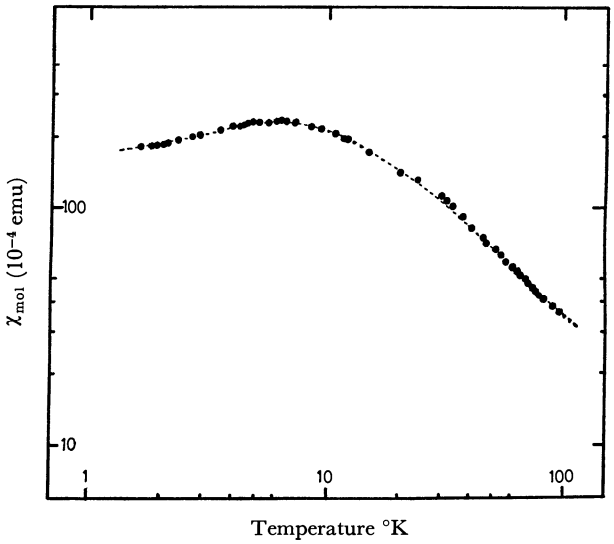

Fig. 1. Magnetic susceptibility of DPNO radical.
●: observed values, ------: calculated values of one-dimensional Heisenberg model

Recently, the magnetic properties of di-*p*-anisyl nitric oxide (DANO) have been shown to be consistent with the nearest-neighbor antiferromagnetic Heisenberg model of a quadratic layer lattice proposed by Duffy, Strandburg and Deck.[9] However, one of the present authors has discussed in detail the magnetic properties of some organic free radicals.[10] In his paper, it was concluded that the neutral organic free radicals with one unpaired electron in a molecule have a one-dimensional antiferromagnetic spin array with a Heisenberg-type isotropic interaction, and was suggested that the DANO radical is a one-dimensional Heisenberg-type antiferromagnet. The present results on the DPNO radical are also consistent with the aforementioned conclusion regarding the neutral organic free radicals.

1) J. Yamauchi, T. Fujito, E. Ando, H. Nishiguchi, and Y. Deguchi, *J. Phys. Soc. Japan*, **25**, 1558 (1968).
2) T. Fujito, H. Nishiguchi, Y. Deguchi, and J. Yamauchi, This Bulletin, **42**, 3334 (1969).
3) J. Yamauchi, H. Nishiguchi, K. Mukai, Y. Deguchi, and H. Takaki, *ibid.*, **40**, 2512 (1967).
4) A. W. Hanson, *Acta Crystallogr.*, **6**, 32 (1953).
5) L. Cambi, *Gazz. Chim. Ital.*, **63**, 579 (1933).
6) H. Wieland and K. Roth, *Ber.*, **53**, 216 (1920).
7) M. Mekata, *J. Phys. Soc. Japan*, **17**, 796 (1962).
8) J. C. Bonner and M. E. Fisher, *Phys. Rev.*, **135A**, 640 (1964).
9) W. Duffy, Jr., D. L. Strandburg, and J. F. Deck, *ibid.*, **183**, 567 (1969).
10) J. Yamauchi, This Bulletin, **44**, 2301 (1971).

BULLETIN OF THE CHEMICAL SOCIETY OF JAPAN, VOL. 44, 3189—3190 (1971)

The Characteristics of Defect Lead Titanate

Shin-ichi SHIRASAKI, Kooichiro TAKAHASHI, and Kazuo MANABE*

National Institute for Research in Inorganic Materials, Honkomagome, Bunkyo-ku, Tokyo

** Tokyo College of Photography, Atsugi, Kanagawa*

(Received April 3, 1971)

$PbTiO_3$ and $BaTiO_3$ have been known as typical ferroelectric materials with perovskite-type structures, the former being characterized by a fairly high Curie temperature (490°C) and by the largest tetragonal lattice strain (0.063) among known perovskite-type ferroelectrics. On the other hand, although many sorts of barium titanate, such as $BaTi_3O_7$, $BaTi_2O_5$, and Ba_2TiO_4, besides the well-studied $BaTiO_3$, have been known, no phase other than $PbTiO_3$ has so far been found in the system of Pb–Ti–O. This means that, during the course of the solid-solid reaction between PbO and TiO_2 at elevated temperatures, one of the reactants present in an excess remains unreacted without forming any compounds other than a single product of $PbTiO_3$. Furthermore, neither an oxygen-excess nor an oxygen-deficient state in $PbTiO_3$ has been found. The present communication will discuss the basic chracterization of the defect lead titanate newly found.

Experimental

All the ceramic samples of defect lead titanate proposed here were prepared by firing noncrystalline lead titanate. The noncrystalline bodies were prepared by adding a titanium tetrachloride aqueous solution to a strongly basic aqueous solution (with the aid of NaOH) of lead acetate under following conditions: with an equimolar ratio of Ti^{4+} and Pb^{2+} quantities (sample A′), with Pb^{2+} in twice the molar quantity of Ti^{4+} (sample B′), and with the latter solution in a large excess (sample C′). All the precipitates thus obtained were thoroughly washed with water until they were free from Na^+. A portion of as-precipitated sample C′ was immersed into a basic aqueous solution of lead acetate for 10 hr and then washed with water (sample D′); the solution was formed by the dissolution of lead acetate into a slightly basic aqueous solution adjusted with the aid of acetic acid and ammonia water. Finally, the noncrystalline samples, A′, B′, C′, and D′ were all fired at 800°C for 1 hr in order to convert them satisfactorily into polycrystalline samples, A, B, C, and D respectively.

Results and Discussion

The results of the chemical analysis of these polycrystalline samples indicated that they all more or less possessed Pb- and oxygen-deficiencies; they can be characterized by the general formula of $(PbO)_x \cdot TiO_2$. Here, it was confirmed that no phases other than the perovskite one were observed, at least on X-ray powder patterns of the samples. The defective structures, however, should be understood as being metastable even if they are stable up to 800°C. A piece of experimental evidence to support the above statement was that all the samples of defect lead titanate, when heated at a considerably higher temperatures (for example, at 950°C) were changed to those with less deficiencies by successively isolating TiO_2 from the original samples.

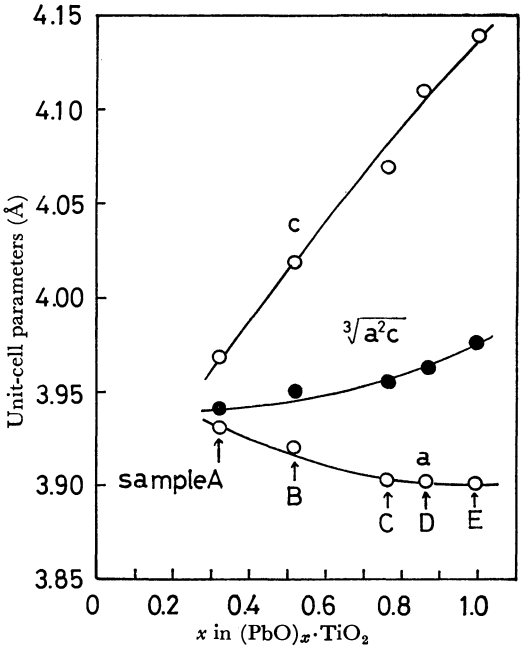

Fig. 1. Unit-cell parameters (a,c and $\sqrt[3]{a^2c}$) as a function of the value x in $(PbO)_x \cdot TiO_2$.

On the other hand, the unit-cell parameters (a,c and $\sqrt[3]{a^2c}$) of each tetragonal lattice varied from one sample to others, depending on the history of the preparation of the samples. The dependence of these parameters on the x value in $(PbO)_x \cdot TiO_2$ is obvious; Fig. 1 depicts this along with the data on a standard sample, E, which was prepared by the solid-solid reaction of an equimolar mixture of PbO and TiO_2 at 1000°C for 1 hr. As may be seen in Fig. 1, with an increase in the degree of the nonstoichiometry between constituent cations, a reducing tendency of $\sqrt[3]{a^2c}$ value is evident. In other words, this fact may be the same as saying that a contraction of the unit-cell volume of the defect lead titanate takes place as a result of the introduction Pb- and/or oxygen-vacancies into the $PbTiO_3$ crystal. It is surprising that considerable amounts of the deficiencies can be introduced into the $PbTiO_3$ crystal while maintaining the perovskite-type structure. At any rate, the present ceramic samples of defect lead titanate may be successfully taken as a new type of ferroelectric material, because they all more or less possess tetragonal lattice strains, $1-c/a$.

Further study was undetaken in order to determine whether or not the defect structures are uniform over the bulk. For this purpose, the degree of the fluctua-

1) J. Mazur, *Nature*, **164**, 358 (1949).
2) W. H. Hall, *J. Inst. Met.*, **75**, 1129 (1949).

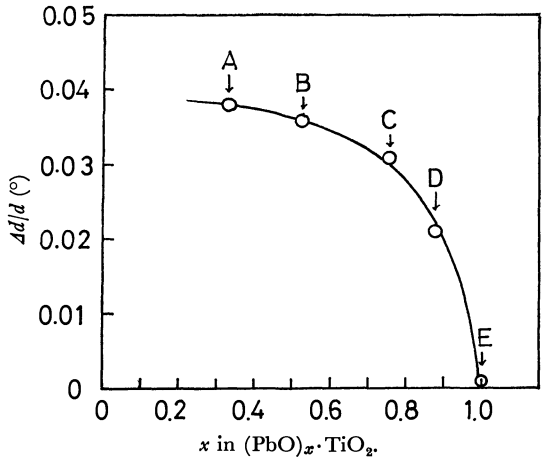

Fig. 2. The fluctuation of interplaner spacings in defect lead titanate.

tion of interplanar spacings, $\Delta d/d$, of each cubic lattice, which appeared when the substance was intentionally held at a temperature (550°C) above the Curie point of the samples, was calculated by observing the reflection angles, θ, and the pure X-ray diffraction broadening, β, with the aid of the relationship:[1,2]

$$\beta = -\frac{\Delta d}{d} \cdot \frac{\sin\theta}{\cos\theta}$$

Practically, when plotting $\beta \cdot \cos\theta$ against $\sin\theta$, the $\Delta d/d$ value was determined from the slope of the straight line obtained. The dependence of the $\Delta d/d$ ratio on the x value is evident, as is illustrated in Fig. 2. Here, from the fact of the presently-observed dependence on x of $\sqrt[3]{a^2c}$ at room temperature, one may expect a further dependence of $\sqrt[3]{a^3}$ or a at 550°C on x. If so, it seems resonable to believe that the fluctuation of interplanar spacings occurs mainly due to a fluctuation of the x value, *i.e.* due to a microscopic inhomogeneity of the defect structures.

In summary, the present lead titanate prepared through the wet process can be characterized by both Pb- and oxygen-deficient structures, and by their inhomogeneities, the degree of which increase with an increase in the over-all degree of the deficiencies.

BULLETIN OF THE CHEMICAL SOCIETY OF JAPAN, VOL. 44, 3190—3191 (1971)

The Effects of the Exciting Energy on the Atomic and Molecular Detachments of Hydrogen in the Photolysis of Simple Molecules

Kinichi Obi, Yuji Ogata, and Ikuzo Tanaka

Department of Chemistry, Tokyo Institute of Technology, Ohokayama, Meguro-ku, Tokyo

(Received April 16, 1971)

Photochemical studies of simple molecules have been mainly concerned with understanding the primary processes, together with their relative yields.[1)]

In this note we wish to report on certain interesting features of the variation in the percentage of the molecular and atomic detachment processes of hydrogen in the photolyses of ethane, ethylene, water, and ammonia with the change in the excitation energy. The experimental data are qualitatively interpreted by a simple theoretical treatment of the RRKM theory.

The primary processes of ethane, ethylene, water, and ammonia are summarized in Table 1. The photolysis of ethylene at 1634 and 1849 Å was carried out using a bromine lamp and a low-pressure mercury lamp respectively. The results of our study of the photolysis of ethylene will be published elsewhere.[2)] In these primary processes, we were most interested in the effect of the exciting energy on the hydrogen elimination primary processes. Figure 1 shows the percentage of the atomic detachment of hydrogen as a function of the excess photon energy, which is the energy difference between the photon energy and the heat of reaction for the atomic elimination. In the case of ethane, the total yield of Reactions (1) and (2) is taken as 100%.

It can clearly be seen in Fig. 1 that there are two kinds of energy dependency in these molecules; one increases its atomic percentage with an excess of energy, such as the cases of ethane and ethylene, while the other shows the oposite trend, such as the cases of water and ammonia. As is shown in Table 1, in the

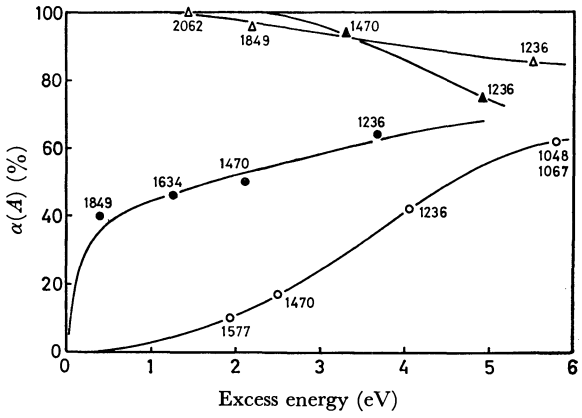

Fig. 1. Dependency of experimental percentage of atomic detachment on excess energy. The numbers in the figure show the wavelength (Å).
○: ethane, ●: ethylene, △: ammonia, ▲: water.

1) J. R. McNesby and H. Okabe, *Advan. Photochem.*, **3**, 157 (1964); J. G. Calvert and J. N. Pitts, Jr., "Photochemistry," Wiley, New York, N. Y. (1966).

2) H. Hara and I. Tanaka, to be published.

Table 1. Primary processes in the photolyses of ethane, ethylene, water and ammonia

	Primary process	ΔH (eV)	Relative yield (%)			
Ethane			1048, 1067Å[a]	1236Å[b]	1470Å[b]	1577Å[c]
(1)	$C_2H_6 + h\nu \longrightarrow C_2H_4 + H_2$	1.4	26	43	78	>90
(2)	$\longrightarrow C_2H_4 + 2H$	5.9	41	31	16	<10
(3)	$\longrightarrow CH_4 + CH_2$	3.8	16	26	6	
(4)	$\longrightarrow CH_3 + CH_3$	3.8	15			
Ethylene			1236Å[d]	1470Å[d]	1634Å[e]	1849Å[e]
(5)	$C_2H_4 + h\nu \longrightarrow C_2H_2 + H_2$	1.8	30	46	54	60
(6)	$\longrightarrow C_2H_2 + 2H$	6.3	70	54	46	40
Water			1236Å[f]	1270Å[g]		
(7)	$H_2O + h\nu \longrightarrow H_2 + O$	5.1	25	6		
(8)	$\longrightarrow H + OH$	5.1	75	94		
Ammonia			1236Å[f]	1849Å[f]	2062Å[h]	
(9)	$NH_3 + h\nu \longrightarrow NH + H_2$	4.1	14			
(10)	$\longrightarrow NH_2 + H$	4.5	86	>96	~100	

a) S.G. Lias, G. J. Collin, R. E. Rebbert, and P. Ausloos, *J. Chem. Phys.*, **52**, 1841 (1970).
b) H. Akimoto and I. Tanaka, *Ber. Bunsenges. Physik. Chem.*, **72**, 134 (1968).
c) I. Tanaka znd H. Akimoto, 7th Informal Photochem. Conf., p. 42 (1966).
d) H. Okabe and J. R. McNesby, *J. Chem. Phys.*, **36**, 601 (1962).
e) See Ref. 2.
f) J. R. McNesby, I. Tanaka, and H. Okabe, *J. Chem. Phys.*, **36**, 605 (1962).
g) L. J. Stief, *ibid.*, **44**, 277 (1966).
h) W. E. Groth, V. Schurath, and R. N. Schindler, *J. Phys. Chem.*, **72**, 3914 (1968).

case of the former the heat of reaction for molecular detachment is much smaller than that for atomic detachment, whereas in the case of the latter the difference between the heats of reaction between the two kinds of detachment is small.

The percentage of the atomic detachment was calculated from the relative rates of the molecular and atomic detachments, which were themselves estimated by the application of the simple RRKM theory to the excited state of the reactant. According to the RRKM theory, the unilmoecular rate constant is expressed as follows:[3]

$$k_E = A\frac{(E-E_a+a^+E_z^+)^{s-1}}{(E+aE_z)^{s-1}} \quad (1)$$

where E is the excess energy of the electronic excited state ($E=E(h\nu)-E_0$, E_0 is the energy of the electronic excited state), E_a is the activation energy, and E_z and E_z^+ are the zero-point energies of the energized molecule and the activated complex respectively. The a and a^+ quantities are empirical correction factors for the energized molecule and the activated complex respectively. The index, s, is the number of the vibrational mode, and A is a constant evaluated from the properties of the species in question.

In this treatment the molecular and atomic detachments are assumed to be competitive processes from the excited state. Thus, the percentage of atomic detachment is given by $\alpha(A)=100\ k_E(A)/(k_E(A)+k_E(M))$, where $k_E(A)$ and $k_E(M)$ represent the rate constants for the atomic and molecular detachment process es respectively. Using Eq. (1), $\alpha(A)$ is expressed as follows:

$$\alpha(A) = \frac{100}{1+A'\left(1+\frac{\Delta E_a-\lambda}{E'-E_a(A)}\right)^{s-1}} \quad (2)$$

3) D. W. Setser and B. S. Rabinovitch, *Can. J. Chem.*, **40**, 1425 (1962).

where $A'=A(M)/A(A)$, $E'=E+a^+(A)E_z^+(A)$, $\Delta E_a=E_a(A)-E_a(M)$, and $\lambda=a^+(A)E_z^+(A)-a^+(M)E_z^+(M)$.

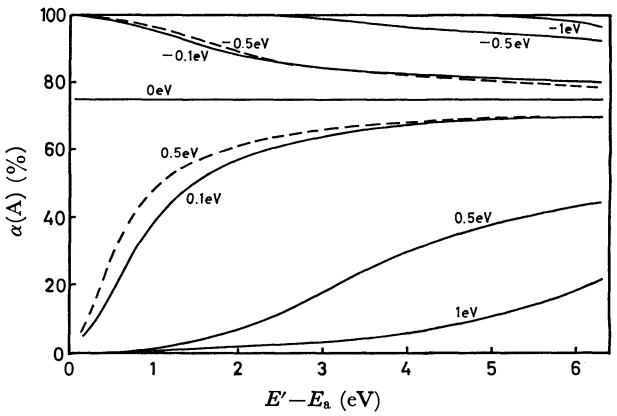

Fig. 2. Dependency of calculated percentage of atomic detachment on excess energy ($E'-E_a$) for various $\Delta E_a-\lambda$ values. ——: $s=18$, – – –: $s=3$.

Assuming $A'=1/3$, at which the percentage of atomic detachment is 75% for a large excess energy, the percentage of atomic detachment was calculated for several values of $\Delta E_a-\lambda$ and s as a function of $E'-E_a$. The results are shown in Fig. 2 for the case of ethane ($s=18$) and also for water ($s=3$), but for the latter only the results for $\Delta E_a-\lambda=\pm 0.5$ eV are shown. As may be seen in Fig. 2, if $\Delta E_a-\lambda$ is positive, the molecular detachment percentage decreases, while if it is negative, it increases with an increase in $E'-E_a$, that is, the photon energy. Comparing these calculated results with the experimental one in Fig. 1, it can be predicted that ethane and ethylene have positive values of $\Delta E_a-\lambda$, while water and ammonia have negative values.

BULLETIN OF THE CHEMICAL SOCIETY OF JAPAN, VOL. 44, 3192 (1971)

The Proton Magnetic Resonance Spectrum of 1,2,3,4-Tetrahydronaphthalene Polymer

Tadashi YONEMITSU, Yasuhiko MATSUKUMA, Kunihiro FURUKAWA, and Genjiro HAZATO

Department of Industrial Chemistry, Faculty of Engineering, Kyushu Sangyo University, Kashii, Fukuoka

(Received April 5, 1971)

The polymerization of naphthalene has been reported by Minato *et al.*[1] The naphthalene polymer was obtained easily by the reaction with anhydrous aluminum chloride. This polymer was estimated to be a 1,2-dihydronaphthalene oligomer. According to the procedure of Minato *et al.*, we also synthesized the naphthalene polymer. The polymer obtained by us was a brown, powdered crystal. This crystal softened and darkened at 50—60°C, melted at about 150°C, and finally carbonized at about 200°C. The molecular weight of the polymer was found to be 1025 by the cryoscopic method. As the molecular weight of $(C_{10}H_8)_8$ is 1024, the average degree of polymerization is 8. Figure 1 shows two structures of the polynaphthalene. The (II) structure seems to be more favorable in both stability and the progress of the reaction. The proton magnetic resonance spectrum of the polymer was obtained on a JNM-MH-100 spectrometer.

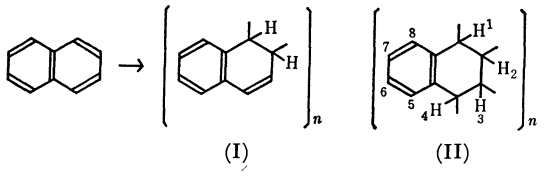

(I) (II)

Fig. 1. The structures of the polynaphthalene and the numbering.

The peaks at 1.84, 2.83, and 7—9 ppm are ascribed to the hydrogens of the 2,3-, 1,4-, and 5,6,7,8-positions respectively. The sharp peak at 7.19 ppm is suspected to be due to $CHCl_3$ in the solvent, $CDCl_3$.

On the other hand, in the NMR spectrum of 1,2-dihydronaphthalene, two peaks have been found, at 5.82 and 6.33 ppm, corresponding to the 3- and 4-positions.[2] Therefore, if the 1,2-dihydro-structure predominates in the polymer, two peaks corresponding to the 3- and 4-positions should appear in the range of 5—7 ppm. Moreover, of course, no peak has been found in that range in tetralin.[3] Therefore, it seems that the polymer we have obtained has the 1,2,3,4-tetrahydro-structure predominantly.

The authors wish to thank Dr. Goto and his coworkers in Japan Electron Optics Laboratory Co., Ltd., for the measurement of the NMR spectrum.

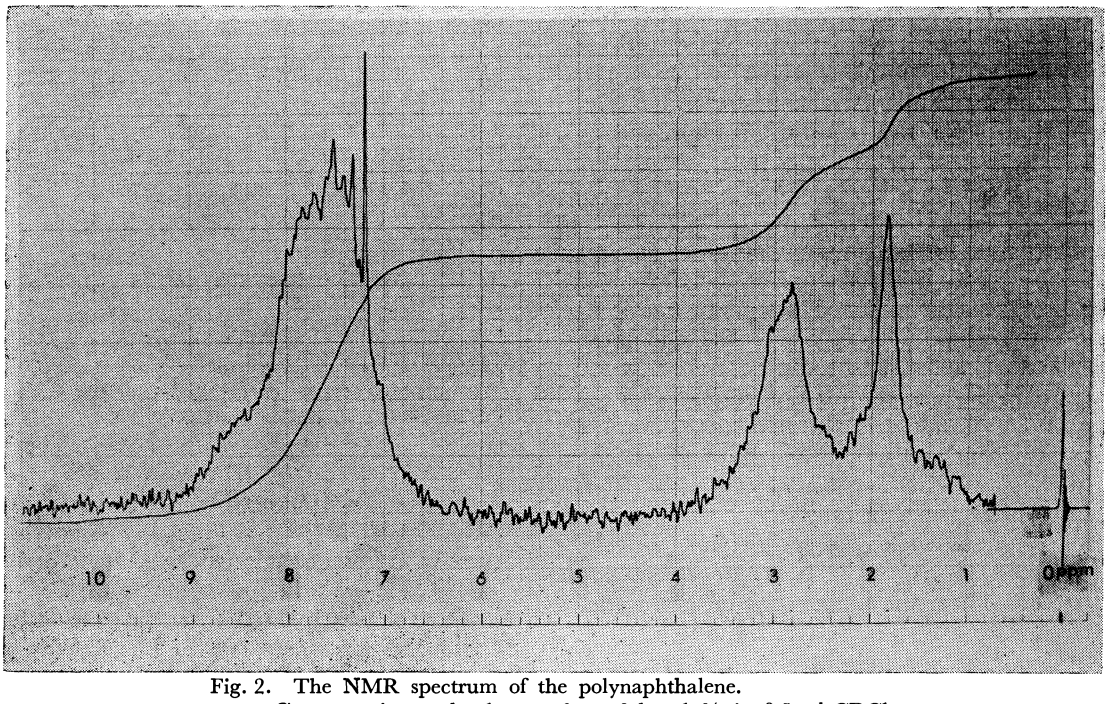

Fig. 2. The NMR spectrum of the polynaphthalene.
Concentration and solvent: about 0.1 mol % in 0.5 m*l* $CDCl_3$
Temperature: 70°C
Internal reference: tetramethylsilane

1) H. Minato, N. Higosaki, and C. Isobe, This Bulletin, **42**, 779 (1969).

2) M. A. Cooper, D. D. Elleman, C. D. Pearce, and S. L. Manatt, *J. Chem. Phys.*, **53**, 2343 (1970).

3) "High Resolution NMR Spectra Catalog," No. 557, Varian Associates, Palo Alto, Calif.

BULLETIN OF THE CHEMICAL SOCIETY OF JAPAN, VOL. 44, 3193—3194 (1971)

Alkoxysilanes. VIII. The Preparation of Alkoxysiloxy Derivatives of Aluminum and Boron

Ichiro KIJIMA, Takeshi YAMAMOTO, and Yoshimoto ABE*

Department of Industrial Chemistry, Faculty of Engineering, Science University of Tokyo, Kagurazaka, Shinjuku-ku, Tokyo

(Received April 26, 1971)

In order to obtain a polymer containing a heterosiloxane linkage in the molecular main chain, we have already reported on the preparation of alkoxysiloxy derivatives of metals (Sb,[1] Ti,[2] Zr,[3] Sn). In the present experimental work, the preparation of the derivatives of aluminum and boron was attempted.

The reaction of triiso-propoxyaluminum or tri-*n*-butyl borate with tri-*t*-butoxysilanol was investigated; it was difficult to isolate the reaction product in 1:1 molar ratio of the silanol to triisopropoxyaluminum by recrystallization and distillation because of its high solubility in solvents or because of its decomposition. The reaction in the 3: 1 molar ratio caused decomposition during the removal of the solvent from the reaction mixture and led to the formation of a gel insoluble in organic solvents. The gas evolved during the decomposition was identified as isobutylene by means of gas chromatography. Therefore, it was considered that, in this reaction, the rupture of the alkoxy group attached to silicon occurred along with alcohol exchange. This reaction is very different from that of the metal alkoxides with the silanol. The difference may be attributed to the property as Lewis acids of aluminum compounds. In the 2:1 molar ratio, however, bis(tri-*t*-butoxysiloxy)-isopropoxyaluminum (I) was isolated by recrystallization (mp 75—76°C). The results of the molecular-weight determination indicated that it was associated. On the other hand, tri-*t*-butoxydi-*n*-butoxy (II) and bis(tri-*t*-butoxysiloxy)*n*-butoxysiloxyboron (III) were easily obtained as viscous liquids, however, it seems difficult to replace the last *n*-butoxy group attached to boron by the butoxysiloxy group because of its steric hindrance.

$$M(OR)_3 + n(Bu^tO)_3SiOH \longrightarrow [(Bu^tO)_3SiO]_nM(OR)_{3-n} + nROH$$

where M=Al, R=Pr^i, and n=2 (I); M=B, R=Bu^n and n=1 (II) or 2 (III)

The reaction of acetylacetonatodiisopropoxyaluminum with the silanol gave bis(tri-*t*-butoxysiloxy)acetylacetonatoaluminum (IV), as in the case of titanium, zirconium, and tin. Bis(tri-*t*-butoxysiloxy)isopropoxyaluminum is associated, while this compound is monomeric (Table 1). The difference seems to be ascribed to the coordination of the carbonyl group in the acetylacetonato to aluminum.[4] These compounds were identified by means of elemental analysis, as is shown in Table 1, and by studying the IR spectra, which were essentially identical and which showed the IR absorption peaks at 1050—1075 (ν_{Si-O-C} and $\nu_{Si-O-Al}$[5]) and 1320 (ν_{B-O-C}), 1500—1600(AcAc) cm^{-1}. The reaction products from bis(acetylacetonato)isopropoxyaluminum, however, were almost all tri(acetylacetonato)-aluminum. In this case, therfore, disproportionation

Table 1. Alkoxysiloxy derivatives of Al and B

Reagents (g)		Product						
						Anal. Found % (Calcd)		
$M(OR)_3$	$(BuO)_3$-SiOH		Yield (%)	Mp, °C Bp °C/mmHg	n_D^{20} or mol wt Found (Calcd)	C	H	Si
5.6	16.5	(I)	36.4	75—76[b]	1300 (613)	52.29 (52.92)	10.18 (9.96)	9.71[c] (9.50)
7.6	8.7	(II)	38.1	125—121.5/2	1.4102	57.22 (57.30)	10.54 (10.75)	6.60 (6.70)
2.7	6.2	(III)	41.0	167—169/1.5	1.4128	54.58 (55.02)	10.80 (10.30)	8.92 (9.22)
5.6[a]	11.8	(IV)	29.3	60—61[b]	710 (685)	54.26 (54.60)	8.97 (9.73)	8.45[d] (8.61)
3.5[a]	8.4	(V)	—	280 (Decomp)	—	49.68 (48.77)	8.95 (8.75)	11.78[e] (11.79)
3.2	2.9	(VI)	—	290/2 (Decomp)	650 (625)	45.00 (45.40)	8.47 (8.52)	12.83 (13.31)

Benzene was used as a solvent. a) (AcAc)Al(OPr^i)$_2$ as reagent. b) Recrystallized from benzene (IV) or *n*-hexane. c) Al%, Found: 3.91 (Calcd: 4.41); d) 8.45 (8.61); e) 8.12 (8.79).

* Present address: Department of Science and Technology, Science University of Tokyo, Yamazaki, Noda, Chiba.

1) Y. Abe and I. Kijima, This Bulletin, **42**, 1148 (1969).

2) Y. Abe and I. Kijima, *ibid.*, **43**, 466 (1970).

3) Presented at the 22nd Annual Meeting of the Chemical Society of Japan, Tokyo, April, 1969.

4) T. R. Patterson, F. J. Pavlik, A. A. Baldoni, and R. L. Frank, *J. Amer. Chem. Soc.*, **81**, 4213 (1959).

5) K. A. Andrianov and N. P. Gashnikova, *Izv. Akad. Nauk, SSSR.*, **1960**, 857.

may occur:

$$(AcAc)Al(OPr^i)_2 + 2(Bu^tO)_3SiOH \longrightarrow [(Bu^tO)_3SiO]_2Al(AcAc) + 2Pr^iOH$$
(IV)

$$3(AcAc)_2Al(OPr^i) + 2(Bu^tO)_3SiOH \longrightarrow 2Al(AcAc)_3 + [(Bu^tO)_3SiO]_2Al(OPr^i) + 2Pr^iOH$$

In order to obtain a polymeric substance, the reaction of acetylacetonatodiisopropoxyaluminum or tri-*n*-butyl borate with di-*t*-butoxy and bis(tri-*t*-butoxysiloxy)silanediol was carried out: with di-*t*-butoxysilanediol, a little tri(acetylacetonato)aluminum and a powder (decomposed at 200°C) soluble in organic solvents were formed, whereas with bis(tri-*t*-butoxysiloxy)silanediol, needle crystals (decomposed at 280°C) almost insoluble in solvents were obtained (V). It was shown, by means of studying the IR spectra and by the elemental analysis, that these substances contained the Si–O–Al bond together with the acetyl-acetonato groups, and that the former had an atom ratio of C: H: Si equal to 6: 13: 1 and that the latter has a unit structure of $[-Al(AcAc)-O-Si[OSi(OBu^t)_3]_2-O-]_n$, although the structures were not confirmed. On the other hand, it was difficult to isolate the products formed by the reaction of tri-*n*-butyl borate with the diols by recrystallization or distillation, however, the results of the study of the IR spectra, the elemental analysis, and the molecular weight determination showed that the raw material obtained by the reaction of the alkoxide with di-*t*-butoxysilanediol was in accordance with the following formula:

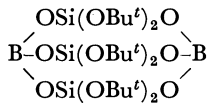
(VI)[6]

Experimental

Materials. The alkoxysilanols were prepared by the method already described.[2,7] Commercially-available aluminum triisopropoxide was redistilled before use. The tri-*n*-butyl borate was obtained by the reaction of boric anhydride with *n*-butyl alcohol according to the procedure of Walton and Rosenbaum;[8] bp 107—109°C/1 mmHg, n_D^{20} 1.4089. The acetylacetonatodiisopropoxyaluminum was afforded by Thomas method;[4] bp 147—148°C/2 mmHg.

Preparation of Compounds (I) and (II). A mixture of metal alkoxide or acetylacetonato chelate, silanol, and benzene was refluxed for 1 hr. The solvent was then removed, and the residue was fractionally distilled *in vacuo* or recrystallized from *n*-hexane or benzene. The results are shown in Table 1.

Reaction of Acetylacetonatodiisopropoxyaluminum with Silanediols. A mixture of 3.5 g (0.014 mol) of the acetylacetonato chelate, 8.4 g (0.014 mol) of bis(tri-*t*-butoxysiloxy)silanediol, and 30 m*l* of benzene was heated. White needle crystals appeared at 70°C; then the mixture was further heated for 30 min. The crystals were filtered and washed with benzene (yield 8.1 g). The analytical data are shown in Table 1.

In another run, a mixture of 4.0 g (0.016 mol) of the chelate, 3.4 g (0.016 mol) of di-*t*-butoxysilanediol, and 30 m*l* of toluene was refluxed for 1 hr. The solvent was then removed, and the residue was recrystallized from *n*-hexane, giving 0.5 g of needle crystals; mp 187—190°C. Found: C, 54.42; H, 6.38; Al, 8.41% (tris(acetylacetonato)aluminum). The filtrate gave a yellow powder (3.7 g) after the removal of the solvent; mp about 200°C (decomposed).

Analysis. The silicon was determined by a method already described. The aluminum was determined to be aluminum oxide after a weighed sample had been decomposed by an aqueous alcohol solution.

6) F. A. Henglein, R. Lang, and K. Scheinest, *Makromol. Chem.*, **18—19**, 102 (1956), *ibid.*, **22**, 103 (1956); B. L. Chamberland and A. G. MacDiarmid, *J. Amer. Chem. Soc.*, **82**, 4542 (1960).

7) Y. Abe and I. Kijima, This Bulletin, **42**, 1118 (1969).

8) J. H. Walton and E. J. Rosenbaum, *J. Amer. Chem. Soc.*, **50**, 1648 (1928).

BULLETIN OF THE CHEMICAL SOCIETY OF JAPAN, VOL. 44, 3195—3196 (1971)

Nicotinonitrile Derivative from 2-Cyano-3-mercapto-3-methylthioacrylamide

Masataka YOKOYAMA

Department of Chemistry, Faculty of Science, Chiba University, Yayoi-cho, Chiba

(Received May 11, 1971)

The reaction of 2-cyano-3-mercapto-3-methylthioacrylamide (**1a**) with carbonyl compounds has been reported.[1] This paper deals with the reaction of **1a** with a cyano compound.

It has been found that 2-imino-4-methylthio-6-methylamino-1,2-dihydronicotinonitrile (**3**) can be isolated in 71% yield by the reaction of **1a** with malononitrile and an aqueous solution of methylamine (30%).

The structure of **3** was established on the basis of spectroscopic evidence and the results of elementary analysis. The NMR spectrum (acetone-d_6) showed a broad NH signal at δ 5.80, a singlet peak for one proton of C(5)–H at δ 5.50, a doublet methyl singal at δ 2.85 (J=5 Hz), and a singlet methyl signal at δ 2.43. On addition of deuterium oxide, the NMR peak of NH disappeared and the doublet methyl signal changed to a singlet. This indicates the presence of the $NHCH_3$ group. The NH stretching bands appeared at 3440, 3400, and 3310 cm^{-1}, and a conjugated CN group occurred at 2200 cm^{-1}. The features of the UV spectrum of **3** were similar to those of 2-aminopyridine,[2] but quite different from those of ethyl 3(2-amino-2-methylaminoethenylthio)-2-cyano-3-methylthioacrylate (**2b**) (see Experimental). Compound **3** might better be written in a pyridone type form to accomodate C(5)–H to δ 5.50.

A plausible mechanism for the formation of **3** is illustrated in Scheme 1 by assuming **2a** as an intermediate. Compound **2b**, corresponding to **2a**, could be isolated by the reaction of ethyl 2-cyano-3-mercapto-3-methylthioacrylate with malononitrile and the aqueous solution of methylamine (30%). Formation of **2b** can be accounted for in the following way:

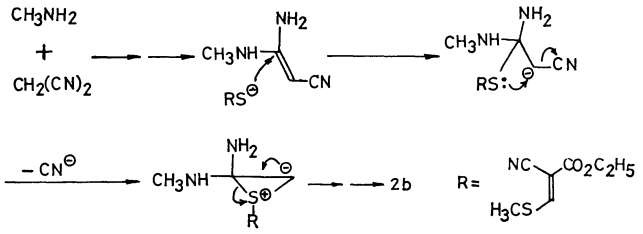

Compound **3** can be formed by the cyclization reaction of **2a**, followed by the loss of an atom of sulfur. A similar desulfuration reaction has been reported on the behavior of a cyclic polysulfide.[3]

Compound **3** was also obtained by refluxing **2b** in alcohol-aqueous ammonia (28%), sulfur being simultaneously eliminated. In the reaction of **1a** with malononitrile and the aqueous solution of methylamine, a small amount of sulfur was detected, while no cyano ion eliminated from malononitrile could be detected by spot test.[4]

Desulfuration of **3** afforded 2-imino-6-methylamino-1,2-dihydronicotinonitrile (**4**). The NMR spectrum (DMSO-d_6) of 4 showed a doublet peak of C(5)–H which caused coupling with that of C(4)–H at δ 5.90

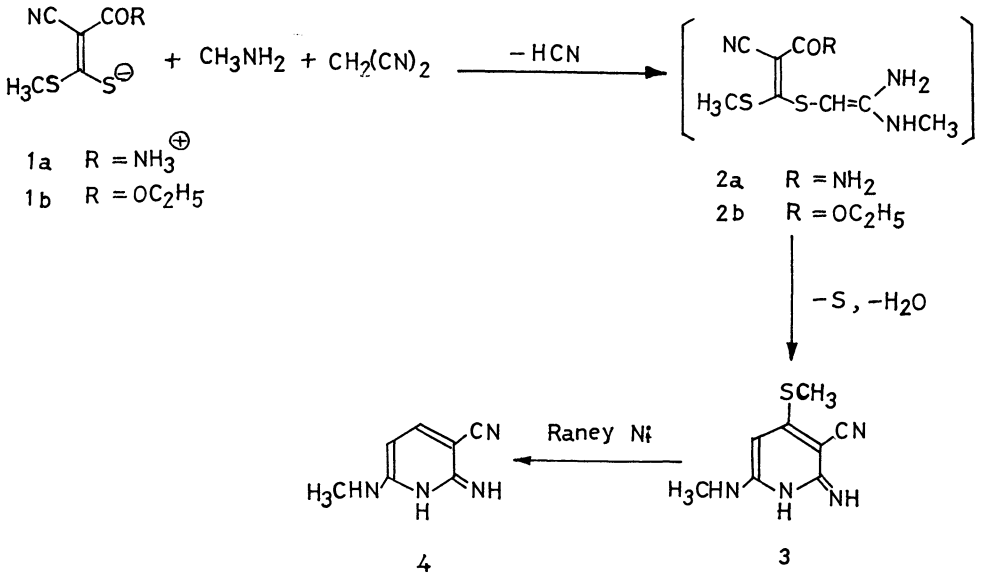

Scheme 1

1) M. Yokoyama, This Bulletin, **44**, 1610 (1971).
2) $UV_{max}^{99\%EtOH}$ 235 mμ (log ε=3.97), 297 (3.51).
3) M. S. Raasch, *J. Org. Chem.*, **35**, 3470 (1970).
4) A dark brown solution containing cuprous sulfate and ammonium sulfide changes to a colorless one by addition of a cyanide ion.

(J=8 Hz), and no peak at δ 2.43 for the methylthio group. Formation of **4** also supports the structure of **3**.

Experimental

Compound **1a** was prepared according to the procedure given in a previous report.[1] The NMR spectra were recorded with a JNM-4H-100 MHz Spectrometer using tetramethylsilane as an internal standard. The IR, UV, and mass spectra were recorded with a Nihon Densi 403G, Hitachi EPS-3T, and Hitachi Double Focus RMU-6E, respectively. Microanalyses were performed at the Institute of Physical and Chemical Research.

Preparation of 2-Imino-4-methylthio-6-methylamino-1,2-dihydronicotinonitrile (3). To a mixture of an aqueous solution of methylamine (30%, 30 m*l*) and **1a** (5 g, 0.03 mol) was gradually added malononitrile (20 g, 0.3 mol) with stirring at room temperature. The reaction mixture immediately started to boil. After 5 min, a colorless crystalline material started to precipitate gradually. After 1 hr, it was filtered, washed with ethanol, and dried. Recrystallization from methanol gave 4 g of colorless needles: yield 71%; mp 223—224°C; $UV_{max}^{99\%EtOH}$ 236.5 mμ (log ε =4.59), 255 (sh, 4.39), 288 (4.10).

Found: C, 49.22; H, 5.14; N, 29.02; S, 16.47%; mol wt, 194 (mass spectrum). Calcd for $C_8H_{10}N_4S$: C, 49.48; H, 5.19; N, 28.85; S, 16.48%; mol wt, 194.19.

A small amount of sulfur was detected from the above filtrate.

Desulfuration of 3. A Raney nickel (Ni: 48%) was activated in the usual way.[5] Compound **3** (3 g, 0.02 mol) was refluxed with the activated Raney nickel (25 g) in ethanol (50 m*l*) for 6 hr. The decolorized reaction mixture was separated from nickel by decantation and centrifugation. The nickel was washed with ethanol and the washings were also centrifuged. The combined alcoholic solution was concentrated to *ca.* 20 m*l* under diminished pressure. The resulting solution was left to stand for 2 weeks. After a small amount of the unreacted **3** was filtered off, the filtrate was allowed to stand for an additional 2 weeks. The second crystalline material (colorless needles) was collected and washed with ethanol: yield 0.1 g; mp 180—181°C; NMR (DMSO-d_6) δ 6.30 (br, 3, NH) δ 5.90 (d, 1, C(4)-H, J=8 Hz) δ 5.50 (d, 1, C(5)-H, J=8 Hz) δ 2.65 (d, 3, CH_3, J=7 Hz); IR (KBr) 3450, 3360, 3130 (s, NH), 2950 (m, CH), 2220 cm^{-1} (s, conj. CN); $UV_{max}^{99\%EtOH}$ 237.5 mμ (logε =4.76), 257 (sh, 4.51), 290 (4.11).

Found: C, 56.69; H, 5.41; N, 37.96%; mol wt, 148 (mass spectrum). Calcd for $C_7H_8N_4$: C, 56.74; H, 5.44; N, 37.82%; mol wt, 148.17.

The NMR absorption of NH disappeared and the doublet methyl signal at δ 2.65 changed to a singlet by addition of deuterium oxide. The structure of the product was thus assigned to 2-imino-6-methylamino-1,2-dihydronicotinonitrile.

Preparation of Ethyl 3(2-Amino-2-methylaminoethenylthio)-2-cyano-3-methylthioacrylate (2b). To a mixture of **1b** (8 g, 0.046 mol) and the aqueous solution of methylamine (30%, 15 m*l*) was slowly added malononitrile (15 g, 0.15 mol) at room temperature. After 30 min, a colorless crystalline material started to precipitate. After 3 hr, the precipitate was collected and washed with ethanol. Recrystallization from methanol gave 3.6 g of colorless plates: yield 29%; mp 177—178°C; NMR (acetone-d_6) δ 5.58 (d, 1, NH, J=4 Hz) δ 4.08 (q, 2, CH_2, J=8 Hz) δ 3.48 (s, 2, NH_2) δ 3.30 (s, 1, CH) δ 2.60 (d, 3, CH_3, J=4 Hz) δ 1.20 (t, 3, CH_3, J=8 Hz); IR (KBr) 3440, 3420, 3180, 3120 (s, NH_2, NH), 2200 (vs, conj. CN), 1660 cm^{-1} (vs, CO); $UV_{max}^{99\%EtOH}$ 228.5 mμ (logε=4.05), 289 (3.58), 345 (4.38).

Found: C, 43.92; H, 5.63; N, 15.30; S, 23.12%; mol wt, 265 (vapor-pressure osmometer, in acetone). Calcd for $C_{10}H_{15}N_3S_2O_2$: C, 43.95; H, 5.53; N, 15.38; S, 23.44%; mol wt, 273.24.

With the addition of deuterium oxide, the NMR absorptions of NH_2 and NH disappeared and the doublet methyl signal at δ 2.60 changed to a singlet.

The author wishes to thank Propessor Dr. Tatsuo Takeshima and Dr. Hiroshi Midorikawa for their kind advice.

5) E. C. Horning, "Organic Syntheses," Coll. Vol. III, p. 181 (1967).

BULLETIN OF THE CHEMICAL SOCIETY OF JAPAN, VOL. 44, 3197—3198 (1971)

Conformations of the Esters. III. The Infrared Carbonyl Absorptions and Conformations of Propionates, Isobutyrates, and Pivalates

Michinori Ōki and Hiroshi Nakanishi

Department of Chemistry, Faculty of Science, The University of Tokyo, Hongo, Bunkyo-ku, Tokyo

(Received May 13, 1971)

In a previous paper,[1] it has been proved that alkyl acetates take only the *s-trans* conformation within their ester group, and it has been suggested that the higher homologs of the esters also have such a conformation. However, in the homologs of carboxylic acids, a conformational heterogeneity will arise if the alkyl chain is properly substituted. The conformational heterogeneity has been reported with mono and dihaloacetates,[2,3] methoxy- and phenoxyacetates,[4,5] α-methoxypropionates, and α-methoxyisobutyrates.[5] However, few authors[6,7] have reported on the conformational heterogeneity of the esters, whose α-carbon is replaced by another carbon group (alkylacetates). The purpose of this note is to present the results of a study of the infrared spectra in the carbonyl region of alkylacetates, and to relate the crabonyl-stretching frequencies with the conformations derived by rotation about the C_{CO}–C_{α} bond.

Experimental

Materials. The required esters were prepared according to the published procedures. The purities of the samples were checked by means of their physical constants, gas-chromatographic results, NMR spectra and infrared spectra.

Apparatus. The infrared spectra were recorded on a Perkin-Elmer 112G single-beam grating spectrometer (3500—3300 cm^{-1}, 1800—1700 cm^{-1}) and a Hitachi EPI-G2 grating infrared spectrophotometer (4000—400 cm^{-1}). The measurement of the spectra and the separation of the bands of esters were carried out as has been described previously.[1]

Results and Discussion

As the model compounds of alkylacetates, some propionates, isobutyrates, and pivalates were chosen. These esters have been reported to have only one carbonyl absorption,[2,3,5,8,9] and no authors have reported the unsymmetric nature of the carbonyl bands of these esters. We measured the carbonyl absorption shapes carefully with a infrared spectrometer of a high resolution. The results are given in Table 1. Clearly, propionates and isobutyrates give bifurcated band in the carbonyl region except for only one case (compound III). These results may be taken as indicating the presence of two conformers if they are proved to be really carbonyl bands. The bifurcation can be attributed neither to the solute-solute interaction nor to the solute-solvent interaction, because the spectra were measured with a solution of a very low concentration and two-peaked absorptions are observed even in carbon tetrachloride. The origin of the bifurcation is also difficult to explain from the standpoint of Fermi resonance for the following two reasons. The solvent effects on the band shapes of the almost all the propionates and isobutyrates are hardly affected at all by solvent polarity. The independency of the relative intensity of the solvent polarity can be attributed to the small difference in the polarities of the conformers. On the other hand, it is well known that in the case of the Fermi resonance, the intensities of the two peaked absorptions of the carbonyl region are dramatically affected by the solvent polarity; in fact, a reversal of the intensity ratio is often observed[10] (see also the case of methyl pivalate). Methyl propionate (I) has car-

Table 1. Carbonyl absorptions of propionates, isobutyrates, and pivalates (c 0.05 mol/l)

	Compound	CS_2 cm^{-1}	ε	CH_3CN cm^{-1}	ε	DMSO cm^{-1}	ε
I	$EtCO_2Me$	1735	148	1731	84		
		1744	702	1739	689		
II	$EtCO_2Et$	1730	127	1723	103		
		1737	841	1733	693		
III	$EtCO_2$ *i*-Pr	1733	790	1729	575		
VI	$EtCO_2$ *t*-Bu	1726	88	1718	76		
		1732	691	1727	562		
V	$EtCO_2$ *t*-Am	1725	117	1716	80		
		1731	891	1725	518		
VI	*i*-$PrCO_2Me$	1733	143	1723	78		
		1740	846	1735	678		
VII	*i*-$PrCO_2Et$	1726	101	1721	90		
		1735	902	1730	749		
VIII	*i*-$PrCO_2$ *i*-Pr	1723	183	1715	43		
		1731	870	1724	709		
IX	*i*-$PrCO_2$ *t*-Bu	1729	183	1716	72		
		1730	998	1724	1102		
X	*t*-$BuCO_2Me$	1722	138	1722	263	1722	527
		1735	1094	1734	387	1732	236
XI	*t*-$BuCO_2CD_3$	1732	501	1726	720		
XII	*t*-$BuCO_2Et$	1728	948	1722	894		
XIII	*t*-$BuCO_2$ *t*-Bu	1725	716[a]	1713	479		

a) in CCl_4 c=0.0004 mol/l

1) Part II: M. Ōki and H. Nakanishi, This Bulletin, **44**, 3144 (1971).
2) T. L. Brown, *Spectrochim. Acta*, **18**, 1615 (1962).
3) H. Laato and R. Isatolo, *Acta Chem. Scand.*, **21**, 2119 (1967).
4) M. L. Josien and C. Castinel, *Bull. Soc. Chim. Fr.*, **1958**, 801.
5) N. Mori, Y. Asano, and Y. Tsuzuki, This Bulletin, **41**, 1871 (1968).
6) A. J. Bowles, W. O. George, and D. B. Cuntiffe-Jones, *Chem. Commun.*, **1970**, 103.
7) S. Ichikawa and T. Shimanouchi, The 21st Annual Meeting of the Chemical Society of Japan, Osaka, April, 1968, and private communication.
8) K. Bowden, N. B. Chapman, and J. Shoter, *Can. J. Chem.*, **41**, 2154 (1963).
9) K. J. Morgan and N. Unwin, *J. Chem. Soc., B*, **1968**, 880.
10) Ref. 1 and the references cited therein.

bonyl overtone absorptions of almost the same shape at 3454 cm^{-1} (ε=0.45) and 3472 cm^{-1} (ε=3.56). These two facts rule out the possibility of the bifurcation of the carbonyl bands being due to the Fermi resonance.

Thus, it is most likely that the bifurcation comes from the presence of at least two conformations. Three stable conformations can arise corresponding to the rotation about the C–O bond in the alcohol part. However, if this is the only cause of the bifurcation, it is difficult to explain why the methyl and *t*-butyl propionates give two absorptions in this region. This consideration leads to the conclusion that the presence of the two bands is most probably attributable to the rotational isomers about the C_{CO}–C_{α} bond, as is shown in Fig. 1.

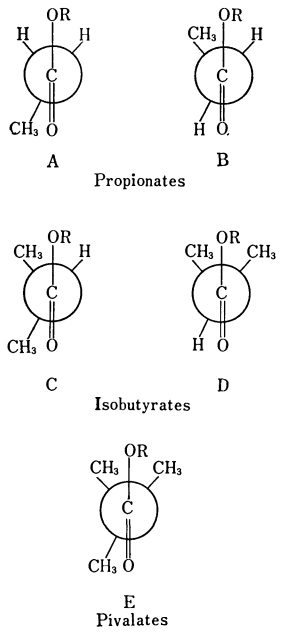

Fig. 1. Possible conformations of alkyl propionate, isobutyrate, and pivalate.

According to the above considerations, pivalate esters should give only one C=O band, because they have only one conformation, E, due to the symmetry of the *t*-butyl group. The results with ethyl and *t*-butyl pivalates conform to this expectation, but methyl pivalate unexpectedly gives a two-peaked band. In order to test the possibility of a Fermi resonance, the C=O absorption spectrum of methyl-d_3 pivalate (XI) was measured. It gives only one symmetrical peak. This necessarily means that the mode of C–H vibration is responsible for the bifurcation of the carbonyl band and strongly suggests that the phenomenon is caused by the Fermi resonance. Auxiliary support for this explanation has been obtained by the dramatic solvent effect on the carbonyl absorptions. Now it is clear that the bifurcation of the carbonyl bands of some simple esters reflects the heterogeneity of the conformations.

There then remains the problem of assigning the two bands to each conformation. Comparing the wave number where the carbonyl absorptions of acetates and pivalates occur, the higher frequency band may be assigned to the C–H and C=O eclipsed forms, B and D. Then it may be taken that these B and D conformers are more stable than the A and C conformers, judging from the integrated intensities of the respective bands. However, it is well known that, for unknown reasons, the C–H and C=O eclipsed conformers are less stable than the C–CH_3 and C=O eclipsed conformers. Therefore, these two contradictory arguments must be settled before establishing the assignments. We do not dare to assign the bands at present, but would like simply to point out the need of further work.

The authors wish to express their hearty thanks to Professor T. Shimanouchi of The University of Tokyo for his helpful discussions.

BULLETIN OF THE CHEMICAL SOCIETY OF JAPAN, VOL. 44, 3198—3199 (1971)

Synthetic Studies of the Flavone Derivatives. XXIII.[1] The Synthesis of Eupatilin

Tokunaru HORIE, Masao TSUKAYAMA, Mitsuo MASUMURA, Kenji FUKUI,* and Mitsuru NAKAYAMA*

Department of Applied Chemistry, Faculty of Engineering, University of Tokushima, Tokushima
**Department of Chemistry, Faculty of Science, Hiroshima University, Higashisenda-machi, Hiroshima*

(Received May 14, 1971)

Eupatilin, isolated from *Eupatorium semiserratum* D C., has been identified as 5,7-dihydroxy-6,3′,4′-trimethoxyflavone (I) on the bases of its spectral data and degradative studies.[2] The present paper will describe the synthesis of I from 2,4-dibenzyloxy-6-hydroxy-3-methoxyacetophenone (II).

The esterification of II with 3,4-dimethoxybenzoyl chloride (III) yielded 2,4-dibenzyloxy-3-methoxy-6-(3,4-dimethoxybenzoyloxy)acetophenone (IV). The IV ester was converted into 2,4-dibenzyloxy-6-hydroxy-3-methoxy-ω-(3,4-dimethoxybenzoyl)acetophenone (V) by the Baker-Venkataraman transformation. The cy-

1) XXII of this series: T. Matsumoto, S. Imai, and K. Fukui, This Bulletin, **44**, 1698 (1971).

2) S. M. Kupchan, C. W. Sigel, R. J. Hemingway, J. R. Knox, and M. S. Udayamurty, *Tetrahedron*, **25**, 1603 (1969).

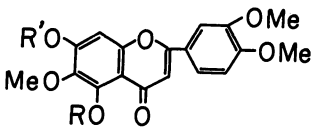

I R=R′=H
VI R=H, R′=C_7H_7
VII R=R′=Ac
VIII R=R′=Et
IX R=H, R′=Et

clodehydration of V with sodium acetate afforded 7-benzyloxy-5-hydroxy-6,3′,4′-trimethoxyflavone (VI). The catalytic hydrogenolysis of VI gave the desired flavone I, which was then easily converted into the diacetate (VII), the diethyl ether (VIII), and the monoethyl ether (IX). The flavone I was shown to be identical with the natural pigment[3] by a mixed-melting-point determination and by IR and UV spectral comparisons.

Experimental[4]

2,4-Dibenzyloxy-3-methoxy-6-(3,4-dimethoxybenzoyloxy)acetophenone (IV). A mixture of the crude II[5] (2.3 g) and III (2.3 g) in anhydrous pyridine (10 m*l*) was heated at 120°C for 2 hr. The cooled reaction mixture was poured into diluted hydrochloric acid, and then extracted with ether. The ether layer was allowed to stand overnight in a refrigerator. The separated crystals were recrystallized from ethyl acetate to give IV; mp 155—157°C (colorless prisms); yield, 800 mg (24%).

Found: C, 70.83; H, 5.53%. Calcd for $C_{32}H_{30}O_8$: C, 70.83; H, 5.57%.

2,4-Dibenzyloxy-6-hydroxy-3-methoxy-ω-(3,4-dimethoxybenzoyl)-acetophenone (V). A mixture of IV (0.9 g), powdered potassium hydroxide (1 g), and anhydrous pyridine (15 m*l*) was heated at 60°C for 4 hr with stirring. The reaction mixture was acidified with diluted hydrochloric acid, and then extracted with ether. The ether layer was allowed to stand overnight in a refrigerator. The separated crystals were recrystallized from ethyl acetate to give V; mp 131—132°C (yellow needles); yield, 450 mg (50%).

Found: C, 70.85; H, 5.33%. Calcd for $C_{32}H_{30}O_8$: C, 70.83; H, 5.57%.

7-Benzyloxy-5-hydroxy-6,3′,4′-trimethoxyflavone (VI). A mixture of V (370 mg), sodium acetate (1 g), and acetic acid (10 m*l*) was heated at 140°C for 4 hr. The reaction mixture was diluted with water, and then extracted with ether. The product was recrystallized from ethyl acetate to give VI; mp 175—177°C (pale yellow plates); yield, 210 mg (71%). UV: λ_{max}^{EtOH} mμ (log ε); 244(4.26), 251.5(4.23), 278 (4.25), 344 (4.39). NMR:[6] ($CDCl_3$) 12.82_s (5-OH).

Found: C, 69.18; H, 5.19%. Calcd for $C_{25}H_{22}O_7$: C, 69.11; H, 5.10%.

5,7-Dihydroxy-6,3′,4′-trimethoxyflavone (Eupatilin) (I). A mixture of VI (150 mg) and palladium charcoal (Pd: 10%; 75 mg) in a mixed solvent of ethyl acetate and methanol (1:1; 80 m*l*) was shaken in an atmosphere of hydrogen for 3 hr. The product was recrystallized from ethyl acetate to give I; mp 241—242°C (yellow prisms); yield, 92 mg (77%). UV: λ_{max} mμ (log ε); (EtOH) 242(4.30), 277(4.29), 345 (4.38); (EtOH–AcONa) 278(4.45), 316(4.20), 376(4.26); (EtOH–$AlCl_3$) 254(4.18), 290(4.24), 352(4.39). NMR: (DMSO) 3.76_s, 3.84_s, 3.87_s (3×MeO); 6.60_s, 6.90_s, 7.09_d (J=9), 7.53_d(J=2), 7.65_q(J=9, 2) (5×Arom.H); 10.5_b, 13.07_s (2×OH) (Natural Pigment:[7] mp 240—241.5°C).

Found: C, 62.51; H, 4.47%. Calcd for $C_{18}H_{16}O_7$: C, 62.79; H, 4.68%.

Diacetate (VII): mp 154—155°C (colorless needles from methanol). UV: λ_{max}^{EtOH} mμ (log ε); 249(4.35), 265_{sh}(4.16),[8] 338(4.40). NMR: ($CDCl_3$) 2.37_s, 2.47_s (2×MeCO); 3.83_s, 3.92_s (6H) (3×MeO); 6.56_s, 6.96_d(J=9), 7.29_s, 7.30_d(J=2.5), 7.49_q(J=9, 2.5) (5×Arom.H).

Found: C, 61.68; H, 4.63%. Calcd for $C_{22}H_{20}O_9$: C, 61.68; H, 4.71%.

Diethyl Ether (VIII): mp 165.5—166.5°C (colorless needles from ethanol). UV: λ_{max}^{EtOH} mμ (log ε); 240(4.34), 266 (4.15), 327(4.42). NMR: ($CDCl_3$) 1.46_t, 1.50_t, 4.14_q (J=7) (2×EtO); 3.87_s, 3.91_s(6H) (3×MeO); 6.51_s, 6.73_s, 6.91_d (J=9), 7.27_d(J=2.5), 7.46_q(J=9, 2.5) (5×Arom. H) (lit,[2] mp 164—166°C).

Found: C, 66.24; H, 6.26%. Calcd for $C_{22}H_{24}O_7$: C, 65.99; H, 6.04%.

Monoethyl Ether (IX): mp 176—177°C (pale yellow needles from ethanol). UV: λ_{max}^{EtOH} mμ (log ε); 244(4.29), 253_{sh} (4.25), 278.5(4.27), 344(4.45). NMR: ($CDCl_3$) 12.80_s(5-OH).

Found: C, 64.80; H, 5.40%. Calcd for $C_{20}H_{20}O_7$: C, 64.51; H, 5.41%.

Acetate of IX: mp 176—177°C (colorless needles from methanol). UV: λ_{max}^{EtOH} mμ (log ε); 240(4.30), 260_i(4.06),[9] 330(4.35).

Found: C, 63.94; H, 5.21%. Calcd for $C_{22}H_{22}O_8$: C, 63.76; H, 5.35%.

3) The natural pigment was kindly supplied by Professor S. M. Kupchan, University of Virginia.

4) All the melting points are uncorrected.

5) K. Fukui, M. Nakayama, and T. Horie, This Bulletin, **42**, 2327 (1969).

6) The NMR spectra were measured with a Hitachi R-20 spectrometer (60 MHz), using tetramethylsilane as the internal standard (δ, ppm): s, singlet; d, doublet; q, quartet; b, broad.

7) The natural pigment was measured in this laboratory.

8) sh=shoulder.

9) i=inflection.

BULLETIN OF THE CHEMICAL SOCIETY OF JAPAN, VOL. 44, 3200 (1971)

Effects of AC Pretreatment on the Formation of Anodic Titanium Oxide Films

Masaki YAMAZAKI,* Mitumoto NAKAGAWA,** and Hiroshi NOZAKI*

*Institute of Industrial Science, The University of Tokyo, Roppongi, Minato-ku, Tokyo

**Department of Applied Chemistry, Faculty of Engineering, Tokai University, Shibuya-ku, Tokyo

(Received May 20, 1971)

Recently, we have reported the formation of electrolytic titanium oxide films in an aqueous solution of barium hydroxide.[1] In this formation, the pretreatment of titanium was done by applying an AC current to titanium in an aqueous solution of sulphuric acid. It has been found that the AC pretreatment is effective in increasing the bath voltage in the anodization of titanium; this pretreatment is also useful in producing good insulating films on the surface of titanium. It would be of interest to know whether a good dielectric film could be formed on titanium by using the AC pretreatment in connection with electrolytic capacitors. Thus, in this work we will report the effects of the AC pretreatment of titanium on the formation of anodic oxide films in an aqueous solution of phosphoric acid.

Two titanium electrodes, 50 mm × 20 mm × 1 mm, were prepared from ST-40 titanium (H, <0.015%; O, <0.20%; N, <0.05%; Fe, <0.20%). One of the electrodes was mechanically polished, while the other was pretreated in a 16 wt% H_2SO_4 solution at 25°C, using AC (50 Hz) at 50 mA/cm², for 2 hr.[1] After these procedures, the surfaces of both electrodes were examined with an optical microscope. The microphotographs obtained are shown in Fig. 1A for the mechanically-polished electrode and in Fig. 1B for the AC-pretreated electrode. Figure 1 shows that the electrode is partially dissolved in the H_2SO_4 solution by the AC pretreatment. This fact was also confirmed by measuring the weight decrease in the titanium electrode during the AC pretreatment.

The anodizations of both the electrodes mentioned above were carried out under the same conditions; the electrodes were anodized in a 13 wt% aqueous solution of phosphoric acid at 25°C with a constnat current density of 3 mA/cm². In these anodizations, the growth of the voltage with the time was examined. The results obtained are shown in Fig. 2. It is obvious from Fig. 2 that the voltage for the AC-pretreated electrode increases rapidly with the time up to 180 V, while the voltage for the mechanically-polished electrode hardly increases at an over 50 V. These results indicate that the AC pretreatment is useful in producing anodic titanium oxide films which have good insulating properties.

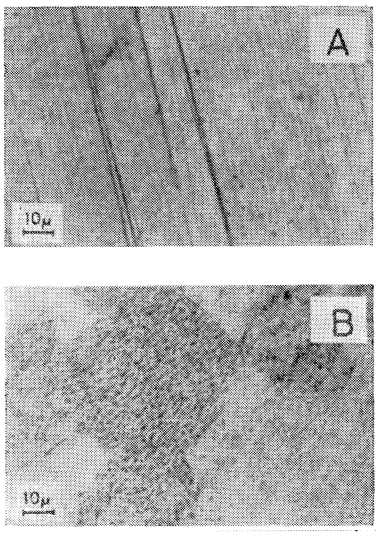

Fig. 1. Microphotographs of the surfaces of titanium electrodes.
A: Mechanically-polished electrode.
B: AC-pretreated electrode.

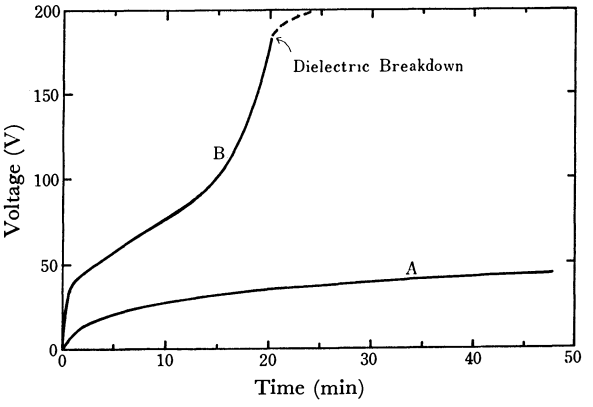

Fig. 2. Bath voltage-time curves for the anodization of titanium at a constant current density of 3 mA/cm².
A: Mechanically-polished electrode.
B: AC-pretreated electrode.

1) a) M. Yamazaki and H. Nozaki, *J. Electrochem. Soc.*, **118**, 400 (1971). b) M. Yamazaki and H. Nozaki, *Kogyo Kagaku Zasshi*, **74**, 1265 (1971). c) M. Yamazaki and H. Nozaki, *J. Phys. Chem.*, **75**, 1279 (1971).

BULLETIN OF THE CHEMICAL SOCIETY OF JAPAN, VOL. 44, 3201—3202 (1971)

Fermentation without Multiplication of Cells Using Microcapsules That Contain Zymase Complex and Muscle Enzyme Extract

Masao KITAJIMA and Asaji KONDO

Central Research Laboratories, Fuji Photo Film Co., Ltd., Asaka-shi, Saitama

(Received May 20, 1971)

In an earlier article, the present authors described that such enzymes as catalase, urease, lipase, and hemoglobin could be microencapsulated into sphere particles from 10 to 1000 μ in diameter by the use of some synthetic polymers, without much loss of enzymatic activity.[1] An enzyme solution was enveloped with a semi-permeable inactive polymer membrane which protected the enzymes, macromolecular protein, from leaking out, but which did not affect the permeation of substrates and products of a low molecular weight.

These enzyme-containing microcapsules are regarded as a kind of immobilized enzymes,[2] but they are essentially different from the others in that the enzymes themselves are intact and retain their normal properties. One of the merits of the encapsulation in comparison to other methods of chemical or physical immobilization is expected to lie in its applicability to multi-enzyme systems.

More than one enzyme of any kind, with reagents if necessary, can be microencapsulated at the same time in a capsule. In this paper we will discuss the microencapsulation of enzyme extracts obtained from yeast (zymase complex) and the muscle of a rabbit, and will investigate alcoholic and lactic fermentation using these microcapsules.

Experimental

Enzyme Extracts. *Zymase Complex*: A freshly-fermented yeast solution (supplied by the Toyo Jozo Co., Ltd.) was treated with a refrigerated cell fractionator (Sorvall-Ribi, RF-1) to destroy the cells. The homogenated solution was centrifuged at 2000 rpm for 30 min, and then the supernatant was filtered with a filter paper to remove the cell wall and the undestroyed cells. The filtrate was turbid and contained plasmic granules.

The Muscle Enzyme Extract. About 100 g of leg muscle of a rabbit was cut into one-centimeter blocks, and then it was homogenated by a homoblender for 15 min while 200 m*l* of a 0.05M pH 7.0 phosphate buffer solution was added. After the fibrous materials had been taken off, the solution was centrifuged at 9000 rpm for 20 min. The supernatant, the enzyme extract, was clear and colorless. All these treatments were carried out at temperatures below 10°C.

Microencapsulation. 3.0 g of an enzyme extract were emulsified in 15 m*l* of a 5% benzene solution of a ladder polymer of sesqui phenylsiloxane (supplied by the Shinetsu Kagaku Co., Ltd.) by the use of a homoblender for 3 min. This W/O-type emulsion was added quickly to 150 m*l* of a 3% gelatine solution phosphate-buffered at pH 7.0 under brisk agitation at 20°C. At this stage, a (W/O)/W-type complex emulsion was formed. The temperature was gradually raised to 37°C over a 1-hr period, after which the agitation was continued for an additional 1.5 hr at the same temperature. The benzene was evaporated gradually during the process so that a hard, solid capsule wall of the silicone was formed around a droplet of the enzyme extract. The microcapsules thus formed were recovered by centrifugation and were washed with the buffer solution three times.

In all the experiments, the amount of the capsules was weighed after incubation and drying in order to minimize the denaturation of the enzymes.

Incubation and Determination of the Reaction Product. *Alcoholic Fermentation*: In a 50 m*l* flask we placed microcapsules containing the zymase complex and 30 m*l* of a 400 mM glucose solution. Then it was put in an air incubator kept at 30°C.

The concentration of the reaction product, ethyl alcohol, was determined by gas chromatography using a Hitachi-Perkin Elmer Model F6-D gas chromatograph. The calibration curve was obtained by the use of an alchohol-water mixture as the standard solution.

Lactic Fermentation: In a test tube we placed about 150 mg of microcapsules containing the muscle enzyme extract, 1 m*l* of 100 mM glucose, 1 m*l* of 1 mM NAD, 1 m*l* of 10 mM ATP, and 2 m*l* of the 50 mM pH 7.0 tris-HCl buffer solution. Then it was incubated in a water bath kept at 39°C.

At the end of the incubation, the microcapsules were removed by filtration, then, to the filtrate obtained above, we added 5 m*l* of a 10% trichloroacetic acid solution. (No preciptitation was observed upon this addition, as there was no free enzyme in the filtrate). After filtration, the amount of the reaction product, lactic acid, was determined according to the Barker and Summerson method.[3] The optical density was measured at 560 nm using a Hitachi Type 139 spectrophotometer. The control solution was prepared by removing the microcapsules from the incubation solution. The calibration curve was prepared by the use of lithium lactate as the standard material.

Results and Discussion

Figure 1 shows a photomicrograph of the microcapsules that contain the zymase complex. Each looks like a ping-pong ball containing the enzyme solution.

Table 1 gives the results for alcoholic fermentation using the microcapsules containing the zymase complex. About 1% of alcohol was produced in 10 days. The reaction rate is calculated as 10—50 μmol of alcohol per gram of capsule per hour. We could not observe any multiplication of yeast cells outside the capsules in any of the experiments.

Table 2 gives the results for the lactic fermentation using microcapsules containing the muscle-enzyme ex-

1) M. Kitajima, S. Miyano, and A. Kondo, *Kogyo Kagaku Zasshi*, **72**, 493 (1969).

2) A. S. Lindsey, *J. Macromol. Sci., Revs. Macromol. Chem.*, **C(1)**, 1 (1969).

3) S. B. Barker and W. H. Summerson, *J. Biol. Chem.*, **138**, 535 (1941).

Table 1. Alcoholic fermentation using the microcapsules that contain the zymase complex

Sample	Diameter (μ)	Weight (mg)	Time (day)	Alc. Conc. (%)	Alcohol (mmol)	Reaction rate (Alc. μmol/ caps-g·hr)
Caps-1	100—500	734	6	0.55	3.6	34
Caps-2	20—200	648	7	0.95	6.2	57
Caps-3	200—800	374	7	0.05	0.3	5.0
Caps-4	100—500	602	11	0.76	5.0	32
Untreated[a)]	—	1.0 (m*l*)	1	0.16	0.11	46[b)]

a) Untreated zymase complex solution.
b) Alc. μmol/m*l*·hr

Table 2. Lactic fermentation using the microcapsules that contain the muscle enzyme extract

Sample	Diameter (μ)	Weight (mg)	Time (hr)	Lactic acid (μmol)	Reaction rate (L.a. μmol/ caps-g·hr)
Caps-1	100—500	168	1	0.14	0.82
Caps-1	100—500	162	40	5.15	0.79
Caps-2	100—500	147	15	0.59	0.27
Caps-3	20—200	180	15	0.17	0.63
Untreated[a)]	—	1.0 (ml)	1	2.82	2.82[b)]

a) Untreated muscle enzyme extract.
b) L.a. μmol/m*l*·hr

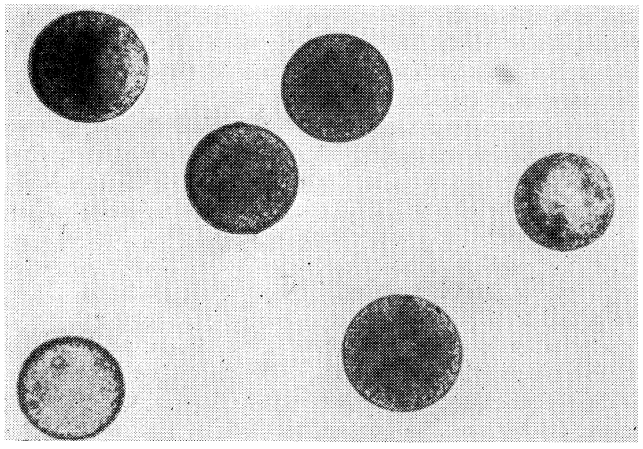

Fig. 1. A photomicrograph of the microcapsules containing the zymase comples.

tract. In these cases, ATP and NAD were added to facilitate the reaction. It is calculated from the results that about 1 μmol of lactic acid is procuced in an hour. The reaction time was chosen according to the sensitivity of the analysis for the products.

As was indicated by Emden, Mielhof, and Parnas, 13 enzymes are necessary to convert glucose into alcohol or into lactic acid. If any one of these enzymes is lost or denatures during the microencapsulation process, the reaction cycle cannot be completed and the final products can not be obtained. Although many encapsulation methods have been reported,[4)] most of them are unsuitable for enzymes. The method described above is believed to be the most suitable one for the encapsulation of enzymes, since no reactive reagent is necessary and the reaction conditions are quite mild throughout the process.

The present authors previously reported that modified red cells that have a reinforced membrane with normal hemoglobin and enzymes in it were obtained by treating red cells with some isocyanates.[5)] These modified cells can also be used as an immobilized multi-enzyme system, since they exibit many complicated enzymatic activities.

The microcapsules obtained here will be useful for the industrial and medical use of enzymes, since they are easy to recover and handle, and can be used in continuous-column reactions that are more complicated than that made possible by the immobilized monofunctional enzymes. It is expected that the enzymes are aligned close to each other in these capsules, so multi-stage reactions can proceed effectively, as in natural cells. It is also expected that they can be used as model samples in studying cellular reactions or membranes.

The authors wish to thank Mr. M. Morishita of the Toyo Jozo Co., Ltd., for kindly supplying the enzyme extracts, and Mr. F. Arai of our research laboratories for the technical assistance.

4) A. Kondo, "Microcapsules," Nikkan Kogyo Shinbun, Tokyo (1970).
5) M. Kitajima, W. Sekiguchi, and A. Kondo, This Bulletin, **44**, 139 (1971).

BULLETIN OF THE CHEMICAL SOCIETY OF JAPAN, VOL. 44, 3203(1971)

Photosensitive Systems Involving Photoconduction and Photochromism

Takao NAKAYAMA, Isamu SHIMIZU, Hiroshi KOKADO, and Eiichi INOUE
Imaging Science and Engineering Laboratory, Tokyo Institute of Technology, Ookayama, Meguro-ku, Tokyo
(Received May 21, 1971)

The photoreversible color changes (photochromism) of spirans are well known. The spectral sensitizing effect of the colored species of spirans upon the photoconduction of zinc oxide has also been observed.[1)]

In this paper, we will discuss some photosensitive systems which show both photochromism and spectral sensitization for photoconduction.

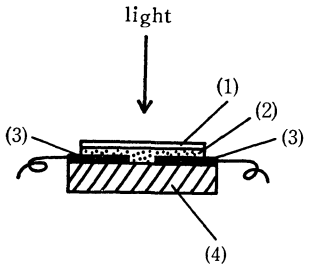

Fig. 1. Experimental arrangement for sp 3 zinc oxide bilayer.
(1) sp 3 evaporated film, (2) zinc oxide powder layer
(3) chromium electrode, (4) glass base

The photosensitive element was formed as is shown in Fig. 1. The photoconductive layer (Fig. 1-(2)) was coated with ZnO powder(0.3 $\mu\phi$)-alcoholic paste on a glass substratum with a pair of Cr-electrodes. After the solvent had been dried from the layer, a photochromic layer (Fig. 1-(1)) was settled upon the layer (Fig. 1-(2)) by the vacuum evaporation of spiran (1,3,3-trimethylspiro[5-chlor-indoline-2,2'-(6'-nitro)benzopyran]).

The photoconductive response of the element was hardly observed in the visible light region, its color was faint yellowish white. An intense color appeared when the element was irradiated with ultraviolet light (365 nm).

The photoconductive response of the photo-colored element was also observed in the visible light region. The spectrum of the photoconduction corresponded to the absorption spectrum of the UV-light-photo-generated colored species of spiran (Curves II and III of Fig. 2). The photocurrent and reflection spectral curves of the element after irradiation with UV light are shown in Fig. 2.

The color of the element was bleached by irradiation with visible light. The photo-bleached element did not show any photocurrent in the visible region. The change between the coloration accompanying spectrally-sensitized photoconduction by UV irradiation and the bleaching of the color by visible light irradiation was repeated several times.

This kind of photochromic and photoconductive element are promising for use with memorized imaging systems.

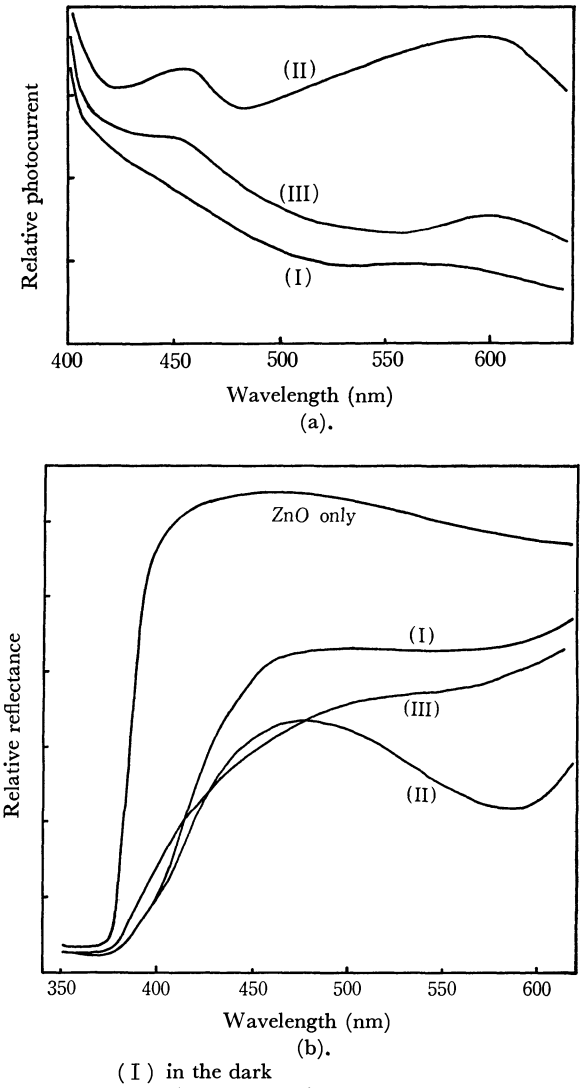

(I) in the dark
(II) after UV light irradiation
(III) same as II after visible light bleaching

Fig. 2. The photocurrent (a) and reflection (b) spectral curves of the element.

1) E. Inoue, T. Nakayama, and H. Kokado, *Kogyo Kagaku Zasshi*, **72**, 2352 (1969).

BULLETIN OF THE CHEMICAL SOCIETY OF JAPAN, VOL. 44, 3204—3205 (1971)

The Isomeric Sulfites of Dihydrofukinolidol

Keizo NAYA, Ichiro TAKAGI,* and Tsuneo KASAI

Department of Chemistry, Faculty of Science, Kwansei Gakuin University, Uegahara, Nishinomiya, Hyogo

(Received May 24, 1971)

We have already elucidated the structure of fukinolide (I) isolated from *Petasites japonicus* Maxim. In this structural study, dihydrofukinolidol (II) was obtained by the hydrogenation of fukinolide I with platinum oxide-acetic acid, followed by alkaline hydrolysis;[1] it was tentatively assigned to the stereoformula II with a 13-β methyl group, considering the approach of the catalyst from the back of the attached site of the ester groups in the hydrogenation process.

This paper will deal with the configurational assignment of the two isomeric sulfites prepared from dihydrofukinolidol II. The isomeric cyclic sulfites derived from the 1,3-diol system have recently been much investigated in order to provide decisive information for the conformational assignment, especially with regard to the correct orientation of the S–O group.[2]

For the purpose of clarifying the 1,3-relationship, including the configurations between the two hydroxyl groups in dihydrofukinolidol II, the compound II, $C_{15}H_{24}O_4$, mp 190—191°C, was treated with thionyl chloride-pyridine to afford a mixture of two isomeric sulfites. The crude product was separated by column chromatography with silica gel-benzene. The faster-running product (III) formed colorless prisms, mp 190.5—191.5°C (dec.), $[\alpha]_D^{22}$ −80° and the slower one (IV), colorless needles, mp 187.5—188.5°C (dec.), $[\alpha]_D^{22}$ −145°. Though the mixed melting point of III and IV showed a slight depression (mp 186.5—187.0°C dec.), both the products were found to possess the same molecular formula, $C_{15}H_{22}O_5S$; both regenerated dihydrofukinolidol II by alkaline hydrolysis, and were converted to the same sulfate by oxidation with perbenzoic acid.

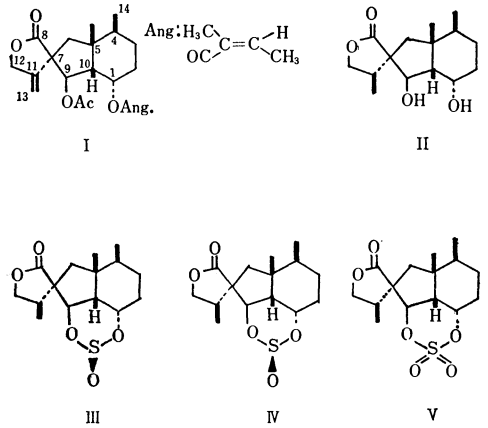

I II III IV V

Fig. 1. Stereoformulas of Fukinolide I, Dihydrofukinolide II, Sulfites III and IV, Sulfate V.

It was suggested that these isomers were derived from the different configurations of the sulfite S=O groups. In addition, the higher melting product III was less soluble in methanol and chloroform. In view of the *cis-trans* isomerism,[3] the compounds III and IV were supposed to have *trans*- and *cis*-characters respectively, according to the above properties (mp, solubility, and adsorption).

Table 1. Comparison of chemical shifts (ppm as δ-values) in the NMR spectra[a] of fukinolidol (I), dihydrofukinolidol (II), sulfites (III) and (IV)

Proton assignment	Compounds I	II	III	IV
1-H	5.10m	4.10m	4.75q (J=6)	5.00m
6-H	1.90d (J=15)	1.50d (J=14)	1.56d (J=14)	1.55d (J=14)
	2.55d (J=15)	2.00d (J=14)	2.04d (J=14)	2.04d (J=14)
9-H	5.77d (J=12)	4.61d (J=11)	5.26d (J=12)	4.45d (J=12)
10-H	2.82dd (J=6, 12)	2.55dd (J=6, 12)	2.95dd (J=7, 13)	3.65dd (J=7, 13)
12-H		4.23t (J=8)	4.35t (J=7.7)	4.35t (J=7.7)
		4.10q (J=8.5, 10)	3.90q (J=8.5, 10)	3.90q (J=8.5, 10)
13-Me		1.15d (J=7)	1.20d (J=7)	1.20d (J=7)
14-Me	0.90d (J=7.5)	0.78d (J=4)	0.88d (J=7)	0.90d (J=7)
15-Me	1.12s	1.00s	1.12s	1.18s

a) NMR spectra were taken in $CDCl_3$ at 60 MHz with TMS standard.

The configurational difference between the two sulfites was well defined by a comparison of the NMR spectra (Table 1 and Fig. 2). The most remarkable difference between the NMR spectra of the two isomers, III and IV, is the strong deshielding of 9-H in III, and of 10-H and 1-H in IV. This contrast may be expected to occur under the influence of the axially-oriented S=O groups in the chair and boat conformations. Furthermore, the compounds III and IV exhibited the IR absorptions of the axial S=O groups[4] at 1190 and 1200 cm^{-1} respectively.

* Present address: Department of Education, Wakayama University, Masago-cho, Wakayama.

1) K. Naya, I. Takagi, M. Hayashi, S. Nakamura, M. Kobayashi, and S. Katsumura, *Chem. Ind.* (London), **1968**, 318.

2) A. T. Rowland, T. B. Adams, H. W. Atland, W. S. Creasy, S. A. Dressner, and T. M. Dyott, *Tetrahedron Lett.*, **1970**, 4405; H. F. Van Woerden and E. Havinga, *Rec. Trav. Chim. Pays-Bas*, **86**, 341 (1967); E. L. Eliel and N. L. Allinger, "Topics in Stereochemistry," Vol. 4, Willey-Interscience, New York (1967), p. 48.

3) E. L. Eliel, "Stereochemistry of Carbon Compounds," McGraw-Hill (1962), p. 326.

4) D. G. Hellier, J. G. Tilett, H. F. Van Woerden, and R. F. M. White, *Chem. Ind.* (London), **1963**, 1956; O. R. S. Edmundson, *Tetrahedron Lett.*, **1965**, 1649.

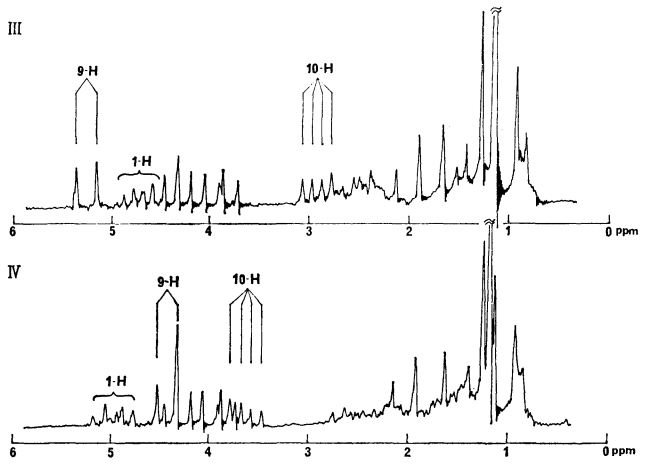

Fig. 2. NMR spectra of sulfites III and IV.

As the absolute configuration of dihydrofukinolidol had been completely established except for the 13β-methyl of the formula II,[5] the above evidence makes possible the assignment of the stereoformula A for III and that of B for IV among the possilbe configurations (A—D, Fig. 3).[6]

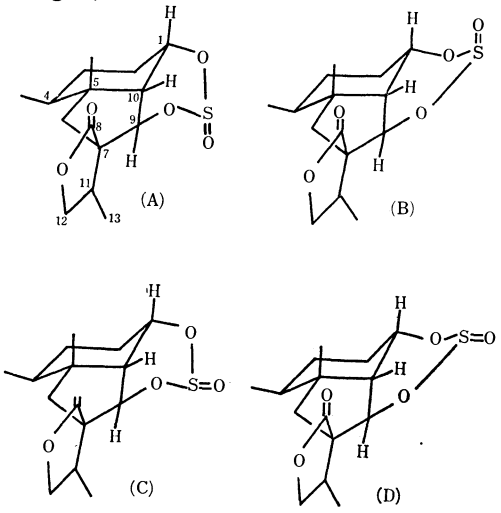

Fig. 3. Possible stereoformulas of sulfites III and IV.

Experimental

All the melting points are uncorrected. The IR spectra were recorded with a JASCO DS-402G spectrophotometer, while the UV spectra were obtained with a Cary Model 14 spectrophotometer. The optical rotations were measured with a Hitachi EPU-2A spectrophotometer. The NMR spectra were determined with a Hitachi R-20A spectrometer, using TMS as the internal standard (δ=0) and $CDCl_3$ as the solvent.

Preparation of Isomeric Sulfites of Dihydrofukinolidol (II). A solution of dihydrofukinolidol[1] (870 mg, mp 190—191°C) in dry pyridine (16 m*l*) was stirred, drop by drop, into a mixture of thionyl chloride (3.4 m*l*) and dry pyridine (16 m*l*) at −35——45°C over a 2 hr period; after the mixture had then been stirred at room temperature for additional 2 hr, the solvent was removed *in vacuo*. The residue was poured into water and extracted with ether. The extract was washed with water and dried over anhydrous sodium sulfate. After the removal of the solvent, the residual solid (1.04 g) was chromatographed over silica gel (20 g); subsequent elution with benzene afforded III (320 mg) as colorless prisms, mp 190.5—191.5°C (dec.) (from ethyl acetate-light petroleum), $[\alpha]_D^{22}$−80° (*c*, 1.0, chloroform); IR (KBr): 1764, 1190 cm^{-1}; tlc (Merck Kieselgel G): R_f, 0.67 (benzene-ethyl acetate, 5: 1).

Found: C, 57.48; H, 6.99; S, 10.41%. Calcd for $C_{15}H_{22}O_5S$: C, 57.30; H, 7.05; S, 10.20%.

Further elution with the same solvent gave IV (240 mg) as colorless needles, mp 187.5—188.5°C (dec.) (from ethyl acetate-light petroleum), $[\alpha]_D^{22}$−145° (*c*, 1.0, chloroform); IR (KBr): 1765, 1200 cm^{-1}; tlc: R_f, 0.48 (benzene-ethyl acetate, 5: 1).

Found: C, 57.57; H, 6.97; S, 10.50%. Calcd for $C_{15}H_{22}O_5S$: C, 57.30; H, 7.05; S, 10.20%. A mixed-melting-point determination with III and IV showed a slight depression (mixed mp 186.5—187.0°C dec.).

Hydrolysis of the Sulfites (III) and (IV). a) The cyclic sulfite III (28 mg) in ethanol (5 m*l*) was added to a 10% potassium hydroxide-methanol solution (3 m*l*), left at room temperature for 2 days, and then warmed at 40—50°C for 10 hr. After acidification with dilute sulfuric acid, the mixture was diluted with water and extracted with ether, washed with a saturated sodium hydrogen carbonate solution and water, and dried over anhydrous sodium sulfate. The subsequent evaporation of the solvent gave II (21 mg) as colorless needles, mp 189—191°C (from ethyl acetate-light petroleum), IR (KBr): 3550, 3460, 1760 cm^{-1}; tlc: R_f, 0.48 (benzene-ethyl acetate, 1: 1).

b) The cyclic sulfite IV (35 mg) was treated as above to give II (22 mg), mp 188—189.5°C (from ethyl acetate-light petroleum). The products from a) and b) showed no melting point depression on admixture with dihydrofukinolidol II, mp 190—191°C.

Oxidation of Cyclic Sulfites with Perbenzoic Acid. a) To a solution of III (20 mg) in chloroform (0.5 m*l*), a solution of 0.117N perbenzoic acid-chloroform (1.6 m*l*) was added; the mixture was then left at room temperature for 16 days. The mixture was extracted with ether, and the extract was washed with a saturated sodium hydrogen carbonate solution and with water. The dried extract was concentrated to afford a solid (19 mg). Chromatography over silica gel (3 g) by means of elution with benzene gave the starting material (8 mg) and an oxidation product V (5 mg); mp 135—138°C (from ethyl acetate-light pertoleum); tlc: R_f, 0.55 (benzene-ethyl acetate, 5: 1).

b) A solution of 0.117N perbenzoic acid-chloroform (3.2 m*l*) was added to a solution of IV (42 mg) in chloroform (1 m*l*), after which the mixture was left at room temperature for 6 days. Working-up as above gave a crude product (71 mg) which was chromatographed on silica gel (5 g) by elution with benzene to furnish crystalline V as colorless leaflets; mp 141.5—142°C (dec.) (from ethyl acetate-light petroleum); tlc: R_f, 0.55 (benzene-ethyl acetate, 5: 1).

Found: C, 54.67; H, 6.63; S, 9.57%. Calcd for $C_{15}H_{22}O_6S$: C, 54.53; H, 6.71; S, 9.67%. The mixed melting point of the two products from a) and b) showed no depression (mixed mp 136—138°C).

The authors wish to thank the Shionogi Research Laboratory, Shionogi & Co., Ltd., for the microanalysis, and the Institute of Food Chemistry for the measurement of the NMR spectra.

5) C. Katayama, A. Furusaki, I. Nitta, M. Hayashi, and K. Naya, This Bulletin, **43**, 1976 (1970).

6) The result of the X-ray analysis connected with this work will soon be presented in this Bulletin.

BULLETIN OF THE CHEMICAL SOCIETY OF JAPAN, VOL. 44, 3206 (1971)

1,8-Dimethylanthracene

Shuzo AKIYAMA and Masazumi NAKAGAWA

Department of Chemistry, Faculty of Science, Osaka University, Toyonaka, Osaka

(Received May 28, 1971)

It has been reported by Lavaux[1] that the Friedel-Crafts reaction of toluene with dichloromethane in the presence of aluminum chloride afforded three compounds with mp 240, 244.5, and 86°C. The last compound has been tentatively assigned to 1,8-dimethylanthracene by Clar.[2]

During the course of synthetic studies of various anthracene derivatives,[3,4] we have prepared 1,8-dimethylanthracene by the reduction of 1,8-bis(bromomethyl)anthracene[4] by means of lithium aluminum hydride in tetrahydrofuran. The resulting hydrocarbon showed mp 128—129°C, and gave satisfactory elemental analysis, infrared, ultraviolet (Fig. 1) and mass spectra. In view of the method of preparation, the hydrocarbon thus obtained should be unequivocally 1,8-dimethylanthracene. Consequently, the hydrocarbon of mp 86°C prepared by Lavaux evidently concerns another dimethylanthracene.

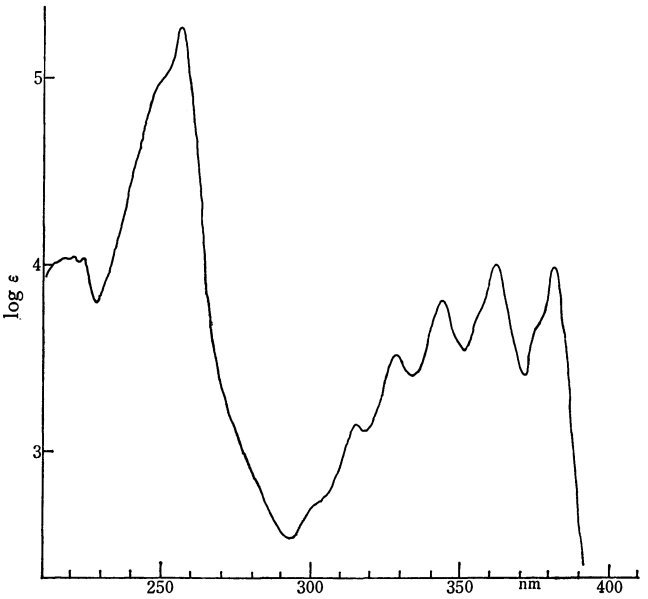

Fig. 1. The electronic spectrum of 1,8-dimethylanthracene.

Experimental

1,8-Dimethylanthracene. A mixture of 1,8-bis(bromomethyl)anthracene[4] (0.728 g, 2 mmol), an excess of lithium aluminum hydride (0.076 g) and tetrahydrofuran (40 m*l*) was stirred at room temperature for 1 hr and then refluxed for 2 hr. The reaction mixture was decomposed by addition of cracked ice and 6N hydrochloric acid (10 m*l*). The organic layer was worked up according to the usual procedure. Removal of the solvent *in vacuo* resulted in a crude material which was re-dissolved in benzene (10 m*l*). The benzene solution was passed through a thin layer of alumina (4 g). Evaporation of the solvent under reduced pressure afforded faint yellow crystals (0.321 g, 78%). Recrystallization twice from ethanol gave colorless plates with blue fluorescence, mp 128—129°C. Found: C, 93.02; H, 6.81%. Calcd for $C_{16}H_{14}$: C, 93.16; H, 6.84%. Mass: 206 (M^+), 191 (M^+-CH_3). Mol. Wt. 206. UV: $\lambda_{max}^{n\text{-hexane}}$ (ε) 220.5 (1100), 223.5 (1100), 256 (18200), 314 (1300), 328.5 (3300), 344.5 (6600), 362 (10300), and 381 nm (9800). IR: 2850—3100, 1520, 1620, 1440, 1380, 900, 876, 780, 740 cm^{-1}.

1) J. Lavaux, *Compt. Rend.*, **139**, 976 (1904).
2) E. Clar, "Aromatic Hydrocarbons," Vol. 1, Academic Press, London and New York, Springer Verlag, Berlin, Göttingen and Heidelberg (1964), p. 299.
3) S. Akiyama and M. Nakagawa, This Bulletin, **33**, 1293 (1960); **35**, 1826 (1962).
4) S. Akiyama and M. Nakagawa, *ibid.*, **44**, 3158 (1971).

BULLETIN OF THE CHEMICAL SOCIETY OF JAPAN, VOL. 44, 3207 (1971)

An Empirical Formula for the Optimum Concentration for Hydrothermal Precipitation

Tominosuke KATSURAI

Department of Electrochemistry, Tokyo Institute of Technology, Ookayama, Meguro-ku, Tokyo

(Received July 6, 1971)

By means of visual autoclaving, *viz.*, visual studies on autoclaving processes with sealed glass tubes, we can easily observe the relation between the concentration of electrolyte solution and the temperature at which onset of turbidity takes place in the solution. It was found that if we plot temperature *vs.* concentration, we obtain a curve concave upward. This means that the incipient stage of hydrothermal precipitation takes place most easily at a certain concentration,[1,2] or that there is an optimum concentration for hydrothermal precipitation.

A simple formula fitting the curve can be obtained if we utilize the distance between solute particles as a unit of concentration. For this purpose let us take the case in which 6.02×10^{23} (Avogadro's number) particles are distributed in equal distance of 12 Å in a 1 *l* volume. The distance corresponds to 1 M solution.

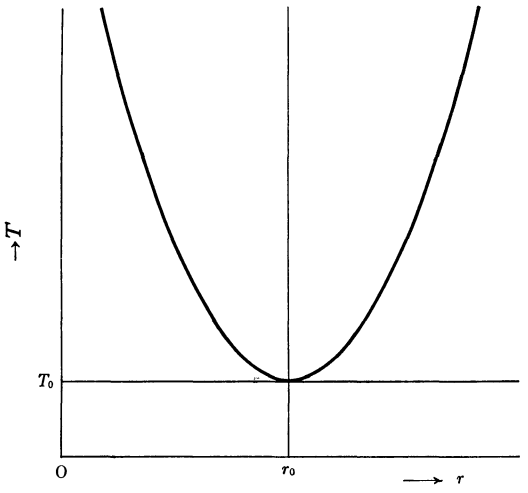

Fig. 1. Relation between inter-solute distance (concentration) and the temperature at which onset of turbidity takes place.

In the usual hydrothermal experiments, concentration is given in terms of mol per liter. The relation between the molar concentration c and the corresponding distance r is given by

$$r = \frac{12}{\sqrt[3]{c}}. \tag{1}$$

By means of this relation, we find that the data of visual autoclaving can be represented by

$$T = T_0 + \alpha(r-r_0)^2, \tag{2}$$

where T=temperature at which onset of turbidity takes place,
T_0 =the lowest temperature at which onset of turbidity takes place,
r =distance between solute particles,
r_0 =the value of r corresponding to T_0,
α =constant.

This is the equation of a parabola with its apex at (r_0, T_0) as shown in Fig. 1. For the sake of illustration, examples are given for aqueous solutions of some compounds.

Compound	T_0 in °C	r_0 in Å	α in Å^{-2}
$AlCl_3$	166	72	0.028
$Ce(NH_4)_2\cdot(NO_3)_6$	107	35	0.069
$ThCl_4$	158	48	0.028
$Th(NO_3)_4$	151	54	0.028

So far there seems to be no theory on hydrothermal precipitation to afford an explicit formula for the relation between r and T. In the meantime, Eq. (2) might be utilized for its simplicity for grasping the process of hydrothermal precipitation.

1) T. Katsurai, *Kolloid-Z.*, **170**, 57 (1960).
2) R. G. Robins, *J. Inorg. Nucl. Chem.*, **29**, 431 (1967).

BULLETIN OF THE CHEMICAL SOCIETY OF JAPAN, VOL. 44, 3208—3209 (1971)

An SCF MO Treatment of Tropone Radical Anion

N. TRINAJSTIĆ
Institute "Rudjer Bošković," Zagreb, Croatia, Yugoslavia

(Received November 18, 1970)

Ikegami and Seto[1] reported on the ESR spectrum of tropone radical anion.

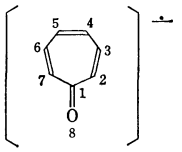

We would like to report our calculations for tropone radical anion using "half-electron" SCF MO method of Dewar *et al.*[2] We also give a comparison between tropone radical anion and the parent compound. Calculations for tropone were performed using Dewar's variant[3] of the original Pople's SCF MO method.[4] Calculated charge densities for tropone and its radical anion and calculated spin densities for tropone radical anion together with spin densities obtained from the observed hyperfine splitting constants[5] are given in Table 1. The

TABLE 1. CALCULATED CHARGE DENSITIES FOR TROPONE AND TROPONE RADICAL ANION, AND CALCULATED AND OBSERVED SPIN DENSITIES FOR TROPONE RADICAL ANION

Ring position	Charge density		Spin density of tropone radical anion	
	Tropone	Tropone radical anion	Calculated	Experimental[a]
1	0.6462	0.5879	0.00	—
2,7	1.0092	1.2585	0.35	0.36
3,6	0.9464	0.9588	0.04	0.004
4,5	0.9854	1.1695	0.21	0.21
8	1.4720	1.6383	0.00	—

a) Y. Ikegami and S. Seto, This Bulletin, **41**, 2225 (1968).

results suggest that spin densities on the stoms 1 and 8 are small or zero, since the highest occupied MO of tropone radical is an antisymmetric orbital. A similar conclusion is reached by HMO calculations[1], but McLachlan's procedure predicted[1] negative spin densities on these atoms even bigger in magnitude than the spin densities on the atoms 3 and 6. This was not tested by ESR study because neither atom 1 nor 8 carries a hydrogen atom. However, both sets of calculations (HMO and McLachlan's procedure)[1] reproduce qualitatively the experimental spin densities, but the quantitative agreement is not so good. If we compare, for example, the ratios of the spin densities on the atoms 2 or 7 and 4 or 5, we obtain the following results.

ρ 2,7/ρ 4,5	Method of calculation
1.56	HMO
2.02	McLachlan's procedure
1.67	our calculations
1.69	experimental value

We would like to add that our calculations included the bond length variations (variable β).[6] This was found[7] recently to be very important in the spin density calculations of the conjugated anion radicals.

TABLE 2. π-ELECTRON CHARGE DENSITY ON OXYGEN IN TROPONE CALCULATED BY VARIOUS AUTHORS

Author	π-Electron charge density (q_0)
Julg and Bonnet[a]	1.335
Inuzuka and Yokota[b]	1.4803
Kuroda and Kunii[c]	1.4714
Hosoya and Nagakura[d]	1.2531
Yamaguchi, Amako, and Azumi[e]	1.1431
Bertelli and Andrews, Jr.[f]	1.280
Our result	1.4720

a) A. Julg and M. Bonnet, *Tetrahedron*, **20**, 2243 (1964).
b) K. Inuzuka and T. Yokota, *J. Chem. Phys.*, **44**, 911 (1966).
c) H. Kuroda and T. Kunii, *Theoret. Chim. Acta* (Berlin), **7**, 220 (1967).
d) H. Hosoya and S. Nagakura, *ibid.*, **8**, 319 (1967).
e) H. Yamaguchi, Y. Amako, and H. Azumi, *Tetrahedron*, **24**, 267 (1968).
f) D. J. Bertelli and T. G. Andrews, Jr., *J. Amer. Chem. Soc.*, **91**, 5280 (1969).

In Table 2 is given π-electron charge distribution on the oxygen atom of tropone calculated by various authors, who all agree that a certain amount of π-electron charge is donated to the oxygen. The unpaired electron in the tropone radical ion, which occupies the π-molecular orbital contributes a certain amount of the charge to the total π-electronic charge densities of each ring carbon atom except for C_1, and to the charge density of the oxygen atoms. Such a charge density distribution may indicate that the polar character of the carbonyl group C_1–O is increased in tropone radical ion.

We have also calculated bond lengths of tropone and its radical anion. The results are given in Table 3. Our calculation of bond lengths of tropone predicts

1) Y. Ikegami and S. Seto, This Bulletin, **41**, 2225 (1968).
2) M. J. S. Dewar, J. A. Hashmall, and C. G. Venier, *J. Amer. Chem. Soc.*, **90**, 1953 (1968).
3) A. L. H. Chung and M. J. S. Dewar, *J. Chem. Phys.*, **42**, 756 (1965); M. J. S. Dewar and G. J. Gleicher, *J. Amer. Chem. Soc.*, **87**, 692 (1965); M. J. S. Dewar and C. de Llano, *ibid.*, **91**, 789 (1969); M. J. S. Dewar and T. Morita, *ibid.*, **91**, 796 (1969).
4) J. A. Pople, *Trans. Faraday Soc.*, **49**, 1375 (1953).
5) Observed hyperfine splitting constants (a_i^H) were converted into spin densities (ρ_i^π) using the relation $\rho_i^\pi = a_i^H / Q_{CH}^H$, where $Q_{CH}^H = 23.7$ Gauss.
6) M. J. S. Dewar and G. J. Gleicher, *J. Amer. Chem. Soc.*, **87**, 685 (1965).
7) H. G. Benson and A. Hudson, *Mol. Phys.*, **20**, 185 (1971).

TABLE 3. CALCULATED AND OBSERVED BOND LENGTHS (in Å)

Bond	Tropone			Tropone radical anion
	Our result	Experiment[a]		
		Kuroda and Kunii	Ogasawara and Kimura	
1,8	1.259	1.270	1.23	1.279
1,2 (1,7)	1.463	1.449	1.45	1.448
2,3 (6,7)	1.355	1.369	1.36	1.392
3,4 (5,6)	1.452	1.431	1.46	1.401
4,5	1.357	1.373	1.34	1.420

a) We wish to thank the referee for information on the important work on the structure of tropone reported at the International Symposium on Non-benzenoid Aromatic Compounds held at Sendai, Japan, in August 1970.

the bond alternation within the seven-membered ring. The results of earlier structural studies on tropone agree with the value of 1.26 ± 0.02 Å for the length of C=O bond, but CC bonds were predicted to be of an equal length (average value being 1.405 ± 0.02 Å).[8] On the other hand, a recent structure determination of 4,5-benzotropone[9] indicated that polyenoid-type bond alternation is present in the tropone moiety. An alternation was found in the tropone ring and experimental bond lengths agree fairly well with our calculated values (Table 3).[10] Apparently tropone is a cyclic polyenoid molecule and it can be regarded as a non-aromatic compound. This was confirmed experimentally[11] and theoretically.[12] Calculated bond lengths (as well as calculated charge densities) of tropone radical anion support representation of its structure as shown below.

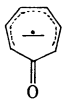

The C=O bond and CC bonds 1,2 and 1,7 are fixed as double and single bonds, respectively, while the remaining CC bonds are aromatic with an average bond length 1.4 Å. This is quite a different structure from that of tropone.

8) See for example: K. Kimura, S. Suzuki, M. Kimura, and M. Kubo, *J. Chem. Phys.*, **27**, 320 (1957).

9) T. Hata, H. Shimanouchi, and Y. Sasada, *Tetrahedron Lett.*, **1969**, 753.

10) M. Ogasawara and M. Kimura reported at the International Symposium on Non-benzenoid Aromatic Compounds held at Sendai, Japan, August 1970 on "The structure of tropone determined by electron diffraction".

11) D. J. Bertelli and T. G. Andrews, Jr., *J. Amer. Chem. Soc.*, **91**, 5280 (1969); D. J. Bertelli, T. G. Andrews, Jr., and P. O. Crews, *ibid.*, **91**, 5286 (1969).

12) Aromatic stabilization (A_s) of tropone is calculated to be only 0.8 kcal/mol. Benzene, for example, has $A_s=20.0$ kcal/mol. Aromatic stabilization was calculated in the manner described by M. J. S. Dewar, A. J. Harget, and N. Trinajstić, *J. Amer. Chem. Soc.*, **91**, 6321 (1969).

SHORT COMMUNICATIONS

The Oxyphenylation of Olefins

Hiroshi Horino and Naoto Inoue
College of General Education, Tohoku University, Kawauchi, Sendai
(Received May 21, 1971)

A number of papers on the aromatic substitution of olefins by the reaction of palladium compounds have been published in recent years.[1-3] In the course of our studies of the aromatic substitution of olefins according to Heck's arylation, a new addition reaction was found in which a phenyl group and an anion part of the protic solvents were added simultaneously to reactant olefins.

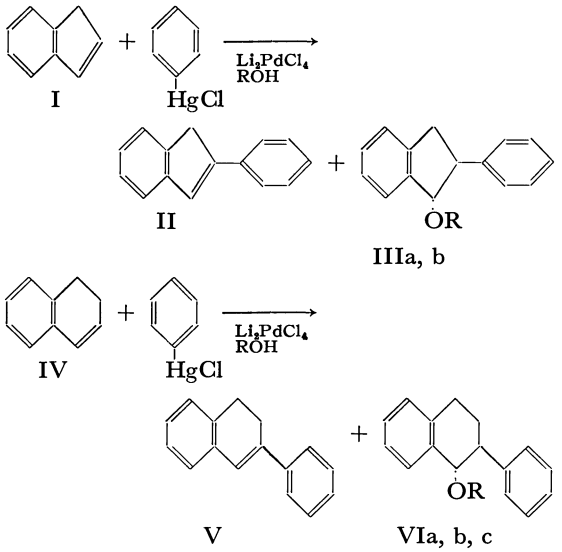

I II IIIa, b IV V VIa, b, c

a: R=H, b: R=$COCH_3$, c: R=CH_3

Table 1. Results of oxyphenylation of olefins in various solvents

Olefin	Solvent	Product	(yield, %)
I	Dioxane–H_2O(1:1)	II(35)[4]	IIIa(50)[a]
I	CH_3COCH_3–H_2O(1:1)	II(28)	IIIa(51)
I	CH_3CO_2H–H_2O(1:1)	II(18)	IIIa(48) IIIb(17)[b]
I	CH_3CO_2H	II(72)	IIIb(7)
I	CH_3COCH_3–H_2O(1:1) CH_3CO_2Na(2 mmol)	II(17)	IIIa(61)
IV	Dioxane–H_2O(1:1)	V(16)[5]	VIa(72)[6]
IV	CH_3CO_2H	V(40)	VIb(14)[6]
IV	CH_3OH	V(16)	VIc(47)[c]

a) Mp 81—82°C, IR(KBr); ν_{OH}=3300—3150 cm^{-1}, NMR(CCl_4); τ 4.95(1H, d, J=6 Hz)
b) Bp 162—165°C/1 mmHg, IR(Neat); $\nu_{C=O}$=1740 cm^{-1}, NMR(CCl_4); τ 8.0(3H), 3.75(1H, d, J=5 Hz).
c) Bp 133—136°C/1 mmHg, IR(Neat); ν_{C-O}=1080 cm^{-1}, NMR(CCl_4); τ 6.88(3H), 5.6(2H, d, J=8 Hz).

The general procedure of the reaction is as follows. A solution of indene (I) (1.2 mmol) or 1,2-dihydronaphthalene (IV) (1.2 mmol), lithium palladium chloride (1 mmol),[2] and phenylmercuric chloride (1 mmol) in the solvents listed in Table 1 was stirred for more than five hours at room temperature.

The reaction products were then separated by chromatography on a silica-gel column. Compound II (or V) was eluted with *n*-hexane, and III (or VI) was eluted with benzene or a mixture of *n*-hexane and benzene (1:1). The isolated products were identified by elementary analysis and by mixed-melting-point tests with authentic samples.[4-7] The addition of sodium acetate (1 or 2 mmol) to a solution of I (1.2 mmol), lithium palladium chloride (1 mmol), and phenylmercuric chloride (1 mmol) in a mixture of acetone and water gave IIIa in a 50 to 60% yield, as is shown in Table 1. The treatment of II or V with a solution of lithium palladium chloride and mercuric chloride in methanol, or with a solution of hydrochloric acid in a mixture of acetone and water, gave only the starting material. The reaction of IIIa or VIa with lithium palladium chloride and mercuric chloride afforded the starting substance. Therefore, it is clear that the oxy compound (III or VI) was not derived from the arylated olefin (II or V), and that II or V was not formed from III or VI.

According to Heck's mechanism,[2] we suggest the following scheme to illustrate the formation of the oxy compounds as well as the arylated olefins.

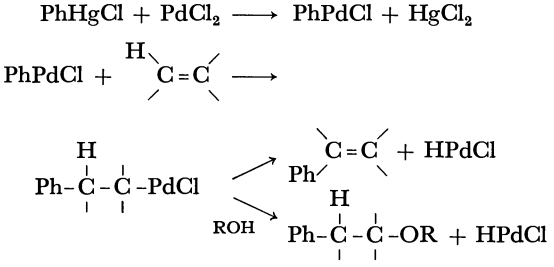

The configurations of the isolated oxy compounds, IIIa, b, and VIa, b, c, were determined to be *trans*.[7]

The extension of this reaction to other simple olefins is now under investigation.

1) Y. Fujiwara, I. Moritani, S. Danno, R. Asano, and S. Teranishi, *J. Amer. Chem. Soc.*, **91**, 1766 (1969); S. Danno, I. Moritani, and Y. Fujiwara, *Tetrahedron*, **25**, 4809 (1969).
2) R. F. Heck, *J. Amer. Chem. Soc.*, **90**, 5518 (1968); R. F. Heck, *ibid.*, **91**, 6707 (1969).
3) K. Garves, *J. Org. Chem.*, **35**, 3273 (1970).
4) J. von Braun and G. Manz, *Ber.*, **62**, 1062 (1929).
5) N. Campbell and D. Kidd, *J. Chem. Soc.*, **1954**, 2154.
6) K. Hanaya, *Nippon Kagaku Zasshi*, **87**, 745 (1966).
7) The hydroboration and oxidation of 2-phenylindene (II)[4] and 2-phenyl-3,4-dihydronaphthalene (V)[5] gave IIIa and VIa[6] respectively, those substances were then acetylated to IIIb and VIb[6] with acetic anhydride and pyridine. The treatment of VIa with sodium hydride and subsequently with methyl iodide afforded VIc.

The Light Resistance of the Flavones and the Flavonols

Makoto KANETA and Noboru SUGIYAMA*
Fukushima Technical College, Fukushima
**Department of Chemistry, Tokyo Kyoiku University, Otsuka, Tokyo*
(Received May 21, 1971)

The plants of *Reseda luteola* (luteolin), *Arthraxon hispidus* (luteolin, arthraxin),[1-3] *Miscanthus tinctorius* (luteolin, arthraxin),[3] *Miscanthus sinensis* (tricin),[3] *Phragmites communis* (tricin),[3] *Allium Cepa* (quercetin), *Myrica rubra* (myricetin), *Sophora japonica* (quercetin), and *Morus bombycis* (morin) have traditionally been used as sources of a natural flavonoid dyestuff, the constituents of which are shown in the respective parentheses above.

Cloth dyed with *Reseda luteola*, *Arthraxon hispidus*, and *Miscanthus tinctorius* has been said to show a high resistance to the light. However, the causes of this have been unknown. The photooxygenation of 3-hydroxyflavones[4] and the photooxidative cyclization of the quercetin derivatives[5] have recently been reported. Since these results seem to suggest that the molecular structure of flavones influences the resistance to the light, the light resistances have been examined by mean of the UV spectra on the following flavones: quercetin (**1**), morin (**2**), arthraxin (**3**), luteolin (**4**), 8-acetyl-5,7-dihydroxy-3′,4′-dimethoxyflavone (**5**),[1] and tricin (**6**). Because of the similarity in the molecular structures of these substances, their molecular extinction coefficients will be considered to be approximately equal.

The ethanol solution of the sample was irradiated with a 200-W high pressure mercury lamp through a Pyrex, water-cooled jacket under bubbling air. The UV spectrum of an aliquot's portion was then recorded at intervals of 3, 5, 8, 18, 37, 49, and 67 hr. The

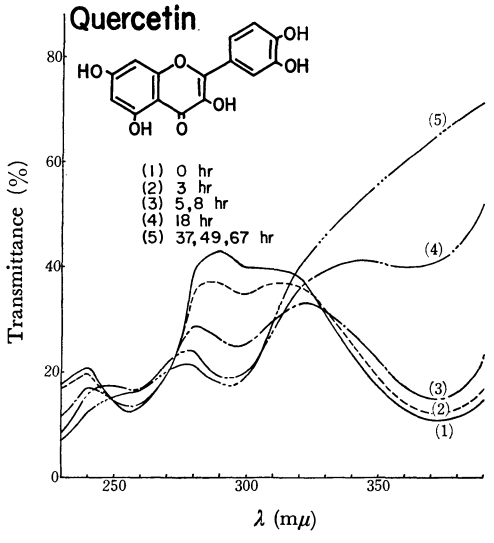

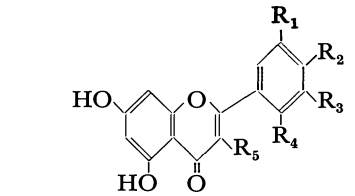

1 R_1,R_2,R_5=OH R_3,R_4=H
2 R_2,R_4,R_5=OH R_1,R_3=H
4 R_1,R_2=OH R_3,R_4,R_5=H
6 R_2=OH R_1,R_3=OMe R_4,R_5=H

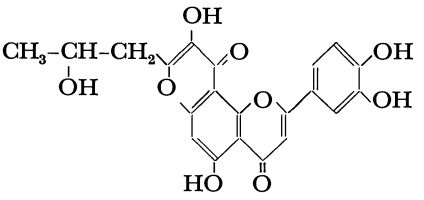

3

resistance to the light was measured in terms of the time required for the disappearance of Band I with the high absorption intensity in the 320—380 nm-region.

As a result, Band I of the UV spectra of **1** and **2** disappeared within 18 to 37 hr, whereas the bands of **4**, **5**, and **6** did so only after 67 hr. Among the bands of **3**, **4**, **5**, and **6**, the band of **3** disappeared in the shortest time. This result seems to indicate that the hydroxyheterocyclic ring attached to the flavone nucleus of **3** is easily decomposed by irradiation, like the pyrone ring of flavonols.

It is thus clear that flavones, in contrast with 3-hydroxyflavones, show a high power of resistance to the light when air is bubbled into its ethanol solution. This agrees with the fact that the dyestuff materials in *Reseda luteola*, *Arthraxon hispidus*, and *Miscanthus tinctorius* are superior to those in the other grasses in point of the resistance to the light.

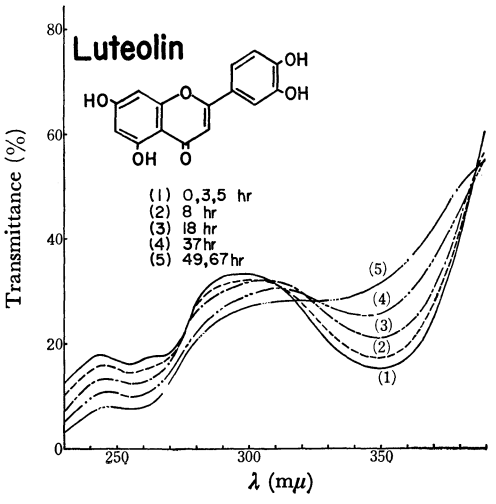

1) M. Kaneta and N. Sugiyama, This Bulletin, **42**, 2084 (1969).
2) M. Kaneta and N. Sugiyama *J. Chem. Soc., C*, **1971**,1982.
3) M. Kaneta and N. Sugiyama, This Bulletin, submitted for publication.
4) T. Matsuura, H. Matsushima, and R. Nakashima, *Tetrahedron*, **26**, 435 (1970).
5) A. C. Waiss, Jr., and J. Corse, *J. Amer. Chem. Soc.*, **87**, 2068 (1965).

Proton Knight Shift in Lithium-Methylamine Solutions

Yoshio NAKAMURA, Mikio YAMAMOTO, Shigezō SHIMOKAWA,* and Mitsuo SHIMOJI

Department of Chemistry, Faculty of Science, Hokkaido University, Sapporo

**Department of Chemistry, Faculty of Engineering, Hokkaido University, Sapporo*

(Received June 28, 1971)

Alkali-metals can be dissolved in liquid methylamine (CH_3NH_2) as in liquid ammonia. We have reported[1,2] that the volume expansion and viscosity of the Li–CH_3NH_2 system can be interpreted by the presence of anion-like solvated electrons trapped by 'cavities', as in alkali metal-ammonia solutions.[3] In this communication we describe the experimental results on the proton Knight shift in the Li–CH_3NH_2 system over a wide range of Li concentration.

The method of preparation of Li–CH_3NH_2 solutions has been described.[1] Solutions were sealed in measuring cells in a vacuum. Nuclear resonance was observed with a JEOL-3H-60 external lock NMR spectrometer in a magnetic field in the vicinity of 14,092G. The Knight shift k is defined[4] as $k=(H_r-H_s)/H_r$, where H_r is the magnetic field for which resonance occurs in the reference solution, and H_s is the magnetic field in sample solution at a fixed frequency. The Knight shift of protons in CH_3- and NH_2-group in CH_3NH_2 was measured as a function of Li concentration. The pure solvent was taken as a reference. Measurements were carried out at 21°C.

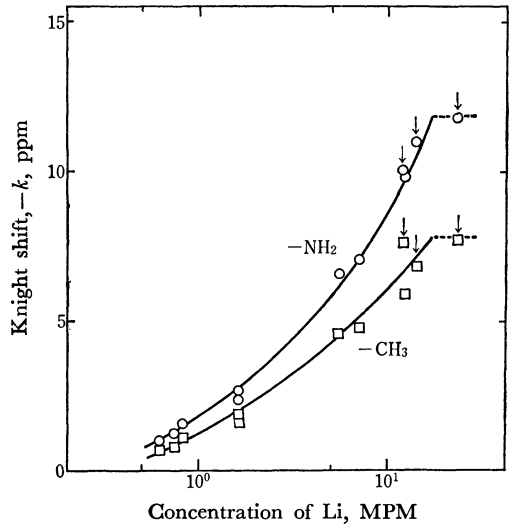

Fig. 1. Proton Knight shift for Li solutions in CH_3NH_2 at 21°C.

The results are shown in Fig. 1. The concentration of the metal is expressed by MPM or mol percentage of metal. The observed Knight shift increases with increasing metal concentration, as for proton and nitrogen in alkali metal-ammonia solutions.[4-6] The shifts are larger for the NH_2-group than for the CH_3-group, which may indicate that the CH_3NH_2 molecules are oriented at the edge of a cavity so that an ammonia-like trap is produced.[7] The values of k for the NH_2-group are of the same order of magnitude as those found in liquid ammonia.[5] It is interesting to see that the observed curve is continuous from low concentration (electrolytic region) to high concentration (metallic region) exhibiting no anomalies at the transition region, which is also in accordance with the observations in ammonia solutions.[5] The broken lines in the figure indicate the saturated solution range determined previously by electrical conductivity measurements.[2] Linewidths were generally around 15 Hz.

It should be noted that the resonance peaks both for CH_3- and NH_2-groups split into unsymmetrical doublets for three samples with high Li concentration, as indicated by arrows in Fig. 1. The width of the split was 8 Hz for the 12.0 MPM solution and almost independent of the metal concentration. Whether this corresponds to two different states of the solvated electrons[3] will be the subject of further investigation. It is also noted that at lower concentrations the sign of k seems to be inverted, though it is negative for the concentration range studied. A supplementary measurement with a saturated solution of the K metal ($\sim 4.7\times10^{-2}$ MPM) shows a positive value of k, +0.07 ppm, for protons in NH_2. A similar result has been observed for the Na-saturated solution, the concentration being about 2×10^{-2} MPM.

1) M. Yamamoto, Y. Nakamura, and M. Shimoji, *Trans. Faraday Soc.*, **67**, 2292 (1971).

2) M. Yamamoto, Y. Nakamura, and M. Shimoji, *ibid.*, in press

3) M. H. Cohen and J. C. Thompson, *Adv. Phys.*, **17**, 875 (1968).

4) D. E. O'Reilly, *J. Chem. Phys.*, **41**, 3729 (1964).

5) T. R. Hughes, *ibid.*, **38**, 202 (1963).

6) J. V. Acrivos and K. S. Pitzer, *J. Phys. Chem.*, **66**, 1693 (1962).

7) H. Blades and J. W. Hodgins, *Can. J. Chem.*, **33**, 411 (1955).

The Reactions of Hot Deuterium Atoms with Ethylene

Yasuhisa SANO and Shin SATO

Department of Applied Physics, Tokyo Institute of Technology, Ookayama, Meguro-ku, Tokyo

(Received June 30, 1971)

The reactions of hot hydrogen atoms with hydrocarbons have been extensively investigated, using recoil tritium from the nuclear reaction.[1,2] The energy with which hydrogen atoms efficiently react with the substrate is not certain, however. Consequently, the photolysis of hydrogen halides and hydrogen sulfide has received renewed attention as the source of hot hydrogen atoms.[3-5]

We have recently studied the 2288 Å photolysis of DI–C_2H_4 mixtures. The excess energy of the D atoms produced ranges from 1.4 to 2.3 eV.[6,7] Since ethylene is a well-known scavenger for thermal hydrogen atoms, it may be one of the most suitable substrates for investigating the hot hydrogen atom-reactions. Nevertheless, very few measurements with this compound have been reported.

The deuterium iodide used was synthesized by heating a mixture of deuterium and iodine on platinized asbestos in a Pyrex tube at 400°C for two days. During the storage of DI gas in the bulb covered with Al-foil, the HI content gradually increased, probably because of the proton-exchange reaction between DI and water in glass or in grease. The initial content of HI was less than 5%; when the content reached over 15%, the DI gas was renewed. The amounts of the products were measured volumetrically with a Toepler pump, and their analyses were made by mass spectrometry.

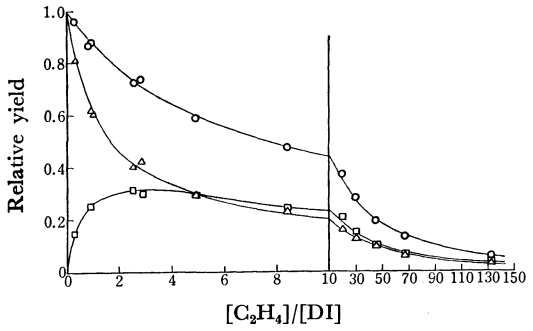

Fig. 1. The relative yields of total hydrogen (○), D_2 (△), and HD (□) as a function of the $[C_2H_4]/[DI]$ ratio. The yield of D_2 in the photolysis of pure DI was taken as unity. Initial DI pressure is 5 Torr and the irradiation time 6 min.

Figure 1 shows the relative yields of total hydrogen, D_2, and HD as a function of the $[C_2H_4]/[DI]$ ratio. The values are corrected for the HI contamination, the isotope effect being disregarded. Every run was sandwiched by the photolysis of pure DI so that the relative yield could be calculated accurately.

The HD formation may be explained in terms of such reactions of hot D atoms with ethylene as:

$$D^* + C_2H_4 \longrightarrow C_2H_3 + HD \quad (1)$$

and/or:

$$D^* + C_2H_4 \longrightarrow C_2H_3D + H \quad (2)$$

followed respectively by:

$$C_2H_3 + DI \longrightarrow C_2H_3D + I \quad (3)$$

and/or:

$$H + DI \longrightarrow HD + I \quad (4)$$

Mass-spectrometric analysis showed that the C_2 fraction in the product contained neither ethane nor acetylene, but C_2H_3D. Table 1 shows the $[C_2H_3D]/[HD]$ ratio as a function of the initial $[C_2H_4]/[DI]$ ratio, the values of which have already been corrected both for the HI contamination and for the C-13 natural abundance.

TABLE 1. THE $[C_2H_3D]/[HD]$ RATIO AS A FUNCTION OF THE INITIAL $[C_2H_4]/[DI]$ RATIO

The irradiation time is 6 min, the estimated conversion of DI being 25%.

$[C_2H_4]/[DI]$	0.27	0.83	2.51	8.35
$[C_2H_3D]/[HD]$	1.5	2.0	1.8	2.0

These results seem to substantiate the occurrence of the hot atom reactions described above. Moreover, the fact that the $[C_2H_3D]/[HD]$ ratio is more than unity suggests that Reaction (2) cannot be ignored in this system. If only Reaction (1) is responsible for the formation of HD, the $[C_2H_3D]/[HD]$ ratio should be less than unity, because a part of the C_2H_3 radicals formed react with the I_2 which is eventually formed in this system and produce no C_2H_3D. On the other hand, if Reaction (2) is more predominant than Reaction (1), the ratio should be more than unity, because a part of the H atoms produced in Reaction (2) react with I_2 and do not contribute to the formation of HD. I_2 molecules are an inevitable product in this system, and the rate constant of the $H+I_2 \rightarrow HI+I$ reaction is known to be more than ten times that of the $H+HI \rightarrow H_2+I$ reaction for the thermalized H atoms.[8]

1) R. Wolfgang, "Progress in Reaction Kinetics," Vol. 3 ed. by G. Porter, Pergamon Press Ltd., Oxford (1965), p. 97.

2) E. K. C. Lee and F. S. Rowland, *J. Phys. Chem.*, **74**, 439 (1970).

3) R. J. Carter, W. H. Hamill, and R. R. Williams, Jr., *J. Amer. Chem. Soc.*, **77**, 6457 (1955).

4) C. C. Chou and F. S. Rowland, *J. Chem. Phys.*, **50**, 5133 (1969).

5) R. G. Gann, W. M. Ollison, and J. Dubrin, *J. Chem. Phys.*, **54**, 2304 (1971).

6) L. E. Compton and R. M. Martin, *J. Phys. Chem.*, **73**, 3474 (1969).

7) A. Kupperman and J. M. White, *J. Chem. Phys.*, **44**, 4352 (1966).

8) J. L. Holmes and P. Rodgers, *Trans. Faraday Soc.*, **64**, 2348 (1968).

A Ternary Rare Earth Boride with a $ThCr_2Si_2$-type Structure

Koichi NIIHARA, Toetu SHISHIDO, and Seishi YAJIMA
The Research Institute for Iron, Steel and Other Metals, Tohoku University, Sendai
(Received July 3, 1971)

In the study of the phase diagram in the yttrium-cobalt-boron system, a ternary compound with a tetragonal unit cell was found to have a composition of 19.8%Y, 40.5%Co, and 39.7%B (by atomic). The stoichiometric composition of YCo_2B_2 is proposed. This is the first compound found in the Y–Co–B system.

The samples were prepared by arc-melting from stoichiometric amounts of Y, Co, and B under purified argon. The purities of the Y, Co, and B used were 99.9%, 99.99%, and 99.9% (by weight) respectively. For homogenizing, the samples were wrapped with tantalum foil, sealed in quartz capsules under a vacuum, and annealed for 150 hr at 800°C. After these heat treatments, the samples were ground in an agate mortar under an inert atmosphere to prevent oxidation and then examined by chemical and X-ray analyses.

TABLE 1. X-RAY POWDER DATA FOR YCo_2B_2
($a=3.561\pm0.003$Å, $c=9.358\pm0.005$Å)

hkl	$d_{obs.}$(Å)	$d_{calc.}$(Å)	$I_{obs.}$	$I_{calc.}$
002	4.678	4.679	5.9	5.4
101	3.319	3.328	48.5	49.2
110	n.obs.	2.518	n.obs.	0.4
103	2.344	2.346	67.6	27.9
004		2.340		30.4
112	2.215	2.217	100.0	110.0
200	1.781	1.781	25.1	30.5
202	n.obs.	1.664	n.obs.	0.1
105	1.656	1.657	10.0	9.7
211	1.570	1.570	10.3	10.7
006	n.obs.	1.560	n.obs.	0.1
213	1.418	1.418	31.1	12.2
204		1.417		23.3
116	1.326	1.326	26.4	23.2
220	1.258	1.259	9.0	12.2
107	1.251	1.252	3.7	3.3
222	n.obs.	1.216	n.obs.	0.3
215	1.213	1.213	7.9	9.9
301	1.177	1.178	4.5	3.2
206	n.obs.	1.173	n.obs.	0.3
008	1.169	1.170	6.0	6.1
310	n.obs.	1.126	n.obs.	0.1
303	1.109	1.109	21.3	5.5
224		1.109		20.4
312	1.094	1.095	16.6	24.1
118	n.obs.	1.061	n.obs.	0.2
217	1.025	1.024	10.0	10.3
305	1.002	1.002	11.3	10.1
321	0.982	0.982	18.5	20.6
226	n.obs.	0.980	n.obs.	1.9
208	0.978	0.978	71.4	94.4

n. obs.=not observed.

The X-ray patterns were taken using Fe radiation with a Debye-Scherrer camera and a diffractometer equipped with an X-ray monochromator. The observed intensities were measured with a Geiger-Müller counter.

The YCo_2B_2 pattern was indexed as tetragonal. As is shown in Table 1, there is a good agreement between the observed and calculated interplanar spacings. The tetragonal unit cell of the YCo_2B_2 structure has the dimensions of $a=3.561\pm0.003$ Å, $c=9.358\pm0.005$ Å, and $c/a=2.628$, and it contains two YCo_2B_2 formula units. Pycnometric-density measurements were also carried out. The experimental and theoretical densities are 6.30 g/cm³ and 6.39 g/cm³ respectively.

The relative intensities were computed assuming that YCo_2B_2 crystallizes isostructurally to the $ThCr_2Si_2$ type,[1-4] which is an ordered ternary version of the $BaAl_4$ type, the two nonequivalent sites of the Al atoms being occupied by different kinds of atoms. The reliability factor, $R=\sum|I_{ob}-I_{cal}|/\sum I_{ob}$, is 0.16. This good agreement between the observed and calculated intensities (Table 1) shows that this is the most probable structure. The space group is number 139, $I4/mmm(D_{4h}^{17})$. The atom locations and the projection of the YCo_2B_2 structure on (010) are shown in Table 2 and in Fig. 1 respectively.

TABLE 2. THE PARAMETER OF ATOM POSITION FOR YCo_2B_2

Tetragonal, $Z=2$, $I4/mmm$ (D_{4h}^{17})			
Equivalent positions $(0,0,0;\ ^1/_2,\ ^1/_2,\ ^1/_2)+$			
2Y	2(a)	(0,0,0)	
4Co	4(d)	$(0,^1/_2,2z;^1/_2,0,2z)$	$z=0.125$
4B	4(e)	$(0,0,z;\ 0,0,\bar{z})$	$z=0.378$

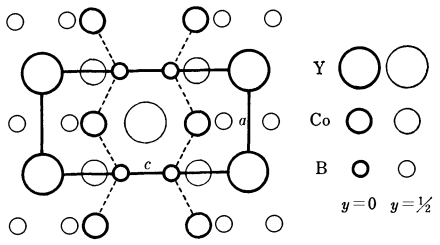

Fig. 1. The projection of YCo_2B_2 structure on (010).

1) Z. Ban and M. Sikirica, *Acta. Crystallogr.*, **18**, 594 (1965).
2) Z. Ban and M. Sikirica, *Z. Anorg. Allg. Chem.*, **356**, 96 (1967).
3) O. I. Bodak, E. I. Gladysheuskii, and P. I. Kripyakeuich, *Izv. Akad. Nauk SSSR, Neorg. Mat.*, **2**, 2151 (1966).
4) O. S. Zarechnyuk, P. I. Kripyakeuich, and E. I. Gladysheuskii, *Sov. Phys. Chem.*, **9**, 706 (1965).

Reaction of Thioboronite. A Convenient Method for the Preparation of β-Hydroxyalkanethioates

Teruaki MUKAIYAMA and Katsuhiko INOMATA

Laboratory of Organic Chemistry, Tokyo Institute of Technology, Ookayama, Meguro-ku, Tokyo

(Received July 17, 1971)

As a part of our study on the reactions of thioboronites, a new and convenient method for the preparation of β-hydroxyalkanethioates by the reaction of carbonyl compounds with ketene was established.

It was reported that nitriles react with thioboronites to form co-ordination complexes, which react with isocyanates or diphenyl ketene to give the corresponding acetamidine or acetaldimine derivatives in fairly good yields.[1,2]

Based on these facts, the analogous reaction of thioboronite with carbonyl compounds and ketene were examined. As an example, equimolar amounts of *n*-butyl di-*n*-butyl thioboronite (1.09 g, 5.1 mmol) and benzaldehyde (0.54 g, 5.1 mmol) in 15 m*l* dry ether were treated with ketene[3] at 0°C for 2 hr. After removal of ether, the oily substance was treated with H_2O–MeOH–H_2O_2 at room temperature. The solution was allowed to stand overnight and MeOH was removed *in vacuo*. The resulting mixture was extracted with ether and the ether layer was washed with 5% solution of sodium bicarbonate and dried over anhydrous sodium sulfate. Ether was evaporated to afford 1.09 g (90%) of *S*-*n*-butyl β-hydroxyhydrocinnamethioate (VIb).

A possible reaction path is outlined in Scheme 1. Initially, an intermediate (III), co-ordination complex,

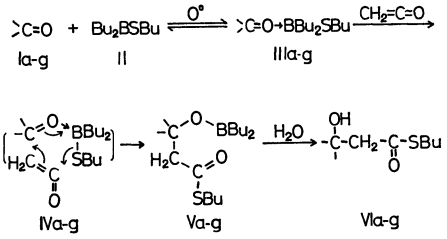

Scheme 1

might be formed from carbonyl compound (I) and thioboronite (II). Ketene will react with the complex to form V through the cyclic transition state (IV). Formation of V was confirmed by the infrared spectrum and hydrolysis to β-hydroxyalkanethioate (VI).

Paetzold and Kosma reported that α,β-unsaturated carboxylic acid chlorides are obtained by a similar reaction of boron chloride with ketene and carbonyl compounds except in the case of benzophenone.[4]

TABLE 1. YIELDS AND PROPERTIES OF β-HYDROXYALKANETHIOATES[a]

	Ia—g	Product	Bp °C (mmHg)	Isolated Yield, %
Ia	$CH_3(CH_2)_2CHO$	VIa	97—98 (4.5)	84
Ib	C_6H_5CHO	VIb	145—146 (4.5)	90
Ic	$C_6H_5CH{=}CHCHO$	VIc	163 (0.18)	90
Id	$(CH_3)_2CO$	VId	82—84 (3.0)	98
Ie		VIe	112—113 (1.5)	91
If	$C_6H_5(C_2H_5)CO$	VIf	139 (3.0)	91
Ig	$(C_6H_5)_2CO$	VIg	b)	94

a) In ether at 0°C for 2 hr.
b) Mp 75.5—76.5°C

The present β-hydroxyalkanethioate synthesis using thioboronite affords the corresponding β-hydroxyalkanethioates in excellent yields from aliphatic, aromatic, and α,β-unsaturated aldehydes and aliphatic, cyclic, and aromatic ketones (including benzophenone, see Table 1). In addition, this reaction has another synthetic utility, since β-hydroxyalkanethioate can be used as an active synthetic intermediate. As an example, the thiol ester can be reduced to aldehyde by unactivated Raney nickel, which indicates the different characteristics of the compound from β-hydroxyalkanoate obtained by Reformatsky reaction.[5]

1) T. Mukaiyama, K. Inomata, and S. Yamamoto, *Tetrahedron Lett.*, **1971**, 1097.
2) T. Mukaiyama, S. Yamamoto, and K. Inomata, This Bulletin, **44**, in press (1971).
3) Prepared by thermal cracking of acetone.
4) P. I. Paetzold and S. Kosma, *Chem. Ber.*, **103**, 2003 (1970).
5) R. L. Shriner, "Organic Reactions," Vol. 1, Wiley, New York, N. Y., (1942), p. 1.

A New Catalyst System for Ammonia Synthesis

Atsumu Ozaki, Ken-ichi Aika, and Humio Hori

Tokyo Institute of Technology, Research Laboratory of Resources Utilization, Ookayama, Meguro-ku, Tokyo

(Received July 20, 1971)

The well-known doubly-promoted iron catalyst (Fe–Al_2O_3–K_2O) has been industrially adopted for ammonia synthesis since the discovery by Mittasch *et al.* in 1910.[1,2] We have studied the role of potash promoter in this catalyst.[3-6] The reaction has been elucidated in terms of adsorbed species as estimated by kinetics and isotope effect and isotopic exchange in nitrogen. The results led to the conclusion that the potash promoter gives rise to a drastic change in the main adsorbed species over iron during the course of ammonia synthesis, from nitrogen atom over pure iron or alumina promoted iron to imino group over the doubly promoted iron, thus enhancing the rate of ammonia synthesis.[3,4] Another effect of the potash promoter is enhancement of the rate of isotopic mixing in nitrogen over iron in the presence of hydrogen.[5,6] These effects of the potash promoter have been interpreted on the basis of its electron-donating nature. If the observed effects by potash are produced by an electron donation to iron, metallic potassium would be more effective owing to its much lower ionization potential. This prediction has been tested and extended to other transition metals.

Catalysts were prepared by impregnating coconut carbon with transition metal chlorides from aqueous solutions, followed by reduction in hydrogen stream at 400°C and by adsorption of potassium vapor at about 400°C. The content of transition metal was 2.5 or 5% wt. of the carbon support. The rate of ammonia synthesis was determined in a closed circulating system equipped with a liquid nitrogen trap using a stoichiometric mixture of hydrogen and nitrogen under 600 mmHg. The reaction temperature ranged from 100 to 400°C.

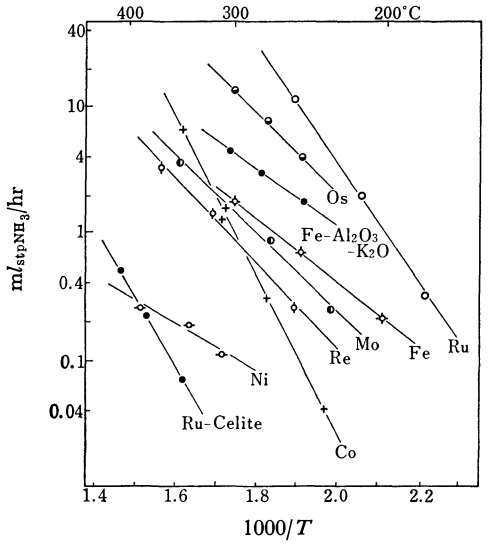

Fig. 1. Arrhenius plots of synthesis rates at a flow rate of 4.5 *l*/hr under 600 mmHg over catalysts of 2.5 g each except Fe–Al_2O_3–K_2O (0.77 g) and Ru-Celite (1.5 g). Os catalyst was prepared from OsO_4.

The results are summarized in Fig. 1 where Arrhenius plots of the rate of ammonia synthesis are shown for several transiton metals, together with previous data on ruthenium celite[7] and the doubly promoted iron.[8] None of these metals, when supported on the coconut carbon without potassium added, showed any activity even at 400°C for the ammonia synthesis, whereas pure iron or ruthenium on Celite can produce ammonia at a measurable rate.[3,7] On the other hand, potassium metal adsorbed on the coconut carbon not impregnated with a transition metal also showed no activity at 400°C, while potassium metal adsorbed on reduced iron remarkably enhanced the rate of ammonia formation. It is thus concluded that potassium metal added enhances the rate of ammonia synthesis on the transition metal.

Figure 1 shows that Ru and Os rank high among the transition metals tested. Fe, Co, Re, and Mo are moderately active, and Ni is much less active. Very little or no activity was detected on Ti, Mn, Rh, and Pd even with adsorbed potassium. The results show that the active catalysts are formed by the metals known to catalyze ammonia synthesis without a promoter such as potassium.[2] In this respect, the effect of potassium is not so specific for the kind of transition metal. But Ru–C–K catalyst has outstanding activity and is able to form ammonia with a rate of 0.037 *ml*·STP NH_3/hr 2.5 g at 146°C and 600 mmHg. This catalyst seems promising for low temperature synthesis of ammonia.

In view of rather low specificity in the effect of potassium, the basic pathway of ammonia formation would be unchanged by the addition of potassium, although the rate determining step might change. The remarkable effect of potassium can be understood if a nitrogen molecule is activated to an anionic intermediate by incorporation of a free electron in a transition metal, simply because an electron transfer from alkali to the transition metal takes place on addition of alkali metal. In agreement with this, sodium, which has a higher ionization potential than potassium, gives a much lower activity than potassium.

1) A. Mittasch, "Advances in Catalysis," Vol. II, Academic Press, Inc., New York (1949), p. 81.
2) W. G. Frankenburg, "Catalysis," Vol. III ed. by P. H. Emmett, Reinhold Pub. Corporation, New York (1955), p. 171.
3) K. Aika and A. Ozaki, *J. Catal.*, **13**, 232 (1969).
4) K. Aika and A. Ozaki, *ibid.*, **19**, 350 (1970).
5) Y. Morikawa and A. Ozaki, *ibid.*, **12**, 145 (1968).
6) Y. Morikawa and A. Ozaki, *ibid.*, in press.
7) K. Aika and A. Ozaki, *ibid.*, **16**, 97 (1970).
8) A. Ozaki, H. S. Taylor, and M. Boudart, *Proc. Royal Soc.*, (London), **258**, 47 (1960).

Codimerization of Ethylene and Styrene Catalyzed by Bis(triphenylphosphine)σ-aryl Nickel(II) Halide-Trifluoroboron Etherate

Noboru KAWATA, Ken-ichi MARUYA, Tsutomu MIZOROKI, and Atsumu OZAKI

Research Laboratory of Resources Utilization, Tokyo Institute of Technology, Ookayama, Meguro-ku, Tokyo

(Received July 31, 1971)

Bis(triphenylphosphine)σ-aryl nickel(II) halide (RNi-$(P\phi_3)_2X$, R=*o*-tolyl, 1-naphthyl, mesityl; X=halide ion; $\phi=C_6H_5$) has been reported to dimerize ethylene selectively, when trifluoroboron etherate coexists with the nickel complex.[1] It has been found that this catalyst system has also a high catalytic activity for the selective codimerization of ethylene and styrene. Rhodium(III) chloride[2] and palladium(II) chloride[3] have been reported to catalyze the codimerization of ethylene and styrene. The former gives 2-phenyl-2-butenes under a high pressure of ethylene and the latter 1-phenyl-butenes. The present catalyst system, however, gives 3-phenyl-1-butene selectively without accompanying 1-phenyl-butenes as is shown in the table. No activity for the codimerization was observed in the absence of trifluoroboron etherate, nor when bis(triphenylphosphine)nickel(II) dibromide was used in place of the σ-aryl nickel complex. The selectivity of codimerization into 3-phenyl-1-butene depends considerably on the σ-aryl ligand of the nickel complex, although catalytic activity seems to be independent of it. When most of styrene was consumed, 3-phenyl-1-butene initially formed was gradually isomerized into *cis*- and *trans*-2-phenyl-2-butenes, and they further reacted with ethylene to form 3-methyl-3-phenyl-1-pentene, causing decrease in the selectivity of the codimerization, while only trace amounts of the isomerized products of 3-phenyl-1-butene were observed in the products obtained under the reaction conditions given in Table 1. The results can be understood by assuming the formation of a nickel hydride, with which π-coordinated styrene is transformed into α-ethylbenzene-nickel intermediate followed by insertion of ethylene to give 3-phenyl-1-butene. The hydrogen source of the nickel hydride was elucidated by means of the dimerization of deutero ethylene.[4]

Table 1. Codimerization of ethylene and styrene

R-Ni$(P\phi_3)_2$Br	Styrene consumed (mmol)	3-Phenyl-1-butene obtained (mmol)	Selectivity[a] (%)
R=*o*-Tolyl	12.7	7.2	58
R=1-Naphthyl	12.9	10.3	80
R=Mesityl	12.7	11.6	91

Nickel complex, 1.0 mmol; $BF_3\cdot O(C_2H_5)_2$, 1.0 mmol; Styrene, 17.4 mmol; CH_2Cl_2, 30 m*l*; temp. 0°C; React. time, 15 min.

a) Based on the styrene consumed. The other products were styrene dimers, *etc.*

The experimental procedure is illustrated by the following ethylene-styrene codimerization. To a solution of bis(triphenylphosphine)-1-naphthyl nickel(II) bromide (1 mmol) in dry methylene chloride (30 m*l*) under nitrogen in a 50 m*l* flask were added trifluoroboron etherate (1 mmol) and styrene (17.4 mmol). The nitrogen gas in the flask had been evacuated at the temperature of liquid nitrogen before ethylene gas (700 mmHg) was introduced at 0°C with vigorous stirring. The temperature of the flask was kept at 0°C for 15 min with continuous supply of ethylene. The reaction was then terminated by adding aqueous sodium hydroxide solution (5 m*l*). Most of the volatile substances such as ethylene, butenes and the solvent were transferred into another flask by means of a liquid nitrogen trap before non-volatile materials were extracted with *n*-hexane. The amounts of non-volatile materials were quantitatively determined by gas chromatography. The results are shown in the table. 3-phenyl-1-butene (phenyl, 2.75 τ(m); CH_2=CH–, 4.0 τ (m), 4.97 τ(d); –CH(–), 6.67 τ(m); $-CH_3$, 8.7 τ(d)) and its isomers isolated by a fractional gas chromatography were identified by NMR spectroscopy, and were also checked by hydrogenation into 2-phenyl-butane with Raney nickel catalyst.

1) K. Maruya, T. Mizoroki, and A. Ozaki, This Bulletin, **43**, 3630 (1970).

2) T. Alderson, E. L. Jenner, and R. V. Kindsey, Jr., *J. Amer. Chem. Soc.*, **87**, 5638 (1965).

3) K. Kawamoto, A. Tatani, T. Imanaka, and S. Teranishi, This Bulletin, **44**, 1239 (1971).

4) T. Kuroki, K. Maruya, T. Mizoroki, and A. Ozaki, *ibid.*, **44**, 2002 (1971)

A Remark on the Unsuitable Use of Nitrobenzene as a Standard Substrate for Homolytic Aromatic Substitution

Hiroyuki OHTA and Katsumi TOKUMARU

Department of Chemistry, Faculty of Science, The University of Tokyo, Hongo, Bunkyo-ku, Tokyo

(Received August 2, 1971)

In homolytic aromatic substitution,[1] reactivities of various aromatic substrates are often determined relative to nitrobenzene[1a,1b,2] or benzene[3] as a standard substrate. We now wish to report that the apparent reactivity of nitrobenzene towards phenyl radicals appreciably changes in the presence of substances carrying transferrable hydrogen atoms such as toluene, ethylbenzene or cyclohexane, showing that nitrobenzene cannot be generally used as a standard substrate for homolytic substitution.

In a mixture of substrates, either phenylhydrazine was treated with nickel peroxide at room temperature[4] or benzoyl peroxide was decomposed at 80°C under nitrogen to generate phenyl radicals and the resulting biaryls were determined by gas chromatography. Whereas the reaction employing phenylhydrazine in nitrobenzene or in toluene gave *o*-, *m*-, and *p*-nitrobiphenyl in a distribution of 58, 7, and 35% or *o*-, *m*-, and *p*-methylbiphenyl in 68, 19, and 13%, respectively,[4] the reaction in a mixture of nitrobenzene and toluene led to a variation in distribution of *o*-, *m*-, and *p*-nitrobiphenyl to 73, 9, and 18% without affecting the distribution of methylbiphenyl isomers. The apparent relative reactivity of toluene to nitrobenzene, k_{PhMe}/k_{PhNO_2}, is 0.69. This is higher than the expected value of 0.33 estimated from the ratio of the reactivities, relative to benzene,[3] of toluene (k_{PhMe}/k_{PhH}, 1.68) and nitrobenzene (k_{PhNO_2}/k_{PhH}, 5.02). The use of benzoyl peroxide as a phenylating source similarly changed the reactivity of nitrobenzene. The value of k_{PhMe}/k_{PhNO_2} is 1.1, distribution of *o*-, *m*-, and *p*-nitrobiphenyl being 71, 11, and 18%, respectively, and that of *o*-, *m*-, and *p*-methylbiphenyl, 63, 22, and 15%, respectively. Likewise, the reactivity of nitrobenzene changed in its mixture with ethylbenzene or cyclohexane.[5]

In order to determine the apparent reactivity, relative to benzene, of nitrobenzene in the presence of toluene, phenylation employing phenylhydrazine was carried out in a ternary mixture of nitrobenzene, toluene, and benzene to show, for nitrobenzene, k_{PhNO_2}/k_{PhH} to be 2.1_1 and partial rate factors, f_o, f_m, and f_p to be 5.1_6, 0.30, and 1.7_5, respectively, and, for toluene, k_{PhMe}/k_{PhH}, f_o, f_m, and f_p to be 1.5_3, 3.0_4, 0.86, and 1.3_6, respectively. On the other hand, phenylation of a binary mixture of nitrobenzene or toluene with benzene was reported to give, concerning nitrobenzene, 5.02, 9.32, 1.16, and 9.05 for k_{PhNO_2}/k_{PhH}, f_o, f_m, and f_p and, concerning toluene, 1.68, 3.30, 1.09, and 1.27 for k_{PhMe}/k_{PhH}, f_o, f_m, and f_p, respectively.[3,6] These results clearly indicate that the presence of toluene, without variation of its reactivity, lowered the apparent reactivity of nitrobenzene, the depression of the partial rate factor of which was the most remarkable for para-position of the nitro group and the least for the ortho-position.

The anomalous behaviour of nitrobenzene could be understood by assuming that nitrophenylcyclohexadienyl radicals resulting from the addition of phenyl radicals to nitrobenzene would, at the expense of transferring their hydrogen atoms to give nitrobiphenyl, abstract hydrogen atoms from a hydrogen donor on their nitro group, as proposed for photo-excited nitrobenzene.[7] Then a precursory radical of *p*-nitrobiphenyl (I) would undergo abstraction to give II more easily than an isomeric radical precursory of *o*-nitrobiphenyl, in which the reactive center might be sterically hindered by the adjacent phenyl group, leading to higher reduction in the yield of *p*-nitrobiphenyl than

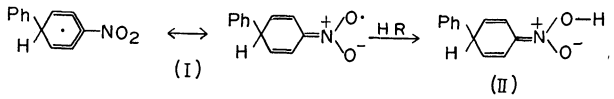

o-isomer. The resulting compound, II or its isomer, subsequently might undergo either dehydration to give nitroso compound which can scavange free radicals[8] without finally producing nitrobiphenyl, or dehydrogenation to nitrobiphenyl or other reactions.

1) As a general reference for homolytic aromatic substitution, see, for example: a) G. H. Williams, "Homolytic Aromatic Substitution," Pergamon Press, Oxford (1960). b) D. H. Hey, in G. H. Williams, ed., "Advances in Free-radical Chemistry," Vol. II, Logos Press, London (1967), p. 47. c) O. Simamura, T. Migita, N. Inamoto, and K. Tokumaru, "Yuriki Hanno," Tokyo Kagaku Dozin, Tokyo (1969), Chapter 11.

2) For example, D. H. Hey, S. Orman, and G. H. Williams, *J. Chem. Soc.*, **1961**, 565.

3) R. Ito, T. Migita, N. Morikawa, and O. Simamura, *Tetrahedron*, **21**, 955 (1965).

4) H. Ohta and K. Tokumaru, This Bulletin, in press.

5) It is to be noticed that decomposition of benzoyl peroxide in a mixture of equal volumes of nitrobenzene and cyclohexane gave cyclohexanol (3% based on the peroxide) and cyclohexanone (1%), both of which were not formed from decomposition in cyclohexane carried out alone in a degassed ampoule. It is also worth mentioning that Prof. T. Migita and his coworkers showed that decomposition of *t*-butyl peroxide in a mixture of toluene and nitrobenzene gave benzoic acid and *t*-butanol in a remarkable yield (private communication).

6) Phenylation using phenylhydrazine and nickel peroxide was found to give similar values to those obtained from phenylation using *N*-nitrosoacetanilide at 20°C.[3]

7) J. W. Weller and G. A. Hamilton, *Chem. Commun.*, **1970**, 1390.

8) G. R. Chalfont, D. H. Hey, K. S. Y. Liang, and M. J. Perkins, *J. Chem. Soc., B*, **1971**, 233.

Lewis Acid Complexes of Diphenylcyclopropenone

Zen-ichi Yoshida and Hideki Miyahara
Department of Synthetic Chemistry, Kyoto University, Yoshida, Kyoto
(Received August 3, 1971)

Condensation reactions of diphenylcyclopropenone (**1**) with active methylene compounds are known to be catalysed by boron trifluoride etherate.[1] Cyclopropenone-Lewis acid complexes could be intermediates, in view of the well known tendency of forming Lewis acid complexes of ketones[2] and the activation of (**1**) by hydrogen chloride[3] or triethyloxonium tetrafluoroborate.[4] In the latter the corresponding intermediates are obviously cyclopropenium cation derivatives.

We wish to report the isolation and the spectral features of 1:1 diphenylcyclopropenone-Lewis acid complexes[5] such as BF_3-complex (**2**), mp 166—167°C and $SbCl_5$-complex (**3**), 216—217°C prepared quantitatively by adding $BF_3 \cdot OEt^2$ to **1** in acetic acid and $SbCl_5$ to **1** in dry methylene dichloride both at room temperature. Both complexes were stable and non-hygroscopic. The structures were determined by analytical (satisfactory for C and H) and spectroscopic (pmr and IR) data and chemical reactions. Hydrolysis of both **2** and **3** liberated diphenylcyclopropenone water complex (**4**) quantitatively. **2** was also obtained from diphenylethoxycyclopropenium tetrafluoroborate after standing for a long time.

Table 1. Phenyl proton chemical shifts (τ in ppm) in $AsCl_3$[a]

Species	ortho[b]	para+meta[b]	(para+meta) −ortho
1	1.83	2.22	0.39
	2.00[c]	2.39[c]	0.39
2	1.70	2.18	0.48
3	1.80	2.14	0.34
4[d]	1.83	2.22	0.39
	2.00[c]	2.39[c]	0.39

a) Taken with a Jeolco C-60-H at room temperature in the concentration range 1.25—5% in $AsCl_3$, except otherwise stated.
b) The center of the corresponding multiplets of AB_2C_2-systems.[7]
c) In $CDCl_3$
d) Water complex prepared according to literature.[8]

Neither concentration effect nor appreciable dissociation of the complexes were observed on the NMR for several hours.

To ascertain the structures of complexes **2** and **3**, the spectra were compared with those of the related species **1** and **4** (Table 1). By complexation with water the IR spectrum changes but not the pmr spectrum (phenyl protons) of **1**. Appreciable lower shifts of 1850 (broad) and 1640 cm^{-1} bands in **1** to 1840 (broad) and 1600 (broad) cm^{-1} bands were observed. It seems likely[9] that 1885 (broad) and 1528 cm^{-1} bands in **2** as well as 1860 (sharp) and 1502 cm^{-1} bands in **3** correspond to 1850 and 1640 cm^{-1} bands in **1**, respectively. This shift may be explained by the order of acidity of Lewis acids ($SbCl_5 > BF_3$).[2] The O–B and O–Sb bonds in the complexes (**2**,**3**) are presumably the electron pair (σ) bond, because even water complex **4** should be formed by energy greater than 8.1 kcal/mol.[11] This is supported by the existence of the strong ν(B–F) 1100 cm^{-1} band[12] due to non-planar BF_3 in **2** and the strong ν(Sb–Cl) 360 cm^{-1} band[13] in **3**. The downfield shifts of (para+meta) protons of the complexes **2** and **3** from those of **1** are 2.4 Hz and 4.8 Hz, respectively, which are comparable with the change between those of 1-phenylcyclohexyl and 1-phenylcyclopentyl cation.[7] The corresponding values for ortho protons of **2** and **3** are 6.0 Hz and 1.8 Hz, respectively. From a comparison of both data it is suggested that an anomalous shielding-effect acts on the ortho-protons in $SbCl_5$ complex. The greater shifts of ortho proton in BF_3 complex than that of (para+meta) might be characteristic influence of strained carbonium ions[7] on phenyl-proton chemical shift. These spectral features might be interpreted in terms of the structure as shown in Fig. 1.

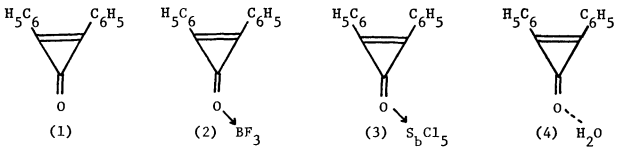

1) Y. Kitahara and M. Funamizu, This Bulletin, **37**, 1897 (1964).
2) D. Cook, *Can. J. Chem.*, **41**, 505 (1963).
3) J. H. M. Hill and M. A. Battiste, *Tetrahedron Lett.*, **1968**, 5537.
4) T. Eicher and A-M. Hansen, *Chem. Ber.*, **102**, 319 (1967).
5) Some metal salt complexes of **1** have been reported.[6] However, they are not of 1:1 type.
6) C. W. Bird and E. M. Briggs, *J. Chem. Soc., A*, **1967**, 1004.
7) D. G. Farnum and G. Mehta, *J. Amer. Chem. Soc.*, **91**, 3256 (1969).
8) F. Toda and K. Akagi, *Tetrahedron Lett.*, **1968**, 3735.
9) The assignment of the IR spectra of 1850 and 1640 cm^{-1} bands in **1** was controversial until the complicated nature of these bands due to strong coupling of several modes was clarified.[10]
10) A. Krebs, B. Schrader, and F. Hofler, *ibid.*, **1968**, 5935.
11) Evaluated as the hydrogen bonding energy of **1** with methanol, see E. Osawa, K. Kitamura, and Z. Yoshida, *J. Amer. Chem. Soc.*, **89**, 3814 (1967).
12) M. Begun and A. A. Palko, *J. Chem. Phys.*, **38**, 2112 (1963).
13) I. R. Beattie and M. Webster, *J. Chem. Soc.*, **1963**, 38.

The Retentive Solvolysis of 1-Phenylethyl Chloride in Binary Mixtures of the Carboxylic Acid with Nitromethane or the Nitrile

Kunio Okamoto, Issei Nitta, Masahiro Dohi, and Haruo Shingu
Department of Hydrocarbon Chemistry, Faculty of Engineering, Kyoto University, Sakyo-ku, Kyoto
(Received July 23, 1971)

It has been previously demonstrated that a nucleophilic co-solvent, such as di-*n*-butyl ether[1] or acetone,[2] intervenes in the acetolysis of 1-butyl-1-*d* *p*-nitrobenzenesulfonate[1] or the methanolysis of 2-octyl *p*-bromobenzenesulfonate,[2] thus affording a by-product derived from the co-solvent and the substrate for the respective solvolyses. We wish now to report on some novel examples which clearly indicate that such intervention leads the S_N1 solvolysis, otherwise inversive, to become a retentive solvolysis.

When the butyrolysis was conducted on optically active 1-phenylethyl chloride (0.10M) in the presence of sodium butyrate (0.100N) at 100°C, in accord with a standard tendency in the S_N1 solvolysis of this system, 1-phenylethyl butyrate with a net (3.5%) inversion of configuration was obtained in an 82% yield, along with styrene in a 14% yield.

In contrast to this, in a binary mixture of butyric acid with acetonitrile (80.0 mol%) the butyrolysis yielded 1-phenylethyl butyrate with a 2.9% *retention* of configuration, accompanied by a predominant (97%) racemization. In addition, a by-product, *N*-1-phenylethylacetamide, isolated from the reaction mixture, when worked-up with water, had a net (3.2%) inverted configuration; this amide may stem from the net-inverted *N*-1-phenylethylacetimidoyl chloride, which was a product of the S_N2-like reaction of the ion-pair intermediate with acetonitrile. These results can be explained by the following reaction scheme, which includes a back-side shielding[3] of the ion-pair intermediate by the C≡N group of acetonitrile and also a subsequent front-side attack of butyric acid on the shielded intermediate:

$$\text{(R)-RCl} \longrightarrow [\text{MeCN}\cdot\overset{+}{\text{R}}\cdot\overset{-}{\text{Cl}}] \xrightarrow{\text{PrCO}_2\text{H}} \text{(R)-RO}_2\text{CPr}$$

$$\downarrow$$

$$\text{(S)-RN=CMe} \xrightarrow{(\text{H}_2\text{O})} \text{(S)-RNHCOMe}$$

$$\text{Cl}$$

Similarly, a net retention of configuration was observed in the propionolysis and in the valerolysis in the binary mixtures of the respective carboxylic acids with acetonitrile. Nitromethane, as a co-solvent, also exhibited a similar retentive function in the butyrolysis. These results are presented in Table 1, along with the first-order solvolysis rate constant for each run.

The nitriles other than acetonitrile (*viz.*, fumaronitrile, malononitrile, and acrylonitrile) were also found to be effective co-solvents in changing the steric course of the butyrolysis from a net inversion to a net retention. In Fig. 1 the extents of the retention (or inversion) of 1-phenylethyl butyrate are plotted against the concentrations of the added nitriles. There is a decided trend towards higher retentions in solvents with higher nitrile concentrations, but there is no simple correlation between the structure of the nitrile and the extent of retention. However, compared with acetonitrile or malononitrile, acrylonitrile and fumaronitrile show no specific effectiveness for the retention; this indicates that their C=C groups are scarcely responsible for the back-side shielding of the ion-pair intermediate.

Table 1. The net steric course and the rates in the solvolysis of 1-phenylethyl chloride (100°C)[a]

Solvent acid	Net steric course for $R'CO_2R$[b]	Net steric course for RNHCOMe[c]	10^5k_1 (sec^{-1})
Acetic	2.94% inv.	—	58.1
Acetic[d]	racem.	2.96% inv.	28.1
Propionic	0.75% inv.	—	5.03
Propionic[e]	2.77% ret.	2.05% inv.	14.1
Butyric	3.53% inv.	—	1.98
Butyric[f]	2.90% ret.	3.22% inv.	6.62
Butyric[h]	0.89% ret.	—	19.2
Valeric	5.94% inv.	—	0.89
Valeric[g]	2.73% ret.	4.69% inv.	7.80

a) In the presence of the sodium salts of the respective acids. b) Yield: 34—82%. c) Yield: 5—10%. d—g) +MeCN (67.9, 68.1, 80.0, and 67.5 mol%, respectively). h) $+MeNO_2$ (79.9 mol%).

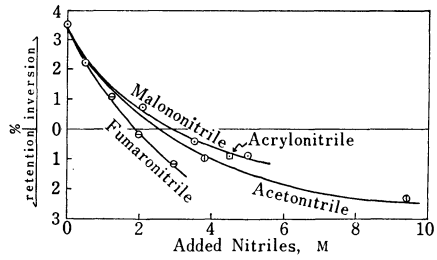

Fig. 1. Extents of retention (or inversion) of 1-phenylethyl butyrate (100°C).

In view of these results, the retentive S_N1 hydrolysis of some aralkyl *p*-nitrobenzoates in the aqueous acetone solvent, found by Goering and his collaborators,[4] may be attributed to the back-side shielding by acetone. Furthermore, our previous observation[5] that the hydrolysis of 1-phenylethyl chloride in aqueous acrylonitrile (97 wt%) affords 1-phenylethyl alcohol with a net (6.3%) retained configuration can be interpreted as involving back-side shielding by acrylonitrile.

1) A. Streitwieser, Jr., and S. Andreades, *J. Amer. Chem. Soc.*, **80**, 6553 (1958).
2) H. Weiner and R. A. Sneen, *ibid.*, **87**, 287 (1965).
3) W. von E. Doering and A. Streitwieser, Jr. *Cf.* A. Streitwieser, Jr., *Chem. Rev.*, **56**, 571 (1956).
4) H. L. Goering and H. Hopf, *J. Amer. Chem. Soc.*, **93**, 1224 (1971), and references cited therein.
5) K. Okamoto, K. Komatsu, and H. Shingu, This Bulletin, **39**, 2785 (1966).

Quenching Cross-Sections of the Metastable Mercury Atom (6^3P_0)

Hiroyuki HORIGUCHI and Soji TSUCHIYA

Department of Pure and Applied Sciences, College of General Education, The University of Tokyo, Meguro-ku, Tokyo

(Received July 9, 1971)

Recently, Callear and McGurk[1] reported that the cross-sections for the deactivation of $Hg(6^3P_0)$ atoms were larger by an order of magnitude than their former data[2] which showed a considerablly less reactivity of $Hg(6^3P_0)$ atoms compared to that of $Hg(6^3P_1)$ atoms. Cambell *et al.*[3] measured the absorption of $Hg(6^3P_0)$ in the gaseous mixture of N_2, quencher and mercury which was excited by the 2537 Å radiation. Their data support the larger cross-sections for quenching $Hg(6^3P_0)$ atoms. We proposed a method[4] to determine the cross-section for each process, $6^3P_1 \rightarrow 6^3P_0$, $6^3P_1 \rightarrow 6^1S_0$, and $6^3P_0 \rightarrow 6^1S_0$, and found that the cross-sections for $6^3P_0 \rightarrow 6^1S_0$ were not so small as Callear and William's results.[2] Recently, we measured the time-history of the 4047 Å absorption of $Hg(6^3P_0)$ after the flash irradiation of the 2537 Å radiation, and observed the cross-section of a reactive molecule for quenching $Hg(6^3P_0)$ atoms. The results are shown in Table 1.

The cross-sections for quenching the 6^3P_0 state are in agreement with the new data of Callear and McGurk[5] within a factor of 5. It is seen from Table 1 that the ratio of the quenching corss-section for the process $6^3P_1 \rightarrow 6^1S_0$ to that for $6^3P_0 \rightarrow 6^1S_0$ is close to 3 except for the case of quenching by N_2, CH_4, or CO_2, which has a larger ratio. Recent results of Vikis and Moser[6] by a chemical method show that the reactivity of $Hg(6^3P_0)$ is much less than that of $Hg(6^3P_1)$, but this is not consistent with the present experiment. Kang Yang[7] proposed that from the conservation of angular momentum, the cross-section of H_2 for quenching $Hg(6^3P_0)$ may be smaller than that of alkane. However, our results differ as has been pointed out by Vikis and Moser.[6] The present results suggest the conclusion that if a molecule has a large cross-section ($\gtrsim 1$ Å^2) for the process $6^3P_1 \rightarrow 6^1S_0$, the corresponding 6^3P_0 cross-section is of the same order of magnitude, and that a molecule with a very small cross-section ($\lesssim 0.1$ Å^2) for quenching the 6^3P_1 state has a much smaller cross-section to deactivate the 6^3P_0 state. If the former case corresponds to the strong coupling between the excited Hg atom and a quenching molecule. the quenching rate of $Hg(6^3P_1)$ would be the same order of magnitude as that of $Hg(6^3P_0)$, because the degeneracy of $^3P_1$ state is removed by a collisional perturbation of a quenching molecule (Q),[8] and the mixing of two states $Hg(6^3P_1)+Q$ and $Hg(6^3P_0)+Q$ occurs in the course of non-adiabatic transition to $Hg(6^1S_0)+Q$. This seems to explain qualitatively the present results for CO, NO, H_2, and D_2.

TABLE 1. QUENCHING CROSS-SECTION (σ^2, Å^2) OF EXCITED MERCURY ATOMS

Quencher	$^3P_1 \rightarrow {}^1S_0$	$^3P_1 \rightarrow {}^3P_0$	$^3P_0 \rightarrow {}^1S_0$		$\sigma^2(^3P_1 \rightarrow {}^1S_0)/\sigma^2(^3P_0 \rightarrow {}^1S_0)$	
	this work	this work	this work	C & M[5]	this work	V & M[6]
N_2	≤ 0.03	0.36	$<8\times10^{-6}$	—	—	—
CO	0.60	2.1	0.21	0.66	2.9	—
NO	20	5	8.0	1.62	2.5	—
H_2	8.3	≤ 0.1	2.1	0.96	3.9	47
D_2	10.0	≤ 0.1	2.9	—	3.4	49
CH_4	0.04	0.03	1.4×10^{-4}	2.86×10^{-4}	290	1400
CO_2	2.48	≈ 0.002	0.035	0.033	71	—

1) A. B. Callear and J. C. McGurk, *Chem. Phys. Lett.*, **6**, 417 (1970).
2) A. B. Callear and G. J. Williams, *Trans. Faraday Soc.*, **60**, 2158 (1964).
3) J. M. Cambell, S. Penzes, H. S. Sandhu, and O. P. Strauz, *Inter. J. Chem. Kinetics*, **3**, 175 (1971).
4) H. Horiguchi and S. Tsuchiya, This Bulletin, **44**, 1213 (1971).
5) A. B. Callear and J. McGurk, *Chem. Phys. Lett.*, **7**, 491 (1970).
6) A. C. Vikis and H. C. Moser, *J. Chem. Phys.*, **53**, 1491 (1970).
7) Kang Yang, *J. Amer. Chem. Soc.*, **89**, 5344 (1967).
8) V. K. Bykhovskii and E. E. Nikitin, *Opt. Spectry.*, **16**, 111 (1964).

Photoinduced Transannular Reaction of 4,5-Octamethylene-1,3-dioxolen-2-one

Tamejiro HIYAMA, Shinsaku FUJITA, and Hitosi NOZAKI
Department of Industrial Chemistry, Kyoto University, Yosida, Sakyo-ku, Kyoto
(Received August 25, 1971)

Recently, 1,3-dioxolen-2-one (vinylene carbonate) has been reported to undergo dimerization[1] or cycloaddition[2] on UV irradiation. However, the photoreaction of compound I[3,4] given in the title proceeded in quite a different way as described below.

A 0.2M solution of I in acetone was irradiated under N_2 with a 200 W high-pressure Hg lamp. The photolysate was distilled to give a mixture of stereoisomers[4] (IIa and IIb, 71% yield) which were isomeric with I as established by means of MS (M^+ *m/e* 196) and elemental analysis. The mixture exhibited an IR band at 1795 cm^{-1} characteristic of a 1,3-dioxolan-2-one system. The NMR signal of the methine proton adjacent to oxygen appeared at δ 4.65—4.75. As separation of IIa and IIb was unsuccessful, the mixture was converted into the corresponding *vicinal* diols (IIIa: IIIb= 5.7: 1). The structure and stereochemistry of IIIa[4] (mp 82—83°C, M^+ *m/e* 170, IR 3400 cm^{-1}) and IIIb[4] (M^+ *m/e* 170, IR 3480 cm^{-1}) were determined as follows. (1) Since the glycol cleavage of IIIa and IIIb with $NaIO_4$ and $KMnO_4$ yielded the same keto acid IV (1735, 1710 cm^{-1}, oxime mp 121—124°C (lit,[5] 124—125.5°C), semicarbazone mp 192—193°C (lit,[5] 195—196°C)), both IIIa and IIIb should have a bicyclo[5.3.0]decane structure. (2) As the oxidation of IIIa and IIIb with *N*-bromosuccimide (NBS)[6] afforded the same ketol V[4] (IR 3460, 1700 cm^{-1}), they shoud have the same mode of ring fusion. (3) The reduction of V with $NaH_2Al(OCH_2CH_2OMe)_2$ (VSH) gave IIIa exclusively: the *trans*-configuration of the *vicinal* hydroxyl groups of IIIa was established on the basis of Cram's rule. (4) The half tosylation of the mixture of IIIa and IIIb followed by reduction with $LiAlH_4$

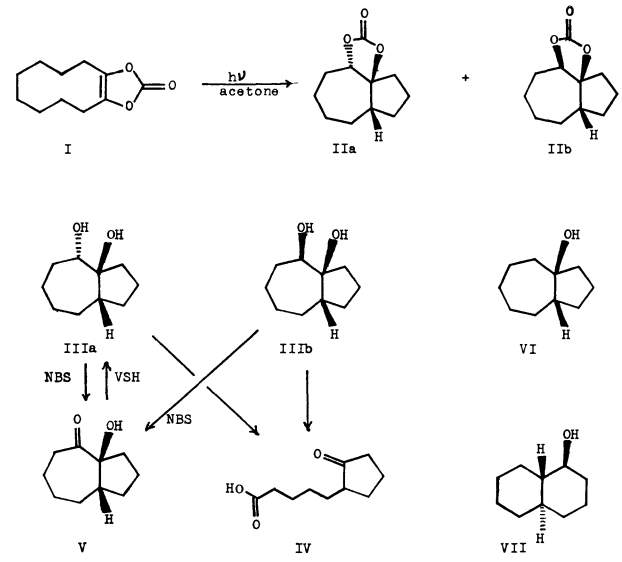

in ether or $NaBH_4$ in dimethyl sulfoxide, afforded *cis*-bicyclo[5.3.0]decan-1-ol (VI)[7] along with *trans*, *trans*-α-decalol (VII).[8] In conclusion, IIIa and IIIb were characterized as *cis*-bicyclo[5.3.0]decane-*trans*-1, 2-diol and its *cis*-diol isomer, respectively.

The transannular reaction of I proceeded as well upon benzene-sensitization. Intramolecular hydrogen-abstraction by the excited olefinic bond in its triplet state and the subsequent recombination of the resulting diradical may account for the new photoreaction.[9] In contrast to the mother compound, the derivative I underwent no cycloaddition to ethylene or acetylene on attempted acetone-sensitized reaction. The intramolecular reaction predominated even in 2-propanol containing benzene sensitizer.

1) W. Hartmann and R. Steinmetz, *Chem. Ber.*, **100**, 217 (1967).
2) a) W. Hartmann, *ibid.*, **101**, 1643 (1968). b) H.-D. Scharf, W. Droste, and R. Liebig, *Angew. Chem.*, **80**, 194 (1968).
3) Compound I (mp 44—45°C, IR 1822, 1731 cm^{-1}, NMR: no olefinic protons) was prepared by the reaction of sebacoin with phosgene in the presence of pyridine or by ethoxycarbonylation of sebacoin and subsequent acid treatment.
4) All the new compounds gave correct data on elemental analyses.
5) W. Herz, *J. Org. Chem.*, **22**, 630 (1957).
6) L. F. Fieser and S. Rajagopalan, *J. Amer. Chem. Soc.*, **71**, 3938 (1949).
7) An authentic sample of VI was prepared by the hydroboration of $\Delta^{1(7)}$-bicyclo[5.3.0]decene.
8) Formation of VII may be ascribed to the base-catalyzed rearrangement of tosylates. Similar rearrangements have been reported, *e.g. cf.* G. Büchi, W. Hofheinz, and J. V. Pauksteils, *J. Amer. Chem. Soc.*, **91**, 6473 (1969).
9) Photoinduced transannular reaction has been reported only in a sterically compressed system of a methylene and an olefinic bond. *Cf.* H.-D. Scharf, *Tetrahedron*, **23**, 3057 (1967); L. Vollner, H. Parler, W. Klein, and F. Korte, *ibid.*, **27**, 501 (1971).

Ultrasonic Study on Aqueous Solutions of Amino Acids

Katsutaka SASAKI and Kiyoshi ARAKAWA

Research Institute of Applied Electricity, Hokkaido University, Sapporo

(Received October 3, 1970)

Ultrasonic experiments for aqueous solutions of amino acids (glycine, *l*-alanine, *l*-valine, and *l*-leucine) were carried out by means of pulse technique in order to study the nature of solute-solvent interactions. The sound velocity and absorption coefficient were determined for aqueous solutions in the frequency range 15–45 MHz, at temperatures 10–30°C. No relaxation frequency was observed in all the solutions. The absorption coefficient for glycine solutions at low concentrations is nearly equal to that for pure water. The result is consistent with the idea that glycine molecules behave as a structure breaker within water. Concerning the concentration dependency of sound velocity and absorption, no appreciable difference is observed in various solutions of amino acids in spite of difference in the size of hydrocarbon side chains in solute molecules. It is concluded that the behavior of *l*-alanine and its higher homologues in water dose not differ from that of glycine.

Recently, a number of studies have been made on the solute-solvent interactions in aqueous solutions.[1,2] Holtzer and Emerson[3] discussed the changes in the structure of water induced by nonelectrolytic solute molecules, based on a simple two state model.[4]

We pointed out from ultrasonic measurements that denaturing agents such as urea, guanidine hydrochloride *etc.* have a "cooperative breaking effect" on the "open-packed structure" or ice-like structure" in water.[5] The cooperative breaking effect of denaturing agents arises from the cooperative nature of structure formation and breaking in water.[6,7]

Since the proposition stated by Frank and Evans,[8] hydrocarbon molecules in water are believed to reinforce the structure (icebergs) around the molecules within water. We showed that 1,3-diethylurea molecules behave as a structure former due to the structure-forming ability of ethyl groups which is in sharp contrast to the behavior of urea and 1,3-dimethylurea molecules as a structure breaker.[9] Hydrophobic bonds which result from the structure-forming ability of hydrocarbon groups in water have been studied by many workers, since it is believed to be an important factor governing the conformation of protein molecules in water.[10,11]

There have been some ambiguities about the behavior of amino acids in water.[12] Tyrell and Zamann[13] reported that there is no appreciable difference between the behavior of glycine and that of *dl*-alanine in water.

On the contrary, Robinson,[14] Tanford[15], and Ellerton *et al.*[16] stated that in aqueous solutions of *l*-alanine and its higher homologues the behaviors of solutes definitely differ from that in glycine solutions.

We have investigated the influences of serveral neutral amino acids upon the structure of water by means of an ultrasonic pulse technique.

Experimental

An ultrasonic pulse method was used for the measurement of absorption coefficient and sound velocity. The apparatus and the procedures were described previously.[17] The sound velocity and absorption coefficient were measured at 5 MHz and in the frequency range 15–45 MHz at temperatures 10–30°C. The data of absorption coefficient were reproducible within ±2% and sound velocity data ±1 m/sec. Samples of glycine, *l*-alanine, *l*-valine, and *l*-leucine were obtained from Nakarai Chemicals Ltd. The shear viscosity in aqueous solutions of these amino acids were measured by means of a capillary viscometer of Ostwald type.

Results

Sound Velocity. The sound velocity data at 5 MHz measured for the aqueous solutions of glycine and *l*-alanine are plotted against temperature in Figs. 1 (a) and (b), respectively, together with the velocity data for pure water by Greenspan and Tschiegg.[18] The velocity *vs.* concentration curves obtained for aqueous solutions of glycine, *l*-alanine, *l*-valine, and *l*-leucine are plotted in Fig. 2 at various temperatures. Concentrations are given in volume %. The concentrations are calculated from the density and weight

1) M. J. Blandamer, D. E. Clarke, N. J. Hidden, and M. C. R. Symons, *Trans. Faraday Soc.*, **64**, 2691(1968); M. J. Blandamer, N, J. Hidden, D. E. Clarke, and N. C. Treloar, *ibid.*, **64**, 3234 (1968): M. J. Blandamer, N. J. Hidden, M. C. R. Symons, and N. C. Treloar, *ibid.*, **65**, 1805(1969).

2) F. Franks and B. Watson, *ibid.*, **65**, 2339(1969); F. Franks and H. T. Smith, *ibid.*, **65**, 2962(1969); F. Franks and D. J. G. Ives, *Quart. Rev.* (London), **20**, 1(1966).

3) A. Holtzer and M. F. Emerson, *J. Phys. Chem.*, **73**, 26 (1969).

4) K. Arakawa and K. Sasaki, This Bulletin, **42**, 303(1969).

5) K. Arakawa, N. Takenaka, and K. Sasaki, *ibid.*, **43**, 636 (1970).

6) H. S. Frank and W-Y Wen, *Discuss. Faraday Soc.*, **24**, 133 (1957).

7) K. Arakawa and K. Sasaki, This Bulletin, **43**, 3048(1970).

8) H. S. Frank and M. W. Evans, *J. Chem. Phys.*, **13**, 507 (1945).

9) K. Sasaki and K. Arakawa, This Bulletin, **42**, 2485(1969).

10) W. Kauzmann, *Advan. Protein Chem.*, **14**, 1 (1959).

11) G. Némethy and H. A. Scheraga, *J. Phys. Chem.*, **66**, 1773 (1962).

12) J. J. Kozak, W. S. Knight, and W. Kauzmann, *J. Chem. Phys.*, **48**, 675 (1968).

13) H. J. V. Tyrell and M. Zamann, *J. Chem. Soc.*, **1964**, 6216.

14) A. L. Robinson, *J. Chem. Phys.*, **14**, 5888 (1946).

15) P. L. Whitney and C. Tanford, *J. Biol. Chem.*, **237**, PC 1735 (1962).

16) H. D. Ellerton, G. Reinfelds, D. E. Mulcahy, and P. J. Dunlop, *J. Phys. Chem.*, **68**, 398 (1964).

17) K. Arakawa and N. Takenaka, This Bulletin, **40**, 2063 (1967).

18) M. Greenspan and C. E. Tschiegg, *J. Res. Nat. Bur. Stand.*, **58**, 249 (1957); *J. Acoust. Soc. Amer.*, **31**, 75 (1959).

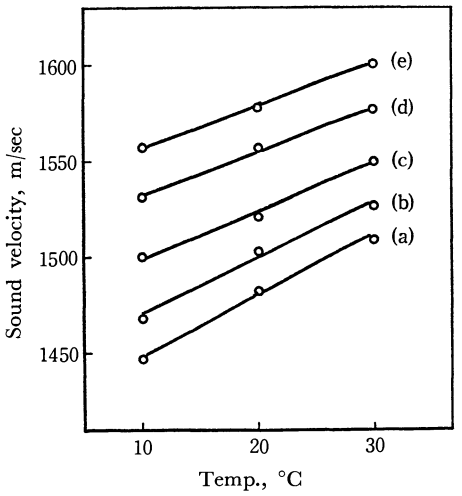

Fig. 1(a). Ultrasonic velocity of aqueous solutions of glycine.
Concn. (M: mol/*l*) (a) pure water, (b) 0.5 M, (c) 1.0 M, (d) 1.5 M, (e) 2.0 M

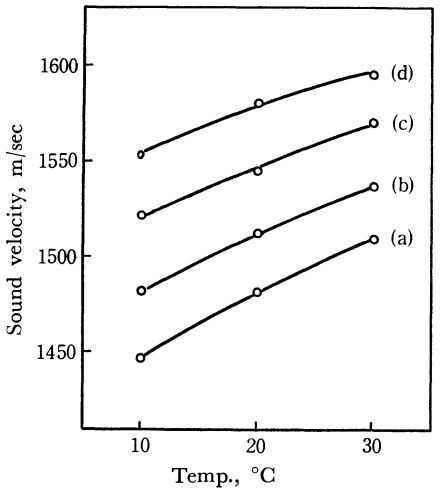

Fig. 1(b). Ultrasonic velocity of aqueous solutions of *l*-alanine.
Concn. (M: mol/*l*) (a) pure water, (b) 0.5 M (c) 1.0 M, (d) 1.5 M

of each amino acid sample in solid state. In Fig. 2, it is shown that the velocity *vs.* concentration relations for solutions of various amino acids form a single composite curve and that the sound velocity is not dependent on the size of hydrocarbon side chain of amino acids.

Ultrasonic Absorption. The absorption coefficient α was measured for the aqueous solutions of glycine in the concentration range 0.5–2.0 mol/*l*, of *l*-alanine in the range 0.5–1.5 mol/*l* of *l*-valine at 0.5 mol/*l* and of *l*-leucine at 0.1 mol/*l*. The frequency dependency of α/f^2 (f, frequency) is shown in Figs. 3 (a), (b), (c), and (d) for each solution. No relaxation frequency was observed for all the solutions tested. This coincides with the result for glycine solutions by Hammes and Pace.[19] In Figs. 4 (a) and (b) we see that at the same concentration for solutions of glycine and

19) G. G. Hammes and C. N. Pace, *J. Phys. Chem.*, **72**, 2227 (1968).

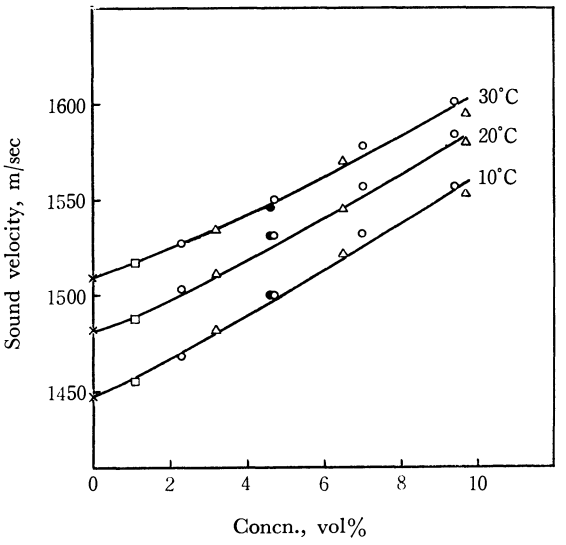

Fig. 2. Concentration dependence of ultrasonic velocity for amino acid solutions.
×, pure water, ○, glycine, △, *l*-alanine, ●, *l*-valine, □, *l*-leucine

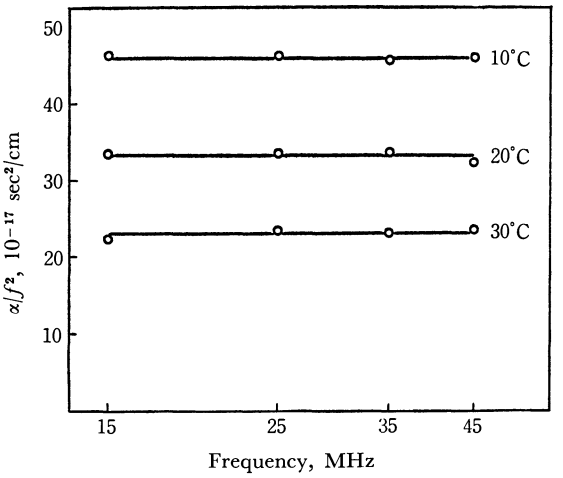

Fig. 3(a). Ultrasonic absorption of aqueous solutions of glycine. (2.0 M glycine)

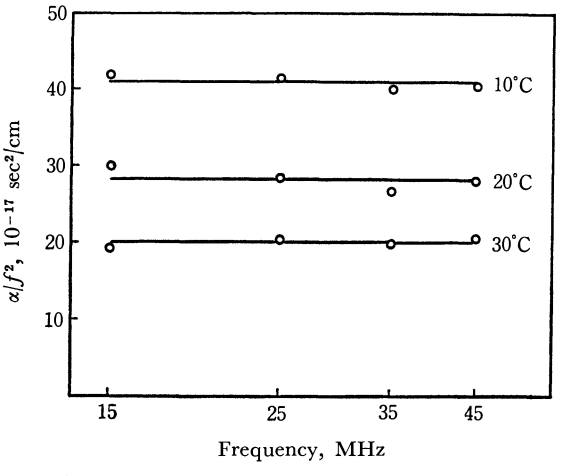

Fig. 3(b). Ultrasonic absorption of aqueous solutions of *l*-alanine. (1.0 M *l*-alanine)

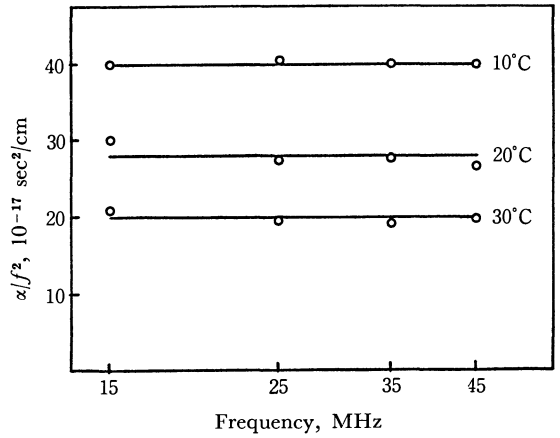

Fig. 3(c). Ultrasonic absorption of aqueous solutions of *l*-valine. (0.5 M *l*-valine)

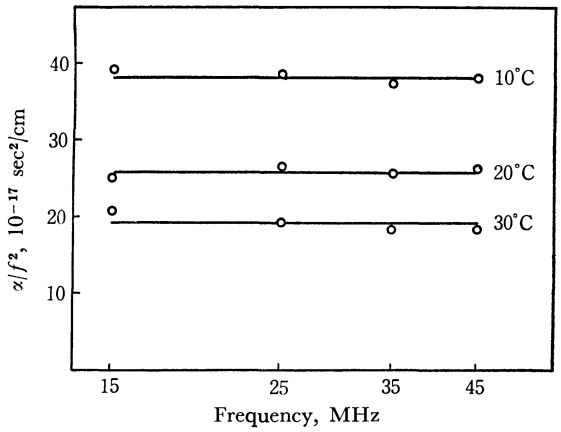

Fig. 3(d). Ultrasonic absorption of aqueous solutions of *l*-leucine. (0.1 M *l*-leucine)

l-alanine, the magnitudes of α/f^2 for both solutions are nearly equal. It is also seen that the magnitudes of of α/f^2 at low concentrations are essentially the same as that of pure water for both solutions. The concentration dependencies of α/f^2 for solutions of four amino acids are compared in Fig. 5. Concentrations are given in volume %. We see that the plot of α/f^2

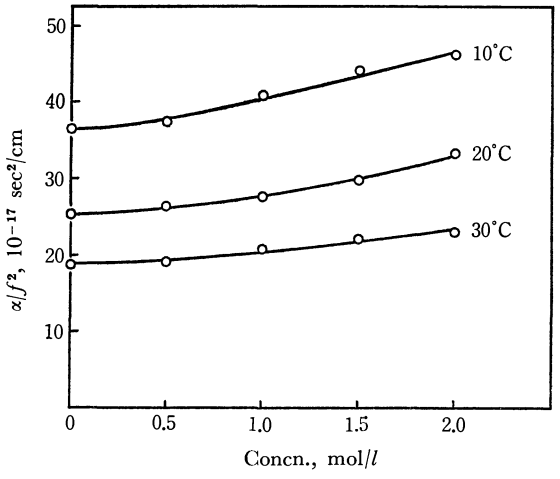

Fig. 4(a). Concentration dependence of ultrasonic absorption for glycine solutions.

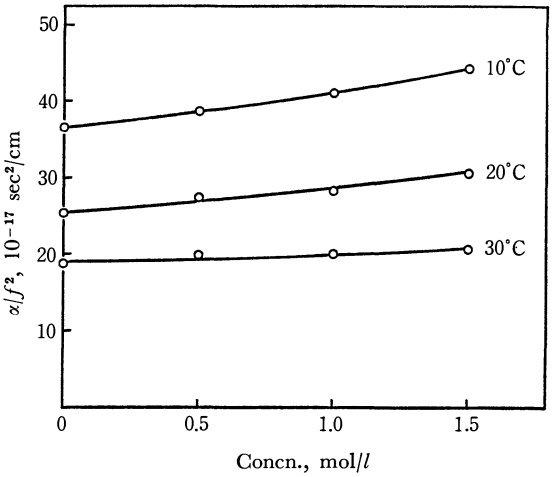

Fig. 4(b). Concentration dependence of ultrasonic absorption for *l*-alanine solutions.

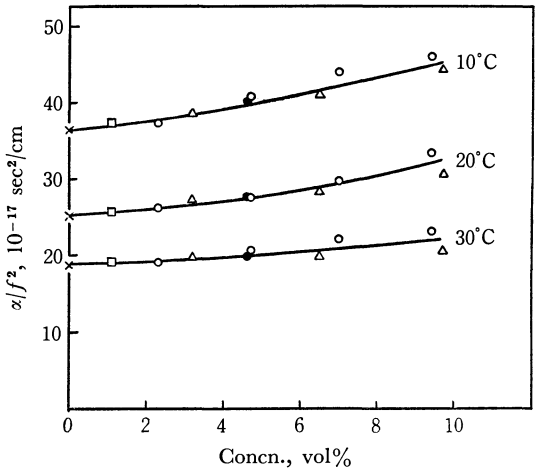

Fig. 5. Concentration dependence of ultrasonic absorption for amino acid solutions.
×, pure water, ○, glycine, △, *l*-alanine, ●, *l*-valine, □, *l*-leucine

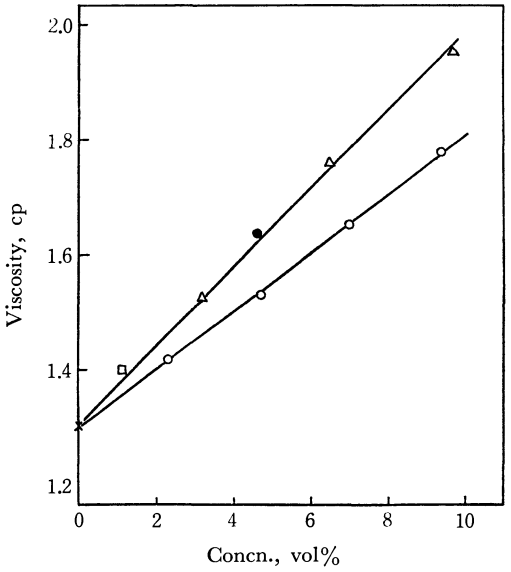

Fig. 6. Viscosity for aqueous solutions of amino acids at 10°C.
○, glycine, △, *l*-alanine, ●, *l*-valine, □, *l*-leucine, ×, pure water

vs. concentration relations for various amino acid solutions forms a single curve at various temperatures. The situation is quite similar to the case of sound velocity shown in Fig. 2. In order to obtain the magnitude of structural absorption $(\alpha/f^2)_{struct.}$ from the data given in Fig. 5, determination of the classical absorption is necessary. The classical absorption is given by

$$(\alpha/f^2)_{shear} = \frac{8\pi^2\eta}{3\rho V^3} \quad (1)$$

where ρ is density, V sound velocity, and η shear viscosity. The values of η were measured for all solutions and given in Fig. 6. Thus, the structural absorption is given in the equation

$$(\alpha/f^2)_{struct.} = (\alpha/f^2)_{obs.} - (\alpha/f^2)_{shear}. \quad (2)$$

The result obtained is shown in Fig. 7.

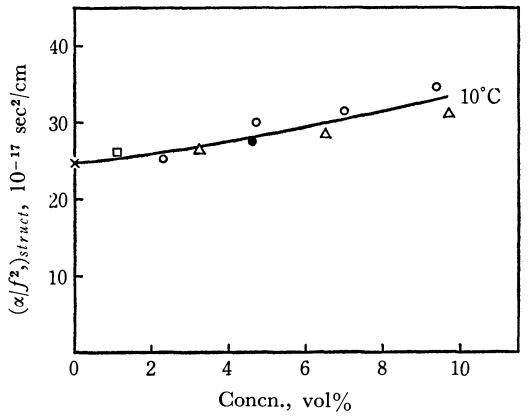

Fig. 7. Concentration dependence of structural absorption for amino acid solutions.
×, pure water, ○, glycine, △, *l*-alanine, ●, *l*-valine, □, *l*-leucine

Discussion

The Effect of Glycine upon the Structure of Water. Robinson *et al.*[20] pointed out from thermodynamical data that glycine behaves as a structure breaker in water while *l*-alanine and higher homologues behave as a structure former. Longsworth[21] supported this view. As for the behaviors of glycine in water, a number of workers have reached the same conclusion that glycine acts as a structure breaker.[13–16,20,21] As seen in Fig. 4 (a), the magnitude of absorption coefficient in an aqueous solution of glycine increases slowly with concentration. The tendency is similar to the case of 1,3-dimethylurea solution, in which the solute molecules behave as a structure breaker.[9] Thus, it might be said that the behavior of glycine in water is essentially similar to that of 1,3-dimethylurea. It seems that glycine molecules break the structure of water though the ability is supposed to be weaker than that of ordinary denaturing agents, such as urea.

The Effect of Side Chain of Amino Acids upon the Structure of Water. It is generally believed that the structure-forming ability of solute molecules in liquid water increases with the size of hydrocarbon side chain.[22,23] However, there has been some controversy concerning the behavior of *l*-alanine and higher homologues of amino acids in water.

Tanford and his collaborators[15,24] pointed out that *l*-alanine and higher homologues behave as a structure former while glycine behaves as a structure breaker. Recently, Spink and Auker[25] supported the view of Robinson, Tanford, and others, based on their thermodynamical data. Kay and Evans[26] also stated that the effect of hydrocarbon side chains of *l*-alanine and higher homologues on the structure in water differs from that of glycine.

On the contrary, Tyrell and Zamann[13] reported on the basis of thermodynamical data that there is no appreciable difference between the behavior of glycine and that of *dl*-alanine in water. This view is supported by the recent study of Kauzmann *et al.*[12]

The results in the present study clearly support the conclusion of Tyrell & Zamann and Kauzmann *et al.* As seen in Figs. 2,5, and 7, the ultrasonic data of sound velocity and absorption form a single curve at each temperature irrespective of the different size of side chains. Thus, it is concluded that the behavior of these four amino acids in water are similar essentially, and the structure-forming effect due to alkyl groups in amino acid molecules are cancelled out by the strong structure-breaking effect due to the dipolar field by zwitter ions ($NH_3^+CHRCOO^-$).

It can therefore be said that amino acids cannot be regarded as good models for studying hydrophobic bonding.[12]

Concluding Remarks

The following conclusion are obtained.

1) The effects of four amino acids on the ice-like structure in water are essentially similar to each other. l-Alanine and its higher homologues do not always behave as a structure former in water.

2) Glycine molecules behave as a weak structure breaker for the ice-like structure in water.

The authors wish to thank Mr. Nobuo Takenaka for his cooperation in performing this study.

20) L. S. Mason, W. F. Offutt, and A. L. Robinson, *J. Amer. Chem. Soc.*, **71**, 1436 (1949).
21) L. G. Longsworth, *ibid.*, **75**, 5706 (1953).
22) D. B. Wetlaufer, S. K. Malik, C. Stoller, and R. L. Coffin, *ibid.*, **86**, 508 (1964).
23) A. Ben-Naim and F. H. Stillinger, *J. Phys. Chem.*, **73**, 900 (1969).
24) Y. Nozaki and C. Tanford, *J. Biol. Chem.*, **238**, 4074 (1963).
25) C. H. Spink and M. Auker, *J. Phys. Chem.*, **74**, 1742 (1970).
26) R. L. Kay and D. F. Evans, *ibid.*, **70**, 2325 (1966).

An ESR Study of NO_2 Adsorbed on Silica Gel Surfaces[1]

Masamoto IWAIZUMI, Shozo KUBOTA, and Taro ISOBE
Chemical Research Institute of Non-Aqueous Solutions, Tohoku University, Sendai
(Received January 22, 1971)

NO_2 adsorbed on silica-gel surfaces shows temperature-dependent ESR spectra, which can be explained by assuming a restricted rotation of the NO_2 molecule, where the preferred axis is the O–O direction. It is concluded from this observation that a hydrogen-bond force between the oxygen of NO_2 and OH groups on the silica-gel surfaces plays a part in the NO_2-silica-gel interaction. It is also estimated, from the observed hyperfine tensor, that the ONO angle may become slightly smaller when NO_2 is adsorbed onto the silica-gel surface from the gas phase.

It is considered that the adsorption of radicals on solid surfaces changes the nature of their motion from that in the gas phase, in solution, or in solid matrices. In many cases of studies of free radicals in adsorbed states, a restricted motion of the molecules has been detected through line-width-broadening effects in the ESR spectra.[2] However, there have been few cases where detailed information about the motion of the radicals or about the nature of the radical-surface interaction has been obtained.

In the present work we examined NO_2 adsorbed on the silica-gel surface by ESR with the aim of getting information about the adsorbed state. We found that NO_2 shows temperature-dependent ESR spectra, which can be explained by the restricted rotation of the molecule, where the preferred axis is the O–O direction. On the basis of this observation, it can be estimated that the NO_2 molecule interacts with the silica-gel surface through a hydrogen bond with OH groups on the silica-gel surface. The change in the molecular structure by adsorption is not large. However it is estimated that the ONO angle may become smaller when NO_2 is adsorbed on the silica-gel surface from the gas phase.

Experimental

The samples for ESR measurements were prepared by letting NO_2 gas be adsorbed on silica-gel surfaces in a vacuum line. The NO_2 used was obtained commercially (The Matheson Co., Inc.) and was dried with P_2O_5. Prior to treatment with NO_2, the silica gel (a Kanto Chemical Co. product for chromatography, 60—80 mesh) was heated for 6 hr at 500—550°C and at 10^{-6} Torr. The silica gel was then exposed to NO_2 gas at about 1 atm at room temperature. After exposing the silica gel to NO_2 for a few minutes, the excess NO_2 was removed by leading the gas into a trap cooled by liquid nitrogen. The ESR spectra were measured by a Hitachi model MES 4001 X-band ESR spectrometer at various temperatures ranging from room temperature to 77°K. The sample was cooled with a gas-flow cooler or with a liquid nitrogen dewar with an unsilvered lower section. The temperature of the sample was monitored by a copper-constantan thermocouple placed just below the sample tube in the cavity.

Results and Discussion

Hindered Rotation of NO_2 on Silica Gel. Figure 1 shows the ESR spectra of NO_2 adsorbed on the silica-gel surface at various temperatures. As Fig. 1 shows, the spectra are temperature dependent. The changes in the spectra were completely reversible upon changes in the temperature. The ESR spectra of NO_2 trapped in various solid matrices have been reported by a number of authors,[3–10] and it has been shown that they can be interpreted in terms of anisotropic hyperfine interaction with the nitrogen nucleus and anisotropic g factors, with the principal axes parallel to the molecular axes. In most of the cases treated in the solid matrices, the hyperfine and g tensors are unsymmetrical, as is to be expected from the molecular geometry. In the present case, however, the ESR spectrum observed at 77°K is interpreted by g and hyperfine tensors which are approximately axially symmetric. This indicates that the radical is rotating about this symmetry axis sufficiently rapidly to give a rotational average about the axis at this temperature. The experimental parameters obtained here are compared in Table 1 with those found in solid matrices. It may be seen from the table that the axis of the rotation is the y axis, *i.e.*, the O–O direction, and that the parameters of the x and z axes are averaged by the rapid rotation of the molecule. As the temperature increases, the absorption peak associated with the y axis disappears and the spectrum tends to become a triplet splitting with equal intensities, indicating that the rotation around the x and z axes becomes important.

According to theoretical calculations of the electro-

1) Presented at the symposium of ESR, Tokyo, October, 1970.

2) For examples a) J. J. Rooney and R. C. Pink, *Proc. Chem. Soc.*, **1961**, 70; *Trans. Faraday Soc.*, **58**, 1632 (1962). b) K. B. Kazanskii, G. B. Pariiskii, I. V. Aleksandrov, and G. M. Zhidomirov, *Solid State Physics (USSR)*, **5**, 649 (1963). c) D. N. Stamires and J. Turkevich, *J. Amer. Chem. Soc.*, **86**, 749 (1964). d) C. M. Muha, *J. Phys. Chem.* **71**, 633, 640 (1967). d) G. B. Carbutt, H. D. Gesser, and M. Fujimoto, *J. Chem. Phys.*, **48**, 4605 (1968).

3) H. Zeldes and R. Livingston, *J. Chem. Phys.*, **35**, 563 (1961).

4) J. Tateno and K. Gesi, *ibid.*, **40**, 1317 (1964).

5) P. W. Atkins, N. Keen, and M. C. R. Symons, *J. Chem. Soc.*, **1962**, 2873.

6) C. Chachaty, *J. Chem. Phys.*, **62**, 728 (1965).

7) W. C. Mosley and W. F. Moulton, *ibid.*, **43**, 1207 (1965).

8) T. J. Schaafsma, G. A. V. D. Velde, and J. Kommandeur, *Mol. Phys.*, **14**, 501 (1968).

9) J.R.Brailsford and J.R.Morton, *J. Magnetic Resonance*, **1**, 575 (1969).

10) P.H.Kasai, W. Weltner, Jr., and E. B. Whipple, *J. Chem. Phys.*, **42**, 1120 (1965).

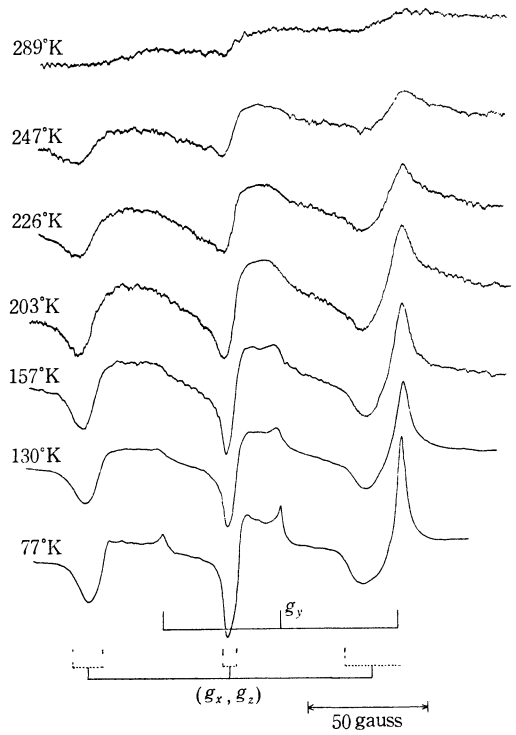

Fig. 1. ESR spectra of NO_2 adsorbed on the silica-gel surface at various temperatures.
Field increases from left to right.

nic structure of the NO_2 molecule,[13-17] it can be considered that a large net negative charge exists in the two oxygen atoms in the molecule. In view of the fact that NO_2 prefers to rotate about the O–O direction on the silica-gel surface, it is reasonable to consider that a hydrogen bond formed between the oxygen of the NO_2 molecule and OH groups on the silica-gel surface may play an important role in the interaction

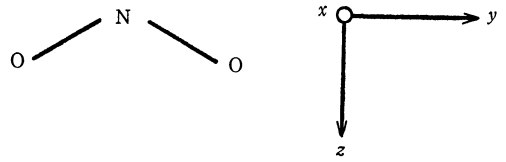

Fig. 2. Coordinate system for NO_2.

of the NO_2 molecule and the silica-gel surface. This model permits the rotation of the NO_2 molecule around the O–O direction. Previously Rozenberg *et al.*[18] pointed out, on the basis of experiments on the adsorption capacity of the silica gel as a function of the dehydration temperature, that the hydrogen-bond force may participate in the adsorption of NO_2 on the silica-gel surface. Our conclusion from the ESR experiments agrees with their result.

Recently, a study of NO_2 adsorbed in synthetic zeolites was reported by Pietrazah *et al.*[19] They observed temperature-dependent ESR spectra and explained them in terms of a hindered rotation of the molecule. However, it has been shown that there was no prefered axis of the rotational freedom for NO_2 adsorbed in synthetic zeolites. It is interesting that the silica-gel system shows a distinct contrast to their results in that, on the silica-gel surface, NO_2 is preferred to rotate about the O–O direction.

Structure of NO_2 on Silica Gel. In the NO_2 molecule, the odd electron is considered mainly to occupy a $4a_1$ molecular orbital constructed from nitrogen $2s$ and $2p_z$, and oxygen $2p_y$ and $2p_z$ atomic orbitals, having the form[5,13-17];

$$\Psi(4a_1) = a_N(2s)\Psi_N(2s) - a_N(2p_z)\Psi_N(2p_z) + a_O(2s)\{\Psi_{O1}(2s) + \Psi_{O2}(2s)\} + a_O(2p_y)\{\Psi_{O1}(2p_y) - \Psi_{O2}(2p_y)\} + a_O(2p_z)\{\Psi_{O1}(2p_z) + \Psi_{O2}(2p_z)\}. \quad (1)$$

Table 1. Magnetic parameters of NO_2 in various media

Medium	g Values			Hyperfine interaction (in MHz)				Reference
				Anisotropic components				
	g_x	g_y	g_z	A_x	A_y	A_z	A_{iso}	
$NaNO_2$(77°K)	2.0057	1.9910	2.0015	−14.77	−22.17	+37.03	+153.2	3
$NaNO_2$(293°K)	2.0059	2.0052	2.0055	− 9.5	−19.0	+28.6	+111.71	4
Ice (77°K)	2.0066	2.0020	2.0022	−17.64	−19.63	+37.55	+159.24	5
Nitromethane (77°K)	2.0047	1.9915	2.0011	−13.8	−22.1	+36.0	+146.4	6
$AgNO_3$ (77°K)	2.0090	1.9978	2.0039	−17.5	−21.8	+37.3	+157.9	7
N_2O_4 (77°K)	2.0054	1.9913	2.0015	−13.75	−19.79	+33.62	+154.61	8
Adsorbed on ZnO (77°K)	2.007	1.994	2.003	− 7.0	−21.1	+28.0	+153.1	11
Adsorbed on silica gel (77°K)	(2.004)[a]	1.9907	(2.004)[a]	(+9.56)[a]	−19.12	(+9.56)[a]	+156.1	This work
NO_2 (gas) (293°K)	2.0062	1.9910	2.0019	−18.73	−19.77	+38.50	+146.5	12

a) Averaged value for x and z components.

11) R. D. Iyengar and V. V. Subba Rao, *J. Amer. Chem. Soc.*, **90**, 3267 (1968).
12) G.R.Bird, J.C. Baird, A.W. Jache, J.A. Hodgson, R.F. Curl, A.C.Kunkle, J.W.Bransford, J.Rastrup-Andersen, and J.Rosenthal, *J. Chem. Phys.*, **40**, 3378 (1964).
13) R.S.Mulliken, *Rev. Mod. Phys.*, **14**, 204 (1942).
14) K.L.McEwen, *J. Chem. Phys.*, **32**, 1801 (1960).
15) K.L.McEwen, ibid., **34**, 547 (1961).
16) M. Green and J. W. Linnett, *Trans. Faraday Soc.*, **57**, 1 (1961).
17) H.Kato, This Bulletin, **37**, 1710 (1964).
18) G. I. Rozenberg and L. I. Kuznetsov-Fetisov, *Tr. Kazan. Khim. Tekhnol. Inst.*, **34**, 12 (1965).
19) T. M. Pietrzak and D. E. Wood, *J. Chem. Phys.*, **53**, 2454 (1970).

The contribution of the nitrogen $2s$ orbital to the $4a_1$ orbital can be estimated from the observed isotropic part of the nitrogen hyperfine splitting constants by the following expression:

$$A_{Iso} = a_N^2(2s)(8\pi/3)g\beta g_N\beta_N\Psi_{N(2s)}(0)^2 \quad (2)$$

with:

$$\Psi_{N(2s)}(0)^2 = 34.0\times 10^{24}\,cm^{-3}.$$

On the other hand, the anisotropic part in the hyperfine interaction of an odd electron in the $2p_z$ component of the $4a_1$ orbital with the nitrogen nucleus can be expressed by the diagonal tensor, A_1, axially symmetric:

$$A_1 = \begin{pmatrix} -\alpha & & \\ & -\alpha & \\ & & 2\alpha \end{pmatrix} = (2/5)a_N^2(2p_z)g\beta g_N\beta_N\langle r^{-3}\rangle \begin{pmatrix} -1 & & \\ & -1 & \\ & & +2 \end{pmatrix}. \quad (3)$$

However, the experimental anisotropic hyperfine tensors obtained for the immobile NO_2 molecules in the solid matrices are usually not axially symmetric but are resolved into two axially symmetric tensors, A_1 and A_2 (symmetric about the x axis). Thus:

$$A_2 + A_1 = (2/5)g\beta g_N\beta_N\langle r^{-3}\rangle \times \left\{a_N^2(2p_x)\begin{pmatrix} +2 & & \\ & -1 & \\ & & -1 \end{pmatrix} + a_N^2(2p_z)\begin{pmatrix} -1 & & \\ & -1 & \\ & & +2 \end{pmatrix}\right\}. \quad (4)$$

A_2 has been explained as arising from the configuration interaction of the ground state with an excited state involving $2b_1 \leftarrow 1b_1$ excitation. When Dousmanis's value[20] for $\langle r^{-3}\rangle_{2p} = 22.5\times 10^{24}\,cm^{-3}$ is used, one can calculate the contribution of the nitrogen $2s$ and $2p_z$ orbitals to the $4a_1$ orbital. From the estimated $a_N(2s)$ and $a_N(2p_z)$, the ONO angle may be calculated, assuming the usual relationship:[21]

$$\angle ONO = 2\cos^{-1}(k^2+2)^{-1/2}, \quad (5)$$

where:

$$k^2 = a_N^2(2p_z)/a_N^2(2s).$$

The experimental hyperfine splitting constants being used, the ONO angle of the NO_2 molecule in the gas phase can be calculated to be 135.5°. In the case of the adsorbed state of the NO_2 molecule treated here, however, we cannot make such a calculation, since the x, y, and z components of the anisotropic hyperfine interaction cannot be obtained separately. However, if we compare the experimental hyperfine coupling constants with the data for NO_2 in the gas phase in Table 1, it is apparent that the magnitude of the isotropic part of the nitrogen hyperfine interaction is larger in the adsorbed state than in the gas phase, while the anisotropic part in the adsorbed state is smaller than those in the gas phase. This suggests that the contribution of the nitrogen $2s$ orbital to the $4a_1$ orbital decreases, and that the nitrogen $2p_z$ contribution may increase by adsorption from the gas phase. It is estimated, therefore, that the ONO angle may decrease by adsorption on the silica gel from the gas phase, although the change in the angle is small, *i. e.*, about 4–5°.

Conclusion

It has been found that NO_2 adsorbed on the silica-gel surface shows temperature-dependent ESR spectra. The low-temperature spectra can be explained as arising from the NO_2 molecule rotating around the O–O direction. As the temperature increases, the spectra indicate that the rotation around the other two axes become important. It is estimated from the observation that a hydrogen-bond force between the oxygen of NO_2 and OH groups on the silica-gel surface plays a part in the NO_2-silica-gel interaction. It has also been shown that the ONO angle might become smaller when NO_2 is adsorbed on the silica-gel surface from the gas phase.

The authors wish to thank Dr. Hiroshi Utsugi for his helpful discussions.

20) G. C. Dousmanis, *Phys. Rev.*, **97**, 967 (1955).
21) C. A. Coulson, *Victor Henri Commemoratif, Contribution a l'Etude de la Structure Moleculaire*, **1948**, p. 15.

On the Factors Determining the Molecular Arrangement in Crystalline Ethylene

Masao HASHIMOTO, Michiko HASHIMOTO, and Taro ISOBE

The Chemical Research Institute of Non-Aqueous Solution, Tohoku University, Sendai

(Received March 30, 1971)

The orientation-dependent potential energy of the ethylene crystal was calculated using a somewhat modified expression for the dispersion energy in the case of non-axially symmetric molecules. It was concluded that the main force which determines the angle between the *bc* plane and the C=C bond axis in the ethylene crystal is the dispersion; on the other hand, it is the quadrupole-quadrupole interaction which determines the angle between the *ab* plane and the C=C bond axis. The expected molecular arrangement in the crystalline ethylene belongs to the space group $P2_1/n$, this is consistent with the conclusion obtained from the spectroscopic data.

Kihara[1-4] has suggested, in his brilliant models, that the molecular arrangement in some molecular crystals depends upon the electrostatic multipole interactions. On the other hand, Craig *et al.*[5,6] concluded that, in the benzene and the naphthalene crystals, the molecular arrangement depends upon a minimization of intermolecular hydrogen-hydrogen repulsions rather than upon the quadrupole-quadrupole and the dispersion energies.

In a previous paper[7] (designated I henceforth), we have found that the electrostatic multipole, the intermolecular hydrogen-hydrogen repulsion, and even the dispersion interaction energies seem to play an important role in determining the molecular arrangement. There remain some ambiguities in determining the factor effective for the molecular arrangement in molecular crystals. Therefore, it is necessary to investigate other molecular crystals from this point of view.

In the present investigation we have studied the refinement of the crystal structure of ethylene, of which both spectroscopic[8-13] and theoretical investigations using the non-bonded atom-atom pair potentials[14] have already been made. We have calculated the orientation dependence of the lattice energy of the crystalline ethylene by means of the same method as before (see I).

It was concluded that the main force which determines the angle between the *bc* plane and the C=C bond axis in the ethylene crystal is the dispersion interaction; on the other hand, it is the quadrupole-quadrupole interaction which determines the angle between the *ab* plane and the C=C bond axis. These results obtained were then compared with the results obtained by the use of the Lennard-Jones-type non-bonded atom-atom interaction potential. All the numerical calculations were made at Computer Center of Tohoku University.

Theoretical

Dispersion Energy. Since the ethylene molecule has a non-axial symmetry, the expression (1) of the dispersion energy for axially-symmetric molecules must be modified:

$$W_{\mathrm{disp}} = -[(A-2B+C)\{\sin\theta\sin\theta'\cos(\phi-\phi') - 2\cos\theta\cos\theta'\}^2 + 3(B-C)(\cos^2\theta+\cos^2\theta') + 2(B+2C)]/R^6, \quad (1)^{15}$$

where $A=e^2\alpha_{\parallel}(QM)_{\parallel}/4$, $B=e^2\alpha_{\parallel}\alpha_{\perp}(QM)_{\parallel}(QM)_{\perp}/2\alpha_{\parallel}(QM)_{\perp}+\alpha_{\perp}(QM)_{\parallel}$, and $C=e^2\alpha_{\perp}(QM)_{\perp}/4$. $(QM)_{\parallel}$ and $(QM)_{\perp}$ are the quantum mechanically-calculable averages (see 1).

In the non-axially symmetrical ethylene molecule, the three components of the molecular polarizability are written in terms of α_x, α_y, and α_z in the cartesian coordinate, where α_z is along the C=C bond; α_y, along the molecular plane, and α_x, along the axis perpendicular to it. $\alpha_{\parallel}$ and $\alpha_{\perp}$ may be expressed as follows:

$$\alpha_{\parallel}=\alpha_z;\ \alpha_{\perp}=(\alpha_x\cos\beta+\alpha_y\sin\beta)/2. \quad (2)$$

β is the angle of the rotation of the molecular plane around the C=C bond axis. In the same way, the modified (QM)'s may be written as follows:

$$(QM)_{\parallel}=(QM)_z;\quad (QM)_{\perp}=\{(QM)_x\cos\beta+(QM)_y\sin\beta\}/2 \quad (3)$$

Then, A, B, and C in Eq. (1) are replaced by new α's and (QM)'s. Thus, Eq. (1) has ben modified to be applicable to the case of non-axial symmetry.

Other Interactions. Quadrupole-quadrupole, the non-additive three body, and the overlap repulsion interactions are treated in exactly the same way as in I. The quadrupole moment of the ethylene molecule used in the present work is $\pm1\times10^{-26}$ e.s.u., which was determined approximately by Smith.[16,17]

The Axilrod and Teller expression for three-body interaction must be modified before it can be applied

1) T.Kihara, *J. Phys. Soc. Japan*, **15**, 1920 (1960).
2) T.Kihara, *Acta Cryst.*, **16**, 1119 (1963).
3) T. Kihara, *ibid.*, **21**, 877 (1966).
4) T. Kihara, *ibid.*, **A26**, 315 (1970).
5) D. P. Craig, R. Mason, P. Pauling, and D. P. Santry, *Proc. Roy. Soc.*, **A286**, 98 (1965).
6) D. P. Craig, P. A. Dobosh, R. Mason, and D. P. Santry, *Discuss. Faraday Soc.*, **40**, 110 (1965).
7) M. Hashimoto, M. Hashimoto, and T. Isobe, This Bulletin, **44**, 649 (1971).
8) C. Brecher and R. S. Halford, *J. Chem. Phys.*, **35**, 1109 (1961).
9) D. A. Dows, *ibid.*, **36**, 2833 (1962).
10) M. Brith and A. Ron, *ibid.*, **50**, 3053 (1969).
11) D. A. Dows, *ibid.*, **36**, 2836 (1962).
12) M. E. Jacx, *ibid.*, **36**, 140 (1962).
13) S. M. Blumenfeld, S. P. Reddy, and H. L. Welsh, *Can. J. Phys.*, **48**, 513 (1970).
14) G. Taddei and E. Giglio, *J. Chem. Phys.*, **53**, 2768 (1970).
15) F. London, *J. Phys. Chem.*, **46**, 305 (1942).
16) W. V. Smith, *J. Chem. Phys.*, **25**, 510 (1956).
17) A. D. Buckingham, *Quart. Rev.*, **13**, 183 (1959).

to the anisotropic molecule. This was done by Stogryn,[18] but the numerically-calculable form was not given there. This will be published elsewhere by the present authors in this series of investigations. At this time, therefore, we will content ourselves with discussing its order of magnitude.

Numerical Calculation

In Table 1, the calculated values of the (QM)'s and α's are indicated. The (QM)'s were calculated as usual (see I), while the α's were calculated by using bond polarizabilities[19].

Table 1. The anisotropies of quantum mechanically calculable average and polarizability of ethylene molecule. The C=C bond axis is along the z-axis

	(QM) a.u.	α cm^3
x	23.882	39.6×10^{-25}
y	18.560	33.8×10^{-25}
z	26.270	54.4×10^{-25}

We start from the structure determined by Bunn.[20] Consider three kinds of molecular rotation. The first is the deflection of the C=C bond axis from the *ab* plane, the second is the deflection of the molecular plane from the *bc* plane, and the last is the rotation of the molecular plane around C=C bond axis. These angles of rotations are indicated in terms of δ, γ, and β respectively (see Fig. 1). In Fig. 1, there are indicated the twelve first neighbour molecules. They are between 4.5 and 6.5 Å away from the central molecule, O. The second neighbours are between 7.4 and 12.9; the third, between 11.1 and 19.4; the fourth, between 15.0 and 25.8, and the fifth, between 19.1 and 32.3 Å, away from the O molecule. We calculated the dispersion and quadrupole-quadrupole interaction energy for the molecules up to fifth neighbours, but the repulsion energy for the first neighbours only.

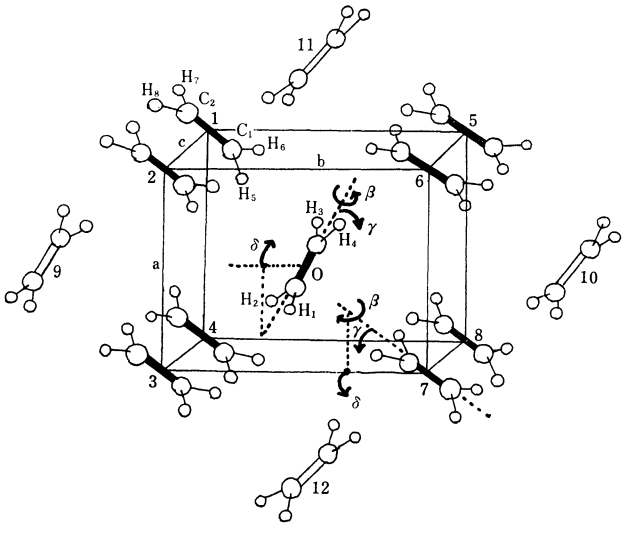

Fig. 1. The starting positions of carbon and hydrogen atoms in crystalline ethylene.
○···carbon atoms; o···hydrogens. a=4.89Å, b=6.46Å, and c=4.14Å.

Results and Discussion

Figure 2 indicates the β-dependency of the interaction energies when δ and γ are fixed at the values of Bunn's structure. The arrows show the values of β, which correspond to Bunn's structure and the spectroscopic structure.[13] From Fig. 2 it may be concluded that the factor determining the molecular orientation around the C=C bond axis is mainly the minimization of the dispersion energy. This confirms the non-axial symmetry of the polarizability of the ethylene molecule about the C=C bond axis.

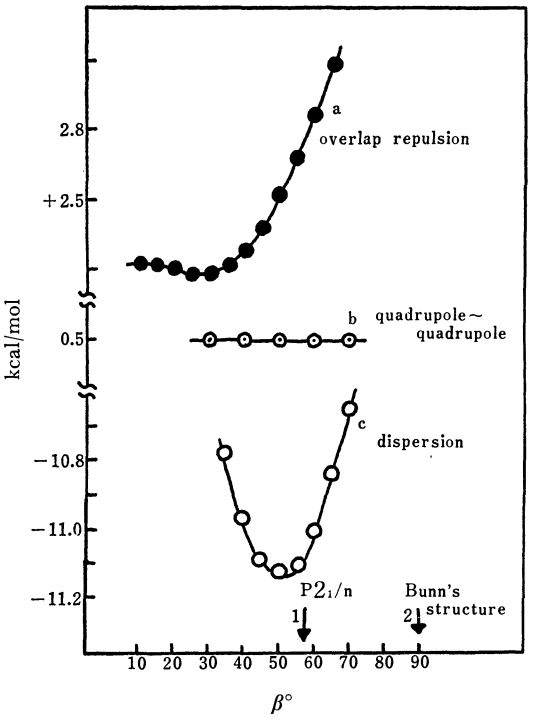

Fig. 2. Variations of interaction energies with the angle of rotation around the C=C bond axis.
a: overlap repulsion; b: quadrupole-quadrupole; c: dispersion interaction.
The arrows 1 and 2 indicate the values correspond to the spectroscopic and Bunn's structures, respectively.

Fixing the β value at the value indicated in Fig. 2, we calculated the δ- and γ-dependencies. The results are indicated in Fig. 3 and 4 respectively. The arrows in these figures also have the same meaning as in Fig. 2. It may be concluded from Fig. 3 that the dispersion interaction mainly determines the angle between the molecular plane and the *bc* plane. We have concluded from Fig. 4 that the angle between the C=C bond axis and the *ab* plane is mainly determined by the quadrupole-quadrupole interactions.

The above conclusions are also confirmed from another point of view. If we approximate the mo-

18) D. E. Stogryn, *J. Chem. Phys.*, **52**, 3671 (1970).
19) J. O. Hirschfelder, C. F. Curtiss, and R. B. Bird, "Molecular Theory of Gases and Liquids," John Wiley & Sons, Inc., N. Y. (1954), p. 951.
20) C. W. Bunn, *Trans. Faraday Soc.*, **40**, 23 (1944).

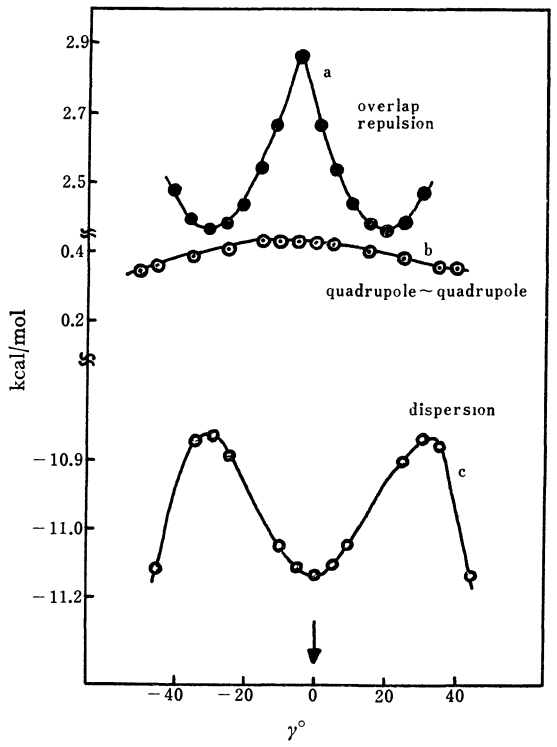

Fig. 3. Variations of interaction energies with the angle of deflection from *bc* plane.
a: overlap repulsion; b: quadrupole-quadrupole; c: dispersion interaction.

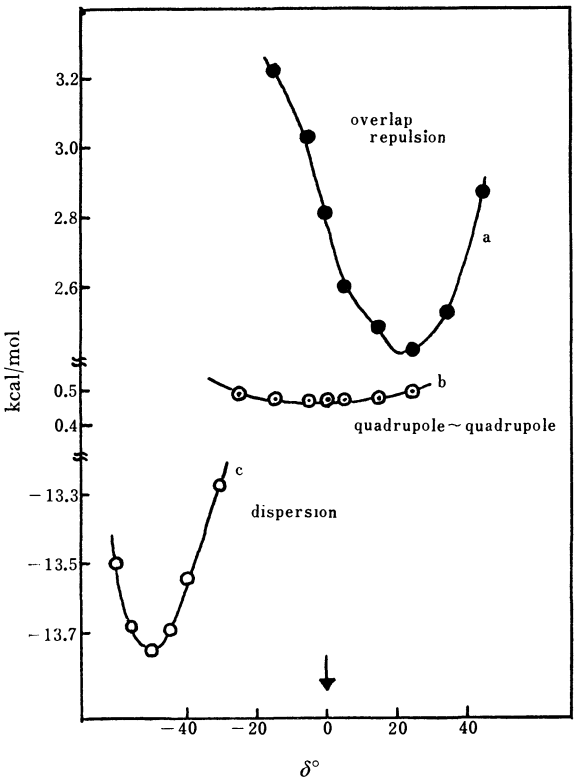

Fig. 4. Variation of interaction energies with the angle of deflection from *ab* plane.
a: overlap repulsion; b: quadrupole-quadrupole; c: dispersion interaction

lecular interaction by the non-bonded atom-atom interaction of the type of Lennard-Jones,

$$v(r) = \sum_j (b_j/r_j^{12} - a_j/r_j^6), \quad (4)$$

where the parameters, a_j and b_j, have been chosen[21] so as to give the best fit with second virial coefficient data of methane. The j summation is extended to all pairs of atoms in the two molecules. Equation (4) is further summed up to fifth neighbours in the crystal.

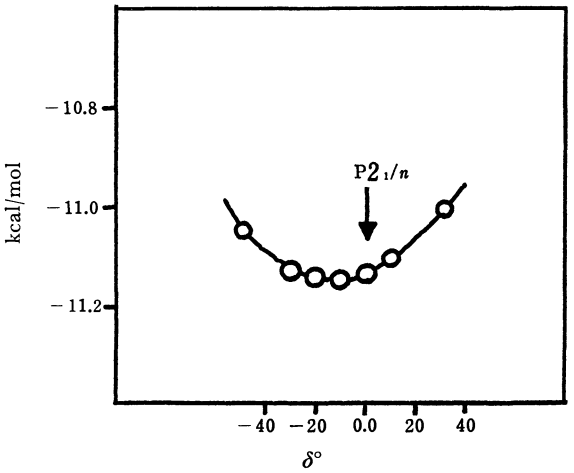

Fig. 5. Variation of Lennard-Jones interaction energy with the angle of deflection from *ab* plane.

Figure 5 indicates the δ-dependency of the $v(r)$. Since the deviation of δ from the experimental value is found to be about 10°, the interaction expressed by Eq. (4) can not explain the experimental δ value. Therefore, quadrupole-quadrupole interaction is necessary to explain the experimental δ value.

It can be concluded from the above results that the main force which determines the angle between the *bc* plane and the C=C bond axis in the ethylene crystal is the dispersion interaction; on the other hand, it is the quadrupole-quadrupole interaction which determines the angle between the *ab* plane and the C=C bond axis. It can also be concluded that the molecular orientation around the C=C bond axis is mainly determined by the dispersion interaction and that the angle of rotation around the C=C axis is nearly equal to the experimental one. This structure belongs to the $P2_1/n$ space group.

The role of the three-body interaction, which is estimated to be of the order of 0.2 kcal/mol if the ethylene molecule has spherical symmetry and which is too large to be neglected, may be important, since it is perhaps strongly orientation-dependent in such anisotropic molecules as ethylene. However, a good estimate of the accuracy of three-body interaction for asymmetric molecules is difficult to make at the present time and must remain a problem for the future.

The authors wish to thank Dr. Masamoto Iwaizumi for his helpful discussions.

21) N. G. Parsonage and R. C. Pemberton, *Trans. Faraday Soc.*, **63**, 311 (1967).

The Ultraviolet Absorption Spectra of Olefins Adsorbed on the Platinum Catalyst

Yuko SOMA

Department of Pure and Applied Sciences, College of General Education, The University of Tokyo, Komaba, Meguro-ku, Tokyo

(Received April 12, 1971)

The ultraviolet absorption spectra of olefins adsorbed on the platinum catalyst supported on silica were studied. By comparing the absorption bands of olefins adsorbed on the platinum catalyst with the chrage-transfer bands of platinum-olefin complexes, the observed bands could be interpreted as being due to the electronic transition from filled platinum 5*d* orbitals to the empty π^* orbital of adsorbed olefins.

The adsorption of olefins on platinum catalysts in relation to hydrogenation has been studied by many workers with various techniques. The structure of adsorbed species on metal catalysts has thus far been elucidated mostly using infrared spectroscopy. Sheppard and his co-workers investigated the adsorption of olefins on a platinum, nickel, or palladium catalyst by infrared spectroscopy, and concluded that the CH_2M–CH_2M type was the structure of the main chemisorbed species on the metal catalysts.[1] By low-energy electron–diffraction studies of ethylene adsorption on the platinum single crystal, Somorjai concluded that ethylene was adsorbed with a C_2H_4 structure on Pt(111) and (100), while Merill explained the adsorbed species on Pt(111) as C_2H_2+2H.[2,3]

Those investigations were concerned with the structure of adsorbed species on the catalyst, knowledge of which was essential to elucidate the reaction mechanism on the catalyst. In addition to this, the understanding of the bonding nature or the electronic interaction between the catalyst and the adsorbed species is very important in the study of the detailed nature of the catalytic reactions.

In the present work, the electronic spectra of olefins adsorbed on the platinum catalyst were studied in an attempt to clarify the bonding nature between adsorbed olefins and the catalyst. The spectra were interpreted as charge-transfer bands due to the electronic transition from platinum to adsorbed olefins; to the author's knowledge, those are the first examples of charge-transfer bands between adsorbed species and the catalyst observed. Thus far, the investigation of the electronic spectra of chemisorbed species has been restricted mostly to the intramolecular transitions and to chemisorbed species on metal oxides.

The ultraviolet absorption spectra of olefins adsorbed on silica-alumina have been studied by Webb and other groups, who have explained them in terms of the carbonium ions on oxides.[4] In this paper, it will be reported that, on a metal catalyst, the situation is different from that on oxides, and that the spectra of adsorbed olefins on a platinum catalyst are closely related to those of platinum-olefin complexes, as is the case with the infrared spectra of adsorbed species on metal catalysts; special reference has been made to the metal complexes including identical species among those chemisorbed.

Experimental

The platinum catalyst was prepared from chloroplatinic acid. Chloroplatinic acid (H_2PtCl_6) containing more than 37% of Pt was supplied by Wako Pure Chemical Industries, Ltd., while the supporting oxide, silica, was obtained from the Degussa Co., Ltd.; their surface areas were 360 m^2/g. Silica was dispersed in an acetone solution of chloroplatinic acid, which was then left standing at room temperature until the solvent had evaporated. The resulting powder (metal content of 1.5% by weight) was pressed to form a disk which was cut in a square platelet (12×20 mm, *ca.* 0.1 mm thick). The platelet was placed in a quartz optical cell connected to a vacuum system, as is shown in Fig. 1.

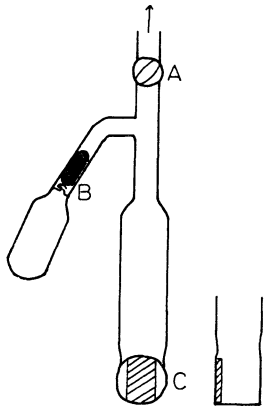

Fig. 1. Optical cell.
A. greaseless cock, B. breakable seal, C. quartz window

The disk was reduced by heat treatment at 350°C in a stream of about 30 cmHg of hydrogen gas for 6 hr and then outgassed at 10^{-6} mmHg at the same temperature for 1 hr to form the catalyst. A silica-supported platinum has been known to reduce the polymerization of olefins as compared with evaporated platinum films. Measured amounts of reaction gases were sealed under a vacuum in a separate compartment attached to the cell through a breakable seal.

The spectra of adsorbed species were recorded in the wavelength range of 250—500 nm with a Hitachi EPS spectrometer by placing a silica disk in the reference beam. At wavelength shorter than 250 nm, the transmission was too small to measure the spectra because of the increased scattering by silica. The spectra of the disks of silica and silica-supported platinum used in these experiments are shown in Fig. 2, the transmission spectra of evaporated platinum film is also shown for comparison.

1) B. A. Morrow and N. Sheppard, *J. Phys. Chem.*, **70**, 2406 (1966), *Proc. Roy. Soc.*, **A311**, 391, 415 (1969).
2) A. F. Morgan and G. A. Somorjai, *J. Chem. Phys.*, **51**, 3309 (1969).
3) D. L. Smith and R. P. Merill, *ibid.*, **52**, 5861 (1970).
4) H. P. Leftin and W. K. Hall, *J. Phys. Chem.*, **66**, 1457 (1962); A. H. Webb, Second International Congress on Catalysis, Reprint II, 65 (1960).

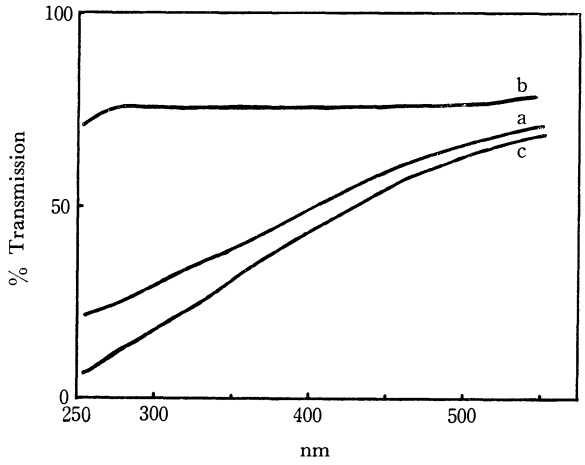

Fig. 2. Spectra of silica disk (a), evaporated film of platinum (b) and silica supported platinum (c).

An ethylene complex of zero-valent platinum, $Pt(PPh_3)_2(C_2H_4)$, was synthesized according to Cook's method.[5] The spectra of this complex were measured in ethylene-saturated cyclohexane, benzene, or an ethyl alcohol solution.

Results

Figures 3–6 show the spectra of adsorbed species in which the back-grounds due to the original catalysts have been subtracted.

When olefins were brought into contact with the platinum catalyst at room temperature, absorption bands immediatly appeared at about 270 and 300 nm, as is shown in Fig. 3 (Curve 1) and Table 1. These bands were stable at least one day if hydrogen was not introduced. After evacuation for 30 sec, the bands changed little. Upon the admission of hydrogen, however, the above bands gradually decreases, and a weak broad band appeared in 340–360 nm (Fig. 3-3). The pressures of olefins and hydrogen were 2–3 cmHg and 5–8 cmHg respectively. The removal of the bands is more rapid for higher olefins; in the case of 1-butene, the bands at 290 and 310 nm disappeared completely 20 min after the admission of hydrogen, whereas in the case of ethylene the bands at 270 and 300 nm remained for 24 hr.

When acetylene was introduced to the catalyst, no bands were observed. On the addition of hydrogen in the cell, spectra similar to those of adsorbed ethylene were observed. As is shown in Fig. 4, the intenisity of the band at 320 nm relative to that of 270 nm was stronger than in the case of ethylene adsorption. These bands decreased slowly on standing, while the weak band in 340–360 nm appeared, as was the case in the olefin hydrogenation.

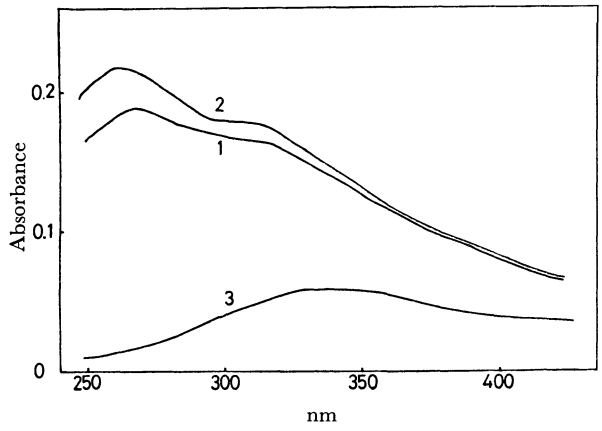

Fig. 3. Spectra of ethylene adsorbed on $Pt\text{-}SiO_2$ at 25°C
1. initial adsorption, C_2H_4 5.23 cmHg
2. addition of 3.57 cmHg of H_2 after evacuating for 30 sec.
3. after overnight hydrogenation

Table 1. Ultraviolet absorption bands of olefins adsorbed on bare platinum surfaces

C_2H_4	270 nm	300 nm
C_3H_6	285	310
$n\text{-}C_4H_8$	290	310
$1\text{-}C_6H_{12}$	295	310

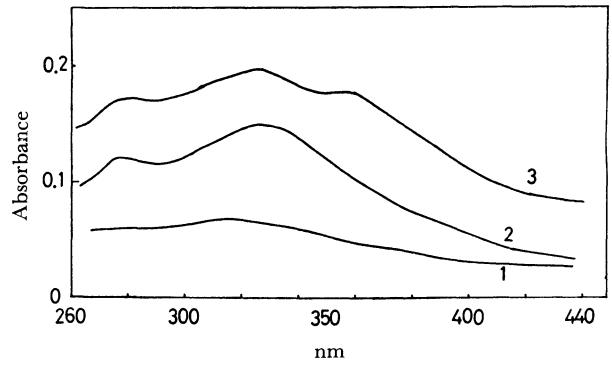

Fig. 4. Spectra of acetylene adsorbed on $Pt\text{-}SiO_2$
1. initial adsorption, C_2H_2 3.77 cmHg
2. addition of 7.60 cmHg of H_2 after evacuating for 30 sec
3. after overnight hydrogenation

When hydrogen was initially adsorbed on a Pt catalyst, a very strong band which was considered to be the absorption due to chemisorbed hydrogen appeared. The band maximum was hidden below 250 nm, and its tail extended to 400 nm, as is shown in Fig. 5. On evacuation for 30 sec and the admission of olefin to the cell at room temperature, the intensity of the absorption bands due to hydrogen remained almost unchanged and weak bands due to olefins around 270 and 300 nm appeared. On standing for a long period, the weak 350 nm band appeared as the intensity of the 270 and 300 nm bands decreased.

At a higher temperature, 90°C, the broad band which might be caused by polymerization of olefins appeared at wavelengths longer than 340 nm.

The spectrum of $Pt(PPh_3)_2(C_2H_4)$ in the ethylene-saturated benzene solution and that of $Pt(PPh_3)_2O_2$ in the benzene solution are shown in Fig. 6. The bands at 276 and 288 nm in the benzene solution appeared at 267 and 288 nm in the cyclohexane solution. The band at a longer wavelength, 288 nm,

5) C. D. Cook and G. S. Jauhal, *J. Amer. Chem. Soc.*, **90**, 1464 (1968).

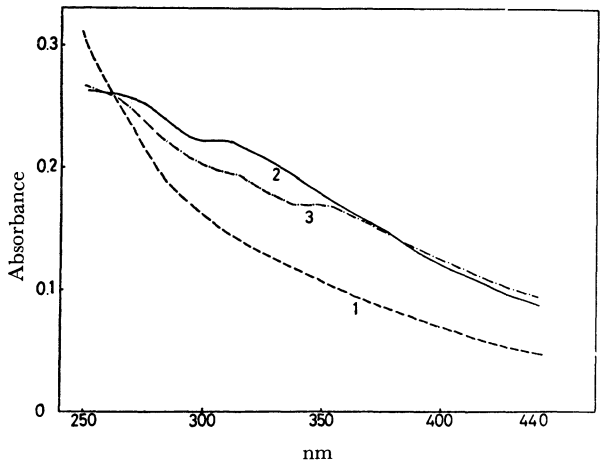

Fig. 5. Spectra of propylene adsorbed on $Pt\text{-}SiO_2$
1. initial adsorption, H_2 6.05 cmHg
2. addition of 2.18 cmHg of C_3H_6 after evacuating for 30 sec
3. after overnight hydrogenation

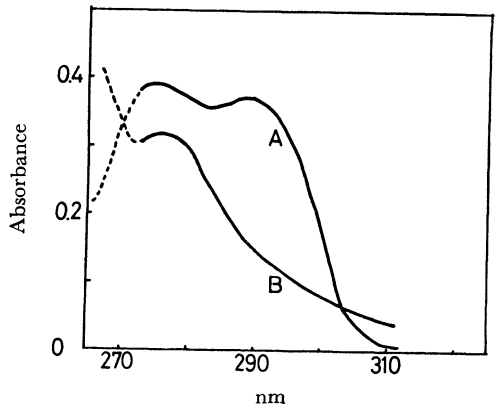

Fig. 6. Spectra of zero-valent platinum complexes
A. $Pt(PPh_3)_2(C_2H_4)$ in ethylene saturated benzene solution
B. $Pt(PPh_3)_2O_2$ in benzene solution

decreased quickly for a few minutes when ethylene had not been saturated in the solution. On the other hand, the band at 276 nm did not change on standing. From the results of the substitution reaction reported by Halpern,[6] it was revealed that the ethylene molecule of $Pt(PPh_3)_2(C_2H_4)$ was quickly replaced by oxygen in solution. Besides, free triphenylphosphine has an absorption band at 260 nm ($\varepsilon=2000$). In connection with these facts, it may be concluded that the band at 288 nm in the benzene solution is a charge-transfer band between platinum and ethylene of $Pt(PPh_3)_2(C_2H_4)$.

Discussion

The spectra of olefin complexes of platinum in the ultraviolet region have scarcely been studied except for those of Zeise's salt, $K^+[PtCl_3(C_2H_4)]^-$. For Zeise's salt, the bands at 299, 267, and 246 nm were assinged to charge-transfer transitions between filled platinum 5*d* orbitals and the empty olefin π^* (antibonding) orbital. The extinction coefficients of the two latter bands, $\varepsilon=3000\ cm^{-1}M^{-1}$, are considerably larger than that of the first one.[7]

In the case of the zero-valent platinum complex, $Pt(PPh_3)_2(C_2H_4)$, a charge-transfer band between platinum 5*d* and the ethylene π^* orbital was observed at 288 nm in the ethylene-saturated cyclohexane solution. Other charge-transfer bands might exist below 250 nm.

The above experimental results of olefin adsorption on platinum suggest that the bands at 270 and 310 nm are due to the absorption related to the adsorbed olefins. The reasons for this are: i) on the admission of olefins, these bands appeared, while they were removed by hydrogenation, and ii) on the admission of acetylene, no absorption bands was observed until hydrogen was introduced. The existence of the olefin structure on the Pt catalyst have been revealed by experiments using infrared spectroscopy or low-energy electron diffraction, as has been indicated in the Introduction.

The infrared spectra of olefin adsorbed on the platinum catalyst have been studied by Sheppard and his collaborators, and a $CH_2M\text{–}CH_2M$-type structure has been proposed as the structure of the main chemisorbed species because the frequencies of the CH stretching vibrations (2920, 2880, 2795 cm^{-1}) are very close to those of saturated hydrocarbons.[1] In the case of ethylene adsorption, this species ($CH_2\text{-}M\text{–}CH_2M$) disappeared after the addition of hydrogen at 20°C, and no spectrum of adsorbed species were detected, but at higher temperatures (95°C) the spectra of the chemisorbed species which was attributed to the existence of the *n*-butyl group persisted after the addition of hydrogen. The spectra of the residual surface species after hydrogenation at room temperature were detected in the case of higher olefins. Thus, the behavior of the ultraviolet spectra observed and the assignments were consistent with those of the infrared spectra of adsorbed olefins.

A comparison of the absorption bands of olefin adsorbed on the Pt catalyst with the charge-transfer bands of olefin complexes of platinum indicates that the bands at 270 and 300 nm are due to the transition between platinum 5*d* and the olefin π^* orbital. The intensities of these bands in the chemisorbed species which correspond to ε of several hundreds

6) J. P. Brick, J. Halpern, and A. L. Pickard, *Inorg. Chem.*, **7**, 2672 (1968), *J. Amer. Chem. Soc.*, **90**, 4491 (1968).

7) R. G. Denning, F. R. Hartley, and L. M. Venazi, *J. Chem. Soc., A*, **1967**, 1322.

8) The number of platinum atoms available in the reaction was estimated using the adsorption data of CO on the Pt-impregenated silica catalyst reported by Hughes,[9] that is, the ratio of the number of CO molecules adsorbed to the number of platinum atoms increased smoothly with the support surface, reaching about 0.6 when the surface area of silica was 360 m^2/g. Assuming that olefin adsorbs on the same sites as CO on platinum, the number of platinum atoms available in the olefin adsorption was reduced to about 10^{18} atoms for a platelet. The extinction coefficients of absorption bands due to adsorbed species were then calculated from the above value.

9) T. R. Hughes, R. J. Houston, and R. P. Sieg, *Ind. Eng. Chem. Process Design Devel.*, **1**, 96 (1962).

of $cm^{-1}M^{-1}$, assuming that all the platinum atoms are involved in the adsorption, are roughly consistent with those of the complexes.[8] The band at 270 nm, which appears at a longer wavelength for the higher olefins, is attributed to the similar transition in ethylene-platinum complexes. The weak band at 350 nm might be due to the occurence of polymerization.

The CH stretching bands of the Pt(0) complex, $Pt(PPh_3)_2(C_2H_4)$, which appear at 3004 and 2964 cm^{-1}, are considerably lower in their frequencies than those of free ethylene, as are those of ethylene adsorbed on the supported platinum catalyst. These experimental facts are consistent with the results of the ultraviolet spectra, suggesting a similarity between the chemisorbed species and the ethylene-Pt complexes.

The fact that the adsorbed species are similar to both the zero-valent and divalent Pt-olefin complexes is not unreasonable, for no clear-cut differences in the bonding between olefin and platinum in the two kinds of salts have yet been revealed to exist.[10,11]

The currently-accepted explanation of the nature of the bonding in metal-olefin complexes is given by the molecular orbital treatment, in which a σ-bond (olefin to metal) and a π-bond (metal-to-olefin back donation) are involved.[11,12] About the relative strengths of the σ and π components of the metal-olefin bond, the work so far suggested that the π-component of the platinum-olefin bond is stronger than the σ-component. The back donation from the central metal atom to the ligand π^* orbital in metal-olefin or metal-acetylene complexes usually reduces the bond order of the π-bonding of the ligand, thence reducing the carbon-carbon stretching frequency. As has been described above, the position of the CH stretching bands of ethylene adsorbed on the supported platinum catalyst and those of ethylene in the Pt(0) complex shift towards those of free ethane, indicating a reduced C=C bond order of ethylene in the chemisorbed species or the complex. A similar reduction in bond order has been reported for the C=C bond of acetylene upon chemisorption on supported platinum or upon the formation of complexes of the $Pt(PPh_3)_2$-(RC=CR′) type.[13,14] Consequently, it may be suggested that the back donation of an electron from platinum to chemisorbed olefins or acetylene plays a fairly important role in the bonding between the metal and the adsorbate.

The author wishes to thank Professor Masaru Nishikawa and Takaharu Onishi for their encouragement and helpful discussions.

10) K. S. Wheelock, J. H. Nelson, L. C. Cusachs, and H. B. Jonassen, *J. Amer. Chem. Soc.*, **92**, 5110 (1970). C. E. Holloway, J. Hulley, B. F. G. Johnson, and G. Lewis, *J. Chem. Soc., A*, **1970**, 1653.

11) F. R. Hartley, *Chem. Rev.*, **69**, 799 (1969).

12) J. W. Moore, *Acta Chem. Scand.*, **20**, 1154 (1966).

13) S. S. Randhava and A. Rehmat, *Trans. Faraday Soc.*, **66**, 235 (1970).

14) E. O. Greaves, C. J. L. Lock, and P. M. Maitlis, *Can. J. Chem.*, **46**, 3879 (1968).

BULLETIN OF THE CHEMICAL SOCIETY OF JAPAN, VOL. 44, 3236—3241 (1971)

The Catalytic Activity and Selectivity of Acidic Metal Salt Catalysts for *n*-Butene Isomerization

Makoto MISONO and Yukio YONEDA

Department of Synthetic Chemistry, Faculty of Engineering, The University of Tokyo, Bunkyo-ku, Tokyo

(Received April 20, 1971)

Double-bond isomerization of *n*-butenes over several supported acidic metal salts such as metal sulfates, perchlorates and phosphates including free acids has been investigated at 60°C with the butene pressure of 14 cmHg. The activity and the selectivity of *cis-trans* isomerization over double-bond migration increased monotonously, as the acid strength of catalysts increased. Acid strength, activity and selectivity of metal salt catalysts increased with the electronegativity of metal ion where free acids were the most strongly acidic and active catalysts ($H^+ > Al^{3+} > Ni^{2+} > Mg^{2+} > Na^+$), and for a given metal ion they increased with the acid strength of the conjugated acid ($ClO_4^- > SO_4^{2-} > PO_4^{3-} > CH_3COO^-$). The activity and selectivity were explained on the basis of a *sec*-butyl carbonium ion mechanism which appears more concerted over weak acids. The active sites for the reaction were suggested to be protonic acid sites closely connected to acid radical.

The simplest and most elementary steps involved in acid catalyzed reactions may be a proton addition to a substrate and its elimination from the protonated complex. It has been established fairly well that the double-bond isomerization of *n*-butenes over most acidic solid catalysts proceeds *via* proton addition to butene followed by its release.[1-3] The *cis-trans* isomerization and the double-bond migration of olefins are referred to as double-bond isomerization, where the hydrocarbon skeleton remains unchanged. Ac-

1) A.Ozaki and K.Kimura, *J. Catal.*, **3**, 395(1964).

2) J. W. Hightower and W. K. Hall, *J. Amer. Chem. Soc.*, **89**, 778 (1967).

3) Y. Kaneda, Y. Sakurai, S. Kondo, E. Hirota, T. Onishi, Y. Morino, and K. Tamaru, The IVth Intern. Congress on Catalysis, Symposium: Mechanism and Kinetics of Complex Catalytic Reactions, Preprint 12, Moscow, 1968.

cording to the presumed mechanism, a proton transfers to butene from the surface of catalyst forming *sec*-butyl carbonium ion, and then a proton goes back to the surface from the ion leaving isomerized or unisomerized butene. The stereoselectivity in the isomerization of 1-butene to 2-butenes over acidic, basic and metal catalysts have been a subject of many investigations,[4,5] but we have found that the selectivity of *cis-trans* isomerization over double-bond migration of 2-butenes was markedly dependent on the acid strength of catalyst.[6] As the acid strength of metal sulfate increased from $MgSO_4$ to $Al_2(SO_4)_3$ and H_2SO_4–SiO_2, the rate of isomerization and the selectivity of *cis-trans* isomerization gradually increased by a factor of 10—10^2. Furthermore, it was demonstrated that the selectivity of each metal sulfate remained almost constant upon changing the preheating temperature, indicating that the nature of metal ion is the predominant factor determining the acid strength of proton on the surface. It was, therefore, possible to estimate the acid strength of the surface of metal sulfate from the electronegativity of metal ion.[7] The estimated acid strength which was qualitatively confirmed using Hammett's indicators showed linear correlations with the catalytic activity and the selectivity of *cis-trans* isomerization.

All these facts prompted us to study further this system in order to find general relationships which connect each other; the nature of the constituent elements of catalyst, the chemical properties of the catalyst surface, the reaction mechanism and the catalytic activity and selectivity. For this purpose, an investigation using a series of catalysts whose chemical nature varies gradually seems useful.

The purposes of the present paper are i) a more precise investigation of the nature of acid sites developing on the surface of the silica-supported metal sulfates and of the relationship between the selectivity and the kinetics of butene isomerization and ii) the extension of the general rules found for metal sulfates to other metal salts.

Experimental

Catalyst Preparation. Silica-supported metal salts were prepared according to the method described before.[6] Silica gel obtained by the hydrolysis of tetraethoxysilane (*ca* 500 m^2/g) was used as support in most cases. Metal sulfates supported on SiO_2 are abbreviated hereafter as Al–S for Al_2SO_4–SiO_2 and Mg–S for $MgSO_4$–SiO_2, *etc.* Unless stated otherwise, the amount of supported metal salts was about 5 wt%.

Butenes, Reaction procedure, Analysis and Acid strength measurement. They were the same as before,[6] except that the circulation systems with the volumes of 124 and 300 m*l* were used in the present work. The catalysts were evacuated for 1 hr at 100°C in reactors preceding the reaction, unless stated otherwise.

Results

Butene isomerization over Al–S and Mg–S. Figure 1 shows the progress of the reaction of *cis*-2-butene over Mg–S (typical weak acid) and Al–S (typical strong acid) plotted according to the first-order equation

$$\ln (x_e - x) = -kt + \ln x_e$$

where x and x_e are the conversion at time t and at equilibrium, respectively. This equation does not hold in rigorous sense, because the averaged rate constant of back reaction from 1-butene and *trans*-2-butene depends on the composition of the products which may vary during the course of reaction (see

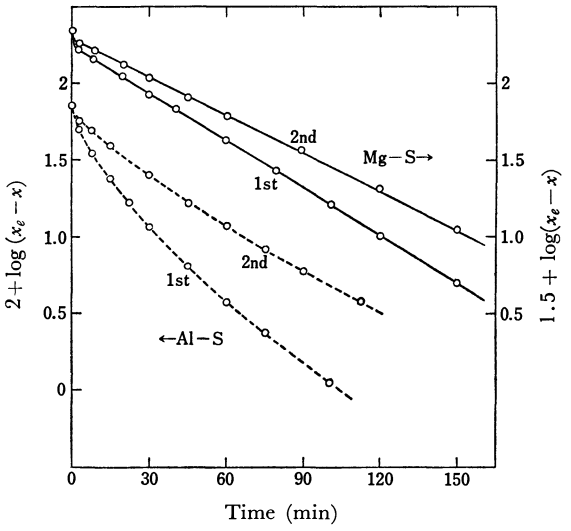

Fig. 1 First-order rate plots for isomerization of *cis*-2-butene over Al-S and Mg-S at 80°C.
Al-S (----, first and second runs), 39 mg
Mg-S (——, first and second runs), 217 mg
Initial pressure: 13.8 cmHg, Circulation system: 124 m*l*

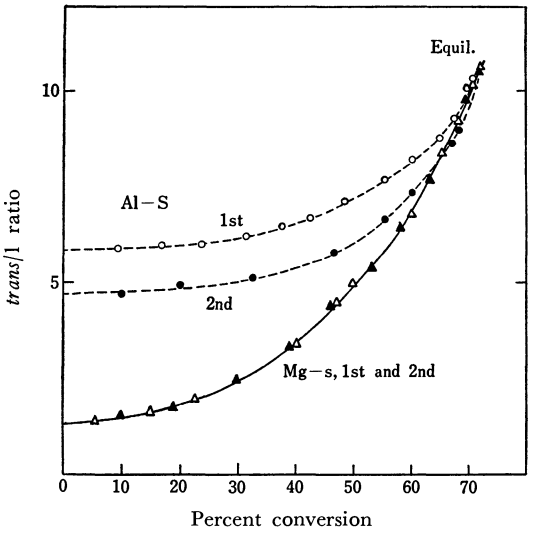

Fig. 2. Composition *vs.* conversion plots for Al-S and Mg-S at 80°C.

4) W. O. Hagg and H. Pines, *J. Amer. Chem. Soc.*, **82**, 2488 (1960).
5) N. F. Foster and R. J. Cvetanovic, *ibid.*, **82**, 4272 (1960).
6) M. Misono, Y. Saito, and Y. Yoneda, *J. Catal.*, **9**, 135 (1967); **10**, 88 (1968).
7) M. Misono, E. Ochiai, Y. Saito, and Y. Yoneda, *J. Inorg. Nucl. Chem.*, **29**, 2685 (1967).

Fig. 2). However, this effect is usually small, so that a linear plot is obtained up to a considerably high conversion, if the reaction is of first order for back and forward directions.[2]

It is seen in Fig. 1 that over Mg–S the reaction follows this equation, except an initial small but rapid deactivation. This plot is very similar to the one obtained by Hightower and Hall over deactivated silica-alumina.[2,8] Repeated runs resulted in little change in the reaction rate over Mg–S. Over Al–S, on the other hand, a rapid and large deactivation occurred at first and it decreased gradually showing a slow time-dependent poisoning, until a nearly constant rate constant was reached after a long period of reaction. The rate at the apparently stationary stage was about half to one-third the initial one.

These trends in deactivation and their contrast between a weak acid and a strong acid catalyst have been observed in the oligomerization of propylene over differently Na-exchanged silica-alumina and Al–S at the temperature range of 100—300°C.[9]

Figure 2 shows the changes in the product composition (given by the *trans*-2-butene/1-butene ratio, *trans*/1) during the course of reaction. The *trans*/1 ratio extrapolated to zero conversion, which was nearly equal to the *cis*/1 ratio obtained from *trans*-2-butene for each catalyst, was high for strong acid catalyst and low for weak acid catalyst, as reported before.[6] The large *trans*/1 ratio for Al–S decreased by the repeated runs as the result of deactivation, while the repeated runs over Mg–S fell on the same line. The end point in Fig. 2 gives the equilibrium ratio of 1:*trans* : *cis*=6 : 66 : 28 (at 80°C). The apparent energies of activation were about 7 kcal/mol for Al–S and about 11 kcal/mol for Mg–S.

Polymerization or coke formation always accompanies the acid catalyzed reaction of olefins.[1,2] Hightower and Hall[2,8] and Brouwer[10] used silica-alumina deactivated by coke formation to obtain reproducible data on the kinetics of butene isomerization. In order to examine the effect of polymerization of butenes (besides the deactivation, there is a possibility of the preferential coke formation of 1-butene which may cause a high *trans*/1 ratio as pointed out by Hightower and Hall[8]), the rates of polymerization of butenes over Al–S and Mg–S were measured by the pressure decrease. Results are summarized as follows: i) pressure decreased more rapidly over Al–S than over Mg–S, reflecting the difference in the extent of deactivation, ii) there was little difference for each catalyst in the rates of pressure decrease among three butene isomers, and iii) the rate of polymerization was less than 10% of the rate of isomerization.

The results of *cis*-2-butene isomerization over silica-supported aluminum sulfate with various aluminum sulfate contents are shown in Fig. 3. The activity increased almost linearly with the aluminum sulfate content up to~3 wt% and then showed saturation at higher content of aluminum sulfate. The selectivity (*trans*/1 ratio), on the other hand, remained almost constant over the whole range of the aluminum sulfate content studied. The acid strength of these catalysts also seems to be constant, as seen from the observed colors of the Hammett indicators over these catalysts

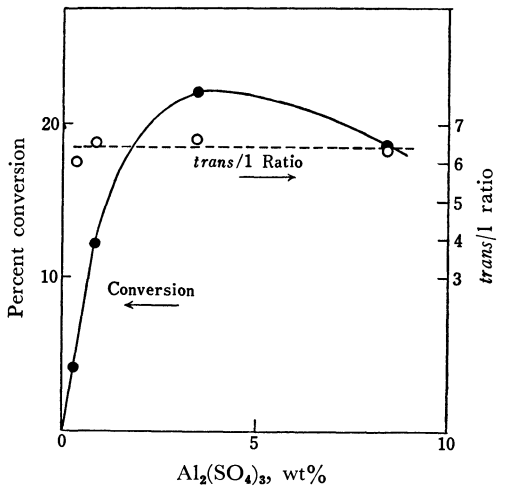

Fig. 3. Effect of amount of supported aluminum sulfate upon catalytic activity and selectivity of *cis*-2-butene isomerization over Al–S at 60°C.

Table 1. The color changes of Hammett's indicators[a]

Catalyst	pK_a of indicator			*trans*/1 ratio
	+1.5[b]	−5.6[c]	−8.2[d]	
$HClO_4$-SiO_2	+	+	+	16—20
$Mg(ClO_4)_2$-SiO_2	+	+	+	7.0
Mg-S	+	−	−	1.2
Al-S (0.3 wt%)	+	+	+	6.0
Al-S (3.5 wt%)	+	+	+	6.6
Al-S-W-2[e]	+	+	+	5.0
Al-S-W-3[e]	+	−	−	2.4
SiO_2[f]	−	−	−	—

a) Acidic colors are indicated by+and basic colors by —.
b) benzeneazodiphenylamine
c) benzalacetophenone
d) anthraquinone
e) see Table 2
f) prepared by hydrolysis of tetraethoxysilane.

Table 2. Effect of extraction of aluminum sulfate from Al-S

Catalyst	Method of extraction	Relative activity	*trans*/1 ratio
Al-S	original	1.0	6.5
Al-S-W-2	extracted by water for 10 min	0.35	5.0
Al-S-W-3	extracted by water several times until the solution became neutral	0.1	2.4
Al-S-W-5	W-3 was left still water overnight	0.05	1.5

8) J. W. Hightower and W. K. Hall, *J. Phys. Chem.*, **71**, 1014 (1967).
9) M. Misono and Y. Yoneda, This Bulletin, **40**, 42 (1967).
10) D. M. Brouwer, *J. Catal.*, **1**, 22 (1962).

as given in Table 1. These facts again support that the selectivity is determined by the acid strength, while the activity by both the acid strength and acid content. Table 2 shows the changes in the activity and the selectivity upon the extraction of aluminum sulfate by water from Al–S. Both of them decreased rapidly upon the repeated washing. This result is in contrast to the fact given in Fig. 3 that the selectivity remained nearly constant upon the variation of the amount of supported aluminum sulfate.

Isomerization of cis-2-*Butene over Silica-supported Metal Salts Other than Metal Sulfate.* The rates of *cis*-2-butene isomerization and the *trans*/1 ratios over silica-supported metal salt catalysts are summarized in Table 3. The rates are given by the conversion at 10 min over 100 mg of catalyst to show the relative activity. Following trends may be remarked in this table: i) For perchlorate salts, the *trans*/1 ratio and the activity increased with the electronegativity of metal ion and the free acid gave the highest values, as observed for metal sulfate catalysts[6] ($H^+ > Ni^{2+} > Mg^{2+} > Na^+$).

Table 3. Isomerization of *cis*-2-butene over various silica-gel supported metal salts at 60°C

Catalyst		Activity[a]	*trans*/1 ratio
Metal sulfate			
Al^{3+}		40	6.5—7.0
Ni^{2+}		10	2.3
Mg^{2+}		2	1.2
Na^+		no reaction	—
Metal perchlorate			
Ni^{2+}	(100)[b]	20	11
	(200)[b]	4	9
	(300)[b]	0.4	8
Mg^{2+}		5	7
Na^+		very low	2
Free acid			
$HClO_4$	(60)[b]	30	16—20
H_2SO_4		40	10
H_3PO_4	(120)[b]	very low	2.5
	(200)[b]	0.1	3
Metal chloride			
Ni^{2+}		very low	1.2
Mg^{2+}		no reaction	—
Metal acetate			
Mg^{2+}		no reaction	—
Others			
Ion exchange resin (Dowex 50W)		—	8—10[c]
p-toluene sulfonic acid		—	8—20[d]

a) % conversion after 10 min over 100 mg of catalyst.
b) Evacution temperature. Others were evacuated at 100°C.
c) Ref. 4.
d) Ref. 6.

ii) For the salts of a given metal ion, they were in the order of the acid strength of the conjugated acid ($ClO_4^- > SO_4^{2-} > PO_4^{3-} > CH_3COO^-$).

iii) As for free acids, both activity and *trans*/1 ratio decreased as $HClO_4 > H_2SO_4 > H_3PO_4$. Over $HClO_4$–SiO_2, *cis*/1 from *trans*-2-butene was ~14 and *cis*/*trans* ratio from 1-butene ~0.7. It is clearly seen that not only the *cis*/1 ratio but also the *trans*/1 ratio exceeded the equilibrium ratio (Fig. 4), although the data rather scattered.[11]

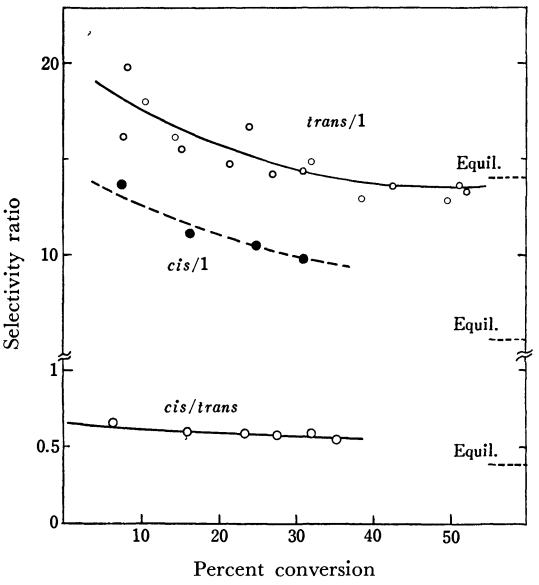

Fig. 4. Composition *vs.* conversion plots of isomerization of butenes over silica-supported perchloric acid at 60°C. *trans*/1 ratio decreased once below the equilibrium ratio due to rapid deactivation and then recovered to the equilibrium one.

iv) Metal chloride and acetate catalysts gave very low or no activity for this reaction.

The acid strength measured by indicators (Table 1) well explains the activity and *trans*/1 ratios as was done in the previous work for metal sulfates.[6] For example, the *trans*/1 ratio increased from 1.2 for Mg–S to 7.0 for $Mg(ClO_4)_2$–SiO_2, where the acid strength of Mg–S was comparable with that of benzeneazodiphenylamine ($pK_A = 1.5$) and $Mg(ClO_4)_2$–SiO_2 was more strongly acidic than anthraquinone ($pK_A = -8.2$).

Finally, the effect of different silica gels as support may be mentioned. Little effect on the activity and the selectivity was observed for the active catalysts such as Al–S. However, there was a little increase in activity in the case of the catalysts having very low activity such as Mg–S and $NiCl_2$–SiO_2 when more acidic silica gel was used as support, although the activities of the supports alone were always much lower than $NiCl_2$–SiO_2.

Discussion

Essential parts of the results obtained previously about the double-bond isomerization of butenes over metal sulfate catalysts were as follows.[6]

i) The acid strength of metal sulfate catalyst was primarily determined by the electronegativity of the

11) Results of several experiments were plotted for *cis*-2-butene isomerization. The scattering of data was due to the rapid deactivation of catalyst, and there existed systematic trend in scattering which will be fully discussed in the forthcoming paper.

constituent metal ion.

ii) The acid strength controls the selectivity of *cis-trans* isomerization over double-bond migration. The activity is determined by both acid strength and content.

iii) The selectivity change was interpreted by the change in the relative rates of proton addition to butene and proton elimination. These rates are expected to vary with acid strength.

The results obtained in the present work for the supported metal perchlorates, sulfates and phosphate (including free acids) (Tables 1 and 3) demonstrate that the acid strength of metal salt catalysts, at least salts of oxy acids, can be controlled not only by changing the metal ion but also by changing the anion. The *trans*/1 ratios and the acid strength given in those tables follow, in general, the expected order of the "intrinsic" acid strength of metal salts. The "intrinsic" acid strength is referred to as the acid strength related directly to the properties of the constituent atoms or groups of the substance. This might be expressed, for example, by the pH of aqueous solution of the metal salts, if one can neglect the leveling effect. If the general trend between the acid strength and the selectivity is applicable to silica-alumina, the *trans*/1 or *cis*/1 ratio over silica-alumina should be as high as those for Al–S and H_2SO_4–SiO_2, since its acid strength is as strong as that of Al–S.[9,12] Reported *trans*/1 or *cis*/1 ratio for silica-alumina ranges from 1 to 7.[1,2,5,8,10] However, it may be noted that Hightower and Hall[8] reported that the *trans*/1 ratio over fresh silica-alumina was about 7, which diminished rapidly down to almost unity by the repeated runs and that most of the previous data were obtained over more or less deactivated catalysts.

Acid Strength and Reaction Mechanism. The selectivity ratio (*trans*/1 or *cis*/1) increased from Mg–S to Al–S with the increase in the catalytic activity. As the equilibrium favors 2-butene formation, secondary isomerization from 1-butene to 2-butene could have effected the high selectivity ratio for active catalysts. However, this possibility can be rejected, since the selectivity ratios higher than the equilibrium ones were found; *e.g.*, *cis*/1 ratios were 14, 10, and 6 for $HClO_4$–SiO_2, H_2SO_4–SiO_2 and Al–S, respectively, where the equilibrium ratio is 5.4, and the *trans*/1 over $HClO_4$–SiO_2 was 16—20, as compared with the equilibrium ratio of 14.4 (Table 3 and Fig. 4). The preferential polymerization of 1-butene as the reason of high *trans*/1 or *cis*/1 ratio suggested by Hightower and Hall[8] is also denied, because this side reaction was less than 10% of the isomerization and little difference was observed among the rates of pressure decrease of three butene isomers. Therefore, the observed selectivity ratio may safely be considered as the ratio of the rates of two paths from a butene isomer. Further, the relationships found among three selectivity ratios for each catalyst, that is, (*trans*/1) (1/*cis*) (*cis*/*trans*)= 1,[4,6] indicate that the reaction orders of isomerizations were nearly identical for each catalyst, so that the observed ratios may be considered as the ratios of the rate constants; *viz.*, *trans*/1, *etc.* are k_{ct}/k_c, *etc.* in the following reaction scheme.

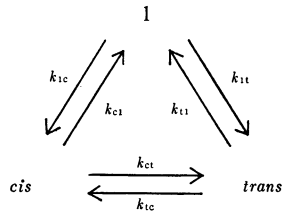

The relative rate constants can be calculated utilizing equilibrium and selectivity ratios as an example for Mg–S at 60°C as follows[4,8]

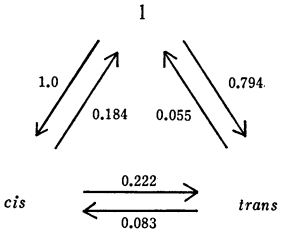

Suppose a simple reaction catalyzed by acid, consisting of a proton addition and elimination,

$$A + H^+ \rightarrow (M) \quad (1)$$

$$(M) \rightarrow B + H^+ \quad (2)$$

where A, B, and M are reactant, product and protonated reaction intermediate, respectively. In step (1), a catalyst acts as an acid and in the next step as a base. As the acid strength increases, the rate will increase initially by the acceleration of step (1) and then diminish upon further increase in the acid strength due to the slow rate of step (2), showing a volcano-type activity pattern.[13,14] This concept may be applied in the present case, since it seems generally accepted that double-bond isomerization of butenes catalyzed by solid acids such as silica-alumina and metal sulfate proceeds through proton addition to form a *sec*-butyl carbonium ion (step(1)) and elimination of proton from the complex (step(2)).[1,2,6,8,10] If one accepts this mechanism, one may expect that over a strong acid the proton addition occurs readily and the carbonium ion is stable. This step would be slow and the ion is unstable over a weak acid. Considering a *sec*-butyl carbonium ion, the proton release from C–H_a would tend to result into *cis*-2-butene formation, from C–H_b into *trans*-2-butene and from one of C–H_c into 1-butene.[8] Since two C_3–H bonds of methylene may be energetically similar and differs from those of methyl (C_1–H_c), it is under-

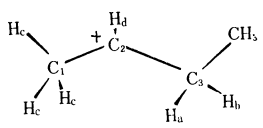

12) J. Take, T. Tsuruya, T. Sato, and Y. Yoneda, to be published.

13) M. Misono, *Shokubai (Catalyst)*, **9**, 252 (1967).

14) O. A. Leffler and E. Grunwald, "Rates and Equilibria of Organic Reactions," John-Wiley and Sons, New York (1963), p. 163.

standable that among various catalysts the *trans*/1 and *cis*/1 ratios were always nearly identical and were different from the *cis*/*trans* ratio which was almost unity.[6]

The changes in 2-/1-butene ratios (*trans*/1 and *cis*/1) may be explained by the variation in the transition state and the relative rates of proton addition and elimination as follows. According to Hammond[15] and Leffler and Grunwald,[14] the transition state of a reaction step more nearly resembles the reactant as the step becomes more exothermic. This postulate calls for, in other words, the transition state of a bond rupture step to involve relatively less bond breakings when the bond is easily broken and relatively more when it is difficult to break. If one applies this postulate to the proton elimination from carbonium ion, the transition state is expected to reflect more the final state, butene, as the ion becomes more stable as over a strong acid. The formation of stable 2-butenes is, therefore, favored over a strong acid. If the carbonium ion is less stable as over a weak acid, the transition state resembles the initial state, the ion, reflecting to a less degree the product, or butene, so that the 2-/1-butene ratio approaches unity. Furthermore, as the acid strength decreases, proton addition would become more difficult and tend to occur almost simultaneously with proton elimination. Then the isomerization reaction will appear more concerted over a weak acid: double-bond migration will increase, relative to *cis-trans* isomerization.

A similar interpretation can be found in the elimination reaction *via* carbonium ion (El mechanism).[16] As the acid strength of a solvent, a nucleophilic reagent or a catalyst decreases, the reaction mechanism changes from El to E2 like mechanism:

$$\text{(El mechanism)}\quad RX + A \rightarrow R^+ + XA$$
$$R^+ \rightarrow \quad R' + H^+$$

By the El mechanism, *sec*-butyl bromide or tosylate gave the butene mixture in the composition of 1 : *trans* : *cis*=5∼7 : 41∼46 : 47∼54 (high 2-/1-butene ratio), while it was 23 : 18 : 59 by E2 mechanism (low 2-/1-butene ratio).[17] When a very unstable carbonium ion is formed as in the elimination of amino group from *sec*-butylamine catalyzed by HNO_2, the composition of butenes was 22 : 25 : 53.[17]

Active Acid Sites for the Double-Bond Isomerization of Butenes. Since 2-/1-butene ratio reflects the acid strength,[6] little variation in the *trans*/1 ratio found upon changing the amount of supported aluminum sulfate (Fig. 3) and the preheating temperature,[6] suggests that a certain and definite interaction between silica gel surface and aluminum sulfate developed the acid sites active for the isomerization. These sites must be protonic (Brönsted type) from the following reasons, although the electronegativity of metal ion which expresses the acid strength of a metal ion as Lewis acid[7] linearly correlated with the selectivity and the catalytic activity.[6]

i) Deuteration of isomerized butenes took place during the reaction over deuterated $NiSO_4$–SiO_2,[1] *p*-toluene sulfonic acid[3] and silica-alumina.[2]

ii) Supported free acids were the most active catalysts and gave the highest *trans*/1 ratios among the series of metal salts of a given acid (Table 3).

iii) $NiCl_2$–SiO_2 and $MgCl_2$–SiO_2 were much less active or inactive as compared to Ni–S or Mg–S. One might be allowed to expect some activity for the formers, if the metal ions themselves are active.

iv) The rate of isomerization decreased upon deuteration of the catalysts (catalyst isotope effect).[18]

This protonic site active for the isomerization is not likely to be a proton in silanol group which may exist and whose acid strength may vary by the metal ion. But it seems to be a proton closely connected to sulfate or perchlorate ion, since 1) the activity and *trans*/1 ratio, as well as the acid strength, strongly depended on the acid strength of anion (Tables 1 and 3), 2) metal chloride catalysts were not active, even though Me–O–Si–OH were reported to exist for these catalysts,[19] and 3) an ion exchange resin (sulfonic acid type)[6] and *p*-toluene sulfonic acid[3] whose acid sites must be SO_3H gave the *trans*/1 ratio and activity as high as H_2SO_4–SiO_2 and $HClO_4$–SiO_2. As the electronegativity represents the power of atom or an ion to attract electron, the role of metal ion may be lowering the electron density of oxygen of –OH, promoting the tendency of the proton to dissociate. The effects of the electronegative group on the acidity was postulated for fluorine treated silanol group.[20] The rapid decrease in the *trans*/1 ratio and the activity upon washing out of aluminum sulfate (Table 2) indicates that the structure of active acid sites is very soluble in water and is, therefore, different from the one reported by Burne et al.[21]

Polymerization on the Surface as the Origin of Deactivation. The pressure decrease observed during isomerization was rapid initially and then the rate reached nearly constant. This process was fast over strong acids and was slow and small over weak acids. These trends closely resemble those found in the case of propylene oligomerization over silica-aluminas with various acid strengths.[9] As in propylene oligomerization and butene isomerization over silica-alumina,[2,8] the polymerization or coke formation from butene is likely to be the primary origin of deactivation in the present case and the acid strength decreased by the deactivation.

The authors are indebted to Professor Y. Saito for helpful discussions. Partial support by the Kawakami Foundation is gratefully acknowledged.

15) G. S. Hammond, *J. Amer. Chem. Soc.*, **77**, 334 (1955).
16) S. Oae, "Elimination Reactions," Tokyo Kagaku Dojin, Tokyo, 1965; J. F. Bunnett, Survey of Progress in Chemistry, Vol. 5 (1969), p. 53.
17) W. B. Smith and W. H. Watson, Jr., *J. Amer. Chem. Soc.*, **84**, 3174 (1962).
18) M. Misono and Y. Yoneda, presented before the 28th Symposium on Catalysis, Osaka, April, 1971; *Shokubai (Catalyst)*, **43**, 22 P. (1971).
19) D. L. Dugger, J. H. Stanton, B. N. Irby, B. L. McConnell, W. W. Cummings, and R. W. Maatman, *J. Phys. Chem.*, **68**, 757 (1964).
20) I. D. Chapman and M. L. Hair, *J. Catal.*, **2**, 145 (1964).
21) K. H. Burne, F. R. Cannings, and R. C. Pitkethly, *J. Phys. Chem.*, **74**, 2197 (1970).

Dependence of ζ-Potential upon Particle Size and Capillary Radius at Streaming Potential Study in Nonaqueous Media[1]

Ayao KITAHARA, Tadashi FUJII, and Seiji KATANO

Science University of Tokyo, Kagurazaka, Shinjiku-ku, Tokyo

(Received April 23, 1971)

The effect of particle size and capillary radius on electrokinetic potential(ζ-potential) was studied in order to check the influence of overlapping of the electrical double layer and radius effect on the measured ζ-potential by the streaming potential method. The streaming potential was measured with varying particle size and capillary radius of glass in the benzene solution of $(C_4H_9)_4NI$. The measurement was carried out over the range where the laminar flow and the Quincke's law hold. The surface conductance was corrected experimentally. ζ-Potential increased with increase of the particle size in the glass column. It was unsuccessful to obtain the ζ-potential independent of the reduced radius of the capillary pore with the Oldham's treatment. ζ-Potential increased with increase of the capillary radius. The increase was elucidated by the Wood's method using the appropriate constants, and the constant ζ-potential which was not affected by the capillary radius was obtained. The value was still different from that obtained by the electrophoretic method, but the difference was considerably small as compared with the previous data.

Electrokinetic potential (ζ-potential) is important as the quantity used in place of surface potential which is necessary to discuss the stability of dispersion or the properties of the electrical double layer, but it is difficult to measure or estimate the ζ-potential on the insulator or the semiconductor. ζ-Potential is usually measured by the electrophoretic method or the streaming potential method. However, the retardation effect and the relaxation effect must be corrected for the former method.[2] The surface conductance and the overlapping of the double layer must be taken into consideration for the latter in order to obtain the proper value. Both values should agree with each other, provided that all proper corrections have been made.

The same system has to be investigated by both methods for comparison, but such study is rare except a few,[3] although the comparison between the streaming potential and the electro-osmosis was done and the coincidence was recognized[4] because of their similar packing column system.

The necessary corrections have to be done for each method to obtain the reliable value of ζ-potential. The correction for the surface conductance was studied for aqueous systems both theoretically and experimentally by Ghosh *et al.*[5] Oldham *et al.* proposed the theory of correcting capillary radius and the surface conductance which was applied successfully to the aqueous and nonaqueous data obtained by other authors.[6] The effect of pore orientation on the cell constant in the pore system of fiber was studied by Mason *et al.* for the streaming potential.[7]

In our laboratory, ζ-potential of the same sample system (barium sulfate powder dispersed in cyclohexane solutions of Aerosol OT) was measured with both the electrophoresis and the streaming potential methods. Both values were widely different.[8] Effects of the surface conductance and the overlapping of the double layer for the streaming potential, which were not corrected, would cause the difference. Fortunately, the thick double layer present in the nonaqueous system makes it easy to study the overlapping.

In this paper, the effect of the overlapping of the double layer was studied experimentally for the nonaqueous system of the particle column and the capillary of glass and data obtained were checked by the present theories. The surface conductance was also corrected experimentally.

Experimental

Samples. A series of spherical glass particles were purchased from the Sugito Seimitsu Glass Co. and further classified with the standard sieves. The diameter range of the samples was tabulated in the 2nd column of Table 1. Glass capillaries of different radii shown in Table 2 were used.

Glass particles were cleaned with mixture of nitric and sulfuric acids and digested on a water bath for 10 hr. After cooling, they were washed repeatedly with de-ionized water until the specific conductivity of the washings was nearly equal to that of the de-ionized water. The particles were dried in an oven at 120°C and extracted with acetone and benzene in turn for 3 hr. They were reheated for 2 hr at 200°C under 10^{-2} mmHg immediately before use. Capillaries were cleaned, washed and dried similarly to the case of particles. After cooling in a desiccator, they were immersed in purified benzene for a while before use.

Benzene used as a solvent was purified and dried from GR grade reagent as usual and finally treated with Molecular Sieves 4A to remove a trace of water, Tetra-*n*-butyl amonium iodide $(C_4H_9)_4NI$ used as an electrolyte in benzene

1) Presented at the 24th Annual Meeting of the Chemical Society of Japan, April, 1971.

2) P. H. Wiersema, A. L. Loeb, and J. Th. G. Overbeek, *J. Colloid Interfac. Sci.*, **22**, 78 (1966).

3) O. Jō and Y. Fujii, *Nippon Kogyo Kaishi* (*J. Mining Inst. of Japan*), **73**, 231 (1957).

4) B. N. Ghosh, *Nature*, **176**, 1080 (1955); *J. Ind. Chem. Soc.*, **39**, 373 (1962); *ibid.*, **39**, 314 (1962).

5) B. N. Ghosh and P. K. Pal, *Trans. Faraday Soc.*, **57**, 116 (1961); B. N. Ghosh, S. P. Moulik, and S. K. Sengupta, *J. Electroanal. Chem.*, **9**, 372 (1965).

6) I. B. Oldham, F. J. Young, and J. F. Osterle, *J. Colloid Sci.*, **18**, 328 (1963).

7) G. B. Biefer and S. G. Mason, *Trans. Faraday Soc.*, **55**, 1239 (1959).

8) A. Kitahara, H. Yamada, Y. Kobayashi, H. Ikeda, and Y. Koshinuma, *Kogyo Kagaku Zasshi*, **70**, 2222 (1967).

Table 1. Particle size of spherical glass particles and reduced capillary radius of glass-packed plug

Sample No.	Diameter (μ)	Reduced radius (μ)
P-1	297—350	20.2
P-2	125—147	13.7
P-3	88—105	12.3
P-4	44—62	7.9
P-5	26—44	5.8

Table 2. Radius of glass capillary

Sample No.	Radius (mm)
C-1	1.45, 1.46, 1.55
C-2	0.95, 1.00, 1.05
C-3	0.44, 0.45
C-4	0.18

was GR grade reagent. The content of water in the benzene solution was below 100 ppm throughout this study.

Apparatus. The streaming potential was measured with an essentially similar apparatus to that used by Dodd *et al.*[9] The cell of the particle system was made of Teflon or glass coated by silicone to prevent surface leakage. Electrodes in the system were perforated stainless steel plates coated by silver. The particle column of 2 $cm^2 \times 0.5$ cm was made by filling about 1.5 g glass particles between both electrodes. The capillary of the length of 25 cm was used as the cell of the capillary system. Platinum wires were placed very closely to both ends of the capillary as electrodes.

Methods. The occurring streaming potential was measured with a vibron voltmeter (DC amplifier of the Takeda Riken Ind. Type TR-85). The electric resistance of the column or capillary filled with the electrolyte benzene solution was measured with a high-resistance measuring apparatus (Modell II-3 of the Hitachi Manufacturing Co.) which can measure up to 10^{15} ohm.

The cell constant of the column or the capillary was determined from the measurement of the conductivity of 0.1 N KCl aq. solution. The measurement was carried out for the same column or capillary after the benzene solution had been thoroughly discharged and washed to avoid the effect of polarization of electrodes. The orientation effect proposed by Mason was not considered because of the sphere particle system.

Results and Discussion

Assurance of Laminar Flow. To ascertain the laminar flow of the solution in the column or capillary, the Darcy's law was examined with the streaming potential apparatus. The law says that

$$V = KP \tag{1}$$

where V is the volume rate of the flowing solution under a driving pressure P and K is the permeability. If the height of the solution column acting as pressure P is h,

$$P = kh (k\text{: constant}), \text{ and } V = -\mathrm{d}h/\mathrm{d}t \ (t\text{: time}) \tag{2}$$

Then Eq. (3) is reduced as follows:

$$\log h = -K't/2.3 + \log h_0, \tag{3}$$

where $K' = kK$ and h_0 is the extrapolated initial height of the solution column. Equation (3) was experimentally confirmed both for the particle column and capillary systems. The relation held over the range of the lower height for the capillary system. The measurement of the streaming potential was carried out within this range. Reynolds number was below 0.1.

Quincke's Law and Time Dependence of Streaming Potential. Next, the applicability of the lineality between the streaming potential (E) and pressure (P) was checked. The Quincke's law was applicable within the pressure range over which the laminar flow was ascertained. The slope of the potential-pressure curve varied with repeated measurements and approached an equilibrium value after 20—24 hr (about 8 measurements), although the constant K' was almost invariable over 24 hr. The time dependence of E/P may be due to cleansing of the wall of the cell and particles or capillary surface and the ion-exchange of particles or capillary. The capillary used once did not show the same streaming potential in repeated experiments. The equilibrium values of E/P were used for the calculation of ζ-potential.

Correction of Surface Conductance. The Helmholtz-Smolchouski's equation taking into consideration of the surface conductance for the capillary radius r is described as follows:

$$\zeta = \frac{4\pi\eta}{D}\frac{E}{P}\left(\kappa_b + \frac{2\kappa_s}{r}\right), \tag{4}$$

where κ_b and κ_s are the bulk and the surface specific conductivity, respectively, and η and D are the viscosity and the dielectric constant of the double layer which are usually substituted by the bulk values. $\kappa_b + \frac{2\kappa_s}{r} = \kappa_c$ for the present nonaqueous system was calculated from the conductivity ($1/R$) of the column or the capillary system filled with the benzene solution of the electrolyte and the cell constant (k_c) whose measurements were described in the experimental part, that is, $\kappa_c = k_c/R$. In the present system, κ_s was much larger than κ_b which had been measured separately in another cell.

Reduced Capillary Radius of Column. The mean reduced capillary radius of the particle column (r) was determined as follows: Poiseuille's law says that

$$V = \frac{n\pi r^4 P}{8\eta l}, \tag{5}$$

where n and l are the number and the length of the capillary, respectively. Ohm's law is expressed as follows:

$$R = \frac{l}{\kappa_b n\pi r^2}. \tag{6}$$

From Eqs. (5) and (6), $r = \sqrt{\frac{8\kappa_b\eta VR}{P}} = \sqrt{8\kappa_b\eta RK}$. (7)

9) C. G. Dodd, J. W. Davis, and F. D. Pidgeon, *J. Phys. Colloid Chem.*, **55**, 684 (1951); R. T. Johnason, P. B. Lorenz, C. G. Dodd, F. D. Pidgeon, and J. W. Davis, *J. Phys. Chem.*, **57**, 40 (1953).

The measurement of r with use of Eq. (7) was carried out with 0.1 N KCl aq. solution. The result was listed on the 3rd column in Table 1.

ζ-Potential of Column System. The change of ζ-potential of the column system with particle size was shown in Fig. 1 for 10^{-5} and 10^{-4} mol/l solutions of $(C_4H_9)_4NI$ in benzene. ζ-potential increased with increase of particle size and appears to approach the saturation value.

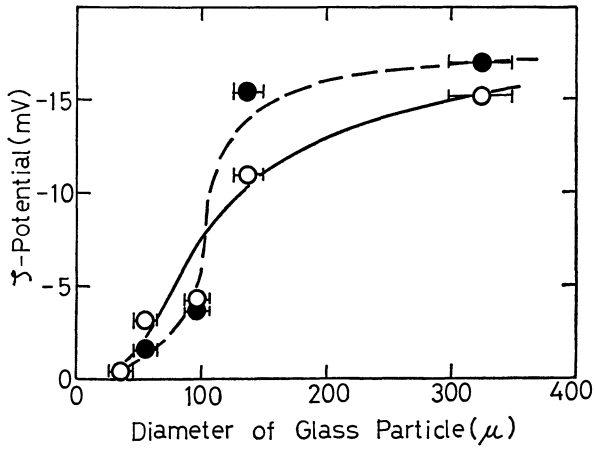

Fig. 1. Change of ζ-potential with particle size of glass in solution of $(C_4H_9)_4NI$ in benzene.
—○—: 10^{-4} mol/l, --●--: 10^{-5} mol/l

The theory proposed by Oldham *et al.*[6] was applied to obtain the ζ-potential independent of particle size. The thickness of the double layer ($1/\kappa$: Debye length) which is necessary for the study was calculated from the data of the specific conductivity.[10] The values were 3.3 μ and 10 μ for 10^{-4} and 10^{-5} mol/l solution system, respectively. The constant ζ-potential independent of the particle size could not be obtained by the Oldham's method. Insufficient reliability of the values of reduced radius for the quantitative calculation and the heterogeneity of pore radius, the contribution of which was investigated by Overbeek *et al.*[11] and by Rutgers *et al.*[12] may be considered as reasons of the failure. Therefore, the measurement for the capillary system was carried out to study the effect of the capillary radius more critically.

ζ-Potential of Capillary System. The contribution of the surface conductance to the total conductance in this system was much larger than that of the bulk conductance similarly to the case of the column system. Hence, the correction by Rutgers *et al.*[13] was improper and inaccurate to do.

ζ-potential calculated from Eq. (4) was depicted against the capillary radius (a) in Fig. 2 for the 10^{-4} mol/l solution of $(C_4H_9)_4NI$ in benzene. It is seen from the figure that ζ-potential depends markedly on the radius, though the data scatter to some extent. Since the value of κa ranges over 55—450 for the capillary system used, the correction of the overlapping of the double layer by the method of Oldham[5] was virtually ineffective to obtain the value independent of the radius.

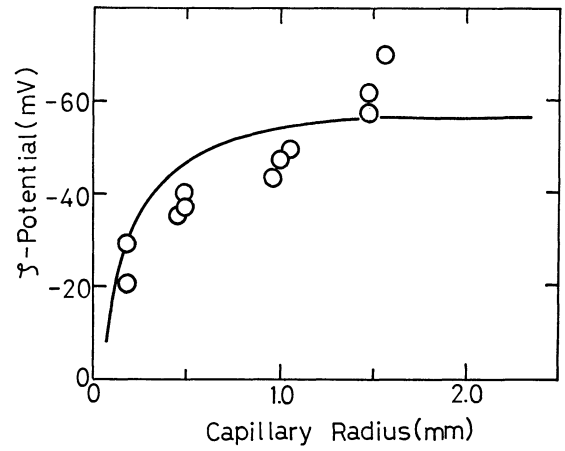

Fig. 2. Change of ζ-potential with capillary radius.
○: Observed values
——: Line by Eq. (9) as $\zeta = -62$ mV, $A = -8.8$ mm

Wood discussed the radius effect over the wide range considering the distribution of charge.[14] The following equation can be obtained from the combination of Eqs. (15), (16), and (22) in the original paper of Wood:

$$\zeta_0 - \frac{2\pi}{Da}\sum_i d_i \Delta M_i = \zeta_{obs}, \tag{8}$$

where ζ_0 and ζ_{obs} are the corrected and observed ζ-potential, respectively, d_i is the distance of the element i from the wall and ΔM_i is the moment of the element. Over the range in which the overlapping of the double layer that should be corrected by the Oldham's method is absent, d_i and ΔM_i have their finite values and they are constant for a fixed concentration of the electrolyte. Then Eq. (8) reduces to Eq. (9):

$$\zeta_0 = \zeta_{obs} + \frac{A}{a}, \tag{9}$$

where A is a constant. This equation was checked with the experimental values in Fig. 3. The linearity between ζ_{obs} and $1/a$ can be approximately recognized. $\zeta_0 = -62$ mV as the corrected ζ-potential and $A = -8.8$ mm were obtained from the least saquares method by the computor. The allowance range of ζ_0 was -62 ± 10 mV from the figure.

Alternatively, the microelectrophoresis of fine glass powders dispersed in the 10^{-4} mol/l solution of $(C_4H_9)_4NI$ in benzene gave -120 mV as the ζ-potential.

10) A. Kitahara, S. Karasawa, and H. Yamada, *J. Colloid Interfac. Sci.*, **25**, 490 (1967); A. Kitahara, T. Komatsuzawa, and K. Kon-no, "Chimie, Physique et Applications Pratiques des Agents deSurface", Vol. II, p. 135, Ediciones Unidas, s.a., Barcelona (1969).

11) J. Th. G. Overbeek and P. W. O. Wijga, *Rec. trav. chim.*, **65**, 556 (1946).

12) A. J. Rutgers and R. Janssen, *Trans. Faraday Soc.*, **51**, 830 (1953).

13) A. J. Rutgers and M. DeSmet, *ibid.*, **43**, 102 (1947).

14) A. L. Wood, *J. Amer. Chem. Soc.*, **48**, 432 (1946).

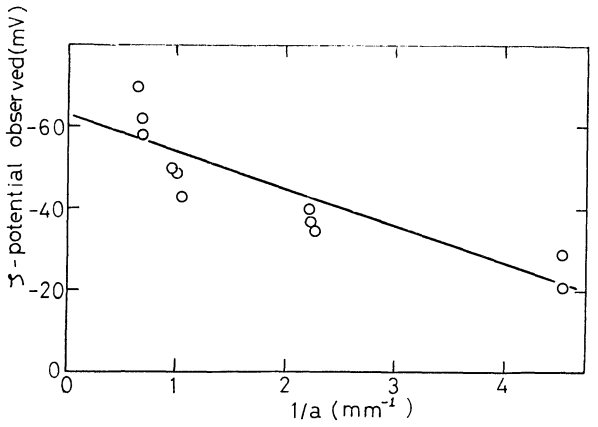

Fig. 3. The relation between ζ-potential observed (ζ_{obs}) and the reciprocal of radius ($1/a$) for the capillary system. The solid line was drawn with use of $\zeta_0 = -62$ mV and $A = -8.8$ mm.

The difference is still present between the value (−120 mV) from the electrophoresis and the one (−62 mV) from the streaming potential. However, difference has been considerably smaller as compared with the large difference of the preceding paper.[8] That is, ζ-potential from the electrophoresis and the streaming potential of barium sulfate powders dispersed in Aerosol OT solution in cyclohexane was +100 mV and +2 mV, respectively. The remaining difference may be elucidated from following reasons. (a) There is minor difference in composition of glass samples used for two methods, causing probable difference in the surface state. (b) There is difference in the washing extent of the surface, because enough washing is done in the process of the streaming potential measurement. (c) The double layer in the nonaqueous system may be distorted by the large local field strength resulting from the high applied potential (40—60 V/cm).

The authors are grateful to the Ministry of Education for the financial support to this study.

BULLETIN OF THE CHEMICAL SOCIETY OF JAPAN, VOL. 44, 3245—3250 (1971)

Acidity Constants of Phenanthrylamines in the Ground, Excited Singlet, and Triplet States

Kinzo Tsutsumi*, Kazuko Aoki, Haruo Shizuka, and Toshifumi Morita

Department of Chemistry, Gunma University, Kiryu, Gunma

(Received May 4, 1971)

Measurements of the acidity constants in the ground ($pK_a(S_0)$), the lowest excited singlet ($pK_a(S_1)$), and triplet states ($pK_a(T_1)$) for 2-, 3-, 4-, and 9-phenanthrylamines have been carried out by spectrophotometry. The pK_a values obtained were in the order of $pK_a(S_0) > pK_a(T_1) > pK_a(S_1)$. The absorption and emission spectra of the phenanthrylamines were compared with the results of the calculations by means of the semi-empirical SCF-MO-CI method. A linear relationship between the pK_a values and the net charge (or charge densities) in the ground and excited states was obtained both experimentally and theoretically.

The basic properties of aromatic compounds have been extensively studied especially for the ground states (S_0). The pK_a values determined experimentally have been satisfactorily explained in terms of the π-electronic energy change accompanied by protonation, and also in terms of the charge density on the atom which attacked by the proton. On the basis of the simple Hückel molecular orbital theory,[1] Coulson and Longuet-Higgins[2] pointed out a linear relation between the pK_a values and the charge densities for the ground states. Does the same thing hold when the self-consistent field molecular orbital theory is used?

Experimental studies on the acid-base properties in the excited states were carried out originally by Förster[3] and developed by Weller,[4] who extended the kinetic method to obtain the acidity constants and who succeeded, with substituted aromatic hydrocarbons, in obtaining the same values as those determined by the Förster cycle. Several workers[3–11] have studied the subject of the acidity constants in the

* Present address: Oyama Technical College, Oyama, Tochigi.

1) E. Hückel. *Z. Physik*, **70**, 204 (1931); **72**, 310 (1931); **76**, 628 (1932).

2) C. A. Coulson and H. C. Longuet-Higgins. *Proc. Roy. Soc.*, **A. 192**, 16 (1947).

3) T. Förster, *Z. Elektrochem.*, **54**, 42, 531 (1950).

4) A. Weller, *ibid.*, **56**, 662 (1952); A. Weller, *Discuss. Faraday Soc.*, **27**, 28 (1959).

5) G. Jackson and G. Porter, *Proc. Roy. Soc.*, **A 260**, 13 (1961).

6) M. K. Kalinowski, Z. R. Grabowski, and B. Pakula, *Trans. Faraday Soc.*, **62**, 918 (1966).

7) E. Vander Donckt and G. Porter, *ibid.*, **64**, 3215 (1968).

8) E. Vander Donckt and G. Porter, *ibid.*, **64**, 3218 (1968).

9) T. Tyulyulkov, F. Fratev, and D. Petkov, *Theoret. Chim. Acta.*, **8**, 236 (1967); T. Tyulyulkov and G. Hiebaum, *ibid.*, **14**, 39 (1969). K. Rotkiewicz and Z. R. Grabowski, *Trans. Faraday Soc.*, **65**, 3263 (1969); J. Bertran, O. Chalvet, and R. Daudel, *Theoret. Chim. Acta*, **14**, 1 (1969).

10) E. Vander Donckt, R. Dramix, J. Naselski, and C. Vogels, *Trans. Faraday Soc.*, **65**, 3258 (1969).

11) J. C. Haylock, S. F. Mason, and B. E. Smith, *J. Chem. Soc.*, **1963**, 4897.

ground and excited states. Summarize those results, the pK_a values in the lowest excited singlet states (S_1) are very much lower than those in S_o, while the pK_a (T_1) values are a little smaller or similar to those in S_1.

In order to explain these results, several discussions have appeared. Jackson and Porter[5] have explained this tendency of pK_a values as resulting from the differences among the electronic structures: the S_0, S_1, and T_1 states have normal, ionic, and radical structures respectively. The pK_a value in the S_1 state was elucidated by the resonance theory.[6-7] An explanation was also made considering the solvation effect on the pK_a values.[8] On the other hand, some theoretical calculations have been reported: they have suggested that the pK_a values in the excited states correlate with the electron-density distribution in the excited states.[9]

These explanations give us interesting suggestions concerning the basic properties in the excited states. No pK_a values of phenanthrylamines, except for those in S_0,[12] have been reported. Little attention has yet been paid to the theoretical consideration concerning these compounds. The purpose of the present paper is to measure these pK_a values for phenanthrylamines and to see if there exists a quantitative correlation between the charge distributions calculated theoretically by the SCF-MO-CI method and the experimental pK_a values in the ground and excited states.

Experimental

Materials. The 2-, 3-, 4-, and 9-phenanthrylamines used were given by Dr. Etsuro Ohta (Gunma University); these compounds were recrystallized twice from benzene. The cyclohexane was purified by passing it through a silica-gel column and by distillation. The methanol and ethanol were Kanto Chemical Co., Ltd., G. R.-grade products and were used without further purification. The buffer solutions used were adjusted using hydrochloric acid and sodium acetate.[13]

Apparatus. The UV absorption spectra were measured by means of a Hitachi 139 spectrophotometer. The fluorescence and phosphorescence spectra were taken with a Hitachi MPF 2A fluorescence spectrophotometer.

The Determination of pK_a Values. The pK_a values in the ground states (S_0) were measured by spectrophotometry at 20°C. The pK_a (S_1) and pK_a (T_1) values were estimated by means of the Förster cycle[3] as in the following relation:

$$pK_a(S_0) - pK_a^* = (\Delta E_{HA} - \Delta E_A)/(2.303RT)$$

where ΔE_{HA} and ΔE_A are the energy differences between the ground and excited states of the protonated and unprotonated molecules respectively. The $pK_a(S_0)$ and pK_a^* ($pK_a(S_1)$ or $pK_a(T_1)$) denote the pK_a values in S_0 and the excited state (S_1 or T_1) respectively. R and T are the gas constant and the absolute temperature respectively. In the present work, the energy difference between the S_0 and S_1 states was evaluated by means of the absorption and fluorescence spectra; the difference corresponds to the O–O transition energy. The energy difference between S_0 and T_1 was estimated by means of the phosphorescence spectra. If the $pK_a(S_0)$ is known, the pK_a^* can then be obtained.

Calculation

The π-electronic structures of some phenanthrylamines were studied by the use of the semi-empirical self-consistent field molecular orbital theory[14,15] combined with the singly excited configuration-interaction calculation. The CI calculation was made by taking 30 configurations of lower energies. The two-center Coulomb repulsion integrals, γ_{ij}, were calculated according to the Mataga-Nishimoto approximation.[16] The one-center Coulomb repulsion integrals, γ_{ii}, were estimated from the corresponding valence-state ionization potentials, (I_i), and electron affinities, (A_i), by the Pariser-Parr method,[14] I_i and A_i being determined from the spectroscopic data using the promotion energies of Hinze and Jaffé.[17] The two-center core resonance integrals, β_{ij}, were evaluated with the Nishimoto-Forster approximation.[18]

Some choices have been made concerning the appropriate I_i value for the nitrogen atom of an amino group. We used three types of parameter values (energies in eV) for the nitrogen atom:

(I) $I_N=28.709$, $\gamma_{NN}=16.757$, core charge=2,[17]

(II) $I_N=27.904$, $\gamma_{NN}=16.428$, core charge (N)=1.957, $I_{C'}=11.5516$, $\gamma_{C'C'}=11.3236$, core charge (C')=1.035.

Here, C' denotes the carbon atom next to the nitrogen atom. These parameter values are taken them Dewar and Morita,[19] who took the sigma polarization effect into account.

(III) $I_N=24.71$, $\gamma_{NN}=13.75$, core charge=2.

These parameter values were determined by Hirota and Nagakura[20] based on doubly-excited configuration interaction calculations.

In the SCF calculations, the variable-β,γ procedure developed by Dewar and Schmeising[21] and later by Nishimoto and Forster[18] was employed. The geometry was assumed to be as follows. All the C–C bond lengths and all the bond angles were taken to be equal to 1.39 Å and 120° respectively. The C–N bond length was assumed to be 1.38 Å. The actual calculation was carried out by an electronic computer, HITAC 5020 E, located at the Computer Center, The University of Tokyo.

12) J. J. Eliot and S. F. Mason, *J. Chem Soc.*, **1959**, 2352.

13) E. *g.*, "Kagaku Benran (The Chemical Index of the Chemical Society of Japan)," (1966), p. 1318.

14) R. Pariser and R. G. Parr, *J. Chem. Phys.*, **21**, 446, 767 (1953).

15) J. A. Pople, *Trans. Faraday Soc.*, **49**, 1375 (1953).

16) N. Mataga and K. Nishimoto, *Z. Physik. Chem.*, **13**, 140 (1957).

17) J. Hinze and H. H. Jaffé, *J. Amer. Chem. Soc.*, **84**, 540 (1962).

18) K. Nishimoto and L. S. Forster, *Theoret, Chim. Acta.*, **3**, 407 (1965); **4**, 155 (1966).

19) M. J. S. Dewar and T. Morita, *J. Amer. Chem. Soc.*, **91**, 796 (1969).

20) F. Hirota and S. Nagakura, This Bulletin, **43**, 1010 (1970).

21) M. J. S. Dewar and H. N. Schmeising, *Tetrahedron*, **5**, 166 (1959); **11**, 96 (1960).

Results

Electronic Absorption Spectra. The absorption spectra of the four phenanthrylamines were measured in cyclohexane at room temperature. Figure 1 shows those absorption spectra. By the substitution of an amino group, the π-electronic structure of phenanthrene was perturbed. The experimental and calculated values for the transition energies and oscillator strengths are listed in Table 1. Table 1 shows that the calculated values are in accordances with those obtained experimentally. No significant effect of the variation of parameters on the transition energies was observed.

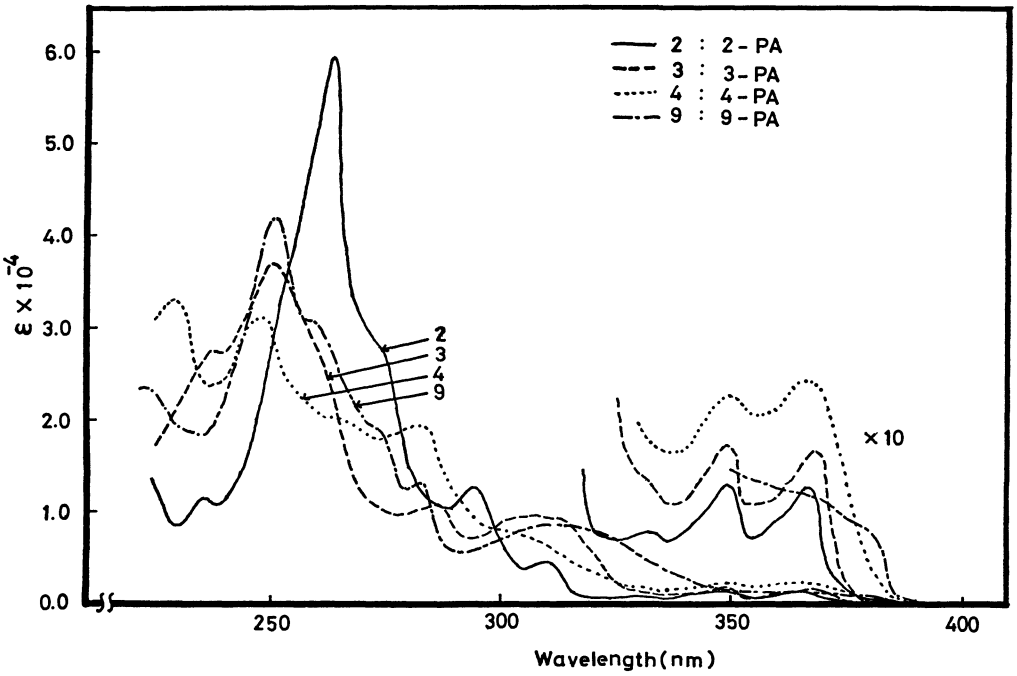

Fig. 1. UV absorption spectra of phenanthrylamines in cyclohexane at 20°C.

Table 1. Transition energies and oscillator strengths

Substance	Obsd.		Calcd(I)		Calcd(II)		Calcd(III)	
	ΔE	f	ΔE	f	ΔE	f	ΔE	f
1-PA	—	—	3.54	0.041	3.53	0.053	3.51	0.068
	—	—	3.99	0.333	3.96	0.325	3.91	0.328
	—	—	4.41	0.042	4.40	0.046	4.38	0.055
	—	—	4.80	0.424	4.77	0.434	4.73	0.402
2-PA	3.55	0.006	3.53	0.013	3.52	0.017	3.50	0.020
	4.00	0.017	4.12	0.119	4.11	0.100	4.10	0.062
	4.21	0.081	4.41	0.041	4.39	0.047	4.37	0.063
	4.52	—	4.70	1.748	4.67	1.775	4.62	1.820
3-PA	3.55	0.007	3.55	0.014	3.55	0.016	3.53	0.022
	4.02	0.111	4.01	0.382	3.98	0.390	3.94	0.417
	4.33	0.087	4.42	0.023	4.41	0.026	4.39	0.030
	4.96	—	4.85	1.244	4.85	1.155	4.84	1.073
4-PA	3.54	0.016	3.51	0.040	3.50	0.047	3.47	0.059
	4.06	0.102	4.05	0.153	4.02	0.133	3.98	0.114
	4.39	0.170	4.38	0.266	4.36	0.323	4.33	0.369
	4.68	—	4.70	0.849	4.69	0.757	4.67	0.606
9-PA	3.36	0.007	3.53	0.025	3.51	0.031	3.49	0.038
	3.91	0.145	3.96	0.334	3.93	0.337	3.88	0.351
	4.38	0.069	4.47	0.039	4.47	0.057	4.46	0.081
	4.52	—	4.78	0.661	4.76	0.412	4.72	0.373

ΔE and f denote the transition energy in units of eV and the oscillator strength respectively. I, II, and III are explained in the text, and PA denotes phenanthrylamine.

Ground-state Acidity Constants, $pK_a(S_0)$. Eliot and Mason[12] have reported the pK_a (S_0) values of phenanthrylamines measured by the potentiometric method. In the present work, the $pK_a(S_0)$ values were determined spectrophotometrically using the buffer solutions. These results are summarized in Table 2.

Table 2. Ground-state acidity constants

Substance	$pK_a(S_0)$		
	(1)[a]	(2)[b]	ΔH[c]
2-PA	4.06	3.60	4.4
3-PA	3.90	3.59	4.4
4-PA	3.18	—	—
9-PA	3.50	3.19	5.6

a) This work.
b) *Cf.* Reference 12.
c) ΔH denotes the enthalpy change in the dissociation of the conjugate acid of the phenanthrylamine in units of kcal/mol. *Cf.* Ref. 12.

The $pK_a(S_0)$ values obtained in the present work are somewhat high ($pK_a \approx 0.36$) in comparison with those reported by Eliot and Mason[12].

Excited Singlet-state Acidity Constants. The absorptions and fluorescence spectra of the four phenanthrylamines(RNH_2) and of their conjugate acids were measured at 20°C in an aqueous methanol solution (5 vol. percent methanol solution) for the parent molecules and in an aqueous methanol solution with sulfuric acid added for the protonated molecules (RNH_3^+). The absorptions and fluorescence spectra of the parent molecules appeared in various regions perturbed by the substituent amino group. However, the spectra of the protonated molecules are similar to that of phenanthrene. For example, the transition energies of the conjugate acid of 2-phenanthrylamine correspond to those of phenanthrene (Table 3) Similar results were obtained for 3-, 4-, and 9-phenanthrylamines. Therefore, the 345 nm (3.5_9 eV) absorption bands of the conjugate acids were assigned to the $^1L_b \leftarrow {}^1A$ transition of the phenanthrene molecule[22] with a maximum at 344 nm(3.6_0 eV). Little effect of the substituent NH_3^+ group on the phenanthryl group was found.

Table 3. Transition energies for the conjugate acid of 2-phenanthrylamine

Excited singlet state	Transition energy (eV)		
	a	b	c
S_1	3.5_9	3.6_0	3.56
S_2	4.2_3	4.2_4	4.09
S_3	4.4_4	4.4_3	4.59
S_4	4.5_4	4.5_2	4.74

a) Experimental data for the conjugate acid of 2-phenanthrylamine.
b) Experimental data of phenanthrene in cyclohexane.
c) Calculated values of phenanthrene in the present work.

The $pK_a(S_1)$ values estimated by the Förster cycle are listed in Table 4.

Triplet-state Acidity Constants. The phosphorescence spectra of the four phenanthrylamines were measured in the rigid methanol-ethanol (1 : 1 mixture in volume) matrices[23] at 77°K. These data are summarized in Table 5. The conjugate acids had the same $T_1 \rightarrow S_0$ transition energies as those of phenanthrene. These results show that the features of the lowest triplet states of the conjugate acids are very similar to those of phenanthrene. The $pK_a(T_1)$ values of protonated PA (RNH_3^+) were also determined by the Förster cycle, as is shown in Table 5. In the present work, the order of the pK_a values of protonated PA is $pK_a(S_0) > pK_a(T_1) > pK_a(S_1)$, as is shown in Tables 2, 4, and 5.

Charge Densities. The charge densities on the nitrogen atom in phenanthrylamines have been estimated by the semi-empirical SCF-MO-CI calculations using the parameters described above. Table 6 shows the calculated charge densities.

Discussion

The lone-pair electron on the amino-nitrogen atom would migrate to the phenanthryl ring much more intensely in the excited singlet state than in the ground state and a little more intensely in the triplet than in the ground state. The calculated results show this is true, as may be seen in Table 6. Accordingly, the basicities would be the largest for the ground state, medium for the lowest triplet state and the least for the lowest excited singlet state. The experimental

Table 4. $S_1 \leftarrow S_0$ transition energies and $pK_a(S_1)$ values of phenanthrylamines

Substance	Absorption (eV)		Fluorescence (eV)		O-O Transition energy (eV)[b]		pK_a (S_1)	ΔH (S_1)[a]
	RNH_2	RNH_3^+	RNH_2	RNH_3^+	RNH_2	RNH_3^+		
2-PA	3.4_8	3.6_0	2.9_2	3.5_7	3.2_0	3.5_8	-2.5_7	-2.4_6
3-PA	3.4_5	3.5_9	3.0_5	3.5_4	3.2_5	3.5_7	-1.6_0	-2.9_8
4-PA	3.4_4	3.5_7	2.7_8	3.5_2	3.1_1	3.5_5	-4.4_9	—
9-PA	3.4_4	3.5_9	2.8_2	3.4_4	3.1_3	3.5_2	-3.2_1	-3.1_6

a) Estimated from the relation: $\Delta H(S_1) = \Delta H(S_0) - (\Delta E_{AH}(S_1) - \Delta E_A(S_1))$, ΔH are in units of kcal/mol.
b) The O-O transition energies were evaluated by means of the absorption and fluorescence spectra.

22) D. S. McClure, *J. Chem. Phys.*, **25**, 481 (1956).
23) H. Shizuka and I. Tanaka, This Bulletin, **42**, 909 (1969).

Table 5. Phosphorescence spectra, $pK_a(T_1)$, and enthalpy changes

Substance	Phosphorescence spectra (nm)		$pK_a(T_1)$	$\Delta H(T_1)$[a] (kcal/mol)
	RNH_2	RNH_3^+		
2-PA	487	453	0.7_2	-0.0_3
3-PA	475	453	1.7_7	1.5_4
4-PA	495	453	-0.3_7	—
9-PA	500	453	-0.9_2	-0.3_3
Phenanthrene	450			

a) Estimated from the relation:
$\Delta H(T_1)=\Delta H(S_0)-(\Delta E_{AH}(T_1)-\Delta E_A(T_1))$.

results indicate this very tendency. Furthermore, as is shown in Table 4, the dissociation of protonated phenanthrylamines in the lowest excited singlet state is an exothermic reaction.

If the chemical non-crossing rule[2] could be applied for the excited states, the linear relation between the charge densities and the excited state pK_a values might be anticipated. Figure 2(a) shows the plot of the pK_a values against the charge densities: a good linear fit is seen for the excited singlet states. Points corresponding to the ground-state pK_a values also

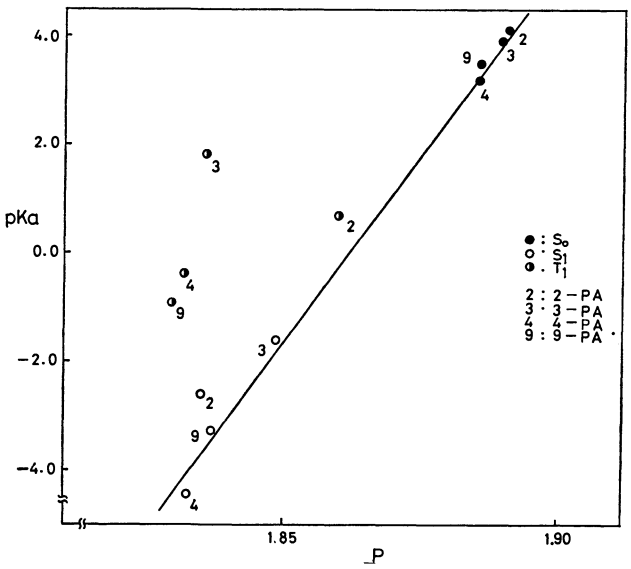

Fig. 2(a). Plot of the pK_a values *vs.* the charge densities. The S_0, S_1, and T_1 denote the ground, the lowest excited singlet, and the triplet states respectively.

lie on the same straight line. Treatment by the least-squares method gives the following equation:

$$pK_a = 133.46P - 248.34 \quad (1.83<P<1.90) \tag{1}$$

for this linear correlation. The slope of the line and the correlation coefficient, except for the plot for the triplet state, are 133.46 and 0.992 respectively. In this plot, we used charge densities calculated using the (II) parameter set, which is based on the consideration of the sigma polarization effect, because the charge densities computed by the (II) parameter set gave a somewhat better linear correlation than those calculated by the (I) and (III) parameter sets.

The enthalpy change (ΔH) in the dissociation of RNH_3^+ (Eq. 2) can be estimated approximately as follows:

$$RNH_3^+ \overset{K_a}{\rightleftharpoons} RNH_2 + H^+ \tag{2}$$

where K_a denotes the equilibrium constant. The enthalpy change can be written as:

$$\Delta H = -RT \ln K_a = (2.303\,RT)pK_a \tag{3}$$

The value of ΔH is approximated by the following equation:

$$\Delta H = I_N - A + C \tag{3'}$$

where I_N is the valence-state ionization potential of the nitrogen atom as determined by the method of Dewar and Morita[19] (see Eqs. (5) and (6); A is the electron affinity of a proton, and C is a constant). Equation (4) is derived from Eqs. (3) and (3'):

$$pK_a^{theo} = \frac{1}{2,303\,RT}(I_N - A + C) \tag{4}$$

$$= \frac{1}{2.303\,RT} I_N + \text{const.}$$

According to Eq. (4), the theoretical pK_a values should be proportional to the valence-state ionization potential of the nitrogen atom.

The estimations of the I_N values were carried out using the following relation[19]:

$$I_N = a + bq + cq^2 \tag{5}$$

where q denotes the total valence-shell electron density, and for the trigonal nitrogen, a, b, and c are equal to −89.402, 24.6265 and −1.4515 respectively. Equation (5) can be also given in the form of Eq. (6):

$$I_N = -10.1622\,Q_\pi - 2.1130\ \text{eV} \tag{6}$$

where Q_π is the net charge on the nitrogen atom; the term of $(Q_\pi)^2$ is disregarded since the $(Q_\pi)^2$ values are very small.

Table 6. Charge densities in the S_0, S_1, and T_1 states

	$P(S_0)$[a]			$P(S_1)$[a]			$P(T_1)$[a]		
	(I)[b]	(II)	(III)	(I)	(II)	(III)	(I)	(II)	(III)
2-PA	1.899	1.891	1.873	1.858	1.835	1.790	1.861	1.860	1.837
2-PA	1.898	1.890	1.872	1.865	1.849	1.810	1.852	1.836	1.796
4-PA	1.894	1.886	1.867	1.849	1.833	1.786	1.847	1.832	1.789
9-PA	1.894	1.886	1.867	1.852	1.837	1.796	1.846	1.830	1.784

a) $P(S_0)$, $P(S_1)$, and $P(T_1)$ denote the charge densities in S_0, S_1, and T_1 states.
b) Meanings of (I), (II), and (III) are described in the text.

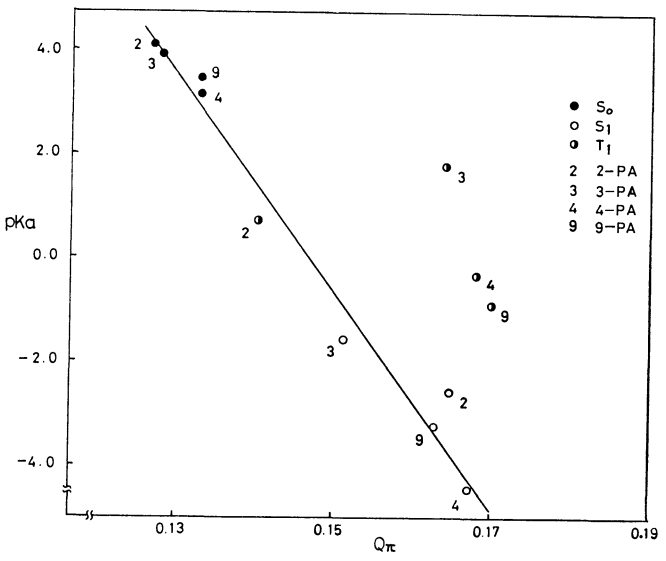

Fig. 2(b). Plot of the pK_a values *vs.* the net charges. The S_0, S_1, and T_1 denote the ground, the lowest excited singlet, and the triplet states respectively.

From the substitution of Eq. (6) into Eq. (4), Eq. (7) is given by:

$$pK_a^{theo} = -\frac{1}{2.303\,RT}(10.1622\,Q_\pi + 2.1130 + A - C) \quad (7)$$

$$= -1.748\times10^2\,Q_\pi + \text{const.}$$

where T equals 293°K.

Therefore, the linear relationship between the pK_a^{theo} values and the net charge Q_π can be derived; the slope of this relationship equals -1.748×10^2, as is described in Eq. (7). Figure 2(b) shows the plot of the experimental pK_a values *vs.* the net charge, Q_π; a good linear relationship is obtained. The following equation is given by the least-squares method:

$$pK_a = -2.05\times10^2\,Q_\pi + 30.322 \quad (8)$$

The slope of the line and the correlation coefficient, except for the plot for the triplet state, are -2.05×10^2 and 0.999 respectively. The slope of the line obtained experimentally is almost the same as that derived by the theoretical method, as is shown in Eqs. (7) and (8).

The pK_a values for the 1-phenanthrylamine can be estimated from the linear relationship in Figs. 2(a) and (b), if the charge densities are known. The estimated pK_a values are shown in Table 7.

Table 7. Estimated pK_a values for the 1-phenanthrylamine

	State	
	S_0	S_1
$P^{a)}$	1.886	1.837
pK_a	3.3_7	-3.1_7

a) P denotes the charge density calculated using the (II) parameter set, as has been described in the text.

The triplet-state pK_a values deviated from linearity. This must be due to some factors such as:

(1) In the present treatment, entropy changes in the dissociation of the conjugate acids are assumed to be constant for the three states of this series of compounds.

(2) The measured pK_a values are for the phosphorescent states. The charge densities to be used in plotting, therefore, should be calculated for the same states. The charge densities in the triplet state calculated by the present method are not precisely equal to those for the phosphorescent state, since the excited molecular orbitals are determined on the basis of the ground-state energy minimization. In order to improve this situation, we tried computations using Roothaan's open-shell procedure based on the minimization of the triplet-state energy.[24] Unfortunately, we were not successful in using it. In the large molecules such as we treated here, the MO energies were very close to each other, and at each stage of iteration an exchange of the MO levels occurred, resulting in no convergence of the charge densities.

Finally, it can be said that a linear relationship between the pK_a values and the net charge (or charge densities) is obtained both experimentally and theoretically in the ground and excited states.

The authors wish to thank Dr. Etsuro Ohta of Gunma University for giving them the phenanthrylamines.

24) C. C. J. Roothaan, *Rev. Mod. Phys.*, **32**. 179 (1960).

Radiotracer Studies on Adsorption of Surface Active Substance at Aqueous Surface. IV. Direct Measurement of Adsorption of Tritiated Nonionic Surfactant

Kazuo TAJIMA, Makio IWAHASHI, and Tsunetaka SASAKI

Department of Chemistry, Faculty of Science, Tokyo Metropolitan University, Setagaya, Tokyo

(Received May 13, 1971)

The radio- and surface-chemically pure nonionic surfactant, $C_{10}H_{21}(CHT)_2O(C_2H_4O)_6H$, was synthesized, and surface tension and adsorbed amount of its aqueous solution were measured directly at the air-solution interface at 30°C. Surface tension was measured by the drop-volume and Wilhelmy plate methods, while adsorbed amount was measured by the radiotracer method. The adsorption isotherm showed saturation values of 2.73×10^{-10} mol/cm^2 above the concentration of about 1/5 of the critical micelle concentration. The observed amount of adsorption was in good agreement with the values calculated from surface tension data measured by the Wilhelmy plate method by applying the Gibbs adsorption isotherm for a single solute system. The time dependence of surface tension of surfactant solution was further discussed, and the inherent time dependence was shown for pure surfactant solution.

Although the surface and bulk properties of the aqueous solution of nonionic surfactant have been studied by many investigators,[1-3] most of them have referred to surfactants of wide homologous distribution. As has been pointed out in a previous paper on adsorption of ionic surfactant,[4] the exact knowledge of adsorption is very important for understanding various phenomena at the air-solution interface. If the radiotracer method using tritiated nonionic surfactant is adopted, the adsorption on aqueous surface can be measured with high accuracy as in the case of ionic surfactant.[5]

In the present paper, tritiated hexaoxyethylenedodecyl ether (3,6,9,12,15,18-hexaoxa-1-triacontanol-19,20-^3H,^3H,; TD(EO)$_6$) was synthesized, and the adsorbed amounts were measured directly at the surface of its aqueous solution by the radiotracer method. The time dependence of the surface tension of this solution was further measured, and the drop-volume and Wilhelmy plate methods were compared with regard to the reliable surface tension value applicable for the Gibbs adsorption isotherm.

Experimental

Materials. TD(EO)$_6$ was synthesized according to the following schema, the details of which will be reported elsewhere.[6] First, tritiated dodecanol (I) was synthesized by the tritiation of dodecenol,[7] and its chemical and radiochemical purities were checked. By the bromination of (I) with hydrogen bromide, tritiated dodecyl bromide was obtained. The product was condensed with trioxyethylene monoalcoholate (II) in the nitrogen atmosphere at about 200°C. The condensation product was extracted with ether and the extract was distilled at 187°C/2 mmHg to give tritiated trioxyethylenedodecyl monoether (III). After chlorination of (III) with thionyl chloride, the product was again reacted with (II) to form TD(EO)$_6$. The crude TD(EO)$_6$ was purified by distillation to remove as completely as possible the lower boiling substances up to about 200°C/2 mmHg. Then the residue was recrystallized repeatedly from absolute hexane at 5—7°C and finally by the chromatography on neutral alumina using mixed solvent of acetone : benzene : methanol in 25 : 24 : 1 volume ratio. Both melting point (25.1°C) and refractive index (n_D^{40} 1.4480) agreed with the published values of 24.9°C and 1.4479, respectively.[8] The surface chemical purity of TD(EO)$_6$ obtained was confirmed by the critical micelle concentration (CMC) determined from a sharp break point of the surface tension *vs.* concentration curve being in agreement with literature value.[9] Water was triply distillated using borosilicate glass apparatus, after being refluxed overnight with the mixture of sulfuric acid and potassium permanganate.

Method and Procedures. The method and apparatus for the measurements of adsorption by a radiotracer technique were previously described in details.[5] The total radioactivity, A_1, on the surface of TD(EO)$_6$ solution which had attained the surface tension equilibrium, and the bulk radioactivity from the interrior of solution, A_2, were measured by a sheet scintillation counter. Radioactivity due to the adsorbed molecules, A_1-A_2, was multiplied by a conversion factor to obtain the amount of adsorption.[5] The surface tension of solution was measured by the drop-volume and Wilhelmy plate methods. In the former method, time required to form each drop was about 5 min. In the latter method, the change of surface tension was automatically recorded up to 24 hr. All measurements were carried out in the atmosphere of saturated humidities in order to prevent the evaporation from the surface of solution. The surface tension of pure water remained constant within the error of ±0.5 dyn/cm for 24 hr. The temperature was maintained at 30 ± 0.2°C.

Results and Discussion

Stability of Aqueous Solution of TD(EO)$_6$. It is well known[10] that the ionic surfactant, for instance

1) M. J. Schick, "Nonionic Surfactants," Marcel Dekker, N. Y. (1967).
2) H. Arai, *J. Colloid Interfac. Sci.*, **23**, 348 (1967).
3) H. Saito and K. Shinoda, *ibid.*, **24**, 10 (1967).
4) K. Tajima, This Bulletin, **44**, 1767 (1971).
5) K. Tajima, M. Muramatsu, and T. Sasaki, *ibid.*, **43**, 1991 (1970).
6) M. Iwahashi and K. Tajima, *J. Labelled Compounds*, to be published.
7) M. Muramatsu, K. Tajima, M. Iwahashi, T. Horiuchi, and K. Masumoto, *ibid.*, to be published.
8) D. Attwood, P. H. Elworthy, and S. B. Kayne, *J. Phys. Chem.*, **74**, 3529 (1970).
9) J. M. Corkill, J. F. Goodman, and R. H. Ottewill, *Trans. Faraday Soc.*, **57**, 1627 (1961).
10) S. P. Harrold, *J. Colloid Sci.*, **51**, 208 (1960).

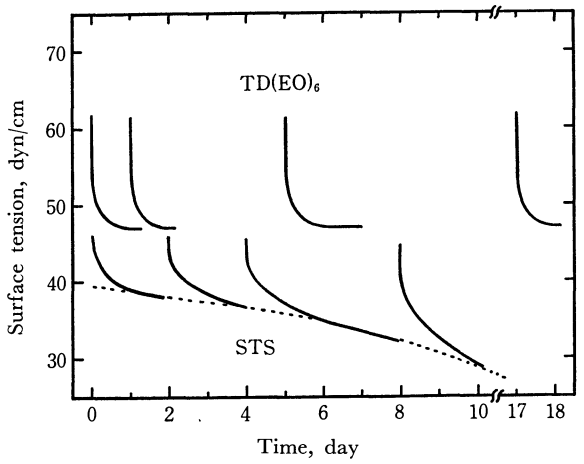

Fig. 1. Time dependence of surface tension for aqueous solution of $TD(EO)_6$ and STS at 30°C.
Upper curves: $TD(EO)_6$, $(5.0\times10^{-6}$ M)
Lower curves: STS, $(1.0\times10^{-3}$ M)
Broken line: progress of bulk hydrolysis

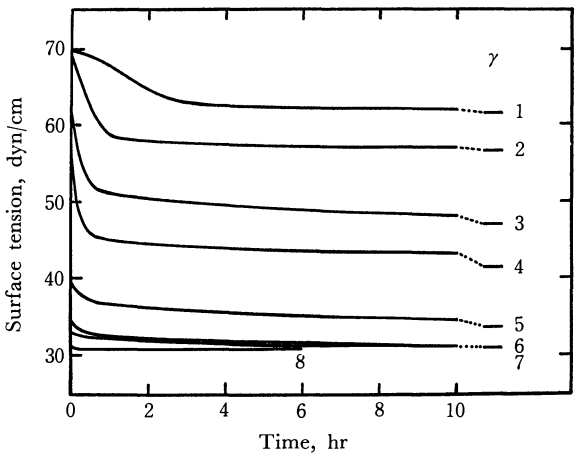

Fig. 2. Time dependence of surface tension of $TD(EO)_6$ solution at 30°C.
γ: equilbrium surface tension.
Concentration of $TD(EO)_6$ $(10^{-5}$ mol/l),
1: 0.020 2: 0.125 3: 0.500 4: 1.00
5: 3.50 6: 5.00 7: 7.50 8: 50.0

sodium tetradecyl sulfate (STS), is readily hydrolyzed in aqueous solution, which has been stocked over 24 hr at room temperature. On the contrary, it is expected that the nonionic surfactants such as polyoxyethylene (EO) alkyl ether consisting of ether bonds, might be more stable in aqueous solution than surfactants having ester bonding like STS. We examined the stability of the aqueous solution of these substances by tracing the time dependence of the surface tension. The results are shown in Fig. 1. The measurements were made for four aqueous solutions of STS and $TD(EO)_6$, successively taken from the respective stock solutions at proper time intervals. In the case of STS, surface tension exhibited a nearly same initial value, and it gradually decreased during the period of 24 hr tending to run along a common broken line, showing no tendency to arrive at equilibrium. The slow decrease of surface tension expressed by the broken line is the indication of hydrolysis taking place in the bulk of the stock solution. On the contrary, surface tension of $TD(EO)_6$ solutions reached to the identical final value after about 24 hr, and the value remained constant even after 17 days. The molecules of $TD(EO)_6$ are chemically stable in aqueous solution which may be stored unchanged for about two weeks at least.

Surface Tension Measurements. Figure 2 shows the typical examples of a time dependence of surface tension for $TD(EO)_6$ solution, where γ shows the equilibrium surface tension. Equilibrium surface tension thus obtained is plotted against the concentration in Fig. 3. The values measured by the drop-volume method are also shown in the same figure for comparison. The surface tension data obtained by the drop-volume method are considerably higher than those by the Wilhelmy plate method. This is due to the slow decrease of surface tension with time, which is pronounced in the dilute solutions. This time dependence also makes the measurement of equilibrium surface tension difficult especially by the drop-volume method. The critical micelle concentration measured by the drop-volume method, CMC′= 8.3×10^{-5} mol/l, is shifted to the higher concentration than that by the Wilhelmy plate method, CMC= 5.2×10^{-5} mol/l. Since the CMC value obtained by the Wilhelmy plate method is more reliable, above discrepancy indicates the fact that the relaxation of surface tension up to about 1 hr is observed even above the CMC up to the concentration of 8.3×10^{-5} mol/l. Since $TD(EO)_6$ exhibits considerable surface activity and considerably lower CMC than STS, a marked time dependence can be expected not only for the solution below the CMC, but also for the solution slightly above the CMC. The latter case may be due to the adsorbing surfactant molecules not being supplied instantaneously from the micelles.

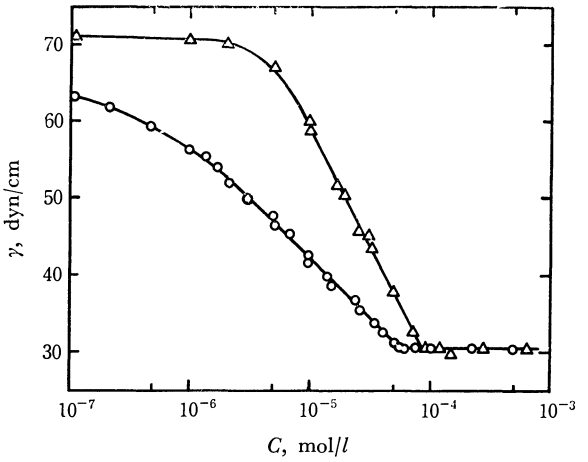

Fig. 3. Surface tension *vs.* concentration of $TD(EO)_6$ solution at 30°C.
○: Wilhelmy plate method
△: drop-volume method

Adsorption Measurement. The adsorption isotherm obtained is shown in Fig. 4. It is found that there is a range of constant adsorption $(2.73\times10^{-10}$ mol/cm^2) above the concentration of about 1/5 of the

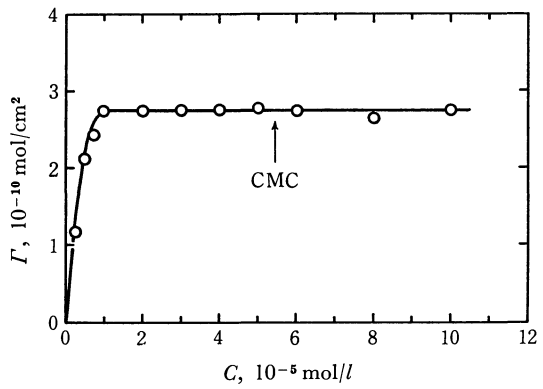

Fig. 4. Adsorption isotherm of $TD(EO)_6$ solution at the air-solution interface at 30°C.

CMC similar to the adsorption isotherm of ionic surfactant with[11] and without[5] salt.

The cross-sectional area per molecule is 60.8 Å^2 in a region of saturated adsorption as shown in Fig. 4. From this value, it is possible to deduce some knowledge concerning the hydrophilic group in the state of adsorption. If the EO groups of the surfactant are in the state of random coil, the relation between the cross-sectional area, S, and the number of EO groups, n, of the molecule is expressed by $S=\pi a^2 n^{2/3}$, where a is a radius of an EO group coil, assumed to be spherical. From the values of $S=60.8$ Å^2 and $n=6$, a cross-sectional area, πa^2, of ethylene glycol group of dodecyl ether is calculated as 18.4 Å^2. This value is very close to the limiting area per molecule, 19.5 Å^2, of ethylene glycol monooctadecyl ether spread at the air-water interface.[12] This confirms the view that the hydophilic groups of polyoxyethylenedodecyl ether are practically in the form of random spherical coils in the adsorbed state. From the measurements of hydration for nonionic surfactant possessing long polyoxyethylene groups, Schott[13] also considered them to be in the form of random coils surrounding the hydrocarbon core of the micelle. Thus, it seems that the EO groups are in a similar state of random coil of close mutual contact both in the state of micelle in the solution and in the state of saturated adsorption at the air-solution interface.

Gibbs Adsorption Isotherm. The experimental confirmation of the Gibbs adsorption isotherm has already been made for aqueous solution of ionic surfactant.[4,5,11] However, in applying the Gibbs isotherm to the solution of ionic surfactant, we have made some non-thermodynamical assumptions such as no hydrolysis in the bulk and surface phases, and the electrical neutrality at the surface for adsorbed species. However, since the aqueous solution of nonionic surfactant does not require such non-thermodynamical assumptions, it seems a most favorable system for applying the Gibbs adsorption isotherm.

The Gibbs adsorption isotherm, for a solution of single solute without any bulk hydrolyses, is expressed as follows;

$$-d\gamma = \Gamma RT\, d\ln C \qquad (1)$$

where γ denotes the equilibrium surface tension, Γ, surface excess and C, concentration of solute. Since the concentration of surfactant used is less than 10^{-4} mol/l, the term of activity coefficient may safely be considered as unity. The adsorbed amounts, calculated from the data of Fig. 3 by applying Eq. (1), are shown by solid lines A and B in Fig. 5. The results calculated from data of surface tension (drop-volume method) *vs.* concentration, measured with the same surfactant by Corkill *et al.*[9] were also shown in the same figure, for comparison. It was seen that the values observed by a radiotracer method are in good agreement with those calculated from the data of the Wilhelmy plate method and not with those from the drop-volume method. Although the values of C and D, which were calculated from the carefully measured data of Corkill *et al.*, are closer to the observed value than that of A, still they are distinctly higher than the observed value. The mean value of C and D, 3.25×10^{-10} mol/cm^2, considered as the value at 30°C, is about 20% higher than the observed value. Therefore, disagreement of the values obtained from the drop-volume method can be ascribed to the application of non-equilibrium surface tension to the Gibbs adsorption isotherm. The deviation of calculated (Wilhelmy) and observed values in concentration below 1×10^{-5} mol/l in Fig. 5, although slight, may be due to the uncertainties for the measurements, of surface tension in extremely low concentration, even for a prolonged measurement of time dependence of surface tension by the Wilhelmy plate method.

A satisfactory agreement between calculated and observed values indicates the validity of the Gibbs adsorption isotherm in the case of ionic surfactant solution.[4,5,11] However, it is important to apply sur-

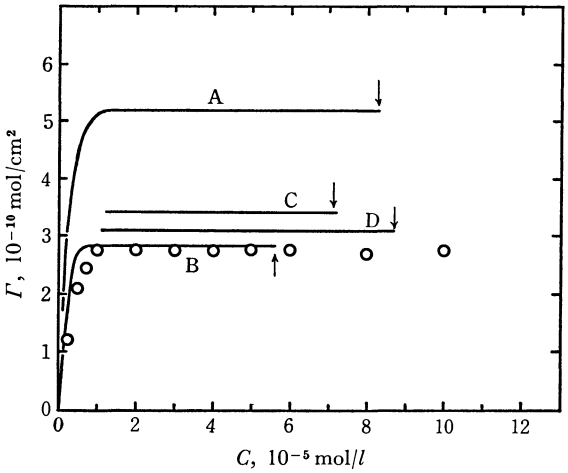

Fig. 5. The test of Eq. (1).
○ : observed value
——: calculated value using data of
(A) drop-volume method (30°C)
(B) Wilhelmy plate method (30°C)
(C) drop-volume method (Corkill, 35°C)
(D) drop-volume method (Corkill, 25°C)
Each arrow shows the CMC.

11) K. Tajima, This Bulletin, **43**, 3063 (1970).
12) R. N. Shukla, M. K. Gharpurey, and A. B. Biswas, *J. Colloid Interfac. Sci.*, **23**, 1 (1967).
13) H. Schott, *ibid.*, **24**, 193 (1967).

face tension values completely in equilibrium, which should be appreciated especially when the time dependence is marked as in the case of polymer surfactant. Also, it should be emphasized that surface tension often deviates largely from the equilibrium value according to the method of measurement as shown in Fig. 3.

Time Dependence of Surface Tension of Surfactant Solution. Corkill *et al.*[9] reported that, with the solution of same surfactant as in the present studies, the equilibrium surface tension is reached almost instantaneously at concentration below the CMC. Razouk and Mysels,[14] in the experiments on film elasticity and surface relaxation, noted reduced increases in the equilibrium surface tension after extensive purification of sodium dodecyl sulfate by foaming, but could not eliminate observed relaxation times of up to 10 min duration. They considered that the relaxation suggested the last traces of impurity not being removed from the system even after the purification by foaming.

In contrast to these statements, slow decrease of the surface tension of pure aqueous surfactant solution has been reported with regard to the solution of hexaoxyethylenedecyl ether,[15] or hexaoxyethylenehexadecyl ether.[16] Also, in the present study, a remarkable time dependence was observed as shown in Fig. 2. Now, there are many reasons to believe that the surface relaxation or the surface tension aging of surfactant solution appears not only in the surfactant solution containing the surface-active impurity, but also in the solution of pure surfactant.

According to the Gibbs adsorption isotherm applied for the solution containing several independent solutes, Eq. (1) gives the total amounts of adsorption of these solutes.[17] Therefore, the calculated amount of adsorption shown as solid line B in Fig. 5 indicates a sum of the amount of adsorption of $TD(EO)_6$ and that of impurities if any. Then, the coincidence of these values with the observed amount of adsorption which corresponds exclusively to radiometrically determined tritium labelled species of $TD(EO)_6$ may be taken as the experimental evidence of the absence of the adsorption of any surface-active impurities. The surface tension decrease with time as shown in Fig. 2 cannot be explained merely by the presence of surface-active impurities as Mysels stated.[18] Further, if the surface relaxation is produced only by the presence of impurity, then the equilibrium surface tension of the solution may not be equal to that of pure surfactant. The "true" surface tension, which the solution of pure surfactant might show, can be obtained by adding the surface tension decrease produced by the impurity to the steady value of surface tension attained after long time, provided that the effect of impurity on the surface tension is additive as Mysels postulated.[18] The surface tension value thus obtained which is practically equal to the surface tension extrapolated to time zero in Fig. 2, is applied to Eq. (1), but adsorbed amount obtained deviated even more largely from the observed value than that calculated from the value of drop-volume method. Therefore, additive effect of impurity on the surface tension is not sufficient to elucidate the time effect.

The explanation of relaxation of surface tension by the existance of impurity cannot exclude the possibility of an inherent time effect attributable to the pure aqueous surfactant solution. In fact, we cannot find any report which distinctly shows the surface tension of aqueous surfactant completely independent of time for all concentrations. On the contrary, many investigators rather believe the inherent relaxation in surface tension of aqueous surfactant solutions, and have proposed several empirical formula expressing surface tension *vs.* time relation or giving equilibrium surface tension by the extrapolation of time to infinity.[19]

Thus, it is certain that aging of surface tension does occur even in aqueous surfactant solution of sufficient purity to show a negligible amount of impurity adsorption.

The authors wish to thank the Ministry of Education for the financial support granted for this research.

14) J. R. Razouk and K. J. Mysels, *J. Amer. Oil Chemists' Soc.*, **45**, 381 (1968).
15) H. Lange, "Proc. Intern. Congr. Surface Activity Cologne," **1**, 279 (1967).
16) P. H. Elworthy and C. B. Macgarlene, *J. Pharm. Pharmacol.*, **14**, 100T (1962).
17) H. Lange, "Nonionic Surfactants," ed. by M. J. Schick, Marcel Dekker, N. Y., (1967), p. 458.
18) K. J. Mysels and A. T. Florence, "Clean Surfaces," ed. by G. Goldfinger, Marcel Dekker, N. Y. (1970), p. 227.
19) A. Boutaric and P. Berthier, *J. Chim. Phys.*, **36**, 1 (1939); H. Lange, "Proc. 3rd Intern. Congr. Surface Activity," **1**, 279 (1960); M. Nakamura and T. Sasaki, This Bulletin, **43**, 3667 (1970).

Infrared Spectra and Lattice Vibrations of $Li_2SO_4 \cdot H_2O$[1]

Shunsuke MESHITSUKA, Hiroaki TAKAHASHI, and Keniti HIGASI

Department of Chemistry, School of Science and Engineering, Waseda University, Shinjuku-ku, Tokyo

(Received May 19, 1971)

Infrared spectra of $Li_2SO_4 \cdot H_2O$ and $Li_2SO_4 \cdot D_2O$ have been measured from 4000 to 30 cm^{-1} at room temperature and liquid-nitrogen temperature. Librational bands of the water of crystallization have been observed and the modes of libration are discussed. The normal coordinate analysis of the crystal as a whole has been performed and the observed bands are interpreted. Translational bands of H_2O and librational bands of SO_4 are also discussed.

The present report deals with a study by infrared spectroscopy and the normal coordinate calculation concerning the vibrations of $Li_2SO_4 \cdot H_2O$ and $Li_2SO_4 \cdot D_2O$ crystals. The investigation was undertaken because of interesting features of the crystals. NMR spectra suggest that the water of crystallization performs a flipping motion around the molecular symmetry axis. There are two different positions for Li ions in a unit cell, one being located close to the water of crystallization and the other tetrahedrally surrounded by the oxygen atoms of the sulfate ions. Some changes in the infrared spectra might take place by variation of temperature on account of this flipping motion of the water of crystallization, and the effect of the environmental difference of the two Li ions might be observed in the infrared spectra.

By the use of X-ray diffraction,[2-4] neutron diffraction[5,6] and NMR spectroscopy,[7-10] several investigators have studied the crystal structure of $Li_2SO_4 \cdot H_2O$ and $Li_2SO_4 \cdot D_2O$, with particular attention to the orientation of the water molecule. Ketudat and Pound concluded from the quadrupole splitting of the deuterium resonance of $Li_2SO_4 \cdot D_2O$ that at room temperature, the water molecule undergoes hindered rotation about the bisector of the D–O–D angle with frequency greater than that of quadrupole interaction.[11] The same conclusion has been reached by other investigators.[12-14] This view is consistent with the large root mean square amplitude of the vibration of the hydrogen atoms observed in the recent neutron diffraction study.[6]

There are only a few works on the infrared[15,16] or Raman spectra[17] of these compounds. The intramolecular vibrations of the SO_4 ion and also the librations of the water molecule have been analyzed to some extent. However, because of the lack of measurements at low temperature the analysis remains still uncertain. There has been no study on the far infrared spectra below 350 cm^{-1}.

Neutron inelastic scattering studies of these compounds have been made by several workers.[18,19] Bajorek *et al.* have observed librational frequencies as well as translational lattice vibrations of the water molecule.[20]

Experimental and Observed Spectra

$Li_2SO_4 \cdot H_2O$ of a special grade (Wako Pure Chemical Industries, Ltd.) was used without further purification.

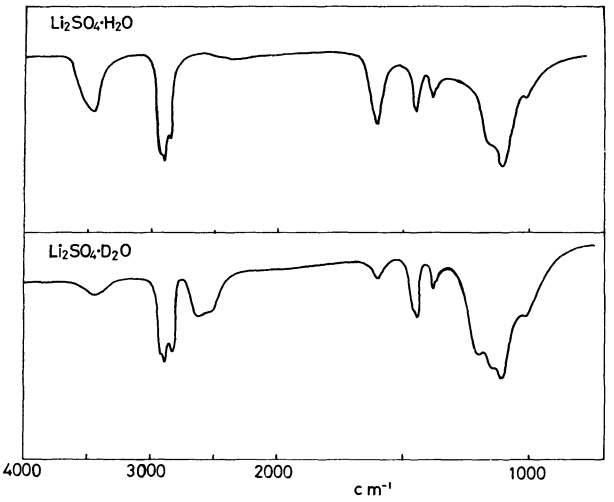

Fig. 1. Infrared spectra of $Li_2SO_4 \cdot H_2O$ and $Li_2SO_4 \cdot D_2O$ in Nujol at room temperature.

1) This work was supported partially by a research grant of the Matsunaga Science Foundation and by the Group Project organized by Science and Engineering Research Laboratory, Waseda University 1969—1970.

2) G. E. Ziegler, *Z. Krist.*, **89**, 456 (1934).
3) A. C. Larson and L. Helmholz, *J. Chem. Phys.*, **22**, 2049 (1954).
4) A. C. Larson, *Acta Cryst.*, **18**, 717 (1965).
5) N. V. Rannev, I. D. Datt, A. B. Tobis, and R. P. Ozerov, *Kristallografiya*, **10**, 914 (1965).
6) H. G. Smith, S. W. Peterson, and H. A. Levy, *J. Chem. Phys.*, **48**, 5561 (1968).
7) M. Soutif and Y. Ayant, *J. Chim. Phys.*, **50**, C 107 (1953).
8) E. Hirahara and M. J. Murakami, *J. Phys. Soc. Japan*, **11**, 239 (1956).
9) M. J. Murakami and E. Hirahara, *ibid.*, **11**, 607 (1956).
10) J. W. McGrath, A. A. Silvidi, and J. C. Carroll, *J. Chem. Phys.*, **31**, 1444 (1959).
11) S. Ketudat and R. V. Pound, *ibid.*, **26**, 708 (1957).
12) T. P. Das, *ibid.*, **27**, 763 (1957).
13) D. F. Holcomb and B. Pedersen, *ibid.*, **36**, 3270 (1962).
14) B. Pedersen and D. F. Holcomb, *ibid.*, **38**, 61 (1963).
15) F. A. Miller, G. L. Carlson, F. F. Bentley, and W. H. Jones, *Spectrochim Acta*, **16**, 135 (1960).
16) J. M. Janik, G. Pytasz, and T. Stank, *Acta Physica Polonica*, **35**, 997 (1969).
17) G. Vassas-Dubuisson, *J. Chim. Phys.*, **50**, C98 (1953).
18) R. J. Prask and H. Boutin, *J. Chem. Phys.*, **45**, 699, 3284 (1966).
19) C. L. Thaper, A. Sequeira, B. A. Dasannacharya, and P. K. Iyengar, *Phys. Stat. Sol.*, **34**, 279 (1969).
20) A. Bajorek, J. A. Janik, J. M. Janik, I. Natkaniec, J. N. Pokotilovsky, M. Sudnik-Hrynkiezicz, V. E. Komarov, R. P. Ozerov, and S. P. Solevev, Proc. of IAEA Symposium on Neutron Inelastic Scattering, Vol. II., p. 143 Vienna (1968).

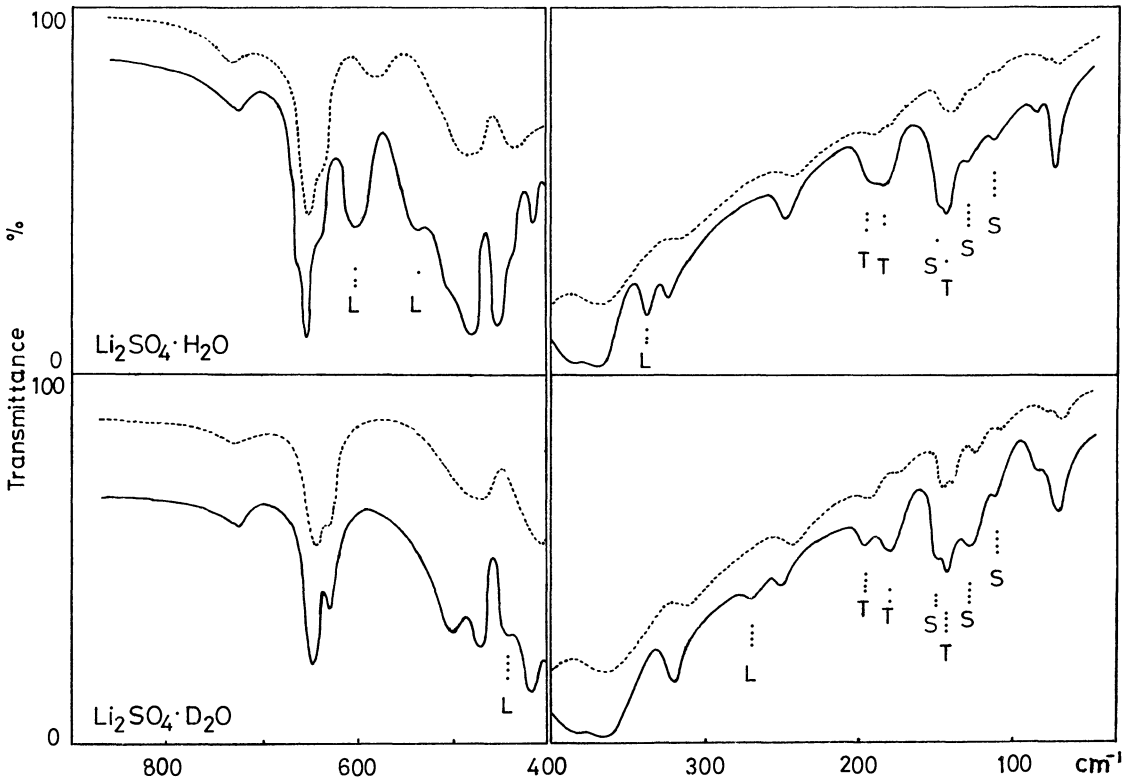

Fig. 2. Infrared spectra of $Li_2SO_4 \cdot H_2O$ and $Li_2SO_4 \cdot D_2O$ in Nujol, ····· 300°K, —— 110°K.
L, T, and S denote a librational band of H_2O, a translational band of H_2O and a librational band of SO_4 respectively.

An infrared spectrophotometer Hitachi EPI-G3 (4000—400 cm^{-1}) and a far infrared spectrophotometer Hitachi FIS-3 (400—30 cm^{-1}) were used. Each measurement was carried out at room temperature and also at liquid nitrogen temperature. The deuterated samples were prepared by gradual recrystallization from a heavy water solution of the anhydrous compound. Although a small amount of light water still remained in the deuterated sample, the heavy water content was sufficiently large for the assignment of infrared bands of $Li_2SO_4 \cdot D_2O$. The observed infrared spectra are shown in Figs. 1-3. By lowering the temperature, all the bands become sharp and intense. At the same time, the bands except for those due to intra-molecular vibrations shift to higher frequencies.

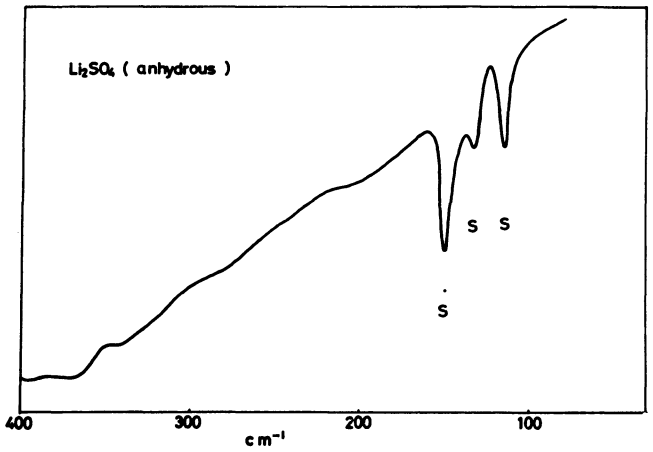

Fig. 3. Infrared spectrum of anhydrous Li_2SO_4 in Nujol at room temperature.
S denotes a librational band of SO_4.

Normal Coordinate Analysis

The crystal structure of $Li_2SO_4 \cdot H_2O$ is $P2_1$–C_2^2 and the crystal parameters are a=5.4537 Å, b=4.8570 Å, c=8.1734 Å, and β=107°22′.[6] A Bravais unit cell contains two $Li_2SO_4 \cdot H_2O$ unit. The optically active lattice vibrations as well as the intra-molecular vibrations were calculated according to the method developed by Shimanouchi *et al.*[21]

A Urey-Bradley type force field was applied to the H_2O molecule and SO_4 ion, and a valence force type potential was used for the interactions within a distance of 3.0 Å between H_2O molecule and SO_4 and Li ions. The bound state of the crystalline water in $Li_2SO_4 \cdot H_2O$ has some characteristic features. The hydrogen atoms of H_2O molecule make hydrogen bondings: one with another water and the other with the oxygen atom of the sulfate ion. One of the lone pairs of the oxygen atom of the water molecule directs toward the Li ion. The other is in the direction toward a hydrogen atom of another H_2O molecule to make a hydrogen bonding. Thus the H_2O molecules constitute a zigzag chain in the crystal by hydrogen bondings.

The potential around the H_2O molecule was assumed to be as shown in Fig. 5 by analogy with the H_2O molecule in ice.[22] In the course of the calculation the interaction coordinates around the H_2O

21) T. Shimanouchi, M. Tsuboi, and T. Miyazawa, *J. Chem. Phys.*, **35**, 1597 (1961).
22) Y. Kyogoku, *Nippon Kagaku Zasshi*, **81**, 1648(1960).

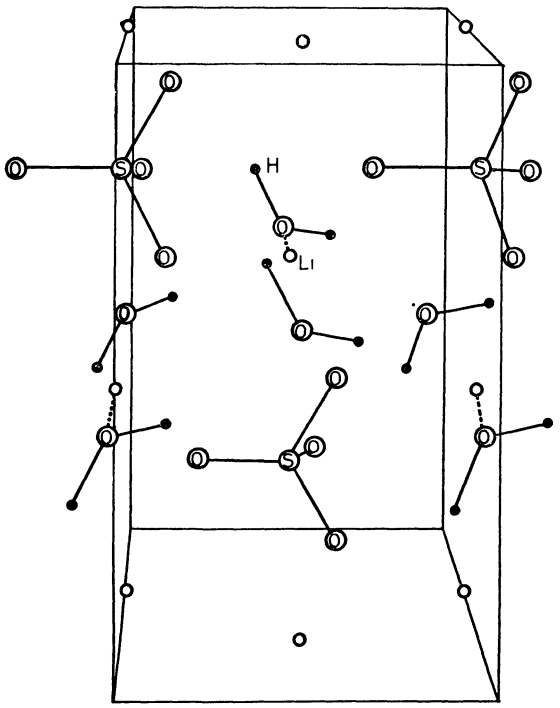

Fig. 4. Crystal structure of $Li_2SO_4 \cdot H_2O$.

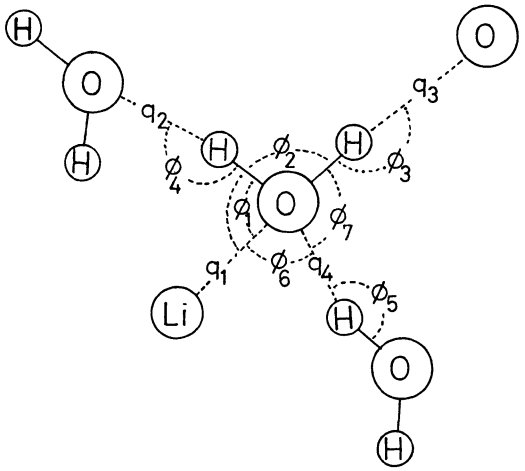

Fig. 5. Coordinates around a H_2O molecule.

molecule are simplified, and Δq(Li···O), Δq(O···H), $\Delta\phi$(Li···O–H), $\Delta\phi$(O–H···O), and $\Delta\phi$(O···Li···O) are used from the following consideration. The coordinate $\Delta\phi$(H–O···H), which is the interaction between the two H_2O molecules in a unit cell, serves to enlarge the frequency splittings between A and B symmetry species. The A and B species, however, are not observed separately so this coordinate is excluded. Further, the coordinate $\Delta\phi$(Li···O···H) is omitted, because this has little effect on the librational frequencies and on the other lattice vibrations. Consequently the potential function in the crystal is expressed as

$$V = V_{intra} + \tfrac{1}{2}\sum_{ij} K_i^1(\Delta q_{ij}(\text{Li}\cdots\text{O}))^2 + \tfrac{1}{2}\sum_{ij} K_i^2(\Delta q_{ij}(\text{O}\cdots\text{H}))^2 + \tfrac{1}{2}\sum_{ij} H_i^1(\Delta\phi_{ij}(\text{Li}\cdots\text{O–H}))^2 + \tfrac{1}{2}\sum_{ij} H_i^2(\Delta\phi_{ij}(\text{O–H}\cdots\text{O}))^2 + \tfrac{1}{2}\sum_{ij} H_i^3(\Delta\phi_{ij}(\text{O}\cdots\text{Li}\cdots\text{O}))^2$$

where V_{intra} denotes the intra-molecular potentials of SO_4 ion and H_2O molecule. K_i^1, K_i^2, H_i^1, H_i^2, and H_i^3 represent the force constants corresponding to the coordinates Δq(Li···O), Δq(O···H), $\Delta\phi$···(Li···O–H), $\Delta\phi$(O–H···O) and $\Delta\phi$(O···Li···O), respectively. The sum was taken over all kinds of internal coordinates i, and all the internal coordinates j for each kind of i in a Bravais unit cell.

Table 1. Force constants

	Distance (Å)	f. c. (mdyn/Å)
K(O-H)	0.95	6.52
K(S=O)	1.48	6.10
H(H-O-H)		0.57
F(H···H)		0.10
H(O=S=O)		0.59
F(O···O)		0.81
$\kappa(SO_4)$		0.25[a]
K(Li···OH_2)	1.91	0.40
K(Li···O)	1.92	0.34
K(Li···O)	1.95	0.22
K(Li···O)	1.99	0.12
K(O···H)	2.00	0.20
K(O···H)	2.78	0.17
K(O···H)	2.97	0.09
H(Li···O-H)		0.15
H(O···Li···O)		0.03
H(O-H···O)		0.01

a) mdyn·Å

Results and Discussion

Intra-molecular Vibrations. Since the site symmetry of sulfate ion in the crystal is C_1, ν_1 becomes infrared active, ν_2 splits into two bands, and ν_3 and ν_4 both split into three bands.[23] The observed spectra are in good agreement with the predictions: ν_1 (1010 cm^{-1}), ν_2 (513 and 478 cm^{-1}), ν_3 (1170, 1155, and 1110 cm^{-1}) and ν_4 (656, 647, and 637 cm^{-1}) at a low temperature. This assignment is also in line with the fact that the frequencies show no frequency shifts on deuteration and little temperature dependence. It is interesting that the splittings of ν_2 and ν_4 become greater on deuteration. The bands at around 1170, 1155, and 1110 cm^{-1} are as strong as other sulfates, and so broad that the positions of the peaks are difficult to determine. Although these bands are considered to be due to the splitting of the stretching mode of the sulfate ion belonging to the F_2 symmetry species, such large splittings have not been obtained by the normal coordinate calculation.

23) nomenclature after G. Herzberg, "Infrared and Raman Spectra of Polyatomic Molecules," Van Nostrand (1945)

Table 2. Frequencies and assignment of $Li_2SO_4 \cdot H_2O$

Obsd (cm^{-1})		Calcd (cm^{-1})		Assignment
300°K	110°K	A	B	
3520	3600	3499	3498	O-H str.
3500	3495	3464	3461	
3475	3455			
1612	1600	1601	1606	H-O-H bend.
1170	1170	1125	1126	SO_4 ν_3
1155	1155	1117	1117	
1110	1110	1114	1115	
1010	1010	1006	1008	SO_4 ν_1
—	656	658	654	SO_4 ν_4
645	647	641	642	
634	637	635	639	
580	600	602	604	H_2O lib.
—	533	541	542	H_2O lib.
—	513	505	505	SO_4 ν_2
475	478	472	474	
432	447	437	437	Li···OH_2 str.
380	387	392	392	Li···O str.
	372	370	369	Li···O str.
—	—	346	346	Li···O str.
—	338	330	337	H_2O lib.
318	325	310	305	O···Li···O bend.
245	249	270	277	O···Li···O bend.
194	196	223	214	H_2O trans.
175	180	174	209	H_2O trans.
145	147	150	161	SO_4 lib.
137	143	130	149	H_2O trans.
123	128	110	100	SO_4 lib.
109	113	96	94	SO_4 lib.
83	84	74	—	
71	72	50	52	

Table 3. Frequencies and assignment of $Li_2SO_4 \cdot D_2O$

Obsd (cm^{-1})		Calcd (cm^{-1})		Assignment
300°K	110°K	A	B	
2600	2610	2565	2564	O-D str.
2550	2560	2497	2493	
	2540			
1195	1195	1165	1172	D-O-D bend.
1150	1150	1125	1125	SO_4 ν_3
1130	1130	1117	1117	
1110	1110	1114	1115	
1010	1010	1006	1008	SO_4 ν_1
—	—	651	649	SO_4 ν_4
643	647	639	640	
629	631	634	636	
490	512	518	521	SO_4 ν_2
465	473	506	509	
423	440	440	437	D_2O lib.
405	420	432	432	Li···OD_2 str.
370	380	394	399	Li···O str.
360	370	367	366	Li···O str.
—	—	363	353	D_2O lib.
—	—	341	342	Li···O str.
315	322	310	305	O···Li···O bend.
—	269	271	277	D_2O lib.
242	249	241	269	O···Li···O bend.
190	194	214	208	D_2O trans.
170	176	172	187	D_2O trans.
142	147	149	161	SO_4 lib.
137	141	129	145	D_2O trans.
122	126	109	98	SO_4 lib.
104	110	96	93	SO_4 lib.
80	82	72	—	
68	66	49	52	

H_2O Librational Modes. The behavior of the water in the crystalline lattice is observed directly by the librational bands which have three characteristic features.

1) The bands are observed in the region between 1100 and 200 cm^{-1}.

2) These frequencies become approximately $1/\sqrt{2}$ on deuteration.

3) The intensities of the bands are very sensitive to temperature change.

Thus the three bands at 600, 533, and 338 cm^{-1} at low temperature are assigned to the librational bands of the water of crystallization in $Li_2SO_4 \cdot H_2O$ crystal. The bands at 600 and 338 cm^{-1} shift respectively to 440 and 269 cm^{-1} on deuteration. The deuterated band corresponding to 533 cm^{-1}, however, seems to be buried under the strong and broad bands at 387 and 372 cm^{-1} of the Li ion. The frequency ratios are 1.35 and 1.26 respectively. Janik *et al.* have observed a band at 835 cm^{-1} and assigned it to a libration of the water molecule.[16] However, we have observed no bands near that frequency.

The librational bands of water of crystallization have been observed in many compounds, but it is difficult to determine the modes of the librational motions experimentally. A normal coordinate analysis is useful for elucidating the behavior of the water molecule in a crystalline lattice.[24-26] The eigen vector (***Lx***) matrix set up by the Cartesian coordinate method shows the displacements of the atoms which correspond to each normal mode. It is seen from this ***Lx*** matrix that the band at 600 cm^{-1} is the rocking mode and the other two bands are mixtures of the wagging and twisting modes. As the values of ***Lx*** depend on the potential field around the water molecule, the interaction coordinates around the water molecule are chosen as thoroughly as possible. The bands at 533 and 338 cm^{-1} can not be observed distinctly until the sample is cooled to liquid nitrogen temperature. This suggests that the bands corresponding to the wagging and twisting motions become diffuse at ordinary temperature as a result of the 180° flipping motion of the water molecule.

H_2O Translational Modes. As the intensities of the bands at 196, 180, and 143 cm^{-1} are very sensitive to temperature change and the frequency shifts are small on deuteration, the bands are assigned to translational lattice vibrations in which water mole-

24) I. Nakagawa, *Spectrochim. Acta*, **20**, 429(1964).
25) K. Fukushima and H. Kataiwa, This Bulletin, **43**, 690 (1970).
26) K. Fukushima, *ibid.*, **43**, 1313(1970).

Table 4. Lattice vibrations of water in $Li_2SO_4 \cdot H_2O$ (low temp.) (cm^{-1})

	IR		Neutron I. S.
	H_2O	D_2O	H_2O
Libration			
rock	600	440	769
wagg + twist	533	—	556
twist + wagg	338	269	343
Translation			
	196	194	235
	180	176	186
	143	141	164

cule moves dominantly. Corresponding to these bands, 235, 186, and 164 cm^{-1} were observed by neutron inelastic scattering.[20]

Bands due to Li Ion. The nature of the metal $\cdots OH_2$ bonds in aquo-complexes has been studied by Nakagawa, and it is proposed that both ionic and covalent characters are involved in the bonds.[24] In this study the band at 432 cm^{-1} is assigned to the $Li\cdots OH_2$ stretching because the frequency shift is small on deuteration and is as sensitive as other lattice vibrations to temperature change. The $Li\cdots OH_2$ stretching force constant (0.40 mdyn/Å) together with the distance (1.91 Å) indicates that this bond may have a considerable covalent character.

The broad and intense bands at 387 and 372 cm^{-1} and the weak bands at 325 and 249 cm^{-1} were assigned to bands due to the Li ion for the following reasons. These bands do not change on deuteration and are less dependent upon temperature than those due to H_2O lattice vibrations. It is strange that the bands at 325 and 249 cm^{-1} are much weaker than those at 387 and 372 cm^{-1}. However, they cannot be explained by combination bands or difference bands. Thus they are assumed to be $O\cdots Li\cdots O$ bending.

SO_4 Librational Modes. The spectrum of the anhydrous sample shows that the bands at 150, 133, and 105 cm^{-1} are markedly sharp and the frequencies correspond to 147, 138, and 113 cm^{-1} respectively in the spectrum of the hydrate. The bands have therefore been assigned to the librational modes of the sulfate ion. It is worthy of notice that the librational frequencies of the sulfate ion have little dependence on the existence of the water of crystallization. The same phenomena have been observed in other compounds in our laboratory. From these considerations the assignment of the vibrations of $Li_2SO_4 \cdot H_2O$ and $Li_2SO_4 \cdot D_2O$ crystals were made as shown in Tables 2 and 3.

The authors wish to express their gratitude to the members of Shimanouchi Laboratory, the University of Tokyo, for use of the computer programs. Thanks are also due to Professor I. Nakagawa, the University of Tokyo, for his helpful suggestions.

BULLETIN OF THE CHEMICAL SOCIETY OF JAPAN, VOL. 44, 3259—3264 (1971)

Adsorption and Decomposition of Formic Acid Adsorbed on Pyrolyzed Polyacrylonitrile

Yutaka KUBOKAWA, Hisashi MIYATA, and Yoshihiko UEGAKI*

Department of Applied Chemistry, University of Osaka Prefecture, Sakai, Osaka

(Received May 21, 1971)

Infrared spectra of various pyrolyzed polyacrylonitrile and of deuterated formic acids (HCOOD, DCOOH, and DCOOD) adsorbed on it were investigated. The effect of pyrolysis temperature upon the decomposition products of formic acid adsorbed on the polymer was studied. It was found that parallelism exists between the concentration of the conjugated nitrile group and the percentage of the decomposition of formic acid adsorbed, leading to the conclusion that the active sites for the decomposition reaction are associated with the conjugated nitrile group in the case of polyacrylonitrile pyrolyzed below 300°C. On the other hand, there was a close correlation between the activity for decomposition and the number of free spins in the polymer pyrolyzed above 350°C.

Since various polymers are used as organic semiconductors, their catalytic activities have been investigated by a number of workers. Manassen and his co-workers[1,2] studied the dehydrogenation reactions catalyzed by pyrolyzed polyacrylonitrile and other polymers with defined structures, and concluded that the quinoid rings in the polymer structure are essential for the dehydrogenation reaction.

However, no detailed study has been carried out on the interaction of the reactants with the polymer under the reaction condition. Information on such interaction seems to be necessary in order to clarify the mechanism of the catalytic reactions on the poly-

* Present address: Industrial Products Research Institute, Shimomaruko, Otaku, Tokyo.

1) J. Manassen and J. Wallach, *J. Amer. Chem. Soc.*, **87**, 2671 (1965).

2) J. Manassen and Sh. Khalif, *ibid.*, **88**, 1943(1966).

mer. In the present work, therefore, infrared spectra of formic acid adsorbed on pyrolyzed polyacrylonitrile and also the spectral changes during the decomposition of formic acid have been investigated. From the results, the catalytic activity of pyrolyzed polyacrylonitrile has been discussed.

Experimental

Materials. Freshly distilled acrylonitrile was dissolved in water and stirred vigorously at 65°C under nitrogen while azobisisobutyronitrile was added. The white polymer thus formed was dissolved in dimethylformamide. By flowing the solution and vaporizing the solvent, a thin film was obtained. The film was cut down to 15×20 mm (about 20 mg), placed in a flame of Pyrex glass and pyrolyzed at 100–400°C in an infrared cell under evacuation. For the catalysts used in the study of the adsorption and decomposition of formic acid, the white polymer was pyrolyzed under evacuation for 3 hr at 150–500°C, the resulting polymer being powdered in a mortar.

Formic acid (Nihon Shiyaku Co. G. R.) was dehydrated by crystallization and vacuum-distilled in the presence of anhydrous copper sulfate. DCOOD (Merck) was used without further purification. DCOOH and HCOOD were prepared by the exchange of DCOOD with H_2O, and of HCOOH with D_2O, respectively.

Apparatus and Procedure. For studies of adsorption and decomposition a conventional constant volume apparatus was used. After the adsorption of formic acid vapor at room temperature, the trap attached to the reaction vessel was immersed in a dry ice-acetone mixture. Decomposition of formic acid adsorbed on the polymer was investigated by measuring the pressure increase due to decomposition. The decomposition products were hydrogen, carbon dioxide and carbon monoxide, being uncondensable at −78°C. After the experiment at room temperature, the temperature of the catalyst was raised in steps, and similar experiments were carried out. Activation energies of decomposition were determined[3,4] by comparison of the rates of decomposition at different temperatures corresponding to the same amount adsorbed. The amount of formic acid desorbed during the decomposition reaction was determined by the pressure increase which took place when the cold trap was warmed to room temperature after the reaction. Analysis of the decomposition products was carried out by gas chromatography using a 2 m silica gel column at 65°C. The isotopic abundance of H_2, HD, and D_2 was determined by a Hitachi RMU-5 mass spectrometer.

The cell used for the infrared spectroscopy of adsorption layer is similar to that used by Peri[5]. All spectra were recorded on a Hitachi EPI-S2 spectrophotometer with a NaCl prism.

Pyrolyzed polyacrylonitrile (about 10 mg) was placed in a quartz tube, evacuated at 100°C, sealed off, and the spectra were recorded on a Nihon Denshi ESR spectrometer 3BX.

3) Y. Kubokawa and H. Miyata, "Proceedings of the Third International Congress on Catalysis", Vol. 2, ed. by W. M. H. Sachtler, G. C. A. Schuit, and P. Zwietering, North-Holland Publishing, Amsterdam (1965) p. 871.

4) Y. Kubokawa and H. Miyata, *J. Phys. Chem.*, **72**, 356 (1968).

5) J. B. Peri, *Discuss. Faraday Soc.*, **41**, 121(1966).

Results and Discussion

Pyrolysis of Polyacrylonitrile. Figure 1 shows the infrared spectra of polyacrylonitrile pyrolyzed at various temperatures. On pyrolysis at 150°C in the region above 1800 cm^{-1}, two sharp bands appeared at about 3000 and 2235 cm^{-1}. With the rise of pyrolysis temperature the band at 3000 cm^{-1} bacame broad and increased in intensity, while the band at 2235 cm^{-1} decreased in intensity. Simultaneously, a sharp band at 2195 cm^{-1} appeared at 200°C, but disappeared completely on raising the temperature up to 350°C. Above the pyrolysis temperature 250°C, the spectrum was opaque in the region below 1600 cm^{-1}. The change in the intensities of the bands at 2235 and 2195 cm^{-1} with pyrolysis temperature is shown in Fig. 2.

As regards the pyrolysis of polyacrylonitrile a number of investigations have been carried out. According to Grassie and Hay,[6] Burlant and Parsons,[7]

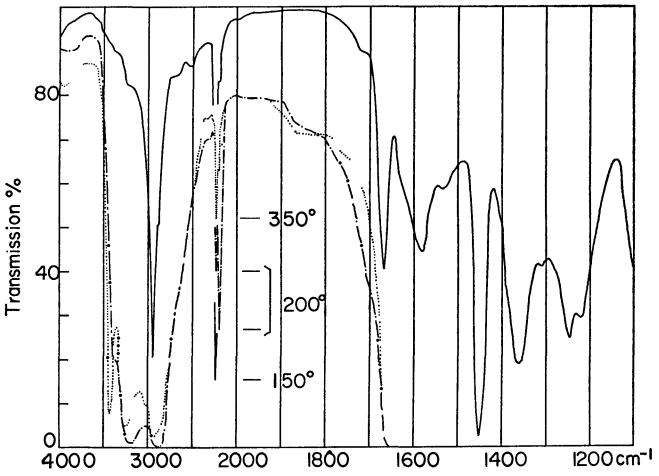

Fig. 1. Infrared spectra of polyacrylonitrile pyrolyzed at 150 (——), 200 (—·—·—), and 350°C (·····).

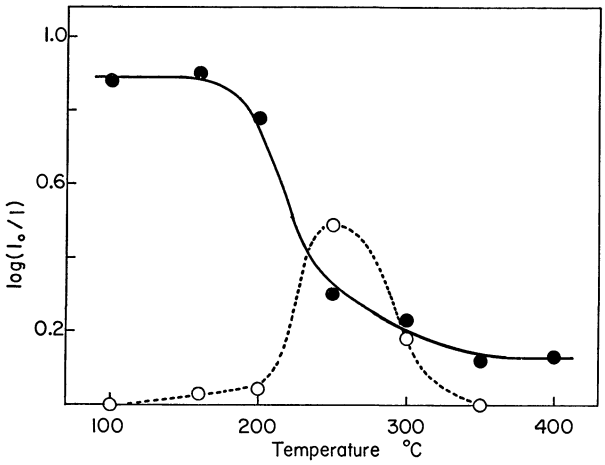

Fig. 2. Change in the band intensities at 2235 (—●—●—) and 2195 cm^{-1} (--○--○--) with pyrolysis temperature.

6) N. Grassie and J. N. Hay, *J. Polym. Sci.*, **56**, 189 (1962).

7) W. J. Burlant and J. L. Parsons, *ibid.*, **22**, 249 (1956).

and Conley and Bieron,[8] the pyrolysis proceeds as follows.

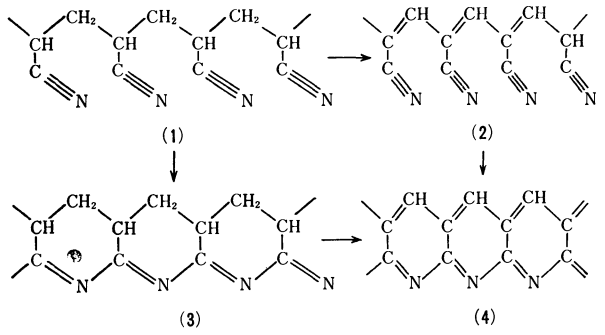

Aromatization of polyacrylonitrile occurs through two parallel processes; **1→2→4** and **1→3→4**. Burlant and Parsons[7] have assigned the bands at 2235 and 2195 cm^{-1} to the alkyl nitrile and to the conjugated nitrile groups, respectively. It follows that the variation in the intensities of both bands with pyrolysis temperature corresponds to the change in the concentration of both nitrile groups. In other words, on pyrolysis of polyacrylonitrile the conjugated nitrile group appears at 200°C. Its concentration passes through a maximum at 250°C and then decreases to almost zero above 350°C. On the other hand, the concentration of the alkyl nitrile group decreases monotonously with increasing pyrolysis temperature. It is seen in Fig. 2 that even above 400°C a small amount of the alkyl nitrile group still remains. Such behavior might be explained by taking into acount the occurrence of the following crosslinking reaction.[6]

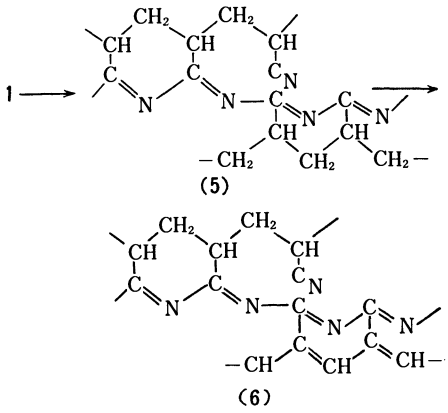

Infrared Study of Interaction of Formic Acid with Pyrolyzed Polyacrylonitrile. It was found that formic acid was not adsorbed on polyacrylonitrile pyrolyzed below 150°C, where there was no band at 2195 cm^{-1} attributable to the conjugated nitrile group. After the adsorption of formic acid the transmission of the polymer decreased in the range from 3400 to 1000 cm^{-1} and the band at 2195 cm^{-1} decreased in intensity.

In order to characterize the interaction of formic acid with pyrolyzed polyacrylonitrile completely, deuterated formic acids were used in infrared measurements. The results obtained with DCOOH are shown

8) R. T. Conley and J. F. Bieron, *J. Appl. Polym. Sci.*, **7**, 1757 (1963)

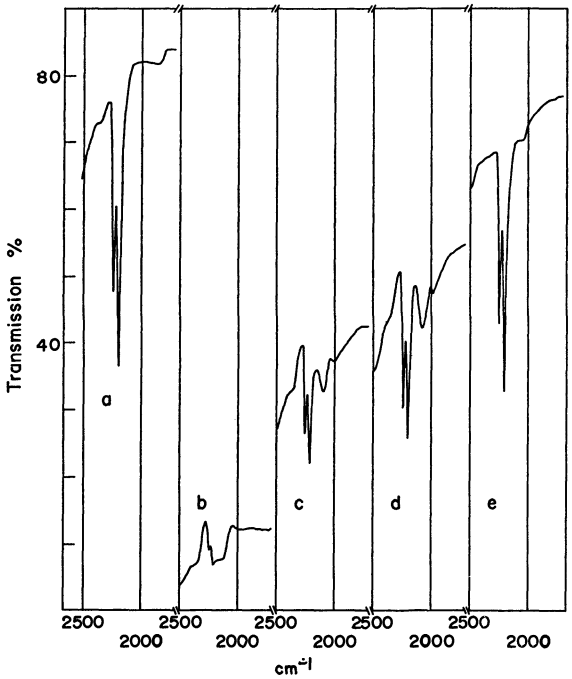

Fig. 3. Infrared spectra of DCOOH adsorbed on polyacrylonitrle pyrolyzed at 240°C.
(a) before adsorption; (b) after adsorption of 6 mmHg DCOOH at 25°C for 2 hr, and removing gas phase; (c) after evacuation at 120°C for 40 min; (d) at 120°C for 2 hr; (e) at 180°C for 1 hr.

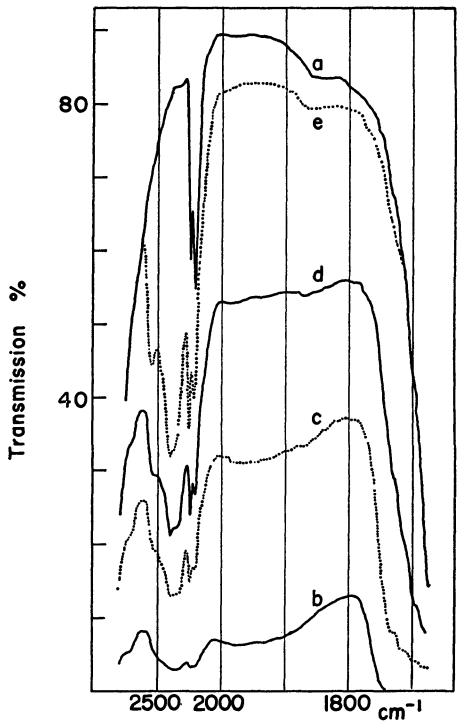

Fig. 4. Infrared spectra of HCOOD adsorbed on polyacrylonitrile pyrolyzed at 240°C.
(a) before adsorption; (b) after adsorption of 9 mmHg HCOOD at 25°C for 2 hr, and removal of gas phase; (c) after evacuation at 120°C for 30 min; (d) at 120°C for 2 hr; (e) at 180°C for 1 hr.

in Fig. 3. We see that a weak band appears at 2100 cm^{-1}. On raising the temperature of the polymer to 120°C, this band shifted to 2070 cm^{-1}, and increased in intensity. It still remained after evacuation for 3 hr at 120°C, and finally disappeared by evacuation at 200°C.

Figure 4 shows the results obtained with the adsorption of HCOOD. The band at 2070 cm^{-1} was not observed. Raising the temperature up to 120°C resulted in a new band at 2380 cm^{-1} having a small shoulder at 2320 cm^{-1} not removed by evacuation at 120°C for 2.5 hr. Even after evacuation at 180°C it still remained, in contrast to the band at 2070 cm^{-1}.

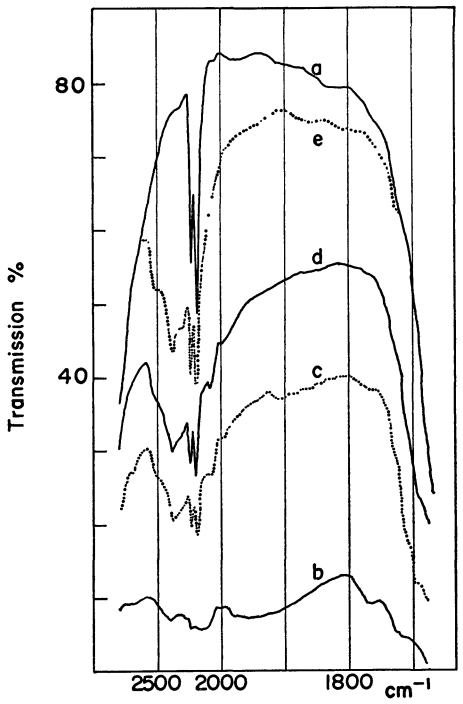

Fig. 5. Infrared spectra of DCOOD adsorbed on polyacrylonitrile pyrolyzed at 240°C.
(a) before adsorption; (b) after adsorption of 6 mmHg DCOOD at 25°C for 2 hr, and removal of gas phase; (c) after evacuation at 120°C for 30 min; (d) at 120°C for 2 hr; (e) at 180°C for 1 hr.

When DCOOD was observed, both bands at 2380 and 2070 cm^{-1} were observed as in Fig. 5. Neither band was removed by evacuation at 120°C, but at 180°C only the band at 2070 cm^{-1} was removed. Such behavior would be expected from the results obtained with DCOOH and HCOOD. Since the bands at 2070 and 2380 cm^{-1} are not observed with undeuterated formic acid, they arise from the interaction of CD and OD groups with the polymer. Considering the fact that pyrolyzed polyacrylonitrile is an efficient hydrogen acceptor as pointed out by Manassen,[1] it is concluded that such an interaction of CD and OD groups involves the D atom transfer to the polymer. Since the frequency of 2070 cm^{-1} belongs to the range of the C–D absorption, it appears that the band at 2070 cm^{-1} originates from the D atom transfer to the C atom in the polymer. Thus, another band at 2380 cm^{-1} can be assigned to the N–D vibration, which was formed by the D atom transfer to the N atom in the polymer.

Decomposition of Formic Acid adsorbed on Polyacrylonitrile pyrolyzed. The temperature of the polymer which had adsorbed a definite amount of formic acid was raised up in steps, at each of which the decomposition of formic acid adsorbed was investigated in the manner described above. Table 1 shows the amounts of formic acid desorbed and those of the decomposition products at various reaction temperatures. It is seen that at lower temperatures the decomposition products consist of carbon dioxide, hydrogen and carbon monoxide, the proportion of carbon dioxide being very large. With the rise of reaction temperature the proportion of hydrogen increases. Such a behavior suggests that at lower temperatures dehydrogenation reaction occurs predominantly, and the hydrogen formed is retained by the polymer. A similar behavior was observed by Manassen in the dehydrogenation of isopropyl alcohol.[1]

The results were obtained with polyacrylonitrile pyrolyzed at 250 and 500°C. The effect of pyrolysis temperature upon the activity of the polymer is shown in Fig. 6. It is seen that decomposition is observed

Table 1. Decomposition of formic acid adsorbed on polyacrylonitrile pyrolyzed at 250 and 500°C

Reaction temp. °C	Amount of HCOOH desorbed ccSTP/g	Activation energy kcal/mol	Total amount of the products ccSTP/g	Distribution of the products (%)		
				CO_2	CO	H_2
(a) pyrolyzed at 250°C						
70	11.5	21.5	1.46	90	1.4	8.6
120	14.7	24.6	5.76	86	2.6	11.4
180	0.58	23.7	4.63	68	2.0	30.0
240	0.00		0.57	70	13.6	17.4
(b) pyrolyzed at 500°C						
70	19.9		1.07	94	6	0
120	3.83		5.35	94	6	0
170	0.17		4.37	81	8	11
260	1.63		4.76	58	13	29
350	0.00		0.98	6	30	64

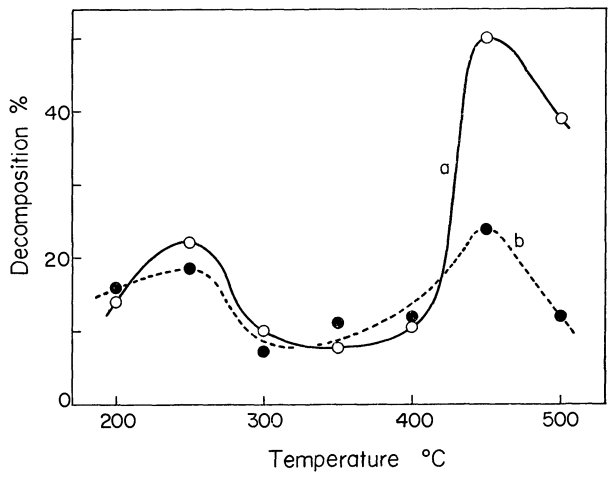

Fig. 6. Effect of pyrolysis temperature upon the activity of the polymer.
(a) 1st experiment (—○—○—), (b) 2nd experiment (--●--●--).

with only polyacrylonitrile pyrolyzed above 200°C. With increasing pyrolysis temperature, the decomposition percent of formic acid increases, showing two maxima at 250 and 450°C. The hydrogen formed during decomposition is retained by the polymer. Its effect upon the activity of the polymer was investigated by repeating the decomposition of formic acid on the same polymer. The results are shown in Fig. 6. The activity is affected slightly or not at all by the retention of hydrogen except for the measurements on the polymer pyrolyzed at higher temperatures.

The results were obtained under conditions where a definite amount (about 40 cc STP/g) of formic acid was introduced and almost all of it was adsorbed on the polymer. Table 2 shows the results for the case where the amount of formic acid introduced was so large that an appreciable amount of formic acid remained in the gas phase (formic acid pressure *ca.* 17 mmHg). It is seen that distributions of the products are almost the same in both cases, although at a reaction temperature above 350°C, the extent to which formation of carbon monoxide occurs is higher in the case when the amount of formic acid adsorbed was 151 cc.

Table 2. Decomposition on formic acid adsorbed in the case of the initial amount of formic acid adsorbed 151.0 ccSTP/g[a)]

Reaction temp. °C	Amount of HCOOH desorbed ccSTP/g	Total amount of the products ccSTP/g	Distribution of the products (%)		
			CO_2	CO	H_2
72	87.9	4.9	95	5	0
130	4.0	14.9	94	6	0
172	5.2	19.1	78	22	0
245	0.1	5.6	42	47	11
340	9.4	6.0	14	58	28

a) Polyacrylonitrile pyrolyzed at 350°C was used.

Hydrogenation and Dehydrogenation of Polyacrylonitrile During the Decomposition of Formic Acid. A comparison of the results in Figs. 2 and 6 shows that there is a parallelism between the concentration of the conjugated nitrile group and the percentage of the decomposition of formic acid adsorbed. Considering that adsorption and decomposition of formic acid take place only on the polyacrylonitrile with the conjugated nitrile group, it is concluded that the active sites for the decomposition of formic acid are associated with the conjugated nitrile group in the case of polyacrylonitrile pyrolyzed below 350°C.

It is concluded that the adsorption of formic acid involves an interaction between the hydroxyl group of formic acid and the conjugated nitrile group in the polymer, leading to the formation of the N–H bond in the temperature range above 120°C.

In addition to the N–H bond formation, the C–H bond formation occurs during the decomposition of formic acid. At present details of the C–H bond formation are not clear. As seen in Table 1, the hydrogen content in the decomposition products increases with increasing reaction temperature, suggesting that the desorption of hydrogen from the polymer takes place. In other words, the polymer hydrogenated during the decomposition of formic acid is dehydrogenated in the higher temperature range. In order to obtain information on the mechanism of dehydrogenation, the decomposition of deuterated formic acid was investigated. On polyacrylonitrile pyrolyzed at 250°C, the isotopic distribution of hydrogen is shown in Table 3. It is seen that considerable quantities of H_2 are produced in the case of DCOOD decomposition. This suggests that some portion of hydrogen desorbed does not originate from formic acid. However, taking into account the fact that the most abundant species is H_2 in the case of HCOOD, while HD in the cases of DCOOH and DCOOD, it may be concluded that a substantial fraction of hydrogen desorbed results from the combination of two hydrogen atoms, one from the CH group of formic acid and the other from the polymer.

Table 3. Isotopic distribution of hydrogen

Reaction temp. °C		Distribution of isotopic hydrogen (%)		
		HCOOD	DCOOD	DCOOH
180	H_2	84	32	9
	HD	16	59	84
	D_2	0	9	7
240	H_2	87	10	19
	HD	13	78	75
	D_2	0	12	6

The activity of the polymer for the decomposition of formic acid should decrease after the reaction, since the nitrile group in the polymer is converted into the NH group after the decomposition reaction. As shown in Fig. 6, however, such a decrease in activity is hardly observed. Such behavior may be explained by assuming that the number of nitrile groups consumed by the reaction is very small compared to the total

TABLE 4. INITIAL RATE OF DECOMPOSITION OF FORMIC ACID

Deuterated formic acid	Initial rate at 120°C (CO_2 formation) mm Hg/min	Ratio
HCOOD	0.482	4.1
DCOOH	0.326	2.8
DCOOD	0.117	1.0

number of nitrile groups available for the reaction. In fact, the amount of formic acid adsorbed on the polymer, 40 ccSTP/g, is very large compared to the amount adsorbed expected from the surface area, (6.1 m^2/g), suggesting that the total number of nitrile groups is accessible to the molecule of formic acid. For example, if all the nitrile groups are available for the reaction, then only 5% of them is consumed by performing the decomposition reaction. Little or no decrease in the activity seems to be explicable.

It seems clear that during the decomposition of formic acid cleavage of the O–H bond as well as of the C–H bond occurs, although details of the latter process remain unknown. In order to obtain information on the rate-determining step for the decomposition reaction, the kinetic isotopic effect of deuterated formic acid was investigated with polyacrylonitrile pyrolyzed at 250°C. As seen in Table 4, the reaction rates decrease in the order HCOOD>DCOOH>DCOOD. It appears, therefore, that cleavage of neither the C–D bond nor the O–D bond is the rate-determining factor in the decomposition reaction.

Relation between the Number of Free Spins of Pyrolyzed Polyacrylonitrile and its Catalytic Activity. As seen in Fig. 6, the polymer pyrolyzed above 350°C exhibits a remarkable activity for the decomposition reaction. Since there are few or no conjugated nitrile groups in such a polymer, its activity is not attributable to the presence of conjugated nitrile groups. It is well-known that the polymer pyrolyzed above 350°C has the quinoid structure,[8,9] which shows the activity for hydrogen acceptor as pointed out by Manassen.[1] It appears, therefore, that the activity for the decomposition reaction arises from the presence of the quinoid structure.

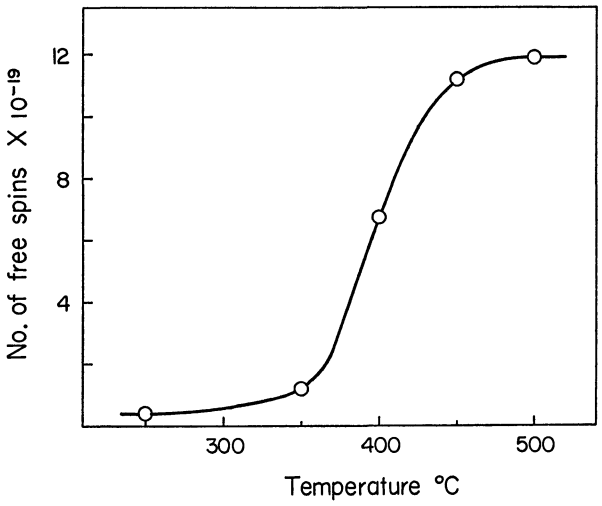

Fig. 7. Number of free spins of polyacrylonitrile pyrolyzed at various temperatures.

The number of free spins of polymer pyrolyzed at various temperatures was measured by ESR. The results are shown in Fig. 7. It is seen that the number increased markedly at temperatures above 350°C, reaching a saturated value around 450°C. A comparison of the results shown in Figs. 6 and 7 suggests that there is a close correlation between the activity for the decomposition and the number of free spins in the polymer. Although the true nature of such a correlation is not clear at present, a similar behavior has been found by Manassen,[1] and Gallard *et al.*[10]

9) M. Becher and H. F. Mark, *Angew. Chem.*, **73**, 641 (1961).
10) J. Gallard, A. R. Pecher, and Ph. Traynard, *J. Catal.*, **13**, 261 (1969).

Measurements of Optical Absorption Spectra under ^{60}Co-γ Irradiation. Aqueous Methylene Blue Solutions Containing Oxygen

Shin-ichi OHNO, Akihisa SAKUMOTO, Teikichi SASAKI, Kiyoshi KAWATSURA, and Katsutoshi FURUKAWA

Japan Atomic Energy Research Institute, Tokai-mura, Ibaraki-ken

(Received May 24, 1971)

Aerated aqueous solutions of methylene blue (MB^+; 3×10^{-7} M) were subjected to ^{60}Co-γ rays in the presence of added methanol, ethanol, or D-glucose at dose rates up to 4×10^{15} eV $g^{-1}s^{-1}$, and the change in the optical absorption spectrum in the 300—700 nm region was studied using a rapid-scan spectrophotometer (scanning speed: 30 ms/100 nm). In the presence of high concentrations ($>10^{-2}$ M) of organic substances, it was found that radiation caused a decrease in the absorption due to MB^+ at 650 nm (the magnitude of the decrease was proportional to the radiation intensity), and that, on the removal of the radiation source, the original absorption spectrum was restored. This was interpreted as meaning that the radiation-produced leuco-form of methylene blue (MBH) was rapidly oxidized by oxygen. The rate constant, $k(MBH+O_2)$, was estimated to be $(0.6\pm0.2)\times10^4$ $M^{-1}s^{-1}$ at neutral pH. In the absence of added organic substances, the permanent decoloration of MB^+ took place; this was interpreted as being due to the reaction of MB^+ with OH-radicals. From the competition kinetic study using 10^{-4} M methanol, the rate constant, $k(OH+MB^+)$, was estimated to be 1.1×10^{10} $M^{-1}s^{-1}$.

Short-lived species in radiation-induced reactions have been studied by pulse-radiolysis techniques,[1] which, in most cases, employ an electron accelerator. On the other hand, much less effort has been made to study the short-lived species during continuous ^{60}Co-γ irradiations. Some reasons for this are: (1) The radiation from available Co-60 sources is, very often, not intense enough to produce measurable concentration of the species to be studied. (2) One must eliminate the radiation effects on the measuring systems, which is more difficult in γ-radiolysis than in electron-beam radiolysis.

We have now constructed an apparatus which can be adopted to a commercially-available spectrophotometer, *e.g.*, a Hitachi rapid-scanning spectrophotometer RSP-2, and which makes it possible to obtain an optical absorption spectrum in the 300-700 nm range of the liquid sample during irradiation up to 4×10^{15} eV $g^{-1}s^{-1}$. The details of the apparatus will be described elsewhere.[2] Here we wish to report the results of such measurements in the case of aerated aqueous solutions of methylene blue.

It is well known that methylene blue in air-free solutions containing various added organic substances loses its color upon irradiation, and that this decoloration can be reversed by the admission of air.[3,4] It is of interest, therefore, to measure the steady-state concentration of methylene blue in aerated solutions during the γ-radiolysis.

Experimental

The radiation source, 15 kCi ^{60}Co, was of a cylindrical type (40 cm in height, 13.4 cm in outer diameter). It was hung on a hoist which could be operated so as to move horizontally at a constant speed (3.3 cm s^{-1}).

The intensity of the radiation energy absorbed by a dilute aqueous solution at a horizontal distance of D cm from the center of the present source is expressed by Eq. (1), on the basis of the Fricke-dosimetry:[5]

$$I\ (\text{eV g}^{-1}\text{s}^{-1}) = 15.6\times10^{17}/D^2 \qquad (1)$$

where $D \geq 20$ cm

The reaction vessel was a 20-cm quartz tube 4.0 cm in internal diameter. The optically-flat windows were attached to the tube ends. The vessel was completely filled with the sample solution through the side arms attached to the vessel.

The reaction vessel was subjected to radiations at a fixed position (see Fig. 1) and at an ambient temperature *ca.* 25°C. The absorption spectra in the range from 330 to 700 nm were obtained using a Hitachi rapid-scanning spectrophotometer RSP-2 (scanning speed: 30 ms/100 nm) and were recorded on an oscilloscope (Hitachi V-018). Variations in the optical density at selected wavelengths could also be recorded as a function of the time.

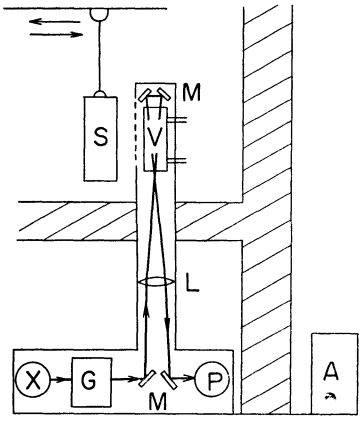

Fig. 1. Schematic drawing of optical arrangement:
X: a 150W Xe-lamp; G: monochrometer (a grating which can rotate for wave-length scanning); L: lens; V: reaction vessel; M: mirrors; P: photomultiplier; A: oscilloscope; S: radiation source. The unit, X, G, and P, makes a Hitachi rapid-scanning spectrophotometer RSP-2.

1) "Pulse radiolysis," Ed. by M. Ebert, Academic Press, London (1965).
2) S. Ohno *et al.*, JAERI-Report, to be published.
3) L. I. Grossweiner, *Radiation Res. Rev.*, **2**, 345(1970).
4) A. J. Swallow, "Radiation Chemistry of Organic Compound," Pergamon Press, London (1960), p. 196."
5) Measurements made by the ^{60}Co-source operating group of the Institute.

All the reagents were of an Analar grade and were used without further purification. The concentration of methylene blue were calculated using an extinction coefficient reported in the literature, *i.e.*, 0.77×10^5 M^{-1}cm^{-1} at 665 nm.[6] The optical path-length of the reaction vessel employed was 40 cm.

Results

Methylene Blue+Ethanol. Figure 2a shows the radiation effects on an optical absorption spectrum of an aerated solution of 3×10^{-7} M methylene blue in the presence of 0.1 M ethanol. Radiation (3.9×10^{15} eV g^{-1}s^{-1}) decreased the absorption at 650 nm by about 30%. However, this bleaching during the irradiation was found to be almost completely reversible, and, on the removal of the radiation source, the original absorption spectrum was restored.

Similar results were obtained when lower concentrations of ethanol (10^{-2} or 10^{-3} M) were used, though the recovery after the removal of the source was 90% when 10^{-3} M ethanol was employed.

Methylene Blue+D-glucose. Aerated aqueous solutions of 3×10^{-7} M methylene blue and 0.1 M D-glucose at various pH values (neutral, 0.1 N H_2SO_4, and 0.01 N NaOH) were examined. All these results were similar to those in the case of 0.1 M ethanol mentioned in the previous section. Both the decrease in absorption during irradiation and the subsequent recovery on removing the source could be repeated several times. The variation in the optical density at 650 nm with the time in the case of methylene blue in aerated 0.01 N NaOH containing 0.1 M D-glucose is shown in Fig. 2b. The radiation source was first brought near the sample (thus causing the decrease in absorption) and then removed from the sample at a constant speed of 3.3 cm s^{-1}.

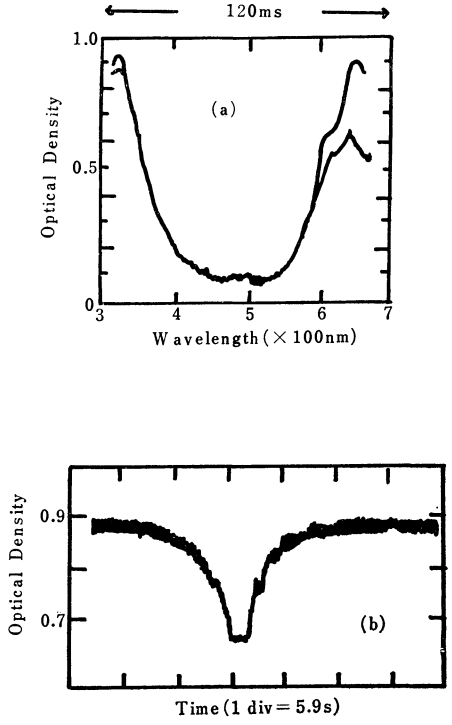

Fig. 2. Radiation effects on absorption spectra of aerated aqueous solutions of 3×10^{-7} M MB$^+$.
(a) 0.1 M ethanol present; Spectrum before irradiation (upper curve) and during the irradiation at dose rate of 3.9×10^{15} eV g^{-1} s^{-1} (lower curve); (b) Decrease in absorption and its recovery accompanying the transfer of the source (see text).

6) J. P. Keene, E. J. Land, and A. J. Swallow, in Ref. 1, p. 227.

Irreversible Bleaching of Methylene Blue. A permanent decoloration of methylene blue occured when it was irradiated in an aerated, or in an argon-saturated, solution containing a low concentration (10^{-4} M) of methanol. The absorption spectra were recorded (*cf.* Fig. 3a) at various intervals after the source was placed at the fixed position (3.9×10^{15} eV g^{-1}s^{-1}). From the results shown in Fig. 3a, one may plot the decrease in the methylene blue concentration with the irradiation time, as in Fig. 3b. This bleaching was found to be irreversible. The initial yield for bleaching was 0.05 molecules per 100 eV of absorbed energy.

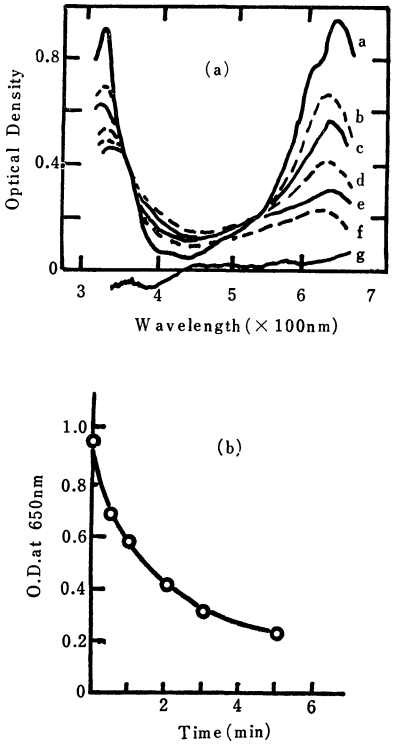

Fig. 3. Spectral change of an aerated solution of (3×10^{-7} M MB$^+$ + 10^{-4} M CH_3OH) with irradiation time at dose rate of 3.9×10^{15} eV g^{-1} s^{-1}.
(a) Spectrum before irradiation(a), and after 0.5(b), 1(c), 2(d), 3(e), and 5(f) min irradiation; Reference solution(g);
(b) Plot of optical density at 650 nm from the above results.

Discussion

When an aerated solution of methylene blue (MB$^+$; see Fig. 4) and high concentrations of organic substances are subjected to irradiation, the reactions which must be considered are very complex. Radiation decomposes water to give H, H_2, e_{aq}^-, H_3O^+,

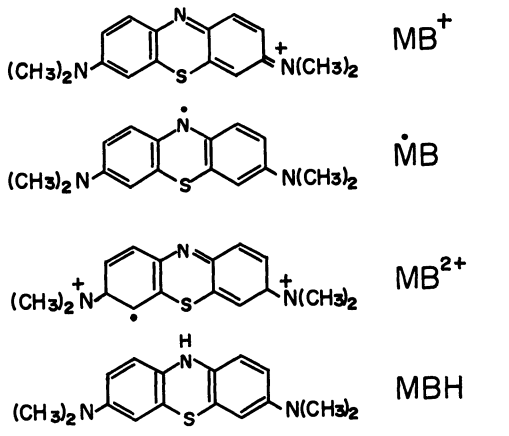

Fig. 4. MB^+ (methylene blue), $\dot{M}B$(semiquinone-form), MB^{2+} (half-oxidized form), and MBH(leuco-form).

OH, and H_2O_2. In aerated solutions where the concentration of oxygen is $\sim 4\times10^{-4}$ M,[7] H and e_{aq}^- will predominantly react with O_2 to yield HO_2 or O_2^-. If the ratio of the concentration of the organic substance to that of MB^+ is high enough, all the OH-radicals react according to:

$$OH + RCH_2OH \rightarrow \dot{R}CHOH + H_2O \quad (2)$$

where RCH_2OH represents ethanol, D-glucose, *etc.* The organic radicals are reducing agents:[3,4]

$$\dot{R}CHOH + MB^+ \rightarrow RCHO + \dot{M}B + H^+ \quad (3)$$

where $\dot{M}B$ represents the half-reduced semi-quinone form of the dye. Such species as $\dot{R}CHOH$ and $\dot{M}B$ may react with themselves (*e.g.*, disproportionation) or with O_2, H_2O_2, O_2^-, or HO_2. These reactions have not yet been fully studied. However, one may assume that reactions involving these radicals are fast. Some relevant rate constants available from the literature are included in Table 1. The present study has failed to observe an absorption due to MB-semiquinone (λ_{max}: 420 nm, $\varepsilon=10{,}400$ $M^{-1}cm^{-1}$),[6] as may be seen from Fig. 2a. This may be because $\dot{M}B$ is too short-lived to attain measurable steady-state concentrations under our experimental conditions. Therefore, it may be concluded that the reversible change in absorption at 650 nm during irradiation is related to the formation of the colorless leuco-base (MBH), which is the fully reduced form of the dye and which is well known to be rapidly oxidized by O_2 to MB^+.[3,4]

Table 1. Some relevant rate constants

Reaction	$k(M^{-1}s^{-1})$	Ref.
$MB^+ + \dot{R}CHOH$ (D-glucose)	2×10^9	12
$MB^+ + e^-_{aq}$	2.5×10^{10}	6
$\dot{M}B + \dot{M}B$ (pH 7)	3.0×10^9	6
$MB^+ + OH$	1×10^{10}	11
$CH_3\dot{C}HOH + O_2$	4.6×10^9	13
$\dot{R}CHOH$ (D-glucose) $+ O_2$	1.6×10^9	13

Rate Constant for ($MBH+O_2$) Reaction. The radiation-induced chemical reactions which finally yield leuco-MB in the present system may be very complicated. However, they all occur in a very short time compared with the time required for the re-oxidation of MBH by O_2. Thus, the reaction sequence forming MBH may be simply expressed as:

$$MB^+ \xrightarrow{G_4 I} MBH \quad (4)$$

where G_4 denotes the 100 eV-yield of MBH in the bulk of the solution, and I, the intensity of the radiation energy absorbed. The re-oxidation of MBH by O_2 may be:

$$MBH + O_2 \xrightarrow{k_{5a}} MB^+ + HO_2^- \quad (5a)$$

Alternatively, it may be:

$$MBH + O_2 \xrightarrow{k_{5b}} \dot{M}B + HO_2 \quad (5b)$$

followed by a further oxidation of $\dot{M}B$, which can be assumed to be much faster than Reaction (5b). In either case, the rate of the disappearance of MBH may be expressed as $k_5[MBH][O_2]$. Thus, for the steady-state concentration of MBH (designated as $[MBH]_s$):

$$d[MBH]/dt = 0 = G_4 I - k_5[MBH]_s[O_2] \quad (6)$$

We also obtain the relation:

$$[MB^+]_0 = [MB^+]_s + [MBH]_s \quad (7)$$

where $[MB^+]_0$ is the initially-added MB^+ concentration, and $[MB^+]_s$, the steady-state MB^+ concentration observed during irradiation. Equation (6) will hold as long as a sufficient amount of the solutes (O_2, organic substance) remains in the solution under the irradiation. This condition will be fulfilled while the total absorbed dose does not exceed 10^{19} eV g^{-1} in the present case (4×10^{-4} M O_2 will be consumed at this dose if it disappears with $G=3$).

The G(MBH) values for deaerated solutions in the presence of sufficient amounts of organic substances have been reported to be 3.3,[8] 2.75,[9] and 2.9.[9] Thus, we may take a value of 3 for the value of G_4 in Eq. (6). The value of $[O_2]$ is 3.7×10^{-4} M for aerated aqueous solutions at 25°C.[7] Thus, one obtains:

$$[MBH]_s = \left(\frac{0.81\times10^4}{k_5}\right)\times I \quad (8)$$

Figure 5 plots the $[MBH]_s$-values *vs.* I. These have been calculated using Eq. (7) and from the measurements of $[MB^+]_s$ at various I values (by varying the distance between the reaction cell and the radiation source) in the (3.7×10^{-7} M MB^++0.1 M ethanol) system. The reasonable fit of the data to a straight line demonstrates the validity of the above scheme. From the slope of the line, one obtains:

$$k_5 = (0.6\pm0.2)\times10^4\ M^{-1}s^{-1} \text{ at neutal pH.}$$

Thus, the half-life of the leuco-form in the present

7) H. Hotta, A. Terakawa, and S. Ohno, This Bulletin, **33**, 442 (1960).

8) E. Hayon, G. Scholes, and J. Weiss, *J. Chem. Soc.*, **1957**, 301.

9) M. J. Day and G. Stein, *Radiation Res.*, **6**, 666(1957).

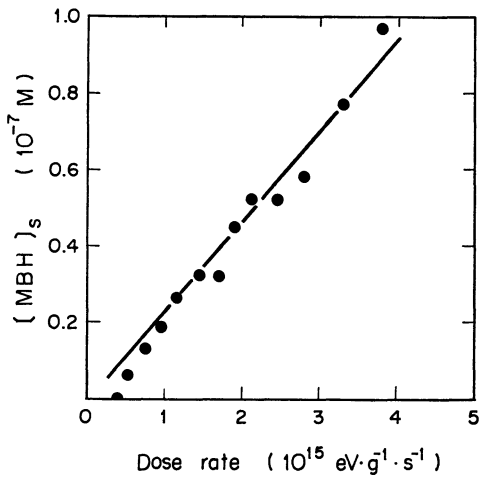

Fig. 5. Steady-state concentrations of leuco-form, $[MBH]_s$, as a function of dose rate, I.

system may be calculated to be $\ln 2/k_5[O_2]=0.3$ s.

Irreversible Decoloration of MB^+. It is generally accepted that the irreversible bleaching of MB^+ occurs by the attack of OH-radicals and that about three OH-radicals are required for one molecule of MB^+ bleached:[3]

$$MB^+ + OH \rightarrow MB^{2+} + OH^- \quad (9)$$

Thus, competition between Reactions (2) and (9) in the (3×10^{-7} M $MB^+ + 10^{-4}$ M CH_3OH) system would lead to the expression:

$$G(-MB^+)_{irrev.} = \frac{G_{OH}}{3}\left(\frac{k_9[MB^+]}{k_9[MB^+] + k_2[CH_3OH]}\right) \quad (10)$$

One may use a value of 0.05 for $G(-MB^+)_{irrev}$ from Fig. 3b, a value of 2.5 for G_{OH},[1] and a value of 5×10^8 $M^{-1}s^{-1}$ for k_2.[10] The value of k_9 is then calculated to be 1.1×10^{10} $M^{-1}s^{-1}$, which is in fair agreement with the value obtained by Hutchinson.[11]

Applicability of the Present Method. The apparatus used in this work may be used to observe the change due to irradiation in the optical absorption spectrum of any transparent material. An optical density change of 0.01 is detectable with the present apparatus. This means that the smallest concentration change which is detectable is approximately 10^{-8} M if a light absorbing species has an extinction coefficient of 10^4 $M^{-1}cm^{-1}$ (optical path-length of the cell: 40 cm). The presence of transient species during a continuous irradiation will be observed if the intensity of radiation is sufficient to produce a steady-state concentration higher than 10^{-8} M. The conditions required for this are determined by means of an equation similar to Eq. (6);

$$GI\times(\text{half-life}) \approx [\text{transient}] \quad (11)$$

With numerical values appropriate to our present work ($G=3$, $I=3.9\times10^{15}$ $eVg^{-1}s^{-1}$, [transient]$=10^{-8}$ M), it may be concluded that optically-absorbing species with a half-life of 0.06 s or longer will be detected and their steady state concentration determined. Provided that the G-value, the rate of generation, is known from other methods (*e.g.*, chemical analyses), information on the rate constant for reactions of the transient and, thus, its lifetime in various media may be obtained.

This method does not utilize kinetic spectroscopy and can be readily used at laboratories with no electron accelerator. However, since the measurable species must have a lifetime of at least 0.06 s, the widespread application of the method cannot be expected at the present moment (*cf.*, the lifetime of the hydrated electron in water, ≈1 ms). Considerable refinement of this method would be possible by, for example, (1) improving the sensitivity of the detection system or (2) employing a larger radiation source. Of these two possibilities, the former one is of more practical interest. One may readily improve the sensitivity by employing a longer optical path-length of the cell. Alternatively, one may employ a highly sensitive detection technique, for example, a lock-in amplifier in conjunction with analyzing light choppers. Attempts to study shorter-lived species by the use of the present spectrophotometer method with some modifications are now in progress in our laboratory.

10) M. Anbar and P. Neta, *Int. J. Appl. Rad. Isotopes*, **18**, 493 (1967).
11) F. Hutchinson, *Radiation Res.*, **9**, 13(1958).
12) E. A. Balazs, J. V. Davies, G. O. Phillps, and D. S. Scheufele, *J. Chem. Soc.*, **1968** C, 1424.
13) G. E. Adams and R. L. Willson, *Trans. Faraday Soc.*, **65**, 2981 (1969).

Thermoelectric Power of the Iodine Complexes of Aromatic Diamines and Thiazines

Mizuka SANO*, Koichi OHNO**, and Hideo AKAMATU***

Department of Chemistry, Faculty of Science, The University of Tokyo, Hongo, Tokyo

(Received May 24, 1971)

The thermoelectric power of *N,N'*-diphenyl-*p*-phenylenediamine·I_2, *N,N'*-di-β-naphthyl-*p*-phenylenediamine·$I_{3.5}$, phenothiazine·I_3, and *N*-methylphenothiazine·I_3 was measured in the temperature range from −35 to 140°C. The observed power for each complex was explained by means of the mechanism of mixed conduction of electrons with holes, and the ratio of electron-conduction to hole-conduction was estimated as a function of temperature. In the iodine complexes of the substituted *p*-phenylenediamines the conductivity due to electrons is found to be larger than that due to holes, while in phenothiazine·I_3 holes contribute more to the conductivity. In *N*-methylphenothiazine·I_3, the hole-conduction is predominant in the higher temperature region and the electron-conduction in the lower temperature region.

Solid electron-donor-acceptor complexes, particularly those involving appreciable contribution from the dative structures, exhibit interesting electric and magnetic properties. *N,N'*-diphenyl-*p*-phenylenediamine (DPPD),[1,2] *N,N'*-di-β-naphthyl-*p*-phenylenediamine (DNPD),[1] phenothiazine (PT),[3], and *N*-methylphenothiazine (MPT)[3] have been reported to form stable iodine complexes. The crystal structure analysis of the iodine complex of DPPD has shown that the iodine atoms are stacked in columns perpendicular to the *ac* plane, and the donor molecules are arranged in layers 3.77 Å apart.[4] The iodine columns are coordinated to NH groups of the donor. The infrared spectrum of phenothiazine-iodine complex has been reported to be identical with that of semiquinoid phenazathionium bromide, indicating that the ground state of the solid complex is dative.[3]

The magnetic properties of these iodine complexes have been reported.[1] They are either diamagnetic or weakly paramagnetic at room temperature. After corrections are made for the diamagnetic contribution and for the paramagnetic one due to paramagnetic impurities, the intrinsic paramagnetic susceptibility is found to decrease slightly with the decrease in temperature. The exchange coupling constant J between ionradicals in a solid has values of 0.05 eV for DPPD·I_2, 0.08 for DNPD·$I_{3,5}$, 0.04 for MPT·I_3, and over 0.1 for PT·I_3.

These complexes show high electrical conductivity but neither photoconductivity nor Hall voltage, so that only the measurement of thermoelectric power seems to be a reliable means of determining the type of conduction. In this paper we present the results on the thermoelectric power measurement of the complexes and an estimation of the ratio of electron-conduction to hole-conduction in the solid.

Experimental

DPPD·I_2, dark green crystals with metallic lustre were obtained by mixing benzene solutions of the diamine and iodine in the stoichiometric ratio. (Found: C, 42.86; H, 3.40; N, 5.70%. Calcd for $C_{18}H_{16}N_2I_2$: C, 42.05; H, 3.14; N, 5.45%).

DNPD·$I_{3.5}$, dark brownish black crystalline powder precipitated on addition of a benzene solution of iodine to a benzene solution of the diamine (Found: C, 38.97; H, 2.17; N, 3.46%. Calcd for $C_{26}H_{20}N_2I_{3,5}$: C, 38.81; H, 2.51; N, 3.48%).

PT·I_3 was prepared by mixing benzene solutions of the components in the stoichiometric ratio.[3] MPT·I_3 was prepared from an ether solution.

A sample powder was sandwiched in a Teflon holder between small disks of platinum supported by two copper cylinders. Each platinum disk was insulated electrically from the copper cylinder with a piece of Teflon sheet. The powder was pressed under the pressure of 100 kg/cm² with an aid of a lever. Thickness of the sample was adjusted to 0.2—0.5 cm. The junctions of copper-constantan thermocouples were soldered to the platinum disks.

Cylindrical electric heaters attached to the upper and lower portions of the copper cylinders were controlled to provide temperature gradient in a sample. For measurements below room temperature the copper cylinders were cooled with dry ice cubes. By this arrangement the temperature dependence of thermoelectric power could be measured in the range from −35 to 140°C. Reference junctions connected to the thermocouples were insulated electrically from one another and placed in an ice-water bath maintained at 0°C.

The thermo-electromotive force (emf) of a sample observed through the copper leads of the thermocouples and that of each thermocouple were measured potentiometrically by use of suitable switching systems. The thermoelectric power Q is calculated by the relation.

$$Q = \Delta V/\Delta T, \quad (1)$$

where ΔV represents the thermo-emf generated in the sample-platinum-copper circuit by the temperature difference ΔT between the sample-platinum junctions. The average temperature of the junctions is taken to be the temperature of sample.

The electrical conductivity of the same sample specimen packed in the Teflon holder was measured by the *DC* method as a function of temperature. The temperature of the specimen was controlled with the aid of a third electric heater in conjunction with a dry ice cooling bath.

* Present address: Department of Materials Science, The University of Electro-Communications, Chofu, Tokyo.

** Present address: The Institute for Solid State Physics, The University of Tokyo, Azabu, Tokyo.

*** Present address: Institute of Materials Science and Engineering, Yokohama National University, Minato-ku, Yokohama.

1) Y. Sato, M. Sano, and H. Akamatu, Proceedings of the Symposium on Molecular Structures, Sapporo (1967), p. 231.

2) V. Hádek, *J. Chem. Phys.*, **49**, 5202 (1968).

3) Y. Matsunaga, *Helv. Phys. Acta*, **36**, 800(1963).

4) J. Huml, *Acta Cryst.*, **22**, 29 (1967).

Results

All the complexes showed high absorption coefficients in the visible and near-infrared spectral regions. The absorption peaks, though broad and poorly defined, were found around 2.2, 1.7, and 1.1 μ for PT·I_3, MPT·I_3, and DPPD·I_2, respectively. The peaks in the near-infrared region are characteristic of solid ionradical salts with strong exchange coupling between ionradical components.[5]

The complexes gave rise to thermo-emf in the order of 10^{-3} V between the platinum electrodes for a temperature difference of about 10°. The absolute thermoelectric power of the complexes was obtained by correcting for the value for copper.[6] The power of each complex was found to be constant at a fixed sample temperature, being independent of the amount of provided temperature gradient around 10° and of the thickness of the sample. Good reproducibility of power was obtained by the rise and fall of temperature within the temperature range. The iodine complex of 4,4′-bis(dimethylamino)-diphenylamine (DADA), however, showed no reproducible power when it was heated up to 40°C.

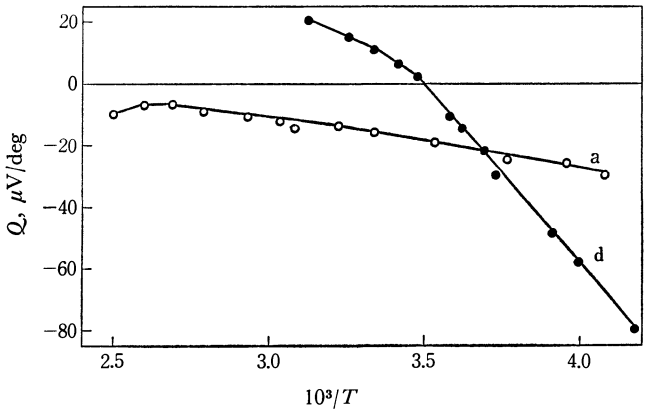

Fig. 1. Thermoelectric powers for (a) DPPD·I_2 and (d) MPT·I_3.

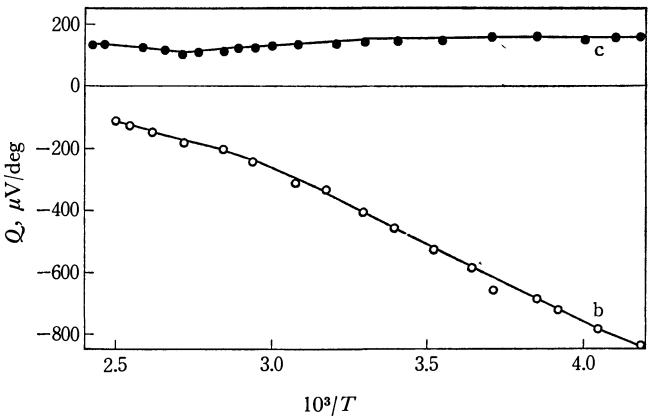

Fig. 2. Thermoelectric powers for (b) DNPD·$I_{3.5}$ and (c) PT·I_3.

Values for the power at 15°C are summarized in Table 1. The sign of power refers to the sign of developed emf at the cold junction. The power for DPPD·I_2, DNPD·$I_{3.5}$, and MPT·I_3 was found to decrease with falling temperature, while that for PT·I_3 changed little with temperature change. The temperature dependence of power is shown in Figs. 1 and 2.

The logarithm of conductivity σ was found to be proportional to the reciprocal of temperature $1/T$ in the entire temperature region, and the activation energy for conduction E_a could be calculated by the formula

$$\sigma = \sigma_0 \exp\left(-\frac{E_a}{kT}\right). \tag{2}$$

The activation energy and specific resistivity ρ at 15°C are summarized in Table 1.

Table 1. Thermoelectric power and specific resistivities at 15°C, and activation energies for conduction

	Q (μV/deg)	ρ (Ω·cm)	E_a (eV)
DPPD·I_2	−20	3.5×10	0.095
DNPD·$I_{3.5}$	−540	5×10^4	0.37
DADA·I	−860	1.3×10^5	—
PT·I_3	+150	1.7×10	0.164
MPT·I_3	+3	2.3×10^2	0.14

Discussion

Johnson and Lark-Horovitz derived the following formula (Eq. (24) in Ref. 7) as a general expression for thermoelectric power of a band-model semiconductor.[7]

$$Q = -\frac{k}{e(n_1c+n_2)}\left[A(n_1c-n_2) - n_1c\ln\left\{\frac{n_1h^3}{2(2\pi m_1kT)^{3/2}}\right\} + n_2\ln\left\{\frac{n_2h^3}{2(2\pi m_2kT)^{3/2}}\right\}\right], \tag{3}$$

where n_1 and n_2 are the densities and m_1 and m_2 the effective masses of conduction electron and hole, respectively. c denotes the mobility ratio μ_1/μ_2, and A the scattering parameter. The parameter comes from the energy of transferring average carrier, and varies somewhat with the scattering process. Scattering theory predicts this quantity varies from 2 for neutral scattering centers to 4 for ionic centers.[8]

In the case where only one type of carrier is present, the expression for the power is obtained from Eq. (3) by dropping the terms pertaining to another type of carrier. Thus we get for electrons

$$Q = -\frac{k}{e}\left[A - \ln\left\{\frac{n_1h^3}{2(2\pi m_1kT)^{3/2}}\right\}\right]. \tag{4}$$

5) Y. Sato, M. Kinoshita, M. Sano, and H. Akamatu, This Bulletin, **42**, 548(1969).

6) A. H. Wilson, "Theory of Metals," 2nd ed., Cambridge Univ. Press, London (1953), p. 207.

7) V. A. Johnson and K. Lark-Horovitz, *Phys. Rev.*, **92**, 226 (1953).

8) T. A. Kontorova, *J. Tech. Phys. Moscow*, **24**, 1291, 1687, 2217 (1954).

Within the limitation of the Boltzmann distribution, the carrier density n_1 can be related to the Fermi level ζ by the equation

$$n_1 = \frac{2(2\pi m_1 kT)^{3/2}}{h^3} \exp\left(-\frac{\varepsilon_1{}^0-\zeta}{kT}\right), \quad (5)$$

where $\varepsilon_1{}^0$ is the energy at the bottom of the conduction band. Substituting Eq. (5) into Eq. (4), we obtain

$$Q = -\frac{k}{e}\left[\frac{\varepsilon_1{}^0-\zeta}{kT}+A\right]. \quad (6)$$

The expression for the power only by holes is given by

$$Q = +\frac{k}{e}\left[\frac{\zeta-\varepsilon_2{}^0}{kT}+A\right], \quad (7)$$

where $\varepsilon_2{}^0$ is the energy at the top of the valence band.

Substitution of both densities of electron and hole into Eq. (3) gives the following expression for mixed conduction of electrons with holes.

$$Q = -\frac{k}{e}\left[\frac{(x-1)}{(x+1)}\left(\frac{E_g}{2kT}+A\right)+\frac{(\varepsilon_1{}^0-\zeta)-(\zeta-\varepsilon_2{}^0)}{2kT}\right], \quad (8)$$

where x denotes the conductivity ratio $n_1\mu_1/n_2\mu_2$, and E_g the forbidden band width.

Explanation of the experimentally obtained curve of the power for each complex was undertaken by means of the formula for the carriers of only one type, on the assumption that the energy difference between the Fermi level and the conduction band $\varepsilon_1{}^0-\zeta$ or the valence band $\zeta-\varepsilon_2{}^0$ is equal to the observed activation energy of conduction E_a. Only the formula including the value of A with negative sign is found to represent the observed power. Theory does not allow a negative A value, so that this type of conduction is ruled out.

In a triethylammonium(TCNQ)$_2$ single crystal the sign of the majority of carriers has been reported to be negative along the c-crystal axis and positive along the a-axis.[9] The result suggests a mixed contribution from both types of carriers to the conductivity in ionradical crystals.

Comparing the expression for mixed conduction

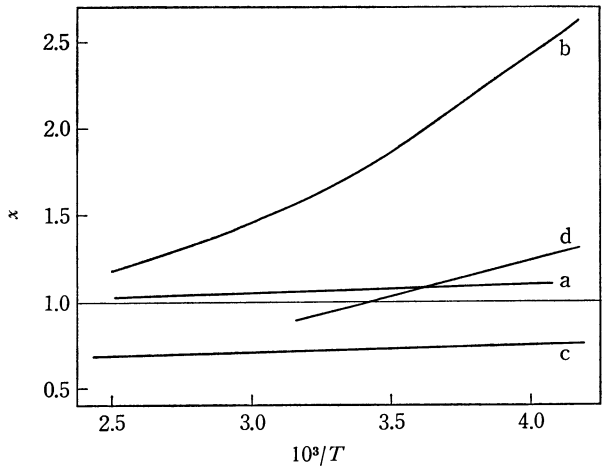

Fig. 3. Conductivity ratios for (a) DPPD·I_2, (b) DNPD·$I_{3.5}$, (c) PT·I_3, and (d) MPT·I_3.

Eq. (8) with the experimentally obtained curve on the assumption that for an ionradical solid the value of A equals 4, as found for ionic scattering centers in ionic crystals, and that the last term in Eq. (8) is negligibly small compared with the first one, one can estimate the conductivity ratio x, and thus determine the type of conduction. In this analysis twice the value for E_a is used for E_g. The conductivity ratio thus obtained is shown in Fig. 3 as a function of temperature. If the electron density n_1 is taken to be equal to the hole density n_2, the value for x corresponds to the mobility ratio μ_1/μ_2. This condition, however, does not seem to hold in the entire range of temperature.

The x values for DPPD·I_2 and DNPD·$I_{3.5}$ are greater than unity, indicating that the conductivity due to electrons is larger than that due to holes. The x-value smaller than unity for PT·I_3 indicates that holes contribute more to the conductivity in the complex. In MPT·I_3, on the other hand, the hole-conduction is predominant in the higher temperature region and the electron-conduction in the lower temperature region. The change of x-value with temperature seems to arise mainly from the different dependence of electron and hole mobilities on temperature.

9) J. P. Farges, A. Brau, D. Vasilescu, P. Dupuis, and J. Néel, *phys. stat. sol.*, **37**, 745(1970).

Solvent Effect on the Vibrational Structures of the Fluorescence and Absorption Spectra of Pyrene

Akira NAKAJIMA

Division of Chemistry, Research Institute of Applied Electricity, Hokkaido University, Sapporo

(Received May 24, 1971)

The anomalously large Ham effect observed in pyrene has been studied in various solvents at room temperature by measuring the fluorescence and absorption spectra. As in the case of benzene, the Ham bands of pyrene were assigned to the 0–0 and a_g-vibration bands. This was confirmed by fluorescence polarization measurement. The correlation of the intensities of the fluorescence and absorption bands to solvent polarities is discussed.

Despite much work on the solvent shifts[1-8] of electronic spectra, comparatively few studies of the solvent effect on their vibrational structures have been carried out. In general the vibrational components in the fine structure of a weak electronic transition are expected to show different intensity behaviors under the action of solvent perturbation.[9] Such a structural change in an electronic band system can be observed remarkably in an electronically forbidden transition containing both vibrationally-induced and forbidden components. However, the phenomenon can rarely be observed in the spectrum of an electronically allowed transition.[9]

Recently the author noticed that the vibrational structures of the fluorescence and absorption spectra of pyrene are markedly altered in various fluid solvents and this effect can be ascribed to the same phenomenon as that known as the Ham effect[10-15] well investigated on benzene. Extensive studies[9,13-18] of the Ham bands in the 2600 Å region of the benzene absorption revealed that the effect is taken to be the appearance of the symmetry forbidden 0–0 progression in the $^1B_{2u}$—$^1A_{1g}$ band system[19,20] affected by dispersion forces between benzene and solvent molecules. As has been demonstrated by Durocher and Sandorfy,[9] and also by Koyanagi,[18] this phenomenon is not restricted to benzene, but can be observed with many benzene derivatives,[9,16,17] naphthalene,[9,16] phenanthrene,[9] *p*-benzoquinone,[18] and perhaps a number of other aromatic molecules.

Most studies on the Ham effect have been performed mainly by the measurements of absorption spectra by adding some amount of highly polarizable substances at relatively low temperatures.[9,10,13,14,16,17] This work was carried out by observing both the fluorescence and the absorption spectra of pyrene in pure solvents at room temperature. When the first absorption band under consideration overlaps the neighboring strong band as in the case of pyrene, the studies by means of fluorescence spectra are advantageous, unless the solvent quenching of fluorescence occurs appreciably.

How the observed effect is to be associated with the solvent properties is a difficult problem of the work.

Experimental

Pyrene was purified by recrystallization, chromatography, zone-refining, and sublimation.

Spectroscopic grade (Dotite Spectrosol) *n*-hexane, cyclohexane, benzene, carbon tetrachloride, acetonitrile, *N,N*-dimethylformamide, and dimethylsulfoxide were obtained from Wako Pure Chemical Industries, Ltd. Spectroscopic grade ethyl ether and tetrahydrofuran were obtained from Kishida Kagaku Co., Ltd. GR grade methanol, ethanol, chloroform, 1,2-dichloroethane, toluene, *p*-dioxane, acetone, and ethyl acetate were purchased from Wako Pure Chemical Industries, Ltd. All these solvents were used without further purification. Isopentane and methylcyclohexane were purified by chromatographic adsorption on silica gel and subsequent fractional distillation. Chlorobenzene of Wako EP grade was dried and fractionally distilled.

The absorption spectra were measured with a Hitachi EPS-3 recording spectrophotometer. The fluorescence spectra were obtained using a Hitachi MPF-2A spectrofluorimeter with sensitivity corrections.[21] The fluorescence polarization spectrum was measured at 77°K in a mixture of methylcyclohexane and isopentane (1 : 1) by use of an apparatus constructed with a Hitachi G-3 grating monochromator and

1) Y. Ooshika, *J. Phys. Soc. Japan*, **9**, 549(1954).
2) E. Lippert, *Z. Naturforsch.*, **10a**, 541 (1955); *Z. Elektrochem.*, **61**, 962(1957).
3) N. Mataga, N. Kaifu, and M. Koizumi, This Bulletin, **29**, 465 (1956).
4) E. G. McRae, *J. Phys. Chem.*, **61**, 562 (1957).
5) H. C. Longuet-Higgins and J. A. Pople, *J. Chem. Phys.*, **27**, 192 (1957).
6) O. E. Weigang, *ibid.*, **33**, 892(1960).
7) S. Basu, "Advances in Quantum Chemistry," Vol. 1, ed. by P-O. Löwdin, Academic Press, New York (1964), p. 145.
8) W. Liptay, *Z. Naturforsch.*, **20a**, 1441(1965).
9) G. Durocher and C. Sandorfy, *J. Mol. Spectry.*, **20**, 410 (1966).
10) J. S. Ham, *J. Chem. Phys.*, **21**, 756 (1953).
11) J. R. Platt, *J. Mol. Spectry.*, **9**, 288 (1962).
12) N. S. Bayliss and L. Hulme, *Australian J. Chem.*, **6**, 257 (1953).
13) S. Leach, R. Lopez-Delgado, and F. Delmas, *J. Mol. Spectry.*, **7**, 304 (1961).
14) S. Leach and R. Lopez-Delgado, "Advances in Molecular Spectroscopy," Vol. 1, ed. by A. Mangini, Pergamon Press, Oxford (1962), p. 419.
15) N. S. Bayliss and N. W. Cant, *Spectrochim. Acta*, **18**, 1287 (1962).
16) G. Durocher and C. Sandorfy, *J. Mol. Spectry.*, **14**, 400 (1964).
17) M. Koyanagi and Y. Kanda, *Spectrochim. Acta*, **20**, 993 (1964).
18) M. Koyanagi, *J. Mol. Spectry.*, **25**, 273(1968).
19) A. Kronenberger, *Z. Physik*, **63**, 494(1930).
20) H. Sponer, G. Nordheim, A. L. Sklar, and E. Teller, *J. Chem. Phys.*, **7**, 207(1939).
21) E. Lippert, W. Nägele, I. Seibold-Blankenstein, U. Staiger, and W. Voss, *Z. Anal. Chem.*, **170**, 1(1959).

a Hitachi EPU-2A prism monochromator.

All the solvents used were confirmed to emit no luminescence having any essential influence on the fluorescence spectra with excitation at about 330 mμ. The concentration of pyrene for fluorescence measurements were of the order of 10^{-5} mol/l. The gas-phase fluorescence was measured with a non-fluorescent square quartz cell containing a small amount of pyrene, evacuated and sealed, in a regulated electric furnace.

Results and Discussion

The spectral changes of pyrene fluorescence in various solvents at room temperature are shown in Figs. 1 and 2. The characteristic bands are named *a*, *b*, *c*, *d*, *e* in the decreasing order of wave number. All the fluorescence spectra were normalized for convenience at 26200 cm^{-1} (band *c*). The vapor-phase spectrum is somewhat diffuse because of the high temperature (180°C) at which it was measured. The bands are observed as shoulders. The relative intensities of the bands *a*, *b*, and *e* increase markedly with the increase of the apparent solvent polarity in going from the gaseous state or a nonpolar solvent such as *n*-hexane to a highly polar solvent such as acetonitrile, while the frequency shifts of these bands are very small and nearly comparable to the experimental error. The slight solvent shifts are in striking contrast to the pronounced solvent enhancement.

The absorption spectra in the region of the first singlet-singlet transition are also shown in Fig. 2. Since no spectral change can be expected to occur, the absorption spectra were not measured in the regions of higher strongly allowed transitions. We see that the fluorescence spectra bear a general mirror-image relationship to the absorption spectra, taking account of the absorption tail of the second intense transition. The first and second absorption bands (corresponding to the fluorescence bands *a* and *b*, respectively) also increase similarly with increasing solvent polarity. It can therefore be accepted that the Ham effect for pyrene takes place

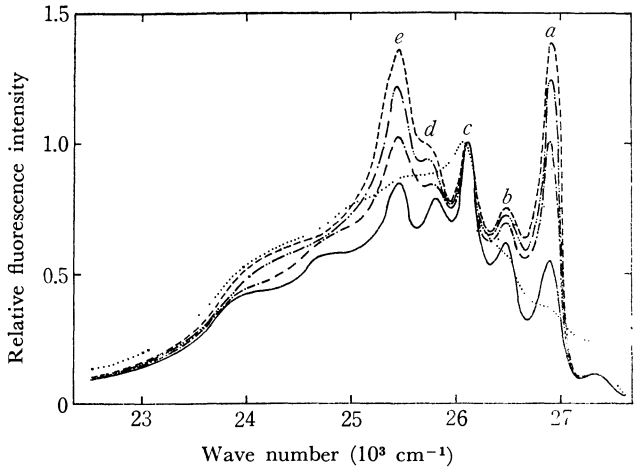

Fig. 1. Fluorescence spectra of pyrene in various solvents. ·····: gaseous state, ——: *n*-hexane, —·—·—: benzene, —··—··—: methanol, -----: acetone.

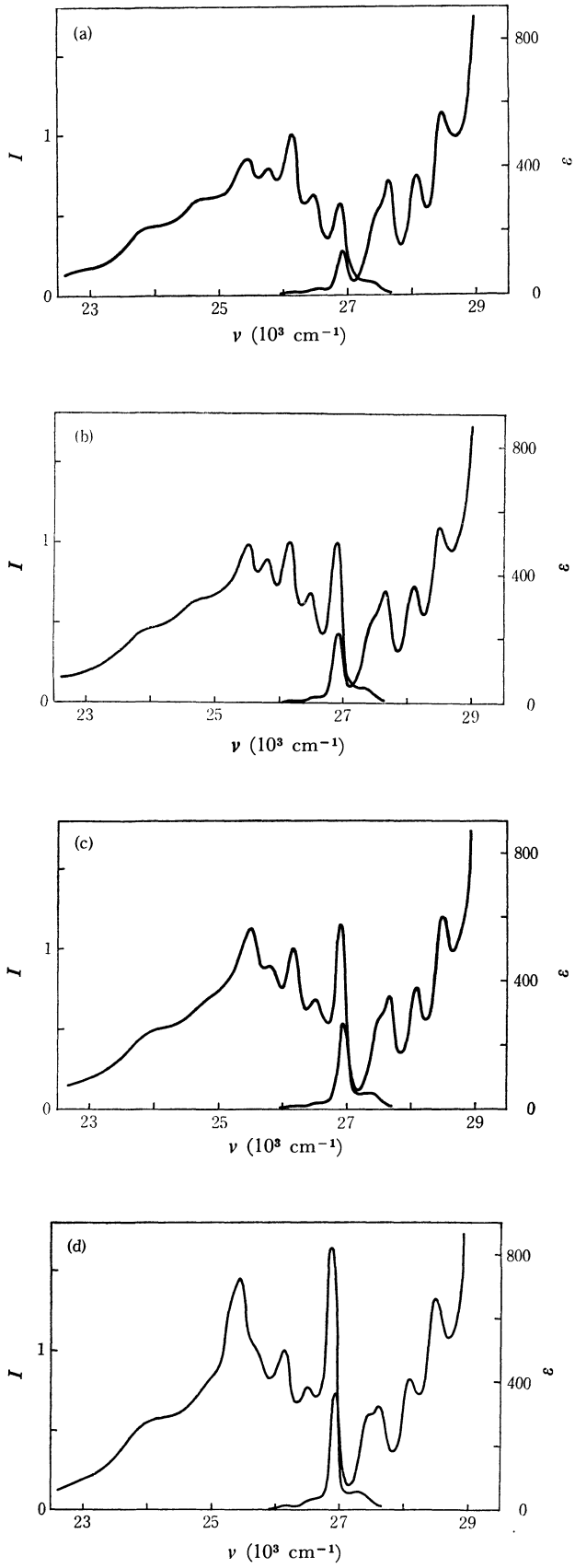

Fig. 2. Fluorescence and absorption spectra in various solvents at room temperature.
(a) cyclohexane, (b) ethyl ether, (c) ethanol, (d) acetonitrile.

TABLE 1. OBSERVED WAVE NUMBERS AND ASSIGNMENT OF VIBRATION BANDS OF FLUORESCENCE

Band	Present work			Klimova[22]	Assignment	
	n-hexane, 25°C (cm^{-1})	methylcyclohexane + isopentane, 77°K (cm^{-1})	Polarization	*n*-hexane, 4°K (cm^{-1})		
a	26880	26880	−0.18	26837	0	0-0
b	26450	26460	+0.01	26431	406	a_g
c	26110	26100	+0.02	26100, 26034	736, 802	?
d	25770	25780	+0.24	25730	1107	b_{1g}
e	25450	25460	+0.03	25432	1405	a_g
		25300		25207, 25201		
(*g*)		25050	+0.16	25027	406+1405	a_g
		24850		24863, 24797		
(*i*)	24690	24670	+0.16	24697, 24630		
(*j*)		24380	+0.27	24326	1107+1405	a_g+b_{1g}
		24210		24200, 24192		
(*l*)		24040	+0.15	24028	1405×2	a_g
(*m*)	23870	23850	+0.20	23801	1405+1631	a_g

to almost the same extent in the absorption and the fluorescence spectra.[22]

As has been suggested,[9] the Ham effect proves to be a helpful tool in vibrational analysis. In analogy with benzene, the solvent-enhanced components can be assigned to the 0–0 band, the a_g-vibration bands and their progressions.[9,14,17,20] From the other vibrationally-induced bands much less influenced by the solvent, information on the mechanism of intensity borrowing due to vibronic coupling[20,23] can be deduced. As given in Table 1, the assignment of the vibrational bands of the fluorescence spectrum was made in reference to the reliable work by Klimova.[24] The band *c*, though strong, could not be assigned.

Based on the presence of the b_{1g}-vibration bands and other evidences,[25–27] Klimova concluded that the first excited singlet electronic state of pyrene (belonging to the point group D_{2h}) has B_{3u} symmetry and the second, B_{2u}.[24] The first singlet transition $^1B_{3u} \leftarrow {}^1A_{1g}$ is, like that of naphthalene,[9] not symmetry forbidden[25] but the contributions to the transition moment cancel each other in a good approximation.

For the sake of confirmation the fluorescence polarization of pyrene[27–29] was measured by the usual photoselection technique.[30] The polarization spectrum together with the low-temperature fluorescence spectrum is illustrated in Fig. 3. It is seen that the weak components are intensified with the increased solvent polarity by cooling and by the additional crystal forces in the rigid matrix.[17,31] The polarization of the main part of the band system is shown to be weakly parallel to the direction of the moment of the second electronic transition. At the wave numbers for the b_{1g}-vibration bands (the *d* band and some bands at lower energies) the polarizations are positive, indicating that the intensity is derived from the neighboring second electronic state with B_{2u} symmetry through coupling with the b_{1g} vibrations.[27] On the other hand, the 0–0 band (*a*) and a_g-vibration bands (*b*, *e*) are negatively polarized against

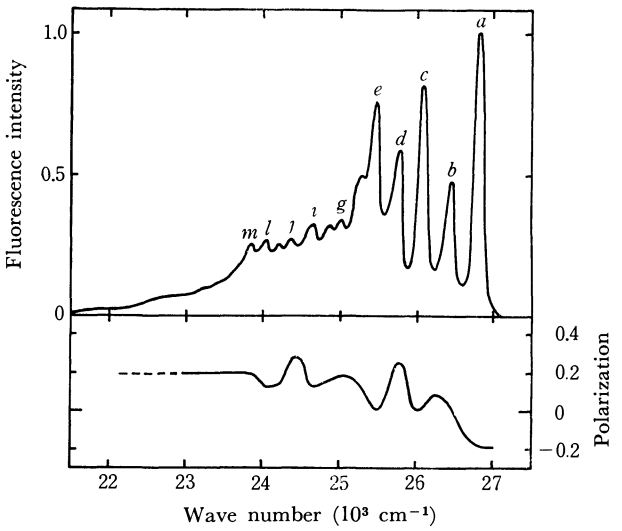

Fig. 3. Polarization and fluorescence spectra of pyrene at 77°K in a methylcyclohexane-isopentane (1 : 1) mixture.
Above: Fluorescence spectrum,
Below: Polarization as a function of wave number with excitation at 30300 cm^{-1}.

22) Since the relative intensities of the fluorescence bands *I* are given as the ratios of their observed intensity to that of the *c* band, the intensity variation of the *c* band in various solvents may be disregarded. However, it can be regarded as small, because the intensity of the third absorption band being a mirror image of the *c* band changes within 20% in the solvents used and most part of this change is affected by the solvent-broadened absorption tail of the second strong transition.

23) D. P. Craig, *J. Chem. Soc.*, **1950**, 59.
24) L. A. Klimova, *Opt. Spectry.*, **15**, 185 (1963).
25) N. S. Ham and K. Ruedenberg, *J. Chem. Phys.*, **25**, 1, 13 (1956).
26) J. Tanaka, *Suppl. Progr. Theoret. Phys.*, No. 12, 183 (1959).
27) H. Zimmerman and N. Joop, *Z. Elektrochem.*, **65**, 138 (1961).
28) R. W. Williams, *J. Chem. Phys.*, **26**, 1186 (1957).
29) R. M. Hochstrasser, *ibid.*, **33**, 459 (1960).
30) A. C. Albrecht, *J. Mol. Spectry.*, **6**, 84 (1961).
31) Y. Kanda, Y. Gondo, and R. Shimada, *Spectrochim. Acta*, **17**, 424 (1961).

the background of positive polarization, in harmony with the assignment of the first excited singlet π state to B_{3u} symmetry.[24,27]

Care should be taken to make a correct symmetry assignment of an electronic state with several different vibrational components by polarization measurements.[27,29] In this sense the solvent-enhanced 0–0 band can play a very significant role.

Considering the relation between the intensities of the Ham bands and the properties of the solvent molecules, the Ham effect might be due to the reduction of molecular symmetry in the field of surrounding solvent molecules or to the distortion of the π electron cloud by the environmental perturbation.[9,12,14,17,18] Confirmation of the cause of the effect is, however, very difficult.

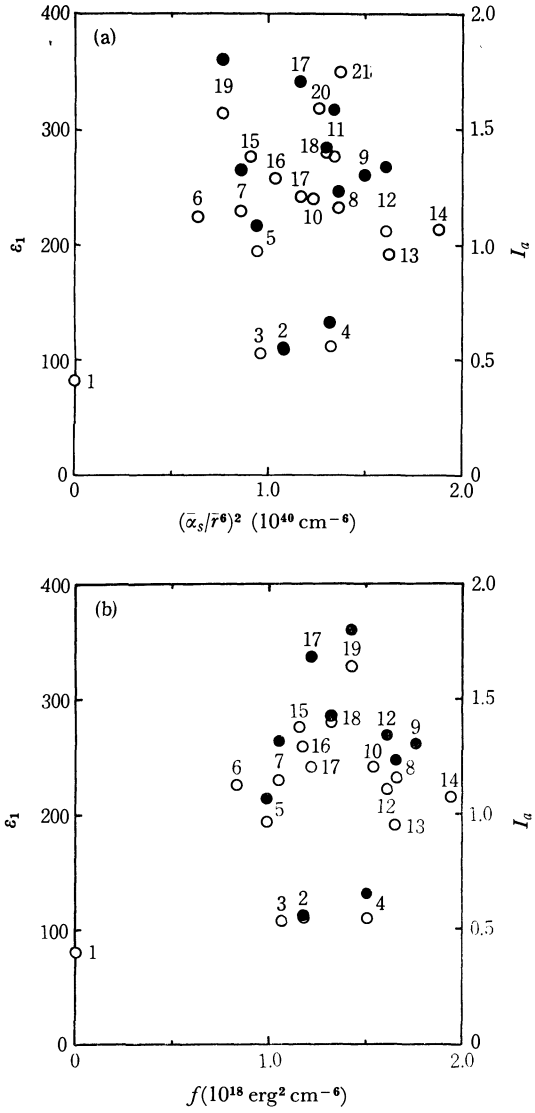

Fig. 4. Plots of the molar extinction coefficient ε_1 of the 0-0 absorption band and the intensity I_a of the a fluorescence band *vs.*
(a) the square of relative dispersion energy and (b) the square of dispersion *plus* induction terms.
1: gas, 2: *n*-hexane, 3: isopentane, 4: cyclohexane, 5: ethyl ether, 6: methanol, 7: ethanol, 8: chloroform, 9: carbon tetrachloride, 10: dichloromethane, 11: dichloroethane, 12: benzene, 13: toluene, 14: chlorobenzene, 15: acetone, 16: ethyl acetate, 17: tetrahydrofuran, 18: dioxane, 19: acetonitrile, 20: *N*,*N*-dimethylformamide, 21: dimethylsulfoxide. ○: fluorescence, ●: absorption.

In the study of the Ham bands of benzene, Koyanagi[17,18] showed a correlation between the apparent molar extinction coefficient of the origin band and the square of the relative quantity relating to dispersion energy $(\bar{\alpha}_s/\bar{r}^6)^2$, where $\bar{\alpha}$ denotes the mean polarizability of the solvent[32] and $\bar{r}$ the mean intermolecular distance between the solute and the solvent molecules.[33,34] Following his theory,[18] the effect of dispersion forces[35] was examined by a similar plot of the molar extinction coefficient ε_1 of the 0–0 band for absorption or the relative intensity I_a of the a band for fluorescence against $(\bar{\alpha}_s/\bar{r}^6)^2$ shown in Fig. 4(a). No perceptible trend can be found among these scattered points. Taking further into account not only the dispersion term[35] including the ionization potentials of the solute and the solvent but also the induction term arising from the interaction between the solvent permanent dipole and the solute induced dipole, the following factor[17,18] was introduced in Fig. 4(b).

$$f = \left\{\left(\frac{3}{2}\cdot\frac{I_p\cdot I_s}{I_p+I_s}\cdot\bar{\alpha}_s + \bar{\mu}^2\right)\Big/\bar{r}^6\right\}^2$$

where I_p and I_s are the ionization potentials[36] of pyrene and the solvent, respectively, and $\bar{\mu}^2$ is the mean square of the solvent dipole moment.[34] The situation, however, is not as improved as might be expected. The errors inherent in the evaluation of the inverse twelfth power of $\bar{r}$ might become serious, but it should be kept in mind that $\bar{r}$ is the proper quantity to be uniquely determined from the molar volumes of the solute and solvent.[37] One possible explanation is that the molecular size of pyrene is several times larger than that of benzene, implying some local interaction between pyrene and the solvent molecules. It is likely that the approximation[18] of a polarizable rigid sphere to a solvent molecule would not be justified in the present system.

Some other attempts have been made to find a correlation. Since it appears that the dielectric constant D of the solvent is of major importance in the enhancement of the bands, it is instructive to plot ε_1 or I_a *vs.* the dielectric factor $(D-1)/(2D+1)$ for the

32) $\bar{\alpha}_s$ was calculated from the refractive index and the molar volume of the solvent.[33,34]

33) The Chemical Society of Japan, ed., "Kagaku Binran," (Handbook of Chemistry), Maruzen, Tokyo (1958).

34) A. Weissberger, E. S. Proskauer, J. A. Riddick, and E. E. Troops, Jr., ed., "Organic Solvents," Technique of Organic Chemistry, Vol. VII, Interscience, New York (1955).

35) F. London, *Z. Physik*, **63**, 245 (1930); *Z. Phys. Chem.*, **B11**, 222 (1930).

36) V. I. Vedeneyev, L. V. Gurvich, V. N. Kondrat'yev, V. A. Medvedev, and Ye. L. Frankevich, "Bond Energies, Ionization Potentials and Electron Affinities," Edward Arnold, London (1966).

37) $\bar{r}$ is a sum of the molecular radii of the solute and the solvent estimated from the respective molecular weight and density.[33] The molecular radius s of a solvent molecule assumed as spherical was calculated by the formula

$$4\pi s^3/3 = 0.7405\, V/N$$

V: molar volume, N: Avogadro number.

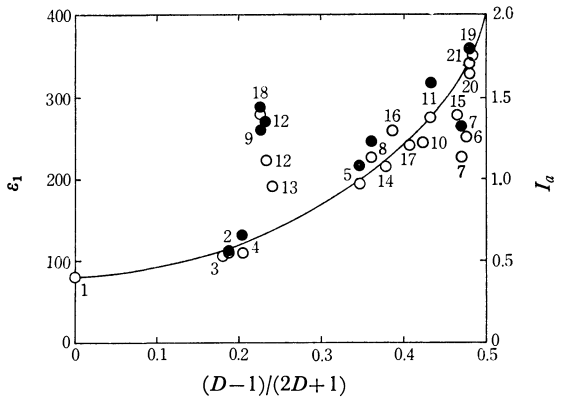

Fig. 5. Plots of ε_1 or I_a *vs.* $(D-1)/(2D+1)$.
See Fig. 4 for the numbering of the points. ○: fluorescence, ●: absorption.

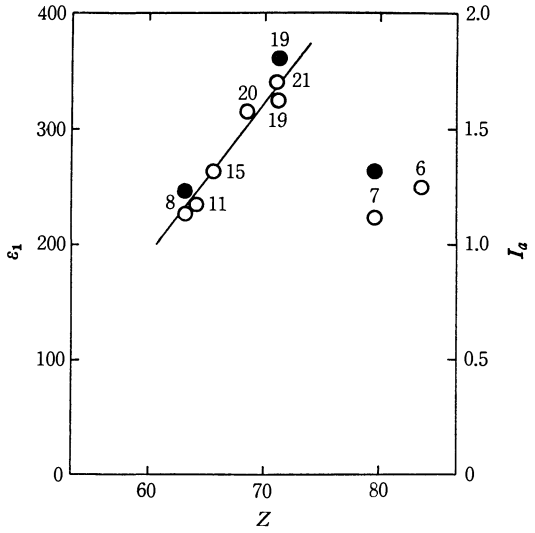

Fig. 6. Relationship between I_a (or ε_1) and the Z-value.
See Fig. 4 for the numbering of the points. ○: fluorescence, ●: absorption.

solvent as shown in Fig. 5. This reveals that there is an appreciably clear relation between them.[38] Moreover, an explicit relationship between the relative fluorescence intensities I_a and Kosower's Z-values[39] can be seen from Fig. 6 for the non-alcoholic polar solvents.

Recently, W. Liptay *et al.*[40] studied the solvent effects on the wave numbers and intensities of the absorption bands of fluorenone and showed the validity of their theoretical relation expressed by means of the ground- and excited-state dipole moments of the solute.[41] In the present case, however, their relation cannot be employed,[42] since pyrene has no dipole in either the excited or ground state.

Accordingly, in view of the appreciable dependence on the solvent dielectric constant, the following quantity was tentatively defined with an adjustable parameter χ:

$$f' = \left(\frac{D-1}{2D+1} - \chi \cdot \frac{n^2-1}{2n^2+1}\right),$$

where n denotes the refractive index of the solvent.[33,34] The case where $\chi=0$ was examined previously. As shown in Fig. 7, assuming that $\chi=0.5$, a rather good correlation was obtained between ε_1 or I_a and f', except for benzene and dioxane which are also known to give an anomalous effect on the frequency shifts of electronic spectra.[40] Other χ-values (*e.g.*, $\chi=1$) and other similar factors appearing in the ordinary solvent shift theories[1-8] have been found to give no better results. Applicability of the quantity given above in the original sense[1-3,8] to the molecule without dipole may, of course, be doubtful. The dielectric nature of solute-solvent interaction in the present system seems to be of significance. No correlation could be found with the energy parameters $\gamma\varepsilon^*$[43] employed in the solution theory[44] based on the cell method.[43] It is only inferred at present that both the dispersive and the inductive interactions involving more complex or microscopic solution structures might be of considerable importance.

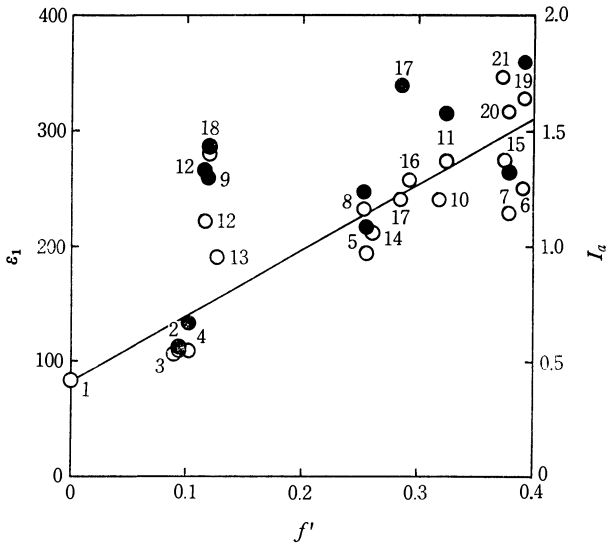

Fig. 7. Plots of ε_1 or I_a *vs.* f'.
See Fig. 4 for the numbering of the points. ○: fluorescence, ●: absorption.

It has been reported by Robinson[45] and Bayliss[46] that the Ham bands of benzene in carbon tetrachloride arise from the intensity borrowed from the solvent. Though the intensities of the Ham bands (and the shifts and broadenings of the spectra) of

38) The relation obtained by plotting ε_1 or I_a against the dielectric constant D itself is less clear.
39) E. M. Kosower, *J. Amer. Chem. Soc.*, **80**, 3253, 3261 (1958).
40) W. Liptay, H. Weisenberger, F. Tiemann, W. Eberlein, and G. Konopka, *Z. Naturforsch.*, **23a**, 377 (1968).
41) W. Liptay, *ibid.*, **21a**, 1605 (1966).
42) According to the formula obtained by W. Liptay,[41] the small remaining term when the ground- and excited-state dipole moments are zero is dependent only on the solvent refractive index.
43) K. Arakawa and O. Kiyohara, This Bulletin, **43**, 975 (1970).
44) J. S. Rowlinson, "Liquids and Liquid Mixtures," Butterworths, London (1969).
45) G. W. Robinson, *J. Chem. Phys.*, **46**, 572 (1967).
46) N. S. Bayliss, *J. Mol. Spectry.*, **31**, 406 (1969).

pyrene in carbon tetrachloride[47] are observed to be relatively large, the contribution by Robinson's mechanism[45] seems to be a smaller fraction of the observed effect.

Extention of this fluorescence study to aromatic molecules other than pyrene is of interest. Experiments in various mixed solvents provide some useful information regarding solvent-solute and, in certain cases, solvent-solvent interactions, in which connection, knowledge of the recent solution theory[44] is helpful. It might be interesting to investigate from similar viewpoints the vibrational structures of phosphorescence spectra[14,48] as well for a variety of compounds in different media.

The author wishes to thank Dr. O. Kiyohara and Prof. K. Arakawa for invaluable discussions. He is also indebted to Messrs. M. Aoi and K. Yamamoto for the instrumental calibrations. Grateful acknowledgements are due to the referee for his kind remarks.

47) Pyrene fluorescence was considerably quenched and a chemical reaction was observed in carbon tetrachloride. A specific interaction seems to take place.

48) Y. Kanda and R. Shimada, *Spectrochim. Acta*, **17**, 7 (1961).

BULLETIN OF THE CHEMICAL SOCIETY OF JAPAN, VOL. 44, 3277—3287 (1971)

Anharmonic Potential Functions of Simple Molecules. I. Direct Numerical Diagonalization of Vibrational Hamiltonian Matrix and Its Application to CO and HCl

Isao SUZUKI

Department of Chemistry, Faculty of Science, The University of Tokyo, Bunkyo-ku, Tokyo

(Received May 27, 1971)

The vibrational energy levels of diatomic molecules are related with the harmonic and anharmonic force constants by solving the vibrational Hamiltonian matrix numerically. The associated rotational levels are computed by two different methods; (1) perturbation treatment which utilizes the wave functions obtained, and (2) direct numerical diagonalization of the vibration-rotation submatrices. This approach, combined with the least-squares procedure, is applied to the determination of anharmonic force constants for CO and HCl molecules. Special attention is paid to the truncation effect of potential functions upon the calculated energy levels. Limitations in the usual perturbation method as well as the applicability of the present method to triatomic molecules are discussed.

The least-squares determination of the harmonic and anharmonic force constants from available spectroscopic data has been attempted for a few simple polyatomic molecules such as CO_2, HCN, OCS, N_2O, H_2O, and HCCH.[1-9] In the above determination, the potential function is expressed in terms of an appropriate coordinate system and is expanded in a power series, the terms quadratic through quartic being retained. The relationships between these force constants and the vibration and vibration-rotation energies are rather complicated; the perturbation technique is usually employed, and the vibration-rotation Hamiltonian of a polyatomic molecule is solved by the successive application of the contact transformations.[10,11] This may be an only approach to finding analytical expressions relating these force constants with energy levels, but some problems concerning its direct use in the least-squares determination of anharmonic force constants remain unsolved: (a) validity of the approximation used, (b) the truncation effect upon the higher order terms, and (c) treatment of anharmonic resonances, especially the handling of weak resonances. If, on the other hand, a proper set of basis wave functions (usually harmonic oscillator wave functions) is chosen, the vibrational Hamiltonian can readily be written down in matrix form, and the vibrational energy levels are obtained through numerical diagonalization. In addition, an orthogonal and normalized wave function can be obtained for each vibrational state as a linear combination of the original basis functions. The components of the eigen vector correspond to the coefficients of the linear combination, from which the rotational energy levels in a given vibrational state are derived by the standard pertur-

1) M. A. Pariseau, I. Suzuki, and J. Overend, *J. Chem. Phys.*, **42**, 2335 (1965).
2) I. Suzuki, *J. Mol. Spectry.*, **25**, 479 (1968).
3) I. Suzuki, M. A. Pariseau, and J. Overend, *J. Chem. Phys.*, **44**, 3561 (1966).
4) T. Nakagawa and Y. Morino, This Bulletin, **42**, 2212 (1969).
5) Y. Morino and T. Nakagawa, *J. Mol. Spectry.*, **26**, 496 (1968).
6) I. Suzuki, *ibid.*, **32**, 54 (1969).
7) M. A. Pariseau, PhD disertation, University of Minnesota (1964).
8) J. Pliva, V. Spirko, and D. Papousek, *J. Mol. Spectry.*, **23**, 331 (1967).
9) I. Suzuki and J. Overend, *Spectrochim. Acta*, **25A**, 997 (1969).
10) H. H Nielsen, *Rev. Mod. Phys.*, **23**, 90 (1951); "*Handbuch* der Physik," S. Flügge, ed. Vol. 37, Springer-Verlag, Berlin (1959).
11) M. Goldsmith, G. Amat, and H. H. Nielsen, *J. Chem. Phys.*, **24**, 1178 (1956); **27**, 838, 845 (1957); **29**, 665 (1958).

bation method. With the use of high speed computers, this second method may yield a more reliable set of harmonic and anharmonic force constants, particularly when it is combined with the least squares procedure.

This line of approach was motivated from the study of the anharmonic potential function for the water molecule, which is expected to have large cubic and quartic cross terms. The direct diagonalization method is, however, first applied to and tested in diatomic molecules, the simplest molecular system with only one vibrational freedom. The vibration-rotation energy levels of a diatomic molecule are given in the form of a double power series,

$$E_{v,J} = \sum_{i,j} Y_{ij}(v+1/2)^i[J(J+1)]^j \quad (1)$$

Dunham[12] derived the relationships between the term values Y_{ij}'s and the force constants (known as the Dunham constants a_i's). The force constants derived from Dunham's equations are compared with those obtained from the present method. Diatomic molecules are probably only molecules, for which force constants higher than quartic can be determined from the presently available data. The least-squares fit to the spectroscopic data has been made with the five parameter potential function (FPPF, quadratic through hexic) as well as the three parameter potential function (TPPF, quadratic through quartic). The truncation effect upon the values of force constants is discussed. The seven parameter potential function (SPPF, quadratic through octic) is also considered in some cases. Two diatomic molecules, CO and $H^{35}Cl$, whose vibrational levels and associated rotational constants have been known precisely up to sufficiently high levels ($v=5$ or $v=6$), are subjected to a detailed investigation. The direct diagonalization method is also attractive in handling polyatomic molecules, since no special treatment is required for the anharmonic resonances.

Hamiltonian

The vibration-rotation Hamiltonian for a diatomic molecule is given as[12]

$$\mathbf{H} = \mathbf{H}_{\mathrm{VIB}} + \mathbf{H}_{\mathrm{ROT}}, \quad (2)$$

$$\mathbf{H}_{\mathrm{VIB}} = (1/2)\omega_e(q^2+p^2) + k_3q^3 + k_4q^4 + k_5q^5 + \cdots \quad (3)$$

$$\mathbf{H}_{\mathrm{ROT}} = B_e(J_x^2+J_y^2)(1-2\gamma^{1/2}q+3\gamma q^2-4\gamma^{3/2}q^3+)\cdots = B_e(J_x^2+J_y^2)\sum_{k=0} R_kq^k . \quad (4)$$

The Hamiltonians as well as all constants are expressed in cm^{-1} units and the operators are dimensionless: $p=\hbar^{-1}(\partial T/\partial q)$, $J_x=\hbar^{-1}P_x$, and $J_y=\hbar^{-1}P_y$. B_e is an equilibrium rotational constant, w_e is a harmonic frequency, and k_i's are anharmonic force constants.[13] The quantity $\gamma=(2B_e/\omega_e)$ represents 'smallness' in perturbation treatment and $R_k=(-1)^k\gamma^{(k/2)}\times(k+1)$ reflects the effect of normal vibration upon the rotational Hamiltonian.

Pure Vibrational Problem. Non-vanishing matrix elements of $(p^2+q^2)/2$, q^3, q^4, q^5, q^6, q^7, and q^8 in the harmonic oscillator wave functions are given in Table A–1 in the Appendix. The contribution of each force constant to the vibrational Hamiltonian matrix $\mathbf{H}_{\mathrm{VIB}}$ might be represented in matrix form, $\mathbf{A}^{(i)}$. The first few nonvanishing elements in each A-matrix are also given in Table A–2 in the Appendix. The final $\mathbf{H}_{\mathrm{VIB}}$ is given as matrix sum

$$\mathbf{H}_{\mathrm{VIB}} = \sum_{i=2} k_i\mathbf{A}^{(i)}, \quad (5)$$

where $k_2=\omega_e$. When n basis functions are chosen, an n by n secular equation in the form of

$$\mathbf{H}_{\mathrm{VIB}}\mathbf{L}_i = \mathbf{L}_i\nu_i \quad (6)$$

is solved for eigen vector L_i and eigen value ν_i. The eigen vectors are normalized to unity: $\mathbf{L}\,\tilde{\mathbf{L}}=\tilde{\mathbf{L}}\,\mathbf{L}=\mathbf{E}$, where $\mathbf{E}$ is a unit matrix.[14]

Vibration-Rotation Energy. The rotational-energy for the vth vibrational state is expressed as

$$E_{v,J} = B_vJ(J+1) - D_vJ^2(J+1)^2, \quad (7)$$

where J is a rotational quantum number. The spacings for rotational energy levels are much narrower than those for vibrational levels, and use of the ordinary perturbation method is justified. Therefore, $\mathbf{H}_{\mathrm{ROT}}$ in Eq. (4) is treated as a perturbing term, and the first-order vibration-rotation energy $E_{v,J}^{(1)}$ is given as

$$E_{v,J}^{(1)} = B_e\langle J|J_x^2+J_y^2|J\rangle\sum_{k=0} R_k\langle v|q^k|v\rangle = B_eJ(J+1)\sum_{k=0} R_k\langle v|q^k|v\rangle . \quad (8)$$

The 'true' wave function for the vth vibrational level is represented as a linear combination of the harmonic oscillator basis functions φ_n's:

$$|v\rangle = \sum_{n=0} a_{vn}|n\rangle \quad (9)$$

Throughout this paper, the indices n and m are used to indicate the harmonic oscillator wave functions $\varphi_n{}^0(q)$ and $\varphi_m{}^0(q)$, and v and v' refer to the true (perturbed) vibrational states. The coefficients a_{vn} are the components of the vth eigen vector. Since φ^0's are normalized and orthogonal, B_v is computed as

$$B_v = B_e\sum_{k=0} R_k\langle v|q^k|v\rangle = B_e[1+\sum_{k=1} R_k\sum_{n,m} a_{vn}a_{vm}\langle n|q^k|m\rangle]. \quad (10)$$

Similarly, the centrifugal distortion constant D_v in Eq. (7) can be obtained by applying the second-order perturbation treatment: $E_{v,J}^{(2)}=\sum_{v\neq v'} H_{vv'}{}^{(1)}H_{v'v}{}^{(1)}/(E_v^{(0)}-E_{v'}{}^{(0)})$.

The alternative method for obtaining the vibration-rotation energy levels is more direct. Since the rotational Hamiltonian $\mathbf{H}_{\mathrm{ROT}}$ for a diatomic molecule is diagonal with respect to the rotational quantum number J, the entire vibration-rotation Hamiltonian matrix is factored into a number of subma-

12) J. L. Dunham, *Phys. Rev.*, **41**, 721 (1932).

13) The force constants k_n's in Eq. (3) are related with the Dunham constants a_m's in the following equation,
$2k_{n+2}=\omega_e\gamma^{n/2}a_n\cdot(n=1,2,3,\cdots)$

14) A similar treatment was carried out by Heilbronner *et al.*[15] but they used a very limited number of basis functions.

15) E. Heilbronner, Hs. H. Guntherd, and R. Gerdil, *Helv. chim. Acta*, **39**, 1171 (1956).

trices, each of which is constituted from the states with identical J values. For non-zero J-values, the terms originated from $\mathbf{H}_{\mathrm{ROT}}$ are treated as effective potential constants which modify the values of k_i in Eq. (3). The values of B_v and D_v are obtained from a direct calculation of vibration-rotation energies. $E_{v,J}$. The B_v values computed from the perturbation method, Eq. (10), are in excellent agreement with those obtained directly. The perturbation method, which is much quicker, is usually used in the present study. The direct method, however, excels the perturbation method when the vibration-rotation wave functions are to be computed. When various vibration-rotation dipole moment matrix elements $R_{v,J}{}^{v',J'}$ are evaluated for CO and HCl, the direct method is used.

Numerical Analysis

The numerical computations have been carried out on a HITAC 5020 E digital computer of the Computation Centre in the University of Tokyo. In order to preserve the desired number of significant figures, double precision arithmetic (64 bits) was used. For most practical purposes, however, the single precision is adequate. The vibrational energy levels and associated rotational constants are taken from the recent high resolution measurements on the vibration-rotation bands of CO and $H^{35}Cl$.[16,17] Their values are listed in Table 1 along with the term values Y_{ij}'s and the potential constants a_n's derived by these authors.

Preliminary Calculation. a) *Number of Basis Functions*: The vibrational energy levels ($v\leqq6$ for CO and $v\leqq5$ for HCl) are calculated from a trial set of the FPPF for both CO and HCl.[18] The number of basis functions is varied from 7 to 50. Convergence of eigen values is appreciably slower in HCl but is completed for the above levels when 30 basis functions are used. Similar results are obtained for the TPPF. Thus, 30 basis functions are used throughout this work, and errors resulting from the truncation of the Hamiltonian matrix are expected to be negligible. A reasonable convergence is obtained for the fundamentals and the first overtones of both CO and HCl and the second overtone of CO with ten basis functions. This implies that the present method is applicable to triatomic molecules. b) *Frequencies*: As shown in Table 1, Rank *et al.* derived the values of the first five force constants from the observed frequencies and rotational constants. The vibrational energy levels for CO and HCl are calculated from these force constants by three different methods, and they are given in Columns (i)–(iii) of Table 2. These energy levels are obtained (i) by direct diagonalization of a 30 by 30 vibrational Hamiltonian matrix, (ii) by the usual second order approximation, where x_e and α_e are given as

$$x_e = (3B_e/2)(5a_1{}^2/4-a_2) = (3/2)(5k_3{}^2/2\omega_e-k_4) \tag{11}$$

and

$$\alpha_e = -(6B_e{}^2/\omega_e)(1+a_1) = -(6B_e{}^2/\omega_e)[1+k_3(2/\omega_eB_e)], \tag{12}$$

and (iii) by using Dunham's formulae[19] (Eq. (15)

Table 1. Observed energy levels and rotational constants (in cm^{-1}) used in the present study
Derived Dunham's Constants a_k and Term Values Y_{ij} are also listed

	(a) CO		(b) HCl	
	v	B_v	v	B_v
$v=0$	0	1.922521	0	10.440254
$v=1$	2143.2740	1.905014	2885.9775	10.136228
$v=2$	4260.0646	1.887513	5667.9841	9.834665
$v=3$	6350.436	1.870010	8346.7816	9.534845
$v=4$	8414.458	1.852513	10922.803	9.236010
$v=5$	10452.170	1.835010	13396.217	8.93743
$v=6$	12463.70	1.817521		
	$Y_{10}=$ 2169.8232	$Y_{01}=$ 1.931274	$Y_{10}=$ 2990.9463	$Y_{01}=$ 10.593416
	$Y_{20}=$ −13.2932	$Y_{11}=$ −0.017507	$Y_{20}=$ −52.8185	$Y_{11}=$ −0.307181
	$Y_{03}=$ 0.0114_4	$Y_{21}=1\times10^{-6}$	$Y_{30}=$ 0.22437	$Y_{21}=$ 0.0017724
			$Y_{40}=$ −0.01218	
	$k_3=-123.47086$	$a_1=-2.6974$	$k_3=-297.6209$	$a_1=-2.3645$
	$k_4=$ 8.70732_9	$a_2=$ 4.5065	$k_4=$ 38.8222_2	$a_2=$ 3.6647
	$k_5=$ -0.48555_1	$a_3=-5.9589$	$k_5=$ -4.1711_1	$a_3=-4.6783$
	$k_6=$ 0.02422_2	$a_4=$ 7.0457	$k_6=$ 0.37099	$a_4=$ 4.9440
	$(\omega_e\fallingdotseq Y_{10})$	$(B_e\fallingdotseq Y_{01})$	$(\omega_e=$ 2991.0904	$B_e=$ 10.593553)

16) D. H. Rank, A. G. St. Pierre, and T. A. Wiggins, *J. Mol. Spectry.*, **18**, 418 (1965).
17) D. H. Rank, B. S. Rao, and T. A. Wiggins, *ibid*, **17**, 122 (1965).
18) The lowest eigen value is usually negative. The energy scale is readjusted so that the ground vibrational level is always at origin.
19) Since these force constants were obtained from Dunham's formulas, the calculated frequencies in (iii) are expected to agree closely with the observed frequencies. The discrepancies found in the actual calculated frequencies are due to neglect of the terms ($\approx B_e{}^3/\omega_e{}^2$) in Y_{20} when Dunham's constants were derived.

Table 2. Comparison of calculated frequencies and rotational constants (in cm^{-1}) by methods (i)—(iv)

	(i) Direct	(ii) 2nd-order	(iii) 4th-order	(iv) Direct[a]	(v) (i)—(ii)	(vi) (i)—(iii)	(vii) (i)—(iv)
(a) CO							
ν_v							
$v=1$	2143.30	2143.24	2143.29	2143.23	6	1	7
$v=2$	4260.22	4259.39	4260.10	4259.81	33	12	41
$v=3$	6350.99	6349.96	6350.51	6349.49	103	48	150
$v=4$	8415.97	8413.45	8414.58	8411.88	252	139	409
$v=5$	10455.69	10450.35	10452.39	10446.33	534	330	936
$v=6$	12470.83	12460.66	12464.00	12451.96	1017	683	1887
B_v							
$v=0$	1.922520	1.922521	1.922521	1.922515	−1	−1	5
$v=1$	1.905025	1.905014	1.905022	1.904984	9	3	41
$v=2$	1.887557	1.887508	1.887524	1.887389	49	34	168
$v=3$	1.870143	1.870001	1.870030	1.869674	142	113	469
$v=4$	1.852824	1.852495	1.852536	1.851771	329	288	1053
$v=5$	1.835653	1.834988	1.835045	1.833596	665	608	2057
(b) HCl							
ν_v							
$v=1$	2887.23	2885.45	2886.44	2883.72	172	79	351
$v=2$	5676.36	5665.27	5669.67	5662.20	1110	670	2416
$v=3$	8380.41	8339.44	8351.02	8280.09	4097	2939	10032
$v=4$	11022.48	10907.98	10931.85	10645.93	11450	9063	37655
$v=5$	13634.86	13370.87	13413.51	13115.58	26399	22135	51928
B_v							
$v=0$	10.440579	10.439966	10.440887	10.439494	613	−308	1085
$v=1$	10.139657	10.132792	10.138699	10.128533	6865	958	11124
$v=2$	9.851493	9.825618	9.840339	9.797745	25875	11154	53748
$v=3$	9.590328	9.518444	9.545806	9.403426	71884	44522	186902
$v=4$	9.375818	9.211127	9.255101	8.365634	—	—	—
$v=5$	9.224414	8.904096	8.968223	8.316344	—	—	—

a) Without hexic off-diagonal matrix elements.

in Ref. 12). The differences (i)–(ii) and (i)–(iii) are given, respectively, in Columns (v) and (vi). They show that these approximation methods break down rapidly in higher vibrational levels. The discrepancies are much larger in HCl, and it is alarming that even for the first overtone of HCl, the calculated frequencies in (ii) and (iii) are off from the exact solution by about 11 and 7 cm^{-1}, respectively.

c) *Rotational Constants.* As given in Eq. (4), the rotational Hamiltonian of a diatomic molecule is expressed as a power series expansion of the dimensionless normal coordinate q, and the terms $k=0$ through $k=6$ are first retained in the present calculation. The calculated values for the rotational constants are given in Columns (i)–(iv) of Table 2. The rotational constants, B_v, may be regarded as the sum of terms $B_v(k)=B_e\cdot R_k\langle v|q^k|v\rangle$. The contribution of each $B_v(k)$ term is listed in Table 3 for the $v=0$, $v=1$, and $v=5$ levels of CO and HCl. The convergence is satisfactory for the low vibrational levels of CO and still good for the $v=5$ level.[20] For HCl, it is satisfactory only for the $v=0$ and $v=1$ levels. It becomes slower in higher vibrational levels. When the least-squares adjustment of force constants is attempted for the HCl molecule, the rotational Hamiltonian is expanded further to the $k=8$ term. Contributions from $B_v(7)$ and $B_v(8)$ are added in Table 3-b.[21]

d) Effect of Off-diagonal Matrix Elements. In the second order perturbation treatment in polyatomic molecules, where harmonic, cubic, and quartic force constants are retained, the off-diagonal contributions of the quartic force constants to the energies are neglected. Only exceptions are the cases in which second order anharmonic resonances are apparent. In the same sense, the off-diagonal contributions of the hexic force constant can be neglected in the fourth order approximation, and the diagonalized results without hexic off-diagonal terms are

20) To estimate the maximum error due to the neglect of higher terms, $B_5(7)+B_5(8)$ is calculated later, which gives 9×10^{-6} cm^{-1}.

21) Even though the terms up to $k=8$ are retained, convergence is slow and unsatisfactory for the higher levels. This forces us to put lighter weights (usually 0.01) on these rotational constants, when the least-squares adjustment is made.

TABLE 3. CONVERGENCE OF ROTATIONAL CONSTANT EXPANSION: $B_v(k)$ VALUES ARE LISTED FOR THE $v=0$, $v=1$, $v=2$, AND $v=5$ LEVELS (in cm^{-1})

(a) CO

	$v=0$	$v=1$	$v=2$	$v=5$
B_v (total)	1.922520	1.905025	1.887557	1.835653
$B_v(0)=B_e$	1.931274	1.931274	1.931274	1.931274
$B_v(1)$	−0.013965	−0.042127	−0.070622	−0.157765
$B_v(2)$	0.005279	0.016361	0.028223	0.068763
$B_v(3)$	−0.000092	−0.000610	−0.001680	−0.008600
$B_v(4)$	0.000024	0.000133	0.000378	0.002264
$B_v(5)$	-0.000000_7	−0.000007	−0.000031	−0.000348
$B_v(6)$	0.000000_2	0.000001	0.000005	0.000076

(b) HCl

B_v (total)	10.440586	10.139765	9.852153	9.238361
$B_v(0)=B_e$	10.593553	10.593553	10.593553	10.593553
$B_v(1)$	−0.268496	−0.814129	−1.365128	−2.804660
$B_v(2)$	0.120556	0.396735	0.724505	1.890411
$B_v(3)$	−0.007246	−0.049633	−0.141149	−0.696959
$B_v(4)$	0.002391	0.015124	0.048392	0.331940
$B_v(5)$	−0.000241	−0.002594	−0.011550	−0.134309
$B_v(6)$	0.000070	0.000710	0.003530	0.058385
$B_v(7)$	−0.000010	−0.000149	−0.000948	−0.024268
$B_v(8)$	0.000003	0.000041	0.000287	0.010321

$B_5(7)+B_5(8)=-0.000009\ cm^{-1}$ for CO.

given in Column (iv) of Table 2. Deviations (i)-(iv) in Column (vii) resemble those in column (v) in the case of CO, and are especially small for the low vibrational levels. As for HCl, the neglect of hexic off-diagonal terms drastically lowered the calculated frequencies. This can be interpreted that the terms like $k_7q^7+k_8q^8$ are necessary to account for the vibrational frequencies of HCl, and the SPPF is also tested in HCl.

Least-Squares Adjustment of Force Constants

Method of Least-Squares. The least-squares corrections to the initial values of force constants are found by solving well-known simultaneous linear equations

$$(\tilde{\mathbf{J}}\mathbf{P}\mathbf{J})\Delta\mathbf{K}=\tilde{\mathbf{J}}\mathbf{P}\Delta\boldsymbol{\nu}. \tag{13}$$

J, **P**, $\Delta\mathbf{K}$, and $\Delta\boldsymbol{\nu}$ have their usual meaning. In the anharmonic potential problem, a finite difference method has been used to evaluate the elements of Jacobian matrix **J**.[1] One advantage in the numerical diagonalization method is that we can use the techniques developed for normal coordinate analysis. From the first order perturbation method,[22] the Jacobian matrix element for the frequency ν_h with a change in the values of k_i is given by

$$\delta\nu_h/\delta k_i=(\tilde{\mathbf{L}}\mathbf{A}^{(i)}\mathbf{L})_{hh}, \tag{14}$$

where $\mathbf{A}^{(i)}$ and **L** are given in Eqs. (5) and (6). The elements for the rotational constant B_v are slightly more complex, Nakagawa and Shimanouchi[23] and Mills[24] evaluated the changes in eigen vectors due to a small change in a force constant k_i. Applying their results to the present case, we have

$$\Psi_v=\Psi_v{}^0+\sum_{v'\neq v}P_{vv'}\Psi_{v'}{}^0, \tag{15}$$

where $P_{v,v'}=\Delta k_i(\tilde{\mathbf{L}}\mathbf{A}^{(i)}\mathbf{L})_{vv'}/(\nu_v{}^0-\nu_{v'}{}^0)$ and $\Psi_{v'}{}^0$'s are the wave functions with $\Delta k_i=0$. As given in Eq. (10), $B_v{}^0$ for $\Delta k=0$ is expressed as

$$B_v{}^0=B_e\sum_{k=0}R_k\langle v|q^k|v\rangle$$

and

$$B_v\approx B_e\sum_{k=0}R_k\langle v|q^k|v\rangle+2\sum_{v'\neq v}P_{vv'}\langle v|q^k|v'\rangle, \tag{16}$$

$$\delta B_v/\delta k_i\approx 2B_e\sum_{k=0}(\delta P_{vv'}/\delta k_i)\langle v|q^k|v'\rangle$$

$$=2B_e\sum_{k=0}R_k\sum_{v'\neq v}(\tilde{L}_0A^{(i)}L_0)_{vv'}\langle v|q^k|v'\rangle/(\nu_v{}^0-\nu_v{}^0) \tag{17}$$

Application to CO and HCl. The least-squares adjustment of force constants has been made for the FPPF as well as the TPPF. The calculation has been made for the latter to see the truncation effect upon the harmonic, cubic, and quartic force constants. The vibrational frequencies and the rotational constants, are used as observational data. The results for CO and HCl are given separately in Tables 4—7. Only a minimum number of data is used to obtain Sets 1 and 2, *i.e.* ν_1, ν_2, B_0, and B_1. Six frequencies ν_1—ν_6 and five rotational constants B_0—B_4 are used in Sets 5 and 6. Sets 3 and 4 are intermediate cases. Sets 1,3, and 5 are obtained by solving a full Hamiltonian, while the quartic off-diagonal matrix elements are ignored in obtaining Sets 2,4, and 6. Similarly, in the FPPF, the hexic off-matrix ele-

22) T. Miyazawa, *Nippon Kagaku Zasshi*, **76**, 1132 (1955).
23) I. Nakagawa and T. Shimanouchi, *ibid.*, **80**, 128 (1965).

Table 4. Converged sets of force constants for CO[a] (in cm^{-1})

NO	NP	NV	NR	OD	SUMD	ω_e	k_3	k_4	k_5	k_6	B_e
1	3	2	2		0.0068	2171.3892	−122.3237	7.4843			
2	3	2	2	α	0.0092	2166.7975	−122.6360	10.1409			
3	3	4	3		0.75	2171.3381	−114.0623	5.6035			
4	3	4	3	α	4.3	2163.4794	−110.5233	7.3836			
5	3	6	5		5.0	2171.2725	−109.7213	4.7350			
6	3	6	5	α	63.0	2158.7036	−107.7104	7.2988			
7	5	6	5		0.0015	2169.8196	−123.5093	8.7279	−0.47603	0.01726	
8	5	6	5	α	0.0045	2169.9376	−122.6191	8.3809	−0.50297	0.05744	
9	6	6	5		0.00016	2169.9191	−123.5529	8.7317	−0.46782	0.01579	1.931241
7′	5	6	5		0.0050	2169.8234	−123.5757	8.7442	−0.47695	0.01722	
8′	5	6	5	α	0.011	2170.1693	−123.6326	8.5976	−0.41933	0.02281	
9′	6	6	5		0.0019[c]	2169.8160	−123.5962	8.7538	−0.47958	0.01747	1.931289
	LIT.[b]					2169.8232	−123.4709	8.7073	−0.48555	0.02422	1.931274

a) NP: number of adjustable parameters, NV and NR: numbers of respective vibrational levels and rotational constants used as data, OD: α in this column indicates that the off-diagonal matrix elements of the highest order force constants are neglected, and SUMD: the sum of weighted squared deviations.
b) See Table 1.
c) The least-squares dispersions of the force constants in Set 9′ are follows; $\sigma(\omega_e)=0.0154$, $\sigma(k_3)=0.0276$, $\sigma(k_4)=0.0052$, $\sigma(k_5)=0.0050$, $\sigma(k_6)=0.00090$, and $\sigma(B_e)=0.000014\ cm^{-1}$.

Table 5. Differences between observed and calculated frequencies and rotational constants (Obsd-Calcd) for CO

Obsd	Sets	1	2	3	4	5	6	7	8	9	7′	8′	9′
v													
$v=1$	2143.274	0	0	−324	1375	−734	4193	−11	−26	3	22	−60	−10
$v=2$	4260.065	0	0	79	17	−801	3409	−23	3	0	14	2	−22
$v=3$	6350.436	3766	−2106	466	−1296	−405	36	−17	19	−3	−7	22	9
$v=4$	8414.458	15608	−8689	−80	606	138	−3244	14	6	10	−17	22	9
$v=5$	10452.170	40525	−22383	2700	9363	350	−3416	21	−38	2	−32	−58	14
$v=6$	12463.700	84591	−45902	−8645	29381	307	3091	0	16	10	0	23	−9
$B_v\times 100$													
$v=0$	192.252	11	−22	−108	−127	−155	−158	0	−7	4	2	8	0
$v=1$	190.501	95	−79	−319	−332	−450	−429	−1	−16	3	3	9	1
$v=2$	188.751	291	−178	−530	−446	−730	−622	−2	−13	1	4	−2	1
$v=3$	187.001	381	−331	−750	−456	−1001	−726	5	3	−3	2	−12	0
$v=4$	185.251	1103	−553	−987	−345	−1267	−726	−8	35	−7	0	11	−2

Differences are given from the last significant figure.

Table 6. Converged sets of force constants for HCl[a] (in cm^{-1})

NO	NP	NV	NR	OD	SUMD	ω_e	k_3	k_4	k_5	k_6	k_7	k_8	B_e
1	3	2	2		0.030	3013.6517	−305.0572	30.3793					
2	3	2	2	α	0.72	2963.8588	−277.7799	44.5324					
3	3	3	3		48.3	3026.2281	−302.1949	27.6823					
4	3	3	3	α	44.9	2950.8328	−269.9356	43.2287					
5	3	5	5		497	3008.0991	−258.4481	17.5360					
6	3	5	5	α	120	2944.6010	−276.0102	47.1034					
7	5	5	5		0.075	2992.0378	−299.6250	39.1738	−3.71343	0.17951			
8	5	5	5	α	0.36	2993.4178	−295.9522	36.3554	−3.45646	0.54440			
9	6	5	5		0.033	2992.2876	−300.2986	39.4324	−3.75365	0.18197			10.594752
10	7	5	5		0.030	2991.8183	−299.0935	39.0356	−3.88475	0.27635	−0.01859	0.00125	
11	8	5	5		0.019[c]	2992.2963	−300.2911	39.4315	−3.87787	0.25233	−0.01401	0.00095	10.595805
	LIT.[b]					2991.0104	−297.6209	38.8222	−4.17110	0.37099			10.593553

a) See Footnote a) of Table 4.
b) See Table 1.
c) The least-squares dispersions of the force constants in Set 11 are as follows; $\sigma(\omega_e)=0.0366$, $\sigma(k_3)=0.0194$, $\sigma(k_4)=0.0078$, $\sigma(k_5)=0.0056$, $\sigma(k_6)=0.0031$, $\sigma(k_7)=0.0018$, $\sigma(k_8)=0.00026$, and $\sigma(B_e)=0.00028\ cm^{-1}$.

Table 7. Differences between observed and calculated frequencies and rotational constants (Obsd-Calcd) for HCl

Obsd	Sets	1	2	3	4	5	6	7	8	9	10	11
v												
$v=1$	2885.978	−13	2	−5236	4581	−7980	8079	64	−240	−18	45	−32
$v=2$	5667.984	−7	−21	4026	−3761	−5872	−710	82	162	10	59	38
$v=3$	8346.728	−35794	33121	1365	978	2857	−5369	−57	122	−85	−68	−48
$v=4$	10922.803	−146606	129416	58504	40064	8751	2643	5	−102	14	26	23
$v=5$	13396.217	−366387	282606	−204103	109902	−4661	−227	−2	54	−31	−4	−3
$B_v\times 100$												
$v=0$	1044.025	156	−813	−24	−1502	−3466	−895	73	−133	9	65	−72
$v=1$	1013.623	−72	256	136	−2190	−9144	−508	55	−135	85	82	78
$v=2$	983.467	−3705	6445	−1685	1331	−13711	3612	−200	294	−98	−67	0
$v=3$	953.467	−13023	18774	−7991	9497	−18091	11010	−550	1332	−393	−278	−18
$v=4$	923.601	−28992	35970	−20550	20974	−23702	18657	−984	3090	−789	−557	−45

Differences are given from the last significant figure.

ments are ignored in Set 8, while a full Hamiltonian is solved for Sets 7 and 9. In Set 9, the equilibrium rotational constant B_e is treated as an adjustable parameter, in other sets its value is fixed (1.931274 cm^{-1} for CO and 10.593553 cm^{-1} for HCl). The relative weights of the rotational constants and vibrational frequencies might affect the outcome. In the present calculation, $B_v\times 10^2$ is usually entered as input data.[25] In Sets 7′–9′ of CO, $B_v\times 10^3$ is used to see the effect due to the change in the relative weight. From the consideration of accuracy in evaluating rotational constants, less weights have to be given to B_3 and B_4 of HCl, usually $B_v\times 10$ being used as data.

Agreement between the calculated and experimental values in HCl is less satisfactory, and the seven parameter potential function (SPPF) is also tested. The results are included in Sets 10 and 11 of Tables 6 and 7. B_e is treated as a variable in Set 11.

Table 8. The calculated and observed frequencies and rotational constants (in cm^{-1}) for isotopic CO and HCl

(a) CO

		Obsd	Calcd (Set 9)
$^{13}C^{16}O$	ν_{0-1}	2096.071	2096.072
	B_0	1.8380	1.8379
	B_1	1.8216	1.8216

(b) HCl

		Obsd	Calcd (Set 7)
$H^{37}Cl$	ν_{0-1}	2883.871	2883.810
	ν_{0-2}	5663.926	5663.849
	B_0	10.4243	10.4238
	B_1	10.1209	10.1207
	B_2	9.8213	9.8224
$D^{35}Cl$	ν_{0-1}	2091.061	2091.148
	ν_{0-2}	4128.433	4128.496
	B_0	5.392261	5.392168
	B_1	5.279816	5.279477
	B_2	5.168106	5.168317
$D^{37}Cl$	ν_{0-1}	2088.073	2088.150
	ν_{0-2}	4122.594	4122.657
	B_0	5.3757	5.3764
	B_1	5.2673	5.2642
	B_2	5.1537	5.1535

Isotopic Species. Only a limited number of data is available for the isotopic species of CO and HCl,[26-28] and no least-squares fit of force constants has been attempted. Within the limit of Born-Oppenheimer approximation, however, the force constants $k_j^{(i)}$ for the isotopic species are related with those in the parent species k_j by means of

$$k_j^{(i)} = k_j(\mu/\mu^{(i)})^{j/4}, \quad (j=2,3,4,\cdots) \tag{18}$$

where μ and $\mu^{(i)}$ are the reduced masses of the parent and isotopic species, respectively. $B_e^{(i)}$ is given as $B_e^{(i)}=(\mu/\mu^{(i)})B_e$.[29] The results are summarized in Table 8, where no significant discrepancies are detected between the calculated and observed frequencies and rotational constants.

Discussion

Force Constants. In CO, the values of the five parameter force constants are not so sensitive to the change of the relative weights, but the effect may be seen in Table 5, where the differences between the observed and calculated frequencies and rota-

24) I. M. Mills, *J. Mol. Spectry.*, **5**, 334 (1960).

25) This is equivalent to weighting the rotational constants a hundred times heavier than the frequencies The frequencies are known with the accuracy of a few thousandths of a wave number. The accuracies of the rotational constants for the low vibrational levels are estimated in the order of 10^{-5} cm^{-1}

26) E. K. Plyler, L. R. Blaine, and E. D. Tidwell, *J. Res. Natl. Bur. Standards*, **55**, 183 (1955).

27) D. H. Rank, D. P. Eastman, B. S. Rao, and T. A. Wiggins, *J. Opt. Soc. Amer.*, **52**, 1 (1962).

28) D. V. Webb and K. N. Rao, *J. Mol. Spectry.*, **28**, 121 (1968).

29) Note that $q=\gamma^{-1/2}\Delta r/r_e=(\Delta r/r_e)(\omega_e/2B_e)^{1/2}$, $B_e=\hbar/(4\pi r_e^2 c\mu)$, and $\omega_e=(1/2\pi)(K_e/\mu)^{1/2}$.

tional constants are listed. Regardless of the choice in the weighting systems, the first three force constants, *i.e.* ω_e, k_3, and k_4 of the FPPF converge to almost the same values. The values of k_5 and k_6 are more sensitive to the handling of data and to the method of calculation. The force constant k_6 converges to a larger value in Set 8. In the perturbation treatment, the off-diagonal contribution of hexic force constant is discarded, since its contribution to the vibrational energy is expected to be small and is of the same order as the diagonal contribution from the neglected higher order terms. As seen from Column (vii) of Table 2, however, the above statement is not adequate for CO and the discrepancy as large as 18 cm^{-1} is found for the $v=6$ level, while the diagonal contribution from k_8 is expected to be less than 1 cm^{-1}. A trial calculation is carried out by using the force constants in Set 9 plus $k_7=-0.001$ cm^{-1} and $k_8=0.0001$ cm^{-1}.[30] The calculated frequencies for the $v=5$ and $v=6$ levels decrease only by 2 and 4 cm^{-1}, respectively. The truncation errors for k_5 and k_6 are much smaller in Set 9, and it is regarded as the best set so far obtained.

From the calculation of the FPPF, we were able to determine the precise values of the first three parameters. ω_e, k_3, and k_4. However, in the potential functions of triatomic molecules from which the present study was initiated, we can hardly expand the potential function beyond quartic terms for parctical reasons. The least-squares adjustment of the TPPF is therefore attempted to seek the most appropriate method and the handling of data to obtain the reasonable values for these three constants. It is clearly seen from Table 4 that the force constants in Sets 1 and 2 are much closer to the values found in the FPPF. The deviations of these force constants from the 'true' values are almost the same in both sets but differing in sign. The average values of the force constants in Sets 1 and 2, $\omega_e=2169.09$, $k_3=-122.48$, and $k_4=8.8126$ cm^{-1}, are much close to the values found in Set 9. These results might be useful when the anharmonic potential functions of polyatomic molecules are dealt with.

The conclusion analogous to the case of CO may be drawn on the converged values of force constants for HCl: the first three force constants in the FPPF, especially those in Sets 7 and 9 converge to almost the same values. As for the TPPF, Sets 1 and 2, in which the minimum number of data is used, yield force constants closer to those in the FPPF. Much closer fit is also obtained when the average values of force constants in Sets 1 and 2 are taken: $\omega_e=2988.76$, $k_3=-291.42$, and $k_4=37.46$ cm^{-1}. However, the values of the first three force constants in Set 8 deviate from those in Sets 7 and 9 by 2—10%. They are much larger than the corresponding deviations found in CO. The overall fit of the calculated frequencies and rotational constants to the experimental values are poorer in HCl. The value $\gamma=(2B_e/\omega_e)$, which is a measure of smallness in perturbation treatment, is 0.007 for HCl in contrast to 0.0017 for CO. The ratio of k_{n+1}/k_n is about 0.01 for CO but close to 0.1 for HCl. This, in conjunction with the relatively large value of γ, makes the convergence much slower. Thus the SPPF where the potential function is expanded to the $k=8$ term was also tested. The results are included in Tables 6 and 7. Since the higher order force constants are considered, the converged values for k_5 and k_6 in Sets 10 and 11 are most reliable, and they are found closer to those found in Sets 7 and 9. This confirms the conclusion drawn earlier on HCl and CO. As far as the FPPF is concerned, the solution of the full vibrational Hamiltonian is preferable.

When the equilibrium rotational constant is treated as an adjustable parameter, a slight increase in the value of B_e serves for the improvement in the least-squares fit. The change in the B_e value is larger in HCl, but the corresponding decrease in the internuclear distance is in the order of 0.0001 Å. Table 9 summarizes the force constants obtained by the ordinary perturbation formulas and by the present method. As far as the general pattern of potential function in diatomic molecule is concerned, the force constants calculated from Dunham's equations, Eq. (15) in Ref. 12, or from the much simpler second-

TABLE 9. THE FIRST THREE FORCE CONSTANTS (in cm^{-1}) OF CO AND HCl DERIVED BY VARIOUS METHODS

(a) CO

	2nd-Order	4th Order	Direct (Set 7)	Direct (Set 9)
ω_e	2169.7574	2169.8232	2169.8234	2169.8160
k_3	−123.4685	−123.4709	−123.5757	−123.5962
k_4	8.7369	8.7073	8.7442	8.7538
B_e	1.931274	1.931274	1.931274	1.931289

(b) HCl

	2nd Order	4th Order	Direct (Set 7)	Direct (Set 9)	Direct (Set 11)
ω_e	2989.9489	2991.0904	2992.0378	2992.2876	2992.2963
k_3	−295.7798	−297.6209	−299.6250	−300.2986	−300.2911
k_4	38.4928	38.8222	39.1738	39.4324	39.4315
B_e	10.592267	10.593553	10.593553	10.594752	10.595815

30) This would be an over estimation for the force constants.

Table 10. The derived force constants from the model potential functions (cm^{-1})

	(a) CO			(b) HCl		
	Set 9	Morse	Exp. Morse	Set 10	Morse	Exp. Morse
ω_e	2169.8160	2169.8160	2169.8160	2991.8183	2991.8183	2991.8183
k_3	−123.5912	−123.5962	−123.5962	−299.0935	−299.0935	−299.0935
k_4	8.7538	8.2138	8.6402	39.4315	34.8839	36.6960
k_5	−0.47958	−0.40102	−0.46369	−3.88475	−2.98917	−3.45629
k_6	0.01747	0.01573	0.01797	0.27635	0.20586	0.27080
k_7				−0.01859	−0.01062	−0.01947
k_8				0.00125	0.00060	0.00108
		A=83592.70	A_1= 124873.08		A=37419.82	A_1= 55898.75
		a=0.113923	a=0.093210		a=0.163588	a= 0.163588
			A_2=−27749.57			A_2=−12421.90

order equations, Eqs (16) and (17), have sufficient accuracies, and errors are probably within a few percent. More careful considerations seem to be necessary for more quantitative arguments, such as spectroscopic detection on the deviations from the Born-Oppenheimer behavior. Dunham's equations are sometimes insufficient for attaining the required accuracy, and the relationship between the spectroscopic term value Y_{ij} and the force constants must be examined carefully. Herman and Ashgarrian[31] tried to explain the discrepancy between the observed and theoretically predicted $Y_{02}(\approx D_e)$ values of HCl from the deviations of Born-Oppenheimer oscillators. Their failure obviously stems from neglect of contributions of the higher order force constants to Y_{02}. A more careful treatment such as given recently by Bunker[32] seems necessary.

As already stated, we have triatomic molecules in mind, and CO may serve as a model for CO_2, and HCl for H_2O. The parameter $\gamma=2B_e/\omega_e$ of CO_2 is less than one third of the corresponding value of CO (0.00058 as compared with 0.00178 of CO), and the least-squares determinatation based on Nielsen's second order perturbation treatment for this molecule[1,2] seems to be adequate. A preliminary calculation shows that the calculated values given in Ref. 2 do not differ significantly from those obtained from the diagonalization method. From the results of HCl, overall difficulties are anticipated for the treatment of anharmonic potential of H_2O. Inclusion of higher order force constants seems to be necessary at least for those related with the hydrogen stretching coordinates. However, some values may be estimated from the lower order force constants by assuming a suitable model potential. The Morse function[33] with two adjustable parameters A and a,

$$V(q) = A[1-\exp(-aq)]^2 \tag{19}$$

is probably the simplest potential for the bond-stretch. These constants can be determined from w_e and k_3 by $a=-2k_3/\omega_e$ and $A=\omega_e^3/8k_3^2$, and higher force constants evaluated from Eq. (19). This is done for CO and HCl, and the results, given in Table 10, show that the bond stretching potential qualitatively follows the pattern of the Morse function[1-3,6] Quantitatively, however, the prediction of the simple Morse function is not very satisfactory. In HCl the k_4 value is about 25% off from the converged one. In order to increase the freedom, the expanded Morse function[34] is also considered;

$$V(q) = \sum_{i=1}^{2} A_i[1-\exp(aq)]^{i+1} \tag{20}$$

The constants A_1, A_2, and a can be determined from ω_3, k_3, and k_4 from the relations

$$\omega_e = 2A_1a^2 \tag{21}$$

$$k_3 = (A_2-A_1)a^3 \tag{22}$$

$$k_4 = (3/2)(7A_1/18) - A_2a^4 \tag{23}$$

which leads to the quadratic equation for a

$$F(a) = a^2 + (36k_3/11\omega_e)a + (24k_4/11\omega_e) = 0. \tag{24}$$

The remaining higher order force constants can be obtained,

$$k_5 = -(1/4)[(A_1-5A_2)]a^5, \tag{25}$$

$$k_6 = (3/4)[(31A_1/270)-A_2]a^6. \tag{26}$$

In the cases for CO and HCl, rigorous solutions for Eq. (24) give imaginary roots for a. However, if we use the value of a which makes the above $F(a)$ minimum $a=-(18k_3/11w_e)$, we have much improved results which are given in the third column of Table 10.

In conclusion, the following remarks can be made. (1) The truncation effect upon the highest order force constant retained in the potential function is in the order of 10—20%, but larger deviations must be tolerated for the hydrogen containing molecules. In the latter, it is preferable to use the FPPF, since the effects of the quintic and hexic force constants to low vibrational levels are not negligible. (2) In order to calculate the rotational constants with accuracies comparable to those attained experimentally, the terms up to $k=6$ should be retained in the rotational Hamiltonian. More terms are necessary for the HCl

31) R. M. Herman and A. Asgharrian, *J. Chem. Phys.*, **45**, 2433 (1966).
32) P. R. Bunker, *J. Mol. Spectry.*, **35**, 306 (1970).
33) P. M. Morse, *Phys. Rev.*, **34**, 37 (1929).
34) A. S. Coolidge, H. M. Jones, and E. L. Vernon, *Phys. Rev.*, **54**, 726 (1938).

molecule. (3) In the TPPF, use of the minimum number of data seems preferable. When the least-squares fit is carried out, solutions with and without the quartic off-diagonal elements must be considered. The results indicate the error limits for these force constants.

The author wishes to express his sincere gratitude to Prof. Takehiko Shimanouchi for his helpful discussion and continuous interest in this work.

Appendix

The non-vanishing matrix elements in the harmonic oscillator representation $\langle n|q^k|n-m\rangle$ are listed in Table A-1. The terms from $k=1$ to $k=8$ are included in the table. The matrix element $\langle n|q^k|n+m\rangle$ can be obtained from the corresponding expression for $\langle n|q^k|n-m\rangle$ by replacing n with $n+m$. Note also that $\langle n|q^2+p^2|n\rangle=2n+1$ and $\langle n|q^2+p^2|n+2\rangle=0$.

In Table A-2, non-vanishing matrix elements of $A_{nm}^{(i)}$ ($n\leq 10$, $m\leq 10$, and $i\leq 8$) are shown.

Table A-1. Non-vanishing matrix elements $(n|q^k|n')$

k	n'	$(n\|q^k\|n')$	k	n'	$(n\|q^k\|n')$
1	$n-1$	$(n/2)^{1/2}$	6	$n-4$	$(3/4)(n-3/2)[n(n-1)(n-2)(n-3)]^{1/2}$
2	n	$n+1/2$	6	$n-6$	$(1/8)[n(n-1)(n-2)(n-3)(n-4)(n-5)]^{1/2}$
2	$n-2$	$[n(n-1)]^{1/2}/2$	7	$n-1$	$(35/8)(n^3+2n)(n/2)^{1/2}$
3	$n-1$	$(3/2)n(n/2)^{1/2}$	7	$n-3$	$(21/8)(n^2-2n+2)[n(n-1)(n-2)/2]^{1/2}$
3	$n-3$	$[n(n-1)(n-2)/8]^{1/2}$	7	$n-5$	$(7/8)(n-2)[n(n-1)(n-2)(n-3)(n-4)/2]^{1/2}$
4	n	$(3/2)(n+1/2)^2+(3/8)$	7	$n-7$	$(1/8)[n(n-1)(n-2)(n-3)(n-4)(n-5)$
4	$n-2$	$(n-1/2)[n(n-1)]^{1/2}$			$\times(n-6)/2]^{1/2}$
4	$n-4$	$(1/4)[n(n-1)(n-2)(n-3)]^{1/2}$	8	n	$(35/8)[(n+1/2)^4+(7/2)(n+1/2)^2+(9/16)]$
5	$n-1$	$(5/2)(n/2)^{1/2}(n^2+1/2)$	8	$n-2$	$(7/4)(2n^3-3n^2+7n-3)[n(n-1)]^{1/2}$
5	$n-3$	$(5/4)(n-1)[n(n-1)(n-2)/2]^{1/2}$	8	$n-4$	$(7/8)(2n^2-6n+7)[n(n-1)(n-2)(n-3)]^{1/2}$
5	$n-5$	$(1/4)[n(n-1)(n-2)(n-3)(n-4)/2]^{1/2}$	8	$n-6$	$(1/4)(2n-5)[n(n-1)(n-2)(n-3)(n-4)(n-5)]^{1/2}$
6	n	$(5/2)(n+1/2)^3+(25/8)(n+1/2)$	8	$n-8$	$(1/16)[n(n-1)(n-2)(n-3)(n-4)(n-5)$
6	$n-2$	$(15/8)(n^2-n+1)[n(n-1)]^{1/2}$			$\times(n-6)(n-7)]^{1/2}$

Table A-2. Non-vanishing matrix elements of $A_{nm}^{(i)}$ ($n\leq 10$, $m\leq 10$, and $i\leq 8$)

n	m	$A_{nm}^{(2)}$	$A_{nm}^{(4)}$	$A_{nm}^{(6)}$	$A_{nm}^{(8)}$	n	m	$A_{nm}^{(3)}$	$A_{nm}^{(5)}$	$A_{nm}^{(7)}$
0	0	0.0	0.0	0.0	0.0	0	1	1.060660	2.651650	9.280777
1	1	1.0	3.0	11.25	52.5	1	2	3.0	11.25	52.5
2	2	2.0	9.0	45.0	262.5	2	3	5.511352	29.08767	176.8225
3	8	3.0	18.0	116.25	840.0	3	4	8.485281	58.33631	445.4773
4	4	4.0	30.0	240.0	2100.0	4	5	11.85854	100.7976	933.8601
5	5	5.0	45.0	431.25	4462.5	5	6	15.58846	158.0496	1727.721
6	6	6.0	63.0	705.0	8452.5	6	7	19.64370	231.5151	2922.001
7	7	7.0	84.0	1076.25	14700.0	7	8	24.0	322.5	4620.0
8	8	8.0	108.0	1560.0	23940.0	8	9	28.63783	432.2190	6932.740
9	9	9.0	135.0	2171.25	37012.5	9	10	33.54102	561.8120	9978.453
10	10	10.0	165.0	2925.0	54862.5					

n	m	$A_{nm}^{(4)}$	$A_{nm}^{(6)}$	$A_{nm}^{(8)}$	n	m	$A_{nm}^{(3)}$	$A_{nm}^{(5)}$	$A_{nm}^{(7)}$
0	2	2.121320	7.954951	37.12311	0	3	0.866025	4.330127	22.73317
1	3	6.123724	32.14955	192.8973	1	4	1.732051	12.99038	90.93267
2	4	12.12436	84.43748	636.5287	2	5	2.738613	27.38613	244.4212
3	5	20.12461	176.0904	1620.0313	3	6	3.872983	48.41229	528.6623
4	6	30.12474	318.3637	3479.4076	4	7	5.123475	76.85213	995.2351
5	7	42.12482	522.5097	6634.6583	5	8	6.480741	113.41296	1701.194
6	8	56.12486	799.7793	11589.784	6	9	7.937254	158.7451	2708.588
7	9	74.12489	1161.4229	18932.784	7	10	9.486833	213.4537	4084.086
8	10	90.12491	1618.6909	29335.659					

n	m	$A_{nm}^{(4)}$	$A_{nm}^{(6)}$	$A_{nm}^{(8)}$	n	m	$A_{nm}^{(5)}$	$A_{nm}^{(7)}$
0	4	1.224745	9.185587	64.29911	0	5	1.936492	20.33316
1	5	2.738613	28.75543	258.7989	1	6	4.743416	66.40783
2	6	4.743416	64.03613	713.8842	2	7	8.874120	155.2971
3	7	7.245688	119.5538	1597.674	3	8	14.49138	304.3189
4	8	10.24695	199.8155	3120.197	4	9	21.73707	532.5581
5	9	13.74773	309.3239	5538.460	5	10	30.74085	860.7439
6	10	17.74824	452.5801	9131.469				

n m	$A_{nm}{}^{(6)}$	$A_{nm}{}^{(8)}$	n m	$A_{nm}{}^{(7)}$	n m	$A_{nm}{}^{(8)}$
0 6	3.354102	46.95743	0 7	6.274950	0 8	12.54990
1 7	8.874120	159.7342	1 8	17.74824	1 9	37.64990
2 8	17.74824	390.4613	2 9	37.64970	2 10	84.18729
3 9	30.74085	799.2622	3 10	68.73864		
4 10	40.60556	1458.167				

The terms contributing to zero point energy, *i. e.* $\omega_e/2$, $(3k_4/4)$, $(15\,k_6/8)$, and $(105\,k_8/16)$, are subtracted from the corresponding diagonal matrix elements.

BULLETIN OF THE CHEMICAL SOCIETY OF JAPAN, VOL. 44, 3287—3292 (1971)

Time-Resolved Fluorescence Studies on Charge Transfer Interactions in 1,2,4,5-Tetracyanobenzene-Toluene Complex[1]

Keiichi EGAWA, Nobuaki NAKASHIMA, Noboru MATAGA,[2] and Chiyoe YAMANAKA*

Department of Chemistry, Faculty of Engineering Science, Osaka University, Toyonaka, Osaka

**Department of Electrical Engineering, Faculty of Engineering, Osaka University, Suita, Osaka*

(Received May 28, 1971)

Time-resolved CT (charge transfer) fluorescence spectra and the fluorescence rise and decay curves at various wavelengths of the CT fluorescence band have been measured for the 1,2,4,5-tetracyanobenzene (TCNB)-toluene system at various temperatures. The results and detailed studies of the effect of solvent polarity on the fluorescene wavenumbers have demonstrated that the relaxation process is due to the change of structure including the surrounding solvent molecules from the Franck-Condon (F.C.) state to the equilibrium (e.q.) state of the excited complex. This relaxation process causes a large Stokes shift of the CT fluorescence.

Although there are numerous investigations on the electron donor-acceptor (EDA) complexes by the absorption spectral measurements, few studies have been carried out on the excited complexes by fluorescence spectral measurements, except for rigid solvents at lower temperatures, because of the fact that the fluorescence yield of the EDA complex in solution at room temperature is extremely small in general.[3] However, somewhat detailed fluorescence studies are possible in the case of TCNB-aromatic hydrocarbon EDA complexes since they are strongly fluorescent in solution at room temperature when the solvent dielectric constant is not large.

It has been observed for the TCNB-toluene EDA complex that the fluorescence lifetime at room temperature is more than 100 nsec which is much longer than the radiative lifetime (~50 nsec) calculated from the intensity of the CT absorption band.[4] Contrary to this, the fluorescence lifetime observed in a rigid state at 77°K is nearly equal to the calculated radiative lifetime.[4] This clearly indicates a considerable change in the structure of the complex during the fluorescence lifetime, where the molecular rearrangement motions including the surrounding solvent molecules occur easily at room temperature but with difficulty at 77°K. The rearrangement relaxation from the F. C. excited state to the e.q. fluorescent state, which can be ascribed to the strong interaction between the excited complex and the surrounding solvent molecules, brings out an extraordinary large Stokes shift of *ca.* 12000 cm^{-1} at room temperature.[4]

In order to elucidate the structure of the excited complex and the dynamical processes of its rearrangement motions we have carried out detailed studies on the effect of temperature and solvent polarity on the fluorescence wave-numbers. We have measured the time resolved fluorescence spectra and the fluorescence rise and decay curves at various fixed wavelengths of the CT fluorescence band of the complex at various temperatures. The results of the time-resolved fluorescence studies gave a direct demonstration of the extensive F.C.→e.q. relaxation process assumed previously.[4]

Experimental

A 337 nm light pulse of nitrogen gas laser was used for the excitation of the complex. The light pulse has a peak output power of 10 kW and duration of 3 nsec. Its repetition rate was *ca.* 50 Hz. Fluorescence emission was observed with a travelling wave-pulsed photomultiplier according to Bennett.[5] The outputs from the photomultiplier with delay line were displayed on an X-Y recorder. Thus, we obtained the time-resolved spectrum at a fixed delay time

1) A preliminary note has been published in *Chem. Phys. Letters*. **8**, 108 (1971).

2) To whom all correspondences should be addressed.

3) a) G.Briegleb, "Elektronen-Donator-Acceptor-Komplexe," Springer-Verlag, Berlin (1962); b) N.Mataga and T. Kubota, "Molecular Interactions and Electronic Spectra," Marcel-Dekker Inc., New York (1970).

4) N.Mataga and Y.Murata, *J. Amer. Chem. Soc.*, **91**, 3144 (1969).

or the time variation of luminescence intensity at a fixed wavelength. Our apparatus was calibrated to obtain correct luminescence quantum spectrum. For the measurement of ordinary luminescence spectrum, an Aminco-Bowman spectrophotofluorometer calibrated to obtain the correct luminescence quantum spectrum was used. The measurement of temperature effect on the fluorescence was conducted by, using a metal dewar with quartz windows. The temperature of the solution in a quartz cuvette placed in the dewar was controlled by a constant flow of cold nitrogen gas. The flow of the gas was controlled by heating liquid nitrogen and the temperature of the solution was measured with a thermocouple. The measurement at 77°K was carried out with a quartz dewar containing a solution in a cuvette immersed in liquid nitrogen. Differential thermal analysis on the phase transition of toluene was made with an apparatus constructed by Prof. S. Seki and his coworkers of this university.

TCNB sample was the same as used before.[4] It was recrystallized from ethanol before use. Benzene and toluene were shaken with sulfuric acid, dried over calcium chloride and after passing through a column of activated alumina, distilled fractionally. *o*- and *m*-xylene were distilled. Cyclohexane and *n*-hexane were passed through a column of activated silica gel, dried over sodium metal and distilled. *o*-Dichlorobenzene and monochlorobenzene were dried over calcium chloride and distilled. Trichloroethylene was distilled. Merck spectrograde tetrachloroethylene was used without further purification. All solutions were deaerated by freeze-pump-thaw cycles.

Results and Discussion

The luminescence spectra of TCNB–toluene system at several temperatures are given in Fig. 1.

When the temperature of the solution is lowered from room temperature to 193°K, the wavelength of the fluorescence band maximum (λ_F^m) shifts from 510 nm to 530 nm. A slight decrease of fluorescence intensity as well as decay time occurs. In the temperature range 183—153°K, where the system is in a supercooled liquid state, the λ_F^m value is approximately constant (~530 nm). A remarkable spectral shift from 530 nm to 450 nm occurs in the temperature range 150—138°K, as indicated partly in Fig. 2. At *ca.* 138°K, the phosphorescence band appears at about 500 nm. It seems probable that, at some temperature around 138°K, the phase transition from the supercooled liquid to the glassy state occurs when the temperature is lowered. At about 146—148°K, the solution is in a quite viscous supercooled liquid state and the fluorescence band with maximum at 490 nm is very broad (with half-value width of *ca.* 6000 cm^{-1}). At lower temperatures (136—77°K) fluorescence band shows further blue shift (λ_F^m=435 nm at 133°K and 420 nm at 77°K).

When the temperature is raised from 77°K, the fluorescence band maximum shows a red shift. An abrupt change in the spectrum as well as in the temperature of the system occurs at 137°K where the phosphorescence intensity becomes much stronger than the fluorescence intensity. We have confirmed by means of differential thermal analysis that this spectral change can be ascribed to the phase change of solution from glassy to crystalline states. The luminescence spectrum of the complex in the crystalline state is shown in Fig. 1. We have confirmed that this luminescence band can be ascribed to the phosphorescence of the complex by means of phosphorescence measurement. The observed phosphorescence decay time was about 2 sec. Thus, the spectra in the crystalline state differ from those in the glassy

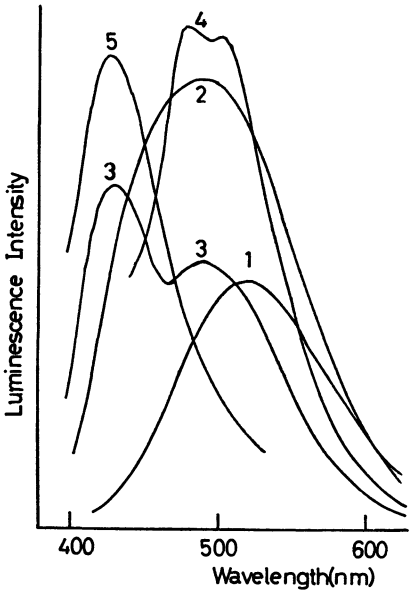

Fig. 1. Luminescence spectra of TCNB-toluene system at various temperatures. [TCNB]=10^{-3} M
1. 260°K (liquid state), 2. 146°K (supercooled liquid state), 3. 113°K (glassy state), 4. 156°K (crystalline state) 5. 189°K (liquid state)

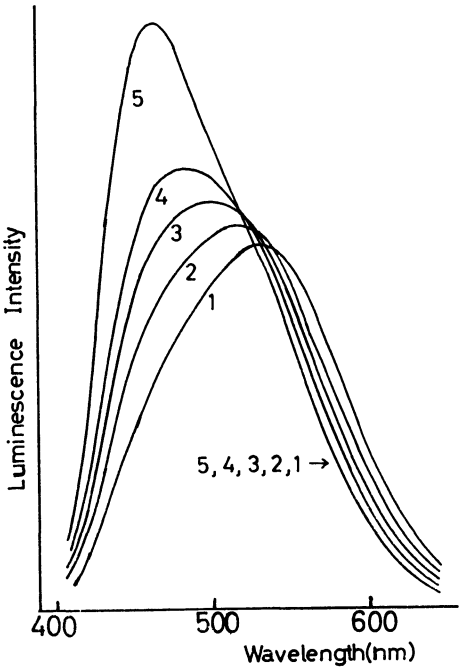

Fig. 2. Spectral change in the temperature range 150—145°K.
1—4: 150—147°K, 5: 145°K.

5) R G. Bennett, *Rev. Sci. Instr.*, **31**, 1275 (1960).

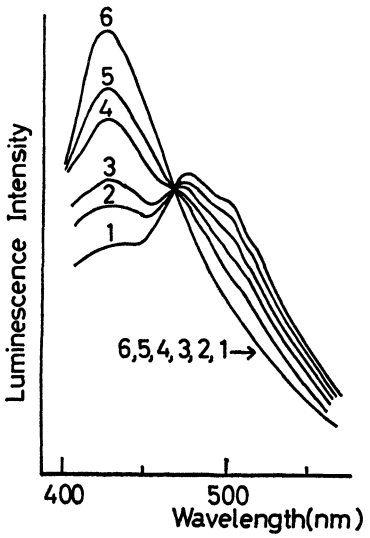

Fig. 3. Spectral change corresponding to the melting of the crystal.
1—3: 182—183°K, 4: 184°K, 5: 185°K, 6: 186°K.

state. In the temperature range 182—188°K, the phosphorescence band with peaks at 475 nm and 500 nm disappears and the fluorescence band appears at 425 nm as shown in Fig. 3. This change corresponds to the melting of the crystal. It should be noted that we can recognize an iso-emissive point at *ca.* 470 nm. At higher temperatures the fluorescence band shows a red shift and λ_F^m value at 243°K is *ca.* 530 nm. When the temperature is raised further, the spectrum shows a blue shift to λ_F^m value of 510 nm at room temperature.

At room temperature, the fluorescence spectra at various delay times from the exciting laser pulse were practically the same, and the fluorescence decay times at various wavelengths of the band were all equal to *ca.* 100 nsec. Analogous results can be observed also in the case of the glassy state at low temperatures (137°—77°K), where the fluorescence decay times at various wavelengths were all equal to *ca.* 50 nsec.

The results indicate that the excited F.C.→e.q. relaxation process of the complex including the surrounding solvent molecules at room temperature is much faster than the time resolving ability (a few nsec) of the apparatus. In the case of the glassy state at low temperatures, however, the observed results seem to indicate that it is impossible for the above relaxation process to occur during the fluorescence lifetime in the rigid state.

If the excited F.C.→e.q. relaxation time becomes comparable to the fluorescence lifetime somewhere between room temperature and the temperature of the glassy state, the fluorescence of the complex should show a time-dependent spectral shift and wavelength-dependent fluorescence rise and decay times. We have actually observed such results in the case of the supercooled liquid state at about 147°K.

As indicated in Fig. 4, the fluorescence decay times at 147°K and at 145°K show remarkable wavelength-dependences and the decay times at long wavelength part of the fluorescence band are much longer than those at short wavelength part of the band. In Fig. 5, we show fluorescence rise and decay curves at 147°K for several different wavelengths. We see

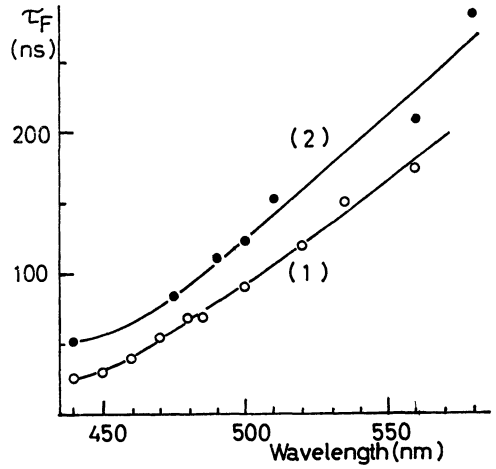

Fig. 4. Wavelength-dependence of the fluorescence decay time in the supercooled liquid state.
1: 147°K, 2: 145°K

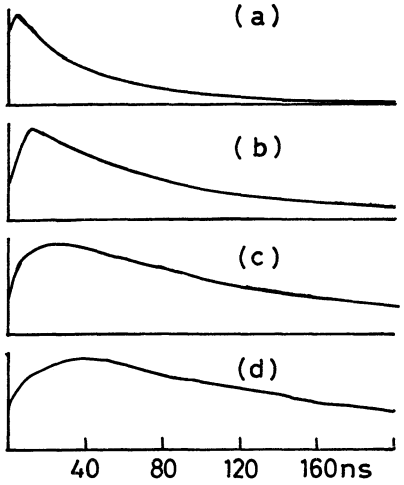

Fig. 5. Rise and decay curves at several wavelengths of the fluorescence band at 147°K.
(a) 460 nm, (b) 500 nm, (c) 540 nm, (d) 580 nm

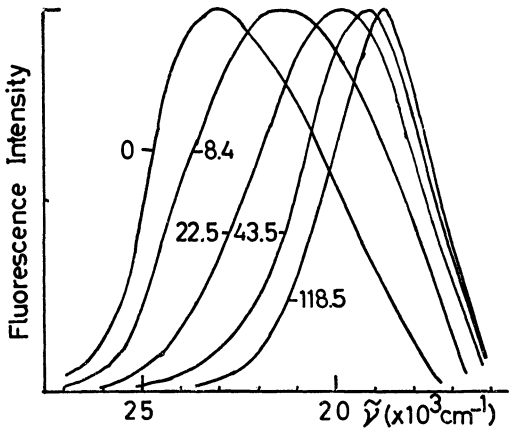

Fig. 6. Time-resolved CT fluorescence spectra of TCNB-toluene system in the supercooled liquid state at 147°K. Times indicated are in nsec after the rise of the laser pulse.

that both the fluorescence rise and decay times are longer at longer wavelengths. Furthermore, as shown in Fig. 6, time-resolved spectra (different spectra at delay times differing from the exciting pulse) have been clearly observed at 147°K.

The above results clearly show that the excited F.C.→e.q. relaxation process in the highly viscous environment at 147°K is much slower than that at room temperature. At 147°K, the relaxation time can be comparable to the decay time of the excited state. Thus, the relaxation process involving the surrounding solvent molecules has been demonstrated.

In Fig. 6, the band shape at the early stage of the fluorescence emission appears to differ considerably from that at the later stage of emission. This might be ascribed to the change in the structure of the complex during the relaxation process. However, it does not seem conclusive since the experimental error is larger at smaller delay times because of the time jitter ($\leq$2 nsec) due to the discharge trigger of the laser tube and smaller emission intensities. At any rate, the change of the structure of the complex should occur somewhere in the course of the excited F.C.→ e.q. relaxation since the radiative lifetime calculated from the absorption intensity is much smaller than the observed decay time.

Recently, the excited singlet-singlet (S_n-S_1) absorption spectra of TCN–Bbenzene and TCNB–toluene complexes have been measured by laser photolysis and by analyzing the reabsorption effect of the CT fluorescence by the excited singlet complexes.[6,7] Since the observed S_n–S_1 absorption spectra are very similar to those of TCNB anion, the electronic structure of the complex in the fluorescent e.q. state has been concluded to be a contact ion-pair.[6,7] Quantum chemical calculations on the TCNB–toluene complex show that the local excitation of TCNB and CT configuration contribute equally to the excited F.C. state while the fluorescent e.q. state has been found to have 99% CT character.[6b] Theoretical calculations have indicated clearly that the complex has the structure given in Fig. 7a in the ground e.q. as well as the excited F.C. states where the intermolecular overlap integral is considerable, while it has a symmetrical overlapping structure (Fig. 7b) in the excited e.q. and ground F.C. states where the intermolecular overlap integral is very small.[6b] Thus the F.C.→e.q. relaxation observed directly in the present work presumably involves a considerable structural change of complex in addition to rearrangements of the surrounding solvent molecules, and the contact ion-pair state seems to have a much longer radiative lifetime than that calculated from absorption intensity.

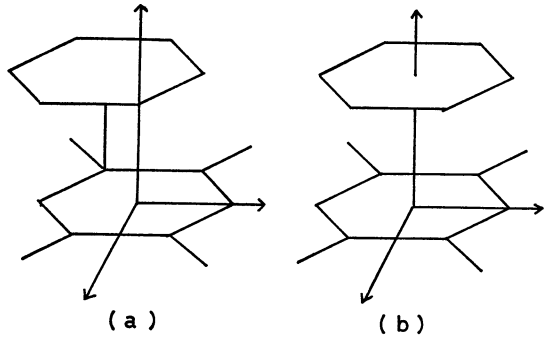

Fig. 7. Possible geometrical configurations of the complex.
a. Ground e. q. and excited F. C. states.
b. Fluorescence e. q. and ground F. C. state.

Since the structural change in the course of the excited F.C.→e.q. relaxation is quite large and the dipole moment of the excited e.q. state seems to be much larger than those in the excited F.C. and ground states, the effect of the solvent polarity on the wavenumbers of the fluorescence band maxima of the complex may be similar to the case of heteroexcimers. Using the theory of dielectric polarization, we can easily show that the wavenumber difference between the absorption and fluorescence band maxima can be given by[8]

$$hc(\tilde{\nu}_a-\tilde{\nu}_f) \cong 2(\Delta f/a^3)(\vec{\mu}_a^2-\vec{\mu}_a\cdot\vec{\mu}_g^{FC}-\vec{\mu}_g\cdot\vec{\mu}_a^{FC}+\vec{\mu}_g^2) - (\Delta f_n/a^3)(\vec{\mu}_a^2-\vec{\mu}_g^{2FC}-\vec{\mu}_a^{2FC}+\vec{\mu}_g^2), \quad (1)$$

$$\Delta f=\frac{\varepsilon-1}{2\varepsilon+1}-\frac{n^2-1}{2n^2+1},\quad \Delta f_n=\frac{n^2-1}{2n^2-1}$$

where a is the cavity radius in Onsager's theory of reaction field, ε and n are the solvent dielectric constant and refractive index, respectively, $\vec{\mu}_a$ and $\vec{\mu}_g$ represent dipole-moments in the excited e.q. and ground e.q. states, respectively, $\vec{\mu}_a^{FC}$ and $\vec{\mu}_g^{FC}$ are dipolemoments in the excited F.C. and ground F.C. states. In the present, the terms with $\vec{\mu}_a^2$ might be much larger than the others in the rhs of Eq. (1). Thus, we have

$$hc(\tilde{\nu}_a-\tilde{\nu}_f) \approx 2(\vec{\mu}_a^2/a^3)\left(\Delta f+\frac{1}{2}\Delta f_n\right). \quad (2)$$

As shown in Fig. 8, Eq. (2) can reproduce experimental results of TCNB–toluene complex in various solvents very well. Since $\tilde{\nu}_a$ value is approximately constant in these systems, the following is valid.

$$hc\tilde{\nu}_f \approx -2(\vec{\mu}_a^2/a^3)\left(\Delta f+\frac{1}{2}\Delta f_n\right) \quad (3)$$

This is the same equation as that applied to the solvent shift of the heteroexcimer fluorescence.

It should be noted that the $(\tilde{\nu}_a-\tilde{\nu}_f)$ value in toluene *i.e.* the value for the TCNB–toluene two component system is included in Fig. 8. We have discussed the possibility of 1 : n ($n\geq2$) complex formation during the lifetime of the fluorescent state in the case of TCNB–benzene and TCNB–toluene systems, in view of the very large Stokes shift.[4] The results in Fig. 8, show that the 1 : n ($n\geq2$) complex formation is improbable, since the observed shift of the fluorescence band can be well explained as due to the electrostatic interaction between the 1 : 1 complex and the solvent molecules.

6) H. Masuhara and N. Mataga, a) *Chem. Phys. Lett.*, **6**, 608 (1970); b) to be published.
7) R. Potashnik and M. Ottolenghi, *Chem. Phys. Letters*, **6**, 525 (1970).
8) See for example, N. Mataga, Y. Kaifu, and M. Koizumi, This Bulletin, **29**, 465 (1956); E. Lippert, *Ber. Bunsenges. Phys. Chem.*, **61**, 962 (1957).

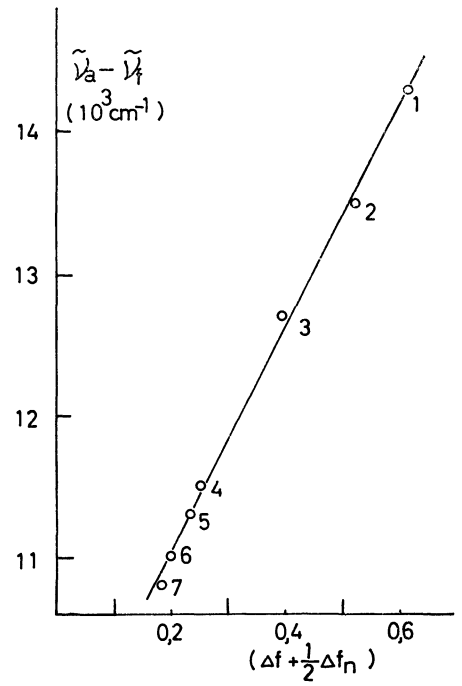

Fig. 8. $(\tilde{\nu}_a - \tilde{\nu}_f)$ *vs.* $(\Delta f + \frac{1}{2}\Delta f_n)$ relation observed for TCNB-toluene complex.
Solvent: 1, *o*-dichlorobenzene; 2, monochlorobenzene; 3, trichloroethylene; 4, toluene; 5, tetrachloroethylene; 6, cyclohexane; 7, *n*-hexane

The results in Fig. 6 can be further analyzed by means of Bakhshiev's equation.[9] The fluorescence intensity at the wavenumber ν and at the delay time t can be written as

$$I(\tilde{\nu}, t) = n(0)B(t) \exp\left[-\int_0^t B(t)dt\right] \cdot \gamma(t) f(\tilde{\nu}, t) \qquad (4)$$

where $n(0)$ is the number of excited molecules at $t=0$, $B(t)$ is the sum of radiative and radiationless transition probabilities, and $\gamma(t)$ is the fluorescence quantum yield. $B(t)$ and $\gamma(t)$ are functions of t in general because of time-dependent structural changes of the system. $f(\tilde{\nu}, t)$ represents the effect of the time-dependent spectral shift on the observed fluorescence rise and decay processes.

If the transition probability and the fluorescence quantum yield is time-independent, *i.e.* the excited F.C.→e.q. relaxation process does not involve the structural change of the complex itself but is caused by the reorientation motions of the surrounding solvent molecules, Eq. (4) can be rewritten as,

$$I(\tilde{\nu}, t) \approx n(0)\frac{1}{\tau_F} \cdot \gamma \exp\left[-t/\tau_F\right] \cdot f(\tilde{\nu}, t)$$
$$= Const \cdot \exp\left(-t/\tau_F\right) \cdot f(\tilde{\nu}, t) \qquad (5)$$

If the change of the structure of the complex occurs at some time in the early stage of the excited F.C.→ e.q. relaxation, the time variation of the fluorescence intensity after that time can be expressed by Eq. (5). $f(\tilde{\nu}, t)$ can be evaluated from the normalized time-resolved spectra as indicated in Fig. 6. The decay time associated with $I(\tilde{\nu}, t)$ can be calculated by means of Eq. (5) assuming an appropriate value for τ_F. In Table 1, the calculated values at various wavelengths taking $\tau_F = 120$ nsec are compared with the observed values. Agreement between the observed and calculated values is rather satisfactory. Almost all parts of the structural change might be completed immediately after the excitation.

9) N. G. Bakhshiev, Y. T. Marurenko, and I. V. Piterskaya, *Opt. Spectry.* (USSR) (English translation) **21**, 307 (1966).

Table 1. Observed and calculated fluorescence decay times for TCNB-toluene system at 147°K

Wavelength (nm)	$\tau_{F,obs}$(nsec)	$\tau_{F,calc}$(nsec)
440	25	30
460	40	50
480	60	60
500	90	90
520	120	105
535	140	130
560	170	135

No relaxation process occurs during the excited state lifetime in the case of the glassy state of TCNB-toluene system. However, we have found out that we can observe a slight time variation of fluorescence spectra in the case of the crystalline state. The crystalline state was formed at 137°K when temperature was raised from 77°K in the glassy state. After the phase transition occurred at 137°K, the temperature was lowered to 77°K or raised to 171°K and the wavelength dependence of the decay times as well as the time-resolved spectra were measured. The results are given in Figs. 9 and 10.

We see that the extent of the wavelength dependent variations of the decay time and the red shift in the time-resolved spectra at 171°K are larger compared to those at 77°K. In general, the extent and the rate of the time-dependent spectral changes in the crystalline state are much smaller than those in the supercooled liquid state at 147°K. This may be due to the fact that the molecular motions responsible for the excited F.C.→e.q. relaxation are much slower in the crystalline state than in the supercooled liquid state at 147°K.

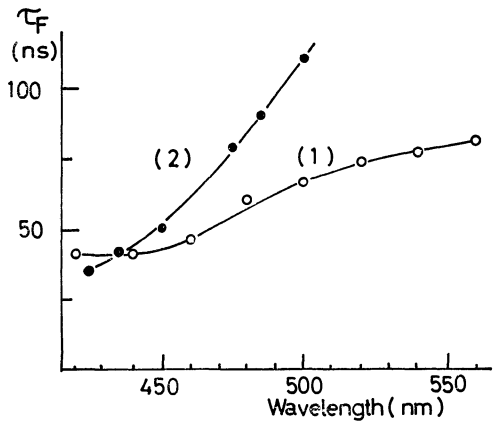

Fig. 9. Wavelength-dependence of the fluorescence decay time in the crystalline state.
1, 77°K; 2, 171°K

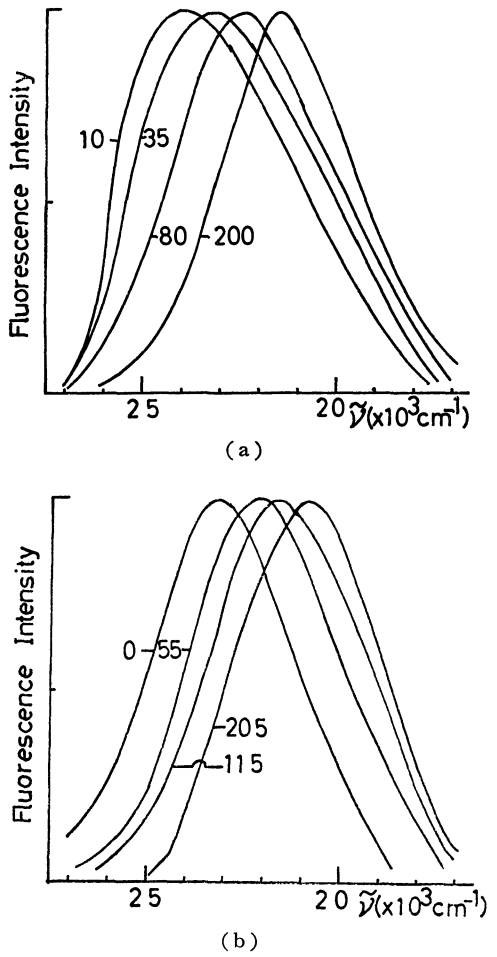

Fig. 10. Time-resolved fluorescence spectra of TCNB-toluene system in the crystalline state. Times indicated are in nsec after the rise of the laser pulse.
a, 77°K; b, 171°K

It seems rather peculiar that the time-dependent spectral changes were not observed in the glassy state, in contrast to the results of the crystalline state. However, since the crystalline state of the TCNB-toluene system was produced by the phase transition from the glassy state at a fairly high temperature, it might be rather soft and contain many defects, which would allow some molecular motions during the excited state lifetime. In the case of TCNB-benzene, TCNB-*o*-xylene and TCNB-*m*-xylene systems, the crystalline state is formed simply by the phase transition from the liquid state when the temperature is lowered. We were not able to observe any wavelength dependence of the fluorescence decay time for these systems in the crystalline state at 77°K. This seems to indicate that the crystals of these systems contain a much smaller amount of defects than the TCNB-toluene system, and it is very difficult for the molecular motions to rise during the excited state lifetime.

Table 2. Observed and calculated fluorescence decay times for TCNB-toluene system in the crystalline state

(A) at 77°K taking $\tau_F = 65$ nsec

Wavelength (nm)	$\tau_{F,obs}$(nsec)	$\tau_{F,calc}$(nsec)
420	40	40
440	40	50
450	45	55
480	60	65
500	65	65
540	75	70

(B) at 171°K taking $\tau_F = 70$ nsec

Wavelength (nm)	$\tau_{F,obs}$(nsec)	$\tau_{F,calc}$(nsec)
425	35	50
450	55	60
475	80	75
500	110	100

We have analyzed the experimental results of Fig. 10 according to Eq. (5), and the results of calculations are shown in Table 2A and 2B. Agreement between the observed and calculated τ_F values is fairly satisfactory. Thus, the model assumed for Eq. (5) appears to be valid approximately in these cases as in the case of relaxation process at 147°K. Probably, a slight structural change in the complex occurs immediately after the excitation even in the crystalline state and only a slight reorientation relaxation of the surrounding solvent molecules occurs during the excited state lifetime.

Concluding Remarks

The extensive relaxation process of excited F.C.→ e.q. in the TCNB-toluene system including the surrounding solvent molecules has been demonstrated by the measurement of the time-resolved fluorescence spectra. The extensive relaxation seems to be initiated by the structural change of the complex due to excitation. Analysis of the time-resolved spectra has indicated that almost all parts of the structure change in the complex occurs immediately after the excitation even in the quite viscous medium at 147°K.

The authors are grateful to Professor S. Seki and his associates of this University for use of the apparatus for differential thermal analysis, and for their helpful discussions concerning the thermal analysis and phase transitions of toluene.

The Electrolytic Conductances of Bis(halogenoacetato)bis-(ethylenediamine)cobalt(III) Ions in Water

Masatoki Yokoi and Kashiro Kuroda*

Department of Chemistry, Faculty of Science, Shinshu University, Matsumoto, Nagano

**Department of Chemistry, Faculty of Science, Ehime University, Matsuyama, Ehime*

(Received May 31, 1971)

The electrolytic conductances of bis(halogenoacetato)bis(ethylenediamine)cobalt(III) perchlorate, $[Co(halac)_2(en)_2]ClO_4$ where Hhalac=CH_3CO_2H, CH_2ClCO_2H, $CHCl_2CO_2H$, CCl_3CO_2H, and CF_3CO_2H were measured in water at 25°C. The equivalent conductances of the solutions ($c=10^{-3}$—10^{-4} mol/l) were obtained from the conductance kinetic runs by extrapolating conductances to time zero. The ionic equivalent conductances of the complex ions were 21.5—17.2 $ohm^{-1}cm^2eq.^{-1}$, and decreased with the increase of the chlorine content in the chloroacetato ligands. Little differences in the ionic equivalent conductances were observed between a pair of cis and trans isomers. The rate constants of the first order aquation of the complexes were estimated.

The electrolytic conductance of a complex ion has often been measured in order to determine (1) the electric charge of the ion, (2) the velocity of substitution reaction such as aquation, and (3) the equilibrium constant of the complex formation or the association constant with a counter ion.

Although many data are available in literature[1], we can hardly find any systematic research which directs out attention to the elucidation of the relation between the conductivity and the structure of complexes. In order to grasp the relation, this study deals with the conductance of bis(halogenoacetato) bis(ethylenediamine)cobalt(III) perchlorate, $[Co(halac)_2(en)_2]ClO_4$, in aqueous solution at 25°C, where Hhalac=CH_3CO_2H, CH_2ClCO_2H, $CHCl_2CO_2H$, CCl_3CO_2H, and CF_3CO_2H.[2] The group of complexes has the following benefits to elucidate the dependence of conductivity on the structure of complexes. They are uni-univalent electrolytes which are the easiest type of electrolyte for theoretical consideration. The *cis*- and *trans*-isomers for various halac have been identified.[3] The size of the complexes increases steadily with the increase of the number of halogene atom in the halac ligands. The counter ion - perchlorate - has little tendency to associate with the complex ions in the range of concentration which were measured ($c=10^{-3}\sim10^{-4}$ mol/l). Their aquation velocities are relatively slow, despite the fact that they belong to the diacido-complex which generally aquates quickly.[4] Thus it is possible to obtain reliable values for equivalent conductance at infinite dilution.

Experimental

Materials. The complexes were prepared by the procedures described previously.[3] They were recrystallized at least twice and washed with absolute ethanol many times in order to remove completely the perchloric acid or sodium perchlorate which were used to precipitate the complexes in recrystallization. They were then dried in a vacuum desiccator over silica gel until the weight of the materials did not change any more. The specific conductance of the water was in a range 6×10^{-7}—7×10^{-7} ohm^{-1} cm^{-1}.

Apparatus and Measurement. A Jones-type bridge was used for the measurements and an alternative current of 10 kc frequency was applied to the bridge. A weighed sample in a small polyethylene dish was dissolved by magnetic stirring in one of two flask-type conductivity cells which had been placed in an oil-thermostat and contained a definite amount of conductivity water (~400 g). The cell constants of the cells were 0.23308 and 0.05355. Immediately after the dissolution, the resistance was measured at definite time intervals. A few complexes were measured in both of the cells, and the agreement of the results was satisfactory. As an example of the measurements, Fig. 1 shows the time-dependence of the specific conductance L of *cis*-$[Co(dclac)_2(en)_2]ClO_4$. We see that the specific conduc-

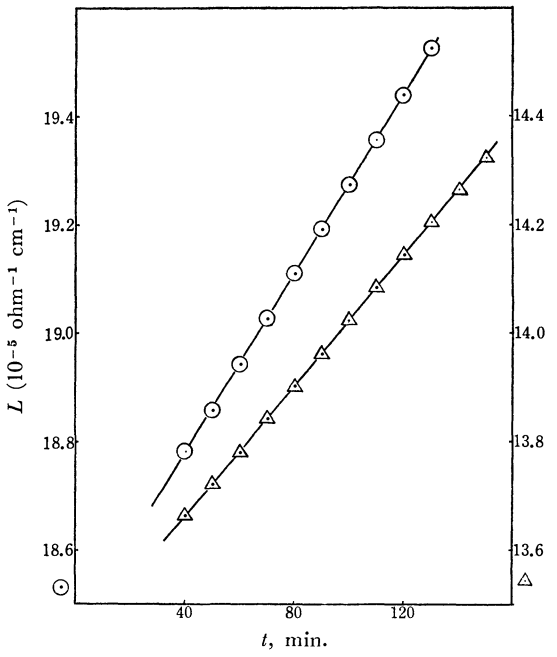

Fig. 1. Variation of specific conductance L of *cis*-$[Co(dclac)_2(en)_2]ClO_4$ solution with time.
⊙ $c=2.272\times10^{-3}$, △ $c=1.638\times10^{-3}$.

1) For example, W. A. Millen, and D. W. Watts, *J. Amer. Chem. Soc.*, **89**, 6858 (1967); S. Katayama and R. Tamamushi, This Bulletin, **41**, 606 (1968), **43**, 2354 (1970).

2) The following abbreviation is used for the halogenoacetato ligands: CH_3CO_2H=Hac, CH_2ClCO_2H=Hmclac, $CHCl_2CO_2H$=Hdclac, CCl_3CO_2H=Htclac, CF_3CO_2H=Htfac.

3) K. Kuroda and P. S. Gentile, This Bulletin **38**, 1362, 1368, 2159 (1965).

4) D. R. Stranks, "Modern Coordination Chemistry," ed. by J. Lewis and R. G. Wilkins, Interscience Publishers Inc., New York, N. Y. (1960), p. 129.

Table 1. Equivalent conductances of the aqueous solutions of $[Co(halac)_2(en)_2]ClO_4$ and related complexes at 25°C

10^4c (mol/l)	Λ (ohm^{-1} cm^2/eq.)	10^4c (mol/l)	Λ (ohm^{-1} cm^2/eq.)
cis-$[Co(ac)_2(en)_2]ClO$		*cis*-$[Co(mclac)_2(en)_2]ClO_4$	
4.648	87.17	2.903	87.14
8.130	86.67	9.310	85.23
14.58	85.63	18.12	84.22
24.98	84.86	30.64	82.71
cis-$[Co(dclac)_2(en)_2]ClO_4$		*cis*-$[Co(tclac)_2(en)_2]ClO_4$	
6.501	83.47	6.660	82.59
10.37	82.66	9.844	82.02
16.38	81.98	23.84	80.70
22.72	81.25		
trans-$[Co(mclac)_2(en)_2]ClO_4$		*trans*-$[Co(dclac)_2(en)_2]ClO_4$	
9.520	84.98	3.645	85.93
13.96	84.46	7.091	85.08
18.33	84.05	8.701	84.90
		13.39	84.36
trans-$[Co(tclac)_2(en)_2]ClO_4$			
3.810	83.32		
9.118	82.21		
12.60	81.80		
cis-$[Co(tfac)_2(en)_2]$acetate		*trans*-$[Co(tfac)_2(en)_2]ClO_4$	
4.868	59.55	4.257	86.27
12.25	58.67	6.832	85.90
22.22	57.76	10.57	85.29
		16.22	84.62
cis-$[Co(mclac)_2(NH_3)_4]ClO_4$		*trans*-$[Co(mclac)_2(NH)_3)_4]ClO_4$	
7.687	89.57	3.183	90.85
8.588	89.43	4.972	90.54
18.76	88.56	12.45	89.80
24.15	88.15	22.97	88.56

tance of all the complexes increased linearly with time in the region 40—100 min. The values obtained within 20 min sometime deviated slightly from the straight line. This can be attributed to the non-homogeneity of the solution, even though all the solid sample dissolved completely in a few minutes. The specific conductance at time zero was extrapolated from the straight line, and the equivalent conductance was calculated.

For each of the complex salts, the measurement was carried out with at least three different concentrations. The equivalent conductances thus obtained are given in Table 1.

Discussion

Dependence on Concentration. The concentration dependence of the equivalent conductance Λ of all the complex salts agreed with the Onsager limiting conductance equation for the uni-univalent salts

$$\Lambda = \Lambda_0 - (\alpha\Lambda_0 + \beta)\sqrt{c}. \quad (1)$$

Thus, from this equation, it is possible to estimate the equivalent conductance at infinite dilution Λ and the ionic equivalent conductance λ_0^+ by subtracting λ_0^-(67.4 for perchlorate and 40.9 for acetate[5]) from Λ_0. These values are summarized in Table 2. The effective ionic radii R^+ are also indicated which are calculated from the following equation,[6] assuming the Stokes law holds in the ionic transportation:

$$R^+ = Fe/1800\pi\eta\lambda_0^+ \quad (2)$$

where F is the Faraday charge, e the electronic charge, and η the viscosity coefficient of water.

Table 2. Limiting conductance of $[Co(halac)_2(en)_2]^+$ and related complexes

	Λ_0	λ_0^+	R^+(Å)	Λ_0	λ_0^+	R^+(Å)
	$[Co(halac)_2(en)_2]ClO_4$					
	cis			*trans*		
ac	88.9	21.5	4.3	—	—	—
mclac	87.7	20.3	4.5	87.4	20.0	4.6
dclac	85.4	18.0	5.1	87.3	19.9	4.6
tclac	84.6	17·2	5.3	84.6	17.2	5.3
tfac	61.2[a]	20.3	4.5	88.0	20.6	4.4
	$[Co(halac)_2(NH_3)_4]ClO_4$					
	cis			*trans*		
mclac	91.7	24.3	3·8	92.4	25.0	3.7

a) acetate

We see that the ionic equivalent conductance decreases and the effective ionic radii increases with increase of the chlorine content in the halac ligand, and that there hardly exists a difference in conductivity between a pair of *cis*- and *trans*-isomers. These results are worthy of discussing.

In a dilute solution, the equivalent conductance of ions depends on the volume or the ionic radii and not on the mass, when the charge of the ions are identical. If actual conductivity of a group of ions is not parallel to the radii of the ions, as in the case of the alkali ions, the cause is attributed to the different degree of the solvent association of ions. Thus, the effective volume of an ion in a solution can be estimated from the conductivity measurement. In the present *cis*- and *trans*-series of the complexes, the association of water molecule (if any) is considered to be identical except at the site of the methyl and the chloromethyl radicals. As the radicals are not hydrophilic, the association at this site would be negligible. Thus, in each series of the complexes, it can be reasonably accepted that the effect of the solvent association does not affect the order of the conductivity of the complexes. Actually, the experimental results showed the normal order expected from the size of the complexes. In the tables, the values of *cis*- and *trans*-$[Co(mclac)_2(NH_3)_4]ClO_4$ are shown for comparison. It is seen that the tetraammine-complexes have a higher conductivity than the corresponding bis(ethylenediamine)-complexes.

Rate of Aquation. The conductivity of the complexes increases with time. This can be undoubtedly attributed to the aquation

5) R. A. Robinson and R. H. Stokes, "Electrolyte Solutions," 2nd ed. Butterworths, London (1959), p. 463.

6) R. M. Fuoss and F. Accascina, "Electrolyte Conductance," Interscience Publishers Inc., New York, N. Y. (1959), p. 60.

$$[Co(halac)_2(en)_2]^+ + H_2O \rightarrow [Co(halac)(H_2O)(en)_2]^{2+} + halac^-.$$

If the conductivity of the resulting halogenoacetatoaquo complexes were known, it would be possible to evaluate accurately the rate of aquation from the time dependence of conductivity. However, the halogenoacetatoaquobis(ethylenediamine)cobalt(III) salts have not been isolated, and the conductivity of the ions are unknown. Thus, an assumption is necessary for the calculation of the rate constant.

The size of the ions which determines the conductivity of this group of complexes can be approximately equal in a reactant bis(halogenoacetato)-complex and the resulting halogenoacetatoaquo-complex, because the replacement of a halogenoacetato ligand by a water molecule does not considerably change the total size of the ion. The resultant ions are divalent. Therefore, it is reasonable to assume that the conductivity of the resultant complex ion is twice as large as that of the corresponding reactant complex ion. The variation of the conductivity with time was examined on this assumption and with λ_0^-'s of the halogenoacetate ions.[7] The plots of log $(L_\infty - L)$ of *cis*-$[Co(ac)_2(en)_2]ClO_4$ *versus* time are shown

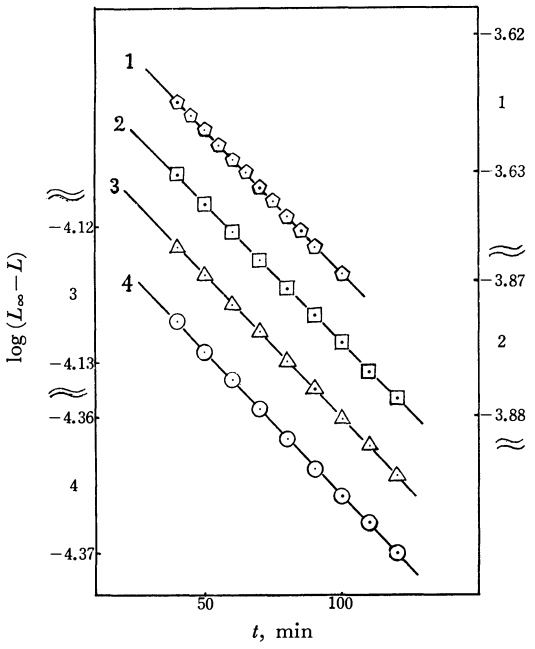

Fig. 2. The plots of log $(L_\infty - L)$ *vs.* time of *cis*-$[Co(ac)_2(en)_2]ClO_4$.
1, $c=2.498\times10^{-3}$, 2, $c=1.458\times10^{-3}$, 3, $c=8.130\times10^{-4}$, 4, $c=4.648\times10^{-4}$.

7) The values of λ_0^- of dichloroacetate and trichloroacetate ions used in the calculation were 37.4 and 35.2, respectively. These values were obtained by the extrapolation of the conductivity data of potassium dichloroacetate and sodium trichloroacetate in aqueous solution at 25°C obtained by one of the authors (M.Y.).

Table 3. First order rate constants of aquation $[Co(halac)_2(en)_2]^+$

	k_1 min^{-1}	k_1 min^{-1}
	$[Co(halac)_2(en)_2]ClO_4$	
	cis	*trans*
ac	4.8×10^{-4}	—
mclac	5.5×10^{-4}	1.2×10^{-4}
dclac	4.9×10^{-4}	1×10^{-5}
tclac	5.2×10^{-4}	1.7×10^{-4}
tfac	5.6×10^{-4}	1.7×10^{-4}
	$[Co(halac)_2(NH_3)_4]ClO_4$	
	cis	*trans*
mclac	4.9×10^{-3}	0.9×10^{-4}

in Fig. 2 as an illustration. The plots are linear. This means that the aquation is a first order reaction similar to the acid-hydrolyses of many analogous complex ions. The first order rate constants obtained by the above procedure are summarized in Table 3. It is interesting to note that the rate constants do not differ considerably among the complexes under the present conditions, *viz.* in the severe neutral solution, although a deviation is observable in *trans*-$[Co(dclac)_2(en)_2]^+$. On the other hand, it has been observed quantitatively in $[Co(halac)(NH_3)_5]^{2+}$ [8] or in the related complexes such as $[Co(aminoacid)(NH_3)_5]^{2+}$ [9] that aquation is accelerated with hydrogen ion depending on the basicity of the halac ligands. A similar behavior was noted qualitatively with this series of complexes (the acidic solution of a complex of the series changes its absorption spectrum faster than the neutral solution). Thus, the aquation (acid hydrolysis) is an acid-catalyzed reaction and the reaction has been supposed to proceed *via* the following path,[8] the larger the basicity of the ligand, the greater being the acceleration of the reaction rate by hydrogen ion.

$$Co\text{-}O\text{-}\overset{\overset{O}{\|}}{C}\text{-}R + H^+ + H_2O \rightarrow Co\text{-}O\text{-}\overset{\overset{OH}{|}}{C}\text{-}R + H_2O$$

$$\rightarrow Co\text{-}OH_2 + O{=}\overset{\overset{OH}{|}}{C}\text{-}R$$

In neutral solution or at a negligible hydrogen ion concentration, the reaction takes place as

$$Co\text{-}O\text{-}\overset{\overset{O}{\|}}{C}\text{-}R + H_2O \rightarrow Co\text{-}OH_2 + {}^-O\text{-}\overset{\overset{O}{\|}}{C}\text{-}R$$

and the rate of the reaction is almost independent of R.

8) K. Kuroda, *Nippon Kagaku Zasshi*, **82**, 572 (1961).
9) K. Ogino, T. Murakami, and K.Saito, This Bulletin, **41**, 1615 (1968)

Two Types of Complexes of *o*-Phenylenediamine with Tetracyanoquinodimethane

Masatake OHMASA*, Minoru KINOSHITA, and Hideo AKAMATU**

Department of Chemistry, Faculty of Science, The University of Tokyo, Hongo, Tokyo

(Received June 3, 1971)

o-Phenylenediamine and tetracyano-*p*-quinodimethane (TCNQ) were shown to form two types of solid complexes with compositions of 1 : 1 and 2 : 1. The 2 : 1 complex is essentially of ionic type, while the 1 : 1 complex is characterized as of non-bonding type from the analysis of its infrared absorption spectrum. It was shown that the difference in type is reflected on the magnetic and electrical properties of these complexes. The ESR absorption or the spin concentration of the 1 : 1 complex changed irreversibly with grinding or heat-treatment (70°C), while no appreciable change was observed in the 2 : 1 complex with these treatments. The electrical resistivity is lower for the 1 : 1 complex than the 2 : 1 complex by a factor of 10^2. From these observations, it is considered that the ground state electronic structure of the 1 : 1 complex is in a similar situation to those of diaminopyrene-chloranil and benzidine-TCNQ complexes.

In a previous paper,[1] the electronic properties of the 2 : 1 complex of *o*-phenylenediamine (*o*-PD) with 7,7,8,8-tetracyano-*p*-quinodimethane (TCNQ) have been discussed as a complex of ionic type. Since then, it was found that the complex of 1 : 1 composition can also be obtained. The ground state character for the 1 : 1 complex was found to be primarily of non-bonding type in contrast to the 2 : 1 complex.

It is of interest to examine and compare the electronic properties of these complexes, since both types can be obtained from the same donor and acceptor. The magnetic and electrical properties of the two complexes were found to differ a great deal from each other.

Experimental

Complex Preparation. *The 2 : 1 Complex*: To a saturated solution of TCNQ in 15 m*l* of dichloromethane was added a solution of 400 mg of *o*-PD in 10 m*l* of dichloromethane at room temperature, and the resulting purple precipitate was collected.

The 1 : 1 Complex: A solution of 610 mg of *o*-PD in 15 m*l* of dichloromethane was added to a solution of 107 mg of TCNQ in 50 m*l* of dichloromethane, and the mixture was cooled to −10°C. Black crystals thus formed were collected.

Measurements. The absorption spectra in the visible and infrared regions, the ESR absorption spectra and the electrical resistivity were measured in a similar manner to that in previous reports[1,2] in which purification of the chemicals was also described.

Results and Discussion

Composition of the Complexes. The chemical composition (donor to acceptor ratio) of the complex was determined from the analysis of the absorption spectra in the UV and visible regions. The results obtained are given in Table 1, the assigned stoichiometric ratios being also listed.

TABLE 1. THE CHEMICAL COMPOSITION OF THE *o*-PD·TCNQ COMPLEXES

Complex	Composition (Donor : Acceptor)	
	Spectral analysis	Assigned stoichiometry
o-PD·TCNQ(1 : 1)	1 : 0.97	1 : 1
o-PD·TCNQ(2 : 1)	1 : 0.47	2 : 1

Characterization of the Complexes. The infrared absorption spectra of both 2 : 1 and 1 : 1 complexes of *o*-PD with TCNQ are shown in Fig. 1, together with the spectra of *o*-PD, TCNQ,[3,4] and lithium salt of TCNQ.

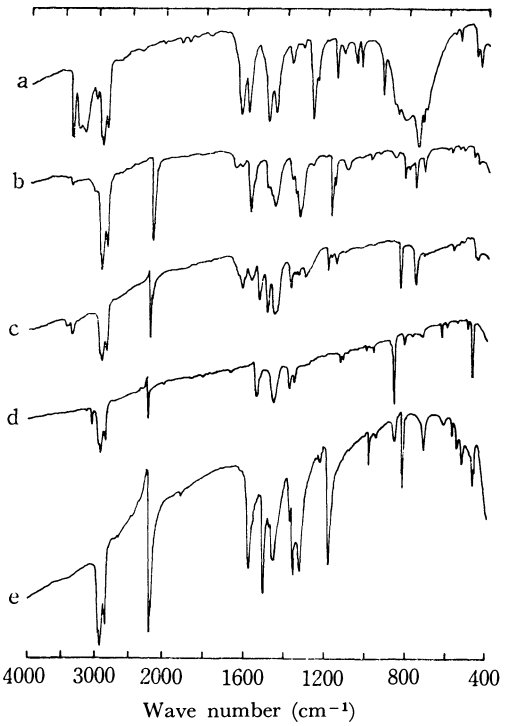

Fig. 1. Infrared absorption spectra of *o*-PD·TCNQ complex and related compounds.
(a) *o*-PD, (b) *o*-PD·TCNQ (2 : 1), (c) *o*-PD·TCNQ (1 : 1), (d) TCNQ, (e) LiTCNQ.

* Present address: The Institute of Physical and Chemical Research, Wako, Saitama.

** Present address: Institute of Materials Science and Engineering, Yokohama National University, Minami-ku, Yokohama.

1) M. Ohmasa, M. Kinoshita, and H. Akamatu, This Bulletin, **41**, 1998 (1968).

2) M. Ohmasa, M. Kinoshita, and H. Akamatu, *ibid.*, **42**, 2402 (1969): **44**, 395 (1971).

The infrared absorption spectrum of the 2 : 1 complex indicates ionic character of the complex. As seen in Fig. 1, the C≡N stretching vibration located at 2223 cm^{-1} in neutral TCNQ is broadened and shifted to 2180 cm^{-1} in the complex. The ring C=C stretching vibration at 1540 cm^{-1} in neutral TCNQ disappears and a new band appears at 1580 cm^{-1}. Another new band is also observed at 1180 cm^{-1}. These features are identical with those of lithium salt of TCNQ, and confirm that the 2 : 1 complex is of ionic type.

Absorption bands of the donor in the 2 : 1 complex also suggest ionic character. An intense band at 1275 cm^{-1} in the spectrum of neutral *o*-PD is assigned to the ring stretching mode involving considerable C–N stretching, because its position and shape are very similar to the corresponding band of aniline.[5] This mode is shifted to 1336 cm^{-1} in the complex and the shift is in the same direction for the same vibrational mode of the *N,N*-dimethyl-*p*-phenylenediamine-TCNQ complex.[1] It is therefore concluded that the 2 : 1 complex is of ionic type. The amine part can be considered to have the form of $(o\text{-PD})_2^+$, because of the neutrality requirement.

In the 1 : 1 complex, the C≡N stretching vibration band is narrow and is located at 2210 cm^{-1}, and the ring stretching mode of TCNQ was observed at 1535 cm^{-1}. The location and the shape of these bands are similar to those of the corresponding bands of neutral TCNQ. The peaks at 1620, 1570, and 1492 cm^{-1} of the complex are identified with those at 1628, 1592, and 1492 cm^{-1} of neutral *o*-PD, respectively. This indicates that the 1 : 1 complex is characterized primarily as of non-bonding type.

The band at 1275 cm^{-1} of neutral *o*-PD, however, was shifted to 1305 cm^{-1} upon complex formation of the 1 : 1 composition. This suggests that the dative structure contributes considerably to the ground electronic state of the complex. In fact, the magnetic and electrical properties of the 1 : 1 complex also seem to reflect this contribution.

The difference in the electronic character can evidently be ascribed to the difference in composition, namely to the difference in the manner of molecular stacking in the crystals. The formation of an ionic complex is governed by the energy needed to charge the component molecules and by the electrostatic energy of the charged lattice. The former is determined by the ionization energy of the donor and the electron affinity of the acceptor, while the latter by Madelung's energy and polarization effects, both of which depend upon the crystal structure of the complex. In our complexes, since the ionization potential of the donor and the electron affinity of the acceptor are the same for both complexes, the electrostatic energy for salt formation seems to favour the crystal structure of the 2 : 1 complex rather than that of the 1 : 1 complex.

It is also of interest to discuss the difference in character of the 1 : 1 complex of *o*-PD·TCNQ and that of the 1 : 1 complex of *p*-phenylenediamine-TCNQ (*p*-PD·TCNQ), since the latter was found to be ionic in contrast to the former.[1] Matsunaga studied the electronic character of a number of complexes and arranged them in a diagram to correlate the character with the relative ionization potentials of donors and the relative electron affinities of acceptors.[6] The complex of *p*-PD·TCNQ is situated in the region of the complexes of non-bonding type, but very near the border line dividing the complexes having non-bonding ground states and those having dative or ionic ground states. The tendency of *p*-PD to form the complexes of dative ground states is suggested to be an exception to his diagram which reflects the effect of the size and shape of the component molecules on the electronic character. Since the ionization potentials of *o*- and *p*-PD are nearly the same,[7] the 1 : 1 complex of *o*-PD·TCNQ is also expected to situate around the border line, but in the region of the non-bonding group. The fact that the *o*-PD·TCNQ complex is found to be actually of non-bonding type verifies, therefore, the validity of the suggestion on the size and shape effects for *p*-PD complexes.

Magnetic and Electrical Properties. The magnetic and electrical properties of the complexes are summarized in Table 2, and the plots of the ESR absorption intensity against temperature are shown in Fig. 2. For both complexes, the intensity increased exponentially with temperature in a higher temperature region. The absorption intensity (I) was analysed in a similar manner to that described for the case of the *p*-PD·TCNQ complex.[1,8,9] The values of the activation energy δ, obtained from the plots of $\ln(IT)$ *vs.* $1/T$

Table 2. Magnetic and electrical properties of the *o*-PD·TCNQ complexes

Complex	Spin concentration[a]	δ (eV)	*g*-Value	$\rho_{15°C}$ (ohm·cm)	*E* (eV)
1 : 1	1×10^{22}	0.11	2.0026	1.0×10^{5}	0.28
2 : 1	7×10^{21}	0.07	2.0028	1.4×10^{7}	0.45

a) Number of electrons contributing to the paramagnetism per one mole of the complex at room temperature, 296°K.

3) T. Takenaka, Preprints of the Symposium on Molecular and Electronic Structure, October, 1969, Fukuoka, Japan.
4) B. Lunelli and C. Pecile, *J. Chem. Phys.*, **52**, 2375 (1970).
5) J. C. Evans, *Spectrochim. Acta*, **16**, 428 (1960).
6) Y. Matsunaga, This Bulletin, **42**, 2490 (1969).
7) The ionization potential of *o*-PD is considered to be larger by about 0.1 eV than that of *p*-PD, because the complexes of *o*-PD with *p*-bromanil and *p*-PD with *p*-bromanil show the charge-transfer band maxima at 646 and 672 mμ, respectively, in carbon tetrachloride.[1]
8) The notation of δ is used here instead of J in Ref. 1.
9) A correction was made for the intensities in the higher temperature region of the 1 : 1 complex by subtracting the intensities obtained by an extrapolation from the lower temperature side to the higher temperature side.

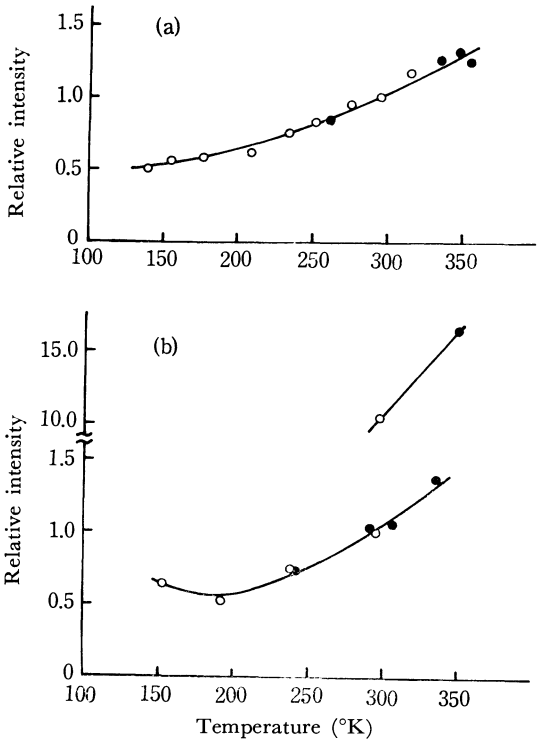

Fig. 2. Variations of ESR absorption intensities with temperature for *o*-PD·TCNQ complexes. Open circles are the points measured when the temperature was lowered, while shaded circles are the points measured when the temperature was raised.
(a) The 2 : 1 complex. The intensity changed reversibly.
(b) The 1 : 1 complex. When the temperature was raised up to 70°C, the intensity increased abruptly. However, when the temperature was lowered from 70°C, the intensity changed with the δ value coincident with that of the lower temperature region.

are given in Table 2.

When the 1 : 1 complex was warmed to 70°C in a vacuum for about 15 minutes, the ESR absorption intensity increased by a factor of 12. This phenomenon was found to be irreversible. However, the value of δ of the sample after heat treatment seems to coincide with that before the heat treatment. The nature of the paramagnetic sites does not seem to change with heat treatment.

The ESR absorption intensity of the 1 : 1 complex increased also by grinding. When the polycrystalline sample was ground in an agatemortar, the line width became slightly broadened and the intensity increased by a factor of about 5. The unpaired electrons observed in the 1 : 1 complex are, therefore, considered to be produced by an electron-transfer from the donor to the acceptor at lattice-defects and/or at the surfaces. The electron-transfer is likely enhanced by such treatments as grinding and heating.

As is seen in Table 2, the value of δ and the spin concentration of the 2 : 1 complex were found to be of the same order as those of the 1 : 1 complex. However, the spin concentration of the former was not affected when the sample was heated up to 82°C. The ESR absorption intensity changed reversibly with temperature as shown in Fig. 2.

The electrical resistivities of these complexes changed with temperature according to the equation $\rho=\rho_0 \times \exp(E/\boldsymbol{k}T)$. The values of the activation energy (E) and the specific resitivity (ρ) at 15°C are given in Table 2. Both $\rho_{15°C}$ and E are higher for the 2 : 1 complex than for the 1 : 1 complex.

The electrical conductivity of the 1 : 1 complex is rather high among the complexes of non-bonding type.[10,11] The complex of 1,6-diaminopyrene with *p*-chloranil[10,12] and the complex of benzidine with TCNQ containing solvent molecules[2,13] also exhibit relatively high conductivity, although they are not ionic in character. These three complexes, have the following common properties. (i) Although they are formed between strong donors and strong acceptors, their ground electronic character is not ionic but non-bonding. (ii) The ESR absorption intensity increases greatly when the crystals are ground into fine powder.[2] (iii) They exhibit relatively high electrical conductivity. These features differ greatly from typical ionic or non-ionic complexes, and seem to indicate that the ground electronic structures of these complexes are in a similar situation to each other. In fact, Matsunaga[6] has pointed out that the complex of 1,6-diaminopyrene with chloranil is located near the border line on his diagram, and such a complex exhibits relatively high conductivity. Our 1 : 1 complex is also located near the border line, and is considered to fall into such a class of complexes.

10) Y. Matsunaga, *Nippon Kagaku Zasshi*, **89**, 905 (1968).
11) M. M. Labes, R. Sehr, and M. Bose, *J. Chem. Phys.*, **33**, 868 (1960).
12) Y. Matsunaga, *Nature*, **211**, 183 (1966).
13) M. Ohmasa, M. Kinoshita, and H. Akamatu, This Bulletin, **44**, 391 (1971).

Magnetic Properties of Diisothiocyanatobis(thiourea)nickel(II) and Related Complexes

Shuji EMORI, Motomichi INOUE, and Masaji KUBO
Department of Chemistry, Nagoya University, Chikusa, Nagoya

(Received June 5, 1971)

The magnetic susceptibilities of diisothiocyanatobis(thiourea)nickel(II), diisothiocyanatobis(*N,N'*-dimethylthiourea)nickel(II), diisothiocyanatobis(2-thioimidazolidinone)nickel(II), diisothiocyanatobis(2-thiopyrrolidone)nickel(II), and diisothiocyanatobis(thioacetamide)nickel(II) were observed between the liquid-helium temperature and room temperature. Except for the second complex, antiferromagnetic interaction operates between one-dimensional nickel chains, within each of which ferromagnetic spin coupling exists. The exchange integrals, J within a chain and J' between chains, were evaluated on the basis of the coupled-double-chain model and the molecular-field model. The absence of interaction between chains in the crystals of the second complex can be accounted for by the presence of bulky *N,N'*-dimethylthiourea molecules between chains. The antiferromagnetic interactions between chains in the crystals of other complexes are attributable to the presence of bridging arrangements between chains, as is indicated by X-ray analysis.

The X-ray crystal analysis of diisothiocyanatobis(thiourea)nickel(II), $Ni(tu)_2(NCS)_2$, was carried out by Nardelli *et al.*,[1,2] who found that nickel ions are bridged by sulfur atoms belonging to thiourea to form linear chains in the crystal, as is shown in Fig. 1. Belova *et al.*[3] determined the magnetic susceptibility of this compound in a range between the liquid-nitrogen temperature and room temperature and suggested the presence of ferromagnetic spin interaction between nickel ions. The compound attracted attention as a model compound for one-dimesional ferromagnets. Flint and Goodgame[4] performed similar studies on a series of compounds with the general formula of $M(tu)_2(NCS)_2$ (M=Mn, Fe, Co, Ni), which had been confirmed by Nardelli *et al.*[5] to be isomorphous with the nickel complex. With decreasing temperature, the observed susceptibilities were found to deviate from the Curie-Weiss law, the deviations being inexplicable by an Ising model with spins $S=1$. However, because of the lack of low-temperature data, no further conclusions could be drawn. On the other hand, the X-ray crystal analyses[6,7] and infrared absorptions[8,9] of $Ni(tim)_2(NCS)_2$ (tim=2-thioimida-

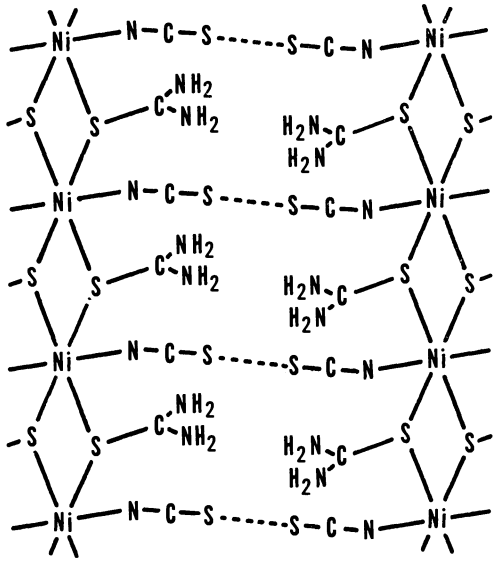

Fig. 1. Structure of $Ni(tu)_2(NCS)_2$.

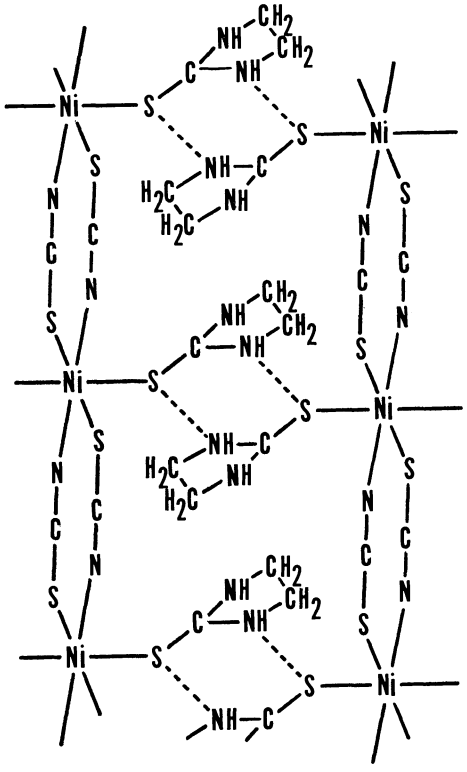

Fig. 2. Structure of $Ni(tim)_2(NCS)_2$.

1) M. Nardelli, A. Braibanti, and G. Fava, *Gazz. Chim. Ital.*, **87**, 1209(1957).
2) M. Nardelli, G. F. Gasparri, G. G. Battistini, and P. Domiano, *Acta Cryst.*, **20**, 349(1966).
3) V. I. Belova, Ya. K. Syrkin, and A. V. Babaeva, *Zh. Neorgan. Khim.*, **6**, 830(1961).
4) C. D. Flint and H. Goodgame, *Inorg. Chem.*, **8**, 1833(1969).
5) M. Nardelli and L. Cavalca, and A. Braibanti, *Gazz. Chim. Ital.*, **87**, 917(1957).
6) M. Nardelli, G. F. Gasparri, A. Musatti, and A. Manfredotti, *Acta Cryst.*, **21**, 910(1966).
7) L. Capacchi, G. F. Gasparri, M. Nardelli, and G. Pelizzi, *ibid.*, **B24**, 1199(1968).
8) G. Yagupsky, R. H. Negrotti, and R. Levitus, *J. Inorg. Nucl. Chem.*, **27**, 2603(1965).
9) P. Domiano, A. G. Manfredotti, G. Grossoni, M. Nardelli, and M. Eleonora, *Acta Cryst.*, **B25**, 591(1969).

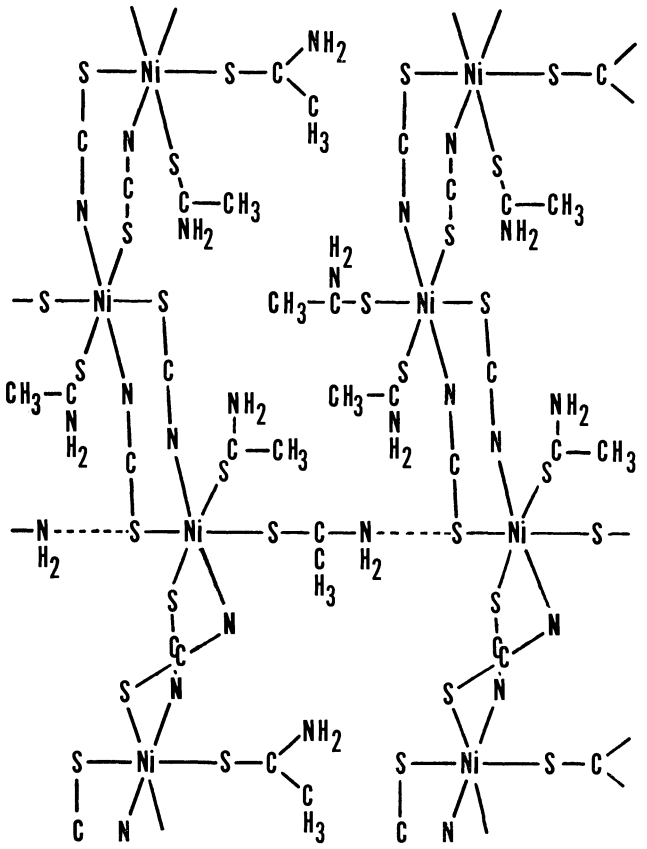

Fig. 3. Structure of $Ni(tam)_2(NCS)_2$.

zolidinone) and $Ni(tam)_2(NCS)_2$ (tam=thioacetamide) indicated that they form crystals with different chain structures, as is shown in Figs. 2 and 3, presumably due to the difference in the donor character of the ligands and the formation of intermolecular hydrogen bonds. These findings suggest that the chain structure of nickel atoms in these compounds do not represent simple one-dimensional ferromagnets, but involve magnetic interactions between chains. The present investigation has been undertaken in order to discuss magnetic interaction within a chain and between chains in these nickel complexes on the basis of the magnetic susceptibilities observed between the liquid-helium temperature and room temperature.

Experimental

Preparation of Materials. The crystals of $Ni(tu)_2(NCS)_2$, $Ni(tim)_2(NCS)_2$, and $Ni(tam)_2(NCS)_2$ were prepared by methods proposed by Nardelli *et al.*[1,10,11] Commercial preparations of thiourea and 2-thioimidazolidinone were allowed to react with nickel(II) thiocyanate. The resulting complexes were recrystallized from water and a 1 : 1 mixture of ethanol and water, respectively. In preparing $Ni(tam)_2(NCS)_2$ in a similar manner, nickel(II) sulfide precipitated during recrystallization. Therefore, a commercial preparation of thioacetamide was purified in advance by recrystallization from benzene, and then allowed to react with nickel(II) thiocyanate. The X-ray powder patterns of these compounds agreed with the data reported in the literature.[1,2,6,7] Found: Ni, 17.84%. Calcd for $Ni(tu)_2(NCS)_2$: Ni, 17.95%. Found: Ni, 15.42%. Calcd for $Ni(tim)_2(NCS)_2$: Ni, 15.48%. Found: Ni, 17.94%. Calcd for $Ni(tam)_2(NCS)_2$: Ni, 18.05%. The crystals of $Ni(dmt)_2(NCS)_2$ (dmt=*N,N'*-dimethylthiourea) were obtained in the same manner as for $Ni(tu)_2(NCS)_2$, using *N,N'*-dimethylthiourea in place of thiourea. Found: Ni, 15.11; C, 25.27; N, 21.77; H, 4.41%. Calcd for $Ni(dmt)_2(NCS)_2$: Ni, 15.32; C, 25.07; N, 21.93; H, 4.22%. For the preparation of $Ni(tpl)_2(NCS)_2$ (tpl=2-thiopyrrolidone), thiopyrrolidone was synthesized by a method reported by Mecke and Mecke[12] and was recrystallized from xylene (fractionated isomeric mixture). A calculated quantity of this starting material was added to a solution of nickel(II) thiocyanate in a 1 : 1 mixture of ethanol and water. The system was heated to dissolve the solid and then filtered. The filtrate was evaporated until crystals separated. Found: Ni, 15.60; C, 32.15; N,14.67 ; H, 3.73%. Calcd for $Ni(tpl)_2(NCS)_2$: Ni, 15.56; C, 31.84; N, 14.86; H, 3.75%.

Magnetic Measurements. Above the liquid-nitrogen temperature, the magnetic susceptibility was determined[13] by the Gouy method, using an Ainsworth recording semimicrobalance, the magnetic field strength amounting to about 3000 Oe. The temperature was determined by means of a copper-constantan thermocouple. In a temperature range of 4.2—80°K, the Faraday method was employed by the use of a torsion balance. The accuracy was estimated to be about ±1.5%. The temperature was measured within an accuracy of ±0.1°K by using an Allen-Bradley carbon thermometer below about 10°K and an Au/Co–Pt thermocouple between 10 and 80°K.

The observed molar susceptibilities have been corrected for diamagnetic contributions from ligands (in 10^{-6} emu/mol): nickel ions, −12;[14] thiocyanate ions, −35;[14] thiourea, −42;[15] *N,N'*-dimethylthiourea, −65;[15] 2-thioimidazolidinone, −61;[14] thiopyrrolidone, −61;[14] and thioacetamide, −42.[16] The temperature-independent paramagnetism was assumed to be equal to 193×10^{-6} emu/mol.[17]

Results

The observed magnetic susceptibilities corrected for diamagnetic contributions and the temperature-independent paramagnetism obey the Curie-Weiss law at high temperatures. The reciprocal susceptibility, $1/\chi$, is plotted in Figs. 4—8 against the temperature, emphasis being laid on data in the low-temperature region, where deviations from the Curie-Weiss law are rather marked. The Weiss constants and

10) M. Nardelli and I. Chierici, *Gazz. Chim. Ital.*, **88**, 248 (1958).
11) M. Nardelli and I. Chierici, *ibid.*, **88**, 359(1958).
12) R. Mecke, Jr., and R. Mecke, Sr., *Chem. Ber.*, **89**, 343 (1956).
13) M. Inoue, S. Emori, and M. Kubo, *Inorg. Chem.*, **7**, 1427 (1968).
14) G. Foëx, "Constantes Sélectionnées, Diamagnétisme et Paramagnétisme," Masson, Paris (1957). P. W. Selwood, "Magnetochemistry," 2nd ed. Interscience Publishers, New York, N. Y. (1956).
15) A. Clow, *Trans. Faraday Soc.*, **34**, 457(1938).
16) A. Clow, *ibid.*, **33**, 894(1937).
17) C. J. Ballhausen, "Introduction to Ligand Field Theory," McGraw-Hill, New York, N. Y. (1962), p. 142.

Table 1. The effective magnetic moment μ_{eff} at room temperature (20°C), the Weiss constant θ, the g-value evaluated from the Curie constants C, and the temperature T_m of the maximum susceptibility of $NiL_2(NCS)_2$

	μ_{eff} (B.M.)	θ (°K)	g	T_m (°K)
$Ni(tu)_2(NCS)_2$[a]	3.36	41.8[f]	2.18	11.0
$Ni(dmt)_2(NCS)_2$[b]	3.31	53.8	2.12	—[g]
$Ni(tim)_2(NCS)_2$[c]	3.11	11.2	2.16	8.3
$Ni(tpl)_2(NCS)_2$[d]	3.10	10.3	2.17	8.4
$Ni(tam)_2(NCS)_2$[e]	3.13	16.2	2.18	—[g]

a) tu: Thiourea. b) dmt: *N,N'*-Dimethylthiourea. c) tim: Thioimidazolidinone. d) tpl: 2-Thiopyrrolidone. e) tam: Thioacetamide.

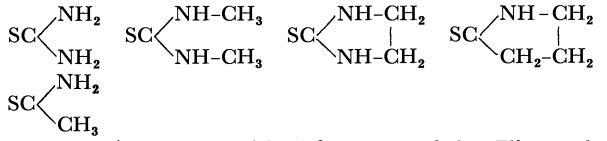

f) The value agrees with 40°K reported by Flint and Goodgame.[4] g) T_m was not observed.

the g-values evaluated from the Curie constants are listed in Table 1. The Weiss constants are positive, indicating that ferromagnetic interaction is predominant.

Discussion

The crystal structure of diisothiocyanatobis(thiourea)nickel(II), $Ni(tu)_2(NCS)_2$, shown in Fig. 1 suggests that the predominant ferromagnetic interaction arises from magnetic interaction through Ni–S–Ni bonds within a one-dimensional nickel chain.

Suzuki *et al.*[18] calculated the parallel susceptibility, χ, of a one-dimensional lattice consisting of Ising spins of $S=1$.

$$\frac{kT\chi}{Ng^2\beta^2}=\frac{1}{2a^2(a+2)}\left[1+\frac{4a^3+5a^2-a+1}{a[(a+a^{-1}-1)^2+8]^{1/2}}\right] \quad (1)$$

where $a=\exp(-2J/kT)$, J is the exchange integral between the nearest neighboring spins in the one-dimensional lattice, T is the absolute temperature, g is the g-value, and β is the Bohr magneton.

Using $g=2.18$, as evaluated from the Curie constant, and assuming $J/k=17$°K, the parallel susceptibility was calculated to be as is shown by a broken curve in Fig. 4. Although the curve well reproduces the experimental data above about 70°K, agreement is poor below this temperature. In addition, the curve of the observed susceptibility shows a maximum at 11.0°K. Accordingly, it is concluded that a weak lateral antiferromagnetic interaction operates between linear chains.

For one-dimensional lattices consisting of spins $S=1/2$, the magnetic susceptibility has been calculated with the Heisenberg model.[19] However, because of the mathematical difficulties involved, rigorous calculations have not been performed for spins greater than 1/2. The series expansion method developed by Rushbrooke and Wood[20] gives a rather poor agreement with the experimental data, because the series converges slowly except at temperatures well above the Néel temperature. Therefore, the following analysis is developed on the basis of the Ising model.

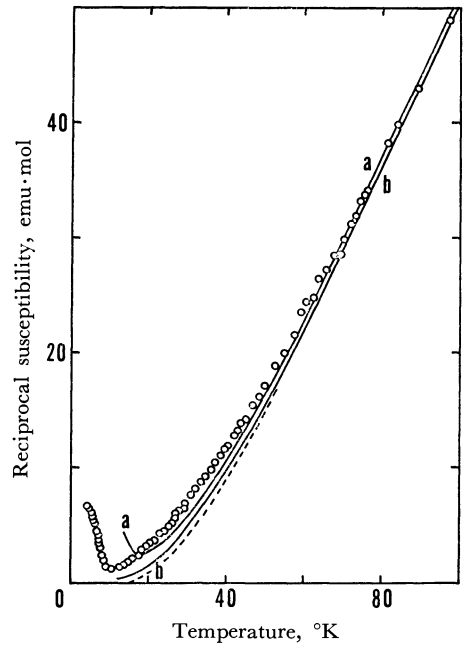

Fig. 4. Reciprocal susceptibility of $Ni(tu)_2(NCS)_2$ as a function of temperature.
Broken curve: Ising model (Eqs. (1) and (2)). Solid curve a: Coupled-double-chain model (Eq. (11)). Solid curve b: Molecular-field model (Eq. (14)).

Although Eq. (1) is rigorous for an isolated one-dimensional lattice, it is difficult to incorporate the effect of interaction between chains into the equation. Therefore, the following alternative method was used. Flint and Goodgame[4] analyzed the susceptibility of $Ni(tu)_2(NCS)_2$ by extending the theoretical equation for the linear Ising model with $S=1/2$ to $S\geq 1$.

$$\chi=\frac{Ng^2\beta^2S(S+1)}{3kT}\exp(j/kT) \quad (2)$$

This equation is based on "reduced" spin magnetic moments capable of orienting only in parallel and antiparallel directions defined as

$$\mu=\frac{1}{2}\left[\frac{S(S+1)}{3/4}\right]^{1/2}g\beta \quad (3)$$

The parameter, j, is related to the exchange integral, J, by[21]

$$j=\frac{S(S+1)}{3/4}J \quad (4)$$

As was pointed out by Flint and Goodgame,[4] Eq. (2) well reproduces the observed susceptibility of

18) M. Suzuki, B. Tsujiyama, and S. Katsura, *J. Math. Phys.*, **8**, 124(1967).
19) J. C. Bonner and M. E. Fisher, *Phys. Rev.*, **135**, A640(1964).
20) G. S. Rushbrooke and P. J. Wood, *Mol. Phys.*, **1**, 257(1958).
21) S. Emori, M. Inoue, M. Kishita, and M. Kubo, *Inorg. Chem.*, **8**, 1385(1969).

Table 2. Exchange integrals, J within a chain and J' between chains, in the crystals of some nickel(II) complexes evaluated by the Ising model (Eq. (1)), the coupled-double-chain model (Eq. (11)), and the molecular-field model (Eq. (14))

	Ising model	Coupled-double-chain model		Molecular-field model	
	J/k (°K)	J/k (°K)	$-J'/J$	J/k (°K)	$-J'/J$
$Ni(tu)_2(NCS)_2$	17	19	0.02_0	19	0.002
$Ni(dmt)_2(NCS)_2$	20	21	0	21	0
$Ni(tim)_2(NCS)_2$	3.0	3.6	0.2_0	3.6	0.27
$Ni(tpl)_2(NCS)_2$	3.0	3.6	0.2_0	3.6	0.28
$Ni(tam)_2(NCS)_2$	4.5	4.6	0.03_3	4.6	—[a]

a) Because T_m was not observed, J' cannot be estimated.

$Ni(tu)_2(NCS)_2$ at high temperatures, but gives poor agreement with it at low temperatures because of the presence of interaction between chains.

For mutually interacting one-dimensional lattices of spins $S=1/2$, theoretical equations have been derived on the basis of a coupled-double-chain model[22,23] as well as a molecular-field model.[24] In the former model, a pair of interacting chains is considered to obtain the magnetic susceptibility given by[23]

$$\frac{kT\chi}{Ng^2\beta^2} = \frac{e^{2K}(e^{K'}R-\sinh^2 K)}{4(R-e^{K'}\sinh 2K)(\cosh^2 K'\cosh^2 2K-\sinh^2 2K)^{1/2}} \tag{5}$$

In this expression,

$$R = \cosh K'\cosh 2K+(\cosh^2 K'\cosh^2 2K-\sinh^2 2K)^{1/2} \tag{6}$$

$$K = j/2kT \tag{7}$$

$$K' = zj'/2kT \tag{8}$$

where j is the exchange integral within a chain, j' is that between chains, and z is the number of nearest chains. In the latter model, antiferromagnetic interaction between Ising chains lying in a plane in parallel to one another is approximated by a molecular field to yield the parallel susceptibility given by[24]

$$\frac{k\chi}{Ng^2\beta^2} = \frac{1}{4}e^{j/kT}\left\{T+T_c\exp\left[\frac{j}{k}\left(\frac{1}{T}-\frac{1}{T_c}\right)\right]\right\}^{-1} \tag{9}$$

where the parameter, T_c, expressing the interaction between chains is equal to the temperature, T_m, of the maximum susceptibility and is related to the exchange integral, j', between chains by

$$j' = -T_c\exp(-j/kT_c) \tag{10}$$

where the first minus sign on the right-hand side takes into account the antiferromagnetic interaction between chains ($j'<0$). Needless to say, Eq. (5) and Eq. (9) lead to Eq. (2) when $K'=0$ and $T_c=0$, respectively.

Equations (5) and (9), which are valid for $S=1/2$, were extended to $S=1$ using the reduced spin model. The former equation leads to

$$\frac{kT\chi}{Ng^2\beta^2} = \frac{2e^{2K}(e^{K'}R-\sinh 2K)}{3(R-e^{K'}\sinh 2K)(\cosh^2 K'\cosh^2 2K-\sinh^2 2K)^{1/2}} \tag{11}$$

where, in accordance with Eqs. (4), (7), and (8), K and K' are given by

$$K = 4J/3kT \tag{12}$$

$$K' = 4zJ'/3kT \tag{13}$$

On the other hand, Eq. (9) is extended to

$$\frac{k\chi}{Ng^2\beta^2} = \frac{2}{3}e^{8J/3kT}\left\{T+T_c\exp\left[\frac{8J}{3k}\left(\frac{1}{T}-\frac{1}{T_c}\right)\right]\right\}^{-1} \tag{14}$$

where T_c is related to the exchange integral, J', between chains by (see Eqs. 4 and 10)

$$J' = -\frac{3}{8}T_c\exp(-8J/3kT_c) \tag{15}$$

As is shown in Fig. 4, the susceptibility of $Ni(tu)_2(NCS)_2$ can be expressed by Eq. (2) above about 70°K with the parameter, j/k, equal to 51°K. This, along with Eq. (4), yields the exchange integral within a chain given by $J/k=19$°K. Using this value for J, and assuming that $J'/J=-0.02$ (Table 2), theoretical calculation was performed on the basis of the coupled-double-chain model (Eq. (11), $z=2$). The result is shown by a solid curve in Fig. 4. The agreement with the experimental data is excellent except for the region near the temperature of the maximum susceptibility.

The susceptibility was calculated theoretically by means of the molecular-field model also (Eq. (14)). As has been mentioned above, the parameter, J, can be evaluated from the data in the high-temperature region as $J/k=19$°K. From this, along with the observed temperature of the maximum susceptibility, T_m ($=T_c=11$°K), J' can be calculated by means of Eq. (15) as $J'/k=0.04$°K. The solid curve b in Fig. 4 shows the results of calculation by means of Eq. (14) using these parameters. The agreement of the theoretical curve with the experimental data is satisfactory. Thus, the ratio, $-J'/J$, of the exchange integral between chains to that within a chain is estimated to be of the order of 0.002—0.02.

The observed positive value for J implies that ferromagnetic interaction exists within a chain. This is anticipated because two orthogonal sp^2 orbitals of a sulfur atom are involved in magnetic interaction through a Ni–S–Ni linkage.

22) R. A. Hunt and D. J. Newman, *J. Phys.*, C Ser. 2, **2**, 75 (1969).
23) M. Inoue and M. Kubo, *J. Magn. Resonance*, **4**, 175 (1971).
24) J. W. Stout and R. C. Chisholm, *J. Chem. Phys.*, **36**, 979 (1962).

On the other hand, the negative value for J' indicates that antiferromagnetic interaction predominates between chains through Ni–NCS···SCN–Ni linkages. In fact, the distance between the nearest sulfur atoms belonging to neighboring chains amounts to 3.45 Å, which is smaller than the sum (3.70 Å) of van der Waals radii.[1,2]

The observed susceptibility of diisothiocyanatobis-(*N*,*N'*-dimethylthiourea)nickel(II), $Ni(dmt)_2(NCS)_2$, shows no maximum in the temperature range investigated (see Fig. 5) and can be reproduced by Eq. (1) with $g=2.12$, as evaluated from the Curie constant and $J/k=20$°K. The exchange integral is not much different from that of $Ni(tu)_2(NCS)_2$ (see Table 2). In addition, the X-ray powder patterns bear a close resemblance to those of $Ni(tu)_2(NCS)_2$, the crystal of which belongs to the triclinic system and yields a very complicated powder spectrum. Accordingly, it is concluded that this compound has one-dimensional nickel chains similar to those in $Ni(tu)_2(NCS)_2$. However, the substitution of thiourea with bulky *N*,*N'*-dimethylthiourea molecules leads to an increase in the distance between chains leading to a decrease in lateral magnetic interaction, and hence to the absence of any maximum in the susceptibility *versus* temperature curve.

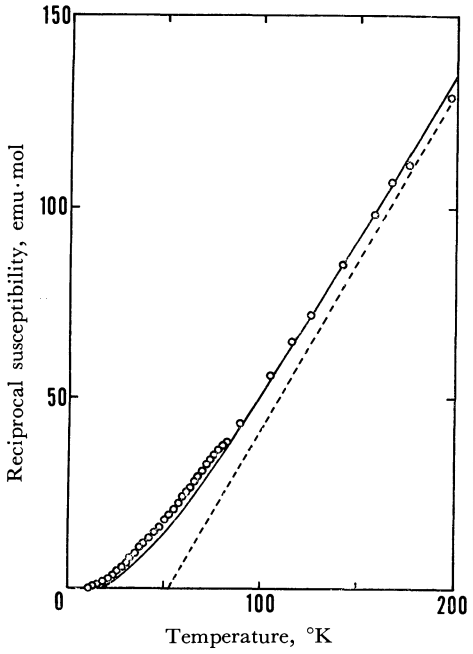

Fig. 5. Reciprocal susceptibility of $Ni(dmt)_2(NCS)_2$ as a function of temperature.
Broken curve: The Curie-Weiss law. Solid curve: Ising model.

The theoretical equation (2) ($j=8J/3$,$J/k=21$°K) based on reduced moments also fits experimental data, as is shown by the solid curve in Fig. 5, which is indistinguishable from the curve of Eq. (1). This indicates that both Eq. (1) and Eq. (2) are good approximations to the susceptibility of linear Ising ferromagnets free from lateral interactions.

Diisothiocyanatobis(2-thioimidazolidinone)nickel(II), $Ni(tim)_2(NCS)_2$, forms one-dimensional lattices of nickel

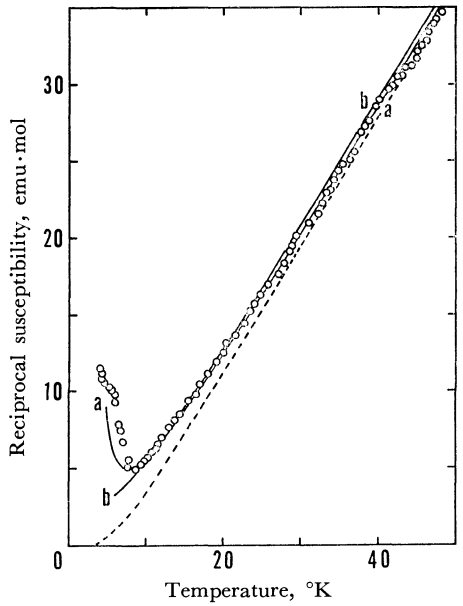

Fig. 6. Reciprocal susceptibility of $Ni(tim)_2(NCS)_2$ as a function of temperature.
Broken curve: Ising model. Solid curve a: Coupled-double-chain model. Solid curve b: Molecular-field model.

atoms through bridging by thiocyanate ions, as is shown in Fig. 2.[6] Although the Weiss constant is positive (Table 1), the susceptibility assumes a maximum value at 8.3°K, below which antiferromagnetic behavior appears. Theoretical calculations (Eq. (1) with $J/k=3.0$°K and Eq. 2 with $J/k=3.6$°K) for isolated Ising chains give broken curves in agreement with each other (*cf.* Fig. 6), but in poor agreement with the experimental data. This indicates that, in addition to ferromagnetic interaction within a chain, antiferromagnetic interaction exists between chains and gives rise to deviations from theoretical calculations for the Ising model, especially at low temperatures. The only conceivable interaction within a chain is superexchange interaction through Ni–N–C–S–Ni linkages, whereas that between chains is an antiferromagnetic superexchange interaction through Ni–S–C–NH···S–Ni linkages lying on a $(0\bar{1}1)$ plane. This is because NH··· S hydrogen bonds exist in the crystals,[6] no other paths being conceivable. From this structure, it can be concluded that $z=2$ in Eq. (15). Theoretical calculations were carried out with Eqs. (11) and (14). Curves calculated with the J'/J ratios listed in Table 2 are shown in Fig. 6. The agreement with the experimental data is excellent.

The temperature dependence of the susceptibility of diisothiocyanatobis(2-thiopyrrolidone)nickel(II), $Ni(tpl)_2(NCS)_2$, bears a striking resemblance to that of $Ni(tim)_2(NCS)_2$, as is shown in Fig. 7. Theoretical calculations analogous to those employed for the latter compound yield the exchange integrals listed in Table 2. The exchange integrals are also close to the corresponding ones of the latter compound. Accordingly, it is concluded that this compound forms crystals similar to those of $Ni(tim)_2(NCS)_2$ shown in Fig. 2. The X-ray powder patterns of the two compounds resemble each other in agreement with the

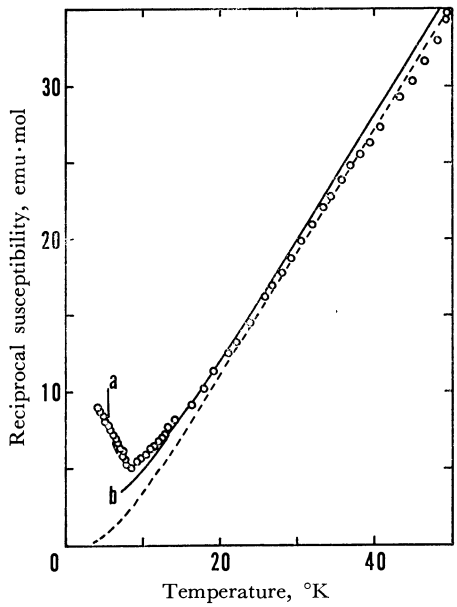

Fig. 7. Reciprocal susceptibility of $Ni(tpl)_2(NCS)_2$ as a function of temperature.
Broken curve: Ising model. Solid curve a: Coupled-double-chain model. Solid curve b: Molecular-field model.

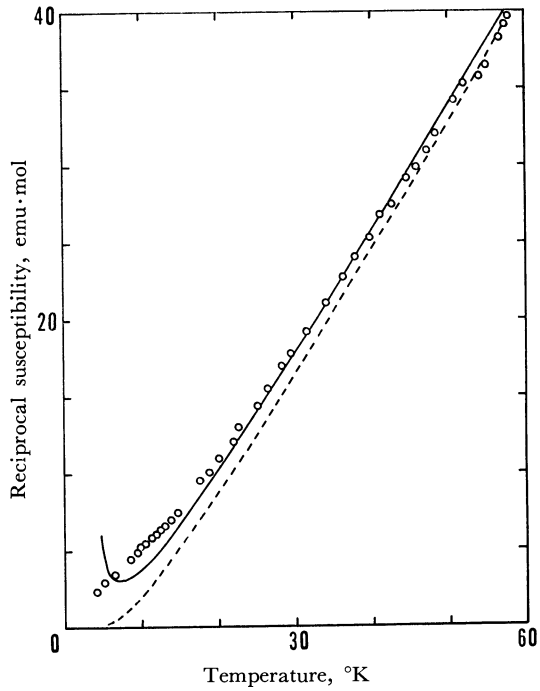

Fig. 8. Reciprocal susceptibility of $Ni(tam)_2(NCS)_2$ as a function of temperature.
Broken curve: Ising model. Solid curve: Coupled-double-chain model.

prediction from magnetic measurements.

The crystal structure[7] of diisothiocyanatobis(thioacetamide)nickel(II), $Ni(tam)_2(NCS)_2$, reveals that nickel atoms are bridged by thiocyanate ions to form one-dimensional chains, as is shown in Fig. 3. However, unlike the case with $Ni(tim)_2(NCS)_2$, two thiocarbonyl groups are coordinated on the *cis* positions of the coordination octahedron of a nickel atom. The one-dimensional chain has a threefold screw axis, and the crystal belongs to the rhombohedral system.

At high temperatures, the observed magnetic susceptibility can be explained by both Eq. (1) and Eq. (2), which coincide with each other, as is shown in Fig. 8. Below 40°K, deviations appear from the theoretical curve. However, no maximum susceptibility was observed in the temperature range investigated. Accordingly, calculations are infeasible with the molecular-field model. With the coupled-double-chain model (Eq. (11) with $z=6$), the exchange integrals, J within a chain and J' between chains, were calculated to be as shown in Table 2. The latter amounts to about 3% of the former. If a single chain is replaced by a resultant spin moment, interactions between chains can be represented by those among such resultant moments in two-dimensional triangular lattice. It has been shown theoretically that antiferromagnetic ordering can never be realized in two-dimensional triangular lattices.[25] This seems to be the reason why no transition to an antiferromagnetic state was observed for this compound.

25) R. M. F. Houtappel, *Physica*, **16**, 425 (1950).

The Catalytic Dehydrohalogenation of Haloethanes on Solid Acids and Bases

Isao MOCHIDA, Yasuhide ANJU, Hiroko YAMAMOTO, Akio KATO, and Tetsuro SEIYAMA

Department of Applied Chemistry, Faculty of Engineering, Kyushu University, Fukuoka

(Received June 7, 1971)

The elimination reactions of haloethanes and halopropanes on solid acids and bases, including a series of metal sulfates supported by silica gel, were studied at 300°C by means of the pulse technique in order to clarify the mechanism of the catalytic dehydrohalogenation. The *trans*-1,2-dichloroethylene/*cis*-1,2-dichloroethylene (*trans*-1,2/*cis*-1,2) selectivities from 1,1,2-trichloroethanes as well as the activities of the metal sulfates supported by silica gel were well correlated with the electronegativities of the metal ions. Generally speaking, the rates of the dehydrochlorination from chloroalkanes were nearly equal to those of the dehydrobromination from bromoalkanes on the solid acids, but the latter were larger than the former on solid bases. The reactivities of the alkylhalides on solid acids and bases were examined from the electronic view-point, and we tried to correlate them with some reactivity indexes. A kinetic isotope effect with regard to hydrogen was observed on solid bases, but not on solid acids, in the dehydrobromination of 1,2-dibromoethane. From these facts, it was concluded that the dehydrohalogenation proceeds through a carbonium-ion mechanism on solid acids and *via* an E2 step-by-step mechanism on solid bases.

It has been reported in previous papers[1] that the dehydrochlorination of 1,1,2-trichloroethane proceeds with different selectivities on solid bases, solid acids, ion-exchanged molecular sieves, chromia, and metal sulfates. The reaction mechanism was discussed on the basis of the linear-free-energy-relationships (LFER) approach, regarding five chloroethanes as well as the *trans*-1,2/*cis*-1,2 selectivities. The selectivity of *trans*-1,2/*cis*-1,2 on the metal sulfate was found not to be related with the electronegativity of the metal ion,[1b] which has been thought to represent the acid strength of the metal sulfate,[2] but to depend on the geometries of the catalysts. The effect of the geometries can be diminished among a series of metal sulfates by using the silica gel as the catalyst support.[3,4]

In the present study, the correlation of the catalytic activities and selectivities with the activities of a series of metal sulfates mounted on silica gel was investigated. At the same time, the reactivities of several haloethanes and halopropanes were measured on typical solid acids, solid bases, and the intermediate in order to obtain more information about the effects of substituents and leaving halogens on the elimination reactivity. The kinetic isotope effect of HBr (DBr) elimination from 1,2-dibromoethane was also measured in order to determine whether or not the C–H bond cleavage was the rate-determining step. A more probable mechanism of the elimination of hydrogen halide may be deduced from these results.

Noller *et al.* have reported that, for dehydrohalogenations over metal salts, the ionic contribution (El-character) increased with the increasing acidity of the cation.[5] They also examined the substituent effect on the reactivity over metal salts.[6] However their studies seem to be lacing in the consideration of the acid-base interaction between catalysts and reagents.

Experimental

Reagents. All the reagents used in this work were obtained from Tokyo Kasei except for 1,2-dibromo-tetradeuteroethane, which was obtained from Merck. They were all of G. R. or E. P. grade and were not purified further.

Catalysts. The catalysts of metal sulfates supported by silica gel were obtained by impregnating silica gel (Wako) with 0.3 meq/g of each metal sulfate (G. R. from the Hayashi Co.), and then dried at 120°C in the atmosphere.[3] The other catalysts were described in the previous papers.[1]

Apparatus and Procedures. The reaction rates and selectivities were measured at 300°C by the pulse technique, as has been described in the previous papers.[1] The catalysts were pretreated in a helium-gas flow for 3 hr at 300°C. The calcination temperature between 300 and 500°C had little effect on either the activity or the selectivity of nickel sulfates on silica gel in the HCl elimination from 1,1,2-trichloroethane, although distinct effects were observed in other reactions.[3,7] The elimination reaction was of nearly first order under the experimental conditions, and the conversion was verified to be a linear function of the reciprocal space velocity (RSV) at low conversions. Thus, the slope of the conversion/RSV gives the apparent rate constant, k (ml/g·min). The details of the experiments were described in the previous papers.[1]

Results

Dehydrochlorination of 1,1,2-Trichloroethane on Metal Sulfates Supported by Silica Gel. The dechlorination and exchange of chlorine with hydrogen took place in addition to the dehydrochlorination on the metal sulfates supported by silica gel in manners similar to those observed on the unsupported metal sulfate.[1b] The dehydrochlorination was of principal concern in the present study because all the other reactions were minor except for the dechlorinations

1) a) I. Mochida, J. Take, Y. Saito, and Y. Yoneda, *J. Org. Chem.*, **32**, 3894 (1967); **33**, 2161, 2163 (1968). b) I. Mochida, A. Kato, and T. Seiyama, *J. Catal.*, **18**, 33 (1970).

2) K. Tanaka and A. Ozaki, *ibid.*, **8**, 1 (1967); K. Tanaka, in "Catalytic Engineering. X. Catalyst Handbook," Chijin Shokan, Tokyo (1967), p. 739.

3) I. Mochida, A. Kato, and T. Seiyama, *J. Catal.*, **17**, 317 (1970).

4) M. Misono, Y. Saito, and Y. Yoneda, *ibid.*, **9**, 135 (1967).

5) P. Andreu, J. Bellorin, G. Cunto, and H. Noller, *Z. Phys. Chem.* (Neue Folge), **64**, 71 (1969).

6) P. Andreu, R. Ballesteros, S. Villaba, J. F. Garcia, and H. Noller, *An. Quim.*, **65**, 931 (1969).

7) K. Tanabe and T. Takeshita, *Advan. Catal.*, **17**, 317 (1967).

on cupric and ferric sulfates.

1) The Catalytic Activity: The products of the dehydrochlorination from 1,1,2-trichloroethane were *trans*-1,2-dichloroethylene, *cis*-1,2-dichloroethylene, and 1,1-dichloroethylene. The catalytic activity varied very much among metal sulfates. The catalytic activities of various supported metal sulfates are shown in Fig. 1 as the function of the electronegativities of the metal ions, the values of which were taken from the literature.[2] Here, the catalytic activity was expressed by the total reaction rate of dehydrochlorination. The logarithms of the reaction rates have a reverse-volcano relationship with the electronegativities of the metal ions except for the thallium ion, although only a few observations were made on the basic side of the catalysts. The minimum activity was found at the silver ion, whose electronegativity was 5.6.

2) The Stereoselectivity: The *trans*-1,2/*cis*-1,2 ratios on the catalysts, the stereoselectivities of this dehydrochlorination, are shown in Fig. 2 as the function of the electronegativities of the metal ions. The logarithms of the ratios are linearly correlated with electronegativities over one and a half orders of magnitude in the ratios. The ratio of 1,1-dichloroethylene/1,2-dichloroethylene (1,1/1,2) was another selectivity of this elimination, although 1,1-dichloroethylene could not be detected on the metal sulfates of high electronegativity. This selectivity was linearly correlated with the *trans*-1,2/*cis*-1,2 selectivity on the same catalyst, as is shown in Fig. 3, where the solid line was that obtained using typical solid acids and bases such as silica-alumina and strontium oxide in a previous paper.[1a] A linear relation was observed in this case, too.

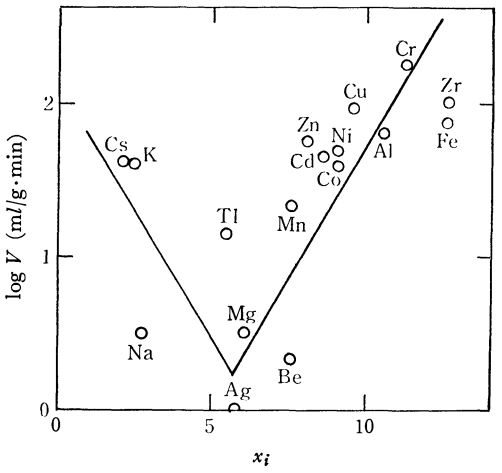

Fig. 1. Catalytic activities of metal sulfates supported by silica gel for the dehydrochlorination of 1,1,2-trichloroethane were plotted against the electronegativities of the corresponding metal ions.
The values of electronegativities, x_i, are taken from Ref. 2.

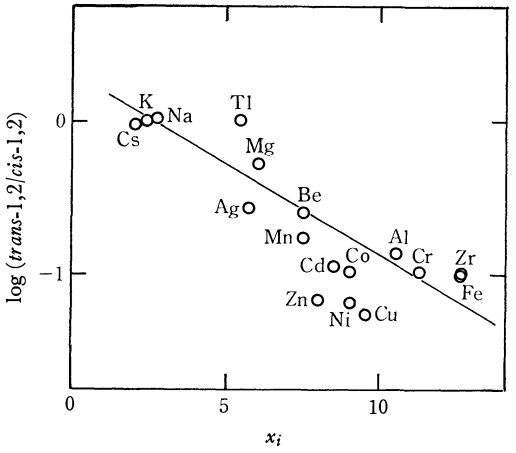

Fig. 2. The *trans*-1,2/*cis*-1,2 selectivities of metal sulfates supported by silica gel were correlated with the electronegativities of the corresponding metal ions.
The values of electronegativities, x_i, are taken from Ref. 2.

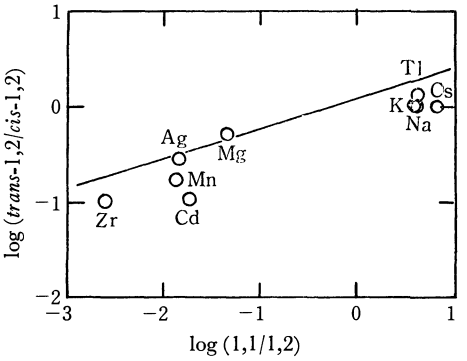

Fig. 3. A correlation between *trans*-1,2/*cis*-1,2 and 1,1/1,2 selectivities from 1,1,2-trichloroethane on metal sulfates supported by silica gel.

3) Reactivity Orders of the Five Chloroethanes: The reactivity orders of the five chloroethanes were 1,1,1-trichloroethane (1,1,1) > 1,1-dichloroethane (1,1) > 1,1,2-trichloroethane into 1,2-dichloroethylene (1,1,2 into 1,2) > 1,1,2,2-tetrachloroethane (1,1,2,2) > 1,2-dichloroethane (1,2) > 1,1,2-trichloroethane into 1,1-dichloroethylene (1,1,2 into 1,1) on nickel, cupric cadmium, and ferric sulfates supported by silica gel, whereas they were 1,1,1>1,1,2,2>1,1,2 into 1,1>

Table 1. Reactivity order of five chloroethanes in dehydrochlorination

a) On sulfates of a high electronegativity.

Reactant / Catalyst	1,1,1	1,1	1,1,2 into 1,2	1,1,2,2	1,2	1,1,2 into 1,1
$NiSO_4$-SiO_2	1910	214	48	2	1.3	0
$CuSO_4$-SiO_2	2575	198	90	6.4	0.5	0
$Fe_2(SO_4)_3$-SiO_2	2490	237	73	6.9	2.7	0
$CdSO_4$-SiO_2	2870	432	45	3.5	1.2	0

b) On sulfates of a low electronegativity.

Reactant / Catalyst	1,1,1	1,1,2,2	1,1,2 into 1,1	1,1	1,1,2 into 1,2	1,2
Tl_2SO_4-SiO_2	219	57	11	5.6	2.6	1.2
K_2SO_4-SiO_2	139	100	31	9.3	7.9	7.5

1) Figures in Table show the reaction rate (ml/min. g).
2) Abbreviations of the reactants and products refer to the text.

1,1>1,1,2 into 1,2>1,2 on potassium and thallium sulfates, as is shown in Table 1. The former reactivity order and the large difference among the reactivities of chloroethanes observed on a metal sulfate of a high electronegativity were like those on a solid acid such as silica-alumina.[1a] On the other hand, the latter reactivity order on a metal sulfate of a low electronegativity was similar to that observed on a basic catalyst such as strontium oxide,[1a] except for the high reactivities of 1,1,1 and 1,1 on such metal sulfates. The reactivity difference between the most and the least reactive chloroethanes on potassium sulfate was only one and a half orders of magnitude. Such a small difference has been observed on the molecular sieve 13X, which was considered to be neutral in the Hammett indicator test.[1a]

Dehydrohalogenation of Haloethanes and Halopropanes on Solid Acids and Bases. *1) Comparison between Dehydrochlorination and Dehydrobromination*: The reactivities of the dehydrohalogenation of several dihaloethanes and monohalopropanes on solid acids and bases are shown in Figs. 4 and 5, where the rates of dehydrochlorination are shown in the abscissa, and those of dehydrobromination, by the ordinate. The dotted lines in both figures show the equal reactivities of the two reactants. The structures of the halides had a considerable effect on the rates over the solid acids. In contrast, only a small effect was observed on the solid bases. The difference was more than five hundred on solid acids, whereas it was less than one hundred on solid bases.

On solid acids, the rates of dehydrochlorination and those of dehydrobromination were nearly equal, as is shown in Fig. 4. The dehydrobromination was two times faster than the dehydrochlorination on solid bases, as is shown in Fig. 5. In any case, it seems from these linear correlations that both dehydrohalogenations, —HCl and —HBr, can be discussed on the common basis of the reaction

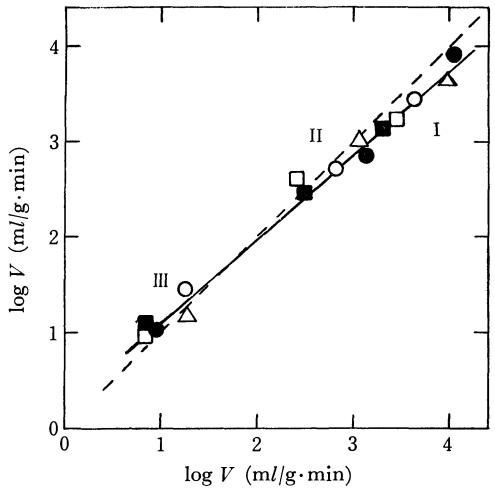

Fig. 4. The reactivities of dehydrochlorination and dehydrobromination on solid acids, ● for silica-alumina, △ for alumina-boria, ■ for nickel sulfate, □ for $NiSO_4$-SiO_2 and ○ for alumina. Group I corresponds to the reactivity regarding iso-PrX, II to *n*-PrX and III to $BrCH_2CH_2X$, where X is chlorine in the case of dehydrochlorination and that is bromine in the case of dehydrobromination.

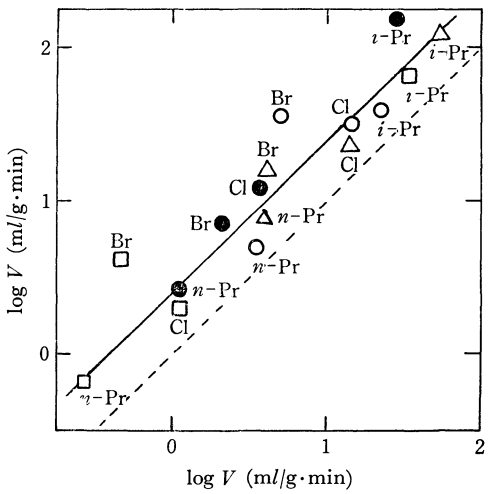

Fig. 5. The reactivities of dehydrochlorination and dehydrobromination on solid bases, ○ for KOH-SiO_2, △ for NaOH-SiO_2, ● for K_2SO_4-SiO_2, □ for SrO. The symbols of Br, Cl, *n*-Pr, and *iso*-Pr, represent the reactivities of dehydrohalogenation of $BrCH_2CH_2X$, $ClCH_2CH_2X$, *n*-PrX, and *iso*-PrX, respectively. (X is Cl or Br)

mechanism, although a discrimination between acidic and basic catalysts is essential.

2) Substituent Effects: The reactivities of *iso*-PrBr, *n*-PrBr, EtBr, 1,2-dibromoethane, and 1-bromochloroethane for dehydrobromination on solid acids are plotted against the Taft's σ^* of the R group in RBr in Fig. 6. The σ^* is thought to represent the electronic effect of the substituent in the saturated compounds.[8] The reactivity decreased monotonously with the increasing σ^*. The correlation seems to consist of two straight lines. The slope of the line through *iso*-, and *n*-propyl bromides and ethyl bromide might indicate the carbonium-ion

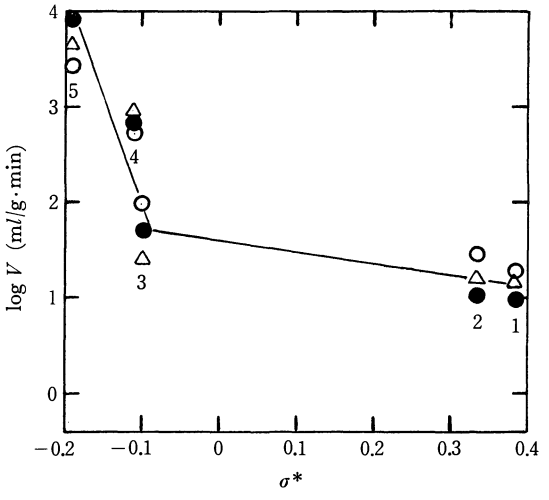

Fig. 6. The reactivities of dehydrobromination on solid acids as a function of σ^*, ● for silica-alumina, △ for alumina-boria and ○ for alumina. The values of σ^* were taken from literature (8). Numbers refer to the reagents, 1; 1-bromo-2-chloroethane, 2; 1,2-dibromoethane, 3; ethyl bromide, 4; *n*-PrBr and 5; *iso*-PrBr.

8) R. W. Taft, "Steric Effects in Organic Chemistry," ed. by M. S. Newman, Wiley, New York (1956), p. 206.

mechanism, because many reactions which are thought to proceed through the carbonium ion give slopes of such a degree.[9] The reactivities of dihaloethanes are too large if the reaction proceeds through the same carbonium-ion mechanism. In reaction of 1-bromo-2-chloroethane, a considerable amount of 1,2-dibromoethane and 1,2-dichloroethane, the products of the halogen exchange reaction, were detected on solid acids. These rather complicated results should be taken into account in the discussion of the reaction mechanism of the elimination.

The NMR chemical shifts were thought to represent the static electron density of the hydrogen. The reactivities on solid bases are compared with the chemical shift of hydrogen to be eliminated in Fig. 7. Except for isopropyl halide, a certain relation can be considered to exist between the reactivity and the chemical shift of the proton, although more adequate reactivity indices should be considered. It may be a dynamic one.[11]

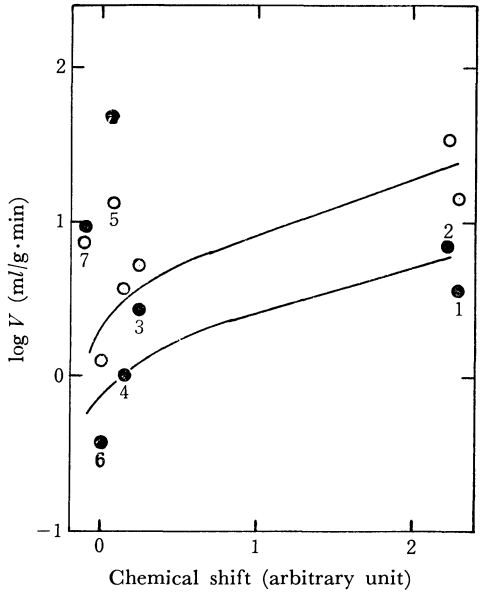

Fig. 7. The reactivities of dehydrohalogenation divided by the symmetry number, the number of its equivalent hydrogen atom, as a function of the NMR chemical shift of hydrogen to be eliminated, ○ for $KOH-SiO_2$ and ● for $K_2SO_4-SiO_2$. The relative values of the abscissa were taken from literature (10). Numbers refer to the reagents, 1; 1,2-dichloroethane, 2; 1,2-dibromoethane, 3; *n*-PrBr, 4; *n*-PrCl, 5; *iso*-PrBr, 6; EtBr, and 7; *iso*-PrCl.

Kinetic Isotope Effect. The kinetic isotope effect in dehydrobromination from 1,2-dibromoethane was measured on solid acids and bases. The rates of dehydrobromination (k_H), those of dedeuterobromination (k_D), and the values of k_H/k_D are shown in Table 2. The maximum theoretical value of k_H/k_D at 300°C is 2.7.[12] The k_H/k_D values on all solid bases except magnesium oxide were greater than 1.5, whereas those on solid acids were nearly unity. Sodium-poisoned alumina had a value of k_H/k_D intermediate between solid acids and bases. This fact may correspond to the amphoteric character of this catalyst.

Table 2. Kinetic isotope effect in dehydrobromination of 1,2-dibromoethane

Catalyst	k_H[1]	k_D[2]	k_H/k_D
SrO	8.6 ±0.2	4.0 ±0.1	2.15±0.11
CaO	0.56±0.04	0.34±0.08	1.65±0.66
MgO	4.8 ±0.6	4.7 ±0.7	1.02±0.24
$KOH-SiO_2$	70±0	44±1	1.59±0.04
$NaOH-SiO_2$	33±2	18±0	1.83±0.12
$K_2SO_4-SiO_2$	14±1	8.5 ±0.3	1.65±0.18
Alumina-NaOH	114±1	87±1	1.31±0.03
Alumina	56±0	57±1	1.00±0.02
$NiSO_4$	14±1	14±2	1.00±0.25
Alumina-boria	22±6	21±4	1.05±0.60
Silica-alumina	11±2	11±3	1.00±0.62
$NiSO_4-SiO_2$	9.7±0.1	7.9±2.8	1.23±0.69

1) The rate of dehydrobromination from 1,2-dibromoethane.
2) The rate of dedeuterobromination from 1,2-dibromotetradeuteroethane.

Discussion

Correlation of Catalytic Activity and Selectivity with the Acid-base Character of Catalysts and a Gradual Change in the Dehydrohalogenation Mechanism. The availability of the electronegativities of the metal ions has been established in many acid-catalyzed reactions.[2-4] The HCl-elimination from 1,1,2-trichloroethane may be included as one such example. The electronegativity of the metal ion was excepted to express the acid strength of the metal sulfate.[2] At higher *Xi* values, the ratio of *trans*-1,2/*cis*-1,2 from 1,1,2-trichloroethane was as small as 0.1, as is shown in Fig. 2, the reactivity order of chloroethanes was also similar to that on typical solid acids. At lower *Xi* values, on the other hand, the ratios are unity, and their plots in Fig. 3 are close to those on typical solid bases, furthermore, the reactivity order is similar to that on solid bases. These facts indicate that the gradual change in the reaction mechanism previously concluded[1] can be applied to this series of catalysts, also.

It is interesting that the catalytic activities *vs. Xi* plots are shaped in a reverse-volcano, with a minimum at the silver ion. 1,2-dichloroethylene was primarily formed on the metal sulfates with the high *Xi* values as is shown in Fig. 1. This product may be explained by the abstraction of 1-chlorine,[13] which

9) J. E. Leffler and E. Gruneald, "Rates and Equilibria of Organic Reactions," Wiely, New York (1963), p. 171; I. Mochida and Y. Yoneda, *J. Catal.*, **7**, 386 (1967); I. Mochida, Y. Anju, A. Kato, and T. Seiyama, This Bulletin, **44**, 2326 (1971).

10) J. W. Emsley, J. Feeney, and L. H. Sutcliffe, "High Resolution Nuclear Magnetic Spectroscopy," Vol. 2, 1120, Pergamon Press, Oxford (1966), p. 672.

11) K. Fukui, H. Kato, and T. Yonezawa, This Bulletin, **34**, 1111 (1961).

12) K. B. Wiberg, *Chem. Revs.*, **55**, 713 (1955).

13)
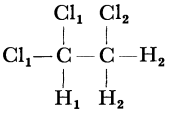

seems to be easily eliminated as an anion by the acidic sites. On the other hand, 1,1-dichloroethylene, that would be produced by the abstraction of the 1-hydrogen[13] easily eliminated as a proton is formed from 1,1,2-trichloroethane on the sulfates with the low *Xi* values. Thus, the gradual change in the reaction mechanism may explain the change in the selectivity according to the acid-base character of the catalyst.

The Mechanism of Dehydrohalogenation on Solid Acids. The fact that no kinetic isotope effect in the dehydrobromination from 1,2-dibromoethane was observed on solid acids indicates that the cleavage of the C–H bond is not involved at or before the rate-determining step. The negative slopes of the lines in Fig. 6 indicate that the reaction intermediate is positively charged. These facts suggest that the active site on solid acids may abstract halogen as an anion. An E2 concerted mechanism has been previously proposed for the HCl elimination on solid acids based on the distribution of the products from 1,1,2-trichloroethane.[1a] The substitution effect shown in Fig. 6 can not be explained by the stabilities of a hypothetical intermediate in an E2 concerted mechanism ($CH_3\overset{-}{C}H\overset{+}{C}H_2$ from $CH_3CH_2CH_2Br$ < $\overset{-}{C}HBr\overset{+}{C}H_2$ from CH_2BrCH_2Br, for example). This fact as well as the absence of any isotope effect rules out the E2 concerted mechanism.

The reactivity order of five chloroethanes on metal sulfates with high *Xi* can be understood on the consideration that the carbonium ion is stabilized by the α-substituted chlorine atom but is unstabilized by the β-substituted chlorine atom.[1a] The equal reactivity between dehydrochlorination and dehydrobromination can also easily be explained by the small free energy differences in $RCl+H^+ \rightarrow R^+ + HCl$ and $RBr+H^+ \rightarrow R^+ + HBr$.[14]

Between two conformations of 1,1,2-trichloroethane, the *trans* form I is more stable than the *cis* one II in a vapor phase,[15] whereas II may be predominant due to strong interaction between electronegative halogen and the acidic surface of solid acids.[3] Whether the *cis* or *trans* elimination is assumed, the stereoselective formation of *cis*-1,2-dichloroethylene can be explained as follows:

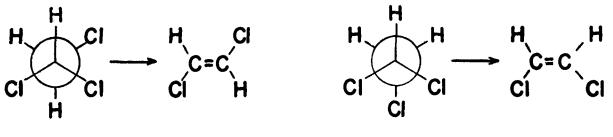

I II

As a explanation of the preferential *cis*-1,2-dichloroethylene formations, which, in some catalysts, are far over the equilibrium value (*cis*-1,2/*trans*-1,2=30,[1b] equilib. one=1.55[16]), this carbonium-ion mechanism containing an electrostatic interaction between acid sites and chlorine atoms may be more adequte than an E2 one.

Alumina has less catalytic activities as to *iso*-Pr and *n*-Pr, but more as to other reactants, than does silica-alumina. Alumina is generally thought to be less active for the carbonium-ion formation, but strikingly more active for some reactions, than is silica-alumina.[17] Therefore, regarding the less reactive reagents, another mechanism should be considered. A homolytic C–Cl cleavage may take to some extent. A considerable exchange of the halogens of 1-bromo-2-chloroethane and the markedly small slope in Fig. 6 may be understood in terms of this additional mechanism.

The Mechanism of Dehydrogenation on Solid Bases. The values of k_H/k_D over unity on solid bases in the elimination of HBr from 1,2-dibromoethane indicate that the C–H bonds were cleaved at or before the rate-determining step. There are three possible mechanisms: that is an E2 concerted, an E2 step-by-step (proton abstraction), or a carbanion mechanism. The dehydrohalogenation selectivity of the preferential elimination of hydrogen bromide from 1-bromo-2-chloroethane on solid bases can be explained in terms of neither the stability of the intermediate in a carbanion mechanism, which is expected from the stabilizing effect of bromine and chlorine on the carbanion ($Br\overset{-}{C}HCH_2Cl > Cl\overset{-}{C}HCH_2Br$), nor the stability of a hypothetical intermediate in an E2 concerted mechanism ($Br\overset{-}{C}H\overset{+}{C}H_2 > Cl\overset{-}{C}H\overset{+}{C}H_2$). Taking account of the higher reactivity of chlorine in comparison with that of bromine, as deduced from the preferential HCl-elimination of 1-bromo-2-chloroethane on solid acids, the selective HBr-elimination on the basic catalyst cannot be explained by an E2 concerted mechanism, either. Thus, both mechanisms must be abandoned. If an E2 step-by-step mechanism with the determining step of the proton abstraction is assumed, the preferential dehydrobromination from 1-bromo-2-chloroethane can be explained in terms of the effect of halogen in the α- and β-positions.[1b] The preferential stereoselectivity of *trans*-1,2 formation from 1,1,2-trichloroethane and the reactivity order of the five chloroethanes on solid bases can also be well explained by the E2 step-by-step mechanism.[1a] The higher reactivity for dehydrobromination than dehydrochlorination on solid bases can be explained from the effect of the halogen of the β-position, and the greater reactivity for the dehydrohalogenation of dihaloethanes may be due to the inductive effect of the halogen of the α-position. All these results may support the idea that the dehydrohalogenation on

14) For example, in the case of R=*n*–Pr, the free energies of formation for compounds are as follows: *n*-PrCl, 8.54 kcal/mol; *n*-PrBr, 14.85; HCl, −23.41; HBr, −13.76 at 300°C. (D. R. Stull, E. F. Westrum, and G. C. Sinke, "The Chemical Thermodynamics of Organic Compounds," Wiley, New York (1968), p. 518).

15) K. Kuratani and S. Mizushima, *J. Chem. Phys.*, **22**, 1405 (1954).

16) K. S. Pitzer and J. L. Hollenberg, *J. Amer. Chem. Soc.*, **67**, 1493 (1954).

17) I. Mochida, J. Take, Y. Saito, and Y. Yoneda, This Bulletin, **41**, 65 (1968); I. Mochida, Y. Anju, A. Kato, and T. Seiyama, *ibid.*, **43**, 2245 (1970).

solid bases proceeds through an E2 step-by-step mechanism, although the reactivity of the haloethane can not yet be quantitatively explained.

The peculiarly high reactivities of *iso*-PrBr and *iso*-PrCl on solid bases cannot be explained by this mechanism. In the dehydrohalogenation of these secondary halides, a carbonium-ion character may increase, because the secondary carbonium ion is easily formed. Noller *et al.* have reported that the dehydrohalogenation of 2-chlorobutane proceeded through a two-step mechanism with a carbonium ion intermediate.[18] This mechanism may be valid in the case of isopropyl halides.

A quantitative explanation of the reactivity must be made next. The MO approach will be useful if its accuracy can be increased.

18) H. Noller, W. Low, and P. Andreu, *Ber. Bunsenges., Phys. Chem.*, **68**, 663 (1964).

BULLETIN OF THE CHEMICAL SOCIETY OF JAPAN, VOL. 44, 3310—3316 (1971)

Dynamic Behaviors of the Electron Donor-Acceptor Complex in its Lowest Excited Singlet State

Hiroshi MASUHARA, Motoo SHIMADA, Nobuyuki TSUJINO, and Noboru MATAGA

Department of Chemistry, Faculty of Engineering Science, Osaka University, Toyonaka, Osaka

(Received June 7, 1971)

Dynamic behaviors of the weak electron donor-acceptor (EDA) complex in its lowest excited singlet state have been investigated by the nsec flash photolysis method and measurements of fluorescence and transient photocurrent. In polar solvents the weak EDA complex in its lowest excited singlet state dissociates spontaneously into ions. The dynamic behaviors of *s*-tetracyanobenzene(TCNB)-benzene and TCNB-toluene complexes were studied in some solvents and the existence of the direct radiationless process at the excited Franck-Condon (FC) state as well as in the course of relaxation process from the excited FC state to the fluorescent state has been confirmed in the case of 1,2-dichloroethane solution. The nature of the intra-complex radiationless processes was discussed on the basis of this result. It has been pointed out that the lifetime of excited states is of crucial importance for understanding the dynamic behaviors of excited weak EDA complexes.

EDA complexes which are fluorescent in solution at room temperature are rather scarce. However, one can observe at room temperature the fluorescence of complexes of some acceptors such as TCNB, tetrachlorophthalic anhydride (TCPA) and pyromelitic dianhydride (PMDA) with hydrocarbon donors.[1-6] From the study of solvent effects on the fluorescence of these complexes, it has been shown that the low fluorescence yield in nonpolar solvents can be ascribed to a small value of radiative rate constant k_f while, in polar solvents, it can be attributed to a large value of radiationless rate constant k_n.[2,3,6] In order to understand the results, the effect of solvent and temperature on fluorescence spectra, fluorescence quantum yield and fluorescence decay times of TCNB complexes were investigated. A small value of k_f was ascribed to the large difference in electronic structure between the fluorescent and ground states.[2] The important role of surrounding environments in the relaxation process, through which the fluorescent state is produced from the excited FC state, was made clear.[2,7,8]

Recently, we have shown that the ionic dissociation of TCNB-toluene complex in the lowest excited singlet state occurs in acetonitrile.[9] Detailed studies on the ionic dissociation of excited EDA complexes may provide useful information for understanding radiationless transitions as well as primary processes of photochemical reactions of EDA complexes. It is well-known that the ionic dissociation of heteroexcimer or the electron transfer in the encounter collision in the excited state can occur easily in polar solvents.[10] However, there are only a few studies on ionic dissociation of the excited EDA complexes which are stable in the ground state.[11,12] In these

1) G. Briegleb, "Electronen-Donator-Acceptor-Komplexe," Springer-Verlag, Berlin, (1962).

2) N. Mataga and Y. Murata, *J. Amer. Chem. Soc.*, **91**, 3144 (1969).

3) T. Kobayashi, K. Yoshihara, and S. Nagakura, Preprint for the Symposium on EDA Complexes, Osaka, 1970.

4) H. M. Rosenberg and E. C. Eimutis, *J. Phys. Chem.*, **70**, 3494 (1966).

5) J. Czekalla and K. O. Mager, *Z. Physik. Chem.* (Frankfurt), **27**, 185 (1961).

6) J. Prochorow and R. Siegoczyński, *Chem. Phys. Lett.*, **3**, 635 (1969).

7) H. Masuhara and N. Mataga, submitted to *Z. Physik. Chem. N. F.*

8) K. Egawa, N. Nakashima, N. Mataga, and C. Yamanaka, *Chem. Phys. Lett.*, **8**, 108 (1971); submitted to this Bulletin.

9) H. Masuhara, M. Shimada, and N. Mataga, This Bulletin, **43**, 3316 (1970).

10) T. Okada, H. Oohari, and N. Mataga, *ibid.*, **43**, 2750 (1970); H. Leonhardt and A. Weller, *Ber. Bunsenges. Phys. Chem.*, **67**, 791 (1963); H. Knibbe, D. Rehm, and A. Weller, *ibid.*, **72**, 257 (1968); O. D. Dmitriefski and A. N. Terenin, *Dokl. Akad. Nauk SSSR*, **151**, 122 (1963); H. Yamashita, H. Kokubun, and M. Koizumi, This Bulletin, **41**, 2312 (1968); K. Kawai, N. Yamamoto, and H. Tsubomura, *ibid.*, **42**, 369 (1969).

11) F. S. Stewart and M. Eisner, *Mol. Phys.*, **12**, 173 (1967); D. F. Ilten and M. Calvin, *J. Chem. Phys.*, **42**, 3760 (1965); E. M. Kosower and L. Lindquist, *Tetrahedron Lett.*, **50**, 4481 (1965); R. F. Cozzes and T. A. Cover, *J. Phys. Chem.*, **74**, 3003 (1970); W. C. Meyer, *ibid.*, **74**, 2118 (1970).

12) R. Potashnik, C. R. Goldschmidt, and M. Ottolenghi, *ibid.*, **73**, 3170 (1969).

studies, the absorption spectra of produced ion radicals were measured by only the conventional flash photolysis method and no direct observation on the primary process of the production of ion radicals in nsec time region was performed. However, the study on the primary processes of ionic photodissociation of EDA complexes is indispensable in order to obtain a correct picture of the dynamic behaviors of excited complexes.

In the present paper the results of our studies on the ionic photodissociation of various weak EDA complexes in various solvents will be described, and the mechanisms of the ionic photodissociation as well as other radiationless processes in these complexes will be discussed in detail.

Experimental

We used a Q-switched ruby laser (Japan Electron Optics, JLR-02A) with out put of *ca.* 1.5 J. The exciting light pulse of 347 nm was produced through ADP frequency doubler with conversion efficiency of *ca.* 8%. The output of an exciting pulse was measured with a ballistic thermopile TRG model 100 (HADRON). The light pulse has a duration of 15—20 nsec. The absorption spectra of ions produced by exciting the complex at the charge-transfer (CT) absorption band were measured photographically by using laser-breakdown sparks in O_2 and Xe gases as spectroflashes.[13] The rise and decay curves of ions were observed by the nsec flash photolysis method we developed. Since a 50 Ω resistor is equipped to photomultiplier to obtain nsec time resolution, a monitoring light intensity falling onto the photomultiplier must be far greater than that of a conventional flash photolysis.[14] We used a Xe flash lamp as monitoring light, the duration of which was adjusted to *ca.* 300 μsec. A block diagram of the present nsec flash photolysis apparatus is shown in Fig. 1. The timing circuit using a cathode-coupled multivibrator makes the adjustment of an exciting pulse to the peak intensity of the monitoring flash lamp easy and linear.[15]

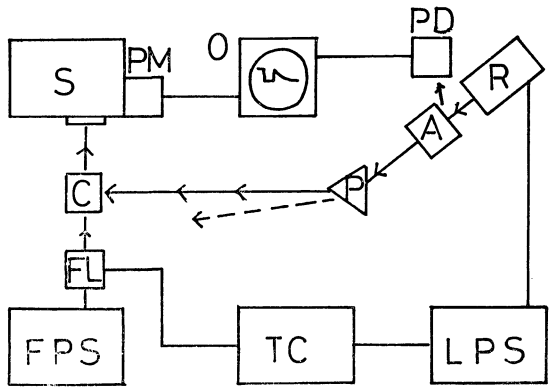

Fig. 1. A block diagram of nsec flash photolysis apparatus. R, ruby; A, ADP frequency doubler; P, separating prism; C, sample cell; LPS, laser power supply; TC, timing circuit; FPS, flash power supply; FL, monitoring flash lamp; S, Nalumi R21 spectrograph; PM, RCA 1P28 or Hamamatsu TV R406 photomultiplier; PD, Hewlet-Packard 5082—4220 photodiode; O, Tektronix 585A synchroscope.

The ion radicals produced were also observed by measuring the photocurrent induced by laser excitation. Although the details of the measurement of the photocurrent will be reported by Taniguchi and Mataga,[16] some fundamental points are given here. Direct irradiation on the electrodes was avoided by focusing the 347 nm pulse. The electrodes were Ni plates of 9 mm × 10 mm set 7 mm apart from each other. To obtain nsec time resolution a 50 Ω resistor was used and the supplied DC voltage between electrodes was adjusted from 90 V to 540 V. The time constant of the electronic circuit is less than 5 nsec. The DC dark current was omitted by using the ac coupling of the input of a Tektronix 585 A synchroscope. For examining the effect of the excitation light intensity on the photocurrent, the normal laser pulse was reduced by using neutral filters composed of wire gauzes. The filters reduced the light intensity to 0.3%, 13%, 32%, and 68%. Some weaker signals of photocurrent were measured by using an Iwatsu cascade amplifier CA-2.

The fluorescence spectra and relative quantum yields of the fluorescence were measured with an Aminco-Bowman spectrophotofluorometer.

The temperature effect on ionic dissociation was studied by measuring the laser-induced photocurrent at various temperatures. The cell for the measurements of photocurrent was fitted into a copper-cellholder, which was coupled to a tank filled with liquid N_2. The whole system was contained in a quartz dewar, the bottom of which is unsilvered to permit photoexcitation. The temperature was measured with a Cu-constantan thermopile and a micro volt meter model AM 1001 (Ohkura Electric Co.).

Acetonitrile, mesitylene, and α-methylstyrene were purified by distillation. Benzene, toluene, and ethyl ether (Merk spectrograde), and ethyl alcohol, isopropyl alcohol, acetone and 1,2-dichloroethane (Nakarai Chemicals, spectrograde) were used without further purification. TCNB, TCPA, and hexamethylbenzene (HMB) were the same as used before.[2] PMDA was purified by repeated recrystallization from ethyl acetate. All the solutions were carefully degassed by the usual method.

Results and Discussion

Absorption Spectra of the Transient Acceptor Anion Produced by Laser Photolysis. The spectra obtained by exciting TCNB-toluene complex to its lowest excited singlet state in acetonitrile solution are shown in Fig. 2. Since the observed transient absorption spectra are identical with those of TCNB anion,[17] it has been proved that the excitation of this complex by light absorption at the CT band leads to the ionic dissociation in acetonitrile solution. This anion decays rather slowly in the course of tens of μsec. Some parts of the produced anions are quite stable and observable even by a usual spectrophotometer. It was not possible to identify the transient spectra of

13) J. R. Novak and M. W. Windsor, *Proc. Roy. Soc. Ser. A*, **308**, 95 (1968).
14) G. Porter and M. R. Topp, *ibid.*, **315**, 163 (1970).
15) J. Millman and H. Taub, "Pulse and Digital Circuits," McGraw-Hill, New York (1966), p. 187.
16) Y. Taniguchi and N. Mataga, Preprint for the Symposium on Photochemistry, Kyoto, 1970.
17) M. Sofue and S. Nagakura, This Bulletin, **38**, 1048 (1965); A. Ishitani and S. Nagakura, *Theor. Chem. Acta* (Berl.), **4**, 236 (1966).

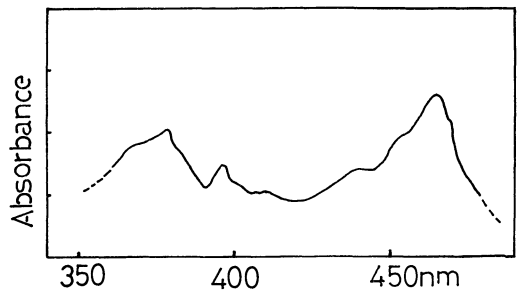

Fig. 2. The transient absorption spectra of the TCNB-toluene-acetonitrile system. Concentration of TCNB, 6×10^{-3} M. Volume ratio of toluene *vs.* acetonitrile, 1 : 2.

toluene cation, which may be ascribed to the fact that the absorption band of cation which lies at *ca.* 460 nm[18] may be hidden behind the strong band of TCNB anion.

We have also made some investigations in other polar solvents, fixing volume ratio of donor solvent *vs.* polar solvent to 1 : 2. The transient spectra due to TCNB anion produced by exciting the TCNB-toluene complex at the CT band were observed also in acetone, isopropyl alcohol and ethyl alcohol. We examined the ionic dissociation of other TCNB complexes by means of the laser photolysis method and observed the absorption spectra of TCNB anion in acetonitrile solution in the cases of TCNB-benzene and TCNB-mesitylene complexes. In the case of the latter, the spectra were also taken by using the fluorescence of cyclohexane solution of tetraphenylbutadiene as a flash light, a technique used by Porter and Topp.[13] Since the fluorescence lifetime of tetraphenylbutadiene is short, the fluorescence light pulse has the same shape in time as an exciting laser pulse. Accordingly, this technique is convenient for observing the species produced rapidly. The acceptor anion was detected also in the cases of TCNB-α-methylstyrene and PMDA-mesitylene complexes with nsec flash photolysis. Thus, the ionic dissociation caused by exciting the CT band in polar solvents has been observed commonly for various weak EDA complexes.

Kinetic Analyses by the Measurements of Fluorescence, Absorption and Photocurrent in Nsec Time Region. The rise and decay curves of acceptor anion were obtained by nsec flash photolysis technique developed in the present work. The oscillograms showing rapid production of acceptor ions in the systems of TCNB-α-methylstyrene-acetonitrile, PMDA-mesitylene-acetonitrile and TCNB-toluene-acetonitrile, are given in Figs. 3, 4 and 5(a), respectively. Such a rapid production of acceptor anion was also observed in the case of TCNB-toluene-acetone. The S_n–S_1 spectra of TCNB-toluene and TCNB-benzene complexes recently reported[7,19,20] are similar to the spectra of TCNB anion. We cannot distinguish the solvated anion from the excited singlet EDA complex having

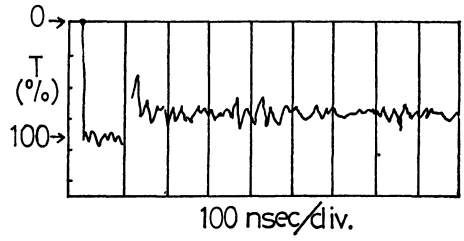

Fig. 3. The rise of TCNB anion produced by exciting the TCNB-α-methylstyrene-acetonitrile system. Observed at 465 nm.

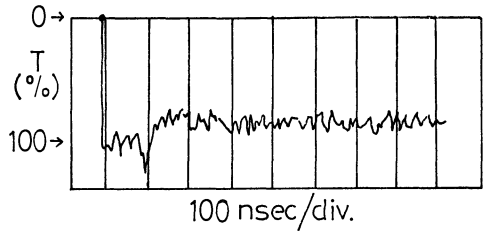

Fig. 4. The rise of PMDA anion produced by exciting the PMDA-mesitylene-acetonitrile system. Observed at 665 nm.

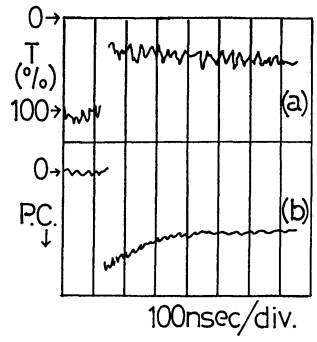

Fig. 5. The kinetic relation between transient photocurrent and transmittance of TCNB anion, produced by exciting the TCNB-toluene-acetonitrile system.
(a) transmittance at 465 nm (b) photocurrent.

the structure of "contact ion-pair"[7,19] by measuring and comparing only the shape of the absorption spectra, although behavior of this anion, *e.g.* the decay processes is different from that of the excited singlet EDA complex.

We have measured the photocurrent induced by laser excitation of weak EDA complexes in various solvents since this may be another useful and important method for examining ionic photodissociation. It has been shown that the obtained photocurrent is due to the dissociated ions, by comparing the rise and decay curves of the photocurrent with those of absorption of acceptor anion. The kinetic relation between transient photocurrent and transient absorption are given in Fig. 5. The rise curve and earlier stage of decay of the photocurrent are almost the same as those of absorption of TCNB anion.[21]

18) T. Shida and H. Hamill, *J. Chem. Phys.*, **44**, 2375 (1966).
19) H. Masuhara and N. Mataga, *Chem. Phys. Lett.*, **6**, 608 (1970).
20) R. Potashnik and M. Ottolenghi, *ibid.*, **6**, 525 (1970).

21) A difference in photocurrent and absorption arises in the later stage of decay. This might be due to secondary reactions as well as the dark current caused by the dark reaction occurring at electrodes because of high applied electric field. The observed photocurrent induced by laser excitation can be ascribed to the dissociated ion radicals.

The rise curve of photocurrent in the case of TCNB-toluene-acetonitrile system and an excitation laser pulse are given in Fig. 6. The shape of the rise curve is the same as that of a time-integrated function of a 347 nm pulse. We have obtained the same results for all the complexes in various solvents at room temperature.

We can observe both the CT fluorescence of TCNB-benzene and the photocurrent due to dissociated ions in the case of 1,2-dichloroethane solution. As indicated in Fig. 7, the fluorescence decay is rather fast corresponding to the rapid production of ions in this solution.

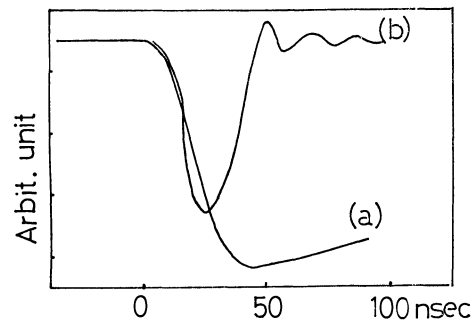

Fig. 6. The rise and decay of photocurrent in the case of the TCNB-toluene-acetonitrile system.
(a) transient photocurrent (b) shape of an exciting pulse.

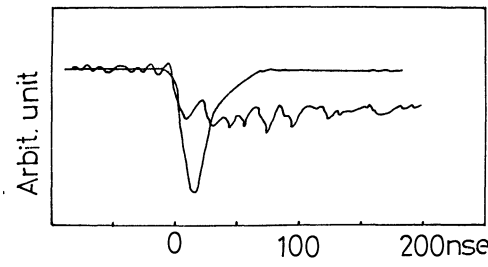

Fig. 7. The kinetic relation between photocurrent and CT fluorescence in the case of the TCNB-benzene-1,2-dichloroethane system.

The photocurrent of aerated TCNB-toluene-acetonitrile system was also measured. It was found that production of TCNB anion in the aerated system was almost the same as that in the degassed system. The decay of ions in aerated solution is, of course, faster than that in degassed solution.

Ionic Dissociation of Weak EDA Complexes in Their Lowest Excited Singlet States. All the results seem to show that ionic dissociation of these complexes occurs in the lowest excited singlet state. However, a two-step process with an excited state as an intermediate and a collision process between excited EDA complexes followed by ionic dissociation should be examined to elucidate the primary process of the dissociation, since a laser pulse is an intense exciting light. First the effect of excitation light intensity on the photocurrent was examined.

In general, the photocurrent density is given by[22]

$$i(t) = \sum_j Z_j e n_j(t) \mu_j E \qquad (1)$$

where Z_j, μ_j, and $n_j(t)$ represent electric charge, mobility, and number of the carrier j in unit volume, respectively. E is an applied electric field. In the present system of weak EDA complexes, the charge carriers are acceptor anions and donor cations, and the equation is reduced to

$$i(t) = en(t)(\mu_{\text{anion}} + \mu_{\text{cation}})E. \qquad (2)$$

Since both ions are simultaneously produced by laser excitation and disappear by recombination reaction, we have

$$\frac{dn}{dt} = aI - bn^2, \qquad (3)$$

where a and b represent rate constants of production and disappearance of ions, respectively. I is an intensity of the exciting pulse.

In the case of EDA complexes in various solvents at room temperature, the dissociation into ion radicals occurs quite rapidly in nsec time region while they decay slowly during time more than ten μsec. Thus the peak photocurrent obtained immediately after excitation is proportional to the concentration of the dissociated ions. The effect of excitation light intensity on the peak photocurrent of TCNB-toluene-acetonitrile system is given in Fig. 8. The linear relation shows that this ionic dissociation is a one-photon process.[23]

The effect of the excitation light intensity on the production of ions has been studied also by means of nsec flash photolysis and measurement of the transient absorption band. The observed results on the TCNB-toluene-acetone system, also indicating a one-photon process, are given in Fig. 9.

We have investigated the temperature effect on ionic dissociation in the case of TCNB-toluene-ethyl alcohol system. The volume ratio of toluene *vs.* ethyl alcohol was set to 1 : 10, in which case a rigid

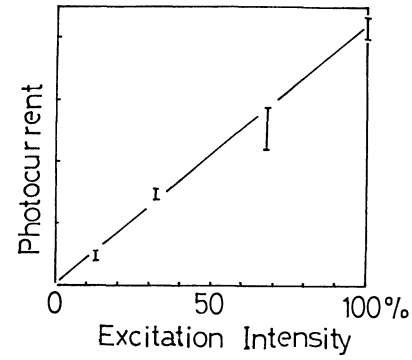

Fig. 8. The effect of exciting light intensity on the peak photocurrent of the TCNB-toluene-acetonitrile system. Optical density at 347 nm is *ca.* 0.1.

22) G. E. Johnson and A. C. Albrecht, *J. Chem. Phys.*, **44**, 3179 (1966); H. S. Pilloff and A. C. Albrecht, *ibid.*, **49**, 4891 (1968); T. Imura, N. Yamamoto, and H. Tsubomura, This Bulletin, **43**, 1670 (1970).

23) The effect of excitation light intensity on ionic dissociation was examined under rather low solute concentration. In the case of high concentration (O. D. at 347 nm ~1.0), a saturation effect of photocurrent was caused by high intensity laser excitation.

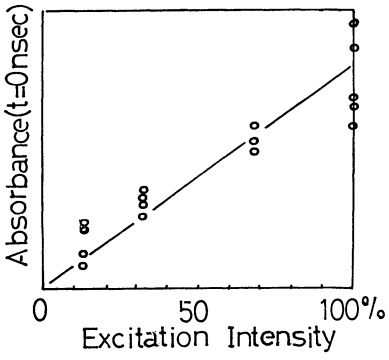

Fig. 9. The effect of exciting light intensity on the transient absorption of TCNB anion produced by irradiating the TCNB-toluene-acetone system. Observed at 462 nm. Optical density at 347 nm is *ca.* 1.0.

glass was formed at liquid nitrogen temperature. Mobility μ and dielectric constant ε of solvent undergo changes with change of temperature. It is well known that mobility μ is proportional to diffusion-controlled rate constant k, which is approximately proportional to T/η,[24] where η and T represent viscosity coefficient and temperature, respectively. Moreover, the relation $\log \eta \sim 1/T$ holds in the case of the glass-forming solvent mixtures.[25] Thus, $\log (i/T)$, where i is the peak photocurrent, should be proportional to $1/T$. It is necessary, however, to correct the peak photocurrent with respect to the dielectric constant of mixed solvent. In the present work, we have neglected the contribution of toluene to dielectric constant of mixed solvent and taken into consideration only the change of dielectric constant of ethylalcohol due to the change of temperature. The results are given in Fig. 10, which shows a linear relation between $\log (i/T)$ and $(1/T)$. This can be ascribed to the fact that the quantum yield of dissociation is constant, independent of temperature, indicating spontaneous dissociation (without activation energy) of this complex in ethyl alcohol.

From the results it can be concluded that the weak EDA complexes (which are stable in the ground state) dissociate spontaneously into ions in their excited CT singlet states in polar solvents.

Dynamic Behaviors of TCNB-Benzene and TCNB-Toluene Complexes in Various Solvents. The dynamic behaviors of excited TCNB-benzene and TCNB-toluene complexes in various solvents were studied in detail, fixing the volume ratio of the donor solvent *vs.* another solvent to 1 : 2. The lifetime and relative quantum yield of fluorescence, exciting the CT band at 347 nm, were measured by the usual method.[2] The relative quantum yields of ionic dissociation were obtained by correcting photocurrent with respect to the strength of applied electric field, the distribution and number of exciting photons, viscosity and dielectric constant of mixed solvents and by comparing the peak photocurrent. Viscosity η and dielectric constant ε of a mixed solvent were

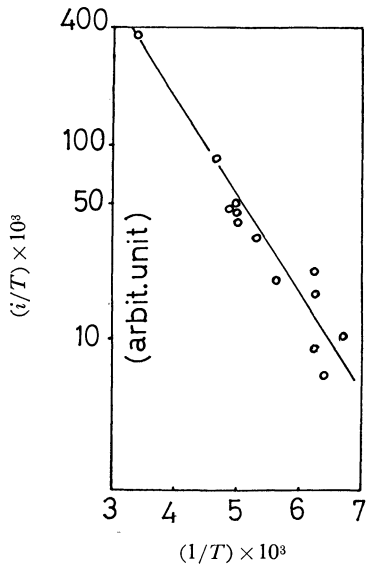

Fig. 10. $\log (i/T)$ *vs.* $(1/T)$ relation observed for the TCNB-toluene-ethanol system.

calculated approximately by equations $\eta=\sum_i v_i\eta_i$ and $\varepsilon=\sum_i v_i\varepsilon_i$, where η_i, ε_i, and v_i represent viscosity, dielectric constant, and volume fraction of the solvent i, respectively.

Estimation of the order of magnitude of the absolute quantum yield of dissociation for the systems of TCNB benzene-acetonitrile and TCNB-α-methylstyrene-acetonitrile was made as follows. (1) The distribution of exciting photons was assumed to be uniform in the effective irradiation spot on the front face of the cell, which was determined from a burned spot on a color sheet produced by a 347 nm pulse. (2) The distribution of the produced TCNB anion in the monitoring portion of the sample cell was averaged. (3) The concentration of the produced anion was calculated, using an optical density of TCNB anion obtained immediately after the excitation (Fig. 5 (a)) and assuming molecular extinction coefficient at 465 nm to be *ca.* 10^4. (4) The quantum yield was put equal to the number of anions divided by the number of exciting photons which were measured to be 1.7×10^{17} per pulse by the TRG 100 thermopile. All the results on TCNB-benzene and TCNB-toluene complexes are listed in Tables 1 and 2.

We see that the decrease of φ_f from benzene to 1,2-dichloroethane solutions is larger than that of τ_f. This result can be explained on the basis of the following two alternative models. (a) The radiative transition probability of fluorescence k_f decreases and the radiationless transition probability increases with the increase of the solvent polarity, due to the strong interaction between the complex and solvent. (b) The direct radiationless process arises from the excited FC state as well as in the course of the relaxation process from the excited FC state to the fluorescent state. This radiationless process as well as the usual one from the fluorescent state increase as the solvent polarity is increased, while the k_f value

24) M. Smoluchowski, *Z. Physik. Chem.*, **92**, 129 (1917).
25) F. Greenspan and E. Fischer, *J. Phys. Chem.*, **69**, 2466 (1965).

TABLE 1. DYNAMIC BEHAVIORS OF TCNB-BENZENE COMPLEX IN ITS LOWEST EXCITED SINGLET STATE

Solvent	ε_{mix}[a]	Fluorescence lifetime	φ_f[b]	φ_{ion}[b]	φ_{nf}[b,c]
Benzene	2.3	~100 nsec	0.009 (1.0)[e]	0	0.91
Ethyl ether	3.7		0.02 (0.23)	0	0.98
1,2-Dichloroethane	7.7	20[d]	0.004 (0.04)	0.001 (0.0015)	0.995
Acetone	14.6			0.035 (0.35)	0.965
Acetonitrile	25.8			0.1 (1.0)	0.9

a) Calculated dielectric constants.
b) φ_f, φ_{ion}, and φ_{nf} represent absolute quantum yields of fluorescence, ionic dissociation, and intra-complex radiationless transition, respectively.
c) φ_{nf} does not contain ionic dissociation and was estimated by the relation $\varphi_{nf}=1-\varphi_f-\varphi_{ion}$.
d) The fluorescence decay curve was observed by exciting the complex with N_2 gas laser. The N_2 laser was the same as that described in Ref. 8.
e) The values in parentheses are relative quantum yields.

TABLE 2. IONIC DISSOCIATION OF TCNB-TOLUENE COMPLEX IN ITS LOWEST EXCITED SINGLET STATE

Solvent	ε_{mix}	Relative quantum yield of ionic dissociation	Appearance of absorption band of TCNB anion
Toluene	2.4	~0	Not observed
Ethyl ether	3.7	~0	Not observed
1,2-Dichloroethane	7.7	0.01	Not observed
Isopropyl alcohol	13.0	0.29	Observed
Ethyl alcohol	17.0		Observed
Acetonitrile	25.8	1.00	Observed

is not affected by the solvent polarity.

On the other hand, the difference in Stokes shift of fluorescence between TCNB-benzene and TCNB-benzene-1,2-dichloroethane systems can be explained by the usual dielectric theory of the solvent shift of fluorescence spectra.[8] This means that the electronic structure of the excited TCNB-benzene complex is independent of the solvent polarity and a constant value of k_f can be expected. Therefore, at the present stage of investigation the larger decrease of φ_f with the increase of solvent polarity from benzene to 1,2-dichloroethane solutions, compared with the decrease of τ_f, may be ascribed to the existence of the direct radiationless process (b).

From Table 1, we can see the increase of φ_{nf} with the increase of solvent polarity from benzene to 1,2-dichloroethane and the increase of φ_{ion} as well as the decrease of φ_{nf} when the solvent is changed from 1,2-dichloroethane to acetonitrile. These results show that solvent polarity plays an important role not only for ionic dissociation but also for intra-complex radiationless transition.

Ionic Dissociation of Various Weak EDA Complexes. We have studied the ionic photodissociation of various EDA complexes in acetonitrile solution. In the case of liquid donors the volume ratio of the donor *vs.* acetonitrile was fixed to 1 : 2. All the results are listed in Table 3, together with the values of the fluorescence lifetime and the result of S_n–S_1 spectral measurement in nonpolar solvents. The yield of ionic dissociation in acetonitrile solution of TCNB complexes with methyl-substituted benzene decreases from benzene to HMB donors. Together with this decrease arises difficulty to observe S_n–S_1 absorption spectra in nonpolar solvents. The S_n–S_1 spectra of TCNB-HMB complex in methylmethacrylate and TCNB-α-methylstyrene systems have not been observed. However, the S_n–S_1 spectra of TCNB-benzene and TCNB-toluene complexes have been observed easily by analyzing the re-absorption of CT fluorescence[7,19,26] and those of TCNB-mesitylene[27] and PMDA-mesitylene complexes by the nsec flash photolysis method. On the other hand, the electronic structure of excited equilibrium state of TCNB complexes has been shown to depend little upon the donor according to our theoretical consideration.[7] Thus, the above results of decreasing dissociation of TCNB complexes with increasing strength of donor appear to contradict the theoretical consideration. The contradiction can be removed by considering the fluorescence lifetimes of these complexes. Those of TCNB-α-methylstyrene and TCNB-HMB complexes in nonpolar solvents seem to be short, since fluorescence decay function is almost the same in shape as an exciting laser pulse. It seems to be difficult to observe the S_n–S_1 spectra of TCNB-α-methylstyrene and TCNB-HMB complexes because of these short lifetimes, and the dissociation yields of these complexes in polar solvents might be low. Short lifetimes may be due to the large value of intra-complex radiationless transition rate constant. This consideration in terms of short lifetime is, of course, related to that given in the above section.

Related and Future Problems. The present results on the process k_f of TCNB-benzene complex in

26) The effect of the re-absorption of CT fluorescence by the excited EDA complex itself was examined in detail. Masuhara and Mataga, This Bulletin, **45**, No. 2 (1972), in press.
27) H. Masuhara and N. Mataga, Preprints for the 24th Annual Meeting of the Chemical Society of Japan, Osaka, 1971.

Table 3. Ionic dissociation of weak EDA complexes in acetonitrile solution

Acceptor	Donor	I_p	φ_{ion}[a]	Absorption of TCNB anion	S_n-S_1 spectra[c]	τ_{fluo}[c]
TCNB	Benzene	9.24 eV	1.0	Observed	Observed	100 nsec
	Toluene	8.82	0.98	Observed	Observed	100
	Mesitylene	8.39	0.46	Observed	Observed	43[3]
	α-Methylstyrene	8.36	0.15	Observed	Not observed	S[d]
	Naphthalene	8.12	Observed			
	HMB	7.85	0.05	Not observed	Not observed	S
	DMA[e]	7.14	Observed			
	TMPD[e]	6.6	Observed[b]			
TCPA	Toluene	8.82	~1.0	Not observed	Not observed	S
PMDA	Mesitylene	8.39	Observed	Observed	Not observed	S

a) Relative quantum yields of ionic dissociation obtained by measurement of photocurrent.
b) The excitation pulse is a 694 nm one of ruby laser.
c) The results in nonpolar solvents.
d) The fluorescence lifetime is short and fluorescence decay function is almost the same in shape as an exciting laser pulse.
e) DMA, *N*,*N*-dimethylaniline; TMPD, tetramethyl-*p*-phenylenediamine.

polar solvents might be related to the CT and electron-transfer mechanism of the fluorescence quenching of aromatic hydrocarbons. One of the authors (N. M.) reported that the stronger decrease of φ_f of the heteroexcimer (HE), formed by an aromatic hydrocarbon and an aromatic amine, compared to the decay time with the increase of solvent polarity may be ascribed to the decrease of k_f and increase of radiationless process as the solvent polarity is increased.[2,10,28] On the other hand, Weller and his co-workers assumed the existence of non-fluorescent solvated ion-pair state as well as the fluorescent HE state and the competition between two processes of formation of these states.[10,29] According to this interpretation, the low value of φ_f of HE in polar solvents is due to the larger probability of the process leading to the non-fluorescent solvated ion-pair state. Our recent study on HE indicates that the assumption of the existence of the non-fluorescent ion-pair state in a solvent, which is not very polar, is fairly reasonable.[16] Although such a non-fluorescent solvated ion-pair state was not assumed explicitly on TCNB-benzene and TCNB-toluene complexes, it may be related to the direct radiationless processes from the excited FC state as well as in the course of the relaxation process from the excited FC state to the fluorescent state.

We have concluded that short lifetimes of rather stronger complexes may be due to the large value of intra-complex radiationless transition rate constant. In this case there might be also a radiationless process due to the degradation from the excited FC state of the complex in addition to the radiationless processes from the fluorescent state. If this degradation process from the excited FC state exists at all, it will be an interesting subject for investigation.

In contrast to our present results where the dissociation of weak EDA complexes occurs in their lowest excited singlet states, the spontaneous dissociation in the lowest CT triplet state of PMDA-mesitylene complex in ether-isopentane solution at low temperature has been reported.[12] The difference may be ascribed to the difference in solvent and temperature, although atomistic mechanism which determines the different way of dissociation is not very clear. We have confirmed that TCNB-α-methylstyrene complex shows a behavior similar to that of other complexes, *i.e.*, it dissociates in the lowest excited singlet state, although its fluorescence behavior is quite peculiar, giving two fluorescence bands in nonpolar solvents.[30] On the other hand, we have recently found a rather slow rise of the laser-induced photocurrent differing from the present results, in the case of PMDA-2-methyltetrahydrofuran complex.[31]

The authors wish to express their thanks to Mr. T. Okada and Mr. Y. Taniguchi for their helpful discussions.

28) N. Mataga, T. Okada, and K. Ezumi, *Mol. Phys.*, **10**, 201, 203 (1966); N. Mataga, T. Odaka, and N. Yamamoto, This Bulletin, **39**, 2562 (1966); N. Mataga and K. Ezumi, *ibid.*, **40**, 1355 (1967); N. Mataga, T. Okada, and N. Yamamoto, *Chem. Phys. Lett.*, **1**, 119 (1967).

29) H. Beens, H. Knibae, and A. Weller, *J. Chem. Phys.*, **47**, 1183 (1967); H. Knibbe, K. Röllig, F. P. Schäffer, and A. Weller, *ibid.*, **47**, 1184 (1967); H. Knibbe, D. Rehm, and A. Weller, *Z. Physik. Chem.* (Frankfurt am Main), **56**, 95, 99 (1967).

30) M. Irie, S. Tomimoto, and K. Hayashi, Preprint for the Symposium on EDA Complexes, Osaka, 1970.

31) M. Shimada, H. Masuhara, and N. Mataga, Preprint for the Symposium on Photochemistry, Tokyo, 1971.

Vibration Spectra and Molecular Structures of *n*-Butyronitrile, β-Chloropropiononitrile, and β-Bromopropiononitrile

Tsunetake FUJIYAMA

Department of Chemistry, Faculty of Science, The University of Tokyo, Bunkyo, Hongo, Tokyo

(Received June 15, 1971)

Infrared and Raman spectra of XCH_2CH_2CN-type molecules (X=CH_3, Cl, and Br) are studied. From the spectral analysis, it is concluded that *trans* and *gauche* isomers coexist in the liquid phase, the *gauche* being more stable. It is also shown that these molecule take *gauche* configurations in the crystalline phase.

In a previous report, the vibration spectra and the molecular structure of succinonitrile were discussed from the point of view of a normal coordinate treatment and the molecular structure.[1] The spectra of succinonitrile in the solid state showed that *trans* and *gauche* forms coexist above −50°C, while only the *gauche* form remains below −50°C. These results are quite different from those of ordinary disubstituted ethanes, such as *n*-butane, 1,2-dichloroethane, and 1,2-dibromoethane, where the stable configuration in the crystalline phase is the *trans* form.[2] In order to ascertain whether this is a phenomenon characteristic of the molecules having cyanide groups, the infrared and Raman spectra of XCH_2CH_2CN-type molecules (X=CH_3, Cl, and Br) were studied.

An empirical rule was proposed by the present author for the relationship between the skeletal deformation vibrations and the molecular configurations of rotational isomers.[3] The validity of this rule was also tested in the present work.

Experimental

Samples. *n*-Butyronitrile was prepared from *n*-butyric acid by the standard method. The product was purified by redistillation; bp 117°C/760 mmHg. The purity was tested by means of gas chromatography.

β-Chloropropiononitrile was synthesised from ethylene cyanohydrin. Thionylchloride was mixed with ethylene cyanohydrin and kept at room temperature for several hours. The mixture was washed with a $NaCO_3$-H_2O solution, dried over calcium chloride, and then distilled; bp 175°C/760 mmHg.

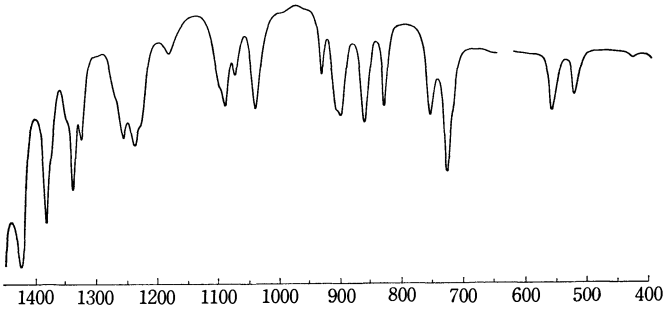

Fig. 1. Infrared spectra of liquid *n*-butyronitrile (room temperature).

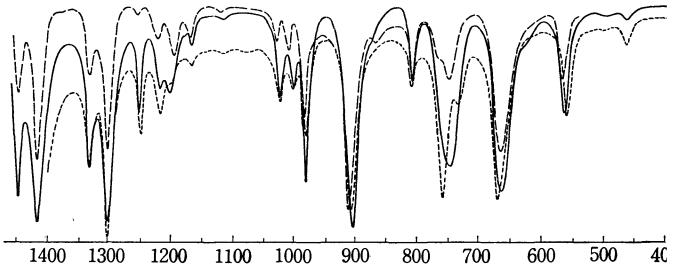

Fig. 2. Infrared spectra of β-chloropropiononitrile (——: liquid, room temperature, ———: glass, −196°C, ----: CS_2 solution).

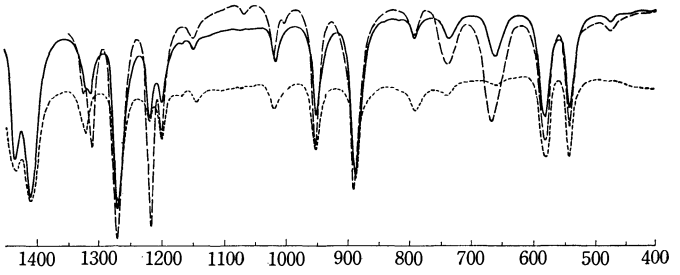

Fig. 3. Infrared spectra of β-bromopropionitrile (——: liquid, room temperature, ----: glass, −196°C, ----: CS_2 solution).

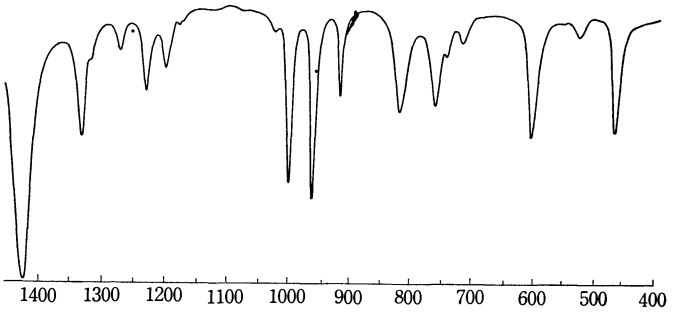

Fig. 4. Infrared spectra of succinonitrile (room temperature).

β-Bromopropiononitrile was also made from ethylene cyanohydrin. Ethylene cyanohydrin was mixed with phosphorous tribromide in ether on an iced-bath and was then kept for 24 hr. The mixture was washed with a $NaCO_3$-H_2O solution, dried over calcium chloride, and distilled; bp 63–65°C/5 mmHg. As the product was rather unstable in the air, freshly-distilled samples were used for the measurements.

Vibration Spectra. The infrared spectra in the NaCl and KBr regions (4000–500 cm^{-1}) were recorded by a Japan Spectroscopic Company 402G grating infrared spec-

1) T. Fujiyama, K. Tokumaru, and T. Shimanouchi, *Spectrochim. Acta*, **20**, 415 (1964).

2) For example, S. Mizushima, Y. Morino, and T. Shimanouchi, *J. Phys. Chem.*, **56**, 324 (1952).

3) T. Fujiyama, This Bulletin, **44**, 1194 (1971).

Table 1. Observed frequencies of liquid XCH_2CH_2CN

$CH_3CH_2CH_2CN$		$ClCH_2CH_2CN$		$BrCH_2CH_2CN$	
Frequency	Mode	Frequency	Mode	Frequency	Mode
100		109		95	t: δ(CCBr)
				123	g: δ(CCBr)
		167	t: δ(CCN), C	158	t: δ(CCN), C
176	g: δ(CCN), C				
188	t: δ(CCN), C	202	g: δ(CCN), C	202	g: δ(CCN), C
		300	t: δ(CCCl)	288	g: δ(CCN), B
		318	g: δ(CCN), B		
360	g: δ(CCN), B	372	t: δ(CCN), B	372	t: δ(CCN), B
373	t: δ(CCN), B				
392	t: $\delta(CCCH_3)$				
430	g: $\delta(CCCH_3)$	465	g: δ(CCCl)		
		494	t: δ(CCC), A	477	t: δ(CCC), A
529	t: δ(CCC), A			544	g: δ(CCC), A
560	g: δ(CCC), A	562	g: δ(CCC), A		
		673	g: ν(C-Cl)	581	g: ν(C-Br)
				685	t: ν(C-Br)
737				745	t: CH_2 rock.
764		752	t: ν(C-Cl)		
			t: CH_2 rock.	797	g: ν(C-CN)
		812	g: ν(C-CN)	820	t: ν(C-CN)
871		880	t: ν(C-CN)		
		908	g: CH_2 rock.	892	g: CH_2 rock.
912	(904, 916 in CS_2)				
940				954	g: CH_2 rock.
		983	g: CH_2 rock.	1003	t: CH_2 rock.
1046		1004	g: CH_2 rock.		
		1077	t: ν(C-C)	1065	t: ν(C-C)
1080					
1095					
1103					
		1116	t: CH_2 twist.	1148	t: CH_2 twist.
		1168	g: CH_2 twist.	1180	g: CH_2 twist.
1182	(1177, 1195 in CS_2)				
		1201	g: CH_2 twist.	1204	g: CH_2 twist.
		1217	t: CH_2 twist.	1224	t: CH_2 twist.
1230					
1260		1252	t: CH_2 wag.		
				1272	g: CH_2 wag.
1275					t:
1300					
		1302	g: CH_2 wag.	1316	t: CH_2 wag.
1327				1324	g: CH_2 wag.
		1332	g: CH_2 wag.		
1340			t:		
1348					
1350					
1385					
1426		1414	CH_2 bend.	1412	CH_2 bend.
1463		1447		1437	

δ; bending, ν; stretching, rock.; rocking, twist.; twisting, wag.; wagging, bend.; bending, t; *trans*, g; *gauche*, A, B, C; see the text.

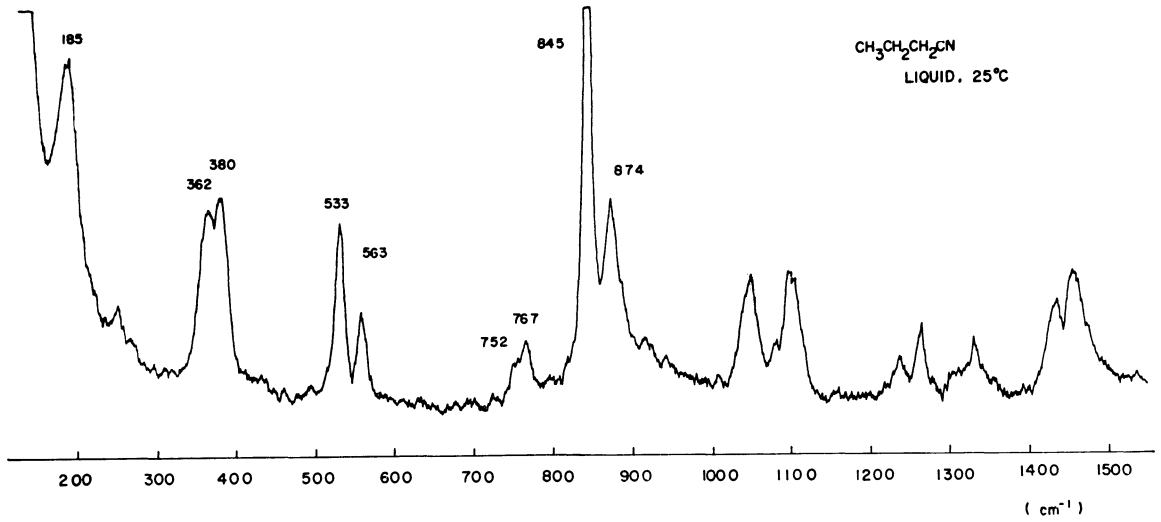

Fig. 5. Raman spectra of *n*-butyronitrile (liquid, room temperature).

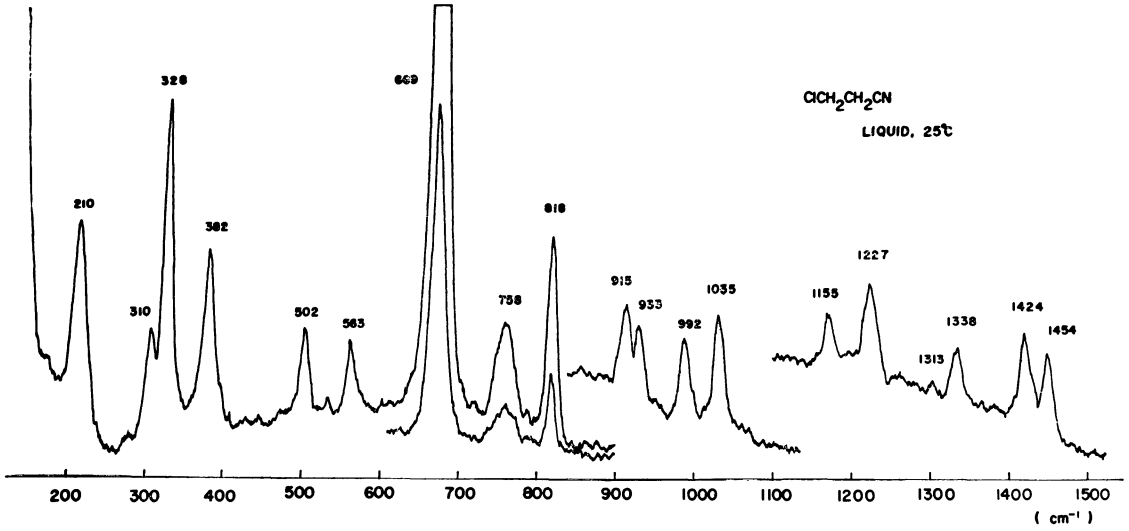

Fig. 6. Raman spectra of β-chloropropiononitrile (liquid, room temperature).

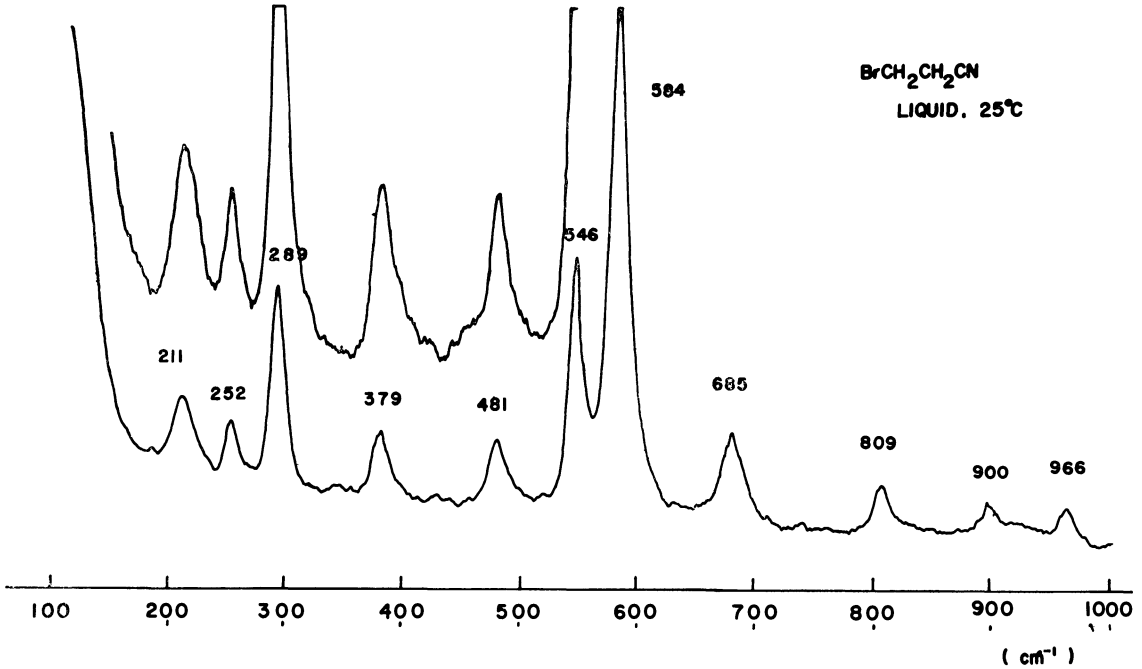

Fig. 7. Raman spectra of β-bromopropiononitrile (liquid, room temperature).

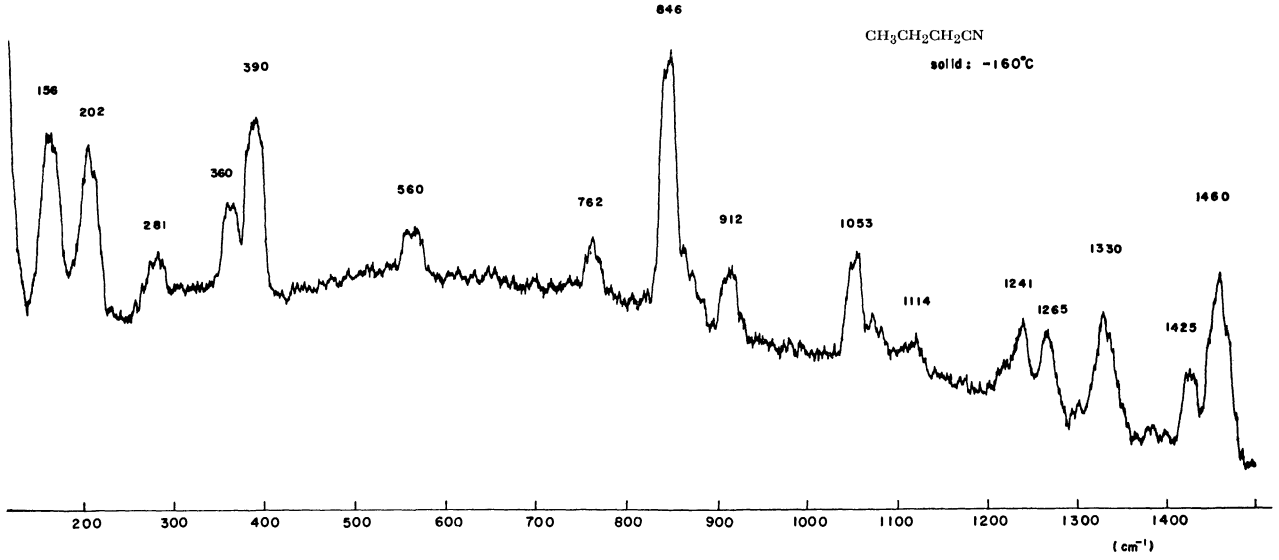

Fig. 8. Raman spectra of crystalline *n*-butyronitrile.

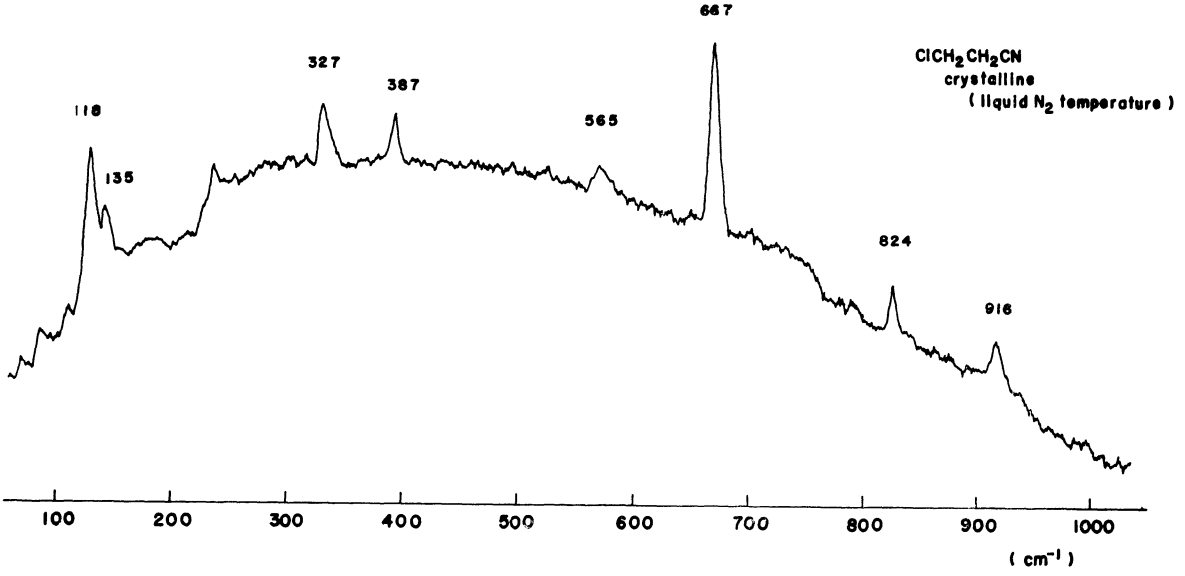

Fig. 9. Raman spectra of crystalline β-chloropropiononitrile.

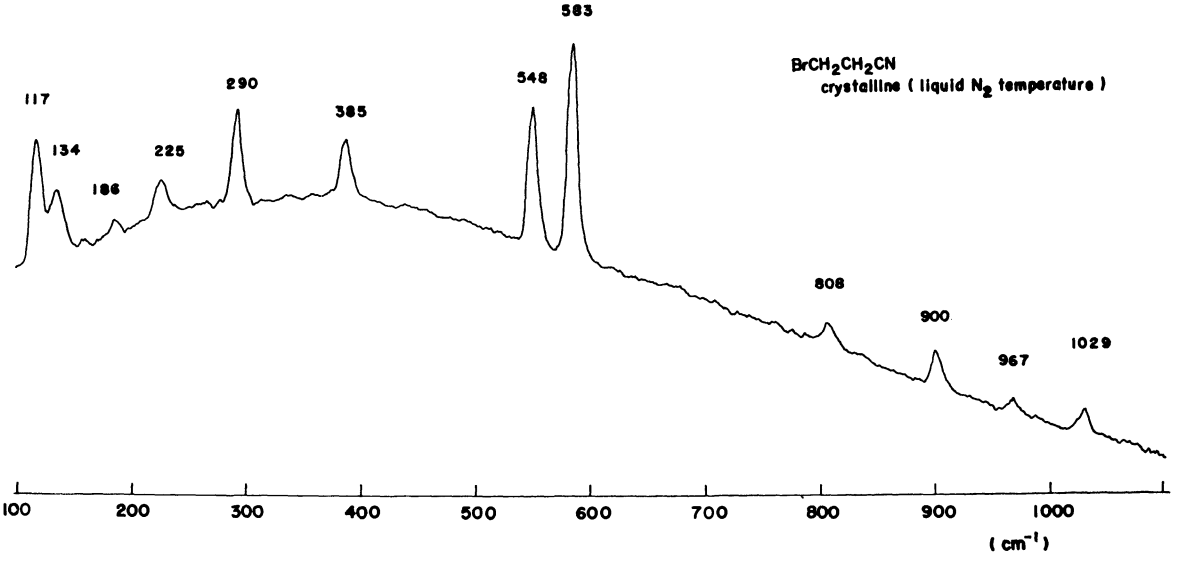

Fig. 10. Raman spectra of crystalline β-bromopropiononitrile.

trometer. A Hitachi FIS-1 far-infrared spectrometer was used for the measurement of the infrared spectra in the lower-frequency region. The Raman spectra were recorded by means of a laser Raman spectrometer which had been designed and constructed in our laboratory.[4] The spectrometer was operated under a resolution of 5–10 cm^{-1}.

The observed frequencies for the liquid sample are summarised in Table 1. The observed infrared spectra of the XCH_2CH_2CN-type molecules in the region of 1400–400 cm^{-1} are shown in Figs. 1–3. For the cases of β-chloropropiononitrile and β-bromopropiononitrile, the spectral changes observed at a low temperature (liquid nitrogen) and in a CS_2 solution are also included. The infrared spectra of succinonitrile observed at room temperature is given in Fig. 4 for comparison. It is important to emphasise that the infrared spectra at low temperatures do not correspond to those of the crystalline phase, although the liquid-nitrogen temperature is lower than the melting points of the samples. The infrared spectra were obtained from films deposited on a cooled (−196°C) potassium chloride window in a conventional low-temperature cell. The deposited film was transparent and the samples were assumed to be in the glassy state. An attempt to obtain the crystalline sample by annealing was unsuccessful.

The Raman spectra for the liquid XCH_2CH_2CN-type molecules in the region of 100–1400 cm^{-1} are shown in Figs. 5–9. The Raman spectra for the crystalline samples are shown in Figs. 6–10. In the case of Raman spectroscopy, annealing is much easier.

Normal Coordinate Treatment

For confirming the vibrational assignment, the normal frequencies of the XCH_2CH_2CN-type molecules were calculated by using the force constants obtained for a series of alkanonitriles[5] and alkylharides.[6] The method of calculation has been described in other papers.[1,7] In the present report, the results of the calculation will not, then, discussed in detail.[8]

Vibrational Assignment and Discussion

Solvent Effect. The *trans* isomer of β-chloropropiononitrile or β-bromopropiononitrile is stabilised more than the *gauche* isomer when the molecule is dissolved in a medium with a small dielectric constant, such as carbon disulfide, because the dipole moment of the *gauche* isomer is larger than that of the *trans* isomer. Thus, the solvent effect on the spectrum is very good experimental evidence for the identification of vibration bands related with rotational isomers.

Two types of absorption bands are found in Figs. 2 and 3. Their relative intensities in a CS_2 solution increase in one type and decrease in the other type. The absorption bands belonging to the former type are assigned to the *trans* isomer, and the other bands, to the *gauche* isomer. In Table 1, the *trans* and the *gauche* bands are indicated by "*t*" and "*g*" respectively.

Low-temperature Spectra. When the infrared spectra of β-chloropropiononitrile and β-bromopropiononitrile at the temperature of liquid nitrogen are compared with those at room temperature, an increase in the relative intensities is observed for the *gauche* bands, while the *trans* bands lose some of their intensities (see Figs. 2 and 3). The Raman spectra of the crystalline samples (see Figs. 6, 8, and 10) definitely determine the location of vibration bands corresponding to either the *trans or gauche* isomer.

Skeletal Deformation Vibrations. Skeletal deformation vibrations and torsional vibrations are expected to occur in the region of 100–700 cm^{-1}. The skeletal deformation vibrations of alkanonitriles can be conveniently classified into three groups.[3] We call them the A, B, and C groups. The B group is composed of pure C–C≡N bending vibrations which occur in the region of 300–400 cm^{-1} with strong intensities. The frequencies related to this vibrational mode are hardly affected by the change in the geometry of the rotational isomers. The A and C groups are composed of the coupled vibrations of C–C≡N bending and C–C–C (or C–C–X) deformation modes, which are localized in the regions of 500—600 cm^{-1} and 100—200 cm^{-1} respectively. The A-type deformation vibrations are good characteristic frequencies with respect to the rotational isomerism. In this group, the vibration of a *trans* isomer has a lower frequency than that of a *gauche* isomer. On the other hand, the C-type deformation-vibration frequencies exhibit rather irregular behaviour because of their coupling with torsional vibrations. In the Raman spectra of Figs. 5—10, we see the bands corresponding to the skeletal deformation vibrations of the A, B, and C types. For example, the Raman bands at 563 and 533 cm^{-1} of *n*-butyronitrile correspond to the A-type deformation vibrations, while the bands at 380 and 362 cm^{-1} and the bands at 185 cm^{-1} correspond, respectively, to the B- and the C-type deformation vibrations.

The spectral changes in the skeletal deformation vibrations on passing from the liquid to the crystalline phase give most reliable experimental evidence for the assignment of the vibration frequencies to the rotational isomers. In the cases of β-chloro- and β-bromopropiononitriles, *trans* and *gauche* bands can easily be identified by referring to the empirical rule of a stretching-vibration frequency of a carbon-halogen bond.[9] A comparison of the spectra in Figs. 6 and 8 shows that the C–Cl stretching vibration at 758 cm^{-1} and the skeletal deformation vibration at 502 cm^{-1} of β-chloropropiononitrile belong to one rotational isomer, while the band at 669 cm^{-1} (the C–Cl stretching) and the band at 563 cm^{-1} (the skeletal deformation) belong to the other rotational isomer. As the C–Cl stretching vibration at 758 cm^{-1} originates from the *trans* isomer, the band at 502 cm^{-1} is assigned to the A-type skeletal deformation vibra-

4) T. Fujiyama and M. Tasumi, *Bunko Kenkyu*, **20**, 28 (1971).
5) T. Fujiyama, This Bulletin, **44**, 89 (1971).
6) M. Tasumi and T. Shimanouchi, *Polym. J.*, **2**, 66 (1971).
7) T. Shimanouchi, *J. Chem. Phys.*, **17**, 245, 734, 848 (1949).
8) The detailed results of the calculation are available upon request.
9) S. Mizushima, T. Shimanouchi, K. Nakamura, M. Hayashi, and T. Tsuchiya, *J. Chem. Phys.*, **26**, 970 (1957).

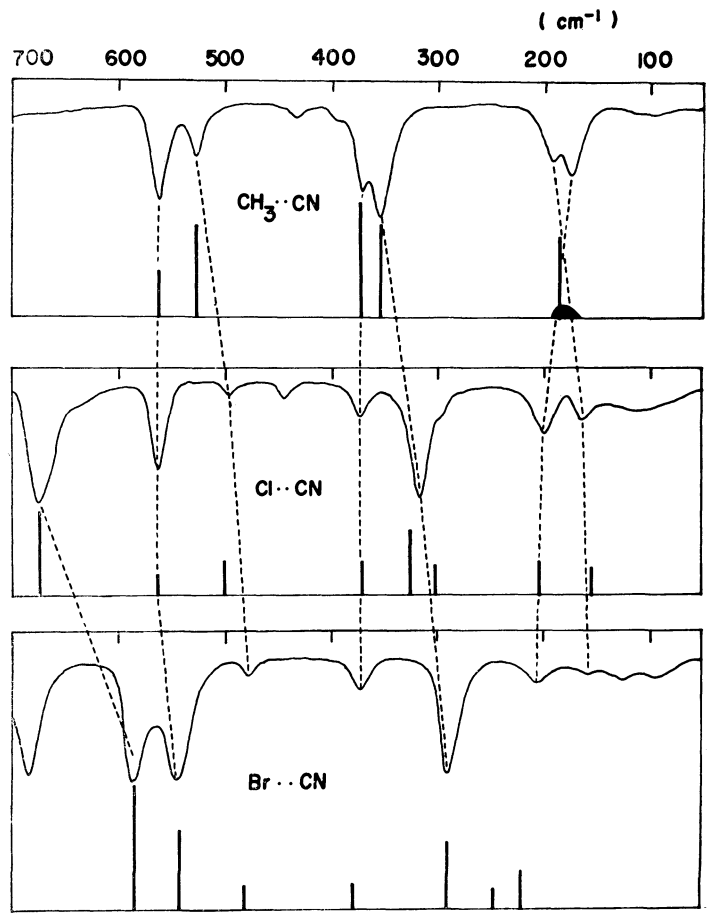

Fig. 11. Comparison of skeletal deformation vibrations of XCH_2CH_2CN (upper curve: infrared, lower bar: Raman).

tion of the *trans* isomer. In the same way, the band at 563 cm^{-1} corresponds to the A-type deformation vibration of the *gauche* isomer, because the 669 cm^{-1} band can definitely be assigned to the C–Cl stretching vibration of the *gauche* isomer. The same situation holds for the bands at 685 and 481 cm^{-1} and for the bands at 584 and 546 cm^{-1} in the case of β-bromopropiononitrile (see Figs. 7 and 10). In the same way, the bands due to the skeletal deformation vibrations can easily be classified for each rotational isomer. The results are summarised in Table 1.

In the case of *n*-butyronitrile, the frequency assignments are based upon the results of normal coordinate treatment and the results of the vibrational assignment for β-chloro- and β-bromopropiononitriles. Two A-type skeletal deformation bands are found, at 533 and at 563 cm^{-1} (see Fig.5). The vibration frequencies are calculated to be 562 cm^{-1} for the *gauche* isomer and 513 cm^{-1} for the *trans* isomer. Thus, the observed frequenciy of 563 cm^{-1} is assigned to the *gauche* isomer, while that of 533 cm^{-1} is assigned to the *trans* isomer. These assignments correspond to those of β-chloro- and β-bromopropiononitrile very well.

The relative intensities of the A-type bands present another confirmation of the assignment. In Fig.11, the infrared and Raman spectra of the XCH_2CH_2CN-type molecules are compared. The relative intensity of the A-type molecules are compared. The intensity of the A-type band of the *gauche* isomer is stronger than that of the *trans* isomer in the infrared spectra, while the *gauche* band decreases in relative intensity in the Raman spectra. This may correspond to the situation that an A-type band of a *trans*-isomer is infrared-inactive if a molecule is of the XCH_2-CH_2X type.

Other Vibrations. The assignments of the other vibrations, namely, the CH_2 deformation vibrations, the C–C stretching vibrations, and the C–CN stretching vibrations, are rather straightforward with the help of the well-established frequency assignments for 1,2-disubstituted ethanes and the results of the calculated normal frequencies. The results are summarised in Table 1. As for *n*-butyronitrile, the identification of the *trans* and *gauche* bands were not definite in this region and, therefore, the observed frequencies were not assigned.

Rotational Isomer. For the three molecules studied, it is ascertained that the *trans* and the *gauche* isomers coexist in the liquid phase. The energy differences between the two rotational isomers in the liquid phase were observed to be about 640, 500, and 420 cal/mol for β-bromopropiononitrile, β-chloropropiononitrile, and *n*-butyronitrile respectively, the *gauche* isomers being more stable. The values of the energy difference are preliminary; a detailed discussion will be reported elsewhere.

The Raman spectra of the crystalline samples show that the *gauche* isomers remain in the crystalline state at the temperature of liquid-nitrogen. The conclusion for *n*-butyronitrile contradicts that of Reference.[10] There was no spectral evidence for the coexistence of the *trans* and *gauche* isomers in the solid state.

The author wishes to acknowledge helpful correspondence with Dr. T. Shimanouchi and Dr. I. Suzuki of The University of Tokyo.

10) J. J. Lucier, E. C. Tuazon, and F. F. Bentley, *Spectrochim. Acta*, **24**, 771 (1968).

BULLETIN OF THE CHEMICAL SOCIETY OF JAPAN, VOL. 44, 3323—3328 (1971)

Theoretical and Experimental Considerations of the Direct Photo-Isomerization and Chemistry of 1,3-Pentadiene

Kozo INUZUKA* and Ralph S. BECKER

Department of Chemistry, University of Houston, Houston, Texas 77004, U. S. A.

(Received June 24, 1971)

Potential energy curves as a function of the angle of twist around single and double bonds have been calculated for piperylene (1,3-pentadiene). Also, direct-excitation *cis*→*trans* photoisomerization and *trans*→methylcyclobutene photochemistry have been investigated as a function of the temperature. The theoretical analysis strongly indicates that the cyclobutene is formed photochemically from the *trans-s-cis* isomer which is created thermally from the *trans*-isomer in the ground state (not by photoisomerization). The temperature-dependency data support this conclusion. The theoretical data also indicate that there is a small barrier to photoisomerization around the double bond in the first excited singlet (and triplet) state. The temperature-dependency data also support this conclusion. The potential energy curves are in harmony with the known emission (none exists), photoisomerization, and internal-conversion data for the *cis*- and *trans*-piperylenes. The emission properties of model cyclic diene steroids are compared with those expected from linear dienes, and the emission results of the former are interpreted within the theoretical framework developed.

The direct photoirradiation of a cyclohexane solution of piperylene at 2537 Å results in the formation of 3-methylcyclobutene and *cis-trans* isomerization as the main reactions.[1] On the other hand, the sensitized photoisomerization of piperylene has also been studied in detail using a variety of sensitizers.[2-5] The experimental data show that there is a photostationary equilibrium between *cis*- and *trans*-piperylene, and also that other photoproducts are produced.[3] The concentration ratio of *cis*- and *trans*-isomers depends on the lowest triplet energy of the sensitizer.[2,5] The theoretical consideration of the photochemical mechanisms appropriate to piperylene are more difficult than in the case of butadiene. The introduction of the methyl group in the terminal carbon atom brings about a steric effect in piperylene, and also the methyl group may have some inductive and resonance effects on the π-electron system of the molecule. In this investigation we made the general assumption that the substitution of a methyl group into the terminal methylene of butadiene does not produce any significant effect on the π-electron structure of butadiene. Therefore, calculated results of the potential energy curves of butadiene can be used to explain the mechanism of the *cis-trans* isomerization of piperylene. However, we have specifically included the non-bonded interaction effect between the methyl group and the other atoms of piperylene at the *cis*-side, at the *trans*-side, and for the form twisted by 90 around the double bond (*vide infra*).

Methods of Calculation

The following numerical values[6] were used for the skeletal structure of *trans*-1,3-butadiene: 1.339 Å for the carbon double bond and 1.480 Å for the central single bond. The value of 123° was assigned to the bond angle, $\angle$CCC. The skeletal structure only was taken into account. All the calculations were carried out within the framework of the general semiempirical SCF-MO-CI method, and the Pariser-Parr approximation was used for the electron repulsion integrals. The resonance integral for the nearest neighbor carbon atom, β_{CC} was treated as a parameter and adjusted to fit the calculated lowest π,π^* state

* Present address of K. I., Department of Applied Science, Tokyo, Electrical Engineering College, Kanda, Chiyoda-ku, Tokyo, Japan. U. S. A. reprint requests should be directed to R. S. B.

1) a) R. Srinivasan, *J. Amer. Chem. Soc.*, **84**, 4141 (1962). b) S. Boue and R. Srinivasan, *ibid.*, **92**, 3226 (1970).

2) G. S. Hammond, J. Saltiel, A. A. Lamola, N. J. Turro, J. S. Bradshaw, D. O. Cowan, R. C. Counsell, V. Vogt, and C. Dalton, *ibid.*, **86**, 3197 (1964).

3) G. S. Hammond, N. J. Turro, and R. S. H. Liu, *ibid.*, **28**, 3297 (1963).

4) G. S. Hammond, N. J. Turro, and P. A. Leermakers, *ibid.*, **83**, 2396 (1962).

5) N. J. Turro, *Photochem. Photobiol.*, **9**, 555 (1969).

6) B. P. Stoicheff, "Advances in Spectroscopy," **1**, (1959), Wiley-Interscience, New York, p. 148.

7) R. Pariser and R. G. Parr, *J. Chem. Phys.*, **21**, 466 (1953).

energy to the experimental value. The β_{CC} for the twisted bond was obtained from the following equation:

$$\beta(\theta) = \beta_{CC} \cos\theta \quad (1)$$

where θ is the angle of twist. All the penetration terms were neglected. In the present paper, calculations concerning the single-bond twist and the terminal double-bond twist were carried out.

In the case of double-bond twisting, the effect of the bond twist upon the electron repulsion integrals was taken into account (*vide infra*). In the case of single-bond twisting, the foregoing concern was neglected because such neglect did not have any significant effect upon the final result. We calculated the state energies of the molecule as it is twisted about the single or double bond using the SCF–MO's obtained. All singly-excited configuration interactions were taken into account (complete single excited-state configurational interaction). Furthermore, in the case of the double-bond twist, all doubly-excited configuration interactions were also taken into account (complete single and double excited-state configurational interaction). The total π-electron energy, E, in the ground state is obtained by:

$$E = E_\pi + E_n \quad (2)$$

where E_π is the energy of the π electrons and where E_n is an effective nuclear interaction term given by Pople:[8]

$$E_n = \sum_{\mu<\nu} Z_\mu Z_\nu / R_{\mu\nu} \quad (3)$$

Z_μ is the effective charge of the atom, μ; unity is used for Z_μ in the present calculation. The potential energy curves for the ground state are obtained by the calculation of the total π electron energy, E, as a function of the angle of twist. The potential energy curves of the excited states, as a function of the angle of twist, are obtained by superimposing the state energies upon the potential curve of the ground state.

Before the calculation of the twisting around the double bond of 1,3-butadiene was carried out, the general SCF–MO–CI method was used to calculate the shape of the potential energy curves for twisted ethylene in order to verify its utility. The calculated potential energy curve of the triplet state[9,10] is in harmony with the experimental results on the photoisomerization of *cis* and *trans*-1,2-dichloroethylene. To produce such potential minima in the excited states of ethylene at 90° (within the framework of the semiempirical SCF–MO–CI with zero differential overlap using the point charge atomic repulsion integral), the following function was used for the atomic repulsion integral of the atoms of the terminal double bond:[12]

$$\gamma_{C=C}(\theta) = \gamma_{C=C}(0) + A(1 - \cos\theta) \quad (4)$$

where the first term corresponds to the planar atomic repulsion integral value, where θ is the angle of twist, and where A is a parameter. All the other atomic repulsion integrals were calculated by the Pariser-Parr equation without any correction. In addition, the twisting around any bond will result in the introduction of $2p\sigma$ components into the atomic repulsion integrals between the *non-nearest* neighbor atoms.[12] This effect will make an atomic repulsion integral value larger than the one with only a pure $2p\pi$ component corresponding to the same bond distance. To take this effect into account, an off-center position was assumed for the location of the center of the atoms involved. As the simplest method, the off-center positions were taken on the same side of the $2p\pi$ orbitals and by some small distance off the center of the atom along the $2p\pi$ atomic-orbital axis. This off-center distance was looked upon as the parameter. The calculation was carried out over the angles from 0° (planar form) to 85° (the nearperpendicular form).

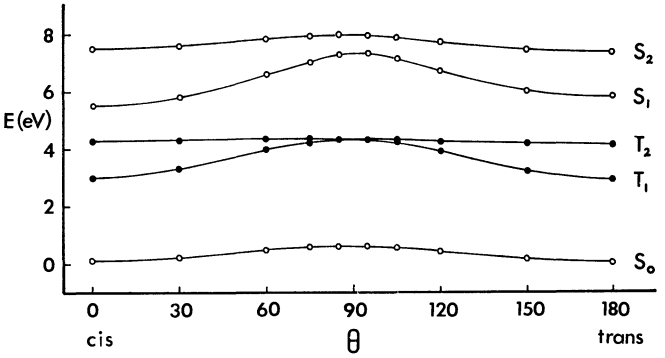

Fig. 1. Potential energy curves for ground and excited states of 1,3-butadiene as a function of angle of twist around the single bond using Eq. (1) ($\beta_{C=C} = -2.70$ eV and $\beta_{C-C} = -2.00$ eV) and including all singly excited configurations.

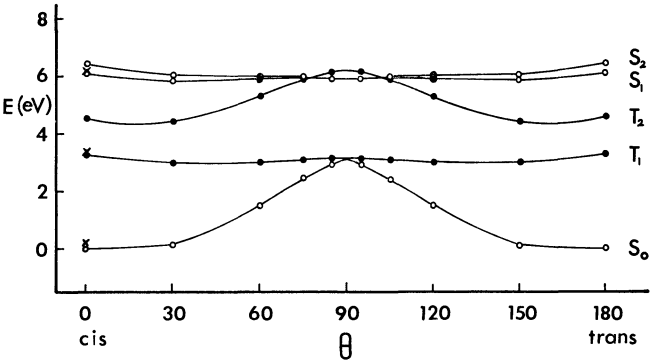

Fig. 2. Potential energy curves for ground and excited states of 1,3-butadiene as a function of angle of twist around a double bond using Eqs. (1) ($\beta_{C-C} = -2.00$ eV and $\beta_{C=C} = -2.70$ eV), (4) ($\gamma_{C=C} = 7.503$ eV and $A = 0.5$ eV), an off-center value of $1.0A$ and including all singly and doubly excited configurations. The X points are the energy values including non-bonding interaction (see text).

8) J. A. Pople, *Trans. Faraday Soc.*, **49**, 1375 (1953).
9) R. G. Parr and B. L. Crawford, *J. Chem. Phys.*, **16**, 526 (1948).
10) R. S. Mulliken and C. C. J. Roothaan, *Chem. Rev.*, **41**, 219 (1947).
11) Z. R. Grabowski and A. Bylina, *Trans. Faraday Soc.*, **60**, 1131 (1969).
12) R. S. Becker, K. Inuzuka, and J. King, *J. Chem. Phys.*, **52**, 5164 (1970); R. S. Becker, K. Inuzuka, J. King, and D. E. Balke, *J. Amer. Chem. Soc.*, **93**, 43 (1971).

The results calculated using these approaches are shown in Figs. 1 and 2.

Results and Discussion

The potential energy curves of 1,3-butadiene twisted around the central bond are shown in Fig. 1.

The potential energy curves resulting from twisting around the double bond are shown in Fig. 2, where these potential energy curves are shown to be symmetric with respect to the twisting angle, 90° since all effects of the hydrogen atoms are neglected. These potential energy curves show that the energies of the T_1, S_1, and S_2 states decrease with an increase in the twisting angle around the double bond. The potential curve for T_1 is almost degenerate with the ground state at 90°. The potential energy curve, T_2, has a maximum at 90°, and it crosses the two potential curves S_1 and S_2 near 80°. The introduction of a methyl group in the position of the terminal hydrogen atom of butadiene will make the potential energy curves of butadiene asymmetric with respect to 90°. The spectroscopic data for the S_1 and T_1 of *cis*- and *trans*-piperylene were used to make a rough estimation of the shape of the potential energy curves of piperylene on the *cis*- and *trans*-sides. The absorption spectra of *cis*- and *trans*-piperylene[13] in an *n*-heptane solution have the $S_0 \rightarrow S_1$ band maxima at 225 nm for the *cis*-form and at 222 nm for the *trans*-form. The difference between the band maximum of the isomers is about 0.1 eV. From the S–T absorption data,[14] the $S_0 \rightarrow T_1$ transition energy of the *trans*-form may be seen to be higher than that of the *cis*-form by about 0.1 eV. The non-bonding interaction energies between the methyl hydrogen atoms and the other atoms of the residual part at the twisting angle, 0, 90, and 180°, using 180° (*trans*) as a reference, were calculated by using Bartell's equations.[15] These values reached their maxima at the *cis*-side (0°) and their minima at 90°. These calculated results show that the non-bonding interaction energy between the methyl group and the residual part of the molecule is negligible for the *trans* (180°) and perpendicular (90°) forms. The non-bonding energy value gave, at most, an energy increase of 0.2 eV for the *cis*-form. As these calculated values correspond to the maximum interaction energy value for each form, the actual non-bonding interaction energy value may be smaller than the value calculated. This calculated value, 0.2 eV, can be superimposed on the calculated ground-state and excited-state potential energy curves of butadiene at 0° (*cis*-form). A consideration of the spectroscopic differences for the $S_0 \rightarrow S_1$ (0.1 eV) and $S_0 \rightarrow T_1$ (0.1 eV) transitions and the non-bonding interaction energy suggests that the lowest excited singlet and triplet states of piperlylene are higher by $\leq$0.1 eV on the *cis*-side than on the *trans*-side (Fig. 2). Therefore, the potential energy curves will be asymmetric around 90° and isomerization should be easier from the *cis*-side than from the *trans*-side (*vide infra*).

The direct irradiation of a mixture of *cis*- and *trans*-piperylene[1] initially gives rise to an increase in the *cis*-piperylene, while the *trans*-piperylene decreases. The 3-methylcyclobutene originates primarily from the *trans* isomer[1] as:

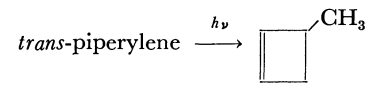

(5)

The following reaction[1] also occurs concurrently:

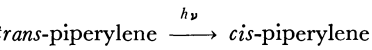

(6)

The irradiation of 1,3-butadiene is known to give rise to cyclobutene.[1,16] This process apparently occurs from the excited singlet state of 1,3-butadiene.[16] This suggestion may also be applicable to the process of the cyclization of piperylene, because the structure of piperylene is parallel to that of 1,3-butadiene. Figure 2 shows that, in the ground-state, twisting around the terminal double bond has a very high potential barrier near 90°. This suggests that the twisting around the terminal double bond of butadiene is very difficult because of the high activation energy. However, the potential curves for the lowest excited singlet and triplet states show that there is a shallow minimum at 30–50° and a small barrier (~0.03 eV) beyond 60° in S_1, and that there is a shallow minimum at 35–60° and a low barrier (~0.1 eV) near 90° in T_1 (Fig. 2). The numerical values for the potential minimum and the barrier height in S_0, S_1, and T_1, and the other states depend on the choice of the parameters; that is, the off-center values, A in Eq. (4) and the approximation used for the electron repulsion integral, *etc.* However, within our present procedure, changes in the magnitude of the parameters for the off-center value and the A value in Eq. (4) result in potential energy curves similar in shape to those in Fig. 2. Those results suggest that a twisted form around the terminal double bond is more stable than the planar forms in S_1 and T_1. Also, Fig. 2 shows that the potential energy curve of T_1 is almost degenerate with that of the ground state, at 90°.[17] This situation in butadiene is very similar to that of piperylene with a slight modification resulting from a slight asymmetry around 90° (*vide supra*). Srinivasan[1] proposed that 3-methylcyclobutene (III) comes primarily from *trans*-piperylene (I). The production of 3-methylcyclobutene from *trans*-piperylene could arise as follows:

13) L. E. Jacobs and J. R. Platt, *J. Chem. Phys.*, **16**, 1137 (1948).
14) R. E. Kellogg and W. T. Simpson, *J. Amer. Chem. Soc.*, **87**, 4230 (1965).
15) L. S. Bartell, *J. Chem. Phys.*, **32**, 827 (1960).
16) R. Srinivasan, *J. Amer. Chem. Soc.*, **85**, 4045 (1963).
17) The calculation was carried out through 0 to 85°. The potential energy curves of both states, S_0 and T_1 are not perfectly degenerated at 85°. Recently Eleveth [*Chem. Phys. Lett.*, **3**, 122 (1969)] carried out the calculation of the state energies of *trans*-butadiene at two twisted angles, 0 and 90°, using the different approach. His result shows that the both states, S_0 and T_1 are nearly degenerate at 90° but they are not perfectly degenerate.

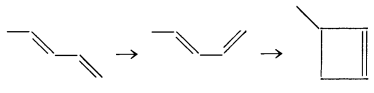

(7)

I II III

The very small production of 3-methylcyclobutene (III) originating from *cis*-piperylene (IV) could occur by the following process:

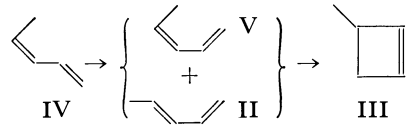

(8)

IV II III

We will now examine the nature of the steps in the reaction (7). Figure 1 suggests that *s-cis*↔*s-trans* isomerization around a single bond of butadiene in the lowest excited states, S_1 and T_1 is difficult. Although there is a potential barrier for *s-cis*↔*s-trans* isomerization in the ground state, its height is quite low relative to those in S_1 and T_1. Figure 1 will be, in principle, also correct for the *s-cis*↔*s-trans* isomerization of piperylene around its single bond. These results thus clearly suggest that (1) the *trans-s-cis* piperylene (II) is not produced from *trans*-piperylene in an excited state, but in the ground state and, (2) that 3-methylcyclobutene is produced from II (*versus* I) photochemically. Furthermore, other recent theoretical research[18] suggests that the concentration of *s-cis*-butadiene in *s-trans* is about 3.2% at room temperature and that its concentration decreases on a decrease in the temperature. Therefore, *trans-s-trans*-piperylene in the ground state will be considered to be in thermodynamic equilibrium with the *trans-s-cis*-piperylene (II).

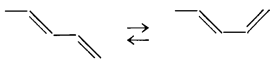

(9)

I II

If *cis*-piperylene were to be the reactant, then reaction (8) would be the appropriate one to consider. The *trans-s-cis*-piperylene (II) is not expected to be produced from IV in the ground state because of the high energy requirement for double-bond isomerization. The *cis-s-cis*-piperylene (V) is not expected to be formed from IV in an excited state for reasons parallel to those given above concerning single-bond isomerization. Furthermore, because of the methyl-hydrogen steric interaction, the equilibrium concentration of the *cis-s-cis*-piperylene (V) produced from IV in the ground state is expected to be very small. Therefore, V will be of very little consequence in the production of the cyclobutene compound. It is potentially possible that (II) could be produced in the excited state of *cis*-piperylene, although the barrier to single-bond isomerization is present. This would involve excited-state double-bond isomerization, followed by a particular coupling, if internal conversion occurred (hot ground state *s-cis*↔*s-trans*); however, this reaction is not expected to occur with any appreciable efficiency. Thus, the formation of 3-methylcyclobutene from *cis*-piperylene is relatively unlikely, and the principal reactant is probably *trans*-piperylene *via* the intermediate (II). The relative importance of the *cis* and *trans* isomers in terms of the quantity of cyclobutene produced from them is in agreement with very recent quantitative findings[1b] published after this investigation was completed. The quantum yield of cyclobutene from the *trans* isomer is ~10 times that from the *cis* isomer.

Further verification exists for the source and mechanism proposed above for the production of the cyclobutene. According to our potential energy curves (Fig. 1), a *s-cis*↔*s-trans* equilibrium in the ground state would depend upon the temperature. That is, the concentration of *trans-s-cis*-piperylene (II) would decrease at low temperatures. Accordingly, the formation of the 3-methylcyclobutene photochemically produced should also *decrease at low temperatures*. The results of the direct irradiation of *cis*- and *trans*-piperylene[19] at different temperatures are shown in Table 1. In this experiment, the formation of 3-methylbutene is found from *trans*-piperylene, but essentially none is observed from *cis*-piperylene. The

Table 1. The photochemistry of piperylenes as a function of temperature

Compound irradiated[a]	Temperature	Irradiation time	% conc.	3-methylcyclobutene
cis-piperylene	21°C	180 min	8.1 (trans)	essentially none observed
	−76°C	180 min	4.0 (trans)	essentially none observed
	21°C[d]	120 min	3.8 (trans)	essentially none observed
	−76°C[d]	120 min	2.1 (trans)	essentially none observed
trans-piperylene	21°C	100 min	—[b]	4.6×[c]
	−76°C	100 min	—[b]	1.5×[c]

a) In *trans*-1,2-dimethylcyclohexane by 200 W mercury arc lamp with Corning 9—54 filter (~220 nm cut-off, >70% transmission 254 nm).

b) It was not possible to determine the quantity of the *cis*-isomer produced. Quantities of *cis* and *trans* isomer determined by gas chromatography.

c) Numbers indicate quantity cyclobutene produced times that of a standard reference signal as determined by gas chromatography.

d) This represents a duplicate run under different experimental arrangements such that the absolute percent concentrations are different. However, note that ratio of the percent concentrations at the two temperatures is the same as that for the preceding set of data.

18) L. M. Sverdlow and E. N. Bolotina, *Russ. J. Phys. Chem.*, **36**, 1502 (1962).

19) J. Guillory, Phillips Pet. Co., Private Communication (1970).

experiment shows that the formation of 3-methylcyclobutene does *decrease with a decrease in the temperature.* Recently, van der Lugt and Oosterhoff[20] performed theoretical calculations concerning the cyclization of *s-cis*-butadiene using a Valence Bond Procedure. Judging from their results,[20] the photocyclization of *s-cis*-butadiene can occur relatively easily from the *s-cis* form in the excited singlet state. According to our experimental and theoretical data (those of others[18,20]), the rate-determining step for the production of the cyclobutene from the *trans* isomer could well involve the formation of II from the *ground state* of *trans*-piperylene (Eqs. (7) and (9)). Also, it is possible that a barrier could exist in the excited state similar to that found for butadiene.[20] An explanation for the difference in the amount of the cyclobutene from the *cis* and *trans* isomers was given earlier.

On the basis of the above discussion and reaction (9), it can be said that, when II is excited and the cyclobutene (III) is produced, the equilibrium between *trans-s-trans-* (I) and *trans-s-cis*-piperylene (II) should be reestablished. Thus, except for minor side reactions, eventually all of the *trans-s-trans*-piperylene (I) should be converted into (II) and the (II) into the cyclobutene (III). This is in agreement with the trend seen experimentally.[1]

In the direct photoisomerization of the piperylene double bond, *cis-trans* isomerization is another important process. The *cis*↔*trans* isomerization of piperylene corresponds to the twisting around the terminal double bond (of butadiene). Figure 2 shows that the twisting of the double bond of butadiene can occur in the lowest singlet state. However, shallow potential energy minima exist at 30–50 and 150–120°, and small potential barriers are present at more highly twisted angles (*cf.* Fig. 2 and above). In the case of butadiene, the potential energy curves are symmetric with respect to 90° if the non-bonding interaction of all the H atoms is neglected. However, in the case of piperylene the effect of the methyl group should make the potential energy curve asymmetric with respect to 90° (*cf.* above and Fig. 2). Thus, we would predict *a temperature dependence for photoisomerization.* Our experimental results (Table 1) show that the *cis*-piperylene→*trans*-piperylene photoisomerization does occur *and that it is temperature-dependent.* Also, the photoisomerization of *trans*-piperylene→*cis*-piperylene can be expected, though it is 20% less than in the *cis*→*trans* process.[1b] These facts suggest that the *cis*-piperylene→*trans*-piperylene isomerization is slightly dominant over the reverse reaction. Therefore, the potential energy curve of the lowest singlet state of piperylene could be slightly asymmetric with respect to 90°. Our potential energy curves do show an asymmetry that would be in agreement with the experimental results (*cf.* above and Fig. 2).

In addition to the formation of the cyclobutene (III), small quantities of 1,3-dimethylcyclopropene have been observed.[1b] However, the quantity is very small compared with the amount of isomerization or even the amount of cyclobutene that results, particularly in the case of the *trans*-piperylene. It has been proposed that cyclopropylmethylene biradical intermediates are important in explaining the formation of the cyclopropene.[1b] Also, it has been proposed that these same intermediates are important,[1b] or are perhaps important,[21] in the photoisomerization of 1,3-dienes. It is salient to point out that, in one case,[1b] the difference in the photochemical reactivity of the *cis* and *trans* piperylenes was based on the fact that no barrier existed between the planar forms and the 90°-twisted forms in the excited singlet state. However, our experimental data (Table 1) strongly suggest that this is not true, at least for the *cis* isomer. Furthermore, our theoretical results indicate that a small barrier exists for twisting in the excited singlet state for both the *cis* and *trans* isomers (*vide supra*). In addition, some asymmetry appears to exist in the potential energy curves (*vide supra*). Finally, very recently serious doubt has been cast on the proposals that cyclopropylmethylene biradical intermediates are important in the photo *cis-trans* isomerization.[22] This doubt has been based on the differences in the concentration dependences for the isomerizations and for the production of the cyclopropenes.[1b]

There are four kinds of processes for the conversion of S_1 to S_0: fluorescence, internal conversion, intersystem crossing (with accompanying emission, internal conversion and photochemistry in triplet states), and photochemistry in S_1. No one has observed emission from a linear 1,3-diene at room temperature; this situation is very similar to that of acrolein, where the total quantum yield of emission is ~0.01[12] (this point will be discussed more later). The total photochemical yields in solution are only about 0.10.[1b] Further, there is a strong indication that ϕ_{IS} is less than 0.1.[21] Thus, in piperylene, internal conversion directly from S_1 to S_0 must have a high quantum yield (~0.80). Figure 2 suggests that fluorescence is unlikely since torsional twisting has essentially no barrier and this latter process is expected to be fast (faster than fluorescence). The spin-orbit coupling is expected to be small in the carbon-hydrogen system except in special cases.[23] Finally, Fig. 2 shows that, as the angle of twist increases, the energy separation between S_1 and S_0 decreases. Thus, the probability of internal conversion *via* vibronic coupling increases as the angle of twist increases from 0 toward 90°. Therefore, the foregoing considerations provide a good qualitative understanding of the experimental results obtained for piperylene. Pertinent to the discussion above, if internal conversion and photochemistry could be restricted, then fluorescence and/or phosphorescence should be observable. Although acrolein exhibits very little emission,[12] model conjugated keto steroids show ϕ_p values of 0.2—0.3.[24]

20) W. Th. A. M. van der Lugt and L. J. Oosterhoff, *J. Amer. Chem. Soc.*, **91**, 6042 (1969).

21) J. Saltiel, L. Metts, and M. Wrighton, *ibid.*, **92**, 3227 (1970).

22) J. Saltiel, private communication, 1971.

23) R. S. Becker, "Theory and Interpretation of Fluorescence and Phosphorescence," Wiley-Interscience New York, N. Y. (1969).

24) G. Marsh, D. R. Kearns, and K. Schaffner, *Helv. Chem. Acta*, **51**, 1890 (1968).

This has been interpreted in terms of the inability of such molecules to isomerize and to torsionally dissipate all of the energy; furthermore, spin-orbit coupling exists as well as vibronic coupling between the $T_{n,\pi}^*$ and $T_{\pi,\pi}^*$ states.[12] Furthermore, ergosterol and lumisterol$_2$ show fluorescence at 80°K.[25] Each of these molecules contain saturated ring systems fused to a cyclohexadiene ring. In these latter two cases, isomerization around a double bond in the excited singlet state should be prohibited and the rigidly bonded steroidal framework should prevent any noticeable torsional dissipation of energy. Thus, a potential energy minimum should exist at some small finite angle and fluorescence should occur. This is in agreement with the experimental results.[25] However, it should be noted that temperature and/or viscosity effects appear to be important since the foregoing steroids apparently do not emit at room temperature[25] even though the quantum yield of photochemistry is less than 1. Studies concerning these steroids and other polyenes are in progress.

Summary

Potential energy curves as a function of the angle of twist around single and double bonds have been calculated for 1,3-butadiene. In addition, these have been modified to apply to piperylene (1,3-pentadiene) by taking into account non-bonding interactions involving the methyl group. The results indicate that substantially higher barriers exist for twisting a single bond in the first excited singlet and triplet states than in the ground state. On the other hand, substantially lower barriers exist in the first excited singlet and triplet states for double-bond twisting compared to that in the ground state. On the basis of these and other considerations, we predicted that (1) cyclobutene should be photochemically produced from the *trans*-piperylene *via* the *trans-s-cis* isomer, (2) a temperature dependence should exist for cyclobutene production from the *trans* isomer because of a barrier to *s-cis-trans* isomerization in the ground state, and a possible barrier in the excited state and (3) very little cyclobutene should be produced from the *cis*-piperylene. All of these predictions are in harmony with the experimental results.

On the basis of the shape of the potential energy curves in the excited singlet (and triplet) states, we predicted that a barrier should exist for the inter photoisomerization of *cis* and *trans* piperylenes. This is verified, at least in part, by the existence of a temperature dependence for the photo *cis*→*trans* process.

On the basis of several pieces of evidence, it does not appear to be necessary to invoke cyclopropylmethylene biradicals as intermediates in the photo *cis-trans* isomerizations of 1,3-dienes.

25) E. Havinga, R. J. Dekock, and M. P. Rappoldt, *Tetrahedron*, **11**, 276 (1969).

BULLETIN OF THE CHEMICAL SOCIETY OF JAPAN, VOL. 44, 3328—3335 (1971)

Charge-Transfer and Proton-Transfer in the Formation of Molecular Complexes. I. The Complex Isomerization of Some Anilinium Picrates by Melting

Gunzi SAITO and Yoshio MATSUNAGA

Department of Chemistry, Faculty of Science, Hokkaido University, Sapporo

(Received July 3, 1971)

o-Chloroaniline, *m*-nitroaniline, 3-nitro-4-methylaniline, and *N,N*-dimethylamino-*p*-benzaldehyde form true phenolates with picric acid. However, their electronic and vibrational spectra were found to be drastically modified by melting. The appearance of a new electronic absorption located near the place where the corresponding *s*-trinitrobenzene complex exhibits the charge-transfer band is noted above the melting point. At the same time, the vibrational bands due to the anilinium ion observed at room temperature are replaced by those due to the aniline. On the basis of these observations, it was concluded that complex isomerization from a true phenolate to a charge-transfer complex takes place by melting in these cases. On the other hand, the spectra of *N,N*-diethylanilinium and *m*-chloroanilinium picrates were shown to remain the same below and above the melting points.

Many years ago, Pfeiffer suggested that the interaction between the two components in a molecular complex could be considered as an interaction between particular force fields to be assigned to some regions of the molecules.[1] If each of the component molecules had more than one type of force field, isomeric molecular complexes could be obtained, depending upon which pair of force fields predominated in the interaction. For example, when an aromatic amine is combined with a polynitrophenol, one type of force field produces an acid-base interaction, and the other, an electron donor-acceptor interaction. The former interaction leads to the formation of true phenolate by proton-transfer, and the latter, to a true molecular compound by charge-transfer (CT). The papers in the present series will deal with the phenomena characteristic of the molecular complexes composed of such bifunctional component molecules.

Hertel has assumed that the progressive weakening

1) P. Pfeiffer, "Organische Molekülverbindungen," 2 Aufl., Verlag von F. Enke, Stuttgart (1927), 341—346.

of the acid-base interaction and strengthening of the donor-acceptor interaction should produce molecular complexes which range in type from true phenolates at one end of the series to true molecular compounds at the other.[2] One may expect the presence of intermediate situations where the same components form either phenolates or CT complexes, depending upon ambient conditions. In fact, several combinations of the components giving such polymorphs were discovered by Hertel. This phenomenon was named "complex isomerism" by this author. The polymorphs differ distinctly from each other in their colors, melting points, molar volumes, phase diagrams, and X-ray diffraction patterns.[2-5] For example, the combination of 1-bromo-2-naphthylamine and picric acid gives a yellow-colored salt at room temperature. The color turns violet-red at 114°C, and then the complex melts at 178°C. The latter temperature is not far from the melting point of the corresponding brilliant red *s*-trinitrobenzene (TNB) complex, 195°C. Further evidence for the change in the type of interaction accompanying the transition has been provided by spectroscopic studies of the polymorphic phases of the two picrates carried out by Briegleb and Delle.[6,7] The infrared spectra of 1-bromo-2-naphthylamine- and 1,6-dibromo-2-naphthylamine-picric acid at room temperature have been shown to have the pattern assigned to NH_3^+ vibrations. When the complexes are heated to 140°C, which is well above the transition points, the intensities of this pattern are markedly diminished and the bands due to the NH_2 group are newly observed. The deep coloration at high temperatures has been attributed to the appearance of CT absorptions. The crystal and molecular structures of the red-colored form of the 1-bromo-2-naphthylamine complex are known.[8]

In principle, the melt of an anilinium picrate is an equilibrium mixture of not only the cation, the anion, and the ion-pair, but also the CT complex and the component molecules. When the equilibrium is favorable to the CT complex and its components, a marked deepening of the color may be observed at the melting point, as if the transition point were elevated to this temperature. A close examination of twenty-four anilinium picrates has revealed that a new phenomenon, complex isomerization by melting, can be observed if the amines are appropriately chosen.

Experimental

Materials. The picric acid and all the aromatic amines used in this work were commercially obtained. The sodium picrate mono hydrate was prepared by the neutralization of the acid with sodium carbonate. The amine hydrochlorides were made by means of a reaction between hydrochloric acid and the amines. They were washed with a small amount of water and then with ether. The anilinium picrates were precipitated by mixing the component compounds separately dissolved in benzene.

Measurements. To measure the reflectance spectra of molten samples, we employed the device proposed by J. Aihara of our laboratory.[9] A powdered sample sandwiched between two quartz plates was mounted on powdered sodium chloride embedded in a brass block. The reflectance given by this arrangement was recorded on a Beckman DK 2A spectroreflectometer. The temperature at the boundary between the quartz plate and the sodium chloride, which is somewhat higher than that of the sample, was regulated as has been described earlier.[10] The measurements are rather qualitative because of the change in the sample thickness and also because of the shift of the baseline caused by heating.

The vibrational spectra of the powdered or molten sample sandwiched between two rock salt plates were examined in the region from 2000 to 4000 cm^{-1} using a Jasco IR-G infrared spectrophotometer equipped with a heating attachment. The temperature near the sample holder was monitored by means of a copper-constantan thermocouple and was kept constant using a Chino temperature-indicating controller, type E 500.

Results and Discussion

A preliminary survey was made by the visual examination of the color change at the melting point. *o*-Bromoanilinium and *o*-iodoanilinium picrates have been known to exhibit complex isomerism; therefore, the anilines having basicities close to or less than those of these two seemed to be the most hopeful component compounds. They are *o*-chloroaniline, *m*-nitroaniline, 3-nitro-4-methylaniline, *N,N*-dimethylamino-*p*-benzaldehyde, and *m*-chloroaniline (see Fig. 11). As expected, all these anilines except the last one were found to form picrates which show a marked color change upon melting. None of the other anilines gave picrates with such behavior.

The o-*Chloroaniline Complex* (*Figs. 1 and 2*). The complex precipitated from a red-colored benzene solution is a pale yellow powder which melts at 138—139°C (134°C by Hertel[2]). The color turns light red upon melting and then returns to yellow upon solidification. As is shown in Fig. 1, the reflectance spectrum at room temperature has a strong absorption below 450 mμ. Upon heating, a red-shift of this band is noted, as is indicated by curve b. Upon melting, a broad band covering the range from 450 to 600 mμ appears. Following the procedure employed by Briegleb and Delle,[7] the CT absorption of an imaginary complex formed between *o*-chloroaniline and picric acid was assumed to be approximated by that of the TNB complex, because the acceptor-strength of picric acid is comparable with that of TNB. The solid TNB complex is red and gives the spectrum shown by curve d. The close similarity

2) E. Hertel, *Ann.*, **451**, 179 (1926).
3) E. Hertel and J. van Cleef, *Ber.*, **61**, 1545 (1928).
4) E. Hertel and K. Schneider, *Z. Phys. Chem. B*, **13**, 387 (1931).
5) E. Hertel and H. Frank, *ibid.*, **27**, 460 (1934).
6) G. Briegleb and H. Delle, *Z. Elektrochem.*, **64**, 347 (1960).
7) G. Briegleb and H. Delle, *Z. Phys. Chem. Neue Folge*, **24**, 359 (1960).
8) E. Carstensen-Oeser, S. Göttlicher, and G. Habermehl, *Chem. Ber.*, **101**, 1648 (1968).
9) J. Aihara, A. Sasaki, and Y. Matsunaga, This Bulletin, **43**, 3323 (1970).
10) C. Dehari, Y. Matsunaga, and K. Tani, *ibid.*, **43**, 3404 (1970).

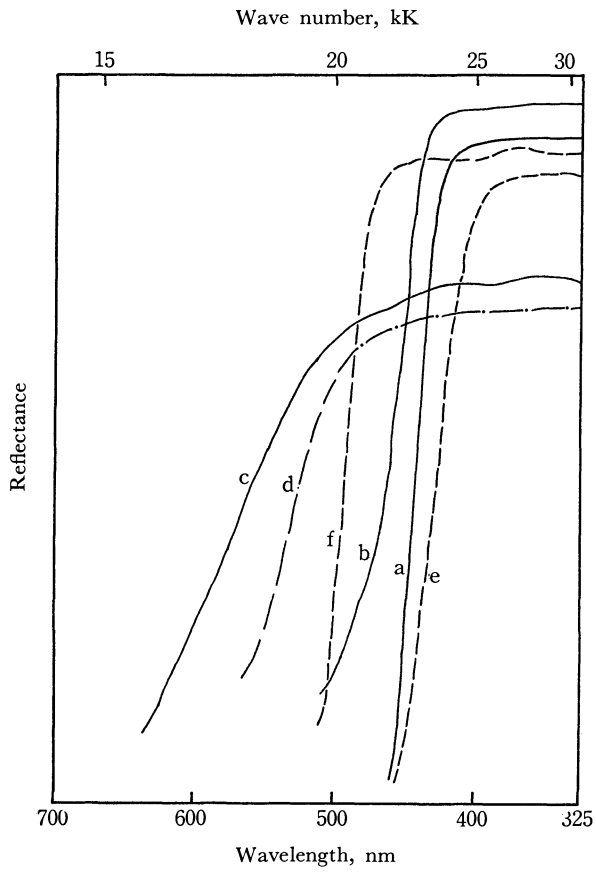

Fig. 1. Reflectance spectra, a) the *o*-chloroaniline-picric acid at room temperature, b) the same a little below the melting point, c) the same in the molten state, d) the TNB complex at room temperature, e) picric acid, and f) sodium picrate.

between curves c and d clearly indicates that the broad band appearing upon the melting of the complex arises from the CT interaction.

In the case of the *N*,*N*-dimethylaniline-TNB complex reported earlier, it was found that the spectrum in the molten state is different from the solid-state spectrum, but much like the one in the dissolved state.[9] Consequently, we attempted to compare the high-temperature spectrum, curve c in Fig. 1, with the spectrum of the corresponding TNB complex in a chloroform solution. Unfortunately, the CT absorption of the *o*-chloroaniline-TNB complex in chloroform was not observable. Nevertheless, the location of its maximum may be estimated by the following method. In our previous work, the energy of the CT absorption maximum of a TNB complex was shown to be larger by 6 kK than that of the corresponding *p*-chloranil complex.[11] Since the CT band of the *o*-chloroaniline-*p*-chloranil complex in a chloroform solution is found at 19.1 kK, the required value may be about 25 kK. This value seems to be a little too high to be compared with curves c and d. Thus, the present results are not in accordance with the observations for the dimethylaniline-TNB complex.

Since *o*-chloroaniline is a weak electron donor and picric acid is a weak acceptor, the resulting CT complex may be expected to be non-ionic. Therefore, the vibrational bands due to the NH_3^+ group must be replaced by those due to the NH_2 group of the amine by melting if complex isomerization occurs. This change will drastically modify the spectrum in the region from 2000 to 4000 cm^{-1}. In Fig. 2, the vibrational spectra of the *o*-chloroaniline complex at room temperature and above the melting point are compared with those of the free amine, its hydrochloride, the free acid, and its sodium salt. All the bands but the one at 3150 cm^{-1} in the complex at room temperature are well approximated by a summation of the bands in the anilinium hydrochloride and those in the sodium picrate. The strong bands appearing near 3600 cm^{-1} in the sodium picrate are not observed in the *o*-chloroaniline complex. They may be assigned to the hydrated water.[12] It is easy to see that the broad bands located at 2040, 2550, and 2820 cm^{-1} in the complex at room temperature constitute the pattern characteristic of the anilinium ion. Although there is no band in the hydrochloride corresponding to the one at 3150 cm^{-1}, Mariella *et al.* have reported that the band appearing in the range from 3150 to 3310 cm^{-1} is characteristic

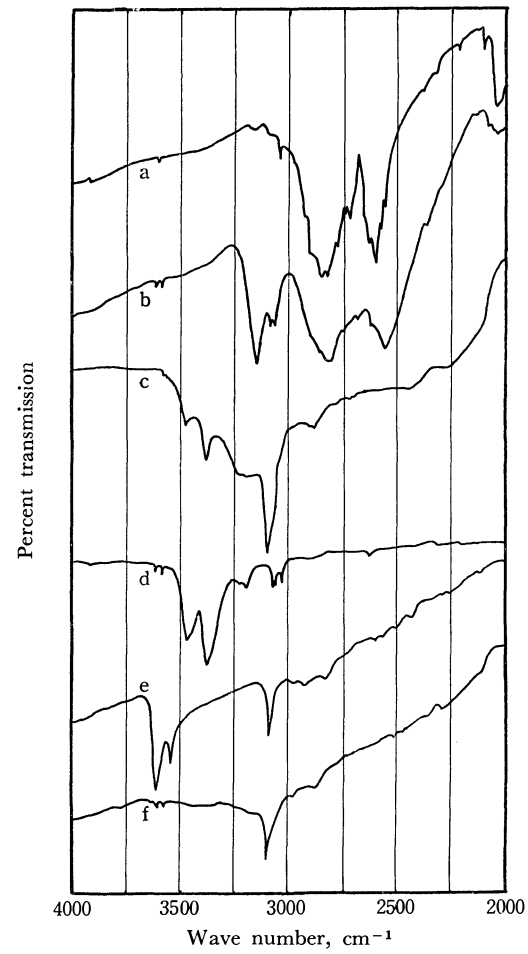

Fig. 2. Vibrational spectra, a) *o*-chloroaniline hydrochloride, b) the *o*-chloroaniline-picric acid at room temperature, c) the same above the melting point, d) *o*-chloroaniline, e) sodium picrate, and f) picric acid.

11) Y. Matsunaga and G. Saito, *ibid.*, **44**, 958 (1971).

12) K. J. Pederson, *J. Amer. Chem. Soc.*, **56**, 2615 (1934).

of the picrates of primary amines. This band has been assigned to a NH_3^+ stretching frequency.[13] The bands in the room-temperature spectrum are not visible in the molten state. The rather weak bands now observable at 3215, 3380, and 3475 cm^{-1} can be ascribed to the amine, and the strong one at 3095 cm^{-1}, to the acid. The weakness of the former bands relative to the latter may be attributed, at least in part, to the vaporization of the amine during the heating. When the anilinium picrate dissociates into its neutral component molecules, the change in the vibrational spectrum may be expected to be the same as that observed. However, the presence of a strong CT band in the melt excludes such an explanation.

It must be noted that the melting point of the *o*-chloroanilinium picrate is essentially the same as that of the corresponding TNB complex—134°C *vs.* the 134.5°C reported by Hertel.[2] Such a coincidence is rather unusual because most anilinium picrates have been known to melt at temperatures higher by 30—70°C than the TNB complexes. Considering the possibility that the picrate isomerizes into the CT complex a little below the melting point, we examined this anilinium picrate by means of a differential scanning calorimeter. At the melting point, two overlapping endothermic peaks were recorded on the thermogram.

The m-*Nitroaniline Complex* (*Figs. 3 and 4*). A red benzene solution is obtained when the yellow component compounds are dissolved together. The complex crystallizes as yellow needles with a melting point of 149–150°C. With this complex, a reversible color change from yellow to red is observed. The reflectance spectrum at room temperature, curve a in Fig. 3, shows that this is an anilinium picrate formed by proton-transfer from the acid to the amine. Upon melting, a broad, strong band with its maximum around 500 mμ or 20 kK appears. As *m*-nitroaniline is rather strongly colored, the spectrum of its melt is presented by curve c for the sake of comparison. The newly-appeared band cannot be attributed to either the amine or the acid. The solid TNB complex gives the spectrum shown by curve d. When curves b and d are compared, it seems to be acceptable that the broad band appearing in the molten complex is a CT absorption. The energy of the CT band in the TNB complex in a chloroform solution is estimated to be 22.7 kK. The band observed with the melt is apparently shifted to the long-wavelength side. The above-mentioned estimation was made on the basis of the energy of the CT band in the *m*-nitroaniline-tetracyanoethylene (TCNE) complex, 14.2 kK, and the average difference in the energy of the CT absorption between TNB complexes and TCNE complexes, 8.5 kK.[11]

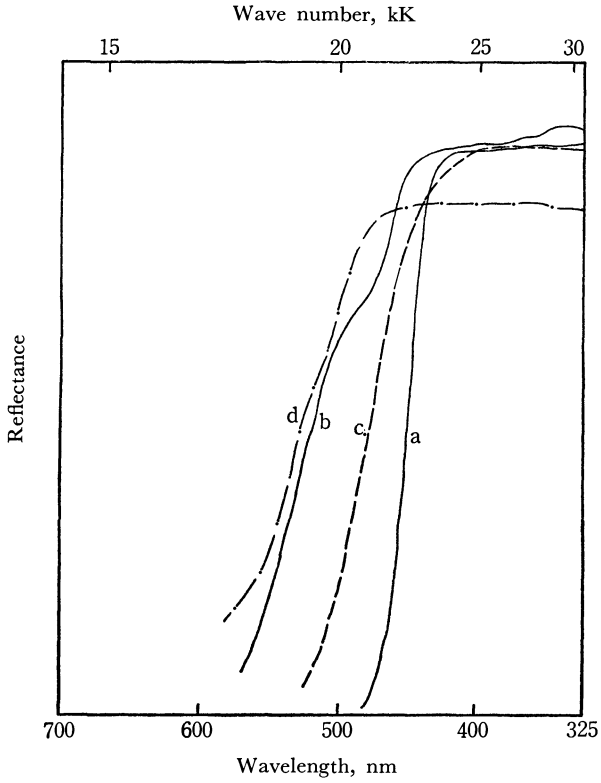

Fig. 3. Reflectance spectra, a) the *m*-nitroaniline-picric acid at room temperature, b) the same above the melting point, c) *m*-nitroaniline in the molten state, and d) the solid TNB complex.

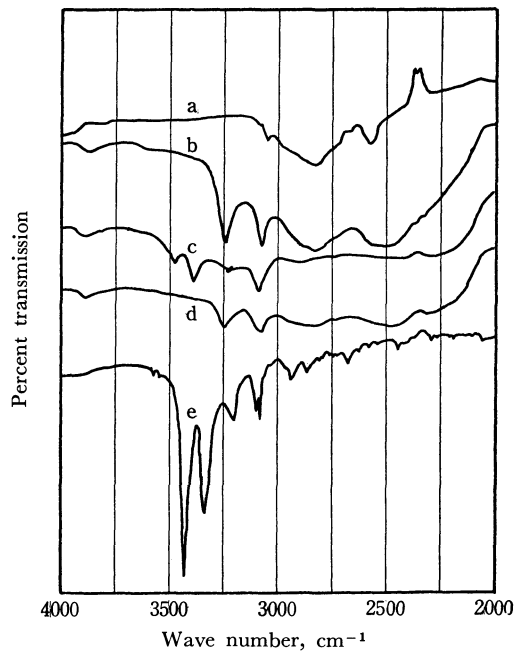

Fig. 4. Vibrational spectra, a) *m*-nitroaniline hydrochloride, b) the *m*-nitroaniline-picric acid at room temperature, c) the same above the melting point, d) the same after solidification, and e) *m*-nitroaniline.

The solid complex exhibits a vibrational spectrum containing two broad bands, located at 2500 and 2850 cm^{-1}, which are characteristic of the anilinium ion (see Fig. 4). The relatively sharp bands appearing at 3388 and 3475 cm^{-1} upon melting correspond well to those in the spectrum of the free amine. The band at 3247 cm^{-1} has no corresponding band in the spectrum of the hydrochloride; however, it is in the range reported by Mariella *et al.* for the picrates of primary amines. The spectrum recorded after

13) R. P. Mariella, M. J. Gruber, and J. W. Elder, *J. Org. Chem.*, **26**, 3217(1961).

solidification is included in Fig. 4 to show how reversible the change is. The hypothesis that this anilinium picrate transforms essentially into a CT complex at the melting point is firmly supported by these pieces of spectroscopic evidence. Finally, we may add that the present complex melts at a temperature about 50°C higher than the TNB complex, which has been reported to melt at 98°C by Sudborough and Beard.[14]

The 3-Nitro-4-methylaniline Complex (Figs. 5 and 6). When the red-colored amine is combined with yellow-colored picric acid, the complex is obtained in the form of yellow needles. The color turns red reversibly upon melting at 156–157°C. The reflectance spectrum was measured a little below and above the melting point. As is shown by curve c in Fig. 5, the molten amine absorbs strongly in the region from 350 to 500 mμ. Therefore, the absorption band characteristic of the complex in the molten state is observed as a shoulder around 525 mμ or 19 kK. This value should be compared with that of 21.1 kK estimated for the energy of the CT absorption of the complex in a chloroform solution. In the room-temperature spectrum of the TNB complex, the CT absorption covers the range from 530 to 600 mμ. The intensity of this band is markedly diminished by melting, as is indicated by curve e. This change

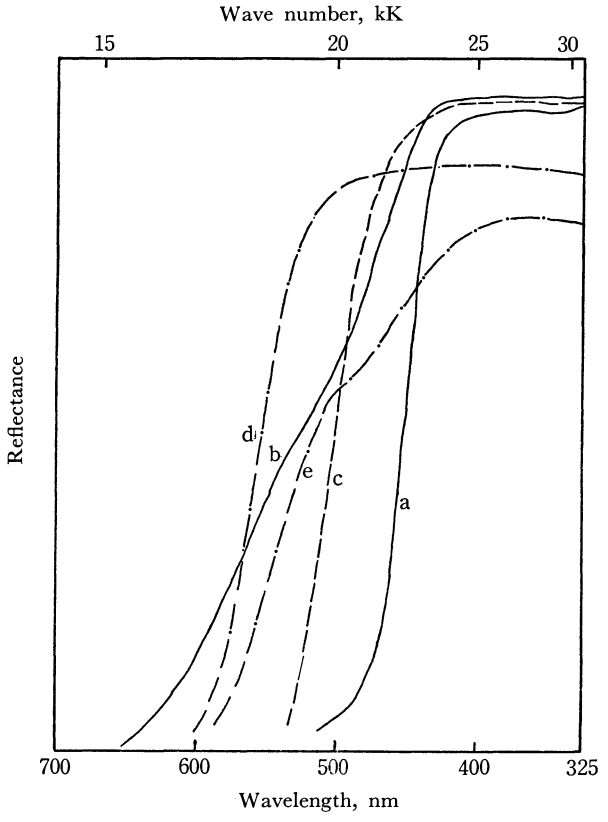

Fig. 5. Reflectance spectra, a) the 3-nitro-4-methylaniline-picric acid a little below the melting point, b) the same above the melting point, c) the amine in the molten state, d) the solid TNB complex, and e) the molten TNB complex.

14) J. J. Sudborough and S. H. Beard, *J. Chem. Soc.*, **97**, 773 (1910).

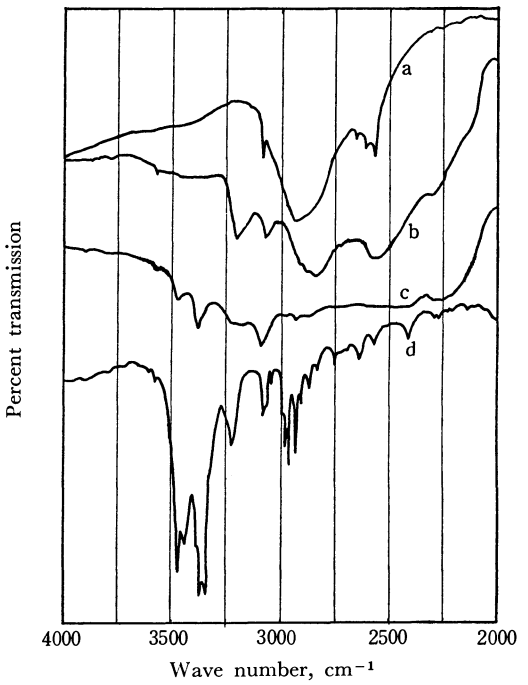

Fig. 6. Vibrational spectra, a) 3-nitro-4-methylaniline hydrochloride, b) the solid 3-nitro-4-methylaniline-picric acid, c) the same in the molten state, and d) the amine.

is possibly to be attributed to the partial dissociation of the molecular complex in the molten state. The resultant spectrum bears a resemblance to curve b.

The vibrational spectrum of the complex is drastically modified by the change in the state, as is shown in Fig. 6. Below the melting point, the two broad bands at 2570 and 2850 cm^{-1} attributable to the anilinium ion dominate. When melted, they are replaced by those at 3390 and 3478 cm^{-1} attributable to the amine. Thus, the spectroscopic observations indicate that the acid-base interaction predominates in the solid complex, and the electron donor-acceptor interaction, in the molten complex. The band near 3100 cm^{-1} remains through the phase change and is to be assigned to picric acid or picrate anion. The absorption characteristic of the picrates of primary amines is observed at 3210 cm^{-1}. The melting point of the TNB complex is found to be 82°C.

The N,N-Dimethylamino-p-benzaldehyde Complex (Figs. 7 and 8). When this white amine and picric acid are dissolved together in benzene, a dark red color develops. Bright yellow prisms crystallize from it. This complex melts at 98—99°C, and it turns red. Upon solidification, the complex turns yellow again. The reflectance spectrum recorded below the melting point, curve a in Fig. 7, is similar to that of sodium picrate; therefore, this complex is considered to be a true phenolate in the solid state. As is shown by curve b, a very pronounced absorption appears upon melting. The maximum seems to be shifted to the long-wavelength side compared with the estimated value for the CT band of the TNB complex in a chloroform solution, 22.0 kK. The spectrum of the reddish brown solid TNB complex is shown by curve c, and that of the melt, by curve d. The larger decrease in

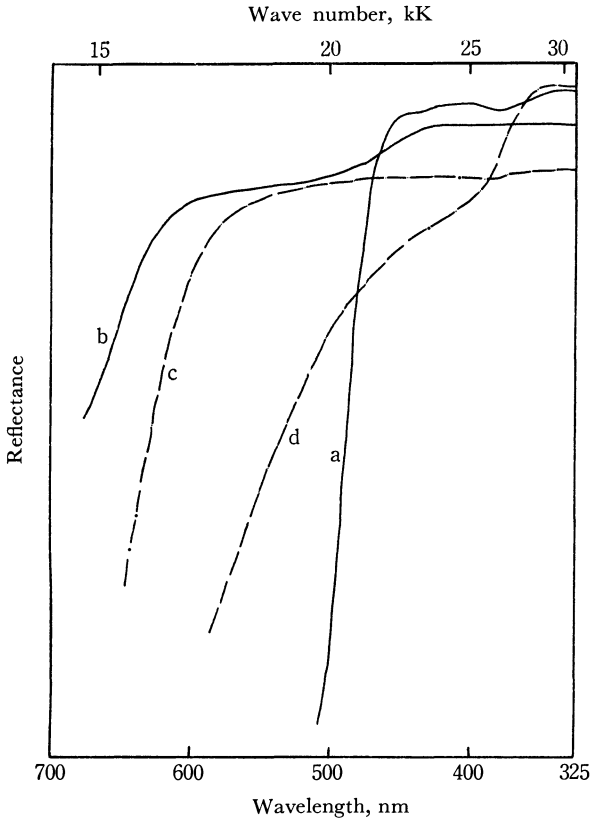

Fig. 7. Reflectance spectra, a) the dimethylamino-*p*-benzaldehyde-picric acid, b) the same in the molten state, c) the solid TNB complex, and d) the same in the molten state.

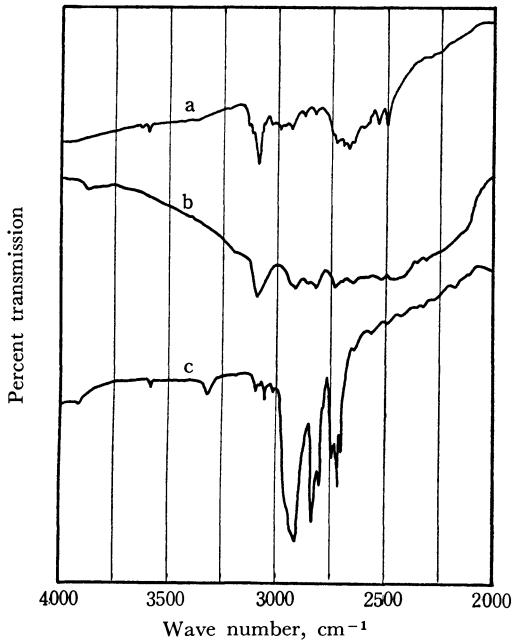

Fig. 8. Vibrational spectra, a) the dimethylamino-*p*-benzaldehyde-picric acid at room temperature, b) the same above the melting point, and c) the amine.

the intensity of the CT band of the TNB complex suggests that this complex dissociates appreciably into its components in the molten state. The similarity between curves b and c is considered to be evidence that the complex in the molten state is of the electron donor-acceptor type.

The vibrational spectra of the solid and molten complexes are presented in Fig. 8. As the amine hydrochloride is not available, the room-temperature spectrum has no reference. According to Mariella *et al.*, tertiary amine picrates have characteristic bands in the range from 2500 to 2670 cm^{-1}.[13] The spectroscopic feature observed at room temperature seems to be of the acid-base interaction. The bands at 2740, 2825, and 2920 cm^{-1} in the melt can be well compared with the strong bands observed in the free amine. Hence, an interaction of the electron donor-acceptor type apparently dominates in the molten complex. The TNB complex melts at 66°C. As is found in many other cases, the melting point of the picrate is definitely higher than this temperature.

The N,N-*Diethylaniline and* m-*Chloroaniline Complexes (Figs. 9 and 10).* For comparison with the complexes mentioned above, we will describe here the spectral behavior of two complexes which do not isomerize at their melting points. *N,N*-Diethylaniline has been chosen as an example because it is one of the strongest bases and also one of the strongest electron donors among the derivatives of aniline. The other example, *m*-chloroaniline, is a base only a little bit stronger than *o*-chloroaniline. Moreover, the electron-donor strengths of these two position isomers are almost equal to each other. Both the diethylaniline and *m*-chloroaniline complexes are yellow in the solid and molten states. The reflectance spectrum of the former complex is shown in Fig. 9. Only a slight shift to the long-wavelength side is observed

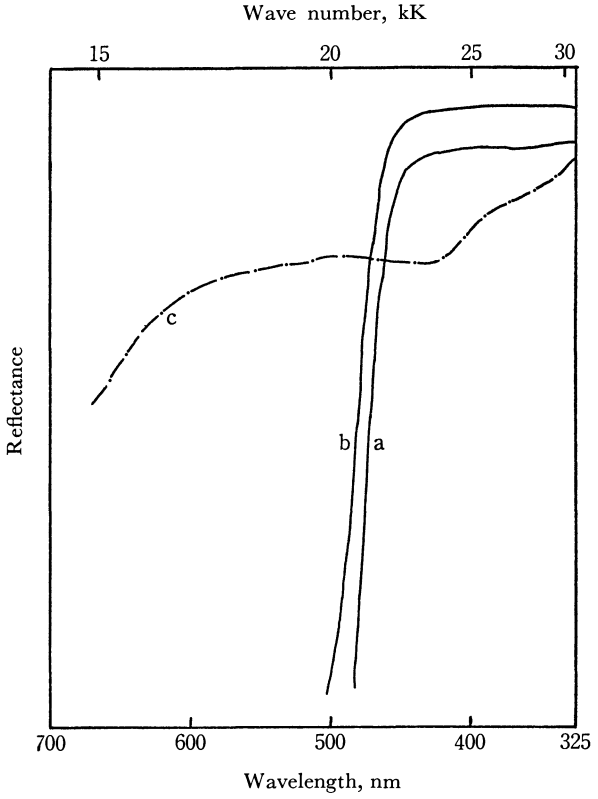

Fig. 9. Reflectance spectra, a) the *N,N*-diethylaniline-picric acid at room temperature, b) the same in the molten state, and c) the TNB complex at room temperature.

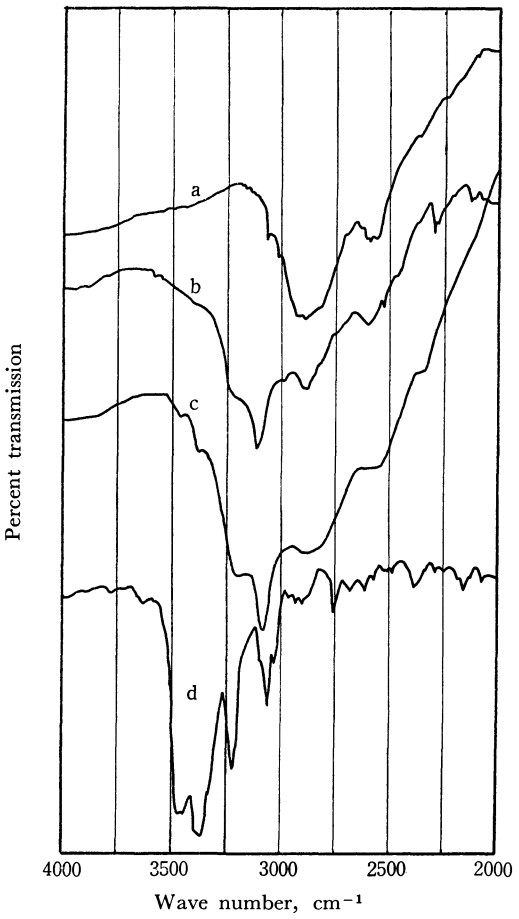

Fig. 10. Vibrational spectra, a) *m*-chloroaniline hydrochloride, b) the *m*-chloroaniline-picric acid at room temperature, c) the same in the molten state, and d) the amine.

when the complex is heated. The spectrum is quite different from that of the corresponding TNB complex. The latter shows a CT absorption covering nearly all the visible region (see curve c).

Figure 10 presents the vibrational spectra of the *m*-chloroaniline complex at room temperature and above the melting point. Both the spectra have two broad strong bands, located at 2575 and 2875 cm^{-1}, which can be compared with those in the amine hydrochloride. The band common to the picrates of primary amines appears at about 3160 cm^{-1}, and the one to be assigned to the picrate ion, at about 3100 cm^{-1}. However, two weak bands visible in the molten complex at 3360 and 3450 cm^{-1} suggest the presence of a small amount of the amine. Nevertheless, it is unquestionable that these complexes are largely of the acid-base type, even in the molten state. The diethylaniline and *m*-chloroaniline complexes melt at 133°C and 173°C (177°C was the value reported by Hertel[2]) respectively. The latter temperature is appreciably higher than the melting point of the corresponding TNB complex, 114.5°C, which is taken from the work by Sudborough and Beard.[14]

General Remarks. When a strong acid is combined with a strong base, the acid-base interaction is expected to predominate. The strength of the former component is expressed by the pK_a, and that of the latter, by the pK_b. As the acid is picric acid throughout the present work, only the pK_b of the amines will be taken into consideration here. On the other hand, the quantity to be considered in the electron donor-acceptor interaction is the ionization potential, I_P, of the amines. As proposed in our previous works,[11,15] the energy of the CT band in the complexes with a common acceptor observed in a chloroform solution will be taken as a measure of I_P. In this work, *p*-chloranil is selected for this purpose. This energy, $h\nu_{CT}$, is approximately given by the $I_P - E_A$ — constant, where E_A is the electron affinity of *p*-chloranil. In Fig. 11, the amines are arranged, with $14 - pK_b = \log[R_1R_2R_3NH^+]/[R_1R_2R_3N][H^+]$ placed on the ordinate, and $h\nu_{CT}$ on the abscissa.[16] We see here that an amine with a high $(14 - pK_b)$ value, that is, a strong base, tends to have a low $h\nu_{CT}$ value, that is, a strong electron donor. As a result, there seems to be a linear relationship between these two quantities, especially among the amines with $(14 - pK_b)$ values higher than 3. The only exception is *N,N*-dimethyl-*o*-toluidine, in which the conjugation between the dimethylamino group and

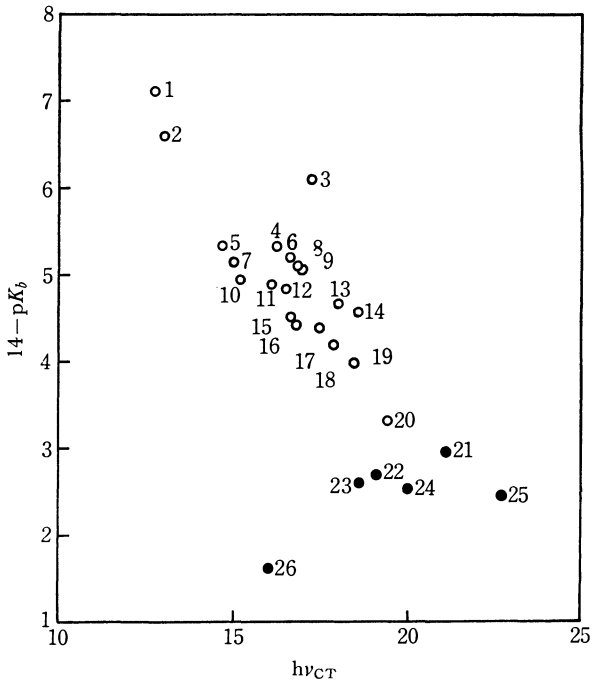

Fig. 11. Plot of $(14 - pK_b)$ of the amines against the energy of the CT band of the *p*-chloranil complexes of : 1, *N,N*-diethyl-*m*-toluidine; 2, *N,N*-diethylaniline; 3, *N,N*-dimethyl-*o*-toluidine; 4, *p*-anisidine; 5, *N,N*-dimethyl-*m*-toluidine; 6, *p*-phenetidine; 7, *N,N*-dimethylaniline; 8, *N*-ethylaniline; 9, *p*-toluidine; 10, *N*-ethyl-*o*-toluidine; 11, 2,4-dimethylaniline; 12, *N*-methylaniline; 13, *m*-toluidine; 14, aniline; 15, *o*-anisidine; 16, *o*-phenetidine; 17, *o*-toluidine; 18, *m*-anisidine; 19, *p*-chloroaniline; 20, *m*-chloroaniline; 21, 3-nitro-4-methylaniline; 22, *o*-chloroaniline; 23, *o*-iodoaniline; 24, *o*-bromoaniline; 25, *m*-nitroaniline; 26, *N,N*-dimethylamino-*p*-benzaldehyde. As to the meaning of open and shaded circles, see text.

15) Y. Matsunaga, This Bulletin, **42**, 2490(1969).
16) D. D. Perrin, "Dissociation Constants of Organic Bases in Aqueous Solution," Butterworths, London (1965), pp. 58—91.

the benzene nucleus may be supposed to be sterically hindered. In their complexes with picric acid, the acid-base interaction is found to predominate in both the solid and molten states. The amines to form such complexes are indicated by open circles. On the other hand, the amines which were found to form CT complexes above the transition or melting points are those with $(14-pK_b)$ values less than 3. In Fig. 11, they are indicated by shaded circles. Furthermore, it must be noted that many of these amines do not fit the relationship mentioned above and tend to be electron donors better than would be expected from the relationship. The results summarized in Fig. 11 reinforce Hertel's view.

In conclusion, it must be pointed out that the possibility of finding monotropic phases, where the four amines studied here and picric acid form CT complexes, still remains. When the red-colored melts are solidified, a part of the solid was often observed to be transitorily red-colored.

BULLETIN OF THE CHEMICAL SOCIETY OF JAPAN, VOL. 44, 3335—3340 (1971)

The Electron Spin Resonance of Binuclear Vanadyl Tartrates

Akinori HASEGAWA, Yoshio YAMADA, and Masaji MIURA

Department of Chemistry, Faculty of Science, Hiroshima University, Higashisenda-machi, Hiroshima

(Received July 9, 1971)

The ESR spectra of aqueous solutions of binuclear vanadyl tartrates remarkably varied with their pH values. This variation was found to be directly correlated with the change in the form of the carboxyl group, *i.e.* whether it was dissociated or acidic. Thus, the frozen solution spectra were observed in water-ethylene glycol at 77°K and analyzed in terms of several magnetic parameters containing the parameter of magnetic dipolar interaction, *D*. From these *D* values, the intramolecular V···V distances were estimated to be *ca.* 4.2, 5.2, and 6.5Å in the solutions at pH 9, 4.8, and 2.8 respectively. Such a remarkable change in the V···V distances as interpreted to be caused by the dissociation of the coordinate bonds between the vanadium atom and the carboxyl oxygen atom and the change in the molecular structure of the tartrates, brought about the change in the form of the carboxyl groups.

The aqueous solutions of vanadyl tartrates give ESR spectra characteristic of a dimeric structure with two unpaired electrons coupled with a spin-exchange interaction.[1] Although the dimeric structure in an aqueous solution had been doubted because of the specific ESR linewidth variation,[2] it has been confirmed by the observations of pairs of satellite lines caused by singlet-triplet transitions, which were allowed because of the mixing of the singlet and the triplet levels.[3-5]

The ESR spectrum of the aqueous vanadyl tartrate solution changes according to the change in the pH value. As to the aqueous solution of vanadyl *dl*-tartrate, fifteen triplet lines were observed, but no satellite lines appeared above pH 6.[1] Two kinds of considerably complicated triplet-state spectra accompanied by satellite lines were observed in the pH ranges from 5 to 3 and from 3 to 2. The values of the spin exchange interaction, J, have been determined to be 1.071×10^{-1} and 5.62×10^{-2} cm^{-1} on the basis of the analysis of the satellite lines for the dimeric species in the pH 3—5 and 2—3 ranges respectively.[4,5] In these two pH ranges, no difference was observed between the aqueous-solution spectrum of vanadyl *dl*-tartrate and that of vanadyl *dd*-tartrate, but a remarkable difference appeared between them above pH 6.[3]

Frozen-solution spectra of vanadyl *dl*- and *dd*-tartrates were observed at pH 7 in a water-ethylene glycol mixture.[6] Their spectra consist of the lines attributable to $\Delta M_s=\pm1$ transitions at $g\approx2$ and to $\Delta M_s=\pm2$ transitions at $g\approx4$, and they are interpreted in terms of the parameter of the magnetic dipolar interaction, D, and the anisotropies of the g value and the hyperfine coupling constant.

However, no interpretation has been given to the structural change of the complex caused by the change in pH. In the present paper, therefore, we attempted to investigate the structural change in these dimeric species by means of ESR, IR, pH titration, and a molecular model.

Experimental

Vanadyl *dl*-tartrate ($Na_4[(VO)_2(d\text{-tart}),(l\text{-tart})]\cdot11H_2O$) and vanadyl *dd*-tartrate ($Na_4[(VO)_2(d\text{-tart})_2]\cdot6H_2O$) were prepared by the method of Tapscott and Belford.[1] pH titrations of the aqueous solutions of these vanadyl tartrates, the pH value of which had been previously adjusted to 2.7 with HCl, were carried out by addition of the aqueous solution of NaOH. The ESR spectra of the solutions of vanadyl *dl*- and *dd*-tartrates at different pH values were measured in the frozen and liquid solution states; the frozen spectra

1) R. E. Tapscott and R. L. Belford, *Inorg. Chem.*, **6**, 735 (1967).
2) R. H. Dunhill and T. D. Smith, *J. Chem. Soc.*, *A*, **1968**, 2189.
3) R. H. Dunhill and M. C. R. Symons, *Mol. Phys.*, **15**, 105 (1968).
4) P. G. James and G. R. Luckhurst, *ibid.*, **18**, 141 (1970).
5) L. C. Dickinson, R. H. Dunhill, and M. C. R. Symons, *J. Chem. Soc.*, *A*, **1970**, 922.
6) R. L. Belford, N. D. Chasteen, H. So, and R. E. Tapscott, *J. Amer. Chem. Soc.*, **91**, 4675 (1969).

were obtained at 77°K in water-ethylene glycol (1 : 1 in volume), and the aqueous solution spectra, at room temperature. The specimens submitted to IR measurements were prepared by freeze-drying the aqueous solutions, the pH values of which had been adjusted to 9, 4.8, and 2.8. The ESR spectra were measured by a spectrometer described elsewhere,[7] and the IR spectra, by the KBr disk method, using a Hitachi EPI-G3 IR spectrometer.

Results and Discussion

The ESR spectra of aqueous vanadyl tartrate solutions depend remarkably upon their pH values, as has been pointed out by several authors.[2-5] Thus, pH titrations of the aqueous solutions were carried out; two inflection points appeared at pH 4.8 and 9, in the pH titration curve of vanadyl *dl*-tartrate, as can be seen in Fig. 1. The same result was also obtained in the case of vanadyl *dd*-tartrate. The amount of NaOH consumed between these two inflection points corresponded to just twice the number of moles of vanadyl tartrate used. All of the four carboxyl groups in a vanadyl tartrate molecule are known to dissociate at pH 9.[1] These facts suggest that, at pH 4.8, two of the carboxyl groups have the acidic form, and the other two have the dissociated form. In the same manner, all of the groups are suggested to have the acidic form at pH 2.8. The change in the ESR spectrum of the aqueous solution was found to be closely correlated with the change in the form of the carboxyl group; different kinds of spectra were observed at pH 2.8, 4.8, and 9, and each of them turned to another upon the pH change in exactly the same manner as was to be expected from the pH titration curve.

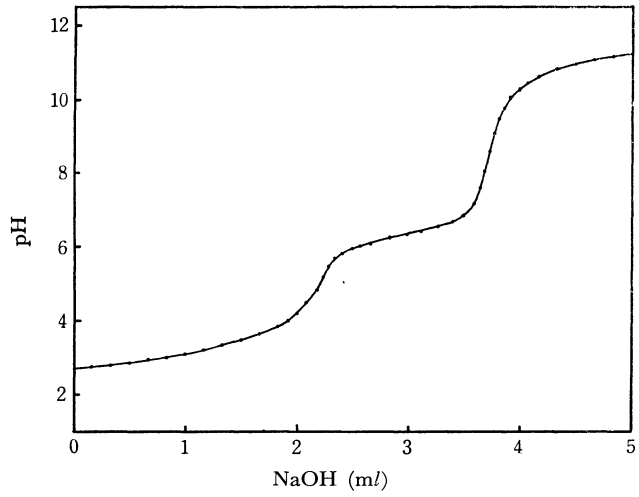

Fig. 1. pH titration curve of 0.085 g vanadyl *dl*-tartrate with aqueous solution of 0.15 N NaOH.

The ESR spectra of the aqueous solutions at pH 2.8, 4.8, and 9 have been well investigated by several authors.[2-5] However, the ESR spectra of the frozen solutions have been studied only at pH 7,[6] where most of carboxyl groups take the dissociated form. Thus, the ESR frozen solution spectra of vanadyl *dl*- and *dd*-tartrates were observed in water-ethylene glycol at pH 9, 4.8, and 2.8; the results are shown in Figs. 2(a)—(d). A difference between the ESR spectrum of vanadyl *dl*-tartrate and that of vanadyl *dd*-tartrate was found in the frozen solution state only at pH 9, as in the case of the aqueous solution state. The spectrum at pH 2.8 is complicated by the presence of hyperfine lines both from the complex corresponding to that obtained at pH 4.8 and from a complex containing a single vanadium nucleus,

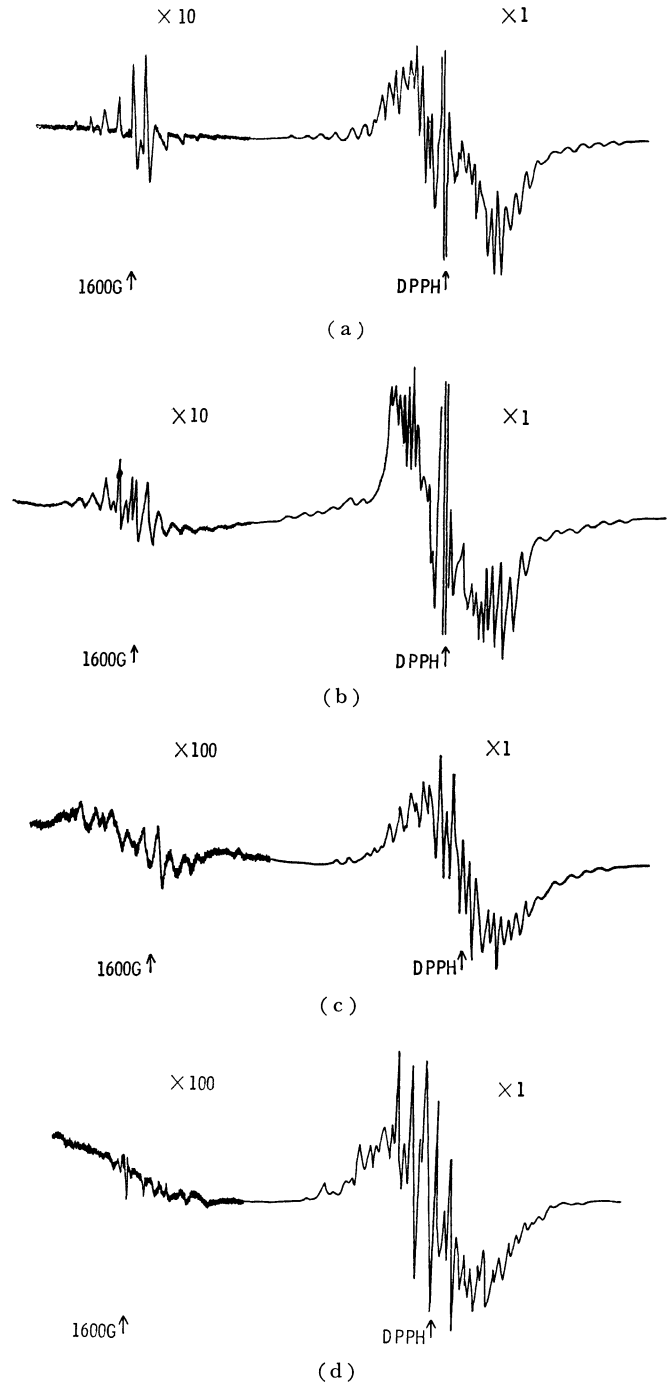

Fig. 2. ESR spectra of frozen solution of vanadyl *dl*-tartrate at (a) pH 9, (c) pH 4.8, and (d) pH 2.8 and of vanadyl *dd*-tartrate at (b) pH 9. Spectra of vanadyl *dd*-tartrate at lower pH values are respectively the same as those of vanadyl *dl*-tartrate.

7) A. Hasegawa and M. Miura, This Bulletin, **40**, 2553 (1967).

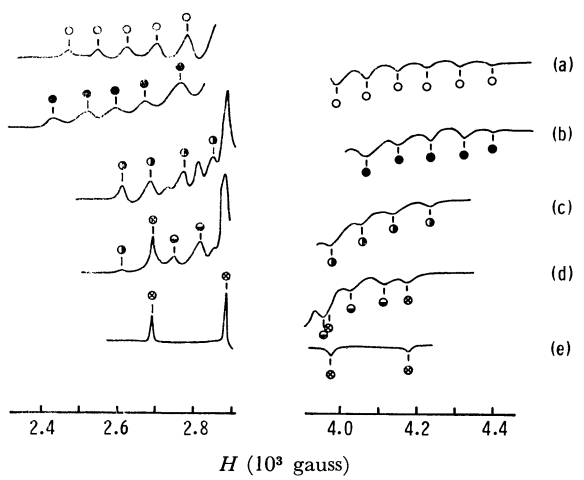

Fig. 3. Expanded view of ESR spectral lines near the both sides of the $\Delta M_s = \pm 1$ transitions of vanadyl *dl*-tartrate at (a) pH 9, (c) pH 4.8, (d) pH 2.8, and (e) pH 1.5 and of vanadyl *dd*-tartrate at (b) pH 9. Letters, (a)~(d), in the following figures have the same meaning as those in this figure. Several symbols in this figure are used to show the assignment of the spectral lines.

which is produced at pH values lower than 2. The ESR spectrum of the frozen solution at pH 1.5 was, therefore, measured in order to subtract it from the spectrum at pH 2.8. Except for the spectrum at pH 1.5, each of these spectra consists of the transition lines of $\Delta M_s = \pm 1$ at $g \approx 2$ and of $\Delta M_s = \pm 2$ at $g \approx 4$. If it is assumed that the ligand field around the vanadium atoms is axially symmetrical and that the two V=O axes in a complex molecule are parallel to each other, these ESR spectra of binuclear complexes can be described by the following spin Hamiltonian:[8,9]

$$\begin{aligned}\mathscr{H} = &\sum_{i=1}^{2} \beta\{g_{\parallel} \boldsymbol{H}_z \cdot \boldsymbol{S}_z^{(i)} + g_{\perp}(\boldsymbol{H}_x \cdot \boldsymbol{S}_x^{(i)} + \boldsymbol{H}_y \cdot \boldsymbol{S}_y^{(i)})\} \\ &+ \sum_{i=1}^{2} \{A_{\parallel} \boldsymbol{I}_z^{(i)} \cdot \boldsymbol{S}_z^{(i)} + A_{\perp}(\boldsymbol{I}_x^{(i)} \cdot \boldsymbol{S}_x^{(i)} + \boldsymbol{I}_y^{(i)} \cdot \boldsymbol{S}_y^{(i)})\} \\ &+ J\boldsymbol{S}^{(1)} \cdot \boldsymbol{S}^{(2)} + \frac{2}{3} D\Big\{\boldsymbol{S}_{z'}^{(1)} \cdot \boldsymbol{S}_{z'}^{(2)} - \frac{1}{4}(\boldsymbol{S}_+^{(1)} \cdot \boldsymbol{S}_-^{(2)} \\ &+ \boldsymbol{S}_-^{(1)} \cdot \boldsymbol{S}_+^{(2)})\Big\} \end{aligned} \quad (1)$$

where the distinction between z and z' originates from the fact that the V=O axis is not necessarily parallel to the V···V axis and where D is a parameter of the magnetic dipolar interaction.

The resonance condition of the $\Delta M_s = \pm 1$ transition between triplet states is given approximately from this spin Hamiltonian, by modifying the relation derived by Glarum and Marshall[9] with anisotropies of the g value and the hyperfine coupling:[8]

$$\begin{aligned} h\nu = g\beta H + K(M^{(1)} + M^{(2)}) \pm \frac{1}{2}\left(J + \frac{2}{3}\gamma D\right) \\ \mp \left\{K^2(\Delta M)^2 + \frac{1}{4}\left(2J - \frac{2}{3}\gamma D\right)^2\right\}^{1/2} \end{aligned} \quad (2)$$

where $$g^2 = g_{\parallel}^2 \cos^2\theta + g_{\perp}^2 \sin^2\theta \quad (3)$$

8) B. Bleaney, *Phil. Mag.*, **42**, 441 (1951).
9) S. H. Glarum and J. H. Marshall, *J. Chem. Phys.*, **47**, 1374 (1967).

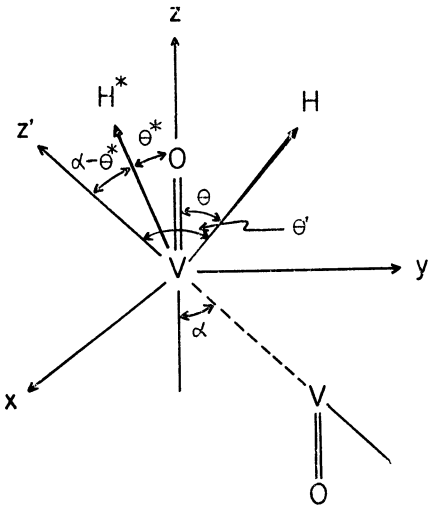

Fig. 4. The relation between two molecular axes and two orientations of the external magnetic field: H is the external magnetic field in a general orientation satisfying Eqs. (2)~(6), and H^*, in the plane containing z and z' axes, is that in the specific orientation giving the maximum resultant splitting satisfying Eqs. (9), (10), and (12).

$$gK = \sqrt{\frac{1}{4}A_{\parallel}^2 g_{\parallel}^2 \cos^2\theta + \frac{1}{4}A_{\perp}^2 g_{\perp}^2 \sin^2\theta} \quad (4)$$

$$\gamma = 3\left(\frac{g_{\parallel}^2 \cos^2\alpha + g_{\perp}^2 \sin^2\alpha}{g^2}\right)\cos^2\theta' - 1 \quad (5)$$

$$\Delta M = |M^{(1)} - M^{(2)}|, \quad (6)$$

where the angles, θ, θ', and α are defined as is shown in Fig. 4. The external magnetic field is, therefore, oriented at the angle of θ to the symmetrical axis with regard to the g value and the hyperfine coupling, *i.e.*, the V=O direction, and at the angle of θ' to the direction at which the maximum magnetic dipolar splitting can be expected, *i.e.*, the V···V direction.

If the assumption,

$$K^2(\Delta M)^2 \ll \left(J - \frac{1}{3}\gamma D\right)^2 \quad (7)$$

is satisfied, Eq. (2) can be simplified as:

$$h\nu = g\beta H + K(M^{(1)} + M^{(2)}) + \gamma D\left(M_s - \frac{1}{2}\right) \quad (8)$$

where $M_s = 1$ or 0. The assumption is satisfied for the frozen solution spectrum at pH 9 because of a large value of J; the J value can be deduced to be about 2×10^{-1} cm^{-1} from the analysis of the linewidth of the triplet spectrum, though the value has not been determined explicitly as yet. The application of Eq. (8) to the spectra at lower pH values is, however, subject to restriction because the J value decreases with the decrease in pH value;[4,5] the derivation of Eq. (8) from Eq. (2) can not be allowed for the transitions corresponding to the large value of $(\Delta M)^2$. Fortunately, even for the spectrum at pH 2.8, the resonance lines due to small values of ΔM, which can be observed near both sides of the $\Delta M_s = \pm 1$ transition spectrum, satisfy the condition of Eq. (7), and the deviation arising from Eq. (8) does not exceed the limits of experimental error. The outermost lines were assigned to the lines of $M^{(1)} = M^{(2)} = \pm 7/2$ with

Table 1. Apparent magnetic parameters

Complex	pH	$\frac{1}{2}A_{\parallel}$* a,b)	D* a)	$g_{\parallel}$* b)	$\frac{1}{2}a_0$ a,c)
Vanadyl *dl*-tartrate	9	72.3	334	1.953	38.3
Vanadyl *dd*-tartrate	9	73.2	335	1.950	40.8
Vanadyl *dl*-tartrate	4.8	74.5	180	1.944	47.6
Vanadyl *dl*-tartrate	2.8	70.1	88	1.941	50.6

a) in unit of 10^{-4} cm^{-1}
b) The second order perturbation is involved in the estimation of these values.
c) These values are not apparent but determined ones.

Table 2. Evaluated values for vanadyl *dl*-tartrate

Complex	pH	$\frac{1}{2}A_{\parallel}$ a)	$\frac{1}{2}A_{\perp}$ a)	D a)	R b)
Vanadyl *dl*-tartrate	9	76.2	19.3	348	4.16

a) in unit of of 10^{-4} cm^{-1}
b) in unit of Å

a maximum resultant splitting due to hyperfine and magnetic dipolar interaction, where the anisotropy of the g value is assumed to be negligible as compared with the anisotropy of the hyperfine coupling constant and with the angular dependency of the magnetic dipolar splitting. The external magnetic field which gives the outermost lines is defined as being oriented at the angles of θ^* to the direction of V=O and $\alpha-\theta^*$ to the direction of the V···V direction, in the plane containing V=O and V···V directions, as can be seen in Fig. 4. The hyperfine coupling constant and magnetic dipolar splitting at this magnetic field direction can be determined approximately from Eq. (8) and from the spectral lines near both the sides of the $\Delta M_s = \pm 1$ transition spectrum, which are shown, with their assignments, in Fig. 3. They are, therefore, shown, neglecting the anisotropy of the g value, by:

$$\frac{1}{2}A_{\parallel}^* = \frac{1}{2}\sqrt{A_{\parallel}^2\cos^2\theta^* + A_{\perp}^2\sin^2\theta^*} \tag{9}$$

and

$$2D^* = D\{3\cos^2(\theta^*-\alpha)\} - 1\} \tag{10}$$

Hereupon, the isotropic coupling constant, $a_0/2$, obtained from the liquid-solution spectrum is connected with the values of $A_{\parallel}$ and $A_{\perp}$ by a well-known relation:

$$\frac{1}{2}a_0 = \frac{1}{3}\left(\frac{1}{2}A_{\parallel} + A_{\perp}\right) \tag{11}$$

On the other hand, the θ^* angle must satisfy the following condition, as can be expected from the maximum resultant splitting:

$$\frac{\partial}{\partial\theta^*}\left[14\times\frac{1}{2}\sqrt{A_{\parallel}^2\cos^2\theta^* + A_{\perp}^2\sin^2\theta^*} + D\{3\cos^2(\theta^*-\alpha)-1\}\right] = 0 \tag{12}$$

As the values of $A_{\parallel}^*/2$ and $2D^*$ can be evaluated from the frozen-solution spectrum, and the value of $a_0/2$, from the liquid-solution spectrum, the θ^* value satisfying Eqs. (9)—(12) can be determined unequivocally provided that the value of α is assumed. Thus, the relation between α and θ^* was calculated from the parameters given in Table 1 by using a computer; the results are shown in Fig. 5. From the value of θ^*,

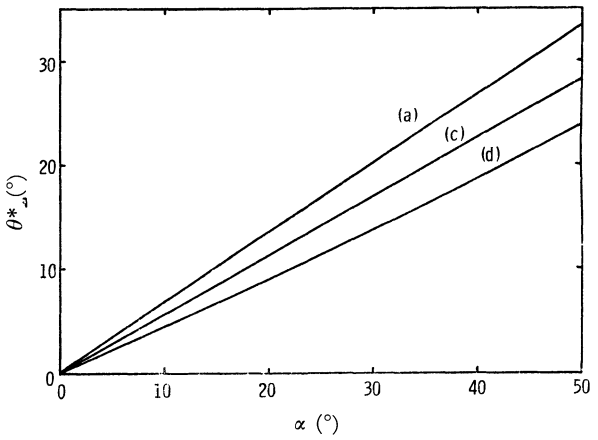

Fig. 5. The relation between α and θ^* for vanadyl *dl*-tartrate. The line for (b) is located slightly higher than that of (a), but almost superimposed with (a) in this figure.

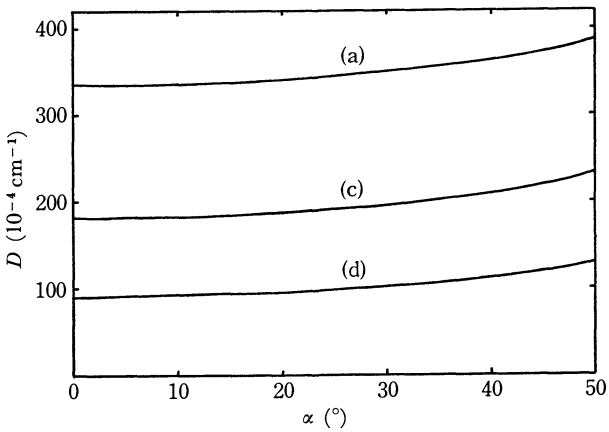

Fig. 6. The relation between α and D for vanadyl *dl*-tartrate. The line for (b) is also located slighly higher than that of (a), but almost superimposed with (a).

in turn, the values of $A_{\parallel}$, $A_{\perp}$, and D were obtained for each value of α. The relation between D and α is shown in Fig. 6.

According to the results of X-ray diffraction,[10] the value of α is 28° for the crystal of vanadyl *dl*-tartrate obtained from the solution at pH 8. When this value is adopted for the complex in the solution of vanadyl *dl*-tartrate at pH 9, the value of θ^* is determined to be 18°58′ from Fig. 5. Thus, the values of $A_{\parallel}/2$, $A_{\perp}/2$, and D determined on the basis of $\alpha=28°$ are given in Table 2. The values of α for other complexes are not yet known but they may be deduced to be not so large.

The intensity ratio of the transition of $\Delta M_s=\pm2$ to that of $\Delta M_s=\pm1$ is proportional to the square of the D value:[11]

$$I_{\Delta M_s=\pm2}/I_{\Delta M_s=\pm1}=\frac{1}{8}\left(\frac{D\sin 2\theta'}{H}\right)^2 \tag{15}$$

It can, therefore, be checked in terms of this relation whether or not the evaluated D value is reasonable. As the intensities of all the $\Delta M_s=\pm1$ transitions are roughly equal in Figs. 2 (a)—(c), the intensities of the $\Delta M_s=\pm2$ transition in these figures may be supposed to be proportional to the square of each D value. The change in the D value evaluated above with the decrease in pH value reasonably explains the observed change in the intensity of the $\Delta M_s=\pm2$ transition, though the D value is an approximate one because of the uncertainty of the α value.

The splitting due to the magnetic dipolar interaction is also approximately shown by:[12]

$$D=\frac{3}{4}g^2\beta^2\frac{\langle 1-3\cos^2\theta'\rangle_{\max}}{R^3} \tag{16}$$

where R is the V···V distance, the θ', the angle between V···V and the magnetic field directions. The value of D (in cm^{-1}) is, therefore, correlated with the V···V distance, R (in Å), by:[6]

$$D=\frac{0.650}{R^3}g^2 \tag{17}$$

When the $D=348\times10^{-4}\,cm^{-1}$ obtained for $\alpha=28°$ was substituted into Eq. (17), the intramolecular V···V distance for the vanadyl *dl*-tartrate at pH 9 was evaluated to be 4.16 Å, where the g value was assumed to be 1.953 (Table 1) as an approximation. The estimated value is very close to the V···V distance determined by means of X-ray diffraction-4.08 Å.[6,10] Although some question is involved in the comparison between the V···V distance in the solution state and that in the crystalline state, the comparison may be significant because a complex molecule is surrounded by eleven water molecules even in the crystalline state.[1] Thus the validity of the procedure for the estimation of the magnetic parameter was confirmed. It is also interesting to compare these results with those which were determined by Belford *et al.* directly from the spectrum observed without such a procedure.[6] The latter values are, by nature, in agreement with those in Table 1. The values of $A_{\parallel}$ and D which were obtained through this procedure, and which are given in Table 2, are larger than those obtained directly from the spectrum.

The relation between R and α was obtained from Fig. 6 and Eq. (16) by the use of the g values in Table 1. The relation depends remarkably upon the value of pH, as can be seen in Fig. 7. The intramolecular V···V distance, which is an approximate value because of the undetermined value of α, changes step by step from *ca.* 4.2 through *ca.* 5.2 to *ca.* 6.5 Å, being closely correlated with the decrease in the pH value, that is, with the change in the form of the carboxyl group.

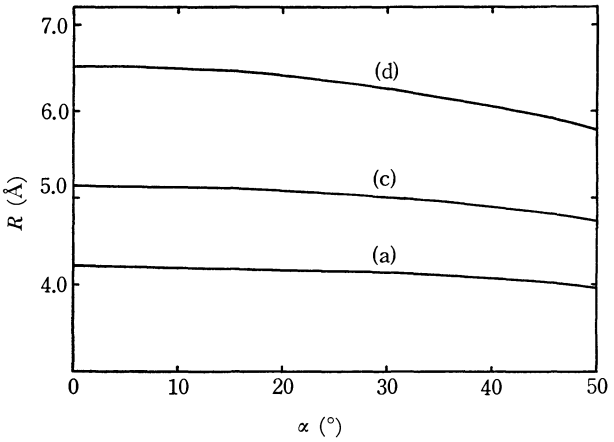

Fig. 7. The relation between α and R for vanadyl *dl*-tartrate. The line for (b) is located a slightly lower than that of (a), but almost superimposed with (a).

When the IR spectra were measured for the complexes in solid forms prepared from solutions of different pH values, the frequency of the absorption due to V=O stretching changed with the change in the pH value; for the vanadyl *dl*-tartrate, 958, 978, and 988 cm^{-1} respectively at pH 9, 4.8, and 2.8, and for vanadyl *dd*-tartrate, 949 cm^{-1} at pH 9, and those at lower pH values were the same as those for vanadyl *dl*-tartrate. Such an increase in the V=O stretching frequency suggests a decrease in the coordination ability of equatorial ligands to the vanadium atom.[13]

It is of great interest to interpret these results in connection with the structural change in these complexes brought about by the change in pH. Such a structural change may be successfully discussed by means of a model of the complex molecule. According to the results of the X-ray diffraction of vanadyl *dl*-tartrate prepared at pH 8,[10] each of two vanadium ions in a molecule of the complex is coordinated with four oxygen atoms, other than the doubly-bonded oxygen atom forming part of the vanadyl ion, two of which are the carboxyl oxygen atom and the alcoholic oxygen atom in a tartrate molecule, and the

10) R. E. Tapscott, R. L. Belford, and I. C. Paul, *Inorg. Chem.*, **7**, 356 (1968).
11) Y. Kurita, *Nippon Kagaku Zasshi*, **85**, 833 (1964).
12) K. W. H. Stevens, *Proc. Roy. Soc.* (London), **A214**, 237 (1952).
13) J. Selbin, L. H. Holmes, Jr., and S. P. McGlynn, *Chem. Ind.* (London), **1961**, 746.

other two of which are those in the other tartrate molecule, as can be seen in Fig. 8. The two quadrilaterals, which are made by combining these four oxygen atoms coordinating to a vanadium atom, slide with one another, resulting in the angle of 28° between V=O and V···V directions and in the distance of 4.08 Å between these vanadium atoms.[6] The molecular model also supports such a structure. For vanadyl *dd*-tartrate at pH 9, the molecular model suggests that the V=O direction is almost parallel to the V···V direction that the V···V distance is approximately equal to that for the vanadyl *dl*-tartrate. With the decrease in the pH value, the carboxyl group in tartrate takes an acidic form and the coordination of the oxygen atoms in this group is weakened. The change in V···V distance, 4.2, 5.2, and 6.5 Å, estimated from the ESR spectrum must be interpreted in terms of a drastic change in the molecular structure. However, there is no molecular model which allows such a change in the V···V distance if four oxygen atoms of tartrates are kept coordinating to each vanadium atom.

Finally, the following structural changes may be suggested for the interpretation of the change in the V···V distance with the pH. The coordinate bond between a vanadium atom and an oxygen atom of a carboxyl group breaks down with the change in the form of the carboxyl group from a dissociated to an acidic one, and the water molecules of the solvent, in turn, participate in the coordination with the vanadium atom. At the same time, the bond between the second and the third carbon atoms in the tartrate molecule rotates, and the rotation about the C–O bond, in which the second or the third carbon atom participates, is also allowed. Furthermore, the length of the coordinate bond remaining may also increase. Thus, at pH 4.8, the dissociation of the two coordinate bonds in a vanadyl tartrate binuclear complex brings about the enlargement of the V···V distance to *ca.* 5.2 Å, and at pH 2.8 the following dissociation of the two coordinate bonds to *ca.* 6.5 Å. This separation of 6.5 Å is possible only for the following structure: the two vanadium atoms are coordinated with oxygen atoms bound to the second and the third carbon atoms in tartrates and are extremely remote from one another, two carboxyl groups in each tartrate molecule are projected out and free from the coordination to the vanadium atom, and two hydrogen atoms are bound to carbon atoms orient to the rather inner part, as can be seen in Fig. 9. The value of α is expected to be small for this complex.

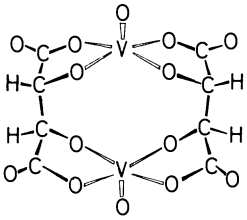

Fig. 8. The structure of the vanadyl *dl*-tartrate in the aqueous solution at pH 9.[1,10]

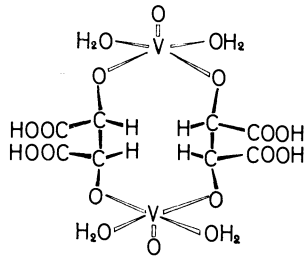

Fig. 9. Proposed structure of the vanadyl *dl*-tartrate in the aqueous solution at pH 2.8.

In such a structure at pH 2.8, two tartrate molecules coordinate to the vanadium atom in the relation of *cis* for vanadyl *dl*-tartrate and of *trans* for vanadyl *dd*-tartrate, as can be expected from the molecular model proposed by Tapscott and Belford.[1,9] If the effect of the difference between the *cis* and *trans* forms on the ESR spectrum is assumed to be weakened by the coordination of the solvent molecules, it can be tentatively accounted for why the ESR spectrum of vanadyl *dl*-tartrate is in close agreement with that of vanadyl *dd*-tartrate at pH 4.8 and 2.8.

In conclusion, the remarkable change in the ESR spectrum of the binuclear vanadyl tartrate complex with the pH has been interpreted in terms of the change in the molecular structure of the complex accompanied by the dissociation of coordinate bonds and the change in the structure of the tartrate molecule.

The authors would like to express their deep gratitude to Professor Junkichi Sohma and Assistant Professor Keiichi Ohno of Hokkaido University for their useful discussions.

The Flow Properties of Hydrophilic Latexes Thickened with Alkali

Yoshio Ito and Shunsuke Shishido
Department of Chemistry, Faculty of Science, Niigata University, Niigata
(Received July 10, 1971)

This paper has aimed at the revelation of the thickening mechanism of a latex on the addition of alkali. Experiments have been made on two kinds of latexes dialyzed thoroughly, *i.e.*, the butadiene-methyl methacrylate copolymer latex and the butadiene-methyl methacrylate-methacrylic acid copolymer latex. The degree of the swelling of the latex particles on the addition of alkali has been correctly obtained and has been connected with the thickenability of the latex. The results provide a more rigorous description than Wesslau's suggestion that the thickening of a latex on the addition of alkali is ascribed to the swelling of the latex particles alone. The reason why NH_4OH is a proper thickener is presented, and the most suitable amount of alkali for the thickening of a latex is discussed.

A hydrophillic polymer latex can be thickened by the addition of alkali. Wesslau[1] has suggested that the increase in the particle size in a latex thickened with NH_3 is responsible for the increase in the viscosity of the latex; however, this suggestion is correct only qualitatively. Therefore, influences of other factors on the viscosity of a latex should be examined, as has been pointed out by several investigators.[2-6]

The present investigation has aimed at the revelation of the flow properties of latexes thickened with alkali.

Experimental and Results

Latexes. A butadiene–methyl methacrylate (B–M) copolymer latex and a butadiene–methyl methacrylate–methacrylic acid (B–M–A) copolymer latex were obtained from the Nihon Gas Chemical Co., Ltd.

Both the latexes used were thoroughly dialyzed with deionized water until their surface tensions were equal or almost equal to that of water. Figure 1 shows the infrared spectra of the copolymer films made from the dialyzed latexes (full line), and from those adjusted to pH 11 with carbonate free sodium hydroxide (dotted line). Table 1 lists the designations of the latexes and the compositions of the copolymers as mol% of the monomers. The particle-size distributions of the latexes used were determined by the measurement of the sizes of about 2000 particles by means

Table 1. Compositions of copolymers of latexes[a]

Latex designation	Mol% of monomers		
	Butadiene	Methyl methacrylate	Methacrylic acid
B-M	55	45	0
B-M-A	50	46.5	3.5

a) The values listed were determined on the basis of the IR-spectral data of Fig. 1.[7]

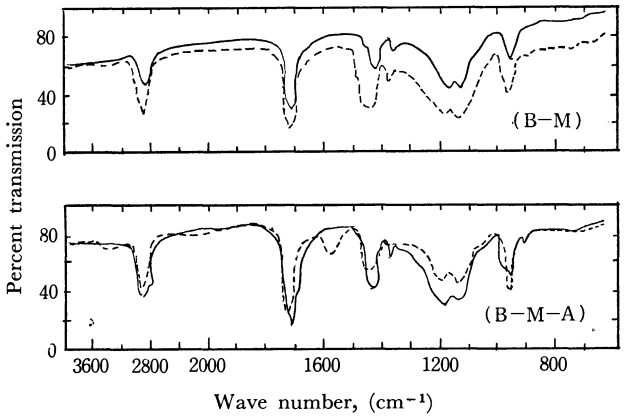

Fig. 1. Infrared spectra of copolymer films. Designations, B-M and B-M-A, are described in Table 1. The full lines and the dotted lines represent the spectra of the films to be made from the dialyzed latexes and those ionized with sodium, respectively.

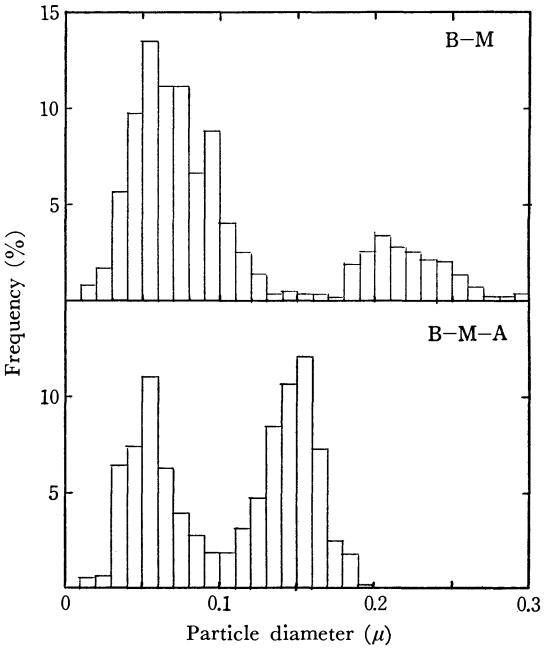

Fig. 2. Particle-size distribution determined with electron microscopy.
The particle frequency is described as a function of diameters.

1) H. Wesslau, *Makromol. Chem.*, **69**, 213 (1963).
2) S. Muroi and K. Hosoi, *Chem. High Polymers*, **26**, 416, 426 (1969).
3) S. Muroi, *J. Appl. Polym. Sci.*, **10**, 715 (1966).
4) S. Muroi and K. Hosoi, *Kogyo Kagaku Zassi*, **69**, 1551 (1966).
5) K. Tyuzyo, Y. Harada, and H. Morita, *Kolloid Z.*, **301**, 155 (1965).
6) S. Muroi, K. Hosoi, and T. Ishikawa, *J. Appl. Polym. Sci.*, **11**, 1963 (1967).

of the electron microscopy[7,8]; they are shown in Fig. 2.

Viscosity. A colloidal suspension such as a latex is generally a non-Newtonian fluid.[9-12] However, when the concentrations of the latexes used were less than 35 wt% on solids, the flow behavior was Newtonian at rates of shear below 8×10^2 sec^{-1}. Consequently, the concentrations in this investigation were limited to 35 wt% on solids as an initial step toward revealing the intricate flow behavior of latexes.

The viscosities were measured with a Ubbelohde-type viscometer for the latexes dialyzed and for those thickened with NH_4OH and NaOH. Figure 3 shows the relations between the specific viscosity (η_{sp}) and the dried-polymer content (wt%) of the latexes. The B–M latex was hardly thickened by the addition of NH_4OH; on the other hand, the B–M–A latex was remarkably thickened with aqueous solutions of NH_4OH and dilute aqueous solutions of NaOH, but hardly thickened with concentrated aqueous solutions of NaOH.

Swelling and Volume Fraction of Latex Particles. The flow properties of suspensions are generally discussed on the basis of the relation between η_{sp} and vol%(ϕ) on solids. However, when the particles of a latex are swollen, the discussion[1] is based on the data of the wt% on the dried polymer because of the difficulty of determining the volume fraction exactly.

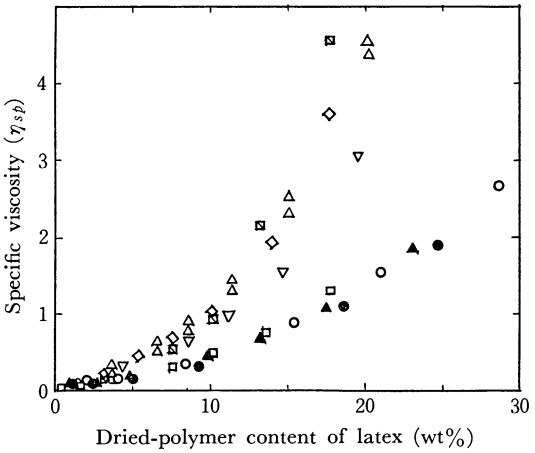

Fig. 3. Influence of thickening with NH_4OH and NaOH on η_{sp}–wt% relationship.
B-M ●: H_2O, ▲: NH_4OH 0.1N
B-M-A ○: H_2O, △: NH_4OH 0.1N, ▽: NH_4OH 1N, □: NaOH 1N, ▨: NaOH 0.1N, ◇: NaOH 0.01N
Above concentrations (N) of NH_4OH and NaOH indicate those in the serum of the latexes. All viscosities were measured at 35.00±0.01°C.

In this investigation, the difficulty was overcome with the determination of the degree of swelling for the latex-film instead of that for the latex-particles.

Making of Latex-films. When a polymer latex is evaporated above the glass temperature of the polymer, it becomes a non-porous film.[13,14] Latex-films of about 0.5 mm in thickness were made by means of the evaporation of the latexes on mercury at 60°C.

Swelling of Latex-films. The degree of swelling may be defined as the ratio of the swollen volume of a polymer film to its volume dried.

The films of the latexes used could be swollen in deionized water or in aqueous solutions of alkali, and then again contracted by drying. It was confirmed that the degrees of swelling were reproducible within ±1% by repetition of the swelling and the contraction; this held for different samples too. From these facts, it was presumed that the degree of swelling of a latex-film is equal to that of the latex particles.

In this investigation, the volume of the film was measured with a Beckman-Toshiba air comparison pycnometer, model 930.

Figure 4 shows the dependence of the degrees of swelling of the latex-films immersed in aqueous solutions of alkali on the alkali content of the solution.

The B–M latex-film was hardly swollen with an increase in the NH_4OH concentrations; the degree of swelling of the B–M–A latex-film was suddenly increased at a moderate concentration of NH_4OH and then slightly decreased with a further increase in the concentration. In the case of the swelling in solu-

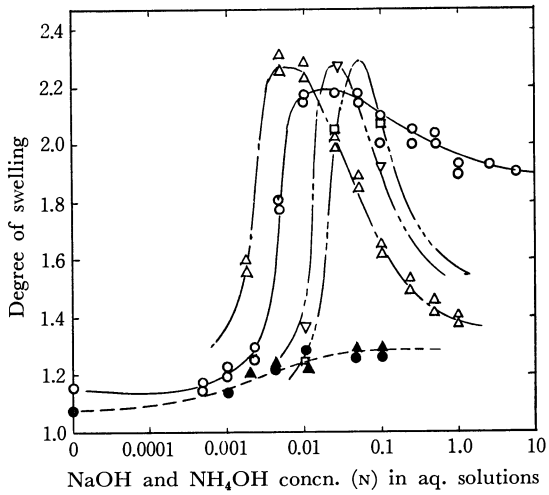

Fig. 4. Degrees of swelling of latex-films immersed in aq. solutions of various alkali concentrations.

Alkali in soln.	Copolymer-film	Wt% of film in soln. of alkali
NH_4OH	------ ●: B-M	1.0
	——— ○: B-M-A	1.0
NaOH	——— ▲: B-M	1.0
	——— △: B-M-A	1.0
	——— ▽: B-M-A	10.0
	——— □: B-M-A	20.1

7) S. Shishido and S. Suzuki, *Chem. High Polymers*, **26**, 451 (1969).
8) K. Kato, *J. Electron Microscopy*, **14**, 219 (1965).
9) M. Moony, *J. Colloid Sci.*, **1**, 195 (1946).
10) S. H. Maron, B. P. Madow, and J. M. Krieger, *ibid.*, **6**, 584(1951); S. H. Maron and B. P. Madow, *ibid.*, **8**, 130 (1953).
11) J. M. Brodnyan and E. L. Kelley, *ibid.*, **20**, 7 (1965).
12) Y. L. Wang, *J. Colloid Interfac. Sci.*, **32**, 633 (1970).
13) T. F. Protzman and G. L. Brown, *J. Appl. Polym. Sci.*, **4**, 81(1960).
14) J. G. Brodnyan and T. Konen, *ibid.*, **8**, 687 (1964).

tions of NaOH, the swelling behavior of the B–M film was similar to that in the case of NH_4OH; the degree of swelling of the B–M–A film was suddenly increased at a moderate concentration and then remarkably decreased with a further increase in the concentration.

It is worth noting that the carboxyl groups in the B–M–A film immersed were equivalent to the alkali content in the solution at the maximum point of swelling.

Discussion

Although the B–M–A latex is more similar to the samples used by Muroi *et al.*[2-4] than to those used by Wesslau[1] in view of the presence of carboxyl groups in the copolymer, this latex, which is unsoluble even in a concentrated NaOH solution, is a suitable sample for an investigation of the flow behavior of a thickened latex, as was proposed by Wesslau.

Equation of Viscosity. The wt% in Fig. 3 may be rewritten as in Fig. 5 in terms of the vol% on the basis of the presumption that when a film and latex-particles of an equal content on solids are thickened with an alkali solution of an identical concentration, the degrees of swelling of both samples are equal.

In Fig. 5, the plots for the B–M latex and the B–M–A latex at 50°C are added.

All the plots were on a curve represented by a full line in this figure and expressed in terms of an empirical formula (1):

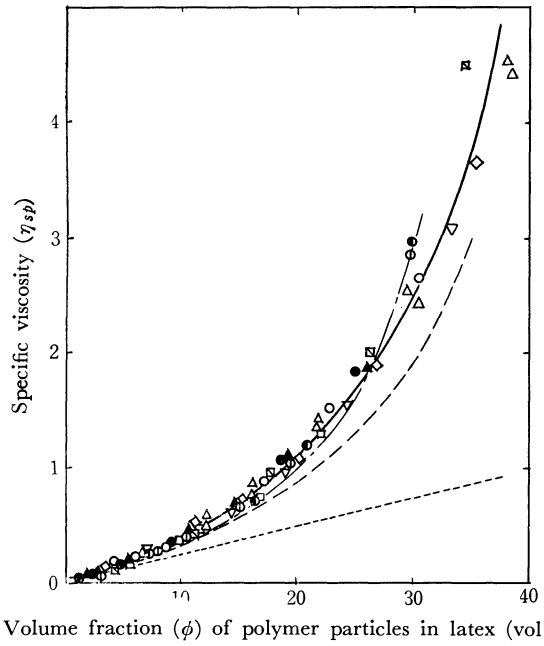

Fig. 5. Relations of η_{sp} and ϕ(vol%) for dialyzed latexes and those thickened.
It is the same with the symbols in Fig. 3 except those of the dialyzed latexes at 50°C, B-M ◐: H_2O and B-M-A ⓘ: H_2O.
——— Einstein's theoretical equation (2)
– – – – Hermans' theoretical equation (3)
------ Einstein's equation at very high dilution (4)

$$\eta_{sp} = (\eta/\eta_0) - 1 = 2.5\phi + 9.6\phi^2 + 31.6\phi^3, \quad (1)$$

where η and η_0 are the viscosities of the latex and its serum, *i.e.*, the dispersing medium, respectively. The broken line represents Einstein's theoretical equation[15] (2), the chain line is Hermans' theoretical equation[16] (3), and the dotted line is Einstein's equation (4) at a very high dilution:

$$\eta/\eta_0 = (1+\tfrac{1}{2}\phi)/(1-2\phi) = 1 + 2.5\phi + 5\phi^2 + 10\phi^3 + 20\phi^4 + \cdots, \quad (2)$$

$$\eta/\eta_0 = 1/(1-2.5\phi) = 1 + 2.5\phi + 6.3\phi^2 + 15.6\phi^3 + 39.0\phi^4 + \cdots, \quad (3)$$

$$\eta/\eta_0 = 1 + 2.5\phi. \quad (4)$$

The (1) empirical formula resembled both the theoretical equations, (2) and (3), and was half-way between Guth-Simha's[17] (5) and Vand's empirical formulae[18] (6), which have often been used:

$$\eta/\eta_0 = 1 + 2.5\phi + 14.1\phi^2 + \cdots, \quad (5)$$

$$\eta/\eta_0 = 1 + 2.5\phi + 7.35\phi^2 + \cdots. \quad (6)$$

The activation energies of flow for both latexes were independent of the concentration and were the same as that for water.

These results suggest that the viscosity of the latex is dependent on that of its dispersing medium and the volume fraction of its particles, and is independent of other factors for the first approximation.

Thickening of Latex with Alkali. As a comparison between the thickenability of the B–M–A latex with alkali in Fig. 3 and the degree of swelling in Fig. 4 shows, the results of the experiment support Wesslau's suggestion.[1] The fact that Eq. (1) was applicable to all the series in Fig. 5 provides a more rigorous description than Wesslau's, though; that is, an increase in the viscosity of a latex on the addition of alkali can be ascribed only to the swelling of the latex-particles.

This conclusion needs to be compared with Muroi's suggestion[2-4] that the dissolution of the surface layers of latex particles containing carboxyl groups and swelling of their cores on the addition of alkali cause the thickening of the latex. The dissolution of the surface layers in his investigation was ascribed to the larger number of carboxyl groups concentrated in the particle surface layers than in the present investigation. Accordingly, the conclusion in the present report does not contradict Muroi's suggestion.

Selection of Alkali for Thickening. It is usually said that the best alkaline thickener is one giving a thickening curve such as B in Fig. 6, and that NH_4OH is the best reagent. These facts can easily be illustrated by a comparison between the curve of the swelling of the B–M–A film with NH_4OH in Fig. 4 and the B-curve in Fig. 6. On the other hand, a

15) T. Katsurai, "Koroido no Riron," Kawaide Shoboo, Tokyo, (1947) p. 46; A. Einstein, *Ann. Physik*, (**4**) **19**, 289(1906), **34**, 591 (1911).
16) J. J. Hermans, "Flow Properties of Disperse Systems," North-Holland, Amsterdam (1953) p.167.
17) E. Guth and R. Simha, *Kolloid-Z.*, **74**, 266 (1936).
18) V. Vand, *J. Phys. Col. Chem.*, **52**, 277 (1949).

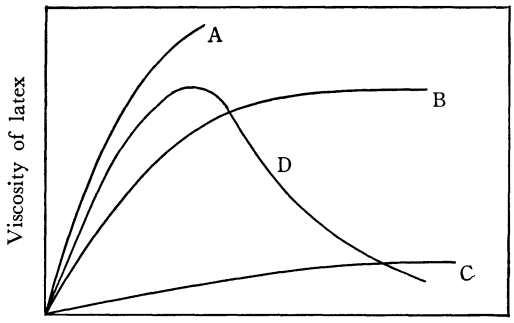

Fig. 6. Thickening of latex on addition of alkaline thickener.

concentrated aqueous solution of NaOH can not be regarded as a good thickener, as is shown in Fig. 3; the D-curve in Fig. 6 is a schematic illustration of this, and it can also be expected from Fig. 4.

The alkali concentration at the maximum value of the degree of swelling, as is shown in Fig. 4, provides information about the most suitable amount of alkali for the thickening of a latex because of the equivalence in the amounts of the carboxyl groups and the alkali ions, as has been described previously.

Particle Size and Its Distribution. Although both the latexes used differed considerably in their particle-size distributions, as is shown in Fig. 2, the $\eta_{sp}\sim\phi$ relations, Eq. (1), were nearly akin to Einstein's relation, Eq. (2), for suspensions of spheres of uniform size. These results suggest that a latex possessing such a size distribution may be regarded as a mono-dispersed system in view of fluid mechanics.

The viscosity of a latex containing a surface-active agent is dependent on the particle size and its distribution.[19] When such latexes are thickened, their flow properties become complex, as has been reported by several investigators.[5,6]

The simpler results obtained in the present investigation may be supposed to be caused by the complete dialysis of the latex.

This research was supported in part by a grant-in-aid for Fundamental Scientific Research from the Ministry of Education, for which the authors are grateful.

19) C. Parkinson, S. Matsumoto, and P. Sherman, *J. Colloid Interfac. Sci.*, **33**, 150 (1970).

BULLETIN OF THE CHEMICAL SOCIETY OF JAPAN, VOL. 44, 3344—3347 (1971)

The Semiconductive Property and the Phase Transition of the $[(C_6H_5)_3PCH_3]^+(TCNQ)_2^{-\cdot}$ Anion Radical Salt. The Entropy Change Due to Electrons and Holes

Yôichi IIDA

Department of Chemistry, Faculty of Science, Hokkaido University, Sapporo

(Received July 16, 1971)

The semiconductive organic crystal of $[(C_6H_5)_3PCH_3]^+(TCNQ)_2^-$ is known to undergo a first-order phase transition at 315.7°K. The discontinuity in the temperature dependence of the electrical conductivity takes place at the transition temperature, above which the populations of the electrons and the holes in the electrical conductivity increase abruptly. A theoretical consideration of the system of conduction carriers in an intrinsic semiconductor was developed in order to evaluate the entropy change of the electrons and holes at the phase transition. For $[(C_6H_5)_3PCH_3]^+$ $(TCNQ)_2^-$, this kind of entropy change was found to be much less than the total entropy change determined from the heat-capacity measurements by Kosaki *et al.* In view of these results, it was concluded that the anomaly in the electrical conductivity was induced by the change in the crystal structure.

There are a few organic semiconductors that are known to undergo phase transitions.[1,2] The phase transitions of such organic semiconductors are particularly interesting, since the anomalies in their electrical conductivities are associated with their phase transitions.

Much attention has been paid to the solid anion radical salts of 7,7,8,8-tetracyanoquinodimethane (TCNQ) because of their high electrical conductivities.[1-4] The phase transition of the TCNQ anion radical salt of methyltriphenylphosphonium, $[(C_6H_5)_3PCH_3]^+(TCNQ)_2^-$, is known to take place at 315.7°K.[1,5-7] Heat-capacity measurements of this phase transition have been made by Kosaki *et al.*[7] The transition has thus been found to be of the first order. The enthalpy and the total entropy change associated with the phase transition were experimen-

1) Y. Iida, M. Kinoshita, M. Sano, and H. Akamatu, This Bulletin, **37**, 428 (1964).

2) Y. Iida, *J. Phys. Soc. Jap.*, **30**, 583 (1971).

3) L. R. Melby, R. J. Harder, W. R. Hertler, W. Mahler, R. E. Benson, and W. E. Mochel, *J. Amer. Chem. Soc.*, **84**, 3373 (1962).

4) W. J. Siemons, P. E. Bierstedt, and R. G. Kepler, *J. Chem. Phys.*, **39**, 3523 (1963).

5) R. G. Kepler, *ibid.*, **39**, 3528 (1963).

6) Y. Iida, M. Kinoshita, A. Kawamori, and K. Suzuki, This Bulletin, **37**, 764 (1964).

7) A. Kosaki, Y. Iida, M. Sorai, H. Suga, and S. Seki, *ibid.*, **43**, 2280 (1970).

tally determined to be 485.18 cal/mol and 1.7206 cal/deg·mol respectively.

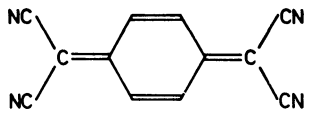

Fig. 1. 7,7,8,8-Tetracyanoquinodimethane (TCNQ).

On the other hand, the discontinuity in the temperature dependence of the electrical conductivity of $[(C_6H_5)_3PCH_3]^+(TCNQ)_2^-$ was observed at the transition temperature, where the electrical conductivity increased abruptly by a factor of about 3.5 in the higher temperature range.[1] This change was found to be reversible. If this anion radical salt belongs to an intrinsic semiconductor, the temperature dependence of the electrical conductivity, σ, below or above the transition temperature can be expressed by:

$$\sigma = \sigma_0 \exp(-E_g/2kT), \tag{1}$$

where E_g is the energy gap between the conduction band and the valence band. The energy gap in the low-temperature phase, E_g, was experimentally determined to be 0.82±0.04 eV, while that in the high-temperature phase, E_g', was thus determined to be 0.60±0.04 eV.[1] An appreciable decrease in the energy gap by about 0.22 eV in the high-temperature phase was found to be caused by the phase transition. Therefore, at the transition temperature, the abrupt increase in the electrical conductivity in the higher temperature range can be understood mostly in terms of the increase in the population of conduction carriers in the high-temperature phase. At this time, the abrupt increase in the electrons and the holes should cause some entropy creation at the phase transition.

The purpose of the present paper is to examine to what extent this kind of entropy change contributes to the total entropy change as determined by the heat-capacity measurements. For this purpose, a general statistical theory for the system of electrons and holes in an intrinsic semiconductor will be developed in the Theoretical section. The entropy change due to the electrons and holes was evaluated when a first-order phase transition takes place in the semiconductor. By applying this theory to the phase transition of $[(C_6H_5)_3PCH_3]^+$ $(TCNQ)_2^-$, we shall investigate the mechanism of the phase transition of this anion radical salt.

Theoretical

Let us consider, in general, the system of an intrinsic semiconductor, where the energy gap between the conduction band and the valence band is assumed to be E_g. In the case of a usual organic semiconductor, the band widths of both the conduction band and the valence band are narrow enough in comparison with the energy gap.[8,9] The carriers for the electrical conduction are excited electrons in the conduction band and holes in the valence band. For an intrinsic semiconductor, the number of the electrons is equal to that of the holes.

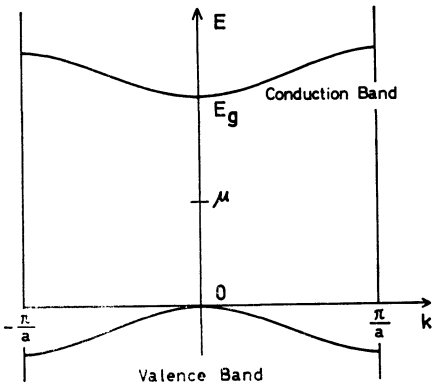

Fig. 2. A schematic representation of the band structure of an intrinsic semiconductor. The zero energy level is taken at the top of the valence band. E_g is the energy gap between the conduction band and the valence band, and μ is the level of the Fermi energy.

Electrons in Conduction Band. First, let us proceed to consider the electrons in the conduction band. It is convenient to describe this system as a grand canonical ensemble.[10] The grand partition function, Z_G, at the temperature T is represented by:

$$Z_G = \sum_{n_i} \exp(-\beta \sum_i \varepsilon_i n_i), \tag{2}$$

$$\varepsilon_i = E_i - \mu, \qquad \beta = \frac{1}{kT}, \tag{3}$$

where the sum with i runs over all the conceived quantum states. In the i th quantum state, E_i is the energy of an electron and n_i represents the number of electrons. μ is the chemical potential (*i.e.*, the Fermi energy). For the Fermi-Dirac statistics, since $n_i=0$ or 1,

$$Z_G = \prod_i (1 + e^{-\beta\varepsilon_i}). \tag{4}$$

The entropy of the system of the electrons in the conduction band, S(electron), can be derived from:

$$S(\text{electron}) = \frac{\partial}{\partial T}\left(\frac{1}{\beta}\ln Z_G\right)_{V,\mu} = k\sum_i \ln(1+e^{-\beta\varepsilon_i}) + T^{-1}\sum_i (e^{\beta\varepsilon_i}+1)^{-1}\varepsilon_i. \tag{5}$$

By using the form of the Fermi-Dirac distribution function of $f_i=1/(e^{\beta\varepsilon_i}+1)$, S(electron) is expressed as:

$$S(\text{electron}) = -k\sum_i [f_i \ln f_i + (1-f_i)\ln(1-f_i)]. \tag{6}$$

The first Brillouin zone in the conduction band is composed of N conduction levels, each of which includes α and β spin states. Then,

$$S(\text{electron}) = -2k\sum_{i=1}^{N} [f_i \ln f_i + (1-f_i)\ln(1-f_i)]. \tag{7}$$

In Eq. (3), the energy of the electron in the conduction band, E_i, and the Fermi energy of the intrinsic semiconductor, μ, are;

8) O. H. LeBlanc, *J. Chem. Phys.*, **33**, 626 (1960); R. G. Kepler, Org. Semicond. Proc. Inter-Ind. Conf., 1 (1962).
9) O. H. LeBlanc, *J. Chem. Phys.*, **35**, 1275 (1961); R. Silbey, J. Jortner, S. A. Rice, and M. T. Vala, Jr., *ibid.*, **42**, 733 (1965).
10) C. Kittel, "Elementary Statistical Physics," John Wiley & Sons, New York (1958).

$$E_i = E_g + \frac{\hbar^2 k_i^2}{2m_e}, \tag{8}$$

$$\mu = \frac{1}{2}E_g + \frac{3}{4}kT\ln\frac{m_h}{m_e}, \tag{9}$$

where $\hbar^2 k_i^2/2m_e$ is the kinetic energy of the electron and is related to the conduction band structure, and where m_e or m_h is the effective mass of the electron or the hole respectively. In the case of usual organic semiconductors, although it is very difficult to determine the precise band structures, the band widths of both the conduction band and the valence band are of the order of kT.[8,9] Since E_g is much larger than kT, one can neglect, in Eq. (8), $\hbar^2 k_i^2/2m_e$ in comparison with E_g, and μ is very nearly equal to $\frac{1}{2}E_g$. By the use of these approximations, the Fermi-Dirac distribution function of f_i is replaced by:

$$f = f_i \approx \frac{1}{\exp(E_g/2kT)+1}, \quad (i=1,2,\cdots, N). \tag{10}$$

Therefore, from Eq. (7), we have:

$$S(\text{electron}) = -2Nk[f\ln f + (1-f)\ln(1-f)]. \tag{11}$$

Holes in Valence Band. The holes in the valence band can be treated in a way similar to that of the electrons in the conduction band. In the case of the holes in the valence band, the Fermi-Dirac distribution function is:

$$f_i = \frac{1}{e^{-(E_i-\mu)/kT}+1}. \tag{12}$$

Here, the energy of a hole, E_i, in the valence band is:

$$E_i = -\frac{\hbar^2 k_i^2}{2m_h}. \tag{13}$$

If we assume that E_g is much larger than $\hbar^2 k_i^2/2m_h$,

$$f = f_i \approx \frac{1}{\exp(E_g/2kT)+1}, \quad (i=1,2,\cdots, N). \tag{14}$$

In this case, the entropy of the system of the holes in the valence band, S(hole), is found to be identical with that of the electrons in Eq. (11).

Entropy Change Associated with a First-order Phase Transition. By summing S(electron) and S(hole), the entropy per mol for the system of the conduction carriers in an intrinsic semiconductor, S(carrier), is then expressed as:

$$\begin{aligned} S(\text{carrier}) &= S(\text{electron}) + S(\text{hole}) \\ &= -4R[f\ln f + (1-f)\ln(1-f)]. \end{aligned} \tag{15}$$

Let us now consider the case when a first-order phase transition takes place in the intrinsic semiconductor at the temperature, T_c. The energy gaps for the low-temperature phase and the high-temperature phase are assumed to be E_g and E_g' respectively. At the transition temperature, the Fermi-Dirac distribution function, f, and the entropy for the system of the conduction carriers, S(carrier), in the low-temperature phase can be derived from the T_c and E_g values by means of Eqs. (10) and (15), while those in the high-temperature phase, f' and S'(carrier), can be derived from the T_c and E_g' values. Therefore, for the system of the conduction carriers, the entropy change, ΔS(carrier), at the phase transition is estimated to be:

$$\Delta S(\text{carrier}) = S'(\text{carrier}) - S(\text{carrier}). \tag{16}$$

Application of the Theory to the Phase Transition of $[(C_6H_5)_3PCH_3]^+(TCNQ)_2^-$

In this section, the above-mentioned theory will be applied to the phase transition of the anion radical salt of $[(C_6H_5)_3PCH_3]^+(TCNQ)_2^-$ at $T_c=315.7$°K. For this anion radical salt, as has been described in the Introduction, the energy gap between the conduction band and the valence band in the low-temperature phase, E_g, is 0.82 ± 0.04 eV, while that in the high-temperature phase, E_g', is 0.60 ± 0.04 eV.[1] Therefore, these values well fulfill the condition that both E_g and E_g' should be considerably larger than kT_c. The notations described in the preceding section will be used for f, S(carrier), f', and S'(carrier). From Eq. (10), f and f' at the transition temperature are evaluated approximately by:

$$f \approx \exp(-E_g/2kT_c), \tag{17}$$

$$f' \approx \exp(-E_g'/2kT_c). \tag{18}$$

Putting the values of f and f' into Eq. (15), we have;

$$S(\text{carrier}) = 3.7\times10^{-5}\ \text{cal/deg·mol}, \tag{19}$$

$$S'(\text{carrier}) = 1.5\times10^{-3}\ \text{cal/deg·mol}. \tag{20}$$

Therefore, for the phase transition of $[(C_6H_5)_3PCH_3]^+(TCNQ)_2^-$, the molar entropy change due to the electrons and holes for the electrical conduction is estimated to be:

$$\Delta S(\text{carrier}) = 1.5\times10^{-3}\ \text{cal/deg·mol}. \tag{21}$$

Discussion

The above-mentioned results clearly indicate that, in the phase transition of $[(C_6H_5)_3PCH_3]^+(TCNQ)_2^-$, the magnitude of $\Delta S(\text{carrier})=1.5\times10^{-3}$ cal/deg·mol is negligibly small in comparison with that of the total entropy change, $\Delta S(\text{obs})=1.7206$ cal/deg·mol, as determined from the heat-capacity measurements.[7] This means that it is quite hopeless to consider the system of the electrons and the holes in the electrical conduction as the main source of entropy creation at the transition. Therefore, most of the total entropy change was found to arise from other sources.

Let us examine the entropy change in the magnetic spins associated with the unpaired electrons on the TCNQ anion radicals. Obviously, the $[(C_6H_5)_3PCH_3]^+(TCNQ)_2^-$ anion radical salt is composed of the diamagnetic counter cations, TCNQ anion radicals, and formally neutral TCNQ molecules.[3-5] The magnetic spins ($S=1/2$) on the TCNQ anion radicals are known to be paired up by an exchange interaction.[5] This system contains a singlet ground state and a triplet exciton state. However, Kepler found a sharp discontinuity in the temperature dependence of the paramagnetic susceptibility of $[(C_6H_5)_3PCH_3]^+(TCNQ)_2^-$ at the transition temperature.[5] Chesnut showed that a certain type of order-disorder transition with respect to the triplet exciton density does occur if one includes in the inter-

action a term which is quadratic in the triplet exciton density, ρ.[11] In this case, the spin entropy change, ΔS(spin), associated with the phase transition is:

$$\Delta S(\text{spin}) = \tfrac{1}{2}R\Delta\rho \ln 3, \quad (22)$$

where $\Delta\rho$ is the change in the triplet exciton density at the transition. In a previous paper,[12] the present author estimated the value of ΔS(spin) for the phase transition of $[(C_6H_5)_3PCH_3]^+(TCNQ)_2^-$ to be 0.13 cal/deg·mol by the use of $\Delta\rho=0.12$, which was calculated from Kepler's data on the discontinuity in the paramagnetic susceptibility at the transition temperature.[5] Although the value of ΔS(spin) is appreciably larger than that of ΔS(carrier), the value of ΔS(spin) is again much less than that of ΔS(obs).

The above-mentioned investigations indicate that the rest of the entropy change, $\Delta S(\text{obs})-\Delta S(\text{carrier})-\Delta S(\text{spin})=1.59$ cal/deg·mol, should be ascribed to the entropy change due to the change in the crystal structure. It is important to note that the magnitude of this residual entropy change amounts to 92.4% of the total entropy change of ΔS(obs). In view of these results, we may conclude that the phase transition of the anion radical salt of $[(C_6H_5)_3PCH_3]^+(TCNQ)_2^-$ at 315.7°K comes mostly from some structural changes. The anomalies in the electrical conductivity and in the paramagnetic susceptibility are probably induced by the change in the crystal structures.

11) D. B. Chesnut, *J. Chem. Phys.*, **40**, 405 (1964).
12) Y. Iida, This Bulletin, **43**, 3685 (1970).

Concluding Remarks

For such semiconductors as $[(C_6H_5)_3PCH_3]^+(TCNQ)_2^-$, where the energy gap is considerably larger than kT, the magnitude of the entropy for the system of the electrons and holes in the electrical conduction is negligibly small, since the distributions of the electrons in the conduction band and of the holes in the valence band are quite limited at the temperature T.

On the other hand, however, the carrier population is very much increased for semiconductors in which the energy gap is comparable to kT. In this case, the magnitude of the entropy for the system of the electrons and holes becomes appreciably large. If these semiconductors undergo phase transitions, this kind of entropy should make a significant contribution to the mechanism of the phase transitions. In addition to the increase in the carrier population, the level of the Fermi energy in Eq. (9) is not located at the center between the conduction band and the valence band. Therefore, Eq. (14) for the holes in the valence band is no longer identical with Eq. (10) for the electrons in the conduction band. Since one cannot neglect the term of $\hbar^2k_i^2/2m_e$ in Eq. (8) or that of $\hbar^2k_i^2/2m_h$ in Eq. (13) in comparison with that of E_g, exact knowledge concerning the band structures of both the conduction band and the valence band will be required in order to evaluate the entropy due to the electrons and the holes.

The author would like to express his appreciation to Professor Akiko Ohno for her helpful discussions.

BULLETIN OF THE CHEMICAL SOCIETY OF JAPAN, VOL. 44, 3347—3352 (1971)

Stability and Extractability of Zinc(II) Thiocyanate Complexes in Several Solvent Extraction Systems

Hiromitsu MORIYA and Tatsuya SEKINE

Department of Chemistry, Science University of Tokyo, Kagurazaka, Shinjuku-ku, Tokyo

(Received March 18, 1971)

The formation and extraction equilibria of zinc(II) complexes with thiocyanate ions have been determined at 25°C. Zinc(II) ions in 1 M sodium perchlorate constant ionic media containing thiocyanate ions at various concentrations have been extracted into chloroform containing β-isopropyltropolone (IPT), into hexane containing trioctylphosphine oxide (TOPO), or into methyl isobutyl ketone (MIBK). The stability constants of the zinc(II) thiocyanate complexes in the aqueous phase were first determined from the decrease in the IPT chelate extraction, and then the distribution constants for the zinc(II) thiocyanate complexes into the latter two solvents were determined. The results were explained by saying that (i) zinc(II) forms the first ($\log \beta_1 = 0.56$), second($\log \beta_2 = 1.32$), and the third($\log \beta_3 = 1.18$) complexes in the above aqueous phase, (ii) TOPO in hexane extracts the second complex as an adduct in the $Zn(SCN)_2(TOPO)_2$ form, (iii) MIBK extracts both the second and the third complexes, and (iv) the addition of sodium perchlorate causes a salting-in effect in the lower-ligand-concentration region. Some discussion was made of the dissociation of ion-pairs in the organic phase.

Since Bock[1] reported a comprehensive study of the solvent extraction of metal ions as thiocyanate complexes, it has been recognized that thiocyanate extraction is an effective method for the separation of various metal ions. The solvent extraction of zinc(II) thiocyanate complexes has been studied both from the analytical and thermodynamical standpoints, and quantitative information about the chemical equilibria has been reported by several authors. Among them, Bock[1] first assumed that both the Zn-

1) R. Bock, *Z. anal. Chem.*, **133**, 110 (1951).

$(SCN)_2$ and $(NH_4)_2Zn(SCN)_4$ complexes are extracted into diethyl ether. Later on, Tribalat and Dutheil[2] determined the distribution of zinc(II) between methyl isobutyl ketone(MIBK) and aqueous 1 M sodium perchlorate constant ionic solutions containing various amounts of thiocyanate ions. They concluded, from an analysis of the distribution data, that all of the first, second, third, and fourth zinc(II) thiocyanate complexes are formed in the aqueous phase and that the $Zn(SCN)_2$ species is extracted into MIBK. The complex formation of zinc(II) in aqueous solutions with thiocyanate ions has been determined by various methods, and the stability constants have been reported.[3]

In the present investigation, the authors have also studied the complex formation of zinc(II) with thiocyanate ions and the extraction of them with trioctylphosphine oxide(TOPO) in hexane or with MIBK. They have determined the stability constants of the thiocyanate complexes in 1 M sodium perchlorate constant ionic media from the changes in the extraction of the divalent zinc ions with the chelating extractant, β-isopropyltropolone(IPT), in chloroform as a function of the thiocyanate concentration in the aqueous phase. Then they measured the extraction of zinc(II) thiocyanate complexes in these aqueous solutions into the two organic solvents, and the complex species in the organic phase were assigned from the distribution data. Some discussion was made of the extraction behavior in these systems and the extractability of each complex.

Experimental

Reagents. A radioactive tracer, zinc-65, was used in order to determine the distribution ratio of zinc(II). It was obtained from the New England Nuclear Co. as a hydrochloric acid solution. The tracer was diluted with a large amount of a 1 M sodium perchlorate solution and stored as the stock solution. The TOPO was obtained from the Dojindo Co. The IPT was obtained from the Takasago Koryo Co. The MIBK was obtained from the Tokyo Kasei Co.; it was washed with dilute perchloric acid, water, and a dilute sodium hydroxide solution respectively, and then several times with water. Sodium perchlorate was prepared from sodium carbonate and perchloric acid and recrystallized three times from water. The other reagents were of an analytical grade and were used without further purification. The concentration of the extractants in the organic solvents was calculated from the amount dissolved in the solvent, while that of the sodium perchlorate or thiocyanate solution was calculated from the weight of the residue left after a certain amount of the solution has been evaporated up in an air-bath at 120°C. The concentration of the thiocyanate solution was also determined by argentimetry.

Procedures. All of the procedures were carried out in a thermostated room at 25±0.5°C. Stoppered glass tubes (volume 20 m*l*) were used for the agitation of the two phases. A certain amount of the sodium thiocyanate solution, the tracer and an acetate buffer (the initial concentration in the aqueous phase was 0.01 M) and the sodium perchlorate solution were added to glass tubes, and then the organic solution was added. The initial concentration of zinc in the aqueous phase was 1×10^{-6} M. The hydrogen-ion concentration for the extraction with IPT was $10^{-3.3}$ to $10^{-5.3}$ M while for the extraction of the thiocyanate complexes, it was 10^{-4} to 10^{-5} M. The initial volume of the two phases was always 5.0 m*l*, and the ionic concentration in the aqueous phase was 1 M unless otherwise noted. The two phases in the tubes were agitated mechanically for about two hours and then centrifuged. A 2 m*l* portion was pipetted from each phase and transferred into small test tubes. The γ-radioactivity of the samples was measured with a well-type(NaI) scintillation counter. A small portion was also taken from the aqueous phase, and the hydrogen-ion concentration was measured potentiometrically by using a solution containing 1.00×10^{-2} M perchloric acid and 9.9×10^{-1} M sodium perchlorate as the standard of $-\log[H^+]$ 2.00 in the 1 M ionic medium.

Statistical

The formation and the stability constant for the "*n*th" zinc(II) complex with thiocyanate ions may be described as follows:

$$Zn^{2+} + nSCN^- \rightleftharpoons Zn(SCN)_n^{2-n}$$

$$\beta_n = \frac{[Zn(SCN)_n^{2-n}]}{[Zn^{2+}][SCN^-]^n} \quad (1)$$

The total concentration of zinc(II) in aqueous solutions containing thiocyanate ions can be described as;

$$[Zn(II)]_{total} = [Zn^{2+}] + [ZnSCN^+] + [Zn(SCN)_2] + [Zn(SCN)_3^-] + \cdots$$
$$= [Zn^{2+}](1 + \sum\beta_n[SCN^-]^n) \quad (2)$$

In the present paper, the subscript "*org*" denotes a chemical species in the organic phase, while the lack of any subscript denotes that in the aqueous phase.

(1) Extraction of Zinc(II) as Chelate Complexes. As was described in a previous paper,[4] the distribution ratios of zinc(II) from an aqueous phase containing no ligand, D_0, and that from an aqueous phase containing a ligand, L^-, can be described as follows if the concentration of the chelating extractant in the organic phase is the same;

$$D[H^+]^2/K_0 = (1+\sum\beta_n[SCN^-]^n)^{-1} \quad (3)$$

where $K_0=D_0[H^+]^2$.

As has been reported, the extracted zinc(II) complex with IPT in the organic phase is described as $ZnA_2(HA)$.[5] However, when the IPT concentration in the organic phase is kept constant, this K_0 should be constant as long as no IPT complexes are formed in the aqueous phase.[4,5] Thus, when the value of K_0 is determined in the absence of the ligand, the stability constants can be determined from this and the distribution ratio measured as a function of the ligand concentration by using Eq. 3.

2) S. Tribalat and C. Dutheil, *Bull. Soc. Chim. France*, **1960**, 160.

3) L. G. Sillén and A. E. Martell, "Stability Constants," Chem. Soc. Spec. Pub. **17**, (1964).

4) T. Sekine, M. Sakairi, F. Shimada, and Y. Hasegawa, This Bulletin, **38**, 847 (1965).

5) T. Sekine and D. Dyrssen, *J. Inorg. Nucl. Chem.*, **26**, 1463 (1964).

(2) Extraction of Zinc(II) as Thiocyanate Complexes. (a) Extraction of Uncharged Thiocyanate Complex: When the uncharged complex in the aqueous phase is extracted with a neutral extractant, E, in the organic phase, it is described as;

$$Zn(SCN)_2 + eE(org)_2 \rightleftarrows Zn(SCN)_2E_e(org)$$

$$Kex_e' = \frac{[Zn(SCN)_2E_e]_{org}}{[Zn(SCN)_2][E]^e_{org}} \quad (4)$$

The distribution ratio of zinc(II) in such a system can be described as;

$$D = \frac{[Zn(SCN)_2]_{org} + [Zn(SCN)_2E]_{org} + [Zn(SCN)_2E_2]_{org} + \cdots}{[Zn^{2+}] + [ZnSCN^+] + [Zn(SCN)_2] + [Zn(SCN)_3^-] + \cdots} \quad (5)$$

By introducing Eqs. (2) and (4) into Eq. (5), we obtain;

$$D = \frac{(1 + \sum^{1+E} Kex_e'[E]^e_{org})\beta_2[SCN^-]^2}{1 + \sum\beta_n[SCN^-]^n} \quad (6)$$

When the concentration of the extractant, E, is kept at b M, the following constant can be defined;

$$K_{DM2} = 1 + \sum Kex_e'b^e = \frac{[Zn(SCN)_2]_{org.total}}{[Zn(SCN)_2]} \quad (7)$$

Then Eq. (6) can be described as;

$$D = \frac{K_{DM2}\beta_2[SCN^-]^2}{1 + \sum\beta_n[SCN^-]^n} \quad (8)$$

(b) Extraction of Both Uncharged Complex and Ion-pairs of Anionic Complexes with Sodium Ions: When the organic solvent is a solvating polar one and extracts the neutral complex, the extraction equilibrium can be described as;

$$Zn(SCN)_2 \rightleftharpoons Zn(SCN)_2(org) \quad (9)$$

The extraction constant for this may also be described by Eq. (7) except that the solvation number of the complex cannot be defined.

The extraction of anionic complexes with sodium ions may also occur. The extraction of the third complex may be described as;

$$Zn(SCN)_3^- + Na^+ \rightleftharpoons NaZn(SCN)_3(org)$$

$$Kex_3'' = \frac{[NaZn(SCN)_3]_{org}}{[Zn(SCN)_3^-][Na^+]} \quad (10)$$

The ion-pair could dissociate in the organic phase;

$$NaZn(SCN)_3(org) \rightleftharpoons Na^+(org) + Zn(SCN)_3^-(org)$$

$$Kdiss(org) = \frac{[Na^+]_{org}[Zn(SCN)_3^-]_{org}}{[NaZn(SCN)_3]_{org}} \quad (11)$$

The concentration ratio of the third complex in the two phases can be described from Eqs. (10) and (11) as;

$$\frac{[NaZn(SCN)_3]_{org} + [Zn(SCN)_3^-]_{org}}{[Zn(SCN)_3^-]} = Kex_3''[Na^+]\left(1 + \frac{Kdiss(org)}{[Na^+]_{org}}\right) \quad (12)$$

In the present study, however, the sodium-ion concentration is kept at 1 M; moreover, as will be described later, that in the organic phase could also be regarded as constant in the lower-ligand-concentration region. Thus, from Eq. (12), an extraction constant can be defined as;

$$K_{DM3} = \frac{[NaZn(SCN)_3]_{org} + [Zn(SCN)_3^-]_{org}}{[Zn(SCN)_3^-]} \quad (13)$$

When both the second and the third complexes are extracted, the distribution ratio may be described as;

$$D = \frac{[Zn(SCN)_2]_{org} + [NaZn(SCN)_3]_{org} + [Zn(SCN)_3^-]_{org}}{[Zn^{2+}] + [ZnSCN^+] + [Zn(SCN)_2] + [Zn(SCN)_3^-] + \cdots} \quad (14)$$

By introducing Eqs. (2), (7), and (13), Eq. (14) can be described as;

$$D = \frac{K_{DM2}\beta_2[SCN^-]^2 + K_{DM3}\beta_3[SCN^-]^3}{1 + \sum\beta_n[SCN^-]^n} \quad (15)$$

(3) Graphic Analysis of the Distribution Data. The zinc(II) IPT chelate distribution data obtained as a function of the thiocyanate concentration and given by a $\log D[H^+]^2K_0^{-1}$ *vs.* $\log[SCN^-]$ plot (*cf.* Eq. (3)) may be treated by a curve-fitting method.[6,7]

When the stability constants for the thiocyanate complexes in the aqueous phase are thus obtained, the extraction data of the zinc(II) thiocyanate complexes with TOPO or MIBK can be determined by using these stability constants as follows.

When only the $Zn(SCN)_2$ complex is extracted into the organic phase, (*cf.* Eq. (8)), the distribution constant can be determined from;

$$K_{DM2} = D(1 + \sum\beta_n[SCN^-]^n)/\beta_2[SCN^-]^2 \quad (16)$$

When both the $Zn(SCN)_2$ and $Zn(SCN)_3^-$ complexes are extracted (*cf.* Eq. (15)), the distribution data can be described as;

$$Y = \log \frac{D(1 + \sum\beta_n[SCN^-]^n)}{[SCN^-]^2} = \log(K_{DM2}\beta_2 + K_{DM3}\beta_3[SCN^-]) \quad (17)$$

When the data are plotted as Y *vs.* $\log[SCN^-]$, they may be fitted by the standard curve[5-7];

$$Y = \log(1 + v), \quad X = \log v \quad (18)$$

and the constants, K_{DM2} and K_{DM3}, can be determined from the curve-fitting and from the β_2 and β_3 values which have already been obtained from the IPT extraction.

Results

The extraction of zinc(II) in a 1 M sodium perchlorate solution into chloroform containing 0.1 M IPT was determined as a function of the hydrogen-ion concentration. The value of the constant, K_0, in Eq. (3) was obtained from the results as;

$$\log K_0 = -8.38$$

It was found that the K_0 value is independent of the hydrogen-ion concentration in the range of $-\log[H^+]$ 3.5 to 5.0 when the IPT concentration in the organic phase is 0.1 M.

Figure 1 shows the decrease in the zinc(II) extrac-

6) T. Sekine and M. Ono, This Bulletin, **38**, 2087 (1965).
7) T. Sekine, M. Sakairi, and Y. Hasegawa, *ibid.*, **39**, 2141 (1966).

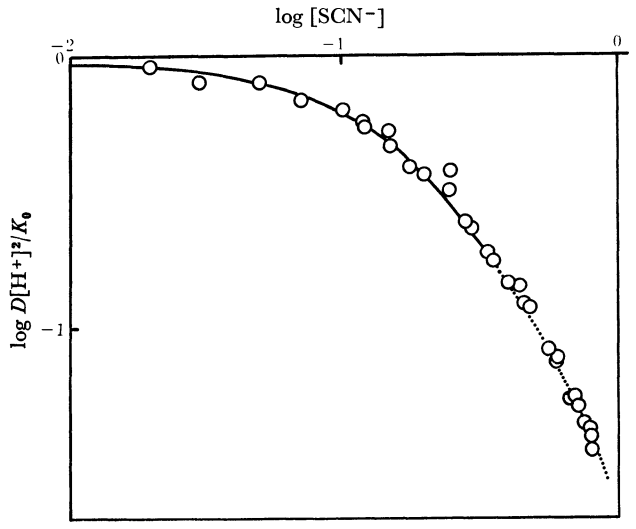

Fig. 1. Decrease in the Zn(II) extraction with IPT as a function of the aqueous thiocyanate concentration. Org. phase; chloroform containing 0.1 M IPT, Aq. phase; 1M Na(SCN, ClO_4). The solid curve is;
$\log D[H^+]^2K_0^{-1} = -\log(1+3.7[SCN^-]+21[SCN^-]^2+15[SCN^-]^3)$

TABLE 1. STABILITY AND DISTRIBUTION CONSTANTS OF Zn(II) THIOCYANATE COMPLEXES IN 1 M Na(SCN, ClO_4) AT 25°C

(a) Stability constants in the aqueous phase.

$\log\beta_1$	$\log\beta_2$	$\log\beta_3$	$\log\beta_4$	Remarks
0.56	1.32	1.18	—	Present work
−0.3	0.5	0.8	1.7	Ref. 2

(b) Distribution constants.

Organic phase	$\log K_{DM2}$	$\log K_{DM3}$
Hexane containing 1.0×10^{-3} M TOPO	1.45	—
MIBK	1.39	3.63

tion with IPT as a function of the thiocyanate concentration in the aqueous phase. This plot was analyzed graphically by using Eq. (3), and the best-fit was obtained when the formation of the first, second, and third complexes was assumed. The stability constants obtained are given in Table 1. The solid curve in Fig. 1 was drawn by using these constants.

Figure 2 gives the distribution ratio of zinc(II) between 1 M Na(SCN, ClO_4) ($-\log[H^+]$ was 4 to 5) and MIBK(closed circles) or hexane containing 1.0×10^{-3} M TOPO(open circles) as a function of the thiocyanate concentration. From these data and the stability constants of thiocyanate complexes in Table 1, the value of Y in Eq. (17) was determined for each plot, these values are given in Fig. 3. It may be seen from Fig. 3 that the values of Y for the TOPO extraction are almost constant in the thiocyanate concentration region from 8×10^{-3} M to 3×10^{-1} M; in other words, the values of K_{DM2} in Eq. (16) are not dependent on the thiocyanate concentration, and thus the only zinc(II) species in the organic phase should be the $Zn(SCN)_2$ complex. It was found that

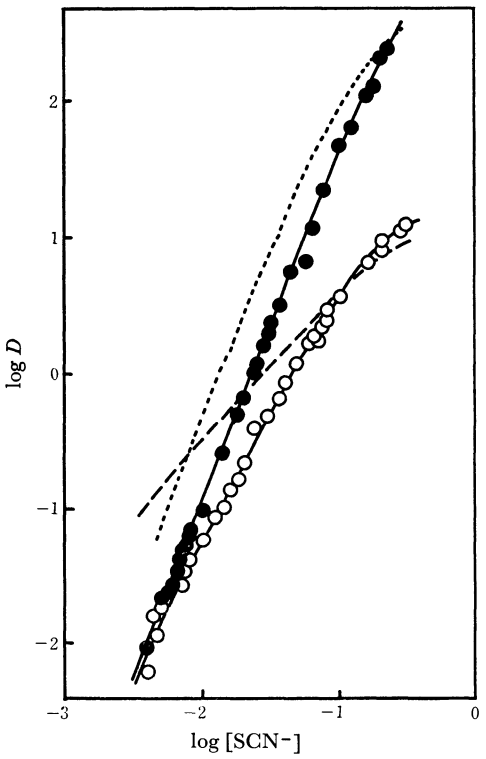

Fig. 2. Extraction of Zn(II) thiocyanate complexes as a function of the aqueous thiocyanate concentration. Org. phase; ○ hexane containing 1.0×10^{-3} M TOPO, ● MIBK, Aq. phase; 1M Na(SCN, ClO_4). The solid curves are;
$\log D=\log 5.8\times10^2[SCN^-]^2/(1+3.7[SCN^-]+21[SCN^-]^2+15[SCN^-]^3)$: ○
$\log D=\log(5.2\times10^2[SCN^-]^2+6.4\times10^4[SCN^-]^3)/(1+3.7[SCN^-]+21[SCN^-]^2+15[SCN^-]^3)$: ●
The broken line and the dotted line show the extraction into hexane containing 1.0×10^{-3} M TOPO or MIBK, respectively, when the aqueous phase is sodium thiocyanate solution containing no sodium perchlorate.

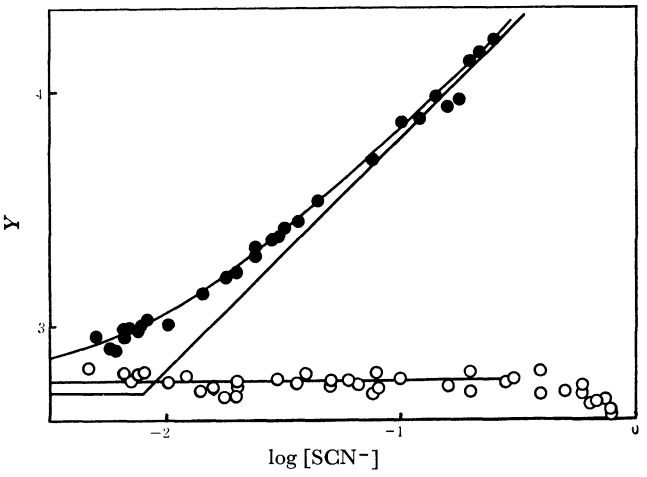

Fig. 3. Graphic analysis of the extraction data (○: TOPO, ●: MIBK).
The ordinate is; $Y=\log D(1+3.7[SCN^-]+21[SCN^-]^2+15[SCN^-]^3)/[SCN^-]^2$
The solid lines are; $Y=2.77$: ○, $Y=\log(5.2\times10^2+6.4\times10^4[SCN^-])$: ●

the distribution ratio between an aqueous phase containing 0.3 M thiocyanate ion and organic phases containing various amounts of TOPO is proportional to

the square of the TOPO concentration in the range of the TOPO concentrations from 2×10^{-4} M to 3×10^{-3} M; thus, the extraction equilibrium can be given by;

$$Zn(SCN)_2 + 2TOPO(org) \rightleftharpoons Zn(SCN)_2(TOPO)_2(org) \quad (19)$$

The distribution constant defined by Eq. (4) ($[Zn(SCN)_2(TOPO)_2]_{org}/[Zn(SCN)_2][TOPO]_{org}$) was obtained as $10^{7.45}$, and that defined by Eq. (7), was $10^{1.45}$ (at 1.0×10^{-3} M TOPO). The solid curve for the TOPO plot in Fig. 2 is a curve calculated by using Eq. (8) and the stability and the distribution constants obtained.

The slope of the extraction curve into MIBK in Fig. 2 is higher than that into hexane containing TOPO; this may be supposed to be due to the extraction of the higher thiocyanate complexes. The value of Y in Eq. (17) was calculated for each plot and plotted against log[SCN$^-$], as is shown in Fig. 3. The plot in Fig. 3 was fitted with the standard curve in Eq. (18). The best-fit curve is shown by the solid curve in Fig. 3. From the parameters of the best-fit curve, the distribution constants in Eqs. (7) and (13) were determined on the basis of Eq. (17). The solid curve for the MIBK plot in Fig. 2 is the curve calculated by using Eq. (15) and the stability and the distribution constants obtained.

Figure 4 shows the percentage distribution of the concentrations of zinc(II) species in the aqueous phase, and those in the hexane phase containing TOPO and in MIBK phase in an equilibrium with the aqueous phase.

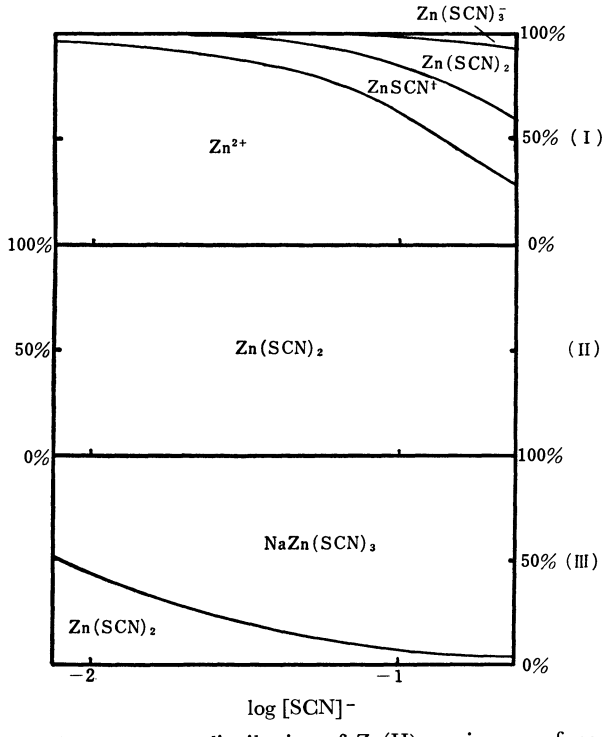

Fig. 4. Percentage distribution of Zn(II) species as a function of the thiocyanate concentration calculated from the constants in Table 1.
(I) 1 M Na(SCN, ClO_4). (II) hexane containing 1.0×10^{-3}M TOPO which is in an equilibrium with (I). (III) MIBK which is in an equilibrium with (I).

The above extractions were always made from the 1 M constant ionic medium. In order to ascertain the effect of the coexisting sodium perchlorate, extraction was also made from sodium thiocyanate solutions containing no sodium perchlorate.

The broken line and the dotted line in Fig. 2 give the extraction curve from these aqueous phases, in which the ionic concentration was not kept constant.

The results described above may be summarized as follows: (i) The extraction curve of zinc(II) in the 1 M Na(SCN, ClO_4) solutions with IPT was explained in terms of the formation of the first, second, and third complexes. The stability of the third complex is not high ($K_3=[Zn(SCN)_3^-]/[Zn(SCN)_2]$ [SCN$^-$] $=10^{-0.14}$). The stability constants given in Table 1 seem to be reasonable because they can explain the zinc(II) thiocyanate extraction with TOPO or MIBK. (ii) The extraction of zinc(II) into hexane containing TOPO was explained in terms of the extraction of the second complex species with two molecules of TOPO. (iii) The extraction of zinc(II) into MIBK was explained in terms of the extraction of the second and the third complexes. (iv) When the aqueous phase contains only sodium thiocyanate, the extraction becomes somewhat higher than that from the constant ionic medium in the region where the thiocyanate concentration is lower than 0.1 M.

Discussion

The extracted ion-pairs, $Na^+Zn(SCN)_3^-$, could dissociate in MIBK. When the dissociation occurs, the extraction of the third complex should be dependent on the sodium concentration in the organic phase, as may be seen from Eq. (12) (the sodium ion concentration in the aqueous phase is kept constant). When the other charged species, such as protons and hydroxide ions, are negligible, the following equation can be written on the basis of the electrical neutrality in the organic phase;

$$[Na^+]_{org} = [ClO_4^-]_{org} + [SCN^-]_{org} + [Zn(SCN)_3^-]_{org} \quad (20)$$

In the present study, the concentration of zinc(II) in the initial aqueous phase is 1×10^{-6} M; this is much lower than the concentration of sodium perchlorate in MIBK (that was estimated to be 1×10^{-2} M[8]). Although no information is availabe about the dissociation of sodium perchlorate and that of the extracted $NaZn(SCN)_3$ ion-pairs, it is most probable that the sodium-ion concentration in the organic phase is constant. Because the concentrations of zinc(II) and sodium thiocyanate in the aqueous phase are much smaller than that of sodium perchlorate under the experimental conditions used in the present study, Eq. (20) can be regarded as $[Na^+]_{org}\simeq[ClO_4^-]_{org}$. Thus the K_{DM3} defined by Eq. (13) could be regarded as a constant in this study.

The stability constants obtained in the present study indicate that they are not very stable. The

8) Y. Hasegawa, T. Ishii, and T. Sekine, This Bulletin, **44**, 275 (1971).

values of the stability constants in the literature[3] are rather scattered. The constants reported in the same ionic medium as in the present study by Tribalat and Dutheil[2] in Table 1 are also somewhat different from the present results; their constant for the first, second, and third complexes are lower than those in the present study, and they estimated a formation of a fourth complex in the same medium which was not found by the present authors.

The extraction curve of zinc(II) from the 1 M Na (SCN, ClO_4) solution into MIBK reported by Tribalat and Dutheil (Fig. 1 in Ref. 2) almost agrees with the results shown in Fig. 2. They analyzed the data by assuming that only the uncharged complex, $Zn(SCN)_2$, is extractable among the four complexes. In the present study, however, it was concluded that both the uncharged complex and the uninegative charged third complex are extracted into the MIBK phase. This assumption seems to be well supported by the extraction data with TOPO in hexane. It may be seen in Fig. 2 that the slope of the plot of the TOPO extraction becomes smaller in the highest-ligand concentration region than that of the MIBK extraction, and the calculated curves from the stability constants obtained by the IPT extraction, shown in Fig. 2 or in Fig. 3, fit the experimental results well.

This seems to agree with the results expected from the nature of the solvents. Hexane containing a small amount (1×10^{-3} M) of TOPO can be regarded as a nonpolar solvent to which the extraction of a polar species such as ion-pairs is unfavorable(although it is possible to extract ion-pairs into a hexane solution of TOPO, especially when the TOPO concentration is high[9]). On the other hand, as has been reported for many MIBK extraction systems,[9-12] the extraction of negatively-charged metal thiocyanate complexes as ion-pairs with cations in the background salt or that of pairs of the sodium ion and the perchlorate ion[8] seems to be very common into this polar and relatively high-dielectric-constant ($\varepsilon=12$) solvent, which also has a great ability of solvation on metal species.

It is remarkable that the log D *vs.* log[SCN^-] plot of the MIBK extraction in Fig. 2 is nearly a straight line with a slope of +2.5. As can be seen from the figures and Eq. (17), this apparent tendency for the log D *vs.* log[SCN^-] plot to be almost a straight line is probably due to the fact that, although the extraction of the uncharged complex does not increase any more in the highest concentration (this is the reason why the slope of the extraction curve with TOPO in Fig. 2 approaches zero), the extraction of the third complex, which increases in the highest region, will still enhance the distribution ratio. When the log D *vs.* log[SCN^-] plot is practically a straight line, in other words, when $\log D=n\log[SCN^-]=c$ where n or c is a constant, it seems to be usually difficult to determine the equilibrium constants, β_n and k_{DMn}, in Eq. (15) simultaneously from the extraction data due to the experimental errors. In the present study, the stability constants, β_n, had already been determined by separate experiments, and, as these constants were available, only the determination of K_{DMn} in Eq. (15) was necessary for the analysis of the equilibrium.

As may be seen in Fig. 2, the extraction curve is different when the aqueous phase is a constant ionic medium and when it contains only sodium thiocyanate. This is probably due in part to the changes in the activity coefficients of the chemical species by the change in the ligand concentration (and, consequently, by the change in the ionic strength); at the same time, it is probable also due to the lower concentration of sodium in the aqueous phase in the MIBK system, as can be seen from Eqs. (10) and (12).

The extraction in analytical work are usually carried out with no control of the activity or in the presence of various other electrolytes in the aqueous phase; in order to make a quantitative analysis of the extraction curves obtained under such conditions, a correction for these factors is indispensable. However, such a correction of the activity (not only of the ligand and metal ions, but also of all the other chemical species connected with the extraction, such as the complexes or the coexisting salts) is usually very difficult; thus, the information available from usual analytical data on the chemical equilibria involved in the systems is of limited use.

The authors are grateful to Mr. Naohiko Ihara of the present laboratory for his experimental aid and invaluable discussions during the work. Part of this work has been carried out in the Laboratory of Analytical and Nuclear Chemistry, Institute of Physical and Chemical Research. The authors are grateful to Professor Nobufusa Saito, the head of the laboratory.

9) T. Sekine, R. Murai, and M. Iguchi, *Nippon Kagaku Zasshi*, **92**, 412 (1971).
10) T. Sekine and T. Ishii, This Bulletin, **43**, 2422 (1970).
11) S. Tribalat and C. Zeller, *Bull. Soc. Chim. France*, **1962**, 2041.
12) Y. Hasegawa, H. Takeuchi, and T. Sekine, This Bulletin, to be published.

Metal Complexes with Amino Acid Amides. III. Geometrical Structures and Electronic Spectra of Bis(α-amino-acid-amidato)palladium(II), -nickel(II) and -copper(II)

Takashi KOMORITA, Jinsai HIDAKA, and Yoichi SHIMURA

Department of Chemistry, Faculty of Science, Osaka University, Toyonaka, Osaka

(Received March 25, 1971)

Square planar complexes of $[ML_2]$ type were synthesized, where M=Pd^{2+} and Ni^{2+} for L=L-valine-, L-phenylalanine- and L-proline-amidate anions, and M=Pd^{2+}, Ni^{2+} and Cu^{2+} for L=L-leucinemethylamidate anion and for L_2=trimethylenediamine-*N*,*N*′-diisobutyric acid amidate dianion; the last ligand is a tetradentate one and gives exclusively *cis* type complexes. *Cis* and *trans* isomers were isolated and identified for each of the L-valinamidato and the L-prolinamidato palladium complexes. All the other complexes were inferred to be *trans* isomers from examination of the electronic absorption and circular dichroism spectra. Common solvent effects of the ligand field bands were clearly observed between the *trans* palladium and *trans* nickel complexes. A similar empirical relationship was also found between the ligand field bands of the *trans* palladium complexes and those of the corresponding *cis* isomers. The spectral behavior of the bis(L-amino-acid-amidato)-copper(II) complexes was not so easily related to that of the corresponding nickel or palladium complexes. The ligand field bands of the palladium, nickel, and copper complexes were tentatively assigned.

In the previous papers of this series,[1,2] square planar bis-chelate complexes of palladium(II), nickel(II) and copper(II) with several α-amino acid amidate ligands were reported. A pair of isomers were prepared for each of bis(L-alaninamidato)- and bis(L-leucinamidato)-palladium(II), but only one isomer was isolated for every nickel(II) and copper(II) complex examined. It has been concluded from the electronic, IR, and NMR spectra that all the complexes cited are of square planar $[M(N)_4]$ type, and that the pairs of palladium(II) complexes are of *cis* and *trans* isomers. The nickel(II) and copper(II) complexes have been considered to be mostly *trans* in solid state or in solution with a few exceptions.

The most interesting fact found in the study of the electronic absorption (AB) and circular dichroism(CD) spectra of these complexes is the similarity of the ligand field bands of the *trans* nickel complexes to those of the corresponding palladium complexes.[1,3] We believe that a comparative study of CD spectra will useful for the elucidation of the electronic structure of square planar complexes. With this view in mind we decided to extend our work to the complexes with additional ligands.

The purpose of the present study is to confirm the previous conclusion concerning the geometrical structures of the bis(α-amino-acid-amidato) complexes, and to investigate their AB and CD spectra more extensively. Bis(α-amino-acid-amidato) type complexes of palladium(II), nickel(II), and copper(II) were prepared with some optically active L-α-amino-acid amides and with a tetradentate ligand which gives *cis* type complexes exclusively.

Experimental

Materials. *1) Ligands*:[4] *Trimethylenediamine*-N,N′-*diisobutyric Acid Amide*: *tndbaH*$_2$: When trimethylenediamine dihydrochloride was used in place of the ethylenediamine analog in Schlesinger's method for ethylenediamine-*N*,*N*′-diisobutyronitrile,[5] trimethylenediamine-*N*,*N*′-diisobutylonitrile was obtained from the ether layer as rhombic plates in good yield. This compound is soluble in ether; mp 90—92°C (uncorr.).

Found: C, 63.68; H, 9.81; N, 26.86%. Calcd for $C_{11}H_{20}N_4$: C, 63.43; H, 9.68; N, 26.90%.

The dinitrile (17.7 g) was suspended in 75 m*l* of concentrated hydrochloric acid under ice cooling and the mixture was allowed to stand overnight at room temperature. The dinitrile was then dissolved. When necessary, hydrogen chloride gas was bubbled into the mixture in order to complete the dissolution. The dihydrochloride salt of the desired compound was obtained as white crystals from the solution by diluting with equivolume of water and cooling in an ice bath. The crystals were filtered off and washed with methanol and then ether. Recrystallization was carried out by concentrating the aqueous solution *in vacuo*. The yield was good.

Found: C, 41.44; H, 8.36; N, 17.37%. Calcd for $C_{11}H_{26}N_4O_2Cl_2$: C, 41.64; H, 8.26; N, 17.66%.

The desired amide $tndbaH_2$ was derived from the dihydrochloride by ion exchange chromatography with Amberlite IRA-410 (OH^--type). This was recrystallized from chloroform and dried at 60°C *in vacuo*. Elongated rectangular plates; mp 140.5—141.5°C (uncorr.).

Found: C, 54.03; H, 9.98; N, 22.88%. Calcd for $C_{11}H_{24}N_4O_2$: C, 54.07; H, 9.90; N, 22.93%.

Other Ligands: L-Valinamide, L-Phenylalaninamide and L-prolinamide were prepared as described elsewhere.[2] L-Leucinemethylamide was prepared according to literature;[6] bp 97—106°C/2 mmHg.

2) $[Pd(tndba)]\cdot 5H_2O$: Forty milliliters of aqueous solution containing 0.75 g of lithium tetrachloropalladate-

1) Part I: T. Komorita, J. Hidaka, and Y. Shimura, This Bulletin, **41**, 854 (1968).

2) Part II: T. Komorita, J. Hidaka, and Y. Shimura, *ibid.*, **42**, 168 (1969).

3) T. Komorita, J. Hidaka, and Y. Shimura, *ibid.*, **42**, 1782 (1969).

4) The following abbreviations are used for ligands: alaaH=alaninamide, leuaH=leucinamide, valaH=valinamide, phalaaH=phenylalaninamide, proaH=prolinamide, leumaH=leucinemethylamide and $tndbaH_2$=trimethylenediamine-*N*,*N*′-diisobutyric acid amide.

5) N. Schlesinger, *Ber.*, **44**, 1135 (1911).

6) A. Rosenberg, *Acta Chem. Scand.*, **11**, 1390 (1957).

(II)[7] was added to a solution of 0.76 g of tndbaH_2 in 35 m*l* of water with stirring. When a clear solution was obtained after stirring for several minutes, the brownish yellow solution was carefully neutralized under pH adjustment with 1 N lithium hydroxide. It took about 100 min for neutralization. The end point was detected when it was observed that the pH was retained at 7.3 for 30 min without further addition of alkali. A crude complex was obtained from the pale yellow solution by concentrating it to near dryness and adding a small amount of ethanol and a large amount of acetone. Purification was performed by ion exchange chromatography with the required amount of 1 : 2 mixture (by volume) of Amberlite IR-120B (H^+-type) and IRA-410 (OH^--type). The eluate was concentrated *in vacuo* below 35°C until the complex began to crystallize and allowed to stand under ice cooling. The pale yellow needles were filtered off, washed with a small volume of cold water twice and dried in air.

Found: C, 30.12; H, 7.34; N, 12.59%. Calcd for $C_{11}H_{32}N_4O_7Pd$: C, 30.11; H, 7.35; N, 12.77%.

3) trans-[*Pd*(L-*vala*)$_2$] *and* cis-[*Pd*(L-*vala*)$_2$]·*0.5*H_2O: Twenty milliliters of aqueous solution containing 1.48 g of lithium tetrachloropalladate(II)[7] was added to a solution of 1.44 g of L-valaH in 20 m*l* of water with stirring. The resulting brown solution was treated with 0.5 N lithium hydroxide in a similar way to that for 2). The pale yellow solution was concentrated *in vacuo* until it became a syrup. Most of the lithium chloride was removed from the syrup by dissolving it in a few m*l* of ethanol and then by extracting it three times with 30 m*l* of ether each time. The same purification procedure was repeated once more. The residual viscous syrup was dissolved in 50 m*l* of 99% ethanol. To this solution, 450 m*l* of ether was added little by little, and the mixture was kept in a refrigerator overnight. After the supernatant solution was removed by decantation, the precipitate was dissolved in 50 m*l* of 99% ethanol again, and reprecipitated carefully from this solution by adding 500 m*l* of ether. At this stage, the crude complex (a *cis-trans* mixture) was obtained as a fine powder, which was washed with ether and dried *in vacuo*. The mixture was fractionally recrystallized by addition of acetone to the concentrated aqueous solution. All fractions of the fibrous crystals, which were washed with a (1 : 10) water-acetone mixture and then with acetone, were collected (1.23 g). Then the contaminated lithium chloride was completely eliminated with an ion exchange column as described in 2). The eluate was concentrated by a rotary evaporator, and then diluted to about one fifth of the saturated concentration. Isolation of the *cis* and *trans* isomers from this solution was performed by fractional crystallization with acetone. Purity of the isomers was checked by the uniformity of the crystals as well as by the reproducibility of the CD spectrum. The *trans* isomer was isolated as glistening fine plates, which had been suspended in the solution at the beginning of crystallization and grew rather slowly. On the other hand, the cis isomer grew more rapidly from the wall of a beaker as prisms, and its aqueous solution was inclined to be supersaturated.

The *trans* isomer: dried over calcium chloride.

Found: C, 35.50; H, 6.24; N, 16.49%. Calcd for $C_{10}H_{22}N_4O_2Pd$: C, 35.67; H, 6.59; N, 16.64%.

The *cis* isomer: dried in the atmosphere.

Found: C, 34.78; H, 6.74; N, 16.15%. Calcd for $C_{10}H_{23}N_4O_{2.5}Pd$: C, 34.74; H, 6.71; N, 16.21%.

7) In practice, lithium chloride and palladium(II) chloride were dissolved in water.

Both isomers are pale yellow, and soluble in water, methanol, ethanol, and *N,N*-dimethylformamide (DMF).

4) trans-[*Pd*(L-*phalaa*)$_2$]: A solution of 1.50 g of L-phalaaH in 25 m*l* of water was slowly added to 60 m*l* of an aqueous solution containing 1.10 g of lithium tetrachloropalladate(II).[7] Together with the brownish precipitate, the whole mixture was subjected to a similar neutralization procedure as in 2). The color of both the precipitate and the supernatant solution then changed to pale yellow. The mixture was continuously stirred for 2 additional hr. Yield of the precipitate, or the desired complex in a crude state, was 1.48 g (82%). This could be recrystallized from a (1 : 2) water-methanol mixture; dried *in vacuo* over phosphorus pentoxide; pale yellow plates; soluble in methanol and ethanol, and slightly soluble in DMF.

Found: C, 50.09; H, 5.17; N, 12.86%. Calcd for $C_{18}H_{22}N_4O_2Pd$: C, 49.95; H, 5.12; N, 12.95%.

5) trans-[*Pd*(L-*proa*)$_2$]·*0.5*H_2O *and* trans-[*Pd*(L-*proa*)$_2$]·CH_3OH: To a solution containing 1.41 g of L-proaH in 40 m*l* of water was added 1.00 g of a powdered palladium(II) chloride, and the suspension was continuously stirred until most of the palladium(II) chloride was dissolved. This took about 40 min. The mixture was then neutralized with an anion exchange resin, Dowex 1×8 (50—100 mesh) of OH^--type. The resin was added little by little with mechanical stirring so that the pH of the mixture was kept under 8. A precipitate was produced at the beginning of the neutralization procedure, but it disappeared as the reaction proceeded. The end point of the neutralization was determined in the same way as in 2). The whole procedure took about 5 hr, and about twice the calculated amount of anion exchange resin was needed. The resin and the residual starting material were discarded by filtration. From the resulting yellow solution, the desired *trans* complex was isolated as a hemihydrate or a methanol adduct. The total yield of the *trans* complexes was 47%, but we could not isolate the *cis* isomer in this procedure.

Hemihydrate: The yellow solution prepared as above was concentrated *in vacuo*. An appropriate amount of acetone was added to the solution and the mixture was cooled in an ice bath. The yellow microcrystals were collected on a glass filter, washed with (1 : 10) water-acetone mixture and acetone, and dried over calcium chloride. Very long plates.

Found: C, 35.62; H, 5.59; N, 16.15%. Calcd for $C_{10}H_{19}N_4O_{2.5}Pd$: C, 35.15; H, 5.60; N, 16.40%.

Methanol Adduct: The yellow solution prepared as above was concentrated to dryness *in vacuo*. The residuals were dissolved in methanol and the methanol solution was concentrated *in vacuo*. The yellow prisms were washed with a small amount of methanol, acetone, and ether, and dried over phosphorus pentoxide *in vacuo*.

Found: C, 35.85; H, 6.00; N, 15.54%. Calcd for $C_{11}H_{22}N_4O_3Pd$: C, 36.23; H, 6.08; N, 15.36%.

Both the hemihydrate and the methanol adduct are soluble in water, methanol, and ethanol.

6) cis-[*Pd*(L-*proa*)$_2$]·*3.5*H_2O: A solution containing 1.48 g of lithium tetrachloropalladate(II)[7] in 60 m*l* of water was mixed with a solution of 1.41 g of L-proaH in 20 m*l* of water. The mixture was neutralized with 0.5 N lithium hydroxide in the same way as that in 2). The yellow solution was concentrated to one fifth of its original volume *in vacuo* and treated with an ion exchange column as in 2), where about twice the calculated amount of resin was used. The first fraction of crystalline products was deposited when the eluate was concentrated to a few m*l*. From the mother liquor two additional fractions were obtained by fractional addition of acetone. Each fraction consisted mainly of

needle crystals and was contaminated by a small amount of plates, or the *trans* isomer. The first two fractions, rich in *cis* isomer, were combined and fractionally recrystallized from the aqueous solution by addition of acetone. The pure *cis* complex consisted of fine yellow needles. Its purity was checked by the CD spectrum as it was difficult to distinguish it from the *trans* complex by their crystal forms only. The sample for elemental analyses was dried in air.

Found: C, 30.28; H, 6.34; N, 14.06%. Calcd for $C_{10}H_{25}N_4O_{5.5}Pd$: C, 30.35; H, 6.37; N, 14.16%.

This complex is soluble in water, methanol, ethanol and DMF. Total yield of the crude complex, contaminated with a small amount of the *trans* isomer, was rather low, 0.71 g (*ca.* 32%). It should be added that considerable amounts of both isomers were separated from the column used in the above preparation when eluted with a concentrated sodium chloride solution.

7) trans-[*Pd(*L-*leuma)*$_2$]: A solution containing 1.32 g of lithium tetrachloropalladate(II)[7] in 70 m*l* of water was added to 80 m*l* of an aqueous solution containing 1.58 g of L-leumaH with stirring. The brown solution was neutralized as in 2) by use of 0.5 N lithium hydroxide. When the resulting solution was concentrated *in vacuo*, the desired complex was deposited as yellow hexagonal plates; yield, 1.85 g (94%). It was recrystallized by concentrating the aqueous solution *in vacuo*. The pure crystals were washed with water and then dried over calcium chloride.

Found: C, 42.53; H, 7.78; N, 14.08%. Calcd for $C_{14}H_{30}N_4O_2Pd$: C, 42.81; H, 7.70; N, 14.26%.

This complex is soluble in water, methanol, ethanol, and DMF.

8) Nickel(II) Complexes: The preparation procedure for these complexes is similar to that for *trans*-bis(L-alaninamidato)nickel(II);[1] an aqueous solution of the ligand (2.2 equivalent amount[8]) and then 1 N sodium hydroxide (2 equiv.) were added to an aqueous solution of nickel(II) acetate (1 equiv.). The desired complex was obtained from the resulting orange colored solution.

[*Ni(tndba)*]·H_2O: The orange yellow solution was concentrated to a small volume (*ca.* 5 m*l*/1 g of the ligand used) and then diluted with a large amount (about 8 times) of ethanol. Sodium acetate and the desired complex were fractionally precipitated from the solution by adding ether gradually. The complex was recrystallized by adding ether to a 95% ethanol solution, the concentration of which had been adjusted to about half as saturated. The sample for elemental analyses was dried over calcium chloride overnight. Deep yellow pillars.

Found: C, 41.43; H, 7.56; N, 16.94%. Calcd for $C_{11}H_{24}N_4O_3Ni$: C, 41.41; H, 7.58; N, 17.56%.

trans-[*Ni(*L-*vala)*$_2$]·$2H_2O$: The complex was obtained by adding methanol and then ether to the concentrated mother solution; dried in air as orange prisms; soluble in water (not very stable), methanol, ethanol, and DMF.

Found: C, 36.95; H, 7.72; N, 16.98%. Calcd for $C_{10}H_{26}N_4O_4Ni$: C, 36.95; H, 8.06; N, 17.24%.

trans-[*Ni(*L-*phalaa)*$_2$]: Recrystallized from a methanol solution by vacuum evaporation; dried *in vacuo* over phosphorus pentoxide; orange plates; soluble in methanol, ethanol and DMF.

Found: C, 56.16; H, 5.85; N, 14.30%. Calcd for $C_{18}H_{22}N_4O_2Ni$: C, 56.14; H, 5.76; N, 14.55%.

trans-[*Ni(*L-*proa)*$_2$]·$2H_2O$: Recrystallized from an aqueous solution by vacuum evaporation; dried over phosphorus pentoxide; orange pillars; soluble in water, methanol, ethanol, and DMF.

Found: C, 37.56; H, 6.96; N, 17.30%. Calcd for $C_{10}H_{22}N_4O_4Ni$: C, 37.42; H, 6.91; N, 17.45%.

trans-[*Ni(*L-*leuma)*$_2$]·H_2O: Recrystallized by adding ether to an ethanol solution; dried over phosphorus pentoxide; orange plates; soluble in methanol, ethanol and DMF, but rapidly decomposed in water.

Found: C, 46.58; H, 8.72; N, 15.45%. Calcd for $C_{14}H_{32}N_4O_3Ni$: C, 46.30; H, 8.88; N, 15.43%.

9) Cu(tndba)·$1.5H_2O$: Copper(II) hydroxide, freshly prepared from 0.93 g of copper(II) sulfate pentahydrate, was added to a solution containing 0.91 g of tndbaH_2 in 15 m*l* of water. The mixture was continuously stirred until a homogeneous red solution was obtained; it took about 100 min. It was filtered and concentrated *in vacuo* until it became a viscous syrup. The syrup was mixed with 2 m*l* of absolute ethanol and then with 150 m*l* of acetone, and allowed to stand in a refrigerator after scratching the vessel with a glass rod. Crystallization proceeded very slowly. Brick-red crystals. The sample for elemental analyses was dried over calcium chloride overnight.

Found: C, 40.19; H, 7.71; N, 16.78%. Calcd for $C_{11}H_{25}N_4O_{3.5}Cu$: C, 39.69; H, 7.57; N, 16.83%.

*10) Cu(*L-*leuma)*$_2$: Copper(II) hydroxide freshly prepared from 0.87 g of copper(II) sulfate pentahydrate was added to a solution of 1.00 g of L-leumaH in 20 m*l* of water. The mixture was stirred for 30 min. The residual copper(II) hydroxide was then filtered off. The violet solution was concentrated *in vacuo* below 35°C until the brick-red crystals of the desired complex began to separate out. The whole mixture was then dissolved in 40 m*l* of ethanol. The complex was precipitated from the solution by slow addition of ether, and recrystallized from its 99% ethanol solution by addition of ether. The crystals were dried over calcium chloride and then over phosphorus pentoxide *in vacuo*. Yield, 0.73 g (60%).

Found: C, 47.64; H, 8.64; N, 15.61%. Calcd for $C_{14}H_{30}N_4O_2Cu$: C, 48.05; H, 8.64; N, 16.01%.

This complex is soluble in water, methanol, ethanol, and DMF.

Measurements. The instruments and solvents employed for measurements of AB and CD spectra were the same as those reported,[2] except for the Shimadzu MPS-50L spectrophotometer used for AB measurements in Nujol mulls. All the measurements were carried out at room temperature.

Both the hemihydrate and the methanol adduct of *trans*-bis(L-prolinamidato)palladium(II) hardly dissolved into DMF, but the AB and CD spectra of the complex in this solvent could be obtained with material prepared by a method analogous to that for *trans*-bis(L-alaninamidato)-palladium(II).[1] The material dissolved somewhat easily in DMF. It was confirmed from its AB and CD spectra in the aqueous and alcoholic solutions and elemental analysis that it is composed of *trans*-[Pd(L-proa)$_2$] and sodium chloride at a mole ratio of about 3 : 1 (Found: C, 34.24; H, 5.30; N, 15.73; Cl, 2.63%.).

Results and Discussion

Spectral data for the complexes newly prepared are given in Tables 1, 2, and 4—7, and in Figs. 1—7 and 9—14. Supplementary data which were obtained for several complexes previously reported are also included in Tables 1, 2 and 4—7. Discussion in this section will be made in reference to the data given in the previous papers for the bis(L-α-amino-

8) 1.1 Equivalent amount for tndbaH_2.

Table 1. AB maxima of the palladium complexes

Complex	Solvent[a]	Maxima[b,c]
trans-[Pd(L-alaa)$_2$]	(Me)	~30sh (2.1) 35.5 (2.44)
trans-[Pd(L-vala)$_2$]	(W)	~30sh (2.1) 35.5 (2.45)
	(Et)	~29sh (2.0) 35.5 (2.46)
	(DMF)	28.1 (2.07) ~35sh (2.6)
trans-[Pd(L-phalaa)$_2$]	(Et)	~29sh (1.95) 35.5 (2.37) {37.4 (2.59), 37.9 (2.70), 38.7sh (2.9)}
	(DMF)	28.4 (2.00) ~35sh (2.5)
trans-[Pd(L-proa)$_2$]·0.5H$_2$O	(W)	~30sh (2.2) 35.5 (2.52)
	(Et)	~29sh (2.1) 35.5 (2.54)
	(DMF)[d]	28.1 (2.04) ~35sh (2.6)
trans-[Pd(L-leuma)$_2$]	(W)	~29sh (2.05) 35.3 (2.43)
	(Et)	28.7 (2.03) ~35.5sh (2.5)
	(DMF)	26.9 (2.03) ~35.5sh (2.6)
cis-[Pd(L-leua)$_2$]·6H$_2$O	(DMF)	~27sh (1.6) ~31sh (2.5) 35.3 (2.79)
cis-[Pd(L-vala)$_2$]·0.5H$_2$O	(W)	~26.7sh (1.3) ~32sh (2.5) 34.8 (2.64)
	(Et)	~26.5sh (1.4) ~31.5sh (2.5) 34.7 (2.65)
	(DMF)	~27sh (1.6) ~31sh (2.5) 35.3 (2.81)
cis-[Pd(L-proa)$_2$]·3.5H$_2$O	(W)	~27sh (1.5) ~31sh (2.3) 35.3 (2.61)
	(Et)	~27sh (1.7) ~31sh (2.3) 35.3 (2.66)
	(DMF)	~27sh (1.8) ~30.5sh (2.3) 35.9sh (2.79)
[Pd(tndba)]·5H$_2$O	(W)	~27sh (1.2) 34.7 (2.59)

a) W=water, Me=methanol, Et=ethanol, and DMF=*N*,*N*-dimethylformamide.
b) Wave numbers are given in 10^3 cm^{-1} unit and the intensities, log ε, in parentheses.
c) sh=shoulder. d) For data, see Experimental.

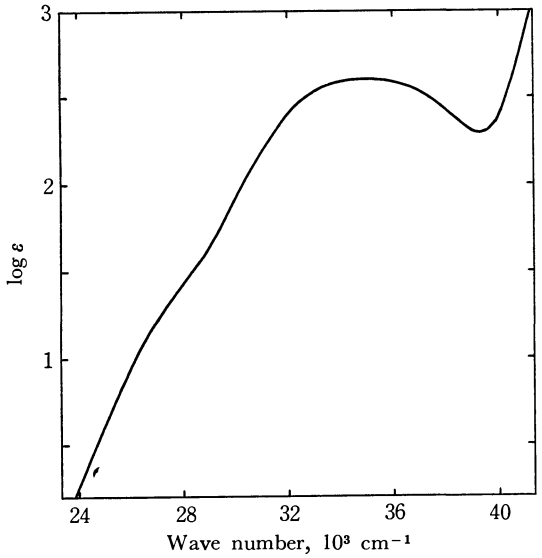

Fig. 1. AB spectrum of [Pd(tndba)] in water.

acid-amidato) complexes. Several AB and CD curves are reproduced in Figs. 5 and 14.

Cis-Trans *Isomerism and Spectral Behavior.* *1) Palladium(II) Complexes*: The absorption spectrum of [Pd(tndba)] given in Fig. 1 and Table 1 is analogous to the spectra of the bis(amino-acid-amidato)palladium(II) complexes, which have been classified into group (B) in Part I.[1] This indicates definitely that the latter complexes have *cis* structures, because the two amino groups of the tndba moiety must be *cis* to each other in the former complex. This is just the conclusion drawn in Part I.[1]

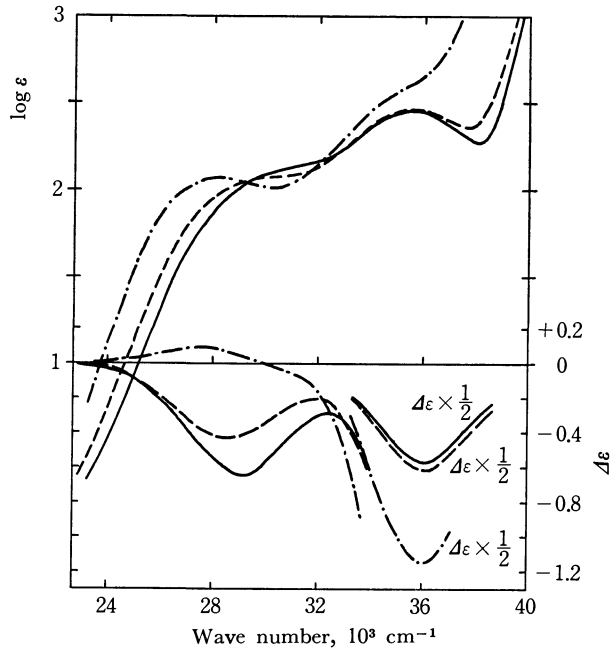

Fig. 2. AB and CD spectra of *trans*-[Pd(L-vala)$_2$] in water (——), in ethanol (----), and in DMF (—·—·).

It was well confirmed by the CD spectra in Table 2, Fig. 4 and Fig. 2 of Ref. 3 that the *trans*-bis(α-amino-acid-amidato)palladium(II) complexes generally have three bands in the ligand field band region: at 26.8—29.2, 31.4—32.3 and 35.5—36.4 kK (kK= 10^3 cm^{-1}). These bands (as well as the corresponding components of AB band) will be called tI, tII and tIII, respectively, in this paper.

TABLE 2. CD EXTREMA OF THE PALLADIUM COMPLEXES

Complex	Solvent	Extrema[a]			
		tI	tII	tIII	Benzenoid
trans-[Pd(L-alaa)$_2$]	(Me)	27.1(−0.03)	31.6(+0.05)	36.4(−0.79)	
trans-[Pd(L-vala)$_2$]	(W)	29.2(−0.65)		36.1(−1.15)	
	(Et)	28.6(−0.43)		36.1(−1.21)	
	(DMF)	27.6(+0.08)		36.1(−2.31)	
trans-[Pd(L-phalaa)$_2$]	(Et)	28.4(−0.32)		36.1(−1.12)	37.4(−1.25) 38.3(−1.17)
	(DMF)	27.2(+0.20)		36.2sh(−2.46)	
trans-[Pd(L-proa)$_2$]·0.5H$_2$O	(W)	28.8(−1.15)		36.3(−1.16)	
	(Et)	28.1(−0.98)	32.0(+0.04)	36.2(−1.74)	
	(DMF)[b]	26.8(−0.39)	31.4(+0.15)	36.0(−3.0)	
trans-[Pd(L-leuma)$_2$]	(W)	28.1(−0.80)	32.3(+0.01)	36.1(−0.85)	
	(Et)	27.3(−0.55)		35.8(−1.15)	
	(DMF)	27.1(+0.26)		35.5(−2.15)	
		c0	cI	cII	cIII
cis-[Pd(L-leua)$_2$]·6H$_2$O	(DMF)	~27sh(−0.06)	29.6(−0.12)	32.4(+0.05)	36.4(−0.58)
cis-[Pd(L-vala)$_2$]·0.5H$_2$O	(W)	~27sh(−0.2)	31.7(—0.96)		35.7(−1.23)
	(Et)	~27sh(−0.2)	30.7(−0.82)		36.1(−1.26)
	(DMF)	~27sh(−0.1)	30.1(−0.28)		36.3(−0.83)
cis-[Pd(L-proa)$_2$]·3.5H$_2$O	(W)	~27sh(−0.2)	30.8(−0.91)		36.8(+0.33)
	(Et)	~27sh(−0.3)	30.7(−0.90)		36.8(+0.12)
	(DMF)	~26.5sh(−0.3)	30.0(−0.62)		36.5(−0.2)

a) Wave numbers are given in 10^3 cm^{-1} unit and the intensities, $\Delta\varepsilon=\varepsilon_l-\varepsilon_d$, in parentheses.
b) For data, see Experimental.

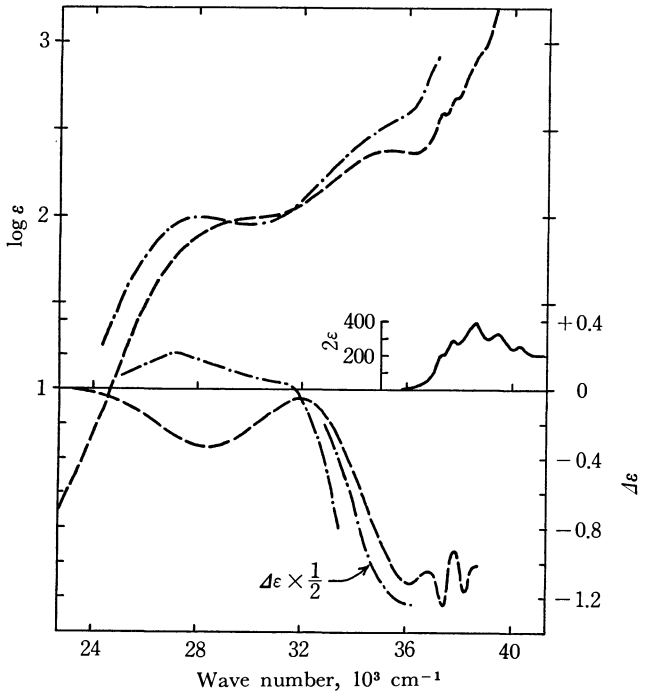

Fig. 3. AB and CD spectra of *trans*-[Pd(L-phalaa)$_2$] in ethanol (———) and in DMF (—·—·), and AB spectrum of L-phalaaH in ethanol (——).

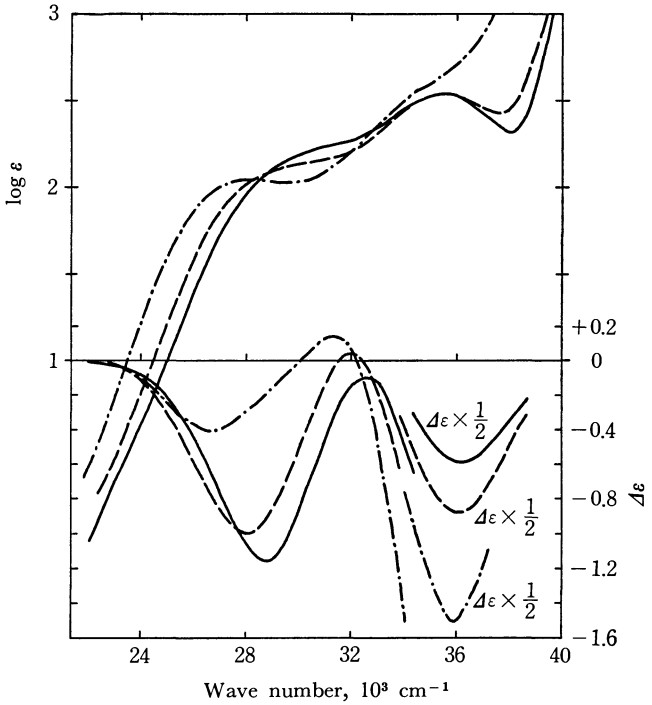

Fig. 4. AB and CD spectra of *trans*-[Pd(L-proa)$_2$] in water (——), in ethanol (———) and in DMF (—·—·).

With respect to the *cis* complexes, four kinds of CD band were observed; these (and the corresponding components of AB band) are labeled c0, cI, cII and cIII as shown in Table 2. Since the situation of the four bands would not differ much among the complexes (Figs. 5—7, and Fig. 2 of Ref. 1), it is conceivable that cII bands are hidden in the CD spectra of all of the *cis* complexes other than the leua complex.

No reliable method for AB and CD band analyses

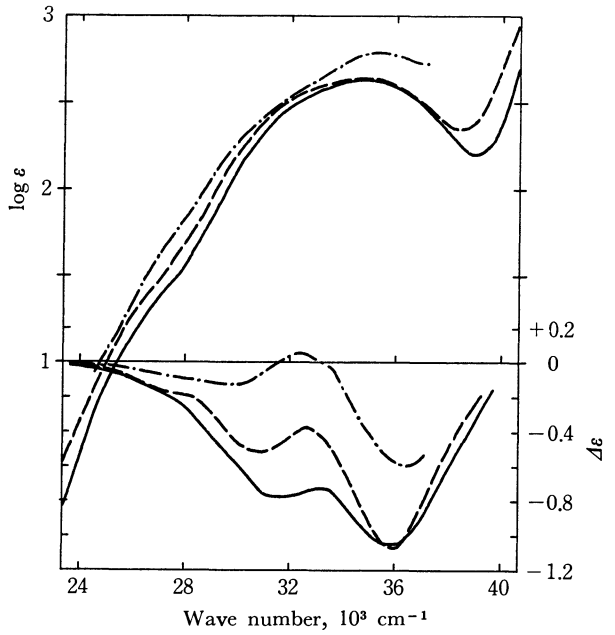

Fig. 5. AB and CD spectra of *cis*-[Pd(L-leua)$_2$] in water (——), in ethanol (– – –), and in DMF (—·—·).

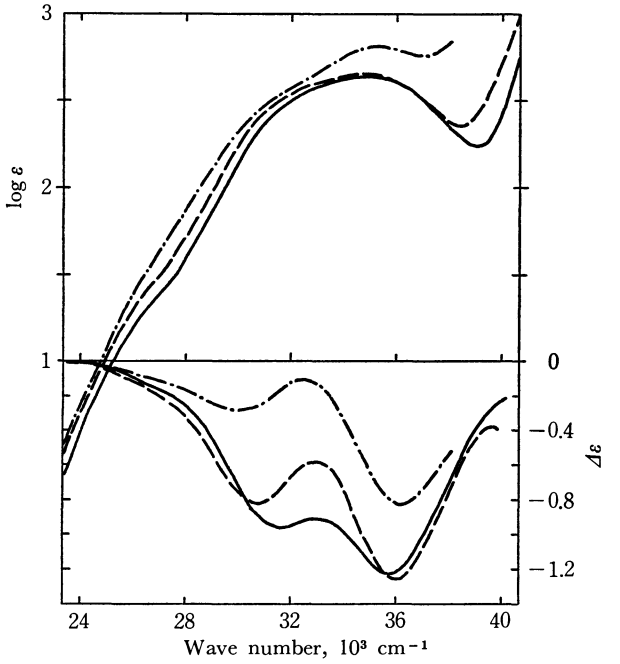

Fig. 6. AB and CD spectra of *cis*-[Pd(L-vala)$_2$] in water (——), in ethanol (– – –), and in DMF (—·—·).

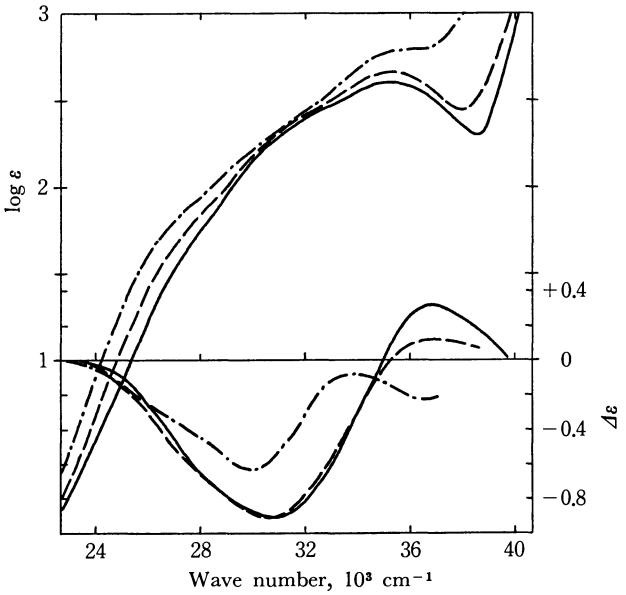

Fig. 7. AB and CD spectra of *cis*-[Pd(L-proa)$_2$] in water (——), in ethanol (– – –), and in DMF (—·—·).

TABLE 3. GENERAL FEATURE OF THE LIGAND FIELD BANDS OF THE PALLADIUM COMPLEXES

Band component	Wave number, 10^3 cm^{-1}	ε
tI	~28.5	~100
tII	~32.3	~100
tIII	~36.0	~300
c0	~27.0	~25
cI	~31.2	~200
cII	~33.3	~150
cIII	~36.0	~350

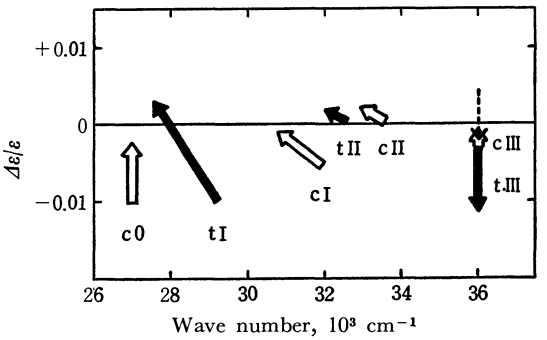

Fig. 8. Changes in the CD of the palladium complexes caused by the change of solvent from water, ethanol to DMF. The broken arrow shows the exceptional behavior of the cIII band of the proa complex.

has so far been established, especially for the bands which contain three or more components with comparable intensities. The results of band analyses given in Table 3 are accordingly somewhat arbitrary, but probable at the present stage since they were obtained from the data for a series of closely related complexes. The molar extinction coefficients estimated for cII and tII are the most unreliable of the numerical values in Table 3 but nevertheless seem to be comparable to those for cI and tI, respectively.

Figure 8 illustrates the general CD behavior exhibited by the palladium complexes as the solvent was changed from water, ethanol to DMF; only a significant deviation from the general CD behavior was found in the cIII band of the proa complex (See Fig. 7).

Two important facts found in Table 3 and Fig. 8 are that characteristics of tI, tII and tIII bands show a close resemblance to those of cI, cII and cIII, respectively, and that the sign inversion for a single CD band is actually caused in the tI and the cIII bands

of a few complexes by change of only the solvent.

2) Nickel(II) Complexes: The CD band with the lowest wave number of the bis(L-amino-acid-amidato)nickel(II) with vala, phalaa or leuma was negative in the alcoholic solution and positive in DMF (Table 5, Figs. 9 and 10, and Fig. 1 of Ref. 3). This is analogous to the behavior exhibited by the tI bands of the *trans* palladium complexes with those ligands (Figs. 2 and 3, and Fig. 2 of Ref. 3). There is a close correspondence between the whole ligand field (AB and CD) spectra of these nickel complexes (Tables 4 and 5) and those of the corresponding *trans* palladium ones. Thus, the three nickel complexes are inferred to be *trans* isomers both in solution and in solid state. It is strongly suggested therefore that the CD band at 24.0 kK corresponds to tIII (Table 5), and the small positive band at 20.8 kK, detected for *trans*-[Ni(L-alaa)$_2$] in methanol,[1] to tII. It may be noted in this connection that the tI CD extrema of the nickel complexes appear to correspond to the AB shoulder (or peak) at about 20.0 kK but that the tIII situates at considerably higher wave number than the AB peak (Tables 4 and 5, Figs. 9—11, Fig. 1 of Ref. 3 and Fig. 4 of Ref. 1).

The CD behavior of the proa complex seems to be an intermediate of the behaviors of the correspond-

Table 4. AB maxima of the nickel complexes

Complex	Solvent or state[a)]	Maxima	
trans-[Ni(L-alaa)$_2$]	(Et)	~20sh	23.3(1.77)
trans-[Ni(L-vala)$_2$]·2H$_2$O			
	(N)	~20sh	23.6
	(Me)	~20sh	23.3(1.75)
	(Et)	~20sh	23.3(1.77)
	(DMF)	~20sh	23.6(1.81)
trans-[Ni(L-phalaa)$_2$]	(N)	~20sh	23.7
	(Me)	~20sh	23.2(1.80)
	(Et)	~20sh	23.1(1.82)
	(DMF)	~20sh	23.5(1.90)
trans-[Ni(L-proa)$_2$]·2H$_2$O			
	(N)	~19sh	23.1
	(W)	~20sh	23.0(1.83)
	(Et)	~20sh	23.1(1.83)
	(DMF)	~20sh	23.4(1.89)
trans-[Ni(L-leuma)$_2$]·H$_2$O			
	(N)	~19sh	23.1
	(Et)	~19sh(1.5)	22.8(1.79)
	(DMF)	19.2(1.52)	23.1(1.83)
[Ni(tndba)]·H$_2$O	(Refl)	~22sh	24.0 ~32sh
	(W)	23.3(1.92)	~32.5sh(1.2)
	(Et)	23.3(1.93)	~31.5sh(1.3)

a) N=Nujol mull, Refl=powder (diffuse reflectance spectrum).

Table 5. CD extrema of the nickel complexes

Complex	Solvent	Extrema	
		tI	tIII
trans-[Ni(L-alaa)$_2$]	(Et)	18.8(−0.04)	24.1(−0.65)
trans-[Ni(L-vala)$_2$]·2H$_2$O			
	(Me)	20.0(−0.32)	24.0(−0.76)
	(Et)	20.1(−0.36)	24.0(−0.81)
	(DMF)	18.8(+0.07)	24.0(−0.80)
trans-[Ni(L-phalaa)$_2$]	(Me)	20.2(−0.28)	24.0(−0.65)
	(Et)	20.1(−0.38)	24.0(−0.68)
	(DMF)	18.9(+0.13)	24.1(−0.75)
trans-[Ni(L-proa)$_2$]·2H$_2$O			
	(W)	20.1(−1.17)	24.4(−0.17)
	(Et)	19.8(−1.13)	24.2(−0.54)
	(DMF)	20.1(−0.68)	24.1(−0.57)
trans-[Ni(L-leuma)$_2$]·H$_2$O			
	(Et)	18.9(−0.40)	23.5(−0.71)
	(DMF)	19.1(+0.35)	23.4(−1.44)

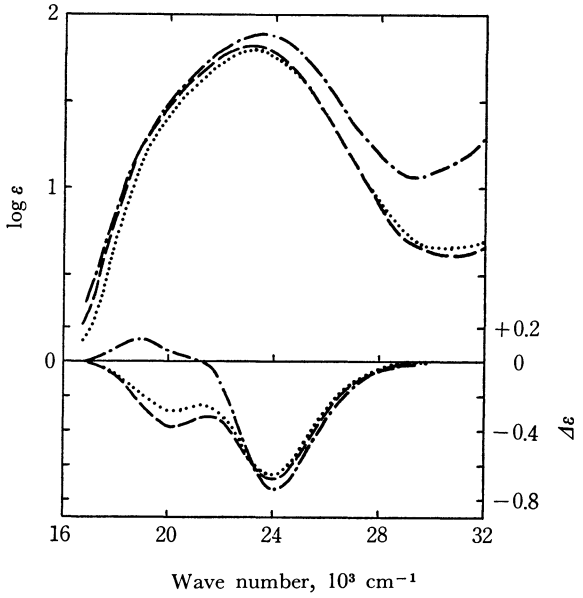

Fig. 9. AB and CD spectra of *trans*-[Ni(L-vala)$_2$] in methanol (·····), in ethanol (———) and in DMF (—·—·).

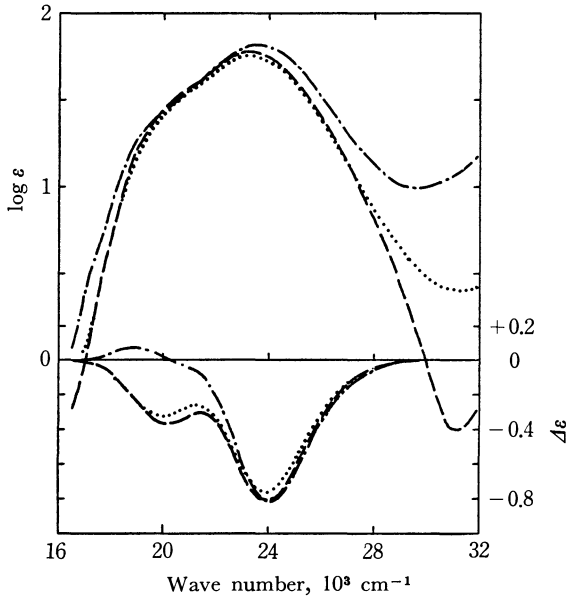

Fig. 10. AB and CD spectra of *trans*-[Ni(L-phalaa)$_2$] in methanol (·····), in ethanol (———) and in DMF (—·—·).

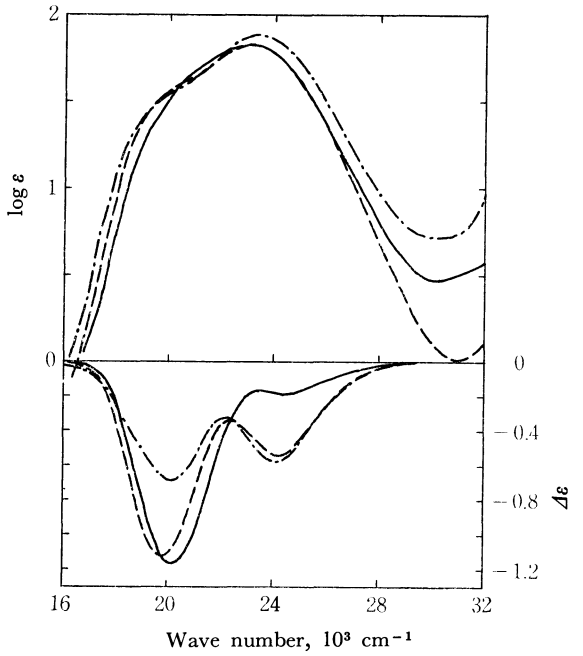

Fig. 11. AB and CD spectra of *trans*-[Ni(L-proa)$_2$] in water (——), in ethanol (— — —), and in DMF (—·—·).

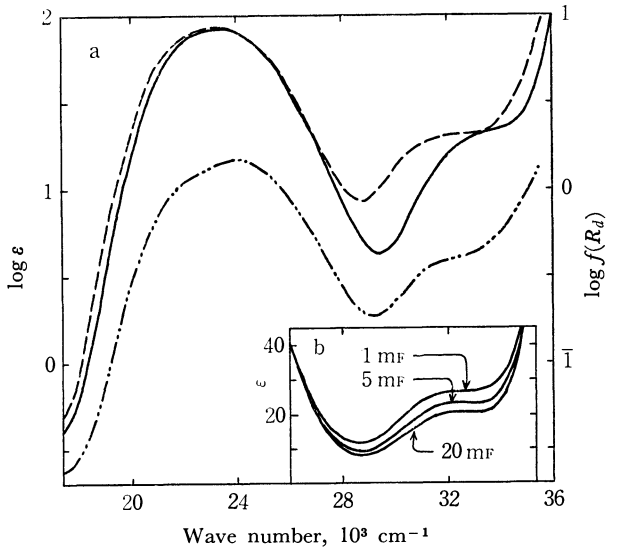

Fig. 12. AB spectrum of [Ni(tndba)]: a, in water (——), in ethanol (— — —), and in solid state (reflectance, —··—··); b, in ethanol.

ing *cis* and *trans* palladium complexes, in the respective solvents (Fig. 11). The wave numbers of the CD extrema, however, do not differ much from those for the other nickel complexes inferred to be *trans* (Table 5). Moreover, the AB spectrum of the proa complex is very similar to spectra of the *trans* complexes and significantly differs from that of the tndba complex, the structure of which is restricted to *cis*-type (Fig. 12). On the whole, it is concluded that the proa complex is also a *trans* isomer. Thus, no *cis* isomer of bis(amino-acid-amidato)nickel(II) has been found so far.

3) Copper(II) Complexes: The six bis(α-amino-acid-amidato)copper(II) complexes showed a broad ligand field band at 18.7—19.5 kK (log ε= 1.67—1.76, except for the proa complex) in aqueous solution.[2] These complexes are considered to be *trans* or to be predominantly so in aqueous and alcoholic solutions. This conclusion is supported to some extent by the following observations; Cu(tndba) is slightly higher either in its intensity or in the wave number than the bis(amino-acid-amidato) complexes. The former has no vague shoulder at its lower wave number side in contrast to the latter (Fig. 13 and Table 6). The spectral difference between the tndba and the bis(amino-acid-amidato) complexes seems to be analogous to that between *cis* and *trans* complexes of palladium(II) or of nickel(II).

The above and the previous[2] discussion concerning the geometrical structure can be applied also to the copper complex with L-leuma in the aqueous, ethanol, and DMF solutions as well as to all the bis(α-amino-acid-amidato)copper(II) complexes dissolved in DMF. Though the leuma complex exhibits the ligand field band at considerably lower wave numbers than the other bis(L-amino-acid-amidato)copper(II) complexes in respective solvents (Table 6), the red shift can be attributed to an effect of the methyl group attached to the amido nitrogen. Actually, similar shifts were also observed in the corresponding *trans* complexes of palladium and nickel (Tables 1 and 4).

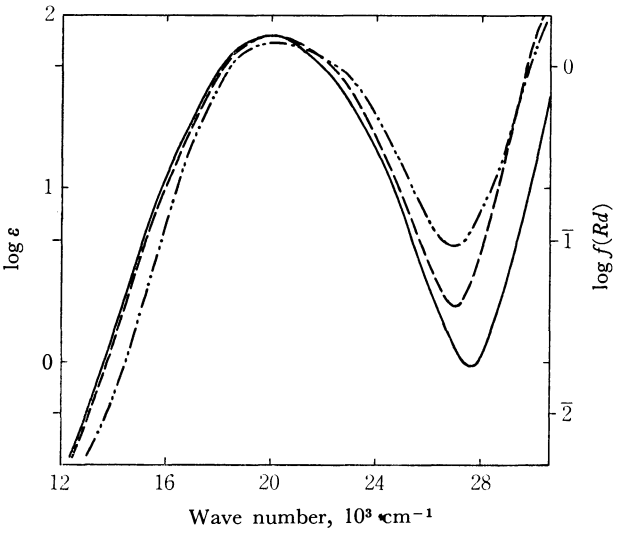

Fig. 13. AB spectrum of Cu(tndba): in water (——), in ethanol (— — —), and in solid state (reflectance, —··—··).

The CD behavior of the bis(L-amino-acid-amidato)-copper(II) complexes is apparently very complicated (Table 7, Fig. 14, and Table 4 of Ref. 2 and Fig. 2 of Ref. 2) in contrast to that of the corresponding nickel or palladium complexes. On the other hand, the shapes and the solvent dependencies of the AB bands of the copper complexes do not differ much from each other (Fig. 14, Fig. 2 of Ref. 2, and Fig. 3 of Ref. 2). It can be accepted that the relative ordering of the components of the band is independent of the kind of ligand. It seems reasonable from an examination of the CD data that the ordering is also independent of the kind of solvent. It is inferred from these considerations that the ligand field band

Table 6. AB data of the copper complexes

Complex	Solvent or state	Maxima	Band-width[a]	Concn.[b]
$Cu(L\text{-vala})_2\cdot 2H_2O$	(DMF)	20.4(1.81)	6.3	2.4
$Cu(L\text{-phalaa})_2$	(DMF)	20.5(1.85)	5.9	2.5
$Cu(L\text{-leuma})_2$	(W)	18.1(1.74) ~29sh(2.1)	6.1	5.0
	(Et)	19.4(1.87) ~27sh(2.2)	6.2	5.0
	(DMF)	~18sh(1.5) 19.9(1.89)	6.7[c]	5.0
$Cu(tndba)\cdot 1.5H_2O$	(Refl)	20.1 ~22.5sh	5.7	—
	(W)	20.0(1.86)	5.2	2.0
	(Et)	20.1(1.88)	5.2	2.0

a) Apparent band-with at half extinction in 10^3 cm^{-1} unit.
b) Concentration in 10^{-3} M unit. c) By extrapolation.

Table 7. CD data of the copper complexes

Complex	Solvent	Extrema			Concn.
$Cu(L\text{-vala})_2\cdot 2H_2O$	(DMF)	14.7(+0.02)	19.0(−0.33)	22.5(+0.05)	5.0
$Cu(L\text{-phalaa})_2$	(DMF)	16.9(+0.02)	20.8(−0.20)		2.5
$Cu(L\text{-leuma})_2$	(W)	16.6(−0.31)	19.8(−0.25)		10
	(Et)	16.1(−0.33)	20.9(−0.18)		10
	(DMF)	15.0(−0.09)	19.9(−0.24)		10

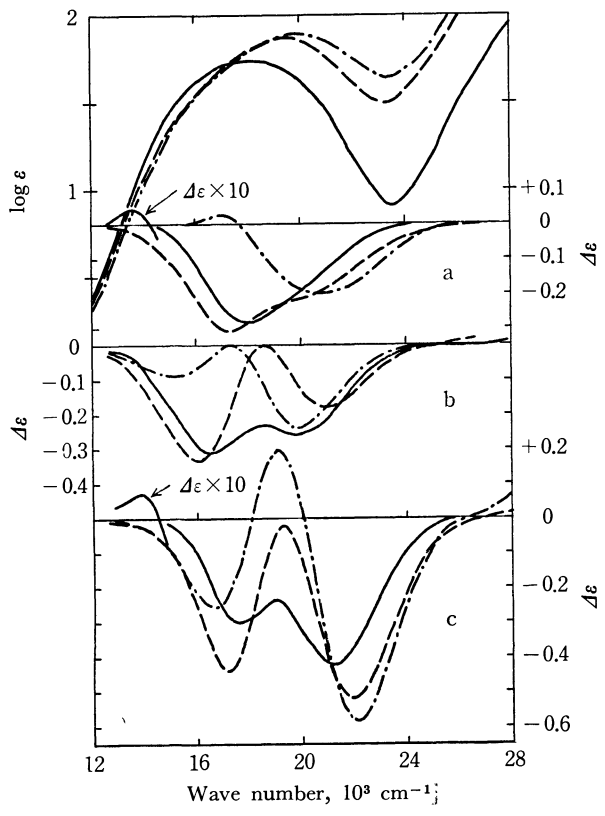

Fig. 14. AB spectrum of $Cu(L\text{-leuma})_2$ and CD spectra of: a, $Cu(L\text{-phalaa})_2$; b, $Cu(L\text{-leuma})_2$; c, $Cu(L\text{-proa})_2$. ——, in water; – – –, in ethanol; —·—·, in DMF.

of the bis(α-amino-acid-amidato)copper(II) complexes generally consists of at least three components which are roughly at 17, 19, and 21—22 kK; these are labeled A, B and C, respectively. Only the leuma complex seems to exhibit each of the three components at lower wave numbers by 0.5—1 kK than the other complexes (Fig. 14b).

A very small positive CD band which is seriously eclipsed by large negative ones was observed at about 14 kK for the copper complexes with L-vala, L-phalaa and L-proa (Figs. 14a and 14c, and Fig. 2 of Ref. 2). The reflectance spectrum of $Cu(L\text{-proa})_2\cdot 2H_2O$ reveals a weak but distinct shoulder at about 13 kK.[2,9] Similar CD bands have been found for bis(L-aminoacidato)copper(II) complexes.[10]

The CD behavior of the proa complex is somewhat specific as discussed in Part II[2] but more or less resembles that of the leuma or of the phalaa complex as demonstrated in Fig. 14.

Nature of the Ligand Field Band. The *trans* palladium as well as the *trans* nickel complexes have three components in the ligand field band; each of the components exhibits a behavior common to both palladium and nickel complexes. Thus, each band labeled tI, tII or tIII for both complexes should be assigned to a common *d–d* transition. Such was the case in the tentative assignment made in Part I.[1] On the other hand, a new kind of CD band, cII, was found in this work for the *cis* palladium complexes other than those previously reported. This requires us to reconsider the band assignment for both *cis* and *trans* palladium complexes.

Three of the possible assignments are listed as the preferable ones in Table 8; the bands labeled with the same Roman numeral are assigned to the transitions derived from a certain transition in D_{4h} symmetry, in each possible assignment of the three, because those bands show a very similar behavior to

9) If the AB and CD bands at 13—14 kK were neither of A, Bnor C, it should be assigned to ν_1; see footnote 11 and the following discussion.

10) T. Yasui, This Bulletin, **38**, 1746 (1965); T. Yasui, J. Hidaka, and Y. Shimura, *J. Amer. Chem. Soc.*, **87**, 2762 (1965).

each other. The assignment for the *trans* complexes in Part I[1] is revived in assignment (1), whereas that for *cis* complexes in (2) apart from cII. However, another possibility (3) is not so easily omitted. The c0 band is assigned to a spin-forbidden transition in every case for the following reasons (*cf.* Ref. 1). First, it has a significantly lower absorption coefficient than the other bands (Table 3). Secondly, it is very unlikely that the band is assigned to ν_1',[11] because it scarcely ever shifts by change of the solvent. Thirdly, it seems that the three bands of the *trans* complexes are reasonably assigned to ν_2, ν_3, and ν_4. From this it follows that ν_2', ν_3', and ν_4', are to be assigned to the three bands other than c0 in the *cis* complexes.

Table 8. Possible band assignments for the palladium and the nickel complexes

Band	Possible assignments[a,b]		
	(1)	(2)	(3)
tI	ν_3	ν_2	ν_2
tII	ν_2	ν_1	ν_3
tIII	ν_4	ν_3, ν_4	ν_4
c0	sf	sf	sf
cI	ν_3'	ν_2'	ν_2'
cII	ν_2'	ν_1'	ν_3'
cIII	ν_4'	ν_3', ν_4'	ν_4'

a) For the definition of the transitions, see footnote 11.
b) sf=a spin forbidden transition.

Let us examine the validity of each of the three assignments. If assignment (2) were valid, the spectral data would indicate that ν_1 is more slightly shifted than ν_2 as the solvent is changed. This is unlikely under a simple ligand field theory. Moreover, the three bands of the *trans* complexes seem to be reasonably assigned to ν_2, ν_3, and ν_4 since only ν_1 is magnetic dipole forbidden.[12] Thus assignment (2) seems unreasonable. Next, assignment (3) is in conflict with the theoretical expectation that the splitting energies would be influenced most seriously between (xz) and (yz) orbitals by the *cis-trans* isomerism. In conclusion, assignment (1) is the most preferable, but still does not seem unambiguous. A similar assignment has been given for bis(β-ketoenolato) copper(II) complexes.[13]

It can be roughly estimated that contributions of interelectronic repulsion energy are less by 3B to ν_3 and ν_4 than to ν_2, where B is Racah's parameter. If assignment (1) is valid, the energy difference $\nu_2-\nu_3$ can be estimated from the experimental results to be some 1000 cm^{-1} for the nickel complexes; this may be smaller than 3B.[14] It is therefore likely that the contributions of ligand field energy to respective transitions are in the order $\nu_2<\nu_3<\nu_4$ for the nickel complexes. The energy order is expected to be realized in the electronic spectra of the corresponding copper complexes as it is, because there is no contribution of interelectronic repulsion energy to any transition in the d^9 chromophore. With respects to the copper complexes, all the A, B and C bands seem to be magnetic dipole allowed. Actually, the largest CD band is A or C in the complexes with phalaa, proa and leuma (Fig. 14), whereas B in those with alaa, leua and vala. Thus three bands A, B, and C may be tentatively assigned, to ν_2, ν_3, and ν_4, respectively.[9] Definitive assignment of ligand field bands has not been given in the CD studies of the copper(II) complexes with optical active amino acids and peptides.[10,15]

The Benzenoid Absorption. A typical band series of phenyl groups was observed in 38000 cm^{-1} (260 mμ) region in both AB and CD spectra of *trans*-bis(L-phenylalaninamidato)palladium(II) in ethanol. These spectra are given in Fig. 3, together with the AB spectrum of L-phenylalaninamide in ethanol (10 mM), and the numerical data in Table 1 and 2. Measurements of the CD spectra were carefully repeated both for the complex and for the ligand, but for the latter $|\Delta\varepsilon|$ was too small ($\lesssim$0.03) in this region to give reliable results. The AB and CD spectra were also measured in an ethanol solution containing the ligand (10 mM) and sodium ethoxide (10 mF). The results, however, were indistinguishable from those without alkali. Though the benzenoid absorption of the complex is overlapped by the other absorption, it seems to be scarcely affected by the complex formation. We conclude from this observation that there is no first order interaction between the phenyl π and the metal d orbitals in the complex. Thus, we exclude the possibility that apical coordination of the phenyl groups exists and causes the about ten times enhanced CD of the benzenoid absorption in the complex.

The 32000 cm^{-1} Band of [Ni(tndba)]. The electronic spectrum of [Ni(tndba)] shows another weak band at about 32000 cm^{-1} (Fig. 12). This band shifted to lower wave numbers when the solvent was changed from water to ethanol. It became slightly more intense when the ethanol solution was diluted (Fig. 12b). Its peak is at a wave number about 9000 cm^{-1} higher than that of the main ligand field band maximum. These characteristics are very similar to those of Band II of bis(α-amino-acid-amidato)copper(II) complexes described in Part II,[2] and hence these two kinds of band seem to have a common origin. However, the following facts appear

11) ν_1, ν_2, ν_3, and ν_4 mean transitions from (z^2), (xy), (xz) and (yz) to (x^2-y^2), and ν_1', ν_2', ν_3' and ν_4' mean those from (z^2), (x^2-y^2), (xz) and (yz) to (xy), respectively, where (k) means a molecular orbital composed mainly of d_k-orbital. The x axis is fixed to be nearly colinear with metal-N(amido) linkage in the *trans* complex, but to bisect N-metal-N angle within each chelate ring in the *cis* complex. The y axis is fixed also within coordination square in both *trans* and *cis* complexes.

12) ν_1 can become magnetic dipole allowed by configuration interaction or mixing of p-orbitals under C_2 symmetry.

13) F. A. Cotton and J. J. Wise, *Inorg. Chem.*, **6**, 917 (1967).

14) The value of B in gaseous Ni^{2+} ion is 1041 cm^{-1}, C. K. Jørgensen, "Absorption Spectra and Chemical Bonding in Complexes," Pergamon Press, Oxford (1962), p. 137.

15) J. M. Tsangaris and R. B. Martin, *J. Amer. Chem. Soc.*, **92**, 4255 (1970).

to be somewhat in conflict with this conclusion: Such a kind of band has not been observed in either the *trans*-bis(α-amino-acid-amidato)nickel(II) complexes or in Cu(tndba), and the intensity of the band of [Ni(tndba)] was not so seriously dependent on concentration and on the kind of solvent (including solid state) as in Band II of the copper complexes.

The authors thank Dr. Seiko Komorita for measurements of the AB spectra in Nujol mulls.

BULLETIN OF THE CHEMICAL SOCIETY OF JAPAN, VOL. 44, 3363—3366 (1971)

The Solvent Effect on the Electron-Transfer Reactions of Cobalt(III) Complexes. The Reduction of the *cis*-Chloro-2-aminoethanolbis(ethylenediamine)cobalt(III) Ion by Iron(II) in Aqueous Solutions of Organic Solvents

Kousaburo Ohashi, Katsumi Yamamoto, Toshio Suzuki, and Yoshimi Kurimura*

Department of Chemistry, Ibaraki University, Mito, Ibaraki

**College of General Education, Ibaraki University, Mito, Ibaraki*

(Received April 7, 1971)

The solvent effect on the reduction of the *cis*-chloro-2-aminoethanolbis(ethylenediamine)cobalt(III) ion by iron(II) was investigated in aqueous solutions of dimethylsulfoxide (DMSO), dimethylformamide (DMF), ethanol, and acetone. The second-order rate constants for the reduction are 4.4×10^{-5} M^{-1}sec^{-1} in the absence of an organic solvent, 1.4×10^{-3} M^{-1}sec^{-1} in 0.20 M_f DMSO, 7.3×10^{-4} M^{-1}sec^{-1} in 0.20 M_f DMF, 1.1×10^{-4} M^{-1}sec^{-1} in 0.20 M_f ethanol, and 1.0×10^{-4} M^{-1}sec^{-1} in 0.20 M_f acetone, at 25°C and at 0.16 M $HClO_4$ and $\sum[ClO_4^-]=0.60$ M (M_f=mol fraction of organic solvent). From the kinetic and spectral data, it is suggested that the increase in the rate upon the addition of an organic solvent may be mainly due to a change in the solvation sphere of the reductant by replacing the water molecules by the organic molecules.

Systematic kinetic investigations of the reductions of the cobalt(III) complexes in the organic solvents and in the organic solvent-water mixtures would provide important information regarding the mechanism of the electron-transfer reactions. Relatively few papers have been reported, however, on the effect of a solvent on the electron-transfer reactions of the metal complexes.

The exchange reactions between $Co(phen)_3^{2+}$ and $Co(phen)_3^{3+}$ in acetone-water[1] and that between iron(II) and iron(III) in isopropanol-water,[2] acetone-water,[3] methanol-water,[3] ethanol-water,[3] 1-propanol-water,[3] and dimethylsulfoxide-water[4] have been investigated. The rates of all these reactions decrease with an increase in the concentrations of the organic solvents.

In some organic solvent-water mixtures, it was found by the present authors that the rates of the reductions of some Co(III)-chloro complexes by iron(II) increase with an increase in the concentration of the nonaqueous solvent, such as dimethylsulfoxide (DMSO), dimethylformamide (DMF), ethanol, and acetone.

In this connection, a rate study of the reduction of the *cis*-chloro-2-aminoethanolbis(ethylenediamine)-cobalt(III) ion by iron(II) was done in organic solvent-water mixtures so as to obtain some information about the effect of the solvent on the electron-transfer reactions.

Experimental

Preparation of Complex. The *cis*-chloro-2-aminoethanolbis(ethylenediamine)cobalt(III) chloride used as the oxidant was prepared in a manner previously reported.[5] The identity and purity of the complex were confirmed analytically and spectrophotometrically. Found: C, 20.68; H, 6.51; N, 20.91. Calcd for $[Co(en)_2(NH_2CH_2CH_2OH]-Cl]Cl_2$: C, 20.79; H, 6.68; N, 20.21.

Materials. Dimethylsulfoxide and dimethylformamide of a spectroscopic grade (Tokyo Kasei) were distilled under reduced pressure. Ethanol and acetone of G. R. grade (Tokyo Kasei) were distilled two times before use.

The preparation of the iron(II) solution and the determinations of the concentrations of hydrogen and perchlorate ions in this solution were carried out by a method similar to that described previously.[6] All the other chemicals used were of a G. R. grade and were used without further purification. The ionic strengths of the solutions were adjusted by the addition of sodium perchlorate solution.

Kinetic Runs. Erlenmeyer flasks containing appropriate amounts of redistilled water, the iron(II) solution, an organic solvent, and a dry complex respectively were kept in a thermostat. The desired volumes of redistilled water and organic solvent were added to the flask containing the dry complex, and the resulting solution was kept in a thermostat for about 30 min. Then, appropriate amounts of the iron(II) solution were added to this solution. A por-

1) B. R. Baker, F. Basolo, and H. M. Neuman, *J. Phys. Chem.*, **63**, 371 (1959).

2) N. Sutin, *ibid.*, **64**, 1766 (1960).

3) R. A. Horne, Ph. D. Thesis, Columbia University, New York, 1955.

4) J. Menashi, W. L. Reynolds, and G. Van Auken, *Inorg. Chem.*, **4**, 299 (1965).

5) S. C. Chan and F. Leh, *J. Chem. Soc., A*, **1967**, 1730.

6) Y. Kurimura, K. Ohashi, T. Ohtsuki, and K. Yamamoto, This Bulletin, **44**, 1293 (1971).

tion of the reaction mixture was transferred rapidly into a 1-cm optical cell placed in a thermostated cell compartment of a Hitachi Model 124 spectrophotometer. The variation in the absorbance of the reaction mixture was recorded automatically in the vicinity of the first absorption maximum of the cobalt(III) complex. The wavelength used for the rate determination was 534 nm.

In all the experiments, the reactions were followed under pseudo-first-order conditions, in which the iron(II) concentration was in great excess with respect to that of the cobalt(III) complex. The pseudo-first-order rate constants, k_p, were calculated from the slope of the log (A_t-A_∞) *vs.* time plots, where A_t and A_∞ are the absorbances at time t and after all the cobalt(III) is reduced to cobalt(II) respectively.

Results

Reduction of cis-$Co(en)_2(NH_2CH_2CH_2OH)Cl^{2+}$ *in an Aqueous Solution.* The pseudo-first-order plots for the iron(II) reduction are shown in Fig. 1. The second-order rate constant, k, for the reaction can be obtained from the slope of the log (A_t-A_∞) *vs.* time plot and a known value of the iron(II) concentration, which is essentially constant under the conditions employed.

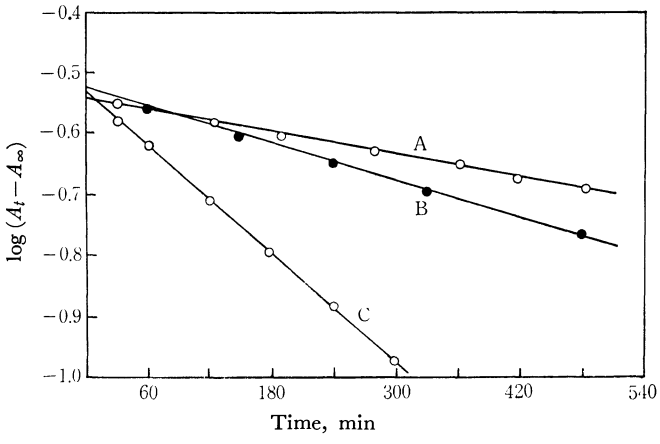

Fig. 1. The pseudo-first-order plots for the reactions of *cis*-$Co(en)_2(NH_2CH_2CH_2OH)Cl^{2+}$ with iron(II) in ethanol-water mixtures.
$[Fe(II)]=0.210$ M, $\sum[ClO_4^-]=0.60$ M, $[HClO_4]=0.16$ M, 25 ± 0.1°C.
A : aqueous solution, $[Co(III)]=4.30\times10^{-3}$ M.
B : 0.20 mol fraction of ethanol, $[Co(III)]=4.62\times10^{-3}$ M.
C : 0.56 mol fraction of ethanol, $[Co(III)]=4.48\times10^{-3}$ M.

Figure 2 shows the dependence of the k_p value on the concentration of iron(II) in aqueous solutions. The linear behavior shown in Figs. 1 and 2 indicates that the rate equation can be expressed by:

$$-\frac{d[Co(III)]}{dt}=k[Co(III)][Fe(II)] \quad (1)$$

The effect of the hydrogen-ion concentration on the rate was examined at a given ionic strength of 0.60 in aqueous solutions. The results indicate that the second-order rate constant is independent of the hydrogen-ion in the concentration region between 0.14 M to 0.43 M.

The effect of the ionic strength on the rate was also examined at a given hydrogen-ion concentration.

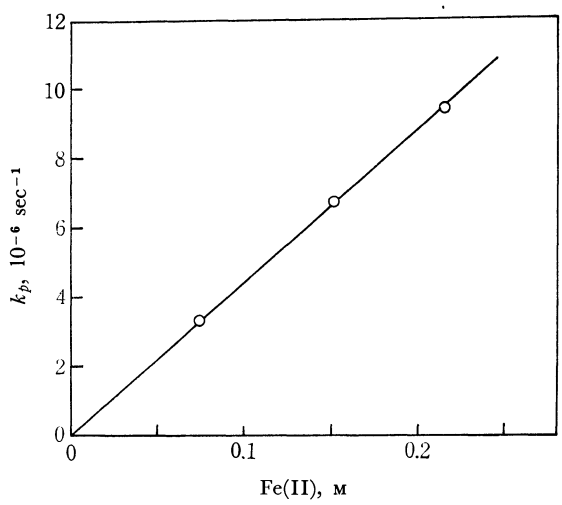

Fig. 2. The dependence of the pseudo-first-order rate constant for the reduction of *cis*-$Co(en)_2(NH_2CH_2CH_2OH)Cl^{2+}$ in aqueous solutions upon iron(II) concentration.
$[Co(III)]=4.30\times10^{-3}$ M, $\sum[ClO_4^-]=0.60$ M, $[HClO_4]=0.16$ M, 25 ± 0.1°C.

Table 1. Effect of ionic strength on the second-order rate constants for the reduction of *cis*-$Co(en)_2(NH_2CH_2CH_2OH)Cl^{2+}$ by iron(II) in aqueous solutions

$\sum[ClO_4^-]$	Rate constant[a] M^{-1} sec^{-1}
0.60	4.38×10^{-5}
1.0	5.07×10^{-5}
2.0	5.78×10^{-5}

a) $[Co(III)]=5.40\times10^{-3}$ M, $[Fe(II)]=0.18$ M, $[HClO_4]=0.20$ M, 25 ± 0.1°C.

A relatively small increase in the rate with an increase in the ionic strength was observed in the hydrogen-ion concentration region investigated. The results are shown in Table 1.

The rate constants and activation parameters for the reduction in an aqueous solution are represented in Table 2, along with the values obtained in an ethanol-water mixture.

Reduction of cis-$Co(en)_2(NH_2CH_2CH_2OH)Cl^{2+}$ *in Some Organic Solvent-Water Mixtures.* The reduction of the Co(III) complex in DMSO-water, DMF-water, ethanol-water, and acetone-water mixtures also obeys the rate expression (1) under the experimental conditions employed.

The second-order rate constants and activation parameters for the reduction at various mol fractions of ethanol are listed in Table 2. With the addition of ethanol to an aqueous solution, the values of the rate constants, $\Delta H^{\neq}$ and $\Delta S^{\neq}$ increase gradually. Such a trend in the rate constants and activation parameters was also observed in the other organic solvent-water mixtures investigated.

The variations in the rate constants with the mol fraction of the organic solvent are illustrated in Fig. 3. In all cases, especially in the cases of DMSO-water and DMF-water, a marked increase in the rates with an increase in the mol fraction of organic

Table 2. The rate constants and activation parameters for the reduction of *cis*-$Co(en)_2(NH_2CH_2CH_2OH)Cl^{2+}$ in ethanol-water mixtures at 25±0.1°C

Mol fraction of ethanol	Rate constant[a] M^{-1} sec^{-1}	$\Delta H^{\neq}$ kcal mol^{-1}	$\Delta F^{\neq}$ kcal mol^{-1}	$\Delta S^{\neq}$ e.u.
0	4.38×10^{-5}	13.2	23.4	−36.4
0.074	7.19×10^{-5}	14.6	23.2	−33.8
0.20	1.12×10^{-4}	15.5	22.8	−30.6
0.32	1.65×10^{-4}	17.8	22.6	−25.6
0.56	3.72×10^{-4}	21.2	22.1	−17.8

a) $[Co(III)]=4.01\times10^{-3}$ M, $[Fe(II)]=0.21$ M, $\sum[ClO_4^-]=0.60$ M, $[HClO_4]=0.16$ M.

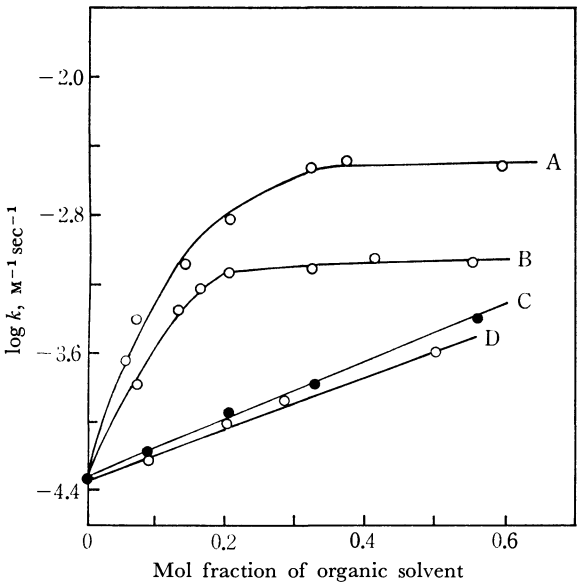

Fig. 3. The plots of logarithmic second-order rate constant *vs.* mol fraction of organic solvent.
$[Co(III)]=4.30\times10^{-3}$ M, $[Fe(II)]=0.086$—0.210 M, $\sum[ClO_4^-]=0.60$ M, $[HClO_4]=0.16$ M, 25±0.1°C
A : dimethylsulfoxide—water
B : dimethylformamide—water
C : ethanol—water
D : acetone—water

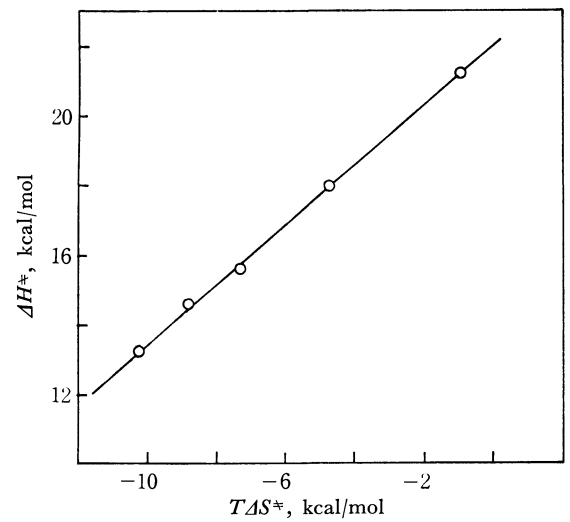

Fig. 4. A plot of $\Delta H^{\neq}$ *vs.* $T\Delta S^{\neq}$ for the iron(II) reduction of *cis*-$Co(en)_2(NH_2CH_2CH_2OH)Cl^{2+}$ in aqueous solution of ethanol.
$\sum[ClO_4^-]=0.60$ M, $[HClO_4]=0.16$ M, 25°C.

solvent is to be seen in this figure. A plot of $\Delta H^{\neq}$ *vs.* $T\Delta S^{\neq}$ at 25°C for the reaction in the ethanol-water mixture gives a straight line with a slope of about 0.85 (Fig. 4). This seems to indicate that there is a certain degree of compensation effect between $\Delta H^{\neq}$ and $T\Delta S^{\neq}$.

Absorption spectra of Ferric Perchlorate in Several Organic Solvent-Water Mixtures. In Fig. 5, the absorption spectra of ferric perchlorate in DMSO-water mixtures are represented. The absorbances of the ferric perchlorate solutions in the mixtures of DMSO, DMF, ethanol, and acetone with water in 0.20 M perchloric acid solutions are plotted as a function of the mol fraction of the organic solvent (Fig. 6). It is apparent from these curves that the addition of DMSO, DMF, ethanol, or acetone to an aqueous solution of ferric perchlorate increases the absorbance of the solution

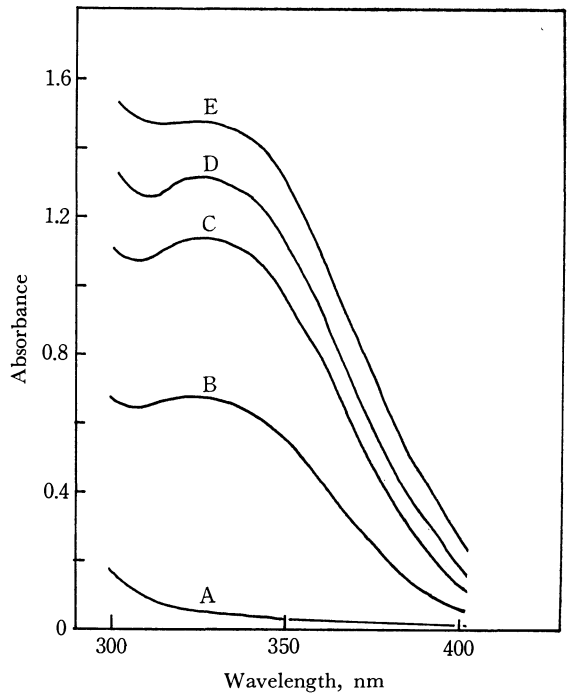

Fig. 5. Absorption spectra of ferric perchlorate in aqueous solution of dimethylsulfoxide.
$[Fe(III)]=1.60\times10^{-5}$ M, $\sum[ClO_4^-]=0.20$ M, $[HClO_4]=0.20$ M, 25°C.
A : aqueous solution.
B : 0.06 mol fraction of dimethylsulfoxide.
C : 0.20 mol fraction of dimethylsulfoxide.
D : 0.37 mol fraction of dimethylsulfoxide.
E : 0.70 mol fraction of dimethylsulfoxide.

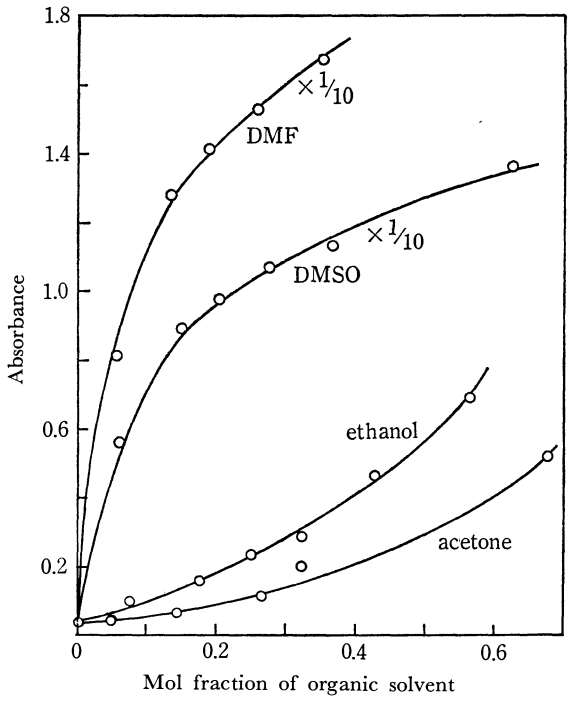

Fig. 6. The plots of absorbance *vs.* mol fraction of organic solvents.
$[Fe(III)]=1.60\times10^{-4}$ M, $\sum[ClO_4^-]=0.20$ M, $[HClO_4]=0.20$ M, at 350 nm, 25°C.

at wavelengths in the vicinity of 350 nm. Such increases in absorbance were also observed previously upon the addition of some alcohols to an aqueous solution of ferric perchlorate.[2,7]

Discussion

The facts that the rate of iron(II) reduction of the *cis*-$Co(en)_2(NH_2CH_2CH_2OH)Cl^{2+}$ is essentially independent of the hydrogen-ion concentration and that the rate is only slightly dependent upon the ionic strength of the solution seem to indicate that the marked increase in the rates with an increase in the concentration of the organic solvent in the organic solvent-water mixtures can not be due mainly to an alternation of the effective hydrogen ion concentration or that of the ionic strength in the media by the addition of organic solvents to aqueous solutions.

The ferrous-ferric exchange reaction proceed about 10^8 times slower in isopropyl alcohol than in water.[2] No specific explanation can be given for this results, however, it has been suggested that the predominant ferrous and ferric species may be quite different in the two solvents.[2] If the reactions have larger differences in configuration in isopropyl alcohol than in water, the reorganization energy may be much greater in alcohol.[2]

Because the coulombic repulsion free energy and outer-sphere reorganization free energy would be increased by a decrease in the macroscopic dielectric constant, and because the macroscopic dielectric constant is decreased with an increase in the organic solvent content, it may be supposed that the rate of the electron-transfer reaction between metal complexes is generally slower in organic solvents than in water, assuming that the same ionic species are present in the two solvents.[8]

In the present system, the anomalous increase in the rate upon the addition of an organic solvent to aqueous solution could not be explained by the effects of coulombic and outer-solvation-sphere reorganization free energy. The addition of an organic solvent to an aqueous solution of ferric perchlorate increases the absorbance of the solution. This increase is similar to that observed on the addition of other alcohols to aqueous solutions of ferric perchlorate.[7] This seems to suggest that some of the water molecules in the coordination-sphere of the ferric ion are replaced by organic solvent molecules. It may be supposed as was mentioned by Sutin,[2] that if the ionization potentials of the organic solvents used here are less than that of water, it would be easier to remove an electron from the solvation shell if the shell contains such organic molecules. This would shift the absorption band of the ferric perchlorate solution toward a longer wavelength and increase the absorbance in the vicinity of 350 nm.[2] Such a replacement of the water molecules by the organic molecules may also be expected in the case of the ferrous perchlorate solution by the addition of an organic solvent to the aqueous solution. In fact, it was suggested that, in a DMSO-water mixture at a higher water concentration, the mixed-ligand complexes, $Fe(DMSO)_{6-n}(H_2O)_n^{2+,3+}$,[4] and in pure DMSO, the DMSO complexes, $Fe(DMSO)_6^{2+,3+}$,[9] are important. On the other hand, the replacement of the ligands in the *cis*-$Co(en)_2(NH_2CH_2CH_2OH)Cl^{2+}$ by the organic molecules during the reaction may be ignored because of the inertness of this complex. The increase in the rate for the present reaction in the organic solvent-water mixtures seems to be contrary in trend to the cases of the electron-exchanges reactions between $Co(phen)_3^{2+}$ and $Co(phen)_3^{3+}$ [1] and iron(II) and iron(III).[4] However, the change in the coordination sphere in the ferrous ions would be one of the most important reasons for the increase in the reactivity upon the addition of organic solvent to the aqueous solutions.

In acidified organic solvent-water mixtures, the main species of iron(II) may be present in the $Fe(OH_2)_{6-a}(OS)_a^{2+}$ form, where OS is the organic solvent molecule. The overall reaction may be given by:

$$cis\text{-}Co(en)_2(NH_2CH_2CH_2OH)Cl^{2+} + Fe(OH_2)_{6-a}(OS)_a^{2+} \rightarrow Co^{2+} + 2en + NH_2CH_2CH_2OH + Cl^- + Fe(III) \quad (2)$$

Although the electron-transfer reaction between *cis*-$Co(en)_2(NH_2CH_2CH_2OH)Cl^{2+}$ and iron(II) would proceed *via* a chloride-bridged activated complex in aqueous solutions,[10] the mechanism for reaction (2) in the organic solvent-water mixtures would not necessarily be same as that for the reaction in aqueous solution.

7) R. A. Horne, *J. Phys. Chem.*, **62**, 509 (1958).
8) R. A. Marcus, *Discuss. Faraday. Soc.*, **29**, 21 (1960).
9) G. Wada and W. Reynolds, *Inorg. Chem.*, **5**, 1354 (1966).
10) Y. Kurimura and K. Ohashi, This Bulletin, **44**, 1797 (1971).

Electron-Transfer Reactions of Multidentate-ligand Cobalt(III) Complexes. III. The Reductions of Several Chloro- and Bromo(nitrilopolycarboxylato)-cobaltate(III) Ions by Iron(II)

Yoshimi KURIMURA, Ikuko MEGURO,* and Kousaburo OHASHI*

College of General Education, Ibaraki University, Mito

**Department of Chemistry, Ibaraki University, Mito*

(Received April 16, 1971)

The reductions of chloro- and bromo(ethylenediaminetriacetatoacetic acid)cobaltate(III), chloro- and bromo(*N*-hydroxyethylethylenediamine-*N*,*N*′,*N*′-triacetato)cobaltate(III), and dichloro(ethylenediaminediacetato)cobaltate(III) ions by iron(II) in perchloric acid solutions obey the second-order rate expression: $-\mathrm{d}[\mathrm{Co(III)}]/\mathrm{d}t = k_c[\mathrm{Co(III)}][\mathrm{Fe^{2+}}]$. The second-order rate constants, k_c, and activation parameters for these reactions were determined spectrophotometrically. For the cases of all the Co(III) complexes investigated, an increase in the rate constant with the hydrogen-ion concentration at a constant ionic strength is expressed by: $\log k_c = \log k_0 + A[\mathrm{H^+}]$, where k_0 and A are constants for the given complex at a constant ionic strength and temperature. The hydrogen-ion dependence can be explained by the difference in the degree of stabilization of the Co(III) anion between that by hydrogen ions and that by sodium ions.

In previous papers, the results of kinetic studies of the electron-transfer reactions of the cobalt(III) complexes of the $CoN_4Cl_2^+$, $CoN_4OH_2Cl^{2+}$ [1] ($N_4=(NH_3)_4$, $(en)_2$, and trien[2]) and CoN_5Cl^{2+} [3] ($N_5=(NH_3)_5$ and tetren[4]) types have been reported. In these studies, the effect of nonbridging ligands on the electron-transfer process were of major interest.

Haim and Sutin[5] found that iron(II) reductions of $Co(HY)Cl^-$ (Y^{4-}=ethylenediaminetetraacetate) proceeds by means of a chloride-bridged inner-sphere mechanism. The behavior of the reaction of $Co(HY)Cl^-$ with iron(II) has also been investigated by Pidcock and Higginson.[6] No kinetic studies of the other monohalogeno- and dihalogeno(nitrilopolycarboxylato)cobaltate(III) complexes have been published, however; the present work on the reaction kinetics was undertaken in order to establish the features of the reaction mechanism.

Experimental

Materials. The stock solution of iron(II) perchlorate was prepared by dissolving iron wire (Mallinckrodt Co. Anala R quality) in a dilute perchloric acid solution. The concentrations of the iron(II), perchrolate, and hydrogen ions were determined by methods similar to those previously reported.[1] All the other reagents used for the preparation of the stock solutions were of a guaranteed reagent quality. Redistilled water was used for the preparation of the reaction mixture.

Preparations of Cobalt(III) Complexes. Sodium chloro- and bromo(ethylenediaminetriacetatoacetic acid)cobaltate(III) (Na[Co(H·EDTA)Cl][7] and Na[Co(H·EDTA)Br][8]), sodium chloro- and bromo(*N*-hydroxyethylethylenediamine *N*,*N*′,*N*′-triacetato)cobaltate(III) (Na[Co(EDTAOH)Cl],[7] and Na[Co(EDTAOH)Br][8]) were prepared by methods similar to those described in the references cited.

Found: C, 28.76; H, 3.82; N, 6.36%. Calcd for Na[Co(H·EDTA)Cl]·0.5H_2O: C, 28.90; H, 3.40; N, 6.74%.

Found: C, 25.29; H, 3.57; N, 5.83%. Calcd for Na[Co(H·EDTA)Br]·H_2O: C, 25.61; H, 3.22; N, 5.97%.

Found: C, 28.59; H, 4.41; N, 6.46%. Calcd for Na[Co(EDTAOH)Cl]·1.5H_2O: C, 28.62; H, 4.32; N, 6.68%.

Found: C, 27.74; H, 4.35; N, 6.29%. Calcd for Na[Co(EDTAOH)Br]·H_2O: C, 26.39; H, 3.77; N, 6.16%.

Sodium dichloro(ethylenediaminediacetato)cobaltate(III). $CoCl_2\cdot 6H_2O$ (4.6 g) and ethylenediaminediacetic acid (3.6 g) were dissolved in 100 m*l* of water. A sodium hydroxide solution (1.6 g in 50 m*l* of water) was then added to the solution, and the Co(II) was oxidized by the addition of 20 m*l* of a 30% hydrogen peroxide solution. Dark blue crystals were obtained after the addition of 100 m*l* of concentrated hydrochloric acid; they were recrystallized from alcohol-water.

Found: C, 22.31; H, 3.49; N, 8.97%. Calcd for Na[Co(EDDA)Cl_2]: C, 22.04; H, 3.08; N, 8.57%.

The electronic spectral data for the complexes are included in Table 1.

Table 1. Spectral data for cobalt(III) complexes

Complex	λ_{max}[a] nm	ε_{max}
Na[Co(H·EDTA)Cl]	583	225
Na[Co(H·EDTA)Br]	594	223
Na[Co(EDTAOH)Cl]	583	207
Na[Co(EDTAOH)Br]	593	210
Na[Co(EDDA)Cl_2]	599	246

a) First absorption maximum.

Kinetic Measurements. The cobalt(III) and iron(II) solutions, both of which contained the necessary amounts of perchloric acid and sodium perchlorate, were kept in a thermostat. The desired volume of the iron(II) solution was then added to the cobalt(III) solution, the solution was transferred to a 1-cm cell which had been placed in a thermostated cell compartment of a Hitachi Model 125 Recording Spectrophotometer, and the absorbance of the reaction mixture in the vicinity of the absorption maximum for the cobalt(III) complex was recorded as a function of the time. Most of the experiments were carried out under second-order conditions. The second-order rate constants,

1) Y. Kurimura, K. Ohashi, T. Ohtsuki, and K. Yamamoto, This Bulletin, **44**, 1293 (1971).

2) en=ethylenediamine and trien=triethylenetetramine.

3) Y. Kurimura and K. Ohashi, This Bulletin, **44**, 1797 (1971).

4) tetren=tetraethylenepentamine.

5) A. Haim and N. Sutin, *J. Amer. Chem. Soc.*, **88**, 5343 (1966).

6) A. Pidcock and W. C. Higginson, *J. Chem. Soc.*, **1963**, 2798.

7) M. L. Morris and D. H. Busch, *J. Amer. Chem. Soc.*, **78**, 5179 (1956).

8) G. Schwarzenbach, *Helv. Chim. Acta*, **32**, 839 (1949).

k_c, for each run were evaluated from the slopes of the usual second-order plots. Some of the Co(EDTAOH)Br$^-$ kinetic runs were carried out under pseudo-first-order conditions. The pseudo-first-order rate constants, k_n, were evaluated from the slopes of the log (A_t-A_∞) *vs.* time plots, where A is the absorbance at time t, and A_∞, the absorbance after all the Co(III) has been reduced to Co(II). The second-order rate constant, k_c, was calculated from the equation $k_c=k_n/[Fe^{2+}]$. For the cases of all the cobalt(III) complexes, the rates of the aquations of the complexes could be neglected as compared to those of the reductions.

Results

Rate Studies at a Given Hydrogen Ion Concentration. In all the cases investigated, the reductions of the Co(III) complexes by iron(II) followed the rate law of $-d[Co(III)]/dt=k_c[Co(III)][Fe^{2+}]$, good second-order plots being obtained in up to 80—95% of the reactions. In addition, all the values of k_c were essentially constants for he given cobalt(III) complex in the region of initial concentrations of iron(II) from 0.0462 to 0.0982 M at a particular hydrogen ion concentration and ionic strength. The second-order rate constants at $[H^+]=0.10$ M and $\Sigma[ClO_4^-]=1.0$ M and at 25°C are summarized in Table 2, along with the activation parameters, which were obtained from temperature dependence of the k_c.

TABLE 2. SECOND-ORDER RATE CONSTANTS[a] AND ACTIVATION PARAMETERS[a] FOR THE REDUCTIONS OF CoZCl$^-$ [b] BY Fe^{2+}

Complex	k_c $M^{-1}sec^{-1}$	$\Delta H^{\neq}$ kcal mol^{-1}	$\Delta S^{\neq}$, eu
Co(H·EDTA)Cl$^-$	1.52[c]	7.8	−31
Co(H·EDTA)Br$^-$	1.23	7.0	−35
Co(EDTAOH)Cl$^-$	1.65	7.5	−33
Co(EDTAOH)Br$^-$	0.73	6.3	−38
Co(EDDA)Cl_2^-	2.36	11	−20

a) Evaluated at $[H^+]=0.10$ M and $\Sigma[ClO_4^-]=1.0$ M and at 25°±0.1°C in $HClO_4$-$NaClO_4$ mediums.
b) Z=H·EDTA^{3-}, EDTAOH^{3-} and EDDACl^{3-}.
c) Rate constant obtained by A. Haim and N. Sutin[5] is 1.9 ± 0.2 $M^{-1}sec^{-1}$ at 25°C, $\Sigma[HClO_4]=2.2$—2.8 M and ionic strength of 3.0 M.

Dependence of the Rate Constant on the Hydrogen-ion Concentration. The hydrogen-ion dependence of the rate constant was examined in the $HClO_4$–$NaClO_4$ medium, in which the ionic strength was maintained at 1.0 M. The values of k_c are slightly increased with an increase in the hydrogen-ion concentration in all cases. The values of the second-order rate constants were found to vary with the hydrogen-ion concentration according to the equation:

$$\log k_c = \log k_0 + A[H^+] \quad (1)$$

where k_0 and A are constants for a given complex and at a constant ionic strength and temperature. The values of log k_c are plotted as a function of the hydrogen-ion concentration in Fig. 1. The k_0 and A values could be obtained from the intercept and slope of the log k_c *vs.* $[H^+]$ plot respectively. These values are summarized in Table 3.

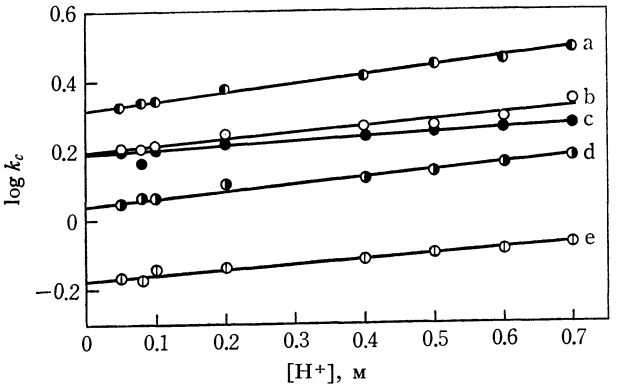

Fig. 1. Dependence of the second-order rate constant upon hydrogen ion concentration.
a : Co(EDDA)Cl_2^- b : Co(EDTAOH)Cl$^-$
c : Co(H·EDTA)Cl$^-$ d : Co(H·EDTA)Br$^-$
e : Co(EDTAOH)Br$^-$
$[Fe^{2+}]=9.73\times10^{-3}$ M, $\Sigma[ClO_4^-]=1.0$ M, $[Co(III)]=2.44\times10^{-3}$—$4.01\times10^{-3}$ M, 25±0.1°C.

TABLE 3. THE VALUES OF k_0 AND A FOR THE Fe^{2+} REDUCTIONS OF CoZX$^-$ AT 25°C[a]

Complex	k_0, $M^{-1}sec^{-1}$	A, $M^{-2}sec^{-1}$
Co(H·EDTA)Cl$^-$	1.54	0.12
Co(H·EDTA)Br$^-$	1.20	0.14
Co(EDTAOH)Cl$^-$	1.57	0.18
Co(EDTAOH)Br$^-$	0.71	0.15
Co(EDDA)Cl_2^-	2.07	0.24

a) Evaluated at $\Sigma[ClO_4^-]=1.0$ M in $HClO_4$—$NaClO_4$ medium and at 25±0.1°C.

Discussion

It has been demonstrated from a direct observation of the transient species of the primary product that the reaction of Co(H·EDTA)Cl$^-$ with Fe^{2+} proceeds *via* a chloride-bridged transition state.[5] Therefore, it is reasonable to assume that the reactions of CoZCl$^-$ (Z=H·EDTA^{3-}, EDTAOH^{3-}, and EDDACl^{3-}) and perhaps CoZBr$^-$ with iron(II) proceed *via* the chloride- and bromide-bridged mechanisms respectively. Such an inner-sphere reaction may be regarded as proceeding through the formation of a bridged activated complex such as $[Co^{III}Z\cdots Cl\cdots Fe^{II}]$.[5] The initial products of the Co(II) and Fe(III) may be the Co(II)-aminopolycarboxylic acid complex and $FeCl^{2+}$ [5] respectively; these substances are unstable and rapidly form Co^{2+} and the Fe(III)-aminopolycarboxylic acid complex respectively under the conditions employed.

The similar effectiveness for the Co(H·EDTA)Cl$^-$ and Co(EDTAOH)Cl$^-$ complexes, and also that for the Co(H·EDTA)Br$^-$ and Co(EDTAOH)Br$^-$ complexes, seem to suggest that there is no appreciable change in the relative effectiveness by replacing the protonated carboxyl group in the Co(H·EDTA)X$^-$ (X=Cl$^-$ and Br$^-$) complex by a $-CH_2OH$ group. The Co(H·EDTA)Br$^-$ and Co(EDTAOH)Br$^-$ complexes are less reactive than the respective corresponding chloride complexes. The smaller effectiveness for the Co(III)-bromo complex compared with that of the corresponding Co(III)-chloro complex has been known in the reduc-

tions of the Co(III) complexes by low reactive reducing agents, such as Fe(II)[9,10] and Eu(II).[11,12] The bridging efficiency seems to depend primarily upon the nature of the reducing agent. This may indicate that the stabilization of the transition state by bond making to the reductants may be of greater importance than bond breaking for the reductants in the reactions investigated.[12]

The higher reactivity for the $Co(EDDA)Cl_2^-$ complex relative to the other complexes investigated may be due to existence of two chloride ions in this complex.

A rate dependence on the hydrogen-ion concentration similar to that expressed by Eq. (1) has been proposed by Pidcock and Higginson,[6] and also there is much experimental evidence for such hydrogen-ion dependence.[6] They ascribed the relatively small increase in the rate constant with an increase in the hydrogen-ion concentration at a constant ionic strength in the iron(II) reduction of $Co(H\cdot EDTA)Cl^-$ to a specific salt effect due to interaction between ions of opposite charges, rather than to a catalysis involving a reaction path in which a proton enters into the transition complex.[6] It was suggested that the increase in the second-order rate constant for the reactions of the $Co(HY)Cl^-$ complex with iron(II) could be ascribed to a greater stabilization of the $Co(HY)Cl^-$ complex by sodium ions than by hydrogen ions.[6]

This explanation seems to applicable to the iron(II) reductions of the $Co(H\cdot EDTA)Br^-$, $Co(EDTAOH)Cl^-$, $Co(EDTAOH)Br^-$, and $Co(EDDA)Cl_2^-$ complexes since all the k_c values for these complexes followed Equation (1) rather than the first-order dependence of the hydrogen ion.

Since the uncoordinated carboxyl group in the $Co(H\cdot EDTA)X^-$ complex are almost all protonated under the conditions employed, and since there is no uncoordinated carboxyl group in the $Co(EDTAOH)X^-$ and $Co(EDDA)Cl_2^-$ complexes, it could hardly be supposed that the reactions of these complexes proceed through a reaction path in which a proton enters into the transition state. On the other hand, there can be no rate dependence upon the hydrogen-ion concentration in the iron(II) reductions of the Co(III) complexes with positive charges, such as CoN_5Cl^{2+} and $CoN_4Cl_2^+$ ($N_5=(NH_3)_5$, $(en)_2NH_3$, and tetren and $N_4=(NH_3)_4$, $(en)_2$, and trien[13]), in the $HClO_4$–$NaClO_4$ medium under conditions of a constant ionic strength and a relatively high hydrogen-ion concentration, because no change in the interactions between the ions of opposite charges, the Co(III) ion and the perchlorate ion, would result from replacing the sodium ions by hydrogen ions.

The values of A, which may be a measure of the difference in the interactions between the cations (H^+ and Na^+) and the reactant Co(III) anion, are almost the same in the cases of the $Co(H\cdot EDTA)Cl^-$, $Co(H\cdot EDTA)Br^-$, $Co(EDTAOH)Cl^-$ and $Co(EDTAOH)Br^-$ complexes, but it is slightly larger for the case of $Co(EDDA)Cl_2^-$. This seems to be ascribable to the greater difference between the degree of the stabilization of this complex by sodium ions and that by hydrogen ions as compared to those of the other Co(III) complexes investigated. The relatively higher values of k_0, ΔH^*, ΔS^*, and A for the $Co(EDDA)Cl_2^-$ may suggest a somewhat different reaction pattern relative to that of the other complexes, for instance, a reaction path including a double chloride-bridged activated complex.

9) H. Diebler and H. Taube, *Inorg. Chem.*, **4**, 1029 (1965).
10) J. H. Espenson, *ibid.*, **4**, 121 (1965).
11) J. P. Candlin, J. Halpern, and D. L. Trim, *J. Amer. Chem. Soc.*, **86**, 1010 (1964).
12) A. G. Sykes, *Adv. Inorg. Chem. Radiochem.*, **10**, 153 (1967).
14) It seems reasonable to assume that these reactions proceed *via* the chloride-bridged activated complexes.[1,2]

Gas-Chromatographic Determination of Ultramicro Amounts of Selenium in Pure Tellurium Metal

Yasuaki SHIMOISHI*

Department of Chemistry, Faculty of Science, Okayama University, Tsushima, Okayama-shi

(Received May 14, 1971)

Selenium (IV) reacts with 4-nitro-*o*-phenylenediamine to form 5-nitropiaselenol, which is detected by means of a gas chromatograph equipped with an electron-capture detector. By this highly sensitive method, the selenium in pure tellurium metal (99.9—99.999%) can easily be determined. Aqua regia oxidizes both selenium and tellurium to the quadrivalent state, and no loss of selenium is found upon this treatment. This method requires only 10—30 mg of a tellurium sample, and the presence of foreign ions does not interfere. It was found that pure tellurium, commercially available, always contains 10^{-3}—10^{-4}% selenium.

Spectrophotometric[1,2] and fluorimetric[3,4] procedures are convenient analytical methods for the determination of traces of selenium. Many organic reagents have been suggested for this purpose, 3,3′-diaminobenzidine[5,6] being widely used. The present author and a coworker[7] have recently proposed a far more sensitive method for detecting selenium in pure sulfuric acid by means of a gas-chromatograph equipped with an electron-capture detector and using 4-nitro-*o*-phenylenediamine. The present paper will describe a gas-chromatographic determination of selenium in pure tellurium. As even about 0.01 μg of selenium can be determined, only a few milligrams of tellurium are needed as the sample. By the oxidation of the pure tellurium with aqua regia, the selenium and the tellurium were converted to the respective quadrivalent states. The selenium in the solution was determined by the gas-chromatographic method using 4-nitro-*o*-phenylenediamine.

Experimental

Reagents. *4-Nitro-o-phenylenediamine Hydrochloride Solution*: This was a 1% acidic solution so stable that the solution could be used after standing for more than 1 week at room temperature.

Stock Selenium(IV) Solution: 351.3 mg of selenium dioxide were dissolved in 250 m*l* of distilled water (1 mg of Se in 1 m*l*). Working solutions were prepared by diluting the stock solution.

Stock Selenium(O) Solution: 3.06 mg of elemental selenium were dissolved in 50 m*l* of carbon disulfide (61.2 μg of Se in 1 m*l*). Working solutions were prepared by diluting the stock solution with carbon disulfide.

Stock Aqua Regia Solution: Concentrated hydrochloric acid and nitric acid were mixed in the volume ratio of three to one. The working solution was the doubly diluted stock solution.

The other reagents were of an analytical reagent grade.

Apparatus. A Shimadzu Model GC-3AE gas chromatograph equipped with an electron-capture detector was used. The glass column (1 m long, 4 mm bore) was packed with 15% SE—30 on 60—80 mesh Chromosorb W. The column and the detector temperature were maintained at 200°C. The nitrogen flow-rate was 48 m*l*/min. A Shimadzu Model 250A recorder was used, and the chart speed was 5 mm/min.

General Procedure. 30 mg of grained pure tellurium was put into a 100-m*l* beaker, and 6 m*l* of aqua regia which has been doubly diluted was added; the solution was then heated in a boiling water bath for 10 min. After cooling, a 3 m*l* portion of concentrated hydrochloric acid was added and the content was transferred to a 100-m*l* separatory funnel and the beaker was rinsed with 10-m*l* of distilled water into the funnel. When the selenium content was too large, an aliquot containing 0.01—0.1 μg of Se was used. Two milliliters of a 1% 4-nitro-*o*-phenylenediamine solution were added and the solution was allowed to stand for 2 hrs. Then, the 5-nitro-piaselenol formed was extracted into 1 m*l* of toluene by shaking for 5 min and the toluene extract was washed with 5 m*l* of 0.2 N sodium hydroxide. Five microliters of the toluene extract were injected into the gas-chromatograph and the peak height was measured.

Results and Discussion

Preparation of the Tellurium Sample. Selenium in the tellurium metal is not present in the form of selenium(IV), but in the elemental form, since the selenium compounds are more readily reduced and less easily oxidized than the corresponding tellurium compounds. Therefore, any selenium in the tellurium must be converted into the 4^+ oxidation state.

In order to dissolve and oxidize both tellurium and selenium to the quadrivalent form, nitric acid, aqua regia or a mixed acid of perchloric acid and nitric acid is usually used. Aqua regia is the most convenient oxidizing reagent, for, unless a considerable excess of nitric acid is used, the basic nitrate and tellurium dioxide are likely to be precipitated. The perchloric acid also lowers the peak height slightly, but the reason is not known. The gas-chromatogram which is obtained with 30 mg of tellurium dissolved in 6 m*l* of aqua regia diluted to two times is shown in Fig. 1. The retention time of 5-nitropiaselenol is four minutes.

Oxidation with Aqua Regia. Usually, when the oxidation of selenium is performed in the presence of hydrochloric acid, a volatile chloride, $SeCl_4$ is formed. This chloride must be responsible for the loss of sele-

* Present address: School for X-ray Technicians, Faculty of Medicine, Okayama University, Shikatacho, Okayama-shi.

1) J. Hoste and J. Gillis, *Anal. Chim. Acta*, **12**, 158 (1955).
2) K. Tôei and K. Ito, *Talanta*, **12**, 773 (1965).
3) J. H. Watkinson, *Anal. Chem.*, **38**, 92 (1966).
4) P. F. Lott, P. Cukor, G. Moriber, and J. Solga, *ibid.*, **35**, 1159 (1963).
5) T. Yuasa, *Japan Analyst*, **10**, 965 (1961).
6) T. Miura and K. Tsutsumi, *ibid.*, **13**, 758 (1964).
7) Y. Shimoishi and K. Tôei, *Talanta*, **17**, 165 (1970).

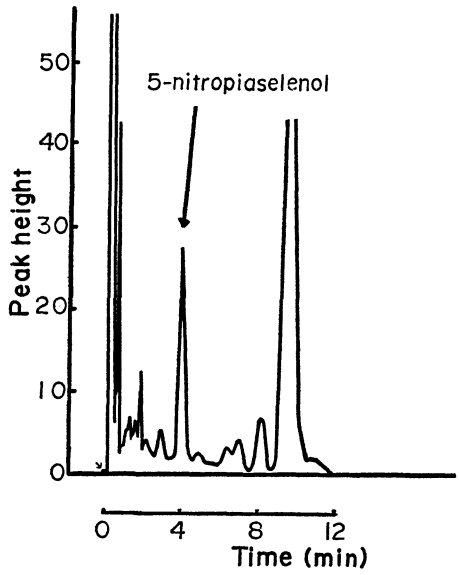

Fig. 1. Gas chromatogram of 5-nitropiaselenol.
Column 15% SE 30/chromosorb W
Carrier gas N_2 (48 m*l*/min)
Temperature 200°C
Range 0.2 V
Sample 5 μl (0.054 μg Se in 30 mg Te)

nium. The effect of the concentration of aqua regia, the oxidation time, and the oxidation temperature are studied to confirm whether or not there is any loss of selenium.

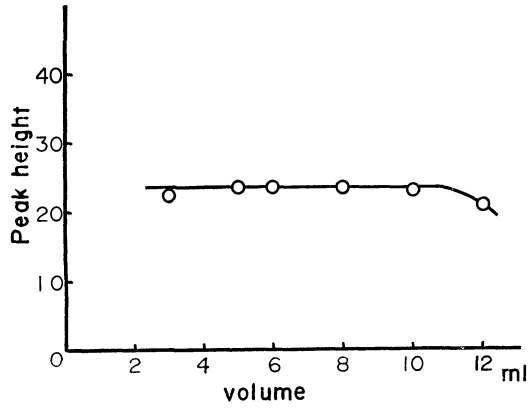

Fig. 2. Effect of the aqua regia concentration (30 mg Te).
Range 0.2 V

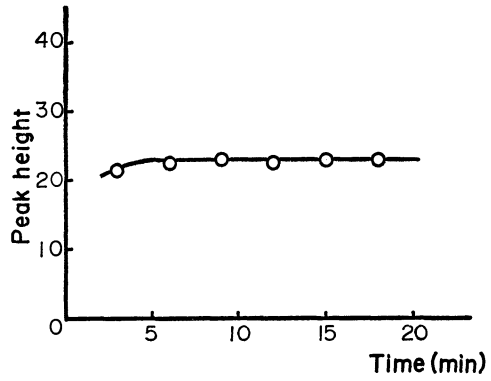

Fig. 3. Effect of the oxidation time (100°C) (30 mg Te).
Range 0.2 V

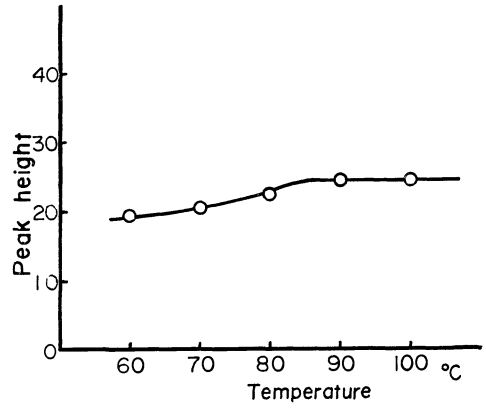

Fig. 4. Effect of the oxidation temperature (30 mg Te).
Range 0.2 V

First of all, the effect of the concentration of aqua regia is studied. It is desirable that the concentration of aqua regia required to oxidize both selenium and tellurium be as low as possible. However, if the volume of the solution is too small, the loss of selenium may occur during oxidation in a boiling water bath. Therefore, doubly-diluted aqua regia is used for the oxidation procedure. The results are shown in Fig. 2. Complete oxidation is performed from 5 to 10 m*l* of aqua regia. Therefore, 6 m*l* of aqua regia, diluted to two times, are used in the following experiments. Next, the oxidation time is measured by heating in a boiling water bath (Fig. 3). As the oxidation is complete from 6 to 18 min, a sufficient oxidation time is 10 min. Lastly, Figure 4 shows the effect of the oxidation temperature. When the oxidation is performed at more than 90°C, the peak height shows the maximum and constant value.

Washing the Toluene Extract with Sodium Hydroxide. When the toluene extract is injected directly, without washing with sodium hydroxide, into the gas-chromatograph, an unknown peak appears overlapping the 5-nitropiaselenol. However, it can easily be removed by washing with a sodium hydroxide solution. Though, usually, the nitro compound is readily dis-

Table 1. Effect of the foreign ions

$\left(\frac{[X]}{[Se]} = 10^4\right)$

Foreign ion (X)	Se recovery Se(0) in CS_2 (μg)	Se recovery in 30 mg Te (μg)
none	0.067 0.062	0.056 0.053
Fe^{3+}	0.066	0.054
Cu^{2+}	0.065	0.054
Ag^{+}	0.066	0.058
Pb^{2+}	0.064	0.057
Hg^{2+}	0.066	0.059
As^{3+}	0.067	0.058
Sb^{3+}	0.060	0.054
Bi^{3+}	0.061	0.054
Fe^{3+} Cu^{2+} Ag^{+} Pb^{2+} As^{3+} Sb^{3+}	0.067	0.053

solved in an alkaline solution, as long as the toluene extract is washed with at least 5 m*l* of a 10^{-3}—1 M sodium hydroxide solution, the unknown acidic substance is removed and no back extraction of 5-nitropiaselenol can be found.

Effect of Foreign Ions. Although the amounts of foreign metals in pure tellurium would be comparable to that of selenium, the effect of a large amount of various ions is examined. No effect is found, even if 10^4 times as many of foreign ions are present, as is shown in Table 1.

Calibration Curve. The calibration curves are made from both a known amount of selenous acid in a hydrochloric acid solution and the elemental selenium dissolved in CS_2 by the above-mentioned procedure. These two curves are parallel to each other (Fig. 5). This results also shows that the oxidation is complete.

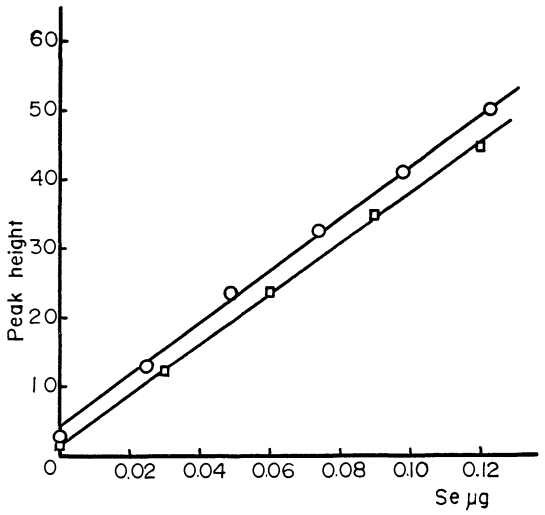

Fig. 5. Calibration curve
Range 0.2 V
—⊖— Se(0) in CS_2
—⊟— Se(IV) as H_2SeO_3

Determination of Selenium in Tellurium. Selenium in 30 mg of commercial pure tellurium was determined by the above-mentioned procedure; the same sample containing a standard addition of elemental selenium was also used for the determination. As its standard addition is always obtained by deducing the former values from the latter values, this method is proved to be suitable and correct for the determination of selenium in pure tellurium metal. The results are shown in Table 2.

TABLE 2. SELENIUM CONTENT IN TELLURIUM

Company	Selenium content in tellurium	
	Analytical reagent grade $\times 10^{-4}$%	Extra pure reagent $\times 10^{-4}$%
A	1.8±0.1	
B	30.0±0.1	22.5±0.2
C	13.5±0.2	7.5±0.1
D	4.0±0.1	31.5±0.2

The mean value of four times mesurement

As the sensitivity of an electron-capture detector tends to vary during operations, a series of experiments should be carried out successively and an unknown content of selenium should be determined along with standard samples which contain similar amounts of selenium. The procedure's outstanding features are that it is simple, highly sensitive, and rapid, and that no special skill is necessary to perform it.

The author is grateful to Professor Kyoji Tôei for his helpful discussions and encouragement.

Spectroscopic Studies of Polynuclear Complexes. III.[1] Characteristics of Some μ-Peroxoammine Cobalt(III) Complexes.

Yoichi SASAKI, Junnosuke FUJITA, and Kazuo SAITO
Department of Chemistry, Faculty of Science, Tohoku University, Sendai

(Received May 20, 1971)

The spectroscopic and chemical properties of various μ-peroxo and μ-superoxo cobalt(III) complexes containing several kinds of polyamine including optically active *l*-propylenediamine (*l*-pn) have been studied. The single bridged μ-peroxo complexes have strong absorption peaks at *ca.* 300 nm, whereas the double-bridged μ-peroxo-μ-amido and μ-peroxo-μ-hydroxo complexes have peaks at *ca.* 350 nm. The μ-superoxo complexes have two absorption peaks in the visible region at *ca.* 700 and 480 nm. The former is remarkably stronger for single-bridged species, but both are of almost equal strength for double bridged species. The complexes $[LNH_3Co(\mu\text{-}O_2^{(2-)})CoNH_3L]^{4+}$ (L; 2en (ethylenediamine), 2*l*-pn, and trien(triethylenetetramine)) are spontaneously converted into $[LCo(\mu\text{-}O_2^{(2-)}, OH)CoL]^{3+}$ in water at room temperature. The en ligands in $[(dien)(en)Co(\mu\text{-}O_2^{(2-)})Co(en)(dien)]^{4+}$ (dien; diethylenetriamine) are replaced by *l*-pn in a few days in aqueous solutions containing an excess of *l*-pn. The absolute configuration of $[(l\text{-pn})_2Co(\mu\text{-}O_2^{(2-)}, OH)Co(l\text{-pn})_2]^{3+}$ is assigned to be $\Delta\Delta$ on the basis of circular dichroism spectrum.

As an extention of our preparative and spectroscopic studies of binuclear cobalt complexes bridged by peroxo or superoxo anions,[1,2] this paper deals with spectroscopic and chemical properties of some binuclear cobalt ammine complexes bridged by peroxo anions. Such complexes have been synthesized by many authors in various ways.[3] Fremy[4] passed air through an ammoniacal solution of cobalt(II) salt and obtained μ-peroxo-decaamminedicobalt(III) ions, $[(NH_3)_5Co(\mu\text{-}O_2^{(2-)})Co(NH_3)_5]^{4+}$, identified by Werner.[5] This compound is readily decomposed to cobalt(II) salt in a neutral solution with evolution of oxygen. Werner[6] prepared a double bridged dicobalt complex $[(NH_3)_4Co(\mu\text{-}O_2^{(2-)},NH_2)Co(NH_3)_4]^{3+}$ from well-known Vortmann's sulfate obtained by passing air through a warm ammoniacal solution of cobalt(II) salt and neutralizing with sulfuric acid. Mori *et al.*[7] obtained the same complex more conveniently and with better yield by warming Fremy's μ-peroxo complex[3] in aqueous ammonia. Recently Gainsford and House, and Duffy *et al.*[8] prepared polyamine derivative of Fremy's μ-peroxo complex,[4] *e.g.* $[(en)_2(NH_3)Co(\mu\text{-}O_2^{(2-)})Co(NH_3)(en)_2]^{4+}$ and $[(trien)(NH_3)Co(\mu\text{-}O_2^{(2-)})Co(NH_3)(trien)]^{4+}$ [9] by adding en or trien to an aqueous solution of $[(NH_3)_5Co(\mu\text{-}O_2^{(2-)})Co(NH_3)_5]^{4+}$ at room temperature. Foong *et al.*[10] obtained a double bridged dicobalt complex $[(en)_2Co(\mu\text{-}O_2^{(2-)},OH)Co(en)_2]^{3+}$ by passing air through an aqueous ethanol solution of cobalt(II) salt and en.

We prepared such binuclear complexes with aims of comparing the ultraviolet and visible absorption spectra with other binuclear complexes given previously,[1,2] and found that some of House's complexes with μ-peroxo bridges undergo rapid spectral change in aqueous solutions even at room temperature. The change seems to be related to an unusual lability of amine type ligands of binuclear complexes with μ-peroxo bridges.

Absorption Spectra of the Complexes. House *et al.*[8] prepared several binuclear complexes of cobalt containing polyamines with peroxo single bridge, including $[(tetren)Co(\mu\text{-}O_2^{(2-)}Co(tetren)]^{4+}$, $[(dien)(en)Co-$

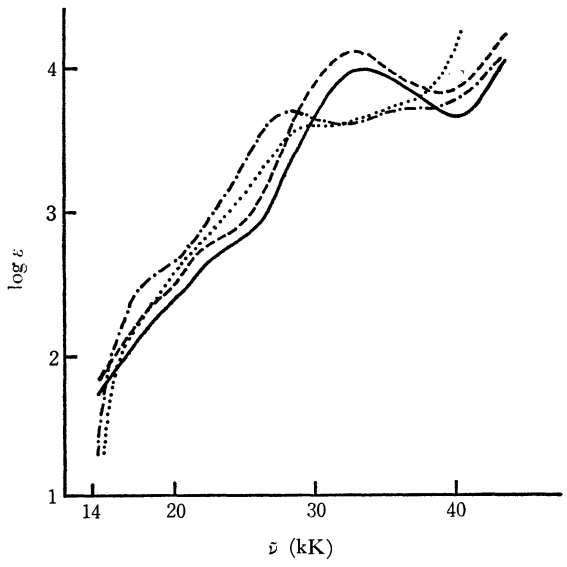

Fig. 1. Absorption spectra of several μ-peroxo dicobalt complexes in water.
——— $[(dien)(en)Co(\mu\text{-}O_2^{(2-)})Co(en)(dien)]^{4+}$
------ $[(tetren)Co(\mu\text{-}O_2^{(2-)})Co(tetren)]^{4+}$
—·—· $[(en)_2Co(\mu\text{-}O_2^{(2-)}, OH)Co(en)_2]^{3+}$
····· $[(en)_2Co(\mu\text{-}O_2^{(2-)}, NH_2)Co(en)_2]^{3+}$

1) Part II of this series, Y. Sasaki, J. Fujita, and K. Saito, This Bulletin, **43**, 3462 (1970).

2) a) Y. Sasaki, J. Fujita, and K. Saito, *ibid.*, **42**, 146 (1969); b) **40**, 2206 (1967); c) Y. Sasaki and J. Fujita, *ibid.*, **42**, 2089 (1969).

3) A. G. Sykes and J. A. Weil, *Progress Inorg. Chem.*, **13**, 1 (1970).

4) E. Fremy, *Ann. Chim. Phys.*, **35**, 257 (1852).

5) A. Werner and A. Mylius, *Z. anorg. Chem.*, **16**, 262 (1898).

6) G. Vortmann, *Monatsh. Chem.*, **6**, 404 (1855); A. Werner, *Ann. Chem.*, **375**, 1 (1910).

7) M. Mori, J. A. Weil, and M. Ishiguro, *J. Amer. Chem. Soc.*, **90**, 615 (1968).

8) a: A. R. Gainsford and D. A. House, *Inorg. Nucl. Chem. Lett.*, **4**, 621 (1968); b: D. L. Duffy, D. A. House, and J. A. Weil, *J. Inorg. Nucl. Chem.*, **31**, 2053 (1969).

9) Abbreviations used in this paper are as follows; en, ethylenediamine; *l*-pn, R(D)(−)D-propylenediamine; dien, diethylenetriamine; trien, trietliylenetetramine; tetren, tetraethylenepentamine.

10) S. W. Foong, J. D. Miller, and F. D. Oliver, *J. Chem. Soc.*, *A*, **1969**, 2847.

$(\mu\text{-}O_2^{(2-)})Co(en)(dien)]^{4+}$, $[(en)_2(NH_3)Co(\mu\text{-}O_2^{(2-)})Co(NH_3)(en)_2]^{4+}$ and $[(trien)(NH_3)Co(\mu\text{-}O_2^{(2-)})Co(NH_3)(trien)]^{4+}$, and gave absorption shoulders in water at 437, 420, 550, and 562 nm with extinction coefficients 619, 557, 247, and 230, respectively, We have prepared *l*-pn derivatives of the second and the third complex $[(dien)(l\text{-pn})Co(\mu\text{-}O_2^{(2-)})Co(l\text{-pn})(dien)]^{4+}$ and $[(l\text{-pn})_2(NH_3)Co(\mu\text{-}O_2^{(2-)})Co(NH_3)(l\text{-pn})_2]^{4+}$ in a similar manner, and measured the absorption spectra of all the six complexes in the region from 200 to 700 nm. All gave absorption maxima at *ca.* 300 nm in freshly

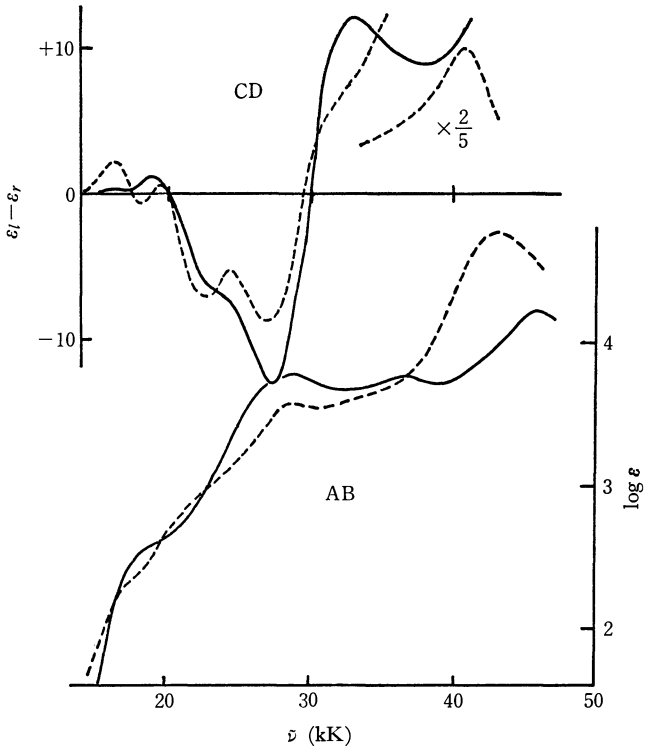

Fig. 2. Absorption (AB) and CD spectra of double-bridged μ-peroxo dicobalt complexes in water.
—— $[(l\text{-dn})_2Co(\mu\text{-}O_2^{(2-)}, OH)Co(l\text{-pn})_2]^{3+}$
---- $\Delta\Delta$-$[(l\text{-pn})_2Co(\mu\text{-}O_2^{(2-)}, NH_2)Co(l\text{-pn})_2]^{3+}$

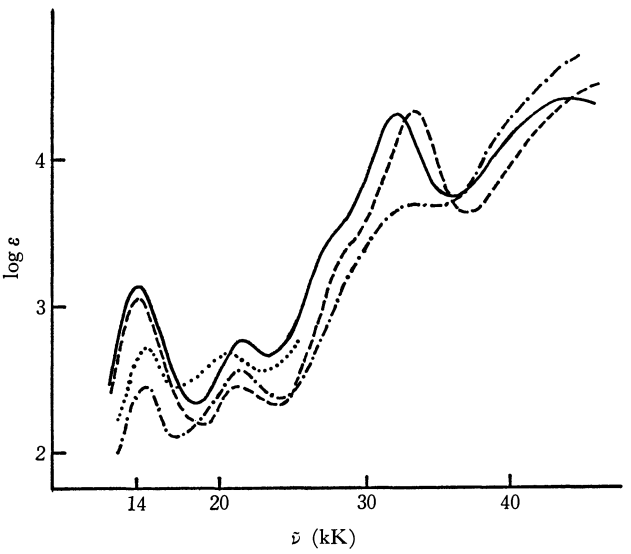

Fig. 3. Absorption spectra of several μ-superoxo dicobalt complexes in 0.01 N perchloric acid.
——— $[(tetren)Co(\mu\text{-}O_2^{(-)})Co(tetren)]^{5+}$
------ $[(en)_2(NH_3)Co(\mu\text{-}O_2^{(-)})Co(NH_3)(en)_2]^{5+}$
—·—· $[(en)_2Co(\mu\text{-}O_2^{(-)}, NH_2)Co(en)_2]^{4+}$
····· $[(en)_2Co(\mu\text{-}O_2^{(-)}, OH)Co(en)_2]^{4+}$ (approximate curve)

prepared solutions. However, the complexes containing ammonia *i.e.* $[(en)_2(NH_3)Co(\mu\text{-}O_2^{(2-)})Co(NH_3)(en)_2]^{4+}$, $[(trien)(NH_3)Co(\mu\text{-}O_2^{(2-)})Co(NH_3)(trien)]^{4+}$ and $[(l\text{-pn})_2(NH_3)Co(\mu\text{-}O_2^{(2-)})Co(NH_3)(l\text{-pn})_2]^{4+}$ underwent rapid spectral change and the absorption maxima shifted to *ca.* 350 nm. The absorption pattern of the other three complexes remained unchanged as shown in Fig. 1.

The double bridged complexes with peroxo and hydroxo bridges, $[(l\text{-pn})_2Co(\mu\text{-}O_2^{(2-)}, OH)Co(l\text{-pn})_2]^{3+}$ and $[(en)_2Co(\mu\text{-}O_2^{(2-)}, OH)\ Co(en)_2]^{3+}$ were prepared according to the method of Foong *et al.*[10] and the absorption spectra were recorded in water. They remained unchanged for more than 24 hr with maxima at *ca.* 350 nm, as seen in Figs. 1 and 2.

TABLE 1. NUMERICAL DATA OF THE ABSORPTION SPECTRUM

(μ-Peroxo complexes in water)	kK (log ε)	kK (log ε)	kK (log ε)
$[(dien)(en)Co(\mu\text{-}O_2^{(2-)})Co(en)(dien)]^{4+}$		24.0 (2.78) s	33.3 (3.98)
$[(dien)(l\text{-pn})Co(\mu\text{-}O_2^{(2-)})Co(l\text{-pn})(dien)]^{4+}$		24.0 (2.73) s	33.2 (4.00)
$[(tetren)Co(\mu\text{-}O_2^{(2-)})Co(tetren)]^{4+}$		24.0 (2.87) s	32.2 (4.10)
$[(en)_2Co(\mu\text{-}O_2^{(2-)}, OH)Co(en)_2]^{3+}$		19.0 (2.59) s	28.0 (3.69)
$[(l\text{-pn})_2Co(\mu\text{-}O_2^{(2-)}, OH)Co(l\text{-pn})_2]^{3+}$		19.3 (2.58) s	28.6 (3.76)
$[(en)_2Co(\mu\text{-}O_2^{(2-)}, NH_2)Co(en)_2]^{3+}$ a)		20 (2.6) s	29.8 (3.59)
(μ-Superoxo complexes in 0.01 N $HClO_4$)			
$[(NH_3)_5Co(\mu\text{-}O_2^{(-)})Co(NH_3)_5]^{5+}$ a)	14.9 (2.92)	20.8 (2.43)	33.6 (4.35)
$[(en)_2(NH_3)Co(\mu\text{-}O_2^{(-)})Co(NH_3)(en)_2]^{5+}$	14.1 (3.05)	21.0 (2.48)	33.1 (4.29)
$[(trien)(NH_3)Co(\mu\text{-}O_2^{(-)})Co(NH_3)(trien)]^{5+}$	14.1 (3.11)	21.3 (2.66)	32.5 (4.29)
$[(dien)(l\text{-pn})Co(\mu\text{-}O_2^{(-)}(Co(l\text{-pn})dien)]^{5+}$	14.0 (3.19)	21.4 (2.79)	32.6 (4.36)
$[(tetren)Co(\mu\text{-}O_2^{(-)})Co(tetren)]^{5+}$	14.1 (3.15)	21.5 (2.78)	31.9 (4.28)
$[(en)_2Co(\mu\text{-}O_2^{(-)}, OH)Co(en)_2]^{4+}$	14.8 (2.72)	20.3 (2.67)	
$[(l\text{-pn})_2Co(\mu\text{-}O_2^{(-)}, OH)Co(l\text{-pn})_2]^{4+}$	14.9 (2.71)	20.7 (2.67)	
$[(en)_2Co(\mu\text{-}O_2^{(-)}, NH_2)Co(en)_2]^{4+}$ a)	14.3 (2.45)	20.8 (2.50)	

s, shoulder. a) from Ref. 2a. (in water)

The spectral data of peroxo bridged complexes are summarized in Table 1. It is seen that the absorption peaks in the ultraviolet region depend on the structure of the bridging part. The single bridged μ-peroxo complexes have absorption maxima at *ca.* 300 nm, whereas the double bridged complexes, μ-peroxo-μ-hydroxo and μ-peroxo-μ-amido, at *ca.* 350 nm.

The absorption spectra of the μ-superoxo complexes corresponding to the μ-peroxo complexes are also shown in Fig. 3 and the data summarized in Table 1. Single bridged μ-superoxo complexes were isolated by the method of House *et al.* Double bridged μ-superoxo-μ-hydroxo complexes were not isolated and their approximate absorption spectra in the visible region were recorded by use of aqueous solutions of the corresponding μ-peroxo-μ-hydroxo complexes in the presence of excessive free chlorine.

The spectral pattern of these μ-superoxo complexes seems to be dependent also on the structure of the bridging part. Single bridged complexes have a distinctive absorption peak at *ca.* 300 nm. They also give absorptions at *ca.* 700 nm (log ε *ca.* 3) and *ca.* 480 nm (log ε, 2.8), the former being stronger. On the other hand, double bridged complexes give absorption peaks at *ca.* 700 and *ca.* 480 nm and their intensities are almost equal (log ε, 2.5). The absorption pattern at *ca.* 300 nm is not clear because of the presence of chlorine.

So far as the complexes given in Table 1 are concerned, the pattern of absorption spectra appears useful for discriminating the structure of the bridging part for both μ-peroxo and μ-superoxo complexes.

Lability of Coordinated Ammines and Amines. As stated previously, the absorption spectrum of $[(en)_2(NH_3)Co(\mu\text{-}O_2^{(2-)})Co(NH_3)(en)_2]^{4+}$ in water changed rapidly and became identical with that of $[(en)_2Co(\mu\text{-}O_2^{(2-)}, OH)Co(en)_2]^{3+}$ prepared by the method of Foong *et al.* within 20 min at room temperature. Such a change indicates that the coordinated ammonia molecules in the single bridged μ-peroxo complexes are easily replaced by water molecules to give double bridged complexes. A similar spectral change was also observed with the corresponding *l*-pn complex. The absorption spectrum of $[(trien)(NH_3)Co(\mu\text{-}O_2^{(2-)})Co(NH_3)(trien)]^{4+}$ in water converges to a pattern with a band at 350 nm with an ε value 5760 (per one complex ion) within *ca.* 40 min, and shows an approximate isosbestic point as seen in Fig. 4. Fallab,[11] Miller and Wilkins[12] reported that $[(trien)Co(\mu\text{-}O_2^{(2-)}, OH)Co(trien)]^{3+}$ showed a band at *ca.* 350 nm, although they did not isolate such species. We also examined the absorption spectrum of this double bridged complex by passing oxygen into an aqueous solution containing trien and cobalt(II) in various molar ratios. The apparent ε values at 350 nm increased with increase in the molar ratio, and approached a constant value 6800, when the ratio was more than 2. Thus it seems that $[(trien)(NH_3)Co(\mu\text{-}O_2^{(2-)})Co(NH_3)(trien)]^{3+}$ also liberates

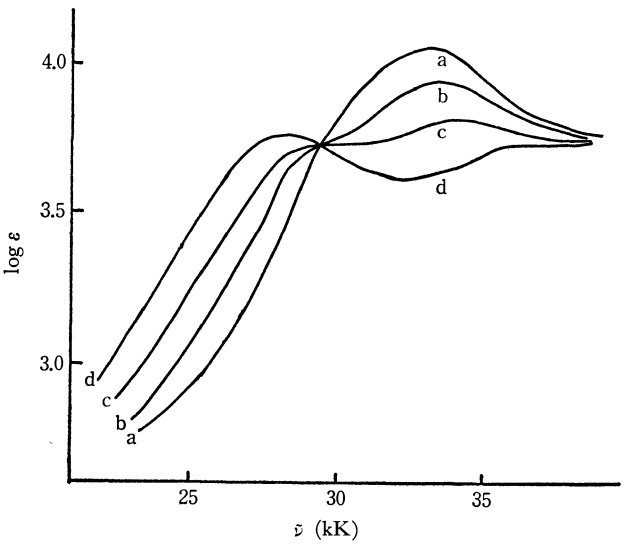

Fig. 4. Change in absorption spectrum of an aqueous solution of $[(trien)(NH_3)Co(\mu\text{-}O_2^{(2-)})Co(NH_3)(trien)]^{4+}$ at room temperature.
a : immediately b : after 5 min
c : after 15 min d : after 45 min

ammonia to form $[(trien)Co(\mu\text{-}O_2^{(2-)}, OH)Co(trien)]^{3+}$ in water at room temperature. All these complexes have various geometrical isomers, but they cannot be distinguished by conventional absorption spectrum measurement.

When a large excess of *l*-pn was added to an aqueous solution of $[(dien)(en)Co(\mu\text{-}O_2^{(2-)})Co(en)(dien)]^{4+}$ at room temperature, circular dichroism

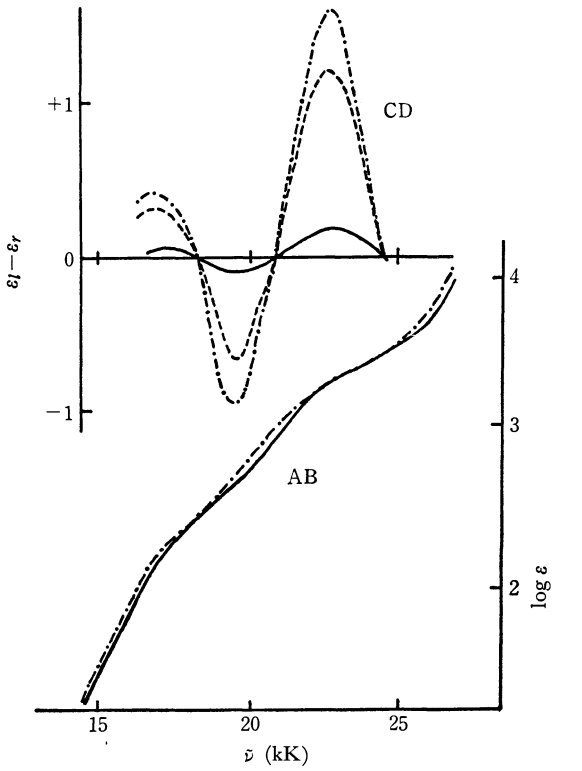

Fig. 5. Change in absorption (AB) and CD spectrum of $[(dien)(en)Co(\mu\text{-}O_2^{(2-)})Co(en)(dien)](ClO_4)_4$ in water containing an excess of *l*-propylenediamine.
—— after 3 hr ---- after 2 days —·—· after 5 days

11) S. Fallab, *Chimia*, **23**, 177 (1969); **24**, 76 (1970).
12) F. Miller and R. G. Wilkins, *J. Amer. Chem. Soc.*, **92**, 2687 (1970).

(CD) appeared as shown in Fig. 5. The CD curve became constant after ten days, while the absorption spectrum remained almost unchanged. When an aqueous solution of synthesized $[(dien)(l\text{-pn})Co(\mu\text{-}O_2^{(2-)})Co(l\text{-pn})(dien)]^{4+}$ was treated with a large excess of en, the CD peak decreased gradually and eventually no CD was observable. These reactions are understood to be ligand substitutions of bidentate en or *l*-pn.

When *l*-pn was added to an aqueous solution of $[(en)_2(NH_3)Co(\mu\text{-}O_2^{(2-)})Co(NH_3)(en)_2]^{4+}$, the absorption and the CD spectrum changed rapidly at room temperature and became identical with those of $[(l\text{-pn})_2Co(\mu\text{-}O_2^{(2-)}, OH)Co(l\text{-pn})_2]^{3+}$ synthesized by modified Foong *et al.*[10] within 20 min. The reaction is much faster than that of the substitution of bidentate ligands mentioned above. On the other hand, substitution of *l*-pn for en in the double bridged complex $[(en)_2Co(\mu\text{-}O_2^{(2-)}, OH)Co(en)_2]^{3+}$ proceeds much slower than that in single bridged μ-peroxo complexes.

Ammonia and amines in uninuclear cobalt(III) complexes are generally believed to be substitution inert.[13] Hence all the observations mentioned above would be understood by considering that the ammonia and amines in the binuclear complexes are unusually labile. Such a lability is not significant in double bridged μ-peroxo-μ-hydroxo complexes and seems to be characteristic of single bridged μ-peroxo complexes. Such a change in lability is more marked for ammonia than for multidentate amines.

Recently Taylor and Sykes[14] reported that $[(NH_3)_4Co(\mu\text{-}OH, NH_2)Co(NH_3)_4]^{4+}$ liberates ammonia in an aqueous solution at a rate 0.46×10^{-4} sec^{-1} (half time 250 min) at 35°C. It was found that the binuclear chromium(III) complex $[(NH_3)_5Cr(\mu\text{-}O)Cr(NH_3)_5]^{4+}$ (rhodochromic salt) liberates one of its ammonia molecules very rapidly at room temperature,[15] and this fact was interpreted as an effect of π-bonding character of chromium oxygen bond.

A more detailed discussion on such an unusual change in lability cannot be made because of insufficient kinetic data. However, some of the properties of binuclear μ-peroxo complexes given in literature[5,8] would be understood by considering the ligand labilising effect in μ-peroxo complexes.

Other Properties of the μ-Peroxo Complexes. All the binuclear μ-peroxo complexes can be oxidized almost quantitatively to the corresponding μ-superoxo complexes by treatment with a slightly acidic aqueous solution containing chlorine. The single bridged μ-superoxo complexes were isolated as perchlorates,[8b] but the double bridged μ-superoxo-μ-hydroxo complexes were not isolated. μ-Peroxo complexes are also oxidized with nitric acid to the corresponding μ-superoxo complexes, but the yield is low.

The μ-peroxo complexes decomposed to cobalt(II) salts in perchloric and sulfuric acid, but always gave small amounts of the μ-superoxo complexes (*ca.* 10% at most). The yield was determined by measuring the intensity of absorption bands at *ca.* 700 nm, which are characteristic of μ-superoxo complexes. When single bridged μ-peroxo complexes were treated with concentrated hydrochloric acid, uninuclear chloropentaamine type complexes were formed.[8,16] On the other hand, μ-peroxo-μ-hydroxo double bridged complexes produced *trans*-dichlorotetraammine type complexes by a similar treatment.

Optical Activity of the Complexes Containing l-Propylenediamine. The absorption and the CD spectra of $[(l\text{-pn})_2Co(\mu\text{-}O_2^{(2-)}, OH)Co(l\text{-pn})_2]^{3+}$ synthesized by a modified Foong *et al.* method[10] and of $\Delta\Delta$-$[(l\text{-pn})_2Co(\mu\text{-}O_2^{(2-)}, NH_2)Co(l\text{-pn})_2]^{3+}$ [2a] are shown in Fig. 2. From a comparison of their well-coinciding CD curves, the μ-peroxo-μ-hydroxo complex seems to have an asymmetric center around both cobalt ions and its absolute configuration can be determined to be $\Delta\Delta$. Hence the $\Delta\Delta$-$[(l\text{-pn})_2Co(\mu\text{-}O_2^{(2-)}, OH)Co(l\text{-pn})_2]^{3+}$ seems to be formed stereospecifically under the given conditions. The CD curve of this complex produced by the hydrolysis of $[(l\text{-pn})_2(NH_3)Co(\mu\text{-}O_2^{(2-)})Co(NH_3)(l\text{-pn})_2]^{4+}$ also suggests a similar stereospecific formation. Further, the $\Delta\Delta$-configuration of this complex is supported by the CD spectrum of its μ-superoxo derivative which was obtained in a slightly acidic solution containing chlorine. We discussed such a stereospecificity of $[(l\text{-pn})_2Co(\mu\text{-}O_2^{(2-)}, NH_2)Co(l\text{-pn})_2]^{3+}$ in a previous paper.[2a] The same steric regulation appears to operate in the formation of μ-peroxo-μ-hydroxo complex.

The complex $[(dien)(l\text{-pn})Co(\mu\text{-}O_2^{(2-)})Co(l\text{-pn})(dien)]^{4+}$ prepared by the method of House *et al.* gives a CD spectrum in water as shown in Fig. 6. The CD changes as indicated and becomes constant

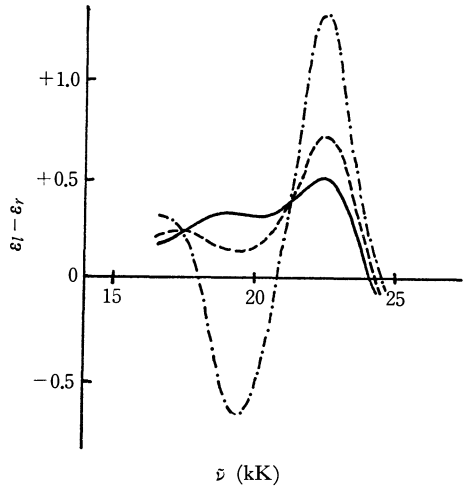

Fig. 6. Change in CD spectrum of an aqueous solution of $[(dien)(l\text{-pn})Co(\mu\text{-}O_2^{(2-)})Co(l\text{-pn})(dien)]^{4+}$ (see text)
—— immediately after solution
---- after 3 hr —·—· after 2 days

13) F. Basolo and R. G. Pearson, "Mechanism of Inorganic Reactions," 2nd Ed., John Wiley and Sons, New York (1967).
14) R. S. Taylor and A. G. Sykes, *J. Chem. Soc., A*, **1970**, 1991.
15) W. K. Wilmarth, H. Graff, and S. T. Gustin, *J. Amer. Chem. Soc.*, **78**, 2683 (1956).
16) A. R. Gainsford and D. A. House, *Inorg. Chim. Acta*, **3**, 33, 367 (1969).

Table 2. Elementary analysis of the complexes

Formulae		C	H	N
$[(en)_2NH_3Co(\mu\text{-}O_2^{(2-)})CoNH_3(en)_2](ClO_4)_4$	Found	12.17	4.53	17.02
$C_8H_{38}N_{10}O_{18}Cl_4Co_2$	Calcd	11.68	4.65	17.04
$[(l\text{-pn})_2NH_3Co(\mu\text{-}O_2^{(2-)})CoNH_3(l\text{-pn})_2](ClO_4)_4$	Found	16.52	5.81	15.98
$C_{12}H_{46}N_{10}O_{18}Cl_4Co_2$	Calcd	16.41	5.28	15.95
$[(trien)NH_3Co(\mu\text{-}O_2^{(2-)})CoNH_3(trien)](ClO_4)_4$	Found	16.47	4.95	15.81
$C_{12}H_{42}N_{10}O_{18}Cl_4Co_2$	Calcd	16.49	4.84	16.02
$[(dien)(en)Co(\mu\text{-}O_2^{(2-)})Co(en)dien)](ClO_4)_4$	Found	16.53	5.21	16.18
$C_{12}H_{42}N_{10}O_{18}Cl_4Co_2$	Calcd	16.49	4.84	16.02
$[dien(l\text{-pn})Co(\mu\text{-}O_2^{(2-)})Co(l\text{-pn})dien](ClO_4)_4\cdot 5H_2O$	Found	16.89	5.01	15.11
$C_{14}H_{56}N_{10}O_{23}Cl_4Co_2$	Calcd	16.96	5.68	14.12
$[(tetren)Co(\mu\text{-}O_2^{(2-)})Co(tetren)](ClO_4)_4$	Found	20.84	5.51	14.98
$C_{16}H_{46}N_{10}O_{18}Cl_4Co_2$	Calcd	20.75	5.01	15.12
$[(en)_2Co(\mu\text{-}O_2^{(2-)}, OH)Co(en)_2](ClO_4)_3$	Found	13.66	4.63	15.77
$C_8H_{33}N_8O_{15}Cl_3Co_2$	Calcd	13.62	4.71	15.88
$[(l\text{-pn})_2Co(\mu\text{-}O_2^{(2-)}, OH)Co(l\text{-pn})_2](ClO_4)_3$	Found	18.37	5.35	14.81
$C_{12}H_{41}N_8O_{15}Cl_3Co_2$	Calcd	18.92	5.43	14.70
$[(en)_2NH_3Co(\mu\text{-}O_2^{(-)})CoNH_3(en)_2](ClO_4)_5$	Found	10.75	4.46	15.50
$C_8H_{38}N_{10}O_{22}Cl_5Co_2$	Calcd	10.43	4.16	15.20
$[(trien)NH_3Co(\mu\text{-}O_2^{(-)})CoNH_3(trien)](ClO_4)_5\cdot H_2O$	Found	14.73	4.80	13.91
$C_{12}H_{44}N_{10}O_{23}Cl_5Co_2$	Calcd	14.54	4.88	14.12
$[(dien)(l\text{-pn})Co(\mu\text{-}O_2^{(-)})Co(l\text{-pn})(dien)](ClO_4)_5$	Found	17.26	5.14	13.78
$C_{14}H_{46}N_{10}O_{22}Cl_5Co_2$	Calcd	16.79	4.63	13.98
$[(tetren)Co(\mu\text{-}O_2^{(-)}Co(tetren)](ClO_4)_5\cdot 2H_2O$	Found	18.04	5.08	12.89
$C_{16}H_{50}N_{10}O_{24}Cl_5Co_2$	Calcd	18.10	4.75	13.19

after *ca.* 2 days at room temperature. The final spectrum is identical with the final pattern (broken line with dot) in Fig. 5, which was formed by the reaction of *l*-pn with $[(dien)(en)Co(\mu\text{-}O_2^{(2-)})Co(en)(dien)]^{4+}$. This μ-peroxo complex can have various geometrical and diastereomeric isomers according to varying chelation of the bi- and terdentate ligand. They have all N_5O type coordination, and change in absorption spectra is not always expected among the isomers. No change in absorption pattern does not deny isomeric change of the complex. It appears, however, that the crystalline $[(dien)(l\text{-pn})Co(\mu\text{-}O_2^{(2-)})Co(l\text{-pn})(dien)]^{4+}$ obtained (see Experimental) has different isomeric composition from its most stable form in aqueous solution, and the CD change in Fig. 6 can be understood as due to some kind of rearrangement in the binuclear complex.

The intensity of CD is of the order of $\Delta\varepsilon = ca. +1.3$ which can be accounted for by either vicinal effect coming from *l*-pn, or by asymmetric configuration in this complex. Apparently the CD indicates some kind of inversion with lapse of time, and this fact may support stereoselective coordination of the ligand. However, the band assignment in this complex still remains uncertain, and nothing decisive as to whether the optically active ligand exhibits stereoselectivity in such a single bridged complex or not can be stated at the present stage.

Experimental

Preparation of the Complexes. The preparation methods of all the complexes are essentially the same as those given in literature.[8,10] The results of elementary analysis are summarized in Table 2.

1) $[(en)_2(NH_3)Co(\mu\text{-}O_2^{(2-)})Co(NH_3)(en)_2](ClO_4)_4$ and $[(trien)(NH_3)Co(\mu\text{-}O_2^{2-})Co(NH_3)(trien)](ClO_4)_4$:
These complexes were prepared by the method of House *et al.*[8] involving substitution of en and trien for ammonias of $[(NH_3)_5Co(\mu\text{-}O_2^{(2-)})Co(NH_3)_5]^{4+}$. They were also prepared directly as follows; cobalt(II) nitrate hexahydrate (2.9 g) and sodium perchlorate (10 g) were dissolved in water (10 m*l*), mixed with ethylenediamine hydrate (2 g) or trien (2 g) in concentrated aqueous ammonia solution (30 m*l*) and bubbled with air for *ca.* 30 min. The brown precipitate was washed with ethanol and ether and air dried (yield *ca.* 3 and 2.5 g, respectively).

2) $[(l\text{-pn})(dien)Co(\mu\text{-}O_2^{(2-)})Co(dien)(l\text{-pn})](ClO_4)_4$:
Cobalt(II) nitrate hexahydrate (2.9 g) and sodium perchlorate (10 g) were dissolved in water (10 m*l*), treated with dihydrochloride of *l*-pn (3 g), dien (1 g) and sodium hydroxide (1.6 g) in water (20 m*l*), and bubbled with air for *ca.* 30 min. The brown precipitate was similarly washed and dried (yield *ca.* 3 g).

3) $[(l\text{-pn})_2(NH_3)Co(\mu\text{-}O_2^{(2-)})Co(NH_3)(l\text{-pn})](ClO_4)_4$:
$[(NH_3)_5Co(\mu\text{-}O_2^{(2-)})Co(NH_3)_5](NO_3)_4\cdot 2H_2O$[5] (1.3 g) was added to a solution of dihydrochloride of *l*-pn (1.5 g), sodium hydroxide (0.8 g) and sodium perchlorate (1.5 g) in water (7.5 m*l*) under constant passage of air. A brown precipitate was formed after 30 min, which was washed and dried in a similar way (yield 0.9 g).

4) $[(dien)(l\text{-pn})Co(\mu\text{-}O_2^{(-)})Co(l\text{-pn})(dien)](ClO_4)_5$:
Crude $[(dien)(l\text{-pn})Co(\mu\text{-}O_2^{(2-)})Co(l\text{-pn})(dien)](NO_3)_4$ was prepared by a similar method to the perchlorate[6] without sodium perchlorate. The brown nitrate was collected after 5 days. This salt (0.6 g) was added to a solution of concentrated hydrochloric acid (1.5 m*l*) and zinc chloride dihydrate (2.5 g) in water (3 m*l*), warmed at 80°C for 30

min and cooled to room temperature. It appears that the peroxo bridge was oxidized to superoxo in the hydrochloric acid solution by the nitrate and precipitated as tetrachlorozincate. The green powder was washed with ethanol, dissolved in a small amount of water containing a trace of nitric acid, and treated with a saturated sodium perchlorate solution. The green crystals were washed with ethanol and ether and air dried (yield 0.4 g).

5) $[(l\text{-}pn)_2Co(\mu\text{-}O_2^{(2-)}, OH)Co(l\text{-}pn)_2](ClO_4)_3$: Cobalt(II) perchlorate (2.4 g) was dissolved in water (10 m*l*) and mixed with *l*-pn (1.5 g) in ethanol (10 m*l*) and water (30 m*l*). Oxygen was passed through this solution for *ca.* 30 min. Yellow crystals precipitated initially dissolved during the course of bubbling. The solution was filtered and kept in a refrigerator for a day. The dark brown crystals were washed with ethanol and ether and air dried (yield *ca.* 1 g).

Propylenediamine was resolved by Dwyer's method.[17]

Measurements. The absorption and the circular dichroism spectra were recorded with a Hitachi 124 double beam recording spectrophotometer and Jasco ORD/UV-5 spectrophotometer with appropriate accessories, respectively.

We are grateful to the Ministry of Education for a Grant-in-aid for our studies on optically active complexes.

17) E. P. Dwyer and F. L. Garvan, *J. Amer. Chem. Soc.*, **81**, 2955 (1959).

BULLETIN OF THE CHEMICAL SOCIETY OF JAPAN, VOL. 44, 3378—3382 (1971)

The Stereochemistry of Nucleophilic Addition. II.[1] The Reformatsky Reaction of Methyl (+)-α-Bromopropionate, 2-Phenylpropanal, and 3-Phenyl-2-butanone

Takashi MATSUMOTO, Isao TANAKA, and Kenji FUKUI

Department of Chemistry, Faculty of Science, Hiroshima University, Higashi-sendamachi, Hiroshima

(Received December 31, 1970)

The Reformatsky reaction of methyl (+)-α-bromopropionate with benzaldehyde was carried out in order to study the reaction mechanism, and two epimeric methyl 3-hydroxy-2-methyl-3-phenylpropionates (IIa and IIb) were obtained in a 59 : 41 ratio. From a comparison of the optical activity of IIb with that of pure (−)-IIb, it was estimated that IIb consists only seven percent of an optically-active compound; this results supports the hypothesis of the enolate anion mechanism. Subsequently, the stereochemistry of this reaction with 2-phenylpropanal (IV) and 3-phenyl-2-butanone (VIII) was studied. The condensation of IV with methyl bromoacetate gave a mixture of the epimeric methyl 3-hydroxy-4-phenylvalerates (Va and Vb), which were separated in a 26 : 74 ratio by means of column chromatography on silica gel. Similarly, VIII was also condensed with methyl bromoacetate to give the epimeric methyl 3-hydroxy-3-methyl-4-phenylvalerates (IXa and IXb) in a 31 : 69 ratio. The configurations of these esters were assigned by correlation with the products of the Grignard reaction, the stereochemistry of which is well known. From the present study, it is clear that the Reformatsky and the Grignard reactions of the carbonyl compound having an asymmetric α-carbon atom proceed in a similar fashion; that is, the entering group predominantly approaches the carbonyl group from the least-hindered side. Therefore, Cram's rule of asymmetric induction can be applied in the stereochemistry of the Reformatsky reaction.

The Reformatsky reaction[2] has long been recognized as a convenient method for preparing β-hydroxy esters, and the stereochemistry of this reaction, as well as that of the Ivanov reaction, has been explained by the hypothesis of an enolate anion mechanism[3-6] involving a cyclic transition state. If the reaction proceeds through the enolate anion intermediate, the condensation of the optically-active α-haloester possessing an asymmetric α-carbon atom, with a carbonyl compound which has no asymmetric carbon atom might be expected to yield a racemate of the corresponding β-hydroxy ester. To obtain further information on this reaction mechanism, we have now studied the condensation of benzaldehyde with methyl (+)-α-bromopropionate (I) in a benzene solution in the presence of zinc. The product (methyl 3-hydroxy-2-methyl-3-phenylpropionate) was separated by means of column chromatography on silica gel to give two epimeric esters; IIa (liquid), $[\alpha]_D^{25}+1.5°$ ($CHCl_3$) and IIb (mp 50.5—51.5°C), $[\alpha]_D^{25}-3.9°$ ($CHCl_3$), in a 59 : 41 ratio. The configurations of the racemates of these major (IIa) and minor (IIb) products had already been identified by Zimmerman and English[7] and Canceill *et al.*[8] as *erythro*- and *threo*-compounds respectively. In order to compare them with the above IIb, optically-pure (−)-IIb was prepared from (±)-*threo*-3-hydroxy-2-methyl-3-phenylpropionic

1) Part I of this series: T. Matsumoto and K. Fukui, This Bulletin, **44**, 1090 (1971). Although the formulas depicted represented only one enantiomer, they are taken to mean a racemate unless otherwise stated.

2) S. Reformatsky, *Ber.*, **20**, 1210 (1887).

3) H. E. Zimmerman and M. D. Traxler, *J. Amer. Chem. Soc.*, **79**, 1920 (1957).

4) E. Toromanoff, *Bull. Soc. Chim. Fr.*, **1962**, 1190.

5) M. Mousseron, M. Mousseron, J. Neyrolles, and Y. Beziat, *ibid.*, **1963**, 1483.

6) H. O. House, "Modern Synthetic Reactions," W. A. Benjamin, New York, N. Y. (1965), p. 242.

7) H. E. Zimmerman and J. English, Jr., *J. Amer. Chem. Soc.*, **76**, 2291 (1954).

8) J. Canceill, J-J. Basselier, and J. Jacques, *Bull. Soc. Chim. Fr.*, **1963**, 1906.

acid (IIIb), mp 97—98°C, in the following manner. (±)-IIIb was resolved by means of cinchonidine, and one of the diastereomeric salts, mp 170—172°C; $[\alpha]_D^{25}$ −87.6° (EtOH), was decomposed with dilute sulfuric acid to give (−)-IIIb, mp 106—107°C; $[\alpha]_D^{25}$ −19.7° (EtOH), which was then further converted by diazomethane to (−)-IIb ($[\alpha]_D^{25}$ −57.1° ($CHCl_3$)). Since (+)-I was recovered with an unchanged specific rotation after it had been refluxed in dry benzene with zinc for 2 hr (the time required for the reaction), it was estimated that a ninety-three-percent racemization occurred in the above condensation. In view of this racemization and the ratio, which was not 50 : 50 in the *erythro*- and *threo*-isomers, the main reaction seems to proceed through the enolate anion mechanism. However, since only a small degree of the optical activity is observed in the products, it is apparent that the reaction partially proceeds by a different reaction mechanism, such as the carbanion mechanism.

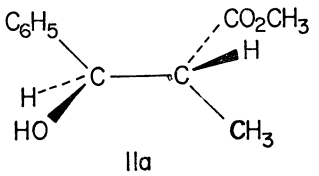

IIa

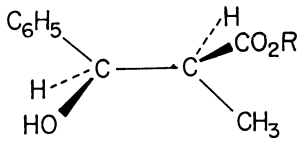

IIb R=CH_3

IIIb R=H

Subsequently, we turned our attention to the study of the stereochemistry of the Reformatsky reaction with carbonyl compounds possessing an asymmetric α-carbon atom, because this type of reaction has been little studied.[9-11] In a previous paper[11] we reported on the stereochemistry of the Reformatsky reaction with 2-alkylcyclohexanones. In this paper we wish to extend the scope of it to non-cyclic carbonyl compounds.

The condensation of 2-phenylpropanal (IV) with methyl bromoacetate in dry benzene in the presence of zinc gave a mixture of epimeric methyl 3-hydroxy-4-phenylvalerates, which were separated by column chromatography to give two oily esters (Va and Vb) in a 26 : 74 ratio. The configurations of these minor (Va) and major (Vb) products were assigned by correlation with the products of the Grignard reaction, the stereochemistry of which is well known. The reduction of Va and Vb with $LiAlH_4$ in ether afforded the corresponding diols, VIa and VIb, respectively. Subsequently, VIa and VIb were subjected to the tosylation with *p*-toluenesulfonyl chloride in pyridine, followed by the reduction of the resulting monotosylates with $LiAlH_4$ in tetrahydrofuran, to give the epimeric 2-phenyl-3-pentanols, VIIa (liquid) and VIIb (mp 39—40°C) respectively. Since Cram and Elhafez[12] had reported the preparation of *threo*- and *erythro*-2-phenyl-3-pentanols by the Grignard reaction of IV with ethylmagnesium bromide or by the reduction of 2-phenyl-3-pentanone with $LiAlH_4$, the condensation of IV with ethylmagnesium iodide was carried out for purposes of direct comparison; the mixture of epimers thus obtained was successfully separated by column chromatography[13] into the *threo* and *erythro* isomers in a 19 : 81 ratio. The alcohols, VIIa and VIIb, were shown to be identical with the authentic *threo* (minor) and *erythro* (major) isomers respectively by comparisons of their IR and NMR spectra.

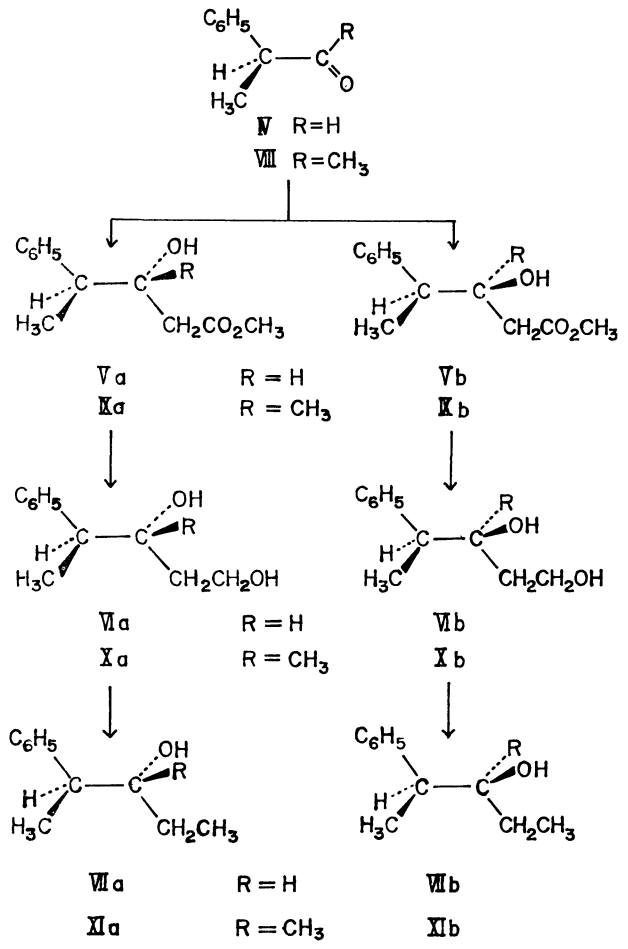

9) W. W. Epstein and A. C. Sonntag, *Tetrahedron Lett.*, **1966**, 791.

10) M. Perry and Y. Maroni-Barnaud, *Bull. Soc. Chim. Fr.*, **1969**, 3574.

11) T. Matsumoto and K. Fukui, This Bulletin, **44**, 1090 (1971).

12) D. J. Cram and F. A. Abd Elhafez, *J. Amer. Chem. Soc.*, **74**, 5828 (1952).

13) The diastereomers were separated by Cram and Elhafez[12] through the use of the phthalic acid ester for the *threo* isomer and the 3-nitrophthalic acid ester of the *erythro* isomer.

Similarly, 3-phenyl-2-butanone (VIII)[14] was also condensed with methyl bromoacetate to give the epimeric methyl 3-hydroxy-3-methyl-4-phenylvalerates (IXa and IXb) in a 31 : 69 ratio. The reduction of the minor (IXa) and major (IXb) esters with $LiAlH_4$ gave the corresponding diols (Xa, mp 76.5—77.5°C and Xb, mp 76—76.5°C), which were

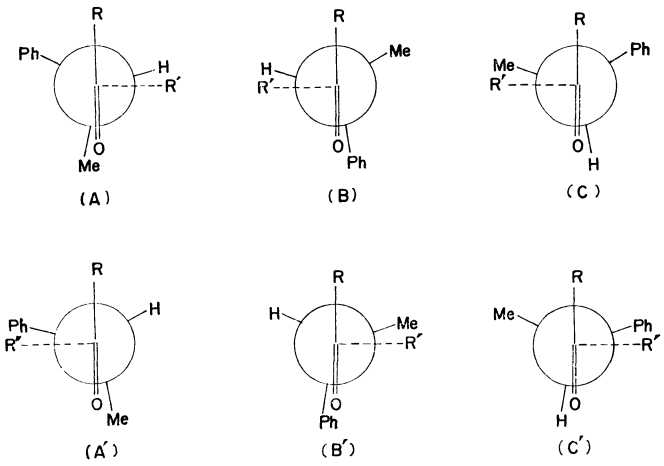

Fig. 1

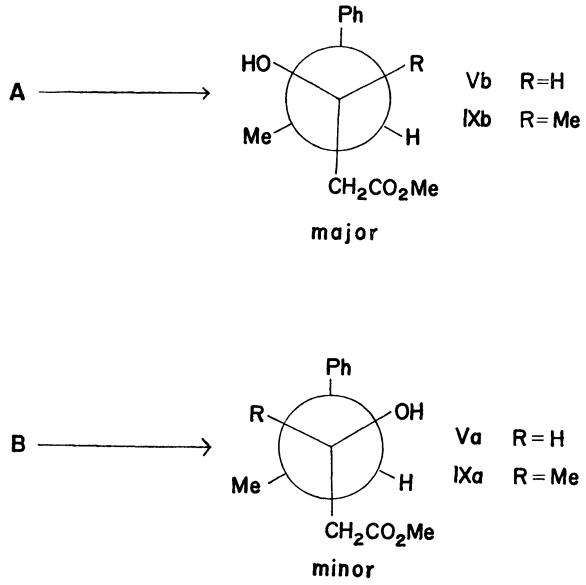

Fig. 2

Table 1. The NMR spectra of Va, Vb, IXa, and IXb in $CDCl_3$

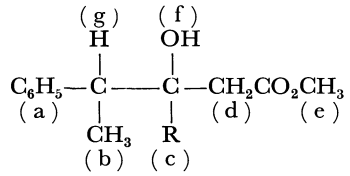

	a	b	c	d	e	f	g
Va R=H	7.33 (s)	1.32 (d, J=7 Hz)	4.2 (m)	2.39 (d, J=5 Hz)	3.67 (s)	2.49 (s)	2.86 (m)
Vb R=H	7.27 (s)	1.38 (d, J=7 Hz)	4.1 (qa, J=6.5 Hz)	2.31 (d, J=6 Hz)	3.63 (s)	2.98 (s)	2.78 (m)
IXa R=CH_3	7.14 (s)	1.33 (d, J=7 Hz)	1.23 (s)	2.37 (s)	3.57 (s)	3.36 (s)	2.80 (qa, J=7 Hz)
IXb R=CH_3	7.11 (s)	1.33 (d, J=7 Hz)	1.17 (s)	2.34 (s)	3.58 (s)	3.44 (s)	2.90 (qa, J=7 Hz)

Table 2. The NMR spectra of VIIa, VIIb, XIa and XIb in $CDCl_3$

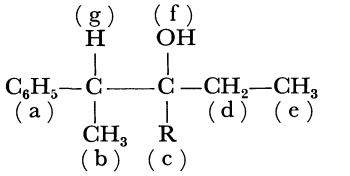

	a	b	c	d	e	f	g
VIIa R=H	7.26 (s)	1.25 (d, J=7 Hz)	3.54 (m)	*ca.* 1.5 (overlap)	0.94 (t, J=6.5 Hz)	1.63 (s)	2.72 (qi, J=7 Hz)
VIIb R=H	7.27 (s)	1.31 (d, J=7 Hz)	3.53 (m)	*ca.* 1.5 (overlap)	0.91 (t, J=6.5 Hz)	1.68 (s)	2.77 (qi, J=7 Hz)
XIa R=CH_3	7.28 (s)	1.28 (d, J=7 Hz)	1.09 (s)	*ca.* 1.4 (overlap)	0.91 (t, J=6.5 Hz)	1.37 (s)	2.83 (qa, J=7 Hz)
XIb R=CH_3	7.26 (s)	1.31 (d, J=7 Hz)	1.03 (s)	*ca.* 1.4 (overlap)	0.91 (t, J=7 Hz)	1.32 (s)	2.81 (qa, J=7 Hz)

14) C. M. Suter and A. W. Weston, *J. Amer. Chem. Soc.*, **64**, 533 (1942).

then further converted to the corresponding 2-phenyl-3-methyl-3-pentanols (XIa and XIb) *via* monotosylates. The Grignard reaction of VIII with ethylmagnesium iodide gave the epimeric alcohols in a 20 : 80 ratio, these minor and major alcohols were also shown by the spectral comparison to be identical with the above XIa and XIb respectively. The six models of transition states for the addition to the carbonyl group directly bonded to asymmetric carbon atom are shown in Fig. 1. The A, B, and C conformations should be more stable than the corresponding A′, B′, and C′ conformations. Of the three (A, B, and C), A is the most stable, while the second most stable conformation is B, as has been reported by Karabatsos.[15] Thus, A and B, where the incoming group, R′, is closest to the smallest group, hydrogen, lead to the major and minor products respectively, as is shown in Fig. 2.

From the present study, it is clear that the Reformatsky and the Grignard reactions with the carbonyl compound possessing an asymmetric α-carbon atom proceed in a similar fashion. Therefore, it may be suggested that Cram's rule[12,15] of asymmetric induction can be applied in the stereochemistry of the Reformatsky reaction. The stereoselectivity of the Reformatsky reaction observed is slightly less than that of the Grignard reaction.

Experimental

All the melting and boiling points are uncorrected. The NMR spectra were taken on a Hitachi Model R-20 NMR spectrometer (60 MHz), using tetramethylsilane as the internal standard. The chemical shifts are presented in terms of δ values; s: singlet, bs: broad singlet, d: doublet, dd: double doublet, t: triplet, qa: quartet, qi: quintet, m: multiplet. The column chromatography was performed on Merck silica gel (0.08 mm).

Methyl (+)-α-Bromopropionate (I). (+)-I (bp 55–56°C/31 mmHg, $[\alpha]_D^{25}$ +68.8° (neat)) was prepared from (+)-lactic acid (30% aqueous solution) by the method of Cowdrey *et al.*[16] The reported physical properties[16] of (+)- and (−)-I are bp 46°C/14 mmHg, $[\alpha]_D$ +19.17°[17] and bp 44°C/12 mmHg, $[\alpha]_D$ −68.57°, respectively.

The Reformatsky Reaction of Benzaldehyde with Methyl (+)-α-Bromopropionate. This reaction was carried out by a method similar to that used with ethyl (±)-α-bromopropionate by Zimmerman and English.[7] The crude product (1.123 g) was directly purified by means of column chromatography on silica gel (80 g). Elution with benzene containing 7% and then 15% ether gave two fractions. The first fraction gave methyl *erythro*-3-hydroxy-2-methyl-3-phenylpropionate (IIa: 503 mg), $[\alpha]_D^{25}$ +1.5° (*c* 0.152, $CHCl_3$) as a colorless oil. NMR in $CDCl_3$: 1.10 (d, J= 7 Hz, $-\overset{|}{C}HCH_3$), 2.74 (m, $-\overset{|}{C}HCH_3$), 3.21 (d, J=4 Hz, $-OH$), 3.52 (s, $-CO_2CH_3$), 4.93 (dd, J=4 and 5.5 Hz, $-\overset{|}{C}HOH$), 7.18 (s, $-C_6H_5$).

Found: C, 68.11; H, 7.20%. Calcd for $C_{11}H_{14}O_3$: C, 68.02; H, 7.27%.

The second fraction gave the *threo*-isomer (IIb: 356 mg), $[\alpha]_D^{25}$ −3.9° (*c* 0.198, $CHCl_3$) as a colorless solid. This was recrystallized from ether containing *n*-pentane to give colorless crystals, mp 50.5—51.5°C, which were shown to be identical with authentic (±)-IIb by a mixed-melting-point determination and by a comparison of their IR spectra. NMR in $CDCl_3$: 0.92 (d, J=7 Hz, $-\overset{|}{C}HCH_3$), 2.74 (qi, J=7 Hz, $-\overset{|}{C}HCH_3$), 3.35 (s, $-OH$), 3.60 (s, $-CO_2CH_3$), 4.61 (d, J=8 Hz, $-\overset{|}{C}HOH$), 7.18 (s, $-C_6H_5$).

Found: C, 68.20; H, 7.33%. Calcd for $C_{11}H_{14}O_3$: C, 68.02; H, 7.27%.

The Resolution of (±)-threo-3-Hydroxy-2-methyl-3-phenylpropionic Acid (IIIb) with Cinchonidine. A solution of (±)-IIIb (1.20 g), mp 97—98°C (lit,[7] mp 96.5—97.5°C) in ethyl acetate was added to a hot solution of cinchonidine (1.96 g) in ethyl acetate (100 m*l*), and then the solution was concentrated to *ca.* 40 m*l*. After the solution had stood at room temperature, the precipitates were collected and then recrystallized from ethyl acetate to give cinchonidine salt as colorless crystals; mp 170—172°C, $[\alpha]_D^{25}$ −87.6° (*c* 0.083, EtOH); yield, 1.22 g.

Found: C, 73.66; H, 7.28; N, 5.80%. Calcd for $C_{29}H_{34}O_4N_2$: C, 73.39; H, 7.22; N, 5.90%.

The cinchonidine salt (1.36 g) was decomposed with dilute sulfuric acid (5%: 20 m*l*) and extracted with ether, and the extract was washed with a saturated sodium chloride solution. After it had been dried over sodium sulfate and the ether had been removed, the residue (425 mg) was recrystallized from benzene to give (−)-IIIb as colorless crystals; mp 106—107°C; $[\alpha]_D^{25}$ −19.7° (*c* 0.094, EtOH).

Found: C, 66.87; H, 6.65%. Calcd for $C_{10}H_{12}O_3$: C, 66.65; H, 6.71%.

The acid, (−)-IIIb, was methylated with ethereal diazomethane to give (−)-IIb, $[\alpha]_D^{25}$ −57.1° (*c* 0.123, $CHCl_3$) or −41.6° (*c* 0.114, EtOH). The IR spectrum was identical with that of authentic (±)-IIb.

The Reformatsky Reaction of 2-Phenylpropanal (IV) with Methyl Bromoacetate. A few drops of a solution of IV (3.22 g) and methyl bromoacetate (5.47 g) in dry benzene (10 m*l*) were stirred, at 80°C, into a mixture of purified zinc powder (2.35 g) and dry benzene (3.0 m*l*). When the exothermic reaction started, the heating bath was removed; the liquid reactants were then added at a rate to maintain the refluxing without further external heating. The total addition required 15 min. The mixture was refluxed for an additional 90 min, cooled, decomposed with a mixture of ice and dilute hydrochloric acid, and then extracted with benzene. The extract was successively washed with aqueous sodium hydrogen carbonate and water, dried over sodium sulfate, and then evaporated. The residue was distilled under a vacuum to give a mixture of epimeric β-hydroxy esters as a colorless oil; bp 147—151°C/10 mmHg; yield, 3.90 g.

The above ester (2.027 g) was chromatographed on silica gel (200 g); subsequently elution with benzene containing 7% and then 10% ether was carried out to give two fractions. The first fraction gave Va (459 mg).

Found: C, 69.15; H, 7.80%. Calcd for $C_{12}H_{16}O_3$: C, 69.21; H, 7.74%.

The second fraction gave Vb (1301 mg).

Found: C, 69.25; H, 7.86%. Calcd for $C_{12}H_{16}O_3$: C, 69.21; H, 7.74%.

Reduction of Va and Vb with $LiAlH_4$. *a)* A solution of Vb (1.300 g) in dry ether (10 m*l*) was added, drop by drop over a 20-min period, to a suspension of $LiAlH_4$ (490 mg)

15) G. J. Karabatsos, *ibid.*, **89**, 1367 (1967).

16) W. A. Cowdrey, E. D. Hughes, and C. K. Ingold, *J. Chem. Soc.*, **1937**, 1227.

17) It seems that the low specific rotation value for (+)-I is due to the contamination of racemate.

in dry ether (5.0 ml). The mixture was refluxed for 2 hr, cooled, poured into a mixture of ice (*ca.* 50 g) and dilute hydrochloric acid (5%: 30 ml), and then extracted with ether. The extract was washed with a saturated sodium chloride solution, dried over sodium sulfate, and then evaporated to give VIb (1.106 g) as an oil which showed no carbonyl absorption band in its IR spectrum and which could be used for the next step without purification. For analysis this was chromatographed on silica gel; elution with benzene containing 50% ether was then carried out.

Found: C, 73.48; H, 9.14%. Calcd for $C_{11}H_{16}O_2$: C, 73.30; H, 8.95%.

b) A solution of Va (343 mg) in dry ether (6.0 ml) was reduced with $LiAlH_4$ (130 mg) by a method similar to that used for VIb; a diol (VIa: 274 mg) was thus obtained as an oil.

Found: C, 73.02; H, 9.22%. Calcd for $C_{11}H_{16}O_2$: C, 73.30; H, 8.95%.

threo- *and* erythro-*2-Phenyl-3-pentanols (VIIa and VIIb).* *a) By the Grignard Reaction*: The Grignard reaction of IV with ethylmagnesium iodide was carried out by a method similar to that of Cram and Elhafez.[12] The crude product (1.054 g: bp 88—107°C/8 mmHg) was purified by means of column chromatography on silica gel (200 g), after which elution was carried out with benzene containing 4% ether to give two fractions. The first fraction gave *threo*-2-phenyl-3-pentanol (VIIa) as an oil (110 mg).

Found: C, 80.31; H, 9.68%. Calcd for $C_{11}H_{16}O$: C, 80.44; H, 9.83%.

The second fraction gave a solid (457 mg) which was then recrystallized from petroleum ether to give the *erythro*-isomer (VIIb) as colorless crystals; mp 39—40°C.

Found: C, 80.20; H, 9.93%. Calcd for $C_{11}H_{16}O$: C, 80.44; H, 9.83%.

b) From VIa and VIb: A mixture of VIb (0.977 g), *p*-toluenesulfonyl chloride (1.034 g), and dry pyridine (10 ml) was allowed to stand at room temperature for 24 hr and was then poured into a mixture of ice and dilute hydrochloric acid (10%: 50 ml). The mixture was extracted with ether, and the extract was washed successively with dilute hydrochloric acid and a saturated sodium chloride solution. After the extract had been dried over sodium sulfate and the ether had been removed, the crude product (0.778 g) was purified by column chromatography on silica gel (60 g) to give monotosylate as an oil; yield, 0.388 g. NMR in $CDCl_3$: 1.28 (3H, d, J=7 Hz, $-\overset{|}{C}HC\underline{H}_3$), 2.42 (3H, s, $-C_6H_4C\underline{H}_3$), 7.22 (5H, s, $-C_6\underline{H}_5$), 7.28 and 7.76 (each 2H, d, J=8.5 Hz, $-C_6\underline{H}_4CH_3$).

Found: C, 64.46; H, 6.66%. Calcd for $C_{18}H_{22}O_4S$: C, 64.65; H, 6.63%.

A solution of the above tosylate (350 mg) in dry tetrahydrofuran (5.0 ml) was stirred, drop by drop over a 20-min period, into a suspension of $LiAlH_4$ (171 mg) in dry tetrahydrofuran (5.0 ml). The mixture was then refluxed for 3 hr, poured into a mixture of ice and dilute hydrochloric acid (5%: 30 ml), and extracted with ether. The extract was washed with a saturated sodium chloride solution, dried, and then evaporated to give an oil (275 mg) which was chromatographed on silica gel (30 g). Elution with benzene containing 3% ether was subsequently carried out to give a solid (138 mg) which was shown to be identical with the above authentic *erythro*-isomer (VIIb) by an IR spectral comparison.

Similarly, the diol VIa was also converted to the *threo*-isomer (VIIa).

The Reformatsky Reaction of 3-Phenyl-2-butanone (VIII) with Methyl Bromoacetate. A ketone (VIII: 4.05 g) was condensed with methyl bromoacetate (4.10 g) in dry benzene in the presence of zinc (1.77 g) by a method similar to that used for V. The product was distilled under a vacuum to give an oil; bp 148—151°C/9 mmHg; yield, 3.37 g.

A portion (2.604 g) of the above product was chromatographed on silica gel (230 g) and separated into two epimeric β-hydroxy esters (IXa: 694 mg and IXb: 1524 mg).

IXa; Found: C, 70.49; H, 8.31%. Calcd for $C_{13}H_{18}O_3$: C, 70.24; H, 8.16%.

IXb; Found: C, 70.45; H, 8.21%. Calcd for $C_{13}H_{18}O_3$: C, 70.24; H, 8.16%.

Reduction of IXa and IXb with $LiAlH_4$. *a)* IXa (1.00 g) was reduced with $LiAlH_4$ by a method similar to that used for VIb. The crude product was recrystallized from *n*-hexane to give Xa as colorless crystals; mp 76.5—77.5°C; yield, 700 mg. NMR in $CDCl_3$: 1.17 (s, $-\overset{|}{\underset{|}{C}}C\underline{H}_3$), 1.32 (d, J=7 Hz, $-\overset{|}{C}HC\underline{H}_3$), 1.78 (qa, J=5 Hz, $-C\underline{H}_2-CH_2OH$), 2.64 (s, $-O\underline{H}$), 2.91 (qa, J=7 Hz, $-\overset{|}{C}\underline{H}CH_3$), 3.86 (t, J=5 Hz, $-C\underline{H}_2OH$), 7.32 (s, $-C_6\underline{H}_5$).

Found: C, 74.29; H, 9.45%. Calcd for $C_{11}H_{14}O_3$: C, 74.19; H, 9.34%.

b) IXb was also reduced with $LiAlH_4$ to give Xb as colorless crystals; mp 76—76.5°C (after crystallization from *n*-hexane). The mixed melting point with Xa (mp 76.5—77.5°C) was 59—61°C. NMR in $CDCl_3$: 1.18 (s, $-\overset{|}{\underset{|}{C}}C\underline{H}_3$), 1.33 (d, J=7 Hz, $-\overset{|}{C}HC\underline{H}_3$), *ca.* 1.70 (m, $-C\underline{H}_2CH_2OH$), 2.55 (bs, -OH), 2.81 (qa, J=7 Hz, $-\overset{|}{C}\underline{H}CH_3$), 3.77 (m, $-C\underline{H}_2OH$), 7.15 (s, $-C_6\underline{H}_5$).

Found: C, 74.40; H, 9.44%. Calcd for $C_{11}H_{14}O_3$: C, 74.19; H, 9.34%.

2-Phenyl-3-methyl-3-pentanols (XIa and XIb). *a) By the Grignard Reaction*: A solution of VIII (9.00 g) in dry ether (20 ml) was added, drop by drop at 0—5°C over a 30-min period, to a Grignard reagent, prepared from magnesium (1.48 g) and ethyl iodide (9.48 g) in dry ether (30 ml). The mixture was stirred at room temperature for 30 min and was then refluxed for 1 hr. After a usual work-up, the product was distilled under a vacuum to give an oil; bp 103—113°C/7 mmHg; yield, 7.92 g. A portion (2.051 g) of the above oil was chromatographed on silica gel (200 g). The elution was carried out with benzene containing 1% and then 5% ether to give the epimeric alcohols (XIa, 225 mg and XIb, 908 mg).

XIa: Found: C, 80.89; H, 10.38%. Calcd for $C_{12}H_{18}O$: C, 80.85; H, 10.18%.

XIb: Found: C, 80.60; H, 10.41%. Calcd for $C_{12}H_{18}O$: C, 80.85; H, 10.18%.

b) From Xa and Xb: By a method similar to that used for VIIb, the two diols (Xa and Xb) were converted to XIa, and XIb respectively, which later substances were shown by a spectral comparison to be identical with the above epimeric alcohols of the Grignard reaction.

Stereochemical Studies in Friedel-Crafts Reactions. I. The Reactions of *cis*- and *trans*-4-Tetrahydrophthalic Acid and Its Dimethyl Ester with Benzene

Kaichiro SUGITA and Shuzi TAMURA

Department of Chemistry, Ritsumeikan University, Kita-ku, Kyoto

(Received January 11, 1971)

The aluminum chloride-catalyzed reactions of *cis*-Δ^4-tetrahydrophthalic acid (**1A**) and its dimethyl ester (**3A**) with benzene gave, stereoselectively, *t*-4-phenyl-*cis*-hexahydrophthalic acid (**2A**) and its dimethyl ester (**12**) respectively. Similarly, the reactions of *trans*-Δ^4-tetrahydrophthalic acid (**1B**) and its dimethyl ester (**3B**) with benzene gave, stereoselectively, *c*-4-phenyl-*trans*-hexahydrophthalic acid (**2B**) and its dimethyl ester respectively, accompanied by a small amount of the *c*-4,*t*-2,*r*-1-isomer. The mechanism can be explained by presuming the interaction of the lone-pair electrons of carbonyl oxygen in the axial carboxyl group with a vacant *p*-orbital of the carbonium ion, which is produced by protonation to the double bond of the cyclohexenes (**1A**, **1B**, **3A**, **3B**).

A number of expensive studies of the directive effect of various remote substituents in hydroboration,[1] oxymercuration,[2] and epoxydation[3] have been reported, but little has been reported on the Friedel-Crafts reaction. Therefore, we have studied the directive effect on the Friedel-Crafts reactions of benzene to the double bond of 4-mono- and 4,5-disubstituted cyclohexenes catalyzed by aluminum chloride. Recently, it was reported[4] that the reaction of *cis*-Δ^4-tetrahydrophthalic acid (**1A**) with benzene catalyzed by aluminum chloride gave quantitatively, 4-phenylhexahydrophthalic acid (**2A**). The stereochemistry of the **2A** acid was not described, however. The present paper will deal with some reactions of benzene with the double bond of such 4,5-disubstituted cyclohexenes as the **1A** acid and its dimethyl ester (**3A**), *trans*-Δ^4-tetrahydrophthalic acid (**1B**), and its dimethyl ester (**3B**).

Results and Discussion

*Configuration of 4-Phenylhexahydrophthalic Acid (**2A**).* The configuration of the acid, **2A**, obtained by the reaction of **1A** with benzene was established on the basis of ring closure, epimerization, and the reaction of 4-phenylhexahydrophthalic acid anhydride (**4A**)[5] with benzene. When the **2A** acid was treated with acetic anhydride or acetyl chloride, the corresponding acid anhydride, **4A**, was obtained in a quantitative yield. Conversely, the hydrolysis of **4A** led to **2A**. The dimethyl ester **12** was converted to a new acid, **2C**, upon treatment with sodium ethoxide, followed by acidification. The **2C** acid is *t*-4,*t*-2,*r*-1-acid with a tri-equatorial structure, which is thermodynamically stable. On the basis of these results, the structure of **2A** was reasonably assumed to be as is shown in Scheme 1.[6]

In order to confirm this *t*-4,*c*-2,*r*-1 configuration of the **2A** acid, the reaction of the **4A** anhydride with benzene was carried out in the presence of aluminum chloride. This reaction gave a mixture of two isomeric keto acids, **5A** and **6A**, both of which were isolated upon fractional recrystallization. The Hunsdiecker reaction of **5A**, followed by treatment with potassium hydroxide in alcohol, gave 4-benzoylbiphenyl.[7] Therefore, the keto acid, **5A**, is 5-phenyl-2-benzoylcyclohexane-1-carboxylic acid. The treatment of **6A** with platinum-black gave 4-phenyl-2-benzylbenzoic acid (**7**). The IR spectrum of **7** shows a strong carbonyl absorption at 1685 cm^{-1}. Its structure was further confirmed by the IR and NMR spectra of the methyl ester, **8**, obtained from **7** and diazomethane. The isomeric keto acid, **5A**, was treated much as **6A** had been to afford the methyl ester **10**. The NMR spectra of the resulting esters exhibited a doublet (J=9.0 Hz[8]) at 8.0 for **8** and a doublet (J=3.0 Hz) at 8.10 ppm for **10**, which were ascribed to Ha in **8** and to Ha′ in **10** respectively.

The bromination of **6A** gave the mono-bromo ketone **11** (γ_{CO} 1680 cm^{-1}), which, on treatment with hydroiodic acid, afforded **6A**. Under similar conditions, **5A** was recovered unchanged. Since the ease of bromination depends on the respective rate of enolization,[9] the difference in behavior of **5A** and **6A** should be attributed to the presence of the axial benzoyl group in **6A** and the equatorial one in **5A**. The methyl ester of **5A** gave a mixture of the **5B** isomeric acid upon epimerization with sodium ethoxide, followed by acid hydrolysis. The recrystallization

1) a) J. Klein, E. Dundelbrum, and D. Avrahami, *J. Org. Chem.*, **32**, 935 (1967); b) D. J. Dasto and F. M. Klein, *ibid.*, **33**, 1468 (1968).

2) H. B. Henbest and B. Nichollis, *J. Chem. Soc.*, **1959**, 227.

3) a) H. B. Henbest, B. Nichollis, W. R. Jackson, R. A. L. Wilson, N. S. Crossley, M. B. Meter, and R. S. McElhinney, *Bull. Soc. Chem. Fr.*, **1960**, 1365; b) N. S. Crossley, A. C. Darby, H. B. Henbest, J. J. McCullough, B. Nicollis, and M. F. Slewart, *Tetrahedron Lett.*, **1961**, 398; c) H. B. Henbest and J. J. McCullough, *Proc. Chem. Soc.*, **1962**, 74.

4) E. Schefczik, *Chem. Ber.*, **98**, 1270 (1965).

5) Since it has been reported that[a,b] the phenyl group had a substantially greater A value than the benzoyl, methoxycarbonyl, and carboxyl groups, it is supposed that the phenyl group in this paper has an equatorial conformation. a) E. L. Eliel, N. L. Allinger, S. T. Angyal, and G. A. Morrison, "Conformational Analysis," Interscience Publishers, New York, N. Y. (1965), p. 236; b) E. W. Garbish, Jr., and D. B. Patterson, *J. Amer. Chem. Soc.*, **85**, 3228 (1963).

6) The possibility of **2D** could not be excluded at this stage, but it was rejected on the basis of subsequent experiments. (*vide infra*).

7) L. M. Long and H. R. Henze, *J. Amer. Chem. Soc.*, **63**, 1939 (1941).

8) J. W. Emsley, J. Feeney, and L. H. Sulchiffe, "High Resolution Nuclear Magnetic Resonance Spectroscopy," Vol. 2, Pergaman Press, Oxford (1966), p. 770.

9) H. E. Zimmerman, *J. Org. Chem.*, **20**, 549(1955).

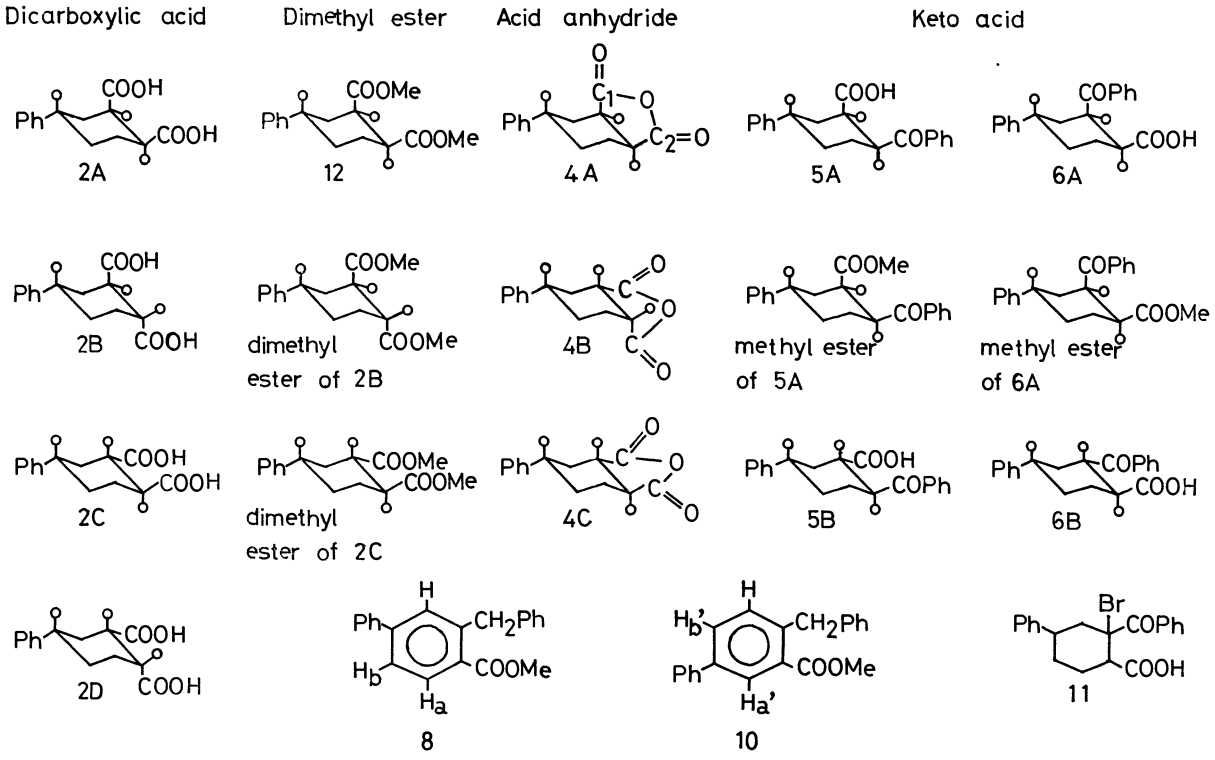

Scheme 1.

of this mixture gave a new acid, **5B**, in a 40% yield. The epimerization of the methyl ester of **6A** similarly gave another new acid, **6B**. These results support the **5A** and **6A** structures shown. Furthermore, the all-equatorial isomers, that is, the **5B** and **6B** keto acids are considered to be *t*-2-benzoyl-*c*-5-phenyl-*r*-1-cyclohexanecarboxylic acid and *t*-2-benzoyl-*t*-4-phenyl-*r*-1-cyclohexanecarboxylic acid respectively.

As is shown in Scheme 1, **6A** was obtained as a result of the attack by benzene an C–1 in **4A**, while **5A** was formed by the reaction of benzene at C–2. When **5A** or **6A** was treated with aluminum chloride in benzene under reflux, both were recovered unchanged. On the basis of the observed reaction of the acid anhydride **4A** with benzene, the configuration of **4A** can reasonably be assumed to be *c*–2, *t*–4, *r*–1 and the alternative structure, **4B**, can be excluded. As the hydrolysis of the acid anhydride **4A** gives the **2A** acid, the configuration of **2A** must be the same as **4A**.

The Reaction of Cyclohexenes with Benzene. The aluminum chloride-catalyzed reaction of various 4,5-disubstituted cyclohexenes with benzene was carried out. The results are shown in Table 1.

The reaction of dimethyl *cis*-Δ^4-tetrahydrophthalate (**3A**) with benzene gave a viscous oil in an 82% yield. The oil proved to be homogeneous on gas-chromatographic analysis and was identified as the dimethyl ester of **2A** by a comparison of the IR spectra. Therefore, the reaction gave, stereoselectively, dimethyl *t*-4-phenyl-*cis*-hexahydrophthalate (**12**) or the dimethyl ester of **2A**. The reaction of *trans*-Δ^4-tetra-

Table 1. Aluminum chloride-catalyzed addition reaction of benzene with 4,5-disubstituted cyclohexene

Cyclohexene	Product	Bp (Mp)	Yield (%)	Product distribution[a] (min)
1B	Crystalline solid[b]	(149—154°C)	90	b)
3A	**12**[c]	153—154°C/3 mmHg (53— 54°C)	82	single peak (69)
3B	Viscous oil[d]	154—155°C/3 mmHg	80	80 (60) : 20 (65)

a) By gas-chromatographic analysis. The ratio was calculated from the peak areas. (retention).

b) Fractional recrystallization from 40% acetic acid gave **2B** (70%), mp 162—164°C, and *t*-4, *t*-2, *r*-1-acid (**2C**) (8%), mp 215—217°C. IR of **2B**: (KBr) 2700—2400 (-OH), 1690 (carboxyl) and 1600 cm^{-1} (aromatic). Found: C, 67.08; H, 6.39%. Calcd for $C_{14}H_{16}O_4$: C, 67.73; H, 6.50%. The dimethyl ester of **2B** was obtained by the treatment of **2B** with diazomethane in ether. IR: (neat) 1730 (ester) and 1605 cm^{-1} (aromatic. NMR: δ ($CDCl_3$) 2.30—1.60 (m, 6, $3CH_2$), 2.95—2.55 (m, 1, CH), 3.45—3.00 (m, 2, 2CH), 3.75 (s, 6, $2CH_3$) and 7.22 ppm (s, 5, aromatic). The *t*-4, *t*-2, *r*-1-acid (**2C**) was identified by a mixed-melting-point determination and by a comparison of its IR spectrum with those of an authentic sample.

c) The product crystallized on cooling. Found: C, 69.74; H, 7.45%. Calcd for $C_{16}H_{20}O_4$: C, 69.54; H, 7.30%.

d) IR: (neat) 1730 (ester) and 1605 cm^{-1} (aromatic). Found: C, 69.75; H, 7.38%. Cald for $C_{16}H_{20}O_4$: C, 69.54; H, 7.30%.

hydrophthalic acid (**1B**) and benzene gave a mixture of acids in a 90% yield, from which **2B** was isolated in a 70% yield and *t*-4-phenyl-*trans*-hexahydrophthalic acid (**2C**) in an 8% yield. Finally, the reaction of dimethyl *trans*-Δ^4-tetrahydrophthalate (**3B**) gave, in an 80% yield, a viscous oil which showed two peaks (area ratio 4 : 1) on gas-chromatography. The GC retention time indicated that the major component was the dimethyl ester of **2B**, and the minor one, the dimethyl ester of **2C**. In short, *trans*-4,-5disusbstituted cyclohexene (**1B**, **3B**) reacted with benzene to give **2B** and the dimethyl ester of **2B** contaminated with the *t*-4,*t*-2,*r*-1-isomer (**2C**, dimethyl ester of **2C**); this is in contrast to the behavior of the *cis*-4,5-disubstituted cyclohexene isomers (**1A**, **3A**). The configuration of the **2B** acid was established on the basis of the analogous epimerization and ring closure described above. The dimethyl ester of **2B** was converted to *t*-4,*t*-2,*r*-1-acid (**2C**) with sodium ethoxide, followed by acidification. This indicated that the **2B** and **2C** acids are stereoisomeric with each other. The **2B** acid was converted to **4A** in a quantitative yield with acetic anhydride, while **2B** was recovered unchanged upon treatment with acetyl chloride. The **2C** acid gave **4A** in a quantitative yield upon treatment with acetic anhydride and gave a new acid anhydride (**4C**) in quantitative yield when treated with acetyl chloride. In spite of the stereochemical differences in these acids (**2A**, **2B**, **2C**) in ring closure, the same product (**4A**) was obtained. In view of these facts, **2B** was identified as *c*-4-phenyl-*trans*-hexahydrophthalic acid having both carboxyl groups in an anti-axial conformation; this should explain the unsuccessful dehydration to anhydride.

Mechanism. It is generally known[10] that the alkylation of aromatics with olefins catalyzed by Lewis acids is initiated by the protonation of the double bond, thus forming a carbonium ion which then reacts with the aromatic rings.

In the presence of a trace amount of water, the protonation of the double bond of *cis*-4,5-disubstituted cyclohexene (**1A**, **3A**) gives a carbonium ion[11] which may be in either one of the two conformations (**13**, **14**) shown in Scheme 2. The conformation of **13** seems to be more stable than **14** since **13** is stabilized by the interaction of the lone-pair electorons of carbonyl oxygen in the axial carboxyl group with the vacant *p*-orbital. On the other hand, **14** does not have an axial carboxyl which might serve to stabilize the carbonium ion. The above explanation may be acceptable in view of the fact that a 1,3-interaction of this type has previously been established.[12,13] Thus, the stereoselective formation of **2A** and **12** can presumably be explained by a route which involves the **15** transition state. Scheme 3 summarizes the reac-

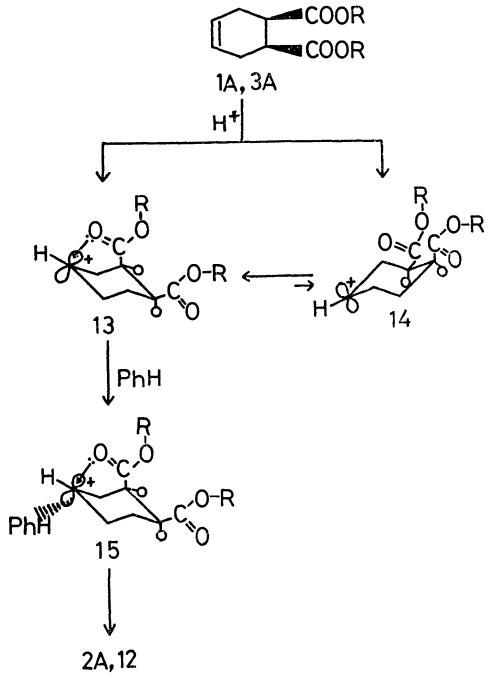

R=H, Me

Scheme 2.

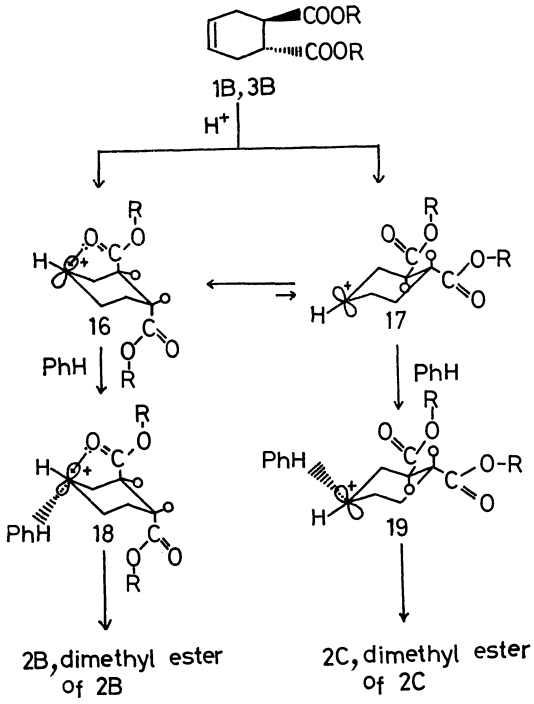

R=H, Me

Scheme 3.

10) S. H. Patinkin and B. S. Friedman, "Friedel-Crafts and Related Reaction," vol. 2, Part 1, ed. by G. A. Olah, John Wiley, New York (1964), p. 3.

11) The ester carbonyl can be coordinated by aluminum chloride:

$$R\text{-}O\diagdown\!\!\diagup C{=}O\cdots AlCl_3 \longleftrightarrow R\text{-}O\diagdown\!\!\diagup C{=}\overset{\oplus}{O}\ \overset{\ominus}{AlCl_3}$$

This coordination may antagonize the above-mentioned carbonium-ion stabilization by *n*-electrons on carbonyl oxygen. Possibly, the stereochemistry involved in the present work suggests that such a coordination is not important in the product-determining step of the Friedel-Carfts reaction.

12) N. Baggett, J. S. Brimacombo, A. B. Foster, M. Stacey, and D. H. Whiffen, *J. Chem. Soc.*, **1960**, 2574.

13) a) B Dobinson and A. B. Foster, *ibid.*, **1961**, 2338; b) N. Baggett, M. A. Bukhari, A. B. Foster, J. Lehamann, and J. M. Webber, *ibid.*, **1963**, 4157.

tion of *trans*-4,5-disubstituted cyclohexenes (**1B**, **3B**). The intermediary carbonium ions can be either bridged, **16**, stabilized by an axial carboxyl group or a usual carbonium ion, **17**. The reaction of benzene with the carbonium ion **16** proceeds in a manner similar to that described in the case of **13** to give the *c*-4,*t*-2,*r*-1 configuration (**2B**, the dimethyl ester of **2B**) stereoselectively. The equatorial attack of benzene and the carbonium ion, **17**, proceeds *via* the most favorable transition state, **19**, in which the two substituents and benzene all occupy equatorial positions, so that the *t*-4,*t*-2,*r*-1 configuration (**2C**, the dimethyl ester of **2C**) is formed.

Experimental[14]

Materials. Commercially-avalilable *cis*-Δ^4-tetrahydrophthalic acid (**1A**) was used. Dimethyl *cis*-Δ^4-tetrahydrophthalate (**3A**) was prepared by the procedure reported by Nazarov and Kucherov;[15] bp 107—109°C/5 mmHg (lit,[15] bp 110—111°C/5mmHg). *trans*-Δ^4-Tetrahydrophthalic acid (**1B**) was prepared by the procedure reported by Nazarov and Kucherov;[15] mp 169—170°C (lit,[15] mp 170—171°C). Dimethyl *trans*-Δ^4-tetrahydrophthalate (**3B**) was prepared by the procedure reported by Nazarov and Kucherov;[15] bp 110—111°C/5mmHg (lit,[15] bp 137°C/20mmHg).

t-*4-Phenyl*-cis-*hexahydrophthalic Acid (**2A**).* This was prepared by the procedure reported by Schefczik;[4] mp 190—191°C (lit,[4] 194°C).

*Reaction of **4A** with Benzene.* Into a solution of **4A** (21.5 g) in dry benzene (87 m*l*), we stirred aluminum chloride (33 g) over a five-minute period below 10°C. Stirring was continued for one hour without further cooling and then for 20 additional minutes under reflux. Then the reaction mixture was poured onto icewater. The evaporation of solvent gave a mixture of carboxylic acids (27 g, 93%), mp 160—186°C. Fractional recrystallization from 95% alcohol gave **5A** (3 g, 11%) and **6A** (18 g, 67%). The recrystallization of **5A** from 85% alcohol gave colorless prisms; mp 182—183°C. IR: (KBr) 2700—2400 (-OH), 1700 (carboxyl), 1680 (Ketone) and 1600 cm^{-1} (aromatic). Found: C, 77.61; H, 6.66%. Calcd for $C_{20}H_{20}O_3$: C, 77.90; H, 6.54%. The recrystallization of **6A** from 95% alcohol gave colorless prisms; mp 202—203°C. IR: (KBr) 2700—2400 (−OH), 1700 (carboxyl), 1680 (ketone) and 1600 cm^{-1} (aromatic). Found: C, 77.82; H, 6.43%. Calcd for $C_{20}H_{20}O_3$: C, 77.90; H, 6.54%.

*The Methyl Esters of **5A** and **6A*** were obtained by the treatment of **5A** and **6A** with diazomethane in ether.

4-Benzoylbiphenyl was prepared by the procedure reported by Long and Henze;[7] mp 100—101°C (lit,[7] 103—104°C).

*4-Benzoylbiphenyl from **5A**.* To a solution of sodium hydroxide (3 g) in water (70 m*l*), **5A** was added (20 g). The mixture was heated to reflux until a clear solution was observed. The solution was cooled to room temperature and filtered. Nitric acid was added, drop by drop, to this filtrate until it reached incipient turbidity. Then a few drops of aqueous sodium hydroxide were added just to clear the solution up again. The slow stirring in of a solution of silver nitrate (13 g) in water (30 m*l*) produced a copious precipitate of the silver salt, which was then collected, washed with water, and carefully dried in a vacuum desiccator. The silver salt was obtained quantitatively. To a suspension of the dry silver salt (20 g) in dry chloroform (100 m*l*), a solution of bromine (9.6 g) in dry chloroform (20 m*l*) was added at room temperature. After this mixture had been refluxed for three hours, a suspension was obtained. After cooling, the suspension was filtered, and the silver bromide in the filter was washed with chloroform. The combined filtrate was washed with an aqueous sodium thiosulfate solution, an aqueous sodium hydroxide solution, water, and brine. Then the solution was dried over anhydrous magnesium sulfate and concentrated under reduced pressure. The distillation of the reaction residue gave an oily product (4 g), bp 220—245°C/2 mmHg. This oil was added to a solution of potassium hydroxide (3 g) in ethyl alcohol (60 m*l*) and refluxed for two hours. Subsequent recrystallization from alcohol gave 4-benzoylbiphenyl (2.5 g, 16%), mp 99—101°C. The structure was confirmed by a mixed-melting-point determination and by a comparison of the IR spectra with those of an authentic sample.[7]

*4-Phenyl-2-benzylbenzoic Acid (**7**).* A mixture of **6A** (1.6 g) and platinum-black (0.5 g) was heated under nitrogen at 305—310°C for four hours. The reaction mixture was then separated and the ether was extracted. The ether layer was treated with 5% sodium hydrogencarbonate and then acid. Recrystallization from alcohol gave **7** (1.0 g, 67%); mp 170—171°C. IR: (KBr) 2700—2400 (-OH), 1685 (carboxyl) and 1600 cm^{-1} (aromatic). Found: C, 84.20; H, 5.52%. Calcd for $C_{20}H_{20}O_2$: C, 84.48; H, 5.67%.

*Methyl Ester of **7** (**8**).* This was obtained by the treatment of **7** with diazomethane in ether. NMR: $\delta(CDCl_3)$ 3.85 (3H, s, CH_3), 4.48 (2H, s, CH_2), 7.20 (5H, s, aromatic), 7.60—7.30 (7H, m, aromatic) and 8.00 ppm (H, d, J= 9 Hz, CH).

*5-Phenyl-2-benzylbenzoic Acid (**9**).* A mixture of **5A** (1.6 g) and platinum-black (0.5 g) was worked up similarly. Recrystallization from alcohol gave **9** (0.8 g, 52%); mp 156—157°C. IR: (KBr) 2700—2400 (-OH), 1695 (carboxyl) and 1600 cm^{-1} (aromatic). Found: C, 84,34; H, 5.77%. Calcd for $C_{20}H_{16}O_2$: C, 84.48; H, 5.67%.

*Methyl Ester of **9** (**10**).* This was obtained by the treatment of **9** with diazomethane in ether. NMR: δ $(CDCl_3)$ 3.80 (3H, s, CH_3), 4.40 (2H, s, CH_2), 7.20 (5H, s, aromatic), 7.70—7.30 (7H, m, aromatic) and 8.10 ppm (H, d, J=3 Hz, CH).

*4-Phenyl-2-benzoyl-2-bromocyclohexane-1-carboxylic Acid (**11**).* To a solution of **6A** (1.0 g) in acetic acid (160 m*l*), bromine (0.8 g) was added at room temperature. The solution was kept at 80°C for 10 min and then cooled. It was poured onto cracked ice and filtered. The precipitate was washed with water and dried. It gave a yellow product (1.1 g); mp 169—175°C. Recrystallization from 80% alcohol gave **11** as colorless prisms (0.9 g, 70%); mp 184—185°C. The melting point of the product was depressed by mixing with **6A**. IR: (KBr) 2700—2400 (-OH), 1700 (carboxyl), 1680 (benzoyl) and 1600 cm^{-1} (aromatic). Found: C, 62.16; H, 4.80%. Calcd for $C_{20}H_{19}OBr$: C, 62.02; H, 4.95%.

*Bromination of **5A**.* The treatment of **5A** with bromine was carried out in a manner similar to that used in the experiment described above except for the condition of acetic acid (50 m*l*). A crystalline material was thus ob-

14) All the melting points and boiling points are uncorrected. The IR spectra were taken on a Hitachi EPI-S spectrometer. The NMR spectra were obtained on a Japan Electron Optics C-60-H spectrometer. The glpc analyses were carried out with a Shimazu GC-4AP appratus using Silicon Grease as the stationary phase.

15) I. N. Nazarov and V. F. Kucherov, *Otdel. Khim. Nauk*, 1954, 329; *cf. Chem. Abstr.*, 49, 5328 (1955).

tained quantitatively; mp 176—180°C. The melting point of the product, without any purification, was identical with that of **5A**. The IR spectra of the product were identical with that of **5A**.

*Debromination of **11** with 47% Hydroiodic Acid.* To a solution of **11** (50 mg) in acetone (3 m*l*), 47% hydroiodic acid (0.1 m*l*) was added. The solution was then kept at about 50°C for three minutes. After the iodine had been destroyed by the addition of a small quantity of sodium thiosulfate, 5 m*l* of water was added to give a precipitate. The precipitate was collected by filtration with water and dried. It gave a white product (35 mg, 88%); mp 197—199°C. The structure of the product, without any purification, was confirmed by a mixed-melting-point determination and by a comparison of the IR spectra with those of **6A**.

*Treatment of **5A** and **6A** with Aluminum Chloride.* This was done similarly except that the reaction time was one hour. In the case of **5A**: **5A** (3.1 g), aluminum chloride (1.5 g) and benzene (10 m*l*). A crystalline material (2.7 g, 87%) was obtained (mp 176—180°C). The recrystallization of the product from 85% alcohol gave colorless prisms, mp 180—181°C. The melting point of the product was not depressed by mixing with **5A**. The IR spectra of the product were identical with those of **5A**. In the case of **6A**: **6A** (3.1 g), aluminum chloride (1.5 g) and benzene (10 m*l*), a crystalline material (2.6 g, 84%) was obtained (mp 194—198°C). The recrystallization of the product from 95% alcohol gave colorless prisms, mp 201—202°C. The melting point of the product was not depressed by mixing with **6A**. The IR spectra of the product were identical with those of **6A**.

Table 2. Epimerization of trisubstituted cyclohexane

Sample[a)]	Product	Mp	Yield (%)
Dimethyl ester of **2A**	**2C**[b)]	220—221°C	400 mg (89)
Dimethyl ester of **2B**	**2C**[b)]	218—219°C	400 mg (89)
5A	**5A**[c)]	180—181°C	450 mg (90)
Methyl ester of **5A**	**5B**[d)]	179—180°C	200 mg (40)
6A	**6B**[e)]	241—242°C	450 mg (90)
Methyl ester of **6A**	**6B**[e)]	240—242°C	400 mg (80)

a) The corresponding methyl ester was obtained by the treatment of diazomethane in ether.

b) Recrystallization from 60% acetic acid gave **2C** of colorless prisms. IR: (KBr) 2700—2400 (-OH), 1705 (carboxyl) and 1600 cm^{-1} (aromatic). Found: C, 67.82; H, 6.41%. Calcd for $C_{14}H_{16}O_4$: C, 67.73; H, 6.50%. The dimethyl ester of **2C** was obtained by the treatment of **2C** with diazomethane in ether. IR: (neat) 1730 (ester) and 1600 cm^{-1} (aromatic). NMR: $\delta(CDCl_3)$ 2.95—1.15 (m, 9, 3CH and $3CH_2$), 3.70 (d, 6, $2CH_3$) and 7.22 (s, 5, aromatic).

c) The structure of the product was confirmed by a mixed-melting-point determination and by a comparison of its IR spectra with those of an authentic sample.

d) It gave a white product (430 mg, 90%); mp 160—174°C. Found: C, 78.03; H, 6.68%. Calcd for $C_{20}H_{20}O_3$: C, 77.90; H, 6.54%. Recrystallization from 80% alcohol gave 5B of white prisms. IR: (KBr) 2800—2500 (-OH), 1700 (carboxyl), 1680 (ketone) and 1600 cm^{-1} (aromatic). Found: C, 77.20; H, 6.68%. Calcd for $C_{20}H_{20}O_3$: C, 77.90; H, 6.54%.

e) Recrystallization from 90% alcohol gave **6B** of colorless prims. IR: (KBr) 2700—2400 (-OH), 1700 (carboxyl), 1680 (ketone) and 1600^{-1} (aromatic). The melting point of **6B** was depressed by mixing with **6A**. The IR spectra of **6B** and **6A** were different in the fingerprint region. Found: C, 77.79; H, 6.62%. Calcd for $C_{20}H_{20}O_3$: C, 77.90; H, 6.54%.

*Aluminum Chloride-catalyzed Reaction of 4,5-Disubstituted Cyclohexene (**1B**, **3A**, **3B**) with Benzene. General Procedure*: Into a solution of 4,5-disubstituted cyclohexene (0.03 M) in dry benzene (0.3 M) we stirred aluminum chloride (0.06 M) over a five-minute period below 10°C. Stirring was continued for one hour without further cooling, and for two additional hours under reflux. Then the reaction mixture was poured onto icewater. The benzene solution was dried over anhydrous magnesium sulfate and evaporated. The product was purified by recrystallization or distillation. The results are given in Table 1.

General Epimerization Procedure: To a sodium ethoxide solution prepared from absolute ethanol (50 m*l*) and sodium ((200 mg) for the dimethyl ester of **2A** (**12**) and the dimethyl ester of **2B**, (100 mg) for **5A**, the methyl ester of **5A**, **6A**, and the methyl ester of **6A**), we added the sample (500 mg). The solution was refluxed for five hours and cooled. After the addition of water (100 m*l*) to the reaction mixture, the resulting mixture was acidified and filtered. The results are shown in Table 2.

*Ring Closure of 4-Phenylhydrophthalic Acid (**2A**, **2B**, **2C**) with Acetic Anhydride or Acetyl Chloride. General Procedure*: A mixture of 4-phenylhexahydrophthalic acid (9.5 g) and acetic anhydride (40 m*l*) or acetyl chloride (40 m*l*) was refluxed for three hours. After the acetic anhydride (25 m*l*) or acetyl chloride (25 m*l*) had been removed from the reaction mixture, the solution was cooled in an ice-box for three days. We thus obtained a crystalline solid. The crystalline solid was washed with light petroleum ether (bp 30—70°C) and purified by recrystallization. The results are shown in Table 3.

Table 3. Ring closure of 4-Phenylhexahydrophthalic acid

Sample	Reagent	Product	Mp	Yield
2A	Acetic anhydride	**4A**[a)]	105—106°C[b)]	quant.
2A	Acetyl chloride	**4A**[a)]	106—107°C[b)]	8.4 g 89%
2B	Acetic anhydride	**4A**[a)]	106—107°C[b)]	quant.
2B	Acetyl chloride	**2B**[c)]	154—159°C[d)]	8.4 g 89%
2C	Acetic anhydride	**4A**[a)]	105—106°C[b)]	quant.
2C	Acetyl chloride	**4C**[e)]	162—163°C[b)]	quant.

a) IR: (Nujol 1850, 1780 (acid anhydride) and 1600 cm^{-1} (aromatic)). Found: C, 73.09; H, 6.13%. Calcd for $C_{14}H_{14}O_3$: C, 73.02; H, 6.37%.

b) Recrystallization from benzene-ligroin.

c) The structure of the product was confirmed by a mixed-melting-point determination and by a comparison of its IR spectra with those of an authentic sample.

d) Crude product.

e) IR: (Nujol) 1865, 1785 and 1600 cm^{-1}. The melting point of **4C** was depressed upon mixing with **4A**. The IR spectra of **4A** and **4C** were different in the fingerprint region. Found: C, 73.09; H, 6.13%. Calcd for $C_{14}H_{14}O_3$: C, 72.74; H, 6.44%.

The authors are very grateful to Professor K. Sisido, Dr. K. Uchimoto, and Mr. T. Imagawa of Kyoto University for their many helpful discussion and suggestions during this work. The authors are also grateful to Dr H. Takahashi, Government Industrial Research Institute, Osaka, for supplying the butadiene, to the Nozaki Laboratory of Kyoto University for the measurement of the NMR spectra, and to Mrs. K. Fujimoto of the Sisido Laboratory for her elemental analyses.

Stereochemical Studies in Friedel-Crafts Reactions. II. The Reactions of 4-Substituted Cyclohexenes with Benzene

Kaichiro SUGITA and Shuzi TAMURA

Department of Chemistry, Ritsumeikan University, Kita-ku, Kyoto

(Received January 11, 1971)

The addition reactions of benzene to the double bonds of 4-substituted cyclohexenes, such as 4-benzoylcyclohexene (**5**), 4-acetylcyclohexene (**6**), methyl 4-cyclohexenecarboxylate (**7**), and 4-cyclohexenecarboxylic acid (**8**) have been studied in the presence of aluminum chloride. In all cases, the reactions gave mainly 1,4-disubstituted cyclohexane with the *trans* configuration stereoselectively. A possible mechanism for this reaction is suggested.

This paper will be concerned with a useful synthetic method for introducing the phenyl group exclusively at the 4-position of the monosubstituted cyclohexene ring by means of the Friedel–Crafts reaction. In the preceding paper[1] of this series, we reported that *cis*- and *trans*-Δ^4-tetrahydrophthalic acid and their dimethyl esters react with benzene in the presence of aluminum chloride to produce the corresponding 1,2,4-trisubstituted cyclohexanes. Thus, *cis*-Δ^4-tetrahydrophthalic acid (**1A**) or its dimethyl ester (**2A**) gives, stereoselectively, *trans*-4-phenyl-*cis*-hexahydrophthalic acid (**3A**) or its dimethyl ester (**4A**) respectively. Meanwhile, *trans*-Δ^4-tetrahydrophthalic acid (**1B**) or its dimethyl ester (**2B**) gives, stereoselectively, *cis*-4-phenyl-*trans*-hexahydrophthalic acid (**3B**) or its dimethyl ester (**4B**).

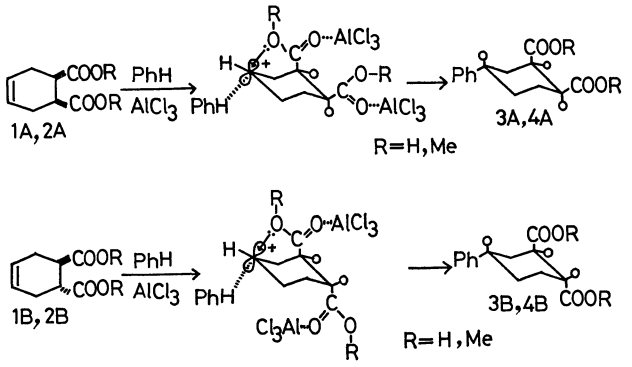

Scheme 1

This finding prompted us to explore the reaction of benzene with carbonium ions which are derived from 4-negatively substituted cyclohexenes. The present paper will describe some addition reactions of benzene to 4-benzoylcyclohexene (**5**), 4-acetylcyclohexene (**6**), methyl 4-cyclohexenecarboxylate (**7**), and 4-cyclohexenecarboxylic acid (**8**) in the presence of aluminum chloride.

Results and Discussion

The results of the reactions of various 4-substituted cyclohexenes with benzene have been summarized in Table 1. The products obtained from 4-substituted cyclohexenes and benzene were found by gas-chromatographic analysis to be composed of two components in all cases. The major components were *trans*-1,4-disubstituted cyclohexanes, whereas the minor components were the *cis*-1,4-disubstituted isomers. All the *trans*-products were identified by a comparison of the spectral and physical data with those of an authentic sample.[2] No 1,3-disubstituted product could be detected.[3]

The semi-crystalline solid obtained from the reaction of 4-benzoylcyclohexene (**5**) and benzene was found to be a mixture of *trans*-4-benzoyl-1-phenyl[4] cyclohexane (**9A**)(96%) and its *cis*-isomer (**9B**)(4%). Since no epimerization of **9A** by sodium ethoxide occurred, the phenyl and benzoyl groups must be diequatorial, *i.e.*, in the *trans* position[5] with respect to each other. On the other hand, the mother-liquid obtained from the reaction of **5** with benzene was converted to pure **9A** by the action of sodium ethoxide. This indicates that **9B** must be the *cis*-isomer. An oily product obtained from the reaction of 4-acetylcyclohexene (**6**) and benzene was found to be a mixture of *trans*-4-acetyl-1-phenylcyclohexane (**10A**) (95%) and its *cis*-isomer (**10B**)(5%). Likewise, methyl 4-cyclohexenecarboxylate (**7**) and benzene were found to be methyl *trans*-4-phenylcyclohexane-1-carboxylate (**11A**)(85%) and its *cis*-isomer (**11B**) (15%).

Thus, the above-mentioned reaction provides a useful method of preparing **9A**, **10A**, and **11A** in good yields. For example, the Friedel-Crafts reaction of **5**, followed by epimerization, gives **9A** in a 90% overall yield.

The reaction of 4-cyclohexenecarboxylic acid (**8**) with benzene gave a mixture of crystalline carboxylic acids in a 94% yield. The mixture of methyl esters obtained by treatment with diazomethane in ether consisted of the *trans* ester (**11A**)(67%) and its *cis*-isomer (**11B**)(33%). When the epimerization of

1) K. Sugita and S. Tamura, This Bulletin, **44**, 3383 (1971).

2) W. S. Johnson and R. D. Offenhauer, *J. Amer. Chem. Soc.*, **67**, 1045 (1945).

3) The results obtained in subsequent experiments suggest that the carbonium ion is formed at the 4-position. Therefore, the carbonium ion is not formed at the 3-position.

4) Since it has been reported[a,b] that the phenyl group has a substantially greater A value than the benzoyl, acetyl, and methoxycarbonyl groups, it is supposed that the phenyl group in this paper has an equatorial conformation. a) E. L. Eliel, N. L. Allinger, S. T. Angyal, and G. A. Morrison, "Conformational Analysis," Interscience Publishers, New York, N. Y. (1965), p. 236. b) E. W. Grabish, Jr., and D. B. Patterson, *J. Amer. Chem. Soc.*, **85**, 3228 (1963).

5) H. E. Zimmerman, *J. Org. Chem.*, **20**, 549 (1955).

Table 1. ALUMINUM CHLORIDE-CATALYZED ALKYLATION REACTION OF BENZENE WITH 4-SUBSTITUTED CYCLOHEXENE

Cyclohexene	Product	Bp	Yield (%)	Product distribution,[a] *trans* : *cis*
(**5**)	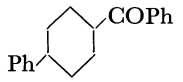	b)	90	96 (54)[d] : 4 (49)
(**6**)	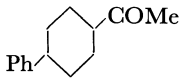	144—148°C/5—6 mmHg	81	95 (28) : 5 (25)
(**7**)	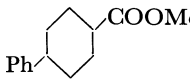	118—121°C/5 mmHg	79	85 (27) : 15 (23)
(**8**)	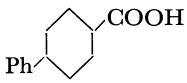	b)	94[c]	67 (26.5) : 33 (24.5)

a) By gas chromatographic analysis. The product ratio was calculated from the peak areas. Dimethyl *cis*-Δ^4-tetrahydrophthalate[1] was used as an internal standard for determination of yields.
b) Semi-crystalline solid.
c) The ratio of the acid was determined as the corresponding methyl ester.
d) Retention time (min).

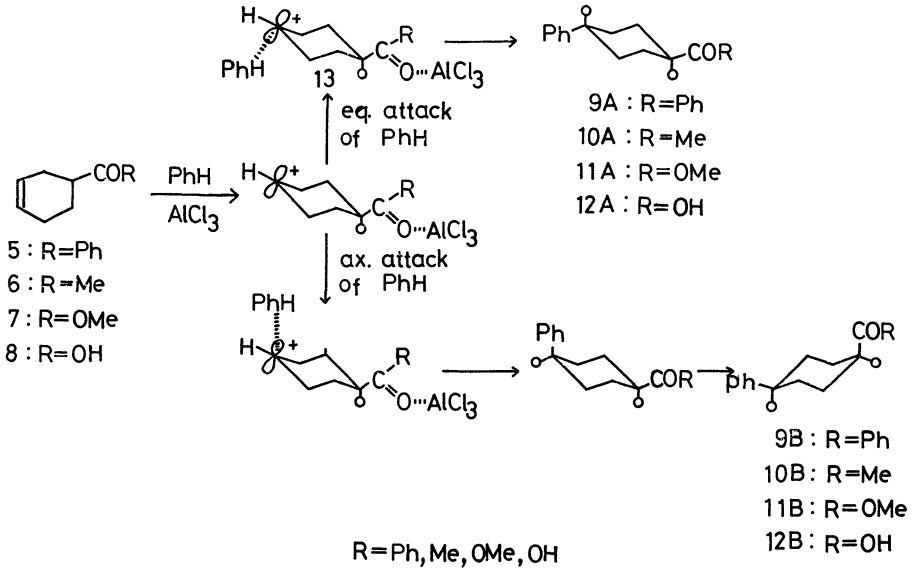

Scheme 2.

the methyl ester was carried out in a manner similar to that described above, the **12A** acid was obtained. The **12A** acid was identified as being in a *trans*-isomer.

Thus, the addition of benzene to the double bond of 4-substituted cyclohexenes (**5**, **6**, **7**, **8**) in the presence of aluminum chloride selectively occurred at the 4-position to the substituent, as is shown in Table 1. These results indicate that the carbonium ion must be produced at the 4-position in these reactions. The equatorial attack of benzene on the carbonium ion should be more favorable than an axial attack, since it leads to a more favorable transition state (**13**) in which the substituent and attacking benzene are both equatorial. Thus, these reactions give rise to predominantly *trans*-1,4-disubstituted products.[6]

6) It may be considered that the result obtained in the present work support the mechanism.

Experimental[7]

Materials. 4-Acetylcyclohexene (**6**) was prepared by the procedure reported by Petrov.[8] Methyl 4-cyclohexenecarboxylate (**7**) and 4-cyclohexenecarboxylic acid (**8**) were prepared by the procedure reported by Klein, Dunkelblum, and Avrahami.[9]

4-Benzoylcyclohexene (5). This was obtained as follows. To a mixture of β-Chloropropiophenone (34 g),

7) All the melting points and boiling points are uncorrected. The IR spectra were taken on a Hitachi EPI-S spectrometer. The NMR spectra were obtained on a Japan Electron Optics C-60-H spectrometer. The glpc analyses were carried out with a Shimazu GC-4AP appratus using Silicone Grease as the stationary phase.

8) A. A. Petrov, *J. Gem. Chem.*, **11**, 309(1941): *cf. Chem. Abstr.*, **35**, 5873 (1941).

9) J. Klein, E. Dinkelblum, and D. Avrahami, *J. Org. Chem.*, **32**, 935 (1967).

potassium acetate (30 g), and toluene (30 ml), butadiene (34 ml) was added in an autoclave. The solution was heated with stirring at 90—92°C for 24 hr. Then the inorganic salt was filtered off after adding toluene. The toluene solution was washed with water, dried over anhydrous magnesium sulfate, and evaporated under reduced pressure. The distillation of the reaction residue gave **5**; bp 125—126°C/5 mmHg (24 g, 63% yield). IR: (neat) 1670 (benzoyl) and 1645 cm^{-1} (olefin). NMR: $\delta(CDCl_3)$ 2.45—1.50 (m, 6, $3CH_2$), 3.50—3.00 (m, 1, CH), 5.80 (t, 2, CH=CH), 7.50—7.25 (m, 3, aromatic), and 8.10—7.75 ppm (m, 2, aromatic). Found: C, 84.45; H, 7.69%. Calcd for $C_{13}H_{14}O$: C, 83.83; H, 7.58%.

4-Acetyl-1-phenylcyclohexane. This was prepared by the procedure reported by Johnson and Offenhauer;[2] mp 55—56°C (lit,[2] 55.1—55.6°C). IR: (Nujol) 1700 (Ketone) and 1600 cm^{-1} (aromatic). NMR: $\delta(CDCl_3)$ 2.05—1.25 (m, 8, $4CH_2$), 2.18 (s, 3, CH_3), 2.75—2.25 (m, 2, 2CH) and 7.20 ppm (s, 5, aromatic).

Methyl 4-Phenylcyclohexane-1-carboxylate. This was prepared by the procedure reported by Johnson and Offenhauer;[2] mp 28—30°C (lit,[2] 29—30°C). IR: (Nujol) 1730 (ester) and 1600 cm^{-1} (aromatic). NMR: $\delta(CDCl_3)$ 2.90—1.20 (m, 10, $4CH_2$ and 2CH), 3.68 (t, 3, CH_3) and 7.22 ppm (s, 5, phenyl).

4-Phenylcyclohexane-1-carboxylic Acid. This was prepared by the procedure reported by Johnson and Offenhauer;[2] mp 200—201°C (lit,[2] 203—204°C).

4-Benzoyl-1-phenylcyclohexane from 4-Phenylcyclohexane-1-carboxylic Acid. A mixture of 4-phenylcyclohexane-1-carboxylic acid (3.3 g) and thionyl chloride (3.5 g) was refluxed for 2 hr and then cooled. The excess thionyl chloride in the reaction mixture was removed under an atmosphere of nitrogen at 30—40°C under reduced pressure. 4-Phenyl-1-chloroformylcyclohexane as a liquid was obtained quantitatively and was used directly, without distillation. To a suspension of aluminum chloride (2.5 g) in dry benzene (17 ml), we vigorously stirred in 4-phenyl-1-chloroformylcyclohexane (3.8 g), drop by drop, below 10°C. Stirring was continued for one hour without further cooling, and then for two more hours under reflux. Then the reaction mixture was poured onto icewater. The benzene solution was separated, washed with water, 5% sodium hydrogencarbonate, and water, dried over anhydrous magnesium sulfate, and evaporated to dryness. A semi-crystalline solid was dissolved in hot *n*-hexane. The solvent was then removed to give *trans*-4-benzoyl-1-phenylcyclohexane (1.0 g, 23% yield); mp 73—79°C. Recrystallization from *n*-hexane gave colorless prisms (0.7 g, 16% yield); mp 95—96°C. IR: (Nujol) 1670 (benzoyl) and 1600 cm^{-1} (aromatic). NMR: $\delta(CDCl_3)$ 2.25—1.40 (m, 8, $4CH_2$), 2.75—2.35 (m, 1, CH), 3.60—3.05 (m, 1, CH), 7.22 (s, 5, aromatic), 7.60—7.35 (m, 3, aromatic), and 8.15—7.80 ppm (m, 2, aromatic). Found: C, 86.33; H, 7.68%. Calcd for $C_{19}H_{20}O$: C, 86.32; H, 7.63%.

Aluminum Chloride-catalyzed Reaction of 4-Substituted Cyclohexene with Benzene. General Procedure: Into a solution of 4-substituted cyclohexene (0.05 mol) in dry benzene (0.5 mol) we stirred aluminum chloride (0.06 mol) over a five-minute period below 10°C. Stirring was continued for one hour without further cooling, and then for two additional hours under reflux. Then the reaction mixture was poured onto icewater. The benzene solution was separated, dried over anhydrous magnesium sulfate, and evaporated to dryness. The product was purified by recrystallization or distillation.

trans-*4-Benzoyl-1-phenylcyclohexane* (***9A***) *from 4-Benzoylcyclohexene* (***5***). The reaction product was recrystallized from *n*-hexane to give **9A** as colorless prisms; mp 96—98°C, 74% yield. The mother liquid was used as the epimerization sample. **9A** was identified · as 4-benzoyl-1-phenylcyclohexane by a mixed-melting-point determination and by a comparison of its IR and NMR spectra with those of an authentic sample.

trans-*4-Acetyl-1-phenylcyclohexane* (***10A***) *from 4-Acetylcyclohexene* (***6***). The product was kept standing in an ice-box for 10 days to separate a crystalline solid (**10A**) (62% yield) from the mother liquid. The mother liquid was used as the epimerization sample. The recrystallization of **10A** from light petroleum ether (bp 30—70°C) gave colorless prisms; mp 54—55°C. **10A** was identified as 4-acetyl-1-phenylcyclohexane by a mixed-melting-point determination and by a comparison of its IR and NMR spectra with those of an authentic sample (Found: C, 82.96; H, 9.12%).

Methyl trans-*4-Phenylcyclohexane-1-carboxylate* (***11A***) *from Methyl 4-Cyclohexenecarboxylate* (***7***). The product was kept standing in an ice-box for 10 days to separate a crystalline solid (**11A**) (27% yield) from the mother liquid (52% yield). The mother liquid was used as the epimerization sample. The recrystallization of **11A** from *n*-hexane gave colorless prisms; mp 29—30°C. **11A** was identified as methyl 4-phenylcyclohexane-1-carboxylate by a mixed-melting-point determination and by a comparison of its IR and NMR spectra with those of an authentic sample (Found: C, 77.20; H, 8.29%).

trans-*4-Phenylcyclohexane-1-carboxylic Acid* (***12A***) *from 4-Cyclohexenecarboxylic Acid* (***8***). The reaction product was recrystallized from 60% aqueous acetic acid to give a crystalline solid; mp 79—124°C. The recrystallization of the crystalline solid from 60% acetic acid gave colorless needles (**12A**) (3% yield); mp 199—200°C. **12A** was identified as 4-phenylcyclohexane-1-carboxylic acid by a mixed-melting-point determination and by a comparison of its IR and NMR spectra with those of an authentic sample. IR: (KBr) 2400—2700 (-OH), 1685 (carboxyl) and

TABLE 2. EPIMERIZATION OF 1,4-DISUBSTITUTED CYCLOHEXANE

Sample	Product	Mp(°C)	Yield	
			mg[f]	%
9A	9A	94— 98	450	90
Mother liquid[a]	9A	92— 96	400	80
10A	10A	51— 55	450	90
Mother liquid[b]	10A[e]	54— 55	400	80
11A	12A	197—200	400	90
Mother liquid[c]	12A	198—201	400	90
d)	12A	195—199	350	80

In all cases, the product obtained was identified by mixed melting point and by comparison of IR spectra with that of authentic sample.

a) From the reaction of **5** with benzene.
b) From the reaction of **6** with benzene.
c) From the reaction of **7** with benzene.
d) Crude product obtained from the reaction of **8** with benzene was converted into its methyl ester by esterification of diazomethane.
e) The product obtained crystallized upon standing in an ice-box. Recrystallization from petroleum ether (bp 30—70°C) gave colorless prisms.
f) Yield from 500 mg of the sample.

1600 cm^{-1} (aromatic) (Found: C, 76.33; H, 7.82%).

General Epimerization Procedure. To a sodium ethoxide solution prepared from absolute ethanol (50 m*l*) and sodium (100 mg), we added the sample (500 mg). The solution was refluxed for five hours and then cooled. After the addition of water (100 m*l*) to the reaction mixture, the resulting mixture was acidified and filtered. The results are shown in Table 2.

The authors are very grateful to Professor K. Sisido, Dr. K. Uchimoto, and Mr. T. Imagawa of Kyoto University for their many helpful discussions and suggestions during this work. The authors are also grateful to Dr. H. Takahashi, Government Industrial Research Institute, Osaka, for supplying the butadiene, to the Nozaki Laboratory of Kyoto University for the measurement of the NMR spectra, and to Mrs. K. Fujimoto of the Sisido Laboratory for elemental analyses.

BULLETIN OF THE CHEMICAL SOCIETY OF JAPAN, VOL. 44, 3391—3395 (1971)

Studies on Separation of Amino Acids and Related Compounds. V. A Racemization Test in Peptide Synthesis by the Use of an Amino Acid Analyzer[1,2]

Nobuo IZUMIYA, Masako MURAOKA, and Haruhiko AOYAGI

Laboratory of Biochemistry, Faculty of Science, Kyushu University, Hakozaki, Fukuoka

(Received March 16, 1971)

Several tripeptides, H-Gly-DL-Ala-B-OH, in which B residues are DL-alanine, L-valine, L-leucine, L-phenylalanine, L-proline, and L-serine have been synthesized and the separation of each glycyltripeptide diastereomers by an amino acid analyzer have been studied. Among six peptides studied, diastereomeric mixtures of H-Gly-DL-Ala-L-Val-OH and H-Gly-DL-Ala-L-Leu-OH were separated completely. A procedure to determine the amounts of LL and DL diastereomer of H-Gly-Ala-Leu-OH by the use of the analyzer was developed, and this procedure was applied to examine the influence of coupling reagents for racemization during coupling of benzyloxycarbonyl-glycyl-L-alanine and L-leucine benzyl ester by several reagents.

To determine the extent of racemization during peptide bond formation several methods have been reported in the literatures.[3] We have attempted to find a convenient racemization test with the application of an automatic amino acid analyzer though Bodanszky and Conklin already reported the use of the analyzer for such purpose.[4] They applied the analyzer for amino acid analysis of acid hydrolysate of a coupling product derived from Ac-L-Ile-OH[5] and H-Gly-OEt, and determined the amounts of L-isoleucine and D-alloisoleucine. Manning and Moore reported the use of the analyzer in the system involving the coupling of *N*-carboxyanhydride of L-leucine and a DL-amino acid.[6]

In this paper we report an accurate procedure to determine the degree of racemization by an amino acid analyzer and the results of the influence of several coupling reagents on the extent of racemization during peptide synthesis.

The proposed scheme for racenization test is shown in Fig. 1. The crude Z-tripeptide-OBz 1 is subjected to hydrogenolysis, the hydrogenated material is submitted to the analyzer, and the amounts of the LL and DL diastereomers are determined.

$$\text{Z-Gly-L-A-OH} + \text{H-L-B-OBzl} \xrightarrow[\text{of A residue)}]{\text{(with partial racemization}} \text{Z-Gly-A-B-OBzl (LL plus DL)} \xrightarrow{H_2\text{-Pd}} \text{H-Gly-A-B-OH (LL plus DL)}$$

Fig. 1. Proposed sequence of synthesis of a diastereomeric mixture.

It was tried previously to discover a convenient system of glycyltripeptide diastereomers for separation by the analyzer.[1] We synthesized the LL and DL isomer of H-Gly-Lys-Glu-OH and similar several tripeptides, with the surmise that a diastereomeric mixture of a polyfunctional neutral tripeptide might be efficiently separated under appropriate conditions. It was observed, however, that all mixtures gave incomplete separation.[1] In the present investigation, we selected rather simple systems involving H-Gly-Ala-B-OH tripeptides in which B could be Ala, Val, Leu, Phe, Pro, and Ser residues.

1) Part IV of this series: M. Muraoka, N. Yoshida, K. Noda, and N. Izumiya, This Bulletin, **41**, 2134 (1968).

2) A part of this work has been briefly communicated: N. Izumiya and M. Muraoka, *J. Amer. Chem. Soc.*, **91**, 2391(1969).

3) For reviews, see: M. Bodanszky and M. A. Ondetti, "Peptide Synthesis," Interscience Publishers, New York (1966), p. 137; T. Kato, H. Aoyagi, M. Waki, N. Mitsuyasu, and N. Izumiya, *Tampakushitsu-Kakusan-Koso*, **16**, 139 (1971).

4) M. Bodanszky and L. E. Conklin, *Chem. Commun.*, **1967**, 773.

5) Abbreviations used: Ac, acetyl; Z, benzyloxycarbonyl; OBzl, benzyl ester; TsOH, *p*-toluenesulfonic acid; HOSu, *N*-hydroxysuccinimide; DCC, dicyclohexylcarbodiimide; NEPIS, *N*-ethyl-5-phenylisoxazolium-3'-sulfonate; EEDQ, *N*-ethoxycarbonyl-2-ethoxy-1,2-dihydroquinoline; TEA, triethylamine; NMM, *N*-methylmorpholine; THF, tetrahydrofuran; DMF, dimethylformamide; MA, mixed anhydride.

6) J. M. Manning and S. Moore, *J. Biol. Chem.*, **21**, 5591 (1968).

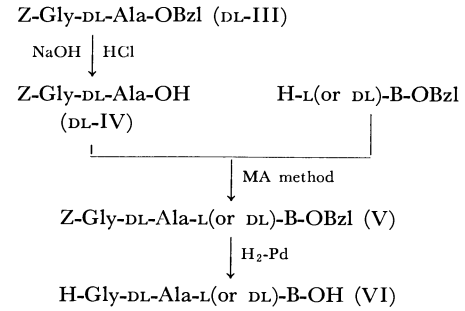

Fig. 2. Synthesis of a crude tripeptide consisting of diastereomers. B; DL-Ala, L-Val, L-Leu, L-Phe, L-Pro or L-Ser residue.

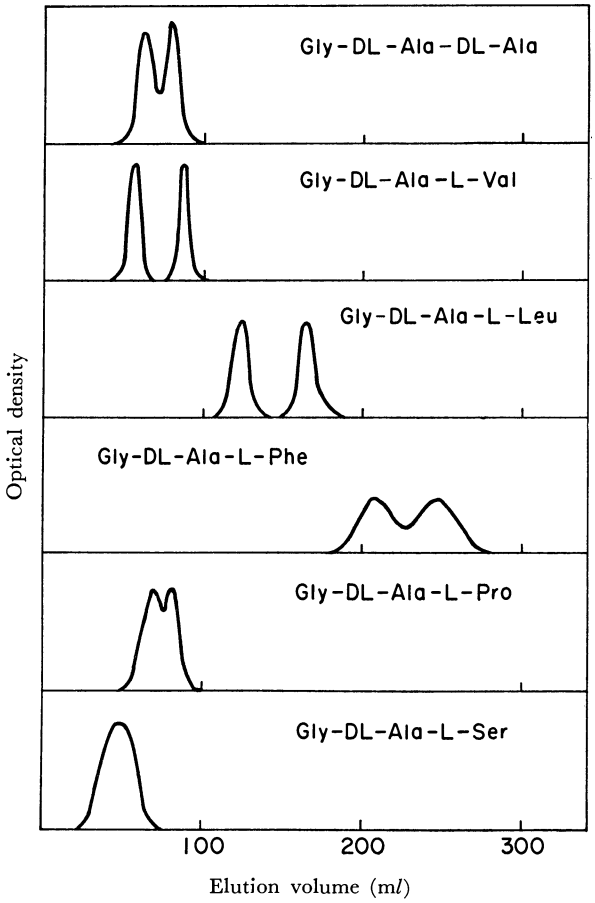

Fig. 3. Elution pattern of H-Gly-DL-Ala-B-OH (VI).

In the previous paper, each pure diastereomer of a tripeptide such as H-Gly-Lys-Glu-OH was prepared, and an artificial mixture of the diastereomers was subjected to separation experiment.[1] In this investigation, a crude tripeptide (VI) consisting of diastereomers was synthesized as shown in Fig. 2 instead of preparation of a pair of pure diastereomers. As shown in Fig. 3, the diastereomeric mixture containing Val or Leu residue as B component was found to be separated completely by the analyzer, and the other mixture containing Ala, Phe, Pro, or Ser separated incompletely.

A diastereomeric mixture of H-Gly-Ala-Leu-OH (IX) was the preferred system for the racemization test (see, Fig. 4) because two peaks of IX were not overlapped with either leucine or H-Gly-Ala-OH

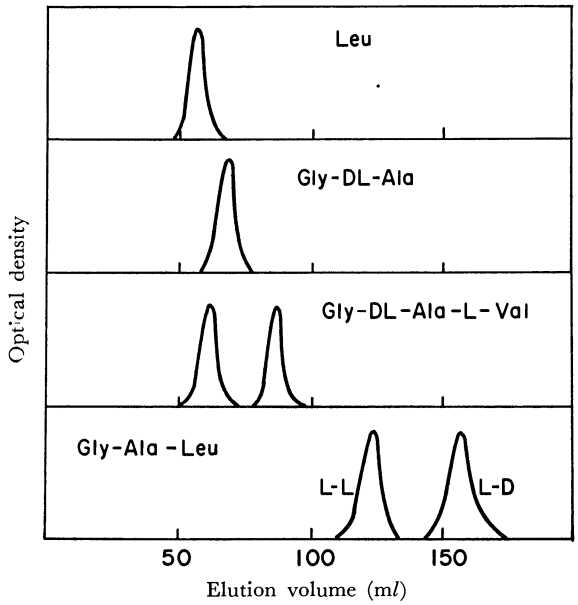

Fig. 4. Elution pattern of amino acid and peptides.

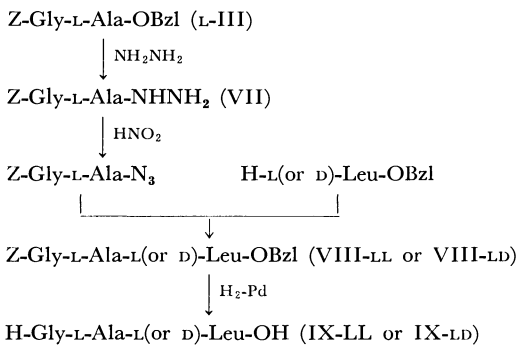

Fig. 5. Synthesis of a pure tripeptide.

which might be contaminated in a final crude tripeptide (see, Fig. 1).[7] A pair of pure diastereomers of IX was prepared as shown in Fig. 5 to be used for identification of two peaks in Fig. 3; the LL isomer was eluted faster than the corresponding LD isomer (Fig. 4).

The limit of detection of the LD contaminated in the LL isomer was studied with an artificial mixture of both isomers. Even when a mixture of the LL isomer (5 μmol) and DL (0.005 μmol) was analyzed, a small peak of the DL could still be recognized. It will be evident that the present method is more sensitive in detecting the slight occurrence of racemization than the Anderson test which has been used widely nowadays.[3]

The present method was applied in the detection of a possible racemization in azide procedure. A crude Z-Gly-Ala-Leu-OBzl obtained from pure Z-Gly-L-Ala-N_3 and H-L-Leu-OBzl was directly hydrogenated, and a part of the filtrate from a hydrogenated mixture was submitted to the analyzer. The material in the filtrate showed only single peak by the LL isomer,

7) Several related amino acids and peptides were subjected to the analyzer; glycine was eluted at 32 ml of effluent volume, alanine at 36 ml, LD isomer of H–Ala–Leu–OH at 126 ml, and its LL isomer at 138 ml.

Table 1. Extent of racemization during peptide bond formation[a)]

No.	Coupling reagent	Additional component	Solvent	Tertiary amine	Reaction time, hr	Reaction temp., °C	Yield of tripeptide (IX-LL plus IX-DL), %	Extent of racemization
1[b)]	Isobutyl chloroformate		THF	TEA	15	25	87	9.5
2	Isobutyl chloroformate		THF	NMM	15	25	91	2.4
3[c)]	Isobutyl chloroformate	HOSu	THF	TEA	2	25	55	1.1
4[c)]	Isobutyl chloroformate	HOSu	THF	NMM	2	25	63	0.2
5	DCC		THF	TEA	48	0	73	22
6	DCC		THF	NMM	48	0	77	21
7[d)]	DCC	HOSu	THF	TEA	48	0	98	0.0
8[c)]	NEPIS		CH_3CN	TEA	24	25	95	1.8
9	NEPIS		CH_3CN	NMM	24	25	72	1.7
10[c)]	EEDQ		THF	TEA	7	25	97	0.2
11	EEDQ		THF	NMM	7	25	91	0.2

a) All components (Z-Gly-L-Ala-OH, H-L-Leu-OBzl, coupling reagent, HOSu and tertiary amine) in the coupling were of equivalent weight.
b) The procedure following that in the literature[10] was noted in detail in the experimental part.
c) The procedure was similar to that described in the literatures: MA,[11] NEPIS,[15] and EEDQ.[16]
d) The procedure reported[12] was slightly modified; the components were of equivalent weight and the temperature was 0°C during the entire reaction.

using a load of up to 6 μmol. The result agreed with the fact that the azide procedure has been considered to be safe to avoid racemization.[3,8]

This procedure was employed to examine the influence of various coupling reagents to racemization, the experiments being summarized in Table 1. In a typical mixed anhydride (MA) method, the coupling yield of Z-Gly-L-Ala-OH and H-L-Leu-OBzl was approximately 87%[9] and the extent of racemization,[4] which is defined as {100[DL isomer]}/{[LL isomer]+[DL isomer]}, was calculated as 9.5. Anderson and his colleagues reported that the extent of racemization was 9 using fractional crystallization in case of the coupling of Z–Gly–L–Phe–OH and H–Gly–OEt.[10] The use of NMM instead of TEA decreased the recemization as 2.4 in this experiment, but Anderson *et al.* reported no isolation of a DL-tripeptide in their experiment.[10] The difference of these results may be due to the differences of the detection method for racemization and of the compounds investigated. The addition of HOSu to the MA system with TEA or NMM decreased the degree of racemization considerably; the results confirm the observation of Anderson and Callahan on the role of HOSu in the MA method.[11]

In the DCC method, the extents of racemization were calculated as 22 and 21 respectively when TEA and NMM were used (Table 1). It was reported previously that the extent of racemization was 9.4 in case of the coupling of Z–L–Leu–L–Phe–OH and H–L–Val–OBu^t,[12] and 9.1—10.6 in case of Z–Gly–L–Phe–OH and H–Gly–OEt.[13] No explanation for the higher degree of racemization observed in our experiment can be offered at the present time. On the contrary the coupling using HOSu and DCC gave no racemate; Weygand *et al.*[12] also reported the occurrence of less than 1% racemization under the similar conditions.

The extent of racemization were calculated as 1.7—1.8 and 0.2 in the applications of NEPIS[14,15] and EEDQ[16] respectively. These results showed similar levels of racemizations observed previously; 3.2 with NEPIS[17] and no detection of a recemate with EEDQ[16] were reported.

A simple and straightforward procedure described in this paper will be a useful test to detect possible

8) The occurrence of racemization have been reported recently even in the case of the azide procedure when unusual reaction condition was applied: G. W. Anderson, J. E. Zimmerman, and F. M. Callahan, *J. Amer. Chem. Soc.*, **88**, 1338 (1966); H. Determann, "Peptides," ed. by H. C. Beyerman, A. Van de Linde, and W. Maassen van den Brink, North-Holland Pub. Co., Amsterdam (1967), p. 73.

9) Yield of 87% was derived from an analysis of H–Gly–Ala–Leu–OH (LL plus DL isomer) by an amino acid analyzer. We assume that the yield of free tripeptide corresponds to approximately that of Z–Gly–Ala–Leu–OBzl (VIII) because the hydrogenation of VIII will proceed quantitatively.

10) G. W. Anderson, J. E. Zimmerman, and F. M. Callahan, *J. Amer. Chem. Soc.*, **89**, 5012 (1967).

11) G. W. Anderson, F. M. Callahan, and J. E. Zimmerman, *ibid.*, **89**, 178 (1967).

12) F. Weygand, D. Hoffmann, and E. Wünsch, *Z. Naturforsch.*, **21b**, 426(1966).

13) G. W. Anderson and F. W. Callahan, *J. Amer. Chem. Soc.*, **80**, 2902(1958).

14) R. B. Woodward, R. A. Olofson, and H. Mayer, *Tetrahedron Suppl.*, **8**, 321(1966).

15) J. Ramachandran and C. H. Li, *J. Org. Chem.*, **27**, 4006 (1962).

16) B. Belleau and G. Malek, *J. Amer. Chem. Soc.*, **90**, 1651 (1968).

17) F. Weygand, A. Prox, and W. König, *Chem. Ber.*, **99**, 1451 (1966).

racemization when a new coupling method is developed in future.

Experimental

R_f of thin-layer chromatography with Merck silica gel G refers to *n*-butanol-acetic acid-pyridine-water (4 : 1 : 1 : 2, vol) system. Benzyl ester toluenesulfonates of L-valine,[18] L-[18] and D-leucine,[19] L-phenylalanine,[18] and L-serine,[20] and H-Gly-DL-Ala-OH[21] were prepared following the literatures.

H-DL-Ala-OBzl·TsOH (I). This was prepared according to the procedure for the L isomer.[18] Yield, 82%, mp 109°C; R_f 0.74 (Found: C, 57.97; H, 6.13; N, 4.13%).

H-L-Pro-OBzl·TsOH (II). A mixture of L-proline, benzyl alcohol, toluenesulfonic acid, and benzene was treated following the general procedure.[18] Yield of II as an oil, 98%; R_f 0.69.

Z-Gly-DL-Ala-OBzl (DL-III). To a chilled solution (−10°C) of Z-Gly-OH (2.1 g) and TEA (1.4 m*l*) in THF (20 m*l*), isobutyl chloroformate (1.31 m*l*) was added. After 10 min, a mixture of I (3.52 g), TEA (1.4 m*l*) and chloroform (20 m*l*) was added to the solution. The reaction mixture was allowed to stand overnight and then evaporated to dryness. After the residual oil was dissolved in ethyl acetate, the solution was washed with 2% hydrochloric acid and 4% sodium bicarbonate, and dried over sodium sulfate. The filtrate was evaporated and the residue was crystallized by addition of petroleum ether. It was recrystallized from ethyl acetate-petroleum ether; yield, 2.54 g (69%); mp 91°C (Found: C, 64.94; H, 5.96; N, 7.52%). Wieland and Heinke prepared this compound by MA method with phosphorus oxychloride; mp 91—92°C.[22]

Z-Gly-L-Ala-OBzl (L-III). This was obtained from Z-Gly-OH and H-L-Ala-OBzl·TsOH as described above. Yield, 62%; mp 77°C; $[\alpha]_D^{25}$ −14.0° (*c* 1, ethyl acetate) (Found: C, 65.07; H, 6.01; N, 7.56%). Gante prepared this compound by a coupling of Z-Gly-OH and N-2,4-dinitrophenyloxycarbonyl-L-Ala-OBzl; mp 77—78°C.[23]

Z-Gly-DL-Ala-OH (DL-IV). To a solution of DL-III (3.7 g, 10 mmol) in methanol (30 m*l*), N sodium hydroxide (12 m*l*) was added. After 2 hr, N hydrochloric acid (12 m*l*) was added and the solution was evaporated. The resulting crystals were collected by aid of cold water. It was recrystallized from ethanol-ether; yield, 1.99 g (71%); mp 182°C (Found: C, 55.56; H, 5.84; N, 9.76%). Clayton *et al.* prepared this compound by a coupling of DL-alanine and a mixed anhydride derived from Z-Gly-OH; mp 183°C.[24]

Z-Gly-L-Ala-OH (L-IV). This was obtained from L-III as described above. Yield, 82%; mp 133°C; $[\alpha]_D^{20}$ −9.8° (*c* 4.4, ethanol) (Found: C, 55.58; H, 5.73; N, 9.81%). This was prepared previously by a coupling of L-alanine and Z-Gly-OH mixed anhydride,[24] and by saponification of Z-Gly-L-Ala-OEt[25]; mp 133°C,[24] 119.5°C;[25] $[\alpha]_D$ −9.5°,[24] −10.2° (ethanol).[25]

Z-Gly-DL-Ala-B-OBzl (B=DL-Ala, L-Val, L-Leu, L-Phe, L-Pro or L-Ser) (V). This compound was prepared from DL-IV (0.28 g, 1 mmol) and a benzyl ester (1 mmol) of an amino acid B as described for the preparation of DL-III. Ethyl acetate solution was dried, and evaporated to yield an oily product (0.3—0.4 g). It contained a compound V indicating R_f 0.94—0.96, and was used for the next step without purification.

H-Gly-DL-Ala-B-OH (VI). A solution of each V (0.3—0.4 g) in 90% acetic acid (5 m*l*) was treated with hydrogen in the presence of palladium black. After several hr, the material with R_f 0.94—0.96 disappeared and a material with R_f 0.21—0.46 appeared; a material in the solution showed R_f 0.21 (H-Gly-DL-Ala-B-OH in which B is L-Ser), 0.31 (DL-Ala), 0.34 (L-Pro), 0.43 (L-Val), 0.44 (L-Phe), and 0.46 (L-Leu). The filtrate from the catalyst was evaporated to dryness. The residual hygroscopic solid was used as such in an experiment with an amino acid analyzer as described later.

Z-Gly-L-Ala-NHNH$_2$ (VII). A solution of L-III (3.7 g) and hydrazine hydrate (2.4 m*l*) in methanol (10 m*l*) was allowed to stand at room temperature for 2 days. It was evaporated and the residual solid was recrystallized from acetone-ether; yield, 2.7 g (92%); mp 134°C; $[\alpha]_D^{25}$ −30.0° (*c* 1, methanol). This was prepared previously from Z-Gly-L-Ala-OEt; mp 133°C,[26] mp 158—160°C.[27]

Z-Gly-L-Ala-L-Leu-OBzl (VIII-LL). To a chilled solution of VII (2.36 g) in acetic acid (50 m*l*) and 2 N hydrochloric acid (10 m*l*), an aqueous solution (5 m*l*) containing sodium nitrite (0.64 g) was added. After 5 min at −5°C, the azide was extracted with ethyl acetate (50 m*l*×3). An organic layer was washed with 10% sodium bicarbonate and dried over sodium sulfate. The filtrate was added to a mixture of H-L-Leu-OBzl·TsOH (3.2 g) and TEA (1.12 m*l*) in DMF (40 m*l*). After 3 days at 0°C, the reaction mixture was evaporated and the residue was dissolved in ethyl acetate. Ethyl acetate solution was washed with 2% hydrochloric acid and 4% sodium bicarbonate, dried, and evaporated. The residual solid was recrystallized from ether-petroleum ether; yield, 2.72 g (70%); mp 102°C; $[\alpha]_D^{25}$ −31.6° (*c*, 1, ethyl acetate).

Found: C, 64.29; H, 7.00; N, 8.47%. Calcd for $C_{26}H_{33}O_6N_3$: C, 64.58; H, 6.88; N, 8.69%.

Z-Gly-L-Ala-D-Leu-OBzl (VIII-LD). Reaction of VII (2.36 g) and H-D-Leu-OBzl·TsOH (3.2 g) as described above yielded 2.48 g (64%) of VIII-LD; mp 125°C; $[\alpha]_D^{25}$ −1.0° (*c* 1, ethyl acetate).

Found: 64.80; H, 6.93; N, 8.49%. Calcd for $C_{26}H_{33}O_6N_3$: C, 64.58; H, 6.88; N, 8.69%.

H-Gly-L-Ala-L-Leu-OH (IX-LL). VIII-LL (1.93 g) was hydrogenated as described for the preparation of VI. The filtrate was evaporated and the resulting crystals were collected by aid of ethanol. It was recrystallized from water-methanol; yield of an air-dried material, 0.93 g (88%); mp 242—245°C (decomp); R_f 0.59; $[\alpha]_D^{25}$ −84.0° (*c* 1, water) (for $C_{11}H_{21}O_4N_3 \cdot 1/4\,H_2O$. Found: C, 50.31; H, 8.22; N, 15.80%; H_2O, 1.65%). The same compound without water of crystallization was prepared previously from Z-Gly-L-Ala-L-Leu-OMe; $[\alpha]_D^{23}$ −87° (water).[27]

18) N. Izumiya and S. Makisumi, *Nippon Kagaku Zasshi*, **78**, 662, 1768(1957).
19) K. Noda, H. Okai, T. Kato, and N. Izumiya, This Bulletin, **41**, 401(1968).
20) H. Voss, *Z. Naturforsch.*, **20b**, 116(1965).
21) R. Shoenheimer, *Z. Physiol. Chem.*, **154**, 203(1926).
22) T. Wieland and B. Heinke, *Ann. Chem.*, **599**, 70(1956).
23) J. Gante, *Chem. Ber.*, **99**, 1576(1966).
24) D. W. Clayton, J. A. Farrington, G. W. Kenner, and J. M. Turner, *J. Chem. Soc.*, **1957**, 1398.
25) B. F. Erlanger and E. Brand, *J. Amer. Chem. Soc.*, **73**, 3508 (1951).
26) M. Bergmann and L. Zervas, *J. Biol. Chem.*, **113**, 341 (1936).
27) R. W. Holley and A. D. Holley, *J. Amer. Chem. Soc.*, **74**, 3069(1952).

H-Gly-L-Ala-D-Leu-OH (*IX*-LD). This was prepared from VIII-LD; yield of an air-dried material, 86%; mp 243—245°C (decomp); R_f 0.57; $[\alpha]_D^{25}$ −29.6° (*c* 0.4, water).

Found: C, 49.20; H, 8.29; N, 15.75%. Calcd for $C_{11}H_{21}O_4N_3 \cdot 1/2H_2O$: C, 49.24; H, 8.27; N, 15.66%. The air-dried sample lost 3.03% of its weight after being dried for 3 hr at 80°C *in vacuo*. Calcd for $1/2H_2O$: 3.35%.

Chromatography of Amino Acids and Peptides by Amino Acid Analyzer. A diastereomeric mixture (VI; approximately 1 μmol) of tripeptide was analyzed by a Hitachi amino acid analyzer, model KLA-3B, under the following conditions: length of column with spherical resin, 0.9×50 cm; solvent, a standard 0.2 M citrate buffer at pH 4.25; flow rate, 60 m*l*/hr; jacket temperature, 55°C. The patterns obtained are shown in Fig. 3. Similarly, amino acids (0.5 μmol), dipeptides (0.5 μmol), and an artificial mixture (1 μmol) of the LL and LD isomer of H-Gly-Ala-Leu-OH (IX) were analyzed; some of the patterns are shown in Fig. 4. It was observed that leucine was eluted at 58 m*l* of effluent volume, H-Gly-DL-Ala-OH at 73 m*l*, IX-LL at 129 m*l*, and IX-LD at 159 m*l*.

Detection of Racemization. *(a) Possible Racemization in Azide Method*: The azide derived from Z-Gly-L-Ala-$NHNH_2$ (VII) was condensed with H-L-Leu-OBzl as described in the preparation of VIII-LL. Ethyl acetate solution was evaporated, the crude Z-Gly-Ala-Leu-OBzl was hydrogenated, the filtrate from the catalyst was evaporated, and a part (6 μmol) of the residue was submitted to the analyzer. The product showed only single peak of IX-LL.

(b) Racemization in MA Method: Similar conditions (temperatures and reaction times) for coupling of Z-Gly-L-Phe-OH and H-Gly-OEt by MA method[9] were applied for the present experiment. To Z-Gly-L-Ala-OH (L-III) (1 mmol) in THF (5 m*l*) was added isobutyl chloroformate. After 12 min at −15°C, a mixture of H-L-Leu-OBzl·TsOH and TEA in THF (5 m*l*) was added, and the reaction mixture was left at 25°C for 15 hr. The mixture was treated as described in the preparation of DL-III, and the ethyl acetate solution was evaporated; yield of a crude solid (VIII), 474 mg. A part (47.4 mg) of VIII was hydrogenated in 90% acetic acid, and the filtrate was evaporated. The residue was dissolved in 0.2 M citrate buffer at pH 4.25 (10 m*l*), and a part (0.7 m*l*) of it was submitted to the analyzer; the yield of H-Gly-Ala-Leu-OH (LL plus DL) from L-III was calculated as 87%, and the extent of racemization was calculated as 9.5. Similar experiment with NMM instead of TEA was carried out, and the yield of the tripeptide and the extent of racemization were calculated (see, Table 1).

(c) Racemization in other Methods: Z-Gly-L-Ala-OH was condensed with H-L-Leu-OBzl by a method using the reagent of DCC, NEPIS or EEDQ. An isolation of crude Z-Gly-Ala-Leu-OBzl (VIII), the hydrogenation of VIII, and an analysis of the hydrogenated material were identical with the procedures described above. The results are summarized in Table 1.

We wish to express our thanks to Dr. K. Noda of this laboratory for his help with an amino acid analyzer and to Professor B. Belleau for the generous gift of EEDQ.

BULLETIN OF THE CHEMICAL SOCIETY OF JAPAN, VOL. 44, 3395—3399 (1971)

Syntheses of (3S, 4R, 15S)-4,15-Dimethyl-1,5-dioxa-3-(3′-formamidosalicylamido)-cyclopentadecane-2,6-dione and Its (15R)-Epimer, New Antimycin Analogs[1]

Mitsuhiro KINOSHITA, Keitaro ISHII, and Sumio UMEZAWA

Department of Applied Chemistry, Faculty of Engineering, Keio University, Koganei-shi, Tokyo

(Received April 16, 1971)

A new type of antimycin analogs, (3S, 4R, 15S)-4,15-dimethyl-1,5-dioxa-3-(3′-formamidosalicylamido)-cyclopentadecane-2,6-dione (**10a**) and its (15R)-epimer (**10b**) have been synthesized. The epimeric fifteen-membered amino-dilactone moieties in **10a** and **10b** were synthesized from a masked L-threonine and *t*-butyl DL-10-hydroxyundecanoate. Each of the separated epimeric amino-dilactones was *N*-acylated with *O*-benzyl-3-nitrosalicylic acid *N*-hydroxysuccinimide ester. Hydrogenation followed by *N*-formylation afforded the antifungal substances, **10a** and **10b**. The 10-*C*-configurations of **10a** and **10b** were determined as "S" and "R", respectively. The (15S)-epimer (**10a**) showed apparently stronger antifungal activity against *Piricularia oryzae* than that of the (15R)-epimer (**10b**).

Recently the total syntheses of dehexyl-deisovaleryl-oxy-antimycin A_1 as a prototype of antimycin A and of antimycin A_3 in a form of the diastereoisomeric mixture have been reported from our laboratory.[2,3]

The most striking characteristic of the structure of antimycin A is its nine-membered dilactone ring linked *via* an amide linkage to 3-formamidosalicylic acid.[4] We now wish to report the syntheses of a new type of antimycin analogs (**10a**) and its epimer (**10b**) which have a fifteen-membered dilactone ring instead of nine-membered ring in antimycin A.

t-Butyl 10-oxoundecanoate (**2**) was prepared from 10-oxoundecanoic acid (**1**)[5] and isobutene by the

1) Part XLI of "Studies on Antibiotics and Related Substances" by Sumio Umezawa.

2) M. Kinoshita and S. Umezawa, This Bulletin, **42**, 854 (1969); *ibid.*, **43**, 897 (1970).

3) M. Kinoshita, M. Wada, and S. Umezawa, *J. Antibiot.* (Tokyo), **22** (11), 580 (1969).

4) F. M. Strong, J. P. Dickie, M. E. Loomans, E. E. van Tamelen, and R. S. Dewey, *J. Amer. Chem. Soc.*, **82**, 1514 (1960). E. E. van Tamelen, J. P. Dickie, M. E. Loomans, R. S. Dewey, and F. M. Strong, *ibid.*, **83**, 1639 (1961).

5) J. Cason, *ibid.*, **68**, 2078 (1946).

same method as previously reported[2] in an 83% yield. Sodium borohydride reduction of **2** in tetrahydrofuran afforded *t*-butyl DL-10-hydroxyundecanoate (**3**) in a 95.8% yield. Catalytic hydrogenation of **2** with Raney Ni W-5 in ethanol also gave 3, however, the yield in this process was low (57.1%).

$CH_3—CO—(CH_2)_8—CO_2R$

1: R=H

2: R=*t*-Bu

↓

$CH_3-CH(OH)-(CH_2)_8-CO_2-Bu^t$

3

↓

$CH_3-CH(OR)-CH(NHCOOCH_2Ph)-CO-O-CH(CH_3)-(CH_2)_8-CO_2R$

4: R=*t*-Bu

5: R=H

The racemic *t*-butyl 10-hydroxyundecanoate (**3**) was allowed to react with excess amount of *N*-benzyloxycarbonyl-*O*-*t*-butyl-L-threonine[6] in the presence of *N*,*N*′-dicyclohexylcarbodiimide (DCCI) and pyridine in ether. The condensation product was purified by silica gel column chromatography with a petroleum ether - diisopropyl ether (2 : 1) system to afford *t*-butyl 10-(*N*-benzyloxycarbonyl-*O*-*t*-butyl-L-threonyloxy)undecanoate (**4**) as a diastereomeric mixture in a 63.5% yield.

De-*t*-butylation of **4** with trifluoroacetic acid gave a free linear ester acid (**5**) which was cyclized in 0.04 M benzene solution by adding 2 moles of trifluoroacetic anhydride at 70°C for 23 hr. The reaction mixture was concentrated and chromatographed on silica gel with a benzene-butanone (30 : 1) system to give from the first and second peaks crystalline cyclization products, **6a** and **6b** in 18.2 and 17.5%, respectively. The products, **6a** and **6b** were found to be the diastereomeric intramolecular cyclization products, namely, the single 15-*C*-epimers of (3S, 4R)-3-(benzyloxycarboxamido)-4,15-dimethyl-1,5-dioxacyclopentadecane-2,6-dione on the basis of elemental analyses, NMR, IR spectra, and molecular weight determinations by mass spectra.

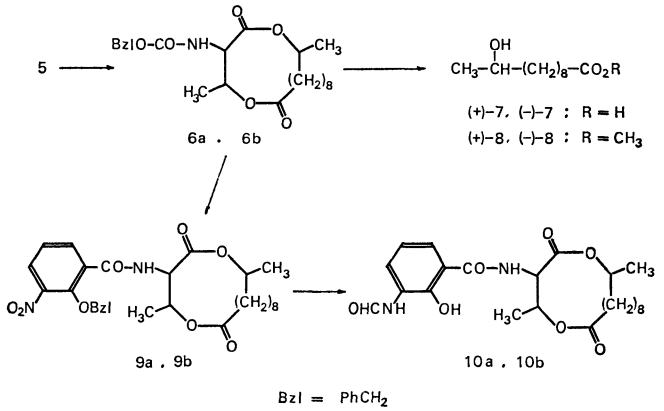

6) E. Schröder, *Ann. Chem.*, **670**, 127 (1963).

The absolute configurations of 15-C-atoms in the epimeric dilactone compounds, **6a** and **6b** were determined as "S" and "R", respectively, by application of Horeau's method[7] to the optical active methyl 10-hydroxyundecanoate, (+)-**8** and (−)-**8**, which were obtained by diazomethane treatment of the crystalline enantiomers, 10-hydroxyundecanoic acids, (+)-**7** and (−)-**7**, derived from **6a** and **6b**, respectively, by the hydrolysis with methanolic sodium hydroxide solution.

The benzyloxycarbonyl groups of **6a** and **6b** were removed by catalytic hydrogenolysis over palladium black in methanol to give the corresponding free amino-dilactones, which were directly *N*-acylated with an active ester, *O*-benzyl-3-nitrosalicylic acid *N*-hydroxysuccinimide ester[2] in tetrahydrofuran.

The crude *N*-acylation products were purified through silica gel columns with a *n*-hexane-ethyl acetate (2 : 1) system to afford the corresponding (3S,4R,15S)-4,15-dimethyl-1,5-dioxa-3-(*O*-benzyl-3′-nitrosalicylamido)-cyclopentadecane-2,6-dione (**9a**) and its (15R) epimer (**9b**) as glassy solids in 89.2 and 86.1% yield, respectively. The structures of **9a** and **9b** were confirmed by their NMR spectra (Table 1).

The compounds, **9a** and **9b** were then hydrogenolyzed over palladium black in methanol to yield the corresponding *N*-(3′-aminosalicyloyl)amidodilactones, which were immediately *N*-formylated with 98% formic acid and DCCI. The crude products were purified by preparative thin-layer chromatography with a *n*-hexane-ethyl acetate (2 : 1) system to afford the title compounds, (3S, 4R, 15S)-4,15-dimethyl-1,5-dioxa-3-(3′-formamidosalicylamido)-cyclopentadecane-2,6-dione (**10a**)(as a crystal) and its (15R)-epimer (**10b**)(as a glassy solid), in 44.7 and 50.7% yield, respectively.

The UV-absorptions of **10a** and **10b** were very similar to those of natural antimycin A and dehexyldeisovaleryloxy-antimycin A_1. The IR-spectra were also similar to those of the natural product and the analog in respect to the characteristic absorptions assignable to ester carbonyl, formamido and aromatic amido groups.

The structures of **10a** and **10b** were further confirmed by the inspection of their NMR spectra (Table 1).

The coupling constants ($J_{3,4}$=2.0) observed in the NMR spectra of the dilactone compounds, **6a**, **6b**, **9a**, **9b**, **10a**, and **10b** (Table 1) are consistent with the partial conformation in which the vicinal threonine-protons, 3–H and 4–H of the fifteen-membered dilactone ring are *gauche*-related. It has recently been reported that in neoantimycin,[8] the vicinal threonine-protons of the fifteen-membered tetralactone ring have a small coupling constant (J=2.5 Hz), similar to that of the dilactone compounds as described above.

Bioassay. The synthetic new antimycin analogs, **10a** and **10b** showed strong inhibition against certain fungi. Minimal inhibitory concentrations

7) A. Horeau, *Tetrahedron Lett.*, **1961**, 506; *ibid.*, **1962**, 965.

8) L. Caglioti, D. Misiti, R. Mondelli, A. Selva, F. Arcamone, and G. Cassinelli, *Tetrahedron*, **25**, 2193 (1969).

Table 1. 60MHz-NMR-spectra of the amino-dilactones
[Splittings,[a] δ(ppm),[b] J(Hz)[c]]

Compounds Protons	6a	6b	9a	9b	10a	10b
15-CH_3	d. 1.22 (6.2)	d. 1.18 (6.2)	d. 1.27 (?)	d. 1.18 (6.2)	d. 1.27 (6.2)	d. 1.24 (6.2)
4-CH_3	d. 1.33 (6.5)	d. 1.31 (6.5)	d. 1.27 (6.5)	d. 1.24 (6.5)	d. 1.36 (6.5)	d. 1.34 (6.5)
3-H	dd. 4.48 (10.0/2.0)	dd. 4.41 (10.0/2.0)	dd. 5.01 (9.5/2.0)	dd. 5.01 (9.5/2.0)	dd. 5.00 (9.5/2.0)	dd. 5.00 (9.5/2.0)
15-H	m. 4.9—5.4	m. 4.8—5.3	m. 5.0—5.4	m. 5.0—5.4	tq. 5.23 (6.2)	m. 4.95—5.35
Ph-CH_2	s. 5.18	s. 5.20	dd. 5.23	dd. 5.28		
4-H	dq. 5.42 (6.5/2.0)	dq. 5.64 (6.5/2.0)	dq. 5.57 (6.5/2.0)	dq. 5.66 (6.5/2.0)	dq. 5.53 (6.5/2.0)	dq. 5.78 (6.5/2.0)
5'-H(Ar)			t. 7.40 (8.0/8.0)	t. 7.40 (8.0/8.0)	t. 6.95 (8.0/8.0)	t. 7.00 (8.0/8.0)
NH(Thr)	d. 5.60 (10.0)	d. 5.30 (10.0)	d. 8.23 (9.5)	d. 7.93 (9.5)	d. 7.13 (9.5)	d. 7.02 (9.5)
4'-H(Ar)			dd. 7.98 (8.0/2.0)	dd. 7.98 (8.0/2.0)	dd. 7.38 (8.0/1.9)	dd. 7.31 (8.0/1.9)
ArNHCHO					s. 7.99	s. 8.13
ArNHCHO					s. 8.56	s. 8.58
6'-H(Ar)			dd. 8.33 (8.0/2.0)	dd. 8.38 (8.0/2.0)	dd. 8.62 (8.0/1.9)	dd. 8.64 (8.0/1.9)
OH(Ar)					s. 12.76	s. 12.76

a) d., doublet; dd., doublet-doublet; m., multiplet; s., singlet; dq., doublet-quartet; t., triplet; tq., triplet-quartet.
b) Internal standard TMS in *ca.* 10% deuteriochloroform solution.
c) In parentheses.

(mcg/ml) of **10a** and **10b** against *Piricularia orizae* were 1.2×10^{-2} and 12.5, respectively.

It is noteworthy that the configurational or conformational difference between the epimeric dilactone structures of **10a** and **10b** may apparently reflect on the striking difference between their antifungal activities.

Experimental

Melting points were determined on a micro hot stage and were uncorrected. Thin-layer chromatography (TLC) was conducted by the use of WAKOGEL B-5 (Wako Pure Chemical Industries, Ltd.). Silica gel column chromatography was carried out by using WAKOGEL C-200 which was activated at 110°C for 1 hr. IR-spectra were recorded on a Hitachi IPI-2 spectrometer, UV-spectra were taken in a Hitachi Perkin-Elmer UV-VIS spectrometer 139. NMR spectra were recorded on a Varian-A-60D spectrometer (TMS as an internal standard) in *ca.* 5—10% (W/V) solution in deuteriochloroform. Optical rotations were measured with a Zeiss Photoelectric Precision Polarimeter 0.005° employing a 0.5 decimeter tube. In general, all concentrations were carried out in a rotary evaporator at reduced pressure below 40°C.

t-*Butyl 10-Oxoundecanoate (2).* To a solution of 10-oxoundecanoic acid (**1**) (11.4 g, mp 55.8—57.0°C) in a mixture of dichloromethane (34 m*l*) and conc. sulfuric acid (0.33 m*l*) was added liquid isobutene (33.4 m*l*) under cooling at −30°C. The stoppered flask was allowed to stand at room temperature for 70 hr. The reaction mixture was processed by the same method as described in the previous paper[2] to give **2** as colorless liquid boiling at 129.5—131°C under 4 mmHg: Yield, 14.6 g (82.8%); n_D^{20} 1.4383; ν_{max}^{liq} 1727 cm^{-1} (C=O and ester).

Found: C, 70.60; H, 11.13%. Calcd for $C_{15}H_{28}O_3$: C, 70.27; H, 11.01%.

t-*Butyl 10-Hydroxyundecanoate (3).* Sodium borohydride (343 mg, 9.08 mmol) was added to a solution of *t*-butyl 10-oxoundecanoate (**2**) (582 mg, 2.27 mmol) in dry tetrahydrofuran (19.3 m*l*) and stirred for 3 hr at room temperature. The reaction mixture was neutralized with 20% H_2SO_4 (1.0 m*l*) and extracted with ether. The combined extracts were washed with $NaHCO_3$ and saturated NaCl solution. After evaporation of the solvent, the residue was distilled under reduced pressure. The fraction boiling at 114—116.5°C/0.03 mmHg was collected: yield, 568 mg (95.8%); n_D^{20} 1.4428; ν_{max}^{liq} 3440 (OH) and 1735 cm^{-1} (ester).

Found: C, 69.40; H, 11.75%. Calcd for $C_{15}H_{30}O_3$: C, 69.72; H, 11.70%.

t-*Butyl 10-*(N-*Benzyloxycarbonyl*-O-t-*butyl*-L-*threonyloxy*)*undecanoate (4).* A solution of *N*-benzyloxycarbonyl-*O*-*t*-butyl-L-threonine (6.00 g, 19.4 mmol) in dry ether (13.1 m*l*) was added dropwise during 40 min to a stirred solution of *t*-butyl 10-hydroxyundecanoate (**3**)(5.00 g, 19.4 mmol), DCCI (4.41 g, 21.4 mmol) and dry pyridine (1.65 m*l*, 19.4 mmol) in dry ether (20 m*l*) cooled to 0°C. Stirring at 0°C was continued for a further 4 hr. After standing at 0°C for 20 hr, to the reaction mixture, DCCI(2.2 g) and dry pyridine(0.83 ml) and then a solution of *N*-benzyloxycarbonyl-*O*-*t*-butyl-L-threonine (3.00 g) in dry ether (6 m*l*) was dropped under stirring at 0°C. Further additions of the threonine derivative (1.0 g×2), DCCI (1.10 g ×2) and dry pyridine (0.413 m*l*×2) in two portions were undertaken in the same procedure as in the preceding additions in 24-hr intervals. After standing at 0°C for 20 hr the precipitate of *N*,*N*'-dicyclohexylurea (5.16 g, 53.7%) was filtered off and the filtrate was treated with acetic acid (1.5 m*l*) under stirring at 0°C for 2 hr. An additional

urea was removed by filtration and the filtrate was washed with 5% $NaHCO_3$ solution, 5% citric acid and saturated NaCl solution, dried over Na_2SO_4, and concentrated to dryness. The syrupy residue (17.31 g) was chromatographed on a silica gel column (1.78 kg, 8.2×65 cm). Elution with a petroleum ether-diisopropyl ether (2 : 1) system gave a straw-colored syrup (6.77 g, 63.5%) as a first fraction which behaved as a homogeneous compound on the tlc using the same solvent system as in the column chromatography: $[\alpha]_D^{23.5}$ −2.5° (*c* 1.63, chloroform); ν_{max}^{liq} 3460, 3360 (NH), 1730 (ester and amide I) and 1505 cm^{-1} (amide II).

Found: C, 68.07; H, 9.40; N, 2.70%. Calcd for $C_{31}H_{51}O_7N$: C, 67.73; H, 9.35; N, 2.55%.

*10-(N-Benzyloxycarbonyl-L-threonyloxy)undecanoic Acid (**5**).* A mixture of **4** (1.72 g) and trifluoroacetic acid (19 ml) was kept at room temperature with occasional swirling for 5 min, after which the reaction mixture was evaporated below 10°C. The residual syrup was then dissolved in ether and again evaporated. This procedure was repeated three times to remove trifluoroacetic acid. The final residue was dried over sodium hydroxide under reduced pressure to afford **5** (1.37 g).

*(3S,4R,15S)-3-Benzyloxycarboxamido-4,15-dimethyl-1,5-dioxacyclopentadecane-2,6-dione (**6a**) and (3S,4R,15R)-3-Benzyloxycarboxamido-4,15-dimethyl-1,5-dioxacyclopentadecane-2,6-dione (**6b**).* A mixture of **5** (1.37 g, 3.13 mmol), dry benzene (78 m*l*) and trifluoroacetic anhydride (0.436 m*l*, 3.13 mmol) was heated at 70°C for 14 hr, after which additional trifluoroacetic anhydride (0.436 m*l*) was added and again heated at the same temperature for 9 hr. The reaction mixture was evaporated and the residue was then dissolved in ether and again evaporated. This procedure was repeated three times to remove trifluoroacetic acid. The final residue was dried over sodium hydroxide in a vacuum to yield a crystalline mass (1.65 g). The product was chromatographed on a silica gel column (400 g, 4.7×53 cm) with benzene-butanone (30 : 1) system to give two fractions corresponding to the first and second elution peaks of the chromatogram. The first fraction gave a crystalline cyclization product **6a** (238 mg, 18.2%); mp 69.7—71.2°C (from ethyl acetate-petroleum ether); $[\alpha]_D^{22}$ +7.1° (*c* 1.7, chloroform); ν_{max}^{KBr} 3440 (NH), 1743 (ester), 1725 (amide I) and 1517 cm^{-1} (amide II).

Found: C, 65.68; H, 7.67; N, 3.44%; M (mass spectrometry), 419.2256; M+1, 420.2311. Calcd for $C_{23}H_{33}O_6N$: C, 65.85; H, 7.93; N, 3.34%; M, 419.2308; M+1, 420.2386.

The second fraction afforded a crystalline cyclization product **6b** (229 mg, 17.5%); mp 135.0—136.0°C (from ethyl acetate-petroleum ether); $[\alpha]_D^{22}$ −33.8° (*c* 1.8, chloroform); ν_{max}^{KBr} 3350 (NH), 1740 (ester), 1715 (amide I), and 1535 cm^{-1} (amide II).

Found: C, 66.16; H, 8.31; N, 3.49%. M (mass spectrometry), 419.2313; M+1, 420.2381. Calcd for $C_{23}H_{33}O_6N$: C, 65.85; H, 7.93; N, 3.34%. M, 419.2308; M+1, 420.2386.

*(+)-10-Hydroxyundecanoic Acid [(+)-**7**].* To a solution of **6a** (100 mg, 0.238 mmol) in methanol (0.48 m*l*) was added 10% aq. NaOH (0.24 m*l*, 0.594 mmol) under ice-cooling and stirred for 4.5 hr at room temperature. The mixture was concentrated, diluted with water and extracted ten times with 1 m*l*-portions of ethyl acetate. The aqueous layer was acidified (pH 4) with 10% H_2SO_4 and extracted with ethyl acetate (1.5 m*l*×4). The dried ethyl acetate layer was evaporated to give a crystalline mass (93.2 mg), which was dissolved in methanol and hydrogenolysed over palladium black.[9] The reduction product was chromatographed on silica gel (6 g) with *n*-hexane-ethyl acetate-acetic acid (20 : 10 : 1) system to afford (+)-**7** (40.9 mg, 85.3%); mp 61.5—63.7°C (from ethyl acetate-petroleum ether); $[\alpha]_D^{21}$ +6.2° (*c* 1.9, chloroform); ν_{max}^{KBr} 3360 (OH), 1712 cm^{-1} (COOH).

Found: C, 65.67; H, 11.12%. Calcd for $C_{11}H_{22}O_3$: C, 65.31; H, 10.96%.

*(−)-10-Hydroxyundecanoic Acid [(−)-**7**].* Saponification of **6b** with 10% aq. NaOH by the same procedure as that used to obtain (+)-**7** from **6a** afforded (−)-**7**; mp 62.0—63.0°C; $[\alpha]_D^{21.2}$ −7.0° (*c* 2.5, chloroform); IR-spectrum of (−)-**7** was identical with that of its enantiomer (+)-**7**.

Found: C, 65.48; H, 11.15%. Calcd for $C_{11}H_{22}O_3$: C, 65.31; H, 10.96%.

*Methyl (+)-19-Hydroxyundecanoate [(+)-**7**].* To a solution of (+)-**7** (18.5 mg) in dry ether (0.6 m*l*) was added excess distilled diazomethane in ether. After 15 min the solution was filtered and the filtrate was evaporated to dryness leaving (+)-**8** as a colorless oil (17.8 mg, 90%). tlc [benzene-acetone (15 : 1)] showed a single spot: $[\alpha]_D^{25}$ +5.6° (*c* 1.8, methanol).

*Methyl (−)-10-Hydroxyundecanoate [(−)-**8**].* The diazomethane treatment of (−)-**7**, similar to that of (+)-**7** gave the enantiomeric methyl ester (−)-**8**: $[\alpha]_D^{25}$ −5.8° (*c* 2.5, methanol).

*Determinations of Absolute Configurations of (+)-**8** and (−)-**8** by Horeau Procedure.* a) α-Phenylbutyric anhydride[10] (50.3 mg, 0.165 mmol) was added to (+)-**8** (18.7 mg, 0.083 mmol) in pyridine (0.5 m*l*). After standing for 18 hr at room temperature, water and benzene were added and the mixture was extracted several times with 0.2 N aq. Na_2CO_3. The extracts were washed with ether, acidified with 6 N HCl and extracted with benzene. The benzene extract was washed with water, dried over Na_2SO_4 and concentrated to dryness. The residue (39.2 mg) had IR and NMR spectra identical with those of racemic α-phenylbutyric acid: $[\alpha]_D^{20}$ −5.0°; $[\alpha]_{546}^{20}$ −6.0°; $[\alpha]_{436}^{20}$ −10.5°; $[\alpha]_{365}^{20}$ −17.7° (*c* 1.96, benzene). Since the recovered α-phenylbutyric acid was levorotatory, the hydroxy ester (+)-**8** has the "S" configuration at its asymmetric center. b) By the same procedure as described in a), the reaction of (−)-**8** (25.2mg, 0.117 mmol) with α-phenylbutyric anhydride (71.2 mg, 0.234 mmol) in pyridine gave a recovered sample (41.5 mg) of α-phenylbutyric acid: $[\alpha]_D^{20.5}$ +4.0°; $[\alpha]_{546}^{20.5}$ +5.3°; $[\alpha]_{436}^{20.5}$ +10.4°; $[\alpha]_{365}^{20.5}$ +18.0° (*c* 2.08, benzene). The configuration at carbinol carbon of (−)-**8**, therefore, is estimated as "R".

*(3S,4R,15S)-4,15-Dimethyl-1,5-dioxa-3-(O-benzyl-3'-nitrosalicylamido)cyclopentadecane-2,6-dione (**9a**).* A solution of **6a** (100 mg, 0.239 mmol) in methanol (3.5 m*l*) was stirred with palladium black (*ca.* 9 mg) for 25 min under bubbling with hydrogen. The filtered reduction mixture was evaporated to yield the free amino-dilactone (65 mg) which showed a single ninhydrin positive spot on tlc with a benzene-acetone (20 : 1) system. The free amino-dilactone (65 mg) was dissolved in dry tetrahydrofuran (1.2 m*l*) and *O*-benzyl-3-nitrosalicylic acid *N*-hydroxysuccinimide ester (88.3 mg, 0.239 mmol) was added. The mixture (pH 6) was kept for 4 hr at room temperature, after which it (pH 5) was allowed to stand for 16 hr at 37°C in an incubator. The reaction mixture (pH 4) was adjusted to pH 6 by the addition of triethylamine and again kept at 37°C for 3 hr. The resulting solution was evaporated to afford a yellow syrup (200 mg)

9) By this hydrogenation process the another saponification product of **6a**, namely *N*-benzyloxycarbonyl-L-threonine, was converted to L-threonine which was easily removed from the title compound by a silica gel column.

10) H. Falk and K. Schlog, *Monatsch. Chem.*, **96**, 276 (1965).

which was purified through a silica gel column (20 g, 1.3×43 cm). Elution with a *n*-hexane - ethyl acetate (2 : 1) system gave the title compound **9a** as a yellow glassy solid: yield 115 mg (89.2%); $[\alpha]_D^{23}$ −16.9° (*c* 1.7, chloroform); $\nu_{max}^{CCl_4}$ 3400 (NH), 1746 (ester), and 1680 cm^{-1} (amide I).

Found: C, 64.64; H, 7.16; N, 4.86%. Calcd for $C_{29}H_{36}O_8N_2$: C, 64.43; H, 6.71; N, 5.18%.

*(3S,4R,15R)-4,15-Dimethyl-1,5-dioxa-3-(O-benzyl-3'-nitrosalicylamido)cyclopentadecane-2,6-dione (**9b**).* The title compound (**9b**) was prepared from **6b** by the same procedure as described for the preparation of the epimer (**9a**) as a yellow glassy solid: yield 86.1%; $[\alpha]_D^{22}$ +35.7° (*c* 1.4, chloroform); $\nu_{max}^{CCl_4}$ 3410 (NH), 1748 (ester), and 1680 cm^{-1} (amide I).

Found: C, 64.69; H, 6.77; N, 5.60%. Calcd for $C_{29}H_{36}O_8N_2$: C, 64.43; H, 6.71; N, 5.18%.

*(3S,4R,15S)-4,15-Dimethyl-1,5-dioxa-3-(3'-formamidosalicylamido)cyclopentadecane-2,6-dione(**10a**).* A solution of **9a** (59.6 mg, 0.109 mmol) in methanol (8 m*l*) was stirred with palladium black under bubbling with hydrogen gas for 30 min. The filtered yellow-green reduction mixture was evaporated to give an orange-red glassy solid (43 mg, 93.9%). The product (43 mg, 0.103 mmol) was dissolved in tetrahydrofuran (1.6 m*l*) and to the solution was added DCCI (22.4 mg, 0.109 mmol) and 98% formic acid (5.4 mg) under ice-cooling. After standing for 23 hr in a refrigerator, the reaction mixture was filtered to remove *N,N'*-dicyclohexylurea (14.7 mg, 60.3%). The orange-red filtrate was evaporated and the crude product (64.8 mg) was purified by preparative thin-layer chromatography (three 20×20 cm-plates) with *n*-hexane - ethyl acetate (2 : 1). The strongest fluorescent band was collected and extracted with ether to afford orange crystals which were recrystallized from ether-petroleum ether (30—40°C) to yield colorless needles of **10a**: yield 21.5 mg (44.2%); mp 124—127.6°C; $[\alpha]_D^{21}$ +49° (*c* 1.1, chloroform); λ_{max}^{MeOH} mμ (log ε), 227 (4.55) and 319 (3.78); $\nu_{max}^{CHCl_3}$ 3430, 3390 (NH), 1740 (ester), 1703 (NHCHO), 1647 (ArCONH), 1613, 1593 (Ar–H) and 1532 cm^{-1} (ArCONH).

Found: C, 61.67; H, 7.23; N, 6.34%. Calcd for $C_{23}H_{32}O_7N_2$: C, 61.59; H, 7.19; N, 6.25%.

*(3S,4R,14R)-4,15-Dimethyl-1,5-dioxa-3-(3'-formamidosalicylamido)cyclopentadecane-2,6-dione (**19b**).* By the same procedure as described for the preparation of **10a**, the title compound (**10b**) was prepared from **9b** as a glassy solid: yield 50.7%; $[\alpha]_D^{22}$+14° (*c* 1.8, chloroform); λ_{max}^{MeOH} mμ (log ε), 227 (4.46) and 319 (3.77); $\nu_{max}^{CHCl_3}$ 3408, 3465 (NH), 1740 (ester), 1707 (NHCHO), 1647 (ArCONH), 1613, 1596 (Ar–H) and 1536 cm^{-1} (ArCONH).

Found: C, 61.32; H, 7.24; N, 5.86%. Calcd for $C_{23}H_{32}O_7N_2$: C, 61.59; H, 7.19; N, 6.25%.

We wish to thank Mr. S. Nakada for the elemental analyses and Mr. M. Wada and Mr. S. Aburagi for their technical assistance. We also wish to thank Professor S. Zen of Kitasato University for the measurement of mass spectra, and Mr. I. Takagi for his microbiological tests.

BULLETIN OF THE CHEMICAL SOCIETY OF JAPAN, VOL. 44, 3399—3405 (1971)

Studies on Aminosugars. XXIX. Syntheses of Nucleosides of 3-Amino-3-deoxy-3-*C*-hydroxymethyl-β-D-ribofuranose[1]

Hiroaki YANAGISAWA, Mitsuhiro KINOSHITA, and Sumio UMEZAWA

Department of Applied Chemistry, Faculty of Engineering, Keio University, Koganei-shi, Tokyo

(Received May 21, 1971)

Reduction of 3-acetamido-3-*C*-carboxy-3-deoxy-1,2-*O*-isopropylidene-α-D-ribofuranose-γ-lactone (**1**) with lithium aluminum hydride or sodium borohydride followed by acetylation gave 3-acetamido-3-*C*-acetoxymethyl-5-*O*-acetyl-3-deoxy-1,2-*O*-isopropylidene-α-D-ribofuranose (**2**). Hyrdolysis of **2** followed by *N*-phthaloylation and *O*-acetylation gave 3-*C*-acetoxymethyl-5-*O*-acetyl-3-deoxy-1,2-*O*-isopropylidene-3-phthalimido-α-D-ribofuranose (**7**), which was acetolyzed and chlorinated to give acylglycosyl chloride (**9**). Condensation of **9** with 6-benzamidopurine followed by aminolysis afforded 9-(3′-amino-3′-deoxy-3′-*C*-hydroxymethyl-β-D-ribofuranosyl)adenine (**11**). 6-dimethylaminopurine, guanine, cytosine and uracil derivatives were similarly synthesized.

In a previous paper[2] we reported the syntheses of branched aminonucleosides which have a new branched amino sugar moiety, 3-amino-3-*C*-carboxy-3-deoxy-D-ribose. As an extension of this work, the syntheses of 9-(3′-amino-3′-deoxy-3′-*C*-hydroxymethyl-β-D-ribofuranosyl)adenine (**11**), 9-(3′-amino-3′-deoxy-3′-*C*-hydroxymethyl-β-D-ribofuranosyl)-6-dimethylaminopurine (**14**), 9-(3′-amino-3′-deoxy-3′-*C*-hydroxymethyl-β-D-ribofuranosyl)guanine (**16**), 1-(3′-amino-3′-deoxy-3′-*C*-hydroxymethyl-β-D-ribofuranosyl)cytosine (**18**) and 1-(3′-amino-3′-deoxy-3′-*C*-hydroxymethyl-β-D-ribofuranosyl)uracil (**20**) are described in the present paper.

It has been found that substitution of 3′-hydroxy group or 3′-hydrogen atom of the sugar moiety of ribonucleosides with some substituents often gives rise to biological activities, *i.e.*, 3′-deoxyadenosine (cordycepin),[3] 9-(3′-amino-3′-deoxy-β-D-ribofuranosyl)-6-dimethylaminopurine[4] and 3′-amino-3′-de-

1) Part XLII of "Studies on Antibiotics and Related Substances" by Sumio Umezawa. A part of this paper was read at the 23rd Annual Meeting of the Chemical Society of Japan, Tokyo, April, 1970. (Abstracts of Papers of the Meeting, Vol. III, p. 1572).

2) H. Yanagisawa, M. Kinoshita, S. Nakada, and S. Umezawa, This Bulletin, **43**, 246 (1970).

3) K. G. Cunningham, W. Manson, F. S. Spring, and S. H. Hutchinson, *Nature*, **166**, 949 (1950).

4) B. R. Baker, J. P. Joseph, and J. H. Williams, *J. Amer. Chem. Soc.*, **77**, 1 (1955).

oxyadenosine[5] have antitumor activities and 3′-*C*-methyladenosine and 3′-*C*-methylcytosine[6] show antiviral activities. In this connection we were interested in transforming the 3′-*C*-carboxyl group of 3′-amino-3′-*C*-carboxy-3′-deoxy-D-ribose moiety in the aminonucleosides[2] to other substituents. We carried out the reduction of the 3′-*C*-carboxyl group to 3′-*C*-hydroxymethyl group.

Synthesis of Sugar Moiety. 3-Acetamido-3-*C*-carboxy-3-deoxy-1,2-*O*-isopropylidene-α-D-ribofuranose-γ-lactone[2] (**1**) was reduced in tetrahydrofuran with lithium aluminum hydride and the reduction product was acetylated with acetic anhydride-pyridine to afford 3-acetamido-3-*C*-acetoxymethyl-5-*O*-acetyl-3-deoxy-1,2-*O*-isopropylidene-α-D-ribofuranose (**2**). It has recently been reported that α-amino and α-acylamino esters were reduced with sodium borohydride to afford the corresponding α-amino and α-acylamino alcohols, respectively, in good yields.[7] The reduction of **1** with sodium borohydride also gave **2** in a good yield.

Compound **2** was treated with a mixture of concentrated sulfuric acid, acetic anhydride and acetic acid in order to obtain the corresponding acetyl sugar which was required for the preparation of nucleoside. The product, whose tlc showed a single spot, had an IR-absorption at 1669 cm^{-1} (amide I), but no absorp tion at 3300—3500 (NH) and 1500—1600 cm^{-1} (amide II). The NMR spectrum of the product showed the presence of four acetyl groups and the absence of N–H proton. These observations and the result of elemental analysis suggested that the structure of the product is 1,2,5-tri-*O*-acetyl-3-deoxy-α-D-ribofuranose-3-spiro-2′-(*N*-acetylaziridine) (**3**). The assignment was also supported by the following reaction. Product **3** was treated with acetic acid as a nucleophile[8] to afford 3-acetamido-1,2,5-tri-*O*-acetyl-3-*C*-acetoxymethyl-3-deoxy-α-D-ribofuranose (**4**) whose structure was confirmed by elemental analysis, IR spectrum [3380 (NH), 1680 (amide I) and 1545 cm^{-1} (amide II)] and NMR spectrum [N–H proton (τ 3.54) and five acetyl groups]. Aziridine formation between 3-amino and 3-*C*-hydroxymethyl groups was also observed on the acetolysis of 3-acetamido-5-*O*-benzyl-3-*C*-benzyloxymethyl-3-deoxy-1,2-*O*-isopropyridene-α-D-ribofuranose (**5**) derived from **2**. The product was assigned as 1,2-di-*O*-acetyl-5-*O*-benzyl-3-deoxy-α-D-ribofuranose-3-*C*-spiro-2′-(*N*-acetylaziridine) (**6**) on the basis of elemental analysis, IR spectrum [1667 cm^{-1} (amide I), no absorption of N–H stretching and amide II] and NMR spectrum (single benzyl group and no N–H proton).

Since the amide-hydrogen in 3-acetamido group of **2** was very reactive in acidic media as described above, the acetamido group of **2** should be favorable for replacement by phthalimido group in order to prevent aziridine formation. Deacetylation of **2** with barium hydroxide followed by phthaloylation with phthalic anhydride-pyridine and *O*-acetylation afforded 3-*C*-acetoxymethyl-5-*O*-acetyl-3-deoxy-1,2-*O*-isopropylidene-3-phthalimido-α-D-ribofuranose (**7**). The NMR spectrum of **7** revealed the presence of two conformers which might be caused by a steric interaction between the bulky phthalimido group, isopropylidene group and acetoxymethyl group. Acetolysis of **7** afforded 3-*C*-acetoxymethyl-1,2,5-tri-*O*-acetyl-3-phthalimido-D-ribofuranose (**8**). Treatment of **8** with hydrogen chloride in ether gave 3-*C*-acetoxymethyl-2,5-di-*O*-acetyl-1-chloro-3-deoxy-D-ribofuranose (**9**), which was immediately used in the next condensation reaction without purification because of its instability.

Synthesis of Nucleosides. Condensation of **9** with benzamidopurine was carried out in the presence of mercuric cyanide and Drierite in nitromethane[9] to afford 6-benzamido-9-(3′-*C*-acetoxymethyl-2′,5′-di-*O*-acetyl-3′-deoxy-3′-phthalimido-D-ribofuranosyl)adenine (**10**).[10] By a similar procedure **9** was condensed with 6-chloropurine, N^2-acetylguanine,[11] and N^4-acetylcytosine[12] to afford 9-(3′-*C*-acetoxymethyl-2′,5′-di-*O*-acetyl-3′-deoxy-3′-phthalimido-D-ribofuranosyl)-6-chloropurine (**12**),[10] 9-(3′-*C*-acetoxymethyl-2′,5′-di-*O*-acetyl-3′-deoxy-3′-phthalimido-β-D-ribofuranosyl)-N^2-acetylguanine (**15**) and N^4-acetyl-1-(3′-*C*-acetoxymethyl-2′,5′-di-*O*-acetyl-3′-deoxy-3′-phthalimido-β-D-ribofuranosyl)-cytosine (**17**), respectively. Although the condensation of **9** with uracil by the mercuric cyanide-nitromethane method and Hilbert-Johnson method[13] was unsuccessful, the desired condensation product, 1-(3′-*C*-acetoxymethyl-2′,5′-di-*O*-acetyl-3′-phthalimido-β-D-ribofuranosyl)uracil (**19**) was obtained with the use of trimethylsilyl method[14] in which 2,4-*O*-bis-(trimethylsilyl)-uracil[15] was used as an activated base.

Positions of the base-sugar linkages in the blocked nucleosides **10**, **12**, **15**, **17**, and **19** were determined by UV spectrometry. The condensation reaction of N^2-acetylguanine with **9** gave predominantly N-9 substituted product.[16] The NMR spectra of the condensation products showed that they were anomeric mixtures except in the case of **19**. The blocked nucleoside of uracil was shown to be the β-anomer

5) B. R. Baker, R. E. Schaub, and H. M. Kissman, *J. Amer. Chem. Soc.*, **77**, 5911 (1955).

6) E. Walton, S. R. Jenkins, R. F. Nut, and F. W. Holly, *J. Med. Chem.*, **12**, 306 (1969).

7) H. Seki, K. Koga, and S. Yamada, *Chem. Pharm. Bull.* (Tokyo), **15**, 1948 (1967).

8) 5,6-Epimino-L-idofuranose and L-altrofuranose are attacked by nucleophiles and the aziridine rings are opened exclusively in the terminal positions. *Cf.* H. Saeki and E. Ohki, *ibid.*, **16**, 2471 (1968).

9) N. Yamaoka, K. Aso, and K. Matsuda, *J. Org. Chem.*, **30**, 149 (1965).

10) The structures of compounds **10**, **12**, and **13**, are represented in Fig. 1 by their β-anomer structures for the sake of convenience.

11) Z. A. Shabarova, Z. P. Polyakova, and M. A. Prokofev, *Zh. Obshch. Khim.*, **29**, 215 (1959).

12) D. M. Brown, A. R. Todd, and S. Varadarajan, *J. Chem. Soc.*, **1956**, 2384.

13) G. E. Hilbert and T. B. Johnson, *J. Amer. Chem. Soc.*, **52**, 4489 (1930).

14) T. Nishimura, B. Shimizu, aad I. Iwai, *Chem. Pharm. Bull.* (Tokyo), **12**, 1471 (1964).

15) T. Nishimura and I. Iwai, *ibid.*, **12**, 352 (1964).

16) S. R. Jenkins, F. W. Holly, and E. Walton, *J. Org. Chem.*, **30**, 2851 (1965).

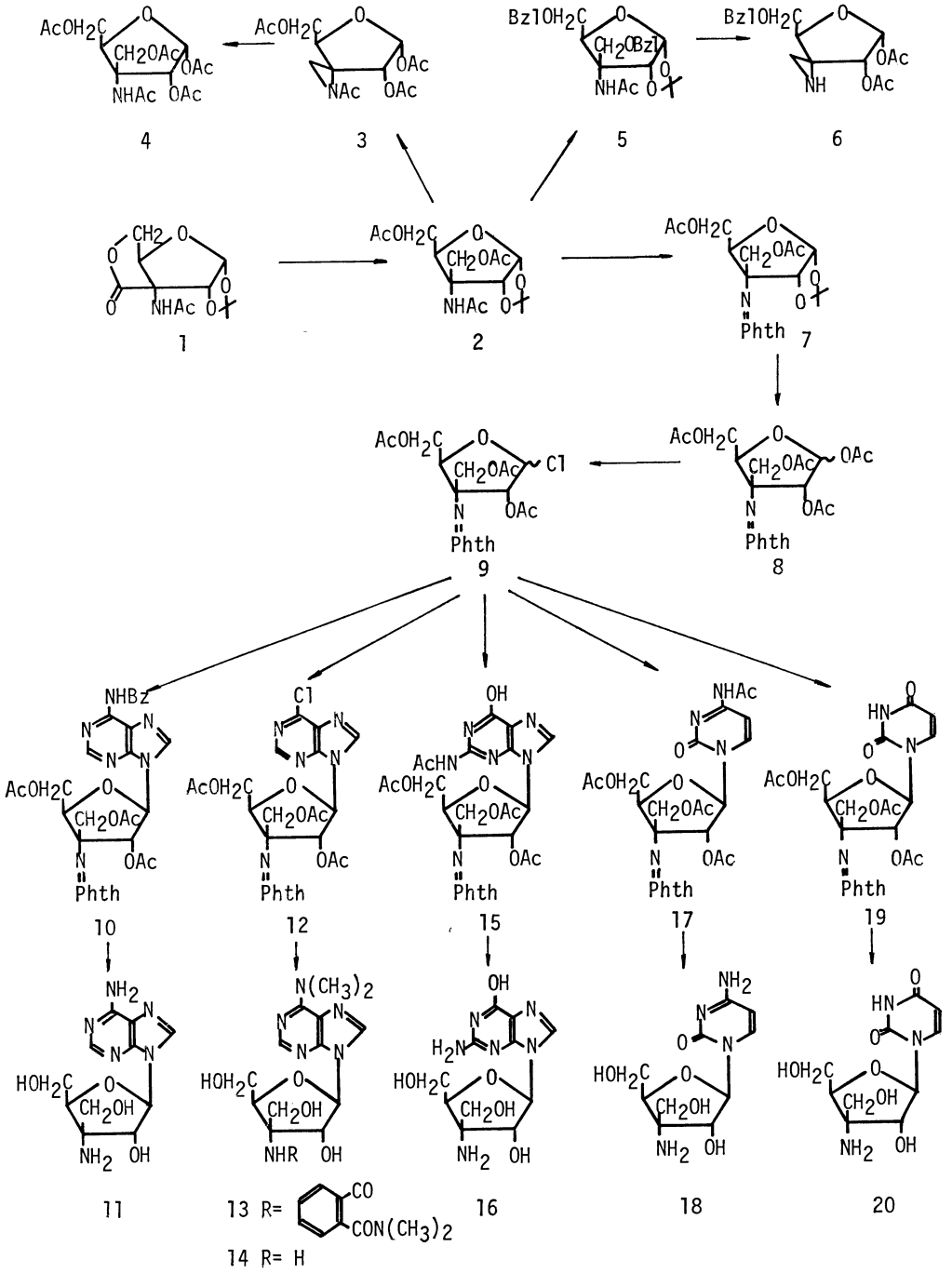

Fig. 1

(**19**). β-Anomer (**15**) was isolated from the anomeric mixture by preparative layer chromatography and β-anomer (**17**) by recrystallization. The blocked nucleoside (**10**)[10] was deacetylated and dephthaloylated with *n*-butylamine-methanol[17] to afford an anomeric mixture of 9-(3′-amino-3′-deoxy-3′-*C*-hydroxymethyl-D-ribofuranosyl)adenine, from which β-anomer (**11**) was isolated. Other blocked nucleosides **15**, **17**, and **19** were similarly deblocked to afford 9-(3′-amino-3′-deoxy-3′-*C*-hydroxymethyl-β-D-ribofuranosyl) guanine (**16**) and 1-(3′-amino-3′-deoxy-3′-*C*-hydroxymethyl-β-D-ribofuranosyl)cytosine (**18**) and 1-(3′-amino-3′-deoxy-3′-*C*-hydroxymethyl-β-D-ribofuranosyl)uracil (**20**), respectively. The blocked nucleoside (**12**)[10] was treated with dimethylamine-methanol to afford 9-[3′-deoxy-3′-(*o*-*N*,*N*-dimethylcarbamoyl) benzamido-3′-*C*-hydroxymethyl-D-ribofuranosyl]-6-dimethylaminopurine (**13**).[10] The product (**13**)[10] was then dephthaloylated with *n*-butylamine-methanol to afford an anomeric mixture of 9-(3′-amino-3′-deoxy-3′-*C*-hydroxymethyl-D-ribofuranosyl)-6-dimethylaminopurine, from which β-anomer (**14**) was isolated by recrystallization.

The NMR spectra of the amino nucleosides **11**, **14**, **16**, **18**, and **20** showed that they contain no anomer.

17) L. Goodman and J. W. Marsico, *J. Med. Chem.*, **6**, 413 (1963).

Their anomeric configurations were determined to be β on the basis of their ORD curves. In general, pyrimidine β-D-nucleosides show positive and purine β-D-nucleosides negative Cotton effects.[18] The ORD curves of the purine nucleosides **11**, **14** and **16** showed negative Cotton effects and those of the pyrimidine nucleosides **18** and **20** showed positive ones. This indicates that all the synthetic branched aminonucleosides have β-configurations.

Examination of the antiviral activity of the branched aminonucleosides (**11**, **14**, **16**, **18** and **20**) is in progress. Compound **11**, namely the 3'-amino-3'-hydroxymethyl derivative of adenosine, has been found to exhibit weak inhibition against *vaccinia Dairen*.

Experimental

Thin layer chromatography (tlc) and preparative layer chromatography (plc) were carried out with the use of silica gel (Daiichi Pure Chemicals Co., Inc.). The prepared plates were activated at 110°C for 1 hr. The spray reagent was 10% sulfuric acid. Silica gel column chromatography was carried out with the use of WAKO-GEL C-200 (Wako Pure Chemical Industries, Ltd.). NMR spectra were taken with a Varian A-60D spectrometer at a frequency of 60 MHz in deuteriochloroform, deuteriodimethyl sulfoxide and deuterium oxide with tetramethylsilane and sodium 2,2-dimethyl-2-silapentane-5-sulfonate as an internal standard. Melting point determination was carried out on a micro hot stage and not corrected.

*3-Acetamido-3-C-acetoxymethyl-5-O-acetyl-3-deoxy-1,2-O-isopropylidene-α-D-ribofuranose (**2**).* *a) Reduction of **1** with Lithium Aluminum Hydride*: A solution of **1** (2.55 g) in tetrahydrofuran (20 m*l*) was added dropwise to a suspension of lithium aluminum hydride (0.99 g) in tetrahydrofuran (24 m*l*) under ice-cooling and stirring for 15 min. The mixture was then stirred in an ice bath for 3 hr and at room temperature for 3 hr. To the reaction mixture was added ethyl acetate (20 m*l*) and 20% aqueous isopropanol (20 m*l*) under ice-cooling and the mixture was stirred at room temperature for 30 min. Isopropanol (150 m*l*) was added to the reaction mixture and the precipitates were separated by centrifuging and washed with isopropanol (80 m*l*×4). The supernatant layer and washings were evaporated to dryness. To the residue was added pyridine (45 m*l*) and acetic anhydride (30 m*l*) and the mixture was kept at room temperature for 15 hr. The reaction mixture was evaporated with toluene, the residue being dissolved in 1 N hydrochloric acid (40 m*l*) and ethyl acetate (80 m*l*). The organic layer was separated, washed with water (20 m*l*) and aqueous sodium bicarbonate solution (20 m*l*) successively, dried over sodium sulfate and evaporated. Trituration of the syrupy residue with diisopropyl ether afforded **2** as a colorless crystal; yield 2.06 g (61.5%). The analytical sample was purified by recrystallization from ethyl acetate-diisopropyl ether: mp 135—136°C; $[\alpha]_D^{23}$+74° (*c* 1.7, ethanol); ν_{max}^{Nujol} 3350, 1743, and 1683 cm^{-1}; τ^{CDCl_3} 3.87 (s, N–H), 4.09 (d, H-1, $J_{1,2}$=4.0 Hz), 7.90 (s, two $OCOCH_3$), 7.98(s, $NCOCH_3$), 8.43 and 8.62 [=$C(CH_3)_2$].

Found: C, 52.37; H, 6.93; N, 4.26%. Calcd for $C_{15}H_{23}NO_8$: C, 52.17; H, 6.71; N, 4.06%.

*b) Reduction of **1** with Sodium Borohydride*: A solution of sodium borohydride (8.9 g) in 50% aqueous ethanol (110 m*l*) was added to a solution of **1**(14.1 g) in ethanol(83 m*l*) and the mixture was refluxed for 15 hr. The reaction mixture was evaporated with toluene to remove a trace of water. Pyridine (120 m*l*) and acetic anhydride (90 m*l*) was added to the residue and the mixture was stirred vigorously at room temperature for 3 hr. The reaction mixture was evaporated and the residue was partitioned between ethyl acetate (200 m*l*) and water (200 m*l*). The organic layer was successively washed with water, aqueous potassium bisulfate solution and aqueous sodium bicarbonate solution. The dried organic layer was evaporated and the residue was triturated with diisopropyl ether to afford **2**: yield 12.5 g (67.5%); mp 135—136°C (from ethyl acetate-diisopropyl ether).

*1,2,5-Tri-O-acetyl-3-deoxy-α-D-ribofuranose-3-C-spiro-2'-(N-acetylaziridine) (**3**).* To a solution of **2** (1.15 g) in a mixture of acetic acid (8 m*l*) and acetic anhydride (8 m*l*) was added dropwise concentrated sulfuric acid (0.8 m*l*) and the mixture was allowed to stand at room temperature for 12 hr. The reaction mixture was shaken with 10% aqueous sodium acetate (40 m*l*) and dichloroethane (20 m*l*). The aqueous layer was further extracted with dichloroethane (10 m*l*×3). The combined extracts were washed with aqueous potassium bicarbonate solution (20 m*l*), dried over sodium sulfate and evaporated to give **3** as a syrup; yield 710 mg (65%). The analytical sample was purified by silica gel column chromatography (ethyl acetate-benzene 1 : 1); $[\alpha]_D^{23}$+61° (*c* 2.1, ethanol); ν_{max}^{Film} 1743, 1669 cm^{-1}; τ^{CDCl_3} 4.43 (d, H-1, $J_{1,2}$=3.2 Hz), 4.64 (d, H-2), 7.86, 7.88, 7.89 and 7.99 (s, $COCH_3$).

Found: C, 50.93; H, 5.77; N, 4.45%. Calcd for $C_{14}H_{19}NO_8$: C, 51.06; H, 5.82; N, 4.25%.

*3-Acetamido-1,2,5-tri-O-acetyl-3-C-acetoxymethyl-3-deoxy-α-D-ribofuranose (**4**).* A solution of **3** (60 mg) in acetic acid (1.5 m*l*) was heated at 55°C for 5 hr, and then evaporated with toluene. The residual syrup was purified through a silica gel column (10 g, 24×1 cm). Elution with ether acetate-benzene (1 : 1 and 3 : 1) afforded **4** as a glass: yield 55 mg (78%); $[\alpha]_D^{22}$ +13° (*c* 2.3, ethanol); ν_{max}^{KBr} 3380, 1753, 1680, and 1545 cm^{-1}; τ^{CDCl_3} 3.54 (s, N–H), 3.86 (d, H-1, $J_{1,2}$=2.7 Hz), 4.46 (d, H-2), 7.83, 7.87, 7.88, 7.93 and 7.97 (s, $COCH_3$).

Found: C, 49.78; H, 5.91; N, 3.64%. Calcd for $C_{16}H_{23}NO_{10}$: C, 49.35; H, 5.95; N, 3.60%.

*3-Acetamido-5-O-benzyl-3-C-benzyloxymethyl-3-deoxy-1,2-O-isopropylidene-α-D-ribofuranose (**5**).* To a solution of sodium (110 mg) dissolved in methanol (6 m*l*) was added **2** (505 mg) and the resulting solution was refluxed for 30 min. After addition of a small amount of ethyl acetate, the solution was evaporated to dryness. The residue was dissolved in anhydrous dimethylformamide (8 m*l*) and to the solution was added freshly dried barium oxide (2.04 g), barium hydroxide octahydrate (0.87 g) and benzyl bromide (2.8 m*l*) under ice-cooling. The mixture was stirred in an ice-bath for 2 hr and then at room temperature for 18 hr. After addition of dichloroethane (20 m*l*) to the reaction mixture, the precipitates were filtered off with a hyflo super cell pad. The filtrate was concentrated to 3—4 m*l* and was diluted with ethyl acetate (15 m*l*). The resulting slurry was warmed, and the precipitates were again filtered off and washed with ethyl acetate. The filtrate and washings were evaporated and the residue was placed on a silica gel column (20 g, 1.8×18 cm) and eluted with benzene-ethyl acetate (3 : 1),

18) J. T. Yang, and T. Samejima, *J. Amer. Chem. Soc.*, **85**, 4039 (1963); T. L. V. Ulbricht, J. P. Jennings, P. M. Scopes, and W. Klyne, *Tetrahedron Lett.*, **1964**, 695; T. Nishimura, B. Shimizu, and I. Iwai, *Biochim. Biophys. Acta*, **157**, 221 (1968).

The eluent containing **5** was evaporated to dryness: a syrup, yield 570 mg (88%); $[\alpha]_D^{17}$ +42° (*c* 3.2, ethanol); ν_{max}^{Film} 3285 and 1654 cm^{-1}; τ^{CDCl_3} 2.70 (s, two C_6H_5), 3.84 (s, N–H), 4.23 (d, H-1, $J_{1,2}$=3.6 Hz), 5.19 (d, H-2), 5.51 (s, two benzyl CH_2), 8.10 (s, N–$COCH_3$), 8.48 and 8.68 [s, =$C(CH_3)_2$].

Found: C, 67.81; H, 6.81; N, 3.34%. Calcd for $C_{25}H_{31}NO_6$: C, 68.00; H, 7.08; N, 3.17%.

*1,2-Di-*O*-acetyl-5-*O*-benzyl-3-deoxy-α-*D*-ribofuranose-3-*C*-spiro-2′-(*N*-acetylaziridine) (**6**).* To a solution of **5** (384 mg) in a mixture of acetic acid (3 m*l*) and acetic anhydride (3 m*l*) was added dropwise concentrated sulfuric acid (0.29 m*l*) and the mixture was kept at room temperature for 12 hr. After addition of 10% sodium acetate solution (20 m*l*), the mixture was extracted with dichloroethane (20 m*l*, 5 m*l*×2) and the extracts were washed with water and aqueous potassium bicarbonate solution and dried over sodium sulfate. After evaporation of the solvent, the residue was purified by silica gel column (10 g, 20×1 cm). Elution with benzene-ethyl acetate (1 : 3 and 1 : 1) gave **6** asasyrup; yield 66 mg (20%); $[\alpha]_D^{17}$ +91° (*c* 1.8, ethanol); ν_{max}^{Film} 1746 and 1667 cm^{-1}; τ^{CDCl_3} 2.66 (s, C_6H_5), 4.47 (d, H-1, $J_{1,2}$= 3.4 Hz), 4.70 (d, H-2), 7.94, 7.98 and 8.04 (s, $COCH_3$).

Found: C, 60.91; H, 6.56; N, 3.81%. Calcd for $C_{19}H_{23}NO_7$: C, 60.47; H, 6.14; N, 3.71%.

*3-C-Acetoxymethyl-5-*O*-acetyl-3-deoxy-1,2-*O*-isopropylidene-3-phthalimido-α-*D*-ribofuranose (**7**).* A mixture of **2** (3.81 g) and barium hydroxide octahydrate (7.62 g) in water (29 m*l*) was refluxed under stirring for 2 hr. Carbon dioxide was passed through the reaction mixture for neutralization. Precipitates were separated by centrifuging and washed with ethanol. The supernatant and washings were evaporated to give a syrup containing colorless crystals. To this was added ethanol (40 m*l*) and the crystals were filtered off and washed with ethanol (10 m*l*). The filtrate and washings were evaporated to afford a syrup (3.01 g). To a solution of the syrup in pyridine (25 m*l*) was added phthalic anhydride (2.46 g) and the mixture was warmed at 50°C for 30 min. Acetic anhydride (25 m*l*) was added and the mixture was further warmed at 50°C for 30 min. The resulting mixture was evaporated and the residue was dissolved in a small amount of benzene and chromatographed on a silical gel column (40 g, 2.8×15 cm). Elution with benzene and benzene-ethyl acetate (10 : 1 and 6 : 1) afforded **7** as a glass: yield 3.34 g (70%). The NMR spectrum of **7** showed that it was a mixture of two conformers (7 : 3) : τ^{CDCl_3} (major) 2.16 (s, C_6H_5), 4.11 (d, H-1, $J_{1,2}$=4.0 Hz), 7.87, 8.01 (s, $COCH_3$), 8.57 and 8.70 [s, –$C(CH_3)_2$]; (minor) 4.07 (d, H-1, $J_{1,2}$=3.9 Hz), 7.87, 7.95 (s, $COCH_3$), 8.57 and 8.67 [s, –$C(CH_3)_2$]; $\nu_{max}^{CHCl_3}$ 1747 and 1725 cm^{-1}; $[\alpha]_D^{17}$+120° (*c* 1.2, ethanol).

Found: C, 58.63; H, 5.66; N, 3.44%. Calcd for $C_{21}H_{23}NO_9$: C, 58.19; H, 5.35; N, 3.23%.

*3-C-Acetoxymethyl-1,2,5-tri-*O*-acetyl-3-deoxy-3-phthalimido-*D*-ribofuranose (**8**).* To an ice-cooled solution of **7** (3.34 g) in a mixture of acetic acid (23 m*l*) and acetic anhydride (23 m*l*) was added concentrated sulfuric acid (1.76 m*l*) under stirring and the mixture was kept at room temperature for 12 hr. The reaction mixture was mixed with powdered sodium acetate trihydrate (18 g) and the resulting slurry was stirred for 30 min. After evaporation at 35°C, the residue was partitioned between water (100 m*l*) and ethyl acetate (70 m*l*). The aqueous layer was further extracted with ethyl acetate (20 m*l*×2). The combined organic layers were washed with aqueous potassium bicarbonate solution (50 m*l*×3) and dried over sodium sulfate. Removal of ethyl acetate and a trace of acetic acid by co-distillation with toluene gave **8** as a glass: yield 2.14 g (58%). An analytical sample was purified by silica gel chromatography with a solvent system, benzene-ethyl acetate (10 : 1) : $[\alpha]_D^{17}$+82° (*c* 2.1, ethanol); $\nu_{max}^{CHCl_3}$ 1750 and 1726 cm^{-1}; τ^{CDCl_3} 2.15 (s, C_6H_4), 3.83 (s, H-1), 4.15 (s, H-2), 7.85, 7.90, 8.06 and 8.08 (s, $COCH_3$).

Found: C, 54.71; H, 4.96; N, 3.04%. Calcd for $C_{22}H_{23}NO_{11}$: C, 55.34; H, 4.86; N, 2.93%.

*3-C-Acetoxymethyl-2,5-di-*O*-acetyl-1-chloro-3-deoxy-*D*-ribofuranose (**9**).* Through a mixture of **8** (2.14 g) and Drierite (2.14 g) in dry ether (100 m*l*) was passed dry hydrogen chloride under ice-salt cooling for 2 hr and the mixture was allowed to stand for 19 hr in a refrigerator. The reaction mixture was evaporated below 30°C and the residual hydrogen chloride was removed by co-distillation with benzene. The TLC of the residue showed that the product **9** (R_f 0.79 with benzene-ethyl acetate 1 : 1) was unstable and a new spot (R_f 0.63) appeared during evaporation. The residue, therefore, was used immediately for the next condensation reaction.

*6-Benzamido-9-(3′-C-acetoxymethyl-2′,5′-di-*O*-acetyl-3′-deoxy-3′-phthalimido-*D*-ribofuranosyl)adenine (**10**).* A solution of **9** [prepared from **8** (2.14 g)] in a small amount of nitromethane was added to a mixture of benzamidopurine (1.07 g), mercuric cyanide (1.14 g) and Drierite (7.00 g) in nitromethane (50 m*l*). After the mixture was refluxed under stirring for 4 hr, the precipitates were filtered off and washed with ethyl acetate. The filtrate and washings were mixed with silica gel (7 g) and evaporated to dryness. The powered residue was placed on a silica gel column (70 g, 2.8×28 cm) and eluted with benzene and benzene-ethyl acetate (1 : 1, 1 : 2 and 1 : 5). The eluent containing **10** was evaporated to afford **10** as an amorphous powder; yield 1.13 g (38%). An analytical sample was obtained by PLC technique with a solvent system, benzene-ethyl acetate (1 : 4) : $[\alpha]_D^{17}$ –31° (*c* 1.39, ethanol); $\nu_{max}^{CHCl_3}$ 1748, 1724, 1610 and 1587 cm^{-1}; λ_{max}^{MeOH} 280 mμ (ε 22300).

Found: C, 58.56; H, 4.70; N, 13.13%. Calcd for $C_{32}H_{28}N_6O_{10}$: C, 58.53; H, 4.30; N, 12.81%.

*9-(3′-Amino-3′-deoxy-3′-C-hydroxymethyl-β-*D*-ribofuranosyl)adenine (**11**).* A solution of **10** (1.13 g) in a mixture of methanol (30 m*l*) and *n*-butylamine (10 m*l*) was refluxed for 19 hr. After evaporation of the resulting solution to dryness, ethyl acetate (50 m*l*) was added to the residue and the mixture was allowed to stand overnight in a refrigerator. The colorless precipitates (440 mg) were separated by filtration and recrystallized from 10% aqueous methanol (20 m*l*): yield 140 mg (27%); mp 230°C; $[\alpha]_D^{14}$ –60° (*c* 1.1, water); RD[19] (c 0.015, water) at 20°C; $[\Phi]_{300}$ –800°, $[\Phi]_{278}$ –1900° (tr); $\lambda_{max}^{H_2O}$ 259mμ (ε 17100), $\lambda_{max}^{0.1NHCl}$ 257 mμ (ε 16100), $\lambda_{max}^{0.1NNaOH}$ 260 mμ (ε 16700); τ^{D_2O} 1.89, 2.17 (s, H-2 and H-8), 4.12 (d, H-1′, $J_{1',2'}$=7.2 Hz) and 5.39 (d, H-2′).

Found: C, 44.91; H, 5.65; N, 28.29%. Calcd for $C_{11}H_{16}N_6O_4$: C, 44.59; H, 5.44; N, 28.37%.

*6-Chloro-9-(3′-C-acetoxymethyl-2′,5′-di-*O*-acetyl-3′-deoxy-3′-phthalimido-*D*-ribofuranosyl)purine (**12**).* A solution of **9** [prepared from **8** (3.46 g)] in a small amount of nitromethane was added to a mixture of 6-chloropurine (1.12 g), mercuric cyanide (1.84 g) and Drierite (10 g) in nitromethane (90 m*l*) under refluxing and stirring. The nitromethane (20 g) was distilled off and the residue was refluxed under stirring for 2 hr. The precipitates were filtered off and washed with ethyl acetate. The filtrate and washings were evaporated with silica gel (7 g) to dryness. The pow-

19) ORD were determined on a JASCO ORD/UV-5 recording spectropolarimeter.

dered residue was placed on a silica gel column (150 g, 3.3×30 cm) and eluted with benzene and benzene-ethyl acetate (10 : 1, 3 : 1, 2 : 1 and 1 : 1), successively. The eluent containing **12** was evaporated to afford a glass; yield 1.92 g (46.3%); λ_{max}^{MeOH} 242 and 266 mμ.

*6-Dimethylamino-9-[3'-deoxy-3'-(o-N,N-dimethylcarbamoyl)-benzamido-3'-C-hydroxymethyl-D-ribofuranosyl]purine (**13**).*[10] A solution of **12** (1.92 g) in 20% dimethylamine-methanol (20 ml) was refluxed for 3.5 hr. The reaction mixture was evaporated to dryness with silica gel (4 g). The powdered residue was placed on a silica gel column (90 g, 2.5×33 cm) and eluted with ethyl acetate and ethyl acetate-ethanol (4 : 1), successively. The eluent containing **13**[10] was evaporated to afford a glass (**13**)[10]; yield 1.18 g (70%). Further purification of the product (200 mg) was carried out by PLC (5 sheets of 0.5 mm×20×20 cm plate) to afford an analytical sample (130 mg): $[\alpha]_D^{20}$ −34° (*c* 3.0, methanol); ν_{max}^{KBr} 3350 and 1596 cm^{-1}; λ_{max}^{MeOH} 275 mμ (ε 20000). The NMR spectrum showed that **13** was an anomeric mixture (β/α=3.5/1): τ^{CD_3OD} (β anomer) 1.73, 1.77 (s, H-2 and H-8), 3.93 (d, H-1', $J_{1',2'}$=7.6 Hz), 4.94 (d, H-2'), 6.50 [s, purine N(CH$_3$)$_2$], 6.85, 7.07 [s, phthaloyl N(CH$_3$)$_2$]; τ^{CD_3OD} (α anomer) 4.08 (d, H-1', $J_{1',2'}$=4.3 Hz), 6.52 [s, purine N(CH$_3$)$_2$], 6.92, 7.17 [s, phthaloyl N(CH$_3$)$_2$].

Found: C, 54.03; H, 6.45; N, 18.94%. Calcd for $C_{23}H_{29}N_7O_6\cdot 1/2\ H_2O$: C, 54.33; H, 5.93; N, 19.27%.

*6-Dimethylamino-9-(3'-amino-3'-deoxy-3'-C-hydroxymethyl-β-D-ribofuranosyl)purine (**14**).* A solution of **13** (200 mg) in 50% *n*-butylamine-methanol (12 ml) was refluxed for 2 days. After evaporation, the residue was partitioned between water (10 ml) and ethyl acetate (10 ml). The aqueous layer was separated, washed with ethyl acetate (10 ml×7) and evaporated to dryness. The NMR spectrum of the glassy residue revealed that it was an anomeric mixture (β/α=3.5/1). The β-anomer (**14**) was separated as crystals from the methanolic solution of the anomeric mixture; yield 62 mg (48%). An analytical sample was obtained by further recrystallization from methanol: mp 172—174°C; $[\alpha]_D^{23}$ −68° (c 2.0, water); RD (*c* 0.017, water) at 20°C, $[\Phi]_{310}$ −800° $[\Phi]_{296}$ −1700° (tr); ν_{max}^{KBr} 3340 and 1600 cm^{-1}; $\lambda_{max}^{H_2O}$ 275.5 mμ (ε 20100), $\lambda_{max}^{0.1NHCl}$ 268 mμ (ε 20000) and $\lambda_{max}^{0.1NNaOH}$ 276 mμ (ε 19600); τ^{D_2O} 1.89, 2.13 (s, H-2 and H-8), 4.06 (d, H-1', $J_{1',2'}$=7.6 Hz), 5.34 (d, H-2') and 6.87 [s, purine N(CH$_3$)$_2$].

Found: C, 47.85; H, 6.45; N, 25.48%. Calcd for $C_{13}H_{20}N_6O_4$: C, 48.14; H, 6.22; N, 25.91%.

*N^2-Acetyl-9-(3'-C-acetoxymethyl-2',5'-di-O-acetyl-3'-deoxy-3'-phthalimido-β-D-ribofuranosyl)guanine (**15**).* To a mixture of N^2-acetylguanine (866 mg), mercuric cyanide (1.14 g) and Drierite (10 g) in nitromethane (100 ml) was added a solution of **9** [prepared from **8** (2.15 g)] in a small amount of nitromethane under refluxing and stirring. After nitromethane (10 ml) was distilled off, the mixture was refluxed for 2 hr under stirring. The precipitates were filtered off and washed with ethyl acetate and the filtrate and washings were evaporated with silica gel (2 g). The residue was placed on a silica gel column (70 g, 3.5×16 cm) and eluted with benzene, benzene-ethyl acetate (10 : 1, 5 : 1, 2 : 1 and 1 : 2), ethyl acetate and ethyl acetate-isopropanol (10 : 1), successively. Evaporation of the eluent containing **15** afforded the anomeric mixtue of **15** as a glass; yield 1.29 g (47%). The product (473 mg) was subjected to PLC (10 sheets of 0.5 mm×20×20 cm plate) with a solvent system, ethyl acetate-isopropanol (10 : 1). The upper bands with R_f value of 0.43 were collected under UV light (365 mμ) and extracted with ethyl acetate-isopropanol (1 : 1) to afford the β-anomer (**15**) as a glass: yield 211 mg (21%); $[\alpha]_D^{25}$ −5° (*c* 4.2, methanol); ν_{max}^{KBr} 3420, 1755, 1726, 1695 (sh), 1610 and 1562 cm^{-1}; λ_{max}^{MeOH} mμ (ε) 242(19800), 255 (18300), 260(18400) and 282 (14000); τ^{CD_3OD} 1.89 (s, H-8), 2.06 (s, phthaloyl C_6H_4), 4.00 (s, H-1' and H-2'), 7.68, 7.90, 7.96 and 8.14 (s, COCH$_3$).

Found: C, 53.08; H, 4.52; N, 13.42%. Calcd for $C_{27}H_{26}N_6O_{11}$: C, 53.11; H, 4.29; N, 13.71%.

The lower bands on PLC afforded a mixture of anomers (α/β=2/1): yield 97 mg (9.6%); τ^{CD_3OD} (α-anomer) 2.71 (s, H-8), 3.37 (d, H-1', $J_{1',2'}$=5.1 Hz) and 3.95 (d, H-2').

*9-(3'-Amino-3'-deoxy-3'-C-hydroxymethyl-β-D-ribofuranosyl)-guanine (**16**).* A solution of **15** (β anomer, 177 mg) in 50% *n*-butylamine-methanol (10 ml) was refluxed for 20 hr. The product (**16**) was deposited as solid in the reaction mixture, separated by centrifuging and washed with methanol; yield 55 mg. Recrystallization from water gave an analytical sample; mp 230°C (colored) but not fused below 300°C; $[\alpha]_D^{23}$ −25° (*c* 1.6, 0.1 N HCl), RD (*c* 0.025, water) at 20°C, $[\Phi]_{320}$ −500°, $[\Phi]_{310}$ −650°(tr); ν_{max}^{KBr} 3380, 3150, 1690, 1653, and 1595 cm^{-1}; $\lambda_{max}^{H_2O}$ 251 mμ (ε 11900) and 274 mμ (ε 8600)(sh), $\lambda_{max}^{0.1NHCl}$ 256.5 mμ (ε 11400) and 275 mμ (ε 8400)(sh), $\lambda_{max}^{0.1NNaOH}$ 258 mμ (ε 9300) and 269 mμ (ε 9500).

Found: C, 40.31; H, 5.60; N, 25.38%. Calcd for $C_{11}H_{16}N_6O_5\cdot H_2O$: C, 40.00; H, 5.49; N, 25.45%.

*N^4-Acetyl-1-(3'-C-acetoxymethyl-2',5'-di-O-acetyl-3'-deoxy-3'-limido-β-D-ribofuranosyl)cytosine (**17**).* A mixture of *N*^{4}-acetylcytosine (0.875 g), mercuric cyanide (1.45 g) and Drierite (10 g) in nitromethane (120 ml) was heated and nitromethane (20 ml) was distilled off at atmospheric pressure. To the resulting mixture was added a solution of **9** [prepared from **8** (2.74 g)] in a small amount of nitromethane under refluxing and stirring. After the second distillation of nitromethane (10 ml), the reaction mixture was refluxed for 2.5 hr under stirring. The precipitates were filtered off and washed with ethyl acetate. Silica gel (2 g) was added to the combined filtrate and washings and evaporated. The residual powders were placed on a silica gel column (50 g, 3.8×17 cm) and eluted with benzene, benzene-ethyl acetate (2 : 1 and 1 : 2), ethyl acetate and ethyl acetate-isopropanol (10 : 1), successively. The eluent containing **17** was evaporated to afford a crystalline solid (1.46 g, 45%). Pure β-anomer (**17**) was obtained by recrystallization of the crystals from ethanol, the first crop 398 mg and the second 252 mg. Total yield 650 mg (45% from the anomeric mixture); mp 268—273.5°C (sintered); $[\alpha]_D^{20}$ +28° (*c* 2.0, dimethyl sulfoxide); ν_{max}^{KBr} 3420, 3140, 1754, 1725, 1662, 1624 and 1560 cm^{-1}; λ_{max}^{MeOH} 242 mμ (ε 22400) and 299 mμ (ε 9000); τ^{DMSO-d_6} 1.75 (d, H-6, $J_{5,6}$=7.6 Hz), 2.77 (d, H-5), 3.65 (d, H-1', $J_{1',2'}$=5.2 Hz), 4.06 (d, H-2'), 7.82, 7.86, 7.88 and 8.26 (s, COCH$_3$).

Found: C, 55.00; H, 4.53; N, 9.68%. Calcd for $C_{26}H_{26}N_4O_{11}$: C, 54.73; H, 4.59; N, 9.82%.

*1-(3'-Amino-3'-deoxy-3'-C-hydroxymethyl-β-D-ribofuranosyl)cytosine (**18**).* A solution of **17** (277 mg) in 50% *n*-butylamine-methanol (10 ml) was refluxed for 15 hr and then evaporated to dryness. The residue was dissolved in ethyl acetate (10 ml) and kept in a refrigerator. The colorless precipitates were collected by filtration and partitioned between water (10 ml) and ethyl acetate (10 ml). The aqueous layer was washed with ethyl acetate (10 ml×5) and evaporated to dryness; yield 123 mg (96%). An analytical sample was obtained reprecipitation from methanol-ethyl acetate; mp 117—120°C; $[\alpha]_D^{27}$ +29° (*c* 3.6, water); RD (*c* 0.029, water) at 20°C, $[\Phi]_{300}$+2700°, $[\Phi]_{289}$+4800 (pk); ν_{max}^{KBr} 3310, 3180 (sh), 1655, 1636 and 1600 (sh)cm^{-1}; $\lambda_{max}^{H_2O}$ 230 mμ (ε 7900) and 270 mμ (ε 8500), $\lambda_{max}^{0.1NHCl}$ 278.5

mμ (ε 11000), $\lambda_{max}^{0.1NNaOH}$ 231 mμ (ε 6900) and 272 mμ (ε 7800); τ^{D_2O} 2.10 (d, H-6, $J_{5,6}$=7.6 Hz), 3.91 (d, H-5), 4.02 d, H-1′, $J_{1',2'}$=6.0 Hz), 5.69 (d, H-2′).

Found: C, 43.65; H, 6.57; N, 18.55%. Calcd for $C_{10}H_{16}N_4O_5 \cdot CH_3OH$: C, 43.41; H, 6.63; N, 18.41%.

*1-(3′-C-Acetoxymethyl-2′,5′-di-O-acetyl-3′-deoxy-3′-phthalimido-β-D-ribofuranosyl)uracil (**19**).* To a solution of **9** [prepared from **8** (3.31 g)] in benzene (10 ml) was added 2,4-di-*O*-trimethylsilyluracil (5.0 g). The mixture was refluxed for 1 hr under stirring and 2,4-di-*O*-trimethylsilyluracil (3.0 g) was then added to this. After the mixture was refluxed for 2 days under stirring, ethanol (40 ml) was added and the resulting slurry was stirred for 30 min. The precipitates were removed by filtration. Silica gel (3 g) was added to the filtrate and evaporated. The residue was placed on a silica gel column (50 g, 3.8×17 cm) and eluted with benzene, benzene-ethyl acetate (5 : 1, 1 : 1, 1 : 2), successively. Evaporation of the eluent containing **19** afforded a pure sample of **19** as a glass; yield 846 mg (23%); $[\alpha]_D^{26}$ +27° (*c* 3.5, methanol); ν_{max}^{KBr} 3410, 1750 (sh), 1720 and 1635 (sh) cm^{-1}; λ_{max}^{MeOH} 242 mμ (ε 13900) and 257 mμ (ε 11600); τ^{CD_3OD} 2.09 (s, phthaloyl C_6H_4), 2.33 (d, H-6, $J_{5,6}$=7.9 Hz), 4.18 (d, H-1′, $J_{1',2'}$=4.4 Hz), 4.21 (d, H-5), 4.40 (d, H-2′), 7.90, 8.07 and 8.18 (s, $COCH_3$).

Found: C, 54.26; H, 4.77; N, 7.43%. Calcd for $C_{24}H_{23}N_3O_{11}$: C, 54.44; H, 4.38; N, 7.93%.

*1-(3′-Amino-3′-deoxy-3′-C-hydroxymethyl-β-D-ribofuranosyl)uracil (**20**).* A solution of **19** (116 mg) in 50% *n*-butylamine-methanol (10 ml) was refluxed for 18 hr. After evaporation the residue was partitioned between water (6 ml) and ethyl acetate (6 ml). The aqueous layer was washed with ethyl acetate (6 ml×7) and evaporated to afford a crystalline solid. To the residue was added isopropanol (6 ml) and the crystals of **20** were collected by centrifuging; yield 27 mg (45.1%). An analytical sample was obtained by recrystallization from water: mp 257.5°C (sintered), 261.5—262°C (decomp.); $[\alpha]_D^{20}$ +13° (*c* 1.0, 0.1 N HCl): RD (*c* 0.025, water) at 20°C, $[\Phi]_{300}$ +800°, $[\Phi]_{278}$ +2900° (pk); ν_{max}^{KBr} 3440, 3365, 1720 and 1680 cm^{-1}; $\lambda_{max}^{H_2O}$ 261.5 mμ (ε 10300), $\lambda_{max}^{0.1NHCl}$ 261 mμ (ε 10500), $\lambda_{max}^{0.1NNaOH}$ 263 mμ (ε 7600); τ^{D_2O} 2.06 (d, H-6, $J_{5,6}$=8.1 Hz), 4.00 (d, H-1′, $J_{1',2'}$=6.5 Hz), 4.04 (d, H-5), 5.69 (d, H-2′) and 6.31 (s, 3′ $-CH_2$).

Found: C, 44.01; H, 5.66; N, 15.13%. Calcd for $C_{10}H_{15}N_3O_6$: C, 43.95; H, 5.53; N, 15.38%.

The authors wish to thank Mr. S. Nakada for microanalyses and Dr. Y. Satoh of Rikkyo University for ORD measurements.

BULLETIN OF THE CHEMICAL SOCIETY OF JAPAN, VOL. 44, 3405—3409 (1971)

The Carboxylation Reaction using Nickel Catalysts. V.[1] The Catalytic Reaction of Propene with Nickel Carbonyl and Nickel Carbonyl-Triphenylphosphine

Sango KUNICHIKA, Yasumasa SAKAKIBARA,* Tadashi OKAMOTO, and Kentaro TAKAGI

Institute for Chemical Research, Kyoto University, Gokasho, Uji, Kyoto

** Chemical Laboratory of Textile Fibers, Kyoto University of Industrial Arts and Textile Fibers, Kyoto*

(Received May 4, 1971)

The carboxylation reaction of propene catalyzed by nickel carbonyl was studied undeer various conditions. Iso- and *n*-butyric acids were obtained in good yields under mild conditions in the presence of a large amount of an organic acid. The catalytic carboxylation area was examined in detail. The carboxylation reaction proceeded smoothly in tetrahydrofuran, acetic acid, and dioxane. The proportion of isobutyric acid was largest in acetic acid (72.5–77.5%). Triphenylphosphine (TPP) had a great effect on the reaction rate, the catalytic reaction area, and the product distribution. On the reaction mechanism, an active species (HNi(CO)(TPP)X) was taken to account for the experimental results.

The preparation of carboxylic acids or their derivatives from unsaturated compounds and carbon monoxide in the presence of metal carbonyls is an important synthetic reaction known well as the carboxylation reaction. Numerous reports have been published on this reaction[2] besides the original works of Reppe *et al.* In our previous studies it was found that the carboxylation of propylne[3] and propadiene[4] in the presence of nickel carbonyl and organic acids takes place smoothly under a low carbon monoxide pressure.

It is said that the carboxylation of olefins except such reactive ones as bicyclo[2,2,1]heptene derivatives needs more stringent reaction conditions than does that of acetylenes.[2] Concerning the carboxylation reaction of olefins catalyzed by nickel catalysts, few detailed investigations have been published; all of them have used much more severe conditions than those for propyne and propadiene reported by us. In this report, the carboxylation of propene using a

1) Part I—IV are designated as follows: I, Y. Sakakibara, This Bulletin, **37**, 1601 (1964). II, S. Kunichika, Y. Sakakibara, and T. Okamoto, *ibid.*, **40**, 885 (1967). III, Y. Sakakibara, T. Okamoto, and H. Kurauchi, *Bull. Inst. Chem. Res., Kyoto Univ.*, **45**, 175 (1967). IV, S. Kunichika, Y. Sakakibara, and T. Nakamura, This Bulletin, **41**, 390 (1968).

2) C. W. Bird, "Transition Metal Intermediates in Organic Synthesis," Logos Press, London (1967), p. 149.

3) S. Kunichika, Y. Sakakibara, and T. Nakamura, This Bulletin, **41**, 390 (1968).

4) S. Kunichika, Y. Sakakibara, and T. Okamoto, *ibid.*, **40**, 885 (1967).

nickel carbonyl catalyst has been investigated in detail with the aim of synthesizing butyric acid under milder conditions than those used in the literature.[5]

$$CH_3CH{=}CH_2 + CO + H_2O \xrightarrow{Ni(CO)_4} CH_3CH_2CH_2CO_2H + (CH_3)_2CHCO_2H$$

The effects on the reaction processes of the reaction temperature, the carbon monoxide pressure, the solvent, and the addition of triphenylphosphine (TPP) were examined. As was seen in the case of the oxo reaction, two isomers were obtained. The nickel carbonyl catalyst and a catalyst system composed of nickel carbonyl and TPP both initiated the reaction smoothly under mild conditions and gave excellent yields of butyric acid. The presence of TPP in the reaction system contributed to obtaining a stable catalytic reaction and had a large influence on the product distribution.

Experimental

Materials. The propene, carbon monoxide, nickel carbonyl, TPP, and other compounds employed in this study were commercial products which were proved to be sufficiently pure by gas chromatography and/or elemental analysis.

Apparatus and Procedures of Carboxylation. A 200-m*l* rotational stirring-type stainless-steel autoclave (used at about 800 rpm) was charged under nitrogen with the solvent, an organic acid, hydroquinone, and a catalyst. The vessel was then cooled to about −40°C and the air was replaced completely by nitrogen. After evacuation, carbon monoxide was introduced until the specified pressure was reached. Then, propene was injected by an injection pump. Two reaction processes, the batch process (A) and the constant pressure process (B), were employed. The (A) process was used to search for the catalytic reaction conditions. The vessel was heated to the specified temperature with stirring, and the fall in the pressure was observed at that temperature. The (B) process was used to collect the kinetic data of the reaction. In this case, the pressure of the vessel was kept constant during the reaction by continuously supplying carbon monoxide from a gas storage tank. The relative reaction rate was calculated roughly from the absorption curve of carbon monoxide in the initial reaction period. The supply of carbon monoxide was stopped during the reaction, after which the vessel was cooled to room temperature. Then, the remaining gas was discharged through a mixture consisting of carbon tetrachloride, bromine, and water to decompose the nickel carbonyl and capture the residual propene.

Analytical Procedures. The reaction products, isobutyric acid and *n*-butyric acid, were determined by gas chromatography using a 2.5-m column of 21% dioctyl sebacate and 4% sebacic acid at 125°C. Acetophenone was used as the internal standard substance. The amount of residual propene trapped as 1,2-dibromopropane was determined gas-chromatographically by a 2.5-m column of 30% dioctyl phthalate at 120°C, using anisole as the internal standard substance. The amount of nickel carbonyl remaining after the reaction was determined by the nickel dimethylglyoxime method.

Results and Discussion

Carboxylation in the Presence of Nickel Carbonyl. At the beginning of this study, some attempts were made to determine the favorable conditions. The results are shown in Table 1. Under the same conditions as those used for the carboxylation of propyne,[3] propene was unreactive and most of the propene and the nickel carbonyl were recovered (Run 1). The reaction under the carbon monoxide pressure using stoichiometric amounts of nickel carbonyl and an organic acid to propene (Run 2) showed a rapid pressure drop at 260°C; this drop indicated that the reaction was under way. In the next run (Run 3), where the amount of nickel carbonyl was reduced to a catalytic amount, the reaction started smoothly. When the amount of organic acid was reduced to a catalytic amount (Run 4), however, virtually no reaction was observed. It became apparent that a large amount of organic acid favored the carboxylation of propene. Therefore, subsequent experiments were carried out in the presence of a large amount of isobutyric acid or acetic acid.

Table 1. Preliminary study[a]

Run No.	Solvent m*l*	C_3H_6 g	$Ni(CO)_4$ g	Cocatalyst g		CO[b] atm	Reaction temp. °C	Reaction period, hr	Remarks
1	CH_3OH	8.4	2.0	H_2O	10	44— 45	160—163	1.5	recovered C_3H_6 96.2%
	70			AcOH	1.8	(10)			recovered $Ni(CO)_4$ 90.6%
2	THF	9.0	9.0	H_2O	25	154—108	260—270	5	
	25			IBA[c]	11.2	(48)			
3	THF	10.2	2.0	H_2O	25	153—140	250—270	5	
	25			IBA	11.2	(48)			
4	THF	13.8	2.0	H_2O	25	164—180	260—277	5.5	
	25			IBA	1.9	(49)			

a) In every case, 0.05 g of hydroquinone was used for the reaction. Reaction process, (A).
b) The range of total pressure during the reaction period is shown. The value on the left shows the initial total pressure and on the right does the final one. The value in parenthesis shows the initial pressure of carbon monoxide at room temperature.
c) IBA; isobutyric acid

5) W. Reppe, *Ann.*, **582**, 1 (1953); H. J. Hagemeyer, US 2739169 (1956); W. F. Gresham and R. E. Brooks, US 2448368 (1949).

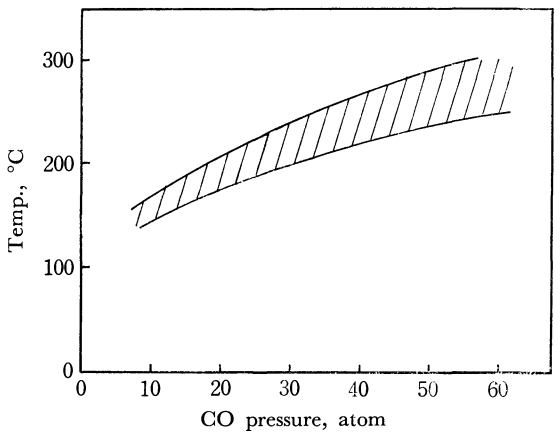

Fig. 1. Catalytic Reaction Area (Relation between the reaction temperature and the initial CO pressure at room temperature).
THF, 25 m*l*; H_2O, 25 m*l*; isobutyric acid, 11.2 g; Nickel carbonyl, 2.0 g; Propene, 4.3—12.5 g; Reaction process, (A).

Catalytic Reaction Area: The catalytic carboxylation using nickel carbonyl was influenced by the reaction temperature and the carbon monoxide pressure. In other words, there is an area of smooth catalytic reaction (afterwards abbreviated as CRA) on the carbon monoxide pressure *versus* reaction temperature diagram. The CRA was examined for the reaction of propene in the presence of a large amount of isobutyric acid: the results are shown in Fig. 1.[6] For a given carbon monoxide pressure, no fall in pressure was observed at temperatures outside of the specified area. That is, all the nickel carbonyl and propene charged were recovered at temperatures below this area; on the other hand, at temperatures above this area, the propene was recovered unchanged, and the nickel carbonyl was decomposed completely. In this region, the catalytic reaction occurred after a short induction period, and almost all the charged nickel carbonyl was recovered after the reaction.

Effect of the Temperature and the Carbon Monoxide Pressure on the Reaction Rate: Several runs were made varying the temperature and the carbon monoxide pressure. The results are shown in Table 2. For the same carbon monoxide pressure, the carboxylation reaction proceeded faster at higher temperatures within CRA. For example, raising the temperature from 160°C to 170°C increased the initial carbon monoxide absorption rate by a factor of 2 (Runs 6 and 7). On the other hand, decreasing the carbon monoxide pressure also accelerated the reaction so much that the rate at 10.5 atm was about two times that at 15 atm (Runs 5 and 7). From these values, it was roughly estimated that the rate is reversely proportional to about a square of the carbon monoxide pressure, as was observed in the case of propyne.[3]

Effect of the Solvent on the Reaction Rate: Six solvents which give a homogeneous solution were ex-

Table 2. Influence of temperature and CO pressure for the carboxylation of propene[a]

Run No.	CO[b] atm	Reaction temp., °C	Reaction period, hr	Relative rate[c]	Recovered $Ni(CO)_4$, %	Recovered C_3H_6, %	Product IBA g (%)[d]	Product NBA[e] g (%)	Product IBA/BA[f] %
5	15	169—171	11.5	1	78.1	25.6	9.3 (71.5)	3.5 (26.0)	72.5
6	10.5	159—165	9.5	1	95.6	36.6	6.0 (54.0)	1.7 (15.6)	77.5
7	10.5	168—172	11.5	2	85.4	27.3	9.3 (72.4)	3.4 (26.1)	73.5
8	8	159—162	7.5	4	82.4	41.7	7.1 (69.6)	2.5 (24.3)	74.1
9	7.5	169—170	1	—	12.4				

a) C_3H_6, 8.4 g; $Ni(CO)_4$, 2.0 g; AcOH, 50 m*l*; H_2O, 10 m*l*; Reaction process, (B).
b) The initial carbon monoxide pressure at room temperature.
c) The initial rate of Run 5 is taken as 1.
d) Yield based on consumed propene.
e) NBA; *n*-butyric acid.
f) BA; the sum of IBA and NBA.

Table 3. Influence of solvents for the carboxylation of propene[a]

Run No.	Solvent[b]	Reaction period, hr	Recovered $Ni(CO)_4$, %	Recovered C_3H_6, %	Product IBA, g (%)	Product NBA, g (%)	Product IBA/BA, %
5	AcOH	11.5	78.1	25.6	9.3 (71.5)	3.5 (26.0)	72.5
10	THF	7.0	62.8	42.3	3.9 (38.6)	2.3 (23.9)	62.5
11	dioxane	9.5	59.4	54.8	2.7 (43.4)	1.2 (11.6)	66.9
12	diglyme	4.2	63.3	56.3	1.3 (16.2)	0.6 (7.8)	67.6
13	dimethyl cellosolve	5.0	93.8	89.5	1.2 (63.1)	0.6 (31.1)	67.1
14	methyl ethyl ketone	6.0	81.9	68.3	1.7 (30.6)	0.8 (15.1)	67.1

a) CO, 15 atm; 170°C; $Ni(CO)_4$, 2.0 g; AcOH, 10 m*l*; H_2O, 10 m*l*; C_3H_6, 8.4 g; Reaction process, (B).
b) Used 40 m*l*.

6) CRA at the low carbon monoxide pressure is especially narrow. The appropriate temperature for 5 atm carbon monoxide pressure could not be found.

TABLE 4. CARBOXYLATION OF PROPENE IN THE PRESENCE OF TPP[a]

Run No.	TPP P/Ni	CO atm	Reaction temp., °C	Reaction period, hr	Relative rate		Recovered	Product		
					[b]	[c]	C_3H_6, %	IBA, g(%)	NBA, g(%)	IBA/BA, %
5	0	15	169—171	11.5		1	25.6	9.3(71.5)	3.5(26.0)	72.5
15	1	7.5	167—172	11.0	1		32.5	5.4(45.1)	3.1(26.0)	63.3
16	2	4	170—173	5.5		2	42.8	3.4(34.0)	4.1(40.6)	45.6
17	2	7.5	168—173	12.0	2.5	1.4	28.7	4.2(33.6)	4.8(38.0)	46.9
18	2	15	169—173	13.0		1	21.7	4.8(34.7)	4.6(33.7)	50.8
19	3	7.5	168—170	11.0	3.5		24.2	4.3(31.8)	5.3(39.8)	44.4
20	2	8	160—163	9.0		1	46.5	3.4(35.0)	3.4(35.0)	50.0

a) C_3H_6, 8.4 g; $Ni(CO)_4$, 2.0 g; AcOH, 50 ml; H_2O, 10 ml; Reaction process, (B).
b) The initial rate of Run 15 is taken as 1.
c) The initial rate of Run 18 is taken as 1.

amined. The results are listed in Table 3. The initial carbon monoxide absorption rates were faster in tetrahydrofuran, acetic acid, and dioxane than those in diglyme, dimethyl cellosolve, and methyl ethyl ketone. For synthetic purposes, acetic acid was the most suitable solvent from the viewpoints of the recovery of nickel carbonyl (high catalytic level), and the yield, and also from the viewpoint of the selectivity of the products, as will be described later.

Product Distribution: Two isomeric butyric acids were obtained by the carboxylation of propene. In Tables 2 and 3, isobutyric acid is shown to have been formed predominantly in every case. Decreasing the temperature tended to increase the proportion of isobutyric acid (Run 6). The solvent also had a considerable effect on the distribution of the two isomers. In acetic acid, the ratio of isobutyric acid to *n*-butyric acid (i/n) was highest. The reported ratios in the literature are i/n=1 by nickel carbonyl,[5] 1/3 by dicobalt octacarbonyl,[7] 2/1 by palladium catalysts,[8] and 1/3 by platinum chloride.[9] The high values obtained here, 2/1—3/1, are thus worthy of note.

Carboxylation in the Presence of Nickel Carbonyl and TPP. A catalyst system composed of nickel carbonyl and TPP was examined, and the results obtained were compared with those obtained using nickel carbonyl alone in order to determine the effect of TPP. The results are summarized in Table 4.

Effect of TPP on CRA: As has been described already, the catalytic carboxylation of propene in the presence of the nickel carbonyl catalyst was possible under the restricted conditions of Fig. 1. The presence of TPP made it possible to perform catalytic carboxylation smoothly under the conditions at which the carboxylation with nickel carbonyl alone did not occur because of the decomposition of the catalyst itself. For example, at 170°C and a carbon monoxide pressure of 7.5 atm, which lies outside the CRA for nickel carbonyl, the catalytic reaction proceeded smoothly in the presence of TPP (Runs 9 and 17). A smooth catalytic reaction was also obtained even at a carbon monoxide pressure of 4 atm (Run 16). This stability of the catalyst system is advantageous from the synthetic point of view.

Effect of TPP on the Reaction Rate: Although the presence of TPP acted to broaden the CRA, it did not accelerate the reaction. At 160°C and a carbon monoxide pressure of 8 atm, the presence of 2 mole equivalents of TPP to nickel carbonyl served to slow down the initial reaction rate to roughly one-fourth that in the absence of TPP (Runs 8 and 20). At 170°C and a carbon monoxide pressure of 15 atm, however, the above two catalyst systems showed approximately equal rates (Runs 5 and 18). Increasing the amount of TPP from 1 to 3 mole equivalents to nickel carbonyl raised the relative rate from 1 to 3.5 (Runs 15, 17, and 19).

Effect of the Carbon Monoxide Pressure on the Reaction Rate: In the presence of 2 mole equivalents of TPP to nickel carbonyl, the decrease in the carbon monoxide pressure raised the reaction rate. This tendency, however, is not so remarkable as that in the absence of TPP. The relative initial rates at carbon monoxide pressures of 15, 7.5, and 4 atm in the presence of 2 mole equivalents of TPP to nickel carbonyl were 1.0, 1.4, and 2.0 respectively (Runs 18, 17, and 16), while in the absence of TPP the initial reaction rate at a carbon monoxide pressure of 10.5 atm was about 2 times that at a carbon monoxide pressure of 15 atm (Runs 5 and 7).

Effect of TPP on the Product Distribution: The presence of TPP had a great influence on the distribution of two isomers. Increasing the ratio of TPP to nickel carbonyl (P/Ni) raised the proportion of *n*-butyric acid, as is shown in Table 4. In connection with such results, it was reported recently that, in the hydroformylation reaction using cobalt[10] or rhodium[11] carbonyl complexes, the presence of phos-

7) A. Matsuda and H. Uchida, This Bulletin, **38**, 710 (1965); F. Piacenti and C. Cioni, *Chem. Abstr.*, **63**, 1137 (1965).
8) J. Tsuji, M. Morikawa, and J. Kiji, *Tetrahedron Lett.*, **1963**, 1437; K. Bittler, N. V. Kutepow, D. Neubauer and H. Reis, *Angew. Chem. Int. Ed. Engl.*, **7**, 329 (1968).
9) L. J. Kehoe and R. A. Schell, *J. Org. Chem.*, **35**, 2846 (1970),
10) E. R. Tucci, *Ind. Eng. Chem., Prod. Res. Develop.*, **7**, 32, 125 (1968); *ibid.*, **8**, 286 (1969); L. H. Slaugh and R. D. Mullineaux, *J. Organometal. Chem.*, **13**, 469 (1968); W. Kniese, J. Hienburg and R. Fischer, *ibid.*, **17**, 133 (1969); F. Piacenti, M. Bianchi. E. Benedetti, and P. Frediani, *ibid.*, **23**, 257 (1970).
11) R. L. Pruett and J. A. Smith, *J. Org. Chem.*, **34**, 327 (1969); J. H. Craddock, A. Hershman, F. E. Paulik, and J. F. Roth, *Ind. Eng. Chem., Prod. Res. Develop.*, **8**, 291 (1969).

phorus compounds gives linear carboxylation products selectively. In the presence of 2 mole equivalents of TPP to nickel carbonyl, the isobutyric acid ratio seemed to increase slightly with an increase in the carbon monoxide pressure (Runs 16, 17, and 18), but the difference in the carbon monoxide pressure initially charged does not fully reflect the total isomer distribution, for the partial pressure of carbon monoxide is not constant during the reaction.

Carboxylation Reaction Path. The active species of catalyst for the carboxylation using nickel carbonyl is speculated to be $HNi(CO)_nX$ (I) (n; maybe 2), which is probably formed by the addition to nickel carbonyl of an active hydrogen compounds (HX) such as hydrogen halide, organic acid, and water. The reaction path is believed to be as follows:[3,12]

$$Ni(CO)_4 + HX \rightleftharpoons HNi(CO)_nX + (4-n)\ CO$$

$$CH_3CH{=}CH_2 + HNi(CO)_nX \rightleftharpoons CH_3\underset{H}{\underset{|}{C}}H\text{-}\underset{Ni(CO)_nX}{\underset{|}{C}}H_2$$

$$CH_3\underset{X(CO)_nNi}{\underset{|}{C}}H\text{-}\underset{H}{\underset{|}{C}}H_2 \quad \overset{CO}{\rightleftharpoons} \quad CH_3CH_2CH_2CONi(CO)_nX$$

$$(CH_3)_2CHCONi(CO)_nX \quad \xrightarrow{H_2O} \quad CH_3CH_2CH_2CO_2H + HNi(CO)_nX$$

$$(CH_3)_2CHCO_2H + HNi(CO)_nX$$

In the presence of TPP, nickel carbonyl would exist as its TPP derivatives formed by replacing some carbon monoxide by TPP, depending on the reaction conditions. The results of the rate and the product distrubution suggest that the active species, different from that in the absence of TPP, also works in the reaction. As recent articles have reported the existence of $HNi[P(C_6H_{11})_3]_2Cl$[13] and $HNi[P(C_6H_{11})_3]_2(OAc)$,[14] it would be reasonable to consider the $HNi(CO)(TPP)X$ (II) species as corresponding to the $HNi(CO)_2X$ (I) of the nickel carbonyl catalyst. Concerning the formation of II, the following scheme may be considered:

$$\begin{array}{ccc} & Ni(CO)_{4-n}(TPP)_n & \\ {\scriptstyle CO \text{ or } TPP}\ \swarrow\!\!\nearrow\ {\scriptstyle HX} & & {\scriptstyle CO \text{ or } TPP}\ \nwarrow\!\!\searrow\ {\scriptstyle HX} \\ HNi(CO)_2X & \overset{\overset{TPP}{\rightleftharpoons}}{\underset{CO}{}} & HNi(CO)(TPP)X \\ (I) & & (II) \end{array}$$

It has been reported that TPP has a strong field-stabilizing power as a ligand.[15] Therefore, both the active species, II, and the Ni-alkyl complexes derived from II would have higher thermal stability than I and its alkyl derivatives. This is in accordance with the finding that, in the presence of TPP, the catalytic carboxylation proceeds under a low carbon monoxide pressure at a high temperature. As for the results of the reaction rate in the presence of TPP, a clear explanation is difficult at the present time. The rate of carboxylation reaction is probably determined by the step of the reaction between propene and the active species, such as I and II.[3] The rate is, then, determined by the reactivity and the concentration of active species. However, their dependence on the reaction conditions is very complicated because of the presence of the many equilibrium steps described in the above scheme. The increase in the proportion of n-butyric acid is caused mainly by two factors, both of which are in good accordance with the effect of TPP on the product distribution. One is the increase in the hydride character of Ni–H,[16] which facilitates the anti-Markownikoff addition to olefin. The other is the steric bulkiness of TPP, which facilitates the formation of the n-alkyl complex rather than that of the more crowded iso-alkyl complex.

The authors wish to thank the Ministry of Education for the financial support of Grant No. 84071.

12) R. F. Heck, "Mechanism of Inorganic Reactions," ed. by R. F. Gould, American Chemical Society, Washington, D. C. (1965), p. 181.

13) M. L. H. Green and T. Saito, *Chem. Commun.*, **1969**, 208.

14) K. Jonas and G. Wilke, *Ang. Chem. Int. Ed. Engl.*, **8**, 519 (1969).

15) M. L. H. Green, "Organometallic Compounds," Vol. II, ed. by G. E. Coates, M. L. H. Green, and K. Wade, Bulter & Tanner, Frome and London (1968), p. 224.

16) TPP has a greater σ-donar character compared with carbon monoxide.

Studies on Hetero-Cage Compounds. II.[1] pK_a Studies on the 3,10-Diazabicyclo[4.3.1]decane System

Tadashi Sasaki, Shoji Eguchi, and Tsutomu Kiriyama

Institute of Applied Organic Chemistry, Faculty of Engineering, Nagoya University, Furo-cho, Chikusa-ku, Nagoya

(Received May 4, 1971)

The pK_a values of pseudopelletierine (**1**), 10-methyl-3,10-diazabicyclo[4.3.1]decan-4-one (**2**), 10-methyl-3,10-diazabicyclo[4.3.1]decane (**3**), 6,8-*exo*-ethanopseudopelloetierine (**4**), 7,9-*exo*-ethano derivatives **5** and **6** of **2** and **3** were measured potentiometrically in water-methyl cellosolve (20 : 80 v/v) at 20°C. The conformational problems in the 3,10-diazabicyclo[4.3.1]decane system were discussed based on the observed pK_a' (pK_{mcs}) values. The characteristic conformational behavior of the monocation (**7**) of **3** was suggested by the higher value of its pK_{mcs} than of **6**.

In a previous publication,[1] we described the synthesis of 10-methyl-3,10-diazabicyclo[4,3.1]decane (**3**) and its 7,9-*exo*-ethano derivative (**6**) by lithium aluminum hydride reduction of 10-methyl-3,10-diazabicyclo[4.3.1]decan-4-one (**2**) and its 7,9-*exo*-ethano derivative (**5**) respectively, both of which were obtained by the Schmidt reaction of pseudopelletierine (**1**) and 6,8-*exo*-ethanopseudopelletierine (**4**), respectively. From the chemical behavior toward methyl iodide and from the NMR spectra, it was shown that the *N*-methyl pyramidal inversion[2] in **3** is allowed, while that in **6** is prohibited by the steric hindrance due to the 7,9-*exo*-ethano bridge, and the *N*-methyl group is forced to take an *anti*-orientation.[3] In this paper, we wish to describe the results of the pK_a studies on these systems.

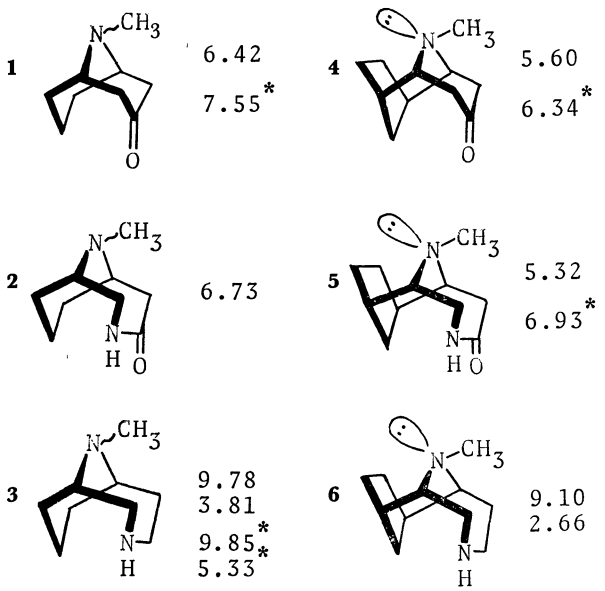

Fig. 1. pK_{mcs} of **1**—**6** (* in water) at 20°C.

The apparent pK_a values of the amines **1**—**6** were measured potentiometrically in water - methyl cellosolve (20 : 80 v/v) at 20°C. The obtained values (pK_{mcs}) are summarized in Fig. 1, in which the values in water (pK_a) are also shown for **1**, **3**, **4**, and **5**.

The pK_{mcs} value of pseudopelletierine was 6.42 which is larger than the value (5.60) of its *exo*-ethano derivative (**4**). The pK_{mcs} value (6.73) of the lactam **2** was also larger than that (5.32) of the corresponding *exo*-ethano lactam **5**. This suggests that the basicity of the *t*-amine is reduced as much as 0.82—1.41 pK unit by the presence of the ethano bridge. This can be ascribed to the more crowdedness in the conjugate acids of **4** and **5** than in those of **1** and **2**. A somewhat similar effect of the steric demand on the amine basicity was also recognized by other workers.[4]

The pK_{mcs} value of **2** was 0.31 larger than that of the ketone **1**, while the value of the ethano-lactam **5** was 0.28 smaller than that of the ethano ketone **4**. This suggests a contradictory effect of the lactam group on the *tert*-amine basicity in **1**—**2** and **4**—**5** series. However, examination of the values of **4** and **5** in water indicates that **5** is a stronger base than **4**. Thus, the basicity of the *t*-amines **2** and **5** might be strengthened by the presence of the lactam group instead of the carbonyl group in **1** and **4**.[5,6]

The tricyclic diamine **6** had two pK_{mcs} values (9.10 and 2.66). In the NMR data of mono salt (**10**)

1) Part I: T. Sasaki, S. Eguchi and T. Kiriyama, *J. Org. Chem.*, **36**, 2061 (1971).

2) For recent reviews on the pyramidal inversion, see a) H. Kessler, *Angew. Chem.*, **82**, 237 (1970); b) A. Lauk, L. C. Allen, and K. Mislow, *ibid.*, **82**, 453 (1970).

3) The prefix *anti* refers to direction with respect to the ethano bridge.

4) For example, see a) H. O. House, P. P. Wickham, and H. C. Müller, *J. Amer. Chem. Soc.*, **84**, 3139 (1962); b) L. A. Paquette and J. W. Heimaster, *ibid.*, **88**, 763 (1966).

5) The basicity promoting effect of the lactam group could be explained by inductive and field effects as well as the ring-size effect. *Cf.* The pK_a value of acetamide (−1.40, 18°C) and cyclohexanone (−6.8, 25°C); J. T. Edward, S. C. R. Meacock, *J. Chem. Soc.*, **1957**, 2000; H. J. Campbell and J. T. Edward, *Can. J. Chem.*, **38**, 2109(1960). For a review on the electronic effects, see C. K. Ingold,"Structure and Mechanism in Organic Chemistry," 2nd Ed., Cornell University Press (1969), Chapter II.

6) The fact that the pK_{mcs} value of **5** is smaller than that of **4** could be explained by the steric hindrance in the solvation. For a similar effect of a carbonyl group on acetolysis rates of 2,6-bridged bicyclo[2.2.1]heptyl and bicyclo[2.2.2]octyl tosylates strengthened by the steric hindrance of the solvation, see R. M. Moriarty, C. R. Romain, and T. O. Lovett, *J. Amer. Chem. Soc.*, **89**, 3927 (1967).

of **6** with trifluoroacetic acid, the chemical shifts of C_2- and C_4-methylene protons adjacent to the *s*-amino group were more deshielded compared to C_1- and C_6-methine protons adjacent to the *t*-amino group.[1] This indicates that the first equivalent of the acid is neutralized by the *s*-amino group in **6** rather than by the *t*-amino group. Hence, the value 9.10 is assigned to pK_{mcs} of the *s*-amino group in **6**, and 2.66 to that of the *t*-amino group. The much smaller value (2.66) of the *t*-amino group in **6** than the values 5.32 and 5.60 of the *t*-amino group in **4** and **5** is apparently explained by the strong inductive- and field-effects of the $-NH_2^+$ group.[5] The assignments are compatible with the fact that the pK_a values of *t*-amines are smaller than those of the corresponding *s*-amines in several monocyclic amines such as pyrrolidine, *N*-methylpyrrolidine, piperidine, *N*-methylpiperidine, morpholine, and *N*-methylmorpholine as summarized in Fig. 2.[7]

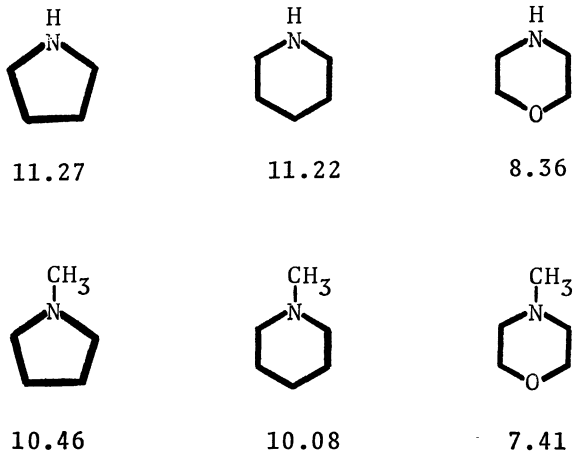

Fig. 2. pK_a of cyclic amines (in water at 25°C).

On the other hand, bicyclodiamine **3** had two pK_{mcs} values (9.78 and 3.81), in which a larger one could be assigned to the *s*-amino group and a smaller one to the *t*-amino group analogously to **6** and other monocyclic *s*- and *t*-amines. The larger pK_{mcs} value of the *s*-amino group in **3** than that in **6**, and the greatly decreased value of the *t*-amino group in **3** compared to **1** and **2** suggest that the monocation of **3** should be more stable than that of **6** for some steric reasons. An inversion of the homopiperazine ring to a boat form is possible in **3**, while in **6**, the presence of the 8,9-*exo*-ethano bridge fixes the N–CH_3 group in *anti*-direction, the inversion of the homopiperazine ring thus, being prohibited. Hence, the monocation of **3** can exist in such a conformation as **7** where the piperazine ring takes the chair-form and the homopiperazine ring takes the boat-form as evidenced by the NMR data of compounds **7** and **9**.[1] A similar

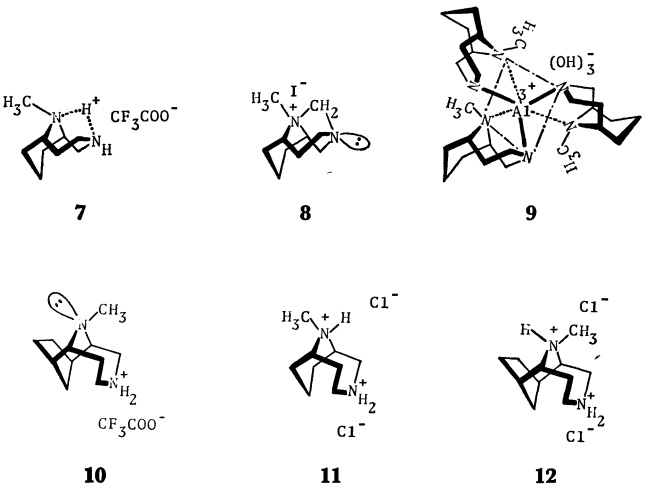

but more drastic conformational effect on the amine basicity has been reported on the bispidine system.[8] *N,N*-Dimethylbispidine (**13**) has a very large pK_a value such as 11.88. This is 1.8 pK unit larger than *N*-methylpiperidine. The stabilizing factors of the monocation might be involved in a very stable adamantane-like conformation such as **14.**

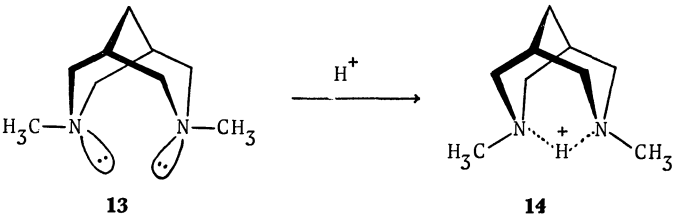

In the bicyclodiamine **3**, the stabilizing effect of the monocation by the *t*-amino group can be fulfilled only by inverting its chair-homopiperazine ring to a boat-homopiperazine ring leading to a strained 1,5-diazabicyclo[3.2.1]octane ring structure instead of a strain-free adamantane form[9] in bispidine **13**. Hence, the increase in the pK_{mcs} value from 9.10 of **6** to 9.78 of **3** is reasonably moderate compared to that of *N*-methylpiperidine to bispidine. Furthermore, the decrease in the second pK_{mcs} value (3.81) or the difference between the two pK_{mcs} values (9.78 and 3.81) seems smaller than that in **13**,[10] but larger than that in piperazine whose pK_a values are reported to be 9.82 and 5.68 at 20°C.[11,12] The abnormally smaller value (2.66) of the *t*-amino group in **6**, how-

7) a) S. Searles, M. Tamres, F. Block, and L. A. Quarterman, *J. Amer. Chem. Soc.*, **78**, 4917(1956); b) "Handbook of Organic Structural Analyses," Ed. by Y. Yukawa, W. A. Benjamin, Inc., New York, N. Y. (1965), p.p. 584–613.

8) J. E. Douglass and T. B. Ratliff, *J. Org. Chem.*, **33**, 355 (1968).

9) Strictly speaking, adamantane is not strain-free, *cf*, P. v. R. Schleyer, J. E. Williams, and K. R. Blanchard, *J. Amer. Chem. Soc.*, **92**, 2377 (1970).

10) The second pK_a value is not reported but even the disalt formation is described to be difficult; Ref. 8.

11) The pK_a value of homopiperazine does not seem to have been reported.

12) G. Schwarzenbach, B. Maissen, and H. Ackermann, *Helv. Chim. Acta*, **35**, 2333 (1952).

ever, is explained by both the electronic effects of $-NH_2^+$ group and the above described steric hindrance of the *exo*-ethano bridge.

A homopiperazine ring seems to be one of the smallest membered ring of diazacyclic compounds that can afford a stable monocation form with one equivalent of acid. Investigation[13] on the proton exchange rate and the *N*-pyramidal inversion rate in *N,N*-dimethylpiperazine monohydrochloride discloses no intermediate formation of a 1,4-diazabicyclo[2.2.1]heptane type monocation in the conversion of *trans*- to *trans**-*N,N*-dimethylpiperazine monohydrochloride, though an organometallic complex formation of bicyclo[2.2.1]heptane skeleton is reported on *N,N*-dimethylpiperazine.[14]

Finally, the stereochemistry of the quaternization in **3** might be discussed briefly.[15] The fact that the basicity of the *s*-amino group is stronger than that of the *t*-amino group in **3**, and the formation of tricyclic diazaundecanium iodide (**8**) from **3** and methylene iodide is facile[1] supports the view that an approach of a proton or methylene iodide from an upper side of the homopiperazine ring in **3** (Fig. 3, A) is more favored to that from a lower side (Fig. 3, B), even if the homopiperazine ring takes a pseudo-chair (a flattened-chair) form due to the steric repulsion between C_8-methylene and $-NH-CH_2-$ groups.[16]

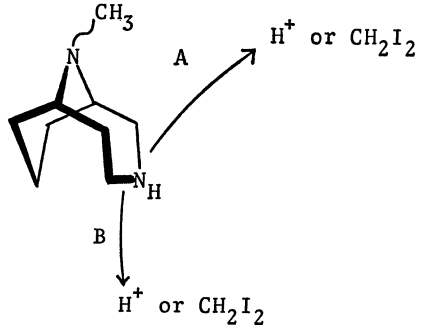

Fig. 3.

Experimental

pK_a measurements were carried out by titrating potentiometrically in an 80% methyl cellosolve-hydrochloric acid solution of each amine ith 0.1 N potassium hydroxide at 20°C. Titration was performed on a Radiometer Model TTl. The 80% methyl cellosolve solution consisted of 4.0 m*l* of methyl cellosolve, 0.6 m*l* of 0.1 N hydrochloric acid, 0.4 m*l* of water, and *ca.* 1.2 mg of each amine.

All the amines used had reported physical constants: pseudopelletierine (**1**), mp 63—65°C (sealed tube) (lit,[17] 63—64°C); 10-methyl-3,10-diazabicyclo[4.3.1]decan-4-one (**2**), mp 164—166°C (lit,[18] 164—166°C); 10-methyl-3,10-diazabicyclo[4.3.1]decane (**3**), mp 43—46°C (sealed tube) (lit,[1] 43—46°C); 6,8-*exo*-ethanopseudopelletierine (**4**), mp 100—102°C (lit,[4b] 103—104°C); 7,9-*exo*-ethano-10-methyl-3,10-diazabicyclo[4.3.1]decan-4-one (**5**), mp 154°C (lit,[1] 154°C); 7,9-*exo*-ethano-10-methyl-3,10-diazabicyclo[4.3.1]-decane (**6**), mp 66—69°C (sealed tube) (lit,[1] 66—69°C).

The authors express their appreciation to Prof. T. Goto and Dr. Y. Kishi for the pK_a measurements.

13) J. L. Sudmeier and G. Occupati, *J. Amer. Chem. Soc.*, **90**, 154 (1968).

14) For example, see G. E. Ryschkewitsch, *ibid.*, **91**, 6535 (1969).

15) a) For a recent review on the quaternization of *t*-amines, see A. T. Bottini, "Selective Organic Transformations," Vol. 1, Ed. by B. S. Thyagarajan, Wiley-Interscience, New York, N. Y. (1970), p.p. 89–142; b) D. R. Brown and J. McKenna, *J. Chem. Soc., B*, **1969**, 570.

16) For a similar repulsion in bicyclo[3.3.1]nonane system, see N. L. Allinger, J. A. Hirsch, M. A. Miller, I. J. Tyminski, and F. A. Van-Catledge, *J. Amer. Chem. Soc.*, **90**, 1199 (1968).

17) Organic Syntheses, Coll. Vol. IV, 1963, p. 816.

18) L. A. Paquette and J. W. Heimaster, *J. Amer. Chem. Soc.*, **88**, 763 (1966).

The Reaction of Nitriles under High Pressure. I. The Formation of Triphenyl-1,3,5-triazine *via* the Equilibrium among Benzonitrile, Alcohols, and Benziminoethers[1]

Masahiro KURABAYASHI, Koshin YANAGIYA, and Masahiko YASUMOTO

The Government Chemical Industrial Research Institute, Tokyo, 6th Div., Mita, Meguro-ku, Tokyo

(Received May 13, 1971)

Benziminoethers were formed from benzonitrile and alcohols to the equilibrium extent, and then 3 mol of benziminoethers were reacted with each other to afford triphenyl-1,3,5-triazine at 2—10 kbar and 100—120°C. The equilibrium shifted toward benziminoether with an increase in the pressure. The equilibrium constant decreased progressively in the order of methanol>ethanol≈*n*-propanol≈*n*-butanol> isopropanol≈*sec*-butanol, which accords with the increasing number of substituents on the α-position of the alcohols. The formation of triphenyl-1,3,5-triazine obeyed the second-order reaction mechanism and was also retarded in the same order. The reaction was found to proceed in the following manner: Benziminoethers produced by the addition of alcohols to benzonitrile dimerize through a rate-determining step and then trimerized into triphenyl-1,3,5-triazine. The apparent activation volume of the formation of triphenyl-1,3,5-triazine amounted to -31 cm^3 mol^{-1} at 110°C when methanol was used as the alcohol. The accelerating effect of the pressure on the formation of triphenyl-1,3,5-triazine is concluded to be mainly caused by the shift of equilibrium toward benziminoether. Three isomers of cyanopyridine were converted in good yields into the corresponding triazines under high pressure.

It is known that nitriles with active hydrogen on the α-position trimerize into trisubstituted-*s*-triazines *via* iminoethers (IE)[2] or amidines.[3] In 1950, Cairns[4] treated many kinds of nitriles with lower alcohols at 70—150°C and 3—8 kbar and thus obtained *s*-triazines in yields of 10—80%. He showed also that the lower the alcohol used the greater the promoting effect. In spite of these interesting findings, he did not describe the mechanism of the reaction nor the role of alcohols, although it had been known that the formation of IE from several alcohols and nitriles is reversible in the presence of alcoxide under atmospheric pressure.[5]

In our first attempt to investigate the reaction of nitriles under high pressure, benzonitrile was chosen as a representative nitrile. The equilibrium constants among benzonitrile, several alcohols, and their iminoethers were determined under high pressure, and the mechanism of the formation of triphenyl-*s*-triazine (TPT) was examined.

Results and Discussion

When the initial ratio of methanol to benzonitrile was widely varied (see Table 1), the plot of the concentration[6] of methylbenziminoether (MBI) against the benzonitrile concentration × methanol concentration gave straight lines (see Fig. 1). This fact indicates the existence of an equilibrium among benzonitrile, methanol, and MBI such as is described beolw;

$$C_6H_5CN + ROH \underset{k_2}{\overset{k_1}{\rightleftharpoons}} C_6H_5C(NH)OR \qquad (1)$$

$$K = k_1/k_2 = [IE]/[C_6H_5CN][ROH], \qquad (2)$$

where k_1 and k_2 are the rate constants for the forward and reverse reactions respectively. The equilibrium constant, K, was determined from Fig. 1 as 0.097 and 0.043 mol^{-1} l at 100°C with methanol under pressures of 7850 and 6000 kg/cm^2 respectively. Figure 2 shows that this equilibrium was established less than ten hours after the initiation of the run with methanol at 100°C and at about 8000 kg/cm^2 and not affected by the progress of the formation of TPT.

The experimental results with several lower alcohols are listed in Table 2. Fairly good agreements are seen between the K values in the right and left small columns, illustrating that the equilibria of Eq. (1) were established with these lower alcohols as well as with methanol under the reaction conditions noted in the table. Though Eq. (1) is a quasi-equilibrium reaction succeeded by the trimerization of IE (mentioned later), it is thought that the K values referred to in this paper agree, within the limits of experimental error, with those of the ideal equilibrium state influenced by no other reaction. K decreased conspicuously when methanol was replaced by ethanol, or when *n*-propanol was replaced by isopropanol. However, the replacement of ethanol by *n*-propanol or *n*-butanol or the replacement of isopropanol by *sec*-butanol did not change the constant appreciably. No IE was produced with *t*-butanol. This fact can easily be understood if one asumes that the forward reaction in Eq. (1) is more strongly retarded by the increasing substitution (either methanol or primary or secondary or tertiary) at the α-position of alcohol than is the reverse reaction.

The natural logarithms of the values of K listed in Tables 2 and 3 are plotted against the pressure and are

---

1) Presented in part at the 12th Meeting of the High-pressure Symposium, Hiroshima, October, 1970.

2) F. C. Schaefer and G. A. Peters, *J. Org. Chem.*, **26**, 2778 (1961); A. Yakubovich, *Chem. Abst.*, **58**, 526, 1256, 13257 (1963); *ibid.*, **62**, 562 (1965).

3) F. C. Scharfer, I. Hechenbleikner, G. A. Peters, and V. P. Wystrach, *J. Am. Chem. Soc.*, **81**, 1466 (1959).

4) T. L. Cairns, N. W. Larchar, and B. C. McKusick, *J. Amer. Chem. Soc.*, **74**, 5633 (1952), U. S. 2503979 (1950).

5) E. K. Marshall and S. F. Acree, *Am. Chem. J.*, **49**, 127 (1913); F. C. Scharefer and G. A. Peters, *J. Org. Chem.*, **26**, 412 (1961).

6) For the calculation of the concentrations, the volume of the reaction medium was assumed to be the sum of the apparent volume of benzonitrile, alcohol, and IE, which were calculated by dividing their quantities as determined in the reaction medium by their specific gravities at 20°C. Under atmospheric pressure, the additivity in volume was found to be nearly constant for mixtures of benzonitrile, methanol, and MBI.

TABLE 1. EFFECT OF THE RATIO OF BENZONITRILE AND METHANOL[a)]

7850 kg/cm²				6000 kg/cm²			
$C_6H_5CN:CH_3OH$ (mol)	Yields (%)[b)]			$C_6H_5CN:CH_3OH$ (mol)	Yields (%)		
	C_6H_5CN	MBI[c)]	TPT[c)]		C_6H_5CN	MBI	TPT
1:79.3	26.5	55.7	7.09	1:61.6	44.8	35.8	2.33
1:39.1	22.7	56.1	15.1	1:29.8	42.2	38.6	6.75
1:25.5	25.2	53.5	19.6	1:18.2	44.1	41.7	8.28
1:19.2	20.1	51.1	25.9	1:12.8	43.5	39.1	13.0
1:12.1	19.1	46.0	31.8	1: 9.64	41.5	37.3	15.3
1:12.2	18.8	46.0	32.0	1: 7.48	42.5	35.7	17.5
1: 8.87	21.3	42.7	36.2	1: 4.78	42.3	31.9	22.9
1: 7.26	17.5	41.4	40.4	1: 3.21	46.2	29.0	21.4
1: 4.66	18.9	45.3	39.8	1: 2.16	52.0	22.5	21.5
1: 3.22	20.7	43.6	37.8	1: 1.42	67.2	19.8	8.56
1: 1.97	28.8	40.0	30.9	1: 0.825	80.7	14.5	1.54
1: 1.29	49.7	34.3	12.8	1: 0.360	89.6	7.53	1.68
1: 0.987	62.3	31.5	9.09				
1: 0.651	69.3	22.4	3.48				
1: 0.328	87.2	13.5	0.55				

a) Reaction conditions: 120°C, 10 hr.
b) Theoretical yield based on benzonitrile.
c) Abbreviations of methylbenziminoether and triphenyl-1,3,5-triazine respectively.

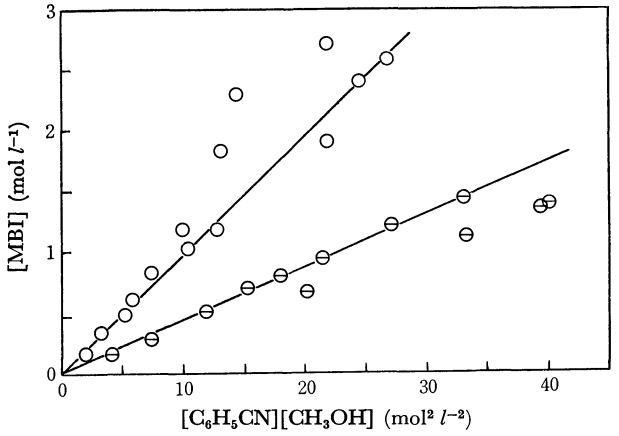

Fig. 1. Relation among the concentrations of components at 10 hr after the initiation of the reaction in the various molar ratio of C_6H_5CN: CH_3OH at 120°C.
○, 7850 kg/cm²; ⊖, 6000 kg/cm².
Deviation from the lineality seems to appear in the range of relatively high yield of TPT. The three points markedly deviating from the 7850 kg/cm² line all belongs to the runs yielding more than 35% of TPT.

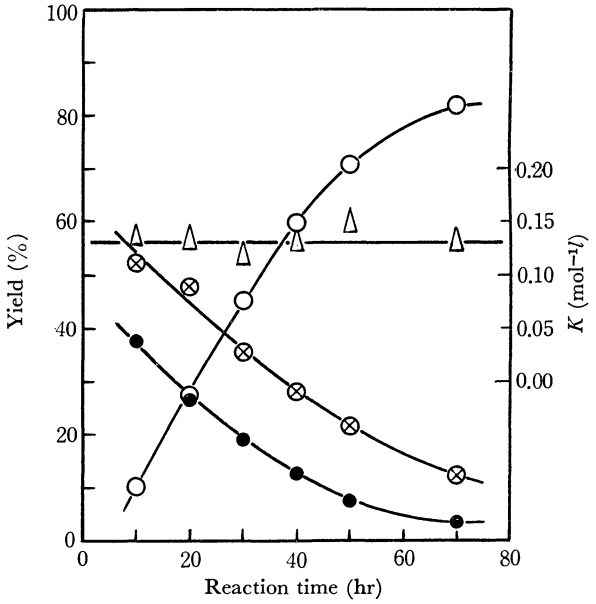

Fig. 2. Time dependence of the composition of the reaction products at the starting ratio of C_6H_5CN: CH_3OH=1: 3.2 (in mol) at 7850 kg/cm² and 100°C.
●, C_6H_5CN; ⊗, MBI; ○, TPT; △, Equilibrium constant, K=[MBI]/[C_6H_5CN][CH_3OH]

shown in Fig. 3. The change in the volume (ΔV) in Eq. (1) is given by the thermodynamic equation for the liquid phase, $\partial \ln K/\partial P = -\Delta V/RT$, and was found, by applying the tangential method to the curves in Fig. 3, to be -17.9 ml mol^{-1} at 120°C and 1 atm. This value is approximately equal to the calculated volume difference, -16.5 ml mol^{-1}, which is the difference between the sums of the molar volumes of the reactants (left side) and the product (right side) of Eq. (1) at 120°C.

The apparent rate of the formation of TPT, v_m (in mol l^{-1} hr^{-1}) is given by:

$$v_m = x/tV_m, \qquad (3)$$

where x is the amount of TPT (in mol) produced in the reaction time, t (in hr), and where V_m is the mean volume of the reaction medium (in l), that is, the arithmetic mean of the initial volume[7] and the volume at time t.[6] The curve with open circles in Fig. 4 shows the $\ln v_m$ values plotted against the reaction pressure; it indicates a marked positive effect of the pressure on the production of TPT. From the thermodynamic equa-

7) The initial volume was obtained by summing the volumes of the components at the initial point, which were calculated from the experimentally-obtained value of K and the starting amounts of the reactants.

TABLE 2. EFFECT OF ALCOHOLS ON THE EQUILIBRIUM CONSTANT, $K=[IE]/[C_6H_5CN][ROH]$[a]

The K value in the left small column of each alcohol in the large column indicates the equiriblium constant obtained for a mixture of alcohol and benzonitrile, and the K value in the right small column indicates the constant obtained for a mixture of the same alcohol and its benziminoether (IE).

Reaction conditions		8000 kg/cm², 100°C, 10 hr						8000 kg/cm², 120°C, 10 hr					
R-OH		CH_3-		C_2H_5-		n-C_3H_7-		CH_3-		C_2H_5-		n-C_3H_7-	
Reactants (g)	C_6H_5CN	2.450	0.046[b]	2.005		1.643	0.030[b]	2.487	0.045[b]	1.955		1.651	0.031[b]
	ROH	2.282	1.693	2.685	1.898	2.904	2.050	2.331	1.684	2.624	1.899	2.893	2.105
	IE		3.490		2.936		2.606		3.421		2.944		2.764
Yields (%)	C_6H_5CN	37.2	35.3	65.8	61.7	89.1	58.1	32.5	30.5	69.5	67.5	74.5	68.8
	IE	52.8	53.7	34.6	30.9	8.27	39.2	40.6	40.4	28.2	27.3	23.7	24.6
	TPT	8.69	11.4	0.57	6.84	0.10	3.43	28.1	30.1	3.15	7.71	1.21	4.67
K ($mol^{-1}l$) $\times 10^{-2}$		11.8	11.5	4.95	4.46	—[c]	—[c]	9.65	9.57	3.70	3.59	3.09	3.34

Reaction conditions		8000 kg/cm², 120°C, 72 hr								
R-OH		n-C_3H_7-		iso-C_3H_7-		n-C_4H_9-		sec-C_4H_9-		t-C_4H_9-
Reactants (g)	C_6H_5CN	1.533	0.027[b]	1.519		1.258	0.011[b]	1.305	0.006[b]	1.959
	ROH	2.729	1.884	2.656	1.805	2.800	1.995	2.817	1.969	4.224
	IE		2.413		2.326		2.374		2.324	
Yields (%)	C_6H_5CN	64.3	56.3	81.6	69.5	63.3	48.7	89.0	85.1	(100)
	IE	19.6	16.8	8.98	8.85	22.9	18.6	7.62	8.03	
	TPT	12.5	23.6	4.06	19.4	11.2	28.7	1.72	4.35	
K ($mol^{-1}l$) $\times 10^{-2}$		3.31	3.09	1.21	1.25	4.64	4.62	1.12	1.12	

Reaction conditions		5000 kg/cm², 120°C, 240 hr											
R-OH		CH_3-		C_2H_5-		n-C_3H_7-		iso-C_3H_7-		n-C_4H_9-		sec-C_4H_9-	
Reactants (g)	C_6H_5CN	1.958	0.036[b]	1.631		1.399	0.024[b]	1.328		1.197	0.009[a]	1.240	0.006[a]
	ROH	1.854	1.357	2.187	1.523	2.451	1.639	2.381	1.765	2.584	1.602	2.675	1.734
	IE		2.675		2.357		2.129		2.146		1.905		2.069
Yields (%)	C_6H_5CN	17.0	14.9	71.5	67.2	75.4	73.0	89.1	90.4	74.5	70.9	91.7	90.9
	IE	11.2	10.7	8.88	8.42	8.74	9.09	3.97	4.24	10.8	9.60	3.56	3.60
	TPT	66.9	69.4	14.9	24.1	11.5	14.2	1.97	5.42	12.4	18.3	1.12	2.19
K ($mol^{-1}l$) $\times 10^{-2}$		3.38	2.71	1.00	0.979	1.26	1.31	0.484	0.500	1.80	1.66	0.488	0.500

a) Reaction conditions: C_6H_5CN:ROH=1:3.2 (in mol).
In the right small column of each alcohol in large columns, the yields were based on benzoyl group.
b) These figures are the calculated values of benzonitrile contained as the impurities in each iminoethers.
c) The reaction time is thought to be deficient for the establishment of the equilibrium state in both or either of the two runs.

TABLE 3. EFFECT OF PRESSURE[a]

Reaction pressure (kg/cm²)	Yields (%)			K ($mol^{-1}l$) $\times 10^{-2}$
	C_6H_5CN	MBI	TPT	
10200	9.94	36.3	54.9	22.0
9160	18.3	45.0	36.9	16.7
7850	33.9	50.3	17.7	11.4
6620	51.3	44.8	7.14	6.96
5500	66.0	31.1	2.82	3.65
4400	81.4	19.4	0.87	1.81
3350	84.4	14.8	0.36	1.31
2340	92.4	9.23	0.0	0.774
1000	95.5	4.33	0.0	0.365
4	98.1	2.31	0.0	0.171
4[a]	97.6	2.03	0.0	0.150

a) Reaction conditions: 110°C, 10 hr, C_6H_5CN:CH_3OH=1:3.2 (in mol).
b) The reaction was carried on for 96 hr in a glass syringe.

tion, $\partial \ln k/\partial P = -\Delta V^*/RT$, the apparent activation volume for the formation of TPT from benzonitrile in the presence of methanol was calculated to be −31.0 ml mol^{-1} at 110°C and 3000—5000 kg/cm². The value of v_m decreased with an increase in the number of substitution on the α-position of the alcohol added, and decreased with an increase in the number of the carbon atoms in the alkyl substituents.

The yield of TPT prepared from a mixture of an alcohol and the benziminoether of the alcohol was larger than that prepared from a mixture of the alcohol and benzonitrile (see Table 2). This fact indicates that IE plays an important role in the formation of TPT. At lower initial mixing ratios of benzonitrile to methanol, a linear relation was obtained between v_m and $[IE]_m$[2 8] as shown in Fig. 5, indicating that

8) $[IE]_m$ is the average value of the concentration of IE at the initial point[7] and after the reaction time t[6].

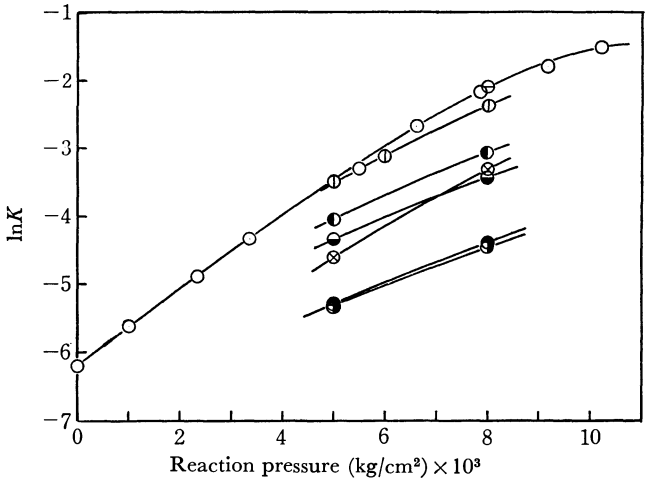

Fig. 3. Plots of the natural logarithm of equilibrium constant K listed in Table 2 *vs.* reaction pressure.

	R-OH	°C		R-OH	°C
⊖	CH_3–	100	◒	*n*-C_3H_7–	120
○	CH_3–	110	◓	*iso*-C_3H_7–	120
⊕	CH_3–	120	◐	*n*-C_4H_9–	120
⊗	C_2H_5–	120	◑	*s*-C_4H_9–	120

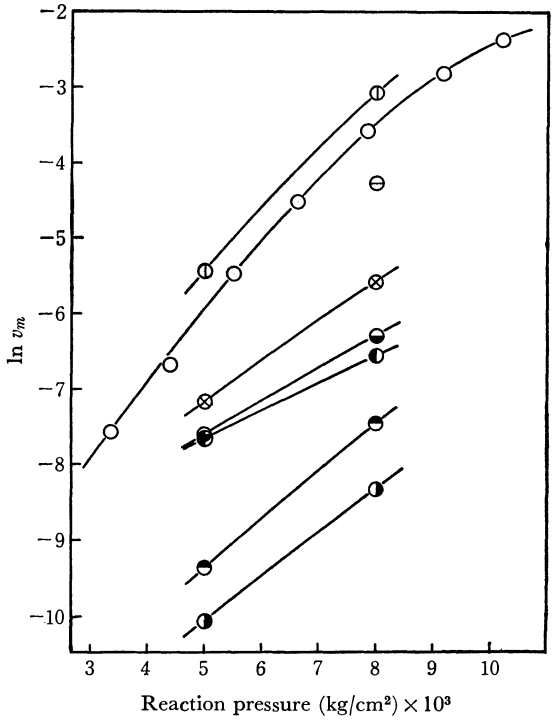

Fig. 4. Plots of the natural logarithm of v_m, which is the mean rate of the formation of TPT in Eq. (3), *vs.* reaction pressure.

	R-OH	°C		R-OH	°C
⊖	CH_3–	100	◒	*n*-C_3H_7–	120
○	CH_3–	110	◓	*iso*-C_3H_7–	120
⊕	CH_3–	120	◐	*n*-C_4H_9–	120
⊗	C_2H_5–	120	◑	*s*-C_4H_9–	120

the formation of TPT is a second-order reaction with respect to the IE concentration. It can be inferred from these results that TPT is formed through a relatively slow dimerization of IE, followed by the cyclization of the dimer with another molecule of IE. The reaction mechanism is given by:

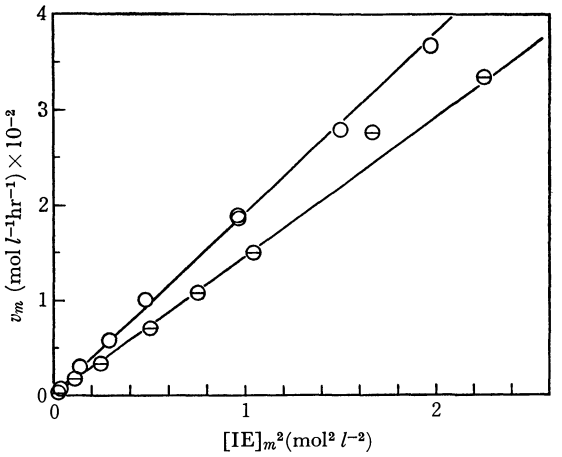

Fig. 5. Relation between the mean rate of the formation of TPT, v_m, and the mean concentration of MBI, $[IE]_m$, in the various initial ratio of C_6H_5CN:CH_3OH at 120°C.
○, 7850 kg/cm²; ⊖, 6000 kg/cm²

The initial concentrations of MBI, $[IE]_i$, was calculated from the data in Table 1 and listed in the following table together with the observed concentrations of it, $[IE]_{obs}$, at ten hours after the initiation of the runs.

7850 kg/cm²

C_6H_5CN:CH_3OH (mol)	$[IE]_{obs}$ (mol/*l*)	$[IE]_i$ (mol/*l*)
1:79.3	0.170	0.212
1:39.1	0.337	0.412
1:25.1	0.484	0.607
1:19.2	0.605	0.778
1:12.1	0.837	1.129
1:8.86	0.835	1.125
1:7.26	1.023	1.423
1:4.66	1.187	1.622

6000 kg/cm²

C_6H_5CN:CH_3OH (mol)	$[IE]_{obs}$ (mol/*l*)	$[IE]_i$ (mol/*l*)
1:61.6	0.140	0.191
1:29.8	0.289	0.389
1:18.2	0.511	0.626
1:12.8	0.657	0.871
1:9.64	0.807	0.930
1:7.48	0.949	1.092
1:4.78	1.212	1.372
1:3.21	1.442	1.560

$$2C_6H_5C(NH)OR \xrightarrow[\text{slow}]{k_3} C_6H_5C(OR)=N-C(NH)C_6H_5 + ROH \quad (4)$$

$$C_6H_5C(OR)=N-C(NH)C_6H_5 + C_6H_5C(NH)OR \xrightarrow[\text{fast}]{k_4} \text{(2-phenyl-4,5-diphenylimidazole)} + 2ROH \quad (5)$$

Here, we propose alkoxybenzimidoylbenzamidine[9] as the structure of the dimer.

If Eq. (4) is the rate-determining step in the formation of TPT, the rate of the formation of TPT is given as:

$$d[TPT]/dt = k_3[IE]^2, \quad (6)$$

9) Yakubovich had obtained a dimer of perfluoroadipo(or glutaro-)iminoether hydrochloride which has a similar structure.[10]

10) A. Ya. Yakubovich, E. L. Zaitseva, R. M. Gitina, U. P. Bazov, I. M. Filatova, and G. I. Braz, *J. General Chem. U. S. S. R.*, **36**, 878 (1966).

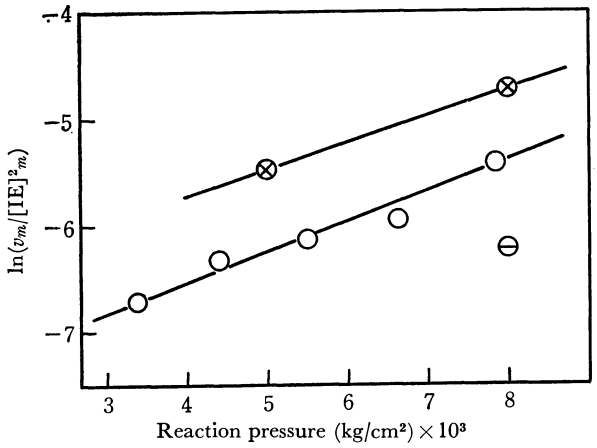

Fig. 6. Plots of $v_m/[IE]_m^2$, which is the rate of Eq. (4) expressed by Eq. (8), *vs.* reaction pressure at 100—120°C for 10 hr in the initial ratio of C_6H_5CN:CH_3OH=1: 3.2.
⊖, 100°C; ○, 110°C; ⊗, 120°C

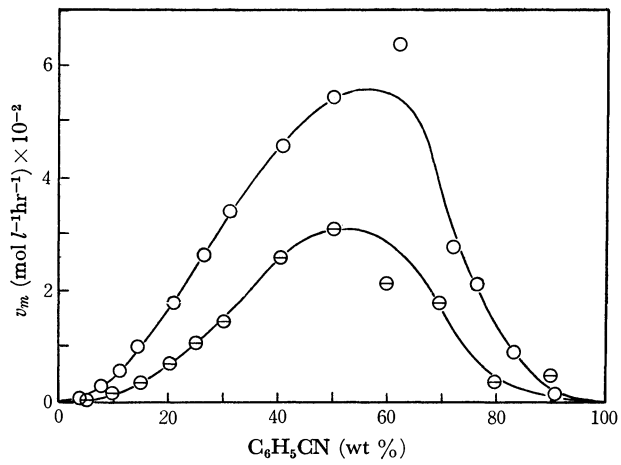

Fig. 7. Relation between the mean rate of the formation of TPT and the initial ratio of C_6H_5CN: CH_3OH at 120°C for 10 hr.
○, 7850 kg/cm² ⊖, 6000 kg/cm²

where k_3 is the rate constant of Eq. (4). From Eq. (3), v_m can be expressed as:

$$v_m \approx d[TPT]/dt \quad (7)$$

and:

$$k_3 \approx v_m/[IE]_m^2 \quad (8)$$

By plotting the natural logarithm of $v_m/[IE]_m^2$ against the reaction pressure (Fig. 6), the activation volume (ΔV^*) of Eq. (4) was determined to be 9 m*l* mol^{-1} in the range of 3000—8000 kg/cm². This indicates that the effect of the pressure on this rate-determining step is relatively small. The marked effect of the pressure on the formation of TPT can, therefore, be mainly ascribed to the fact that pressure shifts the equilibrium of Eq. (1) toward the right.

Figure 7 shows that the value of v_m is at its maximum when the mixing ratio of benzonitrile to methanol is in the range of from 1: 3/2 to 1: 2/3 in weight or from 1: 3 to 1: 2 in molar ratio. The presences of these maxima are expected from Eqs (6) and (2), which mean that the rate of the formation of TPT is proportional to the square of the concentration of IE, *i.e.*, to those of the concentration of benzonitrile and methanol respectively; those facts are important for the effective use of the capacity of the pressure vessel.

As is shown in Table 4, the addition of a small amount of acids stopped the formation of both MBI and TPT, while the addition of bases had little effect on their formation. These results obtained under high pressure differ from those of the commonly-employed synthetic methods, in which a large amount of strong

Table 4. Effect of acids and bases[a]

Starting substances			Yields (%)		
C_6H_5CN: CH_3OH (wt ratio)	Reagents	(mol/C_6H_5CN)	C_6H_5CN	MBI	TPT
1:1			50.2	50.0	3.63
1:0.5			66.1	24.8	2.09
1:1	Hydrogen chloride	0.1			0.0
1:1	Acetic acid	0.1	93.0	0.0	0.0
1:0.85	Pyridine	0.2	74.2	19.9	3.41
1:0.77	Triethylamine	0.2	82.9	6.91	1.03

a) Reaction conditions: 6600 kg/cm², 100°C, 10 hr.

Table 5. Effect of approtic solvents[a]

Reactants (g)		Solvents				Yields (%)			Relative[b] velocities
				Dielectric constants					
C_6H_5CN	CH_3OH	Substances	(g)	(ε_r)	(°C)	C_6H_5CN	MBI	TPT	
2.49	1.25	Dioxane	1.25	2.03	(25)	74.4	20.7	0.02	0.21
2.23	1.12	$(Et_2)O$	1.12	4.34	(20)	76.3	24.2	0.21	0.28
2.43	1.22	$(Me_2N)_3PO$	1.22	30	(20)	72.2	17.2	2.53	2.66
3.17	1.59			(33)[c]	(25)	66.1	24.8	2.09	1.00
2.51	1.26	$C_6H_5NO_2$	1.26	34.8	(25)	69.6	25.5	1.35	1.28
2.52	1.26	$AcN(Me)_2$	1.26	37.7	(20)	59.5	23.8	11.1	12.4
2.50	0.0	$HC(O)N(Me)_2$	2.50	37.7	(20)	107.2	0.0	0.0	0.0
2.46	1.23	$HC(O)N(Me)_2$	1.23	37.7	(20)	64.0	13.3	18.1	18.4
2.51	1.25	AcNHMe	1.26	179	(30)	57.4	23.4	12.2	13.6

a) Reaction conditions: 6600 kg/cm², 100°C 10 hr.
b) $v_m/[IE]_m^2$ are recalculated by taking the value of the run, in which no solvent was added, as unity.
c) Dielectric constants of C_6H_5CN and CH_3OH are 25.2 and 33 respectively, at 25°C.

acids[11-13] or bases[14] are necessary for the direct formation of *s*-triazines from nitriles (having no α-hydrogen). Weakly acidic conditions are also required for the trimerization of IE.[2,10] When a part of the methanol in the initial mixture was replaced by some aprotic solvent, the $v_m/[IE]_m^2$ ratio decreased in the decreasing order of the dielectric constant (see Table 5). These results suggest that the solvation of IE or its dimer, which is expected to be of a considerably polar nature, causes the rate of Eq. (4) to increase.

The procedure mentioned above may be a useful method of preparing various types of IE and trisubstituted-*s*-triazines, because it requires no chemically-reactive catalyst. For example, the three isomers of cyanopyridine were trimerized into the corresponding tripyridyl-*s*-triazines in an almost quantitative yield in the presence of methanol.

Experimental

Materials. Benzonitrile and the six alcohols, all of an EP grade, were carefully dried and distilled. Their water contents were determined by the Karl-Fisher method and were found to be less than 0.02%. The hydrochloride of IE was obtained by Pinner's method by introducing hydrogen chloride into a mixture of benzonitrile and alcohol. The resulting hydrochloride was neutralized, and the IE liberated was extracted and finally distilled. MBI: Yield, 74.5%; bp 61.5—62.3°C/3 mmHg; d_4^{20} 1.0684; n_D^{20} 1.5442; content, 98.7% by gas-liquid phase chromatography (glc). Ethylbenziminoether: 77.0%; 96.2—97.8°C/10 mmHg; 1.0312; 1.5295; 95.7%. *n*-Propyl-: 74.8%; 92°C/4 mmHg; 1.0392; 1.5220; 96.9%. Isopropyl-: 32.6%; 73°C/4 mmHg; 1.0274; 1.5171; 95.0%. *n*-Butyl-: 63.9%; 102—104°C/4 mmHg; 1.0241; 1.5179; 99.6%. *sec*-Butyl-: 21.5%; 86.6°C/2 mmHg; 1.0159; 1.5132; 98.7%. The impurities in IE thus prepared were mainly benzonitrile and/or benzoates. The cyanopyridines were supplied by Koei Chem. Ind., and the melting points of α-, β-, and γ- were 28.3°C, 38.7°C, and 78.6°C respectively.

Reaction Apparatus and Procedure. Collapsible lead capsules with a volume of a few milliliters were filled with the starting materials and put into a Bridgeman-type pressure vessel, in which less than twelve capsules could be placed, and compressed just below the desired pressure by introducing compressed oil from the pressure generator. Then the vessel was quickly heated for 30—40 min until the temperature inside its wall reached just below the desired level; thereafter, the pressure and the temperature were maintained at the desired levels. The reaction pressure was determined by means of a manganin-cell-type assembly corrected by the phase transition pressure of mercury. When the desired reaction time had passed, the temperature of the vessel was reduced to 50°C or less within 30—50 min in order to stop the reaction by cooling the wall with water. Sometimes a glass syringe or a polytetrafluoroethylene capsule was employed; no substantial wall effect was found.

Analysis. For the determination of benzonitrile and IE, glc (Reoplex 400, 4 mm i.d. × 750 mm, 50—250°C, 4°C/min) was employed. The TPT was filtered from the reaction medium, washed in methanol, recrystallized from toluene, and weighed. Solubility correction was made for the calculation of the yield of TPT.

Identification. MBI: A mixture of benzonitrile and methanol (each 2.2 g) was treated at 120°C and at 7800 kg/cm² for 5 hr and then fractionated by glc. The IR spectrum and the retention time of the glc of the fraction (0.5 g) at 150—160°C agreed with those of the authentic sample mentioned above (Found: C, 70.64; H, 6.66; N, 10.86%). The other five preparations of IE were identified by the retention time of glc with the respective authentic samples. TPT: 4.2-g portions of benzonitrile and methanol were similarly treated at 7800 kg/cm² and at 145°C for 3 hr, the product was diluted with methanol and filtered. The TPT (mp 236.8°C; yield, 3.34 g and 79.1%) thus separated was recrystallized from toluene as fine needles (Found: N, 14.14%; mp 237.1°C; mol wt (mass spectroscopy (MS)) 309). The IR spectrum and melting point agreed with those of the authentic sample prepared by the trimerization of benzonitrile in the presence of chlorosulfonic acid.[11] Tris(2-pyridyl)-*s*-triazine: 8.73-g portions of 2-cyanopyridine and methanol were treated at 100°C and at 8000 kg/cm² for 24 hr. The triazine thus produced was completely precipitated by the addition of water (yield, 8.62 g (98.6%)) and was recrystallized from water (Found: C, 69.14; H, 3.92; N, 27.08%; mp 256°C). The melting point and IR spectrum agreed with those of an authentic sample (Tokyo Chem. Ind.; mp 255°C). Tris(3-pyridyl)-: 9.37-g portions of nicotinonitrile and methanol were treated at 100°C and at 8000 kg/cm² for 30 hr. The precipitate was filtered, washed in methanol, weighed 9.08 g (99.1%), and recrystallized from pyridine. Found: C, 68.94; H, 3.92; N, 27.04%; mp 311°C; mol wt (MS), 312; IR, 1580, 1520, 1360 cm⁻¹ for the triazine ring. Calcd for $C_{18}H_{12}N_6$: C, 69.22; H, 3.87; N, 26.91%; mol wt, 312. Tris(4-pyridyl)-: 8.92-g portions of isonicotinonitrile and methanol were treated similarly; the product was filtered and washed in methanol to yield 6.71 g (75.2%). The crude triazine was recrystallized from pyridine. Found: C, 69.29; H, 4.01; N, 26.81%; mp 374°C; mol wt (MS), 312; IR, 1570, 1515, 1370 cm⁻¹. Calcd for $C_{18}H_{12}N_6$: C, 69.22; H, 3.87; N, 26.91%; mol wt, 312. A conciderable amount of an oily matter containing the triazine was also separated.

Mr. Toshiro Minegishi of our Institute cooperated in designing the high-pressure apparatus employed in this study. The authors wish also to express their thanks to Dr. Masasuke Yamada of Koei Chem. Ind. for his gifts of the cyanopyridines used in the present investigation.

11) A. Cook and D. Jones, *J. Chem. Soc.*, **1941**, 278.
12) E. R. Bissell and R. E. Spenger, *J. Org. Chem.*, **24**, 1147 (1959).
13) K. Wakabayashi, M. Tsunoda, and Y. Suzuki, This Bulletin, **42**, 2924 (1969); *ibid.*, **44**, 148 (1971).
14) E. M. Smoline and L. Rapoport, "*s*-Triazines and Derivatives," Interscience Publishers, New York (1959), p. 151.

Conformations of the Esters. V.[1] The Conformations of Carbonates

Michinori Ōki and Hiroshi Nakanishi

Department of Chemistry, Faculty of Science, The University of Tokyo, Hongo, Bunkyo-ku, Tokyo

(Received May 13, 1971)

In alkyl or aryl carbonates, the presence of conformational isomers (*s-cis* and *s-trans*) has been confirmed by infrared and nuclear magnetic resonance spectroscopic techniques. The dipole-moment measurements also support the conclusions obtained from the spectroscopic data.

The conformation of the carbonate has been claimed by Kubo,[2] Thomson,[3] and Longster[4] to be *s-trans-s-trans* on the basis of the data on the dipole moments of dimethyl and diethyl carbonates. In the light of the fact that the *s-cis* conformer can exist together with the *s-trans* in some esters of formic acid which carry the bulky alkyl group,[5] and that carbamates have *s-cis* and *s-trans* conformers,[1] it seemed that it would be interesting to reinvestigate the conformation of carbonates, which are the analogs of esters.

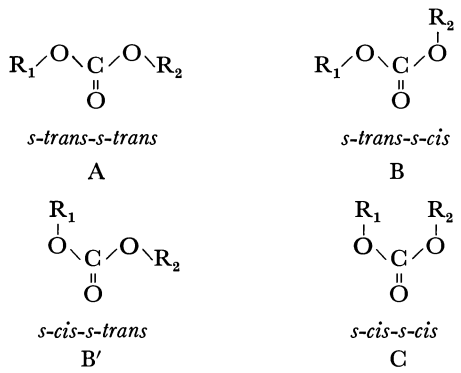

Fig. 1. Four conformational isomers of the carbonate.

In discussing the conformations of carbonates, the four conformers shown in Fig. 1 must be taken into account. C conformer (*s-cis-s-cis*) can be considered to be unimportant, for the repulsion between R_1 and R_2 groups is very large, even if both R_1 and R_2 groups are methyl groups. If the R_2 group is bulkier than the R_1 group ($R_2 > R_1$), the B conformer will be more stable than the B′ conformer, because the length of the C–O_{ether} bond (1.36 Å) is longer than that of C=O (1.20 Å); hence, the repulsion between O_{ether} and R_2 in the B conformer can be expected to be smaller than that between C=O and R_2 in the B′ conformer. As to the chief factors governing the preference of the conformations of the ester, three factors (dipole-dipole interaction, lone pair-lone pair interaction, and the steric repulsion between the carbonyl and the alkyl groups or between the two alkyl groups) were described in an earlier paper.[5] In the carbonates, two additional factors must be taken into account in discussing the conformations: the dipole-dipole interaction between C–O and O–R_2 and the lone pair-lone pair repulsion between two ether oxygens(the so-called "rabbit ear effect",[1,6] (Fig. 2)[7]). With regard to the first factor, the B conformer is favored over the A conformation, in the nonpolar media, while with regard to the second factor, the A conformer is destabilized by the larger repulsion between the two ether oxygens. Therefore, the possibility of the existence of the *s-cis* conformer is larger in the carbonate than in the ordinary ester. The purpose of this paper is to present various sepectroscopic and dipole-moment data to confirm the existence of the *s-trans-s-cis* conformer in some carbonates.

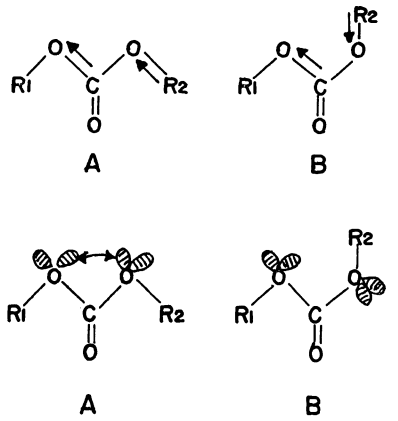

Fig. 2. Additional factors governing the conformations of the carbonate.

Experimental

The dimethyl and diethyl carbonates were of commercial origin and were purified by distillation before measurement. The ethyl methyl carbonate, *t*-butyl methyl carbonate, and 1,1-diethylporpyl methyl carbonate were prepared by pouring the corresponding sodium alkoxide into methyl chloroformate in dry ether with ice-cooling and then distilling under re-

1) Part IV: M. Ōki and H. Nakanishi, This Bulletin, **44**, 3148 (1971).

2) a) M. Kubo, *Sci. Papers. Inst. Phys. Chem. Research., (Tokyo)*, **30**, 169 (1936). b) M. Kubo, Y. Morino, and S. Mizushima, *ibid.*, **32**, 129 (1937).

3) G. Thomson, *J. Chem. Soc.*, **1939**, 1118.

4) G. F. Longster and E. E. Walker, *Trans. Faraday Soc.*, **49**, 228 (1953).

5) M. Ōki and H. Nakanishi, This Bulletin, **43**, 2558 (1970).

6) a) R. O. Hutchins, L. O. Kopp, and E. L. Eliel, *J. Amer. Chem. Soc.*, **90**, 7174 (1968). b) E. L. Eliel, *Kemisk. Tedskrift*, **1969**, No. 6—7, 22. c) E.L. Eliel, *Accounts. Chem. Res.*, **3**, 1 (1970).

7) In a heterocyclic system such as is shown below, Eliel called this lone pair-lone pair interaction the "rabbit ear effect." The A conformation, with an axial methoxy group, is more stable than the B conformation, with an equatorial methoxy group.

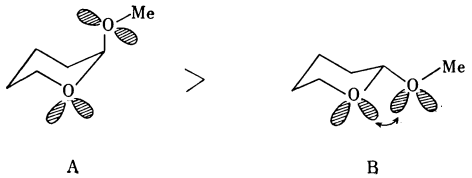

duced pressure. The diisopropyl carbonate, diphenyl carbonate, and bis(2,6-dimethylphenyl) carbonate were prepared from the corresponding alkoxide or phenoxide and phosgene. The methyl phenyl carbonate, 2,6-dimethylphenyl methyl carbonate, methyl 4-nitrophenyl carbonate, and 4-methoxyphenyl methyl carbonate were prepared by pouring methyl chloroformate into a mixture of the corresponding phenol and aqueous sodium hydroxide with ice-cooling.

$MeOCO_2t$-Bu: bp 52—53°C/57mmHg. NMR. (from TMS in benzene) 6.54 (3H, s), 8.63 (9H, s).

$MeOCO_2CEt_3$: bp 104—105°C/57 mmHg. NMR. 6.33 (3H,s), 8.20 (6H,q), 9.17 (9H,t).

i-$PrOCO_2i$-Pr: bp 139—140°C/760 mmHg. NMR.5.13 (2H, mul.) 8.88 (12H, d).

$MeOCO_2C_6H_5$: bp 112°C/23 mmHg. NMR. 2.75 (5H, m), 6.25 (3H, s) (in CCl_4).

$MeOCO_2C_6H_3Me_2$-2,6: bp 135°C/38 mmHg. NMR. 2.92 (3H, s), 6.15 (3H, s), 7.82 (6H, s) (in CCl_4). Found: C, 66.55; H, 6.76%; Calcd for $C_{10}H_{12}O_3$: C, 66.65; H, 6.71%.

$MeOCO_2C_6H_4NO_2$-4: mp 123°C NMR. 6.07 (3H, s).

$MeOCO_2C_6H_4OMe$-4: bp 110—112°C/2 mmHg. Found; C, 59.05; H, 5.24%; Calcd for $C_9H_{10}O_4$: C, 59.34; H, 5.53%.

$C_6H_5OCO_2C_6H_5$: bp 167—168°C/15 mmHg. NMR. 2.75 (10H, m) (in CCl_4).

The purities of the compounds used in this study were checked by studying their infrared spectra and NMR spectra, and by gas chromatography. The infrared spectra were measured on a Perkin Elmer single-beam grating spectrometer and a Hitachi EPI-G2 grating spectrophotometer. The NMR spectra were measured on JNM C-60, JNM-4H-100, and Hitachi R-20B Spectrometers. The dipole moment was measured by the heterodyne beat method, (the inaccuracy was about 0.05D at 1.0D). The calculation of the stability of dimethyl carbonate was carried out by the CNDO/2[8] method, using programs provided by the Computation Center of this University.

Results and Discussion

Nuclear Magnetic Resonance Spectra. In the expectation of obtaining some signs of the existence of A and B conformers, the NMR spectra of t-butyl methyl carbonate and 2,6-dimethylphenyl methyl carbonate were measured at room temperature. These two compounds were selected as the samples because they have a bulky alkyl or aryl group and because the repulsion between C=O and the R group is so large that the possibility of the existence of the *s-cis* conformer is also large. The results were, however, that both gave sharp singlets

Table 1. The change in intensity of NMR peaks of t-butyl methyl carbonate
$MeOCO_2t$-Bu in $CS_2+CH_2Cl_2+C_6H_5CH_3$

	T°C				Chemical shift
	34	−70	−90	−120	τ
CH_3-⟨○⟩-H	1.37	1.31	1.15	1.27	2.86
C_6H_5-CH_3	1.00	1.00	1.00	1.00	7.68
OCH_3	1.29	1.11	0.95	0.84	6.41
$C(CH_3)_3$	3.66	2.53	1.85	1.29	8.41

Table 2. The intensity change of NMR peaks of 2,6-dimethylphenyl methyl carbonate
$MeOCO_2C_6H_3Me_2$-2,6 in $CS_2+CH_2Cl_2$

	T°C				Chemical shift
	34	−70	−90	−100	τ
arom-H	1.00	1.00	1.00	1.00	2.87
OCH_3	1.57	1.34	1.06	0.96	6.04
aom-CH_3	2.22	2.22	1.92	2.07	7.31

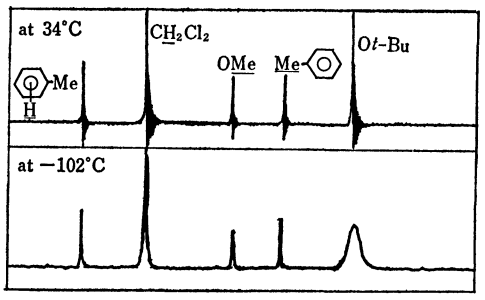

Fig 3. NMR spectra of $MeOCO_2t$-Bu.

for the methoxy groups and did not give any sign of the existence of the two isomers. These results could arise for two reasons: the existence of a single isomer, or rapid exchange between isomers. If the latter is the case, there is a possibility that the singals split at lower temperatures. Thus, the NMR spectra of these compounds were measured at low temperatures in a CS_2–CH_2Cl_2 solvent, with toluene as the internal standard.

The results are shown in Tables 1 and 2 and in Fig. 3. Neither the methoxy nor t-butyl methyl peak separated, even at low temperatures, but the peak of the t-butyl protons became very broad at −102°C. (The height of the t-butyl peak at −102°C is one third of that at 34°C, while the peak height of the methoxy at −102°C is 65% of that at 34°C.) These results can best be interpreted by assuming the presence of two or three conformers in this compound and by assuming that the exchange rate between these conformers is slow enough for the time scale of NMR at this low temperature. Judging from the fact that the broadest peak in t-butyl methyl carbonate at low temperatures is not the methoxy peak but the t-butyl, it may be postulated that the t-butyl group is more mobile, and that the A and B conformations are significant, but not the B′ conformation, because the influence of the anisotropy of the carbonyl must be large in determining the chemical shifts of these protons; the difference in the chemical shifts of the methyl groups in A and B′ conformers is expected to be at least as large as that of t-butyl protons. It may be argued that the difference in the chemical shifts of the methoxy protons in the A and B′ conformers is so small that the peak height decreases only slightly. However, this possibility is seen to be rather unlikely when the average anisotropy effects of the car-

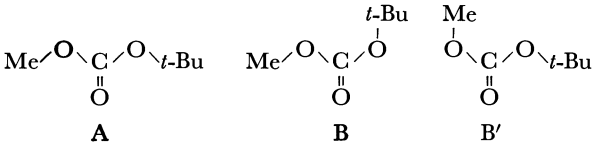

8) a) J. A. Pople, D. P. Satry, and G. A. Segal, *J. Chem. Phys.*, **43**, S 129 (1965). b) J. A. Pople and G. A. Segal, *ibid.*, **43**, S 136 (1965). c) J. A. Pople and G. A. Segal, *ibid.*, **44**, 3289 (1966).

bonyl group to methoxy and *t*-butyl protons are considered. Thus, the contribution of the B′ conformer is small, at least; this consideration conforms with that deduced from the steric effect.

In the case of 2,6-dimethylphenyl methyl carbonate, the situation is somewhat different. The broadest peak at low temperatures is not that of the aromatic methyl but that of the methoxy. These results may again be interpreted by assuming that the anisotropy effect of the carbonyl group is larger for the methoxy methyl than for the aromatic methyl, although there is some difference from the situation of the *t*-butyl methyl carbonate. Therefore, it can be assumed that the main *s-cis* conformation of 2,6-dimethylphenyl methyl carbonate is not B but B′ (Fig. 4). The population of the B conformer is considered not to be significant.

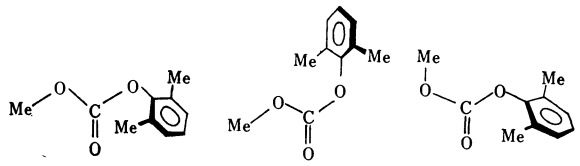

A B B′

Fig. 4. Conformations of 2,6-dimethylphenyl methyl carbonate.

Infrared Spectra of Carbonyl Stretching Vibration Absorption. The infrared spectra of carbonates have been measured by several authors,[9] and it has been reported that carbonates have only one carbonyl absorption.

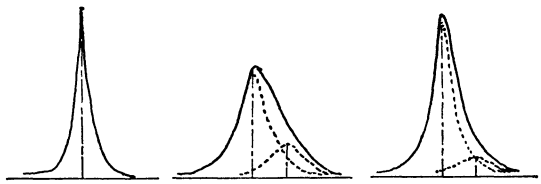

Fig. 5. ν_{CO} absorption of $MeOCO_2t$-Bu in three solvents.

No one has, however, reported about the shape of the carbonyl absorption. However, as has been described in previous papers,[1,5] some formates and carbamates have two carbonyl absorptions and can be assigned to two conformational isomers. From the NMR results on the carbonates, it is expected that a careful reinvestigation of the infrared spectra may produce further evidence for the conformational heterogeneity of the carbonates. Thus, the carbonyl stretching absorption was measured using an instrument with a high resolution. The results follow.

t-Butyl methyl carbonate was found to have an unsymmetrical carbonyl absorption in carbon tetrachloride and acetonitrile. This absorption was graphically separated into two absorptions using Lorenzian curves (Fig. 5). The infrared spectra of carbonyl absorptions of other carbonates were treated similiarly; the results are shown in Table 3.

Carbonates I, II, and III, whose two alkyl groups are relatively samll, all have one symmetrical carbonyl absorption in hexane, carbon tetrachloride, and ace-

Table 3. Carbonyl absorptions of the carbonates

Compound \ Solvent		C_6H_{14} $c=0.02$ mol/l cm^{-1} (ε)	CCl_4 $c=0.0004$ mol/l cm^{-1} (ε)	CH_3CN $c=0.02$ mol/l cm^{-1} (ε)
I	$MeOCO_2Me$	1762.3 (1684)	1756.5 (988)	1755.8 (1400)
II	$EtOCO_2Et$	1752.1 (2089)	1746.3 (956)	1745.2 (1390)
III	$MeOCO_2Et$	1755.3 (1764)	1750.7 (915)	1749.8[a] (1409)
IV	$MeOCO_2t$-Bu	1750.7 (2089)	1739 (73)	1734 (80)
			1744 (891)	1744 (1339)
V	$MeOCO_2CEt_3$		1737 (55)	1734 (150)
			1744 (929)	1744 (1010)
VI	i-$PrOCO_2i$-Pr	1736 (90)	1731 (106)	1727 (52)
		1744 (2258)	1739 (790)	1738 (1403)
VII	$MeOCO_2C_6H_5$	1774 (1500)	1768 (682)	1767 (1131)
		1787 (109)	1779 (73)	1776 (54)
VIII	$MeOCO_2C_6H_3Me_2$-2,6	1771 (2489)	1765 (852)	1763 (1393)
		1783 (178)	1778 (58)	broad
IX	$MeOCO_2C_6H_4NO_2$-4		1774 (825)	1774 (986)
			1788 (67)	1784 (96)
X	$MeOCO_2C_6H_4OMe$-4		1766 (900)	1760 (167)
			1776 (68)	1766 (1952)
XI	$C_6H_5OCO_2C_6H_5$	1777 (187)	1759 (87)	1762 (m)
		1787 (2052)	1784 (845)	1784 (l)
		1799 (249)	1795 (22)	1794 (s)
XII	$(2,6\text{-}Me_2C_6H_3)_2CO_3$		1767 (114)	1762 (50)
			1777 (793)	1773 (1225)

a) Another weak peak exists at 1736 cm^{-1} (ε=66).

9) a) J. L. Hales, J. I. Jones, and W. Kynaston, *J. Chem. Soc.*, **1957**, 618. b) B. M. Galehouse, S. E. Livingstone, and R. S. Nyholm, *ibid.*, **1958**, 3137. c) R. N. Nyquist and W. J. Patts, *Spectrochim. Acta*, **17**, 679 (1961). d) H. Minato, This Bulletin, **36**, 1020 (1963). e) K. V. Krishnamurty, G. M. Harris, and V. S. Sasti, *Chem. Rev.*, **70**, 171 (1970).

tonitrile solvents. However, compounds IV—XII, which have relatively bulky alkyl or aryl groups, show two carbonyl bands in these solvents (compound XI has three absorptions). These results may be interpreted in the following way. In compounds I, II, and III, the steric repulsion between C=O and R_1 or R_2 is small. Thus, these compounds take the conformation, A, which is the most stable. On the other hand, in compounds IV, V, and VI, which have a large alkyl group, the steric repulsion described above becomes serious and the A conformer is so destabilized that the B conformer can exist to a significant extent. The coexistence of the A and B conformers explains the two carbonyl bands. In compound IV ($MeOCO_2t$-Bu), the intensity of the higher wave-number absorption is stronger than that of the lower one. The consideration of the directions of the bond dipoles of C=O and R_2–O[1,5] suggests that the *s-cis* conformer has a higher frequency band than the *s-trans*.[10] Therefore, in *t*-butyl methyl carbonate the B conformer (*s-trans-s-cis*) must be more stable than the A conformer (*s-trans-s-trans*). The solvent effect is found to be such that the intensity of the higher frequency band increases in polar solvents more than in nonpolar solvents. Since the calculated dipole moment of the B conformer (2.1D) is larger than that of the A conformer (0.1D), the results presented here necessarily mean that the B conformer is the one which is prefered in the polar solvents. The situation is somewhat different in compounds VII, VIII, IX, and X from that in compound IV. In these compounds, the intensity of the absorption of the lower wave number is stronger than that of the higher one. In assigning the two absorptions to two conformers in alkyl carbonates, the directions of the two bond dipoles can be considered to be the main factor, whereas in the aryl carbonates, the stability of the resonance canonical structures in addition to the directions of the bond dipoles must be taken into account. Although there are difficulties in assigning the absorptions because of the complexities arising from the steric and electronic effects, the authors would like to assign the tentatively as in the case of dialkyl carbonates. The band at the higher frequency is thus assigned to the *s-cis* conformer. Diphenyl carbonate has three absorptions in the region of carbonyl stretching. Three conformers may be considered: *s-cis-s-cis*, *s-cis-s-trans*, and *s-trans-s-trans*. The interaction between the two benzene rings in the *s-cis-s-cis* conformer will, however, be repulsive, and the repulsion is considered to be too large for the conformer to exist. Therefore, two conformations, *s-cis-s-trans* and *s-trans-s-trans*, will suffice in discussing the conformations of this compound. Thus, one of the bands in the carbonyl region must be attributed to the enhancement of an overtone or combination tone due to the Fermi resonance. Bis-(2,6-dimethylphenyl)carbonate shows two absorptions in which the higher band is stronger. If the analogy of dialkyl carbonate is still applicable, then it can be considered that the *s-cis-s-trans* conformer is to be favored over the *s-trans-s-trans*.

10) This was suggested to be true by the results of the calculation of the bond order of the carbonyl of dimethyl carbonate by the CNDO/2 method.

Surveying the stabilities of these conformers in dialkyl carbonates, alkyl aryl carbonates, and diaryl carbonates, we find that the *s-cis* conformer more stable in the first carbonates, and the *s-trans* conformer is favored in the second carbonates, while in the last the *s-cis* conformer is again more stable, if the above-mentioned assignments are accepted. The origin of these stabilities remains to be explored.

Table 4. Carbonyl overtone of the carbonates

Compound \ Solvent		CCl_4 $c=0.007$ mol/l cm^{-1} (ε)
I	$MeOCO_2Me$	3467 (0.3)
		3492 (4.4)
II	$EtOCO_2Et$	3474 (3.2)
III	$MeOCO_2Et$	3467 (0.5)
		3485 (2.9)
IV	$MeOCO_2t$-Bu	3456 (0.7)
		3476 (5.6)
VIII	$MeOCO_2C_6H_3Me_2$-2,6	3510 (4.9)
		3527 (0.4)

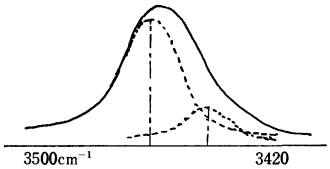

Fig. 6. Infrared spectra of carbonyl overtone of $MeOCO_2t$-Bu in CCl_4.

Infrared Spectra of Carbonyl Overtone. The infrared spectra in the carbonyl overtone region were measured in order to obtain further information about the conformations of the carbonates. The results are shown in Tabel 4 and Fig. 6. *t*-Butyl methyl carbonate (IV) has two absorptions of the carbonyl overtone, and the relative intensities of these two absorptions are almost the same as that of the carbonyl fundamental absorptions. These results suggest that the origin of the bifurcation of the carbonyl band is not the Fermi resonance but the heterogeneity of the conformations, thus supporting the assignment made earlier in this paper. The case of 2,6-dimethylphenyl methyl carbonate(VIII) is the same; the band at a lower frequency is stronger than that at a higher, as is observed in the carbonyl region. Dimethyl carobnate(I) and ethyl methyl carbonate(III), which show only one absorption in the carbonyl fundamental, give, astonishingly, two absorptions, and the intensity of the band at the higher wave number is stronger than that of the lower one, as in the case of *t*-butyl methyl carbonate. It is almost unbelievable that this bifurcation is due to Fermi resonance. Rather, this bifurcation may be explained by considering the existence of two conformers in these carbonates, although they are not detected by the C=O stretching absorption because of the small difference in frequencies. If this postulate is accepted, then in these carbonates with two small alkyl groups, the *s-cis* conformer can be considered from the relative intensity to be more stable than the *s-trans*.

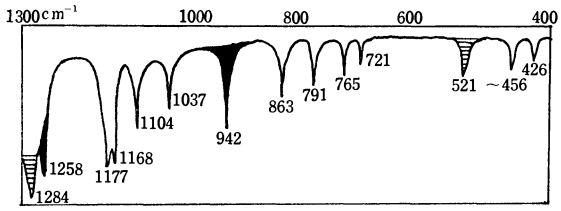

Fig. 7. Solvent effects on infrared spectra of $MeOCO_2t$-Bu in the region of 1300—400 cm^{-1}.
●: increasing band in polar solvent
⊜: decreasing band in polar solvent.

Solvent Effect on the Absorptions in the Region of 1300—400 *cm*$^{-1}$. The B conformer of the carbonate should be more polar than the A conformer, judging from the arrangement of the bond dipoles. This implies that the population of the B conformer will increase in a polar solvent relative to in a nonpolar solvent. Thus, the infrared spectra of *t*-butyl methyl carbonate were measured in various solvents, such as carbon disulfide(2.64),[11] acetone(20.7), chloroform(4.81), *N*,*N*-dimethylformamide(37.7), and dimethyl sulfoxide(48.9), in the region of 1300—400 cm^{-1}. (Fig. 7) The intensities of the absorptions at 942 and 1258 cm^{-1} apparently increase in polar solvents, whereas the intensities of the absorptions at 521 and 1284 cm^{-1} decrease. This apparent solvent effect can be interpreted as implying that *t*-butyl methyl carbonate exist as a conformational mixture, each conformer having a different polarity.

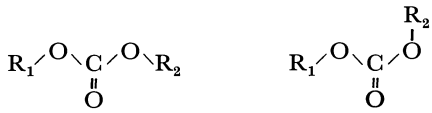

Dipole Moment. The calculated dipole moment values are 0.1D for the A conformer and 2.1D for the B conformer.[12] The dipole-moment values obtained by CNDO/2 calculation are 0.27D for the A conformer, and 2.04D for the B conformer, of dimethyl carbonate. The results obtained with a benzene solution are given in Table 5. *t*-Butyl methyl carbonate (IV) has a little larger dipole moment than the other carbonates at room temperature, and the value at 49°C is smaller than that at 28°C. This temperature dependence of the dipole moment of this compound means that the conformers exist and that the more polar conformer, B or B′, is more stable than the less polar conformer, A. This is in accord with the results obtained from the infrared spectral study. Although it was made clear that the B or B′ conformer is more stable than the A conformer, the observed dipole moment of this compound is in between the two calculated values for the *s-trans* and *s-cis* conformers. The reason for these results may be considered to be an inaccuracy in the calculation of the dipole moments from the bond dipoles, but the twisting of the *t*-butyl group from the plane of the other part of the molecule can be another reason; the latter possibility is supported by the molecular model and by the results obtained with other esters in this laboratory,

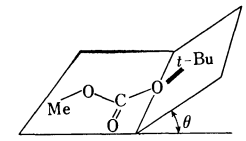

($\theta \neq 0°$). The dipole moment values of compounds I, II, and III are in the range of 0.7—0.9D at room temperature, in between the two calculated values of the A and B conformers.[13] Since these values are colse to that of compound IV, it may be concluded that dialkyl carbonates take two comformations in the liquid phase. This conclusion is supported by the results of an infrared spectroscopic study in the overtone region of the carbonyl stretching, although there remains some ambiguity in the relative populations.

Table 5. Dipole moments of carbonates in benzene

	Compound	μ (D)	T°C
I	$MeOCO_2Me$	0.94	16
		0.91	28
II	$EtOCO_2Et$	0.90	25
III	$MeOCO_2Et$	0.71	28
IV	$MeOCO_2t$-Bu	1.00	28
		0.89	41
		0.80	49

Conclusions

Nuclear magnetic resonance and infrared spectroscopies and dipole-moment techniques have revealed that *t*-butyl methyl carbonate has the A (*s-trans-s-trans*) and B (*s-trans-s-cis*) conformers, the latter being more stable than the former, although the possibility of the existence of the B′ conformer (*s-cis-s-trans*) cannot be ruled out. This is in interesting contrast with the case of *t*-butyl formate, in which the *s-trans* conformer is more stable than the *s-cis*.[5] The difference may be explained by considering the stabilization of the B conformer of the carbonate due to the dipole-dipole interaction between C–O and R–O bonds and the destabilization of the A conformer due to the "rabbit ear effect." Other carbonates also give signs of conformational heterogeneity.

The authors wish to express their hearty thanks to Professor T. Kunii and Mr. K. Morio for their technical assistance in the CNDO/2 calculations.

11) The numbers shown in parentheses are dielectric constants.
12) The calculation was made on the basis of a bond moment value of 0.4D for the C–H bond, a 2.4D value for the C=O bond, and a 0.9D value for the C–O bond.
13) The dipole moments of dimethyl and diethyl carbonates in the gaseous phase were reported by Kubo *et al.*[2] not to change seriously from 55°C to 206°C. The carbonates are, therefore, considered to exist in a *s*-trans conformation only by these authors.

Syntheses of Acylurea Derivatives as Model Compounds for a Highly Specific Organic Reaction

Tadashi ENDO, Shigeru NOGUCHI, and Teruaki MUKAIYAMA

Laboratory of Organic Chemistry, Tokyo Institute of Technology, Ookayama, Meguro-ku, Tokyo

(Received May 14, 1971)

Some types of acylurea derivatives were prepared as model compounds for a highly specific organic reaction by molecular association. When ethyl chloroacetate was treated successively with *o*-aminobenzenethiol (**4**) and chloroacetyl isocyanate (**1**) under mild conditions, triacylurea derivative (**9**) was obtained in total 84% yield. It was found that the use of "amino acid amide and oxalyl chloride" method led to the formation of diacylurea derivative (**11**) in high yield.

Increasing attention has recently been drawn to "molecular interaction" between proteins themselves and between proteins and nucleic acids or lipids in the field of biochemistry. The purine and pyrimidine bases in coenzymes and nucleic acids may play an important role in the control of enzyme reactions by forming hydrogen bonding and charge-transfer complexes with each other or with other biochemical macromolecules in living cells. Acylurea derivatives are regarded as a sort of open chain analogue of the pyrimidine bases. The present paper deals with the fundametal studies on syntheses of acylurea derivatives as model compounds which lead to a specific organic reaction by an intermolecular association.

In preparing acylurea derivatives it was found that the use of acyl isocyanates as carbamoylating reagents is the most effective. The desired acylurea derivatives were obtained in high yields by treatment with amines under mild conditions. Chloroacetyl isocyanate (**1**)[1] readily reacted with ethyl glycinate at 0°C in ether to give 5-chloroacetylhydantoic acid ethyl ester (**2**) in 94% yield.

Nucleophilic substitution at the terminal carbon of **2** was investigated for an introduction of a functional group which can be utilized in the formation of the next acylurea linkage. The aminated product (Y= NH_2) (**3**) could not be isolated by the use of Gabriel

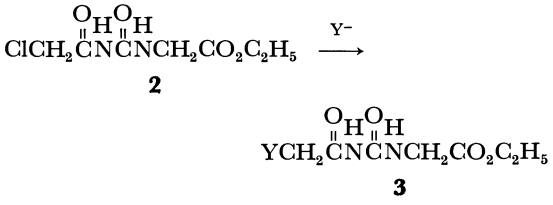

2 **3**

or Sommelet method or by treatment with ammonia[2] in methanol. However, it was found that **2** easily underwent nucleophilic substitution by thiols. Treatment of **2** with benzenethiol, *o*-aminobenzenethiol (**4**), 4-pyridinethiol, and thiobenzoic acid at room temperature in the presence of triethylamine gave the corresponding sulfides in 96, 96, 95, and 88% yields, respectively. Physical properties and analytical data of these sulfides are listed in Table 1. It is of special interest to note that the thiols did not attack the carbonyl carbon of the chloroacetyl group in **2**.

On this basis, it was expected that the successive use of thiols containing the N–H bonds and of **1** would lead to the formation of the desired *polyacylurea* derivatives. An oily product (**5**), easily obtained by the reaction of ethyl chloroacetate with **4** and triethylamine at room temperature, decomposed to give 2*H*-1,4-benzo-

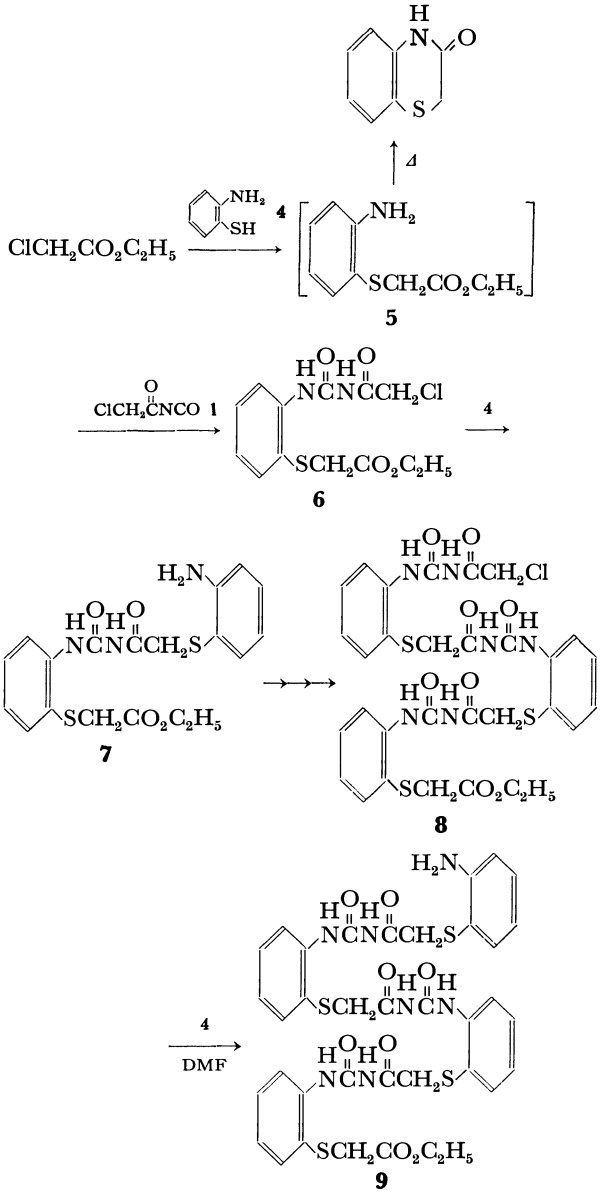

5 **6** **7** **8** **9**

1) A. J. Speziale and L. R. Smith, *J. Org. Chem.*, **27**, 3742 (1962).

2) In this case, chloroacetamide and hydantoic acid ethyl ester were obtained. This may be explained as nucleophilic attack of ammonia on the carbonyl carbon of chloroacetyl group in **2**.

Table 1. Physical properties and analytical data of **3**

Y	Mp, °C	Recrystallization Solvent	Calcd, %				Found, %			
			C	H	N	S	C	H	N	S
C_6H_5S	110—111	Ether	52.70	5.44	9.46	10.80	52.92	5.14	9.31	11.07
o-$NH_2C_6H_4S$	120—121	Benzene	50.16	5.50	13.50	10.28	50.30	5.46	13.59	10.00
$C_6H_5\overset{O}{\overset{\|}{C}}S$	129—130	Ethanol	51.85	4.97	8.64	9.87	51.91	5.05	8.71	9.82
	144—145	Acetone	48.48	5.09	14.14	10.76	48.39	4.94	14.20	11.03

thiazin-3(4*H*)-one in 95% yield when distilled. Thus, compound **5** was converted into the acylurea derivative (**6**), without isolation, on rapid treatment with **1**. Similarly, compound **6** reacted with **4** to afford the amine (**7**). It was found that triacylurea derivative (**9**) was prepared by treatment of **7** successively with **1** and **4**. All processes proceeded almost quantitatively at room temperature. Compound **9** could be isolated in total 84% yield. It should be noted that in contrast to the chloroacetylurea derivatives such as **6** and **8**, **9** is very soluble in organic solvents, especially in dichloromethane, benzene, and acetone. The protons of the methylene groups attached to the sulfur in **7** resonated as two doublets at τ 6.50 and 6.58. However, those of **9** resonated as a singlet at 6.50. The infrared spectrum of **9** showed broader absorptions than that of **7** (Fig. 1).

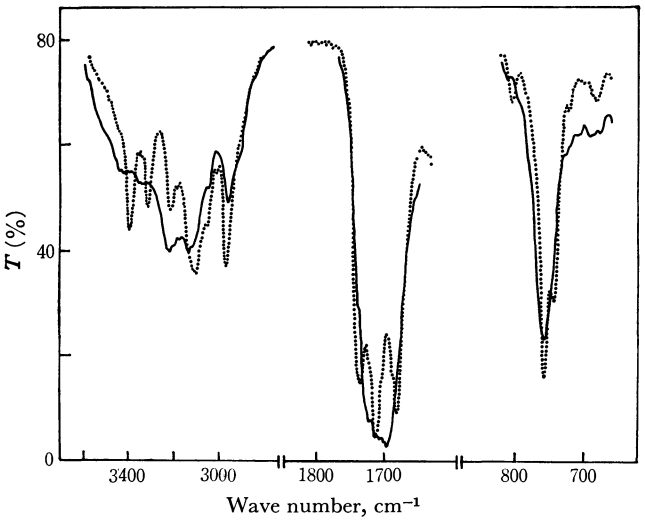

Fig. 1. Infrared spectra of **7** (·····) and **9** (——) in KBr disks.

Preparation of another type of polyacylurea derivatives was studied by the use of amino acid amides on the assumption that amides are easily converted into the corresponding acyl isocyanates[1] when treated with oxalyl chloride. Compound **1** reacted with *p*-aminobenzamide in DMF to give the corresponding acylurea derivative (**10**) in 88% yield. The diacylurea derivative (**11**) was prepared in 70% yield by treatment of **10** first with oxalyl chloride in refluxing acetonitrile and then with ethyl glycinate at room temperature. Compound **11** showed remarkably high decomposition point (323—325°C) and could be recrystallized from DMF-ethanol to give colorless plates.

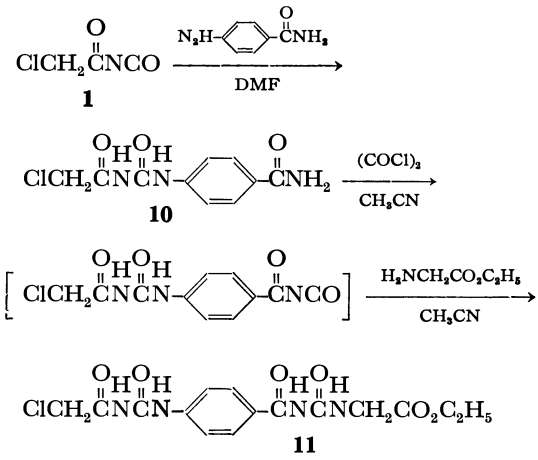

From these results, it seems reasonable to conclude that polyacylurea derivatives could be prepared by the use of either "N–H bond-containing thiol and haloacyl isocyanate" method or of "amino acid amide and oxalyl chloride" method.

Experimental[3]

Materials. Chloroacetyl isocyanate (**1**) was prepared according to the method of Speziale.[1] Benzenethiol, ethyl chloroacetate, *o*-aminobenzenethiol, and *p*-aminobenzamide were all commercial materials and purified by distillation or recrystallization before use. Thiobenzoic acid, 4-pyridinethiol, and ethyl glycinate were prepared in the usual manner.

Preparation of **2** *and* **10**. To a stirred solution of ethyl glycinate (2.10 g, 0.02 mol) in 30 m*l* of ether was added a solution of **1** (2.40 g, 0.02 mol) in 10 m*l* of ether under cooling at 0°C. After stirring had been continued for 1 hr at room temperature, the resulting precipitate of **2** (4.10 g, 94%) was collected by filtration and washed twice with a small amount of ether. Recrystallization from ether gave analytically pure colorless needles, mp 144—145°C (lit,[4] mp 145—146°C). (Found: C, 37.74; H, 4.70; N, 12.86%).

Similarly, **10** was obtained in 88% yield by the reaction of **1** with *p*-aminobenzamide in DMF. Recrystallization from DMF-water gave analytically pure colorless needles, mp 229—230°C (dec.) (lit,[5] mp 236—237°C (dec.)). (Found: C, 47.05; H, 3.84; N, 16.39%).

3) All melting points were uncorrected. The IR spectra were recorded with a Hitachi EPI-G3 Spectrophotometer. The NMR spectra were measured at 100 MHz with a Japan Electron Optics JNM-4H-100 Spectrometer. All the solvents used for reactions were purified by the usual methods.

4) A. H. Corwin and C. I. Damerel, *J. Amer. Chem. Soc.*, **65**, 1974 (1943).

5) W. A. Jacobs and M. Heidelberger, *ibid.*, **39**, 2438 (1917).

Reaction of **2** *with Benzenethiol.* To a solution of **2** (2.23 g, 0.01 mol) in 40 m*l* of acetone was added dropwise a solution of benzenethiol (1.10 g, 0.01 mol) and triethylamine (1.01 g, 0.01 mol) in 10 m*l* of acetone with stirring at room temperature. Stirring was continued for 1 hr at room temperature. After the reaction mixture had been concentrated *in vacuo* to dryness, the residual solid was treated with water for removal of triethylamine hydrochloride. The resulting cyrstals were collected by filtration, washed repeatedly with water and dried over phosphorus pentoxide *in vacuo* to give 2.85 g (96%) of **3** (Y=C_6H_5S). Recrystallization from ether gave white needles.

By a similar procedure the corresponding sulfides were obtained from other thiols. Physical properties and analytical data of these sulfides are listed in Table 1.

Preparation of 2H-1,4-Benzothiazin-(4H)-one. A solution of **4** (2.50 g, 0.02 mol) and triethylamine (2.02 g, 0.02 mol) in 20 m*l* of ether was added to a solution of ethyl chloroacetate (2.45 g, 0.02 mol) in 20 m*l* of ether with stirring at room temperature. A slightly exothermic reaction took place immediately and triethylamine hydrochloride precipitated. Stirring was continued for 1 hr at room temperature. After the reaction mixture had been filtered off, the filtrate was evaporated *in vacuo*. Residual oil (**5**) gave crystals of 2*H*-1,4-benzothiazin-3(4*H*)-one (3.14 g, 95%) with loss of ethanol when heated under reduced pressure. Recrystallization from acetone gave pure colorless needles, mp 175.0—175.5°C (lit,[6] mp 176°C). (Found: C, 58.85; H, 4.15; N, 8.44; S, 19.70%).

Similarly, the oil (**5**) gave 2*H*-1,4-benzothiazin-3(4*H*)-one in 40% yield when allowed to stand for 6 days at room temperature.

Preparation of **6**. To a stirred solution of ethyl chloroacetate (2.45 g, 0.02 mol) in 20 m*l* of ether was added a solution of **4** (2.50 g, 0.02 mol) and triethylamine (2.02 g, 0.02 mol) in 20 m*l* of ether at room temperature. Work-up of the reaction mixture as described above gave the oil (**5**). To a solution of this oil in 30 m*l* of dichloromethane was added a solution of **1** (2.40 g, 0.02 mol) in 20 m*l* of dichloromethane with stirring at room temperature. Stirring was continued for 30 min at room temperature. After removal of dichloromethane, the resulting solid was treated with ether. A white precipitate of **6** (6.30 g, 95%) was collected by filtration and recrystallized from ethanol to give white needles, mp 146.0—146.5°C.

Found: C, 47.43; H, 4.72; N, 8.73; S, 9.94%. Calcd for $C_{13}H_{15}ClN_2O_4S$: C, 47.21; H, 4.57; N, 8.47; S, 9.68%.

Preparation of **9** *and* **7**. A solution of **4** (0.63 g, 0.005 mol) and triethylamine (0.51 g, 0.005 mol) in 10 m*l* of DMF was added to a solution of **8** (3.74 g, 0.005 mol) in 30 m*l* of DMF with stirring at room temperature. Colorless crystals of triethylamine hydrochloride were soon formed. Stirring was continued for 1 hr at room temperature. After evaporation of DMF, the residue was treated with water. The resulting solid was collected by filtration, washed with water, and dried over phosphorus pentoxide *in vacuo* to afford **9** (4.10 g, 98%). Slow addition of ether in small portions to a solution of **9** in dichloromethane gave a white powder, mp 122.0—122.5°C. IR (KBr): 3220 (N–H), 3135 (N–H), 1738 (C=O), 1722 (C=O), 1715 (C=O), 1706 (C=O), 1700 (C=O), and 1696 (C=O) cm^{-1} (see Fig. 1). NMR ($CDCl_3$): τ 8.85 (t, 3H, J=7.0 Hz, CH_3), 6.50 (s, 8H, –S–CH_2–CO–), 5.93 (q, 2H, J=7.0 Hz, –O–**CH_2**–CH_3), and 2.42—3.40 (m, 16H, aromatic protons).

Found: C, 53.37; H, 4.68; N, 11.60; S, 15.18%. Calcd for $C_{37}H_{37}N_7O_8S_4$: C, 53.16; H, 4.46; N, 11.73; S, 15.31%.

Similarly, **7** was obtained in 97% yield by treatment of **6** with **4** and triethylamine in acetone at room temperature. Recrystallization from ethanol gave an analytically pure sample, mp 124.5—125.0°C. IR (KBr): 3405 (N–H), 3325 (N–H), 3225 (N–H), 3110 (N–H), 1736 (C=O), 1712 (C=O), and 1682 (C=O) cm^{-1} (see Fig. 1). NMR ($CDCl_3$): τ 8.87 (t, 3H, J=7.0 Hz, CH_3), 6.58 (d, 2H, J=9.0 Hz, –S–CH_2–CO–), 6.50 (d, 2H, J=10.0 Hz, –S–CH_2–CO), 5.97 (q, 2H, J=7.0 Hz, –O–**CH_2**–CH_3), and 2.42—3.40 (m, 8H, aromatic protons).

Found: C, 54.10; H, 4.94; N, 10.04; S, 15.12%. Cacld for $C_{19}H_{21}N_3O_4S_2$: C, 54.41; H, 5.05; N, 10.02; S, 15.26%.

Preparation of **11**. Oxalyl chloride (1.45 g, 0.012 mol) and **10** (2.56 g, 0.01 mol) were refluxed in 30 m*l* of acetonitrile for 1 hr. Vigorous evolution of hydrogen chloride and carbon monoxide was observed. After the reaction mixture had been concentrated *in vacuo* to dryness for complete removal of the excess of oxalyl chloride, the dark red residue was dissolved in 30 m*l* of acetonitrile. To this solution was added a solution of ethyl glycinate (1.03 g, 0.01 mol) in 10 m*l* of acetonitrile at room temperature with stirring. A slightly exothermic reaction soon took place. Stirring was continued for 30 min at room temperature. After evaporation of the solvent, the residue was treated with ether. The pale yellow crystals of **11** (2.65 g, 70%) were collected by filtration. Repeated recrystallization from DMF-ethanol gave analytically pure colorless plates, mp 323—325°C (dec.). IR (KBr): 3270 (N–H), 3125 (N–H), 1748 (C=O), 1724 (C=O), 1705 (C=O), 1692 (C=O), and 1675 (C=O) cm^{-1}.

Found: C, 47.35; H, 4.69; N. 14.70%. Calcd for $C_{15}H_{17}ClN_4O_6$: C, 46.78; H, 4.45; N, 14.56%.

6) A. W. Hofmann, *Ber.*, **13**, 1234 (1880).

Preparation of Carboxylic Esters and Phosphoric Esters by the Activation of Alcohols[1)]

Oyo MITSUNOBU and Masahiko EGUCHI

Department of Chemistry, College of Science and Engineering, Aoyama Gakuin University, Megurisawa-cho, Setagaya-ku, Tokyo

(Received May 29, 1971)

The reaction of dibenzyl hydrogen phosphate with alcohols in the presence of diethyl azodicarboxylate and triphenylphosphine, followed by catalytic hydrogenation, resulted in the formation of the corresponding alkyl dihydrogen phosphates. When *p*-tolyl dihydrogen phosphate and ethanol were allowed to react with diethyl azodicarboxylate and triphenylphosphine, ethyl *p*-tolyl hydrogen phosphate and diethyl *p*-tolyl phosphate were obtained. On the other hand, dipyridinium *p*-tolyl phosphate gave ethyl *p*-tolyl hydrogen phosphate and di-*p*-tolyl pyrophosphate. The reaction of alkyl *N,N'*-tetraethylphosphorodiamidites with carboxylic acids in the presence of diethyl azodicarboxylate resulted in the formation of corresponding carboxylic esters. When these reactions (benzoylation) were carried out with the use of optically active 2-octanol, 2-octyl benzoate was obtained with inverted configuration.

A number of phosphorylating systems have been devised with a view to preparing phosphate and pyrophosphate diesters by intermolecular dehydration between phosphate monoesters and either an alcohol or a phosphate monoester. In order to bring the phosphate into reaction with an alcohol, most systems employed initial activation of phosphate monoesters by organic dehydrating reagents such as dicyclohexylcarbodiimide,[2)] trichloroacetonitrile[3)] or ketene dimer.[4)] There are, however, few reports on phosphorylation of alcohols which involves initial activation of alcohols.[5-7)]

The present study was carried out with a view to producing esters of phosphoric acid and carboxylic acid *via* activation of alcohols.

Results and Discussion

Preparation of Esters of Phosphoric Acid. Recently, preparation of symmetrical pyrophosphate diesters by means of quinonedibenzimide and tri-*n*-butylphosphine has been reported.[8)] A successful method for the preparation of esters of carboxylic acid by means of triphenylphosphine (**1**) and diethyl azodicarboxylate (**2**) was reported.[9)] The reaction was applied to the phosphorylation of alcohols.

When dibenzyl hydrogen phosphate was treated with a small excess of ethanol in the presence of **1** and **2** at room temperature, followed by catalytic hydrogenation, ethyl dihydrogen phosphate was isolated as its anilinium salt in 92% yield. An exothermic reaction set in as soon as **1** was added to a solution of **2**, dibenzyl hydrogen phosphate and ethanol. It may be reasonable to assume that the reaction intermediate, a quaternary phosphonium salt (**3**),[10)] is protonated to give a second phosphonium salt (**4**). Since ethanol is a

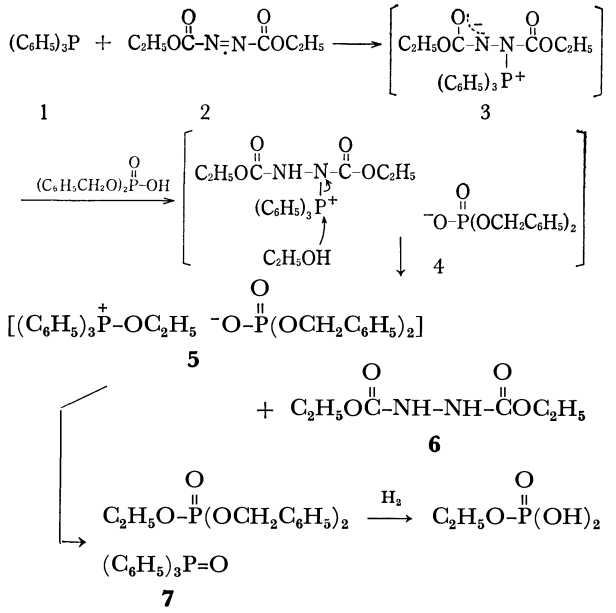

more reactive nucleophile than phosphate anion, **4** primarily undergoes nucleophilic attack by the ethanol to give triphenyl ethoxy phosphonium salt (**5**) and diethyl hydrazodicarboxylate (**6**). The phosphonium salt decomposes into dibenzyl ethyl phosphate and triphenylphosphine oxide (**7**).

When *p*-tolyl dihydrogen phosphate was used in place of dibenzyl hydrogen phosphate in the above reaction, ethyl *p*-tolyl hydrogen phosphate was obtained in a 48% yield along with an undesirable side product, diethyl *p*-tolyl phosphate (23%). Twenty-four percent of *p*-tolyl dihydrogen phsophate was recovered unchanged. The results are summarized in Table 1.

The reaction of dipyridinium *p*-tolyl phsophate with ethanol in the presence of **1** and **2** resulted in the formation of ethyl *p*-tolyl hydrogen phosphate and di-*p*-

1) Presented at the 20th (April 1967) and 23rd (April 1970) meetings of the Chemical Society of Japan.

2) H. G. Khorana and A. R. Todd, *J. Chem. Soc.*, **1953**, 2257.

3) F. Cramer and G. Weimann, *Chem. Ber.*, **91**, 996 (1961).

4) T. Mukaiyama, T. Hata, and O. Mitsunobu, *J. Org. Chem.*, **27**, 1815 (1962).

5) H. G. Khorana, *Can. J. Chem.*, **32**, 227 (1954).

6) F. Cramer, K. Pawelzik, and F. W. Lichtenthaler, *Chem. Ber.*, **91**, 1555 (1958).

7) R. J. W. Cremlyn, *J. Chem. Soc.*, **1961**, 1805.

8) I. Kuwajima and T. Mukaiyama, *J. Org. Chem.*, **29**, 1385 (1964).

9) O. Mitsunobu and M. Yamada, This Bulletin, **40**, 2380 (1967).

10) E. Brunn and R, Huisgen, *Angew. Chem. Intern. Ed. Engl.*, **8**, 513 (1969).

Table 1. Phosphorylation of alcohols by means of diethyl azodicarboxylate and triphenyl phosphine

Starting materials			Products						
$RO\overset{O}{\overset{\|}{}}\!>\!P\text{-}OH$ $R'O$		R″OH	$RO\overset{O}{\overset{\|}{}}\!>\!P\text{-}O^{-}\ H_3\overset{+}{N}C_6H_5$ $R''O$		Yield (%)	MP °C	Anal. %		
R	R′	R″	R	R″				C	H	N
C_6H_5–	H–	C_2H_5–	C_6H_5–	C_2H_5–	41	97—99	Found	56.70	6.27	4.76
							Calcd	56.94	6.15	4.74
C_6H_5–	H–	n-C_3H_7–	C_6H_5–	n-C_3H_7–	59	116—119	Found	57.85	6.54	4.79
							Calcd	58.24	6.53	4.53
p-$CH_3C_6H_4$–	H–	C_2H_5–	p-$CH_3C_6H_4$–	C_2H_5–	48[a]	103	Found	57.84	6.52	4.89
							Calcd	58.24	6.53	4.53
p-$CH_3C_6H_4$–	H–	n-C_3H_7–	p-$CH_3C_6H_4$–	n-C_3H_7–	30	122	Found	59.04	6.97	4.46
							Calcd	59.43	6.86	4.34
$C_6H_5CH_2$–	$C_6H_5CH_2$–	C_2H_5–	H–	C_2H_5–	92	167—170	Found	43.88	6.58	6.80
							Calcd	43.83	6.45	6.39
$C_6H_5CH_2$–	$C_6H_5CH_2$–	n-C_3H_7–	H–	n-C_3H_7–	96	155—157	Found	46.74	7.26	6.34
							Calcd	46.35	6.92	6.01

a) 23.1% of diethyl p-tolyl phosphate was isolated.

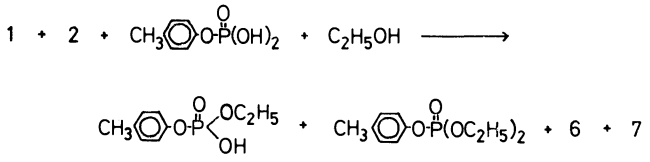

tolyl pyrophosphate as indicated by paper chromatography. Since metaphosphates are generally believed to be reactive intermediates for the phosphorylation of alcohols by means of phosphoric monoesters and dehydrating reagents,[11-14] the result might be explained as follows. The nucleophilic reactivity of the phosphate anion is enhanced by the presence of pyridine[4,15] and the formation of dipolar ion (**8**) takes place. The dipolar ion subsequently decomposed into metaphosphate (**9**) or the trimetaphosphate which gave the phosphate diester and the pyrophosphate diester.

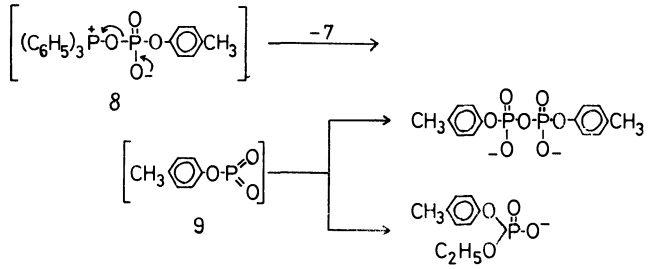

Preparation of Esters of Carboxylic Acid. The above phosphorylation method could not be applied to the phosphorylation and acylation of 2′ and/or 3′-hydroxy groups of nucleosides.[16] Thus, alkyl N,N'-tetraethylphosphorodiamidites prepared from alcohols and N,N'-tetraethylphosphorodiamidous chloride were allowed to react with **2** and carboxylic acids.

When n-propyl N,N'-tetraethylphosphorodiamidite was treated with equimolar amounts of **2** and benzoic acid at room temperature for 3 hr, n-propyl benzoate and diethyl N-(bisdiethylaminophosphoryl) hydrazodicarboxylate were obtained in 78% and 62% yields, respectively. The fact that no rearranged product, isopropyl benzoate, could be detected by NMR spectra indicates the exclusion of a carbonium ion mechanism.

Similarly, various alkyl benzoate and alkyl caproate were obtained. The results are summarized in Table 2.

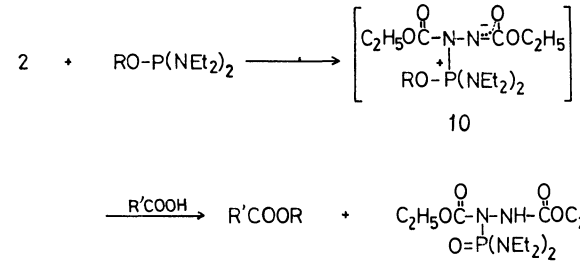

Steric Course of the Reactions. Dealkylation of alkoxyphosphonium salt is generally a simple bimolecular displacement at saturated carbon. Gerrard and Green[17] have shown that the phosphite derived from (+)-2-octanol reacts with ethyl iodide to give octyl iodide with inverted configuration.

In order to clarify the formation of alkoxyphosphonium salts (**5** and **10**) as intermediates in the present reactions, acylation of an optically active alcohol was attempted.

When S-(+)-2-octanol was allowed to react with **1**, **2**, and benzoic acid at room temperature, 2-octyl benzoate was obtained with a specific rotation of $[\alpha]_D$ −39.5°. The reaction of **2** and benzoic acid with R-(−)-2-octyl N,N'-tetraethylphosphorodiamidite derived from R-(−)-2-octanol resulted in the formation of 2-octyl benzoate with a specific rotation of $[\alpha]_D$+32.3°. As the 2-octyl benzoate prepared from S-(+)-2-octanol

11) A. R. Todd, *Proc. Chem. Soc.*, **1962**, 199.
12) P. T. Gilham and H. G. Khorana, *J. Amer. Chem. Soc.*, **80**, 6212 (1958).
13) G. Weimann and H. G. Khorana, *ibid.*, **84**, 4329 (1962).
14) D. M. Brown, J. A. Flint, and N. K. Hamer, *J. Chem. Soc.*, **1964**, 326.
15) F. Cramer and M. Winter, *Chem. Ber.* **92**, 2761 (1959).
16) O. Mitsunobu, K. Kato, and J. Kimura, *J. Amer. Chem. Soc.*, **91**, 6510 (1969).
17) W. Gerrard and W. J. Green, *J. Chem. Soc.*, **1951**, 2550.

and benzoyl chloride showed a specific rotation of $[\alpha]_D$ +38.9°, the present reactions proceeded stereospecifically with inversion of configuration at the alkyl group.

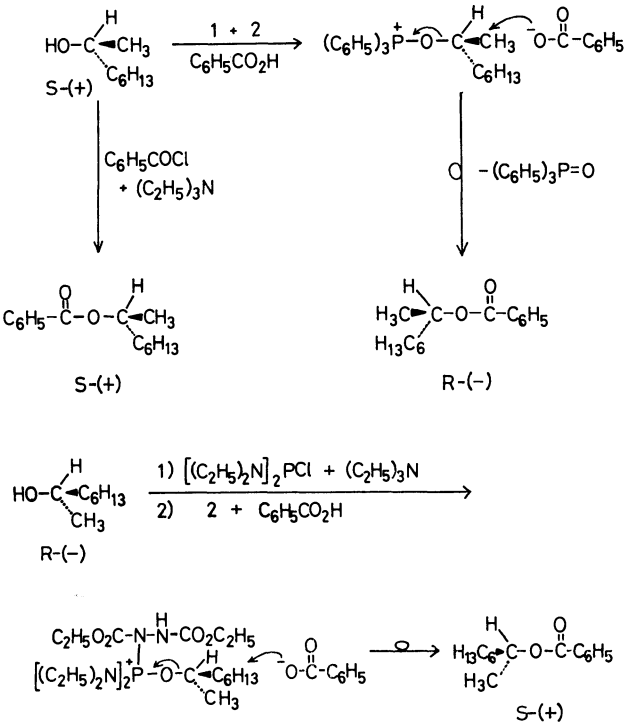

The result can be best explained by assuming the formation of alkoxyphosphonium salts (**5** and **10**). Inversion of the cofiguration takes place on dealkylation. Thus it can be concluded that acylation of alcohols by the present methods involves initial acitvation of alcohols and not of carboxylic acids. Phosphorylation of alcohols may also proceed through an analogous activation process.

Experimental

The IR spectra were measured on a Nippon Bunko IR-G spectrophotometer. The NMR spectra were obtained on a Hitachi Perkin-Elmer R-20 high-resolution spectrometer at 60 MHz, using tetramethylsilane as an internal standard. Optical rotations were measured with JASCO ORD/UV-5.

Reagents. Diethyl azodicarboxylate,[18] dibenzyl hydrogen phosphate,[19] aryl dihydrogen phosphate,[4,20] and S-(+)- and R-(−)-2-octanols[21] were prepared by known procedures. Alkyl *N,N'*-tetraethylphosphorodiamidites were prepared from *N,N'*-tetraethylphosphorodiamidous chloride and alcohols. The alcohols, carboxylic acids, and solvents were purified by ordinary procedures.

Phosphorylation of Ethanol by Means of Dibenzyl Hydrogen Phosphate, Diethyl Azodicarboxylate and Triphenylphosphine. A solution of **1** (1.31 g; 0.005 mol) in 5 m*l* of tetrahydrofuran (THF) was added dropwise to a solution of **2** (0.87 g; 0.005 mol), dibenzyl hydrogen phosphate (1.39 g; 0.005 mol) and ethanol (0.5 m*l*) in 10 m*l* of THF at room temperature under stirring. After the solution was kept standing over night at room temperature, the solvent was removed under reduced pressure. Ethanol (5 m*l*) was added to the residue and undissolved precipitate (mp 128—134°C; 0.42 g) was removed by filtration. Ethanol-water (1: 1; 30 m*l*) was added to the filtrate and the solution was hydrogenated over Pd-C (500 mg) at room temperature and atmospheric pressure. After absorption of hydrogen ceased, the catalyst was filtered off and the solvent was removed under reduced pressure. Water (5 m*l*) and aniline (0.47 g) were added to the residue and undissolved white precipitate, a mixture of **6** and **7** (mp 125—149°C; 1.63 g), was removed by filtration and washed with water. The filtrate and washings were evaporated to dryness to give anilinium ethyl hydrogen phosphate (1.01 g; 91.7%; mp 130—156°C). An analytical sample was obtained by recrystallization from acetonitrile containing a few drops of water, mp 168—170°C. Found: C, 43.88; H, 6.58; N, 6.80. Calcd for $C_8H_{14}NO_4P$: C, 43.83; H, 6.45; N, 6.39.

Phosphorylation of Ethanol by Means of p-*Tolyl Dihydrogen Phosphate, Diethyl Azodicarboxylate, and Triphenylphosphine.* A solution of **1** (10.48 g; 0.04 mol) in 30 m*l* of THF was added dropwise to a solution of **2** (6.96 g; 0.04 mol), *p*-tolyl dihydrogen phosphate (7.52 g; 0.04 mol) and ethanol (5 m*l*) in 50 m*l* of THF at room temperature under stirring. After the solution was kept standing overnight at room temperature, aniline (3.72 g) was added. Paper chromatogram of the reaction mixture showed the existence of a trace of di-*p*-toly pyrophosphate which could not be isolated. Precipitated anilinium *p*-tolyl hydrogen phosphate (2.34 g; 20.8% recovered, mp 176—182°C) was filtered off and the solvent was removed under reduced pressure. Benzene (30 m*l*) was added to the residue and heated to dissolve it. After cooling the solution in a refrigerator, **6** (5.66 g, 80.4%; mp 134—137°C; a mixed melting point with an authentic sample was not depressed) was removed by filtration and the filtrate was concentrated under reduced pressure. The residue was taken up in 20 m*l* of ether and the undissolved precipitate was removed by filtration. The filtrate was washed with water (10 m*l*×5), dried (Na_2SO_4) and distilled to give diethyl *p*-tolyl phosphate (bp 97—100°C at 0.1—0.2 mmHg; 2.26 g; 23.1%; redistillation gave bp 92—95°C at 0.1 mmHg). The diethyl *p*-tolyl phosphate was shown to be identical with the authentic sample by comparison of the infrared spectra (IR (liquid) 1167 (P–OEt), 1280 cm^{-1} (P=O)). From the residue of the fractionation, **7** (mp 145—154°C, after recrystallization from CCl_4) was obtained. The white crystalline compound undissolved in the ether in the above procedure was washed with warm water (100 m*l*) giving **7** (mp 153—156°C; 9.78 g; 88.0%). The washings were evaporated to dryness to give anilinium ethyl *p*-tolyl phosphate (mp 95—120°C; 6.31 g), which was washed with ether and recrystallized from ethyl acetate, mp 103—105°C. A small amount of anilinium *p*-tolyl hydrogen phosphate (0.42 g; 3.7%, mp 175—182°C) was removed by this procedure because it was not soluble in hot ethyl acetate. The yield of the anilinium ethyl *p*-tolyl phosphate was 47.7%.

Found: C, 57.84; H, 6.52; N, 4.89. Calcd for $C_{15}H_{20}NO_4P$: C, 58.24; H, 6.53; N, 4.53.

Ethyl phenyl, phenyl *n*-propyl, and *p*-tolyl *n*-propyl hydrogen phosphates were prepared in an analogous way. They are summarized in Table 1. The corresponding dialkyl aryl phosphates were not isolated.

Reaction of ethyl N,N'-*tetraethylphosphorodiamidite with* n-*caproic acid and diethyl azodicarboxylate.* A solution of ethyl *N, N'*-tetraethylphosphorodiamidite (2.20 g, 0.01 mol) in 15 m*l* of THF was added dropwise to **2** (1.74 g, 0.01 mol) and *n*-

18) N. Rabjohn, "Organic Syntheses." Coll. Vol. III, p. 375 (1955).
19) V. M. Clark and A. R. Todd, *J. Chem. Soc.*, **1950**, 2030.
20) F. Cramer and M. Winter, *Chem. Ber.*, **92**, 2761 (1959).
21) A. W. Ingersoll, "Organic Reactions," Vol. II, ed. by R. Adams, John Wiley and Sons, Inc., New York (1960), p. 376.

Table 2. Preparation of esters of carboxylic acid by means of alkyl *N,N'*-tetraethylphosphorodiamidites and diethyl azodicarboxylate

	Products				
	$R'-\overset{O}{\overset{\|}{C}}-OR$			$C_2H_5OCON(O=P(NEt_2)_2)NHCOOC_2H_5$	
$(Et_2N)_2P-OR$ R	R'	Bp °C/mmHg	Yield (%)	Bp °C/mmHg (mp °C)	Yield (%)
CH_3CH_2-	*n*-$C_5H_{11}-$	58—59/15	54.5	(112—114)	50.8
$CH_3CH_2CH_2-$	*n*-$C_5H_{11}-$	76—78/16	63.0	(109—111)	51.3
CH_3CH_2-	C_6H_5-	94—96/15	90.5	140—142/0.25	49.6
$CH_3CH_2CH_2-$	C_6H_5-	108—110/18.5	77.5	136—142/0.003	62.4
$(CH_3)_2CH-$	C_6H_5-	42—50/2	70.2	128—162/0.32	39.0
$CH_3(CH_2)_2CH_2-$	C_6H_5-	66—68/1	85.3	129—142/0.0025	15.1
$CH_3\underset{\|}{C}H(CH_2)_5CH_3$	C_6H_5-	108—113/1	80.0	(110—113)	25.7
$CH_3\underset{\|}{C}H(CH_2)_5CH_3$ [a]	C_6H_5-	98—100/0.35	54.1 [b]	(110—113)	59.0

a) R-(−) b) S-(+)

caproic acid (1.16 g, 0.01 mol) in 30 m*l* of THF at room temperature. The solution was stirred for 3 hr and concentrated to a sirup. After the sirup was kept standing in a refrigerator overnight, diethyl *N*-(bisdiethylaminophosphoryl)-hydrazodicarboxylate was obtained by filtration: 1.86 g, 50.8%, mp 102—104°C. An analytical sample was obtained by recrystallization from petroleum ether, mp 112—114°C.

Found: C, 45.96; H, 8.39%. Calcd for $C_{14}H_{31}N_4O_5P$: C, 45.89; H, 8.53%. IR(KBr) cm^{-1}: 3170(N–H), 1760, 1730(C=O), 1240(P=O).

The filtrate was distilled to give ethyl caproate, 54.5%, bp 58—59°C/15 mmHg.

Reaction of Ethyl N,N'-*Tetraethylphosphorodiamidite with Benzoic Acid and Diethyl Azodicarboxylate.* A solution of ethyl *N,N'*-tetraethylphosphorodiamidite (2.20 g, 0.01 mol) in 10 m*l* of THF was added dropwise to **2** (1.74 g, 0.01 mol) and benzoic acid (1.22 g, 0.01 mol) in 20 m*l* of THF at room temperature and stirred for 3 hr followed by concentration. After the residue was kept standing overnight in a refrigerator, ethyl benzoate (1.36 g, 90.7%, bp 95—97°C/17 mmHg) and diethyl *N*-(bisdiethylaminophosphoryl)hydrazodicarboxylate (2.29 g, 62.6%, bp 140—142°C/0.25 mmHg) were obtained by distillation.

Similarly, various alkyl benzoates were prepared in good yields as summarized in Table 2. Satisfactory NMR and IR data were obtained for all these esters.

Preparation of R-(−)-2-Octyl N,N'-*Tetraethylphosphorodiamidite.* R-(−)-2-octanol (8.97 g, 0.069 mol) and triethylamine (6.97g, 0.069 mol) in 150 m*l* of benzene were added dropwise to an ice cooled solution of *N,N'*-tetraethylphosphorodiamidous chloride (14.53 g, 0.069 mol) in 150 m*l* of benzene and the mixture was stirred for additional 7 hr. After the mixture was kept standing 2 days, water was added and the benzene layer was separated. The aqueous phase was extracted with benzene. The organic layer was dried by sodium sulfate. The benzene was removed and the residue was distilled to give a 77.5% yield of R-(−)-2-octyl *N,N'*-tetraethylphosphorodiamidite (bp 112—133°C/2 mmHg) which upon redistillation had bp 125—132°C/2 mmHg, $[\alpha]_D-15.0°$ (60.6 mg/cc in ethanol).

Reaction of R-(−)-2-Octyl N,N'-*tetraethylphosphorodiamidite with Benzoic Acid and Diethyl Azodicarboxylate.* A solution of R-(−)-2-octyl *N,N'*-tetraethylphosphorodiamidite (3.05 g, 0.01 mol) in 15 m*l* of THF was added dropwise to a solution of benzoic acid (1.22 g, 0.01 mol) and **2** (1.74 g, 0.01 mol) in 30 m*l* of THF at room temperature. After stirring for 3 hr, the solvent was removed and the residue was kept standing overnight in a refrigerator. A white crystalline compound was collected by filtration and washed with petroleum ether giving diethyl *N*-(bisdiethylaminophosphoryl)hydrazodicarboxylate (2.16 g, 59.0%, mp 110—113°C). The filtrate was distilled to afford S-(+)-2-octyl benzoate (54.1%, bp 96—113°C/0.35 mmHg) which upon redistillation had bp 98—100°C/0.35 mmHg, $[\alpha]_D+33.4°$ (62.0 mg/cc in ethanol).

Reaction of S-(+)-2-Octanol with Benzoic Acid, Diethyl Azodicarboxylate, and Triphenylphosphine. Diethyl azodicarboxylate (0.871 g, 0.005 mol) in 5 m*l* of THF was added dropwise to a solution of **1** (1.31 g, 0.005 mol), S-(+)-2-octanol (0.652 g, 0.005 mol) and benzoic acid (0.611 g, 0.005 mol) in 5 m*l* of THF at room temperature. After the solution was kept standing overnight, the slovent was removed. Ether (5 m*l*) was added to the residue and undissolved white crystalline compound was filtered off. The filtrate was distilled to give a 20.2% yield of 2-octyl benzoate with $[\alpha]_D-39.5°$ (0.032 mol/*l* in THF); bp 114°C/1.5 mmHg.

Preparation of S-(+)-2-Octyl Benzoate. Benzoyl chloride (35.1 mg, 0.0025 mol) in benzene (2 m*l*) was added dropwise to a solution of S-(+)-2-octanol (32.5 mg, 0.0025 mol) and triethylamine (25.2 mg, 0.0025 mol) in benzene (2 m*l*) at room temperature. After removal of triethylammonium chloride by filtration, the residue was distilled to give S-(+)-2-octyl benzoate (380 mg, 65%, bp 97—100°C/0.4 mmHg). Redistillation gave a pure sample, bp 98°C/1 mmHg, $[\alpha]_D+38.9°$ (0.081 mol/*l* in THF).

The authors wish to express their appreciation to Professor Tatsuya Samejima and staff for performing the optical rotation measurements. They also thank Miss Naoko Ikeda for her assistance in a part of the experiments.

Synthesis and the Iodine-Catalyzed Rearrangement of Isohibaene

Masayuki KITADANI, Ken ITO, and Akira YOSHIKOSHI*

College of General Education, Kobe University, Nada-ku, Kobe

**Chemical Research Institute of Non-Aqueous Solutions, Tohoku University, Sendai*

(Received June 3, 1971)

A partial synthesis of isohibaene (VI) starting with nezukol (V) has been accomplished. It involves, as the key step, the intramolecular insertion reaction of a ketocarbene generated by cuprous oxide-catalyzed decomposition of diazoketone (XI) under irradiation. It has been found that isohibaene undergoes rearrangement into a mixture of phyllocladene (XIV) and isophyllocladene (XV) by iodine catalytically.

In a previous paper[1] we (A. Y. and M. K.) reported on iodine-catalyzed skeletal rearrangement equilibrating among (−)-hibaene (I), (+)-kaurene (II), and (+)-isokaurene (III), in which we found hibaene as the most predominant component. The rearrangement was also utilized for the total synthesis of (±)-monogynol[2] (IV).

This paper deals with the transformation of nezukol[3] (V) into isohibaene[4] (VI) and the iodine-catalyzed rearrangement of the latter compound, which is a stereoisomer of hibaene concerning the C_8 and C_{13} positions.

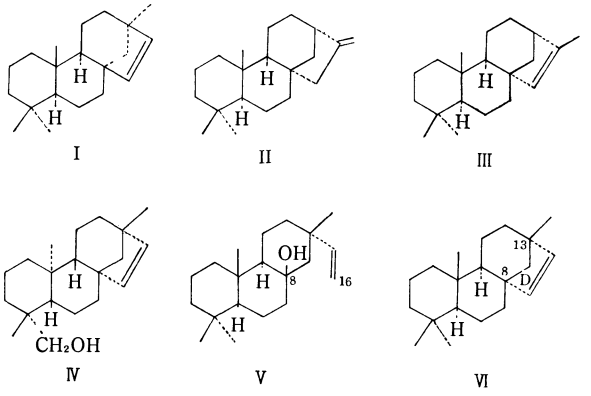

Results and Discussion

A. Synthesis of Isohibaene (VI). For the construction of the five-membered ring (ring D) of isohibaene by forming a bond between C_8 and C_{16} of isopimarane framework (formula V), a copper-catalyzed intramolecular insertion toward a C–H bond[5] as depicted by the step XI→XIIa was seen as a promising process (Scheme 1).

Ozonization of V followed by the reduction of the resulting ozonide with sodium iodide produced hydroxyaldehyde VII along with hydroxy-acid VIII. The former was oxidized with potassium permanganate to obtain VIII. More conveniently, V could be directly oxidized to acid VIII by potassium permanganate in warm acetone. This process gave a better yield. Attempted dehydration of VIII to an unsaturated acid with various dehydrating agents (*e.g.*, thionyl chloride, phosphorus oxychloride, or iodine) resulted in the formation of a complex mixture of products. When VIII was heated in methanol containing a catalytic amount of mineral acid, the acid-catalyzed esterification caused simultaneous dehydration which produced a mixture of the unsaturated esters IXa, IXb, and IXc in the ratio 7 : 2 : 1 (determined by glc). These unsaturated esters were separated by recrystallization and preparative glc, and their structures were assigned as follows. The crystalline ester IXa, the major product, showed no olefinic proton signals in the NMR spectrum and no absorption due to C=C in the IR spectrum. Provided no skeletal rearrangement occurs during the reaction, the double bond of IXa might be located on $\Delta^{8(9)}$. The oily ester IXb, formed in a ratio of 20%, showed a broad olefinic one-proton singlet and absorptions due to a trisubstituted double bond in the NMR and IR spectra, respectively. Hence the structure IXb was

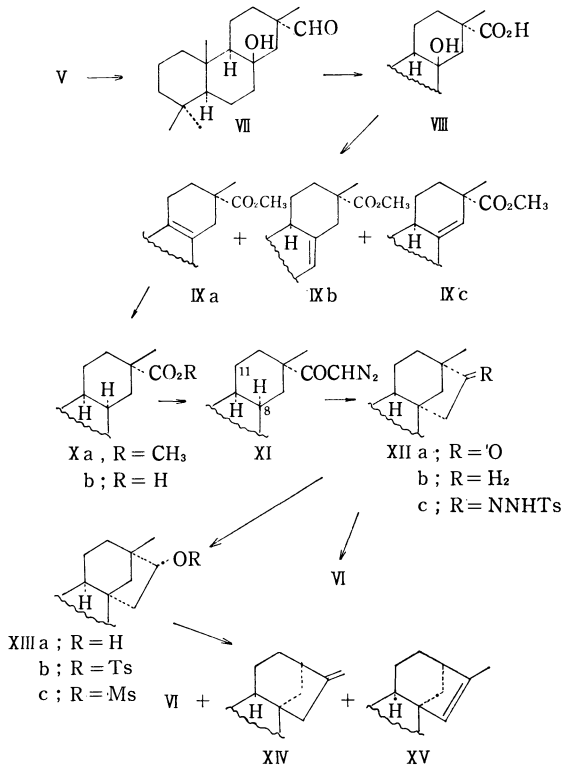

Scheme 1

1) A. Yoshikoshi, K. Kitadani, and Y. Kitahara, *Tetrahedron*, **23**, 1175 (1965).

2) K. Mori, M. Matsui, N. Ikegawa, and Y. Sumiki, *Tetrahedron Lett.*, **1966**, 175; K. Mori and M. Matsui, *Tetrahedron*, **24**, 3095 (1968).

3) M. Kitadani, *Nippon Kagaku Zasshi*, **91**, 664 (1970).

4) For an alternate synthesis of this compound, see E. Wenkert, P. W. Jeffs, and J. R. Mahajan, *J. Amer. Chem. Soc.*, **86**, 2218 (1964).

5) E. Wenkert, B. L. Mylari, and L. L. Davis, *ibid.*, **90**, 3870 (1968).

assignable as the ester. The NMR spectrum of the third ester exhibited a narrow olefinic one-proton singlet, and absorptions due to a trisubstituted double bond were shown in the IR spectrum. Thus, the structure IXc is likely to fit the last ester. The unsaturated ester IXa was hydrogenated in acetic acid over platinum under pressure, and the saturated ester Xa was obtained in 90% yield. Conclusive evidence was not available for the stereochemistry of the saturated ester at this stage. However, the fact that the final product of this synthesis was isohibaene (VI) indicated that the saturated ester had a *trans-anti-cis* stereochemistry. For the preparation of Xa, a mixture of the unsaturated esters IXa—c was similarly hydrogenated and gave a better yield of Xa.

The ester Xa, resistant to alkaline hydrolysis under standard conditions, was heated with potassium hydroxide in boiling ethylene glycol to obtain acid Xb. Treatment of Xb with thionyl chloride gave an acyl chloride, and the latter, without purification, was then converted into a diazoketone by the reaction with diazomethane. The IR spectrum of the product showed strong absorptions due to a diazoketo group at 2140 and 1620 cm^{-1}, and a sharp singlet due to the methine proton located between a carbonyl and a diazo group were observed at δ 5.5 in the NMR spectrum. These spectra supported the view that the product was the desired diazoketone XI.

The intramolecular ketocarbene insertion reaction was effected by addition of the diazoketone XI to boiling cyclohexane in which finely powdered cuprous oxide was suspended, while the reaction mixture was irradiated with a tungsten lamp. A ketone, whose carbonyl group showed absorption at 1740 cm^{-1} in IR was obtained almost quantitatively. In XI, two C–H bonds, *i.e.*, C_8–H and C_{11}–H (axial), toward which the generated ketocarbene may intramolecularly be inserted to form five-membered ketone, were available. Participation of the former bond should lead to the formation of the desired ketone XIIa. The ketone was submitted to the Wolff-Kishner reduction under forced conditions, and the spectra of the resulting hydrocarbon were compared with those of an authentic specimen of isohibane[6] (XIIb). The results including the identity of optical rotation confirmed the hydrocarbon as isohibane. The melting point remained undepressed on admixture with the authentic sample. This demonstrates that the intramolecular ketocarbene insertion toward the *tert.* C–H (C_8–H) bond predominated the attack toward the *sec.* C–H bond (C_{11}-axial H), as has been generally observed in insertion reactions with other carbenes.[7]

Tosylhydrazone XIIc of the ketone was treated with excess methyl lithium to obtain isohibaene (VI), which was identified by comparison of its IR and NMR spectra with those of an authentic specimen. On the other hand, sodium borohydride reduction of ketone XIIa gave alcohol XIIIa, whose hydroxyl group was tentatively assigned to *endo*. Tosylate XIIIb or mesylate XIIIc of the alcohol was heated in collidine affording a mixture of isohibaene (VI), phyllocladene (XIV), and isophyllocladene (XV). XIV and XV were identified by comparison with authentic specimens.

B. Iodine-catalyzed Rearrangement of Isohibaene (VI). Heating isohibaene (VI), phyllocladene (XIV), or isophyllocladene (XV) with a catalytic amount of iodine in boiling xylene caused isomerization of the olefin, and each olefin finally gave a mixture of XIV and XV. In contrast to the rapid isomerization between XIV and XV,[8] isohibaene (VI) rearranged slowly and was exhausted after *ca.* 24 hr. The results on the hibaene-kaurene-isokaurene system[1] and those just mentioned concerning the isohibaene-phyllocladene-isophyllocladene system indicate that the ring system in which the C_8–C_{16} bond is *cis* with regard to the C_{10}-methyl group is thermodynamically most favorable, *viz.*, in equilibrium, hibaene (I) and isophyllocladene (XV) are most stable in respective series (Scheme 2).

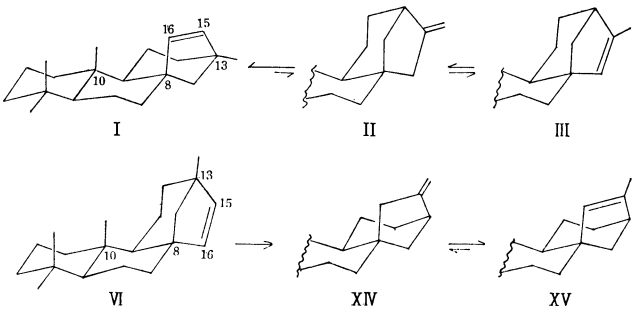

Scheme 2

Experimental

Melting points were uncorrected. IR and UV spectra were run on JASCO Model IR-E and Hitachi Model 124 spectrophotometers, respectively. NMR spectra with carbon tetrachloride as solvent (unless otherwise stated) and tetramethylsilane (δ=0 ppm) as internal standard were taken on a JEOL JNMC-60HL spectrometer, and coupling constants were given in Hz. Mass spectra were obtained by using a Hitachi RMU-6D spectrometer.

Ozonization of Nezukol (V). Excess ozonized air was passed through a solution of nezukol (8.5 g) in ethyl acetate (65 m*l*) at −75°C, and the ozonized solution was treated with sodium iodide (25.5 g) dissolved in acetic acid (85 m*l*). The mixture was allowed to stand overnight at room temperature. Liberated iodine was reduced by the addition of 3% aq. solution of sodium thiosulfate. The resulting solution was concentrated in a vacuum in a bath maintained below 50°C, and the residue was diluted with water. The product was extracted with ether, and the combined extracts were washed with aq. sodium carbonate solution, then with water, and dried over anhydrous magnesium sulfate. Evaporation of the ether left 5.6 g of a semisolid residue, which was recrystallized from ethanol - ether (5:1); 4.85 g (57%) of the hydroxy-aldehyde VII, mp 148—150°C, was obtained as colorless prisms. IR (KBr): 3550, 2725, 1725 cm^{-1}. NMR ($CDCl_3$): 7.33 (1H, s., CHO). M^+=292.

Found: C, 77.90; H, 10.71%. Calcd for $C_{19}H_{32}O_2$: C, 78.03; H, 11.03%.

6) W. Herz, D. Melchior, R. N. Mirrington, and P. J. S. Pauwels, *J. Org. Chem.*, **30**, 1873 (1965).

7) W. Kirmse, "Carbene Chemistry," Academic Press, New York (1964).

8) The iodine-catalyzed isomerization of phyllocladene into isophyllocladene has been reported. L. H. Briggs, B. F. Cain, R. C. Cambie, and B. R. Davis, *J. Chem. Soc.*, **1962**, 1840.

The above sodium carbonate extracts were acidified with mineral acid, and liberated carboxylic acid was extracted with ether. From the extracts, 680 mg (7.6%) of the hydroxy-acid VIII, mp 187—189°C, was obtained as colorless leaflets. IR (KBr): 3560, ~2400, 1678 cm^{-1}.

Found: C, 73.98; H, 10.46%. Calcd for $C_{19}H_{32}O_3$: C, 74.02; H, 10.13%.

Permanganate Oxidation of the Hydroxy-aldehyde VII. To an acetone solution of the hydroxy-aldehyde VII (500 mg) was added potassium permanganate (250 mg) dissolved in water (5 m*l*) over a period of 30 min in an ice-bath. Stirring was continued for an additional 1 hr, and sulfur dioxide was passed through the solution to reduce precipitated manganese dioxide. The resulting solution was filtered and the filtrate was concentrated in a vacuum. The residue was diluted with water and extracted with ether. The extracts were combined, washed with water, and dried. Evaporation of the ether left crystals (500 mg), which were recrystallized from ether - *n*-hexane (1:5) giving hydroxy-acid VIII (498 mg; 94%) metling at 189—190°C.

Permanganate Oxidation of Nezukol (V). Powdered potassium permanganate (11 g) was added portionwise to a stirred solution of nezukol (5.0 g) in acetone (130 m*l*). The temperature of the solution rose gradually. Stirring was continued for an additional 13 hr while the temperature was maintained at 50°C. The reaction mixture was allowed to stand overnight at room temperature. Working up as described above for permanganate oxidation of hydroxy-aldehyde VII gave hydroxy-acid VIII (4.7 g; 90%) melting at 189—190°C.

Unsaturated Esters IXa—c. A suspension of hydroxy-acid VIII (1 g) in dry methanol (15 m*l*) containing concd. sulfuric acid (0.5 m*l*) was refluxed for 30 min. The reaction mixture was poured into water and extracted with ether. The combined extracts were washed with aq. sodium carbonate solution, then with water, and dried. Evaporation of the ether gave a semisolid residue (890 mg), whose glc (20% PEG-20M column) showed three peaks in the ratio of 7:1:2 in elution sequence. Most of the major product IXa, mp 90—91°C, was separated from the residue by recrystallization with methanol as colorless leaflets. IR (KBr): 1720, 1189 cm^{-1}. NMR ($CDCl_3$): 3.64 (3H, s.).

Found: C, 78.94; H, 10.74%. Calcd for $C_{20}H_{32}O_2$: C, 78.89; H, 10.57%.

From the filtrate of the recrystallization, two minor esters were separated by preparative glc (20% PEG-20M column; ϕ, 3 mm×2 m; column temperature, 225°C; hydrogen flow, 30 m*l*/min).

Ester IXb, an oil, corresponded to the last peak in glc. IR (liquid): 1663, 857, 835 cm^{-1}. NMR: 3.63 (3H, s.), 5.38 (1H, br. s., $W_{1/2}=10.5$).

Found: C, 78.65; H, 10.83%. Calcd for $C_{20}H_{32}O_2$: C, 78.89; H, 10.57%.

Another ester IXc was also oily. IR (liquid): 1730, 856, 836 cm^{-1}. NMR: 3.64 (3H, s.), 5.50 (1H, s., $W_{1/2}=4.5$).

Found: C, 78.46; H, 10.89%. Calcd for $C_{20}H_{32}O_2$: C, 78.89; H, 10.57%.

Hydrogenation of the Unsaturated Ester IXa. Freshly prepared Adams' catalyst (1.48 g) suspended in acetic acid (100 m*l*) was activated by treatment with hydrogen in an autoclave. A solution of ester IXa (1.5 g) in acetic acid (100 m*l*) was added to the above suspension, and the mixture was shaken with hydrogen under 50 atm at 30°C for 24 hr. After the catalyst was separated, the solution was concentrated in a vacuum. The residue was dissolved in ether. The solution was washed with aq. sodium carbonate solution and then with water. Evaporation of the organic layer gave a crystalline residue (1.45 g) melting at 85—88°C, whose glc showed two peaks in the ratio of 19:1. Recrystallization of the crude crystals from the methanol solution afforded 1.35 g (90%) of the saturated ester Xa, mp 94—96°C. IR (KBr): 1723 cm^{-1}. NMR: 3.62 (3H, s.).

Found: C, 78.36; H, 10.92%. Calcd for $C_{20}H_{34}O_2$: C, 78.38; H, 11.18%.

A mixture of the unsaturated esters IXa—c provided the saturated ester Xa in 98% yield in a similar manner.

Hydrolysis of the Saturated Ester Xa. A solution of ester Xa (810 mg) and potassium hydroxide (6.4 g) in freshly distilled ethylene glycol (100 m*l*) was refluxed for 30 min. The solution was concentrated to a half volume by distillation, and then cooled down to room temperature. Water (50 m*l*) was added, and carboxylic acid Xb was extracted with chloroform. The crude carboxylic acid (770 mg) was recrystallized from ether - *n*-hexane (4:1) affording 750 mg (97.5%) of colorless prisms, mp 228—230°C. IR (KBr): ~2400, 1695 cm^{-1}.

Found: C, 78.10; H, 10.61%. Calcd for $C_{19}H_{32}O_2$: C, 78.03; H, 11.03%.

Diazoketone XI. A solution of acid Xb (1.012 g), thionyl chloride (20 m*l*), and pyridine (5 drops) in dry ether (45 m*l*) was allowed to stand at room temperature for 24 hr. The solvent and the excess reagent were distilled off in a vacuum, and the residue was redissolved in dry ether (20 m*l*). Excess ethereal diazomethane was added into the above solution over a period of 40 min, and the solution was stirred for 2 hr. After standing overnight the solvent was eliminated. The residue was dissolved in a small volume of ether, and the solution was filtered to remove insoluble substances. The filtrate was allowed to stand at room temperature giving 650 mg of pale yellow crystals, mp 118—121°C. The crystals were collected by filtration, and the filtrate was chromatographed on a silica gel column. An additional amount of diazoketone (400 mg), mp 119—122°C, was obtained by eluting with ether - *n*-hexane (1:4). The combined crystals were recrystallized from petroleum ether to give diazoketone XI (980 mg; 90%) as glossy pale yellow leaflets, mp 122—123°C. UV (cyclohexane): 251 nm (log ε 3.75). IR (KBr): 3150, 2140, 1620 cm^{-1}. NMR ($CDCl_3$): 5.5 (1H, s., $COCHN_2$).

Found: C, 76.23; H, 10.14; N, 8.87%. Calcd for $C_{20}H_{32}ON_2$: C, 76.01; H, 10.21; N, 8.87%.

Ketone XIIa. To a stirred boiling suspension[9] of finely powdered cuprous oxide (5 g) in dry cyclohexane (150 m*l*) was added dropwise a hot solution of diazoketone (2.71 g) in dry cyclohexane (100 m*l*) over a period of 1.5 hr. Stirring was continued overnight at the same temperature. The catalyst was filtered off. Evaporation of cyclohexane left crystals (2.48 g). Recrystallization from *n*-hexane provided ketone XIIa (2.35 g; 95%), mp 145—146°C, as colorless long needles. IR (KBr): 1740 cm^{-1}.

Found: C, 83.65; H, 11.21%. Calcd for $C_{20}H_{32}O$: C, 83.40; H, 11.16%.

An experiment carried out without irradiation gave ketone in a lower yield.

Isohibane (XIIb). Sodium (60 mg) was dissolved in freshly distilled ethylene glycol (3 m*l*); ketone XIIa (280 mg) and anhydrous hydrazine (100 mg) were added to the above solution. The solution was refluxed for 2 days. Water was added, and the product was extracted with ether. The ether layer was washed with water and dried. Crystals (210 mg) obtained by evaporating the ether were chromatographed on an alumina column using petroleum ether - ether (9:1) as an eluting solvent giving isohibane (XIIb). Recrystallization

9) A 375 W tungsten lamp (National) was used for heating.

from *n*-hexane gave colorless needles melting at 76—77.5°C (lit,[6] 65—67°C). $[\alpha]_D$+63.4°C (*c* 0.83, methanol) (lit,[6] $[\alpha]_D$+56°).

Found: C, 87.38; H, 12.65%. Calcd for $C_{20}H_{34}$: C, 87.51; H, 12.49%.

The IR and NMR spectra of the hydrocarbon were identical with those of an authentic specimen.

Tosylhydrazone XIIc. A solution of ketone XIIa (72 mg) and *p*-tosylhydrazine (65 mg) in ethanol (3 m*l*) was refluxed for 1 hr. Water was added, and the product was extracted with ether and dried. A crystalline residue obtained by evaporation of the solvent was chromatographed on an alumina column, and tosylhydrazone (104 mg) was eluted with methanol - ether (1:20). Recrystallization from methanol - ether (5:1) gave crystals (100 mg; 90%) melting at 206—208°C. UV (methanol): 205 (log ε 3.99), 228 (log ε 3.93), 275 (sh.) nm. NMR ($CDCl_3$). 2.44 (3H, s.), 7.30, 7.88 (2H, d., J=8 each, an AB-type).

Isohibaene (VI). A large excess of methyllithium, prepared from methyl iodide and lithium in dry ether, was added to a suspension of tosylhydrazone XIIc (77.3 mg) in dry ether in an ice bath. The suspension changed into a clear solution after 30 min. Stirring was continued for an additional 2 hr at room temperature. The resulting solution was poured on crushed ice and extracted with ether. The ether extracts were dried over anhydrous magnesium sulfate. The semisolid residue obtained by evaporating the ether was recrystallized from methanol. 40 mg (87%) of isohibaene, mp 83—84°C (lit,[5] mp 73—75°C), was obtained. In spite of the fact that the specific rotation observed for our sample, $[\alpha]_D^{25}$+93° (*c* 0.375, methanol) differs from the value reported for isohibaene ($[\alpha]_D$+8°),[5] the IR and NMR spectra of our sample were identical with those of an authentic specimen. IR (KBr): 751, 740 cm^{-1}. NMR: 0.85, 0.88 (3H, s. each), 1.01 (6H, s.), 5.36, 5.51 (1H, d., J=6 each; an AB-type). M^+=272.

Found: C, 88.25; H, 12.10%. Calcd for $C_{20}H_{32}$: C, 88.16; H, 11.84%.

Alcohol XIIIa. Ketone XIIa (628 mg) was dissolved in a 1:1 mixture (20 m*l*) of dry methanol and dry ether, and sodium borohydride (110 mg) was added into the stirred solution in an ice bath. After stirring for 5 hr at the same temperature, the reaction mixture was poured into ice water and extracted with ether. The ether layer was washed with 1N hydrochloric acid, then with water and dried. Ether was evaporated to leave crystals (630 mg), which were recrystallized from methanol to give alcohol XIIIa (625 mg; 96%), mp 130—131°C. IR (KBr): 3490 cm^{-1}. NMR: 3.82 (1H, q., J=10.2 and 5).

Found: C, 82.58; H, 11.80%. Calcd for $C_{20}H_{34}O$: C, 82.69; H, 11.80%.

Tosylate XIIIb. A solution of alcohol XIIIa (1 g) and *p*-toluenesulfonyl chloride (2 g) in dry pyridine (20 m*l*) was allowed to stand for 3 days at room temperature. The reaction mixture was poured into ice-cooled 0.5N hydrochloric acid and extracted with ether. The organic layer was washed with saturated sodium bicarbonate solution, then with water and dried. Evaporation of the solvent left a crystalline residue (1.5 g), which was poured into an alumina column. Elution with ether-petroleum ether (1:5) gave tosylate XIIIb. A pure sample was obtained from petroleum ether by recrystallization as colorless plates (1.35 g; 88%), mp 134—135°C. UV (methanol): 226 (log ε 3.85), 262 (log ε 2.42), 273 (log ε 2.38)nm. IR (KBr): 1598, 1496, 1362, 1188, 1167 cm^{-1}. NMR ($CDCl_3$): 2.46 (3H, s.), 4.42 (1H, q., J=10 and 5), 7.4, 7.9 (2H, d., J=9 each, an AB-type).

Found: C, 73.23; H, 9.30%. Calcd for $C_{27}H_{40}O_3S$: C, 72.94; H, 9.07%.

Mesylate XIIIc. From alcohol XIIIa (450 mg) and mesyl chloride (460 mg), mesylate was obtained in 85% yield in the same manner as for tosylate. After recrystallization from chloroform - petroleum ether (1:5) a pure sample melted at 139—141°C. IR (KBr): 1355, 1180, 1170 cm^{-1}. NMR ($CDCl_3$): 3.0 (3H, s.), 4.61 (1H, q., J=10 and 4.8).

Found: C, 68.75; H, 9.85%. Calcd for $C_{21}H_{36}O_3S$: C, 68.44; H, 9.85%.

Solvolysis of Sulfonates XIIIb and XIIIc. A soultion of tosylate XIIIb (800 mg) and freshly distilled collidine (30 m*l*) was refluxed for 40 hr and then concentrated by distillation. The residue was poured into 1N hydrochloric acid and extracted with ether. The organic layer was washed with saturated sodium bicarbonate solution, then with water and dried. Evaporation of the solvent afforded an oily residue which crystallized on standing. Glc analysis (20% PEG-20M column; φ, 3 mm×2 m; column temperature, 200°C; hydrogen flow, 8.3 m*l*/min) showed three peaks (1.4: 1.2: 1.0 in ratio) at the retention times of 4.0, 4.3, and 5.2 min. The reaction mixture was chromatographed on a 10% silver nitrate-impregnated silica gel column to separate each product. Petroleum ether - ether (9:1) eluted isohibaene (VI), mp 82—83°C (153 mg; 40%), (+)-isophyllocladene (XV; 130 mg; 33%), mp 109—111.5°C, $[\alpha]_D^{25}$+25.6° (lit,[10] mp 111—112°C, $[\alpha]_D$+23°) and (+)-phyllocladene (XIV; 110 mg; 28%), mp 94—96°C, $[\alpha]_D^{25}$+19.3° (lit,[11] mp 98°C, $[\alpha]_D$+16°) in order. Under the same conditions as described above, the retention times of isohibaene, isophyllocladene, and phyllocladene in glc were 4.0, 4.3, and 5.2 min., respectively. Each olefin was identified by comparison of its IR and NMR spectra with those of an authentic specimen.

A result in line with ours was obtained for the solvolysis of mesylate XIIIc.

Iodine-catalyzed Isomerization of Isohibaene, Phyllocladene, and Isophyllocladene. Each olefin was dissolved in dry xylene, and a piece of iodine was added. The solution was refluxed in an oil bath, while monitoring the reaction by 10% silver nitrate-impregnated silica gel tlc using *n*-hexane - ether - benzene (20: 1: 1) as an eluting solvent. Equilibrium between phyllocladene and isophyllocladene was attained in the predominant formation of the latter after about 2 hr, while isohibaene slowly rearranged into a mixture of phyllocladene and isophyllocladene under the same conditions and was exhausted after about 24 hr.

The reaction mixture of each run was vigorously shaken with mercury and then passed through a short alumina column to removed colored materials. The eluate was rechromatographed on a 10% silver nitrate-impregnated silica gel column affording phyllocladene and isophyllocladene in an approximate ratio of 1:3. These isomerization products were identified by their spectra and melting points on admixture with authentic specimens.

The authors would like to thank Professors Ernest Wenkert and Werner Herz for the identification of isohibaene and isohibane, respectively.

10) R. McCrindale and K. H. Overton, "Advances in Organic Chemistry," Vol. 5, p. 100, ed. by R. A. Raphael, E. D. Taylor, and H. Wynberg, Interscience Publishers, New York (1965).

11) A. W. Johnson, T. J. King, and R. J. Martin, *J. Chem. Soc.*, **1961**, 4420.

Studies of Hydroxy Amino Acids. II.[1] The Separation of Diastereoisomers of Hydroxy Amino Acids

Yasuo ARIYOSHI and Naotake SATO

Central Research Laboratories, Ajinomoto Co., Inc., Suzuki-cho, Kawasaki, Kanagawa

(Received June 9, 1971)

It has been found that *erythro*-β-hydroxy-DL-norvaline, *erythro*-β-hydroxy-DL-norleucine, and *threo*-β-hydroxy-DL-leucine form scarcely-soluble compounds in water with α-naphthylphosphoric acid, tetrachlorophthalic acid, and chlorendic acid, respectively. On the other hand, the compounds of their diastereoisomers with the reagents were soluble in water. On the basis of these facts, β-hydroxy-DL-norvaline, β-hydroxy-DL-norleucine, and β-hydroxy-DL-leucine were successfully separated into their diastereoisomers. The configurational assignment of α-amino-β-hydroxy acids without a branched side chain on the γ-carbon atom was established by means of NMR spectroscopy.

α-Amino-β-hydroxy acids are easily obtained by the condensation of copper glycinate with aldehydes or ketones, the method of which was originally proposed by Akabori *et al.*[2] and developed by Mix[3] and by Otani and Winitz.[4] However, this method usually gives a mixture of two diastereoisomeric racemates. Furthermore, the separation of the diastereoisomers is generally so difficult and complicated that only a few methods of doing so have been known. In these methods, β-hydroxy-DL-norvaline and β-hydroxy-DL-norleucine were changed to their copper chelates[3] and β-hydroxy-DL-leucine was converted to its sodium salt.[5]

In the previous paper, the present authors reported the separation of DL-threonine.[1] The separation and the configurational assignment of the diastereoisomers of β-hydroxy-DL-norvaline, β-hydroxy-DL-norleucine, and β-hydroxy-DL-leucine will be described in this paper. *erythro*-β-Hydroxy-DL-norvaline, *erythro*-β-hydroxy-DL-norleucine, and *threo*-β-hydroxy-DL-leucine formed scarcely-soluble compounds in water with α-naphthylphosphoric acid, tetrachlorophthalic acid, and chlorendic acid respectively. The elementary analyses showed that the compound consisted of the amino acid and the reagent in a 1:1 molar ratio, except for the compound with chlorendic acid, of which we failed to obtain an analytical sample. The IR spectra of all the compounds showed the absorption band in a region of 1715—1720 cm^{-1} due to the free carboxyl group as the salt of the amino acids with the strong acids. On the contrary, the compounds of their diastereoisomers with the reagents were soluble in water. These characteristics were successfully used in the separation of the two diastereoisomers of β-hydroxy-DL-norvaline, β-hydroxy-DL-norleucine, and β-hydroxy-DL-leucine.

The precipitates and the mother liquors were individually treated with hydrochloric acid. After removing the liberated reagents by filtration, the *erythro*- and *threo*-forms of the amino acids were recovered from the acidic solutions with an ion-exchange column. The results are summarized in Table 1. The *threo*-forms of β-hydroxy-DL-norvaline and β-hydroxy-DL-leucine also formed comparatively insoluble compounds in water with trimesic acid. These characteristics were also successfully used in the separation of the *threo*-forms of these amino acids, but the separation of the *erythro*-forms failed because of contamination with the *threo*-forms.

TABLE 1. SEPARATION OF THE DIASTEREOISOMERS

Amino acid	Ratio of diastereoisomers		Reagent	Recovery of pure isomers %	
	erythro	*threo*		*erythro*	*threo*
HyNva	53	47	NP	68	64
HyNle	44	56	TCP	71	66
HyLeu	25	75	CA	68	75

Abbreviations used are as follows:
HyNva, β-Hydroxy-DL-norvaline; HyNle, β-Hydroxy-DL-norleucine; HyLeu, β-Hydroxy-DL-leucine; NP, α-Naphthylphosphoric acid; TCP, Tetrachlorophthalic aicd; CA, Chlorendic acid.
To *erythro*-forms of HyNva and HyNle, and *threo*-form of HyLeu, 1.2 equimolar amount of the reagents was used.

α-Amino-β-hydroxy acids with long side chain are difficult to separate into their diastereoisomers by paper or thin-layer chromatography, and a convenient method of determining the configuration has not been found in the literature. The NMR spectra of the diastereoisomers of the amino acids obtained in the investigation were observed at 60 MHz in aqueous solutions, with sodium 2,2-dimethyl-2-silapentane-5-sulfonate as the internal reference.

In an alkaline solution, the chemical shifts of α-CH protons of the *erythro*- and *threo*-forms without a branched side chain on the γ-carbon atom were found in the region of δ 3.30—3.32 ppm and δ 3.13—3.16 ppm respectively (Table 2). However, no such regularity was observed in a neutral or an acidic solution for any of them (Table 2). From these results, it is possible to distinguish the diastereoisomers of α-amino-β-hydroxy acid without a branched side chain on the γ-carbon atom by means of NMR spectroscopy in an alkaline solution. Thus, the ratio of the *erythro*- and *threo*-forms of the synthetic DL-α-amino-β-hydroxy pelargonic acid could be determined to be 30:70 on the basis of the NMR spectrum, though the amino acid could not be clearly separated into its diastereoisomers by paper or thin-layer chromatography.

1) Part 1, Y. Ariyoshi and N. Sato, This Bulletin, **44**, 2787 (1971).
2) M. Sato, K. Okawa, and S. Akabori, *ibid.*, **30**, 937 (1957).
3) H. Mix, *Z. Physiol. Chem.*, **327**, 41 (1961).
4) T. T. Otani and M. Winitz, *Arch. Biochem. Biophys.*, **102**, 464 (1963).
5) Y. Ikutani, T. Okuda, and S. Akabori, This Bulletin, **33**, 582 (1960).

Table 2. Chemical shifts (δ ppm) of α-CH in aqueous solutions

Amino acid	Configuration	Solution		
		alkaline	neutral	acidic
DL-α-Amino-β-hydroxybutyric acid	*erythro*	3.30	3.83	3.92
	threo	3.16	3.58	3.72
β-Hydroxy-DL-norvaline	*erythro*	3.32	3.82	4.22
	threo	3.15	3.62	4–4.2
β-Hydroxy-DL-norleucine	*erythro*	3.32	3.82	3.95
	threo	3.13	3.62	3.85
β-Hydroxy-DL-leucine	*erythro*	3.33	3.90	4.33
	threo	3.32	3.82	4.08
DL-α-Amino-β-hydroxypelargonic acid[a)]	*erythro*	3.29	—	—
	threo	3.13	—	—

a) The compound is insoluble in a neutral or an acidic solution.

Experimental

The melting points are uncorrected. The NMR spectra were obtained with a Varian A-60 or T-60 spectrometer at 60 MHz in aqueous solutions, and chemical shifts are given from sodium 2,2-dimethyl-2-silapentane-5-sulfonate, used as the internal reference. Paper chromatography was carried out by the descending method on Toyo Roshi No. 51 paper with the solvent system of *n*-butanol - methyl ethyl ketone - 28% aqueous ammonia - water (5:3:1:1 v/v). The determination of the diastereoisomers was described in the previous paper.[1] The IR spectra were recorded in Nujol mull with a JASCO IR-S spectrometer.

Preparation of Starting Materials. β-Hydroxy-DL-norvaline, β-hydroxy-DL-norleucine, and DL-α-amino-β-hydroxypelargonic acid were synthesized by the method described by Mix.[3] β-Hydroxy-DL-leucine was obtained according to the method described by Ikutani *et al.*[5] DL-allothreonine and DL-threonine were on hand from the previous investigation.[1]

Salt of Erythro-*β-Hydroxy*-DL-*norvaline with α-Naphthylphosphoric Acid (I).* A solution of 1.3 g of *erythro*-β-hydroxy-DL-norvaline and 3.2 g of disodium α-naphthylphosphate in a mixture of 25 m*l* of water and 1 m*l* of concentrated hydrochloric acid was stored overnight in a refrigerator. The crystals thus formed were collected by filtration; yield, 1.2 g (32%). The compound was recrystallized from aqueous methanol to give **I** as fine crystals; mp 172.5—173.5°C (decomp.). IR: 3360, 3180, 1720, 1595, 1515 cm^{-1}. Found: C, 47.81; H, 6.03; N, 3.74; P, 8.20%. Calcd for $C_{15}H_{20}O_7NP \cdot H_2O$: C, 48.00; H, 5.91; N, 3.73; P, 8.25%.

Salt of Erythro-*β-Hydroxy*-DL-*norleucine with Tetrachlorophthalic Acid (II).* Into a solution of 1.47 g of *erythro*-β-hydroxy-DL-norleucine in 30 m*l* of water, 3.1 g of tetrachlorophthalic acid hemihydrate was dissolved with shaking at room temperature. The crystals precipitated immediately were dissolved by the addition of methanol. The resulting solution was stored overnight in a refrigerator to give **II** as needles; yield, 3.0 g (64%); mp 129.5—130°C (decomp.). IR: 3340, 3200, 1715, 1630, 1535 cm^{-1}. Found: C, 35.85; H, 3.74; N, 2.92; Cl, 30.03%. Calcd for $C_{14}H_{15}O_7NCl_4 \cdot H_2O$: C, 35.84; H, 3.65; N, 3.00; Cl, 30.23%. *threo*-β-Hydroxy-DL-leucine failed to give such a crystalline compound with chlorendic acid in an analytically pure state.

Separation of Diastereoisomers of β-Hydroxy-DL-*norvaline.* A solution of 6.4 g of disodium α-naphthylphosphate and 5.0 g of β-hydroxy-DL-norvaline (*erythro*: *threo*=53: 47) in 55 m*l* of water containing 4 m*l* of concentrated hydrochloric acid was stirred for 2 hr at room temperature, and then stored overnight in a refrigerator. The crystals thus formed were collected by filtration. The IR spectrum of the compound was identical with that of **I**. The crystals were dissolved in a mixture of 50 m*l* of water and 8 m*l* of concentrated hydrochloric acid by warming. The resulting solution was poured onto a column of Dowex 50 W×8 (in the H-form). After washing with water, the amino acid was eluted with 2N ammonium hydroxide (If α-naphthylphosphoric acid crystallized out from the acidic solution, it was filtered off and the filtrate was treated as above). The eluate was filled up to 500 m*l* with water, and 5 μl of it was subjected to quantitative analysis. The solution contained 2.4 g of the *erythro*-form and 0.3 g of the *threo*-form. It was concentrated *in vacuo* to dryness. The residue was crystallized from water - ethanol to give *erythro*-β-hydroxy-DL-norvaline as plates; yield, 1.8 g (68%); mp 247–248°C (decomp.). lit,[3] 245—246°C (decomp.). The compound was confirmed to be a pure *erythro*-form by paper chromatography. (Found: C, 45.38; H, 8.46; N, 10.46%).

The mother liquor excluding the *erythro*-form was poured onto a column of Dowex 50 W×8 (in the H-form) and treated as has been described above. The eluate contained 2.1 g of the *threo*-form and 0.2 g of the *erythro*-form. The eluate was concentrated *in vacuo* and crystallized from water. The *threo*-form was obtained as plates; yield, 1.5 g (64%); mp 218—219°C (decomp.). lit,[3] 217—218°C (decomp.). (Found: C, 45.15; H, 8.44; N, 10.33%). The crystals were confirmed to be pure *threo*-β-hydroxy-DL-norvaline by paper chromatography.

Separation of Diastereoisomers of β-Hydroxy-DL-*norleucine.* A solution of 18.5 g of β-hydroxy-DL-norleucine (*erythro*: *threo*= 44: 56) and 20.8 g of tetrachlorophthalic acid hemihydrate in 185 m*l* of water was stirred for 3 hr at room temperature and then stored overnight in a refrigerator. The crystals (26 g) thus formed were collected by filtration. The IR spectrum of the compound was identical with that of **II**. The crystals were suspended in a mixture of 130 m*l* of water with 10 m*l* of concentrated hydrochloric acid and then boiled under reflux for 30 min. The reaction mixture was stored overnight in a refrigerator. The tetrachlorophthalic acid (17.2 g) thus liberated was filtered off. The filtrate was poured onto a column of Dowex 50 W×8 (in the H-form) and treated in the manner used in the separation of β-hydroxy-DL-norvaline to give the *erythro*-form as plates. Yield, 5.8 g (71%); mp 253—254°C (decomp.). lit,[3] 248—250°C (decomp.). (Found: C, 49.19; H, 8.96; N, 9.54%).

The filtrate (pH 2.70) from the scarcely-soluble compound was acidified to pH 1.20 with concentrated hydrochloric acid and kept for 2 hr at room temperature. The tetrachlorophthalic acid (2.5 g) thus liberated was filtered off. The

filtrate was treated in the manner used in the separation of the *erythro*-form to give the *threo*-form as plates. Yield, 6.8 g (66%); mp 232—233°C (decomp.). lit,[3] 224—226°C (decomp.). (Found: C, 48.90; H, 8.89; N, 9.64%).

*Separation of Diastereoisomers of β-Hydroxy-*DL*-leucine.* A mixture of 10 g of β-hydroxy-DL-leucine (*erythro*: *threo*=25: 75) and 23.8 g of chlorendic acid in 100 m*l* of water was stirred for 2.5 hr at room temperature and then kept overnight in a refrigerator. The scarcely-soluble compound (30.9 g) thus formed was collected by filtration and dissolved in a mixture of 150 m*l* of water and 10 m*l* of concentrated hydrochloric acid by heating. The resulting suspension, containing an oily substance formed during the heating, was stirred at room temperature for 30 min. In the course of stirring, the oily substance turned to crystals, which were then filtered off. The crystals were identified as chlorendic acid by studying the IR spectrum. The filtrate was treated in the manner used in the separation of β-hydroxynorvaline to obtain the *threo*-form as plates. Yield, 5.6 g (75%), mp 232—233°C (decomp.). Recrystallization from water - ethanol raised the melting point to 239—240°C (decomp.). lit, 240—241°C (decomp.),[5] 239—240°C (decomp.).[6] The IR spectrum of the compound was identical with that of the *threo*-form.[7] (Found: C, 48.95; H, 8.96; N, 9.58%).

The filtrate (pH 3.20) from the addition compound was acidified to pH 1.20 with concentrated hydrochloric acid. After standing for 1 hr at room temperature, the chlorendic acid thus liberated was filtered off. The filtrate was treated in the manner used in the separation of the *threo*-form to afford the *erythro*-form as plates. Yield, 1.7 g (68%); mp 241—242°C (decomp.). Recrystallization from water raised the melting point to 249—250°C (decomp.). lit, 255—256°C (decomp.),[5] 253—255°C (decomp.).[6] The compound was obtained as hemihydrate. The IR spectrum of the compound was almost identical with that of the *erythro*-form except for the band due to the water of crystallization.[7] Found: C, 46.27; H, 9.13; N, 9.11%. Calcd for $C_6H_{13}O_3N \cdot 1/2H_2O$: C, 46.14; H, 9.04; N, 8.97%.

The authors are indebted to Miss Yohko Koguchi of our laboratory for the NMR measurements.

6) H. W. Krause, F. W. Wilcke, H. Mix, and W. Langenbeck, *Z. Phys. Chem.*, (Leipzig) **225**, 342 (1964).

7) S. Dalby, G. W. Kenner, and R. C. Sheppard, *J. Chem. Soc.*, **1960**, 968.

BULLETIN OF THE CHEMICAL SOCIETY OF JAPAN, VOL. 44, 3437—3440(1971)

The Synthesis and Photo Reaction of 7,11-Dimethyl-1,6,10-dodecatrien-3-one

Tadahiro KATO, Hideo MAEDA, Mitsuaki TSUNAKAWA, and Yoshio KITAHARA*

Department of Chemistry, Faculty of Science, Tohoku University, Sendai

(Received June 15, 1971)

For the purpose of constructing a pinene skeleton (I), a promising intermediate for the synthesis of bergamotenes (III), the vinyl ketone (II), was synthesized from geranyl bromide (IV) by the application of Meyer's method, followed by a Grignard reaction with vinylmagnesium bromide and subsequent oxidation. The irradiation of II in absolute ether afforded an unexpected keto ether (X) in a low yield; it was characterized by means of a deuterium-exchange reaction and physical methods. No other product except X was isolated from the photoreaction mixture of II.

For the purpose of constructing a pinene skeleton (I) by the photocyclization[1] of olefinic ketone (II), we have synthesized (II) and examined its photoreaction. Compound (I) is a promising intermediate for the synthesis of bergamotenes (III), the structures of which were unequivocally confirmed by an elegant synthesis[2] from β-pinene.

Geranyl bromide (IV), easily obtainable from geraniol by treatment with phosphorous tribromide, was chosen as the starting material. The reaction of the bromide with lithium salt of 2,4,4,6-tetramethyl-5,6-dihydro-1,3-oxazine afforded the coupled product (V) in a 68% yield. The dihydrooxazine (V) was carefully reduced with sodium borohydride to give a fairly unstable tetrahydrooxazine derivative (VI), which, without purification, was hydrolyzed by oxalic acid to give two products, (VII) and (VIII), in 15 and 9% yields respectively.[3] The hydrolysis required the conditions of steam distillation, and the low yield of VII is due to its unstability toward acid at high temperatures. The acyclic aldehyde (VII) is fairly unstable even in a refrigerator under a nitrogen atmosphere.

The reaction of VII with vinylmagnesium bromide afforded the vinyl alcohol (IX) in a 78% yield, this substance was subsequently oxidized with active manganese dioxide to give vinyl ketone (II) in a 60% yield. Compounds (VII), (IX), and (II), especially VII and II, are fairly unstable and should be stored in a refrigerator under a nitrogen atmosphere.

The irradiation of II in absolute ether with a 100-W high-pressure mercury lamp under a nitrogen atmosphere resulted in the formation of several products, from which only a keto-ether (X) was isolated by re-

* To whom inquiries regarding this paper should be addressed.

1) For example, E. J. Corey, J. D. Bass, R. LeMahieu, and R. B. Mitra, *J. Amer. Chem. Soc.*, **86**, 5570 (1964).

2) T. W. Gibson and W. F. Erman, *ibid.*, **91**, 4771 (1969).

3) a) A. I. Meyers, A. Nabeya, H. W. Adickes, and I. R. Politzer, *ibid.*, **91**, 763 (1969). b) J. M. Fitzpatrick, G. R. Malone, I. R. Politzer, H. W. Adickes, and A. I. Meyers, *Organic Preparations and Procedures*, **1** (3), 193 (1969).

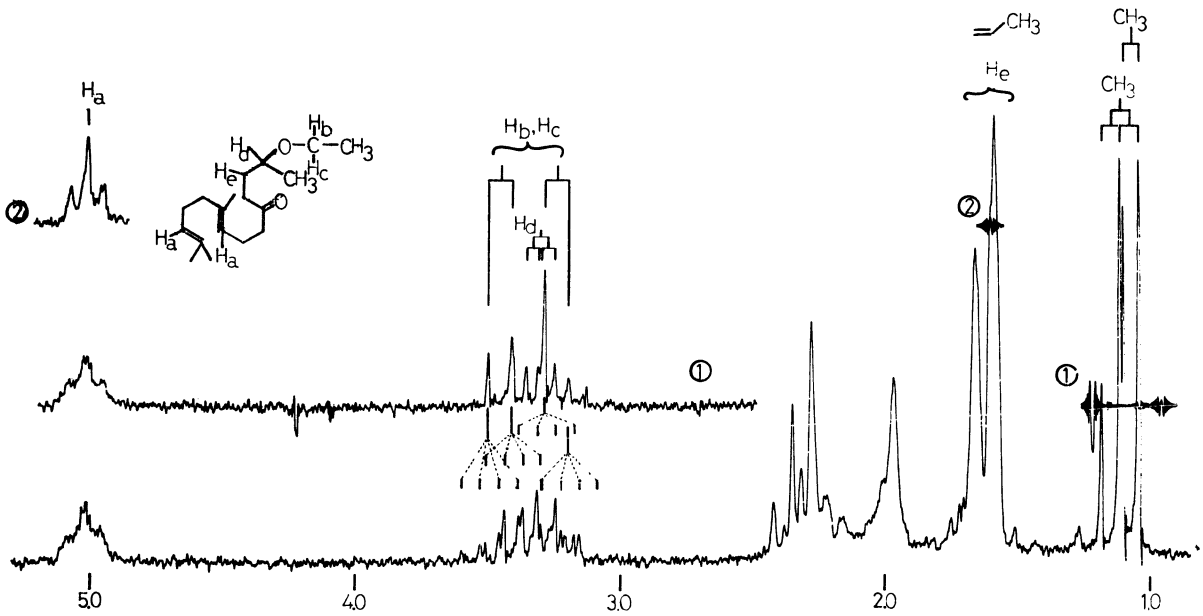

Fig. 1. 100 Mc NMR spectrum of keto ether (X) in CCl_4 plus 10% C_6D_6.

peated column chromatography in a 2% yield.

The gross structure of X was determined on the basis of the following evidence. The active hydrogens of X were replaced by deuterium under alkaline conditions[4] to give the deuterated keto ether. A comparison of the mass spectra of the original and the deuterated keto ether showed that X contained four replaceable hydrogens.

The 100-Mc NMR spectrum[5] of X in CCl_4 plus 10% C_6D_6 (Fig. 1) shows, in addition to two olefinic protons (Ha) at 5.01 and three olefinic methyl groups near 1.60 ppm, complex multiplets between 3.08 and 3.60 due to Hb, Hc, and Hd, a doublet and a triplet of the primary and secondary methyl groups respectively.

The irradiation of both the secondary and primary methyl groups (Fig. 1, ①) causes the multiplets between 3.20 and 3.50 ppm to appear as a pair of doublets centered at 3.45 and 3.24 ppm due to Hb and Hc, and a doublet of doublet at 3.31 (Hd). Simultaneous irradiation at 3.17 and 3.51 converts the triplet and doublet at 1.07 and 1.10 of the primary and secondary methyl groups to sharp singlets and at the same time affects the signals near 1.6 due to the He proton, which appears overlapping with three olefinic methyl groups. Irradiation at 1.60 ppm not only changes the broad multiplet at 5.01 due to olefinic protons (Ha) to a broad triplet (Fig. 1, ②), but also disturbs the multiplets near 3.2 ppm. These decoupling results are best explained in terms of a $-CH_2CH(CH_3)OCH_2CH_3$ grouping and an acyclic geranyl moiety which remains unchanged during the photoreaction.

Although a pinene skeleton could not be constructed by photocyclization, as has been expected at the outset of our study, it was found that the vinyl group of the vinyl ketone (II) is reactive toward ethyl ether under photoirradiation. This reaction may be general, as has been reported[6] recently in the case of conjugated cyclopentenones.

The chemical shifts and coupling modes of Hb, Hc,

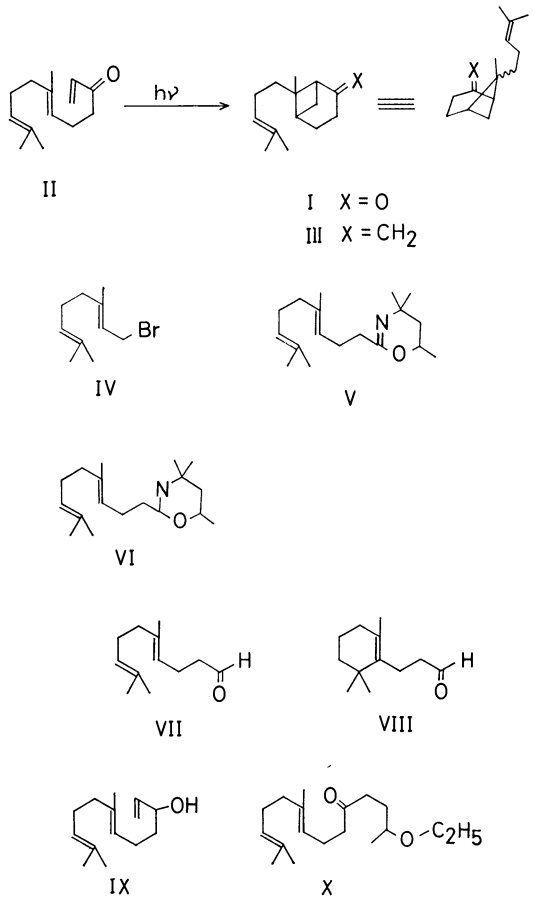

4) B. Nolin and R. N. Jones, *Can. J. Chem.*, **30**, 727 (1952).

5) NMR spectra were measured with Varian T-60 and H-100 spectrometers in carbon tetrachloride if otherwise stated. The Chemical shifts were expressed with ppm from an internal standard of tetramethylsilane.

6) Z. Yoshida, M. Kimura, and I. Tabuse, Symposium of Photochemistry (Japan), symposium paper, p. 100 (1970).

and Hd in X are of interest since they indicate that Hb and Hc are magnetically non-equivalent and that the free rotation near the ether linkage of X is restricted. This may be due to a reason similar to that reported in the case of ethyl isobutyl ether,[7] where the methylene of the ethyl group appaers as an AB of the ABX_3 system.

Experimental

2-(4,8-Dimethyl-3,7-nonadienyl)-4,4,6-trimethyl-5,6-dihydro-1,3-oxazine (V). An ether solution of *n*-butyl lithium (120 m*l*) prepared from *n*-butyl bromide (34.4 g) and lithium (4.3 g) in absolute ether (150 m*l*), was dropped, at −60°C over a one-period into an absolute tetrahydrofuran solution of 2,4,4,6-tetramethyl-5,6-dihydro-1,3-oxazine (18.6 g, 0.13 mol) which had been cooled to −60°C before the addition. After 2 hr stirring at −60——70°C, geranyl bromide (31 g, 0.143 mol) in absolute tetrahydrofuran (40 m*l*) was dropped in over a 30 min period at that same temperature, after which the stirring was continued for a further 30 min. The cooling bath was removed to make the reaction mixture come to room temperature. All the above operations were carried out under a nitrogen atmosphere. The reaction mixture was then poured into ice water. The aqueous solution, after being acidified with 9N hydrochloric acid, was washed with *n*-hexane and then made alkaline by adding a 40% sodium hydroxide solution.

The alkaline solution was extracted with ether, and the ether solution was evaporated to give a residual oil. The residual oil was then purified by distillation to afford a dihydrooxazine derivative (V) (24.4 g, 68% yield); bp 95—97°C/1 mmHg. V: IR (film) 1670 cm^{-1} (*v* C=N–). NMR (*δ*), 1.10 (sharp s, C_4–Me×2), 1.23 (d, J=6.2, C_6–Me), 1.63 (olefinic methyls), 4.02 (m, C_6–H), and 5.13 (olefinic protons). Mass, M^+ 277, Mol Wt ($C_{18}H_{31}NO$) 277.44.

Found: C, 77.49; H, 11.56; N, 4.99%. Calcd for $C_{18}H_{31}NO$: C, 77.92; N, 11.26; N, 5.05%.

2-(4,8-Dimethyl-3,7-nonadienyl)-4,4,6-trimethyl-2,3,5,6-tetrahydro-1,3-oxazine (VI). The dihydrooxazine (V) (30 g, 0.11 mol) was dissolved in 230 m*l* of a mixed solvent of tetrahydrofuran and ethanol (1:1). The solution, after being cooled to −50°C, was carefully neutrallized with 9N hydrochloric acid to pH 7 and sodium borohydride in an aqueous solution [$NaBH_4$(4.25 g, 0.11 mol), H_2O(7 m*l*); 40% NaOH (one drop)] was gradually dropped in over a 30 min period, during which time the solution was kept neutral (pH 6—8) by the occasional addition of 9N hydrochloric acid. After the completion of the addition, the stirring was kept up for an additional hour.

The above operations were carried out at −40——50°C. The reaction mixture was made alkaline by adding a 40% sodium hydroxide solution, and this poured into water. After extraction with ether, the ether solution was washed with a saturated sodium chloride aqueous solution and then dried over anhydrous potassium carbonate. The evaporation of the ether afforded a crude oil (VI) (30.2 g), which, due to its unstability toward heat and silica gel, was used for the next step without purification. IR (film) 3300 cm^{-1}. NMR 1.06, 1.10, and 1.13 (C_4 and C_6-methyls), 1.60 and 1.67 (olefinic methyls), 3.65 (m, C_6-H), 4.13 (t, J=6, C_2–H), and 5.16 (olefinic protons).

5,9-Dimethyl-4,8-decadienal (VII). A mixture of the crude tetrahydrooxazine (VI) (3.05 g), water (30 m*l*), and anhydrous oxalic acid (1.33 g) was steam-distilled under a nitrogen atmosphere, and then the distillate was extracted with ether.

From the ether solution we obtained 1.30 g of oil after an usual work-up. The crude oil was chromatographed on silica gel (20 g) by elution with a mixed solvent of benzene - cyclohexane (1:1) to afford 544 mg of an aldehyde fraction. The aldehyde fraction was then further chromatographed on silica gel (5 g) impregnated with 5% silver nitrate. Successive elution afforded monocyclic aldehyde (VIII) (174 mg) from a benzene - cyclohexane (1:1) mixture and acyclic aldehyde (VII), (287 mg) from an ether eluent. Aldehyde (VII): IR (film) 2750, 1730, 830 cm^{-1}. NMR 1.60 and 1.63 (olefinic methyls), 5.10 (olefinic protons), and 9.80 ppm (bs, aldehyde proton). Mass M^+ 180, Mol wt ($C_{12}H_{20}O$) 180.28. Aldehyde (VIII): IR (film) 2750, 1730 cm^{-1}. NMR 1.00 (sharp s, Me×2), 1.60 (sharp s, olefinic methyl), and 9.83 (bs, aldehyde proton). Mass M^+ 180.

Found: C, 79.90; H, 11.25%. Calcd for $C_{12}H_{20}O$: C, 79.94; H, 11.18%.

Tosyl Hydrazone of VIII. A mixture of the aldehyde (VIII) (73 mg), *p*-tosylhydrazine (100 mg), and methanol (5 m*l*) was stirred overnight at room temperature. The subsequent recrystallization of the crude hydrazone with methanol afforded a pure specimen (85 mg); mp 117°C.

Found: C, 65.26; H, 8.11; N, 8.14%. Calcd for $C_{19}H_{27}N_2O_2S$: C, 65.67; H, 7.83; N, 8.06%.

7,11-Dimethyl-1,6,10-dodecatrien-3-ol (IX). To a tetrahydrofuran solution of vinyl magnesium bromide, prepared from magnesium (200 mg), vinyl bromide (980 mg), and anhydrous tetrahydrofuran (3 m*l*), we added the aldehyde (VII) (477 mg) in anhydrous tetrahydrofuran (6 m*l*) under a nitrogen atmosphere; the reaction mixture was then stirred overnight at room temperature.

The reaction mixture, after being poured into an aqueous ammonium chloride solution, was extracted with ether. From the ether solution we obtained, after an usual work-up, crude oil; this oil was chromatographed on silica gel (16 g) with benzene to give oily vinyl alcohol (IX) (447 mg, 78%). A pure specimen of IX was obtained by rechromatography on silica gel and subsequent distillation. IR (film) 3300, 1670, 1645, 920 cm^{-1}. NMR 1.60 and 1.67 (olefinic methyls), 4.05 (m, CHOH), 5.05—6.13 (five olefinic protons). Mass M^+ 208, Mol wt ($C_{14}H_{24}O$) 208.33.

Found: C, 80.34; H, 11.41%. Calcd for $C_{14}H_{24}O$: C, 80.71; H, 11.61%.

7,11-Dimethyl-1,6,10-dodecatrien-3-one (II). A mixture of the alcohol (IX) (200 mg), active manganese dioxide (2.2 g), and carbon tetrachloride (10 m*l*) was stirred at room temperature overnight. The subsequent removal of the solid and the evaporation of the combined solvents afforded a crude oil (170 mg) which was passed through silica gel (8 g) with a mixed solvent of benzene - cyclohexane (1:1) to give pure ketone (II) (113 mg, 60%). IR (film) 1700 (W), 1680, 1615 cm^{-1}. NMR 1.60 (olefinic methyls), 5.10(b, 2H), and 5.73—6.5(–CH=CH_2 group). Mass M^+ 206, Mol wt ($C_{14}H_{22}O$) 206.32. UV λ_{max}^{MeOH} 324 mμ (64).

Photoreaction of Vinyl Ketone (II). Vinyl ketone (II) (173 mg) in 100 m*l* of absolute ether was irradiated under a nitrogen atmosphere for 8 hr with a 100-W high-pressure mercury lamp. Similarly, 253-, 250-, and 250 mg portions of vinyl ketone were separately irradiated under the same conditions until the starting material disappeared on thin-layer chromatography.

The above reaction mixtures were then combined and passed through 70 g of silica gel by changing the solvents successively. From cyclohexane - benzene (1:1) and benzene -

7) E. Bullock, E. E. Burnell, and B. Gregory, *Chem. Commun.*, **1967**, 193.

isopropylether (4: 1) we obtained 30 mg of the recovered material and 373 mg of a crude oil respectively. The latter was further chromatographed on 5% silver nitrate - silica gel (170 g) with cyclohexane - isopropyl ether (10:1) to give 54 mg of oil, which was then rechromatographed on a short silica-gel column with benzene to afford the pure photoproduct (X) (23 mg). No other product was obtained in a pure form. IR (film) 1715 cm^{-1}. NMR (Fig. 1).

Deuterium Exchange of the Photoproduct (X). The photoproduct (X) and anhydrous sodium carbonate (5 mg) were dissolved in a mixture of CH_3OD (4 m*l*) and D_2O (0.5 m*l*). After the mixture has been refluxed for an hr under a nitrogen atmosphere, the solvents were removed *in vacuo*.

The residue was successively worked up by the addition of CH_3OD (4 m*l*) and D_2O (0.5 m*l*), refluxing, and the subsequent removal of the solvents. The residue was picked up in absolute ether to obtain the deuterated product. Major fragment ions of X and its deuterated product. X: 280(M^+), 234, 191, 165, 151, 136, 121, 111, 98. deuterated X: 284(M^+), 238, 195, 194, 169, 168, 155, 136, 121, 114, 102.

The authors wish to thank Dr. T. W. Gibson (Proctor and Gamble Co.) for his kind information on the cyclization of vinyl ketone (II). They also wish to thank Dr. A. I. Meyers for his sending of copies of the experimental details on the reactions of 5,6-dihydro-1,3-oxazine and its related compounds.

BULLETIN OF THE CHEMICAL SOCIETY OF JAPAN, VOL. 44, 3440—3443 (1971)

The Photochemistry of Large-ring Cycloalkanones[1)]

Kiyohide MATSUI, Takasi MORI, and Hitosi NOZAKI*
Department of Industrial Chemistry, Kyôto University, Kyôto

(Received June 29, 1971)

The photoreactions of 11-, 12-, and 13-membered cycloalkanones (Ia, Ib, and Ic) are described. The major products are *cis*, *trans* isomers of bicyclo[*n*.2.0]alkan-1-ol ($n=7$, 8, and 9; II, III). The stereochemistry and multiplicity of the reactive species have been discussed with emphasis on the effect of the ring size. The Ib cyclododecanone is most readily susceptible to the photochemical cyclization *via* its S_1 state, affording the *cis*-cyclobutanol IIb stereoselectively.

The interest in the effect of the ring size upon transannular reactivity as well as in the syntheses of 1,4-cycloalkanedione[2)] prompted the present authors to investigate the photoreactions of 11-, 12-, and 13-membered cycloalkanones; we have found a remarkable influence of the ring size upon the behavior of the reactive photoexcited species. As is known already, the irradiation of cyclodecanone gives 9-hydroxydecalin or bicyclo[4.4.0]decan-1-ol,[3)] whereas that of cyclododecanone affords bicyclo[8.2.0]dodecan-1-ol.[4)] We first wanted to learn further details on the photoreaction of cyclododecanone (Ib), including its stereochemistry,[5)] and then we proceeded to examine a borderline case, the reaction of cycloundecanone (Ia) and cyclotridecanone (Ic). We obtained the results summarized in Table 1.

The structures of the II and III cyclobutanols were determined to be as shown in Scheme 1. The dehydration of both II and III with thionyl chloride gave a mixture of olefins, VI and VII. The oxidative cleavage of VI with potassium permanganate-sodium metaperiodate led to the known 1,4-diketones, VIII.[2)] The *cis*-hydration of VI by means of hydroboration afforded II. The structure of Va (a *cis*, *trans* mixture) was tentatively assigned on the basis of IR, NMR (two olefin protons), and its catalytic hydrogenation into IVa.

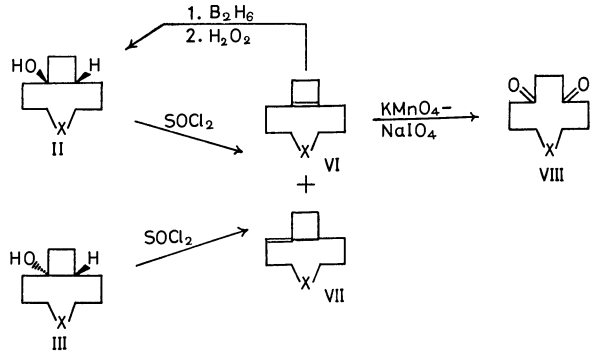

Scheme 1

The cyclobutanol formation was commonly observed in the irradiation of three ketones, Ia, Ib, and Ic, and no other bicyclic product was isolated. However, the reactivity of each ketone was strongly controlled by the ring size, as may be summarized as follows: (1) In a qualitative sense, the reaction of Ib proceeded most rapidly. (2) This ketone, Ib, afforded the best yield of the cyclobutanol derivatives, IIb and IIIb. (3) The highest *cis*/*trans* ratio (II/III) was observed with Ib; the next, with cycloundecanone (Ia), and the lowest,

* To whom reprint requests should be addressed.

1) A part of this work has been described in a preliminary communication: T. Mori, K. Matsui, and H. Nozaki, *Tetrahedron Letters*, **1970**, 1175.

2) T. Mori, K. Matsui, and H. Nozaki, This Bulletin, **43**, 231 (1970).

3) M. Barnard and N. C. Yang, *Proc. Chem. Soc.*, **1958**, 302.

4) a) B. Camerino and B. Patelli, *Experientia*, **20**, 260 (1964). b) K. H. Schulte-Elte and G. Ohloff, *Chimia*, **18**, 183 (1964).

5) The stereochemical aspect of the photochemical cyclization of I_b was briefly descrived by Schulte-Elts (Ref. 3b) in a footnote, with no experimental details. No further report has yet appeared.

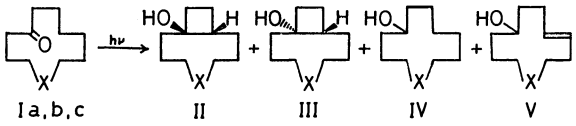

TABLE 1. THE PHOTOLYSIS OF CYCLOUNDECANONE (I_a), CYCLODODECANONE (I_b), AND CYCLOTRIDECANONE (I_c)

	Solvent	Irradiation time (hr)	Recovered I (%)	Product yields (%)				
				II	III	IV	V	unidentified
I_a	benzene	48	8	45	13	trace	8	4
	cyclohexane	48	5	34	9	7	5	3
	2-propanol	48	7	19	8	26	trace	3
	piperylene	144	69	0	0	0	0	trace
I_b	benzene	25	0	70	6	0	0	1
	cyclohexane	8	0	75	12	trace	0	1
	2-propanol	10	0	67	7	12	0	0
	piperylene	119	0	55	0	0	0	trace
I_c	benzene	48	8	36	19	trace[a]		3
	cyclohexane	48	8	37	20	trace[a]		3
	2-propanol	48	8	30	20	3[a]		2
	piperylene	130	21	38	0	0		trace

a) Identification could not be effected because of the small amounts obtained.

with cyclotridecanone (Ic). (4) Cycloundecanone (Ia) was most susceptible to photoreduction to IVa. (5) Only Ia gave unsaturated alcohol, Va.

The presence of piperylene as a triplet quencher drastically reduced the reaction rates. Remarkably, the single product from Ib was, stereoselectively, *cis*-cyclobutanol IIb when the starting material had completely disappeared. Under the same conditions, Ic gave IIc as a sole product; here the reaction proceeded rather sluggishly. In contrast, Ia afforded none of the products, IIa—Va, and decomposed slowly into a tarry product after prolonged irradiation in a piperylene solution.

The photochemical cyclization of open-chain ketones has been the subject of previous investigation,[6] and mechanisms have been discussed by Jeger,[7] Yang,[8] and their co-workers. Some possible explanations of the present case are shown in Scheme 2.

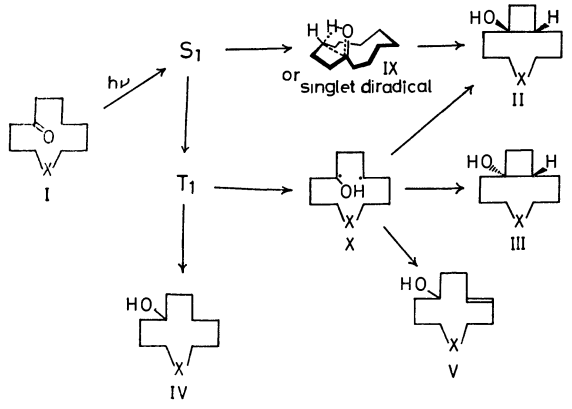

Scheme 2

The stereoselective formation of the *cis*-cyclobutanols, IIb and IIc, on the quenching of Ib (T_1) and Ic (T_1) might be explained by assuming the concerted cyclization of Ib (S_1) and Ic (S_1) through a transition state such as IX or, alternatively, through a singlet diradical intermediate of a similar geometry. The direct cyclization from Ia (S_1) must be conformationally much less favored, as is evident on an inspection of the model. In this case, therefore, Ia (T_1) is the sole active species undergoing transannular cyclization. The cyclotridecanone, Ic, appears to be least porne to cyclization, possibly for conformational reasons.

The selective formation of the IIc *cis*-cyclobutanol under the condition of triplet-quenching may be explained in terms much like those used to explain the IIb formation. The lowest ratio of IIc/IIIc in other solvents indicates that Ic (T_1) is the more important species of the photocyclization in such solvents.

We may conclude that the product distributions are strongly controlled by the transannular proximity of the excited carbonyl group and the reacting methylene proton, which depends on the conformation of the respective ring and, therefore, on the presence or absence of an additional methylene in the long undecamethylene group of Ib. The cyclization of Ib is characterized by the fact that the greatest contribution to the ring closure is made by the excited singlet (S_1). This is in sharp contrast with the open-chain case of ketones and also with 11- and 13-membered cycloalkanones (Ia, Ic).

Experimental

All the temperatures are uncorrected. The NMR spectra were obtained on a JOEL C-60-H spectrometer in CCl_4 solutions, with tetramethylsilane as the internal reference. Chemical shifts are given in ppm from this reference, with a multiplicity of signals in an abbreviated form. The glc

6) D. R. Coulson and N. C. Yang, *J. Amer. Chem. Soc.*, **88**, 4511 (1966), and the references cited there.
7) I. Orban, K. Schaffner, and O. Jeger, *ibid.*, **85**, 3033(1963).
8) N. C. Yang, S. P. Elliot, and B. Kim, *ibid.*, **91**, 7551 (1969).

was performed on HVSG on Chromosorb W, with nitrogen as the carrier gas. The tlc was conducted on Silica-gel G, with *n*-hexane or benzene as the developing solvent. The product yields were calculated on the basis of the peak areas of glc.

Photoreaction of Cycloalkanones (Ia—c). General Procedure: A solution of I (1.00 mmol) in a purified and degassed solvent (20 m*l*) was placed in a Pyrex tube (25 mm in diameter) and covered with nitrogen. Irradiation was effected externally with a high-pressure mercury lamp (200 W). The solution was then evaporated, and the residual oil was distilled. The products were effectively separated from each other by preparative tlc, using benzene or a mixed solvent of *n*-hexane and ether (10: 1) as the eluant. *cis*-Cyclobutanols (II) were more polar than *trans*-isomers (III) on tlc. Monocyclic alcohols (IV, V) were more polar than II and III. Each product was purified by recrystallization or by distillation.

cis-*Bicyclo*[*7.2.0*]*undecan-1-ol (IIa)*. Separation and distillation gave IIa as a colorless solid; mp 42—43°C. IR (Nujol): 3350 cm^{-1} (OH). NMR δ: 1.05—2.60 (m, 19H), 2.75 (s, 1H). Found: C, 78.8; H, 11.8%. Calcd for $C_{11}H_{20}O$: C, 78.5; H, 12.0%.

trans-*Bicyclo*[*7.2.0*]*undecan-1-ol (IIIa)*. The IIIa *trans*-isomer formed a colorless oil. IR (neat): 3470 cm^{-1} (OH). NMR δ: 1.05—2.30 (m, 19H), 2.30—2.80 (m, 1H). Found: C, 78.8; H, 11.7%. Calcd for $C_{11}H_{20}O$: C, 78.5; H, 12.0%.

cis-*Bicyclo*[*8.2.0*]*dodecan-1-ol (IIb)*. A work-up gave IIb as a colorless solid; mp 47—49°C (lit,[4b] mp 48—49°C). IR (Nujol): 3380 cm^{-1} (OH). NMR δ: 1.05—1.70 (m, 16H), 1.70—2.10 (m, 4H), 2.10—2.70 (m, 1H), 2.27 (s, 1H, OH).

trans-*Bicyclo*[*8.2.0*]*dodecan-1-ol (IIIb)*. The IIIb *trans*-isomer was isolated as a colorless oil. IR (neat): 3470 cm^{-1} (OH). NMR δ: 1.05—1.70 (m, 16H), 1.69 (s, 1H, OH), 1.70—2.20 (m, 4H), 2.20—2.75 (m, 1H).

cis-*Bicyclo*[*9.2.0*]*tridecan-1-ol (IIc)*. The IIc *cis*-alcohol formed a colorless solid; mp 45—47°C. IR (Nujol): 3400 cm^{-1} (OH). NMR δ: 0.75—2.30 (m, 23H), 2.74 (s, 1H, OH). Found: C, 79.5; H, 12.5%. Calcd for $C_{13}H_{24}O$: C, 79.5; H, 12.3%.

trans-*Bicyclo*[*9.2.0*]*tridecan-1-ol (IIIc)*. The IIIc *trans*-alcohol was a colorless oil. IR (neat): 3460 cm^{-1} (OH). NMR δ: 1.05—2.15 (m, 23H), 2.10—2.65 (m, 1H). Found: C, 79.7; H, 12.3%. Calcd for $C_{13}H_{24}O$: C, 79.5; H, 12.3%.

Dehydration of II and III. General Procedure:[9] A solution of II or III (2.75 mmol) in dry ether (2.00 m*l*) was stirred, drop by drop, into a solution of thionyl chloride (0.40 m*l*) and pyridine (1.00 m*l*) in dry ether (2.00 m*l*) at 3—5°C. After the reaction had subsided (*ca.* 2 hr), the mixture was poured into ice water and extracted with *n*-hexane. The combined extracts were washed once with water, once with aqueous sodium bicarbonate, and twice more with water. Distillation afforded a mixture of *cis* and *trans* olefins, which were separated by preparative glc (HVSG 2 m, helium).

$\Delta^{1(9)}$-*Bicyclo*[*7.2.0*]*undecene (VIa)*. Separation and distillation gave VIa as a colorless oil in a 31% yield. IR (neat): 1450, 877 cm^{-1}. NMR δ: 0.65—2.65 (m, 14H), 2.68 (s, 4H). Found: C, 87.4; H, 12.2%. Calcd for $C_{11}H_{18}$: C, 87.9; H, 12.1%.

Bicyclo[*7.2.0*]*undec-1-ene (VIIa)*. A work-up gave VIIa as a colorless oil in a 25% yield. IR (neat): 1475, 1450, 869, 792 cm^{-1}. NMR δ: 0.70—2.95 (m, 17H), 4.80—6.15 (m, 1H). Found: C, 87.5; H, 12.2%. Calcd for $C_{11}H_{18}$: C, 87.9; H, 12.1%.

$\Delta^{1(10)}$-*Bicyclo*[*8.2.0*]*dodecene (VIb)*. The VIb olefin was a colorless oil (35% yield). IR (neat): 1465, 1442, 882 cm^{-1}. NMR δ: 1.25—1.85 (m, 12H), 1.95—2.20 (m, 4H), 2.26 (s, 4H). Found: C, 88.0; H, 11.8%. Calcd for $C_{12}H_{20}$,: C, 87.8; H, 12.2%.

Bicyclo[*8.2.0*]*dodec-1-ene (VIIb)*. The VIIb isomer was a colorless oil (28% yield). IR (neat): 1470, 1440, 887, 858, 750, 700 cm^{-1}. NMR δ: 1.15—2.70 (m, 18H), 3.10—3.45 (m, 1H), 4.75—5.15 (m, 1H). Found: C, 87.8; H, 11.9%. Calcd for $C_{12}H_{20}$: C, 87.8; H, 12.2%.

$\Delta^{1(11)}$-*Bicyclo*[*9.2.0*]*tridec-1-ene (VIc)*. This olefin, VIc, was a colorless oil (33% yiled). IR (neat): 1470, 1447, 890, 862, 810, 788 cm^{-1}. NMR δ: 1.15—1.90 (m, 14H), 1.90—2.50 (m, 4H), 2.46 (s, 4H). Found: C, 88.1; H, 12.8%. Calcd for $C_{13}H_{22}$: C, 87.6; H, 12.4%.

Bicyclo[*9.2.0*]*tridec-1-ene (VIIc)*. The VIIc isomer was a colorless oil (27% yield). IR (neat): 1462, 1448, 1010, 970, 887 cm^{-1}. NMR δ: 1.10—2.80 (m, 21H), 4.75—5.15 (m, 1H). Found: C, 88.1; H, 12.7%. Calcd for $C_{13}H_{22}$: C, 87.6; H, 12.4%.

Oxidative Ring Opening of Cyclobutene Derivatives (VIa—c). General Procedure:[10] To a solution of VI (1.00 mmol) in *tert*-butyl alcohol (70 m*l*) there was added a saturated aqueous solution of potassium carbonate (19 mg) and then a stock solution (40 m*l*) which had been freshly prepared from potassium permanganate (20 mg), sodium metaperiodate (1.04 g) and water (40 m*l*). The reaction mixture was stirred for 5 hr and extracted with *n*-hexane, and the extracts were evaporated *in vacuo*. The purification was effected by preparative tlc (Silica-gel G benzene) and distillation or by recrystallization. Each product was identified with an authentic sample.

Hydroboration of Cyclobutene Derivatives (VIa—c). To a solution of VIb (50 mg) in tetrahydrofuran (1.00 m*l*), a tetrahydrofuran solution of diborane (1M, 0.80 m*l*) was added drop by drop, after which the mixture was stirred for a half hour at 0—3°C. Water (1.00 m*l*) was then added carefully, and the mixture was treated with a 3N NaOH solution (1.00 m*l*). To this a 30% H_2O_2 solution was added, drop by drop, at room temperature, and then the whole was allowed to stand overnight. After the subsequent addition of an aqueous NaCl solution, the mixture was extracted with *n*-hexane and the combined extracts were evaporated *in vacuo*. Distillation afforded a colorless solid (43% yield), which was found to be identical with the IIb photoproduct (IR, glc, NMR, and mixed mp). Two other olefins VIa and VIc were treated similarly to afford IIa and IIc respectively.

Cycloundecenol (Va). A mixture containing IVa and Va was separated by preparative tlc (Silica-gel G, benzene). Perfect separation was effected by repeated preparative tlc. (The yield was calculated on the basis of the NMR peak areas of the olefinic protons. This product showed the following spectra in support of the assigned structure. IR (neat): 1645 cm^{-1} (C=C). NMR δ: 0.70—2.50 (m, 16H), 3.20—3.90 (m, 2H), 4.65—5.65 (m, 2H). Found: C, 78.3; H, 11.9%. Calcd for $C_{11}H_{20}O$: C, 78.5; H, 12.0%. The hydrogenation of Va on palladium charcoal afforded saturated monocyclic alcohol. The IR spectrum of its phenylurethane was superimposable on that of authentic cycloundecanol phenylurethane (mp 56—58°C) (literature[11] mp 58—59°C).

The IVa Photoreduction Product. This product was separated by preparative tlc (Silica-gel G, *n*-hexane: ether=

9) G. Darzens, *C. R. Acad. Sci.*, **152**, 1601 (1911).

10) R. U. Lemieux and E. von Rudloff, *Can. J. Chem.*, **33**, 1701 (1955).

11) M. Kobelt, P. Barman, V. Prelog, and L. Ruzicka, *Helv. Chim. Acta*, **35**, 256 (1949).

10: 1) and was found to be identical with authentic cycloundecanol (IR, glc and mp of phenylurethane). The presence of acetone in the photolysate was proven by the formation of 2,4-dinitrophenylhydrazone, mp 123—124°C (from EtOH-H_2O).

The authors are grateful to Prof. K. Sisido for his generous help. They also acknowledge with pleasure financial support from the Ministry of Education, the Japanese Government, and from the Toray Science Foundation.

BULLETIN OF THE CHEMICAL SOCIETY OF JAPAN, VOL. 44, 3443—3445 (1971)

The Preparation of 9-Ethynylanthracene and 9-Ethynyltriptycene and Their Oxidative Coupling

Shuzo AKIYAMA, Fumio OGURA, and Masazumi NAKAGAWA
Department of Chemistry, Faculty of Science, Osaka University, Toyonaka, Osaka

(Received July 1, 1971)

The formation of 9,10-dichloroanthracene by reaction of 9-acetylanthracene with phosphorus pentachloride is described. 9-Ethynylanthracene and 9-ethynyltriptycene have been prepared according to Köbrich's method. The resulting ethynyl compounds have been converted to the corresponding di-ynes using the Eglinton's oxidative coupling reaction.

The treatment of methyl ketone with phosphorus pentachloride followed by dehydrochlorination using a strong base such as sodium amide in liquid ammonia is a general method of preparation of ethynyl compound. However, evolution of acetyl chloride and chlorine was observed on treatment of 9-acetylanthracene with phosphorus pentachloride. A small amount of crystalline 9, 10-dichloroanthracene could be isolated from the viscous oily reaction product. The mechanism for formation of the dichloroanthracene is not yet clear, but considering a similar reaction of anthracene with phosphorus pentachloride to give 9,10-dichloroanthracene,[1] deacetylation and subsequent chlorination seem to be caused by the catalysis of phosphorus pentachloride. The viscous oily product separated from the dichloroanthracene was treated with sodium amide in liquid ammonia. Chromatographic purification of the reaction product yielded unstable yellow crystals contaminated with some chlorine compound. The IR spectrum of the yellow crystals indicates the presence of 9-ethynylanthracene; however, it was not feasible to remove impurity containing chlorine.

Because of these difficulties, the authors adopted the method of Köbrich[2] for the preparation of 9-ethynyl compounds. As indicated in the following scheme, the reaction of 9-anthracenecarboxaldehyde (I_a) in tetrahydrofuran with chloromethylenetriphenylphosphorane (II) yielded a viscous liquid which is presumably a mixture of *cis* and *trans* isomers of the chlorovinyl compound (III_a). The dehydrochlorination of III_a by means of sodium amide in liquid ammonia yielded 9-ethynylanthracene (IV_a) in a reasonable quantity. The rather rapid decomposition of IV_a even in solution contrasts fairly strongly with the stable nature of other arylacetylene. The oxidative coupling of IV_a according to Eglinton's method resulted in 9,9′-dianthryldiacetylene (V_a) which was shown to be identical with an authentic specimen.[3] Using an analogous procedure, 9-triptycenecarboxaldehyde (I_b)[4] was converted to 9-ethynyltriptycene (IV_b). The ethynyl compound (IV_b) was found to be highly stable compound. The oxidative coupling of IV_b gave 9,9′-ditriptycyldiacetylene (V_b) in a quantitative yield as colorless cubes. The recrystallization of V_b could not be performed because of the extremely poor solubility. The material (V_b) gave satisfactory elemental analysis after digestion with a diluted hydrochloric acid. The unusual thermal stability and the extremely poor solubility seem to be attributable to the rigid and bulky cage structure of the terminal triptycene groups.

TABLE 1. HYPOCHROMISM OF 9-SUBSTITUTED TRIPTYCENES
λ IN nm IN ETHANOL

Triptycene		9-Ethynyltriptycene (IV_b)		9-Formyltriptycene (I_b)	
λ	ε	λ	ε	λ	ε
197	62,900	198	59,000	198	62,500
211	64,200	210.5	63,800	212	64,300
270	3,600	269.5	2,800	270.5	2,400
278	4,900	277	3,600	278	3,000

The hypochromism of electronic spectra of triptycene derivatives substituted with electron attractive group at 9-position as compared with that of parent triptycene has been reported by Theilacker and coworkers.[5] As is shown in Table 1, the electronic spectra of I_b and

1) B. M. Mikhailov and M. S. Promyslov, *J. Gen. Chem. (U. S. S. R.)*, **20**, 338 (1950), [*Chem. Abstr.*, **44**, 6408 (1950)].
2) G. Köbrich, H. Trapp, K. Flory, and W. Drischel, *Chem. Ber.*, **89**, 689 (1966).
3) S. Akiyama and M. Nakagawa, This Bulletin, **43**, 3561 (1970).
4) E. C. Kornfeld, P. Barney, J. Blankley, and W. Faul, *J. Med. Chem.*, **8**, 342 (1965).
5) W. Theilacker, K. Albrecht, and H. Uffmann, *Chem. Ber.*, **98**, 428 (1965).

IV_b also show a similar hypochromism in the region of 270—280 nm. However, the strong absorption bands at shorter wavelength region (190—210 nm) exhibit no hypochromism.[6]

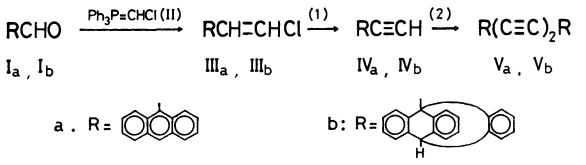

Scheme 1. (1) $NaNH_2$/liq. NH_3; (2) $Cu(OAc)_2$/pyridine-methanol. THF=tetrahydrofuran.

Experimental

All the melting points were uncorrected. The IR and nmr spectra were obtained on a Hitachi EPI-2 and a Varian A-60 spectrometers, respectively. A Hitachi EPS-3T spectrometer was used for the electronic spectroscopy except for short-wavelength region. The spectra below 210 nm were measured on a Zeiss PMQ II, M4Q III spectrometer.[6]

Reaction of 9-Acetylanthracene with Phosphorus Pentachloride. A mixture of 9-acetylanthracene, phosphorus pentachloride, and benzene or phosphoryl chloride was heated under reflux until the evolution of gas ceased (*ca.* 1 hr). The reaction mixture was worked up in the usual manner. The yellow fine needles deposited were filtered to remove the viscous oily material and recrystallized to give pure 9,10-dichloroanthracene. As summarized in Table 2, the increase in the ratio of phosphorus pentachloride to 9-acetylanthracene increases the yield of dichloroanthracene.

Table 2. The formation of 9,10-dichloroanthracene

Run	Acetylanthracene A (g)	PCl_5 B(g)	B/A (molar ratio)	Solvent[a] (ml)	Dichloroanthracene (g)	Yield based on A (%)
1	1.10	1.0	1	b5	0.07	6
2	1.10	2.1	2	b5	0.09	7
3	1.10	5.2	5	b5	0.17	14
4	1.10	1.0	1	p5	0.02	1
5	1.10	9.15	9	p5	0.23	19

a) b=benzene; p=phosphoryl chloride.

Attempted Synthesis of 9-Ethynylanthracene (IV_a). The viscous oily material mentioned earlier was mixed with a small amount of tetrahydrofuran and added to a suspension of sodium amide in liquid ammonia. After 3 hr, ammonium chloride was added to the reaction mixture, and the ammonia was allowed to evaporate. The residue was digested with petroleum ether and subjected to chromatography on alumina. The yellow crystals (mp 54—64°C), thus obtained, were found to be highly unstable and contaminated with chlorine compound.

9-Ethynylanthracene (IV_a). 9-(α-Chlorovinyl)anthracene (III_a): An ethereal solution of *n*-butyllithium (1.04N, 28.8 ml, 0.03 mol) was added to a suspension of chloromethyltriphenylphosphonium chloride[2] (10.70 g, 0.03 mol) over a period of 30 min at −70°C. After, 20 min, a solution of 9-formylanthracene (6.18 g, 0.03 mol) in tetrahydrofuran (100 ml) was added and the cooling bath was removed. The reaction mixture was stirred overnight at room temperature. The solvent was removed under reduced pressure and the viscous oily residue was dissolved in benzene (180 ml). The benzene solution was passed through a short column of alumina (40 g). The filtrate was concentrated and the oily residue was re-dissolved in benzene (40 ml). The benzene solution was percolated through a layer of alumina (20 g). The light yellow liquid obtained by the concentartion of the filtrate was subjected to the following reaction.

Dehydrochlorination of III_a. A solution of the crude III_a in tetrahydrofuran (25 ml) was added over a period of 30 min to a suspension of sodium amide (prepared from 5 g of sodium) in liquid ammonia (200 ml) maintained at −65°C. After the mixture had been stirred for 4 hr, the ammonia was allowed to evaporate. A saturated solution of ammonium chloride was added to the residue under cooling with ice-water. The organic solvent and some part of water were removed under reduced pressure, and extracted with ether (200 ml). Concentration of the extract gave an oily material, which was dissolved in benzene (50 ml) and passed through a short column of alumina (20 g). The oily residue obtained by the concentation of the filtrate was repeatedly digested with petroleum ether (bp 40—60°C, total 800 ml). After triphenylphosphine oxide, which deposited on standing the extract, had been removed by filtration, the filtrate was passed through a thin layer of alumina (10 g) and concentrated to yield yellow crystals (3.65 g, 59% based on I_a). The crystals were re-dissolved in petroleum ether, and the chromatographic purification was repeated 3 times. The final filtrate was chilled in an ice-bath to afford IV_a as light yellow needles, mp 76—76.5°C. IV_a gave orange cuprous and yellow silver acetylides.

Found: C, 94.96; H, 5.00%. Calcd for $C_{16}H_{10}$: C, 95.02; H, 4.98%. IR (KBr-disk): 3290 (−C≡CH) cm^{-1}. NMR (CCl_4): τ 6.16 (s, 1H) (C≡CH), 1.7—2.8 (m, 9H) (aromatic H). UV: $\lambda_{max}^{n\text{-hexane}}$ (log ε) 218 (4.06), 253 (4.96), 259.5 (5.24), 343 (3.54), 360 (3.90), 379 (4.13), 400 (4.31) nm.

9-Ethynyltriptycene (IV_b). 9-(α-Chlorovinyl)triptycene (III_b): The reaction of 9-formyltriptycene[4] (I_b, 5.64 g, 0.02 mol) with chloromethylenetriphenylphosphorane (II) according to the analogous procedure described earlier yielded III_b as a light yellow viscous liqued. Because crystallization was unsuccessful, the liquid was subjected to the subsequent reaction.

Dehydrochlorination of III_b. The dehydrochlorination was performed according to a procedure similar to that used for III_a. The reaction product was digested with benzene (100 ml), and the extract was passed through a short column of alumina (15 g). The light brown liquid obtained from the filtrate was re-digested with petroleum ether (bp 60—80°C, 200 ml). The extract was percolated through a thin layer of alumina (5 g). The colorless crystals (3.35 g, 60% based on Ib) obtained from the filtrate were dissolved in pertoleum ether (bp 40—60°C), and the solution was passed twice through a short column of alumina to yeild colorless cubes. The crystals were recrystallized from benzene-methanol to give pure IV_b as colorless cubes, mp 222.5—223.5°C.

Found: C, 94.73; H, 5.15%. Calcd for $C_{22}H_{14}$: C, 94.93; H, 5.07%. NMR (CCl_4): τ 6.77 (s, 1H) (C≡CH), 4.53 (s, 1H) (bridge head H), 1.83—2.93 (m, 12H) (aromatic H). IR (KBr-disk): 3300 (C≡CH) cm^{-1}.

9,9'-Dianthryldiacetylene (V_a). A mixture of IV_a (0.02 g, 1.1 mmol), cupric acetate monohydrate (5.0 g), pyridine (10 ml) and methanol (1 ml) was stirred for 3 hr at 50°C. The insoluble material was collected by filtration and washed with a small amount of methanol, water, and a small amount of ethanol, successively. The orange tiny cubes (0.20 g, 91%, mp 287—291°C), thus obtained, were dissolved in toluene,

6) The authors are indebted to Professor J. Tanaka of Nagoya University for the measurements of spectra at short wavelength.

and passed through a short column of alumina to give orange cubes, mp 290—292°C which were found to be identical with the authentic sample.[3]

9,9′-Ditriptycyldiacetylene (V_b). The Eglinton's oxidative coupling of analytically pure IV_b (0.60 g) according to a procedure used for V_a gave colorless fine needles in a quantitative yield. The crystals were thoroughly digested with dilute hydrochloric acid to remove inorganic material, and were washed with water, and dried.

Found: C, 95.02; H, 4.81%. Calcd for $C_{44}H_{26}$: C, 95.28; H, 4.72%.

Recrystallization of V_b was infeasible owing to its extremely poor solubility in various organic solvents.

BULLETIN OF THE CHEMICAL SOCIETY OF JAPAN, VOL. 44, 3445—3450 (1971)

Studies on Stable Free Radicals. VI.[1] Synthesis of Substituted 4-Imidazolidinone-1-oxyls

Toshimasa TODA, Syoji MORIMURA, Eiko MORI, Hideo HORIUCHI, and Keisuke MURAYAMA

Central Research Laboratories, Sankyo Co., Ltd., Shinagawa-ku, Tokyo

(Received July 15, 1971)

It was found that the reaction of α-amino nitriles with carbonyl compounds gave the substituted 4-oxoimidazolidines in the presence of basic catalyst. These imidazolidinones were oxidized by hydrogen peroxide: although the imidazolidinones containing an α-hydrogen at the 2- or 5-position gave no radical products, 2,2,5,5-tetrasubstituted imidazolidinones afforded new stable nitroxide radicals. By this method, stable biradicals were also prepared; but, no corresponding stable nitroxide radical was isolated by oxidation of substituted imidazolidine-4-thiones.

Since Rozantsev and Neiman[2] were successful in the preparing of very stable nitroxide radicals, such as 2,2,6,6-tetramethyl-4-oxopiperidine-1-oxyl, interest seems to have increased in the studies of these stable free radicals.[3–6]

We also reported[7] a suitable method for preparing 2,2,6,6-tetramethyl-4-oxopiperidine which afforded a stable nitroxide radical by oxidation.

In present paper, we wish to report that the reaction of α-amino nitriles with aldehydes of ketones in the presence of basic catalyst gave substituted 4-oxoimidazolidines.

Subsequently, we obtained new, stable nitroxide radicals by oxidation of these imidazolidinones; but the imidazolidinones containing an α-hydrogen at 2- or 5-position gave no radical products.

Attempts to prepare corresponding stable nitroxide radicals from substituted imidazolidine-4-thiones failed.

Results and Discussion

Cyclization reaction. Noland *et al.*[8] have reported that cyclohexane-1-spiro-2′-(4′-oxoimidazolidine)-5′-spiro-1″-cyclohexane (IIa) is obtained by self-condensation of 1-amino-1-cyanocyclohexane (IV) catalyzed by sodium ethoxide in ethanol solution containing a small amount of water.

In this method, only two different substituents can be introduced in 2- and 5-positions of the 4-oxoimidazolidine ring (I). In this work, we established a general method for preparing imidazolinones (II) having four different substituents in the 2- and 5-positions.

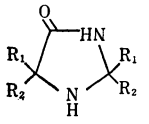

(I)

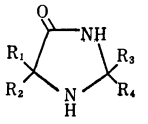

(II)

A crystalline solid was obtained on the reaction of 1-amino-1-cyanocyclohexane (IV) with cyclohexanone in the presence of sodium ethoxide in ethanol solution. This product was identified as IIa by comparison of melting point, IR spectrum and elementary analysis with those of an authentic sample of IIa.[8]

Further, the yield of IIa in this reaction was over 100% based on 1-amino-1-cyanocyclohexane (IV). This result was considered to show that cyclohexanone reacted with the α-amino nitrile, IV to give IIa. The

1) Part V: T. Yoshioka, S. Higashide, S. Morimura, and K. Murayama, This Bulletin, **44**, 2207 (1971).

2) E. G. Rozantsev and M. B. Neiman, *Tetrahedron*, **20**, 131 (1964).

3) E. G. Rozantsev, "Free Nitroxyl Raidcals," Plenum Press, New York, N. Y. (1970), Translated from the Russian, references.

4) A. R. Forrester, J. M. Hay, and R. H. Thomson, "Organic Chemistry of Stable Free Radicals," Academic Press, New York, N. Y. (1968), pp. 180—238, references.

5) K. Murayama, S. Morimura, and T. Yoshioka, This Bulletin, **42**, 1640 (1969).

6) K. Murayama and T. Yoshioka, *ibid.*, **42**, 2307 (1969).

7) K. Murayama, S. Morimura, O. Amakasu, T. Toda, and E. Yamao, *Nippon Kagaku Zasshi*, **90**, 296 (1969).

8) W. E. Noland, R. J. Sundberg, and M. L. Michaelson, *J. Org. Chem.*, **28**, 3576 (1963).

reaction of IV with *n*-butyraldehyde in the presence of a catalytic quantity of aqueous sodium hydroxide afforded similarly the 4-oxoimidazolidine, 1,3-diaza-2-*n*-propyl-4-oxo-spiro[4.5]decane (IIb), as proved by IR spectrum (the presence of carbonyl band at 1691 cm^{-1}) and elementary analysis.

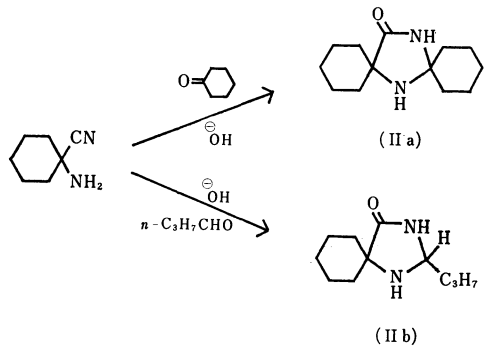

Thus, we confirmed that α-amino nitriles condensed with carbonyl compounds in the presence of a basic catalyst to yield substituted imidazolidinones (II).

The products, IIa—w obtained in this method are listed in Table 1. The structures of these products were confirmed by IR spectra (the presence of carbonyl band at about 1690 cm^{-1}), elementary analysis and the stable nitroxide radicals afforded by oxidation as described in next section.

These imidazolidinones were useful as light stabilizers for synthetic polymers.[9]

Oxidation reaction. Oxidation of the imidazolidinones (II) provided new stable nitroxide radicals (III).

The oxidation[5] of the imidazolidinones were carried out with hydrogen peroxide in the presence of catalytic amount of sodium tungstate and ethylenediaminetetraacetic acid (EDTA) in acetic acid solution.

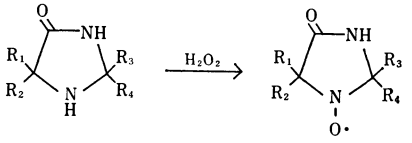

Table 1. Substituted imidazolidinones

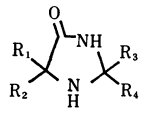

(II)

	Substituents				Yield %	mp °C[B]	Formula	Found %			Calcd %		
	R_1	R_2	R_3	R_4				C	H	N	C	H	N
a	Cyclohexyl		Cyclohexyl		86.6	219—220[a]	$C_{13}H_{22}ON_2$	70.26	9.88	12.57	70.23	9.97	12.60
b	Cyclohexyl		H,	*n*-C_3H_7-	76.4	115—116[b]	$C_{11}H_{20}ON_2$	67.27	10.36	14.16	67.30	10.27	14.27
c	CH_3-	CH_3-	CH_3-	CH_3-	45.9	169—170[c]	$C_7H_{14}ON_2$	58.96	10.11	19.66	59.12	9.92	19.70
d	CH_3-	CH_3-	CH_3-	*i*-C_4H_9-	22.6	126—128[d]	$C_{10}H_{20}ON_2$	65.04	10.88	15.06	65.17	10.94	15.20
e	CH_3-	CH_3-	CH_3-	C_2H_5-	29.5	77— 79[b]	$C_9H_{18}ON_2$	63.43	10.62	16.39	63.49	10.66	16.46
f[A]	CH_3-	CH_3-	Cyclohexyl		90.0	193—194[a]	$C_{10}H_{18}ON_2$	65.77	9.84	15.14	65.89	9.96	15.37
g	Cyclohexyl		Cyclopentyl		70.6	190—191[b]	$C_{12}H_{20}ON_2$	69.25	9.72	13.40	69.19	9.68	13.45
h	Cyclohexyl		H,	*n*-$C_{11}H_{23}$-	23.8	bp170/0.0005	$C_{19}H_{36}ON_2$	73.98	11.55	8.78	73.97	11.76	9.08
i	Cyclohexyl		H,	phenyl	86.2	114.5—115.5[a]	$C_{14}H_{18}ON_2$	72.70	7.88	12.03	73.01	7.88	12.17
j	Cyclohexyl		CH_3-,	3-pyridyl	67.5	147[a]	$C_{14}H_{19}ON_3$	65.77	11.36	16.49	65.83	11.45	16.45
k	Cyclohexyl		TMP[C]		40.5	248.5—249.5[e]	$C_{16}H_{29}ON_3$	68.56	10.47	15.09	68.77	10.46	15.04
l	Cyclohexyl		TMP-oxyl[D]		33.8	198—199[f]	$C_{16}H_{28}O_2N_3$	65.03	9.59	14.08	65.27	9.59	14.27
m	TMP[C]		H,	CCl_3	87.6	190—191[a]	$C_{12}H_{20}ON_3Cl_3$	43.82	6.20	12.62	44.05	6.12	12.85
n	TMP[C]		H,	*p*-Cl-phenyl	68.6	215[d]	$C_{12}H_{24}ON_3Cl$	63.26	7.56	13.20	63.15	7.53	13.28
o	TMP-oxyl[D]		H,	*n*-C_3H_7-	60.6	146—147[a]	$C_{14}H_{26}O_2N_3$	62.49	9.73	15.48	62.65	9.77	15.66
p	TMP-oxyl[D]		Cyclohexyl		44.5	201—202[d]	$C_{16}H_{28}O_2N_3$	65.22	9.57	14.26	65.27	9.59	14.27
q	TMP-oxyl[D]		H,	phenyl	63.5	184—185[a]	$C_{17}H_{24}O_2N_3$	67.46	7.92	13.81	67.52	8.00	13.90
r	TMP-oxyl[D]		H,	*o*-CH-phenyl	88.0	194.5—195.5[d]	$C_{18}H_{26}O_2N_3$	68.40	8.21	13.19	68.32	8.28	13.28
s	TMP-oxyl[D]		H,	*p*-CH_3O-phenyl	81.0	178—179[d]	$C_{18}H_{26}O_3N_3$	64.90	7.81	12.59	65.03	7.88	12.64
t	TMP-oxyl[D]		TMP-oxyl[D]		23.6	261—262[a]	$C_{19}H_{34}O_3N_4$	61.52	9.42	15.14	62.26	9.35	15.29
u	H, phenyl		Cyclohexyl		40.2	176—177[a]	$C_{14}H_{18}ON_2$	72.90	7.91	12.09	73.01	7.88	12.17
v	CH_3-, phenyl		Cyclohexyl		40.0	130—131[b]	$C_{15}H_{20}ON_2$	73.69	8.35	11.21	73.77	8.25	11.21
w	2-CH_3-cyclohexyl		2-CH_3-cyclohexyl		36.0	146—148[a]	$C_{15}H_{26}ON_2$	72.02	10.49	11.22	71.95	10.47	11.19

A): Sodium methoxide was used as catalyst. B) The letters indicate the solvent used for recrystallization as follows: a) ethanol; b) petroleum ether; c) water; d) benzene; e) methanol; f) ethyl acetate.

[C]TMP= 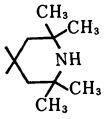

[D]TMP-oxyl= 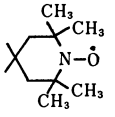

9) K. Murayama, S. Morimura, T. Toda, S. Akagi, T. Kurumada, and I. Watanabe, Brit. 1202298 (1970).

Table 2. Substituted imidazolidinone-1-oxyls

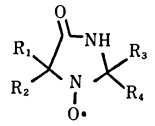

(III)

	Substituents				Yield %	mp °C[A]	Formula	Found %			Calcd %		
	R_1	R_2	R_3	R_4				C	H	N	C	H	N
a	Cyclohexyl		Cyclohexyl		77.6	227—228[a]	$C_{13}H_{21}O_2N_2$	65.93	8.93	11.87	65.80	8.92	11.81
c	CH_3–,	CH_3–	CH_3–,	CH_3–	63.3	225—226[a]	$C_7H_{13}O_2N_2$	53.03	8.33	17.72	53.48	8.34	17.82
e	CH_3–,	C_2H_5–	CH_3–,	C_2H_5–	68.3	114—115[a]	$C_9H_{17}O_2N_2$	58.25	9.29	15.37	58.35	9.25	15.12
f	CH_3–,	CH_3–	Cyclohexyl		89.0	236—237[b]	$C_{10}H_{17}O_2N_2$	61.18	8.71	14.38	60.89	8.69	14.20
l	Cyclohexyl		TMP-oxyl[B]		16.0	191—192[a]	$C_{16}H_{27}O_3N_3$	61.94	8.83	13.58	62.11	8.80	13.58
p	TMP-oxyl[B]		Cyclohexyl		80.8	219.5—220.5[a]	$C_{16}H_{27}O_3N_3$	62.19	8.83	13.49	62.11	8.80	13.58
w	2-CH_3-cyclohexyl		2-CH_3-cyclohexyl		66.5	174—175[a]	$C_{15}H_{25}O_2N_2$	68.05	9.56	10.70	68.41	8.80	10.64

A) Letters indicate the solvent used for recrystallization: a) benzene; b) methanol.

[B]TMP-oxyl =

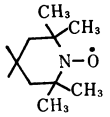

Table 3. The a_N values[a] of substituted imidazolidinone-1-oxyls and piperidine-1-oxyls

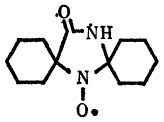 (III a) 14.1	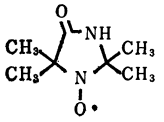 (III c) 14.0	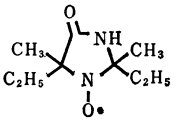 (III e) 13.6	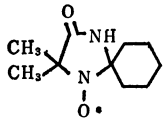 (III f) 14.0	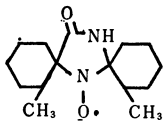 (III w) 14.1
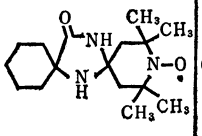 (II l) 15.3	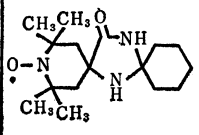 (II p) 15.3	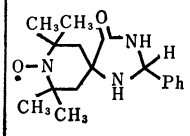 (II q) 15.5	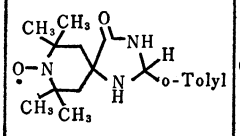 (II r) 15.0	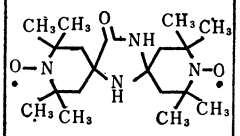 (II t) 15.1 (7.5)

a): measured in 10^{-3} mol/l benzene solution at room temperature, are given in gauss and are accurate to within ±0.1G.

The structures of the products (IIIa—g) were assinged by ESR spectra (triplet lines), elementary analysis and IR spectra in which the carbonyl band of corresponding amines at about 1690 cm^{-1} shifted approximately 20 cm^{-1} toward higher frequency. The nitroxide radicals obtained by the oxidation are listed in Table 2.

These radicals are very stable and no change has occurred on standing at room temperature for several years.

The ESR spectra of these radicals exhibited only three lines, which arise through hyperfine interaction with a ^{14}N nucleus, in evacuated benzene solution. The values of the nitrogen hyperfine splitting are shown in Table 3.

Table 3 indicates that the magnitude of the nitrogen hyperfine splitting in the imidazolidinone-1-oxyl radicals, IIIa,c,e,f, and IIIw, are smaller than that of the derivatives of 2,2,6,6-tetramethylpiperidine-1-oxyl radicals, III,p,q,r, and IIt.

It has been reported[10] that the a_N values of the derivatives of 2,2,6,6-tetramethylpiperidine-1-oxyl, measured in the same solvent, decrease as the carbon atom at the 4-position in the piperidine ring becomes more electron deficient.

Therefore, the fact that the a_N values of the imidazolidinone-1-oxyls are smaller than those of the piperidine-1-oxyls could be considered to be due to the difference of dipolar field effect on the radical moiety between the amide group in imidazolidinone-1-oxyl and the substituents at 4-position in piperidine-1-oxyl.

Furthermore, we were interested in the ESR spectra of bi-nitroxide radicals, IIt, IIIl, and IIIp to determine any intramolecular interaction between the two radical part within a single molecule.

10) R. Briere, H. Lamaire, and A. Rassat, *Bull. Soc. Chim. Fr.*, **1966**, 3273.

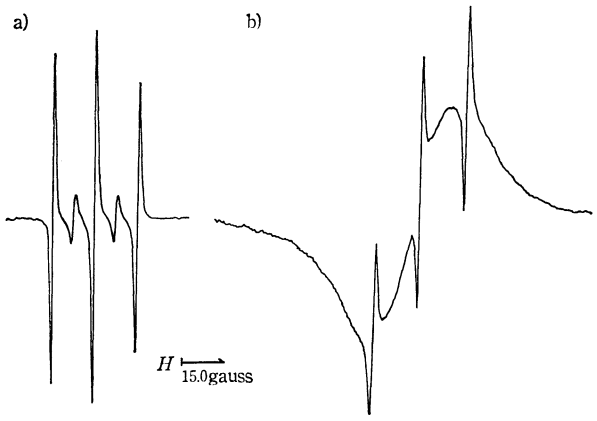

Fig. 1. The ESR spectra of bi-nitroxide radicals.[A)]
A): measured in 10^{-3}mol/*l* benzene solution at room temperature.
a): 2,2,6,6-tetramethylpiperidine-4-spiro-2′-(4′-oxoimidazolidine)-5′-spiro-4″-(2″,2″,6″,6″-tetramethylpiperidine)-1′,1″-dioxyl (IIt).
b): cyclohexane-1-spiro-2′-(4′-oxoimidazolidine)-5′-spiro-4″-(2″,2″,6″,6″-tetramethylpiperidine)-1′,1″-dioxyl (IIIp).
The ESR spectra of IIIl and IIIp are basically very similar.

As shown in Fig. 1a, IIt gave a quintet lines like the spectrum of the carbonate diester of 4-hydroxy-2,2,6,6-tetramethylpiperidine-1-oxyl.[11] The spectra of IIIl and IIIp were more complicated than that of IIt (Fig. 1b).

This suggests that the intramolecular interaction between the two nitroxide radical groups was stronger than in IIt. The ESR studies of these bi-nitroxide radicals are currently under detailed investigation.

In the case of imidazolidinones containing an α-hydrogen adjacent to the secondary amino group, the oxidation products were non-radicals.

Treatment of 1,3-diaza-2-phenyl-4-oxo-spiro[4,5]decane (IIi) with hydrogen peroxide in the presence of sodium tungstate in methanol solution gave white crystals. This product was presumed to be 1,3-diaza-2-phenyl-4-oxo-spiro[4.5]-1-decene-1-oxide (V) from its spectral data (the presence of $\nu_{C=N\to O}$ band[12] at 1588 and 1564 cm^{-1} in IR spectrum and a *m/e* 244 molecular peak in mass spectrum), elementary analysis and the following reaction. The nitroxide, V was converted into 1,3-diaza-2-phenyl-4-oxo-spiro[4.5]decene-1 (VI) on treating with triphenylphosphine. The structure of VI was assigned by IR spectrum (the presence of $\nu_{C=N}$ at 1625 cm^{-1}, mass spectrum (at *m/e* 228 molecular peak) and elementary analysis.

Similarly, 1,4-diaza-2-phenyl-3-oxo-sprio[4.5]-1-decene-1-oxide (VII) and 1,3-diaza-2-*n*-propyl-4-oxo-spiro[4.5]-1-decene-1-oxide (VIII) were obtained by the oxidation of corresponding amines, IIu and IIb, respectively.

This reaction would proceed as shown in Chart 1.

It seems reasonable that the intermediate, nitroxide radical, IX disproportionates to V and X, since dimethylamino radicals disproportionate into dimethylamine and *N*-methylformaldimine.[13] The hydroxylamine, X would regenerate the nitroxide radical, IX by oxidation with hydrogen peroxide.

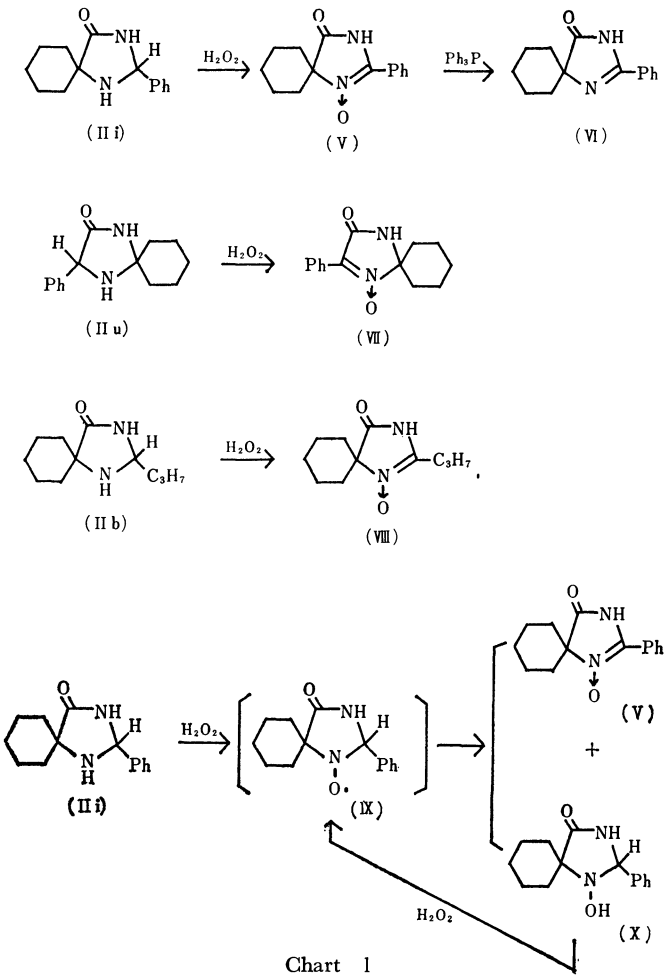

Chart 1

However, it has been reported[14] that norpseudopelletierine containing an α-hydrogen adjacent to a secondary amino group provides a corresponding stable nitroxide radical. In this case, the disproportionation reaction mentioned above, would be hindered by steric factors (Bredt rule).

Oxidation of substituted imidazolidine-4-thiones. We attempted to prepare another stable nitroxide radicals with imidazolidine-4-thione ring.

Rassat *et al.*[15] have suggested the formation of the free radicals of this type in their ESR studies, where they have observed a triplet spectrum on mixing 2,2,5,5-tetramethylimidazolidine-4-thione (XII)[16] and *p*-nitroperbenzoic acid in benzene, but they did not isolate this free radical.

However, we obtained no radical products from the oxidation of imidazolidine-4-thiones.

Treatment of cyclohexane-1-spiro-2′-(imidazolidine-

11) R. Briere, R. M. Dupeyre, H. Lamaire, C. Morat, A. Rassat, and P. Rey, *Bull. Soc. Chim. Fr.*, **1966**, 3290.
12) J. Thesing and W. Sirrenberg, *Chem. Ber.*, **92**, 1748 (1959).
13) D. Mackay and W. A. Waters, *J. Chem. Soc., C*, **1966**, 813.
14) R. M. Dupeyre and A. Rassat, *J. Amer. Chem. Soc.*, **88**, 3180 (1966).
15) G. C. Letourneux, H. Lamaire, and A. Rasst, *Bull. Soc. Chim. Fr.*, **1966**, 3283.
16) F. Asinger, W. Schafer, H. Meisel, H. Kersten, and A. Saus, *Monatsh. Chem.*, **98**, 338 (1967).

4'-thione)-5'-spiro-1''-cyclohexane (XI)[16] with hydrogen peroxide under similar conditions used in the oxidation of IIa gave white crystals. This product was identified as the sulfate of IIa by direct comparison of IR spectrum with that of an authentic sample prepared from IIa and sulfuric acid.

Treatment of XI with perbenzoic acid or excess hydrogen peroxide gave also the sulfate of IIa. Under similar reaction conditions, XII gave the sulfate of IIc.

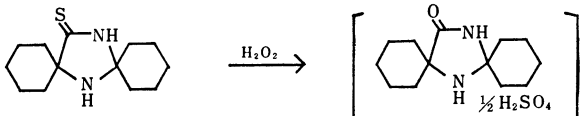

(XI) (IIa)

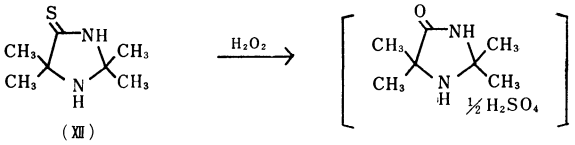

(XII) (IIc)

This reaction would proceed analogously to that in which thiopyrin reacts with hydrogen peroxide in aqueous alkali to give antipyrin and sulfuric acid.[17]

Experimental

Melting points are uncorrected. The IR spectra were determined by means of Nujol mulls and liquid films. The NMR spectra were obtained using a Varian A-60 NMR spectrometer, using tetramethylsilane as the internal standard at 32°C. The mass spectra were obtained using a JEOL-JMS-OIS mass spectrometer. The ESR spectra were recorded on a Hitachi MES 4001 type X-band spectrometer employing 100 kc modulation and the splitting constants were measured relative to aqueous solution of Fremy's salt.

Synthesis of α-Amino Nitriles. α-amino nitriles were prepared from corresponding carbonyl compounds by the Strecker reaction.

4-Amino-4-cyano-2,2,6,6-tetramethylpiperidine. A solution of 2,2,6,6-tetramethyl-4-oxopiperidine[7] (31.0 g, 0.2 mol) in 50 m*l* of methanol saturated with ammonia were added slowly to stirred solution of potassium cyanide (26.0 g) and ammonium chloride (21.5 g) in 200 m*l* of aqueous ammonia (28%) and 60 m*l* of methanol saturated with ammonia at 0—5°C and the solution was stirred at room temperature for 9 hr. The resulting precipitates were removed by filtration and methanolic filtrate was evaporated under reduced pressure at room temperature. The organic layer was extracted with 200 m*l* of methyl ethyl ketone, dried over potassium carbonate and evaporated under reduced pressure to give crude 4-amino-4-cyanotetramethylpiperidine. Recrystallization from petroleum ether gave an analytical sample mp 75—76°C, yield 11.4 g (31.6%). Found: C, 66.45; H, 10.68; N, 23.33%. Calcd for $C_{10}H_{19}N_3$: C, 66.25; H, 10.57; N, 23.18%. IR (cm^{-1}): $\nu_{C\equiv N}$ 2240, ν_{NH} 3470, 3340, 3260, and 3170.

4-Amino-4-cyano-2,2,6,6-tetramethylpiperidine-1-oxyl. In the same manner described above, 34.6 g (0.2 mol) of 2,2,6,6-tetramethyl-4-oxopiperidine-1-oxyl[7] was reacted to give 4-amino-4-cyano-2,2,6,6-tetramethylpiperidine-1-oxyl as a red crystalline solid. Recrystallization from methanol gave an analytically pure sample: mp 129—130°C, yield 15.4 g (40.0%). Found: C, 60.99; H, 9.16; N, 21.42%. Calcd for $C_{10}H_{18}ON_3$: C, 61.19; H, 9.24; N, 21.42%. IR (cm^{-1}): $\nu_{C\equiv N}$ 2200, ν_{NH} 3360, and 3300. ESR (in benzene): a_N= 15.2 gauss.

Cyclization Reactions. In general, the products shown in Table 1 were prepared by the reaction of α-amino nitriles with carbonyl compounds in the presence of catalytic amount of aqueous sodium hydroxide (40%) in ethanol or methanol solution in the manner described below.

Cyclohexane-1-spiro-2'-(4'-oxoimidazolidine)-5'-spiro-1''-cyclohexane (IIa). To a stirred solution of 1-amino-1-cyclohexane (IV) (12.4 g, 0.1 mol) and cyclohexanone (9.8 g, 0.1 mol) in 50 m*l* of methanol was added 1 m*l* of aqueous sodium hydroxide (40%) and the solution was stirred at room temperature for 8 hr. The white product was sepapated (from solution) by filtration, washed with water and ethanol and dried under vacuum. The crude crystals, IIa were recrystallized from ethanol to give an analytically pure sample. IR (cm^{-1}): $\nu_{C=O}$ 1687, ν_{NH} 3300, 3220, and 3020.

Oxidation Reactions. The nitroxide radicals shown in Table II were prepared by oxidation of corresponding substituted imidazolidinones with hydrogen peroxide in a similar way as described previously.[5]

1,3-Diaza-2-phenyl-4-oxo-spiro[4.5]-1-decene-1-oxide (V). To a solution of 9.3 g (40 mmol) of IIi in 50 m*l* of methanol were added 75 mg of EDTA and 50 mg of sodium tungstate and then 20 m*l* of aqueous hydrogen peroxide (30%) with stirring at room temperature. Stirring was continued for 6 days at room temperature. The resulting precipitate was separated by filtration, washed with water and dried *in vacuo* to give 6.0 g (61.5%) of crude crystals, V. The crude crystals, V were recrystallized from methanol to give an analytically pure sample: mp 251—251.5°C. Found: C, 68.35; H, 6.66; N, 11.36%. Calcd for $C_{14}H_{16}O_2N_2$: C, 68.83; H, 6.60; N, 11.47%. IR (cm^{-1}): $\nu_{C=N\to O}$ 1588, 1564, and 1256, $\nu_{C=O}$ 1748. NMR (τ) (in DMF): 7.85—8.35 (10H, broad), 2.34—2.46 (3H, multiplet), 1.27—1.47 (2H, multiplet). Mass spectrum: M^+=244.

1,4-Diaza-2-phenyl-3-oxo-spiro[4.5]-1-decene-1-oxide (VII). From 21.5 g (95 mmol) of IIu, crude crystals, VII were obtained (15.0 g, 65.0%). Recrystallization from methanol gave an analytical sample: mp 259—261°C. Found: C, 68.60; H, 6.60; N, 11.24%. Calcd for $C_{14}H_{16}O_2N_2$: C, 68.83; H, 6.60; N, 11.47%. IR (cm^{-1}): $\nu_{C=N\to O}$ 1555, $\nu_{C=O}$ 1715. NMR (τ) (in DMF): 7.94—8.44 (10H, broad), 2.35—2.47 (3H, multiplet), 1.03—1.23 (2H, multiplet). Mass spectrum: M^+=244.

1,3-Diaza-2-n-propyl-4-oxo-spiro[4.5]-1-decene-1-oxide (VIII). In a similar manner as mentioned above, 6.3 g (32 mmol) of IIb gave 1.8 g (28.6%) of crude crystals, VIII. The crude crystals were recrystallized from cyclohexane to give pure sample: mp 182—183°C. Found: C, 62.99; H, 8.68; N, 13.38%. Calcd for $C_{11}H_{18}O_2N_2$: C, 62.83; H, 8.63; N, 13.32%. IR (cm^{-1}): $\nu_{C=N\to O}$ 1578 and 1242, $\nu_{C=O}$ 1705. Mass spectrum: M^+=210.

1,3-Diaza-2-phenyl-4-oxo-spiro[4.5]decene-1 (VI). A mixture of 3.4 g (14 mmol) of V and 3.7 g (14 mmol) of triphenylphosphine were heated at 270°C for 10 min. The reaction mixture was cooled, dissolved in minimum amount of benzene and chromatographed on a alumina column. Eluting with benzene afforded 2.7 g (87.0%) of VI: mp 178—181°C. Found: C, 74.05; H, 7.63; N, 11.70%. Calcd for $C_{14}H_{16}ON_2$: C, 73.63; H, 7.06; N, 12.27%. IR (cm^{-1}): $\nu_{C=N}$ 1625,

17) R. Kitamura, *Yakugaku Zasshi*, **58**, 676 (1938).

$\nu_{C=O}$ 1714. NMR (τ) (in DMF): 7.95—8.45 (10H, broad), 2.44—2.56 (3H, multiplet), 1.83—2.03 (2H, multiplet). mass spectrum: $M^+=228$. The methanol eluates yielded 1.5 g of triphenylphosphine oxide (mp 156°C) which was confirmed by comparison of IR spectrum with that of an authentic sample.

Sulfate of Cyclohexane-1-spiro-2'-(4'-oxoimidazolidine)-5'-spiro-1''-cyclohexane (IIa). To a solution of 2.4 g (10 mmol) of cyclohexane-1-spiro-2'-(imidazolidine-4'-thione)-5'-spiro-1''-cyclohexane (XI)[15] in 30 m*l* of acetic acid were added 11 mg of EDTA and 9 mg of sodium tungstate and then 30 m*l* of aqueous hydrogen peroxide (30%) at 0—5°C. The solution was stirred at room temperature for additional 1 hr. After the solvent had been evaporated under reduced pressure, a colorless crystalline mass remained. By the recrystallization from ethanol, the sulfate of IIa was obtained as an analytically pure sample: mp 230—231°C, yield 2.4 g (89.0%). Found: C, 57.32; H, 8.54; N, 10.33; S, 5.62%. Calcd for $C_{26}H_{46}O_6N_4S$: C, 57.54; H, 8.85; N, 10.05; S, 5.90%. IR (cm^{-1}): $\nu_{NH_2^+}$ 2000—2600, $\nu_{C=O}$ 1708.

Sulfate of 2,2,5,5-Tetramethyl-4-oxoimidazolidine (IIc). Similarly as described above, 3.2 g (20 mmol) of 2,2,5,5-tetramethylimidazolidine-4-thione (XII)[16] was converted into 2.3 g (60.2%) of sulfate of IIc: mp 236—237°C. IR (cm^{-1}): $\nu_{NH_2^+}$ 2100—2550, $\nu_{C=O}$ 1720.

The authors wish to thank professor Makoto Okawara of the Tokyo Institute of Technology for his valuable comments, Dr. G. Sunagawa, the director of these laboratories for his encouragement and Mr. Tomiji Tsuji for his technical assistance.

BULLETIN OF THE CHEMICAL SOCIETY OF JAPAN, VOL. 44, 3450—3452 (1971)

Charge Migration through Sigma Bonds in a Fragment Ion from 5,5′-Divaleryl-2,2′-spirobiindan under Electron Impact

Akira TATEMATSU, Shinobu NAGA, Hiroshi SAKURAI, Toshio GOTO,* and Hisao NAKATA**,[1]

Faculty of Pharmacy, Meijo University, Showa-ku, Nagoya
**Faculty of Agriculture, Nagoya University, Chikusa-ku, Nagoya*
***Department of Chemistry, Aichi Kyoiku University, Kariya, Aichi*

(Received July 19, 1971)

In order to examine the nature of charge and radical electron migration in mass spectral fragment ions, 5,5′-di-*n*-valeryl-2,2′-spirobiindan (**3**) was prepared and its mass spectrum was measured. The successive loss of two propylene molecules from the molecular ion to give peaks at *m/e* 346 (**b**) and 304 (**c**) was clearly indicated by observing appropriate metastable ion peaks. As the radical electron is one of the prerequisites for these fragmentations to occur, the results demonstrate that the charge and radical electron can migrate through sigma bonds in fragment ion **b**, since the two *n*-valerophenyl groups cannot be brought into close proximity even with C–C bond fission of the spiro ring. While the strongest peak at *m/e* 331 (**a**) is ascribable to the ordinary α-fission of the carbonyl group in **3**, a moderately intense peak at *m/e* 289 (**d**) can adequately be explicable by the similar α-fission of the carbonyl group in ion **b**, the process of which again involves radical electron migration prior to fragmentation.

Electron impact induced fragmentation patterns of organic compounds in a mass spectrometer have been widely rationalized with application of the concept of localized positive charge and localized unpaired electron in the molecular ion.[2] Wachs and McLafferty[3] presented a typical example using a series of substituted 1-(4-*n*-butyrophenyl)-2-phenylethanes (**1**). They suggested that the random removal of an electron from any part of a given molecule was followed by rapid localization of charge and unpaired electron at a particular site. The concept was shown by Howe and Williams[4] not to be inconsistent with the quasi-equilibrium theory of mass spectra.

In certain cases, however, a dynamic distribution of charge appears to operate in fragment ions. For instance, Mandelbaum and Biemann[5] examined mass spectra of 1,3-diphenylcyclopentane derivatives (**2**) of unknown stereochemistry, and concluded that charge would be free to migrate among distant functional groups, and the distribution of charge would be governed by the ionization potentials of the various sites. Kinstle and Oliver[6] also showed that charge would migrate in fragment ions in some instances, though it is difficult to predict the extent of charge mobility in a particular ion.

Although some proposals were made,[7] the precise

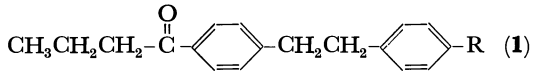

(**1**)

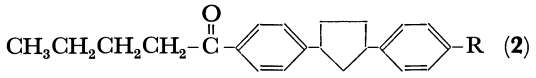

(**2**)

1) To whom the correspondence should be addressed.
2) F. W. McLafferty, *Chem. Commun.*, **1966**, 78. See, also, H. Budzikiewicz, C. Djerassi, and D. H. Williams, "Mass Spectrometry of Organic Compounds," Holden-Day, San Francisco (1967), pp. 9—14.
3) T. Wachs and F. W. McLafferty, *J. Amer. Chem. Soc.*, **89**, 5044 (1967).
4) I. Howe and D. H. Williams, *ibid.*, **90**, 5461 (1968).
5) A. Mandelbaum and K. Biemann, *ibid.*, **90**, 2976 (1968).
6) T. H. Kinstle and W. R. Oliver, *ibid.*, **91**, 1864 (1969).
7) W. Vetter, W. Meister, and W. J. Richter, *Org. Mass Spectrom.*, **3**, 777 (1970).

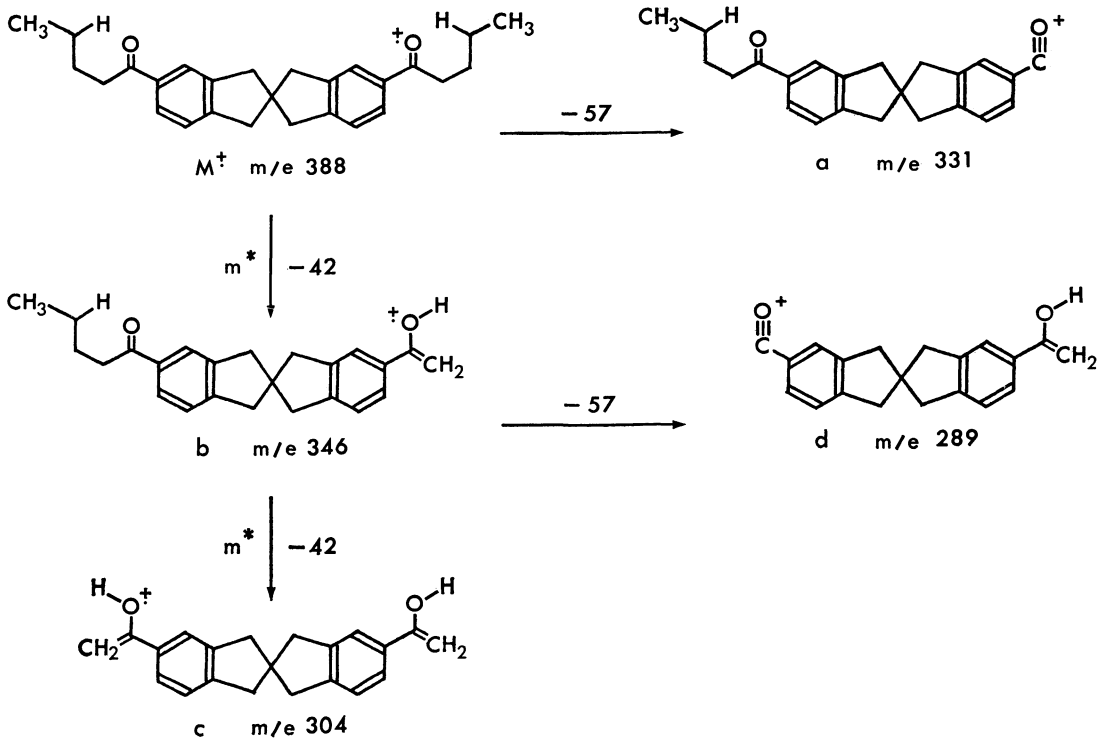

Scheme 1

mechanism of this charge and unpaired electron migration is still unknown. One obvious possibility is that the charge might transfer from one functional group to the other through the space, instead through the sigma bonds, if two groups approach closely enough to permit spatial overlap of their orbitals, as pointed out by Wagner.[8] In order to clarify this point, we have examined the mass spectrum of 5,5′-di-*n*-valeryl-2,2′-spirobiindan (**3**), which apparently cannot be in the conformation that the two phenyl groups approach each other.

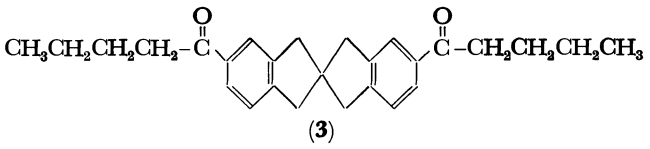

(**3**)

Results and Discussion

5,5′-Di-*n*-valeryl-2,2′-spirobiindan (**3**) was prepared by Friedel-Crafts condensation of *n*-valeryl chloride with 2,2′-spirobiindan, which, in turn, was synthesized from diethyl dibenzylmalonate through 2,2′-spirobiindan-1,1′-dione according to the procedure of Leuchs *et al.*[9,10] The structure of the product was confirmed by IR, UV, and NMR spectral analyses (see, Experimental Section).

The mass spectrum of **3**, shown in Fig. 1, is fairly simple, and the fragmentation sequences are summarized in Scheme 1. As is seen, the molecular ion undergoes two competing fragmentations. An α-fission of the carbonyl group in one of the side chains with loss of a butyl radical produces a peak at *m/e* 331 (ion **a**), whereas the McLafferty cleavage gives a peak at *m/e* 346 (ion **b**). Although the peak at *m/e* 331 is the strongest in the spectrum taken at 70 eV, lowering of impact electron energies resulted the sharp decrease of its intensity relative to that of the ion **b**. This trend is in good agreement with the recent convincing argument[11] on the intensity ratio of peaks from simple cleavage and rearrangement reactions.

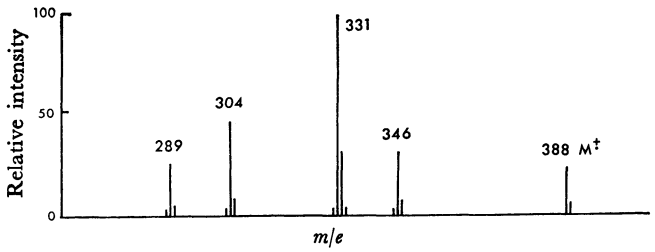

Fig. 1. The mass spectrum of 5,5′-di-*n*-valeryl-2,2′-spirobiindan (**3**).

The most pronounced feature of the spectrum is the appearance of a moderately intense peak at *m/e* 304. The well-defined metastable ion peaks were observed for the processes *m/e* 388 ($M^{+\cdot}$)→*m/e* 346 and *m/e* 346→*m/e* 304, indicating the successive elimination of two propylene molecules from the molecular ion. The exact mass measurement of the *m/e* 304 ion (**c**) (304.150) agreed with the calculated value of $C_{21}H_{20}O_2$ (304.146). With decreasing impact electron energies the intensity ratio of **c**/**b** markedly decreased, and this also suggests the step-wise fragmentation. These results clearly indi-

8) P. J. Wagner, *ibid.*, **3**, 1307 (1970).
9) H. Leuchs and D. Radulescu, *Ber.*, **45**, 189 (1912).
10) H. Leuchs and L. Lock, *Ber.*, **48**, 1432 (1915).
11) P. Brown, *Org. Mass Spectrom.*, **3**, 1175 (1970).

cate that the first McLafferty cleavage of one side chain in **3** was followed by the second McLafferty cleavage of the other side chain. Therefore, the transfer of the ion radical from one site to the other through several sigma bonds is required in the fragment ion **b**, as the radical electron is one of the prerequisites for mass spectral reactions to occur.

There would be three possible routes of formation of ion **d**, since ion **a**, **b**, or **c** could be a precursor ion. A route from ion **a** with elimination of propylene must involve a biradical ion intermediate generated by unpairing of the carbonyl π-electrons and may appear highly improbable.[12] This is also supported by the intensity ratio of **d**/**a** that was almost independent of impact electron energies. The alternative route from ion **c** with loss of a methyl radical may assume ketonization of ion **c** prior to fragmentation, and the process would not be important because enol-keto interconversion in a fragment ion was usually not observed.[13]

The most adequate explanation for the formation of ion **d** is, therefore, from ion **b** with loss of a butyl radical, as indicated in Scheme 1. Although the process is not confirmed by observing an appropriate metastable ion peak, this fragmentation reaction is mechanistically quite feasible, for it merely involves an α-fission of the carbonyl group. Thus, the fragmentation of **b** to **d** is, again, explicable only by assuming the radical electron migration in ion **b**.

Since in our compound **3** the two *n*-valerophenyl groups cannot be brought into close proximity even with C–C bond fission of the spiro ring, the above results clearly demonstrate that the charge and radical electron can migrate through sigma bonds. After completion of the present work, a paper by Lengyel, Uliss, and Mark on the same subject has appeared.[14] Their results are consistent with our. conclusions presented above. It is, however, still unknown whether or not any particular structural limitations and odd- or even-electronic nature of fragment ions can be correlated with the effective charge migration. Studies are in progress in our laboratory to attempt to provide further insight in such problems.

Experimental

All melting points were determined on a Kofler hot stage and are uncorrected. Infrared spectra (IR) were taken as potassium bromide disks using a Nihon Bunko IR-G instrument. Ultraviolet spectra (UV) were measured by a Hitachi EPS-3T spectrophotometer. Nuclear magnetic resonance spectra (NMR) were taken on a Varian A-60 spectrometer, and the peak positions are recorded in ppm from internal tetramethylsilane standard. Mass spectra were measured by a Hitachi RMU-7 mass spectrometer under the following conditions: ionizing voltage 70—14 eV, ion accelerating voltage 1800 V, total emission current 80 μA, ion source temperature 250°C.

5,5′-Di-n-*valeryl-2,2′-spirobiindan (3).* To a solution of 0.46 g of 2,2′-spirobiindan (mp 60—62°C)[9,10] in 10 m*l* of methylene dichloride, 0.55 g of *n*-valeryl chloride and 0.6 g of aluminum chloride were added and the mixture was allowed to stand for 26 hr at room temperature. After the addition of diluted hydrochloric acid under cooling, the mixture was extracted with chloroform. The extracts were combined and evaporated *in vacuo*. The residual brown oil was chromatographed on silica gel. The pure product of **3** was obtained by recrystallization from petroleum ether, mp 73°C, yield 0.56 g, IR (KBr) 1675 cm^{-1} (aromatic ketone); UV λ_{max}^{EtOH} 258 mμ (ε 30200); NMR (CCl_4) 0.94 (6H, deformed t, J=6 Hz), 1.1—2.0 (8H, broad m), 2.83 (4H, t, J=6 Hz), 2.93 (8H, s), 7.16 (2H, d, J=8 Hz), 7.67 (4H, m).

Found: C, 83.61, H, 8.03%. Calcd for $C_{27}H_{32}O_2$: C, 83.46; H, 8.30%.

12) J. Cable, G. W. Adelstein, J. Gore, and C. Djerassi, *Org. mass Spectrom.* **3**, 439 (1970). See, also, F.W. McLafferty, "Interpretation of Mass Spectra," W. A. Benjamin, New York (1966), pp. 138—149.

13) H. Nakata and A. Tatematsu, This Bulletin, **42**, 1678 (1969); J. Diekman, J. K. MacLeod, C. Djerassi, and J. D. Baldeschwieler, *J. Amer. Chem. Soc.*, **91**, 2069 (1969). See, however, D. J. McAdoo, F. W. McLafferty, and J. S. Smith, *ibid.*, **92**, 6343 (1970).

14) I. Lengyel, D. B. Uliss, and R. V. Mark, *J. Org. Chem.*, **35**, 4077 (1970).

Decomposition of Saturated Gaseous Hydrocarbons in Induction-Coupled Argon Plasma Jet

Yukio NISHIMURA, Arata SATOH, Kenjiro TAKESHITA, and Wataru SAKAI*

Research Institute of Industrial Science, Kyushu University, Hakozaki, Fukuoka

**Department of Organic Synthesis, Faculty of Engineering, Kyushu University, Hakozaki, Fukuoka*

(Received August 31, 1970)

The decomposition of methane, ethane, and isobutane has been studied in an induction-coupled argon plasma jet at atmospheric pressure. Methane was decomposed to give mainly acetylene, soot, and hydrogen, and to give the traces of ethylene and ethane. From the dependence of both the conversion of methane and the product distribution on methane feed rate, the input and argon flow rate, it was concluded that methane was not completely mixed with the plasma jet but the decomposition of methane took place mainly in the outer flame of the plasma jet and its surroundings. In the decomposition of ethane, ethylene, and methane were formed in 20—27% and 3—5% selectivity based on carbon, respectively, in addition to acteylene, soot, and hydrogen. In the decomposition of isobutane, propylene was produced in 10—14% selectivity based on carbon, besides the above mentioned products. From these results together with those on propane and *n*-butane,it was suggested that radicals formed by a fission of C–H or C–C bond played the main role in the decomposition of saturated gaseous hydrocarbons in the induction-coupled argon plasma jet.

The thermodynamic calculation of the carbon-hydrogen system at pressures ranging from 0.1 to 10.0 atm suggests that among the products at equilibrium above 2500°K acetylene is the only gaseous hydrocarbon that is stable at room temperature.[1,2] It is also reported that in the reaction of graphite with hydrogen, the formation of acetylene is favored over that of methane and ethylene above 2500°K[3]. On the other hand, in the decomposition of propane[4] and *n*-butane[5] which are charged into the plasms jet countercurrently, methane and ethylene have been obtained in 5—8% and 16—20% selectivity based on carbon, respectively. Furthermore, we assumed in the previous paper[5] that the decomposition of *n*-butane occurred mainly in the outer flame of the plasma jet and its surroundings, and methane and ethylene were formed in the comparatively lower temperature region.

The present paper describes the decomposition of methane, ethane and isobutane, and discusses the region in which the decomposition of hydrocarbons occurs and the decomposition process of saturated gaseous hydrocarbons in the induction-coupled argon plasma jet.

Experimental

Material. Argon was supplied from Osaka Sanso Co. Methane, ethane, and isobutane were obtained from Seitetsu Kagaku Co. (above 99.0% purity) and were used without further purification.

Apparatus and Procedures. Details of the apparatus have been already given in the previous papers.[4,5] Hydrocarbons were countercurrently fed into the induction-coupled argon plasma jet through the spiral coil. The analysis of products was carried out by gas chromatography. Molecular sieve 13X column was used for the separation of hydrogen and methane, and 3% squalane supported on alumina column was used for the analysis of the other gaseous products. The conversion, the selectivity and the yield were calculated on carbon base. The selectivity and the yield of soot were estimated from the carbon balances.

Results and Discussion

Decomposition of Methane. The effect of operating conditions was discussed in terms of the conversion of methane and selectivities of carbon-containing products. Figure 1 shows the effect of methane feed rate on the conversion and the selectivities of carbon-containing products at 9.35±0.01 kW input and 1.56±0.02 *l*/min argon flow rate. Besides the products shown in Fig. 1,

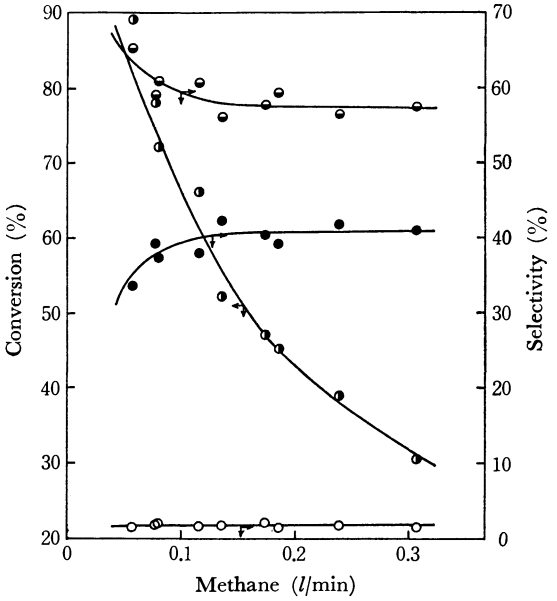

Fig. 1. Effect of methane feed rate on conversion and selectivities of products.
Input: 9.35±0.01 kW, Argon flow rate: 1.56±0.02 *l*/min
-◑- conversion, -◒- C_2H_2, -○- C_2H_4, -●- soot

1) R. F. Baddour and J. L. Blanchet, *Ind. Eng. Chem. Process Des. Develop.*, **1**, 169 (1964).
2) R. E. Duff and S. H. Bauer, *J. Chem. Phys.*, **36**, 1754 (1962).
3) J. T. Clark, "The Application of Plasma for Chemical Processing," ed. by R. F. Baddour and R. S. Timmins, The M. I. T. Press, Cambridge, Massachusetts and London, England (1967), p. 140.
4) Y. Nishimura, K. Takeshita, Y. Adachi, F. Nakashio, and W. Sakai, *Sekiyu Gakkai Shi*, **12**, 698 (1969).
5) Y. Nishimura, M. Nishimura, K. Takeshita, and W. Sakai, *Kogyo Kagaku Zasshi*, **73**, 1974 (1970).

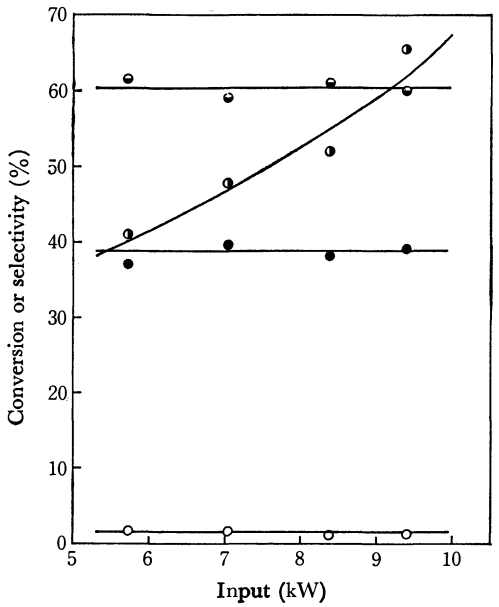

Fig. 2. Effect of input on conversion of methane and selectivities of products.
Feed rate of CH_4: 0.100±0.005 *l*/min,
Argon flow rate: 1.56±0.02 *l*/min
-◑- conversion, -◒- C_2H_2, -○- C_2H_4, -●- soot

a large amount of hydrogen and a trace of ethane were obtained. Acetylene and soot are formed in 56—65% and 34—42% selectivity, respectively, but the selectivity of ethylene reduced to less than 2%, in contrast to the case of the decomposition of *n*-butane in which ethylene was formed in 18—20% selectivity.[5] It is seen from Fig. 1 that the conversion decreases with increasing methane feed rate, while the product distribution reaches almost constant at higher feed rates of methane. A similar dependence of the conversion and the product distribution on hydrocarbon feed rate was also observed

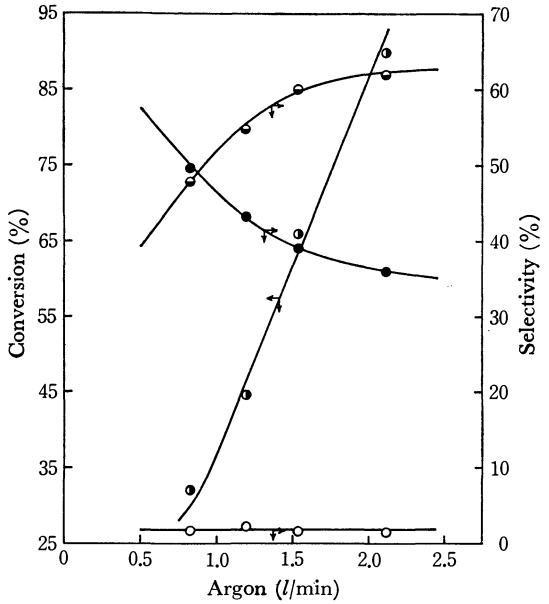

Fig. 3. Effect of argon flow rate on conversion of methane and selectivities of products.
Input: 9.35±0.01 kW, Feed rate of CH_4: 0.100±0.005 *l*/min
-◑- conversion, -◒- C_2H_2, -○- C_2H_4, -●- soot

for the decomposition of propane[4] and *n*-butane.[5] Figure 2 shows the effect of the input at 0.100±0.005 *l*/min methane feed rate and .1.56±0.02 *l*/min argon flow rate. The conversion of methane decreases almost linearly with the lowering of the input, but the product distribution is independent of the imput. On the other hand, it has been reported that in the decomposition of propane[4] and of *n*-butane,[5] the lowering of the input was inclined to decrease the selectivities of acetylene and soot, but to increase those of methane and ethylene. This reflects that more energies are required for the complete decomposition of propane and *n*-butane to atomic carbon and atomic hydrogen compared with that of methane to atomic carbon and atomic hydrogen.

Figure 3 shows the effect of argon flow rate at 0.100± 0.005 *l*/min methane feed rate and 9.35±0.01 kW input. As for *n*-butane,[5] the conversion decreases markedly with reducing argon flow rate. At the same time, the lowering of argon flow rate decreases the selectivity of acetylene and increases that of soot. At argon flow rate below 0.82 *l*/min, the formation of soot tends to be favored over that of acetylene, and from the thermodynamic consideration[1,2] it suggests that the decomposition temperature rises with reducing argon flow rate. On the other hand, as shown in Fig. 4, ArI line (4158

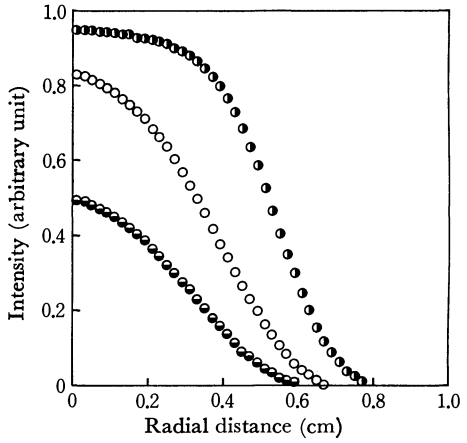

Fig. 4. Radial intensity profiles of ArI (4158 Å) at a distance of 1 cm from methane inlet at various argon flow rate.
-◒- 1.19 *l*/min, -○- 1.56 *l*/min, -◑- 2.12 *l*/min

Å) is observed at a distnace of 1 cm from the methane inlet and its intensity decreases with the lowering of argon flow rate. These results suggest that at the higher argon flow rate, the comparatively high temperature region extends over the neighborhood of the methane inlet and methane can be decomposed in this region. But the decomposition temperature is presumed to be lower in this region than in the upstream of the plasma jet since it has been reported that the temperature of the induction-coupled argon plasma jet dropped toward the downstream of the plasma jet.[6] Therefore, the decomposition at the lower argon flow rate occurs apparently at the higher temperature. These results further suggest that methane is not completely mixed with the plasma jet. That is, from the results stated above together with those on the decomposition of propane[4]

6) T. B. Reed, *J. Appl. Phys.*, **32**, 821 (1961).

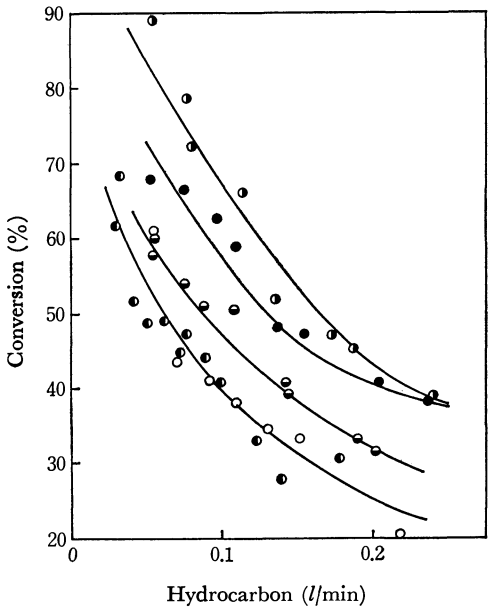

Fig. 5. Variation of conversion with feed rate of hydrocarbons.
Input: 9.35±0.01 kW, Argon flow rate: 1.56±0.02 *l*/min
-◑- CH_4, -●- C_2H_6, -◒- C_3H_8,
-◐- *n*-C_4H_{10}, -○- *i*-C_4H_{10}

and of *n*-butane,[5] we may conclude that saturated gaseous hydrocarbons are not completely mixed with the plasma jet but the decomposition of these hydrocarbons takes place predominantly in the outer flame of the plasma jet and its surroundings under the condition that hydrocarbons are charged into the plasma jet countercurrently.

Decomposition of Ethane and Isobutane. As stated above, the decomposition of methane gave mainly acetylene, soot, and hydrogen with a small amount of ethylene. Consequently, we studied the decomposition of ethane and isobutane in order to know the effect of the structure of hydrocarbons on the conversion, the product distributions and formation processes of methane and ethylene in the decomposition of propane and

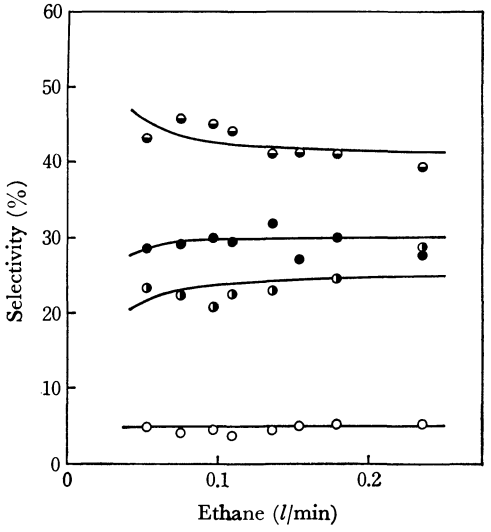

Fig. 6. Effect of ethane feed rate on selectivities of products.
Input: 9.35±0.01 kW, Argon flow rate: 1.56±0.02 *l*/min
-○- CH_4, -◒- C_2H_2, -◑- C_2H_4, -●- soot

Table 1. Selectivities of carbon-containing products in isobutane decomposition

i-C_4H_{10} (*l*/min)	Selectivity of product (%)					
	CH_4	C_2H_6	C_2H_4	C_3H_6	C_2H_2	Soot
0.056	9.7	1.3	10.1	10.7	42.0	26.2
0.073	9.8	2.1	9.5	9.7	45.7	23.2
0.092	9.1	1.3	9.6	10.8	43.4	25.8
0.108	10.1	2.3	10.3	12.6	41.2	23.5
0.131	11.7	1.9	11.3	13.6	37.8	23.7
0.154	11.7	1.5	11.6	13.3	37.1	24.8
0.221	11.3	1.7	11.3	11.6	40.5	23.6

n-butane. Ethane and isobutane were decomposed under the same condition as methane were. Figure 5 shows the variation of conversion of ethane and isobutane with the feed rate of hydrocarbons. Conversions of methane, propane and *n*-butane are included in Fig. 5 for comparison. It is seen from Fig. 5 that the saturated gaseous hydrocarbons become difficult to be decomposed as carbon chains increase and both butane isomers are decomposed in the similar way.

Figure 6 and Table 1 show selectivities of products at various feed rates of ethane and isobutane, respectively. In ethane, appreciable amounts of methane and ethylene are obtained in addition to acetylene, soot, and hydrogen. Especially, ethylene is obtained in 20—27% selectivity. In isobutane, the selectivity of ethylene reduces to 10—12%, but propylene is obtained in 10—14% selectivity and methane is formed in higher selectivity than in the decomposition of ethane, propane,[4]

Table 2. Yields of decomposition products in various hydrocarbons
Hydrocarbon: 0.100±0.005 *l*/min, Ar: 1.56±0.02*l*/min, Input: 9.35±0.01kW

Hydrocarbon	Yield (%)						
	CH_4	C_2H_4	C_2H_6	C_3H_6	C_3H_8	C_2H_2	Soot
CH_4	—	1.0	trace	—	—	40.0	25.5
C_2H_6	2.7	12.8	—	—	—	27.1	20.2
C_3H_8	3.1	8.3	trace	2.9	—	19.8	14.4
n-C_4H_{10}	2.6	8.5	trace	1.1	trace	17.6	10.5
i-C_4H_{10}	4.1	4.0	0.9	5.1	—	16.1	9.3

and *n*-butane.[5] Table 2 illustrates the products and their yields for the decompositions of methane, ethane, propane, *n*-butane, and isobutane at the hydrocarbon feed rate of 0.100±0.005 *l*/min. As is seen from Table 2, the decomposition products and their distributions closely relate with the structure of hydrocarbons. In the decomposition of methane, major products are acetylene, soot, and hydrogen. Acetylene and soot occupy above 98% of carbon-containing products. Thus, methane introduced into the decomposition region is decomposed almost to carbon and hydrogen, and then, acetylene, soot, and hydrogen are formed. That is, the decomposition of methane is assumed to proceed *via* following steps;

$$CH_4 \longrightarrow CH_3 \longrightarrow CH_2 \longrightarrow CH \longrightarrow C_1 \quad (1)$$

$$2C_1 \longrightarrow C_2 \quad (2)$$

$$C_1 + CH \longrightarrow C_2 + H \quad (3)^{7)}$$

$$C_2 + H \longrightarrow C_2H \xrightarrow{H} C_2H_2 \quad (4)$$

$$2CH \longrightarrow C_2H_2 \quad (5)$$

$$nC_1 \longrightarrow C_n \xrightarrow{H} C_nH \quad (6)$$

$$C_1, C_2, \cdots\cdots C_n \longrightarrow C_s \quad (7)$$

$$CH, CH_2, CH_3, C_2H, \cdots\cdots C_nH \longrightarrow C_s + H_2 \quad (8)$$

$$H + H \longrightarrow H_2 \quad (9)$$

where C_s: soot

It is difficult to explain the formation process of ethylene, but it may be concluded that ethylene is formed from carbon and hydrogen under the condition used in this experiment. Saturated hydrocarbons with two or more carbon atoms are decomposed to give appreciably byproducts such as methane, ethylene, or propylene, in addition to acetylene, soot, and hydrogen. If these hydrocarbons are decomposed mostly to carbon and hydrogen, and then, a large portion of methane, ethylene, or propylene is formed, a similar product distribution must be obtained in the decomposition of both *n*-butane and isobutane. The high selectivity of propylene in isobutane decomposition gives the strong support for the intervention of isopropyl radical in the decomposition step.[8] Therefore, it may be concluded that radicals formed by a fission of C–H or C–C bond intervene in the decomposition of saturated gaseous hydrocarbons in the induction-coupled argon plasma jet. That is, these radicals are decomposed to give appreciably methane, ethylene, or propylene, *etc.* at the comparatively lower temperature region in the reaction zone. At the higher temperature region in the reaction zone, these radicals are further decomposed to carbon and hydrogen, and then, acetylene, soot, and hydrogen are produced. For example,

$$C_2H_6 \longrightarrow 2CH_3 \quad (10)$$

$$C_2H_6 \longrightarrow C_2H_5 + H \quad (11)$$

$$C_2H_6 + H \longrightarrow C_2H_5 + H_2 \quad (12)$$

$$C_2H_6 + CH_3 \longrightarrow C_2H_5 + CH_4 \quad (13)$$

$$C_2H_5 \longrightarrow C_2H_4 + H \quad (14)$$

$$C_2H_5 + C_2H_5 \longrightarrow C_2H_4 + C_2H_6 \quad (15)$$

$$CH_3 + H \longrightarrow CH_4 \quad (16)$$

in the decomposition of ethane, methyl and ethyl radicals are formed by the reactions (10), (11), (12), and (13).[9–11] In the lower temperature region, methane and ethylene are formed from these radicals by the reactions (13), (14), (15), and (16). In the higher temperature region, methyl and ethyl radicals are further decomposed to carbon and hydrogen or partly to methyne and methylene radicals, and then, acetylene, soot, and hydrogen are formed through the same process as that for methane decomposition.

7) A. R. Fairbairn, *Proc. Roy. Soc., Ser. A*, **312**, 229 (1969).
8) R. S. Konar, J. H. Purnell, and C. P. Quinn, *J. Chem. Soc., A*, **1967**, 1543.
9) C. P. Quinn, *Proc. Roy. Soc. Ser. A*, **275**, 190 (1963).
10) M. C. Lin and M. H. Back, *Can. J. Chem.*, **44**, 505 (1966).
11) M. C. Lin and M. H. Back, *ibid.*, **44**, 2357 (1966).

NOTES

BULLETIN OF THE CHEMICAL SOCIETY OF JAPAN, VOL. 44, 3457—3458(1971)

Anodic Oxidation of Anthracene in Acetonitrile at a Rotating Ring-disk Electrode

Tetsuaki KIHARA, Kazuo SASAKI,* and Haruo SHIBA
Department of Applied Chemistry, Hiroshima University, Sendamachi, Hiroshima
(Received October 30, 1970)

Although many works have been reported on anodic oxidation of anthracene, there still remains some uncertainty as to its detailed mechanism.

Bard and his coworkers,[1] who studied the reaction in methylene chloride with linear potential sweep technique, reported that the oxidation product undergoes a rapid follow-up chemical reaction. Oxidation in pyridine media[2] gives rise to the formation of 9,10-dihydroanthranyl dipyridinium perchlorate indicating the reaction intermediate to be anthracene dication. The product obtained by the controlled potential electrolysis in acetonitrile was bianthrone.[3]

Anodic oxidation of anthracene has also been studied in relation to electro-chemiluminescence.[4-9] Although many of these studies suggest that it proceeds through two successive one-electron transfer, no definite proof for the formation of one-electron intermediate, anthracene monocation, has been reported. As an only exception, Peover and White,[10] who studied the oxidation of several polycyclic hydrocarbons by means of cyclic voltammetry, stated that a poorly developed cathodic current due to the reduction of anthracene monocation was detectable at high scan-rates. Application of cyclic potential sweep technique is, however, limited by the rate of charge transfer step. If the rate is not rapid enough the current-potential curve observed at high scan-rates becomes deformed and allows no quantitative analysis.

A rotating ring-disk electrode is receiving growing attention[11-14] as a powerful tool for studies of labile intermediates of an electrode reaction. We have attempted to apply this new technique to the reaction concerned.

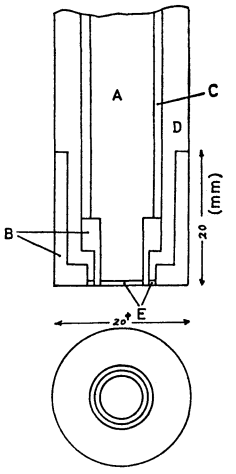

Fig. 1. Cross section of rotating ring-disk electrode. A, shaft (SS45C); B, teflon; C, bakelite; D, copper; E, platinum.

The shape and size to the ring-disk electrode used is schematically shown in Fig. 1. Platinum was used for both ring and disk electrodes. The maximum eccentricity of the electrode caused by rotation was found within 0.01 mm at a periphery of bottom surface. Potentials of both the ring and disk electrodes were independently controlled using a couple of electronic potentiostats. Currents flowing through the electrodes were respectively recorded by two X-Y recorders. The collection efficiency which is defined as the ratio of ring current to disk current was determined experimentally by measuring two representative redox reactions of $Fe(CN)_6^{4-}/Fe(CN)_6^{3-}$ and Cu(I)/Cu(II) couples. The values determined from the two reactions were exactly in agreement with 0.36. These values can be compared to the theoretical one, 0.40, calculated according to the Albery-Bruckenstein's equation.[11] Acetonitrile was used as a solvent and was purified carefully according to the directions of O'Donnell *et al.*[15] 0.1M tetrabutylammonium perchlorate was used as a supporting electrolyte.

Prior to measuring anthracene, the reaction of 9,10-diphenylanthracene (DPA) known to give a stable monocation was studied. Curves A and B in Fig. 2 represent currents flowing through disk and ring elec-

* To whom correspondence should be addressed.

1) J. Phelps, K. S. V. Santhanam, and A. J. Bard, *J. Amer. Chem. Soc.*, **89**, 1752 (1967).
2) H. Lund, *Acta Chem. Scand.*, **11**, 1323 (1957).
3) E. J. Majeski, K. D. Stuart, and W. E. Ohnesorge, *J. Amer. Chem. Soc.*, **90**, 633 (1968).
4) D. M. Hercules, *Science*, **145**, 808 (1964).
5) R. E. Visco and E. A. Chandross, *J. Amer. Chem. Soc.*, **86**, 5350 (1964).
6) E. A. Chandross, J. W. Longworth, and R. E. Visco, *ibid.*, **87**, 3259 (1965).
7) J. M. Bader and T. Kuwana, *J. Electroanal. Chem.*, **10**, 104 (1965).
8) L. R. Faulkner and A. J. Bard, *J. Amer. Chem. Soc.*, **90**, 188 (1968).
9) T. C. Werer, J. Chang, and D. M. Hercules, *ibid.*, **92**, 763 (1970).
10) M. E. Peover and B. S. White, *J. Electroanal. Chem.*, **13**, 93 (1967).
11) W. J. Albery and S. Bruckenstein, *Trans. Faraday Soc.*, **62**, 1920 (1965).
12) P. A. Malachesky, K. B. Prater, G. Petrie, and R. N. Adams, *J. Electroanal. Chem.*, **16**, 41 (1968).
13) A. Damjanovic, M.A. Genshaw, and J. O'M. Bockris, *ibid.*, **114**, 466, 1107 (1967).
14) W. J. Albery and S. Bruckenstein, *Trans. Faraday Soc.*, **62**, 1946, 2596 (1966).
15) J. F. O'Donnell, J. T. Ayres, and C. K. Mann, *Anal. Chem.*, **37**, 1161 (1965).

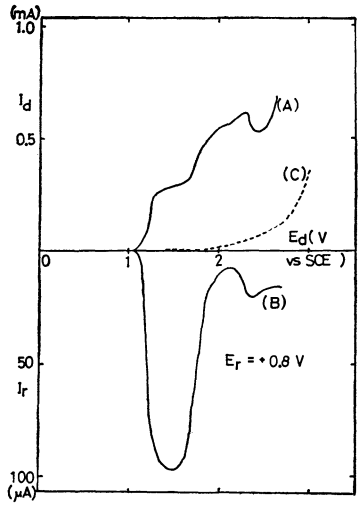

Fig. 2. I-E curves of 9,10-diphenylanthracene.
(A) disk current, (B) ring current with ring potential set at 0.8 V, (C) base current of disk. Solution, 10^{-3}M 9,10-DPA in acetonitril. Supporting electrolytes, 0.1M tetrabutylammonium perchlorate. Rotation speed, 940 rpm. Sweep rate of disk potential, 480 sec/V.

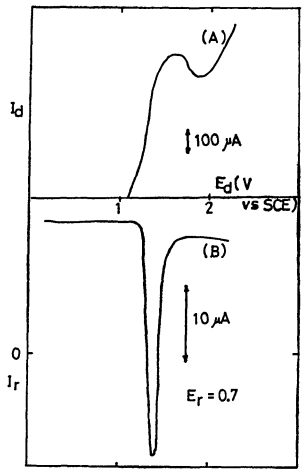

Fig. 3. I-E curves of anthracene.
(A) disk current, (B) ring current with ring potential set at 0.7 V. Solution, 10^{-3}M ANT in acetonitril. Supporting electrolytes, 0.1M tetrabutylammonium perchlorate. Rotation speed, 940 rpm. Sweep rate of disk potential, 40 sec/V.

trodes, respectively, as a function of linearly changing potential of the disk electrode. It should be noted that these curves were obtained by changing the disk potential linearly and fixing the ring potential constant at 0.8 V. Curve C is a background disk current observed in a solution containing no DPA.

The results with DPA can be summarized as follows.

1) DPA is anodically oxidized through two one-electron steps since curve A consists of two waves of approximately equal height.

2) Product at the first wave, DPA monocation, is quite stable and gives rise to a hump-like strong cathodic current at the ring electrode (curve B). The collection efficiency for this species was 0.36.

3) Product at the second anodic wave, DPA dication formed at the potential range of 1.7 to 2.4 V, is labile and undergoes rapid chemical reaction with surroundings. As a result, the ring current diminishes markedly at this potential range.

A small but definite deflection of the disk current appears before the final rise and a corresponding deflection appears also in the ring current. The species responsible for this is uncertain.

Similar curves for unsubstituted anthracene (ANT) are shown in Fig. 3. Disk current exhibits a single wave with the same height as that found in the second wave of DPA. This seems to indicate that the oxidation of ANT proceeds in one step with two electron transfer, $ANT \rightarrow ANT^{2+} + 2e$. However, a sharp rise of cathodic current appearing in the ring current suggests that the electroactive species for this ring current is the monocation of anthracene, ANT^+, rather than its dication. In the case of DPA, the two-electron product was inactive to the ring current. It was reported[16] that the cathodic counterpart of DPA^{2+} appears at a much more negative potential than that of DPA^+. This may be also the case in the oxidation of ANT. A close resemblance in the behavior of ring currents shown in Figs. 2 and 3 strongly suggests that ANT is also oxidized through a consecutive two one-electron steps.

The collection efficiency for the ring-active species, ANT^+, was as low as 0.052 indicating that the species is quite labile. If anthracene monocation undergoes a pseudo-first order reaction during the movement from disk to ring electrode, the fraction f which is collected by the ring electrode can be estimated by the equation

$$f = Ncal\, 2^{-\Delta t/\tau}$$

Transformation of this equation gives

$$\tau = -\Delta t \log 2 / \log (f/Ncal),$$

where $Ncal$ is the calculated collection efficiency, τ the half-life time of anthracene monocation and Δt the mean transit time from disk to ring. Under normal conditions, Δt was estimated to be 0.02—0.1 sec. Corresponding half-life time of ANT^+ is in the range 0.7—3.4×10^{-2} sec. This figure is in agreement with the value estimated roughly as "a few millisecond" by Peover.[10]

16) R. Dietz and B. E. Larcombe, *J. Chem. Soc., B*, **1970**, 1369.

BULLETIN OF THE CHEMICAL SOCIETY OF JAPAN, VOL. 44, 3459—3460(1971)

An Investigation of the Stability Constant of the 2,3-Dihydroxybenzoic Acid Complex with Copper(II)

Hikaru HARADA

Department of Chemistry, Faculty of Science, Tohoku University, Sendai

(Received December 4, 1970)

It has been shown that the stability constants of some metal complexes with tiron (disodium 1,2-dihydroxybenzene-3,5-disulfonate) are larger than those with catechol.[1] This is contrary to what is to be expected from their acid dissociation constants.[2,3]

As this peculiarity seemed to come from the fact that tiron has a negative sulfonic group in the vicinity of the OH group which coordinates to a metal ion, 2,3-dihydroxybenzoic acid (DBA) was used to see whether the COOH group gives any larger stability to the metal-DBA complex. Another problem, however, may rise about this ligand; as DBA is a derivative of salycilic acid with the OH group at the 3 position, there are two possible types of chelation in the complex, namely, the catechol-type and the salycilic acid-type chelate.

Experimental

All the measurenents were carried out by using the same apparatus as was reported previously:[2,4] the reaction vessel and the quartz cell for the measurement of the absorbancy were connected by a Teflon tube. All the reaction solutions were prepared and mixed in a purified nitrogen atmsphere; then the absorbancy and the pH were simultaneously measured. During the measurements, constant-temperature water of 25.0±0.1°C was circulated through the double walls of the reaction vessel. Sodium perchlorate was used to make ionic strength 0.1. The DBA was recrystallized twice from water just before the measurements.

TABLE 1. ACID DISSOCIATION CONSTANTS OF DBA AND RELATED CATECHOL DERIVATIVES

Ligand	pK_{HL}	pK_{H_2L}	pK_{H_3L}
DBA	11.68	9.84	3.10
3,4-Dihydroxybenzoic acid[a)]	11.65	8.89	4.61
Tiron[b)]	11.96	7.89	
Catechol[a)]	12.03	9.32	
3,5-Dinitrocatechol[c)]	9.86	3.32	
3-Nitrocatechol[c)]	11.48	6.50	

a) H. Harada, *Nippon Kagaku Zasshi*, **90**, 267 (1969).
b) Y. Oka, N. Nakazawa, and H. Harada, *ibid.*, **86**, 1158 (1965).
c) K.S. Math, K.A. Venkatachalam, and M.B. Kabadi, *J. Indian Chem. Soc.*, **36**, 65 (1959).

1) H. Harada and Y. Oka, *Nippon Kagaku Zasshi*, **90**, 898 (1969).
2) Y. Oka and H. Harada, *ibid.*, **88**, 441 (1967).
3) This problem has also been pointed out in the paper by R. F. Jameson (*J. Inorg. Nucl. Chem.*, **28**, 2667 (1966)), but no explanation is to be found there.
4) H. Harada, *Nippon Kagaku Zasshi*, **90**, 207 (1969).

Results and Discussion

The acid dissociation constants of DBA were obtained by the method previously used with catechol derivatives.[4] The results are shown in Table 1. The larger K_{H_3L} values and the smaller K_{H_2L} value of DBA than the respective values of 4-carboxy catechol may be due to the formation of a hydrogen bond between the OH and COOH groups of DBA through the H atom of the OH group.

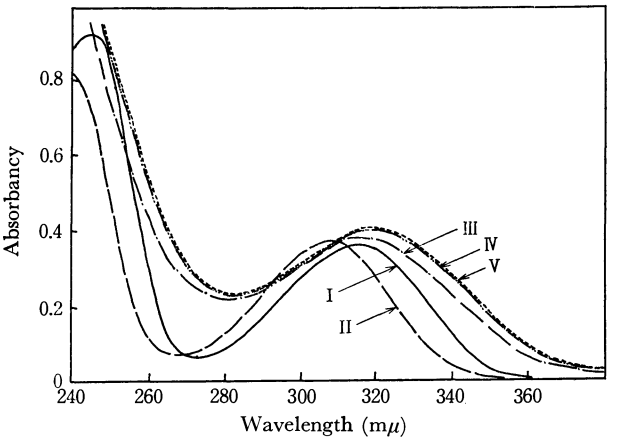

Fig. 1. pH dependence of absorption curve of Cu(II)-DBA system.
pH: I, 2.24 (——)
II, 4.14—4.80 (— —)
III, 5.95 (—·—)
IV, 7.20 (—··—)
V, 7.54 (---------)
concentration:
$Cu(ClO_4)_2$, 1.103×10^{-4} mol/*l*
DBA, 1.103×10^{-4} mol/*l*

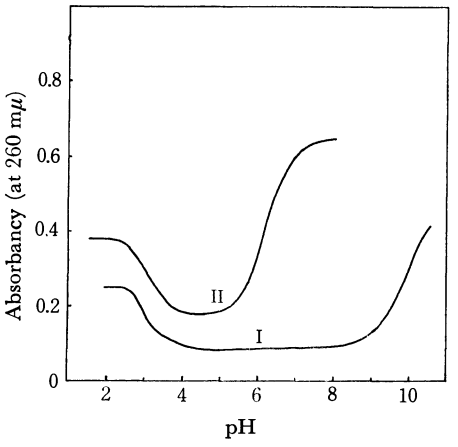

Fig. 2. pH dependence of absorbancy at 260 mμ.
Curve I: DBA
II: Cu(II)+DBA

The stability constant of the Cu-DBA (1: 1) chelate was obtained in a manner to be described below. The absorption spectra of the solution containing the Cu(II) ion and DBA are shown in Fig. 1. The pH-dependence of absorbancy change at 260 mμ is shown in Fig. 2, together with that of the ligand itself.

As is shown in Fig. 2, the decrease in absorbancy at about pH 3 can be ascribed to the dissociation of the carboxyl group of DBA, as was expected from its pK_{H_3L} value.

On increasing the pH, the absorbancy also increased in the pH range from 5.5 to 6.5; this increase was attributed to the formation of the complex.

Here, it is assumed that the Cu-DBA (1: 1) chelate is formed in the pH 5.5—6.5 range according to the following equation:

$$Cu + H_2L = CuL + 2H \quad (1)$$

The equilibrium constant of this reaction may be described as:

$$K_1 = \frac{[CuL][H]^2}{[Cu][H_2L]} \quad (2)$$

When the solution is prepared to make the concentrations of Cu and DBA equal (1.084×10^{-4} mol/l) and when its hydrogen ion concentration is varied, the following equation (reported previously[5]) is obtained:

$$A - a\varepsilon_{H_2L} = a(\varepsilon_{CuL} - \varepsilon_{H_2L}) - [H](A - a\varepsilon_{H_2L})^{1/2}\left(\frac{\varepsilon_{CuL} - \varepsilon_{H_2L}}{K_1}\right)^{1/2} \quad (3)$$

where A is the absorbancy, a is the concentration of the Cu ion and also that of DBA, and ε_{H_2L} and ε_{CuL} are the molar extinction coefficients of DBA and CuL respectively.

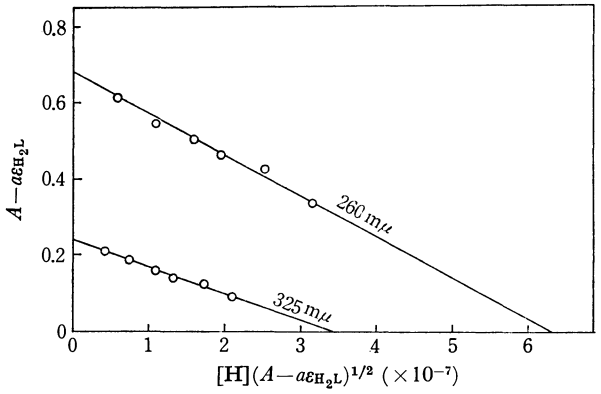

Fig. 3. Relation between $A-a\varepsilon_{H_2L}$ and $[H](A-a\varepsilon_{H_2L})^{1/2}$.
concentration: $Cu(ClO_4)_2$: 1.084×10^{-4} mol/l
DBA: 1.084×10^{-4} mol/l

5) H. Harada, *Nippon Kagaku Zasshi*, **91**, 1064 (1970).

If a plot of $[H](A-a\varepsilon_{H_2L})^{1/2}$ on the right-hand side against $A-a\varepsilon_{H_2L}$ on the left-hand side of Eq. (3) is linear, the variation in absorbancy over the pH 5.5—6.5 range can be considered to be due to the formation of the 1: 1 chelate by means of Eq. (1). Figure 3 indicates that the linear relation holds. The division of the intercept of the line by the square of the slop and again by the concentration of Cu(=DBA), a, gave K_1. The value of K_1, thus obtained was divided by the acid dissociation constant of DBA; then the stability constant of the 1: 1 chelate, k_1, was obtained.

Table 2. Stability constants of Cu(II)-complexes with DBA and related catechol derivatives

Ligand	log k_1
DBA	13.24
Salycilic acid[a)]	10.64
Catechol[b)]	13.50
3,4-dihydroxybenzoic acid[b)]	13.15
Tiron[c)]	14.43
3,5-Dinitrocatechol[d)]	10.45

a) from A. E. Martell and L. G. Sillén, "Stability Constants of Metal Ion Complexes. Section II, Organic Ligands," Chemical Society, London (1964).
b) H. Harada and Y. Oka, *Nippon Kagaku Zasshi*, **90**, 898 (1969).
c) Y. Oka, N. Nakazawa, and H. Harada, *ibid.*, **86**, 1158 (1965).
d) K. S. Math, K. A. Ven Katachalam, and M. B. Kabadi, *J. Indian Chem. Soc.*, **36**, 65 (1959).

As is shown in Table 2, the k_1 value of Cu-DBA is 13.24, which is much nearer to the k_1 value of Cu-catechol (13.50) than to the k_1 value of Cu-salycilic acid (10.64). It can, therefore, be concluded that the DBA in the Cu-complex has a catechol-type-chelation.

When the stability constant of Cu-tiron is compared with that of Cu-DBA, which has a 3-carboxyl group, it can be noticed that Cu-tiron has an appreciably higher value. It seems that the higher stability constant of tiron is not caused by the ordinary substitution effect of the 3-position substituent.

It is supposed that the sulfonic group is more strongly solvated by water than the carboxyl group; hence, the degree of desolvation may also be larger in the sulfonic group when the Cu-chelate is formed. It can perhaps be concluded that the entropy change for the complex formation contributes greatly to the higher stability constant of the Cu-tiron chelate.

BULLETIN OF THE CHEMICAL SOCIETY OF JAPAN, VOL. 44, 3461—3462 (1971)

Formation Constants of Several Copper(II) Alkylthioacetates in a Dioxane-Water Solvent

Akira OUCHI, Toshio TAKEUCHI, and Yayoi OHASHI

Department of Chemistry, College of General Education, The University of Tokyo, Komaba, Meguro-ku, Tokyo

(Received January 14, 1971)

Recently the present authors synthesized and studied the alkylthioacetates of several metals in the solid state.[1-3] Concerning the stability of alkylthioacetato complexes, Irving[4] and Sandell[5] have published the formation constants of some ethylthioacetates of some metals, and Yamasaki[6] has reported on the phenylthioacetates of some metals. Recently Pettit[7] has studied the silver complexes of a series of alkylthioacetic acids and found a linear relation between their stabilities and the Taft σ^* values of their alkyl groups. However, the relation has not yet been examined with regard to the complexes of other metals. Consequently, it seems interesting to furnish the formation-constant data of the copper(II) complexes of a series of alkylthioacetic acids.

Experimental

Materials. *Alkylthioacetic acids*: Methyl-, ethyl-, *n*-propyl-, isopropyl-, *n*-butyl-, isobutyl-, *s*-butyl-, and benzylthioacetic acids were synthesized by the method described in the papers of Larsson[8] and Pettit.[7] They were used after the redistillation under reduced pressure.

1,4-Dioxane: G. R.-grade reagent of the Wako Chemical Co., Ltd. was used after being purified according to the directions of Riddich and Toops.[9]

All other reagents were G. R. reagents of the Wako Chemical Co., Ltd., and were used without any further purification.

General Procedure. The techniques employed were those of Calvin.[10] A Toa Denpa Co. model HM-5A pH meter, a saturated calomel electrode, and a glass electrode were used. All the measurements were made at 30.0 ± 0.1°C. The pH meter was standardized against aqueous buffer solutions (6.86 and 4.00) of the Wako Chemical Co.

The Measurement of the Acid Dissociation Constants: 25 m*l* of dioxane, 5 mmol of potassium nitrate, and 1 mmol of alkylthioacetic acid were diluted to 50 m*l* with water. The sample was titrated with a 1.000N sodium hydroxide standard aqueous solution[11] to record the pH meter reading (B): the B value of the half-neutralization point on the titration curve was thus obtained. pK_D, where K_D is the acid dissociation constant, was obtained by $pK_D=B+(\log U_H^0+\log 1/\gamma)$ where U_H^0 is a conversion factor independent of the ionic concentration and where the γ is the activity coefficient of the strong electrolytes in the solution; they were conveniently obtained by means of the diagram of Uitert.[12]

The Determination of the Formation Constants of the Complexes. 25 m*l* of dioxane, 4 mmol of potassium nitrate, 1 mmol of nitric acid, 0.1 mmol of metal nitrate, and 1 mmol of the ligand were mixed and diluted to 50.00 m*l* with water. The sample was thermostatted more than 4 hr to attain the equilibrium. However, to avoid the effect of decomposition, the sample was titrated within 6 hr after the dissolution. Each run was repeated 4 times, and the average readings were adopted. No precipitation was found during the process ($\bar{n}<2$). The calculation of the formation constants, including the correction for the effect of the dioxane solution, was made as has been described by Calvin,[10] Uitert,[12-14] and Goldberg.[15]

Results and Discussion

A typical run of the data and the results of the calculations are shown in Table 1. The acid dissociation constants obtained, as well as the formation constants of copper(II) complexes of alkylthioacetates are shown in Table 2.

The dissociation constants of these acids are almost all the same. This fact suggests that the inductive effect of the alkyl group does not seriously affect the carboxyl group, as they are separated by a $-S-CH_2-$ group. On the other hand, the coordination ability of sulfur atom should be affected by the alkyl group.

1) A. Ouchi, Y. Ohashi, T. Takeuchi, and Y. Yoshino, This Bulletin, **43**, 1088 (1970).
2) Y. Ohashi, T. Takeuchi, A. Ouchi, and Y. Yoshino, *ibid.*, **43**, 2845 (1970).
3) A. Ouchi, T. Takeuchi, and Y. Ohashi, *ibid.*, **44**, 731 (1971).
4) R. J. Irving and W. C. Fernelius, *J. Phys. Chem.*, **60**, 1427 (1956).
5) A. Sandell, *Acta Chem. Scand.*, **15**, 190 (1961), **24**, 1561, 1718 (1970).
6) K. Suzuki and K. Yamasaki, *J. Inorg. Nucl. Chem.*, **24**, 1093 (1962).
7) L. D. Pettit and C. Sherrington, *J. Chem. Soc., A*, **1968**, 3078.
8) E. Larsson, *Ber.*, **63**, 1347 (1930).
9) J. A. Riddich and E. E. Toops, Jr., "Organic Solvents," 2nd Ed., Interscience Publ. Ltd., London, 1955, p. 371.
10) M. Calvin and K. W. Wilson, *J. Amer. Chem. Soc.*, **67**, 2003 (1945).
11) As the sample was titrated with sodium hydroxide aqueous solution, the concentration of dioxane was not always 50% during the titration. Consequently, the conversion factors of each dioxane concentration were used for each of the calculations, assuming that the total volume was obtained by the addition of both volumes. In these regions the difference of $(U_H^0+\log 1/\gamma)$ per 1% difference of dioxane concentration is about 0.02. Therefore the above correction is enough to keep the calculation error below 0.01, and the difference of pK_D and $\log K$ values in this dioxane concentration region is expected to be below 0.02. In Table 2, the concentration of dioxane was shown as 50%. It is only the approximate concentration where the data were obtained, even though the error from the value at 50% is expected to be below 0.02.
12) L. G. V. Uitert and W. C. Fernelius, *J. Amer. Chem. Soc.*, **76**, 5887 (1954).
13) L. G. V. Uitert and C. G. Haas, *ibid.*, **75**, 451 (1953).
14) L. G. V. Uitert, C. G. Haas, W. C. Fernelius, and B. E. Douglas, *ibid.*, **75**, 455 (1953).
15) D. E. Goldberg, *Chem. Educ.*, **40**, 341 (1963).

Table 1. Titration of 50% dioxane-water solution of copper nitrate (2.00×10^{-3}M), *n*-propylthioglycolic acid (2.00×10^{-2}M), potassium nitrate (8.00×10^{-2}M), and nitric acid (2.00×10^{-2}M) with standard aqueous solution of sodium hydroxide (1.000N)

NaOH (m*l*)	*B*	$\bar{n}$	p(Ch$^-$)
1.050	3.44	0.56	3.47
1.100	3.67	0.86	3.26
1.150	3.85	1.18	3.10
1.200	4.08	1.40	2.90
1.300	4.37	1.92	2.67

B: Readings of the pH meter standardized with aqueous buffer.
(Ch$^-$): Mole concentration of the monovalent chelate anion Ch$^-$.
$\bar{n}$: The number of coordinated ligand molecules per one metal ion.

Table 2. The dissociation constants and the formation constants of copper(II) complexes of alkylthioacetic acids in 50% dioxane[11] at 30°C

Metal Ligands (R=)	H^+ log K_1	Cu^{2+} log K_1	Cu^{2+} log K_2
$C_6H_5\cdot CH_2-$	-5.7_3	3.0	2.4
CH_3-	-5.5_6	3.4	2.7
C_2H_5-	-5.6_6	3.5	2.7
C_3H_7-	-5.6_8	3.5	2.9
$(CH_3)_2CH\cdot CH_2-$	-5.5_5	3.5	2.8
C_4H_9-	-5.6_6	3.6	2.9
$(CH_3)_2CH-$	-5.5_9	3.6	2.8
$(CH_3)(C_2H_5)CH-$	-5.6_6	3.6	2.8

Ligands are $RSCH_2COOH$ where R s are shown in the column above.

The relationship between the formation constants (in log *K*) of the copper complexes and the Taft σ* functions[16] of the substituent, R, for the $R\cdot S\cdot CH_2CO_2H$ ligand is shown in Fig. 1. As is shown in the figure, there is almost a linear relationship between them. This fact also seems to prove the existence of the sulfur-metal bond in the copper complexes, even in the solution.

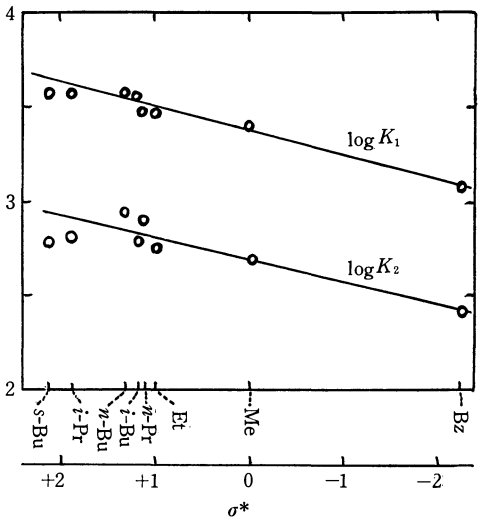

Fig. 1. The relationship between the formation constants of the copper(II) complex and the Taft σ* functions of the substituents R for the ligands $R\cdot S\cdot CH_2COOH$.
R of the ligansd are as follows: Bz : $C_6H_5CH_2$, Me : CH_3, Et : C_2H_5, *n*-Pr : C_3H_7, *i*-Pr : $(CH_3)_2CH$, *n*-Bu : C_4H_9, *i*-Bu : $(CH_3)_2CH\cdot CH_2$, *s*-Bu : $(C_2H_5)(CH_3)CH$

The points of isopropyl- and *s*-butyl-thioacetates, however, all a little lower than the line; this is probably due to the difficulty of the complex formation because of the steric effect of the ligand.

The authors wish to thank Professor Yukichi Yoshino and our colleagues of this laboratory for their helpful discussions.

16) R. W. Taft, Jr., *J. Amer. Chem. Soc.*, **75**, 4231 (1953).

BULLETIN OF THE CHEMICAL SOCIETY OF JAPAN, VOL. 44, 3463—3464(1971)

The Reduction of Some Quinones and Enones by Ferrocene in the Presence of Aluminum Chloride

Yoshimori OMOTE, Ryuichiro KOBAYASHI, Choji KASHIMA, and Noboru SUGIYAMA
Department of Chemistry, Tokyo Kyoiku University, Otsuka, Tokyo

(Received March 3, 1971)

Ferrocene is known to be easily oxidized in the presence of an acid to give ferricinium ion.[1-4] One of us reported that the reaction of ferrocene with fumaroyl chloride in the presence of aluminum chloride did not give 1,2-di(ferrocenylcarbonyl)ethylene, but afforded 1, 2-di(ferrocenylcarbonyl)ethane and β-(ferrocenylcarbonyl)propionic acid.[5] Schaaf and Lenk[6] reported the oxidation of ferrocene in the Friedel-Crafts reaction of ferrocene with some acyl or aroyl chlorides.

We now wish to report our finding that some quinones and enones are reduced by ferrocene in the presence of aluminum chloride to give phenols and saturated ketones respectively.[7] The limitation of the reaction is also examined.

Reduction of Quinones by Ferrocene. Coan *et al.*[8] found the formation of a charge-transfer complex of ferrocene with *p*-benzoquinone or chloranil, but they failed to isolate the complex. We examined the reaction of *p*-benzoquinone with ferrocene in dichloromethane in the presence of aluminum chloride and found that the products were hydroquinone and ferricinium chloride in the molar ratio 1: 1.8. Chloranil and ferrocene afforded tetrachlorohydroquinone and ferricinium chloride in a molar ratio 1: 1.7 under similar conditions.

Thus it might be concluded that two moles of ferrocene react with one mole of a quinone to give two moles of ferricinium ion and one mole of the corresponding hydroquinone.

Reduction of Enones by Ferrocene. The reduction of a variety of enone compounds and other olefinic compounds by ferrocene in the presence of aluminum chloride has been checked. The results are summarized in Table 1 from which it might be concluded that an enedione structure –COCH=CHCO– is essential for the reduction by ferrocene.

As regards stoichiometry of this reaction, the reduction of 1,2-dibenzoylethylene by ferrocene was examined in detail. When 1,2-dibenzoylethylene was brought into reaction with ferrocene in the presence of aluminum chloride in a molar ratio 1: 1: 2 (substrate: ferrocene: aluminum chloride), about half of the substrate was reduced to 1,2-dibenzoylethane, and ferrocene gave ferricinium ion in the molar ratio 1: 1.9 (product: ferricinium ion). This reveals that one mole of an enone whose structure contains –COCH=CHCO– is reduced by two moles of ferrocene.

Table 1. Reducibility of some enones compared with that of some olefinic compounds

RCH=CR′R″

R	R′	R″	Reducibility
C_6H_5CO–	C_6H_5CO–	H–	+
C_6H_5CO–	HOOC–	H–	+
CH_3OCO–	CH_3OCO–	H–	+
C_6H_5–	C_6H_5–	H–	–
–$CH_2CH_2CH_2CH_2$–		H–	–
C_6H_5–	HOOC–	H–	–
CH_3–	HOOC–	H–	–
CH_3CO–	CH_3–	CH_3–	–
FcCO–	C_6H_5–	H–	–

Fc: Ferrocenyl

Experimental

Quinones, Enones and Related Compounds. The following compounds were prepared according to literature: bromosuccinic anhydride,[9] bp_{25} 148°C, β-benzoylacrylic acid,[10] mp 94—95.5°C, 1,2-diacetylethylene,[11] mp 76—79°C, *trans*-1, 2-dibenzoylethylene,[12] mp 108°C, *trans*-β-acetylacrylic acid,[13] mp 125—126°C. Other compounds used were commercial products.

Reduction of p-*Benzoquinone by Ferrocene.* Aluminum chloride (0.39 g, 2.94 mmol) and *p*-benzoquinone (0.11 g, 1.02 mmol) were added into 35 m*l* of dry dichlolomethane and stirred for 5 min. Ferrocene (0.186 g, 1.00 mmol) was then added. After stirring for 80 min at room temperature, the reaction mixture was poured into ice water and the dichloromethane layer was washed with water, dried and evaporated to dryness. The residue was purified by silica-gel chromatography with benzene-ethyl acetate (2: 1) to give hydroquinone (0.079 g, 0.72 mmol), which was identified by comparing with an authentic sample by UV and tlc technique. For comparison, *p*-benzoquinone (0.11 g) was treated in the same procedure as described above but without fer-

1) G. Wilkinson, M. Rosenblum, M. C. Whiting, and R. B. Woodward, *J. Amer. Chem. Soc.*, **74**, 2126 (1952).
2) V. Weinmayr, *ibid.*, **77**, 3009 (1955).
3) M. F. Hauthorne, *J. Org. Chem.*, **21**, 363 (1956).
4) O. N. Suvorova, G. A. Domrachev, and G. A. Razuvaey, *Dokl. Akad. Nauk SSSR*, **183** (4), 850 (1968).
5) N. Sugiyama and T. Teitei, This Bulletin, **35**, 1423 (1962).
6) R. L. Schaaf and C. T. Lenk, *J. Org. Chem.*, **28**, 3238 (1963).
7) During the course of our investigation, the reduction of some enones by ferrocene in the Friedel-Crafts reaction was independently presented at the 2nd Meeting of Non-Benzenoid Aromatic Chemistry by K. Yamakawa and M. Moroe, Abstracts of Papers, p. 68—70, Kyoto, Nov. 22—23 (1968).
8) J.C. Coan, E. Berg, and H.E. Podall, *J. Org. Chem.*, **29**, 975 (1964).
9) R. Anschütz and L. Kinnkut, *Ber.*, **11**, 1221 (1878).
10) D. Papa, E. Swenk, F. Uillani, and E. Klingsberg, *J. Amer. Chem. Soc.*, **70**, 3356 (1948).
11) M. W. Goldberg and P. Müller, *Helv. Chim. Acta*, **21**, 1699 (1938).
12) Organic Syntheses, Vol. 3, p. 248.
13) L. Wolff, *Ann.*, **246**, 246 (1891); H. Schinz, G. Gonbani, and V. Theus, *Helv. Chim. Acta*, **38**, 255 (1955).

rocene, and hydroquinone (0.039 g, 0.36 mmol) was obtained. The net amount of hydroquinone, obtained from the reduction of *p*-benzoquinone by ferrocene is 0.36 mmol.

The aqueous layer from the reaction in the presence of ferrocene was treated with tin(II) chloride acidified with hydrochloric acid to afford ferrocene (0.123 g, 0.66 mmol). The amount of ferrocene was assumed to be equal to that of ferricinium ion. The molar ratio of hydroquinone to ferricinium ion is calculated to be about 1: 1.8.

Reduction of Chloranil with Ferrocene. The same procedure as described above was applied to chloranil, which was found to be not reduced by aluminum chloride without ferrocene. The molar ratio of the obtained tetrachlorohydroquinone to ferricinium ion was about 1: 1.7.

Reduction of Enones and Related Compounds. Aluminum chloride (0.14 g, 1.08 mmol) and a substrate (0.54 mmol) were added into 30 m*l* of dry dichloromethane, and stirred for 5 min. Ferrocene (0.54 mmol) was then added. After stirring for 60 to 120 min, an aliquot was taken out from the reaction mixture, poured into ice water and the organic layer was checked for the reduction product by tlc, UV, or glpc (Table 1). In a control experiment, in which each substrate was treated by aluminum chloride without ferrocene under similar conditions, no reduction product was detected.

Stoichiometric Reduction of 1,2-Dibenzoylethylene by Ferrocene. Aluminum chloride (0.12 g), ferrocene (0.1 g), and 1,2-dibenzoylethylene (0.12 g) were added into 30 m*l* of dry dichloromethane and stirred for 90 min at room temperature. After the reaction mixture was poured into ice water, the dichloromethane layer was washed with water, dried and evaporated to dryness, and the residue was purified by silica-gel chromatography with benzene to afford 1,2-dibenzoylethane[14] (0.054 g). The aqueous layer gave ferrocene (0.078 g) when treated with tin(II) chloride.

Reaction of Ferrocene with Bromosuccinic Anhydride. Dabard[15] reported the preparation of β-ferrocenylcarbonylacrylic acid by the Friedel-Crafts reaction of ferrocene with bromosuccinic anhydride. We examined the same reaction in order to confirm the formation of the reduction product. Ferrocene (0.74 g, 4 mmol), bromosuccinic anhydride (0.72 g, 4 mmol), and aluminum chloride (1.16 g, 8.7 mmol) were added into 30 m*l* of dry dichloromethane, and stirred for 5 hr at room temperature. After methylation of the products with diazomethane and purification by silica-gel chromatography with benzene-ethyl acetate (6: 1), methyl β-ferrocenylcarbonylacrylate (84 mg) and methyl β-ferrocenylcarbonylpropionate (150 mg) were obtained. Boron trifluoride, iron(III) chloride, or titanium(IV) chloride instead of aluminum chloride were examined, but no reaction products were detected.

14) J. B. Conant and R. E. Lutz, *J. Amer. Chem. Soc.*, **45**, 1305 (1923).

15) R. Dabard and B. Gautheron, *Compt. rend., Acad. Sci., Paris*, **254**, 2014 (1962).

BULLETIN OF THE CHEMICAL SOCIETY OF JAPAN, VOL. 44, 3464—3465(1971)

Studies on Rydberg Orbitals. III. Calculation of the 4*s*, 4*p*, and 4*d* Orbitals of Carbon Atom

Haruo Hosoya[1)]

The Institute for Solid State Physics, The University of Tokyo, Roppongi, Minato-ku, Tokyo

(Received March 26, 1971)

Many different approaches to the calculation of Rydberg orbitals of small[2)] atoms and molecules have been undertaken.[3-7)] Apart from its mathematical interest, the information from these studies is useful not only for interpreting the Rydberg spectra but also for estimating, by perturbation calculations, the contribution of Rydberg orbitals of states in several problems such as electronic spectra of charge-transfer complexes and reaction mechanisms.[8)]

The author calculated the 3*s*, 3*p*, and 3*d* orbital wavefunctions and energies of Li(I)-F(I) and their isoelectronic series in their unhybridized Rydberg valence states with the lowest energy,[3)] *e.g.*, for

$$\mathrm{C(I)}\ 1s^2 2s^2 2p 3l,\ V_2\ (l=s, p, d) \tag{1}$$

In this paper the least-STO-basis wavefunctions and orbital energies of carbon 4*s*, 4*p*, and 4*d* orbitals of the valence state

$$\mathrm{C(I)}\ 1s^2 2s^2 2p 4l,\ V_2\ (l=s, p, d) \tag{2}$$

will be reported.

Since the calculation is an extension of the 3 l orbitals, only a brief account is given. The radial part of the least-STO-basis wavefunction 4 l, R_{4l}, has $2(4-l)$ parameters to be optimized (four C_{nl}'s and four μ_{nl}'s).

$$R_{4l} = \sum_{n=l+1}^{4} C_{nl} S(n, \mu_{nl}) \tag{3}$$

where $S(n,\mu_{nl})$ is a normalized Slater type orbital

$$S(n, \mu_{nl}) = (2\mu_{nl})^{n+1/2}\{(2n)!\}^{-1/2} r^{n-1} \exp(-\mu_{nl} r).$$

1) Present address: Department of Chemistry, Ochanomizu University, Bunkyo-ku, Tokyo.

2) By "small" we mean "relatively small but with more than two electrons."

3) H. Hosoya, *J. Chem. Phys.*, **48**, 1380 (1968). Part II of the present series of papers. Most attempts in this problem before 1967 are referred to in this paper.

4) A. U. Hazi and S. A. Rice, *ibid.*, **45**, 3004 (1966); *ibid.*, **48**, 495 (1968).

5) M. B. Robin, R. R. Hart, and N. A. Kuebler, *ibid.*, **44**, 1803 (1966) and related papers.

6) Y. Harada and J. N. Murrell, *Mol. Phys.*, **14**, 153 (1968).

7) T. F. Lin and A. B. F. Duncan, *J. Chem. Phys.*, **48**, 866 (1968); *ibid.*, **51**, 360 (1969).

8) H. Hosoya, "Study on trans-Addition Reaction in Terms of Molecular Orbital Deformation," presented at the "Symposium on Molecular Structures," Sendai, Japan (1963); H. Hosoya and S. Nagakura, This Bulletin, **37**, 249 (1964).

The function R_{4l} should be orthogonal to all the inner orbitals $R_{nl}(n=l+1,\cdots,3;\ 3-l$ conditions). The orbital exponents of the inner loops μ_{nl}'s$(n=l+1,\cdots,3;\ 3-l$ constants) were fixed as in the $3\,l$ calculation. Then by using the normalization condition we are left a single parameter μ_{4l}, which can be determined by optimization process as adopted in the $3\,l$ calculation. The wavefunctions of the $1s$, $2s$, and $2p$ orbitals forming the fixed core potential were taken from the table by Clementi[9] for the ion

$$\text{C(II)}\ \ 1s^2 2s^2 2p,\ V_1\ (=^2\text{P}) \qquad (4)$$

Table 1. Least-STO-basis rydberg orbitals[a] of C(I) $1s^2\ 2s^2\ 2p\ Nl$, V_2 $(N=3,4)$

Orbital Nl	C_{nl}	n	μ_{nl}	−Orbital energy (cm^{-1}) (Quantum defect) Calcd	Obsd
$4s$	−0.032215	1	5.7	12884	12694
	0.128426	2	1.8	(1.08)	(1.06)
	−0.692823	3	0.550		
	1.209454	4	0.328		
$4p$	0.111538	2	1.8	9672	10009
	−0.788364	3	0.465	(0.63)	(0.69)
	1.269707	4	0.297		
$4d$	−0.880863	3	0.340	6909	7031
	1.332636	4	0.230	(0.01)	(0.05)
$3s$[b]	0.055648	1	5.7	29644	30281
	−0.219630	2	1.8	(1.08)	(1.10)
	1.018750	3	0.550		
$3p$[b]	−0.167880	2	1.8	19900	20254
	1.007695	3	0.465	(0.65)	(0.67)
$3d$[b]	1.000000	3	0.340	12281	12402
				(0.01)	(0.03)

a) See Eq. (3). b) Ref. 3.

With these analytical expressions and potential the orbital energy of $4\,l$ electron in the valence state can be calculated for a given μ_{4l} value. Since in this case interaction between the Rydberg electron and core electrons is negligibly small compared to the orbital energy of the Rydberg electron, the orbital R_{4l} giving the lowest orbital energy is close enough to what would be obtained by the Hartree-Fock method. Table 1 gives the wavefunctions, orbital energies and quantum defects of the $4\,l$ orbitals obtained by this optimization procedure and also contains, for the sake of comparison, the least-STO-basis $3\,l$ orbitals.[3]

The observed energy values in Table 1 were obtained by taking the weighted means of all the term values in the Moore table.[10] Although the calculated energy of the $4s$ orbital surpasses the observed value due to several approximations taken, all the results are very close to the observed values. Accuracy of the calculation of Rydberg sates can be better checked with the quantum defects than with the absolute values of the orbital energies. Differences between the observed and calculated values for the $4\,l$ orbitals are as large as those for the $3\,l$ orbitals. As the quantum number of the Ryberg orbital increases, the error due to penetration into the core orbitals will decrease, although the consecutive orthogonalization procedure will pile up the error of the lower members to some extent. Thus this type of calculation of the Rydberg orbitals may be expected to be equally applied to the higher members and also to other systems.

All the calculations were performed in 1967 by using a Facom 202 computer at the Institute for Solid State Physics of the University of Tokyo. Thanks are due to Professor Saburo Nagakura for his interest and criticism.

9) E. Clementi, "Tables of Atomic Functions," IBM Co., San Jose, Calif. (1965).

10) C. E. Moore, "Atomic Energy Levels," U. S. Department of Commerce, Natl. Bur. Stand., Washington, D. C. (1949).

BULLETIN OF THE CHEMICAL SOCIETY OF JAPAN, VOL. 44, 3466—3467 (1971)

Solvent Effect on the Photochemical Oxidation of Phenothiazine with Oxygen

Teiki IWAOKA, Hiroshi KOKUBUN, and Masao KOIZUMI
Department of Chemistry, Faculty of Science, Tohoku University, Katahira, Sendai
(Received March 31, 1971)

The photochemical production of neutral radical in the aerated ethanol solution of phenothiazine (PTH) has been studied by means of steady light experiments, flash technique, and ESR measurements.[1] A reaction scheme proposed is 1) $PTH \xrightarrow{h\nu} PTH^*$, 2) $PTH^* \longrightarrow PTH^T$, 3) $PTH^T + O_2 \longrightarrow PTH\cdots O_2$, 4) $PTH\cdots O_2 \longrightarrow PT\cdot + HO_2\cdot$ in which $PTH\cdots O_2$ was presumed to be a certain type of C–T complex with a lifetime $\sim 6\times 10^{-3}$ sec.

Gilbert,[2] however, has pointed out that the spectrum of the ultimate product resembles that of phenothiazine-5-oxide (5-oxide) and that our transient intermediate might be a radical which gives rise to 5-oxide. In fact our ESR studies were made on 10^{-2}M solutions of PTH while the kinetic studies were chiefly for 10^{-4}M of PTH, so that it might be possible that under the former conditions the main product is radical and under the latter, 5-oxide.

In this note it is demonstrated that the same product, *i.e.* the neutral radical, is produced in the two cases. Further, the solvent effect of the overall reaction and also on the transient intermediate are investigated. The results also support our mechanism.

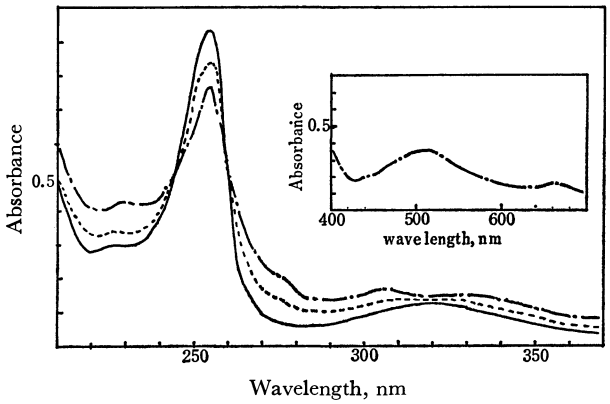

Fig. 1. Spectral change for the ethanol solution of phenothiazine in high concentration (2×10^{-2}M) upon UV illumination.
——; no irradiation ------; 2 hr irradiation
—·—; 12 hr irradiation

First it was reconfirmed that the irradiated solutions of PTH, 2×10^{-2}M in ethanol give an ESR spectrum characteristic of neutral radical which remains unaltered after being kept for more than two hours. When diluted 30 times, the irradiated solutions gave UV spectra as shown in Fig. 1. It is seen that the spectral change is similar to that for the dilute solution.[1] The spectrum in the visible region was taken without dilution.

1) T. Iwaoka, H. Kokubun, and M. Koizumi, This Bulletin, **44**, 341 (1971).
2) B. G. Gilbert, private communication.

Table 1. Quantum yields in various solvents

Solvent	DK	Φ
Acetonitrile	37.5	1.4×10^{-3}
Methanol	32.6	8.0×10^{-3}
Ethanol	24.3	6.0×10^{-3}
n-Butanol	17.8	8.0×10^{-3}
Ethyl ether	4.3	2.0×10^{-2}
Cyclohexane	2.0	2.4×10^{-2}

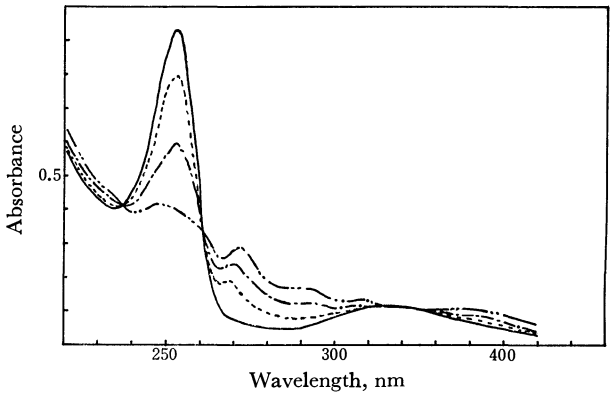

Fig. 2. Spectral change upon illumination (253.7 nm) of phenothiazine solution in the aerated cyclohexane; —— 0 sec, ---- 10 sec, —·— 35 sec, —··— 95 sec, [PTH] $=2.0\times 10^{-5}$M.

The existence of a peak at ~500 nm is consistent with the radical nature of the species.

Table 1 gives the quantum yields of the reaction in several solvents of different polarity. The spectral change is similar in all the solvents and there is no indication of a drastic change in the reaction scheme such as the formation of radical to that of 5-oxide. As an example, the spectral change in the cyclohexane solution is given in Fig. 2. Although ESR measurements were not made for all the cases, the ESR spectrum in the acetonitrile solution of 2×10^{-2}M PTH confirmed that the product is the neutral radical. From Table 1 it is evident that the values of Φ are one order larger in the weakly polar solvents (DK$<\sim$5) than in the polar solvents (DK$>$15); an approximate parallelism exists between Φ and DK.

This may be interpreted as follows. C–T complex is considered in general to be stabilized more or less by the interaction with the solvent molecules in the solvent sphere, and the more polar the solvent molecules, the greater the interaction is expected to be, resulting in a stronger solvation in more polar solvents. Thus the reorientation of molecules in the solvent sphere might be required for any reaction. In the present system it is likely that a more drastic reorientation is necessary for reaction $PTH\cdots O_2 \longrightarrow PT\cdot + HO_2$ than for the backward reaction $PTH\cdots O_2 \longrightarrow PTH + O_2$. It

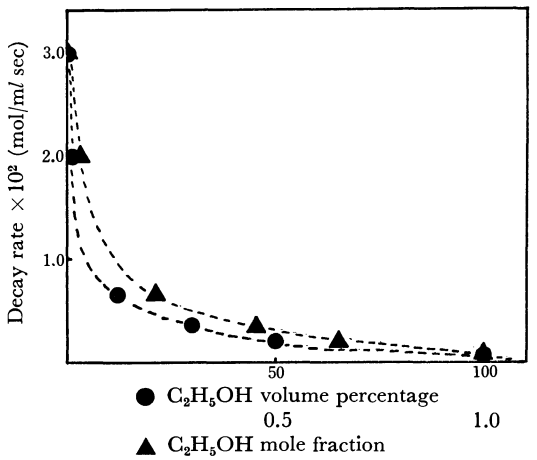

Fig. 3. The rate of disappearance of phenothiazine in the mixed solvent of cyclohexane and ethanol.
[PTH] $=2.0\times10^{-5}$M
light intensity, $I_0=8.7\times10^{-9}$M/sec.cm.

can be expected that the relative ease with which the former reaction occurs becomes smaller in the more polar solvent as was verified by experiment. The change of the decay constant and hence Φ in the mixed solvents of cyclohexane and ethanol given in Fig. 3 can be understood by the above reasoning. Thus a sharp drop in decay rate in the low concentration region of ethanol can be attributed to the selective solvation of the more polar ethanol molecules around PTH, which makes the formation of PT· more difficult.

Table 2 gives the peak positions of the transient spectrum which has been interpreted to be due to C–T complex[1] together with their decay constants. Although it is rather difficult to decide the peak positions accurately due to their low intensity and location at the foot of the original main absorption band, it can be said that in polar solvents (with DK larger than that of pyridine) the peaks are clearly observed around 385—395 nm, while in ethyl acetate, ethyl ether, and cyclohexane they are not observable. This might be due to the blue shift of the peak. The decay constants in these weakly polar solvents were determined from the rise of absorption at 290 nm. It was confirmed that in cases where ~390 nm peaks are observable, their decline and the rise at 290 nm agree well. The decay constants in nonpolar solvents are one order higher than those for polar solvents, indicating that the C–T complex is less stable in these solvents.

Table 2. Solvent effect on the nature of the PTH···O_2 complex

Solvent	DK	Absorption max (nm)	Decay const. (sec^{-1})
Acetonitrile	37.5	385	1.4×10^2
Methanol	32.6	375—385	
Ethanol	24.3	385	1.6×10^2
Acetone	20.7	385	1.5×10^2
n-Butanol	17.8	395	1.2×10^2
Pyridine	12.3	390	7.5×10
Ethyl acetate	6.1	<380	3.9×10^3
Ethyl ether	4.3	<380	$>10^3$
Cyclohexane	2.0	<380	$>10^3$

All the present results support the view that the intermediate is a C–T type complex which yields the neutral radical as a final product. Although simultaneous production of 5-oxide cannot be denied completely, its participation, if it does occur, can be said to be very small. If this were not the case, the spectral change having clear-cut isosbestic points in all the solvents could not be explained.

BULLETIN OF THE CHEMICAL SOCIETY OF JAPAN, VOL. 44, 3468—3469(1971)

β-Substituted α-Cyanoglycidic Esters and Their Reactions

Minoru IGARASHI,*,** Mamoru TAMURA,* and Masae YANAGI*

*Department of Chemistry, Faculty of Science, Ibaraki University, Mito, Ibaraki

**The Institute of Physical and Chemical Research, Wako, Saitama

(Received May 11, 1971)

The reaction of β-alkyl-α-cyanoacrylic esters with hydrogen peroxide was outlined previously as a useful method of synthesizing epoxy nitriles.[1] The applicability of the reaction has now been extended to give β-aryl-α-cyanoglycidic esters from α-cyanocinnamic esters.

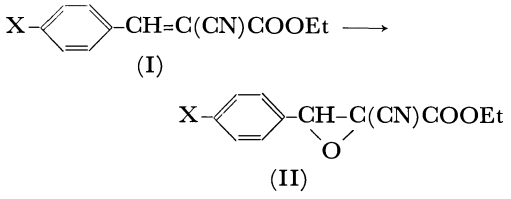

(I) (II)

X: H, Cl, CN, NO_2

Ethyl α-cyanocinnamates (I) were prepared by using the conditions developed by Cope.[2] The epoxidation of these unsaturated esters with hydrogen peroxide proceeded smoothly at 80—85°C without a catalyst. In an ethanolic solution, ethyl α-cyanocinnamate (I, X=H) gave the corresponding epoxy ester (II, X=H) in a 30% yield after 15 hr. Under similar conditions, ethyl α-cyano-β-(*p*-nitrophenyl)acrylate (I, $X=NO_2$) reacted more rapidly with hydrogen peroxide; the epoxy ester (II, $X=NO_2$) was formed in a 96% yield, with the complete consumption of the olefin, after only 1 hr.

The results shown in Table 1 reveal that the electron-withdrawing *p*-substituents accelerate the epoxidation of I, whereas the electron-releasing groups have the reverse effect.

The epoxy compounds obtained above gave unknown products upon hydrolysis with acid or alkali. By the reaction with aqueous ammonia, β-phenyl, β-(*p*-nitrophenyl), and β-(*p*-chlorophenyl)-α-cyanoglycidic esters (II; X=H, NO_2, Cl) gave the corresponding diol amides, accompanied by the epoxy ring opening, and the β-(*p*-cyanophenyl)-α-cyanoglycidic ester (II, X=CN) gave β-(*p*-cyanophenyl)-α-cyanoglycidamide.

Ethyl α-cyano-β,β-dimethylglycidate (III) had previously been synthesized from ethyl α-cyano-β-methylcrotonate.[1] The conversion of III to α-cyano-β,β-dimethylglycidic acid (IV) was effected by alcoholic alkaline hydrolysis. When IV was kept at 140—150°C in an oil bath, decarboxylation took place and the product was the expected 3-methyl-2-oxobutyronitrile (V), which gave the anilide, VI, upon reaction with aniline. The epoxy ester, III, gave the epoxy amide, VII, on treatment with aqueous ammonia.[3] Under similar conditions, the epoxy acid, IV, gave amino-hydroxy acid, VIII.

Experimental

Ethyl α-Cyanocinnamates (I). The unsaturated esters (I, X=H, Cl, CN, NO_2, CH_3, CH_3O, OH) were prepared according to the method of Cope.[2]

Epoxidation of I. *A)* A mixture of I (0.1 mol), 30% hydrogen peroxide (0.2 mol), and ethanol (30 m*l*) was refluxed at 80—85°C on a water bath. To the mixture, water (100 m*l*) was then added, after which it was extracted with chloroform. After the removal of the solvent, the residual oil was distilled to give the epoxy ester (X=H).

B) The reaction was carried out as above. The solution was cooled, and the resulting precipitate was collected by filtration. Recrystallization from ethanol gave the epoxy ester (X=Cl, CN, NO_2).

α-Cyano-β,β-dimethylglycidic Acid (IV). To a solution of ethyl α-cyano-β,β-dimethylglycidata (III)[1] in ethanol, ethanolic potassium hydroxide was added at room temperature. A white precipitate formed during the addition. After the mixture had stood overnight, it was separated by filtration,

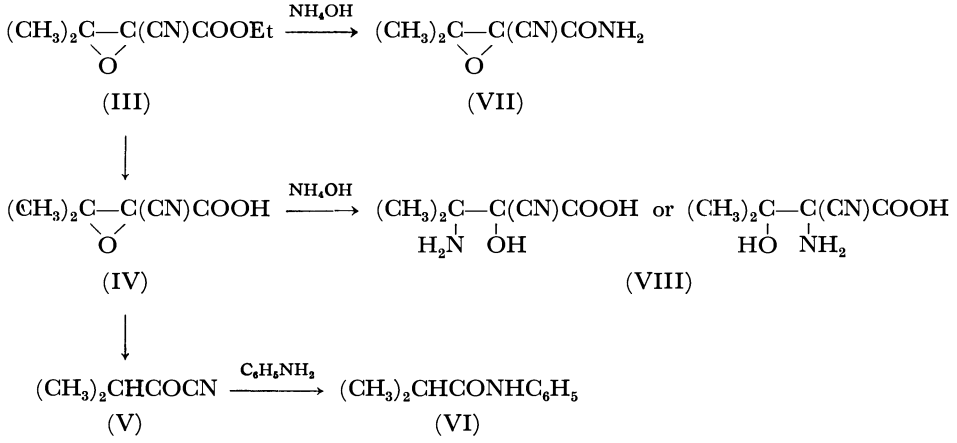

1) M. Igarashi, M. Akano, A. Fujimoto, and H. Midorikawa, This Bulletin, **43**, 2138 (1970).

2) A. C. Cope, *J. Amer. Chem. Soc.*, **59**, 2327 (1937).

3) G. B. Payne, *J. Org. Chem.*, **26**, 663 (1961).

Table 1. Preparation of ethyl β-aryl-α-cyanoglycidates (II) from ethyl α-cyanocinnamates (I)

X	Reaction[a] time, hr	Mp, °C (Bp, °C/mmHg)	Yield (%)	Formula	Calcd (%) C	Calcd (%) H	Calcd (%) N	Found (%) C	Found (%) H	Found (%) N
H	15	(130—133/3)	30	$C_{12}H_{11}O_3N$	66.35	5.10	6.45	65.93	5.31	6.02
NO_2	1	123—124	96	$C_{12}H_{10}O_5N_2$	54.96	3.84	10.68	54.91	3.83	10.65
CN	6	125—127	98	$C_{13}H_{10}O_3N_2$	64.46	4.16	11.57	64.29	4.17	11.57
Cl	15	70	81	$C_{12}H_{10}O_3NCl$	57.27	4.00	5.57	57.22	4.02	5.41
					(Cl, 14.08)			(Cl, 14.01)		
CH_3	15	recovery of I								
OCH_3	15	recovery of I								
OH	15	recovery of I								

a) Reaction temp., 80—85°C

washed with ethanol, and dried. The potassium salt was dissolved in water and neutralized with hydrochloric acid at 0—5°C. After the mixture had stood overnight in an ice box, the resulting precipitate was collected by filtration. The yield was 80%. Recrystallization from benzene gave colorless needles of IV; mp 107°C (decomp) (lit,[3] mp 106—108°C (decomp). Found: C, 50.71; H, 4.84; N, 9.85%).

Reaction of IV with Ammonia. Epoxy acid, IV (1.4 g), was dissolved in concentrated aqueous ammonia (6 ml) and allowed to stand overnight at room temperature. The solution was then concentrated under a vacuum to dryness. Recrystallization from ethanol afforded colorless needles; mp 193°C (decomp). The yield was 1.4 g (89%). The product had an empirical formula in agreement with that of 3-amino-2-cyano-2-hydroxy-3-methylbutyric acid or its isomer, 2-amino-2-cyano-3-hydroxy-3-methylbutyric acid (VIII).

Found: C, 45.95; H, 6.36; N, 18.06%. Calcd for $C_6H_{10}O_3N_2$: C, 45.56; H, 6.37; N, 17.71%.

Decarboxylation of IV. The epoxy acid, IV, was placed with anhydrous sodium sulfate or liquid paraffin in a Claisen flask and heated in an oil bath at 140—150°C until the decarboxylation had ceased. The product was then distilled directly from the reaction flask. Redistillation gave 3-methyl-2-oxobutyronitrile (V); bp 115—120°C (lit,[4] bp 116—118°C) (yield, 45%).

The reaction of a sample of the keto nitrile, V, with aniline gave isobutyranilide (VI); mp 105°C (lit,[5] mp 106—107°C. Found: C, 73.70; H, 8.81; N, 7.74%).

The authors wish to express their hearty thanks to Dr. Hiroshi Midorikawa for his kind advice and encouragement. Thanks are also due to Dr. Haruo Homma and his staff for the microanalyses.

4) W. Tschelinzeff and W. Schmidt, *Ber.*, **62**, 2210 (1929).
5) O. Diels and K. Pflaumer, *ibid.*, **48**, 223 (1915).

BULLETIN OF THE CHEMICAL SOCIETY OF JAPAN, VOL. 44, 3469—3470 (1971)

Copolymerization of Styrene and Liquid Sulfur Dioxide in the Presence of α-Toluenethiol, 1-Butanethiol, or Bromotrichloromethane

Masashi Iino,* Tateo Iguchi, and Niichiro Tokura

Department of Applied Chemistry, Faculty of Engineering, Osaka University, Suita-shi, Osaka

(Received May 12, 1971)

We have carried out copolymerization (telomerization) of styrene and liquid sulfur dioxide (liq. SO_2) in the presence of α-toluenethiol, 1-butanethiol, or bromotrichloromethane by using a radical initiator (AIBN) in order to study of the propagation mechanism in styrene polysulfone formation.

It is well known that aliphatic olefins, such as ethylene and propylene, always form alternate copolymers with SO_2 by a radical initiator. Kharasch and Friedlander obtained telomers (**1** and **2**), by copolymerizing octene-1 and SO_2 in the presence of bromotrichloromethane, but no telomer having $-SO_2Br$ group.[1] Styrene also copolymerizes with SO_2, but unlike aliphatic olefin forms copolymers having various compositions.[2]

$CCl_3CH_2CH(C_6H_{13})Br$

(**1**)

$CCl_3CH_2CH(C_6H_{13})S(O_2)CH_2CH(C_6H_{13})Br$

(**2**)

We have obtained the following telomers (**3**, **4**, and **5**) (the head to tail structure of the first styrene unit in product **5** could not be confirmed) in the case of α-toluenethiol.

$C_6H_5CH_2SCH_2CH_2(C_6H_5)$ (**3**)

$C_6H_5CH_2SStStH$ (**4**)

$C_6H_5CH_2SStS(O_2)StH$ (**5**)

(St=$-CH_2CH(C_6H_5)-$)

* Present address: Chemical Research Institute of Non-Aqueous Solutions, Tohoku University, Sendai.

1) M. S. Kharasch and H. N. Friedlander, *J. Org. Chem.*, **13**, 882 (1948).

2) M. Matsuda and M. Iino, *Macromolecules*, **2**, 216 (1969).

The propagation steps in this chain reaction are considered to be as follows.

$$C_6H_5CH_2S\cdot + CH_2{=}CH(C_6H_5) \longrightarrow \underset{(A)}{C_6H_5CH_2SSt\cdot} \quad (a)$$

$$A + CH_2{=}CH(C_6H_5) \longrightarrow \underset{(B)}{C_6H_5CH_2SStSt\cdot} \quad (b)$$

$$A + SO_2 \longrightarrow \underset{(C)}{C_6H_5CH_2SStSO_2\cdot} \quad (c)$$

$$C + CH_2{=}CH(C_6H_5) \longrightarrow \underset{(D)}{C_6H_5CH_2SStS(O_2)St\cdot} \quad (d)$$

$$A, B, D + C_6H_5CH_2SH \longrightarrow \text{Product, } \mathbf{3}, \mathbf{4}, \mathbf{5} + C_6H_5CH_2S\cdot \quad (e)$$

As in the case of octene-1 – SO_2 system,[1] the telomer with $-SO_2H$ group expected to be formed by termination of (C) radical was not obtained. We carried out copolymerization in the presence of 1-butanethiol or bromotrichloromethane. In these cases also the telomer having $-SO_2H$ group or $-SO_2Br$ (in the case of bromotrichloromethane) group was not obtained. This is probably due to the fact that either the sulfonyl radical is inert to hydrogen abstraction reaction from thiol (and bromine abstraction reaction from bromotrichloromethane) or the life time of sulfonyl radical is very short compared to that of styryl radical at this temperature (60°C).

Structures of products **3**, **4**, and **5** suggest that styrene polysulfone has head to tail structure.

The photo-decomposition of α-toluenethiol or 1-butanethiol in liq.SO_2 was also carried out and only disulfide which was formed by coupling reaction of thiyl radicals was obtained. Sulfone expected to be formed from the reaction of thiyl radical with SO_2 was not obtained.

Experimental

Materials. Styrene, azobisisobutyronitrile (AIBN) and liq. SO_2 were purified by the method described previously.[3] α-Toluenethiol and 1-butanethiol were purified by distillation. Bromotrichloromethane was prepared[4] from bromine and chloroform and distilled just before use.

Telomerization with α-Toluenethiol. 9.0 g (0.09 mol) of styrene, 10.8 g (0.09 mol) of α-toluenethiol, 29.7 g (0.46 mol) of liq. SO_2 and 0.5 g (0.003 mol) of AIBN, were charged in a reaction vessel,[3] and reacted at 60°C for 8 hr. Unreacted liq. SO_2, styrene and α-toluenethiol were then distilled off and the residue was chlomatographed on an alumina column. The liquid obtained by elution with petroleum ether was distilled under a reduced pressure. The distillate (161—164°C/1.5 mmHg) gave 11.8 g (58% yield based on styrene) of **3**, $C_6H_5CH_2SStH$ (St=$-CH_2CH(C_6H_5)-$). Found: C, 79.30; H, 7.04; S, 13.96%. Calcd for $C_{15}H_{16}S$: C, 78.90; H, 7.06; S, 14.04%. NMR (CCl_4): τ, 2.9—3.1 (10H, phenyl), 6.5 (2H, $-CH_2S-$), 7.1—7.7 (4H, $-CH_2CH_2(C_6H_5)$). The residue of the distillation gave about 1 g (6%) of **4**, $C_6H_5CH_2SStStH$, identified as sulfoxide and sulfone by oxidation using $KMnO_4$ in $CHCl_3$. Sulfoxide ($C_6H_5CH_2S(O)$-StStH). Found: C, 78.55; H, 6.89; S, 9.51%. Calcd for $C_{23}H_{24}SO$: C, 79.27; H, 6.94; S, 9.20%. Mp 122—125°C (recrystallized from methanol), IR 1020 cm^{-1} (SO). Sulfone ($C_6H_5CH_2S(O_2)StStH$); mp 102—103°C (recrystallized from methanol), lit,[5] 98—99.5°C, IR 1300, 1120 cm^{-1} (SO_2). Elution with ether gave 0.8 g (4%) of (5), $C_6H_5CH_2SStS$-$(O_2)StH$. Found: C, 69.55; H, 6.03; S, 15.98%; mol wt (mass spectrum) 396. Calcd for $C_{23}H_{24}S_2O_2$: C, 69.66; H, 6.10; S, 16.17%; mol wt 396.6. mp 116.5—118°C, NMR ($CDCl_3$): τ, 2.4—3.1 (m, 15H, phenyl), 5.9—6.1 (quar, 1H, $-CH-$), 6.5 (s, 2H, $C_6H_5C\underline{H}_2-$), 6.4—7.0 (2H, $-S(O_2)CH_2-$), 7.0—7.3 (m, 4H, $-SCH_2-$, $-C\underline{H}_2(C_6H_5)$), showed no methyl group expected from head to head structure of terminal styrene unit.

Telomerization with 1-Butanethiol. 9.0 g (0.09 mol) of styrene 8.3 g (0.1 mol) of 1-butanethiol, 28.7 g (0.45 mol) of liq. SO_2 and 0.5 g (0.003 mol) of AIBN were reacted at 60°C for 30 hr. By the same procedure as in the case of α-toluenethiol, C_4H_9SStH, (7.8 g, 45%), $C_4H_9SStStH$ (about 0.5 g, 4%) and $C_4H_9SStS(O_2)StH$(0.3 g, 2%) were obtained. C_4-H_9SStH. Found: C, 74.41; H, 9.56%. Calcd for $C_{12}H_{18}S$: C, 74.19; H, 9.34%. Bp 88—89°C/<1 mmHg, lit,[6] 96—97°C/1 mmHg. $C_4H_9SStStH$. Speculated from its boiling point (>100°C/<1 mmHg, lit[6] 170°C/1 mmHg), IR spectrum (almost the same as that of C_4H_9SStH) and refractive index (n_D^{25}, 1.5524, lit,[6] 1.5539). $C_4H_9SStS(O_2)StH$. Found: C, 66.05; H, 7.24%. Calcd for $C_{20}H_{26}S_2O_2$: C, 66.26; H, 7.23%. IR 1310, 1130 cm^{-1} (SO_2).

In the reactions using 18 g (0.18 mol) and 36 g (0.36 mol) of styrene, we obtained 0.2 g and 2 g, respectively, of styrene polysulfone other than the products described above.

Telomerization with Bromotrichloromethane. 36.0 g (0.36 mol) of styrene, 40 g (0.2 mol) of CCl_3Br, 168 g (2.6 mol) of liq. SO_2 and 4 g (0.02 mol) of AIBN were reacted at 60°C for 42 hr. By the same procedure as described above, about 20 g (18%) of CCl_3StBr was obtained. We carried out the reaction with various feed compositions, but could not obtain the telomer having $-SO_2Br$ group. CCl_3StBr. Found: C, 35.94; H, 2.50%. Calcd for $C_9H_8BrCl_3$: C, 35.74; H, 2.67%. Mp 51.5°C, lit,[7] 54—55°C.

Photo-decomposition of α-Toluenethiol in Liq. SO_2. A mixture of 10.8 g (0.09 mol) of α-toluenethiol and 28.6 g (0.45 mol) of liq. SO_2, was charged in a quartz vessel, and irradiated with a 300 W mercury lamp (high-pressure) at room temperature for 24 hr. Unreacted SO_2 and α-toluenethiol were distilled off. The residue gave 4.5 g (41% yield based on α-toluenethiol) of $(C_6H_5CH_2S)_2$, identified from IR spectrum of an authentic sample. Only $(C_4H_9S)_2$ was obtained in the case of 1-butanethiol.

3) N. Tokura and M. Matsuda, Kogyo Kagaku Zasshi, **64**, 501 (1961).
4) L. I. Zakharkin, *Chem. Abstr.*, **48**, 547a (1954).
5) H. Miyoshi and R. Oda, *Kogyo Kagaku Zasshi*, **59**, 224 (1956).
6) K. Yamagishi, *Nippon Kagaku Zasshi*, **80**, 1361 (1959).
7) M. S. Kharasch, O. Reinmuth, and W. H. Urry, *J. Amer. Chem. Soc.*, **69**, 1105 (1947).

BULLETIN OF THE CHEMICAL SOCIETY OF JAPAN, VOL. 44, 3471—3472 (1971)

The Reaction of Iodine Azide with Diphenylfulvene

Tadashi SASAKI, Katsumaro MINAMOTO, and Ken USAMI

Institute of Applied Organic Chemistry, Faculty of Engineering, Nagoya University, Furo-cho, Chikusa-ku, Nagoya

(Received May 28, 1971)

Fulvenes, structural isomers of benzenoids, have attracted the interest of organic chemists, especially because of the dual characters between conjugated olefins and aromatics. They give Diels-Alder Adducts in their 1,4-positions[1] as well as substitution products with bromine.[2] We were interested in the introduction of nitrogen atoms into the fulvene skeleton to examine possible modifications of the original chemical features.

Fulvenes might be converted into azides by Hassner's method using iodine azide.[3] Application of this method seems to be of interest since Hassner's documents are limited to mono-olefinic compounds except for 1,3-cyclooctadiene.[3] This paper deals with the elucidation of the structures of the reaction products from diphenylfulvene (**1**) and iodine azide.

The reaction of iodine azide with **1**[4] gave an oily mixture consisting of two diastereoisomeric diazido racemates, complete purification of which was unsuccessful. Treatment of the mixture with two equivalents of dimethyl acetylenedicarboxylate (DAC) gave two crystalline racemates (**3a—b**). The yields and physical constants of the racemates are summarized in Table 1, and their UV spectra given in Fig. 1. Their IR spectra are quite similar except slight differences in the finger print regions. Thus, the spectral similarities confirmed their skeletal and functional identity. Unequivocal assignments of the NMR signals in the region of τ 3.1—3.9 (2 olefinic protons and 2 protons on C_1 and C_2) were impossible due to their ambiguous resolutions.

TABLE 1. YIELDS AND PHYSICAL CONSTANTS OF **3a—b**

	3a	**3b**
Mp (°C)	165—167	162—164
Yield (%)	40	30
ν_{max}^{KBr} cm^{-1}	1730	1730
λ_{max}^{EtOH} nm (log ε)	288 (4.25)	284 (4.15)
	224 (4.35)	222 (4.26)
NMR ($CDCl_3$) τ	2.6—3.1 (10H, Ph)	2.6—3.1 (10H, Ph)
m=multiplet	3.1—3.2 (1H, m)	3.1—3.3 (1H, m)
s=singlet	3.3—3.5 (2H, m)	3.3—3.5 (2H, m)
Ph=phenyl	3.7—3.9 (1H, m)	3.5—3.7 (1H, m)
Me=methyl	6.08 (3H, s, Me)	6.1 (3H, s, Me)
	6.15 (3H, s, Me)	6.15 (3H, s, Me)
	6.26 (3H, s, Me)	6.18 (3H, s, Me)
	6.29 (3H, s, Me)	6.23 (3H, s, Me)

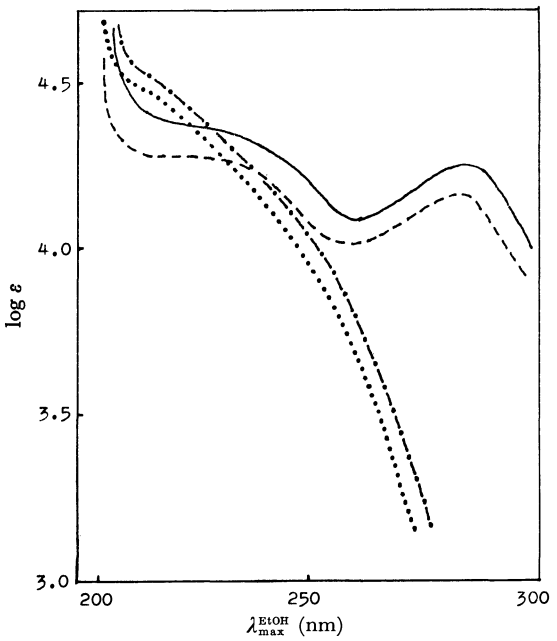

Fig. 1. UV Spectra of **3a** (——), **3b** (----), **4** (-·-·-), and **5** (·····) in EtOH.

Thus, the initial products should be diazido compounds with the same skeleton and π-conjugation system.

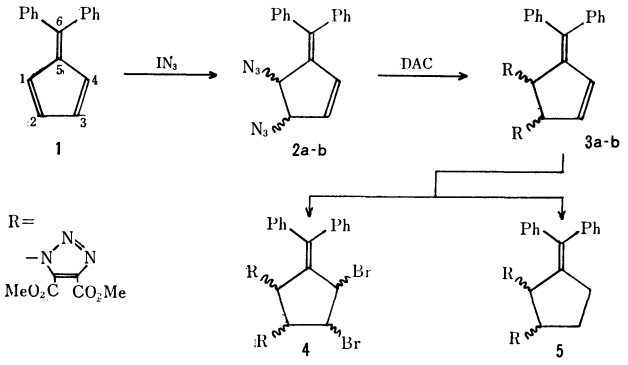

Attempts were made to saturate a double bond in **3a—b** by hydrogenation and bromination for the exclusion of another possible 1,4-adduct (**2'**). Thus, the dibromo compound (**4**) and tetrahydrofulvene (**5**) were obtained from **3b**, whereas the corresponding reaction products from **3b** were intractable. The UV spectra

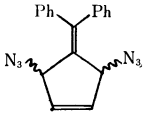

2'

1) For a review on fulvenes, see P. Yates, "Advances in Alicyclic Chemistry," Academic Press, New York-London, **2**, 136 (1968).

2) J. H. Day and C. Pidwerbesky, *J. Org. Chem.*, **20**, 89 (1955).

3) A. Hassner, *Accounts Chem. Res.*, **4**, 9 (1971) and the literatures cited therein.

4) J. L. Kice and F. M. Parham, *J. Amer. Chem. Soc.*, **80**, 3792 (1958).

of **4** and **5** (Fig. 1.) show complete disappearance of the absorption at 288 nm of **3a**, leaving the overlap of absorptions due to the triazole rings and the diphenylethylene group as inflections. It is well-known that 1,1-diphenylethylene absorbs at 250 nm ($\log \varepsilon$ 4.0)[5] and that the extention of a π-conjugation system by a double bond usually causes a bathochromic shift of approximately 30 nm. The absorption at 288 nm coincides with the expected value 280 nm, even assuming some steric restrictions between the diphenylethylene group and one of the triazole rings in **3**. It is anticipated that the saturation of an isolated double bond as in **2** would cause no essential change of a UV spectrum related to a major chromophore as diphenylethylene in **2'**.

It is thus concluded that **3a**—**b** are *cis* and *trans* racemates of 1,2-bis[4,5-bis(methoxycarbonyl)-1*H*-1,2,3-triazolyl]-1,2-dihydro-6,6-diphenylfulvene and **2a**—**b** should be the corresponding steric isomers of the 1,2-diazido compounds. Configurational ascription for each compound is difficult at the present stage.

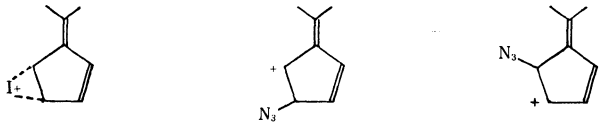

6 7a 7b

Addition of iodine azide to olefins generally results in *trans* addition through the cationic intermediate like **6**.[3] The fact that any addition product having both I and N_3 groups, could not be detected under the present reactions would be rationalized by the marked reaonance stabilization of the intermediate carbonium ion (**7a** or/and **7b**), formed by elimination of I^-, due to the extended conjugation which would involve the polar azide group itself. Thus, the attack of the nucleophilic azide ion on **7a** or/and **7b**, most probably in an S_N1 manner, would yield only one set of *cis* and *trans* isomes (**2a**—**b**) in roughly similar yields. This is in good accordance with our results. At present, it is difficult to say which of **7a** and **7b** was actual or major intermediate.

Experimental

All the melting points are uncorrected. The electronic spectra were measured on a JASCO Model ORD/UV-5 spectrophotometer and the infrared spectra on a JASCO Model IR-S spectrophotometer. The NMR spectra were recorded with a JNM C-60HL NMR spectrometer, TMS being used as an internal standard.

1,2-Diazido-1,2-dihydro-6,6-diphenylfulvene (2a—b). To a stirred suspension of sodium azide (3.0 g, 46 mmol) in dry acetonitrile (20 m*l*) in a methanol-ice bath was slowly added iodine monochloride (3.7 g, 23 mmol) for over 5 min. A solution of diphenylfulvene (**1**) (4.6 g, 20 mmol) in benzene (10 m*l*) was added. The mixture was allowed to attain room temperature and was stirred for additional 24 hr. The red-brown slurry was poured into water (50 m*l*) and the mixture was extracted with ether (3×50 m*l*). The combined ethereal solutions were washed with 5% sodium thiosulfate sloution. It turned out that the dark color of the ethereal layer could not be completely removed even by repeated washing. The ethereal layer was then washed with water, dried over magnesium sulfate and evaporated *in vacuo* to a dark-brown paste, which was chromatographed on a silica gel column (40×2 cm) using benzene as an eluant. A small amount of the starting material was recovered from the first few fractions. TLC with the use of silica gel and benzene showed one major spot with a couple of slower-moving traces. After removal of the benzene *in vacuo*, the residue gave monoclinic needles on standing at −30°C. The crude yield was 80%. IR(KBr): 2120 cm^{-1} (ν N_3). This product was used as such for the next synthesis to evade possible danger of explosion during the course of recrystallization.

1,2-Bis[4,5-bis(methoxycarbonyl)-1H-1,2,3-triazolyl]-1,2-dihydro-6,6-diphenylfulvene (3a—b). To a solution of the diazido mixture (**2a**—**b**) (1 g) in benzene (20 m*l*) was added DAC (1 g, 7 mmol), and the mixture was heated to reflux overnight. After the solvent was evaporated off, the residual paste was applied on a silica gel column (40×2 cm). Elution with benzene removed the excess DAC and unreacted starting material. The column was then eluted with 0.7% ethanol in benzene. The faster-moving fractions gave a pale yellow powder (**3a**) of mp 165—167°C from a mixture of chloroform and methanol. The slower-moving fractions also gave a pale yellow powder of mp 162—164°C from the same solvent.

Found for **3a**: C, 60.32; H, 4.53; N, 13.93%. Found for **3b**: C, 60.12; H, 4.63; N, 13.93%. Calcd for $C_{30}H_{26}N_6O_8$: C, 60.19; H, 4.38; N, 14.04%.

1,2-Bis[4,5-bis(methoxycarbonyl)-1H-1,2,3-triazolyl]-1,2-dihydro-3,4-dibromo-6,6-diphenylfulvene (4). To a stirred cold solution of **3a** (0.5 g, 0.84 mmol) in chloroform (8 m*l*) was added bromine (160 mg, 1 mmol) and the mixture was allowed to stand at room temperature for 2 hr. The dark-brown mixture was evaporated *in vacuo* to give **4** (0.44 g, 70%) as colorless powder, mp 205—207°C (from chloroform-acetone). Beilstein test: positive. IR(KBr): 1720 cm^{-1} (ν C=O). UV spectrum is given in Fig. 1. NMR($CDCl_3$) τ: 2.4—3.0 (m, 10H, 2Ph), 3.0—3.3 (m, 2H, 1- and 2-protons), 4.1—4.4 (m, 2H, 3- and 4-protons), 6.05 (s, 3H, Me), 6.1 (s, 3H, Me), 6.25 (s, 3H, Me), and 6.45 (s, 3H, Me).

Found: C, 47.30; H, 3.54; N, 11.11%. Calcd for $C_{30}H_{26}N_6O_8Br_2$: C, 47.51; H, 3.46; N, 11.08%.

1,2-Bis[4,5-bis(methoxycarbonyl)-1H-1,2,3-triazolyl]-1,2,3,4-tetrahydro-6,6-diphenylfulvene (5). **3a** (0.5 g, 0.84 mmol) was dissolved in acetone (10 m*l*) and hydrogenated in the presence of Pd–C at atmospheric pressure for 5 hr. After standing overnight in hydrogen, the mixture was separated from the catalyst and evaporated *in vacuo* to give **5** as colorless granules, mp 165—167°C (from methanol). Yield: 0.33 g (65%). IR(KBr): 1720 cm^{-1} (ν C=O). For the UV spectrum, see Fig. 1. NMR($CDCl_3$) τ: 2.7—3.2 (m, 10H, 2Ph), 4.0—4.5 (m, 2H, 1- and 2-protons), 6.0—6.2 (broad singlet, 6H, 2Me), 6.25—6.6 (m, 6H, 2Me), 7.2—7.7 (m, 2H), and 7.8—8.2 (m, 2H).

Found: C, 59.48; H, 4.74; N, 13.83%. Calcd for $C_{30}H_{28}N_6O_8$: C, 59.99; H, 4.70; N, 13.99%.

5) R. E. Lyle, E. J. DeWitt, and I. C. Pattison, *J. Amer. Chem. Soc.*, **78**, 61 (1956).

BULLETIN OF THE CHEMICAL SOCIETY OF JAPAN, VOL. 44, 3473—3474(1971)

ESR Studies of the Sulfite Radical Anion

Toshihiko OZAWA, Morio SETAKA, and Takao KWAN
Faculty of Pharmaceutical Sciences, The University of Tokyo, Bunkyo-ku, Tokyo
(Received June 1, 1971)

Rapid-mixing flow techniques coupled with ESR measurements have so far enabled us to identify several unstable radicals formed during chemical reactions.[1-4]

Further work has now been carried out on the oxidation of bisulfite ions in connection with the biologically significant reaction involving sulfite - bisulfite ions.[5] As a result, we found that the sulfite radical anion, SO_3^-, is formed during the reaction of sodium bisulfite with Ce^{4+}. Since the ESR of the sulfite radical anion in aqueous solutions has not yet been reported, we wish briefly to communicate the ESR of the radical anion and its chemical characteristics.

Experimental

The ESR measurements were carried out on a JEOL-P-10 spectrometer (X-band) with 100 kHz field modulation, in conjunction with a JEOL mixer. This apparatus enabled us to detect radicals formed in the reaction time of the order of 5—100 msec. The spectra were recorded at room temperature. The *g*-values were determined relative to DPPH, for which $g=2.0036$. The concentrations of the spins were approximated to the peak-to-peak height of a given signal. Commercial samples of $Ce(NO_3)_4 \cdot 2\ NH_4NO_3$ and $NaHSO_3$ were used without further purification. Each aqueous solution was acidified by sulfuric acid at pH=1. The concentration was 0.01 M for the cerium salt and 0.1 M for the bisulfite in most experiments. Details of the experimental procedure were previously described.[2]

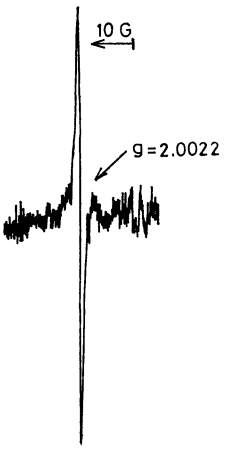

Fig. 1. ESR spectrum of the radical species (SO_3^-) formed during the reaction of Ce^{4+} with $NaHSO_3$ in aqueous solutions.

Results and Discussion

An ESR spectrum characterized by a single line with a nearly isotropic *g*-value was observed, as is shown in Fig. 1, when two solutions, containing Ce^{4+} and HSO_3^- respectively, were subjected to a rapid-mixing flow passing through the ESR cavity. The spectrum was well detectable for reaction times from several to about 100 msec without changing the *g* value (2.0022) and the linewidth of about 2.4 gauss. In view of the strong one-electron oxidizing capability of Ce^{4+}, the sulfite radical anion, SO_3^-, must be formed according to the reaction:

$$HSO_3^- + Ce^{4+} \longrightarrow SO_3^- + H^+ + Ce^{3+} \qquad (1)$$

While no ESR has been reported hitherto with respect to the SO_3^- ion in aqueous solutions, its formation has already been reported for γ-irradiated K_2SO_4 crystals,[6] where an axially symmetric resonance line at the *g*-value of 2.0023—2.0033 has been attributed to the SO_3^- radical anion. The irradiated K_2SO_4 sample gave rise to another spectrum charaterized by a highly anisotropic *g*-tensor (2.0486, 2.0082, 2.0037), which was attributed to the SO_4^- radical anion. The average *g*-value of the SO_4^- is calculated therefrom to be 2.0235, which is much greater than the value observed above. Thus, the spectrum of Fig. 1 can probably be assigned to SO_3^-. This supposition was confirmed by the following observation.

It is well known that pyrosulfite is hydrolyzed according to the reaction:

$$S_2O_5^{2-} + H_2O \longrightarrow 2HSO_3^- \qquad (2)$$

The mixture of Ce^{4+} and pyrosulfite may, then, be expected to produce the SO_3^- radical anion. Experiments have in fact shown that the same signal as that of Fig. 1 was obtained when pyrosulfate and Ce^{4+} were subjected to rapid-mixing flow reactions.

Apart from the ESR measurements, the sulfate radical anion, SO_4^-, is a well established intermediate in the thermal and photochemical decomposition of inorganic persulfates. The one-electron reduction of persulfate ions by Fe^{2+} or Ti^{3+} is known also to produce the radical anion according to:

$$S_2O_8^{2-} + Fe^{2+} \longrightarrow SO_4^{2-} + SO_4^- + Fe^{3+} \qquad (3)$$

Unfortunately, no ESR signal ascribable to the SO_4^- radical anion has been reported in aqueous solutions. However, in the presence of olefinic compounds, the rapid-mixing flow technique has provided ESR evidence for the formation of SO_4^- adducts,[7] suggesting that the

1) M. Setaka, T. Ozawa, Y. Kirino, and T. Kwan, *J. Catal.*, **15**, 209 (1969).
2) T. Ozawa, Y. Kirino, M. Setaka, and T. Kwan, *Nippon Kagaku Zasshi*, **92**, 304 (1971).
3) Y. Kirino and T. Kwan, *Chem. Pharm. Bull.* (Tokyo), **19**, 718 (1971).
4) Y. Kirino and T. Kwan, *ibid.*, **19**, 831 (1971).
5) H. Hayatsu, *J. Amer. Chem. Soc.*, **91**, 5693 (1969).
6) V. V. Gromov and J. R. Morton, *Can. J. Chem.*, **44**, 527 (1966).
7) R. O. C. Norman, P. M. Storey, and P. R. West, *J. Chem. Soc., B*, **1970**, 1087.

SO_4^- radical anion was present, but was very short-lived.

The presence of the SO_2^- radical anion in aqueous solutions of sodium dithionite has also been reported;[8,9] the radical is formed by the monomerization of the dithionite ion:

$$S_2O_4^{2-} \longrightarrow 2SO_2^- \quad (4)$$

We have found an isotropic ESR line for the aqueous solution of sodium dithionite at the g-value of 2.0055; this is in accordance with a recent report.[10] A typical ESR spectrum of SO_2^- is shown in Fig. 2. The signal was fairly stable; it remained for reaction times exceeding one hour at room temperature.

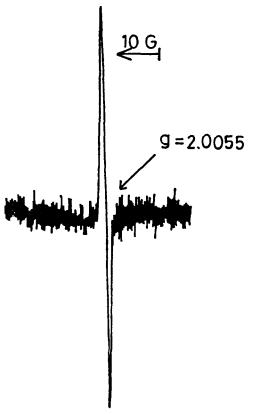

Fig. 2. ESR spectrum of the radical species (SO_2^-) formed in an aqueous solution containing $Na_2S_2O_4$.

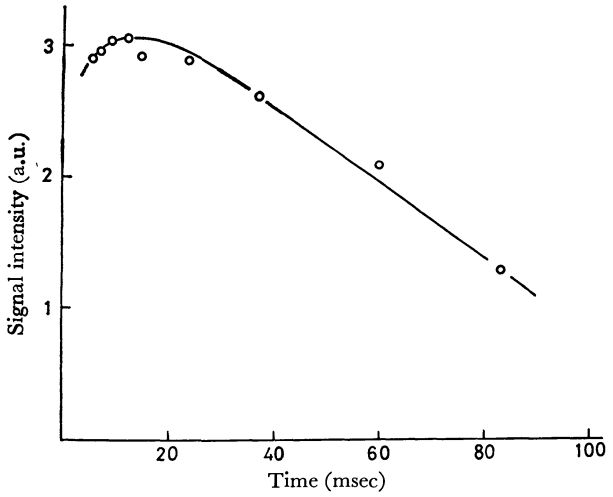

Fig. 3. The signal intensity of SO_3^- *vs.* reaction time relationship.

Figure 3 shows the spin concentrations of SO_3^- against the reaction times. As is shown in Fig. 3, the concentration of SO_3^- reached a maximum at about 10 msec after mixing and gradually decreased thereafter. It was detectable for 100 msec. The stability of the radical anion was, then, distinguishable from that of SO_2^- or SO_4^-. The difference in the thermal stability for SO_3^- and SO_4^- has been noted also in γ-irradiated K_2SO_4 crystals;[6] accordingly, the SO_4^- radical was much less stable than the SO_3^-, which is consistent with the present observation in aqueous solutions. Consequently, the possibility that the spectrum of Fig. 1 could be due to either SO_2^- or SO_4^- can be excluded on the basis of the argument of their stability.

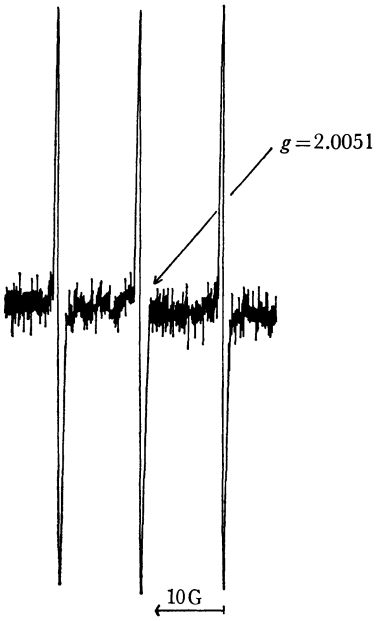

Fig. 4. ESR spectrum of the radical species ($ON(SO_3^-)_2$).

To compare the chemical reactivity of SO_3^- with that of SO_4^-,[7] we further investigated the reaction of SO_3^- with inorganic and organic additives by utilizing the rapid-mixing technique. Some results will be mentioned below. The SO_3^- signal appeared and was stable enough when an ethanol-containing bisulfite was mixed with the Ce^{4+} solution, while the signal was absent when allyl alcohol was substituted for ethanol. These results suggest that the SO_3^- reacts only with olefinic compounds, perhaps forming SO_3^- adducts.

A triplet signal was obtained (Fig. 4) when a $NaNO_2$-containing bisulfite was allowed to react with Ce^{4+}. The signal was exactly the same as that obtainable from potassium nitrosodisulfonate, the Fremy salt ($\cdot O\text{–}N(SO_3K)_2$). This radical may be formed by the one-electron oxidation of the hydroxylamine sulfonate ion, $HON(SO_3^-)_2$, by Ce^{4+} (6). The latter can be formed by the reaction of NO_2^- with HSO_3^- according to (5):[11]

$$NO_2^- + 2HSO_3^- \longrightarrow HON(SO_3^-)_2 + OH^- \quad (5)$$

$$HON(SO_3^-)_2 + Ce^{4+} \longrightarrow ON(SO_3^-)_2 + H^+ + Ce^{3+} \quad (6)$$

The above findings suggest that the SO_3^- radical anion is less reactive than the SO_4^-, the reactivity of which has already been worked out by Norman *et al.*[7] The problem of the relative reactivity of the SO_2^-, SO_3^-, and SO_4^- radical anions awaits further investigations.

8) A. I. Soklakov, *Zh. Strukt. Khim.*, **3**, 559 (1962).

9) S. Lynn, R. G. Rinker, and W. H. Corcoran, *J. Phys. Chem.*, **68**, 2363 (1964).

10) A. Reuveni, Z. Lua, and B. L. Silver, *J. Chem. Phys.*, **53**, 4619 (1970).

11) P. A. Wehrli and F. L. Pigott, *Inorg. Chem.*, **9**, 2619 (1970).

BULLETIN OF THE CHEMICAL SOCIETY OF JAPAN, VOL. 44, 3475—3476(1971)

Aroyl Arenesulfonyl Peroxides. II.[1] Phenylation with Phenyl Radical Generated from Benzoyl *p*-Toluenesulfonyl Peroxide

Ryuki HISADA, Nobumasa KAMIGATA, Hiroshi MINATO, and Michio KOBAYASHI
Department of Chemistry, Tokyo Metropolitan University, Fukazawa, Setagaya-ku, Tokyo

(Received June 10, 1971)

We previously reported that spontaneous decomposition of benzoyl *p*-toluenesulfonyl peroxide (BPT) in benzene gave phenyl *p*-toluenesulfonyl carbonate (yield, 48 mol%), *p*-toluenesulfonic acid (33 mol%), benzoic acid (23 mol%), and biphenyl (1 mol%), and that in the presence of magnesium oxide 44 mol% of biphenyl and 22 mol% of phenyl *p*-toluenesulfonyl carbonate together with *p*-toluenesulfonic acid (57 mol%) and benzoic acid (10 mol%) were produced.[1] It was suggested that the biphenyl obtained was produced by the attack of phenyl radical on benzene. In order to ascertain whether or not the intermediate is phenyl radical, the orientation and the partial rate factors for phenylation with BTP in substituted benzenes were determined. The results will be described in this paper.

Experimental

Materials. Purification of benzene and substituted benzenes[2] and preparations of BTP[1] and the authentic samples of substituted biphenyls[2] have been described previously.

Magnesium oxide was used after heating in a crusible for 2 hr.

Decomposition of BTP. Into a mixture of 300 mmol each of a substituted benzene and benzene (or chlorobenzene), 5 mmol of BTP and 50 mmol of magnesium oxide were added at 10°C. After nitrogen gas was bubbled through the mixture for 20 min, the reaction flask was placed and stirred in a constant-temperature bath at 45.0°C. After 15 hr the reaction mixture was washed with a 5% sodium hydroxide solution to remove acidic products, washed with water, and dried over anhydrous magnesium sulfate. The amounts of the substituted biphenyl isomers were determined gas-chromatographically by the method described previously.[2]

Results and Discussion

The spontaneous decomposition of BTP in benzene was not a simple homolysis, and acid-catalyzed rearrangement to phenyl *p*-toluenesulfonyl carbonate always took place. A detailed study on the mechanism of this rearrangement is being carried out, and the results will be published soon.

When magnesium oxide was suspended in benzene for adsorption of *p*-toluenesulfonic acid produced, the rearrangement was suppressed considerably. In order to check the effect of magnesium oxide on yields of products, decomposition of benzoyl peroxide in benzene

Table 1. Orientations and partial rate factors for phenylation at 45.0°C

PhX	Orientation (%)			Partial rate factors			
	o-	*m*-	*p*-	k_o/k	k_m/k	k_p/k	k_x/k_H
PhOMe	62.3	26.7	11.0	4.75	2.03	1.65	2.53
PhEt	58.0	28.9	13.1	2.28	1.14	1.03	1.31
PhCl	64.6	19.9	15.5	3.92	1.21	1.88	2.02
$PhNO_2$	64.6	9.5	25.9	10.8	1.58	8.66	5.58

a) These data are the average values of two experiments. Errors for orientations are usually 3% except that for *m*-methoxy (6%). Errors for partial rate factors are usually 2% except those for *m*-methoxy (7%) and *p*-methoxy (9%).

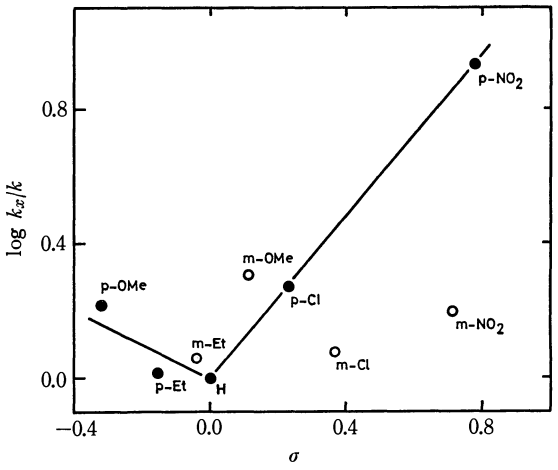

Fig. 1. Hammett's plots for the phenylation at 45.0°C. ●: log k_p/k, ○: log k_m/k $\rho_p = -0.78$ (left half) and $+1.20$ (right half).

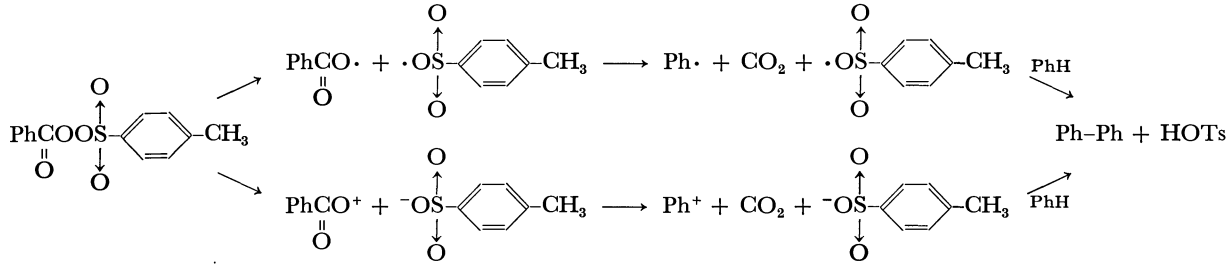

1) For the previous paper in this series, see R. Hisada, H. Minato, and M. Kobayashi, This Bulletin, **44**, 2541 (1971).

2) M. Kobayashi, H. Minato, E. Yamada, and N. Kobori, *ibid.*, **43**, 215 (1970).

in the presence and in the absence of magnesium oxide was studied. Yields of biphenyl, benzoic acid, and phenyl benzoate were the same within experimental error.

The main products of the decomposition of BTP in benzene in the presence of magnesium oxide were biphenyl and *p*-toluenesulfonic acid in addition to the rearranged product, phenyl *p*-toluenesulfonyl carbonate.[1] Biphenyl and *p*-toluenesulfonic acid could arise *via* either phenyl radical or phenyl cation according to the scheme shown above.

The orientations and the partial rate factors for phenylation of substituted benzenes are shown in Table 1. Figure 1 is the Hammett plots of the partial rate factors of *meta* and *para* positions. V-shaped straight lines could be drawn for *para* positions with $\rho=-0.78$ and $+1.20$. Similar results were obtained by the phenylation with phenyl radical produced from benzoyl peroxide ($\rho_p=-1.42$ and $+1.15$ at 80°C)[3] or *N*-nitrosoacetanilide ($\rho_p=-0.39$ and $+1.27$ at 20°C).[4] Both the orientations and the partial rate factors obtained with BTP were quite different from those for phenylation with phenyl cation.[2,5] These data prove that biphenyls are produced by the attack of phenyl radical.

The partial rate factors for *meta* phenylations are not too different from unity except that for the *m*-methoxy position. Experiments were repeated, but the abnormality was reproduced within experimental error. It is possible that nucleophilic anisole and electrophilic BTP have some kind of weak interaction.

3) G. H. Williams, "Homolytic Aromatic Substitution," Pergamon Press, Oxford (1960), pp. 68—73.

4) R. Ito, T. Migita, N. Morikawa, and O. Simamura, *Tetrahedron*, **21**, 955 (1965).

5) M. Kobayashi, H. Minato, and N. Kobori, This Bulletin, **43**, 219 (1970).

BULLETIN OF THE CHEMICAL SOCIETY OF JAPAN, VOL. 44, 3476—3477(1971)

The Determination of the Stability Constant of the Copper(II) Chelate of 2-(*o*-Acetylphenylazo)-1,8-dihydroxynaphthalene-3,6-disulfonic Acid

Shinichi NAGAMORI* and Haruo MIYATA

Department of Chemistry, Faculty of Science, Okayama University, Tsushima, Okayama-shi

(Received June 14, 1971)

We have synthesized the *o*-substituted phenylazochromotropic acids and investigated the effect of substituents on the metal-chelate stabilization. In a previous paper,[1] we reported that the acid dissociation constant of 2-(*o*-acetylphenylazo)-1,8-dihydroxynaphthalene-3,6-disulfonic acid (2-(*o*-acetylphenylazo)chromotropic acid) and the stability constant of its 1:1 chelate with alkaline earth metals could be determined by means of a pH titration method. In the present investigation, the stability constant of the copper(II) chelate was determined spectrophotometrically at 25°C and at an ionic strength of 0.1, with potassium nitrate as the supporting electrolyte. The procedures for the measurements were similar to those described in another previous paper.[2]

The absorption spectra of the reagent and its copper chelate were measured by means of a Hitachi Model EPS-3T recording spectrophotometer; they are shown in Fig. 1. Two sulfonic groups in the reagent are completely dissociated, and the dissociation constant for one of the naphthoic hydroxyl groups was calculated from the absorbance at 566 nm using a Hitachi Model 139 spectrophotometer. The pH measurements were made with a Hitachi-Horiba Model F-5 SS pH meter. The pK_a value is 9.66; Katayama *et al.*[1] have reported that the value is 9.65 by pH titration. The dissociation of another hydroxyl group is very weak because of the strong hydrogen bridge. The reagent thus behaves like a monobasic acid under these experimental conditions. Moreover, the effect of the acetyl group on the pK_a value is unusual, irrespective of its electron-attractive effect. That is, the value of pK_a is higher than 9.19 for the phenylazochromotropic acid.[1]

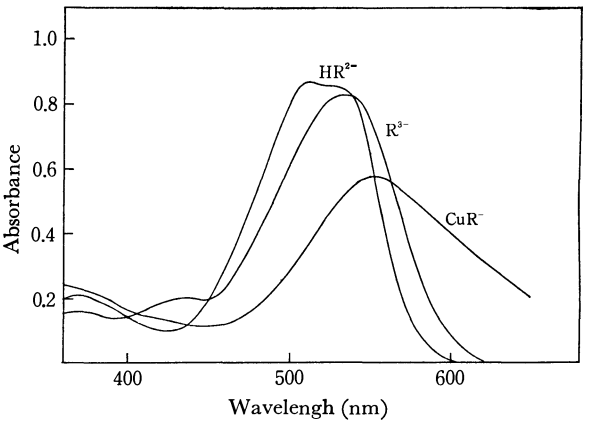

Fig. 1. Absorption spectra of the reagent and its copper chelate.
HR^{2-} at pH 1.0, R^{3-} at pH 12.6, and CuR^{-} at pH 5.57.
ligand concentration, 3.0×10^{-5}M.
copper concentration, 3.0×10^{-3}M.

The chelate formation of this reagent with the copper(II) ion become distinct at a pH of about 5, and the ratio of the reagent to the copper ion, as determined by the continuous-variation method, was 1:1. The stability constant of the copper chelate was calculated

* Present address: Santen Pharmaceutical Co., Ltd., Osaka.

1) T. Katayama, H. Miyata, and K. Tōei, This Bulletin, **44**, 2712 (1971).
2) H. Miyata, *ibid.*, **36**, 385 (1963).

by means of the following equations:

$$HR^{2-} \rightleftarrows H^+ + R^{3-} \quad (1)$$

$$K_a = \frac{[H^+][R^{3-}]}{[HR^{2-}]}$$

$$Cu^{2+} + HR^{2-} \rightleftarrows CuR^- + H^+ \quad (2)$$

$$K' = \frac{[CuR^-]}{[Cu^{2+}][HR^{2-}]} = \frac{[CuR^-]}{(C'_{Cu}-[CuR^-])(C_R-[CuR^-])}$$

$$Cu^{2+} + R^{3-} \rightleftarrows CuR^- \quad (3)$$

$$K = \frac{[CuR^-]}{[Cu^{2+}][R^{3-}]} = \frac{[CuR^-]}{(C'_{Cu}-[CuR^-])\{(K_a/[H^+](C_R-[CuR^-])\}}$$

where

K': the conditional stability constant of the copper chelate

K: the stability constant of the copper chelate

C_R: the total concentration of the reagent, $C_R = [HR^{2-}]+[CuR^-]$

C'_{Cu}[3]: the corrected concentration of copper, $C'_{Cu} = [Cu^{2+}]+[CuR^-]$

$[CuR^-]$: the concentration of the copper chelate.

The calculation procedure has been described in detail in a previous paper.[2] The values of the constants, $\log K'$ and $\log K$, of the copper chelate are listed in Table 1. The plots of the $\log K'$ *vs.* pH are shown in Fig. 2. The slope of this line is equal to 1, showing that the chelate is formed according to Eq. (2). In general, it is considered that the relation between the metal and the reagent is a Lewis-acid-and-base reaction. By comparing the $\log K$ value of the copper chelate with the value of 7.5 of the copper-phenylazochromotropic acid chelate, we can see that the stabilization of the copper chelate with this reagent is possibly due to the increase in the pK_a value of the reagent because of the effect of acetyl group existing in the *ortho* position.

Table 1. Conditional and conventional (first-step) stability constants of the copper(II)-2-(*o*-acetylphenylazo)chromotropic acid chelate at 25°C and at μ=0.1 (KNO_3)

pH	Absorbance at 500 nm	log K'	K	log K
3.68	0.821	2.83	6.51×10^8	
4.05	0.793	3.26	7.35	
4.08	0.791	3.28	7.26	
4.52	0.745	3.65	6.19	
4.54	0.731	3.74	7.17	
4.97	0.658	4.11	6.35	
		average	6.81×10^8	8.8

ligand concentration, 3.0×10^{-5}M.
copper concentration, 6.0×10^{-5}M.
$\varepsilon^{500nm}_{HR^{2-}}=2.80\times10^4$.
$\varepsilon^{500nm}_{CuR^-}=1.01\times10^4$.

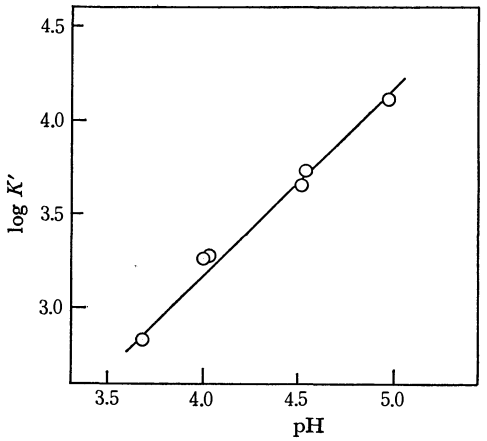

Fig. 2. log K' *vs.* pH.

The authors wish to thank Professor Kyoji Tōei for his kind guidance.

3) This value was corrected for the concentration of copper-acetate complex by using an acetate buffer.

BULLETIN OF THE CHEMICAL SOCIETY OF JAPAN, VOL. 44, 3478—3479(1971)

The Use of Nickel Peroxide as Oxidizing Agent of Phenylhydrazine for the Generation of Phenyl Radicals

Hiroyuki OHTA and Katsumi TOKUMARU

Department of Chemistry, Faculty of Science, The University of Tokyo, Hongo, Bunkyo-ku, Tokyo

(Received June 14, 1971)

It was reported that phenylhydrazine was oxidized with silver oxide,[1] mercuric oxide,[1] and lead tetraacetate[2] to give, probably *via* phenyldiimide, phenyl radicals, which can substitute on aromatic substrates to afford biaryls. These reactions as well as the decomposition of *N*-nitrosoacetanilide have often been employed to generate phenyl radicals at room temperature, though it is not convenient since silver oxide and *N*-nitrosoacetanilide have to be freshly prepared immediately before use and lead tetraacetate must be stored in acetic acid until use. With mercuric oxide, phenylhydrazine undergoes somewhat complicated reactions accompanied by the production of diphenylmercury.[1] In order to find a convenient procedure for the generation of phenyl radicals at room temperature, we investigated the treatment of phenylhydrazine with nickel peroxide, a new oxidizing agent of current interest,[3] on account of its ready availability and its stability during the course of storage. As a result, the reaction was found to be adequate for the present purpose.

Results and Discussion

Gradual addition of phenylhydrazine dissolved in a solvent to a suspension of excess nickel peroxide in the same solvent as above under stirring at room temperature under nitrogen atmosphere gave rise to a mild exothermic reaction with evolution of gas. The reaction carried out in cyclohexane gave benzene (68% yield based on the hydrazine used) together with a small amount of biphenyl (less than 1%). The reaction in carbon tetrachloride afforded chlorobenzene (53.5%), benzene (less than 2%), biphenyl (less than 2%), and hexachloroethane (10.1%). The reaction in benzene gave biphenyl (30%) along with very small amount of 1,4-dihydrobiphenyl (less than 0.2%) and phenol (trace). Treatment of *p*-nitrophenylhydrazine with nickel peroxide in benzene yielded *p*-nitrobiphenyl (34.8%) and nitrobenzene (5.6%).

These results indicate that phenylhydrazine, on treatment with nickel peroxide, gives phenyl radicals, which abstract hydrogen atoms from cyclohexane to afford benzene, or abstract chlorine atoms from carbon tetrachloride to give chlorobenzene[4] and trichloromethyl radicals followed by their dimerization to hexachloroethane.

Formation of biphenyl in benzene is mostly attributable to the substitution of phenyl radicals on benzene, although less than 2% of biphenyl might arise solely from phenylhydrazine moiety without participation of benzene in view of the formation of a small amount of biphenyl in cyclohexane or in carbon tetrachloride. Production of very low yield of 1,4-dihydrobiphenyl suggests that either dihydrobiphenyl does not result appreciably from the reaction or it is once formed but subsequently oxidized to biphenyl by nickel peroxide as demonstrated by a separate experiment. However, the absence of quaterphenyl in addition to the very low yield of dihydrobiphenyl among the products from benzene suggest that phenyl radicals add to benzene to give phenylcyclohexadienyl radicals, which may be oxidized with nickel peroxide to biphenyl rather than disproportionate or dimerize to give biphenyl and 1,4-

TABLE 1. DISTRIBUTION OF ISOMERIC BIARYLS RESULTING FROM THE PHENYLATION OF AROMATIC SUBSTRATES

Substrate	Reaction condition[a]	Biaryls: Total yield[b]	Biaryls: Isomer distribution (%) *o*	*m*	*p*
Toluene	PH–NiPO (1:1)	28	67	19	14
	PH–NiPO (1:3)	34	68	19	13
	NNA[8]		71	18	11
Chlorobenzene	PH–NiPO (1:1)	22	63	20	17
	PH–NiPO (1:3)	30	66	17	17
	PH–Ag_2O[1]		65	22	13
	PH–$Pb(OAc)_4$[2]	38	61	25	14
	NNA[8]		64	21	15
Nitrobenzene	PH–NiPO (1:1)	33	62	7	31
	PH–NiPO (1:3)	48	58	7	35
	PH–$Pb(OAc)_4$[2]	41	60	10	30
	NNA[8]		62	8	30

a) PH, NiPO, and NNA stand for phenylhydrazine, nickel peroxide, and *N*-nitrosoacetanilide, respectively. Figures in parentheses indicate the ratios of moles of phenylhydrazine to g-atoms of nickel peroxide employed.

b) Based on phenylhydrazine used.

1) R. L. Hardie and R. H. Thomson, *J. Chem. Soc.*, **1957**, 2512.

2) J. B. Aylward, *J. Chem. Soc., C*, **1969**, 1663.

3) a) K. Nakagawa, R. Konaka, and T. Nakata, *J. Org. Chem.*, **27**, 1597 (1962). b) R. Konaka, S. Terabe, and K. Kimura, *ibid.*, **34**, 1334 (1969). c) S. Terabe and R. Konaka, *J. Amer. Chem. Soc.*, **91**, 5655 (1969).

4) Formation of chlorobenzene by way of benzenediazonium chloride, though not detected in the present reaction, cannot be completely excluded in view of reports for the detection of benzenediazonium salt in the reaction of phenylhydrazine with lead tetraacetate in dichloromethane[2] and in the decomposition of *N*-nitrosoacetanilide in carbon tetrachloride (W. S. M. Grieve and D. H. Hey, *J. Chem. Soc.*, **1934**, 1797; C. Rüchardt, Chuan-Cheng Tan, and B. Freudenberg, *Tetrahedron Lett.*, **1968**, 4019.

dihydrobiphenyl or tetrahydroquaterphenyl.[5,6] Production of a trace of phenol shows that phenyl radicals are not readily oxidized with nickel peroxide to phenol, in contrast to triphenylmethyl radicals which were reported to suffer oxidation with nickel peroxide to afford triphenylmethanol.[3b]

Oxidation of phenylhydrazine with nickel peroxide in chlorobenzene, nitrobenzene, and toluene gave *o*-, *m*-, and *p*-chloro-, nitro-, or methyl-biphenyl, respectively, the total yields of the respective isomeric biaryls being 30—50%, together with a small amount of biphenyl. The isomer ratios of the biaryls are summarized in Table 1. The increase in the ratio of nickel peroxide to phenylhydrazine from 1 : 1 to 3 : 1 equivalents caused only 1.4 fold increase in the yield of the isomeric biaryls without affecting the distribution among the isomers. The observed ratios of the isomeric biaryls accord well with those obtained from the decomposition of benzoyl peroxide[7] or *N*-nitrosoacetanilide,[8] or the treatment of phenylhydrazine with silver oxide[1] or with lead tetraacetate[2] in aromatic substrates, showing the generation of phenyl radicals from the present reactions.

Experimental

Reagents. Nickel peroxide was determined by iodometric titration,[3a] to contain 0.00323 g-atom of active oxygen per 1 g. Phenylhydrazine was distilled through a spinning band distillation column under reduced pressure and stored in a desiccator under nitrogen.

Solvents. Cyclohexane, benzene, carbon tetrachloride, toluene, and chlorobenzene were purified by conventional methods, and finally distilled through a 1 m high Vigreux column. Nitrobenzene was purified by partial freezing, dried with phosphorus pentoxide and finally distilled.

Authentic Samples. Biphenyl derivatives were prepared and purified by the well-known methods.[9] 1,4-Dihydrobiphenyl was prepared according to the reported procedure.[10]

Reaction of Phenylhydrazine with Nickel Peroxide. In a 100 m*l* three necked round bottomed flask fitted with a nitrogen inlet tube and a reflux condenser was placed 3 g of nickel peroxide and 10 m*l* of a solvent, and the mixture was stirred with a magnetic stirrer in nitrogen stream. After 20 min, 3 mmol of phenylhydrazine dissolved in 10 m*l* of the same solvent as above was gradually added, stirring was continued further 1 hr. The reaction mixture was filtered through a quantitative filter paper on a funnel and the precipitate was successively washed and the combined filtrate and washings were concentrated. No tetrahydroquaterphenyl was precipitated or detected by spectroscopy. The concentrated solution was subsequently examined by gas chromatography.

Reaction of 1,4-Dihydrobiphenyl with Nickel Peroxide. A benzene solution of 1,4-dihydrobiphenyl, 0.315 g, was treated with nickel peroxide, 2.1306 g (6.78 mg atom of active oxygen), under nitrogen and kept to stand overnight and worked up as above. In a control run, the dihydrobiphenyl in benzene was kept to stand without nickel peroxide to confirm that the dihydrobiphenyl was not consumed.

Gas Chromatographic Analysis. A Hitachi K-52 TCD gas chromatograph was used with a 2 m column of 10% silicone grease on chromosorb H for the determination of chlorobenzene, nitrobenzene, and hexachloroethane, with a 2 m column of 10% diisodesyl phthalate on chromosorb P for benzene and a 6 m column of 10% silicone grease on chromosorb H for biaryls.

The authors are indebted to Prof. Osamu Simamura for his encouragement throughout this work and to Dr. Ryusei Konaka, Shionogi Research Laboratory, for the supply of nickel peroxide.

5) Decomposition of benzoyl peroxide in benzene at 80°C carried out in the presence of nickel peroxide was shown to give 1,4-dihydrobiphenyl in a negligible amount and biphenyl in moderately higher yield than without nickel peroxide (O. Simamura and Hiromichi Ohta, private communication).

6) As a general reference for homolytic aromatic substitution, see, for example, D. H. Hey, in G. H. Williams ed., "Advances in Free-radical Chemistry," Vol. II, Logos Press, London (1967), p. 47; O. Simamura, T. Migita, N. Inamoto, and K. Tokumaru, "Yuriki Hanno," Tokyo Kagaku Dozin, Tokyo (1969), Chapter 11.

7) D. H. Hey, S. Orman, and G. H. Williams, *J. Chem. Soc.*, **1961**, 565.

8) R. Ito, T. Migita, N. Morikawa, and O. Simamura, *Tetrahedron*, **21**, 955 (1965).

9) W. E. Bachmann and R. A. Hoffman, "Organic Reactions," Vol. 2, p. 248 (1944).

10) W. Hückel and R. Schwen, *Chem. Ber.*, **89**, 150 (1956).

BULLETIN OF THE CHEMICAL SOCIETY OF JAPAN, VOL. 44, 3480—3481 (1971)

5-Bromo-2,3-benzotropone and its Maleic Anhydride Adduct[1]

Seiji EBINE, Masamatsu HOSHINO, and Takahisa MACHIGUCHI

Department of Chemistry, Faculty of Science and Engineering, Saitama University, Urawa, Saitama

(Received June 17, 1971)

5,7-Dibromo-2,3-benzotropone (I),[2,3] obtained by the dehydrobromination of a tetrabromo derivative of 2,3-benzocycloheptenone, was debrominated on heating with a mixture of acetic and hydrobromic acids at 160°C to give 5-bromo-2,3-benzotropone (II). The position of the bromo substituent in II was established by the following NMR data. The spectrum of II (Fig. 1) contains an AB-type pattern consisting of H-7 at 6.67 ppm (d, $J_{7,6}=12.8$ Hz) and H-6 at 7.19 ppm (dd, $J_{6,7}=12.8$ and $J_{6,4}=2.05$ Hz), with perturbation arising from H-4 at 7.72 ppm (d, $J_{4,6}=2.05$ Hz). 7-Bromo-2,3-benzotropone (III),[4] prepared from 7,7-dibromo-2,3-benzocycloheptenone on treatment with lithium chloride, showed an entirely different NMR spectrum.[5a]

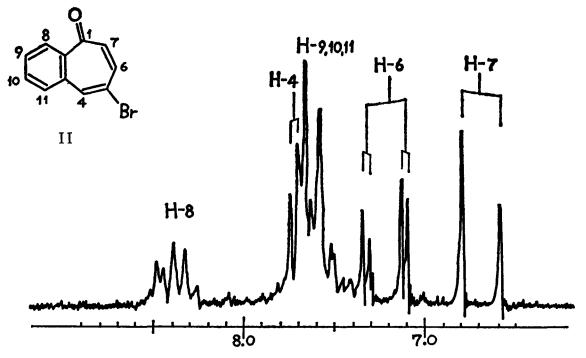

Fig. 1. NMR spectrum in deuteriochloroform at 60 MHz with TMS internal reference.

Chloro-2,3-benzotropone (IV), obtained by the reaction of 1-methoxynaphthalene with dichlorocarbene, has previously been assumed to be a 5- or 7-chloro compound.[6] The NMR spectrum of IV has an AB-type pattern consisting of H-7 at 6.88 ppm (d, $J_{7,6}=13.0$ Hz) and H-6 at 7.15 ppm (dd, $J_{6,7}=13.0$ and $J_{6,4}=1.9$ Hz) perturbed by H-4 at 7.81 ppm (d, $J_{4,6}=1.9$ Hz). The pattern is very similar to that of II, suggesting that IV is also 5-substituted. The dipole moment measurement of II and IV in a benzene solution has supported the above conclusion.[7] The X-ray crystal structure analysis of II and related compounds has also recently been undertaken.[5b]

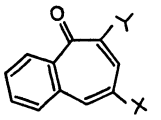

I, X=Y=Br II, X=Br, Y=H
III, X=H, Y=Br IV, X=Cl, Y=H

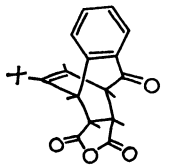

V, X=Br VII, X=Cl

The Diels-Alder reaction of monocyclic troponoids has been studied,[8] and that of benzotroponoids has been briefly reported.[2,9] II underwent a Diels-Alder reaction with maleic anhydride on heating at 160—165°C to give an adduct (V). V was hydrolyzed, on standing in a dilute acetone solution at room temperature, to give the corresponding dicarboxylic acid (VI) which was, in turn, dehydrated with ease on refluxing in a benzene solution to give the original V, proving

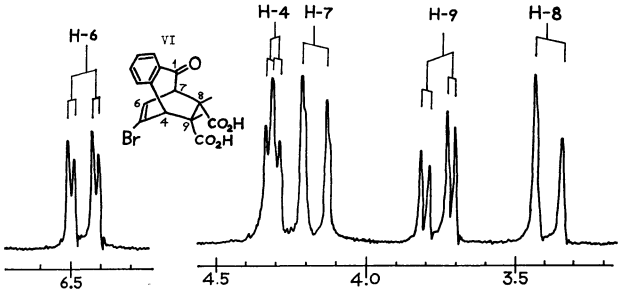

Fig. 2. NMR spectrum in acetone at 100 MHz with TMS internal reference.

1) a) Part IX in a series on 3,4-benzotropolone and related compounds: for Part VIII, see M. Hoshino and S. Ebine, This Bulletin, **43**, 1778 (1970). b) Presented at the 22nd Annual Meeting of the Chemical Society of Japan, Tokyo, April 2, 1969. Preprints III, p. 1468 (No. 16206).

2) S. Ebine, M. Hoshino, and K. Takahashi, This Bulletin, **41**, 2942 (1968).

3) M. C. Woods, S. Ebine, M. Hoshino, K. Takahashi, and I. Miura, *Tetrahedron Lett.*, **1969**, 2879.

4) E. W. Collington, and G. Jones, *Chem. Commun.*, **1968**, 958; *J. Chem. Soc., C*, **1969**, 2656.

5) a) M. Hoshino, S. Ebine, and T. Machiguchi, to be published. b) H. Shimanouchi, T. Hata, and Y. Sasada, Preprints, p. 81, for the International Symopsium on the Chemistry of Nonbenzenoid Aromatic Compounds, Sendai, August 25, 1970.

6) W. E. Parham, D. A. Balon, and E. E. Schweized, *J. Amer. Chem. Soc.*, **83**, 603 (1961); M. K. Saxena and M. M. Bokadia, *J. Indian. Chem. Soc.*, **46**, 855 (1969).

7) T. Shimozawa, S. Kumakura, M. Hoshino, and S. Ebine, This Bulletin, **44**, 565 (1971).

8) T. Nozoe, S. Seto, and T. Ikemi, *Proc. Japan Acad.*, **27**, 655 (1951); E. Sebe, and C. Osako, *ibid.*, **28**, 281 (1952); E. Sebe, and Y. Itsuno, *ibid.*, **29**, 107, 110 (1953); J. Meinwald, S. L. Emerson, N. C. Yang, and G. Büchi, *J. Amer. Chem. Soc.*, **77**, 4400 (1955); O. L. Chapman, and D. J. Pasto, *ibid.*, **81**, 3696 (1959); T. Nozoe, T. Mukai, T. Nagase, and Y. Toyooka, This Bulletin, **33**, 1247 (1960); T. Nozoe, and Y. Toyooka, *ibid.*, **34**, 623 (1961); Y. Kitahara, I. Murata, and T. Nitta, *Tetrahedron Lett.*, **1967**, 3003; S. Ito, H. Takeshita, Y. Shoji, Y. Toyooka, and T. Nozoe, *ibid.*, **1968**, 3215; **1969**, 443; S. Ito, K. Sakan, and Y. Fujise, *ibid.*, **1969**, 775.

9) H. H. Rennhard, G. DiModica, W. Simon, E. Heilbronner, and A. Eschenmoser, *Helv. Chim. Acta*, **40**, 957 (1957).

that VI is a *cis*-dicarboxylic acid. The stereochemistry of VI has now been established on the basis of the following NMR spectral analysis (Fig. 2). An apparent triplet at 4.31 ppm and a doublet at 4.17 ppm collapse to simpler signals on irradiation at an olefinic proton, H-6 at 6.45 ppm, and, alternately, a double doublet ($J_{6,7}$=8.1 and $J_{6,4}$=1.9 Hz) of H-6 collapses to a doublet ($J_{6,7}$=8.1 Hz) on irradiation at 4.31 ppm and to a doublet ($J_{6,4}$=1.9 Hz) on irradiation at 4.17 ppm. The aforementioned triplet and doublet, therefore, are ascribable to H-4 and H-7 respectively. By the use of a similar double-resonance method, an AB-type pattern in the higher field can be assigned to H-8 at 3.40 ppm (d, $J_{8,9}$=9.0 Hz) and H-9 at 3.75 ppm (dd, $J_{9,8}$= 9.0 and $J_{9,4}$=2.6 Hz) perturbed by H-4 (d, $J_{4,9}$=2.6 Hz). It follows, therefore, that, in agreement with the above chemical evidence, VI should be a *cis*-dicarboxylic acid based upon a large value of $J_{8,9}$ and should have an *endo*-configuration based upon a small value of $J_{4,9}$. The *endo-cis*-configuration of VI is further supported by the Nuclear Overhauser Effect (10.4%) observed between H-8 and H-9, and by a small value of $J_{7,8}$ ($\leq$1) not obserbable even in the 100 MHz spectrum, but evidenced by the sharpening of the H-7-doublet on irradiation at H-8, and *vice-versa*. The stereochemistry of V could not be concluded from the NMR spectrum because V failed to give a satisfactory chart because of its difficut solubility, but a facile interconversion between V and VI suggests that V assumes the same *endo*-configuration as VI. V and VI, however, did not undergo Alder-Stein bromolactonization,[10] presumably because of the presence of the 5-bromo substituent. IV reacted with maleic anhydride to afford an adduct (VII), which again failed to give detailed NMR spectral data.

Experimental

5-Bromo-2,3-benzotropone (II). A solution of 200 mg of I[2] in 20 m*l* of 47% hydrobromic acid and 25 m*l* of acetic acid was heated in a sealed tube at 160—165°C for 5 hr. The solution gave a positive potassium iodide-starch test, indicating the presence of free bromine. The hydrobromic and acetic acids were removed by evaporation *in vacuo*, and the residue was recrystallized from methanol to yield 100 mg (76% yield) of II as pale yellow needles melting at 102—103.5°C.

Found: C, 55.99; H, 3.20%. Calcd for $C_{11}H_7OBr$: C, 56.20; H, 3.00%.

I remained unchanged on treatment with hydrochloric acid in the same manner as above.

A solution of 100 mg of II and 70 mg of bromine in 10 m*l* of acetic acid was refluxed for 40 min; the product was then recrystallized from methanol to give 90 mg (67% yield)of I.

Diels-Alder Reaction of 5-Halo-2,3-benzotropones with Maleic Anhydride. The Adducts (V and VII): A mixture of 440 mg of II and 220 mg of maleic anhydride was heated at 160—165°C for 30 min. The mixture was treated with anhydrous ether to remove the excess maleic anhydride, and the crude product (570 mg; 91% yield; mp 220°C dec.) was recrystallized from benzene to give colorless granular crystals of the 5-bromo-2,3-benzotropone-maleic anhydride adduct (V); mp 242°C (dec.).

Found: C, 54.32; H, 2.97%. Calcd for $C_{15}H_9O_4Br$: C, 54.08; H, 2.72%.

A similar treatment of 100 mg of IV[6] with 150 mg of maleic anhydride gave 130 mg (87% yield) of colorless granular crystals of the 5-chloro-2,3-benzotropone-maleic anhydride adduct (VII); mp 217.5—218.5°C.

Found: C, 62.62; H, 3.31%. Calcd for $C_{15}H_9O_4Cl$: C, 62.40; H, 3.14%.

Derivatives of V. a) Dicarboxylic Acid (VI): A solution of 340 mg of V in dilute acetone (35 m*l* of acetone and 20 m*l* of water) was allowed to stand at room temperature for 3 days. On the subsequent evaporation of the solvent below 30°C *in vacuo*, there remained 330 mg (91% yield) of colorless prisms of VI melting at 241—242°C (dec.). The hydrolysis of V with dilute alkali at room temperature gave the same result. VI gave the original V in 90% yield on refluxing in a benzene solution for 1.5 hr.

Found: C, 51.31; H, 3.19%. Calcd for $C_{15}H_{11}O_5Br$: C, 51.30; H, 3.16%.

b) Monomethyl Ester: A solution of 300 mg of V in 160 m*l* of methanol was allowed to stand at room temperature for a day. The subsequent evaporation of the solvent and recrystallization of the residue from dilute acetone (1:1) gave 290 mg (88% yield) of the monomethyl ester as colorless needles; double mp 112°C and 238°C.

Found: C, 50.15; H, 3.94%. Calcd for $C_{16}H_{13}O_5Br \cdot H_2O$: C, 50.15; H, 3.95%.

c) Dimethyl Ester: The methylation of 200 mg of VI with diazomethane in an ether solution afforded 120 mg (55% yield) of the dimethyl ester as colorless granular crystals; mp 113—113.5°C.

Found: C, 53.84; H, 4.07%. Calcd for $C_{17}H_{15}O_5Br$; C, 53.84; H, 3.99%.

10) K. Alder and G. Stein, *Anal. Chem.*, **514**, 4 (1934).

BULLETIN OF THE CHEMICAL SOCIETY OF JAPAN, VOL. 44, 3482—3483 (1971)

Substituent Effects on the NH Proton Chemical Shifts of *p*-Substituted Phenylureas

Yoshihiro ASABE and Yojiro TSUZUKI*

Faculty of Pharmaceutical Sciences, Science University of Tokyo, Ichigayafunagawara-machi, Shinjuku-ku, Tokyo

**Department of Chemistry, Science University of Tokyo, Kagurazaka, Shinjuku-ku, Tokyo*

(Received June 18, 1971)

It has been recognized that the NH proton chemical shifts of substituted anilines[1,2] obey the Hammett's rule as do the side chain CH proton chemical shifts of substituted benzenes.[3] In this study the chemical shifts of the NH protons of *p*-substituted phenylureas were measured to study some correlations between the chemical shifts and vairous substituent constants, and discussions will be given about the substituent effect of *p*-substituent groups on the ureido(–NHCONH$_2$) group.

Dimethyl sulfoxide(DMSO) was chosen as solvent for the reason that DMSO dissolve the samples insoluble in most organic solvents, and also in order to eliminate complication due to the onset of proton exchange among the NH and NH$_2$ groups which provide an additional source of line broadening and coalescence. Under these conditions, the molecules of *p*-substituted phenylureas are isolated from each other and are hydrogen-bonded to the DMSO molecules with which they can not hydrogen exchange.[4–6]

The signals near 6.2 ppm and 3.6 ppm from the reference methyl signal of DMSO are assigned to the NH and NH$_2$ protons respectively and the signals near 4—5 ppm are assigned to the phenyl ring protons. In the phenylureas as well as in formamide, the ^{14}N–H spin-spin coupling is not observed because of the rapid relaxation of ^{14}N quadrupole due to the strong electric field gradients around the N nucleus caused by the CO group.[7] And the NH proton gives only a rather broadening signal due to this ^{14}N–H spin-spin interaction and the quadrupolar effect. For the NH$_2$ protons some difference in chemical shift would be expected between them due to the restricted rotation about the C–N bond, but only a very broadening signal is observed for the above mentioned reasons. It was observed that all the *p*-substituted phenylureas, except the NO$_2$ derivative, show a slight shift towards the higher field with dilution

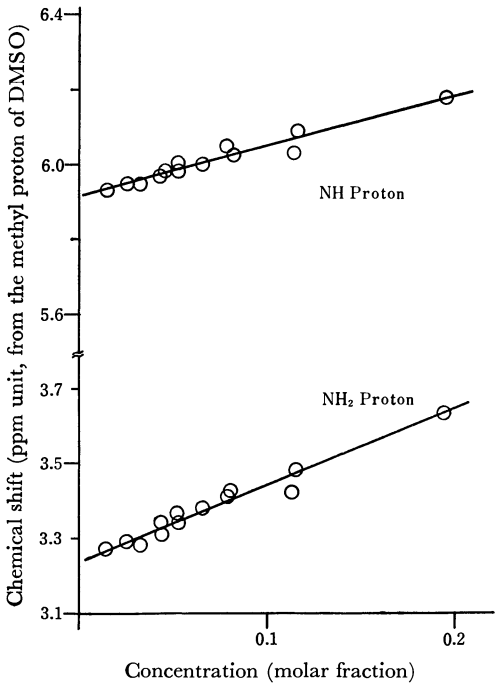

Fig. 1. Plottings of the NH and NH$_2$ proton chemical shift *vs.* concentration (molar fraction) of the phenylurea.

and the chemical shifts show a linear relationship with concentration (Fig. 1). The chemical shifts extrapolated to infinite dilution were obtained by the least square methods.

Now, the following factors may be considered, which affect on the chemical shifts of NH$_2$ and NH protons.

1) Hydrogen bonding and hydrogen exchange.
2) Magnetic anisotropy of the *p*-substituted phenyl group.
3) Variation of the electron density on each N atom.

As mentioned above, the phenylurea molecules in dilute solution exist in a solvated form with the DMSO molecules, and thus the intermolecular as well as intramolecular[8] hydrogen bondings could be ignored. Although detailed studies at various temperatures will be left in future, it is to be allowed from the example by Sunners *et al.*,[5] that the proton exchange is not very important at room temperature. Hence the hydrogen exchange between the NH and NH$_2$ groups may be assumed to be constant. As regards the factor (2), the anisotropic influence of the phenyl ring may predominantly exert

1) T. Yonemoto, W. F. Reynold, H. M. Hutton, and T. Schaefer, *Can. J. Chem.*, **43**, 2668 (1965).
2) L. K. Dyall, *Aust. J. Chem.*, **17**, 419 (1964).
3) Y. Yukawa, M. Sakai, K. Kabazawa, and Y. Tsuno, *Memo. I. S. I. R. Osaka Univ.*, **17**, 185 (1960); C. Heathcock, *Can. J. Chem.*, **40**, 1865 (1962).
4) L. H. Piette, J. D. Ray, and R. A. Ogg, *J. Mol. Spectrosc.*, **2**, 66 (1958), and also J. D. Baldeschwieler and E. W. Randall, *Chem. Rev.*, **63**, 81 (1963).
5) B. Sunners, L. H. Piette, and W. G. Schneider, *Can. J. Chem.*, **38**, 68 (1960).
6) J. W. Emsley, J. Feeney, and L. H. Sutcliffe, "High Resolution Nuclear Magnetic Resonance Spectroscopy," Vol. 1, Pergamon Press, Oxford (1965), p. 554.
7) G. V. D. Tiers and F. A. Bovey, *J. Phys. Chem.*, **63**, 302 (1959); K. Tori, *Ann. Rept. Shionogi Res. Lab.*, **12**, 114 (1962).
8) Intramolecular hydrogen bonding between the NH$_2$ protons and the phenyl ring can be considered.

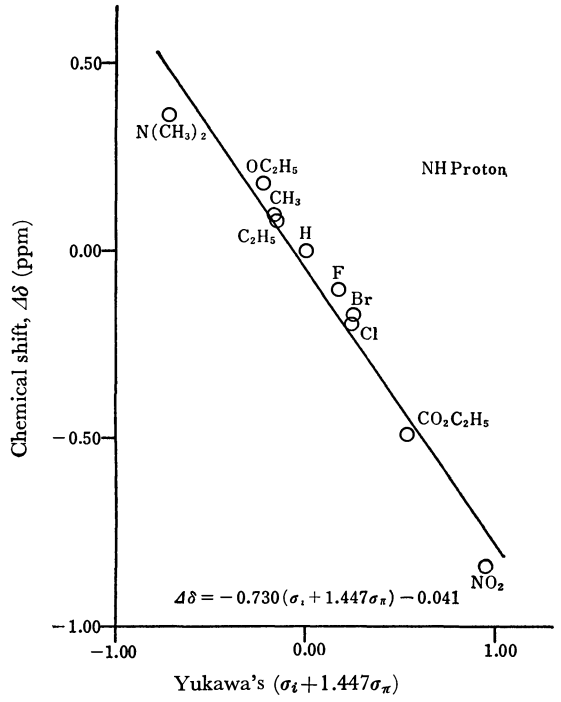

Fig. 2. Correlation of the NH proton chemical shifts and Yukawa's $(\sigma_i+\gamma\sigma_\pi)$ constant.

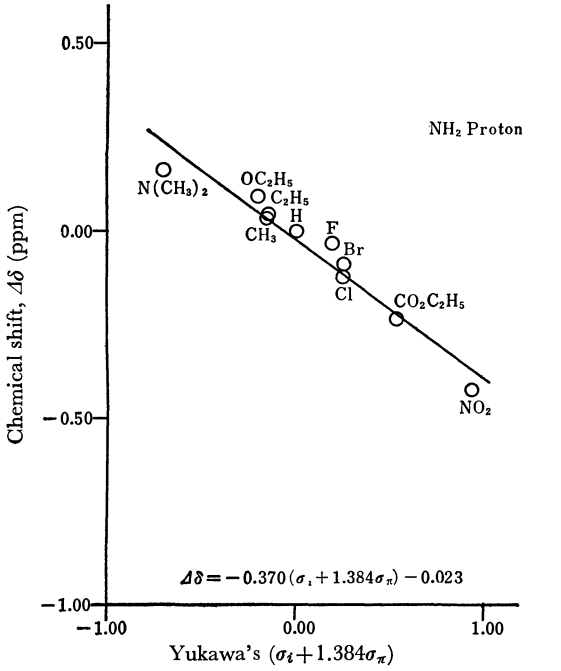

Fig. 3. Correlation of the NH_2 proton chemical shifts and Yukawa's $(\sigma_i+\gamma\sigma_\pi)$ constant.

on the chemical shifts, but the *p*-substituent may be almost ignored sterically and then the anisotropic effect may be considered to be constant. Consequently, only the factor (3), that is, the variation of shielding around the protons by the change of the electron densities on the N atoms is to be considered.

Then, studies were made as to the correlations between the difference of chemical shifts from the standard sample (phenylurea) and the various substituent constants. A fairly good linearity was obtained with Hammett's σ_p values[9] as well as with Taft's $(\sigma_I+2\sigma_R^0)$ values,[10] and the best result with Yukawa's $(\sigma_i+\gamma\sigma_\pi)$ values,[11] but not with other substituent constants. In Figs. 2 and 3 are shown the plottings against Yukawa's $(\sigma_i+\gamma\sigma_\pi)$ values except the I group since the substituent constant can not be estimated. Both the NH and NH_2 protons give a good linear relationship with Yukawa's values, namely, $\Delta\delta=-0.730(\sigma_i+1.447\sigma_\pi)-0.041$ for the NH proton and $\Delta\delta=-0.370(\sigma_i+1.384\sigma_\pi)-0.023$ for the NH_2 proton.

It is, therefore, concluded that the variation of the electron density on the N atom due to the electronic effect of *p*-substituent group determine the NH proton chemical shift. Furthermore, from the fact that the chemical shifts of the NH_2 protons as do the chemical shifts of the NH protons also in accordance with the Hammett's rule, it is confirmed that the N atom of NH_2 group is capable of conjugation with the phenyl ring system through the π-electrons of the CO group.

The ratio of the line slopes(ρ) of the NH proton to that of the NH_2 proton is about 2, that is, the NH proton shows twice as much σ-dependance as the NH_2 proton, and it appears that the H atom of the NH group directly bonded to the phenyl ring ought to be rather more sensitive to the *p*-substituent effect than do the NH_2 protons.

Experimental

Preparation of Samples. The *p*-substituted phenylureas (R-C$_6$H$_4$-NHCONH$_2$) were prepared by the reaction of sodium cyanate with the corresponding anilines in aqueous acetic acid solutions[12] and were purified by recrystallization. The identity and purity was confirmed by the mp determination and also by the IR spectra in a KBr disk.

Measurements. The PMR spectra were measured with a Varian A-60 Spectrometer at 30°C. The spectra were referred to the methyl signal of DMSO, and the chemical shifts were taken in ppm units lower field side from the reference. They were checked and corrected with the water signal of the external standard (in capillary) as a secondary reference. The position of each signal was measured using it's signal peak. A commercial guaranteed reagent was used as solvent (DMSO) and was treated with a molecular sieve before use in order to remove the contaminating water.

9) L. P. Hammett, "Physical Organic Chemistry," Mc-Graw Hill Book Co., New York (1940), Chap. VII.

10) R. W. Taft. Jr., *J. Phys. Chem.*, **64**, 1805 (1959); R. W. Taft. Jr., S. Ehrenson, I. C. Lewis, and R. E. Glick, *J. Amer. Chem. Soc.*, **81**, 5352 (1959); R. W. Taft. Jr., E. Price, I. R. Fox, I. C. Lewis, K. K. Andersen, and G. T. Davis, *ibid.*, **85**, 3146 (1963).

11) Y. Yukawa and Y. Tsuno, *Nippon Kagaku Zasshi*, **86**, 873 (1965).

12) F. Kurzer, "Organic Syntheses," **31**, 8 (1951).

BULLETIN OF THE CHEMICAL SOCIETY OF JAPAN, VOL. 44, 3484—3485 (1971)

Dimerization of Malononitrile by Palladium and Platinum Complex Catalysts

Kuniyuki TAKAHASHI, Akihisa MIYAKE, and Go HATA

Basic Research Laboratories, Toray Industries, Inc., Tebiro, Kamakura, Kanagawa

(Received July 20, 1971)

Previously we reported the palladium catalyzed reactions of 1,3-dienes with active methylene compounds.[1] In the course of the studies a novel catalytic dimerization of malononitrile has been found.

As described in the previous report,[1] malononitrile reacts with butadiene in the presence of a palladium catalyst to give 2,7-octadienyl and bis(2,7-octadienyl)-malononitrile in high yields. However, in the presence of a platinum catalyst, *e.g.*, tetrakis(triphenylphosphine)-platinum(0), the reaction gave only a small amount of the 2,7-octadienyl derivatives, with a large amount of a yellow solid product. The yellow product was insoluble in benzene. The elemental analysis and molecular weight measurement indicated that the product (mp 168—169°C) was a dimer of malononitrile. The dimer exhibited IR absorptions at 3350 and 3230 cm^{-1} (νN–H), 2180 cm^{-1}(νC≡N) and the NMR signals at τ 6.24 (s, 2H), 1.19 and 1.08 (broad, 2H). Its UV spectrum showed the maximum absorption at 274 mμ (ε 14000 in ethanol) due to conjugated double bonds. These spectral characteristics suggest the following structure (I).

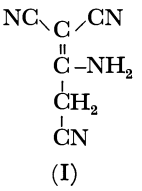

(I)

Carboni[2] prepared the malononitrile dimer (I) for the first time using bases and acids. The IR and NMR spectra of the present product were identical with those of the dimer prepared by the Carboni's method.

Ethyl cyanoacetate also dimerized by the platinum catalyst to give 1-cyano-1,3-diethoxycarbonyl-2-amino-1-propene (II). Ethyl cyanoacetate was not so reactive as malononitrile. The dimer (II) showed IR absorptions at 3420, 3300, and 3230 cm^{-1}(νN–H), 2200 cm^{-1}(νC≡N), and 1740 cm^{-1}(νC=O, ester). The NMR spectrum of II in CCl_4 exhibited signals at τ 8.69 (t, 6H, J=7.0 Hz, –O–C–CH_3), 6.43 (s, 2H, =C–CH_2–CO), 5.80 and 5.77 (two quartet, J=7.0 Hz, –CO–O–CH_2–), 2.55 and 0.68 (broad, 2H, N–H, equal intensities). The maximum absorption of UV spectrum was at 277 mμ (ε 17600 in ethanol).

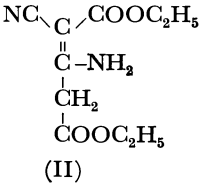

(II)

Tetrakis(triphenylphosphine)platinum is most efficient for the dimerization of malononitrile, but inefficient for the reaction of malononitrile with 1,3-butadiene.[1] A combination of dichloro bis(triphenylphosphine) platinum (II) and sodium phenoxide also showed the catalytic activity. The palladium catalysts, which are quite effective for the reaction of malononitrile with butadiene, was found to be effective for the dimerization reaction of malononitrile, as shown in Table 1, but their activities were low as compared with those of the platinum ones.

It was confirmed that triphenylphosphine or sodium phenoxide alone had no catalytic activity under the present reaction conditions. From the fact that the zerovalent platinum and palladium complexes are effective catalysts, the zerovalent metal atoms appear to play an important role in the catalytic dimerization reactions of malononitrile and ethyl cyanoacetate.

TABLE 1. DIMERIZATION OF MALONONITRILE BY PLATINUM AND PALLADIUM COMPLEXES

Catalyst mmole	Reaction time hr	Dimer yield %
$Pt(Ph_3P)_4$ 0.25	1	82.1
$PtCl_2(Ph_3P)_2$–C_6H_5ONa 0.25	20	80.3
$Pd(Ph_3P)_4$ 0.25	4	39.5
$Pd(Ph_3P)_2$ 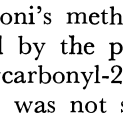 0.25	20	13.6
$PdCl_2(Ph_3P)_2$–C_6H_5ONa 0.25 2.5	20	33.4

malononitrile 0.1 mol, benzene 20 m*l*, 80°C

Experimental

Catalysts. $Pd(Ph_3P)_4$,[3] $Pd(Ph_3P)_2$  ,[4] $PdCl_2(Ph_3P)_2$,[3] $Pt(Ph_3P)_4$,[5] and $PtCl_2(Ph_3P)_2$[5] were prepared by the methods described in the literatures. Sodium phenoxide was prepared by the usual method from sodium metal and phenol.

1) G. Hata, K. Takahashi, and A. Miyake, *Chem. Ind.* (London), **1969**, 1836.

2) R. A. Carboni, D. D. Coffman, and E. G. Howard, *J. Amer. Chem. Soc.*, **80**, 2838 (1958).

3) L. Malatesta and M. Angolleta, *J. Chem. Soc.*, **1957**, 1186.

4) S. Takahashi, K. Sonogashira, and N. Hagihara, *Nippon Kagaku Zasshi*, **87**, 610 (1966).

5) L. Malatesta and C. Cariells, *J. Chem. Soc.*, **1958**, 2323.

Dimerization of malononitrile by $Pt(Ph_3P)_4$. In a two-necked 50 m*l* round-bottomed flask were placed 6.6 g (0.1 mol) of malononitrile, 0.31 g (0.00025 mol) of tetrakis(triphenylphosphine)platinum(0) and 20 m*l* of benzene. The mixture was stirred at 80°C for 1 hr under an argon atmosphere. The precipitated yellow solid was separated by filtration, washed several times with hot benzene and dried to give 5.4 g (82.1% yield) of 1,1,3-tricyano-2-amino-1-propene (I); mp 168—169°C (lit,[2] mp 172—173°C); IR(KBr): 3350, 3230, 2180, 1655, 1555, 1387, 1309, and 906 cm^{-1}; NMR (in hexadeuterodimethyl sulfoxide): 6.24 (s, 2H), 1.19 (broad, 1H), and 1.08 (broad, 1H); UV (in ethanol): λ_{max} 274 mμ (ε 14000). Found: C, 54.42; H, 3.17; N, 42.44%; mol wt, 135.7. Calcd for $C_6H_4N_4$: C, 54.54; H, 3.05; N, 42.41; mol wt, 132.1.

Dimerization of Ethyl Cyanoacetate. The mixture of 11.4 g (0.1 mol) of ethyl cyanoacetate, 0.62 g (0.0005 mol) of tetrakis(triphenylphosphine)platinum(0) and 20 m*l* of benzene was stirred at 80°C for 20 hr. The reaction mixture was fractionally distilled to give 1.8 g (15.8% yield) of 1-cyano-1, 3-diethoxycarbonyl-2-amino-1-propene (II); bp 153—155°C/0.02 mmHg, mp 54—55°C; IR(KBr): 3420, 3300, 3230, 2990, 2200, 1740, 1680, 1630, 1528, 1270, 1185, 1095, 1020, and 785 cm^{-1}; NMR (in carbon tetrachloride): τ 8.69 (t, 6H, J= 7.0 Hz), 6.43 (s, 2H), 5.80 and 5.77 (two quartet, J=7.0 Hz), 2.55 (broad, 1H), and 0.68 (broad, 1H); UV (in ethanol): λ_{max} 277 mμ (ε 17600). Found: C, 53.01; H, 6.22; N, 12.37%; mol wt, 227.3. Calcd for $C_{10}H_{14}N_2O_4$: C, 53.09; H, 6.24; N, 12.37; mol wt, 226.2.

SHORT COMMUNICATIONS

Stereochemical Study of *N,N'*-Dimethylethylenediamine Cobalt(III) Complex *trans*-Dinitrobis(*N,N'*-dimethylethylenediamine)cobalt(III) Ion

Shigenobu YANO, Masahiko SABURI,* and Sadao YOSHIKAWA*

Department of Chemistry, Faculty of Science, Tohoku University, Sendai

**Department of Synthetic Chemistry, Faculty of Engineering, The University of Tokyo, Tokyo*

(Received May 29, 1971)

Recently Buckingham *et al.*[1] prepared *trans,trans*-$[CoX_2(N\text{-Meen})_2]^+$ ($X=Cl^-$, NO_2^-; *N*-Meen=*N*-methylethylenediamine) ion whose *N*-methyl groups are *trans* to each other. They obtained three isomers of the meso (R,S) and the optically active (R,R and S,S) forms, where R and S refer to the chirality of the coordinated nitrogen centers. In these complexes, the nonbonding interactions between the N–CH_3 groups and the N–H groups do not seem to be so large as to exclude their sterically crowded meso isomer. However, in the case of *trans*-$[CoX_2(N,N'\text{-}Me_2en)_2]^+$, where *N,N'*-$Me_2$en denotes *N,N'*-dimethylethylenediamine, strong nonbonding interactions can be expected to be present between the N–CH_3 groups on neighboring ligand molecules. On the other hand, seven isomers are theoretically possible for *trans*-$[CoX_2(N,N'\text{-}Me_2en)_2]^+$ complex owing to the asymmetry of coordinated nitrogen centers, three meso {(RR,SS), (RS,RS), and (RS,SR)} and four optically active {(RR,SR) and (SS,SR), and (RR,RR) and (SS,SS)} forms. Of these, the last two forms in which all four *N*-methyl groups have an equatorial arrangement are likely to be the most favorable sterically.

In order to see the presence of isomerism in the complexes of such type, we investigated *trans*-$[Co(NO_2)_2(N,N'\text{-}Me_2en)_2]I$ as follows.

$Na_3[Co(NO_2)_6]$ (22 g) was allowed to react with a refluxing solution of *N,N'*-Me_2en (10 g) and water for 2 hr. Addition of sodium iodide, then, gave brown crystals of the pure compound. Found: C, 21.06; H, 5.14; N, 18.58%. Calcd for $C_8H_{24}N_6O_4CoI$: C, 21.16; H, 5.33; N, 18.51%. The PMR spectrum of the product in D_2O showed one *N*-methyl singlet (2.2 ppm) and a methylene multiplet (2.4—3.2 ppm) which was regarded to be of AA'BB' pattern by means of iterative analysis.[2] It was shown by PMR study[2] that in aqueous solution *N,N'*-Me_2en chelate rings have a similar *gauche* conformation (Fig. 1). The fact that only one PMR signal of the *N*-methyl group is observed suggests that this complex is assigned to *trans*-$[Co(NO_2)_2(N,N'\text{-}Me_2en)_2]^+$ composed of the most preferred isomers in optically active form. To examine whether it was the unique product under the given conditions, the reaction product of $Na_3[Co(NO_2)_6]$ and *N,N'*-Me_2en was evaporated to dryness and its PMR spectrum was measured in D_2O. An *N*-methyl singlet (2.2 ppm) and a methylene multiplet (2.4—3.2 ppm) were observed. The iodide was successfuly resolved into its optical forms with silver α-bromo-π-camphorsulfonate. It is very likely that all four asymmetric nitrogen atoms in $(-)_{589}$-*trans*-$[Co(NO_2)_2(N,N'\text{-}Me_2\text{-}en)_2]^+$ are of *S*-configuration in view of their CD spectrum as compared with those of some *trans*-dinitrobis(*N*-methylated diamine)cobalt(III) ions which have asymmetric nitrogen atoms with a known configuration.[3]

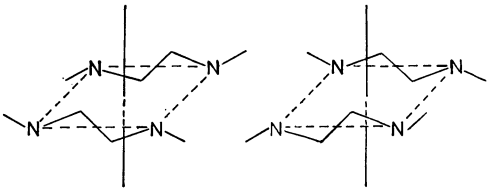

(RR, RR) (SS, SS)

Fig. 1

1) D. A. Buckingham, L. G. Marzilli, and A. M. Sargeson, *J. Amer. Chem. Soc.*, **89**, 3428 (1967).

2) S. Yano, M. Saburi, and Y. Koike, unpublished.

3) M. Saburi, Y. Tsujito, and S. Yoshikawa, *Inorg. Chem.*, **9**, 1476 (1970).

The Oxidation of Chroman-4-ols with Chromic Acid

Shozo YAMAGUCHI, Kuninobu KABUTO, Yoriko KIKUCHI, and Naoto INOUE
College of General Education, Tohoku University, Kawauchi, Sendai

(Received August 2, 1971)

With regard to the oxidation rates with chromic acid of epimeric cyclohexanols(CYHs), it is well known[1] that the axial alcohols are oxidized faster than the equatorial ones and that the bulky substituent adjacent to the hydroxyl group accelerates the reaction. Although isolated studies of the oxidation rates of allyl alcohols are on record,[2] no systematic investigation has yet been reported. We wish to report the oxidation of chroman-4-ols; the results are summarized in the table. Only the most interesting results different from those in the saturated series can be discussed here.

TABLE 1. OXIDATION RATES OF SUBSTITUTED CHROMAN-4-OLS

Compound	Av. rate[a]	k_H/k_D	Preferred conformation of OH[b]	*cis*/*trans*
CR(I)[c]	29.5	5.44	ax'[3]	
cis-2-Me-CR(II)	116	5.30	eq'	10.6
trans-2-Me-CR(III)	10.9		ax'	
cis-2-*i*-Pr-CR(IV)	129		eq'	9.21
trans-2-*i*-Pr-CR(V)	14.0		ax'	
cis-2-Ph-CR(VI)	96.9	4.99	eq'	3.30
trans-2-Ph-CR(VII)	29.4		ax'	
cis-2-*t*-Bu-CR(VIII)	133		eq'	12.1
trans-2-*t*-Bu-CR(IX)	11.0		ax'	
cis-3-Me-CR(X)	61.4	5.12	ax'	3.55
trans-3-Me-CR(XI)	17.3		ax'[3]	
cis-3-Ph-CR(XII)	42.9	5.11	eq'	3.43
trans-3-Ph-CR(XIII)	12.9	5.87	eq'[3]	
cis-3-*t*-Bu-CR(XIV)	16.7	4.11	ax'	3.65
trans-3-*t*-Bu-CR(XV)	4.58		ax'	

a) l/mol sec$\times 10^2$ in 85.5% (by volume) HOAc, 25°C. Rates followed spectrophotometrically at 380 mμ. $[CrO_3]3.00\times10^{-4}$M; $[ROH]2.25\times10^{-4}$M. All data average of 2—4 runs.
b) The conformation of these compounds were determined by NMR.
c) CR: Chroman-4-ol

In this series of compounds, the rates of *cis*-2-substituted chroman-4-ols (2-CRs) are markedly larger, and in *cis*-2- and *trans*-2-CRs the rates are little affected with an increase in the size of the respective substituent. Both *cis*-2- and *cis*-3-CRs react more rapidly than the corresponding *trans* isomers. In all the 2-CRs except 2-Ph-CRs, the ratios of the rates of *cis*/*trans* (9—12) are larger than those of 3-CRs and CYHs. Since the 2-CRs are almost conformationally homogeneous, as is indicated in the table, the above results can be explained to some extent by the fact that the acceleration by the strain relief in the *cis*-2-CRs ($A^{(1,3)}$ strain, *ca.* 1.0 kcal/mol)[3] is greater than that of *trans* ones (*ca.* 0.35 kcal/mol).[4] However, the rate ratio of *cis*/*trans* (*ca.* 3.8), as calculated[4] from the free energy difference (*ca.* 0.65 kcal/mol) between the two isomers, is not so large as the observed value (9—12); consequently, the observed ratio should be attributed to both the stereoelectronic effect[5] and the strain relief.

It is a striking fact that *cis*- and *trans*-3-*t*-Bu-CRs (XIV, XV) show the smallest rates of all the 3-isomers. In the 2-substituted CYHs, the rate ratios of *t*-Bu/Me are 9.3(*trans*)—11(*cis*)[1] due to the presence of a bulky adjacent group. Although similar effects can be expected for the 3-CRs, the ratios are markedly reversed. Since XV exists mostly in the diaxial conformation, it is considered that the *t*-Bu group has little effect on the steric compression of the hydroxyl group, and the ground state can be assumed to be similar to that of *trans*-3-Me-CR(XI). In the transition state, however, the repulsion[4] between the developing carbonyl group and the *t*-Bu group is much larger than that of XI; consequently, XV has the larger activation free energy. This assumption is also supported by the fact that the rates decrease with an increse in the size of the substituent in *trans*-3-CRs.

Contrary to the reactivity anticipated from its preferred conformation, the rate of XIV is quite small compared to that of *cis*-3-Me-CR(X) and *cis*-2-*t*-Bu-CYH ($k=79.7\times10^{-2}$). In the case of strongly hindered alcohols, it has been reported[6] that the formation of the ester is concerned in the rate-controlling step and the rate decreases. In the initial stage of the reaction of XIV, an induction period characteristic of a successive reaction and a smaller isotope effect is observed. These results suggest that the esterification step is connected to some extent with the rate-determining step because of its sterically-crowded situation, in which the hydroxyl group is surrounded by the *t*-Bu group and the hydrogen in a peri-position.

1) E. L. Eliel, S. H. Shroeter, T. J. Brett, F. J. Biros, and J. Richer, *J. Amer. Chem. Soc.*, **88**, 3327 (1966).
2) S. H. Burstein and H. J. Ringold, *ibid.*, **89**, 4722 (1967).
3) S. Yamaguchi, K. Kabuto, Y. Ninomiya, and N. Inoue, This Bulletin, **43**, 3952 (1970).
4) E. L. Eliel, N. J. Allinger, S. J. Angyal, and G. A. Morrison, "Conformational Analysis," John Wiley and Sons, New York (1965), pp. 44, 84, 114.
5) H. Kwart and P. S. Francis, *J. Amer. Chem. Soc.*, **81**, 2116 (1959).
6) von J. Rocek, F.H. Westheimer, A. Eschenmoser, L. Moldvanyi, and J. Schreiber, *Helv. Chim. Acta*, **45**, 2554 (1962).

A Novel Synthesis of Ethyl β-Diethoxyphosphinyl-α,β-unsaturated-carboxylates

Chung-gi SHIN, Yasuchika YONEZAWA, and Juji YOSHIMURA*

Laboratory of Organic Chemistry, Kanagawa University, Kanagawa-ku, Yokohama

**Laboratory of Chemistry for Natural Products, Tokyo Institute of Technology, Ookayama, Meguro-ku, Tokyo*

(Received August 28, 1971)

Although there have been numerous reports on the reaction of aromatic nitro and nitroso compounds with tervalent organophosphorus reagents,[1-5] little attention has been paid to that of aliphatic nitro compound.

In the course of studies on the reaction of ethyl α,β-unsaturated α-nitrocarboxylates (I),[6] we have found that the reaction of I with triethyl phosphite gave ethyl β-diethoxyphosphinyl-α,β-unsaturated-carboxylates (II) in good yield, accompanied by liberation of ethyl nitrite. Only two kinds of vinylphosphonates (IIa and IIb) have recently been prepared by nucleophilic substitution of the corresponding activated vinyl halides with triethyl phosphite as useful synthetic intermediates (Arbusov reaction).[7,8]

When a solution of I (0.1 mol) and triethyl phosphite (0.1 mol) in dry benzene (30 ml) was refluxed for about 3 hr, evolution of gaseous substance took place. Fractional distillation of the reaction mixture gave colorless oil (Table 1). The gaseous substance trapped was identified to be ethyl nitrite by gas chromatography.

The stereochemical assignments of II were made on the basis of independent preparation from vinyl halides and phosphite, and spectroscopic analysis. The vinyl hydrogen signal with J_{P-H}=23.5—28.4 Hz appearing in a lower magnetic field, and that with J_{P-H}=43.5—46.3 Hz in a higher field were assinged to *cis* and *trans*, respectively[9] (Table 2). Consequently, the composition of *cis* and *trans* isomers in II was evaluated from the intensity of the vinyl protons.

From the results it is postulated that the triethyl phosphite reacted nucleophilically to β-position of the nitrocarboxylic esters (aci-form; Ib) and cyclized to afford five membered intermediates (III), and the subsequent concerted reaction in III occurred to give II and ethyl nitrite (Scheme 1). In fact, in the case of isopropyl derivative, an unstable intermediate (bp 95—105°C/0.001 mmHg. Found: N, 4.14%. Calcd for $C_{14}H_{28}NO_7P$: N, 3.97%) was obtained under mild conditions and was decomposed to IIe and ethyl nitrite during the course of redistillation.

Table 1. Boiling points and yields of II

Compound	bp °C/mmHg	Yield(%)
IIb	118—121/2	75.2
IIc	121—123/1.5	67.2
IId	117—122/1	82.0
IIe	119—122/1.5	62.8
IIf	150—152/0.5	65.6

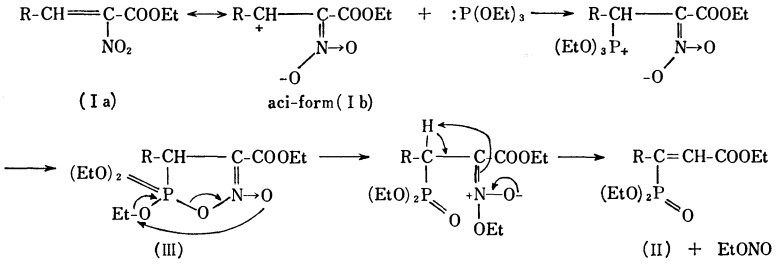

a, R=H; b, R=CH_3; c, R=C_2H_5; d, R=n-C_3H_7; e, R=i-C_3H_7; f, R=C_6H_5

(Scheme 1)

Table 2. NMR[a] and IR[b] spectra of II

Compound	α-H (τ)		β-H (τ)		J_{P-H} (Hz)		COOEt (s)[c]	C=C (w)[d]	P=O (s)	P-O-C (s)	ratio, %	
	cis	*trans*	*cis*	*trans*	*cis*	*trans*					*cis*	*trans*
IIb	3.39	3.51	3.63	3.39	24.5	44.5	1723	1634	1250	1020	70	30
IIc	3.43	3.56	3.67	4.02	25.0	46.3	1725	1630	1250	1025	60	40
IId	3.19	3.34	3.45	3.80	25.0	45.8	1727	1628	1250	1025	70	30
IIe	3.46	3.53	3.71	3.99	28.4	46.3	1722	1620	1250	1020	70	30
IIf	3.18	3.30	3.42	3.73	23.5	43.5	1730	1615	1250	1020	70	30

a; 100 Mc., in CCl_4. b; cm^{-1}, in NaCl. c; s=strong. d; w=weak.

1) J. I. G. Cadogan, *Quart. Rev.*, **22**, 222 (1968).
2) T. Kametani, T. Yamanaka, and K. Ogasawara, *Chem. Commun.* **1963**, 786.
3) P. H. Scott, C. P. Smith, E. Kober, and J. W. Churchill, *Tetrahedron Lett.*, **1970**, 1153.
4) R. J. Sundberg, B. P. Das, and R. H. Smith, *J. Amer. Chem. Soc.*, **91**, 658 (1969).
5) R. J. Sundberg, R. H. Smith, and J. E. Bloor, *ibid.*, **91**, 3392 (1969).
6) C. Shin, M. Masaki, and M. Ohta, This Bulletin, **43**, 3219 (1970).
7) G. Pattenden and B. J. Walker, *J. Chem. Soc.*, **1969**, 531.
8) V. A. Kukuhtin, Yu. Yu. Samitov, and K. M. Kirillova, *Izv. Akad. Nauk, SSSR, Ser. Khim.*, **1962** (2), 356; *Chem. Abstr.*, **67**, 21361s (1967).
9) A. M. Aguiar and D. Daigle, *J. Org. Chem.*, **30**, 2826, 3527 (1965).

Some Short-lived Isotopes of Lanthanum

Akira OHYOSHI,* Emiko OHYOSHI,** Tadaharu TAMAI,*** and Mutsuaki SHINAGAWA****

*Department of Industrial Chemistry, Faculty of Engineering, Kumamoto University, Kumamoto-shi, Kumamoto

**Department of Chemistry, Faculty of Science, Kumamoto University, Kumamoto-shi, Kumamoto

***Research Reactor Institute, Kyoto University, Kumatori-cho, Sennan-gun, Osaka

****Department of Nuclear Engineering, Faculty of Engineering, Osaka University, Suita-shi, Osaka

(Received August 30, 1971)

Because of the difficulty of the rapid isolation of lanthanum from fission product of ^{235}U, the nuclear data on short-lived isotopes of lanthanum, the existence of which has been confirmed, have not yet been reported in detail. In a previous paper,[1] it has been shown that the isolation of lanthanum, cerium, and praseodymium was carried out within 4 min by electromigration at a selected concentration of nitrilotriacetate ions. The time taken for the isolation on lanthanum alone must be much shorter since there is a greater difference in the stabilities of the NTA complexes of lanthanum and cerium as compared with those of other adjacent lanthanide pairs. This method was applied to the rapid isolation of lanthanum isotopes, and some nuclear properties were measured.

A small amount (0.1 m*l*) of 10^{-2}M uranyl nitrate, irradiated for 1 min in KUR at the temperature of dry ice, was diluted by the carrier solution (3×10^{-4}M, 0.4 m*l*) in order to detect the migrating zone of lanthanum by studying color reaction with Arsenazo(III). Using NTA (3.7×10^{-4}M, pH=2.0), the separation was carried out by applying a potential gradient of 80 V/cm for 90 sec. Although this concentration of the ligand ion is lower than the optimum one for the separation of the La-Ce pair,[2] a high mobility is more feasible for separation from other fission products. After detection by color reaction, the γ-ray spectrum of the separated zone was measured with a CAMBERA Ge(Li) detector (30 cc). Starting 4.5 min after the end of irradiation, 20-sec countings were made at 30 sec intervals and each spectrum was recorded on a magnetic tape.

The first and third γ-ray spectra are reproduced in Fig. 1, in which two prominent photopeaks, at 0.395 and 0.541 MeV, may be found to have appreciably short lives. The decay plots of these peak areas are shown in Fig. 2. The half-lives obtained from three runs are given as 40 ± 2 sec for the peak at 0.395 MeV and as 43 ± 3 sec for that at 0.541 MeV. The two other photopeaks, at 0.619 and 0.644 MeV, observed in Fig. 1 were ascribed to the 14 min ^{143}La and the 92 min ^{142}La from their decay rates. No photopeak which should be assigned to particular nuclides of any element other than lanthanum one was found in this experiment.

For short-lived isotopes of lanthanum formed by

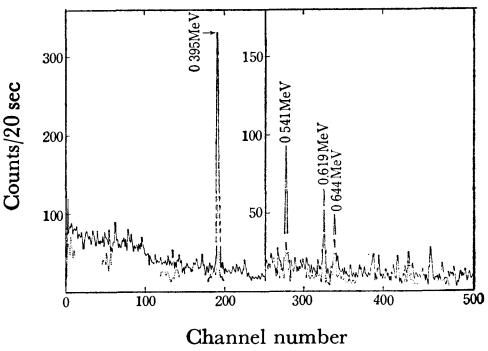

Fig. 1. γ-Ray spectra of La nuclides
—— 270 sec after the end of irradiation
------ 330 sec after the end of irradiation

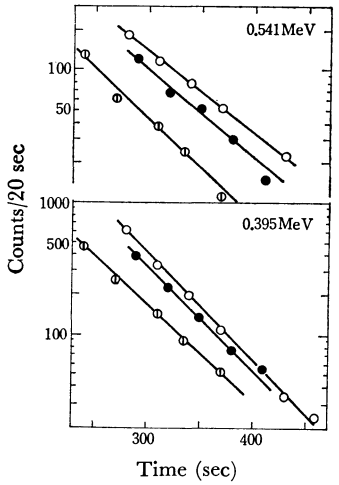

Fig. 2. Decay plots of photopeaks of La nuclide
Experiment No. 1 (○), No. 2 (●), No. 3 (◫)

fission, values of 92 min ^{142}La,[3] 14.0 min ^{143}La,[3] and 41 sec ^{144}La[4] are listed in the literature. For ^{142}La and ^{143}La, both the γ-ray energies and their abundances have been reported, but there have been no data for ^{144}La. As has been described above, a half-life of about 40 sec is given for both photopeaks at 0.395 and 0.541 MeV; therefore, we presumed that these two photopeaks could be attributed to the ^{144}La.

1) E. Ohyoshi, A. Ohyoshi, T. Tamai, and M. Shinagawa, *J. Nucl. Sci. Technol.*, **8** (No. 8), 444 (1971).

2) E. Ohyoshi, This Bulletin, **44**, 423 (1971).

3) M. A. Wakat, "Nuclear Data Tables," Academic Press, New York, Vol. 8, pp. 509, 511 (1971).

4) I. Amarel, R. Bernas, R. Foucher, J. Jastrzebski, A. Johnson, J. Teillac, and H. Gauvin, *Phys. Lett.*, **24B**, 402 (1967).

The Oxidative Coupling of Butyrophenone by Ferric Chloride

Hiroo INOUE, Mitsuya SAKATA, and Eiji IMOTO
Department of Applied Chemistry, College of Engineering, University of Osaka Prefecture, Sakai-shi, Osaka

(Received September 4, 1971)

We wish to report a novel oxidative coupling of enolizable ketone, butyrophenone (I), which takes place thermochemically and photochemically in the presence of ferric chloride, leading to the formation of the γ-diketone, 3,4-benzoylhexane (II), accompanied by chlorination in the α-position of the carbonyl group to give α-chlorobutyrophenone (III).

A solution of 0.22 g (1.34 mmol) of anhydrous ferric chloride in 5 m*l* of I was heated at 70—80°C for 48 hr. During the course of the reaction, ferric chloride was reduced to ferrous chloride in a 67% yield. The two products of II and III were isolated by gas chromatography after work-up; II (yield, 49%) exhibited NMR (CCl_4) signals at 0.7—1.3 (*m*, 6H, CH_3), 1.6—2.1 (*m*, 4H, CH_2), 4.05 and 5.55 (*q* and *t*, 2H, CH), and 6.9—8.0 (*m*, 10H, aromatic protons), and an IR (liquid film) peak at 1680 cm^{-1} (CO). Mass *m/e*; 294 (parent peak).

Found: C, 81.56; H, 7.55%. Calcd for $C_{20}H_{22}O_2$: C, 81.60; H, 7.53%.

III[1] (yield, 31%) exhibited NMR (CCl_4) signals at 1.05 (*t*, 3H, CH_3), 1.7—2.3 (*m*, 2H, CH_2), 4.75 (*t*, 1H, CH), and 7.2—7.9 (*m*, 5H, aromatic protons), and an IR (liquid film) peak at 1693 cm^{-1} (CO).

The yields of II and III, which were calculated by 200×(the number of moles of the product / that of ferric chloride), increased as the reaction time proceeded and then became constant after 3 hr. Over 3 hr, III was not converted to II. When a mixture of 0.11 g (0.58 mmol) of III and 0.063 g (0.48 mmol) of ferrous chloride in 5 m*l* of I was heated at 70°C, II was not obtained, but III was recovered unchanged. These facts indicate that the coupling reaction does not proceed *via* the process involving the reduction of III by ferrous chloride. The yield of II increased with an increase in the concentration of ferric chloride up to the saturation of ferric chloride. Furthermore, the addition of pyridine to the ferric chloride - I system resulted in a decrease in the yield of II. With the molar ratio of pyridine to ferric chloride of 1: 1, III was obtained selectively in a 64% yield.

On the other hand, a solution of 0.21 g (1.27 mmol) of ferric chloride in 5 m*l* of I, which had been placed in a quartz tube, was irradiated with a 100-W high-pressure mercury lamp at a distance of 4 cm under an atmosphere of air at room temperature for 24 hr. During the course of this reaction, white crystals of ferrous chloride precipitated (yield, 83%). The reaction products were II, III, β-chlorobutyrophenone (IV), and acetophenone, which were obtained in 26, 26, 14, and 31% yields respectively. The formation of ethylene was also confirmed by converting the ethylene to 1,2-dibromoethane. Acetophenone and ethylene were produced after the complete conversion of ferric chloride to ferrous chloride. When pyridine was added to the reaction system, with the molar ratio of pyridine to ferric chloride of 1: 1, III, IV, and crotophenone were obtained in 48, 14, and 6% yields respectively after irradiation for 24 hr.

The formation of II and III indicates that the initial step involves the oxidation of the ketone by ferric chloride, thus leading to the α-keto radical. Such a process has been found in the oxidation of ketones by either manganic or ceric ions.[2-4] The α-keto radicals couple with each other to form II or are oxidized by the ferric chloride to give α-chloroketone (III).[5] Further work is in progress and will be reported in the future.

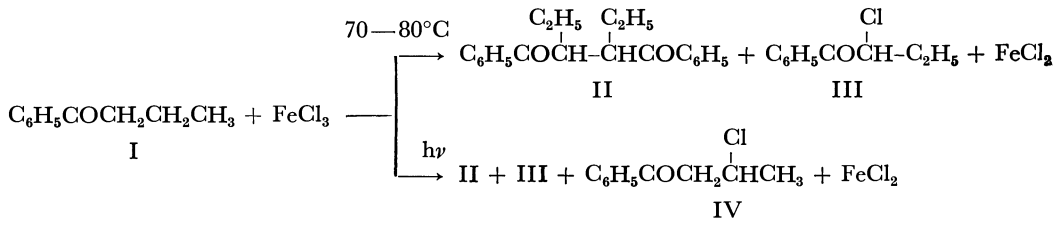

1) F. Asinger, W. Schaefer, and H. Triem, *Monatsh. Chem.*, **97** (5). 1510 (1966); *Chem. Abstr.*, **66**, 28703t(1967).
2) E. I. Heiba and R. M. Dessau, *J. Amer. Chem. Soc.*, **93**, 524 (1971).
3) R. VanHelden and E. C. Kooyman, *Rec. Trav. Chim. Pays-Bas*, **80**, 57 (1961); H. J. den Hertog, Jr., and E. C. Kooyman, *J. Catal.*, **6**, 357 (1966).
4) G. A. Russell and J. Lokensgard, *J. Amer. Chem. Soc.*, **89**, 5059 (1967).
5) J. K. Kochi and D. M. Mog, *ibid.*, **87**, 522 (1965); J. K. Kochi, *Rec. Chem. Progr.*, **27**, 207 (1966).

The Crystal Structure of $(-)_{589}$-Dinitrobis(ethylenediamine)cobalt(III) $(+)_{589}$-Bis(malonato)ethylenediaminecobaltate(III)

Keiji MATSUMOTO and Hisao KUROYA

Department of Chemistry, Faculty of Science, Osaka City University, Sumiyoshi-ku, Osaka

(Received September 10, 1971)

The CD and ORD spectra of $(+)_{589}$-[Co mal_2en]$^-$ (mal=malonate ion) were studied by Douglas and his co-workers.[1] They identified the lowest-frequency CD peak with a negative sign as the *A* component and gave it the *Δ* configuration by making use of Mason's empirical rule.[2] Recently, Judkins and Royer[3] confirmed experimentally Piper's prediction[4] that the sign of the Cotton effect is reversed as the coordination angle(θ) in the chelate ring goes from less than to greater than 90°. This was, however, not taken into account by Douglas *et al.* in applying Mason's rule to $(+)_{589}$-[Co mal_2en]$^-$. In order to reexamine directly the absolute configuration of the complex anion, we have carried out a crystal-structure analysis of $(-)_{589}$-[Co$(NO_2)_2en_2$] $(+)_{589}$-[Co mal_2en].[5,6]

The crystal structure has been determined from the three-dimensional photographic data. The structure was refined by a least-squares method to an *R* factor of 0.101 for 1442 reflections. The absolute configurations of the complex anion as well as of the cation were determined by means of the anomalous dispersion effect of the cobalt atoms for Cu$K\alpha$ radiation. Crystal data: triclinic, space group $P\bar{1}$; $a=10.58(2)$, $b=7.98(1)$, $c=7.99(1)$ Å, $\alpha=122.8(2)$, $\beta=105.3(2)$, $\gamma=74.6(2)°$; $Z=1$ ($D_m=1.81$, $D_c=1.82$ g·cm^{-3}); $\mu=35.9$ cm^{-1} for Ni$K\alpha$.

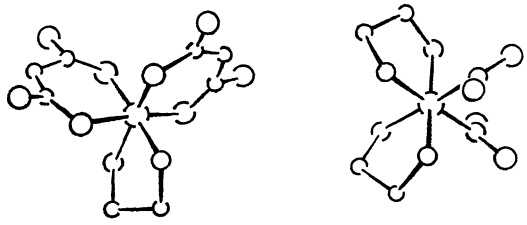

$(+)_{589}$-[Co mal_2en]$^-$ $(-)_{589}$-[Co$(NO_2)_2en_2$]$^+$

Fig. 1. The absolute configurations of the complex ions

The perspective drawings of $(-)_{589}$-[Co$(NO_2)_2en_2$]$^+$ and $(+)_{589}$-[Co mal_2en]$^-$ are presented in Fig. 1. Each of the complex ions has an approximate two-fold axis. The ethylenediamine ligands in both complexes are of the *ob*-conformation. The two six-membered malonate chelate rings are nearly planar, the O–Co–O angle being 96° and greater than the N–Co–N angle in the cobalt(III)-trimethylenediamine chelate ring.[7]

The absolute configuration of $(-)_{589}$-[Co$(NO_2)_2en_2$]$^+$ can be denoted as *Δ* in accordance with the assignment made by those investigating ORD[8] and CD.[2,9,10] It is notable that an empirical rule connecting the absolute configuration of a metal complex and the sign of the Cotton effect of the $^1A_1 \rightarrow A$ electronic transition holds for this complex.

The absolute configuration of $(+)_{589}$-[Co mal_2en]$^-$ has been determined as of *Δ* and is in agreement with the assignment made by Douglas *et al.* Their assignment of the *A* component seems to be correct. However, if Piper's prediction still holds in the case of the trismalonatocobalt(III) complex, the E_a component of $\Delta(+)_{589}$-[Co ox_3]$^{3+}$($\theta<90°$) and that of *Δ* trismalonatocobalt(III) ($\theta>90°$, possibly) will be opposite in sign. The *A* component of the bismalonatocobalt(III) complex derives mainly from the E_a component of the trismalonatocobalt(III) complex.[2] Consequently, the sign of the *A* component of $\Delta(+)_{589}$-[Co mal_2en]$^-$ should be the reverse of that of the E_a component of $\Delta(+)_{589}$-[Co ox_3]$^{3-}$, though these two complexes have the same configuration. Therefore, the assignment of the *A* component by Douglas *et al.* is not entirely satisfactory.

1) B. E. Douglas, R. A. Haines, and J. G. Brushmiller, *Inorg. Chem.*, **2**, 1194 (1963).
2) A. J. McCaffery, S. F. Mason, and B. J. Norman, *J. Chem. Soc.*, **1965**, 5094.
3) R. R. Judkins and D. J. Royer, *Inorg. Nucl. Chem. Lett.*, **6**, 305 (1970).
4) T. S. Piper and A. Karipides, *Mol. Phys.*, **5**, 475 (1962).
5) F. P. Dwyer, I. K. Reid, and F. L. Garvan, *J. Amer. Chem. Soc.*, **83**, 1285 (1961).
6) Recently, the *Δ* configuration of $(+)_{589}$-[Co mal_2en]$^-$ has been worked out for Na$(+)_{546}$-[Co mal_2en]·$2H_2O$ by K. R. Butler and M. R. Show [*Chem. Commun.*, **1971**, 550]. However, we became aware of it after we had submitted the present paper to the Chemical Society of Japan.
7) Y. Saito, T. Nomura, and F. Marumo, This Bulletin, **41**, 530 (1968).
8) T. E. McDermott and A. M. Sargeson, *Aust. J. Chem.*, **16**, 334 (1963).
9) R. D. Gillard and G. Wilkinson, *J. Chem. Soc.*, **1964**, 1368.
10) G. A. Barclay, E. Goldschmied, N. E. Stephenson, and A. M. Sargeson, *Chem. Commun.*, **1966**, 540.

Note on the Formation Constant of the Mono(ethylenediamine)-chromium(III) Complex

Jannik BJERRUM and Ole MØNSTED

Chemistry Department I, Inorganic Chemistry, H. C. Ørsted Institute, University of Copenhagen, Copenhagen, Denmark

(Received September 6, 1971)

In a paper in this journal, Tsuchiya and his co-workers[1] have given values for the 1st formation constant in the chromium(III)-ethylenediamine system. Their procedure was as follows: Aqueous solutions of tris(ethylenediamine)chromium(III) perchlorate to which an excess amount of perchloric acid had been added, were maintained at 25°C for one or two months. On the assumption that equilibrium was established, the solutions containing mono(ethylenediamine) and hexa-aqua ions were then analyzed spectrophotometrically. In this way values of the 1st formation constant were found to be about $10^{16.5}$. As this value in our opinion is much too high, we suspected that the solutions examined by Tsuchiya and his co-workers had not been in equilibrium, and we have, therefore, made similar measurements but at a higher temperature in order to reach equilibrium more rapidly. A solution with the following total concentrations of $[Co\ en_3](ClO_4)_3$ 0.0085M and $HClO_4$ 0.072M was placed in a thermostat at 50°C, and the advancing hydrolysis was followed spectrophotometrically. In our experiment the spectrum changed relatively little over a long period of time in the "equilibrium" range of Tsuchiya and his co-workers, but after the lapse of about three months the spectrum was indistinguishable from that of a solution of the hexa-aquachromium(III) ion. The same was the case with a 0.0096M solution of $Cr(H_2O)_6(ClO_4)_3$, 0.032M in $enH_2(ClO_4)_2$ and 0.022M in $HClO_4$. These results are also consistent with a kinetic study by Garner and his co-workers[2] which implies that the systems studied by Ohta, Matsukawa, and Tsuchiya were not at equilibrium, and that their "equilibrium constants" are not accurate. According to our findings the amount of mono(ethylenediamine) complex not hydrolyzed must be less than one percent of the total chromium. The hydrogen ion concentration in the aquated solution is 0.020M, that of enH_2^+ 0.026M, and by introducing the acid dissociation constants of the last-mentioned ion at 50°C $K_{A,1} \times K_{A,2} = 10^{16.06}$ [3] a simple calculation shows that the 1st formation constant in the chromium(III) ethylenediamine system must be smaller than $\sim 10^{12}$. This value is more than 10^4 times smaller than the value $\sim 10^{16.5}$ given by Ohta, Matsukawa, and Tsuchiya.[1] Tsuchiya and his co-workers[4] have published formation constants for many other chromium(III) complexes but have not made sure that equilibrium is reached by approaching it from both sides. A critical revision of their data therefore seems necessary.

1) M. Ohta, H. Matsukawa, and R. Tsuchiya, This Bulletin, **37**, 692 (1964).

2) R. F. Childers, Jr., K. G. Van der Zyl, Jr., D. A. House, R. G. Hughes, and C. S. Garner, *Inorg. Chem.*, **7**, 749 (1968).

3) F. A. Cotton and F. E. Harris, *J. Phys. Chem.*, **69**, 1203 (1955).

4) This Bulletin, **38**, 1059, 1235 (1965); **39**, 1589 (1966); **41**, 2416 (1968).

Hydrogen-Deuterium Exchange in the Methyl Group of Four Bisdimethylglyoximatocobalt(III) Complexes

Hayami YONEDA,* Ichiro TAKAGI,* and Yukiyoshi MORIMOTO**

*Department of Chemistry, Wakayama University, Masagocho, Wakayama

**Research Laboratories, Fujisawa Pharmaceutical Company, Kashimacho, Higashiyodogawa-ku, Osaka

(Received September 11, 1971)

Organic ligands in chelate compounds are under the influence of the electron-withdrawing effect of a central metal ion, and as a result, proton dissociation from the ligands is more or less facilitated. Thus, hydrogen-deuterium exchange is to be observed in some complexes, when they are dissolved in deuterium oxide. We noticed this kind of exchange from the fact that the intensity of the PMR signal of methylene in malonato chelates dissolved in deuterium oxide decreased with time.[1] Thus, the NMR technique proved to be useful for the study of proton exchange reactions. Several other examples have been found, *i.e.* in the methylene of the glycinatocobalt(III) complex,[2] in the methylene of the palladium Schiff base complex of glycine and pyruvic acid,[3] in the methyl of the acetylacetoneethylenediiminecobalt(III) complex[4] and in the ethylene of the EDTA-cobalt(III) complex.[5]

We would like to report a similar hydrogen-deuterium exchange in the methyl group of a series of bisdimethylglyoximatocobalt(III) complexes of the formula $[CoX_2(dgH)_2]^{+or-}$ in which X is CN^-, NO_2^-, NH_3, or CH_3NH_2. It should be noticed that the exchange rate is dependent on the kind of the axial ligand X.

Figure 1 shows the time change of the PMR spectrum of $[Co(CH_3NH_2)_2(dgH)_2]Cl$ in 2% NaOD deuterium oxide solution at 20°C. The methyl signal of the dimethylglyoximato ligand lies in the middle of the spectrum and shows the intensity decrease and line-broadening with time (Fig. 1, (1), (2), and (3)). This is clearly due to the hydrogen-deuterium exchange

$$-CH_3 \longrightarrow -CH_2D \longrightarrow -CHD_2 \longrightarrow -CD_3$$

The line-broadening is due to the spin-spin coupling between H and D in the intermediates CH_2D and CHD_2.

Thus, the exchange reaction can be followed as the intensity decrease of the methyl signal of the coordinated ligand. The result obtained for the four complexes is shown in Fig. 2. We see that the exchange rate for the free ligand is negligibly small, compared with that of any one of the four complexes tested, and we can conclude that the activation of ligand protons is induced by chelation. It should be pointed out that the exchange in the cyano complex goes very slowly while the exchange in the methylamine complex proceeds fairly fast. Thus, the exchange rate is in the order $CH_3NH_2 > NH_3 > NO_2^- > CN^-$. The half-value periods for these complexes are 7.5 hr for the methylamine, 11 hr for the ammonia, 200 hr for the cyano complexes and more than 1000 hr for the free ligand. The half-value period for the nitro complex lies between those of the ammonia and cyano complexes, but decomposition of the complex prevented determination of the exact value. This exchange rate order is just the reverse of the order of positions of these ligand X in the spectrochemical series. This trend can be interpreted in the following way. Since the activation of ligand protons is induced by the electron-withdrawing effect of a central metal ion, the less positive the effective charge of the metal ion, the smaller the exchange rate of the ligand protons. The smallest exchange rate for the cyano complex is the reflection of the almost complete neutralization of the positive charge of the central metal ion which is caused by the strong coordination of the cyano groups.

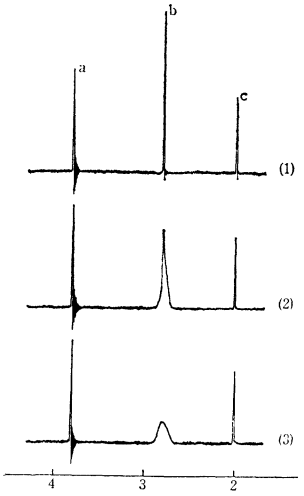

(1) immediately after dissolution
(2) after 2 hr
(3) after 10 hr
a methyl signal of methanol (standard)
b methyl signal of the coordinated dgH^-
c methyl signal of the coordinated methylamine.

Fig. 1. The PMR spectra of $[Co(CH_3NH_2)_2(dgH)_2]Cl$ in 2% NaOD-D_2O solution, measured at 20°C.

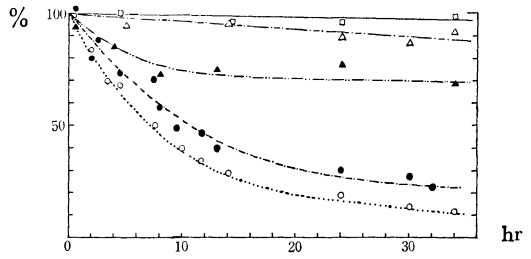

Fig. 2. Plots of the methyl signal intensity of the dimethylglyoximato ligand against time.

dgH^- □, ————
$Na[Co(CN)_2(dgH)_2]$ △, —·—·—·—
$Na[Co(NO_2)_2(dgH)_2]$ ▲, —··—··—··—
$[Co(NH_3)_2(dgH)_2]Cl$ ●, —·—·—·—
$[Co(CH_3NH_2)_2(dgH)_2]Cl$ ○, ----------

1) H. Yoneda and Y. Morimoto, This Bulletin, **40**, 1737 (1967); *Inorg. Chim. Acta*, **1**, 413 (1967).
2) unpublished.
3) H. Yoneda, Y. Morimoto, Y. Nakao, and A. Nakahara, This Bulletin, **41**, 255 (1968).
4) H. Yoneda and Y. Morimoto, *ibid.*, **41**, 2544 (1968).
5) H. Yoneda and Y. Morimoto, *ibid.*, **42**, 1160 (1969).

Syntheses of 3,4-Dideoxy-3-enosides and the Corresponding 3,4-Dideoxy Sugars

Sumio UMEZAWA, Tsutomu TSUCHIYA, and Yasushi OKAZAKI

Department of Applied Chemistry, Faculty of Engineering, Keio University, Koganei-shi, Tokyo

(Received September 16, 1971)

From a biological point of view studies on unsaturated sugars have been drawing attention in recent years, but the introduction of 3,4-unsaturated linkages into sugars is rarely reported. Recently, we described the synthesis of 3′,4′-dideoxykanamycin B,[1] which is active against drug-resistant bacteria, by utilizing a 3,4-unsaturated intermediate. The present work was undertaken to see if a practical method could be worked out for converting aminoglycosidic antibiotics into their unsaturated and dehydroxylated derivatives.

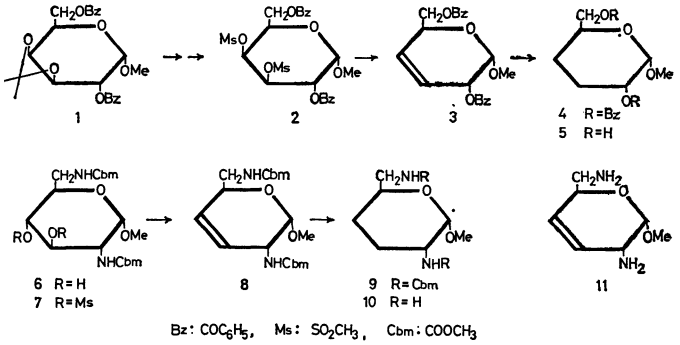

Here we described the syntheses of methyl 3,4-dideoxy-α-D-*erythro*-hexopyranoside (**5**) and methyl 2,6-diamino-2,3,4,6-tetradeoxy-α-D-*erythro*-hexopyranoside (**10**). The syntheses were achieved by way of the corresponding 3,4-unsaturated intermediates. Methyl 3,4-*O*-isopropylidene-α-D-galactopyranoside prepared from methyl α-D-galactopyranoside was benzoylated to give **1**. Removal of the isopropylidene group followed by mesylation gave the corresponding di-*O*-mesyl derivative (**2**). When **2** was treated with sodium iodide and zinc dust in DMF at 130°C for 1.5 hr according to the procedure of Tipson and Cohen[2] and Horton *et al.*,[3] a 3,4-unsaturated derivative, namely, methyl 2,6-di-*O*-benzoyl-3,4-dideoxy-α-D-*erythro*-hex-3-enopyranoside (**3**) was obtained in a yield of 93%, syrup, $[\alpha]_D^{22}$ −17.3° (*c* 1, $CHCl_3$); NMR (in $CDCl_3$): τ 4.05 (2-proton slightly broadened singlet, H-3,4), $J_{1,2}$ 4 Hz, $J_{2,(3,4)} = J_{(3,4),5}$ ~0 Hz. Catalytic hydrogenation of **3** gave methyl 2,6-di-*O*-benzoyl-3,4-dideoxy-α-D-*erythro*-hexopyranoside (**4**), mp 70—71°C, $[\alpha]_D^{22}$ +56.7° (*c* 1, $CHCl_3$). Removal of the protecting groups of **4** gave methyl 3,4-dideoxy-α-D-*erythro*-hexopyranoside (**5**), syrup, $[\alpha]_D^{22}$ +126° (*c* 1.1, water); NMR (in D_2O): τ 5.28 (1-proton doublet, $J_{1,2}$ 3.5 Hz, H-1), τ 7.9—8.6 (4-proton multiplet, H-3,3,4,4).

Methyl 2,6-dideoxy-2,6-dimethoxycarbonylamido-α-D-glucopyranoside (**6**), mp 175—177°C, $[\alpha]_D^{21}$ +108° (*c* 0.7, water) prepared from neamine was mesylated to give the corresponding di-*O*-mesyl derivative (**7**), mp 193—195°C, $[\alpha]_D^{23}$ +94° (*c* 1.5, $CHCl_3$); NMR (in $CDCl_3$): τ 6.77 and 6.90 (each 3-proton singlet, SO_2CH_3). 3,4-Unsaturation was performed likewise in a yield of 90% to give a 3-eno derivative (**8**), mp 157—158°C, $[\alpha]_D^{20}$ −35° (*c* 0.7, methanol); NMR (in $CDCl_3$): τ 4.29 (2-proton slightly broadened singlet, H-3,4), $J_{1,2}$ 4.2 Hz, $J_{2,(3,4)} = J_{(3,4),5}$ ~0 Hz, $J_{2,5}$ ~4 Hz. Catalytic hydrogenation of **8** gave the corresponding tetradeoxy derivative (**9**), syrup, $[\alpha]_D^{19}$ +126° (*c* 0.7, methanol). Removal of the protecting groups of **9** gave methyl 2,6-diamino-2,3,4,6-tetradeoxy-α-D-*erythro*-hexopyranoside (**10**) as needles of monosulfate, mp>180°C, $[\alpha]_D^{22}$ +128° (*c* 1, water). Removal of the protecting groups of **8** gave methyl 2,6-diamino-2,3,4,6-tetradeoxy-α-D-*erythro*-hex-3-enopyranoside (**11**) as needles of monosulfate hemihydrate, mp>180°C, $[\alpha]_D^{22}$ +26° (*c* 1, water); NMR (in D_2O): τ 3.95 (2-proton slightly broadened singlet, H-3,4).

1) H. Umezawa, S. Umezawa, T. Tsuchiya, and Y. Okazaki, *J. Antibiotics*, **24**, 485 (1971).
2) R. Tipson and A. Cohen, *Carbohyd. Res.*, **1**, 338 (1965).
3) E. Albano, D. Horton, and T. Tsuchiya, *ibid.*, **2**, 349 (1966)

The Photoreduction of Polyacenes by Tri-*n*-Butyl Stannane

Itsuo FUJIHARA, Masao OKUSHIMA, Satoshi HIRAYAMA, Shigeru KUSUHARA, and Jiro OSUGI

Department of Chemistry, Faculty of Science, Kyoto University, Sakyo-ku, Kyoto

(Received September 23, 1971)

There have been previous reports on the photoreduction of anthracene derivatives[1] and some polyacenes[2,3] by tri-*n*-butyl stannane. This reaction gives one of the few examples of hydrogen-atom abstraction in a pure π-π^* excited state. Preliminary experiments have shown that the lowest triplet state is susceptible to photoreduction. It is interesting to investigate the mechanism of this reaction and the reactivity of polyacene. Fortunately, the flash-photolysis method gives direct information on the reactivity of the lowest triplet state toward photoreduction. In this communication, we wish to report that some polyacenes were photoreduced in the presence of stannane and that the rate constants of hydrogen abstraction reactions *via* the lowest triplet state were determined by this method.

Prior to kinetical experiments, we investigated the photochemical behavior of deaerated *n*-hexane solutions of polyacenes in the presence of stannane. The samples degassed by repeating a freeze-pump-thaw cycle six times in the dark were irradiated for a series of known time intervals, and the spectral changes were recorded with a Shimadzu SV-50A spectrophotometer for each interval. The results will now be presented. Phenanthrene, naphthacene, 1,2-benzanthracene and chrysene containing stannane were found to lose their characteristic absorption bands in the ultraviolet and the visible regions. For phenanthrene and naphthacene, new bands, which seemed to be assignable to 9,10-dihydrophenanthrene and 5,12-dihydronaphthacene respectively, appeared in the ultraviolet region. However, we haven't yet identified the photochemical products of 1,2-benzanthracene and chrysene. Under the same conditions, though, Brimage and Davidson[3] have recently reported that phenanthrene and 1,2-benzanthracene gave 9,10-dihydrophenanthrene and 7,12-dihydro-1,2-benzanthracene respectively; therefore, we consider that chrysene will be similarly photoreduced to the corresponding dihydro-product.

The flash photolytic experiments were done in deoxygenated benzene solutions of polyacenes containing various concentrations of stannane at room temperature. The decay curves of the lowest triplets after the flash were obtained by observing the transmittance changes at the triplet-triplet-absorption maximum wave lengths: 481 mμ (phenanthrene), 460 mμ (naphthacene), 492 mμ (1,2-benzanthracene), and 570 mμ (chrysene).[4] The apparent rate constants, k, calculated from these curves disregarding the triplet-triplet annihilation, may be related to the photoreduction rate constants, k_r, as follows:

$$k = k_d + k_r[Q]$$

where k_d is the decay constant in the absence of stannane and where $[Q]$ is the concentration of stannane. By plotting k *versus* $[Q]$, the relationship between k and $[Q]$ was found to be almost linear, and from the slopes, we obtained the photoreduction rate constants, $k_r = 1.8\times10^5\,\mathrm{M^{-1}sec^{-1}}$ for phenanthrene (10^{-3}M), $k_r \leqq 10^4\,\mathrm{M^{-1}.sec^{-1}}$ for naphthacene (4×10^{-5}M), $k_r = 1.5\times10^4\,\mathrm{M^{-1}sec^{-1}}$ for 1,2-benzanthracene (10^{-4}M), and $k_r = 1.5\times10^5\,\mathrm{M^{-1}.sec^{-1}}$ for chrysene (10^{-4}M).

On the other hand, Brimage and Davidson[3] obtained $k_r = 4.7\times10^5\,\mathrm{M^{-1}sec^{-1}}$ for phenanthrene and $k_r = 1.8\times10^5\,\mathrm{M^{-1}sec^{-1}}$ for 1,2-benzanthracene using steady illumination; we also got $k_r = 7.1\times10^4\,\mathrm{M^{-1}sec^{-1}}$ for naphthacene and $k_r = 9.4\times10^4\,\mathrm{M^{-1}sec^{-1}}$ for 1,2-benzanthracene by their method.

In comparison with these results, the values obtained by the flash-photolysis method were smaller than those obtained by the steady-state method in any compound. The reason for this is not obvious, but this is a very interesting fact. Particularly, there is a noticeable discrepancy between the values obtained by the two methods for naphthacene. This may suggest that there exists another excited state (or states) which is more reactive than the lowest triplet state. More investigations of the other compounds will offer clear information on the reactive excited states of cata-condensed aromatic hydrocarbons.

1) J. Osugi, S. Kusuhara, and S. Hirayama, *Rev. Phys. Chem. Jap.*, **37**, 94 (1967).

2) J. Osugi, S. Kusuhara, and S. Hirayama, Preprints for the Symposium of Photochemistry, Japan (October, 1968), No. 25.

3) D. R. G. Brimage and R. S. Davidson, *Chem. Commun.*, **1971**, 281.

4) G. Porter and M. W. Windsor, *Proc. Roy. Soc., Ser. A*, **245**, 238 (1958).

Effects of Fluoroborates on the Visible Absorption Spectra of Lanthanum(III)-Alizarin Complexon Chelate[1]

Yoshiki Moriguchi, Tsuneko Kuwabara, and Iwao Hosokawa
Department of Chemistry, Fukuoka University of Education, Munakata-machi, Munakata-gun, Fukuoka
(Received September 27, 1971)

Recently, lanthanum(III) and cerium(III) chelates of alizarin complexon (ALC, 1,2-dihydroxyanthraquinone-3-yl-methylamine-*N*,*N*'-diacetic acid) have been widely utilized as a colorimetric reagent in trace analysis of fluorine since reported by Belcher *et al.*[2] The effectiveness and interesting behavior of the chelates have been described.[3] However, it has been reported that some anions and cations interfere with the determination of fluorine in the ALC method.[4]

We wish to report that, in the presence of potassium tetrafluoroborate (KBF_4) and one of its hydrolysis products, potassium monohydroxytrifluoroborate (KBF_3OH), the visible absorption spectrum of ALC-La chelate changes to that of ALC and this effect is especially remarkable in the presence of KBF_3OH.

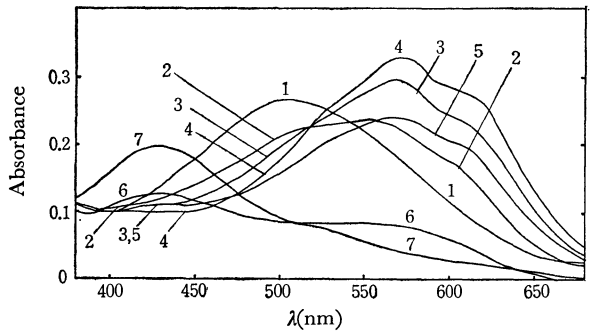

Fig. 1. Effect of KBF_4 on spectrum of ALC-La(III) chelate in acetic acid-sodium acetate buffer (pH 4.65) at 25°C.
1: 5×10^{-5}M ALC-La(allowed to stand for 90 min after adding ALC to $La(NO_3)_3$), 7: 5×10^{-5}M ALC. After adding 5×10^{-3}M KBF_4 to 1, 2: 1 min, 3: 5 min, 4: 11 hr, 5: 5 days, 6: 10 days.

As is shown in Fig. 1, in the presence of 100: 1 molar ratio of KBF_4 to ALC-La chelate, a peak of ALC-La chelate at 505 nm shifts to 572 nm and its spectrum nearly fits that of ALC-La-F ternary complex after 5 min. The spectrum gradually changes and a new peak corresponding to that of ALC appears at 428 nm after 10 days. The changes are accelerated with the rise of reaction temperature and KBF_4 concentration. Thus it is assumed that the effective species on these spectrum changes is not BF_4^- but one or more species of its hydrolysis products as described by the following equations.

$$BF_4^- + OH^- \rightleftharpoons BF_3OH^- + F^- \quad (1)$$

$$BF_3OH^- + OH^- \rightleftharpoons BF_2(OH)_2^- + F^- \quad (2)$$

$$BF_2(OH)_2^- + OH^- \rightleftharpoons BF(OH)_3^- + F^- \quad (3)$$

$$BF(OH)_3^- \rightleftharpoons B(OH)_3 + F^- \quad (4)$$

This is also supported by the results in Fig. 2. KBF_3OH is clearly more effective than KBF_4, that is, its spectrum quickly changes to that of ALC-La-F ternary complex at 20: 1 molar ratio of KBF_3OH to ALC-La chelate, and almost becomes that of ALC after 18.5 hr. The effect of KBF_3OH is also remarkable at 10: 1 molar ratio. It occurs in 40% acetone-water mixed solvent as well as aqueous solution.

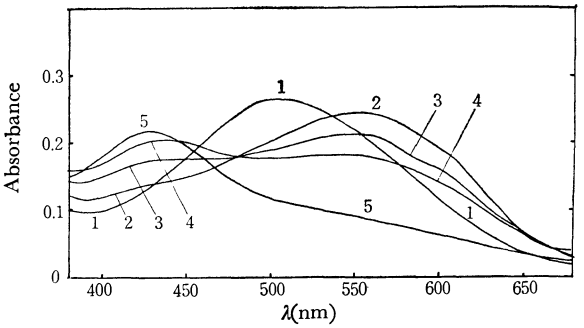

Fig. 2. Effect of KBF_3OH on spectrum of ALC-La(III) chelate in acetic acid-sodium acetate buffer (pH 4.65) at 25°C.
1: 5×10^{-5}M ALC-La(allowed to stand for 90 min after adding ALC to $La(NO_3)_3$). After adding 1.0×10^{-3}M KBF_3OH to 1, 2: 2 min, 3: 6 min, 4: 30 min, 5: 18.5 hr.

Thus we presume that the coexistence of boron has a considerable influence on the ALC method, and dissolved species of fluorine in the presence of boron and its behavior to ALC-La chelate become very important. In a previous paper,[5] we reported that the dissolved state of fluorine in sodium fluoride-boric acid-water system depended on the pH of the solution. The colorimetric determination of fluorine in the ALC method is usually carried out in the pH region 4.5—5. A considerable extent of fluorine in the sample solution is assumed to exist in fluoroborate forms in this region as described in Eqs. (1)—(3), unless boron is previously removed from the sample solution. Thus it seems that fluoroborates interfere with the formation of ALC-La-F ternary complex and are the cause of error in the determination of fluorine.

1) Presented at 23rd Symposium of Analytical Chemistry, Tokushima, 5, June, 1971.
2) R. Belcher, M. A. Leonard, and T. S. West, *J. Chem. Soc.*, **1958**, 2390.
3) For example, I. Hosokawa, *Bunseki Kagaku*, **16**, 1259 (1967).
4) S. S. Yamamura, M. A. Wafe, and J. H. Sikes, *Anal. Chem.*, **34**, 1308 (1962).
5) Y. Moriguchi and I. Hosokawa, *Nippon Kagaku Zasshi*, **92**, 56 (1971).